Can. J. Chem. Downloaded from www.nrcresearchpress.com by 210.87.254.42 on 09/05/12
For personal use only.

Canadian Journal of Chemistry

Published by THE NATIONAL RESEARCH COUNCIL OF CANADA

VOLUME 49 JANUARY 1, 1971 NUMBER 1

Reactions of Alkyl Halides in Fused Salt Media[1]

R. A. BAILEY AND S. F. PREST

Department of Chemistry, Rensselaer Polytechnic Institute, Troy, New York 12181

Received July 13, 1970

Passage of C_1 to C_5 haloalkanes through $SnCl_2$–KCl melts results in halide exchange reactions, alkene formation, and rearrangement (including cyclization) reactions of the organic molecules. Relative reactivities, product distributions and melt composition effects are consistent with a carbonium ion mechanism in which the melt functions as a halide ion acceptor. Some control of product distribution by choice of Lewis acid character of the melt seems possible.

Canadian Journal of Chemistry, **49**, 1 (1971)

While the physical properties of fused salts have been the subject of extensive investigations, reaction chemistry in such media has been studied much less systematically. However, a variety of reactions have been reported, including a number involving substitution, elimination, and other reactions of organic molecules; many of the known examples have been reviewed by Sundermeyer (1). These include halide and pseudohalide exchange, halogenation, and elimination reactions. For the most part they involve small aliphatic or aromatic systems. While some work has involved simple ionic salts such as the alkali halides, most reactions of this type have used low melting systems composed of salts employed as catalysts in more classical reactions, *e.g.* $AlCl_3$–alkali chloride melts and similar systems below 200 °C. These have established the catalytic action of such melts, although the behavior of the molten salt in other systems is not so evident. Generally, little has been done to establish the role of the molten salt in the overall mechanism, or the effect of varying reaction parameters (temperature, melt composition, etc.).

This report considers the reactions of several alkyl halides (C_1 to C_5) in molten KCl–$SnCl_2$ mixtures. Substitution, elimination, and rearrangement reactions were observed, and some beginnings can be made to understand the basic mechanism of the reactions.

Experimental

The reaction system consisted of a vertical cylindrical tube 30 mm in diameter with a fritted Pyrex disc (normally fine porosity) some distance from the lower end. This was enclosed in a cylindrical furnace and the temperature maintained at the desired value by means of an electronic controller. Fisher $SnCl_2.2H_2O$ was dehydrated with acetic anhydride (2), mixed with dry Baker Analyzed KCl, and placed above the frit in the reaction tube. Final purification was effected by passing HCl gas through the salt as the temperature was raised to the desired value. This was followed by a lengthy flush with dry N_2. The organic reactant was added to a flask attached to the lower end of the reaction system, and distilled through the melt aided by a slightly reduced pressure at the exit side. When a constant flow rate had been attained, samples were collected at the exit in liquid nitrogen traps and analyzed by gas chromatography. Care was taken to preheat the reactant vapors to the melt temperature, and to heat the exist system before the traps to prevent product condensation. Proton magnetic resonance and infrared spectroscopy were used when necessary to aid in product identification.

In comparing results, a number of factors must be considered. The melt height was fixed by weight of salt and tube diameter, and was 4.4 cm for the results reported here. The average size of the bubbles passing through the melt was reasonably reproducible for a frit of given porosity, but varied with flow rate. Photographs permitted the average bubble diameter to be estimated as a function of flow rate, and from this and the flow rate the number of collisions of a gas molecule with the melt could be estimated. This was greater at low flow rates, but was of the order of 10^4. It varied somewhat with the reactants, as did the height of froth above the melt during a reaction

[1]Presented in part at the 52nd Conference of the Chemical Institute of Canada, Montreal, May, 1969. Financial support from the National Science Foundation is gratefully acknowledged.

TABLE 1. Reaction products of haloalkanes in 62 mole% $SnCl_2$–KCl at 280 °C

Reactant	Flow rate × 10^2 (mM s^{-1})	Product yield (%) 1-Chloroalkane	2-Chloroalkane	Alkene	Overall
Bromoethane	2	32	—	~4	36
	6	20	—	~2	22
1-Bromopropane	2	17	~2	10	29
	7	7	~1	5	13
1-Chloropropane	2	—	<1	6	<7
1-Iodopropane	2	27	~3	23	53
	7	15	~3	13	31
2-Bromopropane	2	—	68	30	98
	10	—	50	25	75
2-Chloropropane	2	—	—	22	22
1-Bromobutane	2	15	~2	10	27
	7	6	<2	5	<13
1-Chlorobutane	2	—	<1	6	<7
1-Iodobutane	2	15	~4	12	31
	5	12	~1	8*	21
2-Bromobutane	2	—	40	55	95
	8	—	50	40	90
2-Chlorobutane	2	—	—	35	35
1-Bromopentane	2	7	<1	6†	<14

*1-Butene with small amount of 2-butene.
†5% 1-pentene; 1% 2-pentene.

in which a significant amount of the overall process could occur. Therefore, the significance of the following data lies in the relative values and trends rather than in the absolute yield values. While a few reactions approached 100% under these conditions, in general we attempted to operate so as to have only partial reaction so that effects could be detected. Results by no means imply the maximum yield of any product. While a few compounds showed gross decomposition in the melt as evidenced by charring, most recoveries were close to 100%.

The data given in the accompanying Figures and Tables are averaged; variation of the moderate or high yields of ±5% from the results given are typical for runs made under apparently identical conditions. This reflects primarily variation in bubble size. Certain systems showing apparent surface activity of the reactant as indicated by considerable frothing are more erratic.

Results and Discussion

As discussed above, contact times and hence the extent of reaction depend upon flow rate, such that reactivities usually increase with decreasing flow rate. There are occasional exceptions to this, when the yield of one product decreases as a consequence of competition from another; overall reactivities invariably increase as expected. An indication of the magnitude of the flow rate effect is included in the following tables of data.

TABLE 2. Product yields of bromomethanes in 62 mole% $SnCl_2$–KCl, at 280 °C; flow rate, 2 × 10^{-2} mM s^{-1}

Reactant	Products			
$CHBr_3$	$CHBr_2Cl$ 5%	$CHBrCl_2$ 17%	$CHCl_3$ 50%	Overall 72%
CH_2Br_2	CH_2BrCl 10%	CH_2Cl_2 70%	—	80%
CH_2BrCl	CH_2Cl_2 72%			

Substitution and Reactivity Patterns

The relative reactivities of the various compounds studied can be observed from Tables 1–3. Studies on benzyl and allyl bromides were not fully successful due to considerable decomposition and quantitative data are not given, but results indicated the reactivity in the 62 mole% $SnCl_2$–KCl eutectic to be benzyl > allyl > alkyl > aryl (bromobenzene gave essentially no reaction). Within the bromobutanes, the reaction order is tertiary > secondary > iso > primary. These reaction patterns are generally observed with carbonium ion or S_N1 mechanisms (3, 4). The formation of 1-chloroalkanes from the bromo compounds is in the order ethyl > propyl >

Can. J. Chem. Downloaded from www.nrcresearchpress.com by 210.87.254.42 on 09/05/12
For personal use only.

TABLE 3. Product yields from halo-methylpropanes; 62 mole% $SnCl_2$–KCl, at 280 °C; flow rate, 2×10^{-2} mM s^{-1}

Reactant	Products				
	2-Chloro-2-methylpropane	1-Chloro-2-methylpropane	2-Methylpropene	Methyl-cyclopropane	Overall
1-Bromo-2-methylpropane	22%	3%	10%	5%	40%
1-Chloro-2-methylpropane	7%	—	10%	<1%	17%
2-Chloro-2-methylpropane	—	<1%	30%	<1%	30%

butyl > pentyl. This is similar to the order of reactivity in the substitution of thiocyanate and cyanate for chloride in methyl, ethyl, and 1-propyl chloride using melts reported by Packham and Rackley (5), although this may be a very different situation as is indicated by the level of reactivity of benzyl bromide. At a flow rate of 2×10^{-2} mM/s, the ratios of chloride compound formation are 1.9 : 1.1 : 1.0 : 0.5 for bromoethane, 1-bromopropane, 1-bromobutane, and 1-bromopentane, respectively. As a comparison to reactions in more classical media, solvolysis rates in dioxane at 40 °C for the same compounds (6) are in the rather similar ratios 2.2 : 1.2 : 1.0 : 0.9.

The overall reactions of the halopropanes and -butanes follow the order I > Br > Cl. In both the propanes and butanes, product ratios for the substitution, elimination, and rearrangement products were similar for the bromo- and iodo compounds of each series, implying the possibility of a common intermediate. Considerably less rearranged product is formed from the 1-chloro compounds here than in the 1-bromo or 1-iodo systems. This may be explained, since both 2-chlorobutane and 2-chloropropane are more reactive than the 1-chloro compounds, resulting in their being reacted as formed from the latter. As they are less reactive than the parent bromides and iodides, however, they form in proportionately greater yields in these cases.

The completely chlorinated methanes are seen to be the predominant products from the reactions of di- and tri-bromomethane at all flow rates studied (Table 2). The order of reactivity of the individual compounds is $CHBrCl_2$ > $CHBr_2Cl$ > $CHBr_3$. In addition, bromochloromethane is somewhat more reactive than dibromomethane, although an apparent surface active behavior of the latter in the melt makes comparison difficult. Hine and co-workers found that the intermediates of a number of S_N1 solvolysis reactions of halomethanes were stabilized more by chloride than bromide substituents, and thus the reactions were enhanced as observed here (3, 7, 8). All of the above reaction patterns are consistent with a carbonium ion intermediate in the melt or at the melt–vapor interface.

Rearrangement Products

Most primary halides considered here gave some rearranged products (Tables 1 and 3); indeed, 1-bromo-2-methylpropane gave 5–10 times as much rearrangement product, 2-chloro-2-methylpropane, as the expected 1-chloro compound. Rearrangement of secondary halides to primary was slight. Such observations may be explained by the known stabilities of carbonium ions, which are tertiary > secondary > primary. This is indicated both from kinetic data and mass spectrometric formation energies (9). Hence, there would be a net loss in energy for a rearrangement such as

$$CH_3CH_2CH_2^+ \rightarrow (CH_3)_2CH^+$$

This would be even greater in the 1-bromo-2-methylpropane example. Thus, the observed rearrangements would not be surprising if the cation has a sufficient life-time in the melt.

Melt Effects

Variation of melt composition has an appreciable effect on reaction as shown in Table 4, particularly when melts rich in $SnCl_2$ are used. This is understandable on the basis of Lewis acid behavior of the $SnCl_2$, and may be comparable to the behavior of silver and mercuric halides which are used to favor carbonium ion formation in solvolysis reactions of alkyl halides (3, 8). Pure stannous chloride appears readily to accept a halide ion; the pure melt has been shown to be slightly polymeric through chloride bridges (10) and on addition of KCl this structure may be broken down through formation of $SnCl_3^-$ or $SnCl_4^{2-}$ ions in the melt. Conceivably, the melt functions by abstracting a chloride (or bromide)

Can. J. Chem. Downloaded from www.nrcresearchpress.com by 210.87.254.42 on 09/05/12
For personal use only.

TABLE 4. Yield as a function of melt composition, $SnCl_2$–KCl melts, at 295 °C; flow rate, 1×10^{-2} mM s^{-1}

Reactant	Mole% $SnCl_2$	Yield (%) 1-Chloropropane	Yield (%) Propene
2-Chloropropane	100	*ca.* 1	68
	80	*ca.* 1	70
	62	Undetected	50
	50	Undetected	46

Reactant	Mole% $SnCl_2$	Yield (%) 1-Chloropropane	Yield (%) 2-Chloropropane	Yield (%) Propene
1-Bromopropane	100	15	9	31
	80	15	7	28
	62	15	4	16

TABLE 5. Reaction of halopropanes as a function of temperature, 62 mole% $SnCl_2$–KCl; flow rate, 2×10^{-2} mM s^{-1}

Reactant	Temperature (°C)	Yield (%) 1-Chloropropane	Yield (%) 2-Chloropropane	Yield (%) Propene
1-Chloropropane	280	—	<1	6
	295	—	<1	7
	315	—	1	17
1-Bromopropane	280	17	~2	10
	295	15	~3	12
	317	22	~4	20

ion from the organic molecule to produce the complex anion and a carbonium cation. The tendency for this to happen is reduced as the $SnCl_2$ is satisfied by free Cl^- from the KCl, although it is not markedly effected until appreciable KCl has been added. It may be noted that products not detected in 62 mole% $SnCl_2$ may appear with higher $SnCl_2$ concentration, also implying that the carbonium ion has a longer lifetime for reaction in the latter media.

Data in Table 5 show that increasing temperature results in increased reaction. However, changes in melt properties with temperature (*e.g.* viscosity) and their resulting influence on contact times may be equally significant. At temperatures above 330 °C yields decreased, probably because of the change in flow properties of the melt.

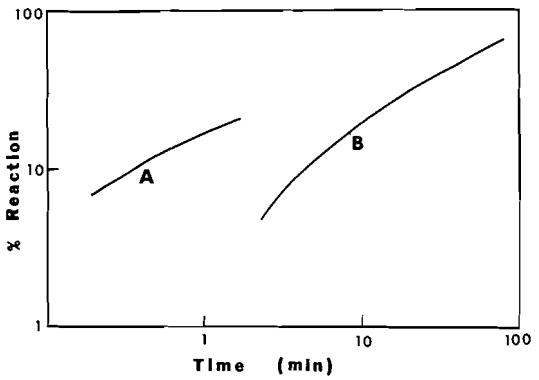

FIG. 1. Comparison of gas phase and molten salt (62 mole% $SnCl_2$–KCl; 317 °C) reaction of 1-bromopropane to give propene. *A*, melt reaction; *B*, gas phase reaction.

Elimination Reactions

Most systems produced unsaturated products corresponding to loss of hydrogen halide from the original molecule, as shown in Tables 1 and 3. That these results are due to melt reactions and not purely thermal decomposition is shown by Fig. 1, which compares the conversion of 1-bromopropane to propene in a gas phase reaction studied by Aguis and Maccoll (11), with our results in the melt. Time refers to the total time in the heated region of our apparatus, which in these experiments was usually much longer than the melt contact time alone. Such results show that the elimination reaction observed in this case is

Can. J. Chem. Downloaded from www.nrcresearchpress.com by 210.87.254.42 on 09/05/12
For personal use only.

Can. J. Chem. Downloaded from www.nrcresearchpress.com by 210.87.254.42 on 09/05/12
For personal use only.

essentially wholly due to reaction with the melt at any reasonable flow rate.

Six chloro-compounds were studied to evaluate the amount of β-elimination of hydrogen in the absence of substitution reactions (Tables 1 and 3). 2-Chloropropane and 2-chlorobutane both give more alkene than the 1-chloro compounds. Also, 2-chlorobutane yields more alkene than does 2-chloro-2-methylpropane, although the overall reactivity of the bromides is in the reverse order. The differences are accountable in terms of the ease of formation of the carbonium ion, since it is well established for S_N1 mechanisms that a secondary carbonium ion is not as stable as a tertiary. Stabilization of the secondary may require a greater shift of electron density from the β-hydrogens, and the stability may then be dependent on the number of such hydrogens available; for example, nine on 2-chloro-2-methylpropane, but five with 2-chlorobutane. If the electron delocalization is greater per hydrogen in the latter, these hydrogens become more acidic and hence more readily available to the bases in the solvent; *i.e.* Cl^-, $SnCl_3^-$ or $SnCl_4^{2-}$.

It is also noted that 1- and 2-butene are formed more readily than propene while ethylene is the most difficult to obtain. This reflects the known values of heats of formation in the series ethylene < propene ~ 1-butene < 2-butene, which has been discussed in equivalent terms by Hughes, Ingold, and Shiner (12). While elimination reactions seem to be understandable on the basis of carbonium ion formation, more data would be required to elucidate all of the details of the reactivities observed.

Reaction Mechanism

We have accounted for the various observations above by means of carbonium ion formation in the melt, or at the melt–vapor interface. Free radical formation should also be considered, particularly in view of the elevated temperatures. Other molten salt reactions in the literature, such as the formation of ethane from methanol and dimethylether (13), may arise through some type of free radical mechanism. A number of compounds investigated in this study, notably α-bromotoluene, tetrabromomethane, and tribromomethane, gave considerable carbonaceous decomposition material in the melt, and produced Sn(IV) compounds which volatilized and were collected with the products. (Sn(IV) was not produced in detectable amounts in the other reactions.) These examples may be cases where homolytic dissociation is a competitive or even favored mode of reaction, but the majority of the reactions reported here are better described by the ionic mechanism.

The following reaction scheme shows the various steps which we believe take place in the reaction of 1-bromopropane

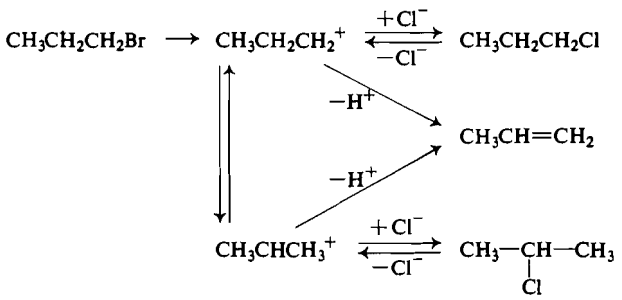

The steps should be reversible but the small bromide ion concentration in the melt ensures that bromide readdition will not be observed. This mechanism implies that 1-chloropropane should be formed from the 2-chloropropane produced, although this may be in small amount since the latter is energetically favored. It is interesting that while this was not seen in the 62% $SnCl_2$–KCl melts it could be observed in pure $SnCl_2$, where the difficulty in removing the chloride from the melt may produce a longer lived cation with more chance for rearrangement.

A similar mechanism is shown below for the reaction of 1-bromo-2-methylpropane. The formation of methylcyclopropane is interesting. Previous preparations from isobutyl compounds have generally been regarded to involve carbanion intermediates (14–16).

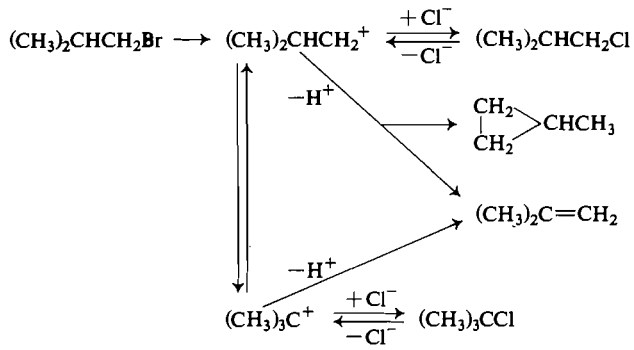

Removal of a proton from $(CH_3)_2CHCH_2^+$ may involve two possible three-centered transition states, leading to methylcyclopropane or 1-butene with the latter being favored.

From the discussion above, it is evident that a number of organic exchange, rearrangement, and elimination reactions can be accounted for by a mechanism involving abstraction of a halide ion from the organic molecule by the melt. To some extent at least, product yields can be controlled by suitable choice of melt and reaction time. Total reaction yields may be high; for most of the reactions discussed here essentially complete utilization of reactant could be achieved by increasing the melt–vapor contact time or introducing more efficient mixing. Yields were reasonably proportional to depth of melt.

1. W. SUNDERMEYER. Angew. Chem. Int. ed. **4**, 222 (1965).
2. G. BRAUER. Handbook of Preparative Inorganic Chemistry. Academic Press, New York. 1963. 728.
3. E. R. THORTON. Solvolysis Mechanisms. Ronald Press Co., New York. 1964.
4. P. M. LAUGHTON and R. E. ROBERTSON. Can. J. Chem. **34**, 1714 (1958).
5. D. I. PACKHAM and F. A. RACKLEY. Chem. Ind. London, 899 (1966).
6. S. OAE and C. A. VANDERWERF. J. Amer. Chem. Soc. **75**, 5037 (1953).
7. J. HINE and D. E. LEE. J. Amer. Chem. Soc. **73**, 22 (1951).
8. J. HINE. Physical Inorganic Chemistry. McGraw-Hill Book Co., New York. 1962.
9. A. STREITWIESER. Chem. Rev. **56**, 571 (1958).
10. J. H. R. CLARK and C. SOLOMONS, J. Phys. Chem. **47**, 1823 (1967).
11. P. J. AGUIS and A. MACCOLL. J. Chem. Soc. 973 (1965).
12. F. H. HUGHES, C. K. INGOLD, and V. SHINER. J. Chem. Soc. 3827 (1953).
13. W. SUNDERMEYER. Chem. Ber. **97**, 1069 (1964).
14. L. FREIDMAN and J. G. BERGER. J. Amer. Chem. Soc. **83**, 492 (1961).
15. W. KIRMS and W. VON E. DOERING. Tetrahedron, **11**, 226 (1960).
16. F. E. CONDON and D. E. SMITH. J. Amer. Chem. Soc. **69**, 965 (1947).

Can. J. Chem. Downloaded from www.nrcresearchpress.com by 210.87.254.42 on 09/05/12
For personal use only.

Exchange Reactions of the *t*-Butyl Cation[1]

S. BROWNSTEIN AND J. BORNAIS
Division of Chemistry, National Research Council of Canada, Ottawa, Canada

Received June 1, 1970

The exchange reaction between *t*-butyl cation and isobutane in sulfur dioxide solution is first order in both species with $E_a = 3.6$ kcal/mole and $\Delta S^{\ddagger}_{298} = -27$ e.u. No reaction is observed, under these conditions, between the *t*-butyl cation and *n*-butane or neopentane. In a similar system the isopropyl chloride – arsenic pentafluoride complex reacts rapidly with *n*-butane to yield propane and the *t*-butyl cation, but does not react with neopentane or cyclopropane. An exchange reaction was also observed between the isopropyl chloride – arsenic pentafluoride complex and propane.

Canadian Journal of Chemistry, 49, 7 (1971)

Can. J. Chem. Downloaded from www.nrcresearchpress.com by 210.87.254.42 on 09/05/12
For personal use only.

Introduction

Most studies of "stable" carbonium ions in solution have been performed with extremely acidic and reactive solvents such as SbF_5–FSO_3H–SO_2 or HF–SbF_5 (1–3). Intramolecular exchange rates have been measured for some species under these conditions by high resolution proton resonance spectroscopy (3, 4). However, the reactivity of the solvents is such that neutral species of similar structure to the carbonium ions are normally not stable, but react to give carbonium ions themselves.

There have been two studies in which the mechanism and thermodynamic activation parameters have been determined for exchange of a carbonium ion with its halide precursor (5, 6). In the first study (5), relatively stable triphenylmethyl cations were employed and the rate-determining step was found to be the dissociation of the triphenylmethyl halide prior to the actual exchange reaction. In the second study (6), the exchange between acetyl fluoride and acetyl hexafluoroarsenate, the exchange was also found to be an S_N1 process in which the rate-determining step appeared to involve a re-arrangement of the acetyl ion formed by dissociation of acetyl hexafluoroarsenate.

There has been considerable interest in reactions of carbonium ions with hydrocarbons since the pioneering paper of Bartlett *et al.* on hydride ion transfer reactions (7). Considerable information on rates and thermodynamic activation parameters on this reaction has been obtained by studies in strongly acidic systems (8, 9). It seemed worthwhile to see if similar kinetic orders to those observed with carbonium ion – halide exchanges would also be found with hydrocarbons. Since the *t*-butyl cation is the most thermally stable of the simple aliphatic carbonium ions the system *t*-butyl cation – isobutane was chosen for the initial studies. Some qualitative studies have been described in which the exchange of the tertiary proton of isobutane was observed (10). The system was such that the concentration of carbonium ion could not be determined. By choosing appropriate conditions it was possible in the present study to produce known, independently variable, concentrations of carbonium ion and of isobutane.

Experimental

Proton resonance spectra were obtained at 100 MHz on a Varian Associates HA 100 D spectrometer. Probe temperatures were calibrated with a copper–constantan thermocouple in a dummy sample tube. Methylene chloride, purified as previously reported (11), was stored over Linde Molecular Sieve 4A in a container on the vacuum line. Arsenic pentafluoride (Ozark-Mahoning) and anhydrous sulfur dioxide (Matheson) were stored over P_2O_5 in bulbs on the vacuum line. Reagent grade *t*-butyl chloride and *iso*-propyl chloride (Eastman Kodak) were used without further purification. An equal volume mixture of methylene chloride and sulfur dioxide was used as solvent in order to obtain a low freezing point along with adequate solubility. The methylene chloride proton signal was used as an internal reference and lock signal, and the peak positions subsequently corrected and reported relative to tetramethylsilane.

The samples were prepared by standard vacuum line techniques, thawed and mixed in a "Dry Ice" bath and quickly inserted into a pre-cooled n.m.r. probe. Kinetic runs were first measured at the lowest temperature and then at increasing temperatures. At the end of the series of measurements the lowest temperature run was repeated to insure that no sample degradation had occurred. The data were fitted by least square techniques and the listed errors are standard deviations.

[1]NRCC No. 11 606.

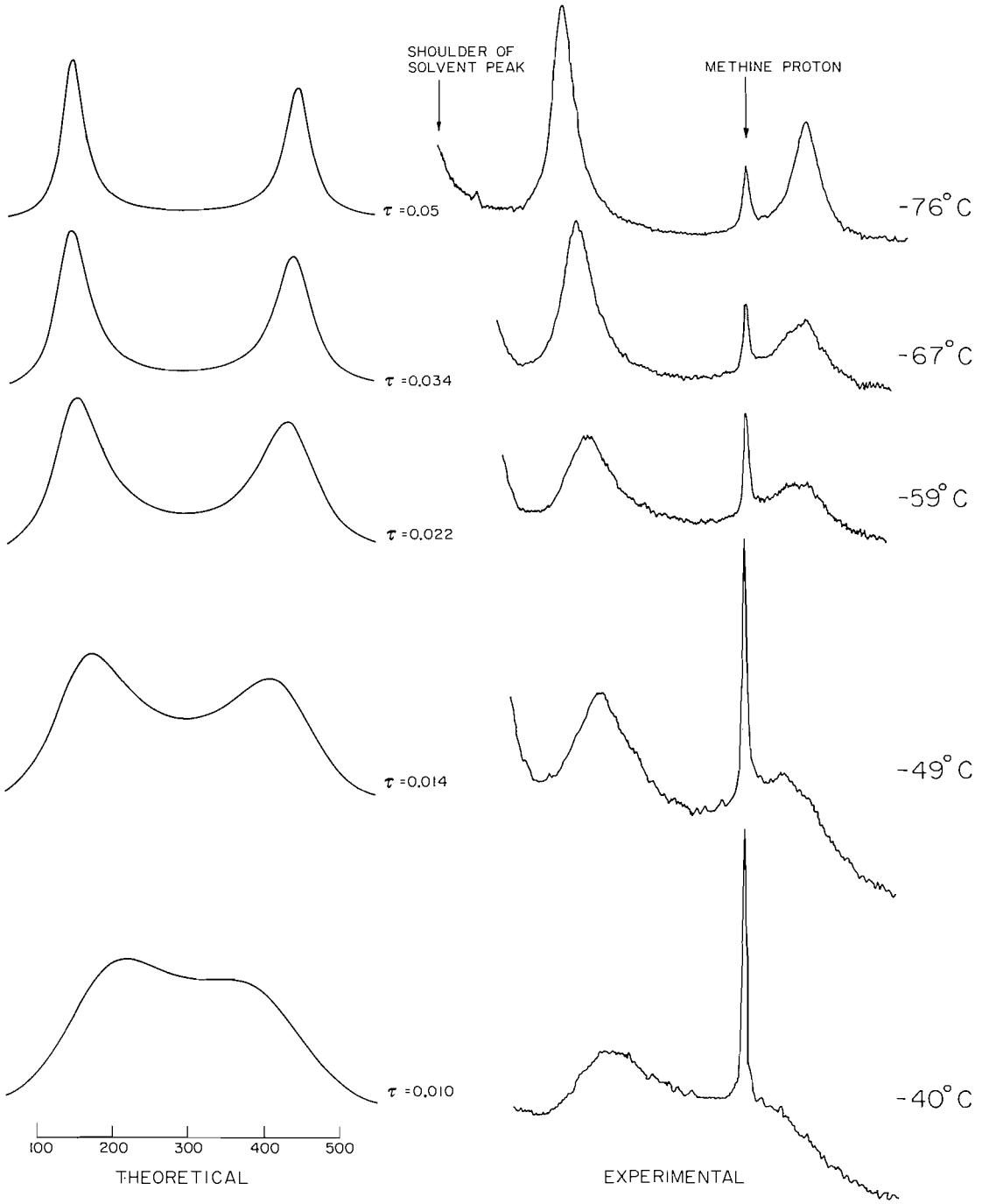

FIG. 1. A comparison of experimental and theoretical spectra of isobutane plus *t*-butyl cation as a function of the exchange rate between them. The scale is in Hz.

Can. J. Chem. Downloaded from www.nrcresearchpress.com by 210.87.254.42 on 09/05/12
For personal use only.

Can. J. Chem. Downloaded from www.nrcresearchpress.com by 210.87.254.42 on 09/05/12
For personal use only.

Results and Discussion

The proton magnetic resonance spectrum of isobutane in a 50% *v/v* solution of sulfur dioxide and methylene chloride, containing twice the concentration of arsenic pentafluoride utilized in the kinetic experiments, has a sharp doublet (J_{H-H} = 7.3 Hz, δ = 0.98 p.p.m. from tetramethylsilane) at −82 °C. With rising sample temperature the two peaks of the doublet broadened and had almost completely merged to a single peak by −40 °C. The peak position moved 0.07 p.p.m. down field in this temperature interval. Presumably there is some type of exchange reaction occurring with residual impurities in the system. However, as can be seen from Fig. 1, this peak broadening corresponds, at any given temperature, to only a very small amount of the observed rate of exchange when the *t*-butyl cation is also present. Therefore, it is possible to obtain moderately accurate kinetic results for the exchange reaction between the *t*-butyl cation and isobutane despite this interfering reaction.

In the solvent system used for this study the *t*-butyl cation displays a sharp single peak whose chemical shift varies from 4.03 p.p.m. at −82 °C to 4.06 p.p.m. at −40 °C. This may be compared with the previously reported values of 3.95 p.p.m. in the solvent system SbF_5–SO_2 and 4.35 p.p.m. in SbF_5 alone (12). By contrast the chemical shift of the precursor, *t*-butyl chloride, is 1.58 p.p.m. These values leave little doubt that it is the *t*-butyl cation, and not a complex, which is being studied.

Since the change of chemical shift difference between the two exchanging *t*-butyl species is only 3 in 300 Hz over the temperature range of interest, a single average value was used for calculation of theoretical spectra. The theoretical spectra were calculated with the same general matrix technique employed previously (13), but with the inclusion of a convolution integral to include the effects of natural line width (14). The decet from the methine proton of isobutane was not included in the theoretical calculations. When the exchange was rapid the peak of this proton was observed as a relatively sharp spike (due to averaging of the spin-coupling) on the side of the isobutane methyl peak. A comparison of typical theoretical and experimental spectra is displayed in Fig. 1.

In the slow exchange limit where the separation between the resonance peaks is considerably greater than the rate of conversion between the two species, it is possible to separately determine the lifetime of each species. However, in the present studies it is only at the slowest exchange rates that this is possible, and even then only in an approximate manner. Therefore, the theoretical spectra have been calculated for the lifetime of the isobutane molecule. This is related to the lifetime of the *t*-butyl cation by the equation

$$[1] \quad \tau_{\text{isobutane}}/C_{\text{isobutane}} = \tau_{t\text{-butyl}}/C_{t\text{-butyl}}$$

regardless of the mechanism of the exchange reaction. The symbols τ and C denote lifetime and concentration, respectively.

The relationship between the lifetime of a species, as determined by magnetic resonance investigations at equilibrium, and rate of change of concentration, measured in conventional kinetic studies, is given by eq. 2.

$$[2] \quad d[Z]/dt = [Z]/\tau_z$$

A perfectly general equation to describe the kinetics of the exchange reaction between the *t*-butyl cation and isobutane is

$$[3] \quad \frac{d[(CH_3)_3CH]}{dt} = c[(CH_3)_3CH]^x[(CH_3)_3C^+]^y$$

where c is the rate constant for the reaction at some particular temperature. Substituting eq. 2

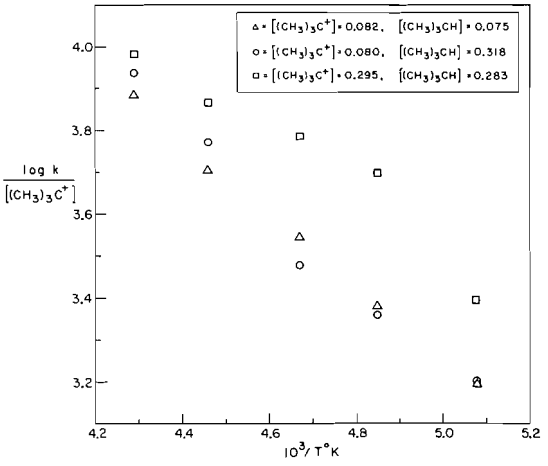

FIG. 2. Temperature dependence of the rate of the exchange reaction between *t*-butyl cation and isobutane.

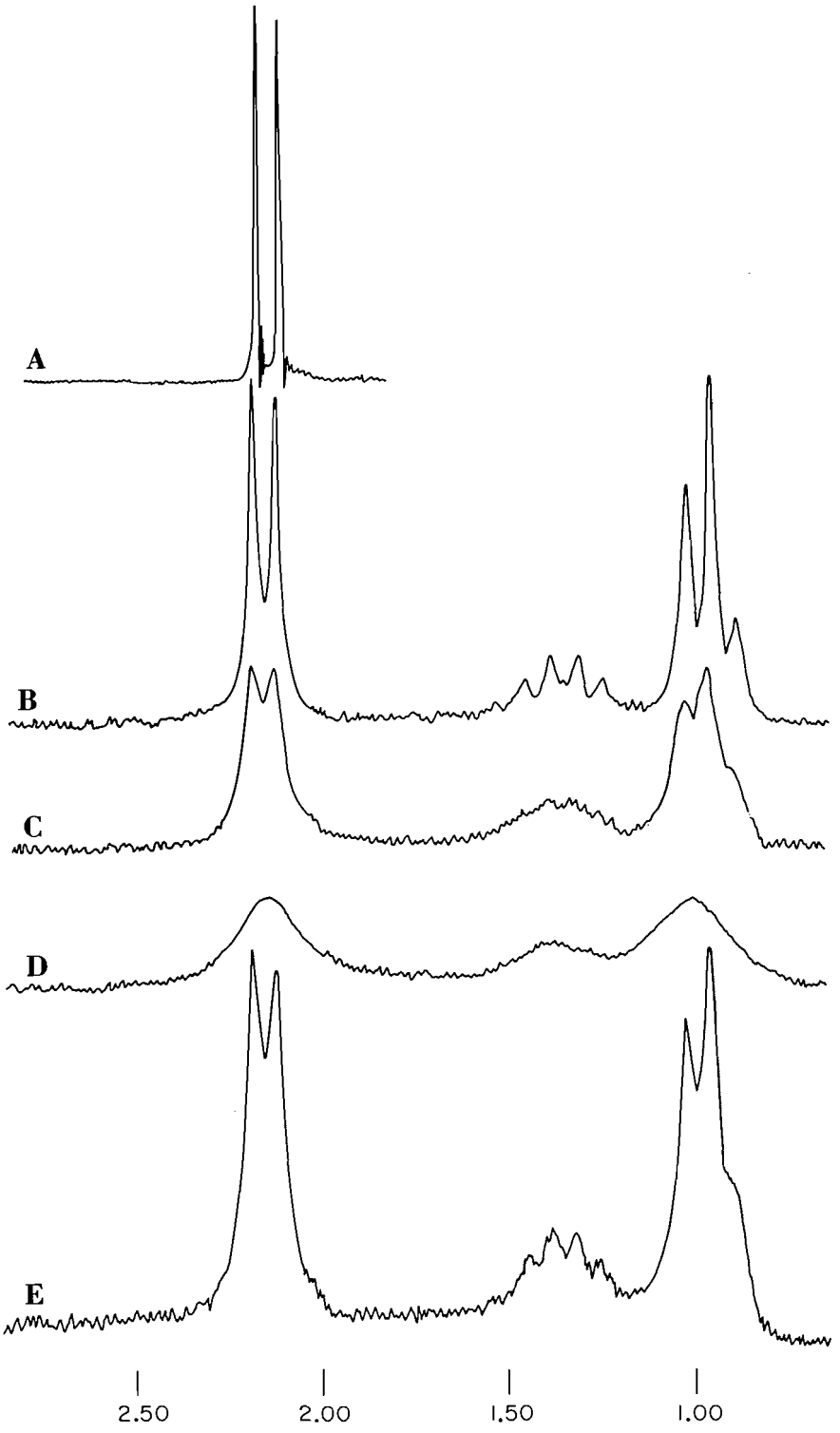

FIG. 3. Proton resonance spectra of the exchanging system isopropyl chloride – arsenic pentafluoride complex plus propane. The scale is p.p.m. from TMS. (*A*) Isopropyl chloride – arsenic pentafluoride complex (0.08 *m*) at −67 °C. (*B*) Isopropyl chloride – arsenic pentafluoride complex (0.082 *m*) and propane (0.086 *m*) at −76 °C immediately after melting and mixing. (*C*) Same solution at −67 °C. (*D*) Same solution at −59 °C. (*E*) Same solution after again cooling to −76 °C.

Can. J. Chem. Downloaded from www.nrcresearchpress.com by 210.87.254.42 on 09/05/12
For personal use only.

Can. J. Chem. Downloaded from www.nrcresearchpress.com by 210.87.254.42 on 09/05/12
For personal use only.

into eq. 3 with $k = 1/\tau$ yields

$$[4] \quad k_{\text{isobutane}} = c[(CH_3)_3CH]^{x-1}\,[(CH_3)_3C^+]^y$$

A plot of log $k/[(CH_3)_3C^+]$ for three of the samples is shown in Fig. 2. From a least squares fit of such a plot for the data from all the samples studied, the Arrhenius energy of activation, E_a, was calculated to be 3.6 ± 0.2 kcal/mole and $\Delta S^{\ddagger}_{298}$ was found to be approximately -27 e.u.

Although there is a large scatter in the rates shown in Fig. 2, the slope for each of the samples is very similar. The concentration of isobutane was varied from 0.075 to 0.318 *m* and of *t*-butyl cation from 0.071 to 0.295 *m*. Over this concentration range, $x - 1 = 0$ and therefore $x = 1$, and the exchange reaction is unimolecular in isobutane. The reaction was also found to be first order in *t*-butyl cation although the limited concentration range experimentally available does not completely exclude the possibility of the reaction being 3/2 order. Some of the scatter in the data of Fig. 2 might be due to the fact that the concentration dependence of the rate is not exactly first order in *t*-butyl cation, but it is primarily due to the difficulties of completely excluding reactive impurities from this very sensitive system (6). Such impurities are likely to reduce the *t*-butyl cation concentration below that calculated and this effect will be most serious at the lower concentrations.

Solutions containing the *t*-butyl cation and *n*-butane showed no evidence of exchange reactions in the temperature region from -82 to -40 °C. The observed spectrum was the sum of those for the individual components. Similarly with neopentane there was no reaction. When *s*-butyl chloride was used as the carbonium ion precursor the *t*-butyl cation was produced and the same results were obtained as with *t*-butyl chloride as a precursor. These results are consistent with previous studies of the rate of *sec*-butyl *t*-butyl cation conversion (15).

The use of isopropyl chloride rather than *t*-butyl chloride gave a solution with a sharp doublet at 2.19 p.p.m. and a septet at 6.10 p.p.m. with a coupling constant of approximately 6.3 Hz between the methyl and methine protons. It is quite unlikely that the isopropyl cation is present since the chemical shifts of the methyl and methine protons are different than those previously reported (16, 17). It seems likely that an isopropyl chloride – arsenic pentafluoride complex is being observed, although the possibility of a rapidly equilibrating system containing a low concentration of carbonium ion cannot be excluded.

This complex was found to exchange rapidly with propane in a system analogous to the system *t*-butyl cation – isobutane. However, it was found that after warming samples containing the isopropyl chloride – arsenic pentafluoride complex, identical spectra were not obtained upon recooling to -76 °C. Some representative results are shown in Fig. 3. Since some decomposition must be occurring upon warming it is not possible to do a kinetic study of this system.

From the results of proton resonance spectroscopy it was observed that the isopropyl chloride – arsenic pentafluoride complex reacts rapidly and completely with *n*-butane to yield the *t*-butyl cation and propane. However, it does not react with neopentane nor cyclopropane at the low temperatures (*ca.* -80 °C) where it is thermally stable.

1. D. BETHELL and V. GOLD. Carbonium Ions, an Introduction. Academic Press, New York. 1967.
2. G. OLAH and A. M. WHITE. J. Amer. Chem. Soc. **91**, 3954 (1969).
3. D. M. BROUWER, C. MACLEAN, and E. L. MACKOR. Discuss. Faraday Soc. **39**, 121 (1965).
4. M. SAUNDERS and J. ROSENFELD. J. Amer. Chem. Soc. **91**, 7756 (1969).
5. H. H. FREEDMAN, A. E. YOUNG, and V. R. SANDEL. J. Amer. Chem. Soc. **86**, 4722 (1964).
6. L. LUNAZZI and S. BROWNSTEIN. J. Amer. Chem. Soc. **91**, 3034 (1969).
7. P. D. BARTLETT, F. E. CONDON, and A. SCHNEIDER. J. Amer. Chem. Soc. **66**, 1531 (1944).
8. D. M. BROUWER and J. M. OELDERIK. Rec. Trac. Chim. **87**, 721 (1968).
9. G. M. KRAMER. J. Amer. Chem. Soc. **91**, 4819 (1969).
10. G. M. KRAMER. J. Org. Chem. **34**, 2919 (1969).
11. A. M. EASTHAM. J. Amer. Chem. Soc. **78**, 6040 (1956).
12. G. A. OLAH, W. S. TOLGYESI, S. J. KUHN, M. E. MOFFATT, I. J. BASTIEN, and E. B. BAKER. J. Amer. Chem. Soc. **89**, 1328 (1963).
13. S. BROWNSTEIN and J. BORNAIS. Can. J. Chem. **46**, 225 (1968).
14. S. BROWNSTEIN, E. C. HORSWILL, and K. U. INGOLD. Can. J. Chem. **47**, 3243 (1969).
15. M. SAUNDERS, E. L. HAGEN, and J. ROSENFELD. J. Amer. Chem. Soc. **90**, 6882 (1968).
16. G. A. OLAH, E. B. BAKER, J. C. EVANS, W. S. TOLGYESI, J. S. MCINTYRE, and I. J. BASTIEN. J. Amer. Chem. Soc. **86**, 1360 (1964).
17. M. SAUNDERS and E. L. HAGEN. J. Amer. Chem. Soc. **90**, 6881 (1968).

Can. J. Chem. Downloaded from www.nrcresearchpress.com by 210.87.254.42 on 09/05/12
For personal use only.

Total Synthesis of (±)-α-Cubebene and (±)-β-Cubebene

EDWARD PIERS,[1] RONALD W. BRITTON, AND WILLIAM DE WAAL
Department of Chemistry, University of British Columbia, Vancouver 8, British Columbia

Received August 10, 1970

An efficient total synthesis of the racemic forms of the novel tricyclic sesquiterpenes α-cubebene (**1**) and β-cubebene (**2**) is described. The key step of this synthesis involved the cupric sulfate catalyzed intramolecular cyclization of the olefinic diazoketone **3**, which produced, in high yield, (±)-β-cubebene norketone (**24**) and (±)-1,6-epi-β-cubebene norketone (**25**), in a ratio of approximately 3:5, respectively.

Canadian Journal of Chemistry, 49, 12 (1971)

On the basis of spectral data, chemical degradation and correlation with known cadinane derivatives, Hirose *et al.* (1–3) have proposed that **1** and **2** correctly represent the structure and absolute stereochemistry of α-cubebene[2] and β-cubebene, respectively, two sesquiterpenes isolated from the commercial oil of cubeb (*Piper cubeba* L.). Structurally, these two natural products contain the bicyclo[3.1.0]hexane moiety and thus represent a novel and interesting variant of the more normal structures found within the cadinane class of sesquiterpenoids. We report in this paper the total synthesis of the cubebenes via a route which fully supports the structural and stereochemical assignments.[3]

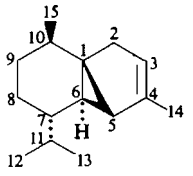

1

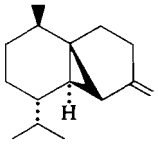

2

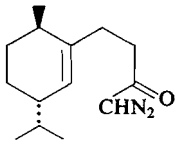

3

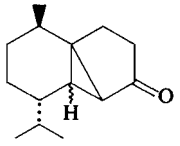

4

The key step of our envisaged synthesis involved the cupric sulfate catalyzed intramolecular cyclization of an appropriately substituted olefinic diazoketone.[4] In particular, it was proposed to prepare and attempt the cyclization of the olefinic diazoketone **3**. Obviously, success of the cyclization would lead to a synthetic intermediate **4** with functionality appropriate for further elaboration to α- (**1**) and β-cubebene (**2**).

Condensation of the commercially available mixture of (±)-menthone and (±)-isomenthone (**5**)[5] (see Scheme 1) with ethyl formate in the presence of sodium methoxide in benzene afforded, in 88% yield, the corresponding hydroxymethylene derivatives **6**. Treatment of the latter under the usual conditions (14) with *n*-butanethiol gave in 89% yield the corresponding *n*-butylthiomethylene derivatives **7**, which, upon reduction with a basic solution of methanolic sodium borohydride provided a quantitative yield of the crude β-hydroxythioenol ether **8**. This material was not purified further, but was immediately subjected to hydrolysis with 1% hydrochloric acid in aqueous acetone. Distillation of the resulting mixture of products produced two major fractions. The first fraction (40%, b.p. 66–68° at 0.35 mm) consisted of the desired α,β-unsaturated aldehydes **10**, while the second fraction (50%, b.p. 120–126° at 0.35 mm) was shown to be the thioenol ether **9**. Normally, the hydrolysis of β-hydroxythioenol ethers of structure similar to compound **8** affords, in good yield, the corresponding α,β-unsaturated aldehyde (15, 16). However, in the present case, although a variety of conditions were used, including the addition of mercuric salts, the isolated yield of the aldehydes **10** did not exceed 40%. Furthermore, various

[1]Fellow of the Alfred P. Sloan Foundation, 1970–1972.

[2]The numbering scheme shown in structure **1** is that normally used for cadinane-type sesquiterpenoids.

[3]For a preliminary report regarding this work, see ref. 4. For another report concerning the synthesis of the cubebenes see ref. 5.

[4]For some previous applications of this type of reaction to terpenoid synthesis, see refs. 6–13, inclusive.

[5]Compounds **5**, **6**, **7**, and **10** represent racemic diastereomeric pairs. Analytical and spectral data of these mixtures were, in each case, in full accord with the structural assignments.

Can. J. Chem. Downloaded from www.nrcresearchpress.com by 210.87.254.42 on 09/05/12
For personal use only.

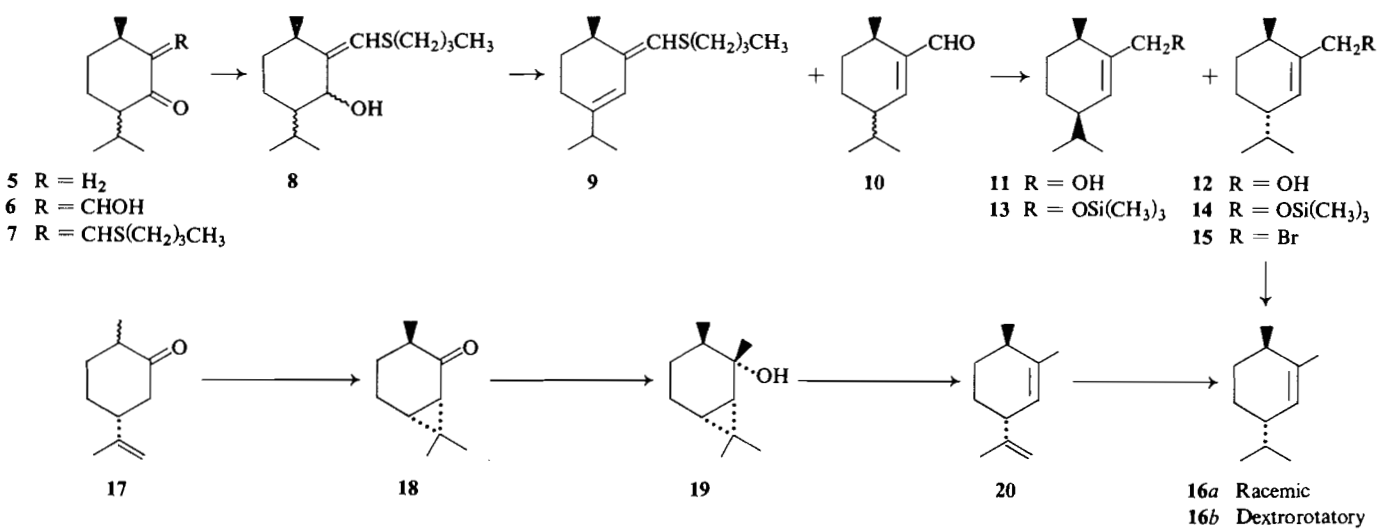

SCHEME 1

Can. J. Chem. Downloaded from www.nrcresearchpress.com by 210.87.254.42 on 09/05/12
For personal use only.

attempts to hydrolyze the thioenol ether **9** to the aldehydes **10** were also unsuccessful.

Reduction of the aldehydes **10** with sodium borohydride afforded, in 91% yield, the corresponding mixture of the alcohols **11** and **12**. To this stage in the synthesis, no attempt had been made to separate the diastereomeric pairs, since all of the intermediates which would have been amenable to separation contained an epimerizable isopropyl group. However, once the aldehyde functionality of **10** had been reduced with sodium borohydride, the possibility for epimerization had been removed. Therefore, attempts were made to separate the mixture of alcohols **11** and **12**.

Gas–liquid chromatographic analysis of this mixture on many different columns at various column temperatures and carrier-gas flow rates failed to reveal any appreciable separation of the two alcohols **11** and **12**. The corresponding acetate derivatives also proved to be extremely difficult to separate. However, the corresponding trimethylsilyl ether derivatives **13** and **14**, which were easily formed in virtually quantitative yield from the alcohols **11** and **12**, were found to separate reasonably well on a preparative Zonyl E-7 column.[6] Preparative g.l.c. thus provided a convenient method for obtaining a sufficient quantity of the pure trimethylsilyl ethers **13** and **14**.

It was important at this stage to ascertain the stereochemistry of the two trimethylsilyl ethers **13** and **14**. Since the ratio of the two compounds in the originally obtained mixture was approximately 1:1, it was impossible to assign the configurations in terms of conformational arguments. Therefore, a chemical proof regarding this point was sought, and the fact that the silyl ether of shorter g.l.c. retention time was indeed the desired *trans* compound **14** was shown as follows.

Hydrolysis of **14** in hot 2% aqueous ethanol gave in, 98% yield, the pure *trans* alcohol **12**, which, upon treatment with phosphorus tribromide in benzene–pyridine at 0° (17), afforded the allylic bromide **15**, in 77% yield. Lithium aluminum hydride reduction of **15** gave a virtually quantitative yield of racemic *trans*-2-methyl-*p*-mentha-2-ene (**16***a*). The spectral properties of this hydrocarbon were in complete accord with the assigned structure.

[6]We are very grateful to Mr. J. Booker, Varian-Aerograph, California, for his help in the selection of a g.l.c. column for this separation.

An unambiguous synthesis of (+)-*trans*-2-methyl-*p*-mentha-2-ene (**16***b*) was carried out as follows (see Scheme 1). The bicyclic ketone (−)-*trans*-caran-2-one (**18**) was prepared from (+)-dihydrocarvone (**17**) according to literature procedures (18, 19), and could be conveniently purified by recrystallization from *n*-hexane at −78°. A sample of **18** purified in this manner exhibited $[\alpha]_D^{22}$ − 181° [lit. $[\alpha]_D^{19}$ − 162.9° (19), − 153° (20)] and in the n.m.r. spectrum showed no signals due to olefinic protons.[7] Reaction of ketone **18** with ethereal methyllithium produced, in high yield, only one product, formulated as **19**. The stereochemistry of the latter was assigned on the basis of the reasonable assumption that the methyllithium would approach the carbonyl group of **18** from the less hindered side, opposite to the sterically bulky *gem*-dimethylcyclopropyl moiety (see ref. 21).

Pyrolysis of the tertiary alcohol **19** in the presence of a small amount of pyridine in a sealed tube at 190–200° for 2 h (19) gave approximately 70% of (+)-*trans*-2-methyl-*p*-mentha-2,8-diene (**20**),[8] which was purified by preparative g.l.c. Hydrogenation of the latter in the presence of the homogeneous catalyst tris(triphenylphosphine)-chlororhodium (22, 23) stopped after the uptake of one equivalent of hydrogen. Isolation of the product afforded (+)-*trans*-2-methyl-*p*-mentha-2-ene (**16***b*), which exhibited i.r. and n.m.r. spectra and g.l.c. retention times identical with those obtained from the racemic compound **16***a*, prepared as described previously. This correlation provided unambiguous evidence for the stereochemistry of our synthetic intermediates **12** and **15** and allowed us to continue with the proposed synthesis of the cubebenes.

Treatment of the allylic bromide **15** (see Scheme 2) with two equivalents of carbethoxymethylenetriphenylphosphorane (24) in refluxing ethyl

[7]The n.m.r. spectrum of samples of **18** which had not been purified by recrystallization clearly showed the presence of small amounts of starting material, (+)-dihydrocarvone (**17**). Furthermore, purification of **18** by preparative g.l.c. or by distillation at temperatures greater than 100° was attended by partial isomerization to **17**. Presumably, these observations account for the fact that our specific rotation value for compound **18** was considerably higher than those previously reported.

[8]This material had to be purified and analyzed immediately, as it tended to autoxidize on standing for even short periods of time. This type of observation had been previously noted by Cocker *et al.* (19) in the case of the analogous compound, (+)-*trans*-*p*-mentha-2,8-diene.

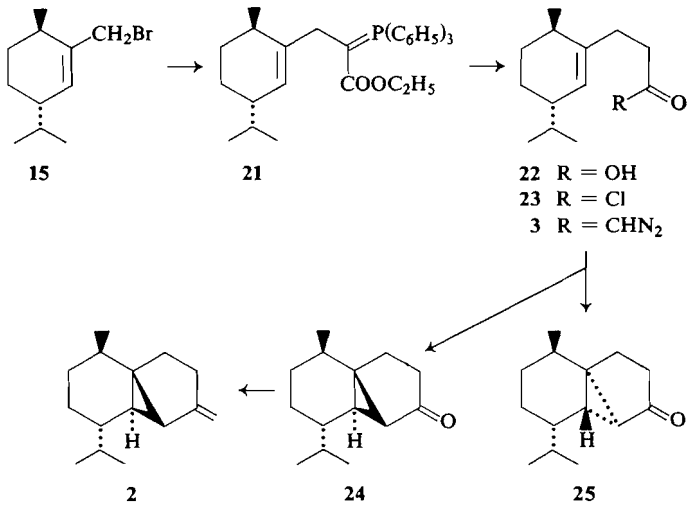

SCHEME 2

acetate for 2.5 h (25) gave, in addition to the crystalline carbethoxymethyltriphenylphosphonium bromide, a virtually quantitative yield of the corresponding alkylated phosphorane **21** as a yellow oil. Hydrolysis of this crude material with 10% potassium hydroxide in refluxing aqueous methanol afforded, in 69% yield, the olefinic carboxylic acid **22**. The stage was now set for the rather simple sequence of reactions which would lead to the formation of the synthetically crucial diazoketone **3**. To this end, **22** was converted into its sodium salt, and the latter was reacted with oxalyl chloride in benzene at 0° to afford the crude acid chloride **23**. When this compound was treated with dry ethereal diazomethane, the corresponding diazoketone **3** was formed almost immediately. The spectral properties of the crude material were in full accord with the assigned structure and it was now possible to attempt the initially proposed cyclization.

When the diazoketone **3** was refluxed in cyclohexane in the presence of cupric sulfate (26) for 1.5 h, a remarkably clean and high-yielding intramolecular cyclization occurred, producing two isomeric ketones, (±)-β-cubebene norketone (**24**) and (±)-1,6-epi-β-cubebene norketone (**25**), in a ratio (g.l.c. analysis) of approximately 3:5, respectively. The minor isomer **24**, upon treatment with methylenetriphenylphosphorane in dimethyl sulfoxide (27), gave a quantitative yield of (±)-β-cubebene (**2**) as a clear, colorless oil. The spectral properties (i.r., n.m.r., u.v., and mass spectrum) of this material were identical with those of natural β-cubebene.[9] Furthermore, the two materials were indistinguishable by g.l.c. Since β-cubebene had already been converted into α-cubebene (1), the synthesis of (±)-β-cubebene (**2**), as described above, also represents a total synthesis of (±)-α-cubebene (**1**).

It should be noted that although the synthetic work described in this paper provides unambiguous evidence regarding the stereochemistry at C-7 and -10 of the two cubebenes **1** and **2**, the nature of the synthesis is such that it supplies no conclusive information concerning the stereochemistry at C-6 of these compounds. However, Hirose *et al.* (3) have presented excellent evidence regarding this point and it thus appears safe to assume that **1** and **2** correctly represent the structure and stereochemistry of α- and β-cubebene, respectively.

Experimental

Melting points, which were determined on a Kofler block, and boiling points are uncorrected. The u.v. spectra were, unless otherwise noted, measured in methanol solution on either a Cary, model 14, or a Unicam, model SP 800, spectrophotometer. Routine i.r. spectra were recorded on a Perkin–Elmer Infracord model 137 spectrophotometer, while all comparison spectra were re-

[9]Natural β-cubebene (**2**) was isolated from Oil of Cubeb, Extra, kindly supplied by Fritzsche Brothers, Inc., New York, N.Y. The i.r. and n.m.r. spectra of this material, isolated by preparative g.l.c., were identical with those kindly supplied by Professor Y. Hirose. In addition, upon ozonolysis, the β-cubebene which was isolated from Oil of Cubeb, Extra, gave the known β-cubebene norketone, m.p. 60–60.5° (lit. m.p. 58.5–59.5° (1)).

Can. J. Chem. Downloaded from www.nrcresearchpress.com by 210.87.254.42 on 09/05/12
For personal use only.

Can. J. Chem. Downloaded from www.nrcresearchpress.com by 210.87.254.42 on 09/05/12
For personal use only.

corded on a Perkin–Elmer model 421 spectrophotometer. The n.m.r. spectra were taken in deuteriochloroform solution on Varian Associates spectrometers, models T-60, A-60, and/or HA-100. Line positions are given in the Tiers τ scale, with tetramethylsilane as an internal standard; the multiplicity, integrated peak areas, and proton assignments are indicated in parentheses. Mass spectrometric measurements were recorded on an AEI, type MS-9, mass spectrometer. The g.l.c. was carried out on an Aerograph Autoprep, model 700. The following columns were employed, with the inert supporting material being 60/80 mesh Chromosorb W in each case: column A, (30 ft × 3/8 in.), 30% Zonyl E-7; column B (20 ft × 3/8 in.), 30% SE-30; column C (10 ft × 1/4 in.), 20% SE-30; column D (10 ft × 3/8 in.), 30% Apiezon J; column E (10 ft × 1/4 in.), 10% Apiezon J; column F (10 ft × 1/4 in.), 20% Carbowax 20 M. The specific column used, along with column temperature and carrier gas (helium) flow-rate (ml/min), are indicated in parentheses. Microanalyses were performed by Mr. P. Borda, Microanalytical Laboratory, University of British Columbia, Vancouver, B.C.

Preparation of Hydroxymethylene Derivatives **6**

To an ice-cooled, stirred suspension of powdered sodium methoxide (135 g, 2.46 moles) in 1500 ml of dry benzene, kept under an atmosphere of dry nitrogen, was added 154 g (1 mole) of a mixture of (±)-menthone and (±)-isomenthone (**5**). The resulting mixture was stirred for 10 min, and then 125 g (1.7 moles) of ethyl formate was added. The mixture was warmed to room temperature and allowed to stand overnight. Water was added, and the layers were separated. The organic layer was extracted with two portions of 10% aqueous sodium hydroxide. The combined aqueous layer and alkaline extracts were cooled, acidified with 6 *N* hydrochloric acid, and thoroughly extracted with ether. The combined extracts were washed with water and dried over anhydrous magnesium sulfate. Removal of the solvent, followed by distillation of the residual oil under reduced pressure, gave 171 g (94%) of the hydroxymethylene derivatives **6** as a pale yellow oil, b.p. 71–73° at 0.2 mm; n_D^{20} 1.4983; u.v. λ_{max} 294 mμ (ε = 7950), λ_{max} (NaOH added) 319 mμ (ε = 17 500); i.r. (film) λ_{max} 6.15, 6.35 μ.

Anal. Calcd. for $C_{11}H_{18}O_2$: C, 72.49; H, 9.95. Found: C, 72.49; H, 10.06.

Preparation of n-Butylthiomethylene Derivatives **7**

A solution of the hydroxymethylene derivatives **6** (137.5 g, 0.755 mole), *n*-butanethiol (75 g, 0.825 mole), and *p*-toluenesulfonic acid (50 mg) in 500 ml of dry benzene was refluxed in a nitrogen atmosphere under a Dean–Stark water separator for 12 h at which time 13 ml of water had been collected. The cooled solution was washed with saturated aqueous sodium bicarbonate, then with water, and finally dried over anhydrous magnesium sulfate. Removal of the solvent gave an oil which, upon distillation under reduced pressure, afforded 170 g (89%) of the *n*-butylthiomethylene derivatives **7**, b.p. 130–136° at 0.35 mm; n_D^{20} 1.5292; u.v. λ_{max} 311 mμ (ε = 13 600); i.r. (film), λ_{max} 6.02, 6.50 μ.

Anal. Calcd. for $C_{15}H_{26}OS$: C, 70.83; H, 10.30; S, 12.61. Found: C, 71.09; H, 10.45; S, 12.30.

Preparation of Aldehydes **10**

To a solution of the *n*-butylthiomethylene derivatives **7** (140.7 g, 0.555 mole) in 1.8 l of methanol was added 21.25 g (0.555 mole) of sodium borohydride dissolved in 55.5 ml of 0.1 *N* sodium hydroxide. The mixture was stirred at room temperature for 2 h then a further 21.25 g (0.555 mole) of sodium borohydride dissolved in 55.5 ml of 0.1 *N* sodium hydroxide was added. After a further 2 h, the methanol was removed at aspirator pressure and the remaining aqueous layer was extracted three times with ether. The ether layers were washed with water then dried over anhydrous magnesium sulfate. Removal of the solvent gave 142 g (100%) of the β-hydroxythioenol ethers **8** as a pale yellow oil, i.r. (film) λ_{max} 3.00, 6.23 μ. This material was used without further purification in the hydrolysis step as described below.

To a solution of the crude alcohol **8** (25.6 g, 0.1 mole) in 500 ml of acetone was added 100 ml of 1% aqueous hydrochloric acid. The resulting mixture was heated on a steam bath for 20 min, then the acetone was removed at water aspirator pressure. The remaining aqueous layer was saturated with sodium chloride and extracted three times with ether. The combined ether layers were washed with water and dried over anhydrous magnesium sulfate Removal of the ether, followed by distillation of the resulting oil under reduced pressure (0.35 mm) gave two fractions: fraction 1, b.p. 66–68°, 6.65 g (40%) consisted of the desired α,β-unsaturated aldehydes **10** as a clear colorless oil, n_D^{20} 1.4878; u.v. λ_{max} 233.5 mμ (ε = 18 750); i.r. (film), λ_{max} 3.75, 5.95, 6.15 μ; n.m.r. τ 0.6 (singlet, 1H, *CH*O), 3.35 (multiplet, 1H, β-vinyl H), 8.82–9.16 (multiplet, 9H, secondary methyls).

Anal. Calcd. for $C_{11}H_{18}O$: C. 79.46; H, 10.91. Found: C, 79.64; H, 10.85.

Fraction 2, b.p. 120–126°, 11.9 g (50%), consisted of the pure thioenol ether **9** as a pale yellow oil, n_D^{20} 1.5363; u.v. λ_{max} 278 mμ (ε = 22 600), λ_{sh} 286 mμ (ε = 21 100); i.r. (film) λ_{max} 6.4, 11.4 μ; n.m.r. τ 4.08 (multiplet, 1H, vinyl H), 4.37 (singlet, 1H, vinyl H), 8.85–9.15 (multiplet, 12H, three secondary methyls and one primary methyl).

Anal. Calcd. for $C_{15}H_{26}S$: C, 75.56; H, 10.99. Found: C, 75.71; H, 11.10.

Preparation of the Mixture of Alcohols **11** *and* **12**

To a solution of sodium borohydride (4.5 g, 0.12 mole in 500 ml of methanol, cooled to 0° in an ice bath, was added a solution of the mixture of aldehydes **10** (20 g, 0.12 mole) in 100 ml of methanol. The reaction mixture was stirred under an atmosphere of nitrogen for 30 min and the methanol was removed at water aspirator pressure. Cold water (200 ml) was added and the aqueous layer was extracted three times with ether. The combined ether extracts were dried over anhydrous magnesium sulfate and the ether was removed at water aspirator pressure. Distillation of the resulting oil under reduced pressure afforded 18.4 g (91%) of the mixture of alcohols **11** and **12**, b.p. 77–78° at 0.25 mm.

Preparation of Trimethylsilyl Ethers **13** *and* **14**

To a solution of the mixture of alcohols **11** and **12** (9 g, 0.053 mole) in 150 ml of dry pyridine was added 30 ml of hexamethyldisilazane and 15 ml of trimethylsilyl chloride.

Can. J. Chem. Downloaded from www.nrcresearchpress.com by 210.87.254.42 on 09/05/12
For personal use only.

The mixture was stirred under an atmosphere of nitrogen for 10 min, then the mixture was filtered and the excess reagents and pyridine were removed at water aspirator pressure. The crude product was distilled under reduced pressure to give 12.2 g (95%) of the mixture of trimethylsilyl ether derivatives **13** and **14**, b.p. 62–63° at 0.35 mm. Analysis of this mixture by g.l.c. (column A, 150°, 200) revealed that the two isomers were present in a ratio of approximately 1:1. Purification of the two isomers was achieved by preparative g.l.c. (column A, 140°, 240). The pure *trans*-isomer **14**, of shorter retention time, was a clear colorless oil and exhibited n_D^{20} 1.4544; i.r. (film) λ_{max} 8.00, 9.4, 11.4, 11.9 μ; n.m.r. τ 4.43 (broad singlet, 1H, vinyl H, $w_{\frac{1}{2}}$ = 4 Hz), 5.92 (unresolved multiplet, 2H, —CH_2—OTMS), 8.99, 9.09, 9.13 (doublets, 9H, secondary methyls, J = 7 Hz), 9.87 (singlet, 9H, Si(CH_3)$_3$).

Mol. Wt. Calcd. for $C_{14}H_{28}OSi$: 240.191. Found (high resolution mass spectrometry): 240.190.

The pure *cis*-isomer **13**, of longer retention time, was a clear colorless oil and exhibited n_D^{20} 1.4540; i.r. (film), λ_{max} 8.03, 9.45, 11.4, 11.9 μ; n.m.r., τ 4.43 (broad singlet, 1H, vinyl H, $w_{\frac{1}{2}}$ = 4 Hz), 5.92 (unresolved multiplet, 2H, —CH_2—OTMS), 8.98, 9.08, 9.13 (doublets, 9H, secondary methyls, J = 7 Hz), 9.87 (singlet, 9H, Si(CH_3)$_3$).

Mol. Wt. Calcd. for $C_{14}H_{28}OSi$: 240.191. Found (high resolution mass spectrometry): 240.191.

Preparation of Alcohol ***12***

The pure *trans*-trimethylsilyl ether **14** (600 mg. 2.5 mmoles) was refluxed in 6 ml of ethanol containing 0.2 ml of water for 2 h. The solvents were removed at water aspirator pressure and the resulting oil was distilled under reduced pressure to afford 413 mg (98%) of the alcohol **12** as a clear colorless oil, b.p. 80° (hot-box) at 0.15 mm; n_D^{20} 1.4825; i.r. (film) λ_{max} 3.0, 6.02, 9.9 μ; n.m.r. τ 4.39 (broad singlet, 1H, vinyl H, $w_{\frac{1}{2}}$ = 5 Hz), 5.92 (unresolved multiplet, 2H, CH_2O—H), 8.22 (singlet, 1H, exchangeable, CH_2OH), 8.98, 9.10, 9.14 (doublets, 9H, secondary methyls, J = 6.8, 6.4, and 6.4 Hz respectively).

Anal. Calcd. for $C_{11}H_{20}O$: C, 78.51; H, 11.98. Found: C, 78.76; H, 12.03.

Preparation of Bromide ***15***

A solution of the alcohol **12** (400 mg, 2.38 mmoles) in 10 ml of benzene containing 0.08 ml of dry pyridine was cooled to 0° in an ice-bath. To this cold stirred solution was added, from a dropping funnel, 312 mg (1.15 mmoles) of phosphorous tribromide in 1.1 ml of dry benzene. The reaction mixture was stirred for 30 min and then diluted with 5 ml of cold dilute aqueous sodium bicarbonate solution. The mixture was extracted with ether and the combined organic layers were dried over anhydrous magnesium sulfate. The solvents were removed at aspirator pressure and the resulting crude product was distilled under reduced pressure to afford 425 mg (77%) of the bromide **15**, b.p. 75° at 0.2 mm; n_D^{20} 1.5027; i.r. (film) λ_{max} 6.08, 8.30 μ; n.m.r. τ 4.30 (broad singlet, 1H, vinyl H, $w_{\frac{1}{2}}$ = 5 Hz), 6.03 (quartet, 2H, $-CH_2Br$, J_{AB} = 10 Hz), 8.95, 9.09, 9.12 (doublets, 9H, secondary methyls, J = 7 Hz).

Anal. Calcd. for $C_{11}H_{19}Br$: C, 57.15; H, 8.28. Found: C, 57.25; H, 8.27.

*(±)-trans-2-Methyl-p-mentha-2-ene (**16a**)*

To a solution of lithium aluminum hydride (50 mg, 1.3 mmoles) in 6 ml of dry tetrahydrofuran was added 300 mg (1.3 mmoles) of the allylic bromide **15**. The mixture was refluxed under an atmosphere of nitrogen for 1.5 h, then cooled to 0°. Water (1 ml) was cautiously added, and the resulting mixture was extracted with ether. The combined ether layers were dried over anhydrous magnesium sulfate and the solvent was removed at water aspirator pressure. Distillation of the resulting oil under reduced pressure gave 188 mg (95%) of (±)-2-methyl-*p*-mentha-2-ene (**16a**) as a clear colorless oil, b.p. 80° (hot-box) at 10 mm; n_D^{20} 1.4602; i.r. (film) λ_{max} 6.93, 7.23, 7.32, 11.5, 11.9 μ; n.m.r. τ 4.87 (broad singlet, 1H, vinyl H, $w_{\frac{1}{2}}$ = 5 Hz), 8.37 (singlet, 3H, vinyl CH_3), 9.05, 9.15, 9.18 (doublets, 9H, secondary methyls, J = 6.6 Hz). This material exhibited spectra (i.r., n.m.r.) identical with those obtained from an authentic sample of (+)-*trans*-2-methyl-*p*-mentha-2-ene (**16b**), the synthesis of which is described below.

Mol. Wt. Calcd. for $C_{11}H_{20}$: 152.156. Found (high resolution mass spectrometry): 152.156.

*(−)-trans-Caran-2-one(**18**)*

A solution of (+)-dihydrocarvone (**17**) (15.2 g, 0.1 mole) in 130 g of 9.4% hydrogen bromide in glacial acetic acid was stirred at room temperature for 15 min, then poured onto 500 g of crushed ice. The resulting mixture was extracted three times with ether and the combined ether extracts were washed with dilute aqueous sodium bicarbonate and water until all of the acetic acid had been removed. The ether layer was dried over anhydrous magnesium sulfate and the ether was removed at water aspirator pressure to afford 23.3 g (100%) of the crude (+)-dihydrocarvone hydrobromide.

To a solution of potassium hydroxide (5.9 g, 0.105 mole) in 250 ml of ethanol at 0° was added the crude hydrobromide (23.3 g, 0.1 mole), and the resulting mixture was stirred for 2 h at 0°. The precipitated potassium bromide was filtered off and the ethanol was removed from the filtrate at water aspirator pressure. Distillation of the resulting oil under reduced pressure gave 12.18 g (80%) of (−)-*trans*-caran-2-one (**18**), b.p. 38–40° at 0.15 mm [lit. b.p. 60° at 1 mm (19)]. This material was crystallized by dissolving it in hexane and cooling the resulting solution to −78° (acetone – Dry Ice). The mother liquors were removed with a pipet and the crystals were warmed to room temperature to give a clear colorless oil. The resulting material was recrystallized under the same conditions and any excess hexane was removed under reduced pressure (vacuum pump, 0.1 mm). A sample of material purified in this way exhibited n_D^{20} 1.4773; $[\alpha]_D^{22}$ −181° (*c*, 1.2 in methanol) [lit. $[\alpha]_D^{19}$ −162.9° (19), −153° (*c*, 5.0) (20)]; i.r. (film) λ_{max} 5.96 μ; n.m.r. τ 8.81, 8.96 (singlets, 6H, tertiary methyls,), 8.98 (doublet, 3H, secondary methyl, J = 6.3 Hz).

Preparation of Alcohol ***19***

To a solution of (−)-*trans*-caran-2-one (**18**) (1.52 g, 0.01 mole) in 50 ml of dry ether was added 15 ml of 2.13

Can. J. Chem. Downloaded from www.nrcresearchpress.com by 210.87.254.42 on 09/05/12
For personal use only.

M ethereal methyllithium (0.032 mole), and the resulting mixture was stirred for 3 days. The excess methyllithium was destroyed by the cautious addition of 2 ml of water, and the ether layer was dried over anhydrous magnesium sulfate. Removal of the ether at water aspirator pressure gave 2.1 g of a pale yellow oil. This material was purified by column chromatography on 60 g of florisil. The fractions eluted with 1:9 ether–hexane and 1:4 ether–hexane were combined to give 1.65 g (98%) of the alcohol **19**, n_D^{20} 1.4800; $[\alpha]_D^{21}$ −9.4° (*c*, 1.0 in methanol); i.r. (film) λ_{max} 2.95, 9.15, 10.95 μ; n.m.r. τ 8.3 (singlet, 1H, exchangeable, O—*H*), 8.74, 8.75, 8.95 (singlets, 9H, tertiary methyls), 9.09 (doublet, 3H, secondary methyl, J = 6.5 Hz).

Anal. Calcd. for $C_{11}H_{20}O$: C, 78.51; H, 11.98. Found: C, 78.63; H, 11.80.

(+)-trans-2-Methyl-p-mentha-2,8-diene (20)

A mixture of the alcohol **19** (836 mg, 5 mmoles) and 0.17 ml of pyridine was placed in a pyrolysis tube and sealed under an atmosphere of nitrogen. The tube was heated in an oil bath at 190° for 2 h after which time it was cooled and carefully opened. The mixture was diluted with ether and dried over anhydrous magnesium sulfate. Removal of the solvents at water aspirator pressure afforded 730 mg of colorless oil. Analysis of this mixture by g.l.c. (column B, 155°, 200) revealed that it consisted of a mixture of 70% (+)-*trans*-2-methyl-*p*-mentha-2,8-diene (**20**) and several minor unidentified components. A sample of **20** purified by preparative g.l.c. (column B, 155°, 200) exhibited n_D^{20} 1.4736; $[\alpha]_D^{20}$ +139.3° (*c*, 3.7 in methanol); i.r. (film) λ_{max} 3.25, 6.08, 11.28 μ; n.m.r. τ 4.72 (broad singlet, 1H, C_3 vinyl H, $w_{\frac{1}{2}}$ = 5 Hz), 5.27 (broad singlet), 2H, CH_3—C=C*H*$_2$, $w_{\frac{1}{2}}$ = 3 Hz), 8.27 (singlet, 6H, vinyl methyls), 8.99 (doublet, 3H, secondary methyl, J = 6.4 Hz).

Anal. Calcd. for $C_{11}H_{18}$: C, 87.93; H, 12.07. Found: C, 88.20; H, 11.85.

(±)-trans-2-Methyl-p-mentha-2-ene (16b)

The hydrogenation of the diene **20** was carried out in benzene at room temperature and atmospheric pressure using tris(triphenylphosphine)chlororhodium (22, 23) as the catalyst. The reaction solution was filtered through a small column of activity II alumina. From 240 mg of **20** there was obtained 225 mg of a clear colorless oil. Analysis of this material by g.l.c. (column C, 110°, 100) showed that it consisted of 80% (+)-*trans*-2-methyl-*p*-mentha-2-ene (**16***b*) and several other minor, unidentified components. A sample of compound **16***b* obtained by preparative g.l.c. (column D, 145°, 200) exhibited n_D^{20} 1.4602; $[\alpha]_D^{22}$ +25.4° (*c*, 0.6 in methanol). This material displayed i.r. and n.m.r. spectra and g.l.c. retention times identical with those obtained from compound **16***a*, prepared as described previously.

Mol. Wt. Calcd. for $C_{11}H_{20}$: 152.156. Found (high resolution mass spectrometry): 152.156.

Preparation of Carboxylic Acid 22

To a hot solution of carbethoxymethylenetriphenylphosphorane (24) (1.28 g, 3.7 mmoles) in 10 ml of ethyl acetate was added 425 mg of the allylic bromide **15** (1.84 mmoles). The resulting mixture was refluxed for 5 h, then cooled and the precipitated carbethoxymethyltriphenylphosphonium bromide (575 mg, 73%) was filtered off. The solvent was removed at water aspirator pressure, and the remaining crude product (**21**) was dissolved in 12 ml of 10% potassium hydroxide in 1:1 methanol–water, and the resulting solution was refluxed for 1 h. The reaction mixture was cooled and the methanol removed at water aspirator pressure. The basic aqueous layer was extracted with ether and then neutralized with 6 *N* hydrochloric acid. The resulting mixture was extracted with ether and the ether extract was dried over anhydrous magnesium sulfate. Removal of the ether followed by distillation of the oily residue under reduced pressure afforded 270 mg (69%) of the carboxylic acid **22** b.p. 120° (hot-box) at 0.15 mm; n_D^{20} 1.4818; i.r. (film) λ_{max} 3.1–3.9, 5.85 μ; n.m.r. τ 4.69 (broad singlet, 1H, vinyl H, $w_{\frac{1}{2}}$ = 4 Hz), 7.40 (singlet, 4H, —CH_2CH_2-CO_2H), 9.00, 9.13, 9.17 (doublets, 9H, secondary methyls).

Anal. Calcd. for $C_{13}H_{22}O_2$: C, 74.24; H, 10.54. Found: C, 74.22; H, 10.53.

(±)-β-Cubebene Norketone (24) and (±)-1,6-Epi-β-cubebene Norketone (25)

The carboxylic acid **22** (242 mg, 1.15 mmoles) was dissolved in aqueous sodium hydroxide (1.32 mmoles), the water was evaporated under reduced pressure, and the residue was dried in a vacuum oven at 70°. A stirred suspension of the resulting dry sodium salt in 20 ml of dry benzene containing 0.02 ml of pyridine was cooled to 0° and 1.5 g (12 mmoles) of oxalyl chloride was added. The reaction mixture was stirred at 0° for 15 min, filtered, and evaporated under reduced pressure (vacuum pump). The solution was kept at 0° during this process. The crude acid chloride **23** (i.r. (film) λ_{max} 5.58 μ; n.m.r. very similar to that of the carboxylic acid **22** except at τ 7.00 (complex multiplet, 4H, —CH_2CH_2COCl)) thus obtained was taken up in 15 ml of dry ether and the resulting solution was added to excess alcohol free ethereal diazomethane which had been dried over potassium hydroxide. The solution was stirred for 15 min and evaporated under reduced pressure affording the crude diazoketone **3**, i.r. (film) λ_{max} 3.27, 4.78, 6.10 μ; n.m.r. τ 4.75 (broad singlet, 2H, vinyl H and COC*H*N_2, $w_{\frac{1}{2}}$ = 4 Hz), 7.64 (singlet, 4H, —CH_2CH_2COCHN_2). The crude diazoketone **3** was dissolved in 30 ml of cyclohexane and cupric sulfate (750 mg) was added. The resulting suspension was refluxed with stirring for 1.5 h after which time the i.r. absorption at 4.78 μ due to the diazoketone **3** had disappeared. The cooled mixture was filtered and the cyclohexane was removed at water aspirator pressure. Distillation of the oily residue under reduced pressure gave 185 mg (78%) of a pale yellow oil, b.p. 100–103° (hot-box) at 0.2 mm. This material was shown by g.l.c. analysis (column E, 190°, 90) to consist of approximately 36% of (±)-β-cubebene norketone (**24**) and 64% (±)-1,6-epi-β-cubebene norketone (**25**). Preparative g.l.c. (column D, 235°, 135) provided pure samples of **24** and **25**. Pure (±)-β-cubebene norketone (**24**) thus obtained exhibited n_D^{20} 1.4940; u.v. λ_{max} 206 mμ (ε = 6150); i.r. (film) λ_{max} 5.85 μ; n.m.r. τ 9.00, 9.05, 9.07 (doublets, 9H, secondary methyls, J = 6.5 Hz).

Anal. Calcd. for $C_{14}H_{22}O$: C, 81.49; H, 10.74. Found: 81.79; H, 10.59.

Can. J. Chem. Downloaded from www.nrcresearchpress.com by 210.87.254.42 on 09/05/12
For personal use only.

Pure (±)-1,6-epi-β-cubebene norketone (**25**) obtained in the same manner exhibited n_D^{20} 1.4984; u.v. λ_{max} 205 mμ (ε = 6280); i.r. (film) λ_{max} 5.82 μ; n.m.r. τ 7.95 (broadened singlet, 4H $w_{\frac{1}{2}}$ = 2 Hz), 8.91 (doublet, 3H, secondary methyl, J = 7 Hz), 8.98 (poorly resolved multiplet, 6H, $CH(CH_3)_2$).

Mol. Wt. Calcd. for $C_{14}H_{22}O$: 206.166. Found (high resolution mass spectrometry): 206.167.

(±)-β-Cubebene (2)

A stirred suspension of sodium hydride (300 mg, 12.5 mmoles) in dry dimethyl sulfoxide (14 ml) was slowly heated under an atmosphere of nitrogen to 75° and kept at this temperature until frothing had ceased (approximately 30 min). The solution was cooled to room temperature and a solution of methyltriphenylphosphonium bromide (5.32 g, 14.8 mmoles) in 8 ml of dimethyl sulfoxide was added. The solution was stirred for 10 min and then a solution of (±)-β-cubebene norketone (**24**) (515 mg, 2.5 mmoles) in 15 ml of dimethyl sulfoxide was added. The reaction mixture was heated to 50° for 6 h, cooled, diluted with water, and then thoroughly extracted with hexane. The combined extracts were washed with water and brine, then dried over anhydrous magnesium sulfate. Removal of the solvent, followed by distillation of the residual oil under reduced pressure afforded 506 mg (99%) of **2** as a clear colorless oil, b.p. 80–82° (hot-box) at 0.2 mm. Analysis of this material by g.l.c. (column F, 170°, 90) revealed that it was only one component and it exhibited n_D^{20} 1.4975; u.v. λ_{max} 208 mμ (ε = 9850); i.r. (film) λ_{max} 3.26, 6.10, 11.72 μ; n.m.r. τ 5.28, 5.47 (unresolved multiplets, 2H, $\diagdown C{=}CH_2$), 9.04, 9.06, 9.10 (doublets, 9H, secondary methyl groups, J = 6.0, 6.5, 6.5 Hz respectively). This material exhibited spectra (u.v., i.r., n.m.r.) and g.l.c. retention times identical with those obtained from authentic β-cubebene, isolated from Oil of Cubeb, Extra (see footnote 9).

Mol. Wt. Calcd. for $C_{15}H_{24}$: 204.187. Found (high resolution mass spectrometry): 204.186.

We thank the National Research Council of Canada and the University of British Columbia Committee on Research for financial support. A National Research Council of Canada Studentship (to W. de W.) and a H. R. MacMillan Family Fellowship (to R.W.B.) are gratefully acknowledged.

1. Y. Ohta, T. Sakai, and Y. Hirose. Tetrahedron Lett. 6365 (1966).
2. Y. Ohta and Y. Hirose. Tetrahedron Lett. 2073 (1967).
3. Y. Ohta, K. Ohara, and Y. Hirose. Tetrahedron Lett. 4181 (1968).
4. E. Piers, R. W. Britton, and W. de Waal. Tetrahedron Lett. 1251 (1969).
5. A. Tanaka, H. Uda, and A. Yoshikoshi. Chem. Commun. 308 (1969).
6. E. Piers, W. de Waal, and R. W. Britton. Chem. Commun. 188 (1968); Can. J. Chem. **47**, 4299 (1969).
7. E. Piers, R. W. Britton, and W. de Waal. Can. J. Chem. **47**, 831 (1969).
8. E. J. Corey and K. Achiwa. Tetrahedron Lett. 1837 (1969).
9. E. J. Corey, K. Achiwa, and J. A. Katzenellenbogen. J. Amer. Chem. Soc. **91**, 4318 (1969).
10. R. M. Coates and R. M. Freidinger. Chem. Commun. 871 (1969).
11. K. Mori and M. Matsui. Tetrahedron Lett. 2729 (1969); Tetrahedron Lett. 4435 (1969).
12. J. J. Plattner, U. T. Bhalerao, and H. Rapoport. J. Amer. Chem. Soc. **91**, 4933 (1969); J. Amer. Chem. Soc. **92**, 3429 (1970).
13. P. A. Grieco. J. Amer. Chem. Soc. **91**, 5660 (1969).
14. R. E. Ireland and J. A. Marshall. J. Org. Chem. **27**, 1615 (1962).
15. R. F. Church, R. E. Ireland, and J. A. Marshall. J. Org. Chem. **27**, 1118 (1962), and references therein.
16. R. E. Ireland and J. A. Marshall. J. Org. Chem. **27**, 1620 (1962), and references therein.
17. W. C. Young and J. F. Lane. J. Amer. Chem. Soc. **59**, 2051 (1937).
18. A. Baeyer. Chem. Ber. **27**, 1915 (1894).
19. W. Cocker, D. P. Hanna, and P. V. R. Shannon. J. Chem. Soc. C, 489 (1968).
20. W. Cocker, P. V. R. Shannon, and P. A. Staniland. J. Chem. Soc. C, 485 (1967).
21. J. W. Daly, F. C. Green, and R. H. Eastman. J. Amer. Chem. Soc. **80**, 6330 (1958).
22. F. A. Jardine and G. Wilkinson. J. Chem. Soc. C, 270 (1967).
23. J. F. Biellmann. Bull. Soc. Chim. Fr. 3055 (1968).
24. O. Isler, H. Gutmann, M. Montavon, R. Ruegg, G. Ryser and P. Zeller. Helv. Chim. Acta, **40**, 1242 (1957).
25. H. J. Bestmann and H. Schulz. Chem. Ber. **95**, 2921 (1962).
26. M. M. Fawzi and C. D. Gutsche. J. Org. Chem. **31**, 1390 (1966), and references therein.
27. E. J. Corey and M. Chaykovsky. J. Amer. Chem. Soc. **87**, 1345 (1965), and references therein.

Can. J. Chem. Downloaded from www.nrcresearchpress.com by 210.87.254.105 on 09/05/12
For personal use only.

Electron Paramagnetic Resonance Study of some Alkyl Substituted Cycloalkenyl Radicals

D. R. GEE[1] AND J. K. S. WAN
Department of Chemistry, Queen's University, Kingston, Ontario
Received August 6, 1970

Well-resolved electron spin resonance (e.s.r.) spectra are reported and analyzed for the radicals produced when samples of solid adamantane doped with alkyl substituted cycloalkenes are γ-irradiated at room temperature.

Canadian Journal of Chemistry, 49, 20 (1971)

Introduction

Pyrolysis experiments (1) revealed the ease with which cycloalkenyl radicals can be generated by removal of one hydrogen atom from cycloalkene molecules. The radicals formed possess unusual resonance stability as no further hydrogen elimination is observed even at temperatures up to 400 °C. Ohnishi *et al.* (2) and Ayscough and Evans (3) subsequently attributed e.s.r. spectra observed following the irradiation of cycloalkene glasses to these cycloalkenyl radicals. These workers concluded that hydrogen elimination preferentially occurred from a carbon atom adjacent to the unsaturated linkage and that the radical generated was stabilized by electron delocalization on three carbon atoms.

In a successful attempt to improve the e.s.r. spectral resolution of these radicals, Helcke and Fantechi (4) generated cyclohexenyl and cycloheptenyl radicals by irradiating polycrystalline thiourea adducts of the parent hydrocarbons with fast electrons. We have recently initiated a systematic study of silver cycloalkenyl radicals in γ-irradiated silver cycloalkene complexes (5), and have extended the study to alkyl substituted olefins. However, a literature search reveals that little e.s.r. information is known about the parent alkyl substituted cycloalkenyl radicals. To extend this study to alkyl cycloalkenyl radicals we found that spectral resolution could be improved by slightly modifying the recently developed technique of Wood and co-workers (6). These workers achieved well resolved isotropic e.s.r. spectra of a series of amino radicals by selective radiation damage of aliphatic amines, deliberately added as impurities to a solid adamantane matrix.

This investigation reports a series of e.s.r. spectra originating from the paramagnetic species generated when samples of polycrystalline adamantane doped with cyclopent-1-ene, 1-methylcyclopent-1-ene, 1-ethyl-cyclopent-1-ene, 1- and 4-methyl-cyclohex-1-ene, 1-methyl-1,4-cyclohexadiene, and 1-methyl-cyclohept-1-ene are each γ-irradiated at room temperature. The factors influencing radical stability and the extent of hyperconjugation between the alkyl substituents and the π conjugated systems are discussed.

Experimental

The cycloalkenes were introduced as impurities into adamantane (Aldrich) by recrystallization of the solid using pure redistilled cycloalkenes (Aldrich) as recrystallizing solvent. Samples of the olefin-containing solids were filtered, dried, and irradiated in air at room temperature in a 19 500 curie source of 1.25 MeV ^{60}Co γ-rays. The dose rate used was approximately 1 Mrad/h and the total dose was 0.2–0.3 Mrad. Electron spin resonance spectra were obtained with an X-band Varian V4502 spectrometer using 100 kc modulation and auxiliary equipment. Microwave power and the modulation amplitude were adjusted to avoid saturation. Simulation of spectra was carried out by an IBM 360/50 computer using a modified version of a program originally made available by the Bell Telephone Laboratory.

Results and Discussion

γ-Irradiation of pure solid adamantane alone leads to a low yield of adamantyl radicals (7). However, when the adamantane samples doped with alkyl cycloalkenes are irradiated at room temperature, no adamantanyl radicals can be detected and formation of other radicals from the alkyl cycloalkene molecules is observed. These radicals probably result from some radiation chemical processes including energy transfer from

[1]Postdoctoral fellow 1969–1970; present address: Department of Chemistry, University of Manchester Institute of Science and Technology, Manchester, England.

Can. J. Chem. Downloaded from www.nrcresearchpress.com by 210.87.254.105 on 09/05/12
For personal use only.

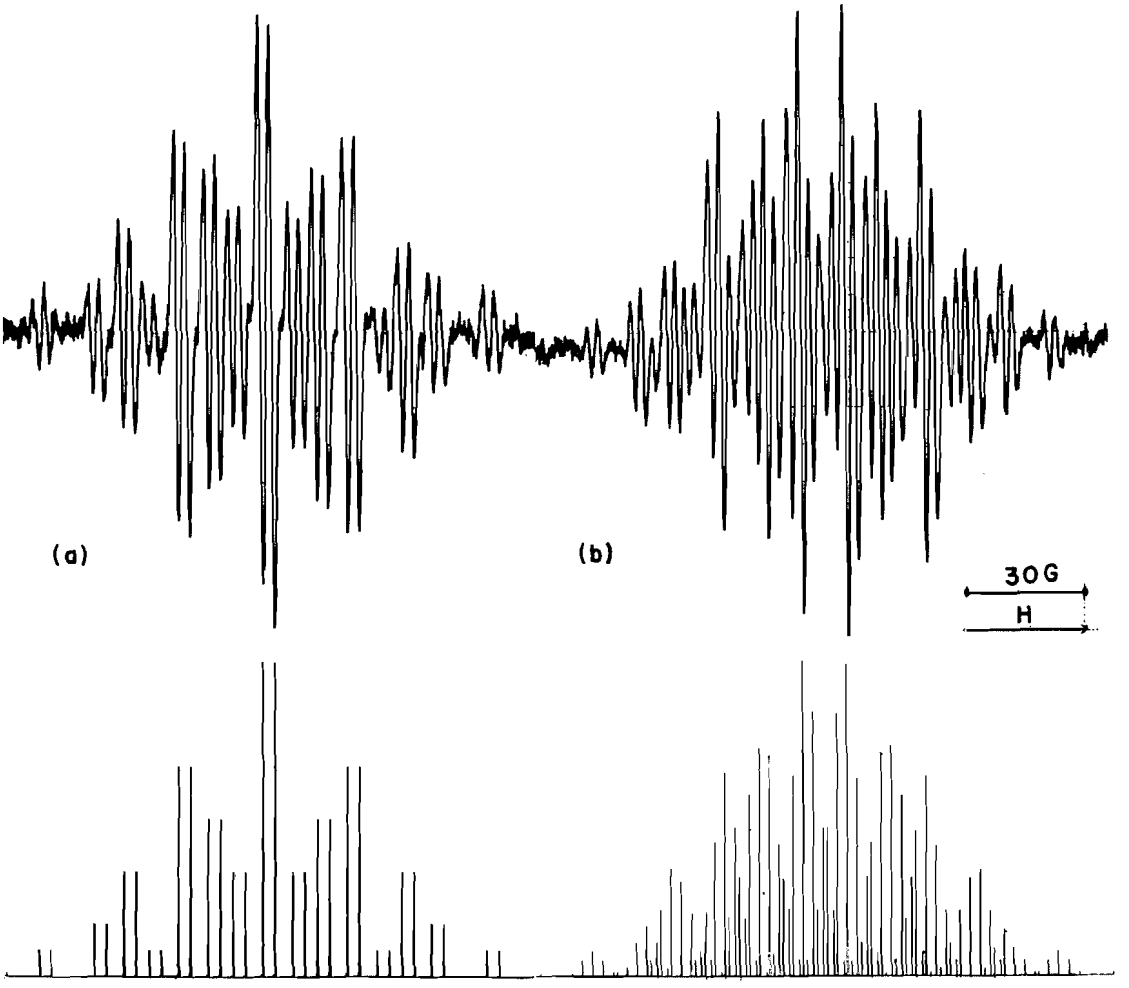

FIG. 1. Electron spin resonance spectra from free radicals trapped in an irradiated adamantane matrix (*a*) 3-cyclopentenyl radical; (*b*) 1-ethyl-3-cyclopentenyl radical.

the matrix to the cycloalkenes. Typical room temperature e.s.r. spectra of these radicals are shown in Figs. 1 to 4.

3-Cyclopentenyl Radical

The improvement of spectral resolution using the adamantane matrix trapping technique enables more accurate assignments than are possible from spectra obtained with irradiated olefin glasses (2, 8). This is demonstrated by the resolution of the small α_2 proton hyperfine splitting in the 3-cyclopentenyl radical (Fig. 1*a*). Assignments for the proton coupling constants of this radical are compared with those of Ohmae *et al.* (2) in Table 1.

Fessenden and Schuler (9) found that each methylene group adjacent to a conjugated π system tends to withdraw approximately 8% of the unpaired spin from the α carbon atoms. Hence, if a value of 0.84 is accepted for the π bonded section of the radical, the individual spin densities at each carbon may be estimated assuming a Q value of 29.6 G for each of the carbon atoms of the allylic system. For the 3-cyclopentenyl radical these calculations yield values of $\rho_{1,3} = 0.47$ and $\rho_2 = -0.1$. If these parameters are used to estimate the magnitude of the methylene proton splittings, a value of 13.8 G is obtained. The experimental coupling constant for these protons was found to be 20.0 G. Helcke and

Can. J. Chem. Downloaded from www.nrcresearchpress.com by 210.87.254.105 on 09/05/12
For personal use only.

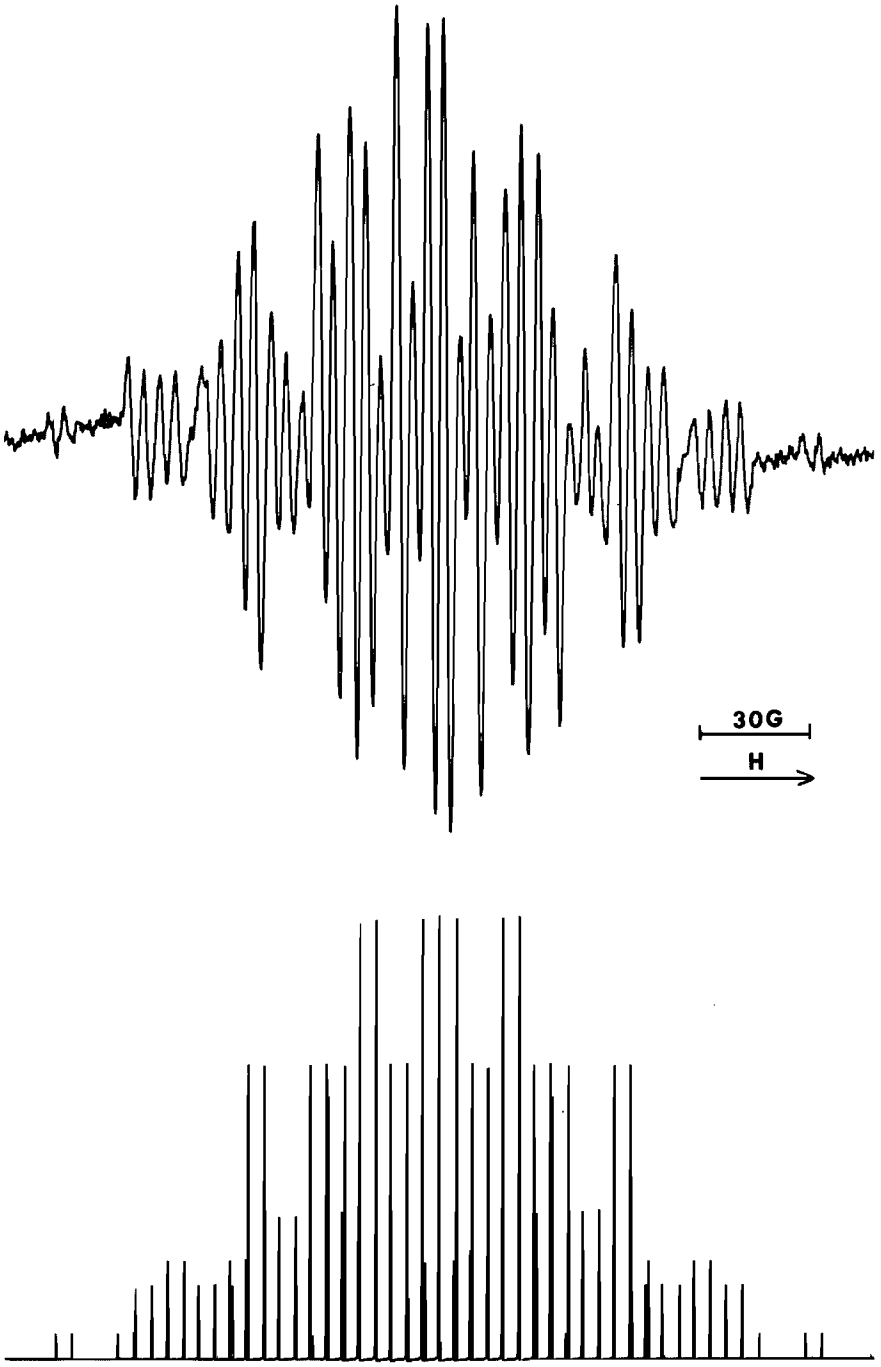

FIG. 2. Electron spin resonance spectra from free radicals trapped in an irradiated adamantane matrix containing 1-methylcyclopent-1-ene.

Can. J. Chem. Downloaded from www.nrcresearchpress.com by 210.87.254.105 on 09/05/12
For personal use only.

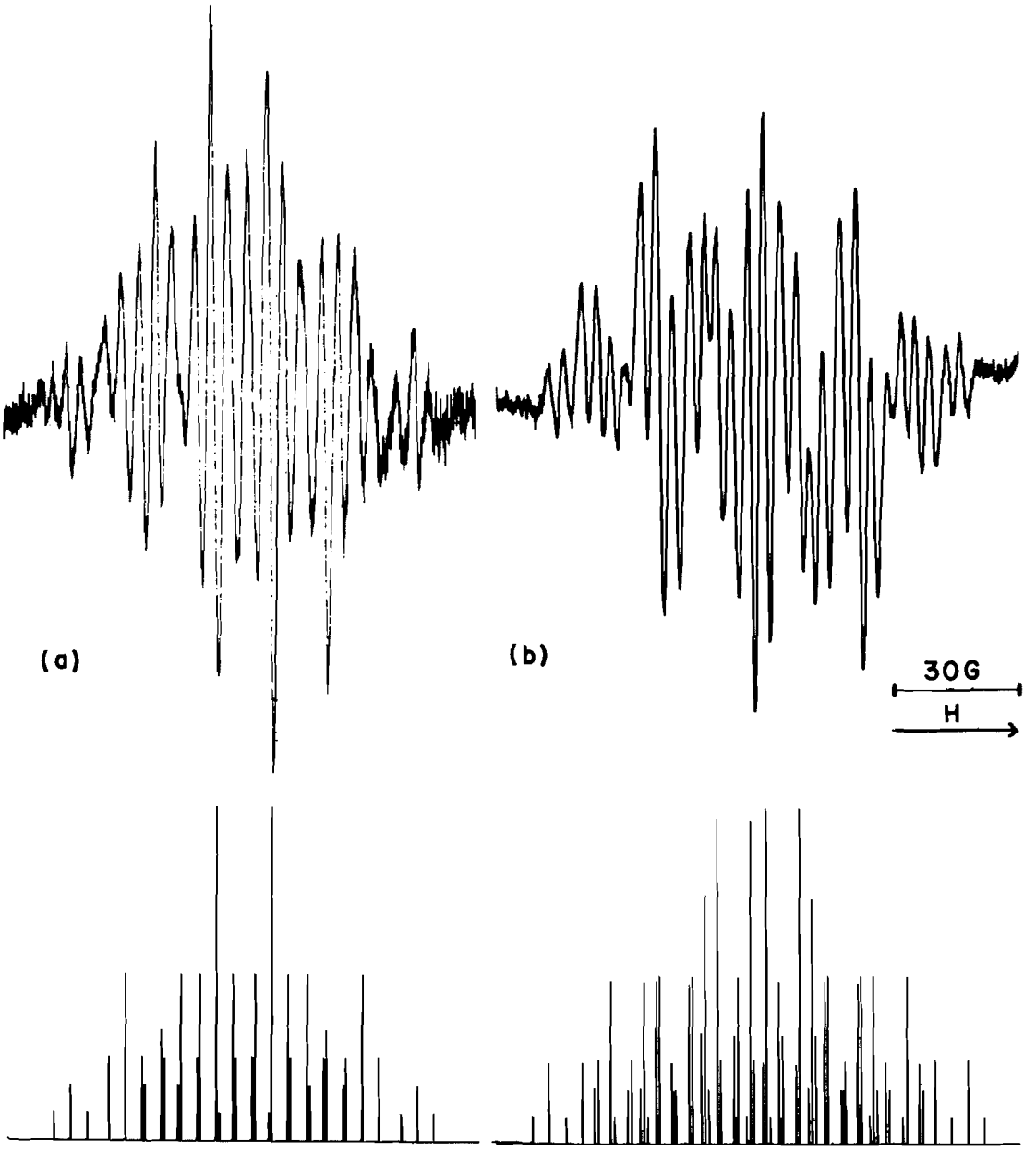

FIG. 3. Electron spin resonance spectra from free radicals trapped in an irradiated adamantane matrix: (*a*) 1-cyclohexenemethyl radical; (*b*) 4-methyl-3-cyclohexenyl radical.

Fantechi (4) observed a similar anomaly with the 3-cyclohexenyl and 3-cycloheptenyl radicals, which they interpreted by suggesting that although the β protons in each radical were equivalent, the rotational averaging which brings this about was not isotropic. The fact that the observed splittings are considerably larger than the isotropic values seems to indicate that the methylene protons are oriented above and below the planar conjugated π system (10, 11). The

Can. J. Chem. Downloaded from www.nrcresearchpress.com by 210.87.254.105 on 09/05/12
For personal use only.

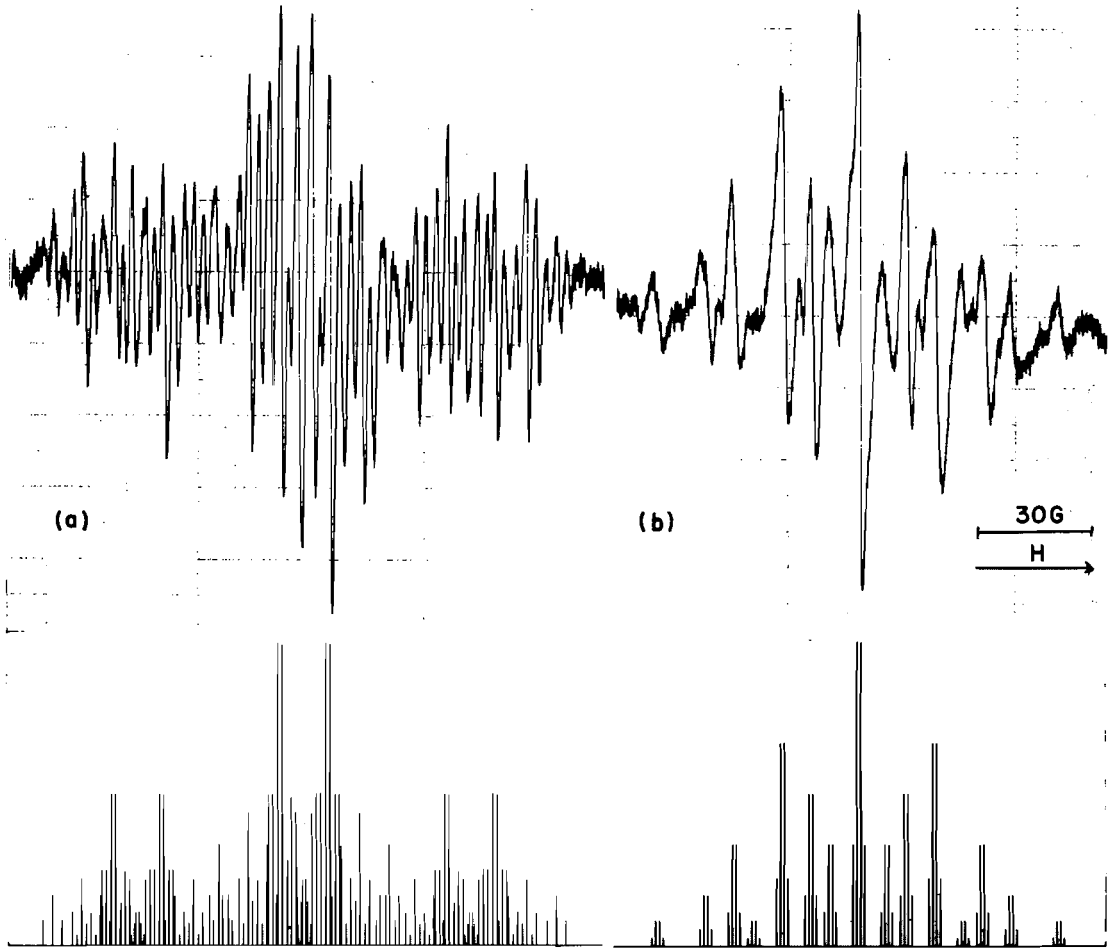

FIG. 4. Electron spin resonance spectra from free radicals trapped in an irradiated adamantane matrix: (*a*) 1-methyl-3-cyclohexadienyl radical; (*b*) 2-methyl-3-cycloheptenyl radical.

work of Fessenden (11) predicts that the magnitude of the β splitting in such a system would indeed approximate to a value of 20 G.

1-Ethyl-3-cyclopentenyl Radical

The spectrum observed (Fig. 1*b*) when samples of adamantane doped with 1-ethyl-cyclopent-1-ene are irradiated may similarly be attributed to the corresponding 1-ethyl-3-cyclopentenyl radical using the hyperfine splitting constants presented in Table 1. A comparison of the splitting constants for this radical and those of the 3-cyclopentenyl radical reveals a decrease in the proton splitting and hence the spin densities at the α carbon atoms. Such a decrease is consistent with the observation of Fessenden and Schuler (9) that methylene groups adjacent to a conjugated π system reduce the unpaired spin density at the α carbon atoms. Since the addition of a substituent at the C_1 carbon atom renders the π conjugated system unsymmetrical, it is no longer possible to estimate accurately the spin density at each α carbon atom. In view of the fact that the proton coupling constants for the four β protons of this 1-ethyl-3-cyclopentenyl radical remain approximately the same as in the unsubstituted radical, it would seem to be reasonable that the spin densities at the C_2 and C_3 carbon positions are not drastically altered. Thus, a value of 13 ± 1 G is to be expected for the coupling constants of the methylene protons adjacent to the π conjugated system (9). The assigned splitting

TABLE 1. Summary of hyperfine coupling constants for substituted 3-cycloalkenyl radicals (G)

Radical	a_1	a_2	a_3	a_β	$a_{(CH_2)}$	$a_{(CH_3)}$
3-Cyclopentenyl	14.0±0.2	3.1	14.0	21.6		
	14.0*	0	14.2*	23.1*		
1-Ethyl-3-cyclopentenyl		2.5	11.4	20.0	13.8	2.6
1-Methyl-3-cyclopentenyl		3.0	11.4	20.4		14.6
4-Methyl-3-cyclohexenyl	14.8	3.9	14.8	25.8		7.8
				8.0		
2-Methyl-3-cycloheptenyl	12.7		12.7	20.0		2±0.8

*Reference 2.

of 1.38 G for the substituent methylene protons in this radical suggests that, in contrast to the β ring protons, the averaging of these protons is essentially isotropic.

1-Methyl-cyclopentenyl Radical

A typical room temperature e.s.r. spectrum of the radical generated when 1-methyl-cyclopentene was irradiated in an adamantane matrix is shown in Fig. 2. Inspection of this spectrum reveals a predominant 1:4:6:4:1 pattern of 20 G spacing characteristic of the four β protons of 3-cycloalkenyl radicals. Spectral analysis on this basis yields the parameters of this 1-methyl cyclopentenyl radical listed in Table 1. The splitting of 14.6 G assigned for the methyl protons compares with the value of 14 ± 1 G expected for the isotropic coupling constants of methylene protons adjacent to a π conjugated system (9, 14).

1-Cyclohexene-methyl Radical

Inspection of the spectrum (Fig. 3*a*) when samples of adamantane containing 1-methyl-cyclohex-1-ene are irradiated reveals a predominant 1:2:1 splitting of 22.0 G. This contrasts with the characteristic 1:4:6:4:1 splitting of the four β protons in 3-cycloalkenyl radicals. We attribute this spectrum to the 1-cyclohexene-methyl radical with the following proton coupling constant assignments. The two β protons have a

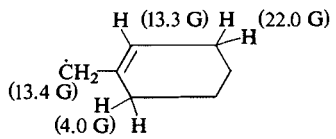

characteristic β splitting of about 22 G (9, 12) whilst the hyperfine splittings of the substituent methylene and the α protons compare with the value of 13.8 G predicted for allylic protons (13).

4-Methyl-3-cyclohexenyl Radical

If an α hydrogen atom is removed from 4-methyl-cyclohex-1-ene, the most likely radicals to result are the 4- and 5-methyl-3-cyclohexenyl radicals. These two isomeric radicals differ as the substituents occupy respectively β and γ positions relative to the allyl system. Since interactions at γ positions are usually very small for hydrocarbons, the assignments for the hyperfine splitting constants for the 5-methyl-3-cyclohexenyl radical would be similar to those of the parent cyclohexenyl radical. Comparison of Fig. 3*b* with reported spectra assigned to the 3-cyclohexenyl radical (2–4) appears to eliminate the 5-methyl-3-cyclohexenyl radical as the species primarily responsible for the spectrum. Computer analysis of Fig. 3*b* on the basis that 4-methyl-3-cyclohexenyl radical is the predominant paramagnetic species yields the spectral parameters presented in Table 1. It appears that the addition of the methyl substituent prevents isotropic averaging of the β protons and effectively locks the β methylene groups with respect to the remainder of the radical. Hence the hyperfine splitting constants observed for the 4-methyl-3-cyclohexenyl radical compare with those quoted for the 3-cyclohexenyl radical at low temperatures (2–4). This indicates that an alkyl substituent at C_4 position does not significantly alter the unpaired spin density on the conjugated system.

1-Methyl-3-cyclohexadienyl Radical

Radiolysis studies (9, 14) on benzene and 1,4-cyclohexadiene yield spectra which have been assigned to the 3-cyclohexadienyl radical. Hence irradiation of samples containing 1-methyl-1,4-cyclohexadiene could presumably lead to formation of either 1-methyl or 2-methyl-3-cyclohexadienyl radicals, depending on the site of the hydrogen atom removal and the relative stability of the radicals formed. Since studies of 1-ethyl-cyclopent-1-ene in the adamantane matrix suggest the removal of a hydrogen atom at C_3 position, our initial attempt to interpret the

Can. J. Chem. Downloaded from www.nrcresearchpress.com by 210.87.254.105 on 09/05/12
For personal use only.

TABLE 2. Hyperfine coupling constants of the 3-cyclohexadienyl and the 1-methyl-3-cyclohexadienyl radicals

Proton splitting parameter	Value (G)	
	3-Cyclohexadienyl*	1-Methyl-3-cyclohexadienyl
a_1	8.99±0.02	
$a_2 = a_4$	2.65	2.50±0.02
a_3	13.04	12.70
a_5	8.99	8.99
$a_{(CH_2)}$	47.70	44.20
$a_{(CH_3)}$		7.85

*Taken from refs. 9 and 14.

major portion of the experimental spectrum in Fig. 4*a* was the 1-methyl-3-cyclohexadienyl radical with coupling constants listed in Table 2. By comparison with the theoretically constructed spectrum, it is conceivable that other radicals other than the 1-methyl-3-cyclohexadienyl radical may also be present.

Whiffen (15) has suggested that the methylene coupling constant of the cyclohexadienyl radical is related to the spin density at the ortho carbon atoms by the expression

$$[1] \qquad a_{(CH_2)} = Q_\beta[\rho_1^{1/2} + \rho_5^{1/2}]^2$$

where ρ_1 and ρ_5 are the spin densities at carbon atoms C_1 and C_5, respectively. Using a value of 35 G (9) for Q_β in this relationship yields a value of +0.284 for ρ_1 in the 1-methyl-3-cyclohexadienyl radical. Thus, the addition of the substituent methyl group appears to reduce the unpaired spin in the allylic system by about 6.6%. Fessenden and Schuler (9) have found a decrease of 8.1% in the spin density for each methylene group attached to the π bonded section of simple allyl radicals. These authors suggest also that the β splitting of the substituent methyl protons are related to the unpaired spin density on the adjacent α carbon atom. Using a Q value of 25.7 G in this relationship, a value of 7.3 G was derived for the methyl protons splitting in the 1-methyl-3-cyclohexadienyl radical. This compares with the experimental assignment of 7.85 G. Thus the tentative identification of this radical appears to be reasonable.

2-Methyl-3-cycloheptenyl Radical

Analysis of the observed spectrum (Fig. 4*b*) when samples of adamantane doped with 1-methyl-cyclohept-1-ene are irradiated, reveals the characteristic β proton splitting of a 3-cycloalkenyl radical (2, 4). Splitting of 13 ± 3 G expected for substituent methyl protons is however not apparent. A comparison of Fig. 4*b* with a spectrum assigned to the 3-cycloheptenyl radical (4) shows that both spectra have the same basic line structure. The hyperfine splitting of 4.5 G assigned to the C_2 protons in the 3-cycloheptenyl (4) is absent from the spectrum of the substituted radical. This seems to suggest that the predominant radical generated when adamantane containing 1-methyl-cyclohept-1-ene is irradiated is the 2-methyl-3-cycloheptenyl radical rather than the expected 1-methyl-3-cycloheptenyl radical.

The tentative assignment for this proposed radical is given in Table 1. Although the methyl substituent renders an accurate estimate of the unpaired spin density of the allylic system difficult, a comparison of the α_1 proton splitting of the substituted and parent radicals, 12.7 and 13.7 G, respectively, shows as expected a lower value for the coupling constant of the substituted radical. The hyperfine splitting of the methyl protons in the substituted radical is not resolved in the experimental spectrum. However, if free rotation of the methyl group is assumed, an estimated methyl protons coupling constant of 2 ± 0.8 G can be derived from the line width of the experimental spectrum. For the 2-methylallyl radical at low temperatures, Kochi and Krusic (16) have assigned a splitting of 3.19 G for the methyl protons. The low value is to be expected from the theoretical consideration of Nakatsuji *et al.* (17). In the absence of a quantitative assessment of the vibronic effects and the thermal motions of the cycloheptyl ring, our assignment of the methyl protons coupling constant in this tentatively identified 2-methyl-3-cycloheptenyl radical appears reasonable.

Conclusions

The predominant radicals formed when samples of solid adamantane doped with alkyl substituted cycloalkenes are irradiated at room temperature are the corresponding cycloalkenyl radicals with the α hydrogen atom removed. The reason for this is undoubtedly the high resonance stability of the allylic system. The site of the hydrogen atom removal and the relative stability of the resulted radicals are dependent upon the ring size and conformation. The major radical formed appears to be one which can most easily

Can. J. Chem. Downloaded from www.nrcresearchpress.com by 210.87.254.105 on 09/05/12
For personal use only.

conjugate with the unsaturated linkage to form a planar configuration.

An alkyl substituent adjacent to the allylic system reduces the total unpaired spin density of the system by about 8%. Alkyl substituents in other positions have much less influence. The extent of hyperconjugation of the substituent methylene protons is determined by the spin density on the carbon atom at which the substituent is attached. The proton coupling constant of the alkyl group of 2-alkyl cycloalkenyl radicals is much smaller than those of the corresponding 1-alkyl cycloalkenyl radicals as the singly occupied π orbital of the 2-alkyl cycloalkenyl radical has a node on the C_2 carbon atom.

The authors are indebted to Mr. L. Fabes and Professors K. E. Russell and J. A. Stone for some helpful discussions. Financial support by the National Research Council of Canada, the Defence Research Board, and the Public Health Department is gratefully acknowledged.

1. A. S. GORDON and S. RUVEN SMITH. J. Chem. Phys. **34**, 331 (1961).
2. S. OHNISHI and I. NITTA. J. Chem. Phys. **39**, 2848 (1963); T. OHMAE, S. OHNISHI, K. KUWATA, H. SUKURAI, and I. NITTA. Bull. Chem. Soc. Japan, **40**, 226 (1967).
3. P. B. AYSCOUGH and H. E. EVANS. Trans. Faraday Soc. **60**, 801 (1964).
4. G. A. HELCKE and R. FANTECHI. Mol. Phys. **18**, 1 (1970).
5. D. R. GEE and J. K. S. WAN. Chem. Commun. 641 (1970); D. R. GEE, K. E. RUSSELL, and J. K. S. WAN. Can. J. Chem. **48**, 2740 (1970); D. R. GEE, K. E. RUSSELL, and J. K. S. WAN. J. Chem. Phys. **53**, 847 (1970).
6. D. E. WOOD and R. V. LLOYD. J. Chem. Phys. **52**, 3840 (1970); D. E. WOOD, R. V. LLOYD, and D. W. PRATT. J. Amer. Chem. Soc. **92**, 4115 (1970).
7. D. R. GEE, L. FABES, and J. K. S. WAN. Chem. Phys. Lett. In press.
8. D. R. SMITH and J. J. PIERONI. J. Phys. Chem. **70**, 2379 (1966); D. R. SMITH, F. OKENKA, and J. J. PIERONI. Can. J. Chem. **45**, 833 (1967); E. BEASLEY and R. S. ANDERSON. J. Chem. Phys. **40**, 2565 (1964).
9. R. W. FESSENDEN and R. H. SCHULER. J. Chem. Phys. **39**, 2147 (1963).
10. E. W. STONE and A. H. MAKI. J. Chem. Phys. **37**, 1326 (1962).
11. R. W. FESSENDEN. J. Chem. Phys. **61**, 1570 (1964).
12. C. CHACHATY. J. Chim. Phys. **64**, 614 (1967).
13. C. HELLER and T. COLE. J. Chem. Phys. **37**, 243 (1962).
14. R. W. FESSENDEN and R. H. SCHULER. J. Chem. Phys. **38**, 773 (1963).
15. D. H. WHIFFEN. Mol. Phys. **6**, 223 (1963).
16. J. K. KOCHI and P. J. KRUSIC. J. Amer. Chem. Soc. **90**, 7157 (1968).
17. H. NAKATSUJI, H. KATO, and T. YONESAWA. Bull. Chem. Soc. Japan, **43**, 698 (1970).

Can. J. Chem. Downloaded from www.nrcresearchpress.com by 210.87.254.105 on 09/05/12
For personal use only.

Can. J. Chem. Downloaded from www.nrcresearchpress.com by 210.87.254.5 on 09/05/12
For personal use only.

The Free Radical Photooximation of Alkanes by Nitrosyl Chloride[1]

MELVYN W. MOSHER
Department of Chemistry, Marshall University, Huntington, West Virginia

AND

N. J. BUNCE[2]
Department of Chemistry, University of Guelph, Guelph, Ontario

Received August 13, 1970

The mechanism of the photooximation of alkanes with nitrosyl chloride has been reinvestigated. The lack of initiation of the reaction with free radical initiators suggests that a free radical chain pathway is not involved. Nevertheless, the relative reactivities of hydrocarbons of different structure and the deuterium isotope effect are very similar to those obtained in chlorinations with elemental chlorine, and in particular, primary and tertiary hydrogens are not inert to photooximation as has been previously supposed. A probable reaction mechanism involves hydrogen abstraction from the substrate by atomic chlorine in a free radical non-chain process. This hydrogen abstraction step is shown not to be significantly reversible.

Canadian Journal of Chemistry, 49, 28 (1971)

The photooximation of alkanes with nitrosyl chloride (1, 2) has recently been the subject of intensive study (3, 4), not least because of its commercial interest (5). In particular cyclohexane may be converted in near quantitative yields to cyclohexanone oxime (6) which is used as a precursor of ε-caprolactam and ultimately nylon 6.

The mechanism of photooximation has been widely considered (7, 8) to be the free radical chain process depicted in Scheme 1.

$$\text{ClNO} \xrightarrow{h\nu} \text{Cl}\cdot + \text{NO}$$

$$\text{Cl}\cdot + \text{RH} \longrightarrow \text{HCl} + \text{R}\cdot$$

$$\text{R}\cdot + \text{ClNO} \longrightarrow \text{Cl}\cdot + \text{RNO}$$

$$\text{RNO} + \text{HCl} \longrightarrow \text{R=NOH.HCl}$$

SCHEME 1

The use of alkanes bearing hydrogens in different environments as substrates gave product ratios entirely different from those observed in free radical chlorinations using molecular chlorine. Although oximes derived from secondary hydrogens were produced almost statistically and in good yield (8), primary (other than primary benzylic) and tertiary positions appeared to be almost inert (3). Likewise alkyl chlorides (8) and aliphatic acids (9) were deactivated at the positions close to the substituent but the effect was more pronounced than that observed for abstraction by atomic chlorine (10, 11). Also, alkyl groups apparently caused steric hindrance to photooximation at nearby secondary sites (3), again in contrast with chlorinations (12). The quantum yield for the production of oximes is of the order of unity, and this, coupled with the unusual product distribution has led Müller and co-workers (3, 13) to question the free radical chain mechanism. They propose either that the reaction takes place by way of free radicals entirely within a solvent cage, or that a nitrosyl chloride molecule photo-activated with energy less than sufficient for complete dissociation is involved in a "4-centered-cage mechanism" (3). Presumably this implies some sort of vibrationally excited species or "hot" ground state. This four-centered process is proposed to be subject to severe steric restrictions and thus is explained the predominant attack at secondary carbon atoms.

The problem with a photooximation mechanism involving vibrationally excited nitrosyl chloride is that, in solution, it would be expected that the lifetime of such species would be very short. In a non-polar solvent the lifetime of vibrationally excited chlorine molecules is estimated at about 10^{-9} s (14), in good agreement with the values 2.6×10^{-9} and 1×10^{-9} s for the lifetimes of vibrationally excited liquid benzene and carbon disulfide, respectively (15). With such a short relaxation time the four-centered mechanism would have to lead to successful reaction at almost every collision if a quantum yield near unity were to be achieved; this would seem to be

[1]Presented in part at the Ninth Informal Conference on Photochemistry, Columbus, Ohio, September 1970.
[2]To whom correspondence should be addressed.

Can. J. Chem. Downloaded from www.nrcresearchpress.com by 210.87.254.5 on 09/05/12
For personal use only.

unlikely in that a four-centered transition state requires a high degree of orientation of the reaction partners and this would presumably not be the case at each encounter.

The purpose of this study was to try to distinguish between the pathway involving photoexcited nitrosyl chloride molecules and a free radical mechanism. The free radical mechanism could be either a chain process (Scheme 1) or a non-chain process (Scheme 2) analogous to the course recently suggested for the mechanism of nitrosation of alkanes by *t*-butyl nitrite (16).

$$\text{ClNO} \xrightarrow{h\nu} \text{Cl}\cdot + \text{NO}$$
$$\text{Cl}\cdot + \text{RH} \longrightarrow \text{HCl} + \text{R}\cdot$$
$$\text{R}\cdot + \text{NO} \longrightarrow \text{RNO} \rightarrow \text{R=NOH}$$

SCHEME 2

Presumably it could also occur entirely within a solvent cage, when it would resemble one of the mechanisms suggested by Müller (3).

Attempts to observe free radicals directly by electron spin resonance (e.s.r.) in solutions undergoing photooximation have been unsuccessful (3); we did not attempt direct observation because the first formed nitrosation product (RNO) is itself photolabile and also gives rise to free radicals (16).

$$\text{RNO} \xrightarrow{h\nu} \text{R}\cdot + \text{NO}$$
$$\text{R}\cdot + \text{RNO} \longrightarrow \text{R}_2\text{NO}\cdot$$

Our experiments were therefore concerned with indirect methods of probing for free radical intermediates. In this paper we present new experimental data which is, we believe, compatible with a free radical mechanism in which hydrogen abstraction is by way of chlorine atoms.

Discussion and Results

In the first series of experiments, attempts were made to promote the reaction by means of free radical initiators. Of the three mechanisms being considered only the free radical chain reaction (Scheme 1) should be capable of being so initiated; successful chemical initiation would exclude an excited state of nitrosyl chloride as an intermediate.

Preliminary experiments showed that at 60° nitrosyl chloride reacts thermally with cyclohexane, cyclohexyl chloride and a little cyclohexanone oxime being produced together with very small amounts of other products. At 100° a very complex mixture is formed though these two compounds are still products. Nitrosyl chloride decomposes reversibly to chlorine and nitric oxide at a reasonable rate at these temperatures (2), as a consequence of the very weak Cl—NO bond (D(Cl—NO) = 38 kcal/mole). We suggest that the thermal reaction gives chlorocyclohexane and cyclohexanone oxime by the following course (Scheme 3).

$$\text{ClNO} \rightarrow \text{Cl}\cdot + \text{NO}$$
$$\text{Cl}\cdot + \text{ClNO} \rightarrow \text{Cl}_2 + \text{NO}$$
$$\text{Cl}\cdot + \text{RH} \rightarrow \text{HCl} + \text{R}\cdot$$
$$\text{R}\cdot + \text{Cl}_2 \rightarrow \text{RCl} + \text{Cl}\cdot$$
$$\text{R}\cdot + \text{NO} \rightarrow \text{RNO} \rightarrow \text{R=NOH}$$

SCHEME 3

When benzoyl peroxide was used as a free radical initiator no cyclohexanone oxime was produced, but 1-chloro-1-nitrosocyclohexane was obtained in addition to cyclohexyl chloride. The quantities of the two major products, however, were little more than in control experiments where the benzoyl peroxide was omitted (see Table 1). The chloronitrosocompound, found in several of these reactions, has been shown (3) to arise by the action of chlorine on the oxime. Several unidentified high boiling materials were also formed in low yield in all these reactions.

The use of azobisisobutyronitrile (AIBN) or phenylazotriphenylmethane (PAT) as initiators was somewhat more efficacious, but even here the "chain length" for the formation of the major products did not exceed unity. It was concluded that in the photochemical oximations the role of the light is not simply to serve as an initiator for a free radical chain, and that Scheme 1 must be no more than a minor reaction pathway.

Previous quantum yield studies are consistent with this conclusion. Quantum yields (for oxime formation) have been found to lie in the range 0.6–1.5 (3, 8, 13, 17). These values[3] clearly do not support a chain mechanism (though they do not exclude one) and are comparable with our "apparent chain lengths".

An important method of implicating a particular free radical as an intermediate in a free radical substitution is to study its discrimination towards hydrogen atoms in different environ-

[3]The value 1.5 has been suggested as being too high.

Can. J. Chem. Downloaded from www.nrcresearchpress.com by 210.87.254.5 on 09/05/12
For personal use only.

TABLE 1. Reactants, major products,[a] and apparent chain length in the reaction between nitrosyl chloride and cyclohexane with free radical initiators

ClNO	Initiator (concentration)		HCl added	Chlorocyclohexane	1-Chloro-1-nitroso-cyclohexane	Cyclohexanone oxime	Temperature (time)	Chain length[b]
0.21	None		None	0.065	Trace	0.0012	58°(48 h)	—
2.16	None		None	0.224	0.100	Trace	80°(36 h)	—
2.16	Bz_2O_2[c]	(0.91)	None	0.263	0.116	None	80°(36 h)	Very short
2.16	Bz_2O_2	(0.71)	None	0.290	0.112	None	80°(36 h)	Very short
1.20	None		1.39	0.055	0.030	Trace	60°(48 h)	—
1.20	AIBN	(0.30)	1.39	0.238	0.100	0.012	60°(48 h)	0.8
1.20	AIBN	(0.41)	1.39	0.272	0.128	0.013	60°(48 h)	0.8
1.39	None		1.97	0.002	0.004	None	56°(12 h)	—
1 39	PAT	(0.041)	1.97	0.026	0.020	0.007	56°(12 h)	1.0
1.39	PAT	(0.035)	1.97	0.020	0.020	0.008	56°(12 h)	1.0
0.70	None		None	0.002	0.002	0.0002	42.5°(6 h)	—
0.70	PAT	(0.065)	None	0.025	0.083	0.010	42.5°(6 h)	0.5
0.98	PAT	(0.093)	None	0.034	0.044	0.063	42.5°(6 h)	0.8
1.26	None		0.99	0.002	0.001	0.0002	42.5°(6 h)	—
1.26	PAT	(0.077)	0.99	0.025	0.083	0.010	42.5°(6 h)	1.5
1.26	PAT	(0.36)	0.99	0.026	0.067	0.010	42.5°(6 h)	0.3

[a]All concentrations are moles/l. Cyclohexane was the solvent.
[b]Chain lengths were calculated by dividing the concentration of the three major products by the concentration of initiator used, after allowing for the amounts of products formed in the control reactions. This assumes an efficiency factor of 0.5 for benzoyl peroxide and AIBN and of 1.0 for PAT.
[c]Benzoyl peroxide.

Can. J. Chem. Downloaded from www.nrcresearchpress.com by 210.87.254.5 on 09/05/12
For personal use only.

ments. In most studies of photooximation the reactivities of different positions in the alkane substrate have been estimated by analysis of the mixture of oximes formed, or the ketones derived from them by hydrolysis. Such determinations assume that the distribution of products reflects the distribution of the initially formed free radicals. This may not be so if the intermediates are labile as is the case for *C*-nitrosocompounds; for example, any tertiary nitrosocompound formed is presumably destroyed, being unable to give an oxime. Neither will it be the case if the products are destroyed; it has been suggested (9) that the lack of observed products from attack on primary hydrogens is a result of further reaction of the product aldoxime (*cf.* the reactivity of aldehydes towards free radicals). Lastly, reversible hydrogen abstraction may distort the distribution of the intermediate radicals initially produced; this phenomenon is well known in free radical brominations (18), and has been observed also in the photocyanation of alkanes by cyanogen chloride (19), a process at least formally analogous to photonitrosation by nitrosyl chloride.[4] The reverse of hydrogen abstraction (reaction 1) could thus modify either of Schemes 1 and 2.

[1] $$HCl + R\cdot \rightarrow RH + Cl\cdot$$

To demonstrate whether reversible hydrogen abstraction was occurring, photoinitiated reactions between nitrosyl chloride and either cyclohexane or 2,3-dimethylbutane in the presence of deuterium chloride and between nitrosyl chloride and a mixture of cyclohexane and perdeuteriocyclohexane were carried out at 0°, at which temperature the solutions of nitrosyl chloride in the alkanes were thermally stable. The alkane was recovered from the reaction mixture and analyzed by mass spectrometry for the deuterium incorporation (or scrambling) which should occur if reaction 1 is taking place (19); in every case the recovered alkane had a mass spectrum identical to that of control material, indicating that no significant degree of reversibility was involved in hydrogen abstraction. A reaction of perdeuteriocyclohexane with nitrosyl chloride in the presence of hydrogen chloride was carried out in the vapor phase to achieve a higher ratio of hydrogen chloride to nitrosyl chloride. Both the excess perdeuteriocyclohexane and the product, perdeuteriocyclohexanone oxime hydrochloride, were analyzed by nuclear magnetic resonance (n.m.r.) but no detectable increase in the amount of ^1H was found in either sample over the amount in the starting material. It would thus appear that reversible hydrogen abstraction is unimportant in photooximation and that the irregularities in the product distributions result from the lability of the first formed products.[5]

In order to obtain a reliable index of the reactivity of the nitrosation intermediate, the reactivities of different hydrocarbon substrates were obtained relative to cyclohexane. The method of relative reactivities, in which a limited amount of reagent competes for two substrates has the advantage in this case that since the disappearance of the substrates is measured, the fate of the intermediates or products is of no consequence (in the absence of reversible hydrogen abstraction). The results of this study, for a variety of alkane structures, are presented in Table 2 together with values for hydrogen abstraction by atomic chlorine for comparison. Photolyses were carried out using both tungsten lamps and a sodium vapor lamp as sources, for it has been suggested that the reaction mechanism changes according to the wavelength of the light used (3).

From an examination of Table 2 the following points may be noted. First, the discrimination of the attacking species towards the different substrates is essentially unchanged whether a sodium vapor lamp or a tungsten lamp is used. Second, the reactive intermediate displays a reactivity towards these substrates very similar to that of atomic chlorine. Third, the non-zero reactivity of tetramethylbutane and 2,3-dimethylbutane indicates that primary and tertiary hydrogens are not inert to the reagent, and we therefore conclude that atomic chlorine is at least a plausible intermediate in the reaction.

Radical reactivities are frequently reported in terms of the selectivity towards primary, secondary, and tertiary hydrogen atoms. In Table 3 are presented the selectivity data for photooxima-

[4]Abstraction of hydrogen from hydrogen chloride by an alkyl radical has also been implicated recently in the chlorination of alkanes by benzoyl hypochlorite (20) and iodobenzene dichloride (21).

[5]Müller and Trense have done similar experiments with bridgehead deuteriated bicyclic compounds (22). They found that the oximes produced had the deuterium content fully conserved. However, since Kooyman and Vegter (23) have indicated that the bridgehead positions of these alkanes are not attacked by free radicals, this observation may not be strictly relevant to this discussion.

TABLE 2. Relative reactivities of several alkanes towards nitrosyl chloride compared with chlorine

Substrate	ClNO[a,b]	ClNO[a,c]	Cl_2[a,b]	Cl_2: literature values		
Cyclohexane[d]	1.00	1.00	1.00	1.00[e]	1.00[f]	1.00[g]
Cyclooctane	1.25(1.10)[h]	1.36	1.04	—	—	—
Cyclopentane	0.81	0.75	0.73	0.83	0.86	0.78
2,3-Dimethylbutane	0.64	0.69	0.67	0.89	0.61	0.87[i]
2,2,3,3-Tetramethylbutane	0.39	0.59	0.33	0.65	—	—
Bicyclo-2,2,1-heptane	0.64	0.79	0.74	0.74	—	0.75[i]
Toluene	0.25	0.32	0.30	—	0.11	—
1-Chlorobutane	0.40	0.45	0.21	0.36	—	0.19[i]

[a]This work, mean value obtained at 0°; for actual values see Experimental section.
[b]Tungsten lamps.
[c]Sodium vapor lamp.
[d]As standard.
[e]Data of ref. 24, 30°, strongly acidic medium.
[f]Data of ref. 25, 40°.
[g]Data of ref. 26.
[h]Bracketed value is from ref. 27.
[i]At 68°.

tion, calculated from the values k(tetramethylbutane), k(cyclohexane), and k(2,3-dimethylbutane) of Table 2, again compared with the values observed for atomic chlorine at 0°. Also presented in Table 3 are values of the deuterium isotope effect for attack on saturated hydrogen by nitrosyl chloride and chlorine; both the selectivity data and the deuterium isotope effect are compatible with the attacking species being atomic chlorine.

From this conclusion follows a definite prediction of the maximum yield of oximes attainable from substrates bearing primary and tertiary, in addition to secondary hydrogens.[6] A survey of the literature using the known selectivity of the chlorine atom indicated that the maximum yield as calculated is never greater than the yield actually obtained (using the data of ref. 4), consistent with the proposed mechanism.

In conclusion, our results with the free radical initiators would seem to exclude a free radical chain mechanism as a major reaction pathway. Studies on the possible reversibility of the attack on the hydrogen atoms indicate that whatever the mechanism, this attack is not significantly reversible. The relative reactivity data, the selectivities derived therefrom, and the deuterium isotope effect are all compatible with the reactive intermediate in the reaction being the chlorine atom, indicating that primary and tertiary hydrogens are not inert to nitrosyl chloride as has been previously supposed. These observations all suggest scheme 2 as a likely course of the reaction; this non-chain free radical process is consistent with the low quantum yield for photooximation and is analogous to the recent proposal by Mackor *et al.* for photonitrosation by *t*-butyl nitrite (16). While these results do not exclude the previously proposed four-centered attack on the alkane by excited nitrosyl chloride, they do remove the necessity for postulating such an intermediate, and indicate that if this intermediate should be involved, its reactivity is comparable with that of atomic chlorine. Whether or not the reaction takes place within a solvent cage or through "free" free radicals cannot be determined on the evidence at hand.

[6]We thank a referee for suggesting this argument to us.

TABLE 3. Selectivity data and secondary deuterium isotope effect for hydrogen abstraction by nitrosyl chloride compared with chlorine, all at 0°

Reagent	Relative selectivity[a]			k_H/k_D[b]
	Primary	Secondary	Tertiary	
ClNO[c]	1	3.8	9.2[e]	1.19
ClNO[d]	1	2.6	4.2[e]	1.20
Cl_2[c]	1	4.5	12[e]	1.28 (1.41)[f]
Cl_2	1	4.5	7.0[g]	1.4[h] 1.3[i]

[a]Per hydrogen.
[b]For actual values see Experimental section.
[c]Tungsten lamps.
[d]Sodium vapor lamp.
[e]Calculated from data of Table 2.
[f]The first value is $k_{C_6H_{12}}/k_{C_5H_{10}} \div k_{C_6D_{12}}/k_{C_5H_{10}}$ using $k_{C_5H_{10}}/k_{C_6H_{12}} = 0.73$ from Table I. The value in brackets uses $k_{C_5H_{10}}/k_{C_6H_{12}} = 0.80$, this being the average of the four quoted values of this quantity from Table 1.
[g]Data of ref. 28.
[h]At 80°; data of ref. 29.
[i]Reference 30, chlorination of toluene at 77°.

Experimental

Nitrosyl chloride was prepared by the action of hydrogen chloride on nitrosyl sulfuric acid, or by the method of Inorganic Syntheses (31, 32). Deuterium chloride was prepared by the action of deuterium oxide on redistilled benzoyl chloride; using standard vacuum

Can. J. Chem. Downloaded from www.nrcresearchpress.com by 210.87.254.5 on 09/05/12
For personal use only.

Can. J. Chem. Downloaded from www.nrcresearchpress.com by 210.87.254.5 on 09/05/12
For personal use only.

line procedures, the deuterium chloride, liberated by stirring the two reagents together for 24 h, was allowed to expand into an evacuated 2 l bulb. The product was fractionated, using a methanol slush bath (−98°) (33). The volatile material after two such fractionations was condensed into acetonitrile, which had previously been dried by the use of molecular sieve, and estimated by alkimetric titration. The hydrocarbon substrates were all commercially available, and were purified by standard procedures when necessary; their purities were ascertained to be > 99.5% by vapor phase chromatography (v.p.c.) before use; perdeuteriocyclohexane was obtained from Stohler Isotope Chemicals. The free radical initiators were available commercially, except for phenylazotriphenylmethane which was prepared by the method of Cohen and Wang (34).

Reactions were carried out in sealed evacuated Pyrex glass ampoules unless otherwise stated. The reaction mixtures to be photoinitiated were placed in a bath of melting ice and photolyzed with two 200 W tungsten lamps or a sodium vapor lamp until colorless, or nearly so. The reactions to be promoted by free radical initiators were protected from the light, and placed in a constant (±3°) temperature bath for an appropriate period. When the reactions were over, the ampoules were cooled to 77 °K and opened. Analysis was by means of v.p.c. using an appropriate column; products were identified by comparison of their v.p.c. retention times with those of authentic materials; samples were collected by preparative v.p.c. and identified by comparison of their infrared (i.r.) spectra with those of authentic samples.

Free Radical Initiated Reactions of Nitrosyl Chloride with Cyclohexane in the Dark

To samples of cyclohexane containing nitrosyl chloride and hydrogen chloride was added the free radical initiator. Control experiments were performed in which the initiator was omitted. The mixtures were degassed by the freeze–thaw method and then sealed. The reaction tubes were wrapped in foil, allowed to thaw, and placed in a constant temperature bath. The tubes were cooled to 77 °K and opened, bromobenzene added as standard and the reaction mixtures were washed once with a solution of sodium thiosulfate (1.0 *M*) to destroy any unreacted nitrosyl chloride and analyzed by v.p.c. (6 ft × ¼ in. SE-30 on 60/80 Chromosorb W programmed from 60 to 200°). The concentrations of the starting materials and the major products are reported in Table 1. Besides those listed in the table there were small amounts of unidentified high boiling materials. When AIBN was used ten such products were present, including bicyclohexyl which was isolated and identified. When PAT was the initiator seven, and with benzoyl peroxide six, such materials were present.

The reactions using benzoyl peroxide as promoter could not be carried out in the presence of hydrogen chloride because benzoyl peroxide reacts with hydrogen chloride (20). After the sodium thiosulfate treatment, these reaction mixtures were dried and the organic layer was saturated with hydrogen chloride then irradiated further, before v.p.c. analysis.

Visible Ultraviolet Spectra of Solutions of Nitrosyl Chloride with Added Hydrogen Chloride

The u.v.–visible spectrum of a solution of nitrosyl chloride in cyclohexane was obtained. The solution was then saturated with dry hydrogen chloride and the u.v.–visible spectrum redetermined. No detectable change was noted.

Nitrosation of Cyclohexane in the Presence of Deuterium Chloride

Two solutions were prepared; these contained nitrosyl chloride (1.40, 1.39 mmole), cyclohexane (1.0, 1.0 mmole), and a 1.16 *M* solution of deuterium chloride in acetonitrile (1.0, 1.0 ml). The homogeneous solutions were degassed and sealed, then irradiated at 0° until colorless. Two samples of cyclohexane were recovered from each solution by preparative v.p.c. (10 ft × ¼ in. 10% Carbowax 20 *M* on 60/80 acid-washed Chromosorb W, 70°), and analyzed by mass spectrometry. The mass spectra were identical to those of authentic samples of cyclohexane.

Nitrosation of 2,3-Dimethylbutane in the Presence of Deuterium Chloride

Two solutions were prepared; these contained nitrosyl chloride (1.36, 1.31 mmole), 2,3-dimethylbutane (1.2, 1.2 mmole), and a 1.16 *M* solution of deuterium chloride in acetonitrile (1.0, 1.0 ml). After a procedure similar to that above, it was found that the recovered hydrocarbon samples had mass spectra identical to that of authentic material.

Nitrosation of a Cyclohexane/Perdeuteriocyclohexane Mixture

(*i*) A mixture of cyclohexane (0.98 mmole) and perdeuteriocyclohexane (1.01 mmole) was saturated with nitrosyl chloride at 0°. The solution was transferred to an ampoule which was evacuated and sealed then irradiated at 0° until colorless. The alkane mixture was recovered by preparative v.p.c. (Carbowax, 100°) and analyzed by mass spectrometry. The mass spectrum was identical to that of the unreacted mixture. (*ii*) To condensed nitrosyl chloride (2.31 mmole) was added a mixture of cyclohexane (1.07 mmole) and perdeuteriocyclohexane (1.01 mmole). The above procedure was followed, but once again with similar results.

Gas Phase Photooximation of Cyclohexane in the Presence of Hydrogen Chloride

A 2 l evacuated bulb was filled with hydrogen chloride to a pressure of 228 mm Hg. The hydrogen chloride was frozen and a mixture of nitrosyl chloride and perdeuteriocyclohexane (2.18 and 23.5 mmole, respectively) was introduced. The reaction bulb was degassed, allowed to warm in the dark until the contents had vaporized, and then irradiated with one 250 W incandescent lamp placed 3 in. away, until the yellow color of nitrosyl chloride was discharged. The hydrogen chloride was now evaporated (methanol slush (33), −98°) and the residue was vacuum transferred into a small flask and methylene chloride added as a standard. The oxime hydrochloride that remained adhered to the walls of the flask was removed by washing with 1 ml of trifluoroacetic acid, then methylene chloride was added as a standard. Analysis by n.m.r. showed that no ^1H over the amount in the starting perdeuteriocyclohexane had been incorporated into either the recovered substrate or the oxime.

Competitive Nitrosation of Several Hydrocarbons

Because of the errors inherent in evaluating the rela-

Can. J. Chem. Downloaded from www.nrcresearchpress.com by 210.87.254.5 on 09/05/12
For personal use only.

tive reactivity relationship

$$k_1/k_2 = \log (RH_0/RH)/\log (SH_0/SH)$$

several determinations were made for each pair of substrates. In each case the accurately weighed solutions were prepared approximately equimolar in cyclohexane, the second alkane, and Freon 113, which served as an inert standard. To *ca.* 2 mmole of condensed nitrosyl chloride was added about twice its volume of the hydrocarbon mixture. The ampoules were evacuated, sealed, and irradiated at 0° until colorless. The original solution was analyzed by v.p.c. (13 ft × ⅛ in. 10% diisodecyl phthalate on 60/80 acid washed Chromosorb W) at an appropriate temperature and the reaction mixtures were then analyzed under identical conditions. The results obtained follow (relative to cyclohexane = 1.00). Those following "*A*" are the nitrosations carried out using nitrosyl chloride and tungsten lamps: those following "*B*" are nitrosations using a sodium vapor lamp, and those following "*C*" are the corresponding values for chlorination with elemental chlorine.

Cyclooctane: *A*: 1.03, 1.27, 1.28, 1.44; *B*: 1.34, 1.35, 1.38, 1.38; *C*: 0.99, 1.02, 1.05, 1.08.

Cyclopentane: *A*: 0.64, 0.66, 0.84, 0.93, 0.95; *B*: 0.73, 0.77, 0.73, 0.78; *C*: 0.71, 0.72, 0.74, 0.77.

2,3-Dimethylbutane: *A*: 0.56, 0.60, 0.63, 0.65, 0.67, 0.75; *B*: 0.66, 0.68, 0.69, 0.74; *C*: 0.61, 0.67, 0.68, 0.70.

2,2,3,3,-Tetramethylbutane: *A*: 0.30, 0.33, 0.34, 0.35, 0.44, 0.48, 0.53; *B*: 0.49, 0.57, 0.63, 0.66; *C*: 0.23, 0.31, 0.38, 0.40.

Bicyclo-2,2,1-heptane: *A*: 0.54, 0.54, 0.62, 0.65, 0.69, 0.71, 0.71; *B*: 0.69, 0.74, 0.84, 0.87; *C*: 0.66, 0.75, 0.76, 0.78.

Toluene: *A*: 0.21, 0.24, 0.24, 0.28, 0.29; *B*: 0.29, 0.31, 0.31, 0.36; *C*: 0.17, 0.17, 0.36, 0.48.

1-Chlorobutane: *A*: 0.24, 0.33, 0.45, 0.48, 0.52; *B*: 0.39, 0.40, 0.43, 0.57; *C*: 0.16, 0.19, 0.23, 0.25.

The deuterium isotope effect was measured by determining the relative reactivity of cyclopentane and perdeuteriocyclohexane in a similar fashion ($k(C_6D_{12}) = 1.00$).

A: 0.85, 0.92, 0.97, 1.11; *B*: 0.82, 0.90, 0.91, 0.97; *C*: 1.03, 1.02, 1.02, 1.03.

No values determined experimentally have been discarded.

We wish to thank our respective Universities and the National Research Council of Canada for financial support. We also thank Dr. D. D. Tanner and the University of Alberta for very kindly obtaining the mass spectra.

1. E. V. Lynn. J. Amer. Chem. Soc. **41**, 368 (1919); E. V. Lynn and O. Hilton. J. Amer. Chem. Soc. **44**, 645 (1922); E. V. Lynn and H. L. Arkley. J. Amer. Chem. Soc. **45**, 1045 (1923).
2. L. J. Beckham, W. A. Fessler, and M. A. Kise. Chem. Rev. **48**, 319 (1951).
3. E. Müller. Pure and Applied Chem. **16**, 153 (1968).
4. M. Pape. Fortschr. Chem. Forschung. **7**, 559 (1967).
5. For references to the patent literature, see ref. 4.
6. E. Müller, H. G. Padeken, M. Salomon, and G. Fiedler. Chem. Ber. **98**, 1893 (1965) and references therein.
7. M. A. Naylor and A. W. Anderson. J. Org. Chem. **18**, 115 (1953).
8. A. Deschamps, P. Baumgartner, and C. Roux-Guerraz. Compt. Rend. **260C**, 4514 (1965).
9. E. Barale and A. Guillemonat. Compt. Rend. **268C**, 1201 (1969).
10. P. S. Fredricks and J. M. Tedder. J. Chem. Soc. 144 (1960).
11. R. S. Davidson. Quart. Rev. **21**, 249 (1967).
12. G. A. Russell and H. C. Brown. J. Amer. Chem. Soc. **77**, 4031 (1955).
13. E. Müller, G. Fiedler, and J. Heiss. Chem. Ber. **101**, 765 (1968) and references therein.
14. B. J. Berne, J. Jortner, and R. Gordon. J. Chem. Phys. **47**, 1600 (1967).
15. K. F. Herzfeld and J. A. Litovitz. Absorption and dispersion of ultrasonic waves. Academic Press, Inc., New York, N.Y. 1959.
16. A. Mackor, J. U. Veenland, and T. J. de Boer. Rec. trav. chim. **88**, 1249 (1969).
17. Toyo Rayon Co. Ltd., French Patent 1,348,005 (1963), Chem. Abs. **60**, 14406d (1964).
18. D. D. Tanner, D. Darwish, M. W. Mosher, and N. J. Bunce. J. Amer. Chem. Soc. **91**, 7038 (1969) and references cited therein.
19. D. D. Tanner and N. J. Bunce. J. Amer. Chem. Soc. **91**, 3028 (1969).
20. N. J. Bunce and D. D. Tanner. J. Amer. Chem. Soc. **91**, 6096 (1969).
21. D. D. Tanner, N. J. Bunce, and M. W. Mosher. Unpublished results.
22. (*a*) E. Müller and U. Trense. Tetrahedron Lett. 2045 (1967); (*b*) 4979 (1967).
23. E. C. Kooyman and G. C. Vegter. Tetrahedron, **4**, 382 (1958).
24. D. D. Tanner and M. W. Mosher. Can. J. Chem. **47**, 715 (1969).
25. C. Walling and M. F. Mayahi. J. Amer. Chem. Soc. **81**, 1485 (1959).
26. G. A. Russell. J. Amer. Chem. Soc. **80**, 4987, 4997 (1958).
27. Y. Shimokawa, S. Wakamtsu, and Y. Ito. Kogyo Kagaku Zasshi, **70**, 1165 (1967); Chem. Abs. **68**, 21400z (1968).
28. C. Walling. Free radicals in solution. John Wiley and Sons, Inc., New York, N.Y. 1957. p. 358.
29. W. H. Urry, quoted by K. B. Wiberg. Chem. Rev. **55**, 713 (1955).
30. W. A. Pryor. Free radicals. McGraw-Hill Book Co., New York, N.Y. 1966. p. 175.
31. G. H. Coleman, G. A. Lillis, and G. E. Goheen. Inorg. Syn. **1**, 55 (1939).
32. J. R. Morton and H. W. Wilcox. Inorg. Syn. **4**, 48 (1953).
33. R. E. Rondeau. Chem. Eng. Data, **11**, 124 (1966).
34. S. G. Cohen and C. H. Wang. J. Amer. Chem. Soc. **75**, 5504 (1953).

Formation, Structure, and Properties of Nitrosonium and Nitronium Fluorosulfate

A. M. QURESHI, H. A. CARTER, AND F. AUBKE[1]
Department of Chemistry, University of British Columbia, Vancouver 8, British Columbia

Received July 27, 1970

The reactions of the nitrogen oxides, N_2O, NO, N_2O_3, $NO_2(N_2O_4)$, and N_2O_5, the oxychlorides ClNO and $ClNO_2$, and the oxyanions NO_2^- and NO_3^- with the fluorosulfonating agents $S_2O_6F_2$ and $BrOSO_2F$ are studied systematically in regard to the formation of nitrosonium and nitronium fluorosulfate. Complex reactions are found when N_2O_3 and N_2O_4 are used as substrates, resulting in mixed or impure products. An explanation involving the intermediate oxidation into N_2O_5 is put forward to explain the results.

The solid products $NOSO_3F$ and NO_2SO_3F are characterized by powder X-ray analysis, infrared and Raman spectroscopy, and their solution behavior in HSO_3F. Whereas $NOSO_3F$ has been found to have an orthorhombic lattice, NO_2SO_3F crystallizes in the monoclinic system. Unit cell parameters are reported. The vibrational spectra are interpreted in terms of ionic compounds $NO^+SO_3F^-$ and $NO_2^+SO_3F^-$. The SO_3F^- anion, however, appears to be perturbed and all the *E* modes are slightly split. No unambiguous evidence for a previously reported non-linear NO_2^+ cation is found. Force constants for this species are calculated assuming $D_{\infty h}$ symmetry.

Both compounds are found to be completely dissociated in HSO_3F as evidenced by conductometry and ^1H and ^{19}F nuclear magnetic resonance (n.m.r.) spectroscopy.

Canadian Journal of Chemistry, 49, 35 (1971)

Can. J. Chem. Downloaded from www.nrcresearchpress.com by 210.87.254.105 on 09/05/12
For personal use only.

Introduction

Peroxydisulfuryl difluoride (1) $S_2O_6F_2$ and bromine(I) fluorosulfate (2, 3) $BrOSO_2F$ have been found in the past (4, 5) to be strong oxidizing and versatile fluorosulfonating agents. While studying their reactivity towards other oxidizing agents we became interested in their reactions with oxides, oxychlorides, and oxyanions of nitrogen.

Previous work has been restricted to the study of the interaction of nitric oxide NO (6, 7) and nitrogen dioxide, (6, 8), NO_2, with $S_2O_6F_2$. Whereas, in the reaction with NO, only nitrosonium fluorosulfate $NOSO_3F$ is formed, according to von Ellenrieder *et al.* (7), in a homogeneous second order reaction, there is some disagreement for the reaction with NO_2. Cady and Roberts (6) find a mixture of nitrosonium and nitronium fluorosulfate together with oxygen as reaction products when NO_2 was present in an excess, according to

$$2NO_2 + S_2O_6F_2 \rightarrow NOSO_3F + NO_2SO_3F + \tfrac{1}{2}O_2$$

The kinetic study (8) indicates a simpler reaction with the sole formation of NO_2SO_3F without oxygen release, where the dissociation of $S_2O_6F_2$ into SO_3F radicals presents the rate controlling step.

It seemed interesting to see whether departure from the gas phase reaction condition could result in a more complex course of reaction and whether an extension to other nitrogen oxides, oxyanions, and oxychlorides as substrates and to $BrOSO_2F$ as reactant would be helpful in rationalizing the findings.

The expected solid reaction products $NOSO_3F$ (9, 10) and NO_2SO_3F (10, 11) have been known for some time; however, both compounds are poorly characterized. Incomplete vibrational spectra (12, 13) are reported and only on NO_2SO_3F is the complete Raman spectrum recorded (14). The unit cell dimensions for $NOSO_3F$ have also been reported (13). Of particular interest to us was the effect of the heterocations NO^+ and NO_2^+ on the SO_3F^- anion, as reflected in the vibrational spectra.

Finally, we were interested in detailed solution studies in the parent acid HSO_3F where formation of the solvated cations NO^+ and NO_2^+ is expected. Conductometry (15) and ^1H (16) as well as ^{19}F n.m.r. should help in comparing both compounds to KSO_3F, which is known (15) to be a strong base in this solvent.

Experimental

Materials

Peroxydisulfuryl difluoride was prepared in a flow reaction of F_2 and SO_3 in an AgF_2 reactor adopted from a report by Cady and Shreeve (17). The $S_2O_6F_2$ used in some of the reactions contained small amounts of $S_2O_5F_2$, disulfuryl difluoride, as an impurity, detectable by ^{19}F n.m.r. Since $S_2O_5F_2$ is found to be inert in these reactions, no attempt at separation was made. Bromine(I) fluorosulfate was prepared as described previously (3).

[1]To whom correspondence should be addressed.

Can. J. Chem. Downloaded from www.nrcresearchpress.com by 210.87.254.105 on 09/05/12
For personal use only.

Nitrous oxide, nitric oxide, and nitrogen dioxide were obtained from Matheson of Canada; the latter two were purified by trap-to trap distillation. Dinitrogen trioxide, N_2O_3, was prepared according to a published method (ref. 18, p. 487). For the preparation of N_2O_5, the method of Harris *et al.* (19) was adopted. Ozone was produced by a T-23 laboratory ozonator made by the Welsbach Corp. Nitrosyl chloride was prepared from KCl (Fisher Scientific Co.) and nitrosyl hydrogen sulfate (ref. 18, p. 511) (Columbia Organic Chemicals). Nitrylchloride was prepared by the interaction of anhydrous nitric acid (ref. 18, p. 491) with chlorosulfonic acid (Matheson, Coleman and Bell) according to Schmeisser (ref. 18, p. 513). Analytical grade KNO_3 and $NaNO_2$ were purchased from Fisher Scientific Co. Fluorosulfuric acid was obtained from Baker and Adamson Co. and purified by double distillation at atmospheric pressure (15). Potassium fluorosulfate, used as reference in the conductometric work, was prepared from KCl and HSO_3F and recrystallized from water. All volatile materials were handled in vacuum lines, equipped with Fisher and Porter teflon stem stopcocks to avoid grease contamination. The purity was checked by melting points, vapor densities, and infrared (i.r.) spectroscopy. A monel reaction vessel equipped with Whitey needle valves was used for the attempted reaction of N_2O with $S_2O_6F_2$. All solids were transferred in a dry nitrogen atmosphere (Vacuum Atmosphere Corporation Dri Lab).

Methods

For all preparations involving the oxyhalides, ClNO and $ClNO_2$, and the oxides, NO, NO_2, (N_2O_4), N_2O_3, and N_2O_5, a standard procedure was used. The reaction vessel consisted of a $\sim$ 100 ml Pyrex flask equipped with a Fisher and Porter teflon stem stopcock and a teflon coated magnetic stirring bar. Weighed amounts of the reactant were added by vacuum distillation with the reaction vessel kept at liquid nitrogen temperature, and the mixture was allowed to warm up slowly in a trichloroethylene cooling bath, initially kept at -85 °C. Reaction occurred when warming up the mixture, $S_2O_6F_2$ was found to react very vigorously with the substrate, while $BrOSO_2F$ appeared to be a milder reactant. Reaction occurred generally in the temperature range of -50 to -20 °C.

The gases non-condensable at liquid nitrogen temperature were removed first and identified mass spectrometrically. All volatile products were removed with the vessel at room temperature and subsequent gentle heating to $\sim$ 40–50 °C. The occurrence of $S_2O_5F_2$ in the volatile fraction was discovered by ^{19}F n.m.r. All steps were closely followed by weight changes.

The reactions of KNO_3 and $NaNO_2$ with $S_2O_6F_2$ were performed in $\sim$ 100 ml Pyrex reaction vessels with flat bottoms and equipped with magnetic stirring bar and Teflon stem valves. A large excess of $S_2O_6F_2$ was used. The amount of oxygen produced was measured with a Toepler pump. The reaction of $NaNO_2$ was found to be quite slow and required heating to $\sim$ 65°. The solid products formed were checked from time to time by Raman spectroscopy in order to follow the course of the reaction more closely. The occurrence of the symmetric NO_2 stretch at 1408 cm^{-1} was taken as evidence for the formation of NO_2SO_3F.

The force constants for NO_2^+ were computed by using a Fortran IV program written by Schachtschneider (46). The harmonic potential function in terms of the internal coordinates is given by the expression

$$2V = k_1\{(\Delta R_1)^2 + (\Delta R_2)^2\} + k\delta(\Delta\theta)^2 + k_{12}(\Delta R_1)(\Delta R_2)$$

where k_1 represents the force between N and O, k_{12} the interaction between the two stretchings, K_δ represents the force associated with bending, and $R_1 = R_2$ is taken to be 1.154 Å (30*b*).

Instrumentation

Infrared spectra were recorded on Perkin–Elmer 137 and 457 spectrophotometers extending the range from 4000–250 cm^{-1}. Silver chloride and KRS-5 (Harshaw Chemicals) were used with Nujol as mulling agent.

Raman spectra were obtained with a Cary 81 spectrophotometer equipped with a Spectro Physics 125 He–Ne laser. Light of 6328 Å wavelength was used at a slit width of 10 cm^{-1}. The samples were contained in flat bottom Pyrex tubes of 5 mm o.d. Proton nuclear magnetic resonance spectra were recorded on a Varian A-60 n.m.r. Spectrometer using HSO_3F as an external reference. ^{19}F n.m.r. spectra were obtained on a Varian HA-100 spectrometer. X-Ray powder photographs were obtained using a General Electric Powder Camera. The Cu–K_α radiation was filtered through nickel. Illford "Illfex" film was used for the spectra. The unit cell dimensions were calculated by least squares analysis of the powder line values using a Fortran IV program written for the IBM 7044 computer.

A Wayne-Kerr Universal Bridge No. B-221A was used for the conductometric studies. Conductivity cells and the cell constant determination have been described previously (3, 15). A Sargent Thermonitor model ST with circulating and heating unit was used in a constant temperature oil bath. The mass spectrum of the non-condensable gas was obtained with an AEI MS9 Mass Spectrometer.

Properties of $NOSO_3F$ and NO_2SO_3F

(a) Analysis

Anal. Calcd. for $NOSO_3F$: N, 9.65; F, 13.1; S, 22.1. Found: N, 9.69; F, 12.8; S, 22.5.

Anal. Calcd. for NO_2SO_3F: N, 10.85; F, 14.73; S, 24.8. Found: N, 11.1; F, 15.0; S, 25.1.

The contents of $NOSO_3F$ in mixtures of both compounds were determined by a $KMnO_4$ titration after hydrolysis.

(b) Melting Points

$NOSO_3F$, +230 °C; NO_2SO_3F, +218 °C.

(c) Densities at 25 °C

$NOSO_3F$, 2.24 (pycnometry), 2.25 (X-ray); NO_2SO_3F, 2.20 (pycnometry), 2.20 (X-ray).

(d) Powder Diagrams

The *d*-spacings together with estimated intensities are listed on the next page.

The following unit cell dimensions are found:

$NOSO_3F$: Space group *Pnma* (D_{2h}) orthorhombic, $a = 8.68 \pm 0.03$ Å, $b = 5.96 \pm 0.016$ Å, $c = 7.35 \pm 0.008$ Å, $\alpha = \beta = \gamma = 90°$, $U = 381.0$ Å^3, $Z = 4$.

NO_2SO_3F: Space group $C_1 2/c_1$ monoclinic, $a = 9.275 \pm 0.004$ Å, $b = 7.00 \pm 0.012$ Å, $c = 7.36 \pm 0.008$ Å, $\alpha = \gamma = 90°$, $\beta = 113.8°$, $U = 437.3$ Å^3, $Z = 4$.

Can. J. Chem. Downloaded from www.nrcresearchpress.com by 210.87.254.105 on 09/05/12
For personal use only.

X-Ray powder data for $NOSO_3F$ and NO_2SO_3F

$NOSO_3F$		NO_2SO_3F	
d-spacing	Relative intensity	*d*-spacing	Relative intensity
6.1287	vw (20)	5.4935	w (30)
5.6409	vs (100)	4.9610	s (80)
4.9466	m (60)	4.2996	vs (100)
4.7121	vs (100)	3.7894	s (70)
4.3632	w (40)	3.5476	m (55)
4.1182	w (35)	3.4015	vs (100)
3.7540	m (65)	3.2522	vw (20)
3.6843	vs (100)	3.1399	vs (95)
3.5069	m (70)	2.7945	s (75)
3.3862	vs (100)	2.7120	s (75)
3.1911	vs (100)	2.6166	vw (20)
2.9591	m (60)	2.4417	w (35)
2.8276	s (70)	2.3008	m (60)
2.6394	s (70)	2.1750	m (60)
2.5464	vw (20)	2.1204	vw (20)
2.3273	w (35)		
2.2319	w (35)	2.0002	vs (90)
2.1987	vw (20)	1.8962	w (35)
2.1349	w (25)	1.8372	vw (25)
2.1129	m (55)	1.8172	vw (20)
1.8933	vw (20)	1.7505	vw (20)
1.8484	w (30)		
1.7966	m (60)		
1.7200	m (65)		
1.6338	w (30)		
1.5894	w (25)		

Results and Discussion

All relevant reactions in this series are listed in Table 1. The following principal features emerge. Substitution of $S_2O_6F_2$ by $BrOSO_2F$ does not lead to a different course of the reaction. Nitric oxide, in agreement with previous work (6, 7) yields nitrosonium fluorosulfate as the sole solid product. On the other side, nitrogen pentoxide forms with both reactants the nitronium fluorosulfate only; the expected amount of oxygen is released. This reaction type has been found previously in the reaction of I_2O_5 and $S_2O_6F_2$ (20). Use of ClNO and $ClNO_2$ as substrates results in a straightforward replacement of chlorine and the formation of nitrosonium and nitronium fluorosulfate, respectively. All these reactions are good and convenient preparative routes to the fluorosulfates. The failure of N_2O to react under the conditions described is not unexpected; the chemical inertness of this species is generally recognized.

All reactions involving N_2O_3 or N_2O_4 as substrates show a greater complexity than suggested either by the kinetic study in the gas phase (8) or the reaction described by Roberts and Cady. Since the reaction of dinitrogen trioxide with $S_2O_6F_2$ should be considered as an exploratory experiment, the exact composition of the starting material was not determined prior to the reaction and contamination with N_2O_4 is a possibility. The main emphasis is placed on the N_2O_4 reactions (5–7).

When a large excess (more than 4:1) of the reactant is present, NO_2SO_3F becomes the main product and only trace amounts of $NOSO_3F$ are found. When, however, N_2O_4 is present in a small excess, formation of both $NOSO_3F$ and NO_2SO_3F in various ratios is found. The postulated ratio (6) of 1:1, however, has never been found; a typical composition is given in Table 1. Generally 10–20% $NOSO_3F$ was found in the solid product.

All reactions 4–7 show the formation of oxygen. Since $S_2O_6F_2$ has been found to be thermally very stable except for the reversible decomposition into SO_3F radicals (21, 22) a decomposition according to: $S_2O_6F_2 \rightarrow S_2O_5F_2 + \frac{1}{2}O_2$ appears under the reaction conditions not very likely. Also, the departure from gas phase behavior is not unexpected, because formation of NO_2SO_3F is found to occur by interaction of the radicals NO_2 and SO_3F (8) with the radical dissociation of $S_2O_6F_2$ as the rate determining step. The concentration of both radicals in the condensed phase should be too low to play any important role.

By analogy to the reaction of KNO_3 and $S_2O_6F_2$, formation of $NOSO_3F$ and NO_2SO_3F would be expected

$$K^+NO_3^- + S_2O_6F_2 \rightarrow KSO_3F + NO_2SO_3F + \tfrac{1}{2}O_2$$

$$NO^+NO_3^- + S_2O_6F_2 \rightarrow NOSO_3F + NO_2SO_3F + \tfrac{1}{2}O_2$$

when one regards N_2O_4 as "nitrosonium nitrate" as indicated by a large number of solvolysis reactions (24). Departure from the expected equimolar amounts can be rationalized by two main routes: (*a*) primary formation of $NOSO_3F$ and partial subsequent oxidation to NO_2SO_3F by $S_2O_6F_2$ or $BrOSO_2F$; (*b*) primary partial oxidation of N_2O_4 to N_2O_5 by $S_2O_6F_2$ or $BrSO_3F$ and then formation of NO_2SO_3F according to routes 8 and 9 of Table 1. The fact that no trace of NO_2SO_3F is found when NO is the substrate is strong evidence against possibility (*a*). The conversion of $NOSO_3F$ into NO_2SO_3F takes place only at temperatures above 70 °C as shown by reaction 14 of Table 1. The reaction of $NaNO_2$ with $S_2O_6F_2$ (17) has been found to proceed via $NOSO_3F$ as a primary

Can. J. Chem. Downloaded from www.nrcresearchpress.com by 210.87.254.105 on 09/05/12
For personal use only.

TABLE 1. Reactions of oxides and oxychlorides of nitrogen with $S_2O_6F_2$ and $BrSO_3F$

Reaction No.	Substrate		Reactant		Temperature (°C)	Solid product		Volatile product	Oxygen (mmol)	Comments
	Compound	Amount*	Compound	Amount*		Compound	Amount*			
1	N_2O	22.7	$S_2O_6F_2$	13.4	60	No reaction		N_2O, $S_2O_6F_2$		
2	NO	Excess (10.3)	$S_2O_6F_2$	4.46	Condensed phase	$NOSO_3F$	8.06	—		
3	NO	8.6	$BrSO_3F$	Excess (14.4)	"	$NOSO_3F$	8.09	Br_2	—	Slight traces of NO_2SO_3F found
4	N_2O_3	Excess (19.8)	$S_2O_6F_2$	15.2	"	$NOSO_3F$, NO_2SO_3F	1.66, 8.06	O_2, $S_2O_5F_2$	—	
5	N_2O_4	Excess (24.2)	$S_2O_6F_2$	9.14	"	$NOSO_3F$ NO_2SO_3F	2.53 14.07	O_2, $S_2O_5F_2$	4.0	
6	N_2O_4	31.0	$S_2O_6F_2$	Excess (52.0)	"	NO_2SO_3F	62.2	$S_2O_5F_2$, O_2	15.5	Very slight traces of $NOSO_3F$ found
7	N_2O_4	67.6	$BrSO_3F$	Excess (290.4)	"	NO_2SO_3F	135.0	$S_2O_5F_2$, Br_2, O_2	1.54	Very slight traces of $NOSO_3F$ found
8	N_2O_5	Excess (19.5)	$S_2O_6F_2$	17.03	"	NO_2SO_3F	33.80	O_2	8.51	
9	N_2O_5	Excess (32.4)	$BrSO_3F$	22.4	"	NO_2SO_3F	22.15	Br_2, O_2	6.09	
10	NOCl	84.7	$S_2O_6F_2$	Excess (91.5)	"	$NOSO_3F$	84.7	Cl_2		
11	NOCl	Excess (38.7)	$BrSO_3F$	27.6	"	$NOSO_3F$	27.6	BrCl		
12	NO_2Cl	Excess (26.5)	$S_2O_6F_2$	11.0	"	NO_2SO_3F	20.0	Cl_2		
13	NO_2Cl	Excess (18.4)	$BrSO_3F$	12.7	"	NO_2SO_3F	12.4	BrCl		
14	$NOSO_3F$	6.26	$S_2O_6F_2$	Excess (29.7)	70°/2 days	NO_2SO_3F	6.259	$S_2O_5F_2$		
15	NO_2SO_3F	13.10	NO	Excess (90.0)	Condensed phase	$NOSO_3F$	—	—		
16	KNO_3	6.64	$S_2O_6F_2$	Excess ~(30.0)	"	KSO_3F, NO_2SO_3F	6.64, 6.64	O_2	3.30	
17	$NaNO_2$	5.06	$S_2O_6F_2$	Excess ~(35.0)	65	$NaSO_3F$, NO_2SO_3F	5.07, 5.07	$S_2O_5F_2$, O_2	2.50	

*In mmol.

TABLE 2. Unit cell dimensions for some nitrosonium and nitronium compounds

Crystal type	Compound	Cell dimensions (Å)			β (deg)	Reference
		a	*b*	*c*		
Orthorhombic	$NOSO_3F$	8.68	5.96	7.35		This work
		8.59	5.99	7.37		13
	KSO_3F	8.62	5.84	7.35		27*
		8.56	5.95	7.33		13
	$NOClO_4$	9.00	5.68	7.23		32
	$NOSO_3OH$	10.682	11.648	10.367		28
Monoclinic	NO_2SO_3F	9.27	7.00	7.36	113.8	This work
	NO_2ClO_4	9.16	7.08	7.30	112.1	33*
	$NOSO_3Cl$	8.997	7.101	7.557	109.8	30*

*Complete structural analysis is reported.

product, detectable by Raman spectroscopy on the incompletely reacted product, to the final product NO_2SO_3F only at $\sim$ 70 °C thus emphasizing the same point.

Therefore, the oxidation of N_2O_4 as the first step becomes a distinct possibility, supported also by reactions 6 and 7 of Table 1 where a large excess of the oxidizer reduces the amount of $NOSO_3F$ to a trace. Any previously reported nitrogen–oxygen polycations such as $N_2O_2^+$ and $N_2O_3^+$ (25) are far too unstable to play any part in the system as final products even though they may be formed as transient species.

In contrast to the conversion of $NOSO_3F$ to NO_2SO_3F which takes place only at elevated temperature, quantitative formation of $NOSO_3F$ from NO_2SO_3F is found, when NO and NO_2SO_3F react at room temperature. Both compounds $NOSO_3F$ and NO_2SO_3F melt sharply at 230 and 218°, respectively. In particular, the first figure is in disagreement with the literature values of 140 (9) and 156–7° (6). For NO_2SO_3F a value of 200 °C is reported (11). Since both fluorosulfates are very moisture sensitive requiring handling in dry nitrogen atmosphere, it seems likely that partial hydrolysis may have been responsible for the low values.

The results of the X-ray diffraction study on powdered polycrystalline samples are listed in Table 2, where a comparison is made with unit cell parameters for related compounds. Previously reported (13) values for $NOSO_3F$ are now slightly refined as done before (27) for KSO_3F (29). Both compounds are isostructural; the parameters show very good agreement and differ from the ones reported for $NOSO_3OH$ (28), which also crystallizes in the orthorhombic system. The unit cell volume of $NOSO_3F$ is, with 381.0 Å^3, slightly larger than for KSO_3F where a value of 370.0 Å^3 is found (27). Even though the interatomic distance for NO^+ (30) of 1.0619 Å is smaller than the ionic radius for K^+ with 1.33 Å according to Pauling (31), it has been argued (32) that the nitrosonium cation when in free rotation and acting as a sphere would have an effective radius of $\sim$ 1.40 Å. This is confirmed in our results and reported previously for the pairs $NOBF_4$ *vs.* KBF_4 (13) and $NOClO_4$ *vs.* $KClO_4$ (32).

On the other hand NO_2SO_3F has been found to crystallize in the monoclinic crystal system and to be isostructural with NO_2ClO_4 (33) with good agreement in the unit cell parameters. Density values derived from the X-ray data show excellent agreement with those found in a pycnometric determination.

The infrared and Raman frequencies for $NOSO_3F$ and NO_2SO_3F are listed in Table 3 together with the corresponding frequencies for KSO_3F and previously published Raman frequencies for NO_2SO_3F (14). Our Raman spectra are shown in Fig. 1. It is interesting to note that the previously reported value for ν_{NO} in $NOSO_3F$ (13) of 2377 cm^{-1} is not confirmed but appears to agree quite well with our value of the asymmetric NO_2 stretching frequency of NO_2^+ in nitronium fluorosulfate of 2390 cm^{-1}. The band contours are in both cases broad. Some minor disagreement is also found with a previous report of the Raman spectrum of KSO_3F (34). We have been unable to find a reported band at 821 cm^{-1} assigned $2\nu_6$, and we find a shoulder at 594 cm^{-1} indicating an unresolved splitting.

As can be seen clearly from Fig. 1 and Table 3, the observed number of vibrational bands does not agree with the expected ones for an unper-

Can. J. Chem. Downloaded from www.nrcresearchpress.com by 210.87.254.105 on 09/05/12
For personal use only.

TABLE 3. Vibrational spectra of KSO_3F, $NOSO_3F$, and NO_2SO_3F*

KSO_3F		$NOSO_3F$			NO_2SO_3F				
							Raman (cm^{-1})		
Raman (cm^{-1})	Assignment	Infrared (cm^{-1})	Raman (cm^{-1})	Assignment	Infrared (cm^{-1})	Assignment	This work	Reference 14	Assignment
					3765vw	$\nu_1 + \nu_{3\ NO_2^+}$			
		2602vw		$2\nu_4$	2735vw	$2\nu_1 + \nu_3$			
		2410vw			2390m b	$\nu_{3\ NO_2^+}$			
		2300ms	2298 s	ν_{NO^+}	2155vw	$2\nu_1$			
		2160vw		$2\nu_1$	1662vw	$\nu_1 + \nu_3$			
		1662vw		$\nu_1 + \nu_3$	1540vw	$2\nu_2$	1408 s	1401	$\nu_{1\ NO_2^+}$
		1300 vs b	1278 w	ν_4	1310s b	ν_4	1308 w	1300	ν_4
1285 w	$\nu_4(E)$	1260	1246 w		1278vs b		1286 w	1280	
1079vs	$\nu_1(A_1)$	1075vs	1077vs	ν_1	1085vs	ν_1	1085vs	1080	ν_1
		835vw		$2\nu_6$	840 w	$2\nu_6$		806	?
745m-wb	$\nu_2(A_1)$	745vs b	755m b	ν_2	750vs	ν_2	745m b	765	
								755	ν_2
								745	
					601 m	$\nu_{2\ NO_2^+}$	602mw	587	$\nu_{2\ NO_2^+}$
594mw sh	$\nu_5(E)$	596m sh	600m sh	ν_5	595m sh	ν_5	589mw	597	ν_5
586 m		591 s	588ms		582m sh				
570 m	$\nu_3(A_1)$	568 s	570ms	ν_3	568 s	ν_3	570 m	563	ν_3
407 s	$\nu_6(E)$	420w sh	416 s	ν_6	412vw	ν_6	417ms	413	ν_6
		405 w	403m sh		405vw		405 m	393	?

*w = weak, vs = very strong, m = medium, b = broad, sh = shoulder, s = strong, vw = very weak.

Can. J. Chem. Downloaded from www.nrcresearchpress.com by 210.87.254.105 on 09/05/12
For personal use only.

Can. J. Chem. Downloaded from www.nrcresearchpress.com by 210.87.254.105 on 09/05/12
For personal use only.

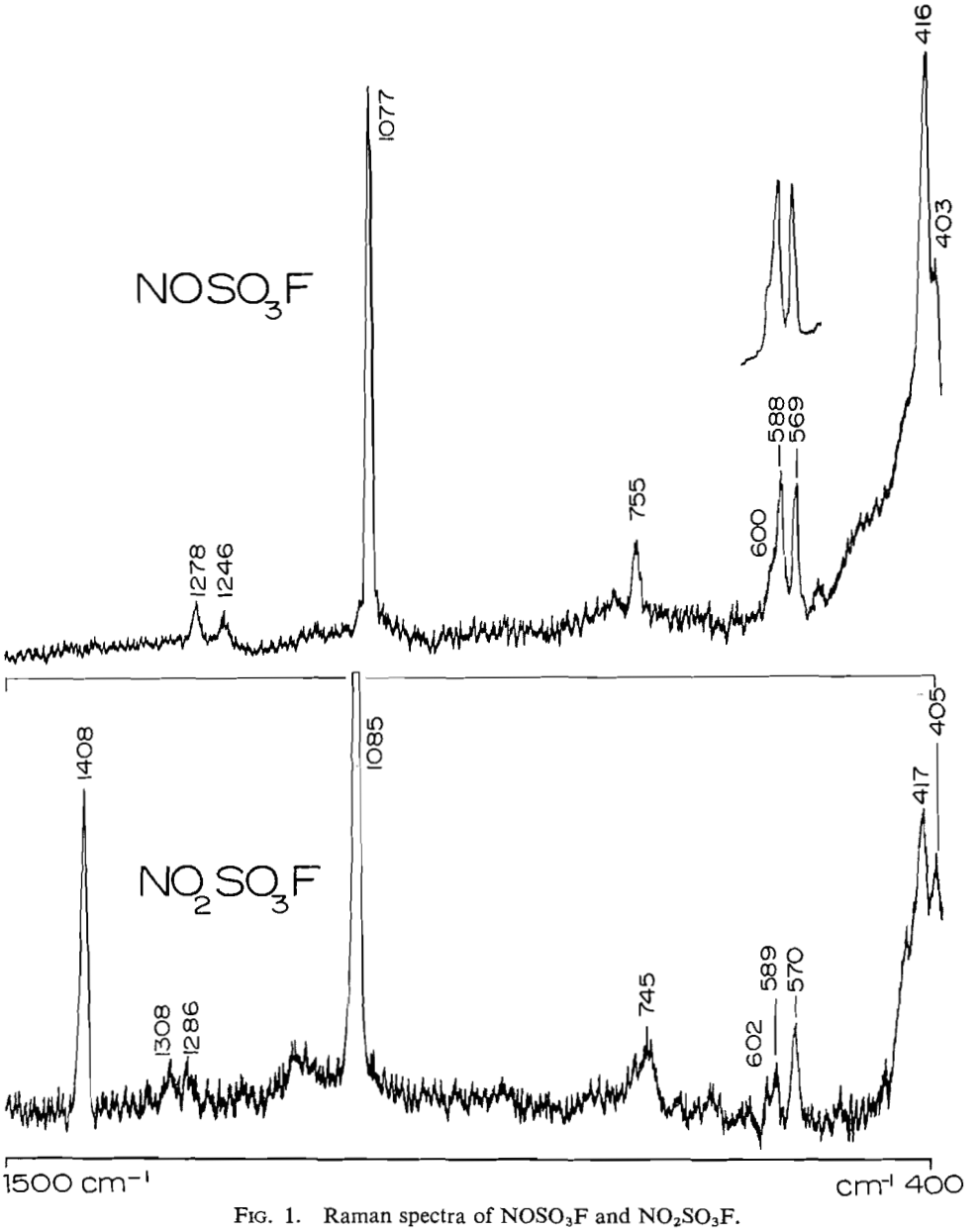

FIG. 1. Raman spectra of $NOSO_3F$ and NO_2SO_3F.

turbed SO_3F^- anion with C_{3v} symmetry. A total of six vibrational modes are expected with three A_1 and three E modes. This situation is best realized for KSO_3F where assignment of the bands is made according to previous work (29, 34–36). Perturbation of the C_{3v} symmetry, *e.g.* covalent interaction over 1 or 2 oxygen atoms will result in a symmetry lowering to C_{2v}. As a consequence all the E modes become split into two components A' and A''. Assuming that such splitting has in fact occurred one can now rationalize the observed spectra for both $NOSO_3F$ and NO_2SO_3F quite nicely. For all but one, ν_4 in $NOSO_3F$ where we were unable to resolve any splitting in the infrared spectrum, a doublet is found, both in the i.r. and the Raman spectra,

TABLE 4. Vibrational frequencies and force constants for the nitronium cation

(*a*) Observed frequencies (cm^{-1})

Compound	ν_1	ν_2	ν_3	Reference
NO_2AsF_6	1404	598	2385	40
NO_2SbF_6	1411	601	2368	40
$(NO_2)_2SnF_6$	1390	602	2392	42
NO_2SO_3F	1405	601	2390	This work
NO_2ClO_4	1396	571	2360	38, 39
NO_2BF_4	1399	590, 605	2380	43
NO_2NO_3	1400	538	2375	41, 45
(CO_2)	1396	660, 653	2344	44

(*b*) Force constants* (mdyn/Å) and calculated frequencies (cm^{-1})

Compound	K_1	K_{12}	K_δ	ν_1	ν_2	ν_3	Reference
NO_2AsF_6	17.44	1.12	0.513	1404	598	2385	This work
NO_2SbF_6	17.41	1.33	0.519	1411	601	2368	"
NO_2SO_3F	17.49	1.10	0.519	1405	601	2390	"
NO_2NO_3	17.32	1.14	0.420				45
CO_2	15.61	1.43	0.570				49

*K_1 = stretching force constant, K_{12} = interaction force constant, K_δ = bending force constant.

clearly visible in the well resolved Raman spectra. The peak separation is found to be between 12 and 32 cm^{-1}, by far smaller than that observed for solid fluorosulfates with bridging or terminal covalent SO_3F groups (37). The splitting of the *E* modes also appears to be slightly more pronounced for NO_2SO_3F than for $NOSO_3F$.

Our interpretation is quite different from the one presented by Vast *et al.* (14). Besides the fact that some factual disagreement exists, the SF stretching mode ν_2 is split into three components, unassigned bands at 393 and 806 cm^{-1} are observed. The following differences emerge: (*1*) except for ν_4 none of the *E* modes is split, and (*2*) a band at 587 cm^{-1} is assigned to $\nu_{2\ NO_2^+}$, which would be Raman forbidden for a linear species with $D_{\infty h}$ symmetry. The conclusion that NO_2^+ in NO_2SO_3F is not linear is mainly based on the author's assignment of the 587 cm^{-1} band. The failure to observe a complete removal of all degeneracies for SO_3F^- is inconsistent with a vibrational study of the isostructural NO_2ClO_4 (38, 39) where for NO_2^+ an ONO bond angle of 175.2 ± 1.40 is reported from X-ray diffraction (33). Here $\nu_{2\ NO_2^+}$ is found at 570 cm^{-1} and the T_d symmetry for ClO_4^- is reduced, resulting in a more complex spectrum.

The assignment for the SO_3F^- anion presented here for NO_2SO_3F seems to be more consistent and compares well with the one for $NOSO_3F$. Assignment of $\nu_{NO_2^+}$ at 601 cm^{-1} is in agreement with previous work in the compounds such as NO_2AsF_6 and NO_2SbF_6 (40) as shown in Table 4, and only in nitronium compounds as in NO_2NO_3 (41) and NO_2ClO_4 (38, 39) is a substantial lowering of $\nu_{2\ NO_2^+}$ found. However, the only substantiated case where the mutual exclusion rule for ν_2 is violated appears to be nitronium perchlorate (38, 39).

Assuming a linear configuration for NO_2^+, we have carried out force constant calculations using a program by Schachtschneider (46) on some NO_2^+ compounds. Excellent agreement between calculated and observed frequencies is observed in all cases; the results are also tabulated in Table 4 and compared to the results of previous force constant calculations on NO_2^+.

The present consistent interpretation of the vibrational spectra for $NOSO_3F$ and NO_2SO_3F, the failure to observe $\nu_{2\ NO_2^+}$ in the Raman spectrum (it may be argued that the Raman band is obscured by $\nu_{5\ SO_3F^-}$) and the good agreement between observed and calculated vibrational frequencies assuming $D_{\infty h}$ symmetry for NO_2^+, cannot be taken as unambiguous proof that this species is strictly linear in NO_2SO_3F. However, the previous claim of non-linearity (14) based on the Raman spectrum seems to be caused by a misinterpretation. A final decision will have to come from a detailed X-ray diffraction study.

The observed small splitting of the *E* modes for the SO_3F^- ion in $NOSO_3F$ and NO_2SO_3F can be explained by either a site symmetry effect or a slight polarization of the anion caused by non-spherical cations. According to Halford (47) C_s and C_2 symmetry is expected for $NOSO_3F$ and

Can. J. Chem. Downloaded from www.nrcresearchpress.com by 210.87.254.105 on 09/05/12
For personal use only.

Can. J. Chem. Downloaded from www.nrcresearchpress.com by 210.87.254.105 on 09/05/12
For personal use only.

NO_2SO_3F, respectively, but this argument should apply to KSO_3F as well, where no splitting is observed except for the weak shoulder at 594 cm^{-1}. The polarization effect appears, therefore, more likely as the cause.

The results obtained in the final part of this investigation are concerned with the solution behavior in fluorosulfuric acid. Both $NOSO_3F$ and NO_2SO_3F are extremely soluble in fluorosulfuric acid, where both behave as strong electrolytes according to

$$NOSO_3F \xrightarrow{HSO_3F} NO^+(solv) + SO_3F^-(solv)$$

$$NO_2SO_3F \xrightarrow{HSO_3F} NO_2^+(solv) + SO_3F^-(solv)$$

The specific conductivity results are shown in Table 5, together with the corresponding values for the standard KSO_3F. Small differences for the 3 solutes are explained by assuming differences in the effective ionic radii of the solvated cations resulting in different mobilities, rather than in incomplete dissociation. At higher concentrations than those normally used in conductivity studies, ^1H and ^{19}F n.m.r. provide good insight into the solution process. Production of SO_3F^- ions will result in a concentration dependent downfield ^1H shift (16) and an upfield shift for the ^{19}F n.m.r. signal. Both are observed and the results are tabulated in Table 6.

Moreover, the Raman spectrum of $NOSO_3F$ shows a strong absorption at 2320 cm^{-1} attributable to the nitrogen–oxygen stretching in NO^+. For NO_2SO_3F in fluorosulfuric acid $\nu_{1\ NO_2^+}$ is found at 1405 cm^{-1}. The observation of a ^{14}N n.m.r. signal for NO_2^+ in solution of HSO_3F has been described and discussed by us previously (48). Both solutes can be used as sources for the nitrosonium or the nitronium cation in HSO_3F, to be used in aromatic substitution reactions.

TABLE 5. Specific conductivities of KSO_3F, $NOSO_3F$, and NO_2SO_3F in HSO_3F at 25.0 °C

Molality × 10^2 (mol/kg)	$K \times 10^4$ (Ω^{-1} cm^{-1})		
	KSO_3F	$NOSO_3F$	NO_2SO_3F
0.00		1.084	1.116
0.25	5.93	6.1	4.87
0.50	11.82	12.4	12.9
0.75	17.80	18.8	19.0
1.00	24.60	24.6	25.1
1.50	35.82	36.8	37.1
2.00	46.81	50.9	47.5
2.50	59.67	60.6	59.5
3.00	71.91	72.2	70.0
3.50	82.30	84.2	81.8
4.00	94.05	93.3	90.0
4.50	105.36	105.2	98.7

*Values taken from a series of measurements by Neering and Thompson (50).

TABLE 6. ^1H and ^{19}F chemical shifts of $NOSO_3F$ and NO_2SO_3F

Compound	Mole fraction (x)	Chemical shift (p.p.m.)	
		$-\delta^1H$	$\delta^{19}F$
KSO_3F	0.01	0.133	0.060
	0.02	0.246	0.115
	0.04	0.463	0.223
	0.06	0.700	0.338
	0.08	0.919	0.431
	0.10	1.150	0.535
$NOSO_3F$	0.01	0.091	0.050
	0.02	0.170	0.101
	0.04	0.381	0.190
	0.06	0.580	0.282
	0.08	0.779	0.410
	0.10	0.961	0.500
	0.12	1.171	0.550
NO_2SO_3F	0.01	0.080	0.035
	0.02	0.165	0.063
	0.04	0.331	0.120
	0.06	0.500	0.185
	0.08	0.672	0.275
	0.10	0.843	0.337
	0.12	1.012	0.380

We are obliged to the National Research Council of Canada for financial support. We thank Mr. P. Borda of this department for the analytical results reported here.

1. F. B. DUDLEY and G. H. CADY. J. Amer. Chem. Soc. **79**, 513 (1957).
2. J. E. ROBERTS and G. H. CADY. J. Amer. Chem. Soc. **82**, 352 (1960).
3. F. AUBKE and R. J. GILLESPIE. Inorg. Chem. **7**, 599 (1968).
4. J. M. SHREEVE and G. H. CADY. J. Amer. Chem. Soc. **83**, 452 (1961).
5. D. D. DESMARTEAU. Inorg. Chem. **7**, 434 (1968).
6. J. E. ROBERTS and G. H. CADY. J. Amer. Chem. Soc. **82**, 353 (1960).
7. G. VON ELLENRIEDER and H. J. SCHUMACHER. Z. Phys. Chem. N.F. Frankfurt, **59**, 151 (1968).
8. G. VON ELLENRIEDER and H. J. SCHUMACHER. Z. Phys. Chem. N.F. Frankfurt, **59**, 157 (1968).
9. W. LANGE. Chem. Ber. **60**, 962 (1927).
10. A. A. WOOLF. J. Chem. Soc. 1053 (1950).
11. D. R. GODDARD, E. D. HUGHES, and C. K. INGOLD. J. Chem. Soc. 2559 (1950).
12. D. J. MILLEN. J. Chem. Soc. 2606 (1950).
13. D. W. A. SHARP and J. THORLEY. J. Chem. Soc. 3557 (1963).
14. P. VAST and M. DEPORCQ-STRATMAINS. Compt. Rend. Acad. Sci. Paris, Ser. C, **267**, 487 (1968).
15. J. BARR, R. J. GILLESPIE, and R. C. THOMPSON. Inorg. Chem. **3**, 1149 (1964).

16. R. J. GILLESPIE and R. F. M. WHITE. Can. J. Chem. **38**, 1371 (1960).
17. G. H. CADY and J. M. SHREEVE. Inorg. Syn. **7**, 124 (1953).
18. G. BRAUER. *Editor* Handbook of Preparative Inorganic Chemistry. Academic Press Inc., New York. 1963.
19. A. D. HARRIS, J. C. TREBELLAS, and H. B. JONASSEN. Inorg. Syn. **9**, 83 (1967).
20. F. AUBKE, G. H. CADY, and C. H. L. KENNARD. Inorg. Chem. **3**, 1799 (1964).
21. F. B. DUDLEY and G. H. CADY. J. Amer. Chem. Soc. **85**, 3375 (1963).
22. E. CASTELLANO, R. GATTI, J. E. SICRE, and H. J. SCHUMACHER. Z. Phys. Chem. N.F. Frankfurt, **42**, 174 (1964).
23. P. W. ATKINS and M. C. R. SYMONS. The Structure of Inorganic Radicals. Elsevier Publishing Company, Amsterdam. 1967. p. 128.
24. C. C. ADDISON. Angew. Chem. **72**, 193 (1960).
25. J. D. S. GOULDEN and D. J. MILLEN. J. Chem. Soc 2620 (1950).
26. F. SEEL and H. SAUER. Z. anorg. allg. Chem. **292**, 1 (1967).
27. K. O'SULLIVAN, R. C. THOMPSON, and J. TROTTER. J. Chem. Soc. A, 2024 (1967).
28. C.-F. LINSTRÖM and J. LÖSCHER. Z. Chem. **9**, 353 (1969).
29. D. W. A. SHARP. J. Chem. Soc. 3761 (1957).
30. (*a*) T. HÖHLE and F. C. HIJLHOFF. Rec. Trav. chim. **86**, 1153 (1967). (*b*) L. E. SUTTON. Tables of Interatomic Distances. The Chemical Society, London. 1958.
31. L. PAULING. The Nature of the Chemical Bond. Third Edition, Cornell University Press. 1960. p. 514.
32. L. J. KLINKENBERG. Rec. Trav. Chim. **56**, 749 (1937).
33. M. R. TRUTER, D. W. J. CRUICKSHANK, and G. A. JEFFREY. Acta Cryst. **13**, 855 (1960).
34. J. GOUBEAU and J. B. MILNE. Can. J. Chem. **45**, 2321 (1967).
35. H. SIEBERT, Z. anorg. allg. Chem. **289**, 15 (1957).
36. R. J. GILLESPIE and E. A. ROBINSON. Can. J. Chem. **40**, 644 (1962).
37. P. A. YEATS, B. L. POH, B. F. E. FORD, J. R. SAMS, and F. AUBKE. J. Chem. Soc. A, 2188 (1970).
38. J. W. NEBGEN, A. D. MCELROY, and H. F. KLODOWSKI. Inorg. Chem. **4**, 1796 (1965).
39. J. R. SOULEN and W. F. SCHWARTZ. J. Phys. Chem. **66**, 2066 (1962).
40. A. M. QURESHI and F. AUBKE. Can. J. Chem. To be published.
41. J. CHEDIN. Compt. Rend. Acad. Sci. Paris, C, **201**, 552 (1935).
42. H. A. CARTER, A. M. QURESHI, J. R. SAMS, and F. AUBKE. Can. J. Chem. **48**, 2853 (1970).
43. J. C. EVANS, H. W. RINN, S. J. KUHN, and G. A. OLAH. Inorg. Chem. **3**, 857 (1964).
44. W. E. OCHSBERG and D. F. HORNIG. J. Chem. Phys. **20**, 1345 (1952).
45. R. TERANISHI and J. C. DECIUS. J. Chem. Phys. **22**, 896 (1954).
46. J. H. SCHACHTSCHNEIDER. Vibrational Analysis of Polyatomic Molecules V and VI, Technical Report No. 231–64, Shell Development Company.
47. R. S. HALFORD. J. Chem. Phys. **14**, 8 (1946).
48. A. M. QURESHI, J. A. RIPMEESTER, and F. AUBKE. Can. J. Chem. **47**, 4247 (1969).
49. H. SIEBERT. Anwendung der Schwingungsspektroskopie in der Anorganischen Chemie, Springer Verlag, Berlin 1966.
50. L. NEERING and R. C. THOMPSON, Unpublished results.

Can. J. Chem. Downloaded from www.nrcresearchpress.com by 210.87.254.105 on 09/05/12
For personal use only.

Can. J. Chem. Downloaded from www.nrcresearchpress.com by 210.87.254.6 on 09/05/12
For personal use only.

Pyrrole Chemistry. Part XI. Some Reactions of the Pyrrole Grignard Reagent with Alkyl Carbonates and Alkyl Thiocarbonates[1]

C. E. LOADER AND HUGH J. ANDERSON
Department of Chemistry, Memorial University of Newfoundland, St. John's, Newfoundland

Received August 5, 1970

The pyrrole Grignard reagent reacts with ethyl thiocarbonates to give good yields of ethyl 2-pyrrolethiocarboxylates.

Diethyl carbonate, by contrast, in accordance with earlier reports gives almost exclusively ethyl 1-pyrrolecarboxylate.

2-Pyrrolecarbonitrile was prepared in good yield from the pyrrole Grignard reagent and ethyl thiocyanate.

Canadian Journal of Chemistry, 49, 45 (1971)

Oddo *et al.* (1) reported that the reaction of the pyrrole Grignard reagent **1** with alkyl chlorocarbonates gave very high yields of the corresponding alkyl 2-pyrrolecarboxylates **2** (eq. 1). Although this method is probably still the most convenient synthesis of 2-pyrrolecarboxylates, other workers have been unable to obtain such high yields (2). Further, the product was usually contaminated with by-products.

[1] 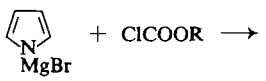

1

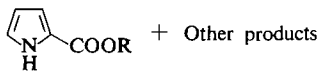

2

The pyrrole Grignard reagent, in common with the alkali metal salts of pyrrole, has been shown to be *N*-metallated (3). In most alkylation reactions this reagent gives predominantly the products of attack at the 2-position of the pyrrole ring. However, depending on the precise reaction conditions (*i.e.* solvents, temperature, time) and also on the alkylating agent, varying amounts of **1**, **2**, **3**, and multiple substitution may occur (4).

Because our work called for the frequent use of the pyrrole Grignard in the synthesis of pyrrole esters and thiolesters we have investigated this aspect of the reaction in some detail.

The pyrrole Grignard reagent reacts with methyl chlorocarbonate to give not only the expected methyl 2-pyrrolecarboxylate but six other products including some methyl 1-pyrrolecarboxylate and methyl 3-pyrrolecarboxylate (4).

[1]Part X. H. J. Anderson and C. W. Huang (17).

The pyrrole salts of the more electropositive metals, of lower co-ordinating ability than magnesium, such as those of sodium and potassium give largely the *N*-acylated pyrroles. The alkali salts would be expected to exist mostly in the ionic form and it seems reasonable to assume that the *N*-acylated products arise from the reaction of the pyrrole anion **3***b*. For the pyrrole Grignard reagent an equilibrium has been suggested involving the ionic **3***a–c* and the covalent **1** species (3). The covalent form would be expected to be more important in the magnesium compound and may be responsible for the differences between the reactions of this and the more ionic alkali metal salts. Hence, presumably the 2- and 3-substituted products arise from the covalent form of the reagent and the 1-substituted products from the ionic form (3).

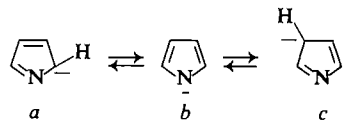

a *b* *c*

3

In the early literature there is a report that contrary to usual results of the acylation of the pyrrole Grignard reagent diethyl carbonate gave almost exclusively ethyl 1-pyrrolecarboxylate rather than the expected ethyl 2-pyrrolecarboxylate (5). We repeated the reaction using both diethyl and dimethyl carbonate and obtained the 1-pyrrolecarboxylates in about 50% yield accompanied by only a trace of the 2-pyrrolecarboxylates. The main by-product was 1,2′-dipyrrolyl ketone and not 1,1′-dipyrrolyl ketone as had been reported (5). As the 1,2′-dipyrrolyl ketone is the main product from the reaction between

Can. J. Chem. Downloaded from www.nrcresearchpress.com by 210.87.254.6 on 09/05/12
For personal use only.

methyl 1-pyrrolecarboxylate and the pyrrole Grignard reagent it is probably formed in the same way in both reactions. Because of our interest in the synthesis of thiolesters we investigated the reaction further using thiol- and thio-carbonates

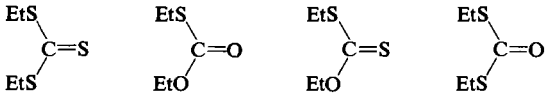

Using literature procedures (6) a series of thiol- and thio-carbonates **4**–**7** were prepared in high yields. Each of the esters was allowed to react with pyrrole Grignard reagent and the products were isolated.

Diethyl trithiocarbonate (**4**) reacted with the pyrrole Grignard reagent to give ethyl 2-pyrroledithiocarboxylate (**8***a*) (43%). There was no apparent formation of 1-substituted products.

8

a R = —CSSEt
b R = —COSEt
c R = —COOEt
d R = —CSOEt
e R = —CN
f R = —$COCH_3$
g R = —$CSNMe_2$

Diethyl thiolcarbonate (**5**) gave a mixture of ethyl 2-pyrrolethiolcarboxylate and ethyl 2-pyrrolecarboxylate. Some 1,2′-dipyrrolyl ketone was also isolated suggesting that 1-pyrrolecarboxylate or 1-pyrrolethiolcarboxylate may be formed which then undergoes further reaction to give the ketone. A trace of ethyl dithiolcarbonate was also isolated, formed by exchange between —OEt and the —SEt groups. Similarly *S*-ethyl ethyl dithiocarbonate (**6**) gave a mixture of ethyl 2-pyrroledithiocarboxylate (**8***a*) and ethyl 2-pyrrolethiocarboxylate (**8***d*) and no 1-substituted products. The symmetrical ethyl dithiolcarbonate (**7**) gave ethyl 2-pyrrolethiolcarboxylate (52%) with virtually no by-products in a very clean reaction. Most of the unused pyrrole could be recovered.

An early report (7) claimed the preparation of ethyl 2-pyrroledithiocarboxylate from the alkylation of the product from the pyrrole Grignard reagent and carbon disulfide. The b.p. disagreed with that observed for the material obtained in our work. We repeated the synthesis and obtained a small yield of a product which was identical to the ethyl 2-pyrroledithiocarboxylate obtained by us from the pyrrole Grignard reagent and ethyl trithiocarbonate, thus the reported b.p. is incorrect.

Phenyl cyanate is reported to react with the pyrrole Grignard reagent to give a poor yield of 2-pyrrolecarbonitrile (**8***e*). The readily available ethyl ester of thiocyanic acid, ethyl thiocyanate, was allowed to react with pyrrole Grignard reagent and the product was found to be 2-pyrrolecarbonitrile (50%) unchanged pyrrole and no other pyrrolic products. This reaction appears to be a useful synthesis of 2-pyrrolecarbonitrile and an improvement on other available methods. However, phenyl thiocyanate gave only a trace of 2-pyrrolecarbonitrile and a large amount of diphenyl disulfide. This is in keeping with the observations of Gronowitz and Hakansson on the reaction of phenyl thiocyanate with alkyl lithium and Grignard reagents (9).

Bean has reported that the acylation of the pyrrole Grignard reagent with ethyl acetate gave only 2-acetylpyrrole (**8***f*) whereas acetyl chloride and acetic anhydride acylate the reagent both in the 2- and 3-positions (10). In a reaction with ethyl thiolacetate the pyrrole Grignard reagent gave only 2-acetylpyrrole. Contamination by 3-acetylpyrrole was negligible as shown by g.l.c. of the crude product, and the yield of pure product was considerably higher than was obtained using ethyl acetate.

Dimethylthiocarbamyl chloride acylated the pyrrole Grignard reagent in the 2-position to give *N*,*N*-dimethyl-2-pyrrolethiocarbamide (**8***g*) in a clean reaction. Again there was no formation of 1-substituted products.

Spectra

The p.m.r. (Table 1) of the methylene group resonances in the *S*-ethyl thiolesters and the dithioesters appears at about 1.3 τ to high field of the *O*-ethyl methylene resonance in esters due to the greater shielding effect of the sulfur atom. The resonances of the ring protons in the thiolesters are closely similar both in shape and chemical shifts to those reported earlier for methyl 2-pyrrolecarboxylate and were quite different to those found in either 1- or 3-pyrrolecarboxylates (11).

Some i.r. spectral data are recorded in the Experimental section.

The 'abnormal' behavior of the alkyl carbon-

TABLE 1. Nuclear magnetic resonance spectra*

Pyrrole **8**		3H	4H	5H	CH_2CH_3	CH_2CH_3
a	2-CSSEt	2.96	3.72	2.96	6.64	8.66
b	2-COSEt	3.02	3.76	3.02	6.96	8.67
d	2-CSOEt	3.15	3.83	3.15	5.37	8.57
e	2-CN	3.12	3.78	3.12	—	—
g	2-CSN(Me)$_2$	3.51	3.71	3.06	6.43(—Me)	
	2-COOMe	3.00	3.70	3.00	6.28(—Me)	

*In $CDCl_3$ with $(CH_3)_4Si$ internal standard. The 3H, 4H, and 5H were multiplets and the methylene resonances were quartets.

ates in their reaction with the pyrrole Grignard reagent offers a useful route to the 1-pyrrolecarboxylates. However, the selectivity of the attack at the 1-position by the alkyl carbonates cannot be extended to the thiol- and thio-carbonates. This appears to stem from differences in the reactivity of the esters. In general the more reactive the acylating agent the less selectivity there is in the attack on the pyrrole Grignard reagent. The alkyl carbonates appear to react only with the pyrrole anion **3***a* whereas the more reactive thiolcarbonates and other common acylating agents are able to react with the undissociated, covalent form of the pyrrole Grignard reagent **1** as well as with the anion **3**.

We are continuing our studies on the preparation and properties of pyrrole thiol- and thiocarboxylates with particular interest in their synthetic uses. Some other aspects of this reaction will be discussed in the next part in this series.

Experimental

Melting points were taken on a Fisher–Johns m.p. block, and are uncorrected. The i.r. spectra were recorded on a Perkin–Elmer 237B spectrophotometer. Mass spectra were recorded on a Hitachi Perkin–Elmer RMU 6E instrument. The p.m.r. spectra were determined on a Varian A-60 spectrometer at 60 MHz. The chemical shifts are in p.p.m. from TMS as an internal standard in $CDCl_3$ unless specified otherwise, and are recorded on the τ scale. Gas chromatograms were run on a Beckman GC-2A chromatograph equipped with a 13½″ column (No. 70008) packed with Apiezon L on fire brick at temperatures between 130 and 220° with helium as the carrier gas. Elemental analyses were determined by Alfred Bernhardt, Mülheim (Ruhr), Germany. Petroleum refers to the fraction b.p. 60–80° unless otherwise stated.

Reaction of Alkyl Carbonates and Alkyl Thiol- and Thiocarbonates with the Pyrrole Grignard Reagent

Dimethyl Carbonate

Dimethyl carbonate (45 g, 1/2 mole) in ether (40 ml) was added dropwise to a stirred solution of pyrrole Grignard reagent (1/2 mole) in ether (180 ml) cooled in an ice bath. The solution turned green and a thick oil was precipitated. The mixture was stirred for 2 h and then allowed to warm to room temperature and stand overnight. The mixture solidified into a thick semi-solid gel. The magnesium complex was decomposed by slow addition of water and then of 2 *N* HCl until a clear mixture was obtained. The organic layer was separated and the aqueous layer was extracted with ether. The organic layer and the ether extracts were combined, washed with water, sodium bicarbonate solution, again with water, and finally dried ($MgSO_4$). The ether was evaporated and the residual liquid was distilled under reduced pressure to give methyl 1-pyrrolecarboxylate, b.p. 55–59°/14 mm, lit. 57–59°/14 mm (12) (26 g, 42%). Some pyrrole (8 g) was recovered in the low boiling fractions. If only 0.25 mole of the dimethyl carbonate were used in the reaction and the mixture was refluxed after the addition, 1,2′-dipyrrolyl ketone was obtained as a major by-product.

In a typical experiment the yields were 1,2′-dipyrrolyl ketone (8 g), m.p. 58–60°, lit. 58.5–60° (11), methyl 1-pyrrolecarboxylate (10.9 g), and recovered pyrrole (5.5 g).

Diethyl Carbonate

Using the same method described above ethyl 1-pyrrolecarboxylate (46%) was obtained together with a trace of 1,2′-dipyrrolyl ketone (~1%). In this case the intermediate magnesium complex did not solidify.

The following experiments were conducted in the same way as the preceding experiment unless otherwise stated using a 100% excess of the pyrrole Grignard reagent in each reaction.

S-Ethyl Ethyl Dithiocarbonate

After the addition of the *S*-ethyl dithiocarbonate the reaction mixture was refluxed for 20 min. The crude product consisted of a mixture of ethyl 2-pyrroledithiocarboxylate and ethyl 2-pyrrolethiocarboxylate in about equal amounts (p.m.r. spectrum). The products were separated by fractional distillation and fractional crystallization from petroleum cooled in a solid CO_2/acetone mixture. The overall yield of products amounted to 39% consisting of ethyl 2-pyrrolethiocarboxylate (15%), b.p. 104–105°/0.2 mm, as a yellow oil; ν_{max}(film) *inter alia* 3375 (N—H str.), 3100 (C—H str.), 2970–2850 (C—H str.), 1541 (C=C str.), and 1220 (O—C str.).

Anal. Calcd. for C_7H_9NOS: C, 54.21; H, 5.85; N, 9.03; S, 20.66. Found: C, 54.35; H, 5.96; N, 8.83; S, 20.76.

The other product was ethyl 2-pyrroledithiocarboxylate (24%), b.p. 119–120°/0.4 mm, lit. b.p. 162–164°/33 mm (7), as a yellow oil; ν_{max}(film) *inter alia* 3473 (N—H str.), 3100 (C—H str.), 2920–2860 (C—H str.), and 1530 (—C=C— str.).

Anal. Calcd. for $C_7H_9NS_2$: C, 49.11; H, 5.30; N, 8.18; S, 37.45. Found: C, 49.27; H, 5.29; N, 8.03, S, 37.32.

Can. J. Chem. Downloaded from www.nrcresearchpress.com by 210.87.254.6 on 09/05/12
For personal use only.

Can. J. Chem. Downloaded from www.nrcresearchpress.com by 210.87.254.6 on 09/05/12
For personal use only.

The yields in this reaction were deceptively low because of the difficulties associated with separating the two products.

Ethyl Thiolcarbonate

The reaction products consisted of about equal parts of ethyl 2-pyrrolethiolcarboxylate and ethyl 2-pyrrolecarboxylate along with traces of 1,2′-dipyrrolyl ketone and 2,2′-dipyrrolyl ketone as indicated by g.l.c. and comparison with authentic samples. Some diethyl carbonate was also present in the reaction products, presumably arising from an exchange reaction of the ethyl thiolcarbonate.

Ethyl Dithiolcarbonate

Ethyl 2-pyrrolethiolcarboxylate was obtained in 62% yield (52% after recrystallization from petroleum) m.p. 28–30°, lit. m.p. 29–29.5° (13). Traces of 1,2′- and 2,2′-dipyrrolyl ketone were also detected in the reaction products (g.l.c.). Repeating the reaction using equimolar amounts of pyrrole Grignard reagent and the dithiolcarbonate the yield fell to 29%.

Ethyl Trithiocarbonate

After the addition of the ethyl trithiocarbonate the mixture was refluxed for 20 min. Ethyl 2-pyrroledithiolcarboxylate (43%) was obtained from the reaction products as a yellow oil, b.p. 119–120°/0.4 mm.

2-Pyrrolecarbonitrile

Ethyl thiocyanate (8.7 g) in ether (15 ml) was added to a stirred solution of the pyrrole Grignard reagent (0.2 mole) in ether (90 ml). The solution warmed up and eventually began to reflux. A green oily precipitate formed and fouled the stirrer blade as it became increasingly solid. The mixture was refluxed for 2 h on a steam bath and then allowed to stand at room temperature overnight. The solid complex was then hydrolyzed with 10% ammonium chloride solution (40 ml) and 2 *N* sulfuric acid (20 ml) and the ether layer was separated. The aqueous layer was extracted with ether and the ether extracts were combined with the ether layer, washed well with water, and dried ($MgSO_4$). The ether was then removed and the liquid residue was fractionally distilled. The fraction b.p. 112–115°/14 mm was 2-pyrrolecarbonitrile (4.6 g, 50%). Literature b.p. 89–90°/1.5 mm (14) identical with authentic material. The low boiling material was unchanged pyrrole and ethyl thiocyanate.

Substitution of phenyl thiocyanate for ethyl thiocyanate in the reaction gave only a trace of 2-pyrrolecarbonitrile. The main product was diphenyl disulfide, m.p. 61°, lit. m.p. 61° (15).

2-Acetylpyrrole

Using the method described by Bean for the preparation of 2-acetylpyrrole from the pyrrole Grignard reagent and ethyl acetate the pyrrole Grignard reagent was reacted with ethyl thiolacetate. The g.l.c. of the dry crude ether extract indicated the absence of the 1-acetyl- and 3-acetyl pyrrole. Distillation of products gave 2-acetylpyrrole in 31% yield, m.p. 88–89°, lit. m.p. 90° (16).

N,N-Dimethyl-2-pyrrolethiocarbamide

Under the same conditions as were used in the preparation of ethyl 2-pyrrolethiolcarboxylate the pyrrole Grignard reagent reacted with dimethylthiocarbamyl chloride to give *N,N*-dimethyl-2-pyrrolethiocarbamide (38%), m.p. 100–100.5°.

Anal. Calcd. for $C_7H_{10}N_2S$: S, 20.79. Found: S, 20.72.

The financial support of the National Research Council of Canada is gratefully acknowledged.

1. B. Oddo. Chem. Abstr. **5**, 686 (1911).
2. P. Hodge and R. W. Rickards. J. Chem. Soc. 2643 (1963).
3. M. G. Reinecke, H. W. Johnson, and J. F. Sebastian. J. Amer. Chem. Soc. **85**, 2859 (1963).
4. K. Schofield. Hetero-aromatic Nitrogen Compounds. Butterworths, London, 1967. p. 106.
5. V. V. Chelintzev and S. G. Karmanov. Chem. Abstr. **9**, 1472 (1915).
6. G. Bulmer and F. G. Mann. J. Chem. Soc. 674 (1945).
7. B. Oddo and C. Alberti. Gazz. Chim. Ital. **68**, 204 (1938).
8. D. Martin and S. Rackow. Chem. Ber. **98**, 3662 (1965).
9. S. Gronowitz and R. Hakansson. Arkiv. Kemi, **17**, 73 (1959).
10. G. P. Bean. J. Heterocycl. Chem. **2**, 473 (1965).
11. H. J. Anderson and C. W. Huang. Can. J. Chem. **45**, 897 (1967).
12. H. J. Anderson and L. C. Hopkins. Can. J. Chem. **42**, 1279 (1964).
13. C. E. Loader and H. J. Anderson. Tetrahedron, **25**, 3879 (1969).
14. H. J. Anderson. Can. J. Chem. **37**, 2053 (1959).
15. Dictionary of Organic Compounds. Vol. III. Eyre and Spottiswoode Ltd., London, 1965. p. 1279.
16. B. Oddo. Ber. **43**, 1012 (1910).
17. H. J. Anderson and C. W. Huang. Can. J. Chem. **48**, 1550 (1970).

Can. J. Chem. Downloaded from www.nrcresearchpress.com by 210.87.254.6 on 09/05/12
For personal use only.

Studies of the Hot Water Extractives of the Bark and Leaves of *Populus deltoides* Bartr.[1,2]

IRWIN A. PEARL AND STEPHEN F. DARLING
The Institute of Paper Chemistry, Appleton, Wisconsin 54911

Received May 12, 1970

The hot water extractives of the fresh smooth green bark and the fresh leaves of a *Populus deltoides* Bartr. tree cut in June and processed by the Waring Blendor technique in ethanol were extracted fractionally with ethyl acetate, and the individual ethyl acetate extracts were fractionated by elution chromatography with water, 20% ethanol, and 50% ethanol on polyamide columns. Important components found in the bark were salicortin, salicin, salicyl alcohol, pyrocatechol, ω-salicyloylsalicin, grandidentatin, grandidentoside, populoside, trichocarposide, and 6-methyldihydroquercetin. Important components found in the leaves were salicortin, salicin, salicyl alcohol, pyrocatechol, 1-*O*-*p*-coumaroyl-β-D-glucoside, populoside, ω-salicyloylsalicin, chrysin-7-glucoside, and a new glucoside, deltoidin, which has been identified as 2-*O*-salicyloylsalicin.

Canadian Journal of Chemistry, 49, 49 (1971)

Introduction

In our continuing investigations on the components of the barks and leaves of *Populus* species, fresh smooth green bark and leaves of a *P. deltoides* Bartr. tree cut in Outagamie County, Wisconsin in June were extracted immediately with ethanol by the Waring Blendor technique (1). The hot water-soluble portions of the ethanol extractives were extracted fractionally with ethyl acetate, and the ethyl acetate-soluble fractions were chromatographed on columns of polyamide and eluted with water followed by 20% ethanol and 50% ethanol as employed in recent studies on the barks of other species (1, 2). As in previous studies, all eluate fractions were monitored by means of t.l.c., concentrated to small volumes, allowed to stand, filtered if crystals separated, and finally freeze dried. Weights of all fractions and of separated crystals were noted, and elution curves were obtained.

Results

Fractional ethyl acetate extraction of the hot water extractives representing 900 g of ovendry bark solids yielded 4.9% of first extract (A) and 1.7% of second extract (B). Similarly, extraction of the hot water extractives representing 700 g of ovendry leaf solids yielded 5.2% of first extract (A) and 2.4% of second extract (B), all on the dry basis.

Data for the polyamide chromatograms of the two ethyl acetate fractions of the bark and leaves are presented in Figs. 1 and 2. The weights noted in these figures are actual weights obtained experimentally from the sample aliquots applied to the polyamide column 50 mm in diameter and 80 cm in length. Major components under the peaks are noted on the figures.

The crystalline compounds noted in the elution curves of Figs. 1 and 2 were identified as described in previous papers as follows: salicin (3), salicortin (1), grandidentatin (4), grandidentoside (5), populoside (5), trichocarposide (6), ω-salicyloylsalicin (7) and 1-*O*-*p*-coumaroyl-β-D-glucose (8). Salicyl alcohol and pyrocatechol were identified under the peaks noted in Figs. 1 and 2 by t.l.c. (9).

Identification of 6-Methyldihydroquercetin

The crystals obtained upon concentration of fractions 126–128 of Fig. 1A were identified as 6-methyldihydroquercetin as follows: the specific color reactions (10) and carbon and hydrogen analyses correspond with the proposed formula. The compound was converted to the corresponding flavonol by a procedure well known to convert dihydroflavonols into flavonols (11). The resulting flavonol exhibited melting point, carbon and hydrogen analysis, and u.v. spectral analysis (10) identical in every respect with those reported for 6-methylquercetin, a flavonol which has been isolated only once (12). Unfortunately, the original authors could not supply us with an authentic sample.

Identification of Chrysin-7-glucoside

The pale yellow crystals which separated from

[1]Paper no. XXVI in the series "Studies on the Barks of the Family Salicaceae" and no. XII in the series "Studies on the Leaves of the Family Salicaceae".

[2]Presented at 3rd Canadian Wood Chemistry Symposium, Vancouver, B.C., June 24–26, 1970.

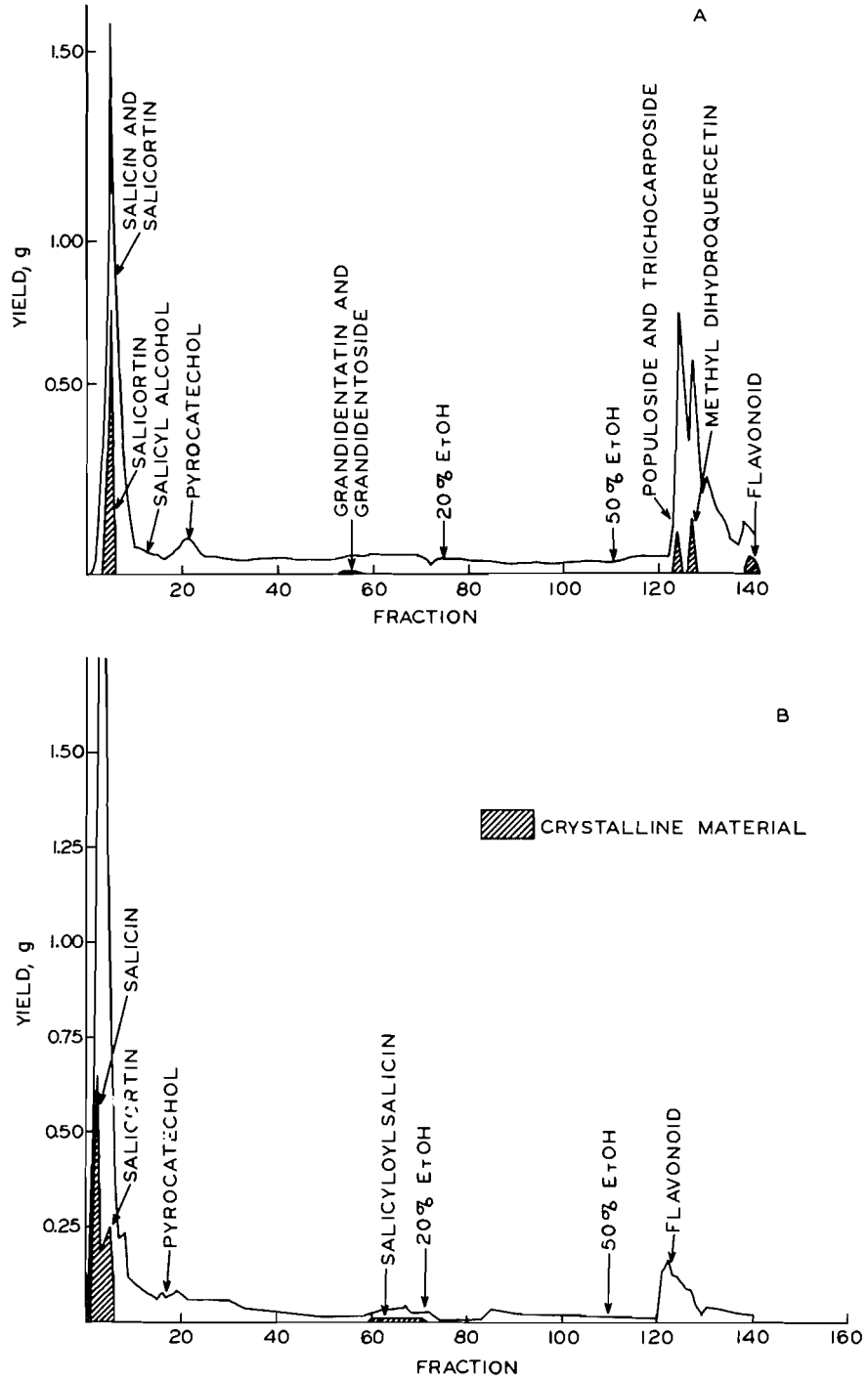

FIG. 1. Polyamide column chromatography of the ethyl acetate extractives fractions from *P. deltoides* bark. Weights of fractions applied to columns: A, 17.5 g; B, 15.5 g.

Can. J. Chem. Downloaded from www.nrcresearchpress.com by 210.87.254.6 on 09/05/12
For personal use only.

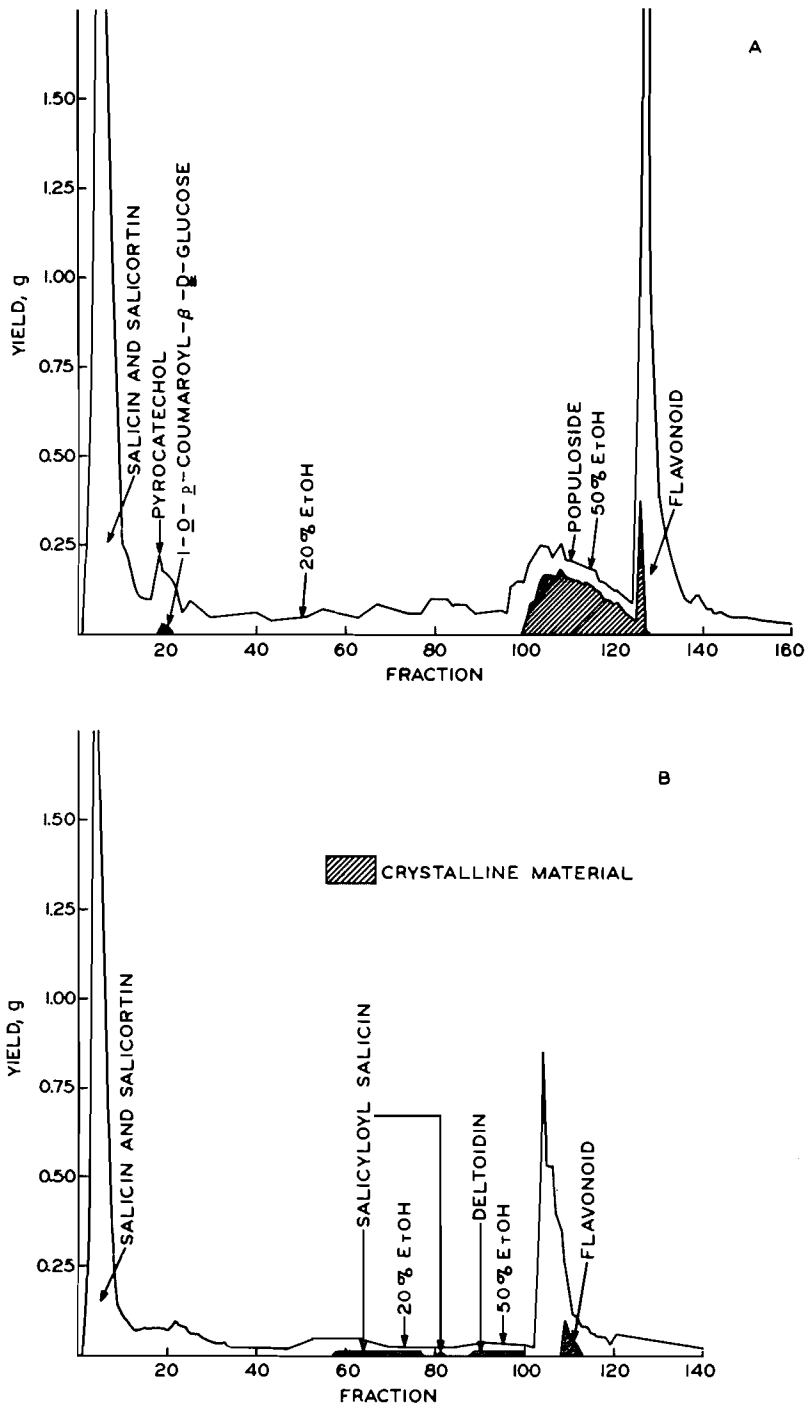

FIG. 2. Polyamide column chromatography of the ethyl acetate extractives fractions from *P. deltoides* leaves. Weights of fractions applied to columns: A, 36.5 g; B, 17.0 g.

Can. J. Chem. Downloaded from www.nrcresearchpress.com by 210.87.254.6 on 09/05/12
For personal use only.

Can. J. Chem. Downloaded from www.nrcresearchpress.com by 210.87.254.6 on 09/05/12
For personal use only.

the concentrated fractions 126 and 127 of Fig. 2A were identified as chrysin-7-glucoside in the following manner. Acid hydrolysis gave 1 mol of chrysin and 1 mol of glucose, and carbon and hydrogen analysis corresponded with a chrysin monoglucoside. Since there are only two possible monoglucosides of chrysin, the identity of the melting point of the new glucoside and that of its acetate with melting points reported for chrysin-7-glucoside and its acetate, respectively (13), together with the fact that the properties of the only other possible compound, chrysin-5-glucoside, are entirely different (14), prove that the new glucoside is chrysin-7-glucoside.

Isolation and Identification of Deltoidin

Recrystallization from dilute ethanol of the crystals which separated from fractions 89–99 of Fig. 2B yielded colorless needles melting at 220–221°. Alkaline hydrolysis yielded salicin and salicylic acid, and analysis indicated a monosalicylic acid ester of salicin. Mass spectrometry of its acetate demonstrated that salicylic acid substitution was on the glucose moiety and suggested 2-*O*-glucose substitution (15). Thus, deltoidin is 2-*O*-salicyloylsalicin or 2-hydroxybenzyl 2-*O*-(2-hydroxybenzoyl)-β-D-glucopyranoside.

Discussion

The data of Figs. 1 and 2 demonstrate the effectiveness of the fractional ethyl acetate extraction technique in preliminary fractionation of the hot water-soluble materials so that crystalline materials can be recovered in relatively pure state from subsequent polyamide chromatography. The data further show that the recovery of crystalline products represented a comparatively small proportion of the total products recovered from the chromatograms. The t.l.c. of filtrates from the crystals noted in Figs. 1 and 2 in all instances indicated more of the specific compound together with one or more components, some in substantial amount. Further fractionations will be necessary to separate these components in order to obtain crystalline compounds for identification.

Salicortin and salicin were the components present in greatest amount in both the bark and the leaves of *P. deltoides*, and each represented several percent of the weight of the dry organs. Although all of these components did not separate from the fractions under the first large peak in all the elution curves, t.l.c. indicated that these fractions comprised essentially only these two components with only traces of other products. If desired, crystalline products could be obtained by chromatography on silica gel as described previously (1).

The yield of crystalline populoside (ω-caffeoylsalicin) obtained from eluate fractions 99–125 of Fig. 2A amounted to almost ½% of the dry leaves. As noted in Fig. 2A, the crystals in each fraction also represented a majority of the weight of each fraction. Thus, it appears that *P. deltoides* leaves are the best available source for this interesting caffeic acid ester of salicin, since it has been found previously only in small quantities in the bark of *P. grandidentata* (16) and the bark of *P. balsamifera* (2).

The spectrum of components found in the barks and leaves of the cottonwood *P. deltoides* Bartr. in the *Aigeiros* section of the *Populus* genus (17) resembles closely the components previously isolated from *P. grandidentata* Michx. in the *Leuce* section (16), whereas marked differences are apparent with the components from the cottonwood *P. trichocarpa* Torr. and Gray and its related *P. balsamifera* L. in the *Tacamahaca* section of the *Populus* genus (2, 6, 9, 18–22).

Although 6-methylquercetin has been isolated from Ponderosa pine bark (*Pinus ponderosa* Laws.) by Kurth *et al.* (12) and named pinoquercetin, its dihydro derivative has not been reported previously. Thus, 6-methyldihydroquercetin is dihydropinoquercetin or 6-methyltaxifolin.

Chrysin-7-glucoside has been isolated from *Prunus aequinoctialis* by Hasegawa (13) who named it aequinoctin and reported a melting point of 245°. The compound was synthesized by Hattori and Shimokoriyama (14) who reported a melting point of 205–210°. Our finding of preliminary congealing at 208–210° with final melting at 244–245° suggests that Hasegawa ignored the preliminary shrinking, and Hattori and Shimokoriyama reported the congealing at 205–210° as the melting point. The present work confirms the identity of the two previously reported compounds.

The acetate of deltoidin was prepared in the usual manner and subjected to mass spectrometry. The major and important peaks of the mass spectrum with their relative intensities are noted in the Experimental. Although deltoidin pentaacetate is an isomer of the acetate of ω-salicyloylsalicin, the mass spectra of the two compounds are entirely different (15). Deltoidin

Can. J. Chem. Downloaded from www.nrcresearchpress.com by 210.87.254.6 on 09/05/12
For personal use only.

pentaacetate does not give the prominent peak at *m/e* 331, which is characteristic of the acetates of all glucosides without glucose moiety substitution (15). Instead of *m/e* 331 and related *m/e* 271 and 211 peaks due to loss of acetic acids from the unsubstituted glucose acetate moiety, deltoidin pentaacetate exhibited a major peak at *m/e* 451 corresponding with an acetylsalicyloyl ester of triacetylglucoseoxonium ion, and demonstrating that salicyloyl substitution in deltoidin is on the glucose moiety.

In an earlier study on the mass spectrometry of phenolic glucosides (15) it was demonstrated that the acetates of phenolic glucosides with aroyl substitution on the 6-*O*-glucose position gave much greater yields of ions corresponding with the loss of two acetic acids and one ketene than did the acetates of those with aroyl substitution on the 2-*O*-glucose position. In the case of monobenzoates of salicin and of ω-salicyloylsalicin, the ion involved was that at *m/e* 231, and the relative intensities were 19.2 and 1.0 for 6-*O*-benzoylsalicin and 2-*O*-benzoylsalicin, respectively, and 38.1 and 1.2 for 6-*O*-benzoyl-ω-salicyloylsalicin and 2-*O*-benzoyl-ω-salicyloylsalicin, respectively. In the mass spectrum of deltoidin pentaacetate, the corresponding peak is that at *m/e* 247. Its relative intensity of 2 suggests 2-*O* substitution on the glucose moiety. It should be noted that these considerations include the assumption that the choice of substitution is only between the 2-*O* and 6-*O* positions on the glucose, since no other type of glucose substitution has been found in naturally occurring phenolic glucosides.

The major fragmentation pattern of deltoidin pentaacetate is pictured in Scheme 1 which accounts for the important peaks in the mass spectrum.

In the fragmentation pattern of Scheme 1 the *m/e* 289 ion derived from the salicyloyltriacetylglucoseoxonium ion *m/e* 409 by loss of two acetic acids is fragmented further by loss of ketene, salicylic acid, and carbon monoxide to give ions *m/e* 247, 109, and 81, respectively, in accordance with the schemes of Biemann *et al.* (23) and Smale and Waight (24). If salicyloyl substitution were on the 6-*O* position of the glucose moiety of deltoidin, loss of two acetic acids from the *m/e* 409 ion could form only the *m/e* 289 ion pictured in Fig. 3.

The ion of Fig. 3 cannot yield an *m/e* 247 ion which can be fragmented further to give the well-known *m/e* 109 and 81 ions as noted in Scheme 1. Although it is entirely possible that the *m/e* 289 ion of Fig. 3 is an end product of fragmentation and that the *m/e* 247 and related ions of the mass spectrum of deltoidin pentaacetate are formed in accordance with a different fragmentation pattern, the fragmentation pattern as noted in Scheme 1 confirms the choice of 2-*O* substitution for the salicyloyl group in deltoidin. Thus, even though not established unequivocally, mass spectrometry suggests that deltoidin is 2-hydroxybenzyl 2-*O*-salicyloyl-β-D-glucopyranoside.

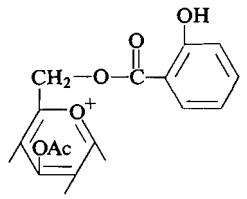

m/e 289

FIG. 3. The *m/e* 289 ion derivable from 2-hydroxybenzyl 6-*O*-salicyloyl-β-D-glucopyranoside.

Experimental

Preliminary Processing of Bark and Leaves

Fresh smooth green bark peeled from the small branches of a 6-year old *Populus deltoides* Bartr. tree cut in Outagamie County, Wisconsin on June 12, 1969 was processed within a few hours after cutting by the Waring Blendor technique (1). A total of 2000 g of fresh bark containing 900 g of oven-dry solids was processed in four equal batches to yield the starting water extractives. In similar manner, the fresh leaves from the same tree were processed at the same time. A total of 2000 g of fresh leaves containing 700 g of oven-dry solids was processed in four equal batches. The actual amounts of ethyl acetate extractives applied to the columns are noted in the results portion.

Isolation and Identification of 6-Methyldihydroquercetin

Upon concentration to small volumes under reduced pressure, eluate fractions 126–128 of Fig. 1A deposited 0.15 g of almost colorless needle rosettes which were recrystallized from ethyl acetate – petroleum ether to give colorless rosettes, melting at 194–195°, $[\alpha]_D^{25}$ + 7.42° (c = 1.3 in 95% ethanol).

Anal. Calcd. for $C_{16}H_{14}O_7$: C, 60.38; H, 4.43. Found: C, 60.37, 60.14; H, 4.43, 4.40.

Color reactions and u.v. spectral analysis (10) indicated a dihydroflavonol with dihydroquercetin type substitution.

Conversion to 6-Methylquercetin

A solution of 40 mg of the dihydroflavonol and 2 g of sodium bisulfite in 10 ml of water containing a little ethanol was boiled under reflux 45 min in accordance with the procedure employed by Kurth (11) for converting dihydroquercetin to quercetin. After cooling, the

Can. J. Chem. Downloaded from www.nrcresearchpress.com by 210.87.254.6 on 09/05/12
For personal use only.

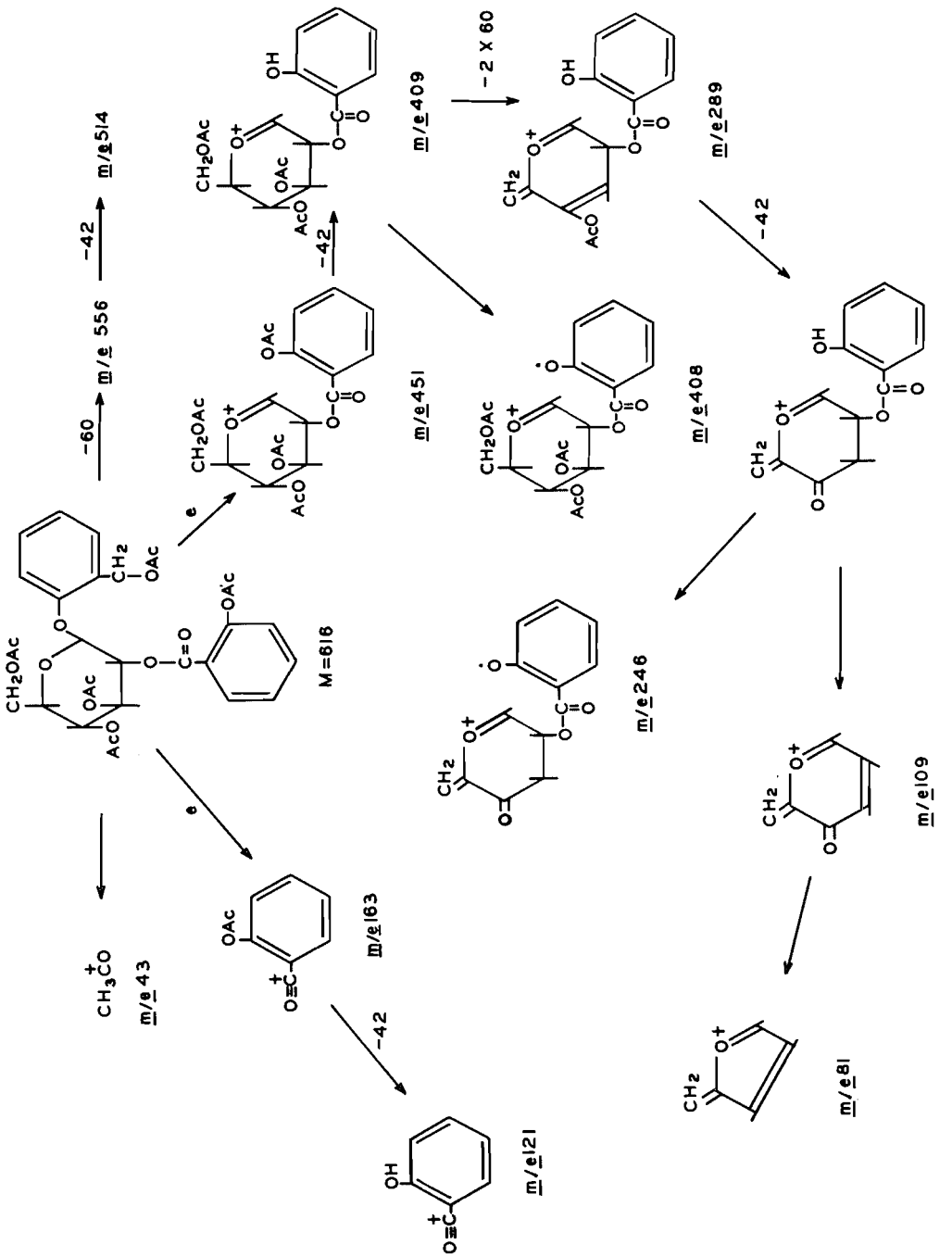

SCHEME 1. Major fragmentation pattern of deltoidin pentaacetate.

Can. J. Chem. Downloaded from www.nrcresearchpress.com by 210.87.254.6 on 09/05/12
For personal use only.

mixture was filtered to yield 21 mg of fine yellow needles, melting at 290–291°.

Anal. Calcd. for $C_{16}H_{12}O_7$: C, 60.76; H, 3.82. Found: C, 60.42, 60.59; H, 3.87, 3.88.

Color reactions and u.v. spectral analysis (10) indicated a flavonol with quercetin type substitution.

Isolation and Identification of Chrysin-7-glucoside

When concentrated, the eluate fractions 126 and 127 of Fig. 2A deposited a total of 0.45 g of pale yellow crystals which were recrystallized from dilute ethanol to give fine, pale yellow needles, melting at 244–245° (after preliminary shrinking at 208–210°).

Hydrolysis with Acid

The pale yellow crystals were hydrolyzed by boiling 5 h under reflux with 3 *N* hydrochloric acid in 20% ethanol. The mixture was cooled and filtered to give yellow needles of chrysin, melting at 282–283° and i.r. absorption spectrum identical with that of authentic chrysin (purchased from Aldrich Chemical Co., Inc., Milwaukee, Wisconsin).

Glucose was identified in the filtrate by paper chromatography.

Chrysin-7-glucoside Pentaacetate

The chrysin glucoside was acetylated with acetic anhydride in pyridine, and the product was recrystallized from 95% ethanol to yield colorless needles, melting at 197–198°, identical with that reported for chrysin-7-glucoside pentaacetate by Hasegawa (13).

Anal. Calcd. for $C_{31}H_{30}O_{14}\cdot H_2O$: C, 57.76; H, 4.81. Found: C, 57.82, 58.02; H, 4.75, 4.77.

Isolation and Identification of Deltoidin

Eluate fractions 89 through 99 of Fig. 2B, upon concentration, deposited a total of 21 mg of colorless crystals which were recrystallized from 50% ethanol to yield colorless needles, melting at 220–221°.

Anal. Calcd. for $C_{20}H_{22}O_9$: C, 59.11; H, 5.46. Found: C, 59.05; H, 5.47.

Deltoidin fluoresces strongly under u.v. and gives a flesh-colored spot on paper when sprayed with DPNA.

Deltoidin was heated 30 min with excess *N* sodium hydroxide solution, and the mixture was cooled, acidified with dilute hydrochloric acid, and extracted with ether. Salicylic acid was identified in the ether extract by paper chromatography and spraying with ferric chloride reagent. Salicin was identified in the aqueous raffinate by t.l.c. on silica gel with 4:1 chloroform–methanol and spraying with sulfuric acid (7).

Deltoidin Pentaacetate

Deltoidin was acetylated with acetic anhydride and pyridine, and the product was recrystallized from ethanol to yield deltoidin pentaacetate as colorless crystals, melting at 140–142°, and having the following major and important *m/e* peaks in its mass spectrum: 43(43), 81(5), 109(10), 120(11), 121(65), 163(100), 169(9), 201(2), 246(2), 247(2), 289(5), 409(1), 451(13), 514(< 1), and 556(< 1).

Mass Spectrum

The mass spectrum was made on a double-focusing Hitachi RMU-6D instrument by direct introduction of the sample with a probe at 180° in the ionizing beam.

Infrared Spectra

The i.r. spectra were obtained with a Perkin–Elmer Model 621 grating i.r. spectrophotometer. Potassium bromide pellets were prepared by hand-grinding with sample before pressing.

The i.r. absorption spectra were determined by Mr. Lowell Sell of The Institute of Paper Chemistry. The mass spectrum was determined by Morgan-Schaffer Corp., Montreal, Quebec. Analyses were performed by Micro-Tech Laboratories, Skokie, Illinois. The authors wish to thank Mrs. Charlotte Robbins for her help in the processing and analytical monitoring required in this investigation.

1. I. A. PEARL and S. F. DARLING. Phytochem. **9**, (1970). (Barks XXI).
2. I. A. PEARL and S. F. DARLING. Phytochem. **8**, 2393 (1969).
3. I. A. PEARL and S. F. DARLING. J. Org. Chem. **24**, 731 (1959).
4. I. A. PEARL and S. F. DARLING. J. Org. Chem. **27**, 1806 (1962).
5. R. L. ERICKSON, I. A. PEARL, and S. F. DARLING. Phytochem. **9**, (1970). (Barks XXV).
6. T. K. ESTES and I. A. PEARL. Tappi, **50**, 318 (1967).
7. I. A. PEARL and S. F. DARLING. Arch. Biochem. Biophys. **102**, 33 (1963).
8. I. A. PEARL and S. F. DARLING. Tappi, **50**, 324 (1967).
9. I. A. PEARL and S. F. DARLING. Phytochem. **7**, 1855 (1968).
10. L. JURD. Spectral Properties of Flavonoid Compounds. *In* Geissman's The Chemistry of Flavonoid Compounds. Macmillan, New York, 1962. p. 107.
11. E. F. KURTH. Ind. Eng. Chem. **45**, 2096 (1953).
12. E. F. KURTH, V. RAMANATHAN, and K. VENKATARAMAN. J. Sci. Ind. Res. (India), **15B**, 139 (1956).
13. M. HASEGAWA. J. Amer. Chem. Soc. **79**, 1739 (1957).
14. S. HATTORI and M. SHIMOKORIYAMA. Acta Phytochim. (Japan), **13**, 109 (1943).
15. I. A. PEARL and S. F. DARLING. Phytochem. **7**, 831 (1968).
16. R. L. ERICKSON, I. A. PEARL, and S. F. DARLING. Tappi, **53**, 240 (1970).
17. FAO Forestry and Forest Products Studies No. 12. Poplars in forestry and land use. Food and Agriculture Organization of the United Nations. Rome, 1958. 511 p.
18. C. R. POTTENGER and I. A. PEARL. Tappi, **49**, 152 (1966).
19. I. A. PEARL and S. F. DARLING. Phytochem. **7**, 825 (1968).
20. I. A. PEARL and S. F. DARLING. Tappi, **51**, 537 (1968).
21. I. A. PEARL and S. F. DARLING. Phytochem. **7**, 1845 (1968).
22. I. A. PEARL and S. F. DARLING. Phytochem. **7**, 1851 (1968).
23. K. BIEMANN, D. C. DEJONGH, and H. K. SCHNOES. J. Amer. Chem. Soc. **85**, 1763 (1963).
24. T. C. SMALE and E. S. WAIGHT. Chem. Commun. 680 (1966).

Can. J. Chem. Downloaded from www.nrcresearchpress.com by 210.87.254.105 on 09/05/12
For personal use only.

The Transmission of Substituent Effects in Transition Metal Complexes

D. R. EATON AND K. L. CHUA
Department of Chemistry, McMaster University, Hamilton, Ontario

Received June 18, 1970

The effect of ligand substitution on bonding to other ligands has been investigated in a series of V(III) complexes. Nuclear magnetic resonance (n.m.r.) contact shifts have been utilized for this purpose. These shifts are interpreted as arising from metal to ligand charge transfer. The results obtained are contrary to those expected from simple considerations of the electron withdrawing or donating abilities of the substituents. Electron withdrawing substituents decrease the charge transfer to the substituted ligand and increase the charge transfer to the remaining ligands. Electron donating substituents have the opposite effect. A simple interpretation is proposed to account for these results. An electron withdrawing substituent on a ligand in the *xy* plane increases the occupancy of d_{xy} which cannot interact with the π system of the ligand in the *xy* plane but which is available for π bonding with the remaining ligands. Effects of this type are to be anticipated whenever the filling of the t_{2g} orbitals is not symmetrical.

Canadian Journal of Chemistry, **49**, 56 (1971)

Introduction

The nature of the bonding in transition metal complexes has been the subject of extensive investigations. A subsection of this field deals with the effect of changes in the structure of one ligand on the bonding to another ligand. The aspect of this latter area which has received the most attention has been the so called "*trans* effect" particularly as it applies to square planar complexes (1). Examples of similar effects in octahedral complexes have also been reported (2) but have been less well documented. The detailed interpretation of the *trans* effect is still to some extent an open question, but in any event a selective transmission of electronic effects through the central metal atom is involved. Our interest in this area derives mainly from a concern with the mechanisms of homogeneous catalysis and of ligand exchange reactions. It is a common finding in this area that rather small changes in the structure of ligands not directly involved in the reaction can considerably change the reaction rates. There is a temptation to try and rationalize results in terms of the concepts of electron withdrawing and donating substituents and of inductive and resonance effects made popular by the organic chemists. In many cases this procedure is less than satisfying. We therefore thought it desirable to undertake some studies aimed at elucidating the details of the transmission of electronic effects in metal complexes. We have in mind here a rather more general phenomenon than the *trans* effect, since changes in one ligand must influence to a greater or a lesser extent the bonding to all other ligands. The work described in the present paper represents one approach to this problem.

The n.m.r. spectra of paramagnetic complexes, when interpretable, offer a very convenient method of studying metal ligand bonding (3). In favorable cases admixture of metal and ligand orbitals leads to delocalization of the unpaired electrons and this is manifested in the form of "contact" shifts of the resonances of ligand protons or other magnetic nuclei. This method can be very sensitive since rather small spin densities give rise to substantial shifts and, for this reason, is particularly suitable for studying the type of problem outlined above. Our choice of system was dictated by some practical limitations of the method. Sharp n.m.r. resonances are only observed if the electron spin relaxation time is short. Vanadium(III) complexes fulfil this condition very well (4). Since we wish to study systems involving a mixture of ligands a multiplicity of resonances is expected and the basic ligand system should therefore be as simple as possible if unambiguous analyses of the spectra are to be made. We have therefore used acetylacetone and simple substituted acetylacetones as ligands. Fortunately data on the effect of substituents on the chelating properties of acetylacetone is available in the literature. Van Uitert *et al.* (5) have measured the pK_d values of a variety of β-diketones and have also measured the formation constants of a large number of β-diketone metal chelates (6). Lintvedt and Holtzclaw (7) have complemented this data with a study of the proton chemical shifts on the enolic protons of β-diketones and have discussed their results in terms of the electron donating or withdrawing abilities of the substituent. In both cases it was concluded that the extreme in electron

withdrawing properties of the compounds examined is exhibited by the hexafluoro-derivative (**1**) and in electron donating properties by the 1,3-diphenyl derivative (**3**) with acetylacetone (**2**) being intermediate.

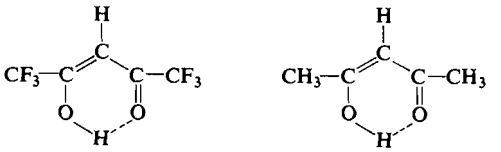

1

2

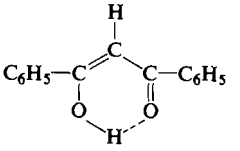

3

Thus the pK_d values of these compounds are 6.0, 12.7, and 13.75, respectively. Recently Lintvedt and Kernitsky (8) have complemented these results with a spectroscopic study leading to similar conclusions. We have therefore chosen to investigate the bonding in mixed complexes involving these three ligands. By using mixed complexes the effect of a substituent on bonding to other ligands can be studied.

Results

The proton magnetic resonance spectrum of tris-(acetylacetonato)vanadium(III) has been reported previously (4, 9, 10). It has also been shown that ligand exchange is relatively fast for a number of β-diketone complexes (11, 12). This is also true for the V(III) compounds. Thus if increasing amounts of hexafluoroacetylacetone are added to a solution in chloroform-*d* of V(III) acetylacetonate a series of n.m.r. spectra are obtained which clearly show lines due to mixed chelates. A typical spectrum is shown in Fig. 1. The resonances due to the original compound gradually disappear and a variety of new lines appear. This result must be attributed to ligand exchange according to the equation

$$V(acac)_3 \underset{acac}{\overset{hfac}{\rightleftharpoons}} V(acac)_2(hfac) \underset{acac}{\overset{hfac}{\rightleftharpoons}} V(acac)(hfac)_2 \underset{acac}{\overset{hfac}{\rightleftharpoons}} V(hfac)_3$$

where acac = acetylacetone; hfac = hexafluoroacetylacetone. Resonance lines at the same frequencies can be obtained either by starting with $V(hfac)_3$ and adding acac or by mixing solutions of $V(acac)_3$ and $V(hfac)_3$. For all these exchange reactions equilibrium appears to have been attained in the time between mixing the solutions and examining in the n.m.r. spectrometer (3 or 4 min). There is however no significant additional broadening of the n.m.r. lines such as would be anticipated if exchange rates were comparable to chemical shifts differences. The lifetime of the mixed complexes therefore lies in the range 10^{-1} to 10^2 s.

The spectrum obtained by mixing equimolar solutions of $V(acac)_3$ and $V(hfac)_3$ is shown in Fig. 2. It may be noted that the lines due to the symmetric chelates are not visible. It appears from this that the equilibrium distribution of ligands is not statistical but that the mixed complexes are favored at the expense of the pure complexes. This result is consistent with the observations of Adams and Larsen (12) and of Pinnavaia and Fay (11) on similar mixed ligand complexes of Zr, Hf, Ce, and Th. Assignments of lines to the individual mixed complexes have been made on the basis of their relative intensities in the various mixtures. Thus on the stepwise addition of hfac to $V(acac)_3$ the two strong lines which appear initially are assigned to the two chemical distinct CH_3 groups in $V(acac)_2(hfac)$. Weaker new lines are assigned to the C—H groups of this compound. On further addition of hfac these lines diminish in intensity and a new set of lines attributable to $V(acac)(hfac)_2$ appears. Finally with a large excess of hfac a single resonance at the correct position for $V(hfac)_3$ is observed. Data on the ^{19}F resonance spectrum was obtained in a similar manner and the resulting assignments for this system are summarized in Table 1. Similar experiments have been carried out with mixtures of $V(acac)_3$ and the diphenyl ligand **3**. In this case the tris chelate cannot be prepared and addition of a rather large excess of the ligand gives no resonances which cannot be assigned to mixed chelates. The separation of the resonances from the different chelates is rather smaller in this case. A spectrum is shown in Fig. 3 and the results are summarized in Table 2. Finally, to complete the series mixtures of $V(hfac)_3$ and diphenyl ligand have been examined and the results are shown in Table 3.

Can. J. Chem. Downloaded from www.nrcresearchpress.com by 210.87.254.105 on 09/05/12
For personal use only.

Can. J. Chem. Downloaded from www.nrcresearchpress.com by 210.87.254.105 on 09/05/12
For personal use only.

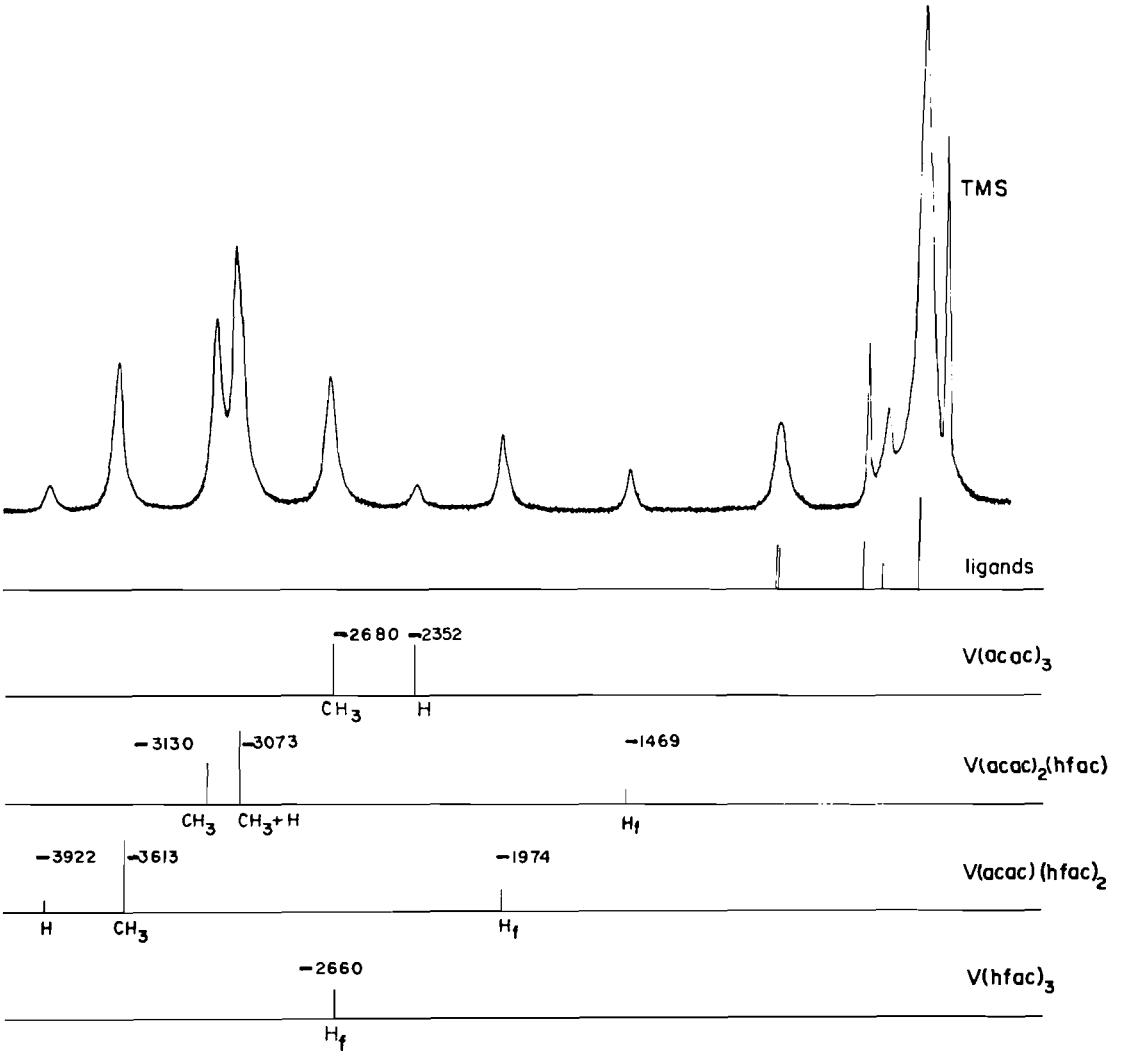

FIG. 1. Nuclear magnetic resonance spectrum and assignments of a mixture of V(III) acetylacetonate and hexafluoroacetylacetone. 60 Mc/s. Solvent $CDCl_3$. Reference TMS internal.

TABLE 1. Chemical shifts (c.p.s.) of mixed complexes with acetylacetone and hexafluoroacetylacetone*

	CH_3		CH(acac)		CH(hfac)		CF_3	
Complex	Observed frequency	Contact shift	Observed frequency	Contact shift	Observed frequency	Contact shift	Observed frequency	Contact shift
$V(acac)_3$	−2680	−2561	−2352	−2025				
$V(acac)_2(hfac)$	−3130	−3073	−3067	−2740	−1469	−1088	+1900	−2734
	−3011	−2954						
$V(acac)(hfac)_2$	−3613	−3494	−3922	−3595	−1974	−1593	+1819	−2815
$V(hfac)_3$					−2660	−2279	+1871	−2763

*Shifts in Hz at 60 Mc/s.

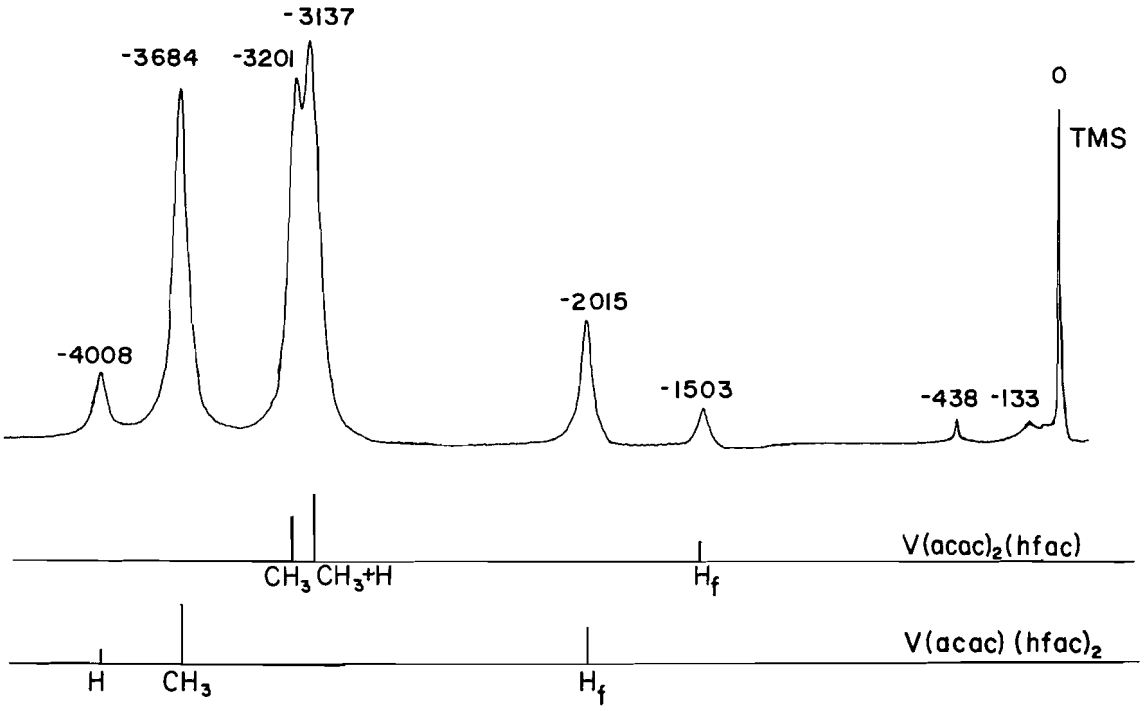

FIG. 2. Nuclear magnetic resonance spectrum of an equimolar mixture of $V(acac)_3$ and $V(hfac)_3$. 60 Mc/s. Solvent $CDCl_3$. Reference TMS internal. This spectrum was obtained at a slightly lower temperature than that in Fig. 1.

TABLE 2. Chemical shifts (c.p.s.) of mixed complexes with acetylacetone and 1,3-diphenyl-1,3-propanedione*

	CH_3		CH(acac)		CH(ϕ–ϕ)	
Complex	Observed frequency	Contact shift	Observed frequency	Contact shift	Observed frequency	Contact shift
$V(acac)_3$	−2667	−2548	−2336	−2009		
$V(acac)_2(ϕ–ϕ)$	−2483	−2364	−2252	−1925	−2893	−2483
$V(acac)(ϕ–ϕ)_2$	−2340	−2221	−2165	−1838	−2757	−2347

*Shifts in Hz at 60 Mc/s.

TABLE 3. Chemical shifts of mixed complexes with hexafluoroacetylacetone and 1,3-diphenyl-1,3-propanedione*

	CH(hfac)		—CH(ϕ–ϕ)		$—CF_3$	
Complex	Observed frequency	Contact shift	Observed frequency	Contact shift	Observed frequency	Contact shift
$V(hfac)_3$	−2689	−2308			+1869	−2765
$V(hfac)_2(ϕ–ϕ)$	−1959	−1578	−4125	−3715	+1843	−2791
$V(hfac)(ϕ–ϕ)_2$			−3518	−3100	+2400	−2194

*Shifts in Hz at 60 Mc/s.

Can. J. Chem. Downloaded from www.nrcresearchpress.com by 210.87.254.105 on 09/05/12
For personal use only.

Can. J. Chem. Downloaded from www.nrcresearchpress.com by 210.87.254.105 on 09/05/12
For personal use only.

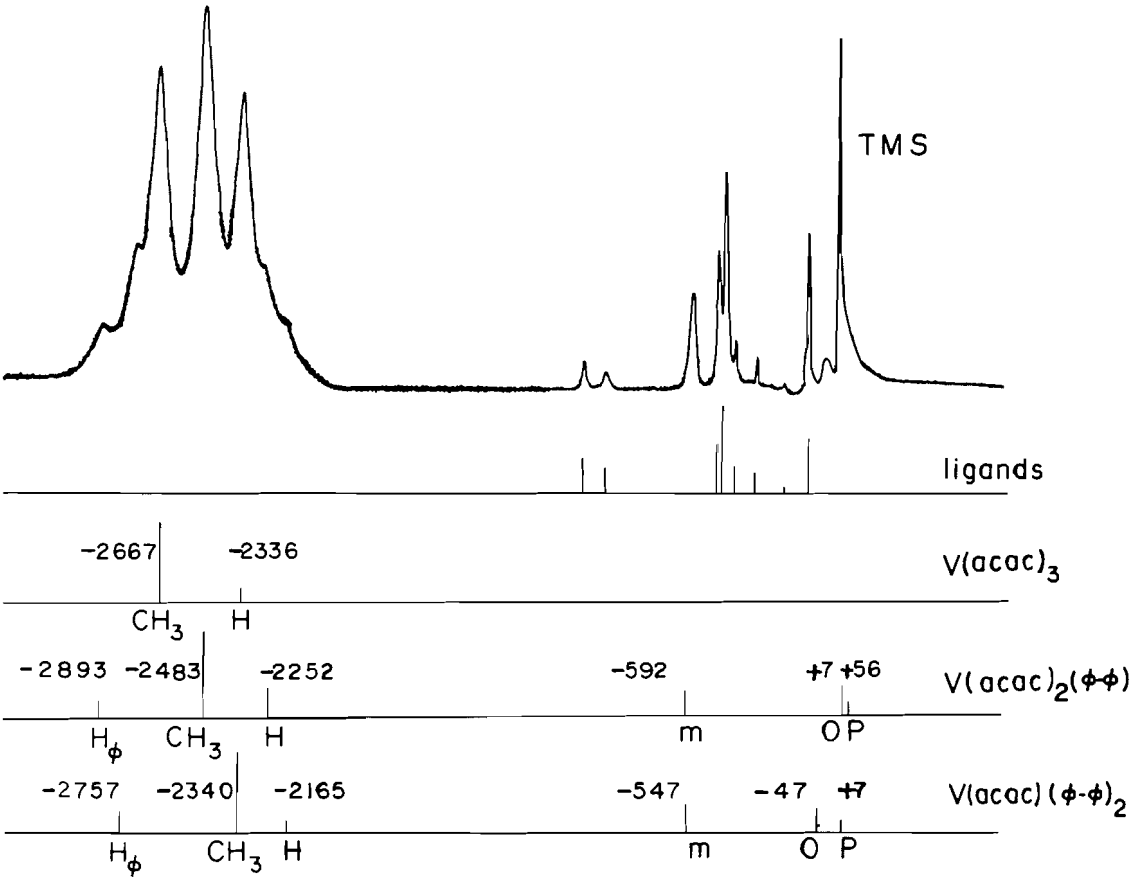

FIG. 3. Nuclear magnetic resonance spectrum and assignments of a mixture of V(III) acetylacetonate and diphenyl ligand. 60 Mc/s. Solvent $CDCl_3$. Reference TMS internal.

TABLE 4. Temperature dependence of n.m.r. lines in V(acac)/(hfac) system*

	$V(acac)_3$		$V(acac)_2(hfac)$		$V(acac)(hfac)_2$		$V(hfac)_3$	
Line	Slope	Intercept	Slope	Intercept	Slope	Intercept	Slope	Intercept
$CH_3(a)$	913×10^3	−480	1082×10^3	−574	1182×10^3	−434		
$CH_3(b)$			1006×10^3	−390				
CH(acac)	729×10^3	−404	1004×10^3	−718	1281×10^3	−653		
CH(hfac)			362×10^3	+105	608×10^3	−429	839×10^3	−506

*Both slope and intercept refer to $\Delta\nu$ vs. $1/T$ plot. Unit of slope is Hz °K, and intercept, Hz.

The temperature dependence of these spectra has also been examined since it has significance to the discussion below. It is found in all cases that the shifts of the n.m.r. frequencies relative to the diamagnetic ligands vary linearly with $1/T$. Some typical plots are shown in Fig. 4. These plots, however, do not pass through the origin. It must be concluded that the shifts cannot be described by a simple Curie law formula. The deviation however is not large. Values for the slopes of these plots, giving a measure of the contact contribution, and of the intercepts, giving a measure of the temperature independent contribution, are shown in Table 4.

The most noteworthy feature of these results is the large effect of ligand substitution on the chemical shifts of other ligands. Thus replacement of CH_3 by CF_3 on one ligand changes the

Can. J. Chem. Downloaded from www.nrcresearchpress.com by 210.87.254.105 on 09/05/12
For personal use only.

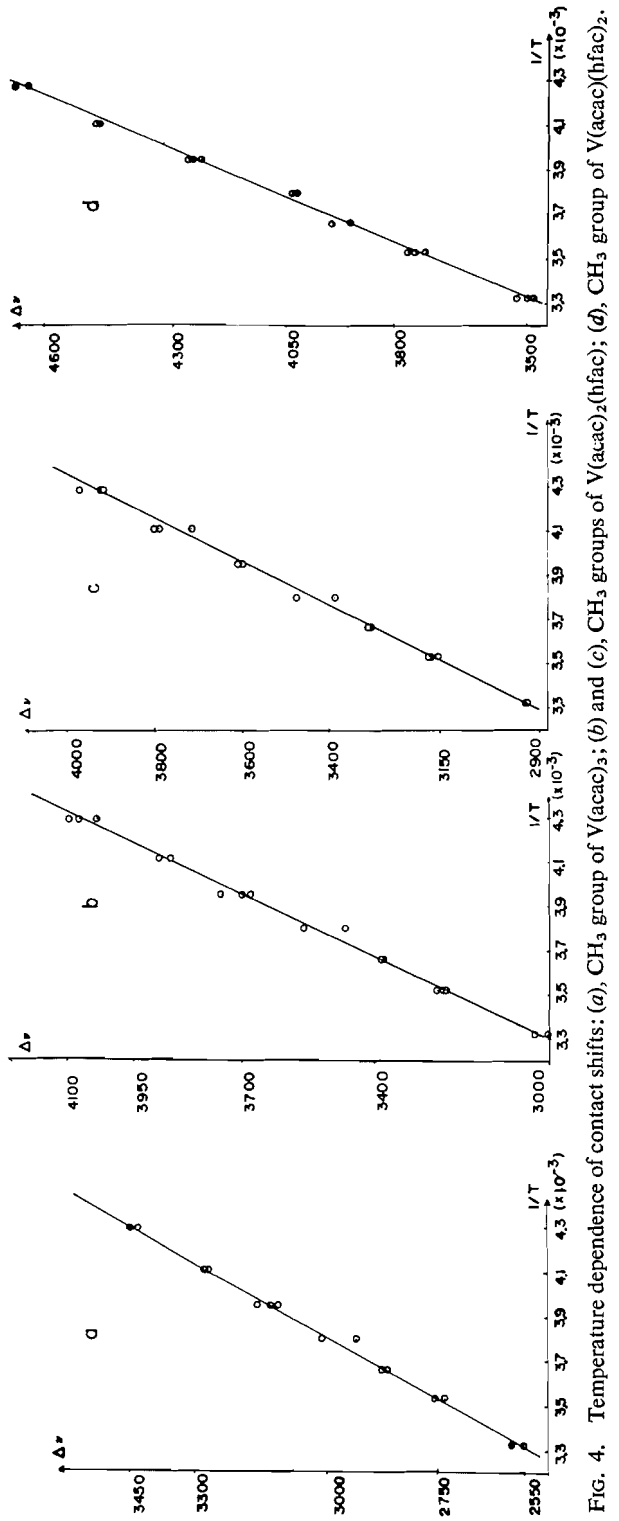

FIG. 4. Temperature dependence of contact shifts: (*a*), CH_3 group of $V(acac)_3$; (*b*) and (*c*), CH_3 groups of $V(acac)_2(hfac)$; (*d*), CH_3 group of $V(acac)(hfac)_2$.

Can. J. Chem. Downloaded from www.nrcresearchpress.com by 210.87.254.105 on 09/05/12
For personal use only.

chemical shifts of the protons on the remaining ligands by 400–800 Hz. Substitution of a second ligand increases the effect to 900–1500 Hz. The direction of the shifts depends on the nature of the substituent. CF_3 substitution increases the shifts of the protons on other ligands, phenyl substitution decreases these shifts. Thus we obviously have a rather sensitive empirical method for studying the transmission of substituent effects through transition metal ions. It would be desirable, however, to interpret these results in terms related to the bonding in the complexes.

Discussion

In order to discuss the present results it is necessary to consider the theory of the d^2 configuration in a little more detail. We first note that in $V(acac)_3$ a trigonal distortion reduces the symmetry from O_h to D_3 splitting the t_{2g} orbital into e and a_1. It is not immediately apparent which of the latter two orbitals will be lower. If e is below a_1 the ground state configuration e^2 gives rise to a $^3A_2$ lower state. If a_1 is below e the resulting a_1e configuration results in a ^3E ground state. At first sight the orbitally degenerate ^3E state appears to offer the more attractive explanation of the observed asymmetric distribution of spin in the mixed chelates. Lin and Orgel (13) have considered a very similar problem of spin distribution in distorted d^8 tetrahedral complexes and devised an elegant explanation based on an orbitally degenerate ground state. A rather minimal modification will adopt this theory to distorted octahedral d^2 complexes. Unfortunately the distorted tetrahedral d^8 complexes which have been examined appear to have non-degenerate ground states (14) and the weight of evidence seems to favor a similar conclusion for the present d^2 complexes.

The main evidence for this latter conclusion is provided by the temperature dependence of the magnetic susceptibility reported in the literature and of the isotropic hyperfine shifts reported in the present paper. Van Vleck (15) first pointed out that if in a situation such as this, the ground state is orbitally degenerate, considerable deviation from Curie law behavior is to be anticipated. All the V(III) distorted octahedral complexes for which susceptibility data have been reported obey the Curie law rather closely. Vanadium alum has been examined most thoroughly (16). At room temperature it has a moment of 2.80 B.M., very close to the spin only value, and departs from Curie law only at very low temperatures. Detailed analysis of the data fits the theory with the inclusion of spin–orbit coupling very well and leaves little doubt that the ground state is $^3A_2$ (17). A value of 2000 cm^{-1} is obtained for the splitting due to the trigonal distortion. $V(acac)_3$ has been examined over the temperature range 80–300 °K (16). It obeys Curie law very well with $\mu = 2.80$ B.M. and a Weiss constant θ of only 2 °C. In fact it appears that the trigonal splitting of many V(III) complexes is very similar and Van Vleck (15) suggests that it may always have a common origin in the Jahn–Teller effect. In any event it seems that the ground state of $V(acac)_3$ must be orbitally non-degenerate. The temperature dependence of the isotropic n.m.r. shifts should parallel that of the magnetic susceptibility. From the plots of Fig. 4 it is apparent that the behavior of the mixed complexes parallels that of $V(acac)_3$ rather closely. It does not seem feasible that there has been any dramatic change in the nature of the ground state on forming mixed chelates, since in each case the shifts vary linearly with $1/T$. The shifts will reflect the behavior of the magnetic susceptibility regardless of their exact origin.

At this point it is perhaps appropriate to briefly review the possibility of a pseudo-contact origin (18) for these shifts. Such an explanation has previously been rejected by all the groups who have examined this problem, but it could be contended that the effect might become important in the mixed chelates because of the lower symmetry and hence larger anisotropy of the g values. We do not favor this possibility but it is difficult to eliminate it entirely. Several authors (17, 19, 20) have calculated the g values expected for a trigonally distorted d^2 complex with an orbitally non-degenerate ground state and some experimental data are available (21). We quote the results of MacFarlane (20) on vanadium corundum as being fairly typical. He found $g_\parallel = 1.919$, $g_\perp = 1.791$, *i.e.*, $\Delta g = 0.12$. For comparison Δg for Co(II) trispyrazolylborate (22), which represents a well established case where pseudo contact effects dominate (23), is 7.5. Thus other things being equal, we can very roughly estimate the expected pseudo-contact contribution to the $V(acac)_3$ shifts as 2% of the observed shifts of Co(II) trispyrazolylborate, *i.e.*, 40–100 c.p.s. at 60 Mc/s. Since there is no evidence that the excited states which determine the g values are signifi-

Can. J. Chem. Downloaded from www.nrcresearchpress.com by 210.87.254.105 on 09/05/12
For personal use only.

cantly lower in energy in the mixed chelates than in $V(acac)_3$ (if they were it should be reflected in an anomalous temperature dependence of the susceptibility and shifts), we conclude that pseudo-contact interactions are unlikely to account for the large effects observed. Further experimental evidence for this conclusion is provided by the relatively small shifts of the phenyl protons in all the phenyl substituted compounds. These also show the characteristic alternation of signs for ortho, meta, and para expected for spin density in the π system but inconsistent with the geometrical dependence of pseudo-contact shifts.

Thus we shall assume that the observed shifts are predominantly contact in origin and arise from delocalization of spin in the π system of the ligand. As such they are determined by the two equations

$$[1] \qquad \frac{\Delta H_i}{H} = \frac{\Delta \nu_i}{\nu} = -a_i \frac{\gamma_e}{\gamma_N} \frac{g\beta S(S+1)}{6S'kT}$$

and

$$[2] \qquad a_i = Q\rho_c$$

In these equations ΔH_i and $\Delta \nu_i$ are the differences due to the paramagnetism in the resonance field or frequency of the nucleus i at applied field H or frequency ν, respectively; a_i is the hyperfine coupling constant of nucleus i; S is the total electron spin and S' the total spin of those unpaired electrons involved in delocalization. In the present case $S' = S = 1$. The hyperfine coupling constants a_i are related to the spin densities in the carbon pπ orbitals (ρ_c) by eq. 2 where Q is approximately constant and equal to -22.5 G for a single aromatic proton and $+27$ G for a methyl group. The other symbols have their usual significance. Thus the problem of interpreting the shifts is reduced to one of calculating the spin densities ρ_c. There are still two possibilities since the spin may reach the ligand by ligand to metal charge transfer, in which case the top bonding ligand π orbital is relevant or by metal to ligand charge transfer which will involve the bottom antibonding π^* orbital. We quote the results of the McLachlan type calculations of Röhrscheid *et al.* (10) for the spin densities in these orbitals since these are the most recent: highest energy π orbital: $\rho_\alpha = \rho_\gamma = +0.0705$, $\rho_\beta = +0.5680$; lowest energy π^* orbital: $\rho_\alpha = \rho_\gamma = +0.5598$, $\rho_\beta = -0.1659$. These results, in conjunction with eqs. 1 and 2, lead to the conclusion that the major delocalization mechanism involves metal-to-ligand charge transfer. It has previously been shown that this type of interpretation gives a consistent picture of the bonding in all the first row transition metal acetylacetonates (4).

Let us now consider the form of the spin containing orbitals in a little more detail. If the complex had O_h symmetry these orbitals would be d_{xy}, d_{xz}, and d_{yz} mixed with a small amount of the appropriate ligand π^* orbitals. The situation for a symmetrical tris chelate has been considered by Orgel (24). The symmetry is reduced to D_3 and without π bonding the orbitals are: a_1, $(1/\sqrt{3})(d_{xy} + d_{xz} + d_{yz})$; e, $(1/\sqrt{2})(d_{xz} - d_{yz})$, $(1/\sqrt{6})(2\,d_{xy} - d_{xz} - d_{yz})$. The ligand π orbitals can be classified as either ψ or χ depending on whether they are symmetric (ψ) or antisymmetric (χ) with respect to reflection in a plane perpendicular to the ligand π system. Examination of the orbitals resulting from a Hückel calculation on the acetylacetonate ligand shows that the highest energy π orbital is ψ and the lowest energy π^* orbital is χ. Orgel (24) has given the correct combinations of these π orbitals which combine with the a_1 and e d orbitals. We note for the present that if the ground state of the complex is orbitally non-degenerate, as we have argued above, the e orbital is doubly occupied and the a_1 orbital unoccupied leading to a symmetrical distribution of the electron spin.

In the mixed chelates in addition to the trigonal distortion mentioned above we must also consider a tetragonal distortion. It is convenient to first consider the case where the tetragonal distortion is very much larger than the trigonal distortion and to let the unique ligand occupy the xy plane. The appropriate symmetry is C_{2v} and the correct d orbitals are: a_1, d_{xy}; a_2, $(1/\sqrt{2})(d_{xz} + d_{yz})$; b_1, $(1/\sqrt{2})(d_{xz} - d_{yz})$. The case corresponds to that of a *cis* complex MA_4B_2 for which crystal field theory shows that the splitting of the orbitals is half as great as for the corresponding *trans* complex with the level order inverted (25). Thus if the ligand in the xy plane provides a larger crystal field than the other ligands, d_{xy} will be the unoccupied orbital and the odd electrons will be concentrated in the xz and yz planes. This will be the case for an electron donating substituent. On the other hand, with an electron attracting substituent, d_{xy} will be the lowest lying orbital and there will be a greater charge density in the xy plane than in xz or yz.

Can. J. Chem. Downloaded from www.nrcresearchpress.com by 210.87.254.105 on 09/05/12
For personal use only.

Consider now the case involving both the trigonal and the tetragonal distortion. C_2 symmetry is conserved and there are two orbitals of a symmetry and one of b symmetry. They correlate with the limiting C_{2v} and D_3 cases as follows

$$\begin{array}{lll} D_3 & C_2 & C_{2v} \\ e \rightarrow & a + b & a \leftarrow a_1 \\ a_1 \rightarrow & a & a \leftarrow a_2 \\ & & b \leftarrow b_1 \end{array}$$

Thus in all cases the unfilled orbital will be of a symmetry and separated from the next lower orbital by an energy large compared with kT as is shown by the Curie law dependence of the shifts. It will, however, vary in character according to the nature of the substituents. If the three chelating ligands are equivalent it will have the form $(1/\sqrt{3})(d_{xy} + d_{xz} + d_{yz})$ *i.e.*, it will have an equal contribution from each d orbital. In the extreme of a very large tetragonal distortion in which the odd ligand provides a strong crystal field the unfilled orbital will be d_{xy}. In the opposite extreme it will be $(1/\sqrt{2})(d_{xz} + d_{yz})$. For intermediate cases either d_{xy} or d_{xz} and d_{yz} will predominate depending on whether the odd ligand provides a stronger or a weaker crystal field than the other two ligands. The second a orbital will always be half-filled and its character will vary in a manner which is complementary to that of the empty orbital. In general the empty orbital will have the form

$$a\, d_{xy} + (\sqrt{1 - a^2}/2)(d_{xz} + d_{yz})$$

and the half-filled orbital the form

$$\sqrt{1 - a^2}\, d_{xy} - (a/\sqrt{2})(d_{xz} + d_{yz})$$

Thus $a = 1$ corresponds to an extreme electron donating substituent, $a = 0$ to an extreme electron withdrawing substituent, and $a = 1/\sqrt{3}$ to the symmetrical case. The parameter a is therefore a measure of the donating or withdrawing properties of the substituent.

In Table 5 matrix elements for the interaction of the various d orbitals in C_2 symmetry with the ligand π orbitals of ψ and χ symmetry are tabulated. If it is assumed that the spin-containing orbitals are predominantly d in character, the coefficients of the ligand orbitals will, by simple perturbation theory, be proportional to these matrix elements. The relative amounts of spin delocalized in the bottom antibonding π-orbital to the different ligands are given in Table 6 for the cases where the ligand A bears either an extreme electron withdrawing or an extreme electron donating substituent. Thus it is predicted that an electron withdrawing substituent such as CF_3 in the compound $V(acac)_2hfac$ should increase the contact shifts of the acac ligands relative to $V(acac)_3$ and decrease those of the hfac ligand relative to $V(hfac)_3$. This is indeed the case. On the other hand, the CH_3 in $V(acac)_2hfac$ may be regarded as an electron donating substituent relative to the hfac and it is predicted that the single (acac) ligand will obtain a disproportionately large share of the spin density. This again agrees with experiment. The arguments for the diphenyl ligand are reversed but entirely analogous.

This interpretation neglects ligand-to-metal charge transfer which it had previously been inferred was less important. In fact if the unfilled orbital in a D_3 complex has a_1 symmetry and if the top filled π orbital of acac has ψ symmetry, ligand-to-metal charge transfer of an α spin cannot occur. In the unsymmetrical chelates it becomes allowed and possibly would have to be taken into account in a quantitative interpretation of the data. It might also be noted that the above model predicts different shifts for the two non-equivalent methyl groups of $V(acac)_2hfac$

TABLE 5. Interaction of d orbitals with ligand orbitals

	d_{xy}	$\frac{1}{\sqrt{2}}(d_{xz} + d_{yz})$	$\frac{1}{\sqrt{2}}(d_{xz} - d_{yz})$
χ_A	0	β	0
$\frac{1}{\sqrt{2}}(\psi_B - \psi_C)$	β	$\beta/\sqrt{2}$	0
$\frac{1}{\sqrt{2}}(\chi_B + \chi_C)$	β	$\beta/\sqrt{2}$	0
ψ_A	0	0	β
$\frac{1}{\sqrt{2}}(\psi_B + \psi_C)$	0	0	$\beta/\sqrt{2}$
$\frac{1}{\sqrt{2}}(\chi_B - \chi_C)$	0	0	$\beta/\sqrt{2}$

TABLE 6. Relative spin delocalized to chelating ligands

Description	*A*	*B*	*C*
Symmetric chelate	1	1	1
Ligand A, extreme electron withdrawing	0	1.5	1.5
Ligand A, extreme electron donating	1.5	0.75	0.75

Can. J. Chem. Downloaded from www.nrcresearchpress.com by 210.87.254.105 on 09/05/12
For personal use only.

since d_{xy} interacts with the $p\pi$ orbitals of the carbonyl groups adjacent to one set of CH_3's and d_{xz} and d_{yz} with the carbonyl groups adjacent to the other set. The splitting of the methyl groups is therefore also a measure of the assymmetry of charge distribution.

These results therefore lead to a consistent picture for the transmission of electronic substituent effects in these octahedral metal complexes. At first sight the experimental results appear to be contrary to the expected substituent effects. Electron attracting substituents such as CF_3 diminish the charge transferred to the substituted ligand and enhance delocalization to the remaining ligands. Electron donating substituents have the opposite effect. However, this result follows naturally from the geometry of the spin containing d_{xy}, d_{xz}, and d_{yz} orbitals. An electron attracting substituent on a ligand in the xy plane tends to concentrate electron density in this plane since d_{xy} is most favorably oriented with respect to the substituted ligand. Electron density in d_{xy} is not available for delocalization to the π system of the ligand in the xy plane for reasons of symmetry but is available to the other two ligands. An electron donating substituent has the opposite effect. The important parameter is the charge density on the oxygen, a conclusion identical to that reached by Lintvedt and Kernitsky (8) from spectroscopic studies of substituent effects. It is interesting to note that these results provide another example of a recurring theme in transition metal bonding, namely the movement of charge in opposite directions in the σ and π bonding systems. The particular mechanism discussed above can, however, only operate for a limited number of d electron configurations since the possibility of an asymmetric distribution of the d electrons is required, the t_{2g} orbitals should not be either filled or half-filled.

We have not attempted to evaluate the mixing parameter a from our experimental results since the theory involves a number of obvious approximations. In particular consideration of only π interactions is a doubtful assumption. We do, however, intend to extend these studies of mixed chelates to include other substituted acetylacetonates and related ligands with the objective of developing at least an empirical scale of substituent effects. Preliminary results in this area are entirely consistent with the results of the present paper.

Experimental

V(III) trisacetylacetonate was obtained from the Research Organic/Inorganic Chemical Co., acetylacetone from Fisher Scientific, hexafluoroacetylacetone from Penninsular Chem. Research Inc., and 1,3-diphenyl-1,3-propanedione from Eastman Organic Chemicals. V(III) trishexafluoroacetylacetonate was prepared by a method analogous to that described by Morris *et al.* (26) for the corresponding aluminum compound.

Vanadium trichloride and hexafluoroacetylacetone dissolved in carbon tetrachloride, were refluxed into dry nitrogen for 45 min. The resulting solution was filtered into nitrogen while hot and the filtrate allowed to cool after which the solvent was removed by vacuum evaporation. The resulting reddish brown solid was purified by recrystallization from carbon tetrachloride. The final product had m.p. 76 °C and was characterized by the single contact shifted resonances in both the H and ^{19}F n.m.r. spectra.

Proton spectra were obtained on a Varian DP 60 instrument using TMS internal reference. ^{19}F spectra were obtained similarly with $CFCl_3$ internal reference. ^{19}F spectra were obtained at 56.4 Mc/s and the shifts converted to 60 Mc/s for comparison with the proton shifts.

All n.m.r. samples were carefully prepared in a dry nitrogen atmosphere. These V(III) complexes oxidize easily to V(IV) and this is manifested in the n.m.r. spectra by excessive broadening of the lines. The n.m.r. line width which is 20–30 c.p.s. in fact provides quite a sensitive probe for the sample purity.

We are indebted to the National Research Council of Canada for financial support of this research.

1. F. Basalo and R. G. Pearson. Mechanisms of Inorganic Reactions. 2nd ed. John Wiley. 1967. p. 351 ff.
2. (*a*) R. J. Myers and J. B. Spencer. J. Amer. Chem. Soc. **86**, 522 (1964). (*b*) A. Wojcicki and F. Basalo. J. Amer. Chem. Soc. **83**, 525 (1961). (*c*) J. Chatt and R. G. Hayter. J. Chem. Soc. 896 (1961).
3. D. R. Eaton and W. D. Phillips. Advan. Mag. Resonance, **1**, 108 (1965).
4. D. R. Eaton. J. Amer. Chem. Soc. **87**, 3097 (1965).
5. L. G. Van Uitert, W. C. Fernelius, and B. E. Douglas. J. Amer. Chem. Soc. **75**, 457 (1953).
6. L. G. Van Uitert, W. C. Fernelius, and B. E. Douglas. J. Amer. Chem. Soc. **75**, 2736 (1953).
7. R. L. Lintvedt and H. F. Holtzclaw. Inorg. Chem. **5**, 239 (1966).
8. R. L. Lintvedt and L. K. Kernitsky. Inorg. Chem. **9**, 491 (1970).
9. A. Forman, G. N. Murrell, and L. E. Orgel. J. Chem. Phys. **31**, 1129 (1959).
10. F. Röhrscheid, R. E. Ernst, and R. H. Holm. Inorg. Chem. **6**, 1315 (1967).
11. T. J. Pinnavaia and R. C. Fay. Inorg. Chem. **5**, 233 (1966).
12. A. C. Adams and E. M. Larsen. Inorg. Chem. **5**, 228 (1966).
13. W. C. Lin and L. E. Orgel. Mol. Phys. **7**, 131 (1964).
14. D. R. Eaton and W. D. Phillips. J. Chem. Phys. **43**, 392 (1965).

15. J. H. VAN VLECK. J. Chem. Phys. **7**, 61 (1939).
16. B. N. FIGGIS, J. LEWIS, and F. MABBS. J. Chem. Soc. 2480 (1960).
17. A. S. CHAKRAVARTY. Proc. Phys. Soc. **74**, 711 (1959).
18. H. M. MCCONNELL and R. E. ROBERTSON. J. Chem. Phys. **29**, 1361 (1958).
19. A. ABRAGAM and M. H. L. PRYCE. Proc. Roy. Soc. Ser. A, **205**, 135 (1951).
20. R. M. MACFARLANE. J. Chem. Phys. **40**, 373 (1964).
21. J. LAMBE and C. KIKUCHI. Phys. Rev. **118**, 71 (1960).
22. J. P. JESSON. J. Chem. Phys. **45**, 1049 (1966).
23. J. P. JESSON. J. Chem. Phys. **47**, 582 (1967).
24. L. E. ORGEL. J. Chem. Soc. 3683 (1961).
25. H. YAMATERA. Bull. Chem. Soc. Jap. **31**, 95 (1958).
26. M. L. MORRIS, R. W. MOSHIER, and R. E. SIEVERS. Inorg. Syn. Vol. IX, 28 (1967).

Can. J. Chem. Downloaded from www.nrcresearchpress.com by 210.87.254.105 on 09/05/12
For personal use only.

Can. J. Chem. Downloaded from www.nrcresearchpress.com by 210.87.254.40 on 09/05/12
For personal use only.

Temperature Dependence of the Diffusion of Carbon Tetrachloride, Chloroform, and Methylene Chloride Vapors in Air by a Rate of Evaporation Method[1]

HARRY WATTS
Exploratory Research Laboratory, Dow Chemical of Canada, Limited, Sarnia, Ontario

Received June 8, 1970

The diffusion coefficients in air of carbon tetrachloride, chloroform, and methylene chloride have been measured over a temperature range from room temperature to close to their boiling points by a modified rate of evaporation method. It was shown that considerable error can occur in diffusion coefficients determined by the rate of evaporation method when gas imperfections are ignored.

Canadian Journal of Chemistry, 49, 67 (1971)

Introduction

Many motives, relating both to the results, and the experimental methods used in obtaining them, prompted the measurements presented in this paper.

Data on the diffusion of chlorinated hydrocarbons through air at elevated temperatures are of value in assessing hazards associated with the use of commercial solvent systems. Recently, Lugg (1) published a monumental investigation of diffusion of 147 compounds in air at 25 °C, which included measurements on several halogenated hydrocarbons. Measurements on chlorinated hydrocarbons at other temperatures appear to be non-existent. The values plotted by McGovern (2) were calculated from theory.

An earlier variation (3) of the rate of evaporation method for determination of vapor diffusion coefficients seemed eminently suitable for adaptation to high temperature operation. Evaluation of this method at high temperatures has been made.

Measurements of diffusion coefficients in a Ney and Armistead type diffusion cell revealed a small, but statistically significant difference between the results of duplicate experiments made in two different diffusion cells (4). The present experiments were designed to enable further investigation of this effect.

In calculation of results of vapor diffusion measurements almost all previous authors have ignored gas imperfections and assumed that the saturated vapor concentration is proportional to the vapor pressure of the liquid. A test of the validity of this assumption seemed desirable and was made.

[1]Contribution No. 180.

Experimental

Materials

Carbon tetrachloride was purified as described previously (5).

Chloroform was treated as described by Francis and McGlashan (6). Gas chromatographic (g.c.) analysis revealed the following impurities: 1,1-dichloroethane, 60 p.p.m.; carbon tetrachloride, 100 p.p.m. Ethanol (100 p.p.m.) was added to inhibit aerial oxidation of the chloroform to phosgene.

Methylene chloride was selected from the production of Dow Chemical of Canada, Limited. The g.c. analysis showed the following impurities: methyl chloride, 50 p.p.m.; chloroform, 80 p.p.m.; vinylidene chloride, 10 p.p.m.

Apparatus

Figure 1 shows a diffusion cell. It consists of a Swagelok reducing union (Crawford Fitting Company) A, drilled to allow a length of Veridia precision bore capillary B to pass through it into a glass bulb C of volume 5 cc. The tube and bulb are sealed in place by Teflon ferrules D. Tubes used in these experiments had internal diameters of 0.200 ± 0.001 and 0.300 ± 0.001 cm and lengths in the range 3–6 cm. The liquid E under study was placed in the bulb to a level just below the lower end of capillary, B. This method of mounting the capillary, which allows interchange of capillaries of different size, constitutes an improvement over earlier cell design (3).

Six cells were suspended in a container as shown in Fig. 2. The glass container, A, was fitted with a perspex lid, B, sealed with a greased O-ring, C. A perspex tube, D, was sealed to the lid, B, to allow an extension hook, E, from an analytical balance to pass into the container. The cells, F, were suspended by wire hooks from six spokes radiating from a rotatable rod, H. For clarity, only two cells are shown. Manipulation of H enabled each cell in turn to be suspended from E and weighed. The outer end of tube D was sealed with a rubber serum cap which was removed during weighing of the cells. A dry air stream was preheated to thermostat temperature by passage through a copper coil immersed in the thermostat and passed through A to flush vapor that had diffused from the cells. This air stream enters at K and exits at L.

Procedure

Cells were filled with the liquid under investigation and the cell assembly was placed in the thermostat. Diffusion

Can. J. Chem. Downloaded from www.nrcresearchpress.com by 210.87.254.40 on 09/05/12
For personal use only.

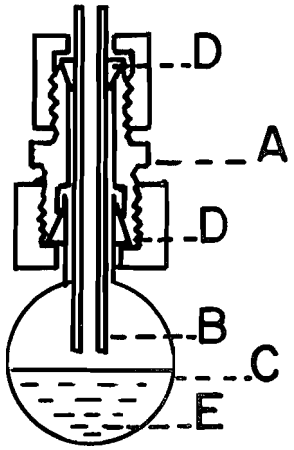

FIG. 1. Diffusion cell. *A*, Swagelok reducing union; *B*, precision bore capillary; *C*, glass bulb; *D*, teflon ferrules; *E*, liquid. Drawing to scale.

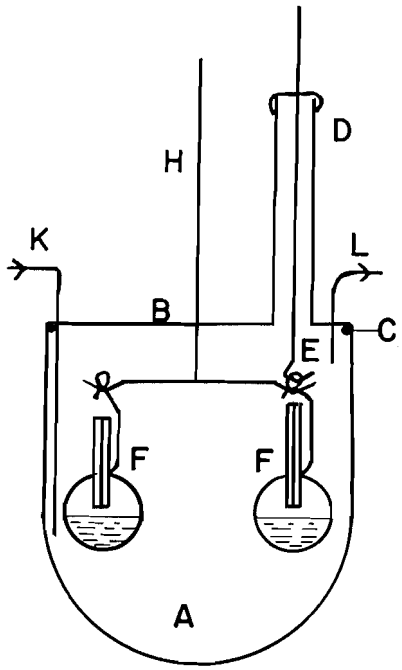

FIG. 2. Cell container. *A*, glass pot; *B*, perspex lid; *C*, O-ring; *D*, perspex tube; *E*, extension hook from balance; *F*, diffusion cell; *H*, rotatable rod; *K*, flushing air entrance; *L*, flushing air exit. Drawing not to scale.

was allowed to proceed overnight to permit steady state conditions to be attained. Each cell was then weighed at the beginning and end of an appropriate measured time interval. Observations were made for two consecutive intervals to ensure that steady state conditions had in fact been obtained. The time was usually between 8 h and 3 days and depended on the nature of the liquid and the temperature. The barometric pressure was recorded at intervals during the experiment and averaged. The thermostat temperature was measured with a quartz thermometer (Hewlett–Packard Company). The total pressure and temperature fluctuations during an experiment were about 2 mm of mercury and 0.02 °K, respectively.

Calculation of Results

The diffusion coefficient of a vapor through air in a rate of evaporation experiment is calculated (7) using the expression

$$[1] \qquad \mathscr{D} = (WL)/(MAct \ln[c/(c - c_s)])$$

In eq. 1, W is the weight of liquid of molecular weight M evaporated in time t, c_s is the saturation concentration of vapor in the air space at the liquid surface while c is the total concentration of air plus vapor, L and A are the length and cross-sectional area of the diffusion path, respectively, and $\mathscr{D}$ is the diffusion coefficient. In the conventional rate of evaporation method the liquid is contained in the bottom of a vertical tube of uniform bore; the same tube thus serves as liquid container and defined diffusion path. Under these conditions L changes with time as the liquid evaporates and appropriate allowance must be made. In the present experimental modification since the diffusion path is a capillary tube the lower end of which protrudes into the vapor space above liquid contained in a bulb, the diffusion path L does not change during the course of an experiment. The apparatus thus resembles a Ney and Armistead type (8) two bulb diffusion cell with one bulb (the atmosphere outside the cell) of infinite size. Thus, as in the Ney and Armistead experiment, it is appropriate to adjust the tube length L for end effects to give an effective length L_{eff}, given by

$$[2] \qquad L_{eff} = L + 0.82d$$

where d is the diameter of the tube.

The assumption of ideality of the air–vapor mixture has been made, almost without exception, by previous workers, who have put

$$[3] \qquad c/(c - c_s) = P/(P - P_s)$$

where P_s is the saturation vapor pressure of the liquid and P is the total pressure, and

$$[4] \qquad c = P/RT$$

where R is the gas constant and T the absolute temperature.

In the present experiments two methods of calculation have been used, in one the assumption of ideality has been made; in the other, corrections for gas imperfections have been made by the method outlined below.

The temperature dependence of the diffusion coefficient for each system studied was obtained by fitting the experimental results to the equation

$$[5] \qquad \mathscr{D} = D_0 T^v$$

where D_0 is a constant and v is, in general, a non-integral exponent.

Correction for Non-Ideality

Ewald, Jepson, and Rowlinson (9) have derived an

Can. J. Chem. Downloaded from www.nrcresearchpress.com by 210.87.254.40 on 09/05/12
For personal use only.

expression giving the mole fraction of the vapor of a solid in a compressed gas with which it is in contact. The same expression would be applicable for a liquid in contact with a gas, provided the solubility of the gas in the liquid is low and insufficient to cause a change in the thermodynamic activity of the liquid. This condition is expected to hold, within experimental error, in the present experiment. Ewald *et al.* gave their derivation only for low mole fractions of vapor. Following their derivation it may be readily shown for the general case that the mole fraction of vapor is given by

$$[6]\quad \ln x_i = \ln (V_M/V_i) + 2B_{ii}/V_i - 2(x_iB_{ii} + x_jB_{ij})/V_M + V_i^L(P_M - P_{is})/RT$$

where the subscripts i and j refer to the vapor and air respectively, x is the mole fraction, the B_{ij} are second virial coefficients, V_M, V_i, and V_i^L are the molar volumes of the air–vapor mixture, the pure saturated vapor, and the pure liquid, respectively.

The molar volumes V_i and V_M are expressed in terms of second virial coefficients

$$[7]\quad V_i = RT/P_{is} + B_{ii}$$

$$[8]\quad V_M = RT/P + (x_i^2B_{ii} + 2x_ix_jB_{ij} + x_j^2B_{jj})$$

In general, experimental values of the second virial coefficients are not available. However, Cruickshank, Windsor, and Young (10) have shown that second virial coefficients for mixtures may be calculated, within experimental error, by the McGlashan–Potter (11) equation

$$[9]\quad B/V^c = 0.430 - 0.886(T^c/T) - 0.694(T^c/T)^2 - 0.0375(n-1)(T^c/T)^{4.5}$$

using the Hudson–McCoubrey (12) combining rules for T_{ij}^c and V_{ij}^c, the critical temperature and volume of the mixture.

$$[10]\quad T_{ij}^c = (T_{ii}^cT_{jj}^c)^{1/2}\left\{\frac{2(I_iI_j)^{1/2}}{I_i + I_j}\right\} \times \frac{2^6 \cdot V_{ii}^cV_{jj}^c}{[(V_{ii}^c)^{1/3} + (V_{jj}^c)^{1/3}]^6}$$

$$[11]\quad V_{ij}^c = 1/8[(V_{ii}^c)^{1/3} + (V_{jj}^c)^{1/3}]^3$$

The parameter n in eq. 9 bears a relationship to molecular size. If the vapor under consideration is a normal hydrocarbon then n is the number of carbon atoms. For other substances, values of n may be estimated by the method of Guggenheim and Wormald (13). For mixtures, a combining rule for n is used (10)

$$[12]\quad n_{ij} = 1/2(n_i + n_j)$$

The procedure in using the above equations to allow for gas imperfections in the calculated diffusion coefficient is as follows. The B_{ii} and B_{jj} are calculated for the vapor and for air using eq. 9, and B_{ij} is calculated using eq. 9 together with pseudo-critical parameters for the mixture obtained from eqs. 10, 11, and 12. Calculations verified that treating air as a single component was justified in that the second virial coefficient for mixtures of carbon tetrachloride and air obtained by treating it as a two-component mixture and as a three-component mixture of carbon tetrachloride, oxygen, and nitrogen differed by about 1%; the effect of this variation in the virial coefficient is well within experimental error on the measured diffusion coefficients. The mole fraction x_i of the vapor was then calculated by an iterative procedure. The mole fraction was assumed to a first approximation to be equal to the partial vapor pressure given by the Antoine equation

$$[13]\quad \log P_x = \alpha - \beta/(\gamma + t)$$

where α, β, and γ are constants and t is the temperature in degrees Celsius. This mole fraction was used in eqs. 8 and 6 to calculate a new value of x_i. The calculation was recycled until the change in x_i during a cycle was less than 0.01%. Then the substitutions

$$[14]\quad c/(c - c_s) = 1/(1 - x_i)$$

and

$$[15]\quad c = 1/V_M$$

were used in eq. 1 to calculate the diffusion coefficient. All calculations were performed on an IBM 360-30 computer. Values of all constants used in the calculations are given in the appendix.

Results

Table 1 gives the constants D_0 and ν in eq. 5 for the three systems studied. The constants of this equation relevant to diffusion coefficients calculated assuming the systems to behave as ideal gases and calculated allowing for gas imperfections are given. The standard deviations given were calculated from the deviations of all the experimental points from the fitted line.

Discussion

Consideration will be given first to the experimental method. Originally, diffusion tubes of length 3, 4.5, and 6.0 cm were used in the diffusion cells, there being one tube of each length of diameter 0.2 and 0.3 cm. An analysis of variance (14) performed on results obtained on these tubes showed that diffusion coefficients measured using 3 cm tubes were significantly lower than those using 4.5 and 6 cm tubes, while there was no significant difference between results obtained on the two longer tubes. Careful examination of the apparatus showed that the short diffusion tubes (A in Fig. 1) did not extend down into the bulb B, but the lower end was inside the neck of the bulb. Thus it is inferred that this result indicates that bad cell geometry had been incorporated in the cells with shorter tubes and, provided cell geometry is satisfactory there is no effect of tube length on diffusion coefficient. It is now believed that the observation

TABLE 1. Constants in eq. 5 for diffusion of stated component in air

Second component	Temperature range (°K)	Number of data	Assumed ideal		Corrected for non-ideality		Standard deviation
			D_0	ν	D_0	ν	
CCl_4	298–348	72	2.996×10^{-6}	1.784	6.667×10^{-6}	1.694	±0.0023
$CHCl_3$	298–328	62	5.830×10^{-6}	1.694	1.438×10^{-6}	1.532	±0.0015
CH_2Cl_2	278–308	20	2.522×10^{-5}	1.462	5.611×10^{-5}	1.351	±0.0019

reported earlier (4) in which the results obtained in two diffusion cells differed significantly was caused by a small difference in cell geometry and not to difference in the lengths of the diffusion tubes. The statistical analysis showed no significant difference between results obtained using tubes of different diameter. After this had been established, all the results obtained with 3 cm tubes were rejected and these tubes were replaced with others of length 5 cm. On all results obtained after that time, no effect of tube length is discernable.

Cells similar in design to the present ones have been used previously by the author (3) to measure diffusion coefficients, and by McKelvey and Hoelscher (15), Fortuin (16), and Altshuller and Cohen (17), to produce low vapor concentrations in an air stream. The two last named groups appear to have had difficulty in obtaining consistent results and preferred to use Stefan's original design of one vertical tube used both as liquid container and diffusion path. No difficulty was experienced in the present work and it is believed that the present method is superior because the diffusion path length is not changing with time. The end correction as used in a Ney and Armistead type (8) apparatus must be applied at both ends of the diffusion tube because there is no forced flow of air streamlining across the top of the tube as in the experiments of Wilke and co-workers (18, 19). In the present experiments the air flow merely serves to flush the diffusate from the cell container. Results obtained using tubes of different lengths and applying the end correction are consistent. With cells of the present design, it is not necessary, as with conventional Stefan diffusion tubes, to extrapolate results obtained with several tube lengths to remove the meniscus effect (18).

The greatest source of error in these experiments is probably fluctuation of atmospheric pressure. Some experiments were performed in which the cell container pressure was controlled with a Cartesian Manostat. The pressure fluctuations were then greater than atmospheric pressure fluctuations except during periods of inclement weather. Therefore, attempts at pressure control were abandoned.

The most striking conclusion to be drawn from the present results is that the assumption of perfect gas behavior is grossly in error. Reference to Tables 1 and 2 shows that neglect of the correction for gas imperfections causes an error of $\sim 2\%$ in the measured diffusion coefficients at 298 °K while at higher temperatures the error rises to 4%. Non-ideality of the vapor–gas mixture has been largely ignored by previous workers on diffusion coefficients measured by the rate of evaporation method. Kohn and Romero mention a correction for non-ideality, but their published results are uncorrected (20). O'Connell, Gillespie, Krostek, and Prausnitz (21) in a recent study of diffusion of water vapor in non-polar gases corrected for gas imperfections using experimental virial coefficients, but they did not mention the magnitude of the error introduced by ignoring these corrections. However, it remains necessary to quote diffusion

TABLE 2. Comparison of experimental and theoretical diffusion coefficients for named component in air

Component	T (°K)	Diffusion coefficients ($cm^2\ s^{-1}$)		
			Experimental	
		Theoretical	Corrected for gas imperfection	Not corrected
CCl_4	298.15	0.0809	0.0759	0.0776
	308.15	0.0851	0.0800	0.0823
	318.15	0.0902	0.0845	0.0872
	328.15	0.0955	0.0889	0.0921
	338.15	0.1008	0.0933	0.0971
	348.15	0.1064	0.0979	0.1023
$CHCl_3$	298.15	0.115	0.0888	0.0909
	308.15	0.123	0.0934	0.0961
	318.15	0.131	0.0981	0.1014
	328.15	0.139	0.1028	0.1069
CH_2Cl_2	288.15	0.0943	0.0970	0.0996
	298.15	0.1006	0.1016	0.1046
	308.15	0.1071	0.1064	0.1098

Can. J. Chem. Downloaded from www.nrcresearchpress.com by 210.87.254.40 on 09/05/12
For personal use only.

TABLE 3. Comparison of diffusion coefficients of vapors in air

Component	Temperature (°K)	$10^2 \times D$ (cm^2 s^{-1}) This work*	Lugg	Mrazek *et al.*
CCl_4	298	7.76±0.08	8.28±0.063	
$CHCl_3$	298	9.09±0.074	8.88±0.187	
	323	10.41		10.6–11.5†
CH_2Cl_2	298	10.46±0.13	10.37±0.13	

*Calculated from fitted curve. Data used for this comparison are not corrected for gas imperfections because no correction was made by Lugg or Mrazek *et al.*
†Range of values over a concentration range.

coefficients both corrected and uncorrected for gas imperfections; the former are needed for theoretical calculations, the latter are needed in some practical problems where it is required to calculate the amount of substance diffusing at a given partial pressure.

Mrazek, Wicks, and Prabhu (22) report measurements of a concentration effect of diffusion coefficients measured by a rate of evaporation method. For the methanol–air system at 55 °C the effect is of the order of 1%. These authors neglected to correct for gas imperfections. In view of the magnitude of corrections for non-ideality demonstrated in the present work, it is difficult to believe that these authors observed anything other than a variation of the magnitude of the non-ideality correction in air–vapor mixtures of different composition at the same temperature. However, the claimed concentration variation of diffusion coefficient was of the order of 9% in the system chloroform–air at 50 °C. Compare this with the present measurements in Table 3. Part of this apparent variation is no doubt due to the neglect of gas imperfections. In the first few experiments with chloroform, the present author used chloroform from which all inhibitor had been removed. It was only when traces of phosgene were detected in the chloroform at the end of an experiment that 100 p.p.m. of ethyl alcohol inhibitor was included in the chloroform. However, the results obtained with uninhibited chloroform were self-consistent and in agreement with those obtained with inhibited chloroform at 298 °K. As the temperature was raised to 328 °K the results with uninhibited chloroform deviated from those obtained with inhibited chloroform and the precision of the results decreased. Comparison of these two sets of results is made in Table 4. The magnitude of the diffusion coefficient obtained by Mrazek *et al.* is very close to that obtained with uninhibited chloroform. Mrazek *et al.* do not give an analysis of their chloroform, but it can only be suspected that they ran into difficulties of which they were unaware. In preparing a chloroform loaded air stream, they passed air through liquid chloroform; under such conditions one may expect any oxidation inhibitor in their chloroform to be rapidly consumed and allow oxidation to occur with subsequent effect on the measured diffusion coefficient. In view of this, their conclusions regarding the magnitude of the concentration dependence of diffusion coefficient in the chloroform–air system must be treated with caution.

Comparison of the present results with those of Lugg (1) is made in Table 3. Lugg did not correct for non-ideality. His results for methylene chloride and chloroform agree with the present results within experimental error. With carbon tetrachloride the agreement is not good. Great care was taken in purification of materials in the present work, while Lugg does not give full details of purity of materials, so the present results are preferred.

Originally it was planned to calculate molecular interaction parameters from the experimental results. Unfortunately, the temperature range is too small to allow calculation of meaningful parameters. Consequently the reverse procedure had been adopted. Interaction parameters for air and the three compounds studied calcu-

TABLE 4. Comparison of diffusion coefficient of $CHCl_3$ in air using $CHCl_3$ with and without oxidation inhibitor

Temperature (°K)	D^* (cm^2 s^{-1}) Inhibited	Uninhibited
298.12	0.0931±0.0006	0.0893±0.001
308.13	0.0957±0.0004	0.0950±0.001
318.17	0.1019±0.00096	0.104 ±0.0039
328.17	0.1057±0.0007	0.120 ±0.0057

*Mean of 6 values at each temperature.

Can. J. Chem. Downloaded from www.nrcresearchpress.com by 210.87.254.40 on 09/05/12
For personal use only.

lated from viscosity measurements and tabulated by Hirschfelder, Curtiss, and Bird (23) have been used to calculate diffusion coefficients at several temperatures. In the calculation the equation (23)

$$[16] \quad D_{12} = 2.628 \times 10^{-5} \frac{(T^3(M_i + M_j)/2M_iM_j)^{1/2}}{P\sigma_{ij}{}^2\Omega_{ij}(T_{ij}{}^*)}$$

was used. Here M is the molecular weight, $\Omega_{ij}(T_{ij})$ is a collision integral at a reduced temperature $T_{ij}{}^* = kT/\varepsilon_{ij}$, and σ_{ij} and ε_{ij}/k are molecular interaction parameters. Values of the collision integral for a Lennard–Jones 6–12 potential function have been tabulated (23). The Hudson–McCoubrey combining rules (12) were used in calculation of σ_{ij} and ε_{ij}/k from values for the pure components. Diffusion coefficients obtained from the smoothed curve through the experimental data are compared with those calculated from theory in Table 2. With methylene chloride the agreement is good, with carbon tetrachloride the agreement is fair, while with chloroform the agreement is bad. Thus molecular interaction parameters obtained from viscosity data for the first two named substances may be used to calculate reasonable values of diffusion coefficients.

The system air – methylene chloride has a low value of the temperature exponent ν, when compared to the other systems and to the average value of 1.75 for many data in the literature (28). The number of data obtained was lower and their standard deviation was higher than with the other systems. Hence, it is believed that this value of ν is probably lower than would be found over a wider temperature range with more data.

Gas chromatographic analyses were performed by C. Kuley. The author is indebted to Professor M. L. McGlashan for a helpful discussion.

1. G. A. Lugg. Anal. Chem. **40**, 1072 (1968).
2. E. W. McGovern. Ind. Eng. Chem. **35**, 1230 (1943).
3. F. Jorgenson and H. Watts. Chem. Ind. 1440 (1961).
4. H. Watts. Trans. Faraday Soc. **60**, 1745 (1964).
5. H. Watts, E. C. W. Clarke, and D. N. Glew. Can. J. Chem. **46**, 815 (1968).
6. P. G. Francis and M. L. McGlashan. Trans. Faraday Soc. **51**, 593 (1955).
7. J. R. Partington. An Advanced Treatise on Physical Chemistry. Vol. 1. Longmans, Green and Co., London. 1949. p. 912.
8. E. P. Ney and F. C. Armistead. Phys. Rev. **71**, 14 (1947).
9. A. H. Ewald, W. B. Jepson, and J. S. Rowlinson. Discuss. Faraday Soc. **15**, 238 (1953).
10. A. J. B. Cruickshank, M. L. Windsor, and C. L. Young. Trans. Faraday Soc. **62**, 2341 (1966).
11. M. L. McGlashan and D. J. B. Potter. Proc. Roy. Soc. London. Ser. A. **267**, 478 (1962).
12. G. H. Hudson and J. C. McCoubrey. Trans. Faraday Soc. **56**, 761 (1960).
13. E. A. Guggenheim and C. J. Wormald. J. Chem. Phys. **42**, 3775 (1965).
14. W. Volk. Applied Statistics for Engineers. McGraw-Hill, New York. 1958. P. 136.
15. J. M. McKelvey and H. E. Hoelscher. Anal. Chem. **29**, 123 (1957).
16. J. M. H. Fortuin. Anal. Chim. Acta, **15**, 521 (1956).
17. A. P. Altshuller and I. R. Cohen. Anal. Chem. **32**, 802 (1960).
18. C. Y. Lee and C. R. Wilke. Ind. Eng. Chem. **46**, 2381 (1954).
19. F. J. Heinzelmann, D. T. Wasan, and C. R. Wilke. Ind. Eng. Chem. Fund. **4**, 55 (1965).
20. J. P. Kohn and N. Romero. J. Chem. Eng. Data, **10**, 125 (1965).
21. J. P. O'Connell, M. D. Gillespie, W. D. Krostek, and J. M. Prausnitz. J. Phys. Chem. **73**, 2000 (1969).
22. R. V. Mrazek, C. E. Wicks, and K. N. S. Prabhu. J. Chem. Eng. Data, **13**, 508 (1968).
23. J. O. Hirschfelder, C. F. Curtiss, and R. B. Bird. Molecular Theory of Gases and Liquids. Wiley, New York. 1954.
24. A. P. Kudchadker, G. H. Alani, and B. J. Zwolinski. Chem. Rev. **68**, 659 (1968).
25. G. Herzberg. Molecular Spectra and Molecular Structure. Vol. I. Spectra of Diatomic Molecules. D. Van Nostrand Company, Inc., Princeton. 1950. Vol. III. Electronic Spectra and Electronic Structure of Polyatomic Molecules. D. Van Nostrand Company, Inc., Princeton. 1966.
26. D. L. Hildenbrand and R. A. McDonald. J. Phys. Chem. **63**, 1521 (1959).
27. R. R. Dreisbach. Physical Properties of Chemical Compounds II. Advances in Chemistry Series Number 22. American Chemical Society, Washington. 1959.
28. E. N. Fuller, P. D. Schettler, and J. C. Giddings. Ind. Eng. Chem. **58**, 19 (1966).

Can. J. Chem. Downloaded from www.nrcresearchpress.com by 210.87.254.40 on 09/05/12
For personal use only.

Can. J. Chem. Downloaded from www.nrcresearchpress.com by 210.87.254.40 on 09/05/12
For personal use only.

Appendix

Data used in calculations

Compound	T_c (°K)		V_c (l mole^{-1})		I (eV)		σ (nm)		ε/k (°K)	n	Antoine constant			
	Value	Reference	Value	Reference	Value	Reference	Value	Reference	(Reference 23)	(Reference 13)	α	β	γ	Reference
CCl_4	556.4	24	0.276	24	11.47	25	0.5881	23	327.0	4.5	6.89405	1219.58	227.16	26
$CHCl_3$	536.4	24	0.239	24	11.42	25	0.3375	23	855.0	4.0	6.90328	1163.0	227.0	27
CH_2Cl_2	510.0	24	0.190[b]	24	11.35	25	0.4759	23	406.0	3.0[d]	7.07138	1134.6	231.0	27
Air	139.3[a]	24	0.0791[a]	24	14.9[c]	25	0.3617	23	97.0	1.0[e]				
O_2	154.74	24	0.074	24	12.2	25								
N_2	126.2	10	0.0846	10	15.576	25								

[a]Calculated from critical parameters for oxygen and nitrogen using Hudson–McCoubrey (12) combining rules.
[b]Value obtained by linear interpolation of values for CH_4, CH_3Cl, $CHCl_3$, and CCl_4 given in ref. 24.
[c]Calculated from values of oxygen and nitrogen assuming that the ionization potential in a mixture is given by $I_m = (x_i I_i + x_j I_j)$. This value used, with the critical parameters for air, in calculation of the virial coefficient of an air – carbon tetrachloride mixture, gave a value in agreement with that obtained by treating the mixture as one of oxygen, nitrogen and carbon tetrachloride. The calculated virial coefficients are insensitive to small changes in ionization potential (12), so any errors in the diffusion coefficients arising from the failure to choose the best value for the ionization potential will be negligible.
[d]Estimated from critical parameters by method given in ref. 13.
[e]Assumed equal to the value for nitrogen (10).

Can. J. Chem. Downloaded from www.nrcresearchpress.com by 210.87.254.40 on 09/05/12
For personal use only.

Diffusion of Methane and Chloromethanes in Air[1]

M. COWIE[2] AND HARRY WATTS
Exploratory Research Laboratory, Dow Chemical of Canada, Limited, Sarnia, Ontario

Received June 8, 1970

The binary gaseous diffusion coefficients of air with methane, methyl chloride, methylene chloride, chloroform, and carbon tetrachloride at 298.2 °K and 1 atm have been determined. A simple diffusion cell was used, in which concentration changes of the diffusing gas were followed by infrared spectrophotometry.

Canadian Journal of Chemistry, 49, 74 (1971)

Introduction

The experimental method described in this paper was developed as a simple technique for determination of the diffusion coefficients of gases and vapors in air. The apparatus was derived from the Ney and Armistead (1) two bulb diffusion cell by making one bulb of infinite size; this bulb in fact was constituted by the atmosphere. Concentration changes of the diffusing gas in the other bulb were followed by infrared (i.r.) spectrophotometry. To evaluate the technique, measurements were made on a number of compounds for which the diffusion coefficients in air were known.

Experimental

Materials

Carbon tetrachloride, chloroform, and methylene chloride were taken from samples used previously (2). Methyl chloride was selected from the production of Dow Chemical of Canada, Limited and contained 17 p.p.m. vinyl chloride; other impurities were below the limits of detection by gas chromatographic analysis (< 10 p.p.m.). Methane (purity 99.95 mole %) was obtained in cylinders from the Phillips Petroleum Company.

Apparatus and Procedure

The diffusion cell is shown schematically in Fig. 1. It consisted of a stainless steel Tee A closed by rock salt windows B which were sealed in place by epoxy resin or by a screw cap fitting and O-rings. Gas contained in the cell diffused out into the atmosphere through the tube C which was mounted in a Swagelok fitting (Crawford Fittings) using Teflon ferrules. Thus the glass and stainless steel tubes used were readily interchangeable. The cell was placed in the beam of a Perkin–Elmer Model 221 IR spectrophotometer and the concentration of gas in the cell determined by scanning an appropriate absorption band. The decrease in concentration of the gas due to diffusion from the cell was followed by repeating the scan of the selected absorption band at suitable time intervals.

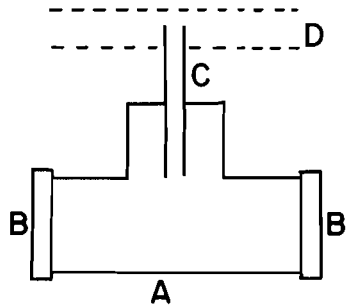

FIG. 1. Schematic diagram of diffusion cell. *A*, Tee piece; *B*, rock salt windows; *C*, capillary tube; *D*, proposed tube of sweep gas. Drawing not to scale.

The best dimensions for the tube C depended upon the cell volume. Two cells of volume 60 ml and 14 ml were used. The length of C was about 6 cm in each cell and the internal diameters were 0.5 cm in the larger and 0.3 cm in the smaller cell. The smaller cell was wrapped in a copper tube through which water from a thermostat at 25 °C was passed. The temperature of the larger cell was determined by measuring the air temperatures near the cell and taking the average. Comparison of results obtained in the two cells showed that the small fluctuations in temperature (± 1 °C) in an air conditioned room were insufficient to cause significant errors with the unjacketed cell.

In the conduct of an experiment, the cell was first charged with air laden with the gas or vapor under study so that the i.r. transmittance at the selected absorption frequency was about 30%. The diffusion was followed until the transmittance became about 70%. Depending on the magnitude of the diffusion coefficient, the duration of an experiment was 3–8 h; about ten scans of the spectrum were made in this time. The barometric pressure was recorded and averaged during each experiment.

Theory and Calculation of Results

The diffusion flux in a system at steady state is given by Fick's first law

$$[1] \qquad J = -\mathscr{D}\frac{\partial c}{\partial x}$$

where J is the flux in moles diffusing through unit

[1]Contribution No. 182.
[2]Vacation student from McMaster University 1968. Present address: Department of Chemistry, University of Alberta, Edmonton, Alberta.

Can. J. Chem. Downloaded from www.nrcresearchpress.com by 210.87.254.40 on 09/05/12
For personal use only.

cross-sectional area in unit time, $\partial c/\partial x$ is the concentration gradient in the direction of diffusion, and $\mathscr{D}$ is the diffusion coefficient. Ney and Armistead (1) derived an expression for calculation of results for their two bulb experiment by solving eq. 1 for the appropriate boundary conditions. Specialization of their expression for the present experiment by setting one bulb volume equal to infinity leads to a triviality. The solution of eq. 1 valid for diffusion from a bulb through a capillary into infinite volume is given below. The method of solution follows closely the derivation of Ney and Armistead and is based on the same assumptions. These are: (*1*) the concentration gradient in the capillary is linear; (*2*) the concentration in the bulb is uniform; (*3*) the concentration outside the bulb is zero; (*4*) at all times the conditions approximate to steady state, *i.e.* the concentration gradient in the tube and the diffusion flux at any instant are those that would be found if the concentration in the bulb was maintained constant at the instantaneous value. The validity of these assumptions has been discussed by Ney and Armistead (1).

If c is the concentration in the bulb and l and A are the length and cross-sectional area, respectively, of the tube

$$[2] \qquad -\mathscr{D}\frac{\partial c}{\partial x} = -\mathscr{D}c/l$$

we can put

$$[3] \qquad J = v/A\,\frac{\delta c}{\delta t}$$

where v is the cell volume and δc is the infinitesimal change in concentration in the cell during the time interval δt. Equating [2] and [3] gives

$$[4] \qquad \frac{\delta c}{\delta t} = -\mathscr{D}Ac/lv$$

Taking the limit $\delta t \to 0$ and integrating gives

$$[5] \qquad \ln c = -\mathscr{D}At/lv + B$$

where B is a constant of integration. Thus a graph of $\ln c$ against t is linear and the slope is $-\mathscr{D}A/lv$.

In the calculation of diffusion coefficients the i.r. transmittance readings were converted to absorbance in the usual way (3), the absorbance of the empty cell was deducted to find that due to the compound. If Beer's law is assumed to hold, the concentration is proportional to the absorbance; conveniently we are spared the need of knowing the proportionality constant because in the calculation of $\mathscr{D}$, we are concerned only in variations of the logarithm of concentration. Here then is one advantage of the present method; it is not necessary to calibrate and determine absolute concentrations of the diffusing gas. Thus we can rewrite eq. 5

$$[6] \qquad \ln \alpha = -\mathscr{D}At/lv + B$$

where α is the i.r. absorbance due to the diffusing gas at time t. In using eq. 6 to calculate diffusion coefficients, the slope of the best straight line through the experimental points was found by a least squares fit.

The usual end correction was made so that the tube length l used in eq. 6 is given by

$$l = l_{act} + 0.82d$$

where l_{act} is the actual tube length and d is the diameter (1).

Results and Discussion

Diffusion coefficients, calculated from these experimental measurements as described in the next section, were corrected to 1 atm pressure in the usual way using the relationship that the diffusion coefficient is proportional to the reciprocal of pressure. Five determinations of the diffusion coefficient were made for each substance. The values were averaged and are given, together with their standard deviations, in Table 1. The frequencies of the i.r. absorption peaks used to follow the diffusion are also given in this table.

The mean diffusion coefficients given in Table 1 agree, within combined experimental errors, with values obtained by other methods in this laboratory (2) and in other laboratories (4, 5), with one exception. The value for carbon tetrachloride is in good agreement with a recent value obtained by one of us (2) but is not in agreement with that of Lugg (5). We prefer our lower value for the following reason. The i.r. method used for measurement of concentration is not suceptible to interference by impurities, provided any i.r. absorption by the impurities occurs at a frequency other than that of the compound under study. The carbon tetrachloride used was of high purity. That the presence of small amounts of impurity is un-

TABLE 1. Diffusion coefficients in air at 298.2 °K and 1 atm pressure

Compound	Infrared frequency (cm^{-1})	Diffusion coefficient		
		This work	Other work	Calculated
CH_4	1310	0.2168 ± 0.0032	0.224[a] (at 294.6 °K)	0.2182 0.2143
CH_3Cl	2985	0.1434 ± 0.0024		0.1297
CH_2Cl_2	1282	0.1042 ± 0.0049	0.1016[b] 0.1037[c]	0.1007
$CHCl_3$	1220	0.0862 ± 0.0015	0.0888[b] 0.0888[c]	0.1152
CCl_4	797	0.0759 ± 0.0017	0.0759[b] 0.0828[c]	0.0801

[a]Reference 4.
[b]Reference 2.
[c]Reference 5.

likely to interfere with the diffusion and affect the magnitude of the measured diffusion coefficient is indicated by several recent studies on diffusion in multicomponent mixtures (see, for example, ref. 6). Impurities can upset measurements by the rate of evaporation method used in determination of the quoted values for carbon tetrachloride (2, 5) because of their effect on vapor pressure, and vapor pressure is used as a measure of concentration of the diffusing substance. Lugg used the rate of evaporation method and did not make the necessary correction (2) for gas imperfections. Had he done so the agreement between his and our results would have been improved but there would still be a discrepancy with carbon tetrachloride. The results from our earlier work (2) corrected to true vapor concentration by allowing for gas imperfections were taken for comparison with our present results because the i.r. method measures true concentration. The surprising agreement between the present value and one earlier value (2) for carbon tetrachloride is regarded as an embarrassing coincidence!

Diffusion coefficients for the compounds studied in this paper were calculated by a kinetic theory equation (7) using the Lennard–Jones 6–12 potential function, for which values of the collision integral have been tabulated (7). In computing values of the molecular interaction parameters for like–unlike interactions, molecular interaction parameters for like–like interactions obtained from viscosity measurements and tabulated by Hirschfelder *et al.* (7) were used in conjunction with the Hudson–McCoubrey combining rules (8) and ionization potentials tabulated by Herzberg (9). The relevant equation and data are given in the Appendix.

For methane, two sets of interaction parameters were given (7) and the diffusion coefficient calculated from each set agrees with the experimental value within experimental error. For methyl chloride the calculated and experimental values agree within about 7%. For carbon tetrachloride, chloroform, and methylene chloride, the agreement is similar to that observed previously. It is not surprising that, of the substances studied, the best agreement between theory and experiment is shown with methane, since it is well established that, within experimental accuracy, methane obeys, while the other substances deviate from, the principle of corresponding states (10).

One experimental disadvantage was discovered in determination of the diffusion coefficient of methane. Initially experiments were made in a cell of length 3.5 cm. With this length, the methane concentration required to obtain an i.r. absorption in the optimum range apparently exceeded the limit for validity of Beer's law for this substance. A plot of the logarithm of the absorbance against time was initially curved and tended asymptotically towards a straight line, the slope of which gave the correct diffusion coefficient; the initial slope of the curve gave about half that value. With a cell of double that path length no such difficulty was encountered. It is apparent that the method includes a built-in test of the assumption of validity of Beer's law for each substance.

The main advantage of the present method is its simplicity. The method is readily adaptable for the study of diffusion in multicomponent mixtures if components are selected having i.r. absorption peaks at different frequencies. With slight modification to the apparatus it would be possible to measure diffusion into gases other than air. All that is required is to pass the outer

Can. J. Chem. Downloaded from www.nrcresearchpress.com by 210.87.254.40 on 09/05/12
For personal use only.

Data used in calculations[a]

Component	σ (nm) (Reference 7)	ε/k (°K) (Reference 7)	Ionization potential (eV) (Reference 9)
CH_4	0.3796 0.3882	144 137	12.99
CH_3Cl	0.3375	855	11.22

[a]Other values as used previously (2).

end of the capillary tube (C in Fig. 1) into a tube, indicated by the dotted lines D in Fig. 1, swept with a flow of the other gas.

Appendix

Diffusion coefficients were calculated using the expression

$$D_{12} = \frac{2.628 \times 10^{-5}[T^3(M_1 + M_2)/2M_1M_2]^{1/2}}{p\sigma_{12}{}^2\Omega_{12}(T_{12}{}^*)}$$

where the subscripts 1 and 2 refer to the two components, D_{12} is the first approximation to the binary diffusion coefficient, M is the molecular weight, T the absolute temperature, p the pressure in atmospheres and $\Omega_{12}(T_{12}{}^*)$ is a collision integral at a reduced temperature of $T_{12}{}^* = kT/\varepsilon_{12}$ and σ_{12} and ε_{12}/k are molecular potential energy parameters characteristic of a 1–2 interaction.

1. E. P. Ney and F. C. Armistead. Phys. Rev. **71**, 14 (1947).
2. H. Watts. Can. J. Chem. This issue.
3. A. D. Cross. Introduction to Practical Infra-red Spectroscopy. Butterworths Scientific Publications, London. 1960.
4. H. F. Coward and E. H. M. Georgeson. J. Chem. Soc. London, 3751 (1937).
5. G. A. Lugg. Anal. Chem. **40**, 1072 (1968).
6. H. Watts. Trans. Faraday Soc. **60**, 1745 (1964).
7. J. O. Hirschfelder, C. F. Curtiss, and R. B. Bird. Molecular Theory of Gases and Liquids. John Wiley and Sons, Inc., New York. 1954.
8. G. H. Hudson and J. C. McCoubrey. Trans. Faraday Soc. **56**, 761 (1960).
9. G. Herzberg. Molecular Spectra and Molecular Structure. III. Structure of Polyatomic Molecules. D. Van Nostrand Company Inc., Princeton. 1966.
10. E. A. Guggenheim and C. J. Wormald. J. Chem. Phys. **42**, 3775 (1965).

Can. J. Chem. Downloaded from www.nrcresearchpress.com by 210.87.254.40 on 09/05/12
For personal use only.

Can. J. Chem. Downloaded from www.nrcresearchpress.com by 210.87.254.5 on 09/05/12
For personal use only.

Anodic Oxidation of Ethylene Glycol on Platinum: a Mechanistic Study[1]

ASHOK K. VIJH[2]
Institute of Research, Hydro-Quebec, Varennes, Quebec

Received April 20, 1970

Anodic oxidation of ethylene glycol (EG) has been examined on platinum in 1 N H_2SO_4 by means of potentiostatic and potentiodynamic techniques. Experimental results consist of steady-state, potential–current relationships, reaction order derivatives, inhibition inflections, potentiodynamic profiles, and product analysis. Reaction mechanism has been proposed by combining these results with the previous information on the adsorption of EG on platinum, and on the pH effects in the anodic oxidation of EG. An analysis of these data has been presented in terms of kinetics under both Langmuir and Temkin conditions of electrode coverage. Inhibition inflections have been interpreted in terms of the kinetic theory of passivation effects proposed by Gilroy and Conway. It has been suggested that a chemical step of the type Pt.EG + Pt.OH → Pt.R + H_2O + Pt is the likely rate-determining-step (r.d.s.). The data indicate that quasi-equilibria prior to the r.d.s. are probably different in the ascending and descending direction of potentials (on the potential–current curves), owing to the presence of different extents of oxygenated (Pt.OH or Pt.O) adsorbed species and the associated effects of coverage on kinetics.

Canadian Journal of Chemistry, **49**, 78 (1971)

Introduction

The electrodic oxidation of various organic substances has been intensively studied in recent years from a fundamental mechanistic point of view (1–12). In the present investigation, an attempt has been made to elucidate the detailed mechanism of anodic oxidation of ethylene glycol on smooth platinum in (aqueous) 1 N H_2SO_4.

Most of the interest in the mechanisms of anodic oxidation of organic compounds has been generated undoubtedly by their possible use as anodic fuels in the fuel cells. The present work, however, was carried out because of the importance of oxidation of ethylene glycol in electrolytic capacitors.

Experimental

The general experimental procedures were similar to those used in our previous work (4) and in other recent work in electrode kinetics (13, 14). Some specific features are listed below, however.

A three-compartment Pyrex cell provided with solution-sealed stop-cocks, gas inlets and outlets, "tru-bore" tubing electrode holders, and other appropriate accessories was used.

Bright platinum working electrodes were sealed into Pyrex in open flame (natural gas and oxygen) and were subsequently degreased in boiling trichloroethylene, cleaned in chromic acid, and thoroughly washed in deionized-distilled water. Bright platinum counter electrodes and hydrogen reference electrodes were used.

A helium atmosphere was always maintained in the working compartment and no electrolysis (even pre-electrolysis) was conducted until all the oxygen had been purged from the working compartment. This procedure eliminated the possibility of formation of traces of H_2O_2 by reduction of dissolved O_2. Commercial helium without further purification was used (15) whereas H_2 gas for the reference compartment was deoxygenated by passing over a palladium catalyst. Optimum pre-electrolysis, both cathodic and anodic, of the 1 N H_2SO_4 was carried out *before* adding the measured amounts of ethylene glycol. Ethylene glycol was comparable to the electronic grade in purity. Sulfuric acid was A.C.S. grade (Allied Chemicals).

An Anotrol potentiostat (Magna Corporation, Model 4700M) was used both for potentiostatic and potentiodynamic work. Potentiodynamic curves were recorded on a Moseley 7035A X–Y recorder (Hewlett–Packard). Circuitries were similar to those described previously and were routine potentiostatic and potentiodynamic configurations (4, 16).

All experiments were carried out at room temperature.

It may be mentioned that in the various graphs to follow, the electrode potentials $E_H(V)$ are in volts and refer to the hydrogen electrode in the *same* solution. In the rate equations and various reaction order derivatives, the electrode potential, $E_H(V)$, has been simply represented by V for the purposes of brevity.

Results

(1) Products of Electrolysis

In agreement with the results of Bagotskii and co-workers (11), it was observed that at room temperature, electro-oxidation of EG does not proceed all the way to CO_2. Non-gaseous products, in which C—C bond in EG is not ruptured, were predominantly formed and were qualita-

[1]This work was carried out in the Research and Development Laboratories of Sprague Electric Company, North Adams, Massachusetts.

[2]Also Visiting Professor in the Energy Center of the National Institute of Scientific Research, University of Quebec at Varennes, Quebec.

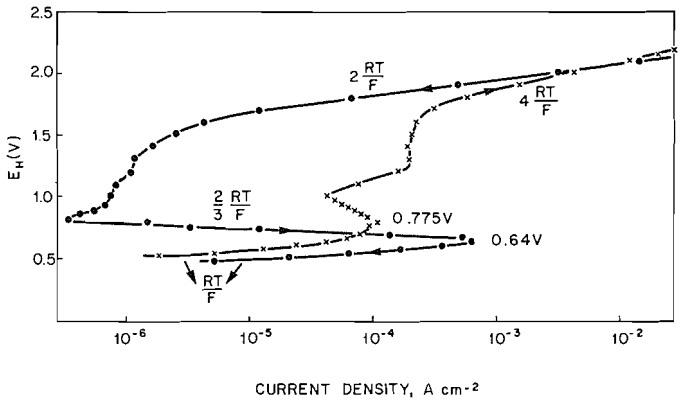

FIG. 1. A steady-state, potentiostatic (point by point), potential – log (current density) relationship on smooth platinum in 1 N H_2SO_4 and 2.5×10^{-1} M ethylene glycol. Helium atmosphere in the working compartment: X, ascending direction potentials; ●, descending direction of potentials.

tively detected (17). In a prolonged electrolysis, the products formed at 0.68 ± 0.02 V were glyoxal and oxalic acid; this confirms the previous observations of Bagotskii and co-workers (11). No formaldehyde, formic acid, glycolaldehyde, acetaldehyde, and acetic acid were detected. Glycolic acid and glyoxalic acid were indicated (17) but could not be confirmed. Attempts to accumulate, and subsequently to isolate, the products of electrolyses for quantitative analyses were unsuccessful because prolonged electrolysis at 0.68 ± 0.02 V (or any other potential for that matter) results in very low current densities, presumably because of long term poisoning effects caused by either intermediate and/or terminal products of electrolysis.

(2) Current–Potential Relationships

In the steady-state, potentiostatic (point-by-point) current–potential relationship the major features, *e.g.*, inhibition inflections and hysteresis effects, were similar to those reported for other electro-organic oxidations by Conway and co-workers (18, 19). The criterion for steady-state was that defined by Wroblowa *et al.* (20), which tends to avoid complications that may arise due to long-term poisoning effects by intermediates and/or products of electrolysis. A typical current–potential relationship has been presented in Fig. 1. In the ascending direction (Fig. 1) a marginal Tafel region of 70 mV is followed by a wide (on the potential scale) inhibition inversion, with a maximum current density of 1×10^{-4} A cm^{-2} in solutions containing 2.5×10^{-1} M EG. The current–potential line in the negative direction of this inhibition inflection extends over too narrow a range of current density to permit the deduction of any negative Tafel slopes. The wide inhibition maximum indicates a Temkin type of adsorption (19) (*i.e.*, activation energy for adsorption changes with coverage) and is consistent with the results of Bagotskii and Vasile'v on electrode coverage (11, 12). This inhibition inflection is followed by a brief increase in rate with increasing potential which, in turn, enters into a transition region, the latter terminating finally into a Tafel region for oxygen evolution (o.e.r.) with anomalously high Tafel slope (220 mV). In the descending direction a Tafel line for o.e.r. with normal slope (130 mV) is followed by a transition region. At 800 mV this transition region enters into a huge (spread over three decades of current density) inhibition inversion "loop" which is narrow and, hence, shows Langmuirian kinetics. The positive Tafel slope of this inhibition inflection is 70 mV and the slope for the negative Tafel line is 40 mV. The ascending and descending curves show a large hysteresis which is usually diagnostic of the presence of oxide and other irreversibly adsorbed species.

It may be added that these current–potential relationships are not vitiated by diffusion effects, which were shown to be unimportant in the oxidation of EG (10).

(3) Reaction Orders

Current–potential relations (ascending directions) as a function of EG concentration have been presented in Fig. 2 for the potential region

Can. J. Chem. Downloaded from www.nrcresearchpress.com by 210.87.254.5 on 09/05/12
For personal use only.

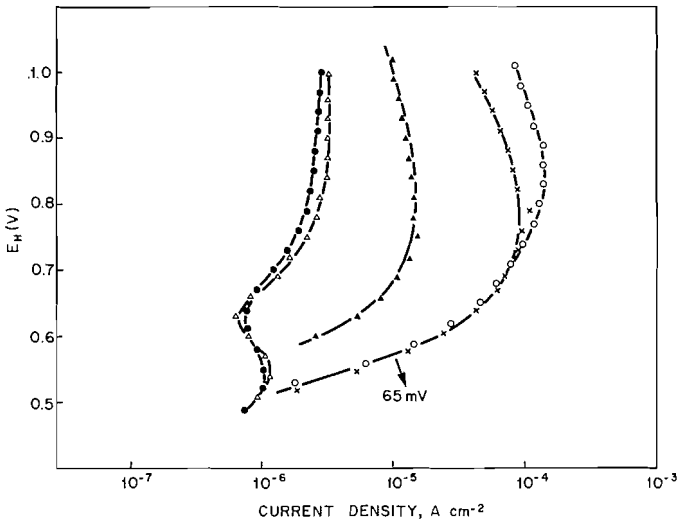

FIG. 2. Steady-state, potentiostatic (point by point) potential – log (current density) relationships in the ascending direction of potentials on platinum in 1 N H_2SO_4 solutions containing the following concentrations of EG: ●, 4.4 × 10^{-3} M; △, 8.8 × 10^{-3} M; ▲, 2.1 × 10^{-2} M; X, 2.5 × 10^{-1} M: ○, 2.1 M. These relationships at potentials more anodic than 1.0 V purposely not shown since no new information relevant to the oxidation of EG can be derived from them.

in which EG is known to undergo significant oxidation, approximately 0.48 to 0.88 V (see Fig. 1). It may be noted that the marginal Tafel line with a slope equal to RT/F is obtained only in solutions with rather high EG concentration. The apparent potentiostatic reaction order, R, *i.e.*, $(\partial \log i/\partial \log c)_{V,\psi,T,\ldots}$ tends to approach zero at 0.5 V. At the potential of maximum current (*ca.* 0.8 V), however, R tends to one (Fig. 3) except for very high EG concentration.

Current–potential relations for the descending direction, as a function of EG concentration, have been presented in Fig. 4. The behavior at the lowest concentration does not fit the systematic trend to Fig. 4, probably because the current densities are very low and approach those of the background electrolyte, thus diminishing the significance of that particular relationship. The values of R obtained from Fig. 4 are fractional and positive (Fig. 5). At the lowest concentrations there is some indication

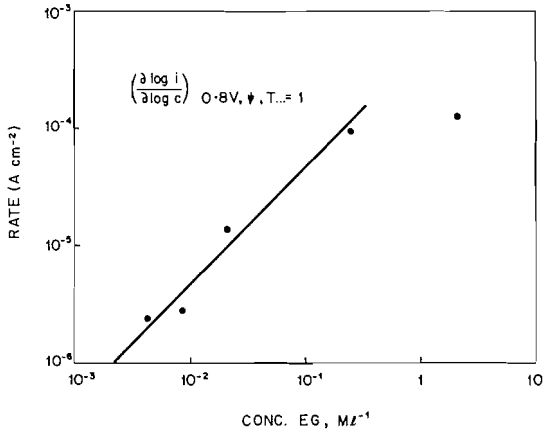

FIG. 3. A plot for obtaining reaction order derivatives, $\partial \log i/\partial \log C$, in the ascending direction of potentials. This plot is based on data in Fig. 2.

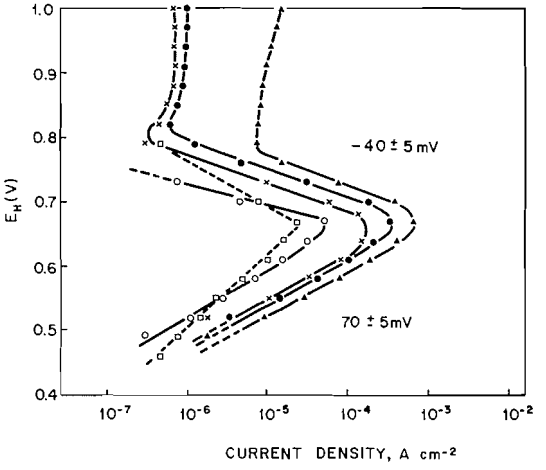

FIG. 4. Steady-state, potentiostatic potential – log (current density) relationships in the descending direction of anodic potentials, at various concentrations of EG listed below: □, 4.4 × 10^{-3} M; ○, 8.8 × 10^{-3} M; X, 2.2 × 10^{-2} M; ●, 2.5 × 10^{-1} M; ▲, 2.1 M.

Can. J. Chem. Downloaded from www.nrcresearchpress.com by 210.87.254.5 on 09/05/12
For personal use only.

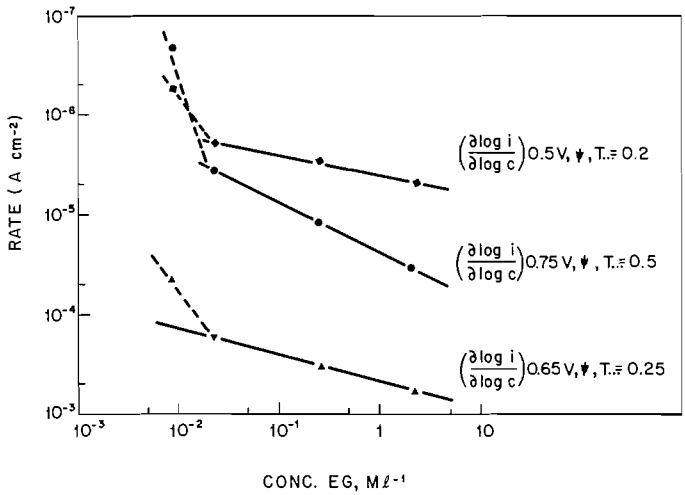

FIG. 5. A plot for obtaining reaction order derivative, $\partial \log i/\partial \log C$, in the descending direction of anode potentials. Primary data used in this plot are contained in Fig. 4.

that R changes significantly but this may be because of the aforementioned difficulty.

The reaction order derivative $(\partial V/\partial \log c)_{i,\psi,T,\ldots}$ obtained from Fig. 4, both for the positive and negative Tafel lines, is also of rather small magnitude, as would be expected. For the positive Tafel line in Fig. 4, the value of $(\partial V/\partial \log c)_{i,\psi,T,\ldots}$ is 14 mV and for the negative Tafel line, 22 mV.

(4) Potentiodynamic Profiles

The peaks observed in the single sweep (from prior steady-state potential) potentiodynamic profiles (Figs. 6 (*a*) and (*b*)) in this system are similar to the current-reversal effects (19) observed in the steady-state, point-by-point, potentiostatic current–potential relationship (Fig. 1). As pointed out previously (7), this would indicate that the potentiodynamic peaks at these sweep rates (16.8 to 720 mV s^{-1}) are probably *kinetic* in origin and are, in fact, inhibition inflections of the type reported by Gilroy and Conway (19). Further, when the potentiodynamic peaks are tested for pseudo-Faradaic nature (plot of peak current *vs.* scan rate) or for diffusion control (peak current *vs.* square root of scan rate) (Fig. 7), *no* linear relation passing through the origin is obtained, thus confirming our conclusion that the potentiodynamic peaks, both in ascending and descending direction, are mainly kinetic in origin.

It is possible to obtain better resolution of the potentiodynamic profiles at certain sweep rates (Fig. 8). In this profile the following important points may be noted.

(*i*) Hydrogen peaks are "masked" and appear as hysteresis.

(*ii*) The huge anodic peak at 0.6 V appears on the descending sweep (1.2 → 0 V) instead of the usual *cathodic* oxide reduction peak. This would show recombinative removal, by a chemical surface reaction, of the oxide (or OH) and the anodic current would arise from the normal Faradaic reaction of glycol oxidation on the bare surface sites remaining after reaction of adsorbed glycol species with the oxide. This situation is somewhat similar to that observed for the oxidation of formic acid (21). The smaller peak around 0.6 V is the same peak but in the ascending (0 → 1.2 V) direction of the sweep.

(*iii*) A tiny, incipient peak around 1.03 V may be noted. From Bagotskii's work (10), this peak would correspond to the oxidation of oxalic acid.

(*iv*) Based on previous work on the anodic oxidation of organic substances (10), the anodic peak on the ascending curve around 0.9 V is the kinetic peak corresponding to the oxidation of EG (with or without coadsorbed oxygenated species, see Discussion).

If, subsequent to the commencement of the first sweep from prior steady-state potential, the potentiostat is driven by the repetitive sweeps, profiles similar to the ones shown in Fig. 9 may be obtained. The *asymmetric* shifts in the large anodic peak produced by repetitive sweeps are believed to have qualitative mechanistic signifi-

Can. J. Chem. Downloaded from www.nrcresearchpress.com by 210.87.254.5 on 09/05/12
For personal use only.

Can. J. Chem. Downloaded from www.nrcresearchpress.com by 210.87.254.5 on 09/05/12
For personal use only.

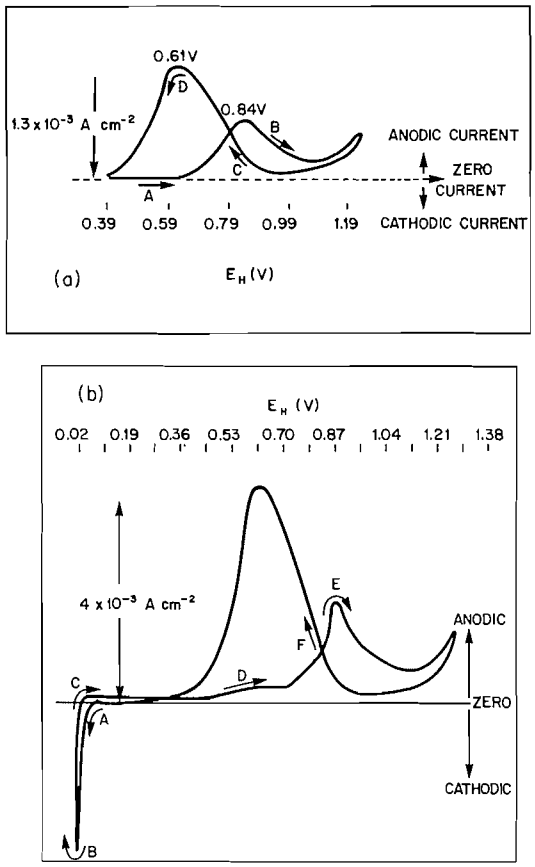

FIG. 6. (*a*) A single sweep potentiodynamic profile (dV/dt = 16.8 mV s^{-1}) triggered from prior steady-state potential (0.39 V) corresponding to complete coverage by ethylene glycol, on platinum in 1 *N* H_2SO_4 containing 2.5 × 10^{-1} *M* EG. (*b*) Similar to Fig. 6(*a*) above except that the steady-state potential prior to the commencement of the single sweep was 60 mV; at this potential the electrode coverage by EG is vanishingly small (see Fig. 10), dV/dt is 50 mV s^{-1}.

cance which will be explained in Discussion section. At potentials more cathodic than 0.1 V, cathodic current appears both in the ascending and descending direction. The position and general shape of the profiles in this region indicates that some current associated with diffusion-controlled oxidation–reduction of intermediate products of electrolysis is probably superimposed on the normal kinetic current. No straightforward quantitative analysis can, however, be extended in this region.

(5) Electrode Coverage

It has been reported by Bagotskii *et al.* (11, 12)

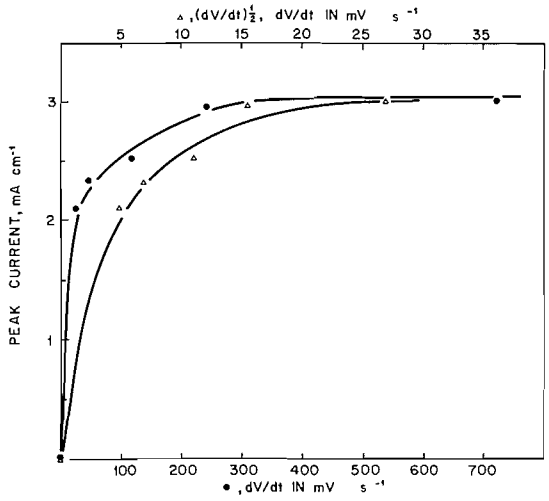

FIG. 7. Plot of peak current *vs.* dV/dt, (●) and $(dV/dt)^{\frac{1}{2}}$, (△) for peak at *ca.* 0.61 V (see Fig. 6*a*).

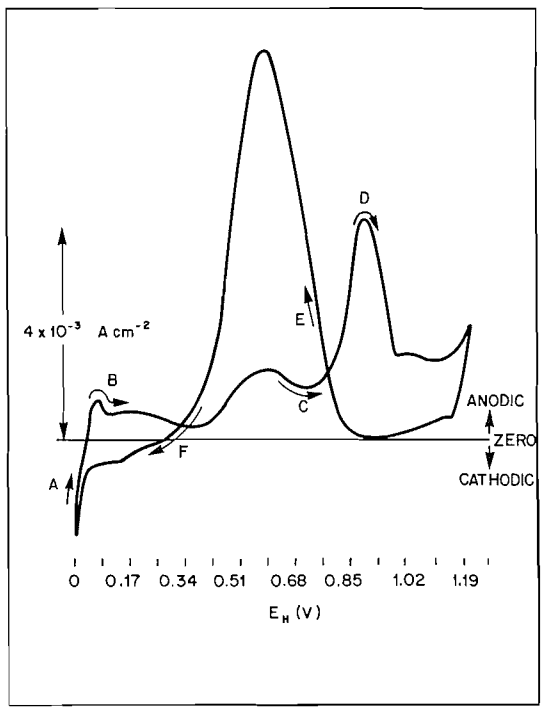

FIG. 8. A single sweep potentiodynamic profile obtained at a sweep rate (240 mV s^{-1}) which yields the maximum resolution of peaks. Steady-state potential prior to the commencement of the sweep was 0 V. A slight incipient anodic peak around 1030 mV, which probably corresponds to the oxidation of oxalic acid (see text and ref. 10), may be noted.

Can. J. Chem. Downloaded from www.nrcresearchpress.com by 210.87.254.5 on 09/05/12
For personal use only.

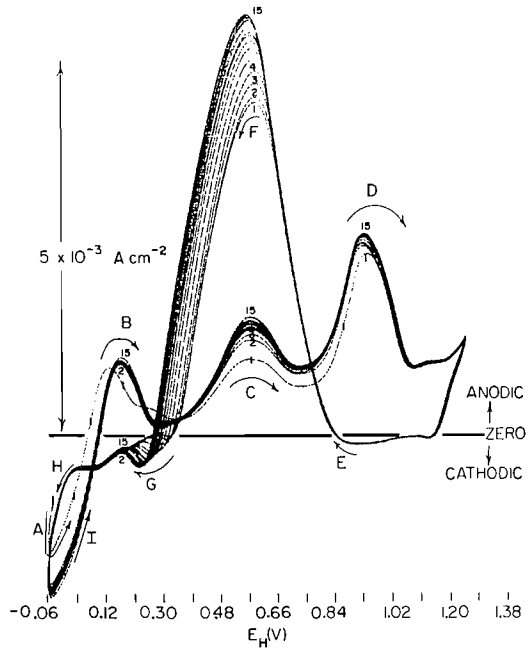

FIG. 9. Similar to Fig. 8 except that after the first sweep triggered from a prior steady-state potential (60 mV) the potentiostat was driven to yield repetitive sweeps. Sweep rate is 354 mV s^{-1}. Numerals refer to the sweep number.

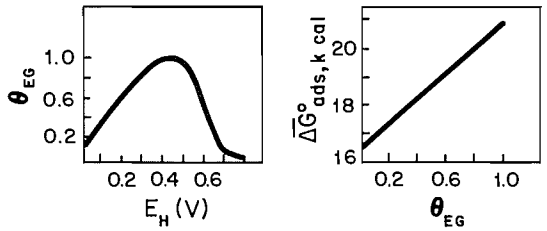

FIG. 10. This figure reproduces Bagotskii's results (ref. 12) on electrode coverage of platinum by EG in 1 *N* H_2SO_4 at 50 °C. EG concentration is 1×10^{-2} *M*. (*a*) Electrode coverage by EG, θ_{EG}, *vs.* electrode potential, E_H; (*b*) apparent standard free energy of adsorption of EG, $\Delta\bar{G}_{ads}^{0}$, as a function of θ_{EG} at 0.4 V and 50 °C. Steady-state adsorption from 1 *N* H_2SO_4 containing 1×10^{-2} *M* EG. The electrode history in this case corresponds to the ascending direction of potentials in our work. It may be noted that adsorption of EG on platinum obeys a Temkin isotherm.

that electrode coverage by EG in this system shows Temkin behavior (Fig. 10); *i.e.*, activation energy for adsorption varies linearly with coverage.

Discussion

(1) Probable Reaction Mechanism

In order to deduce the reaction mechanism, it would be convenient to proceed as follows:

(*i*) Since the Tafel slope for EG oxidation both in the ascending and descending direction (Fig. 1) is *RT/F*, no step which occurs during or after the third charge transfer may be rate-determining (1). It may be readily shown that such a step, if rate-determining under either Langmuir or Temkin conditions of electrode coverage, will result in a Tafel slope equal to or less than *RT/2F*.

(*ii*) Initial charge transfer may not be the r.d.s. since it will result in a Tafel slope equal to *2RT/F*. Further, such a step would require electrode coverage to approach zero, a requirement not sustained by experimental results (Fig. 10).

(*iii*) The observed Tafel slope can arise only under one of the following conditions:

(*a*) When surface diffusion (23) of an adsorbed species is the r.d.s.; such a step, however, is unlikely in the present case since it is important only in metal deposition or occasionally, in the hydrogen evolution reaction.

(*b*) When the rate-determining terminal desorption results in gas evolution which is chemisorbed under Temkin conditions of *activated* adsorption as may be possible in the anodic oxidation of ammonia or hydrazine. This situation is clearly inapplicable in the present case.

(*c*) When an initial charge transfer results in an intermediate adsorbed under Langmuirian conditions, *e.g.*, Pt.OH, which subsequently undergoes a first order chemical heterogeneous step (24) (*cf.* Kolbe reaction in ref. 24). (Note that *kinetically*, this situation would be similar to the Scheme (*A*), Discussion section (*6*), based on Bagotskii's results.)

If the r.d.s. involves only EG as the reactant, the expected kinetics would clearly be Temkin, since adsorption of EG obeys Temkin isotherm (Fig. 10). If, however, the r.d.s. involves another species in addition to EG, the kinetics may become Langmuirian since either the *total* coverage by all species involved in the r.d.s. or the coverage by the second species alone in that case may not obey Temkin kinetics. It is believed that the foregoing modification when applied to generalization (*iii c*) can yield a possible r.d.s. A mechanism consistent with the foregoing considerations is as follows.

Can. J. Chem. Downloaded from www.nrcresearchpress.com by 210.87.254.5 on 09/05/12
For personal use only.

[1] $$Pt + H_2O \rightleftharpoons Pt.OH + H^+ + e \text{ (Langmuir)}$$

[2] $$RH_{solution} + Pt \rightleftharpoons Pt.RH_{d.l.}$$

where RH represents the EG.

[3] $$Pt.RH + Pt.OH \xrightarrow{\text{r.d.s.}} Pt.R + H_2O$$

The reaction products may then be formed in steps subsequent to the r.d.s., with or without participation of PtO.

It is important to note here that from the product analysis, no step involving *fission* of the C—C bond in EG may be postulated as the r.d.s.

(*d*) Alternatively, one could propose a mechanism involving a similar r.d.s. as above (3) but with *two* prior charge transfers leading to potential-dependent Temkin type adsorption of two different reaction intermediates, *viz.*, Pt.OH and Pt.R. The reaction scheme in that case would be as follows

[1] $$Pt + H_2O \rightleftharpoons Pt.OH + H^+ + e \quad \text{(Temkin)}$$

[4] $$Pt + RH \rightleftharpoons Pt.R + H^+ + e \quad \text{(Temkin)}$$

[5] $$Pt.R + Pt.OH \xrightarrow{\text{r.d.s.}} Pt.R' + H_2O + Pt$$

The rate equation in this case would be (22)

[6] $$v_5 = k_5\,\theta_{OH}\,\theta_R \times \exp[\alpha r\theta_{OH/RT}] \exp[\alpha r\theta_{R/RT}]$$

where the various symbols have the usual significance (22, 23). (Note that *kinetically* this mechanism would be identical with Scheme (*B*), Discussion section (*6*), which is based on Bagotskii's results.)

If θ_{OH} and θ_R are determined by potential-dependent quasi-equilibria 1 and 4 (characterized by constants K_1 and K_4), respectively, one obtains (22, 23)

[7] $$\ln K_1 + \ln C_{H_2O} + VF/RT = r\theta_{OH}/RT$$

and

[8] $$\ln K_4 + \ln C_{RH} + VF/RT = r\theta_R/RT$$

or

[9] $$\ln K_1 + \ln K_4 + \ln C_{H_2O} + \ln C_{RH} + 2VF/RT = r(\theta_{OH} + \theta_R)/RT$$

Therefore,

[10] $$\ln v_5 = \ln k_5 + \ln \theta_{OH} + \ln \theta_R + \alpha \ln K_1 + \alpha \ln K_4 + \alpha \ln C_{RH} + \alpha \ln C_{H_2O} + 2\alpha VF/RT$$

It follows that

[11] $$\partial V/\partial \log v_5 = 2.3 \times RT/F$$

[12] $$\partial \log v_5/\partial \log C_{RH} = 0.5$$

[13] $$\partial \log v_5/\partial \log C_{H_2O} = 0.5$$

Since in aqueous acidic solutions, reaction order w.r.t. H_2O will be pseudo-zero order, eq. 13 will be meaningless. However, eq. 13 will assume significance if either the non-aqueous solution contains only small, measured amounts of water or the solution is alkaline; in the latter case eq. 13 will be written as: $\partial \log v_5/\partial \log C_{OH^-} = 0.5$ (13*a*).

Since the adsorption of EG (ascending direction) follows a Temkin isotherm (Fig. 10) and the kinetics in the ascending direction shows Temkin characteristics (Figs. 1, 2), the mechanism proposed in this section is probably more plausible than the one in section (*iii c*). It is important to note, however, that both mechanisms involve a very similar r.d.s. It is possible that in the ascending direction of potentials Temkin kinetics is obeyed (Figs. 1, 2), whereas in the descending direction kinetics becomes Langmuirian (Figs. 1, 4, and 11) because of high surface coverage by oxygenated species. It may be noted that the reaction order predicted for Temkin adsorption (eq. 12) is observed only in the descending direction of potential and not in ascending direction, as would have been expected. No explanation can be offered for this observation at present.

It may be noted that information on the adsorption of EG under conditions corresponding to descending direction of potentials, *i.e.*, in presence of significant amounts of PtO and Pt.OH, is not available. It may not even be possible to obtain such data reliably because of the "chemical" heterogeneous reaction between adsorbed EG and the surface oxide. It is important to emphasize that independent knowledge of adsorption isotherms in the ascending and descending directions is *not* indispensable for the interpretation of present work. This is because indications of Temkin type kinetics in the ascending direction of potentials (Figs. 1, 2) and Langmuirian kinetics in the descending direction (Figs. 1, 4, and 11), are quite strong (19, 23),

Can. J. Chem. Downloaded from www.nrcresearchpress.com by 210.87.254.5 on 09/05/12
For personal use only.

irrespective of the availability of the adsorption isotherms.

(*e*) That the Tafel slope equals 2.3 RT/F may also be predicted on the basis of some other mechanisms; *e.g.*, an electrochemical discharge step as r.d.s. under certain conditions of electrode coverage (24*a*). Such a mechanism is unlikely in the present case since the experimental evidence tends to favor a chemical r.d.s., Discussion section (*5*), in the electrooxidation of a large number of organics, including ethylene glycol.

An examination will now be attempted of the significance of the rest of the results in relation to the foregoing mechanistic proposal.

(2) Inhibition Effects

In the ascending direction of potentials, the negative "Tafel" line following current reversal is too brief to lend itself to quantitative interpretations (Fig. 1). In the descending direction of potentials, however, the inhibition "loop" may be examined theoretically in terms of kinetic theory of passivation effects developed by Gilroy and Conway (19). It has been observed (Fig. 11) that the experimental data fit best, up to a point (marked by arrow in Fig. 11), the inhibition loop predicted for reactions of the type, under Langmuirian conditions of adsorption,

[14] $\quad Pt + Pt.x \rightarrow Pt.Y + Pt.Z$ or $Pt.\overline{Y—Z}.Pt$

with or without the subsequent desorption of Y and Z. Since the fission of C—C bond in EG

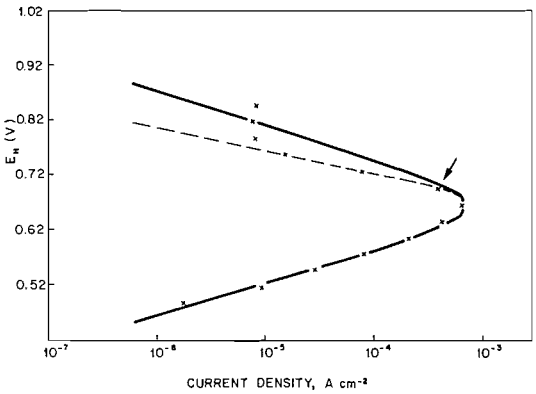

FIG. 11. A typical experimental inhibition inflection (crosses) examined in relation to the theoretical curve of Gilroy and Conway for inhibition, under Langmuirian conditions of adsorption, of the type (see Fig. 2 in ref. 19): Pt.X → Pt.Y—Pt.Z (or $Pt.\overline{Y—Z}.Pt$). Our experimental points refer to the descending potentiostatic curve obtained in solutions containing 2.1 *M* EG (see Fig. 4).

is not indicated in the product analysis, it is preferable to write the right hand side of eq. 14 as $Pt.\overline{Y + Z}.Pt$. At potentials more anodic than 0.7 V, the experimental negative Tafel line departs from the theoretical one and results in a slope of *ca.* 40 mV. Such a deviation from the theoretical curve would indicate that inhibition behavior originating from competitive effects associated with quasi-equilibria of the following type may be important (19)

[1] $\quad Pt + H_2O \rightleftharpoons Pt.OH + H + e$

[15] $\quad 2Pt.OH \rightleftharpoons Pt.O + H_2O + M$

or

[16] $\quad Pt.OH \rightleftharpoons Pt.O + H^+ + e$

It is clear that reactions of the type 15 and 16 are not important below 0.7 V (descending direction) *i.e.*, in the potential range in which, under steady-state, PtO would tend to be reduced.

Langmuirian kinetics in the descending direction of potentials indicated by Fig. 11 would be quite consistent with the r.d.s. suggested in Discussion section *1* (*iii c*).

Further, if the r.d.s. (3) or (5) results in a radical (R or R′ respectively) which is chemisorbed by occupying several surface sites, as indeed is indicated by the results of Bagotskii *et al.* (11, 12), an inhibition of the type

[14] $\quad Pt + Pt.X \rightarrow Pt.\overline{Y + Z}.Pt$ or $Pt.Y + Z.Pt$

would follow (11, 12). Hence, it is concluded that the general features of the inhibition inflection (Fig. 11) are consistent with the suggested r.d.s.

As was mentioned in the Results section, the potentiodynamic peaks (Figs. 6, 8, 9) in general have the same significance as the kinetic inhibition effects depicted in Figs. 1 and 11. It is believed that the inhibition effects (Figs. 1, 4, 6) do not originate from specific adsorption of sulfate ions (25), since Vetter's (26) analysis of Schuldiner's proposal (25) is rather persuasive.

(3) Effect of pH

From the results of Bagotskii *et al.* on the oxidation of several organics, including ethylene glycol (10), a positive value of chemically significant (23) reaction order, $(\partial \log i/\partial \log C_{OH^-})_\phi$, may be concluded. This would be consistent with the r.d.s. proposed here as is clear from eq. 13*a*.

(4) Reaction Orders

The various reaction order derivatives for the

Can. J. Chem. Downloaded from www.nrcresearchpress.com by 210.87.254.5 on 09/05/12
For personal use only.

reactant EG observed in the present investigation are rather complex. The general significance of these derivatives, however, does lend further support to the mechanism suggested here. For example, positive but fractional reaction orders R observed in the descending direction (Fig. 5) would suggest a chemical step as the r.d.s. as proposed here and would be consistent with the value (0.5) predicted by eq. 12.

In the ascending direction, values of R approach zero (Fig. 2) around 0.5 V which is the potential of saturation coverage by EG (Fig. 10), and, hence it is suspected that this R value is probably *pseudo*-zero order. At potentials at which saturation coverage of EG does not obtain, *e.g.*, at 0.8 V (Fig. 10), reaction order R approaches one, except at the highest concentration of EG at which appearance of *pseudo*-zero order again would not be entirely unexpected (Fig. 3). The significance of various reaction orders in the ascending direction of potentials (Figs. 2, 3) is greatly diminished, however, by the fact that the Tafel line, which is rather marginal, is only observed at high EG concentrations (Fig. 2). In the descending direction of potentials, however, satisfactory Tafel lines are obtained at several concentrations (Fig. 4), yielding more meaningful R values which are further discussed below.

An attempt will now be made to estimate the R values from the data of Bagotskii *et al.* and compare it with our values obtained at an approximately comparable electrode potential (0.5 V), in the descending direction of potentials (Fig. 4).

According to Conway *et al.* (22), if the current density i is assumed to be a linear function of θ^n, the apparent potentiostatic reaction order, $(\partial \log i/\partial \log C)_{V,\psi,T,\ldots} = R$, may be written as

$$[17] \qquad R = \frac{\partial \log i}{\partial \log C} = \frac{\partial \log i}{\partial \log \theta}\frac{\partial \log \theta}{\partial \log C}$$

An estimate from the data of Bagotskii *et al.* (11, 12) yields that

$$\left(\frac{\partial \log i}{\partial \log \theta}\right) = 0.6 = n \qquad \text{(ref. 12, Fig. 8)}$$

and

$$\left(\frac{\partial \log \theta}{\partial \log C}\right) = 0.25 \qquad \text{(ref. 11, Fig. 6)}$$

The value of R may thus be deduced as 0.15 from eq. 17. Even though this R value refers to 0.4 V and 50 °C, a qualitatively favorable comparison with our R value (0.2) at 0.5 V and room temperature (Fig. 5) may be made. It may be added that since the coverage by EG is identical at 0.4 and 0.5 V (Fig. 10) and the temperature affects only the time of adsorption necessary to reach a given coverage (11, 12) (a factor irrelevant for steady-state adsorption), such a comparison of R values as attempted here is probably valid.

(5) Miscellaneous Evidence and Arguments Corroborating the Proposed Mechanism

(*i*) There is virtually no oxidation of EG in the potential range 0.3 to 0.5 V (Figs. 1, 2, and 4) even though the electrode is highly covered (Fig. 10). This strongly suggests that virtual absence ($\theta < 0.1$) of steady-state coverage by Pt.OH in this potential range (1) is responsible for lack of significant, steady-state oxidation of EG.

(*ii*) In the ascending direction (Fig. 1), the current reversal commences around 775 mV presumably because the reactant Pt—OH is gradually converted (1) to PtO above *ca.* 800 mV. Similarly in the descending direction (Fig. 1), rate becomes appreciable only in the potential range in which PtO is reduced, probably *via* Pt.OH.

(*iii*) In the repetitive sweep potentiodynamic profiles (Fig. 9) the trend in the shift of the large, kinetic anodic peak qualitatively indicates that, prior to the r.d.s., two quasi-equilibria are probably involved. The extents of departure from equilibrium of these quasi-equilibria, as a result of repetitive sweep, are probably different, hence the asymmetric "half-shifts" in the peak (Fig. 9).

(*iv*) The suggested mechanism which involves a *chemical* r.d.s. is completely consistent with the mechanistic proposals put forward for the oxidation of a large variety of organics by Bockris *et al.* (1), Frumkin and co-workers (6, 9), Brummer (27), and Bagotskii and Vasile'v (10). It seems that a great variety of organics undergo electrodic oxidation through a chemical r.d.s., and hence are quite similar in their kinetic behavior in this particular respect.

(*v*) The conclusion that in electro-organic oxidations, Pt.OH is probably a reactant and PtO a likely inhibitor (Fig. 11) is, again, in agreement with the observations of Bagotskii

Can. J. Chem. Downloaded from www.nrcresearchpress.com by 210.87.254.5 on 09/05/12
For personal use only.

and Vasile'v (10) and Bockris *et al.* (14) based on somewhat different types of arguments. Hence, the conclusions drawn here are sustained by previous mechanistic work on the anodic oxidation of organic compounds.

(6) Comparison with Previous Mechanistic Proposals

Bagotskii and co-workers (11, 12) have proposed a scheme in which four initial dehydrogenations proceed by chemical (rather than electrochemical) dissociation steps and the four adsorbed hydrogen atoms are ionized ("drained off") (18) in a rapid *parallel* reaction. The carbonaceous residue then left on the electrode presumably undergoes oxidation at higher (> 0.5 V) anodic potentials, *i.e.*, at potentials at which significant steady-state oxidation of EG is sustained. The mechanism of Bagotskii *et al.* was based mainly on evidence related to the coulometry (28) of the deposition or ionization of the adsorbed species and decay of rate with time at a given controlled potential. No steady state kinetic data were presented. It may be readily shown, however, that the conclusion of Bagotskii and co-workers can be reconciled with the *kinetic* data obtained in the present investigation. For example, subsequent to the four chemical dehydrogenations of EG, the adsorbed carbonaceous residue, C, may be oxidized by one of the following Schemes

Scheme A

[1] $Pt + H_2O \rightleftharpoons Pt.OH + H^+ + e$ (Langmuir)

[18] $Pt.OH + Pt.C \xrightarrow{\text{r.d.s.}} \text{Products}$

Scheme B

[1] $Pt + H_2O \rightleftharpoons Pt.OH + H^+ + e$ (Temkin)

[16] $Pt.OH \rightleftharpoons Pt.O + H^+ + e$ (Temkin)

[19] $Pt.C + Pt.O \xrightarrow{\text{r.d.s.}} \text{Products}$

Scheme *B* presented here is unlikely, though consistent with the kinetic data, since Pt.O is indicated as an inhibitor rather than a reactant.

In conclusion, it is not possible to distinguish our mechanism from that of Bagotskii and co-workers on the basis of kinetic data presented here. However, in Fig. 10, which is based on results of Bagotskii and co-workers it seems to imply that the adsorption of EG is more or less reversible. If four initial hydrogenations were involved, one would expect to observe a much higher potential-dependence of EG adsorption than is indicated by Fig. 10. From these comments it seems likely that the mechanism proposed by Bagotskii and co-workers is not entirely sound.

It may be added, however, that the open circuit behavior of the system examined previously (11, 12) seems to be explained rather well by the mechanism of Bagotskii and co-workers. It may, therefore, be concluded that no unambiguous mechanistic assignments are possible at present. The proposals put forward by us may hence be regarded only as one of the possible kinetic schemes which seems to be consistent with the available data.

Thanks are due to Dr. R. S. Alwitt and Dr. S. D. Ross for some discussions. Contributions made by Mr. R. W. Santway and Mr. J. Barry to the product analysis are gratefully acknowledged. Dr. J. Parry of Tyco Laboratories is thanked for providing some reprints on the anodic oxidation of ethylene glycol. Helpful comments by Professor B. E. Conway and Dr. P. Lenfant on the rough draft of the manuscript are gratefully acknowledged.

1. J. O'M. Bockris, E. Gileadi, and G. E. Stoner. J. Phys. Chem. **73**, 427 (1969).
2. S. B. Brummer, J. I. Ford, and M. J. Turner. J. Phys. Chem. **69**, 3424 (1965).
3. G. Gilman. J. Phys. Chem. **66**, 2657 (1962); **67**, 78 (1963).
4. B. E. Conway and A. K. Vijh. J. Phys. Chem. **71**, 3637 (1967); **71**, 3655 (1967).
5. M. W. Breiter. J. Electroanal. Chem. **15**, 221 (1967); **14**, 407 (1967); J. M. Moisson-Franckhauser. Rev. de l'Inst. Fran. Du Pétrole, **9**, 728 (1969).
6. A. N. Frumkin and B. I. Podlovchenko. Dokl. Akad. Nauk. SSSR. **150**, 349 (1963).
7. A. K. Vijh. Can. J. Chem. **48**, 197 (1970).
8. M. Fleischman, J. R. Mansfield, and W. F. K. Wynne-Jones. J. Electroanal. Chem. **10**, 511, 522 (1965).
9. B. I. Podlovchenko, O. A. Petry, A. N. Frumkin, and H. Lal. J. Electroanal. Chem. **11**, 12 (1966).
10. V. G. Bagotskii and Y. B. Vasile'v. Electrochim. Acta, **9**, 869 (1964).
11. J. Weber, Y. B. Vasile'v, and V. G. Bagotskii. Electro-khimiya, **2**, 515 (1966). Eng. Transl. by Consultants Bureau, New York.
12. J. Weber, Y. B. Vasile'v, and V. G. Bagotskii. Electro-khimiya, **2**, 522 (1966), Eng. Transl. by Consultants Bureau, New York.
13. B. E. Conway and M. D. Dzieciuch. Can. J. Chem. **41**, 21, 38, 55 (1963).
14. J. O'M. Bockris, H. Wroblowa, E. Gileadi, and B. J. Piersma. Trans. Faraday Soc. **61**, 2531 (1965).
15. E. Yeager and F. Ludwig. *In* Symposium on Electrode Processes. Preprint # 4, A.C.S. Meeting, Miami Beach, April 1967.

16. A. K. VIJH. Ph.D. Thesis. Ottawa University, Ottawa, Canada. 1966.
17. F. FEIGL. Spot Tests. Elsevier Publishing Company, New York. 1956.
18. B. E. CONWAY, N. MARINCIC, D. GILROY, and E. J. RUDD. J. Electrochem. Soc. **113**, 1144 (1966).
19. D. GILROY and B. E. CONWAY. J. Phys. Chem. **69**, 1259 (1965).
20. H. WROBLOWA, B. PIERSMA, and J. O'M. BOCKRIS. J. Electroanal. Chem. **6**, 401 (1963).
21. B. E. CONWAY. *In* Progress in Reaction Kinetics. Vol. 4. *Edited by* G. Porter. Pergamon Press, Oxford. 1967.
22. B. E. CONWAY, E. J. RUDD, and L. G. M. GORDON, Discuss. Faraday Soc. **45**, 87 (1968).
23. B. E. CONWAY. Theory and Principles of Electrode Processes. Ronald Press, New York. 1965; E. GILEADI and B. E. CONWAY. *In* Modern Aspects of Electrochemistry. *Edited by* J. O'M. Bockris and B. E. Conway. Butterworths, London. 1964.
24. A. K. VIJH and B. E. CONWAY. Chem. Revs. **67**, 623 (1967). (*a*) J. W. JOHNSON, H. WROBLOWA, and J. O'M. BOCKRIS. Electrochim. Acta, **9**, 639 (1964).
25. S. SCHULDINER. J. Electrochem. Soc. **116**, 767 (1969); see also; J. P. HOARE. The Electrochemistry of Oxygen. Interscience, New York. 1968.
26. K. J. VETTER and J. W. SCHULTZE. J. Electrochem. Soc. **116**, 824 (1969).
27. S. B. BRUMMER. J. Electrochem. Soc. **113**, 1156 (1966).
28. See, for example, S. GILMAN. *In* Electro-analytical Chemistry. Vol. 2. *Edited by* A. J. Bard. Marcel Dekker. 1967.

Can. J. Chem. Downloaded from www.nrcresearchpress.com by 210.87.254.5 on 09/05/12
For personal use only.

Can. J. Chem. Downloaded from www.nrcresearchpress.com by 210.87.254.6 on 09/05/12
For personal use only.

Spin–Spin Coupling Constants Between Protons and Carbon in 1,3-Dithiole-2-thione and 1,3-Dithiole-2-one. Relationship of *cisoid* H–H to Two-bond ^{13}C–H Couplings in Ethylene Derivatives and Aromatic Compounds

D. M. McKINNON AND T. SCHAEFER
Chemistry Department, University of Manitoba, Winnipeg, Manitoba

Received July 22, 1970

Precise analyses of the p.m.r. spectra of 1,3-dithiole-2-thione and 1,3-dithiole-2-one containing ^{13}C at positions 4 and 2 yield all proton–proton and proton–carbon spin–spin coupling constants. The two-bond proton–carbon couplings are discussed relative to directly bonded proton–carbon couplings in terms of hyperconjugative effects and it is suggested that d orbital participation in sulfur bonding is unimportant in these compounds. A linear correlation of two-bond proton–carbon with *cisoid* proton–proton couplings in some ethylene derivatives and aromatic compounds indicates that the above two compounds behave like ethylene derivatives in this respect, in contrast to benzene, furan, and thiophene. Practical use of the correlation in the analysis of complex ^{13}C resonance spectra is indicated.

Canadian Journal of Chemistry, **49**, 89 (1971)

Introduction

The four-electron molecular orbital treatment of geminal proton–proton coupling in the fragment H—C—H (1), in which inductive and hyperconjugative interactions of a substituent with the fragment orbitals are distinguished, can be qualitatively applied to two-bond carbon–proton couplings in the fragment ^{13}C—C—H. Such an application was made in a study of vinylene carbonate (1,3-dioxole-2-one (**1**)) (2). When $J(^{13}C—C—H)$ is plotted *vs.* $J(^{13}C—H)$ for a number of model compounds significant deviations from the plot are a measure of the hyperconjugative effect of the substituent on $J(^{13}C—C—H)$, the plot itself being a calibration of rehybridization and direct electronegativity (3, 4) effects on $J(^{13}C—H)$ and $J(^{13}C—C—H)$. Calculations in the CNDO/2 approximation of $J(^{13}C—C—H)$ in carbonyl compounds can be qualitatively interpreted in a similar way (5).

The extended Hückel method is not successful in calculating nonbonded carbon–proton coupling constants (6). The CNDO/2 and INDO calculations (7) show promise in reproducing the observed $J(^{13}C—C—H)$. Jameson and Damasco (8) discuss in detail the quantum mechanical basis of $J(^{13}C—C—H)$ in a variety of compounds. Their theory agrees with experiment in predicting a relatively narrow spread of values (9) within each set of bonding situations for the carbon atoms. An exception to the narrow spread of values of $J(^{13}C—C—H)$ occurs for derivatives of ethylene and their theory accounts for this situation as well. Nevertheless, precise agreement between theory and experiment is hardly expected and is not attained for such complex molecules.

Consequently the qualitative approach described for vinylene carbonate is still useful, particularly as it allows a discussion in terms of inductive and hyperconjugative substituent effects, of interest when comparing the results for the title compounds, **2** and **3**, with those for vinylene carbonate (**1**).

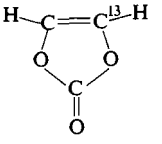

1

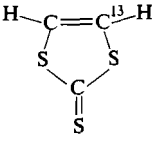

2

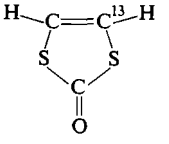

3

In a variation on the above approach we find it useful to compare $J(^{13}C—C—H)$ with *cisoid* $J(H—C—C—H)$ in **1**, **2**, **3**, certain ethylene derivatives, and in benzene, thiophene, and furan. A correlation of these couplings is established below and serves as one measure of aromaticity or potential aromaticity in a compound. In addition, the assignment of $J(^{13}C—C—H)$ couplings in some molecules is bedevilled by complexities (6) and the correlation can be used in a confirming role in such instances.

Experimental

(1) Preparation of Compounds

1,3-Dithiole-2-thione (2)

This was prepared according to the methods of Klingsberg (10). The product was further purified by chromatography on alumina in benzene.

TABLE 1. Proton chemical shifts and coupling constants* in vinylene carbonate (**1**), 1,3-dithiole-2-thione (**2**), and 1,3-dithiole-2-one (**3**)

Parameter	Compound 1	2	3
$J(^{13}C—H)$	220.1	189.50 ± 0.03	190.73 ± 0.03
$J(^{13}C—C—H)$	17.5	4.66 ± 0.02	3.97 ± 0.02
$J(H—C—C—H)$	1.5	7.12 ± 0.02	8.33 ± 0.02
$J(=^{13}C—X—C—H)$†	±9.3	±8.70 ± 0.02	±10.42 ± 0.02
$\nu(^{12}C$ only)‡	421.5	432.64 ± 0.01	410.03 ± 0.02
$\nu(^{13}C$ isotope)§	—	$^{13}C—H$ +0.21 ± 0.02	+0.20 ± 0.02
		$^{13}C=C—H$ +0.15 ± 0.02	+0.14 ± 0.02
		$=^{13}C—S—C—H$ +0.11 ± 0.02	+0.08 ± 0.02

*In Hz.
†This coupling occurs in the molecule containing ^{13}C at position 2.
‡In Hz at 60 MHz to low field of internal TMS. The value for I is from ref. 15 and was measured at infinite dilution in TMS.
§The isotope shifts caused by substitution of ^{13}C for ^{12}C are given in Hz at 60 MHz relative to the proton shifts in the molecule containing only ^{12}C.

1,3-Dithiole-2-one (3)

This was prepared from the corresponding thione **2** by treatment with mercuric acetate as described in (11).

(2) Proton Magnetic Resonance Measurements

Samples were degassed by the freeze–pump–thaw technique and, for reasons of signal to noise ratios, contained only enough carbon disulfide to produce a liquid solution at room temperature. A small amount of tetramethylsilane acted as an internal reference and produced a lock signal for the DA-60 I spectrometer operated in the frequency sweep mode. Peak positions for **2** and **3** were calibrated repeatedly by reading sweep and manual oscillator frequencies and the sign of $J(^{13}C—C—H)$ was found by double resonance measurements as described for vinylene carbonate **2**.

Results and Discussion

(1) Analysis of Spectra

The proton resonance spectra of **2** and **3** are ABX where X = ^{13}C. The observable AB region consists of eight peaks as previously illustrated for **1** (2). With the knowledge of a positive $J(^{13}C—C—H)$ relative to $J(^{13}C—H)$ from the tickling experiments and the further certainty that $J(H—C—C—H)$ is positive (2), these peaks can be unequivocally assigned. A careful ABX analysis gave spectral parameters which reproduced the observed peak positions to within 0.005 to 0.01 Hz of the experimental ones. Consequently confidence can be placed in the isotope shifts of the protons given in Table 1, where the other parameters obtained for **2** and **3** are compared with those of **1**. The sign of $J(^{13}C—X—C—H)$ cannot be determined[1] in the isotropic phase but is almost certainly positive (12).

[1]For the molecules in which ^{13}C occurs at position 2.

(2) $J(^{13}C—C—H)$ Compared with $J(^{13}C—H)$

In the original plot of $J(^{13}C—C—H)$ *vs.* $J(^{13}C—H)$ the reference line was defined by the parameters for ethane, ethylene, acetylene, vinylene carbonate, vinyl bromide, and sym-tetrabromoethane (2). Marked deviations from this line were interpreted in terms of hyperconjugative interaction of substituent orbitals with the $^{13}C—C—H$ fragment orbitals. For reasons of space the plot is not reproduced here. However, the parameters for **2** and **3** fall almost precisely on the reference line of the plot, suggesting no hyperconjugative interaction of sulfur orbitals with the $^{13}C—C—H$ fragment in **2** or **3**. In this respect **2** and **3** are similar to the oxygen analog **1**. If, however, the sulfur 3d orbitals participated to any extent in the bonding a positive deviation from this line might be expected, inasmuch as some of the 3d orbitals for the participating divalent sulfur atoms have the required symmetry.

The present indication of little or no participation of the 3d orbitals from the divalent sulfur agrees with the electron spin resonance data on the 2,4,6-triphenylthiapyryl radical, where the hyperfine splittings can be adequately interpreted without invoking d orbital participation of the divalent sulfur (13). In a similar vein, CNDO/2 calculations on thiophene yield a good fit to the relative magnitudes of H–H and ^{13}C–H coupling constants when 3d, 4s, and 4p orbitals are neglected (14).

(3) $J(^{13}C—C—H)$ Compared with cis $J(H—C—C—H)$

A tentative explanation (8) in terms of substituent effects on resonance integrals has been

Can. J. Chem. Downloaded from www.nrcresearchpress.com by 210.87.254.6 on 09/05/12
For personal use only.

TABLE 2. The *cisoid* J(H—C—C—H) and two-bond $J(^{13}C—C—H)$ values in Hz in some unsaturated compounds

No.	Compound	J(H—C—C—H)	$J(^{13}C—C—H)$	Reference
1	$H_2C=^{13}CH_2$	11.6 ± 0.1	−2.4 ± 0.2	16
2	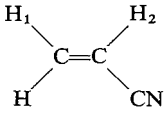	11.65 ± 0.05	(H_1) 0.29 (H_2) −3.67	17
3	*cis*$(C_2H_5OOC)_2CH=CH$	11.9 ± 0.3	(−) 1.5 ± 0.3	18
4	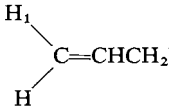	9.92 ± 0.05	(H_1) 1.0 ± 0.3	19
5	**2**	7.12 ± 0.02	4.66 ± 0.02	This paper
6	**3**	8.33 ± 0.02	3.97 ± 0.02	This paper
7	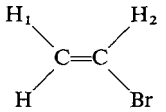	7.27 ± 0.05	(H_1) 7.5 ± 0.5 (H_2) 5.8 ± 0.5	20, 37
8	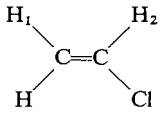	7.16 ± 0.05	(H_1) 7.1 (H_2) 6.8	21, 37
9	*cis* ClCH=CHCl	5.2 ± 0.2	13.3 ± 0.5	22
10	**1**	1.47 ± 0.03	17.5 ± 0.1	2
11	Benzene	7.54 ± 0.05	1.0	12, 34
12	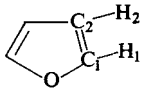	1.75 ± 0.05	(H_1) 14.0 ± 0.1 (H_2) 7.0 ± 0.1	6, 35
13	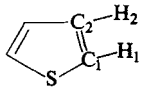	4.7 ± 0.1	(H_1) 4.7 ± 0.1 (H_2) 7.4 ± 0.1	6, 36
14	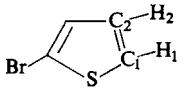	5.5 ± 0.1	(H_1) 3.4 ± 0.1 (H_2) 5.6 ± 0.1	22

given for the relatively wide variation of $J(^{13}C—C—H)$ when both carbon atoms are sp^2 hybridized. For practical purposes, an empirical prediction of this coupling in terms of an experimentally more easily accessible parameter is desirable. In Table 2 *cisoid* J(H—C—C—H) values together with the available $J(^{13}C—C—H)$ values are collected for a series of compounds corresponding to an $sp^2 = sp^2$ situation. In Fig. 1 a plot of J(H—C—C—H) *vs.* $J(^{13}C—C—H)$ displays two correlation lines for these parameters, one for benzene, thiophene, and furan and the other for ethylene derivatives including **1**, **2**, and **3**.

Note that only an average value of $J(^{13}C—C—H)$ is plotted for each compound. For example, in vinyl cyanide the average of the two values involving the protons giving rise to J(H—C—C—H) is plotted in Fig. 1. For allyl bromide only one $J(^{13}C—C—H)$ value is avail-

Can. J. Chem. Downloaded from www.nrcresearchpress.com by 210.87.254.6 on 09/05/12
For personal use only.

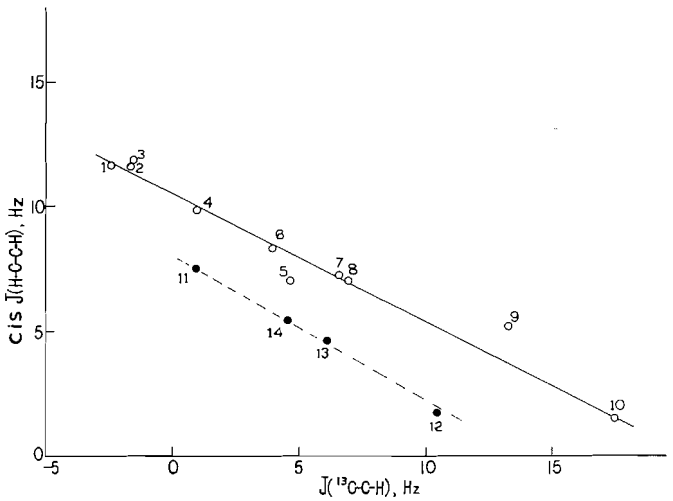

FIG. 1. The carbon–proton coupling over two bonds, $J(^{13}C—C—H)$, is plotted *vs.* the *cisoid* proton–proton coupling over three bonds for the compounds in Table 2. Only one point is given for each compound. (See text for an explanation).

able and is plotted in Fig. 1. Although the theoretical basis underlying the correlations in Fig. 1 is not obvious, their practical use is apparent in the assignment of complex ^{13}C resonance spectra. For example, in cyclic olefins J(H—C=C—H) is strongly dependent on ring size (24–26) and the present correlation allows a prediction of certain two-bond C—H couplings in their ^{13}C spectra. They are predicted to vary widely from the value of -2.4 Hz in ethylene. As another example, the disputed values of the coupling constants in benzoquinone-$^{13}C_2$ could possibly be more firmly assigned (26, 27).

In terms of the present correlations, thiophene and furan are "aromatic", although this is not meant to imply anything about properties such as their reactivity towards electrophiles. Nevertheless, the correlation is interesting in view of the arguments for and against the use of ring currents as a measure of aromaticity (28–33) in thiophene and furan.

Compounds **1**, **2**, and **3** behave much like ethylene derivatives in Fig. 1 although **2** deviates towards the aromatic line. In any case, it seems clear that in these compounds the C=C bond has a mobile bond order near 1, in contrast to benzene, furan, and thiophene. No firm conclusions about the aromatic character of the related 1,2-dithiole-3-ones and thiones could be reached on the basis of chemical shifts or allylic proton couplings (38).

Finally a tentative application to chemical systems of biological interest is suggested by Fig. 1. For example, measurement of the two parameters in a molecule like uridine (**4**), which contains the fragment H—C=C—H in the base, should allow conclusions concerning the delocalization of the π electrons in the base.

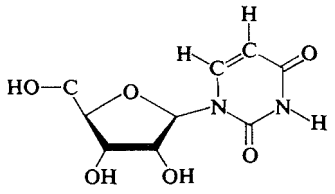

4

(4) Vicinal Carbon–Proton Coupling

In **1**, **2**, and **3**, the vicinal carbon–proton coupling can be represented as in **5** and is analogous to a *trans* coupling. In benzene (**6**) $J(^{13}C—C—C—H) = +7.4$ Hz (12), somewhat

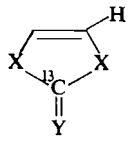

5

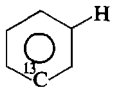

6

smaller than in any of the cases **5**. This may well be a consequence of the higher effective nuclear charge (3) in the radial part of the 2s orbital at

Can. J. Chem. Downloaded from www.nrcresearchpress.com by 210.87.254.6 on 09/05/12
For personal use only.

Can. J. Chem. Downloaded from www.nrcresearchpress.com by 210.87.254.6 on 09/05/12
For personal use only.

the coupled carbon in **1**, **2**, and **3**, arising from the electronegative substituents at that position. Within the sequence **1**, **2**, **3** the effective nuclear charge is smallest in **2** resulting in the lowest $J = 8.7$ Hz. Simple Hückel type molecular orbital calculations (39) indicate larger mobile bond orders for the relevant fragments in **3** than in **2**, suggesting shorter bonds in **3**. It is therefore not surprising (40) to find the large $J = 10.4$ Hz for **3**.

(5) Isotope Shifts of the Proton Resonance

Carbon-13 isotope shifts of up to $+0.007 \pm 0.004$ p.p.m. are observed (41) for directly bonded protons in methane derivatives. A similar shift of $+0.004 \pm 0.003$ p.p.m. occurs in $F(Cl)C{=}C^{13}H_2$ (42). The isotope shifts given in Table 1 for **2** and **3** are the most precise values known to date and decrease from $+0.0035 \pm 0.0004$ p.p.m. for directly bonded protons to 0.0013 ± 0.0004 p.p.m. for a proton separated by three bonds from ^{13}C. Their interpretation for such complex molecules is by no means clear (43).

(6) $J(^{13}C{-}C{-}H)$ and cis $J(H{-}C{-}C{-}H)$ in Cyclopropane

The $J(^{13}C{-}C{-}H)$ value in cyclopropane is -2.55 Hz (44) and *cis* $J(H{-}C{-}C{-}H)$ is 8.97 Hz (45) (one proton bonded to ^{13}C). The point defined by these values would fall very nearly on the benzene line in Fig. 1. This is not to say that cyclopropane is aromatic, although a substantial ring current has been attributed to it (46).

Crecely *et al.* find interesting correlations between long-range C^{13}–H couplings and the vicinal and geminal proton–proton couplings in some monosubstituted cyclopropane derivatives (44) but it is not clear how they relate to the correlation discussed here.

We are grateful to the National Research Council of Canada for financial support.

1. J. A. Pople and A. A. Bothner-By. J. Chem. Phys. **42**, 1339 (1965).
2. K. A. McLauchlan and T. Schaefer. Can. J. Chem. **44**, 321 (1966).
3. D. M. Grant and W. M. Litchman. J. Amer. Chem. Soc. **87**, 3994 (1965).
4. U. Hupbach, H. Frischleder, and H. Helbig. Mol. Phys. **16**, 593 (1969).
5. O. Yamamoto, M. Watabe, and O. Kikuchi. Mol. Phys. **17**, 249 (1969).
6. F. J. Weigert and J. D. Roberts. J. Amer. Chem. Soc. **90**, 3543 (1968).
7. J. A. Pople, J. W. McIver, and N. S. Ostlund. J. Chem. Phys. **49**, 2965 (1968).
8. C. J. Jameson and M. C. Damasco. Mol. Phys. **18**, 491 (1970).
9. G. Miyazima, Y. Utsumi, and K. Takahashi. J. Phys. Chem. **73**, 1370 (1969).
10. E. Klingsberg. J. Amer. Chem. Soc. **86**, 5290 (1964).
11. F. Challenger, E. A. Mason, E. C. Holdsworth, and R. Emmott. J. Chem. Soc. 292 (1953).
12. F. J. Weigert and J. D. Roberts. J. Amer. Chem. Soc. **89**, 2967 (1967).
13. I. Degani, L. Lunazzi, G. F. Pedulli, C. Vincenzi, and A. Mangini. Mol. Phys. **18**, 613 (1970).
14. D. T. Clark. Tetrahedron **24**, 2663 (1968).
15. J. H. Goldstein and G. S. Reddy. J. Chem. Phys. **36**, 2644 (1962).
16. R. M. Lynden-Bell and N. Sheppard. Proc. Roy. Soc. London **269A**, 385 (1962).
17. R. Freeman. J. Chem. Phys. **40**, 3571 (1964).
18. N. Muller. J. Chem. Phys. **37**, 2729 (1962).
19. J. Feeney and P. J. S. Pauwels. Mol. Phys. **14**, 209 (1968).
20. R. M. Lynden-Bell. Mol. Phys. **6**, 537 (1963).
21. F. J. Weigert and J. D. Roberts. J. Phys. Chem. **73**, 449 (1969).
22. G. Govil. J. Chem. Soc. A, 1420 (1967).
23. O. L. Chapman. J. Amer. Chem. Soc. **85**, 2014 (1963).
24. G. V. Smith and H. Kriloff. J. Amer. Chem. Soc. **85**, 2016 (1963).
25. P. Laszlo and P. von R. Schleyer. J. Amer. Chem. Soc. **85**, 2018 (1963).
26. G. Govil. J. Chem. Soc. A, 1416 (1967).
27. G. T. Jones and J. N. Murrell. J. Chem. Soc. A, 421 (1966).
28. J. A. Elvidge and L. M. Jackman. J. Chem. Soc. 859 (1961).
29. H. A. P. De Jongh and H. Wynberg. Tetrahedron. **21**, 515 (1965).
30. D. W. Davies. Chem. Commun. 258 (1965).
31. J. A. Elvidge. Chem. Commun. 160 (1965).
32. R. J. Abraham, R. C. Sheppard, W. A. Thomas, and S. Turner. Chem. Commun. 43 (1965).
33. J. I. Musher. J. Chem. Phys. **43**, 4081 (1965).
34. S. Castellano and R. Kostelnik. Tetrahedron Lett. **51**, 5211 (1967).
35. L. Lunazzi. Mol. Phys. **18**, 413 (1970).
36. D. M. Grant, R. C. Hirst, and H. S. Gutowsky. J. Chem. Phys. **38**, 470 (1963).
37. R. E. Mayo and J. H. Goldstein. J. Mol. Spectry. **14**, 273 (1964).
38. R. F. C. Brown, I. D. Rae, and S. Sternhell. Austral. J. Chem. **18**, 1211 (1965).
39. R. Zahradnik. Advan. Heterocyclic Chem. **5**, 1 (1965).
40. M. A. Cooper and S. L. Manatt. J. Amer. Chem. Soc. **91**, 6325 (1969).
41. S. G. Frankiss. J. Phys. Chem. **67**, 752 (1963).
42. H. M. Hutton and T. Schaefer. Can. J. Chem. **45**, 1111 (1967).
43. H. Batiz-Hernandez and R. A. Bernheim. *In* Progress in Nuclear Magnetic Resonance Spectroscopy. Vol. 3. *Edited by* J. W. Emsley, J. Feeney, and L. H. Sutcliffe. Pergamon Press. Oxford, 1967.
44. K. M. Crecely, R. W. Crecely, and J. H. Goldstein. J. Phys. Chem. **74**, 2680 (1970).
45. V. S. Watts and J. H. Goldstein. J. Chem. Phys. **46**, 4165 (1967).
46. K. Tori and K. Kitahonoki. J. Amer. Chem. Soc. **87**, 386 (1965), and references therein.

Can. J. Chem. Downloaded from www.nrcresearchpress.com by 210.87.254.42 on 09/05/12
For personal use only.

Proton Magnetic Resonance Spectrum of Parafluorotoluene. Sigma and Pi Electron Contributions to $J_p^{H,F}$

R. WASYLISHEN[1] AND T. SCHAEFER
Chemistry Department, University of Manitoba, Winnipeg, Manitoba

Received July 31, 1970

The p.m.r. spectrum of a 15 mole % solution of *p*-fluorotoluene in acetone-d_6 is analyzed at 100 MHz using LAOCN3 and LAME computer programs. The resulting spectral parameters satisfactorily reproduce the methyl proton resonance at 60 MHz. The coupling over six bonds between the fluorine nucleus and the methyl protons is 1.15 ± 0.02 Hz and is taken as a measure of the π electron contribution to the coupling over five bonds between the fluorine nucleus and the proton in *p*-fluorobenzene. The σ electron contribution to this coupling is discussed for some fluorobenzene derivatives and is shown to depend on the electronegativity of the substituents in a manner completely analogous to proton–proton and other proton–fluorine couplings in benzene and pyridine derivatives.

Canadian Journal of Chemistry, 49, 94 (1971)

Introduction

The long-range spin–spin coupling constants between methyl and ring protons in the para position, $^6J_p^{H,CH_3} < 0$, in toluene derivatives arise from a π electron mechanism (1). In a derivative of parafluorotoluene, $J_p^{F,CH_3} > 0$ and has a greater magnitude than J_p^{H,CH_3} in toluene derivatives (2). For a π electron mechanism $J_p^{H,CH_3} \alpha Q_{CH}$ and $J_p^{F,CH_3} \alpha Q_{CF}$, where Q_{CH} and Q_{CF} are the hyperfine interaction constants between an electron in a π orbital on carbon and the proton and fluorine nucleus, respectively (2). But $|Q_{CF}| > |Q_{CH}|$ and $Q_{CF} > 0$, $Q_{CH} < 0$, therefore supporting a π electron mechanism for J_p^{F,CH_3}. A similar conclusion holds for $^4J_p^{F,CH_3}$ in 2-fluoro-3-methylpyridine (3).

The long-range coupling to the methyl protons in benzene derivatives is remarkably insensitive to substituent effects (1–5). Coupling between the ring protons shows a characteristic, probably alternating, dependence on the electronegativity of the substituents (6, 7). The implied inductive effect via the σ system is accentuated for ring proton – ring fluorine couplings, particularly when the electronegative group is situated near the C—F bond (3, 8).

The coupling over five bonds, $^5J_p^{H,F}$, in fluorobenzene derivatives is sensitive to ring substitution, suggesting the presence of a σ electron contribution to $J_p^{H,F}$. A σ contribution can also be inferred from the relative magnitudes and signs of $^5J_p^{H,F}$ and $^6J_p^{F,CH_3}$. The former is small and positive in fluorobenzene but becomes large and negative in the presence of highly electronegative ring substituents. The latter is positive in a fluorotoluene derivative (2) and is much less sensitive to ring substituents.

The purpose of this paper is to establish the π contribution to $^5J_p^{H,F}$ in fluorobenzene and thus to determine the σ contribution to $^5J_p^{H,F}$, known for a series of fluorobenzene derivatives. Hence the p.m.r. spectrum of parafluorotoluene is fully analyzed.

The assumption that coupling constants in the benzene ring can be discussed in terms of σ and π electron contributions is an approximation but it is a natural one to make as long as quantum mechanical calculations, which take all valence electrons into consideration (9), have difficulties in accurately reproducing experimental values, particularly for couplings involving fluorine nuclei. The approximation has been profitably employed in discussing the coupling constants in 2-fluoro-3-methyl pyridine (3) and, more generally, in the interpretation of chemical shifts, nuclear quadrupole frequencies, and the intensities of i.r. spectra of benzene derivatives (10).

Experimental

Parafluorotoluene from Koch–Light was prepared as a degassed, 15 mole % solution in acetone-d_6, containing internal tetramethylsilane (TMS) as an internal reference and locking material. The p.m.r. spectra were recorded at a sweep rate of 0.02 Hz/s in the frequency sweep mode on HA100D and DA60I spectrometers. Ring proton spectra were also recorded while decoupling the methyl protons using an HP4204A audiooscillator. Peak positions were repeatedly calibrated by reading sweep and manual oscillators in the period mode of an HP5323A counter.

[1]Holder of an NRCC bursary, 1970–1971.

Can. J. Chem. Downloaded from www.nrcresearchpress.com by 210.87.254.42 on 09/05/12
For personal use only.

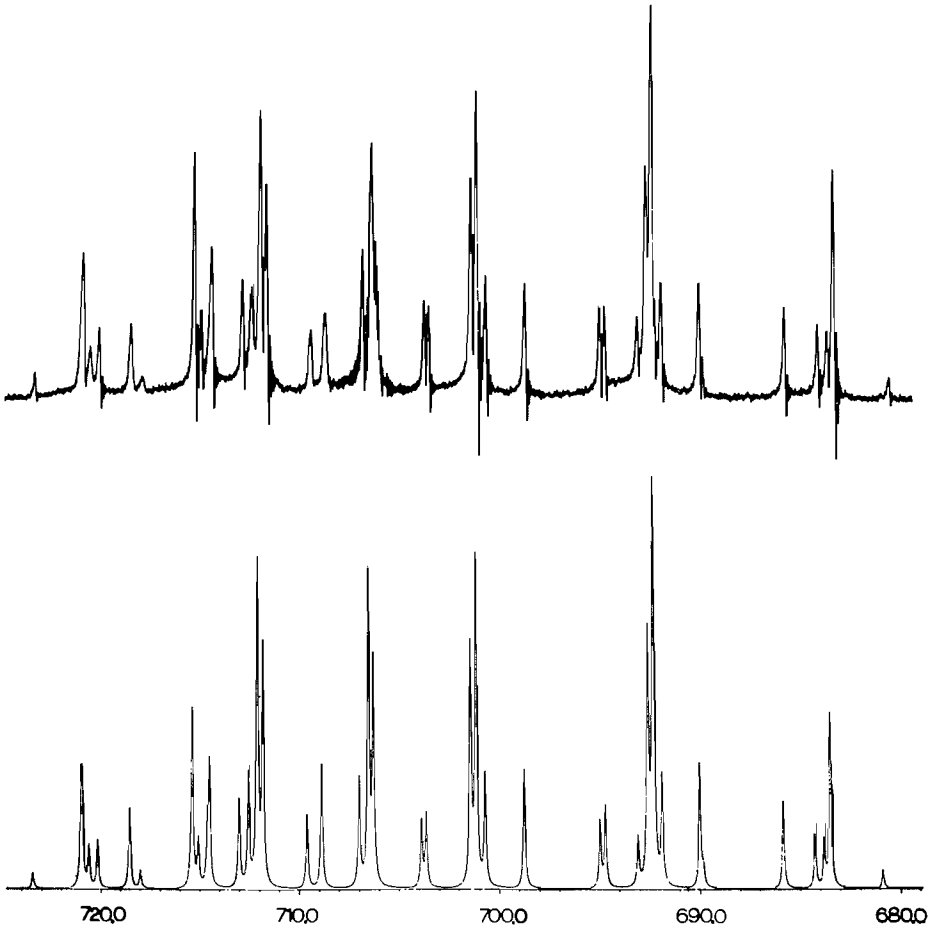

FIG. 1. The observed and calculated ring proton spectrum of a 15 mole % solution of *p*-fluorotoluene in acetone at 100 MHz when the methyl protons are decoupled. The scale is in Hz to low field of internal TMS. The spectrum was taken at a sweep speed of 0.02 Hz/s. The calculated spectrum corresponds to an effective T_2 of 2.80 s and uses the parameters in column 2 of Table 1. Note the unavoidable "beat frequency" in the observed spectrum near 706.5 Hz.

Results and Discussion

(1) Analysis of Spectra

The procedure using LAOCN3 (11) was similar to that adopted by Williamson *et al.* for toluene (4). With the methyl protons decoupled, an iterative fit to the ring proton spectrum was obtained. Initial coupling parameters were estimated from those of benzene, toluene, and fluorobenzene (4, 12, 13). In Fig. 1 the final calculated and observed spectra are displayed at 100 MHz. The iteration was carried out on 45 assigned peaks and column 2 of Table 1 gives the parameters found in this way. The numbering of parameters follows from **1**.

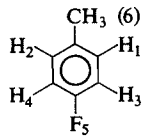

1

Now, because the program accommodates seven spins and because the complete spectrum of **1** is $[AB]_2X_3R$, *i.e.* eight spins, a subspectral analysis was undertaken. The methyl protons are represented by X_3 and therefore the undecoupled ring proton resonance consists of a superposition of four subspectra corresponding to the spin states $\pm 1/2$, $\pm 3/2$ of the composite

TABLE 1. Spectral parameters in Hz for a 15 mole % solution of parafluorotoluene in acetone-d_6

Parameters	LAOCN3			LAME	
	Decoupled spectrum	±1/2 Subspectra	±3/2 Subspectra	All protons assigned	Ring protons assigned*
$\nu(1) = \nu(2)$	712.784(0.004)	712.753(0.002)	712.750(0.002)	712.750(0.002)	712.750(0.001)
$\nu(3) = \nu(4)$	693.300(0.004)	693.272(0.002)	693.277(0.003)	693.272(0.002)	693.272(0.001)
$\nu(6)$	—	226.167(0.002)	—	226.166(0.002)	—
J_{12}	2.379(0.006)	2.389(0.003)	2.379(0.005)	2.390(0.002)	2.390(0.002)
$J_{13} = J_{24}$	8.453(0.005)	8.439(0.003)	8.442(0.004)	8.439(0.002)	8.439(0.002)
$J_{14} = J_{23}$	0.394(0.005)	0.388(0.002)	0.392(0.003)	0.389(0.002)	0.390(0.002)
$J_{15} = J_{25}$	5.421(0.007)	5.426(0.003)	5.424(0.005)	5.431(0.003)	5.431(0.003)
$J_{16} = J_{26}$	—	−0.726(0.002)	−0.721(0.005)	−0.720(0.003)	−0.719(0.002)
J_{34}	2.871(0.006)	2.878(0.003)	2.869(0.005)	2.877(0.003)	2.878(0.002)
$J_{35} = J_{45}$	8.974(0.007)	8.966(0.003)	8.958(0.005)	8.965(0.003)	8.965(0.003)
$J_{36} = J_{46}$	—	0.346(0.002)	0.335(0.005)	0.343(0.002)	0.339(0.003)
J_{56}	—	1.135(0.004)	—	1.149(0.003)	—
The r.m.s. error	0.021	0.014	0.017	0.014	
Largest error	0.040	0.038	0.040	0.045	
Lines assigned	45	101	61	284	
Transitions calculated	48	128	96	416	

*Of 108 calibrated peak positions, seven were not assigned in LAME.

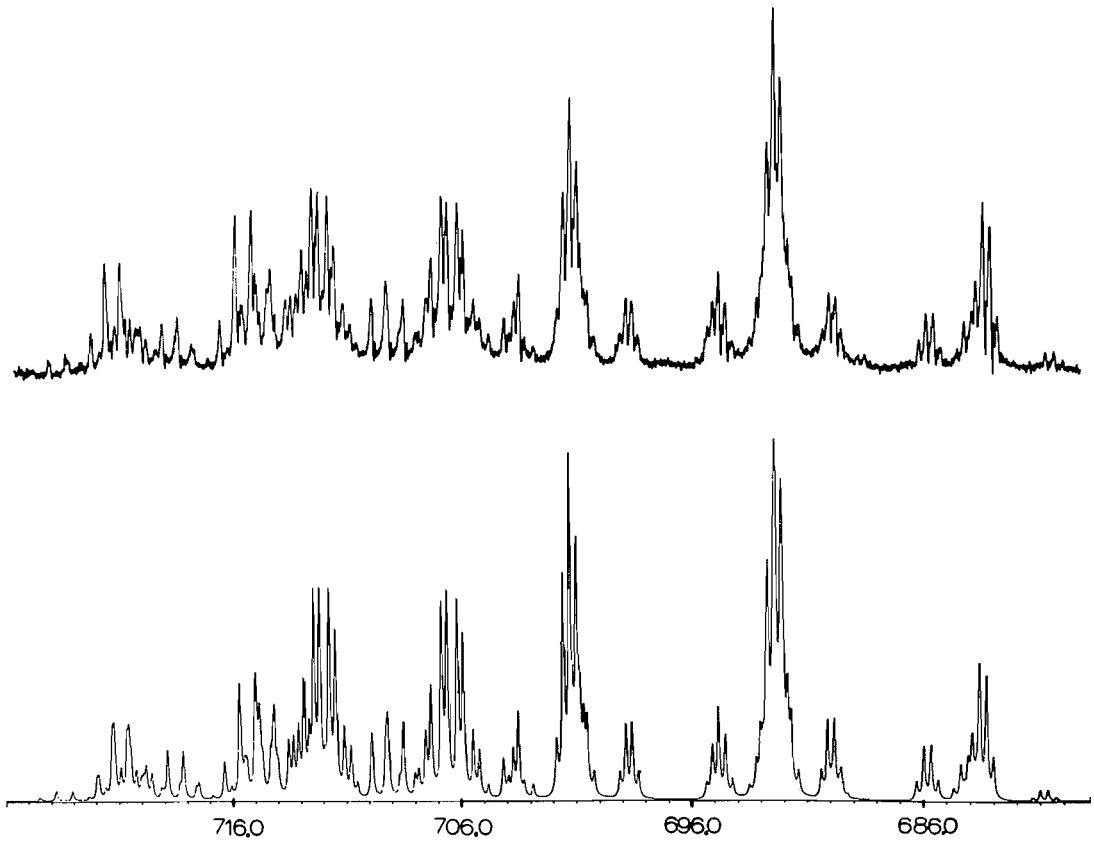

FIG. 2. As in Fig. 1 with methyl protons coupling to the ring protons. The effective T_2 of the calculated spectrum is 2.65 s and the parameters are from columns 3 and 4 of Table 1, weighted 3:1 in favor of the ±1/2 subspectra.

Can. J. Chem. Downloaded from www.nrcresearchpress.com by 210.87.254.42 on 09/05/12
For personal use only.

Can. J. Chem. Downloaded from www.nrcresearchpress.com by 210.87.254.42 on 09/05/12
For personal use only.

spin states of the methyl protons. Of course, the subspectra corresponding to $\pm 1/2$ have three times the intensity of the subspectra corresponding to $\pm 3/2$.

Taking values of $^4J_o^{H,CH_3}$ and $^5J_m^{H,CH_3}$ from toluene (4), the $\pm 1/2$ subspectra were generated and compared to 101 assignable peaks in the ring and methyl proton spectra. An initial value of $^6J_p^{F,CH_3}$ was extracted on a first-order basis from the methyl spectrum. An ensuing iterative fit, allowing the variation of all parameters, gave the results in column 3 of Table 1.

Sixty one peaks from the $\pm 3/2$ subspectra were then assigned and iteration on the ring protons, allowing all parameters to vary, gave the parameters in column 4 of Table 1. The Calcomp plot for the complete ring spectrum is shown in Fig. 2, together with the observed spectrum. The agreement is apparently satisfactory. The probable errors in the parameters are small and multiplication by 8 still yields an acceptably small error estimate in the coupling constants. The parameters obtained from the $\pm 1/2$ subspectra are felt to be more reliable. In Fig. 3, the methyl proton resonance is shown together with the calculated spectrum. The LAME results (see below) are used but the LAOCN3 parameters give substantially the same calculated spectrum.

Comparison of the shift parameters for the decoupled and undecoupled spectra suggests that the decoupling conditions were such as to cause very small (about 0.03 Hz) frequency shifts; due either to the Bloch–Siegert effect or to a bias in the lock signal.

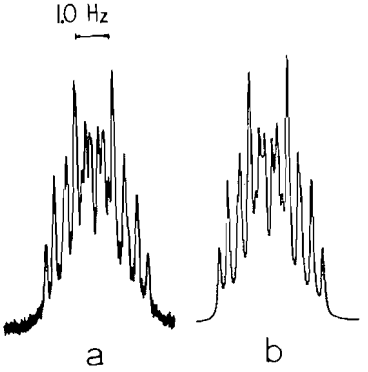

FIG. 3. The experimental and calculated methyl proton spectra at 100 MHz. The experimental spectrum was taken at a sweep speed of 0.01 Hz/s. The effective T_2 of the calculated spectrum was 2.90 s and the parameters are taken from column 5 of Table 1.

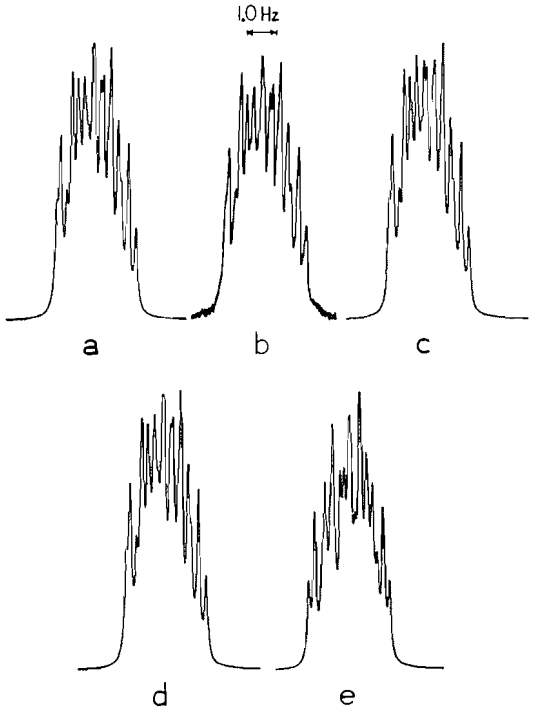

FIG. 4. The experimental methyl proton resonance at 60 MHz, taken at a sweep rate of 0.01 Hz/s, is shown in (*b*). In (*a*) the calculated spectrum is shown using parameters from column 5 of Table 1 but with $J_p^{F,CH_3} = 1.154$ Hz. In (*d*) and (*e*) the same parameters are again used but $J_p^{F,CH_3} = 1.149$ and -1.149 Hz, respectively. In (*c*) the parameters from columns 3 and 4, weighted 3:1 in favor of the $\pm 1/2$ subspectra, are used, $J_p^{F,CH_3} = 1.135$ Hz. In all calculated spectra the effective $T_2 = 2.50$ s.

The parameters obtained from the LAOCN3 analysis were weighted 3:1 in favor of those from the $\pm 1/2$ subspectra and were then employed in the generation of the methyl proton spectrum at 60 MHz (Fig. 4*c*). The observed spectrum at 60 MHz in Fig. 4*b* displays asymmetry about its shift position. The asymmetry depends on the sign[2] of J_p^{F,CH_3}. Although the agreement between calculated and observed spectra is close, it is clear that the positions of a few peaks in the central region of the observed and calculated spectra differ by some hundredths of a Hz.

The reason for the disagreement most likely lies in the value of J_p^{F,CH_3}. Analysis of the proton spectrum at 100 MHz using the computer program LAME (see below) gave $J_p^{F,CH_3} = 1.149$ Hz,

[2]Tickling experiments along the lines described for *p*-fluorobenzaldehyde (14) confirmed the positive sign of J_p^{F,CH_3}.

Can. J. Chem. Downloaded from www.nrcresearchpress.com by 210.87.254.42 on 09/05/12
For personal use only.

an increase of 0.014 Hz over the value obtained from LAOCN3. In Fig. 4*d* the calculated methyl spectrum at 60 MHz now agrees almost perfectly with the observed spectrum in Fig. 4*b*. Increasing J_p^{F,CH_3} by another 0.005 Hz produced somewhat better agreement with the observed spectrum (see Fig. 4*a*). The sensitivity to this parameter indicates to us that the accuracy in J_p^{F,CH_3} is 0.02 Hz, *i.e.*, $J_p^{F,CH_3} = 1.15 \pm 0.02$ Hz.

An analysis using the program LAME (14*a*) was also performed. Transitions are all weighted equally and standard deviations are given in brackets in Table 1. The average deviation between observed and calculated peaks lies near 0.01 Hz. In the correlation matrix (12 parameters) there are four values between 0.2 and 0.3, 11 values between 0.1 and 0.2, and the rest are below 0.1 in magnitude. A relatively large correlation of 0.27 between $J_p^{H,H}$ and $J_o^{H,H}$ can be understood on noting that, as is more easily seen for a case $[AB]_2$, the separation between certain sets of intense peaks is given by $J_p^{H,H} + J_o^{H,H}$.

(2) The Chemical Shifts and Ring Proton–Proton and Ring Proton–Fluorine Couplings

The chemical shifts are solvent dependent (15) and will not be further discussed.

(a) Proton–Proton Couplings

The additivity of substituent effects on $J^{H,H}$ is established, particularly for disubstituted benzenes (12, 16). There is a small solvent effect on some $J_m^{H,H}$ values (17, 18). Loemker and Goldstein analyzed the proton resonance spectrum of fluorobenzene as a 10 mole % solution in acetone (18). An additivity scheme using their parameters and those of benzene and toluene as reported by Williamson *et al.* (4), yields predicted values of *p*-fluorotoluene as follows: $J_{12} = 2.32$, $J_{13} = 8.46$, $J_{14} = 0.40$, $J_{34} = 2.87$ Hz. The excellent agreement between these numbers and those given in Table 1 can be taken as indicating the validity of the present analysis of the spectrum of *p*-fluorotoluene. Note that the initial parameters for our analysis were estimated from the analysis of fluorobenzene in carbon tetrachloride solution and not from the analysis of Loemker and Goldstein in acetone solution.

(b) Ring Proton–Fluorine Couplings

In a 10 mole % solution of fluorobenzene in acetone (18) $J_o^{H,F} = 9.31$ Hz and $J_m^{H,F} = 5.79$ Hz. In *p*-fluorotoluene as a 15 mole % solution in acetone, where the relatively strong solvent dependence of these two couplings (19–21) should be very nearly equal in the two compounds, we have $J_o^{H,F} = 8.96$ Hz and $J_m^{H,F} = 5.43$ Hz. The decrease by 0.35 Hz of both couplings on introduction of the methyl group originates in the electronegativity of CH_3 which is higher than that of H. According to the alternating substituent effect rule (6, 7), $J_o^{H,F}$ increases if X is placed ortho to H or F but should decrease if X is

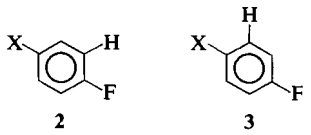

2 **3**

situated meta to H or F in **2**, as we observe. The $J_m^{H,F}$ value in **3** has been observed to decrease in a series of compounds (8), and this behavior is consistent with that of other couplings as is discussed further below.

(3) The Long-range Methyl Couplings

(a) With Ring Protons

These agree to within experimental error with those found in toluene (4) where $J_o^{H,CH_3} = -0.746 \pm 0.026$ Hz and $J_m^{H,CH_3} = 0.356 \pm 0.006$ Hz (errors given are the mean of the difference in the values found from the different subspectra). The conclusions concerning the σ and π electron mechanisms are as recently discussed (1, 4), both couplings having some σ electron contribution in contrast to J_p^{H,CH_3}.

(b) With Fluorine

From Table 1, $J_p^{F,CH_3} = 1.15 \pm 0.02$ Hz in *p*-fluorotoluene. On the assumption that J_p^{F,CH_3} is dominated by a π electron mechanism (2), write

$$[1] \qquad {}^{\pi}J_p^{F,CH_3} \alpha Q_{CF} Q_{CCH}$$

eq. 1, where both hyperfine interaction constants are positive. The Q_{CF} term is composite, varying in magnitude from radical to radical (22–26). In the present connection, the most appropriate Q_{CF} value is one for radicals which approximate as closely as possible to a closed-shell system in the fragment containing the C—F bond. The most likely candidates are the nickel(II) aminotroponeimineate derivatives containing fluorosubstituted phenyl groups (27), where a small spin density from the nickel orbitals is delocalized into the phenyl groups. In such compounds $Q_{CF} = 41.1$ G for the *p*-fluorophenyl derivative (27).

A calibration of the proportionality in eq. 1

TABLE 2. Values of $J_p^{H,F}$ in Hz* in some fluorobenzene derivatives

2-X-Fluorobenzene					3-X-Fluorobenzene			
X	$J_p^{H,F}$	Solvent	E_X†	Reference	X	$J_p^{H,F}$	Solvent	Reference
I	−0.24	CCl_4	2.65	31	H‡	0.20	TMS	18
	−0.24	TMS		8		0.34	Acetone	18
						0.39	CH_3CN	18
CN	−0.24	CCl_4	2.65	31		0.29	CCl_4	18
						0.12	C_6H_{12}	21
Br	−0.64	CCl_4	2.95	31				
	−0.63	TMS		8	I	−0.27	TMS	8
	−0.52	Acetone		33				
					Br	−0.46	TMS	8
Cl	−0.87	CCl_4	3.15	31		−0.63	Acetone	33
	−0.85	TMS		8				
	−0.85	Acetone		33	Cl	−0.59	TMS	8
						−0.47	Acetone	33
NO_2	−0.93	TMS	3.35	8				
	−0.86	Acetone		33	NO_2	−0.53	Acetone	33
F	−1.31	Acetone	3.90	33	F	−0.93	TMS	8
						−0.88	Acetone	33

*The accuracy probably lies between 0.05 and 0.1 Hz.
†The electronegativity, E_X is taken from ref. 39 where $J^{H,H}$ values in benzene derivatives are plotted *vs.* $E_X - E_H = 2.20$.
‡In dimethylformamide (18) $J_p^{H,F}$ is evidently as high as 0.5 Hz.

may be obtained by writing eq. 2, for toluene,

$$[2] \qquad {}^{\pi}J_p^{H,CH_3} \alpha Q_{CH} Q_{CCH}$$

and noting that, by the methyl group replacement technique (28), J_p^{H,CH_3} arises from a π mechanism. Then, assuming that the mobile bond order between C-1 and -4 in toluene, *p*-xylene, and *p*-fluorotoluene does not vary significantly (29), take $Q_{CH} = -22.5$ G (30), $Q_{CF} = 41.1$ G (27), and $J_p^{H,CH_3} = -0.62$ Hz (4). Consequently ${}^{\pi}J_p^{F,CH_3} = -0.62 \times 41.1/-22.5 = 1.16$ Hz.

The close agreement between experiment and model is an indication of the Q_{CF} value appropriate to neutral molecules. It is unlikely that other than a π mechanism is important for a coupling over six bonds. Then −1.15 Hz represents the π electron contribution to J_p^{HF} in fluorobenzene.

(c) Sigma Electron Contribution to $J_p^{H,F}$ in Fluorobenzene Derivatives

On the assumption that the π contribution to $J_p^{H,F}$ is not substantially altered by the substituents in fluorobenzene derivatives[3,4] an assumption which holds to within experimental error for $J_p^{H,H}$ in benzene derivatives (1–5), the σ electron contribution to $J_p^{H,F}$ in fluorobenzene and its derivatives can be discussed as follows. The $J_p^{H,F}$ value in fluorobenzene lies between 0.2 and 0.4 Hz depending on solvent and analytical conditions (13, 20, 21). Writing $J(\text{obs}) = {}^{\pi}J + {}^{\sigma}J$, it follows that ${}^{\sigma}J_p^{H,F} \approx 1.4$ Hz in fluorobenzene.

In Table 2 values of $J_p^{H,F}$ are collected for a few pertinent fluorobenzene derivatives. In Fig. 5, $J_p^{H,F}$ is plotted *vs.* the electronegativity, E_X, of the substituent X in some 2-X fluorobenzenes.

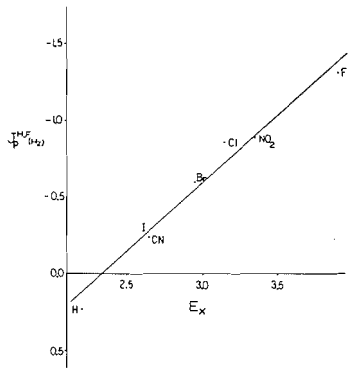

FIG. 5. The $J_p^{H,F}$ value in a number of monosubstituted fluorobenzene derivatives is plotted *vs.* the electronegativity, E_X, of the substituent X. Values are taken from Table 2. The least squares line is given by $J(\text{Hz}) = (-0.882 \pm 0.047)E_X + 2.06 \pm 0.143$. The correlation coefficient, $r = 0.990$.

[3]In 4-fluoro-2-iodotoluene (2) $J_p^{F,CH_3} = 1.28 \pm 0.07$ Hz while preliminary analyses of 2-nitro-4-fluorotoluene and of 3-bromo-4-fluorotoluene in this laboratory show that J_p^{F,CH_3} is constant to within about 0.1 Hz. In pentafluorotoluene, $J_p^{F,CH_3} = 1.4 \pm 0.2$ Hz (32).

[4]Solvent effects on J_p^{F,CH_3} are negligible. Thus we find that even partial protonation of 2-fluoro-5-methylpyridine does not change J_p^{F,CH_3}.

Can. J. Chem. Downloaded from www.nrcresearchpress.com by 210.87.254.42 on 09/05/12
For personal use only.

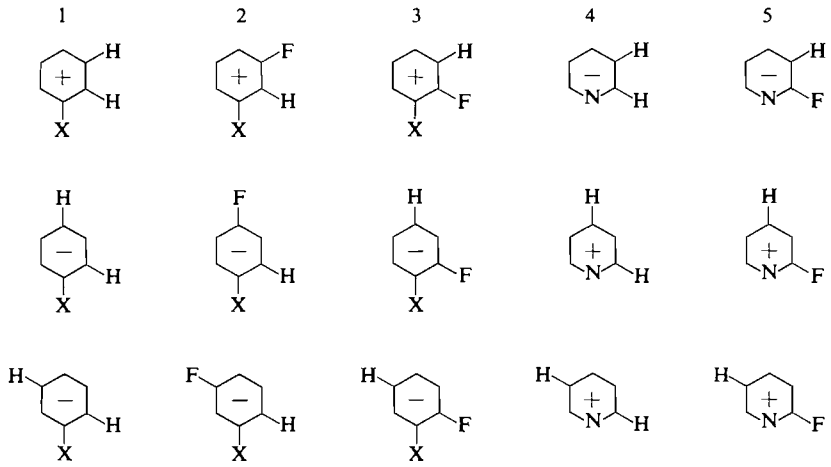

Relative magnitudes of Δ: $\Delta_1 < \Delta_2 < \Delta_3 < \Delta_4 < \Delta_5$

CHART 1

From Table 2 it is apparent that the decrease in $J_p^{H,F}$ as E_X increases is somewhat larger for X placed ortho to F than for X placed ortho to H. Similar plots can be constructed for more heavily substituted fluorobenzenes, data on which can be found in refs. 19, 34–38. The lowest value of $J_p^{H,F}$ is -2.7 Hz in pentafluorobenzene (38).

The data in Table 2 are collected to demonstrate that the observed dependence of $J_p^{H,F}$ on E_X is exactly as expected from previous observations on the E_X dependence of $J_{o,m,p}^{H,H}$ and $J_{o,m}^{H,F}$ in derivatives of benzene, fluorobenzene and pyridine derivatives (3, 6–8, 39). The various J, E_X relationships can be most clearly and economically represented by the diagrams in Chart 1. Let the rate of change of J with E_X be represented by Δ. Then the signs of Δ are as given inside the regular hexagon and the relative magnitudes of Δ are as given at the bottom of Chart 1. In other words, the sign of Δ alternates (6) with the number of bonds separating X from the nucleus involved in the spin–spin coupling. The magnitude of Δ decreases as the number of intervening bonds increases, as predicted on the basis of an inductive effect via the σ system. The alternation has been related (7) to charge alternation predicted by CNDO calculations (40), thus

$$\begin{array}{r} \Delta+\ \Delta\Delta-\ \Delta\Delta\Delta+ \\ X\leftarrow C-C-C- \end{array}$$

In summary, H–F couplings in aromatic compounds show the same qualitative dependence on E_X as do H–H couplings, but the magnitude of the changes is larger for H–F than for H–H couplings. In contrast (41), the analogous F–F couplings behave quite differently.

(4) Sigma or Pi Mechanism for $J_p^{H,H}$ in Benzene

In benzene $J_p^{H,H} = 0.63$ Hz (4), while in toluene $J_p^{H,CH_3} = -0.62$ Hz (4). By the methyl group replacement technique (28) it follows that $J_p^{H,H}$ in benzene itself arises from a π electron mechanism. This conclusion is reinforced by the observation of $J_p^{CH_3,CH_3} = 0.62$ Hz in a derivative of *p*-xylene (1).

Now J_p^{H,CH_3} in toluene derivatives is independent of substituents. For example, $J_p^{H,CH_3} = -0.63$ and -0.59 Hz in 2,6-dichlorotoluene and 3,5-dichlorotoluene respectively,[5] and $J_p^{H,CH_3} = -0.63$ Hz in 2,3,5,6-tetrachlorotoluene (42). Yet $J_p^{H,H}$ decreases, although never to less than 0.2 Hz, on substitution in the benzene nucleus (17). In terms of the present model, the substituent distorts the σ core near the coupled proton leading to a negative σ electron contribution to $J_p^{H,H}$. In other words, the σ electron contribution to $J_p^{H,H}$ vanishes in benzene, is negative in benzene derivatives (apart from compounds like phenyllithium, presumably) and is positive in pyridine derivatives ($J_p^{H,H} = 0.99$ Hz in pyridine (43)). In contrast, the σ and π electron contributions to $J_p^{H,F}$ in fluorobenzene are sizeable but nearly equal in magnitude.

[5]Unpublished work in this laboratory.

Can. J. Chem. Downloaded from www.nrcresearchpress.com by 210.87.254.42 on 09/05/12
For personal use only.

We are grateful to Dr. Roy King and to Dr. C. J. Macdonald for listings and helpful correspondence concerning the computer program LAME and to the authors for a listing of LAOCN3. Financial assistance from the National Research Council of Canada is acknowledged with thanks.

1. C. J. MACDONALD and W. F. REYNOLDS. Can. J. Chem. **48**, 1002 (1970).
2. D. J. BLEARS, S. S. DANYLUK, and T. SCHAEFER. J. Chem. Phys. **47**, 5037 (1967).
3. T. SCHAEFER, S. S. DANYLUK, and C. L. BELL. Can. J. Chem. **47**, 1507 (1969).
4. M. P. WILLIAMSON, R. KOSTELNIK, and S. M. CASTELLANO. J. Chem. Phys. **49**, 2218 (1968).
5. G. KOTOWYCZ and T. SCHAEFER. Can. J. Chem. **44**, 2743 (1966).
6. A. D. COHEN and T. SCHAEFER. Mol. Phys. **10**, 209 (1965).
7. S. CASTELLANO and R. KOSTELNIK. J. Amer. Chem. Soc. **90**, 141 (1968).
8. J. E. LOEMKER, J. M. READ, JR., and J. H. GOLDSTEIN. J. Phys. Chem. **72**, 991 (1968).
9. J. A. POPLE, J. W. MCIVER, and N. S. OSTLUND. J. Chem. Phys. **49**, 2965 (1968).
10. A. R. KATRITZKY and R. D. TOPSOM. Angew. Chem. Int. Ed. **9**, 87 (1970).
11. S. CASTELLANO and A. A. BOTHNER-BY. J. Chem. Phys. 3863 (1964).
12. S. CASTELLANO and R. KOSTELNIK. Tetrahedron Lett. **51**, 5211 (1967).
13. S. CASTELLANO, R. KOSTELNIK, and C. SUN. Tetrahedron Lett. **46**, 4635 (1967).
14. T. SCHAEFER and S. S. DANYLUK. Can. J. Chem. **47**, 4289 (1969).
14a. C. W. HAIGH and J. M. WILLIAMS. J. Mol. Spectrosc. **32**, 398 (1969).
15. T. SCHAEFER and W. G. SCHNEIDER. J. Chem. Phys. **32**, 1218 (1960).
16. J. M. READ, JR., R. W. CRECELY, R. S. BUTLER, J. E. LOEMKER, and J. H. GOLDSTEIN. Tetrahedron Lett. **10**, 1215 (1968).
17. T. SCHAEFER, G. KOTOWYCZ, H. M. HUTTON, and J. W. S. LEE. Can. J. Chem. **46**, 2531 (1968).
18. J. E. LOEMKER and J. H. GOLDSTEIN. Spectrosc. Lett. **1**, 153 (1968).
19. H. M. HUTTON, B. RICHARDSON, and T. SCHAEFER. Can. J. Chem. **45**, 1795 (1967).
20. J. E. LOEMKER, J. M. READ, JR., and J. H. GOLDSTEIN. Mol. Phys. **13**, 433 (1967).
21. T. F. PAGE. Mol. Phys. **13**, 523 (1967).
22. P. H. H. FISCHER and J. P. COLPA. Z. Naturforsch. **24a**, 1980 (1969).
23. M. IWASAKI, S. NODA, and K. TORIYAMA. Mol. Phys. **18**, 201 (1970).
24. N. K. RAY. Chem. Phys. Lett. **3**, 261 (1969).
25. R. H. ALLENDOERFER and A. H. MAKI. J. Amer. Chem. Soc. **91**, 1088 (1969).
26. W. G. ESPERSEN and R. W. KREILICK. Mol. Phys. **16**, 577 (1969).
27. D. R. EATON, A. D. JOSEY, W. D. PHILLIPS, and R. E. BENSON. Mol. Phys. **5**, 407 (1962).
28. R. A. HOFFMAN and S. GRONOWITZ. Arkiv. Kemi, **16**, 471 (1961).
29. D. J. BLEARS, S. S. DANYLUK, and T. SCHAEFER. Can. J. Chem. **46**, 654 (1968).
30. J. A. POPLE, D. L. BEVERIDGE, and P. A. DOBOSH. J. Amer. Chem. Soc. **90**, 4201 (1968).
31. J. ROARK and W. B. SMITH. J. Phys. Chem. **73**, 1046 (1969).
32. R. R. DEAN and W. MCFARLANE. J. Chem. Soc. B, 509 (1969).
33. J. E. LOEMKER, K. M. PRYSE, J. M. READ, JR., and J. H. GOLDSTEIN. Can. J. Chem. **47**, 209 (1969).
34. R. J. ABRAHAM, D. B. MACDONALD, and E. S. PEPPER. J. Chem. Soc. B, 835 (1967).
35. R. G. JONES, R. C. HIRST, and H. J. BERNSTEIN. Can. J. Chem. **43**, 683 (1965).
36. E. LUSTIG and E. A. HANSEN. J. Chem. Phys. **51**, 1839 (1969).
37. E. LUSTIG and P. DIEHL. J. Chem. Phys. **44**, 2974 (1966).
38. R. R. DEAN and W. MCFARLANE. Mol. Phys. **15**, 321 (1968).
39. K. HAYAMIZU and O. YAMAMOTO. J. Mol. Spectrosc. **25**, 422 (1968).
40. J. A. POPLE and M. S. GORDON. J. Amer. Chem. Soc. **89**, 4253 (1967).
41. R. J. ABRAHAM, D. B. MACDONALD, and E. S. PEPPER. J. Amer. Chem. Soc. **90**, 147 (1968).
42. H. ROTTENDORF and S. STERNHELL. Aust. J. Chem. **17**, 1315 (1964).
43. S. CASTELLANO, C. SUN, and R. KOSTELNIK. J. Chem. Phys. **46**, 327 (1967).

Can. J. Chem. Downloaded from www.nrcresearchpress.com by 210.87.254.42 on 09/05/12
For personal use only.

Can. J. Chem. Downloaded from www.nrcresearchpress.com by 210.87.254.40 on 09/05/12
For personal use only.

Nature of the Coordination Bond in Metal Complexes of Substituted Pyridine Derivatives. VI. Electronic Spectra of Some Complexes of Copper(II)

MISS M. TONG AND D. G. BREWER
Department of Chemistry, University of New Brunswick, Fredericton, New Brunswick

Received July 27, 1970

The electronic spectra of some substituted pyridine complexes of copper(II) have been studied. The effects of bonding on the spectroscopic data are discussed, and compared with the R_π values determined from infrared measurements.

Canadian Journal of Chemistry, 49, 102 (1971)

Introduction

The comments of a referee of an earlier paper from this laboratory (1) have prompted us to investigate the electronic spectra of some substituted pyridine complexes of copper(II). König and Schläfer (2, 3) found in the electronic spectrum of $Cupy_2Br_2$ a high intensity band at 410 mμ, which was assigned to the excitation of the metal "d" electron to the empty π-antibonding orbitals of the pyridine. The energy of the metal-to-ligand charge transfer band changes when the oxidizability of the metal or the reducibility of the ligand is altered (4). Thus, in the copper complexes of pyridine with different substituents in the para position, a variation in the energy of the metal-to-ligand charge transfer band is expected.

In our previous paper, a parameter R_π was introduced to indicate the relative π-contribution to the coordination bond in a series of complexes. This parameter was determined from a comparison of the infrared spectra of the metal complex with that of a protonated species where only σ bonding occurs. The extent of "d" orbital splitting in transition metal complexes is also known to be sensitive to metal–ligand π-bonding (5). The question arises as to whether the ligand field splitting parameters would be as sensitive to the substituent on the pyridine ligands as the R_π parameter, and this investigation attempts to answer that query.

Experiment

The method for the preparation of the copper bromide complexes CuL_2Br_2 (L = pyridine, 4-methylpyridine, 4-carbinylpyridine, 4-acetylpyridine, 4-carbomethoxypyridine, 4-cyanopyridine, and 4-nitropyridine) was similar to that reported elsewhere (1).

4-Nitropyridine was prepared and purified according to the procedure of Ochiai (6).

The infrared absorption spectra were recorded on a Beckman IR 12 filter/grating spectrophotometer, using the KBr disc method.

The visible absorption spectra were recorded on a Hitachi Ratio Recording spectrophotometer, model EPS-3T. Most of the selected complex compounds were almost insoluble in ordinary solvents. The spectra of the solid samples were obtained using Nujol mull (7). At room temperature the copper-to-pyridine charge transfer band near 410 mμ appeared as a shoulder and could not be resolved. For this reason, low temperature studies were carried out, using liquid nitrogen, and the two nicely separated peaks as shown in Fig. 1 were obtained. This low temperature method has been described by Rowley and Drago (8).

The position of the absorption peaks was determined by the computer program written by Pitha and Jones (9).

Results

The electronic spectra of all the copper complex compounds showed two absorption peaks

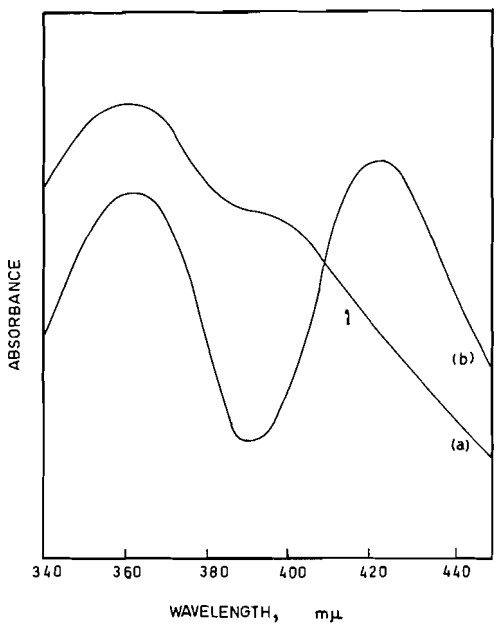

FIG. 1. Electronic absorbance spectra of $Cupy_2Br_2$ in Nujol mull: (*a*) at room temperature; (*b*) at liquid nitrogen temperature.

TABLE 1. Electronic spectral data

Compound	Bromine charge-transfer band (mμ)	Pyridine charge-transfer band (mμ)	d–d Transition (mμ)	R_π	pK_a
$Cu(4\text{-}CH_3py)_2Br_2$	360	407	672 (14 880 cm^{-1})	5.5	6.03*
$Cu(4\text{-}CH_2OHpy)_2Br_2$	361	410	658 (15 200 cm^{-1})	14.5	5.40†
$Cu(py)_2Br_2$	359	416	700 (14 290 cm^{-1})	15.5	5.21*
$Cu(4\text{-}COOCH_3py)_2Br_2$	359	417	691 (14 470 cm^{-1})	32.5	3.49*
$Cu(4\text{-}COCH_3py)_2Br_2$	359	418	690 (14 490 cm^{-1})	36.6	3.50†
$Cu(4\text{-}CNpy)_2Br_2$	360	418	688 (14 530 cm^{-1})	58.6	1.86*
$Cu(4\text{-}NO_2py)_2Br_2$	360	418	683 (14 680 cm^{-1})	60.6	1.39*

*From ref. 10.
†From ref. 1.

between 350 to 420 mμ. For the $Cupy_2Br_2$ complex, the first peak appeared at 359 mμ and remained almost the same for the whole series of complexes with different substituted pyridine ligands, and therefore was assigned as the bromine-to-metal charge transfer band. The second peak, which appeared at 416 mμ and shifted either to lower or higher wavelengths depending upon the substituents, was assigned as the pyridine charge transfer band. This peak was also observed to disappear when pyridine was replaced by ammonia which does not possess any suitable π-acceptor orbitals. A d–d transition band of relatively low intensity appeared in the region between 650 to 700 mμ for all the compounds studied. The ligand field splitting parameter 10 Dq was taken as being equal to the energy of this transition band (3). The electronic spectral data are reported in Table 1, together with the R_π and the pK_a (1, 10) values for each complex compound. R_π values are calculated from the equation: $R_\pi = \nu_{ML} - (1.002\nu_L - 3.60)$ where ν_{ML} and ν_L are the ν_{12} vibration frequencies of the complex and the free ligand, respectively.

Discussion

Dibromobispyridinecopper(II) has been shown to have a distorted octahedral arrangement of ligands around the copper atom, with the pyridine rings *trans* to each other (Fig. 2) (11). The substitution of a functional group in the para position of pyridine should have a very small steric effect. Thus, as a first assumption, we have taken that all the 4-substituted pyridine copper(II) complexes have the same configuration as $Cupy_2Br_2$.

The 10 Dq values shown in Table 1 for the series of CuL_2Br_2 complexes are quite different. It is of interest to consider the origin of such a variation. According to Dunn (12), 10 Dq values

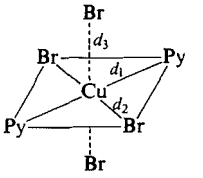

FIG. 2. Structure of $Cupy_2Br_2$: d_1 = 1.99 Å; d_2 = 2.46 Å; d_3 = 3.17 Å.

are influenced by at least four factors: (*i*) purely electrostatic perturbation, (*ii*) the effect of σ-lone pairs belonging to the ligand; that is, the effect of the basic strength of the ligand, (*iii*) the effect of metal-to-ligand π-bonding, and (*iv*) the effect of ligand-to-metal π-bonding. Of all the contributions to 10 Dq, we can neglect (*i*) as we are dealing with the same donor atom. The increase of the basic strength of the ligand would tend to increase the relative magnitude of the σ-bond. On this basis, 4-methylpyridine and 4-carbinylpyridine, which have greater basicity than pyridine, as judged by their pK_a values, will impose a stronger splitting on the copper metal d-orbitals, and should show a higher 10 Dq value than pyridine. This is observed experimentally. However, the 10 Dq value of the 4-carbinylpyridine complex is higher than that of the 4-methylpyridine. This is not expected, since the pK_a value of the latter is higher. It is doubtful, in this case, that the larger 10 Dq value can be attributed to the σ-bonding alone. We suspect that the structure of the complex may also play an important role. Recently, Graddon *et al.* proposed a polymeric octahedral structure for the cobalt(II) complex of 4-carbinylpyridine with the oxygen atom in the carbinyl group taking part in the coordination (13). Whether the same situation occurs in the copper 4-carbinylpyridine bromide complex needs further investigation.

For the compounds containing an electron-

Can. J. Chem. Downloaded from www.nrcresearchpress.com by 210.87.254.40 on 09/05/12
For personal use only.

donating substituent, the effect of π-bonding on the 10 Dq value is expected to be relatively small (1), and any observed variation in 10 Dq can be attributed largely to σ-bonding changes (*i.e.*, basicity) of the ligand. On the other hand, with electron-withdrawing substituents, the π-bonding is expected to be greatly increased at the expense of the σ-bonding, via a synergic mechanism (14). Hence, 10 Dq should be greatly influenced by π-bonding in these particular complexes, *viz.*

$$4\text{-}NO_2py > 4\text{-}CNpy > 4\text{-}COCH_3py > 4\text{-}COOCH_3py > py.$$

Unlike the bromine charge-transfer band, which is not sensitive to the substituents in the pyridine ring, the metal-to-ligand pyridine charge transfer band of the whole series of complex compounds can be divided into two groups. For complexes with electron-donating substituents such as $4\text{-}CH_3py$ and $4\text{-}CH_2OHpy$, which inhibit π-back donation, an increase in the energy of the metal-to-ligand charge transfer band occurred. For complexes with electron-withdrawing substituents, such as $4\text{-}NO_2py$, 4-CNpy, $4\text{-}COCH_3py$, and $4\text{-}COOCH_3py$, which should enhance the π-back donation, no significant change in the energy of the metal-to-ligand charge transfer band can be observed. Hence, one can conclude from the electronic spectral data that there is no π-bonding at all, or that the charge transfer process is insensitive to π-bonding.

If R_π is taken to represent the extent of π-bonding, there is clearly an increase in such bonding from $—CH_3$ to $—NO_2$ as expected. It can be concluded that R_π is a much more sensitive parameter than the others examined.

We are indebted to the National Research Council of Canada for the necessary funds for this investigation.

1. P. T. T. Wong and D. G. Brewer. Can. J. Chem. **46**, 131 (1968).
2. E. König and H. L. Schläfer. Zeit für Phys. Chim. Neue Folge, **26**, 371 (1960).
3. H. L. Schläfer and E. König. Zeit für Phys. Chim. Neue Folge, **30**, 145 (1961).
4. A. B. P. Lever. Inorganic Electronic Spectroscopy. Elsevier Publishing Company, New York. 1968.
5. S. M. Nelson and T. M. Shepherd. Inorg. Chem. **4**, 813 (1965).
6. E. Ochiai. J. Org. Chem. **18**, 534 (1953).
7. J. R. Wasson. Chem. Anal. **56**, 36 (1967).
8. D. A. Rowley and R. S. Drago. Inorg. Chem. **6**, 1092 (1967).
9. J. Pitha and R. N. Jones. Bulletin No. 12. National Research Council of Canada, Ottawa, Canada. 1968.
10. A. Fischer, W. J. Galloway, and J. Vaughan. J. Chem. Soc. 3591 (1964).
11. V. Kupcik and S. Durovic. Czech. J. Phys. **10**, 182 (1960).
12. T. M. Dunn. *In* Modern Coordination Chemistry. *Edited by* J. Lewis and R. G. Wilkins. Interscience Publishers, New York. 1960.
13. D. P. Graddon, K. B. Heng, and E. C. Watton. Aust. J. Chem. **21**, 121 (1968).
14. L. E. Orgel. An Introduction to Transition-Metal Chemistry. John Wiley and Sons, Inc., New York. 1962.

Can. J. Chem. Downloaded from www.nrcresearchpress.com by 210.87.254.40 on 09/05/12
For personal use only.

Can. J. Chem. Downloaded from www.nrcresearchpress.com by 210.87.254.42 on 09/05/12
For personal use only.

Pyrazolines XI.
Determination of the Stereochemical Changes at Carbons-3 and -5 of 1-Pyrazolines on Their Thermal Conversion to Cyclopropanes[1]

D. E. McGreer and J. W. McKinley
Department of Chemistry, The University of British Columbia, Vancouver, British Columbia

Received June 22, 1970

Six 3,3,4,5-tetrasubstituted pyrazolines have been prepared and the product distribution from their pyrolysis reactions have been determined. This has permitted for the first time the unambiguous evaluation of the stereochemical fate of C-3 and -5 of the pyrazolines on conversion to cyclopropanes. A stereoselectivity is noted for these systems which can be related to the structure of the initial pyrazoline. This suggests that the transition state for reaction retains many of the stereochemical factors present in the pyrazoline. Such a condition would be the case for concerted breaking of the two C—N bonds with a developing overlap of the new bonds being formed at the transition state. That this reaction is not restricted by symmetry constraints suggests that the three carbon fragment can act as a symmetric or antisymmetric unit and that these are not separated by more than a few kcal of energy.

Canadian Journal of Chemistry, 49, 105 (1971)

The pyrolysis of pyrazolines leads, by loss of nitrogen, to cyclopropane and olefin products. Van Auken and Rinehart (1) were the first to make a serious attempt to determine a relationship between the stereochemistry in the cyclopropane formed and the pyrazoline used. Since then extensive studies have been made providing varying amounts of information concerning the stereochemical outcome at carbons originally at C-3 or -5 in the pyrazoline. For the present paper we wish to identify the stereochemical fate of C-3 and -5 by the symbols *n* (no information), *r* (retention), or *i* (inversion) and thus *ir* will mean inversion at C-3 and retention at C-5. Results in the literature can be cataloged into three classes.

Class I, with selected examples in Table 1, provides relative stereochemical change at C-3 and -5 of a pyrazoline. This situation is found for systems that have a stereochemical label at C-3 and -5, but nowhere else, as in eq. 1.[2]

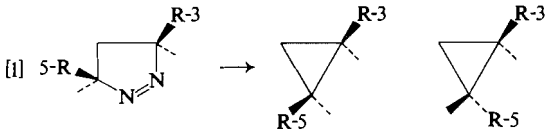

Class II, with selected examples listed in Table 2, provides precise information at one of C-3 or -5 with reference to some other part of the molecule. An example is illustrated in eq. 2.

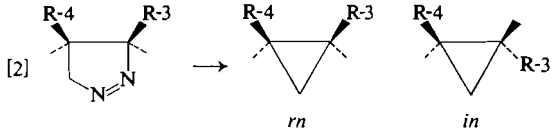

Class III, with selected examples listed in Table 3, provides precise information at both C-3 and -5 and is illustrated by eqs. 3 and 4.

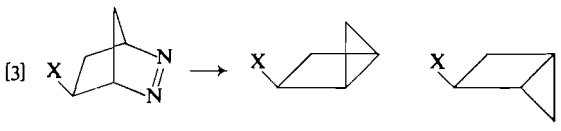

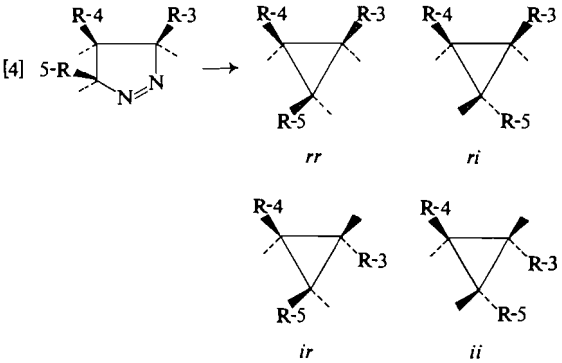

[1]Taken in part from the M.Sc. Thesis of J. W. McKinley (24). Presented in part at the ACS-CIC conference in Toronto, May 1970.

[2]For illustration we have drawn one enantiomer of a racemic pair and have used the *cis* stereoisomer for convenience only. The projection in the Tables corresponds to a view from outside the ring along a line through C-4 and bisecting the N=N group.

TABLE 1. Stereochemistry in cyclopropane products from pyrolysis of 1-pyrazolines in class I

Pyrazoline	Thermal (Δ) photolysis (*hν*)	Products % *cis-*	Products % *trans-*	Products % Other	Reference
C-3 C-4 C-5					
p-anisyl H *p*-anisyl H H H	Δ	43 *rr* or *ii*	57 *ri*	—	2
H H *p*-anisyl *p*-anisyl H H	Δ	7 *ri*	93 *rr* or *ii*	—	2
CH_3 H CH_3 H H H	Δ *hν*	33 *rr* or *ii* 48 *rr* or *ii*	66 *ri* 41 *ri*	1 11	3 4
H H CH_3 CH_3 H H	Δ *hν*	73 *ri* 60 *ri*	25 *rr* or *ii* 26 *rr* or *ii*	2 14	3 4
CH_3O_2C H H CH_3 H CH_3	Δ *hν*	25* *rr* or *ii* 61 *rr* or *ii*	56† *ri* or *ir* 23 *ri* or *ir*	19 16	5 5
CH_3O_2C H CH_3 H H H	Δ *hν*	66* *ri* or *ir* 22 *ri* or *ir*	18† *rr* or *ii* 65 *rr* or *ii*	16 13	5 5

*Methyls *cis*.
†Methyls *trans*.

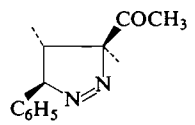

1

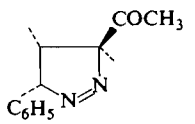

2

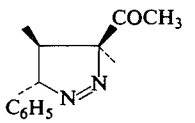

3

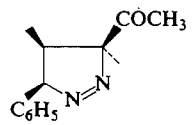

4

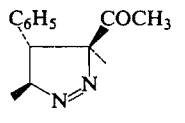

5

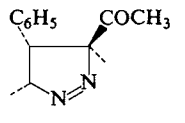

6

The literature to date lacks examples of eq. 4. In the present paper we report on the preparation of six new pyrazolines in this class and report on product analyses from the pyrolysis reaction.

Preparation and Identification of Stereochemistry

Three sets of C-5 epimeric pyrazolines were prepared by (*a*) addition of phenyldiazomethane to 3-methyl-3-pentene-2-one, (*E*)-, (*b*) addition of phenyldiazomethane to 3-methyl-3-pentene-2-one, (*Z*)-, and (*c*) addition of diazoethane to 3-methyl-4-phenyl-3-butene-2-one, (*E*)-.

The pyrazolines prepared according to (*a*)–(*c*) were expected to be **1** and **2**, **3** and **4**, and **5** and **6** respectively since it is known that the addition of diazoalkanes does not affect the stereochemistry of the α and β positions of the unsaturated ketone (1).

Can. J. Chem. Downloaded from www.nrcresearchpress.com by 210.87.254.42 on 09/05/12
For personal use only.

TABLE 2. Stereochemistry in cyclopropane products from pyrolysis of 1-pyrazolines in class II

Pyrazoline	Thermal (Δ) photolysis (*hν*)	Products % *cis*-Δ	Products % *trans*-Δ	Products % Other	Reference
C-3 C-4 C-5					
CH_3 D H	Δ	43 *rn*	43 *in*	4	5
H H H					
CH_3 H H	Δ	42 *in*	42 *rn*	6	5
H D H					
CH_3 CH_3 H	Δ	44 *rn*	35 *in*	21	6
H H H	*hν*	43 *rn*	38 *in*	19	4
CH_3 H H	Δ	46 *in*	22 *rn*	32	6
H CH_3 H	*hν*	25 *in*	41 *rn*	34	4
CH_3O_2C H H	Δ	18* *rn*	12† *in*	70	1
CH_3 CH_3 H	*hν*	80 *rn*	— *in*	20	1
CH_3O_2C CH_3 H	Δ	28* *in*	35† *rn*	27	1
CH_3 H H	*hν*	— *in*	72 *rn*	28	1
CH_3O_2C H H	Δ	31* *rn*	9† *in*	60	7
CH_3 Et H	*hν*	84 *rn*	—	16	7
CH_3O_2C Et H	Δ	11* *in*	72† *rn*	17	7
CH_3 H H	*hν*	— *in*	94 *rn*	6	7

*Alkyl groups *cis*.
†Alkyl groups *trans*.

The pyrazoline assigned structure **5** crystallized from a mixture of **5** and **6** in an ether – petroleum ether solution and was obtained pure. None of the other pyrazolines could be prepared pure. Compounds **3** and **4** were solids and on one occasion could be separated after a crystallization which yielded two crystal sizes, thus the isomers were obtained 95 and 75%[3] pure respectively. Pyrazolines **1**, **2**, and **6** were never crystallized and are assumed to be liquids. In acetone, **1** pyrolyzed at room temperature considerably faster than **2** permitting the isolation of a sample of **2** of 95% purity. Column chromatography on silica gel using ether – petroleum ether (5:95) permitted partial separation of the pyrazolines and in this way **1**, **2**, and **3** were enriched to 85, 62, and 72% purity, respectively.

The identification of pyrazolines **1** to **6** is based on their n.m.r. spectra presented in Table 4, the relative rates of pyrolysis of C-5 epimeric pairs and the proportion of olefin to cyclopropane derivatives in the pyrolysis product.

For a discussion on the use of n.m.r. in this structural determination it is necessary to recognize that pyrazolines adopt a non-planar conformation (**5**) with the plane of the three carbon atoms at an angle (θ) to the plane of C-3, -5, and

[3]Purity in percent refers to the proportion of the two isomers as estimated by n.m.r.

Can. J. Chem. Downloaded from www.nrcresearchpress.com by 210.87.254.42 on 09/05/12
For personal use only.

TABLE 3. Stereochemistry in cyclopropane products from pyrolysis of 1-pyrazolines in class III

Pyrazoline	Products		Reference
	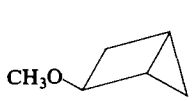	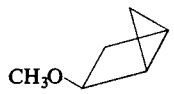	
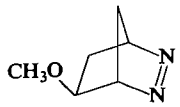	37 *ii*	63 *rr*	9
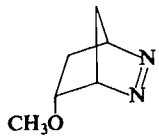	6 *rr*	94 *ii*	9
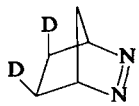	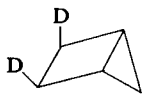	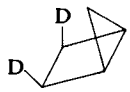	10
	75 *ii*	25 *rr*	

the two nitrogens. 1-Pyrazoline has a potential minimum at 19.7° (11) and pyrazolines held in one conformation have dihedral angles (θ) of 22–31° (3, 5, 8). Thus depending on the substitution pattern we can have principally one conformer or an equilibrium between two conformers which are not necessarily of equal thermodynamic stability. Earlier studies have indicated a preference by bulky groups to adopt the pseudo equatorial positions (5, 12). This factor is strongest for a 3,5-*cis*-disubstituted pyrazoline.

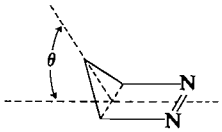

5

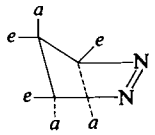

6

Pyrazolines **1**, **3**, and **5** can have three groups pseudo equatorial and are expected to be predominantly in this form. They will, in this form, have the C-4 and -5 hydrogens in a *trans* orientation with a dihedral angle close to 180°, leading to large coupling constants (with a potential maximum of about 11 Hz (7)). Were there an appreciable amount of the other conformer the coupling constant would be reduced to a value of 7–8 Hz corresponding to that for systems with equal conformer populations. Thus coupling constants of 10.4, 9.8, and 8.4 Hz for **1**, **3**, and **5** imply that each of these compounds is predominantly in the conformation shown in Table 4, with the magnitude of θ being greatest for **1** and least for **5**. The coupling of 8.4 Hz for **5** implies either the presence of some of the other conformer or a smaller value of θ.

The presence of two methyls on C-4 in 4,4-dimethyl-1-pyrazoline considerably reduces its rate of pyrolysis (3) by interfering with the loss of nitrogen through a stretching mode perpendicular to the plane of C-3, -4, and -5. In a similar way for pyrazolines locked in one conformation the presence of a pseudo axial group at C-4 would reduce the rate of pyrolysis. Thus the fact that **1** pyrolyzes nine times faster than **2** supports the structural assignment to these compounds. Similarly **3** pyrolyzes more than five times faster than **4**.

Pyrazolines **2**, **4**, and **6** can have only two groups pseudo equatorial and are expected to prefer the conformation with C-3 and -5 having equatorial substituents. There should, however, be more flexibility in these systems. These compounds all have a *cis* orientation between the C-4 and -5 hydrogens. The increased flexibility and the *cis*-orientation are in line with coupling

Can. J. Chem. Downloaded from www.nrcresearchpress.com by 210.87.254.42 on 09/05/12
For personal use only.

TABLE 4. The n.m.r. data for pyrazolines **1** to **6** shown in the conformation expected to be preferred. Signals from pseudo axial groups are underlined

Pyrazoline	$COCH_3$	C-3Me	H-4	H-5	C-4 or C-5Me	$J_{H\text{-}4,H\text{-}5}$
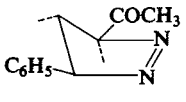 **1**	7.58	8.82	8.08	5.32	8.97	10.4
		$\Delta = 1.24$				
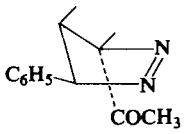 **2**	7.76	8.52	7.29	4.63	9.65	8.5
		$\Delta = 0.76$				
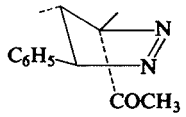 **3**	7.96	8.31	8.4	5.10	9.03	9.8
		$\Delta = 0.53$				
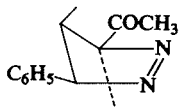 **4**	7.58	8.68	7.7	4.69	9.82	7.5
		$\Delta = 1.10$				
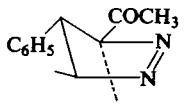 **5**	7.52	8.93	6.78	5.18	8.48	8.4
		$\Delta = 1.41$				
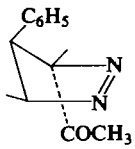 **6**	7.75	8.50	6.27	5.91	8.56	7.0
		$\Delta = 0.75$				

constants of 7–8 Hz and thus coupling constants provide a lead to the assignments of structure.

In addition, however, the above arguments on conformation can be applied to chemical shifts which are principally affected by the anisotropy of the N=N double bond. Groups in the pseudo axial position are placed in the shielding cone of the N=N group and are shifted to higher field. Such groups are emphasized in Table 4 by underlining the observed chemical shift positions and a comparison of values between C-5 epimers is consistent with the structural assignments. The spread in the values of the chemical shifts of the C-5 hydrogen for C-5 epimers can be related to conformer populations. A large angle θ would be expected to increase the shielding of this hydrogen by the azo group as in **1** and **3**. Increased flexibility leading to a mixture of conformers would de-

Can. J. Chem. Downloaded from www.nrcresearchpress.com by 210.87.254.42 on 09/05/12
For personal use only.

Can. J. Chem. Downloaded from www.nrcresearchpress.com by 210.87.254.42 on 09/05/12
For personal use only.

crease this shielding. For comparison we can consider the 4.80 τ position of the C-5 hydrogen in *cis* 3,5-bis(*p*-anisyl)-1-pyrazoline which is rigid with a large θ and the 4.25 τ value for the *trans* isomer which is an equilibrating system with two equally populated conformations. The epimers **5** and **6** do not lend themselves to this treatment as they have the additional factor of a phenyl group on C-4 which in one case is *cis* to the hydrogen at C-5 and the other case is *trans*.

We have estimated the relative magnitude of θ for **1**, **3**, and **5** from coupling constants of the ring hydrogens. An alternative approach using chemical shifts results if we compare chemical shift position of the C-3 methyl to that of the acetyl methyl. The differences (Δ) are recorded in Table 4. We again anticipate that the value for the axial group will be raised by shielding from the azo group and thus a large value for Δ implies that the C-3 methyl is axial and a small Δ implies the C-3 methyl is equatorial, since the C-3 methyl is always to higher field than the acetyl methyl. For comparison the conformationally labile 3-methyl-3-acetyl-1-pyrazoline has a Δ value of 0.84 and *cis* and *trans*-3,5-dimethyl-3-acetyl-1-pyrazoline have Δ values of 0.62 and 0.98. These latter two compounds provide reference points for evaluating the locking of individual conformations. Values of Δ greater than 0.98 imply an axial C-3 methyl and for these compounds the larger value of Δ correlates with larger values of θ. Values of less than 0.62 imply an equatorial C-3 methyl and in these cases the smaller the value of Δ the greater the value of θ. Thus **1** is strongly locked, **3** and **4** are less so, and **2** is likely flexible. It is difficult to evaluate clearly the situation for **5** and **6** due to the presence of the phenyl at C-4 which appears to be shielding the *cis* methyl, however, other evidence (coupling constants, product results, etc.) indicates **5** has a larger value of θ than does **6**.

Olefins from 1-pyrazolines in this series are known to be formed by migration of hydrogen from the pseudo equatorial position at C-4 by a concerted *trans* migration with loss of nitrogen (8). Olefin formation is strongly favored by a phenyl at C-4 and moderately favored by a methyl at C-4. The absence of olefin product from **1**, **3**, and **5** is in accord with a structure favoring a conformation having a methyl or phenyl in the pseudo equatorial position. That **6** on the other hand gives 67% olefin product provides the best evidence for the structural assignment to **5** and **6**.

Pyrolysis Results

Cyclopropanes

There are four cyclopropane products possible from pyrolysis of pyrazolines **1** to **6**. These are listed in Table 5 with the n.m.r. data obtained for the three isolated cyclopropanes. Two of these cyclopropanes do not give the ring opening reaction at temperatures above 250° expected for compounds having a methyl *cis* to an acetyl group (13). The vicinal ring hydrogen coupling constants in this pair are 7.0 and 9.8 Hz identifying them to be **8** and **9** respectively based on the observations of Patel *et al.* (14) that *cis* couplings (8.0–11.2 Hz) are larger than *trans* couplings (5.2–7.0 Hz) for vicinal ring hydrogens.

The coupling constant for the vicinal ring hydrogens of the third isolated cyclopropane was 6.4 Hz, clearly that of a *trans* orientation. Since this compound at 227° readily ring opens it is identified to be **7** and the ring opened products would be **11** and **12**, eq. 5.

[5] 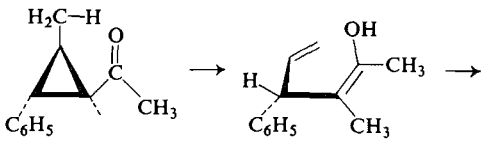

7

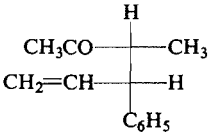

11

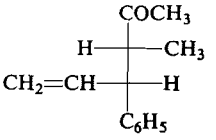

12

The effect of phenyl on a vicinal methyl or acetyl group is one of shielding as seen by the chemical shift positions of the C-1 methyl and acetyl groups. Thus the C-1 methyl of **7** and **9** is to higher field than that of **8** and the C-1 acetyl of **8** is to higher field than that of **7** and **9**. That the phenyl gives a shielding effect is undoubtedly due to the crowding in the molecules which would force the plane of the phenyl group towards a dihedral angle of 90° with the plane of the cyclopropane ring.

There was no evidence for the presence of compound **10** in any of the pyrolysis fractions. Since its presence would be detected by a shift of a chromatographic peak after heating the sample,

TABLE 5. The n.m.r. data in τ units for the 1,1,2,3-tetrasubstituted cyclopropanes

Cyclopropane	C-1 $COCH_3$	C-1 CH_3	C-2 H	C-3 H	C-3 CH_3
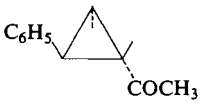 **7**	7.81(s)	8.92(s)	7.15(d) 6.4 Hz	8.6(m)	8.88(d) 6.4 Hz
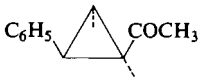 **8**	8.20(s)	8.51(s)	7.99(d) 7.0 Hz	7.66(m)	8.76(d) 6.2 Hz
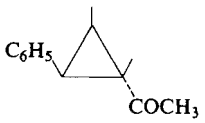 **9**	7.79(s)	8.88(s)	7.19(d) 9.8 Hz	8.2(m)	8.95(d) 6.4 Hz
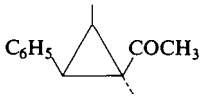 **10**	—	—	—	—	—

due to conversion to a γ,δ-unsaturated ketone, we feel the presence of **10** is in no case greater than 2%.

Olefins

Except for the pyrolysis of **6** olefins are minor products from these pyrazolines. There are four α,β-unsaturated ketones anticipated, two from **1** to **4** and two from **5** to **6**. These four were prepared as *cis,trans* pairs by Wittig procedures. Thus 3-methyl-4-phenyl-3-hexene-2-one (**13**), (*E*)- and (*Z*)- were prepared as a mixture with a β,γ-isomer (50%) by eq. 6. No decision was made on the stereochemistry of these olefins for although the acetyl group might have been expected to give preferential deshielding to the *cis* alkyl group this is not always the case. In **14**, (*E*)- and (*Z*)- (eq. 7) and also in 3-methyl-3-pentene-2-one (14) the shift is in the wrong direction or too small to be observed.

3-Methyl-4-phenyl-3-hexene-2-one (**14**), (*E*)- and (*Z*)-, were prepared by eq. 7. The higher chemical shift for the acetyl resonance at 8.51 (shielding by the *cis* phenyl) in the major product, compared to 7.95 in the minor product, was used to make a tentative structural assignment of the

[6] 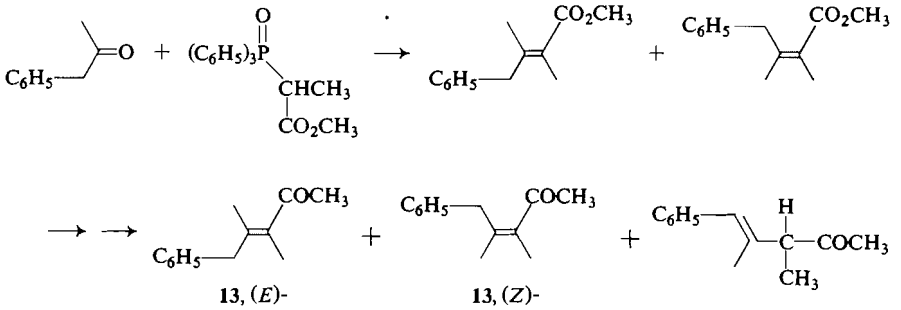

13, (*E*)- **13**, (*Z*)-

Can. J. Chem. Downloaded from www.nrcresearchpress.com by 210.87.254.42 on 09/05/12
For personal use only.

TABLE 6. Product distributions from pyrazolines **1** to **6**

Pyrazoline	Products (%) 7	8	9	10	Other
1	1 *ir*	98 *rr*	— *ri*	— *ii*	1(**13**)
2	12 *ii*	22 *ri*	41 *rr*	— *ir*	25(**13**)
3	91 *rr*	6 *ir*	3 *ii*	— *ri*	—
4	26 *ri*	22 *ii*	45 *ir*	— *rr*	7(**13**)
5	79 *rr*	— *ir*	20 *ri*	— *ii*	—
6	21 *ri*	5 *ii*	6 *rr*	— *ir*	28 **14** *E*- 2 **14** *Z*- 37 **15**

[7]

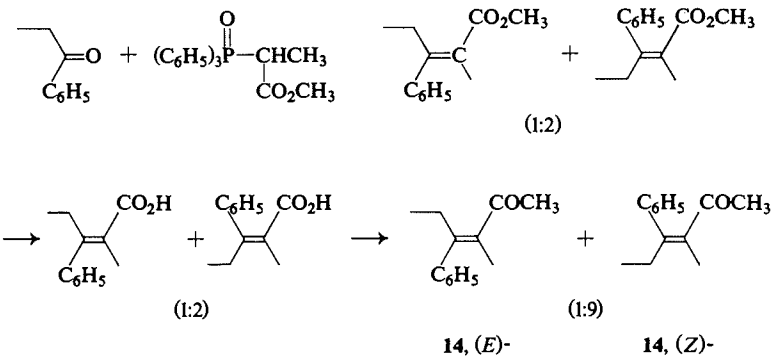

Z configuration to the major product. Similarly the α-methyl of the *E* isomer appears to higher field (8.34 τ) than does that of the *Z* isomer (8.10 τ).

The only β,γ-unsaturated compound detected as a pyrolysis product was 3-methyl-4-phenyl-4-hexene-2-one (**15**) which was isolated admixed with **14** and some other minor components in the pyrolysis of **6**. The presence of **15** was indicated by its n.m.r. spectrum, however, it was not isolated pure and its stereochemistry was not determined.

Table 6 gives the estimated product compositions from pyrazolines **1** to **6** on the basis of product analysis from samples of the following degrees of purity: **1** (85%), **2** (90%), **3** (95%), **4** (75%), **5** (100%), and **6** (72%). The stereochemical results for the cyclopropane products are given in Table 6. The absence of dihydrofurans is noteworthy in view of their formation from other 3-acetyl-1-pyrazolines (12). Their absence is not due to their instability as we have made them by other means. Formation of the olefin **14** (*E*)- as the major α,β-unsaturated olefin from **6** would be consistent with our structural assignment to **6** on the basis of earlier stereochemical studies of the olefin-forming reaction which indicate a concerted migration of hydrogen transoidal to the loss of nitrogen (5, 8).

Discussion

It is clear from the results in Table 6 and earlier results that the conversion of 1-pyrazolines to cyclopropanes is stereoselective. This stereoselectivity can give product with retention at C-3 and -5, retention at one of C-3 or -5 and/or, inversion of C-3 and -5. The stereochemistry in the product lacks the randomness expected for a process proceeding by successive steps in which rotation around single bonds in the intermediate might give mixed stereochemistry in the product. Inversion at one or both of C-3 and -5 has been observed and thus an initial cleavage of the C-3 to N bond followed by S_N2 displacement of nitrogen from C-5 is not indicated.

Stereoselectivity implies concertedness for this reaction and therefore symmetry should play an important role. Bergman and Carter (15) have pointed out that if one assumes little or no interaction by the bonds on C-4 with the breaking bonds then the pyrolysis reaction can be thought of as the reverse of a 2 + 2 cycloaddition of N_2 to a cyclopropane C—C bond. This approach requires a highly strained transition state for

Can. J. Chem. Downloaded from www.nrcresearchpress.com by 210.87.254.42 on 09/05/12
For personal use only.

Can. J. Chem. Downloaded from www.nrcresearchpress.com by 210.87.254.42 on 09/05/12
For personal use only.

formation of product in which the stereochemical change can be *ri* or *ir*.

Presumably product with retained or inverted stereochemistry at both centers would require antarafacial bond formation in the formation of the N_2 unit. In at least one case where *trans* expulsion of nitrogen is called for by symmetry considerations the system has found an alternative path (16) such that the thermal and photochemical processes gave the same stereochemical result.

The tendency for the photochemical process to give the opposite stereochemistry from that of the thermal reaction can be used as a means of detecting symmetry control in a reaction. Existing data on the photochemistry of pyrazolines is given in Tables 1 and 2. Reversal of the stereochemistry is noted for *cis* and *trans*-3,5-dimethyl-3-carbomethoxy-1-pyrazoline. However, in general the data is best summarized by a tendency for the photochemical product to more closely retain the stereochemistry of the starting pyrazoline than does the thermal product. This is in line with the early observations of Van Auken and Rinehart (1).

Good evidence for a trimethylene intermediate has been found for the pyrolysis of alkyl substituted pyrazolines. Calculations of the energy of such a unit for differing central angles show that at small angles the symmetric molecular orbital picture is more stable than the antisymmetric while at greater angles than 100° the antisymmetric form is more stable (17). This calculation makes use of mixing with the C—H orbitals on the middle carbon. That these two symmetry states can be close in energy has been used to explain the stereochemical outcome from *cis* and *trans*-3,5-dimethylpyrazoline (3) and *cis* and *trans*-2,4-dimethylthietanonium salts (18) where both conrotation and disrotation from the trimethylene intermediate are observed.

We wish to propose that a similar interaction between the breaking C—N bonds and the bonds to C-4 can take place before loss of the nitrogen and that steric and substituent factors can force the three carbon unit to act as either a symmetric or antisymmetric component. Thus a variety of stereochemical results are possible in competition with each other. We prefer this proposition to others available since the cyclopropanes are normally formed in competition with olefins which are formed by a concerted symmetry allowed process (5, 8), suggesting therefore that all of the products are formed by symmetry allowed sequences.

Experimental

General

Melting points and boiling points are uncorrected. The i.r. spectra were recorded on a Perkin–Elmer model 137 spectrophotometer. All spectra were measured as liquid films using sodium chloride plates. The 60 MHz magnetic resonance spectra were recorded on either a Varian Associates Model A-60 spectrometer or a Jeolco Model C-60 spectrometer. The 100 MHz n.m.r. spectra were recorded on a Varian Associates Model HR-100 spectrometer. The spectra were run as solutions either in carbon tetrachloride or deuteriochloroform (Merck, Sharp and Dohme) with tetramethylsilane as the internal reference. The v.p.c. units used were an Aerograph Model A-90-P and an Aerograph Model A-90-P3. All columns used were 10′ × 1/4″ unless otherwise indicated. Petroleum ether refers to the fraction boiling between 30–60°.

3-Methyl-3-pentene-2-one, (Z)-

Irradiation of 12 g (0.12 mole) of 3-methyl-3-pentene-2-one, (*E*)- (Aldrich) in 100 ml of ether for 16 h in a silica tube using a Hanovia 450 W lamp (2537 Å) resulted in approximately 25% conversion to the desired *Z* isomer as determined by v.p.c. (didecyl phthalate, 138°, 120 ml per min). The retention times for the *Z* and *E* isomers were 8.6 and 11.0 min, respectively (lit. (12): b.p. 124 and 147°, respectively). The ether was removed and a simple distillation gave a fraction distilling between 131–136° which consisted of a 50:50 mixture of the *Z* and *E* isomers. A further distillation using a Nester and Faust stainless steel spinning-band apparatus gave a fraction distilling from 124–130° which consisted of a 90:10 ratio of the *Z* and *E* isomers, respectively. Final purification by v.p.c. gave 1.8 g (0.18 mole) of greater than 95% purity.

3-Methyl-4-phenyl-3-buten-2-one

The title compound was prepared by the acid condensation of benzaldehyde and methyl ethyl ketone to give a product which melted at 37–40° (lit. (19), m.p. 38–40°).

Addition of Phenyl Diazomethane to 3-Methyl-3-pentene-2-one, (E)-

To an ether solution of 9.8 g (0.1 mole) of 3-methyl-3-pentene-2-one, (*E*)- was added phenyl diazomethane, prepared in 70 ml of petroleum ether from 12 g (0.1 mole) of benzaldehyde hydrazone and 21.6 g (0.1 mole) of yellow mercuric oxide in the presence of 1 ml of saturated potassium hydroxide in ethanol. The solution was left at −5° for 10 days. Pyrazoline formation was followed by use of n.m.r. The ratio of the two pyrazolines **1** and **2** was estimated in the crude reaction mixture as 2:1 respectively. The pyrazolines were stored as a solution in ether – petroleum ether at −5°.

Column chromatography (silica gel, ether – petroleum ether, 5:95 increasing to 10:90) of the crude reaction mixture gave two main fractions, the second of which yielded the pyrazoline mixture of **1** and **2** as a clear

Can. J. Chem. Downloaded from www.nrcresearchpress.com by 210.87.254.42 on 09/05/12
For personal use only.

colorless liquid. Further fractionation gave **1** of 85% purity and **2** of 62% purity. Pyrazoline **2** had the larger R_f value. Partial pyrolysis of 6 g of **1** and **2** in refluxing acetone after 12 h yielded 0.6 g of unreacted **2** of 95% purity.

Anal. Calcd. for $C_{13}H_{16}ON_2$ (as a mixture of **1** and **2**): C, 72.19; H, 7.46; N, 12.95. Found: C, 72.29; H, 7.36; N, 13.11.

The n.m.r. peaks for **1** and **2** in addition to the aromatic resonances at 2.7 τ, are listed in Table 4 and are the basis of their identification.

Addition of Phenyl Diazomethane to 3-Methyl-3-pentene-2-one, (Z)-

To an ether solution of 1.8 g (0.18 mole) of 3-methyl-3-pentene-2-one, (*Z*)- was added phenyl diazomethane (from 3.2 g (0.27 mole) of benzaldehyde hydrazone). The solution was left at −5° for 2 weeks. Pyrazoline formation was followed by n.m.r. The ratio of the two pyrazolines **3** and **4** was estimated in the crude reaction mixture as 2:1 respectively. The pyrazolines **3** and **4** were stored as a solution in ether – petroleum ether at −5°.

Column chromatography (silica gel, ether – petroleum ether, 5:95 increasing to 10:90) of the crude reaction mixture gave two main fractions, the second of which yielded the pyrazoline mixture of **3** and **4** as a white solid. Further fractionation gave **3** of 80% purity and **4** of 50% purity. Pyrazoline **4** had the larger R_f value. On one occasion the pyrazoline mixture being crystallized from ether – petroleum ether (10:90) at −5° yielded two crystal sizes. Separation of these gave **3** of 95% purity and **4** of 75% purity.

Anal. Calcd. for $C_{13}H_{16}ON_2$ (as a mixture of **3** and **4**): C, 72.19; H, 7.46; N, 12.95. Found: C, 72.40; H, 7.40; N, 12.70.

The n.m.r. peaks for **3** and **4**, in addition to the aromatic resonances at 2.7 τ, are listed in Table 4 and are the basis of their identification.

Addition of Diazoethane to 3-Methyl-4-phenyl-3-butene-2-one, (E)-

To an ether solution of 11.2 g (0.07 mole) of 3-methyl-4-phenyl-3-butene-2-one, (*E*)-, was added diazoethane (from 23.4 g (0.20 mole) of *N*-nitroso-*N*-ethyl urea). The solution was left for 1 week at −5° and became clear and colorless. Pyrazoline formation was followed by use of n.m.r. The ratio of the two pyrazolines **5** and **6** was estimated in the crude reaction mixture as 9:1 respectively. The first treatment with diazoethane resulted in about 35% conversion to pyrazoline products. Two more treatments with equal amounts of diazoethane with a one week interval between the second and third treatment were made. The pyrazolines **5** and **6** were stored as a solution in ether – petroleum ether at −5°.

Two weeks after the third treatment the solvent was removed with a rotatory evaporator. The crude reaction product was triturated with petroleum ether to give white crystals. Recrystallization from petroleum ether – ether (95:5) yielded the pure pyrazoline **5** as a white solid: m.p. 65–68°, dec. 107°.

Anal. Calcd. for $C_{13}H_{16}ON_2$: C, 72.19; H, 7.46; N, 12.95. Found: C, 71.96; H, 7.61; N, 12.95.

The n.m.r. peaks for pyrazoline **5**, in addition to the aromatic resonances at 2.8 τ, are listed in Table 4 and are the basis of its identification. The mother liquor from the above recrystallization was shown by n.m.r. to be approximately a 50:50 mixture of the two pyrazolines. The solvent was removed from the mother liquor and then diluted with 10 ml of petroleum ether – ether (95:5) and seeded with pure crystals of the pyrazoline **5**. The solution was left for 1 week at −5°, after which time it was observed that not only additional crystals of **5** were present but also a liquid, presumably the pyrazoline **6**. After the removal of the solid white crystals, the mother liquor was then fractionated by column chromatography (silica gel, petroleum ether – ether, 95:5 increasing to 90:10). Three fractions were used for the product distribution study. The ratio of the two pyrazolines **5** to **6** in the three fractions, as determined by the integration of the two acetyl peaks, was 28:72, 32:68, and 36:64 respectively. By considering successive fractions, it was found that the pyrazoline **6** had the larger R_f value.

Pyrolysis of Pyrazolines 1 and 2 and Product Identification

The following components were identified from the pyrolysis of **1** and **2** either as a neat sample at 100–120° or as a neat sample pyrolyzed in the injector of the v.p.c. The v.p.c. (FFAP, 218°, 120 ml per min) showed 6 peaks with retention times 8.6 (trace), 12.2, 13.6, 16.4, 17.6 (trace), and 20.0 min respectively. The product distribution calculated for each pyrazoline from data in Table 7 is given in Table 6.

The 12.2 min component was isolated and identified to be a mixture of **7**, **11**, and **12** by n.m.r. (CCl_4) peaks at 8.93, 8.86 (d), 7.82, and 7.16 (d) for **7** (66%) and at 9.18 (d), 8.26, and 7.96 for the γ,δ-isomers **11** and **12** (34% total).

The 13.6 min component was isolated and identified as the cyclopropane **8**. The structural assignment was based on the n.m.r. ($CDCl_3$) given in Table 5 plus aromatic hydrogens at 2.8 τ, and i.r. band at 1695 cm^{-1} (carbonyl) with no evidence of a C=C band and by the fact that this compound is stable to thermal rearrangement at 250°.

Anal. Calcd. for $C_{13}H_{16}O$: C, 82.93; H, 8.57. Found: C, 83.06; H, 8.55.

The 16.4 and 17.6 min components could be enriched to about 15% of a fraction with **9** and as such could only be identified by their retention times and the presence of peaks at 6.52 and 6.60 τ in the n.m.r. (CCl_4) attributable to the benzylic protons of 3-methyl-4-benzyl-3-pentene-2-one, (*E*)- and (*Z*)- (**13**).

TABLE 7. Distribution* of products for the pyrolysis† of different ratios of the pyrazolines **1** and **2**

Ratio‡ of **1**:**2**	**7**	**8**	**9**	**13**
85:15	2	91	6	1
74:26	2	86	9	3
51:49	6	66	21	7
38:62	8	54	25	13
10:90	11	30	37	22

*Average of three runs by v.p.c.
†Distribution of products from neat and v.p.c. pyrolysis are identical.
‡Averages of three integrations of the C-5 hydrogens.

Can. J. Chem. Downloaded from www.nrcresearchpress.com by 210.87.254.42 on 09/05/12
For personal use only.

The 20.0 min component was isolated and identified as the cyclopropane **9**. The structural assignment was based on the n.m.r. ($CDCl_3$) given in Table 5 plus aromatic hydrogens at 2.9 τ, an i.r. band at 1690 cm^{-1} (carbonyl) with no evidence of a C=C band, and stability of this compound to thermal rearrangement at 250°.

Anal. Calcd. for $C_{13}H_{16}O$: C, 82.93; H, 8.57. Found: C, 82.89; H, 8.75.

Pyrolysis of Pyrazolines 3 and 4 and Product Identification

The following components were identified from the pyrolysis of **3** and **4** neat at 130–140°. The products of pyrolysis were analyzed using the v.p.c. (FFAP, 218°, 120 ml per min) which showed 6 peaks, with retention times of 8.4 (trace), 12.2, 13.6, 16.4, 18.6 (trace) and 20.0 min respectively. The product distribution calculated for each pyrazoline from data in Table 8 is given in Table 6.

The 12.2 min and 13.6 min components were isolated together. Their retention times and the n.m.r. (CCl_4) showed these to be a mixture of **7**, **11**, **12**, and **8** with peaks at 8.93, 8.87 (d), 7.82, and 7.15 (d) for **7** (65%), 9.19 (d), 8.26, and 7.96 for **11** and **12** (22%), and 8.54 and 8.32 for **8** (13%).

The 16.4 min component was present in only small amounts and therefore could not be isolated. Its retention time does however, fall into the same region as one of the α,β-unsaturated ketones **13**, (*E*)- and (*Z*)-. The fact that on heating the products of pyrolysis at 220° for 2 h resulted in no decrease in this component suggests that it could not be the cyclopropane **10** which under these conditions would rearrange to a pair of γ,δ-olefins.

The 20.0 min component was isolated and identified by n.m.r. (CCl_4) peaks at τ 9.98 (d), 8.92, 7.88, and 7.33 (d) (9.5 Hz) to be the cyclopropane **9**.

Pyrolysis of Pyrazolines 5 and 6 and Product Identification

The following components were identified from the pyrolysis of **5** and **6** neat at 140–145°. The products were analyzed by v.p.c. (FFAP, 208°, 120 ml per min) which showed five peaks with retention times of 12.2 ,13.4, 14.0, 21.0, and 23.5 min respectively. The product distribution calculated for each pyrazoline from data in Table 9 is given in Table 6.

The 12.2 min component was isolated and found to consist of a mixture of olefins. Two of these are identified as the *E*, *Z* pair of 3-methyl-4-phenyl-3-hexene-2-one (**14**) by comparison of the n.m.r. ($CDCl_3$) with that of authentic samples. Peaks attributable to the *E* isomer (42%) at 100 MHz appear at 7.93, 8.35, 9.11 (triplet J = 7.3 Hz), 7.60 (quartet showing long range coupling J = 7.3 Hz), and 2.8 τ. Peaks due to the *Z* isomer (3%) at 100 MHz appear at 8.50, 8.10, and 9.07 τ (triplet J = 7.5 Hz). A further olefin (55%) was tentatively identified as 3-methyl-4-phenyl-4-hexene-2-one, (**15**) on the basis of the following data: i.r. 1715 cm^{-1}; n.m.r. (100 MHz in $CDCl_3$) 7.78 (singlet) acetyl methyl, 8.88 and 8.45 (doublets J = 7.0 Hz) C-3 and -5 methyls respectively, 6.65 (quartet J = 7.0 Hz) C-5 hydrogen, 4.43 (quartet J = 7.0 Hz) vinyl hydrogen, 4.43 (quartet J = 7.0 Hz) vinyl hydrogen, and 2.8 τ (multiplet) aromatic hydrogens. This isomer is assumed to be the *E* isomer based on the mechanism of the olefin-forming reaction. It was not possible to conclude if any of the remaining extraneous peaks in the n.m.r. were due to the other β,γ-isomer 3-methyl-4-phenyl-4-hexene-2-one, (*Z*)- since an authentic sample was not available for comparison.

Anal. Calcd. for $C_{13}H_{16}O$ (olefin mixture): C, 82.93; H, 8.57. Found: C, 83.10; H, 8.71.

Heating the product to over 200° converts the 14.0 min component into the 13.4 min component and this conversion undoubtedly occurs on every pass through the v.p.c. A sample of the 14.0 min component of maximum purity (80%) was indicated to be the cyclopropane **7** by its n.m.r. (CCl_4) given in Table 5 plus aromatic hydrogens at 2.9 τ, i.r. at 1690 cm^{-1}, and its susceptibility to thermal rearrangement.

Anal. Calcd. for $C_{13}H_{16}O$ (mixture of **7**, **11**, and **12**): C, 82.93; H, 8.57. Found: C, 82.83; H, 8.78.

The 13.4 min component had the retention times of the γ,δ-olefins **11** and **12** and was not isolated.

The 21.0 min component was identified as cyclopropane **8** on the basis of its retention time only.

The 23.5 min component was isolated and identified as the cyclopropane **9** by its retention time and n.m.r. (CCl_4) peaks at 9.01 (d), 8.93, 7.89, and 7.30 τ (d) (9.5Hz) which were identical to the same cyclopropane isolated from the decomposition of the pyrazolines **2**, **3**, and **4**.

Rearrangement of Cyclopropane 7 to erythro- and threo-3-Methyl-4-phenyl-5-hexene-2-one (11 and 12)

Four 50 mg samples of the cyclopropane **7** already containing some of the γ,δ-olefins were sealed in Pyrex tubes (2 mm i.d.) and placed in a furnace maintained at 227° for 3.5 h. The v.p.c. (DC 550, 210°, 120 ml per min) indicated that the cyclopropane **7** had completely rearranged to the γ,δ-olefins **11** and **12**. The ratio of the *erythro*-**11** to the *threo*-**12** was estimated by n.m.r. to be 1:2. It was not possible to separate the two γ,δ-isomers by v.p.c. The rearranged products could however be collected as a mixture on the v.p.c. as a clear colorless liquid: i.r. 1723 cm^{-1} (carbonyl stretching frequency); n.m.r. (100 MHz) 7.95 and 8.25 (singlets) acetyl methyls of **11** and **12** respectively, 9.16 and 8.92 (doublets J = 6.9

TABLE 8. Distribution* of products for the pyrolysis of different ratios of the pyrazolines **3** and **4**

Ratio† of **3**:**4**	**7**	**8**	**9**	**13**
25:75	42	18	35	5
58:42	65	12	22	1
95:5	88	7	5	Trace

*Average of three runs by v.p.c.
†Integration of n.m.r. spectra.

TABLE 9. Distribution* of products for the pyrolysis of different ratios of the pyrazolines **5** and **6**

Ratio† of **5**:**6**	Olefins	**7**	**8**	**9**
100:0	0	79	Trace	20
36:64	45	41	2	11
32:68	46	39	3	11
28:72	48	37	4	10

*Average of three runs by v.p.c.
†Average of three integrations of acetyl hydrogens.

Can. J. Chem. Downloaded from www.nrcresearchpress.com by 210.87.254.42 on 09/05/12
For personal use only.

Hz) C-3 methyls of **11** and **12** respectively, 6.60 (triplet $J = 9.0$ Hz) C-4 hydrogens, 7.17 (multiplet of 8 lines) C-3 hydrogens, 4.12 (complex multiplet 40 Hz wide of area one), and 5.03 τ (complex multiplet 32 Hz wide of area two) vinyl hydrogens.

Anal. Calcd. for $C_{13}H_{16}O$: C, 82.93; H, 8.57. Found: C, 8.71; H, 8.75.

Let us assume that the favored conformations for these isomers will have the C-4 and C-3 hydrogens *trans*. This is suggested by the common chemical shift for the hydrogen at C-4 for both compounds and the apparent coupling constant of 9.0 Hz, then the *erythro*-isomer will have the C-3 methyl more shielded and the *threo*-isomer will have the acetyl group more shielded by the phenyl group (20).

Trimethyl α-Phosphonopropionate

Trimethyl α-phosphonopropionate was prepared according to the procedure given by Kinstle (21). The resulting reaction mixture was distilled to give a 31% yield of product distilling from 93–100° at 0.3 mm.

Methyl 2-Methyl-3-benzyl-2-butenoate, (E)- and (Z)-

The procedure according to Kinstle (21) was used. To a slurry of 4.32 g (0.18 mole) of sodium hydride (Ventron) in 200 ml of dry 1,2-dimethoxyethane maintained at 15° was added dropwise in 1 h 35.3 g (0.18 mole) of trimethyl α-phosphonopropionate. After the addition, the grey solution was stirred for 1 h at room temperature and for 5 min at 35°. The solution was cooled to 15° and 24.1 g (0.18 mole) of freshly distilled phenyl acetone (Eastman) was added dropwise over 20 min with rapid stirring. The mixture was warmed to room temperature and stirred vigorously for 15 min and then 20 min at 65°. Ice (300 g) was added with stirring. The mixture was extracted with five 100 ml portions of ether. The combined ether extracts were washed with two 100 ml portions of water to remove the glyme. The ether layer was dried over sodium sulfate and the ether was removed to give 20.8 g (54%) of crude product. The v.p.c. (Ap J, 222°, 120 ml per min) showed at least three products with retention times 18.6, 19.6, and 21.1 min with the first two peaks overlapping considerably. The n.m.r. indicated the presence of both α,β- and β,γ-isomers in approximately a 70:30 ratio respectively. For the α,β- and β,γ-unsaturated esters: i.r. 1715–1740 cm^{-1} (overlapping carbonyl stretching frequencies); n.m.r. (CCl_4) 8.68 (doublet $J = 7.2$ Hz) methyl on C-2 of the β,γ-isomer, 8.0–8.4 (multiplets) vinyl methyls, 6.80 (quartet $J = 7.2$ Hz) hydrogen of C-2 of the β,γ-isomer, 6.54 (broad singlet) benzylic hydrogens of the α,β-isomer, 6.3–6.4 carbomethoxy methyls, 3.65 (broad singlet) vinyl hydrogen, and 2.8–2.9 τ aromatic hydrogens.

Anal. Calcd. for $C_{13}H_{16}O_2$ (mixture of three components): C, 76.43; H, 7.90. Found: C, 76.20; H, 8.10.

*3-Methyl-4-benzyl-3-pentene-2-one (**13**, E- and Z-)*

In a 100 ml flask was refluxed 6 g of the crude esters in 50 ml of 20% sodium hydroxide for 2.2 h (22). The crude reaction mixture was cooled and extracted twice with ether and then acidified with hydrogen chloride. The resulting solution was extracted twice with ether and the ether layer was dried with magnesium sulfate. Removal of ether gave 2.1 g of a white solid containing the crude acids.

The conversion of the acids to the corresponding methyl ketones was done according to the procedure of DePuy *et al.* (23). Into a 50 ml three-necked round bottom flask equipped with a condenser, mechanical stirrer, and nitrogen was placed 2.1 g (0.011 mole) of the crude acids and 25 ml of anhydrous ether. Methyl lithium in ether (0.022 mole) was added dropwise. After the addition, saturated ammonium chloride was added dropwise to destroy the excess methyl lithium. Two clear layers resulted and the ether layer was separated and washed with a saturated ammonium chloride solution, twice with water, and dried over magnesium sulfate. The ether was removed to yield 1.0 g of crude ketone. Bulb-to-bulb distillation yielded 0.8 g (0.004 mole). The yield from the acids was 38% and from phenyl acetone was 8%.

The v.p.c. (FFAP, 218°, 120 ml per min) showed three main peaks with retention times of 15.8, 16.3, and 17.6 min and with an area ratio of 3:1:2 respectively. The α,β to β,γ ratio in the crude reaction mixture was estimated at 50:50 by n.m.r. Thus the 15.8 min component was assumed to be the β,γ-isomer and the latter two peaks to be the α,β-unsaturated ketones **13** (*E*)- and (*Z*)-. These latter peaks had the same retention times as peaks found in the pyrolysis product of pyrazolines **1**, **2**, **3**, and **4**.

The i.r. bands at 1680 and 1685 cm^{-1} were assigned to **13** *E*- and *Z*- and at 1710 cm^{-1} to the β,γ-isomer. The n.m.r. (100 MHz, CCl_4) peaks at 7.81 and 7.82 (singlets) acetyl methyls, 8.25 and 8.26 (singlets) C-3 methyls, 6.54 and 6.59 τ (broad singlets of areas 1:2 respectively) benzylic hydrogens were assigned to the α,β-isomers and peaks at 7.91 (singlet) acetyl methyl, 8.80 (doublet $J = 6.9$ Hz) C-3 methyl, 6.77 (quartet $J = 6.9$ Hz) C-3 hydrogen, and 3.58 τ (broad singlet) vinyl hydrogen were assigned to the β,γ-isomer. Multiplets at 8.08, 8.14, and 8.41 τ (vinyl methyls) could not be clearly assigned.

Anal. Calcd. for $C_{13}H_{16}O$ (mixture of three isomers): C, 82.93; H, 8.57. Found: C, 82.51; H, 8.66.

Methyl-2-methyl-3-phenyl-2-pentenoate, (E)- and (Z)-

The procedure according to Kinstle (21) was used as previously described for the preparation of 25 g (67%) of the esters from 24.1 g of propiophenone. A bulb-to-bulb distillation of the crude reaction product gave a clear colorless liquid whose v.p.c. (FFAP 212°, 120 ml per min) showed one peak with retention time 10.7 min. The n.m.r. indicated that the peak consisted of the expected *E*- and *Z*- α,β-unsaturated esters in a 2:1 ratio: i.r. 1725 and 1735 cm^{-1} (overlapping carbonyl stretching frequencies); n.m.r. 6.29 and 6.77 (singlets) carbomethoxy methyls respectively, 8.32 and 8.00 (singlets) alpha methyls respectively, 9.05 (triplet $J = 3.8$ Hz) C-5 hydrogens, 6.5–6.6 (overlapping quartets) C-4 hydrogens, and 2.9 τ aromatic hydrogens.

Anal. Calcd. for $C_{13}H_{16}O_2$: C, 76.43; H, 7.90. Found: C, 76.02; H, 7.91.

*3-Methyl-4-phenyl-3-hexene-2-one (**14**, E- and Z-)*

Hydrolysis of 17 g of esters by the above procedure gave 1.7 g of solid acids after 24 h reflux: n.m.r. 7.96 and 8.30 (singlets) alpha methyls, 9.06 (triplet $J = 3.8$ Hz) C-5 hydrogens, 7.26 and 7.52 (quartets) C-4 hydrogens, and −0.95 τ (broad singlet) acid proton.

Conversion of 1.5 g of the acids to methyl ketones by the method of DePuy *et al.* (23) gave 160 mg of crude and 120 mg (8.0%) of purified ketones.

The v.p.c. (FFAP 215°, 120 ml per min) showed as the major product two overlapping peaks with retention times of 9.0 and 9.4 min. The n.m.r. indicated that the two ketones **14** *E*- and *Z*- were present in a ratio of 10:90 although the corresponding acids from which they were prepared were in a ratio of 28:72 respectively. Assignment of the structure was based on an assumed shielding by a *cis* phenyl on the α-methyl or acetyl groups. The acetyl peaks were the sharper peaks in the n.m.r. spectrum as the α-methyls had long range coupling to them.

For the ketones **14** *E*- and *Z*- respectively: i.r. 1680–1690 cm^{-1} (overlapping carbonyl stretching frequencies); n.m.r. (CCl_4) (100 MHz) 7.95 and 8.51 (singlets) acetyl methyls, 8.34 and 8.10 (multiplets) alpha methyls, 9.00 and 9.10 (triplets $J = 7.4$ Hz) C-6 hydrogens, and 7.53 τ (quartet $J = 7.4$ Hz) C-5 hydrogens of **14** *Z*-.

Anal. Calcd. for $C_{13}H_{16}O$: C, 82.93; H, 8.57. Found: C, 83.05; H, 8.58.

The authors gratefully appreciate the support received for this work from NRCC and from the Committee on Research of the University of British Columbia.

Thanks are also extended to Miss P. Watson, Mr. R. Burton, and Mr. P. Borda for analytical services.

1. T. V. Van Auken and K. L. Rinehart. J. Amer. Chem. Soc. **84**, 3736 (1962).
2. C. G. Overberger, R. E. Zangaro, and J. P. Anselme. J. Org. Chem. **31**, 2046 (1966).
3. R. J. Crawford and A. Mishra. J. Amer. Chem. Soc. **88**, 3963 (1966).
4. R. Moore, A. Mishra, and R. J. Crawford. Can. J. Chem. **46**, 3305 (1968).
5. D. E. McGreer, N. W. K. Chiu, M. G. Vinje, and K. C. K. Wong. Can. J. Chem. **43**, 1407 (1965).
6. R. J. Crawford and G. L. Erikson. J. Amer. Chem. Soc. **89**, 3907 (1967).
7. R. J. Crawford and L. H. Ali. J. Amer. Chem. Soc. **89**, 3908 (1967).
8. D. E. McGreer and W. S. Wu. Can. J. Chem. **45**, 1398 (1965).
9. E. L. Allred and R. L. Smith. J. Amer. Chem. Soc. **91**, 6766 (1969).
10. W. R. Roth and M. Martin. Tetrahedron Lett. 3865 (1967).
11. J. R. Durig, J. M. Karriker, and W. C. Harris. J. Chem. Phys. **52**, 6096 (1970).
12. D. E. McGreer, N. W. K. Chiu, and M. G. Vinje. Can. J. Chem. **43**, 1398 (1965).
13. D. E. McGreer and N. W. K. Chiu. Can. J. Chem. **46**, 2217 (1968).
14. D. J. Patel, M. E. H. Howden and J. D. Roberts. J. Amer. Chem. Soc. **85**, 3218 (1963).
15. R. G. Bergman and W. L. Carter. J. Amer. Chem. Soc. **91**, 7411 (1969).
16. J. A. Berson and S. S. Olin. J. Amer. Chem. Soc. **92**, 1086 (1970).
17. R. Hoffmann. J. Amer. Chem. Soc. **90**, 1475 (1968).
18. B. M. Trost, W. L. Schinski, and I. B. Mantz. J. Amer. Chem. Soc. **91**, 4320 (1969).
19. M. Stiles, D. Wolf, and G. V. Hudson. J. Amer. Chem. Soc. **81**, 628 (1959).
20. G. H. Schmid. Can. J. Chem. **46**, 3415 (1968).
21. T. H. Kinstle. Ph.D. Thesis. University of Illinois, Urbana, Illinois, 1963.
22. A. I. Vogel. Practical Organic Chemistry. Longmans, Green, and Co. Ltd., New York, N.Y., 1943. p. 921.
23. C. H. DePuy, G. M. Dappen, K. L. Eilers, and R. A. Klein. J. Org. Chem. **29**, 2813 (1964).
24. J. W. McKinley. M.Sc. Thesis. University of British Columbia, Vancouver, British Columbia, 1969.

Can. J. Chem. Downloaded from www.nrcresearchpress.com by 210.87.254.42 on 09/05/12
For personal use only.

Can. J. Chem. Downloaded from www.nrcresearchpress.com by 210.87.254.105 on 09/05/12
For personal use only.

Fluorinated Carbohydrates. Part VII. 2-Deoxy-2-fluorohexopyranosyl Fluorides[1]

L. D. HALL AND R. N. JOHNSON[2]
Department of Chemistry, The University of British Columbia, Vancouver 8, British Columbia

AND

J. ADAMSON[3] AND A. B. FOSTER
Chester Beatty Research Institute, Institute of Cancer Research: Royal Cancer Hospital, Fulham Road, London, S.W. 3, Great Britain

Received June 30, 1970

The ^1H and ^{19}F n.m.r. spectra of the α- and β-anomers of 3,4,6-tri-*O*-acetyl-2-deoxy-2-fluoro-D-glucopyranosyl fluoride and of the corresponding D-manno derivatives have been fully analyzed. The signs of most of the ^{19}F–^1H and of all the ^{19}F–^{19}F couplings have been determined by a heteronuclear double-resonance method. The vicinal ^{19}F–^{19}F couplings are absolutely negative in sign, with $J_{a,a} = -20.0$ Hz, and $J_{a,e}$ and $J_{e,e} = -13.5$ to -18.8 Hz. Sizeable *long-range* couplings (^4J) between an axial fluorine and an axial proton are absolutely positive in sign.

Canadian Journal of Chemistry, 49, 118 (1971)

Introduction

The configurations and conformations of fluorinated carbohydrates can be defined in many cases on the basis of ^1H–^1H couplings, thus enabling a study of the angular and configurational dependencies of vicinal (2–4), geminal (2), and long-range (5) (^4J and ^5J) ^{19}F–^1H couplings.

Extension of this technique to 2-deoxy-2-fluorohexopyranosyl fluorides provides information on the magnitude and absolute sign of vicinal ^{19}F–^{19}F couplings in the four steric relationships possible in a pyranose ring. The purpose of this communication is to report such data for 3,4,6-tri-*O*-acetyl-2-deoxy-2-fluoro-α-D- and β-D-glucopyranosyl fluorides and for the corresponding α-D- and β-D-mannopyranosyl fluorides.

Results and Discussion

Treatment (1) of a solution of 3,4,6-tri-*O*-acetyl-D-glucal in trichlorofluoromethane at $-70°$ with fluoroxytrifluoromethane (6) afforded a mixture of trifluoromethyl 3,4,6-tri-*O*-acetyl-2-deoxy-2-fluoro-α-D-glucopyranoside and the β-D-*manno* isomer and 3,4,6-tri-*O*-acetyl-2-deoxy-2-fluoro-α-D-glucopyranosyl fluoride (**1**) and the β-D-*manno* isomer (**4**). Dissolution of **4** in anhydrous hydrogen fluoride at *ca.* $-10°$ resulted in equilibration (7) to give 3,4,6-tri-*O*-acetyl-2-deoxy-2-fluoro-α-D-mannopyranosyl fluoride (**3**). The fourth difluoride, 3,4,6-tri-*O*-acetyl-2-deoxy-2-fluoro-β-D-glucopyranosyl fluoride (**2**) was obtained by treatment of 2-deoxy-2-fluoro-D-glucose (1) in sequence with acetic anhydride – pyridine, hydrogen bromide – acetic acid, and silver fluoride – acetonitrile. Although the intermediates were not characterized there can be little doubt that the use of hydrogen bromide – acetic acid affords an α-D-glucopyranosyl bromide derivative. Moreover, such compounds are known (2, 7, 8) to react with silver fluoride to give β-D-glucopyranosyl fluorides. Each of the vicinal difluorides **1**–**4** showed a plain positive optical rotary dispersion curve.

The normal ^1H n.m.r. spectra of the difluorides **1**–**4** were reasonably complex and it was not easy to make a direct assignment. Spectra measured

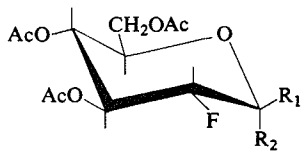

1 $R_1 = H$; $R_2 = F$
2 $R_1 = F$; $R_2 = H$

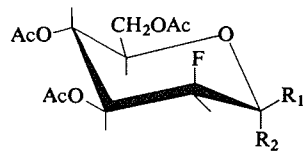

3 $R_1 = H$; $R_2 = F$
4 $R_1 = F$; $R_2 = H$

[1]For a preliminary communication, see ref. 1. This paper also constitutes Part X of a series from U.B.C. entitled "Studies of Specifically Fluorinated Carbohydrates".
[2]U.B.C. Teaching Postdoctoral Fellow, 1968–1970.
[3]A.K. Foundation Postdoctoral Fellow, 1967–1970.

TABLE 1. Chemical shifts* (τ-values, ϕ_c-values†) for the isomeric 3,4,6-tri-*O*-acetyl-2-deoxy-2-fluoro-D-hexopyranosyl fluorides

Compound	H-1	H-2	H-3	H-4	H-5	H-6_1	H-6_2	OAc	F-1†	F-2†
α-D-*gluco* (1)	4.20	5.46	4.46	4.90		5.58—5.94‡		7.93(2) 7.96	151.5	204.5
β-D-*gluco* (2)	4.59	5.54	4.68	4.90	6.11	5.74	5.80	7.94(2) 7.99	140.3	200.9
α-D-*manno* (3)	4.24	5.11	4.73	4.58		5.58—5.94‡		7.90 7.91 7.95	143.4	207.2
β-D-*manno* (4)	4.49	5.10	4.86	4.71	6.14	5.70	5.70	7.88 7.91 7.93	146.4	277.0

*In $CDCl_3$–$CFCl_3$–TMS = 7:2:1.
†Upfield from $CFCl_3$, in p.p.m.
‡Range over which transitions occurred.

TABLE 2. Coupling constants* (Hz) for the isomeric 3,4,6-tri-*O*-acetyl-2-deoxy-2-fluoro-D-hexopyranosyl fluorides

Coupling	Compound			
	α-D-*gluco* (1)	β-D-*gluco* (2)	α-D-*manno* (3)	β-D-*manno* (4)
Proton–Proton				
H_1–H_2	+2.9	+6.1	+2.0	+1.0
H_2–H_3	+9.6	+7.9	+2.5	+2.5
H_3–H_4	9.5	+8.9	10.0	+8.5
H_4–H_5	9.5	9.0	9.0	7.5
H_5–H_{6_1}	†	} Sum, 7.5	†	} Sum, 9.4
H_5–H_{6_2}	†		†	
H_6–H_{6_2}	†	12.0	†	†
Proton–Fluorine				
H_1–F_1	+53.3	+51.7	+48.0	+48.5
H_2–F_2	+48.3	+49.0	+48.5	+49.0
H_2–F_1	+23.8	+11.2	0	+8.0
H_1–F_2	0	+4.0	+4.0	+13.5
H_3–F_2	+12.3	+15.0	+27.0	+22.4‖
H_3–F_1	0.5‡	−1.0	+2.5	0.5‡
H_5–F_1	0§	0	0	0.8
H_4–F_2	0	0	0	+2.0‖
H_5–F_2	0	0	0	0.5‡
(H_{6_1}–F_1 + H_{6_2}–F_1)	0	1.5	0	2.0
Fluorine–Fluorine	−18.8	−15.8	−20.0	−13.5

*All signs are related to the H_1–F_1 coupling, which is known to be absolutely positive (11). All values are first-order splittings which have been shown to be the coupling constants by second-order analysis (see footnote ‖).
†Non-determinable, non-zero coupling.
‡Unresolved coupling; estimate obtained by decrease in half-height width on decoupling.
§All couplings shown as 0 Hz were taken from spin multiplets which showed no detectable changes in the half-height widths of relevant transitions when a powerful decoupling field was applied to the fluorine resonances. Any coupling > 0.2 Hz would have been detected in such an experiment.
‖These are corrected values; the first-order splittings were 21.4 and 3.0 Hz respectively.

with simultaneous irradiation, in turn, of each fluorine resonance enabled a more facile identification of the various ^{19}F–^1H and ^1H–^1H couplings. The spectra shown in Fig. 1 illustrate the success of this approach. The data obtained by first-order analyses of the spectra of the four difluorides are given in Tables 1 and 2.

The structures of the products described above were based on conventional analytical data and, in particular, on the ^1H–^1H coupling constants. From the values of $J_{3,4}$ and $J_{4,5}$ (7.5–10.0 Hz) it is concluded that each of the compounds has an approximate $^4C_1$(D) conformation. The magnitudes of the ^1H–^1H couplings, $J_{2,3}$, provide unequivocal evidence for the configurations assigned at C-2; derivatives in the D-*gluco* series have couplings of 7.9 and 9.6 Hz whereas those in the D-*manno* series have $J_{2,3}$ = 2.5 Hz. In the D-*gluco* series, the values of $J_{1,2}$ provide equally incisive evidence concerning the anomeric con-

Can. J. Chem. Downloaded from www.nrcresearchpress.com by 210.87.254.105 on 09/05/12
For personal use only.

Can. J. Chem. Downloaded from www.nrcresearchpress.com by 210.87.254.105 on 09/05/12
For personal use only.

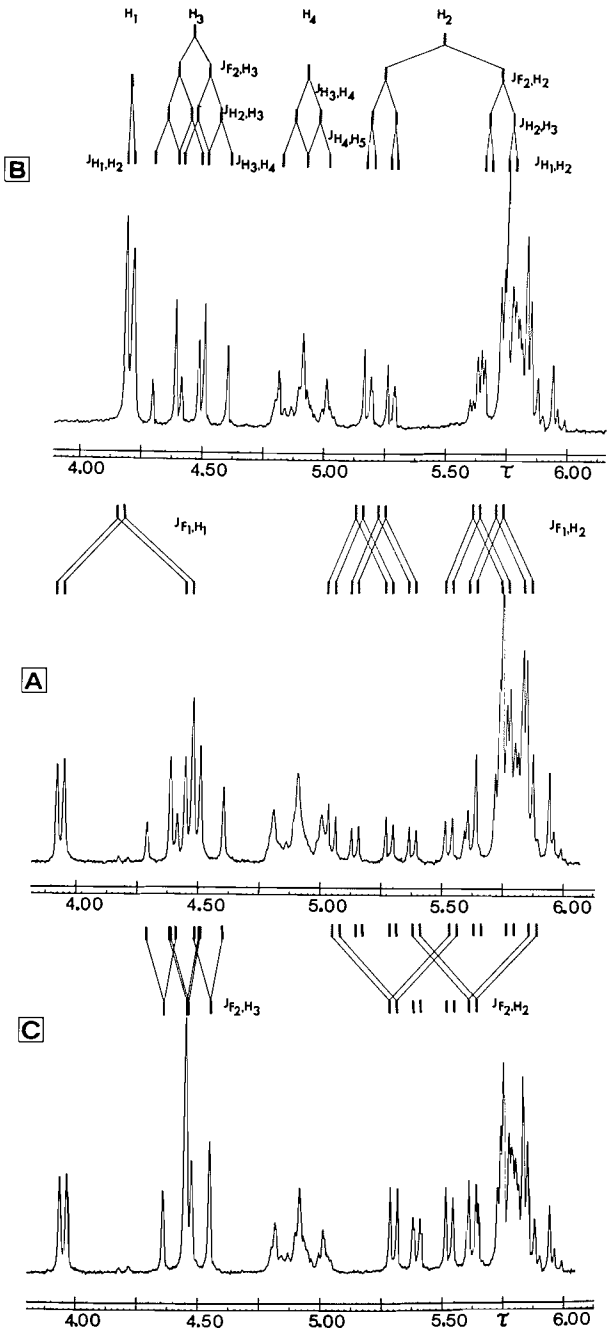

FIG. 1. Partial ^{1}H n.m.r. spectra (100 MHz) of 3,4,6-tri-*O*-acetyl-2-deoxy-2-fluoro-α-D-glucopyranosyl fluoride in deuterochloroform solution. A, Normal spectrum. B, Spectrum with simultaneous irradiation at the F-1 resonance frequency (94, 079, 950 Hz). C, Spectrum with simultaneous irradiation at the F-2 resonance frequency (94, 074, 950 Hz).

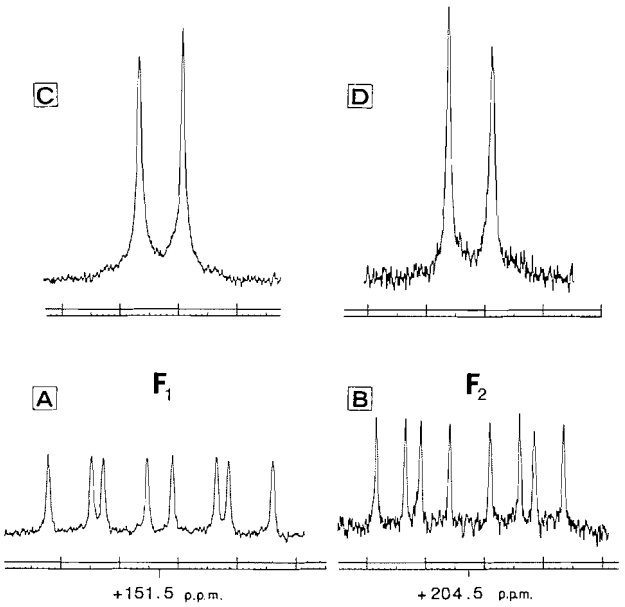

FIG. 2. ^{19}F n.m.r. spectra (94.07 MHz) of 3,4,6-tri-*O*-acetyl-2-fluoro-α-D-glucopyranosyl fluoride in deuterochloroform solution. A, Normal spectrum of the F-1 resonance and B, normal spectrum of the F-2 resonance. The spectra in C and D are the corresponding resonances, measured with simultaneous irradiation of the entire ^1H spectrum using a noise-modulated decoupling field.

figuration; for the α-anomer $J_{1,2}$ = 2.9 Hz and in the β-series, $J_{1,2}$ = 6.1 Hz. Although both of the D-*manno* compounds have similar values for $J_{1,2}$, as expected, it was possible to make a configurational assignment on the basis of the chemical shifts of H-5. In accord with the results of Lemieux and Stevens (9), H-5 of the α-anomer resonated at lower field than did H-5 of the β-anomer.

The magnitudes of the various ^{19}F–^1H couplings were in accord with the same structural assignments (however, see later).

The ^{19}F spectra of the four glycosyl fluoride derivatives were measured in the usual fashion and a typical example is given in Fig. 2A. Although the magnitude of the *vicinal* ^{19}F–^{19}F coupling could be estimated directly from the normal spectrum, it was more convenient to irradiate simultaneously the entire ^1H spectrum, thereby eliminating all the ^{19}F–^1H couplings and enabling a more accurate determination of the ^{19}F–^{19}F coupling; the result of a typical experiment is shown in Fig. 2B.

The signs of many of the ^1H–^1H and ^{19}F–^1H couplings were determined by the "off-resonance" heteronuclear double resonance method previously developed (10) in this laboratory. In this method, a radio-frequency field of moderate strength is placed in the near vicinity of one of the ^{19}F resonances; this results in the selective collapse of individual splittings in the ^1H spectrum. The relative extent of this spin-decoupling effect is a function of the magnitudes and the signs of the individual couplings, and can be interpreted in a reasonably direct fashion. These experiments only give the *relative* signs of the couplings. To convert these to an *absolute* basis it is necessary to refer them to a coupling of known sign; in the present study all signs were related to that of the geminal coupling ($J_{1,F}$) which is known (11) to be absolutely positive in sign.[4]

Before the significance of the ^{19}F parameters of the four glycosyl fluorides is discussed it is important to note that although the ^1H n.m.r. parameters of all these derivatives accord with the assigned structures, there are several marked differences between the coupling constants of the α- and β-anomers of the D-gluco derivatives (**1** and **2**), and of the D-manno derivatives (**3** and **4**), particularly for the latter compounds. For example, the values of $J_{3,4}$ and $J_{4,5}$ are signifi-

[4]For a discussion of this procedure see ref. 12.

Can. J. Chem. Downloaded from www.nrcresearchpress.com by 210.87.254.105 on 09/05/12
For personal use only.

Can. J. Chem. Downloaded from www.nrcresearchpress.com by 210.87.254.105 on 09/05/12
For personal use only.

cantly lower for **4** than for **3**. The same is true for the H_3–F_2 couplings of the two D-*manno* derivatives. It is tempting to suggest that these differences reflect an increase in the population of the $^1C_4$ (D) conformation for the β-anomer (**4**), which would accord with the known, large "anomeric" effect (13) of a C-1 fluorine substituent (14). Attempts to confirm this rationalization by low temperature ^{19}F n.m.r. measurements were unsuccessful; even at −90 °C, no evidence could be obtained for the presence of molecules in the $^1C_4$ (D) conformation. Nevertheless, it is important to bear in mind during the following discussion that the data for the β-anomers might be influenced to some extent by conformational time-averaging, or by conformational distortion of the pyranose ring.

The *vicinal* ^{19}F–^{19}F couplings of derivatives **1**–**4** are of particular interest. It was found that these are all absolutely negative in sign, in contrast to *vicinal* ^1H–^1H and ^{19}F–^1H couplings which are all absolutely positive in sign (12, 15). Furthermore, in marked contrast with the usual observation for *vicinal* ^1H–^1H (16) and ^{19}F–^1H (2–4) couplings where $J_{trans} > J_{gauche}$, the value of the *trans* ^{19}F–^{19}F coupling (**3**, −20.0 Hz) is approximately the same as that of the *gauche* couplings (**1**, −18.8; **2**, −15.8; **4**, −13.5 Hz). It is obvious from this behavior that *vicinal* ^{19}F–^{19}F couplings have some interesting characteristics (1) which merit further investigation; this point will be discussed elsewhere (17).

There does not appear to be any simple rationalization for the values of the ^{19}F chemical shifts, beyond the fact that the anomeric fluorine substituent always gives the lower field resonance of the two. The F-2 shift of the β-D-*manno* derivative is abnormally high for a secondary fluorine substituent[5] since it comes *ca.* 40 p.p.m. to high field of *any* shift we have measured previously for a fluorinated carbohydrate derivative.

Although the magnitude of the H_1–F_1 couplings are smaller for the D-*manno* derivatives than for the D-*gluco* derivatives, an observation which is in accord with previous findings (2), the H_2–F_2 couplings show no similar trend.

It was possible to measure the magnitudes of several long-range ^{19}F-^1H couplings for these derivatives; unfortunately it was not always possible to determine their signs. In accord with previous experience (5) the $^4J_{Fa,Ha}$ coupling between F-1*a* and H-3*a* of the α-D-*gluco* derivative (**1**) is small. However, for the corresponding α-D-*manno* derivative the corresponding coupling is +2.5 Hz. It is not possible to rationalize this behavior unequivocally, although it is tempting to implicate the inversion of configuration at C-2. A $^4J_{Fa,Ha}$ coupling of similar magnitude (+2.0 Hz) occurs between F-2*a* and H-4*a* of the β-D-*manno* derivative (**4**). Again there is the possibility that this reflects an abnormality of the system, since there is other evidence that **4** does not exist wholly in a normal $^4C_1$ (D) conformation. Nevertheless, these two observations of detectable ^4J couplings indicate that some caution may be necessary before such couplings are used for configurational assignments of carbohydrates which have a fluorine substituent attached to a secondary ring-carbon.[6] It should be noted also that several $^5J_{F,H}$ couplings have been found in the n.m.r. spectra of these derivatives and these data will be discussed in detail elsewhere.

Experimental

The general methods used here have been described previously (3).

All n.m.r. spectra were measured with a modified Varian HA-100 instrument as described previously. The noise-modulated heteronuclear decoupling experiments used the same basic components as before (18) with the sole exception of the noise-source; we now use a pseudo-random sequence generator whose effective band-width is controlled by a square-wave function generator, either a Wavetek, model 113 or Heathkit, model IG 82.

*3,4,6-Tri-O-acetyl-2-deoxy-2-fluoro-*β*-D-glucopyranosyl fluoride (2)*

2-Deoxy-2-fluoro-D-glucose (1) (500 mg) was stirred overnight with acetic anhydride (4 ml) and pyridine (2 ml). The mixture was then evaporated *in vacuo* and the syrupy residue was dissolved in hydrogen bromide – glacial acetic acid (5 ml, 45% w/v). After 3 h at room temperature the solution was evaporated *in vacuo*. A solution of the syrupy residue[7] in acetonitrile (5 ml) was

[5]This value was carefully remeasured several times.

[6]Until the present investigation, we had never encountered $^4J_{Fa,Ha}$ couplings in the spectra of glycopyranosyl fluorides; the observed $^4J_{Fe,He}$ couplings for such derivatives were between +3.6 and +4.2 Hz. However, the glycosyl fluorides of deoxy-fluoropyranose sugars examined thus far do show evidence of $^4J_{Fa,Ha}$ couplings.

[7]Note added after submission of manuscript:
In subsequent experiments this compound was characterized as 3,4,6-tri-*O*-acetyl-2-deoxy-2-fluoro-α-D-glucopyranosyl bromide, m.p. 79–80° (from ether), $[\alpha]_D$ +22.9° (*c* 0.7, chloroform). The n.m.r. data ($CDCl_3$), $J_{1,2}$ 3.5, $J_{F,1}$ 0.5 Hz.
Anal. Calcd. for $C_{12}H_{16}BrFO_7$: C, 38.8; H, 4.3; F, 5.1; Br, 21.6. Found: C, 38.9; H, 4.4; F, 5.1; Br, 21.3.

treated with a slurry of silver fluoride (1 g) in acetonitrile (5 ml). The mixture was stirred in the dark for 17 h, silica gel (Merck, 7734, 5 g) was added, and the mixture was evaporated. The residue was added to the top of a column of silica gel and eluted with light petroleum (b.p. 40–60°) – ether (2:1). Evaporation of the combined fractions containing the major product followed by recrystallization of the product from light petroleum – ether afforded the title compound (354 mg, 41%), m.p. 99–101°, $[\alpha]_D^{25}$ + 75° (*c* 1, chloroform), ϕ +2880° (350 nm), +12 300° (200 nm)[*cf.* α-D-*gluco* isomer **1**, ϕ +1560° (300 nm), +18 700° (195 nm)].

Anal. Calcd. for $C_{12}H_{16}F_2O_7$: C, 46.45; H, 5.2; F, 12.3. Found: C, 46.7; H, 5.25; F, 12.2.

3,4,6-Tri-O-acetyl-2-deoxy-2-fluoro-α-D-mannopyranosyl fluoride (3)

3,4,6-Tri-*O*-acetyl-2-deoxy-2-fluoro-β-D-mannopyranosyl fluoride (650 mg) was stirred with anhydrous hydrogen fluoride (5 ml) at 0 – −10° for 15 min, then at room temperature for 10 min. The solution was poured into saturated aqueous sodium hydrogen carbonate (50 ml) and the product, extracted with chloroform (3 × 50 ml) in the usual manner, crystallized on trituration with light petroleum. Recrystallization from light petroleum (b.p. 60–80°) – ether afforded the title compound (504 mg, 77%), m.p. 89–90°, $[\alpha]_D^{25}$ +27°, ϕ +3800 (200 nm)[*cf.* β-D-*manno* isomer (**2**), ϕ +3600° (200 nm)].

Anal. Calcd. for $C_{12}H_{16}F_2O_7$: C, 46.45; H, 5.2; F, 12.3. Found: C, 46.4; H, 5.3; F, 12.2.

It is a pleasure for one of us (L.D.H.) to thank the National Research Council of Canada for their generous financial support, especially for the equipment which forms the basis of the heteronuclear decoupler. This work was supported in part by a grant (No. 352) from N.A.T.O. and by grants to the Chester Beatty Research Institute (Institute of Cancer Research: Royal Cancer Hospital) from the Medical Research Council of Great Britain and the Cancer Research Campaign.

1. J. ADAMSON, A. B. FOSTER, R. H. HESSE, and L. D. HALL. Chem. Commun. 309 (1969); L. D. HALL, R. N. JOHNSON, J. ADAMSON, and A. B. FOSTER. Chem. Commun. 463 (1970).
2. L. D. HALL and J. F. MANVILLE. Can. J. Chem. **47**, 1 (1969); Chem. Commun. 37 (1968).
3. A. B. FOSTER, R. HEMS, and L. D. HALL. Can. J. Chem. **48**, 3937 (1970).
4. J. S. BRIMACOMBE, A. B. FOSTER, R. HEMS, J. H. WESTWOOD, and L. D. HALL. Can. J. Chem. **48**, 3946 (1970).
5. A. B. FOSTER, R. HEMS, L. D. HALL, and J. F. MANVILLE. Chem. Commun. 158 (1968).
6. D. H. R. BARTON, L. S. GODINHO, R. H. HESSE, and M. M. PECHET. Chem. Commun. 804 (1968).
7. D. H. BRAUNS. J. Amer. Chem. Soc. **45**, 833 (1923); F. MICHEEL and A. KLEMER. Advan. Carbohyd. Chem. **16**, 85 (1961).
8. B. HELFERICH and R. GOOTZ. Ber. **62**, 2505 (1929); F. MICHEEL, A. KLEMER, and R. FLITSCH. Ber. **91**, 663 (1958).
9. R. U. LEMIEUX and J. D. STEVENS. Can. J. Chem. **43**, 2059 (1965).
10. L. D. HALL and R. N. JOHNSON. To be published.
11. E. L. MACKOR and D. MACLEAN. J. Chem. Phys. **44**, 64 (1966). R. A. BERNEIM and B. J. LAVERY. J. Amer. Chem. Soc. **89**, 1279 (1967).
12. L. D. HALL and J. F. MANVILLE. Carbohyd. Res. **9**, 11 (1969).
13. S. J. ANGYAL. *In* Conformational Analysis. E. L. ELIEL, N. L. ALLINGER, S. J. ANGYAL, and G. A. MORRISON. Interscience Division, John Wiley and Sons, Inc., New York, 1965.
14. L. D. HALL and J. F. MANVILLE. Can. J. Chem. **47**, 19 (1969).
15. L. D. HALL and J. F. MANVILLE. Carbohyd. Res. **8**, 295 (1968).
16. M. KARPLUS. J. Chem. Phys. **30**, 11 (1959); J. Amer. Chem. Soc. **85**, 2870 (1963).
17. L. D. HALL and R. N. JOHNSON. To be published.
18. R. BURTON and L. D. HALL. Can. J. Chem. **48**, 59 (1970).

Can. J. Chem. Downloaded from www.nrcresearchpress.com by 210.87.254.105 on 09/05/12
For personal use only.

Can. J. Chem. Downloaded from www.nrcresearchpress.com by 210.87.254.40 on 09/05/12
For personal use only.

A New Tetrahydroprotoberberine Alkaloid from *Corydalis caseana* A. Gray

C. K. YU AND D. B. MACLEAN
Department of Chemistry, McMaster University, Hamilton, Ontario
AND
R. G. A. RODRIGO AND R. H. F. MANSKE
Department of Chemistry, University of Waterloo, Waterloo, Ontario

Received June 12, 1970

The isolation and structure of a new tetrahydroprotoberberine alkaloid from *C. caseana* is reported. This alkaloid, named caseanadine, has a phenolic hydroxyl at C-1 and methoxyls at C-2, -9, and -10. Its structure has been deduced from an analysis of its p.m.r. mass, and i.r. spectra. The alkaloid has a substitution pattern different from other members of this group of alkaloids of established structure.

Canadian Journal of Chemistry, 49, 124 (1971)

An examination of *C. caseana* was reported in 1938 by Manske and Miller (1) who isolated ten alkaloids. Five of them were known at that time, namely, protopine, allocryptopine, bicuculline, corypalmine, and scoulerine. Of the alkaloids of unassigned structure caseanine (F-36) is now known to be identical with *l*-tetrahydropalmatine, casealutine (F-32) to be identical with isocorypalmine and F-34 to be identical with cryptopine (2). The alkaloids designated F-33 and F-35 have been named caseamine and caseadine, respectively, and have been shown to be tetrahydroprotoberberines with a novel substitution pattern (3, 4). Of the ten alkaloids of known structures six are tetrahydroprotoberberines, three are of the protopine type, and one is a phthalide isoquinoline.

We report here a new alkaloid, $C_{20}H_{23}NO_4$, m.p. 170° from this source to which we assign the trivial name, caseanadine (**1**). The u.v. spectrum has λ_{max}(MeOH) 282 mμ and the i.r. spectrum $\nu_{max}(CHCl_3)$ 3540 cm^{-1} (OH absorption) and bands in the region 2700–2800 cm^{-1} (Bohlmann bands). The spectral properties are not inconsistent with a tetrahydroprotoberberine. The mass spectrum of caseanadine shows a molecular ion at *m/e* 341 (100) as expected and fragment ions at *m/e* 326 (7), 310 (20), 178 (8), 176 (6), 164 (82) and 149 (38). This pattern is characteristic of tetrahydroprotoberberines (5) substituted with two methoxyl groups in ring D and with one hydroxyl and one methoxyl group in ring A as in structure I. Unfortunately, the mass spectrum does not define the sites of substitution in rings A and D.

The 100 MHz p.m.r. spectrum of caseanadine in $CDCl_3$ is shown in Fig. 1. The spectrum con-

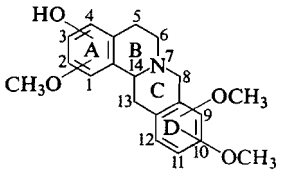

I

firms the presence of four aromatic protons and three methoxyl groups. The presence of the doublet centered near 4.2 δ is characteristic of protoberberines in which ring D carries an oxygen substituent at C-9 (5). This signal constitutes one-half of an AB quartet associated with the protons at C-8. The other half of this signal is obscured in this spectrum by the methoxyl signals. The aromatic region definitely shows one AB system with indications that another may also be present.

The partial spectrum of caseanadine (Fig. 2) in DMSO-d_6 was more informative, particularly in the aromatic region. The presence of two AB systems is clearly discernible there and thus the substituents in ring A must be at the 1,2- or 3,4-positions. The previous demonstration that caseamine and caseadine have substituents at the 1- and 2-position suggests that caseanadine may be similarly substituted in ring A. The presence of two AB quartets in the aromatic region along with the p.m.r. evidence that C-9 carries an oxygen substituent defines the substitution in ring D. Thus caseanadine may be represented as in II where $R_1 + R_2 = H + CH_3$. The assignment of the OH group to C-1 rests on decoupling evidence on caseanadine and on an examination of the p.m.r. spectrum of its *O*-acetyl derivative **2** shown in Fig. 3.

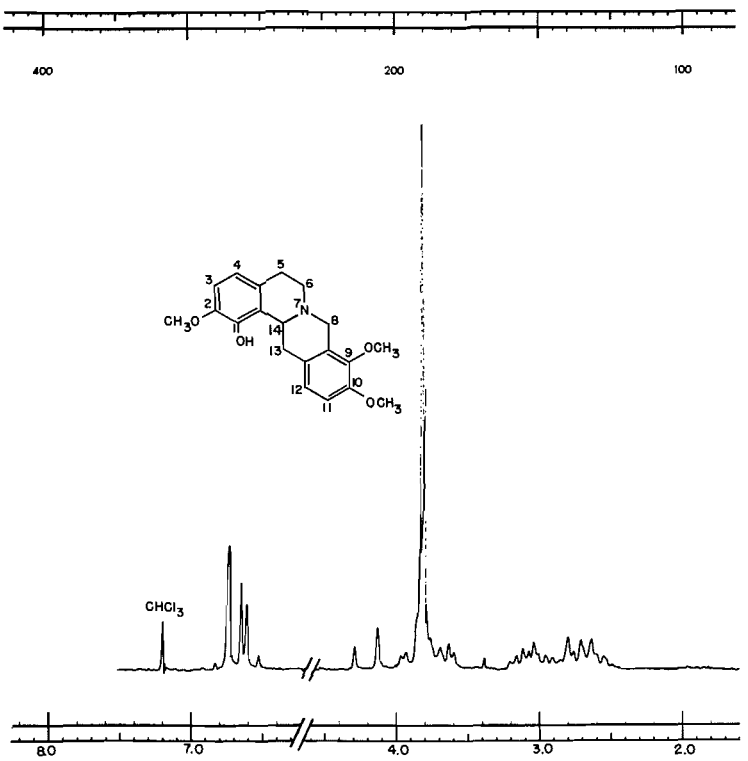

FIG. 1. The 100 MHz p.m.r. spectrum of caseanadine (**1**) in $CDCl_3$.

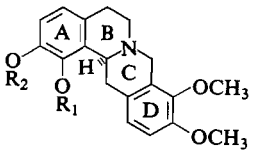

II

$R_1 + R_2 = H + CH_3$

The p.m.r. spectrum of **2** shows that two aromatic protons have shifted downfield in **2** and, therefore, they must be in the ring carrying the *O*-acetyl group. The chemical shift of the remaining (ring D) protons has not changed appreciably. Moreover, it is obvious from the height of the signals that the lowest field proton of **2** is the highest field proton of **1**. The magnitude of the shift (*ca.* 0.4 p.p.m.) is expected for a proton para to a phenolic hydroxyl group which has undergone acetylation (6). The high field signal of **1** and the low field signal of **2** are both broader (less sharp) than the proton to which they are coupled. This suggests that these protons are broadened by ortho-benzylic coupling whereas the protons to which they are coupled are less strongly long-range coupled to meta and/or para protons (7). Double irradiation experiments lend support to the assignment of structure I ($R_1 = H$; $R_2 = CH_3$).

Irradiation of **2** in the region 280–324 Hz from TMS caused the low field proton to sharpen relative to that proton to which it is directly coupled. The effect is most pronounced in the region 294–310 Hz from TMS. The effect is shown in Fig. 4*a*. A similar effect is observed in **1** when the solution in DMSO-d_6 is subjected to irradiation in the region 265–284 Hz as shown in Fig. 4*b*. The signals which are under irradiation in both systems must be one or other of the signals associated with the protons at C-5 or -13. With the orientation of substituents of structure II irradiation at C-13 would not affect the protons of ring A. The only other benzylic proton which can be long-range coupled to the aromatic protons of ring A is situated at C-14. This proton has not been assigned in this spectrum but since it is benzylic and alpha to nitrogen one would expect to find it at lower field than 3 p.p.m. from TMS. In the

Can. J. Chem. Downloaded from www.nrcresearchpress.com by 210.87.254.40 on 09/05/12
For personal use only.

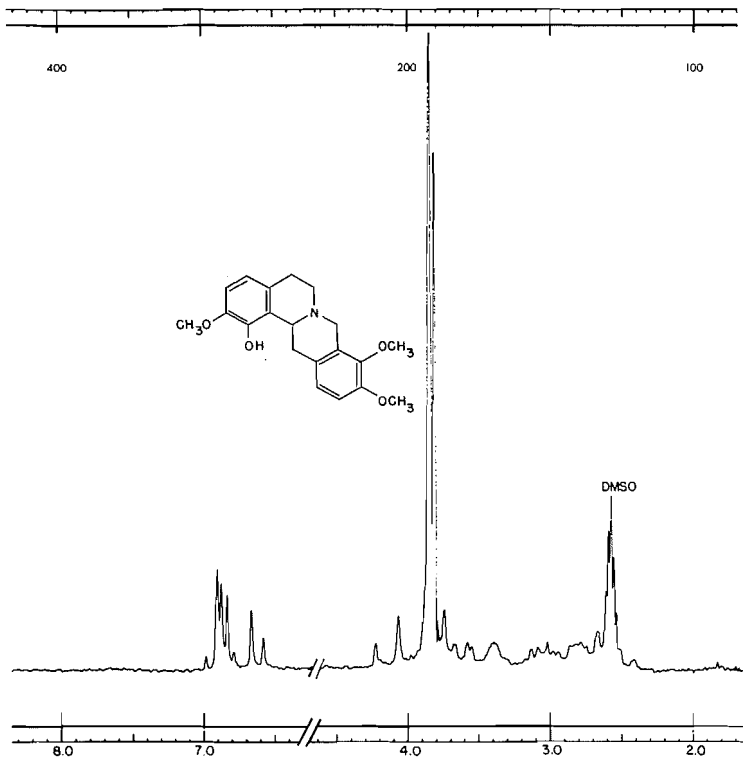

FIG. 2. The 100 MHz p.m.r. spectrum of caseanadine (**1**) in DMSO-d_6.

13-methylprotoberberines this proton is clearly defined and appears in the region 3.7 ± 0.1 (8).

The alternative structure, III, although unlikely on biogenetic grounds, must also be considered. If III were the correct structure, the low field proton of the AB quartet of **2** in ring A would be that at C-1, and the high field proton of the AB quartet of **1** in ring A would be that at C-1.

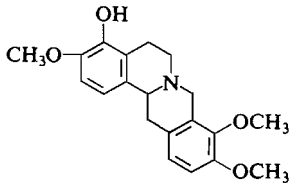

III

Irradiation at C-5 would affect the proton at C-1 less than that at C-2 since meta-benzylic coupling is weaker than para (7), a circumstance which is contrary to the observed result. In any event, in structure III the proton at C-1 would be expected to be broader, even after irradiating C-5, than that at C-2 because it would still be ortho-benzylic coupled to C-14. Such is not the case. Nevertheless, the irradiating field may be affecting the protons at C-13. These protons will not be long-range coupled to C-1 but irradiation at C-13 might increase the area of the proton at C-1 through a nuclear Overhauser effect (9) and give the misleading impression that a decoupling had occurred. An examination of the peak width at half height definitely shows a decoupling of the low field aromatic proton of **2** and the high field aromatic proton of **1**. For **1** the width at half height of the high field aromatic proton is 1.9 Hz in the uncoupled spectrum, and in the decoupled spectrum, 1.0 Hz. For the other half of the AB quartet the figures were 1.4 and 1.0 Hz. Only structure II (R = H; R_2 = CH_3) is compatible with these observations.

Thus, the decoupling experiments establish the orientation of the substituents in ring A. A *trans*-quinolizidine conformation of rings A and B in caseanadine is indicated by the presence of Bohlmann bonds in its i.r. spectrum (10). The large negative optical rotation of caseanadine in $CHCl_3$ suggests the absolute configuration shown in the diagram in which the C-14 hydrogen has an α-orientation (11).

Can. J. Chem. Downloaded from www.nrcresearchpress.com by 210.87.254.40 on 09/05/12
For personal use only.

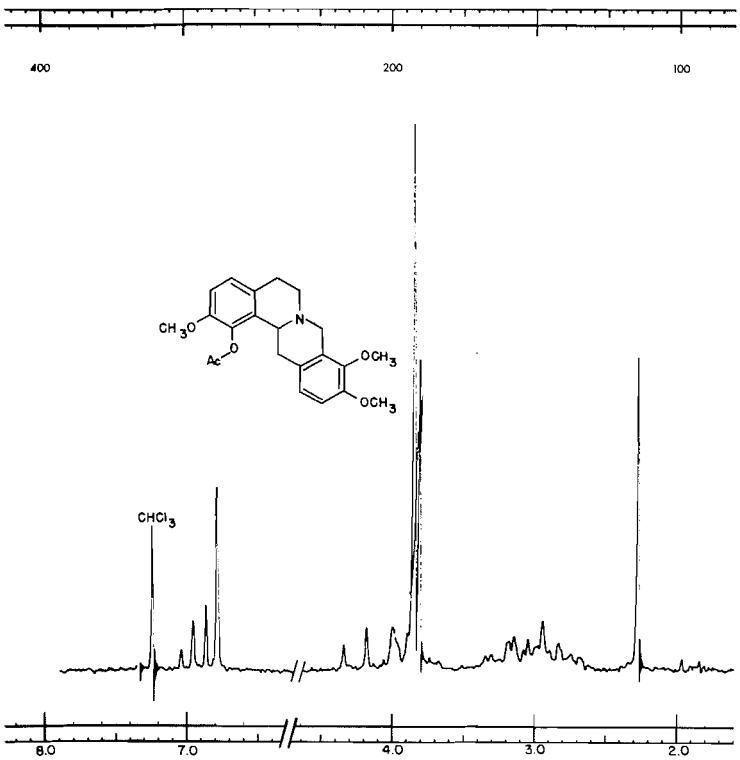

FIG. 3. The 100 MHz p.m.r. spectrum of *O*-acetylcaseanadine (**2**) in $CDCl_3$.

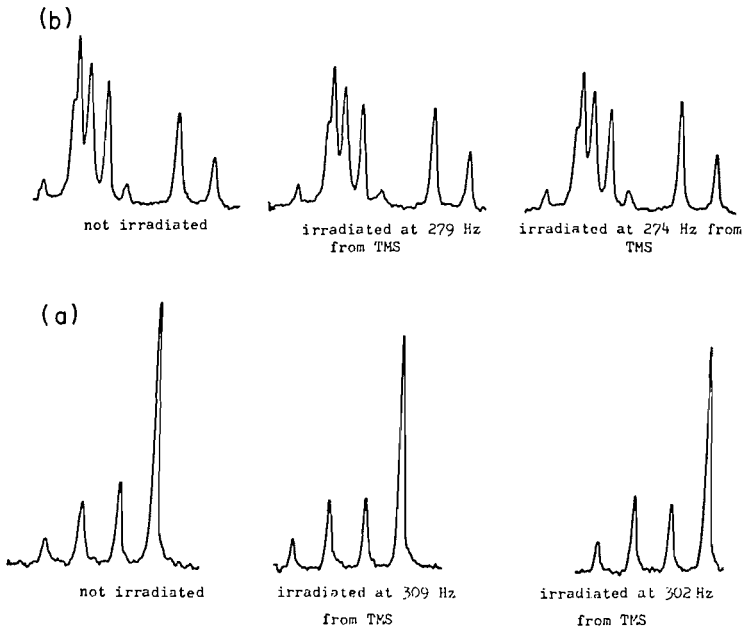

FIG. 4. (*a*) Double irradiation of *O*-acetylcaseanadine. (*b*) Double irradiation of caseanadine.

Can. J. Chem. Downloaded from www.nrcresearchpress.com by 210.87.254.40 on 09/05/12
For personal use only.

Can. J. Chem. Downloaded from www.nrcresearchpress.com by 210.87.254.40 on 09/05/12
For personal use only.

Experimental

Methods

Mass spectra were recorded on a CEC 21-110B double-focusing mass spectrometer. For high resolution work spectra were recorded on plates and accurate mass measurements were made using perfluorokerosene as a marker (12).

The p.m.r. spectrum was recorded using the frequency sweep mode of a Varian HA-100 spectrometer. Samples were dissolved in $CDCl_3$ using added TMS as the internal locking signal. Chemical shifts were measured relative to TMS using a V4315 frequency counter incorporated in the instrument. Double irradiation was achieved by employing a Hewlett–Packard 201C audiogenerator at the desired frequency. A Beckmann IR 10 spectrometer was used to record i.r. spectra and a Cary 14 spectrometer was used for the u.v. spectrum.

Isolation of Caseanadine

The mother liquor from which the tetrahydropalmatine (caseanine) had been removed (1) as completely as possible (both as the free base and as its hydrochloride) was again taken up in dilute hydrochloric acid. The clarified solution was basified with excess potassium hydroxide and the liberated bases taken up in ether. Much of the ether from the dried (KOH) solution was removed by evaporation. From the concentrated solution a mixture of bases separated in the course of several days. There was a fraction sparingly soluble in warm methanol which proved to consist largely of protopine and allocryptopine. The moderately soluble base consisted of fine flat needles (melting not sharply at 151°) which when recrystallized from methanol changed to less soluble stout prisms which when placed in a melting point bath at 150° melted at 170° with some shrinking at 165° $[\alpha]_D(CHCl_3) = -212°$.

Anal. Calcd. for $C_{20}H_{23}NO_4$: C, 70.4; H, 6.8; N, 4.1. Found: C, 71.0; H, 6.6; N, 4.4.

Accurate mass measurement of the molecular ion gave the following result: calcd. for $C_{20}H_{23}NO_4$, 341.1627; found, 341.1657.

O-Acetylcaseanadine

Caseanadine (10 mg) was dissolved in acetic anhydride (2 ml) and pyridine (0.5 ml). The mixture was allowed to stand at room temperature for 12 h when it was evaporated to dryness under reduced pressure. The residue, after neutralization, was dissolved in ether, washed several times with aqueous sodium carbonate, and the solution dried over anhydrous potassium carbonate. The residue obtained upon evaporation of the solvent failed to crystallize. The t.l.c. showed only one spot which had a different R_f value from the starting material. The p.m.r. spectrum, Fig. 3, demonstrates the presence of the *O*-acetyl group and clearly indicates the absence of unacetylated material. The mass spectrum has a molecular ion at *m/e* 385 (55) with major fragment ions at *m/e* 164 (100) and 149 (53). Insufficient material was available for a combustion analysis. Accurate mass measurement of the molecular ion gave the following result: calcd. for $C_{22}H_{25}NO_5$, 383.1733; found, 383.1685.

We thank the National Research Council of Canada for financial support of this work. We wish to acknowledge the assistance and advice of J. K. Saunders with the p.m.r. measurements.

1. R. H. F. Manske and M. R. Miller. Can. J. Res. **16B**, 153 (1938).
2. R. H. F. Manske and W. R. Ashford. Alkaloids, **4**, 77 (1954).
3. C.-Y. Chen, D. B. MacLean, and R. H. F. Manske. Tetrahedron Lett. 349 (1968).
4. M. P. Cava, M. V. Lakshmikantham, and M. J. Mitchell. J. Org. Chem. **34**, 2665 (1969).
5. C.-Y. Chen and D. B. MacLean. Can. J. Chem. **46**, 2501 (1968).
6. R. J. Highet and P. F. Highet. J. Org. Chem. **30**, 902 (1965).
7. D. T. Wittiak, D. R. Patel, and Y. Lin. J. Amer. Chem. Soc. **89**, 1908 (1967).
8. C. K. Yu. Unpublished results, McMaster University, Hamilton, Ontario.
9. F. A. L. Anet and A. J. R. Bourn. J. Amer. Chem. Soc. **87**, 5250 (1965).
10. F. Bohlmann. Chem. Ber. **91**, 2157 (1958).
11. H. Corrodi and E. Hardegger. Helv. Chim. Acta, **39**, 889 (1956).
12. K. Biemann. Pure Appl. Chem. **9**, 95 (1964).

Studies on the Decomposition of Tetra-alkylammonium Salts in Solution. IV. The α-Deuterium Secondary Isotope Effect

E. C. F. Ko AND K. T. Leffek
Department of Chemistry, Dalhousie University, Halifax, Nova Scotia

Received June 18, 1970

The secondary deuterium isotope effect is reported for the decomposition of benzyl-α-d_2-phenyldimethylammonium bromide in both chloroform and acetone solvent, over a temperature range of 25 to 30°. The magnitudes of the rate ratios are compared to literature values for S_N1 reactions, from which it is concluded that the mechanism of the decomposition involves a carbonium ion or ion-pair. The variation of the isotope effect with solvent is rationalized in terms of specific solvent interaction with the benzyl group.

Canadian Journal of Chemistry, **49**, 129 (1971)

Can. J. Chem. Downloaded from www.nrcresearchpress.com by 210.87.254.42 on 09/05/12
For personal use only.

Introduction

Previous papers (1–3) have presented evidence that the thermal decomposition of quaternary ammonium iodides and bromides, which contain a benzyl group, decompose completely in chloroform and acetone solvents to yield a benzyl halide and a tertiary amine, by a mechanism which was described as an "ionic internal nucleophilic substitution (1)". This mechanism is envisaged as an essentially unimolecular process and the reaction gives first order kinetics when the rate constant is evaluated with respect to the concentration of the ammonium ion, as distinct from that of the ammonium halide ion-pair, in which latter form most of the substrate exists under the experimental conditions. The transition state of the reaction may contain, in addition to the ammonium ion itself, some anions and solvent molecules, but the covalency change is postulated to involve only the carbon atom of the benzyl group and the nitrogen atom.

If this postulate is true, the substitution of the two hydrogen atoms attached to the benzyl carbon by deuterium should result in a change in the rate of reaction of the same order of magnitude as is observed for α-deuteration in typical S_N1 reactions. When the secondary α-deuterium isotope effects were first observed in 1957 (4–6), they were immediately recognized (6) as an additional diagnostic test for the unimolecular and bimolecular mechanisms in nucleophilic substitutions. Subsequent work, particularly in the solvolysis reactions of methyl compounds (7–9) established the test more firmly.

The basis of the secondary α-deuterium isotope effect test of mechanism is as follows. Isotope effects on rates of reactions result from changes in vibrational frequencies which involve the isotopically substituted atom. The effect of α-deuteration is assumed to be dominated by changes in the bending modes of vibration of C—H and C—D, between the initial and transition states. In an S_N1 reaction the transition state is less crowded than the initial state, therefore the frequencies of the bending modes of vibration of C—H and C—D are decreased during the activation process and this decrease is less for the deuterated compound since C—D has a lower zero-point energy ($\sum \frac{1}{2}h\nu_i$) than C—H in the initial state. Thus the difference in the zero-point energies between the two compounds is less in the transition state than in the initial state, which gives the deuterated compound a larger energy of activation and a smaller rate constant. The isotope effect, quoted as k_H/k_D, is therefore greater than unity (normal) for S_N1 reactions.

The same argument when applied to an S_N2 reaction, in which the transition state is more crowded than the initial state predicts an increase in the frequencies of the bending vibrations during activation and values of k_H/k_D less than unity (inverse).

Reviews of these isotope effects in 1961 by Weston (10) and by Seltzer (11) showed that reactions usually considered S_N1 gave free energy of activation differences $\Delta\Delta G^{\ddagger}$ ($= RT/n$ ln k_H/k_D, where n is the number of deuterium atoms) in the range of 55 to 80 cal/mole. Seltzer (11) concluded that the limiting value for an S_N1 reaction was $k_H/k_D = 1.12$ at 105 °C ($\Delta\Delta G^{\ddagger} \simeq 85$ cal/mole^{-1}) and used this criterion to deduce the mechanism of a non-solvolytic decomposition reaction. This value has been accepted generally (12–14).

Can. J. Chem. Downloaded from www.nrcresearchpress.com by 210.87.254.42 on 09/05/12
For personal use only.

However, the approximate nature of the theory is shown by the observation of small normal isotope effects (up to $\Delta\Delta G^{\ddagger} = 27$ cal/mole^{-1}) for some non-solvolytic S_N2 reactions (15–19), but despite this, there is a clear difference in magnitude between the two mechanisms.

Results and Discussion

Rate constants for the decomposition of normal and deuterated tetra-alkylammonium bromides at various temperatures are presented in Table 1. The rate ratios, k_H/k_D in the right hand column, which show only a slight dependence on temperature, are approximately 1.25 in chloroform solvent and 1.20 in acetone solvent. Since there are two deuterium atoms present in the molecule, the magnitude of the isotope effect is $\Delta\Delta G^{\ddagger} \simeq 70$ cal/mole^{-1} in chloroform and 57 cal/mole^{-1} in acetone. These values are considerably larger than the largest observed normal isotope effect for non-solvolytic S_N2 reactions and, at least in chloroform, quite close to the S_N1 limiting value of 85 cal/mole^{-1}. Previous measurements made on α-deuterated benzyl compounds gave $k_H/k_D = 1.25$ at 50 °C for the solvolysis of benzyl-1,1-d_2 *p*-toluenesulfonate in acetic acid (6), corresponding to $\Delta\Delta G^{\ddagger} = 72$ cal mole^{-1}, as opposed to $k_H/k_D = 1.05$ at 40 °C or $\Delta\Delta G^{\ddagger} = 15$ cal mole^{-1} for the radiochloride exchange with benzyl-1,1-d_2 chloride in *N,N* dimethylformamide solvent (17). Also, Shiner *et al.* (14) have recently reported α-deuterium isotope effects on the rates of solvolysis of several benzyl derivatives in a number of solvent mixtures and correlated the magnitude of the effects with mechanism.

TABLE 1. Rate data for the decomposition of benzyl-α-d_2-phenyldimethylammonium bromide and its normal analogue in solution

Temperature (°C)	$10^5\ k_H$* (s^{-1})	$10^5\ k_D$* (s^{-1})	k_H/k_D
Chloroform solvent			
30	1.72	1.37	1.25_5
35	3.20	2.56	1.25_0
40	6.05	4.84	1.25_0
45	12.2	9.72	1.25_5
50	23.3	18.2	1.25_9
55	44.0	35.3	1.24_6
60	85.8	68.9	1.24_5
Acetone solvent			
30	1.41	1.18	1.19_4
35	2.84	2.37	1.19_8
40	5.53	4.60	1.20_2
45	11.5	9.36	1.22_8
50	22.1	18.1	1.22_1
55	40.1	33.3	1.20_4

*Specific first order rate constant.

In comparison with the above values, the results in Table 1 strongly favor a transition state for the ammonium ion decomposition in which a carbonium ion is being formed, although this carbonium ion may have an extremely short life-time before it forms an ion-pair with a bromide ion. Alternatively, if an appropriate definition of an ion-pair is assumed the transition state may be pictured as a loose solvent-separated ion-pair, but in either case the results require that the anion is not involved in covalency change during the activation process.

The activation parameters and their standard deviations are reported in Table 2 together with the isotope effects on these parameters. The latter were calculated by fitting the observed rate ratios to eq. 1 by the method of least squares. It

$$[1]\quad \log_{10} k_H/k_D = \frac{(\Delta H_D^{\ddagger} - \Delta H_H^{\ddagger})}{2.303RT} - \frac{(\Delta S_D^{\ddagger} - \Delta S_H^{\ddagger})}{2.303R}$$

may be seen that the entropy contribution to the free energy of activation difference is larger than that of the enthalpy. This does not invalidate the above argument made in terms of free energy of activation since it has been shown by Wolfsberg and Stern (20) using model calculations, that secondary deuterium isotope effects entirely in the entropy term may be accommodated by the transition state theory provided the appropriate changes in vibrational frequencies take place during the reaction. However, the results in Table 2 give rise to a feeling that perhaps a model for a reaction which ignores the solvent completely makes too gross an approximation. On the other hand the nature of solvation effects on secondary isotope effects is, at present time, suited only to an empirical approach.

Table 1 shows that there is a significant difference between the rate ratios in the two solvents, with the more polar acetone giving the smaller isotope effect. This difference, in comparison to solvent effects on α and β deuterium isotope rate effects already reported (12, 13, 18, 21–25) is large, but not exceptionally so.

TABLE. 2. Activation parameters for the decomposition of benzylphenyldimethylammonium bromide and isotope effects for the benzyl-α-d_2 analogue

Solvent	$\Delta H_H^{\ddagger}$(kcal mole^{-1})	$\Delta S_H^{\ddagger}$(cal mole^{-1} deg^{-1})	$(\Delta H_D^{\ddagger} - \Delta H_H^{\ddagger})$*	$(\Delta S_D^{\ddagger} - \Delta S_H^{\ddagger})$*
$CHCl_3$	26.3 ± 0.4	6.1 ± 1.1	0.031 ± 0.03	−0.35 ± 0.1
$(CH_3)_2CO$	26.8 ± 0.2	7.5 ± 0.7	−0.134 ± 0.09	−0.80 ± 0.3

*Calculated from k_H/k_D values given in Table 1, using method of least squares.

Several years ago Shiner and Verbanic (26) recognized the difficulty of explaining large solvent effects on isotope rate effects without invoking specific solvation at the site of isotopic substitution. In the ammonium ion decomposition there must be a specific interaction between the α-hydrogen (or deuterium) atoms or the benzyl carbon atom and the solvent molecules to give the different isotope effect for the two solvents, because if it were merely a matter of general solvation of the positive charge, the rate ratio would be larger in acetone than in chloroform. Since this is not the case, it is postulated that a specific interaction contributes a component to the observed isotope effect. It has been postulated by Weiner and Sneen (27, 28) that under some conditions during nucleophilic substitution reactions, acetone is sufficiently nucleophilic to interact with the substrate molecule to form an unstable intermediate. If this postulate were extended to the present work, the interaction would be between the carbonyl group and the benzyl carbon atom, rather than the hydrogens attached to the benzyl carbon atom. The experimental observations do not allow a sufficiently precise definition of the interaction to distinguish between these two similar alternatives, but the isotope effects do clearly show that the α-hydrogens are involved in an important manner. Bearing this in mind, an explanation of the solvent effect on the rate ratio may be formulated in the following way, using "α-hydrogen interaction" as a description of the involvement of the acetone, since this allows the argument to be put most succinctly.

The interaction between the α-hydrogen (deuterium) atoms and the solvent will be stronger the more positive the charge on these atoms. This charge on the α-hydrogen atoms increases during the activation process as the positive charge is transferred from the nitrogen to the benzyl carbon atom. Since C—D releases electrons under the influence of a positive charge to a greater extent than C—H (29), the α-hydrogen-solvent interaction is greater for the deuterium compound than for the hydrogen compound. Also, this interaction is greater in the transition state than in the initial state. Thus, the entropy of the deuterium system will be lower than that of the hydrogen system and the difference between the two systems will be less in the transition state than in the initial state. Therefore, the contribution to $(\Delta S_D^{\ddagger} - \Delta S_H^{\ddagger})$ from this source is positive. Since this effect should be larger in the more polar solvent, this positive contribution to $\Delta\Delta S^{\ddagger}$ renders the observed value in Table 2 for acetone less negative than it otherwise would be, compared to the value for chloroform. The less negative value in turn yields a smaller positive $\Delta\Delta G^{\ddagger}$ for acetone and hence a smaller rate ratio.

This type of solvent effect is, of course, a minor component of the overall isotope effect which results from the quite substantial positive values of $\Delta\Delta G^{\ddagger}$ noted earlier.

Thus, the α-deuterium isotope effect is consistent with the type of transition state envisaged in the previous work (1–3) and its variation with the solvent may be explained reasonably in terms of a specific solvent participation in the reaction.

Experimental

Toluene-α-d_3 was purchased from Merck, Sharpe and Dohme of Canada Limited and converted into benzyl-α-d_2 bromide by *N*-bromosuccinimide containing a trace of benzoyl peroxide. The preparation was carried out on a 1 g scale using the conditions given by Johnstone and Stevens (30). A nearly quantitative yield was obtained and the product was purified by distillation; boiling range 135–138° at 22 mm Hg.

Benzyl-α-d_2-phenyldimethylammonium bromide was prepared from the deuterated benzyl bromide and dimethylaniline and purified by recrystallization as described previously (3); melting range 155–157°.

The purification of the solvents and the procedure for the kinetic measurements and calculation of results were exactly the same as in the earlier work (1, 3).

Can. J. Chem. Downloaded from www.nrcresearchpress.com by 210.87.254.42 on 09/05/12
For personal use only.

The authors are grateful for financial support by the National Research Council of Canada.

1. K. T. LEFFEK and F.H-C. TSAO. Can. J. Chem. **46**, 1215 (1968).
2. J. T. BURNS and K. T. LEFFEK. Can. J. Chem. **47**, 3725 (1969).
3. E. C. F. KO and K. T. LEFFEK. Can. J. Chem. **48**, 1865 (1970).
4. W. H. SAUNDERS, JR., S. ASPERGER, and D. H. EDISON. Chem. Ind. 1417 (1957).
5. A. STREITWIESER, JR., and R. C. FAHEY. Chem. Ind. 1417 (1957).
6. K. MISLOW, S. BORCIC, and V. PRELOG. Helv. Chim. Acta, **40**, 2477 (1957).
7. R. R. JOHNSON and E. S. LEWIS. Proc. Chem. Soc. 52 (1958).
8. J. A. LLEWELLYN, R. E. ROBERTSON, and J. M. W. SCOTT. Can. J. Chem. **38**, 222 (1960).
9. S. HARTMAN and R. E. ROBERTSON. Can. J. Chem. **38**, 2033 (1960).
10. R. E. WESTON, JR. Ann. Rev. Nuc. Sci. **11**, 439 (1961).
11. S. SELTZER. J. Amer. Chem. Soc. **83**, 2625 (1961).
12. V. J. SHINER, JR., W. E. BUDDENBAUM, B. L. MURR, and G. LAMATY. J. Amer. Chem. Soc. **90**, 418 (1968).
13. A. STREITWIESER JR., C. L. WILKINS, and E. KIEHLMAN. J. Amer. Chem. Soc. **90**, 1598 (1968).
14. V. J. SHINER, JR., M. W. RAPP, and H. R. PINNICK, JR. J. Amer. Chem. Soc. **92**, 232 (1970).
15. K. T. LEFFEK. Can. J. Chem. **42**, 851 (1964).
16. C-Y. WU and R. E. ROBERTSON. Chem. Ind. 1803 (1964).
17. B. ÖSTMAN. J. Amer. Chem. Soc. **87**, 3163 (1965).
18. S. SELTZER and A. A. ZAVITSAS. Can. J. Chem. **45**, 2023 (1967).
19. G. E. JACKSON and K. T. LEFFEK. Can. J. Chem. **47**, 1537 (1969).
20. M. WOLFSBERG and M. J. STERN. Pure Appl. Chem. **8**, 325 (1964).
21. E. S. LEWIS, J. C. BROWN, and W. C. HERNDON. Can. J. Chem. **39**, 954 (1961).
22. E. S. LEWIS and C. E. BOOZER. J. Amer. Chem. Soc. **76**, 791 (1954).
23. G. J. FRISONE and E. R. THORNTON. J. Amer. Chem. Soc. **90**, 1211 (1968).
24. L. HAKKA, A. QUEEN, and R. E. ROBERTSON. J. Amer. Chem. Soc. **87**, 161 (1965).
25. C. C. LEE and E. W. C. WONG. Tetrahedron, **21**, 539 (1965).
26. V. J. SHINER, JR., and C. J. VERBANIC. J. Amer. Chem. Soc. **79**, 373 (1957).
27. H. WEINER and R. A. SNEEN. J. Amer. Chem. Soc. **85**, 2181 (1963).
28. H. WEINER and R. A. SNEEN. J. Amer. Chem. Soc. **87**, 287 (1965).
29. E. A. HALEVI. Prog. Phys. Org. Chem. **1**, 109 (1963).
30. R. A. W. JOHNSTONE and T. S. STEVENS. J. Chem. Soc. 3346 (1960).

Can. J. Chem. Downloaded from www.nrcresearchpress.com by 210.87.254.42 on 09/05/12
For personal use only.

Can. J. Chem. Downloaded from www.nrcresearchpress.com by 210.87.254.105 on 09/05/12
For personal use only.

Photolysis of Acyl Group IV Metalloids: the Formation of Silyl Radicals

A. G. Brook, P. J. Dillon, and R. Pearce
Department of Chemistry, University of Toronto, Toronto 181, Ontario

Received August 12, 1970

The photolyses of several acylsilanes and one acylgermane in carbon tetrachloride have been shown to involve Norrish Type I cleavage of the metalloid–acyl bond to give metalloidal radicals. These radicals readily abstract chlorine from the solvent.

Canadian Journal of Chemistry, **49**, 133 (1971)

Recently, the photolyses of acetyltriphenylsilane and (−)-acetyl-1-naphthylphenylmethylsilane in carbon tetrachloride were shown to involve the formation of silyl radicals which subsequently abstracted halogen from the solvent, in the latter case with significant retention of optical configuration (1). In other studies it was demonstrated that photolysis of acylsilanes in alcohols proceeded via a siloxycarbene intermediate (2).

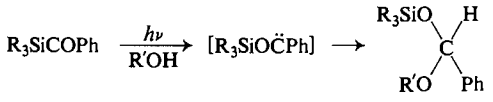

In order to further investigate the apparent duality of the reaction pathway (radical or siloxycarbene formation) a more detailed investigation was begun; the photolysis of a variety of acylsilanes in carbon tetrachloride is reported here.

The photolysis of acetyltrimethylsilane in carbon tetrachloride produced trimethylchlorosilane (99%), acetyl chloride (67%), 1,1,1-trichloropropanone (30%), and hexachloroethane (61%). These results are in accord with those found previously for acetyltriphenylsilane (1). The nature of the products suggests that acetyl and trimethylsilyl radicals are formed by Norrish Type I cleavage of the acyl–silicon bond followed by reactions of the radicals with the solvent, as shown in Scheme 1.

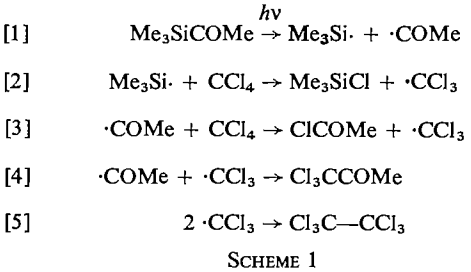

Scheme 1

If Scheme 1 adequately describes the overall process, then the sum of the yields of acetyl chloride and 1,1,1-trichloropropanone, representing products derived from the acetyl radical, and the sum of the yields of 1,1,1-trichloropropanone and hexachloroethane, representing products derived from the trichloromethyl radical, will each be 100%. These were found to be 97 and 91% respectively.

The possible occurrence of other minor reactions was briefly investigated. Hexamethyldisilane, which would result from a combination of trimethylsilyl radicals, trimethylsilane from hydrogen abstraction, and trichloromethyltrimethylsilane from cross-combination of radicals, could not be detected in the reaction mixture. It can be concluded therefore, that the reaction pathways depicted in Scheme 1 adequately describe the photolysis of acetyltrimethylsilane in carbon tetrachloride.

The yields of 1,1,1-trichloropropanone, acetyl chloride and hexachloroethane were found to be temperature dependent, the yield of trichloropropanone being observed to decrease with increasing temperature while the yields of acetyl chloride and hexachloroethane increased with increasing temperature, as shown in Table 1. These observations are explained if the activation energy for the abstraction of chlorine by the acetyl radical, step 3, Scheme 1, is greater than that for the radical combination reactions, steps 4 and 5, as would be expected.

Table 1. Yields of photolysis products at various temperatures

	Temperature (°C)		
Product	−23	0	76
Me_3SiCl	100	99	99
Cl_3CCOMe	38	30	14
MeCOCl	63	67	74
Cl_6C_2	48	61	63

TABLE 2. Products of photolyses in carbon tetrachloride

Acylmetalloid*	Products
$Me_3SiCOEt$	Me_3SiCl (~ 100%), EtCOCl (53%), Cl_6C_2 (54%), Cl_3CCOEt (yield undetermined)
$Et_3SiCOMe$	Et_3SiCl (94%), MeCOCl (65%), $MeCOCCl_3$ (35%), Cl_6C_2 (64%)
n-$Pr_3SiCOMe$	*n*-Pr_3SiCl, MeCOCl, $MeCOCCl_3$, Cl_6C_2 (yields undermined)
n-$Bu_3SiCOMe$	*n*-Bu_3SiCl, MeCOCl, $MeCOCCl_3$, Cl_6C_2 (yields undetermined)
$Me_3SiCOPh$	Me_3SiCl (87%), PhCHO, PhCOCl, Cl_6C_2
$Ph_3SiCOPh$	No reaction
$Ph_3GeCOPh$	Ph_3GeCl (94%), PhCOCl (91%), Cl_6C_2 (98%)
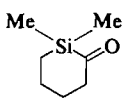	$Me_2ClSi(CH_2)_4COCl$ (48%), $Me_2ClSi(CH_2)_4COCCl_3$ (14%),† Cl_6C_2 (yield undetermined)

*In all photolyses 0.2 g of acylmetalloid was irradiated in 5 ml of dry carbon tetrachloride at 0° under nitrogen for about 1–2 h using a low pressure 100 W mercury lamp.
†Yields are those of product isolated by fractional distillation.

The photolysis of a number of other acylsilanes and one acylgermane in carbon tetrachloride were also investigated and analogous results were obtained for all other acylmetalloids studied (except benzoyltriphenylsilane), as shown in Table 2.

When benzoyltrimethylsilane was photolyzed, benzaldehyde was found, presumably because the benzoyl radical abstracts hydrogen from the trimethylsilyl group. This is supported by the observation that no benzaldehyde was formed in the photolysis of benzoyltriphenylgermane, where only aromatic protons are available. Acetaldehyde was not observed in the reactions involving the acetyl radical.

Benzoyltriphenylsilane was inert to photolysis even over prolonged periods of time. This is in marked contrast to its rapid photochemical decomposition in the presence of alcohols (2) and its unique behavior is not understood. Benzoylsilanes and benzoylgermanes exhibit an $n \rightarrow \pi^*$ absorption maximum at about 420 mμ, whereas acetylsilanes and acetylgermanes have a maximum at about 380 mμ. The energy absorbed appears sufficient to cause rupture of the silicon–acetyl bond on one hand, but is insufficient to break the silicon–benzoyl bond. Since the carbon–germanium bond is considerably weaker than the silicon–carbon bond, the photolytic decomposition of benzoyltriphenylgermane is not unexpected. This explanation of the above observations does not, however, satisfactorily explain the photolysis of benzoyltrimethylsilane, whose absorption maximum is virtually identical to that of benzoyltriphenylsilane.

The reaction of the cyclic acylsilane, 1,1-dimethyl-1-silacyclohexan-2-one, is noteworthy. Preliminary investigations of the photolytic decompositions of cyclic acylsilanes in a variety of media have indicated that cyclic siloxycarbenes are involved (3–5). The products obtained on photolysis of the silacyclohexanone in carbon tetrachloride are 5-(chlorodimethylsilyl)pentanoyl chloride and 1,1,1-trichloro-6-(chlorodimethylsilyl)hexan-2-one as expected from a simple Norrish Type I cleavage of the silicon–carbonyl bond followed by reactions as in Scheme 1; thus siloxycarbenes do not appear to be involved under these conditions.

From the preceding results it appears that aliphatic acylsilanes when photolyzed in carbon tetrachloride undergo Norrish Type I cleavage exclusively: further work is underway to establish more clearly the factors which determine whether siloxycarbene formation or Norrish Type I cleavage will occur in other solvents.

Experimental

General

The n.m.r. spectra were recorded on either a Varian A-60 or A56/60 instrument using carbon tetrachloride. The i.r. spectra were obtained on a Perkin–Elmer Model 237-B IR Spectrometer. The u.v. spectra were obtained

Can. J. Chem. Downloaded from www.nrcresearchpress.com by 210.87.254.105 on 09/05/12
For personal use only.

TABLE 3. Analysis and physical properties of new acyclic acylsilanes

Acylmetalloid	Boiling point (°C)	n_D^{20}	Analyses (%) Calculated C	Calculated H	Found C	Found H
$Me_3SiCOCH_2CH_3$	140/760 mm	1.4191	55.32	10.83	55.05	10.98
$Et_3SiCOMe$	180/760 mm	1.4426	60.69	11.46	60.48	11.68
n-$Pr_3SiCOMe$	110/5 mm	1.4456	65.93	12.07	65.90	12.10
n-$Bu_3SiCOMe$	84/15 mm	1.4496	69.35	12.47	69.60	12.59

TABLE 4. The i.r. and u.v. spectra of acylsilanes

Acylmetalloid	ν (C=O)	λ (ε)
$Me_3SiCOMe$	1647	388 (93), 372 (126), 358 (100) 346 (62), 333 (34), 323 (18)
$Me_3SiCOC_2H_5$	1646	382 (115), 366 (126), 352 (100), 340 (60), 328 (32), 317 (14)
$Et_3SiCOMe$	1644	390 (101), 372 (131), 360 (102), 343 (63), 335 (35), 322 (15)
n-$Pr_3SiCOMe$	1644	389 (97), 374 (128), 360 (98), 347 (61), 334 (32), 322 (15)
n-$Bu_3SiCOMe$	1643	382 (115), 366 (126), 352 (100), 340 (60), 328 (32), 317 (14)

on a Unicam SP800 Spectrometer. A Varian Aerograph Series 200 Gas Chromatograph was used for product analysis with a 20′ × 1/4″ aluminum column containing 20% SE30 on Chromasorb B. The photolysis employed a PAR-38 100 W mercury floodlamp.

Preparation of Acylmetalloids

All acylmetalloids were prepared by previously described methods (6–8). Physical data of new acylmetalloids are listed in Table 3 and spectroscopic data are given in Table 4.

Photolysis of Acylmetalloids in Carbon Tetrachloride

Products were identified by i.r. and n.m.r. spectroscopy, and by v.p.c., each product being identified by comparison of the retention time of an authentic sample with that of the appropriate peak in the v.p.c. Trichloromethyltrimethylsilane was prepared for comparison purposes by the method of Bamford and Pant (9). Its absence in the photolysate of acetyltrimethylsilane in carbon tetrachloride was demonstrated by v.p.c. Yields of all products were determined using an internal standard and the peak-weight method.

In the case of the cyclic acylsilane, the photolysate from the acylsilane (3.75 g) in CCl_4 (300 ml) was evaporated and the residual liquid was distilled on a semi-micro, spinning-band column to give 5-(chlorodimethylsilyl)pentanoyl chloride, 2.7 g (48%), b.p. 48–50°/0.12 mm, and somewhat impure 1,1,1-trichloro-6-(chlorodimethylsilyl)hexan-2-one, 1.1 g (14%), b.p. 73–74°/0.10 mm.

Anal. Calcd. for $ClMe_2Si(CH_2)_4COCl$: C, 39.44; H, 6.62; Cl, 33.26. Found: C, 39.23; H, 6.84; Cl, 33.40. The i.r. (film): 5.56 (C=O) μ.

Anal. Calcd. for $ClMe_2Si(CH_2)_4COCCl_3$: C, 32.45; H, 4.77; Cl, 47.89. Found: C, 33.21; H, 4.78; Cl, 46.89. The i.r. (film): 5.70 (C=O) μ.

We are indebted to the National Research Council of Canada for support of this research and for a scholarship to P.J.D.

1. A. G. BROOK and J. M. DUFF. J. Amer. Chem. Soc. **91**, 2118 (1969).
2. A. G. BROOK and J. M. DUFF. J. Amer. Chem. Soc. **89**, 454 (1967).
3. J. B. PIERCE. Ph.D. Thesis. University of Toronto, Toronto, Ontario, 1966.
4. H. KUCERA. M.Sc. Thesis. University of Toronto, Toronto, Ontario, 1968.
5. A. G. BROOK. *In* Advances in organometallic chemistry. Vol. 7. Academic Press, New York, 1968. p. 95.
6. A. G. BROOK, J. M. DUFF, P. F. JONES, and N. R. DAVIS. J. Amer. Chem. Soc. **89**, 431 (1967).
7. E. J. COREY, D. SEEBACH, and R. FREEDMAN. J. Amer. Chem. Soc. **89**, 434 (1967).
8. A. G. BROOK, M. QUIGLEY, G. J. D. PEDDLE, N. V. SCHWARTZ, and C. M. WARNER. J. Amer. Chem. Soc. **82**, 5102 (1960).
9. W. R. BAMFORD and B. C. PANT. J. Chem. Soc. (C) 1470 (1967).

Can. J. Chem. Downloaded from www.nrcresearchpress.com by 210.87.254.105 on 09/05/12
For personal use only.

Can. J. Chem. Downloaded from www.nrcresearchpress.com by 210.87.254.5 on 09/05/12
For personal use only.

Chlorination of Pyrroles. Part I

D. G. DURHAM AND A. H. REES
Department of Chemistry, Trent University, Peterborough, Ontario

Received June 5, 1970

Formylation of 1-phenylpyrrole gave mainly the 2-aldehyde which was converted to the methyl ester. Chlorination produced the 4- and 5-monochloro, the 4,5-dichloro and the 3,4,5-trichloro derivatives and 2-methoxycarbonyl-5-oxo-1-phenyl-2,3,4-trichloro-3-pyrroline which were identified spectroscopically. The mass spectral cracking patterns of the chloropyrrole esters have been interpreted.

Canadian Journal of Chemistry, 49, 136 (1971)

The natural occurrence of chloropyrroles such as pyoluteorin (**1**) (1, 2) and the pyrrolnitrins (**2**) (3–7) led us to investigate the chlorination of some pyrroles including 2-methoxycarbonylpyrrole (8) and 2-methoxycarbonyl-1-phenylpyrrole (**3**, X = Y = Z = H, R = COOMe) (9) which we now report.

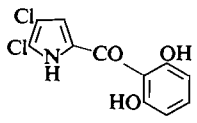

1

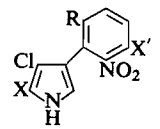

2

3

Formylation (10) of 1-phenylpyrrole gave a 14:1 mixture of 2- and 3-aldehydes. The 2-isomer was converted (8) to the acid **3** (X=Y=Z=H, R = COOH) and its methyl ester. Chlorination of this ester with varying amounts of chlorine in acetic acid gave mixtures of products plus starting material. Attempts to resolve these mixtures were only successful by g.l.c. Chlorination (2 equiv) gave products identified as the 4-chloro (8%), 5-chloro (20%), 4,5-dichloro (40%), and 3,4,5-trichloro (25%) esters by consideration of their n.m.r. and mass spectra. Esters without a 5-chloro substituent had n.m.r. spectra in which the phenyl protons resonated as a singlet (Table 1).

The mass spectra suggest a 1- to 2-phenyl shift (see Scheme 1).

A similar breakdown was observed in the mass spectra of the esters **3** (R = COOMe) after loss of OMe then CO. The esters also lost the methoxycarbonyl group with hydrogen transfer giving M-58 ions **3** (R = H), Table 2, a pathway also observed in 2-methoxycarbonyl furans (11).

We also record *m/e* 77 (Ph^+) and regard its intensity as a measure of the electrophilic character of the pyrrole ring.

Chlorination of ester **3** (X = Y = Z = H, R = COOMe) with four molar equivalents of chlorine gave a product $C_{12}H_8Cl_3NO_3$ having carbonyl absorption at 1770 (α-chloroester) and 1740 (lactam) cm^{-1}. Following known chlorination of pyrrole (12), we assigned to the above compound the structure **8**. There was no indication of chlorination in the phenyl ring.

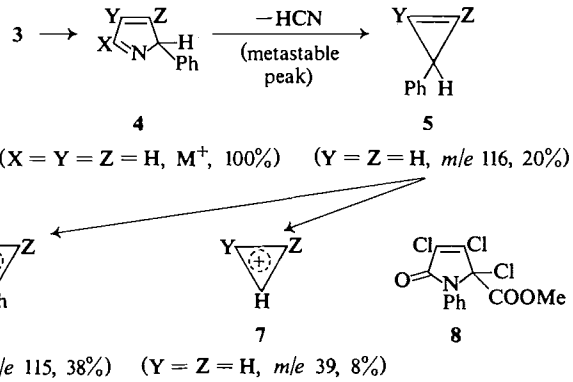

4 (X = Y = Z = H, M^+, 100%) **5** (Y = Z = H, *m/e* 116, 20%)

6 (Y = Z = H, *m/e* 115, 38%) **7** (Y = Z = H, *m/e* 39, 8%) **8**

SCHEME 1

TABLE 1. The n.m.r. spectra of *N*-phenylpyrrole, its aldehydes, and chloroesters*

1-Phenyl protons		2	3	4	5
2.65 s		3.05 m	3.75 m	3.75 m	3.05 m
2.65 s	*CHO*	0.45	3.05 m	3.71 m	3.05 m
2.6 s		2.44 m	*CHO* 0.28	3.34 m	3.0 m
2.7 s	COO*Me*	6.34	3.2 m	3.84 m	3.04 m
2.7 m	COO*Me*	6.34	2.98 d	3.78 d	Cl
			← J = 4.5 Hz →		
2.7 s	COO*Me*	6.32	3.15 d	Cl	3.1 d
			← J = 1.5 Hz →		
2.7 m	COO*Me*	6.38	3.06 s	Cl	Cl
2.7 m	COO*Me*	6.35	Cl	Cl	Cl
2.55 s	COO*Me*	6.16	Cl	Cl	=O
	Cl				

*Run in $CDCl_3$ with TMS internal standard on the JEOLCO C6OHL, τ values quoted.

TABLE 2. Mass spectra of 2-methoxycarbonyl-1-phenylpyrroles*

Chloro	M^+	M-31	M-58	M-86	M-162	Ph^+(*m/e* 77)
Nil	201 90	170 100%	143 12	115 40	39 11	14
4-	235; 237 100% 38	204; 206 75 24	177; 179 6 2	149; 151 7 2	73; 75 3 2	16
5-	235; 237 100% 35	204; 206 88 30	177; 179 8 3	149; 151 3 1	73; 75 10 3	17
4,5-Di-	269; 271; 273 100% 64 10	238; 240; 242 50 35 5	211; 213 4 3	183; 185 2 1	107; 109 5 3	24
3,4,5-Tri-	303; 305; 307; 309 100% 99 32 4	272; 274; 276; 278 50 45 14 1	245; 247; 249 6 5 1		141; 143; 145 6 6 2	40

*Run at 70 eV on the A.E.I. M.S.12 using the direct insertion probe, peaks under 1% omitted.

Experimental

The g.l.c. was done on a Dynatronics Instrument Corp. Chrom-Alyzer-100 with 8′ × ¼″ column of 30% SE 30 silicone, using helium at 235°.

Formylation of 1-Phenylpyrrole

1-Phenylpyrrole, 10 g, was formylated (10) giving 70% distilled 2-aldehyde which after g.l.c. had ν_{max} (film) 1665, 1600, 1530, 1500, 1330 cm^{-1}; mass spectrum *m/e*, (relative intensity) 171 (100), 170 (50), 115 (15), 93 (40), 78 (12), 77 (10), 51 (12), 39 (6).

The 2-aldehyde was characterized as its semicarbazone, m.p. 181–183°, crystallized from methanol, depressed in mixed m.p. with the semicarbazone of **3** (X = Y = R = H, Z = CHO) below.

Anal. Calcd. for $C_{12}H_{12}N_4O$: C, 63.15; H, 5.3; N, 24.5. Found: C, 63.0; H, 5.2; N, 24.6.

The pure 3-aldehyde was obtained by preparative g.l.c. with ν_{max} (film) 1670, 1595, 1535, 1510, 1260, 1200 cm^{-1}. Mass spectrum 171 (95), 170 (100), 115 (15), 77 (13), 51 (12), 39 (7). The semicarbazone had m.p. 188–190° recrystallized from methanol.

Anal. Calcd. for $C_{12}H_{12}N_4O$: C, 63.15; H, 5.3; N, 24.5. Found: C, 63.5; H, 5.3; N, 24.2.

Preparation of 2-Methoxycarbonyl-1-phenylpyrrole

The 2-aldehyde, 11 g, in 100 ml methanol was oxidized (8) giving 9.4 g, 85% of acid, m.p. 164–166°, crystallized from benzene [lit. (9) m.p. 165°]. Esterification with diazomethane gave the ester, m.p. 87–88°, crystallized from light petroleum [lit. (9) m.p. 88°], ν_{max} (Nujol) 1700, 1595, 1270, 1120, 1040, 950, 810 cm^{-1}; u.v. max 264 mμ (ε 24 900).

Chlorination of 3 (X = Y = Z = H, R = COOMe)

Chlorination (2 mol) in acetic acid (8), gave after evaporation of the solvent, a mixture of chloroesters. This was taken up in ether and the solution washed with sodium bicarbonate solution, then with water, and dried ($MgSO_4$). After concentration the residue was resolved by g.l.c. giving the following products:

5-Chloro-2-methoxycarbonyl-1-phenylpyrrole (3, X=Cl, Y = Z = H, R = COOMe), an oil which could not be induced to crystallize, ν_{max} (film) 1715, 1595, 1275, 1150 cm^{-1}.

Anal. Calcd. for $C_{12}H_{10}ClNO_2$: C, 61.3; H, 4.3; Cl, 14.9; N, 5.95. Found: C, 61.5; H, 4.35; Cl, 15.0; N, 5.75.

4-Chloro-2-methoxycarbonyl-1-phenylpyrrole (3, Y=Cl, X = Z = H, R = COOMe), prisms, m.p. 78–80°, recrystallized from light petroleum, ν_{max} (Nujol) 1710, 1595, 1260, 1140, 950, 810 cm^{-1}.

Anal. Calcd. for $C_{12}H_{10}ClNO_2$: C, 61.3; H, 4.3; Cl, 14.9; N, 5.95. Found: C, 61.4; H, 4.4; Cl, 14.0; N, 6.1.

Can. J. Chem. Downloaded from www.nrcresearchpress.com by 210.87.254.5 on 09/05/12
For personal use only.

4,5-Dichloro-2-methoxycarbonyl-1-phenylpyrrole (3, X = Y = Cl, Z = H, R = COOMe), plates, m.p. 97–99°, recrystallized from light petroleum, ν_{max} (Nujol) 1710, 1595, 1270, 1020, 955, 830 cm^{-1}; u.v. max 275 mμ (ε 20 400).

Anal. Calcd. for $C_{12}H_9Cl_2NO_2$: C, 53.4; H, 3.4; Cl, 26.2; N, 5.2. Found: C, 53.3; H, 3.4; Cl, 26.4; N, 5.2.

2-Methoxycarbonyl-1-phenyl-3,4,5-trichloropyrrole (3, X = Y = Z = Cl, R = COOMe), prisms, m.p. 79–81°, recrystallized from light petroleum, ν_{max} (Nujol) 1710, 1595, 1280, 840 cm^{-1}.

Anal. Calcd. for $C_{12}H_8Cl_3NO_2$: C, 47.3; H, 2.65; Cl, 34.9; N, 4.6. Found: C, 47.5; H, 2.7; Cl, 35.1; N, 4.65.

Chlorination (4 mol) as described above, gave **8** which came out of the ether solution, needles, m.p. 132–135°, recrystallized from aqueous ethanol: u.v. max 227 mμ (ε 13 500), n.m.r. Table 1; mass spectrum *m/e*, 319 (M^+, 22), 77 (100).

Anal. Calcd. for $C_{12}H_8Cl_3NO_3$: C, 45.0; H, 2.5; Cl, 33.2; N, 4.4. Found: C, 45.0; H, 2.5; Cl, 33.0; N, 4.4.

We wish to thank Trent University for a Graduate Studentship (to D.G.D.) and the National Research Council of Canada for general support.

1. R. TAKEDA. J. Amer. Chem. Soc. **80**, 4749 (1958); Bull. Agr. Chem. Soc. Japan, **23**, 126, 165 (1959).
2. K. BAILEY and A. H. REES. J. Chem. Soc. (D), 1284 (1969); Can. J. Chem. **48**, 2257 (1970).
3. K. ARIMA, H. IMANAKA, M. KOUSAKA, A. FUKUDA, and G. TAMURA. Arg. Biol. Chem. **28**, 575 (1964).
4. K. ARIMA, H. IMANAKA, M. KOUSAKA, A. FUKUDA, and G. TAMURA. J. Antibiot. (Japan), Ser. A, **18**, 201 (1965).
5. H. NAKANO, S. UMIO, K. KARIYONE, K. TANAKA, T. KISHIMOTO, H. NOGUCHI, I. UEDA, H. NAKAMURA, and Y. MORIMOTO. Tetrahedron Lett. 737 (1966). Chem. Pharm. Bull. **17**, 559 (1969).
6. M. HASHIMOTO and K. HATTORI. Chem. Pharm. Bull. **14**, 1314 (1966).
7. M. HASHIMOTO and K. HATTORI. Bull. Chem. Soc. (Japan), **39**, 410 (1966).
8. P. HODGE and R. W. RICKARDS. J. Chem. Soc. 2543 (1963).
9. A. PICTET and A. STEINMANN. Chem. Ber. **35**, 2532 (1902).
10. R. M. SILVERSTEIN, E. E. RYSKIEWICZ, C. WILLARD, and R. C. KUEHLER. J. Org. Chem. **20**, 668 (1955).
11. R. GRIGG, M. V. SARGENT, D. H. WILLIAMS, and J. A. KNIGHT. Tetrahedron, **21**, 3441 (1965).
12. G. MAZZARA. Gazz. **32** II, 28 (1920). I. T. MILLAR, H. D. SPRINGALL, and N. V. SIDGWICK. The organic chemistry of nitrogen. 3rd Edition. Clarendon Press, Oxford, 1966. p. 629.

Can. J. Chem. Downloaded from www.nrcresearchpress.com by 210.87.254.5 on 09/05/12
For personal use only.

Can. J. Chem. Downloaded from www.nrcresearchpress.com by 210.87.254.6 on 09/05/12
For personal use only.

Structure of Fumarophycine

M. CASTILLO, J. K. SAUNDERS, AND D. B. MACLEAN
Department of Chemistry, McMaster University, Hamilton, Ontario
AND
N. M. MOLLOV AND G. I. YAKIMOV
Institute of Organic Chemistry, Bulgarian Academy of Science, Sofia, Bulgaria

Received August 12, 1970

Fumarophycine, an alkaloid derived from *Fumaria officinalis* of Bulgarian origin, is shown by spectroscopic methods to be a new member of the spiroisoquinoline group. It has been related by chemical methods to the alkaloid, fumaritine, of known constitution.

Canadian Journal of Chemistry, 49, 139 (1971)

The alkaloids of *Fumaria officinalis* were first examined by Manske (1) in 1938. More recently he has reported (2) the isolation of two other minor alkaloids from this source. Alkaloids belonging to the protoberberine (1), protopine (1), and the spiroisoquinoline (3–5) groups are now known to be elaborated by this species. A few years ago Mollov *et al.* (6) examined *F. officinalis* of Bulgarian origin from which fumarophycine, **1**, was isolated as the major alkaloid along with smaller amounts of protopine, cryptopine, and sinactine. They assigned to fumarophycine the formula, $C_{22}H_{23}NO_6$, and from its properties inferred that it was a new alkaloid. By p.m.r. spectroscopy, it was shown that fumarophycine had a methylenedioxy group, an *O*-methyl group, a phenolic hydroxyl group, an alcoholic *O*-acetyl group, an *N*-methyl group and four aromatic protons. Alkaline hydrolysis of fumarophycine gave a compound of the expected mass while methylation with diazomethane gave *O*-methylfumarophycine thus confirming the character of the *O*-acetyl and hydroxyl functions. Further examination of fumarophycine using high resolution mass spectrometry and 100 MHz p.m.r. spectroscopy has enabled us to assign its structure.

The mass spectrum of fumarophycine provided the first clue that it was a new representative of the spiroisoquinoline group of alkaloids. In the high mass region besides a molecular ion peak at *m/e* 397 (25)[1] there were peaks at 355 (26), M-C_2H_2O, 354 (100), M-C_2H_3O, and 337 (48), M-$C_2H_4O_2$. The most significant peak in the spectrum appeared at *m/e* 192 (6) of composition $C_{11}H_{14}NO_2$. Previous examination (5, 7) of the mass spectra of spiroisoquinoline alkaloids containing a hydroxyl group in the spiro system has shown that they fragment to dihydroisoquinolinium ions and these ions are often the most intense in the spectra. The low intensity of this ion, to which we assign structure *a*, in the case of fumarophycine, is not surprising since the hydroxyl group is acetylated. Fragmentation to give *m/e* 192 could occur only after loss of ketene. Thus from its mass spectrum and from its origin it appears that fumarophycine is another example of the spiroisoquinoline group of alkaloids as represented in partial structure *b*. The methoxyl and hydroxyl groups are placed in ring A because of the composition of ion *a*. The mass spectrum does not, however, provide any information concerning the substitution pattern. It was necessary, therefore, to turn to p.m.r. spectroscopy which has been used so successfully with other members of this series (3–5, 7, 8) to confirm the structure and to define the substitution pattern and the relative stereochemistry.

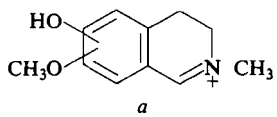

a

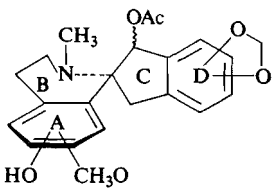

b

[1]Ion intensities are given in brackets. The composition of the ions has been established by accurate mass measurement.

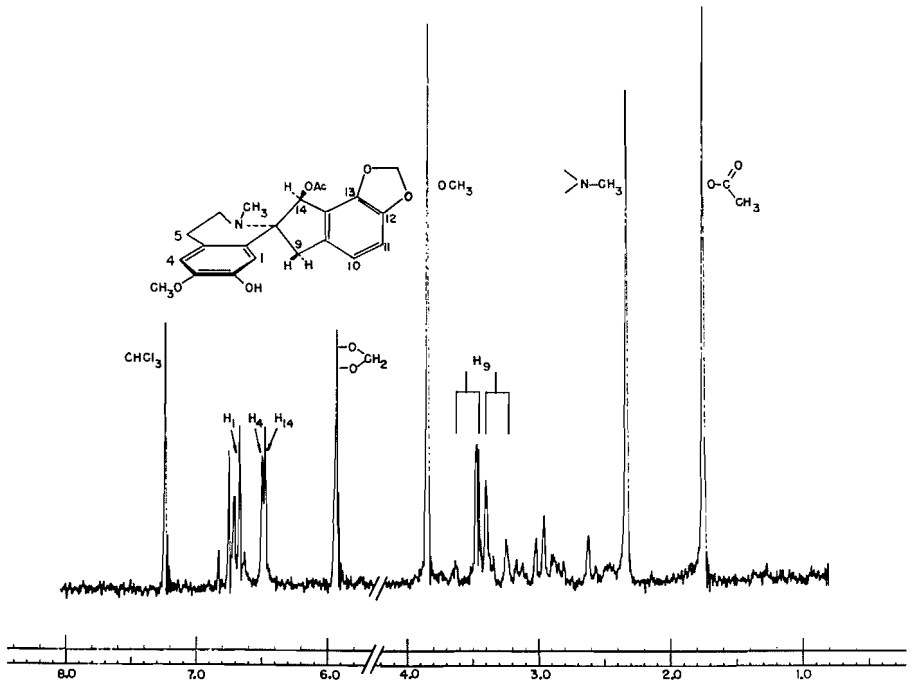

FIG. 1. The 100 MHz p.m.r. spectrum of fumarophycine.

The 100 MHz p.m.r. spectrum of fumarophycine, Fig. 1, has confirmed the original assignment of substituent groups made by Mollov *et al.* Thus, we find a signal of area 2 at 5.94 δ assigned to the methylenedioxy group and three singlets of area 3 at 1.74, 2.32, and 3.94 which are assigned, respectively, to acetyl-methyl, *N*-methyl and *O*-methyl groups. In the region 2.32 to 3.94 δ there are signals corresponding to six aliphatic protons. Two of these are present as an AB quartet, δ H_A = 3.32, H_B = 3.55, J_{AB} = 16 Hz. These signals are assigned to the benzylic protons at C-9. The remaining four protons in this region may be attributed to those at C-5 and -6. In the region 6.0–7.0 δ there are signals corresponding in area to five protons. Two of these are present as an aromatic AB quartet, δ H_{10} = 6.66, H_{11} = 6.79, $J_{H_{10}H_{11}}$ = 8.0 Hz while the other three are singlets at 6.67, 6.50 and 6.48 δ representing the protons at C-1, -4, and -14 respectively. The assignment of these signals to specific protons in the system is based on measurement of nuclear Overhauser effects (n.O.e.) (9).

The n.O.e. measurements were used in the elucidation of the structure of other alkaloids of this ring system (4, 5, 7, 8). When this technique was applied to **1**, the following results were obtained. Irradiation of the signal at 2.32 δ (*N*-CH_3) resulted in an increase of area of 25% for the signal at 6.48 δ. Accordingly, we can assign the latter signal to the proton geminal to the acetoxy group at C-14 and at the same time we have established its relative stereochemistry. Irradiation at the center of the benzylic AB quartet increased the area of the signal at 6.67 δ by 25% which permits assignment of this singlet to the proton at C-1. The singlet at 6.50 δ must then be attributed to C-4. This has been confirmed by the observation that there is an increase in area of 8% for this signal on irradiation of the axial proton at C-5 (3.50 δ). There is no observable change in area of the signal at 6.67 δ as a result of this latter irradiation. The assignment of the methoxyl group at C-3 is based on the evidence that irradiation of the methoxyl signal at 3.94 δ increases the area of the signal at 6.50 δ by 24% but does not affect the signal at 6.67 δ. Finally we are able to assign the protons of the aromatic AB quartet to C-10 and -11. Irradiation of the

Can. J. Chem. Downloaded from www.nrcresearchpress.com by 210.87.254.6 on 09/05/12
For personal use only.

protons of the benzylic AB quartet increased the area of the signal at 6.66 δ by 20%. This is compatible with the observation that the higher field doublet of this AB quartet is broader than its lower field counterpart, a reflection of the fact that ortho-benzylic coupling is stronger than meta (10).

The presence of the acetyl group in fumarophycine has deshielded the proton at C-1 relative to non-acetylated analogues (5). Moreover, the relatively high field absorption of the acetyl-methyl suggests that it is shielded by one or other of the aromatic rings (probably ring A) of this system. Similar effects have been observed in the spectrum of diacetyl ochrobirine (8).

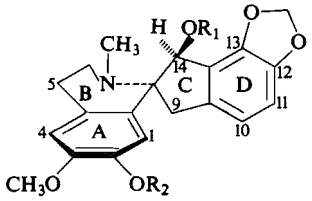

1 R_1 = Ac; R_2 = H
2 R_1 = H; R_2 = H
3 R_1 = Ac; R_2 = Ac
4 R_1 = H; R_2 = CH_3

The p.m.r. data are thus compatible with the spiroisoquinoline structure and indeed demonstrate that **1** is the only satisfactory formulation of fumarophycine. It is, therefore, a derivative of fumaritine **2** (5) whose structure has been confirmed by synthesis (11). We were able to establish a direct relationship by converting both **1** and **2** by acetylation to the common derivative **3**. The i.r. and p.m.r. spectra of **3** prepared from **1** and **2** were identical in all respects.

One feature of the chemistry of fumarophycine remains unresolved. In their initial report Mollov *et al.* (6) reported on the alkaline hydrolysis of fumarophycine to fumarophycinol, m.p. 128–30°, and its subsequent methylation with diazomethane to *O*-methylfumarophycinol, m.p. 134–137°. According to the structure which has been established for fumarophycine, fumarophycinol would be expected to be identical with fumaritine and *O*-methylfumarophycinol with fumaricine (**4**) but they were not. For each pair the melting points were different, the mass spectra were virtually identical, but the p.m.r. spectra, although similar, showed minor but distinct differences. The reason for these differences has not been established and their investigation must await the availability of further supplies of the alkaloid.

Experimental

Methods

Mass spectra were recorded on a CEC 21-110B double-focusing mass spectrometer. For high resolution work spectra were recorded on plates and accurate mass measurements were made using perfluorokerosene as a marker (12).

The p.m.r. spectrum was recorded using the frequency sweep mode of a Varian HA-100 spectrometer. Samples were dissolved in $CDCl_3$ using added TMS as the internal locking signal. Chemical shifts were measured relative to TMS using a V4315 frequency counter incorporated in the instrument. Double irradiation was achieved by employing a Hewlett–Packard 201C audiogenerator at the desired frequency.

Fumarophycine

The isolation and properties of this compound have been described (6). The molecular formula of fumarophycine has been confirmed by high resolution mass spectrometry.

Mol. Wt. Calcd. for $C_{22}H_{23}NO_6$: 397.153. Found: 397.154.

O-Acetylfumarophycine

Fumarophycine (10 mg) was dissolved in acetic anhydride (5 ml) containing pyridine (0.1 ml) and the mixture was allowed to stand at room temperature for 24 h. The excess anhydride and pyridine were evaporated under reduced pressure, the residue triturated in aqueous sodium carbonate, and the suspension extracted several times with chloroform. The chloroform extract was dried over sodium sulfate, and evaporated to a residue which was purified by preparative t.l.c. on silica gel using $CHCl_3$:MeOH = 99:1 to develop the plate. The residue obtained upon elution could not be induced to crystallize but on an analytical thin layer plate it showed only a single spot. The mass spectrum showed a molecular ion at *m/e* 439. The i.r. spectrum had two bands in the carbonyl region at 1730 and 1760 cm^{-1} attributed to alcoholic *O*-acetate and phenolic *O*-acetate groups, respectively. The p.m.r. spectrum of **2** is similar to that of **1** but shows a new peak attributed to the methyl of the phenolic-*O*-acetate group. The principal peaks are

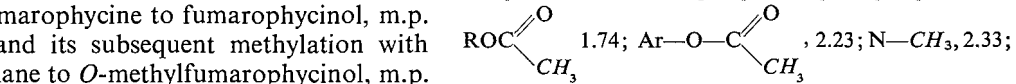

OCH_3, 3.79; and methylenedioxy, 5.96 δ.

O,O-Diacetylfumaritine

Fumaritine was acetylated in the same manner as fumarophycine and the product worked up and purified as described above. Its properties were identical in all respects with those of *O*-acetylfumarophycine.

This work was supported at McMaster by the National Research Council of Canada.

Can. J. Chem. Downloaded from www.nrcresearchpress.com by 210.87.254.6 on 09/05/12
For personal use only.

1. R. H. F. MANSKE. Can. J. Research **16B**, 438 (1938).
2. R. H. F. MANSKE. Can. J. Chem. **47**, 1103 (1969).
3. J. K. SAUNDERS, R. A. BELL, C.-Y. CHEN, D. B. MACLEAN, and R. H. F. MANSKE. Can. J. Chem. **46**, 2873 (1968).
4. J. K. SAUNDERS, R. A. BELL, C.-Y. CHEN, D. B. MACLEAN, and R. H. F. MANSKE. Can. J. Chem. **46**, 2876 (1968).
5. D. B. MACLEAN, R. A. BELL, J. K. SAUNDERS, C.-Y. CHEN, and R. H. F. MANSKE. Can. J. Chem. **47**, 3593 (1969).
6. N. M. MOLLOV, G. I. YAKIMOV, and P. P. PANOV. C. R. Acad. Bulg. Sci. **20**, No. 6, 557 (1967).
7. R. H. F. MANSKE, R. RODRIGO, D. B. MACLEAN, D. E. F. GRACEY, and J. K. SAUNDERS. Can. J. Chem. **47**, 3585 (1969).
8. R. H. F. MANSKE, R. G. A. RODRIGO, D. B. MACLEAN, D. E. F. GRACEY, and J. K. SAUNDERS. Can. J. Chem. **47**, 3589 (1969).
9. F. A. L. ANET and A. J. R. BOURN. J. Amer. Chem. Soc. **87**, 5250 (1965).
10. D. T. WITTIAK, D. B. PATEL, and Y. LIN. J. Amer. Chem. Soc. **89**, 1908 (1967).
11. T. KISHIMOTO and S. UYEO. J. Chem. Soc. (C), 2600 (1969).
12. K. BIEMANN. Pure Appl. Chem. **9**, 95 (1964).

Can. J. Chem. Downloaded from www.nrcresearchpress.com by 210.87.254.6 on 09/05/12
For personal use only.

Nuclear Magnetic Resonance Study of Several Derivatives of 1,3,5,7-Tetramethyltricyclo[5.1.0.0^{3,5}]octane. Stereochemical Assignments by Nuclear Overhauser Enhancements[1]

M. GORDON, W. C. HOWELL, C. H. JACKSON, AND J. B. STOTHERS
Department of Chemistry, University of Western Ontario, London 72, Ontario

Received July 22, 1970

Measurements of the nuclear Overhauser enhancements in the title series permit unequivocal assignments of the 6-substituent in a series of 1,3,5,7-tetramethyltricyclo[5.1.0.0^{3,5}]octan-2-ones and derivatives. Supporting evidence provided by long-range coupling interactions through four σ-bonds is also presented. The proton shifts in these systems appear to depend primarily on the degree of steric hindrance; this aspect is discussed.

Canadian Journal of Chemistry, **49**, 143 (1971)

Can. J. Chem. Downloaded from www.nrcresearchpress.com by 210.87.254.6 on 09/05/12
For personal use only.

Introduction

The synthesis of 1,3,5,7-tetramethyltricyclo-[5.1.0.0^{3,5}]octan-2,6-dione (**1**) by acid-catalyzed decomposition of the dipyrazoline, formed from duroquinone and diazomethane, has been described (1) and the stereochemistry of the cyclo-

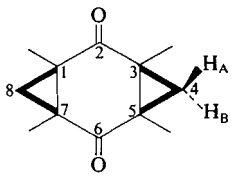

1

propyl rings established as *syn* by partial reduction to two diastereomeric ketoalcohols, **2** and **3**. The stereochemical assignments for the latter, however, were not made since unequivocal evidence was lacking. It is the purpose of this paper to report results of a detailed n.m.r. study of these ketoalcohols and several derivatives which allow us to complete the configurational assignments. Determinations of certain nuclear Overhauser enhancements (n.O.e.) (2) and some long-range coupling constants provide unequivocal evidence for the conclusions presented. The chemical transformations investigated in this study are summarized in Scheme 1, which illustrates the routes employed to prepare 12 new derivatives of the little known tricyclo[5.1.0.0^{3,5}]-octane system. For convenience and clarity the stereochemistry of the various members in this series is indicated in Scheme 1, while the experimental basis of these assignments is discussed later.

[1]This paper represents Part XXII in the series on n.m.r. studies; Part XXI, A. W. Brinkmann *et al.* (25).

Results

Chemical Transformations

The reduction of **1** with one equivalent of sodium borohydride gave a mixture of keto-alcohols, **2** and **3**. After separation by column chromatography, **2** was esterified with acetyl chloride in benzene containing some pyridine to give **4**, the corresponding ketoacetate; treatment of **4** with alcoholic potassium hydroxide, under reflux, regenerates **2**. Catalytic reduction of **1** also yields a mixture of ketoalcohols, **2** and **3**, but **3** predominates. In the manner first described, **3** gives the corresponding ketoacetate **5**; upon refluxing **3** in acetic acid or acetic acid/acetic anhydride, however, ketoacetate **4** is formed exclusively. Treatment of either **2** or **3** with thionyl chloride in benzene leads to the formation of the same chloroketone, **6**; similarly, reaction with phosphorus tribromide in benzene yields one bromoketone, **7**.

A mixture of diols is obtained by borohydride reduction of **2** from which the major component, **8**, is readily separable by t.l.c. Both **8** and **9** can be esterified to the corresponding acetates, **10** and **11**, with retention of configuration at C-2 and -6. Borohydride reduction of **4** yields the hydroxyacetate, **12**, whose structure was confirmed by acetylation to **10**. In contrast to the behavior of **2**, borohydride reduction of **3** yields a single diol, **9**, identical to the minor component formed from **2**. Similarly, reduction of **5** with excess sodium borohydride gave a single hydroxyacetate, **13**, which may be acetylated to give **11**.

In an attempt to obtain a monofunctional derivative of this tricyclo[5.1.0.0^{3,5}]octane system, reductions of the bromoketone, **7**, were investigated. Sodium in *t*-butyl alcohol causes ring opening to form 1,3,5,7-tetramethylbicyclo-

Can. J. Chem. Downloaded from www.nrcresearchpress.com by 210.87.254.6 on 09/05/12
For personal use only.

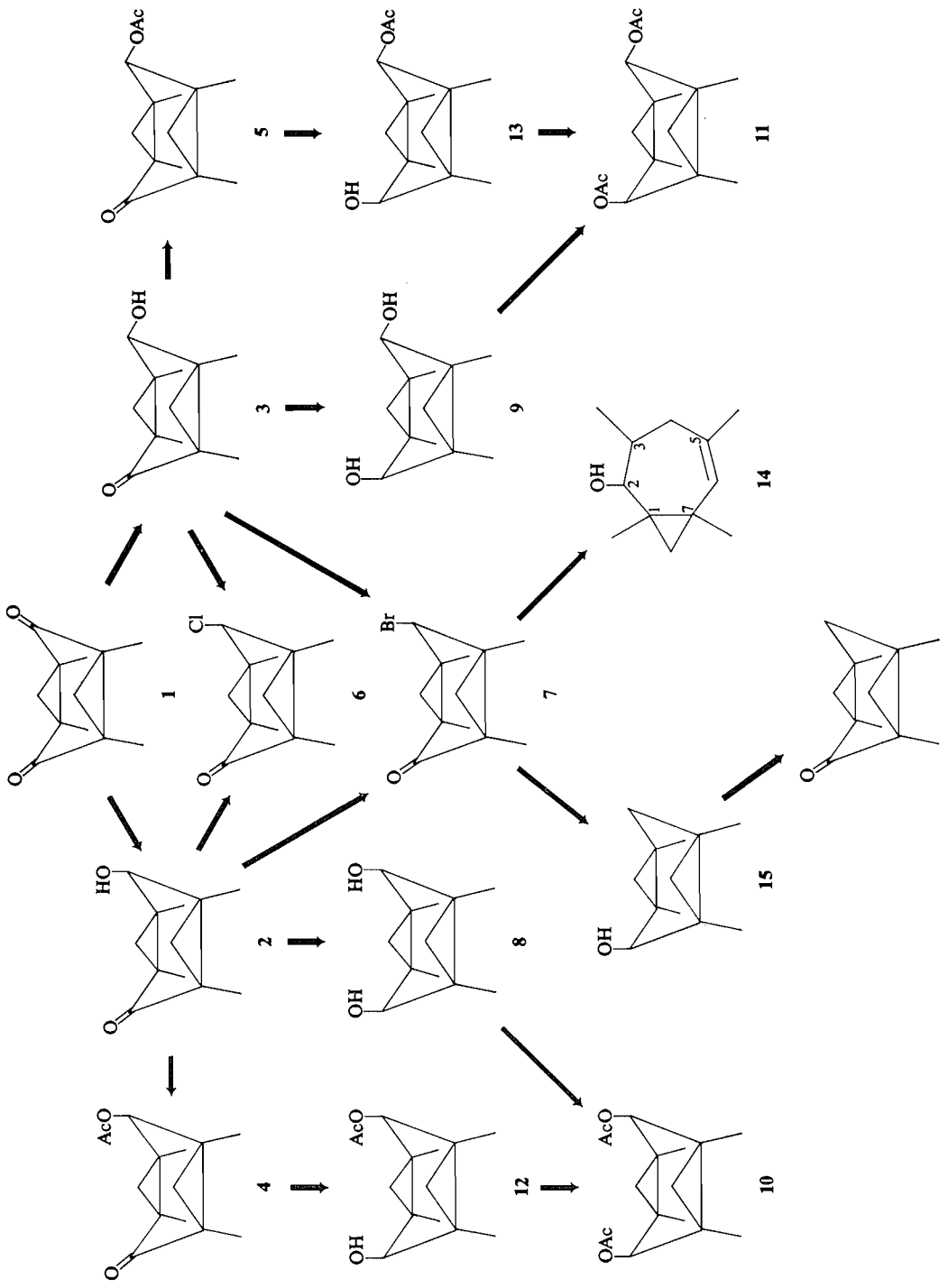

SCHEME 1

TABLE 1. The n.m.r. parameters for several 1,3,5,7-tetramethyltricyclo[5.1.0.0^{3,5}]octanes (δ, p.p.m. from TMS; J in Hz)

	Chemical shifts					Coupling constants			
Compound	H_A	H_B	H_X*	H_Y*	CH_3	J_{AB}	J_{AX}	J_{BX}	J_{BY}
1	2.08	0.81			1.30	5.6_6	—	—	
2	1.67	0.45	4.01		1.26, 1.35	5.7_7	0.2_3	0.9_9	
4	1.73	0.48	5.61		1.19, 1.29 2.20(OAc)	5.7_6	0.1_5	0.9_8	
6	1.71	0.61	4.43		1.30, 1.38	5.9_1	—	0.9_8	
7	1.68	0.65	4.53		1.30, 1.38	5.9_3	0.1_0	1.0_0	
3	1.74	0.53	4.13		1.27, 1.35	5.9_4	—	0.1_0	
5	1.68	0.55	5.72		1.12, 1.24 2.09(OAc)	6.1_0	—	—	
8	0.75	−0.20	3.93	3.93	1.20				
9	0.97	−0.02	3.83	4.07	1.28, 1.32				
10	1.13	−0.08	5.57	5.57	1.03 2.13(OAc)	5.8_7	0.1_5	0.6_8	0.1_5
11	1.05	0.10	5.47	4.93	1.12, 1.18 2.13(OAc)	5.9_5	0.2_0	—	0.2_5
12	0.95	−0.13	5.55	3.93	1.03, 1.20 2.13(OAc)				
13	0.88	−0.08	5.50	4.03	1.00, 1.30 2.08(OAc)				
15	0.58	0.19	1.66† 1.97†	3.97	1.13, 1.27	5.1_0	—	0.5_3	—
16	1.48	0.46	1.82‡ 2.76‡		1.16, 1.23	5.5_2	0.4_0	0.8_1	

*X and Y indicate C-6 and -2, respectively.
†Geminal coupling, 14.4_8 Hz.
‡Geminal coupling, 14.5_8 Hz.

[5.1.0]oct-5-en-2-ol, **14**, whose structure and stereochemistry may be ascertained from its proton spectrum and that of the product obtained by reaction in *t*-butyl alcohol-*d*, as discussed below. Reaction of **7** with excess sodium borohydride in aqueous *t*-butyl alcohol, however, yields, as the major product, the alcohol, **15**, which may be oxidized with manganese dioxide to the corresponding ketone, **16**. It is interesting that reduction of **16** with lithium aluminum hydride yields a single alcohol, **15**. In contrast, Winstein and coworkers (4) found that reduction of the closely related ketone, **17**, gives both epimeric alcohols in a 1:1 ratio.

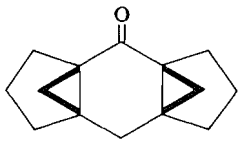

17

Proton Spectra

The proton spectra of the series **1–13** are similar. Each exhibits an AB pattern for the cyclopropyl methylene protons, two singlets for the two pairs of methyl groups on quaternary carbon (except the symmetrical cases) and signals for the methine protons at C-6 (and C-2). In these systems, δ_{AB} is relatively large, in the range 0.95–1.21 p.p.m., with J_{AB} 5.52–6.10 Hz. The methine signals for the series **2**, **4**, **6**, **7**, and **10**, appear as triplets with $J \sim 1.0$ Hz indicating long-range coupling with the cyclopropyl methylene protons. Accordingly one-half of the AB pattern, the B portion at higher field, exhibits these small splittings which may be eliminated by spin decoupling. In some cases a smaller long-range coupling of the A portion is also apparent, J 0.1–0.2 Hz. Detailed n.m.r. studies were not carried out on **12** and **13**, while the relative insolubilities of **8** and **9** in chloroform, the solvent used for all other analyses, precluded extensive n.m.r. examination. The proton spectral data for the tricyclic derivatives are collected in Table 1.

Discussion

The exclusive formation of **4** by acetolysis of **3** bears direct analogy with the findings of Winstein and coworkers (3) for the closely related system, **18**. Solvolysis of either of the epimeric acetates, **18**, gave the same mixture of epimeric alcohols,

Can. J. Chem. Downloaded from www.nrcresearchpress.com by 210.87.254.6 on 09/05/12
For personal use only.

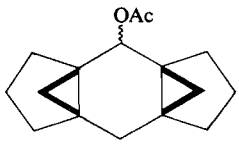

18

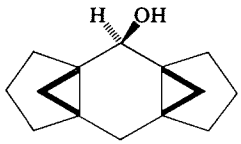

19

one of which constitutes more than 99% of the mixture and was assigned structure **19**, with the hydroxyl group *cis* to the cyclopropyl rings. In fact **18** is one of the most reactive secondary ester systems yet reported indicating the formation of a remarkably stable carbonium ion, a biscyclopropylcarbinyl system. In methanolic potassium hydroxide, only partial saponification occurs along with the formation of a substantial amount of solvolysis product, the methyl ether corresponding to **19** (4). Undoubtedly a similar carbonium ion, or mixture of ions, is generated in the present system. The formation of a single haloketone from either epimeric alcohol, **2** or **3**, is additional evidence of the intermediacy of this species.

The remarkable reactivity of this system suggested possible routes to monofunctional derivatives. A variation of the carbonium-ion trapping method (5) was successful whereby solvolysis of the bromoketone, **7**, in aqueous *t*-butyl alcohol containing a large excess of sodium borohydride leads to the monoalcohol, **15**. To minimize alcoholysis, the bulky *t*-butyl alcohol was chosen enabling the intermediate to be efficiently trapped by borohydride ion. Simple reduction of **7** with sodium in *t*-butyl alcohol, however, leads to **14** apparently following a reaction course analogous to the 1,4-homoelimination found by Winstein (6) for the dichloro derivative, **20**, which, with lithium/*t*-butyl alcohol in tetrahydrofuran, gives 1,3,5,7-tetramethylbicyclo[5.1.0]octa-2,5-diene, **21**.

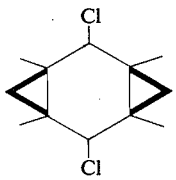

20

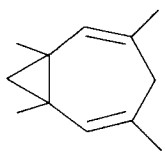

21

The structure and probable conformation of **14** can be assigned from its proton spectrum which contains two singlets δ 1.03, 1.08 for methyl groups on quaternary C-1 and -7 and two doublets, δ 1.01 (J 7 Hz), 1.71 (J 1 Hz), also assignable to methyl groups, on saturated carbon (Me—C_3—H) and on the olefin carbon (C-5), respectively. The small coupling for the latter is indicative of a trisubstituted double bond and, as confirmation, a single olefinic proton (C-6), δ 5.32, was shown to be coupled to the 1.71 p.p.m. methyl signal by spin decoupling. An AB pattern typical of the cyclopropyl methylene protons is clearly apparent, δ_A 0.44, δ_B 0.26, J_{AB} 4.5 Hz, as is the hydroxyl signal, confirmed by deuterium exchange. In addition, a doublet centered at δ 2.65 with J = 10 Hz may be assigned to a carbinyl proton, H—C_2—O. Complex patterns in the region 2.4–2.7 and 1.4–1.9 p.p.m. were shown to arise from one and three additional protons respectively. Synthesis of **14** using *t*-butyl alcohol-*d* gives a product whose spectrum confirms the assignments of the carbinyl proton and shows that a second position is deuterated since the higher field multiplet decreases in intensity. These results are in accord with a two-step process whereby the initial product is the unsaturated enol, **22**, which upon ketonization (with incorporation of a deuterium atom) is reduced to the unsaturated alcohol, 1,3,5,7-tetramethylbicyclo[5.1.0]oct-5-en-2-ol (**14***a*) with a total incorporation of two deuterium atoms. The protons at C-2 and -3 appear to be *trans*-diaxial, or nearly so, because of the 10 Hz vicinal coupling found for the carbinyl proton. In addition, its relatively high shielding, δ 2.65, compared to that, for example, in the ketoalcohols, **2** and **3**, δ 4.01 and 4.13, respectively, suggests that this proton is lying over the olefinic bond. The well-known long-range shielding effect of the olefinic bond tends to shield nuclei in this orientation (7). Inspection of molecular models indicates a likely conformation may be represented as **14***b*, although **14***c* would appear to have smaller destabilizing nonbonded interactions. It would also retain the diaxial disposition of the C-2 and -3 protons, but there would be no explanation for the pronounced upfield shift of the carbinyl proton. The assignment of the relative orientation of the hydroxyl and cyclopropyl groups in **14***a* follows from the results for the other derivatives but this stereochemistry is not established. Alternatively the unsaturated bicyclic alcohol may have structure **14***d* for which there are also two conformations corresponding to **14***b* and *c*;

Can. J. Chem. Downloaded from www.nrcresearchpress.com by 210.87.254.6 on 09/05/12
For personal use only.

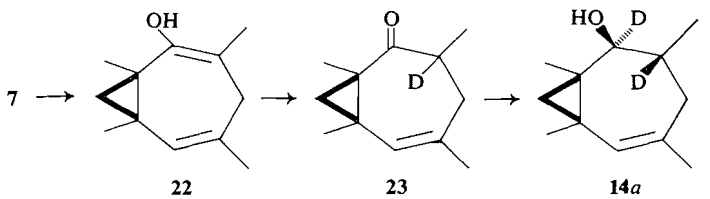

22 23 14*a*

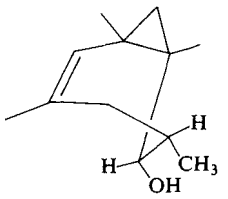

14*b*

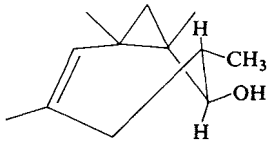

14*c*

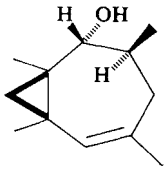

14*d*

the boat-like form similarly places the carbinyl proton over the double bond while retaining its *trans*-diaxial disposition relative to the C-3 proton. The much smaller shift difference between the cyclopropyl protons, δ_{AB} 0.18, compared to that in the tricyclic systems suggests that the deshielding influence of closely neighboring protons has been eliminated so that one of these protons is not sterically crowded.

The use of n.O.e. measurements to determine the relative orientations of protons in a wide variety of molecules is becoming increasingly popular (2, 8–10). It has been amply demonstrated that closely-neighboring protons provide a major mechanism for spin-lattice relaxation of each proton such that saturation of one of the neighbors causes an increase in the integrated intensity of the other's absorption. Thus the spatial relationship of various nonequivalent protons in a given molecule may be determined. The present system seems ideally suited for n.O.e. measurements since the methine proton at C-6 (-2) which is *trans* to the cyclopropyl rings must lie close to the vicinal methyl groups with the *cis*-methine proton further removed. Consequently, differential n.O.e. results may be expected for these protons in **2**–**16** such that the orientation of the oxygen function may be unequivocally established. Similarly, a distinction between the cyclopropyl methylene protons should be possible since the proton *cis* to the methyl groups should be affected more than its geminal partner. It has been shown (9), however, that the n.O.e. for a methylene proton caused by saturation of vicinal or further separated protons is small because the major relaxation occurs by interaction with its geminal neighbor. In any event the enhancement is sufficient to determine unequivocally the relative orientations. For the present series, the n.O.e. results are listed in Table 2.

From these results it is apparent that the n.O.e. for the carbinyl methine protons in the epimeric alcohols, **2** and **3**, and acetates, **4** and **5**, differ appreciably. The much larger values for **2** and **4** confirm the *cis* orientation of the oxygen functions with respect to the cyclopropyl rings. The even larger enhancements in the chloro- and bromoketones, **6** and **7**, are strong evidence for the assigned stereochemistry although the epimers are not available for direct comparisons. Similarly the high field B proton of the cyclopropyl methylene group is appreciably affected by saturation of the methyl protons. The one exception, **4**, is

Can. J. Chem. Downloaded from www.nrcresearchpress.com by 210.87.254.6 on 09/05/12
For personal use only.

TABLE 2. The n.O.e. results for several tricyclooctanes

Compound	Nuclear Overhauser enhancements*			
	$H_X\{CH_3\}$	$H_B\{CH_3\}$	$H_B\{H_A\}$	$H_A\{H_B\}$
1		17	19	19
2	16	10		
3	8	9		
4	33	1		
5	14	13		
6	39	9		
7	34			
10	32	24		
11	29			
	(29)†			
15			10	7
16	28		15	
	(6)‡			

*Expressed as % increase in integrated intensity upon saturation of the interacting nuclei; $H_i\{H_j\}$ denotes observations of H_i with saturation of H_j.
†Bracketed value found for C-2 methine proton.
‡Bracketed value found for C-6 methylene proton *cis* to the cyclopropane rings.

puzzling but an explanation is not evident to us. It must be noted, however, that the high field portion of the AB pattern exhibits the larger long-range coupling with the methine proton strongly indicating that this proton is indeed *cis* to the methyl groups (see below). The fact that significant enhancements are found for the methine protons *trans* to the methyl groups in **3**, **5**, and **16** clearly shows that appreciable relaxation occurs via the methyl protons, but the much larger n.O.e. in each epimeric case (**2**, **4**, and **16**) confirms the assignments. In the extreme case, **11**, the n.O.e. is the same for both the *cis* and *trans* methine protons indicating that the central ring must be nearly planar. It seems reasonable that the geometry of the six-membered ring depends on the nature of the 2- and 6-substituents and the variations in the n.O.e. results may be taken as evidence for this idea. Unfortunately it is not possible to derive even semi-quantitative estimates of the ring geometry from the available data. It is interesting that the geminal proton enhancements, *i.e.* $H_A\{H_B\}$ etc., are somewhat smaller than those found for a variety of methylene groups in other systems (9); the values for the C-6 methylene protons in **16** were found to be 19 and 24% for the upfield and downfield protons, respectively. These results, with those in Table 2, indicate that other pathways also make substantial contributions to the overall relaxation for these protons.

The long-range coupling constants of *ca.* 1 Hz (J_{BX}) exhibited by the *trans* C-6 proton with the upfield cyclopropyl proton constitute confirmatory evidence for the assignments in **2**, **4**, **6**, **7**, **10**, **14**, and **15**. These are four-bond couplings through a saturated network for which it is known that the maximum interaction occurs for a "W" configuration (11, 12) which is closely approached for the *trans* methine proton and the cyclopropyl proton *cis* to the methyls. It is expected that the long-range interaction between the remaining cyclopropyl methylene proton and the *trans* C-6 proton (J_{AX}) will be much smaller; the results in Table 1 (J_{AX}) are in complete agreement with this expectation. The J_{BX} values for **3** and **5**, on the other hand, are very small, $\leqslant 0.1$ Hz, indicating that the relative orientation of the cyclopropyl and methine protons does not approach the "W" configuration; analogous results are well documented (11–14). It is interesting that the long-range couplings in **11**, having both *cis* and *trans* acetoxyl groups, are almost equal but small, 0.2 Hz. These data indicate that the central six-membered ring has a geometry appreciably different from that in the other disubstituted tricyclic systems. It may be suggested that this ring is flatter in **11** since the *cis*-diacetate exhibits a long-range coupling of 0.7 Hz, significantly smaller than that in **2**, **4**, **6**, or **7**, and one would expect appreciable steric interaction between the *cis* acetoxyl groups. In addition, the n.O.e. results for **11** show no difference between the *cis* and *trans* methine protons (Table 2). The larger couplings in the keto derivatives indicate that the carbonyl group tends to hold the central ring in a geometry more favorable for long-range interactions through the four σ-bonds. The smaller values for monoalcohol **15** may arise because of somewhat greater flexibility of the six-membered ring.

Although the geminal coupling constants, J_{AB}, for the cyclopropyl methylene groups vary, 5.1–6.1 Hz, no correlation with a specific structural feature is evident; the values are in the usual range for three-membered ring compounds (15). The J_{gem} values for the methylene groups in the monofunctional derivatives, **15** and **16**, are 14.5 and 14.6 Hz, respectively, indicating that no major changes in ring geometry or electron density occur in these H—C_6—H bonds with a change in hybridization at C-2 (16).

Although the chemical shift data, in themselves, do not provide unequivocal evidence on the basis of which stereochemical assignments can be deduced, some interesting trends are apparent.

One of the cyclopropyl methylene protons in

Can. J. Chem. Downloaded from www.nrcresearchpress.com by 210.87.254.6 on 09/05/12
For personal use only.

Can. J. Chem. Downloaded from www.nrcresearchpress.com by 210.87.254.6 on 09/05/12
For personal use only.

the ketone derivatives absorbs at significantly lower field than those of the saturated compounds. This is the proton *trans* to the methyls as shown by the foregoing results. The nearly orthogonal relationship between the planes of the carbonyl group and the cyclopropane ring has been postulated to result in orbital overlap between these two groups (17–19). Ground-state electron withdrawal by this mechanism may account for the downfield shifts as well as the low carbonyl stretching frequencies observed (**1**, $\nu_{CO}(CHCl_3)$ 1667 cm^{-1}; **15**, 1641 cm^{-1}; cyclohexane-1,4-dione, 1727 cm^{-1} (20); cyclohexanone, 1710 cm^{-1} (21)). This interaction is consistent with the observation of the enormous accelerating effect of the cyclopropyl groups in the hydrolysis of **18** and the corresponding *p*-nitrobenzoates (3). One would expect, however, that an electronic effect of this nature would affect both methylene protons nearly equally, but only one is appreciably shifted to lower field; this downfield shift of one of the cyclopropyl protons, however, is explicable in terms of a dispersion effect. In this tricyclic skeleton the cyclopropyl protons *trans* to the methyl groups are closely-lying neighbors and it is known that the close approach of neighboring protons leads to a deshielding of each (22). It has been noted above that δ_{AB} is very much smaller, 0.18 p.p.m., in the ring-opened bicyclic derivative, **14**, which is consistent with the above since the bicyclic system is not constrained to a form in which another proton is in close proximity to one of the cyclopropyl protons. The possible contribution of the carbonyl group, owing to its anisotropy, to the differential shift of one of the cyclopropyl protons cannot be neglected but it is difficult to account for the observed trend in terms of the usual model of its long-range shielding effect (7); the situation is not improved by the use of a recent modification (23) of this model. In each case, the models predict either a shielding effect at the "inner" cyclopropyl protons or a weak deshielding effect, depending on the geometry of the central ring, which is either planar or a flattened boat to judge from the n.O.e. data.

The shifts of the *trans* proton at C-6 in the keto derivatives are unexceptional although these protons absorb at higher field than the *cis* protons in the corresponding isomers (*cf.* **2** *vs.* **3**, **4** *vs.* **5**, **16**). The downfield shift probably arises from steric interaction of the *cis* C-6 protons with the two neighboring cyclopropyl protons (22) since such an interaction would increase δ_{AB} for the cyclopropyl methylene group. In the saturated systems, the *cis* methine proton appears at higher field than the corresponding *trans* hydrogen. It seems likely that in the saturated compounds there is an increase in ring flexibility which allows the cyclopropane rings to move further apart than in the ketones. If this is the case, models indicate that the *trans* C-6 proton is much closer to the C-5 and -7 methyl groups than the *cis* proton is to the cyclopropyl hydrogens; thus, steric interaction between the *trans* proton and the methyl hydrogens would account for the observed downfield shift. It should be noted that the compounds in which this effect can be observed possess both 2- and 6-substituents. In the monoalcohol, **15**, the trend is reversed indicating that nonbonded interaction between the 2- and 6-substituents affects the geometry of the central ring appreciably.

Experimental

Proton Spectra

The chemical shifts were determined on a Varian A-60 spectrometer using dilute solutions in chloroform and are accurate to ±0.05 p.p.m. The coupling constants and n.O.e. were obtained on degassed chloroform solutions containing small amounts of TMS as a standard and some benzene to provide a "locking" signal for the Varian HA-60IL spectrometer. The coupling constants reported are the average of at least three scans at a 50 Hz sweep width and were calibrated using a Hewlett-Packard 5245L counter; these are judged to have a precision of ±0.05 Hz. All integrated intensities were the average of at least ten determinations obtained by irradiating, using low power, the appropriate resonant frequencies and blank regions of the spectrum. The enhancements reported are accurate to ±3%.

Materials

1,3,5,7-Tetramethyltricyclo[5.1.0.0^{3,5}]octan-2,6-dione (1)

The dipyrazoline (1.5 g), formed from reaction of diazomethane and duroquinone in ether (1), was dissolved in glacial acetic acid (50 ml) and treated with 70% perchloric acid (30 drops). After effervescence had ceased, the reaction mixture was poured into water and **1** was isolated by extraction with chloroform. The crude crystalline product (1.1 g) was recrystallized from petroleum ether (60–80°) to give 0.46 g (40%) of **1**, m.p. 143.5–145° (lit. (1): m.p. 144–145°).

Ketoalcohol 3

Diketone **1** (1.92 g) dissolved in absolute ethanol (75 ml) containing platinum oxide (0.29 g) was hydrogenated, using a Parr apparatus, at 44 p.s.i. for 29 h. Chromatography on alumina with benzene:ether (93:7) as eluant gave a mixture of ketoalcohols **2** and **3** but further elution with ether gave a solid (0.83 g) which was recrystallized from benzene to give ketoalcohol **3** (0.63 g, 33%) m.p. 166–167° (lit. (24): 167–168°).

Can. J. Chem. Downloaded from www.nrcresearchpress.com by 210.87.254.6 on 09/05/12
For personal use only.

Ketoalcohol **2**

To diketone **1** (1.14 g) dissolved in isopropyl alcohol (50 ml) was added 50% aqueous isopropyl alcohol (10 ml) containing sodium borohydride (0.07 g) and the mixture stirred for 6.5 h. After evaporation of the isopropyl alcohol and addition of water, the product was isolated by extraction with chloroform followed by chromatography on alumina. After the unreacted starting material (0.1 g) was eluted with benzene:hexane (4:1), elution with benzene:ether (92:8) gave a solid (0.73 g) which was recrystallized from benzene to yield the ketoalcohol **2** (0.63 g, 54%) m.p. 159–160° (lit. (24): 160–161°). With ether as eluant a mixture of ketoalcohols **2** and **3** was recovered from the alumina column.

cis-Diol **8**

Reduction of ketoalcohol **2** with excess sodium borohydride gave a mixture of diols **8** and **9** (80:20). Chromatography, on alumina, followed by recrystallization from benzene afforded the major product, **8**, m.p. 185.5–186.5°.

Anal. Calcd. for $C_{12}H_{20}O_2$: C, 73.43; H, 10.27. Found: C, 73.41; H, 10.25.

trans-Diol **9**

Similarly sodium borohydride reduction of ketoalcohol **3** gave *trans*-diol **9** exclusively, m.p. 168–173°.

Anal. Calcd. for $C_{12}H_{20}O_2$: C, 73.43; H, 10.27. Found: C, 73.26; H, 10.28.

Hydroxyacetate **12**

Reduction of ketoacetate **4** with excess sodium borohydride gave the hydroxyacetate **12** as the major product, m.p. 140.5–141.5°.

Anal. Calcd. for $C_{14}H_{22}O_3$: C, 70.55; H, 9.31. Found: C, 70.19; H, 9.54.

Hydroxyacetate **13**

In an analogous manner, sodium borohydride reduction of **5** yielded hydroxyacetate **13** as the major component, m.p. 96.5–97.5°.

Anal. Calcd. for $C_{14}H_{22}O_3$: C, 70.55; H, 9.31. Found: C, 70.48; H, 9.22.

Monoalcohol **15**

To bromoketone **7** (0.25 g) dissolved in *t*-butyl alcohol (10 ml) was added, with stirring, 10 ml of 50% aqueous *t*-butyl alcohol containing sodium borohydride (0.6 g). The mixture was stirred at room temperature for 1 h and then poured into water. After extraction with chloroform and concentration of the extracts, a colorless material (0.13 g) was extracted with cold hexane which crystallized from *n*-pentane to give monoalcohol **15**, m.p. 74–75°.

Anal. Calcd. for $C_{12}H_{20}O$: C, 79.94; H, 11.18. Found: C, 79.87; H, 11.39.

The residue of the chloroform extract was identified as *cis*-diol **8**.

Monoketone **16**

Manganese dioxide (1.5 g) was added to an ethereal solution of **15** (0.39 g in 20 ml ether) and the mixture stirred for 39 h at room temperature. After removal of the solids by filtration and evaporation of the ether, **16** (0.16 g), m.p. 85–86°, was obtained in 43% yield by recrystallization from hexane.

Anal. Calcd. for $C_{12}H_{18}O$: C, 80.85; H, 10.18. Found: C, 80.93; H, 10.01.

Acetylation of **2**, **3**, **8**, **9**, **12** *and* **13**

Acetyl chloride (1.5 ml) was added dropwise to a cold (~0°) solution of **2** (0.29 g) in benzene (15 ml) and pyridine (3 ml). After the addition was complete the mixture was warmed to room temperature and allowed to stand for 1 h. The product was isolated by extraction with chloroform followed by chromatography on alumina with benzene:hexane (4:1) as eluant. Recrystallization from 60–80° petroleum ether gave ketoacetate **4** (0.32 g) m.p. 123–124° in 88% yield. (lit. (24): 124.5–125.5°).

The above procedure with ketoalcohol **3** gave **5** m.p. 135.5–137° (lit. (24): 135.5–136°).

The diacetates, **10** and **11**, were obtained in two ways, *viz.* from either the corresponding diol or hydroxyacetate. Acetylation of *cis*-diol **8** gave **10**, m.p. 137.5–138.5°.

Anal. Calcd. for $C_{16}H_{24}O_4$: C, 68.54; H, 8.63. Found: C, 68.48; H, 8.59.

Similarly the *trans*-diacetate **11**, m.p. 49.5–50.5°, was obtained from *trans*-diol **9**.

Anal. Calcd. for $C_{16}H_{24}O_4$: C, 68.54; H, 8.63. Found: C, 68.93; H, 8.60.

Chloroketone **6**

To a cold (~5°) solution of **2** (0.23 g) in benzene (10 ml) was added a solution of thionyl chloride (5 ml) in benzene (10 ml) after which the solution was warmed to room temperature and allowed to stand for 2 h. Concentration of the reaction mixture gave a residue which was recrystallized from petroleum ether (60–80°) to yield chloroketone **6** (0.18 g, 73%) m.p. 139.5–141°.

Anal. Calcd. for $C_{12}H_{17}OCl$: C, 67.78; H, 8.06; Cl, 16.67. Found: C, 67.27; H, 7.75; Cl, 16.68.

Chlorination of ketoalcohol **3**, in a similar manner gave the same chloroketone.

Bromoketone **7**

Phosphorous tribromide (3 ml) was added to a cold solution of **2** (0.26 g) in benzene (25 ml) and the mixture allowed to stand overnight at room temperature. Chloroform extraction of the reaction mixture yielded a product which was recrystallized from hexane:benzene (100:1) to give bromoketone **7** (0.30 g, 88%) m.p. 151.5–153°.

Anal. Calcd. for $C_{12}H_{17}OBr$: C, 56.06; H, 6.67; Br, 31.08. Found: C, 56.43; H, 6.24; Br, 31.35.

In this way **7** was also prepared from **3**.

Sodium/t-Butyl Alcohol Reduction of Bromoketone, **7**

Small pieces of sodium metal (0.20 g) were added to a solution of **7** (0.17 g) in *t*-butyl alcohol and the mixture stirred under nitrogen at room temperature for 1.5 h. Fresh sodium metal (0.10 g) was added and stirring under nitrogen continued for a further 2.5 h. Work-up in the usual manner, *i.e.* chloroform extraction and chromatography on alumina, yielded, with 50:50 benzene:hexane as eluant, monoalcohol, **14**, in 66% yield after recrystallization from hexane, m.p. 120.5–121.5°.

Anal. Calcd. for $C_{12}H_{20}O$: C, 79.94; H, 11.18. Found: C, 79.40; H, 11.02.

This procedure with *t*-butyl alcohol-*d* afforded **14***a* partially deuterated at C-1 and -2.

We are grateful for financial support provided by the National Research Council of Canada in the form of operating grants and a studentship (C.H.J.). We also acknowledge the technical assistance of Miss P. M. Pellitt with some of the preliminary n.m.r. work.

1. W. C. HOWELL, M. KTENAS, and J. M. MACDONALD. Tetrahedron Lett. 1719 (1964).
2. F. A. L. ANET and A. J. R. BOURN. J. Amer. Chem. Soc. **87**, 5250 (1965).
3. L. BIRLADEANU, T. HANAFUSA, B. JOHNSON, and S. WINSTEIN. J. Amer. Chem. Soc. **88**, 2316 (1966).
4. L. BIRLADEANU, T. HANAFUSA, and S. WINSTEIN. J. Amer. Chem. Soc. **88**, 2315 (1966).
5. H. C. BROWN and H. M. BELL. J. Org. Chem. **27**, 1928 (1962); J. Amer. Chem. Soc. **85**, 2324 (1963).
6. S. WINSTEIN. Personal communication.
7. L. M. JACKMAN and S. STERNHELL. Applications of n.m.r. spectroscopy in organic chemistry. 2nd Edition. Pergamon Press, New York, 1969. p. 88 *ff*.
8. M. C. WOODS, H.-C. CHIANG, Y. NAKADAIRA, and K. NAKANISHI. J. Amer. Chem. Soc. **90**, 522 (1968).
9. R. A. BELL and J. K. SAUNDERS. Can. J. Chem. **46**, 3421 (1968); J. K. SAUNDERS and R. A. BELL. Paper presented at the 52nd C.I.C. Conference, Montreal, Quebec, May 1969.
10. R. A. ARCHER and P. V. DEMARCO. J. Amer. Chem. Soc. **91**, 1530 (1969).
11. S. STERNHELL. Rev. Pure Appl. Chem. **14**, 15 (1964).
12. S. STERNHELL. Quart. Rev. **23**, 236 (1969).
13. Y. OSAWA and M. NEEMAN. J. Amer. Chem. Soc. **85**, 2856 (1963).
14. F. P. JOHNSON, A. MELERA, and S. STERNHELL. Aust. J. Chem. **19**, 1523 (1966).
15. D. J. PATEL, M. E. H. HOWDEN, and J. D. ROBERTS. J. Amer. Chem. Soc. **85**, 3218 (1963).
16. J. A. POPLE and A. A. BOTHNER-BY. J. Chem. Phys. **42**, 1339 (1965).
17. W. G. DAUBEN and G. H. BEREZIN. J. Amer. Chem. Soc. **89**, 3449 (1967).
18. E. M. KOSOWER and M. ITO. Proc. Chem. Soc. 25 (1962).
19. L. D. HESS, J. L. JACOBSON, K. SCHAFFNER, and J. N. PITTS, JR. J. Amer. Chem. Soc. **89**, 3684 (1967).
20. M. V. BHATT, G. SRINIVASAN, and P. NEELAKANTAN. Tetrahedron, **21**, 291 (1965).
21. D. H. WHIFFEN and H. W. THOMPSON. J. Chem. Soc. 1005 (1946).
22. R. J. ABRAHAM and J. S. E. HOLKER. J. Chem. Soc. 806 (1963); R. S. NEALE and E. B. WHIPPLE. J. Amer. Chem. Soc. **86**, 3130 (1964); B. V. CHENEY. J. Amer. Chem. Soc. **90**, 5386 (1968).
23. G. J. KARABATSOS, G. C. SONNICHSEN, N. HSI, and D. J. FENOGLIO. J. Amer. Chem. Soc. **89**, 5067 (1967).
24. J. M. MACDONALD. Ph.D. Thesis. University of Western Ontario, London, Ontario. 1964.
25. A. W. BRINKMANN, M. GORDON, R. G. HARVEY, P. W. RABIDEAU, J. B. STOTHERS, and A. L. TERNAY, JR. J. Amer. Chem. Soc. **92**, 5912 (1970).

Can. J. Chem. Downloaded from www.nrcresearchpress.com by 210.87.254.6 on 09/05/12
For personal use only.

Can. J. Chem. Downloaded from www.nrcresearchpress.com by 210.87.254.6 on 09/05/12
For personal use only.

Mechanism of Sulfonation of 4-Hydroxyazobenzene

E. BUNCEL AND W. M. J. STRACHAN
Department of Chemistry, Queen's University, Kingston, Ontario

AND

H. CERFONTAIN
Laboratory for Organic Chemistry, Nwe Achtergracht 129, University of Amsterdam, The Netherlands

Received April 8, 1970

The mechanism of sulfonation of 4-hydroxyazobenzene and of 4-hydroxyazobenzene-4′-sulfonic acid in concentrated sulfuric acid media is examined through rate correlations and comparison is drawn with sulfonation of alkyl- and halogenobenzenes by means of log k *vs.* log $a_{H_2S_2O_7}$ plots. It is concluded that several mechanisms are operative in the hydroxyazobenzene system and that the curvature of the plot is the result of a change in rate-determining step from σ-complex formation to proton abstraction.

Canadian Journal of Chemistry, 49, 152 (1971)

As part of a study concerned with elucidation of the Wallach rearrangement processes (1), the kinetics of sulfonation of 4-hydroxyazobenzene were determined for the 90–100% H_2SO_4 region (2). In Scheme 1 are shown the various processes which were observed in the spectral study with 4-hydroxyazobenzene (2). In 90% H_2SO_4 the substrate is present completely in its monoprotonated form **1** ($pK_a^1 - 1.0$, corresponding to 99.9% protonation in 55% H_2SO_4). There are two consecutive sulfonation processes (Scheme 1, reactions *1* and *2*) yielding the mono-sulfonic acid **3** and disulfonic acid **5**,[1] and three concurrent equilibria (reactions *3*, *4*, and *5*) involving the diprotonated species **2**, **4**, and **6**. In 100.0% H_2SO_4 reaction 1 has a half-life of 5 min at 25°, while reaction 2 has a half-life of 28 h (2). Now the Wallach rearrangement of azoxybenzene to 4-hydroxyazobenzene in 99.99% H_2SO_4 occurs with a half-life of 20 s at 25°, with a somewhat faster rate expected in 100.0% H_2SO_4 (3). Hence spectral examination of azoxybenzene in 100.0% H_2SO_4 some minutes after mixing reflects merely the processes of Scheme 1 undergone by the already formed 4-hydroxyazobenzene (4).

The mechanism of the sulfonation reactions was commented on briefly in a previous paper (2). A reaction scheme was presented showing electrophilic attack by SO_3 on mono-protonated 4-hydroxyazobenzene (**1**) as the initial step. The non-reactivity toward sulfonation of diprotonated substrate **2** was further indicated by the extended linearity of the rate–H_0 plot when account for diprotonation was taken by plotting log $k_{obs} - \log c_{SH^+}/(c_{SH^+} + c_{SH_2^{++}})$ *vs.* H_0.

In this paper we treat in greater depth the mechanism of the sulfonation processes. An analysis is made of rate correlations on the basis of attack by various possible electrophilic species, the formation of two σ-complex intermediates, and subsequent product-forming steps in which various bases may abstract a proton from aryl carbon. Results from previous work (2) have been re-calculated according to a revised H_0 scale (5).

The generalized kinetic scheme (*cf.* ref. 6) on the basis of which the sulfonation of 4-hydroxyazobenzene may be considered is shown in Scheme 2. The reactive substrate **1** is denoted by ArH. There are two distinct σ-complex intermediates **7** and **8** (transfer of SO_3 from the electrophile YSO_3 to **1** yields **7** whereas transfer of SO_3H^+ from ZSO_3H^+ yields **8**), which lead to product species **9** and **10** by proton abstraction processes. Intermediates **7** and **8** are joined through a rapidly attained equilibrium process *e* by means of an acid/base pair such as H_2SO_4/HSO_4^- or $H_3SO_4^+/H_2SO_4$, and the product species **9** and **10** are similarly interconnected in process *f*. The rate-determining steps may be either attack by electrophile on **1** (reactions *a* and *b*), or proton abstraction from the σ-complexes (reactions *c* and *d*), or a combination of these. Electrophilic species to be considered in the sulfonation processes are SO_3, H_2SO_4,

[1]The spectral identification of the disulfonic acid product did not enable a complete structural proof to be deduced. Assignment of orientation in reaction *2* is hence tentative (2).

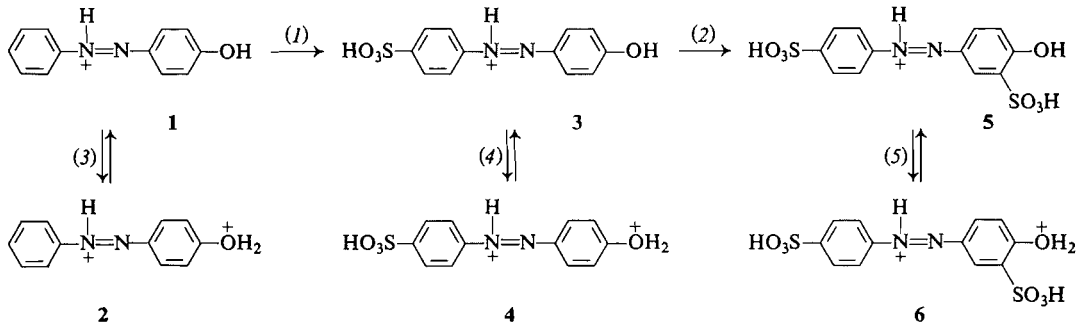

SCHEME 1

$H_2S_2O_7$, HSO_3^+, $H_3SO_4^+$, and sulfuric acid solvates of these (5–12). Basic species in this system are then HSO_4^-, H_2SO_4, and $HS_2O_7^-$ (5).

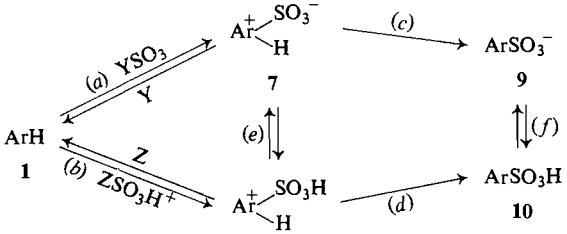

SCHEME 2

Rate correlations for sulfonation were made considering as sulfonation mechanism eq. 1 in which X is the electrophilic species and B the

$$[1]\quad ArH + X \underset{-1}{\overset{1}{\rightleftharpoons}} Ar\begin{matrix}X\\H\end{matrix} \xrightarrow{B,\ 2} ArX + BH^+$$

proton-abstracting base. Assuming that the σ-complex intermediate (ArXH) is present in steady-state concentration, one obtains an expression relating the variables of eq. 1 to the observed pseudo first-order rate constant for reaction (k_{obs}). In eq. 2, k_{SH^+} signifies reaction via the monoprotonated substrate, *i.e.* $k_{obs} = k_{SH^+} \cdot c_{SH^+}/(c_{SH^+} + c_{SH_2^{++}})$; the *a* terms signify activities, and the *f* terms activity coefficients.

$$[2]\quad k_{SH^+} = \frac{k_1 k_2 a_X a_B}{k_{-1} + k_2 a_B} \cdot \frac{f_{ArH}}{f^{\ddagger}}$$

Equation 2 may be simplified under two limiting conditions. In the first case, step 1 in eq. 1 is rate-determining, *i.e.* $k_2 a_B \gg k_{-1}$, and eq. 3 results. In the second case, step 2 in eq. 1 is rate determining and eq. 4 results.

$$[3]\quad k_{SH^+} = \frac{k_1 a_X f_{ArH}}{f_1^{\ddagger}}$$

$$[4]\quad k_{SH^+} = \frac{k_1 k_2 a_X a_B f_{ArH}}{k_{-1} f_2^{\ddagger}}$$

The activities of the various entities (X and B) in solution can be related to the known values of $a_{H_2SO_4}$ (13), a_{H_2O} (13), and $a_{HSO_4^-}$ (14), through equilibria applicable to the sulfuric acid – water system. These equilibria, and the various assumptions necessary in the derivations, have been previously described (5, 6, 15, 16). One thus obtains relationships shown in eqs. 5–8.[2]

$$[5]\quad a_{SO_3} = K_1 \frac{a_{H_2SO_4}}{a_{H_2O}}$$

$$[6]\quad a_{H_2S_2O_7} = K_2 \frac{a_{H_2SO_4}^2}{a_{H_2O}}$$

$$[7]\quad a_{HSO_3^+} = K_3 \frac{a_{H_2SO_4}^2}{a_{H_2O} a_{HSO_4^-}} = K_3' \left(\frac{a_{H_2SO_4}}{a_{H_2O}}\right)^{3/2}$$

$$[8]\quad a_{H_3SO_4^+} = K_4 \frac{a_{H_2SO_4}^2}{a_{HSO_4^-}} = K_4' \left(\frac{a_{H_2SO_4}^3}{a_{H_2O}}\right)^{1/2}$$

The kinetic data for sulfonation may be tested against rate expressions which can be derived for various sequences and X/B combinations in Scheme 2, on the basis of one of the limiting conditions, eqs. 3 and 4. We have considered a number of such "intuitively reasonable" reaction paths and X/B combinations and derived the appropriate rate expressions, in each case plot-

[2]Assuming that $a_{HSO_4^-}/a_{H_3O^+} \simeq 1$ (*cf.* refs. 14, 16) in > 80% H_2SO_4 it follows that $a_{HSO_4^-} = K_5 a_{H_2O}^{\ddagger} a_{H_2SO_4}^{\ddagger}$.

Can. J. Chem. Downloaded from www.nrcresearchpress.com by 210.87.254.6 on 09/05/12
For personal use only.

TABLE 1. Consideration of reaction pathways and rate correlations for sulfonation of 4-hydroxyazobenzene and 4-hydroxyazobenzene-4′-sulfonic acid according to Scheme 2

Function plotted against $\log k_{SH^+}$	Reaction pathway tested in Scheme 2		
	X*	B†	Predicted slope‡
A $\log a_{H_2SO_4}$	$H_3SO_4^+$ (fast)	HSO_4^-	2.0
B $\log a_{H_2SO_4}/a_{H_2O}$	SO_3 (slow)		1.0
	HSO_3^+ (slow)		1.5
C $\log a_{H_2SO_4}^2/a_{H_2O}$	$H_2S_2O_7$ (slow)		1.0
	SO_3 (fast)	H_2SO_4	1.0
	HSO_3^+ (fast)	HSO_4^-	1.0
D $\log a_{H_2SO_4}^3/a_{H_2O}$	$H_3SO_4^+$ (slow)		0.5
	SO_3 (fast)	HSO_4^-	0.5
	$H_2S_2O_7$ (fast)	H_2SO_4	1.0

*Specifies the X entity in paths *a* or *b* of Scheme 2 and whether reaction by X is the slow (eq. 3) or the fast (eq. 4) step. When X is SO_3 or HSO_3^+ the paths are restricted to (*a*) and (*b*) respectively but with the other electrophiles either reaction path is possible in theory.
†The basic entity is specified only when proton abstraction, processes *c* or *d*, is rate-limiting (eq. 4).
‡See eqs. 5–8 and footnote 2.

ting a function against $\log k_{SH^+}$.[3] Such plots assume the constancy of various equilibrium K's and of activity coefficient ratios of $f_{ArH}/f^{\neq}$ over the acid range tested. The functions plotted and the reaction pathways so tested are given in Table 1.

The actual plots corresponding to functions A–D of Table 1 are all curved, for both substrates (**1** and **3**); typical plots are shown in Fig. 1 and discussed further below. It can hence be concluded that no single kinetic expression fits the rate data exactly, which suggests that the sulfonation process does not follow a single mechanism throughout the acid range studied for either substrate, or that assumptions concerning constancy of activity coefficient ratios and equilibrium constants may be invalid. The plot which is most nearly linear is the $\log k_{SH^+}$ *vs.* H_0 plot for sulfonation reaction *1* of Scheme 1. However no mechanistic significance is attached to this finding (19, 20).

As an alternative to the analytical approach described above, one may gain insight into mechanisms by comparison with systems in which the reaction pathway has been established with some confidence. Extensive studies of aromatic sulfonation processes have recently been described (21–23). The mechanism proposed (14, 21–23) for the sulfonation of alkyl- and halogenobenzenes in sulfuric acid, which is applicable to the present system, is discussed according to Scheme 2 and Fig. 1. At low sulfuric acid concentrations the rate-limiting step is (*b*) with $H_3SO_4^+$ as the electrophile and the product is formed via steps *e* and *c* with HSO_4^- as the proton abstracting agent. At higher sulfuric acid concentration the rate-limiting step is again (*b*) but the electrophile becomes $H_2S_2O_7$ and the product is again mainly formed via steps *e* and *c*. At yet higher acid concentrations, which are still below 100% H_2SO_4, step *e* becomes in part rate-determining because of the sharp decrease in the ratio $a_{HSO_4^-}/a_{H_2SO_4}$ (22), being preceded by electrophilic attack by $H_2S_2O_7$, path *b*. At even higher acid concentrations the sulfonic acid product **10** will be formed by the sequence (*b*), X = $H_2S_2O_7$, and (*d*), B = H_2SO_4 rather than HSO_4^-, because of a further decrease in $a_{HSO_4^-}/a_{H_2SO_4}$; furthermore the rate of step *d* will increase relative to that of step $-b$ and this will lead to an increase in $d(\log k)/d(\log a_{H_2S_2O_7})$.

For 4-hydroxyazobenzene in the region of 94–99.7% H_2SO_4 the graph of $\log k_{SH^+}$ *vs.* $\log a_{H_2S_2O_7}$ (Fig. 1) is linear with a slope of 0.79 instead of the unit slope required according to path *b* with X = $H_2S_2O_7$ rate-limiting (*cf.* C in Table 1). This behavior is similar to that observed for benzene (12), bromobenzene (23), chlorobenzene (22), and *p*-nitrotoluene (8).[4] With 4-

[3]The $\log k_{SH^+}$ values of ref. 2 have been recalculated using the combined H_0 scales of Jorgenson and Hartter (17) and Gillespie and Robinson (5) to evaluate the extent of diprotonation. The pK_a^2 values (18) have been adjusted accordingly to −11.1 for **1** ⇄ **2** and −12.0 for **3** ⇄ **4**. The usual expression, $\log c_{SH_2^{++}}/c_{SH^+} = pK_a^2 - H_0$, was used to calculate the term $\log c_{SH^+}/(c_{SH^+} + c_{SH^{++}})$ which operates on $\log k_{obs}$.

[4]Account has been taken of the slight protonation of *p*-nitrotoluene (9% in 99% H_2SO_4). The reported pK_a value (9*a*) has been adjusted according to the new H_0 scale (5).

Can. J. Chem. Downloaded from www.nrcresearchpress.com by 210.87.254.6 on 09/05/12
For personal use only.

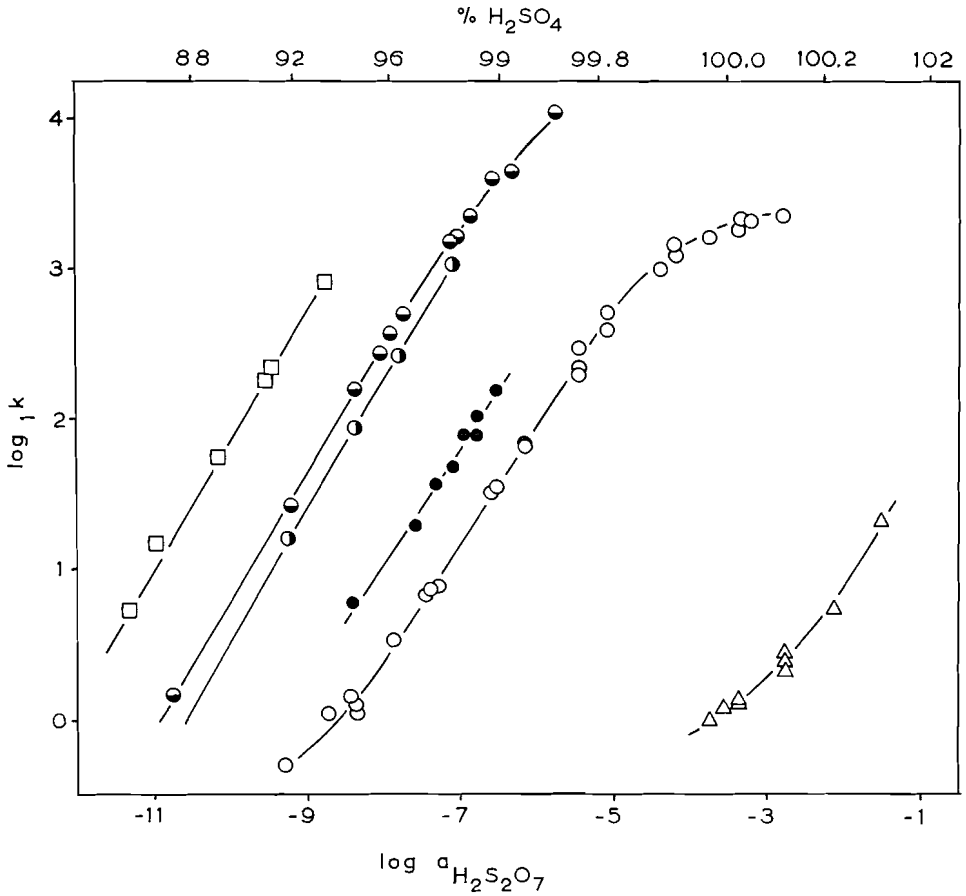

FIG. 1. Correlations of pseudo first-order rate constants (s^{-1}) for sulfonation at 25° with log $a_{H_2S_2O_7}$. (The $a_{H_2S_2O_7}$ data for 97–101% H_2SO_4 were taken from ref. 21; the variation in $a_{H_2S_2O_7}$ at lower acid concentrations was calculated by eq. 6).

Substrate	Ordinate	Slope	Reference
□ Benzene	log k + 5	0.86	12
◒ Chlorobenzene	log k_{para} + 5	0.88–0.5	22
◑ Bromobenzene	log k_{para} + 5	0.88	23
● *p*-Nitrotoluene (96.5°)	log k_{SH+} + 7	0.80	8
○ 4-Hydroxyazobenzene	log k_{SH+} + 5	0.79–0.15	2
△ 4-Hydroxyazobenzene-4′-sulfonic acid	log k_{SH+} + 5	0.40–0.87	2

hydroxyazobenzene and chlorobenzene, the slope d(log k)/d(log $a_{H_2S_2O_7}$) decreases at acid concentrations >99.8 and >98% H_2SO_4 respectively, indicating that step *e*, Scheme 2, with B = HSO_4^- becomes in part rate-determining at these acid concentrations. The decrease in slope below 94% H_2SO_4, if significant, may be explained in terms of additional formation of σ-complex **8** by step *b* with $H_3SO_4^+$ as the electrophile. The increase in slope observed for 4-hydroxyazobenzene-4′-sulfonic acid in the region of 100% H_2SO_4 is similar to that observed for *p*-difluorobenzene in the region of 99% H_2SO_4 (23). It may also be explained similarly, *i.e.*, in terms of a decrease in the rate of step $-b$ with B = HSO_4^-, relative to that of step *d* with B = H_2SO_4.

In summary, the principal process in the sulfonation of 4-hydroxyazobenzene is concluded to be rate-determining electrophilic attack by $H_2S_2O_7$ with formation of intermediate complex **8**. Below 94% H_2SO_4, electrophilic attack by

Can. J. Chem. Downloaded from www.nrcresearchpress.com by 210.87.254.6 on 09/05/12
For personal use only.

$H_3SO_4^+$ may also be important. However, in ~100% H_2SO_4 and above, proton abstraction becomes in part rate-limiting.

Financial support of this work by the National Research Council of Canada (E.B. and W.M.J.S.) is gratefully acknowledged.

1. E. BUNCEL. *In* Mechanisms of molecular migrations. B. S. Thyagarajan, *editor*. John Wiley and Sons, Inc., Interscience Publishers, Inc., New York, 1968.
2. W. M. J. STRACHAN and E. BUNCEL. Can. J. Chem. **47**, 4011 (1969).
3. E. BUNCEL and W. M. J. STRACHAN. Can. J. Chem. **48**, 377 (1970).
4. E. BUNCEL, W. M. J. STRACHAN, R. J. GILLESPIE, and R. KAPOOR. Chem. Commun. 675 (1969).
5. R. J. GILLESPIE and E. A. ROBINSON. *In* Non-aqueous solvent systems. T. C. Waddington, *editor*. Academic Press, London, 1965.
6. (*a*) H. CERFONTAIN. Mechanistic aspects in aromatic sulfonation and desulfonation. Interscience Publishers, Inc., New York, 1968. (*b*) H. CERFONTAIN and C. W. F. KORT. Mechanisms of reactions of sulfur compounds. Intrascience Foundation, **3**, 23 (1968).
7. C. K. INGOLD. Structure and mechanism in organic chemistry. Bell and Sons, London, 1953. p. 299.
8. W. A. COWDREY and D. S. DAVIES. J. Chem. Soc. 1871 (1949).
9. (*a*) J. C. D. BRAND, W. C. HORNING, and M. B. THORNLEY. J. Chem. Soc. 1374 (1952). (*b*) J. C. D. BRAND, A. W. P. JARVIE, and W. C. HORNING. J. Chem. Soc. 3844 (1959).
10. V. GOLD and D. P. N. SATCHELL. J. Chem. Soc. 1635 (1956).
11. M. KILPATRICK, M. W. MEYER, and M. L. KILPATRICK. J. Phys. Chem. **64**, 1433 (1960).
12. A. W. KAANDORP, H. CERFONTAIN, and F. L. J. SIXMA. Rec. Trav. Chim. **81**, 969 (1962).
13. W. F. GIAUQUE, E. W. HORNING, J. E. KUNZLER, and T. R. RUBIN. J. Amer. Chem. Soc. **82**, 62 (1960).
14. C. W. F. KORT and H. CERFONTAIN. Rec. Trav. Chim. **87**, 24 (1968).
15. P. A. H. WYATT. Trans. Faraday Soc. **56**, 490 (1960).
16. E. B. ROBERTSON and H. B. DUNFORD. J. Amer. Chem. Soc. **86**, 5080 (1964).
17. M. J. JORGENSON and D. R. HARTTER. J. Amer. Chem. Soc. **85**, 878 (1963).
18. W. M. J. STRACHAN, A. DOLENKO, and E. BUNCEL. Can. J. Chem. **47**, 3631 (1969).
19. F. A. LONG and M. A. PAUL. Chem. Rev. **57**, 935 (1957).
20. J. F. BUNNETT and F. P. OLSEN. Can. J. Chem. **44**, 1917 (1966).
21. C. W. F. KORT and H. CERFONTAIN. Rec. Trav. Chim. **88**, 1298 (1969).
22. C. W. F. KORT and H. CERFONTAIN. Rec. Trav. Chim. **86**, 865 (1967).
23. C. W. F. KORT and H. CERFONTAIN. Rec. Trav. Chim. **88**, 860 (1969).

Can. J. Chem. Downloaded from www.nrcresearchpress.com by 210.87.254.6 on 09/05/12
For personal use only.

Can. J. Chem. Downloaded from www.nrcresearchpress.com by 210.87.254.5 on 09/05/12
For personal use only.

Structure of the Acetone–Indanedione Adduct

STEPHEN J. KUHN
Exploratory Research Laboratory, Dow Chemical of Canada, Limited, Sarnia, Ontario

AND

IAN D. RAE
Department of Chemistry, Monash University, Clayton, Victoria, 3168, Australia

Received June 10, 1970

A compound formed by condensation of 2 mol of indanedione and 2 of acetone is shown to have structure **2**. This reinterpretation, largely based on p.m.r. and i.r. evidence, is supported by the structures assigned to an enol acetate and a dihydro derivative of **2**.

Canadian Journal of Chemistry, **49**, 157 (1971)

The product, $C_{24}H_{18}O_3$, of base-catalyzed condensation between acetone and indane-1,3-dione has recently been assigned structure **1** (1). We wish to offer a reinterpretation of the p.m.r. and i.r. spectroscopic data for this compound which requires its formulation as **2**. New structures are also assigned to derivatives of **2** which help to confirm our reinterpretation.

Degradation of the condensation product by hydroxylamine and subsequent hydrolysis of the intermediate dioximes yields **3** and indane-1,3-dione, see Scheme 1. The reaction sequences show that the degradation product would be the same whether the original adduct had structure **1** or **2**. A comparison of the n.m.r. spectra of **3** and the original adduct provides a vital clue to the structure of the adduct. In the transformation of **1** to **3** the resonance position of the aromatic protons should be most affected; however, they remain virtually undisturbed. The

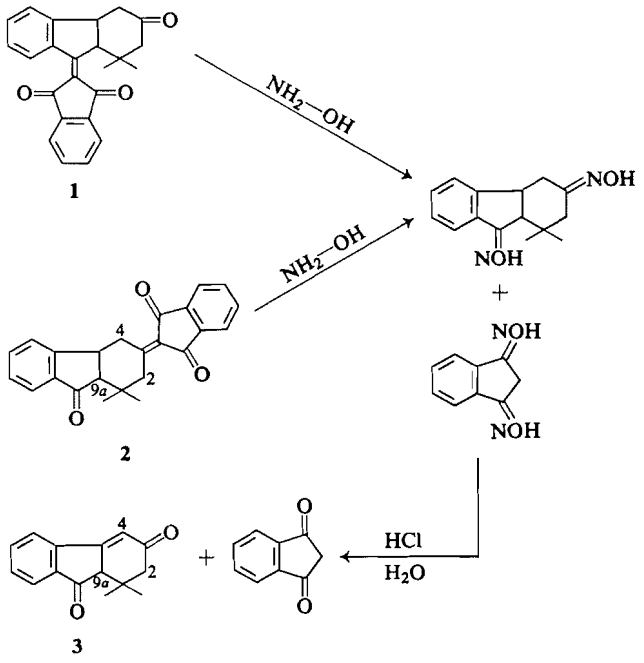

SCHEME 1

Can. J. Chem. Downloaded from www.nrcresearchpress.com by 210.87.254.5 on 09/05/12
For personal use only.

protons whose resonance positions are most affected are the olefinic H-4 (shifted from 8.78 to 6.53 p.p.m.) and one of the H-2 pair (shifted from 4.06 to 2.4 p.p.m.) as would be expected in the transformation of **2** to **3**. This identifies C-3, and not C-9 (in structure **3**) as the point of attachment for the indanedionyl moiety.

The geometry of the cyclohexene ring in **2** is such that the olefinic proton and one of the C-2 methylene protons are almost in the plane of the indanedione moiety and thus suffer pronounced deshielding. The other methylene proton is pseudo-axial and shows long-range coupling to the olefinic proton (2, 3). Substitution in the tetrahydrofluorene skeleton of **2** involves first the replacement of the 9*a*-proton, the new substituent (CH_3, Br) occupying this pseudo-axial position (1). Bromination also introduces a second substituent, replacing one of the methylene protons at C-2. The remaining aliphatic proton is allylic and adjacent to a bromine atom, but proximity to the carbonyl is also required to rationalize its extreme chemical shift (6.5 p.p.m.; the downfield shift of 2.44 p.p.m. on bromination is close to that predicted by Shoolery's rules (4)). Thus the second bromine must also occupy a pseudo-axial position (partial structure **4**) where the unfavorable steric interaction with the other bromine is apparently preferable to the dipole–dipole interaction which a pseudo-equatorial bromine would have with the nearby carbonyl (*cf.* the axial haloketone rule (5)). The long-range coupling to H-4 is now exhibited by the pseudo-equatorial C-2 proton but so little is known about the dependence of such couplings on geometry and electronegativity that the significance of such an observation in structural terms is quite low (2).

A comparison of the i.r. spectra of the original adduct and the degradation product **3** also provides some useful information about the structure of the original adduct. The i.r. spectrum of the original adduct has three strong bands in the carbonyl region at 1716, 1680, and 1679 cm^{-1}. The i.r. spectrum of the degradation product **3** has two bands in the carbonyl region at 1718 and 1655 cm^{-1}. The band in compound **3** at 1718 cm^{-1} is assigned to a tetrahydro fluorenone type of carbonyl (7, 8) and the band at 1655 cm^{-1} to the conjugated cyclohexene carbonyl group. Structure **1** for the original adduct has no fluorenone type of carbonyl group. The band at 1716 cm^{-1} could be due to one of the indanedionyl carbonyl groups; however, the band did not disappear on the removal of the indanedionyl group in the transformation of the original adduct to **3**. These results also indicate that **2** is the correct structure for the original adduct.

An enolacetate of the original adduct has been prepared by reaction with acetic anhydride in the presence of *p*-toluenesulfonic acid monohydrate. A singlet at 8.93 p.p.m. in its p.m.r. spectrum is assigned to the olefinic proton H-4 and its chemical shift indicates that the acetate formation did not take place on groups on C-3 forming either **6** or **6***a*.

In the structure **6** the indanedionyl moiety, free to rotate from the plane of the olefinic system, would no longer exert the powerful deshielding effect on proton C-4. The destruction of the carbonyl group on C-3 in the transformation of **1** to **6***a* would also change the shielding of H-4 considerably. Structure **5** is in complete agreement with the p.m.r. spectrum of the enolacetate; however structure **6***b* derived from structure **1** should also be discussed. A comparison of the i.r. spectra of the original adduct and its enolacetate again provides some useful information. The strong carbonyl band in the original adduct at 1716 cm^{-1} is completely missing from the i.r. spectrum of the enolacetate and a new band at 1779 cm^{-1} corresponding to a vinyl ester type of carbonyl appears. The indanedionyl carbonyls appear as a single strong band at 1680 cm^{-1} in the enolacetate. These results indicate that the enolacetate formation takes place on a carbonyl other than the indanedionyls, thus supporting structure **5** for the enolacetate and structure **2** for the original adduct. The *gem*-dimethyl and methylene protons of **5** give rise to a slightly broadened singlet in the p.m.r. spectrum at 40 °C (1.37 and 3.47 p.p.m. respectively), indicating a conformational averaging process in the six-membered ring.

Reduction of compound **2** with sodium dithionite gives a mixture of at least two new compounds, but equilibration of the mixture with strong base produces largely the one product to which we assign structure **7** (R = H). The definitive resonances in the p.m.r. spectrum of this compound are those of the 9*a*-proton (2.88 p.p.m.) and the olefinic proton at C-4 (6.15 p.p.m.), the chemical shift of the latter indicating

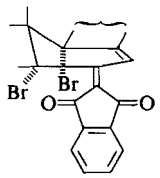

4

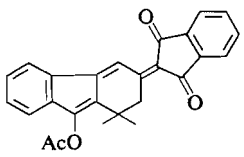

5

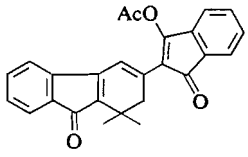

6

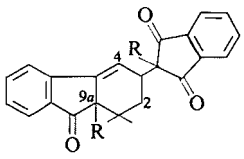

7

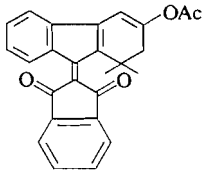

6a

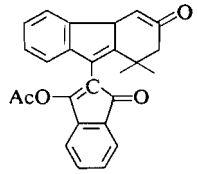

6b

that the two portions of the molecule are no longer coplanar. Due to the near equality of $J_{3,4}$, $J_{4,9a}$, and $J_{3,9a}$ (each approximately 2 Hz) these two resonances are apparent triplets and mutual decoupling experiments serve to reduce each to a clean doublet. The C-3 proton gives rise to a complex multiplet centered at 3.25 p.p.m., superimposed on which is the signal of the proton of the indane-1,3-dione moiety. This latter and the 9*a*-proton triplet are removed on deuteration to give **7** (R = D) in which the C-4 proton gives rise to a doublet ($J_{3,4}$ approximately 2 Hz).

Experimental

The preparation of the acetone–indanedione condensation product and some of its derivatives has been described in an earlier paper (1).

Reduction of **2** *by Sodium Dithionite*

The amount of sodium dithionite prescribed by Geita and Vanags (6) for the reduction of **2** resulted in incomplete reduction. Using a large excess of reducing agent led to complete reduction of **2** in good yield.

A mixture of 5 g of **2** and 25 g of sodium dithionite in 400 cc of 50% aqueous ethyl alcohol was heated under reflux for 3 h. After cooling the reaction mixture was diluted with 2000 ml of cold water and the precipitate was filtered. The product was crystallized from ethyl alcohol, m.p. 157–161 °C. Yield 4.5 g.

Anal. Calcd. for $C_{24}H_{20}O_3$: C, 80.9; H, 5.6. Found: C, 81.0; H, 5.45.

The n.m.r. spectrum of the reduction product indicates that it is a mixture of **7** and its isomer. Equilibration, by dissolving 3 g of the reduction products in a solution of 10 g of potassium hydroxide in 50 ml of 50% methanol and heating the mixture at 40 °C for 30 min, followed by filtration and pouring of the filtrate into excess 10% aqueous acetic acid results in a product which consists of 90% of **7** and has m.p. 170–172 °C.

Anal. Calcd. for $C_{24}H_{20}O_3$: C, 80.9; H, 5.6. Found: C, 80.8; H, 5.65.

Preparation of the Enolacetate of **2**

A solution of 2 g of **2** and 1 g of *p*-toluenesulfonic acid monohydrate in 60 ml of acetic anhydride was distilled slowly through an empty column until most of the acetic anhydride had been removed (4 h). After cooling, 25 ml of water was added to the residue and it was extracted with ether. Evaporation of the ether gave 1.9 g of brick red product, the m.p. 258–259 °C.

Anal. Calcd. for $C_{26}H_{20}O_4$: C, 78.8; H, 5.02. Found: C, 78.75; H, 5.1.

Deuteration of **7**

To a solution of 5.5 g of $NaOCH_3$ in 30 ml of CH_3OD–D_2O (1:1 volume) was added 2 g of **7**. Upon shaking a homogeneous solution was obtained, which was poured into a solution of 15 g of CH_3COOD in 30 g of D_2O. The yellow precipitate was filtered, washed twice with 5 ml of D_2O and dried (m.p. 168–171 °C). The dry product weighed 1.8 g. The n.m.r. spectrum of the compound showed that proton 9*a* and the indanedionyl pro-

Can. J. Chem. Downloaded from www.nrcresearchpress.com by 210.87.254.5 on 09/05/12
For personal use only.

ton had been exchanged by deuterium. The indanedionyl deuterium was very labile and slowly exchanged with protium when exposed to atmospheric moisture.

1. S. J. KUHN. Can. J. Chem. **47**, 1461 (1969).
2. S. STERNHELL. Quart. Rev. (London), **23**, 236 (1969).
3. M. BARFIELD and B. CHAKRABARTI. Chem. Rev. **69**, 757 (1969).
4. L. M. JACKMAN. Applications of nuclear magnetic resonance spectroscopy in organic chemistry. Pergamon Press, Oxford, 1959. p. 59.
5. E. L. ELIEL. Stereochemistry of carbon compounds. McGraw-Hill Book Company, Inc., New York, 1962. pp. 240 and 422.
6. L. GEITA and G. VANAGS. Latv. PSR Zinat. Akad. Vestis, Kim. Ser. 57–63 (1969).
7. H. O. HOUSE. J. Amer. Chem. Soc. **82**, 2561 (1960).
8. H. O. HOUSE and R. G. CARLSON. J. Org. Chem. **29**, 74 (1964).

Can. J. Chem. Downloaded from www.nrcresearchpress.com by 210.87.254.5 on 09/05/12
For personal use only.

Magnetic Resonance Studies of Metal Olefin Complexes. II. Electron Spin Resonance Spectra of γ-Irradiated Silver Complexes with Cyclohexadienes and 1-Methyl Cyclopentene

D. R. GEE[1] AND J. K. S. WAN
Department of Chemistry, Queen's University, Kingston, Ontario

Received August 31, 1970

Electron spin resonance studies of silver cycloalkenyl radicals by γ-irradiation of polycrystalline silver cycloalkene complexes have been extended to include the effect of alkyl substitution at the double bond, the effect of conjugation in cyclic diolefins and the effect of anions, on the formation of these silver cycloalkenyl radicals.

Canadian Journal of Chemistry, 49, 160 (1971)

Introduction

Studies (1, 2) of the stability of silver alkene and 1-alkyl alkene complexes indicate that both steric and basicity effects are important. Uncertainty remains as to whether the steric effects of the 1-alkyl substituent result in a weaker metal–olefin bond or only a larger entropy change for the system upon complex formation. In contrast, Quinn and Van Gilder's infrared studies (3) suggest that a stronger silver–olefin interaction accompanies the increased basicity of cycloalkenes which have an alkyl group at the double bond. Dewar (4) further postulates that there may also be a weakening of the π component of the coordination bond concurrent with the strengthening of the σ component by the electron donating alkyl substituent. This latter effect may be relatively unimportant, as it is thought (5) that the σ component of the coordinate bond predominates in silver olefin complexes.

Factors other than olefin basicity and the steric effects of substituents which can affect the stability of the silver complexes include the strength of interaction between cations and anions (1), and the effect of conjugation in diolefin complexes on weakening of the coordination bond (6).

As a parallel study to silver olefin complexes, we have initiated a systematic investigation of silver alkenyl radicals generated by γ-irradiation of the parent complexes (7–9). In the present report we have extended our studies of silver alkenyl radicals to include silver 1-methylcyclopentenyl radical and the corresponding uncomplexed 1-methyl-cyclopentenyl radical, the silver cyclohexadienyl radicals generated from the 1,3- and 1,4-cyclohexadiene silver perchlorate and silver tetrafluoroborate complexes.

Experimental

All cycloalkenes were obtained from Aldrich. Anhydrous silver perchlorate and silver tetrafluoroborate were supplied by Alfa Inorganic and Ozark Mahoning, respectively. 1,4-Cyclohexadiene-3,3,6,6-d_4 was prepared by the method of Campbell (10). The silver complexes were prepared using the methods of Comyns and Lucas (11) and Quinn and Van Gilder (12). Silver analyses of all these complexes were within 0.02% of the values predicted. Sample irradiation has been described previously (8). Electron spin resonance (e.s.r.) spectra were

[1]Postdoctoral fellow 1969–1970; present address: Department of Chemistry, University of Manchester Institute of Science and Technology, Manchester, England.

ton had been exchanged by deuterium. The indanedionyl deuterium was very labile and slowly exchanged with protium when exposed to atmospheric moisture.

1. S. J. KUHN. Can. J. Chem. **47**, 1461 (1969).
2. S. STERNHELL. Quart. Rev. (London), **23**, 236 (1969).
3. M. BARFIELD and B. CHAKRABARTI. Chem. Rev. **69**, 757 (1969).
4. L. M. JACKMAN. Applications of nuclear magnetic resonance spectroscopy in organic chemistry. Pergamon Press, Oxford, 1959. p. 59.
5. E. L. ELIEL. Stereochemistry of carbon compounds. McGraw-Hill Book Company, Inc., New York, 1962. pp. 240 and 422.
6. L. GEITA and G. VANAGS. Latv. PSR Zinat. Akad. Vestis, Kim. Ser. 57–63 (1969).
7. H. O. HOUSE. J. Amer. Chem. Soc. **82**, 2561 (1960).
8. H. O. HOUSE and R. G. CARLSON. J. Org. Chem. **29**, 74 (1964).

Can. J. Chem. Downloaded from www.nrcresearchpress.com by 210.87.254.40 on 09/05/12
For personal use only.

Magnetic Resonance Studies of Metal Olefin Complexes. II. Electron Spin Resonance Spectra of γ-Irradiated Silver Complexes with Cyclohexadienes and 1-Methyl Cyclopentene

D. R. GEE[1] AND J. K. S. WAN
Department of Chemistry, Queen's University, Kingston, Ontario

Received August 31, 1970

Electron spin resonance studies of silver cycloalkenyl radicals by γ-irradiation of polycrystalline silver cycloalkene complexes have been extended to include the effect of alkyl substitution at the double bond, the effect of conjugation in cyclic diolefins and the effect of anions, on the formation of these silver cycloalkenyl radicals.

Canadian Journal of Chemistry, 49, 160 (1971)

Introduction

Studies (1, 2) of the stability of silver alkene and 1-alkyl alkene complexes indicate that both steric and basicity effects are important. Uncertainty remains as to whether the steric effects of the 1-alkyl substituent result in a weaker metal–olefin bond or only a larger entropy change for the system upon complex formation. In contrast, Quinn and Van Gilder's infrared studies (3) suggest that a stronger silver–olefin interaction accompanies the increased basicity of cycloalkenes which have an alkyl group at the double bond. Dewar (4) further postulates that there may also be a weakening of the π component of the coordination bond concurrent with the strengthening of the σ component by the electron donating alkyl substituent. This latter effect may be relatively unimportant, as it is thought (5) that the σ component of the coordinate bond predominates in silver olefin complexes.

Factors other than olefin basicity and the steric effects of substituents which can affect the stability of the silver complexes include the strength of interaction between cations and anions (1), and the effect of conjugation in diolefin complexes on weakening of the coordination bond (6).

As a parallel study to silver olefin complexes, we have initiated a systematic investigation of silver alkenyl radicals generated by γ-irradiation of the parent complexes (7–9). In the present report we have extended our studies of silver alkenyl radicals to include silver 1-methylcyclopentenyl radical and the corresponding uncomplexed 1-methyl-cyclopentenyl radical, the silver cyclohexadienyl radicals generated from the 1,3- and 1,4-cyclohexadiene silver perchlorate and silver tetrafluoroborate complexes.

Experimental

All cycloalkenes were obtained from Aldrich. Anhydrous silver perchlorate and silver tetrafluoroborate were supplied by Alfa Inorganic and Ozark Mahoning, respectively. 1,4-Cyclohexadiene-3,3,6,6-d_4 was prepared by the method of Campbell (10). The silver complexes were prepared using the methods of Comyns and Lucas (11) and Quinn and Van Gilder (12). Silver analyses of all these complexes were within 0.02% of the values predicted. Sample irradiation has been described previously (8). Electron spin resonance (e.s.r.) spectra were

[1]Postdoctoral fellow 1969–1970; present address: Department of Chemistry, University of Manchester Institute of Science and Technology, Manchester, England.

Can. J. Chem. Downloaded from www.nrcresearchpress.com by 210.87.254.40 on 09/05/12
For personal use only.

obtained with a Varian V4502 spectrometer and auxiliary equipment. Simulation of spectra was done on an IBM 360/50 computer using a modified version of a program made available by the Bell Telephone Laboratory.

Results and Discussion

Silver 1-Methyl-Cyclopentyl Radical

To study the effect of alkyl substitution at the double bond of silver cycloalkenyl radicals, a large number of other alkyl substituted cycloalkene–silver complexes have been included in this study. However, most of them either decompose under γ-irradiation or lead to only unresolved single broad-line e.s.r. spectra. Only the silver 1-methyl-cyclopent-1-ene was stable enough and gave reasonably resolved e.s.r. spectra.

The e.s.r. spectra observed when silver perchlorate 1-methyl-cyclopentene complex was irradiated almost certainly results from Ag^+ 1-methyl-3-cyclopentyl radical (8). Computer analysis of the experimental spectra on this basis yields the parameters presented in Table 1.

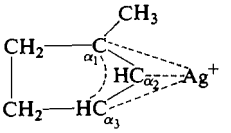

TABLE 1. Summary of hyperfine coupling constants for Ag^+ 1-methyl-3-cyclopentenyl radical

Splitting constant	Value (G)	
	Ag^+ 1-methyl cyclopentenyl	Ag^+ cyclopentenyl*
$a_H(\alpha_1)$		10.9
$a_H(\alpha_2)$	2.5±0.3	3.0
$a_H(\alpha_3)$	7.1	10.9
$a_H(\beta)$	20.4	22.0
a_{CH_3}	11.9	
a_{Ag}	38.5	30.5
Spin density on Ag%	5.8	4.6

*Taken from ref. 8.

The experimental β proton coupling constants of this silver 1-methyl-cyclopentyl radical compare with those assigned to the uncomplexed methyl cyclopentenyl radical (13). This appears to support previous observations that little ring distortion occurs in the complexation (3, 14).

A comparison of the derived spin densities on the silver ion for the substituted and unsubstituted Ag^+ methyl-cyclopentenyl radicals (Table 1) reveals an increase in silver spin density with alkyl substitution. If, as presently seems probable, the spin density on the silver ion arises primarily from spin polarization of the σ coordinate bond, it would appear that our results indicate that methyl substitution at the double bond brings about a stronger interaction between the alkenyl and the silver ion. Quinn and Van Gilder (3) from their infrared observations of the perturbation in $\nu_{C=C}$ of the olefin, upon complex formation, have reached a similar conclusion for the parent silver complexes. Thus the effect of the electron donating methyl substituent is to increase olefin basicity and give a stronger coordinate bond. Steric effect, however, probably accounts for previous reports (2, 5) that 1-methyl substituted olefins form complexes less stable than the unsubstituted olefins.

Further inspection of the changes in proton coupling constants of the complexed radical (Table 1) reveals an apparent increase in the asymmetry of the spin distribution on the cycloalkenyl part of the radical. In a nuclear magnetic resonance (n.m.r.) study of the parent complexes Quinn and Van Gilder (3) have suggested that the deshielding effect of the methylene protons adjacent to the double bond is due to the positioning of the silver ion closer to the carbon-2. Such explanation can be applied also to the results of the silver methyl cyclopentenyl radical.

Silver Cyclohexadienyl Radicals

A number of silver complexes of conjugated olefins, including benzene, have been studied. Only silver cyclohexadienyl complexes led to reasonably resolved e.s.r. spectra.

A typical room temperature e.s.r. spectrum observed when either $AgClO_4$– or $AgBF_4$–1,4-cyclohexadiene is irradiated is shown in Fig. 1*a*. Similar spectra were obtained with the irradiated silver 1,3-cyclohexadiene complexes. Thus, it appears that the radicals generated in both isomers have essentially the same structure, probably the silver cyclohexadienyl radical.

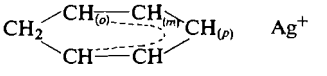

Computer analysis of the experimental spectra on the basis of this silver cyclohexadienyl radical yields the parameters presented in Table 2. Despite the small asymmetric linewidth variation

Can. J. Chem. Downloaded from www.nrcresearchpress.com by 210.87.254.40 on 09/05/12
For personal use only.

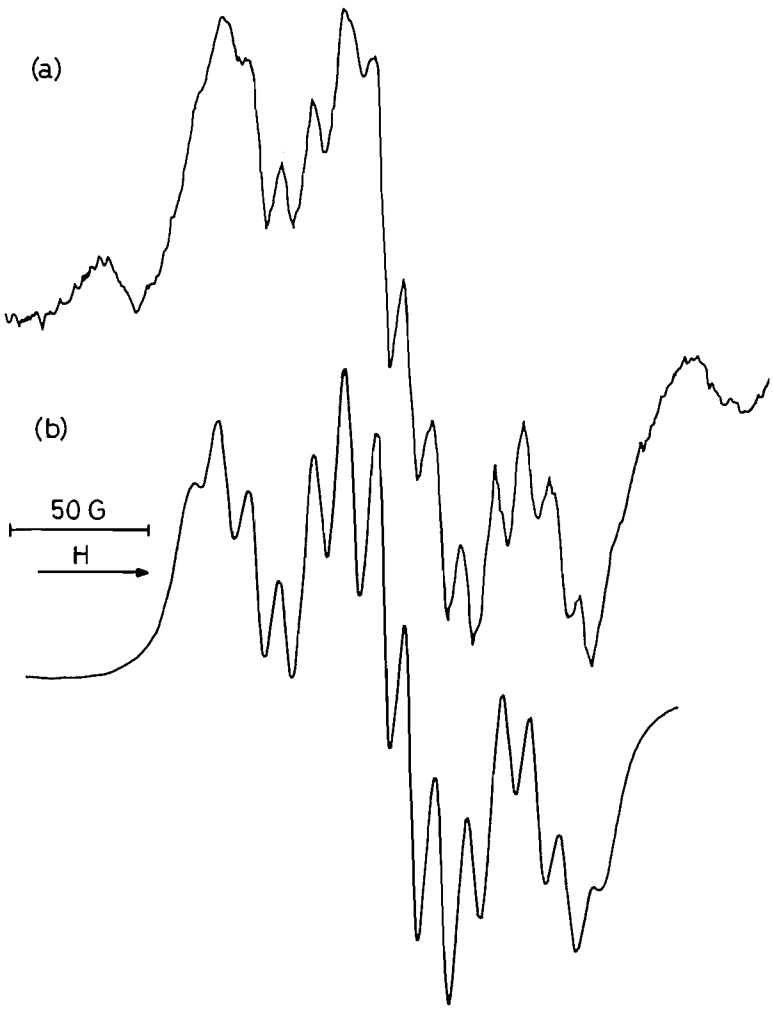

FIG. 1. Electron spin resonance spectra of γ-irradiated silver perchlorate 1,4-cyclohexadiene complex: (*a*) experimental spectrum; (*b*) computer simulated spectrum of Ag^+ cyclohexadienyl radical.

in the experimental spectrum, reasonable agreement is observed when computed spectra simulated using the data in Table 2 are compared with those obtained experimentally. The broad outer lines in the experimental spectra in Fig. 1*a* were only observed with the perchlorate as anion and may be due to some other trapped radicals. To confirm the spectral assignments, the silver complex of cyclohexadiene-3,3,6,6-d_4 was studied. The deuterated spectra agree with the assignments using an a_D/a_H ratio of 0.1535.

The proton coupling constants of the silver cyclohexadienyl radical are essentially identical with the values for the uncomplexed cyclohexadienyl radical (15). Again this indicates that little ring distortion occurs in the complexed radical. The derived spin density of $3.0 \pm 0.3\%$ on the silver ion of the silver cyclohexadienyl radicals compares with the value of 3.4% estimated for silver cyclohexenyl radical (8). This suggests that some small weakening of the coordinate bond occurs probably as a result of the conjugation in the cyclodienyl system. Similar observations of the parent silver complexes have been reported (6).

X-Ray data for the silver cyclooctatetraene (16) and silver benzene complexes (17) indicate that the silver ion in these complexes is positioned

TABLE 2. Spectral parameters for Ag^+ cyclohexadienyl radicals

Splitting constant	Value (G)			
	1,3-Cyclohexadiene $AgClO_4$	1,3-Cyclohexadiene $AgBF_4$	1,4-Cyclohexadiene $AgClO_4$	1,4-Cyclohexadiene $AgBF_4$
a_{Ag}	18.5±0.4	19.0	21.2	21.8
$a_{(CH_2)}$	45.2	45.2	45.0	45.0
$a_{H(o)}$	8.9	8.9	8.9	8.9
$a_{H(m)}$	2.6	2.6	2.6	2.6
$a_{H(p)}$	13.0	13.0	13.0	13.0
Spin density on Ag%	2.8	2.8	3.2	3.2

above the plane of the ring. If the silver ion also occupies a similar position in the silver cyclohexadienyl radical, it would explain the small difference in the derived spin densities of the silver ion in the radicals formed from 1,3- and 1,4-cyclohexadienes, as greater orbital overlap would be expected with the more symmetrical parent 1,4-cyclohexadiene. Our results also indicate the formation of these silver cyclohexadienyl radicals being independent of the anion, at least for the ClO_4 and the BF_4 anions.

The authors are indebted to Dr. A. Rudge for some technical assistance, and to Dr. H. W. Quinn of the Dow Chemical Company of Canada, Sarnia, for sending some preprints of his work. Financial support from the National Research Council of Canada and the Defence Research Board is gratefully acknowledged.

1. H. W. QUINN and J. H. TSAI. Advan. Inorg. Radiochem. **12**, 217 (1969).
2. C. D. M. BEVERIVIJK, G. J. M. VAN DER KERK, A. J. LEUSINK, and J. G. NOLTES. Organometal. Rev. A, **5**, 215 (1970).
3. H. W. QUINN and R. L. VAN GILDER. Can. J. Chem. **47**, 4691 (1969).
4. M. J. S. DEWAR. Bull. Soc. Chim. France, **18**, C74 (1951).
5. J. G. TRAYHAM and J. R. OLECHOUSKI. J. Amer. Chem. Soc. **81**, 571 (1959).
6. M. A. MUHS and F. T. WEISS. J. Amer. Chem. Soc. **84**, 4697 (1962).
7. D. R. GEE and J. K. S. WAN. Chem. Commun. 641 (1970).
8. D. R. GEE, K. E. RUSSELL, and J. K. S. WAN. Can. J. Chem. **48**, 2740 (1970).
9. D. R. GEE, K. E. RUSSELL, and J. K. S. WAN. J. Chem. Phys. **53**, 847 (1970).
10. J. R. CAMPBELL. Ph.D. thesis. Queen's University, Kingston, Ontario. 1969.
11. A. E. COMYNS and H. J. LUCAS. J. Amer. Chem. Soc. **79**, 4339 (1957).
12. H. W. QUINN and R. L. VAN GILDER. Can. J. Chem. **48**, 2434 (1970).
13. D. R. GEE and J. K. S. WAN. Can. J. Chem. This issue.
14. H. HOSOYA and S. NAGAKWA. Bull. Chem. Soc. Japan, **37**, 249 (1964).
15. R. W. FESSENDEN and R. H. SCHULER. J. Chem. Phys. **39**, 214 (1963) and **38**, 773 (1963).
16. F. SCOTT MATHEWS and W. N. LIPCOMB. J. Amer. Chem. Soc. **80**, 4745 (1958).
17. H. G. SMITH and R. E. RUNDLE. J. Amer. Chem. Soc. **80**, 5075 (1958).

Erratum: Dipole moments, charge-transfer parameters, and ionization potentials of the methyl-substituted benzene–tetracyanoethylene complexes

R. K. CHAN AND S. C. LIAO
Department of Chemistry, University of Western Ontario, London, Ontario

Received October 7, 1970

(Ref. Can. J. Chem. **48**, 299 (1970))

Canadian Journal of Chemistry, **49**, 163 (1971)

Equation 27 on p. 304 should read as follows:

$$C_1 = E_A + \frac{e^2}{r} + X + W_0$$

Can. J. Chem. Downloaded from www.nrcresearchpress.com by 210.87.254.40 on 09/05/12
For personal use only.

Can. J. Chem. Downloaded from www.nrcresearchpress.com by 210.87.254.105 on 09/05/12
For personal use only.

Reaction of Methyl-lithium with Phosphonitrilic Fluorides: a Novel Orientation Pattern

N. L. PADDOCK[1] AND T. N. RANGANATHAN
Department of Chemistry, University of British Columbia, Vancouver 8, British Columbia
AND
S. M. TODD
Department of Chemistry, University of Manchester, Manchester 13, England

Received October 9, 1970

The reaction of methyl-lithium with the phosphonitrilic fluorides $(NPF_2)_{3-5}$ follows a predominantly geminal course, the third and fourth substituents in the tetrameric ring entering antipodally to the first two. This behavior, and the competitive occurrence of an addition reaction, is attributed to the π-inductive effect of the substituents on a delocalized homomorphic π-system.

Canadian Journal of Chemistry, **49**, 164 (1971)

Although many investigations have been carried out on the orientation of substituents entering the phosphonitrilic ring and the structural changes which they induce, there has hitherto been no attempt to relate the observed pattern to the structure of the π-electron system. We have investigated the point directly through a study of the reactions of the phosphonitrilic fluorides $(NPF_2)_{3-5}$ (which measurements of ionization potentials (1) show to have a strongly developed π-system) with methyl-lithium in diethyl ether (which should introduce no π-conjugative or steric (2) complications). A novel orientation pattern is found for the methylation of $N_4P_4F_8$ in that, as indicated by ^1H and ^{19}F n.m.r. spectroscopy, geminal di-substitution is followed predominantly by antipodal entry of the third substituent, as shown. Both findings are unexpected on electrostatic grounds. The methyl group would be expected to be electron-releasing relative to fluorine, causing the second substituent to enter antipodally to the first, as in the amination of $N_4P_4Cl_8$ (3). On the other hand, where geminal di-substitution at P-1 has an electrostatic origin, as in the substitution of chlorine by fluorine in $N_4P_4Cl_8$ (4), the third substituent enters at P-2. The course of methylation of $N_4P_4F_8$, distinct from both these patterns, can be understood in terms of the effect of π-inductive interactions on the atomic π-charges; by analogy with the bimolecular substitution reactions of phosphoryl compounds, reactivity is expected to correlate (inversely) with electron density of the reaction center (5). The induced charges (6) are given in Table 1 for six- and eight-membered rings. Since $\delta\alpha$ is negative, the charges have the same sign as the tabulated values, and, from this cause alone, a second nucleophilic substitution should take place principally at P-1, as found. The substitution of the third group can be expected to occur where the π-induced negative charge is least, *i.e.* at P-3 if the electronegativity difference between the π-orbitals at P and N is great enough. The recognition of this orientation effect, with a similar basis to that of substitution in the benzene ring, reinforces the conclusions of a study of bond length inequalities (7).

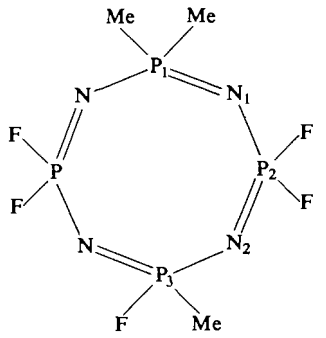

Methylation of $N_3P_3F_6$ also takes place geminally, but a competitive addition reaction

[1]To whom correspondence should be addressed.

TABLE 1. Mutual atom polarizabilities* $\pi_{s,1} = \partial q_s/\partial\alpha_1$

	Atom(s)	ρ	1(P-1)	2(N-1)	3(P-2)	4(N-2)	5(P-3)
N_3P_3	Homomorphic	1	+0.309	−0.126	+0.003	−0.063	
	Homomorphic	2	+0.182	−0.078	−0.002	−0.022	
	Heteromorphic	1	+0.252	−0.085	−0.041	0	
	Heteromorphic	2	+0.158	−0.063	−0.016	0	
N_4P_4	Homomorphic and heteromorphic	1	+0.273	−0.096	−0.023	−0.006	−0.023
		2	+0.166	−0.068	−0.010	−0.003	−0.004

*Hückel molecular orbital calculations, $\alpha_N = \alpha_p + \rho\beta$.

prevents the formation of simple N_3P_3 derivatives containing more than two methyl groups and, in the reaction with $N_5P_5F_{10}$, reduces the yield of $N_5P_5Me_{10}$; by contrast, a good yield (~70%) of $N_4P_4Me_8$ is obtainable from $N_4P_4F_8$. Exhaustive methylation of $N_3P_3F_6$, followed by treatment with methyl iodide, gives a product of composition $N_3P_3Me_{11}Li$, in which each phosphorus atom evidently carries three methyl groups. Table 1 shows that the positive charge on P-1 induced by two methyl groups is highest in the six-membered ring and for homomorphic interactions (8) and the addition of a third methyl group to P-1 is most likely in this case. For the N_5P_5 ring ($\rho = 1$), $\pi_{1,1} = 0.305$ (homomorphic) and 0.283 (heteromorphic). Experimentally, the relative importance of the substitution reaction, as measured by the yields of methylphosphonitriles $(NPMe_2)_n$ increases in the order $n = 3, 5, 4$, the order of decreasing $\pi_{1,1}$ (homomorphic). Insofar as the orientational effects are those of the uppermost π-system, the chemical and physical (1) results agree with the assignment of its symmetry type as homomorphic.

We thank the National Research Council of Canada for financial support, and the University of British Columbia for a University Graduate Fellowship (to T.N.R.).

1. G. R. BRANTON, C. E. BRION, D. C. FROST, K. A. R. MITCHELL, and N. L. PADDOCK. J. Chem. Soc. A, 151 (1970).
2. C. W. ALLEN and T. MOELLER. Inorg. Chem. **7**, 2177 (1968).
3. K. JOHN, T. MOELLER, and L. F. AUDRIETH. J. Amer. Chem. Soc. **82**, 5616 (1960); **83**, 2608 (1960).
4. J. EMSLEY and N. L. PADDOCK. J. Chem. Soc. A, 2590 (1968).
5. R. F. HUDSON. Adv. Inorg. Chem. Radiochem. **5**, 347 (1963).
6. C. A. COULSON and H. C. LONGUET-HIGGINS. Proc. Roy. Soc. London, Ser. A, **191**, 39 (1947).
7. W. C. MARSH, T. N. RANGANATHAN, J. TROTTER, and N. L. PADDOCK. Chem. Commun. 815 (1970).
8. D. P. CRAIG. J. Chem. Soc. 997 (1959).

Can. J. Chem. Downloaded from www.nrcresearchpress.com by 210.87.254.105 on 09/05/12
For personal use only.

Can. J. Chem. Downloaded from www.nrcresearchpress.com by 210.87.254.40 on 09/05/12
For personal use only.

Canadian Journal of Chemistry

Published by THE NATIONAL RESEARCH COUNCIL OF CANADA

VOLUME 49 JANUARY 15, 1971 NUMBER 2

The Crystal Structure of a Thiathiophthen Nitrogen Isostere, 3,5-Epidithio-2,5-diphenyl-2,4-pentadienylidene-3-aminoquinoline

F. LEUNG AND S. C. NYBURG

Department of Chemistry, University of Toronto, Toronto 181, Ontario

Received August 11, 1970

The crystal structure of a thiathiophthen nitrogen isostere (7) has been solved by X-ray analysis. The crystal belongs to the triclinic system with unit cell dimensions: $a = 11.275(11)$, $b = 9.558(10)$, $c = 10.797(10)$ Å, $\alpha = 92.50(10)$, $\beta = 116.98(10)$, $\gamma = 92.61(10)°$. There are two molecules per unit cell, space group $P\bar{1}$. The data were collected by diffractometer with Cu$K\alpha$ radiation. The structure was solved by symbolic addition procedures, and fully refined anisotropically using full-matrix least squares to an R factor of 6.3%.

The S—S and S—N bond lengths were found to be 2.364 and 1.887 Å, respectively. This reveals the partial bonding character between S...S...N atoms.

Canadian Journal of Chemistry, 49, 167 (1971)

Introduction

The crystal structure determination of the symmetric molecule 2,5-dimethyl-thiathiophthen **1** in 1958 (1) revealed an anomalous S...S distance of 2.36 Å, substantially longer than a single bond (2.08 Å) and far shorter than a van der Waals contact (*ca.* 3.5 Å). Similar anomalous distances have been found in a large number of other molecules containing at least one S atom at the end of an "open" five-membered ring, for example, in the unsymmetric thiathiophthen derivatives **2** (2) and **3** (3) and in the selenium and oxygen isosteres **4** (4) and **5** (5).

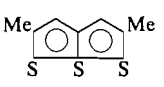

1

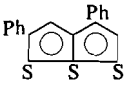

2

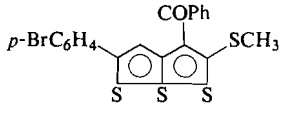

3

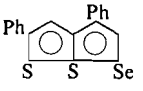

4

Derivatives of thiathiophthen usually show in the crystal one short (2.12–2.22 Å) and one long (2.45–2.57 Å) S...S distance unless crystallographic symmetry is required. At one time it was thought that 2,5-dimethylthiathiophthen, **1**, although required crystallographically to be symmetric, may have been a statistically disordered assembly of asymmetric molecules. A re-examination of its crystal structure in this laboratory, however, indicates that this is not so (6).

The nitrogen isosteres **6** have recently been synthesized by Klingsberg (7) and it is of some interest to know whether there is an S...N interaction in these molecules. A preliminary report showing that there is such an interaction has been published (8).

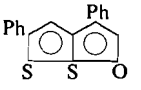

5

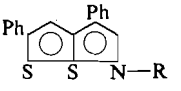

6

Experimental

The specimen of 3,5-epidithio-2,5-diphenyl-2,4-pentadienylidene-3-aminoquinoline (7) supplied by Klingsberg was recrystallized as red prisms from nitromethane.

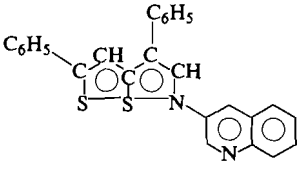

7

The unit cell dimensions were determined from diffractometer measurements and refined by a least squares procedure.

Can. J. Chem. Downloaded from www.nrcresearchpress.com by 210.87.254.40 on 09/05/12
For personal use only.

$C_{26}S_2N_2H_{18}$ f.w. = 422.6.

Triclinic, $a = 11.275(11)$, $b = 9.588(10)$, $c = 10.797(10)$ Å, $\alpha = 92.50(10)$, $\beta = 116.98(10)$, $\gamma = 92.61(10)°$, $V = 1033.2$ Å^3, $Z = 2$, $D_c = 1.36$ g/cc, $D_m = 1.35$ g/cc, space group $P\bar{1}$ (No.2), $\mu = 23.7$ cm^{-1}, (CuKα, $\lambda = 1.5418$ Å).

The intensities were collected at room temperature on a Picker four circle automatic diffractometer (Ni-filtered, Cu radiation), and all independent reflections with $\sin\theta < 0.9063$ were measured in 2θ scan mode. A total of 3522 reflections were measured, of which 149 were unobservably weak.

Structure Determination

The structure was solved by obtaining phases from the normalized structure factor magnitudes using the symbolic addition procedure (9). A comparison between the theoretical and experimental statistical averages and distributions of the $|E|$'s shown in Table 1 clearly indicates that the crystal belongs to a centrosymmetric space group.

The signs of 447 reflections with $|E|$ greater than 1.5 were determined using the Σ_2 equation

$$sE_h \simeq s \sum_{k,} E_k E_{h-k}$$

(where "s" means "the sign of"). The starting phases were those of three origin-specifying reflections and five others given the symbolic phases of Table 2. There are numerous Σ_2 relationships indicating $c = d =$ positive, $a = b = e$. If a is positive, all the signs determined would be positive, which is an improbable solution, therefore an E-map with a assigned negative was computed. This E-map unambiguously revealed the whole structure.

Refinement

The atomic coordinates as read from the E-map were refined by full-matrix least squares using the XFLS variant of ORFLS (10). Using atomic scattering factors derived from Hartree–Fock wave functions (11) and hydrogen positions from a difference Fourier map, refinement reached an ultimate conventional R of 0.063. Hydrogen atoms were given anisotropic temperature factors of the atoms to which they are bonded. Final F_o and F_c values have been placed in the Depository for Unpublished Data.[1] The positional and thermal parameters with standard

TABLE 1. Statistical averages and distribution of normalized structure factor amplitudes

Parameter	Value: Experimental	Value: Theoretical (centric)
$\langle\|E\|\rangle$	0.803	0.798
$\langle\|E^2 - 1\|\rangle$	0.997	0.968
$\langle E^2\rangle$	1.017	1.000
$\|E\| \geq 3.0$	0.5%	0.3%
$\|E\| \geq 2.0$	5.1%	5.0%
$\|E\| \geq 1.0$	31.2%	32.0%

TABLE 2. Initial phases for symbolic addition procedure

hkl	$\|E\|$	Phase
$\bar{6}\,5\,\bar{6}$	3.30	+
2 2 7	3.51	+
$\bar{1}\,2\,2$	3.99	+
2 8 $\bar{6}$	3.02	*a*
$\bar{2}\,2\,1$	2.72	*b*
1 1 $\bar{5}$	2.52	*c*
$\bar{9}\,1\,9$	2.68	*d*
2 4 8	3.22	*e*

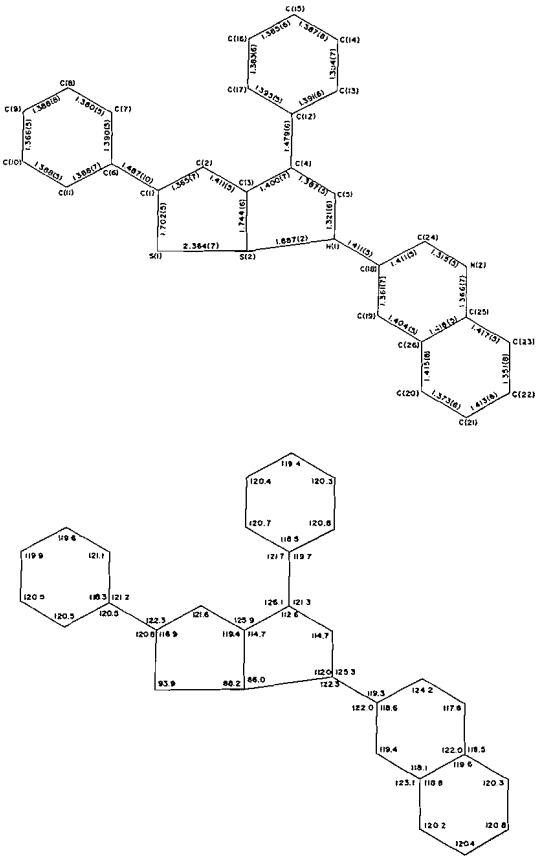

FIG. 1. Bond lengths and angles.

[1]Photocopies may be obtained free of charge, upon request, from the Depository of Unpublished Data, National Science Library, National Research Council of Canada, Ottawa, Canada.

Can. J. Chem. Downloaded from www.nrcresearchpress.com by 210.87.254.40 on 09/05/12
For personal use only.

TABLE 3. Fractional atomic coordinates (e.s.d's in parentheses)

Atom	x	y	z
S(1)	0.35070(7)	0.81318(8)	−0.19642(8)
S(2)	0.39773(7)	0.67840(7)	−0.00299(7)
N(1)	0.45454(22)	0.57091(23)	0.15395(22)
N(2)	0.32025(26)	0.41265(28)	0.37165(26)
C(1)	0.51345(27)	0.86898(27)	−0.14115(28)
C(2)	0.60446(27)	0.82361(28)	−0.01777(27)
C(3)	0.56593(26)	0.73252(27)	0.05907(27)
C(4)	0.65190(25)	0.67693(27)	0.18384(27)
C(5)	0.58510(27)	0.58683(29)	0.23249(29)
C(6)	0.55218(28)	0.96603(27)	−0.22277(28)
C(7)	0.68266(32)	0.98033(34)	−0.20397(32)
C(8)	0.71967(40)	1.07489(38)	−0.27543(39)
C(9)	0.62490(40)	1.15569(37)	−0.36939(39)
C(10)	0.49581(37)	1.14112(34)	−0.39071(34)
C(11)	0.45857(33)	1.04621(31)	−0.31878(31)
C(12)	0.79832(26)	0.70639(28)	0.26040(26)
C(13)	0.88000(30)	0.59604(34)	0.30956(30)
C(14)	1.01663(31)	0.62152(40)	0.38874(33)
C(15)	1.07400(31)	0.75815(39)	0.42167(33)
C(16)	0.99380(30)	0.86855(39)	0.37138(33)
C(17)	0.85732(29)	0.84325(33)	0.29171(30)
C(18)	0.36382(26)	0.49567(27)	0.18767(26)
C(19)	0.24147(26)	0.44320(29)	0.08837(30)
C(20)	0.02719(30)	0.31028(34)	0.03191(38)
C(21)	−0.05222(33)	0.23968(37)	0.07800(43)
C(22)	−0.00748(35)	0.22669(36)	0.22193(42)
C(23)	0.11461(32)	0.28174(32)	0.31651(39)
C(24)	0.39770(31)	0.47973(33)	0.32887(29)
C(25)	0.19875(28)	0.35596(28)	0.27252(30)
C(26)	0.15495(26)	0.37039(26)	0.12844(28)
H(2)	0.7027(35)	0.8553(35)	0.0228(35)
H(5)	0.6374(33)	0.5300(35)	0.3178(36)
H(7)	0.7503(37)	0.9233(38)	−0.1418(38)
H(8)	0.8111(41)	1.0779(40)	−0.2699(41)
H(9)	0.6522(40)	1.2242(38)	−0.4156(41)
H(10)	0.4211(40)	1.1963(39)	−0.4549(40)
H(11)	0.3635(37)	1.0454(36)	−0.3344(36)
H(13)	0.8427(35)	0.4940(39)	0.2921(36)
H(14)	1.0742(36)	0.5496(41)	0.4167(39)
H(15)	1.1690(36)	0.7794(40)	0.4712(37)
H(16)	1.0417(36)	0.9662(42)	0.3972(39)
H(17)	0.7994(35)	0.9168(37)	0.2580(36)
H(19)	0.2092(32)	0.4599(35)	−0.0125(36)
H(20)	−0.0054(34)	0.3377(37)	−0.0760(42)
H(21)	−0.1487(37)	0.1981(41)	0.0056(42)
H(22)	−0.0739(38)	0.1776(40)	0.2522(45)
H(23)	0.1537(36)	0.2634(37)	0.4287(43)
H(24)	0.4905(35)	0.5214(38)	0.4081(34)

deviations as obtained in the least squares refinement are given in Tables 3 and 4. The β_{ij} in Table 5 are the coefficients in the expression

$$\exp(-(\beta_{11}h^2 + \beta_{22}k^2 + \beta_{33}l^2 + 2\beta_{13}hl + 2\beta_{12}hk + 2\beta_{23}kl))$$

The bond distances and angles in the molecule are shown in Fig. 1, the average standard deviations of the angles being 0.5°.

Discussion

The S...S distance of 2.364(7) Å is almost identical to that found in 2,5-diphenyl- and in 2,5-dimethyl-thiathiophthen. Apparently (12) the S...S distance can span the range from 2.0 to 2.6 Å.

The S—N bond length seems to be greater than that found in **8** (13), **9** (14), and **10** (15) which are 1.632, 1.663, and 1.740 Å for S(2)—N(1), respectively. The C(5)—N(1) distance compares favorably with the value obtained in *s*-triazine (16), where the C—N distance was found to be 1.319 Å.

The interior angles at C(3), C(4), and C(5) in the five-member ring S(2), C(3), C(4), C(5), N(1) are substantially less than the 120° expected for

TABLE 4. Thermal parameters × 10^5 (e.s.d's in parentheses)

Atom	β_{11}	β_{22}	β_{33}	β_{12}	β_{13}	β_{23}
S(1)	730(12)	1223(16)	948(14)	−42(10)	165(9)	374(11)
S(2)	651(11)	949(13)	855(13)	−105(9)	266(9)	26(9)
N(1)	787(37)	915(41)	687(36)	−100(30)	310(30)	156(30)
N(2)	1064(44)	1359(52)	903(43)	−358(38)	393(36)	189(37)
C(1)	890(45)	758(44)	853(46)	54(35)	400(38)	83(36)
C(2)	807(43)	890(48)	773(44)	82(36)	366(36)	119(36)
C(3)	736(41)	782(45)	774(43)	31(34)	300(35)	55(35)
C(4)	731(43)	804(47)	829(46)	−1(35)	333(36)	75(37)
C(5)	796(44)	951(51)	878(46)	−38(37)	394(37)	47(38)
C(6)	996(47)	755(44)	818(45)	62(36)	437(38)	44(36)
C(7)	1057(53)	1201(60)	1085(56)	32(44)	558(45)	177(46)
C(8)	1526(68)	1304(68)	1498(70)	−18(54)	931(59)	252(55)
C(9)	1682(76)	1205(66)	1446(72)	126(56)	974(63)	290(54)
C(10)	1565(69)	1137(61)	1133(59)	234(51)	739(53)	321(48)
C(11)	1242(56)	929(51)	948(51)	220(43)	536(44)	204(41)
C(12)	761(42)	952(48)	682(41)	20(35)	312(34)	165(36)
C(13)	963(49)	1191(58)	937(51)	210(43)	411(41)	337(43)
C(14)	882(51)	1721(73)	1012(56)	256(49)	371(43)	455(51)
C(15)	769(47)	1833(76)	977(54)	−24(48)	305(41)	227(51)
C(16)	762(47)	1628(70)	1138(58)	−158(46)	374(43)	122(50)
C(17)	800(45)	1116(53)	987(51)	−122(38)	389(40)	54(41)
C(18)	787(42)	836(45)	777(45)	−81(35)	336(36)	131(36)
C(19)	730(44)	929(51)	904(49)	−19(37)	282(38)	53(39)
C(20)	764(47)	1181(61)	1481(68)	−169(43)	323(46)	−3(51)
C(21)	872(54)	1317(70)	1879(83)	−177(49)	408(54)	92(60)
C(22)	1098(59)	1192(64)	1957(82)	4(49)	797(59)	386(58)
C(23)	1029(54)	1041(57)	1612(70)	−156(44)	682(51)	278(49)
C(24)	1056(52)	1354(61)	770(49)	−354(44)	367(41)	206(42)
C(25)	899(46)	821(47)	1030(50)	−77(37)	437(40)	132(38)
C(26)	740(42)	736(45)	910(48)	26(35)	280(37)	75(36)

sp^2 hybridization and this indicates the presence of an S—N attraction or exceptional interatomic forces.

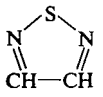

8

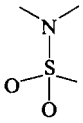

9

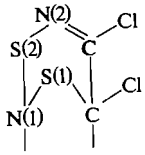

10

The molecule may be considered as a resonance hybrid of both dithiole (**11***a*) and isothiazole, (**11***b*), bearing in mind that this "single-bond

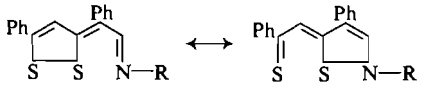

11*a* **11***b*

no-bond" concept fails to explain the unequal S—S lengths in the unsymmetrical thiathiophthen derivatives **2** and **3** and even more so in the symmetrical molecule **12** recently reported by Johnson and Paul (17).

The nature of the bonding in these compounds is not well understood although some theories have been proposed (18, 19). The bond between

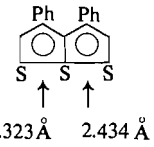

12

TABLE 5. Difference in electronegativity (23), Δ, and S—S bond length, *L*

System	Δ	*L* (Å)	Reference number
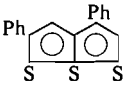	0.0	2.51	2
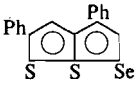	0.1	2.49	4
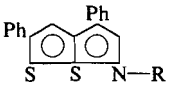	0.5	2.36	This work
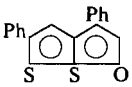	1.0	2.09	5

Can. J. Chem. Downloaded from www.nrcresearchpress.com by 210.87.254.40 on 09/05/12
For personal use only.

TABLE 6. Best least squares planes of the form $AX + BY + CZ = D$, where X, Y, Z are real orthogonal coordinates, X along x and Z along z*

(a) Coefficients

Plane	Description	A	B	C	D
1	"Thiathiophthen moiety"	0.4254	−0.7474	−0.5103	−3.0101
2	Phenyl ring attached to C(1)	0.1683	−0.6621	−0.7303	2.9173
3	Phenyl ring attached to C(4)	0.5577	0.0064	−0.8300	2.1123
4	3-Quinolyl group	0.5210	−0.8512	−0.0635	−2.5074

(b) Angles between normals to planes (degrees)

Plane	1	2	3	4
1	0	20.10	49.00	27.10
2			45.91	45.77
3				70.26

the sulfur atoms in these systems is weak and small differences in intermolecular forces acting on the atoms might be the cause of differences in observed bond lengths. A detailed analysis of intermolecular forces may give a clue to this question.

The S...S distances and difference of electronegativities between S and X for the S...S...X systems with similar diphenyl substitution are shown in Table 5. The S...S distance decreases as the difference in electronegativity increases. This may be due to an increase in ionic character of the S...S interaction, an effect which could be confirmed by structural analyses of similar compounds having X elements with a range of electronegativities.

The bond lengths in the quinolyl ring agree extremely well with those found in 5-acetoxy-6-methoxy-8-nitroquinoline (20). In no case does the difference in bond length exceed 2.5σ and the average is only 1.0σ. Neither this latter structure nor ours give such good bond length agreement with those cited for 8,8′-dibromo-2,2′-methylenediquinoline (21) and even less with those cited for 1-methyl-2-quinolone (22) where a predominant quinolinium-type contribution is suspected to be present.

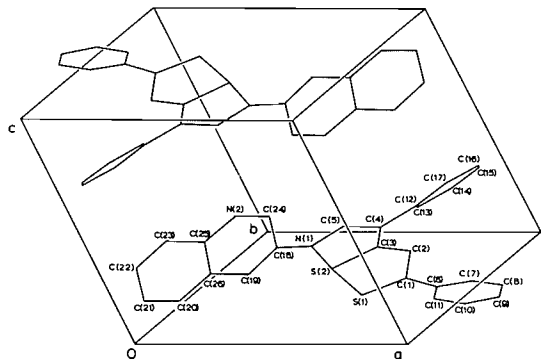

FIG. 2. Packing of molecules in the unit cell.

Coefficients for the best least squares planes through (*i*) the "thiathiophthen moiety" (S(1), S(2), N(1), C(1), C(2), C(3), and C(5)), (*ii*) the two phenyl rings, and (*iii*) the quinolyl group are listed in Table 6. In no case does the maximum deviation from planarity exceed 0.03 Å. Doubtless the interaction between hydrogen atoms at C(2) and C(17) causes the phenyl ring at C(4) to be twisted 49° from the central ring plane (Table 6). On the other hand, interaction between hydrogen atoms at C(2) and C(7) at C(5) and C(24) is weaker so that the phenyl ring at C(1) and the quinolyl ring are twisted only 20 and 27°, respectively.

The packing of the molecules in the unit cell is shown in Fig. 2. There are no especially short intermolecular contacts.

We are grateful to Dr. E. Klingsberg for supplying the crystals and to Mr. J. C. Rylaarsdam for help with the diagrams. F.L. was in receipt of a Province of Ontario Graduate Fellowship during this work, which was generously supported by the National Research Council of Canada.

1. S. BEZZI, M. MAMMI, and G. GARBUGLIO. Nature, **182**, 247 (1958).
2. A. HORDVIK, E. SLETTEN, and J. SLETTEN. Acta Chem. Scand. **20**, 2001 (1966).
3. S. M. JOHNSON, M. G. NEWTON, I. C. PAUL, R. J. S. BEER, and D. CARTWRIGHT. Chem. Commun. 1170 (1967).
4. J. H. VAN DEN HENDE and E. KLINGSBERG. J. Amer. Chem. Soc. **88**, 5045 (1966).
5. A. HORDVIK. Private communication.
6. F. LEUNG and S. C. NYBURG. Chem. Commun. 137 (1969).
7. E. KLINGSBERG. J. Org. Chem. **33**, 2915 (1968).

Can. J. Chem. Downloaded from www.nrcresearchpress.com by 210.87.254.40 on 09/05/12
For personal use only.

8. F. LEUNG and S. C. NYBURG. Chem. Commun. 707 (1970).
9. J. KARLE and I. L. KARLE. Acta Cryst. **21**, 849 (1966).
10. R. D. ELLISON. XFLS, An extensively modified version of ORFLS (Report ORNL-TM-305, Oak Ridge National Laboratory, 1962). Unpublished.
11. D. T. CROMER and J. B. MANN. Acta Cryst. A**24**, 321 (1968).
12. J. SLETTEN. Chem. Commun. 688 (1969).
13. F. A. MOMANY and R. A. BONHAM. J. Amer. Chem. Soc. **86**, 162 (1964).
14. L. M. TREFONAS and R. MAJESTE. J. Hetero. Chem. **2**, 80 (1965).
15. A. C. HAZELL. Acta Chem. Scand. **21**, 415 (1967).
16. P. J. WHEATLEY. Acta Cryst. **8**, 224 (1955).
17. P. L. JOHNSON and I. C. PAUL. Chem. Commun. 1014 (1969).
18. K. MAEDA. Bull. Chem. Soc. Japan, **33**, 1466 (1960); **34**, 785, 1166 (1961).
19. R. GLEITER and R. HOFFMANN. Tetrahedron, **24**, 5899 (1968).
20. M. SAX and R. DESIDERATO. Acta Cryst. **23**, 319 (1967).
21. J. VAN THUIJL and C. ROMERS. Acta Cryst. **20**, 899 (1966).
22. M. CALLERI and J. C. SPEAKMAN. J. Chem. Soc. A, 1644 (1969).
23. L. PAULING. The Nature of the Chemical Bond. 3rd. ed. Cornell University Press, Ithaca, New York. 1960.

Can. J. Chem. Downloaded from www.nrcresearchpress.com by 210.87.254.40 on 09/05/12
For personal use only.

Can. J. Chem. Downloaded from www.nrcresearchpress.com by 210.87.254.42 on 09/05/12
For personal use only.

Extractive-photometric Investigation of Cadmium Chelates of 4-(2-Thiazolylazo)-resorcinol (TAR)

O. NAVRATIL[1] AND R. W. FREI[2]

Chemistry Department, Dalhousie University, Halifax, Nova Scotia

Received June 15, 1970

A quantitative interpretation of the extractive distribution of cadmium chelates of TAR (= H_2A) between liquid organic and water phases has been made and two groups of extractable species have been determined: (*a*) uncharged complexes of the type CdA in which co-ordinated water is replaced by suitable uncharged organic base (2,9-dimethyl-1,10-phenanthroline) and (*b*) charged complexes CdA_2^{2-} which are extracted as ionic pairs in the presence of charged organic bases.

The evaluation of the character of the bases and the effect of p*H* and the nature and concentration of other inorganic anions are presented.

Canadian Journal of Chemistry, 49, 173 (1971)

N-heterocyclic azodyes have been used in the analytical chemistry of heavy and noble metals because of their great sensitivity and better selectivity when compared with isocyclic azodyes. The derivatives of thiazolylazophenols have often been preferred because of their easier preparation (1, 2). For extractive applications, reagents with one —OH group have been primarily utilized because they form uncharged complexes. Although the derivatives of resorcinol (*i.e.*, 4-(2-thiazolylazo)-resorcinol (TAR) and 4-(2-pyridylazo)-resorcinol (PAR)) have been employed widely as chelatometric indicators because of their ability to form colored complexes with many metal ions, they have not been used in extraction procedures. The reason for this is the charge of the complexes which results from the preferential dissociation of the —OH group on the resorcinol in the position *para* to the azo group. An exception is palladium, which has been extracted with PAR (3, 4) and TAR (5) using ethyl acetate or isoamyl alcohol as solvents. Pd–PAR or Pd–TAR 1:1 chelate complexes were extracted from sulfuric acid medium.

In the present work attention is focused on the extractive-photometric investigation of some heavy metal chelates of TAR with a view toward further electrophoretical studies of these charged complexes.

Experimental

Solutions and Reagents

Aqueous stock solutions of the metal ions Cu^{2+}, Ni^{2+}, Co^{2+}, Cd^{2+}, Zn^{2+}, Pb^{2+}, Fe^{2+}, and Mn^{2+} were prepared and if necessary a small amount of hydrochloric or sulfuric acid was added to prevent hydrolysis. Stock solutions of tetramethylammonium iodide (Me_4NI), tetra-*n*-propylammonium bromide (Pr_4NBr), tetra-*n*-butylammonium iodide (Bu_4NI), tetra-*n*-hexylammonium bromide (Hex_4NBr), tetra-*n*-hexylammonium iodide (Hex_4NI), tetra-*n*-heptylammonium chloride (Hep_4NCl), ethylhexadecyldimethylammonium bromide ($EtHdMe_2NBr$), trimethylphenylammonium chloride (Me_3PhNCl), 1,3-diphenylguanidine (DPG) (all Eastman Organic Chemicals), tetraphenylarsonium chloride (Ph_4AsCl), tri-*n*-octylamine (TOA) (both Aldrich), tri-*n*-butylamine (TBA) (British Drug Houses), cetylpyridinium chloride (CPCl) (Fisher Scientific), and 2,9-dimethyl-1,10-phenanthroline (DMphen) (Frederick Smith Chem.) were prepared from weighed amounts dissolved in benzene, chloroform, methylisobutyl-ketone (MIBK), isoamyl alcohol (IAOL), or water. TAR (Aldrich) was dissolved in 0.05 *M* ammonium hydroxide solution. Chloroacetate, acetate, borate, and ammonia – ammonium chloride buffers were used over the p*H* range 1.9 to 10; the concentration of the inorganic solutions of the water phase was always 0.03 *M* except for the study of the dependency of the equilibrium ratio of the metals on the analytical concentration of the interfering inorganic anions. All chemicals and reagents used were of analytical reagent grade quality.

Apparatus

Transmission spectra were measured with a Bausch and Lomb Spectronic 505 recording spectrophotometer in the visible region using 1 cm glass cuvettes. The atomic absorption spectrophotometer (Perkin–Elmer Model 290) with Cd, Co–Cr–Cu–Mn–Ni, and Zn–Ca hollow cathodes was used for the measurement of the metal concentrations in water and organic phases. For p*H* measurements of the aqueous phase a Radiometer p*H* meter 28 (Denmark) was used.

Procedure

Four to five ml of water phase containing $5 \times 10^{-5} - 5 \times 10^{-4}$ *M* solution of the metal ion, a solution of $5 \times 10^{-4} - 5 \times 10^{-3}$ *M* TAR, buffer solution, and masking agents were shaken with an equal volume of organic solvent containing $1 \times 10^{-4} - 1 \times 10^{-2}$ *M* organic base. To establish equilibrium these systems were shaken for 2–3.5 h in test tubes with ground glass stoppers in a homemade rotator, using 1.5 turns/s. This time

[1]On leave from the University of Brno, Czechoslovakia.
[2]To whom correspondence is to be addressed.

interval was sufficient to establish equilibrium in all systems. After separating the layers, an aliquot part was taken from the organic phase for spectrophotometric measurements, or from both phases for atomic absorption measurements. The concentration of the metals present in each liquid phase was determined with the use of calibration curves.

The distribution of TAR alone between benzene or IAOL and aqueous buffer solutions was studied spectrophotometrically as described above. A definite volume of a solution of 0.12 *M* NaOH was added to an aliquot of the water phase (or organic phase after evaporation to dryness) so that TAR (= H_2A) was completely transformed to the anionic form A^{2-}. Its concentration was measured against a water blank, using suitable calibration curves.

Results and Discussion

The distribution of TAR

The acid dissociation constants of TAR were determined spectrophotometrically to be $pk_{a(para)} = 6.23$ and $pk_{a(ortho)} = 9.44$ (6) according to the equations below

$$k_{a(para)} = \frac{[H^+_{para}][HA^-]}{[H_2A]} = 10^{-6.23} \quad k_{a(ortho)} = \frac{[H^+_{ortho}][A^{2-}]}{[HA^-]} = 10^{-9.44}$$

Thus the —OH group in para position to the azo group is more acidic

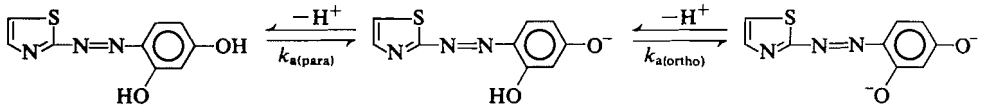

and since it does not participate directly in the formation of the metal chelate it must be responsible for the negative charge of the complex in neutral and alkaline media. The solubility of the reagent is probably better in a more polar organic solvent; the experimental results obtained by the authors show the value[3] of $Q_{H_2A} = [H_2A]_0/[H_2A]$ to be 19.8 in the system benzene – 0.03 *M* aqueous buffer solution and 1211 in the buffer – isoamyl alcohol system.

The distribution of TAR between aqueous buffer solution and benzene given by eqs. 1 and 2

[1] $$q_{H_2A} = \frac{[H_2A]_0}{[H_2A] + [HA^-] + [A^{2-}]}$$

or

[2] $$q_{H_2A} = -\frac{Q_{H_2A}[H^+]^2}{[H^+]^2 + k_{a(para)}[H^+] + k_{a(para)}k_{a(ortho)}}$$

and the theoretical distribution curve calculated according to eq. 2 is shown in Fig. 1. Experimental values obtained by spectrophotometric measurements agree well with the theoretical values.

The Extraction of Cd(II)–TAR Complexes

Assuming that the highest coordination number of Cd(II) is six and A^{2-} is a tridentate ligand, we can postulate that 1:1 CdA and 1:2 CdA_2^{2-} complexes are formed. Although the CdA complex is neutral, it is normally poorly extractable because of the presence of water molecules which can occupy free coordination sites on the metal. The extraction of such a complex is, however, possible when the coordinated water is replaced by a suitable organic reagent or organic solvent. For the extraction of the CdA_2^{2-} complex, on the other hand, the major problem is the elimination of the negative charge. This can be achieved with the addition of a suitable organic cation, which results in the formation of an extractable ion association complex.

The cadmium ion was chosen for an investigation of both types of extractable complexes (A and B) because of the good sensitivity of this metal when using atomic absorption spectrophotometry for determination.

[3]The equilibrium concentration of the compound X in the organic phase is expressed as $[X]_0$ and that in the water phase as [X].

Can. J. Chem. Downloaded from www.nrcresearchpress.com by 210.87.254.42 on 09/05/12
For personal use only.

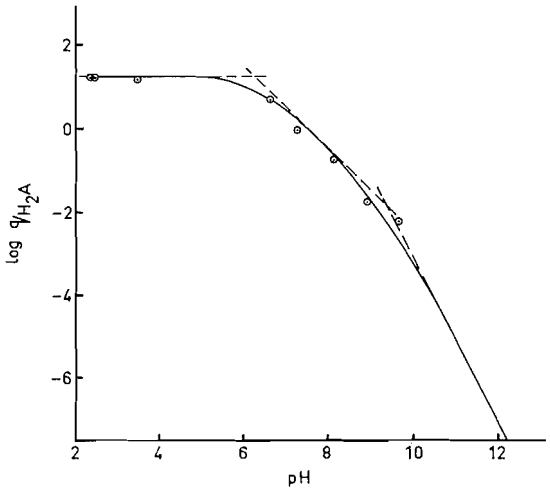

FIG. 1. Effect of pH of the water phase on the distribution of H_2A between benzene and 0.03 M buffer solutions. The curve represents calculated values, the intersection of broken lines represents theoretical values of $pk_{a(para)}$ and $pk_{a(ortho)}$; ○ are experimental points.

(A) A quantitative description of the extraction of cadmium when using DMphen as a suitable uncharged organic base can be made with the assumption of the following distribution equilibria

[3] $$Cd^{2+} + H_2A \rightleftharpoons CdA + 2H^+ \qquad K_1 = -\frac{[CdA][H^+]^2}{[Cd^{2+}][H_2A]}$$

[4] $$Cd^{2+} + 2H_2A \rightleftharpoons CdA_2^{2-} + 4H^+ \qquad K_2 = \frac{[CdA_2^{2-}][H^+]^4}{[Cd^{2+}][H_2A]^2}$$

[5] $$CdA + DMphen \rightleftarrows CdA(DMphen) \qquad k_{ad1} = \frac{[CdA(DMphen)]}{[CdA][DMphen]}$$

The number of coordinated water molecules in the CdA complex is neglected.

[6] $$CdA(DMphen) \rightleftarrows \{CdA(DMphen)\}_0 \qquad Q_{CdA(DMphen)} = \frac{[CdA(DMphen)]_0}{[CdA(DMphen)]}$$

[7] $$Cd^{2+} + y DMphen \rightleftarrows Cd(DMphen)_y^{2+} \qquad k_{ad2} = \frac{[Cd(DMphen)_y]}{[Cd^{2+}][DMphen]^y}$$

For the extraction of cadmium as a CdA(DMphen) complex the distribution of Cd is given as

[8] $$q_{Cd} = \frac{[CdA(DMphen)]_0}{[Cd^{2+}] + [CdA] + [CdA_2^{2-}] + [CdA(DMphen)] + [Cd(DMphen)_y^{2+}]}$$

where $y = 1$–3. Then

[9] $$q_{Cd} = \frac{Q_{CdA(DMphen)} k_{ad1} K_1 [DMphen][H_2A]}{[H^+]^2\{1 + \frac{[H_2A]K_1}{[H^+]^2}(1 + [DMphen]k_{ad1}) + \frac{[H_2A]^2 K_2}{[H^+]^4} + k_{ad2}[DMphen]^y\}}$$

Typical extraction curves for the dependency of the log equilibrium ratio of Cd ($= q_{Cd}$) on pH are shown in Fig. 2. It can be seen that log q_{Cd} values increase with a slope of 2.0 ∓ 0.2 in the low pH range, then pass through a maximum and decrease with a slope of -1.7 ∓ 0.3 with higher pH values. Each interval of the value of the slope of the pH-extraction curve depends on the predominant species in the water phase and can be described by the term in brackets in the denomi-

Can. J. Chem. Downloaded from www.nrcresearchpress.com by 210.87.254.42 on 09/05/12
For personal use only.

nator of eqs. 8 and 9, *e.g.* $Cd^{2+} \rightarrow CdA(DMphen) \rightarrow CdA_2^{2-}$. The extraction maximum on the curve is equal to the maximum of the concentration of the CdA(DMphen) species; it can also be observed in the same p*H* region when the system Cd^{2+}–TAR is used with IAOL as an organic phase without DMphen (see Fig. 2). On the other hand, when benzene is present as organic phase without DMphen, the extraction of Cd is negligible in all the p*H* region ($\log q_{Cd} < -2.5$). This fact indicates that the complex CdA is probably hydrated and non-extractable into benzene. Taking into account that the water molecules can be replaced by the relatively polar IAOL molecules, we can assume the extractable complex to be $CdA(IAOL)_r$.

The formation of the $Cd(DMphen)_y^{2+}$ species also plays an important role, and the same effect can be observed as described recently by Hamilton and Freiser (7). First the extraction of Cd is observed to increase with an increase in DMphen concentration. At a concrete concentration level the extraction curve shifts to the right because of a formation of the unextractable $Cd(DMphen)_2^{2+}$ and $Cd(DMphen)_3^{2+}$ complexes. As a consequence, the last term in the lower part of eq. 9 cannot be neglected.

(*B*) When ionic associates are formed as a result of the presence of a charged organic base, the following equilibria can be formulated (K_{as} = association constant, Q = partition coefficient)

[10] $$B^+ + X^- \rightleftarrows (B^+, X^-) \qquad K_{as,BX} = \frac{[(B^+, X^-)]}{[B^+][X^-]}$$

[11] $$(B^+, X^-) \rightleftarrows (B^+, X^-)_0 \qquad Q_{BX} = \frac{[(B^+, X^-)]_0}{[(B^+, X^-)]}$$

X^- is the inorganic anion present in the water phase.

[12] $$2B^+ + CdA_2^{2-} \rightleftarrows (2B^+, CdA_2^{2-}) \qquad K_{as,BCdA} = \frac{[(2B^+, CdA_2^{2-})]}{[B^+]^2[CdA_2^{2-}]}$$

[13] $$(2B^+, CdA_2^{2-}) \rightleftarrows (2B^+, CdA_2^{2-})_0 \qquad Q_{BCdA} = \frac{[(2B^+, CdA_2^{2-})]_0}{[(2B^+, CdA_2^{2-})]}$$

Then the distribution of Cd in the presence of charged organic base is given by

[14] $$q_{Cd} = \frac{[(2B^+, CdA_2^{2-})]_0}{[Cd^{2+}] + [CdA] + [CdA_2^{2-}]}$$

assuming that the concentration of the ionic associates in the water phase can be neglected (*e.g.* the value of Q_{BCdA} is very high).

From the equilibria mentioned above, the following equation for the distribution of cadmium can be written

[15] $$q_{Cd} = \frac{Q_{BCdA} K_{as,BCdA} K_{as,BX}^{-2} Q_{BX}^{-2} K_2 [(B, X)]_0^2 [H_2A]^2 [H^+]^{-4} [X^-]^{-2}}{1 + K_1[H_2A][H^+]^{-2} + K_2[H_2A]^2[H^+]^{-4}}$$

Equation 15 does not take into account the possible formation of Cd–X complexes which could take place at higher concentrations of X^-; it does, however, indicate that q_{Cd} is proportional to $[(B^+, X^-)]_0^2$ and to $[X^-]^{-2}$ when the p*H* of the water phase remains constant.

The Effect of Composition and Concentration of Organic Bases on the Extraction of Some M^{II}–TAR Complexes

In general, the extraction of ionic pairs is favored when the solvent molecules of the extracting agent and the oppositely charged part of the complex are similar in character; this results in a higher value of $Q_{BCdA} \times K_{as,BCdA}$. Various types of organic bases were examined and the values of equilibrium ratios of Cd, Co, and Ni when using 1×10^{-2} *M* solutions of organic bases in benzene, isoamyl alcohol, or MIBK are presented in Table 1.

Comparing the character of the bases investigated, we can conclude that the extraction of Cd, Co, and Ni improves with an increase in chain length of the alkyl group in the alkylammonium base. Best results are obtained with the systems Hep_4NCl–benzene and CPCl–IAOL. The use of ternary amines (TOA, TBA) and also

Can. J. Chem. Downloaded from www.nrcresearchpress.com by 210.87.254.42 on 09/05/12
For personal use only.

Can. J. Chem. Downloaded from www.nrcresearchpress.com by 210.87.254.42 on 09/05/12
For personal use only.

TABLE 1. Effect of organic base on extraction of Cd, Co, and Ni*

Base	Solvent	log q_{Cd}	log q_{Co}	log q_{Ni}
Me_4NI	Benzene	−2.69	< −2.0	< −2.0
Pr_4NBr	Benzene	−1.63	−1.6	−1.6
Bu_4NI	Benzene	−1.60	−1.0	−1.2
Hex_4NBr	Benzene	2.56	>2.0	>2.0
	IAOL	0.78	1.0	1.0
Hex_4NI	Benzene	1.94	⩾2.0	⩾2.0
	IAOL	1.52	1.4	1.2
	MIBK	1.10	—	—
Hep_4NCl	Benzene	2.84	—	—
Me_3PhNCl	Benzene	−3.43	< −2.0	< −2.0
DPG	Benzene	−2.81	< −2.0	< −2.0
	IAOL	−0.32	−1.6	−1.8
TBA	Benzene	−2.00	⩽ −2.0	< −2.0
TOA	Benzene	−2.69	< −2.0	< −2.0
CPCl	IAOL	2.2	1.8	2.0
$EtHdMe_2NBr$	IAOL	1.11	1.2	1.0
Ph_4AsCl	IAOL	0.18	0.6	0.7

*$c_{Cd} = 1 \times 10^{-4}$ *M*, $C_{Co,Ni} = 2 \times 10^{-4}$ *M*, $c_{TAR} = 1.25 \times 10^{-3}$ *M*, ammonia - ammonium chloride buffer (p*H* 9.4).

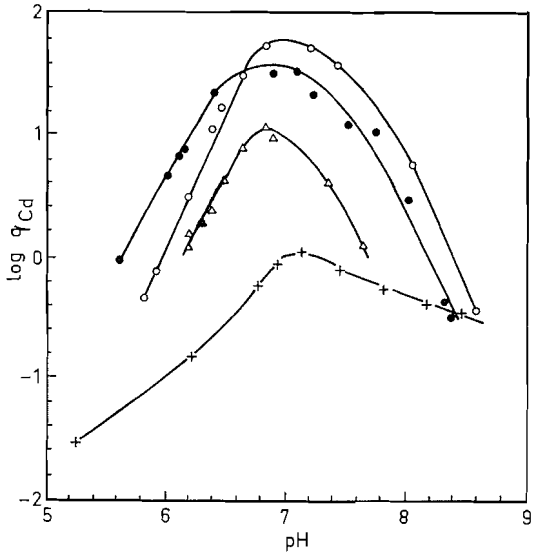

FIG. 2. Effect of p*H* of the water phase on the distribution of cadmium between solution of DMphen in benzene and IAOL only and 0.03 *M* water buffer solution. $c_{H_2A} = 1 \times 10^{-3}$ *M*; $c_{Cd} = 1 \times 10^{-4}$ *M*; c_{DMphen}: ○, 1×10^{-3} *M*; ●, 1×10^{-4} *M*; △, 2.5×10^{-5} *M*; +, IAOL only, without DMphen.

DPG is not satisfactory because of their inability to form charged cations in alkaline medium. The dependence between log q_{Cd} and the analytical concentration of the base is presented in Fig. 3. The limiting values of the slopes for the straight plots are $+2.0 \mp 0.2$ in all cases. Thus the dependence between q_{Cd} and $[(B,X)]_0$ from eq. 15 is valid and complexes of the type ($2B^+$, CdA_2^{2-}) are extracted in all systems.

The Effect of the Nature and Concentration of Inorganic Anions

It is known that the nature and concentration of inorganic anions influence the extractability of ionic pairs because of their different hydration (8). A competitive extraction according to eqs. 10 and 11 can take place, resulting in a decrease of free base in the system.

The influence of the analytical concentration of some inorganic anions on the extractability of Cd, when using a 1×10^{-2} *M* solution of CPCl in IAOL, is shown in Fig. 4. The limiting value of the slopes of these curves is equal to -2.0 ∓ 0.2 for SCN^-, ClO_4^-, and I^-. The good agreement between the theoretical and the experimental values of the slopes can be explained by the low hydration numbers of these anions (9), *e.g.* by the relatively constant distance between anion and cation in the extractable ionic pair. On the other hand, the hydration of the other anions investigated is not negligible and consequently the conditions for their extraction as ionic pairs are more complicated. Similar observations have been made with a Cd–TAR benzene chloride system as described in the following section.

The Effect of the Analytical Concentration of TAR

The dependence between log q_{Cd} and log c_{H_2A} in natural water phase is shown in Fig. 5. The slope of the straight line is 2.0 ∓ 0.1 in accordance with eq. 15, because at a constant p*H* of the water phase, c_{H_2A} is directly proportional to $[H_2A]$.

Can. J. Chem. Downloaded from www.nrcresearchpress.com by 210.87.254.42 on 09/05/12
For personal use only.

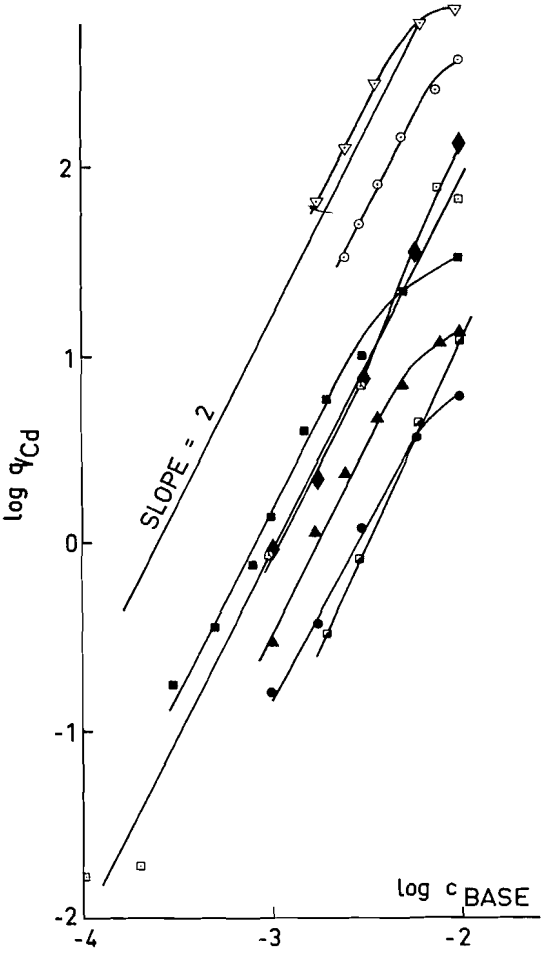

FIG. 3. Effect of the analytical concentration of the organic bases on the distribution of cadmium between 0.03 M ammonia – ammonium chloride buffer solution and different organic solvents. $c_{H_2A} = 1.25 \times 10^{-3}$ M, $c_{Cd} = 1 \times 10^{-4}$ M. Hex_4NBr: ○, benzene; ●, IAOL. Hex_4NI: □, benzene; ■, IAOL; ◪, MIBK. $EtHdMe_2$-NBr: ▲, IAOL. CPCl: ◆, IAOL. Hep_4NCl: ▽, benzene.

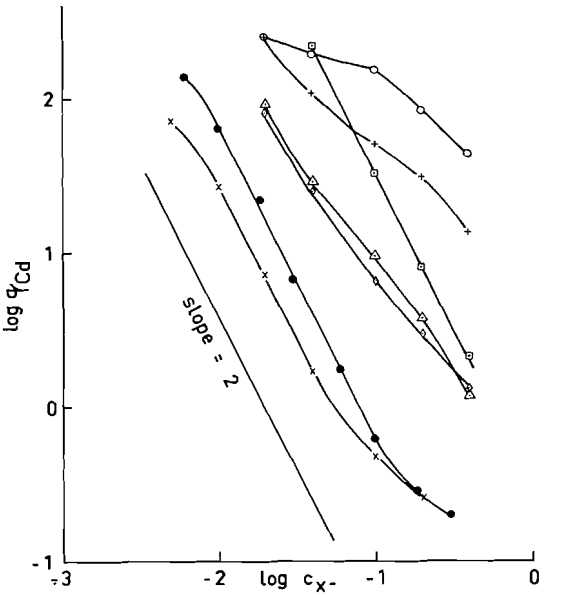

FIG. 4. Effect of the analytical concentration of some inorganic anions on the distribution of cadmium between 0.03 M buffer solutions and 1×10^{-2} M solution of CPCl in IAOL. $c_{H_2A} = 2 \times 10^{-3}$ M, $c_{Cd} = 2 \times 10^{-4}$ M. ○, SO_4^{2-}; +, Cl^-; □, I^-; △, Br^-; ◇, NO_3^-; ●, ClO_4^-; ×, SCN^-.

The Effect of pH of the Water Phase

As shown in Fig. 6, the pH–extraction curves have different characteristics for the CPCl–IAOL and Hep_4NCl–benzene systems. The first one is in quantitative agreement with eq. 15 after subtraction of the corresponding portion for the extractable cadmium in the system Cd–H_2A–IAOL only (blank curve). The extractability of the second system is practically independent of pH due to the formation of a competitive extractable anionic chloro complex.

The explanation of these phenomena probably depends on an evaluation of the association and equilibrium constants according to eqs. 10 and 11. The magnitude of these constants on the other hand evidently depends on the dielectric constants of the solvents, on the size and charge of the species formed, and on the ionic strength of the water phase (10). The behavior of the other bivalent heavy metals is different; only zinc interferes seriously as can be seen in Table 2.

Conclusions

The systems studied in this work can be utilized in analytical chemistry depending on the nature

TABLE 2. The extraction of some bivalent metals with the Hep_4NCl benzene system in acidic medium*

Metal	%E
Cd^{2+}	98.9
Zn^{2+}	20.0
Ni^{2+}	0.6
Co^{2+}	Negligible
Cu^{2+}	”
Mn^{2+}	”
Fe^{2+}	”
Pb^{2+}	”

*$c_{Hep_4NCL} = 1 \times 10^{-2}$ M, $c_M = 2 \times 10^{-4}$ M, $c_{Cl^-} = 0.02M$, p$H = 4.6$, H_2A is absent.

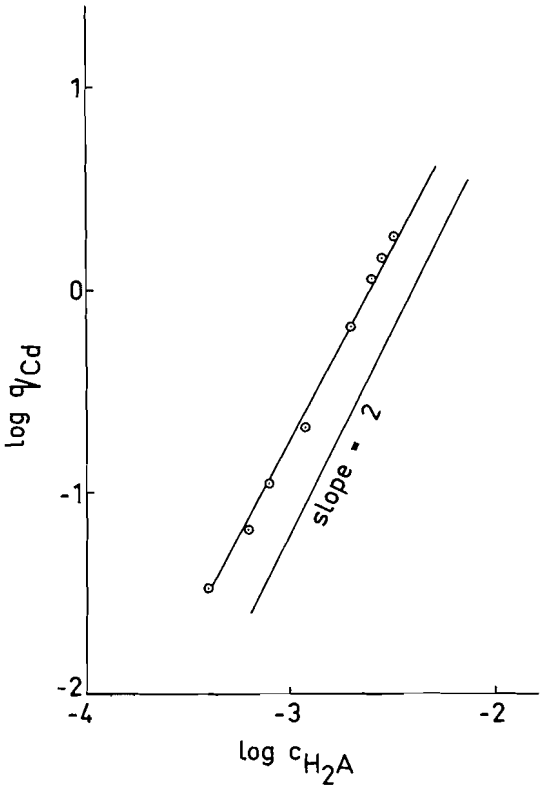

FIG. 5. Effect of the analytical concentration of H_2A on the distribution of cadmium between 0.03 *M* buffer solutions and 1×10^{-2} *M* CPCl solution in IAOL. $c_{Cd} = 8 \times 10^{-5}$ *M*, p*H* of the water phase = 6.99.

of the water phase. Cadmium can be separated directly from acidic water solutions by extraction with solutions of suitable tetraalkylammonium salts in benzene. When TAR is used in alkaline water phase medium, the group of bivalent heavy metals or especially soluble amine complexes can be extracted preferentially as ion association complexes and determined in the organic phase with the aid of suitable instrumental methods.

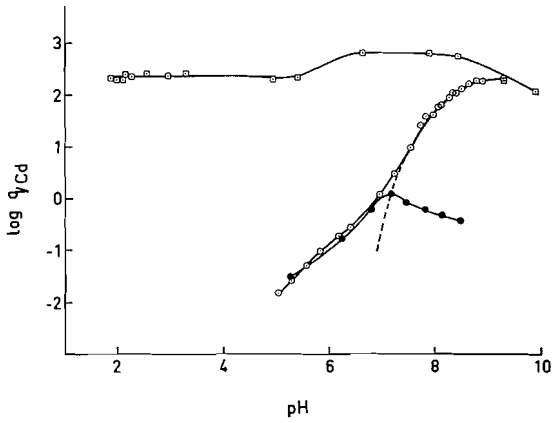

FIG. 6. Effect of p*H* of the water phase on distribution of cadmium between 0.03 *M* chloride buffer solutions and IAOL, CPCl–IAOL, and Hep_4NCl – benzene systems. $c_{Cd} = 2 \times 10^{-4}$ *M*, $c_{H_2A} = 2 \times 10^{-3}$ *M*. ○, 1×10^{-2} *M* solution of CPCl in IAOL; ●, IAOL only. ----, differential curve; □, 1×10^{-2} *M* solution of Hep_4NCl in benzene.

This work was supported by grants from the National Research Council and the Department of Energy, Mines, and Resources of Canada.

1. M. LANGOVA-HNILICKOVA and L. SOMMER. Folia fac. sci. nat. univ. Purkynianae brun. **9**, 1 (1968).
2. R. G. ANDERSON and G. NICKLESS. Anal. **92**, 207 (1967).
3. H. FLASCHKA and J. HICKS. Microchem. J. **11**, 517 (1966).
4. V. M. IVANOV. Zh. anal. Khim. **22**, 763 (1967).
5. LIN HUI KAI, CHEN KUANG-YI, and CHENG FAN-CHENG. Hua Hsueh Tung Pao, 365 (1966). Chem. Abstr. **66**, 25818.
6. M. HNILICKOVA and L. SOMMER. Talanta, **13**, 667 (1966).
7. H. G. HAMILTON and H. FREISER. Anal. Chem. **41**, 1310 (1969).
8. R. M. DIAMOND and D. G. TUCK. Progr. Inorg. Chem. **2**, 109 (1970).
9. Y. MARCUS and A. S. KERTES. Ion Exchange and Solvent Extraction of Metal Complexes. Wiley–Interscience, 1969. p. 29.
10. G. H. MORRISON and H. FREISER. Solvent Extraction in Analytical Chemistry. J. Wiley, New York, 1957. p. 30.

Can. J. Chem. Downloaded from www.nrcresearchpress.com by 210.87.254.42 on 09/05/12
For personal use only.

Can. J. Chem. Downloaded from www.nrcresearchpress.com by 210.87.254.6 on 09/05/12
For personal use only.

^{18}O Transfer in the System Thiosulfate–Sulfite–Water: an Example of a Set of Consecutive Reversible First Order Rate Processes

R. H. Betts and S. Libich
Department of Chemistry, University of Manitoba, Winnipeg 19, Manitoba

Received June 30, 1970

The rate and mechanism of transfer of oxygen between thiosulfate ion and water, in the presence of sulfite, has been investigated with ^{18}O-enriched $Na_2S_2O_3$. The principal path, for the conditions examined, is via sulfur atom transfer between sulfite and thiosulfate, accompanied by oxygen atom transfer between sulfite and the solvent water. The latter path is suppressed at high p*H*, and oxygen transfer from thiosulfate proceeds to the sulfite stage only. At intermediate p*H*, the two processes have comparable rates, and the kinetics show the behavior expected for a system of consecutive, reversible first order processes. Under these conditions sulfite is observed to behave as a true intermediate, first accumulating ^{18}O from thiosulfate, and then releasing it to the solvent water.

Canadian Journal of Chemistry, 49, 180 (1971)

Introduction

The isotopic exchange reaction of sulfur in the aqueous system sulfite–thiosulfate was examined some years ago by Ames and Willard (1). The outer sulfur of thiosulfate is transferred to sulfite at a measurable rate, the reaction being first order in both sulfite and thiosulfate, and zero order with respect to hydrogen ion. It will at once be evident that transfer of the outer S from thiosulfate converts the donor ion to sulfite, and the acceptor ion to thiosulfate. In effect this is equivalent to transfer of oxygen from one species to the other. More recently, oxygen transfer between water and thiosulfate has been examined over a limited range of temperature and p*H* (2). The reaction is observable, but slow *e.g.*, half-time of 20–30 h at p*H* 6.0, and at a temperature of 80 °C. In view of the known S atom transfer process [1], addition of sulfite would be expected to provide an alternate path for transfer of oxygen between thiosulfate and water, provided that the sulfite–water oxygen exchange process [2] is reasonably rapid

[1] $$*OSS + SO \rightarrow *OS + SSO$$

[2] $$*OS + H_2O \rightarrow OS + H_2O*$$

(OSS represents thiosulfate and SO the appropriate sulfite species). The authors of ref. 2 have found no evidence of this coupled path, in that addition of 0.01 *M* sulfite to 0.1 *M* ^{18}O-thiosulfate produced no noticeable acceleration of oxygen transfer. They suggested that the apparent lack of catalysis by sulfite was due to the slowness of the sulfite–H_2O exchange reaction. However, a recent study of the kinetics of the sulfite–water exchange in this laboratory (3) shows that for the conditions of temperature and p*H* used in (2), oxygen exchange between these latter species is very rapid, and indeed the oxygen in H_2O and sulfite would be always at isotopic equilibrium for the time scale (hours) used in ref. 2.

To resolve this discrepancy, we have studied the kinetics of oxygen transfer in the system thiosulfate–sulfite–water, using ^{18}O-labelled thiosulfate, over the p*H* region from 3 to 13, and for sulfite–thiosulfate ratios from 0.75 to 4.0. The results confirm that the sulfur atom transfer process (reaction 1) provides an important route for interchange of oxygen between thiosulfate and water. As is outlined more fully below, the results at appropriate p*H* values provide a most interesting illustration of a system of reversible, consecutive first order rate processes. Such systems have been examined theoretically a number of times, but to the best of our knowledge, no actual chemical systems of this kind have been described heretofore.

Experimental

Enriched water (1.6 atom%, ^{18}O obtained from Yeda Research and Development Co., Ltd.) was redistilled from alkaline permanganate. Water of normal isotopic composition used in our experiments was doubly distilled. Sodium sulfite was anhydrous certified A.C.S. Fisher. All other chemicals were of reagent grade, and used without further purification. ^{18}O-enriched sodium thiosulfate was prepared from sodium sulfite and sulfur according to the method of Hargreaves and Dunningham (4). A mixture of sodium sulfite, ^{18}O-labelled water, and sulfur in a molar ratio of $\sim$1:5:1.5 (excess sulfur was used) was heated at approximately 80 °C for 60 h. Sulfite rapidly reaches isotopic equilibrium with the labelled water and reacts with sulfur to form $Na_2S_2O_3 \cdot 5H_2O$. This material is a liquid above 48 °C, in which the other materials present are insoluble. It was filtered through a sintered glass filter at 50 °C, and the separated liquid $Na_2S_2O_3 \cdot 5H_2O$ dehydrated under vacuum at 90–100 °C. Iodometric

Can. J. Chem. Downloaded from www.nrcresearchpress.com by 210.87.254.6 on 09/05/12
For personal use only.

analysis of the product indicated it to be 99% $Na_2S_2O_3$ and less than 1% Na_2SO_3. The isotopic oxygen composition was found to be 1.24 atom% ^{18}O. This labelled material was used without further purification.

Kinetic runs were done in the following way. The water was freed of dissolved oxygen by bubbling with argon (Matheson H.P.) before adding sulfite, to prevent the oxidation of the latter. Then concentrated HCl or NaOH was added as required to obtain the desired p*H*, and ^{18}O-$Na_2S_2O_3$ was then added. This solution was then placed in a water bath held at 50.3 °C, the temperature used for all experiments. In some experiments, the p*H* measurements were made at room temperature on duplicate solutions made up with unlabelled anhydrous sodium thiosulfate, while in other experiments the labelled solutions were used directly. A Model 801 Orion p*H* meter was used.

At timed intervals, 1–2 ml aliquots were removed, the p*H* adjusted to 11–12, and sulfite was precipitated and centrifuged down as $SrSO_3$ by addition of an aqueous solution of $SrCl_2$. The remaining solution was adjusted to p*H* 4.7 with acetate, and thiosulfate recovered by adding excess 0.5 *M* Cu(II) tetrapyridine acetate solution. This reagent ($CuPy_4Ac_2$) is made simply by adding excess pyridine to a solution of Cu(II) acetate. Cu(II) oxidizes thiosulfate to tetrathionate and the latter precipitates with excess $CuPy_4Ac_2$ as $CuPy_4S_4O_6$ (5). This precipitate filters readily, and when washed with ether or acetone gives an anhydrous product. Blank experiments with ^{18}O-labelled water showed that this procedure for isolating thiosulfate from solution caused not more than 3% induced exchange of the oxygen in the salt with the solvent oxygen.

In some experiments, thiosulfate was recovered as BaS_2O_3 precipitate after the sulfite had been removed as $SrSO_3$. The BaS_2O_3 precipitate, however, proved difficult to handle, since precipitation was very slow; often requiring addition of alcohol to encourage precipitation. Moreover, this salt is difficult to dehydrate.

The isotopic composition of the sulfite, tetrathionate, or thiosulfate was determined using the method of Shakhashiri and Gordon (6), in which the oxygen of the salt is converted to CO_2 by heating it with AgCN under vacuum for 2 h at 500 °C. The CO_2 thus formed was purified by sublimation from an *n*-pentane slush bath (−130 °C) to a bulb cooled in liquid nitrogen.

Isotopic analysis of CO_2 was done with a Varian-Mat GD-150 isotope ratio mass spectrometer. The relative abundance of ^{18}O in each sample was measured directly as a so-called *P*-factor on this instrument, defined as the ratio of abundance of carbon dioxide of mass 46 to that for masses 44 + 45.

Results and Discussion

In an aqueous solution of thiosulfate and sulfite, there are several possibilities of ^{18}O exchange among the various species. The direct exchange of ^{18}O between thiosulfate and water has been shown to be quite slow (2) and for the experimental conditions and times used here this possibility can be neglected. The remaining ^{18}O exchange possibilities can be represented by eqs. 1 and 2 above, with corresponding exchange rates R_1 and R_2. Now if thiosulfate only is labelled with ^{18}O initially, then one has a system of two consecutive reversible first order reactions with respect to ^{18}O exchange.

The following definitions are required. $x = [S_2O_2O^{*2-}], y = [SO_2O^{*2-}], z = [H_2O^*], X = 3[S_2O_3^{2-}]$, $Y = 3[SO_3^{2-}]$, and $Z = [H_2O]$; where x, y, and z represent the molar concentrations of the ^{18}O-labelled species. Because the ^{18}O level was low ($\sim 1\%$), doubly labelled oxyanions can be neglected. The quantities X, Y, and Z represent the concentration of ^{16}O in g-atoms l^{-1} of the indicated species.

Noting that for each sulfur atom transferred at a rate R_1, there are three oxygen atoms transferred (see footnote to Table 1), the rates of ^{18}O transfer are readily shown to be given by eqs. 3–5

$$[3] \quad \frac{dx}{dt} = R_1 \frac{y}{Y} - R_1 \frac{x}{X}$$

$$[4] \quad \frac{dy}{dt} = R_1 \frac{x}{X} - R_1 \frac{y}{Y} - R_2 \frac{y}{Y} + R_2 \frac{z}{Z}$$

$$[5] \quad \frac{dz}{dt} = R_2 \frac{y}{Y} - R_2 \frac{z}{Z}$$

It is convenient to recast eqs. 3–5 in terms of the corresponding experimental *P*-factors, defined as follows

$$P_x = k \frac{x}{X},$$

$$P_y = k \frac{y}{Y}$$

and

$$P_z = k \frac{z}{Z}$$

(The term k in these definitions is a proportionality constant, the same for each definition, which allows for the fact that the *P*-factor is only a relative and not an absolute measure of the corresponding $^{18}O/^{16}O$ ratio. It allows *e.g.*, for instrumental calibration, and for the statistical factor of 2 involved in ^{18}O assay via CO_2 mass spectrometry. It is cancelled out in the following differential equations, and also out of the *F* values following eq. 13.) Substituting appropriately for x, y, and z in eqs. 3–5, one has

$$[6] \quad \frac{dP_x}{dt} = \frac{R_1}{X}(P_y - P_x)$$

Can. J. Chem. Downloaded from www.nrcresearchpress.com by 210.87.254.6 on 09/05/12
For personal use only.

$$[7] \quad \frac{dP_y}{dt} = \frac{R_1}{Y}(P_x - P_y) - \frac{R_2}{Y}(P_y - P_z)$$

$$[8] \quad \frac{dP_z}{dt} = \frac{R_2}{Z}(P_y - P_z)$$

The general solution of such a set of coupled rate equations has been given in the literature (7–12). The two methods of solving such coupled rate equations are: (*a*) converting these equations into second order differential equations of a single component and solving the resulting second order equation by standard methods, refs. 7–9, or (*b*) the above set of coupled differential equations can be solved in closed form, refs. 10–12. We have used the second method and specifically followed the procedure given in ref. 12 because equations for P_x, P_y, and P_z can be obtained conveniently by this method.

The general solution of eqs. 6–8 can therefore be written simply as

$$[9] \quad P_i = A_i' e^{-\lambda_1 t} + A_i'' e^{-\lambda_2 t} + A_3$$

where P_i represents P_x, P_y, or P_z as appropriate; A_i' and A_i'' are constants of integration satisfying initial conditions and $A_3 = P_\infty$ (the equilibrium isotopic ratio in all components at infinite time (eq. 17 below). λ_1 and λ_2 are the same for P_x, P_y, or P_z and can be given in terms of the reaction rates R_1 and R_2 and of the concentrations of the components X, Y, and Z as given by eqs. 10 and 11.

$$[10] \quad \lambda_1 = \frac{1}{2}\left\{\frac{R_1}{X} + \frac{R_1 + R_2}{Y} + \frac{R_2}{Z} + \left[\left(\frac{R_1}{X} + \frac{R_1 + R_2}{Y} + \frac{R_2}{Z}\right)^2 - 4R_1R_2\left(\frac{X + Y + Z}{XYZ}\right)\right]^{1/2}\right\}$$

$$[11] \quad \lambda_2 = \frac{1}{2}\left\{\frac{R_1}{X} + \frac{R_1 + R_2}{Y} + \frac{R_2}{Z} - \left[\left(\frac{R_1}{X} + \frac{R_1 + R_2}{Y} + \frac{R_2}{Z}\right)^2 - 4R_1R_2\left(\frac{X + Y + Z}{XYZ}\right)\right]^{1/2}\right\}$$

Equations 9–11 describe the variation of the isotopic ratios in thiosulfate, sulfite, and water as a function of time. Because water is overwhelmingly the main species, its isotopic composition is not a sensitive indicator of the exchange process and so was not measured.

The kinetics of reactions 1 and 2 have been studied previously (1, 3). Reaction 1 has a first order dependence on thiosulfate and sulfite, and zero order dependence on $[H^+]$, whereas reaction 2 has a first order dependence on sulfite, and is second order in $[H^+]$. Clearly there is available a greater degree of experimental control on R_2 than on R_1, since the former can be varied by many orders of magnitude, with respect to R_1, simply by alteration of the p*H*. Experimental measurements were made in the p*H* region 2.75 to 13, with the results up to p*H* 9.6 summarized in Table 1.

It is convenient and useful to consider all the results in four groups, distinguished by the p*H* region. Each of these groups will now be discussed separately for sulfite and thiosulfate concentrations of the order of 0.5 *M*.

Case 1

In the p*H* range 5 to 10 the exchange of oxygens between water and sulfite is extremely rapid so that $R_2 \gg R_1$. Therefore only the rate of oxygen atom transfer between thiosulfate and water is experimentally measurable by our method. Sulfite acts as a catalyst to exchange oxygen atoms between thiosulfate and water at a rate governed by the sulfur atom transfer between thiosulfate and sulfite as measured by Ames and Willard (1). Sulfite and water form a common pool of oxygen atoms which exchange with the oxygen atoms of thiosulfate. In this region of p*H* the sulfite is in ^{18}O isotopic equilibrium with water so $P_y = P_z$ at all times. Since no ^{18}O is lost from the system the following relation holds for infinite time

$$[12] \quad P_\infty(X + Y + Z) = XP_x + (Y + Z)P_y$$

Equation 12 can be used to eliminate P_y from eq. 6, and the resulting equation can be integrated directly to give

$$[13] \quad \ln\left[\frac{P_x + P_\infty}{P_{x_0} - P_\infty}\right] = -R_1\frac{X + Y + Z}{X(Y + Z)}t$$

Here, P_{x_0} is the isotopic ratio in thiosulfate at zero time; P_x is the isotopic ratio in thiosulfate at time t; and P_∞ is the isotopic ratio in thiosulfate or in any of the other components at infinite time. In terms of the *P*-factors, the fraction exchanged, *F*, can be defined as

$$F = (P_{x_0} - P_x)/(P_{x_0} - P_\infty)$$

hence

$$(P_x - P_\infty)/(P_{x_0} - P_\infty) = (1-F)$$

TABLE 1. Summary of data on oxygen transfer between thiosulfate and water in the presence of added sulfite at 50.3 °C

Run number	$[S_2O_3^{2-}]$ (M)	$[SO_3^{2-}]$ (M)	pH	$R_1 \times 10^5$ (g-atoms O l^{-1} s^{-1})	$k_1 \times 10^4$ ($l\,m^{-1}\,s^{-1}$)
1*	0.20	0.50	9.59	6.15	2.05
2*	0.20	0.50	7.31	6.10	2.03
3*	0.20	0.50	6.93	6.60	2.20
4*	0.20	0.50	6.44	6.30	2.10
5*	0.20	0.50	4.80	5.79	1.94
6*	0.20	0.50	7.60	6.37	2.11
7†	0.20	0.50	6.90	5.97	1.99
8†	0.20	0.50	6.90	6.20	2.07
9†	0.20	0.50	6.90	5.88	1.95
10†	0.20	0.50	6.90	5.60	1.87
11†	0.20	0.50	7.32	6.08	2.04
12†	0.20	0.50	7.32	6.42	2.14
13*	0.40	0.30	9.59	7.74	2.15
14†	0.30	0.40	9.60	6.75	1.88
15*‡	0.20	0.80	9.59	14.6	3.05
16*‡	0.50	0.50	9.59	20.2	2.71
17†‡	0.50	0.50	7.3	24.9	3.30
18*	0.20	0.50	2.75	19.5	6.47

*Thiosulfate recovered as $CuPy_2S_4O_6$.
†Thiosulfate recovered as BaS_2O_3.
‡Note higher ionic strength for these experiments. ($R_1 = 3k_1[SO_3^{2-}][S_2O_3^{2-}]$. k_1 in ref. 1 is given in terms of S atom transfer; for each such event, 3 oxygen atoms, in effect, transfer.

and eq. 13 is in the form of a conventional McKay relation (13). Equation 13 is also identical to an equation derived by Takaishi (7) for exchange processes involving an intermediate complex.

Plots of log $(1 - F)$ *vs.* time show linear behavior as illustrated in Fig. 1 for run No. 1 in Table 1. From the slopes of such plots, R_1 has been determined. Using the kinetic equation determined by Ames and Willard given by [14]

$$[14] \qquad R_1 = 3\,k_1\,[S_2O_3^{2-}]\,[SO_3^{2-}]$$

values of k_1 shown in Table 1 have been calculated. As a comparison the rate constant k_1 calculated from the data of Ames and Willard is 3.44×10^{-4} $l\,m^{-1}$ s^{-1} at 50 °C and for ionic strength of 2.0. Evidently the sulfur atom transfer process accounts very well for the interchange of oxygen between thiosulfate and water over this region of pH.

Case 2

At a p$H > 11$, oxygen exchange between sulfite and water is effectively stopped (3). The only oxygen exchange is between thiosulfate and sulfite, via S atom transfer. The McKay equation (13) for ^{18}O exchange between these two species is given by eq. 15

$$[15] \qquad \ln \frac{P_x - P_\infty}{P_{x_0} - P_\infty} = -R_1 \frac{X + Y}{XY}\,t$$

where P_x and P_{x_0} have the same definition as in case 1 but P_∞ now refers to the ^{18}O isotopic equilibrium between *thiosulfate and sulfite only*, as given by eq. 16

$$[16] \qquad P_\infty = \frac{XP_{x_0} + YP_{y_0}}{(X + Y)}$$

A plot of log $(1 - F)$ *vs.* time for an experiment done at pH 13 is illustrated in Fig. 2. The good linearity of this plot is proof that oxygen in H_2O is not involved in any way. From the slope of this plot, R_1 was calculated as 5.75×10^{-5} g-atoms oxygen l^{-1} s^{-1}. This is in good agreement with the data of Table 1, in which the thiosulfate exchange with water was catalyzed by sulfite, and R_1 was calculated from eq. 13. Evidently sulfur atom transfer is still the main process responsible for oxygen exchange. The insensitivity of this process to pH is to be expected from the work of Ames and Willard (1).

Case 3

In the pH range 10 to 11 both R_1 and R_2 are within one or two orders of magnitude of each other. Thiosulfate and sulfite are exchanging oxygen atoms at a rate R_1 and sulfite is simultaneously exchanging oxygen atoms with water at a rate R_2. Since the ^{18}O isotopic label begins in thiosulfate, the ^{18}O exchange in this system can best be described as two consecutive reversible first order reactions represented by eqs. 1 and 2. The analytical solution of these equations has

Can. J. Chem. Downloaded from www.nrcresearchpress.com by 210.87.254.6 on 09/05/12
For personal use only.

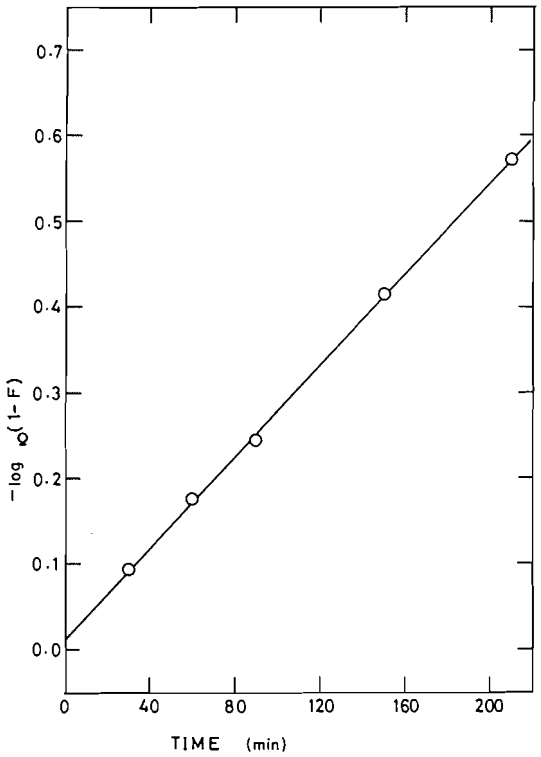

FIG. 1. Fraction of ^{18}O exchange between thiosulfate and water catalyzed by sulfite at pH = 9.6 (see eq. 13).

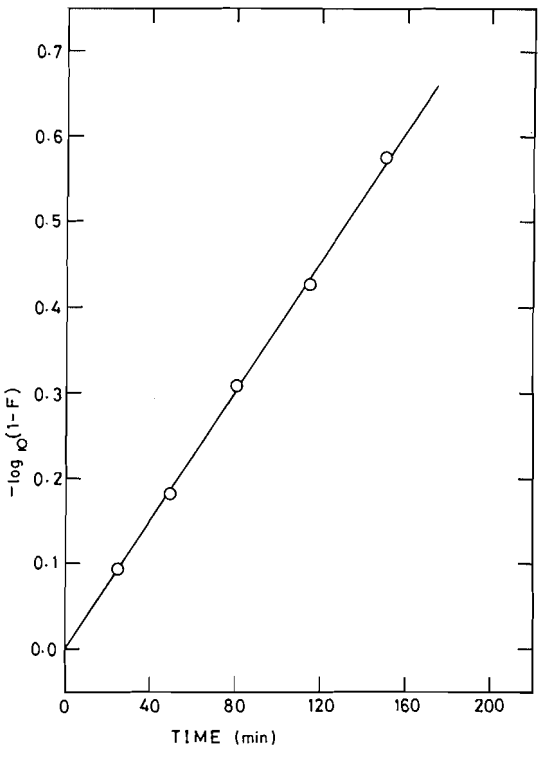

FIG. 2. Fraction of ^{18}O exchange between thiosulfate and sulfite at pH 13 (see eq. 15), 0.2 M $S_2O_3^{2-}$, 0.5 M SO_3^{2-}.

already been discussed and the general solution is given by eq. 9.

A graphical method can be used to evaluate λ_1, λ_2, A_x', and A_x'' in eq. 9, provided that R_1 and R_2 are sufficiently different so that λ_1 and λ_2 will differ by at least an order of magnitude. If $(P_x - P_\infty)$ is plotted against time on semi-log paper, then at sufficiently long times the curve should become a straight line, the exponential term with the smaller λ factor in eq. 9 being the main component at long times. The slope of this line segment will give the value of the smaller of the two λ's. If this line segment is extrapolated back to zero time and the ordinates of all points on this extrapolated line are now subtracted from the ordinates of the corresponding points on the original curve, and the resulting values replotted as before *vs.* time, a straight line should result corresponding to the other exponential term in eq. 9. The slopes of these two resolved lines give λ_1 and λ_2 and the intercepts give the pre-exponential factors, A_x' and A_x''. From this information R_1 and R_2 can be calculated. The data for $(P_y - P_\infty)$ can be treated in a similar way, and should give the same set of values for λ_1 and λ_2, and appropriate values for A_y' and A_y''.

To indicate the validity of this analysis, an experiment was done at pH 10.8, $[S_2O_3^{2-}] = [SO_3^{2-}] = 0.5$ M, a condition for which R_2 is expected to be less than R_1, but not zero. The ^{18}O level in both thiosulfate and sulfite was determined experimentally as a function of time, *i.e.*, values of P_x and P_y were obtained. (The quantity P_z (^{18}O level in H_2O) was not followed, because as indicated earlier, this quantity does not change appreciably during the experiment.) Experimental values of P_x and P_y are shown in Fig. 3. In this figure, the upper result shows the fall in level of ^{18}O in thiosulfate as the reaction proceeds. The lower curve shows very clearly the corresponding initial rise in ^{18}O abundance in sulfite. A transient equilibrium is reached, as expected, followed by a decrease as the sulfite–water exchange proceeds towards isotopic equilibrium.

Plots of $(P_x - P_\infty)$ and $(P_y - P_\infty)$, on a logarithmic scale, *vs.* time, are shown in Fig. 4, together with resolution of the curves into straight

Can. J. Chem. Downloaded from www.nrcresearchpress.com by 210.87.254.6 on 09/05/12
For personal use only.

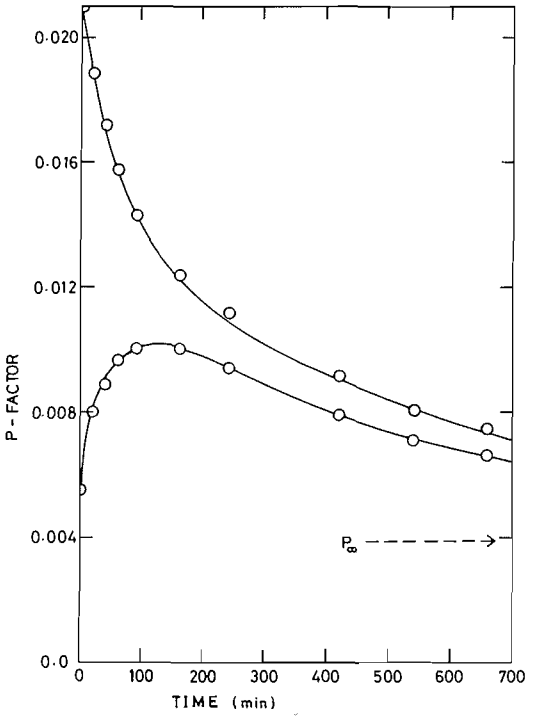

FIG. 3. Variation of ^{18}O in thiosulfate (upper curve) and sulfite (lower curve) as a function of time at pH 10.8. Open circles are experimental points and the lines are drawn from eqs. 18 and 19.

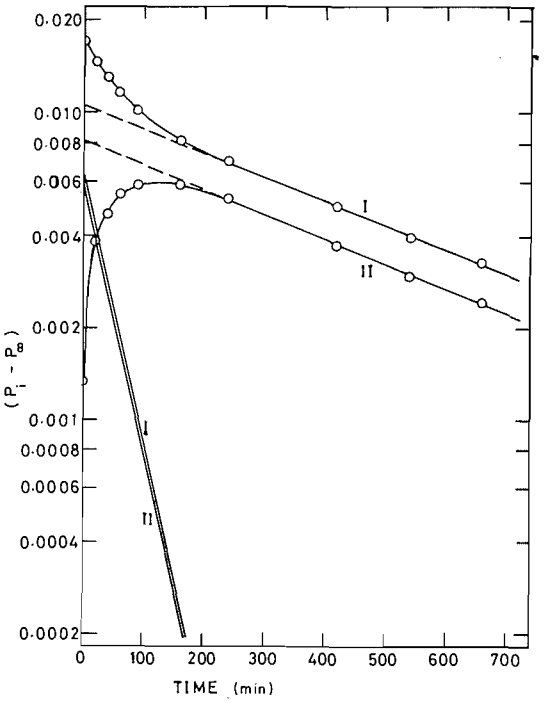

FIG. 4. *I*, Data from measurement of ^{18}O content of thiosulfate; *II*, ^{18}O content of sulfite. The corresponding straight line portions show the resolution of the two exponential terms (see text).

line components corresponding to the individual exponential terms comprising the curves as described above. The two sets of data lead to consistent values for λ_1 and λ_2, namely $\lambda_1 = 0.0193\ \text{min}^{-1}$, $\lambda_2 = 0.00182\ \text{min}^{-1}$, from the $(P_x - P_\infty)$ results, and $\lambda_1 = 0.0195\ \text{min}^{-1}$ $\lambda_2 \approx 0.00186\ \text{min}^{-1}$ from the $(P_y - P_\infty)$ results. The quantities A_i' and A_i'' have been determined from the intercepts of the straight lines in Fig. 4 P_∞ was calculated from eq. 17.

$$[17] \qquad P_\infty = \frac{XP_{x_0} + YP_{y_0} + ZP_{z_0}}{X + Y + Z}$$

where P_{x_0} was the initial isotopic ratio in the thiosulfate at the start of the experiment and P_{y_0} and P_{x_0} are isotopic ratios for naturally occurring sulfite and water. The equations for variation of P_x and P_y as a function of time under our experimental conditions become

$$[18] \quad P_x = 0.0042 + 0.0065\, e^{-0.0194t} + 0.0106\, e^{-0.00184t}$$

$$[19] \quad P_y = 0.0042 - 0.0060\, e^{-0.0194t} + 0.0082\, e^{-0.00184t}$$

Values of λ and t are in consistent units of min^{-1} and min, respectively.

In Fig. 3 the open circles represent experimental values whereas the solid lines are drawn from eqs. 18 and 19. The fit is very satisfactory.

From the average values of λ_1 and λ_2 determined in Fig. 4 and given above, R_1 and R_2 can be calculated from eqs. 20 and 21

$$[20] \qquad \lambda_1 + \lambda_2 = \frac{R_1}{X} + \frac{R_1}{Y} + \frac{R_2}{Y} + \frac{R_2}{Z}$$

and

$$[21] \qquad \lambda_1\lambda_2 = R_1R_2\,\frac{X + Y + Z}{XYZ}$$

from which $R_1 = 2.13 \times 10^{-4}$ g-atoms oxygen $l^{-1}\ s^{-1}$ and $R_2 = 1.00 \times 10^{-4}$ g-atoms oxygen $l^{-1}\ s^{-1}$. From this value of R_1, k_1 (eq. 14) has been calculated as 2.82×10^{-4} l $\text{mole}^{-1}\ s^{-1}$ which agrees with the values in Table 1 for similar thiosulfate and sulfite concentrations.

The value of R_2 (the rate of the sulfite–water exchange) derived in this analysis is not directly comparable to the data for this quantity from

Can. J. Chem. Downloaded from www.nrcresearchpress.com by 210.87.254.6 on 09/05/12
For personal use only.

Can. J. Chem. Downloaded from www.nrcresearchpress.com by 210.87.254.6 on 09/05/12
For personal use only.

ref. 3 because of the large differences in the experimental conditions (ionic strength, sulfite concentration) between the two sets of results. Our best estimate of R_2 from ref. 3, extrapolated to the present conditions, is $\sim 1.4 \times 10^{-5}$ g-atom oxygen l^{-1} s^{-1}, in not unreasonable agreement with the value reported above.

Case 4

In the acid region (pH < 4) thiosulfate by itself becomes increasingly unstable (14). However, in the presence of sulfite which in this pH region is mainly in the forms bisulfite and sulfurous acid (sulfur dioxide), the thiosulfate is stabilized and no sulfur appears even after several hours. In the absence of sulfite, precipitation of sulfur occurs within seconds. The unexpected stability of the thiosulfate in this acid medium may be related to the process

$$[22] \quad H^+ + HSO_3^- + S_2O_3^{2-} \rightleftharpoons SO_2 \cdot S_2O_3^{2-} + H_2O$$

Spectroscopic evidence for the complex $SO_2 \cdot S_2O_3^{2-}$ has been found by Battaglia and Miller (15). Addition of thiosulfate to sulfite in a sufficiently acid medium produces a yellow color in the solution and this is thought to be due to the molecular complex shown in eq. 22.

The rate of oxygen atom transfer between thiosulfate and water is clearly accelerated at low pH, as is shown by run No. 18 in Table 1 made at a pH of 2.75. The value of k_1 is 6.46×10^{-4} l m^{-1} s^{-1} and this is 3 times greater than for equivalent runs at higher pH. This acceleration at low pH may be due to direct exchange between thiosulfate and water; Pryor and Tonellato (2) indicate that this process is accelerated by a decrease in pH. Alternatively, the sulfur atom transfer process may show some slight dependence on pH; the work of Ames and Willard (1) did not go below pH 4.5. Also thiosulfate may decompose and the sulfur produced may react with the sulfite thus producing thiosulfate with an ^{18}O isotopic ratio equal to that of the water with which the sulfite is in equilibrium. Radioactive sulfur exchange measurements between sulfite and thiosulfate in acid medium are required to check for the presence of the latter processes.

Conclusion

Evidently the sulfur atom transfer process of Ames and Willard (1) has an important role in the kinetics of oxygen transfer between thiosulfate and sulfite. The subsequent oxygen transfer from sulfite to water then occurs, depending on the pH of the system. The kinetics of the overall process are as predicted from independent studies of the two separate systems. Because of the differing kinetic orders of the two parts of the system, with respect to $[H^+]$, the overall kinetics can be varied at will. At each end of the pH range, the usual first order kinetics of simple isotopic exchange reactions is observed, while in the mid-region, one has two consecutive processes occurring at not dissimilar rates. This leads to the reversible consecutive first order behavior illustrated in Figs. 3 and 4.

We are unable to state with precision the exact reason for the disagreement between this work and that in ref. 2, inasmuch as there are some numerical inconsistencies in the earlier work. We would suggest, however, that the conditions chosen there (low concentration of sulfite relative to thiosulfate) were not such as to allow the S atom transfer process to be clearly identified in the presence of the concurrent direct exchange of oxygen between water and thiosulfate.

This work was supported financially by the National Research Council of Canada.

1. D. P. Ames and J. E. Willard. J. Amer. Chem. Soc. **73**, 164 (1951).
2. W. A. Pryor and U. Tonellato. J. Amer. Chem. Soc. **89**, 3379 (1967).
3. R. H. Betts and R. H. Voss. Can. J. Chem. **48**, 2035 (1970).
4. L. Hargreaves and A. C. Dunningham. J. Soc. Chem. Ind. **42**, 147T (1923).
5. G. Heinze. Z. Anorg. Allgem. Chem. **276**, 146 (1954).
6. B. Z. Shakhashiri and G. Gordon. Talanta, **13**, 142 (1966).
7. T. Takaishi. Bull. Chem. Soc. Japan, **42**, 1266 (1969).
8. A. Gellhorn, M. Merrell, and R. M. Rankin. Amer. J. Physiol. **142**, 407 (1944).
9. G. E. Francis, W. Milligan, and A. Wormall. Isotopic Tracers, University of Toronto Press, Toronto. 1959.
10. F. A. Matsen and J. L. Franklin. J. Amer. Chem. Soc. **72**, 3337 (1950).
11. R. A. Alberty and W. G. Miller. J. Chem. Phys. **26**, 1231 (1957).
12. A. A. Frost and R. G. Pearson. Kinetics and Mechanism 2nd ed. John Wiley & Sons, Inc., New York. 1965.
13. H. A. C. McKay. Nature, **142**, 997 (1938).
14. R. H. Dinegar, R. H. Smellie, and V. K. LaMer. J. Amer. Chem. Soc. **73**, 2050 (1951).
15. C. W. Battaglia and W. J. Miller. Photogr. Sci. Eng. **12**, 46 (1968).

The Radiolysis of Gaseous DCl[1,2]

D. K. JARDINE AND D. A. ARMSTRONG
Department of Chemistry, University of Calgary, Calgary, Alberta

AND

A. W. BOYD AND C. WILLIS
Physical Chemistry Branch, Chalk River Nuclear Laboratories, Atomic Energy of Canada Limited, Chalk River, Ontario

Received August 26, 1970

The value of $G(D_2)$ from the radiolysis of gaseous DCl is 7.4 ± 0.3 at dose rates of 10^{15} and 10^{27} eV g^{-1} s^{-1}. The yield of hydrogen (D_2, H_2, or HD) from electron reactions and the unscavengeable yield are, within experimental error, the same as in HCl. However, fewer thermal hydrogen atoms are formed in primary processes and a greater proportion of the electrons produce clustered negative ions ($(DCl)^-_{(c)}$) than in HCl. The magnitude of $k_{D+DCl}/k_{D+Cl_2} = 2.9 \times 10^{-3}$ at 288 °K is a factor of three smaller than k_{H+HCl}/k_{H+Cl_2} at the same temperature.

Canadian Journal of Chemistry, 49, 187 (1971)

Can. J. Chem. Downloaded from www.nrcresearchpress.com by 210.87.254.42 on 09/05/12
For personal use only.

Introduction

The effects of isotopic substitution on the primary radiolysis yields and on the ion and radical reactions are of considerable interest. For studying these effects the system used should be one in which the fundamental radiolytic processes are well known and understood. Gaseous hydrogen chloride is such a system. The use of SF_6 and chlorine as scavengers for electrons and hydrogen atoms has led to determinations of the yields of these species and to the mechanism for radiolysis (1). Both the yields and the mechanism have been confirmed by irradiations at very high dose rates (2).

This paper is a report of the experimental values for the yields of electrons and thermal deuterium atoms obtained in the radiolysis of DCl with the above scavengers using both high and low dose rates. The significance of these yields with respect to the primary processes occurring in DCl and HCl are not discussed in the present paper but will be presented in a subsequent publication.

Experimental

The apparatus and techniques were the same as those previously described. The Febetron 705 pulsed electron accelerator at Chalk River Nuclear Laboratories was used for the high dose rate irradiations (2). Dosimetry was based on the nitrogen yields from N_2O with $G(N_2)$ taken as 12.4 (3). The dose in DCl was calculated from the ratio of electron stopping powers of DCl and N_2O. Low dose rate irradiations were carried out with a 120 kVp Phillips X-ray machine at the University of Calgary as in the earlier work with HCl (1). In this case dosimetry was based on the hydrogen yields from HCl. The dose rate per mole in DCl was taken as identical to that in HCl under the same conditions.

The deuterium chloride was guaranteed 99% minimum purity as supplied by Merck, Sharp and Dohme of Montreal. It was preirradiated and sublimed at −125 °C before use. All irradiation cells and vacuum lines were treated with DCl for at least 24 h prior to the radiolysis experiments. The Cl_2 and SF_6 were freed of permanent gases before use.

The isotopic composition of the product gas from the Febetron irradiations was determined with a C.E.C. 21-610 mass spectrometer. It averaged 93 ± 3% deuterium. Radiolysis of a 50:50 mixture of HCl and DCl indicated an enrichment by a factor of two in the H content of the product hydrogen (*i.e.* D_2, H_2, or HD). Hence it appears that the DCl content of the starting material is in the range 95 to 98% and there is no significant contamination of the DCl. The doses in the Febetron irradiations were 1.6 Mrads, in the X-ray irradiations 1–20 krads.

Results

Radiolysis in the Absence of Scavengers

Four determinations of the hydrogen yield from the X-radiolysis of DCl at ~600 Torr were made at 273 and 296 °K. The mean value, which is taken as $G(D_2)$, was 7.4 ± 0.2. The mean value of 12 determinations in the Febetron radiolysis at 288 °K and 1200 Torr was 7.5 ± 0.4. As in the radiolysis of HCl (2) the hydrogen yield is unaffected by the change from the X-ray dose rate (~10^{15} eV g^{-1} s^{-1}) to the much larger Febetron dose rate (~10^{27} eV g^{-1} s^{-1}).

[1]AECL No. 3754.
[2]Based on part of the Ph.D. dissertation of D. K. Jardine.

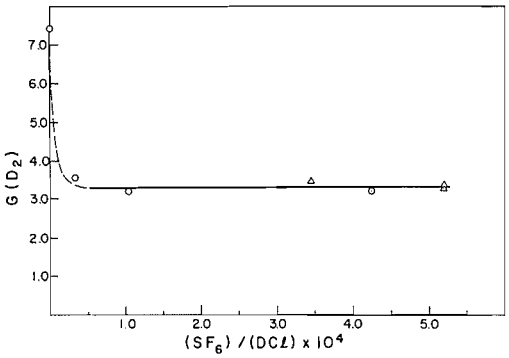

FIG. 1. The effect of SF_6 on the yield of D_2 in the radiolysis of DCl. ○, Febetron radiolysis at 10^{27} eV g^{-1} s^{-1}, 1200 Torr, and 290 ± 3 °K. △, X-radiolysis at 10^{15} eV g^{-1} s^{-1}, 600 Torr, and 290 ± 3 °K.

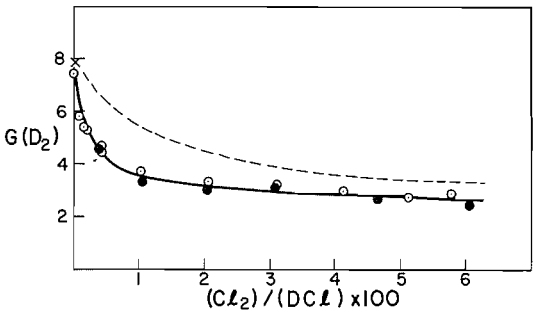

FIG. 2. The effect of Cl_2 on the yield of D_2 in the Febetron radiolysis of DCl at 1200 Torr and 288 °K. ○, 10^{27} eV g^{-1} s^{-1}; ⊙, 5×10^{26} eV g^{-1} s^{-1}; ---, results with HCl (2).

Effect of SF_6

Figure 1 shows the plateau yield obtained in the presence of SF_6. Values are included for irradiations at both high and low dose rates. The net reduction in $G(D_2)$ is 4.1. Within the experimental error of ±0.2 molecule per 100 eV, this is equal to the value of $G_{ionization} = G_e = 4.0 \pm 0.1$ calculated from W for DCl. The latter quantity is identical to W for HCl (= 25.0 ± 0.4 eV (4)).

Effects of Chlorine

The effects of chlorine were studied under three different sets of conditions: (*a*) Febetron radiolysis at 288 °K, (*b*) X-radiolysis at 273 °K, and (*c*) X-radiolysis at 196 °K. The results are presented in Figs. 2, 3, and 4, respectively. The dashed lines show the effects of Cl_2 in HCl under similar conditions. Comparative data for the radiolysis of HCl are included (1, 2). The G values for $(Cl_2)/(DCl)$ ratios below 3×10^{-5} at 196 °K were obtained from the slopes of hydrogen concentration *vs.* dose plots for the radiolysis of DCl, which initially contained no chlorine. These G values are shown on the left hand side of Fig. 4, which has an expanded scale. The other data on this figure and the values in Figs. 2 and 3 were derived by irradiating synthetic mixtures of Cl_2 and DCl.

Discussion

Previous studies (1, 2, 5) have shown that the important primary reactions in irradiated gaseous HCl are as follows

[1] $$HCl \rightsquigarrow HCl^+ + e \qquad (G_{ionization} = 4.0 \pm 0.1 = G_e)$$

[2] $$HCl^+ + HCl \rightarrow H_2Cl^+ + Cl$$

[3] $$e + HCl \xrightarrow{[3b]} (HCl)^-_{(c)} \xrightarrow{[6]} H \text{ (or } H_2 \text{ directly)} \quad (G(HCl)^-_{(c)} = 2.5)$$
$$e + HCl \xrightarrow{[3c]} H \quad (G_\beta = 1.5) \quad (G_\gamma = 1.8) \quad G_{\beta+\gamma} = 3.3$$
$$G_{H'} = 5.8 \pm 0.2 \quad (= \text{Total scavengeable yield of } H_2) = G_e + G_\gamma$$

[4] $$HCl \rightsquigarrow Cl + H$$

[5] $$HCl \rightsquigarrow Cl + H \qquad G_{H''} = 2.2 \pm 0.2 \ (= \text{Unscavengeable yield of } H_2)$$

Can. J. Chem. Downloaded from www.nrcresearchpress.com by 210.87.254.42 on 09/05/12
For personal use only.

Can. J. Chem. Downloaded from www.nrcresearchpress.com by 210.87.254.42 on 09/05/12
For personal use only.

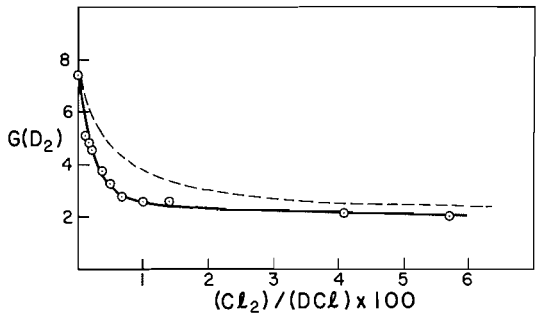

FIG. 3. The effect of Cl_2 on the yield of D_2 in the X-radiolysis of DCl at 600 Torr and 273 °K. Dose Rate 10^{15} eV g^{-1} s^{-1}. ---, results with HCl (1).

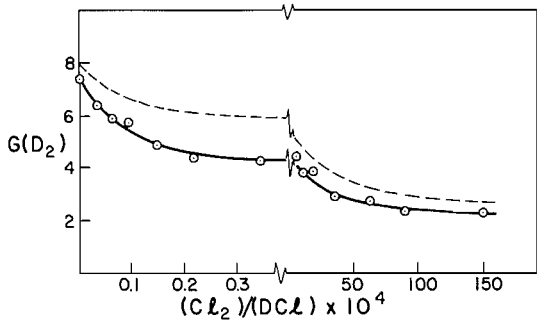

FIG. 4. The effect of Cl_2 on the yield of D_2 in the X-radiolysis of DCl at 400 Torr and 196 °K. Dose rate 10^{15} eV g^{-1} s^{-1}. ---, results with HCl (1).

Reactions 4 and 5 are dissociative excitation giving either thermal hydrogen atoms or unscavengeable (hot) hydrogen atoms (H). All the unscavengeable hydrogen atoms result from [5] with a yield of $G_{H''} = 2.2 \pm 0.2$ but reaction 4 contributes only part, *i.e.*, $G_\gamma = 1.8$, of the total thermal hydrogen atom yield.

The ionic reactions are complex. The capture of thermal electrons (reaction 3) can be explained in terms of the following reactions (5, 6)[3]

$$[3a] \qquad e + 2\,HCl \rightleftarrows (HCl)_2^{-*}$$

$$[3b] \qquad (HCl)_2^{-*} + HCl \rightarrow (HCl)_2^{-} + HCl$$

$$[3c] \qquad (HCl)_2^{-*} + HCl \rightarrow H + Cl^- \cdot 2HCl$$

On the basis of high pressure mass spectral data for ions in other polar gases, it has been assumed that H_2Cl^+, Cl^-, and $(HCl)_2^-$ all become clustered. This is indicated by the subscript (c). The clustered $(HCl)_2^-$ ion, *i.e.* $(HCl)^-_{(c)}$ has a lifetime $> 2 \times 10^{-7}$ s with respect to reaction 6 (2)

$$[6] \qquad (HCl)^-_{(c)} \rightarrow H + HCl_2^-{}_{(c)} \text{ or } H_2 + Cl_2^-{}_{(c)}$$

at room temperature, so this reaction occurs at the X-ray dose rate where the mean ion combination lifetime is ~ 10 ms. As shown, its yield is $G(HCl)^-_{(c)} = 2.5$. At the Febetron dose rate the ion combination lifetime is less than 10 ns (2). Chemical evidence (2) shows that under these conditions $(HCl)^-_{(c)}$ forms thermal H atoms in reaction 7

$$[7] \qquad H_2Cl^+_{(c)} + (HCl)^-_{(c)} \rightarrow H + xHCl$$

In the absence of hydrogen atom scavengers all thermal hydrogen atoms, H, undergo reaction 8

$$[8] \qquad H + HCl \rightarrow H_2 + Cl$$

leading to a total hydrogen yield of $G(H_2) = G(HCl)^-_c + G_\beta + G_\gamma + G_{H''} = 2.5 + 1.5 + 1.8 + 2.2 = 8.0 \pm 0.3$. The yield $G_{H''}$ of unscavengeable hydrogen has been attributed to reactions of hot hydrogen atoms, H, formed in reaction 5. Molecular chlorine is produced in reaction 9

$$[9] \qquad Cl + Cl + M \rightarrow Cl_2 + M$$

In the remainder of this paper DCl reactions are indicated by inserting D after the number of the corresponding HCl reaction.

Effect of SF_6

The net reduction in $G(D_2)$ caused by SF_6 is equal to G_e and is the same as the reduction of $G(H_2)$ from HCl (4.0 ± 0.1 molecules per 100 eV). Thus it is clear that in both systems the net stoichiometry *one electron → one molecule of hydrogen* is maintained.

Effects of Chlorine

Figure 5 shows a reciprocal plot of the data from the chlorine experiments in the Febetron radiolysis at 288 °K based on a competition between Cl_2 and DCl for the scavengeable hydrogen forming species. The total yield of these, $G_{D'}$, given by the intercept of the reciprocal plot is 5.0.

Subtraction from the total Febetron yield $G(D_2) = 7.5$ gives a value of 2.5 for the unscavengeable yield, $G_{D''}$. The values of $G_{D''}$ derived from the high chlorine concentrations in Figs. 3 and 4 are 2.0 and 2.2, respectively, for

[3] * denotes an undeactivated complex.

TABLE 1. Radiolysis yields from DCl and HCl

	DCl	HCl
G(total product)	7.4	8.0
$G_{\text{Ionization}} = G_e$ (from W)	4.0	4.0
Product yield from electrons	4.1	4.0
Total scavengeable yield	$G_{D'} = 5.2$	$G_{H'} = 5.8$
Unscavengeable yield	$G_{D''} = 2.2$	$G_{H''} = 2.2$
Yield of scavengeable negative ion	$G_{(DCl)_{(c)}^-} = 3.1$	$G_{(HCl)_{(c)}^-} = 2.5$
Yield of thermal H atoms		
(*a*) From reaction 3*c*	$G_{\beta D} = 0.9$	$G_{\beta} = 1.5$
(*b*) From reaction 4	$G_{\gamma D} = 1.2$	$G_{\gamma} = 1.8$
Rate constant ratios	$(k_{D+DCl}/k_{D+Cl_2})_{290\ °K} = 2.9 \times 10^{-3}$	$(k_{H+HCl}/k_{H+Cl_2})_{290\ °K} = 1.07 \times 10^{-2}$
	$(k_{3bD}/k_{3cD})_{196\ °K} = 3.4$	$(k_{3b}/k_{3c})_{196\ °K} = 1.7$
	$(k_{6D}/k_{11D})_{196\ °K} = 6 \times 10^{-5}$	$(k_6/k_{11})_{196\ °K} = 8 \times 10^{-5}$

*G_e has an uncertainty of ± 0.1 per 100 eV. All other yields have a relative uncertainty of 0.2 per 100 eV.

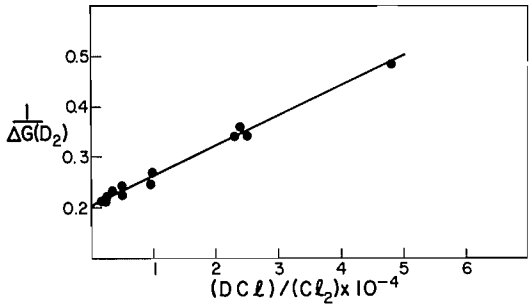

FIG. 5. Reciprocal plot of the reduction in the D_2 yield in DCl–Cl_2 mixtures at a dose rate of 10^{27} eV g^{-1} s^{-1} at 288 °K.

X-irradiations, where the total yield $G(D_2) = 7.4$. From the three results we take $G_{D''} = 2.2$ and $G_{D'} = 5.2$, each with an uncertainty of ± 0.3. $G_{\gamma D}$ can be derived from the yield $G_{D'}$ $(= G_e + G_{\gamma D})$ giving $G_{\gamma D} = 1.2$. These yields are compared with the corresponding yields for HCl in Table 1.

If it is assumed that in the Febetron irradiations chlorine and DCl are competing only for thermal D atoms, *viz.*

[8D] $\quad D + DCl \rightarrow D_2 + Cl$

[10D] $\quad D + Cl_2 \rightarrow DCl + Cl$

then k_{8D}/k_{10D} can be shown from the slope and intercept of the reciprocal plot in Fig. 5 to be 2.9×10^{-3} at 288 °K. This is in excellent agreement with $2.8_7 \times 10^{-3}$ calculated from the expression

$$\frac{k_{D+DCl}}{k_{D+Cl_2}} = \frac{1}{12.9} \exp\left(-\frac{1887 \text{ cal mol}^{-1}}{RT}\right)$$

This expression was derived by Wood and White (7) from the experimentally determined temperature dependence of k_{H+HCl}/k_{H+Cl_2}, using transition state theory. It is not likely to be seriously in error, and the good agreement provides strong evidence that at Febetron dose rates chlorine scavenges only thermal D atoms. This observation parallels that for HCl (2). It means that under Febetron conditions all electrons form thermal deuterium atoms and is taken as evidence for reaction 7D

[7D] $\quad D_2Cl^+_{(c)} + (DCl)^-_{(c)} \rightarrow D + x DCl$

The total yield of thermal D atoms $G_{D'}$ is thus equal to G_e plus the yield of thermal deuterium atoms $G_{\gamma D}$ formed directly in reaction 4D. The yield of the latter, 1.2, is significantly less than $G_{\gamma} = 1.8$ in HCl. This is in fact the main source of the difference in total product yields between the two gases, and it will be considered in a later paper on primary processes.

The results in Fig. 4 show that the scavenging of chlorine in the X-radiolysis at 196 °K is composite as was the case for HCl (1) under these conditions. The initial reduction to a plateau at $G(D_2) = 4.3$ is attributed to the scavenging of the negative ion $(DCl)^-_{(c)}$ formed in DCl reactions which are analogous to [3*a*] and [3*b*].

[3*a*D] $\quad e + 2DCl \rightarrow (DCl)_2^-{}^*$

[3*b*D] $\quad (DCl)_2^-{}^* + DCl \rightarrow (DCl)_2^- + DCl$

As in HCl this postulated intermediate must either form product

[6D] $\quad (DCl)^-_{(c)} \rightarrow D + (DCl_2)^-_{(c)}$ or $D_2 + Cl_2^-{}_{(c)}$

$\quad\quad + DCl \downarrow$

$\quad\quad D_2$

or can be scavenged by chlorine

Can. J. Chem. Downloaded from www.nrcresearchpress.com by 210.87.254.42 on 09/05/12
For personal use only.

[11D] $(DCl)^-_{(c)} + Cl_2 \rightarrow Cl_2^-{}_{(c)}$ or $Cl + Cl^-_{(c)}$

A competition treatment of the data in the left hand side of Fig. 4 gives $k_{6D}/k_{11D} \sim 6 \times 10^{-5}$ at 196 °K as opposed to 8×10^{-5} for k_6/k_{11} at the same temperature

[11] $(HCl)^-_{(c)} + Cl_2 \rightarrow Cl_2^-{}_{(c)}$ or $Cl + Cl^-_{(c)}$

The yield of $(DCl)^-_{(c)}$, 3.1, is the total hydrogen yield less the yield of 4.3 from the first plateau of Fig. 4. This is larger than the yield of $(HCl)^-_{(c)}$, 2.5. The fact that isotopic substitution favors reaction 3*b* over 3*c* is probably due to the greater strength of the DCl bond, which has to be broken in forming Cl^- ($D_{DCl} = 103$ kcal mole^{-1} *vs.* $D_{HCl} = 102$ kcal mole^{-1} (8)), thus slowing down [3*c*].

The results for chlorine at 273 °K do not clearly fall into two distinct scavenging regions, but they cannot be interpreted purely in terms of a competition for D atoms. An analysis of the kind conducted for HCl (1) was not attempted. However, the data do indicate a value of about 10^{-3} for k_{6D}/k_{11D} at this temperature. Hence, k_{6D}, like k_6, must have an activation energy of ~ 5 kcal mole^{-1} (1).

1. R. S. DAVIDOW and D. A. ARMSTRONG. J. Chem. Phys. **48**, 1235 (1968) and references therein.
2. C. WILLIS, A. W. BOYD, and D. A. ARMSTRONG. Can. J. Chem. **47**, 3783 (1969) and references therein.
3. C. WILLIS, O. A. MILLER, A. E. ROTHWELL, and A. W. BOYD. Advan. Chem. Ser. **81**, 539 (1968).
4. D. E. WILSON and D. A. ARMSTRONG. To be published.
5. D. E. WILSON and D. A. ARMSTRONG. Radiat. Res. Rev. **2**, 297 (1970).
6. G. R. A. JOHNSON and J. L. REDPATH. Trans. Faraday Soc. **66**, 861 (1970).
7. G. O. WOOD and J. M. WHITE. J. Chem. Phys. **52**, 2613 (1970).
8. G. HERZBERG. Spectra of Diatomic Molecules. Van Nostrand, New York. 1965.

Can. J. Chem. Downloaded from www.nrcresearchpress.com by 210.87.254.42 on 09/05/12
For personal use only.

The Electronic Spectra of Tetragonal Chromium(III) Complexes

M. KEETON, B. FA-CHUN CHOU, AND A. B. P. LEVER
The Department of Chemistry, York University, Downsview, Ontario

Received April 30, 1970

Methods for processing the electronic spectra of tetragonal chromium(III) complexes are briefly reviewed. New criteria for assigning the spectra of these complexes are introduced and the data processed to yield a series of crystal field and molecular orbital parameters. The validity of these are discussed with particular reference to the apparent π bond contribution in the chromium ligand bonds. It is concluded that the bonding is better described in ionic rather than covalent terms.

Canadian Journal of Chemistry, 49, 192 (1971)

Can. J. Chem. Downloaded from www.nrcresearchpress.com by 210.87.254.6 on 09/05/12
For personal use only.

Introduction

There has been considerable interest recently (1–9) in the study of the electronic spectra of tetragonal complexes with a $^{n}B_{1g}$ (in D_{4h}) ground term, ($^{n}A_{2g}$ in O_h). In particular, studies have been made of a wide series of chromium(III) (1–6) and nickel(II) (1, 7–9) complexes. This paper concerns itself primarily with the methods available to interpret the spectra of tetragonal chromium(III) complexes in terms of chemically useful parameters.

Calculation

Three basic approaches are available.

(*i*) Crystal field theory (2) which parametrizes the data in terms of the radial integrals *Dq*, *Ds*, and *Dt* and the interelectronic repulsion parameter *B*(2). *Dq* may be further factored into the in-plane crystal field strength Dq_{xy} and the out-of-plane, or axial, field strength Dq_z. This is a four variable approach and there are generally four observable d–d transitions, thus a complete solution is possible but cannot be readily checked. Knowledge of the in-plane and out-of-plane field strengths is very convenient (1).

(*ii*) A strong field approach which parametrizes the data in terms of the one electron energy separation of the d orbitals (1). This is also a four parameter theory, *viz.* Δ_1 = splitting of the t_{2g} level, Δ_2 = separation of the d_{xy} and $d_{x^2-y^2}$ orbitals (also equal to $10Dq_{xy}$), and Δ_3 = splitting of the e_g level, and the repulsion parameter *B*.

Approaches (*i*) and (*ii*) may be directly related by the relationships already published (1), but are not strictly homomorphous because there are constraints placed upon the values of the radial integrals by the crystal field theory, whilst no such constraints are placed upon the one electron splitting energies.

(*iii*) Various semi-empirical molecular orbital approaches have been applied. Some years ago McClure (10) discussed the splitting of the octahedral d levels by the distortion in terms of the parameters dσ and dπ, describing the differences in the σ and π bonding of the ligands, respectively. More recently the orbital angular overlap model (11–16) has been tentatively applied (1) to these systems. This treatment utilizes five parameters, $e_{\sigma L}'$, $e_{\pi L}'$, $e_{\sigma Z}'$, $e_{\pi Z}'$, and *B* (for a complex with ligands L and Z). This is inconvenient when there are only four observables, unless one of these parameters may be set to zero (as can frequently occur) or can be independently determined. These overlap parameters are directly related to the McClure parameters by the equations (1)

$$d\sigma = (3/4)(e_{\sigma Z}' - e_{\sigma L}') \text{ and } d\pi = e_{\pi Z}' - e_{\pi L}'$$

If these parameters are chemically significant, they can provide valuable insight into the nature of the chemical bond in these non-cubic systems. Further sophistication is possible, *e.g.* *B* could be factored into B_{xy} and B_z, but in the absence of further independent data, such an analysis would not be profitable.

Given an assignment of the spectrum, any or all of the above parameters may generally be determined. However, an unambiguous assignment is rarely possible. Several approaches to the problem of assignment have been made.

Four transitions are generally observed, arising from the lifting of the degeneracy of the orbital triplets (in octahedral symmetry), *viz.*

$$\nu_1\ {}^4E_g^a \leftarrow {}^4B_{1g}$$
$$\nu_2\ {}^4B_{2g} \leftarrow {}^4B_{1g}$$
$$\nu_3\ {}^4E_g^b \leftarrow {}^4B_{1g}$$
$$\nu_4\ {}^4A_{2g}^a \leftarrow {}^4B_{1g}$$

where the numerals 1–4 do not necessarily imply

Can. J. Chem. Downloaded from www.nrcresearchpress.com by 210.87.254.6 on 09/05/12
For personal use only.

order of increasing energy. ν_1 and ν_2 derive from the $^4T_{2g}$ level in O_h symmetry, whilst ν_3 and ν_4 derive from $^4T_{1g}$(F). Transitions to the components $^4E_g{}^c$ and $^4A_{2g}{}^b$ derived from $^4T_{1g}$(P) occur at much higher energies (around 40 000 – 45 000 cm^{-1}) and are rarely observed.

The transition ν_2 is equal to $10Dq_{xy}$ and is approximately constant in a series of complexes CrL_4Z_2 when L is kept constant and Z is varied. It can, therefore, be easily identified in the spectrum. The separation between ν_1 and ν_2 is, to first order, $35/4Dt$ and Dt is related to the in-plane and out-of-plane field strengths via (17)

$$[1] \qquad Dt = (4/7)(Dq_{xy} - Dq_z)$$

Since the first order energy of ν_1 is $10Dq - (35/4)Dt$, and the sign of Dt is generally identifiable through expression 1, assignment of ν_1 to the band on the low or high energy side of ν_2 (according to whether the in-plane field is greater than or less than the out-of-plane field strength, respectively) is generally unambiguous. The inclusion of off-diagonal terms into the energy through configurational interaction between the various E_g levels will very rarely invert this sequence (2). Thus we are left with a decision regarding assignment of the two high energy bands to $A_{2g}{}^a$ and $E_g{}^b$.

A number of approaches to this problem have been proposed. Perumareddi (2) generally requires that k ($= Ds/Dt$) is positive although he points out that negative values of k cannot be ruled out. Positive values of k lead to the energy order $^4E_g{}^b > {}^4A_{2g}{}^a$ (if Dt is positive which is the case for all compounds under consideration here). There is no theoretically justifiable reason to assume that k is always positive, and indeed, negative values have now been unambiguously observed (5, 6). Dubicki and Martin (4) deduce the signs of $d\sigma$ and $d\pi$ through consideration of the chemical nature of the ligands concerned, and thereby can in most, but not all, cases, arrive at an unambiguous assignment.

Here we do not put any constraints on the signs of the parameters (except perhaps for Dt, whose sign is almost invariably unequivocal) but merely require that the parameters obtained for a series of closely related complexes be internally consistent. Thus the calculations are carried out for both possible assignments and the results compared for consistency.

Ideally single crystal polarized spectra or magnetic circular dichroism spectra should be obtained to unequivocally identify the transitions. In fact two polarized light studies have been reported (5, 18) and these provide a firm basis for the final assignments.

A first order calculation ignoring any configurational interaction between the E_g or between the A_{2g} states has been shown to be inadequate, yielding misleading results for most parameters (1). Earlier (1) we had proposed including configurational interaction between the two lowest E_g levels ($E_g{}^a$ and $E_g{}^b$) but ignoring interaction with $E_g{}^c$, (and also ignoring the interaction of $A_{2g}{}^a$ with $A_{2g}{}^b$) since these were felt to be of too high an energy to interfere. Comparison of those results with the data reported here utilizing the secular determinants (1, 2), which take into account all configurational interaction within the E_g and A_{2g} sets, reveals that this last approximation is also inadequate for most parameters. It is sufficient to evaluate Dq_z very accurately, but provides misleading values of most other parameters and in particular grossly underestimates B. Thus all the data reported here are derived from the complete configuration interaction matrices.

A computer program was written to solve the matrices for all the parameters (using the interrelationships previously reported (1)) for both possible assignments, I, $E_g{}^b > A_{2g}{}^a$, II, $E_g{}^b < A_{2g}{}^a$. The final parameters were used to recalculate the input energies and the difference between the input and output energies printed as a measure of the exactness of the fit. In virtually all cases a perfect fit was achievable. *A good fit cannot be taken as evidence of a correct assignment.*

In order to distinguish one assignment from the other, a parameter is needed which is sensitive to the choice of assignment, and for whose value and sign we have a chemically intuitive grasp. The parameter $d\pi$, and $e_{\pi L}{}'$ derived therefrom, fulfils these criteria. In order to use the five-parameter theory with only four observables, we have written $e_{\pi en}{}'$ and $e_{\pi NH_3}{}'$ as zero, since the amines do not possess any orbitals capable of a π interaction with the chromium ion.

Table 1 lists the orbital angular overlap parameters $e_{\sigma L}{}'$ and $e_{\pi L}{}'$ calculated via both assignments for the complexes under discussion. Since the assignments of the $Cren_2Cl_2{}^+$ and $Cren_2F_2{}^+$ spectra are known from single crystal polarized spectra (5, 18) these assignments (italicized in the table) are assumed to be correct and are used as the basis for discussion. Note that these

TABLE 1. Orbital angular overlap data from assignments I and II

Ion	I ($^4E_g{}^b > {}^4A_{2g}{}^a$)		II ($^4A_{2g}{}^a > {}^4E_g{}^b$)	
	e_σ'	e_π'	e_σ'	e_π'
$Cren_2F_2^+$	7233(en) 4914(F)	0(en) −317(F)	*7233(en)* *7811(F)*	*0(en)* *2016(F)*
$Cren_2Cl_2^+$	*7333(en)* *5558(Cl)*	*0(en)* *900(Cl)*	7333(en) 6354(Cl)	0(en) 1571(Cl)
$Cren_2Br_2^+$	7566(en) 5341(Br)	0(en) 1000(Br)	7566(en) 6417(Br)	0(en) 1986(Br)
$Cren_2(H_2O)_2^{3+}$	7490(en) 5887(H_2O)	0(en) 101(H_2O)	7490(en) 7459(H_2O)	0(en) 1370(H_2O)
$Cren_2(OH)_2^+$	6640(en) 4046(OH)	0(en) −1278(OH)	6640(en) 7553(OH)	0(en) 1391(OH)
$Cr(H_2O)_4F_2^+$	5935(H_2O) 4510(F) 7627(H_2O) 6205(F)	101*(H_2O) −490(F) 1370*(H_2O) 779(F)	5935(H_2O) 6817(F) 7627(H_2O) 8510(F)	101*(H_2O) 1270(F) 1370*(H_2O) 2539(F)
$Cr(NH_3)_4F_2^+$	6967(NH_3) 4931(F)	0(NH_3) −275(F)	6967(NH_3) 7453(F)	0(NH_3) 1751(F)

*Assumed assignments in italics are known to be correct from single crystal polarized spectra studies (5, 18).

complexes are assigned in the reverse sense to one another. Assignment I is preferred for the bromide complex since Br^- is expected to be a better π donor than the Cl^- ion, but should surely be more similar to the latter than to F^-. Moreover assignment II requires Br^- to be a better σ donor than Cl^- towards chromium(III), which in view of the hardness of this metal ion is not expected (4).

In the case of the hydroxyl complex, $Cren_2(OH)_2^+$, assignment I is immediately eliminated since it is inconceivable that the hydroxyl ion be a π acceptor to chromium(III) (negative $e_{\pi Z}'$), assignment II is therefore accepted; this implies that the hydroxyl group is a slightly better π donor towards chromium(III) than the bromide ion, which is not too unreasonable (but see below). Assignment II then follows for the aquo complex $Cren_2(H_2O)_2^{3+}$, since the π characteristics of H_2O and OH (in view of polarization by the Cr(III) ion) are surely not so disparate that assignment I could be accepted. Assignment II for the $Cr(NH_3)_4F_2^+$ species follows by comparison with the ethylenediamine fluoride complex. The reverse assignment yields a negative value for $e_{\pi F}'$ inconsistent with the ethylenediamine fluoride data.

In the case of the aquo-fluoride, none of the orbital angular overlap parameters can be written as zero, so one must be assumed. We arbitrarily choose to assume that $e_{\pi(H_2O)}' = 1370$ cm^{-1} as derived above (Table 1). The parameters derived from assignment II are then more consistent with previous data than those from assignment I (this predicts very low values for both e_F' parameters). Note that had assignment I for $Cren_2(H_2O)_2^{3+}$ been accepted and the much lower value of $e_{\pi(H_2O)}'$ been used in the case of the aquo-fluoride, both assignments would give inconsistent and low values of the e_F' parameters. Additional support for the correctness of assignment II for the aquo-fluoride follows from the observation of a band near 37 000 cm^{-1} in its spectrum (19). Assignment II predicts (Table 3) the components of the $^4T_{1g}$(P) term (in O_h symmetry) to lie near 37 000 cm^{-1}, whilst assignment I predicts them to lie above 38 000 cm^{-1}.

Comparison of our assignments with those of Dubicki and Martin (4), who, as indicated above, used different criteria for assignment, show agreement for the assignments of $Cren_2Cl_2^+$, $Cren_2F_2^+$, and $Cr(H_2O)_4F_2^+$. Their treatment, however, failed to unequivocally assign the spectra of $Cren_2Br_2^+$ and $Cren_2(H_2O)_2^{3+}$. There is also agreement with the previous assignment (6) for $Cr(NH_3)_4F_2^+$. The assignments quoted here supersede those presented earlier (1) which are, in part, in error.

The parameters calculated from the data (Table 2) assuming these assignments are shown in Table 3.

Can. J. Chem. Downloaded from www.nrcresearchpress.com by 210.87.254.6 on 09/05/12
For personal use only.

TABLE 2. Assigned transition energies for some *trans*-CrX_4Z_2 complexes*

Ion	$^4E_g{}^a$	$^4B_{2g}$	$^4A_{2g}{}^a$	$^4E_g{}^b$	$^4A_{2g}{}^b$	$^4E_g{}^c$	Reference number
$Cren_2F_2{}^+$	18 500	21 700	29 300	25 300	*40 427*	*43 595*	19
$Cren_2Cl_2{}^+$	17 300	22 000	25 300	26 500	*40 051*	*41 787*	18
$Cren_2Br_2{}^+$	16 950	22 700	24 200	25 970	*39 412*	*41 386*	4
$Cren_2(OH)_2{}^+$	18 250	19 920	30 300	25 190	*39 217*	*43 214*	3
$Cren_2(H_2O)_2{}^{3+}$	19 680	22 470	29 670	27 470	*43 299*	*45 549*	3
$Cr(H_2O)_4F_2{}^+$	16 300	17 400†	25 500	22 700	*36 053*	*37 614*	4
$Cr(NH_3)_4F_2{}^+$	18 100	20 900	28 200	24 700	*39 437*	*42 233*	6

*The data were obtained from the references indicated. The energies for the $^4A_{2g}{}^b$ and $^4E_g{}^c$ transitions, indicated in italics, are calculated from the parameters in Table 2. They are generally too high in energy to be observed. Note however that $Cr(H_2O)_4F_2{}^+$ does (19) have a band at 37 000 cm^{-1} in agreement with calculation. The parameters in Table 3 fit these transition energies exactly.
†This band was not observed. We assume it on the basis that the crystal field strength of water in $Cr(H_2O)_6{}^{3+}$ is 1740 cm^{-1}.

Before discussing these results and their chemical significance, it is worth considering the probable errors which may be present in these parameter values.

In utilizing the equations for this system one makes the implicit assumption that the band energies employed represent electronic transition energies. In fact they are known to be vibronic in origin. In consequence the actual electronic energies will differ from observed energies by the vibrational component; in addition the neglect of spin–orbit coupling will cause additional error. Moreover, the bands are not always sharp so that estimation of the true band energy from the experimental spectrum may involve some error (which, however, may be minimized by use of low temperature data). These errors will influence the values of the final parameters and in order to estimate these errors a calculation of the data for $Cren_2Cl_2{}^+$ was made in which all the input energies were allowed to vary, individually, or in concert, by ± 200 cm^{-1}. The following data ensued from the 81 resulting calculations: *Ds*, 175–333, mean 254 cm^{-1}; *Dt*, 461–553, mean 509; $e_{\sigma Cl}{}'$, 5341–5761, mean 5556; $e_{\sigma en}{}'$, 7277–7400, mean 7339; $d\pi$, 660–1105, mean 891; $d\sigma$, -1147–-1509, mean -1334; Dq_z, 1252–1372, mean 1310; *B*, 619–726, mean 670; Δ_1, -1320–-2205, mean -1780; Δ_3, 3059–4024, mean 3557, cm^{-1}.

In the case of $d\pi$ the two extreme values, 660 and 1105 cm^{-1}, were isolated solutions, the other 79 roots lying within 19% of the mean.

These results, and similar data with other sets of input energies, suggest that the smaller parameters may be in error by some 10%, perhaps more in the case of *Ds* and $d\pi(\Delta_1)$ and any parameters with very small values. The larger molecular orbital parameters may be in error by several hundred wavenumbers, but this only represents an error of some 5%. The confidence in a given parameter value may be improved by consideration of a series of related complexes and by measurement of a given complex in different physical states. Where possible this is done here. Of course error is undoubtedly introduced by the simplicity of the basic assumptions made for this treatment (*e.g.* exclusion of overlap with the ligands) and the absolute value of any parameter should not be regarded too seriously. However, it may be hoped that the relative variations in a parameter from one ligand to another do have real chemical significance.

Bearing this in mind, the variation of the parameter $e_{\pi L}{}'$ may be written

[2] $\quad en < Cl^- \leqslant Br^- < OH^- \simeq H_2O < F^-$

and the variation in $e_{\sigma L}{}'$

[3] $\quad Br^- \simeq Cl^- < en \simeq H_2O \simeq OH^- < F^-$

These series are similar to those presented by Glerup and Schäffer (6) except that they find that OH^- and F^- are interchanged in both series. These authors based their series on the spectra of the complexes $Cr(NH_3)_4X_2{}^+$ but have not reported detailed calculations.

The internal consistency of the data is exemplified by noting that parameters obtained for a given ligand in one complex are essentially unaltered in other complexes with the same ligand, within the limits of the errors discussed above. For example, the value of Dq_z, which incidentally is comparatively insensitive to small errors in the input energies, for the fluoride ion is precisely the same in the three fluoro complexes studied.

It is evident that chromium(III) interacts much more strongly with oxygen ligands and the fluoride ion than it does with the amines or the heavier halogens. This indicates strong class *A*

Can. J. Chem. Downloaded from www.nrcresearchpress.com by 210.87.254.6 on 09/05/12
For personal use only.

Can. J. Chem. Downloaded from www.nrcresearchpress.com by 210.87.254.6 on 09/05/12
For personal use only.

TABLE 3. Crystal field and molecular orbital parameters (cm^{-1})

Ion	Ds	Dt	Δ_1	Δ_3	$e_{\pi L}'$	$e_{\sigma L}'$	$e_{\pi Z}'$	$e_{\sigma Z}'$	$d\pi$	$d\sigma$	B	Dq_L	Dq_Z	Assignment
$Cren_2F_2^+$	−741	361	−4030	−1160	0*	7233	2016	7811	2016	434	692	2170	1537	II
$Cren_2Cl_2^+$	250	510	−1800	3550	0*	7333	900	5558	900	−1331	670	2200	1307	I
$Cren_2Br_2^+$	350	610	−2000	4450	0*	7567	1000	5341	1000	−1668	560	2270	1202	I
$Cren_2(OH)_2^+$	−658	161	−2780	−1830	0*	6640	1391	7553	1391	684	778	1992	1709	II
$Cren_2(H_2O)_2^{3+}$	−382	318	−2740	60	0*	7490	1370	7459	1370	−22	744	2247	1689	II
$Cr(H_2O)_4F_2^+$	−586	115	−2330	−1770	1370*	7626	2539	8510	1169	662	700	1740	1537	II
$Cr(NH_3)_4F_2^+$	−640	317	−3505	−970	0*	6967	1751	7453	1751	365	667	2090	1535	II

*Assumed. The parameters are defined in the text. The parameters given here reproduce exactly the transition energies quoted in Table 3. Using an alternate source of data for the first two compounds (4) yields $e_{\pi F}' = 2159$ and $e_{\pi Cl}' = 740$ cm^{-1}. Δ_1 the splitting of the t_{2g} level (in O_h symmetry) is positive when the xz, yz pair of orbitals lies lower than xy. Δ_3 the splitting of the e_g level (in O_h symmetry) is positive when the z^2 orbital lies lower than $x^2 - y^2$. Note that the definition (1) of Ds and Dt differs in sign from the definitions used by some other authors (2, 4, 5). Assignment I, $^4E_g^b > {}^4A_{2g}^a$; II, $^4E_g^b < {}^4A_{2g}^a$.

Can. J. Chem. Downloaded from www.nrcresearchpress.com by 210.87.254.6 on 09/05/12
For personal use only.

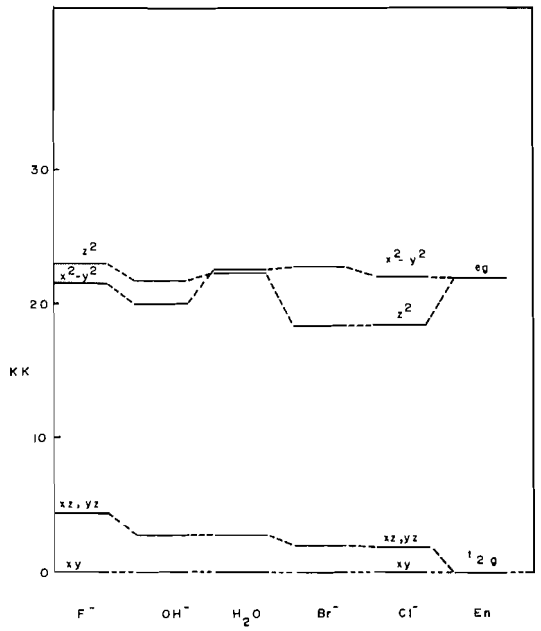

FIG. 1. One electron d orbital energy levels in the complexes $Cren_2X_2^{n+}$, where X = F, Cl, Br, OH, H_2O, or X_2 = en.

behavior for the ion as expected. The high position of the F^- ion in the σ bonding series should not, therefore, be too surprising. Its high position in the π bonding series is however puzzling at first sight.

To clarify this point a plot was made (Fig. 1) of the splitting of the $t_{2g}(\Delta_1)$ and $e_g(\Delta_3)$ levels (in O_h symmetry) by the tetragonal field. The splitting of the t_{2g} level arises purely as a consequence of the difference in π bond capability between the two ligands, whilst the splitting of the e_g set reflects the differences in σ bonding (1). The energy of the d_{xy} orbital was arbitrarily set at zero in all complexes since its energy, to first order, should be unaffected by changes in the axial ligand. It is clear from Fig. 1 there is a general trend that as the splitting of the t_{2g} level decreases (left to right) the splitting of the e_g level also decreases and changes sign in the center of the diagram. This diagram reinforces the view evident from the series 2 and 3 that the strongly σ bonding ligands are also the strongly π bonding ligands.

These data need not necessarily be interpreted in terms of a covalent metal–ligand interaction; indeed an ionic interaction seems more credible. If a ligand were bound strongly to the chromium atom through a covalent σ bond, its effective charge would be made so positive that it is unlikely it could simultaneously function as a good π donor. In other words transfer of charge to the chromium atom through a σ mechanism will inhibit transfer to charge *in the same direction* by a π mechanism. On the other hand this apparent behavior would be expected if the bonding is essentially ionic. Polarization of the ligand by the chromium(III) ion can take place leading to a splitting of the chromium d orbitals which could be described via crystal field theory. The ligand σ electrons and the ligand π electrons may each be considered to repel chromium d electrons (20). The latter would be less effective than the former since the distance of the ligand π orbitals from the origin (chromium atom) will be greater than for the ligand σ orbitals. In the tetragonal situation a splitting of the e_g and t_{2g} levels will occur as a consequence of the differences in the σ and π charge localizations in the two ligands. Such a description reproduces qualitatively the results presented here; indeed one can go further by predicting that the smallest ligand, F^-, will give the largest splitting of $\Delta_1(t_{2g})$ simply because it is closest to the metal. This is seen to be the case.

Thus although the semi-empirical molecular orbital parameters might infer that the fluoride ion, and to a lesser extent the hydroxyl ion and water, are involved in strong π bonding to the chromium atom, (5) this is probably not the case. The energy parameters are probably quite correct within the errors described above, but their interpretation must be treated with caution. These data have been used (6) to more quantitatively set up a two-dimensional spectrochemical series, first described by McClure (10), which would simultaneously demonstrate the σ and π characteristics of a given ligand. Whilst such a diagram can be physically constructed using dσ and dπ values (or Δ_1 and Δ_3 (6)), the conclusion from this work must be that these parameters do not necessarily infer anything about the extent of σ or π *covalent* interaction.

This is not to exclude the possibility of chromium(III) forming strong covalent bonds to a ligand. With perhaps the cyanide ion it may do so. Unfortunately a *trans* dicyanide chromium tetraammine complex has not yet been synthesized. The existence of *cis* dicyanide derivatives, however, may reflect the presence of covalent π bonding.

A recent comparison of the electron spin

Can. J. Chem. Downloaded from www.nrcresearchpress.com by 210.87.254.6 on 09/05/12
For personal use only.

resonance (e.s.r.) spectra of the CrF_6^{3-} and $Cr(CN)_6^{3-}$ ions (21) provides support for these studies by concluding that whilst both the CN and F ligands contribute π orbital density to the description of the molecular orbital primarily involving the metal t_{2g} orbitals, no overlap is necessary in the fluoride case to reproduce the e.s.r. parameters, whilst overlap is required in the case of cyanide. In other words the bonding is ionic. Similar conclusions have been reached in the e.s.r. studies of other fluoro complexes of the first row transition metals (20), where ionic π contributions have been apparent.

The data and sources thereof are given in Table 2. They were processed in part with an IBM 360/50 computer and in part by a CDC 6400 computer.

Method of Calculation

The data were analyzed by a program which processed them by the following general procedure. The energies were solved for *Dq*, *Ds*, *Dt*, and *B* using first order equations, *i.e.* neglecting configurational interaction. Since these are linear (1) the solutions are trivial. These first order parameters were then inserted back into the calculation and used to solve the secular determinants, inclusive of configurational interaction (22), for the transition energy roots. These roots were compared with the input transition energies, and an absolute standard deviation calculated. Each of the input parameters was then individually incremented and the calculation iterated to minimize the absolute standard deviation.

Given time and sufficiently small increments a perfect fit to the data could generally be obtained. This procedure was facilitated by the fact that it was not usually necessary to increment 10 *Dq* since it was a direct observable from the spectrum ($^4B_{2g} \leftarrow {}^4B_{1g}$ transition energy). Moreover the range of possible values for *B* is quite small (region 500–800 cm^{-1}). Other techniques for solution of the secular determinants were tried, but this appeared to be the most economic in computer time. This procedure is more reliable than a possibly shorter but more involved minimum seeking routine in that provided the increments in the parameters are small (*i.e.* less than 50 cm^{-1}) convergence into false minima is avoided.

The program which computed the errors in the parameters followed the same routine. However, in view of the very large number of calculations involved (81 for one set of input energies), the parameters were not iterated to a perfect fit. Instead the parameters were printed when the absolute standard deviation of output transition energies from the input energies was less than 100 cm^{-1}.

We are indebted to the National Research Council of Canada for financial assistance and to Dr. Bryan Hollebone for useful discussions.

1. A. B. P. LEVER. Coord. Chem. Rev. **3**, 119 (1968).
2. J. R. PERUMAREDDI. Coord. Chem. Rev. **4**, 73 (1969).
3. W. A. BAKER and M. G. PHILLIPS. Inorg. Chem. **5**, 1042 (1965).
4. L. DUBICKI and R. L. MARTIN. Aust. J. Chem. **22**, 839 (1969).
5. L. DUBICKI, M. A. HITCHMAN, and P. DAY. Inorg. Chem. 9, 188 (1970).
6. J. GLERUP and C. E. SCHÄFFER. Progress in Coordination Chemistry. *Edited by* M. Cais. Elsevier, Amsterdam. 1968. p. 500.
7. D. A. ROWLEY and R. S. DRAGO. Inorg. Chem. **6**, 1092 (1967); 7, 795 (1968).
8. D. M. L. GOODGAME, M. GOODGAME, M. A. HITCHMAN, and M. J. WEEKS. J. Chem. Soc. A, 1769 (1966).
9. G. R. BRUBAKER and D. H. BUSCH. Inorg. Chem. **5**, 2114 (1966).
10. D. S. MCCLURE. Advances in the Chemistry of the Coordination Compounds. *Edited by* S. Kirschner. McMillan Co., New York. 1961. p. 498.
11. C. K. JØRGENSEN, R. PAPPALARDO, and H. H. SCHMIDTKE. J. Chem. Phys. **39**, 1422 (1963).
12. C. K. JØRGENSEN and H. H. SCHMIDTKE. Z. Phys. Chem. **38**, 118 (1963).
13. W. G. PERKINS and G. A. CROSBY. J. Chem. Phys. **42**, 407 (1965).
14. H. H. SCHMIDTKE. Z. Naturforsch. **19a**, 1502 (1964).
15. C. E. SCHÄFFER and C. K. JØRGENSEN. Mol. Phys. **9**, 401 (1965).
16. C. E. SCHÄFFER and C. K. JØRGENSEN. Mat. Fys. Medd. Dan. Vid. Selsk. **34**, No. 13 (1965).
17. R. A. D. WENTWORTH and T. S. PIPER. Inorg. Chem. **4**, 709 (1965).
18. S. YAMADA. Coord. Chem. Rev. **2**, 83 (1967).
19. T. Y. CHIA and E. L. KING. Discuss. Faraday Soc. **29**, 109 (1960).
20. S. SUGANO and R. G. SHULMAN. Phys. Rev. **130**, 517 (1963).
21. A. WOLBERG. J. Chem. Phys. **51**, 2765 (1969).
22. A. B. P. LEVER. Inorganic Electronic Spectroscopy. Elsevier Publ. Co., Amsterdam. 1968. Appendix V.

La réaction des nitrilotriacétates métalliques avec la proline

J. Israeli et J. R. Cayouette
Département de Chimie, Université de Moncton, Moncton, New Brunswick

Reçu le 9 juillet 1970

On a calculé à partir des courbes de titrages pH métriques les constantes de formation des complexes mixtes resultant de la réaction des nitrilotriacétates métalliques avec la proline. Les constantes de formation des complexes mixtes suivent la série de Irving–Williams.

La réaction de formation des complexes mixtes est une réaction exothermique; on en a déterminé l'enthalpie et l'entropie. La grande diminution d'entropie qui accompagne la formation des complexes mixtes de cuivre(II) a été interpretée par l'effet Jahn–Teller.

Canadian Journal of Chemistry, 49, 199 (1971)

Can. J. Chem. Downloaded from www.nrcresearchpress.com by 210.87.254.42 on 09/05/12
For personal use only.

Introduction

La réaction des nitrilotriacétates métalliques avec des coordinats bidentés a été observée pour la première fois dans ce laboratoire (1); nous avons également étudié d'une façon systématique la formation des complexes mixtes qui resultent de la réaction des nitrilotriacétates métalliques avec les acides aminés (2–4). Des études similaires ont été rapportées récemment par d'autres chercheurs (5–8).

Comme suite à nos recherches antérieures, nous avons étudié dans ce travail la réaction des nitrilotriacétates métalliques avec la proline, acide aminé contenant un groupement amine secondaire cyclisé. Petit-Ramel et Pâris (9, 10) a rapporté l'existence du cuivre(II) – glycinate-prolinate et il semble que ce soit le seul complexe mixte contenant la proline que l'on connaisse.

Partie expérimentale

Une force ionique de 0.1 M a été maintenue constante à l'aide du nitrate de potassium. Par conséquent toutes les constantes que nous utilisons dans ce travail sont des constantes de concentration et se rapportent à cette force ionique.

Le pH a été mesuré avec l'aide d'un pH mètre "Radiometer Model 26" qui a été calibré avec des solutions tampons ayant des pH connus à différentes températures. La concentration des protons a été calculé par la formule $a_{H^+} = C_{H^+} f$ et pour l'évaluation de f on a utilisé la formule de Davies (11).

Résultats

On a titré à l'aide de la soude un mélange équimoléculaire de nitrate métallique ($Me(NO_3)_2$) de nitrilotriacétate disodique (HX^{2-}) et de proline (LH). La Fig. 1 reproduit de titrages réalisés à une température de 25 °C.

Soit "a" le nombre de moles de soude ajouté par mole de métal. La Fig. 1 montre l'existence

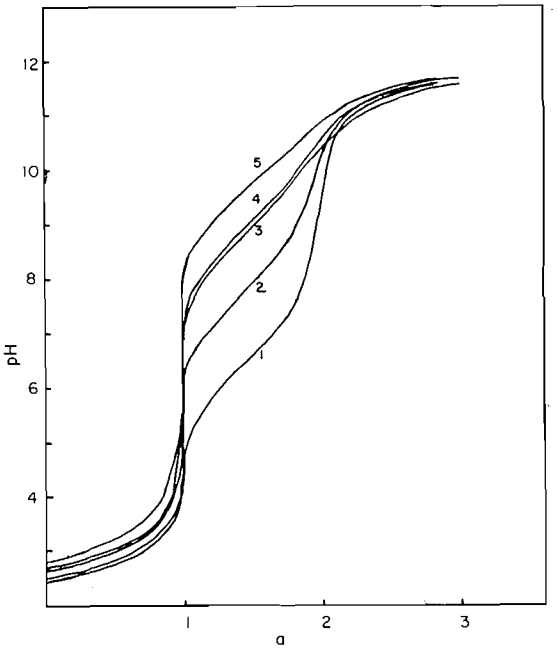

Fig. 1. Titrage par la soude d'un mélange équimoléculaire de nitrate métallique 0.01 M en présence du nitrilotriacétate disodique 0.01 M et de proline 0.01 M à une force ionique de 0.1 M KNO_3 et à la température de 25 °C. Le nombre de moles de soude ajouté par mole de métal est dénoté par "a". *1*, Me = Cu; *2*, Me = Ni; *3*, Me = Zn; *4*, Me = Co; *5*, Me = Cd.

de deux points d'inflexion situés respectivement à $a = 1$ et à $a = 2$.

Jusqu'à $a = 1$, il se forme le nitrilotriacétate métallique MeX^-, et entre $a = 1$ et $a = 2$, il se forme le complexe mixte suivant la réaction

$$[1] \qquad MeX^- + LH \rightarrow MeXL^{2-} + H^+$$

Pour calculer la constante de formation K_f du complexe mixte, on a utilisé les points expérimentaux situés entre $a = 1$ et $a = 2$ et pour

Can. J. Chem. Downloaded from www.nrcresearchpress.com by 210.87.254.42 on 09/05/12
For personal use only.

cette région nous avons employé les équations suivantes qui ont été démontré auparavant (2–4)

$$[2] \quad (\mathrm{L}) = \frac{(2-a)C_{\mathrm{Me}} + (\mathrm{OH}^-) - (\mathrm{H}^+)}{(\mathrm{H}^+)/K_a}$$

$$[3] \quad K_f(\mathrm{L}) + 1 = \frac{C_{\mathrm{Me}}}{(\mathrm{L})\left\{1 + \frac{(\mathrm{H}^+)}{K_a}\right\}} = y$$

Dans ces formules, K_a est la constante de dissociation de la proline.

On voit donc qu'un graphique de y en fonction de (L) doit donner une droite de pente égale à K_f, et dont l'ordonnée à l'origine est 1. Dans toutes nos expériences, nous avons vérifié cette formule, et on a toujours obtenu une ordonnée à l'origine égale à 1. Les travaux furent effectués à des concentrations initiales $C_{\mathrm{Me}} = C_{\mathrm{HX}} = C_{\mathrm{HL}}$ variant de 0.02 à 0.001 M.

Dans le Tableau 1, on donne le pK_a de la proline à différentes températures.

Dans le Tableau 2, on donne le logarithme de la constante de formation des complexes mixtes à différentes températures, comme l'enthalpie et l'entropie de la réaction de formation des complexes mixtes.

L'enthalpie de la réaction de formation des complexes mixtes a été calculée en multipliant par R la pente de la droite représantant $\ln K_f = f(1/T)$.

Pour calculer l'entropie Jones (12) a recommandé d'utiliser la relation

$$(\partial \Delta G^0/\partial T)_P = -\Delta S^0$$

Pour cuivre – nitrilotriacétate-prolinate on a fait un graphique de $-\Delta G^0 = f(T)$ et on a obtenu une droite dont la pente est égale a ΔS^0. L'energie libre a été calculé par la formule

$$\Delta G^0 = -RT \ln K$$

Dans le cas du Ni(II), Zn(II), Co(II) et Cd(II), il était impossible d'utiliser cette méthode pour calculer l'entropie parce que l'intervalle de variation de ΔG^0 est du même ordre de grandeur que l'erreur expérimentale de ΔG. Par conséquent pour ces cas, on a calculé à chaque température l'entropie à partir de la relation $\Delta G^0 = \Delta H^0 - T\Delta S^0$, et la valeur moyenne est donnée dans le Tableau 2. Comme l'a indiqué Jones (12), ces valeurs d'entropies, obtenues par cette méthode pour Ni, Co, Zn, Cd, sont moins précises.

TABLEAU 1. pK_a de la proline à différentes températures et à μ = 0.1 M KNO_3

t (°C)	pK_a
15	10.64±0.01
25	10.41±0.01
50	9.86±0.01
70	9.39±0.01

Auparavant (1) nous avons déterminé les constantes de formation des complexes mixtes qui résultent de la réaction des nitrilotriacétates métalliques avec la glycine à une force ionique 0.5 M KNO_3. Hopgood et Angelici (6) a redéterminé ces constantes à une force ionique 0.07 M KNO_3.

Dans ce travail nous avons redéterminé ces constantes à 25 °C et à une force ionique 0.1 M KNO_3 Dans ces conditions pour la glycine pK_a = 9.54 ± 0.01. Le Tableau 3 rassemble nos résultats.

Discussion

Les constantes de formation des complexes mixtes contenant la proline, suivent la série de Irving–Williams (13) et on peut les placer dans l'ordre

Cu > Ni > Zn > Co > Cd

La réaction conduisant à la formation des complexes mixtes est une réaction exothermique et les enthalpies de la réaction suivent le même ordre que les constantes de stabilité.

La réaction de formation du complexe mixte de cuivre est plus exothermique que la réaction de formation du complexe mixte de nickel. D'après Yatsimirskii (14) ceci indique que pour le cuivre il y a une grande stabilisation par l'effet Jahn–Teller. De ce fait, les groupements axiaux liés au métal central s'éloignent de celui-ci, et par conséquent ces groupements peuvent être solvatés par le solvant. Le processus de solvatation des groupements axiaux conduit à une diminution de l'entropie de la réaction. D'après les valeurs du Tableau 2, on voit que pour le cuivre l'entropie de la réaction de formation du complexe mixte est assez négative (−12 u.e./mole).

Une phénomène semblable a été rapporté par Nancollas (8) pour la réaction de formation du complexe mixte cuivre(II) – éthylènediaminediacétate – éthylènediamine à partir de l'éthylène-

TABLEAU 2. Constantes de formation des complexes mixtes contenant la proline, et enthalpies et entropies de la réaction de formation de ces complexes mixtes; $\mu = 0.1\ M\ KNO_3$

Métal	log K_f 15 °C	25 °C	50 °C	70 °C	$-\Delta H°$ (kcal/mole)	$\Delta S°$ (u.e./mole)
Cu(II)	6.47±0.02	6.24±0.02	5.59±0.02	5.02±0.02	10.9±0.4	−12.0±0.5
Ni(II)	5.11±0.04	4.99±0.04	4.62±0.04	4.27±0.04	6.5±0.5	+ 0.9±0.3
Zn(II)	4.14±0.05	3.98±0.05	3.68±0.05	3.38±0.05	5.7±0.3	− 0.8±0.2
Co(II)	3.95±0.05	3.85±0.05	3.56±0.05	3.23±0.05	5.5±0.4	− 0.8±0.3
Cd(II)	3.15±0.05	3.05±0.05	2.83±0.05	2.62±0.05	3.9±0.2	+ 0.9±0.2

TABLEAU 3. Constantes de formation des complexes mixtes résultant de la réaction des nitrilotriacétates métalliques avec la glycine à 25 °C et à $\mu = 0.1\ M\ KNO_3$

Métal	log K_f
Cu(II)	5.26±0.02
Ni(II)	4.41±0.04
Zn(II)	3.59±0.05
Co(II)	3.38±0.05
Cd(II)	3.05±0.05
Mn(II)	1.80±0.10

diamine et cuivre(II) – éthylènediaminediacétate. Nancollas a suggéré que la formation du complexe mixte est accompagnée par la libération de deux groupements carboxyliques et par leur solvatation simultanée.

Dans le cas des complexes mixtes contenant la proline, il est difficile de savoir si les deux groupements carboxyliques proviennent de nitrilotriacétate seulement, ou si un carboxyle provient du nitrilotriacétate et l'autre de la proline.

Si K_f(proline) dénote la constante de formation des complexes mixtes contenant la proline et si K_f(glycine) dénote la constante de formation des complexes mixtes contenant la glycine, on peut écrire pour eux la relation linéaire suivante

$$\log K_f(\text{proline}) = 1.5 \log K_f(\text{glycine}) - 1.5$$

Les complexes mixtes contenant la proline sont plus stables que les complexes mixtes contenant la glycine, car la stabilité des complexes mixtes augmente avec la basicité du coordinat.

L'un de nous (J.I.) remercie le Conseil National de Recherches du Canada pour une subvention de recherche grâce à laquelle il a pu accorder une bourse à J. R. Cayouette.

1. J. ISRAELI. Can. J. Chem. **41**, 2710 (1963).
2. J. ISRAELI et M. CECCHETTI. Talanta, **15**, 1031 (1968).
3. J. ISRAELI et M. CECCHETTI. J. Inorg. Nucl. Chem. **30**, 2709 (1968).
4. J. ISRAELI et M. CECCHETTI. Can. J. Chem. **46**, 3821 (1968).
5. N. E. JACOBS et D. W. MARGERUM. Inorg. Chem. **6**, 2038 (1967).
6. D. HOPGOOD et R. ANGELICI. J. Amer. Chem. Soc. **90**, 2508 (1968).
7. G. SHARMA et J. P. TANDON. J. Inorg. Nucl. Chem. **32**, 1273 (1970).
8. G. DEGISCHER et G. H. NANCOLLAS. Inorg. Chem. **9**, 1259 (1970).
9. M. PETIT-RAMEL et R. M. PÂRIS. Bull. Soc. Chim. Fr. 2791 (1968).
10. M. PETIT-RAMEL et R. M. PÂRIS. C.R. Acad. Sci. Paris, Ser. C, **266**, 1368 (1968).
11. C. W. DAVIES. Electrochemistry. Philosophical Library, New York. 1968. p. 60.
12. M. M. JONES. Elementary Coordination Chemistry. Prentice-Hall. 1964. p. 438.
13. H. IRVING et R. J. P. WILLIAMS. J. Chem. Soc. 3192 (1953).
14. K. B. YATSIMIRSKII. Zhur. Neorg. Khim. **1**, 2451 (1956).

Can. J. Chem. Downloaded from www.nrcresearchpress.com by 210.87.254.42 on 09/05/12
For personal use only.

Dimethylgermanium Dinitrate

D. POTTS AND A. WALKER
Department of Chemistry, Scarborough College, University of Toronto, 1265 Military Trail, West Hill, Ontario
Received July 20, 1970

Dimethylgermanium dinitrate has been prepared by the reaction of dimethylgermanium dichloride and nitrogen pentoxide in carbon tetrachloride. The properties of this compound have been investigated and compared with those of other known Group IVA alkyl nitrates. The vibrational spectra show that the nitrato groups are covalently bound to the germanium in a unidentate manner. Ultraviolet spectra and conductivity measurements indicate that the compound behaves as a 1:2 electrolyte in water and dimethyl sulfoxide but is a non-electrolyte in methyl cyanide, nitromethane, and ethyl acetate. The complexes $Me_2Ge(NO_3)_2 \cdot py$ and $Me_2Ge(NO_3)_2 \cdot 2,2'dipy$ have been prepared and the infrared spectra of these compounds indicate considerable weakening of the germanium–nitrato bonds.

Canadian Journal of Chemistry, 49, 202 (1971)

Can. J. Chem. Downloaded from www.nrcresearchpress.com by 210.87.254.6 on 09/05/12
For personal use only.

Following our work on $Et_2Pb(NO_3)_2$ (1) and $MeSn(NO_3)_3$ (2), it was of interest to us to investigate the organo-nitrate chemistry of germanium, since the only organogermanium nitrate known to date is trimethylgermanium nitrate (3), and this compound has not been characterized completely.

We first attempted to prepare dimethylgermanium dinitrate by the reaction of liquid dinitrogen tetroxide on tetramethylgermanium in ethyl acetate, since this was the synthetic route used in the preparation of $Et_2Pb(NO_3)_2$ (1) and $Me_2Sn(NO_3)_2$ (4). After removal of solvent and excess tetroxide, the product was always an oil, probably a mixture of the mono and dinitrato species. Our work on $MeSn(NO_3)_3$ (2) suggested that dimethylgermanium dinitrate might be obtained by reacting the dichloride analogue with either dinitrogen tetroxide or dinitrogen pentoxide in carbon tetrachloride. The reaction using dinitrogen tetroxide did give the required product but the reaction was slow and the yield poor. The reaction with dinitrogen pentoxide, however, proceeded smoothly yielding white needle-like crystals of dimethylgermanium dinitrate which, after filtration and washing with cold carbon tetrachloride, were easily purified by sublimation in vacuo at 60 °C.

This paper discusses some of the chemical and physical properties of dimethylgermanium dinitrate, particularly those useful for comparison with other Group IVA alkyl nitrato complexes.

Results and Discussion

Dimethylgermanium dinitrate is a stable white crystalline solid, in contrast to the methylgermanium halides and trimethylgermanium nitrate, all of which are liquids at room temperature. Like the tin analogue (4), it is very hygroscopic, but it is more volatile than $Me_2Sn(NO_3)_2$, subliming rapidly at 60 °C/10^{-2} mm. The compound is readily soluble in water and many polar organic solvents and, like $Sn(NO_3)_4$ (5) and $MeSn(NO_3)_3$ (2) but in contrast to $Me_2Sn(NO_3)_2$ (4), is appreciably soluble in some non-polar organic solvents such as chloroform and carbon tetrachloride. These solubility properties support the spectroscopic evidence of highly covalent nitrato groups in dimethylgermanium dinitrate. The lack of reactivity of the compound towards diethyl ether, acetone, and Nujol is consistent with Raman spectroscopic evidence of unidentate nitrate groups (5). When heated gently in air the compound melts liberating dinitrogen tetroxide; but when heated strongly it explodes, leaving a white residue.

Vibrational Spectra

The observed infrared and Raman bands together with suggested assignments are presented in Table 1. The appearance of Raman bands in the 1300 cm^{-1} region and the fact that the Raman band in the 1600 cm^{-1} region is very weak is characteristic of the pattern observed for all compounds known to contain unidentate nitrate groups, and quite unlike that observed for those compounds containing known symmetrically bidentate nitrate groups (6). Consequently the nitrate bands are assigned in accordance with Addison and Logan (7) assuming a unidentate nitrato structure. The Ge—CH_3 vibrational modes are assigned following Griffiths (8).

The splitting of the bands in the 1300 and 900 cm^{-1} regions is undoubtedly due to vibrational coupling of the two nitrato groups, as was

Can. J. Chem. Downloaded from www.nrcresearchpress.com by 210.87.254.6 on 09/05/12
For personal use only.

TABLE 1. Vibrational spectra of dimethylgermanium dinitrate*

Infrared (cm^{-1})	Raman (cm^{-1})	Assignment
2890 vw		Asym. C—H stretching
2870 vw		Sym. C—H stretching
1692 w		(1290 + 394)
1610 s	1582 vw	Asym. NO_2 stretching
1415 w		Asym. CH_3 deformation
1290 s, sp	1322 w	Sym. NO_2 stretching
1275 s, sp	1307 w	
1258 m, sh	1252 m	Sym. CH_3 deformation
930 s, sp	990 w	N—O stretching
908 m	975 m	
840 m		CH_3 rocking
815 sh		
782 m, sp	783 w	NO_3 out-of-plane rocking
	722 w	Sym. NO_2 bending
695 w	704	Asym. NO_2 bending
660 w	669 m	Asym. Ge—C stretching
600 w	601 vs	Sym. Ge—C stretching
394 s, sp	370 s	Ge—O stretching
247 m, sp	248 m	Ge—O bending

*s = strong, m = medium, w = weak, v = very, sh = shoulder, sp = sharp.

observed for diethyllead dinitrate (1) and dimethyltin dinitrate (4), and is consistent with a pseudo tetrahedral structure for $Me_2Ge(NO_3)_2$. The two germanium–carbon stretching frequencies required for such a structure are also observed. The asymmetric NO_2 stretching frequency is not split, but as this band is rather broad, the two expected bands may not be sufficiently resolved.

The strong bands at 394 cm^{-1} infrared (i.r.) and 370 cm^{-1} Raman (R) are assigned to Ge—O stretching modes.

The bands at 247 cm^{-1} (i.r.) and 248 cm^{-1} (R) are too high to be assigned to GeC_2 bending vibrations (8), and are thus conditionally assigned to Ge—O bending and torsion modes. The fact that the asymmetric and symmetric Ge—C stretching modes occur at somewhat higher frequencies as compared to the analogous bands for Me_2GeCl_2 (8) indicates that the germanium is more electropositive in the nitrato compound.

Ultraviolet Spectra

The ultraviolet spectra of solutions of dimethylgermanium dinitrate in water and dimethyl sulfoxide are shown in Fig. 1. The observed peak at 302.5 mμ (ε = 14.35) for the aqueous solution corresponds to the dissociation of the molecule yielding two nitrate ions in solution (9). In contrast to $Me_2Sn(NO_3)_2$ (4) and $Et_2Pb(NO_3)_2$ (1), the aqueous solution of $Me_2Ge(NO_3)_2$ did not change upon boiling. The spectrum of the dimethyl sulfoxide solution has a peak at 312.5 mμ (ε = 9.75) and this is also consistent with the presence of two nitrate ions per mole (9). Again in contrast to the tin and lead analogues, this solution was found to be stable with respect to time.

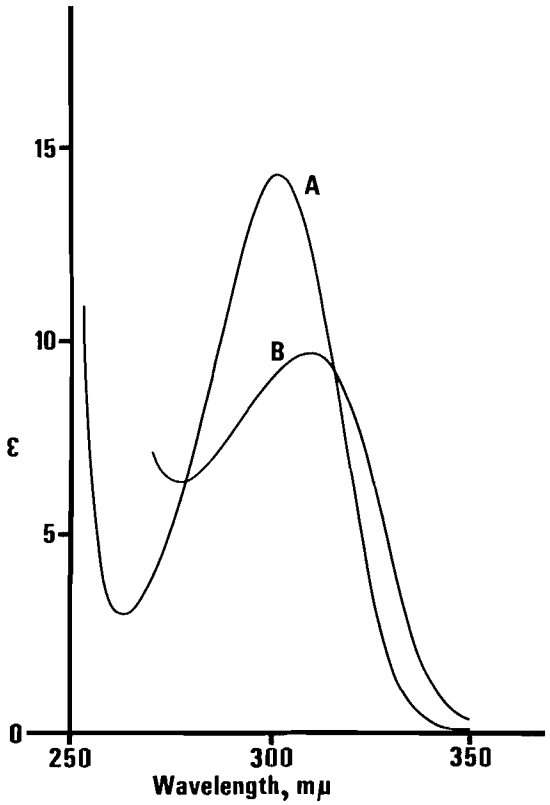

FIG. 1. Ultraviolet spectra of solutions of dimethylgermanium dinitrate at 25 °C. *A*, water; *B*, dimethyl sulfoxide.

Figure 2 shows the ultraviolet solution spectra of dimethylgermanium dinitrate in methyl cyanide, ethyl acetate, and methanol. The spectra are typical of those obtained for solutions of many covalent metal nitrates in these solvents, indicating considerable metal-nitrate interaction (9). They are in general the same as those obtained for $Me_2Sn(NO_3)_2$ (4), and for fresh solutions of $Et_2Pb(NO_3)_2$ (1), although the extinction coefficients are somewhat lower in the present case. The peak maxima occur at 270.0 mμ in all three solvents, and the extinction coefficients are 14.56, 18.02, and 16.18 in methyl

TABLE 2. Molar conductivities of $Me_2Ge(NO_3)_2$ in various solvents at 25 °C

H_2O		DMSO		MeOH		MeCN		$MeNO_2$	
M concn. $\times 10^3$	M cond. (ohm^{-1} cm^2)	M concn. $\times 10^3$	M cond. (ohm^{-1} cm^2)	M concn. $\times 10^3$	M cond. (ohm^{-1} cm^2)	M concn. $\times 10^3$	M cond. (ohm^{-1} cm^2)	M concn. $\times 10^3$	M cond. (ohm^{-1} cm^2)
1.01	784	0.858	74.5	1.07	171	0.947	0.458	1.59	3.76
3.43	794	2.91	68.1	2.93	120	5.45	0.577	5.35	0.243
9.32	792	6.08	63.4	4.99	98.4	9.20	0.543	12.03	1.03
14.1	787	9.66	59.5	8.77	79.3	13.6	0.328	19.4	0.874
18.9	782	17.4	53.8	17.3	60.3	17.7	0.104	28.9	0.650

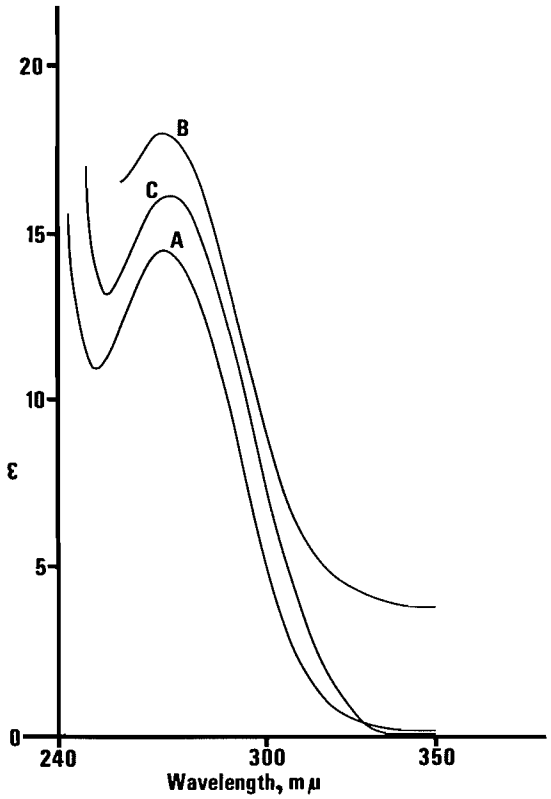

FIG. 2. Ultraviolet spectra of solutions of dimethylgermanium dinitrate at 25 °C. *A*, methyl cyanide; *B*, ethyl acetate; *C*, methyl alcohol.

cyanide, ethyl acetate, and methanol, respectively. These solutions were stable with respect both to time and refluxing.

Conductivities

The molar conductivities of dimethylgermanium dinitrate in water, dimethyl sulfoxide, methanol, methyl cyanide, and nitromethane are listed in Table 2. The low conductivity of methyl cyanide and nitromethane solutions indicate that $Me_2Ge(NO_3)_2$ is virtually a non-electrolyte in these solvents (10). The molar conductivities of aqueous solutions greatly exceed the expected value for a 1:2 electrolyte (*ca.* 240 ohm^{-1} cm^2 at 0.001 *M*) (4). These solutions are very acidic and the high conductivities are attributed to hydrolysis similar to that found for dimethyltin dinitrate (4). However, the conductivity values for the germanium solutions are much higher than those found for tin, the latter having a molar conductivity of 403 ohm^{-1} cm^2 at 0.001 *M* (4). This result is consistent with the greater acidity of the Me_2Ge^{2+} ion. By comparison it was found that the Et_2Pb^{2+} ion is only hydrolyzed in hot aqueous solutions (1). The conductivities of dimethyl sulfoxide solutions are very similar to those obtained for $Me_2Sn(NO_3)_2$ (4) and indicate that $Me_2Ge(NO_3)_2$ is a 1:2 electrolyte in this solvent. The values obtained in methanol show concentration dependence typical of weak electrolyte behavior. Therefore while in very dilute solutions (0.001 *M*) the conductivity indicates some degree of ionization ($AgNO_3$ in MeOH has a molar conductivity of 94.20 ohm^{-1} cm^2 at a concentration of 0.00168 *M* (11)), at the concentration used for the u.v. spectrum (0.0412 *M*) considerable association is evident.

Molecular Weight

The molecular weight of $Me_2Ge(NO_3)_2$ was determined cryoscopically in nitrobenzene and found to be 238.6 (theoretical monomeric value = 226.7).

Pyridine and 2,2'-Dipyridyl Complexes

The two adducts $Me_2Ge(NO_3)_2$·py and $Me_2Ge(NO_3)_2$·dipy were obtained as white precipitates from chloroform solutions containing $Me_2Ge(NO_3)_2$ and excess ligand. Since the six coordinate dipyridyl adduct is formed readily, it is interesting that only a mono adduct is formed between $Me_2Ge(NO_3)_2$ and pyridine. Present work in this laboratory has shown that

Can. J. Chem. Downloaded from www.nrcresearchpress.com by 210.87.254.6 on 09/05/12
For personal use only.

TABLE 3. Infrared spectra of $Me_2Ge(NO_3)_2py$ and $Me_2Ge(NO_3)_2dipy$, ligand bands omitted*

Band (cm^{-1})		
$Me_2Ge(NO_3)_2py$	$Me_2Ge(NO_3)_2dipy$	Assignment
1430 s, br	1408 s, br	Asym. NO_2 stretching
1290 s, br	1300 s, br	Sym. NO_2 stretching
1008 w	980 sh	N—O stretching
870 w, br	860 m, br	CH_3 rock
822 s, sp	822 m, sp 804 s, sp	NO_3 out-of-plane rock
a	760 w	Sym. NO_2 bending
720 w, sp	715 w, sp	Asym. NO_2 bending
630 m	629 m, sh	Asym. Ge—C stretching
595 w, sh	a	Sym. Ge—C stretching
363 m, br	375 w	Ge—O stretching

*s = strong, m = medium, w = weak, br = broad, sh = shoulder, sp = sharp, a = obscured by ligand absorption.

$Me_2Sn(NO_3)_2$ forms the analogous complexes $Me_2Sn(NO_3)_2 \cdot py$ and $Me_2Sn(NO_3)_2 \cdot dipy$. Pyridine and 2,2′-dipyridyl adducts with Group IVA alkyl nitrates are presently being studied in detail. The pyridine adduct is very hygroscopic, whereas the dipyridyl adduct is only slightly hygroscopic.

The principal infrared bands and their assignments for the two complexes are presented in Table 3. By comparison with similar chloro complexes the bands due to pyridine and dipyridyl were clearly identified and are not included in the table. The lower values for the splitting between the asymmetric and symmetric NO_2 stretching frequencies and the higher values for the N—O stretching frequencies as compared to $Me_2Ge(NO_3)_2$, indicate that the metal–nitrate bonds are much weaker in both adducts. The somewhat lower values for the Ge—O stretches in the adducts also indicate weaker metal–nitrate interaction.

Experimental

Dimethylgermanium Dinitrate

Dinitrogen pentoxide was prepared by a gas phase reaction between dinitrogen tetroxide and ozone. Dimethylgermanium dichloride (6.6 g) was added to a solution of dinitrogen pentoxide (13.5 g) dissolved in carbon tetrachloride (60 ml). The dichloride dissolved immediately in the reaction mixture and after stirring for ½ h white crystals were precipitated from the solution. The mixture was stirred for 24 h and the crystals were separated by filtration. After sublimation in vacuo at 60 °C, pure $Me_2Ge(NO_3)_2$ (5.3 g) was obtained as a white crystalline solid. Extreme care was taken to exclude moisture throughout the entire procedure.

Anal. Calcd. for $Me_2Ge(NO_3)_2$: C, 10.6; NO_3^-, 54.7; Ge, 32.02. Found: C, 10.1; NO_3^-, 54.0; Ge, 32.58.

$Me_2Ge(NO_3)_2py$

Pyridine (5.0 ml, 0.062 mol) in chloroform (5 ml) was added to a solution containing dimethylgermanium dinitrate (1.05 g, 0.00463 mol) in chloroform (10 ml). A white precipitate was formed immediately, accompanied by the evolution of heat. After cooling, the precipitate was filtered and washed twice with dry petroleum ether. Moisture was again carefully excluded from the apparatus. The pyridine adduct obtained (1.15 g) was a white powdery solid.

Anal. Calcd. for $Me_2Ge(NO_3)_2py$: C, 27.49; NO_3^-, 40.55; Ge, 23.74. Found: C, 27.08; NO_3^-, 40.64; Ge, 23.33.

$Me_2Ge(NO_3)_2dipy$

2,2′-Dipyridyl (0.922 g, 0.00591 mol) dissolved in chloroform (5 ml) was added to a solution of $Me_2Ge(NO_3)_2$ (0.528 g, 0.00233 mol) in chloroform (10 ml). The white precipitate, which formed immediately, was filtered and washed first with dry chloroform and then with dry petroleum ether. The yield of the white powdery solid was 0.66 g.

Anal. Calcd. for $Me_2Ge(NO_3)_2dipy$: C, 37.64; H, 3.69; N, 14.64. Found: C, 37.48; H, 3.84; N, 14.53.

For the compounds $Me_2Ge(NO_3)_2$ and $Me_2Ge(NO_3)_2py$, nitrate was determined gravimetrically as nitron nitrate, germanium was determined gravimetrically as GeO_2 using the technique employed by Rochow (12), and carbon was determined by the Van Slyke wet oxidation method. Due to the extreme difficulty found in oxidizing the carbon in these compounds, it was necessary to mix 1.5 g KIO_3 with the sample before the addition of the Van Slyke oxidation mixture. All other analyses were carried out by microanalytical laboratories. Pyridine was dried by allowing it to sit 24 h over calcium hydride followed by distillation onto molecular sieves. Other solvents were dried by standard techniques.

Infrared spectra were recorded using a Beckman I.R. 12 spectrophotometer. Spectra of $Me_2Ge(NO_3)_2$ were taken in carbon tetrachloride and carbon disulfide using variable path length cells with silver chloride windows. Far infrared spectra (200–400 cm^{-1}) were taken in carbon tetrachloride using 0.1 mm polyethylene liquid

Can. J. Chem. Downloaded from www.nrcresearchpress.com by 210.87.254.6 on 09/05/12
For personal use only.

cells. All other spectra were obtained with Nujol or halocarbon mulls using KRS-5 plates.

Raman spectra were determined on the solid phase using a Spex monochromator and the red line of a krypton laser.

Ultraviolet spectra were recorded using a Cary #14 spectrophotometer using fused silica cells and dried spectroscopic solvents.

Conductivities were recorded with a Beckman model RC-18 bridge system, and a cell following the design of Greiner (13).

We wish to thank the National Research Council of Canada for supporting this work and for a Studentship to D.P.

1. D. POTTS and A. WALKER. Can. J. Chem. **47**, 1621 (1969).
2. J. R. FERRARO, D. POTTS, and A. WALKER. Can. J. Chem. **48**, 711 (1970).
3. M. SCHMIDT and I. RUIDISCH. Chem. Ber. **95**, 1434 (1962).
4. C. C. ADDISON, W. B. SIMPSON, and A. WALKER. J. Chem. Soc. 2360 (1964).
5. C. C. ADDISON and W. B. SIMPSON. J. Chem. Soc. 598 (1965).
6. G. S. BROWNLEE. Ph.D. Thesis. University of Nottingham, Nottingham. 1969.
7. C. C. ADDISON and N. LOGAN. Advances in Inorganic and Radiochemistry. Vol. 4. Academic Press. 1964. p. 72.
8. J. E. GRIFFITHS. Spectrochim. Acta, **20**, 1335 (1964).
9. C. C. ADDISON and D. SUTTON. J. Chem. Soc. A, 1524 (1966).
10. C. C. ADDISON, B. J. HATHAWAY, N. LOGAN, and A. WALKER. J. Chem. Soc. 4308 (1960).
11. R. E. BUSBY and V. S. GRIFFITHS. J. Chem. Soc. 902 (1963).
12. E. G. ROCHOW. J. Amer. Chem. Soc. **69**, 1729 (1947).
13. R. H. GREINER. Fusion, p. 11, Nov. 1960.

Can. J. Chem. Downloaded from www.nrcresearchpress.com by 210.87.254.6 on 09/05/12
For personal use only.

Nitrogen Bridged Osmium–Ruthenium Complexes

CLIVE M. ELSON, J. GULENS, AND JOHN A. PAGE
Department of Chemistry, Queen's University, Kingston, Ontario
Received August 14, 1970

The formation of $[(H_2O)(NH_3)_4Ru—N_2—Os(NH_3)_5]^{4+}$ by the reaction of *cis*-$Ru(NH_3)_4(H_2O)_2^{2+}$ and $Os(NH_3)_5N_2^{2+}$ has been studied over the range 15–45 °C. The reaction followed second order kinetics with $k_f = 1.2 \times 10^{-1}\ M^{-1}\ s^{-1}$ at 25.0 °C and $E_a = 16.8 \pm 0.1$ kcal/mole. Measurement of equilibrium concentrations gave $K_{eq} = 4 \times 10^3\ M^{-1}$ at 25.0 °C.

The (4+) dimer was stable but removal of the excess *cis*-$Ru(NH_3)_4(H_2O)_2^{2+}$ reactant by oxidation at −0.10 V was followed by dimer decomposition. The breakup obeyed simple first order kinetics with $k_r = 2.9 \times 10^{-5}\ s^{-1}$ at 25.0 °C.

Oxidation of the (4+) dimer at +0.10 V gave a stable (5+) dimer. Removal of the excess $Os(NH_3)_5N_2^{2+}$ reactant at +0.30 V was followed by decomposition of the (5+) dimer giving $Os(NH_3)_5N_2^{2+}$ and $Ru^{III}(NH_3)_4X_2$. The decomposition again obeyed first order kinetics with $k_1 = 1.5 \times 10^{-5}\ s^{-1}$ at 25.0 °C. The (5+) dimer has an intervalence – transfer absorption band at 755 nm and is characterized as $[X(NH_3)_4Ru^{III}—N_2—Os^{II}(NH_3)_5]^{5+}$.

The studies were carried out in an aqueous H_2SO_4–K_2SO_4 electrolyte of p*H* 3.3, $\mu = 0.30$.

Canadian Journal of Chemistry, 49, 207 (1971)

Introduction

The formation of the binuclear complex, $[(NH_3)_5Ru—N_2—Ru(NH_3)_5]^{4+}$ in which the nitrogen group bridges the two metal atoms was first reported by Taube and co-workers (1). An analogous dimeric ruthenium(II) aquo-tetraammine (2) and a mixed ruthenium(II) pentaammine aquo-tetraammine species (3) are now known and the kinetics and energetics of formation of these complexes have been studied (3).

The nitrogen bridged binuclear osmium(II) pentaammine complex is not known. However, Allen and Stevens have prepared the unsymmetrical complexes, $[(NH_3)_5Ru—N_2—Os(NH_3)_5]^{4+}$ and $[(NH_3)_5Ru—N_2—Os(NH_3)_5]^{5+}$ (4). In this paper we report on the characterization and kinetics of formation and decomposition of the related nitrogen bridged osmium pentaammine – ruthenium aquo-tetraammine complexes.

Experimental

The experimental methods, apparatus, and the preparation of the *cis*-$Ru(NH_3)_4Cl_2 \cdot Cl$ have been previously described (3). The near-infrared spectra were recorded on a Cary 14 spectrophotometer. The reactions were carried out in an aqueous K_2SO_4–H_2SO_2 electrolyte ($\mu = 0.30$, pH = 3.3 at 25 °C). The potentials reported (V) are in volts relative to a saturated potassium chloride calomel electrode.

The $Os(NH_3)_5N_2 \cdot Cl_2$ was prepared from $(NH_4)_2OsCl_6$ (Engelhard Os-40) by the method of Allen and Stevens (5). The purity of the product was established spectrophotometrically using Taube's value of the extinction coefficient ($\varepsilon = 2.5 \times 10^4$ at 208 mm) (6). The initial product was found to be only 60–70% $Os(NH_3)_5N_2 \cdot Cl_2$, but this was increased to 85–90% by a second reflux with hydrazine hydrate. The purity was also established by coulometry (7); the $Os(NH_3)_5N_2^{2+}$ underwent a clean oxidation at +0.32 V ($n = 1.0 \pm 0.1$) on Pt in a 0.08 *M* $MeSO_3H$ electrolyte. The extinction coefficients actually used in this work are reported in Table 1.

Results

(1) $[(H_2O)(NH_3)_4Ru—N_2—Os(NH_3)_5]^{4+}$

The reactant, *cis*-$Ru(NH_3)_4(H_2O)_2^{2+}$ (A), was prepared by controlled potential electrolysis of weighed amounts of *cis*-$Ru(NH_3)_4Cl_2 \cdot Cl$ on a Hg cathode at −0.50 V under Ar. The reaction was initiated by the addition of $Os(NH_3)_5N_2 \cdot Cl_2$(M) to the Ru(II) solution. The Hg electrode was kept at its reducing potential and the Ar atmosphere maintained throughout the subsequent reaction; the background current remained negligible.

The initial concentration of M was determined spectrophotometrically. With time, an absorbance peak developed at 257 nm while the peak at 208 nm (due to M) decreased. A well defined isosbestic point appeared at 227 nm. The peak at 257 nm is assigned to the complex $[(H_2O)(NH_3)_4Ru—N_2—Os(NH_3)_5]^{4+}$ (D(4+)) having both metals in the +2 oxidation state: *i.e.* D(2,2). The reaction can be represented by

$$A + M \xrightarrow{k_f} D(4+)$$

The concentration of M was followed by the decrease in absorbance at 208 nm allowing for the contribution of the product. The second

TABLE 1. Extinction coefficients: H_2SO_4–K_2SO_4 electrolyte

Complex	Extinction coefficient 208 nm	246 nm	257 nm
$Os(NH_3)_5N_2^{2+}$	2.5×10^4*	2.0×10^3	1.6×10^3
$Os^{III}(NH_3)_5X$†	1.0×10^3	4.5×10^2	—
cis-$Ru(NH_3)_4(H_2O)_2^{2+}$	8.30×10^2	—	4.70×10^2
cis-$Ru^{III}(NH_3)_4X_2$‡	1.08×10^3	5.34×10^2	5.30×10^2
$[(H_2O)(NH_3)_4Ru—N_2—Os(NH_3)_5]^{4+}$	3.3×10^3§	—	5.1×10^4‖
$[X(NH_3)_4Ru^{III}—N_2—Os^{II}(NH_3)_5]$¶	4.8×10^3	3.7×10^4	—
$X = SO_4^{2-}$ or HSO_4^- or H_2O			

*Reference 6.
†Coulometric oxidation of $Os(NH_3)_5N_2.CL_2$.
‡Coulometric oxidation of *cis*-$Ru(NH_3)_4(H_2O)_2^{2+}$.
§Equated to extinction coefficient of (4+) dimer at 306 nm.
‖Derived from ratio of decrease in absorbance at 208 nm to increase in absorbance when $Os(NH_3)_5N_2^{2+}$ reacted with Ru(II).
¶Coulometric oxidation of (4+) dimer.

TABLE 2. Rate constants for (4+) dimer formation

Temperature (°C)	C_A^0 ($M \times 10^3$)	C_M^0 ($M \times 10^3$)	k_f (M^{-1} s^{-1} × 10)	Number of points	Reaction time (min)	Correlation coefficient
14.9	1.88	0.565	0.48_0	21	101	1.000
16.7	1.48	0.526	0.53_3	14	66	1.000
25.0	0.951	0.638	1.2_5	10	48	0.998
25.0	1.01	0.536	1.2_0	15	56	1.000
35.1	0.893	0.531	3.1_2	15	37	0.993
39.6	0.425	0.285	4.7_4	10	20	0.997
45.2	0.410	0.310	7.5_4	5	10	0.979

order rate constant was evaluated by least square fits on plots of

$$(C_A^0 - C_M^0)^{-1} \times \ln[C_M^0(C_A^0 - C_M^0 + C_M)/C_A^0 C_M]$$

vs. time and the results, over a range of temperatures, are tabulated in Table 2. The plots were linear over the stated reaction times, although at the higher temperatures a negative curvature was observed at longer times as the back reaction became significant. The rate of reaction was demonstrated to be dependent on the initial concentrations of both A and M. A good Arrhenius plot was obtained and gave, by least squares fitting, $E_a = 16.8 \pm 0.1$ kcal/mole and $\Delta S^{\ddagger} = -6 \pm 0.5$ e.u.

One kinetic run at 25.0 °C was allowed to proceed for 30 h under the stated conditions. After approximately 17 h the concentrations of M and D(4+) stabilized; past this point from 17 to 30 h there was a small decrease (~3%) in the absorbances at 208 and 257 nm. The concentrations of M and D(4+) were calculated from simultaneous equations for the absorbance at the two wavelengths, and assuming equilibrium at 17 h gave

$$K_{eq} = \frac{C_{D(4+)}}{C_A \cdot C_M} = \frac{C_{D(4+)}}{(C_A^0 - C_{D(4+)})(C_M)} = 4.2 \times 10^3\ M^{-1}$$

The decomposition of the dimer was followed in another series of experiments. The reaction was allowed to proceed as before, but when an appreciable concentration of dimer had been formed the reaction was reversed by switching the electrode potential to −0.10 V. This potential will oxidize the excess A to *cis*-ruthenium(III) tetraammine (3) but is not sufficiently oxidizing to attack either nitrogen species

$$D(4+) \xrightarrow{k_r} A + M$$

$$A \xrightarrow[-0.10\ V]{-e} Ru(III)$$

The electrode was maintained at −0.10 V after the excess Ru(II) had been oxidized and past this point the absorbance at 257 nm decreased and that at 208 nm increased. A well defined isosbestic point was observed at 227 nm. The concentrations of M and D(4+) were calculated from the simultaneous equations at the two wavelengths; the sum of their calculated

TABLE 3. Rate constants for dimer decomposition at 25 °C

Dimer	C_M^0 ($M \times 10^3$)	C_D^0 ($M \times 10^3$)	k_r ($s^{-1} \times 10^5$)	Number of points	Reaction time (min)	Correlation coefficient
(4+)	0.249	0.315	2.9_0	19	140	0.999
	0.214	0.336	2.9_2	17	180	0.999
(5+)	—	0.281	1.5_1	22	480	1.000

concentrations was constant throughout the run. The first order rate constant for the decomposition was evaluated by plotting ln ($C_{D(4+)}$) *vs.* time. The plots were linear for the time studied; this represented the decomposition of approximately 30% of the initial (4+) dimer. The values of k_r are given in Table 3.

If the equilibrium constant for the formation of the (4+) dimer is calculated as the ratio of k_f to k_r, then at 25 °C

$$K_{eq} = \frac{k_f}{k_r} = \frac{1.2 \times 10^{-1}\ M^{-1}\ s^{-1}}{2.9 \times 10^{-5}\ s^{-1}} = 4.1 \times 10^3\ M^{-1}$$

This value agrees closely with that obtained from the assumed equilibrium concentrations.

(2) $[(H_2O)(NH_3)_4Ru—N_2—Os(NH_3)_5]^{5+}$

Further electrolysis of the solution containing the (4+) dimer, M and Ru(III) using a Pt electrode at +0.10 V under Ar gave a clean oxidation of the dimer. The oxidation consumed 1.0 faraday per mole based on the initial concentration of dimer, and was accompanied by a decrease in absorbance and a shift in the maximum from 257 to 246 nm. The reaction was reversible and the (4+) dimer could be quantitatively regenerated at a Hg electrode at −0.15 V, a more reducing potential. The reaction can be represented as

$$\underset{D(4+)}{[(H_2O)(NH_3)_4Ru—N_2—Os(NH_3)_5]^{4+}} \underset{+e\ -0.15\ V}{\overset{-e\ +0.10\ V}{\rightleftharpoons}} \underset{D(5+)}{[(H_2O)(NH_3)_4Ru—N_2—Os(NH_3)_5]^{5+}}$$

However, the coulometry does not indicate the distribution of oxidation states in the (5+) dimer. It is possible that the aquo group on the ruthenium may be replaced by a SO_4^{2-} or HSO_4^- from the electrolyte if the ruthenium is in the (3+) state. The (5+) dimer also exhibited an absorbance maximum at 755 nm ($\varepsilon \sim 2 \times 10^3$).

The decomposition of the (5+) dimer was also examined. The solution containing the (5+) dimer, M and Ru(III) was further oxidized using the Pt electrode at +0.30 V, under Ar. This potential will oxidize M to an Os(III) species (7). Upon "completion" of the electrolysis the working electrode was disconnected. From this point, it was observed that the absorbance at 246 nm decreased while that at 208 nm increased. A well defined isosbestic was obtained at 224 nm. The reaction can be represented

$$D(5+) \underset{Ar}{\overset{k_r'}{\rightarrow}} M + Ru(III)$$

so that the (5+) dimer decomposes to $Os(NH_3)_5N_2^{2+}$ and *cis*-$Ru^{III}(NH_3)_4X_2$. The first order rate constant was evaluated by plotting ln ($C_{D(5+)}$) *vs.* time and the plot was linear over 30% decomposition of the (5+) dimer. The sum of the concentrations of D(5+) and M was constant over the time studied. The value of k_r' is given in Table 3.

Attempts to prepare the (5+) dimer by direct reactions were unsuccessful. The pairs of reactants, *cis*-$Ru^{III}(NH_3)_4X_2$ with $Os(NH_3)_5N_2^{2+}$, and $Os(NH_3)_5(H_2O)^{3+}$ with *cis*-$Ru(NH_3)_4(H_2O)N_2^{2+}$ were mixed together in the 0.08 *M* $MeSO_3H$ electrolyte, but there was not any detectable increase in absorbance at 246 nm on prolonged standing at room temperature.

Discussion

The $Os(NH_3)_5N_2^{2+}$ nucleophile and *cis*-$Ru(NH_3)_4(H_2O)_2^{2+}$ substrate have been shown to react with overall second order kinetics to produce the (4+) dimer. The kinetics can be interpreted in terms of a displacement mechanism (S_N2) or a dissociative mechanism (S_N1) with the implications stated previously (3) still applying. The rate of reaction at 25.0 °C of the $Os(NH_3)_5N_2^{2+}$ nucleophile with the substrate ($1.2 \times 10^{-1}\ M^{-1}\ s^{-1}$) was found to be about twice as fast as those previously reported (3) for the nucleophiles $Ru(NH_3)_5N_2^{2+}$ ($0.68 \times 10^{-1}\ M^{-1}\ s^{-1}$) and *cis*-$Ru(NH_3)_4(H_2O)N_2^{2+}$ ($0.72 \times 10^{-1}\ M^{-1}\ s^{-1}$) with the same substrate. The activation energies and entropies of activation are of the same order for all three nucleophiles.

The increased nucleophilicity of the nitrogen group bound to osmium can be explained by the stronger π-donating ability of Os(II) compared to that of Ru(II).

The one electron oxidation of the (4+) dimer to produce a stable species that can be reversibly reduced, indicates the (5+) species is still a simple dimer. The band at 246 nm of the (5+) dimer is assigned to the charge-transfer absorption $t_{2g} \rightarrow \pi^*$. The lower energy absorption at 755 nm can be interpreted as a heteronuclear intervalence-transfer absorption (IT) (3,2) $\rightarrow$ (2,3)* (8) where the "odd" electron in the 5+ complex preferentially resides on one of the metals. This is analogous to the arguments of Creutz and Taube (9) who have reported that

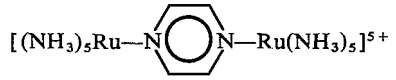

exhibits an IT band at 1570 nm. However, the observed decomposition of the (5+) dimer to give only Os(II) and Ru(III) species is not conclusive proof that the odd electron in the dimer resides exclusively on the Os center; the localization could take place in the decomposition step.

An attempt was made to locate the "odd" electron by an anation experiment. The (4+) and (5+) dimers of the osmium pentaammine with both the tetraammine and pentaammine of ruthenium were prepared in a non-complexing 0.08 *M* $MeSO_3H$ electrolyte. Both of the (4+) dimers exhibited absorbance peaks at 257 nm. The $[(H_2O)(NH_3)_4Ru—N_2—Os(NH_3)_5]^{5+}$ exhibited peaks at 246 and 770 nm, and the $[(NH_3)_5Ru—N_2—Os(NH_3)_5]^{5+}$ at 246 and 758 nm. Anation of the (5+) dimers by a 1000 fold excess of Cl^- shifted the peak of the (5+) dimer of the ruthenium tetraammine to 803 nm, and the peak of the (5+) dimer of the ruthenium pentaammine to 775 nm. There was not any appreciable shift (< 2 nm) in the higher energy band of either dimer.

The greater shift of the near-infrared band of the (5+) dimer of the ruthenium tetraammine can be ascribed to a Cl^- substitution of the aquo group on the ruthenium (9). This suggests that in the (5+) dimer there is a ruthenium(III) center, since the tendency of non π-acceptor ligands to substitute on a ruthenium(II) center is small (10). In a similar case Taube and Creutz have shown (9) that in 2 *M* NaCl, the (D_2O) group of

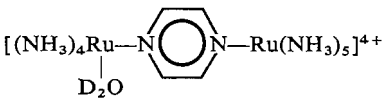

is substituted only after oxidation of the tetraammine center to ruthenium(III).

Therefore, in the sulfate electrolyte, the (5+) dimer is presumably $[X(NH_3)_4Ru^{III}—N_2—Os^{II}(NH_3)_5]$.

The authors are greatly indebted to Dr. A. D. Allen and J. R. Stevens for their part in this work. A fellowship (C.M.E.) from the Province of Ontario and both a scholarship (J.G.) and grant from the National Research Council of Canada are gratefully acknowledged.

1. D. F. Harrison, E. Weissberger, and H. Taube. Sci. **159**, 320 (1968).
2. A. D. Allen, T. Eliades, R. O. Harris, and P. Reinsalu. Can. J. Chem. **47**, 1605 (1969).
3. Clive M. Elson, I. J. Itzkovitch, and John A. Page. Can. J. Chem. **48**, 1639 (1970).
4. C. V. Senoff. Chem. Can. **21** (9), 31 (1969).
5. A. D. Allen and J. R. Stevens. Chem. Commun. 1147 (1967).
6. Hans A. Scheidegger, John N. Armor, and Henry Taube. J. Amer. Chem. Soc. **90**, 3263 (1968).
7. Clive M. Elson, J. Gulens, I. J. Itzkovitch, and John A. Page. Chem. Commun. 875 (1970). COM 754, received May 15th 1970.
8. G. C. Allen and N. S. Hush. Progr. Inorg. Chem. **8**, 357 (1967).
9. Carol Creutz and Henry Taube. J. Amer. Chem. Soc. **91**, 3988 (1969).
10. Peter C. Ford. Coordin. Chem. Rev. **5**, 75 (1970).

Can. J. Chem. Downloaded from www.nrcresearchpress.com by 188.143.235.115 on 09/06/12
For personal use only.

Application of Paramagnetic Shift Reagents in Nuclear Magnetic Resonance Studies of Complex Alcohols and Amines[1]

ELAINE GILLIES,[2] W. A. SZAREK, AND M. C. BAIRD
Department of Chemistry, Queen's University, Kingston, Ontario

Received June 9, 1970

The effects of Co(acetylacetonate)$_2$, Ni(acetylacetonate)$_2$, and Cu(ethyl acetoacetate)$_2$ on the nuclear magnetic resonance spectra of a variety of alcohols and amines have been studied. Changes are produced in the spectra, which are useful for assigning the signals.

Canadian Journal of Chemistry, 49, 211 (1971)

Introduction

The effects of paramagnetic transition metal ions on chemical shifts in ^{1}H nuclear magnetic resonance (n.m.r.) spectra have been the subject of intensive study for about ten years. In cases where there are no chemical interactions, the resonance positions of the protons in solution are shifted to higher fields by the magnetic fields resulting from the presence of the paramagnetic ions. This susceptibility shift is given (2) by the expression

$$[1]\quad \Delta\nu = \left[\chi - \chi_0 - \frac{\chi_0(d_0 - d_s)}{m}\right]\frac{2\pi\nu_0 m}{3}$$

where $\Delta\nu$ is the change in chemical shift from the diamagnetic position, χ is the mass susceptibility of the paramagnetic compound, χ_0 is the mass susceptibility of the solvent, d_0 is the density of the solvent, d_s is the density of the solution, m is the mass of the paramagnetic compound in 1 ml of solution, and ν_0 is the probe frequency of the spectrometer. Evans (2) has described a procedure, based on eq. 1, for determining the paramagnetic susceptibilities of transition metal compounds.

In cases where an organic molecule coordinates to a paramagnetic transition metal ion, the n.m.r. spectrum is usually dominated by electron spin – nuclear spin interactions.[3] The Fermi contact shift arises when unpaired electron spin density is delocalized from the metal ion into the molecular orbitals of the coordinated ligand. The result is that the n.m.r. spectra of paramagnetic complexes often show much larger variations in the shielding of the different hydrogen nuclei than is normally found for diamagnetic molecules. The magnitude of the contact shift, $\Delta\nu_i$, is given by the equation

$$[2]\quad \frac{\Delta\nu_i}{\nu_0} = -A_i\frac{\gamma_e}{\gamma_N}\frac{g\beta S(S+1)}{3kT}$$

where ν_0 is the probe frequency of the spectrometer, A_i is the isotropic electron spin – nuclear spin coupling constant, usually observed in electronic spin resonance (e.s.r.) spectra, γ_e and γ_N are the gyromagnetic ratios of the electron and nucleus, respectively, g is the Landé factor, β is the Bohr magneton, and S is the total electron spin. In cases where proton contact shifts occur as a consequence of electron delocalization into a ligand π-molecular orbital, A_i is proportional to the π-electron spin density of the ith carbon atom, and contact shift data are very useful in elucidating the nature of metal–ligand bonding and mechanisms of spin delocalization (4).

In cases where the g tensor of the metal complex is not isotropic, dipolar interactions between the magnetic dipoles of the unpaired electrons and those of the nuclear spins occur. The resulting pseudocontact shifts depend only on the geometry of the molecule and do not involve covalent metal–ligand interactions. Pseudocontact data have been used in ion-pair formation and solvation studies (5).

As mentioned above, the ^{1}H n.m.r. spectra of many paramagnetic molecules cover a much larger range than do those of diamagnetic molecules, resonance frequencies often being 100–200 p.p.m. from the diamagnetic positions. Where the electronic relaxation times are favorable, reasonably narrow line widths occur, and the spectra of complex molecules can often be interpreted on a first-order basis.

Recently a number of publications have appeared describing attempts to use paramagnetic

[1]For a preliminary communication, see ref. 1.
[2]Née Elaine Dent.
[3]For a comprehensive review of the phenomena described here, see ref. 3.

Can. J. Chem. Downloaded from www.nrcresearchpress.com by 188.143.235.115 on 09/06/12
For personal use only.

ions to simplify and aid in the interpretation of the ^1H n.m.r. spectra of complex organic molecules. On the basis of contact shifts induced by $NiBr_2 \cdot 3H_2O$, Zaev *et al.* (6) have suggested assignments in the ^1H n.m.r. spectra of several substituted pyrazoles. Changes induced by metal ions in the n.m.r. spectra of biologically important molecules such as lysozyme (7) and cholesterol (8) have also been noted, although few definite assignments could be made in either case. We are engaged in a systematic investigation of the possible uses of a number of paramagnetic transition metal complexes in the simplification and interpretation of the n.m.r. spectra of complex organic molecules such as carbohydrates. In order to establish a firm basis for investigations of complex molecules, we have studied in detail the effect of $Co(acac)_2$ (acac = acetylacetonate) on the n.m.r. spectra of solutions of a wide variety of compounds containing hydroxyl groups. Some results have already been communicated (1); we now report full details of our work to date.[4]

Experimental

The compounds $Co(acac)_2$ (9), $Ni(acac)_2$ (10), and Cu(ethyl acetoacetate)$_2$ (11) were prepared as described in the literature. The violet-red cobalt compound is stable in the solid state, but oxidizes slowly in solution to give orange Co(III) compounds; thus only freshly prepared solutions of $Co(acac)_2$ were used. Most of the organic compounds were purchased from commercial sources, and were not purified unless their n.m.r. spectra indicated the presence of impurities.

The general procedure followed was to observe the n.m.r. spectra of the hydroxyl compound in $CDCl_3$ in the presence of varying concentrations of $Co(acac)_2$. The solutions of the hydroxyl compounds varied in concentration from 0.2 to 1 *M*, with preference being given to the higher concentration, although in any one set of measurements the concentration was kept constant. The concentration of the metal complexes varied from 1×10^{-6} to 0.3 *M*, depending on the effect on the spectrum. The spectra were measured on Varian T-60 and A-60 spectrometers with tetramethylsilane (TMS) as both internal and external standard.

Results

Solutions of $Co(acac)_2$ in $CDCl_3$ are pale pink in color; addition of alcohols does not change the color noticeably. For 1*M* ethanol solutions containing cobalt concentrations of greater than about 0.005 *M*, the susceptibility shifts (*i.e.* the difference between the internal and external TMS references) are measurable and increase linearly with increasing cobalt concentration up to at least 0.3 *M* $Co(acac)_2$. This relationship is to be expected if the magnetic properties of the cobalt complex do not change over the concentration range studied, and thus it seems likely that the nature of the cobalt species remains unchanged.

On adding increasing amounts of $Co(acac)_2$ to a solution of a saturated alcohol in $CDCl_3$, quite drastic and systematic changes take place in the n.m.r. spectrum, both in the chemical shifts and in the line widths. These changes are illustrated in Fig. 1, which shows the effects that $Co(acac)_2$, in the concentration range 0.010 to 0.152 *M*, has on a 1*M* solution of ethanol in $CDCl_3$. It can be seen that the hydroxyl resonance broadens and moves upfield beyond the internal TMS line at quite low cobalt concentrations. The methylene lines, on the other hand, broaden and lose their resolution to the same extent only at higher concentrations of $Co(acac)_2$, moving downfield at a slower rate as well. The methyl triplet, although obviously affected more than the internal TMS line, broadens the least of the ethanol resonances, moving slightly upfield only at relatively high cobalt concentrations. The extent of the susceptibility shift is indicated by the external TMS lines imposed on the spectra.

The effects described above were observed in almost all of the examples of saturated alcohols. Only the magnitude and the direction of the hydroxyl resonances varied unpredictably; deuterated samples were used whenever necessary, to avoid ambiguities. Unfortunately, only the resonances due to α-CH_n groups appear to change their chemical shifts to any great extent, thereby making only their identification possible; β- and γ-CH_n resonances generally shift very little (20–30 Hz), and to higher field. We have found, however, that the line broadening effect *is* attenuated along a saturated organic molecule. This broadening, which may be attributed to the proximity of the unpaired electrons on the cobalt ion, has the effect of destroying the fine structure of the α-CH_n resonance and changing it to a broad, featureless band at such low cobalt concentrations that the spectrum of the rest of the molecule is still quite well resolved. As the cobalt concentration is increased, the β-CH_n resonance loses its fine structure, then the γ-CH_n resonance, and so on.

[4]Since submitting this manuscript, a report appeared on another shift reagent [tris(dipivalomethanato) europium] for use in nuclear magnetic resonance spectroscopy; see ref. 19.

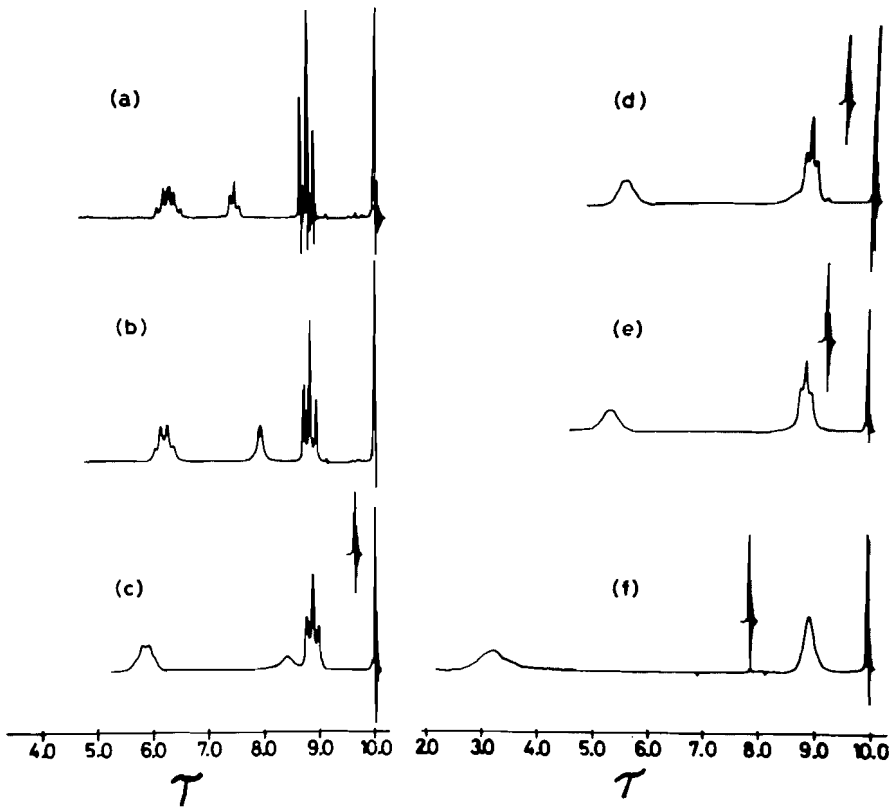

FIG. 1. Perturbation of the nuclear magnetic resonance spectrum of ethanol (1*M* in $CDCl_3$) by $Co(acac)_2$. Concentrations of $Co(acac)_2$: (*a*) 0, (*b*) 0.010 *M*, (*c*) 0.0276 *M*, (*d*) 0.0404 *M*, (*e*) 0.0512 *M*, and (*f*) 0.152 *M*. The susceptibility shift is indicated by the external tetramethylsilane lines imposed on the spectra.

A number of alcohols have been studied as described above, and it appears that there is a correlation between the structure of the alcohol and the contact shift of the α-CH_n group as the concentration of $Co(acac)_2$ is increased. Our results are summarized in Fig. 2, in which the chemical shift change ($\Delta\nu$) of the α-CH_n resonances of a series of alcohol solutions 1 *M* in $CDCl_3$ is plotted against the concentration of $Co(acac)_2$. It can be seen that the straight-chain alcohols shift the fastest, while isopropyl alcohol and *sec*-butyl alcohol, which have methyl groups on the α-carbon atom, shift the slowest. Isobutyl alcohol, which has branching at the β-carbon atom, is intermediate. In all of these cases the α-CH_n resonance lies in the region τ6–7, and is readily distinguished from the other aliphatic proton lines at higher fields. The latter resonances, in all cases, retain their fine structure up to at least 0.05 *M* $Co(acac)_2$, at which concentration the α-CH_n resonances are invariably a broad, featureless band. The chemical shifts of the β-, γ-, etc. CH_n resonances do not change significantly relative to internal tetramethylsilane, presumably because of a lack of Fermi contact interactions, and nothing apparently can be gained from inspection of this part of the spectrum.

The trends noted above are followed by a number of polyfunctional alcohols. In cases such as 2-methoxyethanol, 2-(2-ethoxyethoxy)-ethanol, ethylene glycol, 1,3- and 1,4-butanediol, 2-hydroxymethyltetrahydrofuran, and 2-hydroxymethyltetrahydropyran, the presence of more than one oxygen atom causes considerable overlap of the proton resonances. On addition of $Co(acac)_2$ to solutions of these compounds, resonances corresponding in intensity to the number of α-CH protons present shifted downfield in each case.

Allyl alcohol, benzyl alcohol, and phenol exhibited behavior quite different from the simple aliphatic compounds. In all three cases there were rapid shifts both upfield and downfield.

As a check on the influence of other functional

Can. J. Chem. Downloaded from www.nrcresearchpress.com by 188.143.235.115 on 09/06/12
For personal use only.

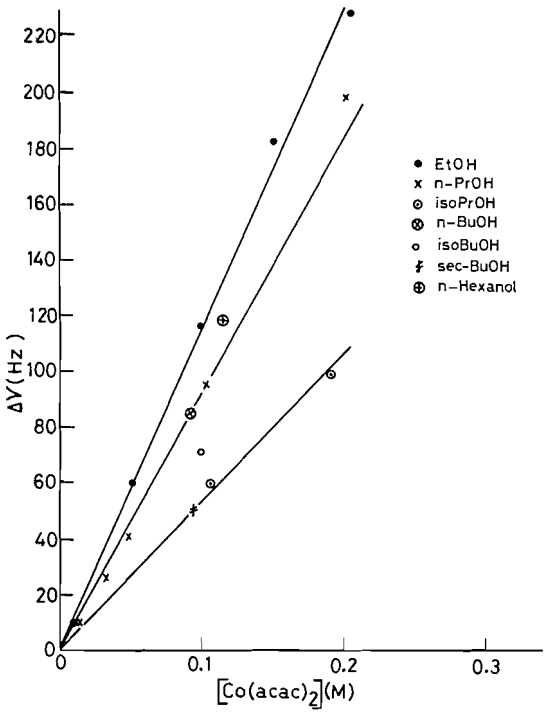

FIG. 2. Dependence of the change in chemical shift ($\Delta\nu$) of the α-CH_n resonances of saturated alcohols (1 *M* in $CDCl_3$) on the concentration of $Co(acac)_2$.

groups, we have also run the n.m.r. spectra of $CDCl_3$ solutions of dimethyl sulfoxide, ethyl methyl ketone, diethyl ether, tetrahydrofuran, 1,4-dioxane, 1,3,5-trioxane, 1,2-dimethoxyethane, and diglyme in the presence of $Co(acac)_2$. Although some of the oxygen donors form yellow solutions with $Co(acac)_2$, in all cases the lines shift to somewhat higher field and remain relatively narrow. Thus these functional groups should not affect the influence that $Co(acac)_2$ has on the spectra of compounds containing hydroxyl groups. Solutions of $Co(acac)_2$ and ethyl sulfide turn deep orange, suggesting a chemical reaction; the solutions remain paramagnetic, although there appears to be little effect on the n.m.r. spectra, either on the line widths or the chemical shifts.

Amines, however, behave very similarly to alcohols. On adding $Co(acac)_2$ to a solution of triethylamine, the methylene quartet moves downfield and loses its fine structure at about the same rate as does that of ethanol. The methylene quartet of diethylamine moves downfield even faster. Obviously amino groups will interfere with any investigations of compounds containing hydroxyl groups, and the influence of $Co(acac)_2$ on the ^1H n.m.r. spectra of amines is being examined further.

The effects of some other paramagnetic complexes on the n.m.r. spectra of amines and hydroxylic compounds were also investigated. Contact shifts with $Ni(acac)_2$ are approximately as large as with $Co(acac)_2$, although β-CH_n resonances tend to move slightly downfield rather than upfield. Line broadening is much more noticeable with $Ni(acac)_2$, however, with the result that loss of resolution of fine structure is much more pronounced.

No contact shifts were observed using Cu(ethyl acetoacetate)$_2$ either with alcohols or amines. In the case of ethanol, at least, the line broadening effects are much greater than those with $Co(acac)_2$. In the case of amines, the attenuation of the line broadening by the copper compound is rather remarkable. The presence of 5.6×10^{-3} *M* Cu(ethyl acetoacetate)$_2$ in a 1 *M* solution of triethylamine causes complete loss of resolution of the methylene quartet, leaving a broad band. The methyl resonance, on the other hand, is still a very well-resolved triplet. The effect of the copper compound on diethylamine is even more drastic and is illustrated in Fig. 3. The presence of only 3×10^{-5} *M* copper completely destroys the methylene resolution, although the methyl triplet is virtually unaffected and still exhibits ringing. When the copper concentration is raised to 6.2×10^{-4} *M*, the methylene resonance has virtually disappeared into the baseline, a change which is complete when the copper concentration is 3.4×10^{-3} *M*, although the methyl resonance is still an easily recognized triplet.

Discussion

In the presence of a Lewis base, the cobalt and nickel acetylacetonates exist as the labile monomers *trans*-$M(acac)_2L_2$ (M = Co, Ni; L = Lewis base) (12).

$$[3] \qquad M(acac)_2 + 2L \rightleftharpoons M(acac)_2L_2$$

Since the exchange of ligands L between complexed and uncomplexed sites is rapid on the n.m.r. time scale, the spectra are time-averaged, the various proton resonances being shifted from their normal diamagnetic values by an amount which is proportional to the concentration of the paramagnetic compound. Thus as $Co(acac)_2$ is added to a solution of a potential ligand, in this

Can. J. Chem. Downloaded from www.nrcresearchpress.com by 188.143.235.115 on 09/06/12
For personal use only.

Can. J. Chem. Downloaded from www.nrcresearchpress.com by 188.143.235.115 on 09/06/12
For personal use only.

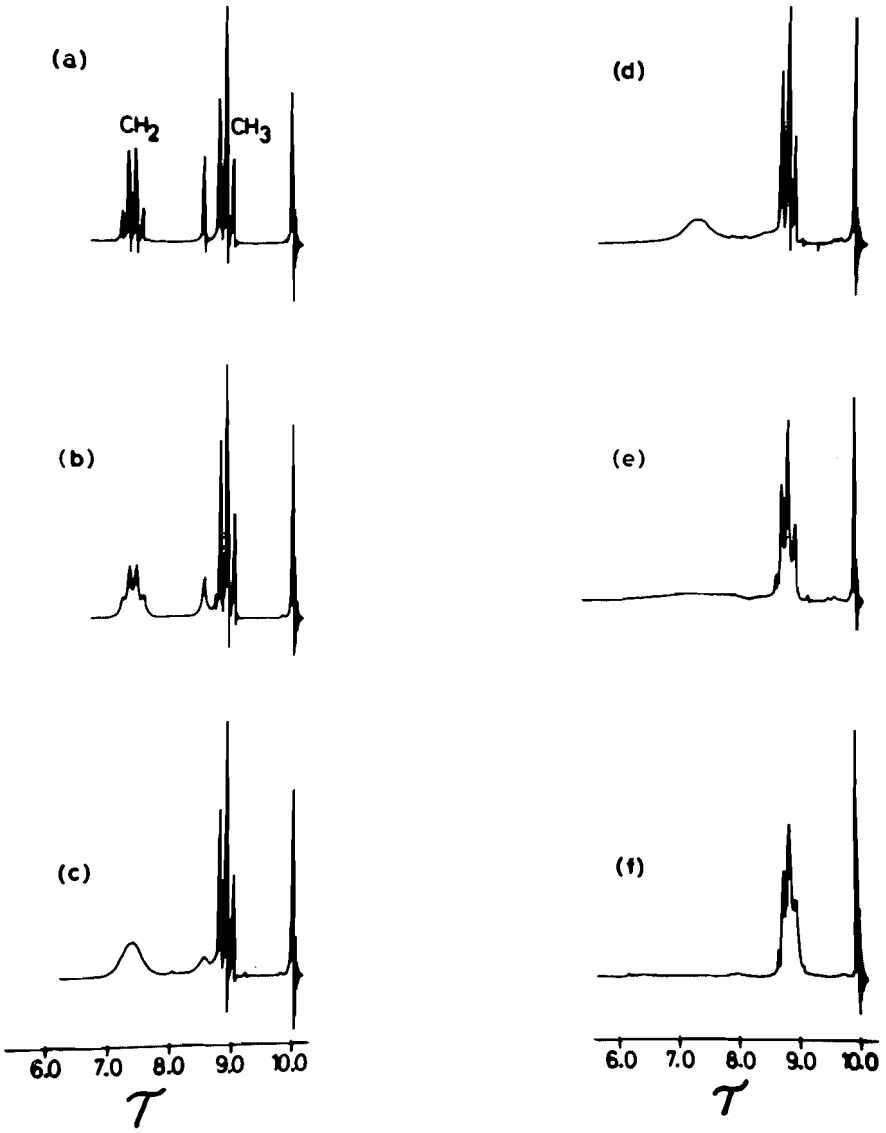

FIG. 3. Perturbation of the nuclear magnetic resonance spectrum of diethylamine (1 M in $CHCl_3$) by Cu(ethyl acetoacetate)$_2$. Concentrations of Cu(ethyl acetoacetate)$_2$: (*a*) 0, (*b*) ~ 6.0×10^{-6} M, (*c*) ~ 3.0×10^{-5} M, (*d*) ~ 6.2×10^{-5} M, (*e*) 6.2×10^{-4} M, and (*f*) 3.4×10^{-3} M.

work an alcohol, the proton resonances of L shift towards the resonance positions of the complex $Co(acac)_2L_2$. A number of reports have been published on the ^1H n.m.r. spectra of the complexes $Co(acac)_2L_2$ and $Ni(acac)_2L_2$ where L is pyridine (13), piperidine (13), α-, β-, and γ-picolines (13), aryl phosphines, arsines, amines, sulfides, halides, and isonitriles (14), substituted anilines (15), substituted pyridine *N*-oxides (16, 17) and quinoline *N*-oxides (18). No contact shifts were observed with bromobenzene, tris-*o*-tolylphosphine, triphenylarsine, triphenylamine, benzonitrile, and diphenyl sulfide (13). Contact shift data have been generally interpreted in terms of spin delocalization from the metal to the ligands L and it has been found that, as expected, both σ- and π-delocalization mechanisms can operate.

The correlation of the contact shift of the α-CH_n group of the saturated alcohols with structure (Fig. 2) is probably a result of steric interactions. It is seen that the contact shift is approximately the same for all the straight-chain alcohols, but is decreased somewhat when an alkyl substituent is on the β-carbon atom and decreased still further when substitution occurs on the α-carbon atom. The substituents probably have the effect of destabilizing the metal–ligand bond, thereby shifting the equilibrium of eq. 3 to the left. Since the observed contact shift is a weighted average of the chemical shifts of free and complexed L, a decrease in equilibrium constant will lead to smaller contact shifts.

Our results with compounds containing other functional groups as potential Lewis bases suggest that only amines will interfere. Although some of the ethers undoubtedly interact with $Co(acac)_2$, only slight shifts to higher field appear to occur. Ether linkages two or three carbon atoms away from a hydroxyl group may lead to chelation, but we have no evidence for such behavior at present.

The relatively large contact shifts with amines are probably a result of the much greater basicity of amines as compared with alcohols. Thus the equilibrium in eq. 3 will lie farther to the right, resulting in a greater proportion of the ligand being complexed and hence a larger contact shift. The difference between di- and triethylamine is probably a result of steric factors, although a great deal of work with nitrogen donors remains to be done. The effect of Cu(ethyl acetoacetate)$_2$ on the methylene resonance of diethylamine is quite remarkable, and work is now in progress to see if the result is general for secondary amines. It may be that different metal complexes will be specific for different functional groups.

The authors thank the National Research Council of Canada for financial support of this research and Mr. T. B. Grindley for carrying out some of the preliminary work.

1. W. A. Szarek, E. Dent, T. B. Grindley, and M. C. Baird. Chem. Commun. 953 (1969).
2. D. F. Evans. J. Chem. Soc. 2003 (1959).
3. D. R. Eaton and W. D. Phillips. Advan. Mag. Resonance, **1**, 103 (1965).
4. D. R. Eaton and W. D. Phillips. Advan. Mag. Resonance, **1**, 112 (1965).
5. D. R. Eaton and W. D. Phillips, Advan. Mag. Resonance, **1**, 147 (1965).
6. E. E. Zaev, V. K. Voronov, M. S. Shvartsberg, S. F. Vasilevsky, Yu. N. Molin, and I. L. Kotljarevsky. Tetrahedron Lett. 617 (1968).
7. C. C. McDonald and W. D. Phillips. Biochem. Biophys. Res. Commun. **35**, 43 (1969).
8. C. C. Hinckley. J. Amer. Chem. Soc. **91**, 5160 (1969).
9. J. B. Ellern and R. O. Ragsdale. Inorg. Syn. **11**, 84 (1968).
10. F. A. Cotton and J. P. Fackler, Jr. J. Amer. Chem. Soc. **83**, 2818 (1961).
11. D. P. Graddon. J. Inorg. Nucl. Chem. **14**, 161 (1960).
12. D. P. Graddon. Coordination Chem. Rev. **4**, 1 (1969).
13. J. A. Happe and R. L. Ward. J. Chem. Phys. **39**, 1211 (1963).
14. W. D. Horrocks, Jr., R. C. Taylor, and G. N. Lamar. J. Amer. Chem. Soc. **86**, 3031 (1964).
15. R. W. Kluiber and W. D. Horrocks, Jr. Inorg. Chem. **6**, 430 (1967).
16. R. W. Kluiber and W. D. Horrocks, Jr. Inorg. Chem. **5**, 152 (1966).
17. R. W. Kluiber and W. D. Horrocks, Jr. J. Amer. Chem. Soc. **87**, 5350 (1965).
18. R. W. Kluiber and W. D. Horrocks, Jr. J. Amer. Chem. Soc. **88**, 1399 (1966).
19. J. K. M. Sanders and D. W. Williams. Chem. Commun. **422** (1970).

Can. J. Chem. Downloaded from www.nrcresearchpress.com by 188.143.235.115 on 09/06/12
For personal use only.

Can. J. Chem. Downloaded from www.nrcresearchpress.com by 210.87.254.42 on 09/05/12
For personal use only.

The Heats of Solution and Related Thermodynamic Properties of Sodium Chlorate in Water and Water–Dioxane Mixtures

A. N. CAMPBELL AND O. BHATNAGAR[1]

Department of Chemistry, University of Manitoba, Winnipeg, Manitoba

Received August 17, 1970

The heats of solution of sodium chlorate in water, and in several water–dioxane mixtures, have been determined experimentally at concentrations of salt ranging from 0.01 molal to saturation. For the dilute region, a direct method was used but for the concentrated range the method was that of diluting the saturated solution. The free energy decreases due to dilution have been calculated from previously determined activity coefficients. Using these data, the entropy changes have been evaluated.

The graph of heat of solution *vs.* concentration of sodium chlorate passes through a minimum for the solutions more concentrated in dioxane, but not for water and weak dioxane mixtures. A tentative explanation of this is offered.

Canadian Journal of Chemistry, 49, 217 (1971)

The present paper is a continuation of the work on the electrical and thermodynamic properties of solutions of sodium chlorate and of lithium chlorate in water and in water–dioxane mixtures, which has been carried out in this laboratory over the last few years (1). In a recent paper (2) Campbell and Oliver reported the mean molal activity coefficients of sodium chlorate and of lithium chlorate in water, in 44.5 wt. % dioxane–water and in 64.5 wt. % dioxane–water. In the present work we have determined the heats of solution of $NaClO_3$ over the entire solubility range in water and in various water–dioxane mixtures, including those solvent mixtures, for which we had previously determined the activity coefficients.

These data have enabled us to determine the excess free energy and entropy of solution. A comparison of these thermodynamic data for the various solutions illustrates the effect of varying dielectric constant on the excess free energy and entropy of solution.

Experimental

Purity of Chemicals

The methods of purification have been described previously (2). The purified dioxane had a refractive index of $n_D^{25} = 1.4203$ and a density of 1.0283 g/cc. The accepted literature values are $n_D^{25} = 1.42025$ (3) and $d = 1.02804$ (4). The water, obtained by passage through an ion-exchange column, had a specific conductance of 2×10^{-7} mhos/cm.

Heats of Solution

The heats of solution were determined by two different methods, one applied to the dilute range and the other to the concentrated range. The heats of solution in the dilute range were determined in an apparatus which is represented in Fig. 1. Heats of solution in the concentrated range were determined as heats of dilution of the saturated solution, using an apparatus previously described (5). Such results are dependent for their accuracy upon the reliance which can be placed upon the

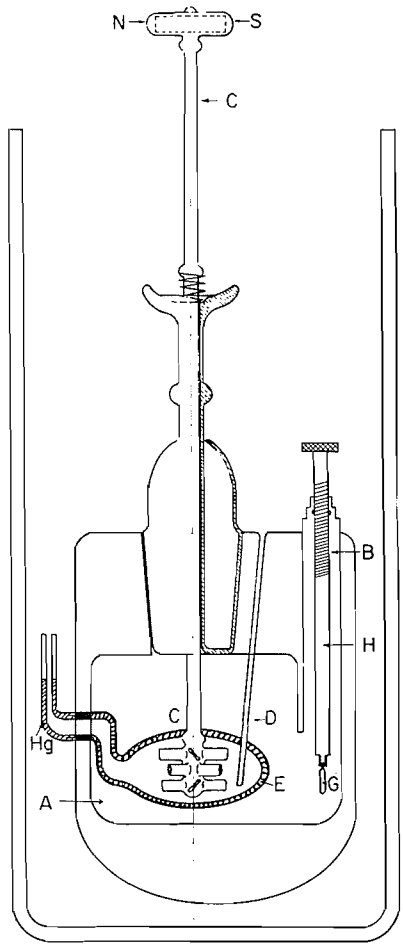

FIG. 1. Double-walled glass calorimeter.

[1]Postdoctorate Fellow.

Can. J. Chem. Downloaded from www.nrcresearchpress.com by 210.87.254.42 on 09/05/12
For personal use only.

direct determination of heat of solution in, say, 1 *m* solution. We found that our results by both methods lay on one smooth curve.

The calorimeter used for direct determination (Fig. 1) consists of a double-walled glass vessel of total capacity about 80 cc. The space between the inner and outer walls is evacuated and silvered. The inner compartment is divided into two parts, A and B. Part A is fitted with standard taper joint and a silvered glass stopper, which carries an exit tube housing the magnetic stirrer, C. The blades of the stirrer are bent in such a way as to create a whirlpool around the stirrer, which sucks solid salt into this area very quickly, ensuring quick solution of the salt. Compartment A also carries a thermistor well, D, for temperature sensing. The heating element, E, consists of platinum wire (resistance = 2 ohms approximately) and is sealed into a glass tube. Compartment B contains an ampoule, G, and a crushing device, H, consisting of a teflon screw. The ampoules are made from 6 mm Pyrex tubing, blown to 1 cm diameter, and 5 cm long. The ampoules are sealed under vacuum and attached to the teflon screw with polyethylene tubing. Screwing down the crushing device causes the ampoule to break.

The accuracy of the calorimeter was tested by determining the heat of reaction of THAM (tris(hydroxymethylamino) methane) with 0.1 *N* HCl. We obtained a value of 7136 ± 22 cal/mole, slightly higher than the reported value of 7104 cal/mole (6). We claim an overall accuracy of 1% for our results.

Results

The direct experimental results are reproduced in Table 1, which gives the direct heats of solution, heats of dilution, and derived heats of solution, as functions of molality and of $m^{1/2}$.

The derived thermodynamic quantities were obtained as follows. Campbell and Oliver (2) have reported the activity coefficients of $NaClO_3$ in water, in 44.5% dioxane and in 64.5% dioxane – water mixtures. They found that the mean molal activity coefficients could be represented by the equation

$$[1] \quad \ln\gamma = -Sm^{1/2} + Bm + Cm^{3/2} - Dm^2$$

where γ is the mean molal activity coefficient of the solute, S is the Debye–Hückel limiting slope, and B, C, and D are adjustable constants. The latter were evaluated from the experimental data, as described by Campbell and Oliver (2). In the absence of experimental work leading to γ values in the dilute region, we used the above equation to calculate γ in the dilute region. The activity coefficients were then used to calculate the excess free energy decrease of solution and from this the entropy change or $T\Delta S$ values, in the usual way. These values are reproduced in Table 2. The limiting or standard heats of solution ΔH^0, were obtained by plotting experimental ΔH's of solution against $m^{1/2}$ and extrapolating to $m = 0$. The results are expressed graphically in Fig. 2. Since sodium chlorate is insoluble in pure dioxane, experimental measurements were impossible but a reasonable value of ΔH^0 for pure dioxane was obtained from the so-called heat of transfer (ΔH_{trans}). This represents the difference between the heat of solution ΔH^0 in pure water and in a given dioxane–water solvent. The heats of transfer were evaluated for dioxane–water mixtures and these were plotted against the dielectric constant of the mixture. From this plot the value of ΔH_{trans} from water to pure dioxane was found to be 4660 cal/mole from which the ΔH^0 value for pure dioxane results as 620 cal/mole. The values of ΔH^0 for the mixed solvents, obtained in the above way, are also to be found in Table 2.

Discussion

Foz and Colomina (7) report a ΔH^0 value of 5.29 kcal/mole, as against our value of 5.28 kcal/mole. In obtaining their ΔH^0 value, however, Foz and Colomina plotted experimental ΔH values against m, the molality. A better procedure, and that adopted by us, is to plot ΔH against $m^{1/2}$. When the data of Foz and Colomina are treated in this way, a result of $\Delta H^0 = 5.40$ kcal/mole is obtained, a value somewhat higher than ours. The results of Foz and Colomina are higher than ours.

The plots of ΔH *vs.* $m^{1/2}$ are straight lines for pure water and for 44.5% dioxane but 50.0, 64.5, and 70.0% dioxane – water mixtures give curves passing through a minimum, and this minimum becomes more pronounced with increasing dioxane content, that is, with lower dielectric constant. According to theory, in the absence of ionic association, the experimental plot should lie above the limiting slope but this behavior is only observed with pure water as solvent. In all the dioxane–water mixtures, the experimental curves lie below the limiting slope, the deviation being more pronounced with increasing dioxane content, that is, with decreasing dielectric constant. Ionic association of course increases in the lower dielectric constant media.

Figure 3 is a plot of ΔH, ΔG, and $T\Delta S$ *vs.* m, for water and for two mixed solvents. The values of limiting ΔH and $T\Delta S$ decrease with decreasing dielectric constant but the value of the free energy

Can. J. Chem. Downloaded from www.nrcresearchpress.com by 210.87.254.42 on 09/05/12
For personal use only.

TABLE 1. Integral heats of solution of $NaClO_3$ in water

Heats of solution			Heats of dilution and derived heats of solution					Data of Foz and Colomina (7)		
m (mole/kg)	$m^{1/2}$	ΔH solution (kcal/mole)	m_1 (mole/kg)	$m_1{}^{1/2}$	m_2 (mole/kg)	ΔH dilution (cal/mole)	ΔH solution (kcal/mole)	m (mole/kg)	$m^{1/2}$	ΔH (kcal/mole)
(0.0000)	(0.0000)	(5.280)								
0.0082	0.0905	5.210	3.9280	1.9819	0.6888	954	3.510	0.1122	0.3349	5.238
0.0107	0.1034	5.206	4.2258	2.0556	0.7994	944	3.456	0.2011	0.4484	5.214
0.0818	0.2860	5.096	5.4050	2.3248	0.8011	1123	3.276	0.3505	0.5920	5.127
0.1042	0.3228	4.979	6.2415	2.4982	1.2849	1016	3.166	0.7977	0.8931	4.951
0.1579	0.3973	4.876	7.4623	2.7317	4.2258	415	3.041	1.3472	1.1606	4.772
0.2452	0.4951	4.811	8.7920	2.9651	3.9280	574	2.936	2.0027	1.4151	4.568
0.4086	0.6392	4.657	9.3403	3.0562	2.9075	816	2.898	2.7416	1.6557	4.380
0.6893	0.8302	4.464						3.5220	1.8767	4.209
0.8003	0.8945	4.400						4.4077	2.0994	4.046
0.9149	0.9565	4.380						5.3722	2.3178	3.900
1.0096	1.0047	4.306						6.3555	2.5210	3.778
1.0831	1.0407	4.224						7.7722	2.7878	3.668
1.2859	1.1339	4.180						8.5499	2.9240	3.576
1.4856	1.2188	4.083								
1.6202	1.2728	4.132								
1.8020	1.3423	3.996								
2.9062	1.7047	3.714								

Can. J. Chem. Downloaded from www.nrcresearchpress.com by 210.87.254.42 on 09/05/12
For personal use only.

TABLE 1 (*Continued*)

Integral heats of solution of $NaClO_3$ in 44.5% dioxane – 55.5% water

Heats of solution			Heats of dilution and derived heats of solution				
m (mole/kg)	$m^{1/2}$	ΔH solution (kcal/mole)	m_1 (mole/kg)	$m_1^{1/2}$	m_2 (mole/kg)	ΔH dilution (cal/mole)	ΔH solution (kcal/mole)
(0.0000)	(0.0000)	(4.920)					
0.0104	0.1019	4.862	1.4773	1.2154	0.2410	507	4.081
0.0319	0.1786	4.720	1.8241	1.3505	0.8885	292	3.988
0.1201	0.3465	4.686	2.2355	1.4951	0.3648	676	3.890
0.2402	0.4901	4.589	2.7342	1.6535	0.3660	758	3.804
0.3652	0.6043	4.566	3.4137	1.8476	1.2411	441	3.722
0.6583	0.8113	4.442					
0.7726	0.8789	4.396					
0.9495	0.9744	4.263					
1.3089	1.1440	4.145					

Integral heats of solution of $NaClO_3$ in 50% dioxane – 50% water

Heats of solution			Heats of dilution and derived heats of solution				
m (mole/kg)	$m^{1/2}$	ΔH solution (kcal/mole)	m_1 (mole/kg)	$m_1^{1/2}$	m_2 (mole/kg)	ΔH dilution (cal/mole)	ΔH solution (kcal/mole)
(0.0000)	(0.0000)	(4.060)					
0.0249	0.1578	4.192	1.6150	1.2708	0.1610	479	3.810
0.1125	0.3354	4.221	1.9555	1.3983	0.2062	559	3.713
0.1376	0.3709	4.254	2.3502	1.5330	0.7299	619	3.621
0.2056	0.4534	4.272	2.7751	1.6658	0.6290	698	3.602
0.3978	0.6307	4.379	3.3216	1.8225	1.3396	347	3.565
0.5180	0.7197	4.357					
0.6298	0.7931	4.301					
0.7509	0.8665	4.195					
0.9742	0.9870	4.078					
1.1754	1.0841	3.989					

Can. J. Chem. Downloaded from www.nrcresearchpress.com by 210.87.254.42 on 09/05/12
For personal use only.

TABLE 1 (*Concluded*)

Integral heats of solution of $NaClO_3$ in 64.5% dioxane – 35.5% water

Heats of solution			Heats of dilution and derived heats of solution				
m (mole/kg)	$m^{1/2}$	ΔH solution (kcal/mole)	m_1 (mole/kg)	$m^{1/2}$	m_2 (mole/kg)	ΔH dilution (cal/mole)	ΔH (kcal/mole)
(0.0000)	(0.0000)	(3.000)					
0.0122	0.1104	3.245	1.4703	1.2125	0.4514	439	3.551
0.0377	0.1941	3.271	1.6062	1.2673	0.4623	457	3.523
0.0441	0.2100	3.464	2.0695	1.4385	0.9624	335	3.425
0.0713	0.2670	3.567	2.3750	1.5411	1.1305	271	3.381
0.1067	0.3266	3.665	2.7334	1.6532	1.3820	214	3.366
0.1236	0.3515	3.793					
0.1622	0.4027	3.885					
0.2666	0.5163	4.085					
0.2668	0.5163	4.042					
0.3144	0.5607	3.977					
0.3839	0.6195	4.025					
0.4156	0.6446	3.946					
0.5203	0.7213	3.990					
0.6269	0.7917	3.873					
0.7554	0.8691	3.881					
0.8971	0.9471	3.767					
0.9618	0.9807	3.741					

Integral heats of solution of $NaClO_3$ in 70% dioxane – 30% water

Heats of solution			Heats of dilution and derived heats of solution				
m (mole/kg)	$m^{1/2}$	ΔH solution (kcal/mole)	m_1 (mole/kg)	$m_1{}^{1/2}$	m_2 (mole/kg)	ΔH dilution (cal/mole)	ΔH solution (kcal/mole)
(0.0000)	(0.0000)	(2.440)					
0.0228	0.1508	2.806	1.2181	1.1036	0.9871	87	3.173
0.0539	0.2321	2.969	1.4428	1.2011	0.6586	245	3.165
0.0937	0.3061	3.203	1.7766	1.3329	0.8010	185	3.135
0.1004	0.3168	3.143	1.9426	1.3936	0.7730	244	3.096
0.1594	0.3992	3.456					
0.1924	0.4386	3.401					
0.2944	0.5425	3.467					
0.3846	0.6201	3.547					
0.4860	0.6971	3.481					
0.5417	0.7360	3.461					
0.6548	0.8092	3.404					
0.7602	0.8719	3.341					
0.7896	0.8886	3.301					
0.9472	0.9732	3.230					

Can. J. Chem. Downloaded from www.nrcresearchpress.com by 210.87.254.42 on 09/05/12
For personal use only.

TABLE 2. Summary of thermodynamic properties

	100% water				44.5% dioxane – 55.5% water				64.5% dioxane – 35.5% water			
m (mole/kg)	γ	ΔG (kcal/mole)	ΔH (kcal/mole)	$T\Delta S$ kcal/mole)	γ	ΔG (kcal/mole)	ΔH (kcal/mole)	$T\Delta S$ (kcal/mole)	γ	ΔG (kcal/mole)	ΔH (kcal/mole)	$T\Delta S$ (kcal/mole)
0.01	0.915	−5.56	5.19	10.75	0.755	−5.79	4.86	10.65	0.526	−6.21	3.22	9.43
0.05	0.825	−3.78	5.07	8.85	0.579	−4.20	4.77	8.97	0.288	−5.02	3.47	8.49
0.10	0.772	−3.03	4.98	8.01	0.500	−3.55	4.71	8.26	0.207	−4.59	3.65	8.24
0.30	0.688	−1.87	4.76	6.63	0.392	−2.54	4.55	7.09	0.107	−4.07	3.96	8.03
0.50	0.645	−1.34	4.60	5.94	0.355	−2.05	4.44	6.49	0.096	−3.59	3.98	7.57
0.70	0.617	−0.99	4.67	5.46	0.334	−1.72	4.35	6.07	0.084	−3.35	3.90	7.25
0.90	0.597	−0.73	4.36	5.09	0.319	−1.48	4.27	5.75	0.077	−3.16	3.79	6.95
1.00	0.589	−0.63	4.32	4.95	0.313	−1.33	4.24	5.62	0.074	−3.09	3.74	6.83
1.25	0.570	−0.40	4.20	4.60	0.298	−1.17	4.16	5.33	0.068	−2.94	3.64	6.58
1.50	0.555	−0.22	4.13	4.35	0.286	−1.00	4.08	5.08	0.063	−2.79	3.56	6.35
1.75	0.543	−0.06	4.02	4.08	0.273	−0.87	4.02	4.89	0.060	−2.67	3.49	6.16
2.00	0.538	+.09	3.96	3.87	0.264	−0.76	3.95	4.71	0.058	−2.55	3.44	5.99
2.25	0.533	+.22	3.86	3.64	0.255	−0.66	3.90	4.56	0.057	−2.43	3.40	5.83
2.50	0.525	+.32	3.82	3.50	0.248	−0.57	3.85	4.42				
2.75	0.519	+.42	3.74	3.32	0.245	−0.47	3.80	4.27				
3.00	0.515	+.52	3.69	3.17	0.239	−0.39	3.76	4.15				
3.50	0.508	+.68	3.58	2.90	0.239	−0.21	3.70	3.91				
4.00	0.506	+.84	3.50	2.66	0.251	−0.00	3.63	3.63				
*0.00		−5.70	5.28	10.98		−6.00	4.92	10.92		−6.50	3.00	9.50
					Constants of eq. 1 $S = 3.1545$, $B = 3.6769$ $C = -2.1478$, $D = 0.4626$				Constants of eq. 1 $S = 7.2091$, $B = 8.5792$ $C = -5.2046$, $D = 1.2282$			

*Extrapolated values corresponding to $\Delta H°$, $\Delta G°$, and $T\Delta S°$.

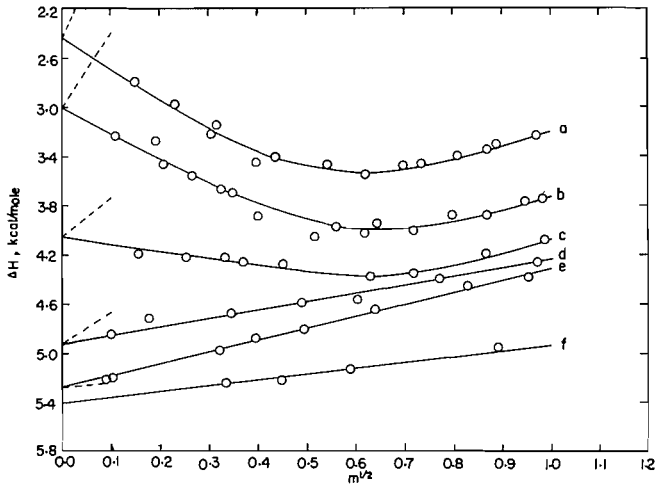

FIG. 2. Heats of solution (ΔH) *vs.* $m^{1/2}$ of $NaClO_3$ in water and water dioxane mixtures. (*a*) 70% dioxane – 30% water; (*b*) 64.5% dioxane – 35.5% water; (*c*) 50% dioxane – 50% water; (*d*) 44.5% dioxane – 55.5% water; (*e*) water; (*f*) the data of Foz and Colomina (7).

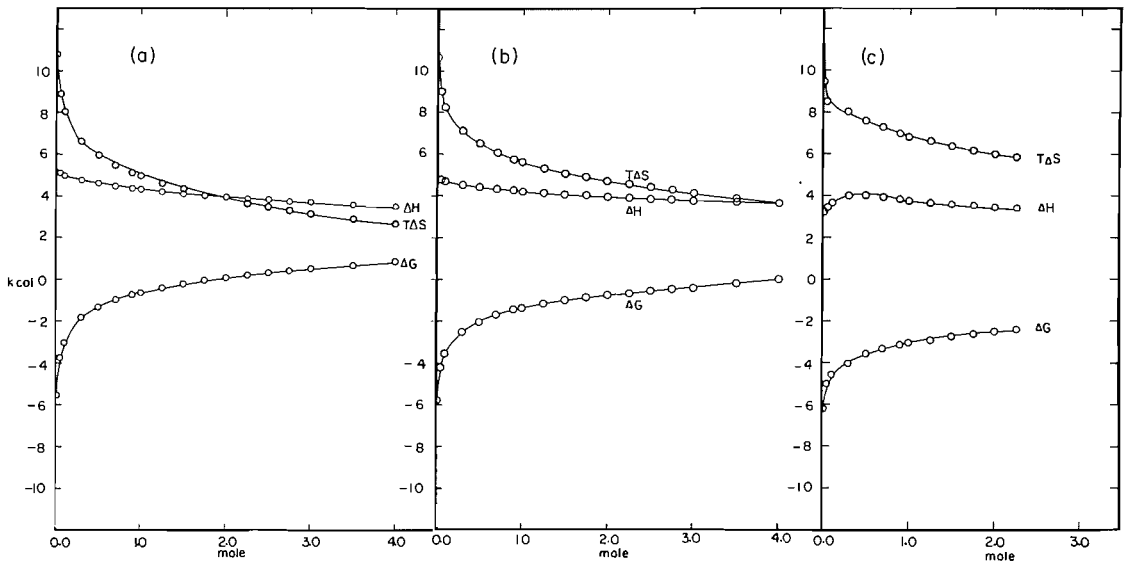

FIG. 3. (*a*) Plot of ΔH, ΔG, and $T\Delta S$ for water; (*b*) plot of ΔH, ΔG, and $T\Delta S$ for 44.5% dioxane – 64.5% H_2O; (*c*) plot of ΔH, ΔG, and $T\Delta S$ for 64.5% dioxane – 35.5% H_2O.

change increases. The lower values of ΔH^0 may be accounted for on the supposition that, as the content of dioxane increases, fewer hydrogen bonds, per mole of solvent, are broken.

The fact that a minimum occurs in the ΔH plot on three of the five curves, *viz.*, those for 50.0, 64.5, and 70.0% dioxane, may possibly be due to dioxane playing the major role in solvating the ions in the dilute region, while the process is reversed as the concentration of salt increases, the solvation then being principally a water solvation. The curves for the concentrated (salt) range are similar to those in water and 44.5% dioxane, where, presumably, the solvation is principally hydration. At first sight, this explanation seems unlikely, in view of the lower dielectric

Can. J. Chem. Downloaded from www.nrcresearchpress.com by 210.87.254.42 on 09/05/12
For personal use only.

constant of pure dioxane. Hyne (8), however, has shown that the addition of electrolyte to dioxane–water mixtures greatly increases the micro dielectric constant above its bulk value. However this may be, one can hardly avoid the conclusion from purely arithmetical considerations that dioxane solvation (low value of ΔH) must predominate in solutions low in salt, if the dioxane content is greater than 44.5%.

We thank our glass-blower, Mr. Bryn Easterbrook, for construction of the apparatus as well as helpful suggestions for its design.

1. A. N. CAMPBELL, E. M. KARTZMARK, and B. G. OLIVER. Can. J. Chem. **44**, 925 (1966); B. G. OLIVER and A. N. CAMPBELL. Can. J. Chem. **47**, 4207 (1969).
2. A. N. CAMPBELL and B. G. OLIVER. Can. J. Chem. **47**, 2671 (1969).
3. P. R. FREY and E. C. GILBERT. J. Amer. Chem. Soc. **59**, 1344 (1937).
4. H. SCHOTT. J. Chem. Eng. Data, **6**, 19 (1961).
5. A. N. CAMPBELL, E. M. KARTZMARK, and S. C. ANAND. Can. J. Chem. **48**, 1579 (1970).
6. R. J. IRVING and I. WASDO. Acta Chem. Scand. **18**, 195 (1964).
7. O. R. FOZ and M. COLOMINA. Anales De Fisica Quimica, **45B**, 137, (1949).
8. J. B. HYNE. J. Amer. Chem. Soc. **85**, 304 (1963).

Can. J. Chem. Downloaded from www.nrcresearchpress.com by 210.87.254.42 on 09/05/12
For personal use only.

Can. J. Chem. Downloaded from www.nrcresearchpress.com by 210.87.254.6 on 09/05/12
For personal use only.

A Technique for Determining Proton Chemical Shifts arising from Ring Current Effects: the Conformations of Triply Ortho-substituted Diphenyl Ethers[1]

J. J. BERGMAN AND W. D. CHANDLER
Department of Chemistry, University of Saskatchewan, Regina, Saskatchewan

AND

R. Y. MOIR
Department of Chemistry, Queen's University, Kingston, Ontario

Received July 22, 1970

A double-difference technique, making it possible to obtain that part of proton chemical shifts that originates in the shielding by the second ring in diphenyl compounds, is discussed. Evidence in support of the theory comes from the chemical shifts of aromatic ring protons in a family of triply ortho-substituted diphenyl ethers. The conformations of these ethers appear to be independent of the ortho-substituent, X ($X \neq H$), and the COC angle is shown to be approximately 120°.

Canadian Journal of Chemistry, 49, 225 (1971)

Studies of aromatic conformation rely heavily upon the magnetic anisotropy of the benzene ring. Separation of this effect from the others that influence the chemical shift of proton magnetic resonance (p.m.r.) signals has been difficult, and most of the previous studies (*e.g.*, ref. 1) have been content with qualitative or empirical evaluations. This paper describes a method for determining the "other ring" contribution quantitatively for diphenyl ethers.

In a previous paper (1) it was shown by nuclear magnetic resonance (n.m.r.) spectral analysis that triply ortho-substituted diphenyl ethers derived from metameconine (**1***a–c*) adopt the asymmetric, "H_a-inside" conformation as their principal conformation (Fig. 1). This conclusion was inferred from the observation that the n.m.r. signal from H_a occurs 0.27 to 0.38 p.p.m. to higher field in the diphenyl ethers than in the corresponding anisoles (**2***a–c*). At the same time, the signals from H_b and H_c are 0.13 to 0.18 and 0.067 to 0.20 p.p.m. to higher and lower field respectively when a similar comparison is made. H_a and H_b must see more of the ring current-induced shielding field of the metameconine ring than does H_c and the "H_a-inside" conformation of Fig. 1 accounts for this fact nicely. It was shown in the same paper that the two ortho-hydrogens of **1***d* are magnetically equivalent, indicating that the two "H-inside" conformations are exchanged at such a rate that the average lifetime is less than the lifetime of proton spin states.

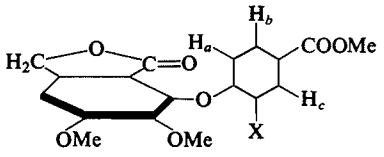

FIG. 1. "H_a-inside" conformation of triply ortho-substituted diphenyl ethers derived from metameconine.

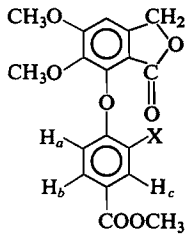

1

1*a*: X = NO_2; **1***b*: X = NH_2
1*c*: X = I; **1***d*: X = H

In theory, it should be possible to determine the average conformation with greater precision than

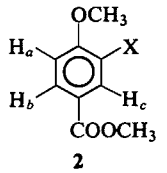

2

2*a*: X = NO_2; **2***b*: X = NH_2
2*c*: X = I; **2***d*: X = H
2*e*: X = OCH_3; **2***f*: X = Cl
2*g*: X = CN

[1]Much of this work is taken from the Ph.D. Thesis of W. D. Chandler, Queen's University, Kingston, August 1965 and was presented at the National Meeting of the Chemical Institute of Canada, in Montreal, June, 1965.

Can. J. Chem. Downloaded from www.nrcresearchpress.com by 210.87.254.6 on 09/05/12
For personal use only.

was done in the previous work, since the "other-ring" shielding is highly conformation dependent. The conformation, or geometrical relationship of the two rings, can, except for the carbon–oxygen bond lengths, be described in terms of three angular parameters. These are the COC bond angle and the two angles defining the rotation of each ring relative to the plane containing the COC bond. Every conformation will fix the geometric relation of H_a, H_b, and H_c to the other ring and, by the use of some appropriate model (2–5), the "other-ring" shielding at these protons could be calculated. If, at the same time, there were a method of extracting the "other-ring" shielding for each of H_a, H_b, and H_c from their chemical shifts, these experimental values could be related to the calculated ones and the average conformation deduced. There would be three equations, one for each of the three protons, to calculate the three unknown angles. In practice, such a procedure would be difficult for two reasons: (*i*) the "other-ring" shielding must be averaged over weighted values of the angles as the n.m.r. spectrum is obtained for a mobile system. Doing this averaging could be a formidable task unless reasonable guesses were made as to the limits to be imposed on the angles; (*ii*) the total chemical shift is dependent upon a number of factors, the magnetic anisotropy of the second ring being only one of them.

The next section describes a method of extracting the "other-ring" effects from experimental chemical shifts.

First-order, Double-difference Method

The discussion is restricted to the determination of "other-ring" effects for protons of triply ortho-substituted diphenyl ethers such as **1***a*–**1***c*. Our method requires that the related disubstituted ether (**1***d*) and anisoles (**2***a*–**2***d*) be available for comparison.

Let $\delta_{DX}{}^j$ be the chemical shift observed for the *j*th ring proton (H_a, H_b, or H_c) in a diphenyl ether such as **1***a*–**1***c*, *i.e.* with X not hydrogen. The simplest possible theory would be that this chemical shift could be thought of as made up of independent contributions from: (*i*) the substituent X, $\delta_X{}^j$, (*ii*) the rest of the molecule but not including "other-ring" shielding, $\delta_D{}^j$, and (*iii*) the "other-ring" shielding, $\delta_{\omega X}{}^j$, which depends on conformation. Thus,

$$\delta_{DX}{}^j = \delta_X{}^j + \delta_D{}^j + \delta_{\omega X}{}^j$$

In practice this model was found to work well enough to inspire confidence in the approach, but considerable improvement was obtained by the introduction of a parameter $\delta_{D,X}{}^j$, which expresses the fact that the contributions of D and X are not quite independent. With this term added the working equation is [1].

$$[1] \qquad \delta_{DX}{}^j = \delta_D{}^j + \delta_X{}^j + \delta_{D,X}{}^j + \delta_{\omega X}{}^j$$

As shown later this very simple model satisfied several experimental tests. For the anisoles such as **2***a*–**2***c*

$$[2] \qquad \delta_{AX}{}^j = \delta_A{}^j + \delta_X{}^j + \delta_{A,X}{}^j$$

where $\delta_{AX}{}^j$ is the chemical shift of the *j*th proton in the appropriately substituted anisole. Subtracting [2] from [1] for the same X and *j* gives

$$[3] \quad \delta_{DX}{}^j - \delta_{AX}{}^j = (\delta_D{}^j - \delta_A{}^j) + (\delta_{D,X}{}^j - \delta_{A,X}{}^j) + \delta_{\omega X}{}^j$$

When X = H (**1***d* and **2***d*) eq. 3 becomes

$$[4] \quad \delta_{DH}{}^j - \delta_{AH}{}^j = (\delta_D{}^j - \delta_A{}^j) + (\delta_{D,H}{}^j - \delta_{A,H}{}^j) + \delta_{\omega H}{}^j$$

The difference between [3] and [4] gives the double-difference eq. 5.

$$[5] \quad \Delta_X{}^j \equiv (\delta_{DX}{}^j - \delta_{AX}{}^j) - (\delta_{DH}{}^j - \delta_{AH}{}^j) = (\delta_{D,X}{}^j - \delta_{A,X}{}^j) - (\delta_{D,H}{}^j - \delta_{A,H}{}^j) + (\delta_{\omega X}{}^j - \delta_{\omega H}{}^j)$$

Were it not for the two non-linear terms, $\Delta_X{}^j$ would be a direct experimental measure of the difference in "other-ring" shielding for diphenyl ethers with X = H and X ≠ H, and if the assumption were made that $\delta_{\omega X}{}^j$ is independent of the substituent X, then eq. 5 would predict $\Delta_X{}^j$ to be a constant throughout a given family. Although the number of compounds in family **1** was limited, the observation (1) that $\Delta_X{}^j$ varies with X far beyond experimental error suggests that $\delta_{\omega X}{}^j$ is not substituent independent, or that the non-linear terms are important or both.

Equation 5 may be further simplified if use is made of the separability postulate.[2] The interaction shifts are written as

$$[6] \qquad \delta_{Y,Z}{}^j = I_Y{}^j I_Z{}^j$$

[2]A discussion of this postulate is given by Leffler and Grunwald (6) under the theory of extrathermodynamic relationships.

Can. J. Chem. Downloaded from www.nrcresearchpress.com by 210.87.254.6 on 09/05/12
For personal use only.

the product of separate parameters for each part, provided that the interaction is small or has a direction that remains approximately constant for the family to be compared. Then eq. 5 becomes

$$[7]\quad \Delta_X{}^j = (I_D{}^j I_X{}^j - I_A{}^j I_X{}^j) - (I_D{}^j I_H{}^j - I_A{}^j I_H{}^j) + (\delta_{\omega X}{}^j - \delta_{\omega H}{}^j)$$

$$[8]\quad \Delta_X{}^j = (I_X{}^j - I_H{}^j)(I_D{}^j - I_A{}^j) + (\delta_{\omega X}{}^j - \delta_{\omega H}{}^j)$$

The use of [8] is made difficult by the two X-dependent terms on the right side. However, if $\delta_{\omega X}{}^j$ were independent of X (X ≠ H), a plot of $\Delta_X{}^j$ *vs.* $I_X{}^j - I_H{}^j$ would result in a straight line whose intercept on the $\Delta_X{}^j$ axis would be the desired $\delta_{\omega X}{}^j - \delta_{\omega H}{}^j$ for a mythical diphenyl ether with the same conformation as the other ethers (X ≠ H) but for which the electronic properties of X would be the same as those of H. The problem with this analysis is that the interaction parameters $I_X{}^j$ are not known.

There have been attempts to correlate the chemical shifts of aromatic protons with substituent parameters such as Hammett's σ values (7), and *d* values of Martin and Dailey (8), and *Q* values (9–11).[3] Since all of these parameters have been used to explain non-additive chemical shifts with some success, it is not unreasonable to assume that the $I_X{}^j$ parameters might be related in some way to them. If a linear relationship were to hold, the following equations would be obtained.

$$[9]\quad \Delta_X{}^a = A(d_m{}^X - d_m{}^H) + (\delta_{\omega X}{}^a - \delta_{\omega H}{}^a)$$
$$\Delta_X{}^a = B(\sigma_m{}^X - \sigma_m{}^H) + (\delta_{\omega X}{}^a - \delta_{\omega H}{}^a)$$

$$[10]\quad \Delta_X{}^b = C(d_p{}^X - d_p{}^H) + (\delta_{\omega X}{}^b - \delta_{\omega H}{}^b)$$
$$\Delta_X{}^b = D(\sigma_p{}^X - \sigma_p{}^H) + (\delta_{\omega X}{}^b - \delta_{\omega H}{}^b)$$

$$[11]\quad \Delta_X{}^c = F(d_o{}^X - d_o{}^H) + (\delta_{\omega X}{}^c - \delta_{\omega H}{}^c)$$
$$\Delta_X{}^c = G(Q^X - Q^H) + (\delta_{\omega X}{}^c - \delta_{\omega H}{}^c)$$

where *A*, *B*, *C*, *D*, *E*, *F*, and *G* are all constants. Since the σ, *d*, and *Q* parameters are known or can be calculated, an experimental way is open to test the double-difference theory and its underlying assumptions and, at the same time, to obtain "other-ring" shielding data.

[3]W. B. Smith, private communication. For purposes of this work the *Q* values for NH_2 and NO_2 were taken to be −0.7 and 6.3, respectively (11).

Results

To test the method outlined above a new series of triply ortho-substituted diphenyl ethers (**3**) was prepared. This particular series was chosen because (*i*) it was easier to synthesize than the corresponding metameconine series (**1**) and (*ii*) the two trichlorophenyl ring protons are equivalent, can easily be identified, and their signal does not interfere with the *ABC* pattern of the other three aromatic protons.

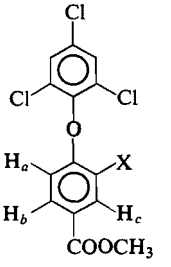

3

3*a*: X = NO_2; **3***b*: X = NH_2
3*c*: X = I; **3***d*: X = H
3*e*: X = OCH_3; **3***f*: X = Cl
3*g*: X = CN

The n.m.r. spectrum of each ether was taken along with that of the corresponding anisole (**2**) at ambient temperature. In all cases concentration effects were minimized. To insure accuracy of the chemical shift data, the aromatic region of each spectrum was reproduced to within ±0.2 Hz by an *ABC* or *AA'BB'* calculation. The experimental values for $\Delta_X{}^j$ are given in Table 1.

An excellent linear, least-squares correlation was obtained from a plot[4] of $\Delta_X{}^b$ against σ_p (Fig. 2), with a standard deviation of 0.005 p.p.m.

TABLE 1. $\Delta_X{}^j$ values for the diphenyl ether series **3***

X	$\Delta_X{}^a$ (p.p.m.)†	$\Delta_X{}^b$ (p.p.m.)†	$\Delta_X{}^c$ (p.p.m.)†
NO_2	−0.419‡	−0.107†	0.165
NH_2	−0.408	−0.167	0.118
I	−0.398	−0.140	0.097
CN	−0.375	−0.110	0.128
Cl	−0.402	−0.132	0.112
OCH_3	−0.382	−0.143	0.132

*In solution in chloroform-*d*.
†The estimated experimental error is ±0.007 p.p.m.
‡The δ values were measured relative to tetramethylsilane so as to increase as the applied magnetic field decreases. The negative sign indicates that H_a and H_b are more shielded in the diphenyl ether than in the corresponding anisole.

[4]σ values have been taken from reviews by Jaffé (12) and Ritchie and Sager (13).

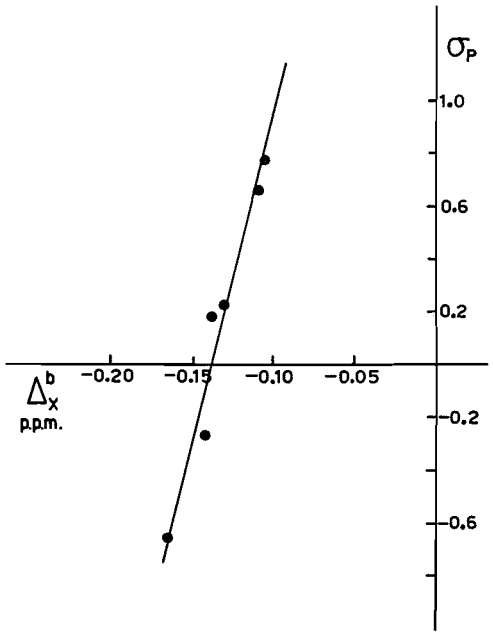

FIG. 2. Plot of $\Delta_X{}^b$ *vs.* σ_p.

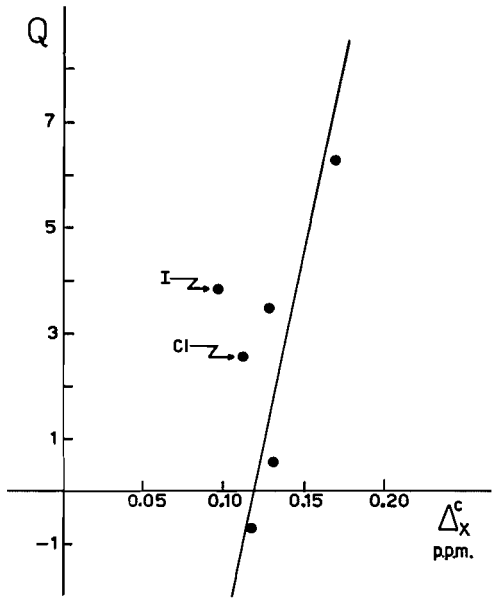

FIG. 3. Plot of $\Delta_X{}^c$ *vs.* Q.

and a correlation coefficient of 0.97. Using $\sigma_p{}^H = 0.00$ and the equation for the line ($\Delta_X{}^b = -0.149 + 0.0395\sigma_p{}^X$), $\delta_{\omega X}{}^b - \delta_{\omega H}{}^b$ was calculated to be -0.140 ± 0.002 p.p.m., well within the estimated experimental error. By comparison, the average value, $\bar{\Delta}_X{}^b$, for the six compounds studied is -0.133 p.p.m. with a standard deviation of 0.020 p.p.m. As expected, the correlation between $\Delta_X{}^b$ and d_p was equally good, since d_p and σ_p themselves correlate well (8). It would seem that there is an experimental justification for the approach used for H_b.

There is a poorer correlation between $\Delta_X{}^c$ and Q (Fig. 3) or d_o with the points for X = I and X = Cl deviating from the best straight line drawn for the other four substituents by 0.03 to 0.05 p.p.m. Without these two points the standard deviation is 0.010 p.p.m. and the correlation coefficient is 0.89. Using the known value for Q^H, $\delta_{\omega X}{}^c - \delta_{\omega H}{}^c$ was calculated to be 0.135 ± 0.003 p.p.m., again within experimental error. With all six points included, the standard deviation increased to 0.018 p.p.m. while $\delta_{\omega X}{}^c - \delta_{\omega H}{}^c$ was 0.123 ± 0.008 p.p.m. The average value for the six compounds is 0.125 p.p.m. with a standard deviation of 0.023 p.p.m. The inability of substituent parameters to account for the chemical shifts of protons ortho to I and, to a lesser extent, to Cl, is well known (7, 8). However, the present deviation of 0.05 p.p.m. is lower than that observed by these single-difference techniques. In light of the earlier work on substituent parameters, it is surprising that the CN group does not also cause a large deviation.

$\Delta_X{}^a$ does not correlate with either σ_m (Fig. 4) or d_m within experimental error although there is a trend of $\Delta_X{}^a$ becoming slightly less negative with decreasing σ_m and with increasing d_m. The standard deviation from a straight line is 0.018 p.p.m. with a correlation coefficient of 0.06. By comparison, the average value $\bar{\Delta}_X{}^a = -0.396$ p.p.m. with a standard deviation of 0.017 p.p.m. It is this average value that will be used in subsequent discussion of $\delta_{\omega X}{}^a - \delta_{\omega H}{}^a$.

It is understandable that $\Delta_X{}^a$ would give such poor correlation with substituent parameters as H_a, because of its proximity to the trichlorophenyl ring, would be most affected by deviations from an X-independent conformation; small variations would be less significant for H_b and H_c. In addition, d_m and σ_m vary over a smaller range than do the corresponding ortho and para parameters used for the six substituents. Considering the inherent errors in the substituent parameters and the reasonably small variations in the $\Delta_X{}^j$ values, it is satisfying that the correlations for H_b and H_c are as good as they are.

Can. J. Chem. Downloaded from www.nrcresearchpress.com by 210.87.254.6 on 09/05/12
For personal use only.

Can. J. Chem. Downloaded from www.nrcresearchpress.com by 210.87.254.6 on 09/05/12
For personal use only.

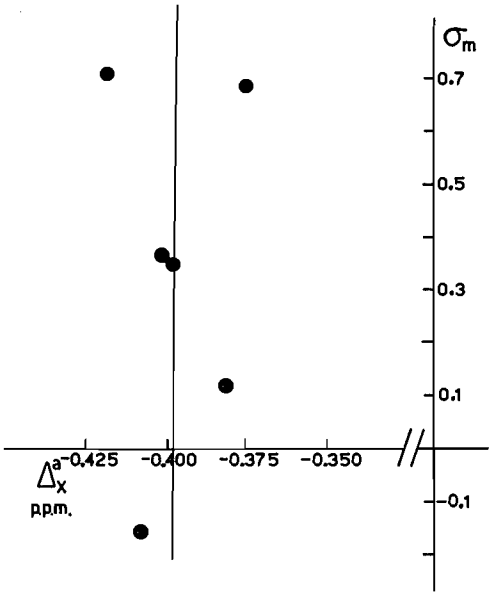

FIG. 4. Plot of $\Delta_X{}^a$ *vs.* σ_m.

Further evidence in favor of the theory can be obtained from a more explicit consideration of the conformations involved. If each diphenyl ether in series **3** (X ≠ H) adopts only the "H_a-inside" conformation[5] then

$$[12] \qquad \delta_{\omega X}{}^j = \lambda_0{}^j$$

where $\lambda_0{}^j$ is the "other-ring" shielding in that conformation, assuming that the COC bond angle and other parameters do not vary with X. To account for the equivalency of H_a and X, and H_b and H_c when X = H where $\lambda_\pi{}^j$ is the "other-

$$[13] \qquad \delta_{\omega H}{}^j = (\lambda_0{}^j + \lambda_\pi{}^j)/2$$

ring" shielding for the jth proton in the "H_a-outside" conformation (the ring has been rotated through 180°). At this level of approximation

$$[14] \qquad \delta_{\omega X}{}^j - \delta_{\omega H}{}^j = (\lambda_0{}^j - \lambda_\pi{}^j)/2$$

Since H_b and H_c would exchange places in a rotation of the X-containing ring through 180°, $\lambda_0{}^b = \lambda_\pi{}^c$ and $\lambda_\pi{}^b = \lambda_0{}^c$. Therefore,

$$[15] \quad \delta_{\omega X}{}^b - \delta_{\omega H}{}^b = (\lambda_0{}^b - \lambda_\pi{}^b)/2 = (\lambda_\pi{}^c - \lambda_0{}^c)/2 = -(\delta_{\omega X}{}^c - \delta_{\omega H}{}^c)$$

[5]Evidence from variable temperature n.m.r. studies (to be presented in a later paper) indicates this assumption is valid.

The experimental data show that the relationship expressed by [15] is observed, as $\delta_{\omega X}{}^c - \delta_{\omega H}{}^c = 0.135 \pm 0.003$ p.p.m. and $\delta_{\omega X}{}^b - \delta_{\omega H}{}^b = -0.140 \pm 0.002$ p.p.m. Thus the model has passed an important test that is independent of any particular theory for the source of the magnetic anisotropy in aromatic rings.

The data obtained for series **3** indicate that the double-difference technique works well and that the assumption that the ether conformation is independent of X is a reasonable one.

Determination of Conformation

The three angular parameters θ, φ, and ψ necessary to fix the conformation of a diphenyl ether can be defined as follows: θ is the COC bond angle, φ is the angle the ring containing H_a, H_b, and H_c makes with the COC plane, and ψ is the angle the trichlorophenyl ring (the "other-ring") makes with the plane perpendicular to the COC plane but containing the CO bond. Such a definition means that when the molecule is in the "H_a-inside" conformation (Fig. 1), both φ and ψ are zero. The signs of φ and ψ are set as being positive for counterclockwise rotation when viewed along the respective CO bonds toward the oxygen.

If z_j and ρ_j are the coordinates defining the distance of H_j above the plane of the trichlorophenyl ring and the distance in the plane of the ring from its center, respectively (Fig. 5), then it is a straightforward matter to derive expressions for these coordinates in terms of the three angular parameters.

Although it represents an oversimplification, it is, nonetheless, instructive to see what happens if both φ and ψ are set equal to zero ("H_a-inside" conformation). In such a conformation, the shielding at H_a and H_b becomes a maximum. Using the appropriate calculated values of ρ and

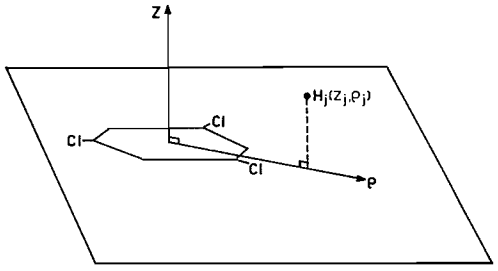

FIG. 5. Coordinate system relative to the center of the trichlorophenyl ring of series **3**.

Can. J. Chem. Downloaded from www.nrcresearchpress.com by 210.87.254.6 on 09/05/12
For personal use only.

TABLE 2. "Other-ring" shielding values calculated for the "H_a-inside" conformation*

θ	λ_0^a (p.p.m.)	λ_0^b (p.p.m.)	λ_0^c (p.p.m.)
110	−2.722	−0.358	0.038
115	−2.026	−0.284	0.047
120	−1.500	−0.222	0.056
130	−0.811	−0.126	0.067

*$\phi = \psi = 0$. See Fig. 1.

z, and the ring current shielding tables of Johnson and Bovey (4) the "other-ring" shielding shift has been calculated for each ring proton. These values, which are presented in Table 2 for four different θ's, are the λ_0^j used in eqs. 12 to 15 (the subscript 0 means that $\phi = 0$). For purposes of obtaining this datum, the CO length, L, was taken to be 1.28 Å, the value found by Toussaint (14) for 4,4′-dibromodiphenyl ether. Tables supplied by Farnum and Wilcox (5) gave similar values for λ_0^j although they are larger in magnitude by 10 to 20% than those obtained using the tables of Johnson and Bovey.

Since $\delta_{\omega X}^j - \delta_{\omega H}^j$ would be $(\lambda_0^j - \lambda_\pi^j)/2$ for the "H_a-inside" conformation (from eq. 14), these have been calculated for the same COC angles and are shown in Table 3.

On the basis of a pure "H_a-inside" conformation, the three calculated values for $\delta_{\omega X}^j - \delta_{\omega H}^j$ are not internally consistent for any COC angle, θ, when compared with the experimental ones (−0.396, −0.140, and 0.135 p.p.m.). For example, if the experimental and calculated values for $\delta_{\omega X}^b - \delta_{\omega H}^b$ or $\delta_{\omega X}^c - \delta_{\omega H}^c$ are matched, θ would have to be in the neighborhood of 120°. At this angle, the calculated $\delta_{\omega X}^a - \delta_{\omega H}^a$ is more than twice the experimental −0.396 p.p.m. Common sense suggests that the actual conformation must account for librations in the angles φ and ψ even if H_a is "inside". How large these librations should be and how the infinite number of conformations generated by them should be averaged to give an average value of $\delta_{\omega X}^j - \delta_{\omega H}^j$ is difficult to judge.[6] However, the use of equations for z and ρ and tables of ring shielding parameters shows that as φ and ψ increase from zero, the shielding drops off far more rapidly for H_a than for either H_b or H_c. For example, with $\theta = 120°$, if $\phi = \psi = 15°$, $\delta_{\omega X}^j - \delta_{\omega H}^j$ would be −0.46, −0.12, and 0.12 p.p.m. for $j = a$, b, and c, respectively. This assumes that when X = H, the two "H-inside" conformations with $\phi = 15$ and 165° are still equally probable to account for magnetic equivalence. Thus it is quite reasonable to have $\theta = 120°$ and $\delta_{\omega X}^j - \delta_{\omega H}^j = -0.40$, −0.14, and 0.14 p.p.m. provided that ϕ_{av} and ψ_{av} are sufficiently large.[7]

TABLE 3. $(\lambda_0^j - \lambda_\pi^j)/2$ calculated for the "H_a-inside" conformation*

θ	$(\lambda_0^a - \lambda_\pi^a)/2$ (p.p.m.)†	$(\lambda_0^b - \lambda_\pi^b)/2$ (p.p.m.)	$(\lambda_0^c - \lambda_\pi^c)/2$ (p.p.m.)
110	−1.454	−0.198	0.198
115	−1.107	−0.165	0.165
120	−0.844	−0.139	0.139
130	−0.500	−0.096	0.096

*$\phi = \psi = 0$. See Fig. 1.
†λ_π^a is approximately 0.190 p.p.m. regardless of the value of θ.

Although no estimates of the COC bond angle have been made previously for diphenyl ethers as highly substituted as those used in this study, Toussaint (14) estimated the angle in solid 4,4′-dibromodiphenyl ether to be 123° by X-ray studies and Leonard and Sutton (15) obtained a value of 116 ± 4° for diphenyl ether itself from dipole moment studies. The present work suggests an angle not larger than 120° but probably greater than 115°, surprisingly in good agreement with the literature when one considers the simplicity of the model used.

Besides the previously mentioned simplifications, the ring current picture is itself a classical model and may not adequately give a three-dimensional representation of the associated magnetic field. The π-current is undoubtedly more dispersed than the two currents separated by 1.28 Å in the Johnson–Bovey model (the Farnum–Wilcox, double torroidal-shell model predicts a slightly larger value for θ). How substituents such as three chlorines affect the ring current is, of course, unknown but the possibility of the effect being substantial cannot be ruled out.

Finally, although a specific series of diphenyl ethers was studied, any group of diphenyl com-

[6]Work is presently underway on computer averaging of the possible conformations to obtain better estimates of $\delta_{\omega X}^j - \delta_{\omega H}^j$ to compare with the experimental values.

[7]$\delta_{\omega X}^a - \delta_{\omega H}^a$ can be made equal to −0.40 p.p.m ($\theta = 120°$) if the conformation is taken to be 70% pure "H_a-inside" and 30% "H_a-outside". However, $\delta_{\omega X}^b - \delta_{\omega H}^b$ would then be −0.05 p.p.m., a value far too low to be acceptable. Also see footnote 5.

Can. J. Chem. Downloaded from www.nrcresearchpress.com by 210.87.254.6 on 09/05/12
For personal use only.

pounds could have been used provided that a corresponding group of monophenyls was also available. An extension to benzophenones, diphenylmethanes, and diphenyl sulfides is presently underway.

Experimental

All nuclear magnetic resonance (n.m.r.) data reported were recorded using a Varian A-60-A spectrometer on a scale of 100 Hz sweep width, calibrated by means of a side-band method. All the lines in the aromatic 3- and 4-proton region were reproduced to within ±0.2 Hz by means of *ABC* or *AA'BB'* calculations done by means of the computer. $\Delta_X{}^J$ values were obtained as follows: the aromatic proton chemical shifts were measured on the corrected 100 Hz sweep width relative to a generated side-band of tetramethylsilane as an internal standard (2% *v/v*) and the four appropriate shifts were used to calculate $\Delta_X{}^J$. Because tetramethylsilane was used as the standard for shift measurements, negative values of $\Delta_X{}^J$ indicate that the *j*th proton was more shielded in the diphenyl ether than in the corresponding anisole. All the compounds were dissolved in chloroform-*d* at a concentration less than 9 mg/0.5 ml. No concentration effects were noticed provided the concentration was kept below this value. In many cases no concentration effects were noticed at all.

Melting points were determined on a Kofler, micro hot stage apparatus and are reported uncorrected.

The preparation and properties of the following have been described previously (1, 17): methyl 4-methoxy-3-nitrobenzoate (**2***a*); methyl 3-amino-4-methoxybenzoate (**2***b*); methyl 3-iodo-4-methoxybenzoate (**2***c*); methyl 4-methoxybenzoate (**2***d*); methyl 3,4-dimethoxybenzoate (**2***e*); 2-(4′-carbomethoxy-2′-nitrophenoxy)-1,3,5-trichlorobenzene (**3***a*); 2-(2′-amino-4′-carbomethoxyphenoxy)-1,3,5-trichlorobenzene (**3***b*); 2-(4′-carbomethoxy-2′-iodophenoxy)-1,3,5-trichlorobenzene (**3***c*); 2-(4′-carbomethoxyphenoxy)-1,3,5-trichlorobenzene (**3***d*); 2-(4′-carbomethoxy-2′-methoxyphenoxy)-1,3,5-trichlorobenzene (**3***e*).

Methyl 3-Chloro-4-methoxybenzoate (2f)

3-Chloro-4-hydroxybenzoic acid (0.5 g, m.p. 170–172°) was dissolved in 2 *N* aqueous sodium hydroxide (20 ml) and dimethyl sulfate (5 ml) was added. Additional base was added as needed to maintain a basic solution. The solution was allowed to stand overnight before being acidified with dilute hydrochloric acid to produce 3-chloro-4-methoxybenzoic acid (0.48 g), m.p. 114–115° (uncorrected). The methylated acid was refluxed for 10 h with methanol (30 ml), methyl iodide (3.0 ml), potassium carbonate (0.6 g), and a little water. Dilution of the solution with water gave the crude product (0.4 g) which was recrystallized from ligroin (b.p. 100–115°) as long white needles, m.p. 94–95° (uncorrected). A literature value of 94–95° is reported for this compound (16).

Methyl 3-Cyano-4-methoxybenzoate (2g)

Methyl 3-amino-4-methoxybenzoate (3.6 g) was dissolved in 6 *N* hydrochloric acid. After the solution had been cooled to below 5°, sodium nitrite (1.5 g) was added in small amounts with stirring. A solution of cuprous cyanide was prepared as follows: To a solution of copper sulfate (6.25 g) and sodium chloride (1.62 g) in hot water (20 ml), a solution of sodium bisulfite (1.32 g) and sodium hydroxide (1.75 g) in water (10 ml) was added. The precipitated cuprous chloride was filtered, washed well with absolute ethanol and ether, and was suspended in water (20 ml). Sodium cyanide (3.25 g) in water (5 ml) was added and the resulting solution cooled to 5°. Toluene (50 ml) was poured on top of the cuprous chloride solution before the cold diazonium salt solution, previously brought to neutral by the addition of sodium carbonate, was added slowly and with vigorous stirring. An immediate reaction occurred to yield an orange-red coloration. When addition was complete, the mixture was kept in ice for 0.5 h and then was left at room temperature for an additional 12 h. The toluene was evaporated and the dark residue collected (4.3 g). This material was recrystallized twice from ligroin (b.p. 100–115°), was sublimed and the sublimate was recrystallized from ligroin as a slightly yellow product, m.p. 125–126° (uncorrected). The infrared spectrum showed a peak due to CN stretching.

Anal. Calcd. for $C_{10}H_9NO_3$: C, 62.82; H, 4.74; N, 7.33. Found: C, 62.43, 62.75; H, 4.55, 4.53; N, 7.91, 7.63.

2-(4′-Carbomethoxy-2′-chlorophenoxy)-1,3,5-trichlorobenzene (3f)

(*a*) 2-(4′-Carbomethoxy-2′-iodophenoxy)-1,3,5-trichlorobenzene (5.0 g) was refluxed with cuprous chloride (1.0 g, prepared as outlined under preparation of **2***g*) in dimethylformamide (50 ml) for 12 h. The mixture was poured into an aqueous solution of acidic ferric chloride. Although the viscous oil that formed would not solidify, it was collected by decanting the water solution and was crystallized from hot ethanol (95%) as dark crystals (1.12 g). Two more crystallizations from ethanol (95%) gave white crystals, m.p. 97–99°. An n.m.r. spectrum of this sample showed the presence of a small amount of the iodo starting material. The analytical sample was prepared by crystallizing the material from petroleum ether (b.p. 37–50°), ligroin (b.p. 100–115°), aqueous ethanol and diethyl ether – petroleum ether (1:1), m.p. 97–100° but the iodo impurity could not be removed completely this way.

Anal. Calcd. for $C_{14}H_8O_3Cl_4$: C, 45.94; H, 2.20; Cl, 38.74. Found: C, 44.62, 44.77; H, 2.05, 1.97; Cl, 36.96, 37.28. This analysis indicates about 8–9% of the iodo starting material.

The n.m.r. data reported for this compound were obtained from the analytical sample.

(*b*) 2-(2′-Amino-4′-carbomethoxyphenoxy)-1,3,5-trichlorobenzene (5.9 g) was dissolved in glacial acetic acid (40 ml). This solution was added slowly to a second solution of sodium nitrite (1.38 g) in sulfuric acid (20 ml) with the temperature kept below 35°. After 2 h the mixture was added to a solution of cuprous chloride (8.0 g, prepared as outlined under preparation of **2***g*) in hydrochloric acid (10 ml). Frothing occurred initially but after 2 h the reaction subsided. Dilution with water produced a gummy residue which was dissolved in hot ethanol and

filtered, and the filtrate cooled to produce an oil. The oil could be crystallized from methanol only with much difficulty. Two further crystallizations from methanol yielded yellowish crystals, m.p. 96–99°. The infrared spectrum was essentially identical to that of the product produced by method (*a*) although there were traces of some impurity. The yield by this method was so low as to make it impractical to use it as a preparative procedure.

2-(4′-Carbomethoxy-2′-cyanophenoxy)-1,3,5-trichlorobenzene (3g)

2-(4′-Carbomethoxy-2′-iodophenoxy)-1,3,5-trichlorobenzene (5.0 g) was refluxed for 4 h with cuprous cyanide (1.11 g) in dimethylformamide (50 ml). The mixture was poured into a solution of ferric chloride (6.0 g) in dilute hydrochloric acid (50 ml). A gum was formed initially but this soon solidified. One recrystallization from ethanol (95%) gave long brown prisms (2.4 g), m.p. 126–128° (uncorrected), whose infrared spectrum showed absorption due to CN stretching. A further recrystallization from ethanol gave the analytical sample, m.p. 129–130° (uncorrected).

Anal. Calcd. for $C_{15}H_8O_3NCl_3$: C, 50.50; H, 2.26; N, 3.93; Cl, 29.84. Found: C, 50.69, 50.93; H, 2.10, 2.15; N, 3.93, 4.32; Cl, 29.39, 29.52.

Support of the work and the grant of a Scholarship to one of us (W.D.C.) by the National Research Council of Canada are gratefully acknowledged.

1. W. D. CHANDLER, W. MACF. SMITH, and R. Y. MOIR. Can. J. Chem. **42**, 2549 (1964).
2. J. A. POPLE. J. Chem. Phys. **24**, 1111 (1956).
3. J. S. WAUGH and R. W. FESSENDEN. J. Amer. Chem. Soc. **79**, 846 (1957); **80**, 6687 (1958).
4. C. E. JOHNSON and F. A. BOVEY. J. Chem. Phys. **29**, 1012 (1958).
5. D. G. FARNUM and C. F. WILCOX. J. Amer. Chem. Soc. **89**, 5379 (1967).
6. J. E. LEFFLER and E. GRUNWALD. Rates and equilibria of Organic Reactions. John Wiley and Sons, Inc., New York. 1963. Chap. 6.
7. H. SPIESECKE and W. G. SCHNEIDER. J. Chem. Phys. **35**, 731 (1961).
8. J. S. MARTIN and B. P. DAILEY. J. Chem. Phys. **39**, 1722 (1963).
9. F. HRUSKA, H. M. HUTTON, and T. SCHAEFER. Can. J. Chem. **43**, 2392 (1965).
10. W. B. SMITH and J. L. ROARK. J. Amer. Chem. Soc. **89**, 5018 (1967).
11. J. L. ROARK and W. B. SMITH. J. Phys. Chem. **73**, 1043 (1969).
12. H. H. JAFFÉ. Chem. Rev. **53**, 191 (1953).
13. C. D. RITCHIE and W. F. SAGER. Prog. Phys. Org. Chem. **2**, 323 (1964).
14. O. J. TOUSSAINT. Bull. Soc. Roy. Sci. Liège, **15**, 86 (1946).
15. N. J. LEONARD and L. E. SUTTON. J. Amer. Chem. Soc. **70**, 1564 (1948).
16. K. AWERS. Ber. **30**. 1475 (1897).
17. W. D. CHANDLER and R. Y. MOIR. Can. J. Chem. To be published.

Can. J. Chem. Downloaded from www.nrcresearchpress.com by 210.87.254.6 on 09/05/12
For personal use only.

The Triplet State of Borazine

W. F. YOUNG, F. GREIN, J. PASSMORE, AND I. UNGER
Department of Chemistry, University of New Brunswick, Fredericton, New Brunswick

Received August 5, 1970

An attempt has been made to experimentally locate the triplet state of borazine. Borazine vapor was added to benzene vapor excited at 2580 Å. Borazine vapor has no effect on the first excited singlet state of benzene but does strongly quench the triplet state. A comparison of the experimental findings with theoretical predictions has been carried out.

Canadian Journal of Chemistry, 49, 233 (1971)

Can. J. Chem. Downloaded from www.nrcresearchpress.com by 210.87.254.6 on 09/05/12
For personal use only.

Introduction

The borazine molecule is remarkably similar to the benzene molecule. However, while there exists a considerable amount of literature dealing with the photochemistry of benzene (1–4), very little is known about the photochemical behavior of borazine (5). Borazine begins to absorb at about 2000 Å (6) and excitation in this region does not lead to dissociation (7) or emission, although the excited species may undergo certain reactions, such as deuterium exchange (5), which do not involve ring cleavage.

Theory predicts the triplet state of borazine to be at about 130 kcal. To date no experimental data have been forthcoming to substantiate this point. This communication describes an attempt to experimentally locate the triplet state of borazine.

Experimental

Materials

Biacetyl, from Aldrich Chemical Company, was stored in a blackened bulb and was purified by bulb-to-bulb distillation *in vacuo*. Fluorometric grade benzene from Hartman-Leddon Company was used without further purification. Borazine was prepared and purified according to the method of Hohnstedt and Haworth (8), but at lower yields. The purity of the product was estimated at about 98% from its infrared spectrum and vapor phase chromatography. The ultraviolet spectrum of up to 50 Torr of borazine was obtained by use of a Jarrell-Ash one meter 15° Robin Vacuum U.V. dual beam spectrophotometer. Above 2000 Å the spectrum was completely featureless (9). Below 2000 Å the spectrum was similar to that reported in the literature (6). All materials were thoroughly degassed before use.

Equipment

The high vacuum system employed was grease and mercury free equipped with Hoke packless metal diaphragm valves. Pressures were measured by means of a spiral gauge obtained from the National Research Council of Canada (NRCC) in Ottawa. The cell was a flow-through cuvette type, 1 cm × 1 cm × 4.5 cm. Samples in this cell were mixed by means of a circulating pump obtained from NRCC; all experiments were carried out at room temperature (27 °C). A modified Aminco-Bowman spectrofluorometer (spf.) was used for all emission measurements. Details about the spf. have been described previously (10).

When mixtures containing borazine, at pressures exceeding 30 Torr, and biacetyl were allowed to stay in the system for a short while ($\simeq$30 min), a heavy material was deposited on the walls of the vacuum line and some uncondensable gas was produced. These phenomena were observed with or without exposure to light. In order to minimize such effects fresh samples were always used with mixing, recording of the emission being performed as rapidly as possible ($\simeq$5 min).

Theoretical

Several s.c.f.–c.i. (self-consistent-field configuration-interaction) calculations, based on the Pariser–Parr–Pople (P.P.P.) approximation, have been reported in the literature. The results of Perkins and Wall (11) and Chalvet, Daudel, and Kaufman (12) are reproduced in Table 1. Chalvet *et al.* performed several sets of computations, differing in the choice of parameters. Only the set which is in best agreement with the observed u.v.-absorption spectrum has been selected for inclusion in Table 1. In rows 3 and 4 of Table 1 we report two representative sets of results from computations done in this laboratory. Details will be published elsewhere. In both cases the parameters were chosen according to P.P.P. methods with further adjustments to yield about 6.5 and 7.2 eV for the singlet transitions from the ground state to the $^1A_2'$ and $^1E'$ states of borazine, respectively. In the first case (row 3), the starting π-electron charges were taken to be one unit for both boron and nitrogen; in the second case (row 4), the starting charges for boron were zero, for nitrogen two units (uncharged model). It was found easier to work with the uncharged model, which also gave ionization energies in reasonable agreement with

TABLE 1. Electronic transition energies (in eV) from ground state of borazine

Reference	Transition energy to excited state					
	$^1A_2'$	$^1A_1'$	$^1E'$	^3A	^3A	$^3E'$
Perkins *et al.* (11)	6.58	7.26	7.51	6.58	6.88	6.58
Chalvet *et al.* (12)	6.509	5.74	7.145	5.74	5.822	5.781
This work	6.51	7.80	7.30	6.03	6.51	6.05
This work	6.52	7.84	7.18	5.57	6.53	5.92
Observed	6.5	?	7.2	—	—	—

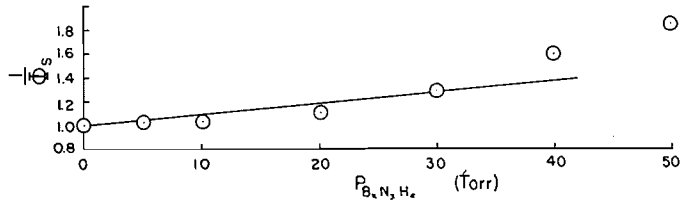

FIG. 1. Plot of $1/\Phi_s$ *vs.* borazine pressure, benzene pressure = 20 Torr, biacetyl pressure = 0.15 Torr, λ_{ex} = 2580 Å.

the observed one (11.5 eV calculated *vs.* 10.3 eV observed).

Of main interest are the calculated energies of the lowest triplet state. According to Table 1 they lie between 5.57 and 6.58 eV. Our calculations favor a value of 5.6 to 5.7 eV, or about 130 kcal/mole. In no case could a triplet excitation energy below 5.5 eV, or 127 kcal/mole, be obtained.

It may be noted in passing that our calculations place the excited $^1A_1'$ state above the $^1E'$ state. Similarly, one of the ^3A states comes out much higher in energy than the $^3E'$ state.

Results and Discussion

Essentially two types of experiments were carried out. (*a*) The effect of increasing pressures of borazine on the relative quantum yield of fluorescence of benzene excited at 2580 Å (band pass 40 Å) and hence the singlet yield was monitored. Table 2 summarizes the results, basically borazine has no effect on the first excited state of benzene. (*b*) The effect of borazine on the relative triplet quantum yield of benzene, excited at 2580 Å, was examined. Since benzene does not exhibit any phosphorescent emission in the gas phase the sensitized emission of biacetyl technique (13) was used to monitor the triplet yield of benzene. Borazine strongly quenches the triplet state of benzene, and $1/\Phi_s$ (the reciprocal of the relative sensitized emission yield of biacetyl) *vs.* borazine obeys a linear relationship (see Fig. 1). In order to be sure that the above phenomenon is not some sort of artifact due to the possible reaction between biacetyl and borazine, the effect of borazine on biacetyl excited at 4360 and 3650 Å was examined, the results are given in Fig. 2. Borazine has no effect on the emission yield of biacetyl excited directly at 4360 Å and increases the emission yield of biacetyl excited at 3650 Å. The above observations indicate that borazine has much the same effect as other vibrational quenchers have on the photochemical behavior of biacetyl (2, 14).

These experimental findings indicate that the triplet state of borazine lies at an energy not higher than 112 kcal, which is the maximum energy a benzene triplet would have if inter-

TABLE 2. Effect of borazine on the relative fluorescence yield of 20 Torr of benzene excited at 2580 Å

$B_3N_3H_6$ pressure (Torr)	BiA pressure (Torr)	$\Phi_{f,rel}$
0	0	1.0
10	0	1.0142
20	0	0.9882
30	0	0.9753
50	0	0.9089
0	0.15	1.0
5	0.15	0.9928
10	0.15	0.9622
20	0.15	0.9484
30	0.15	0.9622
40	0.15	0.9677
50	0.15	0.9743

Can. J. Chem. Downloaded from www.nrcresearchpress.com by 210.87.254.6 on 09/05/12
For personal use only.

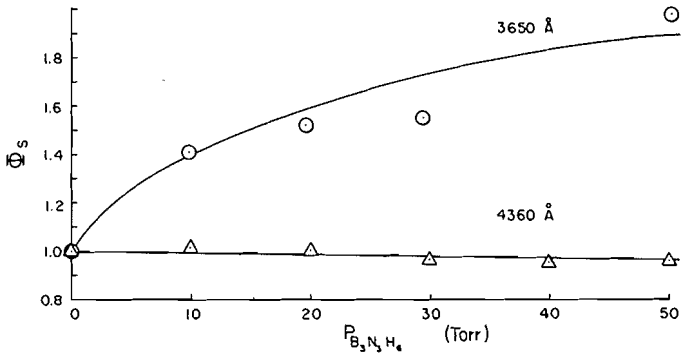

FIG. 2. The effect of borazine on the relative emission yield of 9.1 Torr of biacetyl excited directly at 3650 and 4360 Å.

system crossing, in that molecule, occurs from upper vibrational levels of the singlet. A kinetic scheme consistent with the experimental observations is given below. This scheme is by no means complete; however, since at 2580 Å, 80% of the benzene molecules which have absorbed light either fluoresce or crossover to the triplet state (15), the scheme should account for most of the major processes.

$$[1a] \quad B + h\nu \rightarrow B^s$$

$$[1] \quad B^s \rightarrow B + h\nu_f$$

$$[2] \quad B^s \rightarrow B^t$$

$$[3] \quad B^t + BiA \rightarrow BiA^t$$

$$[4] \quad B^t + BN \rightarrow BN^t + B$$

$$[5] \quad BiA^t \rightarrow BiA + h\nu_p$$

$$[6] \quad BiA^t \rightarrow BiA$$

$$[7] \quad BN^t \rightarrow BN$$

In the above scheme, B, BiA, and BN represent benzene, biacetyl, and borazine respectively, s denotes a molecule in the singlet state and t a molecule in the triplet state. Fluorescent emission is represented by $h\nu_f$ while phosphorescent emission is denoted by $h\nu_p$. Application of the steady state treatment to this scheme yields

$$[8] \quad \frac{1}{\Phi_s} = \frac{(k_5 + k_6)(k_1 + k_2)(k_3[\mathrm{BiA}] + k_4[\mathrm{BN}])}{k_5 k_3 k_2 [\mathrm{BiA}]}$$

Since the biacetyl pressure was held constant in all experiments eq. 8 predicts that a plot $1/\Phi_s$ *vs.* [BN] should be linear and is confirmed experimentally.

The data also indicate that the lifetime of the borazine triplet must be considerably shorter than the lifetime of the benzene triplet. If this were not the case then borazine triplets, having been formed in reaction 4, could transfer energy to biacetyl by a reaction such as

$$[9] \quad BN^t + BiA \rightarrow BiA^t + BN$$

and one would not observe any quenching of the sensitized emission of biacetyl which is contrary to the experimental observations.

The authors are grateful to the National Research Council of Canada for financial support.

1. W. A. NOYES, JR. and I. UNGER. Advan. Photochem. **4**, 49 (1966).
2. J. G. CALVERT and J. N. PITTS. Photochemistry. J. Wiley and Sons, Inc., New York. 1966.
3. M. NISHIKAWA and P. K. LUDWIG. J. Chem. Phys. **52**, 107 (1970).
4. G. M. BREWER and E. K. C. LEE. J. Chem. Phys. **51**, 3131 (1969) and references therein.
5. M. P. NADLER and R. F. PORTER. Inorg. Chem. **8**, 599 (1969).
6. J. R. PLATT, H. B. KLEVENS, and G. W. SCHAEFFER. J. Chem. Phys. **15**, 598 (1947).
7. G. LEE and R. F. PORTER. Inorg. Chem. **6**, 648 (1967).
8. L. F. HOHNSTEDT and D. T. HAWORTH. J. Amer. Chem. Soc. **82**, 89 (1960).
9. L. E. JACOBS, J. R. PLATT, and G. W. S. SCHAEFFER. J. Chem. Phys. **16**, 116 (1948).
10. F. W. AYER, F. GREIN, G. P. SEMELUK, and I. UNGER. Ber. Bunsenges. Phys. Chem. **72**, 283 (1968).
11. P. G. PERKINS and D. H. WALL. J. Chem. Soc. A, 235 (1966).
12. O. CHALVET, R. DAUDEL, and J. J. KAUFMAN. J. Amer. Chem. Soc. **87**, 399 (1965).
13. H. ISHIKAWA and W. A. NOYES, JR. J. Chem. Phys. **37**, 582 (1962).
14. S. H. NG, G. P. SEMELUK, and I. UNGER. Ber. Bunsenges. Phys. Chem. **74**, 29 (1970).
15. W. A. NOYES, JR. and D. A. HARTER. J. Chem. Phys. **46**, 674 (1967).

Can. J. Chem. Downloaded from www.nrcresearchpress.com by 210.87.254.6 on 09/05/12
For personal use only.

Can. J. Chem. Downloaded from www.nrcresearchpress.com by 210.87.254.40 on 09/05/12
For personal use only.

Fluorinated Carbohydrates. Part VIII. Studies of Some 3-Deoxy-3-fluoro-D-pyranosyl Fluorides[1]

L. D. HALL AND R. N. JOHNSON[2]
Department of Chemistry, The University of British Columbia, Vancouver 8, British Columbia

AND

A. B. FOSTER AND J. H. WESTWOOD
Chester Beatty Research Institute, Institute of Cancer Research; Royal Cancer Hospital, Fulham Road, London, S.W.3, Great Britain

Received August 26, 1970

Detailed analyses have been made of the ^1H and ^{19}F n.m.r. spectra of the α- and β-anomers of 2,4,6-tri-*O*-acetyl-3-deoxy-3-fluoro-D-glucopyranosyl fluoride and of 2,4-di-*O*-acetyl-3-deoxy-3-fluoro-β-D-xylopyranosyl fluoride. The $^4J_{F,F}$ couplings demonstrate a stereospecific dependence with $^4J_{a,a} = +10.4$, $^4J_{a,e} = +1.0$, and $^4J_{e,e} = -3.0$ Hz.

Canadian Journal of Chemistry, 49, 236 (1971)

Introduction

In the previous paper of this series we utilized (1) a series of 2-deoxy-2-fluoro-D-hexopyranosyl fluorides as model systems to determine the angular dependence of vicinal (^3J) ^{19}F–^{19}F couplings. We now describe a parallel investigation which enables us to comment on the stereospecific dependencies of long-range (^4J), ^{19}F–^{19}F couplings.

The derivatives chosen were the α- (**1**) and β-anomers (**2**) of 2,4,6-tri-*O*-acetyl-3-deoxy-3-fluoro-D-glucopyranosyl fluoride and 2,4-di-*O*-acetyl-3-deoxy-3-fluoro-β-D-xylopyranosyl fluoride (**3**) which were prepared by standard procedures (see Experimental).

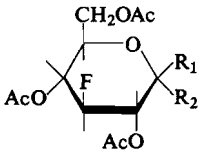

1 $R_1 = H$; $R_2 = F$
2 $R_1 = F$; $R_2 = H$

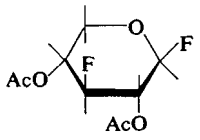

3

Results and Discussion

The ^1H n.m.r. spectra of derivatives **1–3** were analyzed in the usual fashion, using ^1H–{^{19}F} decoupling experiments to confirm the source and magnitude of the individual ^{19}F–^1H coupling constants. The resultant data are summarized in Tables 1 and 2.

The ^1H–^1H and ^{19}F–^1H couplings of the α-D-*gluco*-derivative (**1**) are all consistent with the anticipation that this derivative should favor the $^4C_1$ (D) conformation **A**. The data for the

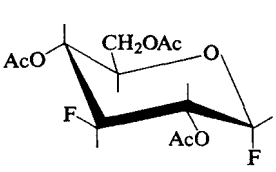

A

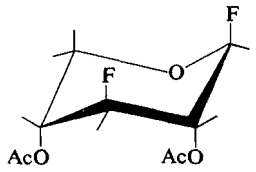

B

corresponding β-anomer (**2**) also accord reasonably well with the $^4C_1$ (D) conformation, although the values of $J_{2,3}$ and $J_{3,4}$ are smaller than the corresponding values for **1**. Possibly the strong "anomeric effect" (2) of the fluorine substituent at C-1 results (3) in local flattening of the pyranose ring in the O_5—C_1—C_2 region; it seems somewhat unlikely that this derivative is undergoing an overall conformational inversion to the $^1C_4$ (D) conformation because the value of $J_{4,5a}$ is identical to that of the α-anomer (**1**).

In accord with expectation (3), the data for the β-D-*xylo* derivative (**3**) indicate that this derivative favors almost exclusively the $^1C_4$ (D) conformation **B**. That the vicinal ^1H–^1H couplings of **3** are all somewhat smaller than those previously reported (3) for 2,3,4-tri-*O*-acetyl-β-D-xylopyranosyl fluoride may indicate that **3** has a somewhat higher preference for the $^1C_4$ (D) conformation; however, the change in the elec-

[1]This paper also constitutes Part XI of a series from U.B.C. entitled "Studies of Specifically Fluorinated Carbohydrates".

[2]University of British Columbia Postdoctoral Teaching Fellow, 1968–1970.

TABLE 1. Chemical shifts (τ-values, ϕ_c-values*)

Compound	H-1	H-2	H-3	H-4	H-5_a	H-5_e	H-6_1	H-6_2	OAc	F-1	F-3
α-D-*gluco* (**1**)†	4.27	4.98	5.21	4.71	5.93	—	5.74	5.86	7.88 7.92 7.94	149.8	201.1
β-D-*gluco* (**2**)‡	4.73	4.80	5.43	4.69	6.21	—	5.76	5.79	7.90 7.94 7.95	138.8	196.0
β-D-*xylo* (**3**)†	4.59	*ca.* 5.0	5.35	*ca.* 5.0	5.69	6.28	—	—	7.91 7.92	137.7	195.7

*In p.p.m. to high field of $CFCl_3$.
†In $CDCl_3$:$CFCl_3$:TMS = 60:25:15.
‡In $CDCl_3$:$CFCl_3$:TMS = 65:20:15.

TABLE 2. Coupling constants (Hz)

	Compound		
Coupling constant	α-D-*gluco* (**1**)	β-D-*gluco* (**2**)	β-D-*xylo* (**3**)
H_1–H_2	+2.6	+6.0	2.7
H_2–H_3	9.5	+7.7	+4.7
H_3–H_4	9.5	+8.5	+4.7
H_4–H_{5_a}	9.5	+9.5	3.0
H_{5_a}–H_{6_1}	} Sum = 6.5	} Sum = 7.8	—
H_{5_a}–H_{6_2}			—
H_{6_1}–H_{6_2}	12.5	12.4	—
H_4–H_{5_e}	—	—	3.5
H_{5_e}–H_{5_a}	—	—	12.8
$^4J_{H,H}$ coupling	*	*	†
H_1–F_1	+52.2	+51.5	49.8
H_3–F_3	51.5	+51.3	+45.5
H_2–F_1	+22.6	+10.8	7.7
H_2–F_3	+14.5	+15.0	+12±0.5
H_4–F_3	13.5	+13.5	+12±0.5
H_3–F_1	1.0	0	0.1–0.2‡
H_{5_a}–F_1	0.5	0	0.5
H_{5_e}–F_1	—	—	0
H_1–F_3	+4.0	0	0
H_{5_a}–F_3	1.0‡	−1.0	+2.5
H_{5_e}–F_3	—	—	0.3‡
F_1–F_3	+1.0	−3.0	+10.4

*None resolved.
†H_1–H_3 = 0.5 Hz; H_3–H_{5_e} = 0.8 Hz.
‡Unresolved coupling; detected by heteronuclear decoupling.

tronegativity of the C-3 substituent cannot be discounted.

The magnitudes of the ^4J, ^{19}F–^{19}F couplings were readily obtained from the ^{19}F spectra, using noise-modulated ^{19}F–{^1H} decoupling (4) to eliminate all the proton couplings.

Attempts were made to determine the signs of the ^{19}F–^{19}F couplings by experiments based (5) on the well known, selective irradiation method (6). A radiofrequency field was placed in the near vicinity of one of the fluorine resonances and its effects on the ^1H resonances followed as a function of the separation between the decoupling frequency and the fluorine resonance frequency. The extent of collapse of individual splittings depends not only on the magnitudes, but also on the signs of the individual splittings.

It proved possible to follow unequivocally the selective collapses observed in the ^1H spectra of both the α-D-*gluco* (**1**) and the β-D-*xylo* (**3**) derivatives. In the former case, the $^4J_{F,F}$ coupling proved to have the same sign as the F_1–H_1 and F_3–H_1 couplings and is thus *absolutely positive* in sign (7, 1). For compound **3** the $^4J_{F,F}$ coupling had the same sign as the F_3–H_{5_a} coupling and is thus also *absolutely positive* in sign (1). It proved

Can. J. Chem. Downloaded from www.nrcresearchpress.com by 210.87.254.40 on 09/05/12
For personal use only.

Can. J. Chem. Downloaded from www.nrcresearchpress.com by 210.87.254.40 on 09/05/12
For personal use only.

more difficult to follow the experiments made with the β-D-*gluco* derivative (**2**), but the spectra obtained were most readily interpreted on the basis of an *absolutely negative* sign for the $^4J_{Fe,Fe}$ coupling, or, more specifically, for the F_1–F_3 coupling opposite in sign to the F_3–H_2 coupling.

While this study was in progress Abraham (8) reported an analysis of the $^4J_{F,F}$ couplings of perfluorinated cyclohexanes and propanes. His conclusions are summarized in Table 3, together with the couplings obtained from derivatives **1**–**3**. It is noteworthy that even though the absolute magnitudes of couplings of the fluoro-sugars are different from those reported by Abraham, the *relative* magnitudes in the two series are identical. In particular, the "1,3-diaxial" relationship appears to lead to the largest couplings. It is evident that the magnitude of a $^4J_{F,F}$ coupling is dependent on the relative orientations of the fluorine substituents and of the nature of nearby substituents. Since the diaxial arrangement of the two fluorine substituents leads to a positive coupling whereas the diequatorial relationship leads to a negative coupling, it is likely that some molecular geometries may lead to near-zero $^4J_{F,F}$ couplings. Until further details of these dependencies are available, it would seem unwise to use $^4J_{F,F}$ as the sole basis for conformational or configurational assignments. For example, the $^4J_{Fe,Fe}$ coupling of Abraham (8) and the $^4J_{Fa,Fa}$ coupling of this investigation have almost the same absolute magnitude. That it is mandatory to determine the sign of such ^4J couplings is exemplified by the opposite sign of these couplings.

The heteronuclear decoupling experiments described above automatically provided evidence concerning the signs of several of the ^1H–^1H and ^{19}F–^1H couplings. These signs are listed in Table 2; all of them are in accord with previous determinations (1, 9, 10).

Experimental

The n.m.r. experiments were performed with a modified (4) Varian HA-100 instrument, following previously established procedures.

Melting points are uncorrected. Optical rotations were determined on ~1% solutions in chloroform using a Perkin–Elmer 141 polarimeter. The t.l.c. was performed on Kieselgel (Merck) 7731 and detection with concentrated sulfuric acid. Column chromatography was effected on Kieselgel 7734. Light petroleum refers to the fraction b.p. 40–60°.

TABLE 3. Magnitudes and signs of ^4J, ^{19}F–^{19}F couplings (Hz)

Couplings	Abraham (ref. 6)	This study
Axial:axial	+26	+10.4
Axial:equatorial	0	+1
Equatorial:equatorial	−10	−3

2,4-Di-O-acetyl-3-deoxy-3-fluoro-β-D-*xylopyranosyl Fluoride (3)*

3-Deoxy-3-fluoro-D-xylose (11) was treated with pyridine – acetic anhydride in the usual way to give a product which, after elution from Kieselgel with ether – light petroleum (b.p. 40–60°) (1:1), was shown to be a mixture of 1,2,4-tri-*O*-acetyl-3-deoxy-3-fluoro-α- and β-D-xylopyranoses on the basis of n.m.r. data ($CDCl_3$): α-anomer, H-1, triplet, τ 3.74 ($J_{1,2} \sim 4$, $J_{F,3} \sim 4$ Hz); β-anomer, H-1, doublet, τ 4.29 ($J_{1,2} \sim 7$ Hz). The α,β-mixture crystallized from ethanol – light petroleum to give material of m.p. 90–100°.

A solution of the α,β-mixture (753 mg) in a 45% solution (6 ml) of hydrogen bromide in glacial acetic acid was kept at room temperature for 1 h. Examination by t.l.c. (ether – light petroleum, 1:1) showed that no starting material remained but also indicated that the product apparently had decomposed on the silica plate. For this reason, after removal of solvents at *ca.* 30°/1–3 mm, the crude xylosyl bromide was not purified by chromatography on silica. However, the n.m.r. spectrum ($CDCl_3$), which showed only one anomeric proton signal (triplet, τ 3.30, $J_{1,2} \sim 4$, $J_{F,1} \sim 4$ Hz), was consistent with the anticipated structure 2,4-di-*O*-acetyl-3-deoxy-3-fluoro-α-D-xylopyranosyl bromide.

The crude bromide (700 mg) was dissolved in dry acetonitrile (10 ml) and stirred with silver monofluoride (1.2 g) at room temperature for 1 h, with the exclusion of light. The t.l.c. (ether – light petroleum, 1:1) then showed one major and traces of minor products. The filtered mixture was then concentrated in the presence of a small amount of Kieselgel and the residue was added to the top of a column of Kieselgel. Elution with ether – light petroleum (1:1) gave the major product (300 mg, 46% overall yield) which was crystallized from chloroform – light petroleum (b.p. 60–80°) to give the title compound **3**, m.p. 58°, $[\alpha]_D^{20}$ −67°.

Anal. Calcd. for $C_9H_{12}F_2O_5$: C, 45.4; H, 5.05; F, 16.0. Found: C, 45.4; H, 5.1; F, 15.9.

2,4,6-Tri-O-acetyl-3-deoxy-3-fluoro-α-D-*glucopyranosyl Fluoride (1)*

Anhydrous hydrogen fluoride (20 ml) was poured on to a mixture of 1,2,4,6-tetra-*O*-acetyl-3-deoxy-3-fluoro-α- and β-D-glucopyranoses (2 g) (obtained by treatment of 3-deoxy-3-fluoro-D-glucose with pyridine – acetic anhydride in the usual manner). The solution was stored for 20 min at *ca.* −10° and then at room temperature for 10 min. After pouring into a well-stirred water–chloroform mixture, the chloroform solution was neutralized with saturated aqueous sodium hydrogen carbonate, dried ($MgSO_4$), and concentrated. Examination of the residue by t.l.c. (ether – light petroleum, 2:1) showed four components. Elution of the mixture from Kieselgel

Can. J. Chem. Downloaded from www.nrcresearchpress.com by 210.87.254.40 on 09/05/12
For personal use only.

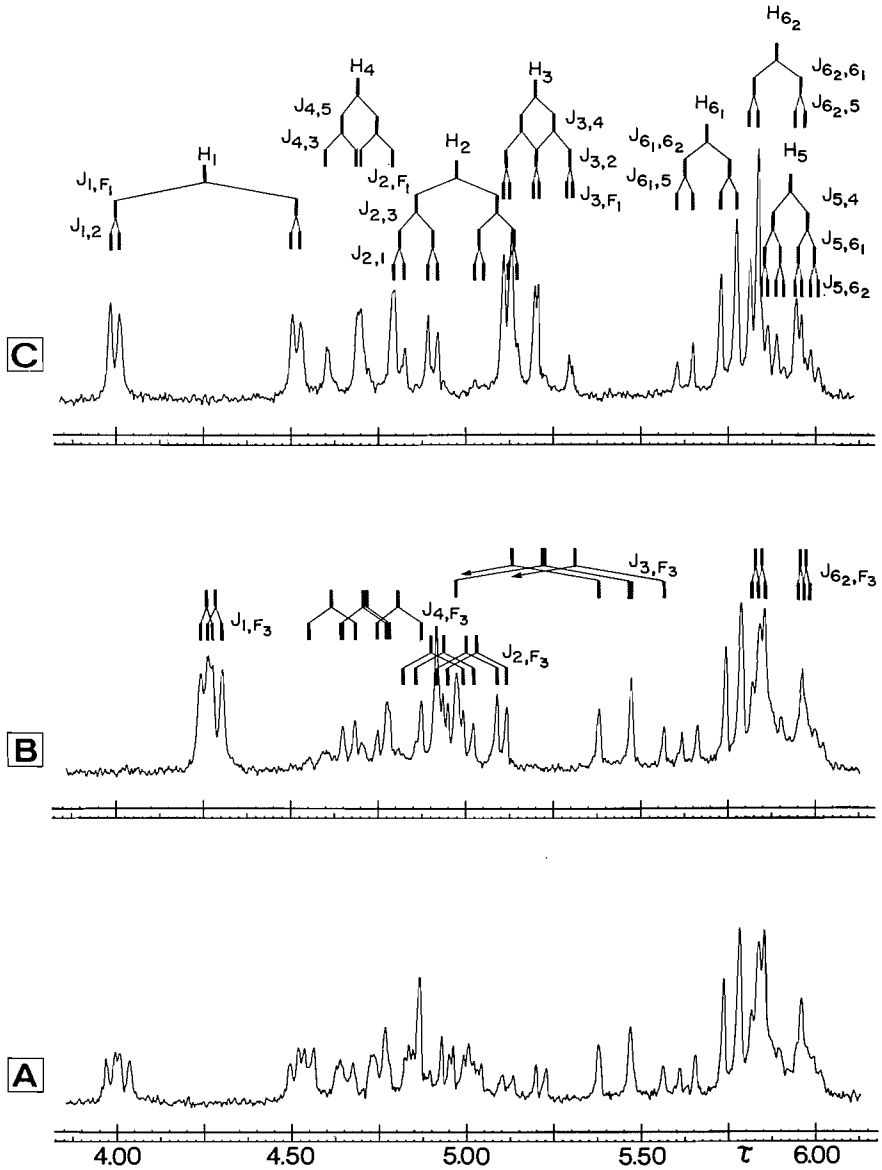

FIG. 1. Partial ^{1}H n.m.r. spectra (100 MHz) of 2,4,6-tri-*O*-acetyl-3-deoxy-3-fluoro-α-D-glucopyranosyl fluoride (**1**) in $CDCl_3$:$CFCl_3$:TMS (60:25:15) solution. A, Normal spectrum B, spectrum with simultaneous irradiation at the F-1 resonance frequency (94 079 960.0 Hz). C, spectrum with simultaneous irradiation at the F-3 resonance frequency (94 075 160.0 Hz). A diagrammatic representation of the first-order assignment is given.

with the same solvent mixture gave the title compound **1** (673 mg, 38%), b.p. 155–165° (bath)/0.1 mm, $[\alpha]_D^{23}$ +76°.

Anal. Calcd. for $C_{12}H_{16}F_2O_7$: C, 46.4; H, 5.2; F, 12.3. Found: C, 46.4; H, 5.4; F, 12.1.

2,4,6-Tetra-O-acetyl-3-deoxy-3-fluoro-β-D-*glucopyranosyl Fluoride (2)*

A solution of 1,2,4,6-tetra-*O*-acetyl-3-deoxy-3-fluoro-α-D-glucopyranose (**10**) (1.1 g) in a 45% solution (4 ml) of hydrogen bromide in acetic acid was stored at room temperature, and monitored by t.l.c. (ether – light petroleum, 1:1). After 90 min, no starting material remained and a major product (R_F *ca.* 0.6) was detected. The solution was evaporated at <40°/0.5 mm and final traces of solvent were removed by distillation of toluene from the residue which was then eluted from Kieselgel with ether – light petroleum (1:1). The major, chro-

matographically homogeneous product (850 mg, 73%) failed to crystallize and slowly decomposed at room temperature. The n.m.r. spectrum was consistent with the structure 2,4,6-tri-*O*-acetyl-3-deoxy-3-fluoro-α-D-glucopyranosyl bromide. The splitting of the signal for H-1 (triplet, $J_{1,2} \sim 4$, $J_{F,1} \sim 4$ Hz; *cf.* $J_{F,1} \sim 4$ Hz for 1,2,4,6-tetra-*O*-acetyl-3-deoxy-3-fluoro-α-D-glucopyranose) was indicative of the α-configuration.

To a stirred solution of freshly prepared glycosyl bromide (850 mg) in dry acetonitrile (2 ml) was added silver monofluoride (1.5 g). After 1 h, the solution was filtered, concentrated under diminished pressure, and the residue was eluted from Kieselgel with benzene–ether (9:1). The major product (550 mg, 77%) was recrystallized from ethanol – light petroleum to give the title compound, m.p. 79.5–80°, $[\alpha]_D^{25}$ +6°.

Anal. Calcd. for $C_{12}H_{16}F_2O_7$: C, 46.5; H, 5.2; F, 12.3. Found: C, 46.4; H, 5.2; F, 12.7.

Spectral Assignments and Analyses

The assignments of the spectra were based on matching of multiplet spacings and were confirmed by ^1H–{^{19}F} heteronuclear spin-decoupling experiments. A typical example is shown in Fig. 1.

Distinction between the resonances of H-5$_e$ and -5$_a$ of the β-D-*xylo* derivative **3** was based primarily on the magnitude of the coupling between H-3 and *one* of the H-5 protons, assigned thereby as H-5$_e$. Further evidence in support of this assignment can be derived from a comparison of the H-5$_e$ and -5$_a$ shifts of **3** (τ 6.28 and 5.69, respectively) with the corresponding shifts of those of 2,3,4-tri-*O*-acetyl-β-D-xylopyranosyl fluoride (τ 6.26 and 5.72).

It is a pleasure for one of us (L.D.H.) to thank the National Research Council of Canada for their generous financial support. This investigation was also supported by grants to the Chester Beatty Research Institute (Institute of Cancer Research: Royal Cancer Hospital) from the Medical Research Council of Great Britain and the Cancer Research Campaign (formerly the British Empire Cancer Campaign for Research), and from N.A.T.O., grant No. 352.

1. L. D. HALL, R. N. JOHNSON, J. ADAMSON, and A. B. FOSTER. Can. J. Chem. **49**, 118 (1971).
2. R. U. LEMIEUX. *In* Molecular rearrangements. Part 2. *Edited by* P. de Mayo. Interscience, New York, 1964.
3. L. D. HALL and J. F. MANVILLE. Can. J. Chem. **47**, 19 (1969).
4. R. BURTON and L. D. HALL. Can. J. Chem. **48**, 59 (1970).
5. W. R. CULLEN, L. D. HALL, and R. N. JOHNSON. To be published.
6. W. A. ANDERSON and R. FREEMAN. J. Chem. Phys. **37**, 85 (1962); R. FREEMAN and W. A. ANDERSON. J. Chem. Phys. **37**, 2053 (1962).
7. E. L. MACKOR and D. MACLEAN. J. Chem. Phys. **44**, 64 (1966); A. BERNHEIM and B. J. LAVERY. J. Amer. Chem. Soc. **89**, 1279 (1967).
8. R. J. ABRAHAM. J. Chem. Soc. (B), 1022 (1969).
9. L. D. HALL and J. F. MANVILLE. Carbohyd. Res. **8**, 295 (1968); **9**, 11 (1969).
10. A. B. FOSTER, R. HEMS, L. D. HALL, and J. F. MANVILLE. Chem. Commun. 158 (1968).
11. A. B. FOSTER, R. HEMS, and J. M. WEBBER. Carbohyd. Res. **5**, 85 (1967).

Can. J. Chem. Downloaded from www.nrcresearchpress.com by 210.87.254.40 on 09/05/12
For personal use only.

Synthesis of 6-Hydroxyfulvenes. I. Acid-catalyzed Rearrangements[1,2]

A. W. McCulloch, B. Stanovnik,[3] D. G. Smith, and A. G. McInnes
Atlantic Regional Laboratory, National Research Council of Canada, Halifax, Nova Scotia

Received July 9, 1970

New syntheses of 2-carbomethoxy-, 2-carboxy-3-carbomethoxy-, 2,3-dicarboxy-, and 2,3-dicarbomethoxy-4,6-dimethyl-6-hydroxyfulvenes are described.

Canadian Journal of Chemistry, 49, 241 (1971)

Can. J. Chem. Downloaded from www.nrcresearchpress.com by 210.87.254.6 on 09/05/12
For personal use only.

Fulvenes have long aroused interest because of their natural occurrence, distinct chemical behavior, and bright colors (1–5). In this note we wish to report new syntheses of some 6-hydroxyfulvene derivatives. Compounds of this type are useful intermediates in the synthesis of several nonbenzenoid cyclic conjugated systems (3, 6).

We describe the preparation of 2,3-dicarboxy-, 2-carboxy-3-carbomethoxy-, and 2,3-dicarbomethoxy-4,6-dimethyl-6-hydroxyfulvenes (**3***a–c*) and of 2-carbomethoxy-4,6-dimethyl-6-hydroxyfulvene (**3***d*). All four compounds (**3***a–d*) were prepared by acid-catalyzed rearrangement of the bromolactonic acid **2***a* or its methyl ester **2***b*, while **3***c* was also prepared by acid-catalyzed rearrangement of the oxaquadricyclane **4**. The experimental conditions and yields are summarized in Table 1.

Compound **2***a* was prepared by bromination of the Diels–Alder *exo* adduct **1** of 2,5-dimethylfuran and maleic anhydride in aqueous base, as described by Woodward and Baer and Zefirov *et al.* (7). The latter group have found that **2***a* in the presence of H_2SO_4 in methanolic 2,4-dinitrophenylhydrazine rearranges to give the 2,4-dinitrophenylhydrazone derivative of the keto form of **3***c*. We have found that the bromolactonic acid **2***a* rearranges in the presence of HBr or H_2SO_4 in $CHCl_3$ to give an almost quantitative yield of the fulvene **3***a*, while its monomethyl ester **2***b* undergoes a similar rearrangement to yield **3***b*. Even more remarkable is the spontaneous conversion of **2***a* (or **2***b*) to **3***a* (or **3***b*) *in the solid state*. Crystals of **2***a* (or **2***b*) evolve hydrogen bromide over a period of two to three months at room temperature eventually ending up as green crystals of **3***a* (or **3***b*). The conversion is complete in about 3 weeks if crystals of **2***a* (or **2***b*) are kept in an atmosphere saturated with HBr. The above rearrangements undoubtedly proceed by initial protonation of the lactone carbonyl followed by a concerted intramolecular rearrangement with elimination of HBr to give the cyclopentadiene skeleton (see Scheme 1). Enolization then yields the substituted 6-hydroxyfulvene The stability of the latter is due to the ability of the substituents to form a strong hydrogen bonded network.

TABLE 1. Products obtained after 24 h at room temperature

Starting material	Acid/solvent	Products (%)				
		2*b*	**3***a*	**3***b*	**3***c*	**3***d*
2*a*	$HBr/CHCl_3$		95			
2*a*	$H_2SO_4/CHCl_3$		77			
2*a*	HBr/CH_3OH				47	34
2*a*	H_2SO_4/CH_3OH	90				
	excess H_2SO_4/CH_3OH	20			60	20
2*b*	$HBr/CHCl_3$	95				
2*b*	$H_2SO_4/CHCl_3$			60		
2*b*	HBr/CH_3OH				95	
2*b*	H_2SO_4/CH_3OH	85				
	excess H_2SO_4/CH_3OH				90	
2*a*	HBr/MeOH/0°/40 h				32	12
	HBr/MeOH/60°/18 h				20	30
4	H_2SO_4/CH_2Cl_2/25°/20 m				37	

The elimination of HBr does not appear to be rate determining since the conversion of **2***a* to **3***a* is not accelerated by pyridine. Moreover, rearrangement (in the solid state) of **2***a* occurs much more readily than that of **2***b*; intramolecular protonation of the lactone carbonyl can only occur in **2***a* indicating that this step is important in initiating reaction.

If the bromolactonic ester **2***b* was treated with excess HBr or H_2SO_4 in *methanol* rather than $CHCl_3$, rearrangement was accompanied by

[1]Issued as NRCC No. 11599.
[2]This work was reported in part at the 48th Annual Conference of the Chemical Institute of Canada, which was held in Montreal in May, 1965.
[3]NRCC Postdoctorate Fellow, 1964–1965.

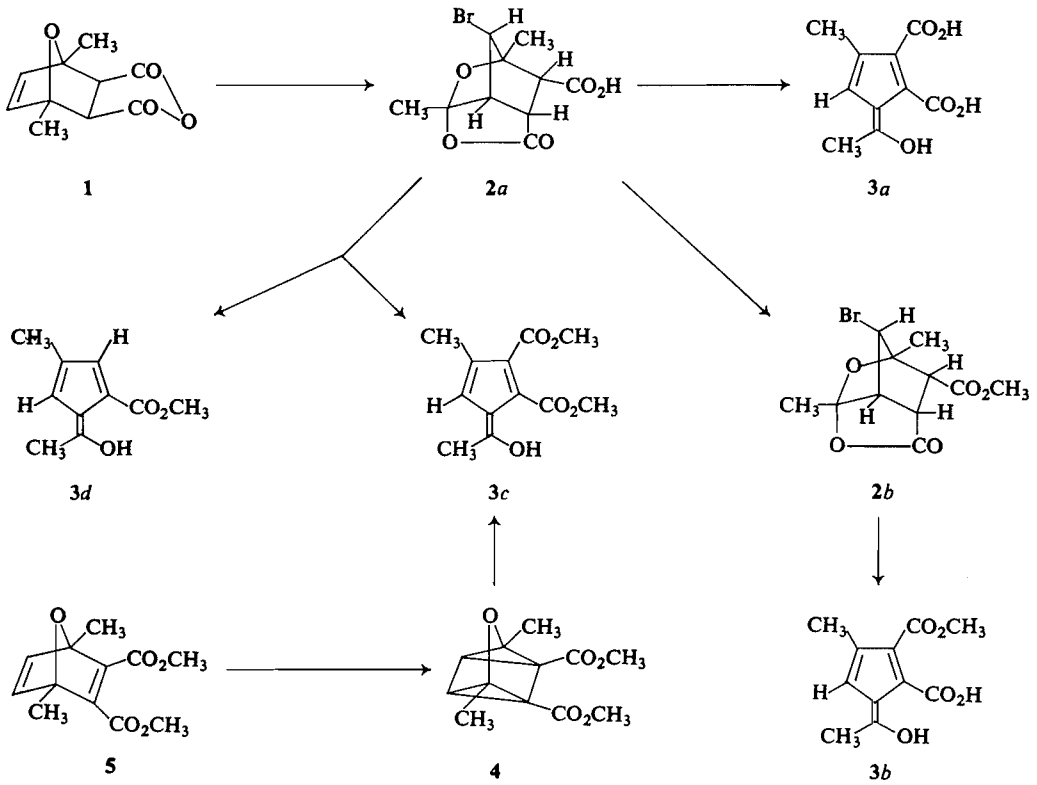

esterification to give the fulvene diester **3c**. In the case of **2a**, however, this change in solvent resulted in its conversion to **3d** as well as **3c**. The ratio of these products was temperature dependent, an increase in temperature favoring the formation of **3d** (see Table 1). Conversion of **2a** to **3d** occurs by the decarboxylative elimination process shown in Scheme 2.

The fulvene diester **3c** has also been obtained (37%) by acid-catalyzed cleavage and rearrangement of the oxaquadricyclane **4**. Prinzbach and Vogel have recently reported that this same conversion is promoted by CuCl, and that some substituted oxaquadricyclanes may be isomerized thermally to 6-hydroxyfulvenes (8).

Structures of 3a–d

The structures of the fulvenes **3a–d** were elucidated on the basis of their analytical and spectral data (see Experimental and Table 2). All four compounds show i.r. absorptions for very strongly hydrogen-bonded hydroxyl and also for bonded carboxy or carbomethoxy carbonyl groups as expected of 6-hydroxyfulvenes with carbonyl substituents at C-2 (3, 9–12). Their u.v. spectra are compatible with fulvene structures (1, 2).

The p.m.r. spectra (Table 2) of **3a**, *b*, and *c* show characteristic signals (quartets) for a single fulvene ring proton coupled to the protons of an allylic methyl group. In addition each shows

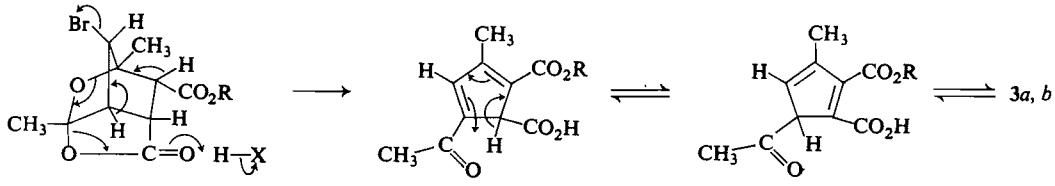

SCHEME 1

Can. J. Chem. Downloaded from www.nrcresearchpress.com by 210.87.254.6 on 09/05/12
For personal use only.

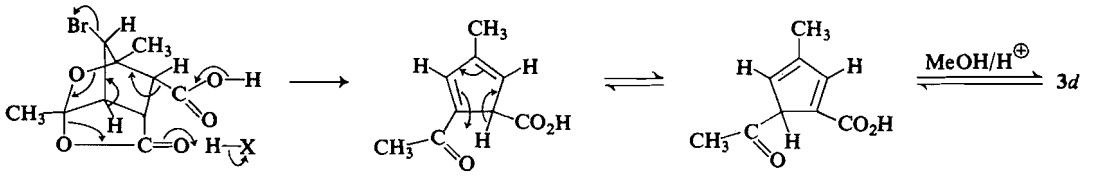

SCHEME 2

TABLE 2. Proton magnetic resonance data for **3***a–d**

Compound **3**	Chemical shifts (τ) C-2 R_1	C-3 R_2	C-4 CH_3	C-5 H	C-6 CH_3	C-6 OH	$J_{p,q}$(Hz) H_5,CH_3	H_3,H_5
a $R_1 = R_2 = CO_2H$†		−0.84, b‡	7.68, d	3.08, q	7.40, s	−9.71, s	0.9	—
b $R_1 = CO_2H$; $R_2 = CO_2CH_3$§		6.00, s	7.71, d	3.17, q	7.38, s	−9.70, s	0.8	—
c $R_1 = R_2 = CO_2CH_3$§		6.13, s	7.97, d	3.29, q	7.56, s	−5.70, s	1.1	—
d $R_1 = CO_2CH_3$; $R_2 = H$§	6.13, s	2.82, d	7.95, d	3.27, m	7.60, s	−5.15, s	1.1	2.3

*The compound had the following general structure:

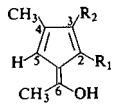

†In tetrahydrofuran-d_8.
‡b = broad, s = singlet, d = doublet, m = multiplet.
§In $CDCl_3$.

a singlet for the methyl group at C-6 with a chemical shift in agreement with those reported (10, 13–16) for methyl groups in a similar environment. Enolic hydroxyl groups at C-6 in fulvenes carrying a carbonyl substituent at C-2 are known to form very strong hydrogen bonds. The hydrogen-bonded hydroxyl protons have characteristically low chemical shifts, *e.g.* −8.87 τ (8–10, 13, 16, 17). In **3***c* the signal for this proton appears at −5.70 τ, while in **3***a* and *b* it appears at −9.71 τ!

The p.m.r. spectrum of **3***d* (Table 2) shows characteristic signals for carbomethoxy, allylic methyl, C-6 methyl, and enolic hydroxyl, as well as for *two* fulvene ring protons. The proton at C-5 appears as a sextet, being coupled to both the allylic methyl hydrogens (J = 1.1 Hz) and to the proton at C-3 ($J_{3,5}$ = 2.3 Hz). The value of $J_{3,5}$ is consistent with values previously reported for 2,4-couplings in similarly substituted fulvenes (10). Supporting evidence for the structure of **3***d* was obtained from its mass spectrum. Loss of methanol from the parent ion (*m/e* 180 → 148) is a characteristic of 2-carbomethoxyfulvenes (10). (A similar loss of methanol was observed in the spectrum of **3***c*.) The i.r. absorption for a hydrogen-bonded carbonyl at 1626 cm^{-1} confirms that the carbomethoxy and enolic hydroxyl groups have the steric relationship shown in **3***d*. The evidence cited above indicates that these compounds (**3***a–d*) exist predominantly in solution in enolic form, a finding in accord with those obtained previously (*cf.* 3, 9, 17) for similar systems possessing a carbonyl substituent at C-2.

We had hoped that this procedure might offer a general route to the 6-hydroxyfulvene system. However the method is subject to certain limitations, the chief of these being (*a*) that it requires the formation of a bromolactonic derivative of type **2**, and (*b*) that the strongly acidic nature of the reaction mixture may cause decomposition of the starting material or reaction product. These difficulties have been overcome by the development of a general, photochemical synthesis of 6-hydroxyfulvenes from adducts of type **5**; this will be the subject of a future communication.

Experimental

The u.v. spectra were determined using a Beckman DK-2 ratio recording spectrophotometer and i.r. spectra with Perkin–Elmer 237 or 521 spectrometers. The p.m.r. spectra were recorded using a Varian A-60A spectrometer, with tetramethylsilane as internal standard.

Can. J. Chem. Downloaded from www.nrcresearchpress.com by 210.87.254.6 on 09/05/12
For personal use only.

Can. J. Chem. Downloaded from www.nrcresearchpress.com by 210.87.254.6 on 09/05/12
For personal use only.

The bromolactonic acid **2***a* and its methyl ester **2***b* were prepared according to the methods of Woodward and Baer and Zefirov *et al.* (7). The oxaquadricyclane **4** was prepared from the appropriate Diels–Alder adduct under conditions similar to those reported by Prinzbach *et al.* (18).

2,3-Dicarboxy-4,6-dimethyl-6-hydroxyfulvene (3a)

(i) By Reaction of 2a with HBr in $CHCl_3$

The bromolactonic acid, **2***a*, (2.91 g, 0.01 mol) was suspended in 10 ml or dissolved in 30 ml alcohol-free $CHCl_3$. The suspension or solution was saturated with HBr and allowed to stand overnight at room temperature. The green solid product was filtered and washed with a small amount of $CHCl_3$. Crystallization from a large volume of benzene gave yellow prisms (2.0 g, 95%), m.p. 128–129°. The i.r. spectrum (KBr) showed absorptions for bonded hydroxyl (broad band centered at 3000 cm^{-1}) and carboxyl carbonyl (medium intensity band at 1650 cm^{-1}) groups; $\lambda\lambda_{max}$ (EtOH): 243 (ε 11 500), 332 (ε 12 100), 384 mμ (ε 5500); $\lambda\lambda_{max}$ ($CHCl_3$): 342 (ε 11 200), 390 mμ (ε 4200).

Anal. Calcd. for $C_{10}H_{10}O_5$: C, 57.14; H, 4.80; O, 38.06. Found: C, 57.40; H, 4.98; O, 37.60.

(ii) By Reaction of 2a with H_2SO_4 in $CHCl_3$

Compound **2***a* (500 mg) was stirred with a 30% excess of concentrated H_2SO_4 (235 mg) in alcohol-free $CHCl_3$ (10 ml) overnight at room temperature. The product (276 mg, 77%) which was filtered and washed with H_2O and $CHCl_3$, was identical to that isolated in (*i*) above.

(iii) Solid State

The elimination of HBr from **2***a* took place also in the solid state, conversion to **3***a* being complete in about 2 months. If the solid compound was allowed to stand in an atmosphere of HBr the reaction was complete in 3–4 weeks.

2-Carboxy-3-carbomethoxy-4,6-dimethyl-6-hydroxyfulvene (3b)

(i) By Reaction of 2b with HBr in $CHCl_3$

Compound **2***b* (3.05 g, 0.01 mol) was dissolved in alcohol-free $CHCl_3$ (15 ml) and the solution saturated with HBr and allowed to stand overnight at room temperature. The fulvene **3***b*, (1.7 g, 76%) crystallized from solution. Crystallization from benzene gave greenish prisms, m.p. 97–98°. Compound **3***b* shows no OH stretching absorption when examined as a dilute (0.005 *M*) solution in CCl_4. However, after replacement of exchangeable hydrogens with deuterium, the hydrogen-bonded OH groups were observed as an OD stretching vibration at 2334 cm^{-1}. The carbonyl region (KBr) was complex with an envelope rather than well-defined bands; $\lambda\lambda_{max}$ (EtOH): 255 (ε 12 200), 332 mμ (ε 17 000); $\lambda\lambda_{max}$ ($CHCl_3$): 343 (ε 16 700), 392 mμ (ε 5600).

Anal. Calcd. for $C_{11}H_{12}O_5$ (mol. wt. 224): C, 58.92; H, 5.40; O, 35.68. Found (224 (osmometer)): C, 59.07; H, 5.33; O, 35.74.

(ii) By Reaction of 2b with H_2SO_4 in $CHCl_3$

Treatment of **2***b* (896 mg) with a 100% excess of concentrated H_2SO_4 (800 mg) in $CHCl_3$ (10 ml) for 24 h at room temperature caused 60% conversion to **3***b*.

Reaction in the solid state was complete in about 3 months.

2,3-Dicarbomethoxy-4,6-dimethyl-6-hydroxyfulvene (3c)

(i) By Reaction of 2b with HBr or H_2SO_4 in CH_3OH

Compound **2***b* (200 mg) was dissolved in CH_3OH (8 ml) and the solution saturated with HBr and allowed to stand overnight at room temperature. The yellow–green solution was then poured into $CHCl_3$ and washed with H_2O. Drying and evaporation gave **3***c* as a yellow oil (164 mg, 95%).

Compound **2***b* (450 mg) was dissolved in CH_3OH (10 ml) and a 12-mol excess of concentrated H_2SO_4 (2.0 g) added. The mixture was stirred overnight at room temperature, then worked-up as above to give a yellow oil (318 mg, 90%). In the presence of lower concentrations of H_2SO_4 conversion to **3***c* was slow. Compound **3***c* was obtained as a yellow oil, $n_D^{25} = 1.5713$. Molecular ion mass: Calcd. for $C_{12}H_{14}O_5$, 238. Found: *m/e* 238. Characteristic i.r. absorptions (liq. film): broad band centered at 2950 (bonded OH), 1726 (non-bonded C=O), 1618 cm^{-1} (bonded C=O); $\lambda\lambda_{max}$ (EtOH): 247 (ε 9400), 327 mμ (ε 10 400); $\lambda\lambda_{max}$ ($CHCl_3$): 323 (ε 7650), 379 mμ (ε 3500).

Compound **3***c* was also obtained together with **3***d* by reaction of **2***a* with HBr or H_2SO_4 in CH_3OH (see below).

(ii) By Reaction of the Oxaquadricyclane 4 with H_2SO_4

Compound **4** (2.40 g) was dissolved in CH_2Cl_2 (100 ml) and concentrated H_2SO_4 (500 mg) added to the stirred, ice-cold solution, which immediately darkened in color. After stirring at room temperature for 20 min the mixture was poured into ice water. After drying, evaporation from the organic layer gave a dark brown residue (2.51 g). Chromatography on silicic acid ($CHCl_3$ as eluant) gave **3***c* as a bright yellow oil (892 mg, 37%) identical in all respects to the product isolated above.

2-Carbomethoxy-4,6-dimethyl-6-hydroxyfulvene (3d)

(*i*) Compound **2***a* (4.0 g) was dissolved in CH_3OH (25 ml) and the ice-cold solution saturated with HBr. The mixture was allowed to stand at room temperature overnight, and was then poured into $CHCl_3$ and washed with H_2O. Drying and evaporation of the organic layer gave an orange–red oil. Preparative t.l.c. (silica gel G, $CHCl_3$ as eluant) gave two yellow materials, with R_f values of 0.35 and 0.8. The fraction of R_f 0.8 afforded **3***d* as a bright yellow oil (851 mg, 34%) which solidified on cooling, m.p. 16–17°. Molecular ion mass: Calcd. for $C_{10}H_{12}O_3$, 180. Found: *m/e* 180. Characteristic i.r. absorptions (liq. film): broad band centered at 2900 (bonded OH), 1626 cm^{-1} (bonded C=O); $\lambda\lambda_{max}$ (EtOH): 237 (ε 16 600), 314 (ε 10 950), 373 mμ (ε 5200); $\lambda\lambda_{max}$ ($CHCl_3$): 317 (ε 11 500), 376 mμ (ε 5400).

The fraction of R_f 0.35 gave the fulvene diester **3***c* as a yellow oil (1.54 g, 47%), identified by p.m.r.

(*ii*) Compound **2***a* (500 mg) was dissolved in CH_3OH (10 ml) and a large excess (2.2 g) of concentrated H_2SO_4 added. The mixture was stirred overnight at room temperature. After work-up as in (*i*) above, a yellow–orange oil was obtained, p.m.r. analysis of which showed approximately 20% conversion to **3***d*, with *ca.* 20% **2***b* and 60% **3***c*.

In the presence of lower concentrations of H_2SO_4 the conversions to **3***c* and *d* were slower, **2***b* being the major product.

(iii) Effect of Temperature

Samples (500 mg) of **2***a* were dissolved in CH_3OH (15 ml). The solutions were then saturated with HBr (*i*) at 0°, with ice-cooling, and (*ii*) at reflux temperature (60°). The reactions were carried out at these temperatures and were then worked-up as above and the products separated by preparative t.l.c. The yields obtained are given in Table 1.

We wish to thank Mrs. M. G. Flack and J. van Ingen for technical assistance and D. J. Embree for recording the mass spectra.

1. E. D. BERGMANN. *In* Progress in organic chemistry. Vol. 3. Butterworths, London, 1955. p. 81.
2. J. H. DAY. Chem. Rev. **53**, 167 (1953).
3. K. HAFNER, K. H. HÄFNER, C. KÖNIG, M. KREUDER, G. PLOSS, G. SCHULZ, E. STURM, and K. H. VÖPEL. Angew. Chem. Int. Ed. **2**, 123 (1963).
4. E. D. BERGMANN. Chem. Rev. **68**, 41 (1968). P. YATES. Adv. Alicyclic Chem. **2**, 59 (1968).
5. D. H. Lo and M. A. WHITEHEAD. Tetrahedron, **25**, 2615 (1969).
6. K. HAFNER, W. BAUER, and G. SCHULZ. Angew. Chem. Int. Ed. **7**, 806 (1968).
7. N. S. ZEFIROV, R. A. IVANOVA, R. M. KETCHER, and Y. K. YUREV. Zh. Obshch. Khim. **35**, 61 (1965). *cf.* R. B. WOODWARD and H. BAER. J. Amer. Chem. Soc. **70**, 1161 (1948).
8. H. PRINZBACH and P. VOGEL. Helv. Chim. Acta, **52**, 396 (1969).
9. K. HAFNER, H. E. A. KRAMER, H. MUSSO, G. PLOSS, and G. SCHULZ. Chem. Ber. **97**, 2066 (1964).
10. R. F. CHILDS, R. GRIGG, and A. W. JOHNSON. J. Chem. Soc. (C), 201 (1967).
11. K. HAFNER, G. SCHULZ, and K. WAGNER. Ann. (Justus Liebig's), **678**, 39 (1964).
12. K. HAFNER, K. H. VÖPEL, G. PLOSS, and C. KÖNIG. Ann. (Justus Liebig's), **661**, 52 (1963).
13. R. E. BOZAK and K. L. RINEHART. J. Amer. Chem. Soc. **84**, 1589 (1962).
14. W. B. SMITH and B. A. SHOULDERS. J. Amer. Chem. Soc. **86**, 3118 (1964).
15. M. L. HEFFERNAN and A. J. JONES. Aust. J. Chem. **19**, 1813 (1966).
16. R. C. ALLGROVE and U. EISNER. Tetrahedron Lett. **6**, 499 (1967).
17. D. LLOYD and N. W. PRESTON. J. Chem. Soc. (C), 2464 (1969).
18. H. PRINZBACH, P. VOGEL, and W. AUGE. Chim. (Aarau), **21**, 469 (1967).

Can. J. Chem. Downloaded from www.nrcresearchpress.com by 210.87.254.6 on 09/05/12
For personal use only.

Can. J. Chem. Downloaded from www.nrcresearchpress.com by 210.87.254.40 on 09/05/12
For personal use only.

Spiroalkylation of some Homophthalimides and Oxindoles with 1-Bromo-2-chloroethane

D. E. HORNING, G. LACASSE, AND J. M. MUCHOWSKI[1]
Bristol Laboratories of Canada, Candiac, Quebec

Received August 6, 1970

The base-induced alkylation of 4-unsubstituted homophthalimides with 1-bromo-2-chloroethane produced the spirocyclopropane compounds **4**. The structures of these compounds were supported by their spectral properties and by their susceptibility towards cleavage of the three-membered ring with secondary amines.

Under similar conditions, 3-unsubstituted oxindoles also yielded spirocyclopropane compounds **7**, but 4-hydroxycarbostyril gave the 4-*O*-alkylated compound **8** instead.

Canadian Journal of Chemistry, 49, 246 (1971)

In connection with another problem, it was found necessary to prepare 4,4-disubstituted homophthalimides of type **2** (Y = Cl, Br; X = H, Cl). Since Fournier and Decombe (1) had reported that the triethylamine-induced alkylation of homophthalimides (**1**, R = H, alkyl, aryl) with 1,2-dibromoethane afforded the spiro compounds **3**, we attempted to avoid this reaction pathway by operating under conditions which would be expected to favor the formation of **2**. When a dimethyl formamide (DMF) solution of 2-methylhomophthalimide (**1**, R = CH_3; X = H) containing potassium carbonate or sodium hydride was treated with a large excess of 1-bromo-2-chloroethane, a halogen free compound with the same m.p. as that reported for **3** (R = CH_3; X = H) was produced (Table 2). The n.m.r. spectrum (Figs. 1 and 3) was completely inconsistent with this structure and uniquely compatible with that of the spiro cyclopropane **4** (R = CH_3; X = H) (see Scheme 1). The four-proton multiplet centered at δ 1.85 (Fig. 3 and Table 1) was of the AA′BB′ type with a pattern very similar to that observed for the methylene hydrogens of 1-phenylcyclopropane-1-carboxylic acid (2). The low field multiplet at δ 8.17 (Fig. 1) was assigned to H-8 of the aromatic ring which had been deshielded by the adjacent carbonyl group. The chemical shift of this proton was almost the same as that observed (δ 8.08) for the analogous proton in the starting material and essentially identical to that of H-8 in 2,4,4-trimethylhomophthalimide (δ 8.16, Fig. 2). The absorption at δ 6.74 (Fig. 1) was attributed to H-5 on the expectation that a proton situated above the plane of a cyclopropane ring would experience shielding relative to its "normal" position (3). This characteristic upfield shift (Δ > 20 Hz in comparison to the analogous proton in 2-methylhomophthalimide

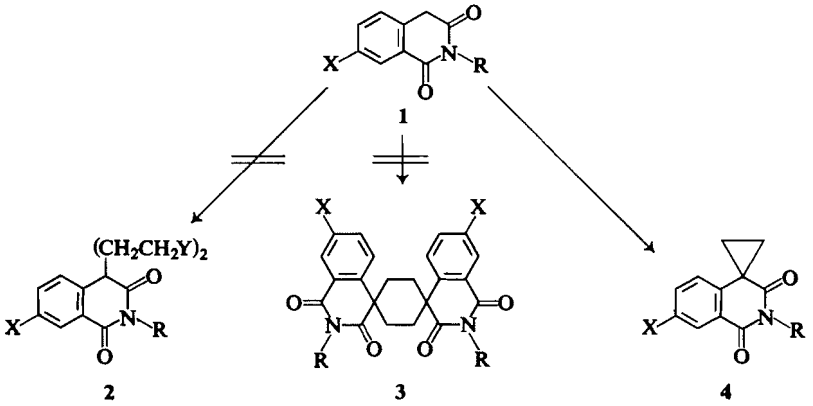

SCHEME 1

[1]To whom enquiries concerning this paper should be addressed.

TABLE 1. Chemical shifts and coupling constants for the cyclopropane hydrogens of 2-methyl-4,4-dimethylenehomophthalimide in Hz

H_A*	H_B	L†	N	K	M	J_{gem}	J_{trans}	J_A‡	J_B
95.7	126.5	±11.75§	3.58	19.80	±0.2	−4.1§	7.7	10.0	9.8

*H_A and H_B were assigned arbitrarily to the high and the low field portions of the spectrum, respectively. We are currently examining this system for the presence of a n.O.e. between H-5 and the adjacent cyclopropane protons. If a positive effect is observed, an unambiguous assignment of the A and B protons will be possible (see ref. 13 for example). See NOTE ADDED IN PROOF below.

†For the significance of the terms K, L, M, N, etc. see ref. 2.

‡$J_A = J_{AA'} : J_B = J_{BB'}$.

§All but one of the calculated and observed transition energies agreed to within ±0.2 Hz. The calculated position for line no. 4 was 0.5 Hz on the low field side of the measured value. Since transitions 3, 4, and 7 appeared as a singlet with w_H = 1.6 Hz, it was not possible to gauge the significance of this discrepancy. For the calculated spectrum and coupling constants L was taken as a negative and M as a positive quantity. See ref. 2 for details.

NOTE ADDED IN PROOF: Irradiation of the low field half of the cyclopropane absorption did not significantly affect the integrated intensity of any of the aromatic protons. In contrast, saturation of the high field portion of the cyclopropane resonance resulted in a 16% increase in the integrated intensity of the δ 6.74 multiplet (*i.e.* H-5, see Fig. 1). Therefore H_A can now be unambiguously assigned to the two cyclopropane hydrogens directed toward the aromatic ring, in agreement with our original arbitrary assignment (see footnote†, Table 3).

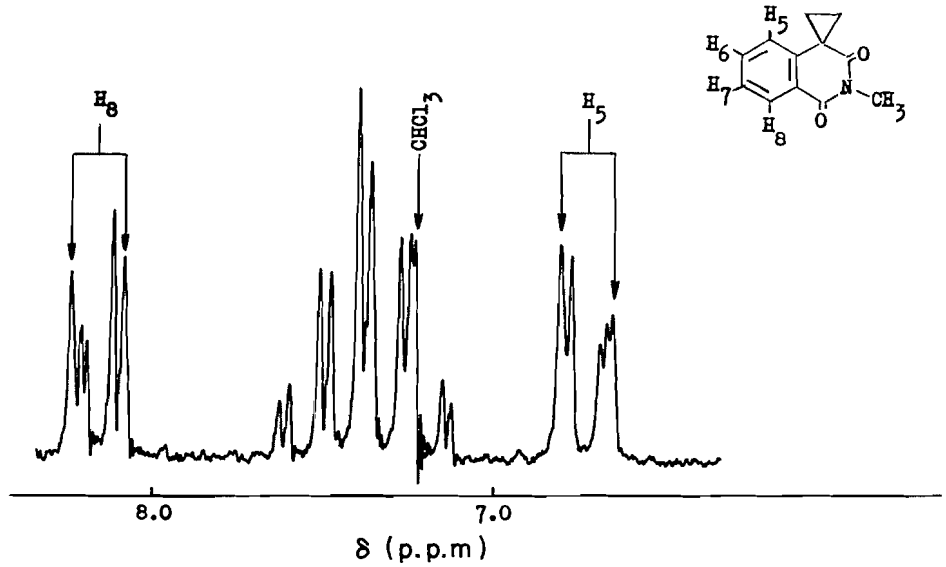

FIG. 1. The n.m.r. spectrum of the aromatic protons of 2-methyl-4,4-dimethylenehomophthalimide.

or in 2,4,4-trimethylhomophthalimide) which has recently been recorded for similarly constituted systems without comment (4), was even more clearly observed (Δ = 29 Hz) for the 7-chloro derivative of **4** (R = CH_3; X = Cl, see Figs. 4 and 5).

In addition to the n.m.r. and i.r.[2] spectral properties and the correct elemental analysis and molecular weight (Rast), the structure of **4** (R = CH_3; X = H) was supported by its reactions with secondary amines. As a cyclopropane-bearing carbanion stabilizing substituents, the ring cleavage of this compound was anticipated (6) and demonstrated to be especially facile. An excess of dimethylamine in DMF (65°) rapidly produced the air sensitive amine ***5a*** (Scheme 2) which was characterized as its stable hydrobromide salt. Its structure was substantiated by its elemental analysis and spectral characteristics. In particular, the n.m.r. spectrum of the free base had a broad (w_H = 13 Hz, probably due to slow exchange) absorption centered at δ 3.96 due to the single proton at C-4, which was rapidly exchanged with deuterium oxide. Neither the salt nor the free base showed any evidence of an i.r. absorption in the 3100–3650

[2]The spirocyclic homophthalimides described herein (Table 2) possessed a medium intensity absorption at 1708 ± 10 cm^{-1} and a strong band at 1665 ± 5 cm^{-1}; all of the other homophthalimides possessed similar absorptions at 1673 ± 10 and 1719 ± 10 cm^{-1}. Hall and Zbinden (5) reported absorptions at 1728 ± 1 and 1672 ± 4 cm^{-1} for two six-membered imides.

Can. J. Chem. Downloaded from www.nrcresearchpress.com by 210.87.254.40 on 09/05/12
For personal use only.

Can. J. Chem. Downloaded from www.nrcresearchpress.com by 210.87.254.40 on 09/05/12
For personal use only.

TABLE 2. Yields and properties of some spirocyclic homophthalimides and related compounds

Compound no.	R	X	% Yield* Base A†	% Yield* Base B†	Melting point (°C)	Crystallization solvent	% Calculated C	% Calculated H	% Calculated N	% Found C	% Found H	% Found N
4	H	H	—‡	50	206–207§	Acetonitrile	70.58	4.85	7.48	70.70	4.90	7.43
4	CH_3	H	53–62	69–79	169–171§	Cyclohexane:benzene (3:1)	71.62	5.51	6.96	71.38	5.58	7.04‖
4	CH_3	Cl	—‡	75	172–173	Benzene:cyclohexane (1:1)	61.15	4.27	5.94	61.27	4.30	5.95
4	C_2H_5	H	56–63	78.5	136–138	Cyclohexane	72.54	6.09	6.51	72.74	6.04	6.36
4	C_6H_5	H	—‡	56.5	195–197§	Benzene	77.75	4.98	5.32	77.63	4.97	5.34
7	CH_3	—	64	—¶	82–84	Cyclohexane	76.27	6.40	8.09	76.11	6.38	8.04**
7	CH_2CH_2Cl	—	30–35	—¶	42.5–44††	Hexane	65.01	5.45	6.32	65.15	5.42	6.27
8	—	—	—‡	48–56	226–227	Acetonitrile	59.07	4.51	6.26	58.98	4.51	6.22

*Yields refer to once crystallized products.
†Base A = sodium hydride; base B = potassium carbonate (see Experimental section).
‡Reaction with this base not attempted.
§Melting points reported (1) for **3**, R=H, CH_3, and C_6H_5 (X=H in all cases) were 212, 172, and 195°, respectively.
‖Molecular weight (Rast): Calcd. for $C_{12}H_{11}NO_2$: 201.2. Found: 192.
¶Potassium carbonate did not effect the desired cycloalkylation reaction.
**Molecular weight (Rast): Calcd. for $C_{11}H_{11}NO$: 173.2. Found: 183.
††Sublimed at 40°/0.001 mm before analysis. On standing a higher melting form (m.p. 74–75°) was obtained; later preparations gave only the high melting modification.

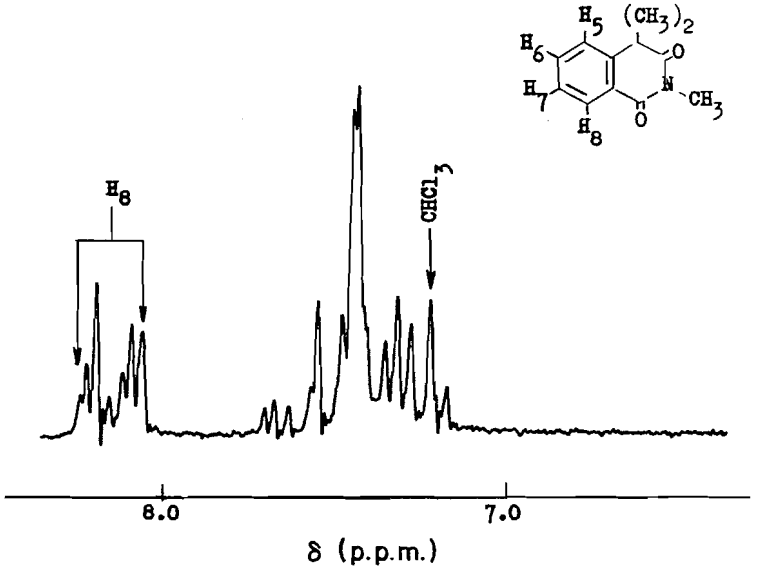

FIG. 2. The n.m.r. spectrum of the aromatic protons of 2,4,4-trimethylhomophthalimide.

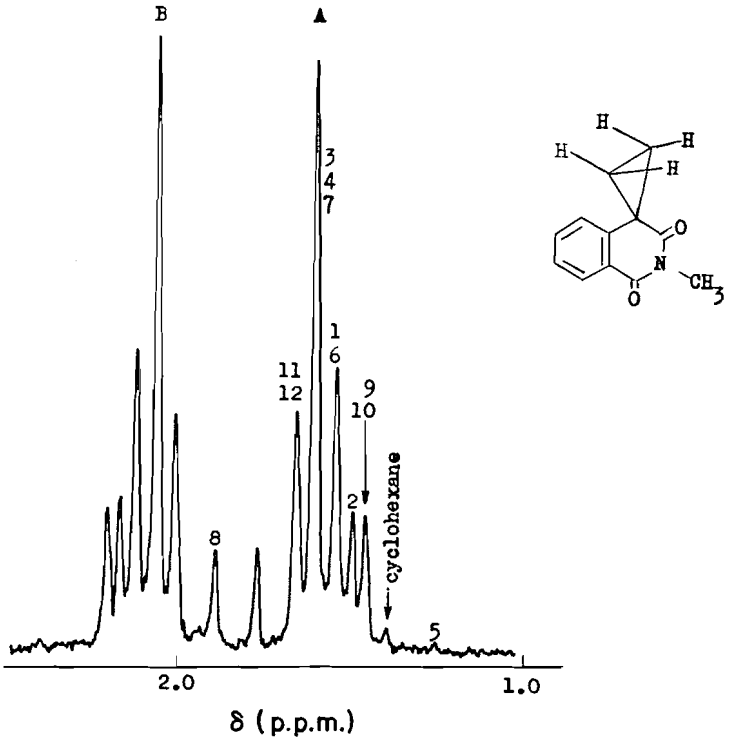

FIG. 3. The n.m.r spectrum of the cyclopropane hydrogens of 2-methyl-4,4-dimethylenehomophthalimide.

Can. J. Chem. Downloaded from www.nrcresearchpress.com by 210.87.254.40 on 09/05/12
For personal use only.

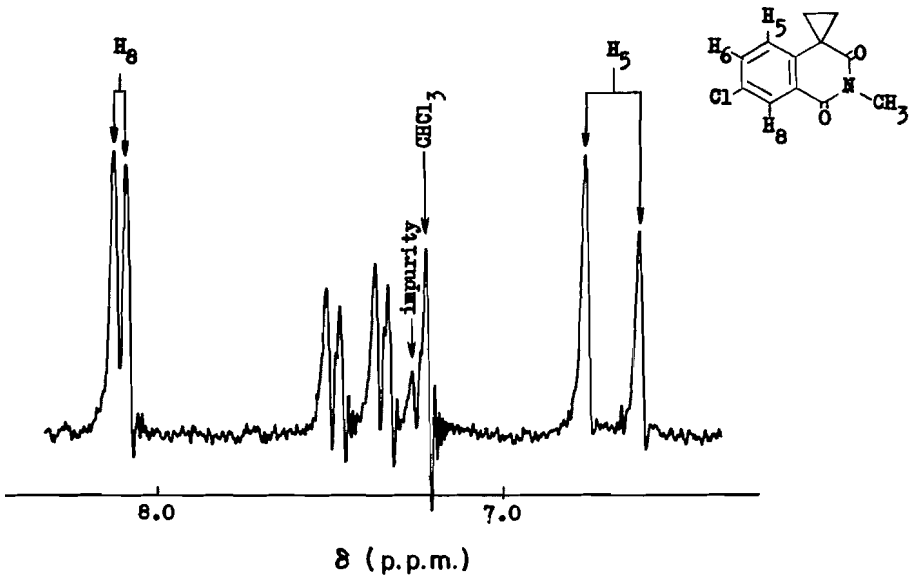

FIG. 4. The n.m.r. spectrum of the aromatic protons of 2-methyl-4,4-dimethylene-7-chlorohomophthalimide.

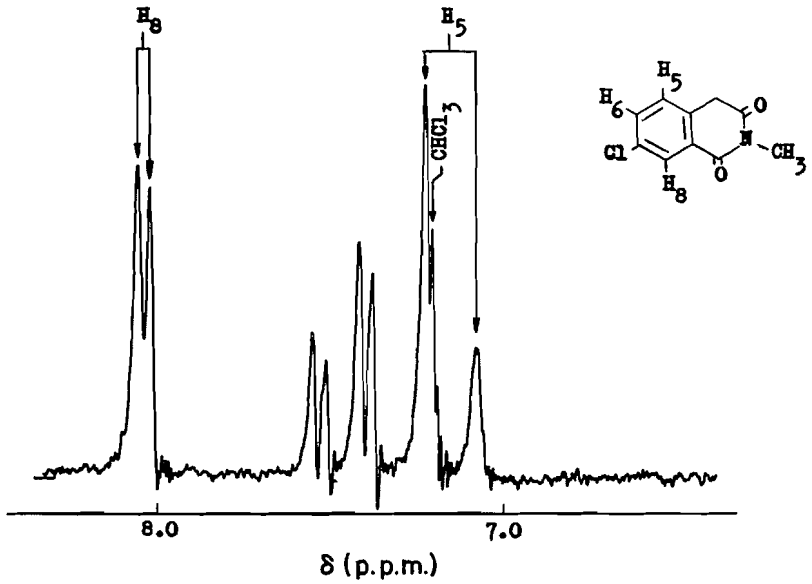

FIG. 5. The n.m.r. spectrum of the aromatic protons of 2-methyl-7-chlorohomophthalimide.

cm^{-1} region. On standing in air, the base was transformed in part to the hydroxy compound **6***a*. The presence of an hydroxyl moiety was indicated by a broad band at 3270 cm^{-1} in the i.r. spectrum of the hydrobromide salt, and a diffuse (w_H = 40 Hz) absorption easily exchangeable with D_2O centered at δ 5.98 in the n.m.r. spectrum of the free base. The hydroxy compound **6***a* is the product which would be expected from reduction of an hydroperoxide by a tertiary amine (7). 1-Dimethylamino-3-phenyloxindole has been reported to undergo an analogous aerial oxidation (8). Scission of the cyclopropane ring was also accomplished with refluxing piperidine,

Can. J. Chem. Downloaded from www.nrcresearchpress.com by 210.87.254.40 on 09/05/12
For personal use only.

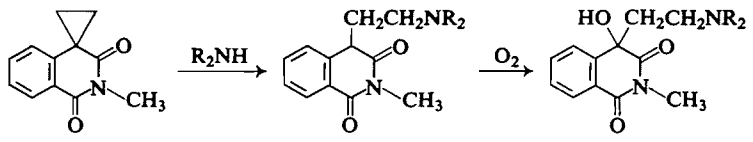

5
a R = CH_3
b R = $(CH_2)_5$

6
a R = CH_3
b R = $(CH_2)_5$

SCHEME 2

and the base thus obtained (**5***b*) was also rapidly oxidized by air to the hydroxy compound **6***b*. The *N*-ethyl compound (**4**, R = C_2H_5; X = H) underwent the same cleavage reaction with secondary amines, but the products were not fully characterized.

The base-promoted alkylation of several other homophthalimides with 1-bromo-2-chloroethane also yielded compounds to which cyclopropane structures were assigned (Table 2) principally on the basis of the similarity of their n.m.r. spectra (Table 3) to that of **4** (R = CH_3; X = H). Two members of this group (**4**, R = H, C_6H_5; X = H; see Table 2) also had melting points which were close to those reported (1) for the alleged spiro compounds (**3**, R = H, C_6H_5; X = H). On the basis of the observations described herein, it is highly probable that all of these latter structures will have to be revised.

The alkylation reaction was extendable to oxindole and 1-methyloxindole. The products (**7***a*, *b*)[3] were assigned the spiro cyclopropane structures **7** mainly by analogy, since, in this case, the n.m.r. spectra were much less definitive than observed in the homophthalimide series. Although the cyclopropane hydrogens still appeared as an AA'BB' pattern, the upfield shift of the adjacent aromatic proton (H-4) was no longer observed. This latter effect was presumably a consequence of the increased tilting of the plane of the cyclopropane ring away from the adjacent Ar—H bond. An attempt to cycloalkylate 4-hydroxycarbostyril in the usual manner gave instead only 4-(2-chloroethoxy)carbostyril (**8**), the structure of which was readily apparent from its elemental analysis and spectral properties (see Tables 2 and 3).

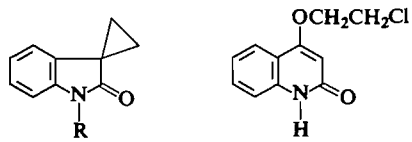

7
a R = CH_2CH_2Cl
b R = CH_3

8

[3]The cycloalkylation of the oxindole compounds could only be effected with sodium hydride as the base. Under these conditions oxindole did not lend itself to selective *C*-alkylation, therefore the reaction was carried out in a manner such that only **7***a* was produced (excess sodium hydride).

Experimental

The melting points were recorded in a Gallenkamp melting point apparatus and are not corrected. The i.r. spectra were measured as solutions in chloroform or solid dispersions in mineral oil with a Perkin–Elmer 237-B grating spectrophotometer or a Unicam SP-200G i.r. spectrophotometer.

Homophthalic acid was purchased from the Aldrich Chemical Co. and oxindole and *N*-methyloxindole were prepared by catalytic reduction of the corresponding isatins (9).

Preparation of the Homophthalimides (1)

The following general procedures were found to be more reproducible and to give products of better purity than the usual literature methods (*e.g.*, 10, 11).

(a) Low Boiling Amines (Water Soluble)

Homophthalic acid (0.1 mol), was dissolved with stirring in a solution of the primary amine (1.0 mol) in *ca.* 150 ml of water; brief heating was sometimes necessary to obtain a clear solution. The solution was evaporated to dryness *in vacuo* and 250 ml of xylene was added to the residue. The vigorously stirred mixture was heated under reflux while the water was collected and periodically removed from an attached Dean–Stark apparatus. When the evolution of water had ceased (reaction periods ≤ 18 h), the solvent was removed *in vacuo* and the residue was crystallized from the appropriate solvent.

2-Methyl-7-chlorohomophthalimide was obtained in this way in 76% yield (pure), m.p. 116–118°.

Anal. Calcd. for $C_{10}H_8NO_2Cl$: C, 57.29; H, 3.84; N, 6.68. Found: C, 57.34; H, 3.91; N, 6.71.

(b) High Boiling and/or Water Insoluble Amines

Homophthalic acid (0.1 mol) was added with vigorous stirring to a solution of the amine (0.4 mol) in 250 ml of xylene. The mixture was heated at reflux temperature

Can. J. Chem. Downloaded from www.nrcresearchpress.com by 210.87.254.40 on 09/05/12
For personal use only.

Can. J. Chem. Downloaded from www.nrcresearchpress.com by 210.87.254.40 on 09/05/12
For personal use only.

TABLE 3. The n.m.r.* spectra of some spirocyclic homophthalimides and related compounds

Compound no.	R	X	Cyclopropane hydrogens†			Aromatic hydrogens			Other
			δ_A	δ_B	Peaks in each half	H-5	H-6,7	H-8	
4‡	H	H	1.70	1.94	5	7.09	7.58	8.14	11.53(NH)
4	CH_3	H	1.60	2.11	7	6.74	7.22	8.17	3.35(NCH_3)
4	CH_3	Cl	1.58	2.11	7	6.67	7.41	8.09	3.34(NCH_3)
4	C_2H_5	H	1.60	2.12	6	6.81	7.47	8.26	1.24(t)§, 4.08(q)[N—C_2H_5]
4	C_6H_5	H	1.64	2.16	6	6.78	7.35‖	8.20	—
7	CH_3	—	1.47	1.70	5	—	7.00¶	—	3.24(NCH_3)
7	CH_2CH_2Cl	—	1.50	1.73	5	—	7.00¶	—	3.71(quin)**, 4.07(quin)[NCH_2CH_2Cl]
8	—	—	4.08††	4.35††	6	—	7.42¶	—	5.88(H_3), 11.30(NH)

*The n.m.r. spectra were recorded with a Varian A-60A spectrometer as *ca.* 0.9 *M* solutions in deuteriochloroform (unless speeified otherwise) and are expressed in p.p.m. (δ) from internal tetramethylsilane.

†The cyclopropane hydrogens appeared as a multiplet of the AA'BB' type. The A part of the spectrum was arbitrarily assigned to the two cyclopropane hydrogens directed toward the aromatic ring. See NOTE ADDED IN PROOF at end of Table 1.

‡Measured in perdeuteriodimethylsulfoxide.

§q = Quartet; quin = quintet: t = triplet.

‖Center of a complex multiplet which included the five *N*-phenyl hydrogens.

¶Center of a complex multiplet.

**These protons appeared as an A_2B_2 pattern with $J/\nu_0\delta = 0.34$.

††Methylene protons of the 2-chloroethoxy side chain.

Can. J. Chem. Downloaded from www.nrcresearchpress.com by 210.87.254.40 on 09/05/12
For personal use only.

with separation of water as above. The work up procedure was the same as that described above.

The pure yields of the homophthalimides obtained by methods *a* and *b* ranged from 70–90%. The melting points and other physical properties of these compounds agreed with the literature values.

General Conditions for the Cycloalkylation Reaction

(a) Sodium Hydride as the Base

A 55% dispersion of sodium hydride in mineral oil (50 mmol)[4] was washed free of the carrier with hexane and layered with 100 ml of dry DMF. The mixture was stirred at 0° in a nitrogen atmosphere while the solid homophthalimide or oxindole (25 mmol) was added portionwise. When the evolution of gas had become slow, 1-bromo-2-chloroethane (250 mmol) was added dropwise at 0° at a rate such that excessive foaming was avoided (*ca.* 1/2 h). The cooling bath was removed, and stirring at room temperature under a slight positive pressure of nitrogen was continued for 12–24 h. The deeply colored solution was poured into a large volume of water and the product was extracted into benzene. The extract was washed well with water, dried over sodium sulfate, and evaporated *in vacuo*. The spirocyclic homophthalimides were usually obtained crystalline and were then recrystallized from a suitable solvent. The oxindoles gave oils from which the desired spiro compound was isolated by column chromatography on neutral alumina (Fluka, activity II).

(i) 1-Methyloxindole gave an oil (*ca.* 2 g from a 10 mmol scale reaction) which was chromatographed on 100 g of alumina (packed in benzene) using methylene chloride as the eluant. The first 100 ml of the eluate was discarded, the next 130 ml contained the product which was then further purified by crystallization.

(ii) The reaction with oxindole also gave an oil (2.4 g from a 15 mmol scale reaction). The product was obtained from the mixture by dry column chromatography (12) on 200 g of alumina using chloroform as the eluant (50 ml fractions). The product was found in fractions 2–7.

(b) Potassium Carbonate as the Base

To a stirred mixture of the homophthalimide (50 mmol) and potassium carbonate (90–100 mmol) in 100 ml of dry DMF was added 500 mmol of 1-bromo-2-chloroethane. The mixture was stirred at room temperature under a positive pressure of nitrogen for 18–48 h. The deeply colored mixture was poured into water and extracted with benzene [ethyl acetate for **4** (R = H = X)] and after the usual manipulations the crude product was purified by crystallization. In the case of **4** (R = C_6H_5; X = H) it was necessary to isolate the product by chromatography of the mixture on alumina (30 g/g of substrate) using chloroform as the eluant.

*Ring Cleavage of **4** (R = CH_3, X = H) with Secondary Amines*

(a) Dimethylamine

Nitrogen was bubbled through 50 ml of DMF, contained in a pressure bottle, for 10 min and then dimethylamine was passed into the solvent until 9.0 g (200 mmol) had been absorbed. The cyclopropane (2.00 g) was added, the bottle was sealed and placed in an oil bath at 65°. After 1.5 h the solution was cooled to room temperature and nitrogen was passed through the solvent to remove the dimethylamine (*ca.* 10 min). The solution was concentrated to 15 ml at 60°/20 mm and the resultant was diluted with 15 ml of water and 10 ml of 48% hydrobromic acid. The solution was concentrated to about 5 ml *in vacuo* and then it was diluted with water and made basic with sodium carbonate solution (200 g/l). The mixture was extracted with dichloromethane, the extract was dried over sodium sulfate and evaporated *in vacuo* (eventually at 60°/0.01 mm). All operations on the free base were performed as rapidly as possible to minimize aerial oxidation. The oil (1.693 g) was converted to its hydrobromide salt in ether and this was crystallized from acetonitrile. The first crop (945 mg) of crystalline material was fairly pure **5***a* (m.p. 196–200°). Addition of ether (to turbidity) to the mother liquor gave 1.05 g of a mixture (m.p. 170–200°) which was fractionally crystallized from acetonitrile. The mixture was thus separated into a small amount (128 mg) of the very insoluble 4-hydroxy compound **6***a* (m.p. 227–230°) and 436 mg (200–205°) of the more soluble **5***a*.

Three recrystallizations of the lower melting salt from acetonitrile gave pure **5***a*, m.p. 203–205°.

Anal. Calcd. for $C_{14}H_{18}N_2O_2 \cdot HBr$: C, 51.40; H, 5.85; N, 8.55. Found: C, 51.17; H, 5.93; N, 8.54.

The i.r. spectrum (Nujol mull) of the salt had absorptions at 2700 (br), 2605, 2480, 1717, and 1675 cm^{-1}.

The n.m.r. spectrum of the free base ($CDCl_3$) had singlets at δ 2.03 (*N*-dimethyl group) and 3.29 (ring *N*-methyl) and multiplets centered at δ 2.23 (four methylene protons), 3.96 (methine proton at C-5, w_H = 13 Hz), 7.44 (H-5 to -7) and 8.13 (H-8). The absorption at δ 3.96 was easily exchanged with D_2O.

The high melting salt was thrice recrystallized from acetonitrile, but the m.p. (227–230°) remained unchanged. This material (**6***a*) could be obtained in much larger amounts if **5***a* was left (as the free base) in an open vessel for 2–3 days. Only **6***a* could be isolated (as the insoluble hydrobromide salt) from the mixture thus obtained.

Anal. Calcd. for $C_{14}H_{18}N_2O_3 \cdot HBr$: C, 48.99; H, 5.58; N, 8.16. Found: C, 48.93; H, 5.60; N, 8.25.

The i.r. spectrum (Nujol mull) of the salt of **6***a* had absorptions at 3270, 2670 (br), 2460 (br), 1725, and 1675 cm^{-1}.

The n.m.r. spectrum ($CDCl_3$) of the free base had singlets at δ 2.33 (*N*-dimethyl group), 3.34 (ring *N*-methyl), and 5.98 (OH; w_H = 40 Hz), and complex multiplets centered at δ 2.17 (four methylene protons), 7.58 (H-5 to -7) and 8.14 (H-8).

(b) Piperidine

Piperidine (20 ml) was deoxygenated as before, then 2.00 g of the cyclopropyl compound was added and the solution was heated at reflux temperature (nitrogen atmosphere for 1/2 h. The work-up procedure was the same as that described above but no precautions were taken to minimize exposure to air. The mixture of bases (2.10 g) was separated by fractional crystallization of the hydrobromide salts from acetonitrile. The less soluble higher melting (the various crops had melting points which ranged from 255 to 268°) fractions (total of 988 mg) contained mainly the product of aerial oxidation (*i.e.* **6***b*). The lower melting (melting points ranged from 205–209°), more soluble fractions consisted of fairly pure **6***a* (total of 837 mg).

[4]Sodium hydride (75 mmol) was used for oxindole.

After three crystallizations from acetonitrile the higher melting material (*6b*) had m.p. 271–272°.

Anal. Calcd. for $C_{17}H_{22}N_2O_3 \cdot HBr$: C, 53.27; H, 6.05; N, 7.31. Found: C, 53.06; H, 6.04; N, 7.33.

The i.r. spectrum (Nujol mull) had bands at 3370, 2725, 2660, 2550, 1725, and 1674 cm^{-1}.

The more soluble salt (*6a*) was crystallized once from acetonitrile and twice from 2-propanol. The m.p. was then 207–209°.

Anal. Calcd. for $C_{17}H_{22}N_2O_2 \cdot HBr$: C, 55.59; H, 6.31; N, 7.63. Found: C, 55.30; H, 6.34; N, 7.54.

The i.r. spectrum (Nujol mull) had absorptions at 2660 (br), 2560, 1718, and 1677 cm^{-1}.

The Overhauser effect was measured with a Varian HA-100 spectrometer by Dr. H. J. Koch and Mr. R. Simoneau at the Department of Chemistry, McGill University, Montreal, Quebec. We thank Professor A. S. Perlin for making the service available to us.

1. (*a*) C. FOURNIER and J. DECOMBE. C.R. série C. **264**, 210 (1967); (*b*) C. FOURNIER and J. DECOMBE. Bull. Soc. Chim. Fr. 364 (1968).
2. H. M. HUTTON and T. SCHAEFER. Can. J. Chem. **41**, 2429 (1963).
3. D. J. PATEL, M. E. HOWDEN, and J. D. ROBERTS. J. Amer. Chem. Soc. **85**, 3218 (1963).
4. G. F. KOSER and W. H. PIRKLE. J. Org. Chem. **32**, 1992 (1967).
5. H. K. HALL and R. ZBINDEN. J. Amer. Chem. Soc. **80**, 6428 (1958).
6. J. M. STEWART and H. H. WESTBERG. J. Org. Chem. **30**, 1951 (1965).
7. C. W. KAPP and E. G. E. HAWKINS. J. Chem. Soc. 4106 (1953).
8. R. F. MEYER. J. Org. Chem. **30**, 3451 (1965).
9. J. M. MUCHOWSKI. Can. J. Chem. **47**, 857 (1969).
10. N. P. BUU-HOI, G. SAINT-RUF, and J. C. BOURGEADE. J. Heterocycl. Chem. **5**, 545 (1968).
11. B. R. HARRIMAN, R. S. SHELTON, M. G. VAN CAMPEN, and M. R. WARREN. J. Amer. Chem. Soc. **67**, 1481 (1945).
12. (*a*) B. LOEV and K. M. SNADER. Chem. Ind. 15 (1965); (*b*) B. LOEV and M. M. GOODMAN. Chem. Ind. 2026 (1967).
13. F. A. L. ANET and A. J. R. BOURN. J. Amer. Chem. Soc. **87**, 5250 (1965).

Can. J. Chem. Downloaded from www.nrcresearchpress.com by 210.87.254.40 on 09/05/12
For personal use only.

Can. J. Chem. Downloaded from www.nrcresearchpress.com by 210.87.254.42 on 09/05/12
For personal use only.

Effects of Centrifugal Distortion and Nuclear Quadrupole Coupling in the Microwave Spectrum of Vinyl Chloride

M. C. L. GERRY

Department of Chemistry, The University of British Columbia, Vancouver 8, British Columbia

Received August 31, 1970

Both *a*- and *b*-type rotational transitions have been measured up to $J = 30$ for the two most abundant isotopic species of vinyl chloride, in the frequency region 8–18 GHz. These have enabled refinement of the rotational and chlorine nuclear quadrupole coupling constants, and evaluation of all first order centrifugal distortion constants. From the quadrupole coupling constants it is concluded that the field gradient around the C—Cl bond is somewhat more symmetric than previously reported. A comparison is made between the centrifugal distortion constants obtained from the microwave spectrum and those calculated using infrared data.

Canadian Journal of Chemistry, 49, 255 (1971)

Introduction

Several aspects of the microwave spectrum of vinyl chloride have appeared previously. In the first study (1) nuclear quadrupole coupling was observed and measured for the first time in the rotational spectrum of an asymmetric rotor. Subsequently Kivelson, Wilson, and Lide (K.W.L.) (2) observed low J *a*-type R branches of several isotopic species, which yielded internuclear parameters, more accurate chlorine nuclear quadrupole coupling constants, and the molecular dipole moment. More recently Savariraj (3) measured some low J *a*-type and *b*-type transitions, and after accounting partially for centrifugal distortion, obtained a value for the rotational constant A in the ground vibrational state.

This article presents the assignment and measurement of a large number of *a*- and *b*-type transitions to high values for J for the two most abundant isotopic species. Using these transitions the rotational and nuclear quadrupole coupling constants have been refined, enabling some further structural information to be obtained. Also, good values for all first order centrifugal distortion constants have been obtained, permitting comparison with those calculated from a force field obtained solely from vibrational data.

Experimental

Transitions were measured in the frequency region 8–18 GHz, using a 100 kHz Stark modulated spectrometer having a 10 ft X-band cell. The spectrometer was of conventional design, except that the source was a phase stabilized Hewlett-Packard 8400B Microwave Spectroscopy Source. This source permitted broad banded frequency sweeps with chart presentation of absorption lines, which considerably eased initial searches for transitions. For accurate measurements the source, phase stabilized, was swept manually through the absorption lines. All measurements were made at room temperature at sample pressures of 1–10 μ. The sample was obtained from the Matheson Company and used without further purification.

Observed Spectrum and Assignment

Initially the rigid rotor spectrum of vinyl chloride, with transitions split by nuclear quadrupole coupling, was predicted using previously published rotational and nuclear quadrupole coupling constants (2, 3). After a general search for transitions over the complete frequency range studied, the prediction enabled several previously unreported low J transitions to be identified easily. Using these transitions in turn, and the methods of analysis given in the following sections, refined rotational and quadrupole coupling constants and preliminary centrifugal distortion constants were obtained; these gave further predictions of higher J transitions. Several of these were identified after detailed investigation of the appropriate frequency regions, and yielded improved distortion constants, as well as satisfactory predictions and assignments up to $J = 30$. The quadrupole coupling patterns confirmed all assignments.

The observed frequencies and their assignments, hypothetical unsplit frequencies, transition frequencies calculated using the measured rotational and centrifugal distortion constants, and the distortion corrections are given in Tables 1 and 2 for $CH_2CH^{35}Cl$ and $CH_2CH^{37}Cl$, respectively. The average deviations for observed and calculated frequencies are 0.03 MHz for $CH_2CH^{35}Cl$ and 0.04 MHz for $CH_2CH^{37}Cl$.

TABLE 1. Ground state rotational transitions* of $CH_2CH^{35}Cl$ (MHz)

Transition	$F'-F''$	Observed frequency	Unsplit line†	Calculated frequency‡	Distortion correction§
$1_{01}-0_{00}$	$\frac{3}{2}-\frac{3}{2}$	11 463.79	11 475.23	11 475.18	−0.01
	$\frac{5}{2}-\frac{3}{2}$	11 478.12			
	$\frac{1}{2}-\frac{3}{2}$	11 489.50			
$2_{12}-3_{03}$	$\frac{7}{2}-\frac{9}{2}$	15 821.36	15 823.87	15 823.90	−0.65
	$\frac{3}{2}-\frac{5}{2}$	15 826.74			
	$\frac{5}{2}-\frac{7}{2}$	15 827.76			
$5_{14}-5_{15}$	$\frac{7}{2}-\frac{7}{2}$	8 768.08	8 769.03	8 769.05	−0.98
	$\frac{13}{2}-\frac{13}{2}$	8 768.44			
	$\frac{9}{2}-\frac{9}{2}$	8 769.53			
	$\frac{11}{2}-\frac{11}{2}$	8 769.93			
$5_{05}-4_{14}$	$\frac{9}{2}-\frac{7}{2}$	9 032.68	9 033.77	9 033.73	−1.29
	$\frac{11}{2}-\frac{9}{2}$	9 033.14			
	$\frac{7}{2}-\frac{5}{2}$	9 034.17			
	$\frac{13}{2}-\frac{11}{2}$	9 034.57			
$6_{15}-6_{16}$	$\frac{9}{2}-\frac{9}{2}$	12 274.12	12 275.02	12 275.00	−1.83
	$\frac{15}{2}-\frac{15}{2}$	12 274.41			
	$\frac{11}{2}-\frac{11}{2}$	12 275.60			
	$\frac{13}{2}-\frac{13}{2}$	12 275.85			
$7_{16}-7_{17}$	$\frac{11}{2}-\frac{11}{2}$	16 362.46	16 363.35	16 363.33	−3.15
	$\frac{17}{2}-\frac{17}{2}$	16 362.71			
	$\frac{13}{2}-\frac{13}{2}$	16 363.92			
	$\frac{15}{2}-\frac{15}{2}$	16 364.22			
$10_{29}-11_{1,10}$	$\frac{23}{2}-\frac{25}{2}$, $\frac{17}{2}-\frac{19}{2}$	8 343.08	8 343.32	8 343.32	17.72
	$\frac{21}{2}-\frac{23}{2}$, $\frac{19}{2}-\frac{21}{2}$	8 343.58			
$14_{2,12}-14_{2,13}$	$\frac{25}{2}-\frac{25}{2}$, $\frac{31}{2}-\frac{31}{2}$	8 779.15	8 779.33	8 779.37	−14.10
	$\frac{27}{2}-\frac{27}{2}$, $\frac{29}{2}-\frac{29}{2}$	8 779.52			
$15_{2,13}-15_{2,14}$	$\frac{27}{2}-\frac{27}{2}$, $\frac{33}{2}-\frac{33}{2}$	11 355.37	11 355.58	11 355.62	−20.34

Can. J. Chem. Downloaded from www.nrcresearchpress.com by 210.87.254.42 on 09/05/12
For personal use only.

TABLE 1. (*Continued*)

Transition	$F'-F''$	Observed frequency	Unsplit line†	Calculated frequency‡	Distortion correction§
	$\frac{29}{2}-\frac{29}{2}$	11 355.78			
	$\frac{31}{2}-\frac{31}{2}$				
$16_{2,14}-16_{2,15}$	$\frac{29}{2}-\frac{29}{2}$	14 413.78	14 414.04	14 414.11	−28.58
	$\frac{35}{2}-\frac{35}{2}$				
	$\frac{31}{2}-\frac{31}{2}$	14 414.30			
	$\frac{33}{2}-\frac{33}{2}$				
$17_{2,15}-17_{2,16}$	$\frac{31}{2}-\frac{31}{2}$	17 990.24	17 990.49	17 990.50	−39.21
	$\frac{37}{2}-\frac{37}{2}$				
	$\frac{33}{2}-\frac{33}{2}$	17 990.74			
	$\frac{35}{2}-\frac{35}{2}$				
$17_{2,15}-18_{1,18}$	$\frac{31}{2}-\frac{33}{2}$	16 984.70	16 985.56	16 985.52	−7.52
	$\frac{37}{2}-\frac{39}{2}$				
	$\frac{33}{2}-\frac{35}{2}$	16 986.43			
	$\frac{35}{2}-\frac{37}{2}$				
$18_{2,16}-19_{1,19}$	$\frac{33}{2}-\frac{35}{2}$	15 574.48	15 575.34	15 575.33	−17.28
	$\frac{39}{2}-\frac{41}{2}$				
	$\frac{35}{2}-\frac{37}{2}$	15 576.21			
	$\frac{37}{2}-\frac{39}{2}$				
$18_{3,16}-19_{2,17}$	$\frac{39}{2}-\frac{41}{2}$	17 987.51	17 987.60	17 987.60	113.74
	$\frac{33}{2}-\frac{35}{2}$				
	$\frac{37}{2}-\frac{39}{2}$	17 987.71			
	$\frac{35}{2}-\frac{37}{2}$				
$19_{2,17}-20_{1,20}$	$\frac{35}{2}-\frac{37}{2}$	15 057.32	15 058.20	15 058.22	−30.77
	$\frac{41}{2}-\frac{43}{2}$				
	$\frac{37}{2}-\frac{39}{2}$	15 059.08			
	$\frac{39}{2}-\frac{41}{2}$				
$20_{2,18}-21_{1,21}$	$\frac{37}{2}-\frac{39}{2}$	15 448.12	15 448.98	15 449.00	−48.52
	$\frac{43}{2}-\frac{45}{2}$				
	$\frac{39}{2}-\frac{41}{2}$	15 449.84			
	$\frac{41}{2}-\frac{43}{2}$				

Can. J. Chem. Downloaded from www.nrcresearchpress.com by 210.87.254.42 on 09/05/12
For personal use only.

TABLE 1. (*Continued*)

Transition	$F'-F''$	Observed frequency	Unsplit line†	Calculated frequency‡	Distortion correction§
$21_{2,19}-20_{3,18}$	$\frac{45}{2}-\frac{43}{2}$ $\frac{43}{2}-\frac{41}{2}$ $\frac{41}{2}-\frac{39}{2}$ $\frac{39}{2}-\frac{37}{2}$	12 780.63‖**	12 780.63	12 780.62	−188.50
$21_{2,19}-22_{1,22}$	$\frac{39}{2}-\frac{41}{2}$ $\frac{45}{2}-\frac{47}{2}$	16 754.74	16 755.62	16 755.62	−71.06
	$\frac{41}{2}-\frac{43}{2}$ $\frac{43}{2}-\frac{45}{2}$	16 756.50			
$22_{3,19}-23_{2,22}$	$\frac{41}{2}-\frac{43}{2}$ $\frac{47}{2}-\frac{49}{2}$	11 107.49	11 107.90	11 107.91	78.54
	$\frac{43}{2}-\frac{45}{2}$ $\frac{45}{2}-\frac{47}{2}$	11 108.32			
$25_{3,22}-25_{3,23}$	$\frac{53}{2}-\frac{53}{2}$ $\frac{51}{2}-\frac{51}{2}$ $\frac{49}{2}-\frac{49}{2}$ $\frac{47}{2}-\frac{47}{2}$	9 361.24‖**	9 361.24	9 361.19	−68.36
$26_{3,23}-26_{3,24}$	$\frac{55}{2}-\frac{55}{2}$ $\frac{53}{2}-\frac{53}{2}$ $\frac{51}{2}-\frac{51}{2}$ $\frac{49}{2}-\frac{49}{2}$	11 648.26‖**	11 648.26¶	11 648.23	−90.52
$26_{2,25}-25_{3,22}$	$\frac{53}{2}-\frac{51}{2}$ $\frac{51}{2}-\frac{49}{2}$	10 063.62‖	10 064.03¶	10 063.69	−80.84
	$\frac{55}{2}-\frac{53}{2}$ $\frac{49}{2}-\frac{47}{2}$	10 064.44‖			
$27_{3,24}-27_{3,25}$	$\frac{51}{2}-\frac{51}{2}$ $\frac{57}{2}-\frac{57}{2}$ $\frac{53}{2}-\frac{53}{2}$ $\frac{55}{2}-\frac{55}{2}$	14 345.39‖**	14 345.39¶	14 345.33	−118.19
$27_{2,26}-26_{3,23}$	$\frac{55}{2}-\frac{53}{2}$ $\frac{53}{2}-\frac{51}{2}$	15 869.18‖	15 869.60¶	15 869.12	−71.66
	$\frac{57}{2}-\frac{55}{2}$ $\frac{51}{2}-\frac{49}{2}$	15 870.02‖			
$28_{3,25}-28_{3,26}$	$\frac{53}{2}-\frac{53}{2}$ $\frac{59}{2}-\frac{59}{2}$	17 494.62‖	17 494.75¶	17 494.61	−152.29

Can. J. Chem. Downloaded from www.nrcresearchpress.com by 210.87.254.42 on 09/05/12
For personal use only.

TABLE 1. (*Concluded*)

Transition	F'–F''	Observed frequency	Unsplit line†	Calculated frequency‡	Distortion correction§
$27_{4,24}$–$28_{3,25}$	$\frac{55}{2}-\frac{55}{2}$, $\frac{57}{2}-\frac{57}{2}$	17 494.88‖			
	$\frac{57}{2}-\frac{59}{2}$, $\frac{55}{2}-\frac{57}{2}$, $\frac{53}{2}-\frac{55}{2}$	17 912.70‖	17 912.70¶	17 913.11	379.53
$29_{4,25}$–$30_{3,28}$	$\frac{51}{2}-\frac{53}{2}$, $\frac{61}{2}-\frac{63}{2}$, $\frac{55}{2}-\frac{57}{2}$	14 937.01‖	14 937.23¶	14 937.45	282.24
	$\frac{59}{2}-\frac{61}{2}$, $\frac{57}{2}-\frac{59}{2}$	14 937.45‖			

*Estimated uncertainty is ±0.05 MHz, except where otherwise indicated.
†Hypothetical unsplit frequencies with hyperfine structure removed.
‡Frequency calculated using the rotational constants and centrifugal distortion constants obtained in the analysis.
§Deviation between the calculated frequency of the adjacent column and that calculated using the derived rotational constants in a rigid rotor approximation.
‖Not used in the analysis for quadrupole coupling constants.
¶Not used in the distortion analysis.
**Estimated uncertainty is ±0.1 MHz.

Nuclear Quadrupole Coupling

The nuclear quadrupole energy of an asymmetric rotor having one quadrupolar nucleus may be written to first order as (4)

$$[1]\quad E_Q = \frac{f(I,J,F)}{J(J+1)}\chi_{aa} \times [3\langle P_a^2\rangle - J(J+1) + (\langle P_a^2\rangle - W)\eta/b_p]$$

where $f(I,J,F)$ is Casimir's function (5); b_p is Wang's asymmetry parameter; $W = W(b_p)$ is the Wang reduced energy; $\langle P_a^2\rangle$ is the average value of the square of the angular momentum about the a-principal inertial axis. If χ_{gg} is the component of the quadrupole coupling tensor along the g-principal inertial axis, η is defined by $\eta\chi_{aa} = \chi_{bb} - \chi_{cc}$. A least squares fit was made to χ_{aa} and $\eta\chi_{aa}$ in this equation using all resolved groups having $J \leqslant 25$ for both isotopic species. The results are shown in Table 3. It is seen that the values for χ_{aa} are in excellent agreement with earlier values (2), whereas the values for η are rather different. Nevertheless, the ratio $\chi_{cc}(^{35}Cl)/\chi_{cc}(^{37}Cl) = 1.2649 \pm 0.0042$;[1] this agrees well with the ratio of the quadrupole moments of the two isotopes (1.2688), as is expected for a planar molecule.

With the assumption that one principal axis of the chlorine quadrupole tensor coincides with the C—Cl bond, and using the structural data of K.W.L. (2), the coupling constants were transformed from the inertial axis system to the principal axis system (z parallel to the C—Cl bond, y perpendicular to the molecular plane). The principal values of the quadrupole coupling tensor thus obtained are $\chi_{xx} = 38.37$ MHz, $\chi_{yy} = 31.52$ MHz, and $\chi_{zz} = -69.89$ MHz. These values are somewhat different from those obtained previously (2); in particular the difference $\chi_{xx} - \chi_{yy} = 6.85$ MHz is rather less.

The three main contributing resonance structures of vinyl chloride are probably

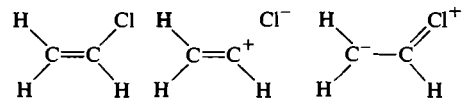

1 2 3

Goldstein (6) has shown that the difference $\chi_{xx} - \chi_{yy}$ is related to the number of electrons lost from chlorine as a result of double bonding, δ, with $\delta = (\chi_{xx} - \chi_{yy})/164.6$. In turn δ may be

[1]All errors reported are for confidence limits of 95%.

Can. J. Chem. Downloaded from www.nrcresearchpress.com by 210.87.254.42 on 09/05/12
For personal use only.

TABLE 2. Ground state rotational transitions* of $CH_2CH^{37}Cl$ (MHz)

Transition	F'–F''	Observed frequency	Unsplit line	Calculated frequency	Distortion correction
1_{01}–0_{00}	$\frac{3}{2}-\frac{3}{2}$	11 235.78	11 244.81	11 244.76	−0.01
	$\frac{5}{2}-\frac{3}{2}$	11 247.08			
	$\frac{1}{2}-\frac{3}{2}$	11 256.10			
5_{14}–5_{15}	$\frac{7}{2}-\frac{7}{2}$	8 432.88	8 433.67‡	8 433.70	−0.93
	$\frac{13}{2}-\frac{13}{2}$	8 433.23			
	$\frac{9}{2}-\frac{9}{2}$	8 434.06			
	$\frac{11}{2}-\frac{11}{2}$	8 434.40			
6_{15}–6_{16}	$\frac{9}{2}-\frac{9}{2}$	11 804.88	11 805.65	11 805.67	−1.74
	$\frac{15}{2}-\frac{15}{2}$	11 805.18			
	$\frac{11}{2}-\frac{11}{2}$	11 806.09			
	$\frac{13}{2}-\frac{13}{2}$	11 806.38			
7_{16}–7_{17}	$\frac{11}{2}-\frac{11}{2}$, $\frac{17}{2}-\frac{17}{2}$	15 737.28	15 737.87	15 737.88	−2.99
	$\frac{13}{2}-\frac{13}{2}$, $\frac{15}{2}-\frac{15}{2}$	15 738.43			
10_{29}–$11_{1,10}$	$\frac{23}{2}-\frac{25}{2}$, $\frac{17}{2}-\frac{19}{2}$	11 668.88	11 669.06	11 669.05	16.54
	$\frac{21}{2}-\frac{23}{2}$, $\frac{19}{2}-\frac{21}{2}$	11 669.27			
$13_{1,12}$–$12_{2,11}$	$\frac{29}{2}-\frac{27}{2}$, $\frac{27}{2}-\frac{25}{2}$, $\frac{25}{2}-\frac{23}{2}$, $\frac{23}{2}-\frac{21}{2}$	17 395.13†	17 395.12	17 395.06	−38.36
$14_{2,12}$–$14_{2,13}$	$\frac{25}{2}-\frac{25}{2}$, $\frac{31}{2}-\frac{31}{2}$	8 137.66	8 137.78	8 137.84	−12.94
	$\frac{27}{2}-\frac{27}{2}$, $\frac{29}{2}-\frac{29}{2}$	8 137.91			
$15_{2,13}$–$15_{2,14}$	$\frac{27}{2}-\frac{27}{2}$, $\frac{33}{2}-\frac{33}{2}$	10 533.37	10 533.50	10 533.52	−18.68
	$\frac{29}{2}-\frac{29}{2}$, $\frac{31}{2}-\frac{31}{2}$	10 533.63			

Can. J. Chem. Downloaded from www.nrcresearchpress.com by 210.87.254.42 on 09/05/12
For personal use only.

TABLE 2. (*Continued*)

Transition	F'–F''	Observed frequency	Unsplit line	Calculated frequency	Distortion correction
$16_{2,14}$–$16_{2,15}$	$\frac{29}{2}-\frac{29}{2}$	13 381.42	13 381.61	13 381.68	−26.27
	$\frac{35}{2}-\frac{35}{2}$				
	$\frac{31}{2}-\frac{31}{2}$	13 381.80			
	$\frac{33}{2}-\frac{33}{2}$				
$17_{2,15}$–$17_{2,16}$	$\frac{31}{2}-\frac{31}{2}$	16 717.09	16 717.27	16 717.33	−36.09
	$\frac{37}{2}-\frac{37}{2}$				
	$\frac{33}{2}-\frac{33}{2}$	16 717.46			
	$\frac{35}{2}-\frac{35}{2}$				
$17_{2,15}$–$18_{1,18}$	$\frac{31}{2}-\frac{33}{2}$	17 898.46	17 899.15	17 899.11	−4.53
	$\frac{37}{2}-\frac{39}{2}$				
	$\frac{33}{2}-\frac{35}{2}$	17 899.85			
	$\frac{35}{2}-\frac{37}{2}$				
$19_{2,17}$–$20_{1,20}$	$\frac{35}{2}-\frac{37}{2}$	15 381.39	15 382.05	15 382.07	−25.20
	$\frac{41}{2}-\frac{43}{2}$				
	$\frac{37}{2}-\frac{39}{2}$	15 382.72			
	$\frac{39}{2}-\frac{41}{2}$				
	$\frac{41}{2}-\frac{43}{2}$				
$19_{3,17}$–$20_{2,18}$	$\frac{39}{2}-\frac{41}{2}$	9 105.04†	9 105.04	9 105.01	139.72
	$\frac{37}{2}-\frac{39}{2}$				
	$\frac{35}{2}-\frac{37}{2}$				
$21_{2,19}$–$22_{1,22}$	$\frac{39}{2}-\frac{41}{2}$	16 330.78	16 331.45	16 331.44	−61.82
	$\frac{45}{2}-\frac{47}{2}$				
	$\frac{41}{2}-\frac{43}{2}$	16 332.11			
	$\frac{43}{2}-\frac{45}{2}$				
$22_{3,19}$–$23_{2,22}$	$\frac{41}{2}-\frac{43}{2}$	15 025.84	15 026.15	15 026.12	79.23
	$\frac{47}{2}-\frac{49}{2}$				
	$\frac{43}{2}-\frac{45}{2}$	15 026.46			
	$\frac{45}{2}-\frac{47}{2}$				
	$\frac{47}{2}-\frac{47}{2}$				
$25_{3,22}$–$25_{3,23}$	$\frac{53}{2}-\frac{53}{2}$	8 366.02†§	8 366.02	8 365.96	−60.52
	$\frac{49}{2}-\frac{49}{2}$				
	$\frac{51}{2}-\frac{51}{2}$				

Can. J. Chem. Downloaded from www.nrcresearchpress.com by 210.87.254.42 on 09/05/12
For personal use only.

TABLE 2. (*Concluded*)

Transition	F'–F''	Observed frequency	Unsplit line	Calculated frequency	Distortion correction
$26_{3,23}$–$26_{3,24}$	$\frac{49}{2}-\frac{49}{2}$ $\frac{55}{2}-\frac{55}{2}$ $\frac{51}{2}-\frac{51}{2}$ $\frac{53}{2}-\frac{53}{2}$	10 420.68†§	10 420.68‡	10 420.57	−80.26
$27_{3,24}$–$27_{3,25}$	$\frac{51}{2}-\frac{51}{2}$ $\frac{57}{2}-\frac{57}{2}$ $\frac{53}{2}-\frac{53}{2}$ $\frac{55}{2}-\frac{55}{2}$	12 848.39†§	12 848.39‡	12 848.23	−105.00
$27_{2,26}$–$26_{3,23}$	$\frac{55}{2}-\frac{53}{2}$ $\frac{53}{2}-\frac{51}{2}$	12 534.99†	12 534.32‡	12 535.01	−80.83
	$\frac{57}{2}-\frac{55}{2}$ $\frac{51}{2}-\frac{49}{2}$	12 535.64†			
$28_{3,25}$–$28_{3,26}$	$\frac{53}{2}-\frac{53}{2}$ $\frac{59}{2}-\frac{59}{2}$ $\frac{55}{2}-\frac{55}{2}$ $\frac{57}{2}-\frac{57}{2}$	15 689.20†§	15 689.20‡	15 688.95	−135.58
$28_{2,27}$–$27_{3,24}$	$\frac{57}{2}-\frac{55}{2}$ $\frac{55}{2}-\frac{53}{2}$	17 900.88†	17 901.21‡	17 900.79	−68.52
	$\frac{59}{2}-\frac{57}{2}$ $\frac{53}{2}-\frac{51}{2}$	17 901.53†			

*Estimated uncertainty is ± 0.05 MHz, except where otherwise indicated. For an explanation of column headings see Table
†Not used in the analysis for quadrupole coupling constants.
‡Not used in the analysis for centrifugal distortion constants.
§Estimated uncertainty is ± 0.1 MHz.

TABLE 3. Chlorine nuclear quadrupole coupling constants in vinyl chloride

Molecule	χ_{aa} (MHz)	η*
$CH_2CH^{35}Cl$	−57.13±0.11†	0.1034±0.0009
$CH_2CH^{37}Cl$	−45.15±0.11	0.1039±0.0014

*$\eta = (\chi_{bb} - \chi_{cc})/\chi_{aa}$.
†Errors given are for confidence limits of 95%.

regarded as approximately defining the double bond character, or the fractional contribution of **3**. In the present case $\delta \sim 0.04$, indicating a rather smaller contribution of **3** than 0.06 given previously. Using well known methods (5) structures **1** and **2** were found to have fractional contributions 0.73 and 0.23, respectively. In view of the approximations made in these calculations, most notably the neglect of overlap, these values must be regarded as very approximate.

Rotational Constants and Centrifugal Distortion

The first order energy expression for a semi-rigid asymmetric rotor may be written as (7)

$$[2] \qquad E = E_R + E_D$$

$$[3] \qquad E_R = \tfrac{1}{2}(B + C)J(J + 1) + [A - \tfrac{1}{2}(B + C)]\,W(b_p)$$

Can. J. Chem. Downloaded from www.nrcresearchpress.com by 210.87.254.42 on 09/05/12
For personal use only.

TABLE 4. Ground state spectroscopic constants (MHz) of vinyl chloride

Parameter	Value	
	$CH_2CH^{35}Cl$	$CH_2CH^{37}Cl$
A	56 839.704 ±0.144*	56 756.744 ±0.308
B	6029.954 ±0.016	5903.562 ±0.034
C	5445.235 ±0.016	5341.209 ±0.034
τ_{aaaa}	−4.868 ±0.043	−4.871 ±0.089
τ_{bbbb}	−0.01649 ±0.00022	−0.01572 ±0.00043
τ_{aabb}	0.1474 ±0.0030	0.1454 ±0.0055
τ_{abab}	−0.04840 ±0.00043	−0.04710 ±0.00086

*Errors reported are for confidence limits of 95%.

[4] $$E_D = \tfrac{1}{4} \sum_{\alpha,\beta} \tau'_{\alpha\alpha\beta\beta} \langle P_\alpha^2 P_\beta^2 \rangle$$

Here E_R is the rigid rotor energy and E_D is the first order centrifugal distortion correction. In eq. 4 the coefficients $\tau'_{\alpha\alpha\beta\beta}$ are related to the centrifugal distortion constants by $\tau'_{\alpha\alpha\alpha\alpha} = \tau_{\alpha\alpha\alpha\alpha}$ and $\tau'_{\alpha\alpha\beta\beta} = \tau_{\alpha\alpha\beta\beta} + 2\tau_{\alpha\beta\alpha\beta}$; α and β can be a, b, or c. Expressions for the average values of the angular momentum operators in the rigid asymmetric rotor basis have been given elsewhere (8, 9).

Although nine distinct coefficients appear in eq. 4, at most only five combinations of these can be evaluated to first order from a rotational spectrum (9). For the particular case of a planar molecule like vinyl chloride, relations exist (10) which enable this number to be reduced to four.[2] A least squares fit of the spectrum was made to three rotational constants and the four centrifugal distortion constants τ_{aaaa}, τ_{bbbb}, τ_{aabb}, τ_{abab}. Linear variations of the rotational constants were allowed. No attempt was made to include second order or P^6 terms. It has been shown, however, that good distortion constants are obtainable using the first order expression if the analysis excludes high J transitions (10). This procedure has been adopted in the present case, and the analysis has included transitions with $J \leq 25$.

Table 4 gives the ground state rotational constants and centrifugal distortion constants for both isotopic species. The rotational constants obtained are in good agreement with those of earlier work (2, 3). The centrifugal distortion constants are similar for both isotopic species, and differ substantially from those given previously (3). As a check the analysis were carried out using transitions with $J \leq 20$; the results agreed with those of Table 4 within experimental error.

The centrifugal distortion constants can be calculated from the inverse force constant matrix using the following equation (11)

[5] $$\tau_{\alpha\beta\gamma\delta} = -\frac{A\Delta}{I_{\beta\beta} I_{\gamma\gamma}} R \sum_{i,j} (J^\circ_{\alpha\beta})_i (F^{-1})_{ij} (J^\circ_{\gamma\delta})_j$$

The quantities $(J^\circ_{\alpha\beta})_i = (\partial I_{\alpha\beta}/\partial S_i)_0$ are the partial derivatives of the components of the inertia tensor with respect to the ith internal coordinate. A, Δ are rotational constants in MHz; $I_{\beta\beta}$, $I_{\gamma\gamma}$ are principal moments of inertia in a.m.u. Å^2; $R = 2h \times 10^{17}$ with h in erg s. If the derivatives have units of a.m.u. Å and a.m.u. Å^2 rad^{-1} for a stretch and a bend, respectively, and the force constants have units of mdyn Å^{-1}, mdyn Å rad^{-2}, and mdyn rad^{-1} for a stretch, a bend and a stretch bend interaction, respectively, then the $\tau_{\alpha\beta\gamma\delta}$ are in MHz.

El-Sabban and Zwolinski (12) have recently published a set of force constants using vibrational data from the normal isotopic species and the seven deuterated species. It is interesting to compare centrifugal distortion constants calculated from their results with those obtained experimentally. In their analysis they used a valence force field where the in-plane internal coordinates were the changes in the five bond distances and the four X—C=C angles, with X being Cl or H, and the out-of-plane coordinates were roughly a CH_2 wag, a CHCl wag, and a C=C twist. The derivatives of the components of the inertia tensor with respect to these coordi-

[2]Strictly these relations are valid for a rigid planar body, and thus require the use of equilibrium rotational constants. Since these are not available, the ground state rotational constants A and B were used, and the rotational constant C adjusted to make the inertial defect identically zero.

Can. J. Chem. Downloaded from www.nrcresearchpress.com by 210.87.254.42 on 09/05/12
For personal use only.

TABLE 5. Comparison of observed and calculated centrifugal distortion constants (MHz) of $CH_2CH^{35}Cl$

Parameter	Observed	Calculated	
		Using all force constants	Using diagonal force constants
τ_{aaaa}	−4.868	−5.10	−3.86
τ_{bbbb}	−0.01649	−0.0174	−0.0152
τ_{aabb}	0.1474	0.158	0.128
τ_{abab}	−0.04840	−0.0537	−0.0461

nates were obtained according to the methods of Kivelson and Wilson (11). Only the derivatives with respect to the in-plane coordinates were found to be non-zero. Using these derivatives the centrifugal distortion constants for CH_2-$CH^{35}Cl$ were evaluated using all the force constants of El-Sabban and Zwolinski, and also using only the diagonal force constants. The values obtained are compared with the experimental values in Table 5.

The agreement between the observed values and those calculated using all the force constants is fairly good. The agreement when the diagonal force constants are used is in general rather worse, though clearly a good approximation is obtained. Evidently the distortion constants are much more sensitive to the diagonal than to the off diagonal elements, with the latter having a comparatively minor effect, though giving better values. One should, however, be careful in drawing any conclusions from the improved agreement when all the force constants are used, for there are still discrepancies between the observed and calculated values. Some of the interaction constants, notably those between C=C stretching and both C—Cl stretching and C=C—Cl bending, were unobtainable in the normal coordinate treatment, and could well affect the centrifugal distortion constants.

Support of the National Research Council of Canada is gratefully acknowledged.

1. J. H. GOLDSTEIN and J. K. BRAGG. Phys. Rev. **75**, 1453 (1949).
2. D. KIVELSON, E. B. WILSON, JR., and D. R. LIDE, JR. J. Chem. Phys. **32**, 205 (1960).
3. G. A. SAVARIRAJ. Ann. Soc. Sci. Bruxelles, **80**, 88 (1966).
4. C. FLANAGAN and L. PIERCE. J. Chem. Phys. **38**, 2963 (1963).
5. C. H. TOWNES and A. L. SCHAWLOW. Microwave Spectroscopy. McGraw-Hill, New York. 1955.
6. J. H. GOLDSTEIN. J. Chem. Phys. **24**, 106 (1956).
7. D. KIVELSON and E. B. WILSON, JR. J. Chem. Phys. **20**, 1575 (1952).
8. R. L. COOK. J. Chem. Phys. **42**, 2927 (1965).
9. J. K. G. WATSON. J. Chem. Phys. **46**, 1935 (1967).
10. L. PIERCE, N. DICIANNI, and R. H. JACKSON. J. Chem. Phys. **38**, 730 (1963).
11. D. KIVELSON and E. B. WILSON, JR. J. Chem. Phys. **21**, 1229 (1953).
12. M. Z. EL-SABBAN and B. J. ZWOLINSKI. J. Mol. Spectry. **27**, 1 (1968).

Can. J. Chem. Downloaded from www.nrcresearchpress.com by 210.87.254.42 on 09/05/12
For personal use only.

5,6-Dehydrolupanine, a New Alkaloid, and Lupanine from *Thermopsis rhombifolia* (Nutt.) Richards

Y. D. Cho and R. O. Martin

Department of Biochemistry, University of Saskatchewan, Saskatoon, Saskatchewan

Received February 23, 1970[1]

In addition to the alkaloids originally reported in flowering plants of *T. rhombifolia*, lupanine (**3**) and a new major alkaloid were isolated from 6 week old plants. This new alkaloid has been characterized as 5,6-dehydrolupanine (**7**).

Canadian Journal of Chemistry, 49, 265 (1971)

Can. J. Chem. Downloaded from www.nrcresearchpress.com by 210.87.254.6 on 09/05/12
For personal use only.

Introduction

In their original investigation of the alkaloids of *T. rhombifolia*, using dried flowering plants, Manske and Marion (1) reported the presence of the pyridone bases cytisine, *N*-methylcytisine, anagyrine (rhombinine) (**1**), thermopsine (**2**), and rhombifoline. There has been no report of the occurrence in this species of either lupanine (**3**) or sparteine (**4**), reported widespread in other thermopsis species (2, 3).

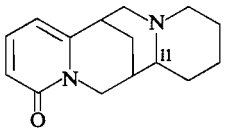

1 (11 R)
2 (11 S)

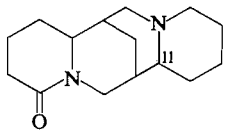

3 (11 R)
6 (11 S)

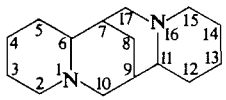

4

The most widely accepted view concerning the biosynthesis of these alkaloids is that sparteine, formed from lysine via cadaverine, is oxidized to lupanine which in turn may be further oxidized to the pyridone base anagyrine (4, 5). Though never discussed this latter conversion presumably occurs via an intermediate dehydrolupanine. Interestingly, in contrast to several dehydrolupanines (C=C in C or D ring)[2] accessible through chemical methods (6–8), the only such natural compounds reported are a dehydrolupanine from *Lupinus albus* (9) to which, however, no assignment has been made of the position of unsaturation (10) and a reportedly different dehydrolupanine from *L. perennis* L. (11).

As an integral part of our studies on the biosynthesis of these alkaloids from $^{14}CO_2$, we examined the alkaloid extracts of fresh plants from 1–10 weeks of age by means of t.l.c. and g.l.c. By 5 weeks of age an alkaloid, designated as BNC-1, whose g.l.c. behavior differed from that of any of the known alkaloids previously reported in this species, was evident. Analysis of these extracts, at various time intervals after pulse labelling of 5–7 week old plants with $^{14}CO_2$, by g.l.c.–combustion – continuous counting and t.l.c.–autoradiography as described previously for our work with the *Conium* alkaloids (12), showed **3** to be the earliest labelled alkaloid, followed by BNC-1 and then **1**. This "chronology" of appearance of ^{14}C in these bases suggested BNC-1 might be the expected, though never proposed dehydrolupanine, intermediate between **1** and **3**, thus deserving of further investigation. Also the surprising finding of what appeared to be lupanine as the earliest formed alkaloid made confirmation of its occurrence an identity by chemical means desirable.

Discussion

An examination of the basic extract of fresh 6 week old plants of *T. rhombifolia* by t.l.c., g.l.c., and mass spectrometry of individual g.l.c. fractions confirmed the presence of the five quinolizidine alkaloids originally reported in dried flowering plants. In addition, traces of lupanine (**3**), and a new major constituent, having distinctive g.l.c. behavior (Fig. 1) were isolated.

This latter compound called BNC-1 gave a mass fragmentation pattern (Fig. 2B) remarkably similar to that reported for aphyllidine (**5**) (13)

[1]Revision received September 9, 1970.
[2]Rings designated from left to right as A, B, C, D.

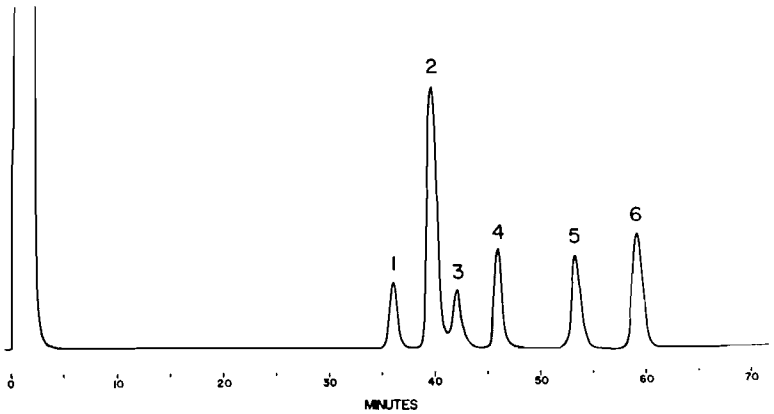

FIG. 1. Gas–liquid chromatogram of the crude alkaloid extract of 6 week old *thermopsis rhombifolia*; (1) alkaloid BNC-1; (2) *N*-methylcytisine; (3) cytisine; (4) rhombifoline; (5) thermopsine; (6) anagyrine.

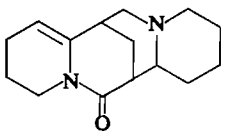

5

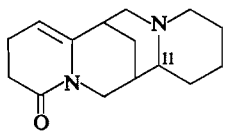

7

and its molecular formula, $C_{15}H_{22}N_2O$. However, its mild catalytic hydrogenation gave **3** ($C_{15}H_{24}N_2O$) as the sole reduction product which was readily distinguishable by its mass spectrum from isolupanine (**6**), as well as the isomeric 10-oxo-sparteine (aphylline), epiaphylline, and 17-oxo-sparteine (13), showed it to be a dehydrolupanine. The problem to be resolved then, was the location of the double bond, the C-11 position being excluded because **6** would have been the expected reduction product (6). Comparison with a sample of authentic 11,12-dehydrolupanine showed BNC-1 to clearly differ in its t.l.c. behavior (Table 1), u.v. spectrum, and sensitivity to air oxidation. The failure of formic acid to reduce BNC-1 could not, owing to the low basicity of the lactam nitrogen (14), rule out the double bond being within the lactam ring at C-5.

The u.v. spectrum of BNC-1 (λ_{max} 250 mμ, $\log_\varepsilon$ 3.8) was similar to that of **5** (15) and indicative of the vinyl amide grouping as in **7**. Such a grouping was further suggested by the i.r. spectrum, which exhibited a strong ν_{max} at 1635 cm^{-1} ($\nu_{C=O}$), only slightly higher than for **5**, and between that of **3** (1622 cm^{-1}) and the corresponding pyridone, **1** (1652 cm^{-1}) (16).

A single olefinic proton (symmetrical 1H triplet, τ 5.10, $J \simeq 4$ Hz), at the low end of the range expected for the vinyl amine grouping (17), was present in the n.m.r. spectrum of BNC-1 but not in that of **3**. In addition, the signal (1H doublet, τ 5.6, $J \simeq 13$ Hz) arising from the strongly deshielded equatorial proton of the geminal pair at C-10 (*peri* to the C=O group) in **5** (18, 19), was somewhat more shielded in BNC-1 (1H doublet, τ 6.00, $J \simeq 12$ Hz). An even stronger shielding effect has been observed on the chemical shift of the analogous pair of protons at C-2 (*peri* to the C=O group) in aphyllidine. This pair is equivalent (2H singlet, τ 6.34 (19)), and has been attributed to a deformation of the A ring by the double bond thus displacing these protons relative to the anisotropic magnetic field of the carbonyl group. It is doubtful that any long range interaction from a double bond in the D ring could account for this effect on these protons in either **5** or **7**.

The apparent ease of hydrolysis of BNC-1 (>10×) compared to **3**, is consistent with a strain producing ring deformation expected from the introduction of a double bond into the C-5 position, evident from a molecular model of **7**. This should be contrasted to the lack of appreciable difference in stability between **5**, and its dihydroderivative, aphylline, both of which hydrolyze with difficulty compared to even **3** (20). This ease of hydrolysis accounted for its variable and often poor recovery from plants in early studies. In fact more recently, BNC-1 has been found to exceed the concentration of *N*-methylcytisine in plants 5–6 weeks of age.

Can. J. Chem. Downloaded from www.nrcresearchpress.com by 210.87.254.6 on 09/05/12
For personal use only.

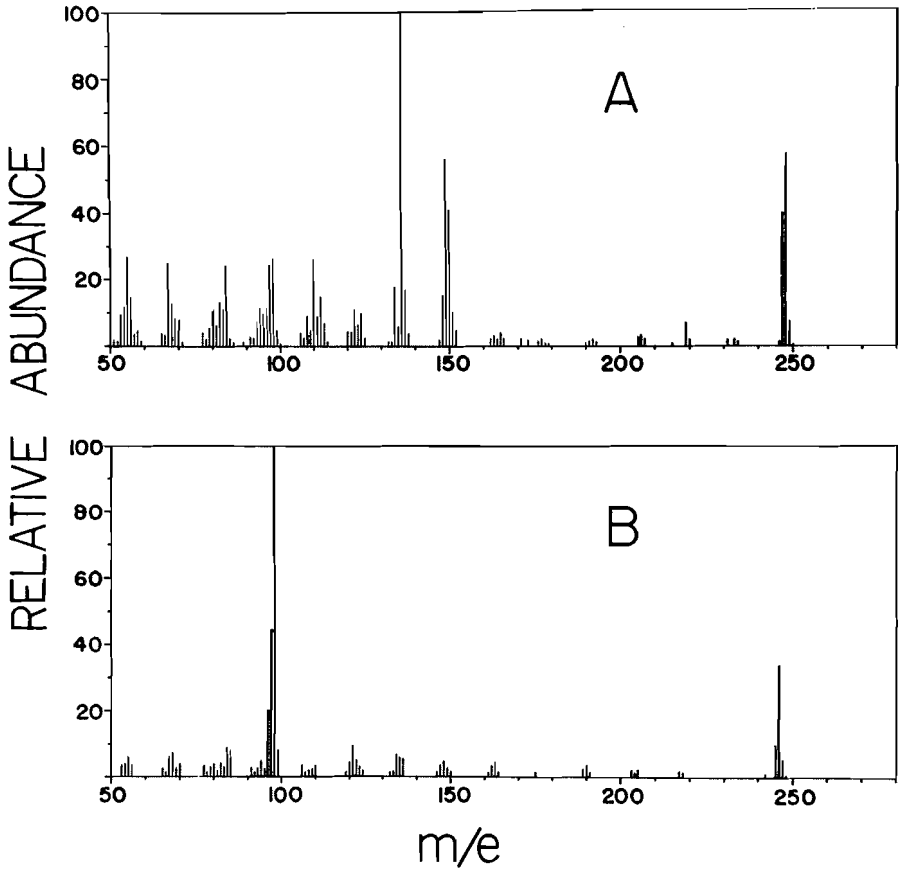

FIG. 2. Mass fragmentation pattern (70 eV) of lupanine (A) and alkaloid BNC-1 (B).

TABLE 1. Chromatographic properties of standard alkaloids and those of 6 week old *Thermopsis rhombifolia* eluted from g.l.c.

Compound	Gas–liquid chromatography*			R_f on t.l.c. system		
	R_t (min)	Peak† no.	%‡	A	B	C
Lupinine	4.4	—	—	0.23	0.56	0.58
Sparteine	7.0	—	—	0.08	0.67	0.44
BNC-1	36.2	1	9	0.83	0.75	0.53
11,12-Dehydrolupanine§	—	—	—	<0.05	—	0.33
Isolupanine	40.0	—	—	0.79	0.71	0.50
N-Methylcytisine	40.2	2	37	0.61	0.59	0.13
Lupanine	41.5	—	0.7‖	0.72	0.74	0.48
Cytisine	42.2	3	8	0.28	0.19	0.12
Rhombifoline	46.1	4	14	0.85	0.68	0.41
Thermopsine	53.5	5	15	0.78	0.68	0.23
Anagyrine	59.5	6	17	0.69	0.64	0.19
Lupaninic acid§	—¶	—	—	<0.05	—	0.33
Hydrolyzed BNC-1§	—¶	—	—	<0.05	—	0.19

*Ten percent QF-1 column, see text for conditions.
†Numbers correspond to those in Fig. 1.
‡Percent of total plant alkaloid calculated from relative g.l.c. peak areas.
§Acetate salt; hydrochlorides for last two compounds.
‖After large scale separation from cytisine by preparative t.l.c.
¶Not eluted.

Can. J. Chem. Downloaded from www.nrcresearchpress.com by 210.87.254.6 on 09/05/12
For personal use only.

Can. J. Chem. Downloaded from www.nrcresearchpress.com by 210.87.254.6 on 09/05/12
For personal use only.

Having located the unsaturation between C-5 and -6 in ring A, **7**, its pronounced effect on altering the mass fragmentation of the parent lupanine skeleton can be rationalized by two considerations. First, the double bond at C-5 greatly reduces the possibility of the two cleavage reactions between C-6 and -7, considered to lead to the two major fragments at *m/e* 136 and 149 in the spectrum of **3** (13). This has been clearly observed when comparing the mass spectrum of **5** (*m/e* 98 (base peak) and 136, RA 10%) with its dihydroderivative, aphylline (*m/e* 136 (base peak) and 98, RA 45%) (13). Second, the lowering of the ability of N-1 to stabilize a positive charge, resulting from the interaction of its lone pair of electrons with the adjacent p-orbitals of the carbonyl and olefinic groups, would have the effect that the major center of charge localization would be expected on N-16, favoring the formation of the major fragment at *m/e* 98 ($C_6H_{12}N^+$) by either of two paths analogous to those occurring with **5** (13) or **1** (21).

On the basis of this cumulative evidence we therefore assigned to alkaloid BNC-1 the structure of 5,6-dehydrolupanine (2-oxo-5,6-dehydrosparteine) (**7**), which in addition to being the "missing link" between anagyrine and lupanine, both also present in this particular species, is the first fully characterized naturally occurring dehydrolupanine.

Given the hydrolytic instability of this compound it is unlikely it would have been recovered by most isolation procedures commonly used, without the special precautions now described. Also its occurrence in quantity only in young plants at a particular stage of development, means it would not be noticed in most alkaloid studies, which utilize older, flowering, and frequently dried plants. Of interest is our failure to detect any isolupanine although the corresponding pyridone, thermopsine, is present. Likewise the apparent absence of sparteine from this species is not an isolated instance in this genus (3) in which it has been reported widespread (2) and should be compared to its rare occurrence in the closely related genus *Baptisia* (22).

Experimental

All solvents were reagent grade, redistilled through a 70 cm column filled with glass helices.

Chromatographic and Spectroscopic Methods

Thin Layer Chromatography

The t.l.c. was carried out using three systems: (A) silica gel G (E. Merck) developed with chloroform/methanol/-concentrated ammonia 90:9:1 (v/v/v); (B) aluminum oxide, basic (Woelm binderless) developed with benzene/-acetone/methanol (34:3:3 (v/v/v); (C) cellulose (Machery Nagel, MN pulver 300) developed with *n*-butanol/concentrated HCl/water 70:7.5:13.5 (v/v/v). Tanks were lined with filter paper. Chromatograms, air dried for 1 h were viewed under u.v. light to locate pyridone alkaloids, then sprayed with iodoplatinate reagent (23) to visualize all alkaloid areas.

Gas–Liquid Chromatography

The g.l.c. was carried out using an F & M (Hewlett Packard Corp.) Model 400 gas chromatograph, equipped with an exit splitter and a single hydrogen flame detector. Columns were U-shaped pyrex glass tubes (1.3 m × 4 mm i.d.) filled with Chromosorb W (AW, DMCS treated, 70–80 mesh) coated with 10% QF-1 by the filtration method of Horning *et al.* (24) and conditioned for 48 h at 240°. The injector was held at 230°; the column, initially at 140°, 5 min after injection of the sample was programmed at a rate of 2°/min to a maximum of 230°; He flow 40 ml/min. Other columns utilized were 5% XE-60 (22) and 5% SE-30. Collection of individual effluent peaks for spectroscopic examination, rechromatography, etc. was achieved by inserting clean capillary tubes (10 × 1.8 mm o.d.) into the exit port. To determine the extent of liquid phase "bleeding" which might contaminate the collected compound, a generous blank was collected from the g.l.c. from 1 min prior to expected peak emergence to 1 min past the usual peak end, which was then introduced as a sample into the mass spectrometer. A maximum column temperature of 210° was not exceeded when collecting compounds for mass spectra. A more detailed description of these chromatographic and collection methods, applied to a wider range of lupin alkaloids, will be presented elsewhere (25).

Spectroscopic Methods

All integer mass spectra were recorded at 70 eV, using an AEI M.S. 12 instrument. Samples contained in capillary tubes were directly inserted by means of a probe into the ion source. High resolution mass spectra were kindly carried out by Prof. A. M. Hogg of the Department of Chemistry, University of Alberta, Edmonton, Alberta. The u.v. absorption spectra, on samples collected from g.l.c. in preweighed capillaries, and eluted with 95% ethanol, were determined using a Cary model 14 instrument. The i.r. spectra were determined in dry $CHCl_3$, using a Beckman IR-8 instrument. The n.m.r. spectra were determined in $CDCl_3$ with tetramethylsilane as an internal reference, using a Varian HA 100 instrument.

Reference Compounds

The chromatographic behavior of the following compounds, homogeneous on all three t.l.c. systems and on g.l.c. (QF-1 and SE-30 columns) are summarized in Table 1. All gave mass spectra in agreement with those previously published (13, 21) and were free of any extraneous fragments above the molecular ion. The mass

Can. J. Chem. Downloaded from www.nrcresearchpress.com by 210.87.254.6 on 09/05/12
For personal use only.

spectra of the free base forms were identical, before and after g.l.c., and differed from the salt form mainly by exhibiting a more abundant molecular ion.[3]

Commercial cytisine, thermopsine, lupanine perchlorate, and sparteine sulfate (converted to monoperchlorate salt) were recrystallized to give melting points in agreement with literature values (1, 27). Anagyrine hydrobromide, a gift of Prof. T. J. Mabry, Department of Chemistry, University of Texas, had g.l.c. behavior as previously reported (22). Lupinine, a gift of Prof. E. Wenkert, Department of Chemistry, Indiana University, had a satisfactory melting point. *N*-Methylcytisine, a gift of the S. B. Penick Co., showed g.l.c. behavior relative to cytisine as previously reported (22) and was purified by that means.

Isolupanine was synthesized in 60% yield by catalytic reduction of thermopsine (28) and purified by g.l.c. Its mass spectrum was very similar to lupanine: *m/e* 136 (base peak); 149, RA 60%, but with a more abundant molecular ion, *m/e* 248, RA 90%. Rhombifoline was synthesized in 70% yield from cytisine and but-3-enyl bromide (29) and purified by t.l.c. (system A), then by g.l.c. Mass spectra (M^+) *m/e* 244.1572 calculated for $C_{15}H_{20}N_2O$, 244.1576; base peak, *m/e* 58. Lupaninic acid was prepared in 90% yield by hydrolysis of lupanine and purified by preparative paper chromatography (30). 11,12-Dehydrolupanine was synthesized in quantitative yield (t.l.c.) by mercuric acetate oxidation of lupanine and isolated as the acetate salt (pale yellow gum) (6); λ_{max} (shoulder 235 nm). Due to the nature of the sample, accurate weight determination necessary for extinction coefficient calculation was not possible. The free base was too sensitive to air oxidation to prepare a suitable sample for g.l.c., or mass spectrometry. Catalytic reduction in glacial acetic acid over PtO_2, 25°, atmospheric pressure for 1 h gave >90% of a product identical with isolupanine on t.l.c.

Isolation and Characterization of Plant Alkaloids

Extraction

Five hundred grams of freshly harvested, 6 week old plants of *T. rhombifolia*, grown from locally collected seeds in a controlled environment chamber, were extracted immediately. Whole plants washed free of vermiculite were homogenized for 5 min in 4 l of 1% HCl in 95% ethanol and allowed to stand overnight at 5°. The filtered extract was evaporated to near dryness *in vacuo* at 20–25°. The dark green residue was suspended in water, filtered, alkalinized to p*H* 11–12 with cold 10 *N* NaOH, and extracted 3× with 1.5 volumes of CH_2Cl_2. The combined CH_2Cl_2 extracts were extracted 3× with equal volumes of 0.25 *N* HCl. The combined aqueous acid extract was cooled to 5°, alkalinized to p*H* 11 with cold 10 *N* NaOH and extracted 3× with 1.5 volumes of CH_2Cl_2. The pooled CH_2Cl_2 extract was dried over anhydrous Na_2SO_4 and the solvent removed *in vacuo* at 20°. The pale yellow total alkaloid residue, 25 mg, was redissolved in 1 ml of methanol and stored under nitrogen at 0°. Recovery as determined by g.l.c. peak areas of all the reference alkaloids by this scheme was greater than 90%, as indicated by a pilot extraction of a mixture of known amounts of each alkaloid. It was necessary to keep the aqueous extracts cold during p*H* changes owing to the hydrolytic instability of alkaloid BNC-1.

Identification and Estimation of Alkaloids

The g.l.c. of aliquot portions of the total alkaloid extract indicated the presence of at least six components (see Fig. 1) whose relative percentages were estimated from their respective peak areas (Table 1). The t.l.c. on system A revealed the presence of at least five components. Tentative identifications, made following co-chromatography with reference compounds, indicated the presence of all the compounds previously reported (1) and in addition the earliest component to be eluted from the g.l.c., designated as BNC-1 (before *N*-methylcytisine) which did not correspond to any standard available. The chromatographic behavior of all the plant alkaloids and reference compounds is summarized in Table 1. Confirmation of identity and purity of each g.l.c. peak was made by comparison of mass fragmentation patterns of individual components (20–50 μg), collected from the g.l.c. with those of authentic reference compounds collected in the same way. In all cases "clean" spectra were obtained identical to the appropriate standard with the exception of the early portion of the cytisine peak which had mass fragments at *m/e* 248, 149, and 136, none of which are present in the spectra of cytisine and in a ratio of 6:6:10, characteristic of lupanine.

Lupanine

To confirm the presence of lupanine, 10% of the total alkaloid extract was chromatographed (preparative) on system A, the region above *N*-methylcytisine eluted with methanol and injected into the g.l.c. In addition to alkaloids BNC-1, rhombifoline, thermopsine and anagyrine, a small peak (4–5% relative to thermopsine) corresponding to lupanine was detectable, which when collected gave a mass spectrum identical to that for lupanine (see Fig. 2A). No sign of sparteine was seen on the preparative chromatograms.

Alkaloid BNC-1

The earliest component to be eluted from the g.l.c., after collection, appeared unchanged on reinjection onto the same column and homogeneous on XE60 and SE30 columns and on all three t.l.c. systems. By repeated collection of this component from successive injections of aliquot portions of 2/3 of the total alkaloid extract into the g.l.c., 2–3 mg of a colorless liquid was obtained. Its mass spectrum is shown in Fig. 2B; M^+ at *m/e* 246 and base peak at *m/e* 98. Precise mass analysis of the peaks at *m/e* 246 (M^+) and 98 showed them to have the following compositions: (M^+) measured 246.1733; calcd. 246.1732 for $C_{15}H_{22}N_2O$; *m/e* 98 measured 98.0974; calculated 98.0970 for $C_6H_{12}N$; λ_{max}(EtOH) 250 nm (log ε 3.8); λ_{max} 2920 and 2840 (m) (methylene CH) and 1635 cm^{-1} (s) ($\nu_{C=O}$). The n.m.r.: τ 5.1 t (1H, J = 4 Hz), 6.00 d (1H, J = 12 Hz).

Catalytic Hydrogenation of BNC-1

A slow stream of hydrogen was passed through a

[3]The mass spectra of rhombifoline, isolupanine, and thermopsine, not previously reported, will be published elsewhere in digital and bar graph form together with those of the above and a number of related compounds (26).

solution of 0.5 mg of BNC-1 in 1.5 ml ethanol over 0.1 mg of 5% Pd/C at room temperature and atmospheric pressure. The catalyst was removed by filtration and the solvent removed *in vacuo* below 30°. The residue, redissolved in methanol and analyzed by g.l.c. and three t.l.c. systems, contained only a single product corresponding to lupanine, with no sign of the easily distinguished starting material for isolupanine. The mass spectrum of a sample collected from g.l.c., compared with that of a parallel sample of authentic lupanine, confirmed lupanine as the sole reduction product. The absence of extraneous peaks confirmed the purity of the original BNC-1 sample.

Attempted Formic Acid Reduction of BNC-1

To 490 μg (2μmol) of BNC-1 in a capillary tube (g.l.c. collection) 4 μmol of 97% formic acid was added. The tube after heat sealing was incubated at 65° for 2 h. The tubes were cooled, the contents washed out with water, made alkaline with cold 10% NaOH, and extracted into CH_2Cl_2. Aliquot portions of the CH_2Cl_2 extract, after volume reduction were analyzed by g.l.c. and on three t.l.c. systems which showed only unchanged starting material to be present.

Acid Hydrolysis of BNC-1 and Lupanine

Hydrolysis of BNC-1, its hydrogenation product, and lupanine were carried out directly in capillary tubes containing 125 μg (0.5 μmol) of each compound collected from g.l.c. by introducing 20 μl of 0.5 *N* HCl (10 μmol), heat sealing the tubes, and incubating at 60° for 1 h. The tubes were opened and the contents analyzed directly by t.l.c. in systems A and C. In addition to the starting compounds only a single product of lower R_f was detected in each case. The hydrolysis product of lupanine and reduced BNC-1 had R_f values identical with lupaninic acid, whereas that of BNC-1 was of even lower R_f in system C. (See Table 1.) The degree of hydrolysis, estimated from relative spot areas was 60% for BNC-1 and 5% for its hydrogenation product and lupanine.

We thank Mr. T. Mazurek of the Prairie Regional Laboratory, National Research Council of Canada for the n.m.r. spectra and the National and Medical Research Councils of Canada for their support of this work.

1. R. H. F. Manske and L. Marion. Can. J. Res. B **21**, 144 (1943).
2. M. F. Cramner and B. L. Turner. Evol. **21**, 508 (1967).
3. E. Balcar-Skrzydlewska and B. Borkowski. Abhand. Deutsch. Akad. Wiss. Berlin Kl. Chem. Geol. Biol. #3, 265 (1966).
4. I. D. Spenser. Compr. Bioch. **20**, 231 (1968).
5. E. Leete. *In* Biogenesis of natural products. 2nd Edition. P. Bernfeld, *Editor*. Pergamon Press, Oxford, 1967. p. 953.
6. L. Marion and N. J. Leonard. Can. J. Chem. **29**, 355 (1951).
7. O. E. Edwards, F. H. Clarke, and B. Douglas. Can. J. Chem. **32**, 235 (1954).
8. K. H. Shin, L. Fonzes, and L. Marion. Can. J. Chem. **43**, 2012 (1965).
9. E. Nalborczyk. Bull. Acad. Pol. Sci., Ser. Sci. Biol. **9**, 409 (1961).
10. T. Nalborczyk. Bull. Acad. Pol. Sci., Ser. Sci. Biol. **16**, 317 (1968).
11. M. Rink and H. Schafer. Arch. Pharm. **287**, 290 (1964).
12. S. M. C. Dietrich and R. O. Martin. Biochem. **8**, 4163 (1969).
13. D. Schumann, N. Neuner-Jehle, and G. Spiteller. Monatsh. Chem. **99**, 390 (1968).
14. N. J. Leonard and R. R. Sauers. J. Amer. Chem. Soc. **79**, 6210 (1957).
15. A. W. Sangster and K. L. Stuart. Chem. Rev. **65**, 69 (1965).
16. L. Marion, D. A. Ramsay, and R. Jones. J. Amer. Chem. Soc. **73**, 305 (1951).
17. D. H. Williams and I. Fleming. Spectroscopic methods in organic chemistry. McGraw-Hill, London, 1966. p. 128.
18. M. Wiewiorowski, O. E. Edwards, and M. D. Bratek-Wiewiorowska. Can. J. Chem. **45**, 1447 (1967).
19. F. Bohlmann and D. Schumann. Tetrahedron Lett. 2705 (1965).
20. A. S. Sadykov, A. I. Ishbaev, and Kh. A. Aslanov. Dokl. Akad. Nauk. S.S.S.R. **155**, 865 (1964).
21. N. Neuner-Jehle, H. Nesvadba, and G. Spiteller. Monatsh. Chem. **95**, 687 (1964).
22. M. F. Cranmer and T. J. Mabry. Phytochem. **5**, 1333 (1966).
23. R. Mumer and M. Machebouef. Bull. Soc. Chim. Biol. **31**, 144 (1949).
24. E. C. Horning, W. J. A. Vanden Heuvel, and B. G. Creech. Methods of Biochemical Analysis, **11**, 82 (1963).
25. Y. D. Cho and R. O. Martin. J. Chromatogr. Submitted.
26. Y. D. Cho and R. O. Martin. Arch. of Mass Spectral Data. In press.
27. L. Marion and S. W. Fenton. J. Org. Chem. **13**, 780 (1948).
28. A. P. Orekhov, S. S. Norkina, and H. Gurevich. Chem. Ber. **66**, 625 (1933).
29. W. F. Cockburn and L. Marion. Can. J. Chem. **30**, 92 (1952).
30. B. Malek and H. Auterhoff. Planta, **8**, 179 (1960).

Can. J. Chem. Downloaded from www.nrcresearchpress.com by 210.87.254.6 on 09/05/12
For personal use only.

Can. J. Chem. Downloaded from www.nrcresearchpress.com by 210.87.254.5 on 09/05/12
For personal use only.

Nucleophilic Substitution on S_4N_4. Reactions with Benzylamines

YUKIHIKO SASAKI AND FREDRIC P. OLSEN
Department of Chemistry, McMaster University, Hamilton, Ontario

Received May 29, 1970

Reactions of benzylamines with tetrasulfur tetranitride lead to benzylidenimine polysulfides, ammonia, *N*-benzylidene benzylamines, and some free sulfur. The stoichiometric equation has been established. The reaction is quite sensitive to structural changes and appears limited to ring substituted benzylamines. The benzylidenimine polysulfides undergo thermal decomposition to sulfur and triphenyl-*s*-triazine and react with benzylamine to give benzylammonium polysulfides, ammonia, and *N*-benzylidene benzylamine. The benzylammonium polysulfides decompose in air to sulfur, hydrogen sulfide, and benzylammonium thiosulfate.

Canadian Journal of Chemistry, 49, 271 (1971)

Tetrasulfur tetranitride is quite reactive toward nucleophilic substitution. Reactions with phosphines (1–3), Grignard reagents (4, 5), ammonia (6, 7), amines (8), cyanide ion (1), and diazomethanes (9) have been reported. Although the products differ considerably from one reaction to another, they generally arise from attack of the nucleophile on sulfur with destruction of the sulfur nitrogen ring system. Formulas of products from a few of these reactions are supported by both elemental analysis and molecular weight determinations, but for some only an elemental analysis is reported; in a few cases there is neither. Seldom is the structure of the product unambiguously determined with both. Overall stoichiometries have only rarely been investigated and, not surprisingly, a composite picture of nucleophilic substitution on tetrasulfur tetranitride has not emerged.

Closely related nucleophiles often appear to behave differently. Although ammonia (6, 7) is reported to give an ammoniate of composition $S_2N_2 \cdot NH_3$, generally formulated as $H_2N—S—\overset{-}{N}—\overset{+}{S}=NH$, secondary amines are reported to give thiobisamines. Thus, dimethylamine gave bisdimethylamine monosulfide and piperidine gave bispiperidine monosulfide (8). Benzylamine on the other hand was reported by Schenck (8) to give ammonia, sulfur, and triphenyl-*s*-triazine when reacted on a steam bath but the thioamide of thiobenzoic acid, **1**, at room temperature. The stoichiometry given in eq. 1 was proposed. A material identical to **1** was subsequently

[1] $6C_6H_5CH_2NH_2 + 3S_4N_4 \rightarrow$

$$6C_6H_5—\overset{\overset{S}{\|}}{C}—N=S + 8NH_3 + 2N_2$$

1

isolated from the reaction of sulfur with benzylamine in the presence of lead(II) oxide (10). Based on a molecular weight determination, structure **1** was discarded in favor of **2** or possibly **3**. An authentic sample of **3** subsequently pre-

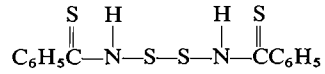

2

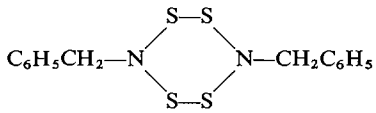

3

pared from benzylamine and sulfurmonochloride, however, had different properties (11). The structure of Schenck's material remains in doubt (11*b*). A reaction between tetrasulfur tetranitride and phenylhydrazine was reported to lead to sulfur, nitrogen, and ammonia. The stoichiometry given in eq. 2 was proposed although benzene was not isolated.

[2] $12C_6H_5NHNH_2 + 3S_4N_4 \rightarrow$

$$12S + 8NH_3 + 12C_6H_6 + 14N_2$$

The work described herein was undertaken with the aims of clarifying the structure of the benzylamine tetrasulfur tetranitride product, of establishing the overall stoichiometry for the reaction, and of determining if this reaction was applicable to other primary amines or to phenylhydrazine.

Results and Discussion

Characterization of Products

When tetrasulfur tetranitride and benzylamine were mixed as described by Schenck (8) [about 1 mol of tetrasulfur tetranitride to 7 mol of

Can. J. Chem. Downloaded from www.nrcresearchpress.com by 210.87.254.5 on 09/05/12
For personal use only.

amine], an exothermic reaction was observed. This was accompanied by several color changes and the evolution of ammonia. Yellow needles which appeared to be identical to the material described by Schenck were obtained on washing the product with ice cold methanol and constituted the major crystalline product. The elemental analysis corresponded quite closely to the composition $(C_7H_6NS_2)_x$, and the molecular weight (osmometric in benzene) showed x to be 2 in agreement with Levi's observations (10) on the material isolated from the reaction of sulfur with benzylamine in the presence of lead(II) oxide. The properties of this yellow solid were, however, inconsistent with both of Levi's proposed structures, **2** and **3**, and also with **1**. It should have been formulated as benzylidenimine tetrasulfide, **4**, based on the following evidence.

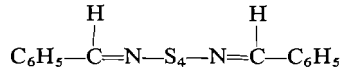

4

The n.m.r. spectrum, Fig. 1, showed a sharp singlet at -7.87 p.p.m. and a multiplet at -7.05 to -7.48 p.p.m. Integration indicated one proton for the singlet and five protons for the multiplet (phenyl group). This eliminated structures **1** and **3** but did not rule out **2** although it would be rather surprising to have found such a sharp singlet for a thioamide proton (usually at least 0.5 p.p.m. wide). The i.r. spectrum showed no N—H stretching absorption (nothing above 3100 cm^{-1}) thus eliminating **2**. There was, however, a weak band at 1630 cm^{-1} assignable to a C=N stretch, *i.e.* structure **4**.

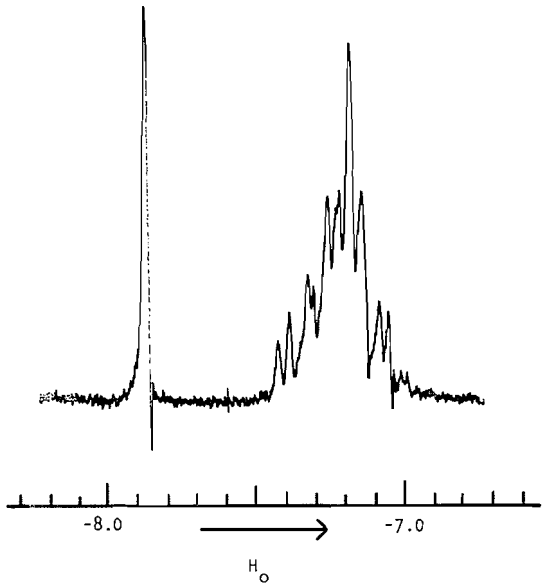

FIG. 1. The n.m.r. spectrum of benzylidenimine tetrasulfide.

Furthermore, two analogous compounds were isolated from the same reaction mixture whose n.m.r. spectra were quite similar to **4**. They both had one sharp singlet of area one downfield from a phenyl multiplet of area five. Elemental analyses and molecular weights along with n.m.r. confirmed that these compounds had the same organic component as **4** but that three and two sulfur atoms replaced the four in **4**. Table 1 lists n.m.r. chemical shifts in various known compounds with a benzylidenimine group. The benzylidenic protons in these compounds lie between -7.73 and -8.61 p.p.m. The chemical shifts of the low field singlets for the three compounds isolated from the reaction of tetrasulfur tetranitride with benzylamine, Table 2, also lie in this region. Thus, the chemical shifts are in good agreement with the benzylidenimine structure. The last compound in Table 2, an analogous monosulfide prepared from *p*-chlorobenzylamine and tetrasulfur tetranitride, is of particular interest. Its n.m.r. spectrum is very similar to that of **4** with a sharp singlet downfield of the phenyl multiplet (areas 1:4). The elemental analysis showed only one sulfur atom per two nitrogen atoms. With a molecular weight near 322, the n.m.r. spectrum requires this compound to have equivalent organic components. There is only one possible symmetrical structure with one sulfur which satisfies all of the requirements: *p*-chlorobenzylidenimine monosulfide. The similarity in n.m.r. spectra then requires similar structures for the other materials. Pyrolysis of benzylidenimine tetrasulfide to elemental sulfur, benzonitrile, and triphenyl-*s*-triazine also supports structure **4**.

A similar arylimine disulfide (but disubstituted on both benzylidene carbons) has been previously prepared (14) by reaction of sulfur monochloride with the phenyl magnesium bromide – benzonitrile adduct. The assignment of structure was based mainly on chemical evidence including the method of synthesis and the observed hydrolysis to benzophenoneimine hydrochloride and sulfur monochloride with concentrated hydrochloric acid.

TABLE 1. The n.m.r. chemical shifts for various known compounds with benzylidenimine protons

Compounds	C_6H_5— (p.p.m.)	H | —C=N— (p.p.m.)	Solvents
$C_6H_5CH{=}N{-}N{=}CHC_6H_5$	−7.30 to −7.90	−8.52	CCl_4 (12*a*)
$C_6H_5CH{=}N{-}\underset{\displaystyle H}{\underset{\vert}{N}}{-}C_6H_5$	−6.50 to −7.70	−7.73	Acetone (12*b*)
$CH_3OC_6H_4CH{=}N{-}N{=}CHC_6H_4OCH_3$	−6.83 to −7.82	−8.61	$CDCl_3$ (12*c*)
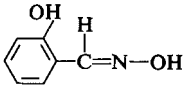	−6.75 to −7.45	−8.18	$CDCl_3$ (13)
$C_6H_5CH{=}N{-}CH_2C_6H_5$	−7.16 to −7.80	−8.22	CCl_4*
p-$ClC_6H_4CH{=}N{-}CH_2C_6H_4Cl$-*p*	−7.32 to −7.92	−8.44	$CDCl_3$*
p-$CH_3OC_6H_4CH{=}N{-}CH_2C_6H_4OCH_3$-*p*	−6.58 to −7.80	−8.10	$CDCl_3$*

*This work.

TABLE 2. Selected constants for arylimine polysulfides $Y{-}C_6H_4CH{=}N{-}S_x{-}N{=}CHC_6H_4{-}Y$

Y	*x*	Infrared (cm^{-1}) C=N	Infrared (cm^{-1}) S—N	Thin-layer chromatography* R_f	Nuclear magnetic resonance H | —N=C—	Nuclear magnetic resonance Phenyl
H	4	1630	853	0.46†	−8.02§ −7.87‖	−7.12 to −7.55 −7.05 to −7.48
	3	1658	850	0.40†	−8.42‖	−7.32 to −7.88
	2	1655	853	0.36† (0.24)†	−8.14‖ (−8.61)‖	−7.24 to −7.84
	1					
p-CH_3O	4	1670	863	0.73‡ (0.68)‡	−7.95§	−6.67 to −7.95¶
	3					
p-Cl	4	1640	853	0.49†	−7.98§	−7.23
	1	1640	852	0.28†	−8.65§	−7.44 to −7.87

*( ) Not fully characterized.
†Carbon disulfide.
‡Methylene chloride.
§Deuterochloroform.
‖Carbon tetrachloride.
¶Methoxy at −3.85.

Stoichiometry of the Reaction

Schenck's (8) proposed reaction, corrected to the benzylidenimine tetrasulfide structure, is given in eq. 3. When a five-fold excess of acid

[3] $S_4N_4 + 2C_6H_5CH_2NH_2 \rightarrow N_2 + C_6H_5CH{=}N{-}S_x{-}N{=}CHC_6H_5 + (4 - x)S + 2NH_3$

(5 HCl/S_4N_4) was used to trap the ammonia, the acid solution was basic at the end of the reaction. More than 5 mol of ammonia per mol of nitride was evolved rather than the 2 required by eq. 3. Formation of benzylidenimine tetrasulfide from benzylamine represents oxidation; taking nitrogen to retain its −3 oxidation state in ammonia, sulfur must be reduced. The change in formal oxidation state for sulfur is from +3 in S_4N_4 to $+\frac{1}{2}$ in benzylidenimine tetrasulfide, a change of $2\frac{1}{2}\,e^-$/sulfur, or $10\,e^-/S_4N_4$. Oxidation of benzylamine represents a $2\,e^-$ change or $4\,e^-$/benzylidenimine tetrasulfide. An additional $6\,e^-$ oxidation product is required. Schenck's scheme used the conversion of two nitrogen atoms of S_4N_4 to elemental nitrogen for this

Can. J. Chem. Downloaded from www.nrcresearchpress.com by 210.87.254.5 on 09/05/12
For personal use only.

Can. J. Chem. Downloaded from www.nrcresearchpress.com by 210.87.254.5 on 09/05/12
For personal use only.

purpose. It seems quite likely from the large quantity of ammonia evolved, however, that *all* of the nitrogen of S_4N_4 goes to ammonia. Since 80–85% of the sulfur has been accounted for already, the additional oxidized product must arise from the benzylamine. Column chromatography gave this product, *N*-benzylidene benzylamine. The latter is formally derivable from benzylamine by a $2\,e^-$ oxidation to benzylidenimine and subsequent elimination of ammonia between this product and benzylamine. Thus, 3 mol of *N*-benzylidene benzylamine would be required to account for the missing $6\,e^-$ oxidation. One might then formulate the overall reaction as eq. 4 where the three *N*-benzylidene

[4] $$S_4N_4 + 8C_6H_5CH_2NH_2 \rightarrow C_6H_5CH{=}N{-}S_x{-}N{=}CHC_6H_5 + 7NH_3 + 3C_6H_5CH{=}N{-}CH_2C_6H_5 + (4 - x)S$$

benzylamines are needed to complete the reduction of sulfur. Four moles of ammonia would arise from the four nitrogens of the nitride and the remaining three would result from formation of the 3 mol of *N*-benzylidene benzylamine. This equation was tested by reacting benzylamine and tetrasulfur tetranitride in an 8:1 molar ratio and attempting quantitative isolation of all products. The coefficients from eq. 4 (1:8:1:7:3) were found experimentally to be 1.0:8.0:1.0:6.8:2.8. The stoichiometry given in eq. 4 was therefore quite closely approximated. With a large excess of benzylamine (22:1 molar ratio), benzylidenimine polysulfides were not obtained. The yield of *N*-benzylidene benzylamine increased considerably, and an orange solid identified as benzylammonium polysulfide was obtained in addition to a small amount of benzylammonium thiosulfate. These products were also observed when benzylidenimine polysulfides were reacted with benzylamine. With less than 8 mol of amine per mol of nitride, eq. 4 was still observed, but the quantity of arylimine polysulfides produced decreased in proportion to the quantity of amine used. When the 8:1 stoichiometric reaction was followed by n.m.r. spectroscopy, the final products were found to be present along with the starting materials even in the very early stages of the reaction (5 min). The concentration of the final products increased, and the concentration of the reactants decreased as time passed; the reaction was completed in about 15 h at room temperature. No peaks were observed at any time other than those corresponding to products and reactants, and notwithstanding several color changes, it appears unlikely that any *long-lived* intermediates are present between the starting tetrasulfur tetranitride and benzylidenimine polysulfides. Therefore, the reaction as represented by eq. 4 describes the course of nucleophilic substitution on tetrasulfur tetranitride by benzylamine and offers a synthetic route to arylimine polysulfides with mono substituted α-carbons.[1] The mechanism is not clear, but all of the nitrogen of the tetrasulfur tetranitride goes to ammonia, and the nucleophile becomes bound only to sulfur. Clearly several steps are required with an early step being partially ionic since the reaction is at least ten fold slower in non polar solvents (see next section). The reaction might be better thought of as a redox process than as a nucleophilic substitution.

Synthetic Application

Since the reaction as run was heterogeneous and would not be useful for solid amines, the effect of various solvents was investigated. Benzene resulted in a very slow reaction (if any); only unreacted starting materials were present after 24 h. Acetone resulted in rapid consumption of tetrasulfur tetranitride and amine; however, this appeared to be a Willgerodt–Kindler reaction (15, 16).[2] Several amine solvents were found to give benzylidenimine polysulfides, but the yields were lower than in the absence of solvent. Yields of benzylidenimine polysulfides were 52% in dimethylformamide, 60% in pyridine, and 91% in triethylamine compared to the quantitative reaction observed in the absence of these solvents. Triethylamine, therefore, appears usable when necessary but offers no advantage over the *neat* reaction. Both *p*-methoxy and *p*-chlorobenzylamine were found to undergo a reaction analogous to eq. 4. With the former, the sulfur containing species were *p,p'*-dimethoxybenzylidenimine tetrasulfide in 77% yield and the apparent trisulfide in about 5% yield. The yield of *N*-(*p*-methoxybenzylidene)*p*-methoxybenzylamine was quantitative. With *p*-chlorobenzylamine the yield of polysulfides and of *N*-(*p*-chlorobenzylidene)-

[1]See however following paper.

[2]Although tetrasulfur tetranitride has not previously been examined as a sulfur source under Willgerodt-Kindler conditions, its reactivity in this sense is probably not too surprising (17).

Can. J. Chem. Downloaded from www.nrcresearchpress.com by 210.87.254.5 on 09/05/12
For personal use only.

p-chlorobenzylamine was 79%, and some mono sulfide was isolated along with the tetrasulfide. An additional 14% of elemental sulfur was also obtained. Free sulfur could arise by decomposition of the tetrasulfide to the observed monosulfide or by decomposition of some precursor. *p*-Nitrobenzylamine gave approximately 48% of elemental sulfur and no other tractable product. The *p*-nitro group is most likely involved directly in a competing reaction[3] of some sort since both *p*-chloro and *p*-methoxybenzylamines gave acceptable yields of aryliminepolysulfides. α-Methylbenzylamine did not lead to an analogous arylimine polysulfide while allylamine resulted in an apparent polymer. The reaction is therefore quite sensitive to small structural changes, and its synthetic usefulness appears limited to the reactions of ring substituted benzylamines.

With phenylhydrazine (8:1 molar ratio) the products were diphenyl disulfide, diphenyl monosulfide, elemental sulfur, and ammonia. In this reaction approximately 2 mol of ammonia per mol of tetrasulfur tetranitride were evolved. Thus, nitrogen gas must have been formed directly from tetrasulfur tetranitride to complete reduction of the sulfur. Had a reaction analogous to that with benzylamine occurred to give $C_6H_5N{=}N{-}S_x{-}N{=}NC_6H_5$, followed by breakdown of this product to the observed phenylsulfides and nitrogen, 7 mol of ammonia per mol of tetrasulfur tetranitride should still have been evolved. The phenylhydrazine reaction is therefore quite different from that with benzylamine and appears best formulated as in eq. 5. The yield of diphenyl-

$$[5]\quad S_4N_4 + 2C_6H_5\overset{\displaystyle H}{\underset{|}{N}}{-}NH_2 \rightarrow 2NH_3 + C_6H_5S_xC_6H_5 + 3N_2 + (4-x)S$$

polysulfides isolated in the presence of triethylamine based on eq. 5 was 74% (55% disulfide and 19% monosulfide). Here also the nucleophile becomes bonded only to sulfur, but the nitrogen is obtained in a different oxidation state than in the benzylamine reaction.

Reactions of Benzylidenimine Tetrasulfide

A mass spectrum of benzylidenimine tetrasulfide failed to show the parent peak. Instead, fragments such as S_x^+ ($x = 1$–8) and $C_6H_5CN^+$ were observed. The sulfur species with $x > 4$ must come from thermal decomposition and subsequent reactions rather than fragmentation, and the whole mass spectrum therefore probably represents pyrolysis products. Schenck (8) reported triphenyl-*s*-triazine as a product from the reaction of tetrasulfur tetranitride with benzylamine at steam bath temperature. Levi (10) was unable to reproduce this work in refluxing benzene. Consequently, the thermal decomposition of benzylidenimine tetrasulfide was investigated. Benzylidenimine tetrasulfide, heated to 105 °C (just above the m.p.) *in vacuo*, gave triphenyl-*s*-triazine, hydrogen sulfide, elemental sulfur, and benzonitrile as the main products along with a basic gas presumed to be ammonia. Thus, the main decomposition is described by eq. 6. The yield of sulfur based on eq. 6 was 82%,

$$[6]\quad C_6H_5CH{=}N{-}S_4{-}N{=}CHC_6H_5 \rightarrow H_2S + 2/x(C_6H_5CN)_x + 3S$$

and 67% of the total nitrogen was isolated in the form of either triphenyl-*s*-triazine or benzonitrile. Ammonia must arise from another reaction in competition with eq. 6. This decomposition was not observed in refluxing benzene and appeared to occur only at or above the m.p.

Photolysis of benzylidenimine tetrasulfide resulted in decomposition to lower polysulfides and elemental sulfur as shown in eq. 7. Benzyl-

$$[7]\quad C_6H_5CH{=}N{-}S_4{-}N{=}CHC_6H_5 \xrightarrow{h\nu} C_6H_5CH{=}N{-}S_{4-x}{-}N{=}CHC_6H_5 + xS \quad (x = 1\text{–}3)$$

idenimine monosulfide is very likely produced in this reaction. Although not isolated and fully characterized, the presence of this material is fairly certain from n.m.r. spectra (benzylidenimine type proton at −8.61 p.p.m.) and t.l.c. (R_f of 0.24, color observed when sprayed with silver nitrate solution was nearly identical to the other three benzylidenimine polysulfides and developed at the same rate) of the photolysis mixture.

Since benzylidenimine tetrasulfide was not isolated from tetrasulfur tetranitride in the presence of excess benzylamine, the reaction of the polysulfide with benzylamine was investigated. Benzylidenimine tetrasulfide reacted readily with benzylamine to give a deep reddish solution. Addition of anhydrous ether precipitated an orange solid which resembled the benzylammonium hexasulfide prepared by Levi (19) from sulfur, benzylamine, and hydrogen sulfide.

[3]See for example ref. 18.

Can. J. Chem. Downloaded from www.nrcresearchpress.com by 210.87.254.5 on 09/05/12
For personal use only.

Its n.m.r. spectrum supported this structure. A sample left in the air for a few days decomposed slowly with the evolution of hydrogen sulfide to sulfur and benzylammonium thiosulfate. The thiosulfate presumably arose by air oxidation of either the polysulfide or of one of its intermediate hydrolysis products. Thiosulfates have been previously isolated from sulfur with butylamine and from sulfur with ethylenediamine (20). In these cases the thiosulfates were thought to form concurrently with, rather than from, the polysulfides. Our results demonstrate that in the benzylamine system thiosulfates are a simple air oxidation/hydrolysis product of the benzylammonium polysulfides.

When a sample of benzylammonium polysulfide was dissolved in methanol, it decomposed quite rapidly to hydrogen sulfide, benzylamine and sulfur. The molar ratio of benzylamine to sulfur was 1:3.2 requiring an average sulfur chain length between 7 and 8. Levi's designation (19) of a similar material as a *hexa*sulfide was based on this type of quantitative decomposition to hydrogen sulfide, sulfur, and benzylamine.[4] Similar orange solids were prepared by Levi's (19) method and were also found to result from the reaction of either sulfur or heptasulfurimide with benzylamine. Heptasulfurimide has been previously (21) found to react with a large number of amines. In the case of propylamine, Richter (21) was able to demonstrate the presence of the propylammonium cation in solution although the anion was not identified. Our results would suggest that the anion was a polysulfide or possibly a thiosulfate if the solutions were not kept free of air. (Reactions between sulfur and benzylamine form the basis of the following paper.)

Sulfur chain lengths obtained by analysis of the products from the sulfur–amine, heptasulfurimide–amine, and benzylidenimine tetrasulfide – amine routes tended to vary from one preparation to another. In general, values ranged between 6 and 7 although values as high as 8–9 were occasionally obtained. Several samples of these materials were subjected to pyrolysis and in all cases gave hydrogen sulfide, sulfur, thiobenzamide, 3,5-diphenyl-1,2,4-thiadiazole, and dibenzyl polysulfides. Occasionally, 1,2-diphenyl ethane or *N*-benzylthiobenzamide was also isolated. The ratio of these materials tended to vary from one benzylammonium polysulfide preparation to another with sulfur rich species (free sulfur and dibenzylpolysulfides) predominating by a greater amount compared to sulfur-poor species (diphenylethane, *N*-benzylthiobenzamide, and 3,5-diphenyl-1,2,4-thiadiazole) in those cases where analysis suggested longer sulfur chains. While we cannot be certain that the starting material is free of *uncombined* sulfur in all cases, we favor a variable chain length polysulfide formulation with an average sulfur chain length of between 6 and 7 being most common for the product from the sulfur–benzylamine route in the absence of added hydrogen sulfide and also from the benzylidenimine polysulfide – benzylamine route. The polysulfides when heated with excess benzylamine gave *N*-benzylthiobenzamide. This material has also been obtained in high yield by heating sulfur in benzylamine directly (22). Its formation by heating polysulfides in benzylamine could well arise indirectly by this route, *i.e.*, decomposition to hydrogen sulfide, benzylamine, and free sulfur and subsequent reactions of the latter.

Spectra of Benzylidenimine Polysulfides

The chemical shift in the proton n.m.r. spectra of the methylene group in alkyl polysulfides, $RCH_2S_xCH_2R$, has been reported to be quite sensitive to sulfur chain length (23, 24). For dimethyl-di-*t*-butyl- and dibenzylpolysulfides the absorption moves to lower field as the number of sulfur atoms in the chain increases while for methyl chloro polysulfides, CH_3S_xCl, the methyl absorption moves to higher field as the number of sulfurs increases (23, 24). The difference in chemical shifts between two members of a series generally tended to become smaller as the sulfur chain length increased in all series although the tetra- and pentasulfides appeared closer than expected in the methyl series. For the unsubstituted benzylidenimine polysulfides, the chemical shifts of the benzylidene protons (Table 2) did not vary with sulfur chain length in a consistent manner. The tetrasulfide was at highest field,

[4]Elemental analysis leading to percent composition does not distinguish between a benzylammonium polysulfide (chain length 6–7) and a benzylammonium hydrogen sulfide (with a chain length of 3–3.5); however, a polysulfide on thermal decomposition would lead to hydrogen sulfide and benzylamine in molar ratios of 1:2 while a benzylammonium hydrogensulfide would give these materials in a 1:1 molar ratio. Levi's (19) observed values of 1:1.97 and 1:2.07 eliminate this latter possibility.

followed by the disulfide, the trisulfide, and at lowest field the (presumed) monosulfide. It is apparent that estimating sulfur chain lengths from relative chemical shifts alone is dangerous where these shifts have not been independently established by some other method. The R_f values (Table 2) appear to be a better criterion for this purpose. These increase monotonously as the number of sulfurs increase in all cases.

The i.r. spectra of the benzylidenimine polysulfides were complex; however, all showed weak absorption between 1640 and 1670 cm^{-1} as well as fairly strong absorption between 850–865 cm^{-1}. These regions, summarized in Table 2, represent C=N and N—S stretching frequencies. The intensity of the C=N absorption is known to be quite variable (25). Oximes generally give very weak C=N stretching absorptions.[5] For all benzylidenimine polysulfides prepared, the C=N stretching absorptions were observed to be weak. The sulfur–nitrogen stretching frequencies have been found (27) to be related to the sulfur–nitrogen bond lengths by the empirical eq. 8,

$$[8] \qquad r_{NS} = 0.0483\mu_{NS} + 1.099$$

where μ_{NS} = i.r. stretch in μ; r_{NS} = bond length. The sulfur–nitrogen bond lengths estimated from this equation are fairly constant at 1.66 Å for all of the imines prepared. This is somewhat shorter than the normal single bond length of 1.76 Å found in sulfamic acid (28) or the single bond covalent radii sum of 1.74 Å (29) but is longer than the N—S bond in tetrasulfur tetranitride (1.62 Å) (30). These data suggest that the N—S bond in the benzylidenimine polysulfides has at least some double bond character. The bond order is estimated as about 1.5 from the empirical relationship between i.r. stretching frequency and bond order given by Chapman and Waddington (31). If these empirical relationships hold for the benzylidenimine polysulfides, the suggested increase in bond order could be interpreted as evidence for $d\pi$–$p\pi$ double bonding between the Schiff's base and the adjacent sulfur.

Ultraviolet absorption spectra for the unsubstituted benzylidenimine polysulfides are shown in Fig. 2. The tetrasulfide showed three maxima at 243 ($\varepsilon = 1.8 \times 10^4$), 303 ($\varepsilon = 2.3 \times 10^4$), and 333 m$\mu$ ($\varepsilon = 1.0 \times 10^4$). The trisulfide showed only two obvious maxima at 242 ($\varepsilon = 1.3 \times 10^4$) and 309 m$\mu$ ($\varepsilon = 2.4 \times 10^4$) while the disulfide had maxima at 294 ($\varepsilon = 2.8 \times 10^4$) and 304 m$\mu$ ($\varepsilon = 2.9 \times 10^4$). These spectra do not closely resemble those of either typical alkyl polysulfides (32, 33) or typical Schiff's bases (34). Judging from the increase in extinction coefficients in the 300 mμ region for the

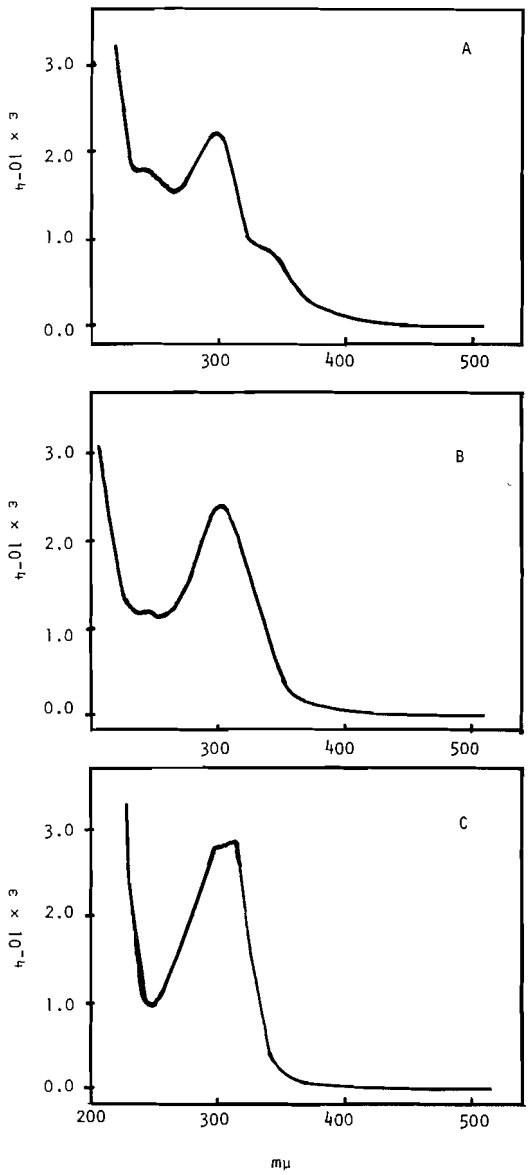

FIG. 2. Electronic absorption spectra of benzylidenimine polysulfides in methanol; (A) tetrasulfide; (B) trisulfide; (C) disulfide.

[5]Acetophenoneoxime shows a C=N stretching absorption whose molar extinction coefficient is almost 1/20 the value in the corresponding Schiff's base (26).

Can. J. Chem. Downloaded from www.nrcresearchpress.com by 210.87.254.5 on 09/05/12
For personal use only.

lower sulfides, it appears likely that three absorptions occur in each compound becoming more clearly separated as the sulfur chain length increases. It does not seem profitable to speculate on the probable origin of these transitions at this time.

Experimental

General

Melting points were obtained on a Thomas Hoover capillary melting point apparatus and are uncorrected. Proton n.m.r. spectra were recorded on a Varian Model T-60 spectrometer and are relative to internal tetramethyl silane. Elemental analyses were performed by Schwarzkopf Microanalytic Laboratories, Woodside, New York. Molecular weight measurements were carried out on a Mechrolab Model 301A Vapor Pressure Osmometer with dibenzyl disulfide as reference and benzene as solvent. The i.r. spectra were recorded on a Beckman IR5 spectrometer and u.v. spectra on a Cary Model 14 using methanol as solvent. The dry box was a Vacuum Atmospheres Corporation Dry Lab Model HE-43 equipped with Dry Train Model HE-93B. The t.l.c.'s were obtained on 0.1 mm air dried silica gel plates using carbon disulfide or methylene chloride as eluent and sulfur as a reference. Chromatography grade silica gel (100–200 mesh) was used for column chromatography keeping the weight of absorbent to that of the mixture near 50:1.

Materials

Tetrasulfur tetranitride was prepared from sulfur monochloride and ammonia as previously described (35). Recrystallization from benzene afforded pure material of m.p. 178 °C dec. *p*-Nitrobenzylamine was prepared from potassium phthalimide and *p*-nitrobenzylbromide as previously described (36, 37). Its n.m.r. spectrum in deuterochloroform showed three absorptions: −1.72 p.p.m. (broad singlet, 2.2 H, $—NH_2$), −4.05 p.p.m. (singlet, 2.0 H, $—CH_2—$), and −7.36 to −8.34 p.p.m. (multiplet, 4.1 H, $—C_6H_4—$). The m.p. of the hydrochloride salt was 249–250 °C [lit. 250 (38) and 256 °C (39)]. Solvents used for chromatography were U.S.P. grade, and sulfur was "precipitated" grade. Other materials were reagent grade and were used without further purification.

Reactions of Sulfur with Benzylamine; Identification of Products

Tetrasulfur tetranitride (1.99 g, 10.8 mmol) was placed in a 100 ml three-necked flask with a magnetic stirring bar. A rubber serum stopper was placed at one of the necks and another was connected to a cylinder of dry nitrogen. The third neck was connected to a gas washing bottle containing 50.0 mg equiv of hydrochloric acid in about 250 ml of water. Benzylamine was degassed under vacuum, and 8.0 ml (73 mmol) was introduced through the rubber serum stopper by syringe. The reaction was stirred at room temperature while a continuous flow of nitrogen was maintained through the apparatus. The tetrasulfur tetranitride dissolved in the benzylamine to give an orange solution which gradually changed to dark green and after 30 min to yellow-brown. These color changes were accompanied by evolution of heat and ammonia, the latter continuing for at least 5 h. After 14 h the reaction mixture solidified to a yellow chunk. At this point the hydrochloric acid solution was found to be basic. The reaction mixture was separated by chromatography. Hexane eluted about 20 mg of sulfur identified by its m.p. and R_f value. Pure benzylidenimine tetrasulfide (about 2.5 g), obtained from the column by elution with 13% benzene in hexane, was recrystallized from hot methanol to give yellow needles of m.p. 100.5–102 °C.

Anal. Calcd. for $C_{14}H_{12}N_2S_4$ (mol. wt.: 336): C, 49.97; H, 3.59; N, 8.32; S, 38.11. Found (332): C, 49.54; H, 3.67; N, 8.70; S, 37.70.

Benzylidenimine tri- and disulfides were also eluted by 13% benzene in hexane but were not cleanly separated on the column. Appropriate enriched fractions were combined and were further purified by fractional recrystallization from methanol. The trisulfide (about 200 mg) gave white needles of m.p. 125–126 °C.

Anal. Calcd. for $C_{14}H_{12}N_2S_3$ (mol. wt.: 304): C, 55.23; H, 3.97; N, 9.20; S, 31.59. Found (306): C, 55.07; H, 4.12; N, 8.98; S, 32.04.

The disulfide (about 400 mg) was recrystallized from methanol to give nearly colorless white needles of m.p. 100–100.5 °C.

Anal. Calcd. for $C_{14}H_{12}N_2S_2$ (mol. wt.: 272): C, 61.74; H, 4.44; N, 10.28; S, 23.54. Found (271): C, 61.16; H, 4.20; N, 10.41; S, 23.74.

Elution with 20% ether in benzene gave *N*-benzylidene benzylamine (about 1.9 g) as an oil with a b.p. near 105 °C at 0.1 mm Hg. The n.m.r. and i.r. spectra were identical to those of an authentic sample prepared from benzylamine and benzaldehyde (40). Benzaldehyde (about 2.0 g) was eluted by 40% ether in benzene and was identified by comparison of its n.m.r. and i.r. spectra with those of an authentic sample. A quantity of benzylamine was obtained from the column on elution with 50% methanol in ether. Since an n.m.r. spectrum of the crude reaction mixture prior to chromatography did not indicate the presence of either benzylamine or benzaldehyde, these materials must form by hydrolysis of *N*-benzylidene benzylamine on the column.

Quantitative Reaction at a Molar Ratio of 1:8

The reaction was repeated as above using 922 mg (5.01 mmol) of tetrasulfur tetranitride and 4.4 ml (40.3 mmol) of benzylamine. The gas washing bottle contained 50.0 mg equiv of hydrochloric acid. After 20 h of stirring the hydrochloric acid was diluted to 500 ml. A 25.0 ml aliquot required 8.20 ml of 0.100 *N* sodium hydroxide solution for neutralization. The products were separated by washing with ice cold methanol to give 1.21 g of benzylidenimine tetrasulfide contaminated with small amounts of sulfur and benzylidenimine tri- and disulfides. The methanol was removed *in vacuo* to give 3.26 g of oil. The t.l.c. indicated this oil to be mainly *N*-benzylidene benzylamine with a small amount of benzylidenimine tetrasulfide. An n.m.r. spectrum gave the molar ratio of these two as 9.1 to 1.0. Total yields of products were therefore: ammonia, 33.6 mmol; *N*-benzylidene benzylamine, 2.74 g (14.0 mmol); sulfur and benzylidenimine polysulfides together expressed as tetrasulfide, 1.73 g (5.15 mmol).

Can. J. Chem. Downloaded from www.nrcresearchpress.com by 210.87.254.5 on 09/05/12
For personal use only.

Can. J. Chem. Downloaded from www.nrcresearchpress.com by 210.87.254.5 on 09/05/12
For personal use only.

Excess Benzylamine

Tetrasulfur tetranitride (500 mg, 2.72 mmol) and 6.4 ml of benzylamine (59 mmol) were stirred under a dry nitrogen atmosphere. The solution went through the orange and green stages, became orange and then blood red. After 24 h it was reddish brown and quite viscous. Upon addition of anhydrous ether a reddish solution containing an orange solid was obtained; some hydrogen sulfide was evolved. The orange solid was filtered, and the red ether solution was evaporated to give 5.75 g of material which when chromatographed yielded *N*-benzylidene benzylamine (1.78 g), sulfur (130 mg), benzaldehyde (1.95 g), benzylammonium thiosulfate (210 mg), and a quantity of benzylamine. The orange solid melted with decomposition at 90–97 °C in an evacuated sealed tube and decomposed continuously in air with evolution of hydrogen sulfide. After several days in air it was a mixture of sulfur and a white solid which after recrystallization from methanol had a m.p. of 173–174 °C. This material in aqueous solution gave a white precipitate with lead acetate; with silver nitrate it gave a yellowish precipitate which soon turned brown; with barium chloride it gave a white precipitate which was soluble in dilute hydrochloric acid but not in acetic acid; it readily discolored permanganate and was therefore identified as a thiosulfate. The n.m.r. spectrum in deuterium oxide showed three peaks consistent in chemical shift and areas with those expected for the phenyl, ammonium (exchanging with water), and methylene peaks of a benzylammonium ion. Its i.r. spectrum showed a strong NH stretch at 3280 cm^{-1}. Calcd. for benzylammonium thiosulfate 8.80% N, found 8.53% N.

Reactions with p-Chlorobenzylamine; Identification of Products

Tetrasulfur tetranitride (533 mg, 2.90 mmol) and 2 ml of *p*-chlorobenzylamine (16 mmol) were reacted as above. After 24 h the thick yellow paste was separated by chromatography. Hexane eluted about 70 mg of sulfur. Elution with 20% benzene in hexane gave about 570 mg of *p*-chlorobenzylidenimine tetrasulfide which was recrystallized from methanol to give yellow needles of m.p. 114.5–116 °C.

Anal. Calcd. for $C_{14}H_{10}N_2S_4Cl_2$ (mol. wt.: 405): C, 41.48; H, 2.49; N, 6.91; Cl, 17.49; S, 31.64. Found (395): C, 41.56; H, 2.65; N, 6.91; Cl, 17.38; S, 31.80.

p-Chlorobenzylidenimine monosulfide (about 240 mg) was eluted by 50% benzene in hexane and after recrystallization from methanol gave yellow needles of m.p. 146.2–146.8 °C.

Anal. Calcd. for $C_{14}H_{10}N_2SCl_2$ (mol. wt.: 309): C, 54.38; H, 3.26; N, 9.06; Cl, 22.93; S, 10.37. Found (322): C, 54.15; H, 3.25; N, 9.56; Cl, 22.86; S, 10.88.

N-(*p*-Chlorobenzylidene)-*p*-chlorobenzylamine was eluted by 100% benzene and was recrystallized from methanol to give thin white plates of m.p. 62–65 °C.

Anal. Calcd. for $C_{14}H_{11}NCl_2$ (mol. wt.: 264): C, 63.66; H, 4.20; N, 5.30; Cl, 26.84. Found (281): C, 63.57; H, 4.18; N, 5.31; Cl, 26.58.

At Molar Ratio of 1:8

When 344 mg (1.87 mmol) of tetrasulfur tetranitride was reacted with 2.11 g (14.9 mmol) of *p*-chlorobenzylamine, the products obtained were sulfur, 33 mg (1.03 mmol), *p*-chlorobenzylidenimine tetrasulfide, 598 mg (1.48 mmol), and *N*-(*p*-chlorobenzylidene)-*p*-chlorobenzylamine, 1.17 g (4.43 mmol). *p*-Chlorobenzylidenimine monosulfide was found in only trace amounts along with two other materials which appeared to be the di- and trisulfides based on their R_f values of 0.38 and 0.30 *vs.* 0.49 and 0.25 for the tetra- and monosulfides, respectively.

Reactions with p-Methoxybenzylamine; Identification of Products

Tetrasulfur tetranitride (542 mg, 2.94 mmol) and 2.0 ml (16 mmol) of *p*-methoxybenzylamine were reacted as above. After 24 h the solidified product was washed with ice cold methanol to give 710 mg (1.79 mmol) of *p*-methoxybenzylidenimine tetrasulfide which on recrystallization from absolute ethanol gave yellow plates of m.p. 112–113 °C.

Anal. Calcd. for $C_{16}H_{16}N_2S_4O_2$ (mol. wt.: 396): C, 48.46; H, 4.07; N, 7.06; S, 32.34. Found (391): C, 48.59; H, 4.24; N, 7.10; S, 32.66.

The methanol solution was concentrated, and the products were dissolved in chloroform from which 93 mg of a white solid of m.p. 230 °C precipitated. This material was identified as *p*-methoxybenzylammonium thiosulfate based on n.m.r. and chemical analyses as described for benzylammonium thiosulfate. The remaining yellow oil was purified by column chromatography to give an additional 140 mg of *p*-methoxybenzylidenimine tetrasulfide (eluted by 5% ether in benzene), 620 mg of anisaldehyde (eluted by 100% ether) identified by comparison of its n.m.r. and i.r. spectra with those of an authentic sample, and *p*-methoxybenzylamine (eluted by 80% methanol in ether) which was identified by its n.m.r. spectrum.

At Molar Ratio of 1:8

When 2.00 g (10.8 mmol) of tetrasulfur tetranitride was reacted with 10.9 ml (87 mmol) of *p*-methoxybenzylamine and the product was washed with ice cold methanol, 3.13 g of *p*-methoxybenzylidenimine tetrasulfide remained. Upon cooling to about −20 °C, 372 mg of a yellow solid precipitated. This material was a roughly equal mixture of *p*-methoxybenzylidenimine tetrasulfide and a new *p*-methoxybenzylidenimine polysulfide of $R_f = 0.68$ *vs.* 0.73 for the tetrasulfide. Attempted recrystallization of this material led to a mixture of these two materials with a third, *p*-methoxybenzylidenimine polysulfide. The original solvent from which these solids were obtained was removed *in vacuo* to give 8.45 g of oil. A part of this material when chromatographed gave mainly anisaldehyde and *p*-methoxybenzylamine. The n.m.r. spectrum before chromatography did not show any aldehyde, however. When the balance was distilled under reduced pressure, a yellow oil was obtained at 175–180 °C and 0.1 mm Hg which crystallized to a solid of m.p. 36.5–37.5 °C, lit. (41) 37–38 °C for *N*-(*p*-methoxybenzylidene)-*p*-methoxybenzylamine. The n.m.r. spectrum (a singlet at −3.62, 3.0 H, CH_3O—; a broad singlet at −4.58, 4.1 H, —CH_2—; a multiplet at −6.58 to −7.80, 4.1 H, —C_6H_4—; and a broad singlet at −8.10 p.p.m., 1.0 H, H—C=N) was consistent with that expected for this material. Total yields were therefore

Can. J. Chem. Downloaded from www.nrcresearchpress.com by 210.87.254.5 on 09/05/12
For personal use only.

3.32 g (8.37 mmol) of *p*-methoxybenzylidenimine tetrasulfide, 180 mg (0.49 mmol) of *p*-methoxybenzylidenimine trisulfide[6] and 8.45 g (33.1 mmol) of *N*-(*p*-methoxybenzylidene)-*p*-methoxybenzylamine.

p-Nitrobenzylamine

Tetrasulfur tetranitride (500 mg, 2.72 mmol) was reacted as above with 2.0 g (13 mmol) of *p*-nitrobenzylamine. The reaction mixture became very viscous, and 2 ml of dimethylformamide (the minimum amount to allow the mixture to be stirred) was added. After 12 h the product, a very viscous dark brown gum, was dissolved in hot methanol. From this solution 166 mg of elemental sulfur (5.19 mg atoms) precipitated. The mother liquor contained a viscous tar whose n.m.r. spectrum showed no peaks downfield from the phenyl multiplet. Characterization of this material was not undertaken.

d,l-α-Methylbenzylamine

Tetrasulfur tetranitride (656 mg, 3.56 mmol) was reacted as above with 2 ml of α-methylbenzylamine (16 mmol). The reaction mixture became brownish red, and a basic gas was evolved. After stirring for 24 h, the viscous product was dissolved in methanol and cooled to 0 °C whereupon 160 mg (5.0 mg atoms) of sulfur precipitated. Attempted chromatographic separation led to a number of fractions of viscous dark brown materials but none had the singlet methyl peak required for a benzylidenimine type of product. Distillation, recrystallization and preparative scale t.l.c. failed to give tractable, single component products.

Allylamine

Tetrasulfur tetranitride (501 mg, 2.72 mmol) was reacted as above with allylamine (2 ml, 27 mmol). Ammonia was evolved fairly rapidly, and the color passed through orange to dark brown; after 6 h it had become very viscous. The excess allylamine was removed *in vacuo* leaving a dark brown tar which was insoluble in ether, benzene, hexane, and alcohol. This was assumed to be polymeric and was not further characterized.

Phenylhydrazine

Tetrasulfur tetranitride, 514 mg (2.80 mmol), was placed in a flask equipped as in the benzylamine reaction and cooled to 0 °C. The gas washing bottle contained 7.00 mg equiv of hydrochloric acid in about 70 ml of water. Phenylhydrazine (2.15 g, 19.9 mmol) was added to the flask and immediately solidified. On warming to about 20 °C it remelted, and the temperature of the exothermic reaction which ensued was maintained below 25 °C by periodic cooling. The solution became orange, then brilliant yellow-orange, and eventually yellow. After 6 h gas evolution had ceased. After 12 h the reaction was stopped, and the solution in the acid trap was diluted to 100 ml. A 50 ml aliquot required 4.45 ml of 0.075 *N* potassium hydroxide solution for neutralization. The products were separated by column chromatography. Hexane eluted 221 mg (6.90 mg atoms) of elemental sulfur. Elution with 15% benzene in hexane gave 196 mg of a white solid which was recrystallized from methanol to give diphenyl disulfide of m.p. 59–60 °C, lit. (42) 60–61 °C, and molecular weight by mass spectrum of 218 (Calcd. for $C_{12}H_{10}S_2$, 218). The n.m.r. and i.r. spectra were identical to those of authentic diphenyldisulfide. Elution with 20% benzene in hexane gave 122 mg of diphenyl monosulfide as a colorless oil. The mass spectrum showed an apparent molecular ion of mass 186 (Calcd. for $C_{12}H_{10}S$, 186). The n.m.r. and i.r. spectra were identical to those of the authentic material. Elution with more polar solvents gave considerable amounts of multicomponent mixtures of viscous red materials which were not characterized. A similar reaction of 504 mg (2.74 mmol) of tetrasulfur tetranitride and 2 ml (20.4 mmol) of phenylhydrazine in 5 ml of triethylamine for 30 h at 0 °C with work-up as above led to 95 mg (2.97 mg atoms) of elemental sulfur, 326 mg (1.49 mmol) of diphenyl disulfide, and 99 mg (0.53 mmol) of diphenyl monosulfide

Pyrolysis of Benzylidenimine Tetrasulfide

Benzylidenimine tetrasulfide (711 mg, 2.12 mmol) was placed in a 100 ml flask, evacuated to 7×10^{-4} mm Hg, sealed, and heated in an oil bath to 105 °C. As the solid fused, some gas evolution was observed, and an oil boiled off and condensed on the walls of the flask above the oil bath level. After 7 h the mixture was cooled, the flask was opened, and a basic gas was detected by p*H* paper. Hydrogen sulfide was also detected by wet lead acetate paper. The non-volatile products were separated by column chromatography. Pure hexane eluted 222 mg (6.6 mg atoms) of elemental sulfur. Elution with 13% benzene in hexane gave 45 mg of unreacted benzylidenimine tetrasulfide (0.13 mmol). Elution with 20% benzene in hexane gave 234 mg (0.76 mmol) of triphenyl-*s*-triazine (R_f 0.14, silica gel – carbon disulfide with sulfur = 0.80). Recrystallization from a hexane–benzene mixture gave colorless needles of m.p. 234.5–235 °C [lit. (43) 235–235.4 °C]. The i.r. spectrum of this material was identical to that of authentic triphenyl-*s*-triazine (43). A 1:1 mixture of benzene and hexane eluted 59 mg (0.57 mmol) of benzonitrile identified by comparison of its i.r. and n.m.r. spectra with those of an authentic sample.

Benzylidenimine Tetrasulfide with Excess Benzylamine

Benzylidenimine tetrasulfide (510 mg, 1.52 mmol) was dissolved in 2.71 g (25 mmol) of benzylamine under a dry nitrogen atmosphere and stirred for 24 h.[7] The reaction mixture was placed in a dry box and anhydrous ether was introduced into the reaction mixture and stirred well. An orange solid precipitated which was filtered and washed with ether. This solid decomposed in air with the evolution of hydrogen sulfide and melted at 93–96 °C dec. in an evacuated sealed tube. Nitrogen analysis gave 6.67%. Calcd. for $C_{14}H_{10}N_2S_6$, 6.85 and for $C_{14}H_{10}N_2S_7$, 6.37%. An n.m.r. spectrum in dry dimethyl-d_6-sulfoxide showed three peaks: −3.96 (singlet, 1.7 H, $—CH_2—$), −6.32 (broad singlet, 3.4 H, $—NH_3$) and

[6]The assignment of this material as the trisulfide rests on the R_f value and on the decomposition to tetrasulfide and a new material, probably the disulfide. Disproportionation of unsubstituted benzylidenimine trisulfide to di- and tetrasulfides was observed when samples were left in solution for long periods of time.

[7]A reaction run without a dry nitrogen atmosphere led to benzylammonium thiosulfate.

Can. J. Chem. Downloaded from www.nrcresearchpress.com by 210.87.254.5 on 09/05/12
For personal use only.

−7.00 p.p.m. (broad singlet, 5.0 H, C_6H_5—). The filtrate was concentrated to give an oily material. This was separated by column chromatography to give 55 mg of sulfur (1.7 mg atoms), 425 mg (2.2 mmol) of *N*-benzylidene benzylamine, 310 mg (2.9 mmol) of benzaldehyde, and a substantial quantity of benzylamine. A sample of the orange solid was placed in an evacuated sealed tube (weight not recorded) in the dry box and heated to 170–180 °C for 12 h. A strong odor of hydrogen sulfide (confirmed by wet lead acetate paper) was noted when the tube was cooled and opened. The non-volatile products were separated by column chromatography. Hexane eluted 73 mg (2.3 mg atoms) of elemental sulfur. Elution by 20–40% benzene in hexane gave 120 mg (about 0.4 mmol) of dibenzyl-polysulfides with sulfur chain lengths of 2–6 inclusive.[8] Elution with benzene gave 66 mg (0.27 mmol) of 3,5-diphenyl-1,2,3-thiadiazole which after recrystallization from ethanol had a m.p. of 89–90 °C [lit. (44) 89–90 °C]. This was further identified by mixed m.p. (undepressed) and comparison of its i.r. and n.m.r. spectra with those of an authentic sample prepared from thiobenzamide and iodine (44). Ether eluted 37 mg (0.16 mmol) of *N*-benzylthiobenzamide of m.p. 85 °C [lit. (45) 84–85 °C]. This was identified by mixed m.p. (undepressed) and comparison of its i.r. and n.m.r. spectra with those of the authentic material prepared from sulfur and benzylamine (45). Elution with 30% methanol in ether gave 72 mg (0.53 mmol) of thiobenzamide which was recrystallized from benzene to give a m.p. of 113–114 °C [lit. (46) 115–116 °C]. The mixed m.p. with an authentic sample prepared from benzonitrile and hydrogen sulfide (46, 47) was undepressed, and the i.r. and n.m.r. spectra were identical.

A sample of benzylammonium hexasulfide was prepared from benzylamine, sulfur, and hydrogen sulfide as previously described (19). It melted at 96 °C in an evacuated sealed tube and was an orange solid which decomposed slowly in air with evolution of hydrogen sulfide to give eventually elemental sulfur and benzylammonium thiosulfate. The n.m.r. spectrum of this material was virtually superimposable on that of the material obtained from the benzylidenimine tetrasulfide reaction.

Benzylamine with Sulfur

Benzylamine (5 ml, 45.8 mmol) was added to 1.08 g (33.8 mg atoms) of sulfur, and the mixture was stirred for 24 h under a nitrogen atmosphere. Anhydrous ether was added and stirred well. An orange solid remained undissolved (1.94 g) which melted at 93–94 °C in an evacuated sealed tube. Nitrogen analysis gave 6.54% (*i.e.*, between a hexa- and heptasulfide).

A sample was subjected to a Soxhlet extraction with anhydrous ether in the dry box for 24 h and was found to be completely decomposed into sulfur, benzylamine, and (presumably) hydrogen sulfide. A sample left in air evolved hydrogen sulfide and became a yellowish solid. This was dissolved in methanol to leave some elemental sulfur. The methanol solution was found to contain mainly benzylammonium thiosulfate. Another sample added to methanol evolved hydrogen sulfide and deposited 344 mg (10.7 mg atoms) of sulfur. The methanol solution contained 357 mg (3.3 mmol) of benzylamine. A sample (not weighed) was heated for 12 h at 170–180 °C in an evacuated sealed tube. The products obtained on chromatography were: sulfur, 188 mg (5.9 mg atoms); 1,2-diphenylethane, 74 mg (0.41 mmol); dibenzylpolysulfides (a mixture of tri-, tetra-, penta- and hexasulfides), 88 mg (about 0.35 mmol);[8] 3,5-diphenyl-1,2,3-thiadiazole, 127 mg (0.53 mmol); and thiobenzamide, 40 mg (0.29 mmol).

A sample of the benzylammonium polysulfide (568 mg) was dissolved in 8 ml of benzylamine and refluxed for 3 h during which time the dark reddish brown color slowly changed to pale yellow, and vigorous hydrogen sulfide evolution was observed. The reaction mixture was dissolved in hot hexane, and upon cooling 600 mg (2.7 mmol) of *N*-benzylthiobenzamide of m.p. 86 °C was obtained.

Heptasulfurimide with Benzylamine

Benzylamine (4.2 ml, 38.6 mmol) was added to 1.00 g (4.18 mmol) of heptasulfurimide under a dry nitrogen atmosphere. The solution immediately became blue and after a few minutes dull green and then reddish. After 10 h the dark red solution was placed in the dry box, and an aliquot was removed and heated in a free flame until it boiled. The red color became pale yellow and evolution of hydrogen sulfide was observed. After cooling it solidified and was recrystallized from hexane to give *N*-benzylthiobenzamide of m.p. 84 °C. The remainder was stirred with anhydrous ether in the dry box. About 400 mg of an orange solid precipitated. This was filtered and washed with anhydrous ether to give a material of m.p. 95–97 °C dec. Nitrogen analysis gave 5.82%; calculated for benzylammonium *octa*sulfide, 6.06 and for the *nona*sulfide, 5.67%. This material, in contrast to the previous samples, was not stable even in the dry box; it slowly became dark brown and looked "wet". In air it decomposed with the evolution of hydrogen sulfide to give sulfur and benzylammonium thiosulfate. A sample (not weighed) was pyrolyzed in an evacuated sealed tube as before and gave: sulfur, 174 mg (5.4 mg atoms); dibenzylpolysulfides (a mixture of di-, tetra- and pentasulfides), 214 mg (0.86 mmol);[8] 3,5-diphenyl-1,2,3-thiadiazole, 127 mg (0.53 mmol); and thiobenzamide, 40 mg (0.29 mmol).

This work was carried out under a grant from the National Research Council of Canada.

1. E. Fluck, M. Becke-Goehring and G. Dehoust. Z. Anorg. Allg. Chem. **312**, 60 (1961).
2. H. L. Krauss and H. Jung. Z. Naturforsch. **16B**, 624 (1961).
3. E. Fluck and R. M. Reinisch. Z. Anorg. Allg. Chem. **328**, 165 (1964).
4. J. Weiss and H. Piechaczek. Z. Naturforsch. **18B**, 1139 (1963).
5. A. Meuwsen. Chem. Ber. **64**, 2301 (1931).
6. O. Ruff and E. Geisel. Chem. Ber. **37**, 1573 (1904).
7. M. Becke-Goehring and R. Schwarz. Z. Anorg. Allg. Chem. **296**, 3 (1958).
8. R. Schenck. Ann. **290**, 171 (1896).
9. E. Fluck. Z. Anorg. Allg. Chem. **312**, 195 (1961).
10. T. G. Levi. Gazz. Chim. Ital. **61**, 294 (1931).

[8]The chain length and average composition was estimated from n.m.r. spectra. See ref. 24.

11. (*a*) M. BECKE-GOEHRING and H. JENNE. Chem. Ber. **92**, 1149 (1959); (*b*) J. S. POND. Ph.D. Thesis. University of Minnesota, Minneapolis, Minnesota, 1964.
12. (*a*) NMR Spectra Catalog. Sadtler Research Laboratories, Philadelphia, Pennsylvania, 1967, Spectra No. 702; (*b*) Spectra No. 3606; (*c*) Spectra No. 4516.
13. NMR Spectra Catalog Vol. 1. Varian Associates, Palo Alto, California, 1962, Spectra No. 156.
14. O. EXNER. Collect. Czech. Chem. Commun. **28**, 3150 (1963).
15. M. CARMACK and M. A. SPIELMAN. Organic reactions. Vol. III. John Wiley and Sons, Inc., New York, N.Y., 1946. pp. 83.
16. F. ASINGER and H. OFFERMANNS. Synthesen mit Ketonen, Schwefel und Ammoniak bzw. Aminen und Chemisches Verhalten der Reaktionsprodukte. Westdeutscher Verlag, Koln und Opladen, 1966.
17. B. MILLIGAN and J. M. SWAN. J. Chem. Soc. 2969 (1959).
18. V. M. MAR'YANOVSKII, A. M. SIMONOV, and V. V. FIRSOV. Zh. Org. Khim. **5**, 2196 (1969).
19. T. G. LEVI. Gazz. Chim. Ital. **60**, 975 (1930).
20. M. G. VORONKOV and A. YA. LEGZDYN. J. Org. Chem. U.S.S.R. **3**, 446 (1967).
21. G. P. RICHTER. Ph.D. Thesis. University of Minnesota, Minneapolis, Minnesota, 1968.
22. F. H. MCMILLAN. J. Amer. Chem. Soc. **70**, 868 (1948).
23. J. R. VAN WAZER and D. GRANT. J. Amer. Chem. Soc. **86**, 1450 (1964).
24. D. GRANT and J. R. VAN WAZER. J. Amer. Chem. Soc. **86**, 3012 (1964).
25. L. J. BELLAMY. The infra-red spectra of complex molecules. John Wiley and Sons, Inc., New York, N. Y., 1962. pp. 271.
26. M. J. FABIAN and M. LEGRAND. Bull. Soc. Chim. Fr. 1461 (1956).
27. A. J. BANISTER, L. F. MOORE, and J. S. PADLEY. Spectrochim. Acta, **23A**, 2705 (1967).
28. R. L. SASS. Acta Cryst. **13**, 320 (1960).
29. F. A. COTTON and G. WILKINSON. Advanced inorganic chemistry. Interscience Publishers, New York, N. Y., 1967. pp. 115.
30. B. D. SHARMA and J. DONOHUE. Acta Cryst. **16**, 891 (1963).
31. D. CHAPMAN and T. C. WADDINGTON. Trans. Faraday Soc. **58**, 1679 (1962).
32. J. TSURUGI and T. NAKABAYASHI. J. Org. Chem. **24**, 807 (1959).
33. T. NAKABAYASHI, J. TSURUGI, and T. YUBUTA. J. Org. Chem. **29**, 1236 (1964).
34. L. N. FERGUSON and G. E. K. BRANCH. J. Amer. Chem. Soc. **66**, 1467 (1944).
35. E. G. ROCHOW. Inorganic syntheses. Vol. VI. McGraw Hill Book Co. Inc., New York, N.Y., 1960. pp. 124.
36. S. GABRIEL. Chem. Ber. **20**, 2224 (1887).
37. O. L. BRADY and L. KLEIN. J. Chem. Soc. 874 (1927).
38. H. R. ING and R. H. F. MANSKE. J. Chem. Soc. 2348 (1926).
39. F. R. GOSS, C. K. INGOLD, and I. S. WILSON. J. Chem. Soc. 2440 (1926).
40. A. T. MASON and G. R. WINDER. J. Chem. Soc. **65**, 191 (1894).
41. R. JUDAY and H. ADKINS. J. Amer. Chem. Soc. **77**, 4559 (1955).
42. K. G. ALLUM, J. A. CREIGHTON, J. H. S. GREEN, G. J. MINKOFF, and L. J. S. PRINCE. Spectrochim. Acta, **24A**, 927 (1968).
43. R. D. SPENCER and B. H. BEGGS. Anal. Chem. **35**, 1633 (1963).
44. G. KRESZE, A. HORN, R. PHILIPPSON, and A. TREDE. Chem. Ber. **98**, 3401 (1965).
45. F. H. MCMILLAN. J. Amer. Chem. Soc. **70**, 868 (1948).
46. K. KINDLER. Ann. **431**, 187 (1923).
47. A. W. HOFMANN. Chem. Ber. **2**, 645 (1869).

Can. J. Chem. Downloaded from www.nrcresearchpress.com by 210.87.254.5 on 09/05/12
For personal use only.

Reactions of Benzylamine with Sulfur

YUKIHIKO SASAKI AND FREDRIC P. OLSEN
Department of Chemistry, McMaster University, Hamilton, Ontario
Received May 29, 1970

A five-step sequence has been established for the room temperature reaction of sulfur with benzylamine. Benzylamine polysulfides and benzylidenimine polysulfides occur as interconverting intermediates in this system. The final products are benzylammonium polysulfides, ammonia, and *N*-benzylidene benzylamine.

Canadian Journal of Chemistry, 49, 283 (1971)

Can. J. Chem. Downloaded from www.nrcresearchpress.com by 210.87.254.5 on 09/05/12
For personal use only.

Primary amines have been successfully employed in the Willgerodt–Kindler reaction (1, 2) where, in addition to the usual products, they can lead to novel types of compounds. Thus, acetophenone at elevated temperatures gives thioamides (1, 2) but at room temperature (in the presence of 0.25 g atoms of sulfur per mol of ketone) gives a Schiff's base (3). When the quantity of sulfur is increased, the yield of Schiff's base decreases, and at a sulfur to ketone ratio of 8:1 the heterocyclic compound 8-alkylamino-8-phenyl-1,2,3,4,5,6-hexathiocane-7-thione (**1**) results (4, 5). Primary amines are

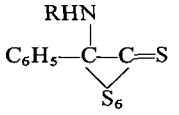

1

known to catalyze various reactions of sulfur with organic substrates. Aniline, for example, shows an accelerating effect on the rate of vulcanization of natural rubbers (6–8). Mercaptans, unreactive toward elemental sulfur at low temperatures, readily evolve hydrogen sulfide in the presence of butylamine (9, 10) providing a convenient route to alkyl disulfides. By adjusting the molar ratio of mercaptan to sulfur, the sulfur chain length in the product can be changed fairly selectively up to the tetrasulfide (10). *n*-Butyl- and other amines may function as catalysts in the dehydrogenation of heterocyclic compounds with elemental sulfur (11, 12).

The mechanism of the Willgerodt–Kindler reaction remains unclear, notwithstanding a considerable amount of work. Most of the proposed mechanisms (1, 2, 9, 13–17) have considered the first step to be attack either by the amine at the carbonyl carbon or by sulfur at the α-carbon to the carbonyl group. This step is generally thought to be followed by migration of the functional group or groups along the carbon chain with eventual irreversible oxidation at the end of the chain giving the final product. These mechanisms remain rather speculative, and none has considered the possibility of any reaction between sulfur and the amine. More detailed information about the interaction of sulfur with amines, a reaction which is known to occur even at room temperature (18, 19), appears vital to any understanding of the Willgerodt–Kindler reaction and the various other reactions involving amines as catalysts in sulfur reactions. The work described herein was undertaken with the aim of establishing the nature of the room temperature reactions between sulfur and benzylamine.

Results and Discussion

A Proposed Reaction Scheme

Purified tertiary amines have been demonstrated to be inert to sulfur under normal conditions (18, 20, 21) but to give trialkylammonium polysulfides when hydrogen sulfide is added (22). Primary and secondary amines also lead to alkylammonium polysulfides with hydrogen sulfide and sulfur (22) although here the same products result even in the absence of added hydrogen sulfide (23, 24). Levi (25) has proposed reactions 1 and 2 to account for these observations.

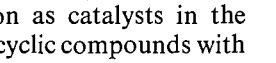

[1] $2R_2NH + S_{y+1} \rightarrow R_2N{-}S_y{-}NR_2 + H_2S$

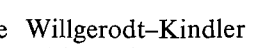

[2] $H_2S + (x-1)S + 2R_2NH \rightarrow (R_2NH_2^+)_2S_x^{2-}$

Spectroscopic and conductometric measurements (18) have confirmed the presence of alkylammonium polysulfides in both the primary and secondary amine systems. The e.s.r. data have been interpreted (26) in terms of polythiobisamines, and these materials have been isolated from several secondary amine – sulfur reactions car-

Can. J. Chem. Downloaded from www.nrcresearchpress.com by 210.87.254.5 on 09/05/12
For personal use only.

ried out in the presence of a hydrogen sulfide scavenger (25, 27). It therefore seems reasonable to assume that since primary amines form polysulfide ions, they should also form polythiobisamines. The product isolated from benzylamine (the only primary amine reported to lead to a well-defined product) and sulfur in the presence of lead(II) oxide was not the benzylamine polysulfide, however, but rather its oxidation product, benzylidenimine tetrasulfide (28, 29).

Benzylamine *di*sulfide was consequently prepared and evaluated as a possible intermediate in this reaction. This material decomposed quite readily when exposed to small amounts of benzylamine at room temperature. Even in the absence of base it was stable for only a few hours. After an induction period (5–5½ h with no change), it underwent fairly rapid (~1 h) autocatalytic decomposition. The products of these decompositions were *N*-benzylidene benzylamine and ammonia along with smaller amounts of benzylidenimine tetrasulfide, benzylammonium polysulfides, and sulfur. When the autocatalytic decomposition was monitored by n.m.r., benzylamine and benzylidenimine tetrasulfide were observed to form, to increase to a maximum concentration, and then to decrease in amount as the concentration of *N*-benzylidene benzylamine increased. The ratio of benzylamine to benzylidenimine tetrasulfide formed in the early stages was near 4:1. These results suggested a base catalyzed redox type disproportionation of benzylamine disulfide as per eq. 3. The benzylamine produced would be expected to catalyze further decomposition of the benzylamine disulfide leading to the observed autocatalysis. As described in the preceding paper (29), benzylidenimine tetrasulfide reacts with benzylamine to give benzylammonium polysulfides, *N*-benzylidene benzylamine, and ammonia. This reaction would occur as the concentration of benzylidenimine tetrasulfide and benzylamine increased during the decomposition and would thus account for the observed products. Since benzylidenimine tetrasulfide was obtained from the decomposition of benzylamine *di*sulfide, benzylamine polysulfides could be intermediates in the reaction of benzylamine with sulfur. When sulfur, benzylamine disulfide, or benzylidenimine tetrasulfide was dissolved in an excess of benzylamine, a reddish-brown solution formed, and ammonia was evolved. From all of these solutions benzylammonium polysulfides and *N*-benzylidene benzylamine were isolated. Thus, these possible intermediates all lead to the same final products.

[3] $$3C_6H_5CH_2\overset{H}{\underset{|}{N}}—S_2—\overset{H}{\underset{|}{N}}CH_2C_6H_5 \rightarrow 4C_6H_5CH_2NH_2 + C_6H_5\overset{H}{\underset{|}{C}}{=}N—S_4—N{=}\overset{H}{\underset{|}{C}}C_6H_5 + 2S$$

Equations 4 to 8 are consequently proposed to account for the benzylamine-sulfur system[1] where [6] is base catalyzed and [7] is catalyzed by sulfide ion. The latter point seems justified since only small amounts of *N*-benzylidene benzylamine and ammonia were produced from benzylidenimine tetrasulfide and benzylamine in the presence of lead(II) oxide, a sulfide ion scavenger.

[4] $$(a+1)S + 2C_6H_5CH_2NH_2 \rightleftharpoons H_2S + C_6H_5CH_2\overset{H}{\underset{|}{N}}—S_a—\overset{H}{\underset{|}{N}}CH_2C_6H_5$$

[5] $$H_2S + (x-1)S + 2C_6H_5CH_2NH_2 \rightarrow (C_6H_5CH_2NH_3^+)_2S_x^{2-}$$

[6] $$3C_6H_5CH_2\overset{H}{\underset{|}{N}}—S_a—\overset{H}{\underset{|}{N}}CH_2C_6H_5 \rightarrow 4C_6H_5CH_2NH_2 + C_6H_5CH{=}N—S_b—N{=}CHC_6H_5 + (3a-b)S$$

[7] $$C_6H_5CH{=}N—S_b—N{=}CHC_6H_5 + 2C_6H_5CH_2NH_2 \rightleftharpoons 2C_6H_5CH{=}NH + C_6H_5CH_2\overset{H}{\underset{|}{N}}—S_b—\overset{H}{\underset{|}{N}}CH_2C_6H_5$$

[8] $$C_6H_5CH{=}NH + C_6H_5CH_2NH_2 \rightarrow NH_3 + C_6H_5CH{=}N—CH_2C_6H_5$$

In [4], benzylamine reacts with sulfur to give a benzylamine polysulfide and hydrogen sulfide. This is written as an equilibrium since tetraalkylamine polysulfides are known (30) to react with hydrogen sulfide to give amines and elemental sulfur. In eq. 5, the hydrogen sulfide formed in [4] reacts with more sulfur and benzylamine to give benzylammonium polysulfides (one of the final products). Both eqs. 4 and 5 are based on analogy with Levi's (25) work on secondary amines. Davis and Nakshbendi (18)

[1]In eqs. 4–8 *a*, *b*, and *x* represent the number of sulfur atoms in the various polysulfide chains; *b* is generally 4 and less commonly 3, 2, or 1; *x* is generally 6–7; no estimate for *a* is available.

Can. J. Chem. Downloaded from www.nrcresearchpress.com by 210.87.254.5 on 09/05/12
For personal use only.

have proposed an alternative mechanism (reactions 9 and 10) for the initial steps in the interaction of sulfur with a secondary amine which does not involve free hydrogen sulfide. The primary amine analogue of **2** could well be present

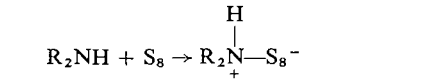

[9] $R_2NH + S_8 \rightarrow R_2\overset{+}{N}(H)—S_8^-$

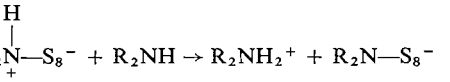

[10] $R_2\overset{+}{N}(H)—S_8^- + R_2NH \rightarrow R_2NH_2^+ + R_2N—S_8^-$

2

in our system as an intermediate which could react with more amine to give benzylamine polysulfide and alkylammonium polysulfides as per eqs. 11 and 12. The sum of eqs. 9 to 12, given by [13], is the same as the sum of [4] and [5].

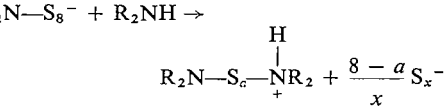

[11][2] $R_2N—S_8^- + R_2NH \rightarrow R_2N—S_a—\overset{+}{N}(H)R_2 + \frac{8-a}{x}S_x^{-2}$

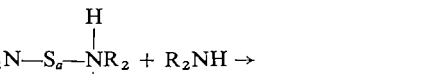

[12] $R_2N—S_a—\overset{+}{N}(H)R_2 + R_2NH \rightarrow R_2N—S_a—NR_2 + R_2NH_2^+$

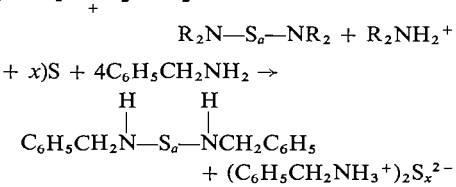

[13] $(a + x)S + 4C_6H_5CH_2NH_2 \rightarrow C_6H_5CH_2\overset{H}{N}—S_a—\overset{H}{N}CH_2C_6H_5 + (C_6H_5CH_2NH_3^+)_2S_x^{2-}$

For simplicity only, since it is not possible to distinguish between these two mechanisms on the basis of the work described here, the scheme will be based on eqs. 4 and 5. It should be emphasized, however, that eqs. 9–12 offer an equally good alternative to [4] and [5] (see also reference 31). In eq. 6, the benzylamine polysulfides formed in [4] are proposed to decompose to benzylamine, sulfur, and benzylidenimine polysulfides as observed experimentally for benzylamine *di*sulfide. Since sulfur and benzylamine are produced in this step, eqs. 4–6 will be repeated. In eq. 7, the benzylidenimine polysulfides produced in [6] are proposed to react with benzylamine in the presence of sulfide ion to give benzylamine polysulfides and benzylidenimine. Exchange of one amine for another has been previously observed in alkylamine polysulfides. Thus, when *N*-methylaniline disulfide is mixed with aniline or when aniline disulfide is mixed with *N*-methylaniline, exchange occurs quite rapidly at room temperature[3] to give the five species shown in eq. 14. By analogy, exchange of imine for amine in the presence of the excess benzylamine is

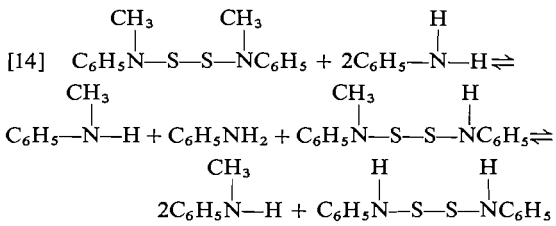

[14] $C_6H_5\overset{CH_3}{N}—S—S—\overset{CH_3}{N}C_6H_5 + 2C_6H_5—\overset{H}{N}—H \rightleftharpoons C_6H_5—\overset{CH_3}{N}—H + C_6H_5NH_2 + C_6H_5\overset{CH_3}{N}—S—S—\overset{H}{N}C_6H_5 \rightleftharpoons 2C_6H_5\overset{CH_3}{N}—H + C_6H_5\overset{H}{N}—S—S—\overset{H}{N}C_6H_5$

expected to occur here with the benzylidenimine polysulfides. The benzylidenimine proposed as a product in this exchange is known (32) and is quite reactive toward nucleophiles. It has been previously proposed (33) to react with benzylamine to give *N*-benzylidene benzylamine and ammonia as per [8]. Catalysis by sulfide ion as proposed in eq. 7 appears to be fairly common in sulfur-amine reactions (20, 21). Since benzylamine polysulfides are produced in [7], all steps will be repeated until all the sulfur is converted to benzylammonium polysulfides or all the benzylamine is converted to *N*-benzylidene benzylamine and ammonia. The proposed scheme is obviously complex with benzylamine polysulfides and benzylidenimine polysulfides involved in a cyclical catalytic sense. The interrelationship between the various compounds is shown in Fig. 1.

Quantitative Assessment of the Proposed Reaction Scheme

The proposed scheme described by Fig. 1 (reactions 4–8) accounts for the observed products using intermediates which are known independently to lead to these products. Each of the steps is based on analogy with a known reaction in a similar system. The intricate relationship between the compounds makes it impossible, however, to study any one step independently of the others. Nevertheless, a number of quantitative predictions can be derived from this scheme which are subject to experimental test. Before deriving these predic-

[2]From the charge balance it is apparent that $(8 - a)/x$ must equal 1 in this particular equation (*i.e.*, $a + x = 8$).

[3]J. C. Barrick and F. P. Olsen, unpublished observations.

Can. J. Chem. Downloaded from www.nrcresearchpress.com by 210.87.254.5 on 09/05/12
For personal use only.

tions, three useful relationships are noted. First, all hydrogen sulfide formed in the presence of benzylamine (since hydrogen sulfide is formed only from benzylamine, it cannot be formed in the absence of benzylamine) goes immediately to benzylammonium polysulfides. Therefore, in the absence of a sulfide scavenger, eqs. 4 and 5 may always be combined (added) to eliminate hydrogen sulfide as in [13]. Second, since benzylidenimine was neither isolated nor detected, it must react with benzylamine fairly rapidly compared to the various other reactions in the system. Here again, benzylidenimine is formed only from benzylamine and hence cannot be formed in the absence of benzylamine (alternatively and equally good, equilibrium [7] may lie fairly far to the left). Equations 7 and 8 may consequently be combined to eliminate benzylidenimine (twice [8] added to [7]) to give [15]. Finally, it should be noted that the benzylamine polysulfides formed in [7] have

[15] $$C_6H_5CH{=}N{-}S_b{-}N{=}CHC_6H_5 + 4C_6H_5CH_2NH_2 \rightarrow C_6H_5CH_2\overset{H}{\underset{|}{N}}{-}S_b{-}\overset{H}{\underset{|}{N}}CH_2C_6H_5 + 2NH_3 + 2C_6H_5CH{=}NCH_2C_6H_5$$

a different sulfur chain length than those formed in [4]. Since the chain length is variable in both places, this does not pose a chemical problem. However, the combination of equations is very much simpler if these two materials can be related. Equation 16 is postulated for this purpose. This equation is solely a computational

[16] $$C_6H_5CH_2\overset{H}{\underset{|}{N}}{-}S_b{-}\overset{H}{\underset{|}{N}}CH_2C_6H_5 \rightarrow C_6H_5CH_2\overset{H}{\underset{|}{N}}{-}S_a{-}\overset{H}{\underset{|}{N}}CH_2C_6H_5 + (b-a)S$$

artifact and need not reflect a real chemical process. Indeed, free sulfur could be formed or consumed in eqs. 6 or 7. It could also be formed by decomposition of (or consumed by addition to) either benzylamine polysulfides or benzylidenimine polysulfides or by any combination of these four processes. The result is the same and is accounted for by [16].

Stoichiometry of the Overall Reaction of Sulfur with an Excess of Benzylamine

An overall equation for the reaction of sulfur with excess benzylamine may be obtained by

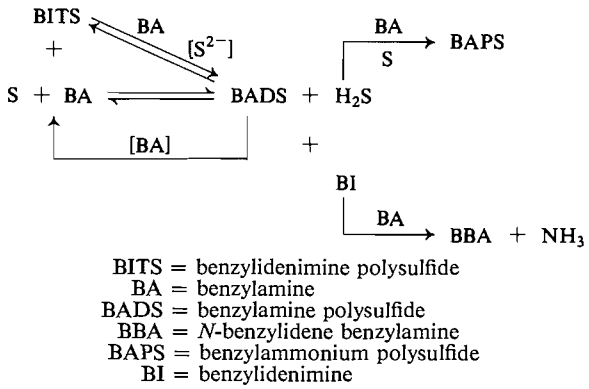

FIG. 1. Reaction of sulfur with benzylamine.

combining eqs. 4 through 8 to eliminate all intermediates. Benzylamine polysulfides may be eliminated by adding eq. 6 to three times [13] to give [17]. The benzylidenimine polysulfides may

[17] $$(3x+b)S + 8C_6H_5CH_2NH_2 \rightarrow C_6H_5CH{=}N{-}S_b{-}N{=}CHC_6H_5 + 3(C_6H_5CH_2NH_3^+)_2S_x^{2-}$$

now be eliminated from [17] by the following procedure. First, eq. 15 is combined with [16] to correct the sulfur chain lengths and then (after multiplying by three) combined with [6] to give (after dividing by a common factor of 2) [18]. Equation 18 when combined with [17] gives

[18] $$C_6H_5CH{=}N{-}S_b{-}N{=}CHC_6H_5 + 4C_6H_5CH_2NH_2 \rightarrow 3NH_3 + 3C_6H_5CH{=}NCH_2C_6H_5 + bS$$

(after dividing by $3x$) the predicted overall stoichiometric reaction, [19]. The quantities of

[19] $$S + \frac{4}{x}C_6H_5CH_2NH_2 \rightarrow \frac{1}{x}C_6H_5CH{=}NCH_2C_6H_5 + \frac{1}{x}NH_3 + \frac{1}{x}(C_6H_5CH_2NH_3^+)_2S_x^{2-}$$

benzylamine, *N*-benzylidene benzylamine, ammonia, and benzylammonium polysulfide required to react with or formed from one gram atom of sulfur are functions of x, the number of sulfurs in the benzylammonium polysulfide chain. Since this is known (29) to be between 6 and 7, an "acceptable range" for each coefficient is predicted. A known quantity of sulfur was therefore reacted with a *known excess* of benzylamine. The ammonia evolved was collected in an acid trap and determined by back titration. The

Can. J. Chem. Downloaded from www.nrcresearchpress.com by 210.87.254.5 on 09/05/12
For personal use only.

TABLE 1. Test of eq. 19

Compounds	Coefficients Found*	Calculated $x = 6$	Calculated $x = 7$
Sulfur	(1.00)	(1.00)	(1.00)
Benzylamine	0.670	0.667	0.573
N-Benzylidene benzylamine	0.163	0.167	0.143
Ammonia	0.150	0.167	0.143
Benzylammonium polysulfide if $x = 6$	0.161	0.167	—
$x = 7$	0.150	—	0.143

*± 5% of value shown.

benzylammonium polysulfides were precipitated by addition of ether, dried, and weighed. The total combined weight of *N*-benzylidene benzylamine and residual benzylamine was determined, and the molar ratio of these two materials was obtained by integration of an n.m.r. spectrum to give the absolute quantities of *N*-benzylidene benzylamine formed and of benzylamine consumed. Thus, each of the four coefficients in [19] is experimentally measurable. Table 1 compares the experimental values with those calculated for $x = 6$ and 7. The results for all four materials are in quite good agreement with those predicted based on eq. 19.

Reaction of Sulfur with Benzylamine in the Presence of a Sulfide Scavenger

Steps 4 and 6 together should be subject to examination independently of the others by adding a sulfide scavenger to suppress the sulfide catalyzed reaction 7. Combination of [4] and [6] (three times [4] added to [6]) gives the stoichiometric eq. 20 where the hydrogen sulfide produced is removed by the lead oxide to give lead sulfide and water rather than reacting as per [5]. When

[20] $$(b + 3)S + 2C_6H_5CH_2NH_2 \rightarrow C_6H_5\overset{H}{\overset{|}{C}}{=}N{-}S_b{-}N{=}\overset{H}{\overset{|}{C}}C_6H_5 + 3H_2S$$

sulfur and benzylamine were allowed to react in triethylamine in the molar ratio of 7 to 2 (*i.e.*, $b = 4$), the yield of benzylidenimine polysulfides isolated was 90 ± 2% based on [20]. The products consisted of benzylidenimine tetra-, tri-, di-, and monosulfides in molar ratios of approximately 16:2:2:1. The balance of the starting material was converted to *N*-benzylidene benzylamine along with some benzylidenimine benzylamine sulfide (the unsymmetrical mixed amine imine monosulfide). The same reaction in benzene gave a similar yield and distribution of products, but the reaction time was almost ten fold longer. When the benzylamine to sulfur ratio was increased, the average sulfur content of the benzylidenimine polysulfides formed decreased, and the total yield of polysulfides based on [20] decreased somewhat. The decrease appeared to be due to incomplete blocking of reaction 7 since *N*-benzylidene benzylamine formation was increased considerably as was the quantity of benzylidenimine benzylamine monosulfide. The latter is most likely an intermediate in the exchange reaction as shown in eq. 21. Thus,

[21] $$C_6H_5\overset{H}{\overset{|}{C}}{=}N{-}S_b{-}N{=}\overset{H}{\overset{|}{C}}C_6H_5 + C_6H_5CH_2NH_2 \rightleftarrows C_6H_5\overset{H}{\overset{|}{C}}{=}N{-}S_b{-}\overset{H}{\overset{|}{N}}CH_2C_6H_5 + C_6H_5CH{=}NH$$

eq. 20 appears to remain valid. Changing the molar ratio of sulfur to benzylamine leads mainly to variation in the numerical value of *b*.

Reactions of Benzylidenimine Tetrasulfide with Excess Benzylamine

This situation is nearly covered by eq. 18 above. The *b*S formed in [18] should react in the presence of the excess benzylamine according to [19]. Adding [18] to [19] multiplied by *b* eliminates the sulfur to give [22]. Since the starting material is the tetrasulfide, $b = 4$ and the overall stoichiometric eq. 23 results. The coefficients based

[22] $$C_6H_5CH{=}N{-}S_b{-}N{=}CHC_6H_5 + \frac{4(b + x)}{x}C_6H_5CH_2NH_2 \rightarrow \frac{b}{x}(C_6H_5CH_2NH_3^+)_2S_x^{2-} + \frac{3x + b}{x}(C_6H_5CH{=}N{-}CH_2C_6H_5 + NH_3)$$

[23] $$C_6H_5CH{=}N{-}S_4{-}N{=}HCC_6H_5 + \frac{(16 + 4x)}{x}C_6H_5CH_2NH_2 \rightarrow \frac{4}{x}(C_6H_5CH_2NH_3^+)_2S_x^{2-} + \frac{4 + 3x}{x}[NH_3 + C_6H_5CH{=}N{-}CH_2C_6H_5]$$

on the reaction of 1 mol of benzylidenimine tetrasulfide with excess amine are determined by the average sulfur chain length of the benzylammonium polysulfide produced. The products

Can. J. Chem. Downloaded from www.nrcresearchpress.com by 210.87.254.5 on 09/05/12
For personal use only.

TABLE 2. Test of eq. 23

Compounds	Coefficients		
	Found*	Calculated	
		$x = 6$	$x = 7$
Benzylidenimine tetrasulfide	(1.00)	(1.00)	(1.00)
Benzylamine	6.67	6.67	6.28
N-Benzylidene benzylamine	3.57	3.67	3.58
Ammonia	3.37	3.67	3.58

*±5% of values shown.

were separated as described for the reaction of sulfur with excess amine. Table 2 shows the experimental coefficients for *N*-benzylidene benzylamine, ammonia, benzylammonium polysulfide, and benzylamine along with those predicted from eq. 23 for $x = 6$ and 7. These results show eq. 23 to provide a good quantitative description of the experimental facts.

Benzylidenimine tetrasulfide exposed to benzylamine in the presence of lead(II) oxide gave only equilibration of the sulfur chain length as well as small amounts of several benzylidenimine benzylamine polysulfides again presumably via reaction 21.

Autocatalytic Decomposition of Benzylamine Disulfide

In the autocatalytic decomposition of benzylamine disulfide, the final products are *N*-benzylidene benzylamine and ammonia along with smaller quantities of benzylammonium polysulfides, benzylidenimine tetrasulfide, and elemental sulfur. Two assumptions are inherent in the derivation of the previous equations. Equations 4–8 must of course hold, and there must be an excess of benzylamine (not necessary for [20] only). In the decomposition of benzylamine disulfide, benzylidenimine polysulfides, and sulfur are produced in the presence of a *limited amount* of benzylamine. Since the latter reacts with both of the former, it is necessary to consider the relative rates of the two processes, a factor which is not relevant to the previous derivations. Two limiting cases can be imagined: (*i*) where benzylamine reacts with sulfur very much faster than with benzylidenimine polysulfides, and (*ii*) where benzylidenimine polysulfides react much faster than sulfur.

Case (i) Following decomposition according to [6], the reaction of $(3a - b)$ sulfurs with 4 benzylamines according to [13] must be considered. For the values of a, b, and x relevant to this case ($a = 2$ since the starting material is the disulfide, $b \sim 4$ and $x = 6$–7), it is apparent that $3a - b < a + x$. Therefore, reaction 13 is limited by the quantity of sulfur present and not by the quantity of benzylamine. Multiplying [13] by $(3a - b)/(a + x)$ and adding this result to [6] eliminates the sulfur and leads to [24].

$$[24]\quad \frac{3x+b}{a+x}\,C_6H_5CH_2\overset{H}{\underset{|}{N}}\!-S_a-\overset{H}{\underset{|}{N}}CH_2C_6H_5 \rightarrow C_6H_5CH{=}N-S_b-N{=}CHC_6H_5 + \frac{4x-8a+4b}{a+x}\,C_6H_5CH_2NH_2 + \frac{3a-b}{a+x}\,(C_6H_5CH_2NH_3^+)_2S_x^{2-}$$

The remaining benzylamine will now react with the benzylidenimine polysulfides. This should be according to [15]. However, it is first necessary to correct for the differing sulfur chain lengths, *i.e.*, eq. 15 is added to [16] to give [25].

$$[25]\quad C_6H_5CH{=}N-S_b-N{=}CHC_6H_5 + 4C_6H_5CH_2NH_2 \rightarrow C_6H_5CH_2\overset{H}{\underset{|}{N}}\!-S_a-\overset{H}{\underset{|}{N}}CH_2C_6H_5 + (b-a)S + 2NH_3 + 2C_6H_5CH{=}NCH_2C_6H_5$$

However, this equation is not consistent with the assumption that reaction of sulfur with benzylamine is rapid. Since sulfur is formed in the presence of benzylamine, eq. 25 must be modified to allow for reaction of the sulfur with benzylamine. This can be done by multiplying [13] by $(b - a)/(a + x)$ and then adding [25]. The result, [26], now gives the fate of the remaining benzylamine present in [24].

$$[26]\quad C_6H_5CH{=}N-S_b-N{=}CHC_6H_5 + \frac{4(x+b)}{a+x}\,C_6H_5CH_2NH_2 \rightarrow 2(NH_3 + C_6H_5CH{=}NCH_2C_6H_5) + \frac{x+b}{a+x}\,C_6H_5CH_2\overset{H}{\underset{|}{N}}\!-S_a-\overset{H}{\underset{|}{N}}CH_2C_6H_5 + \frac{b-a}{a+x}\,(C_6H_5CH_2NH_3^+)_2S_x^{2-}$$

Equations 26 and 24 may now be combined to eliminate benzylamine by multiplying [26] by $(x - 2a + b)/(x + b)$ and adding this to [24] to

Can. J. Chem. Downloaded from www.nrcresearchpress.com by 210.87.254.5 on 09/05/12
For personal use only.

give (after dividing out a common factor of 2) eq. 27. Since the starting material is the disulfide,

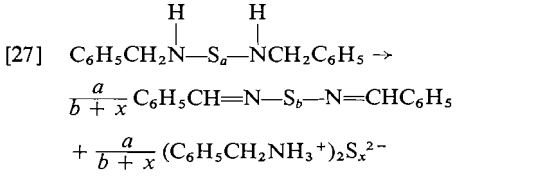

[27] $C_6H_5CH_2\overset{H}{\underset{|}{N}}—S_a—\overset{H}{\underset{|}{N}}CH_2C_6H_5 \rightarrow$
$\frac{a}{b+x}C_6H_5CH{=}N—S_b—N{=}CHC_6H_5$
$+ \frac{a}{b+x}(C_6H_5CH_2NH_3^+)_2S_x^{2-}$
$+ \frac{x-2a+b}{b+x}(NH_3 + C_6H_5CH{=}NCH_2C_6H_5)$

$a = 2$, and since only benzylidenimine tetrasulfide was observed experimentally among the products in this reaction, $b = 4$. Substituting these for a and b in [27] gives [28] as the predicted overall stoichiometric reaction for case (*i*).

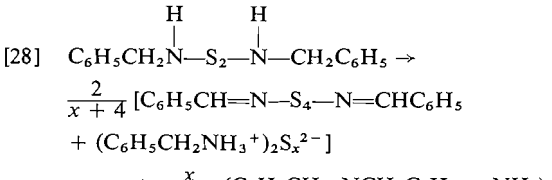

[28] $C_6H_5CH_2\overset{H}{\underset{|}{N}}—S_2—\overset{H}{\underset{|}{N}}—CH_2C_6H_5 \rightarrow$
$\frac{2}{x+4}[C_6H_5CH{=}N—S_4—N{=}CHC_6H_5$
$+ (C_6H_5CH_2NH_3^+)_2S_x^{2-}]$
$+ \frac{x}{x+4}(C_6H_5CH{=}NCH_2C_6H_5 + NH_3)$

Case (ii) Returning to eq. 6, the benzylamine produced now reacts exclusively with the benzylidenimine polysulfides according to [15]. The latter must be modified (added to [16]) to correct the sulfur chain length and may then be added to [6] to give (after dividing out a common factor of 2) eq. 29.

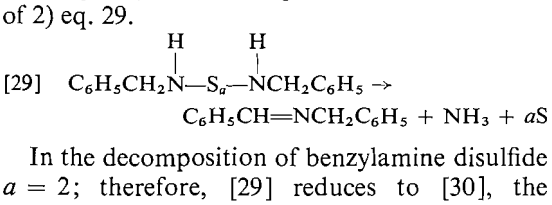

[29] $C_6H_5CH_2\overset{H}{\underset{|}{N}}—S_a—\overset{H}{\underset{|}{N}}CH_2C_6H_5 \rightarrow$
$C_6H_5CH{=}NCH_2C_6H_5 + NH_3 + aS$

In the decomposition of benzylamine disulfide $a = 2$; therefore, [29] reduces to [30], the predicted stoichiometric equation for this case.

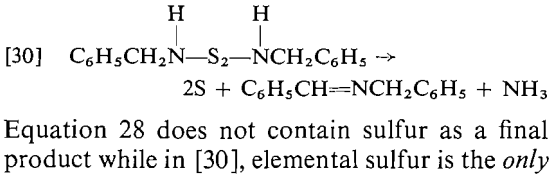

[30] $C_6H_5CH_2\overset{H}{\underset{|}{N}}—S_2—\overset{H}{\underset{|}{N}}CH_2C_6H_5 \rightarrow$
$2S + C_6H_5CH{=}NCH_2C_6H_5 + NH_3$

Equation 28 does not contain sulfur as a final product while in [30], elemental sulfur is the *only* sulfur-containing species. Experimentally, 38% of all the sulfur present went to elemental sulfur. Therefore neither of these two limiting cases holds. The intermediate case may be approximated by combining eqs. 28 and 30 and taking the fraction of sulfur obtained as a product (f_S = mg atoms of elemental sulfur produced/total mg atoms of sulfur present in all forms) as a measure of the relative importance of these two extreme cases (*i.e.*, f_S[30] added to $(1 - f_S)$[28]) as in [31]. Equation 31 predicts the ratio of benzylidenimine tetrasulfide to benzylammonium polysulfide as well as the ratio of benzylidenimine

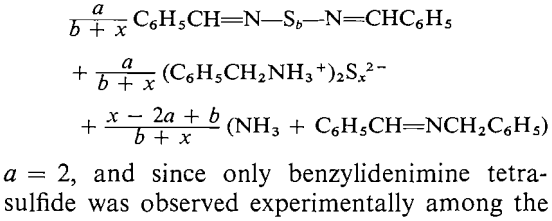

[31] $C_6H_5CH_2\overset{H}{\underset{|}{N}}—S_2—\overset{H}{\underset{|}{N}}CH_2C_6H_5 \rightarrow 2f_SS$
$+ \frac{2(1-f_S)}{x+4}[C_6H_5CH{=}N—S_4—N{=}CHC_6H_5$
$+ (C_6H_5CH_2NH_3^+)_2S_x^{2-}]$
$+ \frac{x+4f_S}{x+4}(C_6H_5CH{=}NCH_2C_6H_5 + NH_3)$

benzylamine to ammonia to be 1:1. Experimentally these two ratios were found to be 0.99 ± 0.05 and 1.02 ± 0.05 in excellent agreement with [31]. The ratio of *N*-benzylidene benzylamine *plus* ammonia to benzylammonium polysulfide *plus* benzylidenimine tetrasulfide is predicted by [31] to be $(x + 4f_S)/2(1 - f_S)$. Since experimentally $f_S = 0.38$, this ratio should be 6.1 for $x = 6$ and 6.9 for $x = 7$. The experimental value was $\sim 10 \pm 3$. The probable error is quite large, but the agreement appears acceptable.[4]

p-Methoxybenzylidenimine Tetrasulfide with Amine

Two kinds of *N*-benzylidene benzylamines are expected as products from the reaction of *p*-methoxybenzylidenimine tetrasulfide with unsubstituted benzylamine according to eqs. 4–8. When eq. 7 is written for the reaction of *p*-methoxybenzylidenimine polysulfide with unsubstituted benzylamine and added to twice [8] (*p*-methoxybenzylidenimine reacting with unsubstituted benzylamine), the result is [32]. All

[32] $CH_3OC_6H_4CH{=}N—S_b—N{=}CHC_6H_4OCH_3$
$+ 4C_6H_5CH_2NH_2 \rightarrow$
$2CH_3OC_6H_4CH{=}NCH_2C_6H_5$
$+ 2NH_3 + C_6H_5CH_2\overset{H}{\underset{|}{N}}—S_b—\overset{H}{\underset{|}{N}}CH_2C_6H_5$

the *p*-methoxy substituent has now been converted to final products and the newly formed unsubstituted benzylamine polysulfides decompose via [6]. After correcting for the sulfur chain

[4]The 38% of sulfur isolated is apt to be too low rather than too high since sulfur has some solubility in *N*-benzylidene benzylamine. If the quantity of sulfur isolated were to be increased (as it probably should be) by only a few milligrams, the agreement would improve considerably.

length in [6] by adding three times [16], three times [32] may be added leading to the situation shown in [33]. Since there is an excess of benzyl-

[33] $3CH_3OC_6H_4CH{=}N{-}S_b{-}N{=}CHC_6H_4OCH_3 + 8C_6H_5CH_2NH_2 \rightarrow C_6H_5CH{=}N{-}S_b{-}N{=}CHC_6H_5 + 2bS + 6NH_3 + 6CH_3OC_6H_4CH{=}NCH_2C_6H_5$

amine, the sulfur in [33] reacts as per [19], and the benzylidenimine polysulfides as per [23]. Adding eq. 22 to 33 and this in turn to $2b$ times eq. 19 gives (after dividing out a common factor of 3) the predicted overall stoichiometric equation as in [34]. Since the starting material is the tetra-

[34] $CH_3OC_6H_4CH{=}N{-}S_b{-}N{=}CHC_6H_4OCH_3 + \frac{4(b+x)}{x} C_6H_5CH_2NH_2 \rightarrow \frac{b}{x}(C_6H_5CH_2NH_3^+)_2S_x^{2-} + \frac{3x+b}{x} NH_3 + \frac{x+b}{x} C_6H_5CH{=}NCH_2C_6H_5 + 2CH_3OC_6H_4CH{=}NCH_2C_6H_5$

sulfide, $b = 4$, and [34] reduces to [35].

[35] $CH_3OC_6H_4CH{=}N{-}S_4{-}N{=}CHC_6H_4OCH_3 + \frac{(16+4x)}{x} C_6H_5CH_2NH_2 \rightarrow 2CH_3OC_6H_4CH{=}NCH_2C_6H_5 + \frac{4+x}{x} C_6H_5CH{=}NCH_2C_6H_5 + \frac{4+3x}{x} NH_3 + \frac{4}{x}(C_6H_5CH_2NH_3^+)_2S_x^{2-}$

The ratio of *N*-(*p*-methoxybenzylidenimine) benzylamine to *N*-benzylidenimine benzylamine should be $2:[(4+x)/x]$ or 1.20 to 1.27 where $x = 6$ to 7. The products, obtained after removal of the benzylammonium polysulfides, were hydrolyzed with dilute hydrochloric acid. As required by eq. 35 the benzylammonium polysulfides and *all* of the benzylamine formed by hydrolysis of the *N*-benzylidene benzylamine were unsubstituted; *all* of the *p*-methoxy substituent was present in the aldehydes formed from the *N*-benzylidene benzylamines. Not all of the aldehyde was substituted however; the ratio of anisaldehyde to benzaldehyde was 1.29 ± 0.10 in excellent agreement with that predicted in eq. 35.

Conclusions

Using a polysulfide chain length of 6–7 as established independently (29) for the benzylammonium polysulfides, all aspects of each of the five eqs. 19, 20, 23, 31, and 35, derived from the proposed scheme (reactions 4–8), have been quantitatively confirmed experimentally. The reaction scheme with a benzylidenimine polysulfide – benzylamine polysulfide "cycle" is therefore considered to provide a satisfactory explanation of the reactions of sulfur with benzylamine. Although the scheme has been established only for benzylamine, it nevertheless seems reasonable to expect that other primary amines might follow a similar overall reaction sequence. It has been previously shown (23, 24) that sulfur with a few primary amines, such as butylamine and ethylenediamine, gives alkylammonium polysulfides. Since sulfur is reduced by these amines, the amines must be oxidized, presumably to either the alkylamine polysulfides, alkylidenimine polysulfides, or Schiff's bases.

A detailed mechanistic interpretation cannot be formulated for each of the steps (eqs. 4–8) at this time but an early step is probably ionic since the rate of formation of benzylidenimine tetrasulfide from benzylamine and sulfur in the presence of the sulfide scavenger was considerably faster in polar solvents than in non-polar solvents. Step 5 is obviously ionic as is the analogous step 9 in the Davis (18) mechanism. The observed base catalysis in step 6 most probably involves the weakly acidic N—H protons. This is consistent with the isolation (25, 27) of tetraalkylamine polysulfides from sulfur and secondary amines where the absence of a second N—H would block step 6. The autocatalytic decomposition of benzylamine disulfide which produced a limited amount of benzylamine in addition to sulfur and benzylidenimine polysulfides provides some indication of the relative rates of steps 4 and 7 (because these appear to be equilibria, steps 5, 6, and 8 may also contribute, however) since the latter two materials compete for the limited amount of benzylamine formed. Apparently, step 4 (along with 5 and 6) is about 50% faster than 7 (along with 8). The final step, 8, is very likely a reversible nucleophilic addition of benzylamine to the imine carbon followed by a proton shift and elimination of ammonia.

The reaction of primary amines with sulfur in the presence of lead(II) oxide has some potential synthetic importance in the preparation of imine polysulfides. Sulfur is obviously a more convenient starting material than tetrasulfur tetranitride (29). The reaction conditions are quite

Can. J. Chem. Downloaded from www.nrcresearchpress.com by 210.87.254.5 on 09/05/12
For personal use only.

Can. J. Chem. Downloaded from www.nrcresearchpress.com by 210.87.254.5 on 09/05/12
For personal use only.

mild, and the rate is reasonably rapid. If this synthesis is applicable to other primary amines, it could provide a convenient route for the conversion of primary amines to aldehydes or ketones which could be readily obtained by hydrolysis of the imine polysulfides.

Experimental

Instrumentation, solvents and chromatography were as previously described (29).

Benzylamine Disulfide

Freshly distilled sulfur monochloride (1.9 ml, 23.6 mmol) in 100 ml of anhydrous ether was added dropwise to 10.0 ml (91.7 mmol) of benzylamine in 500 ml of anhydrous ether in a 1 l three-necked flask equipped with a stirrer and calcium chloride drying tube. A white precipitate of benzylammonium chloride formed rapidly and was separated by filtration. The solvent was removed *in vacuo* to give a pale yellow, creamy oil. This oil was dissolved in hexane at 30–40 °C and on cooling to ice temperature precipitated a white solid. Further recrystallization from pentane gave pure benzylamine disulfide of m.p. 52.5–53 °C.

Anal. Calcd. for $C_{14}H_{16}N_2S_2$ (mol. wt.: 276): C, 60.83; H, 5.83; N, 10.13; S, 23.20. Found (270): C, 60.93; H, 5.53; N, 9.94; S, 23.42.

Evaporation of the mother liquor gave 3.0 g of oil whose n.m.r. spectrum indicated the presence of benzylamine disulfide, *N*-benzylidene benzylamine, and other unidentified materials.

The n.m.r. spectrum of benzylamine disulfide showed absorptions at −2.75 (broad, —NH), −4.09 (singlet, —CH_2—), and −7.05 p.p.m. (singlet, phenyl-) with relative areas of 1.00:1.91:4.92, respectively. The i.r. spectrum showed N—H stretching at 3334 cm^{-1} and S—N stretching at 850 cm^{-1}. An R_f value could not be obtained since the material decomposed on the silica gel plate. Pure benzylamine disulfide kept under vacuum in a drying apparatus at room temperature for 5–6 h decomposed to a mixture of benzylidenimine polysulfides, *N*-benzylidene benzylamine, and sulfur. It could be stored at −20 °C for several weeks, but decomposition eventually began even at this temperature. The impure material could be kept for a much longer period. When benzylamine disulfide was heated in a m.p. capillary to 75 °C and cooled, the oil solidified and remelted at 53 °C. When it was heated above 100 °C, however, decomposition occurred with evolution of gas. A t.l.c. of the decomposition product showed sulfur, benzylidenimine tetra-, tri-, and disulfides, and *N*-benzylidene benzylamine.

The course of the room temperature decomposition of benzylamine disulfide was monitored by n.m.r. spectroscopy. Approximately 260 mg of pure material was stirred under a nitrogen atmosphere. Periodically a 25–30 mg aliquot was withdrawn, dissolved in 0.5 ml of deuterochloroform and an n.m.r. spectrum was taken. After 3 h no change was apparent. After 5 h some benzylamine was visible (about 5%). After 6 h approximately 85% of the disulfide remained. After an additional ½ h (total elapsed time: 6½ h) nearly 95% of the disulfide was decomposed, and benzylamine and benzylidenimine tetrasulfide were prominent in molar ratios of approximately 4:1. A small amount of *N*-benzylidene benzylamine was also observable at this time. After 8 h the n.m.r. showed mainly *N*-benzylidene benzylamine, small amounts of benzylidenimine tetrasulfide and the benzylammonium cation (presumably the polysulfides). A spectrum after 13 h was unchanged from that at 8 h.

Benzylidenimine Benzylamine Monosulfide

Sulfur (984 mg, 30.7 mg atoms), lead(II) oxide (9.10 g, 40.7 mmol), and 10 ml of benzene were placed in a 100 ml three-necked flask equipped with a water condenser, a serum rubber stopper, a cylinder of dry nitrogen gas, and an outlet to a gas washing bottle with about 250 ml of aqueous hydrochloric acid solution (containing 50.0 mg equiv of acid). The benzylamine used was degassed under vacuum, and 3.4 ml (31.2 mmol) was introduced through the serum stopper by syringe. The reaction mixture was stirred for about 20 h with a continuous slow flow of dry nitrogen. The acid solution was diluted to 500 ml, and a 5.00 ml aliquot required 4.53 ml of 0.100 *N* sodium hydroxide for neutralization. Ammonia (4.7 mmol) had therefore been evolved. The lead sulfide was removed by filtration and was thoroughly washed with ether and benzene. The combined solvents were removed, the remaining oil was weighed, and an n.m.r. spectrum integrated. This led to the following distribution of materials: benzylidenimine tetrasulfide, 910 mg (2.7 mmol); benzylidenimine disulfide, 260 mg (1.0 mmol); benzylidenimine benzylamine monosulfide, 700 mg (2.9 mmol); *N*-benzylidene benzylamine, 1.12 g (5.7 mmol); and unreacted benzylamine, 100 mg (0.9 mmol). These data rest on the assumed structure of benzylidenimine benzylamine monosulfide. This material was isolated, and its structure was confirmed as follows. The crude oil was taken up in about 50 ml of methanol and chilled. Benzylidenimine tetrasulfide precipitated (850 mg) and was discarded. Then, 260 mg of benzylidenimine disulfide (contaminated with some tetrasulfide) precipitated in several successive fractions which were collected and discarded. After several days at −20 °C, 350 mg of a white crystalline material precipitated. This material was recrystallized from methanol to give benzylidenimine benzylamine monosulfide of m.p. 58.5–59 °C.

Anal. Calcd. for $C_{14}H_{14}N_2S$ (mol. wt.: 242): C, 69.39; H, 5.82; N, 11.56; S, 13.23. Found (249): C, 69.6; H, 5.30; N, 11.74; S, 13.65.

An n.m.r. spectrum in carbon tetrachloride showed four absorptions: a singlet at −7.77 (1.0 H, benzylidene proton), a multiplet at −7.07 to −7.67 (10.2 H, phenyl rings), a doublet at −4.30 (2.0 H, J = 5.5 c.p.s., methylene protons), and a broad triplet at −3.66 p.p.m. (1.0 H, proton on nitrogen). The i.r. spectrum in carbon tetrachloride showed bands assignable to N—H stretching at 3360 cm^{-1}, C=N stretching at 1645 cm^{-1}, and S—N stretching at 853 cm^{-1}. The R_f value on silica gel with carbon disulfide as eluent was 0.15 *vs.* 0.80 for sulfur. This material was also formed when benzylidenimine tetrasulfide and benzylamine were mixed in the presence of lead(II) oxide. For example, 1.00 g (2.98 mmol) of benzylidenimine tetrasulfide stirred for 5 h with 3.9 ml (35.7 mmol) of benzylamine and 2.71 g (12.2 mmol) of

Can. J. Chem. Downloaded from www.nrcresearchpress.com by 210.87.254.5 on 09/05/12
For personal use only.

lead(II) oxide in 15 ml of benzene led on chromatography to: 37 mg (1.2 mg atom) of sulfur, 170 mg (0.51 mmol) of benzylidenimine tetrasulfide, 110 mg (0.37 mmol) of benzylidenimine trisulfide, 90 mg (0.33 mmol) of benzylidenimine disulfide, 25 mg (0.10 mmol) of benzylidenimine benzylamine sulfide, 75 mg of two other unsymmetrical amine–imine polysulfides which were not fully characterized, and 480 mg (2.5 mmol) of *N*-benzylidene benzylamine. Ammonia (2.4 mmol) was evolved.

Quantitative Experiments; Sulfur with Excess Benzylamine

Sulfur (640 mg, 20.0 mg atoms) was placed in a three-necked flask equipped with a stirrer, gas washing bottle, nitrogen inlet, and rubber serum stopper. The gas washing bottle contained 7.50 mg equiv of hydrochloric acid. Benzylamine (2.90 g, 27.1 mmol) was introduced through the serum stopper, and the flask was stirred at room temperature under a slow continuous flow of nitrogen. After 4 h the reaction was complete, and anhydrous ether was added. The mixture was stirred for 2 h, and the orange solid which precipitated was filtered and washed with anhydrous ether. When this solid was dried in air, evolution of hydrogen sulfide was observed. When the solid was free of ether, it weighed approximately 960 ± 30 mg. The weight was not accurate due to continuous decomposition with evolution of hydrogen sulfide, about 35 mg weight loss per 20 min. The m.p. was 90–96 °C dec. in an evacuated sealed tube. After 2 days in air, it had decomposed into sulfur and benzylammonium thiosulfate. The combined ether extract was evaporated under reduced pressure at about 35–40 °C to give 2.42 g of oil containing benzylamine, *N*-benzylidene benzylamine, and benzylammonium polysulfide. The integrated n.m.r. spectrum led to the following distribution of products: benzylamine, 1.47 g (therefore 1.43 g, 13.4 mmol, consumed); *N*-benzylidenebenzylamine, 640 mg (3.26 mmol); benzylammonium polysulfides, 1.31 g (total; 3.22–2.98 mmol for $x = 6$ and 7, respectively). The acid solution in the gas washing bottle was diluted to 500 ml, and a 50.0 ml aliquot required 4.50 ml of 0.100 *N* sodium hydroxide solution for neutralization. Therefore, 3.00 mg equiv of ammonia were evolved.

Sulfur and Benzylamine in the Presence of a Sulfide Scavenger

Sulfur (1.03 g, 32.2 mg atoms), 3.49 g (15.6 mmol) of lead(II) oxide, 1 ml (9.17 mmol) of benzylamine, and 10 ml of triethylamine were stirred together under a dry nitrogen atmosphere at room temperature. Within 2 h the reaction mixture had become quite black. After 24 h it was filtered, and the lead sulfide was washed thoroughly with ether and benzene. The combined filtrate was concentrated to give 1.41 g of solid. This was dissolved in carbon disulfide, and its n.m.r. spectrum was recorded. Integration gave the relative amounts of the five components (whose identities were verified by t.l.c.) and led to the following data: benzylidenimine tetrasulfide, 1.06 g (3.16 mmol); benzylidenimine trisulfide, 0.11 g (0.37 mmol); benzylidenimine disulfide, 0.11 g (0.41 mmol); benzylidenimine monosulfide,[5] 0.043 g (0.18 mmol); *N*-benzylidene benzylamine, 0.080 g (0.41 mmol). An analogous reaction in benzene using identical quantities required 1 week for complete reaction of the sulfur and led to the following data: tetrasulfide, 1.13 g (3.36 mmol); trisulfide, 0.14 g (0.46 mmol); disulfide, 0.027 g (0.10 mmol); monosulfide,[5] 0.071 g (0.30 mmol); *N*-benzylidene benzylamine, 0.125 g (0.64 mmol).

A similar reaction with 1.02 g (31.9 mg atoms) of sulfur, 7.53 g (33.8 mmol) of lead oxide, and 2.2 ml (20.1 mmol) of benzylamine in 3 ml of benzene led to the data below: tetrasulfide, 0.26 g (0.77 mmol); trisulfide, 0.12 g (0.39 mmol); disulfide, 0.59 g (2.2 mmol); benzylidenimine benzylamine monosulfide, 0.34 g (1.4 mmol); and *N*-benzylidene benzylamine, 0.95 g (4.9 mmol).

Benzylidenimine Tetrasulfide with Excess Benzylamine

Benzylidenimine tetrasulfide (1.02 g, 3.03 mmol) was placed in a 100 ml three-necked flask equipped as described above. The gas washing bottle contained 15.00 mg equiv of hydrochloric acid. Benzylamine (6.6 ml, 60.5 mmol) was introduced through the serum stopper. After 6 h the reaction was complete. The acid solution was diluted to 500 ml, and a 50.0 ml aliquot required 4.82 ml of 0.100 *N* sodium hydroxide solution for neutralization. Therefore, 10.2 mg equiv of ammonia were evolved. The reaction mixture was diluted with 50 ml of anhydrous ether, and the orange solid which precipitated was filtered and washed with anhydrous ether. The combined ether solutions were concentrated *in vacuo* at 40–50 °C to give 6.41 g of oil containing only *N*-benzylidene benzylamine and unreacted benzylamine. The weight and integrated n.m.r. spectrum indicated the amounts of these two products to be: benzylamine, 4.32 g (therefore 2.15 g, 20.2 mmol, consumed) and *N*-benzylidene benzylamine, 2.10 g (10.8 mmol).

Decomposition of Benzylamine Disulfide

Benzylamine disulfide (248 mg, 0.90 mmol) was stirred under a slow flow of nitrogen gas. The outlet was connected to a gas washing bottle containing 1.00 mg equiv of aqueous hydrochloric acid. The white solid changed slowly to a yellow oil which contained a solid. The precipitate was filtered and washed with small amounts of anhydrous ether to give 22 mg (0.69 mg atoms) of elemental sulfur. The solvent was removed *in vacuo* to give 196 mg of an oil whose n.m.r. spectrum showed three materials: benzylidenimine tetrasulfide, *N*-benzylidene benzylamine, and benzylammonium ion (presumably the polysulfide) in molar ratios of 2.0:20.5:2.0, respectively. From these data the yields of products were calculated to be:[6] benzylidenimine tetrasulfide, 24 mg (0.071 mmol); *N*-benzylidene benzylamine, 142 mg (0.73 mmol); benzylammonium polysulfide, 31 mg (0.071 mmol). The acid solution was diluted to 500 ml, and a 200 ml aliquot required 1.14 ml of 0.100 *N* sodium hydroxide for neutralization. Therefore, 0.715 mmol of ammonia was evolved.

p-Methoxybenzylidenimine Tetrasulfide

p-Methoxybenzylidenimine tetrasulfide was prepared from *p*-methoxybenzylamine and tetrasulfur tetranitride as previously described (29). After recrystallization from methanol it had a m.p. of 112–113 °C. A 734 mg (1.85 mmol) sample was placed in a 100 ml round-bottom flask with a magnetic stirring bar, and 1.4 ml (12.8 mmol)

[5]Not fully characterized, see ref. 29.

[6]Benzylammonium polysulfide was assumed to be the heptasulfide. These numbers do not change more than 5% if the hexa- or octasulfide is assumed.

Can. J. Chem. Downloaded from www.nrcresearchpress.com by 210.87.254.5 on 09/05/12
For personal use only.

of benzylamine was added. The reaction mixture was stirred under a nitrogen atmosphere for 5 h whereupon a t.l.c. showed the absence of *p*-methoxybenzylidenimine tetrasulfide. About 60 ml of anhydrous ether was introduced into the reaction mixture and stirred for 1 h. An orange solid precipitated from the yellowish solution which was filtered and washed with anhydrous ether. It melted at 95–97 °C dec. and, when kept in the air for a few days, decomposed to sulfur and a thiosulfate with the evolution of hydrogen sulfide. An n.m.r. spectrum of the thiosulfate taken in deuterium oxide showed three absorptions corresponding to a benzyl CH_2 group, an NH_3^+ group, and a phenyl complex. No absorption corresponding to a *p*-methoxy methyl group was detected. The orange solid was, therefore, unsubstituted benzylammonium polysulfide. The combined ether extracts were concentrated *in vacuo*, and the n.m.r. spectrum of the resulting oil showed a complicated phenyl region between −6.85 and −8.04 p.p.m., a broad NH_2 peak at −1.87 p.p.m., a methoxy methyl group at −3.47 p.p.m., the CH_2 of benzylamine at −3.87 p.p.m., an unresolved CH_2 doublet for mixed *N*-benzylidene benzylamine at −4.74 p.p.m., and the unresolved CH triplets for mixed *N*-benzylidene benzylamine at −8.21 p.p.m. This mixture was refluxed for 4 h with 50 ml of 5% hydrochloric acid. After cooling the mixture was extracted with ether (ether extract I). The aqueous layer was neutralized with base and extracted with ether (ether extract II). Ether extract II was dried and concentrated to give a large quantity of oil. The n.m.r. spectrum of this material, taken in deuterochloroform, showed only benzylamine. No trace of a methoxy methyl group could be detected. Ether extract I was dried and the ether removed *in vacuo* to give an oil whose n.m.r. spectrum showed two aldehyde peaks: anisaldehyde at −9.87 p.p.m. and benzaldehyde at −10.00 p.p.m. as well as the *p*-methoxy methyl absorption at −3.74 p.p.m. and a complex phenyl region. The ratio of the two aldehyde peaks, anisaldehyde to benzaldehyde, was approximately 1.5 to 1. However, the ratio increased with the time of evaporation (of the ether) presumably due to selective loss of the more volatile benzaldehyde. A more accurate ratio was obtained from the n.m.r. spectrum of the crude reaction mixture (before hydrolysis). Integration of the combined overlapping CH_2 peaks for the two kinds of *N*-benzylidene benzylamines at −4.74 p.p.m. relative to the methoxy methyl peak at −3.47 p.p.m. gave 40.3:34.0. The relative amount of the *p*-methoxy derivative was therefore 1/3 of 34.0 or 11.3, and the total relative amount of both kinds of Schiff's bases was 1/2 of 40.3 or 20.1. The relative amount of the unsubstituted material was therefore 20.1 less 11.3 or 8.8. The ratio of *p*-methoxy substituted to unsubstituted *N*-benzylidene benzylamine was therefore 11.3/8.8 or 1.29 ± 0.10.

This work was carried out under a grant from the National Research Council of Canada.

1. M. Carmack and M. A. Spielman. *In* Organic reactions. Vol. III. John Wiley and Sons, New York, N.Y., 1946. p. 83.
2. F. Asinger and H. Offermanns. Synthesen mit Ketonen, Schwefel und Ammoniak bzw. Aminen und Chemisches Verhalten der Reaktionsprodukte. Koln und Opladen, Westdeutscher Verlag, 1966.
3. F. Asinger and K. Halcour. Monatsh. Chem. **95**, 24 (1964).
4. F. Asinger, H. W. Becker, W. Schäfer, and A. Saus. Monatsh. Chem. **97**, 301 (1966).
5. F. Asinger and H. Offermanns. Angew. Chem. Int. Ed. **6**, 907 (1967).
6. G. D. Kratz, A. H. Flower, and C. Coolidge. Ind. Eng. Chem. **12**, 317 (1920).
7. W. Scott and C. W. Bedford. Ind. Eng. Chem. **13**, 125 (1921).
8. G. Petry and W. Scheele. Kaut. Gummi. Kunstst. **20**, 518 (1967).
9. F. H. McMillan and J. A. King. J. Amer. Chem. Soc. **70**, 4143 (1948).
10. B. D. Vineyard. J. Org. Chem. **32**, 3833 (1967).
11. F. Asinger, W. Schäfer, H. Meisel, H. Kersten, and A. Saus. Monatsh. Chem. **98**, 338 (1967).
12. F. Asinger, W. Schäfer, and H. Triem. Monatsh. Chem. **97**, 1510 (1966).
13. F. Asinger, W. Schäfer, K. Halcour, A. Saus, and H. Triem. Angew. Chem. Int. Ed. **3**, 19 (1964).
14. F. Asinger, H. Offermanns, and A. Saus. Monatsh. Chem. **100**, 724 (1969).
15. J. A. King and F. H. McMillan. J. Amer. Chem. Soc. **68**, 632 (1946).
16. M. Behforouz. Diss. Abst. **26**, 6365 (1966).
17. W. G. Dauben, R. P. Ciula, and J. B. Rogan. J. Org. Chem. **22**, 362 (1957).
18. R. E. Davis and H. F. Nakshbendi. J. Amer. Chem. Soc. **84**, 2085 (1962).
19. A. P. Zipp and S. G. Zipp. Sulfur Inst. J. 2 (1968).
20. P. D. Bartlett, E. F. Cox, and R. E. Davis. J. Amer. Chem. Soc. **83**, 103 (1961).
21. P. D. Bartlett, A. K. Colter, R. E. Davis, and W. R. Roderick. J. Amer. Chem. Soc. **83**, 109 (1961).
22. H. Krebs, E. F. Weber, and H. Balters. Z. Anorg. Allg. Chem. **275**, 147 (1954).
23. M. G. Voronkov and A. Ya. Legzdyn. J. Org. Chem. U.S.S.R. **3**, 446 (1967).
24. T. G. Levi. Gazz. Chim. Ital. **60**, 975 (1930).
25. T. G. Levi. Gazz. Chim. Ital. **61**, 286 (1931).
26. W. G. Hodgson, S. A. Buckler, and G. Peters. J. Amer. Chem. Soc. **85**, 543 (1963).
27. H. Jenne and M. Becke-Goehring. Chem. Ber. **91**, 1950 (1958).
28. T. G. Levi. Gazz. Chim. Ital. **61**, 294 (1931).
29. Y. Sasaki and F. P. Olsen. Can. J. Chem. This issue.
30. R. W. Saville. J. Chem. Soc. 2880 (1958).
31. R. MacColl and S. Windwer. J. Phys. Chem. **74**, 1261 (1970).
32. T. L. Tolbert and B. Houston. J. Org. Chem. **28**, 695 (1963).
33. M. Pesez and J. Bartos. Bull. Soc. Chim. Fr. 1122 (1963).

Oxydation lente du cétène en phase gazeuse. I. Réaction à "hautes températures"

PIERRE MICHAUD[1] ET CYRIAS OUELLET
Département de Chimie, Université Laval, Québec 10, Québec

Reçu le 30 juin 1970

La combustion lente du cétène en phase gazeuse a été étudiée en régime statique dans un réacteur en Vycor de 30 × 4 cm, pour différents mélanges cétène–oxygène entre 280 et 500 °C à partir d'une pression totale de 20 mm Hg. Continuant les travaux de Barnard et Kirschner, nous avons mis en évidence deux domaines de combustion lente. Ce premier article présente les résultats cinétiques et analytiques relatifs au domaine des "hautes températures" (380–500 °C). La réaction est autocatalytique, l'énergie globale d'activation est de l'ordre de quelques kilocalories par mole. Les principaux produits sont le monoxyde de carbone, le formaldéhyde, l'eau, et l'anhydride carbonique. On ne décèle pas d'éthylène. Nous proposons un schéma réactionnel en chaînes, dans lequel le formaldéhyde est l'agent de ramification dégénérée:

$$CH_2O + O_2 = HCOOH + O$$
$$O + CH_2O = \cdot CHO + \cdot OH$$

The slow combustion of ketene in the gas phase was studied by the static method in a 30 × 4 cm Vycor cylinder between 280 and 500 °C at pressures above 20 mm Hg. Extending the work of Barnard and Kirschner, we have established the existence of two types of slow combustion of ketene corresponding to two temperature ranges. In this first paper, we describe the kinetic and analytical results obtained in the higher temperature range (380–500 °C). The reaction is autocatalytic and shows a low temperature coefficient corresponding to a few kilocalories per mole. The main products are carbon monoxide, formaldehyde, water, and carbon dioxide. No ethylene was detected. We suggest a chain reaction in which formaldehyde is the intermediate responsible for degenerate branching:

$$CH_2O + O_2 = HCOOH + O$$
$$O + CH_2O = \cdot CHO + \cdot OH$$

Canadian Journal of Chemistry, 49, 294 (1971)

Introduction

Comme le constate Salooja (1), le cétène intervient souvent comme produit intermédiaire dans la combustion de nombreux dérivés oxygénés d'hydrocarbures. Par exemple, dans le cas de l'oxydation lente de l'acétone à 498 °C, l'initiation $CH_3—CO—CH_3 + O_2 = \dot{C}H_2—CO—CH_3 + \cdot HO_2$ est suivie par la décomposition du radical $\dot{C}H_2—CO—CH_3$ instable à cette température $\dot{C}H_2—CO—\dot{C}H_3 = CH_2CO + \cdot CH_3$, le cétène étant ensuite lui-même consommé par l'oxygène (2). Le seul travail au sujet de la combustion lente du cétène est celui de Barnard et Kirschner (3) qui ont surtout étudié la réaction à haute température (475 °C); ces auteurs trouvent que les principaux produits de combustion sont le monooxyde de carbone, le formaldéhyde, l'eau, et l'anhydride carbonique, et proposent un schéma cinétique de réactions en chaînes propagées par les radicaux $\cdot OH$ et $\cdot HO_2$, l'agent de ramification étant le formaldéhyde $CH_2O + O_2 = \cdot CHO + \cdot HO_2$. Dans un travail préliminaire, nous avons déterminé la limite inférieure d'explosion, les limites de flammes froides uniques et multiples, et la limite inférieure de combustion lente pour des mélanges stoechiométriques cétène–oxygène ($CH_2CO:O_2 = 1:2$) (4). Nous présentons les résultats cinétiques et analytiques relatifs à la combustion lente du cétène dans le domaine des "hautes températures" ($\theta > 380$ °C) en complétant les résultats de Barnard et Kirschner et dans le domaine des "basses températures" ($\theta < 350$ °C) qui n'a pas été décrit par ces auteurs. Nous proposons des schémas cinétiques qui expliquent la plupart de nos résultats expérimentaux.

Méthode expérimentale

(A) Appareillage

La combustion du cétène est étudiée par la méthode statique, dans un cylindre de Vycor (30 cm × 4 cm) maintenu à une température constante (± 1 °C); le seul traitement préalable du réacteur est un lavage à l'acide nitrique concentré suivi d'un rinçage soigneux à l'eau distillée. Tout le montage adjacent au réacteur est muni de robinets en Teflon Delmar et chauffé à une température d'environ 100 °C, pour éviter toute condensation ou polymérisation. La réaction est suivie par enregistrement de la variation de pression mesurée par une jauge magnétique (Pace Engineering Co.) et par le prélèvement d'échantillons à différents temps en vue de l'analyse.

[1]Boursier post-doctorat, Division de Chimie, Conseil National de Recherches du Canada, Ottawa, Canada.

Can. J. Chem. Downloaded from www.nrcresearchpress.com by 210.87.254.105 on 09/05/12
For personal use only.

Can. J. Chem. Downloaded from www.nrcresearchpress.com by 210.87.254.105 on 09/05/12
For personal use only.

(B) Gaz employés

Le cétène est préparé selon la méthode de Fisher *et al.* (5), par pyrolyse de l'anhydride acétique 99% + 3 (Matheson, Coleman et Bell) sur un ruban de chromel A porté à 500 °C, et sous une pression de 500 mm Hg. Après distillation fractionnée et purification, le cétène est conservé dans une ampoule à l'obscurité et à −196 °C pour éviter toute polymérisation. La pureté du cétène a été contrôlée en comparant le spectre i.r. de notre produit à celui publié par Drayton et Thompson (6), et par c.p.g. sur une colonne de célite modifiée par 20% de dinonylphtalate; il ne contient en particulier pas de traces d'éthylène et autres hydrocarbures, les impuretés principales (< 0.3%) étant l'acide et l'anhydride acétiques. Nous utilisons de l'oxygène médical 99.6% + 3 (Ohio). Le formaldéhyde est préparé par chauffage modéré du paraformaldéhyde.

(C) Analyse

Après un certain temps de réaction, les produits de combustion sont détendus dans un ballon d'analyse de 250 cm^3 préalablement évacué et sont analysés par c.p.g. (chromatographe F/M, modèle 700, modifié pour l'introduction des gaz, muni de détecteurs à conductivité thermique et ionisation de flamme). Le monoxyde de carbone, le méthane, l'oxygène résiduel et l'hydrogène sont analysés sur une colonne de tamis moléculaire 5A à 25 °C, l'anhydride carbonique sur une colonne de gel de silice à 60 °C et le cétène sur une colonne de célite modifiée par 20% de dinonylphtalate à 25 °C. Les autres produits de combustion (eau, méthanol, acétaldéhyde, et acétone) sont analysés sur une colonne de brique pilée modifiée par 20% de carbowax 400 à 50 °C, ou de célite modifiée par 20% de diglycérol à 100 °C. Les acides, le formaldéhyde et les peroxydes sont piégés à −80 °C dans une ampoule amovible contenant 10 cm^3 d'eau distillée: les acides sont titrés par une solution de soude *N*/100 sous atmosphère d'azote, en présence de phénolphtaléine; le formaldéhyde est mesuré par la méthode spectrophotométrique de Bricker et Johnson (7) et les peroxydes sont dosés par la méthode iodométrique de Cullis et Newitt (8).

Résultats

(A) Résultats cinétiques

Les variations de pression en fonction du temps (ΔP *vs.* t) ont été enregistrées pour différents mélanges cétène–oxygène ($0.5 \leq CH_2CO:O_2 \leq 2$) entre les températures de 280 et 500 °C et à partir d'une pression totale de 20 mm Hg. Pour obtenir des résultats reproductibles, il est nécessaire de "passiver" le réacteur par une série d'expériences préliminaires et d'employer un protocole standard de manipulation; la reproductibilité est de l'ordre de 5% à 420 °C, étant beaucoup plus difficile à obtenir à basse température (vers 300 °C). Après une période d'induction plus ou moins longue pendant laquelle ΔP est nulle, la pression augmente suivant une courbe en "S" caractéristique (fig. 1). Nous avons défini sur ces enregistrements manométriques quatre principaux paramètres cinétiques: ΔP_∞ = augmentation maximum de pression (mm Hg); P_0 = pression totale à $t = 0$; $(dP/dt)_{max}$ = vitesse maximum de la réaction (mm Hg/s); t_{max} = temps auquel la vitesse maximum est atteinte (s); ϕ = constante d'accélération (s^{-1}), exprimant l'accélération initiale exponentielle de la pression.

Jusqu'à $t = t_{max}$, la pression croît suivant $\Delta P = Ne^{\phi t}$, où N est une constante. L'augmentation maximum de pression est proportionnelle à la pression initiale ($\Delta P_\infty = \alpha.P_0$); le coefficient α passe par un maximum pour un rapport $CH_2CO:O_2$ voisin de l'unité et il varie en fonction des pressions partielles du cétène et de l'oxygène de la façon représentée sur la fig. 2. L'ordre global (relatif à P_0) et les ordres par rapport à CH_2CO et à O_2 sont donnés au tableau 1 et sont en bon accord avec ceux déterminés par Barnard et Kirschner à 475 °C.

Le tableau 2 présente des valeurs de $(dP/dt)_{max}$, de t_{max}, et de ϕ pour quelques réactions à différentes températures. On en tire des valeurs de l'énergie d'activation apparente qui varient un peu selon le paramètre utilisé pour les calculer (tableau 3), mais qui permettent quand même de

TABLEAU 1. Ordres partiels et global d'après différents paramètres

	n_{CH_2CO}	n_{O_2}	n_{P_0}
$(dP/dt)_{max}$	1.5 (1.7)*	1.2 (1.2)*	3.0 (3.0)*
$1/t_{max}$	1.4	1.1	2.1
ϕ	1.0	1.2	2.1

*Valeurs trouvées par Barnard et Kirschner (3).

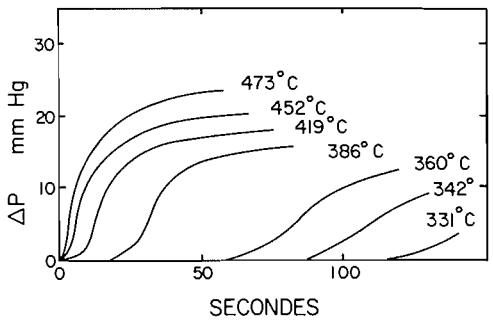

FIG. 1. Courbes de pression à diverses températures pour des mélanges 1 CH_2CO : 2 O_2 à P_0 = 95.0 mm Hg.

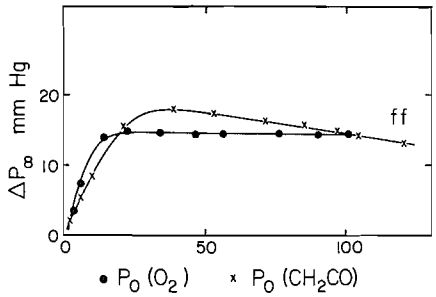

FIG. 2. Augmentation totale de la pression en fonction des pressions partielles initiales des réactifs à 420 °C, jusqu'aux flammes froides ff. La pression de l'un des réactifs est constante à 38 mm Hg.

TABLEAU 2. Influence de la température sur les paramètres de vitesse. Mélange 1 $CH_2CO : 2\ O_2$. $P_0 = 59$ mm Hg

θ (°C)	$(dP/dt)_{max}$ (mm Hg/s)	t_{max} (s)	ϕ (s^{-1})
497	0.95	6.5	0.87
452	0.80	13.8	0.52
420	0.74	23.2	0.34
388	0.65	39.5	0.24
340	0.40	132.	0.10
330	0.14	214.	0.05

tirer une conclusion d'ensemble: la réaction est affectée d'un coefficient de température petit aux températures supérieures, tel que l'ont déjà constaté Barnard et Kirschner, mais grand aux températures inférieures. La transition, qui se situe vers 370 °C, induit à penser qu'on a affaire à des mécanismes différents.

L'addition d'hélium abaisse très légèrement la vitesse de la réaction, alors que le ralentissement est beaucoup plus marqué si le rapport surface/volume du réacteur augmente. La surface du réacteur exerce des effets importants et en particulier des revêtements de chlorure de potassium et d'oxyde de plomb inhibent fortement la combustion lente.

(B) Résultats analytiques

Les principaux produits de la combustion lente à 420 °C sont le monoxyde de carbone, le formaldéhyde, l'eau, et l'anhydride carbonique, accompagnés de traces de méthane, d'hydrogène, de méthanol, d'acide acétique, d'acétaldéhyde, et de peroxyde d'hydrogène (fig. 3) qui sont essentiellement les produits trouvés par Barnard et Kirschner (3). L'augmentation ΔP de la pression est une bonne mesure de l'avancement de la réaction, sauf pendant la période d'induction où

TABLEAU 3. Energies d'activation apparentes d'après trois paramètres. Mélange 1 $CH_2CO : 2\ O_2$. $P_0 = 59$ mm Hg

	Energie d'activation (kcal $mole^{-1}$)	
Paramètre	370–500 °C	300–360 °C
$(dP/dt)_{max}$	4.3±0.3	42.0±2.0
t_{max}	16.0±0.3	32.0±1.0
ϕ	10.8±0.6	40.0±2.0

le cétène et l'oxygène sont consommés pour donner principalement du formaldéhyde. Les bilans sont satisfaisants surtout lorsque la réaction est bien avancée (tableau 4). La fig. 4 indique comment varient les pressions finales des réactifs et des produits principaux avec le rapport $CH_2CO:O_2$, la pression totale étant constante.

Le résultat le plus caractéristique est relatif au formaldéhyde; sa pression varie parallèlement à la vitesse dP/dt de la réaction et suit au début de la combustion la même croissance exponentielle que $\Delta P = Ne^{\phi t}$, la constante d'accélération étant égale à $3.4 \times 10^{-1}\ s^{-1}$ à 420 °C. L'addition de formaldéhyde à l'instant initial, en quantité égale à la concentration maximum, supprime totalement la période d'induction, la combustion débutant avec la vitesse maximum (fig. 5), alors que l'addition au temps t_{max} et après celui-ci n'a pas d'influence. La pression maximum de formaldéhyde croît linéairement avec la pression initiale de cétène $(P_{CH_2O})_{max} = 0.32\ P_{CH_2CO}$ et diminue très légèrement avec celle d'oxygène. On voit au tableau 5 que la vitesse maximum de la réaction et la concentration maximum de formaldéhyde varient parallèlement l'une à l'autre entre 420, et 500 °C. Le facteur de température relatif à $(CH_2O)_{max}$ est de 4.6 ± 0.3 kcal $mole^{-1}$.

Nous avons déduit des résultats analytiques les énergies globales d'activation relatives aux vitesses de consommation du cétène et d'oxygène et à la vitesse de formation du monoxyde de carbone, soit respectivement 5.1, 6.0, et 5.2 kcal/mole.

Discussion

La transition que nous observons vers une température de 370 °C (tableaux 2 et 3), indique certainement le passage d'un mécanisme de combustion à "hautes températures" (380–500 °C), à un mécanisme à basses températures (280–350 °C). Cette transition est confirmée par

Can. J. Chem. Downloaded from www.nrcresearchpress.com by 210.87.254.105 on 09/05/12
For personal use only.

Can. J. Chem. Downloaded from www.nrcresearchpress.com by 210.87.254.105 on 09/05/12
For personal use only.

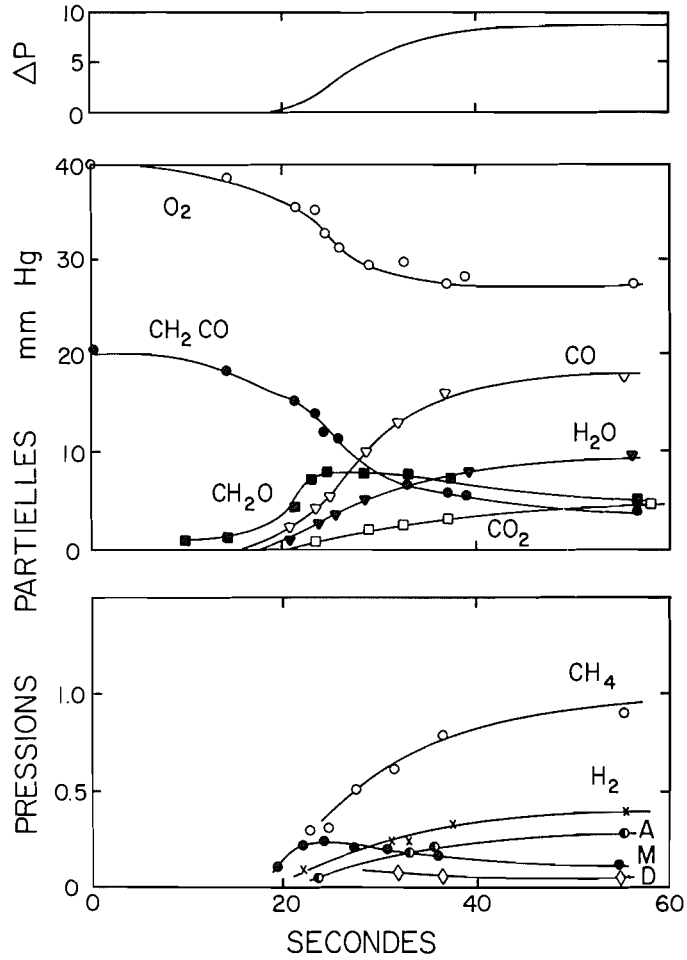

FIG. 3. Variations de la pression et de la composition durant la réaction d'un mélange 1 CH_2CO : 2 O_2 à

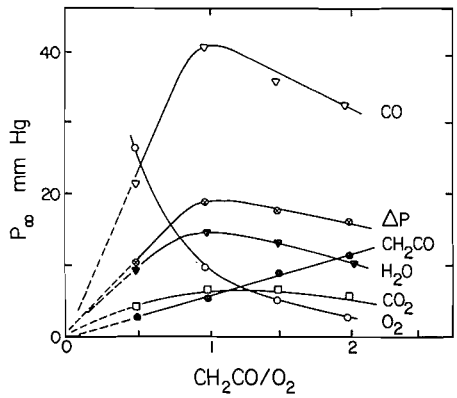

FIG. 4. A 420 °C et 59 mm Hg, influence du rapport CH_2CO/O_2 sur les valeurs finales de ΔP et des pressions partielles.

l'étude du diagramme d'explosion (4); la pression P_c et la température T_c sur la limite d'explosion obéissent à la relation $\ln P_c = A/T_c + B$, qui est représentée par un couple de deux droites qui se coupent pour $\theta = 375$ °C, et d'autre part, la température de 370 °C correspond à la pression minimum du lobe de flamme froide unique (9).

Tous les résultats que nous avons décrits indiquent que la combustion lente du cétène est une réaction en chaînes ramifiées probablement dégénérées:

(*a*) La réaction débute après une période d'induction, l'augmentation consécutive de pression étant exponentielle jusqu'au temps t_{max}.

(*b*) Nous avons observé des flammes froides et l'analyse un peu avant le passage de la flamme

Can. J. Chem. Downloaded from www.nrcresearchpress.com by 210.87.254.105 on 09/05/12
For personal use only.

TABLEAU 4. Bilans de pression et d'atomes pour un mélange 1 CH_2CO : 2 O_2 à 420 °C

t (s)	$P_{obs.}$ (mm Hg)	$P_{calc.}$ (mm Hg)	O (mm at)	C (mm at)	H (mm at)
0	59.0	59.0	98.4	39.3	39.3
14	59.1	57.3	95.4	37.3	38.2
20	59.5	57.1	92.2	37.1	41.2
25	62.0	59.5	91.4	36.3	44.9
37	66.6	68.9	99.3	37.9	45.6
56	68.5	68.7	98.6	35.2	40.9
82	69.2	69.5	98.3	35.9	39.5

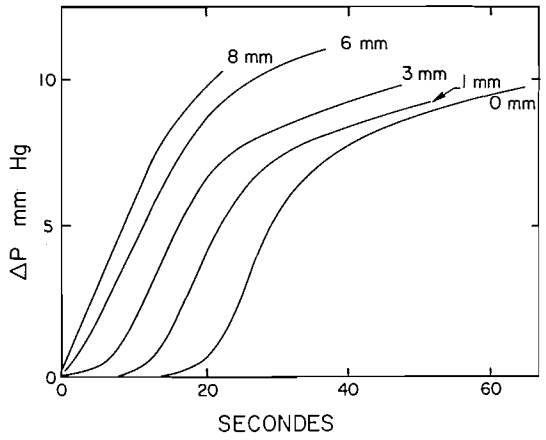

FIG. 5. Effets de l'addition de diverses quantités de formaldéhyde à 420 °C. Mélange 1 CH_2CO : 2 O_2, P_0 = 59 mm Hg.

TABLEAU 5. Vitesses maxima et pressions maxima de formaldéhyde à diverses températures

θ (°C)	$(dP/dt)_{max}$ (mm Hg s^{-1})	$(P_{CH_2O})_{max}$ (mm Hg)
497	1.04	11.0
452	0.95	8.8
420	0.88	7.6
388	0.83	6.7

montre que le formaldéhyde est alors en concentration importante (9).

(*c*) La concentration en formaldéhyde varie parallèlement à la vitesse de la réaction et son addition à l'instant initial en quantité égale à sa concentration maximum supprime totalement la période d'induction (fig. 5).

(*d*) Les paramètres cinétiques dépendent d'une fonction compliquée des concentrations en cétène et en oxygène, la constante d'accélération $\phi = 3.4 \times 10^{-1}\ s^{-1}$ étant de l'ordre de celle associée à une réaction en chaînes ramifiées.

Trois modes d'initiation semblent a priori possibles. Le premier est la réaction invoquée dans la pyrolyse ou la photolyse du cétène (éq. 1).

[1] $$CH_2CO = :CH_2 + CO$$
$$\Delta H_1 = 77 \pm 3 \text{ kcal/mole}$$
avec $\Delta H_f^0(CH_2CO) = -14.8$ kcal/mole,
$\Delta H_f^0(CO) = -26.4$ kcal/mole,
et $\Delta H_f^0(:CH_2) = 88 \pm 3$ kcal/mole (10)

Non seulement cette réaction est fortement endothermique, mais les radicaux $:CH_2$ qu'elle produit peuvent réagir non seulement avec l'oxygène, mais aussi avec le cétène pour donner de l'éthylène (11). Or, on n'a pu déceler aucune trace d'éthylène entre 250 et 500 °C. Le second mode d'initiation (éq. 2) possible est:

[2] $$CH_2CO + O_2 = \cdot CHCO + HO_2^{\cdot}$$
$$\Delta H_2 = 59 \pm 3 \text{ kcal/mole}$$

ΔH_2 a été calculée en supposant que D^0 ($\cdot CH{=}CO$) = $D^0(CH_2{=}CO)$ = 77 ± 3 kcal/mole et en prenant ΔH_f^0 ($:\!CH$) = 142 kcal/mole (10). Le radical ·CHCO a été postulé par Young (12) et plus récemment par Becker *et al.* (13) dans l'étude spectroscopique des flammes du système $\cdot H + O_2 + CH_2CO$.

Le troisième mode d'initiation possible est l'addition d'oxygène sur la double liaison du cétène, processus semblable à celui invoqué dans le cas de la combustion des hydrocarbures éthyléniques (14). Dans cette réaction (éq. 3)

[3] $CH_2CO + O_2 \rightarrow$

$$\begin{pmatrix} CH_2{-}C{=}O \\ | \quad\quad | \\ O{-}{-}O \end{pmatrix} \rightarrow CH_2O + CO_2 \quad [a]$$
$$\rightarrow \cdot OH + \cdot CHO + CO \quad [b]$$

la formation du superoxide est probablement exothermique. Cet intermédiaire peut se décomposer en $CH_2O + CO_2$ comme en [3*a*], ce qui correspondrait à la formation de très petites

		ΔH kcal/mole
	Initiation:	
[3*b*]	$CH_2CO + O_2 = \begin{pmatrix} CH_2—CO \\ \vert \quad \vert \\ O——O \end{pmatrix} = \cdot OH + \cdot CHO + CO$	4 ± 2
	Propagation P_1:	
[4]	$CH_2CO + \cdot OH = CH_2O + \cdot CHO$	-16 ± 2
[5]	$\cdot CHO + O_2 = CO + HO_2^{\cdot}$	-26
[6]	$\cdot CH_2CO + HO_2^{\cdot} = CO + CH_2O + \cdot OH$	-35 ± 2
	Propagation P_2:	
[7]	$CH_2CO + \cdot OH = H_2O + \cdot CHCO$	-13 ± 3
[8]	$\cdot CHCO + O_2 = 2\ CO + \cdot OH$	-82 ± 3
	Ramification et attaque de CH_2O:	
[9]	$CH_2O + O_2 = HCOOH + :O$	~ 0
[10]	$CH_2O + :O = \cdot CHO + \cdot OH$	-15 ± 2
[11]	$CH_2O + \cdot OH = H_2O + \cdot CHO$	-33 ± 2
[12]	$CH_2O + HO_2^{\cdot} = H_2O_2 + \cdot CHO$	-4 ± 2
	Le principal mode de terminaison:	
[13]	Probablement la destruction de $HO_2\cdot$ sur la paroi.	

SCHÉMA 1

quantités de ces substances durant la période d'induction avec une exothermicité d'environ -107 kcal/mole très suffisante pour donner du formaldéhyde excité (20) comme il s'en produit dans les flammes froides. On peut concevoir que le transfert de cette énergie crée les premiers centres actifs radicalaires, mais on ne saurait distinguer expérimentalement cette alternative de la réaction 3*b* que nous proposons pour l'initiation. Cette réaction a, sur les réactions 1 et 2, l'avantage d'être affectée d'une faible endothermicité, $\Delta H_{3b} = 4 \pm 2$ kcal/mole, ce qui permet de supposer que son énergie d'activation globale est nettement inférieure à celles des deux autres.

Les radicaux ·OH produits dans l'initiation peuvent propager deux chaînes. L'une d'elles, [4], [5], et [6], rend compte de l'accumulation de formaldéhyde et de monoxyde de carbone dans les premiers temps de la réaction; l'autre, par les réactions 7 et 8, indique un mode de formation de l'eau et un rôle possible du radical ·CHCO. Cependant, lorsque la concentration de formaldéhyde sera suffisamment élevée, l'attaque de cette espèce par les radicaux ·OH provenant de la ramification constituera le mode de propagation le plus important [10], [11], et [5].

Pour expliquer la formation des produits principaux, nous proposons donc le schéma 1.

Si l'on tient compte de ce que le formaldéhyde s'oxyde suivant la réaction globale $CH_2O + 1/2\ O_2 = CO + H_2O$ (15), la somme de cette réaction et des réactions d'initiation [3] et de propagation P_1 et P_2 est compatible avec nos résultats analytiques, puisqu'elle conduit à

$$4\ CH_2CO + 3.5\ O_2 = 2\ CH_2O + 5\ CO + 2\ H_2O + CO_2$$

ce qui correspond à $P_{CO} = 2\ \Delta P$, $P_{H_2O} = 0.8\ \Delta P$, et $P_{CO_2} = 0.4\ \Delta P$, alors que nos analyses nous ont donné respectivement $P_{CO} = 2\ \Delta P$, $P_{H_2O} = 1\ \Delta P$, et $P_{CO_2} = 0.4\ \Delta P$.

Pour ce qui est de la ramification, le formaldéhyde, formé par les réactions 4, 6, et 16, est le seul produit qui réunit tous les critères d'agent de ramification dégénérée. La faible énergie d'activation à l'époque où la vitesse est maximum indique déjà que la réaction de ramification doit être affectée d'une énergie d'activation peu élevée. Cette énergie peut être calculée à partir de nos données (4, 9) sur la limite inférieure d'explosion. On sait que dans le cas d'une explosion en chaînes avec rupture sur une paroi efficace la pression P_c à la limite inférieure, obéit à la loi

$$P_c \propto e^{E_r/2RT}$$

E_r étant l'énergie d'activation de la ramification

Can. J. Chem. Downloaded from www.nrcresearchpress.com by 210.87.254.105 on 09/05/12
For personal use only.

Can. J. Chem. Downloaded from www.nrcresearchpress.com by 210.87.254.105 on 09/05/12
For personal use only.

		ΔH kcal/mole
[17]	$CH_2CO + \cdot OH = \begin{pmatrix} CH_2—CO \\ \quad\quad\ \vert \\ H—O \end{pmatrix} = \cdot CH_3 + CO_2$	-56 ± 1
[18*a*]	$\cdot CH_3 + CH_2CO = \mathit{CH_4} + \cdot CHCO$	2 ± 4
[18*b*]	$\cdot CH_3 + CH_2O = \mathit{CH_4} + \cdot CHO$	
[19]	$HO_2^{\bullet} + CH_2CO = CH_3O\cdot + CO_2$	-81
[20]	$CH_3O\cdot + CH_2CO = \mathit{CH_3OH} + \cdot CHCO$	± 3
[21]	$CH_2CO + \cdot OH = \begin{pmatrix} H_2C—CO \\ \quad\quad\ \vert \\ O—H \end{pmatrix} = CH_2O + CO + \cdot H$	4
[22]	$\cdot H + CH_2CO = H_2 + \cdot CHCO$	2 ± 3
[23]	$CH_2CO + H_2O = CH_3COOH$	-31
[24]	$HO_2^{\bullet} + CH_2CO = \mathit{H_2O_2} + \cdot CHCO$	17
[25]	$HO_2^{\bullet} + CH_2O = \mathit{H_2O_2} + \cdot CHO$	-4

SCHEMA 2

(16). Nous avons trouvé (9) que notre limite obéit à la relation

$$[14] \qquad \ln P_c = A/T_c + B$$

et que $A = 1470 \pm 20$ °K, ce qui conduit à $E_r = 5.9 \pm 0.1$ kcal/mole. Nous ne pouvons retenir la réaction de ramification habituellement invoquée:

$$[15] \qquad CH_2O + O_2 = \cdot CHO + HO_2^{\bullet}$$

dont l'énergie d'activation est égale à au moins 32 kcal/mole (17) en phase gazeuse et à au moins la moitié de cette valeur dans l'hypothèse où la réaction aurait lieu sur la paroi. C'est pourquoi nous proposons le mécanisme de ramification de Knox et Norrish (18), soit les réactions 9 et 10, la première s'effectuant suivant [9*a*] et [9*b*].

$$[9a] \qquad \cdot CHO + O_2 = HCO_2^{\bullet} + :O$$

$$[9b] \qquad HCO_2 + CH_2O = HCOOH + \cdot CHO$$

Ce processus de ramification est compatible avec une énergie d'activation de 6 kcal/mole. Cette hypothèse a été récemment reprise par Yang et Gray (19) dans une théorie expliquant les phénomènes d'explosion et de flammes froides. En particulier la réaction 16 affectée d'une exothermicité $\Delta H_{16} = -99$ kcal/mole serait suffisante pour porter le formaldéhyde à l'état excité (20) dans les flammes froides du cétène.

$$[16] \quad CH_2CO + :O = \begin{pmatrix} CH_2—CO \\ \diagdown\ \diagup \\ O \end{pmatrix} = CH_2O + CO$$

Pour éviter de faire appel à des atomes d'oxygène libres, on pourrait remplacer la réaction 9 par

$$CH_2O + O_2 = [P] = \cdot H + CO_2 + \cdot OH$$

où [P] serait un intermédiaire peroxydique hypothétique. Cette réaction est exothermique par environ 5 kcal/mole.

La terminaison des chaînes, compte-tenu des effets de surface observés, est sans doute hétérogène et, parmi les radicaux, $HO_2^{\bullet}$ est le plus susceptible de se détruire sur la paroi, en particulier recouverte de chlorure de potassium ou d'oxyde de plomb (21).

Parmi les produits mineurs, nous avons décelé à 420 °C, de petites quantités de méthane, de méthanol, d'hydrogène, d'acide acétique, d'acétaldéhyde, et de peroxyde d'hydrogène. Il est probable que les réactions du schéma 2 interviennent dans la formation de ces composés.

A cette température élevée, les radicaux méthyle ont une bonne chance (22) d'abstraire un hydrogène selon [18], réaction concurrencée par leur réaction avec l'oxygène pour former le radical peroxydique qui se décompose en formaldéhyde et radical hydroxyle. Une partie des atomes d'hydrogène réagissant en [22] provient vraisemblablement de la décomposition de radicaux $\cdot CHO$ et $HO_2^{\bullet}$. Nous avons mesuré (9) la vitesse de la réaction du cétène avec l'eau [23] à 360 °C. Quant au peroxyde d'hydrogène, il ne peut pas jouer un rôle important comme agent de

Can. J. Chem. Downloaded from www.nrcresearchpress.com by 210.87.254.105 on 09/05/12
For personal use only.

ramification, car sa décomposition homogène est beaucoup plus lente que sa destruction sur la paroi à la température de nos expériences (23).

Nous avons traité notre schéma cinétique par l'approximation des états quasi-stationnaires, en analysant d'abord le début de la combustion pendant la période d'induction et ensuite la réaction au temps t_{max} où la vitesse est maximum.

Première étape: période d'induction

Il se forme principalement du formaldéhyde et du monoxyde de carbone, ces formations faisant intervenir surtout les réactions d'initiation [3] et de propagation P_1 [4], [5], et [6]. On suppose que la vitesse de consommation du formaldéhyde est contrôlée par celle de la ramification représentée par la somme des réactions 9 et 10, soit

[26] $2\,CH_2O + O_2 = HCOOH + \cdot CHO + \cdot OH$

pour simplifier la notation. Le paramètre qui décrit le mieux l'évolution de la réaction durant cette période est la constante d'accélération ϕ qui exprime la croissance exponentielle de la pression et de la concentration de formaldéhyde. L'approximation des états quasi-stationnaires, soit

$$d[\cdot OH]/dt = d[\cdot CHO]/dt = d[HO_2^{\bullet}]/dt = 0$$

avec $d[CH_2O]/dt \neq 0$, puisque le formaldéhyde s'accumule durant cette période, conduit à la relation

$$[27] \qquad [CH_2O] = \frac{n_0}{a_{26}}(e^{\phi t} - 1)$$

où n_0 = taux de la réaction d'initiation, $a_{26} = k_{26}[O_2]$, et

$$\phi \text{ (théorique)} \propto k_6 k_{26} k_{13}^{-1} [CH_2CO][O_2]$$

Nous retrouvons le fait que la croissance de la concentration du formaldéhyde est exponentielle et nous devons pouvoir identifier cette constante ϕ (théorique) à la constante d'accélération expérimentale ϕ. Nous trouvons effectivement que ϕ dépend des pressions partielles de cétène et d'oxygène suivant des ordres voisins de l'unité (tableau 1). L'énergie globale d'activation relative à ϕ doit être égale à $E_6 + E_{26} - E_{13} = 10.8 \pm 0.6$ kcal/mole (tableau 3). Rappelons que l'énergie d'activation de la ramification telle que déterminée d'après la limite inférieure d'explosion est $E_{26} \simeq 6$ kcal/mole. Comme $E_{13} \sim 0$, nous obtenons $E_6 = 4.8 \pm 0.6$ kcal/mole, valeur plausible puisque $\Delta H_6 = -35 \pm 2$ kcal/mole.

Deuxième étape: calcul de la concentration maximum de formaldéhyde et de la vitesse maximum de consommation du cétène au temps t_{max}

Au temps t_{max}, nous ne pouvons plus négliger la propagation P_2 ni la consommation du formaldéhyde par les radicaux $\cdot OH$ et $HO_2^{\bullet}$ dans les réactions 11 et 12. Au maximum de vitesse, le taux de production de centres actifs par la réaction d'initiation est négligeable par rapport au taux de leur production par la réaction de ramification, la seule dont il faut tenir compte. En faisant cette simplification, on trouve, pour la concentration maximum du formaldéhyde

$$[28] \quad [CH_2O]_{max} \propto \left[\frac{k_4\,k_6}{k_{11}k_{12}}\right]^{1/2} [CH_2CO],$$

et pour la vitesse maximum de consommation du cétène

$$[29] \quad -\frac{d}{dt}[CH_2CO]_{max} \propto \frac{k_6 k_{26}}{k_{13}}\left(\frac{k_4 k_6}{k_{11}k_{12}}\right)^{1/2}[CH_2CO]^2[O_2]$$

Nous retrouvons le fait expérimental que la pression maximum atteinte par le formaldéhyde est proportionnelle à la pression du cétène dans le mélange initial mais ne dépend pas de celle de l'oxygène. L'expression [29] est en accord avec l'ordre global de 3 par rapport à la vitesse maximum trouvé expérimentalement (tableau 1) et avec le fait que l'ordre partiel est plus grand par rapport au cétène que par rapport à l'oxygène.

Nous avons vu que $E_6 = 5$ kcal/mole et $E_{26} \simeq 6$ kcal/mole et il va de soi que $E_{13} \sim 0$. En appliquant la relation empirique de Polanyi, $E \simeq 11.5 - 0.25\ |\Delta H|$, nous obtenons les valeurs approximatives $E_{11} = 3.5$ et $E_{12} = 10.5$ kcal/mole. L'énergie globale d'activation relative à $(P_{CH_2O})_{max}$ doit s'identifier à $\frac{1}{2}(E_4 + E_6 - E_{11} - E_{12}) = 4.5$ kcal/mole en excellent accord avec la valeur expérimentale de 4.3 kcal/mole, si l'on fait $E_4 = 18$ kcal/mole. Avec cette même valeur de E_4, l'énergie globale d'activation par rapport à la vitesse maximum de consommation du cétène est $(E_6 + E_{26} - E_{13}) + \frac{1}{2}(E_4 + E_6 - E_{11} - E_{12}) = 15.5$ kcal/mole, valeur qui est forte par rapport à celle de 5 kcal/mole mesurée,

mais qui reste dans l'intervalle des valeurs inscrites au tableau 3.

Ce travail a été financé par une subvention du Conseil National de Recherches du Canada et par une bourse du gouvernement canadien à P.M.

1. K. C. SALOOJA. Combust. Flame, **10**, 17 (1966).
2. J. A. BARNARD ET T. W. HONEYMAN. Proc. Roy. Soc. **A279**, 236 (1964).
3. J. A. BARNARD ET E. KIRSCHNER. Combust. Flame, **11**, 496 (1967).
4. P. MICHAUD, J. LEBEL, ET C. OUELLET. Combust. Flame, **12**, 395 (1968).
5. G. FISHER, A. F. MACLEAN, ET G. SCHNIZER. J. Org. Chem. **18**, 1055 (1953).
6. L. G. DRAYTON ET A. W. THOMPSON. J. Chem. Soc. **2**, 1416 (1948).
7. C. E. BRICKER ET H. R. JOHNSON. J. Anal. Chem. **17**, 400 (1945).
8. C. F. CULLIS ET E. J. NEWITT. Proc. Roy. Soc. **A237**, 531 (1956).
9. P. MICHAUD. Thèse. Université Laval, Québec, Québec, 1969.
10. S. W. BENSON. J. Chem. Educ. **42**, 502 (1965).
11. R. L. RUSSEL ET F. S. ROWLAND. J. Amer. Chem. Soc. **90**, 1671 (1968).
12. R. J. YOUNG. J. Chem. Soc. **3**, 2909 (1958).
13. H. K. BECKER, D. KLEY, ET R. J. NORSTROM. 12th International Symposium on Combustion. Pittsburgh, Pennsylvania, 1969. p. 405.
14. A. J. HARDING ET R. G. W. NORRISH. Proc. Roy. Soc. **A212**, 291 (1952).
15. J. F. GRIFFITHS ET G. SKIRROW. Oxid. Combust. Rev. **3**, 47 (1969).
16. F. S. DAINTON. Chain reactions: an introduction. Second edition. Methuen and Co. Ltd., London, 1966.
17. N. S. ENIKOLOPYAN. 7th International Symposium on Combustion. Butterworths London, 1959. p. 157.
18. J. H. KNOX ET R. G. W. NORRISH. Proc. Roy. Soc. **A221**, 151 (1954).
19. C. H. YANG ET B. F. GRAY. J. Phys. Chem. **73**, 3395 (1969).
20. A. D. WALSH. Trans. Faraday Soc. **43**, 305 (1947).
21. G. H. N. CHAMBERLAIN, D. E. HOARE, ET A. D. WALSH. Discuss. Faraday Soc. **14**, 89 (1953).
22. S. W. BENSON. Foundations of chemical kinetics. McGraw-Hill, New York, 1960. p. 296.
23. (*a*) P. A. GIGUERE ET J. D. LIU. Can. J. Chem. **35**, 283 (1957). (*b*) D. BRATTEN ET R. R. BALDWIN. International 8th Symposium on Combustion. Williams and Wilkins, Baltimore, Maryland, 1962.

Can. J. Chem. Downloaded from www.nrcresearchpress.com by 210.87.254.105 on 09/05/12
For personal use only.

Can. J. Chem. Downloaded from www.nrcresearchpress.com by 210.87.254.5 on 09/05/12
For personal use only.

Oxydation lente du cétène en phase gazeuse. II. Réaction à "basses températures"

PIERRE MICHAUD[1] ET CYRIAS OUELLET
Département de Chimie, Université Laval, Québec 10, Québec

Reçu le 30 juin 1970

Nous avons étudié la combustion lente du cétène entre 280 et 350 °C. La différence fondamentale avec la combustion lente de "hautes températures" est la présence de peroxydes (surtout d'hydroperoxydes) et l'absence de méthane. Les produits principaux: formaldéhyde, monoxyde de carbone, eau, et anhydride carbonique demeurent les mêmes. Nous proposons un schéma en chaînes ramifiées par la décomposition homogène: $CH_3OOH = CH_3O\cdot + \cdot OH$.

The slow combustion of ketene was investigated in the low-temperature range 280–350 °C. It differs from the reaction at higher temperatures chiefly by the presence of peroxides (mostly hydroperoxides) and the absence of methane. The main products: formaldehyde, carbon monoxide, water, and carbon dioxide are the same in both cases. A reaction scheme is proposed, which involves degenerate branching through the decomposition of methyl hydroperoxide: $CH_3OOH = CH_3O\cdot + \cdot OH$.

Canadian Journal of Chemistry, 49, 303 (1971)

Introduction

Dans la partie I (Oxydation lente du cétène en phase gazeuse: réaction à "hautes températures" (1)), nous avons mis en évidence un domaine de combustion lente de "basses températures" 280 °C < θ < 350 °C. Cet article décrit les résultats cinétiques et analytiques relatifs à cette région.

Méthode expérimentale

L'appareil et la préparation du cétène ont été décrits dans la partie I: en particulier, la combustion est étudiée dans le même réacteur de Vycor. La différence fondamentale entre les deux domaines de combustion lente est la présence à basses températures de peroxydes parmi les produits de combustion. Ceux-ci ont été dosés par la méthode de Cullis et Newitt (2) qui permet de déterminer quantitativement les peracides, le peroxyde d'hydrogène et les hydroperoxydes. Cette méthode nous a indiqué qu'environ 90% des peroxydes sont des hydroperoxydes, 10% des peracides et H_2O_2.

Résultats

(A) Résultats cinétiques

La reproductibilité est plus difficile à obtenir qu'à "hautes températures", principalement pour les longues périodes d'induction. Les enregistrements sont des courbes en "S", sauf certaines variations singulières, pour lesquelles l'accélération initiale exponentielle est suivie par un arrêt apparent de la combustion par consommation de la totalité de l'oxygène (fig. 1). Il ne peut s'agir de flammes froides, puisque celles-ci sont toujours suivies par une montée consécutive de la pression (3) mais peut-être du "pic d'arrêt" mis en évidence par Lucquin (4); ce phénomène ne s'observe que pour des mélanges riches en cétène ($CH_2CO:O_2 > 1.1$) et dans un intervalle de températures relativement restreint (autour de 300 °C).

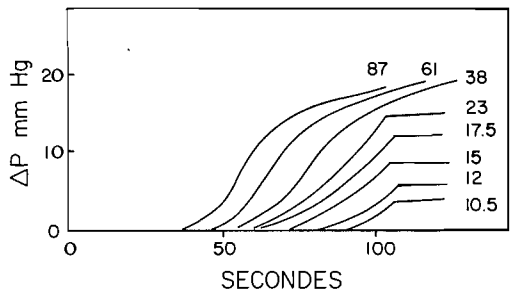

FIG. 1. Enregistrements manométriques à 330 °C pour différentes pressions initiales $P_0(O_2)$ inscrites sur les courbes, la pression initiale de cétène étant $P_0(CH_2CO)$ = 38 mm Hg dans tous les cas.

Les paramètres cinétiques ΔP_∞, $(dp/dt)_{max}$, t_{max}, et ϕ (définis dans partie I), ont été étudiés en fonction de la pression totale P_0 et des pressions partielles de cétène et d'oxygène. ΔP_∞ est proportionnel à P_0, ($\Delta P_\infty = \alpha \cdot P_0$), le coefficient α passant par un maximum pour $CH_2CO:O_2 \geqslant 1:1$. Les ordres globaux et partiels sont différents à 330 °C de ceux calculés à 420 °C et sont inscrits dans le tableau 1.

(B) Résultats analytiques

Nous avons analysé en détail les produits de la combustion lente d'un mélange stoechiométrique cétène–oxygène à 330 °C (fig. 2). Les bilans sont satisfaisants surtout lorsque la réac-

[1]Boursier post-doctorat, Division de Chimie, Conseil National de Recherches du Canada, Ottawa, Canada.

Can. J. Chem. Downloaded from www.nrcresearchpress.com by 210.87.254.5 on 09/05/12
For personal use only.

TABLEAU 1. Ordres n par rapport à CH_2CO, à O_2 et à la pression initiale P_0

	n		
	CH_2CO	O_2	P_0
$(dp/dt)_{max}$	2.1	0.5	2.6
$1/t_{max}$	1.6	0.6	2.0
ϕ	1.0	0.5	1.0

TABLEAU 2. Bilans atomiques durant la réaction d'un mélange 1 CH_2CO:2O_2 à 330 °C

t (s)	P_{exp} (mm)	P_{calc} (mm)	O (mm atm)	C (mm atm)	H (mm atm)
0	59.0	59.0	98.3	39.3	39.3
109	59.0	55.5	92.4	34.1	35.9
195	60.5	57.6	93.5	32.6	37.2
222	63.9	66.1	100.8	36.8	39.1
278	67.0	68.5	98.0	38.5	35.1
380	67.2	70.7	101.3	40.7	36.6

tion est bien avancée (tableau 2). Les pressions partielles de cétène et d'oxygène décroissent linéairement avec l'augmentation ΔP de la pression à partir de la fin de la période d'induction (fig. 3), ce qui permet de prendre dp/dt comme mesure de la vitesse de la réaction. Les principaux produits de combustion sont les mêmes qu'à 420 °C, la différence principale étant la présence de peroxydes (surtout des hydroperoxydes), l'absence de méthane et la présence de traces d'acétone. La formation de méthanol est plus importante qu'à 420 °C. Le formaldéhyde atteint très vite une pression stationnaire de l'ordre de 8 mm Hg et son addition à l'instant initial n'a pas d'effet sur la vitesse de la combustion, contrairement à son influence à 420 °C.

Discussion

Les résultats cinétiques et analytiques indiquent que la combustion du cétène à 300 °C est une réaction en chaînes ramifiées. L'intermédiaire responsable de la ramification ne semble pas être le formaldéhyde puisque sa concentration demeure stationnaire jusqu'au moment où le cétène a été entièrement consommé (fig. 2). De plus l'addition de formaldéhyde n'affecte ni la période d'induction, ni la vitesse maximum de la réaction. Les longues périodes d'induction que nous obtenons (de l'ordre de centaines de secondes), ainsi que la région de détonation mise en évidence sur le diagramme d'explosion (3),

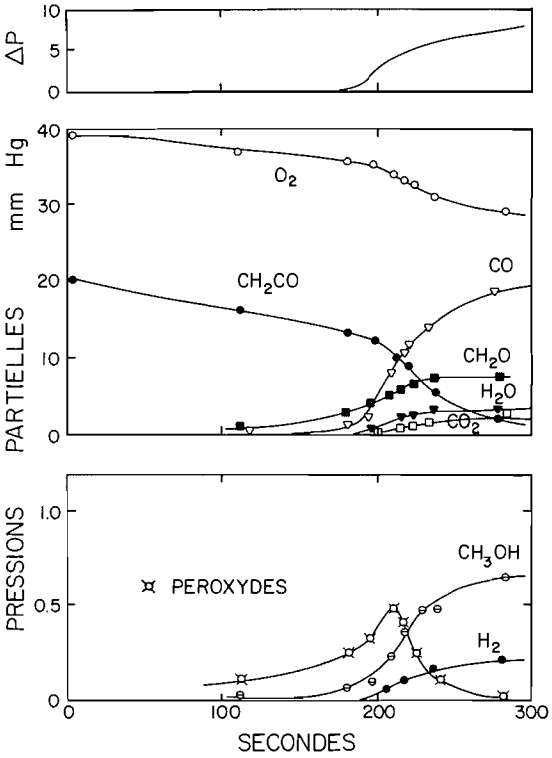

FIG. 2. Evolution de la pression et de la composition durant l'oxydation lente à 330 °C d'un mélange 1 CH_2CO:2 O_2 de pression initiale 59 mm Hg.

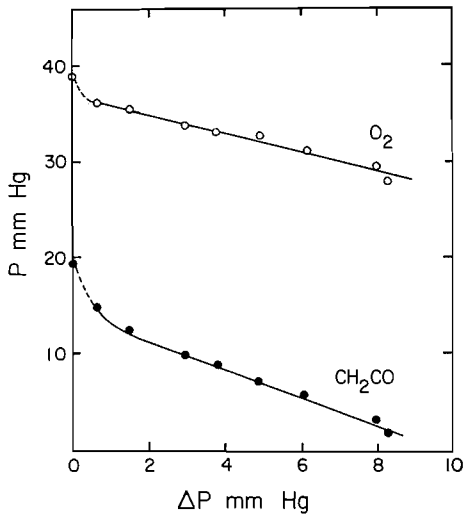

FIG. 3. Consommation des réactifs en fonction de ΔP comme mesure de l'avancement de la réaction à 330 °C d'un mélange 1 CH_2CO:2 O_2 de pression initiale 59 Hg mm.

Can. J. Chem. Downloaded from www.nrcresearchpress.com by 210.87.254.5 on 09/05/12
For personal use only.

doivent être associées à la formation de peroxydes. Le temps de vie moyen de l'agent de ramification est approximativement égal à $1/\phi$, ϕ étant la constante d'accélération: à 330 °C, $\phi = 0.048\ s^{-1}$, d'où un temps de vie de 21 s. Norrish (5) a montré que le temps de vie moyen est égal au rapport de la concentration stationnaire de l'intermédiaire à sa vitesse maximum de formation; la concentration maximum de peroxydes est de 0.6 mm Hg, leur vitesse de formation 0.023 mm Hg/s, d'où un temps de vie de 26 s en bon accord avec la valeur déterminée précédemment. Parmi les peroxydes, nous avons identifié H_2O_2, des peracides et surtout des hydroperoxydes (90%). Le H_2O_2 en très faible concentration ne semble pas être l'agent de ramification car sa vitesse de décomposition homogène est faible à une température de l'ordre de 300 °C, et sa décomposition thermique à des températures inférieures à 400 °C est surtout hétérogène (6, 7). Les peracides pouvant être présents (acides performique et peracétique) ont des temps de vie de l'ordre de 10^{-1} à 10^{-2} s à 330 °C (8), et la valeur que nous avons calculée (21–26 s) est de l'ordre du temps de vie d'un hydroperoxyde (9). Fisher et Tipper (10) trouvent que le temps de vie de l'hydroperoxyde de méthyle est de 30 s à 395 °C, Barnard et Honeyman (11) trouvent 75 s à 284 °C.

Ces considérations, en plus de l'absence de méthane et de la concentration plus élevée de méthanol à 330 °C, nous suggèrent que CH_3OOH est l'agent de ramification probable à cette température:

[32] $CH_3OOH \rightarrow CH_3O\cdot + \cdot OH$

[17] $\cdot OH + CH_2CO \rightarrow CH_3\cdot + CO_2$

suivie par l'oxydation des radicaux $\cdot CH_3$

[30] $\cdot CH_3 + O_2 + M = CH_3O_2\cdot + M$

[31] $CH_3O_2\cdot + CH_2CO = CH_3OOH + \cdot CHCO$

les radicaux $CH_3O_2\cdot$ ayant à 330 °C un temps de vie suffisamment long pour abstraire un atome d'hydrogène (12). La ramification homogène [32] contrôlant la vitesse de la combustion, en particulier au maximum de vitesse, l'énergie globale d'activation de 42 ± 2 kcal/mole (mesurée comme la variation de $(dp/dt)_{max}$ avec $1/T$) est en accord avec la valeur de $E_{30} = 38.5$ kcal $mole^{-1}$ déterminée par Barnard et Cohen (12).

Rappelons que, dans le domaine de hautes températures, c'est le formaldéhyde qui est l'agent de ramification. La combustion lente du cétène est donc une réaction qui passe d'un mécanisme aldéhydique à un mécanisme peroxydique par un changement modéré de la température.

L'analyse du schéma réactionnel complet est très compliquée, et nous proposons une suite de réactions qui s'applique raisonnablement bien au début de la réaction, en faisant les remarques suivantes:

(1) Les produits principaux sont dans la phase initiale le formaldéhyde, le monoxyde de carbone et les peroxydes (CH_3OOH), l'eau et l'anhydride carbonique s'accumulant relativement tard.

(2) La formation de H_2O_2 est plus importante qu'à 420 °C et la terminaison homogène [33].

Le schéma réactionnel est le schéma 1:[2]

		$\Delta H°$ kcal/mole
[3*a*]	$CH_2CO + O_2 = \begin{matrix} CH_2—C^{O} \\ \vert \quad \vert \\ O \quad —O \end{matrix} \rightarrow CH_2O + CO_2$	−107
[3*b*]	$\rightarrow \cdot CHO + \cdot OH + CO$	4 ± 2
[4]	Propagation $CH_2CO + \cdot OH \rightarrow CH_2O + \cdot CHO$	−16 ± 2
[5]	P_1 $\cdot CHO + O_2 \rightarrow CO + \cdot HO_2$	−27 ± 4
[6]	$CH_2CO + \cdot HO_2 \rightarrow CH_2O + CO + \cdot OH$	−35 ± 2
[17]	Propagation $CH_2CO + \cdot OH \rightarrow \cdot CH_3 + CO_2$	−56 ± 1
[30]	P_3 $\cdot CH_3 + O_2 + M \rightarrow CH_3O_2\cdot + M$	−27 ± 1
[31]	$\cdot CH_3O_2 + CH_2CO \rightarrow CH_3OOH + \cdot CHCO$	7 ± 3
[8]	$\cdot CHCO + O_2 \rightarrow 2CO + \cdot OH$	−82 ± 3
[32]	Ramification $CH_3OOH \rightarrow CH_3O\cdot + \cdot OH$	−40 ± 1
[33]	Terminaison $HO_2\cdot + HO_2\cdot \rightarrow H_2O_2 + O_2$	−43 ± 1

Schéma 1

[2]Les numéros des réactions font suite à ceux de l'article précédent (1).

L'approximation des états quasi-stationnaires et des considérations cinétiques nous conduisent (13) à

$$[CH_3OOH]^{1/2} = \frac{k_6 \cdot k_{17}[CH_2CO]}{k_4 \cdot (k_{32}k_{33})^{1/2}} (1 - e^{-k_{32}t/2})$$

Ce résultat présente l'intérêt de prévoir l'allure de la formation du peroxyde en fonction du temps, et permet d'évaluer approximativement la constante k_{32}. D'après nos résultats analytiques (tableau 2), il faut un temps de 210 s pour que la concentration des peroxydes atteigne les 9/10 de leur concentration maximum, d'où

$$\frac{k_{32}}{2} \cdot 210 \sim 2.1 \text{ et } k_{32} \sim 2.10^{-2}\ s^{-1}$$

Cette valeur est en accord avec la détermination de Barnard et Cohen (12) qui trouvent

$$k_{32} = 4.3 \times 10^{12}\ e^{\cdot -38500/RT}$$

pour la décomposition homogène de CH_3OOH, soit $\sim 4 \times 10^{-2}$ à 330 °C.

Ce travail a été financé par une subvention du Conseil National de Recherches du Canada, et l'un de nous (P.M.) remercie le gouvernement canadien pour l'attribution d'une bourse.

1. P. MICHAUD et C. OUELLET. Can. J. Chem. Ce numéro.
2. C. F. CULLIS et E. J. NEWITT. Proc. Roy. Soc. **A237**, 531 (1956).
3. P. MICHAUD, J. LEBEL et C. OUELLET. Combust. Flame, **12**, 395 (1968).
4. M. LUCQUIN. J. Chim. Phys. **55**, 827 (1958).
5. R. G. W. NORRISH. Discuss. Faraday Soc. **10**, 269 (1951).
6. P. A. GIGUÈRE et I. D. LIU. Can. J. Chem. **35**, 283 (1957).
7. D. E. HOARE, J. B. PROTHEROE, et A. D. WALSH. Trans. Faraday Soc. **55**, 548 (1959).
8. C. A. MACDOWELL et J. B. FARMER. 5th Symposium International on Combustion. Rheinhold Publishing Corporation, New York, 1955. p. 453.
9. A. D. KIRK et J. H. KNOX. Trans. Faraday Soc. **56**, 1296 (1960).
10. J. P. FISHER et C. F. H. TIPPER. Trans. Faraday Soc. **59**, 1174 (1963).
11. J. A. BARNARD et T. W. HONEYMAN. Proc. Roy. Soc. **A279**, 248 (1964).
12. J. A. BARNARD et A. COHEN. Trans. Faraday Soc. **64**, 396 (1968).
13. P. MICHAUD. Thèse de doctorat. Université Laval, Québec, Québec, 1969.

Can. J. Chem. Downloaded from www.nrcresearchpress.com by 210.87.254.5 on 09/05/12
For personal use only.

Alkaloids of *Tabernaemontana psychotrifolia* H.B.K.

R. H. BURNELL AND J. D. MEDINA
Département de chimie, Université Laval, Québec, Québec
Received June 23, 1970

A new alkaloid $C_{20}H_{24}N_2O$ (taberpsychine) obtained from Venezuelan *T. psychotrifolia* is shown to have structure **5**. The Hofmann degradation products of taberpsychine and its dihydro derivative are discussed. Two other bases isolated are affinine and 16-epi-vobasinic acid, the latter for the first time as a natural product.

Canadian Journal of Chemistry, 49, 307 (1971)

Can. J. Chem. Downloaded from www.nrcresearchpress.com by 210.87.254.6 on 09/05/12
For personal use only.

Extraction of *Tabernaemontana psychotrifolia* H.B.K.[1] yielded three principal alkaloids but the abundance of the major base taberpsychine, $C_{20}H_{24}N_2O$, and the fact that it could not be readily placed in a "skeletal" group by mass spectrometry made it the principal area of interest.

The u.v. spectrum of taberpsychine shows absorption typical of an indole moiety, with no substituents other than the "normal" ones at position 2 and 3. The i.r. spectrum confirms the presence of the aromatic nucleus and of the indolic NH, but the absence of absorption due to hydroxyl or carbonyl groups fails to provide information concerning the nature of the oxygen atom present. Since neither acetylation nor mild oxidation reactions produced any change in the molecule, the oxygen atom was, by exclusion, assumed to be ethereal.

The n.m.r. spectrum affords evidence about the remainder of the molecule, including the functionality of the second nitrogen atom. A broad quartet at 5.38 δ (J = 6.5 Hz) integrating for one proton, accompanied by a doublet of doublets for three protons at 1.68 δ (J = 6.5 and 2.0 Hz respectively) is evidence for an ethylidene side chain. Decoupling experiments (Fig. 1) left no doubt about this and at the same time localized the origin of the small coupling observed in the methyl signal and also of the broadening of the quartet for the olefinic proton. Irradiating the methyl signal, the broad lower field part (H in Fig. 1) of an AB quartet (3.60 and 2.93 δ, J = 14 Hz) becomes a sharp doublet; while irradiating this broad doublet (3.60 δ) the disappearance of the small splitting of the methyl group signal is observed (this also sharpens the quartet for the olefinic proton). This AB quartet is found in a region typical for protons at carbon atoms adjacent to nitrogen, permitting the placing of the ethylidene side chain in the sequence shown in **1**, with the methylene group adjacent to the basic nitrogen atom responsible for the AB quartet discussed above. A singlet at 2.53 δ integrating for three protons must be assigned to a methyl group on the basic nitrogen (since the indolic nitrogen bears no substituent). The spectrum also confirms the presence of four aromatic protons (4H multiplet 7.07–7.66 δ) and the indolic NH (singlet 8.42 δ).

Another feature in the n.m.r. spectrum is a pair of doublets at 5.13 δ (J = 10 and 2 Hz) integrating for one proton. The signal is only ascribable to a proton adjacent both to an aromatic moiety and an oxygen atom. The splitting pattern suggests that it is also adjacent to a methylene.

Zinc dust distillation of taberpsychine, following a small scale method described by Biemann and Spiteller (1) coupled with gas-chromatographic analysis of the volatile distillate showed the major product to be 3-ethylpyridine (direct comparison in the gas chromatograph with an authentic sample and n.m.r. spectrometry of the material recovered). The product could only *be formed from the part of the molecule containing the basic nitrogen* and since the analogous pyridinium ion is observed as one of the major peaks in the fragmentation in the mass spectrum (122 m/e) the basic nitrogen atom is located in a six-membered ring.

Hydrogenation of taberpsychine afforded a dihydro derivative, $C_{20}H_{26}N_2O$, in which the ethylidene side chain was no longer present as shown by the n.m.r. spectrum, while a signal due to a methyl group on a saturated carbon appeared as a triplet at 0.98 δ (J = 7 Hz).

[1]The identification was made by, and a herbareum specimen is filed at, the Botanical Gardens, Caracas, Venezuela.

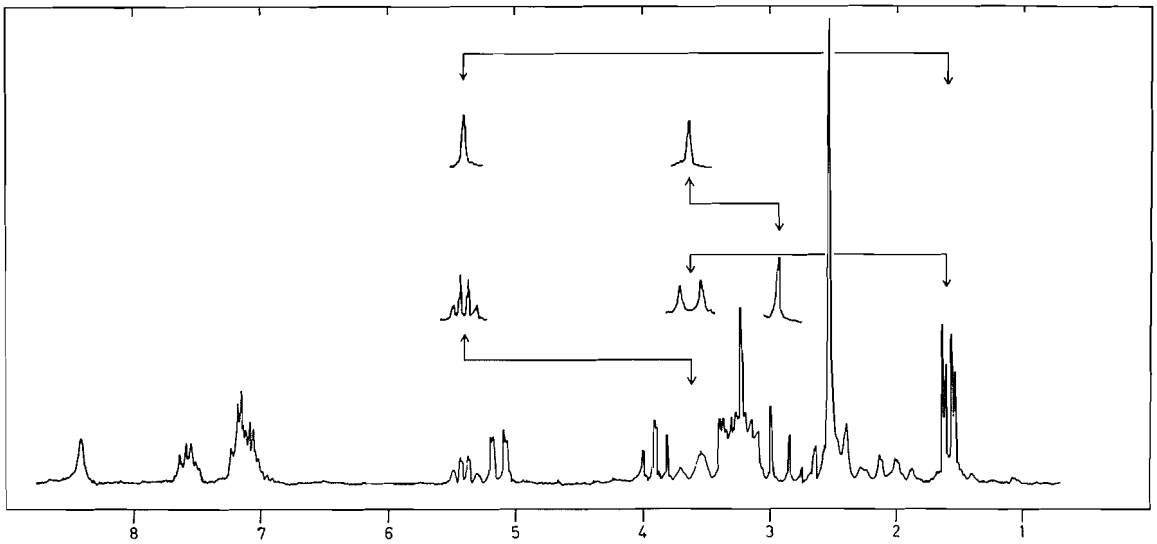

FIG. 1. The n.m.r. spectrum (100 MHz) of taberpsychine in deuteriochloroform (TMS = 0 p.p.m.). Double irradiations are indicated by the double headed arrows.

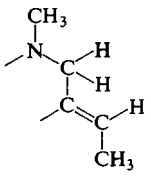

1

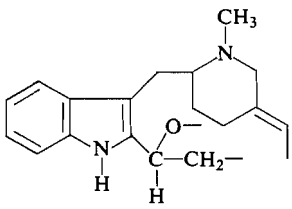

2

The methiodide of the dihydro derivative undergoes Hofmann degradation with potassium tertiobutoxide to give a major product, $C_{21}H_{28}N_2O$, whose u.v. spectrum indicates the presence of a double bond conjugated to the indole chromophore (2, 3). The presence of this new double bond is corroborated by the n.m.r. spectrum of the dihydrotaberpsychine-methine, in which one finds the signals for two olefinic protons at 6.69 (doublet J = 12 Hz) and 5.55 δ (doublet of doublets J = 12 and 8 Hz) as the low field AB part of an ABX system (see Fig. 2). The fact that the double bond introduced during this reaction is conjugated with the aromatic moiety and the assumption of a very likely tryptamine biogenesis allows the linkage of the two units as shown in partial structure **2** and also places the oxygen atom on the carbon attached to position 2 of the indolic portion. A methylene group can be placed adjacent to the carbon bearing the oxygen atom on the basis of the pattern for the proton adjacent to both the aromatic residue and oxygen (doublet of doublets J = 10 and 2 Hz).

Spin decoupling experiments (Fig. 2) on dihydrotaberpsychine-methine provided information concerning the missing linkage of the oxygen atom. In effect, it demonstrated that the X part (1H) of the ABX system involving the vinyl protons introduced by the degradation, is also coupled to an A′B′ system (doublet 4.21 δ, J = 11 Hz and triplet 3.79 δ, J = 11 Hz) appearing in a region typical for protons adjacent to oxygen. The Hofmann product must therefore contain the sequence:

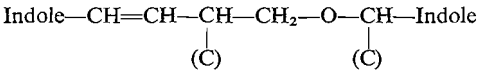

and this observation is only compatible with the partial structure for the methine shown by **3**.

The molecular formula of the base indicates a pentacyclic structure. The additional ring must involve the methylene group shown and only one point of attachment remains (at the starred carbon) since the nature and number of protons at all other positions has been demonstrated in the discussion above, thus the complete structure for the major Hofmann product is given as **4** in which the configuration of the *C*-ethyl residue must be as shown, arising from hydrogen addition to the more exposed face of the molecule, and hence the

Can. J. Chem. Downloaded from www.nrcresearchpress.com by 210.87.254.6 on 09/05/12
For personal use only.

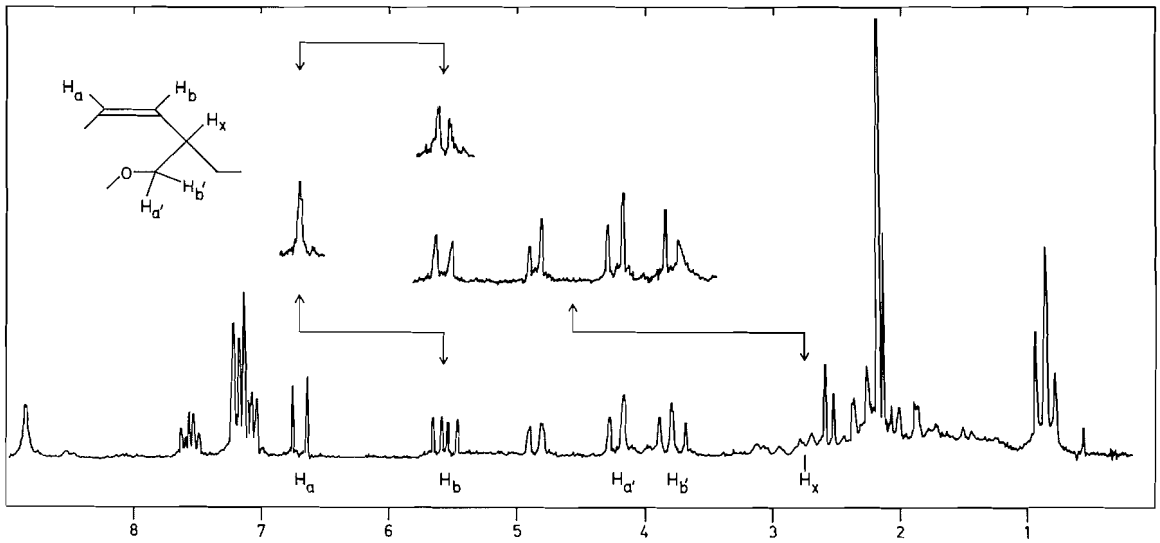

FIG. 2. The n.m.r. spectrum (100 MHz) of dihydrotaberpsychine methine in deuteriochloroform (TMS = 0 p.p.m.).

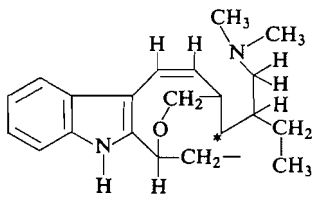

3

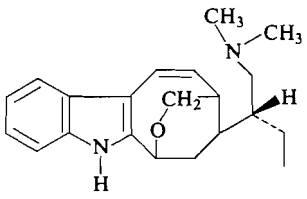

4

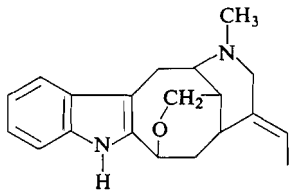

5

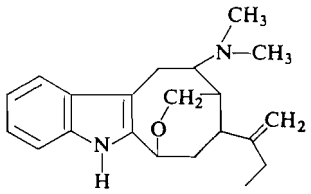

6

structure of taberpsychine is **5** which is compatible with all spectral data.[2]

A minor product from the Hofmann degradation of dihydrotaberpsychine methiodide was also isolated although it could not be induced to crystallize. The n.m.r. spectrum shows a pair of doublets (4.98 and 5.63 δ, J = 1 Hz) typical of a terminal methylene group, which together with the preceding evidence permitted the formulation of the material as structure **6**.

Once the structure of taberpsychine had been elucidated, the result obtained from the Hofmann degradation performed on the methiodide of taberpsychine itself could be rationalized, whereas before a rather complex n.m.r. spectrum had rendered its interpretation difficult. This degradation, effected using the same conditions as for the dihydro compound already discussed, af-

[2]After our preliminary report on taberpsychine (P. R. Benoin *et al.* (6)) we were informed that the alkaloid anhydrovobasindiol had been ascribed the same structure (M. Hesse, personal communication). In a subsequent publication (J. J. Dugan *et al.* (7)) the two alkaloids are shown to be identical.

Can. J. Chem. Downloaded from www.nrcresearchpress.com by 210.87.254.6 on 09/05/12
For personal use only.

Can. J. Chem. Downloaded from www.nrcresearchpress.com by 210.87.254.6 on 09/05/12
For personal use only.

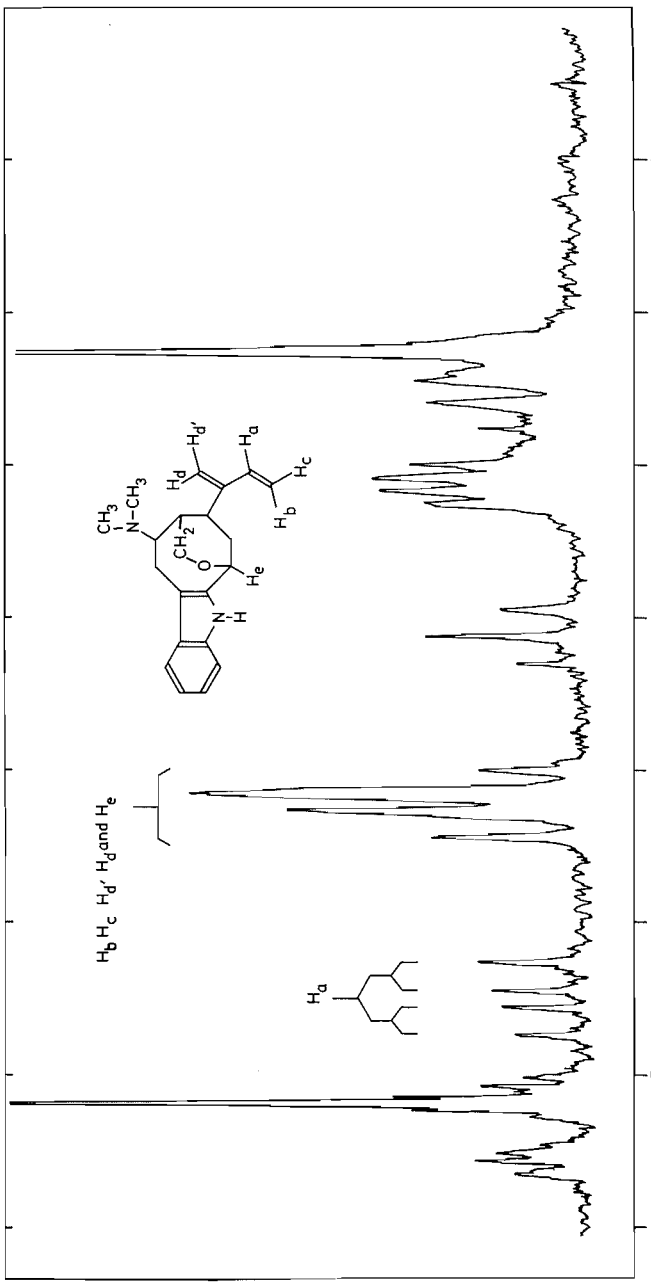

FIG. 3. The n.m.r. spectrum (60 MHz) of taberpsychine methine in deuteriochloroform (TMS = 0 p.p.m.).

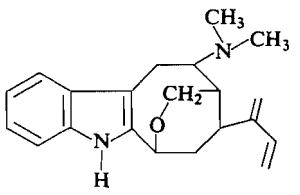

7

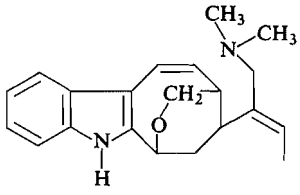

8

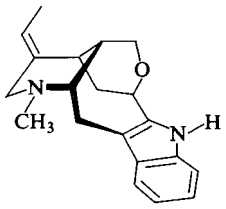

9

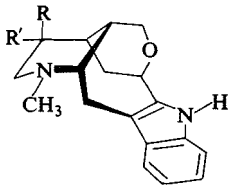

10

a R = H; R′ = Et
b R = Et; R′ = H

forded a major product, $C_{21}H_{26}N_2O$, whose u.v. spectrum shows the presence of a conjugated diene in addition to the original indole residue. The n.m.r. spectrum of this taberpsychine-methine shows a complex (5H) pattern in the region where the absorption for olefinic protons is expected (see Fig. 3). The pattern is further complicated by the presence in the same area, of the absorption due to the C-3 proton adjacent to the aromatic ring and the oxygen atom. The product obtained by hydrogenation of the methine showed two saturated *C*-methyl signals in the n.m.r. spectrum hence the conjugated diene could only be formed by elimination of one of the protons in the methyl group and migration of the double bond to open the piperidine ring, leaving the nitrogen attached to the eight-membered ring. The structure of this degradation product was assigned as shown in **7**. A very minor product of this Hofmann degradation was observed by t.l.c. but could not be isolated. This is probably the isomer of the diene as depicted in **8**.

The problem of the stereochemistry of taberpsychine is almost reduced to a question of absolute stereochemistry, since once the configuration at one of the asymmetric centers is fixed, the closing of the rings determines the configuration at the other centers. Thus the alkaloid has either the stereochemistry shown in structure **4** or its complete mirror image. The vinylogous Hofmann degradation of taberpsychine methiodide to give the diene **7** is understandable since the two activated "benzylic" protons at C-6 are not suitably disposed to allow facile *trans*-elimination. Examination of molecular models of taberpsychine suggests that the hydrogenation of the exocyclic double bond would be specifically from that face of the molecule which would lead to an equatorial ethyl group as in **10***a*. Hydrogenation from the other face, which should give the axial ethyl residue (as in **10***b*) is seriously hindered by the eight-membered ring and the aromatic system. The results of the Hofmann degradation of the methiodide of the dihydrotaberpsychine **10***a* show that the predominant reaction involves the elimination of one of the protons at C-6 adjacent to the indole ring. It would be difficult to rationalize this observation on the basis of structure **10***b* where the equatorial hydrogen substituent, introduced by hydrogenation, is stereochemically well situated for a *trans*-elimination.[3]

Another alkaloid obtained from *T. psychotrifolia* analyzed for $C_{20}H_{24}N_2O_2$ and its particular u.v. spectrum [λ_{max} 224 (10 000) and 318 (12 000)] permitted its classification as an α-acyl indole.

The i.r. spectrum confirms the presence of the

[3]We realize that the structural elucidation of taberpsychine is based almost entirely on spectral evidence. Although we had a large amount of alkaloid available for degradative studies, some 40 different experiments aimed at the isolation of other degradation products failed (J. D. Medina (8)).

Can. J. Chem. Downloaded from www.nrcresearchpress.com by 210.87.254.6 on 09/05/12
For personal use only.

Can. J. Chem. Downloaded from www.nrcresearchpress.com by 210.87.254.6 on 09/05/12
For personal use only.

carbonyl group (strong band 1650 cm^{-1}) as well as that of the aromatic moiety and the indolic NH. This spectrum also shows the presence of a hydroxyl group. The n.m.r. spectrum was difficult to perform due to the only slight solubility of the base in most organic solvents, but the problem was partly solved by the use of a hot saturated chloroform solution. The spectrum showed the presence of a methyl group attached to the basic nitrogen (singlet 2.53 δ) and of a methyl group on a tri-substituted double bond (1H quartet 5.40 δ, $J = 6$ Hz and 3H triplets 1.68 δ, $J = 6$ Hz).

Acetylation of the base with acetic anhydride in pyridine at room temperature gives a monoacetate (molecular weight by mass spectrometry 366) and while this product is rather unstable it could be characterized spectrally. The i.r. spectrum proves that it is an *O*-acetyl derivative (peaks at 1745 and 1235 cm^{-1}) and the n.m.r. spectrum reveals that the acetyl methyl is unusually shielded (3H singlet 1.77 δ). The most useful information, however, is given by the mass spectra since that of the base itself shows two major peaks at 152 and 122 *m/e* while in the acetate one finds a new peak at 194 *m/e* (42 mass units from 152 *m/e*).

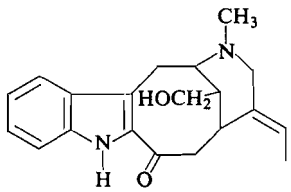

11

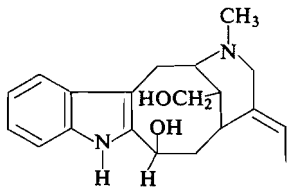

12

The structure proposed, which is justified by the mass spectrum is identical with that proposed for affinine **11**, (4) and although the physical constants given in the literature for the latter were misleading, the base is in fact affinine and this was confirmed by reduction by sodium borohydride to vobasinediol **12**.

That the stereochemistry at C-16 is as shown can be readily seen from the extreme shielding of the acetyl methyl (3H singlet 1.77 δ) observed in the n.m.r. spectrum of the *O*-acetyl derivative. In vobasine, the same shielding is observed for the methyl of the ester group, this appearing at 2.63 δ.

A third alkaloid, $C_{20}H_{22}N_2O_3$, is a high melting compound (m.p. 295° dec.) only sparingly soluble in most organic solvents which suggested it to be a salt. However, no anion was detectable pointing to an internal salt or amino acid. The u.v. spectrum of the base [λ_{max} 238 (13 100) and 316 (20 000) mμ] is that of an α-acyl indole and the i.r. spectrum presents two very typical bands in the region for carbonyl groups. One of them at 1650 cm^{-1} is assigned, in agreement with the u.v. spectrum, to a keto group on C-3 conjugated to the indole moiety and the other at 1610 cm^{-1}, a very strong band which is only compatible with a carboxylate carbonyl. The n.m.r. spectrum (performed in 2% D_2SO_4 in D_2O solution) shows the presence of an *N*-methyl group (3H singlet at 3.00 δ, displaced to lower field due to the quaternization of the basic nitrogen) and of an exocyclic ethylidene chain (1H quartet 5.93 δ and 3H doublet 1.68 δ, $J = 7$ Hz) in addition to the absorption expected from the indolic residue.

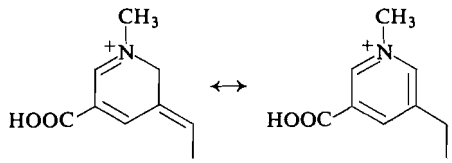

13

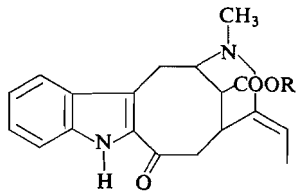

14

a R = H
b R = CH_3

The mass spectrum of the base presents its principal peak at 122 *m/e*, very typical fragmentation in the mass spectrometric degradation of vobasine-like alkaloids. Another important peak is that at 166 *m/e* (44 mass units = COO from

Can. J. Chem. Downloaded from www.nrcresearchpress.com by 210.87.254.6 on 09/05/12
For personal use only.

122) which coupled to the evidence for the presence of an acidic residue in the molecule, leads to the conclusion that the latter is attached to the six-membered ring producing the pyridinium ion **13** in the fragmentation.

Based on this evidence the alkaloid was assigned structure **14***a*, which is that of 16-epi-vobasinic acid previously prepared by Renner (5) but never before reported as a natural product. All spectral data are in agreement with this structure, including the fragmentation in the mass spectrum.

Confirmation for the structure is provided by methylation of the base by prolonged treatment with diazomethane. The i.r. spectrum of the product obtained shows the absorption typical of esters (1740 cm^{-1}), while the n.m.r. spectrum shows it is a methyl ester (3H singlet 3.53 δ). The position of the absorption for the methyl group of the ester in the spectrum determines the stereochemistry at C-16, as being epimeric to that in vobasine where the same absorption shows the methyl group of the ester to be very shielded (3H singlet 2.63 δ) presumably because it lies immediately above the electronic cloud of the aromatic ring.

The methylated derivative **14***b* presents the same physical properties, and the i.r., n.m.r., and mass spectra are identical with those of *16-epi-vobasine* given in the literature (5).

Experimental

Melting points are uncorrected. Unless otherwise stated, the conditions and instruments employed for the various spectra were as follows: u.v., ethanol solutions (ε in parentheses); i.r., KBr pellets, Beckmann I.R.4; n.m.r., deuteriochloroform solutions with tetramethylsilane protons taken as 0 p.p.m., Varian A 60; mass spectra, AEI MS-9 and Varian M-66 spectrometers.

Extraction and Isolation of the Alkaloids

The ground trunk bark (6.5 kg) was extracted with methanol, until the alcoholic extract gave a negative reaction with Vassler's reagent. Evaporated to dryness this extract yielded a brown tar, which was triturated five times with 200 ml fractions of 2% hydrochloric acid. The acidic solution was then continuously extracted with chloroform to separate non-basic materials. From this chloroform, after concentration and cooling, was obtained the soluble hydrochloride of *taberpsychine* (6.627 g).

The aqueous solution was then basified with ammonia and again continuously extracted with chloroform. The chloroform containing the basic material yielded, on cooling, a black powder (1.505 g) which was filtered, redissolved in 2% hydrochloric acid, and extracted once with chloroform. This chloroform was discarded and the aqueous solution neutralized with ammonia then extracted with chloroform four times. The chloroform was taken to dryness and the white amorphous *16-epi-vobasinic* acid (454 mg) was obtained.

The chloroform solution containing the bases was evaporated to dryness to give a semi-solid tar (61 g; total crude bases: 68.08 g). Part of the crude bases (10 g) was dissolved in acetone–ethanol and on slow evaporation a fine precipitate was obtained. Filtered and washed with cold acetone, it resulted in a mixture of 16-epi-vobasinic acid and affinine (300 mg). Both materials are virtually insoluble in all solvents, but affinine is slightly soluble in hot methanol and so the mixture was separated by boiling the solid in methanol and filtering while hot. Affinine (180 mg) precipitated from the methanol solution as an amorphous solid.

Another portion of the crude base (25 g) was submitted to a countercurrent distribution with acetate buffer, p*H* 3.4 (25 ml), using chloroform as stationary phase (25 ml), for a total of 50 transfers.

Fractions 1 to 7 (10 g) contained only neutral material and were not investigated further. Fractions 18 to 40 (12.7 g) yielded taberpsychine. Fractions 41 to 50 (1.22 g) yielded affinine.

Taberpsychine

The base was recrystallized from acetone and sublimed for analysis, m.p. 208° (dec.), $[\alpha]_D$ −243°; λ_{max} 222 (33 100), 272 (sh. 6500), 280 (7500), and 286 mμ (6650); ν_{max} 3241 (NH), 2747 (*N*-methyl), 744 and 728 cm^{-1} (aromatic).

The n.m.r. spectrum δ: 1H singlet 8.42 (NH); 4H multiplet 7.07–7.66 (aromatic); 1H broad quartet 5.38, J = 6.5 Hz, and 3H doublet of doublets, J = 6.5 and 2.0 Hz (ethylidene side chain); 3H singlet 2.53 (*N*-methyl); 1H doublet of doublets 5.13, J = 10 and 2 Hz (C_3—H); 2H AB quartet 2.93 and 3.60, J = 14 Hz (C-21 methylene). Mass spectrum: 308.1849 (M^+; $C_{20}H_{24}N_2O$ requires 308.1887), 293, 279, 154, 130, 122, 121, 108, 107 *m/e*.

Anal. Calcd. for $C_{20}H_{24}N_2O$: C, 77.9; H, 7.8; N, 9.1; O, 5.2. Found: C, 77.9; H, 8.0; N, 9.0; O, 5.2.

Taberpsychine Methiodide

Taberpsychine (409 mg) was dissolved in acetone (10 ml) and methyl iodide (0.5 ml) added. The solution was refluxed for a few min and then cooling gave white needles of taberpsychine methiodide which was recrystallized from acetone, m.p. 272–274° (dec.); λ_{max} 222 (34 400), 276 (sh. 7200) and (7800) mμ; ν_{max} 3170 (NH), 2830 (*N*-methyl), and 780 (aromatic) cm^{-1}.

The n.m.r. spectrum δ : 1H singlet 8.35 (NH); 4H multiplet 7.00–7.87 (aromatic); 1H broad quartet 5.43, J = 7 Hz, and 3H broad doublet 1.65, J = 7 Hz (ethylidene side chain); 3H singlet 3.28, and 3H singlet 3.03 (2 *N*-methyls); 1H doublet of doublets 5.23, J = 10 and 2 Hz (C_3—H). Anal. Calcd. for $C_{21}H_{27}N_2OI$: C, 56.0; H, 6.0; N, 6.2; O, 3.6; I, 28.2. Found: C, 55.7; H, 5.8; N, 6.4; O, 3.9; I, 28.1.

Can. J. Chem. Downloaded from www.nrcresearchpress.com by 210.87.254.6 on 09/05/12
For personal use only.

3-Ethyl Pyridine from Taberpsychine

Sublimed taberpsychine (194 mg) was mixed with dried zinc dust (1 g) and heated in a sealed tube at 280° for 3 h. A yellow distillate obtained in the cooler part of the tube protruding from the block was dissolved in methanol and analyzed in the gas chromatograph [Apiezon L 10%]. The spectrum shows two peaks (3:1 ratio) with retention times of 6 and 12.5 min respectively at a column temperature of 130° and increasing at the rate of 1°/min, which were identified by direct comparison as corresponding to 3-ethyl pyridine and 3-methyl-5-ethyl pyridine respectively. The major fraction was recovered and dissolved in deuterated chloroform. The n.m.r. spectrum δ : 2H multiplet 8.27–8.47 (H-2 and -6); 1H broad doublet 7.40, J = 8 Hz (H-4); 1H quartet 7.03 and 7.13 J = 8 Hz (H-5); 2H quartet 2.62, J = 7 Hz, and 3H triplet 1.22, J = 7 Hz (ethyl chain).

Dihydrotaberpsychine

Taberpsychine (1.210 g) was dissolved in ethanol (100 ml) and platinum oxide (500 mg) added together with glacial acetic acid (10 ml). After shaking for 50 h in an atmosphere of hydrogen (50 p.s.i.), the catalyst was filtered off and the alcoholic solution evaporated to dryness under reduced pressure. The resulting brown foam was redissolved in 2% hydrochloric acid, basified with ammonia, and extracted four times with chloroform which was evaporated to dryness. The product (1.150 g) was dissolved in acetone and the dihydrotaberpsychine obtained as white crystals, m.p. 191–193°; λ_{max} 223 (34 100), 277 (sh. 9000), 284 (9800), and 293 (8300) mμ; ν_{max} 3271 (indole NH), 2788 (*N*-methyl), 745 and 726 aromatic cm^{-1}

The n.m.r. spectrum δ : 4H multiplet 7.00–7.80 (aromatic); 1H doublet of doublets 5.12, J = 10 and 2 Hz (C_3—H); 3H singlet 2.53 (*N*-methyl); 3H triplet 0.98, J = 7 Hz (methyl in saturated ethyl side chain). Mass spectrum: 310 (M^+), 295 (M-15), 279 (M-31), 265, 251, 195, 180, 170, 168, 155 *m/e*. (M^{++}), 144, 138, 130, 124, 122, 108 *m/e*.

Anal. Calcd. for $C_{20}H_{26}N_2O$: C, 77.4; H, 8.4; N, 9.0; O, 5.2. Found: C, 77.2; H, 8.4; N, 8.9; O, 5.4.

Dihydrotaberpsychine Methiodide

Dihydrotaberpsychine (650 mg) was dissolved in acetone (15 ml) and methyl iodide (2.5 ml) was added to the warm solution. The mixture was boiled for 5 min and then allowed to cool. The amorphous dihydrotaberpsychine methiodide obtained was recrystallized from acetone, m.p. 255–258° (dec.); λ_{max} 221 (55 200), 275 (sh. 10 900), 284 (11 700), and 292 (10 400) mμ.

Anal. Calcd. for $C_{21}H_{29}N_2OI$: C, 55.8; H, 6.5; N, 6.2; O, 3.5; I, 28.1. Found: C, 55.7; H, 6.5; N, 6.3; O, 3.6; I, 28.3.

Dihydrotaberpsychine-methine

Dihydrotaberpsychine methiodide (550 mg) was suspended in *tert*-butyl alcohol (15 ml) and a solution (25 ml) of potassium (1 g) in *tert*-butyl alcohol added slowly. The mixture was refluxed for 24 h, then evaporated to dryness under reduced pressure, the residue was redissolved in water and the aqueous solution extracted four times with chloroform. The dihydrotaberpsychine-methine (418 mg) was obtained as a pale yellow foam which was crystallized from acetone and sublimed for analysis, m.p. 153–155°; λ_{max} 229.5 (38 500), 271 (12 000), 284 (11 400), and 294 (sh. 9000) mμ; ν_{max} 3250 (indole NH), 2820 and 2760 (*N*-methyl), 745 and 730 (aromatic) cm^{-1}.

The n.m.r. spectrum δ : 1H singlet 8.84 (indole NH); 4H multiplet 7.00–7.64 (aromatic); 1H doublet 6.69, J = 12 Hz (C_6—H) and 1H doublet of doublets 5.55, J = 12 and 8 Hz (C_5—H), both being the low field portion of an ABX system; 1H doublet of doublets 4.84, J = 12 and 2Hz (C_3—H); AB part of a second ABX system; 1H doublet 4.21, J = 11 Hz and 1H triplet 3.79, J = 11 Hz (methylene adjacent to oxygen in the oxide ring); 6H singlet 2.20 (*N*-dimethyl); 3H triplet 0.87, J = 7 Hz (methyl on saturated ethyl side chain). Mass spectrum: 324 (M^+), 310, 295, 280, 266, 194, 185, 180, 169, 168, 162 (M^{2+}), 156, 137, 130, 124, 58 *m/e*. Mol. wt. by mass spectrometry: 324.2175. $C_{21}H_{28}N_2O$ requires: 324.2202.

A minor product which could not be induced to crystallize was identified by means of its n.m.r. spectrum as the other isomer of dihydrotaberpsychine-methine (structure **6**). The n.m.r. spectrum δ : principal feature was a pair of doublets at 4.97 and 5.63, J = 2 Hz due to a terminal methylene.

Hydrogenation of Dihydrotaberpsychine-methine

Dihydrotaberpsychine-methine (400 mg) was dissolved in ethanol (50 ml), platinum oxide (150 mg) and glacial acetic acid (15 ml) were added, and the mixture left hydrogenating for 24 h (50 p.s.i.). The reaction mixture was then filtered and evaporated to dryness under reduced pressure. The residue was dissolved in water, basified with ammonia, and extracted with chloroform yielding a yellow foam (340 mg). This foam was dissolved in acetone and the crystalline derivative obtained was recrystallized from the same solvent, m.p. 184–186°; λ_{max} 224.5 (46 000), 279 (sh. 11 050), 285 (12 000), and 293 (10 300) mμ; ν_{max} 3250 (indole NH), 2750 (*N*-methyl) and 740 (aromatic) cm^{-1}.

The n.m.r. spectrum δ : 1H broad singlet 9.23 (indole NH); 4H multiplet 6.92–7.73 (aromatic); 1H broad doublet 5.10, J = 10 Hz (C_3—H); 6H singlet 2.20 (*N*-methyls); 3H triplet 0.85, J = 7 Hz (methyl in saturated ethyl side chain). Mass spectrum: 326.2362 (M^+; $C_{21}H_{30}N_2O$ requires: 326.2358), 282, 281, 268, 226, 225, 180, 168, 156, 144, 130 *m/e*.

Anal. Calcd. for $C_{21}H_{30}N_2O$: C, 77.3; H, 9.3; N, 8.6; O, 4.9. Found: C, 77.5; H, 9.2, N, 8.4; O, 5.1.

Taberpsychine-methine

Taberpsychine methiodide (1.687 g) was suspended in *tert*-butyl alcohol and a solution (25 ml) of potassium (1 g) in *tert*-butyl alcohol added. The suspension was refluxed for 18 h and then taken to dryness under reduced pressure, redissolved in water and extracted with ether to give a brown foam (1.200 g). After redissolving the foam in ether and reducing the solution to a small volume, taberpsychine-methine crystallized selectively (589 mg). Recrystallization was from ether, m.p. 194–196° (dec.); λ_{max} 224 (46 300), 278 (sh. 8800), 284 (9200), and 292.5 (8100) mμ; ν_{max} 3270 (indole NH), 3075 (aromatic), 2766 (*N*-methyl), 1590, 740 and 725 (aromatic) cm^{-1}.

The n.m.r. spectrum δ : 1H broad singlet 8.18 (NH);

Can. J. Chem. Downloaded from www.nrcresearchpress.com by 210.87.254.6 on 09/05/12
For personal use only.

4H multiplet 6.98–7.64 (aromatic); 1H doublet of doublets 6.40 and 6.51, $J = 18$ and 11 Hz (H_a); 1H doublet 5.28, $J = 18$ Hz (H_b); 1H doublet 5.21, $J = 11$ Hz (H_c); 2H doublet 5.22, $J = 8$ Hz (2-H_d); 1H doublet 5.09, $J = 11$ Hz (C_3—H); 6H singlet 2.27 (2-*N*-methyl). Mass spectrum: 322 (M^+), 278 (M-N(CH_3)$_2$), 215, 194, 183, 180, 168, 156, 136, 130 *m/e*.

Anal. Calcd. for $C_{21}H_{26}N_2O$: C, 78.2; H, 8.1; N, 8.7; O, 5.0. Found: C, 78.1; H, 8.0; N, 8.5; O, 5.0.

A minor product was observed by t.l.c. but could not be isolated. This is probably the other isomer formed in small quantity.

Hydrogenation of Taberpsychine-methine

Taberpsychine-methine (429 mg) was dissolved in ethanol (50 ml) containing acetic acid. Platinum oxide (200 mg) was added and the mixture shaken for 18 h under hydrogen (50 p.s.i.). The solution was then filtered, evaporated to dryness under reduced pressure, and the residue redissolved in water, basified with ammonia, and extracted with ether. The ether was evaporated to dryness and a white foam (400 mg) was obtained. The tetrahydro compound was crystallized from acetone–ether and sublimed, m.p. 153–155°; λ_{max} 225 (29 300), 278 (7500). 284.5 (8100), and 293 (7050) mμ; ν_{max} 3250 (indole NH), 2766 (*N*-methyl), 740 and 730 (aromatic) cm^{-1}.

The n.m.r. spectrum δ : 1H broad singlet 8.82 (indole NH); 4H multiplet 6.97–7.73 (aromatic); 1H broad doublet 5.12, $J = 10$ Hz (C_3—H); 6H singlet 2.35 (*N*-methyls); 3H triplet 1.25, $J = 9$ Hz, and 3H doublet 0.93, $J = 6$ Hz (saturated methyls).

Anal. Calcd. for $C_{21}H_{30}N_2O$: C, 77.3; H, 9.3; N, 8.6; O, 4.9. Found: C, 77.2; H, 9.3; N, 8.3; O, 4.9.

Affinine

The very insoluble base was recrystallized from a large volume of ethanol and sublimed for analysis, m.p. 273–275° (dec.); λ_{max} 236 (sh. 13 200) and 320 (13 400) mμ; ν_{max} 3150 (broad, NH and OH), 2800 (*N*-methyl), 1650 (3-keto), 740 (aromatic) cm^{-1}.

The n.m.r. spectrum δ : 1H broad singlet 9.80 (indole NH); 4H multiplet 7.00–7.83 (aromatic); 1H broad quartet 5.40, $J = 6$ Hz, and 3H broad doublet 1.68, $J = 6$ Hz (ethylidene side chain); 3H sharp singlet 2.53 (*N*-methyl). Mass spectrum: 324 (M^+), 293 (M-CH_2OH), 158, 152, 122, 108 *m/e*.

Anal. Calcd. for $C_{20}H_{24}N_2O_2$: C, 74.0; H, 7.5; N, 8.6; O, 9.9. Found: C, 73.8; H, 7.5; N, 8.5; O, 10.0.

Affinine Acetate

Affinine (150 mg) was dissolved in pyridine (5 ml) and an excess of acetic anhydride (1 ml) added. The mixture was left standing overnight at room temperature. Methanol was then added to hydrolyze the excess anhydride and the solution evaporated to dryness under reduced pressure. The residue was redissolved in water, basified with ammonia, and the aqueous solution extracted with chloroform. The product is very unstable and decomposes while in solution, so crystallization was not possible. However i.r., n.m.r., and mass spectra indicate that it is indeed monoacetate of the base; λ_{max} (qualitative) 223 (shoulder), 237 (shoulder), and 319 mμ; ν_{max} 3300 (indole NH), 1745 and 1235 (O-acetyl), 1650 (3-keto), 1575 and 740 (aromatic) cm^{-1}.

The n.m.r. spectrum δ : 1H singlet 9.80 (indole NH); 4H multiplet 7.00–7.84 (aromatic); 1H broad quartet 5.40, $J = 6$ Hz and 3H doublet 1.67, $J = 6$ Hz (ethylidene side chain); 3H singlet 2.53 (*N*-methyl); 3H singlet 1.77 (*O*-acetyl). Mass spectrum: 366 (M^+), 306 (M-acetic acid), 293 (M-CH_3COOCH_2), 263, 194, 158, 122 *m/e*.

Vobasinediol (from Affinine)

Affinine (110 mg) was suspended in absolute methanol (25 ml), an excess of sodium borohydride (100 mg) was added, and the mixture left standing overnight at room temperature. Water (200 ml) was then added and the aqueous solution extracted with ether. After evaporation to a small volume, colorless needles of vobasinediol (100 mg) were obtained and sublimed for analysis, m.p. 244–245° (dec.), $[\alpha]_D$ −60° (methanol); λ_{max} 224 (21 600), 283 (6100), and 291 (5400) mμ; ν_{max} 3300 (NH and OH), 2280 (*N*-methyl), 740 (aromatic) cm^{-1}.

The n.m.r. spectrum δ : 1H singlet 9.75 (indole NH); 4H multiplet 6.90–7.62 (aromatic); 1H broad quartet 5.47, $J = 7$ Hz and 3H broad doublet 1.68, $J = 7$ Hz (ethylidene side chain); 1H broad doublet 5.27, $J = 6$ Hz C_3—H); 3H singlet 2.43 (*N*-methyl). Mass spectrum: 326 (M^+), 308 (M-H_2O), 293 (M-H_2O-15), 277 (M-H_2O-CH_2-OH), 183, 180, 154, 152, 136, 130, 122 *m/e*.

Anal. Calcd. for $C_{20}H_{26}N_2O_2$: C, 73.6; H, 8.0; N, 8.6; O, 9.8. Found: C, 73.6; H, 8.0; N, 8.4; O, 9.7.

16-epi-Vobasinic Acid

The base was recrystallized several times from large volumes of hot ethanol, m.p. 295° (dec.); λ_{max} 238 (13 100) and 316 (20 000) mμ; ν_{max} 3105 (indole NH), 1650 (3-keto), 1610 (carboxylate), and 753 (aromatic) cm^{-1}.

The n.m.r. spectrum δ : (in 2% D_2SO_4/D_2O solution) 4H multiplet 6.88–7.77 (aromatic); 1H broad quartet 5.93, $J = 7$ Hz and 3H broad doublet 1.68, $J = 7$ Hz (exocyclic ethylidene); 3H singlet 3.00 (*N*-methyl on quaternary nitrogen. Mass spectrum: 338 (M^+), 293 (M-COOH), 180, 166, 158, 122 *m/e*.

Anal. Calcd. for $C_{20}H_{22}N_2O_3$: C, 71.0; H, 6.6; N, 8.3; O, 14.2. Found: C, 70.8; H, 6.6; N, 8.0; O, 14.4.

16-epi-Vobasine (from 16-epi-Vobasinic Acid)

16-epi-Vobasinic acid (200 mg) was suspended in dry methanol (20 ml) and ethereal diazomethane solution (20 ml) added. The mixture was refluxed overnight on a water bath. The solution was then evaporated to dryness and redissolved in ether. 16-epi-Vobasine (190 mg) crystallized on slow evaporation and was recrystallized from ether, m.p. 185–187°; λ_{max} 237 (10 550) and 320 (12 000) mμ; ν_{max} 3300 (indole NH), 2750 (*N*-methyl), 1740 (methyl ester), 1645 (3-keto) and (aromatic) cm^{-1}.

The n.m.r. spectrum δ : 1H broad singlet 9.57 (indole NH); 4H multiplet 7.00–7.83 (aromatic); 1H broad quartet 5.51, $J = 7$ Hz and 3H broad doublet 1.73, $J = 7$ Hz (exocyclic ethylidene); 3H singlet 3.53 (methyl ester); 3H singlet 2.52 (*N*-methyl). Mass spectrum: 352 (M^+), 293 (M-$COOCH_3$), 180, 166, 158, 122 *m/e*.

Anal. Calcd. for $C_{21}H_{24}N_2O_3$: C, 71.6; H, 6.9; N, 8.0; O, 13.6. Found: C, 71.5; H, 6.8; N, 8.0; O, 13.6.

We thank the National Research Council of Canada for financial assistance and the Instituto Venezolano de Investigaciones Cientificas for an Overseas Bursary (to J.D.M.). We are indebted to G. Agostini (Botanical Gardens, Caracas, Venezuela) for assistance with identifying and collecting the plant material.

1. K. BIEMANN and G. SPITELLER. J. Amer. Chem. Soc. **84**, 4578 (1962).
2. J. SZMUSZKOVICZ. J. Amer. Chem. Soc. **82**, 1180 (1960).
3. J. M. BRUCE. J. Chem. Soc., 2366 (1959).
4. J. A. WEISBACH, R. F. RAFFAUF, O. RIBEIRO, E. MACKI, and B. DOUGLAS. J. Pharm. Sci. **52**, 350 (1963).
5. U. RENNER, D. A. PRINS, A. L. BURLINGAME, and K. BIEMANN. Helv. Chim. Acta. **46**, 2186 (1963).
6. P. R. BENOIN, R. H. BURNELL, and J. D. MEDINA. Tetrahedron Lett. 807 (1968).
7. J. J. DUGAN, M. HESSE, V. RENNER, and H. SCHMID. Helv. Chim. Acta. **52**, 701 (1969).
8. J. D. MEDINA. Ph.D. Thesis. Université Laval, Québec, Québec. 1968.

Can. J. Chem. Downloaded from www.nrcresearchpress.com by 210.87.254.6 on 09/05/12
For personal use only.

Kinetics of Thermal Decomposition of Aqueous Perchloric Acid

M. Patricia Henderson, Viola I. Miasek, and T. W. Swaddle[1]
Department of Chemistry, The University of Calgary, Calgary 44, Alberta

Received August 27, 1970

Thermal decomposition of 1.1–6.6 *m* aqueous perchloric acid at 295–322° yields oxygen, chlorine, and a small quantity of hydrochloric acid. The initial rates of decomposition have been measured, using a perchlorate ion activity electrode, and show 3.5 order dependence on the stoichiometric perchloric acid concentration; the corresponding rate coefficient and activation energy at 300.0° are $3.1 \times 10^{-7}\ m^{-2.5}\ s^{-1}$ and 84 kcal $mole^{-1}$, respectively. The order of reaction with respect to time is less than 3.5 and depends upon the initial perchloric acid concentration; this effect is due to acceleration of the decomposition by the reaction products, notably chloride ion. It is suggested that the rate-determining step in the decomposition of aqueous perchloric acid is the reaction of two undissociated $HClO_4$ molecules to give H_2O, ClO_3, and ClO_4.

Canadian Journal of Chemistry, 49, 317 (1971)

Can. J. Chem. Downloaded from www.nrcresearchpress.com by 210.87.254.40 on 09/05/12
For personal use only.

Perchloric acid is used extensively in physical studies of phenomena in aqueous solution, since it is the strongest of the common acids and also because its anion has remarkably little tendency to form complexes with metal ions. The aqueous acid is, however, thermodynamically unstable ($\Delta G^0 = -26.3$ kcal/$mole^{-1}$ at 25° for the hypothetical 1 *m* solution (1)) with respect to decomposition to oxygen, chlorine, and water, and it is clear that the kinetics of this decomposition must be known if the acid is to be used in extending studies of aqueous electrolyte solutions to high temperatures.

Accordingly, the present study was designed primarily to provide empirical rate data on the decomposition of aqueous perchloric acid as a function of temperature, and over a concentration range which would include the commonly-chosen "swamping electrolyte" values, 1–6 *m*. A literature search for such information was unsuccessful, although it has been reported (2) that no chlorine, DOCl, $DClO_2$, or $DClO_3$ can be detected spectroscopically in 1 *m* $DClO_4$ after several days in a titanium vessel with sapphire windows at 250°. On the other hand, the decomposition of 83–100% $HClO_4$ has received considerable attention (3–8), as has the decomposition of $HClO_4$ vapor (9–12).

Experimental

All the stock chemicals used in this study were "Baker Analyzed" reagent grade, with the exception of ammonium nitrate (Matheson, Coleman and Bell) and sodium nitrate (Fisher Certified reagent). The perchloric acid (72%) was used without further purification; the experimental results were independent of the manufacturer's batch. Lithium perchlorate trihydrate was made from lithium carbonate and perchloric acid. Distilled water was passed through Barnstead deionizer and organic removal cartridges before use. Red mercuric oxide was used as the primary standard in acidimetry. Spectrophotometric measurements were made using a Cary Model 15 spectrometer.

The pressure vessels used consisted of a cylindrical body (2.54 cm i.d. × 4.60 cm o.d.) of ATL-40 commercially pure titanium, 0.2% palladium alloy (Atlas Titanium, Welland, Ontario), with a plug of the same material, such that the cavity volume was 62.0 cm^3. The seal between plug and body was effected with a Teflon gasket contained between two Ti–0.2%Pd rings, after the manner of Gill and Marshall (13). Retaining pressure was applied to the plug through a bearing ring which transmitted the thrust of six bolts located in the top of the externally-fitted stainless-steel screw cap.

The Ti–0.2%Pd alloy was selected because of its high resistance to attack by chlorine in the presence of water, together with its low susceptibility to crevice corrosion (which is a particularly serious hazard where Teflon gaskets are used and where chloride ion may be present) (14). However, it was found that 6 *m* $HClO_4$ attacked the metal appreciably at 300°, with the production of an orange solution containing titanium, evidently in the form of the familiar Ti(IV)–peroxy complexes. Accordingly, the vessels were fitted with silica liners with loosely-fitting caps, for the purpose of kinetic studies involving $HClO_4$ at high temperatures; attack of the titanium by the gaseous reaction products was then negligible except when chloride ion was added in large amounts to the $HClO_4$, in which case very high chlorine pressures were developed and some $TiCl_4$ fumes were observed on opening the vessels. The volume occupied by the silica liner and its cap was 14.2 cm^3, and the capacity of the liner was about 30 ml.

Thermostating of the pressure vessels was achieved with a Blue M Conwate CW-160HF-1 forced-convection oven. The reaction temperature was measured with an iron–constantan thermocouple in conjunction with a Leeds–Northrup 742523-All potentiometer. A Thermoelectric Icell provided the cold-junction reference temperature (0.00 to 0.05°), and the hot junction was en-

[1]To whom correspondence should be addressed.

Can. J. Chem. Downloaded from www.nrcresearchpress.com by 210.87.254.40 on 09/05/12
For personal use only.

closed in a thin-walled Pyrex sheath and immersed in Dow-Corning 560 silicone fluid contained in a dummy pressure vessel. The thermocouple was standardized frequently, either against a platinum resistance thermometer traceable to N.B.S., or against Fisher T-421 Ther-Metric fusion-point standards (notably anthraquinone, triple point 284.59 ± 0.05°).

With correct positioning of the pressure vessels in the oven and adequate stability of the room temperature, the reaction temperatures were constant within ±0.2° or better in the course of a kinetic experiment; where larger temperature uncertainties are stated, these reflect differences in the absolute value of the thermoregulator set-point from one set of experiments to another.

A Lauda NS-HT thermostat bath was used for calibrations against the platinum resistance thermometer, and for some experiments involving sampling of the gaseous reaction products. The latter employed the same pressure vessels but with the usual plug replaced by one having a long stem protruding 10 cm beyond the pressure vessel cap. This plug, of Ti–0.2% Pd alloy, had a narrow axial bore which led to a stainless-steel high-pressure valve; the upper part of the plug stem extended out of the bath and was cooled with circulating water so as to protect the valve from corrosion. However, decomposition of the best available bath oils (Lauda Ultratherm 330S Circulating Fluid, and Dow Corning 560 Silicone Fluid) was so extensive when operating at 300° that the NS-HT bath could be used only for a few brief experiments and calibrations.

In a typical kinetic run, 20.0 ml aliquots of perchloric acid solution, of which both the hydrogen-ion and perchlorate contents had been measured, were placed in the silica liners, capped, and sealed in the pressure vessels under a nitrogen atmosphere. The vessels were placed in the overheated oven, so that the oven and vessel temperatures converged more rapidly upon the set-point. Thermal equilibrium was achieved in less than 50 min even at 322°, but the reaction time was reckoned from the time at which the monitored dummy vessel was within 5° of the set-point (in effect, 35–40 min after insertion of the vessels). After a chosen reaction time, a vessel would be removed from the oven and chilled rapidly with cold water. The vessels were opened cautiously in the hood, the compressed gaseous products (chlorine and oxygen) being allowed to dissipate before removal of the screw-cap, and the contents of the liner and the condensate in the pressure vessel were transferred quantitatively to 50 ml graduated flasks and made to the mark with water.

After dilution so that $0.01\ M < [ClO_4^-] < 0.10\ M$, the ionic strength was adjusted to 1.0 M with sodium nitrate, and the pH was made to about 5 with the minimum amount of concentrated NaOH solution, added with a syringe burette. The perchlorate ion concentration was then determined with an Orion 92-81 perchlorate ion activity electrode in conjunction with a Beckman Research Model pH Meter and an Orion 90-02 double junction reference electrode in which the outer chamber was filled with 10% NH_4NO_3 solution.

The sample was thermostated (20.5 ± 0.1°) and gently stirred magnetically while reading the electromotive force (e.m.f.); most of the dissolved chlorine escaped to the air, and in any event did not affect the electrode response. The e.m.f. reading was converted to perchlorate ion concentration using a calibration curve which had been set up in the same way with five standard $HClO_4$ solutions spanning the range 0.01–0.10 M; plots of e.m.f. *vs.* log $[ClO_4^-]$ were invariably linear to a high degree, but a fresh calibration curve was necessary for each set of measurements. The stoichiometric perchlorate concentration so determined was accurate to ±2.0% or better, but other factors such as leakage of gases during the kinetic runs could have introduced greater uncertainties. In general, triplicate kinetic measurements agreed to within ±3.0%. Concentrations were measured on the molar scale, for convenience, and subsequently converted (where possible) to the molal scale, using the density data of Markham (15) as adapted by Robertson (16).

Hydrogen ion concentrations were measured in a similar way, prior to pH adjustment, using a Beckman Futura 39311 glass electrode.

Potentiometric titration of perchlorate with tetraphenylarsonium chloride (17) was also tried, using the Gran method (18), but the procedure was no more accurate and much less convenient than the direct-reading method, and in any event standardization of the arsonium salt solution is necessary.

The chloride ion contents of some samples were determined using an Ag/AgCl electrode, although the residual chlorine in the solution affected the electrode response. Nevertheless, it was established that chloride ion was not a major reaction product; such HCl as was present in the solutions at 20° probably came from reactions 1 and 2.

$$[1] \qquad Cl_2 + H_2O \rightleftharpoons HOCl + H^+ + Cl^-$$

$$[2] \qquad 2HOCl \rightarrow 2HCl + O_2$$

Attempts were made to follow the decomposition of $HClO_4$ by iodometric titration of the chlorine produced, but the reproducibility of the results was poor and the yields of chlorine were less than those expected on the basis of the corresponding perchlorate concentrations. These inconsistencies arose partly from the hydrolysis of chlorine to HOCl and HCl, but mainly from leakage of gases from the reaction vessel on chilling, which often lead to gasket failure. There was no evidence of high-temperature leakage in any of the experiments referred to in this report.

Results

Reaction Products

The absence of chlorine gas, and the absence of a detectable increase in $[Cl^-]$ or a decrease in $[H^+]$ or $[ClO_4^-]$, showed that 4 m $HClO_4$ does not undergo significant thermal decomposition in 13 h at 250°; at 300°, however, much chlorine was produced in the same time. The absorption spectrum of the latter solution showed a pronounced maximum at 325 mμ which is characteristic of aqueous chlorine (19), but the absence of other features in this region of the

Can. J. Chem. Downloaded from www.nrcresearchpress.com by 210.87.254.40 on 09/05/12
For personal use only.

spectrum indicated that ClO_2, ClO_2^-, and $HClO_2$ were not present in significant amounts (20).

Chloride ion was present in the decomposed $HClO_4$ solutions to the extent of 4% or less of the total chlorine in the decomposition products. This can be accounted for in terms of equilibrium 1, which is rather rapidly established at room temperature and for which the equilibrium quotient is $4 \times 10^{-4}\ M^2$ at 25° (21). Reaction 1 is endothermic ($\Delta H^0 = 5.06$ kcal mole^{-1}) at 25°, but the data of Connick and Chia (21) suggest $\Delta C_p^0 = -95$ cal deg^{-1} mole^{-1} at 25°, and, if this does not change greatly with temperature, it can be argued that equilibrium 1 will lie even further to the left at 300°. Thus, the chloride concentrations at 300° will remain rather small, despite the high pressures of chlorine gas developed in $HClO_4$ decompositions.

The direct vapor-phase hydrolysis of chlorine to HCl and oxygen is not favored thermodynamically at 300° (22, 23). However, HCl and O_2 may be the main products of aqueous $HClO_4$ decomposition at the critical temperature (24).

In the decomposition of pure aqueous $HClO_4$, the decrease in perchlorate ion content to a stoichiometric concentration c was invariably accompanied by a corresponding decrease in the hydrogen ion concentration to an amount exceeding c but not greater than 1.06 c. The slight excess of $[H^+]$ over $[ClO_4^-]$ is evidently a consequence of reactions 1 and 2, and it was therefore necessary to follow the progress of the decomposition of aqueous $HClO_4$ by analyzing for the stoichiometric perchlorate concentration, c. It is, however, clear that the overall stoichiometry of decomposition is

$$[3] \qquad 4H^+ + 4ClO_4^- \rightleftharpoons 2H_2O + 2Cl_2 + 7O_2$$

Kinetics of Decomposition of Aqueous Perchloric Acid

Preliminary results obtained at 300° showed that the *apparent* order of reaction with respect to *time* was dependent upon the initial concentration of c_0 of the perchloric acid. Thus, the perchlorate concentrations plotted against time in Fig. 1 refer to $c_0 = 6.61\ m$ and require an order of 2.6 in stoichiometric perchloric acid with respect to time, while the corresponding order is 1.5 when $c_0 = 2.26\ m$ (as is illustrated by the typical linear plot of $c^{-0.5}$ *vs.* time in Fig. 2). Similarly, at 306°, the apparent order with respect to time was 2.0 for $c_0 = 3.60\ m$, and at all temperatures studied the order was 1.5 when $c_0 = 2.26\ m$. These apparent orders of reaction are purely empirical and do not necessarily have any theoretical significance; they do, however, represent the experimental data adequately to at least 80% completion of reaction.

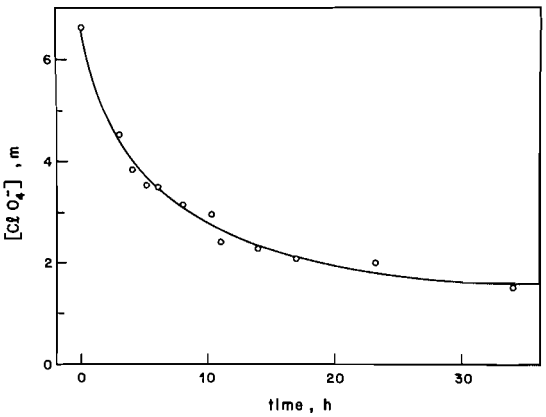

FIG. 1. Decomposition of 6.61 m perchloric acid at 300.0°.

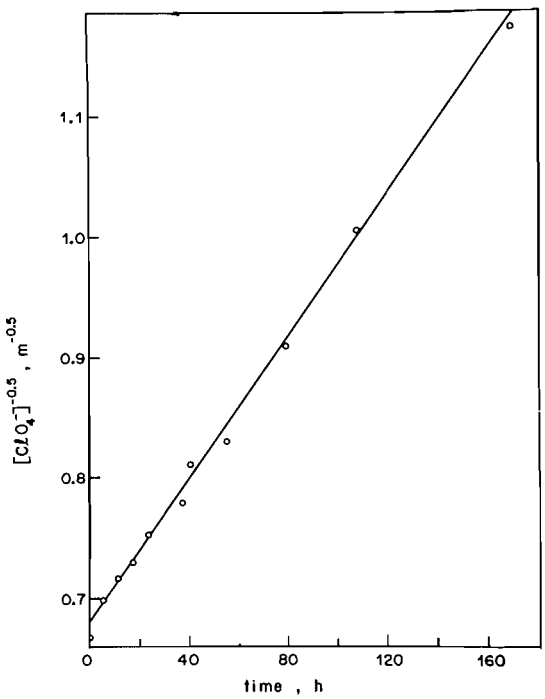

FIG. 2. Apparent 1.5-order kinetics of decomposition of 2.26 m perchloric acid at 300.0°.

Can. J. Chem. Downloaded from www.nrcresearchpress.com by 210.87.254.40 on 09/05/12
For personal use only.

TABLE 1. Initial rates of decomposition of aqueous perchloric acid

c_0, m	Temperature (°C)	$-dc/dt$ (m s^{-1}) as $c \rightarrow c_0$
6.61	300.0	2.2×10^{-4}
5.06	300.0	8.7×10^{-5}
3.59	300.0	2.3×10^{-5}
2.26	300.0	5.6×10^{-6}
1.09	300.0	5.3×10^{-7}
4.63	306.5	1.7×10^{-4}
3.60	306.0	5.1×10^{-5}
2.26	306.0	9.8×10^{-6}
1.02	306.5	1.1×10^{-6}

These results are typical of reactions in which the products cause acceleration of the reaction rate (25), and it is therefore necessary to determine the *true* order of the initial decomposition reaction (*i.e.*, the order with respect to *concentration*) by graphical estimation of the initial rate of decomposition, $-dc_0/dt$, as a function of the initial perchloric acid concentration c_0. The estimation of initial rates is subject to rather large uncertainties, as will be obvious from Fig. 1 (this being a worse case than most), but log–log plots of the data of Table 1 show very clearly that the order of reaction is 3.50 ± 0.05, at 300 and 306° at least

$$[4] \qquad -dc/dt = k_{3.5}c^{3.5}$$

where $k_{3.5}$ has the weighted mean values of 3.1×10^{-7} $m^{-2.5}$ s^{-1} at 300° and 5.7×10^{-7} $m^{-2.5}$ s^{-1} at 306.0°, the error limits being ±10% in either case.

In view of the difficulty of determining the initial rates of decomposition with sufficient accuracy from the sharply curved plots of c *vs.* time, the activation energy E was calculated using the *apparent* (1.5-order) rate coefficients for a fixed initial molality (2.26 m) of the acid. It is immaterial, for this purpose, that the apparent order with respect to time has no theoretical validity. We can write

$$[5] \qquad \ln(-dc_0/dt) = \ln k' + n' \ln c_0 = \ln k + n \ln c_0$$

where n and n' are the true and apparent reaction orders, and k and k' are the corresponding rate coefficients, respectively. Then,

$$[6] \qquad \ln k = (n' - n) \ln c_0 + \ln k' = \text{constant} + \ln k'$$

so that a plot of $\ln k'$ against $1/T$ will have the same slope as the Arrhenius plot for the true reaction order, so long as n' is independent of temperature and represents the data accurately.

Values of $k'_{1.5}$ over a 27° range of temperature are listed in Table 2. These, and all other data given in this article (except where otherwise stated), refer to 20.0 ml samples with a gas space of 27.8 cm^3 at 20°. Strictly speaking, a correction should be applied to the molalities measured at 20° for water removed into the vapor phase at high temperatures. This cannot be done with great accuracy, since the vapor pressure of water in aqueous $HClO_4$ at high temperatures is not accurately known, but we have assumed that it is the same fraction of the vapor pressure of pure water at high temperatures (26) as at 25° (27) and we have calculated the increase Δm in molality expected for 2.26 m $HClO_4$ at high temperatures, due allowance being made for the decrease in vapor volume brought about by expansion of the liquid phase (26). Estimates of Δm are listed in column 3 of Table 2; it will be seen that Δm is barely outside the experimental error, and accordingly we have chosen to ignore it except in column 4 of Table 2. The latter data show that the activation energy E for the thermal decomposition of dilute aqueous perchloric acid is $84._2$ kcal mole^{-1}, with a possible uncertainty of ±2 kcal mole^{-1}. The $k'_{1.5}$ data are reproduced by eq. 7 to within the experimental error

$$[7] \qquad \log_{10} k'_{1.5} = 26.37 - (18\,400/T)$$

The above analysis assumes that the decomposition of $HClO_4$ occurs in the solution, and not the vapor, phase. This supposition was shown to be correct by partially decomposing 15, 20, and 25 ml aliquots of 2.26 m $HClO_4$ at 306.0° for identical periods of time. The vapor spaces in the three vessels would be 26.3, 19.2, and 12.0 cm^3, and the relative rates of disappearance

TABLE 2. Apparent 1.5-order rate coefficients, $k_{1.5}'$, for $c_0 = 2.26$ m

Temperature (°C)	$10^6 k_{1.5}'$ ($m^{-0.5}$ s^{-1})	Δm (%)	$10^6 k_{1.5}^{corr.}$ ($m^{-0.5}$ s^{-1})
321.5±0.3	26.2	4.3	25.7
312.3±0.2	9.1	3.6	9.0
306.0±1.0	4.4_1	3.5	4.3
304.3±0.2	3.1_4	3.4	3.0_9
300.0±1.0	1.64	3.3	1.61
294.5±0.3	0.87	3.2	0.86

Can. J. Chem. Downloaded from www.nrcresearchpress.com by 210.87.254.40 on 09/05/12
For personal use only.

of $HClO_4$ should therefore have been about 1.4:1.0:0.6 if decomposition of $HClO_4$ vapor, in equilibrium with the dissolved acid, were the main contributor to the reaction rate (the negligible $HClO_4$ content of the condensate formed outside the liner proved that most of the $HClO_4$ remains in solution even at 322°). In fact, the reaction rates were rather similar and actually showed the opposite trend, if any at all (*e.g.*, after 90.8 h, the perchlorate concentrations remaining in the 20 and 25 ml samples were 0.507 and 0.490 *m*, respectively).

Addition of broken silica glass, such that the area of silica in contact with the solutions was more than doubled, produced no significant changes in the percentage decompositions per given time interval, within the experimental error. Thus, in 35.3 h, at 306.0°, 15 ml of 2.26 *m* $HClO_4$ decomposed to 1.26 *m* in the presence of about 5 ml crushed silica, while the corresponding figure for 20 ml of the same acid without added silica was 1.25 *m*; similarly, after 73.0 h, the corresponding data were 0.65 and 0.69 *m*. It may therefore be concluded that the reaction is a homogeneous one, in solution.

Thus far, the reaction order has been expressed in terms of the stoichiometric $HClO_4$ concentration; if the acid is completely dissociated, however, this order will represent the sum of the orders with respect to $[ClO_4^-]$ and $[H^+]$. The reaction rate is directly proportional to the hydrogen-ion concentration raised to some power, since 2.26 *m* $LiClO_4$ underwent no decomposition (within the limits of detection) under conditions which brought about more than 50% decomposition of 2.26 *m* $HClO_4$.

The results of series of experiments at 300.0° and roughly constant ionic strength ($[H^+] + [Li^+] = [ClO_4^-] = 2.2\ m$) are summarized in Table 3 in terms of extrapolated initial perchlorate decomposition rates. A plot of log $(-dc_0/dt)$ *vs.* log $[H^+]_0$ indicates an order of 1.2 (or 1.17 ± 0.06) with respect to hydrogen ion.

In order to check the order of reaction with respect to perchlorate ion directly, or to learn how the $HClO_4$ decomposition rate responds to changes in the ionic strength, one must find an inert, non-basic, anionic substitute for perchlorate ion with a low tendency to ion-pairing, so that the ionic strength or the acidity can be maintained at will. Of the common anions, only the hydrogen sulfate ion, HSO_4^-, behaves as a univalent, non-basic, non-acidic ion between 300 and 400° (28), and a solution, 2 *M* in $LiClO_4$ and 3 *M* in $NaHSO_4$ at 20°, showed no decomposition after 55 h at 294.5°.

TABLE 3. Initial rates of decomposition of $LiClO_4$–$HClO_4$* at 300.0° as a function of initial hydrogen ion concentration, $[H^+]_0$

$[H^+]_0$ (*m*)	$[ClO_4^-]_0$ (*m*)	$10^6 \times -dc/dt$ ($m\ s^{-1}$) at zero time
0.277	2.067	0.51
0.555	2.167	1.19
1.133	2.254	2.85
2.256	2.256	5.5

*$[H^+] + [Li^+] = [ClO_4^-] \approx 2.2\ m$.

The effect of added $NaHSO_4$ on the rate of decomposition of 2 *M* (20°) $HClO_4$ is illustrated by the data of Table 4, which show that a modest but definite "medium" or "ionic strength" effect causes the rate of $HClO_4$ decomposition to decrease as the electrolyte concentration increases.

Semi-quantitative experiments, in which the extent of decomposition of 3.5 *m* $HClO_4$ at 300.0° was compared with that of 2.26 *m* $HClO_4$/1.2 *m* $H[HSO_4]$ mixture, and 6.61 *m* $HClO_4$ with 2.26 *m* $HClO_4$/4.3 *m* $H[HSO_4]$, confirmed that the true order of reaction with respect to perchlorate ion was roughly 2 at these concentrations of electrolytes.

When lithium chloride was added to the $HClO_4$ before thermal decomposition, greatly increased yields of chlorine were obtained, and much H^+ and Cl^- were consumed. The rate of loss of perchlorate was accelerated by the addition of moderate amounts of chloride. The decomposition of 2 *M* (25°) $HClO_4$ at 294.5° in 23.3 h showed the same general features as the data for 55 h listed in Table 5.

It should be noted, from Table 5, that the decrease $\Delta[H^+]$ in hydrogen-ion concentration equals the sum of $\Delta[ClO_4^-]$ and $\Delta[Cl^-]$, within the experimental uncertainty. The apparent near-

TABLE 4. Effect of 3.0 *M* (20°) $NaHSO_4$ on the rate of decomposition of 2.05 *M* (20°) perchloric acid at 294.5°

Elapsed time (h)	% ClO_4^- decomposed, 2 *M* $HClO_4$	% ClO_4^- decomposed, 2 *M* $HClO_4$/3 *M* $NaHSO_4$
55	23	20
109	42	28
165	47	33

TABLE 5. Decomposition of 2 *M* $HClO_4$ in 55 h in the presence of added LiCl at 294.5°*

$[H^+]_0$	$[ClO_4^-]_0$	$[Cl^-]_0$	$[H^+]_{55}$	$[ClO_4^-]_{55}$	$[Cl^-]_{55}$	$\Delta[H^+]$	$\Delta[ClO_4^-]+\Delta[Cl^-]$	$\Delta[Cl^-]/\Delta[ClO_4^-]$
2.11	2.11	0.00	1.72	1.73	0.017	0.39	0.36	—
2.08	2.08	0.56	1.10	1.56	0.034	0.98	1.05	1.0
2.06	2.09	1.04	0.65	1.60	0.065	1.41	1.46	2.0
2.13	2.04	1.63	0.26	1.57	0.220	1.87	1.88	3.0
2.10	2.08	1.99	0.15	1.60	0.513	1.95	1.96	3.1
2.11	2.08	4.03	0.08	1.59	2.505	2.03	2.01	3.1

*Concentrations are in *M* units, determined experimentally at 20°; subscripts refer to time in hours.

constancy of $\Delta[ClO_4^-]$ in the presence of added chloride is presumably fortuitous; acceleration by chloride is evidently compensated for by reductions in the reaction rate caused by the rapid exhaustion of the hydrogen ion content. The effect of chloride ion requires the presence of hydrogen ion, since it was found that 2 *M* (25°) $LiClO_4$ containing 2 *M* (25°) LiCl underwent no detectable loss of perchlorate or evolution of chlorine in 55 h at 294.5°.

Discussion

The initial rate of decomposition of dilute aqueous $HClO_4$ decreases approximately threefold for each 10° decrease in temperature, and approximately ten-fold for each halving of the initial concentration of $HClO_4$. These large effects are reflections of the unusually high activation energy (84 kcal $mole^{-1}$) and order of reaction (3.5) with respect to the substrate. Since the initial rate of decomposition of 1 *m* $HClO_4$ is small (5×10^{-7} *m* s^{-1}) at 300°, it can be stated that the rate is negligibly small for 1 *m* $HClO_4$ at 250° and for the 0.2 *m* acid at 300°, as far as experiments of about a day's duration are concerned. Perchloric acid may therefore have considerable utility in physico-chemical studies of high temperature aqueous solutions, although direct attack by $HClO_4$ on oxidizable solute species such as transition-metal ions may limit its applicability.

The observed non-integral orders of reaction with respect to hydrogen ion (about 1.2) and perchlorate ion (by difference, about 2.3) prevent the unambiguous assignment of a reaction mechanism. The reaction was found to be somewhat retarded by high concentrations of inert electrolyte ($NaHSO_4$), and so the overall molecularity of reaction with respect to the stoichiometric $HClO_4$ concentration is probably 4. The orders of reaction with respect to H^+ and ClO_4^- separately are each greater than 1, and it is probable that the molecularity is 2 with respect to each of these species. The "ionic strength" concept, used in deriving the order in H^+, may not be reliable at these high temperatures, at which the product of the solvent dielectric constant and the absolute temperature has less than half its room temperature value; this is particularly unsatisfactory since the substrate ($HClO_4$) comprised most or all of the electrolyte present in many of the experiments. There is also the possibility that the perchloric acid is appreciably associated near 300°.

However, if we assume that the molecularities with respect to H^+ and ClO_4^- are both 2, then the stoichiometric mechanism is probably

$$[8] \qquad H^+ + ClO_4^- \overset{K}{\rightleftharpoons} HClO_4$$

$$[9] \qquad 2HClO_4 \xrightarrow{\text{slow}} \text{intermediates} \xrightarrow{\text{fast}} H_2O + Cl_2 + \tfrac{7}{2}O_2$$

Values of the association constant *K* of $HClO_4$ are not accurately known even for temperatures below 100°; the available estimates are conflicting (27, 29), but it seems that not more than 1% of the $HClO_4$ in the solutions used in the present study could be associated at 25°. Reaction 8 is likely to be endothermic with a positive molal heat capacity change, so that association could be extensive in the temperature range of interest (295–322°). However, for the much weaker acid HCl, *K* is only about 30 m^{-1} at 306° (30), while sulfuric acid (which, as $H[HSO_4]$, is a close analogue of $H[ClO_4]$) is recognized (28) to behave as a strong uni-univalent electrolyte between 300 and 400°. It therefore seems reasonable to assume that only a small fraction of the $HClO_4$ is associated at 295–322°, so that the mechanism of reactions 8 and 9 would give rise to a fourth-order rate law.

Can. J. Chem. Downloaded from www.nrcresearchpress.com by 210.87.254.40 on 09/05/12
For personal use only.

Can. J. Chem. Downloaded from www.nrcresearchpress.com by 210.87.254.40 on 09/05/12
For personal use only.

The nature of reaction 9 is a matter for speculation, since we detected no intermediates. The reversible condensation of two $HClO_4$ molecules to give water and the relatively unstable anhydride Cl_2O_7 has been suggested (3, 4, 6, 7) for the decomposition of 83–100% $HClO_4$, but Pearson (31) considers this improbable, and besides it is scarcely likely to be relevant to dilute aqueous $HClO_4$.

The rate of homogeneous pyrolysis of $HClO_4$ vapor is first order in molecular $HClO_4$, and has an activation energy of 45.1 kcal mole^{-1}, which is close to the HO—ClO_3 bond energy of 48.3 kcal mole^{-1} (9); in contrast, the H—$OClO_3$ bond energy is 112 kcal mole^{-1} (32), and the O—ClO_3H energy is over 105 kcal mole^{-1} (5). It is therefore highly probable that reaction 10 is the rate-determining step in the homogeneous gas-phase pyrolysis of $HClO_4$.

[10] $$HClO_4 \rightarrow HO\cdot + \cdot ClO_3$$

This is supported by Fisher's demonstration (11) that ClO is a major reaction intermediate, along with some ClO_2; these probably originate from ClO_3 and ClO_4. The rapid reactions following [10] are probably [11] through [16].

[11] $$HClO_4 + \cdot OH \rightarrow H_2O + ClO_4\cdot$$

[12] $$ClO_4\cdot \rightarrow ClO_2 + O_2$$

[13] $$ClO_2 \rightarrow Cl\cdot + O_2$$

[14] $$2Cl\cdot \rightarrow Cl_2$$

[15] $$\cdot ClO_3 \rightarrow \cdot ClO + O_2$$

[16] $$2\cdot ClO \rightarrow Cl_2 + O_2$$

In contrast to the gas-phase reaction, the decomposition of dilute aqueous $HClO_4$ appears to be bimolecular in undissociated $HClO_4$, and we therefore propose that the rate-determining step in solution involves association of two $HClO_4$ molecules through interaction of their strong —$O^{\delta-}H^{\delta+}$ dipoles. The resulting geometry will be favorable to the elimination of H_2O and the formation of the fragments $\cdot ClO_3$ and $\cdot ClO_4$ (reaction 17) which would subsequently decompose rapidly to oxygen and chlorine via reactions 12 through 16.

[17] $$O_3Cl—OH + H—OClO_3 \xrightarrow{\text{slow}} ClO_4\cdot + \cdot ClO_3 + H_2O$$

It will be seen that this is the same as the probable gas-phase mechanism outlined above, except that the sequential reactions 10 and 11 have coalesced into a single synchronous step. It also resembles the condensation mechanism favored by Zinoviev *et al.* (3, 4, 6, 7), except that independent ClO_3 and ClO_4 fragments are the products of the initial step, rather than Cl_2O_7.

If the H—OH bond energy is taken to be 117 kcal mole^{-1}, then the minimal activation energy for step 17 in the gas phase is 43 kcal mole^{-1}; in solution, the polar molecule $HClO_4$ would be further stabilized relative to the products of step 17, so that the activation energy for this step may be 50 kcal mole^{-1} or more. The enthalpy change of reaction 8 at about 300° can only be guessed at, but it will almost certainly be quite endothermic, and, by analogy with HCl (for which ΔH^0 is about 17 kcal mole^{-1} (30) for association of the aqueous acid), we can anticipate that $10 < \Delta H^0 < 25$ kcal mole^{-1}. Hence, for a mechanism in which reaction 8 (taken *twice*) is followed by the rate-determining step 17, we can expect an overall activation energy greater than 70 and perhaps as much as 100 kcal mole^{-1}; the observed value is 84 kcal mole^{-1}.

The addition of chloride ion to aqueous perchloric acid must reduce the free H^+ concentration at high temperatures by forming molecular HCl (30), yet it is observed that the decomposition of $HClO_4$ is actually faster when chloride is added. Evidently, a direct reaction can occur between HCl and ClO_4^- (or possibly $HClO_4$). The data of Table 5 show that, if enough chloride is present, three moles of chloride are consumed for each mole of perchlorate decomposed. The stoichiometry of the chloride-dependent pathway is therefore,

[18] $$4H^+ + 3Cl^- + ClO_4^- = 2Cl_2 + 2H_2O + O_2$$

It will be noted that, regardless of what fraction of the decomposition goes by reaction 18, the change in hydrogen ion concentration, $\Delta[H^+]$, is given by eq. 19, which is verified by the data of Table 5.

[19] $$\Delta[H^+] = \Delta[Cl^-] + \Delta[ClO_4^-]$$

Reaction 18 is best accounted for by the mechanistic sequence [20]–[23], which, like the gas-phase pyrolysis scheme of Fisher (11), involves the rapid decomposition of ClO_3 to ClO and oxygen. Other plausible mechanisms which do not involve this step give the wrong overall stoichiometry. Reaction 23 will be complex.

$$[20]\quad H^+ + HCl + ClO_4^- \xrightarrow{\text{slow}} Cl^\cdot + H_2O + {}^\cdot ClO_3$$

$$[21]\quad 2Cl^\cdot \xrightarrow{\text{fast}} Cl_2$$

$$[22]\quad ClO_3^\cdot \xrightarrow{\text{fast}} ClO^\cdot + O_2$$

$$[23]\quad ClO^\cdot + 2HCl \xrightarrow{\text{fast}} H_2O + \tfrac{3}{2}Cl_2$$

The observed acceleration of the decomposition of pure aqueous $HClO_4$ by its own decomposition products (specifically Cl_2) can be attributed, at least in part, to the production of small amounts of chloride by reactions 1 and 2. It might be noted that bromide (33) and iodide (34) ions both can cause reduction of aqueous $HClO_4$ at temperatures as low as 100–135°.

We thank Dr. J. M. Simmie for the mass spectra, and Drs. P. W. M. Jacobs and W. E. Jones for supplying copies of otherwise unobtainable articles. We are grateful to the National Research Council of Canada for an operating grant.

1. D. D. Wagman, W. H. Evans, V. B. Parker, I. Halow, S. M. Bailey, and R. H. Schumm. Selected Values of Chemical Thermodynamic Properties. N.B.S. Technical Note 270-3, Washington, D.C., 1968.
2. W. C. Waggener, A. J. Weinberger, and R. W. Stoughton. Appl. Spectrosc. **22**, 545 (1968).
3. A. E. Missan and A. M. Sukhotin. Russ. J. Inorg. Chem. **4**, 276 (1959).
4. A. A. Zinoviev and A. B. Tsentsiper. Russ. J. Inorg. Chem. **4**, 329 (1959).
5. A. B. Tsentsiper. Russ. J. Inorg. Chem. **4**, 493 (1959).
6. A. A. Zinoviev and V. P. Babaeva. Russ. J. Inorg. Chem. **6**, 138 (1961).
7. V. P. Babaeva and A. A. Zinoviev. Russ. J. Inorg. Chem. **8**, 288 (1963).
8. V. P. Babaeva and A. A. Zinoviev. Dokl. Akad. Nauk SSSR, **149**, 592 (1963).
9. J. B. Levy. J. Phys. Chem. **66**, 1092 (1963).
10. D. J. Sibbett and J. M. Lobato. Investigation of the Mechanism of Combustion of Composite Solid Propellants. Aerojet Report No. 1782, Aerojet-General Corp., Azusa, California, April 1960.
11. I. P. Fisher. A Mass Spectrometric Study of the Thermal Decomposition of Perchloric Acid and Chlorine Dioxide. Technical Report No. 66/13, Rocket Propulsion Establishment, Westcott, England, November 1966; Trans. Faraday Soc. **63**, 684 (1967).
12. G. A. Heath and J. R. Majer. Trans. Faraday Soc. **60**, 1783 (1964).
13. J. S. Gill and W. L. Marshall. Rev. Sci. Instr. **32**, 1060 (1961).
14. Titanium Design Data Book for the Chemical Processor. Titanium Metals Corp. of America, 233 Broadway, New York, N.Y. pp. 13, 23, 64.
15. A. E. Markham. J. Amer. Chem. Soc. **63**, 874 (1941).
16. E. B. Robertson. Ph.D. Thesis. University of Alberta, Edmonton, Alberta. 1964.
17. R. J. Baczuk and R. J. DuBois. Anal. Chem. **40**, 685 (1968).
18. A. Liberto and M. Mascini. Anal. Chem. **41**, 676 (1969).
19. W. C. Fergusson, L. Slotin, and D. W. G. Styles. Trans. Faraday Soc. **32**, 956 (1936).
20. C. C. Hong and W. H. Rapson. Can. J. Chem. **46**, 2061 (1968).
21. R. E. Connick and Y.-T. Chia. J. Amer. Chem. Soc. **81**, 1280 (1959).
22. A. E. Korvezee. Rec. Trav. Chim. Pays-Bas, **50**, 1092 (1931).
23. A. R. Gordon and C. Barnes. J. Phys. Chem. **36**, 2292 (1932).
24. E. V. Jones and W. L. Marshall. Reactor Chemistry Division Annual Report ORNL-4229-UC-4, Oak Ridge National Laboratory, Oak Ridge, Tennessee. 1967. p. 90.
25. K. J. Laidler. Reaction Kinetics. Vol. 1. Pergamon Press, Oxford, England. 1963. pp. 18–19.
26. N. E. Dorsey. Properties of Ordinary Water-Substance. Reinhold Publishing Corp., New York, N.Y. 1940.
27. R. Haase, K.-H. Dücker, and H. A. Küppers. Ber. Bunsenges. Phys. Chem. **69**, 97 (1965).
28. A. S. Quist, W. L. Marshall, and H. R. Jolley. J. Phys. Chem. **69**, 2726 (1965).
29. J. W. Akitt, A. K. Covington, J. G. Freeman, and T. H. Lilley. Trans. Faraday Soc. **65**, 2701 (1969).
30. A. E. Martell and L.-G. Sillén. Stability Constants. Chemical Society Special Publication No. 17, London, 1964. p. 272.
31. G. S. Pearson. Advan. Inorg. Radiochem. **8**, 177 (1966).
32. I. P. Fisher. Trans. Faraday Soc. **64**, 1852 (1968).
33. W. R. Crowell, D. M. Yost, and J. D. Roberts. J. Amer. Chem. Soc. **62**, 2176 (1940).
34. E. Kahane and T. Tomesco. Compt. Rend. **201**, 1195 (1935).

Can. J. Chem. Downloaded from www.nrcresearchpress.com by 210.87.254.40 on 09/05/12
For personal use only.

Reactions of Some Allylic and Propargylic Halides with Nucleophiles Analogous to Those Present in Proteins and Nucleic Acids

J. Bryan Jones and David W. Hysert[1]

Lash Miller Chemical Laboratories, Department of Chemistry, University of Toronto, Toronto 181, Ontario

Received June 12, 1970

The relative alkylating capabilities of crotyl chloride, allyl bromide, and 1-bromo-2-butyne with respect to compounds containing thiol, imidazole, primary amino, and methylthio functions representative of those present in cysteine, histidine, lysine and methionine residues have been studied using 2-bromoacetophenone as the reference alkylating agent.

Canadian Journal of Chemistry, 49, 325 (1971)

Can. J. Chem. Downloaded from www.nrcresearchpress.com by 210.87.254.5 on 09/05/12
For personal use only.

The use of reagents capable of effecting chemical modifications of proteins (including enzymes and immunoglobulins) and nucleic acids has proven of great value in recent years (1–5). However, although the spectrum of modifications which can now be achieved is quite broad it is clear that there remains considerable scope for improving the functional group- and stereospecificity (or selectivity) of such reagents.

In this regard we have initiated a programme designed to explore and evaluate the feasibility of incorporating *cis*- and/or *trans*-ethylenic and acetylenic bonds into alkylating functions in order to exploit their unique geometrical properties with respect to specific and stereochemically controlled protein or nucleic acid modifications.[2]

The types of compounds considered first were among the simplest which could be chosen, *viz.* those containing one ethylenic or acetylenic bond only. Although most of the alkylating groups which had already proven useful (1–5) would be expected to be quite reactive when attached to simple unsaturated carrier moieties of this kind, it was decided initially to evaluate the hitherto biologically untried alkylating agents of the allylic and propargylic halide types.

The compounds selected as being representative of allylic and propargylic halides were crotyl bromide (**1**), crotyl chloride (**2**), allyl bromide (**3**), and 1-bromo-2-butyne (**4**). 2-Bromoacetophenone (**5**) was also included in the survey for comparison purposes and as a reference reagent whose utility and rates of reaction with certain protein nucleophiles had been established previously (2). The protein nucleophiles which should be most susceptible to alkylation by the above reagents under conditions of physiological p*H* are cysteine thiol, histidine imidazole, lysine ε-amino, and methionine methylthio groups. However, since in previous related studies, difficulties in isolating and identifying products had arisen when appropriate amino acid derivatives models had been used, it was decided to carry out the first experiments using even simpler model compounds containing functions analogous to those of the amino acids of interest in order to simplify the structural analyses involved. In addition, on the basis of past experience (7, 8) it was felt that delineation of the range of reactions to be expected and the provision of p.m.r. spectra for reference purposes would prove invaluable in the design and analyses of the subsequent amino acid and protein alkylation experiments. The model compounds chosen[3] were, respectively, α-toluene thiol (**6**), imidazole (**7***a*), and *N*-methylimidazole (**7***b*),[4] benzylamine (**8**) and benzyl methyl sulfide (**9**).

The guanidinium group of arginine (pK_a 11.6–12.1 (1)) was also considered, using guanidine (**10**) as the model, even though *in vivo* it is always largely protonated and thus retains very little nucleophilic character. However, it was felt that by using a suitably constructed bridge, *exo*-arginine residues on appropriate proteins might

[1]Abstracted in part from the M.Sc. thesis of D. W. H., University of Toronto, Toronto, Ontario, 1968.

[2]The potential of the geometry of the acetylenic bond with respect to the design of enzyme probes has recently been recognized independently by Latif and Kaiser (6).

[3]The factors considered in choosing these model nucleophiles included the similarity of their pK_a's to the corresponding *in vivo* group, and the ease with which the p.m.r. spectra of the possible products could be interpreted (7, 8).

[4]*N*-methylimidazole also provided a model for the guanine residues of DNA and RNA since compounds capable of effecting its *N*-alkylation should also react with N-7 of guanine (7).

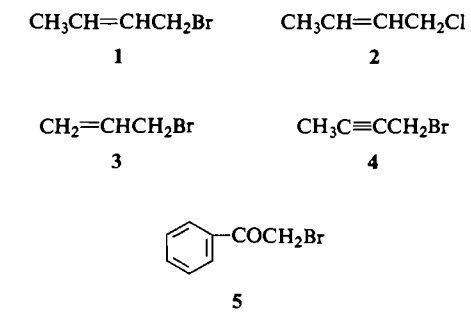

be brought into close enough proximity with an alkylating function for any unfavorable rate of the alkylation reaction to be counterbalanced sufficiently for significant modification to be achieved. That such a possibility was not unreasonable was substantiated by the successful active site and other arginine modifications reported recently (3) using dicarbonyl reagents.[5]

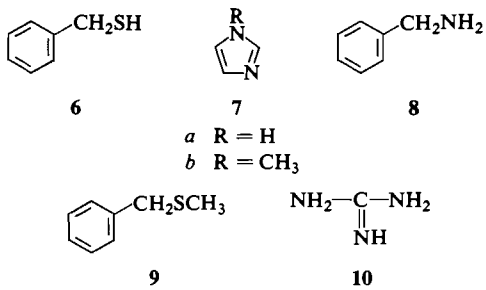

All of the compounds **1**–**10** were available commercially except for 1-bromo-2-butyne which was readily prepared by bromination of 2-butyn-1-ol. Unfortunately, after the investigation had been under way for some time it became necessary to discontinue the studies on crotyl bromide (**1**) since its tendency to isomerize to a mixture containing 15% of 3-bromo-1-butene at equilibrium (9) precluded the collection of any reproducible data. Attention was therefore concentrated on a comparison of the relative alkylating abilities of crotyl chloride (**2**), allyl bromide (**3**), 1-bromo-2-butyne (**4**), and 2-bromoacetophenone (**5**). No attempt was made at this preliminary stage to separate the *cis* and *trans* isomers present in the commercial crotyl chloride since both isomers have been shown to undergo nucleophilic substitution at approximately the same rates (10).

The experimental procedures followed were relatively straightforward and most of the reactions studied proceeded as expected and do not warrant individual discussion. Accordingly the relevant data for the reactions of crotyl chloride, allyl bromide, 1-bromo-2-butyne, and 2-bromoacetophenone with α-toluenethiol, imidazole, *N*-methylimidazole, benzylamine, and benzyl methyl sulfide have been summarized in Chart 1 and Table 1. As Table 1 shows, no attempt was made at this stage to carry out the reactions in aqueous media approximating more closely the expected *in vivo* conditions in order to avoid the complications which would undoubtedly have arisen from competitive hydrolysis of the alkylating agents (11).

The alkylations of α-toluenethiol all proceeded very smoothly in the presence of 1 equiv of base to give easily isolable products in high yields. Further alkylation of the sulfide products **11***a*–*d* to give sulfonium salts did not occur under the mild reaction conditions employed.

The reactions with imidazole (**7***a*) and *N*-methylimidazole (**7***b*) were rather more difficult to control owing to the ease with which the primary alkylation products **12** reacted with a second mole of alkylating agent to give the bisalkylated salts **13**. The mono-alkylated products were relatively easily isolated and characterized; in contrast, compounds **13** and **14** were much less tractable and proved no exception to the general rule that doubly alkylated imidazolium salt derivatives are difficult to purify (12–15). In fact owing to the extremely deliquescent natures of the series of salts **13** and **14** only the 2-bromoacetophenone products **13***d* and **14***d* could be satisfactorily isolated and characterized and the structural assignments of **13***a*–*c* and **14***a*–*c* were made mainly on the basis of their p.m.r. spectra. The purest samples of the imidazolium salts **13***a*–*c* were obtained by the appropriate alkylation of the corresponding mono-alkylated compounds **12***a*–*c*.

The benzylamine reactions presented no problems and each of the mono- and bisalkylated derivatives were isolated without difficulty. However, since the phenacyl compounds **15***d* and **16***d* were known to be unstable as the free

[5]These reactions occur most readily at p*H* 8–9 and an initial nucleophilic attack of a carbonyl group by the guanidinium moiety is implicit in such modifications.

Can. J. Chem. Downloaded from www.nrcresearchpress.com by 210.87.254.5 on 09/05/12
For personal use only.

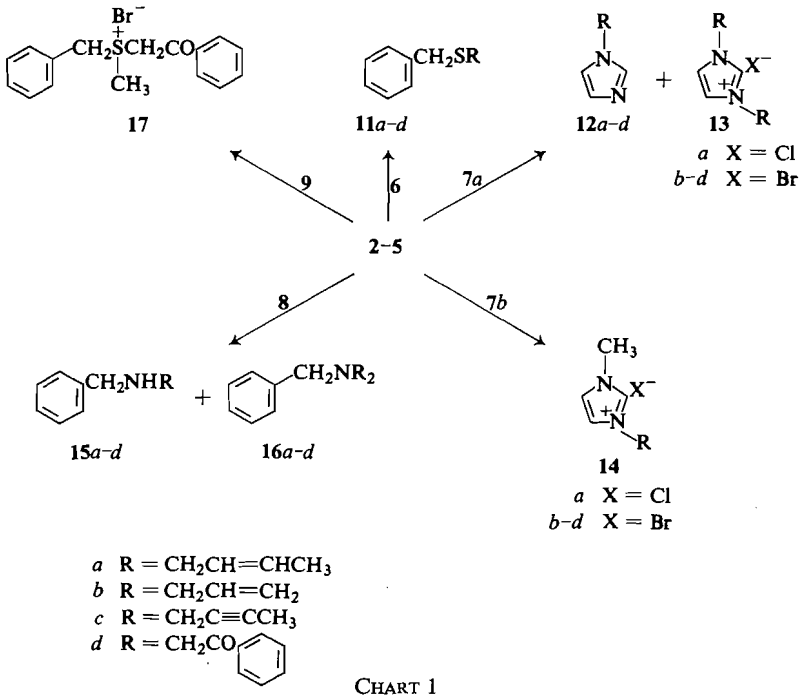

CHART 1

bases (16) they were isolated as the hydrobromide salts.

Although as expected from its ability to alkylate the α-chymotryptic methionine 195 residue (2), 2-bromoacetophenone reacted smoothly with benzyl methyl sulfide (**9**) to give the corresponding sulfonium salt **17**, no such products could be isolated upon treatment of **9** with crotyl chloride, allyl bromide or 1-bromo-2-butyne under reaction conditions varying from mild (organic solvents, 25°) to vigorous (neat reactants, sealed tube, 150°). The inaccessibility of the latter compounds is perhaps not surprising in view of the well documented instability of simple sulfonium salts in general (17) and of unsaturated derivatives in particular (18) and in retrospect it appears that benzyl methyl sulfide was not a suitable choice as a model for the methionine *S*-methyl group.[6]

The reasons for including the guanidinium group in this survey have been outlined earlier and in order to provide an estimate of the difficulties which might be expected with the current series of alkylating agents the reaction of the most reactive of them, 2-bromoacetophenone, with the model nucleophile guanidine was studied as a function of p*H*.[7] In aqueous methanol no reaction occurred until a p*H* of 11 was approached and at p*H* 11.7 at 25° rapid, multiple (ten products by t.l.c.), reactions occurred. However, on lowering the reaction temperature to 0° a crystalline product was isolated and from the melting behavior and the spectroscopic properties of the material it was concluded that the product was the result of base-catalyzed Darzens condensation of 2-bromoacetophenone. On recrystallization of the mixture from ethanol under equilibrating conditions, the higher melting, thermodynamically more stable, *cis* (21) isomer, m.p. 154–155.5°, of 4-bromo-2,3-epoxy-3-phenylbutyrophenone was obtained exclusively. Since no reaction of guanidine with 2-bromoacetophenone could be induced at p*H*

[6]This view is substantiated by the subsequent observations that the *S*-methyl group of *N*-acetylmethionine is readily alkylated by both allyl bromide, 1-bromo-2-butyne, and 2-bromoacetophenone (19).

[7]Very few guanidine alkylations have been reported in the literature and for most of these vigorous reaction conditions were found to be necessary. However, recently it has been demonstrated that using suitably reactive reagents, such as 5-chloro-3-methyl-4-nitro-2-pyrazoline, alkylation of guanidine is facile under very mild conditions (20).

Can. J. Chem. Downloaded from www.nrcresearchpress.com by 210.87.254.5 on 09/05/12
For personal use only.

Can. J. Chem. Downloaded from www.nrcresearchpress.com by 210.87.254.5 on 09/05/12
For personal use only.

TABLE 1. Summary of the products and yields obtained and the conditions used for the reactions of the nucleophilic compounds **6–9** with alkylating agents **2–5**

Nucleophile	Alkylating agent [mol equiv]	Reaction conditions	Products (yield)*
α-Toluenethiol (**6**)	Crotyl chloride (**2**) [1.0]	MeOH(25°) with 1 equiv NaOH	**11***a* (88%)
	Allyl bromide (**3**) [1.0]	,,	**11***b* (85%)
	1-Bromo-2-butyne (**4**) [1.0]	,,	**11***c* (94%)
	2-Bromoacetophenone (**5**) [1.0]	Ether (0°) with 1 equiv Et_3N	**11***d* (quantitative)
Imidazole (**7***a*)	Crotyl chloride [1.0]	MeOH (65°) with 1 equiv $NaHCO_3$	**12***a* (37%); **13***a* (41%)†
	,, ,, [0.2]	,,	**12***a* (80%)
	Allyl bromide [1.0]	MeOH (25°) with 1 equiv $NaHCO_3$	**12***b* (30%); **13***b* (23%)†
	,, ,, [0.2]	,,	**12***b* (94%); **13***b* (5%)†
	1-Bromo-2-butyne [1.0]	,,	**12***c* (35%); **13***c* (26%)†
	,, [0.2]	,,	**12***c* (83%); **13***c* (15%)†
	2-Bromoacetophenone [1.0]	MeOH(25°)	**12***d* (32%); **13***d* (59%)
	,, [2.0]	,,	**12***d* (10%); **13***d* (90%)†
	,, [0.1]	MeOH (25°) with 1 equiv $NaHCO_3$	**12***d* (94%)
N-Methylimidazole (**7***b*)	Crotyl chloride [1.0]	MeOH(65°)	**14***a* (68%)†
	Allyl bromide [1.0]	MeOH(25°)	**14***b* (89%)†
	1-Bromo-2-butyne [1.0]	,,	**14***c* (91%)†
	2-Bromoacetophenone [1.0]	,,	**14***d* (98%)
Benzylamine (**8**)	Crotyl chloride [1.0]	MeOH (65°)	**15***a* (15%); **16***a* (35%)
	Allyl bromide [1.0]	Ether (25°)	**15***b* (36%); **16***b* (35%)
	1-Bromo-2-butyne [0.5]	,,	**15***c* (27%); **16***c* (43%)
	2-Bromoacetophenone [1.2]	MeOH (25°)	**15***d* (8%); **16***d* (54%)
Benzyl methyl sulfide (*9*)	Crotyl chloride	Varied	—
	Allyl bromide	,,	—
	1-Bromo-2-butyne	,,	—
	2-Bromoacetophenone [1.0]	Benzene or aqueous acetone (25°)	**17** (51%)

*All yields quoted are absolute and have not been corrected for any recovered starting materials.
†Yield estimated by p.m.r.

values below those at which the latter began to undergo the self-condensation reaction no further studies on guanidine were carried out.

From the preparative reactions summarized in Table 1 the relative reactivities of the alkylating agents **2**–**5** with each of the model compounds **6**, **7***a*, **7***b*, and **8** appeared to be in the order 2-bromoacetophenone ≫ allyl bromide > 1-bromo-2-butyne ≫ crotyl chloride.

Summary and Conclusions

The data obtained indicate that, although chloro compounds probably react too slowly to be of much value, allylic and propargylic bromides (and presumably iodides) are of potential value for alkylating cysteine sulfhydryl, histidine imidazole, and lysine amino groups. In addition differences between the rates of reaction of functional groups such as those of the bromides **3** and **4** and the bromomethylketone **5** may enable selective or sequential *in vivo* modifications to be achieved.

Further structural, rate of reaction, and p*H* dependence studies on the above and more conjugated alkylating agents with amino acid derivatives, and on polyunsaturated bifunctional reagents as probes for proteins and nucleic acids are in progress.

Experimental

Melting points were determined on a Fisher–Johns apparatus and are uncorrected. The g.l.c. analyses were performed on an F and M 400 chromatograph fitted with glass columns containing 3.8% SE-30 or 1% NPGS on Diatoport S. The t.l.c. was carried out on Silica gel G with chloroform – methanol – ammonium hydroxide (90:15:1, v/v/v) as the developing solvent and using iodine vapor visualization. The various spectral data reported were obtained on Varian A-60 and HA-100, Perkin–Elmer 237B and 350, MS-902 or CEC 21-490, and Unicam SP 800 instruments. Tetramethylsilane was used as the internal reference for all p.m.r. spectra. All reactions were monitored by t.l.c. or g.l.c. and solvent evaporations were effected by rotary evaporation.

Materials

1-Bromo-2-butyne was prepared in 54% yield from but-2-yn-1-ol (Columbia Organic Chemicals) by the method of Ashworth *et al.* (22). All other required compounds were purchased from Fisher or Aldrich and each was repurified by fractional (including spinning band) distillation or recrystallization until the physical properties *viz.* m.p. or b.p. (and when necessary, refractive index), t.l.c., g.l.c., i.r., and p.m.r. spectra, indicated the absence of impurities.

Alkylation of α-Toluenethiol (6)[8]

(a) With Crotyl Chloride (2)

Crotyl chloride (1.81 g, 20 mmol) was added dropwise at 25° to a stirred solution of α-toluenethiol (2.48 g, 20 mmol) in methanol (30 ml) containing 10 *N* aqueous sodium hydroxide (2ml, 20 mmol). After 24 h the reaction mixture was diluted with ether (100 ml) and the precipitated sodium chloride removed by filtration. The ethereal filtrate was washed with saturated aqueous sodium chloride (50 ml), then dried ($MgSO_4$), and evaporated. Fractional distillation of the residual oil gave benzyl crotyl sulfide (**11***a*, 3.09 g, 87%), b.p. 86°/0.5 Torr (lit. (23) b.p. 137–139°/18 Torr); p.m.r. ($CDCl_3$) δ 1.64–1.74 (3H, m, CH_3C=), 2.94–3.06 (2H, m, SCH_2C=), 3.64 (2H, s, $C_6H_5CH_2S$), 5.42–5.62 (2H, m, —CH=CH—), and 7.32 p.p.m. (5H, s, C_6H_5).

(b) With Allyl Bromide (3)

From 1 molecular equiv each of allyl bromide and α-toluenethiol under the above conditions for 1 h was obtained in 77% yield allyl benzyl sulfide (**11***b*), b.p. 117–118°/14 Torr (lit. (24) b.p. 115–116°/14 Torr); p.m.r. ($CDCl_3$) δ 2.95 (2H, d of q, J = 1.7 Hz, SCH_2CH=CH_2), 3.58 (2H, s, $C_6H_5CH_2S$), 4.9–5.7 (3H, m, CH=CH_2), and 7.26 p.p.m. (5H, m, C_6H_5).

(c) With 1-Bromo-2-butyne (4)

One molecular equivalent each of 1-bromo-2-butyne and α-toluenethiol for 10 h yielded 78% of benzyl but-2-ynyl sulfide (**11***c*), b.p. 82–83°/0.1 Torr; u.v. (CH_3OH) 267 (ε 204) and 261 (ε 321) nm; p.m.r. ($CDCl_3$) δ 1.82 (3H, t, J = 2 Hz, CH_3C≡), 3.03 (2H, q, J = 2 Hz, ≡CCH_2S), 3.81 (2H, s, $C_6H_5CH_2S$), and 7.2–7.4 p.p.m. (5H, m, C_6H_5).

Anal. Calcd. for $C_{11}H_{12}S$: C, 74.94; H, 6.86; S, 18.19. Found: C, 74.98; H, 6.76; S, 18.20.

(d) With 2-Bromoacetophenone (5)

Equimolar amounts of 2-bromoacetophenone, α-toluenethiol, and triethylamine were mixed in ether at 0° to give, after work-up, 2-(benzylthiol)acetophenone (**11***d*, quantitative yield), plates from ethanol, m.p. 88.5–90° (lit. (25) m.p. 89°); p.m.r. ($CDCl_3$), δ 3.66 (2H, s, $C_6H_5CH_2S$), 3.75 (2H, s, SCH_2CO), 7.26–7.64 (8H, m, aromatic), and 7.92–8.04 p.p.m. (2H, d of d, J = 2.7 Hz, ortho aromatic protons).

Alkylations of Imidazole (7a)

As indicated by Table 1 the alkylations of imidazole were carried out in methanol solutions with varying molar proportions of reagents, and both in the presence and absence of sodium bicarbonate. The conditions outlined below for the crotyl chloride reactions[8] are representative of those used to prepare the reference samples of the individual products used in the analyses summarized in Table 1.

[8]Since the alkylation procedures are similar within each series of reactions only the crotyl chloride reaction is fully described for any nucleophile. The total data obtained are summarized in Table 1. The p.m.r. data are reported in full for each product since the chemical shift values and splitting patterns observed were sufficiently characteristic to be of value during subsequent analyses of the products of reactions of amino acids and proteins. When not recorded, i.r. and u.v. data were as expected.

Can. J. Chem. Downloaded from www.nrcresearchpress.com by 210.87.254.5 on 09/05/12
For personal use only.

Can. J. Chem. Downloaded from www.nrcresearchpress.com by 210.87.254.5 on 09/05/12
For personal use only.

(a) With Crotyl Chloride (2)

Crotyl chloride (3.2 g, 35 mmol) in methanol (35 ml) was added dropwise with stirring during 3.5 h to a refluxing mixture of imidazole (11.9 g, 175 mmol) and sodium bicarbonate (2.95 g, 35 mmol) in methanol (35 ml). Following further heating under reflux for 24 h the reaction mixture was evaporated and the residue dissolved in water (60 ml) and extracted with chloroform (3 × 20 ml). The chloroform extract was washed with saturated aqueous sodium chloride (25 ml), then dried ($MgSO_4$), and evaporated. Fractional distillation of the oil obtained yielded *N*-crotylimidazole (**12***a*, 2.55 g), b.p. 52–54°/0.15 Torr; p.m.r. (CCl_4) δ 1.65–1.82 (3H, m, CH═CHC*H*$_3$), 4.38–4.58 (2H, m, NC*H*$_2$CH═), 5.57–5.63 (2H, m, CH$_2$C*H*═C*H*CH$_3$), 6.77 (1H, t, J = 1 Hz, CH═C*H*NCH$_2$), 6.87 (1H, s, C*H*═CHNCH$_2$), and 7.26 p.p.m. (1H, s, N═C*H*—N).

Anal. Calcd. for $C_7H_{10}N_2$: C, 68.81; H, 8,25; N, 22.94. Found: C, 69.17; H, 8.14; N, 22.97.

Subsequent reaction of *N*-crotylimidazole (1.0 g, 9 mmol) with crotyl chloride (0.82 g, 9 mmol) at 60° for 1 h gave *N,N'*-dicrotylimidazolium chloride (**13***a*, 94% by p.m.r.[9]); p.m.r. (DMSO-d_6) δ 1.5–1.8 (6H, m, CH═CH-C*H*$_3$), 4.5–4.8 (4H, m, NC*H*$_2$CH═), 5.2–5.7 (4H, m, CH$_2$C*H*═C*H*CH$_3$), 7.25 (2H, d, J = 1 Hz, $\overset{+}{N}$CH═C-*H*N), and 9.78 p.p.m., (1H, broad s, $\overset{+}{N}$C*H*N).

(b) With Allyl Bromide (3)

Allyl bromide (1 equiv), imidazole (5 equiv), and sodium bicarbonate (1 equiv) in methanol at 25° for 4 days yielded *N*-allylimidazole (**12***b*, 96%), b.p. 40–42°/0.1 Torr; p.m.r. ($CDCl_3$) δ 4.5 (2H, d of t, J = 6.1 Hz, NC*H*$_2$CH═), 5.0–6.2 (3H, m, C*H*═C*H*$_2$), 6.90 (1H, t, J = 1 Hz, NCH═C*H*NCH$_2$), 7.05 (1H, d, J = 1 Hz, NC*H*═CHNCH$_2$), and 7.47 p.p.m. (1H, s, N═C*H*N); mass spectrum *m/e* (relative intensity) 108 P (51), 41 (100).

Anal. Calcd. for $C_6H_8N_2$: C, 66.64; H, 7.46; N, 25.91. Found: C, 66.42; H, 7.78; N, 25.74.

From *N*-allylimidazole (1 equiv) and allyl bromide (1 equiv) in methanol at 25° for 1 week was obtained 88% of *N,N'*-diallylimidazolium bromide[9] (**13***b*), p.m.r., (DMSO-d_6) δ 5.12 (4H, d of t, J = 6.1 Hz, $\overset{+}{N}$C*H*$_2$CH═), 5.31–5.56 (4H, m, CH$_2$CH═C*H*$_2$), 5.98–6.42 (2H, m, CH$_2$C*H*═CH$_2$), 8.09 (2H, d, J = 2 Hz, $\overset{+}{N}$C*H*═C*H*N), and 9.78 p.p.m. (1H, t, J = 2 Hz, $\overset{+}{N}$═CHN).

(c) With 1-Bromo-2-butyne (4)

1-Bromo-2-butyne (1 equiv), imidazole (5 equiv), and sodium bicarbonate (1 equiv) in methanol at 25° for 4 days afforded *N*-(but-2-ynyl)imidazole (**12***c*, 83%) b.p. 59–59.5°/0.1 Torr; p.m.r. ($CDCl_3$) δ 1.81 (3H, t, J = 2 Hz, C*H*$_3$C≡), 4.65 (2H, q, J = 2 Hz, NC*H*$_2$C≡), 7.04 (1 H, t, J = 1 Hz, NCH═C*H*NCH$_2$), 7.07 (1 H, d, J = 1 Hz, NC*H*═CHNCH$_2$) and 7.59 p.p.m. (1H, s, N═C*H*N); mass spectrum *m/e* (relative intensity) 120 P (100).

Anal. Calcd. for $C_7H_8N_2$: C, 69.98; H, 6.71; N, 23.32. Found: C, 69.66; H, 6.66; N, 23.24.

One equivalent each of *N*-(but-2-ynyl)imidazole and 1-bromo-2-butyne in methanol at 25° for 1 week yielded 94% of *N,N'*-di(but-2-ynyl)imidazolium bromide (**13***c*),[9] p.m.r. (DMSO-d_6) δ 1.89 (6H, t, J = 3 Hz, CH$_3$C≡), 5.32 (4H, q, J = 3 Hz, $\overset{+}{N}$C*H*$_2$C≡), 7.99 (2H, d, J = 2 Hz, $\overset{+}{N}$C*H*═C*H*N), and 9.75 p.p.m. (1H, t, J = 2 Hz, $\overset{+}{N}$═C*H*N).

(d) With 2-Bromoacetophenone (5)

2-Bromoacetophenone (1 equiv) and imidazole (10 equiv) alone in methanol at 25° for 20 h gave (following sodium bicarbonate treatment during work-up) *N*-(2-oxo-2-phenylethyl)imidazole (**12***d*, 94%), spars from benzene m.p. 119–120°; p.m.r. ($CDCl_3$) δ 5.38 (2H, s, C$_6$H$_5$COC*H*$_2$N), 6.95 (1H, t, J = 1 Hz, NCH═C*H*-NCH$_2$), 7.14 (1H, s, NC*H*═CHNCH$_2$), 7.4–7.7 (4H, m, meta and para aromatic and N═C*H*—N), and 8.03 p.p.m. (2H, d of d, J = 2.8 Hz, ortho aromatic). Mass spectrum *m/e* (relative intensity) 186 P (20) and 104 (100).

Anal. Calcd. for $C_{11}H_{10}N_2O$: C, 70.95; H, 5.41; N, 15.05. Found: C, 71.13; H, 5.32; N, 14.87.

N,N'-Di(2-oxo-2-phenylethyl)imidazolium bromide (**13***d*) was obtained in 59% yield from the reaction of equimolar proportions of 2-bromoacetophenone and imidazole in methanol at 25° for 24 h. Following sodium bicarbonate treatment during the work-up procedure, it was obtained as needles (from ethanol) m.p. 258–259°, p.m.r. (DMSO-d_6), δ 6.31 (4H, s, $\overset{+}{N}$C*H*$_2$CO), 7.70–7.86 (6H, m, meta and para aromatic), 7.93 (2H, d, J = 1 Hz, $\overset{+}{N}$C*H*═C*H*N), 8.13, 8.21 (4H, 2d, J = 1 Hz, ortho aromatic), and 9.30 p.p.m. (1H, t, J = 1 Hz, $\overset{+}{N}$═C*H*N).

Anal. Calcd. for $C_{19}H_{17}N_2O_2Br$: C, 59.23; H, 4.45; N, 7.27; Br, 20.74. Found: C, 59.48; H, 4.64; N, 7.15; Br, 20.82.

Alkylations of N-Methylimidazole (7b)

(a) With Crotyl Chloride (2)

A solution of *N*-methylimidazole (2.0 g, 24 mmol) and crotyl chloride (2.20 g, 24 mmol) in methanol (25 ml) was heated under reflux for 11 h. Evaporation of the solvent yielded quantitatively *N*-crotyl-*N'*-methylimidazolium chloride (**14***a*) as a deliquescent[9] solid, p.m.r. (DMSO-d_6) δ 1.6–1.9 (3H, m, CH═CHC*H*$_3$), 3.98 (3H, s, $\overset{+}{N}$—C*H*$_3$), 4.8–5.1 (2H, m, $\overset{+}{N}$C*H*$_2$CH═CHCH$_3$), 5.6–6.2 (2H, m, C*H*═C*H*CH$_3$), 8.0 (2H, d, J = 1Hz, $\overset{+}{N}$C*H*═C*H*N), and 9.84 p.p.m. (1H, broad s, $\overset{+}{N}$═C*H*N).

(b) With Allyl Bromide (3)

Equimolar allyl bromide and *N*-methylimidazole in methanol at 25° for 7 days gave *N*-allyl-*N'*-methylimidazolium bromide (**14***b*) as a low melting deliquescent, solid (89%),[9] p.m.r. (DMSO-d_6) δ 4.0 (3H, s, C*H*$_3\overset{+}{N}$), 5.05 (2H, d of t, J = 6. 1 Hz, $\overset{+}{N}$C*H*$_2$CH═CH$_2$), 5.28–5.53 (2H, m, CH═C*H*$_2$), 5.95–6.36 (1H, m, CH$_2$C*H*═CH$_2$), 8.01 (2H, d, J = 2 Hz, $\overset{+}{N}$C*H*═C*H*N), and 9.64 p.p.m. (1H, broad s, $\overset{+}{N}$═C*H*N).

[9]Owing to the extremely deliquescent properties of the bisalkylated imidazolium salts and of the alkylated *N*-methylimidazole derivatives (**12–15**) no further purification of this compound was possible.

Can. J. Chem. Downloaded from www.nrcresearchpress.com by 210.87.254.5 on 09/05/12
For personal use only.

(c) With 1-Bromo-2-butyne (4)

One equivalent each of 1-bromo-2-butyne and *N*-methylimidazole in methanol at 25° for 7 days afforded a 91% yield of the low melting, deliquescent, *N*-(but-2-ynyl)-*N'*-methylimidazolium bromide (**14***c*), p.m.r. (DMSO-d_6) δ 1.91 (3H, t, J = 3 Hz, $\overset{+}{N}CH_2C{\equiv}CCH_3$), 3.98 (3H, s, $CH_3\overset{+}{N}$), 5.31 (2H, q, J = 3 Hz, $\overset{+}{N}CH_2C{\equiv}CCH_3$), 7.96 (2H, d, J = 2 Hz, $\overset{+}{N}CH{=}CH\overset{+}{N}$), and 9.62 p.p.m. (1H, broad s, $\overset{+}{N}{=}CH\overset{+}{N}$).

(d) With 2-Bromoacetophenone (5)

2-Bromoacetophenone (1 equiv) and *N*-methylimidazole (1 equiv) were reacted in methanol solution at 25° for 6 h. *N*-Methyl-*N'*-(2-oxo-2-phenylethyl)imidazolium bromide (**14***d*) was obtained in 98% yield as prisms from acetonitrile/tetrahydrofuran, m.p. 153–154° (lit. (26) m.p. 153–155°), p.m.r. (DMSO-d_6) δ 4.0 (3H, s, $CH_3\overset{+}{N}$), 6.31 (2H, s, $\overset{+}{N}CH_2CO$), 7.59–8.00 (5H, m, meta and para aromatic and $\overset{+}{N}CH{=}CH\overset{+}{N}$), 8.15 (2H, d of d, J = 6.1 Hz, ortho aromatic), and 9.4 p.p.m. (1H, s, $\overset{+}{N}{=}CH\overset{+}{N}$).

Alkylations of Benzylamine

(a) With Crotyl Chloride (2)

Crotyl chloride (9.06 g, 0.1 mol) and benzylamine (10.7 g, 0.1 mol) were dissolved in methanol (50 ml) and the solution was heated at 60° for 4 days. Following solvent evaporation, the residue was dissolved in aqueous sodium hydroxide (10% w/v, 100 ml) and the resulting solution was extracted with ether (3 × 75 ml). The combined ether extract was washed with saturated aqueous sodium chloride (50 ml), dried ($MgSO_4$), and evaporated. Fractional (spinning band) distillation of the residual oil gave *N*-crotylbenzylamine (**15***a*, 2.4 g), b.p. 81°/1.5 Torr (lit. (27) b.p. 95°/12 Torr), p.m.r. ($CDCl_3$) δ 1.27 (1H, s, N*H*), 1.5–1.7 (3H, m, =CH—CH_3), 3.1–3.3 (2H, m, NCH_2CH=), 3.72 (2H, s, $C_6H_5CH_2N$), 5.5–5.7 (2H, m, —C*H*=C*H*—), and 7.30 p.p.m. (5H, s, C_6H_5).

The pot residue was dissolved in ether (35 ml) and was then treated with aqueous sodium hydroxide (10% w/v, 50 ml) and benzenesulfonylchloride (2.5 g) (to remove any remaining primary or secondary amino compounds) and the ethereal solution was separated and washed with aqueous sodium hydroxide solution (10% w/v, 5 × 25 ml). The organic layer was then extracted with aqueous hydrochloric acid (3 × 25 ml) and the acid solution was washed with ether (25 ml) and was then brought to p*H* 12 with solid sodium hydroxide. Extraction with ether (3 × 25 ml), followed by evaporation of the dried ($MgSO_4$) ether solution and fractional distillation yielded *N,N'*-dicrotylbenzylamine (**16***a*, 3.8 g), b.p. 75°/0.1 Torr, p.m.r. ($CDCl_3$), δ 1.5–1.7 (6H, m, =CHCH_3), 2.9–3.1 (4H, m, NCH_2CH=), 3.47 (2H, d, J = 2 Hz, $C_6H_5CH_2N$), 5.4–5.6 (4H, m, —C*H*=C*H*—), and 7.1–7.4 (5H, m, C_6H_5); mass spectrum *m/e* (relative intensity), 215 P (24) and 91 (100).

Anal. Calcd. for $C_{15}H_{21}N$: C, 83.66; H, 9.83; N, 6.51. Found: C, 83.73; H, 9.70; N, 6.77.

(b) With Allyl Bromide (3)

A solution containing equimolar amounts of allyl bromide and benzylamine in ether was kept at 25° for 5 days and was then filtered to remove benzylamine hydrochloride. Treatment of the filtrate with dry HCl gave *N*-allylbenzylamine (**15***b*, 36%) as its hydrochloride salt, needles from ethanol–ether, m.p. 144–145° (lit. (28) m.p. 143–144°); the free base had b.p. 63°/0.75 Torr (lit. (28) b.p. 70–79°/5.5 Torr), p.m.r. ($CDCl_3$) δ 1.32 (1H, s, N*H*), 3.19 (2H, d of t, J = 6.1 Hz, NCH_2CH=CH), 3.7 (2H, s, $C_6H_5CH_2N$), 5.0–5.3 (2H, m, CH=CH_2), 5.7–6.1 (1H, m, C*H*=CH_2), and 7.28 p.p.m. (5H, m, C_6H_5).

The ether filtrate from the original reaction was worked-up as for the crotyl chloride reaction (except that the Hinsberg sulfonation step was omitted) and yielded (after spinning band fractionation) 37% of *N,N'*-diallylbenzylamine (**16***b*), b.p. 73°/1.0 Torr (lit. (29) b.p. 89°/4 Torr); p.m.r. ($CDCl_3$) δ 3.06 (4H, d of t, J = 6.1 Hz, NCH_2CH=), 3.55 (2H, s, $C_6H_5CH_2N$), 5.0–5.3 (4H, m, CH=CH_2), 5.7–6.1 (2H, m, C*H*=CH_2) and 7.2–7.4 (5H, m, C_6H_5).

(c) With 1-Bromo-2-butyne (4)

The mono-(**15***c*) and bis-(**16***c*) alkylated products were obtained directly from the first fractional (spinning band) distillation of the mixture obtained from the reaction of 1-bromo-2-butyne (1 equiv) and benzylamine (1 equiv) in ether at 25° for 5 days. *N*-(But-2-ynyl) benzylamine (27%) had b.p. 89–90°/1.2 Torr; p.m.r. ($CDCl_3$) δ 1.4 (1H, s, N*H*), 1.77 (3H t, J = 2 Hz, ≡CCH_3), 3.31 (2H, q, J = 2 Hz, NCH_2C≡), 3.8 (2H, s, $C_6H_5CH_2N$), and 7.2–7.4 p.p.m. (5H, m, C_6H_5).

Anal. Calcd. for $C_{11}H_{13}N$: C, 82.97; H, 8.23; N, 8.80. Found: C, 82.88; H, 8.25; N, 8.84.

N,N'-Di(but-2-ynyl)benzylamine (43%) had b.p. 99°/0.17 Torr; p.m.r. ($CDCl_3$) δ 1.81 (6H, t, J = 2 Hz, ≡CCH_3), 3.33 (4H, q, J = 2 Hz, NCH_2C≡), 3.76 (2H, s, $C_6H_5CH_2N$), and 7.2–7.5 p.p.m. (5H, m, C_6H_5), mass spectrum *m/e* (relative intensity) 211 P (4) and 43 (100).

Anal. Calcd. for $C_{15}H_{17}N$: C, 85.26; H, 8.11; N, 6.63. Found: C, 84.79; H, 7.98; N, 6.95.

(d) With 2-Bromoacetophenone (5)

From 2-bromoacetophenone (1 equiv) and benzylamine (1 equiv) in methanol at 25° for 10 h, the hydrobromide of *N,N'*-di(2-oxo-2-phenylethyl)benzylamine (**16***d*) was obtained directly by filtration in 54% yield. It formed fine prisms from ethanol m.p. 197–198° (lit. (30) m.p. 196–197°); p.m.r. (DMSO-d_6) δ 4.58 (2H, s, $C_6H_5CH_2\overset{+}{N}$), 5.14 (4H, s, $\overset{+}{N}CH_2CO$), 7.29–7.83 (1H, m, aromatic), 7.93 (2H, d, J = 1 Hz, ortho aromatic), and 8.01 p.p.m. (2H, d, J = 1 Hz, ortho aromatic).

Anal. Calcd. for $C_{23}H_{22}NO_2Br$: C, 65.10; H, 4.99; N, 3.30; Br, 18.84. Found: C, 64.92; H, 5.24; N, 3.35; Br, 18.70.

The original filtrate was evaporated and the residue dissolved in hot aqueous hydrobromic acid (p*H* 4, 70 ml). On cooling, the filtered solution yielded 8% of the hydrobromide of *N*-(2-oxo-2-phenylethyl)benzylamine (**15***d*), fine needles from aqueous ethanol, m.p. 201–202° (lit. (30) m.p. 201–202°); p.m.r. (DMSO-d_6) δ 4.28 (2H, s, $C_6H_5CH_2\overset{+}{N}$), 4.89 (2H, s, $\overset{+}{N}CH_2CO$), 7.41–7.88 (8H, m, aromatic), 8.05 (1H, d, J = 1 Hz, ortho aromatic), and 8.13 p.p.m. (1H, d, J = 1 Hz, ortho aromatic).

Anal. Calcd. for $C_{15}H_{16}NOBr$: C, 58.83; H, 5.21; N, 4.58; Br, 26.10. Found: C, 59.04; H, 5.42; N, 4.57; Br, 26.27.

Alkylation of Benzyl Methyl Sulfide (9)

Attempted alkylations with (*a*) crotyl chloride, (*b*) allyl bromide, and (*c*) 1-bromo-2-butyne under a variety of conditions were unsuccessful.

(d) With 2-Bromoacetophenone (5)

Benzyl methyl sulfide (2.1 g, 15 mmol) and 2-bromoacetophenone (3.0 g, 15 mmol) were dissolved in benzene (10 ml) and after keeping the mixture for 4 days at 7°, the solid produced was filtered off, and washed with acetone. Recrystallization from methanol/2-propanol gave fine needles of benzyl-(2-oxo-2-phenylethyl)methyl sulfonium bromide (17, 2.6 g), m.p. 118–119° (lit. (31) m.p. 118°); p.m.r. (CF_3COOH) δ 3.03 (3H, s, $CH_3\overset{+}{S}$), 4.88 (2H, s, $C_6H_5CH_2\overset{+}{S}$), 5.29 (2H, s, $C_6H_5COCH_2\overset{+}{S}$), and 7.4–8.2 p.p.m. (10H, m, C_6H_5).

Attempted Alkylation of Guanidine with 2-Bromoacetophenone

Aqueous sodium hydroxide (1 ml of 10 *N*, 10 mmol) was added to a suspension of guanidine hydrochloride (0.96 g, 10 mmol) in methanol (15 ml) at 0° and the mixture was then filtered to remove sodium chloride. 2-Bromoacetophenone (2 g, 10 mmol) in cooled (0°) methanol (10 ml) was then added to the stirred filtrate and after keeping for 6 h at 0°, the reaction mixture was filtered. The crystalline solid (0.43 g) obtained was shown by p.m.r. (see Discussion) to consist of a mixture of *cis*- and *trans*-4-bromo-2,3-epoxy-3-phenylbutyrophenone. Three recrystallizations from ethanol afforded the pure *cis*-isomer as spars, m.p. 154–155° (lit. (21) m.p. 160–161°); i.r. (KBr) 1679 (CO), 1227 (C—C) and 919 cm^{-1} (C—C); p.m.r. (DMSO-d_6), δ 3.9 (1H, d, J = 11 Hz, $BrCH_A$), 4.75 (1H, d, J = 11 Hz, $BrCH_B$), 5.1 (1H, s, $OCHCO$), and 7.18–8.0 p.p.m. (10H, m, C_6H_5); mass spectrum *m/e* (relative intensity) 316 P (4) and 223 (100).

Anal.[10] Calcd. for $C_{16}H_{13}O_2Br$: C, 60.58; H, 4.13; Br, 25.20. Found: C, 60.61; H, 4.41; Br, 25.15.

Guanidine hydrobromide was recovered from the reaction mixture in 74% yield.

We thank the National Research Council of Canada and the National Cancer Institute of Canada for their generous support and for the award (to D.W.H.) of an NRCC Science Scholarship.

[10]The elemental analytical data were obtained prior to the recognition of this material as a known compound. They are included as further corroboration of the correctness of the structure assignment.

1. W. C. J. Ross. Biological Alkylating Agents. Butterworth's, London, England, 1962.
2. B. R. Baker. Design of active site directed irreversible enzyme inhibitors. John Wiley and Sons, Inc, New York, N.Y., 1967.
3. B. L. Vallee and J. F. Riordan. Ann. Rev. Biochem. **38**, 733 (1969).
4. E. Haber. Ann. Rev. Biochem. **37**, 497 (1968).
5. S. J. Singer. Adv. in Prot. Chem. **22**, 1 (1967).
6. N. Latif and E. T. Kaiser. J. Org. Chem. **34**, 3653 (1969).
7. J. B. Jones and J. M. Young. Can. J. Chem. **48**, 1566 (1970) and previous papers.
8. J. B. Jones and J. N. Barker. Can. J. Chem. **48**, 1574 (1970).
9. B. D. England. J. Chem. Soc. 1615 (1955).
10. L. F. Hatch and S. S. Nesbitt. J. Amer. Chem. Soc. **72**, 727 (1950); **73**, 358 (1951). L. F. Hatch and P. R. Noyes. J. Amer. Chem. Soc. **79**, 345 (1957).
11. *cf.* R. H. Dewolfe and W. G. Young. Chem. Rev. **56**, 753 (1956).
12. A. Pinner and R. Schwartz. Ber. **35**, 2441 (1902).
13. J. Sarasin and E. Wegmann. Helv. Chim. Acta, **7**, 720 (1924).
14. K. von Auwers and N. Mauss. Ber. **61**, 2411 (1928).
15. E. R. Shepard and H. A. Shonle. J. Amer. Chem. Soc. **69**, 2269 (1947).
16. M. Busch and G. Hefele. J. Prakt. Chem. **191**, 425 (1911).
17. F. E. Ray and I. Levine. J. Org. Chem. **2**, 267 (1937).
18. G. B. Butler and B. M. Benjamin. J. Amer. Chem. Soc. **74**, 1846 (1952).
19. J. B. Jones and D. W. Hysert. To be published.
20. J. Zauhar and B. F. Ladouceur. Can. J. Chem. **46**, 1079 (1968).
21. C. L. Stevens and V. J. Traynelis. J. Org. Chem. **19**, 533 (1954).
22. P. J. Ashworth, G. H. Whitham, and M. C. Whiting. J. Chem. Soc. 4633 (1957).
23. H. J. Backer and G. J. de Jong. Rec. Trav. Chim. **70**, 377 (1951).
24. I. J. Buchi, M. Prost, H. Eichenberger, and R. Lieberherr. Helv. Chim. Acta, **35**, 1527 (1952).
25. C. Wahl. Ber. **55B**, 1449 (1922).
26. V. Boekelheide and N. A. Fedoruk. J. Amer. Chem. Soc. **90**, 3830 (1968).
27. C. Mannich and O. Hieronimus. Ber. **75B**, 49 (1942).
28. S. L. Shapiro, V. A. Parrino, and L. Freedman. J. Amer. Chem. Soc. **81**, 2220 (1959).
29. G. B. Butler and R. L. Bunch. J. Amer. Chem. Soc. **71**, 3120 (1949).
30. A. T. Mason and G. R. Winder. J. Chem. Soc. 1355 (1893).
31. H. Boehme and W. Krause. Chem. Ber. **82**, 426 (1949).

Can. J. Chem. Downloaded from www.nrcresearchpress.com by 210.87.254.5 on 09/05/12
For personal use only.

Can. J. Chem. Downloaded from www.nrcresearchpress.com by 210.87.254.6 on 09/05/12
For personal use only.

The Mass Spectrometry of *para*-Substituted Benzyl Nitrates

P. J. SMITH[1]
Department of Chemistry, Bishop's University, Lennoxville, Quebec

Received[2] August 5, 1969

The mass spectra of several *para*-substituted benzyl nitrates have been measured at 70 and 15 eV. The major fragmentation pathways have been established using deuterium labelling and measurement of metastable peaks. The formation of the *para*.$Y.C_6H_4.CH_2O^+$ ions from the parent ions approximately correlate with the Hammett sigma constants. A hydrogen–deuterium isotope effect of approximately 1.8 was found for the loss of hydrogen (deuterium) from the $C_6H_5CHDO^+$ ion at 10 eV.

Canadian Journal of Chemistry, **49**, 333 (1971)

Introduction

A detailed study of the mass spectra of aliphatic organic nitrate esters has recently been reported (1, 2). No observable parent ion was found for any of the straight-chain esters up to ten carbon atoms. The major fragments were found to arise from cleavage of the carbon–carbon bond adjacent to the nitrate group to give an *m/e* 76 peak ($CH_2ONO_2^+$), from fission of the carbon–oxygen bond leading exclusively to the RCH_2^+ ion, and from cleavage of the oxygen–nitrogen bond to give an *m/e* 46 peak (NO_2^+). There was no observable fragment ion corresponding to oxygen–nitrogen bond rupture leading to the RCH_2O^+ ion. The principal cleavages of an *n*-alkyl nitrate are summarized in reaction 1.

$$[1]\quad RCH_2^+ \overset{b}{\leftarrow} [R\overset{a}{-}CH_2\overset{b}{-}O\overset{c}{-}NO_2]^{\ddagger} \overset{c}{\rightarrow} NO_2^+ \; m/e\ 46$$
$$\downarrow a$$
$$CH_2ONO_2^+ \; m/e\ 76$$

Results and Discussion

The present study was carried out on a series of *para*-substituted benzyl nitrates with the aim of establishing and comparing their fragmentation patterns with those of the aliphatic compounds. The nitrate esters were synthesized as described in the Experimental Section and all were shown to be thermally stable at the operating conditions of the mass spectrometer. The spectra were determined at both 70 and 15 eV for the *p*-CH_3, *p*-H, *p*-Cl, and *p*-CF_3 compounds and the major fragments are shown in Table 1. The benzyl nitrates, unlike the aliphatic esters, all exhibit a fairly intense parent ion, particularly at the lower ionization voltage. The major fragmentation pathways lead to the $P - 46$ ion (loss of nitrite), $P - 62$ ion (loss of nitrate), and the $p.Y.C_6H_4^+$ and $C_6H_5^+$ ions.

The fragmentation process of oxygen–nitrogen bond rupture leading to loss of nitrite from the parent ion and the formation of the $P - 46$ ions, reaction 2, unlike that of the aliphatic compounds where no $P - 46$ peak was observed, is a favored pathway for the decomposition of the benzyl

$$[2]\quad p.Y.C_6H_4.CH_2ONO_2^{\ddagger} \rightarrow p.Y.C_6H_4.CH_2O^+ + NO_2^{\cdot}$$

nitrate esters. This process, in fact, leads to the base peak in the mass spectrum of the *p*-trifluoromethyl compound determined at 15 eV. The corresponding α-d_2 esters, $p.Y.C_6H_4.CD_2ONO_2$, fragmented also to the $P - 46$ ions, $p.Y.C_6H_4.CD_2O^+$.

The decomposition of the $P - 46$ ions, p-$Y.C_6H_4.CH_2O^+$, is of some interest. For all the compounds studied, both undeuterated and α-dideuterated, peaks were observed in the mass spectra corresponding to the loss of one H (or D) from the $p.Y.C_6H_4CH_2(D_2)O^+$ ion to give the benzaldehyde-like $P - 47$ (or $P - 48$) ion which subsequently loses another H (or D) to give a $P - 48$ (or $P - 50$) peak. These processes are represented in reaction 3. The $p.Y.C_6H_4.C{\equiv}O^+$

$$[3]\quad p.Y.C_6H_4.CH_2(D_2)O^+ \xrightarrow{-H\ (or\ D)} p.Y.C_6H_4.CH(D)O^+ \xrightarrow{-H\ (or\ D)} p.Y.C_6H_4.C{\equiv}O^+$$

[1]Present address: Department of Chemistry and Chemical Engineering, University of Saskatchewan, Saskatoon, Saskatchewan.

[2]Revision received August 31, 1970.

TABLE 1. Mass spectra of some *p*-substituted benzyl nitrates*

	p-CH_3		*p*-H		*p*-Cl		*p*-CF_3	
m/e	70 eV	15 eV	70 eV	15 eV	70 eV	15 eV	70 eV	15 eV
28	4		3		32		22.5	
29	6		9		17		64	
30	6.5		7		11.5		39	
39	23.5		11		8		13	
46	5		5		8.5		53	35
50	6.5		12		26.5		27.5	
51	13		31		20		25	
65	30	5.5	5					
69							12	
75					28.5		19	
77	37.5	27.5	100	100	100	100	16.5	
78	7	3.5	11.5	9	11	10	7.5	
79	3.5		25	40				
91	100	100	22	21.5				
92	9	9.5	2	3				
93	17	26						
95							16	
105	23	21	11	13				
106	2.5	3	5	17.5				
107			9	38				
111					62.5	60		
112					6.5	7		
113					37	48		
114					3.5	5		
115					6	11		
119	11	10.5						
120	3	6						
121	14	51						
125					26	25	7	
126					3	5	8	
127					9	10	55.5	41
139					16	18		
140					5	13		
141					23	66		
142					4	11		
143					6.5	22		
145							100	84
146							10	10
147							10	22
153			16	57				
159							34.5	40
167	21.5	67						
173							23	38
174							19	78
175							22	100
176							2.5	12
187					21.5	73		
188					3	8		
189					7.5	25		
221							7.5	37

*Peaks having an abundance of 1% or greater relative to the base peak as given in the Table.

ions were produced in all cases by the preferential loss of the α-hydrogens from the $P - 46$ ions since the $p.Y.C_6H_4.CD_2O^+$ ions decomposed by the loss of two and four mass units to give the $p.Y.C_6H_4.C{\equiv}O^+$ ions with no loss of a hydrogen radical being observed.[3] Both $C_6H_5CH_2O^+$ and $C_6H_5CD_2O^+$ led to the ion, $C_6H_5C{\equiv}O^+$, at *m/e* 105 which decomposed to $C_6H_5^+$ by the loss of carbon monoxide as evidenced by the metastable peak at 56.5 (105 → 77).

Another decomposition pathway for the $p.Y.C_6H_4.CH_2O^+$ ions is confirmed by metastable peaks in the spectra of benzyl nitrate and its α-d_2 analogue. This route is similar to that proposed by Shannon (4) for the decomposition

[3]Eliel *et al.* (3) obtained a similar result in a study of the formation of the $C_6H_5CO^+$ ion from benzyl alcohol.

Can. J. Chem. Downloaded from www.nrcresearchpress.com by 210.87.254.6 on 09/05/12
For personal use only.

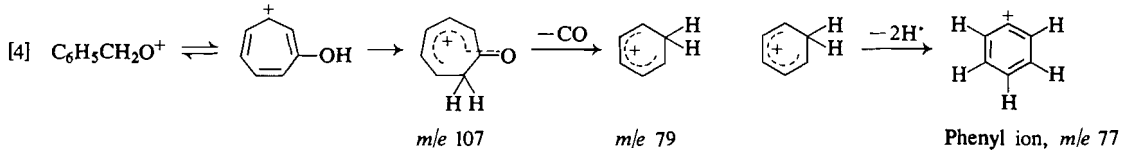

m/e 107 *m/e* 79 Phenyl ion, *m/e* 77

of benzyl alcohol and is represented in reaction 4 for the $C_6H_5CH_2O^+$ ion.

The loss of carbon monoxide from the $C_7H_7O^+$ ion, *m/e* 107, to give *m/e* 79 is confirmed by the observation of a metastable peak at 58.3 (107 → 79). Similarly, the $C_6H_5CD_2O^+$ ion loses CO to give a peak at *m/e* 81, $m^* = 60.3$ (109 → 81). The $C_6H_7^+$ ion, *m/e* 79, loses two hydrogen atoms to give the phenyl ion, $C_6H_5^+$, as confirmed by a metastable peak at 75.1 (79 → 77). The corresponding deuterated ion, $C_6H_5D_2$, *m/e* 81, loses one deuterium[4] to give *m/e* 79, $m^* = 77.1$ (81 → 79). The $C_6H_5D^+$ ion, *m/e* 79, subsequently decomposes to *m/e* 77, the base peak in the spectrum, $m^* = 75.1$ (79 → 77).

The phenyl ion,[5] *m/e* 77, derived from both the undeuterated and deuterated benzyl nitrate lost C_2H_2 to give *m/e* 51, $m^* = 33.8$ (77 → 51), indicating that deuterium was not scrambled into the ring during the fragmentation processes although it must be considered that the statistical factor, which favors loss of H over D, might lead to a very weak metastable ion corresponding to the loss of C_2HD.[6]

The formation of the $p.Y.C_6H_4^+$ ions can occur by two pathways other than that represented in reaction 3 for the decomposition of the $p.Y.C_6H_4.CH_2O^+$ ions. Firstly, the neutral formaldehyde molecule can be lost from the $p.Y.C_6H_4.CH_2O^+$ ions, reaction 5

[5] $p.Y.C_6H_4.CH_2O^+ \rightarrow p.Y.C_6H_4^+ + CH_2{=}O$

and secondly, the cleavage of the carbon–carbon bond adjacent to the nitrate function[7] leads also to the $p.Y.C_6H_4^+$ ions, reaction 6.

[6] $p.Y.C_6H_4.CH_2ONO_2^{\ddagger} \rightarrow p.Y.C_6H_4^+ + {}^{\cdot}CH_2ONO_2$

Metastable peaks, corresponding to these two processes, did not appear in the spectra of benzyl nitrate and its α-d_2 analogue.

The "benzyl" ion, $p.Y.C_6H_4.CH_2^+$, a significant ion in the spectra of all the compounds studied, is produced by cleavage of the carbon–oxygen bond, reaction 7.

[7] $p.Y.C_6H_4.CH_2ONO_2^{\ddagger} \rightarrow p.Y.C_6H_4.CH_2^+ + NO_3$

In no case was a peak observed at *m/e* 62 corresponding to the NO_3^+ ion in agreement with the results obtained from the aliphatic nitrate ester study. For all the compounds, the α-d_2 analogues gave peaks corresponding to the $p.Y.C_6H_4CD_2^+$ ions and as well $C_6H_5CHDONO_2$ fragmented to the *m/e* 92 ion, $C_6H_5CHD^+$.

The spectrum of $C_6H_5CH_2ONO_2$ revealed a strong metastable peak at 46.4 (91 → 65) corresponding to the loss of acetylene from the "benzyl" ion. Similarly, $C_6H_5CD_2ONO_2$ gave two weak metastable peaks; one at 46.8 (93 → 66) corresponding to the loss of C_2HD from $C_6H_5CD_2^+$ and the other at 48.3 (93 → 67), resulting from the loss of C_2H_2. These results suggest that deuterium is scrambled in the "benzyl" ion via the tropylium ion (5), and that the benzyl ions, $p.Y.C_6H_4.CH_2^+$ can best be represented by the structure

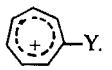

The fragmentation process, illustrated in reaction 2, was studied with the view of determining whether a hydrogen–deuterium isotope effect exists for the loss of hydrogen from the $C_6H_5CHDO^+$ ion, reaction 8. The mass spectrum

[8] $C_6H_5CHDONO_2^{\ddagger} \rightarrow C_6H_5CHDO^+ \xrightarrow{k^H} C_6H_5CDO^+$, $C_6H_5CDO^+ \xrightarrow{k^D} C_6H_5CHO^+$

of $C_6H_5CHDONO_2$ was obtained at low ionization voltage (10 eV, nominal) in order to minimize

[4] A peak at *m/e* 80 corresponding to the loss of a hydrogen from $C_6H_5D_2^+$ is not observed.

[5] The stability of this ion is indicated by the fact that it is a major fragment (Table 1) even for the *para*-substituted compounds where loss of *para*-substituent is necessary for its formation.

[6] Benzyl nitrate α-d_1 gave $C_6H_5CHDO^+$ ion, *m/e* 108, which lost CO to give *m/e* 80 which also decomposed to the phenyl ion, *m/e* 77.

[7] In no case was a peak observed at *m/e* 76 corresponding to the $CH_2ONO_2^+$ ion, which is a prominent ion in the spectra of the aliphatic nitrates (1).

Can. J. Chem. Downloaded from www.nrcresearchpress.com by 210.87.254.6 on 09/05/12
For personal use only.

Can. J. Chem. Downloaded from www.nrcresearchpress.com by 210.87.254.6 on 09/05/12
For personal use only.

subsequent fragmentation from the above ions and, in fact, only the four ions represented above appeared in the mass spectrum. The isotope effect[8] was measured using the ratio of peak heights for $C_6H_5CDO^+$ and $C_6H_5CHO^+$ ions after appropriate corrections for ^{13}C. The value for k^H/k^D was determined to be approximately 1.8 and is somewhat less than that found for *N*-methyl-3-cyano-1,4-dihydropyridine-4-*d*, 7.85 at 11.2 eV (6).

An interpretation of the magnitude of the isotope effect obtained in the present study, however, is difficult since the origin of an isotope effect obtained from electron bombardment reactions is somewhat obscure (6). It is suggested that a study of the possible effect of *para*-substituent on the magnitude of the hydrogen–deuterium isotope effect[9] might shed some light on the factors which contribute to the isotope effects encountered in mass spectral fragmentations.

The elegant technique of kinetic substituent effects (7–11) has recently been used for the assignment of ion structures and for the detailed elucidation of fragmentation pathways. Consequently, it was decided to investigate the effect of *para*-substituents on the fragmentation of the parent ion of the nitrate esters to the $p.Y.C_6H_4.CH_2O^+$ ions at both 70 and 15 eV. The results are shown in Table 2 where Z is defined as $[P - NO_2]^+/[P]^+$ and Z_0 refers to the unsubstituted compound.

Since the substituent is retained, and consequently a correlation of Z values with rates is not expected (10), an approximate Hammett plot is obtained when log Z/Z_0 is plotted against Hammett's sigma values, Fig. 1. It is possible that part of the apparent rate reduction by electron-donating substituents could be due to the accompanying reduction in ionization potentials

TABLE 2. Relative intensities for the loss of $NO_2^\cdot$ from *para*-substituted benzyl nitrates at 70 and 15 eV

para-Substituent	Z/Z_0 for loss of $NO_2^\cdot$	
	70 eV	15 eV
CH_3	1.2	1.2
H	1.0	1.0
Cl	1.5	1.3
CF_3	4.8	4.3

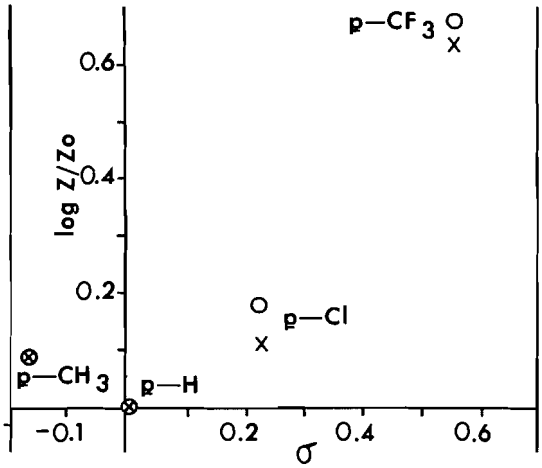

FIG. 1. log Z/Z_0 *vs.* σ constants for fragmentation of $p.Y.C_6H_4.CH_2ONO_2$ ions to $p.Y.C_6H_4.CH_2O^+$ ions; ×, 70 eV; ○, 15 eV.

(12) producing a larger fraction of molecular ions with less than the activation energy for dissociation, thus decreasing the Z values (see ref. 13 for a critical review on the correlation of substituents with rates). This effect would be very important at low voltage. The approximate constancy of the Z/Z_0 ratios in Table 2, however, for changes in ionization voltage from 70 to 15 eV, indicates that at least in part the fragmentation process is aided by electron-withdrawing substituents. It is expected that the Hammett correlation would improve at ionization voltages near the appearance potential where decomposition of the $p.Y.C_6H_4CH_2O^+$ ions is negligible.

Experimental

Materials

Benzyl Nitrate

This was prepared from benzyl chloride and silver nitrate in acetonitrile (14). The product, purified by fractional distillation from silver nitrate and calcium carbonate, was obtained in 60% yield, b.p. 62–62.5°/1 mm (ref. 14, b.p. 45°/0.5 mm).

[8]The possibility of scrambling in the $C_6H_5CHDO^+$ ion exists with deuterium being incorporated into the ring. That scrambling is probably unimportant is shown from the spectrum of $C_6H_5CD_2ONO_2$ where a peak corresponding to the loss of hydrogen from the $C_6H_5CD_2O^+$ ion is not observed. Furthermore, both benzyl nitrate and benzyl nitrate α-d_2 gave $C_6H_5C{\equiv}O^+$ which decomposed to *m/e* 77, $C_6H_5^+$, since both compounds gave a metastable peak at 56.5 (105 → 77).

[9]A. N. Bourns and P. J. Smith (results to be published) found that k^H/k^D varied with *para*-substituent for the reaction of 2-arylethylammonium salts with ethoxide ion in ethanol at 40°; $k^H/k^D = 4.15$ for *p*-CF_3 and 2.64 for *p*-OMe.

p-Methylbenzyl Nitrate

This was prepared from *p*-methylbenzyl bromide and silver nitrate by the same procedure used for benzyl nitrate (14). The product was obtained in 42% yield, b.p. 72.0–73.5°/1 mm (ref. 15, 78°/0.6 mm).

p-Chlorobenzyl Nitrate

This was prepared from *p*-chlorobenzyl chloride and silver nitrate by the same procedure used for benzyl nitrate (14). The product was obtained in 75% yield, b.p. 107–107.1°/8 mm.

Anal.[10] Calcd. for $C_7H_6ClNO_3$; C, 44.82; H, 3.22. Found: C, 44.76; H, 3.25.

p-Trifluoromethylbenzyl Nitrate

This was prepared from *p*-trifluoromethylbenzyl bromide[11] and silver nitrate by the same procedure used for benzyl nitrate (14). The product was obtained in 57% yield, b.p. 83.5–84°/2.5 mm.

Anal. Calcd. for $C_8H_6O_3NF_3$; C, 43.45; H, 2.73; F, 25.78. Found: C, 43.37; H, 2.58; F, 25.73.

Benzyl Nitrate α-d_2

This compound was prepared using the procedure described by Buncel and Bourns (14). Benzyl α-d_2 alcohol was synthesized and found to be better than 99% $C_6H_5CD_2OH$ by nuclear magnetic resonance (n.m.r.) analysis. Benzyl nitrate α-d_2 was prepared from the above alcohol in two steps, b.p. 45°/0.5 mm (ref. 14, b.p. 45°/0.5 mm). Benzyl nitrate α-d_2 was shown to be better than 99% deuterated in the benzylic position by n.m.r. analysis.

Benzyl Nitrate α-d_1

This compound was prepared using the procedure described by Buncel and Bourns (14). Benzyl α-d_1 alcohol was prepared by reduction of purified benzaldehyde with lithium aluminum deuteride and was shown to contain 1.02 hydrogens in the benzylic position by n.m.r. analysis. Benzyl nitrate α-d_1 was prepared from this alcohol in two steps, b.p. 45°/0.5 mm (ref. 14, b.p. 45°/0.5 mm). Benzyl nitrate α-d_1 was shown to have 1.01 hydrogens in the benzylic position by n.m.r. analysis.

p-Methylbenzyl Nitrate α-d_2

This compound was prepared using the procedure described by Buncel and Bourns (14). *p*-Methylbenzyl alcohol α-d_2 was synthesized and shown to be completely deuterated at the benzylic position by n.m.r. analysis. *p*-Methylbenzyl nitrate α-d_2 was prepared from the above alcohol in two steps, b.p. 72.5–73.0/1 mm (ref. 15, 78°/0.6 mm). This nitrate ester was shown to be better than 99% deuterated in the benzylic position by n.m.r. analysis.

p-Trifluoromethylbenzyl Nitrate α-d_2

This compound was prepared by the procedure described by Buncel and Bourns (14). *p*-Trifluoromethylbenzyl alcohol α-d_2 was synthesized and shown to be completely deuterated at the benzylic position by n.m.r. analysis. *p*-Trifluoromethylbenzyl nitrate α-d_2 was prepared from the above alcohol in two steps, b.p. 83.8–84°/2.5 mm. This compound was shown by n.m.r. analysis to be better than 99% deuterated in the benzylic position.

Mass Spectra

Most mass spectra were obtained with a Consolidated Electrodynamics Corp. Model 21-104 mass spectrometer. The samples were introduced by a CEC all glass inlet system, at 60°, into the source maintained at 90°. The spectra were recorded at 70 and 15 eV at an ionization current of 10 μA. The metastable spectra were run on an MS-12 mass spectrometer with these samples introduced directly into the source at 80°. The spectra were run at an accelerating voltage of 8 kV and an ionization voltage of 70 eV and ionization current of 10 μA.

Test of the Thermal Stability of the Organic Nitrate Esters

The fragmentation patterns of all the compounds studied did not vary on changes of inlet and source temperatures of 30° from those reported above. In addition, a sample of each of the esters studied was heated at 100° for 30 min in an evacuated sealed tube and no change in its n.m.r. and mass spectra was found.

The author would like to thank Mrs. Carol Pollock who synthesized several of the undeuterated nitrate esters. Financial support from the National Research Council of Canada is gratefully acknowledged.

1. R. T. M. Fraser and N. C. Paul. J. Chem. Soc. B, 659 (1968).
2. R. T. M. Fraser and N. C. Paul. J. Chem. Soc. B, 1407 (1968).
3. E. L. Eliel, J. D. McCollum, S. Meyerson, and P. N. Rylander. J. Amer. Chem. Soc. **83**, 2481 (1961).
4. J. S. Shannon. Aust. J. Chem. **15**, 265 (1962).
5. H. M. Grubb and S. Meyerson. *In* (F. W. McLafferty, ed.) Mass Spectrometry of Organic Ions. Academic Press, New York. 1963. pp. 516–519 and literature cited therein.
6. B. J. S. Wang and E. R. Thornton. J. Amer. Chem. Soc. **90**, 1216 (1968).
7. M. M. Bursey and F. W. McLafferty. J. Amer. Chem. Soc. **88**, 29 (1966).
8. M. M. Bursey and F. W. McLafferty. J. Amer. Chem. Soc. **89**, 1 (1967).
9. F. W. McLafferty and T. Wachs. J. Amer. Chem. Soc. **89**, 5043 (1967).
10. M. M. Bursey. Org. Mass Spectrom. **1**, 31 (1968).
11. P. Brown. J. Amer. Chem. Soc. **90**, 2694 (1968).
12. T. W. Bentley, R. A. W. Johnstone, and D. W. Payling. J. Amer. Chem. Soc. **91**, 3978 (1969).
13. I. Howe, D. H. Williams, and R. G. Cooke. Org. Mass Spectrum. **2**, 137 (1969).
14. E. Buncel and A. N. Bourns. Can. J. Chem. **38**, 2457 (1960).
15. J. W. Baker and D. M. Easty. J. Chem. Soc. 1193, 1208 (1952).
16. P. J. Smith and A. N. Bourns. Can. J. Chem. **48**, 125 (1970).

[10]Elemental analysis was performed by Galbraith Laboratories, Inc., Knoxville, Tennessee.

[11]For the synthesis of this compound see ref. 16.

Can. J. Chem. Downloaded from www.nrcresearchpress.com by 210.87.254.6 on 09/05/12
For personal use only.

Applications of Quantum Chemistry. I. Energetics and Bonding in Conjugated Free Radical Chains[1]

N. C. BAIRD
Department of Chemistry, University of Western Ontario, London, Ontario
Received August 28, 1970

The heats of formation at 25 °C and the equilibrium carbon–carbon bond lengths are calculated by the neglect of nonbonded differential overlap molecular orbital theory for a series of conjugated, acyclic free radicals containing from one to nine unsaturated carbon atoms. The total bonding energies in the radicals exceed the values expected from polyene bond terms by 5–9 kcal/mol, depending on the length and branching of the chain.

Canadian Journal of Chemistry, 49, 338 (1971)

Can. J. Chem. Downloaded from www.nrcresearchpress.com by 210.87.254.40 on 09/05/12
For personal use only.

Introduction

Although considerable experimental difficulties are associated with the determination of thermodynamic properties of free radicals, the potential utility of such information continues to spur considerable research in this field. Heats of formation (ΔH_f) of hydrocarbon free radicals are useful (*1*) in deducing the nature of the bonding in open-shell systems, (*2*) in calculations of the rates of homolytic gas-phase reactions (*1*), and (*3*) in the estimation of the energies of twisted triplet states of polyenes (2), etc.

Recently, Dewar *et al.* (3) have shown that accurate ΔH_f's for hydrocarbon free radicals can be calculated using the same molecular orbital theories which have proven so successful in reproducing the ΔH_f's of closed-shell organic molecules. In this paper, a π electron s.c.f.-l.c.a.o.-m.o. method is used to explore the thermochemistry and bonding in acyclic, conjugated free radicals containing from one to nine sp^2-hybridized carbon atoms.

Method of Calculation

The molecular orbital theory employed herein is a variant of the n.n.d.o. (neglect of nonbonded differential overlap) method reported previously (4). The bonding energy and the equilibrium bond lengths in each free radical are evaluated by deducing the optimum set of π electron molecular orbitals via the "half-electron" procedure (3); the total bonding energy associated with the carbon–carbon and the carbon–hydrogen single bonds is evaluated empirically from Morse functions (4).

[1]Research supported by the National Research Council of Canada.

The n.n.d.o. theory used here differs from that previously reported only in several of the semi-empirical parameter values; the new version yields more accurate energies and geometries than did the old:

(*i*) The equilibrium $C(sp^2)$–$C(sp^2)$ single bond energy is taken as 88.8 (rather than 88.0) kcal/mol.

(*ii*) The two-center component β (in eV) of the resonance integral between carbon atoms separated by distance R (in Å) is now

$$\beta = -105.202/\exp(1.985R)$$

(*iii*) The bond lengths R are made self-consistent with the simple bond order matrix **P** (no overlap populations included) by

$$R = 1.496 - 0.2021\mathbf{P}$$

In all cases, *initial* bond lengths of 1.4 Å and idealized bond angles of 120° were assumed.

Results and Discussion

The calculated heats of formation for eight conjugated free radicals are listed in the fourth column of Table 1. The agreement between the calculated and experimental ΔH_f's is excellent (within 2 kcal/mol) for the three radicals, methyl,[2] allyl, and pentadienyl, for which measurements are available. In the case of the branched free radicals (**4**, **6**, and **7**), there exists steric interactions between hydrogen atoms separated by three carbon–carbon bonds of the same type that destabilize *cis*-butadiene by 2 kcal/mol

[2]Note that the ΔH_f of CH_3 (along with those of ethylene, *trans*-butadiene, benzene, naphthalene, and anthracene) was used to fit the parameters. The r.m.s. error in the ΔH_f is reduced from 1.4 to 0.5 kcal/mol for this series by use of the new parameterization.

TABLE 1. Thermochemistry at 25 °C of free radicals (kcal/mole)

Radical	Source	ΔH_f of radical: Experimental	Calculated	Adjusted*	ΔH_f†	ΔH‡
CH_3 (1)	CH_4	34.3§‖	34.1	34.1	−17.9	104.1
(2)		41.4§	43.0	43.0	4.9	90.2
(3)		52.9§	54.4	54.4	18.1	88.4
					25.2	81.3
(4)		—	57.0	59.0	18.1	93.0
(5)	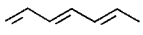	—	67.6	67.6	31.4¶	88.3
	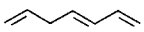				38.9¶	80.8
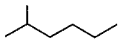 (6)	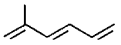	—	70.8	72.8	31.7¶	93.2
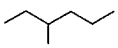 (7)	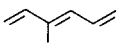	—	67.5	71.5	31.7¶	91.9
(8)	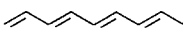	—	81.4	81.4	44.6¶	88.9
	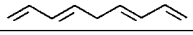				52.6¶	80.9

*ΔH_f's of 4, 6, and 7 corrected for steric interactions. See text for details.
†From ref. 7 unless indicated otherwise.
‡ΔH for the reaction RH → R + H, where ΔH_f(H) = 52.1 kcal/mol.
§See ref. 8.
‖See ref. 9.
¶Extrapolated from the ΔH_f's (see note † above) of the series ethylene, *trans*-butadiene, propene, 2-methylbutadiene, and 1-*trans*-3-pentadiene.

relative to the *trans* conformation (5). Since such effects are not included in the present molecular orbital treatment, an empirical correction of the above magnitude has been applied where applicable (column five of Table 1). Given the calculated ΔH_f's in Table 1, the C—H and C—C bond dissociation enthalpies in a wide variety of closed-shell hydrocarbons can be determined, provided the ΔH_f of the latter is known or can be estimated. As an example of this application, the heats of reaction from various reactants (column 2 of Table 1) to the conjugated radicals are listed in the last column of Table 1.

The trends in the theoretical ΔH_f's (Table 1) and in the calculated bond lengths (Table 2) yield an interesting insight into the bonding in conjugated free radicals. The change in the ΔH_f when an additional double bond is joined to an unbranched radical increases with chain length, and eventually converges to the value of $\sim$ 14 kcal/mol found in closed-shell polyenes

$$\Delta\Delta H_f(C_3 - C_1) = 8.9 \text{ kcal/mol}$$
$$\Delta\Delta H_f(C_5 - C_3) = 11.4 \text{ kcal/mol}$$
$$\Delta\Delta H_f(C_7 - C_5) = 13.2 \text{ kcal/mol}$$
$$\Delta\Delta H_f(C_9 - C_7) = 13.8 \text{ kcal/mol}$$

Thus the unbranched radicals having three, five, seven, and nine carbon atoms are stabilized by 5.1, 7.7, 8.5, and 8.7 kcal/mol relative to the *effective* double and single bond energies operative in polyenes. Combining the stabilization in allyl with the known single-bond rotation barrier of $\sim$ 5 kcal/mol in *trans*-butadiene (6) leads to the prediction that the barrier to rotation about a carbon–carbon bond of $\sim$ 10 kcal/mol in the allyl free radical.

Can. J. Chem. Downloaded from www.nrcresearchpress.com by 210.87.254.40 on 09/05/12
For personal use only.

Can. J. Chem. Downloaded from www.nrcresearchpress.com by 210.87.254.40 on 09/05/12
For personal use only.

TABLE 2. Calculated carbon–carbon bond lengths

Radical number	Bond*	Length (Å)
2	1–2	1.390
3	1–2	1.366
	2–3	1.424
4	1–2	1.394
	2–3	1.474
	3–4	1.342
	2–5′	1.393
5	1–2	1.356
	2–3	1.441
	3–4	1.395
6	1–2	1.395
	2–3	1.472
	3–4	1.348
	4–5	1.470
	5–6	1.343
	2–7′	1.393
7	1–2	1.342
	2–3	1.472
	3–4	1.427
	4–5	1.421
	5–6	1.368
	3–7′	1.370
8	1–2	1.351
	2–3	1.452
	3–4	1.378
	4–5	1.416

*In branched radicals, the carbon atoms are numbered starting from the left of the diagram in Table 1 and along the all *trans* backbone. The primed numbers refer to atoms branched off this backbone.

The calculated bond distances in the unbranched radicals further emphasize the decreasing importance of additional electron delocalization in the longer chains. There is a marked tendency for the terminal bonds to acquire full polyene "double bond" character and for the penultimate bonds polyene "single bond" character; for example the C_9 free radical is well represented by the single structure

The extent of bond alternation is more pronounced in the radicals **4** and **6** which are both branched at the 2 position. The bonding in these systems simulates that of an allyl radical joined at its "inactive" middle carbon to ethylene and to butadiene, respectively, by a polyene-like single bond, since the bond distances are well characterized by the structures

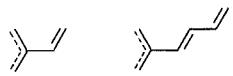

This interpretation is supported by the energetics of the free radicals, since the increases in the ΔH_f upon adding two and four carbon atoms to allyl in this manner are calculated as +14.0 and +27.8 kcal/mol, respectively, which are essentially identical to the values calculated for addition of double bonds to ethylene of +14 and +28 kcal/mol. Similarly, the bond lengths in the seven-carbon radical branched at the 3-position simulate those of a polyene unit joined at an inactive position of the pentadienyl radical

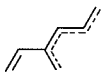

The calculated energy for this system is, however, almost 1 kcal/mol greater than expected for this structure.

1. S. W. BENSON. Thermochemical Kinetics. John Wiley and Sons, Inc., New York. 1968.
2. N. C. BAIRD. Mol. Photochem. **2**, 53 (1970).
3. (*a*) M. J. S. DEWAR, J. A. HASHMALL, and C. G. VENIER. J. Amer. Chem. Soc. **90**, 1953 (1968). (*b*) N. C. BAIRD and M. J. S. DEWAR. J. Chem. Phys. **50**, 1262 (1969).
4. N. C. BAIRD. Mol. Phys. **18**, 39 (1970).
5. J. G. ASTON. Discuss. Faraday Soc. **10**, 73 (1951).
6. J. G. ASTON, G. SZASZ, H. W. WOOLLEY, and F. G. BRICKWEDDE. J. Chem. Phys. **14**, 67 (1946).
7. J. D. COX and G. PILCHER. Thermochemistry of Organic and Organometallic Compounds. Academic Press, New York. 1970.
8. D. M. GOLDEN and S. W. BENSON. Chem. Rev. **69**, 125 (1969).
9. N. A. GAC, D. M. GOLDEN, and S. W. BENSON. J. Amer. Chem. Soc. **91**, 3091 (1969).

Chemistry of the Aminochromes. Part XIV. Noradrenochrome[1,2]

W. S. POWELL[3,4] AND R. A. HEACOCK[5,6]
Department of Biochemistry, Faculty of Medicine, Laval University, Quebec 10, Quebec

Received July 30, 1970

The preparation, in pure crystalline form, of noradrenochrome and its monosemicarbazone, together with some of their more important properties is described.

Canadian Journal of Chemistry, 49, 341 (1971)

Can. J. Chem. Downloaded from www.nrcresearchpress.com by 210.87.254.6 on 09/05/12
For personal use only.

Despite the fact that adrenochrome, the important red quinonoid oxidation product of adrenaline, has been known in crystalline form since 1937 (1), noradrenochrome (**1**), the corresponding aminochrome (*cf.* refs. 2, 3) obtained from noradrenaline (**2**), has not been fully characterized in the solid state. The properties of solutions containing variable amounts of **1** prepared by the oxidation of solutions of **2** have been described fairly extensively (*cf.* refs. 2, 3). These solutions may also have contained other substances, such as unchanged **2** and its initial, uncyclized oxidation product, noradrenaline quinone (4, 5). Noradrenochrome (**1**) has been obtained as "red rings on the side of the flask" after solutions containing **1**, prepared by the oxidation of **2** with silver oxide in acetonitrile (6), were concentrated to dryness *in vacuo*. However, the preparation of crystalline **1** has not yet been reported. This note describes the preparation, characterization, and properties of this interesting oxidation product of noradrenaline (**2**).

Noradrenochrome (**1**) can be obtained as a deep reddish-violet crystalline solid on careful concentration, at low temperatures, of its solutions in methanol, prepared by oxidation of suspensions of **2** (free base) by silver oxide. Extreme care must be taken to remove all traces of silver from the solutions containing **1** prior to their concentration. This has been achieved by filtration of the solution, firstly through a bed of anhydrous sodium sulfate (*cf.* 7) and

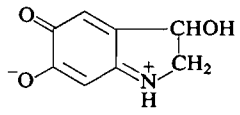

1

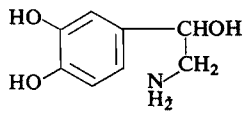

2

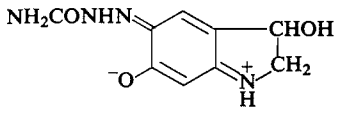

3

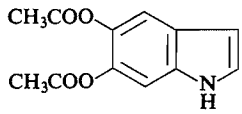

4

secondly through a Dowex-1 (Cl^-) resin bed (*cf.* 8). There appeared to be no advantage in centrifuging the solution (*cf.* 9) prior to crystallization of the aminochrome.

A crystalline derivative of **1**, the monosemicarbazone **3**, has been prepared directly from the aminochrome. This compound has not previously been described in the literature. The aminochrome monosemicarbazones have considerable importance in medicine as haemostatic agents (*cf.* refs. 3, 10).

Noradrenochrome (**2**) can be easily reduced in aqueous solution by ascorbic acid (*cf.* refs. 2, 3) to 5,6-dihydroxyindole, which can readily be isolated as its diacetyl derivative (*i.e.* **4**).

Experimental

The melting points were determined on either a Leitz Hot-Stage instrument or a Fisher–Johns apparatus and are uncorrected. The i.r., u.v., n.m.r., and mass spectra were determined on Perkin–Elmer model 237, Bausch and Lomb 505, Varian A-60-A, and Dupont/C.E.C. 21-110B instruments respectively.

Noradrenochrome (1)

Freshly prepared silver oxide (22.5 g) was added to a suspension of L-noradrenaline base (5 g, Schuchardt) in

[1]Part XIII, see ref. 14.
[2]NRCC No. 11605.
[3]Graduate Student, Department of Chemistry, Dalhousie University, Halifax, Nova Scotia.
[4]Holder of an NRCC Scholarship.
[5]Professeur Visiteur: Département de Biochimie, Faculté de Médecine, Université Laval, Québec 10, Québec (1969/1970).
[6]Permanent address (R.A.H.) to which correspondence and reprint requests should be sent: National Research Council of Canada, Halifax, Nova Scotia.

dry methanol (500 ml) at 32°. The reaction mixture was vigorously shaken for 6 min at this temperature (it was possible to maintain the temperature at 32° without external heating due to the mildly exothermic nature of the reaction), after which time it was filtered firstly through an anhydrous sodium sulfate bed (height = 2 cm; diameter = 11 cm) and secondly through a Dowex-1 × 8 (Cl^-) resin[7] bed (height = 3 cm; diameter = 10 cm). The filtrate was concentrated below 20° *in vacuo* to small bulk (*ca.* 30 ml), until crystals began to form in the solution. Noradrenochrome was obtained in dark reddish-violet needles [150 mg (3%); totally decomposed without melting by 105°] on filtration of the solution; $\lambda_{max}(H_2O)$ nm(ε): 217(22 350), 293(8580), 488(3190); ν_{max}(KBr): 3320 (sh), 3120, 1676, 1663, 1622, 1580, 1530 cm^{-1}.

Anal. Calcd. for $C_8H_7NO_3$: C, 58.18; H, 4.24; N, 8.48. Found: C, 58.39; H, 4.08; N, 8.56.

Noradrenochrome Monosemicarbazone (3)

Semicarbazide hydrochloride (27 mg) in acetate buffer (1.5 ml) at p*H* 5 was added to a stirred solution of noradrenochrome (20 mg) in water (1.5 ml). The crude monosemicarbazone (15 mg) was obtained in brownish-orange needles after the solution had been allowed to stand at room temperature for 1.5 h. Pure noradrenochrome monosemicarbazone [9 mg (34%); totally decomposed without melting by 221°] was obtained in fine orange needles after recrystallization of the crude product from water; λ_{max}(0.1 *N* HCl): nm(ε): 373(29 000); $\lambda_{max}(H_2O)$ nm(ε): 440(sh), 351(27 000); λ_{max}(0.1 *N* NaOH) nm(ε): 441 mμ (27 700).

Anal. Calcd. for $C_9H_{10}N_4O_3$: C, 48.65; H, 4.54; N, 25.22. Found: C, 48.84; H, 4.46; N, 25.03.

Reduction of Noradrenochrome (1) by Ascorbic Acid (cf. 11); Preparation of 5,6-Diacetoxyindole (4)

Ascorbic acid (400 mg) was added to a mixture of noradrenochrome (75 mg) in water (5 ml) and peroxide-free ether (15 ml). The system was vigorously shaken until the red color was totally discharged (about 1 min). The ether phase was removed and dried (Na_2SO_4) and a mixture of acetic anhydride (2 ml) and dry pyridine (2 ml) added. After removal of the ether *in vacuo* the reaction mixture was allowed to stand at room temperature for 2 h, and was then evaporated to dryness *in vacuo*. The residue was dissolved in CH_2Cl_2 (15 ml) and washed in turn with the following reagents: 0.1 *N* HCl (15 ml), saturated aqueous sodium bicarbonate (3 × 15 ml), and water (2 × 15 ml). The CH_2Cl_2 solution was dried (Na_2SO_4) and on evaporation to dryness gave a white crystalline solid (47 mg), which gave 5,6-diacetoxyindole [38 mg (36%), m.p. 139–142°] on recrystallization from heptane containing a small quantity of benzene, lit. m.p. 139–140° (12), 130–133° (13). The n.m.r., τ($CDCl_3$): 1.6 (broad s, *N*—H), 2.74 (s, H_4), 2.96 (s, H_7), 3.08 (t, H_2), 3.70 (t, H_3), 7.73 (s, CH_3). After shaking with D_2O the peak at τ 1.6 disappeared and the triplets at τ 3.08 and 3.70 collapsed to doublets ($J_{2,3}$ = 2.7 Hz).[8] Mass spectrum: $M^{+\cdot}$ 233.0684 ± .0007; Calcd. for $C_{12}H_{11}NO_4$ 233.06881.

The authors wish to express their thanks to Dr. L. Babineau (Department of Biochemistry, Faculty of Medicine, Laval University) for providing the necessary space and facilities in his laboratories to enable this research to have been carried out. The n.m.r. spectrum was obtained by courtesy of Dr. R. Burnell (Department of Chemistry, Faculty of Science, Laval University). The mass spectrum was recorded by Mr. D. Embree (A.R.L.).

1. D. E. Green and D. Richter. Biochem. J. **31**, 599 (1937).
2. R. A. Heacock. Chem. Rev. **59**, 181 (1959).
3. R. A. Heacock. Advan. Heterocycl. Chem. **5**, 205 (1965).
4. A. Kodja and S. Bouchilloux. C. R. Soc. Biol. **153**, 1407 (1959).
5. A. Kodja and S. Bouchilloux. Biochim. Biophys. Acta, **41**, 345 (1960).
6. P. Marquardt and E. Carl. Naturwiss. **39**, 210 (1952).
7. H. Sobotka and J. Austin. J. Amer. Chem. Soc. **73**, 3077 (1951).
8. R. A. Heacock, C. Nerenberg, and A. N. Payza. Can. J. Chem. **36**, 853 (1958).
9. A. Feldstein. Sci. **128**, 28 (1958).
10. H. Sobotka, N. Barsel, and J. D. Chanley. Fortschr. Chem. Org. Naturst. **14**, 217 (1957).
11. G. L. Mattok and R. A. Heacock. Can. J. Chem. **42**, 484 (1964).
12. R. A. Heacock, M. E. Mahon, and B. D. Scott. Can. J. Chem. **39**, 231 (1961).
13. R. J. S. Beer, K. Clarke, H. G. Khorana, and A. Robertson. J. Chem. Soc. 2223 (1948).
14. W. Powell and R. A. Heacock. Can. J. Chem. **47**, 2102 (1969).

[7]The Dowex resin was pretreated by the method described in the literature (8).

[8]Long range coupling between H_3 and H_7 was also apparent, although the coupling constant ($J_{3,7} \simeq 0.7$ Hz) was difficult to measure accurately.

Can. J. Chem. Downloaded from www.nrcresearchpress.com by 210.87.254.6 on 09/05/12
For personal use only.

Hydrocarbon Complexes of Iron Carbonyls Formed Photochemically in Argon Matrices at 17 K

M. J. NEWLANDS AND J. F. OGILVIE
Department of Chemistry, Memorial University of Newfoundland, St. John's, Newfoundland

Received August 5, 1970

Irradiation of pentacarbonyliron with ethene in an argon matrix gives $(C_2H_4)Fe(CO)_4$, while ethyne reacts with the carbonyl under similar conditions to give a complex of 1-buten-3-yne.

Canadian Journal of Chemistry, 49, 343 (1971)

Matrix isolation coupled with absorption spectrometry has recently been shown to be a convenient method for the study of photochemical reactions of transition metal carbonyl derivatives (1). Products were detected which could not be prepared by standard thermal methods.

Further studies with ethene and normal and deuterated ethyne have now been carried out. A mixture of the hydrocarbon and pentacarbonyliron in an argon matrix (proportions ~10:1:100) at 17 K has been subjected to photolysis by radiation from a mercury lamp filtered to exclude wavelengths < 312 nm and between 417 and 676 nm.

Reaction of ethene with pentacarbonyliron during irradiation produces carbon monoxide and a monoalkene complex, $(C_2H_4)Fe(CO)_4$, a compound previously prepared by a high-pressure reaction (2).

A comparison of the important new bands in the vibrational spectrum (Perkin–Elmer 225, CsI optics), with the fundamental wave numbers previously reported appears in Table 1. Further irradiation leads to new bands, such as 1490 and 1218 cm^{-1}, which may indicate loss of further carbon monoxide from the alkene complex.

TABLE 1. Comparison of wave numbers of $(C_2H_4)Fe(CO)_4$ in argon matrix and gas

Gas (2)	Ar matrix
3090	*
3024	*
2088	2090
2007	2009
1986	1992
1511	1508
1446	*
1200	1195
942	*
704	711
	635
	608

*Masked by remaining ethene.

Reactions of ethyne with iron carbonyls yield complex mixtures of products under conventional conditions (3). In the present experiments, spectrometric changes during photolysis indicate production of 1-buten-3-yne, which complexes with the iron via the alkyne group only. The principal evidence for this comes from new bands for $C_2H_2(C_2D_2)$ at 1709 (1560), co-ordinated C≡C vibration (4); 1547 (1462), uncoordinated C=C (5); 912 (796), methylene wag of vinyl group (5); and 672 (531) cm^{-1}, CH bending vibration of C≡CH group which is presumably no longer linear. Dimerization of ethyne to 1-buten-3-yne in the presence of copper(I) salts was discovered by Nieuwland *et al.* about 1930 (6), but the present work appears to have provided the first evidence for a complex of 1-buten-3-yne with a metal other than copper. Photolysis of ethyne itself, either gaseous or solid, requiring light of wavelength < 257 nm, produces 1-buten-3-yne as a minor by-product and then only under special conditions (7).

We thank the National Research Council of Canada and the Research Corporation of New York for financial assistance.

1. J. F. OGILVIE. Chem. Commun. 392 (1970).
2. H. D. MURDOCH and E. WEISS. Helv. Chim. Acta, **46**, 1588 (1963).
3. G. E. COATES, M. L. H. GREEN, and K. WADE. Organometallic Compounds. Vol. II. Methuen and Co. Ltd., London, 1968. Chapt. 8, and references cited therein.
4. D. M. ADAMS. Metal-ligand and related vibrations. Edward Arnold Ltd., London, 1967. pp. 186–188; K. NAKAMOTO. Characterization of organometallic compounds by infrared spectroscopy. *In* Characterization of organometallic compounds. Pt. 1. *Edited by* M. Tsutsui. Interscience Publishers, New York, 1969. p. 129.
5. L. J. BELLAMY. The infrared spectroscopy of complex molecules. 2nd Edition. Methuen and Co. Ltd., London, 1958.
6. J. A. NIEUWLAND, W. S. CALCOTT, F. B. DOWNING, and A. S. CARTER. J. Amer. Chem. Soc. **53**, 4197 (1931).
7. B. L. DUNICZ. J. Amer. Chem. Soc. **63**, 2461 (1931).

Can. J. Chem. Downloaded from www.nrcresearchpress.com by 210.87.254.105 on 09/05/12
For personal use only.

Photochemistry of Steroid 4-en-3-one 11α-Nitrites. A Novel Synthesis of A-Nor-B-homo Steroids

HANS REIMANN AND OLGA Z. SARRE
Schering Corporation, Bloomfield, New Jersey 07003

Received September 25, 1970

Photolysis of some 11α-hydroxysteroid 4-en-3-one nitrites afforded 1-oximinosteroid 4-en-3-ones and 9*a*-methyl-B(9*a*)-homo-A-norsteroid 3(5),9*a*-dien-2-ones. Chemical and physical evidence for the latter, as well as a plausible mechanism for the transformation, is presented.

La photolyse de quelques nitrites dérivés d'hydroxy-11α oxo-3 Δ^4-stéroides a fourni des oximino-1 oxo-3 Δ^4-stéroides et des oxo-2 $\Delta^{3(5),9}$ méthyl-9*a* B(9*a*)-homo A-norstéroides. Des preuves physiques et chimiques de la nature de ces derniers composés ainsi qu'un mécanisme plausible pour cette transformation sont aussi présentés.

Canadian Journal of Chemistry, **49**, 344 (1971)

Since the original publication by Barton and coworkers (1), the photolysis of organic nitrites has provided many interesting and sometimes unexpected transformation products (2). In general, the Barton reaction in the steroid series has been directed to the functionalization of axial angular methyl groups, starting with suitably oriented nitrite esters. It appeared, however, that it should be possible to involve a ring methylene group in hydrogen abstraction by an alkoxy radical, generated from an equatorial nitrite group located so as to permit the formation of a six-membered transition state. This communication reports the photolysis of nitrite esters of some 11α-hydroxysteroid 4-en-3-ones, resulting in attack at C-1.[1]

Irradiation of 11α-hydroxy-4-pregnene-3,20-dione nitrite (**1***a*, obtained as a gum from the free alcohol by reaction with nitrosyl chloride in pyridine) in toluene afforded two major products. One of these was identified as the expected product of the Barton reaction, 11α-hydroxy-1-oximino-4-pregnene-3,20-dione (**2***a*),[2] m.p. 238–240° dec.; $[\alpha]_D$ +3.5° (chloroform); λ_{max}(MeOH) 238 nm (ε 12 900); λ_{max}(NaOH) 365 nm; λ(Nujol) 2.80, 3.04, 5.88, 6.02, 6.18, 10.5 μ; δ 0.67 (s, 18-H_3), 1.51 (s, 19-H_3), 2.12 (s, 21-H_3), 5.90 (broad s, 4-H) p.p.m.[3] The second major product was assigned structure **3***a* (R = H), 11α-hydroxy-9*a*-methyl-B(9*a*)-homo-A-nor-3(5),9*a*-pregnadien-2-one, on the basis of its physical and spectroscopic properties as well as chemical transformations.[4] Compound **3***a* (R = H) (m.p. 170–171°; $[\alpha]_D$ −220°; λ_{max}(MeOH) 306 nm (ε 17 900); λ(Nujol) 2.95, 5.90, 6.03, 6.43 μ) contained no nitrogen and analyzed well for $C_{21}H_{28}O_3$. The molecular formula was supported by the mass spectrum, molecular ion at *m/e* 328 and a prominent peak due to loss of H_2O at *m/e* 310. The n.m.r. spectrum was interpretable on the basis of the assigned structure, δ 0.71 (s, 18-H_3), 2.01 (s, 19-H_3), 2.17 (s, 21-H_3), 2.94 (s, 1-H_2), 4.17 (t of d, J = 10 and 5 Hz, 11β-H), 5.91 (broad s, 3-H) p.p.m. The compound was purified via its acetate (**3***a*, R = $COCH_3$), m.p. 168–170°; $[\alpha]_D$ −186° (chloroform); λ_{max}(MeOH) 303 nm (ε 17 500); λ(Nujol) 5.75, 5.86, 5.98, 6.03, 6.40, 8.0 μ; mass spectrum, no molecular ion, but prominent peak at *m/e* 310;

[1] *cf.* The reaction of 11α-hydroxysteroids with lead tetraacetate (3). The photolysis of an 11α-nitrite in a ring A saturated triterpene was recently used in the synthesis of β-amyrin (4).

[2] All new crystalline compounds gave satisfactory analytical values. Physical measurements were performed under the direction of Dr. M. Yudis. The n.m.r. spectra were recorded in deuteriochloroform solution with TMS as internal standard. Rotations were measured in dioxane unless otherwise noted.

[3] The chemistry of 1-oximino-steroid 4-en-3-ones such as **2***a* will be reported elsewhere.

[4] The 9*a*-methyl-B(9*a*)-homo-A-nor-3(5), 9*a*-dien-2-one steroid system has very recently been described as the product of a complex reaction sequence (5).

Can. J. Chem. Downloaded from www.nrcresearchpress.com by 210.87.254.105 on 09/05/12
For personal use only.

δ 0.76 (s, 18-H_3), 1.73 (s, 19-H_3), 2.03 (s, acetate), 2.15 (s, 21-H_3), 2.94 (s, 1-H_2), 5.96 (s, 3-H) p.p.m., from which it was readily regenerated by saponification with potassium hydroxide in aqueous methanol. Attempts to dehydrate the alcohol **3***a* (R = H) under a variety of conditions were unsuccessful; however, the acetate **3***a* (R = $COCH_3$) readily underwent pyrolytic elimination in mineral oil at about 350° to afford the 3(5),9*a*,9(11)-trien-2-one (**4**), m.p. 145–146°; $[\alpha]_D$ +57°; λ_{max}(MeOH) 215 (ε 6200), 233–238 (ε 6500), 314 nm (ε 18 300); λ(Nujol) 5.85, 5.92, 6.07, 6.37 μ; mass spectrum, molecular ion *m/e* 310; δ 0.68 (s, 18-H_3), 2.01 (s, 19-H_3), 2.15 (s, 21-H_3), 2.98 (s, 1-H_2), ~5.80 (m, 11-H), 5.92 (s, 3-H) p.p.m. Compound **4** on hydrogenation with palladium on calcium carbonate in benzene consumed 2 mol of hydrogen, giving the conjugated cyclopentenone derivative (**5**), m.p. 175–176°; λ_{max}(MeOH) 236 nm (ε 16 000); λ(Nujol) 5.85, 5.89 (sh), 6.22 μ; δ 0.65 (s, 18-H_3), 0.70 (d, J = ~7 Hz, 19-H_3), 2.11 (s, 21-H_3), 5.91 (m, 3-H) p.p.m. The stereochemistry of **5** at C-9, -9*a*, and -10 has not been established; it is presumed that hydrogenation from the α-face may be preferred.

The photolysis of an 11α-nitrite was also carried out, *inter alia*, in the 17α-methyltestosterone series. The requisite starting material, 11α,17β-dihydroxy-17α-methyl-4-androsten-3-one 17-acetate 11-nitrite (**1***b*, R′ = $COCH_3$), m.p. 143–144° dec.; $[\alpha]_D$ +27°; λ_{max}(MeOH) 239 nm (ε 18 200); λ(Nujol) 5.78, 5.98, 6.13, 6.22, 7.87, 7.95 μ, was prepared from 11α-hydroxy-17α-methyltestosterone by diacetylation, selective hydrolysis at C-11, and reaction with nitrosyl chloride. Irradiation of **1***b* (R′ = $COCH_3$) afforded the 1-oxime (**2***b*, R′ = $COCH_3$), m.p. 258–259° dec.; $[\alpha]_D$ −125°; λ_{max}(MeOH) 239 nm (ε 13 800), λ_{max}(NaOH) 365 nm; λ($CHCl_3$) 2.81, 3.0, 5.80, 5.97, 6.20, 7.9 μ, and the A-nor-B-homo compound (**3***b*, R = H, R′ = $COCH_3$), m.p. 259–262° dec.; $[\alpha]_D$ −285°; λ_{max}(MeOH) 307 nm (ε 17 300); λ(Nujol) 3.01, 5.75, 5.95, 6.10, 6.38, 7.9, 8.0 μ, as the major products. Acetylation of **3***b* (R = H, R′ = $COCH_3$) gave the 11,17-diacetate (**3***b*, R = R′ = $COCH_3$), m.p. 180–181°; λ_{max}(MeOH) 218 (ε 7000), 303 nm (ε 17 500); λ(Nujol) 5.76, 5.92, 6.10, 6.40, 8.0 μ, while saponification afforded the diol (**3***b*, R = R′ = H), m.p. 232–233° dec.; $[\alpha]_D$ −311°; λ_{max}(MeOH) 216 (ε 6900), 308 nm (ε 17 200); λ(Nujol) 3.0 (broad), 6.00, 6.10, 6.42 μ, which was converted to the 11-acetate (**3***b*, R = $COCH_3$, R′ = H), m.p. 186–190°; λ_{max}(MeOH) 218 (ε 7800), 304 nm (ε 17 000); λ(Nujol) 2.91, 5.76, 5.96, 6.37, 8.0 μ.

The products of the photolysis may be rationalized on the basis of the C-1 radical **A**, which may combine with NO to yield the 1-oxime **2**, or alternatively proceed to the A-nor-B-homo compound **3** via the C-4 radical **B** by loss of the C-1 hydrogen with cleavage of the C_5—C_{10} bond.

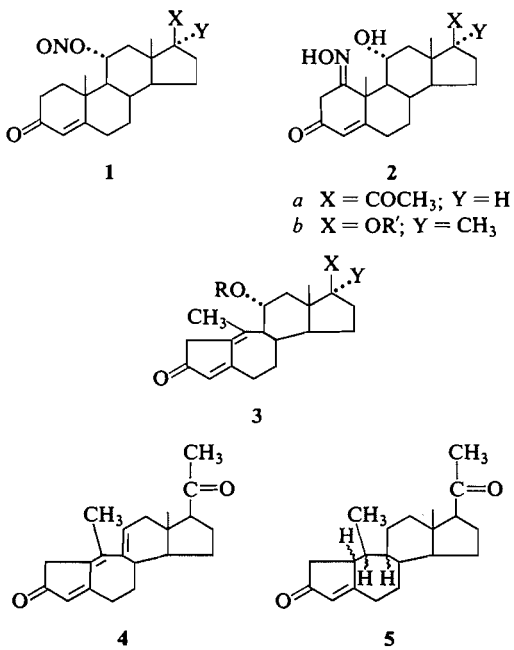

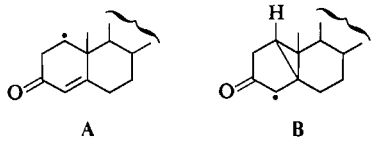

1. D. H. R. Barton, J. M. Beaton, L. E. Geller, and M. M. Pechet. J. Amer. Chem. Soc. **82**, 2640 (1960).
2. For reviews see (*a*) A. L. Nussbaum and C. H. Robinson. Tetrahedron, **17**, 35 (1962); (*b*) M. Akhtar. *In* Advances in Photochemistry. Vol. 2. Interscience Publishers, New York, N.Y., 1964. p. 263.
3. J. Kalvoda, G. Anner, D. Arigoni, K. Heusler, H. Immer, O. Jeger, M. Lj. Mihailović, K. Schaffner, and A. Wettstein. Helv. Chim. Acta, **44**, 186 (1961).
4. D. H. R. Barton, E. F. Lier, and J. F. McGhie. J. Chem. Soc. (C), 1031 (1968).
5. M. Lj. Mihailović, Lj. Lorenc, J. Faršek, H. Nešović, G. Snatzke, and P. Trška. Tetrahedron **26**, 557 (1970).

Can. J. Chem. Downloaded from www.nrcresearchpress.com by 210.87.254.42 on 09/05/12
For personal use only.

Canadian Journal of Chemistry

Published by THE NATIONAL RESEARCH COUNCIL OF CANADA

VOLUME 49 FEBRUARY 1, 1971 NUMBER 3

Infrared Studies of Water in Crystalline Hydrates: $LiI.3H_2O$[1]

GEORGE BRINK[2] AND MICHAEL FALK

Atlantic Regional Laboratory, National Research Council of Canada, Halifax, Nova Scotia

Received September 14, 1970

The infrared spectra of undeuterated and partially deuterated $LiI.3H_2O$ were recorded between 4000 and 1000 cm^{-1}. The splitting of the fundamentals of isotopically dilute HDO indicates that the water molecules are distorted and form one strong, linear OH...I^- hydrogen bond and one weak, non-linear hydrogen bond. The non-equivalence of the two hydrogens of the water molecule disagrees with the space group $P6_3mc$-C_{6v}^4 for this hydrate, proposed on the basis of X-ray diffraction studies. It is concluded that the space group, including hydrogens, is one of lower symmetry, $P6_3$-C_6^6. The gradual broadening and convergence of the HDO fundamentals at increasing temperature is explained by increasing librational motion of the water molecules.

Canadian Journal of Chemistry, 49, 347 (1971)

Introduction

The crystal structure of $LiI.3H_2O$ was examined in 1928 by Hendricks, who reported a hexagonal unit cell with $a = 7.45$ Å and $c = 5.45$ Å, two formula units per unit cell and space group $P6_3mc$-C_{6v}^4 (1). West re-examined the structure in 1934, confirmed the space group, and derived approximate atomic coordinates for iodine, oxygen, and lithium (2). According to West the structure of $LiI.3H_2O$, like that of $LiClO_4.3H_2O$, has the space group $P6_3mc$ (2). In both hydrates the water oxygens (O_w) lie on planes of symmetry, and are coordinated to two lithium cations and, through hydrogen bonds, to two anions.

In the case of $LiClO_4.3H_2O$ the basic structure proposed by West has been confirmed. The proton positions have been located and the presence of weak hydrogen bonds established by Raman spectroscopy (3), nuclear magnetic resonance (4), neutron diffraction (5, 6), and infrared spectroscopy (7). The structure of $LiI.3H_2O$, on the other hand, does not appear to have been further studied in the past 36 years and the proton positions are unknown. As a part of our research program on the infrared spectra and structure of water in crystalline hydrates (7–9), we have now investigated $LiI.3H_2O$.

[1]NRCC No. 11 633.

[2]NRCC Postdoctorate Fellow, 1968–1970.

Experimental

$LiI.3H_2O$ was obtained from Alpha Inorganics, Beverley, Mass. Because of the plasticity and lack of cleavage of this hydrate, it is not possible to grind it and the usual techniques of sample preparation employing Nujol mulls and KBr pellets cannot be used. Instead, thin films of $LiI.3H_2O$ on CaF_2 plates were used, prepared as follows: a drop of a nearly saturated solution of LiI in H_2O or in a mixture of H_2O and D_2O, heated to about 35°, was placed between two warm CaF_2 plates,[3] forming a capillary film. The plates were allowed to cool to room temperature, then slid apart, producing a thin film of saturated solution on each plate. Gentle evaporation of such films under a stream of dry nitrogen in a room maintained at about 20% relative humidity produced clear polycrystalline films of $LiI.3H_2O$. The films had a melting point of 75.4°, in good agreement with the literature value of 75.5° (10). At higher humidities the crystals deliquesced rapidly. At lower humidities (*e.g.* over concentrated H_2SO_4) the crystals were dehydrated to lower hydrates.[4]

[3]AgCl plates could not be used because they are attacked by aqueous LiI.

[4]We have obtained the spectra of the lower hydrates by controlled dehydration of the trihydrate. The dihydrate was obtained by exposing the trihydrate films to a partial vacuum of about 0.01 mm Hg for 20 min. The observed melting point was 77.9° [$LiI.2H_2O$, m.p. 78° (10)]. The main absorption bands of the dihydrate above 1000 cm^{-1} (the transmission cut-off of the CaF_2 plate) are: OH stretching at 3390 and 3470 cm^{-1}, HOH bending at 1604 cm^{-1} with a shoulder at 1620 cm^{-1}, and its overtone $2\nu_2$ at 3219 cm^{-1}. When the films were exposed to a vacuum of about 0.001 mm Hg, a spectrum of what may be the monohydrate was obtained: OH stretching at 3480 and 3412 cm^{-1}, HOH bending at 1612 cm^{-1}, $2\nu_2$ overtone at 3210 cm^{-1}. The above spectra were recorded at room temperature.

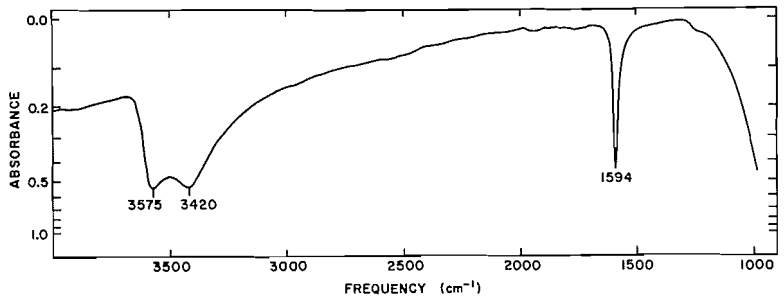

FIG. 1. Spectrum of undeuterated $LiI.3H_2O$ on a CaF_2 substrate at room temperature.

Isotopically dilute HDO was used in this study since it has a far simpler vibrational spectrum than H_2O or D_2O and hence is preferable in structural studies (11–13). The D:H ratios in the hydrate were taken to be twice the ratio of the area of the OD stretching band to the area of the OH stretching band in the spectrum of the parent solution (14, 15). The HDO concentration was about 6%, assuming a random distribution of H and D. It was not practical to work with lower HDO concentrations in view of the extremely thin films used.

Spectra were recorded on a Perkin–Elmer model 521 spectrophotometer, as described in ref. 7. In low-temperature experiments, the hydrate films were protected from dehydration by a thin film of Nujol or halocarbon oil.

Results

The spectrum of undeuterated $LiI.3H_2O$ at room temperature is shown in Fig. 1. The bands at 3575 and 3420 cm^{-1} are due to OH stretching. The band at 1594 cm^{-1} is due to HOH bending. The small band near 1250 cm^{-1} is probably due to the overtone of the librational frequencies near 625 cm^{-1}, which are not accessible because of the absorption of the CaF_2 window. At $-175°$ the OH stretching bands are better resolved and occur at 3586 and 3409 cm^{-1}; the HOH bending is at 1590 cm^{-1} and its overtone, $2\nu_2$, at 3170 cm^{-1}.

Figure 2 shows the bands due to OD stretching and HOD bending fundamentals of isotopically dilute HDO in $LiI.3H_2O$ in the temperature range $+25$ to $-175°$. At low temperatures both fundamentals give rise to doublets, separated by 110 cm^{-1} for OD stretching and 20 cm^{-1} for HOD bending. Increasing temperature causes a gradual broadening and convergence of the doublets. At room temperature the two OD stretching bands are still separated by about 60 cm^{-1} while the two components of the HOD bending are no longer resolved.

Discussion

Site Symmetry of H_2O and the Space Group of $LiI.3H_2O$

West (2) placed the oxygen atom, O_w, of the water molecule of $LiI.3H_2O$ in the 6(*c*) equipoint, which has the symmetry m-C_s (16). The six water molecules must then be equivalent; this is confirmed by the single HOH bending fundamental in Fig. 1. The two hydrogen atoms of the water molecule are unlikely to lie *on* the mirror plane passing through O_w, Li′, and Li″, as this would lead to a planar four-fold coordination about the water oxygen. The expected, approximately tetrahedral coordination places the hydrogen atoms *off* the mirror plane, as shown by the dotted lines in Fig. 3*B*, and renders them equivalent by symmetry.

The splitting of the HDO fundamentals shows, however, that the water molecules are distorted and their two hydrogens non-equivalent (8, 17). The infrared spectra thus suggest that the planes of symmetry are in fact absent, as far as the hydrogen positions are concerned. Therefore, the space group of $LiI.3H_2O$ *including hydrogens* is not $P6_3mc$-$C_{6v}{}^4$, but one of lower symmetry, $P6_3$-$C_6{}^6$.

Hydrogen Bonding in $LiClO_4.3H_2O$ and in $LiI.3H_2O$

In $LiClO_4.3H_2O$, the O . . . O_w. . . O angle is 125° (2), only 16° wider than the usual H—O_w—H angle of about 109° in crystals. Neutron diffraction studies (5, 6) have shown that the two O_w—H bonds assume symmetric orientations with respect to the Li′—O_w—Li″ plane. This leads to two equivalent hydrogen bonds, O_w—H′. . . O′ and O_w—H″. . . O″, which are slightly non-linear, the O—H . . . O angle being about 160° (Fig. 3*A*). The absence of splitting of the HDO fundamentals in the infrared spectrum

Can. J. Chem. Downloaded from www.nrcresearchpress.com by 210.87.254.42 on 09/05/12
For personal use only.

Can. J. Chem. Downloaded from www.nrcresearchpress.com by 210.87.254.42 on 09/05/12
For personal use only.

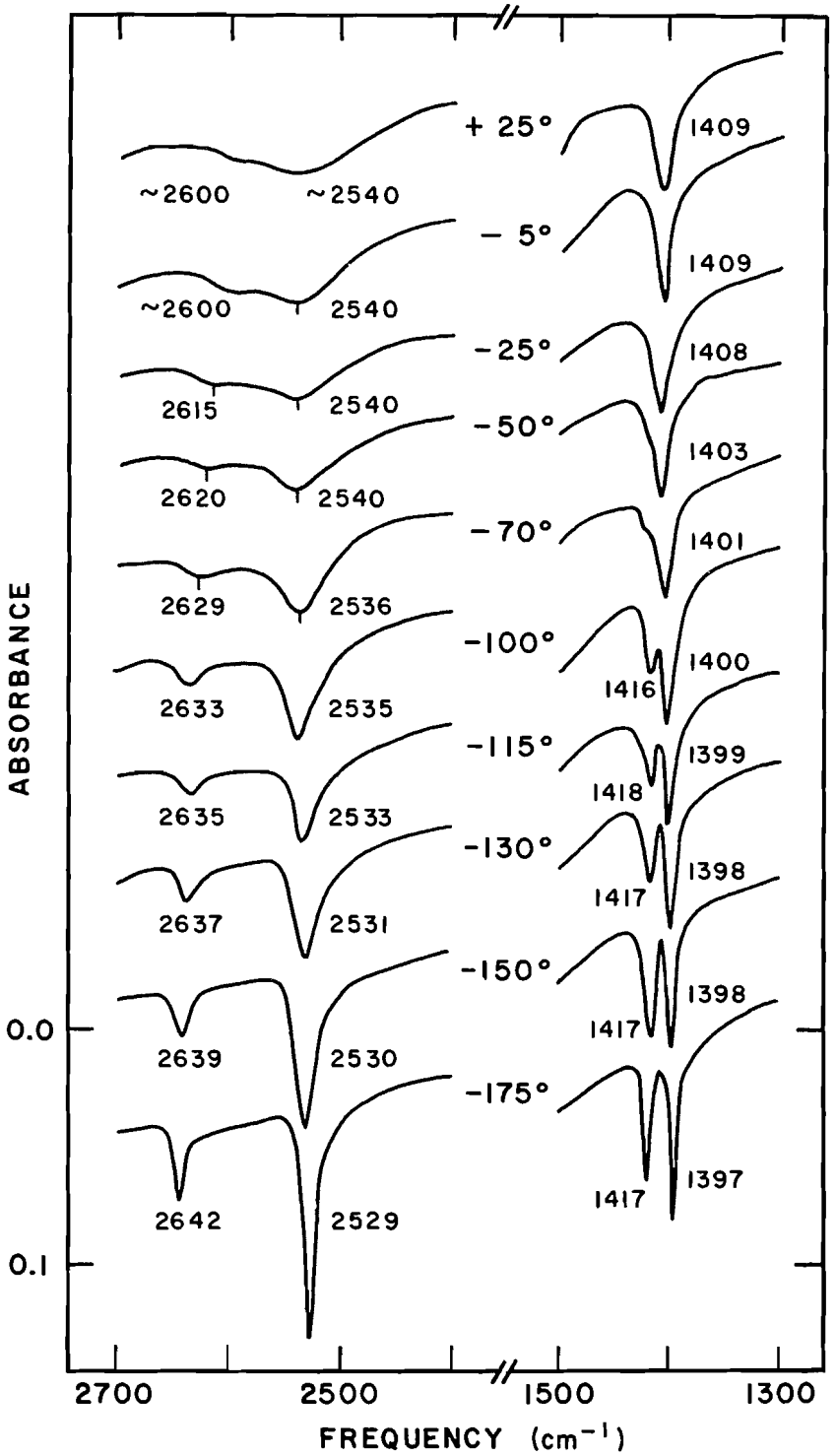

FIG. 2. Spectrum of partially deuterated LiI.3H$_2$O (H:D = 97:3) in the OD stretching and HOD bending regions at various temperatures.

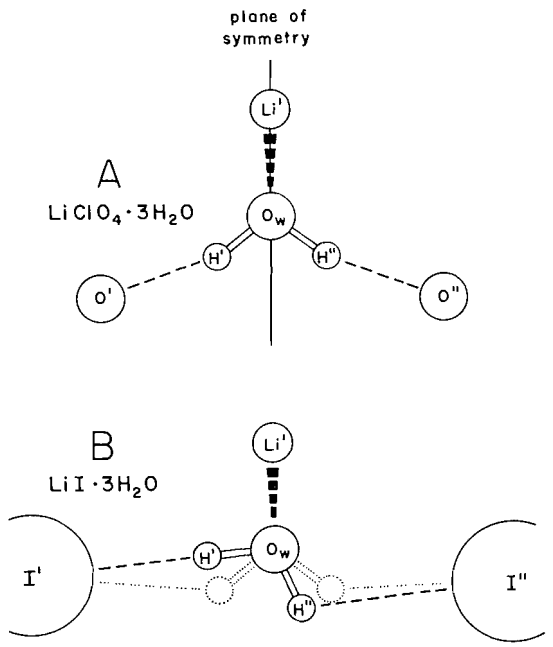

FIG. 3. The environment of the water molecule in $LiClO_4.3H_2O$ and $LiI.3H_2O$, viewed down the six-fold axis which passes through Li′ and Li″ (eclipsed). Heavy atom positions are from West (2); hydrogen atom positions are discussed in the text.

of this hydrate is a particularly sensitive confirmation of the equivalence of O_wH' and O_wH'' (7).

In $LiI.3H_2O$, if we accept West's coordinates for the heavy atoms (2), the I′. . . O_w. . . I″ angle is about 169°, much wider than the usual H—O_w—H angle of 109°. If the O_w—H bonds of the water molecules were oriented symmetrically with respect to the Li′—O_w—Li″ plane, as in $LiClO_4.3H_2O$, the angles O_w—H′. . .I′ and O_w—H″. . . I″ would be 140° and the two hydrogen bonds highly non-linear (Fig. 3*B*, dotted lines). Alternatively, the water molecules may be oriented in such a way as to form two unequal OH . . . I hydrogen bonds. In the extreme case, one bond would be linear and the other extremely non-linear, with an OH . . . I angle of about 103°, as shown by full lines in Fig. 3*B*. There are two equivalent ways in which a water molecule can achieve this configuration: the linear bond may be formed with either I′ or with I″.

The splitting of the HDO fundamentals in partially deuterated $LiI.3H_2O$ shows that in this hydrate, in contrast to $LiClO_4.3H_2O$, the orientation of least energy is asymmetric. At the lowest temperature, −175°, the water molecules appear to adopt the extreme configuration of Fig. 3*B*. The OD stretching frequency of 2529 cm^{-1} corresponds to a relatively strong hydrogen bond, which must be nearly linear, while the frequncy of 2642 cm^{-1} corresponds to an extremely weak bond, which must be non-linear. The two possible asymmetric orientations are of equal energy and are separated by a small potential maximum; they probably occur statistically throughout the crystal. At low temperatures, when only the lower librational energy levels are occupied, each water molecule has one strongly bonded and one weakly bonded OH group. With increasing temperature the higher energy levels of the libration of the water molecule about the axis parallel to the six-fold axis of the crystal become increasingly occupied. This libration will tend to bend and thus weaken the stronger OH . . . I bond and at the same time straighten and thus strengthen the weaker OH . . . I bond. The resulting gradual reorientation causes the observed shifting together and broadening of the HDO doublets. Librational levels which lie above the central maximum of the double-well potential correspond to states in which the water molecule is *on the average* symmetrically oriented. Thus, at sufficiently high temperatures a coalescence of the HDO doublets may be expected. This coalescence does not occur for the OD stretching fundamental of partially deuterated $LiI.3H_2O$, but appears to arise for partially deuterated $Ba(ClO_4)_2.3H_2O$ and $NaClO_4.H_2O$, for both of which the split HDO fundamentals merge into a single broad band before the dehydration temperature is reached (7).

1. S. B. HENDRICKS. Amer. J. Sci. **15**, 403 (1928).
2. C. D. WEST. Z. Kristallogr. **88**, 198 (1934).
3. L. COUTURE-MATHIEU and J. P. MATHIEU. Acta Crystallogr. **5**, 571 (1952).
4. N. M. ALEKSANDROV and E. PETRZHAK. Zh. Strukt. Khim. **6**, 527 (1965).
5. I. D. DATT, N. V. RANNEV, and R. P. OZEROV. Kristallografiya, **13**, 261 (1968).
6. A. SEQUEIRA and I. BERNAL. *In* Molecular Dynamics and Structure of Solids. *Edited by* R. S. Carter and J. J. Rush. N.B.S. Spec. Publ. 301. 1969. p. 249.
7. G. BRINK and M. FALK. Can. J. Chem. **48**, 2096 (1970).
8. V. SEIDL, O. KNOP, and M. FALK. Can. J. Chem. **47**, 1361 (1969).
9. T. A. FORD and M. FALK. J. Mol. Struct. **3**, 445 (1969).
10. Gmelins Handbuch der anorganischen Chemie, **20**, 452 (1960).

Can. J. Chem. Downloaded from www.nrcresearchpress.com by 210.87.254.42 on 09/05/12
For personal use only.

11. R. D. WALDRON. J. Chem. Phys. **26**, 809 (1957).
12. T. T. WALL and D. F. HORNIG. J. Chem. Phys. **43**, 2079 (1965).
13. M. FALK and T. A. FORD. Can. J. Chem. **44**, 1699 (1966).
14. C. A. SWENSON. Spectrochim. Acta, **21**, 987 (1965).
15. H. R. WYSS and M. FALK. Can. J. Chem. **48**, 608 (1970).
16. International Tables for X-Ray Crystallography, Vol. 1. Kynoch Press, Birmingham. 1952.
17. J. SCHIFFER. Ph.D. Thesis, Princeton University, Princeton, New Jersey. 1963.

Can. J. Chem. Downloaded from www.nrcresearchpress.com by 210.87.254.42 on 09/05/12
For personal use only.

Can. J. Chem. Downloaded from www.nrcresearchpress.com by 210.87.254.105 on 09/05/12
For personal use only.

Electron Spin Resonance Study of Surface Defects of Silica Gel Formed by Gas Discharges[1]

K. HUKUDA[2] AND Y. AMENOMIYA
Division of Chemistry, National Research Council of Canada, Ottawa, Canada

Received July 27, 1970

Surface defects of silica gel formed by a microwave electric discharge in a stream of oxygen and of nitrogen have been studied by means of electron spin resonance (e.s.r.) spectroscopy. The magnetic center is identified as a hole trapped by a surface oxygen atom which is formed by the removal of a hydrogen atom from a hydroxyl group. The principal values of the **g**-tensor were found to be $\mathbf{g}_{xx} = 2.037$, $\mathbf{g}_{yy} = 2.008$, and $\mathbf{g}_{zz} = 2.002$, respectively, where the direction of x-axis was taken along the O—Si bond. The center has a weak hyperfine interaction with a hydrogen nucleus of an adjacent hydroxyl group. The hyperfine splitting is 15 Oe.

Canadian Journal of Chemistry, 49, 352 (1971)

Introduction

Since the early work of Kazanskii *et al.* (1) on hydrogen atoms trapped on the surface of silica gel, a number of attempts have been made to detect e.s.r. signals of atoms and free radicals adsorbed on solid surfaces. This type of work provides useful information on the structure of solid surfaces which aids our understanding of the catalytic activity of solids. Recently, particular interest has been shown in e.s.r. signals with three different components of **g**-tensor (we call this kind of center a three-**g**-value center hereafter). Kasai (2) reported a set of principal **g**-values, 2.0046, 2.0090, and 2.057, for O_2^- on barium zeolite, and 2.0016, 2.0066, and 2.113 for O_2^- on sodium zeolite. Wang and Lunsford observed similar spectra on various kinds of alkaline earth zeolites (3). Iyengar *et al.* obtained a set of **g**-values, 1.980, 2.002, and 2.024, on rutile (4) and attributed this signal to O_2^+ species. However, Iyengar and Kellerman later revised their earlier assignment to a species containing nitrogen and oxygen (5). In the present work e.s.r. measurements of three-**g**-value centers which are formed on the surface of silica gel by a microwave electric discharge in a stream of gas have been made in an attempt to obtain information on the surface properties of oxide catalysts.

Experimental

The silica gel which was used was obtained by grinding Cab-O-sil M-5 with water. The gel was dried in an oven overnight at 110 °C, and finally calcined in air for 3 h at 600 °C. The silica gel thus prepared was crushed and screened to 28–32 mesh. About 30 mg of the powder was placed at the bottom of a U-shaped discharge tube such as shown in Fig. 1. After evacuation, oxygen or nitrogen gas was permitted to flow through the tube at a flow rate of about 0.0002 mol/min at a pressure of 2 Torr. The discharge cavity shown in the same figure was fed with an incident microwave power of 60 W at 2450 MHz from a Microtron 200 generator (Electro-medical Supplies Ltd.). After operation of the discharge for 500 s, the tube was evacuated at room temperature and about 4 Torr of helium was admitted in order to shorten the time required for changing the sample temperature. The silica gel was then dropped into the bottom of the quartz tube (Fig. 1) for e.s.r. measurement. A Varian X-band spectrometer was used with a rectangular TE_{012} sample cavity. The temperature of measurement was varied from −196 to 127 °C.

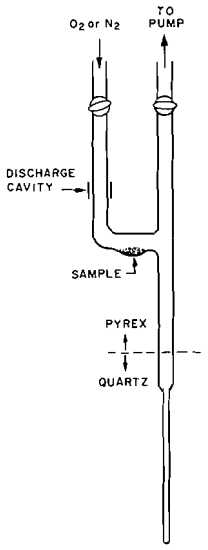

FIG. 1. Discharge tube.

[1]NRCC No. 11 652.
[2]National Research Council of Canada Visiting Scientist. Present address: Department of Physics, Faculty of Science, Kyushu University, Fukuoka, Japan.

Can. J. Chem. Downloaded from www.nrcresearchpress.com by 210.87.254.105 on 09/05/12
For personal use only.

A deuterated silica gel which was used for comparison purposes was prepared by contacting silica gel which had been previously evacuated for 10 min at 800 °C, with the saturated vapor of D_2O for several days at room temperature.

Results and Discussion

Figure 2 shows typical e.s.r. spectra obtained at various temperatures after discharge in the oxygen stream at room temperature. The shape of the spectrum is sensitive to the temperature of measurement (sample temperature), as is clear from Fig. 2. At any given temperature, however, the spectrum was reproduced with a somewhat reduced intensity after a heating-and-cooling cycle. The discharge in the nitrogen stream gave similar results to those shown in Fig. 2, indicating that the formation of centers did not require the presence of oxygen in the gas phase. Since the same spectrum was obtained independent of which gas was used, most of the present experiments were carried out with an oxygen stream.

When the sample was heated above room temperature after the discharge, the intensity of the spectrum measured at liquid nitrogen temperature decreased without changing its shape, as mentioned above. Figure 3 shows the first-order plot of the intensity against time. The figure indicates that there are two different processes involved in the decay of the centers, and the activation energies were found to be 11.3 kcal/mol for the faster and 13.2 kcal/mol for the slower decay, respectively.

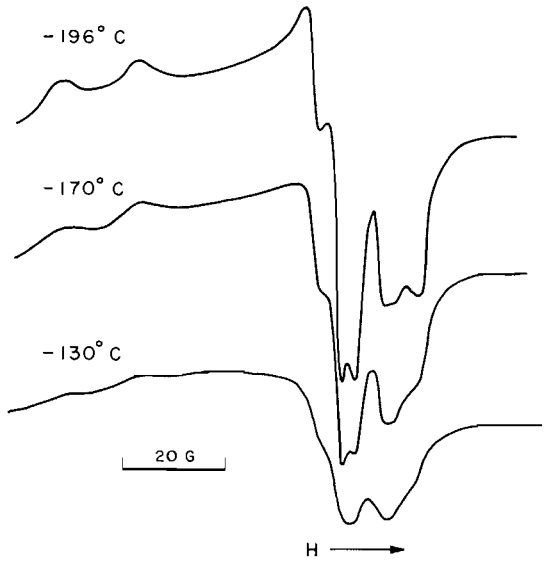

FIG. 2. Typical e.s.r. spectra obtained at various temperatures. Discharge was carried out in O_2 stream at room temperature.

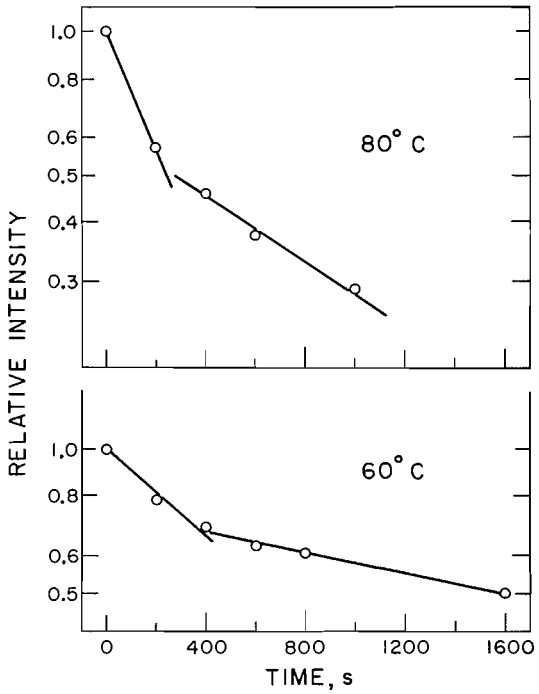

FIG. 3. Variation of spectral intensity with time.

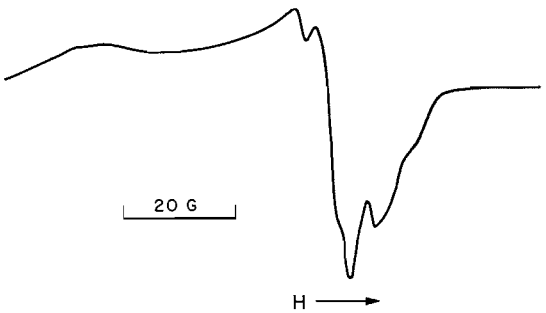

FIG. 4. Spectrum of deuterated silica gel obtained at −196 °C.

A spectrum obtained with the deuterated sample is shown in Fig. 4. It is apparent that the shape of the spectrum is different from that of the undeuterated sample shown in Fig. 2. In particular, the two small peaks of the undeuterated sample appearing at low magnetic field became a single broad peak when the sample was deuterated. This fact suggests that there is a hyperfine interaction with a hydrogen nucleus existing on an adjacent site, and the spectrum of

Can. J. Chem. Downloaded from www.nrcresearchpress.com by 210.87.254.105 on 09/05/12
For personal use only.

undeuterated sample consists of two hyperfine components. It is reasonable that the hyperfine components should not be separated for the deuterated silica gel, since the spin of deuterium nucleus is 1 and the magnetic moment is 3.25 times smaller than that of the proton. In addition, the deuterated sample would not have been fully deuterated, so that the peak appearing at low magnetic field is very broad as a result of the superposition of hyperfine components of both H and D atoms. If this is the case, the splitting of the two peaks in the undeuterated sample should remain unchanged even if the measurement is made at a different microwave frequency. On the other hand, the splitting should be proportional to the frequency, if the two components are due to two kinds of centers with different **g**-values. Measurements were therefore made with a Q-band spectrometer, whose frequency was about 4 times larger than that of the X-band, and it was found that the two small peaks became a single broad peak with a half-width of 37 Oe. The results may be explained as follows. The magnetic centers are formed on the silica gel surface which has far more defects compared to the bulk of the solid. The existence of various crystal surfaces in the solid results in the formation of several kinds of surface sites with different crystal field environments, causing a spread of **g**-values and broadening of the peak. The effect of broadening should be greatest for the peak at the lowest magnetic field where the difference in **g**-value from that of free spin is largest. Since the line broadening due to the distribution of **g**-values is magnified in the higher frequency measurement, the two peaks in the X-band spectrum would become a single unresolved peak in the Q-band spectrum. From the Q-band spectrum the distribution range of the largest principal component of the **g**-tensor was roughly estimated to be 2.039 to 2.035.

As already mentioned, the present results indicate that the e.s.r. spectrum obtained with the undeuterated silica gel has two hyperfine components as a result of interaction with a hydrogen nucleus in a neighboring hydroxyl group. It also seems reasonable to assume that there are in addition magnetic centers which are not in close proximity with hydroxyl groups and which therefore give similar signals but without interaction with protons. In other words, the observed spectrum consists of three elementary spectra, two hyperfine components and the other without the interaction. Using the shape function $g(H)$ of an elementary spectrum, the shape function $f(H)$ of the observed spectrum is expressed as

$$f(H) = g(H - \tfrac{1}{2}\Delta H) + g(H + \tfrac{1}{2}\Delta H) + \alpha g(H)$$

where ΔH is the hyperfine splitting and α is a coefficient determined from the population ratio between interacting and non-interacting centers. ΔH was determined as 15 Oe from the separation of the two small peaks appearing at low magnetic field (Fig. 2). With this value for ΔH and taking 0.5 as α and also assuming the elementary spectrum as shown in Fig. 5(*a*), a simulated spectrum is obtained as shown by the solid line in Fig. 5(*b*) where the observed spectrum is also indicated by a broken line. Although some parts of the simulated spectrum differ from the observed one, the agreement is considered satisfactory, particularly with regard to the position of peaks. We could get better agreement if we added another spectrum with an axially symmetric **g**-tensor and adjusted the value of α. However, this is too

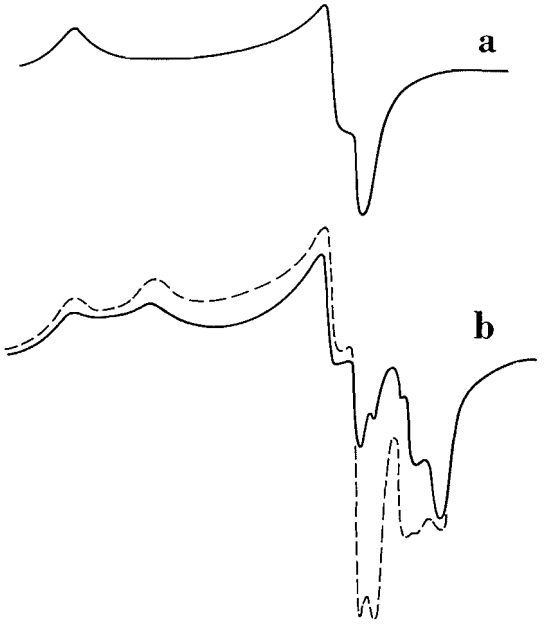

FIG. 5. Comparison of simulated spectrum with observed one. (*a*) Elementary spectrum, (*b*) simulated spectrum (solid curve), and observed spectrum (broken curve).

Can. J. Chem. Downloaded from www.nrcresearchpress.com by 210.87.254.105 on 09/05/12
For personal use only.

speculative at this stage. $\alpha = 0.5$ used in the simulation means that only 25% of total magnetic centers lack a hydroxyl group in their neighboring sites. This is not unreasonable for the present silica gel which was not dehydrated at high temperatures. In conclusion, it seems certain that the magnetic centers formed by the discharge have a **g**-tensor with three different principal values. The **g**-values of the centers were $\mathbf{g}_{xx} = 2.037$, $\mathbf{g}_{yy} = 2.008$, and $\mathbf{g}_{zz} = 2.002$, respectively, and the hyperfine splitting was 15 Oe as already mentioned.

The **g**-tensor obtained above is close to that of the O_2^+ species trapped in alkali halide crystals (6). Similar spectra were observed on the surface of alkaline earth zeolites (3) and the center was identified as adsorbed O_2^-. In the present study, however, both O_2^+ and O_2^- are ruled out because the center could be formed by a nitrogen gas discharge with almost the same efficiency as by an oxygen gas discharge. The present **g**-values are also close to those obtained with hydroxyl radicals in solid ice (7). However, hydroxyl radical is stable only at low temperatures (8–10), and it is unlikely that these radicals are trapped stably on solid surface at such a high temperature as employed in the present experiments (room temperature). Moreover, the hyperfine splitting obtained here is almost a half of that reported on the hydroxyl radical.

The e.s.r. signal at -196 °C disappeared when the sample was heated at temperatures above 100 °C for several minutes. It reappeared if the sample was subjected to a discharge again, but its intensity became very weak after the procedure was repeated two or three times. It was necessary to expose the silica gel to saturated water vapor for several days to recover the signal intensity. This fact indicates that the existence of hydroxyl groups on the surface is essential to the formation of the centers. It is therefore postulated that hydrogen atoms are removed from hydroxyl groups during a discharge, thus producing on the surface $\mathrm{O{-}\overset{|}{\underset{|}{Si}}{-}}$ with a trapped hole on the oxygen.

We can roughly estimate the **g**-values for this particular center by a similar method to that employed by Kurita and Gordy (11) for $\mathrm{S{-}\overset{|}{\underset{|}{C}}{-}}$ radicals. For the calculation of **g**-shift,

$$\Delta\mathbf{g}_{vv} = -\sum_i 2\lambda\langle\psi_0|L_v|\psi_i\rangle\langle\psi_i|L_v|\psi_0\rangle/(E_i - E_0)$$

it is assumed that the hole is in the π orbital of oxygen as ground state, and that one of the sp_2 hybrids forms a σ bonding orbital with Si. It is further assumed that the energy of the state in which the hole exists in the bonding σ orbital is very high. Taking the x-axis along the O—Si bond and the z-axis perpendicular to the sp_2 hybrid plane, the **g**-shifts from the free electron value are obtained as

$$\Delta\mathbf{g}_{xx} = -2\lambda/\Delta E$$

$$\Delta\mathbf{g}_{yy} = -2\lambda/3\Delta E$$

$$\Delta\mathbf{g}_{zz} = 0$$

where λ is the spin–orbit coupling constant of oxygen and ΔE is the energy difference between the ground state and the excited state in which the hole is in one of the nonbonding sp_2 hybrids. The ratio of $\Delta\mathbf{g}_{xx}/\Delta\mathbf{g}_{yy}$ is about 3 from the above calculation, while the observed ratio is 5.8. With $\lambda = -150\ \mathrm{cm}^{-1}$ and the observed value of $\Delta\mathbf{g}_{xx} = 0.035$, ΔE is calculated to be $8.6 \times 10^3\ \mathrm{cm}^{-1}$. Further deductions will not be made because the above model is an oversimplified one and also no value of ΔE is available for comparison. The model is, however, consistent with the observation that the center has one large principal value of the **g**-tensor and two smaller values close to the **g**-value of the free electron and the value of ΔE calculated is thought to be a reasonable order of magnitude.

The hyperfine splitting of 15 Oe may appear to be small compared with that of other compounds containing hydrogen. However, this value means that the fractional occupancy of the hole on the hydrogen s orbital is about 3%, which is considered to be a reasonable value if we assume a hydrogen bond between the center and an adjacent hydroxyl group. Coulson and Danielsson calculated the contribution of a covalent structure to such bonding to be several percent (12). Further experimental evidence is, however, needed to confirm this point.

The authors wish to express their sincere thanks to Dr. C. V. Stager of McMaster University, Hamilton for the measurements which he kindly made with a Q-band

spectrometer. Thanks are also due to Drs. K. F. Preston and J. R. Morton of these laboratories for the use of the e.s.r. spectrometer and for the loan of vacuum facilities.

1. V. B. KAZANSKII, G. B. PARIISKII, and V. V. VAEVODSKII. Kinetika i Kataliz, **1**, 539 (1960).
2. P. H. KASAI. J. Chem. Phys. **43**, 3322 (1965).
3. K. M. WANG and J. H. LUNSFORD. J. Phys. Chem. **74**, 1512 (1970).
4. R. D. IYENGAR, M. CODELL, J. S. KARRA, and J. TURKEVICH. J. Amer. Chem. Soc. **88**, 5055 (1966).
5. R. D. IYENGAR and R. J. KELLERMAN. J. Catal. **12**, 107 (1968).
6. C. JACCARD. Phys. Rev. **124**, 60 (1961).
7. J. A. BRIVATI, M. C. R. SYMONS, D. J. A. TINLING, and D. O. WILLIAMS. J. Chem. Soc. A, 719 (1969).
8. M. S. MATHESON and B. SMALLER. J. Chem. Phys. **23**, 521 (1955).
9. S. SIEGEL, L. H. BAUM, and J. M. FLOURNOY. J. Chem. Phys. **32**, 1249 (1960).
10. S. SIEGEL, J. M. FLOURNOY, and L. H. BAUM. J. Chem. Phys. **34**, 1782 (1961).
11. Y. KURITA and W. GORDY. J. Chem. Phys. **34**, 282 (1961).
12. C. A. COULSON and U. DANIELSSON. Arkiv fur Fysik, **8**, 239 (1954).

Can. J. Chem. Downloaded from www.nrcresearchpress.com by 210.87.254.105 on 09/05/12
For personal use only.

Free Radicals by Mass Spectrometry. XLIII. Ionization Potentials and Ionic Heats of Formation for Vinyl, Allyl, and Benzyl Radicals[1]

F. P. LOSSING
Division of Chemistry, National Research Council of Canada, Ottawa, Canada

Received August 27, 1970

Using an energy-resolved electron beam, ionization potentials for the following free radicals have been measured: vinyl 8.95 V, allyl 8.07 V, benzyl 7.27 V. For vinyl and allyl ions new measurements of thresholds for dissociative ionization give $\Delta H_f(C_2H_3^+) = 266$ kcal/mol and $\Delta H_f(C_3H_5^+) = 226$ kcal/mol, leading to neutral radical heats of formation $\Delta H_f(C_2H_3) = 59.6$ kcal/mol and $\Delta H_f(C_3H_5) = 40$ kcal/mol. The data for benzyl radical and ion give ΔH_f(benzyl cation) = 213 kcal/mol.

Canadian Journal of Chemistry, 49, 357 (1971)

Can. J. Chem. Downloaded from www.nrcresearchpress.com by 210.87.254.5 on 09/05/12
For personal use only.

Introduction

The ionization potential values available for vinyl, allyl, and benzyl free radicals were measured some years ago, using conventional mass spectrometer ion sources. It is now well-known that, as a result of low resolution in energy, ionization thresholds determined in this way are generally higher than the adiabatic IP by 0.1–0.7 V, the error becoming larger with unfavorable Franck–Condon factors in the threshold ionization region. Recent electron impact measurements, either by the Retarding Potential Difference (RPD) method or by the use of true energy-resolved electron beams, are in satisfactory agreement with the more precise results obtainable by photoionization (PI) or photoelectron spectroscopy. The results of a recent study (1) of the ionization potentials of C_1–C_4 alkyl radicals, using an energy-resolved electron beam from a two-stage double-hemispherical energy selector, show that good agreement now holds among the IP values for these radicals as measured by the RPD method, photoionization, and monoenergetic electron impact, even in cases where the ionization efficiency curves in the threshold region are decidedly non-linear. The present work reports new IP values for vinyl, allyl, and benzyl radicals using a monoenergetic electron beam with an energy width at half-height of about 0.07 V.

For vinyl and allyl radicals, appearance potentials for formation of the corresponding $C_2H_3^+$ and $C_3H_5^+$ ions in dissociative ionization of suitable compounds have also been obtained. Heats of formation of the ionic and neutral species have been derived, and compared with available literature data. The situation is more complicated for benzyl ion, since $C_7H_7^+$ ions formed by dissociative ionization processes have almost certainly the tropylium ion structure (2, 3).

Experimental

The measurements were carried out using the electron energy selector, ionization chamber, ion extractor, and quadrupole mass filter previously described (4). Radicals were produced in sufficient concentrations by pyrolysis of suitable compounds (see below) at pressures of about 10^{-3} Torr in a fused-silica capillary furnace (5). Performance characteristics of this apparatus for some simple molecules (6) and radicals (1, 7) have been reported previously.

Results and Discussion

Vinyl Radical and Ion

In earlier measurements on vinyl radical (8) the radical was produced by the pyrolysis of methylvinyl mercury. In the present work the radicals were obtained more conveniently and in somewhat better yield from the pyrolysis of divinylsulfone.

[1] $(CH_2{=}CH)_2SO_2 \rightarrow 2\,CH_2{=}\dot{C}H + SO_2$

Some C_2H_2 and C_2H_4 were also formed by secondary reactions. Contributions from these species to the *m/e* 27 peak were shown to be negligible with electron energies in the range used for measuring the threshold ionization of C_2H_3 radical.

A typical threshold ionization curve for C_2H_3 radical is shown in Fig. 1, along with that for krypton added to the gas stream for calibration of the energy scale. This curve appears to exhibit one or more short linear sections, possibly corresponding to vibrational levels of the $C_2H_3^+$ ion.

[1]NRCC No. 11 667.

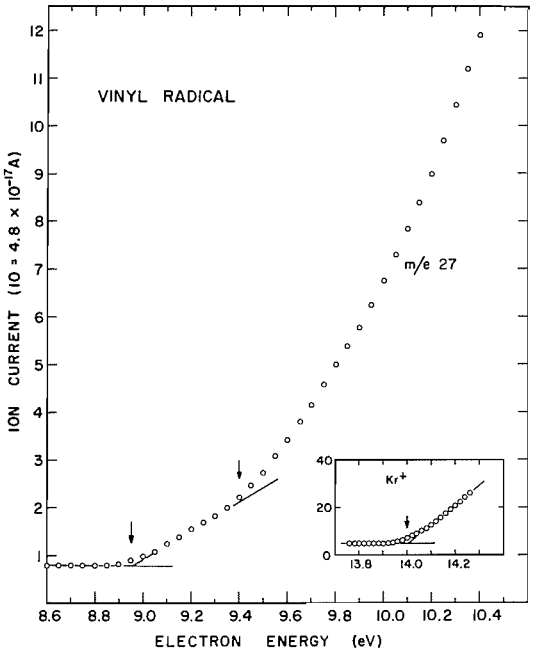

FIG. 1. Threshold ionization curve for vinyl radical produced by pyrolysis of divinyl sulfone.

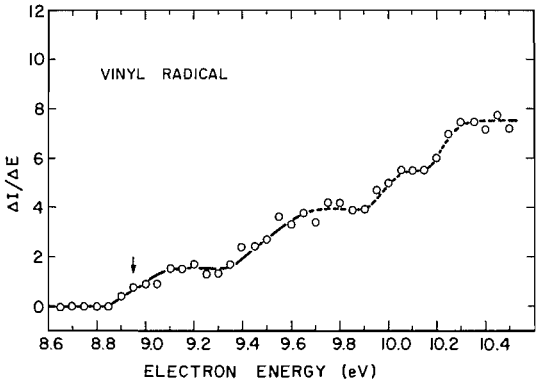

FIG. 2. First differential curve for vinyl radical ionization. The arrow marks the ionization potential obtained from Fig. 1.

The reality or otherwise of this structure may be judged from Fig. 2, which gives the first derivative of the data points of Fig. 1. No smoothing was employed. Extrapolation of the first "linear" segment of Fig. 1 gives 8.95 V for the ionization potential of C_2H_3 radical. An upward break at around 9.4 V appears to correspond to the earlier values of 9.35–9.45 V obtained for IP(C_2H_3) using conventional ion sources (8, 9). Owing to lack of energy resolution in the earlier measurements, the lowest segment of the curve was not observed. It is difficult to say whether the present result represents the true adiabatic IP, or whether it should be considered merely an upper limit. From Fig. 1 it appears improbable that the curve extends below 8.95 V but this possibility cannot be entirely ruled out.

There appears to be no other literature value, either experimental or theoretical, for this ionization potential aside from the earlier low resolution results cited above. It may be noted for comparison that this value for the ionization potential of vinyl is 0.9 V lower than that of CH_3 radical (9.84 V) and about 0.6 V higher than that of C_2H_5 radical (8.38 V) (1). Current theoretical treatments for ionization energies of radicals appear to be insufficiently reliable to enable an estimate for IP(C_2H_3) to be made.

Three recent measurements of the photoionization threshold for the dissociative process

[2] $$C_2H_4 + h\nu \rightarrow C_2H_3^+ + H + e$$

have been made, giving the appearance potential AP($C_2H_3^+$) as 13.80 V (10), 13.37 ± 0.03 V (11), and 13.25 ± 0.05 V (12). It seems probable that the lowest value is to be preferred. From standard heat of formation data this value gives $\Delta H_f(C_2H_3^+) = 266$ kcal/mol. The reason for the difficulty in measuring this threshold, even by the usually precise PI method, is the low probability for $C_2H_3^+$ ion formation near the energy threshold, resulting from the competing process

[3] $$C_2H_4 + h\nu \rightarrow C_2H_2^+ + H_2 + e$$

for which the appearance potential is slightly lower (10, 12). Earlier electron impact values for AP($C_2H_3^+$) are in the range 14.00–14.06 V using a conventional ion source (8, 13) and 14.10 ± 0.15 V using RPD electron impact (14). In view of this difficulty no attempt was made to remeasure this appearance potential in the present work. As an alternative, the appearance potentials for $C_2H_3^+$ ion formation from vinyl chloride and vinyl bromide were examined. The curves found for $C_2H_3^+$ ion formation from these compounds exhibited a feature not observed for other fragment ions examined so far with this apparatus. As can be seen in Fig. 3, the ionization efficiency curve for $C_2H_3^+$ production showed a "tail" of low $C_2H_3^+$ yield, having a nearly linear form, followed by an abrupt upward break corresponding to a sudden large increase in $C_2H_3^+$ yield. Comparison with the shape of the krypton standard curve indicates that this break is at

Can. J. Chem. Downloaded from www.nrcresearchpress.com by 210.87.254.5 on 09/05/12
For personal use only.

Can. J. Chem. Downloaded from www.nrcresearchpress.com by 210.87.254.5 on 09/05/12
For personal use only.

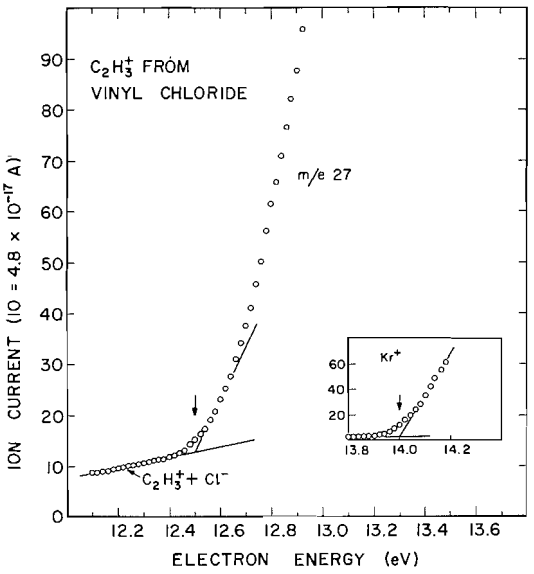

FIG. 3. Appearance potential curve for formation of $C_2H_3^+$ ion from vinyl chloride. The arrow marks the onset for the production of $C_2H_3^+$ and neutral Cl atom.

about 12.5 V. It seems probable that the "tail" can be associated with the ion pair process

[4] $$C_2H_3Cl + e \rightarrow C_2H_3^+ + Cl^- + e$$

and that the upward break corresponds to the threshold for the process

[5] $$C_2H_3Cl + e \rightarrow C_2H_3^+ + Cl + 2e$$

with this assumption, $AP(C_2H_3^+) = 12.5$ V gives $\Delta H_f(C_2H_3^+) = 268$ kcal/mol. A curve of nearly identical form was obtained for vinyl bromide, with an upward break at 11.9 V, corresponding to $\Delta H_f(C_2H_3^+) = 266$ kcal/mol. These results are in good agreement with the photoionization value (12) of $\Delta H_f(C_2H_3^+) = 265.9$ kcal/mol. No definite value could be obtained for the onset of the "tail" portion of the $C_2H_3^+$ curves, owing to the low probability for this process and the uncertainty as to the true shape of its ion yield curve.

From $\Delta H_f(C_2H_3^+) = 266$ kcal/mol and $IP(C_2H_3) = 8.95$ V one gets $\Delta H_f(C_2H_3) = 59.6$ kcal/mol, corresponding to a bond dissociation energy $D(C_2H_3—H) = 99.2$ kcal/mol. Aside from the earlier electron impact work, which is based on erroneously high values for $AP(C_2H_3^+)$ and $IP(C_2H_3)$, experimental data for this bond are rather sparse. A pyrolytic study of divinyl mercury using the toluene carrier technique gave $D(C_2H_3—H) \sim 102.5$ kcal/mol (15, 16) with a rather large uncertainty. From unpublished results on the reaction of HI with vinyl iodide, Golden and Benson (17) deduced $D(C_2H_3—H) \geqslant 108 \pm 2$ kcal/mol, corresponding to $\Delta H_f(C_2H_3) \geqslant 68.4$ kcal/mol. Assuming the value of $\Delta H_f(C_2H_3^+) = 266$ kcal/mol to be correct, this heat of formation for C_2H_3 would require $IP(C_2H_3)$ to be $\leqslant 8.57$ V, about 0.4 V lower than the presently reported value. This discrepancy is large enough to raise the question as to whether the $C_2H_3^+$ ion formed at the dissociation threshold for ethylene and vinyl halides has some other minimum energy configuration differing substantially from the "vinyl" structure.

Allyl Radical and Ion

A good yield of allyl radical was obtained by the pyrolysis of allylmethyl nitrite, prepared from a sample of 3-butene-1-ol. A threshold ionization curve for allyl radical is given in Fig. 4. The curve exhibits one or perhaps two breaks above the threshold, which is at 8.07 V with a probable uncertainty of about ± 0.03 V. A first differential curve for these data points is given in Fig. 5, which shows clearly a second "step" at 8.22 V and just possibly a third at about 8.45 V. Earlier

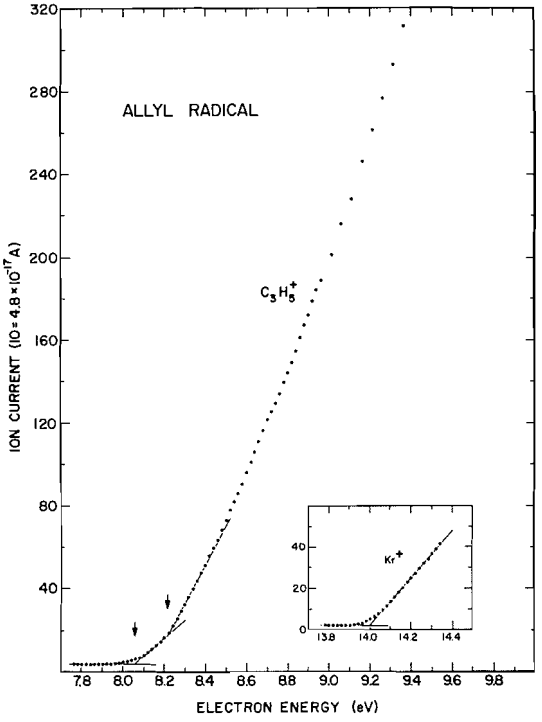

FIG. 4. Threshold ionization curve for allyl radical, produced by pyrolysis of allylmethyl nitrite.

Can. J. Chem. Downloaded from www.nrcresearchpress.com by 210.87.254.5 on 09/05/12
For personal use only.

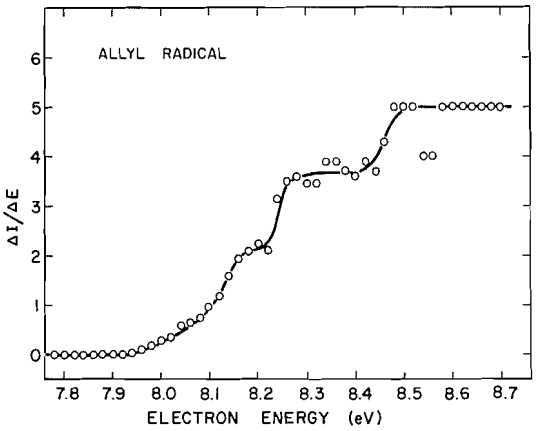

FIG. 5. First differential curve for allyl radical ionization, showing two and possibly three "steps".

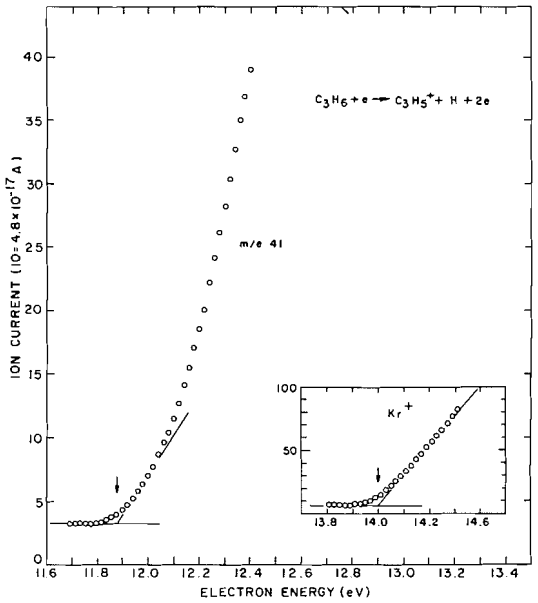

FIG. 6. Threshold curve for formation of $C_3H_5^+$ ion from propylene. Curves for $C_3H_5^+$ formation from 1- and 2-butene were of the same form.

measurements of 8.16 V (18) and 8.15 V (9) for IP(allyl) using conventional ion sources presumably correspond approximately to an unresolved maximum Franck–Condon factor at an energy of about 8.2 V. With some reservations, one can assign the onset at 8.07 V to the adiabatic IP. The presence of another "segment" below this value looks improbable but cannot be entirely ruled out.

The appearance potentials for $C_3H_5^+$ fragment ion from propylene, 1- and 2-butene were also measured. The efficiency curves were all of the apparently structureless type shown in Fig. 6. The estimated thresholds are given in Table 1, along with some earlier values measured by conventional methods (19) and by a second differential ionization method (20). No photon impact or RPD electron impact values for $C_3H_5^+$ appear to have been published. From standard heats of formation these appearance potentials lead to $\Delta H_f(C_3H_5^+) = 226$ kcal/mol with a probable uncertainty of 1 or 2 kcal/mol. Subtracting IP(allyl) = 8.07 V gives ΔH_f(allyl) = 40 ± 2 kcal/mol, in reasonable agreement with recent measurements by kinetic methods of 41 ± 1 kcal/mol (17, 21). Appearance potential data for $C_3H_5^+$, as collected in a recent compilation (22), give a wide range of values of $\Delta H_f(C_3H_5^+)$, from 216 to more than 260 kcal/mol. This indicates that although *m/e* 41 is a relatively abundant ion in the mass spectra of many hydrocarbons and allyl derivatives, its formation is not a particularly simple process (23).

Benzyl Radical and Ion

A reasonably good yield of benzyl radical was obtained by the pyrolysis of benzylmethyl nitrite at moderate furnace temperatures (24)

$$C_6H_5CH_2CH_2ONO \rightarrow C_6H_5CH_2CH_2\dot{O} + NO$$

$$C_6H_5CH_2CH_2\dot{O} \rightarrow C_6H_5\dot{C}H_2 + CH_2O$$

The threshold ionization curve for benzyl radical (Fig. 7) was strongly curved, and showed no evident structure over the first 2.5 V portion. In the absence of any linear or quasi-linear section at the onset, an extrapolation to a well-defined threshold cannot be made. A comparison of the curved foot in the inset of Fig. 7 with the curvature of the foot of the krypton standard curve, resulting from the 0.07 V energy half-width, indicates that the onset of the benzyl curve cannot be lower

TABLE 1. Appearance potentials for $C_3H_5^+$ ion formation

Compound	AP (V)	$\Delta H_f(C_3H_5^+)$ (kcal/mol)	Previous AP (V)
Propylene	11.88	226.8	12.11[a]
1-Butene	11.28	226.1	11.73[a], 11.4[b]
2-Butene	11.33	225.6	11.60[a]

[a]Reference 19.
[b]Reference 20.

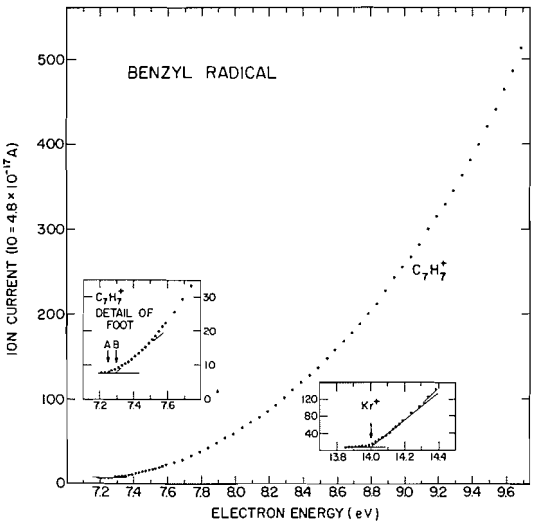

FIG. 7. Threshold ionization curve for benzyl radical, produced by pyrolysis of benzylmethyl nitrite. Points *A* and *B* are estimated lower and upper limits for the onset of ionization.

than point *A* (7.25 V) nor higher than point *B* (7.30 V). The best way to express this result is as the limit IP(benzyl) $\leqslant 7.27 \pm 0.03$ V. This is appreciably lower than the value of 7.76 V obtained earlier by electron impact in a conventional ion source; evidently the curvature of the foot of the benzyl curve was seriously underestimated in the earlier measurement. There is, however, an unresolved discrepancy between the present value, and a value of 7.63 ± 0.02 obtained by photoionization (25, 26). There seems no reason to suspect in either experiment that isomerization of benzyl radicals to tolyl or cycloheptatrienyl radicals, which are less stable than benzyl, has occurred. In any case, the IP of cycloheptatrienyl, 6.237 V (26, 27) is much lower than either of the experimental values for benzyl. The ionization potential of tolyl radical, $CH_3C_6H_4$, is probably not too different from that of toluene[2] and consequently too high to be a source of confusion in these experiments. The possibility of a real difference between the electron and photon impact experiments does exist, although it is rather unlikely. Ionization of benzyl radical by electron impact could conceivably occur through formation of a discrete excited neutral state, which then rearranges and ejects an electron to form tropylium ion.

[2]Compare, for instance IP(phenyl) and IP(benzene) (ref. 22).

$$C_6H_5CH_2 + e \rightarrow C_6H_5CH_2^* + e$$

$$C_6H_5CH_2^* \rightarrow C_7H_7^+ \text{ (tropylium)} + e$$

Formation of the excited state $C_6H_5CH_2^*$ by photon impact could be spin-forbidden, making this mechanism inoperative or improbable for photoionization.

It is of interest in this respect, particularly in view of the well-known isomerization (2, 3)

[6] $$\text{benzyl}^+ \rightarrow \text{tropylium}^+$$

to calculate heats of formation for these two ionic species from the current data. Taking IP(cycloheptatrienyl) = 6.24 V (26, 27), $D(C_7H_7—C_7H_7)$ in ditropenyl = 1.85 ± 0.05 V (26), and ΔH_f(ditropenyl) = 94.6 kcal/mol (28), one obtains ΔH_f(cyclo-$C_7H_7^+$) = 212 kcal/mol. A slightly lower value for $\Delta H_f(C_7H_7^+)$, 209 kcal/mol, has been suggested from a measurement of the enthalpy of dissociation of bitropenyl (29). Taking ΔH_f(benzyl) = 45 kcal/mol (16) and IP(benzyl) = 7.27 V, one obtains $\Delta H_f(C_6H_5CH_2^+)$ = 213 kcal/mol. On this basis, reaction 6 is thermoneutral or only slightly exothermic. This result is surprising in view of the universality of this reaction for benzyl ion and its analogs (3), and tends to support the possibility that the present electron impact IP for benzyl is too low because of some rearrangement as suggested above.

1. F. P. LOSSING and G. P. SEMELUK. Can. J. Chem. **48**, 955 (1970).
2. P. N. RYLANDER, S. MEYERSON, and H. M. GRUBB. J. Amer. Chem. Soc. **79**, 842 (1957).
3. H. M. GRUBB and S. MEYERSON. *In* Mass Spectrometry of Organic Ions. *Edited by* F. W. McLafferty. Academic Press, New York. 1963. Chap. 10.
4. K. MAEDA, G. P. SEMELUK, and F. P. LOSSING. Intern. J. Mass Spectry. Ion Phys. **1**, 395 (1968).
5. J. B. FARMER and F. P. LOSSING. Can. J. Chem. **33**, 861 (1955).
6. F. P. LOSSING and G. P. SEMELUK. Intern. J. Mass Spectry. Ion Phys. **2**, 408 (1969).
7. T. MCALLISTER and F. P. LOSSING. J. Phys. Chem. **73**, 2996 (1969).
8. A. G. HARRISON and F. P. LOSSING. J. Amer. Chem. Soc. **82**, 519 (1960).
9. D. BECK and O. OSBERGHAUS. Z. Phys. **160**, 406 (1960); D. BECK. Discuss. Faraday Soc. **36**, 56 (1963).
10. R. BOTTER, V. H. DIBELER, J. A. WALKER, and H. M. ROSENSTOCK. J. Chem. Phys. **45**, 1298 (1966).
11. B. BREHM. Z. Naturforsch. **21***a*, 196 (1966).
12. W. A. CHUPKA, J. BERKOWITZ, and K. M. A. REFAEY. J. Chem. Phys. **50**, 1938 (1969).
13. C. LIFSHITZ and F. A. LONG. J. Phys. Chem. **67**, 2463 (1963).
14. J. E. COLLIN. Bull. Soc. Chim. Bel. **71**, 15 (1962).

Can. J. Chem. Downloaded from www.nrcresearchpress.com by 210.87.254.5 on 09/05/12
For personal use only.

15. A. F. TROTMAN-DICKENSON and G. J. O. VERBEKE. J. Chem. Soc. 2580 (1961).
16. J. A. KERR. Chem. Rev. **66**, 465 (1966).
17. D. M. GOLDEN and S. W. BENSON. Chem. Rev. **69**, 125 (1969).
18. F. P. LOSSING, K. U. INGOLD, and I. H. S. HENDERSON. J. Chem. Phys. **22**, 621 (1954).
19. I. OMURA. Bull. Chem. Soc. Jap. **34**, 1227 (1961); **35**, 1845 (1962).
20. G. G. MEISELS, J. Y. PARK, and B. G. GIESSNER. J. Amer. Chem. Soc. **92**, 254 (1970).
21. D. M. GOLDEN, A. S. RODGERS, and S. W. BENSON. J. Amer. Chem. Soc. **88**, 3196 (1966).
22. J. L. FRANKLIN, J. G. DILLARD, H. M. ROSENSTOCK, J. T. HERRON, and K. DRAXL. Ionization Potentials, Appearance Potentials, and Heats of Formation of Gaseous Positive Ions. National Bureau of Standards, Washington. June 1969.
23. G. G. MEISELS, J. Y. PARK, and B. G. GIESSNER. J. Amer. Chem. Soc. **91**, 1555 (1969).
24. F. P. LOSSING and J. B. DE SOUSA. J. Amer. Chem. Soc. **81**, 281 (1959).
25. F. A. ELDER. Ph.D. Thesis, Department of Physics, University of Chicago, Chicago, Illinois. 1968.
26. F. A. ELDER and A. C. PARR. J. Chem. Phys. **50**, 1027 (1969).
27. B. A. THRUSH and J. J. ZWOLENIK. Discuss. Faraday Soc. **35**, 196 (1963).
28. A. G. HARRISON, L. R. HONNEN, H. J. DAUBEN, JR., and F. P. LOSSING. J. Amer. Chem. Soc. **82**, 5593 (1960).
29. G. VINCOW, HYP J. DAUBEN, JR., F. R. HUNTER, and W. V. VOLLAND. J. Amer. Chem. Soc. **91**, 2823 (1969).

Can. J. Chem. Downloaded from www.nrcresearchpress.com by 210.87.254.5 on 09/05/12
For personal use only.

X-Ray Induced Polymerization of Gaseous Vinyl Chloride. Effect of Additives

JACQUES GROSSOLEIL AND JAN A. HERMAN
Department of Chemistry, Laval University, Quebec, Quebec

Received August 17, 1970

The X-ray induced polymerization in the gas phase of pure vinyl chloride and of its mixtures with O_2, NO, SF_6, NH_3, CH_3NH_2, H_2O, HCl, and C_2H_2 were examined. About 75% of the polymerization proceeds via a radical mechanism. The experiments indicate that most of the additives are deactivating chain transfer agents. Gel permeation chromatography showed that the polymer is activated by X-ray absorption during the time it takes to fall to the bottom of the irradiation cell, and forms a branched polymer.

Canadian Journal of Chemistry, 49, 363 (1971)

Can. J. Chem. Downloaded from www.nrcresearchpress.com by 210.87.254.105 on 09/05/12
For personal use only.

Introduction

It is generally accepted that the radiation-induced polymerization of gaseous vinyl chloride is an example of a radical mechanism (1, 2). Our previous work (3) on the X-ray induced polymerization of vinyl chloride, in particular the kinetic consideration of the initiation and termination processes, seemed, at first sight, compatible with a free radical mechanism. There was an initial acceleration period and a post-polymerization effect, which could hardly be explained except by a radical mechanism. On the other hand, the propagation rate of the so-called "stationary-rate-regime", which is first power dependent on the dose-rate, was explained by assuming a hindered termination process (3).

To the above example of the radical polymerization, one can contrast the radiation-induced polymerization of gaseous isobutene, which proceeds by an ionic mechanism (4, 5). However, some experimental observations are common to both systems, *iso*-C_4H_8 and C_2H_3Cl. An example is the increase in the rate of polymerization with dose-rate according to a first order relation, which was invoked by Okamoto *et al.* (4) as an argument for the ionic polymerization process in isobutene. Recently Williams *et al.* (6) showed that a termination involving a transfer of the active species to an impurity or a scavenger, such that the reaction product is nonpropagating, will give a first power dependence on the dose-rate, and the mechanism will apply indistinguishably to ionic or radical polymer chain propagation. In the gas phase the role of such impurities or scavengers may be filled by the numerous radiation-induced decomposition products, which are sometimes formed with relatively high yields. This, together with the observation (7) of continuous acceleration of the propagation-rate of radiation-induced polymerization of vinyl chloride in the presence of an electric field, and of the action of nitric oxide, which even at relative important concentrations (~ 7 mol%) does not completely stop the polymerization, led us to reconsider some of our previous conclusions, and to give special attention to the possibility of some ionic mechanisms. Recent work on ion–molecule reactions shows the existence of some short chain reactions in the gaseous vinyl chloride (8, 9), although it seems doubtful to associate ionic propagation measured at 10^{-2} Torr and polymer formation at pressures of several hundred Torr.

Therefore we have carried out new experiments on the radiation-induced polymerization of gaseous vinyl chloride in order to obtain a better understanding of the mechanisms responsible for the polymer formation. The approach was twofold: measurement of the rate of polymerization in the presence of suitable additives, some of them being recognized as ionic scavengers (NH_3) or electron capturers (SF_6), and characterization of the polymer by its chain length and composition.

Experimental

The experimental device was the same as that described previously (3), with modifications to allow precise mea-measurements of the polymerization-rate at the very beginning and at the end of the irradiation. Essentially, the experimental device is a manostat composed of an irradiation cell, F, a mercury manometer with an electrical control, M, and a calibrated container, C, whose volume can be adjusted by a controlled admission of mercury, Fig. 1. The changes in the volume are transposed into electrical signals by a variable resistance connected to the container. In the present work the irradiation cell was a 1 l stainless steel or glass cylindrical vessel with its principal axis horizontal. As before (3), the X-rays

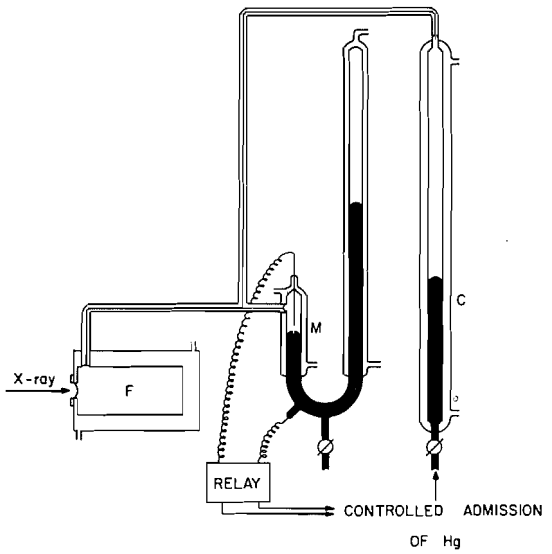

FIG. 1. The experimental design.

from a "Machlett OEG 60" tube penetrate horizontally into the irradiation cell through a thin aluminum window (0.06 mm thick, 22 mm diameter). In this way the polymer falls to the bottom and is outside the directly irradiated volume. The sensitivity of the manostat at 1 atm corresponds to the pressure change resulting from a variation of temperature of less than 0.01 °C. The whole manostat was therefore placed in a thermostatic bath whose temperature could be kept constant within 0.02 °C. The compensation of the pressure changes could be recorded automatically both by expansion and by contraction of the volume. Such recording is very useful when measuring the volume changes at the beginning of the experiments when the gas expands by absorption of the energy from X-rays. In this way, the induction periods, if any, could be accurately observed.

Each irradiation experiment was carried out on a freshly prepared mixture of the monomer and the additive. When a series of irradiation experiments of vinyl chloride with increasing quantities of a particular additive was finished, the irradiation cell was demounted and thoroughly cleaned. The solid polymer from some series of experiments was collected and used for further studies. In order to obtain reproducible results (because of the slow establishment of the adsorption equilibrium), gases freshly admitted to the irradiation cell were always kept several hours (usually over-night) at the temperature of the thermostatic bath before the beginning of the irradiation.

Vinyl chloride from Matheson Company was purified by trap-to-trap distillation at the temperature of liquid nitrogen and stored in a 6 l container from which it was taken for irradiation experiments. The only impurity detected by gas chromatography was C_2HCl in quantities less than 10 p.p.m. Oxygen was prepared by pyrolysis of analytical grade $KMnO_4$. Nitric oxide from Matheson was purified further by the method of Forst and Rice (10). Other additives, SF_6, NH_3, CH_3NH_2, HCl, and C_2H_2, obtained from Matheson Company, were purified by trap-to-trap distillation at −185 °C and distilled water was previously degassed by the thawing–freezing technique before its mixing with the monomer.

The dose-rate was estimated from the $P\Delta V$ measurements at the pressure and the temperature of the experiment and at the very beginning of the irradiation. The absorption of the X-rays by the gas and the walls increases instantaneously the temperature inside the irradiation cell (a few tenths of a degree depending upon the intensity of X-ray and pressure of the gas), and the corresponding increase of the volume was recorded. It was impossible to establish the ratio of the energy absorbed by the gas and by the walls, therefore only an approximate value of the dose-rate could be calculated by comparison with $G(—C_2H_3Cl)$ published by Herman and Hupin (3); in the present study it was around 2.8×10^{17} eV g^{-1} min^{-1}. The total dose absorbed ranged between 10^{19} and 10^{20} eV, which allowed the maximum conversion of the monomer to be maintained under 1.5%.

The infrared spectrum of the solid polymer in KBr was taken on a Perkin–Elmer 621 spectrophotometer. The molecular weight distribution was determined by gel permeation chromatography (Waters Associates Inc.). The lack of suitable poly(vinyl chloride) standards of low molecular weight (< 20 000) forced us to calibrate our polymer samples against polystyrene standards. However, the calibration curves for higher molecular weights (> 50 000) from polystyrene and poly(vinyl chloride) standards coincide; hence we assume that the error in molecular weight determination against polystyrene standards is small. The polymer was dissolved in tetrahydrofuran.

Results

The radiation-induced polymerizations were conducted at constant pressure, 77 ± 0.3 cm Hg, and constant temperature, 19.8 ± 0.02 °C. In some experiments the X-ray intensity was varied in order to measure the dependence on the dose-rate. In all experiments the polymerization started immediately the X-rays were switched on and the rate of the monomer disappearance was constant during the whole time of irradiation. At the end of irradiation the pressure dropped suddenly as the gas cooled and this corresponded on the recorded curve to a rapid decrease of the volume, but we did not notice any slow exponential decrease of the volume which could be attributed to the post-polymerization. These two facts, (*a*) the constant rate of monomer disappearance over the whole time of irradiation and (*b*) the apparent lack of a post-polymerization, are in contradiction with what has already been published (3). The negative temperature coefficient of the polymerization-rate was again

Can. J. Chem. Downloaded from www.nrcresearchpress.com by 210.87.254.105 on 09/05/12
For personal use only.

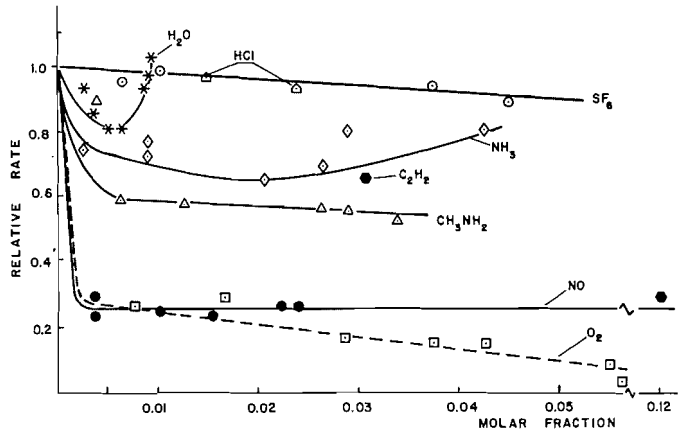

FIG. 2. Relative polymerization-rates of gaseous vinyl chloride mixed with various additives, irradiated by X-rays.

noted, in agreement with other works (11, 12). However, the polymerization-rate of the pure vinyl chloride depends on the condition of the surface; it increases (*ca.* 10%) when the surface of the cell is coated with previously deposited poly(vinyl chloride). This surface effect, operating either for stainless steel or glass walls, is responsible for the poor reproducibility of the polymerization-rate for pure C_2H_3Cl in a freshly cleaned irradiation cell.

The decrease of the volume during radiation-induced polymerization is taken as a measure of the polymer formation. This is in fact a lower limit, because one should take into account the increase of the number of molecules within the system due to the accumulation of the decomposition products resulting from radiolysis. However, in the conditions of the present experiments the total yield of the decomposition products is less than 3% of the $G(-C_2H_3Cl) \sim 500$ of the monomer disappearance. Hence, we can assume that within 2% the rate of monomer consumption represents the polymerization. The effect of increasing quantities of NO, O_2, H_2, NH_3, CH_3NH_2, SF_6, HCl, and C_2H_2 on the polymerization-rate of vinyl chloride is shown in Fig. 2. Nitric oxide and oxygen were used as radical scavengers, whereas ammonia, methylamine and SF_6 were added as ion or electron interceptors. The mean value of the rate of disappearance of the pure monomer is 6.4 μmol/min for either glass or stainless steel cells coated with the deposit of the polymer. Oxygen and nitric oxide have the most pronounced effect on the rate; amounts as small as $\sim 2 \times 10^{-3}$ mole-fraction are sufficient to decrease by $\sim 75\%$ the initial polymerization-rate. After this sharp decrease of polymerization-rate, further additions of O_2 or NO have different effects; increasing amounts of oxygen slowly diminish the rate of polymerization of the monomer, whereas NO does not further alter the attained rate. The action of CH_3NH_2 and NH_3 are less pronounced; they decrease the rate by ~ 40 and $\sim 31\%$, respectively. It is worthwhile to record that with increasing amounts of ammonia the polymerization-rate increases slightly. This effect is much more pronounced in the presence of water vapor. Here the polymerization-rate passes through a minimum at $\sim 7 \times 10^{-3}$ mole-fraction of H_2O and then increases rapidly to values which are higher than the polymerization-rate of pure vinyl chloride. The action of SF_6, which is added to C_2H_3Cl as competitor for electron capture, is weak, but noticeable. During the radiolysis of C_2H_3Cl the main decomposition products are HCl and C_2H_2 and their yields per 100 eV of absorbed energy are around 10, and 1.5, respectively (13). In two experiments we added small amounts of HCl (Fig. 1) to verify if the polymerization is retarded by this compound. The results indicate that HCl has the same effect as SF_6. On the other hand a molar fraction of $\sim 3 \times 10^{-2}$ of acetylene diminishes by $\sim 35\%$ the polymerization-rate (Fig. 2). In order to obtain more information, we carried on some experiments in which equal quantities of SF_6 and NH_3 were mixed at the same time with C_2H_3Cl. For the system SF_6 (0.028) + NH_3 (0.025) the relative polymerization-rate dropped to 0.61,

Can. J. Chem. Downloaded from www.nrcresearchpress.com by 210.87.254.105 on 09/05/12
For personal use only.

Can. J. Chem. Downloaded from www.nrcresearchpress.com by 210.87.254.105 on 09/05/12
For personal use only.

while for the mixture SF_6 (0.052) + NH_3 (0.048 mole-fraction) the relative rate was 0.69.

In the present study, the polymerization-rate, V, for pure vinyl chloride can be represented by the following expression

$$V = k\,P^{1.2}\,I^{1.07}$$

where I stands for X-ray intensity. This expression agrees in respect to the intensity dependence with a similar one obtained by Herman and Hupin (3) for the "regime rate" of polymerization. The presence of additives diminishes the value of the exponent of the intensity factor to around 0.83 ± 0.05, and seems to be relatively independent of the nature of the additive.

The infrared (i.r.) spectrum of the pure poly(vinyl chloride) resembles that described by Krimm (14), but in addition there is always a weak band at 1720 cm^{-1}. This absorption band is characteristic of the carbonyl group, $R-\overset{\overset{O}{\|}}{C}-R$, especially if a halogen atom is linked to an adjacent carbon (15). During radiolysis of the pure vinyl chloride the formation of a carbonyl group in the polymer is impossible; neither the traces of oxygen adsorbed on the metallic walls nor on the glass walls of the irradiation cell could contribute to such an extent to the 1720 cm^{-1} band. The only plausible explanation of the origin of this band is the instantaneous oxidation of free bonds of the polymer when the cell is opened for removing the products and cleaning. This agrees with the observation of Hupin (7), that the oxygen is adsorbed after irradiation by the freshly formed polymer. The i.r. spectrum of poly(vinyl chloride) formed in irradiated C_2H_3Cl + H_2O also has the 1720 cm^{-1} weak band of the carbonyl group. In the case of vinyl chloride irradiated in the presence of O_2, the i.r. spectrum of the polymer shows a very strong 1720 cm^{-1} band. The polymer i.r. spectra of C_2H_3Cl irradiated in the presence of NH_3 or SF_6 indicate some bands characteristic of the N, or S and F atoms, respectively. In the case of the polymer formed in the presence of ammonia there are medium intensity absorption bands at 3150 and 3050 cm^{-1}, which might be assigned to $-NH_2$ and —NH stretching of amides (16). There is another strong band at 1408 cm^{-1}, but its assignment is uncertain. The system C_2H_3Cl + SF_6 gives a red polymer, whose i.r. spectrum shows additional bands at 820, 840, and 870 cm^{-1}, at which the assignment is uncertain, but which most probably belong to the —C—S—F group. The i.r. spectra of polymers of both systems, C_2H_3Cl + NH_3 and C_2H_3Cl + SF_6 show also a very weak carbonyl group band at 1720 cm^{-1}, which means that in these systems some free bonds persist after irradiation.

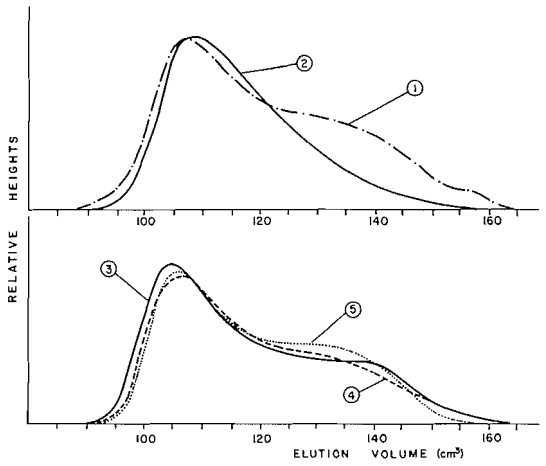

FIG. 3. Gel permeation chromatograms of poly(vinyl chloride) formed from pure C_2H_3Cl and its mixture with various additives. (*1*), pure C_2H_3Cl irradiated by X-rays; (*2*), pure C_2H_3Cl irradiated by β-rays; (*3*), C_2H_3Cl + H_2O; (*4*), C_2H_3Cl + SF_6; (*5*), C_2H_3Cl + NH_3.

Much information can be obtained from analysis of the polymer by gel permeation chromatography (g.p.c.). Figure 3 shows the shape of the g.p.c. chromatograms for polymers formed during irradiation of pure vinyl chloride or the mixtures with additives. In Table 1 are represented the number average, $\overline{M}_n$, and the weight average, $\overline{M}_w$, molecular weight calculated by the method of Smith (17) as modified by Chen (18). The values of $\overline{M}_n$ obtained by the g.p.c. method are comparable with those already published (3) which were established by a cryoscopic method. The ration $\overline{M}_w/\overline{M}_n$ defines the polydispersity index of the polymeric material (column 5 of Table 1). For comparison we include the results of polymerization of pure gaseous C_2H_3Cl by 0.54 MeV β-rays from a ^{90}Sr source (curve 2 in Fig. 3). It can be seen that in the latter case the $\overline{M}_n$ is higher by a factor ~ 2 and consequently the polydispersity index is lower. Obviously the reason for that is the reduced tailing of the low molecular weight polymer compared to the

TABLE 1. Molecular weights calculated from g.p.c. distribution curves

System	Number average molecular weight $\overline{M}_n$	Average degree of polymerization d.p.	Weight average molecular weight $\overline{M}_w$	Polydispersity index
C_2H_3Cl irradiated by ^{90}Sr β-rays in Pyrex cell	1730	27.5	7340	4.2
C_2H_3Cl irradiated by X-rays in Pyrex cell	900	14.5	6520	7.2
C_2H_3Cl irradiated by X-rays in S.S.* cell	860	13.8	5500	6.4
$C_2H_3Cl + SF_6$ irradiated by X-rays in S.S. cell	970	15.5	6390	6.5
$C_2H_3Cl + NH_3$ irradiated by X-rays in S.S. cell	960	15.4	4850	5.8
$C_2H_3Cl + H_2O$ irradiated by X-rays in S.S. cell	920	14.7	6050	7.7

*S.S. = stainless steel.

TABLE 2. Chemical analysis of solid polymer

System	Percentage of C	H	Cl	Other atoms
C_2H_3Cl (Theoretical)	38.43	4.84	56.73	—
$(C_2H_3Cl)_n$	38.46	4.93	56.59	—
$C_2H_3Cl + SF_6$	37.22	4.61	52.76	S : 2.03
$C_2H_3Cl + NH_3$	37.12	4.95	55.25	N : 1.60
$C_2H_3Cl + H_2O$	38.59	4.69	55.57	O : 1.15

poly(vinyl chloride) formed in X-ray irradiation (curve 1 in Fig. 3). The g.p.c. chromatograms are very much alike for the polymers formed by X-ray irradiation of both pure C_2H_3Cl and with added scavengers. All of them show a flat broad component spread over low molecular weights as far as the trimer and dimer. The low molecular weight component is only slightly related to the nature of the additive. Only ammonia shows an effect, the amount of the low molecular weight component increasing relative to the high molecular weight polymer (Fig. 3 and Table 1).

Table 2 gives the results of the chemical analysis of the solid polymer.

Discussion

Criticism of The Previous Work

The results of the present studies disagree on several points with the previous data by Herman and Hupin (3). In contrast to (3) we do not find any evidence for an initial acceleration of the polymerization-rate, and a relatively important post-polymerization. The absence of the first effect can easily be explained by the improved design of the automatic regulator of the manostat. The post-polymerization effect in (3) was confused with the establishment of the adsorption equilibrium. In fact, there must be a small post-polymerization, as shown by the fixation of O_2 on free bonds of the polymer when opening the cell but this effect was overestimated in (3). We have already stressed that the adsorption equilibrium is reached very slowly. Now, as soon as the X-rays impinge on the walls a desorption occurs which is reversed when irradiation is stopped. It is this readsorption which was erroneously taken as a post-polymerization. Therefore, the hypothesis of an important hindered termination process of the polymerization (3) cannot be retained and another explanation of the observed phenomena must be sought.

Present Studies

We shall start with the study of the solid polymer, because it indicates some important aspects of the polymerization processes. The g.p.c. chromatograms show a high polydispersity index either for the polymer prepared from pure vinyl chloride, or for mixtures of C_2H_3Cl with additives (Table 1). Even if the polydispersity index tends to be overstated by the g.p.c. method (18), the shape of the chromatograms suggests that we are dealing with a polymer formed in more than one process. The peak corresponding to ~ 110 cm^3 of eluted volume (Fig. 3) results most probably from one process, while the broad shoulder on the right side of the peak arises from another process. Huang and Westlake (19) were able to show for the γ-ray induced polymerization of liquid styrene at low temperatures, that a bimodal molecular weight distribution corresponds to two different polymerization processes.

Can. J. Chem. Downloaded from www.nrcresearchpress.com by 210.87.254.105 on 09/05/12
For personal use only.

Can. J. Chem. Downloaded from www.nrcresearchpress.com by 210.87.254.105 on 09/05/12
For personal use only.

The comparison of the molecular weight distribution curves of the polymer formed in β-ray irradiation (curve 2) with that of the polymer formed in the X-ray experiment (curve 1) is particularly interesting. The curve 2 is unimodal and the broad shoulder (which exists on all chromatograms of polymer formed in X-ray experiments) has disappeared. Now, the initiation and the propagation mechanisms of polymerization are the same for both β- and X-ray irradiation. Therefore, the hypothesis that the component corresponding to ~ 110 cm^3 results from radical mechanisms and the broad shoulder from ionic processes (or vice-versa) cannot be accepted, because molecular weight distribution curves should be practically the same for both kinds of radiation. However, there are two other possible explanations: (*a*) the intensity effect and (*b*), irradiation of the polymer during the time it takes to fall to the bottom of the irradiation cell. The intensity of the X-ray source being about 4 orders of magnitude higher than our ^{90}Sr β-ray irradiation facilities, there is an increased probability of termination of polymeric chains by primary radicals. In this case one expects that the molecular weight distribution would conserve the shape of curve 2, but might be shifted toward lower molecular weight, *i.e.* to higher elution volume. Figure 2 shows that this is not the case and, therefore, the intensity alone cannot explain the existence of the broad shoulder component characteristic of X-ray irradiations. It seems that the hypothesis of irradiation of the polymer is the best answer. The mass-absorption coefficient of X-rays by the solid polymer being much higher that that of the gaseous monomer (roughly in the ratio of densities of solid poly(vinyl chloride) to gaseous C_2H_3Cl) the probability of X-ray absorption by the polymer is quite high and leads to the formation of free sites, which can initiate lateral chains on an isolated linear polymer. Indeed, poly(vinyl chloride) is known to cross-link under ionizing radiation (20). At the same molecular weight a branched polymer has a smaller average dimension than a linear macromolecule and it will be eluted with lower molecular weight linear polymers, and should be found in the tail of the molecular weight distribution curve. This hypothesis is strengthened by the fact that at room temperature the polymer does not dissolve entirely in a mild solvent, such as *o*-dichlorobenzene, suggesting that some branched material is present after irradiation. Obviously, β-ray induced polymerization cannot behave in a similar way. If the assumption is correct, it implies an underestimation by the g.p.c. method of the number average molecular weight, $\overline{M}_n$ and the average degree of polymerization, $\overline{\text{d.p.}}$, and explains the deviation between the present measurements (Table 1) and the previously reported value, $\overline{\text{d.p.}} = 18.2$ (3).

The i.r. spectra and the chemical analysis of the polymers formed from C_2H_3Cl mixed with SF_6, NH_3, or H_2O, show in each case fragments of the additive incorporated into the polymer chain. None of these additives can initiate polymerization, therefore, their presence in the polymer can only proceed from chain transfer. If this is correct and assuming one only additive fragment per macromolecule, it is possible to calculate the average degree of polymerization from chemical analysis data. The following values are found: $\overline{\text{d.p.}} \approx 25$ for the $C_2H_3C + SF_6$ system, $\overline{\text{d.p.}} \approx 22$ for $C_2H_3Cl + H_2O$, and $\overline{\text{d.p.}} \approx 15$ for $C_2H_3Cl + NH_3$. These confirm, in general, the average degree of polymerization measured by the g.p.c. and cryoscopic methods. In the case of the mixture of vinyl chloride with ammonia the $\overline{\text{d.p.}}$ seems low. It is possible that in this case there is, on the average, more than one nitrogen atom per macromolecule and it might indicate that ammonia reacts with poly(vinyl chloride) in different processes.

The additives used in this study can intervene in three different ways: (*a*) scavenging action of free radicals, (*b*) interception of positive or negative (electrons) ions, and (*c*) chain transfer process. In the last case one can distinguish between an active chain transfer and a deactivating chain transfer. We have already assumed that additives are acting in a chain transfer as well as in their characteristic scavenging role. The addition of less than 0.005 molar fraction of oxygen or nitric oxide has a very pronounced effect, the relative polymerization-rate being reduced by $\sim 75\%$. The possibility of charge transfer between parent ion, $C_2H_3Cl^+$ (ionization potential, i.p. = 10.0 eV) (21) and oxygen (i.p. = 12.07 eV) (22, 23) must be ruled out; it follows then that the observed decrease of the rate results from radical processes. In the case of NO (i.p. = 9.25 eV) (23) a charge transfer from the vinyl chloride ion is possible, in principle, but there is no evidence for it when a comparison is

Can. J. Chem. Downloaded from www.nrcresearchpress.com by 210.87.254.105 on 09/05/12
For personal use only.

made to the scavenging action of oxygen (Fig. 2). Therefore, we assume that at the pressure of *ca.* 77 cm Hg about 25% of the polymerization is accounted for by a non-radical mechanism. A further addition of O_2 to the system influences the rate of this non-radical part of polymerization, while NO has no effect (Fig. 2). The reason for this is the oxygen induced decomposition of C_2H_3Cl which gives an important increase in HCl formation, which in turn acts as a retarder of the polymerization, (13). Apparently, NO does not decompose the monomer, but instead it reacts efficiently with Cl atoms to form nitrosyl chloride (7).

If some ionic species are precursors or initiators of polymerization, then the addition of SF_6 would compete for thermal electrons, and we would expect to observe an initial rapid decrease of the polymerization-rate followed by a plateau when all electrons of interest are scavenged. Such behavior is not observed. There is only a slow steady decrease of the relative polymerization-rate with increasing concentration of SF_6 (Fig. 2). There is still the possibility that the polymer electron-attachment coefficient is much higher than that of the SF_6. Lee (24) showed that the greater the number of Cl atoms substituted to the alkyl group the higher the probability of electron attachment. No matter what the electron-attachment process is, it seems that the action of SF_6 is not related to the anionic polymerization of gaseous C_2H_3Cl. Moreover, experiments with irradiation of $C_2H_3Cl + NH_3 + SF_6$ systems suggest that SF_6 is acting as a neutral species and not as a negative ion, because the polymerization-rate in such systems decreases by an amount which is the sum of the independent action of each of the additives alone. We assume, therefore, that the steady slow decrease of the rate with increasing additive concentration results from a deactivating chain transfer. This is partly confirmed by the chemical analysis and the i.r. spectra of the polymer.

It is important to note that HCl acts exactly in the same manner as SF_6, and we assume that here we are also dealing with a deactivating chain transfer process. At atmospheric pressure $G(HCl) \sim 10$ in γ-ray irradiated gaseous vinyl chloride (13) and, assuming that this value is approximately the same for 50 kV X-ray irradiation, the accumulation of HCl within the system might have a non-negligible effect on polymerization as a chain transfer agent. The next important radiolysis product of gaseous C_2H_3Cl is acetylene, $G(C_2H_2) \sim 1.5$. In Fig. 2 we see that the addition of 0.03 molar fraction of C_2H_2 decreases the polymerization-rate by around 35%, which is high compared to the $\sim 6\%$ decrease by a similar amount of HCl. Acetylene is known to be a deactivating chain transfer agent (25) and its retarding action suggests that it behaves in the same manner in the present system. The combined actions of C_2H_2 and HCl as deactivating chain transfer agents are most probably the reason for the low degree of polymerization of vinyl chloride in the gas phase, and they may be considered as limiting the polymerization-rate in the absence of all other additives.

In contrast to isobutene (4) the evidence from the use of additives such as ammonia or methylamine is not conclusively in favor of a cationic polymerization. The charge exchange reaction between vinyl chloride ion and ammonia (i.p. = 10.15 eV)(26) is possible if the parent ion has a small energy excess of around 0.2 eV. However, charge transfer processes of this kind might be much slower than the bimolecular reaction between $C_2H_3Cl^+$ and the monomer for which the rate constant is around 1×10^{-11} cm^3 molecule^{-1} s^{-1} (8). Therefore, the initial drop of the relative polymerization-rate with addition of small quantities of NH_3 is probably due to interception of radical species able to initiate polymerization. In the case of methylamine (i.p. = 8.97 eV) (27) a charge transfer process from the $C_2H_3Cl^+$ is much more favored than with NH_3. A contribution from such a process might be included in the initial rapid decrease of the rate, which is substantially higher than that for the $C_2H_3Cl + NH_3$ system. After the initial rapid drop of the rates in the presence of NH_3 or CH_3NH_2, more of these additives induces a slow decrease of the polymerization (Fig. 2) which we attribute to a deactivating chain transfer. In the case of the $C_2H_3Cl + NH_3$ system an increase of the polymerization-rate can be noticed beginning at 0.025 molar fraction of NH_3. A tentative explanation of this might be the consumption of HCl by NH_3 in the reaction for formation of ammonium chloride. The increase of polymerization-rate by NH_3 is also seen during irradiation of vinyl bromide (25), and we account for this effect by the interception of HBr, which is a powerful deactivating chain transfer agent. The $C_2H_3Cl + H_2O$

Can. J. Chem. Downloaded from www.nrcresearchpress.com by 210.87.254.105 on 09/05/12
For personal use only.

system shows effects, which might be linked with the hydration of ionic species and HCl removal. However, we are unable, for the time being, to give any evidence for such processes.

Chain transfer will lead to retardation of polymerization if the radical product of the transfer reaction has a low reactivity towards the monomer. A kinetic scheme for such retarded polymerization in the present case is given below, in which M, S, P_r represent monomer, additive (retarder), and polymer, and $R_i^{\cdot}$, $R_p^{\cdot}$, and $R_b^{\cdot}$ initial, and propagating, linear and branched radicals (and ions), respectively.

$$[1a] \qquad M \xrightarrow{\text{X-ray}} R_i^{\cdot}$$

$$[1b] \qquad R_i^{\cdot} + S \rightarrow RS^{\cdot} \text{ (inactive)}$$

$$[1c] \qquad R_i^{\cdot} + M \rightarrow R_{i+1}^{\cdot}$$

$$[1d] \qquad R_p^{\cdot} + M \rightarrow R_{p+1}^{\cdot}$$

$$[1e] \qquad R_p^{\cdot} + S \rightarrow P_r + S'^{\cdot} \text{ (inactive)}$$

$$[1f] \qquad P_r \xrightarrow{\text{X-ray}} R_b^{\cdot}$$

$$[1c'] \qquad R_b^{\cdot} + M \rightarrow R_{b+1}^{\cdot}$$

$$[1e'] \qquad R_b^{\cdot} + S \rightarrow P_r + S'^{\cdot} \text{ (inactive)}$$

$$[1g] \qquad R_p^{\cdot} + R_s^{\cdot} \rightarrow P_{p+s} \text{ or } P_p + P_s$$

$$[1h] \qquad R_p^{\cdot} + S^{\cdot} \rightarrow P_p$$

The reaction 1*b* is operating only in systems where additives are mixed with the monomer. In particular the rate dependence on intensity of irradiation is affected by this reaction. A rigorous treatment of scheme 1 without the initiation by irradiated polymer [1*f*] was given by Kice (28). Subsequently, Allen *et al.* (29) and Jenkins (30) used a similar treatment. The kinetic expression for the propagation-rate is quite cumbersome and its use is limited to special experimental conditions. Due to the further complexity in introducing the propagation by activated polymer [1*f*], we do not try to establish a quantitative expression for the propagation-rate. We assume that in the absence of any additives, the role of the retarder S is played by C_2H_2 and HCl. On the other hand, additives such as NH_3 or CH_3NH_2, besides their retarding action, scavenge the $Cl^{\cdot}$ atoms which result from the decomposition of the excited C_2H_3Cl or C_2H_4Cl molecules. The latter molecule results from the addition of H atoms to the double bond of the monomer (31). In our opinion the $Cl^{\cdot}$ atoms are responsible in part for the initiation of the polymerization. Such initiation is in competition, of course, with the formation of the HCl.

This work was made possible through the financial assistance of the National Research Council of Canada. The authors are indebted to Miss H. R. Chen for illuminating discussions and to Dr. R. Lanthier for PVC standards used in the g.p.c. calibration. We are also grateful to Mr. F. Bouchard and Mr. G. Marier for technical assistance.

1. W. Mund, M. van Meerssche, and J. Momighy. Bull. Soc. Chim. Belg. **62**, 109 (1953).
2. A. Chapiro. Radiation Chemistry of Polymeric Systems. Interscience, New York. 1962. p. 219.
3. J. A. Herman and P. M. Hupin. Can. J. Chem. **41**, 1578 (1963).
4. H. Okamoto, K. Fueki, and Z. Kuri. J. Phys. Chem. **71**, 3222 (1967).
5. Ff. Williams. Fundamental of Radiation Chemistry. *Edited by* P. Ausloos. Interscience, New York. 1968. p. 554.
6. Ff. Williams, K. Hayashi, K. Ueno, K. Kayashi, and S. Okamura. Trans. Faraday Soc. **63**, 1501 (1967).
7. P. M. Hupin. Ph.D. thesis. Laval University, Quebec City, Quebec. 1963.
8. J. A. Herman, J. J. Myher, and A. G. Harrison. Can. J. Chem. **47**, 647 (1969).
9. B. M. Hughes, T. O. Tiernan, and J. H. Futrell. J. Phys. Chem. **73**, 829 (1969).
10. W. Forst and K. O. Rice. Can. J. Chem. **41**, 562 (1963).
11. J. R. Puig and R. H. Bretton. *Cited by* A. Chapiro in ref. 2.
12. M. Koisumi, K. Nakutsuka, and S. Kato. Bull. Chem. Soc. Jap. **27**, 185 (1954).
13. This laboratory. Unpublished results.
14. S. Krimm. Fortschr. Hochpolym.-Forsch. **2**, S. 51 (1960).
15. C. Cherrier. Compt. Rend. **225**, 997 (1947).
16. R. Norman and C. Sandorfy. Chemical Applications of Spectroscopy. *Edited by* W. West. Interscience Publ., New York. 1956. p. 518.
17. W. N. Smith. J. Appl. Polym. Sci. **11**, 639 (1967).
18. H. R. Chen. M.Sc. thesis. Laval University. 1969.
19. R. Y. Huang and J. F. Westlake. Polymer Lett. **7**, 713 (1969).
20. A. Chapiro. Radiation Chemistry of Polymeric Systems. Interscience, New York. 1962. p. 352.
21. J. Momigny. Nature, **199**, 1179 (1963).
22. B. Brehm. Z. Naturforsch. **21**, 196 (1966).
23. A. J. Nicholson. J. Chem. Phys. **39**, 954 (1963).
24. T. G. Lee. J. Phys. Chem. **67**, 360 (1963).
25. S. Munari, G. Castello, and S. Russo. Chim. Ind. Milan, **47**, 26 (1965).
26. K. Watanabe. J. Chem. Phys. **26**, 542 (1957).
27. K. Watanabe and J. Mottl. J. Chem. Phys. **26**, 1773 (1957).
28. J. L. Kice. J. Amer. Chem. Soc. **76**, 6274 (1954).
29. P. W. Allen, F. M. Merrett, and J. Scanlan. Trans. Faraday Soc. **51**, 95 (1955).
30. A. D. Jenkins. Trans. Faraday Soc. **54**, 1885 (1958).
31. A. M. Rennert and M. H. J. Wijnen. Ber. Bunsenges. Phys. Chem. **72**, 222 (1968).

Substituent Effects on the Orientation of Diels–Alder Reactions. II

CIRILL SCHMIDT,[1,2] S. D. SABNIS,[2,3] EDITH SCHMIDT, AND D. K. TAYLOR
Department of Chemistry, University of Prince Edward Island, Charlottetown, Prince Edward Island

Received July 22, 1970

The competitive ortho directing (c.o.d.) influence of a 1-methoxy group and a 4-methyl was studied in the Diels–Alder addition of 1-methoxy-1,3-pentadiene (**1**) to 2,6-dimethylbenzoquinone (**2**). It was found that the c.o.d. influence of a terminally located methoxy is stronger than the effect of a terminal methyl group in the diene since only adduct **3** could be isolated. The influence of non-terminal substituents compared to terminal substituents in the diene appears to be insignificant. This was demonstrated by obtaining only adduct **5** from the addition of 3-ethoxy-1,3-pentadiene (**4**) with 2,6-dimethylbenzoquinone (**2**). The following order of c.o.d. influence was suggested in the diene relative to a methyl group in the dienophile $OCH_3 > CH_3 > H$.

Canadian Journal of Chemistry, 49, 371 (1971)

Recently a novel approach was initiated to investigate the mechanism of Diels–Alder reactions by determining the ratios of the two possible adducts III and IV formed from 1,4-unsymmetrically disubstituted dienes I and 2,6-disubstituted quinones II, eq. 1 (1). Such an experimental design allows a convenient variation of electronic density at the four carbon atoms involved in the formation of the two σ bonds. The following order of ortho[4] orienting influence was suggested by varying the substituents in the diene (X and Y) relative to a methyl in the dienophile ($Z = CH_3$) as defined by eq. 1 (1).

The purpose of the present communication was to extend this study to the internal competition between an alkoxy and a methyl group at the two terminal positions of a diene. It was found previously that a terminal acetoxy group is approximately four times more powerful as an ortho orientor than a terminal methyl group (1). Since the methoxy group is a more efficient mesomeric electron donor than an acetoxy group, it was of interest to examine the reaction of 1-methoxy-1,3-pentadiene (**1**) with 2,6-dimethylbenzoquinone (**2**), eq. 2.

Another aspect of the present study was to inquire about the influence of an alkoxy group at a terminal position in comparison to the effect of the same group when located at a non-terminal position. Thus the addition of 2-ethoxy-1,3-pentadiene (**4**) with 2,6-dimethylbenzoquinone (**2**) was studied, eq. 3.

Results and Discussion

(a) The Reaction of 1-Methoxy-1,3-pentadiene (1) with 2,6-Dimethylbenzoquinone (2)

The desired diene **1** was obtained by the catalytic pyrolysis of 1,1,3-trimethoxy-pentane (**7**) using a continuous flow system, eq. 4. The methoxy acetal was prepared from the readily available 2-penten-1-al (**6**) (2) by the standard procedure (3). In spite of numerous attempts, the yield of the pyrolitic reaction could not be improved beyond 20% by us under a variety of conditions.

Diene **1** appeared to be homogeneous in v.p.c. and had the appropriate mass and spectroscopic properties. It is assumed that diene **1** possessed a *trans,trans* geometry since it participated in the Diels–Alder reaction without difficulty. The addition of diene **1** to quinone **2** led to the isolation of the crystalline adduct **3** in a 60% yield based on quinone **2**. The components were reacted in benzene at 120° in a sealed tube for 24 h. In refluxing benzene the reaction did not proceed to a significant extent. Its structure follows from its spectroscopic properties, especially its 100 MHz n.m.r. spectrum. The one-proton doublet situated at (τ) 6.15, $J = 5$ Hz is assigned to the hydrogen at C-1, whereas a second, clearly defined doublet at 6.83, ($J = 8$ Hz, 1H) is assigned to the proton at C-4*a*. Had this compound had the alternative orientation corresponding to **8**, the signal at 6.15 should have been a triplet.

[1]To whom inquiries and requests for reprints should be sent.

[2]A part of this work was carried out on the premises of University of New Brunswick, Fredericton, New Brunswick.

[3]Present address: 48 Benham Hall Lane, Bombay-4, India.

[4]The terms ortho, meta, and para refer to the relative positions of the angular substituent to the two groups contained in the cyclohexene ring of the Diels–Alder adduct.

[1] 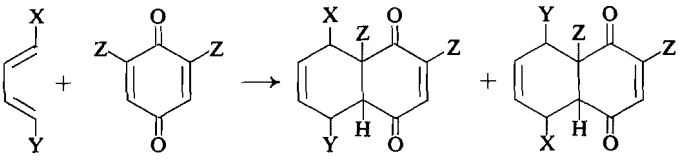

I II III IV

$COOCH_3 > OCOCH_3 > CH_3$

[2] 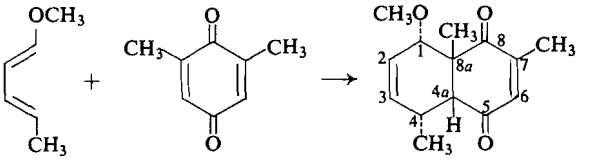

1 2 3

[3] 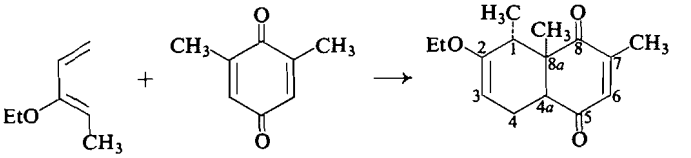

4 2 5

[4] 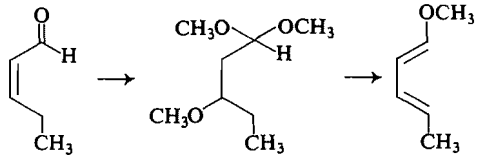

6 7 1

The remainder of the clearly resolved n.m.r. signals is in agreement with the proposed structure. Our attempts had been unsuccessful to detect any trace of the alternatively oriented adduct **8** or **9** which could have been formed by the elimination of methanol from adduct **8**. The cross conjugated compound **9** was encountered while studying the addition of 1-acetoxy-1,3-pentadiene (1). The stereochemistry of adduct **3** is assigned in compliance with the vast number of known diene additions (4).

It can therefore be concluded that a terminal methoxy group is a more powerful ortho orientor than a terminal methyl group relative to a methyl group in the dienophile.

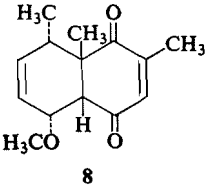

8

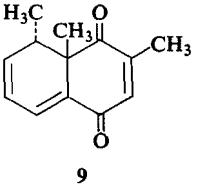

9

(b) The Reaction of 3-Ethoxy-1,3-pentadiene (4) with 2,6-Dimethylbenzoquinone (2)

The readily available diene **4** (3) was reacted with 2,6-dimethylbenzoquinone (**2**) in refluxing benzene for 24 h. Only one adduct, **5**, was isolated in 70% yield as an oil, having the appropriate spectroscopic properties. The enol–ether **5** was hydrolyzed with aqueous acetic acid at room temperature furnishing the crystalline unsaturated triketone **10**, m.p. 110–112°, in 80% yield.

The 100 MHz n.m.r. spectrum of **10** reveals the structure of adduct **5**. A one proton triplet centered at 7.02 could be assigned to the hydrogen at C-4*a*. This proton, α to a ketone, should be therefore adjacent to a methylene group.

Had the unsaturated triketone **10** been derived from the alternatively oriented Diels–Alder adduct **12** → **13**, the one-proton signal located at 7.02 should have been a doublet. It should be pointed out that the signal at 7.02 (1H) cannot be due to the hydrogen at C-1 in compound **10** since this signal should have appeared as a quadruplet. Furthermore the same signal cannot be attributed to the hydrogen at C-4 in the alternatively oriented triketone **13** because this should have appeared

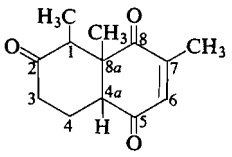

10

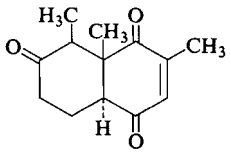

11

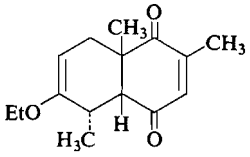

12

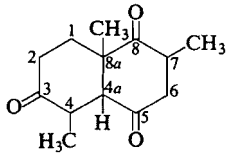

13

as a multiplet. This assignment was further confirmed by a decoupling experiment. Decoupling at the 1-methyl doublet position 8.8, $J = 7$ Hz, 3H did not affect the one proton triplet at 7.02.

When the unsaturated triketone **10** was heated at 100 °C for 3 h it isomerized to the crystalline **11** melting at 145°. Although the i.r. spectra of **10** and **11** are identical, their n.m.r. spectra are markedly different. In the case of the low melting compound **10**, the methyl signals appeared at 8.52, (s, 3H, angular methyl), 8.80 (d, 3H, $J = 7$ Hz, 1-methyl), and at 7.97 (s, 3H, 7-methyl). The respective signals for **11** appeared at 8.87 (s, 3H, angular methyl), 9.25 (d, 3H, 1-methyl), and at 7.96 (s, 3H, 7-methyl). These data suggest that these two compounds are *cis–trans* isomers with respect to the ring junction.

On examination of Dreiding models it can be seen that the angular methyl group of **10** is located in the deshielding zone of C-8 keto group. Accordingly, the same group in **11** should be shielded. The secondary 1-methyl group exhibited a considerable (0.45 p.p.m.) change in its n.m.r. signal. Since, however, the latter group is likely to be influenced by the anisotropies of two keto groups (at C-2 and -8) it would be unjustified to comment on the stereochemistry of the 1-methyl group on this basis. Tentatively the secondary methyl group is assumed to be equatorial in **10** and **11**. The stereochemistry of adduct **5** is assigned in accordance with the *endo–cis* addition rules (4).

It appears therefore that a terminal methyl group is a significantly better ortho orientor than a hydrogen. Furthermore a 3-alkoxy group has no influence on the outcome of orientation in comparison to terminal substituents in the diene.

It is well-known that the addition of 2-substituted dienes to an unsymmetric dienophile leads to a high para/meta isomer ratio (5). If such an orienting influence had been operational in this case, adduct **12** should have been formed in preference to the exclusively formed compound **5**. This finding is in agreement with the large number of cases studied (4). Nevertheless it was of interest to ascertain the overwhelming influence of terminal substituents compared to the effect of non-terminal groups at the inception of these investigations.

From the two Diels–Alder additions studied it can be concluded that the ortho directing influence of terminal substituents follows the order: $OCH_3 > CH_3 > H$.

The study of further critically chosen Diels–Alder additions is in progress.

It is believed that a knowledge of orientation preferences will lead to a better understanding of the mechanism of Diels–Alder reactions.

Experimental[5]

1,1,3-Trimethoxy-pentane (7)

A solution of 1 l of absolute methyl alcohol and 250 ml of trimethyl orthoformate was acidified with 0.5 ml of absolute methyl alcohol which was previously saturated with dry hydrochloric acid gas. To this solution 265 g of 2-pentene-1-al (2) was dripped in at 5° in 1 h. The reaction mixture was allowed to stand for 24 h. The solution was neutralized with sodium methylate dissolved in methyl alcohol (universal indicator paper). The excess methanol and a part of the trimethyl orthoformate were distilled off at atmospheric pressure using a Vigreux column while the temperature rose to approximately 100°. The residue was fractionated at 100 mm Hg. After discarding 25 ml of forefraction, 260 g of product was collected at 79–83° corresponding to a 50% yield. The residue was not distillable at this pressure. Mass spectrum (70 eV) *m/e*: 162 (molecular ion), 147 (base peak); i.r. (CCl_4) 2950, 1460, 1380, 1100 cm^{-1}; u.v. end absorption; n.m.r. ($CDCl_3$) τ 9.07 (t, 3, CH_3—CH_2), 8.38 (m, 2, CH_3—CH_2—), 7.82 (m, 2, CH_2 at C-2), 6.77 (s, 3, CH_3O), 5.69 (m, 1, C*H*—OCH_3 at C-3), 4.64 (t, 1, C*H*—$(OCH_3)_2$).

Anal. Calcd. for $C_8H_{18}O_3$: C, 59.20; H, 11.19. Found: C, 59.10; H, 11.06.

[5]All melting points were taken on a Fisher–Johns melting point apparatus and are uncorrected. The elemental analyses were carried out by Pascher Mikroanalytical Laboratorium, Bonn, West Germany, and Schwarzhopf Mikroanalytical Laboratory, Woodside, N.Y. The i.r. spectra were recorded on a Perkin–Elmer Model 137B infracord spectrophotometer. The u.v. spectrograms were taken on a Coleman Hitachi Model 124 double-beam grating spectrophotometer. The n.m.r. spectra were recorded on a Varian Associates 56.4 MHz spectrophotometer. The mass spectra were obtained with a Hitachi Perkin–Elmer Model RMS-4 spectrometer.

1-Methoxy-1,3-pentadiene (1)

One hundred grams of 1,1,3-trimethoxy-pentane (7) was dripped into a pyrolyzer at 300° in 45 min using dry nitrogen as the carrier gas. The pyrolyzer consisted of a 35 cm long pyrex tube (diameter 12 mm) which was heated with a coil of Nichrome wire regulated with a powerstat. The catalyst was prepared by soaking pyrex glass wool in a saturated solution of potassium bisulfate and heating at 400° in an oven.

The products were collected in two consecutive Dry Ice – acetone cooled traps which contained pentane and 5% sodium bicarbonate solution. The pentane solution of the products was washed four times with saline then dried with magnesium sulfate. The pentane was removed by atmospheric distillation, then the residue (60 g) was fractionated. After collecting 30 g of forefraction 18 g of the product was distilled at 122°/760 mm Hg. This fraction was further purified with the help of preparative gas chromatography furnishing 11 g of diene **1** (18.5%).[6] Several attempts were made to improve the yield with $KHSO_4$ and NaH_2PO_4 as catalysts at various temperatures without success. Mass spectrum (70 eV) *m/e* 98 (parent peak), 77 (base peak); i.r. (CCl_4) 2950, 1630, 1250 cm^{-1}; u.v.$_{max}$ (95% C_2H_5OH) 237 mμ (ε 20 000); n.m.r. ($CDCl_3$) τ 8.27 (d, 3, J = 7 Hz), CH_3—CH═), 6.66 (s, 3, CH_3O—), 4.26 (m, 4, olefinic protons).

Anal. Calcd. for $C_6H_{10}O$: C, 73.55; H, 10.27. Found: C, 73.42; H, 10.36.

cis-1,4,4a,5,8,8a-Hexahydro-1α-methoxy-4α,7,8,8aβ-trimethyl-5,8-dioxonaphthalene (3)

A solution of 1 g of 1-methoxy-1,3-pentadiene and 1 g of 2,6-dimethylbenzoquinone in 5 ml of benzene was heated at 120° for 18 h in a sealed tube. After evaporating the benzene, the residue was subjected to vacuum distillation at 0.1 mm Hg. The unreacted quinone (390 mg) sublimed at 70°. The brown residue was then chromatographed on silica gel plates by developing with benzene–ether (9:1). Besides some starting material (53 mg) one product (586 mg) was isolated in crystalline form corresponding to a 60% yield based on the amount of consumed quinone. It was recrystallized from benzene–pentane, m.p. 72–73 °C. Mass spectrum (70 eV) *m/e* 234 (parent peak), 159 (base peak); i.r. (CCl_4) 2900, 1690, 1630, 1100 cm^{-1}; u.v.$_{max}$ (95% C_2H_5OH) 242 mμ (ε 10 500); n.m.r. (CCl_4) τ 9.01 (s, 3, angular CH_3), 8.83 (d, 3, J = 6.0 Hz, 4-CH_3), 8.03 (s, 3, 7—CH_3), 7.36 (m, 1, C*H*—CH_3), 6.83 (d, 1, J = 8 Hz, proton at C-4*a*), 6.63 (s, 3, CH_3O), 6.15 (d, 1, J = 5 Hz, C*H*—OCH_3), 4.20 (m, 2, protons at C-2, 3), 3.40 (m, 1, proton at C-6).

Anal. Calcd. for $C_{14}H_{18}O_3$: C, 71.68; H, 7.73. Found: C, 71.52; H, 7.74.

cis-1,4,4a,5,8,8a-Hexahydro-2-ethoxy-1α,7,8aβ-trimethyl-5,8-dioxonaphthalene (5)

A solution of 14 g of 3-ethoxy-1,3-pentadiene (**4**) (3) and 8 g of 2,6-dimethylbenzoquinone (**2**) in 100 ml of dry benzene was refluxed under anhydrous conditions for 24 h. After evaporating the benzene and a part of the diene by distilling at atmospheric pressure the brown residue was fractionated *in vacuo*. The unreacted quinone (1.5 g) was recovered by sublimation then 8.45 g of adduct **5** was collected at 114–120°/0.2–0.35 mm Hg corresponding to a 70% yield based on the amount of consumed quinone. The residue of distillation amounted to about 1 g. The oily product appeared homogeneous in t.l.c. and v.p.c.; i.r. (CCl_4) 2900, 1680, 1625, 1450, 1170 cm^{-1}; u.v.$_{max}$ (95% C_2H_5OH) 242 mμ (ε 11 500); n.m.r. (CCl_4) τ 8.89 (d, 3, J = 7 Hz, 1-methyl), 8.7 (t, 3, CH_3—CH_2O—), 8.62 (s, 3, angular methyl), 8.00 (s, 3, 7-methyl), 6.3 (q, 2, CH_3—CH_2O—), 5.63 (m, 1, olefinic at C-3), 3.30 (s, 1, olefinic at C-6). Adduct **5** was analyzed in terms of crystalline triketones **10** and **11**.

cis-1,2,3,4,4a,5,8,8a-Octahydro-1α,7,8aβ-trimethyl-2,5,8-trioxonaphthalene (10)

A solution of 10 g of enol ether **5** in 120 ml of acetic acid–water (3:1) was allowed to stand at room temperature for 3 h. After the removal of solvents *in vacuo* the orange colored residue was recrystallized from ether, furnishing 6.5 g (73%) of triketone **10**, m.p. 110–112°; i.r. ($CHCl_3$) 2900, 1715, 1680, 1625, 1200 cm^{-1}; u.v.$_{max}$ (95% C_2H_5OH) 242 mμ (ε 11 500); n.m.r. ($CDCl_3$) τ 8.8 (d, 3, J = 7 Hz, 1-methyl), 8.52 (s, 3, angular methyl), 7.97 (s, 3, 7-methyl), 7.02 (t, 1, proton at C-4*a*), 3.35 (s, 1, olefinic).

Anal. Calcd. for $C_{13}H_{16}O_3$: C, 70.80; H, 7.32. Found: C, 70.77; H, 7.24.

trans-1,2,3,4,4a,5,8,8a-Octahydro-1α,7,8aβ-trimethyl-2,5,8-trioxonaphthalene (11)

When the hydrolysis of **5** was carried out at 100° for 2 h, triketone **11** was obtained. Alternatively triketone **10** could be isomerized to triketone **11** under the same conditions, m.p. 145°; i.r. ($CHCl_3$) 2900, 1715, 1680, 1625, 1200 cm^{-1}; u.v.$_{max}$ (95% C_2H_5OH) 242 mμ (ε 11 500); n.m.r. ($CDCl_3$) τ 9.25 (d, 3, J = 8 Hz, 1-methyl), 8.87 (s, 3, angular methyl), 7.96 (s, 3, 7-methyl), 3.33 (s, 1, olefinic).

Anal. Calcd. for $C_{13}H_{16}O_3$: C, 70.80; H, 7.32. Found: C, 70.79; H, 7.30.

The financial assistance of the National Research Council of Canada is gratefully acknowledged. Special thanks are due to Professor Z. Valenta of University of New Brunswick, Fredericton, New Brunswick, for drawing our attention to this problem and for helpful discussion. We also thank the University of Prince Edward Island for granting an undergraduate research scholarship to Mr. D. K. Taylor in the summer of 1969. We are also grateful to Drs. T. Durst and R. Fraser of University of Ottawa, Ottawa, Canada, for 100 MHz n.m.r. spectra.

1. CIRILL SCHMIDT. J. Org. Chem. **35**, 1324 (1970).
2. R. GRUNANGER and D. GRECO. Gazz. Chim. Ital. **88**, 296 (1958).
3. L. H. SARETT and R. M. LUKES. J. Amer. Chem. Soc. **74**, 1393 (1952).
4. A. S. ONISHCHENKO. Diene synthesis. Israel Program of Scientific Translations. Jerusalem, 1964.
5. J. SAUER. Angew. Chem. Int. Ed. Engl. **6**, 16 (1967).

[6]An Aerograph Model A-90-P (thermal conductivity detector) was used.

Can. J. Chem. Downloaded from www.nrcresearchpress.com by 210.87.254.6 on 09/05/12
For personal use only.

The Photolysis in Acidic Aqueous Solutions of the Monooxalato-bisethylenediamine Chromium(III) Cation and the Bisoxalatomonoethylenediamine Chromate(III) Anion: Photolysis Modes and Quantum Yields

A. D. KIRK, K. C. MOSS, AND J. G. VALENTIN
Department of Chemistry, University of Victoria, Victoria, British Columbia

Received August 17, 1970

The photolysis reactions of the complex ions $[Cr(en)_2ox]^+$ and $[Cren(ox)_2]^-$ have been studied in the p*H* range $1 \rightarrow 3$ and at temperatures from 0 to 25 °C. It has been found that both ions photoaquate to a monodentate protonated ethylenediamine complex which then undergoes further aquation thermally with loss of the ethylenediamine ligand. Quantum yields for these aquations were measured for irradiation into the ligand field bands, the values obtained being 0.18 and 0.02, respectively. The results are discussed in terms of known empirical correlations for Cr(III) complexes. Assuming these reactions may occur from the $^4T_{2g}$ state as precursor, arguments are presented that the correlation between quantum yield and ΔE may depend on mixing of the $^4T_{2g}$ and ^2E_g states, and its effect on the intersystem crossing rate constant.

Canadian Journal of Chemistry, 49, 375 (1971)

Introduction

During the last decade there has been a growing interest in the solution photochemistry and the luminescence of complex ions. For some metals, patterns of behavior have begun to emerge and some empirical correlations have been noted. Both subjects have recently been reviewed (1–4).

Perhaps the most suitable transition metal complexes for these studies are those of Cr(III), since they are often thermally substitution inert, their photoreactions are uncomplicated by redox processes, they have well-defined and understood spectroscopic states, and they have well-understood luminescence behavior (5). The main limitations on research on Cr(III) complexes are difficulties of preparation of many of the compounds with two or more different ligands, the thermal instability in solution of some, and the difficulties of analysis and identification, particularly of closely related isomers.

Previous work on the photolysis of Cr(III) complexes has suggested that the complexes with O_h symmetry show quantum yields that generally decrease together with ΔE, the spacing between the $^4T_{2g} \leftarrow {}^4A_{2g}$ and $^2E_g \leftarrow {}^4A_{2g}$ absorption band maxima (6, 7) or, as is roughly equivalent, the average field strength of the ligands (referred to as the ΔE correlation). For non-O_h chromium(III) complexes Adamson (8) has suggested that the mode of photoaquation can be predicted from the rules.

"(*1*) Consider the six ligands to lie in pairs at the ends of three mutually perpendicular axes. That axis having the smallest average crystal field will be the one labilized, and the total quantum yield will be about that for an O_h complex of the same average field.

(*2*) If the labilized axis contains two different ligands, then the ligand of greater field strength preferentially aquates. This may be a type of *trans* effect.

(*3*) The discrimination implied by rules *1* and *2* will occur to a greater extent if it is the L_1 rather than the L_2 band that is irradiated."

The present work comprises a study of the photochemistry of the pair of complex ions $[Cr(en)_2ox]^+$ and $[Cren(ox)_2]^-$. Together with the ion $[Cr(en)_3]^{3+}$ studied by Schläfer and Geiss (9), and the ion $[Cr(ox)_3]^{3-}$ studied by Spees and Adamson (10), and Porter *et al.* (11), these comprise a series of ions for which the validity of the ΔE correlation for progressive substitution of one ligand by another may be examined. It was also hoped that studies of the mode of photolysis would give information on the validity of Adamson's Rules for these ions.

Previous work on $[Cr(ox)_3]^{3-}$ placed an upper limit of 10^{-3} on the photoaquation yield for this complex, although a wavelength-independent yield of 0.08 was found for photoracemization. Schläfer and Geiss showed that $[Cr(en)_3]^{3+}$ underwent photoaquation with a wavelength independent quantum yield of 0.37. No photoracemization yield was reported although racemization was found in the thermal reaction (15*b*). The reaction was followed both by spectropho-

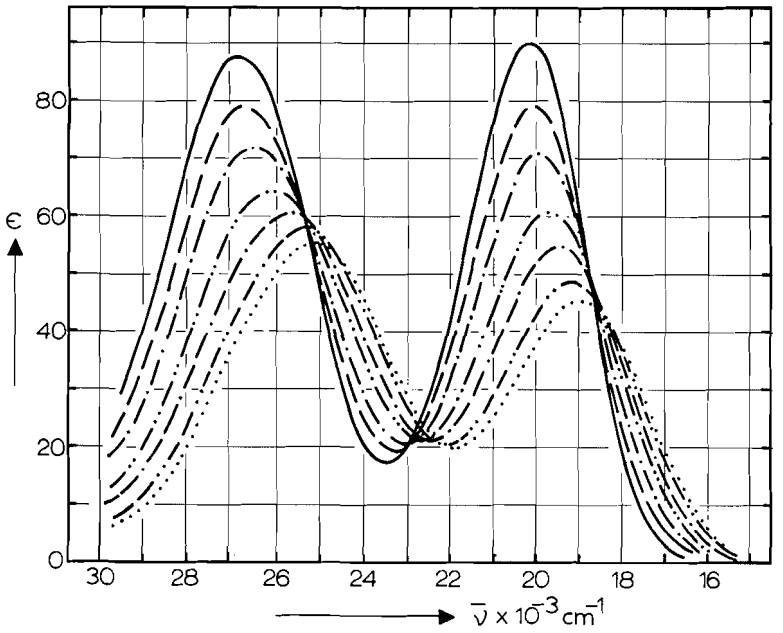

FIG. 1. Spectral changes in the photolysis of $[Cr(en)_2ox]^+$. pH = 1.0, temperature = 25 °C.

tometry and by the pH change during photolysis. The conclusion reached by these authors was that the initial product of the photoreaction was the monodentate protonated ethylenediamine complex $[Cr(en)_2(enH)(H_2O)]^{4+}$ (complexes containing this ligand will hereafter be referred to as enH complexes) which then underwent thermal aquation to give the product $[Cr(en)_2(H_2O)_2]^{3+}$, stated to be predominantly *cis*. The intermediate species was not, however, isolated from the solution and of its properties, only the calculated extinction coefficients at the photolysis wavelengths were obtained. Other workers have reported relatively stable complexes containing monodentate protonated ethylenediamine (12), ethylenetriamine (13), and recently oxalate (14). Background information to this study was also provided by the previous studies of the thermal aquations of $[Cr(en)_3]^{3+}$ (15), *cis*-$[Cr(en)_2(H_2O)_2]^{3+}$ (16), and $[Cren(ox)_2]^-$ (17).

Results

The Photolysis Modes of $[Cr(en)_2ox]^+$ and $[Cren(ox)_2]^-$

Both of these complexes were observed to undergo thermal aquation with loss of ethylenediamine (17) in acid solution at room temperature, the rate being faster for $[Cren(ox)_2]^-$. On photolysis with light corresponding to absorption either in the $^4T_{2g} \leftarrow {}^4A_{2g}$ and $^4T_{1g} \leftarrow {}^4A_{2g}$ ligand field bands (pseudo O_h symmetry), similar but recognizably different spectral changes were observed. Neither for the photochemical nor for the thermal reactions of either complex was any free oxalate observed in the reacted solutions.

The spectral changes on photolysis, Figs. 1 and 2, showed that for both complexes ethylenediamine aquation was occurring, but the disappearance of the isosbestic points after the initial reaction clearly showed that secondary processes were occurring. When slightly acid solutions were photolyzed (pH 2 → 3) the pH was observed to rise, and post-irradiation proton uptake also occurred. Thin-layer chromatography of the photolyzed solutions (18) showed the presence of $[Cren(H_2O)_2ox]^+$ and $[Cr(H_2O)_2(ox)_2]^-$ as products of the two photoreactions.

The above results were rationalized when the thermally unstable species $[Cren(enH)(H_2O)ox]^{2+}$ and $[Cr(enH)(H_2O)(ox)_2]^0$ were isolated from the respective photolyzed solutions by ion-exchange chromatography at 0 °C. $[Cr(enH)(H_2O)(ox)_2]^0$ was also isolated in smaller amounts from thermally reacted solutions of $[Cr(en)(ox)_2]^-$.

No evidence was found for any other type of

Can. J. Chem. Downloaded from www.nrcresearchpress.com by 210.87.254.6 on 09/05/12
For personal use only.

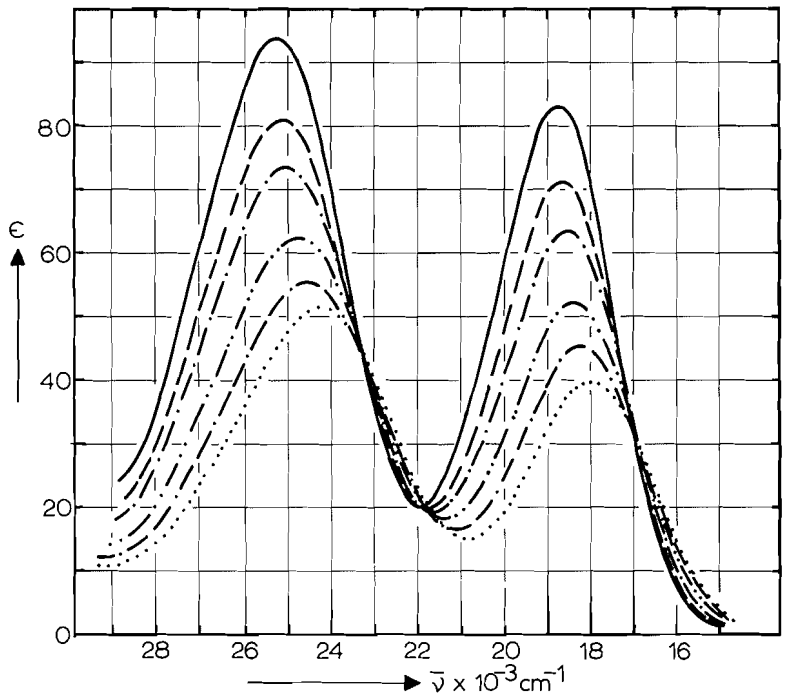

FIG. 2. Spectral changes in the photolysis of $[Cren(ox)_2]^-$. pH = 1.0, temperature = 25 °C.

photoreaction, although, as is discussed later, photoracemization remains a possibility. Thus at pH < 4, and provided conditions are chosen to minimize any secondary photolysis, the modes of the thermal and photochemical reactions can be written,

$$[1] \quad [Cr(en)_2ox]^+_{aq} + H^+ \xrightarrow[k_1]{\phi_1} [Cr(en)(enH)(H_2O)ox]^{2+}_{aq}$$

$$[2] \quad [Cr(en)(enH)(H_2O)ox]^{2+}_{aq} + H^+ \xrightarrow[k_2]{} [Cren(H_2O)_2ox]^+_{aq} + enH_2^{2+}$$

$$[3] \quad [Cren(ox)_2]^-_{aq} + H^+ \xrightarrow[k_3]{\phi_2} [Cr(enH)(H_2O)(ox)_2]^0_{aq}$$

$$[4] \quad [Cr(enH)(H_2O)(ox)_2]^0_{aq} + H^+ \xrightarrow[k_4]{} [Cr(H_2O)_2(ox)_2]^-_{aq} + enH_2^{2+}$$

$[Cr(en)(enH)(H_2O)ox]^{2+}$ Spectrum and Thermal Aquation

This compound was separated from the reaction solution by chromatography on Rexyn 102 at 0 °C, eluted by 10^{-2} M HCl after the other complexes present had been eluted with 10^{-3} M HCl. In Fig. 3 the absorption spectrum of this enH complex is compared with the species $[Cr(en)_2ox]^+$ and $[Cr(en)(H_2O)_2ox]^+$. It is seen, as is expected from ligand field theory and analogy with the ammine complexes, that the spectrum is intermediate both in regard to wavelengths of the band maxima and extinction coefficients. This is entirely consistent with the replacement of one $-NH_2$ group of the ethylenediamine ligand by water. The extinction coefficients were obtained by chromium analysis on the eluted fraction. In addition, the spectrum is very similar to that obtained by calculation (see caption to Fig. 3) from the spectral changes in a rapid photolysis at high intensity.

Spectrophotometric attempts to measure the rate of thermal aquation of the enH complex at pH 1.0 and 21 °C did not yield precise values, due to the thermal instability of the product $[Cren(H_2O)_2ox]^+$, but the order of magnitude of k_2

Can. J. Chem. Downloaded from www.nrcresearchpress.com by 210.87.254.6 on 09/05/12
For personal use only.

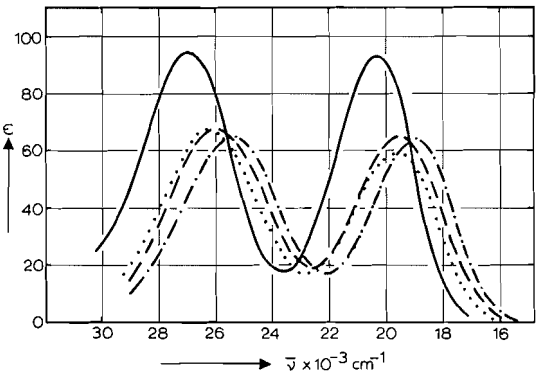

FIG. 3. Comparison of spectra of $[Cr(en)_2ox]^+$ (—) and (·-·-·) $[Cren(H_2O)_2(ox)]^+$ with the product (---) of $[Cr(en)_2ox]^+$ photolysis at p*H* 2 and 0 °C.
This figure also shows the spectrum of the product, (···), calculated as follows. With the full visible light from the lamp to give high intensity, $[Cr(en)_2ox]^+$ was photolyzed and the extent of its decomposition measured from the p*H* change assuming reaction to the monodentate enH complex. The spectrum was then calculated from the final observed spectrum assuming that $[Cr(en)(enH)(H_2O)(ox)]^{2+}$ was the sole product complex.

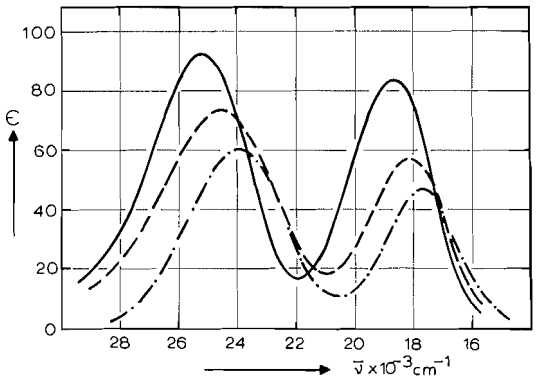

FIG. 4. Comparison of spectra of $[Cren(ox)_2]^-$ (—) and $[Cr(H_2O)_2(ox)_2]^-$ (·-·-·) with the product (---) of $[Cren(ox)_2]^-$ photolysis at p*H* 2.0 and 0 °C.

was $1.0 \rightarrow 5.0 \times 10^{-5}$ s^{-1}. Furthermore, none of this enH complex could be isolated by ion exchange chromatography from the thermal reaction. This is consistent with our observations that $k_2 > k_1$. The rough value $k_1 = 0.5 \times 10^{-5}$ s^{-1} was calculated from the spectral changes in the thermal reaction on the assumption that the thermal reaction leads directly to the bisaquo complex and free ethylenediamine. To our knowledge, no complete kinetic study of the thermal aquation of $[Cr(en)_2ox]^+$ has been carried out, probably due to this complication of $[Cren(H_2O)_2ox]^+$ instability, so no precise comparisons are possible.[1]

$[Cr(enH)(H_2O)(ox)_2]^0$ Spectrum and Thermal Aquation

The complex $[Cr(enH)(H_2O)(ox)_2]^0$ was separated from the reaction solution by chromatography on Dowex 1-X8, eluted with 10^{-3} *M* $NaClO_4$ at 0 °C. Figure 4 shows that the spectrum is again intermediate to the starting material and the bisaquo complex, as to be expected for the replacement of one $—NH_2$ group of the ethylenediamine ligand by water.

This enH complex showed, however, a more complex time-dependence of its absorption spectrum. As the solution warmed to 21 °C in the spectrophotometer cell, and before the onset of aquation to yield free enH_2^{2+} and the bisaquo complex (a process easily recognizable by the band shifts to the red and the slight lowering of the extinction coefficients), a rapid spectral change was observed. This consisted of a rise of about 33% in the extinction coefficients of the bands, without shifts in the wavelengths of the maxima. (Simple temperature dependence of the extinction coefficients was excluded as a cause.) Constant temperature measurements at 0 °C gave a first order rate constant of about 7×10^{-5} s^{-1} for the process at this temperature. On the basis of the nature of the spectral change and the value of the rate constant found, we consider the process to be a *cis/trans* equilibration of the reaction product $[Cr(enH)(H_2O)(ox)_2]^0$.

By analogy with the spectra of known *cis/trans* pairs the increase in extinction coefficients suggests that the initial product is predominantly in the *trans* configuration. This conclusion requires that the photoaquation reaction proceeds predominantly with stereochemical change. This finding may support Schläfer and Wasgestian's results with $[Cr(NH_3)_5Cl]^{2+}$ (28) should future work confirm the *cis* configuration of the product $[Cr(NH_3)_4(H_2O)Cl]^{2+}$ reported there.[2]

[1]Subsequent to submission of this manuscript, the authors became aware of such a study which confirms our conclusions and our values of k_1 and k_2 (31).

[2]This *cis* configuration has recently been confirmed by Bulzani (32).

Can. J. Chem. Downloaded from www.nrcresearchpress.com by 210.87.254.6 on 09/05/12
For personal use only.

TABLE 1. Photoaquation quantum yields for $[Cr(en)_2ox]^+$ and $[Cren(ox)_2]^-$ photolysis in mol einstein^{-1}

Complex	Wavelength (nm)	Temperature (°C)	Quantum yield by pH*	Quantum yield by Spectrophotometry
$[Cr(en)_2ox]^+$	400	0	0.20 ±0.02	0.19 ±0.05†
		15	0.16 ±0.02	
		23	0.18 ±0.02 0.17 ±0.02	
	540	0		0.21 ±0.06†
		15	0.12 ±0.02	
		23	0.14 ±0.02 0.16 ±0.02	
(The upper limit for the quantum yield of free oxalate was 0.002)				
$[Cren(ox)_2]^-$	400	0	0.020±0.006	
		15	0.020±0.006 0.030±0.010	
		23		0.012±0.006‡
	540	15	0.020±0.006	
		23		0.018±0.008§
(The upper limit for the quantum yield of free oxalate was 0.001)				

*pH = 3.0.
†Average of 3 runs; pH = 1.0, T = 3 °C.
‡Average of 5 runs; pH = 1.0, T = 25 °C.
§Average of 3 runs; pH = 1.0, T = 25 °C.

Kinetic analysis of the spectral changes subsequent to this *trans* to *cis* equilibration yields a value of 0.94×10^{-5} s^{-1} for the first order rate constant k_4 at 21.5 °C and p*H* 2. This result is in excellent agreement with that of Schläfer and co-workers who obtained $k_4 = 1.0 \times 10^{-5}$ s^{-1} at 20.0 °C and p*H* 1.1 from a kinetic analysis of the thermal aquation of $[Cren(ox)_2]^-$ (17).

Quantum Yields of the Photoaquation Reactions

Having identified the reaction modes, and having the spectra of all the complexes involved, it became possible to measure the quantum yields of photoaquation by means of either the proton uptake or the spectral changes. Because the latter were small, the more precise values are generally obtained by the first method. Mainly due to the relatively low light intensities obtainable when using interference filters to produce monochromatic radiation, in both complexes significant corrections had to be made for thermal reaction during the photolysis. These corrections ranged from 10 to 40% for the bisethylenediamine–monooxalato complex and from 30 to 200% for the monoethylenediamine–bisoxalato complex, depending on the temperature of the experiment. Despite these large magnitudes the quantum yields were satisfactorily consistent, but the statistical uncertainty in the quantum yields is consequently large.

The results are tabulated in Table 1, which includes for comparison those yields obtained by the spectrophotometric methods. The agreement between the two methods is satisfactory. Within ±10% uncertainty, the data reveal no trends suggesting a large temperature variation of quantum yield for either complex, and no variations with p*H*. It appears from the results for $[Cr(en)_2ox]^+$ that there may be some effect of wavelength, the quantum yield perhaps being somewhat larger in the $^4T_{1g} \leftarrow {}^4A_{2g}$ band. More reliable data on these questions would demand much greater experimental precision. For the purpose of the ensuing discussion it will be taken that the bisethylenediamine–monooxalato complex has a constant photoaquation quantum yield under these conditions of 0.18, while the quantum yield of the monoethylenediamine–bisoxalato complex is a constant value of about 0.02. Table 1 shows also the maximum quantum yields for any free oxalate production from the two complexes.

No experiments were carried out to investigate any photoracemization processes in these complexes. Such measurements would be extremely difficult. In particular one would wish to separate the changes in rotation arising from the photo-

Can. J. Chem. Downloaded from www.nrcresearchpress.com by 210.87.254.6 on 09/05/12
For personal use only.

Can. J. Chem. Downloaded from www.nrcresearchpress.com by 210.87.254.6 on 09/05/12
For personal use only.

aquation process from those due to true inversion of configuration. Even were that possible, one could then not unequivocally assign any such rotation to a particular mechanism, such as thermal re-chelation of monodentate oxalate intermediates to the starting materials.

Discussion

For the bisethylenediamine–monooxalato complex the photoaquation mode is entirely ethylenediamine and is therefore the same as the rate-controlling first step in the thermal reaction. As stated, our measurements of the rate of the latter suggest that for the thermal process at 21 °C, $k_1 < k_2$ so that the intermediate enH complex can not be present in large amounts in the thermal reaction. As shown, however, the relatively stable compound is obtained easily by photolysis, with $\phi = 0.18$.

We recognize that the absence of free oxalate in the photolyzed solution does not eliminate the possibility of oxalate photolysis to give an intermediate of structure $[Cr(en)_2(H_2O)(oxH)]^{2+}$. (Experiments with solutions of $[Cr(H_2O)_2(ox)(oxH)]^0$ prepared according to Chang (14) showed no reaction in the test for oxalate.) However, such a process would result in the take-up of protons without observable spectral changes (since ox^{2-} and H_2O have equivalent ligand field strengths) and the quantum yields measured by the two methods (pH and spectrophotometric) would be in disagreement, the pH quantum yield being higher by the amount of any such oxalate aquation. For $[Cr(en)_2ox]^+$ such a disagreement is not observed. In addition, were such an intermediate reasonably stable at 0 °C, one would have expected to find it in the chromatographic separations. That such an intermediate is likely to be stable is suggested by the findings of Chang (14) for the complexes $[Cr(H_2O)_2(ox)(oxH)]^0$ and $[Cr(H_2O)_2mal(malH)]^0$ (mal = malonate).

The possibility remains of an additional primary process occurring, whereby a monodentate oxalate intermediate is initially produced but instead of protonating re-chelates to the original complex. Such a process might be thought detectable by photoracemization studies but we have not attempted them because of the difficulty of such experiments for a complex which also photoaquates, and the ambiguities of interpretation pointed to earlier.

Similar arguments can be made for the monoethylenediamine bisoxalate complex. The quantum yield data allow some possibility of a small oxH product yield but nevertheless the chromatographic evidence is against the presence of such a species. Again the yield of oxalate aquation allowable by the data may be small due to immediate thermal re-chelation of a monodentate species.

Because of the ambiguity created by possible re-chelation of primary products, discussions of the photolysis modes in terms of Adamson's rules are not really justified. For the bisethylenediamine compound the reaction mode is the same as for the thermal reaction and is consistent with Adamson's rules. For $[Cren(ox)_2]^-$ the only certain process observed is the same as the thermal reaction but is not the oxalate aquation predicted by Adamson's rules. However, it appears that the low quantum yields of oxalate aquation in all these complexes may be determined by strong bonding between Cr(III) and the bidentate oxalate ion. The example serves to illustrate the importance of purely chemical factors in influencing the overall reaction mode of excited states.

Consideration of the overall photoaquation yields for the series of complexes from $[Cr(en)_3]^{3+}$ to $[Cr(ox)_3]^{3-}$ supports the ΔE correlation for progressive ligand exchange. The only other series of O_h complexes for which similar information is available is the $[Cr(NH_3)_x(H_2O)_{6-x}]^{3+}$ series (6), and there, although it may be of minor significance, no measurements of water exchange were made.

It has been previously suggested that the ΔE correlation has its origin in thermal back reaction from the doublet state shortening the lifetime of this supposedly photochemically active state (6). Schläfer has suggested alternatively that it is due to some inherent property of the states themselves (7). Now recent work by Porter (19) shows that at least for reineckate ion the quartet state may be photochemically active, as had been earlier suggested by Adamson (8). This suggests the possibility of a more direct reason for the ΔE correlation, residing in reaction from quartet states.

Figure 5 shows the typical idealized energy level diagram for an O_h Cr(III) complex and defines rate constants for various radiative and non-radiative processes. Assuming that some

Can. J. Chem. Downloaded from www.nrcresearchpress.com by 210.87.254.6 on 09/05/12
For personal use only.

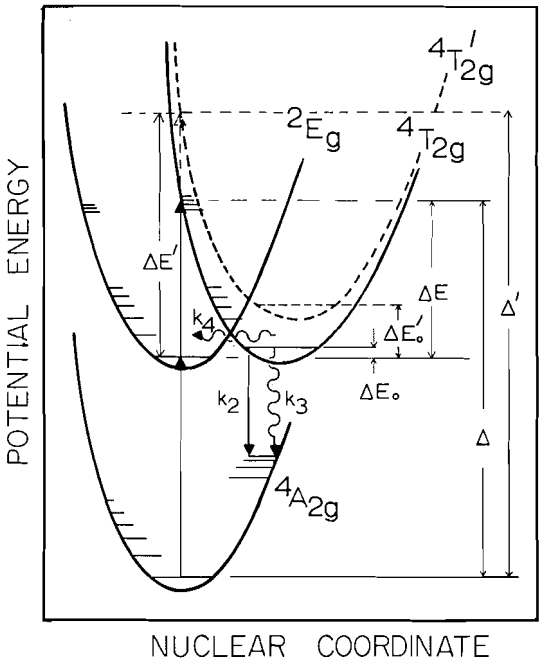

FIG. 5. Potential energy diagram for a Cr(III) complex ion. The rate constants shown are for radiative transition of $^4T_{2g}$ to the ground state, k_2; non-radiative transition of $^4T_{2g}$ to the ground state, k_3; and intersystem crossing from $^4T_{2g}$ to ^2E_g, k_4. The diagram also shows diagrammatically the relation between ΔE_0, ΔE, and Δ, the primed values being for the $^4T_{2g}$ state of a complex with a larger Δ value.

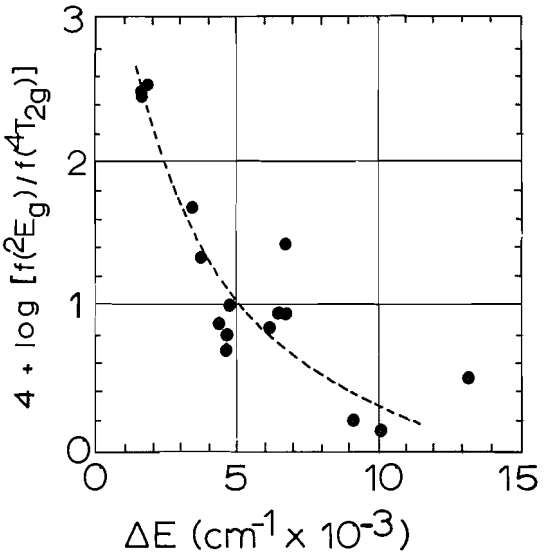

FIG. 6. Plot of $\log_{10} f(^2E_g \leftarrow {}^4A_{2g})/f(^4T_{2g} \leftarrow {}^4A_{2g})$ *vs.* ΔE, $\Delta E = E(^4T_{2g} \leftarrow {}^4A_{2g}) - E(^2E_g \leftarrow {}^4A_{2g})$. The ratio of the oscillator strengths of the $^2E_g \leftarrow {}^4A_{2g}$ and $^4T_{2g} - {}^4A_{2g}$ transitions has been taken as a measure of the extent of mixing of the $^4T_{2g}$ and ^2E_g states by spin–orbit coupling. The plot demonstrates a crude correlation of the extent of such mixing with ΔE.

fraction a, of the rate constant k_3 represents photochemical reaction from the $^4T_{2g}$ state as precursor, then the quantum yield of reaction is

$$\phi_r = a.k_3/(k_2 + k_3 + k_4)$$

It is clear from this expression that if arguments can be presented to suggest that k_4 increases rapidly as ΔE decreases, while at the same time, a, k_2, and k_3 have values insensitive to ΔE, then the decrease in ϕ_r with ΔE can be rationalized.

That k_4 does increase with decreasing ΔE can be supported both theoretically and in terms of indirect experimental evidence. From the theory of radiationless transitions one may relate k_4, the intersystem crossing rate constant, to the first order mixing of the pure $^4T_{2g}$ and ^2E_g states by spin–orbit coupling. Thus its magnitude will depend inversely on the square of the energy difference ΔE_0 between the zeroth levels of these states (20). As we have tried to show in Fig. 5, this ΔE_0 should increase together with $\Delta E = E(^4T_{2g}) - E(^2E_g)$ as Δ increases.

Unfortunately not enough data on intersystem crossing rates in Cr(III) complexes is available to make a direct test of this correlation possible. However, the process discussed here parallels the radiative transition $^2E_g \leftarrow {}^4A_{2g}$, which in first order theory borrows its intensity from the $^4T_{2g} \leftarrow {}^4A_{2g}$ transition by the same mixing of the states $^4T_{2g}$ and ^2E_g. Thus indirect support is obtained when one views the plot in Fig. 6, based on data from Table 2, of $\log f(^2E_g \leftarrow {}^4A_{2g})/f(^4T_{2g} \leftarrow {}^4A_{2g})$ *vs.* ΔE. The plot supports the contention that the extent of mixing of the two states is an inverse function of ΔE. Since there is no theoretical or experimental reason to propose a dependence of a, k_2, or k_3 on ΔE, it is therefore reasonable to ascribe the variation of ϕ_r with ΔE to the variation of k_4. As ambiguous direct support for the foregoing thesis we quote the recent work of Webb and Patterson (21), who find that for three Cr(III) complexes, $(k_3 + k_4)$, the total rate constant for non-radiative removal of $^4T_{2g}$ states increases with decreasing ΔE.

To obtain the further correlation of ϕ with Δ one must correlate Δ and ΔE. This does not appear at first sight likely since ΔE may be approximately written

TABLE 2. Transition energies, oscillator strength ratios (27), and quantum yields of photoreaction for chromium(III) complexes

Complex ion	$E(^4T_{2g} \leftarrow {}^4A_{2g})$ ($cm^{-1} \times 10^{-3}$)	$E(^2E_g \leftarrow {}^4A_{2g})$ ($cm^{-1} \times 10^{-3}$)	ΔE^* ($cm^{-1} \times 10^{-3}$)	$\frac{f(^2E_g \leftarrow {}^4A_{2g})}{f(^4T_{2g} \leftarrow {}^4A_{2g})} \times 10^4$	ϕ_a†
$[Cr(CN)_6]^{3-}$	26.40	13.15	13.25	3.0	0.1‡
$[Cr(phen)_3]^{3+}$	23.80	13.70	10.10	1.4	
$[Cr(dipyr)_3]^{3+}$	22.00	13.75	9.25	1.6	
$[Cr(en)_3]^{3+}$	21.74	14.95	6.79	9.0	0.37
$[Cr(pn)_3]^{3+}$	21.74	14.93	6.81	27	
$[Cr(tn)_3]^{3+}$	21.55	14.99	6.56	8.9	
$[Cr(NH_3)_6]^{3+}$	21.51	15.49	6.02	7.7	0.26
$[Cr(NH_3)_5H_2O]^{3+}$	20.80	15.22	5.58		0.15
$[Cr(NH_3)_5F]^{2+}$	19.93	15.14	4.79	11.4	
$[Cr(NH_3)_5Cl]^{2+}$	19.55	14.85	4.70	5.0	0.38§
$[Cr(NH_3)_5Br]^{2+}$	19.23	14.82	4.41	7.4	
$[Cr(NCS)_6]^{3-}$	17.67	13.01	4.66	6.3	0.26
$[Cr(ox)_3]^{3-}$	17.48	14.68	3.80	21.4	0.1 (rac.)
$[CrenF_4]^-$	17.45	14.97	3.48	47.5	
$[Cr(imid)_6]^{3+}$	16.05	14.42	1.63	289.6	
$[Cr(ur)_6]^{3+}$	16.05	14.43	1.62	297	0.10
$[Cr(atp)_6]^{3+}$	15.90	14.04	1.86	332	

*$\Delta E = E(^4T_{2g} \leftarrow {}^4A_{2g}) - E(^2E_g \leftarrow {}^4A_{2g})$.
†Quantum yield of photoaquation, from ref. 3.
‡From refs. 29 and 30.
§From ref. 9.

$$\Delta = \Delta - 9B - 3C$$

$$\Delta - 21B; \text{ if } C = 4B$$

where B and C are the Racah parameters.

However, an examination of the data for some complexes in Table 2 shows very good correlation between ΔE and Δ. Thus either the ratio C/B or the values of B and C generally vary in a compensatory manner with Δ. Table 2 shows that on the basis of the presently limited data on the photochemistry of octahedral Cr complexes, the correlation of Δ or ΔE with the quantum yield of reaction is good. Exceptions appear to be hexocyanochromate(III) and other complexes such as the trisphenanthroline complex where π bonding may stabilize the complexes.

Experimental

(A) Preparations

$K[Cren(ox)_2].2H_2O$ was prepared as described by Schläfer *et al.* (17)

Anal. Calcd. for $K[Cren(ox)_2].2H_2O$: Cr, 14.3; C, 19.8; H, 3.3; N, 7.7. Found: Cr, 14.8; C, 20.5; H, 3.2; N, 7.9.

$[Cr(en)_2ox]Cl.H_2O$ was prepared as described by Bushra and Johnson (22).

Anal. Calcd. for $[Cr(en)_2ox]Cl.H_2O$: Cr, 16.6; C, 23.0; H, 5.8; N, 17.8. Found: Cr, 16.4; C, 23.3; H, 6.2; N, 17.8.

$[Cren(H_2O)_2ox]Br.H_2O$ was prepared as described by Werner (23).

Anal. Calcd. for $[Cren(H_2O)_2ox]Br.H_2O$: Cr, 15.6; C, 14.4; H, 4.2; N, 8.4. Found: Cr, 15.6; C, 14.3; H, 4.1; N, 8.4.

$[Cren(enH)(H_2O)ox]^{2+}$ or $[Cr(enH)(H_2O)(ox)_2]^0$ were prepared by photolyzing acidic solutions of $[Cr(en)_2ox]Cl$ or $K[Cren(ox)_2]$, respectively, at 0 °C, with visible light and separating the photolysis products by chromatography.

(B) Solutions

All photolysis solutions were prepared at the run temperature in semi-darkness. For spectrophotometric determinations 1.0×10^{-2} M solutions of complex at pH 1.0 were used. In addition, the $[Cren(ox)_2]^-$ solutions were 0.15 M in ClO_4^- and $[Cr(en)_2ox]^+$ solutions were 0.10 M in Cl^-. For pH runs 1.0×10^{-2} M solutions of complex at pH 3.0 were used. All solutions for pH runs were 0.10 M in KCl.

(C) Photolysis Apparatus

A P.E.K. 1000 W A-H6 water-cooled high pressure mercury lamp was used as a light source. A Calflex-C heat reflecting filter together with filtraflex B-20 interference filters (Rolyn Corp.) were used for wavelength selection. The 400 nm filter had a half-band-width of 5 nm and the 540 nm filter, 7 nm.

The photolysis cell was positioned in a constant temperature bath (±0.1 °C) equipped with a double quartz window to admit the light beam. The face of the photolysis cell was masked to eliminate the possibility of any cell wall effects of the type reported by Lee and Seliger (24).

(D) Actinometry

2.0×10^{-2} M solutions of $K[Cr(NH_3)_2(NCS)_4]$ at its natural pH were used as chemical actinometers (25). In the spectrophotometric runs the actinometer cell was placed directly behind the sample cell so that intensity

Can. J. Chem. Downloaded from www.nrcresearchpress.com by 210.87.254.6 on 09/05/12
For personal use only.

Can. J. Chem. Downloaded from www.nrcresearchpress.com by 210.87.254.6 on 09/05/12
For personal use only.

monitoring was integral for the transmitted light. In the p*H* runs about 8% of the filtered light beam was reflected by a 45° quartz window on to a photocell. The output of the photocell was used to monitor the intensity of the lamp during each run. The photocell was calibrated at the two wavelengths used with 2.0×10^{-2} *M* solutions of $K[Cr(NH_3)_2(NCS)_4]$.

(E) Chromatography

Thin-layer chromatographic separations of $[Cren(H_2O)_2ox]^+$ from $[Cr(en)_2ox]^+$ and $[Cr(H_2O)_2(ox)_2]^-$ from $[Cren(ox)_2]^-$ have been previously described (18).

Ion exchange column chromatography on a jacketed column at 0 °C was used for separation of the components of the photolysis solutions. On Rexyn 102, $[Cr(en)_2ox]^+$ and $[Cr(en)(H_2O)_2ox]^+$ eluted first with 10^{-3} *M* hydrochloric acid, after which $[Cr(en)(enH)(H_2O)(ox)]^{2+}$ eluted with 10^{-2} *M* hydrochloric acid. On Dowex 1-X8 $[Cr(enH)(H_2O)(ox)_2]$ eluted first with 10^{-3} *M* sodium perchlorate, followed by $[Cren(ox)_2]^-$ and finally $[Cr(H_2O)_2(ox)_2]^-$.

The extinction coefficients of the enH complexes were found by measuring the absorbance spectra of the separated components and then analyzing the solutions for Cr(III) as described below (Section I).

(G) Spectrophotometric Determination of Thermal Kinetics

The thermal aquation rates of the monodentate protonated ethylenediamine complexes were found by observing spectral changes at constant temperature. The complexes were separated from the photolysis solution by ion exchange chromatography and the time dependence of their spectrum followed using an Unicam SP-700 ultraviolet–visible spectrophotometer equipped with a constant temperature cell compartment.

(H) Oxalate Analysis

All analyses for free oxalate in the photolysis solutions were made using the method of Buriel-Marti *et al.* (26) with the following modification: 4 ml of the Fe(III) salicylate solution was pipetted into a 10 ml volumetric flask and 3 ml of the photosolution added. The solution was made up to 10 ml and the absorbance read at 19 500 cm^{-1}. The method was calibrated by adding to the reagent 3 ml aliquots of 2.0×10^{-2} *M* $K[Cren(ox)_2].2H_2O$ containing known amounts of free oxalate.

The Fe(III) salicylate reagent gave a negative response when tested with a monodentate oxalate complex. Equal excesses of $[Cr(H_2O)_2(oxH)(ox)]^0$ (13) and potassium oxalate were added to separate solutions of the Fe(III) salicylate reagent. The potassium oxalate completely decolorized the Fe(III) salicylate reagent indicating a positive test for oxalate. The $[Cr(H_2O)_2(oxH)ox]^0$ produced no color change other than that due to dilution.

(I) Chromium Analysis

All Cr(III) analyses were made using an alkaline peroxide oxidation technique. The solution to be analyzed was made alkaline with ammonia and a small excess of H_2O_2 was added. The solution was heated on a steam bath for 20 min, additional ammonia being added to ensure alkalinity. The solution was then diluted to a known volume, the absorbance of the resulting $[CrO_4]^-$ measured at 373 nm and compared to a previously prepared calibration curve for $K[CrO_4]$.

The authors are grateful for the financial support of the National Research Council of Canada and the University of Victoria Faculty Research Fund by grants-in-aid of research (A.D.K and K.C.M) and for an NRCC Bursary (J.G.V).

1. E. L. Wehrey. Quart. Rev. London, **28**, 251 (1967).
2. A. W. Adamson *et al.* Chem. Rev. **68**, 541 (1968).
3. D. Valentine. Advances in Photochemistry. *Edited by* W. A. Noyes *et al.* Interscience Publishers, New York, **6**, 123 (1968).
4. P. D. Fleischauer and P. Fleischauer. Chem. Rev. **70**, 199 (1970).
5. L. S. Forster. Transition Metal Chemistry. *Edited by* R. L. Carlin. Interscience Publishers, New York, **5**, 1 (1969).
6. M. R. Edelson and R. A. Plane. Inorg. Chem. **3**, 231 (1964).
7. H. L. Schläfer. J. Phys. Chem. **69**, 2201 (1965).
8. A. W. Adamson. J. Phys. Chem. **71**, 798 (1967).
9. H. L. Schläfer and W. Geiss. Z. Phys. Chem. Frankfurt, **65**, 107 (1969).
10. S. T. Spees and A. W. Adamson. Inorg. Chem. **1**, 531 (1962).
11. G. B. Porter, J. G. W. Doering, and S. Karanka. J. Amer. Chem. Soc. **84**, 4027 (1962).
12. H. D. K. Drew. J. Chem. Soc. 2328 (1932).
13. D. K. Lin and C. S. Garner. J. Amer. Chem. Soc. **91**, 6637 (1969).
14. J. C. Chang. Inorg. Nucl. Chem. Lett. **5**, 587 (1969).
15. (*a*) H. L. Schläfer and O. Kling. Z. Phys. Chem. N.F. **16**, 1 (1958). (*b*) H. L. Schläfer and H. Seidel. Z. Phys. Chem. N.F. **16**, 14 (1958).
16. H. L. Schläfer and R. Kollrack. Z. Phys. Chem. N.F. **18**, 348 (1958).
17. (*a*) H. L. Schläfer *et al.* Z. Phys. Chem. N.F. **24**, 307 (1960). (*b*) H. L. Schläfer. J. Inorg. Nucl. Chem. **13**, 101 (1960).
18. A. D. Kirk, K. C. Moss, and J. G. Valentin. J. Chromat. **36**, 332 (1968).
19. G. B. Porter. To be published.
20. A. Messiah. Quantum Mechanics. North Holland Publ. Co., Amsterdam, **2**, 735 (1962).
21. D. L. Webb and L. K. Patterson. To be published.
22. E. Bushra and C. H. Johnson. J. Chem. Soc. 1937 (1939).
23. A. Werner. Ann. **405**, 212 (1914).
24. J. Lee and H. H. Seliger. J. Chem. Phys. **40**, 519 (1964).
25. A. W. Adamson and E. Wegner. J. Amer. Chem. Soc. **88**, 394 (1966).
26. F. Buriel-Marti *et al.* Anal. Chem. **25**, 583 (1953).
27. H. U. Zander. Ph.D. Thesis, University of Frankfurt, Frankfurt, Germany. 1969.
28. H. L. Schläfer and H. F. Wasgestian. Z. Phys. Chem. **57**, 3 (1968).
29. A. Chiang and A. W. Adamson. J. Phys. Chem. **72**, 3827 (1968).
30. H. F. Wasgestian. Z. Phys. Chem. N.F. **67**, 39 (1969).
31. H. Gausman. Ph.D. Thesis. University of Frankfurt, Frankfurt, Germany. 1966.
32. V. Balzani. Private communication.

Biosynthesis of Lobinaline[1, 2]

R. N. GUPTA AND IAN D. SPENSER
Department of Chemistry, McMaster University, Hamilton, Ontario

Received July 9, 1970

The biosynthesis of lobinaline (**1**) in intact plants of *Lobelia cardinalis* L. was studied by tracer methods. The incorporation data are consistent with the view that the alkaloid is formed by dimerization of α-phenacylpiperidine (**3**), whose piperidine nucleus is derived from lysine via a nonsymmetrical intermediate, and whose sidechain originates, as an intact C_6–C_2 unit, from phenylalanine via cinnamic acid.

Canadian Journal of Chemistry, 49, 384 (1971)

Can. J. Chem. Downloaded from www.nrcresearchpress.com by 210.87.254.5 on 09/05/12
For personal use only.

Introduction

The cardinal flower, *Lobelia cardinalis* L., so called for its brilliant scarlet bloom, is one of the more spectacular North American wild flowers. Lobinaline (**1**), the major alkaloid of this plant species, was isolated by Manske (2) in 1938. Its structure was determined some 30 years later (3, 4, 5).

Visual dissection of its nucleus (dotted line) leads to two fragments, C_6–C_2–C_5N, whose skeleton corresponds to that of some simpler Lobelia alkaloids, 8-phenylnorlobelol (**4**) (6) and 8-phenyllobelol (**5**) (6), which occur in *Lobelia inflata*. Even though such monomeric structures have not hitherto been found in *L. cardinalis*, the hypothesis is biogenetically attractive, that the lobinaline skeleton originates by dimerization of a suitably functionalized C_6–C_2–C_5N monomer. Indeed, such a suggestion was made (7) long before the structure of lobinaline had been established.

The origin of the C_6–C_2–C_5N alkaloids of *Lobelia inflata* has not been investigated. However, the biosynthesis of sedamine (**5**), a base which differs from 8-phenyllobelol only in the configuration at C-2′, has been studied in *Sedum acre* (1, 8, 9). It was established that the piperidine nucleus of sedamine arises from lysine via a nonsymmetrical intermediate, and that the C_6–C_2 sidechain is derived as an intact unit from phenylalanine (Scheme 1).

The objectives of the present study of lobinaline biosynthesis were to identify primary precursors and to test whether the alkaloid does indeed originate by dimerization of a monomer related to sedamine, such as α-phenacylpiperidine (**3**).

Methods and Results

In 11 tracer experiments, specifically labelled samples of phenylalanine, cinnamic acid, benzoic acid, lysine, and α-phenacylpiperidine were administered by the wick method to intact plants of *Lobelia cardinalis* L. when these were in full bloom. In each experiment lobinaline (**1**) was extracted from the aerial parts of the plants and was purified to constant radioactivity as the *N*-acetyl derivative (**2**). The details of these experiments are recorded in Table 1.

The labelled samples of acetyllobinaline (**2**) obtained from individual feeding experiments were degraded, by reactions described in the Experimental section, into the degradation products shown in Scheme 2. The specific activities of the degradation products are listed in Tables 2, 4, and 6 (indicated limits are standard deviation of the mean).

The samples of acetyllobinaline derived from 3-^{14}C-phenylalanine (expt. 2) and 3-^{14}C-cinnamic acid (expt. 5) yielded *p*-nitrobenzoic acid whose specific activity was half that of the intact alkaloid, and whose label was confined to the carboxyl carbon (*i.e.* C-5 and/or C-7 of lobinaline) (*p*-nitrobenzoic acid minus *p*-nitroaniline) (Table 2). The acetyllobinaline derived from the sample of 2,3-$^{14}C_2$-phenylalanine of known isotope distribution (see Experimental) (expt. 3) yielded *p*-nitrobenzoic acid whose specific activity, relative to that of the intact alkaloid, corresponded to the fraction of radioactivity at C-3 of the doubly labelled precursor (Table 3).

Activity from 2-^{14}C-phenylalanine (expt. 1) and from 2-^{14}C-cinnamic acid (expt. 4) was also

[1]This paper is dedicated to Professor Kurt Mothes, Director Emeritus of the Institute of Plant Biochemistry, German Academy of Sciences, Halle, West Germany on the occasion of his 70th birthday.

[2]A preliminary account of part of this work has been published (1).

FOR ERRATA SEE
V.49 ... IS 7 ... P. 2374

Can. J. Chem. Downloaded from www.nrcresearchpress.com by 210.87.254.5 on 09/05/12
For personal use only.

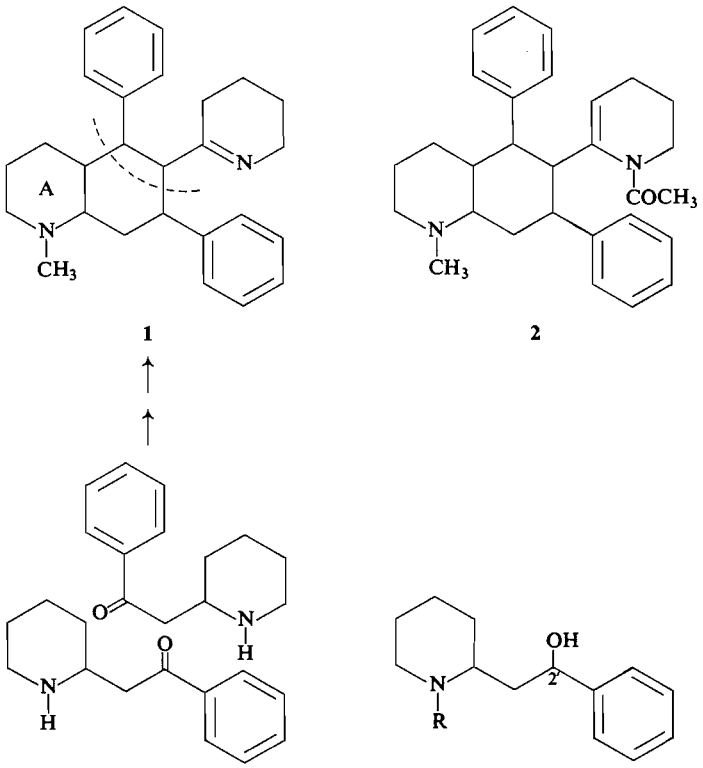

incorporated into lobinaline. These samples of the alkaloid were not degraded, since all attempts to develop reactions suitable for extracting the presumed labelled centers, C-6 and -8, were unsuccessful. Acetyllobinaline isolated after administration of carboxyl-^{14}C-benzoic acid (expt. 6) was essentially inactive.

Radioactivity from 6-^{14}C-lysine (expts. 7 and 8) was recovered in the degradation fragments derived from the heterocyclic nuclei of lobinaline. Succinic acid, β-alanine, and a mixture of β-alanine and *N*-methyl-β-alanine, each showed a specific activity corresponding to approximately half that of the intact alkaloid (Table 4).

The same fragments, isolated from the acetyllobinaline from 2-^{14}C-lysine (expt. 9), were devoid of radioactivity, as was the formaldehyde (C-2) obtained from this sample of the alkaloid (Table 4).

The activity of the formaldehyde (C-2) obtained in an early experiment from 6-^{14}C-lysine-derived acetyllobinaline corresponded to one

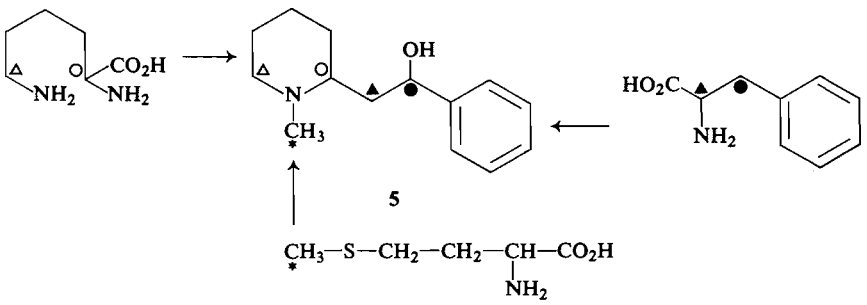

SCHEME 1. Incorporation of labelled precursors into sedamine (8).

Can. J. Chem. Downloaded from www.nrcresearchpress.com by 210.87.254.5 on 09/05/12
For personal use only.

TABLE 1. Incorporation of labelled compounds into lobinaline

Expt. no.	Compound administered	Nominal: Specific activity (mCi mmol^{-1})	Nominal: Total activity (mCi)	Date	Plants: No.	Plants: Dry weight (g)	Days	Acetyllobinaline: Yield (mg)	Acetyllobinaline: Specific activity (counts min^{-1} mmol^{-1}) $\times 10^{-4}$
1	2-^{14}C-DL-Phenylalanine*	1.1	0.1	September 1965	6	37	3	192	0.65 ± 0.02
2	3-^{14}C-DL-Phenylalanine†	10	0.1	September 1964	6	55	6	324	1.59 ± 0.05
3	2,3-$^{14}C_2$-DL-Phenylalanine‡			August 1966	15	156	3	956	5.21 ± 0.10
	from 2-^{14}C-DL-Phenylalanine§	1.8	0.1						
	from 3-^{14}C-DL-Phenylalanine‖	4.5	0.1						
4	2-^{14}C-Cinnamic acid¶	1.7	0.1	August 1965	8	23	3	60	2.02 ± 0.05
5	3-^{14}C-Cinnamic acid**	0.6	0.1	September 1965	12	46	3	270	3.95 ± 0.07
6	Carboxyl-^{14}C-Benzoic acid*	10	0.1	August 1965	8	26	4	91	0.06 ± 0.01
7	6-^{14}C-DL-Lysine††	2.3	0.05	September 1964	6	33	3	169	30.18 ± 0.70
8	6-^{14}C-DL-Lysine†	2.6	0.1	August 1966	6	68	3	260	29.47 ± 0.50
9	2-^{14}C-DL-Lysine‖	3.3	0.1	November 1966	8	87	3	480	13.58 ± 0.25
10	6-^{3}H,2-^{14}C-DL-Lysine‡			August 1968	10	90	3	215	19.74 ± 0.18 (^{14}C)
	from 6-^{3}H-DL-Lysine‖	6.9×10^3	0.8						
	from 2-^{14}C-DL-Lysine¶	1.3	0.1						
11	6-^{14}C-α-Phenacylpiperidine‡	1.0	0.075	September 1968	8	102	3	530	99.45 ± 1.03

*Volk Radiochemical Company.
†Commissariat à l'Énergie Atomique, France.
‡See Experimental.
§Nuclear Research Chemicals Inc.
‖New England Nuclear.
¶Tracerlab.
**Merck, Sharpe and Dohme.
††Calbiochem.

Can. J. Chem. Downloaded from www.nrcresearchpress.com by 210.87.254.5 on 09/05/12
For personal use only.

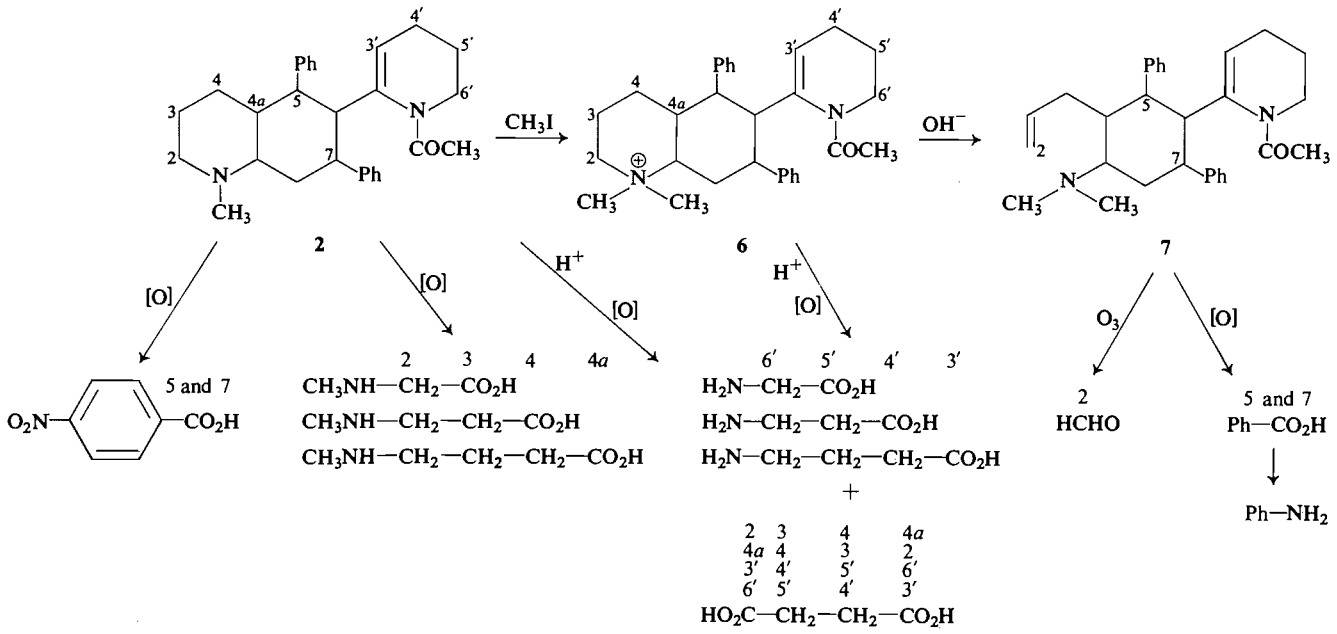

SCHEME 2. Degradation of acetyllobinaline.

TABLE 2. Incorporation of phenylpropanoid precursors into lobinaline

Precursor: Expt. no.:	3-^{14}C-DL-Phenylalanine 2		3-^{14}C-Cinnamic acid 5		2,3-$^{14}C_2$-DL-Phenylalanine 3	
Product	SA*	RSA†	SA	RSA	SA	RSA
Acetyllobinaline	1.59 ± 0.05	100 ± 3	1.64 ± 0.04‡	100 ± 2	5.21 ± 0.10	100 ± 2
p-Nitrobenzoic acid	0.76 ± 0.04	48 ± 3	0.78 ± 0.02	48 ± 2	1.43 ± 0.03	28 ± 1
p-Nitroaniline	0.01 ± 0.002	0.3 ± 0.1	0.01 ± 0.002	1 ± 0.3	—	

*Specific activity (counts min^{-1} $mmol^{-1}$) × 10^{-4}.
†Relative specific activity: percent (acetyllobinaline = 100).
‡Obtained from the original acetyllobinaline, specific activity (3.95 ± 0.07) × 10^4 counts min^{-1} $mmol^{-1}$, by dilution with inactive acetyllobinaline.

TABLE 3. Incorporation of 2,3-$^{14}C_2$-phenylalanine into lobinaline (expt. 3); distribution of label in precursor and product

Precursor	RSA*	Product	RSA*
2,3-$^{14}C_2$-Phenylalanine	100 ± 2†	Acetyllobinaline (2α ± 2β)	100 ± 2‡
3-^{14}C-	56 ± 2†	*p*-Nitrobenzoic acid (β)	28 ± 1‡
$\frac{\text{2,3-}^{14}C_2\text{-Phenylalanine}}{\text{3-}^{14}\text{C-}}$ = 1.78 ± 0.08		$\frac{\text{Acetyllobinaline (2α ± 2β)}}{\text{2 × p-Nitrobenzoic acid (2 × β)}}$ = 1.82 ± 0.05	

*Relative specific activity, percent.
†See Experimental.
‡See Table 2.

quarter of the activity of the intact alkaloid (expt. 7). Modification of the degradation procedure in more recent work (expt. 8) led to formaldehyde containing 40% of the total activity. This discrepancy is discussed below.

Acetyllobinaline, obtained from the experiment with 6-^{3}H,2-^{14}C-lysine (expt. 10), showed a $^3H/^{14}C$ ratio identical with that of the doubly labelled precursor. The $^3H/^{14}C$ ratio of the pipecolic acid, isolated from the same plants, was approximately 20% higher (Table 5).

The distribution of radioactivity within the acetyllobinaline derived from 6-^{14}C-α-phenacylpiperidine (expt. 11) (Table 6) was similar to that of the alkaloid sample derived from 6-^{14}C-lysine (expt. 8).

Discussion

Lysine and phenylalanine, the primary metabolites which supply the skeleton of sedamine (**5**) also serve as precursors of lobinaline (**1**). The mode of incorporation of each of these substrates into sedamine (Scheme 1) was deduced unequivocally on the basis of a chemical degradation which permitted isolation of individual carbon atoms in such a way that the total activity of the intact alkaloid was accounted for in terms of activity at individual sites (8). Chemical degradation of lobinaline, on the other hand, was only partial. Due to the inertness of the alkaloid towards a wide variety of reagents (*cf.* ref. 3), sustained attempts to devise reactions capable of yielding degradation products representing C-6, -8, -8*a*, and -2′ failed to give useful results. Even though the interpretation of some of the incorporation data therefore rests on indirect argument, the conclusions are, for the most part, unambiguous.

The results of the experiments with phenylpropanoid precursors (expts. 1–5) are consistent with the view that an intact C_6–C_2 unit, derived from phenylalanine, is incorporated into each of the two "halves" of lobinaline, in analogy with the mode of entry of the phenylalanine-derived fragment into sedamine (Scheme 1).

Label from 3-^{14}C-phenylalanine (expt. 2) and from 3-^{14}C-cinnamic acid (expt. 5) is confined to the carboxyl group of the degradation product, *p*-nitrobenzoic acid, whose specific activity was half that of lobinaline in both experiments (Table 2).

Lobinaline contains two *C*-phenyl groups. *Provided that the yield of p-nitrobenzoic acid derived from each of these two moieties is equal*, isolation of a sample of this acid, with a specific activity half that of the original lobinaline, accounts for the total activity of the alkaloid and indicates that either one or both of the two

Can. J. Chem. Downloaded from www.nrcresearchpress.com by 210.87.254.5 on 09/05/12
For personal use only.

Can. J. Chem. Downloaded from www.nrcresearchpress.com by 210.87.254.5 on 09/05/12
For personal use only.

TABLE 4. Incorporation of lysine into lobinaline

Precursor:	6-^{14}C-DL-Lysine						2-^{14}C-DL-Lysine	
Expt. no.:	7				8		9	
Product	SA*	RSA†	SA	RSA	SA	RSA	SA	RSA
Acetyllobinaline	6.63 ± 0.11‡	100 ± 2	2.26 ± 0.03‡	100 ± 1	7.76 ± 0.20‡	100 ± 3	13.58 ± 0.25	100 ± 2
Formaldehyde (C-2) (as dimedone derivative)	[1.63 ± 0.04	25 ± 1]§	—		3.06 ± 0.05	39 ± 1§	0.002 ± 0.006	0
Succinic acid	—		1.02 ± 0.04	45 ± 2	4.00 ± 0.11	51 ± 2		
Mixed DNP-amino acids‖	—		1.13 ± 0.04	50 ± 2	4.07 ± 0.05	52 ± 2	0.05 ± 0.01	0
DNP-β-Alanine	—		—		4.27 ± 0.07	55 ± 2	—	
Benzoic acid	0.01 ± 0.003	0	—		—		—	

*Specific activity (counts min^{-1} $mmol^{-1}$) × 10^{-4}.
†Relative specific activity: percent (acetyllobinaline = 100).
‡Obtained from the original sample of acetyllobinaline (Table 1) by dilution with inactive carrier.
§See Discussion.
‖For the calculation of the molar specific activity the molecular weight of DNP-β-alanine was used.

Can. J. Chem. Downloaded from www.nrcresearchpress.com by 210.87.254.5 on 09/05/12
For personal use only.

TABLE 5. Incorporation of 6-^{3}H,2-^{14}C-DL-lysine (expt. 10)

	$^3H/^{14}C$ Ratio
6-^{3}H,2-^{14}C-DL-Lysine	14.9 ± 0.5
Acetyllobinaline	14.4 ± 0.1
Pipecolic acid	16.8 ± 0.1

C_6–C_1 units are specifically derived from phenylalanine. The relative specific activity of the two units is not necessarily the same, but distribution of activity must be such that the relationship, relative specific activity at C-5 plus relative specific activity at C-7 equals 100, is obeyed. However, the two *C*-phenyl moieties of lobinaline lie in different chemical environments. There is therefore no *a priori* reason why *p*-nitrobenzoic acid should arise at the same rate from the two sites. Since oxidation of lobinaline is not necessarily complete, it is more likely that the two sites produce different amounts of degradation product, and that these yields differ somewhat from experiment to experiment. *If on oxidation each of the two sites yields a different quantity of p-nitrobenzoic acid*, the resultant product will have a specific activity corresponding to half that of the intact alkaloid either purely fortuitously,[3] or only if each of the two sites, C-5 and -7, contains one half of the total activity of the original lobinaline.

Even though we incline towards the last mentioned interpretation of the results, the other possibilities cannot be entirely ruled out on the basis of the present results.[4]

[3]Thus, *e.g.*, *p*-nitrobenzoic acid of the observed specific activity would be obtained from a sample of lobinaline containing 10% of its activity at C-5 and 60% at C-7, provided that four times as much *p*-nitrobenzoic acid is contributed to the final product by C-7 as is supplied by C-5. Under such circumstances the total activity of the intact alkaloid is not accounted for in the *p*-nitrobenzoic acid.

[4]Mention should be made of an attempt, albeit unsuccessful, to show by means of mass-spectroscopy whether both or only one of the phenyl nuclei of lobinaline had acquired label. A major mass-spectrometric fragment (*m/e* 186) of lobinaline has been related to a segment of the molecule (5), which happens to correspond to one of the two "biogenetic halves" of lobinaline. Mass spectrometry of labelled lobinaline, obtained from a feeding experiment with [ring $^2H_5$]-phenylalanine, should demonstrate whether the molecular ion of lobinaline was accompanied by a signal M + 10 or M + 5, and whether the fragment, *m/e* 186, was accompanied by a corresponding fragment, *m/e* 191. A feeding experiment with [ring $^2H_5$]phenylalanine was carried out but the deuterium content of the lobinaline which was isolated was too low to yield the desired information (*cf.* footnote 7).

The remaining ambiguity might have been dispelled, had we succeeded in perfecting degradations of lobinaline, capable of isolating C-6 and/or C-8, the presumed centers of activity in lobinaline derived from 2-^{14}C-phenylalanine (expt. 1) and 2-^{14}C-cinnamic acid (expt. 4). Attempts to isolate α-picolinic acid, whose carboxyl group would have represented C-6, by aromatization of the piperideine nucleus followed by oxidation (3), failed to yield more than traces of the desired product. Equally futile were attempts to gain access to C-8, as the 2-carboxyl group of quinolinic acid, by demethylation of lobinaline (3) followed by dehydrogenation (3) and oxidation. Another possible approach to C-8, exhaustive methylation at N-1, which led, via **6** and **7** (*cf.* ref. 5), to a neutral methine, *m/e* 473, presumably **8** (two possible positions of the double bond shown by dotted lines), was also abandoned because of low yields.

Even though specific incorporation of label from 2-^{14}C-phenylalanine and 2-^{14}C-cinnamic acid into the predicted sites of lobinaline was therefore not demonstrated, the results of two further experiments are, nevertheless, consistent with the view that intact C_6–C_2 units derived from phenylalanine are incorporated into the alkaloid.

The labelling pattern established by partial degradation (Table 2), within the lobinaline obtained from plants to which intermolecularly labelled 2,3-$^{14}C_2$-phenylalanine of known distribution of radioactivity was administered (expt. 3), was found to correspond to that of the precursor (Table 3). Such a numerical relation-

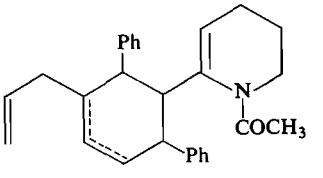

8

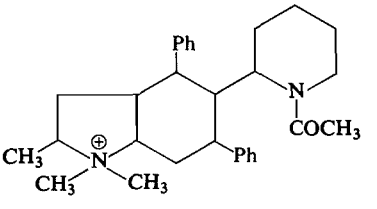

9

TABLE 6. Incorporation of 6-^{14}C-α-phenacylpiperidine into lobinaline (expt. 11)

Product	Specific activity (counts min^{-1} $mmol^{-1}$) $\times 10^{-4}$	Relative specific activity
Acetyllobinaline (diluted)	5.81 ± 0.06	100 ± 1
Formaldehyde (C-2) (as dimedone derivative)	2.30 ± 0.06	40 ± 1
Succinic acid	2.63 ± 0.08	45 ± 1
DNP-β-alanine	3.09 ± 0.06	53 ± 1

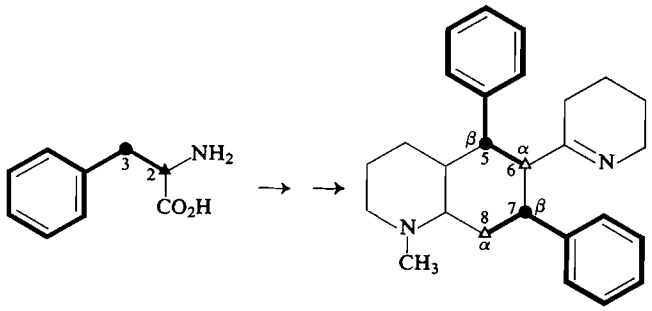

SCHEME 3. Incorporation into lobinaline of an intact C_6–C_2 unit derived from phenylalanine.

ship is as demanded by the hypothesis that intact C_6–C_2 units are incorporated and is most unlikely to be coincidental. The lack of incorporation of a C_6–C_1 precursor (expt. 6) is also consistent with this view.

Even though not entirely conclusive, the weight of evidence from expts. 1–6 favors the conclusion that, as in the case of sedamine, intact C_6–C_2 units supply the predicted moieties of lobinaline (Scheme 3).

The results of the experiments with labelled lysine (expts. 7–10) demonstrate that, in analogy with the biosynthesis of sedamine (8), a C_5N unit, derived from lysine by way of a nonsymmetrical intermediate, is incorporated into the piperidine nucleus of each of the two "halves" of lobinaline, and that each of the two "halves" of the molecule contains one half of the total activity (Table 4).

An early degradation result (July 1966) appeared to lead to a different conclusion. Formaldehyde, generated by ozonolysis of the Hofmann degradation product **7** (in the presence of unchanged lobinaline, see Experimental) obtained from lobinaline derived from 6-^{14}C-lysine, contained one quarter of the activity of the intact alkaloid (expt. 7, Table 4). This result demonstrated non-random entry of label from lysine into the alkaloid. Since it was presumed that the formaldehyde was derived solely from C-2 of lobinaline, the result appeared to indicate that four of the carbon atoms of the alkaloid were labelled. On this basis it might have been tempting to infer that the four labelled centers were C-2, -8*a*, -2′, and -6′, and that lysine had been incorporated into each of the two "halves" of lobinaline via a symmetrical intermediate. To provide further evidence in support of such an inference, confirmatory results had to be generated. At that time none of the crucial carbon atoms, other than C-2, were accessible. Evidence was sought in another way. If lysine had indeed entered by way of a symmetrical intermediate and activity from 6-^{14}C-lysine was distributed equally over four sites of lobinaline, it was an essential corollary that the same four sites would be labelled analogously when 2-^{14}C-lysine served as the precursor. Yet the formaldehyde derived from a sample of lobinaline isolated from the feeding experiment with 2-^{14}C-lysine (expt. 9) was completely inactive (Table 4). The earlier inference, that two symmetrical C_5N units had entered lobinaline, thus became untenable, since incorporation of the lysine-derived unit into ring A had clearly taken place in a non-symmetrical manner. The results might be plausibly interpreted to mean that the two "halves" of lobinaline were unequally labelled, and that they were therefore derived from related but unequal precursor units (10).

Can. J. Chem. Downloaded from www.nrcresearchpress.com by 210.87.254.5 on 09/05/12
For personal use only.

Can. J. Chem. Downloaded from www.nrcresearchpress.com by 210.87.254.5 on 09/05/12
For personal use only.

It became increasingly obvious that compelling evidence on the mode of incorporation of lysine into lobinaline would emerge only if the resistance of the molecule to degradation could be broken and degradation fragments could be obtained from each of the two hetero-rings, accounting for the total activity of the intact alkaloid. Success appeared assured when, on careful oxidation of lobinaline, a mixture of amino acids was obtained, from which β-alanine, contaminated with a little *N*-methyl-β-alanine, was isolated as the major component (Scheme 2). The specific activity of this mixture, obtained from the lobinaline derived from 6-^{14}C-lysine (expt. 7, Table 4), was half of that of the original alkaloid.

This result can be interpreted in a variety of ways, on the basis of arguments analogous to those adduced in the interpretation of the data obtained in the experiment with 3-^{14}C-phenylalanine, above. The most likely, though by no means the only, explanation of the activity pattern found in the amino acid mixture was that each of the components of the mixture, β-alanine and *N*-methyl-β-alanine, were equally labelled, presumably at the C-atoms derived, respectively, from C-6′ and -2 of the original alkaloid, and that the two "halves" of lobinaline contained equal activity. This inference, which was supported by the observation that succinic acid obtained in the same degradation also showed a specific activity corresponding to one half that of the alkaloid, was in direct contradiction to the earlier result, that formaldehyde (thought to be derived solely from C-2) showed only one quarter of the initial activity. This result thus became suspect. The mode of incorporation of 6-^{14}C-lysine into lobinaline was therefore reinvestigated (expt. 8).

Succinic acid, and the mixture of the *N*-dinitrophenyl derivatives of β-alanine and *N*-methyl-β-alanine, obtained from the oxidation of this sample of lobinaline, again contained approximately one half of the activity of the intact alkaloid. So did a pure sample of *N*-dinitrophenyl-β-alanine, obtained by oxidation of the corresponding lobinaline methohydroxide (**6**) (Scheme 2). Since β-alanine represents C-6′, -5′, -4′, of the piperideine nucleus of lobinaline,[5] it follows that this fragment contains one half of the total activity of the alkaloid, presumably[6] at C-6′.

The other half of the activity of the intact alkaloid would be expected to reside at C-2. This carbon is contained in the degradation fragment, *N*-methyl-β-alanine. Since the specific activity of the mixture of β-alanine and *N*-methyl-β-alanine and that of β-alanine corresponded to approximately one half that of the intact alkaloid, *N*-methyl-β-alanine must also contain approximately one half the original activity. This activity is presumably contained at C-2, the carbon which is the source of the formaldehyde obtained on degradation. Yet, in the earlier experiment with 6-^{14}C-lysine (expt. 7), this formaldehyde had contained one quarter, rather than one half of the total activity. A modified procedure for the ozonolysis of the Hofmann product involving shorter exposure to ozonized oxygen yielded formaldehyde which contained approximately 40, and not 25%, of the activity of the original alkaloid. It must be concluded that in the course of the oxidation formaldehyde is generated not only from C-2, but also from one of the *N*-methyl groups of the methine base **7** or of the contaminating acetyllobinaline, presumably by way of the corresponding *N*-oxides. The inactive formaldehyde so produced then causes lowering of the specific activity of the formaldehyde derived from C-2. This contamination with inactive formaldehyde can be minimized but cannot be entirely prevented. Analogous findings in the course of the osmium tetroxide–periodate oxidation of a similarly ^{14}C-labelled Hofmann product have recently been reported (11).

The evidence from expts. 7–9 indicates that activity from ^{14}C-lysine is equally divided between the two "halves" of lobinaline, and that the two heterocyclic rings are derived from lysine via a non-symmetrical intermediate (Scheme 4). Non-symmetrical incorporation of lysine is confirmed by the result of the experiment with 6-^{3}H,2-^{14}C-lysine (expt. 10). The ^{3}H/^{14}C ratio of this doubly labelled precursor was maintained in lobinaline (Table 5), indicating that loss of tritium relative to carbon had not occurred in the course of biosynthesis. Symmetrical incorporation of a lysine-derived precursor would have

[5]The possibility cannot be excluded, however, that β-alanine may originate also from ring A (C-2, -3, -4) of lobinaline, as a consequence of oxidative demethylation.

[6]Further degradation of the β-alanine was precluded by lack of material.

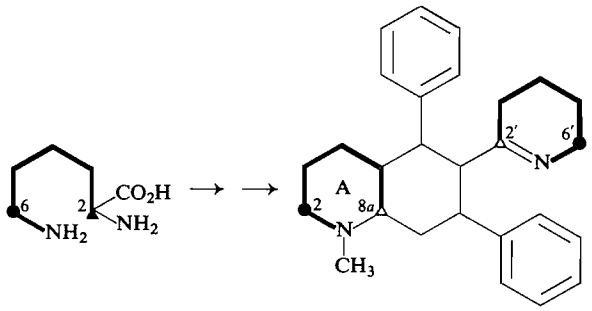

SCHEME 4. Incorporation into lobinaline of a C_5N unit derived from lysine.

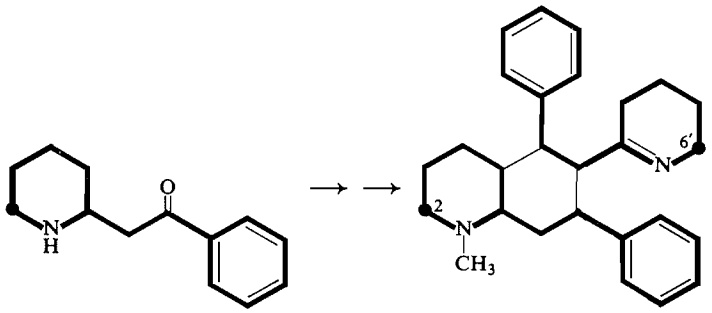

3

SCHEME 5. Incorporation into lobinaline of α-phenacylpiperidine.

placed C-6 of lysine at C-2′, as well as at C-6′ of lobinaline. Since C-2′ does not carry a hydrogen atom, such symmetrical incorporation would have demanded loss of tritium, relative to ^{14}C.

Incorporation of lysine, as well as of phenylalanine, into lobinaline, thus takes place in complete analogy with the entry of the two substrates into sedamine. Furthermore, it appears that the lysine-derived C_5N unit and the phenylalanine-derived C_6–C_2 unit enter both "halves" of lobinaline at the same rate, since in every experiment in which a degradation was performed, approximately half of the activity of the intact alkaloid was recovered in fragments representing each of the two "halves" of lobinaline.

The evidence is thus entirely consistent with the notion that lobinaline is, from the point of view of its biosynthesis, a modified dimer of a C_6–C_2–C_5N unit, related to sedamine.

A final experiment strengthened this view. 6-^{14}C-α-Phenacylpiperidine (3) (12) was administered to *L. cardinalis* (expt. 11). Partial degradation of the highly radioactive lobinaline which was isolated indicated, within the limitations of the degradation procedures discussed earlier, that both "halves" of the molecule were labelled at the predicted sites (C-2 and -6′) (Scheme 5), and that each of these sites carried one half of the activity of the precursor[7] (Table 6). The hypothesis that lobinaline originates from a monomer unit related to α-phenacylpiperidine demands exactly such a distribution of activity. The results here reported support this hypothesis.

Experimental

Isolation of Lobinaline

The dried aerial parts[8] of *Lobelia cardinalis* L. (40 g) were powdered in a blender (Osterizer Galaxie 10), the powder was moistened with aqueous ammonia (2 *M*, 25 ml), the mixture was allowed to stand for 1 h, and was continuously extracted with ether for 36 h. The ether extract was then extracted with hydrochloric acid (2 *M*, 5 × 5 ml). The acid extract was repeatedly washed with ether (10 ml portions), until the ether extract was no

An attempt to demonstrate, by mass-spectrometry, incorporation of ^{15}N from ^{15}N-α-phenacylpiperidine (prepared (*cf.* ref. 12) from ε-^{15}N-DL-lysine) failed to yield conclusive results. The ^{15}N content of the lobinaline which was obtained was too low for direct mass-spectrometric demonstration of heavy species.

[8]Preliminary experiments showed that the roots of the plant contained negligible amounts of the alkaloid.

Can. J. Chem. Downloaded from www.nrcresearchpress.com by 210.87.254.5 on 09/05/12
For personal use only.

Can. J. Chem. Downloaded from www.nrcresearchpress.com by 210.87.254.5 on 09/05/12
For personal use only.

longer colored. The acid solution was made strongly alkaline by addition of potassium hydroxide solution (10% w/v), and the basic components were extracted into hexane (5 × 30 ml). The combined hexane extract was dried (sodium sulfate) and the solvent evaporated, yielding crude lobinaline as a dark semicrystalline solid. Attempted purification of lobinaline by chromatography on alumina and crystallization as the hydrochloride (5) or the free base (3) was accompanied by significant losses of material.

Purification was achieved by conversion to acetyllobinaline. The crude product was refluxed with acetic anhydride for 5 min and solvent was evaporated *in vacuo*. The residue was dissolved in water, the aqueous solution was washed with ether and made alkaline by addition of aqueous potassium hydroxide (10% w/v). The mixture was extracted with ether (3 × 20 ml), the ether extracts were dried, solvent was evaporated, and the residue was recrystallized from hexane and sublimed at 190–200° and 3×10^{-3} mm. Acetyllobinaline (350 mg), m.p. 158–159°, was obtained (mass spectrum *m/e* 428). Reported m.p. 159–160° (3).

p-Nitrobenzoic Acid by the Oxidation of Acetyllobinaline

A mixture of acetyllobinaline (175 mg) and concentrated nitric acid (5 ml) was heated on the steam bath until nitric acid had evaporated. The residue was dissolved in sodium hydroxide solution (5% w/v, 10 ml), finely powdered potassium permanganate (1.2 g) was added, and the mixture heated overnight with continuous stirring. The mixture was cooled and acidified with dilute sulfuric acid, a stream of sulfur dioxide was passed through, and the solution was then extracted with ether. The ether extract was washed with water, dried, and evaporated. The residue was crystallized from aqueous methanol and sublimed at 120–125° and 5×10^{-3} mm, yielding a crystalline solid (40 mg), m.p. 239–240°, mass spectrum *m/e* 167, identical (mixture m.p., i.r. spectrum) with an authentic sample of *p*-nitrobenzoic acid.

p-Nitroaniline from p-Nitrobenzoic Acid (13)

p-Nitrobenzoic acid (50 mg) was dissolved in chloroform (5 ml), and a mixture of oleum (10%, 2.5 ml) and concentrated sulfuric acid (0.5 ml) was added, followed by sodium azide (5 mg). The mixture was refluxed 3 h with rapid stirring, cooled, and poured onto crushed ice (25 g). The chloroform layer was separated and rejected. The aqueous layer was made alkaline with sodium hydroxide (1 *M*) and extracted with ether (3 × 10 ml). The ether layer was washed with water, dried, and the solvent was evaporated. The residue was sublimed at 130–140° and 3×10^{-3} mm, yielding *p*-nitroaniline (25 mg) melting at 147–148°.

Hofmann Degradation of Acetyllobinaline

Acetyllobinaline (200 mg) was dissolved in dry acetone (4 ml), methyl iodide (2 ml) was added, and the mixture was allowed to stand 48 h at room temperature, and was then evaporated to dryness, yielding a foamy residue which did not crystallize. The residue was repeatedly triturated with ether, and the ether extracts containing unreacted acetyllobinaline were decanted. The residue was dissolved in hot aqueous methanol (50% v/v) and freshly precipitated silver oxide (300 mg) was added. The mixture was allowed to stand 4 h in the dark, solid was filtered off, the filtrate and washings were combined, solid potassium hydroxide (1 g) was added, and the solvent was evaporated.

Basic components were recovered from the residue by high vacuum sublimation at 190–200° and 5×10^{-3} mm. The sublimate was a mixture of unchanged acetyllobinaline (~70%) and the methine base (7) (~30%). In a pilot experiment the latter was separated by the general method described for the purification of methine bases derived from *trans*-decahydroquinoline systems (14). The mixture was refluxed 6 h with a solution containing acetic anhydride (2.5 ml) and glacial acetic acid (2.5 ml). The solvents were then evaporated, the residue was dissolved in water, and the solution made alkaline with potassium hydroxide (1 *M*), and was extracted with ether to remove unreacted acetyllobinaline. The aqueous layer was saturated with potassium iodide and extracted with chloroform, and the solvent evaporated. A quaternary salt, presumably 9 (*cf.* ref. 14) (n.m.r. spectrum: *C*-methyl, doublet, centered at 1.6 p.p.m.) remained. It was dissolved in hot water, freshly precipitated silver oxide was added, and the hot solution was left for 2 h in the dark. Solid was filtered off, the solution was evaporated, and the residue was heated *in vacuo*. The methine base 7 (*cf.* ref. 5) sublimed at 150–180° and 3×10^{-3} mm as a gummy mass which did not crystallize (mass spectrum, molecular ion *m/e* 442).

This separation was not used in the degradation of labelled samples. The mixed crude bases were dissolved in a mixture of ethyl acetate (3 ml) and acetic acid (2 ml). The solution was cooled in ice/salt mixture and ozonized oxygen was passed, in early experiments for 15 min, and in more recent runs for less than 5 min. The solution was then diluted with water (40 ml), zinc dust (50 mg) was added, and the mixture was concentrated until 25 ml distillate had been collected.

5,5-Dimethyl-1,3-cyclohexanedione (dimedone) (25 mg) was added to the distillate which was then allowed to stand at room temperature overnight. Formaldehyde dimethone (10 mg), which crystallized when the solution was concentrated, was recrystallized from aqueous methanol, and after sublimation at 120–140° and 3×10^{-3} mm melted at 186–187°.

The reaction mixture remaining after removal of formaldehyde by distillation was made alkaline by addition of aqueous sodium hydroxide (1 *M*), and was then extracted with ether. The ether extract was dried, solvent was evaporated, and water (20 ml) and powdered potassium permanganate (1 g) were added to the residue. The mixture was heated 24 h under reflux with constant stirring. The mixture was cooled and acidified (1 *M* sulfuric acid) and sulfur dioxide was passed until all manganese dioxide had dissolved. The solution was extracted with ether (3 × 10 ml), the extract was washed with water (1 ml), dried and evaporated, the residue was sublimed at 60° and 5×10^{-3} mm, and the sublimate was crystallized from aqueous methanol. Resublimation yielded benzoic acid (10 mg), m.p. 120–121°.

β-*Alanine from Acetyllobinaline*

(a) Chromic Acid Oxidation of Acetyllobinaline

Acetyllobinaline (200 mg) was suspended in aqueous sulfuric acid (5 ml, 30% v/v) and the mixture was refluxed for 1 h with continuous stirring. Chromic acid (1 g) in

Can. J. Chem. Downloaded from www.nrcresearchpress.com by 210.87.254.5 on 09/05/12
For personal use only.

water (1.5 ml) was then added and refluxing was continued for 36 h with stirring.

Excess chromic acid was destroyed by addition of a few drops of methanol and the mixture was continuously extracted with ether for 24 h. The ether extract was worked-up for succinic acid, the residue was diluted with water (100 ml), and worked-up for amino acids.

The ether layer was extracted with water (5 × 1 ml), the aqueous extract was washed with ether (2 ml) and was then evaporated to dryness. The residue was sublimed at 110–130° and 5×10^{-3} mm, yielding succinic acid (5 mg), m.p. 181–182°, identical with an authentic sample.

The aqueous solution containing the residue remaining after extraction of the chromic acid oxidation mixture with ether was heated on the steam bath and neutralized (p*H* 6–7) by addition of hot barium hydroxide solution. After 1 h the mixture was filtered, the precipitate was washed with hot water (3 × 10 ml), and the combined filtrate and washings were concentrated, treated with charcoal and filtered. Sodium carbonate (25 mg) and methanolic 2,4-dinitrofluorobenzene (10% v/v, 1 ml) was added, and the mixture was allowed to stand at room temperature with occasional stirring. The solution whose p*H* was still above p*H* 8 was extracted with ether, and the extract discarded. The solution was then acidified with hydrochloric acid (2 *M*) and was extracted with ether. The ether extract was dried, solvent was evaporated under reduced pressure, and the residue was heated at 80° and 3×10^{-3} mm to remove 2,4-dinitrophenol by sublimation. The deep yellow residue was dissolved in chloroform (0.5 ml) and the solution was applied to two plates (20 × 20 cm) coated with silica gel (2 mm thickness). Development with benzene/pyridine/acetic acid 80:20:2 (15) led to the appearance of three well separated major bands, whose R_f value corresponded to those of authentic samples of the *N*-dinitrophenyl derivatives of glycine (R_f 0.28), β-alanine (R_f 0.72), and γ-aminobutyric acid (R_f 0.82). A minor band of higher R_f value was not identified.

The band corresponding to *N*-dinitrophenyl-β-alanine was scraped off the plate and eluted thoroughly with methanol. The methanol was evaporated, the residue was dissolved in hydrochloric acid (1 ml, 1 *M*) and the solution extracted with ether (3 × 5 ml). The ether extract was washed with water (1 ml) and dried (sodium sulfate), the solvent evaporated, and the residue sublimed at 150–160° and 3×10^{-3} mm.

The sublimate did not crystallize. Its mass spectrum showed, in addition to the expected molecular ion of *N*-dinitrophenyl-β-alanine, *m/e* 255, a signal at *m/e* 269, presumably due to *N*-dinitrophenyl-*N*-methyl-β-alanine. The sublimate was esterified by treatment with diazomethane in ether. The n.m.r. spectrum of the product in deuterochloroform showed a singlet (3.03 p.p.m.) characteristic for *N*-methyl. The mixture of the *N*-dinitrophenyl derivatives of β-alanine and *N*-methyl-β-alanine, or of their methyl esters, resisted all attempts at separation by thin layer, column, or gas–liquid chromatography.

(b) Chromic Acid Oxidation of Acetyllobinaline Methohydroxide

Methyl iodide (2 ml) was added to a solution of acetyllobinaline (300 mg) in acetone (2 ml), the mixture was allowed to stand 48 h at room temperature and was then evaporated to dryness. The residue was triturated with ether to remove unreacted acetyllobinaline. The residue was dissolved in hot aqueous methanol (5 ml, 50% v/v), freshly precipitated silver oxide (400 mg) was added, and the mixture was kept in the dark for 4 h. Solid was filtered off and washed with hot water (2 × 5 ml), and filtrate and washings were combined and evaporated, yielding a residue which was dissolved in aqueous sulfuric acid (5 ml, 30% v/v) and refluxed 1 h with continuous stirring. Chromic acid (1 g) in water (1.5 ml) was then added and refluxing was continued for 36 h with stirring.

Further work-up of the reaction mixture was as described in the case of the direct chromic acid oxidation of acetyllobinaline, above. Succinic acid was isolated from the ether soluble fraction of the oxidation mixture. Amino acids, present in the aqueous layer, were converted into their *N*-dinitrophenyl derivatives, which were separated by thin layer chromatography, as described above. Three major bands were again observed.

The band corresponding to *N*-dinitrophenyl-β-alanine was scraped off the plate and eluted thoroughly with methanol. The methanol was evaporated, the residue was dissolved in dilute hydrochloric acid, and the solution extracted with ether. The ether extract was washed with a little water, the solution was dried (sodium sulfate), the solvent was evaporated and the residue sublimed at 150–160° and 3×10^{-3} mm, yielding *N*-dinitrophenyl-β-alanine (10 mg), m.p. 142–144° (reported m.p. 145–146° (16)), which was further purified by crystallization from a mixture of methanol and ether, followed by resublimation (mass spectrum, molecular ion *m/e* 255).

N-2,4-Dinitrophenyl Derivatives

Authentic samples of the *N*-dinitrophenyl derivatives of ω-amino acids, which were required for comparison with the samples derived from acetyllobinaline, were obtained as follows.

N-Dinitrophenylglycine, N-Dinitrophenyl-β-alanine, and N-Dinitrophenyl-γ-aminobutyric Acid

These samples were commercial products (Sigma Chemical Co.).

N-Dinitrophenyl-N-methyl-β-alanine

3-Methylaminopropionitrile (420 mg, Aldrich Chemical Co.) was dissolved in methanol (5 ml), and sodium hydroxide (1 *M*, 5.2 ml) was added. The mixture was refluxed 6 h, the solvents were then evaporated and the residue triturated with ether to remove unchanged nitrile or amide. The residue was then dissolved in water (5 ml) and the solution was brought to p*H* 10 by addition of a few drops of 1 *M* hydrochloric acid. Methanolic 2,4-dinitrofluorobenzene (10% v/v, 5 ml) was added and the mixture was allowed to stand 2 h at room temperature with occasional shaking. Water was added, the solution was extracted with ether, and the ether extract rejected. The aqueous solution was acidified and extracted with ether, the ether extract was washed with water, dried over anhydrous sodium sulfate, and concentrated. *N-Dinitrophenyl-N-methyl-β-alanine* crystallized spontaneously, and was further purified by sublimation at 5×10^{-3} mm and 130–140°, m.p. 142–143°. Mass spectrum, molecular ion *m/e* 269.

Can. J. Chem. Downloaded from www.nrcresearchpress.com by 210.87.254.5 on 09/05/12
For personal use only.

Anal. Calcd. for $C_{10}H_{11}N_3O_6$: C, 44.61; H, 4.12; N, 15.61. Found: C, 44.45; H, 4.05; N, 15.37.

N-Dinitrophenyl-N-methyl-γ-aminobutyric Acid

A mixture of *N*-methyl-2-pyrrolidone (500 mg, Aldrich Chemical Co.) and concentrated hydrochloric acid (2 ml) was refluxed 4 h. The solution was evaporated to dryness and the residue was repeatedly extracted with ether to remove unchanged starting material, and was then recrystallized from methanol/ether (17). The *N*-methyl-γ-aminobutyric acid hydrochloride so obtained was converted, by the standard procedure outlined above, into *N-dinitrophenyl-N-methyl-γ-aminobutyric acid*, m.p. 104–105°, after recrystallization from aqueous methanol. Mass spectrum, molecular ion *m/e* 283.

Anal. Calcd. for $C_{11}H_{13}N_3O_6$: C, 46.64; H, 4.63; N, 14.84. Found: C, 46.87; H, 4.57; N, 14.74.

Methyl Esters of N-Dinitrophenyl-ω-amino Acids (cf. ref. 18)

The *N*-dinitrophenyl-ω-amino acid (20 mg) was dissolved in methanol (5 ml), a solution of diazomethane in ether was added, and the mixture was allowed to stand at room temperature overnight. Solvents were evaporated under reduced pressure and the dark red oily residue was dissolved in chloroform (0.5 ml) and applied to a column (1 × 10 cm) packed with neutral alumina, activity I. The product was eluted with benzene, the eluate was concentrated to dryness, and the residue crystallized from methanol and sublimed at $\sim 10^{-3}$ mm.

The following esters were prepared:

Methyl 3-[2,4-dinitrophenylamino]propionate (methyl ester of *N*-dinitrophenyl-β-alanine) m.p. 97°; mass spectrum, molecular ion *m/e* 269.

Anal. Calcd. for $C_{10}H_{11}N_3O_6$: C, 44.61; H, 4.12; N, 15.61. Found: C, 44.49; H, 3.98; N, 15.46.

Methyl 4-[2,4-dinitrophenylamino]butyrate (methyl ester of *N*-dinitrophenyl-γ-aminobutyric acid) m.p. 52°; mass spectrum, molecular ion *m/e* 283.

Anal. Calcd. for $C_{11}H_{13}N_3O_6$: C, 46.64; H, 4.63; N, 14.84. Found: C, 46.43; H, 4.60; N, 15.07.

Methyl 3-[N-2,4-dinitrophenyl-N-methylamino]propionate (methyl ester of *N*-dinitrophenyl-*N*-methyl-β-alanine) m.p. 103°; mass spectrum, molecular ion *m/e* 283, n.m.r. spectrum, *N*-methyl, singlet 3.03 p.p.m.

Anal. Calcd. for $C_{11}H_{13}N_3O_6$: C, 46.64; H, 4.63; N, 14.84. Found: C, 46.77; H, 4.71; N, 15.04.

Methyl 4-[N-2,4-dinitrophenyl-N-methylamino]butyrate (methyl ester of *N*-dinitrophenyl-*N*-methyl-γ-aminobutyric acid) oily, mass spectrum, molecular ion *m/e* 297.

Administration of Labelled Compounds to Lobelia cardinalis

Plants of *Lobelia cardinalis* L. were obtained from Sheridan's Nursery, Port Credit, Ontario. Plants in full bloom were used in all feeding experiments. The labelled compound was dissolved in distilled water (10 ml), and equal portions of the solution were administered to individual plants by aspiration into the stem through a cotton wick. In most experiments the plants were kept in contact with tracer for 3 days. The labelled compounds which were administered to the plants in separate experiments are listed in Table 1.

The sample of doubly labelled phenylalanine (expt. 3) was prepared by mixing [2-^{14}C]-DL-phenylalanine (Nuclear Research Chemicals Inc., 9.3 mg, total activity $(4.75 \pm 0.17) \times 10^7$ c.p.m., specific activity $(0.84 \pm 0.03) \times 10^9$ c.p.m. mmol^{-1}) and [3-^{14}C]-DL-phenylalanine (New England Nuclear, 3.7 mg, total activity $(6.07 \pm 0.22) \times 10^7$ c.p.m., specific activity $(2.71 \pm 0.10) \times 10^9$ c.p.m. mmol^{-1}). This gave intermolecularly labelled [2,3-$^{14}C_2$]-DL-phenylalanine (13.0 mg, total activity $(10.82 \pm 0.28) \times 10^7$ c.p.m., specific activity $(13.73 \pm 0.34) \times 10^8$ c.p.m. mmol^{-1}), with a specific activity at C-2 of $(6.03 \pm 0.22) \times 10^8$ c.p.m. mmol^{-1} ($43.9 \pm 1.9\%$) and a specific activity at C-3 of $(7.70 \pm 0.27) \times 10^8$ c.p.m. mmol^{-1} ($56.1 \pm 2.4\%$).

The sample of doubly labelled lysine (expt. 10) was prepared by mixing [2-^{14}C]-DL-lysine (Tracerlab, 14.5 mg, nominal total activity 0.1 mCi) and [6-^{3}H]-DL-lysine (New England Nuclear, 0.021 mg, nominal total activity 0.8 mCi. The ^{3}H/^{14}C ratio of the sample (Table 5) was determined by liquid scintillation counting.

The sample of [6-^{14}C]-α-phenacylpiperidine (expt. 11) was prepared from [6-^{14}C]-DL-lysine (Commissariat à l'Énergie Atomique, France) by the method described in an earlier paper (12).

Isolation of Labelled Lobinaline and Pipecolic acid from L. cardinalis

Labelled lobinaline was isolated from the dried stems and leaves of the plants used in each of the 11 tracer experiments. Chemical and radiochemical yields are summarized in Table 1.

Radioactive pipecolic acid was isolated by carrier dilution from plants of *L. cardinalis* to which 6-^{3}H,2-^{14}C-DL-lysine had been administered. The dried plant material was first extracted with ether to isolate lobinaline (see above), and was then further extracted with methanol (12 h). Solvent was evaporated, and unlabelled pipecolic acid (250 mg) was added to the residue which was then extracted with water (5 × 5 ml). Pipecolic acid was then re-isolated by a method described in an earlier publication (19).

Determination of Radioactivity

Radioactivity was assayed, on samples of finite thickness on aluminum planchettes, with a gas-flow system (Model 4342, Nuclear Chicago). The usual corrections for background and self-absorption were applied. The counting efficiency for ^{14}C was approximately 30%. For plating, a 1% solution of collodion in dimethylformamide was used as the solvent. In the cases of benzoic and *p*-nitrobenzoic acid, a drop of a 5% solution of sodium hydroxide in 50% aqueous methanol was added to prevent loss by evaporation.

The ^{3}H/^{14}C ratios were measured by liquid scintillation counting (Mark I liquid scintillation computer, Model 6860, Nuclear Chicago). Activity due to ^{3}H and ^{14}C was determined simultaneously, by external standardization counting with ^{133}Ba. Samples were dissolved in methanol or methanol–water and the solution was dispersed in a solution of Liquifluor (Nuclear Chicago) diluted 25 times with toluene. Duplicate samples of each compound were counted under comparable conditions of quenching. For highly quenched samples the confidence limits of the quench correction curves were ±5%.

Confidence limits shown in the Tables are standard deviation of the mean.

We are greatly indebted to Dr. M. M. Robison, CIBA Pharmaceutical Company, Summit, New Jersey, for a most generous sample of lobinaline. This investigation was supported by a grant from the National Research Council of Canada.

1. R. N. GUPTA and I. D. SPENSER. Chem. Commun. 893 (1966).
2. R. H. F. MANSKE. Can. J. Res. **16** B, 445 (1938).
3. M. M. ROBISON, W. G. PIERSON, L. DORFMAN, B. F. LAMBERT, and R. A. LUCAS. Tetrahedron Lett. 1513 (1964); J. Org. Chem. **31**, 3206 (1966).
4. M. M. ROBISON, B. F. LAMBERT, L. DORFMAN, and W. G. PIERSON. J. Org. Chem. **31**, 3220 (1966).
5. D. M. CLUGSTON, D. B. MACLEAN, and R. H. F. MANSKE. Can. J. Chem. **45**, 39 (1967).
6. H. WIELAND, W. KOSCHARA, E. DANE, J. RENZ, W. SCHWARZE, and W. LINDE. Ann. Chem. **540**, 103 (1939); C. SCHÖPF and T. KAUFFMANN. Ann. Chem. **608**, 88 (1957).
7. R. ROBINSON. The Structural Relations of Natural Products. Clarendon Press, Oxford, 1955. p. 67.
8. R. N. GUPTA and I. D. SPENSER. Can. J. Chem. **45**, 1275 (1967).
9. R. N. GUPTA and I. D. SPENSER. Phytochem. **9**, 2329 (1970).
10. J. R. GEAR and I. D. SPENSER. Nature, **191**, 1393 (1961).
11. A. R. BATTERSBY, P. BOHLER, M. H. G. MUNRO, and R. RAMAGE. Chem. Commun. 1066 (1969).
12. R. N. GUPTA and I. D. SPENSER. Can. J. Chem. **47**, 445 (1969).
13. A. I. VOGEL. A Textbook of Practical Organic Chemistry. 3rd Edition. Longmans, Green & Co., Ltd., London, 1956. p. 919.
14. J. MCKENNA and A. TULLEY. J. Chem. Soc. 945 (1960).
15. D. WALZ, A. R. FAHMY, G. PATAKI, A. NIEDERWIESER, and M. BRENNER. Exper. **19**, 213 (1963); G. PATAKI. Techniques of Thin-Layer Chromatography in Amino Acid and Peptide Chemistry. Revised edition. Ann Arbor Science Publishers Inc., Ann Arbor, Mich., 1968. p. 133.
16. K. R. RAO and H. A. SOBER. J. Amer. Chem. Soc. **76**, 1328 (1954).
17. S. M. MCELVAIN and J. F. VOZZA. J. Amer. Chem. Soc. **71**, 897 (1949).
18. C. M. FLETCHER, A. G. LOWTHER, and W. S. REITH. Biochem. J. **56**, 106 (1954).
19. R. N. GUPTA and I. D. SPENSER. J. Biol. Chem. **244**, 88 (1969).

Can. J. Chem. Downloaded from www.nrcresearchpress.com by 210.87.254.5 on 09/05/12
For personal use only.

Can. J. Chem. Downloaded from www.nrcresearchpress.com by 210.87.254.42 on 09/05/12
For personal use only.

Polarographic Observations of some Iron Organometallic Compounds in Acetonitrile

J. H. BRECKENRIDGE,[1] H. W. VANDENBORN, AND W. E. HARRIS
Department of Chemistry, University of Alberta, Edmonton, Alberta

Received[2] August 29, 1969

Polarography in acetonitrile is useful for the study of the electrochemical behavior of organometallic compounds because acetonitrile is a suitable solvent for this class of compounds and provides a wide potential range over which their electrochemical behavior can be investigated. This inquiry was undertaken to enhance the understanding of the chemistry of these compounds. The polarographic behavior of three related iron compounds was studied and attempts were made to identify the products of the electrochemical reactions.

Canadian Journal of Chemistry, 49, 398 (1971)

Experimental

Reagent-grade acetonitrile was purified by distillation from sodium hydride followed by distillation from phosphorous pentoxide. Tetraethyl ammonium perchlorate was prepared according to ref. 1, recrystallized four times from water, and dried over phosphorous pentoxide.

The purified acetonitrile was stored in a glass container under helium and was metered into a polarographic cell with a Metrohm piston buret through a glass and teflon system. Oxygen was removed from the acetonitrile by bubbling helium previously saturated with acetonitrile through it.

Polarograms were obtained by using a three-electrode system and a Metrohm Polarecord equipped with an infrared (i.r.) compensator. The supporting electrolyte, tetraethyl ammonium perchlorate, was used at a concentration of 0.05 *M*. The reference electrode was a Ag/0.01 *M* $AgNO_3$ electrode in acetonitrile. The reference electrode was isolated from the solution by a small piece of porous glass sealed in glass tubing with silicone rubber cement (G.E. Silicone Seal). The working counter electrode was a platinum wire sealed in glass. The polarographic cells were flat-bottom glass tubes about 7 cm long and 2.8 cm in diameter. The supporting electrolyte and compound were weighed into the cell, then the cell was flushed with helium and a known volume of acetonitrile metered into it.

The same apparatus was also used to control the potential of a mercury-pool electrode for coulometric measurements. The solution was stirred with a magnetic stirrer. The counter working electrode was isolated behind two glass frits. Electrical connection between the working counter electrode and the solution was maintained through acetonitrile saturated with electrolyte (approximately 0.5 *M*). The total corrent passed was determined with the aid of a hydrazine coulometer (2).

Infrared spectra were determined with 1-mm KBr cells and a Perkin–Elmer 337 infrared spectrophotometer. Spectra in the far i.r. were obtained with Nujol mulls, polyethylene cells, and a Beckman IR-11 spectrophotometer.

[1]Present address: Selkirk College, Castlegar, Box 1200, British Columbia.

[2]Revision received September 3, 1970.

Polarographic Results

The polarographic behavior of cyclopentadienecarbonylhydridobis(trichlorosilyl)iron (**1**) in

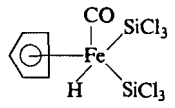

1

acetonitrile was examined. This compound is known (3) to ionize in acetonitrile according to the equation

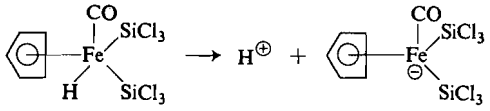

In the polarogram for this compound shown in Fig. 1*A* two waves with half-wave potentials of about −1.5 and −2.4 V are evident. The diffusion current for both these waves is a linear function of concentration. The diffusion current for the first wave decreases as the electrolyte concentration is increased, whereas the diffusion current for the second increases as the concentration is increased. This behavior is consistent with the theory that the first wave is due to the reduction of a positive species and the second, to a negative species.

A graph of potential against log $i/(i_d - i)$ for the first and second waves had slopes of −0.13 and −0.14 V. This suggests that the polarographic reductions at the electrode were not reversible.

Coulometric measurements indicate that the first wave is a one-electron reduction (the experimental value for n was found to be 0.99). Decom-

Can. J. Chem. Downloaded from www.nrcresearchpress.com by 210.87.254.42 on 09/05/12
For personal use only.

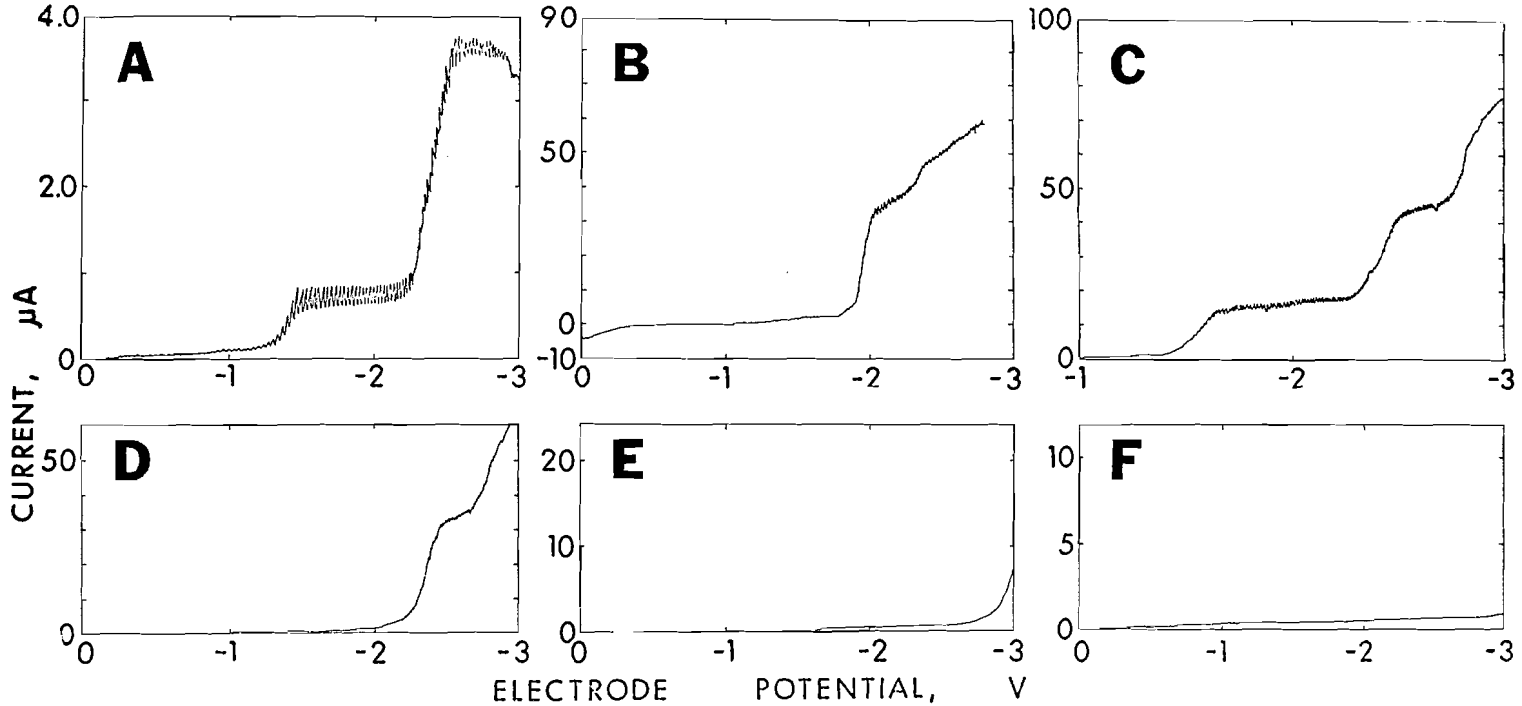

FIG. 1. Polarograms taken in acetonitrile with 0.05 *M* tetraethylammonium perchlorate with a Ag/0.01 *M* $AgNO_3$ reference electrode. *A*, compound **1**; *B*, compound **3**; *C*, compound **3** after ½ h of coulometric reduction at −2.05 V; *D*, compound **3** at end of coulometric reduction at −2.05 V; *E*, compound **3** at end of coulometric reduction at −2.6 V; *F*, background current of acetonitrile with 0.05 *M* Et_4NClO_4.

position occurred during the coulometric reduction at −2.4 V, but relatively large values for the number of electrons were signified from the approximate data obtained. Estimates based on the Ilkovic equation and the diffusion currents at known concentrations indicated a value for n of about 6 or 7 for the second wave.

On the basis of the polarographic and coulometric evidence it seems reasonable to conclude that the first wave results from a reduction of a solvated proton and the second from reduction of the ion

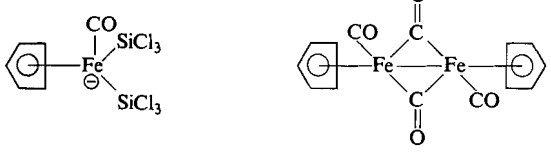

2

Bis(dicarbonylcyclopentadienyliron) (**2**) yielded a single well-defined polarographic wave with a half-wave potential of −1.84 V. The diffusion current was a linear function of concentration and the number of electrons was equal to two. The product of the reduction was not the expected ion

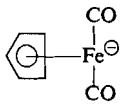

One product, a fine black powder exceedingly high in iron, was presumably iron. The other product was most likely the cyclopentadienyl ion. As demonstrated by Fig. 1*B*, a typical polarogram for cyclopentadienedicarbonyltrichlorosilyliron

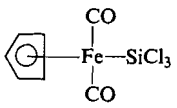

3

(**3**) has two polarographic waves. The first wave has a half-wave potential of −1.93 V. The second, which is poorly defined, has a half-wave potential of about −2.4 V. The magnitude of the second wave is a linear function of concentration, whereas the diffusion current for the first wave becomes less than linear at higher concentrations. Plots of diffusion current against the square root of the height of the mercury column indicated that both waves were diffusion-controlled. For the first wave typical coulometric values for n were 2.2 and for the second about 0.9; these values were reproducible to about 5%. During coulometric runs on the first polarographic wave the reduction current did not decline exponentially, as one would expect, but increased for about the first half hour. This unusual behavior was attributed to the formation and reduction of hydrogen chloride (see below).

Figure 1*C* shows a polarogram taken 30 min after beginning a coulometric reduction at a potential of −2.05 V (the top of the first polarographic wave). Only a small fraction of the original wave at −1.93 V remains, and now a well-defined wave exists at −2.4 V and a completely new wave has appeared at −1.4 V.

The new wave at −1.4 V was found to be due to a volatile chlorine compound that could be removed from the solution by passing helium through it. The condensed gas coming out of the cell (acetonitrile together with the volatile compound) tested positively for chloride. The half-wave potential agrees with that reported for hydrogen chloride (4) and hydrogen chloride can be blown out of an acetonitrile solution (4). From these observations it was concluded that the compound was hydrogen chloride.

Chloride ions yield a well-developed anodic wave in acetonitrile. This wave was used to determine whether or not chloride is released during the electrolysis of **3**. It was found that about two chloride ions (probably one from direct electrochemical reduction and subsequently another by chemical reaction of the reduction product to form hydrogen chloride) are released during coulometric reduction at −2.05 V and an additional chloride is released during the coulometric reduction at −2.4 V. Coulometric reduction at the half-wave potential −1.95 V gave the same results as for reduction at −2.05 V.

Infrared Examination of the Products of Coulometric Reduction

The changes in the infrared spectrum of **3** during its coulometric reduction were obtained by examining the solution at regular intervals. Compound **3** has carbonyl frequencies at 2040 and 1990 cm^{-1} in acetonitrile as solvent. These frequencies are virtually identical to those reported by Jetz and Graham (5) with hexane as solvent. The trichlorosilyl group gives two doublets, at 595 and 586 cm^{-1} and at 520 and

Can. J. Chem. Downloaded from www.nrcresearchpress.com by 210.87.254.42 on 09/05/12
For personal use only.

Can. J. Chem. Downloaded from www.nrcresearchpress.com by 210.87.254.42 on 09/05/12
For personal use only.

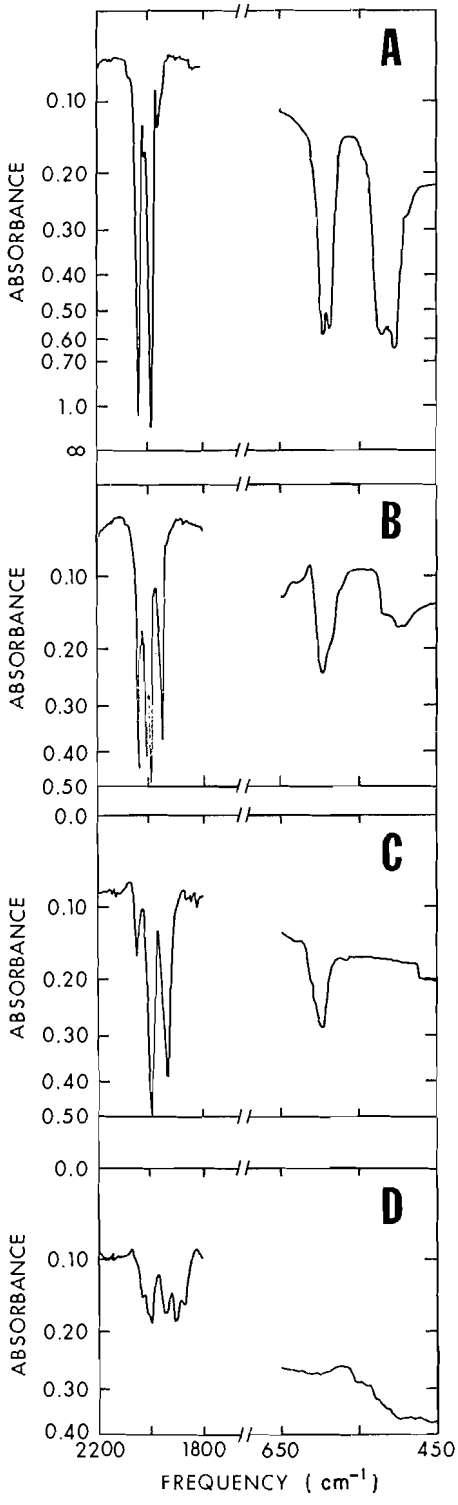

505 cm^{-1} (Fig. 2*A*). After ½ h of coulometry one of the trichlorosilyl doublets became a shoulder on a single new peak at 600 cm^{-1}, and the other became a small broad peak. At the end of the coulometric reduction at −2.05 V only the new peak at 600 cm^{-1} remained (Fig. 2*C*). If the coulometric reduction was continued at a higher voltage, *i.e.*, at −2.6 V, which is in the region of the diffusion current for the second wave, further changes in the spectrum could be observed. The intensity of the carbonyl peaks at 2010 and 1950 cm^{-1} decreased, and the trichlorosilyl peak at 600 cm^{-1} disappeared (Fig. 2*D*).

Compound **3** was also examined spectroscopically in the far infrared region. A peak was observed at 304 cm^{-1}. After coulometric reduction at −2.05 V this peak split into two new peaks at 350 and 280 cm^{-1}. These two peaks disappeared after the coulometric reduction was continued at the higher voltage of −2.6 V. No assignments for these absorption bands are suggested at this time.

The $SiCl_2$ and $SiCl_3$ groups are known (6) to give two peaks, in the regions of 450–530 and 540–600 cm^{-1}. The SiCl group, however, gives only one peak, in the region of 460–660 cm^{-1}. From these infrared and polarographic observations it seems reasonable to conclude that the polarographic wave with half-wave potential at −1.93 V for compound **3** results from the electrochemical removal of a chlorine atom attached to the silicon and the reduction of hydrogen chloride, which is formed by a chemical reaction that removes the second chlorine from the silicon atom. The effect of the loss of the two chlorine atoms is to cause a downward shift in the carbonyl peaks. The single new peak at 600 cm^{-1} suggests that one chlorine atom remains attached to the silicon atom after coulometric reduction at −2.05 V. The disappearance of the peak at 600 cm^{-1} after further reduction at −2.6 V suggests that the polarographic wave with half-wave potential −2.4 V results from the removal of the remaining chlorine atom. Removal of this last chlorine atom probably results in some decomposition of the product because the intensity of the carbonyl peaks decreased. At this stage the

FIG. 2. Infrared spectra of compound **3** taken at intervals during coulometric reduction. *A*, before any reduction; *B*, after ½ h of reduction of −2.05 V; *C*, end of coulometric reduction at −2.05 V; *D*, end of coulometric reduction at −2.6 V.

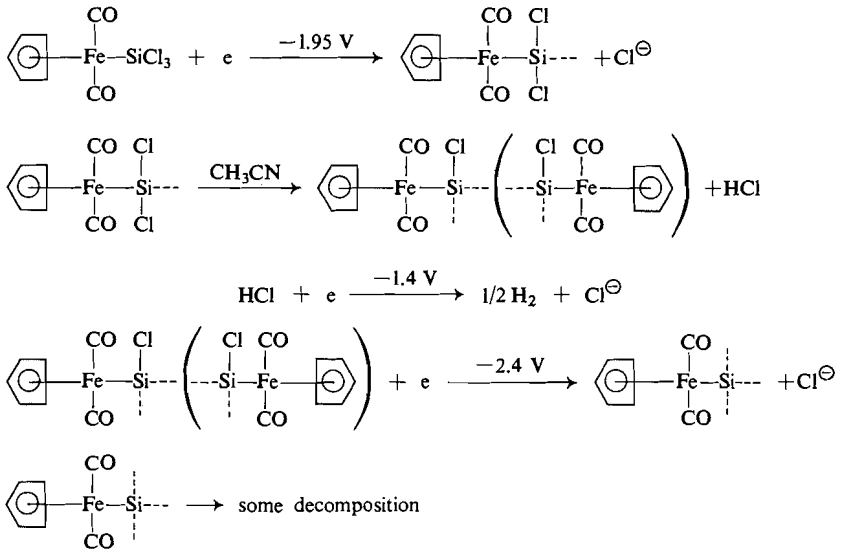

FIG. 3. Possible mechanism and suggested products formed during reduction of compound **3**.

solution was a clear bright orange with no precipitate present.

On the basis of the experimental observations it seems reasonable that in all three of the compounds **1**, **2**, and **3**, each cyclopentadiene and chloride ion can accept one electron during electroreduction. The electroreductions of **1** and **2** seem straightforward; the reduction of **3**, however, is complicated by side reactions because the number of electrons was not a whole number. The source of hydrogen to form hydrogen chloride as a product of the electroreduction of **3** is probably acetonitrile. Traces of water are not involved here because the water content of the acetonitrile was negligibly low. If 1 to 2% of water was added to the acetonitrile, hydrogen chloride was not formed as one of the products of electroreduction at −2.05 V and the number of electrons, *n*, remained at 2. Also in the presence of a small amount of water there was little or slow hydrolysis of the trichlorosilane groups. After coulometric reduction of **3** at −2.6 V, an irreversible polarographic wave at highly negative potentials still remained (Fig. 1*D*). At potentials more negative than −2.6 V coulometric reduction leads to decomposition of the compound, and a fine black suspension was obtained as product.

Figure 3 proposes a possible mechanism for the electroreduction. The overall reaction at −1.95 V is consistent with infrared evidence and the chloride content of the solution after coulometry. It is suggested that the initial product of the reduction may further react to form a new compound with an Si—Si bond. Compound **2** can be ruled out as a possible product of the reduction at −2.4 V because of its incompatible spectral and electrochemical characteristics.

We wish to thank W. Jetz, who synthesized and donated the iron compounds essential to this study.

1. I. M. KOLTHOFF and J. F. COETZEE. J. Amer. Chem. Soc. **79**, 870 (1957).
2. J. J. LINGANE. Electroanalytical Chemistry, 2nd ed. Interscience Publishers Inc., New York. 1958. p. 456.
3. W. JETZ. Private communication.
4. J. F. COETZEE and I. M. KOLTHOFF. J. Amer. Chem. Soc. **79**, 6110 (1957).
5. W. JETZ and W. A. G. GRAHAM. J. Amer. Chem. Soc. **89**, 2773 (1967).
6. N. A. CHUMAEVSKII. Opt. Spect. **10**, 33 (1961).

Can. J. Chem. Downloaded from www.nrcresearchpress.com by 210.87.254.42 on 09/05/12
For personal use only.

Can. J. Chem. Downloaded from www.nrcresearchpress.com by 210.87.254.6 on 09/05/12
For personal use only.

Addition of Iodonium Nitrate to Unsaturated Hydrocarbons

U. E. DINER
Research Council of Alberta,[1] *Edmonton 7, Alberta*

AND

J. W. LOWN
Department of Chemistry, University of Alberta, Edmonton 7, Alberta

Received August 25, 1970

Iodonium nitrate in chloroform–pyridine at room temperature undergoes a *trans* stereospecific electrophilic addition to alkenes to form (*i*) iodoaliphatic nitrate esters, (*ii*) iodoalkane pyridinium nitrates, or (*iii*) alkene pyridinium iodides depending on the substrate. The addition is sensitive to steric hindrance effects and anti-Markovnikov addition is commonly encountered. In similar additions to conjugated dienes 1,2-additions in a Markovnikov fashion to form 1:1 adducts of type (*ii*) are the rule. Terminal acetylenes give alkynyl iodides in fair yield.

Canadian Journal of Chemistry, 49, 403 (1971)

Investigations of the scope and mechanism of addition of pseudo-halogens (iodine isocyanate, iodonium azide, nitrosyl acetates, *N,N*-dichlorourethan) have attracted considerable attention and have proved of synthetic utility in the preparation of aziridines and β-halocarbamates (1–7).

In a preliminary communication we reported the addition of iodonium nitrate (generated *in situ* by the reaction of iodine chloride with silver nitrate in chloroform–pyridine solution) to some monoolefins, a reaction which gave (*i*) iodoaliphatic nitrate esters, (*ii*) iodoalkane pyridinium nitrates, or (*iii*) alkene pyridinium iodides depending on the substrate (8). These reactions extended the range of known pseudo-halogen additions and complemented the recent report by Hassner *et al.* of the reaction of nitryl iodide with alkenes (9).

In a continuation of our investigations we report reactions of iodonium nitrate with (*a*) dienes, conjugated and unconjugated, cyclic and acyclic; (*b*) acetylenic compounds; and we provide further details of the reactions with (*c*) acyclic and cyclic alkenes, terminally and nonterminally unsaturated.

Reactions with Acyclic Terminal Alkenes

Simple alkenes upon reaction with iodonium nitrate gave only products of the type shown in eq. 1. Only in the case of 1-hexene however was

[1] $\text{>C=C<} + (\text{I·2Py})^{+}\text{NO}_3^{-} \xrightarrow[\text{Pyridine}]{\text{CHCl}_3} \text{>C(ONO}_2\text{)—C(I)<}$

the adduct predicted from considerations of carbonium ion stability (*i.e.* corresponding to Markovnikov addition) the sole product in the reaction, when 1-iodo-2-hexanol nitrate was produced in 83% yield. This and similar structures were confirmed by zinc–copper couple reduction, followed by treatment of the resulting iodohydrin with lithium aluminum hydride (procedure A, see eq. 2). The alcohol produced was identical with an authentic sample of 2-hexanol.

[2] 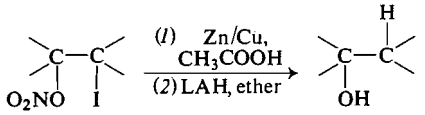

Steric factors appear to play an important role directing the approach of the nitrate ion to the initially formed iodonium ion in the case of 3,4-dimethyl-1-hexene leading to a mixture of 70% Markovnikov and 30% anti-Markovnikov[2] addition (see Table 4). In the assignment of structures to these and similar products in this study by n.m.r. spectroscopy it was observed that methine protons alpha to an ONO_2 group absorb in the range 4.8–5.4 δ, whereas protons alpha to an iodo function absorb in the range 4.0–5.0 δ (10). Fowler *et al.* have shown that methylene protons alpha to an iodo function absorb at 3.0–3.5 δ (11). In our work methylene hydrogens alpha to

[1]Research Council of Alberta Contribution No. 498.

[2]In our previous communication the reported figures were 40% Markovnikov and 60% anti-Markovnikov. That was the ratio observed after distillation of the crude oil. Repetition of the experiment, and careful distillation to avoid loss and decomposition of material produced a mixture with the composition indicated above. The influence of the methyl groups is still apparent with the formation of 30% of the product derived from steric effects.

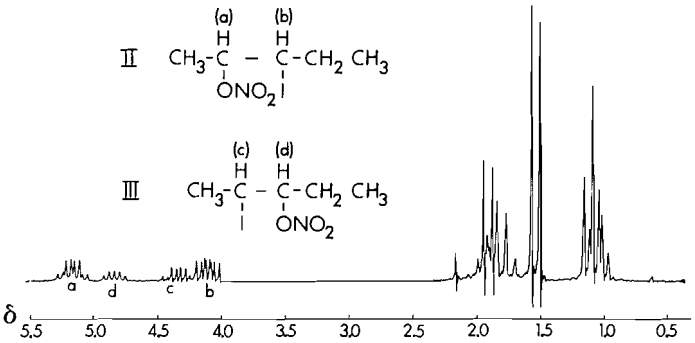

FIG. 1. The n.m.r. spectrum of 3-iodo-2-pentanol (II) and 2-iodo-3-pentanol (III) nitrates (isomeric mixture in $CDCl_3$ (100 MHz).

an iodo group absorbed close to 3.5 δ. For example, the n.m.r. spectrum of 1-iodo-2-hexanol nitrate showed δ ($CDCl_3$): 0.7–1.2 (m, 9H, CH_3, 3(CH_2)), 3.35 (d, 2H, CH_2I), and 4.9 (m, 1H, $CHONO_2$).

In the case of 3,3-dimethyl-1-butene steric hindrance by the *tert*-butyl group to the approach of the nitrate ion is the overriding factor and the ester with the nitrate group at the primary position **1** is the only product obtained as clearly demonstrated by the n.m.r. spectrum. Procedure A produced pure 3,3-dimethylbutan-1-ol as shown by the n.m.r. spectrum and comparison of its g.l.c. retention time with that of an authentic sample.

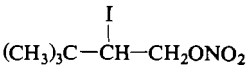

1

Reactions with Acyclic Non-terminal Alkenes

cis-2-Pentene afforded a mixture of 3-iodo-2-pentanol and 2-iodo-3-pentanol nitrates in a 70:30 ratio as shown by the n.m.r. spectrum (Fig. 1) corresponding to a preferential attack by the nitrate ion at the less hindered carbon of the iodonium ion intermediate. The assignments in the n.m.r. spectrum made on the basis of the empirical chemical shift observations mentioned above are shown in Fig. 1. The structural assignments were confirmed by hydrogenolysis of the isomeric iodopentanol nitrates by (*a*) zinc–copper in acetic acid or (*b*) electrolytic reduction in a buffer at p*H* 4.7 at −0.9 V *vs.* saturated calomel electrode at a mercury cathode. Reduction of the iodohydrins with lithium aluminum hydride produced a mixture of the corresponding 2-pentanol and 3-pentanol, the composition of which (70:30) was determined by g.l.c. by comparison with mixtures of authentic 2-pentanol and 3-pentanol.

When iodonium nitrate in chloroform–pyridine was added to more highly substituted olefins, in addition to the expected iodonitrate ester, the formation of iodopyridinium salts was observed. 2-Methyl-2-butene gave *N*-[2-(2-methyl-3-iodo) butyl]pyridinium nitrate (**2**) in 75% yield and 2,3-dimethyl-2-butene gave the analogous iodopyridinium nitrate **3** in 47% yield. As can be seen in Table 5 the chemical shift of methyl groups α to the pyridinium and iodine groups is very similar.

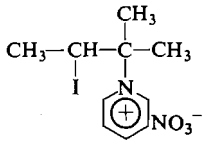

2

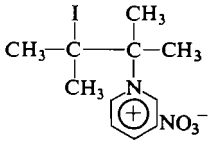

3

In the case of **3** for example, the starting olefin presented a sharp signal in the n.m.r. spectrum at δ 1.6. The iodo pyridinium nitrate (**3**) on the other hand showed two sharp signals at δ 2.08 and 2.05.

The analogous addition of bromonium nitrate to 2-methyl-2-butene gave as the major product the bromonitrate ester **4** together with only a small yield of the corresponding bromopyridinium nitrate **5**.[3] With ethyl vinyl ether, another example in which the carbonium ion involved is considerably stabilized, the pyridine competes successfully (12) with the nitrate ion for the

[3]It may be noted that when I is replaced by Br, the chemical shift of the α methyl group moves upfield about 0.3 p.p.m. *N*-[2-(2-Methyl-3-bromo)butyl]pyridinium nitrate, prepared with bromonium nitrate in a similar way, showed in the n.m.r. δ [$(CD_3)SO$]: 1.6 (d, 3H, J = 7 Hz, CH_3—C—Br); 1.82(s, 6H, $(CH_3)_2$—C—N^+); and 4.9 (q, 1H, J = 7 Hz, CH—Br). The separation between the two sets of methyl groups was now very clear, the methyl group α to the bromine atom being 0.22 p.p.m. upfield from the —CH_3 groups α to the pyridinium group.

Can. J. Chem. Downloaded from www.nrcresearchpress.com by 210.87.254.6 on 09/05/12
For personal use only.

Can. J. Chem. Downloaded from www.nrcresearchpress.com by 210.87.254.6 on 09/05/12
For personal use only.

iodonium ion giving *N*-[1-(1-ethoxy-2-iodo)ethyl]pyridinium nitrate as the exclusive product.

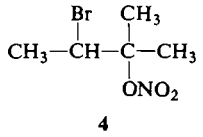

4

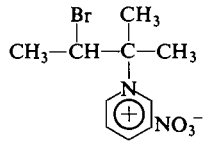

5

Reactions with Cyclic Monounsaturated Compounds

Addition of iodonium nitrate to cyclic olefins allows an examination of the stereochemistry of the reaction. Cyclohexene gave two products the first of which, the iodoalkane nitrate obtained in 50–60% yield showed in the n.m.r. the following significant absorptions, 4.17 (m, 8 lines, 1H, C*H*—I, $J_{1,2} = 10$, $J_{2,3a} = 9$, $J_{2,3e} = 5$ Hz); 5.15 (m, 8 lines, 1H, *C*HONO$_2$, $J_{1,2} = 10$, $J_{1,6a} = 9$, $J_{1,6e} = 5$ Hz) which demonstrates a *trans* stereospecific addition leading to a *trans* diequatorial conformation **6**. Closely related electrophilic additions to alkenes have been demonstrated to be *trans* stereospecific (11, 13). This conformation

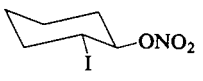

6

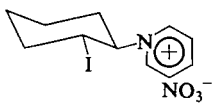

7

was insensitive to changes in solvent polarity ($CDCl_3$, CCl_4, C_6H_6, CD_3CN) (14). In this reaction the corresponding iodo pyridinium salt **7** was obtained in 40% yield. The n.m.r. spectrum showed δ [$(CD_3)_2SO$]: 4.9 (m, 2H, C*H*I and C*H*—N^+), 2.5 (m, 4H, —CH_2—CHI and CH_2—CH—N^+), and 2.1 (m, 4H, 2(CH_2)). The signals corresponding to the pyridinium ring appeared at δ 8.35, 8.8, and 9.35 as three multiplets integrating in the ratio of 2:1:2.

Similarly cyclopentene reacted with iodonium nitrate to give 2-iodo-cyclopentanol nitrate in 54% yield and *N*-(2-iodocyclopentyl)pyridinium nitrate in 43% yield.

Norbornene gave the expected iodonitrate ester **8** in approximately 60% yield. However no iodopyridinium salt was produced. Instead, the nortricyclanyl iodide **9** was formed in 40% yield together with a corresponding amount of the pyridinium nitrate (see eq. 3). Even after several distillations **8** and **9** could not be obtained analytically pure. However the n.m.r. and mass spectra were consistent with the structures proposed. Reduction of **8** by procedure A afforded norborneol consisting of 90% of the *endo* isomer and 10% of the *exo* isomer, the n.m.r. spectrum and g.l.c. retention times of which corresponded to those of authentic samples.

[3] 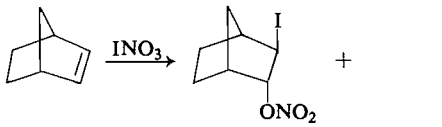

8

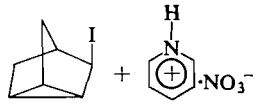

9

The n.m.r. of **9** was consistent with the structure proposed; δ ($CDCl_3$): 3.8 (s, 1H, *C*HI); 2 (m, 2H, 2—*CH*); and 1.4 (m, 6H, 2(CH_2), 2—*CH*). It compared well with the n.m.r. of authentic nortricyclanyl-bromide.

Reaction with 2,3-dihydropyran produced *trans*-equatorial *N*-(3-iodo-tetrahydropyranosyl) pyridinium nitrate (**10**), the n.m.r. spectrum of which (anomeric proton) δ in $(CD_3)_2SO$, 6.38 (d, 1H, $J_{1,2} = 10$Hz) closely resembles that of similar substances reported by Lemieux and Morgan (15). In contrast to the case of cyclohexene

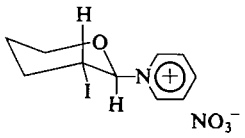

10

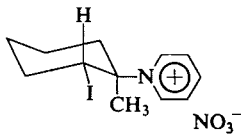

11

the corresponding iodonitrate ester could not be isolated, in keeping with the finding that compounds which give rise to very stable carbonium ion intermediates react preferentially to give the iodopyridinium nitrate salts. This is demonstrated by contrasting the reaction of cyclohexene (*vide supra*) with that of 1-methylcyclohexene in which the only isolable product was the *N*-[1-(1-methyl-2-iodocyclohexyl)]pyridinium nitrate (**11**) in 25% yield. The fact that the pyridinium group becomes attached to the more highly substituted carbon on an olefinic bond was established by an X-ray crystallographic study of *N*-[2-(2-methyl-3-iodobutyl)]pyridinium nitrate (**2**) formed from 2-methyl-2-butene which showed

Can. J. Chem. Downloaded from www.nrcresearchpress.com by 210.87.254.6 on 09/05/12
For personal use only.

the pyridinium ring attached to the tertiary carbon (16). A complete report on the structure determination will be published elsewhere.

Reactions with Unconjugated Dienes

In all cases upon reaction of an unconjugated diene with 1 equiv of iodonium nitrate only one double bond reacted, giving the iodoalkene nitrate ester and/or the iodoalkene pyridinium nitrate depending on the degree of substitution in the substrate. For example 1,5-hexadiene gave a 1:1 adduct with the characteristic n.m.r. absorption for the $-CH_2I$ and $CHONO_2$ groups: 2.0 (m, 4H, 2(CH_2), 3.35 (d, 2H, CH_2I), 5.15 (m, 3H, $=CH_2$ and $CHONO_2$), and 5.6 (m, 1H, =CH). Accordingly structure **12** was assigned to

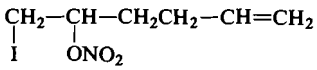

12

this product, corresponding to Markovnikov addition. 1,4-Cyclohexadiene behaved in a similar way to other unconjugated alkenes and gave 5-iodocyclohexene-4-ol nitrate **13** in 27% yield and *N*-[4-(5-iodocyclohexenyl)]pyridinium nitrate **14** in 24% yield. Reaction of 4-vinylcyclohexene

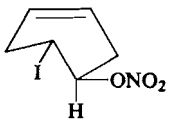

13

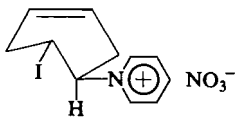

14

with iodonium nitrate allows an examination of competition in the electrophilic addition to acyclic and cyclic alkenes within the same model. The products proved to be the iodonitrate ester **15** in 25% yield and the iodopyridinium salt **16** in 27% yield corresponding exclusively to addition in the ring. The alternative structure for **15** in which addition takes place to the vinyl group may be immediately excluded because of the absence in 3.5–3.0 δ region of the n.m.r. spectrum of a signal characteristic of $-CH_2I$. The comparable alternative structure for **16** may also be excluded because in no case in additions to a monosubstituted alkene has a pyridinium compound been observed in significant amounts (see above).[4] It should be noted that the positions of the iodine and nitrate groups in **15** and the iodine and pyridinium groups in **16** on the 1–2 cyclohexane bond cannot be assigned unambiguously. The marked preference for electrophilic additions in this case to the cyclic olefinic bond may be ascribed to the greater stability of the resulting iodonium ion.

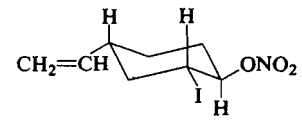

15

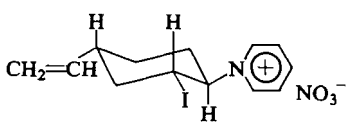

16

Reaction of norbornadiene with iodonium nitrate produced two products corresponding to cross-ring interaction, *i.e.* tricyclo [2.2.1.$0^{2,6}$]-3-iodoheptan-5-ol nitrate **17** (in 64% yield after distillation) and the corresponding iodopyridinium salt **18**, *N*-[3-(5-iodonortricyclanyl)]pyridinium

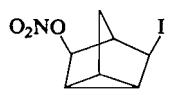

17

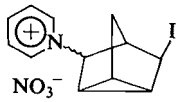

18

nitrate in 10% yield. The n.m.r. spectrum of **17** showed no olefinic protons and was consistent with a tricyclane structure. The structure of **17** was confirmed by reduction with zinc–copper couple in acetic acid at room temperature followed by reduction with zinc dust in acetic acid to nortricyclanol as verified by comparison with an authentic sample (17). It may be noted that reduction could not be effected using procedure A in this particular example. Examination of the n.m.r. spectrum of **18** showed it to consist of a mixture of two isomers **18***a* and *b*, the former

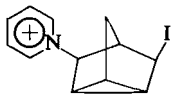

18*a*

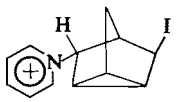

18*b*

having the same configuration as that of the major product **17**. The above reaction resembles the addition of iodine isocyanate to 5-methylenenorbornene reported by Hassner and coworkers (18) and also resembles products obtained by Grimwood and Swern (19).

[4]In the case of 3,4-dimethylhex-1-ene and 3,3-dimethylbut-1-ene a very small amount of pyridinium salts was observed and isolated. This will be discussed in a subsequent publication.

Can. J. Chem. Downloaded from www.nrcresearchpress.com by 210.87.254.6 on 09/05/12
For personal use only.

Reactions with Conjugated Dienes

In all the examples studied of addition to conjugated dienes only the iodopyridinium salts were obtained and they corresponded exclusively to 1,2-addition of one equivalent of iodonium nitrate. In these cases the carbonium ion involved is allylic and the sole formation of the pyridinium salt is consistent with the observation that this is the major type of product obtained when a stable carbonium ion is involved as observed in the case of monoolefins discussed above.

2,4-Hexadiene produced a 70% yield of *N*-[4-(5-iodo-2-hexenyl)]pyridinium nitrate (**19**). The

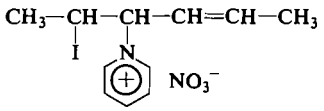

19

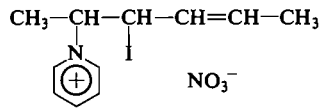

20

possibility of a 1,4-addition was discounted since the n.m.r. spectrum showed two well-separated doublets at δ 2.0 and 1.75 with $J = 7$ and 5 Hz respectively, corresponding to two methyl groups in quite different environments, whereas other model compounds show that methyl groups alpha to an iodo group have similar chemical shifts to methyl groups alpha to a pyridinium group.

The n.m.r. spectrum is consistent with either the Markovnikov structure **19** or the anti-Markovnikov structure **20**. However structure **19** is preferred from mechanistic considerations since the pyridine would be expected to attack the more stable allylic cationic center.

2,3-Dimethyl-1,3-butadiene afforded *N*-[3-(4-iodo-2,3-dimethyl)butenyl]pyridinium nitrate **21** in 62% yield. The n.m.r. spectrum of the product

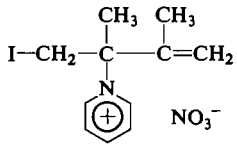

21

was again consistent with a 1,2-addition because it showed an AB quartet characteristic of the terminal vinylic protons centered at 5.28 and 5.41 δ. The former is assigned to the proton *cisoid* to the methyl group because of further long range coupling to the methyl group (20).

Styrene falls naturally in this group and gave two products, *N*-[1-(1-phenylethenyl)]-pyridinium iodide (**22**) as the major product in 75–80% yield together with 10% of the iodonitrate ester **23**. Compound **23** could not be isolated analytically

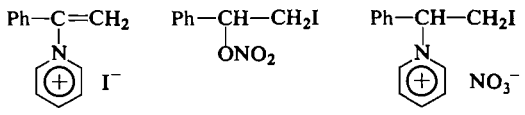

22 **23** **24**

pure, because it suffers extensive decomposition when distilled. However n.m.r. and mass spectrometry evidence was consistent with the assigned structure. Treatment of **23** with an excess of pyridine at room temperature afforded **22** in good yield, presumably by way of pyridine-catalyzed elimination of hydrogen iodide from the intermediate **24**. This suggests but does not prove that the pyridinium salts like **22** described in this study are formed by nucleophilic displacement of the nitrate ion by pyridine from the corresponding initially formed iodo-nitrate esters.

Isoprene also gave an iodopyridinium salt **25** as the only isolable product in 30% yield. In this particular reaction a considerable amount of tars were produced and the salt obtained was difficult to crystallize.

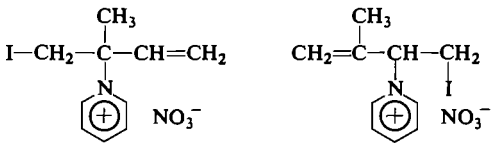

25*a* **25*b***

The n.m.r. spectrum, Fig. 2, showed an ABB′ system for the vinylic protons clearly demonstrating the marked preference for 1,2-addition. The n.m.r. spectrum similarly confirms **25*a*** and eliminates **25*b*** for this sample. In only one instance was this pure isomer obtained. Further runs produced a mixture of **25*a*** and *b* in the ratio of 70:30. The n.m.r. spectrum of **25*b*** was similar to that of **25*a*** except for an ICH_2 absorption at δ 4.42 and a CH_3 absorption at δ 2.07.

Similarly 1,3-cyclohexadiene gave the pyridinium salt **26** in 60% yield. The reasons for the marked preference for 1,2-additions in the case of conjugated dienes are not clear at this time.

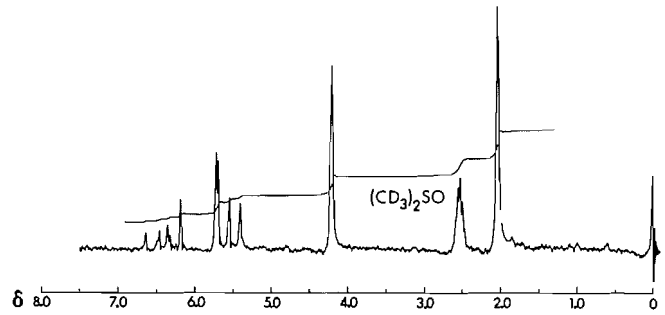

FIG. 2. The n.m.r. spectrum of **25***a* in $(CD_3)_2SO$ (60 MHz).

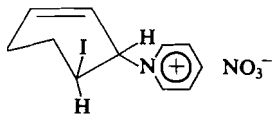

26

Reactions with Acetylenic Compounds

As expected, non-terminal acetylenes were unreactive towards electrophilic addition of iodonium nitrate. However terminal acetylenes reacted readily to give alkynyl iodides according to eq. 4.

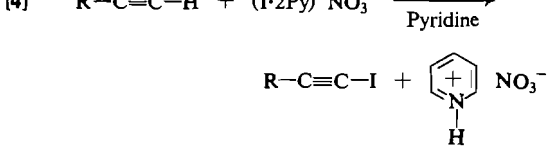

[4] $R-C\equiv C-H + (I\cdot 2Py)^+NO_3^- \xrightarrow[\text{Pyridine}]{CHCl_3} R-C\equiv C-I +$ pyridinium NO_3^-

Pyridinium nitrate was obtained in stoichiometric quantity indicating complete replacement of the acidic proton of the acetylene. Some tar formation took place with a consequent decrease in yield of product. The structures of the iodoacetylenes were fully consistent with the analytical and spectral data. The chemistry of this class of compounds has recently been reviewed (21). The terminal iodo compounds produced in this way are summarized in Table 1.

Experimental

Melting points were determined on a Fisher–Johns apparatus and are uncorrected. The i.r. spectra were recorded on a Perkin–Elmer model 221 spectrophotometer. The n.m.r spectra were recorded on Varian A-60 and A-100 analytical spectrometers. The spectra were measured on approximately 10–15% (w/v) solutions in $CDCl_3$ or $(CD_3)_2SO$ with tetramethylsilane as a standard. Line positions are reported in p.p.m. from the reference. Mass spectra were obtained with a Perkin–Elmer model 270 gas chromatograph–mass spectrometer. The ionization energy, in general, was 70 eV.

The g.l.c. analyses were performed with an F and M model 700 gas chromatograph; various columns packed with polar and non-polar liquid phases were used to check the chromatograms obtained.

General Procedure for the Reaction of Iodonium Nitrate with Unsaturated Hydrocarbons

Silver nitrate, 6.8 g, (0.04 mol) was dissolved in a mixture of 30 ml of chloroform and 15 ml of reagent grade pyridine. Iodine monochloride, 6.5 g (0.04 mol), in 15 ml of chloroform, was added dropwise to the stirred solution. The silver chloride produced was filtered off and washed with 10 ml of pyridine, and 0.04 mol of the olefin added at once to the yellow filtrate. The mixture was stirred at room temperature for 3 h. Then ether was added to the solution, the oily precipitate (if any), collected, and the ethereal solution evaporated in a rotary evaporator. The oil obtained after evaporation was distilled, the product obtained being the iodo-nitrate ester.

The precipitate which was insoluble in ether was washed several times with ether, whereupon it became a solid. The following procedure (B) was found satisfactory

TABLE 1. Iodoacetylene compounds

	Alkynyl iodide			
1-Alkyne	Yield (%)	Boiling point (°C/mm)	Molecular ion	Reference
1-Octyne	40*	58/0.7	236	22
Phenylacetylene	60	73/0.7	228	23
Methylacetylene	45	100/700†	166	22, 24

*Anal. Calcd. for $C_8H_{13}I$: C, 40.70; H, 5.55. Found: C, 41.10; H, 5.54. Literature b.p. 95–97° at 7.5 mm.
†Literature b.p. 110° at 760 mm.

Can. J. Chem. Downloaded from www.nrcresearchpress.com by 210.87.254.6 on 09/05/12
For personal use only.

Can. J. Chem. Downloaded from www.nrcresearchpress.com by 210.87.254.6 on 09/05/12
For personal use only.

for these compounds. This solid was dissolved in a beaker in a small amount of a 50:50 mixture of ethanol – isopropyl alcohol. Ether was added until the solution became slightly cloudy. This beaker was then placed inside a bigger one, containing a small amount of ether. This bigger beaker was covered with Saran wrap, sealed with an elastic band wrapped around, and finally put in the refrigerator. The crystals obtained, (iodo pyridinium salt) were filtered off, washed with ether, and dried. In a few instances, when the iodo pyridinium salt was difficult to purify and very dark in color (contamination with iodine and tarry materials), the purification was carried out by chromatography on silica gel, eluting with $CHCl_3$, 5% CH_3OH in $CHCl_3$ (v/v), 10% CH_3OH in $CHCl_3$ (v/v), and 30% CH_3OH in $CHCl_3$ (v/v), the iodo pyridinium salt being collected with the last mixture of solvents.

The analytical and spectral data for the iodoaliphatic nitrate esters, and iodoalkane pyridinium nitrate salts thus obtained are summarized in Tables 2–5.

Formation of the Iodo Alkynes

The procedure was similar to that explained above. Addition of ether to the reaction mixture resulted in the precipitation of an equivalent amount of pyridinium nitrate that was filtered off. The remaining liquid was evaporated in the rotary evaporator and the residual oil distilled.

General Procedure for the Electrolytic Reduction of the Iodo-nitrate Esters

The iodo-nitrate ester (0.02 mol) was dissolved in 75 ml of acetate buffer, p*H* 4.7, and 175 ml of isopropyl alcohol. This solution was electrolyzed at −0.9 V *vs.* saturated calomel electrode over a period of 16 h, after which time there was no more material reducible at −0.9 V.

Then the solution was poured into water, extracted with ether, the ether extract washed with dilute sodium bicarbonate solution, dried ($MgSO_4$), and evaporated. The residual oil was distilled and the collected iodohydrin, without further purification, reduced with lithium aluminum hydride.

General Procedure for the Zinc–Copper Couple Reductions

The iodo-nitrate ester (6 mmol) was added dropwise to a stirred mixture of 1.5 g of zinc–copper couple (Alfa Inorganics) in 25 ml of acetic acid at room temperature,[5] and left stirring overnight. Then, the solid was filtered off, the liquid poured into a mixture of ether–water and solid sodium bicarbonate added in portions until the solution was completely neutralized. The ether layer was removed, the aqueous layer extracted with more ether, the two ethereal portions combined, then dried ($MgSO_4$) and evaporated. The resulting liquid (about 90% pure by g.l.c.) showed no covalent nitrate absorption in the i.r. spectrum but the presence of the OH group. Without further purification it was then reduced with excess lithium aluminum hydride and the resulting alcohols identified by comparison of their retention times and i.r. and n.m.r. spectra with those of authentic samples.

Reduction of the Tricyclo [2.2.1.$0^{2,6}$]-3-iodopentan-5-ol with Zinc Dust in Acetic Acid – Ether

The iodo alcohol (1.7 g) was dissolved in 10 ml of ether and 10 ml of acetic acid. Zinc dust (1 g) was added and the reaction mixture refluxed overnight, allowed to cool, filtered, and poured into a mixture of ether–water. Solid sodium bicarbonate was added in portions until the solution was completely neutralized. The ether layer was washed with water saturated with sodium chloride, dried, and evaporated. The residual oil (0.84 g) proved it to be a mixture of 90% of nortricyclanol and 10% nortricyclyl acetate by g.l.c. (17). This mixture was then dissolved in methanol containing a small amount of sodium methoxide, refluxed for 5 h, and the solvent evaporated. The residue was taken up with petroleum ether (b.p. 40–60°), the petroleum ether washed with water, dried ($MgSO_4$), and evaporated. Pure nortricyclanol (0.4 g, 50% yield) was obtained, identical with an authentic sample.

Preparation of the N-[2-(2-Methyl-3-bromo)butyl)]-pyridinium Nitrate ***5*** *and the Corresponding Bromo-nitrate Ester* ***4***

The procedure and molar quantities was similar to that used for the preparation of the iodo pyridinium salts, except that bromine was used instead of iodine chloride. After the addition of ether to the reaction mixture, no oily precipitate was observed. The organic liquid was then concentrated in a rotary evaporator and 7 g of a brown oil was obtained that separated into two layers. These two phases were separated, and the upper layer (5.3 g) was placed in the refrigerator for 3 days. A few crystals formed, which were filtered off and the residual liquid distilled. Three grams of product **4** were obtained (35% yield), b.p. 30 °C at 0.3 mm.

Anal. Calcd. for $C_5H_{10}NO_3Br$: C, 28.32; H, 4.75; N, 6.60. Found: C, 28.43; H, 4.93; N, 6.47.

The n.m.r. of **8** showed δ ($CDCl_3$): 4.7 (q, 1H, *CH*—Br, J = 7 Hz); 1.65—1.77 (s, d, 9H, $3CH_3$).

The second layer produced 120 mg of crystals upon cooling that were combined with the first crop. Recrystallization was performed according to procedure B and 100 mg of **5** were obtained.

Anal. Calcd. for $C_{10}H_{15}N_2O_3Br$: C, 41.25; H, 5.19; N, 9.62. Found: C, 40.83; H, 5.27; N, 9.20.

*Purification of N-[1-(1-Phenylethenyl)]pyridinium Iodide (****22****)*

The crude crystalline product was dark and contaminated with considerable amounts of pyridinium nitrate which were difficult to remove by the recrystallization procedure described above. Therefore 1 g of the crude material was dissolved in H_2O (10 ml) and 0.5 g of solid potassium carbonate added. The aqueous solution was extracted with ether, the ether discarded, and the solution acidified to p*H* = 7 with dilute nitric acid. The aqueous layer was evaporated to dryness *in vacuo* and the residual solid taken up in ethanol. The ethanol solution was concentrated *in vacuo* and 0.42 g of pure **22** obtained, m.p. 155–158°.

Anal. Calcd. for $C_{13}H_{12}NI$: C, 50.50; H, 3.91; N, 4.53. Found: C, 50.10; H, 3.71; N, 4.31.

[5]If the preparation is done on a larger scale, it is advisable to cool the reaction mixture in an ice bath.

Can. J. Chem. Downloaded from www.nrcresearchpress.com by 210.87.254.6 on 09/05/12
For personal use only.

TABLE 2. Iodo-nitrate esters

Alkene	Iodo-nitrate ester	Boiling point (°C/mm)	Yield (%)	Formula	Observed			Calculated			Molecular ion
					C	H	N	C	H	N	
Hex-1-ene	1-Iodohexan-2-ol nitrate	80/0.5	83	$C_6H_{12}NO_3I$	26.35	4.79	4.73	26.39	4.42	5.12	—
cis-Pent-2-ene	3-Iodopentan-2-ol nitrate 2-Iodopentan-3-ol nitrate	45/0.2*	75	$C_5H_{10}NO_3I$	23.38	3.99	5.18	23.18	3.89	5.41	M-ONO_2 197
3,3-Dimethylbut-1-ene	2-Iodo-3,3-dimethylbutanol nitrate	55/0.2	70	$C_6H_{12}NO_3I$	26.37	4.80	4.70	26.39	4.42	5.12	M-ONO_2 211
3,4-Dimethylhex-1-ene	1-Iodo-3,4-dimethylhexane-2-ol nitrate 2-Iodo-3,4-dimethylhexane-1-ol nitrate	93–97/0.5	75	$C_8H_{16}NO_3I$	32.30	5.60	4.37	31.90	5.35	4.65	301
Cyclohexene	2-Iodocyclohexanol nitrate	113/1.3	60	$C_6H_{10}NO_3I$	26.84	3.87	4.98	26.58	3.72	5.16	271
Cyclopentene	2-Iodocyclopentanol nitrate	96/1	54	$C_5H_8NO_3I$	23.54	3.24	5.20	23.36	3.13	5.45	M-I 130
Norbornene†	2-Iodonorborneol nitrate	83/0.3	60	$C_7H_{10}NO_3I$	30.55	3.50	4.33	29.70	3.56	4.95‡	M-I 156
1,5-Hexadiene	6-Iodohex-1-en-5-ol nitrate	62/0.35	85	$C_6H_{10}NO_3I$	26.51	3.34	4.89	26.59	3.72	5.16	271
Norbornadiene	Tricyclo[2.2.1.$0^{2,6}$]-3-iodopentane-5-ol nitrate	75/0.08	64	$C_7H_8NO_3I$	30.05	3.18	5.05	29.92	2.87	4.93	M-ONO_2 219
1,4-Cyclohexadiene	5-Iodocyclohexen-4-ol nitrate	50/0.5	27	$C_6H_8NO_3I$	26.91	3.23	5.22	26.79	3.00	5.20	M-I 142
4-Vinylcyclohex-1-ene	2-(1)-Iodo-4-vinylcyclohexanol nitrate	89/0.4	25	$C_8H_{12}NO_3I$	32.91	4.05	4.20	32.83	3.96	4.71	M-I 170
Styrene	2-Iodo-1-phenylethanol nitrate	110/1	10	—	—	—	—	—	—	—	293

*Isomeric mixture.
†Nortricyclanyl iodide was produced in 40% yield, b.p. 40°/0.15mm. Molecular ion 220. See text.
‡See text.

Can. J. Chem. Downloaded from www.nrcresearchpress.com by 210.87.254.6 on 09/05/12
For personal use only.

TABLE 3. Iodo pyridinium salts

Alkene	Iodo pyridinium salt	Melting point (°C)	Yield (%)	Formula	Observed			Calculated		
					C	H	N	C	H	N
Cyclohexene	*N*-(2-Iodocyclohexyl)pyridinium nitrate	145–150	40	$C_{11}H_{15}N_2O_3I$	37.77	4.80	7.97	37.73	4.32	8.00
Cyclopentene	*N*-(2-Iodocyclopentyl)pyridinium nitrate	Oil	43	$C_{10}H_{13}N_2O_3I$	34.13	3.96	8.94	35.73	3.89	8.33
1-Methylcyclohex-1-ene	*N*-[1-(1-Methyl-2-iodocyclohexyl)]pyridinium nitrate	70	25	$C_{12}H_{17}N_2O_3I$	39.24	4.71	8.27	39.57	4.70	7.69
2,3-Dimethylbut-2-ene	*N*-[2-(2,3-Dimethyl-3-iodobutyl)]pyridinium nitrate	105(dec.)	47	$C_{11}H_{17}N_2O_3I$	37.79	4.50	7.85	37.51	4.86	7.95
2-Methylbut-2-ene	*N*-[2-(2-Methyl-3-iodobutyl)]pyridinium nitrate	121–123	75–80	$C_{10}H_{15}N_2O_3I$	35.38	4.63	8.01	35.50	4.47	8.28
Norbornadiene	*N*-[3-(5-Iodonortricyclanyl)]pyridinium nitrate	118–125(dec.)	10	$C_{12}H_{13}N_2O_3I$	40.31	3.80	8.20	40.02	3.64	7.78
1,4-Cyclohexadiene	*N*-[4-(5-Iodocyclohexenyl)]pyridinium nitrate	156–157(dec.)	24	$C_{11}H_{13}N_2O_3I$	37.80	3.96	7.90	37.95	3.76	8.04
4-Vinylcyclohex-1-ene	*N*-[1(2)-2(1)-Iodo-4-vinylcyclohexyl)]pyridinium nitrate	93–98	26.5	$C_{13}H_{17}N_2O_3I$	41.75	4.70	—	41.50	4.55	7.44
2,4-Hexadiene	*N*-[4-(5-Iodo-2-hexenyl)]pyridinium nitrate	116–117(dec.)	70	$C_{11}H_{15}N_2O_3I$	37.77	4.34	8.13	37.73	4.32	8.00
Isoprene	*N*-[2-(2-Methyl-1-iodobutenyl)pyridinium nitrate	111–116	30	$C_{10}H_{13}N_2O_3I$	35.26	3.97	8.43	35.73	3.90	8.33
1,3-Cyclohexadiene	*N*-[3-(4-Iodocyclohexenyl)]pyridinium nitrate	118	60	$C_{11}H_{13}N_2O_3I$	38.20	3.74	7.80	37.95	3.76	8.04
2,3-Dimethyl-1,3-butadiene	*N*-[3-(4-Iodo-2,3-dimethylbutenyl)pyridinium nitrate	106–108	57	$C_{11}H_{15}N_2O_3I$	37.70	4.03	7.91	37.73	4.32	8.00
Ethyl vinyl ether	*N*-[1-(1-Ethoxy-2-iodo)ethyl]pyridinium nitrate	66–69	75	$C_9H_{13}N_2O_4I$	31.70	3.70	8.50	31.78	3.85	8.23
Dihydropyran	*N*-(3-Iodotetrahydropyranosyl)pyridinium nitrate	113–116	72	$C_{10}H_{13}N_2O_4I$	33.80	3.70	7.81	34.10	3.72	7.95
Styrene	*N*-[1-(1-phenylethenyl]pyridinium iodide	155	40	$C_{13}H_{12}NI$	50.90	4.00	—	50.50	3.91	4.53

TABLE 4. Spectroscopic properties of the iodo-nitrate esters

Compound	δ (CDCl$_3$) I—*CH*<	>*CH*—ONO$_2$	*I*—CH$_2$—	O$_2$N—O—*CH*$_2$—	Olefinic hydrogens	Methine and methylen hydrogens
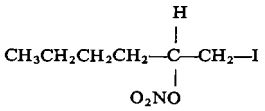	—	4.9 (1H)m	3.35 (2H)d J = 5.5 Hz			1.3 (9H)m
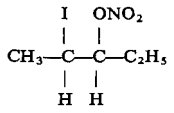	See Fig. 1					
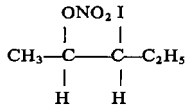						
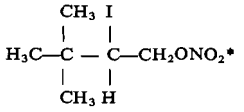	4.17 (1H)t			4.8 (2H)d		
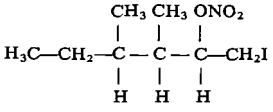	4.8	5.0 (1H)m	3.4 (0.7H)m	4.4 (0.3H)m		2–0.8 (13H)m
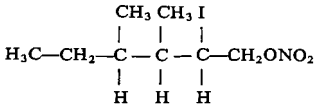						
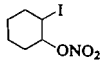	4.17 (1H)m	5.15 (1H)m				1.7 (8H)m
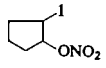	4.2 (1H)m	5.4 (1H)m				2 (6H)m
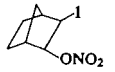	3.75 (1H)m	5.5 (1H)m				2.8–1.3 (8H)m
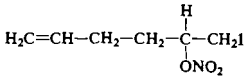		4.9 (1H)m	3.35 (2H)d J = 5.5 Hz		5.6 5.15 (1H)m (2H)m	2 (4H)m
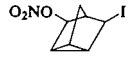	4.25 (1H)m	5.03 (1H)m				2.5 1.75 (1H)m (5H)m
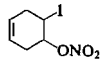	4.38 (1H)m	5.27 (1H)m			5.6 (2H)m	2.7 (4H)m
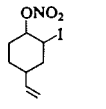	4.5 (1H)m	4.9 (1H)m			5.7 5.15 (1H)m (2H)m	2.0 (7H)m

*The methyl groups present a singlet at δ 1.15.

Can. J. Chem. Downloaded from www.nrcresearchpress.com by 210.87.254.6 on 09/05/12
For personal use only.

Can. J. Chem. Downloaded from www.nrcresearchpress.com by 210.87.254.6 on 09/05/12
For personal use only.

TABLE 5. Spectroscopic properties of iodo pyridinium nitrates

Compounds*	δ ((CD$_3$)$_2$SO)							
	CH—I	*CH*—N+	*CH*$_3$—C—I	*CH*$_3$—C—N+	Olefinic hydrogens	+N—*CH*—O—R	Methine and methylene hydrogens	Other groups
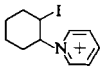	4.9 (1H)m	4.9 (1H)m					2.1 (8H)m	
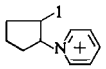	4.6 (1H)m	5.2 (1H)m					2.1 (6H)m	
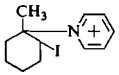	4.85 (1H)m			2.05 (3H)s			2.3 (4H)m 1.7 (4H)m	
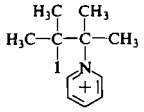			2.08 (3H)s	2.05 (3H)s				
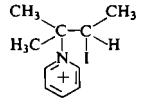	5.1 (1H)q J = 7 Hz		1.9 (3H)s J = 7 Hz	1.97 (6H)s				
	4.3 (0.56H)s 3.8 (0.44H)s	5 (1H)s					2.75 (1H)s 1.95 (4H)m 1.1 (1H)m	
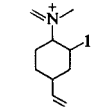	4.9 (1H)m	5.1 (1H)m			6.3 (2H)m 5.35 (1H)m		2.2 (6H)m	*HC*—C≡C 2.85 (1H)m
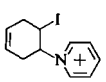	5 (1H)m	5.2 (1H)m			5.65 (2H)m		2.9 (4H)m	

Can. J. Chem. Downloaded from www.nrcresearchpress.com by 210.87.254.6 on 09/05/12
For personal use only.

TABLE 5. (*Concluded*)

Compounds*	δ ((CD$_3$)$_2$SO)							
	CH—I	*CH*—N+	*CH*$_3$—C—I	*CH*$_3$—C—N+	Olefinic hydrogens	+N—*CH*—O—R	Methine and methylene hydrogens	Other groups
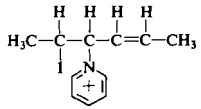	4.9 (1H)m	5.75 (1H)m	2.0 (3H)d J = 7 Hz		6.1 (1H)m 5.85 (1H)m			*CH*$_3$—C≡C 1.75 (3H)d J = 5 Hz
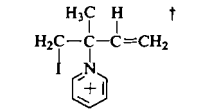 †	4.2 (2H)s			2.03 (3H)s	6.3 (1H)m 5.6 (1H)d 5.5 (1H)d J = 11 Hz J = 17 Hz			
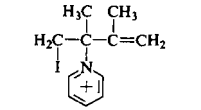	4.3 (2H)s			2.03 (3H)s	5.41 (1H)d 5.28 (1H)s			*CH*$_3$—C≡C 1.63 (3H)m
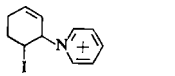	4.85 (1H)m	5.8‡ (2H)m			6.3 (1H)m		2.35 (4H)m	
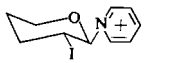	4.8 (1H)m					6 38 (1H)d J = 10 Hz	4.2 (3H)m 2.2 (3H)m	—*CH*$_3$—CH$_2$
ICH$_2$—CH—OEt 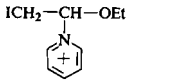	3.82 (2H)d J = 5 Hz					6.23 (1H)t J = 5 Hz	3.62 (2H)m	1.2 (3H) J = 6 Hz
Ph—C=CH$_2$ § 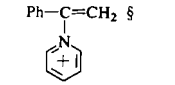					6.13 (1H)d J = 3 Hz 6.5 (1H)d J = 3 Hz			Phenyl H 7.5 (5H)m

*Unless otherwise indicated the counter ion was nitrate.
†See Figure 2.
‡Includes one of the olefinic protons.
§Counter ion was iodide.

The authors are grateful to Dr. R. M. Elofson for valuable discussions during the course of this work, and also for carrying out the electrolytic reduction. They thank J. McCutcheon and J. Forsythe for able technical assistance. The National Research Council of Canada provided partial support to J. F. during the summer of 1970.

1. L. Birckenbach and M. Linherd. Chem. Ber. **63**, 2544 (1930); **64**, 961 and 1076 (1931).
2. G. Drefahl and K. Ponsold. Chem. Ber. **93**, 519 (1960).
3. G. Drefahl, K. Ponsold, and G. Kollner. J. Prakt. Chem. **23**, 136 (1964).
4. C. G. Gebelein and D. Swern. J. Org. Chem. **33**, 2758 (1968).
5. T. A. Foglia and D. Swern. J. Org. Chem. **31**, 3625 (1966).
6. H. C. Hamann and D. Swern. Tetrahedron Lett. 3303 (1966).
7. A. Hassner and C. C. Heathcock. Tetrahedron Lett. 1125 (1964).
8. U. E. Diner and J. W. Lown. Chem. Commun. 333 (1970).
9. A. Hassner, J. E. Kropp, and G. J. Kent. J. Org. Chem. **34**, 2628 (1969).
10. J. W. Emsley, J. Feeney, and L. H. Sutcliffe. High resolution nuclear magnetic resonance spectroscopy. Vol. 2, Pergamon Press, London, 1966. p. 672.
11. F. W. Fowler, A. Hassner, and L. A. Levy. J. Amer. Chem. Soc. **80**, 2077 (1967).
12. P. R. Wells. Chem. Rev. **63**, 212 (1963).
13. R. G. Guy, R. Bonnett, and D. Lanigan. Chem. and Ind. 1702 (1969).
14. R. U. Lemieux and J. W. Lown. Can. J. Chem. **42**, 893 (1964).
15. R. U. Lemieux and A. R. Morgan. Can. J. Chem. **43**, 2205 (1965).
16. M. N. G. James. Biochemistry Department, University of Alberta, Edmonton, Alberta. Unpublished results.
17. J. Meinwald, J. Crandall, and W. E. Hymans. Org. Syn. **45**, 74.
18. A. Hassner, R. P. Hoblitt, C. Heathcock, J. E. Kropp, and M. Lorber. J. Amer. Chem. Soc. **92**, 1326 (1970).
19. B. E. Grimwood and D. Swern. J. Org. Chem. **32**, 3665 (1967).
20. L. M. Jackman and S. Sternhell. Applications of nuclear magnetic resonance spectroscopy in organic chemistry. 2nd Edition. Pergamon Press, New York, N.Y., 1969. p. 323.
21. K. M. Smirnov, A. P. Tomilov, and A. I. Shchekotikhin. Russian Chem. Revs. 326 (1967).
22. H. G. Viehe. Chemistry of acetylenes. Marcel Dekker, New York, N.Y. 1969. p. 739.
23. T. H. Vaughn and J. A. Nieuwland. J. Amer. Chem. Soc. **55**, 2150 (1933).
24. F. F. Cleveland and M. J. Murray. J. Chem. Phys. **11**, 450 (1943).

Can. J. Chem. Downloaded from www.nrcresearchpress.com by 210.87.254.6 on 09/05/12
For personal use only.

Can. J. Chem. Downloaded from www.nrcresearchpress.com by 210.87.254.40 on 09/05/12
For personal use only.

Theory of Ionic Conduction in Solids Based on the Homogeneous Generation of Defect Pairs and Its Application to Anodic Oxidation

M. J. DIGNAM AND D. F. TAYLOR
Department of Chemistry, University of Toronto, Toronto 181, Ontario

Received August 19, 1970

The theory for ionic conduction in solids based upon the homogeneous, field-assisted generation of defect pairs is developed in a general, three dimensional form, and its range of applicability is examined. At high field strengths the equations reduce to those of the so-called high field Frenkel defect theory, proposed originally by Bean, Fisher, and Vermilyea. At low field strengths, the steady-state expression reduces to the well-known conduction equation derived originally by Mott for ionic conduction in the alkali halides. At intermediate field strengths, more complicated relationships obtain. The homogeneous generation of defect pairs, whether field or current assisted, is shown to be inapplicable as a mechanism for the high field anodic oxidation of the valve metals, since either type of theory predicts unacceptable behavior for the mean free path of the mobile defects. Any such conduction mechanism can be acceptable only for the case of thick films ($\gg 10^4$ Å).

Canadian Journal of Chemistry, 49, 416 (1971)

Introduction

In 1956, Bean, Fisher, and Vermilyea (1) proposed a theory to account for the complex kinetics of formation of anodic oxide films on the valve metals (principally Ta, Al, Nb). The theory was subsequently clarified in certain details, first by Dewald (2) in 1957, and then by Young (3) in 1959. It was Young who named it the high field Frenkel defect theory. The essential features of this theory are summarized in the following paragraph.

The applied electric field is assumed to act on lattice cations in the oxide film reducing the activation energy for the formation of Frenkel defects (interstitial cations and cation vacancies). The interstitial cations so generated are assumed to move in the direction of the applied field, which acts to reduce the activation energy for the transport motion as well as that for defect formation. The vacancies, assumed immobile, function as traps for the mobile interstitials, and are assigned a characteristic capture cross-section for this recombination process. Under conditions of constant field strength and temperature, a steady-state concentration of defect pairs is ultimately established in which the rate of field-assisted generation of defect pairs is equal to the rate of their recombination. Under these steady-state conditions, the ion current density is a function of the field strength alone for a given temperature. On changing the current density or field strength suddenly, however, the concentration of defect pairs adjusts slowly, and the approach toward a new steady-state condition produces field or ion-current transients.

This theory has been shown to account for the functional form of many of the data pertaining to the anodic oxidation of the valve metals. However, it fails to account for both the form of the observed constant field transients and the transport number data (4, 5).

The purpose of this paper is twofold: first, to derive from the basic model proposed by Bean *et al.* more general ionic conduction equations, and second, to show that this model cannot be applied to valve metal anodic oxidation.

Field Assisted Generation of Defect Pairs

In order to simplify the problem somewhat, it is assumed at the outset that the positions occupied by the lattice cations (from which the Frenkel defects are generated) represent centers of symmetry in the solid, at least with respect to the potential energy surface for displacement of these lattice cations. From elementary rate theory, the probability that a given lattice cation will enter an interstitial position along a path within the infinitesimal solid angle $\sin\theta d\theta d\phi$, where θ is the polar angle and ϕ the longitudinal angle (normal spherical polar coordinates) is given by $\nu_{\theta,\phi} \exp[-U_{\theta,\phi}(E_{\theta,\phi})/kT] \sin\theta d\theta d\phi$ where $E_{\theta,\phi}$ is the component of the electric field in the (θ,ϕ) direction, $U_{\theta,\phi}(E_{\theta,\phi})$ is the net activation energy in this direction, and $\nu_{\theta,\phi}$ is the corresponding frequency factor. The direct functional dependence of $U_{\theta,\phi}$ on (θ,ϕ) and the functional form of $\nu_{\theta,\phi}$ will reflect the structural symmetry. Thus in this case, where the origin is

Can. J. Chem. Downloaded from www.nrcresearchpress.com by 210.87.254.40 on 09/05/12
For personal use only.

assumed to be a center of symmetry,

$$\nu_{\theta,\phi} = \nu_{\pi-\theta,\phi+\pi}$$

and

$$U_{\theta,\phi}(E_{\theta,\phi}) = U_{\pi-\theta,\phi+\pi}(-E_{\pi-\theta,\phi+\pi})$$

Taking $\theta = 0$ as the direction of the applied field, the total probability of lattice dissociation in any direction, P_+, is given by

$$[1]\quad P_+ = \int_{-1}^{1}\int_{0}^{2\pi} \nu_{x,\phi} \exp\left[-U_{x,\phi}(Ex)/kT\right] d\phi\, dx$$

where E is the electric field strength and $x \equiv \cos\theta$. This integral can be expressed as the sum of two integrals for $-1 \leqslant x \leqslant 0$ and $0 \leqslant x \leqslant 1$. If the limits of integration on the first of these two terms are changed to (0, 1) by substituting $-x$ for x, on applying the symmetry conditions in the form

$$\nu_{-x,\phi} = \nu_{x,\phi+\pi}$$

and

$$U_{-x,\phi}(-Ex) = U_{x,\phi+\pi}(-Ex)$$

one obtains

$$[2]\quad P_+ = \int_{0}^{1}\int_{0}^{2\pi} \nu_{x,\phi} \exp\left[-U_{x,\phi}(Ex)/kT\right] d\phi\, dx + \int_{0}^{1}\int_{0}^{2\pi} \nu_{x,\phi+\pi} \exp\left[-U_{x,\phi+\pi}(-Ex)/kT\right] \times d\phi\, dx$$

Since $\nu_{x,\phi}$ and $U_{x,\phi}$ (Ex) must be periodic functions of ϕ of period 2π or a sub-multiple of 2π, the integrals in eq. 2 differ only in the sign of the parameter E. Making the substitution

$$[3]\quad \nu_1 \exp\left[-W_1(E)/kT\right] = \int_{0}^{1}\int_{0}^{2\pi} \nu_{x,\phi} \exp\left[-U_{x,\phi}(Ex)/kT\right] d\phi\, dx$$

where ν_1 is the weighted mean value of $\nu_{x,\phi}$, the weighting factor being $\exp\left[-U_{x,\phi}(Ex)/kT\right]$, and $\exp\left[-W_1(E)/kT\right]$ is the mean value of $\exp\left[-U_{x,\phi}(Ex)/kT\right]$, eq. 2 becomes

$$[4]\quad P_+ = \nu_1\left[\exp\left[-W_1(E)/kT\right] + \exp\left[-W_1(-E)/kT\right]\right]$$

As $U_{x,\phi}(Ex)$ will in general be a polynomial function of Ex (6), and most likely also somewhat temperature dependent, no significant increase in function complexity is introduced through the averaging process of eq. 3. In fact, one would expect that for any given E, $U_{x,\phi}(Ex)$ would display one or more pronounced minima on variation of (x,ϕ), the number depending on the rotational symmetry order of the structure about the $x = 1$ ($\theta = 0$) axis (specified by the direction of the field). In this case, W_1 would reflect very closely the function $U_{x,\phi}$ at the minima. Setting W_1 equal to $U_{x,\phi}$ at the minimum or saddle point, and ν_1 equal to $\nu_{x,\phi}$ at the same point, corresponds to the usual approximation made in treating thermally activated kinetic processes.

The rate of formation of defect pairs per unit volume, dn_+/dt, can now be written in the form

$$[5]\quad dn_+/dt = (N-n)\nu_1\left\{\exp\left[-W_1(E)/kT\right] + \exp\left[-W_1(-E)/kT\right\}\right.$$

where N is the number of cation lattice positions per unit volume and n the number of cation vacancies.

Ion Flux and Defect Recombination

Proceeding in a manner exactly analogous to that of the section above, the flux density of ions in a direction within the solid angle $\sin\theta d\theta d\phi$ is given by

$$[6]\quad d^2J_{\theta,\phi} = ma_{\theta,\phi}\nu_{\theta,\phi}{}^1 \exp\left[-U_{\theta,\phi}{}^1(E\cos\theta)/kT\right] \sin\theta d\theta d\phi$$

where m is the number of interstitial cations per unit volume, and $a_{\theta,\phi}$ is the mean distance travelled in the (θ,ϕ) direction per activation. Assuming as before that the interstitial positions are centers of symmetry, the net flux in the direction of the field, J, is given by

$$[7]\quad J = m\int_{0}^{1}\int_{0}^{2\pi} xa_{x,\phi}\nu_{x,\phi}{}^1\{\exp\left[-U_{x,\phi}{}^1(Ex)/kT\right] - \exp\left[-U_{x,\phi}{}^1(-Ex)/kT\right]\} d\phi\, dx$$

Upon making the substitution

$$[8]\quad \nu_2 \exp\left[-W_2(E)/kT\right] = \int_{0}^{1}\int_{0}^{2\pi} xa_{x,\phi}\nu_{x,\phi}{}^1 \exp\left[-U_{x,\phi}{}^1(Ex)/kT\right] d\phi\, dx$$

eq. 7 becomes

$$[9] \qquad J = ma\nu_2\{\exp[-W_2(E)/kT] - \exp[-W_2(-E)/kT]\}$$

where $a\nu_2$ is the weighted mean value of $a_{x,\phi}\nu_{x,\phi}{}^1$, the weighting factor being $x \exp[-U_{x,\phi}{}^1(Ex)/kT]$, and $\exp[-W_2(E)/kT]$ is the mean value of $x \exp[-U_{x,\phi}{}^1(Ex)/kT]$.

Defining $\sigma_{x,\phi}(E)$ as the capture cross-section of a cation vacancy for an interstitial moving in the (x,ϕ) direction, the rate of recombination of defect pairs per unit volume within the solid angle $\sin\theta d\theta d\phi$ is given by $n\sigma_{x,\phi}(E)d^2J_{x,\phi}$ provided the vacancies are immobile. On substituting from eq. 6, integrating over all values of (x,ϕ), and applying the symmetry condition, the total rate of recombination of defect pairs per unit volume is obtained as

$$[10] \quad (dn_-/dt) = mn\int_0^1\int_0^{2\pi}\sigma_{x,\phi}(E)a_{x,\phi}\nu_{x,\phi}{}^1\{\exp[-U_{x,\phi}{}^1(Ex)/kT] + \exp[-U_{x,\phi}{}^1(-Ex)/kT]\}\,d\phi\,dx$$

Defining σ through eq. 11

$$[11] \qquad \sigma a\nu_2 \exp[-W_2(E)/kT] = \int_0^1\int_0^{2\pi}\sigma_{x,\phi}(E)a_{x,\phi}\nu_{x,\phi}{}^1 \exp[-U_{x,\phi}{}^1(Ex)/kT]\,d\phi\,dx$$

eq. 10 becomes

$$[12] \qquad dn_-/dt = mn\sigma a\nu_2\{\exp[-W_2(E)/kT] + \exp[-W_2(-E)/kT]\}$$

By solving for σ from eqs. 11 and 8, it can be seen that this parameter is the weighted mean value of $\sigma_{x,\phi}(E)/|x|$, the weighting function being $|x|a_{x,\phi}\nu_{x,\phi}{}^1 \exp[-U_{x,\phi}{}^1(E|x|)/kT]$. For values of E which are not too small, the weighting function will be a maximum for $|x|$ close to one, and fall off rapidly with decreasing $|x|$. Under these conditions, σ will be very nearly the capture cross-section for motion in the field direction. As a direct result of the coulombic attraction between the defect pairs, $\sigma_{x,\phi}(E)$ would be expected to depend somewhat on both field strength and temperature. Even in the absence of such dependence, however, σ should show a field and temperature dependence introduced through the averaging procedure. This effect should be small compared to the temperature and field variation inherent in $\sigma_{x,\phi}(E)$.

Steady-State Ionic Conduction

For specimens sufficiently thick that space charge effects may be neglected (7), under steady-state conditions $n = m$ and $dn_+/dt = dn_-/dt$ so that from eqs. 5 and 12

$$[13] \qquad n^2 = \frac{(N-n)\nu_1}{\sigma\nu_2 a}\,\frac{e^{-W_1(E)/kT} + e^{-W_1(-E)/kT}}{e^{-W_2(E)/kT} + e^{-W_2(-E)/kT}}$$

$W_j(E), j = 1$ or 2, may be represented by the following expression (6)

$$[14] \qquad W_j(E) = \phi_j\left[1 - \frac{\mu_j{}^*E}{\phi_j} + \frac{1}{C_j}\left(\frac{\mu_j{}^*E}{\phi_j}\right)^2 + \cdots\right]$$

where ϕ_j is the zero field activation energy, $\mu_j{}^*$ the activation dipole in the limit of low field strength, and C_j a dimensionless constant.

(I) Very High Field Strengths

For $(\mu_j{}^*E/kT) \gg 1, j = 1, 2$, eq. 13 reduces to

$$[15] \qquad n^2 = \frac{(N-n)\nu_1}{\sigma\nu_2 a}\,e^{-[(W_1(E)-W_2(E))/kT]}$$

and from eq. 9

$$[16] \qquad i = nqa\nu_2\,e^{-W_2(E)/kT}$$

where i is the ion current density and q the charge on the mobile ion. Elimination of n from eqs. 15 and

Can. J. Chem. Downloaded from www.nrcresearchpress.com by 210.87.254.40 on 09/05/12
For personal use only.

16 leads to the following steady-state equation for high field ionic conduction, provided $N \gg n$

$$[17] \qquad i = q\left(\frac{N\nu_1\nu_2 a}{\sigma}\right)^{\frac{1}{2}} e^{-[W_1(E)+W_2(E)]/2kT}$$

If terms of order 3 or higher in the field strength are ignored, eq. 17 may be written as

$$[18] \qquad i = q\left(\frac{N\nu_1\nu_2 a}{\sigma}\right)^{\frac{1}{2}} e^{-\phi/kT} e^{[(\mu^*E/kT)(1-\mu^*E/C\phi)]}$$

where $\mu^* = (\mu_1^* + \mu_2^*)/2$, $\phi = (\phi_1 + \phi_2)/2$ and

$$\frac{1}{C} = \frac{1}{2C_1}\frac{(\mu_1^*/\mu^*)^2}{(\phi_1/\phi)} + \frac{1}{2C_2}\frac{(\mu_2^*/\mu^*)^2}{(\phi_2/\phi)}$$

Equation 18 is essentially the same as that proposed by Bean *et al.* (1), except for the inclusion of the quadratic field term.

(II) Intermediate Field Strengths

For $\phi_j \gg \mu_j^* E \gtrsim kT, j = 1, 2$, the quadratic field term is negligible and eqs. 13 and 14 reduce to

$$[19] \qquad n^2 = \frac{(N-n)\nu_1}{\sigma\nu_2 a} e^{-(\phi_1-\phi_2)/kT}\frac{\cosh(\mu_1^* E/kT)}{\cosh(\mu_2^* E/kT)}$$

and eqs. 9 and 14 can be combined to give

$$[20] \qquad i = 2nqa\nu_2 \sinh(\mu_2^* E/kT) e^{-\phi_2/kT}$$

so that when n is eliminated (assuming $N \gg n$)

$$[21] \qquad i = 2q\left(\frac{N\nu_1\nu_2 a}{\sigma}\right)^{\frac{1}{2}} e^{-(\phi_1+\phi_2)/2kT} \sinh\left(\frac{\mu_2^* E}{kT}\right)\left[\frac{\cosh(\mu_1^* E/kT)}{\cosh(\mu_2^* E/kT)}\right]^{\frac{1}{2}}$$

(III) Low Field Strengths

For $\mu_j^* E/kT \ll 1$, eqs. 19 and 21 reduce to

$$[22] \qquad n^2 = \frac{(N-n)\nu_1}{\sigma\nu_2 a} e^{-(\phi_1-\phi_2)/kT}$$

$$[23] \qquad i = 2nqa\left(\frac{\mu_2^* E}{kT}\right) e^{-\phi_2/kT}$$

hence

$$[24] \qquad i = 2q\left(\frac{N\nu_1\nu_2 a}{\sigma}\right)^{\frac{1}{2}}\frac{\mu_2^* E}{kT} e^{-(\phi_1+\phi_2)/2kT}$$

It is interesting to note that for low field strengths, n is independent of field strength, hence the defects must be generated by thermal activation alone. Thus at low field strength, n will be equal to the equilibrium value, and

$$[25] \qquad K_d = \frac{n^2}{N(N-n)} = \frac{\nu_1}{\sigma\nu_2 aN} e^{-(\phi_1-\phi_2)/kT}$$

where K_d is the equilibrium constant for the formation of defect pairs. Since

$$[26] \qquad \left[\frac{\partial(k \ln K_d)}{\partial(1/T)}\right]_V = -\Delta U_d^0$$

where ΔU_d^0 is the standard internal energy of formation of a defect pair, and since $\sigma, \nu_1, \nu_2, a, \phi_1$, and

Can. J. Chem. Downloaded from www.nrcresearchpress.com by 210.87.254.40 on 09/05/12
For personal use only.

ϕ_2 may be considered essentially temperature independent under conditions of constant volume,

[27] $$\phi_1 - \phi_2 = \Delta U_d^0$$

Noting that $kT \ln K_d = -\Delta A_d^0 = -\Delta U_d^0 + T\Delta S_d^0$ and that $\mu_2^* = qa/2$ (6, 8), a combination of eqs. 24, 25, and 27 leads to

[28] $$i = (\nu_2 N q^2 a^2/kT) E \exp[\Delta S_d^\circ/2k] \exp\{-[(\Delta V_d^\circ/2) + \phi_2]\}$$

This expression is the same as that obtained by Mott and Gurney (9) for low field ionic conduction in the alkali halides, except that in that case, N is the concentration of ion pairs in the crystal and ΔS_d^0 and ΔU_d^0 refer to the formation of Schottky defects at constant volume.

Turning briefly once again to ionic conduction under conditions of very high field strengths, it should be emphasized that the equations which have been derived in the previous sections are equivalent to those of Bean, Fisher, and Vermilyea (1) not only for the steady-state, but for transient situations as well. Upon making the assumption that the film is electrically neutral ($m = n$), the ion-current density is given by eq. 9 as

[29] $$i = qna\nu_2 \, e^{-W_2(E)/kT}$$

and an expression for the net rate of formation of defect pairs per unit volume can be obtained from eqs. 5, 9, and 12

[30] $$\frac{dn}{dt} = (N - n)\nu_1 \, e^{-W_1(E)/kT} - \frac{n\sigma i}{q}$$

Except for the inclusion of a quadratic field term in $W_j(E)$, $j = 1, 2$, eqs. 29 and 30 are identical to those given by Dewald (2) to describe the transient behavior of anodic oxide films on valve metals.

Mean Free Path of Mobile Defects

For any conduction model in which the mobile defects are generated within the transport medium, motion in the direction of the field can be characterized by a mean free path, λ. The net flux of defects is simply the product of their rate of formation and the mean distance travelled by each defect in the field direction before annihilation. Hence λ is related to J and (dn_+/dt) through the equation

[31] $$J = \lambda (dn_+/dt)$$

For high field conditions in which ionic motion against the field direction can be ignored, the rate of defect annihilation is simply given by

[32] $$(dn_-/dt) = n\sigma J$$

where n is the volume concentration of trapping sites and σ their capture cross-sectional area. Combining eqs. 31 and 32 gives

[33] $$\lambda = \frac{1}{n\sigma}\left(\frac{dn_-}{dt} \Big/ \frac{dn_+}{dt}\right)$$

which for the conditions $(dn_+/dt = dn_-/dt)$ reduces to the familiar relation for the steady-state mean free path

[34] $$\lambda_s = 1/n\sigma$$

Equations 31 to 34 are valid, independent of the particular mechanism of formation of the mobile defects so long as they are generated homogeneously throughout the transport medium. Equations 9 and 12 yield eq. 32 in the high field limit, and elimination of λ from eqs. 31 and 34 combined with eqs. 5 and 15 gives eq. 17, as expected.

(I) Steady-State Conditions

For the particular case of high field generation of defect pairs, eqs. 15 and 34 combine to give

Can. J. Chem. Downloaded from www.nrcresearchpress.com by 210.87.254.40 on 09/05/12
For personal use only.

[35] $$\lambda_s = \left(\frac{\nu_2 a}{N\nu_1\sigma}\right)^{\frac{1}{2}} e^{[W_1(E)-W_2(E)]/2kT}$$

Recalling that $\phi = (\phi_1 + \phi_2)/2$, λ_s can be expressed as

[36] $$\lambda_s = \left(\frac{\nu_2 a}{N\nu_1\sigma}\right)^{\frac{1}{2}} e^{-[(\mu_1^{*2}/C_1\phi_1)-(\mu_2^{*2}/C_2\phi_2)]E^2/2kT} e^{(\phi-\phi_2)/kT} e^{-(\beta_s-\beta_2)E}$$

where $W_1(E)$ and $W_2(E)$ have been expanded according to eq. 14, and

[37] $$\beta_2 = -\frac{1}{kT}\left(\frac{\partial W_2(E)}{\partial E}\right)_T$$

$$\beta_s = -\frac{1}{2kT}\left[\frac{\partial[W_1(E) + W_2(E)]}{\partial E}\right]_T$$

The coefficient of E^2 in eq. 36 is small, and E is a very slowly changing function of i. This exponential factor is therefore essentially constant over a wide range of current densities and will subsequently be represented by the symbol A.

In the same way eq. 17 becomes

[38] $$i = i_0 e^{-\phi/kT} e^{\beta_s E}$$

where i_0 is again essentially constant and is given by

[39] $$i_0 = q\left[\frac{N\nu_1\nu_2 a}{\sigma}\right]^{\frac{1}{2}} e^{[(\mu_1^{*2}/C_1\phi_1)+(\mu_2^{*2}/C_2\phi_2)]E^2/2kT}$$

Thus a steady-state expression for the mean free path which does not depend explicitly on E can be obtained from eqs. 36 and 38

[40] $$\lambda_s = \left(\frac{\nu_2 a}{N\nu_1\sigma}\right)^{\frac{1}{2}} A\left[\exp\left[\frac{\phi(\beta_2/\beta_s) - \phi_2}{kT}\right]\right]\left[\frac{i_0}{i}\right]^{(\beta_s-\beta_2)/\beta_s}$$

From a consideration of the physical system, λ_s cannot be smaller than one jump distance, nor as large as one-half the film thickness; *i.e.*

[41] $$X/2 > \lambda_s \gtrsim 3 \text{ Å}$$

Since an equation of the form of [17] fits steady-state data for anodic film formation on tantalum, a typical valve metal, for films at least as thin as a few hundred Å, and over a substantial range of temperature and field strength (10), it is clear that the following conditions must hold

[42] $$(\beta_s - \beta_2)/\beta_s \ll 1$$

$$[\phi(\beta_2/\beta_s) - \phi_2]/kT \ll 1$$

otherwise λ_s would be a rapidly varying function of current density and temperature, and this is precluded by condition 41. For example, if the high field Frenkel defect theory (or essentially this theory involving other defect pairs) were correct then β_s and β_2 would correspond to the steady-state and transient differential field coefficients defined in [43]

[43] $$\beta_s = \frac{\partial \ln i}{\partial E}\left(\text{limit } \frac{dE}{dt} \to 0\right)$$

$$\beta_2 = \frac{\partial \ln i}{\partial E}\left(\text{limit } \frac{dE}{dt} \text{ large}\right)$$

For the anodic oxidation of tantalum, β_s/β_2 is approximately equal to 3 (6) so that from eq. 40 λ_s is

Can. J. Chem. Downloaded from www.nrcresearchpress.com by 210.87.254.40 on 09/05/12
For personal use only.

proportional to the current density to the power $-2/3$. Young's data for tantalum (10) shows adherence to the conduction equation for a film 600 Å in thickness over a three decade range in current density. This corresponds to a two decade range in the steady-state mean free path, and from [41] such a range in λ_s for $X = 600$ Å is only just possible. However, for the equations derived on the basis of homogeneous generation of defect pairs to be a good approximation, the steady-state mean free path must in fact be substantially less than $X/2$, otherwise it will not be controlled entirely by kinetic phenomena within the film, but will be greatly influenced by the film thickness. Accordingly, for a film 600 Å thick, λ_s must be between about 3 and 30 Å for the high field homogeneous generation theory to be valid. To account for the data, however, λ_s must vary by a factor of 10^2, so that on this basis alone the high field Frenkel defect theory (or a modified form of it involving other defect pairs) may be ruled out as a possible mechanism.

Young has proposed a model for high field ionic conduction in valve metals in which the mobile defects are generated by an avalanche mechanism, homogeneously, and at a rate proportional to J^2 (11). This gives, with condition 41, the result $\lambda \propto 1/J$ for both steady-state and transient conditions, which requires that λ_s vary by a factor of 10^3 for a film 600 Å thick, a totally impossible condition. Indeed it is highly improbable that any conduction mechanism based on homogeneous generation of defects, and involving a defect concentration dependent on E and/or J, will satisfy condition 41 within the accessible range of experimental conditions for films even as thick as 10^4 Å.

Further evidence against the applicability of this class of mechanism to the valve – metal oxide system can be found in the series of galvanostatic transient measurements carried out by Tvarusko on very thin (10–100 Å) films of tantalum oxide (12). Chemically polished tantalum wires were anodized galvanostatically in a 1% H_3PO_4 aqueous electrolyte at current densities of 0.4 and 4 $\mu A/cm^2$ for various but very short periods of time before the current was doubled. The voltage "overshoots" observed were similar in all respects to those obtained by Dewald with much thicker (> 200 Å) tantalum oxide films formed in dilute sulfuric acid (2). Upon analysis, it was found that the excess field values (2) were independent of film thickness even for the thinnest films, and in fact these values were almost identical to those of Dewald. All calculations led to the conclusion that the situation in very thin films of the order of 10–20 Å is not essentially different from that in thicker films. To be consistent with the theory of high field generation of defect pairs, arguing as above, these data require that the steady-state mean free path vary by a factor of $(20)^{2/3} \simeq 7.4$ for a film 10–20 Å thick. Similarly, for Young's avalanche theory, λ_s must be assumed to vary by a factor of 20. In both cases, the requirement is at variance with condition 41.

(II) Transient Conditions (Constant Current)

Ignoring charging currents, the ratio of λ just before to that just after the abrupt increase in cell current in the experiments described above is given from eqs. 32 and 33 as

$$\frac{\lambda_1}{\lambda_m} \simeq \left(\frac{J_1}{J_2}\right)\left(\frac{dn_+}{dt}\right)_m \Big/ \left(\frac{dn_+}{dt}\right)_1 \qquad [44]$$

since n cannot change instantaneously.

In actual fact, the ion flux cannot be switched instantly from J_1 to J_2, primarily on account of charging current transients. These are much faster than ion current transients for the valve – metal oxide systems, so that the approximation made in eq. 44 will be a good one for these systems. Referring specifically to the high field theory of defect generation, the corresponding fields can be related through eqs. 17, 37, and 43 giving

$$E_m - E_1 \simeq (1/\beta_2) \ln (J_2/J_1) \qquad [45]$$

and from eqs. 5 and 37 the ratio of the volume rates of defect generation is obtained as

$$\left(\frac{dn_+}{dt}\right)_m \Big/ \left(\frac{dn_+}{dt}\right)_1 \simeq e^{(2\beta_s - \beta_2)(E_m - E_1)} \qquad [46]$$

Thus for this special case of galvanostatic field transients and the tantalum–oxide system,

Can. J. Chem. Downloaded from www.nrcresearchpress.com by 210.87.254.40 on 09/05/12
For personal use only.

$$[47] \qquad \frac{\lambda_m}{\lambda_1} \simeq \left(\frac{i_1}{i_2}\right)^{2[(\beta_s-\beta_2)/\beta_2]} \simeq \left(\frac{i_1}{i_2}\right)^4$$

The corresponding equation for Young's avalanche theory is

$$[48] \qquad \lambda_m/\lambda_1 = i_1/i_2$$

Equation 47 predicts that for a voltage overshoot experiment in which the current density is doubled, the transient mean free path should vary by a factor of 16. Dewald's data for thicker films ($\sim$ 300 Å) produce an even more surprising result, since he found that the observed phenomena were independent of the ratio (i_2/i_1) for values of this ratio as high as 40. From eq. 47, this would correspond to a reduction in the transient mean free path by a factor of approximately 4×10^{-7}! If λ as well as λ_s were assumed to satisfy the inequality, [41], the above result would clearly rule out the high field theory even for very thick films. We are not in general entitled to make this assumption, however, since under conditions in which λ is time dependent, it can no longer be identified with the mean distance travelled by a mobile defect in one lifetime. Thus, although eq. 31 defines λ unambiguously for both steady-state and transient conditions, λ can only be interpreted as a true mean free path for conditions in which λ is time independent. The arguments presented here against both the theory involving the high field generation of defect pairs and that involving an avalanche mechanism must therefore rest on the behavior predicted for λ_s. On this basis alone, both theories show gross internal contradictions when examined against the data.

The situation is essentially unaltered if allowance is made for motion of the other member of the defect pair. Generation of the defects is of course unaffected, but an equation corresponding to eq. 9 must be introduced to describe the motion of the oppositely charged species in the reverse direction. There will be characteristic a_3, ν_3, and W_3 terms for this motion, and these parameters will not in general be equal to a_2, ν_2, and W_2. In fact, it is highly unlikely that the two activation energies for defect transport will be similar enough to allow a significant contribution from both sources. The capture cross-section for the recombination process will remain unchanged, but the increase in relative velocity must be taken into account by using the vectorial difference of the two fluxes in equations such as eq. 32. The conduction equations of the previous section must become correspondingly more complicated, and a second mean free path is required. However, the mean free path as defined and discussed in this section is simply the sum of those required in the more complicated theory involving dual modes of charge transport, and consequently the arguments presented against rate control through the field or current assisted homogeneous generation of defects are generally valid.

Summary

The so-called high field Frenkel defect theory for ionic conduction in solids has been extended to a more general form, and its range of applicability has been examined. Expressions have been derived for conduction under high-, intermediate-, and low-field conditions. These equations were found to coincide with those derived previously by other authors for the high and low field cases. The homogeneous field-assisted generation of defect pairs was shown to be inapplicable as a mechanism for the anodic oxidation of a typical valve metal, tantalum. Irreconcilable contradictions arose when the predictions of such a theory regarding the steady-state mean free path of the mobile defects were examined against experimental data. In a similar manner the mechanism for defect generation by an ionic avalanche process controlled by the current was shown to be unacceptable under the same circumstances.

In so far as high field ionic conduction through thin films ($\lesssim 10^4$ Å) is concerned, it is highly improbable that the concentration of mobile defects is controlled by homogeneous generation within the film. If for some accessible temperature and current density the conditions for homogeneous generation should fortuitously be met, altering the current density or temperature by a relatively small amount would almost certainly alter the predicted steady-state mean free path to lie outside its permitted range. It must be concluded that any conduction mechanism based on the homogeneous generation of

Can. J. Chem. Downloaded from www.nrcresearchpress.com by 210.87.254.40 on 09/05/12
For personal use only.

defects where the concentration of these defects is directly dependent on E and/or i can be justified only for the case of relatively thick ($\gg 10^4$ Å) films.

The authors are grateful to the National Research Council of Canada for supporting this research and for a scholarship (D.F.T.).

1. D. P. Bean, J. C. Fisher, and D. A. Vermilyea. Phys. Rev. **101**, 551 (1956).
2. J. F. Dewald. J. Phys. Chem. Solids, **2**, 55 (1957).
3. L. Young. Can. J. Chem. **37**, 276 (1959).
4. M. J. Dignam. J. Electrochem. Soc. **112**, 729 (1965).
5. M. J. Dignam and P. J. Ryan. Can. J. Chem. **46**, 549 (1967).
6. M. J. Dignam and D. B. Gibbs. J. Phys. Chem. Solids, **30**, 375 (1969).
7. M. J. Dignam and P. J. Ryan. Can. J. Chem. **41**, 3108 (1963).
8. M. J. Dignam. J. Phys. Chem. Solids, **29**, 249 (1968)
9. N. F. Mott and R. W. Gurney. Electronic Processes in Ionic Crystals. Oxford University Press. 1948. Chap. II, Sections 1 and 5.
10. L. Young. Proc. Roy. Soc. London, **A258**, 496 (1960).
11. L. Young. Proc. Roy. Soc. London, **A263**, 395 (1961).
12. A. Tvarusko. U.S. At. Energy Comm. NP-16828 (1966).

Can. J. Chem. Downloaded from www.nrcresearchpress.com by 210.87.254.40 on 09/05/12
For personal use only.

Structure of Lycoctamone and its Analogues[1,2]

M. H. Benn,[3] J. D. Connolly,[3] O. E. Edwards, L. Marion, and Z. Stojanac[3]

Biochemistry Laboratory, National Research Council of Canada, Ottawa, Canada

Received June 22, 1970

The lactams derived from the lycoctonine family of diterpenoid alkaloids undergo acid-catalyzed dehydration of the *vic*-glycol system to produce pinacolones. More vigorous acid treatment converts these to 'lycoctamone' analogues, which are now shown to be α,β unsaturated aldehydes containing in addition an inert allylic alcohol system. Proof of structure and a mechanism for the formation of these compounds involving bond migration and fission are presented. A steric driving force for the reaction leading to these compounds is suggested. Lycoctamone and its analogues are of potential value in the stepwise degradation of the lycoctonine skeleton for biosynthetic studies.

Canadian Journal of Chemistry, 49, 425 (1971)

Can. J. Chem. Downloaded from www.nrcresearchpress.com by 210.87.254.5 on 09/05/12
For personal use only.

The structure and stereochemistry illustrated in **1** was established for the alkaloid lycoctonine[4] by X-ray crystallography (1). Most of the previously described chemistry was soon shown to be consistent with this structure (2–7). However, the nature of one intriguing transformation product, 'lycoctamone' (8), eluded us until p.m.r. observations corrected misconceptions about the functional groups.

Mild acid treatment of the lactam **2** (R = OH) derived from lycoctonine gave the pinacolic dehydration product anhydrooxolycoctonine[5] (**3**, R_1 = OH, R_2 = OCH_3) (Scheme 1). More vigorous treatment with acid converted both **2** and **3** to lycoctamone (8). This compound was still a δ lactam (ν_{max} 1610 cm^{-1}) and contained one readily-acetylated and one hindered hydroxyl, and two methoxyl groups. Spectral evidence (λ_{max} 245 (ε 10 000) and 310 mμ ε 160); ν_{max} 1661 cm^{-1}) and catalytic hydrogenation disclosed the presence of an α,β unsaturated carbonyl system in lycoctamone.

The primary hydroxyl group was not involved in the formation of lycoctamone, since 18-*O*-methyl-oxolycoctonine (**4**) and 18-deoxy-oxolycoctonine (**5**) which have no oxygen on that carbon, gave exactly parallel products.

Both 18-*O*-methyl-6-demethoxyoxolycoctonine (**6**) and oxodelpheline (**7**) (6) gave lycoctamone analogues with the loss of $C_2H_8O_2$. This is the same loss as for the conversion of oxolycoctonine to lycoctamone, hence the function on C-6 is not involved in the reaction.

Since 1-deoxyoxodelcosine (**8**) gave a lycoctamone analogue with loss of CH_6O_2, the hydroxyl on C-14 is involved but the function on C-1 is not. The participation of the C-14 function was confirmed when oxobrowniine (**9**), was treated with acid. Again loss of CH_6O_2 was observed giving the precise analogue (brownamone) of lycoctamone. By elimination we conclude that the other *O*-methyl group lost in formation of the lycoctamones was on C-16.

The fact that the pinacolic dehydration product **3** gave lycoctamone at least as efficiently as the parent glycol oxolycoctonine, and that this was true also of anhydro compounds (pinacones) corresponding to **4** and **6**, suggested that the molecule of water lost in formation of the lycoctamones came from the glycol and that the anhydro compounds (pinacones) were intermediate in the reaction.

It had been concluded earlier (8) that lycoctamone was a trisubstituted α,β unsaturated ketone (ν_{max} 246 mμ) and that it contained only one double bond. Analysis of its n.m.r. spectrum has shown both these conclusions to be incorrect.

The presence of an aldehyde function was indicated by a one-hydrogen singlet at τ 0.25 in the spectrum of lycoctamone and a comparable signal in the spectra of all the analogues which were studied. In the spectra of the dihydro derivatives, in which the conjugated double bond was reduced, the aldehyde proton resonated at τ 0.50 and as expected the signal was now a doublet

---

[1]Issued as NRCC No. 11628.

[2]Presented in part at the I.U.P.A.C. Symposium on the Chemistry of Natural Products, Kyoto, Japan, April 12–18, 1964.

[3]NRCC Postdoctorate Fellow.

[4]The revised numbering suggested by Dr. J. W. Rowe for the aconane skeleton has also been adopted by Professors S. W. Pelletier and K. Wiesner.

[5]In order to accord with general usage in the Delphinium and Aconite alkaloids we use the name oxolycoctonine for the lactam which we had previously called lycoctonam.

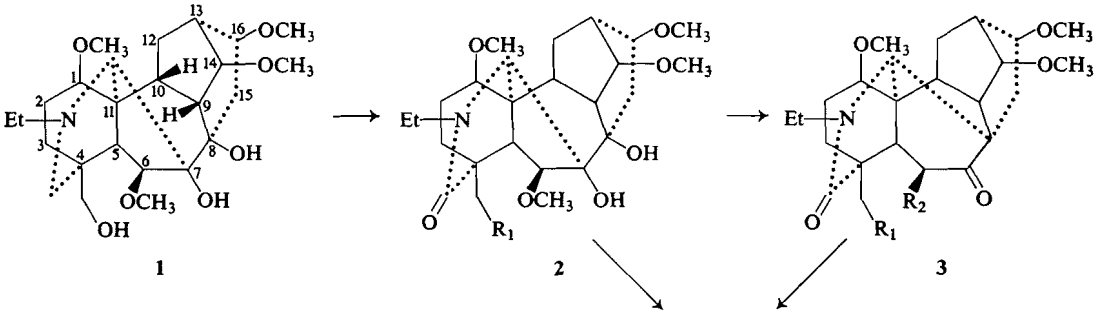

1 2 3

$C_{23}H_{31}NO_6$

Lycoctamone

(R_1 = OH; R_2 = OCH_3)

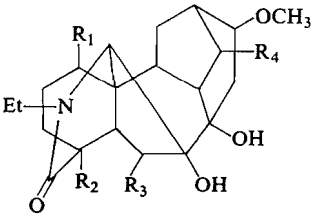

4 $R_1 = R_3 = R_4 = OCH_3$, $R_2 = CH_2OCH_3$
5 $R_1 = R_3 = R_4 = OCH_3$, $R_2 = CH_3$
6 $R_1 = R_4 = OCH_3$, $R_2 = CH_2OCH_3$, $R_3 = H$
7 $R_1 = R_4 = OCH_3$, $R_2 = CH_3$, $R_3 = OH$
8 $R_1 = H$, $R_2 = R_3 = OCH_3$, $R_4 = OH$
9 $R_1 = R_2 = R_3 = OCH_3$, $R_4 = OH$.

SCHEME 1

with J = 3Hz. The alcohols (lycoctamols) derived by sodium borohydride reduction of the aldehyde function of 18-deoxylycoctamone and des(oxymethylene)lycoctamone (**16**) had a broad ($w_{1/2}$ = 4 Hz) two-hydrogen singlet at τ 5.85, shifted downfield on esterification. Finally, the presence of the weak i.r. band at 2730 cm^{-1}, a positive Angeli–Remini test for aldehyde, a positive hydrogen sulfide – sodium pentacyanoammine ferroate (9) test for an α,β unsaturated aldehyde, and dehydration of the oxime of 18-deoxylycoctamone to a nitrile confirmed that lycoctamone and its analogues were α,β unsaturated aldehydes.

Inspection of the n.m.r. spectrum of lycoctamone[6] revealed the presence of three vinyl hydrogens. A broad ($w_{1/2}$ = 6 Hz) one-hydrogen signal near τ 3.4 in lycoctamone was shifted upfield to near τ 4.6 in the products of sodium borohydride reduction of the aldehyde function (lycoctamol). Hence this arises from a β hydrogen of an α,β unsaturated aldehyde system in lycoctamone. In accord with this the signal was absent in dihydrolycoctamone. A second double bond was indicated by a pair of one-hydrogen singlets at τ 4.68 and 4.73 in the spectrum of lycoctamone, and nearly identical signals in that of the other lycoctamone analogues. This pair of signals was absent in tetrahydrolycoctam, in which both double bonds had been reduced and the aldehyde oxygen removed by hydrogenolysis. The double bond carrying these protons was resistant to hydrogenation. An indication of the nature of this double bond came from the i.r. spectra of lycoctamone. A medium-intensity band appeared quite consistently near 910 cm^{-1}; this and a weak band near 3100 cm^{-1} suggested that it was an exocyclic methylene group. The n.m.r. signals for the two vinyl hydrogens asso-

[6]The following comments about lycoctamone spectra apply to the analogues derived from compounds **4** to **9** as well.

Can. J. Chem. Downloaded from www.nrcresearchpress.com by 210.87.254.5 on 09/05/12
For personal use only.

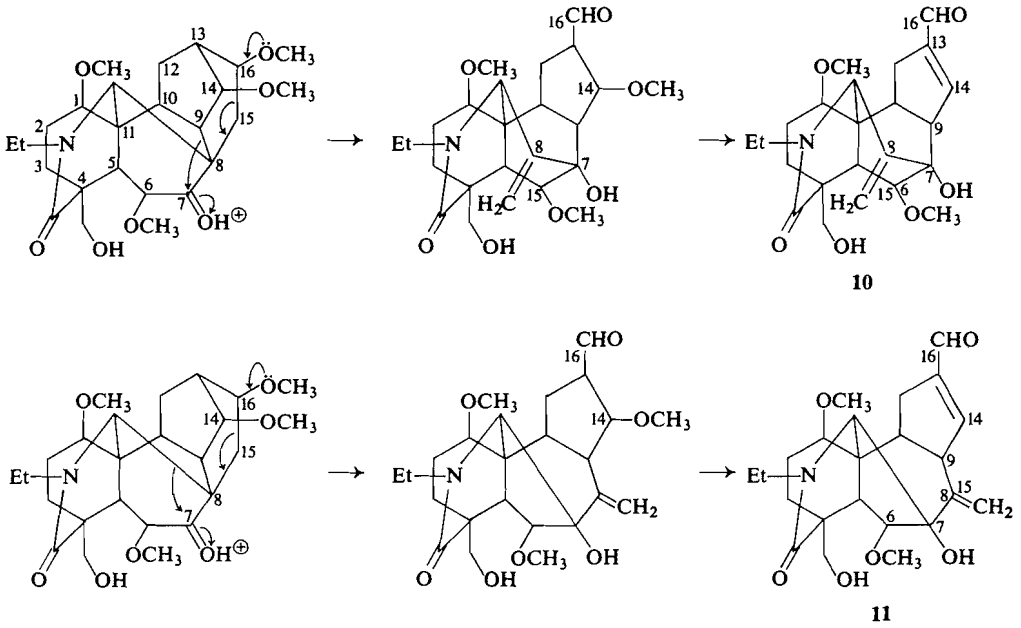

SCHEME 2

ciated with it were at rather low field for non-conjugated terminal methylene (τ 5.4), but did not exclude this possibility.[7]

The u.v. maximum of lycoctamone was at long wavelength (*ca.* 245 mμ) for an unsaturated aldehyde, but was not far from that of cyclopent-1-enal (ν_{max} 238 mμ). The i.r. peak for the carbonyl of cyclopent-1-enal (ν_{max} ($CHCl_3$) 1675 cm^{-1}) was at a low wave number, similar

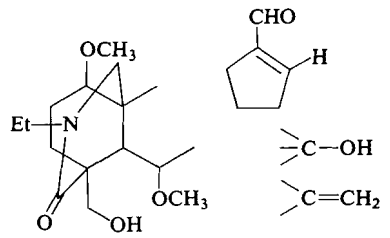

FIG. 1. Suggested systems contained in the lycoctamone analogues.

to that of lycoctamone. In addition the aldehyde hydrogen of cyclopent-1-enals gave n.m.r. signals near τ 0.28 (*cf.* lycoctamone at τ 0.25), at significantly lower field than that of cyclohex-1-enal (τ 0.66) and other conjugated unsaturated aldehydes (10).[8] We hence tentatively concluded that the lycoctamone analogues contained the systems illustrated in Fig. 1.

On the assumption that anhydrolycoctonam (2) was an intermediate in the formation of lycoctamone, mechanistic considerations (Scheme 2) led to postulation of two alternative structures, **10** and **11**, for lycoctamone, both of which contained the required functional groups. It seemed unlikely that **11** would have survived the acid reaction conditions and the subsequent basic hydrolysis of the monoacetate since there is no obvious reason why the terminal double bond would not move into conjugation. In addition the marked inertness of the isolated double bond to catalytic hydrogenation and osmylation (see below) are not accounted for by **11**. The three dimensional representation of **10**, however, (see **12**) shows the terminal methylene to be markedly shielded by other rings. Hence **10** ≡ **12** was a good working hypothesis for the structure of lycoctamone. The proximity of the terminal methylene group and the double bond of the cyclopentenal system is illustrated in more detail in **13**. The overlap of π orbitals could possibly

[7]The action of ozone on lycoctamone and dihydrolycoctamone (conjugated olefin reduced) in chloroform gave formaldehyde. However, the diagnostic value of these observations was made very uncertain when it was shown that delcosine gave formaldehyde under these conditions. Presumably oxidation of methoxy groups to formaldehyde takes place.

[8]We thank Professor J. B. Stothers for informing us of his observations prior to publication.

Can. J. Chem. Downloaded from www.nrcresearchpress.com by 210.87.254.5 on 09/05/12
For personal use only.

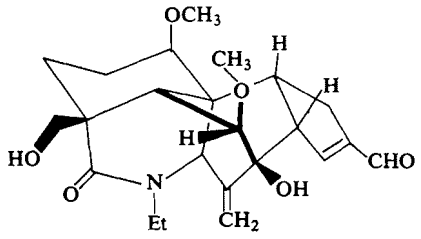

12

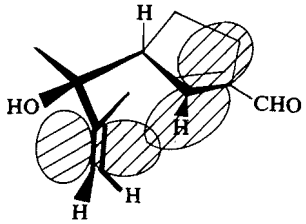

13

account for the bathochromic shift of the $\pi \rightarrow \pi^*$ absorption in lycoctamone relative to cyclopentenal ($\Delta\lambda = +7$ mμ) since the positive charge on C-14 would thereby be delocalized.

A test of the plausibility of structures **10** or **11** was provided by treating 14-deoxyoxobrowniine (**14**) with acid. As expected, pinacolic dehydration product and a mixture of non-conjugated aldehydes (dihydrobrownamones) (ν_{max} ($CHCl_3$) 2730 and 1720 cm^{-1}, n.m.r. signals around τ 0.5) were produced. The aldehydes were sensitive, and decomposed on attempts to separate them by repeated chromatography. This prevented precise correlation with the dihydrobrownamone produced by catalytic hydrogenation of brownamone. However, the analysis and spectral evidence indicated that they were the C-13 epimers of structure **15** (Scheme 3) if lycoctamone was correctly represented by **10**.

With structure **10** as a working hypothesis, an effort was made to establish the structure of lycoctamone and its analogues. First, attempts were made to prove the presence of the cyclopentenal system and the presence of a terminal methylene group and associated tertiary allylic alcohol. Later, attempts were made to interrelate these two sets of functions.

Des(oxymethylene)lycoctamone (**16**) was reduced over palladium to the dihydro compound **17** (Scheme 4). This was converted to the methyl ketone **18** by methyl magnesium iodide and subsequent oxidation. Trifluoroperacetic acid oxidation of **18**, followed by alkaline hydrolysis of the product and oxidation of the resulting secondary alcohol gave an epoxy ketone **19**. This had ν_{max} ($CHCl_3$) 1730 cm^{-1} which did not convincingly demonstrate its cyclopentanone character. The low frequency could however be rationalized if the epoxide had the most likely configuration illustrated in **19**. The unshared electrons on the oxide oxygen would be close enough to reduce the restoring force in a polarizing vibration of the C=O group, and so lower the cyclopentanone carbonyl stretching frequency.

A second sequence of steps gave more rigorous proof of the cyclopentenal system. Wolff–Kishner reduction of deoxymethylene lycoctamone gave under varying conditions three olefins.

The terminal olefin **20** was the major product of the reduction when performed at 180°. Relatively pure olefin **21** was obtained by conversion of the aldehyde to the ethylene thioketal, followed by Raney-nickel desulfurization. Wolff–Kishner reduction at 200° produced all three olefins, and at 220° **22** became a major product. Further, when a mixture of the three olefins was heated at 220° with potassium hydroxide in

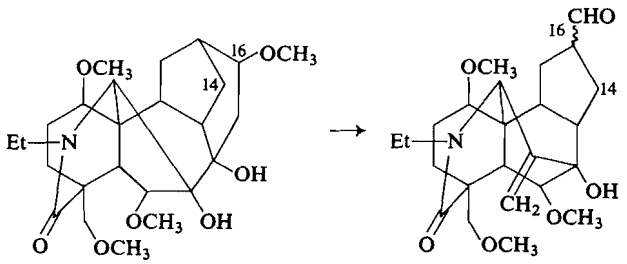

14 15

SCHEME 3

Can. J. Chem. Downloaded from www.nrcresearchpress.com by 210.87.254.5 on 09/05/12
For personal use only.

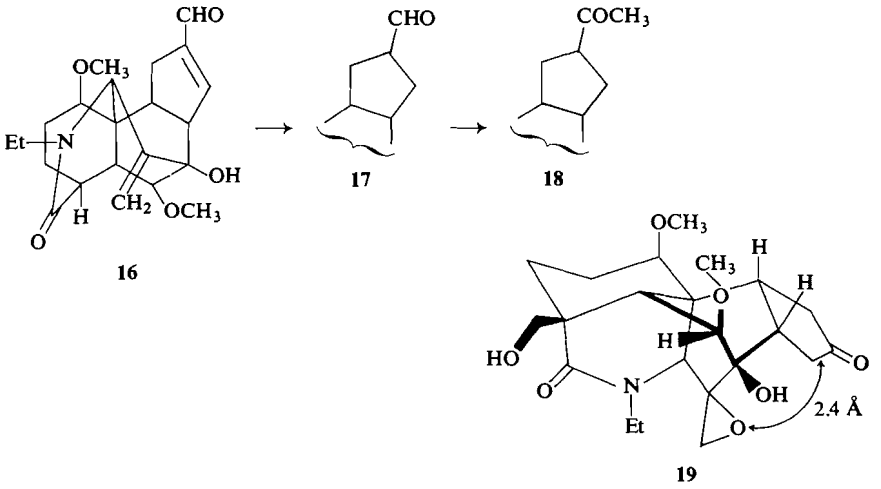

SCHEME 4

triethyleneglycol, **20** and **21** were converted almost completely into **22**. The illustrated structures (Scheme 5) account beautifully for the chemistry of these olefins. Oxidation of **20** gave a ketone **23** with ν_{max} (CCl_4) 1742 cm^{-1}, finally confirming the cyclopentenal character of lycoctamone. Hydroboration of **21** and **22** gave alcohols but only the one form **21** could be readily oxidized to a ketone. This ketone was internally hydrogen bonded (ν_{max} (CCl_4) 3420 and 1718 cm^{-1} at high dilution) in perfect accord with structure **24**.

The n.m.r. spectrum of olefin **22** showed the presence of one vinyl hydrogen (in addition to those of the terminal methylene). Hence the hydroboration product should be the secondary alcohol **25**. Both the isomerization of **21** to **22** and the resistance of alcohol **25** to oxidation can be accounted for on steric grounds. In olefin **21**, repulsive interaction of the 17, 1α and 12α hy-

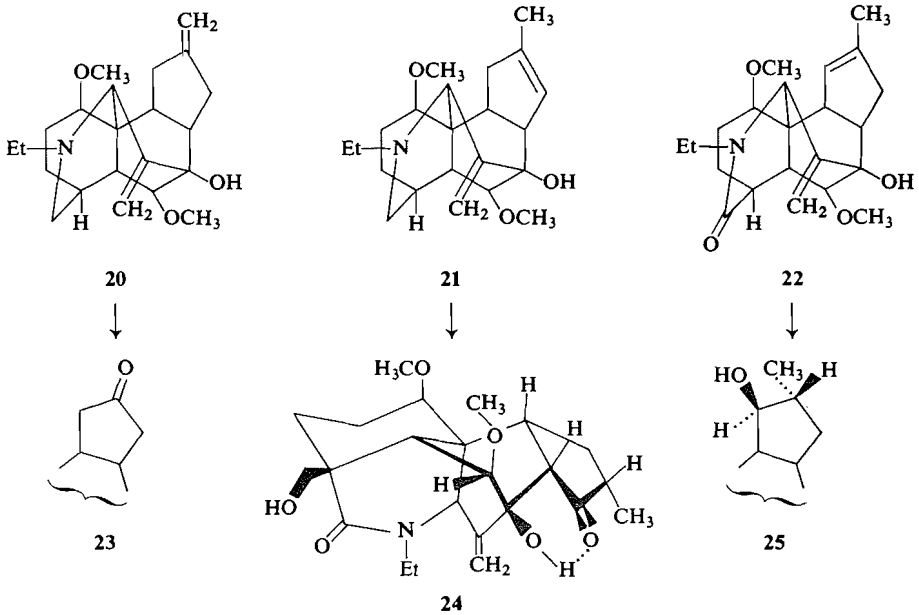

SCHEME 5

Can. J. Chem. Downloaded from www.nrcresearchpress.com by 210.87.254.5 on 09/05/12
For personal use only.

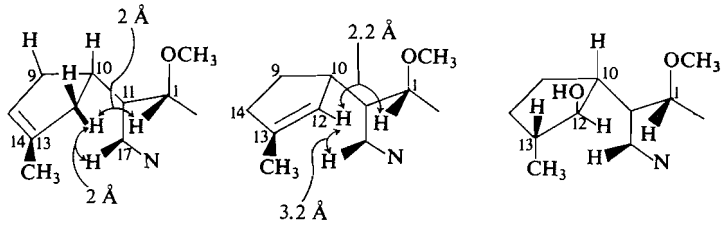

A B C

drogens is marked (in a Courtauld model the hydrogen atoms nearly touch, *i.e.* the inter-hydrogen distance is *ca.* 2 Å) (see **A**). In addition the vinyl hydrogen and 7-hydroxyl are eclipsed. These interactions are relieved on isomerization to **22** (see **B**). The hydroboration product **25** has the 12α-hydrogen very encumbered (see **C**) and relatively inaccessible to the base required to complete chromic acid oxidation (11).

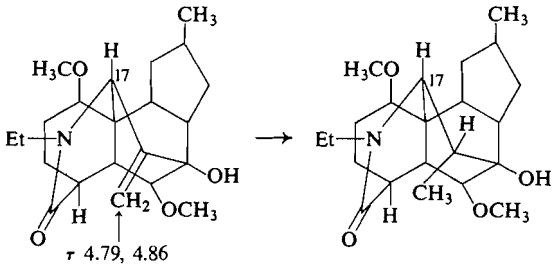

26 **27**

SCHEME 6

In order to simplify study of the hindered terminal double bond of the lycoctamones, the cyclopentenal system was converted by hydrogenolysis over palladium in acetic acid to the methylcyclopentane. The product from lycoctamone, dihydrolycoctam, was inert to osmium tetroxide – sodium periodate combination. However, both it and des(oxymethylene)dihydrolycoctam (**26**) still gave vinyl hydrogen signals in their n.m.r. spectra. Des(oxymethylene)dihydrolycoctam could be hydrogenated further over platinum in ethanol to a saturated lactam **27** (tetrahydrodes(oxymethylene)lycoctam) (Scheme 6). The increased complexity of the signals above τ 8.5 in the n.m.r. spectrum of the fully hydrogenated product suggested that a new methyl group had been produced but the integrated intensities were not decisive. In a further set of reactions, **26** was converted to the epoxide **28** using trifluoroperacetic acid. Analysis, the change in chemical shift of the methylene hydrogens shown on the figures in Scheme 7, and the further chemical reactions of **28** were consistent with this formulation. Vigorous lithium aluminum hydride reduction of **28** gave a basic diol,

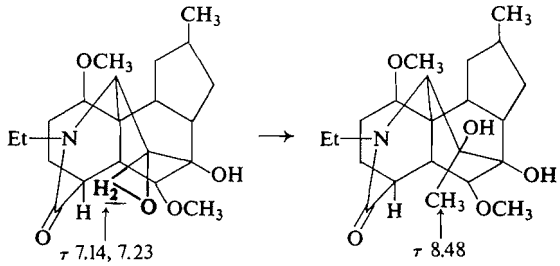

28 **29**

SCHEME 7

which could be oxidized by permanganate to the lactam **29**. The new methyl group gave a sharp signal at τ 8.48 as expected. The diol took up 1.3 mol of lead tetraacetate in 2 h giving a mixture of ketones and an ester (ν_{max} 1710 and 1745 cm^{-1}). The n.m.r. spectrum of the mixture showed the presence of an acetoxy group (τ 7.52) and two methyl ketone groups (epimers?) at τ 7.89 and 8.00. The diketone was not isolated in a pure state however since internal aldol condensations and/or epimerizations rapidly converted it to a mixture. One compound was isolated from this mixture and found to have the composition and physical properties expected for the internal aldol-condensation product **30**. The presence of extra low-field hydrogen signals (one-hydrogen doublet entered at τ 5.94, J = 9 Hz), corresponding to a hydrogen on C-6, excludes aldol condensation onto this carbon.

The presence and environment of the allyl alcohol thus corresponds exactly to that in structure **10**.

A spin decoupling study of the n.m.r. spectrum of des(oxymethylene)lycoctamone gave results in agreement with structure **16**. A broad ($w_{1/2}$ 5 Hz)

Can. J. Chem. Downloaded from www.nrcresearchpress.com by 210.87.254.5 on 09/05/12
For personal use only.

Can. J. Chem. Downloaded from www.nrcresearchpress.com by 210.87.254.5 on 09/05/12
For personal use only.

one-hydrogen signal at τ 5.76 should correspond to the hydrogen on C-17. A doublet at τ 6.75 and 6.80 seemed likely to arise from the hydrogen on C-6. Irradiation at τ 8.14 collapsed the doublet to a singlet and sharpened the signal at τ 5.78. This is consistent with resonance of the 5-hydrogen at τ 8.14. Long range W plan coupling with the 17-hydrogen (J = 3 Hz) is to be expected (12) (see formula **31**).

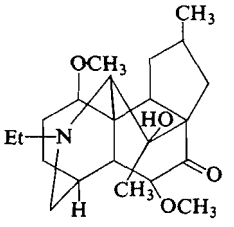

30

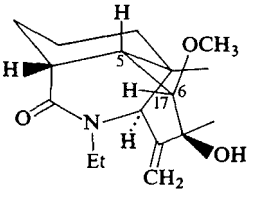

31

Attempts to directly relate the functions on the cyclopentane ring to the allyl alcohol system failed. However the internal hydrogen bonding observed for ketone **24** not only provides evidence for the assumed relationship, but it is incompatible with a corresponding ketone derived from structure **11**. In addition, the hydrogen on C-17 in dihydrodes(oxymethylene)lycoctam (**26**) was at τ 5.88. In the tetrahydro derivative **27** this hydrogen resonated at τ 6.40 close to that for des(oxymethylene)oxolycoctonine itself (τ 6.30). This large chemical shift is consistent with the allylic relation between the 17-hydrogen and the double bond as in **10**, but cannot be accounted for on the basis of structure **11**. In addition, the spectra of the aldol condensation product **30** (ν_{max} 1716 cm^{-1}; a three-hydrogen singlet at τ 8.42) are accounted for by this structure but not with the alternative ones **32** or **33** corresponding to structure **11**. In particular, the carbonyl stretching frequency of aldols similar to **32** was around 1742 cm^{-1} (des(oxymethylene)-iso compound) (3, 13), and a methyl ketone

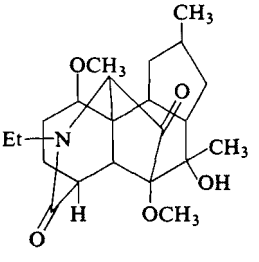

32

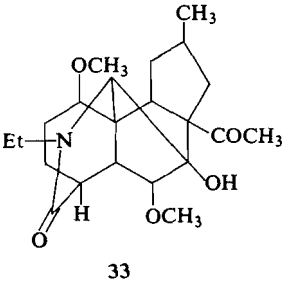

33

function as in **33** has its methyl signal near τ 7.85.

In view of the above evidence and the arguments advanced earlier about the expected instability of **11**, we conclude that lycoctamone has structure **10**.

The driving force for the unusual and deep-seated change leading to lycoctamone would seem to be steric in origin since the primary fission product has no obvious electronic stabilization. A likely possibility for the driving force was relief of the repulsive interactions of the 1,3-diaxial oxygen substituents at C-14 and -16. However, this is not a dominant factor since 14-deoxyoxobrowniine (**14**) underwent the reaction with facility.

Notable relief of repulsive interactions between substituents on C-18 and the 6-hydrogen and between the 6-methoxyl and the 9-hydrogen is illustrated in the transition from the anhydro

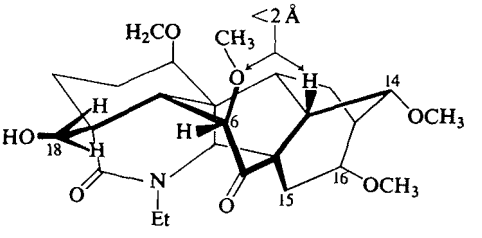

34

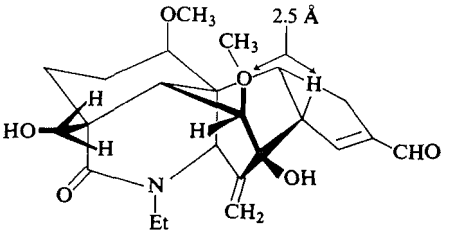

35

compound **34** to lycoctamone **35**. As expected if these interactions provided much of the driving force for the reaction, replacement of the 4-substituent by hydrogen (des(oxymethylene)oxylycoctonine) makes the reaction much more difficult. Very little unsaturated aldehyde was produced under the usual acid conditions, but in 5 h, at room temperature in concentrated sulfuric acid, approximately 50% of des(oxymethylene)lycoctamone was produced. The removal of the 6-methoxyl group (18-*O*-methyl-6-

Can. J. Chem. Downloaded from www.nrcresearchpress.com by 210.87.254.5 on 09/05/12
For personal use only.

demethoxyanhydrooxolycoctonine, **3**, R_1 = OCH_3, R_2 = H) made the reaction even more sluggish. After 5 h in concentrated sulfuric acid only 25% of lycoctamone analogue was produced. The fragmentation must be well advanced in the transition state so that relief of the abovementioned interactions is felt. Both Dreiding and Courtauld models demonstrate that considerable angle distortion of bonds exists in the anhydro compounds. This can be noticed readily if the 15–16 bond is coupled last. It is likely that some of the driving force for the rearrangement to the lycoctamones also arises from this strain.

It is, at first sight, surprising to find an allyl alcohol as product of an acid-catalyzed reaction. However because of the bridgehead position of the allylic hydroxyl, the only likely course of further reaction would be protonation of the terminal methylene followed by rearrangement to a methyl ketone. The fact that this takes place slowly, if at all, we attribute to the proximity of the methylene group to the more basic amide and α,β unsaturated aldehyde systems which must compete successfully for available protons.

The lycoctamone analogues are potentially very valuable in studies of biosynthesis of the lycoctonine family of diterpenoid alkaloids, since labelling on C-18 and -19 could readily be examined.

Experimental

The i.r. spectra were taken on a Perkin–Elmer model 21 prism spectrometer, and are of Nujol mulls unless otherwise specified. The n.m.r. spectra were obtained on Varian HA-60 and A-60 instruments in deuterochloroform unless specified, with tetramethylsilane as internal standard unless otherwise indicated. Rotations were in absolute ethanol unless the solvent is given. Chromatography was on Woelm neutral alumina and t.l.c. on silica gel plates.

Lycoctamone

This gave positive Angeli–Rimini and Tollens tests for aldehyde, and a positive test for an α,β unsaturated aldehyde (9). Weak bands at 2720 (—CHO) and 3090 cm^{-1} (=CH_2) were present in the i.r. spectrum of a carbon tetrachloride solution of lycoctamone acetate. The n.m.r. spectrum of lycoctamone ($CDCl_3$) had a sharp one-hydrogen signal at τ 0.25 (CHO), a broad one-hydrogen signal centered at τ 3.24 (HC=C—C=O), two one-hydrogen signals at τ 4.68 and 4.73 (=CH_2), and two methoxyl signals at τ 6.28 and 6.54.

Dihydrolycoctamone

Lycoctamone (135 mg) was added to 20 ml of 95% ethanol containing 20 mg of palladium black presaturated with hydrogen. In 25 min, uptake of hydrogen ceased (6.94 ml at N.T.P., 1.17 mol). The product crystallized from a concentrated acetone solution, m.p. 125–128°. It had only end absorption in the u.v., and ν_{max} ($CHCl_3$) 1615 and 1721 cm^{-1}. It gave positive Tollens and Angeli–Rimini tests but a negative test for α,β unsaturated aldehyde (9). Its n.m.r. spectrum had a one-hydrogen doublet at −134 Hz from solvent chloroform (J = 4 Hz) and two one-hydrogen singlets at +113 and +119 Hz from the chloroform signal.

Anal. Calcd. for $C_{23}H_{33}NO_6 \cdot 2H_2O$: C, 60.64; H, 8.19. Found: C, 60.25; H, 7.81.

Parent ion at *m/e* 419, Calcd. for $C_{23}H_{33}NO_6$: 419

Dihydrolycoctamone monoacetate, prepared by reduction of lycoctamone acetate as above had m.p. 190–194°.

Anal. Calcd. for $C_{25}H_{35}NO_7$: C, 65.05; H, 7.64. Found: C, 64.94; H, 7.63.

Attempted Oxidation of Dihydrolycoctam

A solution of 80 mg of dihydrolycoctam (8) and 30 mg of osmium tetroxide in 3 ml of 80% acetic acid – 20% water was left for 1 h at room temperature. To this was added 100 mg of sodium paraperiodate in 10 ml of 80% acetic acid. After 5 h at room temperature the solvent was removed *in vacuo*, the residue dissolved in methylene chloride, and acid removed by extracting with sodium carbonate solutions. The neutral product (80 mg) had an n.m.r. spectrum nearly identical to that of dihydrolycoctamone. A trace of carbonyl-containing product was indicated by a band at 1700 cm^{-1}.

Ozonolysis of Dihydrolycoctamone

A stream of ozonized oxygen was bubbled into a solution of 5 mg of dihydrolycoctamone in 7 ml of chloroform for 10 min. The chloroform was then evaporated *in vacuo* and the residue taken up in 4 ml of water. Steam distillation was carried out until 5 ml of distillate collected. This gave a rich violet color with chromatropic acid reagent. A blank with reagents was negative.

Ozonolysis of Delcosine

Ozonized oxygen was bubbled for 15 min into a solution of 20 ml of delcosine in 8 ml of acetic acid. After addition of 8 ml of water, the mixture was steam distilled. The distillate gave the characteristic violet color with chromatropic acid reagent.

18-O-Methyllycoctamone

A solution of 80 mg of 18-*O*-methylanhydrooxolycoctonine (14) in 1.5 ml of acetic acid containing 0.2% sulfuric acid was heated for 2 h at 115°. The cooled mixture was added to 5 ml of ice-water, and the resulting solution made alkaline with ammonia. Extraction with chloroform gave 80 mg of product, which was adsorbed from benzene onto 2 g of neutral alumina, activity III. Benzene eluted 14 mg of amorphous material, then benzene–chloroform mixtures eluted 62 mg which crystallized from acetone. After recrystallization and sublimation at 180°, 5×10^{-4} mm, the product had m.p. 227–228°, and λ_{max} 245 mμ (ε 12 000).

Anal. Calcd. for $C_{24}H_{33}NO_6$: C, 66.80; H, 7.71; 3 OCH_3, 21.57. Found: C, 66.52; H, 7.45; OCH_3, 21.98.

The compound gave n.m.r. signals at τ 0.05 (1H), 3.22 (1H), a two-hydrogen pair at τ 4.7 and 4.73, and three three-hydrogen signals at τ 6.28, 6.50, and 6.59.

Can. J. Chem. Downloaded from www.nrcresearchpress.com by 210.87.254.5 on 09/05/12
For personal use only.

18-O-Methyl-6-demethoxylycoctamone

18-*O*-Methyl-6-demethoxyanhydrolycoctonam (14) (69 mg) was dissolved in 1 ml of concentrated sulfuric acid, the solution left for 5 h at room temperature, then poured onto crushed ice. The aqueous solution was made alkaline using concentrated ammonium hydroxide, then the product extracted into chloroform. The 45 mg of readily extracted product was adsorbed from benzene onto 1 g of alumina, activity II. Benzene (30 ml) eluted 16 mg of undesired product. Benzene–chloroform (3:1, 10 ml) eluted 9 mg of an approximately 3:7 mixture of starting material and desired product, and a further 10 ml of solvent eluted 9 mg of the lycoctamone analogue. The compound was sublimed at 195°, 1×10^{-3} mm. It then had ν_{max} 3380, 1682, and 926 cm^{-1}. It melted over a wide range, mainly 235–243°.

Anal. Calcd. for $C_{23}H_{31}NO_5$ (mol. wt. 401): 2 OCH_3, 15.29. Found (parent ion at *m/e* 401 with an impurity at *m/e* 415): OCH_3, 16.93, 16.88.

The yield estimated from the i.r. maximum was approximately 21%. Prolonging the time of reaction to 20 h reduced the yield to approximately 11%.

18-Deoxyoxolycoctonine (5)

The yield was markedly improved over the previous report (15). 18-deoxylycoctonine (1.03 g) in 5 ml of dry pyridine was added to a mixture of 800 mg of chromium trioxide in 12 ml of pyridine. The reaction mixture was shaken overnight, concentrated to half-volume under reduced pressure (bath at 45°), then poured onto 50 ml of crushed ice. After acidification with 3 *N* sulfuric acid, remaining oxidizing agent was reduced by bubbling in sulfur dioxide. The product was extracted into chloroform (6 × 25 ml). The chloroform layer, after washing with water then drying over sodium sulfate, was evaporated, leaving 860 mg of glassy residue. This was adsorbed from benzene onto 10 g of neutral alumina, activity II. Benzene and benzene–chloroform eluted 860 mg of product which crystallized from acetone–hexane to give 703 mg of colorless prisms, m.p. 166–169°.

18-Deoxylycoctamone

A solution of 758 mg of 18-deoxyoxolycoctonine (5) in 10 ml of 0.2% sulfuric acid in acetic acid was heated at 115° for 1.5 h. The sulfuric acid was neutralized by addition of sodium carbonate, then the bulk of the acetic acid evaporated under reduced pressure. The residue was taken up in water, the product extracted into chloroform and this solution washed free of acid with sodium carbonate solution. The product recovered from the chloroform was adsorbed from benzene onto 16 g of alumina, activity III. Benzene (50 ml) and benzene–chloroform (1:1) eluted 12 mg which was discarded. Benzene–chloroform (1:1, 80 ml) and benzene–chloroform (1:3, 60 ml) eluted 658 mg which yielded 204 mg of deoxylycoctamone. Rechromatography of the mother liquor on 6.6 g of alumina activity IV gave more product. The eluates with benzene and benzene–chloroform (1:1) crystallized, yielding a further 170 mg of 18-deoxylycoctamone. After recrystallization from acetone it melted at 240–244°, and had $[\alpha]_D$ + 361° (*c*, 2.3 in $CHCl_3$), λ_{max} 244 (ε 16 600), 308 mμ (ε 288), and ν_{max} 3600, 3500, 3300, 1671, and 1620 cm^{-1}.

Anal. Calcd. for $C_{23}H_{31}NO_5 \cdot H_2O$: C, 65.85; H, 7.94. Found: C, 66.10; H, 7.60.

The compound had n.m.r. signals at −282 (1H, sharp), −115 (1H, broad), −32 (1H), and −28 (1H) Hz relative to external water.

When 172 mg of 18-deoxyoxolycoctonine was dissolved in 1.5 ml of concentrated sulfuric acid and the solution left at room temperature for 5 h, the product contained no starting material or anhydro compound. Chromatography on alumina enabled isolation of 59 mg of 18-desoxylycoctamone.

Oxime: m.p. 255–260°, λ_{max} 244 mμ, (ε 13 800).

Anal. Calcd. for $C_{23}H_{32}N_2O_5$: N, 6.73. Found: N, 6.65.

The oxime was dehydrated by 1 h refluxing with acetic anyhydride, giving a 50% yield of crude nitrile (ν_{max} 2120 cm^{-1}) after chromatography on alumina. After recrystallization from acetone–hexane the nitrile had m.p. 235–238°, ν_{max} 2240 cm^{-1}.

Anal. Calcd. for $C_{23}H_{30}N_2O_4$: C, 69.32; H, 7.59; N, 7.03. Found: C, 69.31; H, 7.47; N, 7.05.

18-Deoxylycoctamol

A solution of 80 mg of 18-deoxylycoctamone and 80 mg of sodium borohydride in 5 ml of methanol was left at room temperature for 45 min. Fifteen milliliters of 2 *N* sulfuric acid were added, and the product extracted into chloroform. After removal of the chloroform the 80 mg of glassy residue was taken up in acetone–hexane. It crystallized in the form of small prisms m.p. 205–210°. After two recrystallizations from this solvent mixture it had m.p. 230–232°. It had only strong end absorption in the u.v., and ν_{max} 3430, 3360, 1123, and 908 cm^{-1}. Its n.m.r. spectrum had vinyl hydrogen signals at 112 Hz (broad one-hydrogen singlet), and a poorly resolved doublet centered at 128 Hz (two hydrogens). It had a two-hydrogen signal at 190 Hz attributable to a $—CH_2OH$ group (all chemical shifts relative to internal chloroform).

Brownamone

Oxobrowniine (16), m.p. 165–168° (600 mg) was dissolved in 20 ml of 0.2% (v/v) sulfuric acid in acetic acid. The solution was heated in a bath held between 115 and 123° for 2.5 h, then concentrated to small volume under reduced pressure. After addition of 10 ml of water it was adjusted to p*H* 8 using 4% sodium carbonate solution. Thorough extraction with methylene chloride gave 660 mg of product. This was hydrolyzed by 25 min refluxing with 50 ml of 5% potassium hydroxide in 50% aqueous methanol, giving 581 mg of hydrolysate. This was adsorbed from benzene onto 17 g of neutral alumina, activity III. Benzene (90 ml), chloroform in benzene (50 ml 10%, 50 ml 20%) eluted 35 mg of ketonic material. Chloroform in benzene (30–50%) eluted 158 mg of pure brownamone and 70 mg of less pure material. The estimated total yield was 208 mg (39%). The product had m.p. 222–230° with some crystals remaining until 240°; ν_{max} (Nujol) 3400, 1678, 1616, 934 cm^{-1} and λ_{max} 244 mμ, (ε 11 900). Its n.m.r. spectrum had signals at τ 0.25 (1H singlet), 3.34 (1H, $w_{1/2}$ 5 Hz), 4.81 (1H), 4.87 (1H), 5.80 (1H doublet, J = 3.5 Hz), 6.36 (3H), 6.59 (3H), 6.68 (3H), 8.87 (3H triplet, J = 7 Hz).

Anal. Calcd. for $C_{24}H_{33}O_6N$: C, 66.80; H, 7.71. Found: C, 66.89; H, 7.62.

Can. J. Chem. Downloaded from www.nrcresearchpress.com by 210.87.254.5 on 09/05/12
For personal use only.

*14-Deoxyoxobrowniine (**14**)*

14-Dehydrooxobrowniine (16) m.p. 167–171° (979 mg) was dissolved in 25 ml of triethylene glycol and 7 ml of 95% hydrazine. The solution was heated at 140° for 1 h, 4 g of potassium hydroxide was cautiously added, then the bath temperature raised during 40 min to 190°. The bath was maintained at 190–200° for 4 h, then at 200–210° for 1 h. After cooling, the mixture was diluted with 35 ml of water and extracted repeatedly with methylene chloride. The 923 mg of white froth remaining after removal of the methylene chloride was adsorbed from benzene on 18.5 g of neutral alumina, activity III. Benzene, benzene–chloroform, and chloroform eluted 650 mg of nearly pure 14-deoxyoxobrowniine which, however, did not crystallize. After distillation at 200°, 5×10^{-4} mm, it had ν_{max} 1615 cm^{-1}.

Anal. Calcd. for $C_{25}H_{39}O_7N$: C, 64.49; H, 8.44. Found: C, 64.64; H, 8.63.

*Dihydrobrownamone (**15**)*

A solution of 234 mg of 14-deoxyoxobrowniine in 20 ml of 0.2% (v/v) sulfuric acid in glacial acetic acid was heated at 115° for 100 min. The bulk of the acetic acid was evaporated under reduced pressure, the residue taken up in 5 ml of water, then sufficient solid sodium carbonate added to bring the p*H* to 8. Thorough extraction with methylene chloride gave 203 mg of product. This was hydrolyzed by 30 min reflux with 5% potassium hydroxide in 50% aqueous methanol. The 165 mg of hydrolysate was adsorbed on 3.3 g of grade III neutral alumina. Benzene (50 ml) eluted 10 mg of ketonic material. Chloroform in benzene (1:4 to 3:1) eluted the desired product (90 mg) with some contamination at both ends. The estimated total yield of dihydrobrownamone was 79 mg (31%). After recrystallization from ether–pentane the compound had m.p. 146–156°, ν_{max} ($CHCl_3$) 3570, 3420, 2730, 1720 and 1630 cm^{-1}. Its n.m.r. spectrum had three signals at τ 0.43, 0.52, and 0.57 (—CHO), two one-hydrogen signals at τ 6.28 and 6.40 (=CH_2), and a split six-hydrogen signal at τ 6.67 (two methoxyl groups). Attempts to separate the aldehyde epimers by further chromatography resulted in destruction of the sensitive compound. The compound was dried 2 h at 100° *in vacuo*.

Anal. Calcd. for $C_{24}H_{35}O_8N$: C, 66.49; H, 8.14. Found: C, 66.28; H, 8.09.

The action of 12 *N* sulfuric acid at 100° for 2 h on 14-deoxyoxobrowniine gave a mixture containing pinacolic dehydration product and dihydrobrownamone. The yield of the latter was estimated by i.r. spectroscopy to be approximately 30%.

*1-Deoxyoxodelcosine (**8**)*

One gram of 1-dehydrooxodelcosine (17), m.p. 225–227°, was added to a mixture of 25 ml of triethylene glycol and 10 ml of hydrazine. After 70 min heating at 140°, potassium hydroxide (4 g) was added cautiously. The temperature was raised to 190° during 1 h, excess hydrazine being swept out of the condenser by dry nitrogen. The bath temperature was maintained at 185–190° for 4 h. The cooled reaction mixture was then diluted with 30 ml of water and the product extracted into methylene chloride. The methylene chloride layers were washed with water, dried, and distilled, giving 875 mg of product. This was adsorbed from benzene onto 18 g of alumina, activity III. Benzene (50 ml) eluted a fore-run of 15 mg. Chloroform (100 ml) eluted 750 mg of quite pure 1-deoxyoxodelcosine. This was rechromatographed on 15 g of alumina, activity III. Chloroform (150 ml) eluted 688 mg of product which crystallized readily. After three recrystallizations from benzene–hexane it melted at 225–235°. It appeared to be strongly hydrated, and only slowly lost water on drying. After 2 h at 110°, 1×10^{-2} mm, it gave a low carbon value.

Anal. Calcd. for $C_{24}H_{32}O_7N$: C, 63.83; H, 8.26. Found: C, 62.72; H, 8.13.

*Action of Sulfuric Acid on **8***

1-Deoxyoxodelcosine (208 mg) was dissolved in 4 ml of concentrated sulfuric acid at room temperature. After 5 h crushed ice was added, the solution made alkaline with saturated sodium carbonate solution, and the product extracted into chloroform. The 83 mg of froth recovered from the chloroform was adsorbed from benzene on 1.7 g of alumina, activity III. The benzene eluates (30 ml) were discarded. Benzene–chloroform (15 ml, 1:1) eluted 30 mg of the desired product. After crystallization from benzene–hexane it lost solvent at 95° with partial melting, resolidified, and melted at 154–157°. After 24 h drying over P_2O_5 under 1×10^{-2} mm it was analyzed.

Anal. Calcd. for $C_{23}H_{31}O_5N$: C, 68.80; H, 7.78. Found: C, 69.18; H, 7.59.

The compound had ν_{max} 3340, 2730, 1683, 1616, and 935 cm^{-1}, and λ_{max} 243 mμ, (ε 10 600). The yield of the α,β unsaturated aldehyde was estimated spectroscopically to be 22%.

The yield of unsaturated aldehyde when 1-deoxyoxodelcosine was heated for 3 h at 100° in 12 *N* sulfuric acid was estimated spectroscopically to be 12%.

*Des(oxymethylene)lycoctamone (**16**)*

Des(oxymethylene)lycoctonam (15) (1.01 g) was dissolved with stirring in 8 ml of concentrated sulfuric acid. After 5 h at room temperature the solution was poured onto crushed ice, and the product extracted into methylene chloride. The organic layers were washed free of acid using sodium carbonate solution, dried, and distilled, giving 706 mg of froth. This was adsorbed from benzene on 14 g of alumina, activity III. Benzene, and benzene–chloroform (1:1) eluted fairly pure des(oxymethylene)-lycoctamone. After recrystallization from acetone–hexane this gave 330 mg, m.p. 198–201° (237–241° in an evacuated capillary); $[\alpha]_D$ + 288° (*c*, 1.04). It had ν_{max} 246 mμ, (ε 10 700) and ν_{max} 3380, 1675, 1621, and 913 cm^{-1}.

Anal. Calcd. for $C_{22}H_{29}NO_5$: C, 68.19; H, 7.54; 2 OCH_3, 16.02. Found: C, 68.68; H, 7.67; OCH_3, 15.89.

Its n.m.r. spectrum had signals at τ 0.27 (1H), 3.37 (1H), 4.80 (1H), 4.87 (1H), 5.76 (1H), 6.50 (OCH_3), 6.68 (OCH_3), a one-hydrogen doublet (?) centered at 6.79 (J = 3.5 Hz), and a triplet centered at 8.89 (J = 7 Hz) (N—C_2H_5).

Treatment of des(oxymethylene)lycoctonam with 0.1% sulfuric acid in acetic acid at 110° for 1.5 h gave a product which had no maximum at 246 mμ.

*Dihydrodes(oxymethylene)lycoctamone (**17**)*

When hydrogenated over presaturated 30% palladium-on-charcoal in ethanol des(oxymethylene)lycoctamone

Can. J. Chem. Downloaded from www.nrcresearchpress.com by 210.87.254.5 on 09/05/12
For personal use only.

absorbed consistently 1.2 mol of hydrogen. Chromatography of the product on neutral alumina, activity IV, gave a very readily (20% benzene in chloroform) eluted hydrogenolysis product, followed by a mixture of two dihydro products. The yield of the latter was approximately 81%. The mixture had m.p. 125–137° after recrystallization from acetone–ether–hexane; $[\alpha]_D$ 116° (*c*, 1.14 in chloroform).

Anal. Calcd. for $C_{22}H_{31}O_5N$: C, 67.84; H, 8.02. Found: C, 68.01; H, 8.22.

Hydrogenation of des(oxymethylene)lycoctamone over palladium black gave 1.05–1.17 mol uptake. The dihydro compound from this reduction had m.p. 125–128° after recrystallization from acetone–pentane. It had ν_{max} ($CHCl_3$) 1720 and 1605 cm^{-1} and only end absorption in the u.v.

Methyl Carbinols from Dihydrodes(oxymethylene)lycoctamone (17)

Dihydrodes(oxymethylene)lycoctamone mixture (272 mg) in dry ether–chloroform mixture was added to an excess of methyl magnesium iodide in ether. The mixture was refluxed for 3 h, then left overnight at room temperature. The excess reagent was decomposed with dilute sulfuric acid, and the product extracted into chloroform. This mixture (300 mg) was chromatographed on neutral alumina, activity IV. After a weakly adsorbed fore-run, carbinol 1 was eluted with 50% chloroform–benzene giving 45 mg, m.p. 179–182°, $[\alpha]_D$ 112° (*c*, 0.9).

Anal. Calcd. for $C_{23}H_{35}O_5N$: C, 68.12; H, 8.70. Found: C, 68.02; H, 8.52.

Elution with chloroform and methanol in chloroform gave carbinol 2, 100 mg, m.p. 190–192°, $[\alpha]_D$ 109° (*c*, 1.28).

Anal. Calcd. for $C_{23}H_{35}O_5N{\cdot}H_2O$: C, 65.22; H, 8.81. Found: C, 66.23; H, 8.10.

Mol. wt. Calcd. for $C_{23}H_{35}O_5N$: 405. Parent ion at *m/e* 405.

Methyl Ketone 18

The mixture of methyl carbinols (72 mg) was left for 15 h in excess chromium trioxide – pyridine at room temperature, dilute sulfuric acid was added, and sulfur dioxide bubbled in until a clear green solution was obtained. This was extracted with chloroform to give 65 mg of product. The t.l.c. showed the presence of two similar products, whose ratio was not noticeably changed by 2 h exposure to potassium hydroxide in methanol. The mixture was chromatographed on grade IV neutral alumina, giving 57 mg of readily-eluted methyl ketones. The middle fractions crystallized from ether–hexane giving 23 mg, m.p. 149–151°, $[\alpha]_D$ 100° (*c*, 1.2); ν_{max} 1700, 1620 cm^{-1}.

Anal. Calcd. for $C_{23}H_{33}O_5N$: C, 68.46; H, 8.24. Found: C, 68.31; H, 8.09.

The mother liquors and the other ketone-rich fractions gave nearly identical i.r. spectra, so were combined for Baeyer–Villiger oxidation.

Epoxy Diol

A mixture of the methyl ketones (**18**) (254 mg) was treated with excess trifluoroperacetic acid in methylene chloride, the solution refluxed for 1 h, then left at room temperature for 3–4 h. Aqueous sodium sulfite was added, then the methylene chloride layer separated and washed with sodium carbonate solution. The product was hydrolyzed by 1 h refluxing with potassium hydroxide in ethanol. After removal of the alcohol under reduced pressure the residue was taken up in dilute acid and extracted with chloroform, giving 156 mg of product. This gave two main spots on t.l.c. Concentration of the aqueous layers followed by further extraction gave 50 mg of more polar products. The main product was chromatographed on alumina, activity IV. The least polar compound, eluted with benzene–chloroform mixtures and chloroform, crystallized readily from chloroform–ether giving 70 mg, m.p. 232–235°, $[\alpha]_D$ 62 (*c*, 0.98), ν_{max} ($CHCl_3$) 1625 cm^{-1}. Its n.m.r. spectrum had a 1H signal near τ 5.8 superimposed on the *N*-ethyl quartet (CHOH), a 1H singlet at τ 6.09 (C-15 hydrogen) and two 1H singlets at τ 7.2 and 7.3 (H_2C C).

Anal. Calcd. for $C_{21}H_{31}O_6N$: C, 64.10; H, 7.94. Found: C, 64.23; H, 7.69.

The second major product was not obtained pure.

Epoxy Ketol 19

Crystalline epoxy diol (21 mg) was left overnight with 25 mg of chromium trioxide in pyridine. The 21 mg of product had a weak carbonyl peak near 1725 cm^{-1} in carbon tetrachloride. The t.l.c. showed the presence of considerable unchanged alcohol. Repetition of the oxidation on the mixture increased the carbonyl intensity; however unchanged alcohol was still present and semi-crystalline, but not completely pure, ketone was obtained. Oxidation of the epoxy diol with chromium trioxide in acetic acid or Kiliani reagent gave mixtures of carbonyl compounds, probably because of opening of the epoxide ring.

Olefin 20

Des(oxymethylene)lycoctamone (320 mg) in ethylene glycol (10 ml) and hydrazine hydrate (10 ml) was heated at 120° for 1 h. Potassium hydroxide (900 mg) was added and the reaction temperature raised to 180–190° for 4 h. The solution was cooled, acidified with 6 *N* hydrochloric acid, and extracted with chloroform. The product (316 mg) crystallized on standing. Its n.m.r. spectrum showed the presence of a large proportion of the exocyclic olefin **20**. The t.l.c. showed mainly one spot which was resolved into three on silica–$AgNO_3$ plates. The main spot was the one with the lowest R_f, corresponding to the exocyclic olefin **20**, while the other spots corresponded to olefins **21** and **22**. After recrystallization from chloroform–acetone, 140 mg of nearly pure **20** was obtained (m.p. 212–216°). A second recrystallization from the same solvent gave a sample with m.p. 222–224°, $[\alpha]_D$ 142° (*c*, 1.06 in chloroform).

Anal. Calcd. for $C_{22}H_{31}O_4N$: C, 70.75; H, 8.37. Found: C, 70.96; H, 8.57. The sample had ν_{max} (Nujol) 3300, 1622 cm^{-1} and gave n.m.r. signal at τ 4.6 (1H), 4.75 (1H), and 5.26 (2H).

Olefin 21

Des(oxymethylene)lycoctamone (70 mg) was dissolved in a chloroform–ether mixture, then ethane dithiol (0.2 ml) and redistilled BF_3 etherate (0.2 ml) added. The reaction mixture was left at room temperature for 2 h. Excess aqueous sodium hydroxide (4 *N*) was added and the solution extracted with ether. The ether extract was washed with 4 *N* aqueous NaOH, then with water. The

Can. J. Chem. Downloaded from www.nrcresearchpress.com by 210.87.254.5 on 09/05/12
For personal use only.

product (70 mg) crystallized from $CHCl_3$–ether–hexane; m.p. 182–184°; $[\alpha]_D$ +244° (*c*, 0.8 in $CHCl_3$).

Anal. Calcd. for $C_{24}H_{33}NO_4S_2$: C, 62.19; H, 7.18. Found: C, 61.95; H, 7.43.

Thioketal (45 mg) in acetone was refluxed for 6 h with excess deactivated Ni(R). The Ni(R) was filtered off and washed six times with hot acetone. The product (30 mg) crystallized on standing and was purified by preparative t.l.c. It was recrystallized from $CHCl_3$–ether–hexane, m.p. 171–173°; $[\alpha]_D$ +213° (*c*, 0.55 in $CHCl_3$).

Anal. Calcd. for $C_{22}H_{31}NO_4$: C, 70.75; H, 8.37. Found: C, 70.98; H, 8.71.

The n.m.r. spectrum of the product had a strong signal at τ 8.30 (CH_3—C=C). The t.l.c. on silica gel – silver nitrate showed the presence of a small amount of olefin **22**, with olefin **21** as the main product.

High Temperature Wolff–Kishner Reduction (Olefin 22)

Des(oxymethylene)lycoctamone (100 mg) in ethylene glycol (5 ml) and hydrazine hydrate (4 ml) was heated for 1½ h. Potassium hydroxide (400 mg) was added and the reaction mixture heated at 220° for 4 h. Work-up as usual yielded crystalline material (95 mg). The t.l.c. on silica gel – silver nitrate showed this to be a mixture of all three olefins as before but with an increased amount of the least polar one (**22**).

The mixture (95 mg) was heated in ethylene glycol (5 ml) with KOH (2.5 g) for 2 h at 220°. The product was a yellow oil (60 mg) and showed two shots on an ordinary plate. Separation by preparative t.l.c. yielded two crystalline fractions, the less polar being the required olefin fraction (40 mg). The more polar (20 mg) compound had no vinyl proton signals in its n.m.r. spectrum and was set aside (this was also formed to some extent in the gentler Wolff–Kishner reduction). The olefin fractions were shown by t.l.c. on a silica gel – silver nitrate plate to be almost pure olefin **22**. This crystallized from acetone–ether–hexane mixture, and had m.p. 176–186°. After one recrystallization it had m.p. 186–189° and $[\alpha]_D$ +52° (*c*, 1.02 in $CHCl_3$).

Anal. Calcd. for $C_{22}H_{31}NO_4$: C, 70.75; H, 8.37. Found: C, 70.36; H, 8.82. The n.m.r. spectrum showed signals at τ 4.52 (1H), 4.65 (1H), 4.95 (1H) and 8.39 (3H).

A mixture of olefins from Wolff–Kishner reduction at 180° was shaken with H_2 in ethanol over 10% palladium-on-charcoal; approximately 1 mol of H_2 was taken up in 3 min. The product crystallized spontaneously and on silica gel – silver nitrate plates showed mainly one spot with none of the olefins remaining. It crystallized from $CHCl_3$–ether–hexane to give m.p. 185–192°. Its n.m.r. spectrum still contained the signals for the exocyclic methylene group (C-18) and was indistinguishable from that of dihydrodes(oxymethylene)lycoctam.

Oxidation of Olefin 20

The exocyclic olefin (30 mg) in ether (3 ml) and pyridine (3 ml) was treated with OsO_4 (3 mg) overnight at room temperature. The osmate ester was destroyed by stirring with aqueous sodium bisulfite for 20 min. The crude diol (25 mg) obtained by extraction with $CHCl_3$ was dissolved in MeOH (5 ml) and treated with sodium periodate (30 mg) in water at 5° for 3 h. Water was added and the solution extracted with $CHCl_3$ to yield crude ketone **23** (20 mg) which crystallized from an acetone–ether–hexane mixture giving 10 mg with m.p. 224–228° and $[\alpha]_D$ +141° (*c*, 0.69 in $CHCl_3$).

Anal. Calcd. for $C_{21}H_{29}NO_5$: C, 67,18; H, 7.79. Found: C, 67.61; H, 8.00. The ketone had ν_{max} (CCl_3) 1742 (cyclopentanone) and 1647 cm^{-1} (lactam) and n.m.r. peaks at τ 4.52 (1H) and 4.77 (1H) (exocyclic methylene).

Ketone 24

Olefin **21** (140 mg) contaminated with some olefin **19** was treated with excess diborane in tetrahydrofuran under nitrogen for 12 h. After removal of the solvent the residue was refluxed for 5 min with ethanol containing hydrogen peroxide and potassium hydroxide. The product was contaminated with "polymeric" material, but was purified by chromatography on alumina (activity III). The more readily eluted alcohol **25** (25 mg, m.p. 217–223°) was followed by the desired alcohol from **21**. This appeared to be a mixture of stereoisomers due to attack of diborane on both sides of the ring. It crystallized from acetone–hexane as rods, m.p. 150–166°, ν_{max} (CCl_4) 3650, 3530, and 1643 cm^{-1}. After sublimation it analyzed for a hemi-hydrate.

Anal. Calcd. for $C_{22}H_{33}NO_5 \cdot \frac{1}{2}H_2O$: C, 65.97; H, 8.56. Found: C, 65.66; H, 8.76.

The alcohols from **21** were oxidized with pyridine – chromium trioxide complex. A benzene solution of the product was filtered through a short column of alumina, activity III. The material recovered from the benzene crystallized but was apparently a mixture of epimers with m.p. 145–158°. After recrystallization from acetone–hexane and sublimation, a fraction with m.p. 161–165.5° was obtained. The bulk of the product analyzed correctly for ketone **24**.

Anal. Calcd. for $C_{22}H_{31}O_5N$: C, 67.84; H, 8.02. Found: C, 67.74; H, 7.94.

The ketone had ν_{max} (CCl_4) 3420, 1735 (shoulder), 1724, and 1645 cm^{-1}, unchanged at higher dilution. Its n.m.r. spectrum contained the two-hydrogen signal characteristic of the exocyclic methylene group.

Alcohol 25

Olefin **22** (m.p. 187–190°, 120 mg) was hydrated as described for olefin **21**. After one recrystallization from alcohol and two from acetone–hexane, alcohol **25** separated as prisms, m.p. 223–224°, $[\alpha]_D$ 124° (*c*, 0.77). It had ν_{max} ($CHCl_3$) 3560, 3440 and 1630 cm^{-1}. It was sublimed for analysis.

Anal. Calcd. for $C_{22}H_{33}O_5N$: C, 67.49; H, 8.50. Found: C, 67.24; H, 8.66.

The n.m.r. spectrum showed signals at δ 4.62 and 4.75 (>C=CH_2), 5.7 (d, OH), 5.82 (1H), 6.53 (OCH_3), 6.60 (OCH_3), 6.79, 6.85 (d?, 2H), 7.56 (OH), 8.87 (3H triplet, J = 7 Hz) and 8.97 and 9.04 (3H doublet). Another sample with identical rotation and i.r. and n.m.r. spectra melted at 233–236°.

The alcohol was only acetylated to a small extent after 16 h at room temperature in 1:1 acetic anhydride – pyridine mixture. It was inert to chromium trioxide – pyridine and potassium dichromate in acetic acid. Jones reagent (19) in acetone at room temperature produced some ketone (ν_{max} ($CHCl_3$) 1726 cm^{-1}) but much of the alcohol was converted to acids.

Can. J. Chem. Downloaded from www.nrcresearchpress.com by 210.87.254.5 on 09/05/12
For personal use only.

Dihydrodes(oxymethylene)lycoctam (26)

When hydrogenated over 30% palladium-on-charcoal in acetic acid, des(oxymethylene)lycoctamone took up 1.8 mol of hydrogen. The product gave mainly one spot on t.l.c. with R_f identical to the minor product from the reduction over platinum in acetic acid (see below). Chromatography on alumina, activity IV, gave pure material as the first eluted substance. When recrystallized from chloroform–hexane it had m.p. 189–195°; $[\alpha]_D$ 130° (*c*, 0.71). Its n.m.r. spectrum had the pair of one-hydrogen singlets at τ 4.70 and 4.75 characteristic of the exocyclic methylene group, and a new methyl doublet centered at τ 9.05 (J = 5 Hz). The hydrogen on C-15 gave a sharp singlet at τ 5.88. After sublimation it had m.p. 203–206°; ν_{max} (CCl_4) 3545, 1641 cm^{-1}.

Anal. Calcd. for $C_{22}H_{33}O_4N$: C, 70.37; H, 8.86. Found: C, 71.67; H, 8.72.

Hydrogenation of the dihydro compound over platinum in acetic acid gave a product with R_f on t.l.c. identical with that of tetrahydrodes(oxymethylene)lycoctam.

Tetrahydrodes(oxymethylene)lycoctam (27)

Des(oxymethylene)lycoctamone (130 mg) in acetic acid was shaken for 15 h with Adam's platinum catalyst and hydrogen. The product gave two main spots on t.l.c. A repetition of the hydrogenation resulted in a small uptake of hydrogen and some reduction in intensity of the spot with higher R_f. The products were separated by chromatography on alumina into two hydrogenolysis products and a more polar mixture presumably having primary alcohol functions. The least polar compound still had vinyl hydrogens in its n.m.r. spectrum and had ν_{max} 910 cm^{-1} (=CH_2) (see dihydrodes(oxymethylene)lycoctam).

The second product eluted (57 mg) had m.p. 208–214° after sublimation and $[\alpha]_D$ 24° (*c*, 0.82).

Anal. Calcd. for $C_{22}H_{35}O_4N$: C, 69.99; H, 9.35; N, 3.71. Found: C, 70.29; H, 9.10; N, 3.91.

Its n.m.r. spectrum had no vinyl hydrogen signals. The hydrogen on C-15 now gave a broad ($w_{1/2}$ Hz) singlet at τ 6.40.

Epoxy Compound 28

Dihydrodes(oxymethylene)lycoctam (20 mg) was treated with excess trifluoroperacetic acid in methylene chloride in the presence of sodium dihydrogen phosphate. The reaction mixture was stirred for 30 min, refluxed for 1 h then stirred for 4 h at room temperature. The excess peracid was reduced by aqueous sodium sulfite and the organic layer washed free of acid using aqueous sodium carbonate. The product gave one main spot on t.l.c. Chromatography on grade IV alumina gave 8 mg of crystals, m.p. 200–205°, $[\alpha]_D$ 75° (*c*, 0.91). This was sublimed for analysis.

Anal. Calcd. for $C_{22}H_{33}O_5N$: C, 67.49; H, 8.50. Found: C, 67.52; H, 8.41. The n.m.r. spectrum showed a quartet centered at τ 5.75, J = 7 Hz (N—CH_2—CH_3), a doublet at τ 6.1 (J = 3.5 Hz, 15-H), τ 6.51 and 6.69 (two OCH_3), and two 1H singlets at τ 7.14 and 7.22 (hydrogens on C-18).

Reduction of the Epoxy Compound 28

A solution of 330 mg of epoxide in 20 ml of dry dioxan containing *ca.* 1 g of lithium aluminum hydride in suspension was refluxed for 17 h. The product was separated into basic (310 mg) and neutral (18 mg) components. The base gave two spots on t.l.c. The more polar of the two was obtained nearly free of the less polar by chromatography on alumina, activity IV (eluted with benzene and chloroform). After sublimation, the dihydroxy base melted at 189–190°.

Anal. Calcd. for $C_{22}H_{37}O_4N$: C, 69.62; H, 9.83. Found: C, 69.67; H, 9.29.

Permanganate Oxidation of the Dihydroxy Base

A solution of 220 mg of the base in a mixture of 10 ml of acetone, 5 ml of acetic acid, and 1 ml of water was oxidized by addition of 540 mg of potassium permanganate over a period of 3 h. The neutral product (210 mg) was chromatographed on alumina, activity III. Chloroform and methanol in chloroform eluted 98 mg of **29** which crystallized from acetone as square prisms, m.p. 210–218° (47 mg).

Anal. Calcd. for $C_{22}H_{35}O_5N$: C, 67.14; H, 8.97. Found: C, 67.23; H, 8.96. It had ν_{max} ($CHCl_3$) 1625 cm^{-1} and $[\alpha]_D$ +21° (*c*, 0.63 in $CHCl_3$). Its n.m.r. spectrum had a 2H quartet at τ 5.70, a one-hydrogen doublet at 6.23 (J = 2 Hz, C-15 hydrogen), methoxyl signals at τ 6.60 and 6.71, and a new methyl singlet at τ 8.48.

The other more readily eluted neutral products (using up to 70% chloroform in benzene) were not characterized, but contained the *N*-acetyl compound (ν_{max} 1670 cm^{-1}), a second lactam (ν_{max} 1630 cm^{-1}), and probably the desethyl lactam.

Lead Tetraacetate Oxidation of 29

Compound **29** in a saturated solution of lead tetraacetate in acetic acid (1 mg of **29** per ml) reduced 0.68 mol of oxidant in 40 min, 1.26 mol in 2 h, and 1.46 mol in 20 h. Preparative oxidations were run under these conditions for 1.5 h. The n.m.r. spectrum of the crude product had a signal at τ 5.40 (N—CHC=O), and sharp signals at τ 7.52, 7.89, and 8.00. The product (200 mg) chromatographed on alumina, activity III. Only the early eluate (40–60% chloroform in benzene) crystallized, giving 30 mg. After sublimation this melted at 140–146° and had $[\alpha]_D$ −5° (*c*, 1.3 in $CHCl_3$) and ν_{max} ($CHCl_3$) 1716, 1627 cm^{-1}.

Anal. Calcd. for $C_{22}H_{33}O_5N$: C, 67.49; H, 8.50. Found: C, 67.30; H, 8.27.

The n.m.r. spectrum showed signals at τ 5.95 (15-hydrogen), a doublet at τ 5.88 and 6.10, two three-hydrogen signals at τ 6.43 and 6.70, and a three-hydrogen signal at τ 8.42. This agrees with structure **30**.

We thank Dr. K. H. Palmer, who first prepared 18-deoxylycoctamone, Mr. R. Lauzon for i.r. spectra, Mr. H. Seguin for microanalyses, and Mr. M. Lesage and Mr. J. Nicholson for n.m.r. spectra.

1. M. Przybylska and L. Marion. Can. J. Chem. **34**, 185 (1956).
2. O. E. Edwards, L. Marion, and D. K. R. Stewart. Can. J. Chem. **34**, 1315 (1956).
3. O. E. Edwards, L. Marion, and K. H. Palmer. J. Org. Chem. **22**, 1372 (1957).
4. O. E. Edwards, M. Los, and L. Marion. Can. J. Chem. **37**, 1996 (1959).
5. Z. Valenta and I. G. Wright. Tetrahedron, **9**, 284 (1960).

6. R. C. COOKSON and M. E. TREVETT. J. Chem. Soc. 3864 (1956).
7. O. E. EDWARDS, L. MARION, and K. H. PALMER. Can. J. Chem. **36**, 1097 (1958).
8. O. E. EDWARDS, L. MARION, and R. A. MCIVOR. Can. J. Chem. **32**, 708 (1954).
9. F. FEIGL. Spot tests in organic analysis. Elsevier, New York, N.Y., 1960. p. 233.
10. R. E. KLINCK and J. B. STOTHERS. Can. J. Chem. **44**, 45 (1966).
11. R. STEWART. Oxidation mechanisms. W. A. Benjamin, New York, N.Y., 1964. p. 33.
12. N. S. BHACCA and D. H. WILLIAMS. Applications of n.m.r. spectroscopy in organic chemistry. Holden-Day Inc., San Francisco, California, 1964. p. 115.
13. O. E. EDWARDS and L. MARION. Can. J. Chem. **32**, 195 (1954).
14. V. SKARIC and L. MARION. Can. J. Chem. **39**, 1579 (1961).
15. O. E. EDWARDS and L. MARION. Can. J. Chem. **30**, 627 (1952).
16. M. H. BENN, M. A. M. CAMERON, and O. E. EDWARDS. Can. J. Chem. **41**, 477 (1963).
17. V. SKARIC and L. MARION. Can. J. Chem. **38**, 2433 (1960).
18. K. BOWDEN, I. M. HEILBRON, E. R. H. JONES, and B. C. L. WEEDON. J. Chem Soc. 39 (1946).

Can. J. Chem. Downloaded from www.nrcresearchpress.com by 210.87.254.5 on 09/05/12
For personal use only.

Can. J. Chem. Downloaded from www.nrcresearchpress.com by 210.87.254.42 on 09/05/12
For personal use only.

Secondary Kinetic Isotope Effects in Bimolecular Nucleophilic Substitutions. IV. The Temperature Dependence of the Deuterium Effect for the Reaction of *N,N*-Dimethyl-d_6-aniline and Methyl *p*-toluenesulfonate. Correlation of Isotope Effects on Activation Parameters[1,2]

K. T. Leffek and A. F. Matheson[3]
Chemistry Department, Dalhousie University, Halifax, Nova Scotia

Received August 27, 1970

The temperature dependence of the isotope effect for the reaction of dimethylaniline and dimethyl-d_6-aniline with methyl *p*-toluenesulfonate in nitrobenzene solvent has been measured, yielding the result, $(\Delta H_D^{\ddagger} - \Delta H_H^{\ddagger}) = -134 \pm 30$ cal mole^{-1}, $(\Delta S_D^{\ddagger} - \Delta S_H^{\ddagger}) = -0.15 \pm 0.09$ cal mol^{-1} degree^{-1}.

This result has been compared with 15 other temperature dependence studies by plotting $\Delta\Delta H^{\ddagger}$ per D atom *vs.* $T\Delta\Delta S^{\ddagger}$ per D atom. The points fall on two clearly separated straight lines. A similar correlation is found for a plot of $\Delta\Delta G^{\ddagger}$ per D atom *vs.* $\Delta\Delta H^{\ddagger}$ per D atom.

The significance of the correlation is discussed and a possible rationalization, in terms of mechanism and particularly the role of the solvent is given.

Canadian Journal of Chemistry, 49, 439 (1971)

Introduction

Kaplan and Thornton (1) have studied the effect of deuterium substitution for the methyl hydrogens of *N,N*-dimethylaniline on the rate of the quaternization reaction of the amine with methyl *p*-toluenesulfonate in nitrobenzene solvent at 51°. From frequency change considerations and force constant model calculations, they concluded that steric interactions yielded the most satisfactory explanation of their results. This implies that the isotope effect is a rate change brought about primarily by a difference between the enthalpies of activation for the normal and deuterated species, rather than a difference between the entropies of activation. The only temperature dependence study of a secondary deuterium isotope effect on this type of reaction was carried out by Leffek and MacLean (2) who found that the rate change resulting from the deuteration of methyl iodide in its reaction with 2-picoline in benzene was due entirely to an entropy effect. It seemed of interest, therefore, to carry out a temperature dependence study on the isotope effect for *N,N*-dimethyl-d_6-aniline and methyl *p*-toluenesulfonate.

[1]Presented in part at the International Conference on the Mechanisms of Reactions in Solution at the University of Kent at Canterbury, England, July 20–24, 1970.

[2]Based on a thesis submitted by A. F. Matheson in partial fulfillment of the requirements for the degree of Doctor of Philosophy at Dalhousie University, 1969.

[3]Present address: Uniroyal Research Centre, Guelph, Ontario.

Results and Discussion

Since the isotope effect measured by Kaplan and Thornton (1) at 51° was about 12% ($k_H/k_D = 0.88_3$), it was necessary to determine the rate ratio over a wide temperature range in order to be sure that a small change in the rate ratio with temperature would be detected. Table 1 shows the rate constants for the reaction of dimethylaniline and its deuterated analogue with methyl *p*-toluenesulfonate in nitrobenzene solution over a range of temperatures from 30 to 120°. The value reported by Kaplan and Thornton (1) is included and was used together with the present results to calculate the activation parameter differences by the least squares method. Equation 1 yielded $(\Delta H_D^{\ddagger} - \Delta H_H^{\ddagger}) = -134 \pm 30$ cal mol^{-1} and $(\Delta S_D^{\ddagger} - \Delta S_H^{\ddagger}) = -0.15 \pm 0.09$ cal mol^{-1} deg^{-1}.

$$[1] \quad \ln \frac{k_H}{k_D} = \frac{(\Delta H_D^{\ddagger} - \Delta H_H^{\ddagger})}{RT} - \frac{(\Delta S_D^{\ddagger} - \Delta S_H^{\ddagger})}{R}$$

The isotope effect is seen to be mainly an enthalpy effect, supporting the interpretation offered by Kaplan and Thornton (1) and also the argument presented earlier by Brown and McDonald (3), that nonbonded interactions play a major role in the inverse effects found for Menschutkin reactions where the positions of isotopic substitution are in the tertiary amine. The zero-point

TABLE 1. Second order rate constants and isotopic rate ratios for the reaction of dimethyl and dimethyl-d_6-aniline with methyl *p*-toluenesulfonate in nitrobenzene solvent.

Temperature (°C)	Dimethylaniline	Number of runs	$10^5 k_2$ (1 mol^{-1} s^{-1})	k_H/k_D
30.10	d_0	2	0.883	0.86_2
	d_6	2	1.024	
40.08	d_0	1	2.11	0.85_7
	d_6	1	2.46	
51.29	d_0	3	5.06	0.88_3*
	d_6	3	5.73	
60.03	d_0	2	9.66	0.89_3
	d_6	2	10.81	
70.04	d_0	2	18.75	0.88_4
	d_6	2	21.1	
79.88	d_0	3	37.5	0.90_2
	d_6	2	41.6	
90.15	d_0	1	71.6	0.88_4
	d_6	1	81.0	
99.85	d_0	2	122.3	0.90_0
	d_6	2	135.9	
109.50	d_0	3	219	0.89_2
	d_6	3	246	
120.50	d_0	4	391	0.91_7
	d_6	4	427	

*Reference 1.

energy approximation predicts an increase in the separation of the vibrational zero-point energy levels between the normal and deuterated molecules on attainment of the transition state, when the positions of isotopic substitution experience a more crowded environment, *i.e.* $E_D - E_H$ ($=\Delta\Delta H^{\ddagger}$) is negative. Such a situation holds in the present reaction if the initial aniline is considered to consist of an almost planar, trigonal conformation about the central nitrogen atom. Spectroscopic and theoretical evidence in support of this assumption is available (4, 5). In the transition state, the change towards a tetrahedral structure about the nitrogen atom will bring the methyl (deuteromethyl) groups into closer proximity with one another, with an accompanying increase in deformation frequencies. Kaplan and Thornton's i.r. assignments (1) for the normal and deuterated anilines and the corresponding product quaternary ammonium salts appear to indicate that the stretching frequencies are affected to only a minor degree.

Correlation of Isotope Effects on Activation Parameters

A major problem in the study of secondary deuterium isotope effects lies in the lack of understanding of the relative variations in the isotope effects on the enthalpy and entropy of activation. Individual cases have been explained in terms of physical-organic concepts (6) or in theoretical terms (7), but no general correlations have been made. For this reason a plot of $\Delta\Delta H^{\ddagger}$ ($=\Delta H_D{}^{\ddagger} - \Delta H_H{}^{\ddagger}$) per D atom *vs.* $T\Delta\Delta S^{\ddagger}$ per D atom was made as shown in Fig. 1, from the data available in the literature, which are summarized in Table 2. The value of T was selected as 300 °K. The use of $T\Delta\Delta S^{\ddagger}$ rather than the entropy of activation which Leffler used (8) allows a direct comparison of the contributions from the enthalpy and entropy of activation to the free energy of activation isotope effect. The selected reactions all involve relatively straight-forward nucleophilic substitution at a saturated carbon atom, for which the temperature dependence study has been made using at least three different temperatures. Reactions in which σ–π overlap with the forming carbonium ion have been postulated (9) and reactions involving free radical formation (10), have not been included.

A clear separation of reactions under consideration is seen in Fig. 1, which are labelled

Can. J. Chem. Downloaded from www.nrcresearchpress.com by 210.87.254.42 on 09/05/12
For personal use only.

Can. J. Chem. Downloaded from www.nrcresearchpress.com by 210.87.254.42 on 09/05/12
For personal use only.

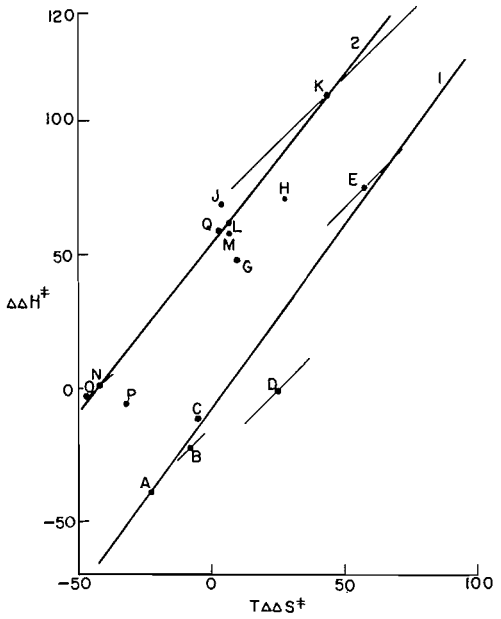

FIG. 1. Correlation of the enthalpy and entropy contributions to the secondary deuterium isotope effect at 300 °K for nucleophilic substitution reactions at saturated carbon. The letters refer to the reactions in Table 2.

series 1 and series 2 for the set with the lower $\Delta\Delta H^{\ddagger}$ and the set with the higher $\Delta\Delta H^{\ddagger}$, respectively.

Before considering these linear free energy relationships further, it is necessary to examine their meaningfulness. Leffler has intensively studied the relationship between $\Delta H^{\ddagger}$ and $\Delta S^{\ddagger}$ for selected reaction series of structurally similar substrates and demonstrated that for many such systems an isokinetic relationship (8)

$$\delta\Delta H^{\ddagger} = \beta\,\delta\Delta S^{\ddagger}$$

holds where β is a constant with the dimensions of absolute temperature. Leffler and Grunwald (11) and several others (12–15) have considered the possibility that the linear relationship between enthalpy and entropy of activation may be accounted for solely in terms of experimental error, since $\Delta H^{\ddagger}$ and $\Delta S^{\ddagger}$ are not independent parameters so that an error in one yields a corresponding error in the other (16). This leads to an error contour about a given point which is not the usual circle but an elongated ellipse with the long axis inclined to the entropy co-ordinate at a slope equal to the mean experimental temperature (11). Thus an error in $\Delta H^{\ddagger}$ will only displace a given point along the correlation line and will not produce a set of scattered points. These observations may give rise to doubts concerning the meaningfulness of $\Delta H^{\ddagger}$ *vs.* $\Delta S^{\ddagger}$ plots in which all the points fall on a single straight line, but they cannot account for the separation of a correlation into two parallel lines.

In Fig. 1, the circles indicate only the position of the experimental points, but some error limits are illustrated as lines through certain points. In

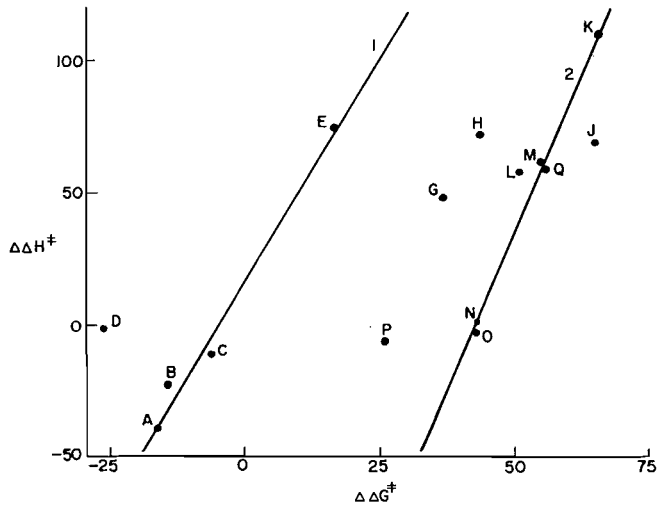

FIG. 2. Correlation of the secondary deuterium isotope effect on the enthalpy of activation with its effect on the free energy of activation for nucleophilic substitution reactions at saturated carbon. The letters refer to the reactions in Table 2.

Can. J. Chem. Downloaded from www.nrcresearchpress.com by 210.87.254.42 on 09/05/12
For personal use only.

TABLE 2. Activation parameter differences for secondary deuterium isotope effects in nucleophilic substitutions at saturated carbon

Reaction	Substrate	Nucleophile	Solvent	$\Delta\Delta H^*$ per D (cal mol^{-1})	$^*T\Delta\Delta S^*$ per D (cal mol^{-1})	Reference
A	CD_3I	CN^-	H_2O	−39	−23	18
B	CH_3OTs†	$(C_6H_5)N(CD_3)_2$	$C_6H_5NO_2$	−22	−8	This work
C	CD_3I	$S_2O_3^{2-}$	H_2O	−11	−5	19
D	CD_3I	2(CH_3) pyridine	C_6H_6	−1	+25	2
E	$C_6H_5.C_6H_5CH_2\overset{+}{N}CD_3.C_3H_5$ I^-	—	$CHCl_3$	+75	+58	20
F	$(CH_3)_2CDCCl(CH_3)_2$	H_2O	80% aqueous C_2H_5OH	+580	+444	30
G	cyclo$C_5H_9CH_2CD_2ONs$§	H_2O	25% aqueous dioxane	+48	+10	21
H	cyclo $C_5H_9CH_2CD_2ONs$§	CH_3COOH	CH_3COOH	+72	+28	21
J	$C_2H_5CD_2CH(CD_3)OTs$†	CH_3COOH	CH_3COOH	+69	+4	22
K	cyclo $C_3H_5.CD_2Cl$	H_2O	H_2O	+110	+44	23
L	$(CD_3)_3CCl$	H_2O	H_2O	+58	+7	24
M	$(CD_3)_3CCl$	H_2O	50% aqueous C_2H_5OH	+62	+7	24
N	$(CD_3)_2CHOMs$‖	H_2O	H_2O	+1	−42	6
O	$(CD_3)_2CHOTs$†	H_2O	H_2O	−3	−47	6
P	$(CD_3)_2CHBr$	H_2O	H_2O	−6	−32	6
Q	1(OCH_3), 2(CD_3)− 2 chloropropane	H_2O	H_2O	+59	+3	25

*T is 300 °K.
†*p*-Toluenesulfonate.
§*p*-Nitrobenzenesulfonate.
‖Methanesulfonate.

Can. J. Chem. Downloaded from www.nrcresearchpress.com by 210.87.254.42 on 09/05/12
For personal use only.

the examples showing error limits, the limits are those obtained as standard deviations in $\Delta\Delta H^{\ddagger}$ and $\Delta\Delta S^{\ddagger}$ by application of the usual least squares treatment to a series of rate ratios measured at a series of different temperatures. Wiberg (16) has warned that in these circumstances it is the maximum error which should be considered, but this is rather difficult to estimate in an objective manner. Therefore, the objective standard deviation is shown which may be multiplied by 2 or 3 to estimate the maximum error.

Exner (14) has shown that apart from the problem of large errors in $\Delta H^{\ddagger}$ and $\Delta S^{\ddagger}$, a purely random set of rate constants measured at two different temperatures will yield activation parameters which show a correlation coefficient of 0.998. Exner demonstrated that meaningful correlations may be established between $\Delta H^{\ddagger}$ and $\Delta S^{\ddagger}$ indirectly by plotting log k at one temperature against log k at a second temperature, or by plotting the activation energy against log k. The latter test has been applied to the present case by plotting $\Delta\Delta H^{\ddagger}$ against $\Delta\Delta G^{\ddagger}$ and is shown in Fig. 2. The scales of both Figs. 1 and 2 exclude reaction F (Table 2) but this point is so far removed from the others that it could be correlated with either or both series of reactions. Thus, it is concluded that a genuine compensatory effect between $\Delta\Delta H^{\ddagger}$ and $\Delta\Delta S^{\ddagger}$ exists irrespective of the position of deuteration. This emphasizes the unitary nature of secondary deuterium isotope effects with respect to the site of isotope substitution and demonstrates the triviality of the division of the effects into α-, β-effects, etc. Such a classification is useful, but should not be allowed to obscure the fact that the rate changes which result upon isotopic substitution come about through changes in vibrational frequencies of the molecule and that these changes are merely interpreted by attaching names to them such as hyperconjugation, induction, steric effects, etc.

The validity of the zero-point energy approximation, which assumes that $\Delta\Delta H^{\ddagger}$ is the major contributor to $\Delta\Delta G^{\ddagger}$ and hence to the rate ratio, is clarified by the correlation in Fig. 1. The slopes of approximately 1.3 show that $\Delta\Delta H^{\ddagger}$ increases more rapidly than does the compensating $T\Delta\Delta S^{\ddagger}$ term within each series. The series 1 line passes very close to the origin (at $T\Delta\Delta S^{\ddagger} = 0, \Delta\Delta G^{\ddagger} \cong -7$ cal mol^{-1}), so that $\Delta\Delta H^{\ddagger}$ provides the larger contribution to $\Delta\Delta G^{\ddagger}$ for all but the very small normal and inverse isotope effects. However, since the series 2 line does not pass through the origin, the $T\Delta\Delta S^{\ddagger}$ term is approximately equal to or larger than the $\Delta\Delta H^{\ddagger}$ contribution, for $\Delta\Delta G^{\ddagger}$ values ranging from approximately -40 to $+40$ cal mol^{-1} per D atom. The corresponding rate changes for such isotope effects can be large for molecules containing several deuterium atoms, *e.g.* the solvolysis of isopropyl-β-d_6 compounds in water (points labelled N, O, and P in Fig. 1) exhibit rate ratios of about 1.3–1.5 (6).

Although the two sets of reactions do not correspond to their molecularity (*i.e.* S_N2 or S_N1), the reactions of series 1 are predominantly S_N2 and most of those of series 2 have considerable S_N1 character. However, a more distinct difference between the two series is that one set consists exclusively of solvolytic reactions while the other contains non-solvolytic reactions. Thus, the most obvious external source of the shift from series 1 to series 2 is the solvent and its behavior on passage from the ground state to the transition state, which, in the majority of the latter cases, involves a reaction center with a degree of electron deficiency. Therefore, it is proposed that the distinction between the two series is engendered by a more effective increase in solvation on passage to the transition state for the reactions in series 2 compared to those in series 1, because of the vulnerability of their carbon centers to solvent approach.

It is of interest to consider to what extent an unsolvated model for the reactions is capable of explaining the separation of the two series. A simple approach is to consider the separation as an entropy shift, *i.e.* series 2 is characterized by more negative $T\Delta\Delta S^{\ddagger}$ terms than series 1. Wolfsberg and Stern (17) have carried out theoretical calculations starting from general eq. 2 in which the symbols have their standard

$$[2]\quad k_H/k_D = \left[\frac{M_D}{M_H}\cdot\frac{M_H^{\ddagger}}{M_D^{\ddagger}}\right]^{3/2}\left[\frac{\Pi I_D}{\Pi I_H}\cdot\frac{\Pi I_H^{\ddagger}}{\Pi I_D^{\ddagger}}\right]^{1/2} \times \prod^{3N-6}\frac{e^{-\frac{1}{2}h\nu_D/kT}}{e^{-\frac{1}{2}h\nu_H/kT}}\cdot\prod^{3N^{\ddagger}-7}\frac{e^{-\frac{1}{2}h\nu_H^{\ddagger}/kT}}{e^{-\frac{1}{2}h\nu_D^{\ddagger}/kT}} \times \prod^{3N-6}\frac{(1-e^{-h\nu_D/kT})^{-1}}{(1-e^{-h\nu_H/kT})^{-1}} \times \prod^{3N^{\ddagger}-7}\frac{(1-e^{-h\nu_H^{\ddagger}/kT})^{-1}}{(1-e^{-h\nu_D^{\ddagger}/kT})^{-1}}$$

meanings (17). Following Wolfsberg and Stern, eq. 2 may be abbreviated to eq. 3 where MMI

$$[3]\quad k_H/k_D = (\mathrm{MMI}) \times (\mathrm{ZPE}) \times (\mathrm{EXC})$$

TABLE 3. Calculated $\Delta\Delta S^{\ddagger}$ contributions from mass and moment of inertia changes for trigonal transition states

C–Y distance (Å)	C–X distance (Å)	Mass of X (a.w.u.)	$\Delta\Delta S_I{}^{\ddagger}$	$\Delta\Delta S_M{}^{\ddagger}$ (cal mol^{-1} deg^{-1})	$\Delta\Delta S_{MMI}{}^{\ddagger}$
2.5	1.5	120.5	−0.440	−0.031	−0.471
2.5	2.5	120.5	−0.443	−0.031	−0.474
2.5	3.5	120.5	−0.443	−0.031	−0.474
2.5	2.5	60.25	−0.438	−0.020	−0.458
2.5	2.5	120.5	−0.443	−0.031	−0.474
2.5	2.5	180.75	−0.442	−0.037	−0.479
—	—	—	+0.927	+0.479	+1.406

represents the mass, moment of inertia term of eq. 2, ZPE, the zero-point energy term, and EXC, the excitation of vibrations term. If the EXC is approximated to unity

$$[4] \qquad k_H/k_D = (\text{MMI}) \times (\text{ZPE})$$

or

$$[5] \qquad \ln k_H/k_D = \ln (\text{MMI}) + \ln (\text{ZPE})$$

When eq. 5 is compared to eq. 1 the entropy contribution to the isotope effect

$$\Delta\Delta S^{\ddagger} = -R \ln (\text{MMI})$$

or

$$[6] \quad \Delta\Delta S^{\ddagger}{}_{MMI} = -\frac{R}{2} \ln \left[\frac{\Pi I_D \, \Pi I_H{}^{\ddagger}}{\Pi I_H \, \Pi I_D{}^{\ddagger}}\right] - \frac{3R}{2} \ln \left[\frac{M_D \, M_H{}^{\ddagger}}{M_H \, M_D{}^{\ddagger}}\right]$$

Thus $\Delta\Delta S_{MMI}{}^{\ddagger}$ can be estimated from the geometry of a model reaction and the assumed geometry for the corresponding transition state. Wolfsberg and Stern have made such calculations for a variety of models (17), two of which have been developed here. The basic S_N2 reaction between a nucleophile X and a substrate CH_3Y has been considered, in which the C—Y bond distance is taken as 2.00 Å and the atomic weight of Y as 120.5, *i.e.* CH_3Y is similar to CH_3I. The substrate was treated as tetrahedral and the transition state as a trigonal bipyramid, with $X\hat{C}Y = 180°$ and $H\hat{C}H = 120°$. Table 3 shows the effect of varying the transition state structure and it may be seen that altering the mass of the attacking nucleophile X and its distance from the carbon atom have very little effect on $\Delta\Delta S_{MMI}{}^{\ddagger}$, which remains virtually constant at -0.47 cal mol^{-1} deg^{-1}.

In contrast to this, the last line of Table 3 shows that a hypothetical transition state consisting of a trigonal CH_3 group unassociated with either X or Y yields a $\Delta\Delta S_{MMI}{}^{\ddagger}$ of $+1.41$ cal mol^{-1} deg^{-1}. This is one extreme of the range of possible transition states for S_N1 reactions, the other being the tetrahedral CH_3Y, identical to the initial state which gives an (MMI) of unity (17) and, therefore, $\Delta\Delta S_{MMI}{}^{\ddagger}$ equal to zero.

These calculations show that S_N1 reactions should exhibit a positive $\Delta\Delta S^{\ddagger}$ provided that the approximation (EXC) = 1 is valid, which may not always be the case (17). Nevertheless, in semi-quantitative terms, $\Delta\Delta S^{\ddagger}$ would be expected to correlate with mechanism.

Inspection of Table 2 and Fig. 1 reveals that negative $T\Delta\Delta S^{\ddagger}$ terms are found in series 1 for those reactions which are S_N2 with the exception of that for reaction D, which does not fall on the line. In series 2, the most negative entropy terms are found for the three *sec*-propyl compounds studied, although both primary and tertiary compounds are seen to yield positive entropy terms. There is no doubt that solvation effects will modify the predictions of Table 3 to a marked degree, especially in the solvolytic reactions, so the agreement between the experimental values and those of Table 3 is no worse than is to be expected. It is concluded that the unsolvated model, although useful in itself, is insufficient to fully account for the separation of the reactions into two series.

Experimental

Materials

N,N-Dimethylaniline was refluxed with acetic anhydride in a 2:1 ratio by weight for 3 h, then distilled at atmospheric pressure (26). The amine was then fractionally redistilled under vacuum and the middle fraction was collected and stored in an opaque container over calcium hydride and under nitrogen.

N,N-Dimethyl-d_6-aniline was prepared via trimethyl-d_9 phenylammonium iodide as described by Kaplan and Thornton (1). The deuterium source was methyl-d_3 iodide from Merck, Sharpe and Dohme of Canada, Ltd. The

Can. J. Chem. Downloaded from www.nrcresearchpress.com by 210.87.254.42 on 09/05/12
For personal use only.

Can. J. Chem. Downloaded from www.nrcresearchpress.com by 210.87.254.42 on 09/05/12
For personal use only.

overall yield was about 75%. An n.m.r. spectrum of a neat sample of product showed no signal for the methyl hydrogens and a mass spectrometric analysis gave 96.7% of d_6 product and 3.3% of d_5 product.

Commercial methyl tosylate was distilled *in vacuo* and the middle cut retained.

Trimethylphenylammonium tosylate was prepared by refluxing an equimolar mixture of methyl tosylate and *N,N*-dimethylaniline in benzene for 1 h. The reaction mixture was then stoppered and allowed to stand overnight. The white product was washed with anhydrous ether, twice recrystallized from isopropanol and stored under vacuum over phosphorus pentoxide. The yield was 75%, m.p. 160–161° (lit. (1) 160–161°).

Nitrobenzene solvent was dried over anhydrous calcium sulfate and distilled at atmospheric pressure, boiling range 210.5–211°.

Kinetic Measurements

The reaction rates were measured by following the change in conductivity with time using a Wayne–Kerr Universal bridge, model B 221 and cells manufactured by LKB—Producter AB (Sweden) of about 5 ml capacity and cell constant approximately 0.1 cm^{-1}. The oil filled constant temperature baths maintain the quoted temperatures to $\pm 0.01°$ at the lower temperatures and $\pm 0.02°$ at the higher temperatures.

The cells were washed with acetone, water, and acetone again and dried by a stream of nitrogen for 2 min before use. Calibration curves were obtained for concentration *vs.* conductivity of trimethylphenylammonium tosylate at each temperature. A stock solution of tosylate was prepared by weight and the conductances determined for a series of ten diluted solutions. The dilutions were made using the mechanical titrimeter built by Martin *et al.* (27), which had been calibrated by Kulin (28). Two of the calibration curves are illustrated in Fig. 3. The calibration curves obtained with undeuterated trimethylphenylammonium tosylate were also applied to the deuterated analogue, assuming that the isotope effect on the conductivity was negligible. This was checked experimentally and found to be true for the salt *N*-methyl-d_3-pyridinium iodide.

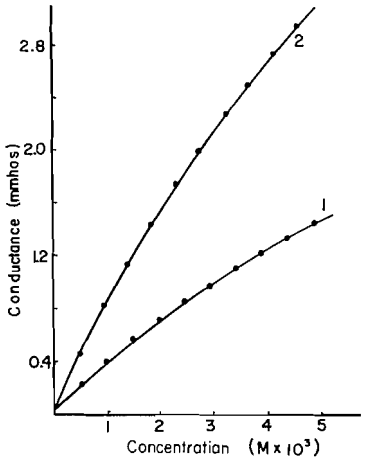

FIG. 3. Calibration graphs of concentration *vs.* conductance for trimethylphenylammonium tosylate in nitrobenzene. Curve 1 at 40° and curve 2 at 120°.

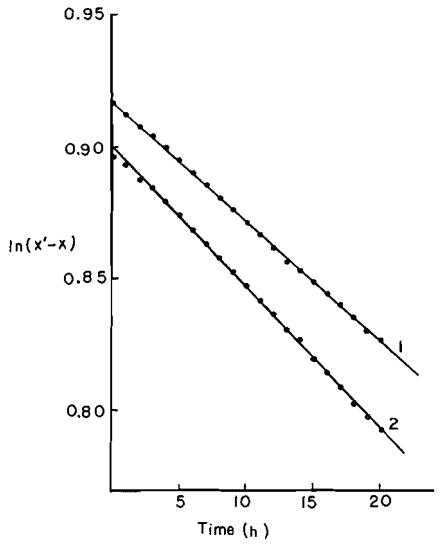

FIG. 4. Guggenheim plots for the reactions of dimethylaniline (1) and dimethyl-d_6-aniline (2) with methyl tosylate at 40° in nitrobenzene.

The kinetic runs were carried out under pseudo–first order conditions with initial concentrations of methyl tosylate and *N,N*-dimethylaniline approximately 0.1 and 3×10^{-3} *M* respectively. The first order rate constants were calculated by the Guggenheim method (29) by a least squares method applied to 21 conductivity readings made in each of the first and third half-lives of the reaction. Second order rate constants were found by division of the first order constant by the initial methyl tosylate concentration, corrected for solvent expansion to the appropriate temperature. Two runs are illustrated in Fig. 4.

The authors are grateful for financial support by the National Research Council of Canada and, specifically, for an NRCC Studentship to A.F.M. The loan of the mechanical titrimeter by Dr. R. E. Robertson, University of Calgary, Calgary, Alberta (formerly of NRCC, Ottawa), is also gratefully acknowledged.

1. E. D. KAPLAN and E. R. THORNTON. J. Amer. Chem. Soc. **89**, 6644 (1967).
2. K. T. LEFFEK and J. W. MACLEAN. Can. J. Chem. **43**, 40 (1965).
3. H. C. BROWN and G. J. MCDONALD. J. Amer. Chem. Soc. **88**, 2514 (1966).
4. J. C. D. BRAND, D. R. WILLIAMS, and T. J. COOK. J. Mol. Spectrosc. **20**, 193 (1966).
5. C. A. COULSON. Valence. Oxford University Press, London, 1961. p. 262.
6. K. T. LEFFEK, R. E. ROBERTSON, and S. E. SUGAMORI. Can. J. Chem. **39**, 1989 (1961).
7. M. WOLFSBERG and M. J. STERN. Pure and Appl. Chem. **8**, 325 (1964).
8. J. E. LEFFLER. J. Org. Chem. **20**, 1202 (1955).
9. C. C. LEE and E. W. C. WONG. Can. J. Chem. **43**, 2254 (1965).

10. A. A. ZAVITSAS and S. SELTZER. J. Amer. Chem. Soc. **86**, 1265 (1964).
11. J. E. LEFFLER and E. GRUNWALD. Rates and equilibria of organic reactions. John Wiley and Sons, Inc., New York, N.Y. 1963. Chapt. 9.
12. R. C. PETERSEN, J. H. MARKGRAF, and S. D. ROSS. J. Amer. Chem. Soc. **83**, 3819 (1961).
13. C. D. RITCHIE and W. F. SAGER. Progress in Phys. Org. Chem. **2**, 323 (1964).
14. O. EXNER. Coll. Czech. Chem. Commun. **29**, 1094 (1964).
15. O. EXNER. Nature **201**, 488 (1964).
16. K. B. WILBERG. Physical organic chemistry. John Wiley and Sons, Inc., New York, N.Y. 1964. p. 378.
17. M. WOLFSBERG and M. J. STERN. Pure and Appl. Chem. **8**, 225 (1964).
18. A. V. WILLI and C. M. WON. J. Amer. Chem. Soc. **90**, 5999 (1968).
19. A. V. WILLI and C. M. WON. Can. J. Chem. **48**, 1452 (1970).
20. K. T. LEFFEK and F. H-C. TSAO. Can. J. Chem. **46**, 1215 (1968).
21. C. C. LEE and E. W. C. WONG. Tetrahedron, **21**, 539 (1965).
22. E. S. LEWIS and C. E. BOOZER. J. Amer. Chem. Soc. **76**, 791 (1954).
23. C-Y. WU and R. E. ROBERTSON. Chem. and Ind. 195 (1966).
24. L. HAKKA, A. QUEEN, and R. E. ROBERTSON. J. Amer. Chem. Soc. **87**, 161 (1965).
25. K. T. LEFFEK, R. E. ROBERTSON, and S. E. SUGAMORI. Unpublished work.
26. A. I. VOGEL. Practical organic chemistry. Longmans, Green and Co., Toronto, Ontario. 1954. p. 550.
27. S. MARTIN, R. E. ROBERTSON, and G. C. BENSON. J. Sci. Instrum. **41**, 237 (1964).
28. E. L. KULIN. M.Sc. Thesis. Dalhousie University, Halifax, Nova Scotia. 1969.
29. E. A. GUGGENHEIM. Phil. Mag. **2**, 538 (1926).
30. V. J. SHINER, Jr. J. Amer. Chem. Soc. **76**, 1603 (1954).

Can. J. Chem. Downloaded from www.nrcresearchpress.com by 210.87.254.42 on 09/05/12
For personal use only.

Cinétique de l'oxydation du sous-oxyde de carbone en phase gazeuse

JEAN LEBEL[1] ET CYRIAS OUELLET
Département de Chimie, Université Laval, Québec 10, Québec

Reçu le 10 juillet 1970

Nous avons étudié la combustion lente et explosive du sous-oxyde de carbone, par la méthode statique, à des pressions inférieures à 500 mm Hg et à des températures de 560 à 680 °C. La réaction se fait en deux temps, [*a*] et [*b*]. La réaction *b* étant inhibée par C_3O_2. L'oxydation lente [*a*] est suivie

[*a*] $$C_3O_2 + 2O_2 = 2CO + CO_2 + O_2$$

[*b*] $$2CO + O_2 = 2CO_2$$

de l'oxydation [*b*] explosive ou lente selon que l'on est en-dessous ou au-dessus de la limite supérieure d'explosion du système $CO–O_2$. Au-dessus d'une autre limite de pression, le mélange $C_3O_2–O_2$ explose sans retard. La présence de H_2O accélère la réaction *a* et abaisse les limites d'explosion. L'oxydation lente a une énergie d'activation globale de 34 kcal/mol. Nous proposons une chaîne propagée par

$$C_3O_2 + O = C_2O + CO_2$$

$$C_2O + O_2 = 2CO + O$$

et ramifiée selon

$$CO_2^* + O_2 = CO_2 + O + O$$

dans une chaîne énergétique responsable de l'explosion.

The slow and the explosive combustion of carbon suboxide has been studied by the static method at pressures below 500 mm Hg and temperatures ranging from 560 to 680 °C. Reaction occurs in two distinct phases, [*a*] and [*b*], where [*b*] is inhibited by C_3O_2. The slow oxidation [*a*] is followed by

[*a*] $$C_3O_2 + 2O_2 = 2CO + CO_2 + O_2$$

[*b*] $$2CO + O_2 = 2CO_2$$

oxidation [*b*] which is explosive at the lower pressures but slow above the upper pressure limit for $CO–O_2$. Above another, higher pressure limit, the $C_3O_2–O_2$ mixture explodes without delay. Water accelerates reaction *a* and lowers the pressure limits. Reaction *a* shows an over-all activation energy of 34 kcal/mol. We suggest that chain propagation takes place according to

$$C_3O_2 + O = C_2O + CO_2$$

$$C_2O + O_2 = 2CO + O$$

and that an energy chain leads to the branching reaction

$$CO_2^* + O_2 = CO_2 + O + O$$

responsible for explosion.

Canadian Journal of Chemistry, **49**, 447 (1971)

Introduction

On connaît peu de choses sur la combustion du sous-oxyde de carbone. Clusius et Huber (1) ont montré que ce composé brûle avec une flamme bleue dans l'air sec et avec une flamme jaunâtre et fuligineuse dans l'air humide; ils ont aussi déterminé les limites d'allumage par étincelle de mélanges de plusieurs compositions. von Weyssenhoff *et al.* (2) ont trouvé qu'à la température ordinaire, le sous-oxyde ne réagit pas avec l'oxygène moléculaire, mais qu'il réagit lentement avec l'ozone et très rapidement avec l'oxygène atomique selon deux mécanismes donnant l'un 3 CO et l'autre CO_2 et le radical C_2O. La réaction du sous-oxyde avec l'oxygène atomique et celles de C_2O avec l'oxygène moléculaire et avec quelques autres composés ont été étudiées en détail par Liuti *et al.* (3), Williamson et Bayes (4), et Willis et Bayes (5). Lebel *et al.* (6) ont mis en évidence l'inhibition de l'explosion du système $CO–O_2$ par le sous-oxyde.

Nous avons entrepris une étude systématique de l'oxydation du sous-oxyde par l'oxygène moléculaire à hautes températures et des rapports entre cette réaction et l'oxydation du

[1]Adresse actuelle: Centre d'études universitaires, Rimouski, Québec.

monoxyde de carbone. Dans nos expériences, nous avons pris soin d'éviter la polymérisation et la présence de composés hydrogénés.

Méthode expérimentale

La réaction a été étudiée par la méthode statique dans un cylindre en Vycor de 22 × 4.5 cm dont la température était maintenue constante et uniforme à ±1 °C près dans un four. Environ 30 min avant chaque expérience, on introduisait les quantités désirées de sous-oxyde et d'oxygène dans un ballon auxiliaire en évitant que ces gaz ne soient contaminés par de la vapeur de mercure. On détendait rapidement la quantité voulue de ce mélange dans le réacteur, où sa pression était mesurée par un capteur électro-magnétique de marque Pace (modèle P7) et enregistrée au cours de la réaction. Entre les expériences, on maintenait dans le réacteur chaud un vide de l'ordre de 10^{-4} mm durant au moins 30 min.

On préparait le sous-oxyde de carbone par déshydratation de l'acide malonique selon la technique de Long *et al.* (7) telle que modifiée par Batchelor *et al.* (8). Après l'avoir redistillé plusieurs fois, on le conservait à −196 °C à l'obscurité pour l'empêcher de se polymériser. On contrôlait sa pureté en prenant le spectre i.r., le spectre de masses et des chromatogrammes; d'après ces essais, les quantités d'anhydride carbonique et d'acide acétique étaient dans tous les cas nettement inférieures à 0.1%. L'oxygène employé était de marque Ohio pour fins médicales. Nous croyons que nos mélanges réactionnels étaient "secs", c'est-à-dire exempts d'impuretés hydrogénées, puisque l'addition de petites quantités d'eau affectait de façon disproportionnée les limites d'explosion, comme on le verra plus loin.

Pour analyser les gaz durant la réaction, on aspirait un échantillon dans une boucle d'où il était entraîné par un flux d'hélium dans un chromatographe de marque F & M, modèle 700, le tout à la température de la chambre. Sur tamis moléculaire 5 Å, on séparait l'oxygène et le monoxyde de carbone avec des temps de retention respectifs de 4.8 et 16.5 min. Le sous-oxyde de carbone et l'anhydride carbonique étaient séparés sur brique pilée contenant 23% d'Apiezon M, selon les indications de Hirt et Palmer (9), avec des temps de retention respectifs de 9.2 et 3.5 min dans nos colonnes.

Résultats

(a) Comportement général et limites d'explosion

Bien que l'oxydation complète du sous-oxyde en anhydride carbonique ne comporte aucune variation de pression, la réaction débute dans tous les cas par une augmentation de pression. Selon la température, la composition du mélange et la pression, cette variation de pression suit l'un des cours illustrés sur la fig. 1. Il s'agit, dans ce cas, d'une famille de réactions, à 653 °C, de mélanges contenant tous du sous-oxyde à la même pression initiale de 24.6 mm Hg, mais de l'oxygène à différentes pressions initiales. En

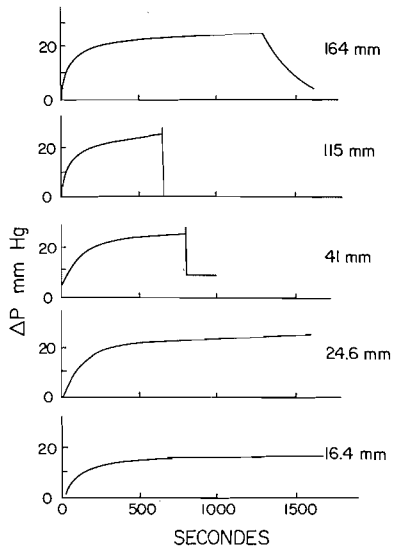

FIG. 1. Variations de pression au cours de réactions à 653 °C de mélanges où la pression initiale de C_3O_2 est de 24.6 mm Hg, celle d'oxygène étant inscrite vis-à-vis chaque courbe.

examinant de bas en haut les courbes de cette figure, on voit que si la pression initiale de l'oxygène ne dépasse pas celle du sous-oxyde, la pression totale atteint un plateau et reste stationnaire. S'il y a un excès d'oxygène, la montée de pression est suivie d'une explosion accompagnée d'une lueur bleuâtre. Avec un grand excès d'oxygène. l'augmentation de pression se termine par une baisse lente qui débute soudainement. Tout se passe comme si la réaction s'effectuait en deux temps, l'étape

$$[1] \qquad C_3O_2 + 2O_2 = 2CO + CO_2 + O_2$$

devant se terminer avant que ne débute la suivante:

$$[2] \qquad 2CO + O_2 = 2CO_2$$

En effet, sur la courbe du bas, on voit que la hausse de pression est égale à la pression initiale d'oxygène, 16.4 mm, qui limite l'étendue de la réaction 1. Sur la courbe suivante les deux réactifs ont la même pression initiale de 24.6 mm et la réaction 1 est complète, se soldant par un accroissement de pression de 24.6 mm, c'est-à-dire que $\Delta P_f = P_0(C_3O_2)$. La troisième courbe est obtenue en présence d'un excès modéré d'oxygène. Dès que la réaction 1 est terminée avec $\Delta P_f = 24.6$ mm, le mélange CO–O_2 explose, mais il ne reste pas assez d'oxygène pour

que la combustion soit complète. Sur la courbe suivante, $P_0(O_2) > 2P_0(C_3O_2)$, on trouve encore $\Delta P_f = 24.6$ mm, et dans ce cas la combustion explosive de CO, réaction 2, est complète et la pression du système revient à sa valeur initiale. Si l'on accroît encore la pression d'oxygène, on atteint une région où la combustion du monoxyde par l'oxygène en excès est une réaction lente qui débute soudainement; on se trouve au-dessus de la limite supérieure d'explosion du mélange CO–O_2. On voit donc que les réactions 1 et 2 constituent deux étapes bien distinctes, la deuxième n'étant franchie qu'après la disparition pratiquement complète du sous-oxyde. Ce dernier est un inhibiteur puissant (6, 10).

Il est intéressant de noter la ressemblance entre nos résultats et ceux de James et Laffitte (11) et de Cusin et James (12) sur la combustion du cyanogène. Cette réaction se fait aussi en deux étapes, la première étant une accumulation de monoxyde selon

$$(CN)_2 + 2O_2 = 2CO + N_2 + O_2$$

suivie de sa combustion explosive.

Enfin, il existe une pression au-dessus de laquelle l'allure de la réaction change radicalement. L'accroissement de pression, au lieu de débuter à une vitesse maximum pour aller vers un plateau, prend une allure autoaccélérée comme dans les courbes de la fig. 2 et dégénère en explosion après un temps très bref qui se confond avec la période d'échauffement des gaz.

La fig. 3 représente les régions où l'on observe ces divers types de réaction avec des mélanges de composition $1C_3O_2:2O_2$. La région A est celle où l'on obtient des explosions à long retard attribuables à la combustion [2] du monoxyde accumulé durant l'étape 1. Dans la région B, la combustion à long retard du monoxyde est lente. La région C est celle où le mélange C_3O_2–O_2 explose sans retard. Sans préjuger des

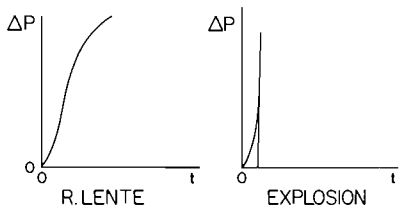

FIG. 2. Allures de la variation initiale de pression au voisinage de la limite d'explosion.

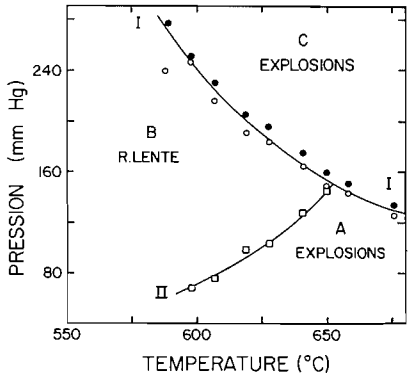

FIG. 3. Domaines de réactions lentes et d'explosions pour un mélange de composition $1C_3O_2:2O_2$.

mécanismes de ces types de réaction, nous appelons la courbe I (fig. 3) limite inférieure d'explosion du mélange C_3O_2–O_2 et la courbe II limite supérieure d'explosion du mélange CO–O_2–CO_2 provenant de l'étape [1]. On voit que ces deux limites se recoupent à 653 °C pour le mélange de composition $1CO_3O_2:2O_2$.

Si l'on porte les logarithmes des pressions limites contre $1/T$, on obtient les droites de la fig. 4 représentant la limite inférieure d'explosion du sous-oxyde et la limite supérieure d'explosion du monoxyde en présence du CO_2 provenant de la réaction 1.

Les limites représentées sur la fig. 3 sont celles de mélanges $1C_3O_2:2O_2$. Les changements de composition entraînent des déplacements importants de ces limites; nous en avons noté, mais n'en avons pas fait une étude systématique.

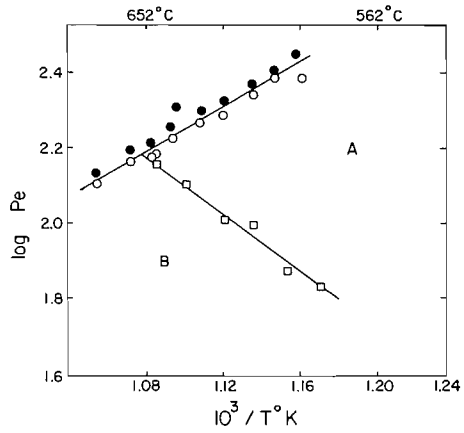

FIG. 4. Droites d'Arrhénius tirées des limites de la fig. 3.

Ces effets de composition expliquent que certains de nos résultats semblent, à première vue, être en désaccord avec les données de la fig. 3. Par exemple, la réaction représentée au sommet de la fig. 1 s'effectuant à 653 °C à une pression totale de 188.6 mm Hg, serait une explosion immédiate si le mélange avait la composition 1:2. D'autre part, ces déplacements de limites ont rétréci le champ de certaines séries d'expériences à composition variable.

Il est reconnu que l'addition de composés hydrogénés affecte les limites d'explosion de mélanges $CO–O_2$ (13) si ces derniers sont suffisamment secs. Nous avons d'abord remarqué que des traces d'hydrogène accélèrent la combustion lente du sous-oxyde et abaissent sa limite inférieure d'explosion. Nous avons aussi ajouté de l'eau et avons constaté que 1 mm d'eau exerçait un effet égal à celui de 12 mm. Pour des raisons de commodité, nous avons travaillé en présence d'une pression partielle d'eau égale à 5 mm, introduite dans le réacteur avant le mélange $1C_3O_2:2O_2$. On retrouve, dans ces conditions, des courbes de pression de mêmes allures que celles de la fig. 1, mais fortement accélérées, et les limites d'explosions sont abaissées de quelque 100 °C et 100 mm, comme on le constate en comparant la fig. 5 à la fig. 3. On voit, en particulier que la limite d'explosion que nous croyons être la limite supérieure du système $CO–O_2$ est largement décalée vers les basses températures, phénomène déjà connu (13). Il est remarquable que par sa position et par son apparence de rebroussement à 575 °C, cette limite semble s'apparenter à la deuxième limite d'explosion du système $H_2–O_2$ dans la région où celle-ci s'incurve vers la troisième limite. Il

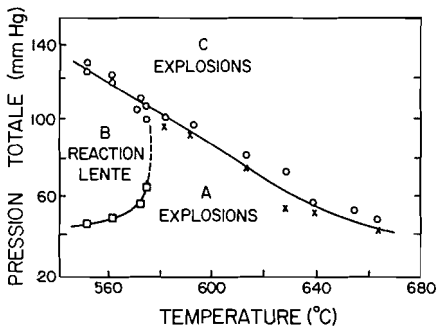

FIG. 5. Domaines de réactions lentes et d'explosions pour un mélange $1C_3O_2:2O_2$ en présence de 5 mm Hg de H_2O.

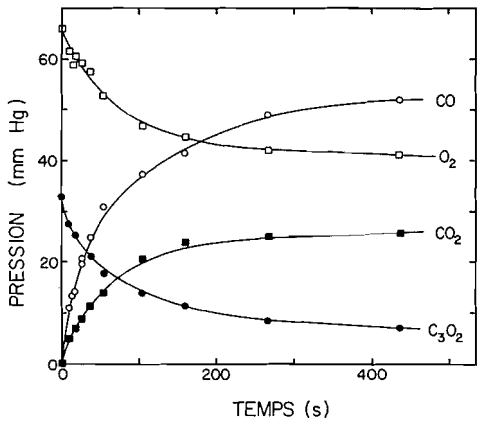

FIG. 6. Variations des pressions partielles durant l'oxydation à 632 °C d'un mélange $1C_3O_2:2O_2$ de pression initiale 99.8 mm Hg.

n'est pas impossible, étant donné que des atomes d'oxygène sont produits dans la chaîne d'oxydation de C_3O_2, qu'un nouveau mode de ramification tel que

$$CO + O + H_2O = CO_2 + H + OH$$

entre en jeu (14).

(b) Cinétique de la réaction lente

Cette section contient la description des résultats cinétiques obtenus sur la réaction 1, l'oxydation lente du sous-oxyde de carbone. Les résultats se rapportant à l'oxydation lente du monoxyde de carbone au-dessus de sa limite supérieure d'explosion seront décrits dans un autre article (15).

La fig. 6 montre l'évolution des espèces chimiques durant l'oxydation lente à 632 °C d'un mélange $1C_3O_2:2O_2$ de pression initiale $P_0 =$ 99.8 mm Hg. Cette réaction est l'une de celles qui sont suivies d'une combustion explosive du monoxyde de carbone par l'oxygène résiduel. Des familles de courbes semblables à celle-ci ont été obtenues par chromatographie à partir d'échantillons de mélanges gazeux à 632, 645, 652, et 671 °C. Dans tous ces cas et à tous instants durant ces réactions, les produits étaient dans un rapport de concentrations constant: $(CO)/(CO_2) = 2.0$ à la précision des mesures près. De plus, les variations de pression totale et partielles obéissaient à l'éq. 3, ce qui vérifie

$$[3] \quad \Delta P = -\Delta P_{C_3O_2} = -\Delta P_{O_2} = +\Delta P_{CO_2} = +0.5\Delta P_{CO}$$

TABLEAU 1. Variation de la vitesse initiale V_0 en fonction de la pression initiale P_0 de C_3O_2; $\theta = 631$ °C, P_0 de $O_2 = 162$ mm Hg

P_0 (mm)	P_0^2 (mm^2)	V_0 (mm s^{-1})	P_0^2/V_0
28.2	795	1.43	555
15.3	235	0.417	562
9.2	85	0.129	660
4.7	22	0.0513	430
3.9	15.2	0.0242	620

que cette première phase de phénomène est uniquement l'oxydation du sous-oxyde suivant l'éq. 1, et en particulier qu'il ne se forme pas d'autre produit, par exemple un polymère qui se déposerait dans la canalisation près du réacteur.

Ces constatations nous ont permis d'utiliser les mesures de pression pour l'étude de la cinétique de la réaction lente [1].

Nous avons d'abord mesuré les valeurs $V_0 = (dP/dt)_0$ des taux initiaux d'accroissement de pression en prenant les pentes à l'origine. On voit au tableau 1 que V_0 varie comme le carré de la pression partielle initiale de C_3O_2 dans une série de réactions à 631 °C où la pression initiale de O_2 était partout de 162 mm Hg. Pour la série de réactions à 653 °C du tableau 2, la pression initiale de C_3O_2 est de 24.6 mm Hg et l'on voit que V_0 varie comme la racine carrée de la pression initiale de O_2. Une autre série de réactions à 653 °C à composition initiale constante $1C_3O_2{:}2O_2$ a montré que V_0 varie comme la pression initiale à la puissance 2.5. On peut donc écrire, pour nos mélanges "secs", l'éq. 4. En

$$[4] \qquad -d(C_3O_2)/dt = k(C_3O_2)^2(O_2)^{1/2}$$

désignant les pressions partielles initiales par $A = P_0(C_3O_2)$ et $B = P_0(O_2)$ et en tenant

TABLEAU 2. Variation de la vitesse initiale V_0 en fonction de la pression initiale P_0 de O_2; $\theta = 653$ °C, P_0 de $C_3O_2 = 24.6$ mm Hg

P_0 (mm)	$P_0^{1/2}$ (mm$^{1/2}$)	V_0 (mm s^{-1})	$P_0^{1/2}/V_0$
164	12.8	0.537	23.8
115	10.7	0.448	24.0
49.2	7.0	0.323	21.8
41.0	6.4	0.311	20.5
32.8	5.7	0.233	24.5
24.6	4.9	0.222	22.4
16.4	4.0	0.171	23.6
8.2	2.8	0.113	25.4

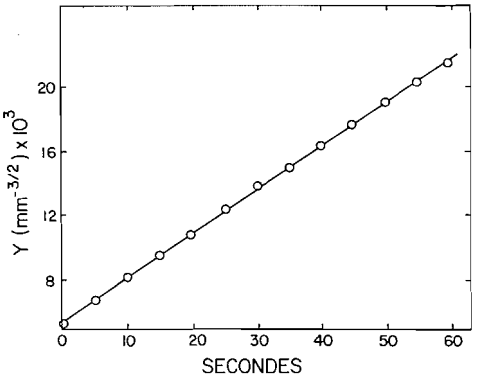

FIG. 7. Représentation de l'éq. 5 d'après les données obtenues lors de la réaction à 652 °C d'un mélange $1C_3O_2{:}2O_2$ de pression initiale 66 mm Hg.

compte de l'éq. 3, on écrit [4] sous la forme

$$d(\Delta P)/dt = k'(A - \Delta P)^2(B - \Delta P)^{1/2}$$

Dans le cas où l'oxygène est en excès, $(B > A)$, l'intégration donne l'éq. 5. Sur la fig. 7, on a

$$[5] \quad \frac{1}{B-A}\left[\frac{(B-\Delta P)^{1/2}}{(A-\Delta P)} - \frac{1}{2}\left(\frac{2.3}{(B-A)^{1/2}} \times \log\frac{(B-\Delta P)^{1/2}+(B-A)^{1/2}}{(B-\Delta P)^{1/2}-(B-A)^{1/2}}\right)\right] = k't$$

porté les valeurs du membre de gauche de cette équation (désigné par la lettre Y) en regard du temps, en insérant les valeurs de ΔP et de t obtenues lors d'une réaction à 652 °C avec un mélange où $A = 22$ et $B = 44$ mm Hg, soit $(1C_3O_2{:}2O_2)$. On voit que l'éq. 5 est bien vérifiée durant une bonne partie de la réaction; il en est ainsi quelles que soient les valeurs relatives de A et de B. Au-delà d'environ 60% de conversion, la droite s'incurve vers le bas, ce que nous attribuons à l'influence des produits. La pente de cette droite est la valeur de k'. Dans le cas de la réaction de la fig. 6, nous obtenons $k' = 2.7 \times 10^{-4}$ mm Hg$^{-3/2}$ s^{-1}. Plus loin, nous remplacerons k' par k (l/mol)$^{3/2}$ s^{-1}.

Il faut noter que l'ordre global de 2.5 a été obtenu dans tous les cas où notre mélange était "sec". Avec des mélanges moins purs (contenant probablement des traces d'eau ou d'acide acétique) l'ordre global devenait égal à 2, l'ordre par rapport au sous-oxyde s'abaissant à 1.5 tandis que l'ordre par rapport à l'oxygène restait de 0.5.

Nous avons calculé l'énergie d'activation

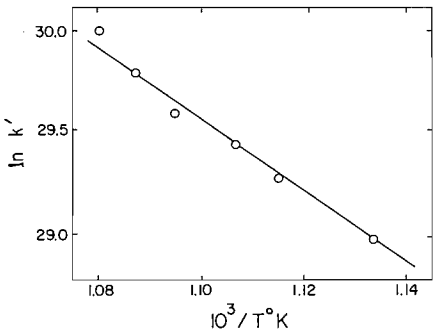

FIG. 8. Droite d'Arrhénius obtenue à partir des valeurs k' de l'éq. 5.

globale de deux façons. D'après les vitesses initiales $V_0 = (dP/dt)_0$ à différentes températures, on obtient $E = 33$ kcal/mol. D'autre part, nous avons pris les valeurs de k' d'après l'éq. 5 pour des réactions à différentes températures et en avons tiré les valeurs de la constante k de l'éq. 4 en termes des concentrations, par conversion des unités et corrections pour l'effet de température. La droite d'Arrhénius de la fig. 8, où k est exprimée en $(l/mol)^{3/2}\ s^{-1}$, nous a donné $E = 35$ kcal/mol. Incidemment, la concordance entre ces deux valeurs confirme la validité de l'éq. 5. Pour le facteur préexponentiel A dans $k = Ae^{-E/RT}$, on obtient la valeur $A = 2.3 \times 10^{21}\ (l/mol)^{3/2}\ s^{-1}$.

(c) Effets d'additifs et de surface

Les effets d'additifs sont très variés (10). L'argon n'affecte pas la vitesse initiale V_0, mais abrège la période d'induction τ de l'explosion, donc favorise l'explosion de $CO–O_2$ en présence d'une petite concentration résiduelle de C_3O_2. L'addition de CO_2 n'affecte pas non plus V_0, mais retarde l'explosion de $CO–O_2$. Par exemple, dans une réaction à 653 °C où $P_0(C_3O_2 + 3O_2) =$ 196 mm Hg, l'addition de 49 mm Hg de CO_2 a porté la période d'induction τ de 1163 à 1763 s. L'effet de l'addition de CO au mélange $C_3O_2–O_2$ initial est complexe; ce gaz abaisse la limite d'explosion de $C_3O_2–O_2$, accroît légèrement la vitesse initiale V_0 d'oxydation de C_3O_2 et abrège la période d'induction τ de l'explosion de $CO–O_2$, comme le montre le tableau 3. De plus, en présence de quantités importantes de CO, l'ordre de la réaction relatif à C_3O_2 passe de 2.0 à 1.5. Enfin, un effet inattendu: en présence de CO, l'augmentation de la concentration initiale de C_3O_2 entraîne un accroissement de la

TABLEAU 3. Effets de l'addition de CO à un mélange initial où $P_0(C_3O_2) = 32.8$, $P_0(O_2) = 164$ mm Hg, et $\theta = 631$ °C

$P_0(CO)$ (mm)	V_0 (mm s^{-1})	τ (s)
0.0	1.43	980
13.4	1.62	538
20.2	1.74	581
27.3	2.10	571
40.6	2.27	402
50.6	1.99	221

vitesse initiale V_0 mais aussi un prolongement important de la période d'induction τ, tandis qu'en l'absence de CO, la période τ est d'autant plus courte que la vitesse initiale est plus grande. Ceci s'explique si l'on considère que durant la réaction 1, CO s'accumule et C_3O_2 s'épuise jusqu'à ce que le rapport $(CO)/(C_3O_2)$ atteigne la valeur critique à laquelle il y a explosion. Ainsi, l'addition de CO hâte l'explosion et l'addition de C_3O_2 la retarde. Les divers effets de l'addition de H_2O ont été décrits plus haut.

L'addition de NO_2 inhibe fortement l'oxydation de C_3O_2, comme le montre la fig. 9. Il est difficile de dire si l'effet observé est attribuable à NO ou à NO_2, ce dernier étant fortement dissocié à 661 °C, car on se trouve ici en présence d'un excès d'oxygène. On sait (4) qu'à 25 °C, NO réagit sur le radical C_2O 135 fois plus vite que l'oxygène moléculaire. Il est donc vraisemblable qu'il agisse comme capteur de C_2O dans la chaîne d'oxydation de C_3O_2, tandis qu'il a peu d'effet sur celle de CO.

Pour étudier l'influence du rapport surface/-volume, nous avons utilisé trois cylindres de Vycor identiques de 4.5 × 22 cm, l'un vide, les

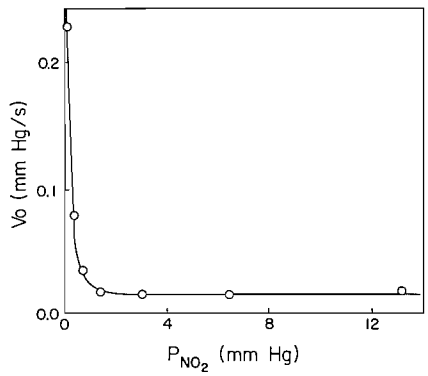

FIG. 9. Inhibition par NO_2 de l'oxydation lente de C_3O_2.

autres contenant des tubes de Vycor courts. Les rapports obtenus étaient respectivement S/V = 1.1, 3.2, 5.0 cm^{-1}. Une série d'expériences (10) à des pressions allant de 12 à 130 mm de mélanges $1C_3O_2$:$2O_2$ à 661 °C ont montré que la vitesse initiale V_0 décroît quand S/V croît, la vitesse variant grosso-modo comme la racine carrée du diamètre. De plus, l'ordre global de la réaction pour chacun des réacteurs passe de 2.4 pour S/V = 1.1 cm^{-1}, à 2.0 pour S/V = 3.2 cm^{-1}, et à 1.8 pour S/V = 5.0 cm^{-1}. La limite inférieure d'explosion d'un mélange $1C_3O_2$:$2O_2$ à 671 °C est passée de 130 mm Hg dans le réacteur ordinaire de S/V = 1.1 cm^{-1} à 250 mm Hg dans celui de S/V = 3.2 cm^{-1}, l'explosion devenant immédiate et violente.

Discussion

Nous proposons le schéma réactionnel 1 ci-dessous.

		$\Delta H°$ 1000 °K kcal/mol
[i]	$C_3O_2 + O_2 + M \rightarrow 3CO + O + M$	4
[i']	$C_3O_2 \xrightarrow{\text{paroi}} C_2O + CO$	86
[6]	$C_3O_2 + O \rightarrow C_2O + CO_2$	−42
[7]	$C_2O + O_2 \rightarrow 2CO + O$	−82
[8]	$CO + O \rightarrow CO_2^*$	12
[9]	$CO_2^* + CO \rightarrow CO_2 + CO^*$	−2
[10]	$CO^* + O_2 \rightarrow CO_2 + O$	−146
[11]	$CO_2^* + O_2 \rightarrow CO_2 + O + O$	−19
[12]	$C_2O + O_2 \rightarrow CO_2 + CO$	−211
[13]	$C_3O_2 + O \rightarrow 3CO$	−117
[14]	$C_2O + CO \rightarrow C_3O_2$	−86
[15]	$O \xrightarrow{\text{paroi}}$	
[16]	$C_2O \xrightarrow{\text{paroi}}$	

SCHEMA 1

Les enthalpies de ces réactions ont été obtenues à partir des données de Kybett *et al.* (16) sur C_3O_2 et de celles de Willis et Bayes (5) et de Becker et Bayes (17) sur le radical C_2O, et converties à 1000 °K. Pour les enthalpies de formation à 1000 °K, nous adoptons $\Delta H_f^0(C_3O_2)$ = −10 kcal/mol et $\Delta H_f^0(C_2O)$ = 98 kcal/mol. La pyrolyse de C_3O_2, [i'], doit être affectée d'une variation d'enthalpie de 86 kcal/mol. D'autre part on a trouvé (18, 19) pour la pyrolyse homogène, des énergies d'activation de 56 et de 61 kcal/mol. Pour expliquer nos résultats, nous supposons que la pyrolyse de C_3O_2 sur la paroi est beaucoup plus importante que celle en phase gazeuse dans les conditions de nos expériences. Nous avons calculé pour notre réaction 1 ΔH_1^0 = −127 kcal/mol, de sorte que l'effet d'auto-échauffement n'intervient probablement pas aux vitesses ordinaires, mais contribue sans doute à déclencher l'explosion.

(a) L'oxydation lente

Au début de l'oxydation lente de C_3O_2 selon [1], il n'y a pas encore de CO dans le système. Il se forme du CO et du CO_2 par le cycle des réactions de propagation [6] et [7]. Le fait que les produits restent dans la proportion $(CO)/(CO_2)$ = 2 jusqu'à la disparition quasi complète de C_3O_2 signifie que C_3O_2 est un capteur d'atomes O beaucoup plus efficace que CO ($k_6 \gg k_8$). Dès qu'il ne reste plus de C_3O_2, les atomes O deviennent disponibles pour attaquer le CO suivant la chaîne énergétique des réactions 8 à 11. Cette vue simplifiée d'un mécanisme "tout ou rien" est justifiée parce que le début de l'oxydation de CO se manifeste toujours par une cassure nette de la courbe de pression et aussi parce que les analyses de quelques échantillons prélevés quelques secondes avant cette cassure n'on révélé que des traces de C_3O_2.

Les ordres apparents de 2 relatif à C_3O_2 et 1/2 relatif à O_2 [4], ainsi que l'abaissement de ces ordres par l'augmentation du rapport surface/volume, nous ont conduits à admettre que l'initiation résulte de deux réactions: une oxydation homogène par choc triple, [i] et une pyrolyse hétérogène [i']. De plus, nous postulons des terminaisons homogènes [12], [13], et [14] et hétérogène [15] et [16]. Les concentrations des atomes O et des radicaux C_2O sont infimes au cours de la réaction lente; c'est pourquoi nous n'avons pas inclus, parmi les modes de terminaison, leurs recombinaisons dont les taux seraient négligeables par rapport à ceux des réactions 12, 13, et 14. D'autre part, comme les terminaisons hétérogènes sont toutes linéaires, elles n'affectent pas l'ordre de la réaction, mais seulement la vitesse et les limites d'explosion. Nous les avons omises pour simplifier le calcul des états stationnaires.

Si les deux modes d'initiation [i] et [i'] sont

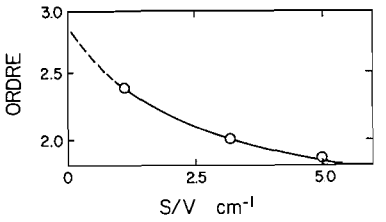

FIG. 10. Variation de l'ordre global de l'oxydation lente en fonction du rapport surface/volume.

importants, on doit s'attendre à ce que les ordres, en particulier l'ordre global de la réaction, dépendent de la valeur du rapport surface/volume, comme nous l'avons déjà constaté. Les ordres que nous avons observés expérimentalement dans nos trois réacteurs sont représentés sur la fig. 10 en fonction de S/V. L'ordre tend vers $n = 3$ pour un réacteur hypothétique à $S/V = 0$ (absence de parois), c'est-à-dire dans le cas d'une initiation purement homogène.

Incluons les deux modes d'initiations, négligeons les terminaisons sur la paroi et posons $k_7 \gg k_{12}$ (puisque $(CO)/(CO_2) = 2$ reste constant). La concentration stationnaire des atomes d'oxygène s'écrit alors

$$(O)_{stat.} = \frac{k_i k_6 (O_2)(M) + k_i' k_7}{k_7 k_{13} + k_{12} k_6}$$

La constance du rapport 2 des produits implique aussi que $k_6 \gg k_{13}$, de sorte que la dest truction de C_3O_2 dans l'oxydation lente espratiquement attribuable à la seule réaction 6 et donne l'éq. 17. En l'absence d'initiation hétérogène, le terme $k_i'(C_3O_2)$ serait nul et l'ordre apparent serait $n = 3$, comme pour le cas $S/V = 0$ sur la fig. 10. Par contre, pour des

$$[17] \quad \frac{-d(C_3O_2)}{dt} = \frac{k_7 k_6}{k_7 k_{13} k_{12} k_{16}} \times [k_i(C_3O_2)(O_2)(M) + k_i'(C_3O_2)]$$

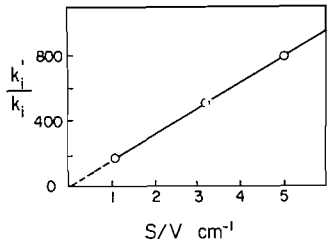

FIG. 11. Importances relatives des réactions d'initiation [i] et [i'] en fonction du rapport surface/volume.

valeurs élevées de S/V, le terme $k_i'(C_3O_2)$ prédominerait et l'ordre tendrait vers $n = 1$, comme l'indique la même figure. Pour préciser cette prédiction qualitative, nous avons calculé les valeurs du rapport k_i'/k_i pour lesquelles une courbe $\log V_0$ *vs.* $\log P_0$ (où V_0 = vitesse initiale et P_0 = pression totale initiale) donne les ordres $n = 2.4$, 2.0, et 1.8 obtenus expérimentalement dans nos trois réacteurs. Ces valeurs sont $k_i'/k_i = 180$, 550, et 850 respectivement. La validité de ce calcul est confirmée par la fig. 11, où l'on voit que l'importance de l'initiation hétérogène (k_i') est proportionnelle à S/V et, en particulier, que $k_i' \to 0$ quand $S/V \to 0$.

(b) Les explosions

Nous avons distingué deux sortes d'explosion: l'explosion retardée du mélange CO–O_2–CO_2, qui correspond à la région A de la fig. 3; et l'explosion immédiate du mélange C_3O_2–O_2, qui correspond à la région C. Dans l'un et l'autre cas, l'explosion résulte d'une accélération de la réaction par la ramification [11] ce qui implique que le mécanisme dominant est la chaîne énergétique des réactions 8 à 11.

Dans le cas de l'explosion retardée, les facteurs qui empêchent la réaction de s'auto-accélérer sont la capture des atomes O par C_3O_2 selon [6] et [10], mais aussi la désactivation de CO_2* et de CO* par le CO_2 présent, effet que nous n'avons pas inscrit dans notre schéma, et peut être aussi la recombinaison homogène [14] étudiée par Palmer et Cross (20), tant qu'il reste un peu de C_3O_2.

L'explosion du mélange C_3O_2–O_2 doit faire intervenir l'ensemble des chaînes radicalaire et énergétique. La limite inférieure dépendra du taux net de production d'atomes O, qui peut s'écrire

$$d(O)/dt = -k_8(CO)(O) + k_{10}(CO^*)(O_2) + 2k_{11}(CO_2^*)(O_2) - k_6(C_3O_2)(O) + k_7(C_2O)(O_2) - k_{15}(O)$$

En remplaçant dans cette équation (CO*), (CO_2*), et (C_2O) par leurs concentrations stationnaires, on obtient l'expression du facteur net de ramification, [18]. Dans le membre de

$$[18] \quad \phi = \frac{k_{11} k_{13} (CO)(O_2)}{k_9(CO) + k_{11}(O_2)} - \frac{k_6(C_3O_2)[k_{14}(CO) + k_{16}]}{k_7(O_2) + k_{10}(CO) + k_{16}} - k_{15}$$

droite de cette équation, le premier et le troisième termes, pris seuls, donnent la valeur de ϕ pour la combustion de système $CO–O_2$. Le deuxième terme, qui est négatif, exprime l'action inhibitrice de C_3O_2 sur l'oxydation de CO.

Durant l'oxydation lente de C_3O_2, le deuxième terme décroît à mesure que C_3O_2 disparaît par les réactions 6 et 7, en même temps que le premier terme croît à mesure qu'il se forme du CO. La valeur de ϕ devient de moins en moins négative et atteint $\phi \simeq 0$, valeur critique à laquelle le mélange explose. Il se peut d'ailleurs qu'à certaines températures et compositions, la somme du premier et troisième termes reste négative après la disparition du deuxième; dans ce cas le CO s'oxyde lentement. L'équation 18 montre que la limite d'explosion dépend des concentrations d'une façon compliquée. On peut cependant dire que le deuxième terme n'influe pas sur la limite d'une explosion retardée, puisqu'il s'annule, $(C_3O_2) = 0$, avant qu'elle ne se produise.

Aux pressions et températures les plus élevées, il se peut que l'oxydation lente du C_3O_2 soit auto-accélérée, vraisemblablement par auto-échauffement. Dans ce cas, la décroissance du deuxième terme serait accélérée et, fournissant le CO, provoquerait une croissance accélérée du premier terme. L'effet thermique aidant, le système s'acheminerait rapidement vers $\phi = 0$ et l'explosion, qui serait celle d'un mélange $CO–O_2$. Ce serait le cas de la limite inférieure d'explosion du système $C_3O_2–O_2$ (courbe I de la fig. 3). En réalité, cette appellation désignerait un état de choses où l'explosion de $CO–O_2$ est atteinte sans retard.

Il est possible que les deux sortes d'explosion soient attribuables à la même réaction de ramification [11]. Si l'on désigne par B, l'énergie d'activation de cette réaction, on peut exprimer les coefficients de température des limites inférieure et supérieure d'explosion par les équations

$$P_{\text{inf.}} = C/d\, e^{B/2RT}$$

$$P_{\text{sup.}} = C'\, e^{-(B-E)/RT}$$

où C et C' sont des constantes, d est le diamètre du réacteur, E est l'énergie d'activation d'une terminaison homogène, et B, l'énergie d'activation de la réaction de ramification. Les pentes des droites de la fig. 4 nous donnent les valeurs expérimentales $B/2 = 14$ kcal/mol pour la limite inférieure d'explosion de $C_3O_2–O_2$ et $B - E = 24$ kcal/mol pour la limite supérieure d'explosion de $CO–O_2$. Donc, pour $C_3O_2–O_2$, $B = 28$ kcal/mol, ce qui est en accord avec la valeur citée par Dainton (21) $B > 25$ kcal/mol pour $CO–O_2$ et représente probablement l'énergie d'activation de la ramification [11]. Pour la limite supérieure d'explosion de $CO–O_2$, nous arrivons à la même valeur $B = 28$ kcal/mol en attribuant à la recombinaison la valeur plausible $E = 4$ kcal/mol. Il semble donc que les explosions des systèmes $C_3O_2–O_2$ et $CO–O_2$ impliquent le même processus de ramification [11]. Rappelons que la limite inférieure d'explosion du système $C_3O_2–O_2$ est très sensible au rapport surface/volume, ce qui implique des terminaisons hétérogènes importantes, malgré la pression relativement élevée, et sans doute aussi un gradient de température résultant de l'oxydation rapide de C_3O_2. Dans ces conditions, il n'est pas invraisemblable que la limite inférieure d'explosion du système $CO–O_2$ en présence d'un inhibiteur puissant (C_3O_2) se situe à une pression supérieure à celle de la limite supérieure d'explosion du système $CO–O_2$ non inhibé.

Nous remercions le Conseil National de Recherches du Canada de son aide financière.

1. K. CLUSIUS et M. HUBER. Helv. Chim. Acta, **32**, 2400 (1949).
2. H. VON WEYSSENHOFF, S. DONDES, et P. HARTECK. J. Amer. Chem. Soc. **84**, 1526 (1962).
3. G. LIUTI, C. KUNZ, et S. DONDES. J. Amer. Chem. Soc. **89**, 5542 (1967).
4. D. G. WILLIAMSON et K. D. BAYES. J. Amer. Chem. Soc. **89**, 3390 (1967).
5. C. WILLIS et K. D. BAYES. J. Amer. Chem. Soc. **88**, 3203 (1966).
6. J. LEBEL, P. MICHAUD, et C. OUELLET. J. Phys. Chem. **72**, 3678 (1968).
7. D. A. LONG, F. S. MURFIN, et R. L. WILLIAMS. Proc. Roy. Soc. (London), **A223**, 251 (1954).
8. J. S. P. BATCHELOR, E. FURBY, et K. L. WILKINSON. At. Energy Res. Estab. (Gr. Brit.). Rep. R-3942, 1962.
9. T. J. HIRT et H. B. PALMER. Anal. Chem. **34**, 164 (1962).
10. J. LEBEL. Thèse. Université Laval, Québec, Québec. 1969.
11. H. JAMES et P. LAFFITTE. Rev. Inst. Fr. Pétrol. **13**, 349 (1958). H. JAMES. Rev. Inst. Fr. Pétrol. **12**, 1241 (1957); **13**, 83 (1958).
12. F. CUSIN et H. JAMES. J. Chim. Phys. **58**, 162 (1961).
13. A. S. GORDON. J. Chem. Phys. **20**, 340 (1952). P. G. DICKENS, J. E. DOVE, et J. W. LINNETT. Trans. Faraday Soc. **60**, 539 (1964).
14. G. J. MINKOFF et C. F. H. TIPPER. Chemistry of Combustion Reactions. Butterworths, London, 1962. p. 79. D. E. HOARE et A. D. WALSH. Trans. Faraday Soc. **50**, 37 (1954).
15. J. LEBEL et C. OUELLET. A paraître.

16. B. D. KYBETT, G. K. JOHNSON, C. K. BARKER, et J. L. MARGRAVE. J. Phys. Chem. **69**, 3603 (1965).
17. K. H. BECKER et K. D. BAYES. J. Chem. Phys. **48**, 653 (1968).
18. H. B. PALMER et T. J. HIRT. J. Amer. Chem. Soc. **84**, 113 (1962).
19. H. RIJEWSKI, J. TROE, et H. GG. WAGNER. Z. physik Chem. N.F. **68**, 321 (1969).
20. H. B. PALMER et W. D. CROSS. Carbon, **3**, 475 (1966).
21. F. S. DAINTON. Chain reactions. Methuen, London, 1966. p. 162.

Can. J. Chem. Downloaded from www.nrcresearchpress.com by 210.87.254.6 on 09/05/12
For personal use only.

Proton Magnetic Resonance Studies of Ionic Solvation in Ion-Exchange Resins. Part II

H. D. SHARMA[1] AND N. SUBRAMANIAN
Department of Chemistry, University of Waterloo, Waterloo, Ontario

Received July 7, 1970

The proton magnetic resonance spectra of anion-exchange resin Dowex AG1 of various crosslinkages ranging from X1 to X10 in the F^-, Cl^-, Br^-, I^-, NO_3^-, and ClO_4^- forms have been recorded and the values of the molal chemical shift, $\delta^0_{X^-}$, are found to be -0.035, 0.026 (assumed), 0.035, 0.045, 0.037, and 0.058 p.p.m./mol, respectively, for the anions. These values are generally lower compared to those observed in corresponding aqueous solutions, indicating that ion–solvent interactions are similar in both the resin matrix and the aqueous solution but there is probably increased ion association in the resin phase. The effective hydration numbers have been deduced from the temperature dependence measurements of proton chemical shifts for the alkali-metal ions and for a few anions in various crosslinkages of Dowex AG 50W and Dowex AG1 resins. The values of the hydration number decrease as the crosslinkage increases for the alkali-metal ions. The decrease in the hydration number at high crosslinkage is attributed to ion association in the resin phase. The reversal of selectivity in K^+/Cs^+ system below X16 in the sulfonated resin is explained on the basis of decrease in the hydration of K^+ form of resin compared to that of Cs^+ form, consistent with the experimental observations. The electrostatic interactions between the counterion and fixed group and ions and solvent in the resin phase have been discussed in the light of the proposed models.

Canadian Journal of Chemistry, 49, 457 (1971)

Introduction

A considerable body of experimental data has been obtained in connection with equilibria and kinetics in ion-exchange resin (1–3). Several models have been proposed to interpret and to predict the selectivity of ions when in equilibrium with their respective solutions. The model proposed by Gregor pictures the ion-exchanger as consisting of two parts, an un-crosslinked polyelectrolyte with solvent and the cross linking. Selectivity for an ion is considered to arise primarily because of differences in the partial molal volumes of the counterions in the resin phase (4). The other models rely on the electrostatic interactions between the counterion and the fixed group and the ion–solvent interactions (5–7). In all these models ion-pair formation and ionic hydration is recognized as of key importance to explain the observed swelling pressures and selectivity of ions under a variety of conditions. An excellent review has been presented by Reichenberg and Diamond and Whitney in ref. 2. However, there is very little direct experimental evidence to support or disprove the basic assumptions on which the models are based. Glueckauf and Kitt obtained the hydration numbers of cations in the resin phase by a method based on thermodynamical considerations (8).

Nuclear magnetic resonance (n.m.r.) has proved to be a versatile technique in studying ionic solvation in aqueous and non-aqueous solutions of electrolytes (9–11). More recent studies in this connection concern the determination of solvation numbers of ions in solution (12–16). Of these, two approaches are particularly suitable for aqueous solutions of alkali and alkaline earth salts, *viz.*, (*a*) effect of concentration (17) and (*b*) effect of temperature (14–16) on the proton chemical shift of water. The n.m.r. spectra of suspensions of ion-exchange resins should shed light on the structure of the "internal electrolyte solution". This has been verified by the investigations of Gordon (18) and Choppin and co-workers (19). It has been shown by us that the effect of ion concentration and temperature on the chemical shifts of interior water can be conveniently studied in a quantitative manner in sulfonated cation-exchange resins (20). The "effective hydration numbers" for alkali-metal ions were calculated from the temperature dependence of the chemical shift. Recently, similar results have been reported by Creekmore and Reilley (21). We have extended these studies to both anion- and cation-exchange resins of various cross linkages and ionic forms. The hydration numbers calculated from the experimental results have been discussed in terms of the "models" to rationalize the observed selectivity coefficients for ions.

[1]To whom all correspondence should be addressed.

Can. J. Chem. Downloaded from www.nrcresearchpress.com by 210.87.254.6 on 09/05/12
For personal use only.

Experimental

All the resins used in this work were procured from Bio-Rad Laboratories, Richmond, California. Dowex AG 50W (X1 to X16) cation-exchange resins (with sulfonate anion on a polystyrene lattice) were obtained in the H^+ form while the anion-exchanger Dowex AG1 (X1 to X10) (with quaternary ammonium group on a polystyrene lattice) and Bio-Rex 9 (with pyridinium group on a polystyrene lattice) were in their Cl^- form. After necessary conditioning, these were converted to the required ionic forms by the column method. Special care was taken to ensure complete conversion and removal of all excess of the electrolyte used in the process. Bio-Rex 63 (a cation-exchange resin with phosphonate anion on a polystyrene lattice) and Bio-Rex 70 (another cation-exchange resin with carboxylate anion on an acrylic lattice), supplied in the Na^+ form, were used as such after conditioning. 200–400 mesh beads were used throughout except for Dowex AG 50W (X1) and Dowex AG1 (X1) resins where only 50–100 mesh was available. However, the bead size, while affecting the signal width, had little effect on the observed chemical shift (20).

Water contents of the resins in their various ionic forms and crosslinkages were determined by the Karl Fischer technique. This method has been shown to be very rapid and reliable for both cation- (22) and anion- (23) exchange resins and yields values of water contents with an accuracy of $\pm 2\%$.

The capacities of cation-exchange resins were determined as described previously (20). For the anionic resins, the capacities were found in the chloride form as follows (24). A given weight of the air-dried resin of known water content was transferred to a column. A very large excess of 0.5 *N* KNO_3 solution was passed through the column and the concentration of the liberated chloride ions in the effluent was estimated by Mohr titration. Doubly distilled, deionized water was used throughout and the salts were all of the highest purity commercially available.

The proton magnetic resonance (p.m.r.) spectra of aqueous suspensions of resins were recorded on a Varian A-60 spectrometer. The temperature of the sample was controlled with a Varian V-6040 temperature controller. The details of the spectral measurements are given in our earlier paper (20).

Results

The p.m.r. spectrum of a well-settled aqueous suspension of an ion-exchange resin usually consists of two signals arising from water protons inside and outside the resin environment (18). Compared to pure water and solutions of diamagnetic salts, the line widths are larger due to susceptibility considerations and heterogeniety of the resin phase (18). The chemical shift between the external and internal water peaks is defined, as before, by $\delta = \Delta\nu/60$ (p.p.m.), where $\Delta\nu = (\nu_{ext\,H_2O} - \nu_{int\,H_2O})$ c.p.s. *i.e.*, a positive value of δ would mean that the internal water peak is upfield with respect to the external water peak. The p.m.r. spectra of aqueous suspensions of Dowex AG1 (X1 to X10) in the F^-, Cl^-, Br^-, I^-, NO_3^-, and ClO_4^- forms were recorded at 25 °C. If the chemical shifts of the internal and external water protons were very close, the overlapping peaks were resolved by a hybrid analog-digital computer routine using an IBM 360/44 computer. The observed δ values are plotted against the ionic molalities, *m*, in Fig. 1.

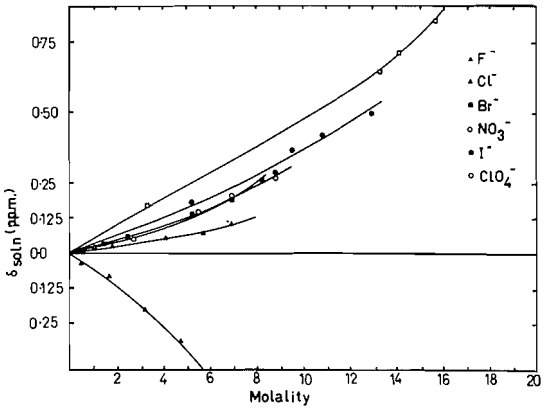

FIG. 1. Chemical shift as a function of ionic concentration for Dowex AG1 resin at 25 °C.

The influence of temperature on the proton chemical shift of internal water, δ_{soln}, was studied in Dowex AG 50W resins of crosslinkage 4, 8, and 16 in the Na^+, K^+, Rb^+, Cs^+, and NH_4^+ forms. Similar temperature–shift data were also obtained for a few anionic forms of Dowex AG1. The change in the observed δ values with increase in temperature for the NH_4^+ form of Dowex AG 50W (X8) is shown in Fig. 2 as a typical case.

For each ionic form, the δ_{soln} value at a given temperature with respect to gaseous ethane, δ_{soln}^{ethane}, was evaluated from the experimental δ values and by following the procedure described previously (20). The coefficient, $\delta_{soln}^{ethane}/dT$ (p.p.m./°C), was then obtained as the slope of a least square plot of δ_{soln}^{ethane} *vs.* temperature (Table 1). For the ClO_4^- form, the temperature studies could not be carried out beyond 40 °C. When heated to 50 °C and above, irreversible decomposition of the resin sets in as was indicated by irreproducible δ values.

Discussion

Susceptibility Corrections

In the p.m.r. studies of aqueous solutions, it

Can. J. Chem. Downloaded from www.nrcresearchpress.com by 210.87.254.6 on 09/05/12
For personal use only.

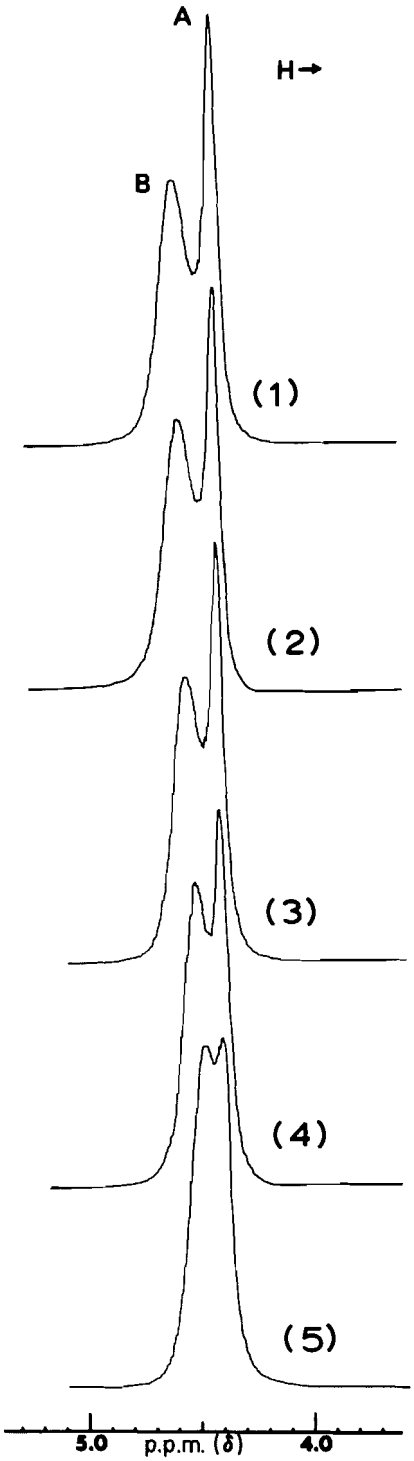

FIG. 2. Effect of temperature on the proton magnetic resonance spectrum of a suspension of AG 50W (X8) (200–400 mesh) resin in the NH_4^+ form: (*1*) 15 °C, (*2*) 25 °C, (*3*) 32 °C, (*4*) 40 °C, and (*5*) 50 °C; *A*, "internal" water peak; *B*, "external" water peak.

was found necessary to correct for the bulk diamagnetic susceptibility contributions from the ionic species present (17, 25). In the resin system, additional contribution can be expected from the organic part of the resin particle. It was seen by us, however, that when the spectra of sulfonated cation-exchangers were recorded without allowing the resin beads in the n.m.r. tube to settle down, a third line appeared as a shoulder on the high field side of the "external" water line (20). The very sharp third resonance line was assigned to the protons of the "bulk" water. A similar observation was made with the anion-exchanger as well. The spectra of well-shaken suspensions of AG1 resin in the F^- and ClO_4^- forms are reproduced in Fig. 3.

It is significant that, for a given ionic form and crosslinkage, δ is independent of the bead size (20). On the other hand, the shift between "bulk" and "external" water, whose value varies from 2 to 10 c.p.s., is found to be a function of the nature of the counterion (being maximum for Cs^+), the crosslinkage and the size (and, therefore, the density) of the resin. This latter shift is a result of susceptibility effects. Whereas the bulk water molecules are farther removed from the resin, the external water is actually held as a tightly bound sheath around the resin surface. The rate of exchange between the two kinds of water is lower than the n.m.r. time scale (17). While considering the δ values, it is therefore reasonable to assume that there is, so to speak, a built-in susceptibility correction in the system and to omit any further such correction. The fact that the resin beads are spherical provides additional justification for neglecting the susceptibility effect (26, 27).

Factors Influencing the Chemical Shift

In order to interpret the observed δ values, we need to consider the effect of (*a*) the organic matrix, (*b*) the fixed ionic group, and (*c*) the counterion on the structure of the internal water. The nature and concentration of the counterion strongly influence the position of the internal water proton signal, but the contribution from the other two factors still remains uncertain.

TABLE 1. Effective hydration numbers of Dowex AG 50W and Dowex AG1 resins in various ionic forms and crosslinkages

Resin	Ionic form	Cross-linkage	Ionic molality (m)	$d\delta_{soln}^{ethane}/dT$ (p.p.m./°C)	h (±0.5–1.0)
Dowex AG 50W	NH_4^+	4	3.3	0.00830	2.2
		8	5.7	0.00792	1.7
		16	10.3	0.00716	1.4
	H^+	2	1.8	0.00923	0.6
		8	4.8*	0.00761*	2.0* (2.9)
	Na^+	4	3.3*	0.00690*	4.8* (3.0)
		8	5.3*	0.00635*	3.6* (2.9)
		16	8.7	0.00632	2.2
	K^+	4	3.9*	0.00662*	4.4*
		8	6.2	0.00633	3.0 (2.7)
		16	11.1	0.00597	1.9
	Rb^+	4	3.9	0.00754	3.0
		8	6.3	0.00678	2.6 (2.6)
		16	10.1	0.00622	1.9
	Cs^+	4	3.7	0.00787	2.7
		8	6.2*	0.00699*	2.4* (3.2)
		16	9.5	0.00615	2.1
Dowex AG1	ClO_4^-	1	3.3	0.00930	0.6
		4	13.3	0.00823	0.6
		10	15.6	0.00823	0.5
	F^-	2	1.7	0.01010	~0.0
		4	3.1	0.00900	1.1
		10	4.7	0.00814	1.8
	Br^-	8	(5.8)	—	— (1.3)
	I^-	4	9.5	0.00696	1.6
		8	(8.9)	—	— (1.2)
		10	12.9	0.00809	0.7
	NO_3^-	4	5.48	0.00829	1.3

*Values from previous work, ref. 20. Values in parentheses from ref. 16.

(a) The Organic Matrix

Gordon has reported a high field shift of the resonance signal of carbon-bound protons present inside the cation- and anion-exchange resins (18). He attributes this effect to the diamagnetic anisotropy of the polystyrene matrix. According to Gordon (18) and Choppin and co-workers (19), similar high field shift of resonance line is likely also for water protons. However, it can be seen from Fig. 1 that as $m \to 0$, $\delta \to 0$; *i.e.*, at zero ionic concentration, internal and external water protons have identical chemical shifts. A similar observation was made earlier for the cation-exchange resins (20). If the matrix does in fact shift the interior water line upfield, extrapolation to $m = 0$ would have resulted in a positive intercept. Since this is not observed for the several ionic forms investigated, it can be concluded that, for hydroxylic protons, matrix contribution from anomalous magnetic susceptibility to the experimentally observed δ value is negligible.

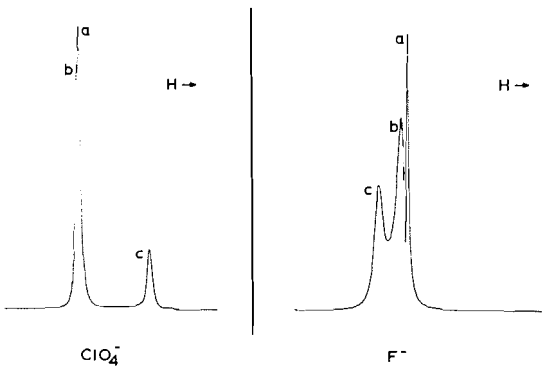

FIG. 3. Proton magnetic resonance spectra of suspensions of ClO_4^- and F^- forms of Dowex AG1 (X8) (200–400 mesh) in water (without allowing the resin particles to settle down): (*a*) "bulk water", (*b*) "external" water, and (*c*) "internal" water signals.

(b) The Fixed Ionic Group

It has been suggested that the ion attached to the resin matrix may not affect the water proton

Can. J. Chem. Downloaded from www.nrcresearchpress.com by 210.87.254.6 on 09/05/12
For personal use only.

Can. J. Chem. Downloaded from www.nrcresearchpress.com by 210.87.254.6 on 09/05/12
For personal use only.

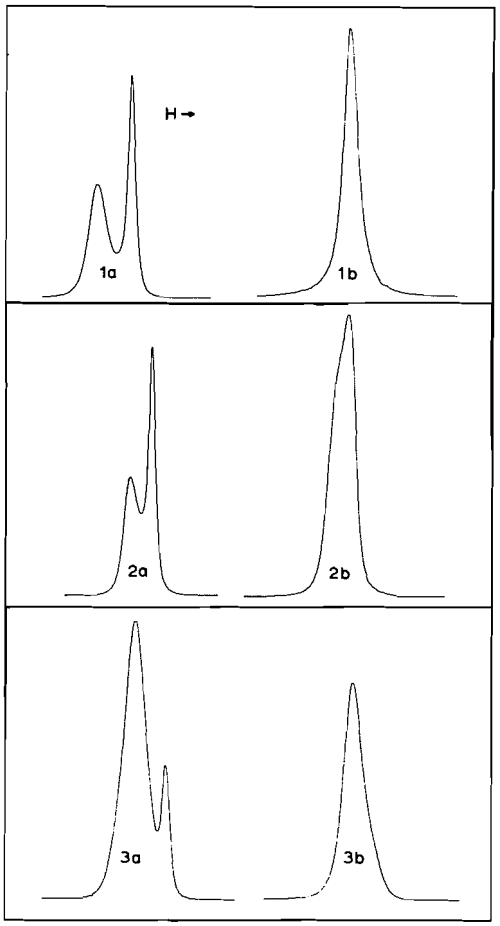

FIG. 4. Comparison of p.m.r. spectra of ion-exchange resins with different fixed ionic groups: (*1a*) Dowex AG 50W (X8), Na^+ and (*1b*) Bio-Rex 63, Na^+; (*2a*) Dowex AG 50W (X8), Na^+ and (*2b*) Bio-Rex 70, Na^+; (*3a*) Dowex AG1 (X1), I^- and (*3b*) Bio-Rex 9, I^-.

shift (28). If it were indeed so, the ion-exchange system should offer an excellent means of determining the "absolute" shift characteristic of the counterion, since, as mentioned above, the observed shifts are free from the matrix and susceptibility effects. With a view to examining the influence of the fixed ionic function, the p.m.r. spectra of the following pairs of resins were recorded (Fig. 4): (*i*) Na^+ form of Dowex AG 50W (X8) ($m = 5.26$) and Bio-Rex 63 ($m = 4.8$); (*ii*) Na^+ form of Dowex AG 50W (X4) ($m = 3.25$) and Bio-Rex 70 ($m = 3.3$), and (*iii*) I^- form of Dowex AG1 (X1) ($m = 5.2$) and Bio-Rex 9 ($m = 6.2$). The observed dissimilarity in values for each pair of resins may be due to the difference in the $\delta^0_{X^-}$ value characteristic of the fixed ion and/or due to the difference in the extent of ion association between the fixed group and the counterion. The contribution towards δ from these two factors cannot be separated particularly in weak acid and weak base resins.

Concentration Dependence of δ for Anion-exchange Resins

The variation of δ with the ionic concentration in the resin phase has already been considered for the cation-exchange resins (20). The shift data were analyzed following Hindman's treatment of water proton chemical shift in aqueous solutions of uni–uni electrolytes (17). The same procedure is followed for the anion-exchange resins. It is assumed that the experimentally observed δ values can be related to the molality of the resin salt according to the equation

$$[1] \qquad \delta = \delta^0_{salt}(m) + B(m)^2$$

where, δ^0_{salt} is δ/m as $m \to 0$ and B, a constant, depends on the nature of the salt. At infinite dilution, δ^0_{salt} can be considered to be the sum of $\delta^0_{M^+}$ and $\delta^0_{X^-}$, the cationic and anionic molal shifts, respectively. The δ^0_{salt} values were evaluated for the halide, nitrate, and perchlorate ions in Dowex AG1 resin from least square plots of δ *vs.* m and are reported in Table 2.

Hindman (17) reported a value of 0.026 p.p.m./mol for Cl^- in aqueous solutions, based on the scale $\delta^0_{NH_4^+} = 0$. Since the $\delta^0_{M^+}$ values in the resin were obtained earlier using the same scale, and since our purpose is to compare the molal shifts observed in the two systems, we assume, for consistency, that $\delta^0_{Cl^-} = 0.026$ p.p.m./mol in the resin. If there is ion-pair formation in the Cl^- form this value is expected to be lower. The experimentally observed value of δ^0_{salt} for the Cl^- form of Dowex AG1 is 0.008 p.p.m./mol. Consequently, the quaternary ammonium cation of the resin is assigned a $\delta^0_{M^+}$ value of -0.018 p.p.m./mol. Based on this value, $\delta^0_{X^-}$ were obtained for the other anions.

The anion molal shifts in the resin are compared with those found in aqueous solution in Table 2. The signs and the order of the shifts are seen to be identical in the two systems, while $|\delta^0|$ values are uniformly lower in the resin phase, thus complementing earlier observations on the molal shifts for the cations (20). $\delta^0_{X^-}$ values for Br^- and NO_3^- ions in the resin are close to the corresponding values in aqueous solution within the limits of experimental error. The larger

TABLE 2. Comparison of molal chemical shifts for anions in ion-exchange resin and in aqueous solution at 25 °C

Anion	Molal shift (p.p.m.) Ion-exchange δ^0_{salt}	Ion-exchange $\delta^0_{X^-}$	Aqueous solution $\delta^0_{X^-}$ (Hindman, ref. 17)
F^-	−0.053	−0.035	−0.075
Cl^-	0.008	0.026 (assumed)	0.026*
Br^-	0.017	0.035	0.053
I^-	0.027	0.045	0.069
NO_3^-	0.019	0.037	0.046
ClO_4^-	0.040	0.058	0.091

*Value based on $\delta^0_{NH_4^+} = 0$ scale.

differences in the case of I^- and ClO_4^- ions may very well be due to error resulting from extrapolation. The aqueous solution values for these ions have been computed from δ–m plots for NaI and NH_4ClO_4 solutions in the concentration region 0–4.5 and 0–2 m, respectively. On the other hand, the lowest concentration limit attainable in the resin is 5.2 m for I^- and 3.3 m for ClO_4^-.

Amongst the anions, the largest difference in the $\delta^0_{X^-}$ value is observed for F^-. This resembles a similar observation made with the H^+ form of the cation-exchange resin, for which $|\delta^0_{ion\text{-}ex} - \delta^0_{aq.\ soln}|$ was found to be maximum (20). In these two cases, ion-pair formation in the resin matrix is very likely as a result of the small ionic size. ^{19}F chemical shifts in the resin have been interpreted recently as indicating possible association of F^- with the resin ion (21).

Differences in the magnitude of the two sets of molal chemical shifts are only to be expected in view of the additional factors encountered in the resin system. The enormous osmotic pressure present within the resin bead, the physical presence of the intertwining hydrocarbon matrix and the immobility of the fixed ion will affect, in some way, the structure of the internal water. Considering these additional effects, there appears to be a similarity in the magnitude of the ionic molal shifts. This can be taken to indicate that either the various extraneous effects cancel each other or the electrostatic interactions of ions with water and between themselves predominantly influence the observed chemical shift of the water protons. Finally, the result that resin $|\delta^0|$ values are consistently lower for both cations and anions as compared to the ones in homogeneous aqueous solutions may be regarded as evidence of enhanced ion–ion interactions.

Effect of Temperature

Malinowski *et al.* have deduced "effective hydration numbers" for electrolytes from the results of change of proton chemical shift with temperature in aqueous solutions (14–16). By assuming that the chemical shift of water molecules hydrating the ions is not influenced by change in temperature, they have related the effective hydration number, h, to the rate of change of δ with temperature in pure water and in solution. In the present work, the temperature coefficient data obtained for some cation- and anion-exchange resins listed in Table 1 are likewise treated. The "effective hydration numbers" so obtained are included in Table 1. Values of h from our earlier work (20) and those reported independently by Creekmore and Reilley (21) are also included in the Table for comparison.

If indeed $\delta^0_{NH_4^+} = 0$, as assumed previously (17), it is satisfactory to set $d\delta_{NH_4^+}/dT$ equal to zero, or, in effect, $h_{NH_4^+} = 0$ (this may not be correct, but NH_4^+ ion does not perturb the water structure and therefore the p.m.r. signal remains unaffected (17)). For ammonium resinates, the observed hydration numbers can thus be assigned to the fixed sulfonate group (Table 1). From these values and the equation (15)

$$[2] \qquad h = n_+h_+ + n_-h_-$$

the values of h_+ for H^+ and the alkali-metal ions can be evaluated. The number of moles of cations and anions formed when one mole of salt dissociates, n_+ and n_-, are both unity for all cases

Can. J. Chem. Downloaded from www.nrcresearchpress.com by 210.87.254.6 on 09/05/12
For personal use only.

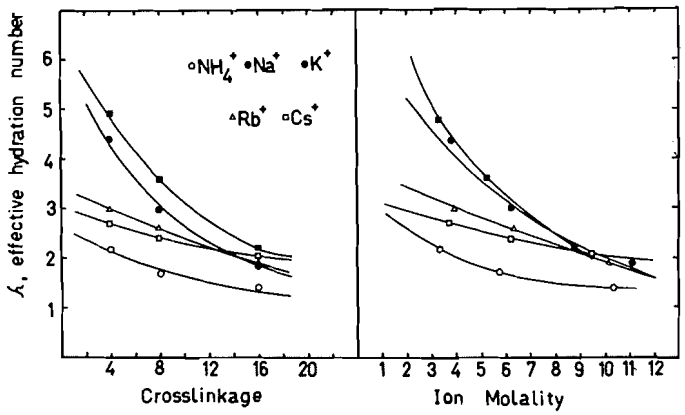

FIG. 5. Effective hydration numbers of ammonium and alkali metal resinates as (*a*) function of crosslinkage (*b*) function of molality in Dowex AG 50W resin.

considered here. It can be seen that the average values of h_+ when extrapolated to resin of crosslinkage of 0 (Fig. 5) (linear extrapolation is strictly not valid. The values of h for resin of crosslinkage 2 could not be determined since Δv is very small), are nearly equal to the ones found in aqueous solutions (Table 3). The h_+ values for Na^+, K^+, and Rb^+ decrease as the crosslinkage of the resin increases. It is inconceivable that the hydration number of Na^+ can be ~ 1 in resin of X16 when "free solvent" is present in the resin matrix. We attribute the lowering of hydration numbers of the above mentioned ions to increased ion association in the resin phase. Further evidence for ion association is derived from the fact that if the hydration number does not change with concentration of the electrolyte, then the $\delta_{soln}{}^{ethane}$ *vs.* temperature lines for all concentrations of the electrolyte should converge to a fixed point (14). It can be seen from Fig. 6 that the lines for all the crosslinkages meet at one point for Cs^+ form and not for Na^+ form. Creekmore and Reilley have reported an increase in ^{23}Na line width with increase in crosslinkage (21), which has also been interpreted in terms of ion association of Na^+ with the fixed group in the resin matrix. Our preliminary experiment with Cs^+ form of resin of crosslinkage 12 indicates that the ^{133}Cs n.m.r. signal is clearly observable and the line width is ~ 500 Hz. This may be indicative of the fact that the solvation of Cs^+ ions is not affected significantly in the resin phase with change in crosslinkage from 4 to 16. Since there is evidence for ion association in the resin phase for Na^+ with the fixed group, the hydration number as shown in Table 1, cannot be assigned to individual ions but they can be considered as number of molecules of water associated with the counterion and the fixed group (resinate) together. The effect of hydration of resinates on ion-exchange selectivity will be discussed later.

The comments on the hydration numbers for the anions in the anion-exchange resin are of a similar nature. It is assumed that the hydration number for the fixed quaternary ammonium ion

TABLE 3. Hydration numbers of alkali metal ions at infinite dilution in ion-exchange resins and in aqueous solution

	Hydration number at infinite dilution, h^0_+		
	Ion-exchange resin		
Ion	p.m.r. method	Thermodynamic method ref. 8	Aqueous solution (Hindman, ref. 17)
Li^+	—	3.3	4.0
Na^+	4.0	1.5	3.1
K^+	3.2	0.6	2.1
Rb^+	1.5	—	1.6
Cs^+	0.9	0.0	1.0

Can. J. Chem. Downloaded from www.nrcresearchpress.com by 210.87.254.6 on 09/05/12
For personal use only.

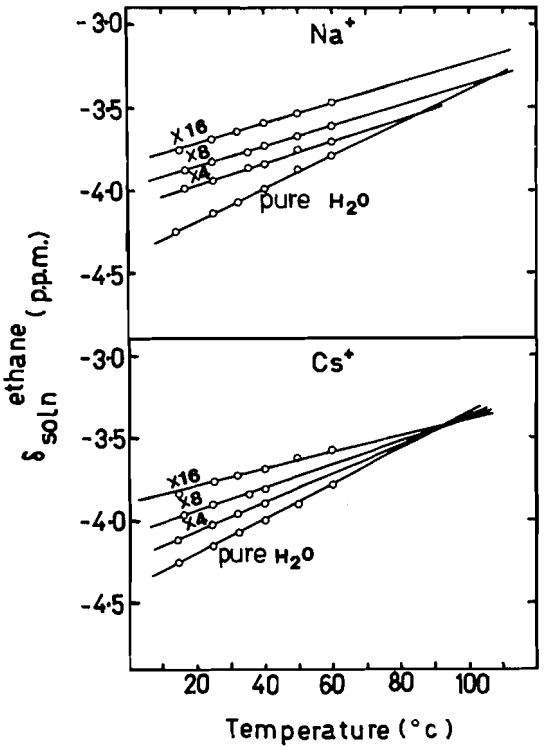

FIG. 6. Temperature dependence of "internal" water chemical shift for (*a*) Na^+ and (*b*) Cs^+ forms of Dowex AG 50W for various crosslinkages. Pure water line is from ref. 14.

is zero (16) and that the hydration numbers obtained by the temperature dependence of the chemical shift (Table 1) are due to counterions. As expected, the hydration numbers for the anions are lower compared to those for the cations. The observations of Creekmore and Reilley (21) on the n.m.r. signal of ^{19}F in the resin phase indicate considerable ion association of the counterion with the fixed group inside the resin matrix. The hydration numbers follow the order $ClO_4^- < I^- < Br^- \leqslant NO_3^- < F^-$. The variation of h values with increasing crosslinkage is less pronounced.

Ionic Hydration and Ion-exchange Selectivity

The molal selectivity coefficient $K_{B/A}$ for two competing univalent ions A and B can be depicted by (1)

$$[3] \quad \ln K_{B/A} = \ln (\bar{\gamma}_A/\bar{\gamma}_B) + \ln (\gamma_B/\gamma_A) + (\pi/RT)(v_A - v_B)$$

where $\bar{\gamma}$ and γ are the mean activity coefficients of ions denoted by the subscript in the resin and aqueous phases, respectively. π = swelling pressure, and v = partial molar volume of ions. In a dilute solution γ_A and γ_B approach unity and thus can be neglected. $\bar{\gamma}_A$ and $\bar{\gamma}_B$ for ions cannot be determined by any direct method. According to Gregor's postulates, the activity coefficient of ions in the resin phase can be related to the solvation of the counterion and the fixed group and to the swelling pressure as follows

$$[4] \quad \ln K_{B/A} = (\pi/RT)(\bar{v}_A - \bar{v}_B)$$

where $\bar{v}_A$ and $\bar{v}_B$ are the hydrated molar volumes of ions in the resin phase. If the rationale behind the Malinowski's method is correct, we can estimate the partial molar volumes of the ions from their respective hydration numbers. For low crosslinked resin $\bar{v}$ follows the order $Na^+ > K^+ > Rb^+ > Cs^+$ and hence we obtain the selectivity sequence of ions as $Cs^+ > Rb^+ > K^+ > Na^+$. For Dowex AG 50W X16, the hydration number of counterions follows the order $Rb^+ < K^+ < Cs^+ < Na^+$. $\bar{v}$ will be in the order $Cs^+ > Rb^+ > K^+ \geqslant Na^+$ if effective radii of the cations are taken into account for estimating the $\bar{v}$ values. The selectivity sequence will then be $Na^+ \geqslant K^+ > Rb^+ > Cs^+$, which is contrary to the experimental observations (2). However, if we consider the hydrated volume of the resinate (experimental evidence exists for ion association), $\bar{v}$ perhaps follows the order $Rb^+ > K^+ > Cs^+ > Na^+$ (radius of cation has much less influence on $\bar{v}$), and hence the observed selectivity sequence can be predicted. Moreover, the reversal in the selectivity of Cs^+ and K^+ (2) *i.e.* change in sign of $\ln K_{Cs/K}$ at crosslinkage of 15 can be predicted from Fig. 5. The selectivity sequences predicted by Eisenman (7) from his observations on the electrode glasses of varying composition can also be predicted from the degree of hydration of the resinates, *i.e.* the predicted selectivity sequences for the alkali-metal ions for the sulfonated resins are $Cs^+ > Rb^+ > K^+ > Na^+$, below X12; $Rb^+ > Cs^+ > K^+ > Na^+$ from X12–X14; and $Rb^+ > K^+ > Cs^+ > Na^+$ from X15–X20.

Similarly, from Table 1, the selectivity sequence for the anions in Dowex AG1 can be predicted as $ClO_4^- > I^- > Br^- \sim NO_3^- > F^-$, which is the observed sequence (2).

Gregor's theory presents a simplified approach towards the interpretation of ion-exchange equi-

Can. J. Chem. Downloaded from www.nrcresearchpress.com by 210.87.254.6 on 09/05/12
For personal use only.

Can. J. Chem. Downloaded from www.nrcresearchpress.com by 210.87.254.6 on 09/05/12
For personal use only.

libria. Its applicability has been demonstrated by modifying the concept of hydrated volume of ions inside the resin phase and not counterion alone. As stated earlier, Gregor considered the solvation of both the fixed group and the counterion. This is the first time that some experimental results have been obtained to demonstrate the applicability of the theory. Unfortunately, the selectivity sequences for ions other than alkali-metal ions can hardly be rationalized, for example $\bar{v}$ for NH_4^+ is lower than that of Cs^+ and thus NH_4^+ should be preferred in the resin phase which is contrary to the experimental observations. Similarly the sequences for alkyl ammonium ions cannot be rationalized. It probably fails to account for the selectivity of large, poorly solvated ions.

A mechanistic approach based on ion–ion and ion–solvent interactions in the resin phase has been suggested (5–7). These interactions are considered to be electrostatic in nature for a fixed grouping of low field (sulfonic acid or quaternary ammonium groups). Hydration of ions is recognized as of key importance in terms of energetics rather than hydrated volume. For complete discussion of the ion-exchange selectivity we refer to articles by Reichenberg and Diamond and Whitney in ref. 2. The selectivity coefficient is related to the net free energy change in the ion-exchange equilibrium when the resin is in contact with solution of ions A and B.
Thus

$$[5] \quad \ln K_{B/A} = -\Delta G_{B/A}{}^0/RT = -(1/RT)[(\overline{\Delta G}_h{}^B - \overline{\Delta G}_h{}^A) - (\Delta G_h{}^B - \Delta G_h{}^A) + (\overline{\Delta G}_{el}{}^B - \overline{\Delta G}_{el}{}^A)]$$

where $\overline{\Delta G}_h$ and ΔG_h are free energy of hydration of the ions depicted by superscripts in the resin and aqueous phase respectively. $\overline{\Delta G}_{el}$ is electrostatic free energy of ion interacting with the fixed group. Our experimental observations indicate that large changes in ΔG values are involved even for alkali-metal ions when they are taken up into the resin phase from dilute solutions. The subject of ion hydration and ion pairing has been treated extensively (29–31) but there is no satisfactory theoretical treatment to calculate the free energy change for these equilibria wherein the dielectric constant of the medium is not known. The selectivity coefficients can only be predicted qualitatively. However, it is difficult to rationalize the selectivity of large ions in resins of low crosslinkage. Recent observations of Zundel from infrared (i.r.) spectra of polystyrenesulfonic acid of 5% crosslinkage indicate that large ions can form a lattice type structure inside the resin matrix (32). The electrostatic free energy is further lowered (Madelung factor). This type of structure is formed if the fixed groups are separated by appropriate distance. If they are too close together, the lattice type of structure cannot exist and thus a reversal in selectivity is expected. The lattice type structure can also permit larger "free water" content in the matrix. Polyvalent ions similarly orient themselves in the resin matrix to maximize the electrostatic free energy (32). The ion-exchange selectivity depends not only on hydration of ions but also on the orientation of counterion with respect to the fixed groups and the polarizability of ions (specific interactions). Zundel has further shown from i.r. spectra that the ions like Ag^+, Tl^{3+}, Hf^{4+} have greater interaction with the fixed groups.

The total water content of the resin in a given ionic form can be regarded as the sum of "bound" and "free" water molecules (1)

$$[6] \quad H_2O_{(t)} = H_2O_{(b)} + H_2O_{(f)}$$

all quantities referring to 1 g resin in H^+ form. Since $H_2O_{(b)}$ is given by $(h \times Q \times 18/1000)$ where Q is the capacity in meq/g, and knowing $H_2O_{(t)}$, it is possible to determine $H_2O_{(f)}$. The amounts of "free" water calculated in this way for Dowex AG 50W in some alkali-metal forms are found in Table 4. It is surprising to note that the free water is almost constant for a given crosslinkage of resin for alkali-metal ion forms. The free water is probably present to minimize the repulsion between the fixed group. The concept of "free" water has some bearing on the mobility of ions in the resin phase. It is indeed postulated that "free" water aids the transport of ions in the matrix.

Finally, mention should be made of the apparent anomalous behavior of the resin in H^+ and F^- forms. In both these cases, increase in ion molality results in an increase of hydration number. Kaminsky observed anomalous temperature effects on the viscosity of aqueous solutions of structure-forming ions like Li^+ and Mg^{2+} and attributed this to the long range ordering of water molecules (33). It is also interesting to note that temperature effect on

TABLE 4. Total, bound, and free water in Dowex AG 50W resins of different ionic forms and crosslinkages

Ion	Cross-linkage	$H_2O_{(t)}$ (g)	$H_2O_{(b)}$ (g)	$H_2O_{(f)}$ (g)
Na^+	4	1.62	0.45	1.17
	8	0.99	0.34	0.65
	16	0.55	0.19	0.36
K^+	4	1.35	0.42	0.93
	8	0.84	0.28	0.56
	16	0.44	0.17	0.27
Rb^+	4	1.36	0.28	1.08
	8	0.82	0.24	0.58
	16	0.47	0.17	0.30
Cs^+	4	1.42	0.26	1.16
	8	0.84	0.22	0.62
	16	0.51	0.18	0.33
NH_4^+	4	1.60	0.21	1.39
	8	0.92	0.16	0.76
	16	0.67	0.12	0.55

proton chemical shifts yields lower values of h for LiCl and $MgCl_2$ as compared to CsCl and $CaCl_2$, respectively (16). It appears that this technique for the determination of hydration number generally tends to give rather unexpected values for structure-forming ions. It is likely that the cause for these deviations can be traced to the assumptions involved in the derivation of the relationship of temperature dependence of the chemical shift. More experimental evidence in both aqueous and resin systems (for the structure forming ions) is necessary before any definite conclusion can be drawn.

Conclusions

Proton magnetic resonance can be effectively used as a probe to investigate the perturbations of the internal water structure in the ion-exchange resins caused by the matrix and the fixed and counterions. The concentration–chemical shift and temperature–chemical shift data obtained lend themselves to reasonable quantitative treatments similar to those employed by Hindman and Malinowski in the study of aqueous electrolyte solutions. Insight into ion–water, ion–ion, and water–water interactions might be gained by comparing such parameters as δ^0_{ion} and h in the two systems. Experimental evidence up to this point seems to support the original concept of ion-exchange resins as concentrated aqueous electrolyte (34). Further, it is hoped that a knowledge of the parameters such as those reported in this work might prove useful in interpreting the experimentally observed ionic selectivities, rate of uptake of ions etc., in the ion-exchange resin.

The authors thank the National Research Council of Canada for providing financial support for this work and for the award of a Post-Graduate scholarship to N.S. We are grateful to Dr. R. C. Vasishth, Research Director, Reichhold Chemicals (Canada) Ltd., Weston, Ont. for making available to us the use of the Varian A-60 spectrometer.

1. F. HELFFERICH. Ion Exchange, McGraw-Hill Book Co., Inc., New York. 1962.
2. J. A. MARINSKY (*Editor*). Ion Exchange. Vol. 1. Marcel Dekker Inc., New York. 1966. Chaps. 7 and 8.
3. H. D. SHARMA, R. E. JERVIS, and L. W. MCMILLAN. J. Phys. Chem. **74**, 969 (1970).
4. H. P. GREGOR. J. Amer. Chem. Soc. **70**, 1293 (1948); **73**, 642 (1951).
5. J. L. PAULEY. J. Amer. Chem. Soc. **76**, 1422 (1954).
6. F. E. HARRIS and S. A. RICE. J. Phys. Chem. **61**, 1360 (1957).
7. G. EISENMANN. Biophys. J. Suppl. **2** (2), 259 (1962).
8. E. GLUECKAUF and G. P. KITT. Proc. Roy. Soc. London, Ser. A, **228**, 322 (1955).
9. J. F. HINTON and E. S. AMIS. Chem. Rev. **67**, 367 (1967).
10. J. BURGESS and M. C. R. SYMONS. Quart. Rev. London, **22**, 276 (1968).
11. C. DEVERELL. Progr. N.M.R. Spectrosc. **4**, 235 (1969).
12. Z. LUZ and S. MEIBOOM. J. Chem. Phys. **40**, 1058, 1066 (1964).
13. T. J. SWIFT and W. G. SAYRE. J. Chem. Phys. **44**, 3567 (1966).
14. E. R. MALINOWSKI, P. S. KNAPP, and B. FEUER. J. Chem. Phys. **45**, 4274 (1966).
15. P. S. KNAPP, R. O. WAITE, and E. R. MALINOWSKI. J. Chem. Phys. **49**, 5459 (1968).
16. R. W. CREEKMORE and C. N. REILLEY. J. Phys. Chem. **73**, 1563 (1969).
17. J. C. HINDMAN. J. Chem. Phys. **36**, 1000 (1962).
18. J. E. GORDON. J. Phys. Chem. **66**, 1150 (1962).
19. R. H. DINIUS, M. T. EMERSON, and G. R. CHOPPIN. J. Phys. Chem. **67**, 1178 (1963).
20. T. E. GOUGH, H. D. SHARMA, and N. SUBRAMANIAN. Can. J. Chem. **48**, 917 (1970).
21. R. W. CREEKMORE and C. N. REILLEY. Anal. Chem. **42**, 725 (1970).
22. H. D. SHARMA and N. SUBRAMANIAN. Anal. Chem. **41**, 2063 (1969).
23. H. D. SHARMA and N. SUBRAMANIAN. Anal. Chem. **42**, 1287 (1970).
24. A. I. VOGEL. Textbook of Quantitative Inorganic Analysis. John Wiley and Sons, Inc., New York. 1967.
25. B. P. FABRICAND and S. GOLDBERG. J. Chem. Phys. **34**, 1624 (1961).
26. J. A. POPLE, W. G. SCHNEIDER, and H. J. BERNSTEIN. High Resolution Nuclear Magnetic Resonance. McGraw-Hill Book Co., New York. 1959.
27. K. FREI and H. J. BERNSTEIN. J. Chem. Phys. **37**, 1891 (1962).
28. J. P. DE VILLIERS and J. R. PARRISH. J. Polym. Sci. Part A, **2**, 1331 (1964).

Can. J. Chem. Downloaded from www.nrcresearchpress.com by 210.87.254.6 on 09/05/12
For personal use only.

29. R. W. GURNEY. Ionic Processes in Solution. McGraw-Hill Book Co., Inc. 1953.
30. D. F. C. MORRIS. Structure and Bonding. Vol. 4. Springer-Verlag, Inc., New York. 1968. p. 63.
31. E. GLUECKAUF. *In* Chemical Physics of Ionic Solutions. (*Editors*). B. E. Conway and R. G. Barradas. John Wiley and Sons, Inc. 1964. p. 67.
32. G. ZUNDEL. Hydration and Intermolecular Interaction. Academic Press, New York. 1969. Chap. IV.
33. M. KAMINSKY. Discuss. Faraday Soc. **24**, 171 (1957).
34. W. C. BAUMAN and J. EICHHORN. J. Amer. Chem. Soc. **69**, 2830 (1947).

Can. J. Chem. Downloaded from www.nrcresearchpress.com by 210.87.254.6 on 09/05/12
For personal use only.

Can. J. Chem. Downloaded from www.nrcresearchpress.com by 210.87.254.40 on 09/05/12
For personal use only.

The Crystal Structure of $KIO_3.HIO_3$

LILIAN Y. Y. CHAN AND F. W. B. EINSTEIN
Department of Chemistry, Simon Fraser University, Burnaby 2, British Columbia

Received June 11, 1970

The crystal structure of potassium hydrogen di-iodate (bi-iodate) $KIO_3.HIO_3$ was determined from three dimensional X-ray data collected by counter methods. The structure was refined by full-matrix least-squares techniques to a conventional R factor of 5.0% for the 1392 observed reflexions. The salt crystallizes in the monoclinic space group $P2_1/c$ with eight formula units in a cell of dimension $a = 7.028(1)$ Å, $b = 8.203(1)$ Å, $c = 21.841(3)$ Å, $\beta = 98.03(1)°$.

The iodate units are all basically pyramidal; weak interionic I—O contacts complete a very distorted octahedral environment around three iodine atoms. There is a capped octahedral (7-coordinate) environment around the remaining iodine atom. The I—O bonds are in the range 1.75–1.82 Å and the I—OH bonds are 1.91 and 1.95 Å; variations in length can be correlated with differences in the degree of involvement in (*a*) hydrogen bonding and (*b*) interaction with adjacent iodine atoms.

Canadian Journal of Chemistry, 49, 468 (1971)

Introduction

The crystal structure of α-iodic acid, HIO_3, was studied by Rogers and Helmholz (1) and was found to contain pyramidal IO_3 groups. Later, a neutron diffraction study by Garrett (2) showed the hydrogen bonding in the structure to consist of infinite chains of the type, ...H—IO_3...H—IO_3...H—IO_3. It was also pointed out (1) that three more distant oxygen atoms completed a distorted octahedron around the central iodine atom. Dasent and Waddington (3) studied the infrared spectra of a number of iodates; among them potassium hydrogen di-iodate, $KIO_3.HIO_3$. It was found that for this compound, the spectrum was complex and the bands could not be assigned satisfactorily from a simple structural model. They concluded therefore that two types of iodate groups were present. We have carried out an X-ray crystal structure analysis of $KIO_3.HIO_3$ in order to ascertain firstly the nature of the hydrogen bonding and secondly to examine the differences in the iodate groups including the interactions between oxygen and iodine atoms of neighboring iodate ions.

Experimental

Colorless potassium hydrogen di-iodate crystals were obtained by crystallizing equimolar quantities of HIO_3 and KIO_3 from hot water. Weissenberg photographs of the zones *h*0*l*, *h*1*l*, *h*2*l* using CrK_α radiation, together with precession photographs of the zones *hk*0, 0*kl* and several other general *hkl* zones using MoK_α radiation, showed systematic absences for *h*0*l*: $l = 2n + 1$ and 0*k*0: $k = 2n + 1$. This combined with the Laue group, 2/*m*, indicated unambiguously the space group $P2_1/c$.

Crystal Data

$KIO_3.HIO_3$

Monoclinic, f.w. = 390, space group $P2_1/c$ with $a = 7.028(1)$, $b = 8.203(1)$, $c = 21.841(3)$ Å, $\beta = 98.03(1)°$ and $V = 1246.8$ Å^3. $D_m = 4.17(10)$ g/cm^3 (Berman density balance determination), $D_x = 4.16$ g/cm^3, $Z = 8$, $F(000) = 1392$, $\mu(MoK_\alpha) = 108.7$ cm^{-1}.

All data were collected using a plate-shaped crystal fragment of dimensions 0.54 × 0.19 × 0.05 mm mounted with the *b* axis (the direction of greatest elongation) parallel to Φ. The largest crystal face was the {100}; the remaining faces were not identified on account of the irregular crystal shape. Cell constants were determined by applying a least-squares fit to 30 general high angle reflexions. $MoK_{\alpha1}$, $K_{\alpha2}$, and K_β measurements were used in three independent refinements whose results did not differ significantly. The values quoted were that based on $MoK_{\alpha2}$, $\lambda = 0.713543$ Å, at 22 °C. The numbers in parentheses are the least-squares estimated standard errors.

Reflexion intensities for the unique set of data were manually measured with Niobium-filtered MoK_z radiation, $\lambda = 0.7107$ Å, using a scintillation detector with pulse-height analysis. Measurements were made using a 1.2° takeoff angle with a symmetrical θ–2θ scan of 1.6° width (carried out at a rate of 4°/min). Background counts of 12 s were measured at both scan limits. Of the 1644 intensities recorded in the range $0° < 2\theta < 45°$, 1392 were above 2σ and were considered as observed reflexions. ($\sigma = \sqrt{N}$ where N is the scan count plus the total of both background counts.) Three standard reflexions were measured every 3 h and retained a constancy within 1% over the entire data collection. Coincidence losses were checked by measurement of outstanding reflexions together with some of intermediate intensities at lower incident beam strength; since a constant relationship was found, no coincidence losses were assumed. An experimental absorption curve in Φ was determined at $\chi = 90°$; the intensity varied symmetrically about $\Phi = 0$. Approximate absorption corrections were applied to the intensity data according to this experimental curve and then Lorentz and polarization

Can. J. Chem. Downloaded from www.nrcresearchpress.com by 210.87.254.40 on 09/05/12
For personal use only.

factors were applied to give structure factors in the usual manner.

Structure Determination

The density and space group requirements could only be met by having eight formula units per unit cell, each asymmetric unit consisting of two formula units. From the unsharpened three-dimensional Patterson function it was possible to assign positions for four independent iodine atoms. These atomic coordinates, with isotropic temperature factors of 2.0 Å^2, were used to phase the structure factors. One cycle of full-matrix least-squares refinement of these atomic positions and individual isotropic temperature factors was carried out. The function minimized was $\Sigma\omega(|F_o| - |F_c|)^2$ where ω was chosen to be unity. The conventional R-factor (defined as $(\Sigma|F_o| - |F_c|)/\Sigma|F_o|$) dropped from 0.49 to 0.30. A three-dimensional electron-density map was computed from which two potassium atomic positions were located. Two cycles of least-squares refinement on these atomic positions and isotropic temperature factors brought the R-factor down to 0.20. At this point, an electron density difference map revealed twelve oxygen atoms around the iodine atoms and in one cycle of least-squares refinement the agreement improved to 0.132.

An examination of the structure factors F_o and F_c at this stage showed that the experimental absorption curve applied was too severe and it was modified to be less so. The R-factor improved spectacularly to 0.071. After two cycles of full-matrix least-squares refinement varying all isotropic and coordinate parameters, the agreement was 0.058. At this point, some of the low angle reflexions appeared to be affected by extinction. An isotropic extinction parameter E_c was introduced such that the following expression was minimized by the least-squares procedure

$$\sum \omega \left(F_o - \frac{F_c}{1 + E_c \times I} \right)^2$$

where I is the uncorrected intensity and $\omega = 1$. (The final value of E_c was 0.0000841(53).) The R-factor dropped to 0.054, while all the temperature factors were held isotropic. An electron density difference map showed as its largest feature that all four iodine atoms were moving anisotropically. Two cycles of least-squares refinement including anisotropic temperature factors for the four iodine atoms brought the value of R down to 0.050 and showed further shifts negligible. Whilst the anisotropic thermal motion and extinction parameters might well contain errors due to the approximate absorption corrections, the values obtained were physically reasonable. The improvement obtained from introducing these variables was sufficiently large to justify them on Hamilton's criterion (4). Until completion of the refinement, $\omega = 1$ had been used throughout. This choice was justified on the basis of an examination of trends for $\Sigma\omega\Delta^2/n$ as a function of $\sin\theta/\lambda$ and $|F_o|$, where $\Delta = |F_o| - |F_c|$ and n = total number of reflexions. For the final cycle, ω was given a constant value (0.1307) such

TABLE 1. Atomic parameters for $KIO_3.HIO_3$

Atom	Coordinates			B (Å^2)
	x	y	z	
I(*1*)	0.1688(2)	0.1045(2)	0.6573(1)	*
I(*2*)	0.2314(2)	0.3873(2)	0.4998(1)	*
I(*3*)	0.6678(2)	0.3679(2)	0.6563(1)	*
I(*4*)	0.6524(2)	0.8605(2)	0.6359(1)	*
K(*1*)	0.2498(7)	0.8765(7)	0.5034(2)	1.60(9)
K(*2*)	0.1444(7)	0.6136(7)	0.6715(2)	1.79(9)
O(*11*)	0.0531(21)	0.2675(18)	0.6925(7)	1.41(28)
O(*12*)	0.0150(22)	0.9416(20)	0.6691(7)	1.92(30)
O(*13*)	0.0986(22)	0.1429(20)	0.5758(7)	2.04(30)
O(*21*)	0.0014(21)	0.3560(19)	0.4534(7)	1.62(28)
O(*22*)	0.3192(22)	0.5407(20)	0.4524(7)	1.82(29)
O(*23*)	0.3501(22)	0.2093(19)	0.4744(7)	1.65(29)
O(*31*)	0.4159(23)	0.3994(22)	0.6383(8)	2.25(31)
O(*32*)	0.6475(22)	0.2708(20)	0.7347(7)	1.88(30)
O(*33*)	0.7410(23)	0.5658(20)	0.6851(8)	2.14(32)
O(*41*)	0.4045(21)	0.8058(19)	0.6276(7)	1.37(27)
O(*42*)	0.6645(20)	0.9027(19)	0.7243(7)	1.40(27)
O(*43*)	0.6229(22)	0.0612(20)	0.6086(7)	1.90(30)

Atom	U_{11}†	U_{22}	U_{33}	U_{12}	U_{13}	U_{23}
I(*1*)	96(7)	164(8)	173(8)	−41(7)	11(6)	−15(7)
I(*2*)	135(8)	157(8)	109(8)	−7(7)	19(6)	−5(7)
I(*3*)	112(8)	128(8)	173(8)	0(6)	17(6)	5(7)
I(*4*)	101(8)	120(8)	173(8)	2(6)	25(6)	19(7)

*Anisotropic thermal parameter used for iodine atoms (Å)^2 × 10^4.

†These values were obtained from $\beta_{ij} = 2\pi^2 b_i b_j U_{ij}$ where β_{ij} appear as a temperature effect through $\exp[-(\beta_{11}h^2 + 2\beta_{12}hk + \ldots)]$ in the structure factor expression and b_i are the reciprocal lattice vectors.

Can. J. Chem. Downloaded from www.nrcresearchpress.com by 210.87.254.40 on 09/05/12
For personal use only.

that the error of fit, $[\Sigma\omega(|F_o| - |F_c|)^2/(N_o - N_v)]^{\frac{1}{2}}$, where $(N_o - N_v)$ = number of observations − number of variables, was 1.00. This gave 'correct' standard errors for the coordinate and temperature parameters as absolute weights were used.

An electron density difference map computed after the refinement was complete showed no positive peaks greater than 0.7 e/Å^3 though a negative trough of −1.2 e/Å^3 was found.

The scattering factors used throughout including anomalous scattering for iodine and potassium atoms, were taken from the "International Tables for X-ray Crystallography" (5).

The major programs used were our modifications of the NRCC Data Reduction Program, the University of Canterbury (New Zealand) versions of ORFLS, ORFFE, and FORDAP. Calculations were carried out at the Simon Fraser University Computing Centre on an IBM 360/50.

Table 1 gives the final atomic parameters. The least-squares estimated standard errors are listed in parentheses. Table 2 lists the relevant interatomic distances and angles, the standard errors in parentheses include errors from cell dimensions and those estimated from the variance–covariance matrix calculated during the last cycle of least-squares refinement. Table 3 lists the $|F_o|$ and F_c for each measured reflexion where $|F_c| = |\sqrt{A^2 + B^2}|$ and F_c has the sign of A since, in general, B is small. Accidentally unobserved reflexions are indicated as negative $|F_o|$ and were given the value of $\sigma/2$. Figure 1 shows the packing of the ions within the unit cell viewed down the a^* axis.

Structure Description and Discussion

(I) Environment of the Iodine Atoms

For each of the iodine atoms, there are three oxygen atoms at a distance of ~1.8 Å from the central iodine atom, forming a distorted pyramidal arrangement. The I—O bond lengths vary from 1.753 to 1.952 Å.

In addition to these expected covalent bonds, there are extensive oxygen–iodine contacts ranging from 2.4 to 3.4 Å between neighboring iodate ions. Iodine atoms are found to have two types of environment.

(a) Distorted Octahedron

Around I(*1*), I(*3*), and I(*4*), there are three short I—O contacts of ~1.8 Å as well as three long I...O contacts of ~2.6 Å for I(*3*) and I(*4*) and ~3.0 Å for I(*1*). These six oxygen atoms form a distorted octahedron about the central iodine atom. A similar environment around the iodine atom is also found in αHIO_3 (1).

(b) Distorted Capped-Octahedron

Each iodate group, based on I(*2*), has in addition to the three covalently bonded oxygen atoms, four more distant contacts (~3.0 Å)

TABLE 2. Interatomic distances and angles

(*a*) I—O bond distances

Predicted formal bond order	Contacts	Observed bond length (Å)	Average length (Å)*
2	I(*3*)—O(*31*)	1.778(17)	
	I(*3*)—O(*33*)	1.791(17)	1.777(17)
	I(*4*)—O(*41*)	1.784(15)	
	I(*4*)—O(*43*)	1.753(17)	
1⅔	I(*2*)—O(*21*)	1.818(15)	
	I(*2*)—O(*22*)	1.792(16)	
	I(*2*)—O(*23*)	1.807(15)	1.796(21)
	I(*1*)—O(*11*)	1.793(15)	
	I(*1*)—O(*12*)	1.759(16)	
	I(*1*)—O(*13*)	1.808(16)	
1	I(*3*)—O(*32*)	1.911(17)	1.932
	I(*4*)—O(*42*)	1.952(15)	

*The standard errors in the average values are estimated from the internal consistency and show no significant difference between bonds of predicted orders 1⅔ and 2.

(*b*) Interionic contacts (I—O and K—O < 3.5 Å)

Type of contact		Distance*	Symmetry relationship†	Average distance
I(*1*)	O(*31*)	3.04	1	
	O(*41*)	3.08	1*a*	3.18
	O(*33*)	3.43	4	
I(*2*)	O(*13*)	2.84	1	
	O(*21*)′	2.93	2	
	O(*31*)	3.12	1	3.03
	O(*22*)′	3.24	2	
I(*3*)	O(*22*)	2.50	2	
	O(*43*)	2.72	1	2.69
	O(*11*)	2.84	1*b*	
I(*4*)	O(*23*)	2.47	2	
	O(*12*)	2.64	1*b*	2.60
	O(*33*)	2.68	1	
K(*1*)	O(*13*)	2.80	2*a*	
	O(*13*)	2.98	1*c*	
	O(*21*)	2.83	2	2.88
	O(*22*)	3.04	1	
	O(*23*)	2.87	2	
	O(*23*)	2.91	1*c*	
	O(*41*)	2.84	1	
	O(*43*)	2.77	2	
K(*2*)	O(*11*)	2.96	1	
	O(*12*)	2.84	1	
	O(*21*)	2.78	2	
	O(*31*)	2.76	1	2.83
	O(*32*)	2.68	4	
	O(*33*)	2.92	1*d*	
	O(*41*)	2.69	1	
	O(*42*)	3.02	4	

*Standard errors in these distances are all less than ±0.02 Å.
†Key for symmetry relationship: (1) x, y, z; (1*a*) $x, y-1, z$; (1*b*) $x+1, y, z$; (1*c*) $x, y+1, z$; (1*d*) $x-1, y, z$; (2) $\bar{x}, \bar{y}, \bar{z}$; (2*a*) $\bar{x}-1, \bar{y}, \bar{z}$; (2*b*) $\bar{x}, \bar{y}-1, \bar{z}$; (3) $x, \frac{1}{2}+y, \frac{1}{2}-z$; (4) $\bar{x}, \frac{1}{2}-y, \frac{1}{2}+z$.

Can. J. Chem. Downloaded from www.nrcresearchpress.com by 210.87.254.40 on 09/05/12
For personal use only.

(*c*) Angles in degrees around iodine atoms

	I(*2*)		I(*1*)		I(*3*)		I(*4*)	
I—O Contacts involved	Bonding O	Angle	Bonding O	Angle	Bonding O	Angle	Bonding O	Angle
Both I—O < 2.00 Å	O(*21*), O(*22*)	97.7(7)	O(*11*), O(*12*)	100.4(7)	O(*31*), O(*32*)	93.6(8)	O(*41*), O(*42*)	93.6(7)
	O(*22*), O(*23*)	100.3(7)	O(*12*), O(*13*)	100.7(8)	O(*32*), O(*33*)	96.7(8)	O(*42*), O(*43*)	99.0(7)
	O(*23*), O(*21*)	97.7(7)	O(*13*), O(*11*)	102.3(8)	O(*33*), O(*31*)	100.0(8)	O(*43*), O(*41*)	97.7(8)
2.40 Å < both I—O < 3.5 Å	O(*21*)′, O(*22*)′	106.8	O(*31*), O(*41*)	105.7	O(*22*), O(*43*)	86.1	O(*22*), O(*33*)	98.6
	O(*21*)′, O(*13*)	93.5	O(*41*), O(*33*)	96.3	O(*22*), O(*11*)	101.0	O(*23*), O(*12*)	101.6
	O(*13*), O(*22*)′	109.0	O(*31*), O(*33*)	100.6	O(*11*), O(*43*)	83.9	O(*33*), O(*23*)	87.4
	O(*21*)′, O(*31*)	79.3						
	O(*22*)′, O(*31*)	55.1						
	O(*13*), O(*31*)	65.3						
One I—O < 2.00 Å	O(*21*), O(*22*)′	165.1	O(*11*), O(*41*)	167.0	O(*31*), O(*11*)	170.7	O(*41*), O(*12*)	170.0
2.40 Å < One I—O < 3.5 Å	O(*22*), O(*13*)	179.0	O(*12*), O(*31*)	176.7	O(*32*), O(*22*)	172.4	O(*42*), O(*23*)	176.3
	O(*23*), O(*21*)′	172.1	O(*13*), O(*33*)	172.9	O(*33*), O(*43*)	169.7	O(*43*), O(*33*)	172.7
	O(*21*), O(*13*)	83.2	O(*11*), O(*31*)	76.6	O(*31*), O(*22*)	85.0	O(*41*), O(*23*)	88.2
	O(*21*), O(*21*)′	78.4	O(*11*), O(*33*)	77.6	O(*31*), O(*43*)	89.4	O(*41*), O(*33*)	89.0
	O(*22*), O(*22*)′	77.0	O(*12*), O(*33*)	79.3	O(*32*), O(*11*)	79.5	O(*42*), O(*33*)	77.7
	O(*22*), O(*21*)′	87.0	O(*12*), O(*41*)	77.6	O(*32*), O(*43*)	86.5	O(*42*), O(*12*)	77.1
	O(*23*), O(*22*)′	100.0	O(*13*), O(*31*)	78.9	O(*33*), O(*22*)	90.9	O(*43*), O(*12*)	85.5
	O(*23*), O(*13*)	79.2	O(*13*), O(*41*)	90.7	O(*33*), O(*11*)	87.0	O(*43*), O(*23*)	84.3
	O(*31*), O(*21*)′	139.8						
	O(*31*), O(*22*)	114.0						
	O(*31*), O(*23*)	100.1						

(*d*) O—O interionic distances (< 3.00 Å) and selected angles (degree)

Type	Distance or angle	Symmetry relationship
O(*22*)—O(*31*)	2.94*	1
O(*23*)—O(*43*)	2.89	2*b*
O(*12*)—O(*42*)	2.91	1*d*
O(*33*)—O(*42*)	2.97	1
O(*11*)—O(*42*)	2.73†	2*b*
O(*42*)—O(*32*)	2.71†	3
I(*3*)—O(*32*)—O(*42*)	107.1(8)	
I(*4*)—O(*42*)—O(*32*)	95.6(7)	
I(*4*)—O(*42*)—O(*11*)	120.9(8)	
I(*1*)—O(*11*)—O(*42*)	104.9(7)	
O(*32*)—O(*42*)—O(*11*)	99.5(7)	

*Standard deviations in these distances are less than ± 0.03 Å.
†Hydrogen bonded O . . . HO distances.

forming a distorted capped-octahedron around the iodine atom. Two of these weaker contacts are provided from a crystallographically equivalent (centro-symmetrically related) iodate I(*2*) ion. The remaining two arise from oxygen atoms of other independent iodate ions.

(II) Description of K^+ Ion Environment

Each potassium ion has eight near-neighboring oxygen atoms, K^+—O being 2.67–3.04 Å. Each ion has a similar environment which can best be described as a distorted square antiprism.

(III) Crystal Packing

The overall structure may be considered to consist of $(IO_3...HIO_3...HIO_3)^-$, $(IO_3...IO_3)^{2-}$, and K^+ ions packed together electrostatically. Rogers and Helmholz (1) had originally interpreted the structure of αHIO_3 as being held together by bifurcated hydrogen bonds. Later, Wells (6) re-examined the structure and concluded that it was better described as infinite $HIO_3...HIO_3...$ chains; this model was confirmed by Garrett's (2) neutron diffraction work. $KIO_3.HIO_3$ may be regarded as containing a fragment of this chain, which suggests that chains of this type have some inherent stability.

The packing density of oxygen atoms in $KIO_3.HIO_3$ is less than those found for other structures containing the iodate ion. The volume per oxygen atom is 26.0 $Å^3$ compared with 21.8 in ceric iodate monohydrate (7), 20.8 in HIO_3, 24.7 in sodium iodate, and about 16 in a closest packed oxygen structure. The oxygen atoms in $KIO_3.HIO_3$ do not form a closest packed arrangement, a result which is hardly surprising.

The Covalent I—O Bonds

The twelve independent I—O bonds (range 1.75 to 1.95 Å) show two significantly longer I—O bonds, namely I(*5*)—O(*42*) = 1.952 and I(*3*)—O(*32*) = 1.911 Å. These can reasonably be expected to be the hydroxylic oxygen atoms (the final electron density difference map showed peaks in suitable positions for hydrogen atoms but these peaks were no larger than other spurious non-atomic peaks). Further support for this interpretation is provided by the distances of O(*42*)—O(*32*) = 2.708 and O(*42*)—O(*11*) = 2.731 Å. These are fully consistent with the O—H stretching frequency in the infrared spectrum (3) which would predict an OH...O length of 2.7 Å on the basis of existing empirical correlations (8, 9). Also from these I—O and O—O distances, one concludes that O(*42*) acts both as a hydrogen bond donor and acceptor, whereas O(*32*) acts as hydrogen bond donor alone. The interatomic angles in Table 2*d* show reasonable agreement with this conclusion.

The I—O bonds of order 1 in O_2I—OH are significantly different from those of formal bond order $1\frac{2}{3}$ (in the IO_3^-, 1.80 Å) which do not, however, differ significantly from those of bond order 2 (in the HIO_3 molecule, 1.78 Å). Two factors are likely to mask these fractional differences between multiple bonds, firstly involvement as hydrogen bond acceptors, and secondly, variations in the weak donation of the oxygen atoms lone pair of electrons to an adjacent iodine atom's empty d orbitals. The latter effect may well be a crucial one in this structure, since the high effective charge on the iodine atom makes it strongly electrophilic.

The Weak I—O Interactions

The relatively high charge (5+) and electronegative environment of the iodine atom may be responsible for contraction of the d orbitals allowing them to provide suitable overlap with the oxygen p orbitals, as pointed out by Mitchell (10). This would provide an explanation of the extensive, weak I--O interactions found in $KIO_3.HIO_3$; in addition, for the XO_3^- species, one would expect acceptor strength to decrease in the series X = I, Br, Cl, as I is the most polarizable and thus has the highest effective positive charge.

It is worthwhile comparing the weak I—O interactions between the IO_3^- and the HIO_3 species listed in Table 2. In the IO_3^- ions

Can. J. Chem. Downloaded from www.nrcresearchpress.com by 210.87.254.40 on 09/05/12
For personal use only.

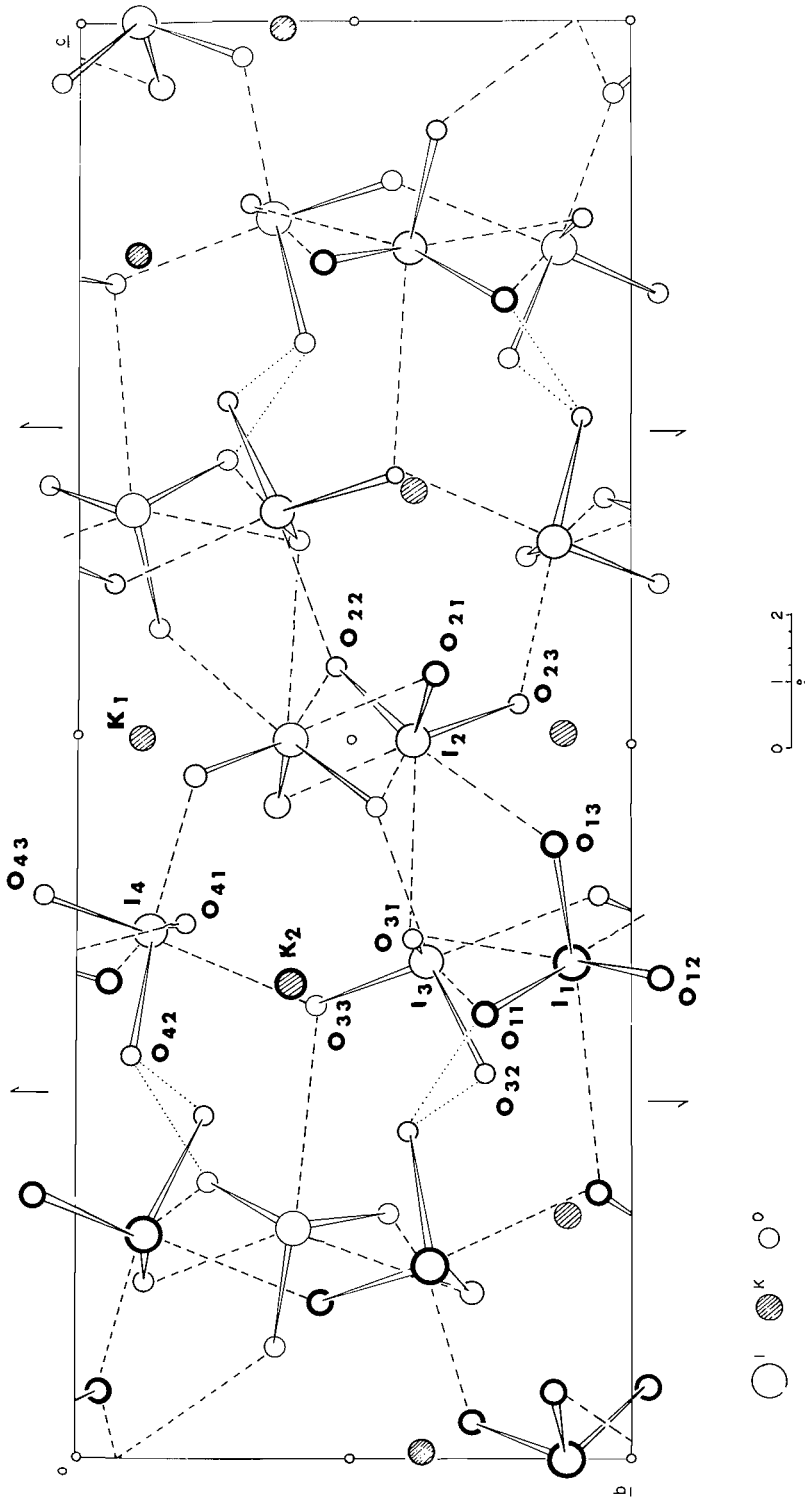

FIG. 1. Crystal structure of $KIO_3.HIO_3$ viewed down the a^* axis. (Dotted lines indicate hydrogen bonds, dashed lines weak I---O interactions.)

Can. J. Chem. Downloaded from www.nrcresearchpress.com by 210.87.254.40 on 09/05/12
For personal use only.

Can. J. Chem. Downloaded from www.nrcresearchpress.com by 210.87.254.40 on 09/05/12
For personal use only.

Table 3. Measured and calculated structure factors
(scale = 0.5 x $F_{absolute}$)

H	L	OBS	CALC
**** H = 0 ****			
0	2	16	28
0	4	205	-230
0	6	669	715
0	8	295	293
0	10	207	-203
0	12	303	290
0	14	329	294
0	16	-21	-9
0	18	161	147
0	20	212	179
0	22	71	62
1	1	31	35
1	2	55	-58
1	3	188	207
1	4	110	126
1	5	180	195
1	6	-10	-14
1	7	-11	-9
1	8	59	-65
1	9	-14	6
1	10	193	183
1	11	171	166
1	12	92	79
1	13	44	27
1	14	206	-187
1	15	-17	13
1	16	76	63
1	17	117	102
1	18	177	159
1	19	121	99
1	20	162	-129
1	21	61	53
1	22	68	-60
1	23	32	38
2	0	-7	25
2	1	110	-130
2	2	24	22
2	3	47	-65
2	4	-10	-4
2	5	123	143
2	6	53	61
2	7	91	97
2	8	43	-32
2	9	235	-231
2	10	-12	12
2	11	41	-41
2	12	68	70
2	13	152	179
2	14	-16	-5
2	15	86	-74
2	16	-16	-16
2	17	139	-115
2	18	81	74
2	19	75	64
2	20	44	33
2	21	62	52
2	22	-16	-6
3	1	19	20
3	2	142	-121
3	3	46	-56
3	4	-11	22
3	5	130	-146
3	6	92	100
3	7	-11	13
3	8	170	-172
3	9	47	48
3	10	72	81
3	11	174	-161
3	12	96	96
3	13	55	-77
3	14	169	-151
3	15	111	100
3	16	31	20
3	17	77	-61
3	18	194	167
3	19	179	-151
3	20	156	-126
4	0	128	125
4	2	24	-31
4	4	168	-167
4	6	223	234
4	8	31	36
4	10	128	-136
4	12	54	57
4	14	87	88
4	16	83	-78
4	18	-14	-14
4	20	188	-171
4	22	103	95
5	1	211	-165
5	3	103	100
5	5	114	-119
5	7	141	139
5	9	126	-128
5	11	140	151
5	13	95	-106
5	15	177	-169
5	17	84	-78
5	19	76	-85
5	21	202	180
5	23	164	-84
6	0	59	52
6	2	355	341
6	4	62	-59
6	6	124	-117
6	8	53	53
6	10	174	-166
6	12	92	-87
6	14	-14	0
6	16	84	-78
6	18	31	-34
6	20	179	-169
6	22	68	-60
6	24	32	-33
7	1	182	194
7	3	23	-24
7	5	216	-225
7	7	55	-55
7	9	114	-450
7	11	61	-96
7	13	73	-21
7	15	82	-74
7	17	111	-102
7	19	48	-46
7	21	52	-31
8	0	205	-200
8	2	82	-81
8	4	39	-10
8	6	136	-142
8	8	140	-140
8	10	54	-55
8	12	140	171
8	14	28	-2
8	16	158	-162
8	18	59	-101
8	20	42	73
9	1	86	-88
9	3	151	-159
9	5	158	-162
9	7	59	-101
9	9	128	123
9	11	56	55
9	13	418	416
9	15	84	-81
9	17	140	-166
9	19	37	34
9	21	141	-137
10	0	59	-60
10	2	34	-40
10	4	168	-167
10	6	188	-178
10	8	142	141
10	10	-10	-10
10	12	115	-116
10	14	221	-226
10	16	126	-128
10	18	42	44
10	20	-9	-8
11	1	22	17
11	3	17	-14
11	5	202	-196
11	7	118	-118
11	9	102	-104
11	11	52	51
11	13	126	-128
11	15	27	-29
11	17	76	-85
11	19	66	-61
12	0	46	-60
12	2	90	-96
12	4	78	-75
12	6	-9	11
12	8	90	-91
12	10	37	41
12	12	17	-12
12	14	46	-44
12	16	-12	19
12	18	183	183
12	20	-12	8
13	1	39	40
13	3	151	148
13	5	81	79
13	7	30	30
13	9	56	-75
13	11	56	-57
13	13	81	-81
13	15	50	-47
13	17	69	-66
13	19	86	95
14	0	92	87
14	2	62	59
14	4	29	-35
14	6	66	68
14	8	-12	8
14	10	51	59
14	12	17	19
14	14	24	-18
14	16	84	-98
14	18	58	64
15	1	45	49
15	3	38	-27
15	5	23	-15
15	7	54	53
15	9	62	-58
**** H = 5 ****			
0	0	82	76
0	2	56	-60
0	4	44	46
0	6	162	160
0	8	37	35
0	10	88	-82
0	12	119	123
0	14	79	82
1	0	-10	6
1	1	30	-33
1	2	10C	-94
1	3	154	153
1	4	92	-84
1	5	67	72
1	6	-11	-19
1	7	100	-101
1	8	59	53
1	9	100	106
1	10	75	-76
1	11	146	150
1	12	100	-102
1	13	69	-69
1	14	24	23
1	15	25	20
2	0	28	28
2	1	241	-232
2	2	54	53
2	3	219	217
2	4	56	-59
2	5	238	-239
2	6	21	21
2	7	277	-284
2	8	110	114
2	9	99	99
3	1	117	-111
3	3	73	67
3	5	112	-102
3	7	-11	-78
3	9	268	-266
3	11	2	2
3	13	186	-186
3	15	51	54
3	17	-7	7
3	19	102	-104
3	21	111	-115
4	0	144	144
4	2	115	116
4	4	-12	18
4	6	275	280
4	8	88	-85
4	10	69	-77
4	12	73	73
4	14	111	-115
4	16	-12	11
4	18	374	374
4	20	31	-31
5	1	42	-37
5	3	40	-36
5	5	35	-35
5	7	69	-66
5	9	31	-30
5	11	56	-57
5	13	81	-81
5	15	47	-47
5	17	78	-74
5	19	99	-92
6	0	-12	2
6	2	127	-118
6	4	49	-47
6	6	38	-27
6	8	23	-15
6	10	54	53
6	12	62	-58
**** H = 6 ****			
0	0	96	-96
0	2	458	-446
0	4	112	-102
0	6	55	55
0	8	268	-266
0	10	2	2
0	12	144	144
0	14	-78	-78
0	16	186	-186
0	18	51	54
0	20	-73	71
1	1	32	27
1	3	115	116
1	5	18	18
1	7	275	280
1	9	88	-85
1	11	76	-77
1	13	-11	-7
1	15	69	71
1	17	73	73
1	19	-11	-1
2	0	50	-51
2	2	102	-104
2	4	111	-115
2	6	-12	11
2	8	374	374
2	10	17	-12
2	12	152	154
2	14	29	-35
2	16	-12	10
2	18	183	183
2	20	-12	8
3	1	59	51
3	3	81	79
3	5	30	30
3	7	81	-75
3	9	56	51
3	11	32	-33
3	13	81	-81
3	15	157	160
3	17	91	87
3	19	56	54
4	1	45	49
4	3	36	-33
4	5	62	58
4	7	37	31
4	9	132	-136
4	11	101	103
4	13	118	120
4	15	25	-22
4	17	88	-82
4	19	119	123
5	0	23	20
5	2	22	-18
5	4	92	-84
5	6	67	72
5	8	119	-114
5	10	33	-31
5	12	28	28
5	14	44	42
5	16	22	-18
5	18	13	13
6	1	25	23
6	3	10	10
6	5	60	-55
6	7	72	-76
6	9	103	100
6	11	41	46
6	13	97	-97
6	15	56	-67
6	17	119	-114
6	19	73	-72
7	2	97	-98
7	4	66	-68
7	6	56	-50
7	8	20	-25
7	10	29	-29
7	12	79	-75
7	14	78	-81
8	1	65	-63
8	3	38	-39
8	5	21	-25
8	7	85	81
8	9	-12	-2
8	11	47	51
8	13	86	-82
8	15	77	-75
8	17	65	-67
**** H = 7 ****			
0	0	127	-132
0	2	20	-18
0	4	17	9
0	6	89	-88
1	0	-11	-1
1	1	48	50
1	2	-11	-7
1	3	26	-29
1	4	39	38
1	5	162	-161
2	0	34	35
2	1	327	329
2	2	62	-60
2	3	59	-62
2	4	-11	1
3	0	-11	3
3	1	49	-41
**** H = 8 ****			
0	2	125	-112
0	4	142	129
0	6	114	113
0	8	230	-225
0	10	87	-89
0	12	217	229
0	14	-12	-7
0	16	77	-76
0	18	84	84
0	20	124	113
0	22	70	-63
1	1	116	-103
1	2	38	37
1	3	80	78
1	4	-7	11
1	5	69	63
1	6	159	159
1	7	208	-208
1	8	142	146
1	9	114	119
1	10	-10	-20
1	11	142	152
1	12	-10	-3
1	13	179	-189
1	14	172	188
1	15	-12	-14
1	16	-12	9
1	17	195	184
1	18	76	-65
1	19	83	-78
1	20	73	75
1	21	124	-109
1	22	118	103
1	23	172	146
2	1	244	231
2	2	19	18
2	3	765	772
2	4	76	-76
2	5	49	-50
2	6	-5	14
2	7	15	-16
2	8	42	-44
2	9	57	-63
3	7	37	39
3	8	168	-172
3	9	99	99
3	10	164	-164
3	11	32	27
3	12	115	116
3	13	-12	18
3	14	275	280
3	15	88	-85
3	16	76	-77
3	17	-11	-7
3	18	69	71
3	19	-13	-1
3	20	-12	12
**** H = 9 ****			
0	2	-8	-16
0	4	189	-184
0	6	-11	4
0	8	93	95
1	1	84	80
1	2	48	41
1	3	88	-89
1	4	45	-43
1	5	36	-31
1	6	136	-137
1	7	51	49
1	8	-9	-5
1	9	190	-190
1	10	45	-42
1	11	-10	-3
1	12	129	-131
1	13	104	108
1	14	76	-79
1	15	164	-156
1	16	40	42
1	17	74	-77
1	18	51	-59
1	19	246	254
1	20	101	-103
1	21	95	-56
1	22	59	-43
2	1	600	-622
2	2	22	19
2	3	281	-268
2	4	20	20
2	5	244	239
2	6	-7	-52
2	7	332	-321
2	8	20	-16
2	9	467	-399
2	10	46	42
2	11	104	105
2	12	35	-33
2	13	124	-125
2	14	25	-17
2	15	337	-338
2	16	-12	12
2	17	25	-35
2	18	-12	16
2	19	41	-49
2	20	-12	-16
2	21	156	-165
3	1	-9	-1
3	2	32	29
3	3	82	84
3	4	172	-167
3	5	-9	0
3	6	163	-155
3	7	-9	-3
3	8	-10	10
3	9	115	116
3	10	72	-71
3	11	53	-50
3	12	184	-184
3	13	85	-89
3	14	96	96
3	15	46	-45
3	16	97	-101
3	17	26	-21
3	18	193	-190
3	19	111	-111
4	0	232	240
4	2	39	44
4	4	138	138
4	6	124	119
4	8	127	-119
4	10	132	-123
4	12	96	-96
4	14	242	-238
4	16	155	155
4	18	28	28
**** H = 10 ****			
0	2	-8	-16
0	4	134	142
0	6	-11	4
0	8	93	95
1	1	84	80
1	2	48	41
1	3	88	-89
1	4	45	-43
1	5	36	-31
1	6	136	-137
1	7	51	49
1	8	-9	-5
1	9	190	-190
1	10	45	-42
1	11	-10	-3
1	12	129	-131
1	13	104	108
1	14	76	-79
1	15	164	-156
1	16	40	42
1	17	74	-77
1	18	51	-59
1	19	246	254
1	20	101	-103
1	21	95	-56
1	22	59	-43
2	1	600	-622
2	2	22	19
2	3	281	-268
2	4	20	20
2	5	244	239
2	6	-7	-52
2	7	332	-321
2	8	20	-16
2	9	467	-399
2	10	46	42
2	11	104	105
2	12	35	-33
2	13	124	-125
2	14	25	-17
2	15	337	-338
2	16	-12	12
2	17	25	-35
2	18	-12	16
2	19	41	-49
2	20	-12	-16
2	21	156	-165
3	1	-9	-1
3	2	32	29
3	3	82	84
3	4	172	-167
3	5	-9	0
3	6	163	-155
3	7	-9	-3
3	8	-10	10
3	9	115	116
3	10	72	-71
3	11	53	-50
3	12	184	-184
3	13	85	-89
3	14	96	96
3	15	46	-45
3	16	97	-101
3	17	26	-21
3	18	193	-190
3	19	111	-111
4	0	232	240
4	2	39	44
4	4	138	138
4	6	124	119
4	8	127	-119
4	10	132	-123
4	12	96	-96
4	14	242	-238
4	16	155	155
4	18	28	28
**** H = 11 ****			
0	2	-8	-16
0	4	134	142
0	6	-11	4
0	8	93	95
1	1	84	80
1	2	48	41
1	3	88	-89
1	4	45	-43
1	5	36	-31
1	6	136	-137
1	7	51	49
1	8	-9	-5
1	9	190	-190
1	10	45	-42
1	11	-10	-3
1	12	129	-131
1	13	104	108
1	14	76	-79
1	15	164	-156
1	16	40	42
1	17	74	-77
1	18	51	-59
1	19	246	254
1	20	101	-103
1	21	95	-56
1	22	59	-43
2	1	600	-622
2	2	22	19
2	3	281	-268
2	4	20	20
2	5	244	239
2	6	-7	-52
2	7	332	-321
2	8	20	-16
2	9	467	-399
2	10	46	42
2	11	104	105
2	12	35	-33
2	13	124	-125
2	14	25	-17
2	15	337	-338
2	16	-12	12
2	17	25	-35
2	18	-12	16
2	19	41	-49
2	20	-12	-16
2	21	156	-165
3	1	-9	-1
3	2	32	29
3	3	82	84
3	4	172	-167
3	5	-9	0
3	6	163	-155
3	7	-9	-3
3	8	-10	10
3	9	115	116
3	10	72	-71
3	11	53	-50
3	12	184	-184
3	13	85	-89
3	14	96	96
3	15	46	-45
3	16	97	-101
3	17	26	-21
3	18	193	-190
3	19	111	-111
4	0	232	240
4	2	39	44
4	4	138	138
4	6	124	119
4	8	127	-119
4	10	132	-123
4	12	96	-96
4	14	242	-238
4	16	155	155
4	18	28	28
**** H = 12 ****			
0	2	-8	-16
0	4	134	142
0	6	-11	4
0	8	93	95
1	1	84	80
1	2	48	41
1	3	88	-89
1	4	45	-43
1	5	36	-31
1	6	136	-137
1	7	51	49
1	8	-9	-5
1	9	190	-190
1	10	45	-42
1	11	-10	-3
1	12	129	-131
1	13	104	108
1	14	76	-79
1	15	164	-156
1	16	40	42
1	17	74	-77
1	18	51	-59
1	19	246	254
1	20	101	-103
1	21	95	-56
1	22	59	-43
2	1	600	-622
2	2	22	19
2	3	281	-268
2	4	20	20
2	5	244	239
2	6	-7	-52
2	7	332	-321
2	8	20	-16
2	9	467	-399
2	10	46	42
2	11	104	105
2	12	35	-33
2	13	124	-125
2	14	25	-17
2	15	337	-338
2	16	-12	12
2	17	25	-35
2	18	-12	16
2	19	41	-49
2	20	-12	-16
2	21	156	-165
3	1	-9	-1
3	2	32	29
3	3	82	84
3	4	172	-167
3	5	-9	0
3	6	163	-155
3	7	-9	-3
3	8	-10	10
3	9	115	116
3	10	72	-71
3	11	53	-50
3	12	184	-184
3	13	85	-89
3	14	96	96
3	15	46	-45
3	16	97	-101
3	17	26	-21
3	18	193	-190
3	19	111	-111
4	0	232	240
4	2	39	44
4	4	138	138
4	6	124	119
4	8	127	-119
4	10	132	-123
4	12	96	-96
4	14	242	-238
4	16	155	155
4	18	28	28
**** H = 13 ****			
0	2	-8	-16
0	4	134	142
0	6	-11	4
0	8	93	95
1	1	84	80
1	2	48	41
1	3	88	-89
1	4	45	-43
1	5	36	-31
1	6	136	-137
1	7	51	49
1	8	-9	-5
1	9	190	-190
1	10	45	-42
1	11	-10	-3
1	12	129	-131
1	13	104	108
1	14	76	-79
1	15	164	-156
1	16	40	42
1	17	74	-77
1	18	51	-59
1	19	246	254
1	20	101	-103
1	21	95	-56
1	22	59	-43
2	1	600	-622
2	2	22	19
2	3	281	-268
2	4	20	20
2	5	244	239
2	6	-7	-52
2	7	332	-321
2	8	20	-16
2	9	467	-399
2	10	46	42
2	11	104	105
2	12	35	-33
2	13	124	-125
2	14	25	-17
2	15	337	-338
2	16	-12	12
2	17	25	-35
2	18	-12	16
2	19	41	-49
2	20	-12	-16
2	21	156	-165
3	1	-9	-1
3	2	32	29
3	3	82	84
3	4	172	-167
3	5	-9	0
3	6	163	-155
3	7	-9	-3
3	8	-10	10
3	9	115	116
3	10	72	-71
3	11	53	-50
3	12	184	-184
3	13	85	-89
3	14	96	96
3	15	46	-45
3	16	97	-101
3	17	26	-21
3	18	193	-190
3	19	111	-111
4	0	232	240
4	2	39	44
4	4	138	138
4	6	124	119
4	8	127	-119
4	10	132	-123
4	12	96	-96
4	14	242	-238
4	16	155	155
4	18	28	28
**** H = 14 ****			
0	2	-8	-16
0	4	134	142
0	6	-11	4
0	8	93	95
1	1	84	80
1	2	48	41
1	3	88	-89
1	4	45	-43
1	5	36	-31
1	6	136	-137
1	7	51	49
1	8	-9	-5
1	9	190	-190
1	10	45	-42
1	11	-10	-3
1	12	129	-131
1	13	104	108
1	14	76	-79
1	15	164	-156
1	16	40	42
1	17	74	-77
1	18	51	-59
1	19	246	254
1	20	101	-103
1	21	95	-56
1	22	59	-43
2	1	600	-622
2	2	22	19
2	3	281	-268
2	4	20	20
2	5	244	239
2	6	-7	-52
2	7	332	-321
2	8	20	-16
2	9	467	-399
2	10	46	42
2	11	104	105
2	12	35	-33
2	13	124	-125
2	14	25	-17
2	15	337	-338
2	16	-12	12
2	17	25	-35
2	18	-12	16
2	19	41	-49
2	20	-12	-16
2	21	156	-165
3	1	-9	-1
3	2	32	29
3

Can. J. Chem. Downloaded from www.nrcresearchpress.com by 210.87.254.40 on 09/05/12
For personal use only.

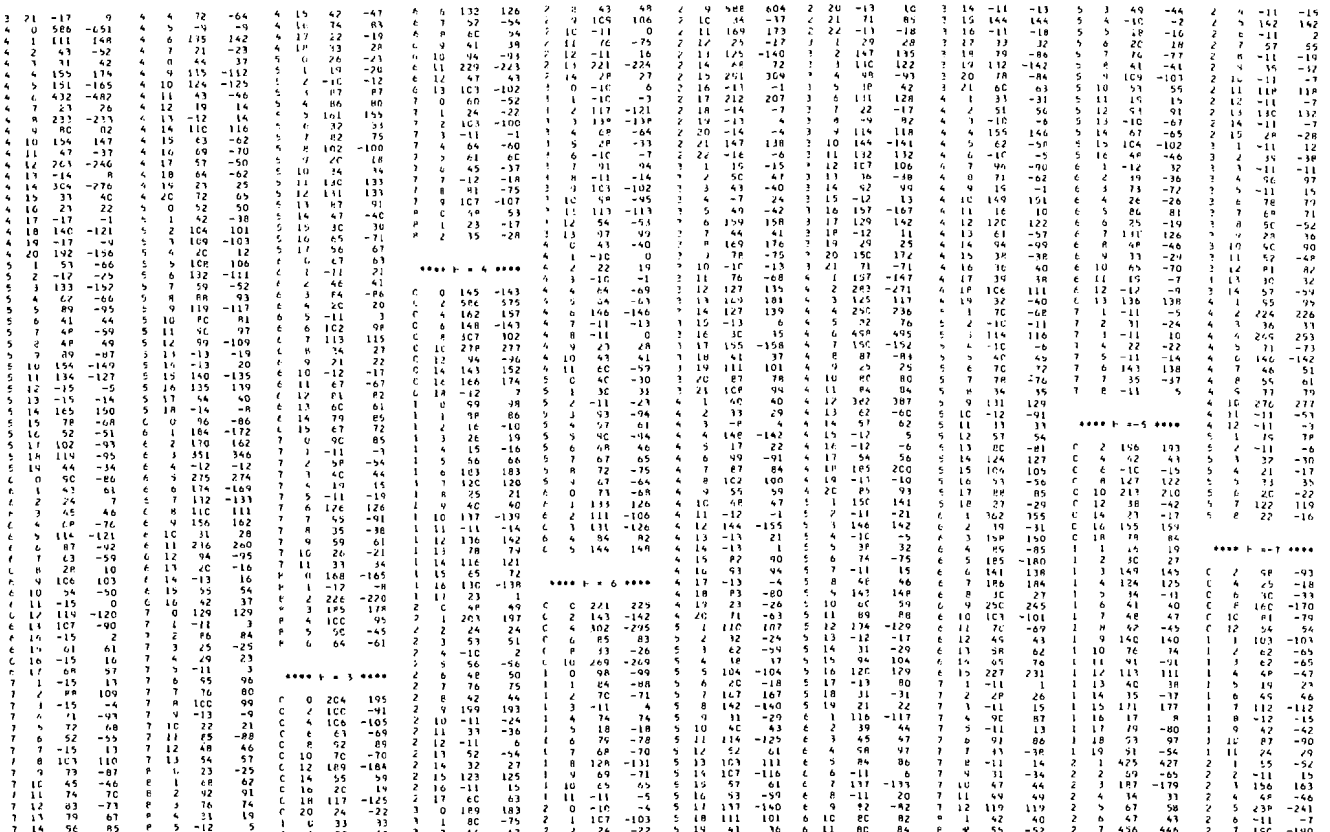

(involving I(*1*) and I(*2*)), the average I...O distances are invariably longer than those for the HIO_3 molecules (I(*3*) and I(*4*)). These differences may be explained in terms of the negative charge of the IO_3^- ion being more localized on the iodine atom than in the case for the HIO_3 molecule. Hence, the negative oxygen atoms would find it easier to approach, and donate, to the vacant empty 5d orbitals of the more electropositive iodine atom in HIO_3.

We propose that the lone pair on the iodine atom is situated in between the longer I—O contacts in the case of the distorted octahedral environment. If such is the case, one would not expect a head-on approach of an oxygen atom directly towards a lone pair position as is found in a regular capped octahedron. In fact, the approach of the distorted capped oxygen atom O(*31*) to I(*2*) is considerably displaced towards one side of the triangle formed by O(*21*)′, O(*22*)′, and O(*13*). This suggests that the lone pair of I(*2*) in the I(*2*)–I(*2*) dimer has more s character than the other iodine atoms.

The thermal motion for the different atoms in $KIO_3.HIO_3$ is in general low, even after approximate absorption corrections have been made. None of the iodine atoms show markedly anisotropic motion and in the absence of any sound physical model to base corrections on, we have used interatomic distances uncorrected for anisotropic thermal movement. The corrections would be small in any event, and susceptible to the errors in our treatment of absorption. The small amount of thermal motion may be attributed to the ionic nature of the crystals together with the hydrogen bonding giving a stable 3-dimensional structure. It is also consistent with the hardness and difficulty in cleaving crystals.

Note added in proof

Dr. K. Rieckhoff and Mr. R. Ninnis have kindly examined a sample of $KIO_3 \cdot HIO_3$ and have detected a strong second harmonic effect indicating that, as in the parent structures KIO_3 and HIO_3, a crystallographic center of symmetry is lacking. This result is in agreement with the piezoelectric effect recently reported (11). It might be expected that the deviations from centrosymmetry arise mainly through the hydrogen bonding.

We wish to thank Dr. D. G. Tuck of this Department for suggesting the problem and for his interest in its solution. We are grateful to Dr. F. R. Ahmed and Dr. B. R. Penfold who kindly supplied their computer programs. Our thanks are also due to the National Research Council of Canada as without their financial support this work could not have been carried out.

1. M. T. Rogers and L. Helmholz. J. Amer. Chem. Soc. **63**, 278 (1941).
2. B. S. Garrett. Struct. Rep. **18**, 393 (1954).
3. W. E. Dasent and T. C. Waddington. J. Chem. Soc. A, 2429 (1960).
4. W. C. Hamilton. Statistics in Physical Sciences. Ronald Press Company, 1964. p. 217.
5. International Tables for X-ray Crystallography. Vol. 3, Sect. 3.3, 1965.
6. A. F. Wells. Acta Cryst. **2**, 128 (1949).
7. J. A. Ibers. Acta Cryst. **9**, 225 (1956).
8. K. Nakamoto, M. Margoshes, and R. E. Rundle. J. Amer. Chem. Soc. **77**, 6480 (1955).
9. W. C. Hamilton and J. A. Ibers. Hydrogen Bonding in Solids. Benjamin Inc. 1968. p. 87.
10. K. A. R. Mitchell. Chem. Rev. **69**, 157 (1969).
11. G. Kemper and Aafje Vos. Acta Cryst. **B26**, 302 (1970).

Can. J. Chem. Downloaded from www.nrcresearchpress.com by 210.87.254.40 on 09/05/12
For personal use only.

The Raman Spectra of the Chlorofluorosilanes in the Gaseous, Liquid, and Solid State; Anomalous ^{35}Cl, ^{37}Cl Isotope Intensity Effects in the Splitting of the Totally Symmetrical SiCl Stretching Mode in $SiCl_3F$ and $SiCl_2F_2$

K. HAMADA,[1] G. A. OZIN, AND E. A. ROBINSON

University of Toronto, Lash Miller Chemical Laboratories and Erindale College, Toronto 181, Ontario

Received July 17, 1970

The Raman spectra of the chlorofluorosilanes are reported in their various phases together with vibrational assignments of the normal modes. The ^{35}Cl–^{37}Cl isotope lines of the totally symmetrical SiCl stretching modes in $SiCl_3F$ and $SiCl_2F_2$ were partially resolved in the solid and liquid phases and their intensities were found to be approximately normal in the liquid state but may show deviations in the solid state. Possible reasons for this behavior are discussed and the results are compared with similar effects observed for CCl_3F and $CHCl_3$.

Canadian Journal of Chemistry, 49, 477 (1971)

Can. J. Chem. Downloaded from www.nrcresearchpress.com by 210.87.254.42 on 09/05/12
For personal use only.

Introduction

One of the advantages of laser Raman spectroscopy is that highly reactive or hygroscopic materials can be studied in all-glass cells and in certain favorable cases in all three phases. A change in structure with phase is thus easily detected and, by studying the species in the gas phase, spectra can be obtained free from interfering effects that often make the spectra of solids and liquids difficult to interpret.

Using argon-ion and krypton-ion laser excitation we have been able to obtain excellent quality spectra in the gas, liquid, and solid phases for most of the chlorofluorosilanes; the vibrational data for which has previously been incomplete (1, 2). As far as can be certain the Raman spectra of $SiCl_2F_2$ and $SiClF_3$ have not been previously reported and our gas phase data for SiF_4, $SiClF_3$, $SiCl_2F_2$, and $SiCl_3F$ are new.

Experimental

The chlorofluorosilanes were prepared according to the method of Booth and Swinehart (3) through a Swartz type reaction. Silicon tetrachloride was partially fluorinated using antimony trifluoride with antimony pentachloride as a catalyst, and the chlorofluorosilanes were separated by means of trap-to-trap distillation and low temperature fractionation. The separate fractions were found to be sufficiently pure for spectroscopic examination as the peak intensities of impurity bands, were always less than 5% of the strongest band in the fraction under investigation. Raman spectra were recorded on a Spex 1401 spectrometer using a Carson argon ion laser (2 W at 4880 or 5145 Å) or krypton-ion laser (200 mW at 5682 or 6471 Å) for excitation. For measurements at low temperature the cell used was similar to that previously described (5).

[1]Present address: Faculty of Education, Nagasaki University, Nagasaki, Japan.

Results and Discussion

The vibrational modes for the tetrahedral molecules SiF_4 (T_d), $SiClF_3$ (C_{3v}), $SiCl_2F_2$ (C_{2v}), and $SiCl_3F$ (C_{3v}) are such that all modes are expected to be Raman active.

The Raman spectra of the chlorofluorosilanes are shown in Tables 1, 2, and 3 together with polarization data for the liquids and gases. The vibrational assignments are straightforward for $SiCl_3F$ and $SiClF_3$ by analogy with the recently published liquid phase Raman spectra of the bromofluorosilanes (4) and are also shown in Tables 1, 2, and 3. In the case of $SiCl_2F_2$ some ambiguity lies in the assignment of the three low frequency deformations of symmetry type b_1, b_2, and a_2 but the two a_1 type deformations in $SiCl_2F_2$ are easily identified since their lines will be polarized and the symmetrical SiF_2 deformation is expected to be at a higher frequency than the corresponding $SiCl_2$ deformation.

In the spectrum of $SiCl_3F$ three doublets occur at 946 and 935, 640 and 620, and 476 and 467 cm^{-1}, respectively, all of which may be interpreted as due to Fermi resonance. Thus, for example, in the solid phase 946 (a_1) is in resonance with 2×467 ($a_1 \times a_1 = a_1$), 640 (e) is in resonance with $467 + 168$ ($a_1 \times e = e$), and 467 (a_1) is in resonance with 2×238 ($a_1 \times a_1 = a_1$).

An interesting feature of the present study relates to the ^{35}Cl, ^{37}Cl isotope splitting, an effect well known for ν_1 of the tetrahedral MCl_4 species (M = C, Si, Ge, Sn, Ti, and P), ν_1 of planar

TABLE 1. The Raman spectrum of $SiCl_3F$ in the gaseous, liquid, and solid states

Assignment (C_{3v})			Solid (−196 °C) (cm^{-1})	Liquid (25 °C) (cm^{-1})	Gas (25 °C/600 mm) (cm^{-1})
a_1	ν_1	ν_s (SiF)	946 vw	940 w (p)	947 vw (p)
	$2\nu_2$		935 vw	918 vw sh (p)	916 vw (p)
e	ν_4	ν_{as} ($SiCl_3$)	640 w	646 vw	638 w br
	$\nu_2+\nu_5$		620 w	626 w	
	$2\nu_3$		476 vw sh	473 vvw	477 vvw sh (p)
a_1	ν_2	ν_s ($SiCl_3$)	467 s	463 s (p)	464 s (p)
e	ν_5	δ_{as} (SiClF)	278 mw br	276 mw	283 mw
a_1	ν_3	δ_s ($SiCl_3$)	238 mw	235 m (p)	240 m (p)
e	ν_6	δ_{as} ($SiCl_3$)	168 ms	165 ms	166 m

*s = strong; m = medium; w = weak; v = very; sh = shoulder; br = broad; p = polarized.

TABLE 2. The Raman spectrum of $SiCl_2F_2$ in the gaseous, liquid, and solid states

Assignment (C_{2v})			Solid (−196 °C) (cm^{-1})	Liquid (25 °C) (cm^{-1})	Gas (25 °C/600 mm) (cm^{-1})
b_1	ν_6	ν_{as} (SiF_2)	964 w	985 vw	987 vw
a_1	ν_1	ν_s (SiF_2)	897 mw	906 w (p)	915 w (p)
b_2	ν_9	ν_{as} ($SiCl_2$)	658 w 647 w	650 w	638 w
a_1	ν_2	ν_s ($SiCl_2$)	517 s	517 s (p)	520 s (p)
a_1	ν_3	δ_s (SiF_2)	320 m	322 ms (p)	324 mw (p)
b_1	ν_7	δ_{as} (SiF_2)	314 m	307 w sh	303 w
a_2	ν_5	δ (FSiCl)	273 mw	275 w	279 w
b_2	ν_8	δ_{as} ($SiCl_2$)	214 mw 206 w	210 w	210 w
a_1	ν_4	δ_s ($SiCl_2$)	176 ms	176 m (p)	174 mw (p)

TABLE 3. The Raman spectrum of $SiClF_3$ in the solid and gaseous states and SiF_4 in the gaseous state

$SiClF_3$					SiF_4		
Assignment			Solid (−196 °C) (cm^{-1})	Gas (25 °C/600 mm) (cm^{-1})	Assignment		Gas (25 °C/600 mm) (cm^{-1})
e	ν_4	ν_{as} (SiF_3)	985 w	1004 vw	f_2	ν_3	1025 w br
a_1	ν_1	ν_s (SiF_3)	876 w	878 w (p)	a_1	ν_1	800 s (p)
a_1	ν_2	ν_s (SiCl)	591 s	593 s (p)			
a_1	ν_3	δ_s (SiF_3)	347 m	351 mw (p)	f_2	ν_4	389 mw br
e	ν_5	δ_{as} (SiClF)	~255 vw	—	e	ν_2	268 w br
e	ν_6	δ_{as} (SiCl)	223 m	222 w			

BCl_3, ν_5 of $CHCl_3$, and ν_1 of Si_2Cl_6 (5). The observed intensities of the component lines constituting the multiplets are generally found to be in satisfactory agreement with those theoretically predicted from the abundances of the chlorine isotopes; however, in one or two cases, notably in solid $CHCl_3$ (−196 °C), anomalous isotope intensities have been observed (6).

The calculations of isotope intensities are generally based on the first order approximation that the intensity of a line associated with a particular isotope arrangement is proportional to the probability of forming that molecular arrangement. For example, the chlorine isotope splitting of the SiCl totally symmetrical stretching mode in Si_2Cl_6 has been observed (5); five of the expected seven components were observed at −196 °C and their intensities found to be in satisfactory agreement with those predicted on the above model. The remaining two were expected to be too weak to be detected.

In the present study we have observed the chlorine isotope splitting for solid $SiCl_3F$ and $SiCl_2F_2$ at −196 °C, and for the liquids at 25 °C. The Raman data are consistent with the expected symmetries (C_{3v} and C_{2v}, respectively) in both the solid and liquid phases and the observed frequencies and gross intensities remain essentially

Can. J. Chem. Downloaded from www.nrcresearchpress.com by 210.87.254.42 on 09/05/12
For personal use only.

Can. J. Chem. Downloaded from www.nrcresearchpress.com by 210.87.254.42 on 09/05/12
For personal use only.

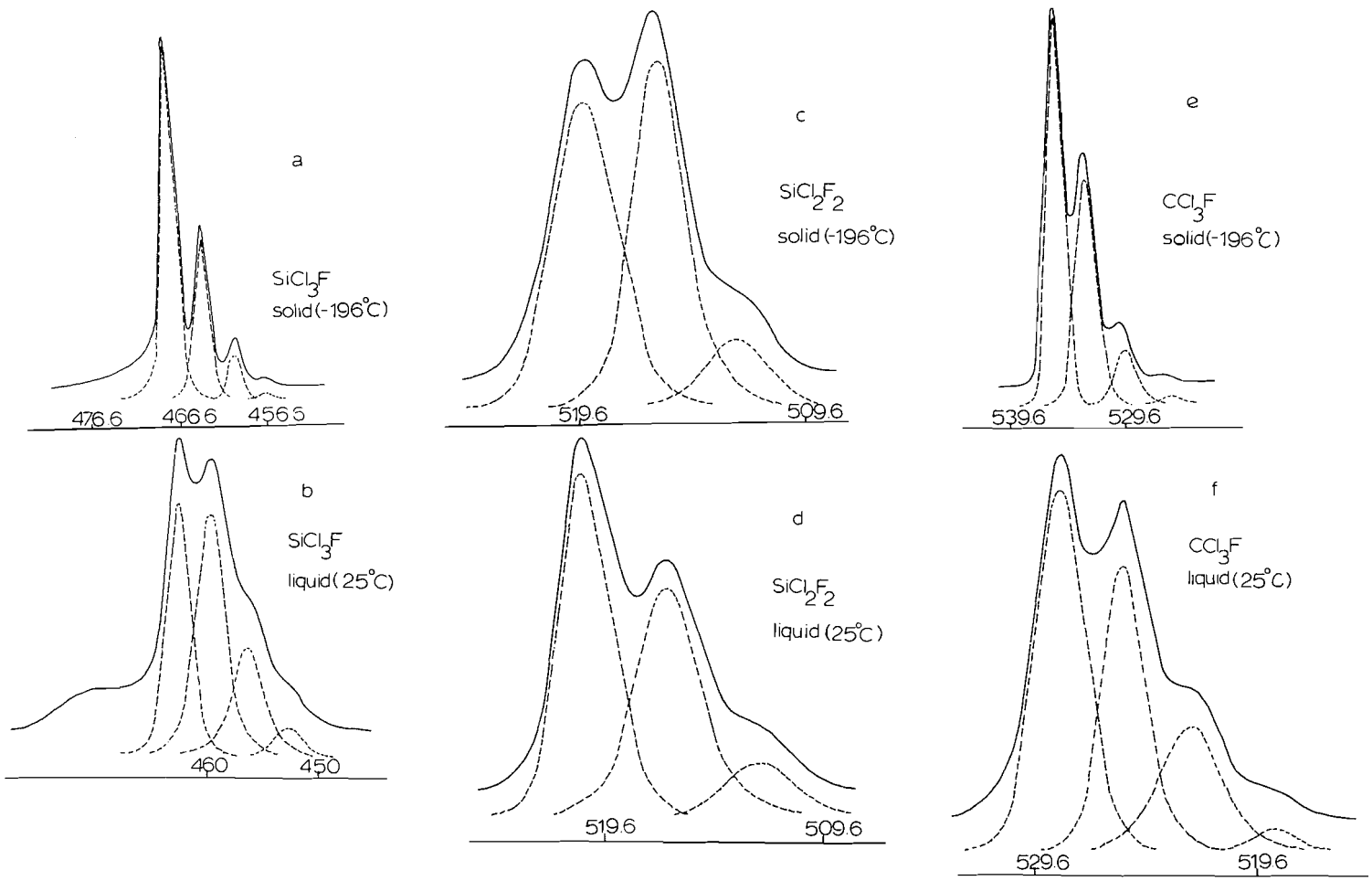

FIG. 1. ^{35}Cl, ^{37}Cl isotope splitting in the a_1 MCl stretching mode of (*a*) solid $SiCl_3F$ (−196 °C), (*b*) liquid $SiCl_3F$ (25 °C), (*c*) solid $SiCl_2F_2$ (−196 °C), (*d*) liquid $SiCl_2F_2$ (25 °C), (*e*) solid CCl_3F (−196 °C), and (*f*) liquid CCl_3F (25 °C).

TABLE 4. Correlation of a C_{3v} molecule through the site symmetry C_s and into the crystal $D_{2h}{}^{16}$

C_{3v} (Free molecule 4 in unit cell)	C_s (Site symmetry) [Correlating about $\sigma(\times z)$]	$D_{2h}{}^{16}$ (Unit cell)
$4\times a_1$	$4a'$	$a_g+b_{2g}+b_{1u}+b_{3u}$
$4\times e$	$4a'$	$a_g+b_{2g}+b_{1u}+b_{3u}$
	$4a''$	$b_{1g}+b_{3g}+a_u+b_{2u}$

unchanged between phases. However, the chlorine isotope lines for the a_1 SiCl stretching modes in $SiCl_3F$ and $SiCl_2F_2$ are found to be approximately normal in the liquids but show deviations in the solids. The observed intensities are shown in Fig. 1, together with the individual peaks obtained by use of a Dupont curve resolver.

In the case of $SiCl_3F$ (*cf.* CCl_3F), the solid state intensities clearly show deviations (Fig. 1*a*) from the theoretical values 28.8:28.2:19.2:1.0. However, the liquid state intensities for the species $Si^{35}Cl_3F$, $Si^{35}Cl_2{}^{37}ClF$, $Si^{35}Cl^{37}Cl_2F$, and $Si^{37}Cl_3F$ are approximately in agreement with the theory (Fig. 1*b*). It is interesting to note that the isotope component intensity ratios in solid $CHCl_3$ (5), $SiCl_3F$, and CCl_3F (Fig. 1*a* and 1*e*) for the symmetrical MCl stretching modes, are all *closely similar.*

If the crystal structures of CCl_3F and $SiCl_3F$ are isomorphous with that of the known structure of crystalline $CHCl_3$ ($P_{nma}[D_{2h}{}^{16}]$), with four molecules in the primitive unit cell (7), then correlation splitting of the a_1 MCl stretching mode to give similar intensities of the isotopic components is reasonable. The anomalous intensities of the isotope components in CCl_3F and $SiCl_3F$ can then be attributed to an unresolved factor group splitting. For site symmetry C_s the correlation shown in Table 4 would be expected.

In the case of $SiCl_2F_2$ the three predicted components of the totally symmetrical stretching mode due to the isotope species $Si^{35}Cl_2F_2$, $Si^{35}Cl^{37}ClF_2$, and $Si^{37}Cl_2F_2$ were partially resolved. The expected intensity ratios 9.40:6.13:1.00 were approximately observed in the liquid phase (Fig. 1*d*) but again the ratios of the intensities in the solid state (Fig. 1*c*) were anomalous. These probably result from a similar phenomenon to that described for solid $SiCl_3F$ and solid CCl_3F, that is, unresolved factor group splitting.

The authors are grateful to the Defence Research Board of Canada and the National Research Council of Canada for financial support.

1. J. GOUBEAU, F. HAENSHKE, and A. RUOFF. Z. Anorg. Chem. **366**, 113 (1969).
2. J. STOKR and B. SCHNEIDER. Chem. Listy, **48**, 336 (1954); **52**, 985 (1958).
3. H. A. BOOTH and C. F. SWINEHART. J. Amer. Chem. Soc. **57**, 1333 (1935).
4. M. L. DUBOIS, M. B. DELHAYE, and F. WALLART. Comp. Rend. **269**, 260 (1969).
5. G. A. OZIN. J. Chem. Soc. A, 2952 (1969).
6. H. F. SHURVELL. Raman Newsletter, **18**, 8 (1970).
7. R. FOURNE and M. RENAUD. Comp. Rend. **263B**, 19 (1966).

Can. J. Chem. Downloaded from www.nrcresearchpress.com by 210.87.254.42 on 09/05/12
For personal use only.

Can. J. Chem. Downloaded from www.nrcresearchpress.com by 210.87.254.5 on 09/05/12
For personal use only.

Synthesis and Structure of 3-Methyl-1-phenyl-4-sulfhydrylbenzylidene-5-thiopyrazolone

R. F. LANGLER
Department of Chemistry, Dalhousie University, Halifax, Nova Scotia

Received August 25, 1970

The synthesis of 3-methyl-1-phenyl-4-sulfhydrylbenzylidene-5-thiopyrazolone (**4**) is reported. It is a potential sequestering agent as well as a new example of a β-dithiocarbonyl compound. The structure of **4** is unambiguously established by conversion to 4-benzoyl-3-methyl-1-phenyl-5-pyrazolethiol (**3**).

Canadian Journal of Chemistry, **49**, 481 (1971)

In recent years, there has been an increasing interest in the application of sulfur-containing ligands to trace-metal analysis. A number of successful syntheses of both monothio (1–4) and dithio analogs (5–7) of the β-dicarbonyl chromophore have been reported. I now report the preparation of a new β-dithiocarbonyl system.

A 4-acyl pyrazole substrate was selected because of the well established value of these systems as sequestering agents (8, 9).

Treatment of 4-benzoyl-5-chloro-3-methyl-1-phenylpyrazole (**2**) or 4-benzoyl-3-methyl-1-phenyl-5-pyrazolethiol (**3**) with phosphorus pentasulfide in hot toluene gives 3-methyl-1-phenyl-4-sulfhydrylbenzylidene-5-thiopyrazolone (**4**) in 10 and 15% yields respectively (see Scheme 1).

The i.r. spectrum of **4** exhibits a broad, weak absorption band at 2400 cm^{-1} which does not change upon dilution, in accord with an intramolecularly H-bonded thiol. The n.m.r. spectrum displays a sharp singlet at -0.1 τ (1H) which is

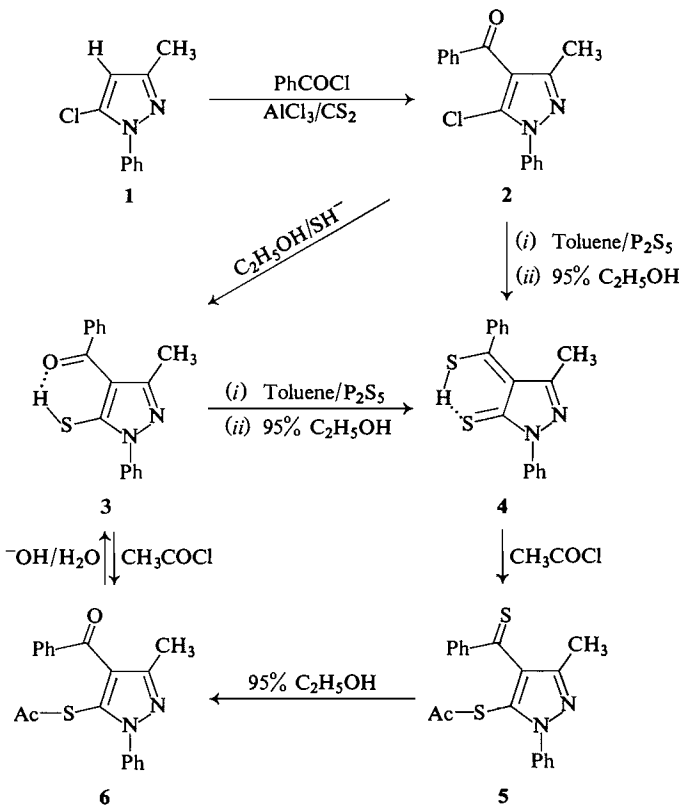

SCHEME 1

Can. J. Chem. Downloaded from www.nrcresearchpress.com by 210.87.254.5 on 09/05/12
For personal use only.

readily removed from the spectrum when the sample is shaken with D_2O, thus further substantiating the thiol moiety. Also evident in the n.m.r. are a broad signal centered at 2.4 τ (10H) and a singlet at 8.2 τ (3H) assigned to the two phenyl rings and the C-3 methyl group respectively.

The high resolution mass spectrum of **4** shows the molecular ion at *m/e* 310.0586 ($C_{17}H_{14}N_2S_2$) and an abundant ion at *m/e* 121.0113 (C_7H_5S) in agreement with a thiobenzoyl group. Other abundant ions occur at *m/e* 309 ($M^{\cdot+}$-H), 277 ($M^{\cdot+}$-SH), 105 (PhN_2^+), 77 ($C_6H_5^+$), and 51 ($C_4H_3^+$) all of which were determined at low resolution. The loss of a hydrogen radical ($M^{\cdot+}$-1) and an ·SH radical ($M^{\cdot+}$-33) from the molecular ion are processes observed in the mass spectrum of enethiolphenone **3** and have been observed in other enethiol systems (1).

The u.v. spectrum of **4** exhibits maxima at 235 (ε 15 900), 310 (ε 5600), and 538 nm (ε 228), the latter of which shifts to 450 nm (ε 3480), in the presence of dilute sodium hydroxide. Hopefully, this base-induced hypsochromic shift will prove useful in characterizing other β-dithiocarbonyl compounds. No analogous shift is observed in the u.v. spectrum of enethiolphenone **3**.

When the red crystalline dithiopyrazole **4** is refluxed in acetyl chloride, the blue, oily monoacetate **5** is obtained. Its i.r. spectrum displays an intense enethiolacetate carbonyl bond (4) at 1720 cm^{-1}. The n.m.r. spectrum of this dithioacetate exhibits two sharp singlets (3H each) at 7.9 and 7.8 τ confirming monoacetylation.

The mass spectrum of the acetylated dithio adduct **5** does not show a molecular ion but is essentially identical to that of **4** with an additional ion at *m/e* 43 (CH_3CO^+). The u.v. spectrum displays maxima at 595 (ε 100), 310 (ε 10 000), and 232 nm (ε 20 000).

By momentarily refluxing the dithioacetate **5** in 95% ethanol a quantitative conversion to the colorless crystalline monothioacetate **6** is accomplished. The i.r. spectrum of **6** shows intense absorption bands at 1720 and 1660 cm^{-1} in agreement with enethiolacetate and enaminophenone functions respectively. The n.m.r. spectrum exhibits two methyl singlets at 7.9 and 7.7 τ. A high resolution mass spectrum established the molecular ion as 336.0929 a.m.u. ($C_{19}H_{16}N_2O_2S$) showing no ion at *m/e* 121 and displaying abundant ions at *m/e* 105 ($C_7H_5O^+$, $C_6H_5N_2^+$) and 43 (CH_3CO^+). The mass spectrum of **6** is essentially identical to that of **3** with an additional ion at *m/e* 43.

Since the instability of thioketones is well established (10), the mild hydrolysis of **5** to **6** lends chemical support to the formulation of **5** as a thiophenone.

The monothio acetate **6** may also be conveniently prepared by treating **3** with acetyl chloride, thus unambiguously establishing the skeleta of **6**, **5**, and **4** and conclusively establishing **4** as the desired dithioketo system.

The facile conversion of the monothioacetate **6** to the enethiolphenone **3** in dilute aqueous sodium hydroxide provides chemical evidence for the formulation of **6** (and therefore **5**) as an *S*-acetate, since this functional group is particularly unstable to base (11).

The n.m.r. resonance positions of the C-3 methyl group in the chlorophenone **2**, the enethiolphenone **3**, and the dithiopyrazole **4** are 7.5, 7.9, and 8.2 τ respectively. This can be interpreted to indicate progressively decreasing π-electron density along the C_4—C_5 bond of the pyrazole nucleus, thereby resulting in progressively lesser deshielding of the C-3 methyl group by the π-system of the ring. Hence, I have formulated the dithiopyrazole as tautomer **4**. Such a formulation is in accord with expectation. Tautomeric forms involving a thiophenone are essentially precluded by the instability of thioketones (10). Further, thioamides are generally quite stable (12) and the resonance energy of the pyrazole nucleus appears to be rather small (9) so that the ring itself provides little energy for enolization of the thiolactam thiocarbonyl.

If the residue from the reaction of chlorophenone **2** with phosphorus pentasulfide is recrystallized from 95% ethanol, excess reagent is hydrolyzed, generating H_2S *in situ*, and red crystals of **4** are obtained in 10% yield. If, however, the residue is washed with several aliquots of 2½% sodium hydroxide solution, no dithiopyrazole **4** is obtained but the enethiolphenone **3** is isolated from the wash solution in 10% yield. Since dissolution of pure dithiopyrazole **4** in aqueous sodium hydroxide does not result in the formation of any enethiolphenone **3**, it is reasonable to propose that some intermediate is formed between P_2S_5 and chlorophenone **2**, which is then decomposed upon work-up to give products

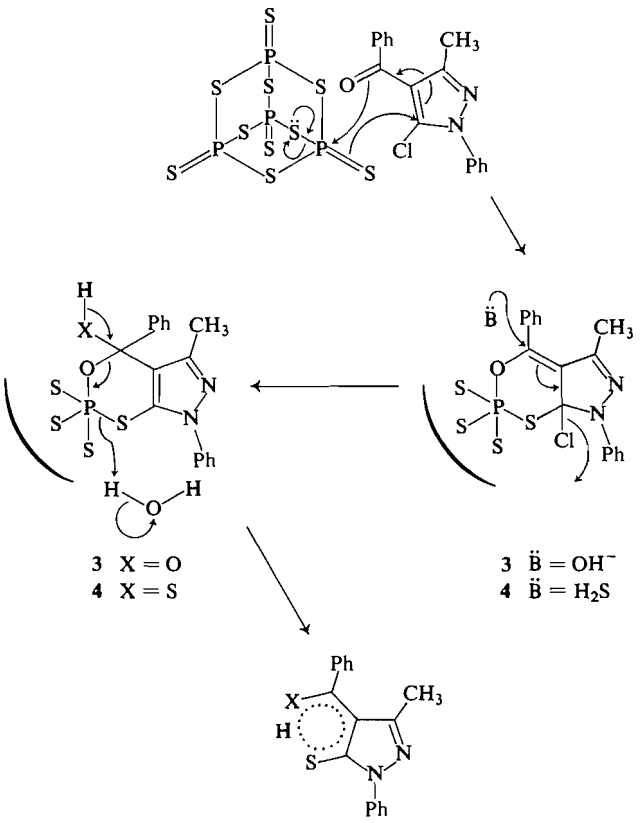

SCHEME 2

dependent upon the nucleophiles present in solution. A proposed mechanism is depicted in formula Scheme 2.

Experimental

General

The i.r. spectra were recorded on a Baird Associates Model 4-55 Double-beam spectrophotometer. The mass spectra were determined with a Bell and Howell/CEC 21-110B spectrometer. The n.m.r. spectra were obtained on a Varian A-60 instrument using TMS as internal standard. The u.v. spectra were recorded using a Coleman Model 124 Hitachi Double Beam spectrophotometer. Melting points were determined on a Fisher–Johns melting point apparatus and are uncorrected. The t.l.c. was carried out on plates of silica gel G (A. G. Merck).

Preparation of 4-Benzoyl-5-chloro-3-methyl-1-phenylpyrazole (2)

The chlorophenone **2** is prepared as described by Michaelis and Rojahn (13) from the chloropyrazole **1** (14). The preparation requires reflux of the appropriate compounds (*vide* formula Scheme 1), in CS_2 for 18 h. If the procedure is modified by allowing the CS_2 to evaporate after refluxing for 15 min, and heating the dry reaction mixture for 5–6 h at 70 °C, the yield, after basification and ether extraction, is 83% as opposed to the reported yield of 65–70%.

Preparation of 3-Methyl-1-phenyl-4-sulfhydrylbenzylidene-5-thiopyrazolone (4)

Purified phosphorus pentasulfide[1] (10 g) (15) and either 4-benzoyl-5-chloro-3-methyl-1-phenylpyrazole (**2**) or 4-benzoyl-3-methyl-1-phenyl-5-pyrazolethiol (**3**) (6 g) (16, 17) were heated in distilled toluene (50 ml) for 3.5 h at 100 °C. The toluene was decanted, evaporated, and the residue recrystallized from 95% ethanol (25 ml). Red needles (650 mg) were obtained after recrystallization to constant m.p. (128–130 °C). The product was homogeneous on t.l.c. (R_F, 0.45) using benzene as eluant. The i.r. bands were present ($CHCl_3$) 2400 and 1600 cm^{-1}; λ_{max} (EtOH) 235 (ε 15 900), 310 (ε 5600) and 538 nm (ε 228). The n.mr. spectrum ($CDCl_3$) showed signals at τ −0.1 (1H, D_2O exchangeable), 2.4 (10H), and 8.2 (3H). The high resolution mass spectrum confirmed the formula as $C_{17}H_{14}N_2S_2$ (molecular ion *m/e* 310.0586).

Preparation of 5-Mercaptoacetyl-3-methyl-1-phenyl-4-thiobenzoylpyrazole (5)

The dithiopyrazole **4** (100 mg) was refluxed in freshly

[1]Reagent grade CS_2 should be used for the preparation of purified P_2S_5 as described in this reference.

Can. J. Chem. Downloaded from www.nrcresearchpress.com by 210.87.254.5 on 09/05/12
For personal use only.

distilled acetyl chloride (10 ml) for 1 h. The acetyl chloride was evaporated to give the blue, oily dithioacetate **5**. This oil exhibited two spots on t.l.c. The major spot (R_F, 0.60) using chloroform for elution was due to **5**. The secondary spot proved to be identical with authentic **6** when double spotted. The i.r. bands ($CHCl_3$) were present at 1720 and 1600 cm^{-1}; λ_{max} (EtOH) 232 (ε 20 000), 310 (ε 10 000) and 595 nm (ε 100).

The n.m.r. spectrum ($CDCl_3$) showed signals at τ 2.3 (10H), 7.8 (3H), and 7.9 (3H).

Preparation of 4-Benzoyl-5-mercaptoacetyl-3-methyl-1-phenylpyrazole (6)

Enethiolphenone **3** (100 mg) was refluxed in freshly distilled acetyl chloride (10 ml) for 1 h. Evaporation of the acetyl chloride, and recrystallization of the residue from benzene/low boiling petroleum ether gave colorless crystals (m.p. 114–115 °C).

The recrystallized product was homogeneous on t.l.c. (R_F, 0.45), using chloroform as eluant. The i.r. bands were present ($CHCl_3$) at 1720, 1660, and 1600 cm^{-1}; λ_{max} (EtOH) 210 (ε 22 000), 260 (ε 16 000) and 270 nm (ε 10 000). The n.m.r. spectrum ($CDCl_3$) displayed signals at τ 2.4 (10H), 7.7 (3H), and 7.9 (3H). The high resolution mass spectrum confirmed the formula as $C_{19}H_{16}N_2O_2S$ (molecular ion *m/e* 336.0929).

Hydrolysis of 5

5-Mercaptoacetyl-3-methyl-1-phenyl-4-thiobenzoylpyrazole (**5**) (44 mg) was heated in boiling 95% ethanol for 2 min. The ethanol was evaporated and the residue recrystallized from benzene/low boiling petroleum ether to give **6** (40 mg). Identity with authentic **6** (*vide supra*) was established by t.l.c., n.m.r., i.r., and a mass spectrum. No depression of m.p. was observed when the sample was admixed with authentic **6**.

Basic Hydrolysis of 6

4-Benzoyl-5-mercaptoacetyl-3-methyl-1-phenylpyrazole (**6**) (52 mg) was added to a solution of methanol (2 ml) – 2½% aqueous sodium hydroxide (8 ml) and the solution gently refluxed. As solid **6** dissolved, the solution turned yellow. After 1 h the solution was acidified and extracted with ether. The ether (dried over $MgSO_4$) was evaporated to give crude enethiolphenone **3** (42 mg).

After recrystallization from 95% ethanol, identity was established with authentic **3** by mixed m.p., t.l.c. and n.m.r. spectra.

It is a pleasure to express my sincere gratitude to Dr. D. E. Ryan, who initiated and supported this research, and to Dr. C. A. Armour for his interest and encouragement. Special thanks are extended to both Mr. D. J. Embree, who obtained the mass spectra, using the mass spectrometric facilities of the Atlantic Regional Laboratories of the National Research Council of Canada, Halifax, and to Dr. D. L. Hooper of Dalhousie University who ran the n.m.r. spectra.

1. S. H. H. Chaston, S. E. Livingstone, T. N. Lockyer, V. A. Pickles, and J. S. Shannon. Aust. J. Chem. **18**, 673 (1965).
2. F. Duus and S. O. Lawesson. Ark. Kem. **29**, 127 (1968).
3. F. Duus, P. Jakobsen, and S. O. Lawesson. Tetrahedron, **24**, 5323 (1968).
4. F. Duus, E. B. Pedersen, and S. O. Lawesson. Tetrahedron, **25**, 5703 (1969).
5. U. Schmidt. Ber. **92**, 1171 (1959).
6. R. Mayer and S. Scheithauer. Ber. **100**, 1413 (1967).
7. J. Cavalla. J. Chem. Soc. 4664 (1962).
8. B. S. Jensen. Acta. Chem. Scand. **13**, 1347 (1959).
9. B. S. Jensen. Acta. Chem. Scand. **13**, 1668 (1959).
10. E. E. Reid. Organic chemistry of bivalent sulfur. Vol. III. Chemical Publishing Co., 1960. p. 159.
11. E. E. Reid. Organic chemistry of bivalent sulfur. Vol. IV. Chemical Publishing Co., 1962. p. 31.
12. E. E. Reid. Organic chemistry of bivalent sulfur. Vol. IV. Chemical Publishing Co., 1962. p. 45.
13. A. Michaelis and C. Rojahn. Ber. **50**, 737 (1917).
14. A. Michaelis and R. Pasternak. Ber. **32**, 2398 (1899).
15. W. Baker, J. Harborne, and W. Ollis. J. Chem. Soc. 1303 (1952).
16. A. Michaelis. Ann. **361**, 251 (1908).
17. E. Lehmann. Ann. **361**, 283 (1908).

Can. J. Chem. Downloaded from www.nrcresearchpress.com by 210.87.254.5 on 09/05/12
For personal use only.

Can. J. Chem. Downloaded from www.nrcresearchpress.com by 210.87.254.5 on 09/05/12
For personal use only.

Dibenzo[*a*,*d*]cycloheptene and Related Compounds. III.[1] The Synthesis of Some Analogues of Methadone Containing the Dihydrodibenzo[*a*,*d*]cycloheptene and the Tetrahydrodibenzo[*a*,*d*]cyclooctene Ring Systems

D. E. HORNING AND J. M. MUCHOWSKI[2]
Bristol Laboratories of Canada, Candiac, Quebec

Received July 6, 1970

The synthesis and spectral properties of some two- and three-carbon ortho-bridged analogues of the analgesic methadone are described. These compounds were devoid of analgesic activity.

Canadian Journal of Chemistry, 49, 485 (1971)

Methadone (**1**, R = CH_3), a clinically useful narcotic analgesic (2), was first prepared by Bockmuhl and Ehrhart (3) during the second World War. Although considerable effort has been devoted to structural modification of this molecule (3–6; see especially ref. 4, pp. 969–986), most of the synthetic activity has been confined to the preparation of conformationally flexible open chain systems much like methadone itself. Structures **2** (7), **3** (8), **4** (ref. 4, pp. 985–986, and refs. 9, 10), **5** (11), and **6** (12) represent notable departures from this trend.[3]

We wished to prepare analogues of **1** in which the mobility of the aliphatic portion of the molecule was essentially unaltered, but wherein the rotational freedom of the phenyl groups was intermediate between that of methadone and structures **3**–**6**. A study of Dreiding models indicated that the two- and three-carbon ortho-bridged compounds **7** (n = 2, 3) were capable of adopting several conformations in which the angle between the planes of the aromatic rings closely resembled that observable in a number of the conformations readily accessible to methadone. The preparation of **7** (n = 2, 3) for evaluation as analgesics therefore was of considerable interest, and the synthesis of these compounds was achieved in the manner described in Scheme 1.

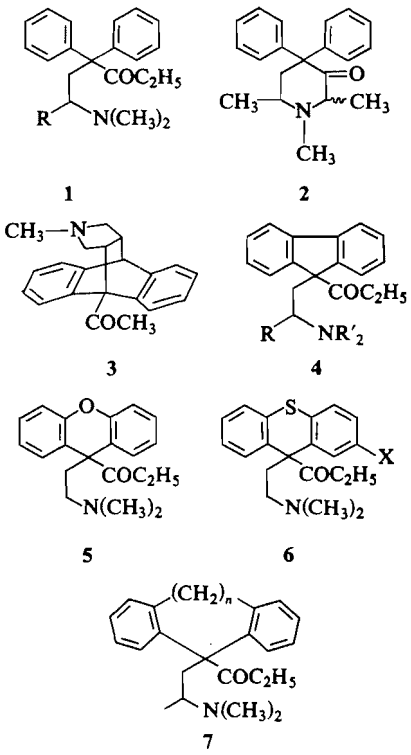

The alkylation of the cyanides **8** with 3-bromo-2-(tetrahydropyran-2-yloxy)-propene (THP = tetrahydropyran-2-yl), generated *in situ* (13), followed by acidic hydrolysis of the intermediate enol ethers, produced the keto nitriles **9**, which in turn were converted to the methadone-type nitriles **12** by a Leuckart reaction[4] with dimethylformamide and formic acid. The transformation

[1]For Part II see ref. 1.

[2]To whom enquiries concerning this paper should be addressed.

[3]Compound **2** was said (7) to be "quite toxic" and did not exhibit "promising analgesic activity", **3** had 1/20 of the activity of morphine (1/25 methadone) in mice on subcutaneous administration (8), **4** (R = R′ = CH_3) was described (9) as showing "slight analgesia at 0.5–5 mg/kg", **5** was reported (11) to possess "1/5 of the analgesic activity of morphine (1/6 methadone) when used on experimental animals", and **6** (X=H, Cl) was not active (12) in mice or rats at 10 mg/kg (subcutaneous).

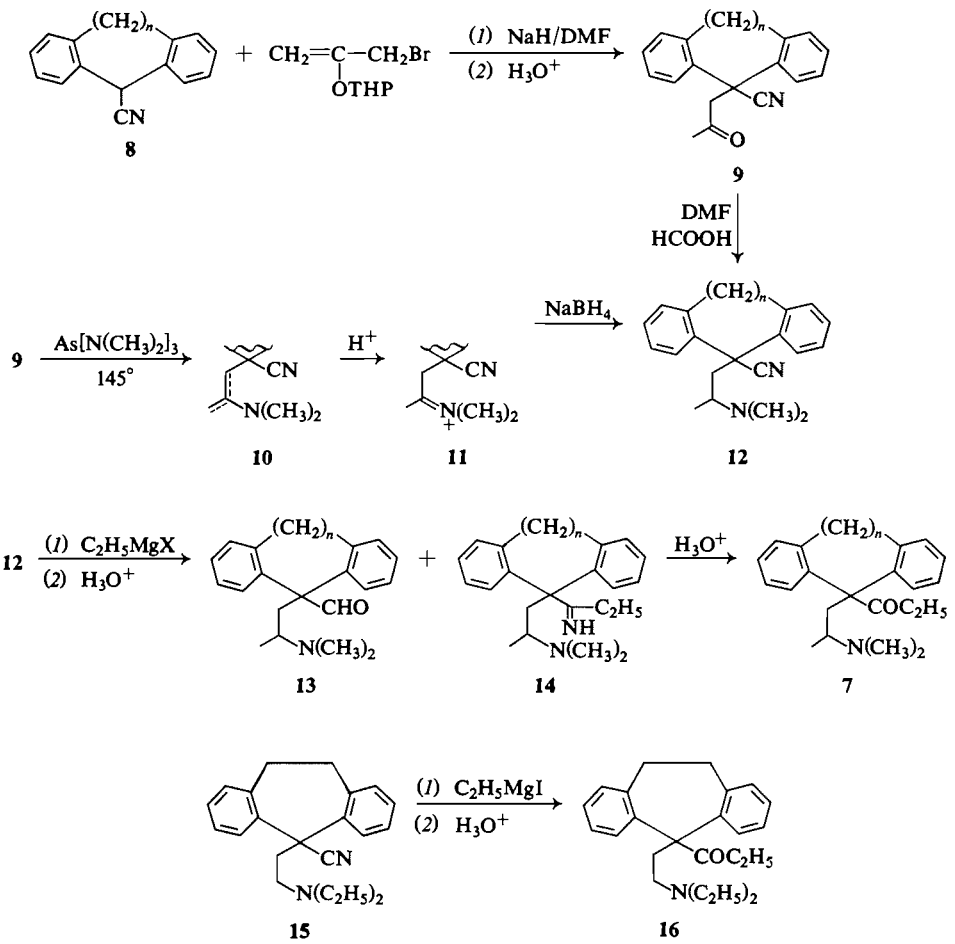

SCHEME 1

of **9** to **12** could also be effected[4] by the borohydride reduction of the quaternary imminium tosylates **11** derived from the corresponding enamines **10** and anhydrous *p*-toluenesulfonic acid. These enamines were obtained when the keto nitriles **9** and *tris*-dimethylamino arsine were heated together at 145°. When the nitriles **12** were treated with an excess of an ethyl Grignard reagent at 90°, mixtures of the reduction products **13** and the expected imines **14** were produced in both cases. The relative proportions of these products depended on the ethyl halide which was used for the preparation of the Grignard reagent; for example, with **12** ($n = 2$), ethylmagnesium iodide gave approximately equal amounts of the aldehyde and the imine, while ethylmagnesium bromide produced a 2:1 imine–aldehyde mixture. While the reduction of hindered nitriles to aldehydes by secondary and tertiary Grignard reagents is known (14), the reaction does not appear to have been described for primary Grignard reagents. The increase in the proportion of the aldehyde **13** ($n = 2$) when ethylmagnesium iodide was substituted for ethylmagnesium bromide is comparable to that observed for the reduction of ketones to the corresponding alcohols by Grignard reagents (15). The behavior of the nitrile **12** ($n = 3$) was atypical in the sense that the relative amount of the aldehyde was greater for ethylmagnesium bromide. The hydrolysis of the imines **14** to the ketones **7** was accomplished under relatively mild conditions (*e.g.* see ref. 17) by heating an aqueous solution of the hydro-

[4]When this work was nearing completion, a patent was issued (16) which described the application of essentially identical synthetic approaches to methadone-type nitriles.

Can. J. Chem. Downloaded from www.nrcresearchpress.com by 210.87.254.5 on 09/05/12
For personal use only.

Can. J. Chem. Downloaded from www.nrcresearchpress.com by 210.87.254.5 on 09/05/12
For personal use only.

TABLE 1. Yields and physical constants of some methadone analogues and related compounds

Compound	*n*	% Yield*	Melting point* / Boiling point	% Calculated C	% Calculated H	% Calculated N	% Found C	% Found H	% Found N
9	2	74–82	157–158† 161–162	82.88	6.22	5.09	82.62	6.22	5.30
9	3	66–77	109–111	83.01	6.62	4.84	82.76	6.48	4.83
12	2	53–82‡	152–154§	70.03	6.64	7.10	69.98	6.77	7.06
12	3	25–32	76.5–77.5‖	82.92	8.23	8.80	82.95	8.29	8.87
13	2	18–25	92–93¶	82.04	8.20	4.56	82.01	8.11	4.54
7	2	25–41	140–145/0.01	82.34	8.71	4.18	82.42	8.79	4.14
7	3	15–27	150/0.005	82.47	8.94	4.01	82.78	8.86	4 09
16	2	50	140–150/0.01	82.47	8.94	4.01	82.58	8.90	4.09

*Yields refer to once crystallized or distilled products; the physical constants are those of the analytically pure compounds.
†This compound exhibited a double melting point.
‡Yield of amine.
§Melting point, and analysis of the acid oxalate salt.
‖After sublimation at 70 °/0.005 mm.
¶After sublimation at 80 °/0.005 mm.

TABLE 2. Spectral properties of some methadone analogues and related compounds

Compound	Infrared (cm^{-1})*	Nuclear magnetic resonance (δ)†
9 ($n = 2$)	2239,1707,1730	2.00(s,3H), 3.27(m,4H), 3.62(s,2H), 7.25(m,6H), 8.14(m,2H)‡
9 ($n = 3$)	2236,1715(sh),1727	1.62(m,2H), 1.85(s,3H), 2.54(m,4H), 3.69(d,2H),§ 7.18(m,7H), 7.75(m,1H)
12 ($n = 2$)	2235‖	0.75(m,3H),¶ 1.83(s,6H), 2.42(m,3H), 3.16(m,3H), 7.07(m,6H), 7.98(t,2H)**
12 ($n = 3$)	2233	0.55, 0.94(doublets 3H, $J = 6.6, 6.1$)††, 1.60(m,2H), 1.91, 2.06(singlets, 6H)††, 2.54(m,4H), 7.09(m,7H), 7.80(m,1H)
13 ($n = 2$)	1718	0.78(d,3H, $J = 6.0$), 1.83(s,6H), 2.53(m,3H), 3.22(s,4H), 7.32(m,8H), 9.79(s,1H)
7 ($n = 2$)	1713‖,‡‡	0.57(d,3H, $J = 6.4$), 0.77(t,3H, $J = 7.1$), 1.81(s,6H), 2.25(m,5H), 3.14(m,4H), 6.97(m,1H), 7.24(m,7H)
7 ($n = 3$)	1708‖,‡‡	0.57(m,3H, $J \approx 5$)§§, 0.82(t,3H,$J = 7.3$), 1.72(m,2H), 2.00(s,6H), 2.70(m,9H), 7.21(m,8H)
16	1710‖	0.75(q,6H, $J = 7.2$), 0.78(q,3H, $J = 7.1$), 2.18 (m,10H), 3.12(s,4H), 7.12(s,8H)

*Measured in chloroform (unless specified otherwise) with a Perkin–Elmer 237B grating spectrophotometer, or a Unicam SP-200G infrared spectrophotometer.
†Recorded with a Varian A-60A spectrometer in $CDCl_3$ containing tetramethylsilane as an internal standard; the solute concentration was about 10% by weight.
‡d = Doublet, m = multiplet, q = quartet, s = singlet, t = triplet; J values given in Hz.
§Two singlets, probably because of the proximate asymmetric carbon.
‖Measured as neat liquids.
¶Two overlapping doublets ($J \approx 4.5$) centered at 44 and 48 Hz.
**Width at half height (w_H) = 4 Hz.
††The resonances at δ 0.94 and 1.91 were due to an impurity (30–40%). They were also found in some samples of 7 ($n=3$) which were not rigorously purified.
‡‡The hydrochloride salts absorbed ($CHCl_3$) at 1707 ($n=2$) and 1708 ($n=3$) cm^{-1} respectively.
§§See footnote ¶¶ in Table 3.

TABLE 3. The n.m.r. parameters of methadone and some methadone analogues

Compound	Form	Chemical shift (Hz)*			
		Aryl	$N(CH_3)_2$	$CHCH_3$	$COCH_2CH_3$
1†	Base	439‡	127	29($J = 6.5$)§	50($J = 7.0$)
	HCl	446‡	165($J = 5$–5.5)‖	42($J = 6.5$)	50($J = 7.0$)
7 ($n = 2$)	Base	424†	108	34($J = 6.4$)¶	46($J = 7.1$)
	HCl	424**($w_H = 6$)	144($J = 5.0$)††	52.5($J \approx 6.0$)‡‡	49($J \approx 7.0$)‡‡
7 ($n = 3$)	Base	434**($w_H = 6$)§§ 418**($w_H = 20$)‖‖	120	34($J \approx 5$)¶¶	49($J = 7.3$)
	HCl	433**($w_H = 7$)§§ 398**($w_H = 10$)‖‖	160($J = 5.0$)[a]	35($J = 6.6$)	47($J = 7.2$)

*Solvent $CDCl_3$; solute concentration *ca.* 10% by weight.
†Data taken from ref. 17.
‡Narrow singlets.
§In methadone nitrile this absorption appeared at 54 Hz ($J = 6.5$).
‖Center of triplet formed by two overlapping doublets.
¶Doublet contained fine structure.
**Center of multiplet.
††Two doublets centered at 135 and 152 Hz, addition of D_2O caused collapse to a singlet at 144 Hz.
‡‡These absorptions overlapped to give a deformed triplet. After D_2O exchange a doublet ($J = 6.2$) at 51 Hz and a triplet centered at 49 Hz. ($J = 7.2$) was obtained.
§§Integrated intensity, 7H.
‖‖Integrated intensity, 1H.
¶¶Two doublets with fine structure centered at 33 and 35 Hz.
[a] Two doublets centered at 159 and 161 Hz, addition of D_2O caused collapse to a singlet at 163 Hz.

bromide salts at reflux temperature for *ca.* 2.5 days.

One example, **16**, of a compound related to normethadone (**1**, R = H) was prepared from the known (18) nitrile **15** and ethylmagnesium iodide.

The yields and physical constants of some of the above compounds are contained in Table 1, the n.m.r. and i.r. spectral data are compiled in Tables 2 and 3.

On the basis of physical and chemical evidence, Casy ((19) and refs. therein) proposed that the favored conformation of methadone and its salts in solution was probably represented by structure **17**. The non-equivalence of the *N*-methyl

Can. J. Chem. Downloaded from www.nrcresearchpress.com by 210.87.254.5 on 09/05/12
For personal use only.

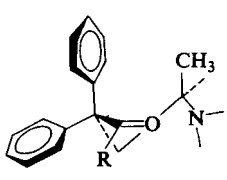

17

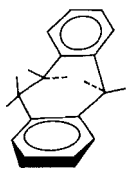

18

19

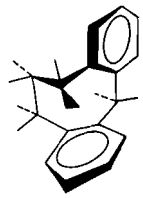

20

groups in the n.m.r. spectrum of methadone salts and the high field n.m.r. absorption of the secondary methyl group (in comparison to that of the corresponding nitrile for example; see Table 3) in methadone and its salts were consistent with this proposal.

An examination of Dreiding models of the seven- and eight-membered analogues of methadone (**7**, $n = 2, 3$) showed that the acyclic portions of these molecules could readily adopt a chair-like conformation virtually identical to that of methadone.[5] Furthermore, the flexible tetrahydrodibenzo[*a*,*d*]cyclooctene system in **7** ($n = 3$) could assume conformations varying from the favorable with aryl planes intersecting at 110° (*i.e.* **19**), to the relatively unfavorable with nearly (within 25°) bisecting aryl planes (*i.e.* **20**). On the other hand, the comparatively rigid dihydrodibenzo[*a*,*d*]cycloheptene system of **7** ($n = 2$) adopted a boat-like conformation (*i.e.* **18**)[6] with the aryl planes tilted about 60° from coplanarity.

One of the more salient observations to be made from the data shown in Table 3 was the similarity of the n.m.r. spectra of methadone free base and the eight-membered analogue **7** ($n = 3$). In addition, hydrochloride salt formation in this compound resulted in the anticipated downfield shift and non-equivalence of the *N*-methyl groups like that observed for methadone. In contrast to methadone, however, the chemical shift of the secondary methyl group[7] was not significantly altered on salt formation. This indicated that the expected deshielding was compensated for by an increase in aromatic shielding, perhaps as a result of a decrease in the conformational mobility of the acyclic portion of the molecule (see below). The non-equivalence of the *N*-methyl groups[8] and the unchanged chemical shift of the secondary methyl group in the salt, both were in support of a strong hydrogen bond between the carbonyl oxygen atom and the protonated amino group, probably in a conformation similar to that depicted by **17**.

The n.m.r. spectra of the seven-membered compound (**7**, $n = 2$) and methadone free base also showed similarities, but the *N*-dimethyl group was much more shielded than for methadone. Salt formation again produced the expected downfield shift of the *N*-dimethyl group but in this case the non-equivalence ($\Delta = 17$ Hz) of the *N*-methyl groups was much more dramatic. In addition, as for methadone, protonation of the dimethylamino group resulted in a concomitant deshielding of the secondary methyl hydrogens, but the magnitude of this shielding was larger than for methadone. The high field position of the *N*-dimethyl group in the base and the salt was interesting and was evidence for a conformation in which both *N*-methyl groups were specially shielded by the aromatic features of the molecule. This observation when viewed in conjunction with the high field position of the secondary

[5]The acyclic portions of the xanthene and thioxanthene compounds, **5** and **6**, and normethadone (**1**, $R = CH_3$) had about the same conformational mobility, but the aryl groups in **1** were restricted to within 35 ° of coplanarity.

[6]Two identical boat conformers, which differed only in the relative dispositions of the 5-substituents, were possible.

[7]The secondary methyl groups for several of the compounds listed in Tables 2 and 3 did not appear as simple doublets separated by J_{H-CH_3} (*e.g.* see footnotes ¶ and §§, Table 2). This phenomenon was probably due to virtual coupling (20) between the secondary methyl group and the β-methylene function. In these cases, the J_{H-CH_3} coupling constants should be viewed as being very approximate.

[8]A referee has pointed out that the non-equivalence of the *N*-methyl groups in the salts of methadone and **7** ($n = 2, 3$) is dependant on the proximity of the dimethylammonium group to an asymmetric carbon, and conformational preferences, and that pronounced chemical differences are evidence for marked conformational preferences (see ref. 21). In this connection, it is worth noting that salts of methadone nitrile do not show non-equivalent *N*-methyl groups. Further, the evidence for an intramolecular hydrogen bond in a conformation such as **17** for methadone salts is based on reactivity and i.r. data (see (19) and refs. therein), and pk_a measurements (23*b*), in addition to the n.m.r. studies cited above. Lastly, the above conformation is found in crystalline methadone hydrobromide as shown by X-ray data (see (19) and refs. therein).

Can. J. Chem. Downloaded from www.nrcresearchpress.com by 210.87.254.5 on 09/05/12
For personal use only.

Can. J. Chem. Downloaded from www.nrcresearchpress.com by 210.87.254.5 on 09/05/12
For personal use only.

methyl group (lower than methadone, but still shielded in comparison to the nitrile **12** (n = 2)), make it unlikely that **7** (n = 2) and methadone possess similar conformations.

Any apparent conformational similarities between **7** (n = 2, 3) and methadone were not mirrored by their physiological activities in laboratory animals (mice) since neither the seven- nor the eight-membered analogues had detectable analgesic activity (Eddy hot plate test) at dose levels of 150 and 50 mg/kg by the oral and subcutaneous route respectively.[9]

Portoghese has proposed (22, 23) that **21** may represent the manner in which methadone interacts with the "analgesic receptor" (⊖ represents an anionic site; ⊠ denotes an H-bonding proton donor dipole). Compounds **3–7**, and **16** clearly cannot adopt a conformation with bisected aryl planes as in **21** although **7** (n = 3) could approach

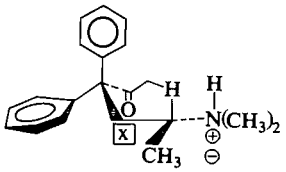

21

it. The lack of analgesic activity in compounds **7** (n = 2, 3) and **16** would seem to be consistent with the existence of such a conformation (*i.e.* **21**) at the receptor level.[10]

Experimental

The melting points were determined in a Gallenkamp melting point apparatus and are not corrected.

A solution of anhydrous *p*-toluenesulfonic acid was prepared by distilling off the benzene–water azeotrope from a benzene solution of *p*-toluenesulfonic acid monohydrate. The acid concentration was determined by titration of an aliquot with standard sodium hydroxide solution (phenolphthalein).

5-Cyano-10,11-dihydro-5*H*-dibenzo[*a*,*d*]cycloheptene (**8**, n = 2) and 12-cyano-5,6,7,12-tetrahydrodibenzo[*a*,*d*]-cyclooctene (**8**, n = 3) were prepared according to a published procedure (1).

The term "carbonate solution" used throughout the Experimental section refers to an aqueous solution of sodium carbonate (200 g/l).

*5-Cyano-5-acetonyl-10,11-dihydrodibenzo[a,d] cycloheptene (**9**, n = 2)*

A 60% dispersion of sodium hydride in mineral oil (2.00 g, 50 mmol) was freed of the carrier with hexane, covered with DMF (50 ml), and cooled to 0°. A solution of 1,3-dibromo-2-(tetrahydropyran-2-yloxy)propane (9.0 g, 30 mmol (13)) in dry DMF (10 ml) was added all at once and the cooling bath was removed. At 10°, hydrogen evolution became vigorous; the temperature was not allowed to exceed 25°. After 45 min, when gas evolution had become slow, the mixture was cooled to 0° or less, and the solid nitrile (**8**, n = 2; 4.38 g, 20 mmol) was added portion-wise while maintaining the temperature at 0°. The cooling bath was removed, and after 3.5 h at room temperature the solution was poured into a large volume of water. The product was extracted into benzene, the extract was dried over sodium sulfate and evaporated *in vacuo*. The oily enol ether was taken up in a solution consisting of methanol (180 ml) and 10% hydrochloric acid (20 ml), and heated at reflux temperature for 1 h. The solution was evaporated to a small volume *in vacuo* the residue was diluted with a large volume of water and the product was extracted into dichloromethane. The extract was dried over sodium sulfate, the solvent was removed *in vacuo* and the residue was crystallized from 2-propanol. The yield of product, m.p. 155–157°, was 4.07–4.51 g (74–82%). On recrystallization this material melted at 157–158°, resolidified, and then melted again at 161–162°.

*12-Cyano-12-acetonyl-5,6,7,12-tetrahydrodibenzo-[a,d]cyclooctene (**9**, n = 3)*

This compound, prepared in the same way as the corresponding seven-membered compound, was obtained in 66–77% yield.

*5-Cyano-5-(2-dimethylamino)propyl-10,11-dihydrodibenzo[a,d]cycloheptene (**12**, n = 2)*

(1) Leuckart Method

The ketone (2.75 g, 10 mmol), DMF (40 ml), and 90% formic acid (2 ml), were heated together at 190° in a stainless steel bomb for 42 h. The cooled solution was diluted with water, made alkaline with carbonate solution, and then extracted with benzene. The benzene phase was alternately extracted with 10% hydrochloric acid and water, dried over sodium sulfate, and evaporated *in vacuo*. The solid residue was crystallized from 2-propanol to give the recovered ketone, m.p. 156–157° then 160–161° (706–980 mg). The combined aqueous and acid extract from above was made alkaline with carbonate solution and the product was extracted into dichloromethane. The extract was dried over sodium sulfate and evaporated *in vacuo* giving an oil (1.53–1.84 g, 78–82% based on ketone consumed) which crystallized on standing. It was sufficiently pure to be used directly in the Grignard reaction. The acid oxalate, prepared in the manner described below, had m.p. 150–152°.

*(2) Borohydride Reduction of the Quaternary Imminium Tosylate **11** (n = 2)*

A mixture of the ketone (10 mmol) and *tris*-dimethylaminoarsine ((24); 2 ml, 2.25 g, 10.8 mmol) was heated

[9]The compounds were administered orally as dispersions (Tween) in water and subcutaneously as aqueous solutions of the non-crystalline hydrochloride salts. The activities were double checked to exclude possible animal variations. Compound **16** was inactive at an oral dose of 150 mg/kg.

[10]On the other hand, the significant activity shown by **3** and **5** is an enigma which will probably have to be accounted for in terms of some other mode of substrate–receptor interaction. It would also be of interest to determine if the thioxanthene compounds **6** (inactive at 10 mg/kg) had analgesic activity at the dose levels at which compounds **3** and **5** were reported to be active (10–40 mg/kg).

Can. J. Chem. Downloaded from www.nrcresearchpress.com by 210.87.254.5 on 09/05/12
For personal use only.

briefly at 200° to form a melt, and the melt was then placed in an oil bath at 145° until the evolution of dimethylamine was complete (10 min). To the cooled glass was added dry benzene (50 ml) and the mixture was stirred to effect solution of the enamine (i.r. 1614 cm^{-1} (neat)). To the stirred mixture was added a solution of anhydrous *p*-toluenesulfonic acid in benzene (75 ml; 6 mg/ml). After 1.5 h the solvent was removed *in vacuo*, dry DMF (75 ml) was added to the residue, and the mixture was cooled to 0° with stirring. Sodium borohydride (1.5 g) was added portionwise, and then stirring was continued at 0° for 0.5 h. The mixture was poured into ice-water containing some salt, this was shaken with benzene, filtered through Celite to break the emulsion, and the organic phase was separated and combined with a benzene extract of the aqueous phase. The extract was washed well with water, dried over sodium sulfate, and the solvent was removed *in vacuo*. The residual amine borane (i.r., 2375 cm^{-1}(neat)) was dissolved in 75% acetic acid (200 ml) containing 10% hydrochloric acid (2 ml), and the solution was heated on a steam bath for 2.5 h. The solvent was removed *in vacuo*, the residue was diluted with water, made basic with carbonate solution, and extracted with benzene. The organic phase was extracted with 10% hydrochloric acid, the acid phase was made alkaline with carbonate solution, and the liberated base was extracted into dichloromethane. The extract was dried over sodium sulfate and evaporated *in vacuo* leaving an oil (1.61–1.92 g, 53–63% yield) which usually crystallized on standing. It was further purified by conversion to the acid oxalate in 2-propanol. The yield of this salt, m.p. 149–152° was 40–49% based on the starting ketone. The pure base could be recovered from the oxalate in greater than 95% yield.

*12-Cyano-12-(2-dimethylamino)propyl-5,6,7,12-tetrahydrodibenzo[a,d]cyclooctene (**12**, n = 3)*

(a) Method 1

The Leuckart reaction was carried out in the same way as for the seven-membered ketone, however it was necessary to purify the cyano amine by dry column chromatography (25) on neutral alumina [Fluka, activity II, ratio of alumina to compound = 200 (by weight), elution solvent, 1% methanol in chloroform (v/v)] to free it of a more polar impurity. The yield of the pure amine was 14% based on starting material taken or 26% based on unrecovered starting material.

(b) Method 2

The reaction was carried out precisely as for the seven-membered compound except that the crude product was purified by dry column chromatography (neutral alumina, activity II) to remove two more polar side products. The column was developed with 2% methanol in chloroform. The amine, m.p. 75–77°, identical to that prepared by method 1, was obtained in 25–32% yield.

*5-Formyl-5-(2-dimethylamino)propyl-10,11-dihydrodibenzo[a,d]cycloheptene (**13**, n = 2) and 5-Propionyl-5-(2-dimethylamino)propyl-10,11-dihydrodibenzo[a,d]cycloheptene (**7**, n = 2)*

The cyano amine (**12**, $n = 2$) was reacted with 2 molar equiv. of ethylmagnesium bromide exactly as described by Attenburrow *et al.* (26). The reaction mixture was decomposed with 20% hydrobromic acid, and the acid phase was made alkaline with carbonate solution and extracted with dichloromethane. The extract was dried over sodium sulfate and evaporated *in vacuo* leaving an oil (2.3 g from 2.26 g of the nitrile) which was taken up in 20% hydrobromic acid (50 ml). Magnesium chloride hexahydrate (10 g) was added and after 12 h the solid was collected by filtration. It was immediately slurried in carbonate solution, and the liberated base was extracted into dichloromethane. The extract was dried over sodium sulfate and evaporated *in vacuo* leaving the crude crystalline aldehyde. This material was sublimed at 90°/0.005 mm to give the pure aldehyde m.p. 92–93° (410 mg, 18%). When ethylmagnesium iodide was used the yield of this product was 25%.

The acidic filtrate from above was made alkaline with carbonate solution and extracted with dichloromethane. The usual manipulations gave the imine (**14**, $n = 2$, i.r., 1640 cm^{-1}(neat), 1.41 g) which contained a trace of the aldehyde as shown by i.r. spectroscopy. Hydrogen bromide gas was bubbled through an ethereal solution of this mixture, the whole was evaporated *in vacuo*, and the residue was taken up in water (300 ml) and heated at reflux temperature for 48–66 h. The solution was made alkaline with carbonate solution and the liberated base was extracted into dichloromethane. After the usual work-up, the oily base was evaporatively distilled at 140–150°/0.005 mm to give a viscous oil (1.00 g, 41%). When ethylmagnesium iodide was used the yield of this base was 25%. We were not able to prepare any crystalline derivatives of this compound (*e.g.* oxalate, hydrochloride, hydrobromide, tartarate, etc.). For n.m.r. purposes, the hydrochloride was prepared by the addition of a dichloromethane solution of the base to a three-fold excess of dry hydrogen chloride in the same solvent. The solution was evaporated to dryness *in vacuo*, dichloromethane was added to the residue, and the solvent was again removed. This process was repeated two additional times and the solid foam thus obtained was dried *in vacuo* over calcium chloride for 12 h.

*12-Formyl-12-(2-dimethylamino)propyl-5,6,7,12-tetrahydrodibenzo[a,d]cyclooctene (**13**, n = 3) and 12-Propionyl-12-(2-dimethylamino)propyl-5,6,7,12-tetrahydrodibenzo[a,d]cyclooctene (**7**, n = 3)*

The Grignard reaction on the nitrile was carried out as for the corresponding seven-membered compound. The aldehyde–imine mixture was easily separated by dry column chromatography on neutral alumina (activity II) using 2% methanol in chloroform as the eluant. When ethylmagnesium iodide was used the yield of the oily aldehyde (i.r. 1723 cm^{-1}(neat)) was 26%. The aldehyde was not characterized further. The crude imine was produced in 38% yield (i.r. 1638 cm^{-1}(neat)). If ethylmagnesium bromide was used the yield of the aldehyde rose to 42% while that of imine dropped to 31%.

The imine was hydrolyzed in the usual manner. The crude product was evaporatively distilled at 150°/0.005 mm to give 15–27% of the pure ketone (based on starting nitrile). This base also did not give any crystalline salts with the usual acids. The hydrochloride salt (solid foam) was prepared in the same way as described for the seven-membered compound above.

*5-Cyano-5-diethylaminoethyl-10,11-dihydrodibenzo-[a,d]cycloheptene (**15**)*

This compound was prepared by the dropwise addition

of a toluene solution of *N,N*-diethyl-2-chloroethylamine to a solution of the nitrile (**8**, $n = 2$) in *t*-butanol containing sodium *t*-butoxide. The pure amino nitrile (80% yield) had physical constants in agreement with those reported by Davis *et al.* (18).

*5-Propionyl-5-diethylaminoethyl-10,11-dihydrodibenzo[a,d]cycloheptene (**16**)*

The reaction of **15** with ethylmagnesium iodide was carried out exactly as described by Attenburrow *et al.* (26) with the exception that the decomposition of the Grignard reaction mixture was carried out with 20% hydrobromic acid. The base was evaporatively distilled at 140–150°/0.01 mm to give a clear viscous oil (50% yield).

We thank Dr. T. Conway of these laboratories, and Professor B. Belleau of the University of Ottawa, Ottawa, Canada, for invaluable discussions concerning several aspects of this paper. We wish to thank Dr. R. Berman and J. C. Vigeant of the Pharmacology Division of these laboratories for making the mouse activity data on compounds 7, ($n = 2, 3$) and **16** available to us. The n.m.r. spectra were recorded by G. Lacasse whose efforts in this regard are gratefully acknowledged.

1. K. Ackermann, J. Chapuis, D. E. Horning, and J. M. Muchowski. Can. J. Chem. **47**, 4327 (1969).
2. R. A. Hardy, Jr. and M. G. Howell. Analgetics. *Edited by* G. deStevens. Academic Press, New York, N.Y., 1965. p. 234–236.
3. M. Bockmuhl and G. Ehrhart. Ann. **561**, 52 (1948).
4. O. J. Braenden, N. B. Eddy, and H. Halbach. Bull. Wld. Hlth. Org. **13**, 937 (1955).
5. P. A. J. Janssen. Synthetic analgesics. Part I. Diphenylpropylamines. Pergamon Press, London, 1960. p. 50–60.
6. P. A. J. Janssen and C. A. M. Van Der Eycken. Drugs affecting the central nervous system. *Edited by* A. Burger. Marcel Dekker, Inc., New York, N.Y., 1968. p. 48–51.
7. F. F. Blicke and J. Krapcho. J. Amer. Chem. Soc. **74**, 4001 (1952).
8. S. Lecolier. Chim. Ther. **3**, 34 (1968).
9. D. Shapiro. J. Org. Chem. **14**, 839 (1949).
10. D. Ginsberg and M. Baizer. J. Amer. Chem. Soc. **71**, 1500 (1949).
11. E. Kasztreiner and L. Vargha. Act. Chim. Acad. Sci. Hung. **32**, 473 (1962); Chem. Abstr. **58**, 11317 (1963).
12. J. F. Muren. J. Med. Chem. **13**, 140 (1969).
13. D. E. Horning, G. Kavadias, and J. M. Muchowski. Can. J. Chem. **48**, 975 (1970).
14. (*a*) H. S. Mosher and W. T. Mooney. J. Amer. Chem. Soc. **73**, 3948 (1951). (*b*) E. J. Blanz, Jr. and H. S. Mosher. J. Org. Chem. **23**, 492 (1958). (*c*) N. Rabjohn and E. L. Crow. J. Org. Chem. **28**, 2907 (1963).
15. H. J. Shine. J. Chem. Soc. 8 (1951).
16. J. F. Cavalla, R. Simpson, and A. C. White. Br. Pat. No. 1 124 682, 1968; Chem. Abstr. **70**, 28671*p* (1969).
17. P. Ofner and E. Walton. J. Chem. Soc. 2158 (1950).
18. M. A. Davis, S. O. Winthrop, J. Stewart, F. A. Sunahara, and F. Herr. J. Med. Chem. **6**, 251 (1963).
19. A. F. Casy. J. Chem. Soc. B, 1157 (1966).
20. F. A. L. Anet. Can. J. Chem. **39**, 2262 (1961).
21. M. van Gorkum and G. E. Hall. Quart. Rev. **22**, 14 (1968).
22. (*a*) P. S. Portoghese. J. Med. Chem. **8**, 609 (1965). (*b*) P. S. Portoghese. J. Med. Chem. **12**, 839 (1969).
23. P. S. Portoghese. J. Pharm. Sci. **55**, 865 (1966).
24. H. V. Hirsch. Chem. Ber. **100**, 1289 (1967).
25. (*a*) B. Loev and K. M. Snader. Chem. and Ind. 15 (1965). (*b*) B. Loev and M. M. Goodman. Chem. and Ind. 2026 (1967).
26. J. Attenburrow, J. Elks, B. A. Hems, and K. N. Speyer. J. Chem. Soc. 510 (1949).

Can. J. Chem. Downloaded from www.nrcresearchpress.com by 210.87.254.5 on 09/05/12
For personal use only.

Can. J. Chem. Downloaded from www.nrcresearchpress.com by 210.87.254.6 on 09/05/12
For personal use only.

Oligoribonucleotide Synthesis. II.[1] Preparation of 2′-*O*-tetrahydropyranyl Derivatives of Adenosine and Cytidine Necessary for Insertion in Stepwise Synthesis

THOMAS NEILSON AND EVA S. WERSTIUK
Department of Biochemistry, McMaster University, Hamilton, Ontario

Received July 30, 1970

The syntheses of N^6-benzoyl-2′-*O*-tetrahydropyranyladenosine (**2**) and N^4-benzoyl-2′-*O*-tetrahydropyranylcytidine (**11**) and their corresponding 5′-*O*-*p*-methoxytrityl derivatives, **3** and **12** respectively, are described. Compounds **2**, **3**, **11**, and **12** are the protected derivatives of adenosine and cytidine required for insertion into a new oligoribonucleotide synthesis. Compound **2** was prepared from the known 2′-*O*-tetrahydropyranyladenosine by perbenzoylation followed by de-*O*-benzoylation. Compound **11** is prepared from cytidine by the following sequence: orthoacetate protection of the 2′- and 3′-hydroxyls; benzoylation of the 5′- and N^4-positions; orthoacetate ring opening provided a mixture of the 2′- and 3′-monoacetates from which the major, 3′-*O*-acetyl-N^4,5′-*O*-dibenzoylcytidine (**7**) was isolated; dihydropyran treatment on the 2′-hydroxyl of **7** and subsequent selective deacylation studies were carried out. Specific de-*O*-acylation gave **11**.

Canadian Journal of Chemistry, 49, 493 (1971)

Synthesis of oligoribonucleotides of defined length and sequence is essential for the investigation of the many remaining problems surrounding the phenomenon of protein synthesis, in particular, the nature of transfer RNA binding sites in aminoacyl synthetases and ribosomes. Although enzymic synthesis can supply a few oligonucleotides of this type, at present only chemical synthesis is potentially capable of supplying all possible combinations. Additional advantages inherent in chemical synthesis stem from its ready extension to the preparation of analogues, for example, changing the bases of any given sequence, say one at a time.

No synthetic material longer than a triribonucleotide has been made by purely chemical means following the preparation of the 64 triplets by Lohrmann *et al.* (2). Their approach was relatively laborious and tended to be inefficient resulting often in yields of a few o.d. units. Two developments however, have encouraged further interest in this general area.

(*a*) Ready solubility of tertiary phosphates in non-polar solvents means that relatively large quantities of intermediates can be handled by silica gel chromatography (3–5). Consequently the slower DEAE–cellulose chromatographic procedures can be by-passed, at least until after the various protecting groups have been removed late in overall synthesis.

(*b*) Removal of the *O*-tetrahydropyranyl grouping can be accomplished using mild mineral acid (p*H* 2) (6) with negligible isomerization of the diphosphate ester linkage. Consequently certain acid-labile protecting groups can also be used to protect the hydroxyl groups of the ribofuranoside ring.

A new stepwise oligoribonucleotide synthesis incorporating these salient features has been developed (1) and its relative convenience illustrated by the synthesis of uridyl[3′–5′]uridyl[3′–5′]uridine (UpUpU) from 2′-*O*-tetrahydropyranyluridine. To show the general nature of this synthetic procedure, 2′-*O*-tetrahydropyranyl derivatives of adenosine, cytidine, and guanosine must be available to allow preparation of oligonucleotides of any sequence. Although the uracil base requires no protection, the amino groups of adenine, cytosine, and guanine must be protected to ensure efficient 3′–5′ diphosphate coupling. *N*-Aroyl groups, in particular *N*-benzoyl and anisoyl, are most often used for this purpose.

In this communication we describe the synthesis of protected intermediates, N^6-benzoyl-2′-*O*-tetrahydropyranyladenosine (**2**) and N^4-benzoyl-2′-*O*-tetrahydropyranylcytidine (**11**) and their corresponding 5′-*O*-*p*-methoxytrityl derivatives, **3** and **12** (the latter pair destined to become the precursors of the 5′-terminal nucleoside unit of an oligoribonucleotide). Subsequent stepwise incorporation of these compounds into a linear sequence by diphosphate coupling will provide synthesis of protected oligoribonucleotides

[1]For part 1 see ref. 1.

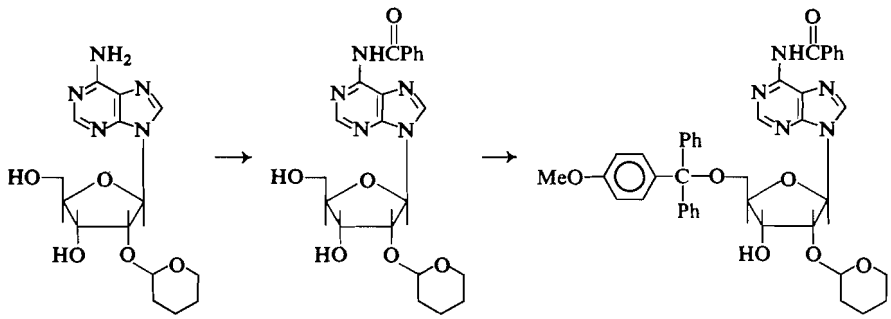

1 2 3

containing any predetermined sequence of uridine, adenosine, and cytidine.

2′-*O*-Tetrahydropyranyladenosine (**1**) was prepared by the method of Griffin *et al.* (6). The better crystallizing lower R_F diastereoisomer was used in subsequent conversions to ensure complete and specific blocking of the 2′-position of adenosine. This will guarantee high fidelity in all future 3′–5′ internucleotidic linkages.

Benzoylation of **1** in pyridine followed by careful de-*O*-benzoylation (7) gave N^6-benzoyl-2′-*O*-tetrahydropyranyladenosine (**2**) in 87% yield as a solid foam. Treatment of **2** with 1 equiv of *p*-anisylchlorodiphenylmethane in pyridine gave the expected N^6-benzoyl-5′-*O*-*p*-methoxytrityl-2′-*O*-tetrahydropyranyladenosine (**3**) in 88% yield.

Treatment of 2′,3′-*O*-methoxyethylidenecytidine (**5**) (8) with benzoyl chloride in pyridine gave N^4,5′-*O*-dibenzoyl-2′,3′-*O*-methoxyethylidenecytidine (**6**) in 95% yield over two steps from cytidine (4). Treatment with 5% acetic acid opened the cyclic orthoacetate ring system to give a mixture of the 3′- and 2′-*O*-acetyl derivatives, **7** and **8**. The p.m.r. data indicated an approximate 3:1 mixture of the isomers. Fractional crystallization gave 3′-*O*-acetyl-N^4,5′-*O*-dibenzoylcytidine in 35% yield. The p.m.r. data of the 3′-*O*-acetate, **7**, agreed with the empirical rules established by Fromageot *et al.* (9).

Deacylation studies on **7** showed that it was possible to remove the protecting groups selectively. Half-saturated methanolic ammonia treatment for 2.5 h at ambient temperature gave 85% yield of the N^4,5′-*O*-dibenzoylcytidine (**9**). Sodium hydroxide (0.5 *N*) treatment on **7** in ethanol–pyridine solution gave N^4-benzoylcytidine in 57% yield. Prolonged methanolic ammonia exposure on **7** for 2 days at ambient temperature gave cytidine (**4**) in 69% yield. Such mild conditions for the removal of an *N*-benzamido group should prove useful in an oligoribonucleotide deblocking procedure.

Reaction of **7** with dihydropyran and *p*-toluenesulfonic acid in anhydrous dioxan gave the corresponding 2′-*O*-tetrahydropyranyl derivative which on immediate de-*O*-acylation using methanolic ammonia, gave a diastereoisomeric mixture of N^4-benzoyl-2′-*O*-tetrahydropyranylcytidine (**11**). Silica gel column chromatography separated this mixture into low R_F (high melting) and high R_F (low melting) components in 30 and 34% yields respectively. Treatment of **11** (low R_F) with 1 equiv of *p*-anisylchlorodiphenylmethane in anhydrous pyridine gave the expected N^4-benzoyl-5′-*O*-methoxytrityl-2′-*O*- tetrahydropyranylcytidine (**12**) in 96% yield.

A further check on exclusive 2′-*O*-tetrahydropyranyl substitution of cytidine was provided by preparing **11** from 3′-*O*-acetyl-N^4-benzoyl-5′-*O*-methoxyacetylcytidine (**15**). The isolation of **15** and its 2′-isomer **16** as crystalline solids has been reported (10), thorough p.m.r. and chemical studies on this pair being carried out to ascertain their substitution pattern. Unfortunately no preparative data exist for these compounds and so **15** was prepared in the following manner.

Cytidine (**4**) was converted to its N^4-benzoyl derivative **10** in 59% yield by reaction of benzoic anhydride in methanol. Trimethyl orthoacetate treatment of **10** in anhydrous acidic conditions gave N^4-benzoyl-2′,3′-*O*-methoxyethylidinecytidine (**13**) as a glass in 90% yield. Reaction of **13** with methoxyacetic acid[2] activated by triiso-

[2]This constitutes a convenient general method for esterification as it uses the more stable and more readily available free carboxylic acids rather than their corresponding acid chlorides or anhydrides.

Can. J. Chem. Downloaded from www.nrcresearchpress.com by 210.87.254.6 on 09/05/12
For personal use only.

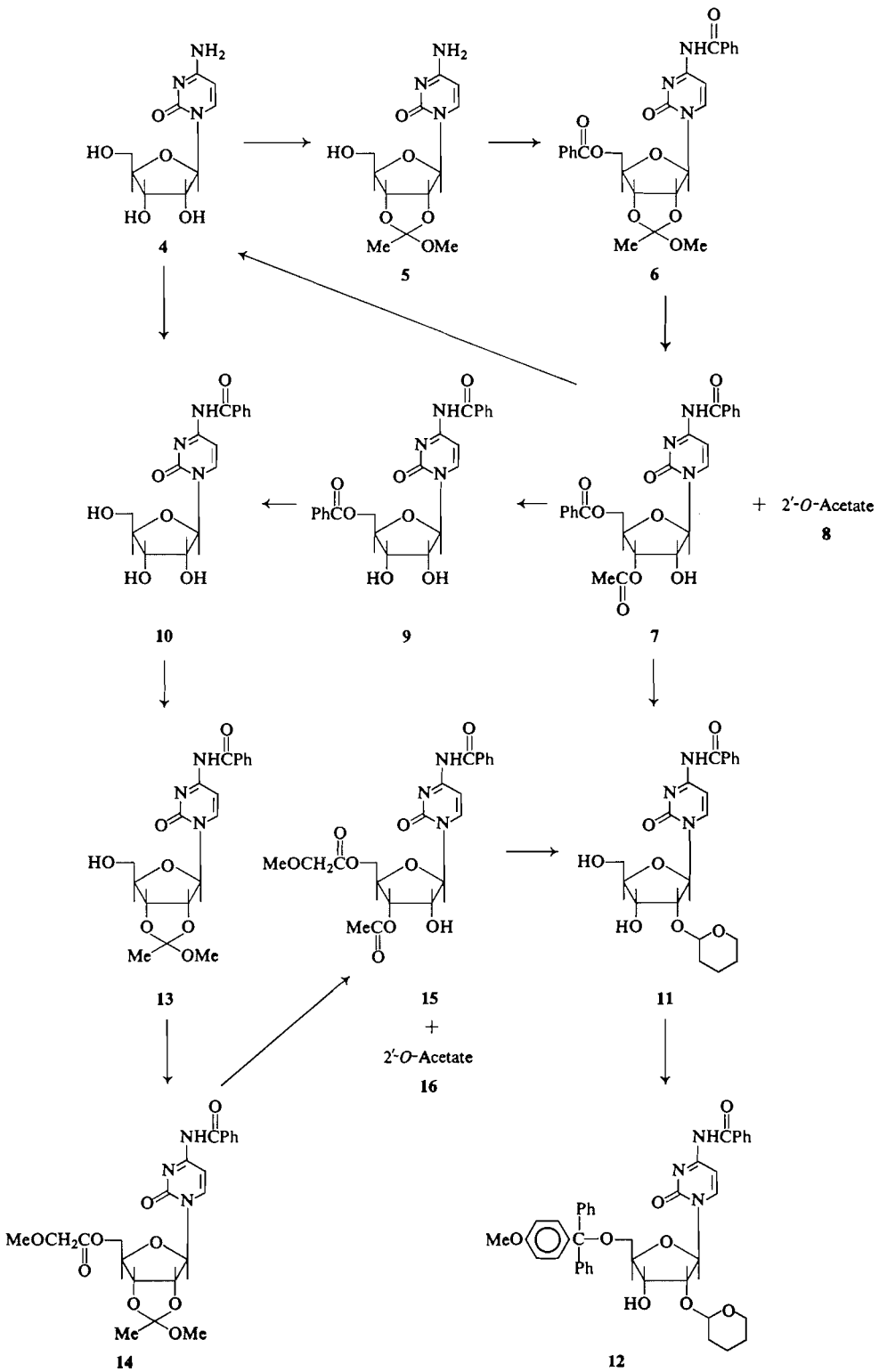

Can. J. Chem. Downloaded from www.nrcresearchpress.com by 210.87.254.6 on 09/05/12
For personal use only.

Can. J. Chem. Downloaded from www.nrcresearchpress.com by 210.87.254.6 on 09/05/12
For personal use only.

propylbenzenesulfonyl chloride in pyridine gave the corresponding 5′-*O*-methoxyacetate (**14**) as a solid foam. Orthoacetate ring opening of **14** using aqueous 5% acetic acid solution gave the expected mixture of 2′- and 3′-*O*-acetate isomers **15** and **16** in 33% yield over the last two steps. Fractional crystallization of this mixture gave a sample of pure 3′-*O*-acetate (**15**). Condensation of **15** with dihydropyran and subsequent methanolic ammonia treatment gave a diastereoisomeric mixture of N^4-benzoyl-2′-*O*-tetrahydropyranylcytidine (**11**) which on silica gel column chromatography gave identical samples of the components obtained by the route described above.

Thus, suitably protected intermediates are available for insertion into the stepwise synthesis (1). Work describing the triphosphate coupling reactions and subsequent deblocking procedures to give oligoribonucleotides of predetermined sequence and length is in progress.

Experimental

Melting points were taken on a Gallenkamp hot-block melting point apparatus and are uncorrected. The p.m.r. spectra were recorded on a Varian T60 spectrometer in 10–15% (w/v) DMSO-d_6 – D_2O solutions, and line positions are reported in p.p.m. from the reference (TMS). Mass spectra were determined on an Associated Electrical Industries MS-9 double focusing high resolution mass spectrometer. Silica gel (Baker Analyzed Reagent) was used for column chromatography; and Analtech prescored silica gel plates were employed for t.l.c. The plates were developed in 5 or 10% methanol in methylene chloride mixtures.

N^6-Benzoyl-2′-O-tetrahydropyranyladenosine (2)

The lower R_F component of the diastereoisomeric mixture of 2′-*O*-tetrahydropyranyladenosine (**1**) was prepared from adenosine (6). Compound **1** (1 g) was dissolved in anhydrous pyridine (10 ml) and the solution cooled to 0°. Benzoyl chloride (2 ml) was added dropwise, the reaction mixture stirred for 2 h, and then allowed to return to ambient temperature whereupon pyridine hydrochloride separated. The use of t.l.c. in 5% CH_3OH–CH_2Cl_2 showed the reaction to be complete (R_F 0.1 → 0.9). Ice (2–3 g) was added and the quenching allowed to proceed for 20 min. The mixture was poured into water (100 ml) and the solution extracted with methylene chloride (3 × 50 ml). The combined extracts were washed with water (2 × 50 ml) and evaporated *in vacuo* to give an oil. The crude tribenzoate was dissolved in a solution mixture of ethanol (15 ml) and pyridine (8 ml). A sodium hydroxide (2*N*) solution (16 ml) and additional ethanol (16 ml) were added. The de-*O*-benzoylation was allowed to proceed for *only* 5 min, then Dowex-50 resin (pyridinium form) was added to the reaction mixture until the solution p*H* was approximately 7. The t.l.c. in 5% CH_3OH–CH_2Cl_2 showed complete conversion (R_F 0.9 → 0.3). The resin was removed by filtration and the filtrate was reduced to a third of its volume by evaporation *in vacuo* whereupon it was extracted by methylene chloride (4 × 20 ml). The combined extracts were washed with water (2 × 25 ml) and evaporated *in vacuo* to a solid foam, the last traces of pyridine being removed by co-distillation *in vacuo* with toluene (2 × 20 ml). This foam was subjected to silica gel column chromatography and N^6-benzoyl-2′-*O*-tetrahydropyranyladenosine was obtained as a solid foam (1.13 g, 87%) upon elution with 2% CH_3OH–CH_2Cl_2. Crystallization could not be effected but the material was sufficiently pure for further conversions.

The p.m.r. spectrum showed signals (δ TMS) at 8.82 and 8.78 (2H, 2 singlets; 2 and 8 protons of adenine); 7.95 (2H, multiplet; *o*-benzoate protons); 7.55 (3H, multiplet; other benzoate protons); 6.26 (1H, doublet $J \sim 6$ Hz; 1′-anomeric proton); 4.88 (1H, triplet $J \sim 5$ Hz; 3′-sugar proton); 4.73 (1H, singlet; THP acetal proton); 4.42 and 4.11 (1H each, multiplets; 2′- and 4′-sugar protons); 3.72 (4H, multiplet; *O*-methylene of THP and 5′-sugar protons); and 1.60 p.p.m. (6H, multiplet; *C*-methylene THP protons).

Anal. Calcd. for $C_{22}H_{25}N_5O_6$ (mol. wt. 455.46): N, 15.3. Found: N, 14.7. The mass spectrum of N^6-benzoyl-2′-*O*-tetrahydropyranyladenosine (recorded at 250–260°, probe 1) showed a strong M^+ peak at 455 *m/e*; and further peaks at 426 (M-29, loss of CHO); 351 (M-104, loss of C_6H_5CO—); 266 (M-189, loss of C_6H_5CO— and THP); 136, 135 (M-319, and M-320 respectively, loss of C_6H_5CO—, THP and ribose).

N^6-Benzoyl-5′-O-p-methoxytrityl-2′-O-tetrahydropyranyladenosine (3)

N^6-Benzoyl-2′-*O*-tetrahydropyranyladenosine (280 mg) was dissolved in anhydrous pyridine (2 ml) and methylene chloride (10 ml). *p*-Anisylchlorodiphenylmethane (280 mg, 1.1 equiv) was added and the reaction mixture was sealed and left overnight in the dark at ambient temperature. The t.l.c. in 5% CH_3OH–CH_2Cl_2 showed the reaction was complete (R_F 0.3 → 0.9). The reaction was quenched with ethanol (2 ml) and poured into water (25 ml). The mixture was extracted with methylene chloride (3 × 25 ml). The combined extracts were washed with water (3 × 25 ml) and evaporated *in vacuo* to a gum, the last traces of pyridine being removed by co-distillation *in vacuo* with toluene (2 × 20 ml). Column chromatography on silica gel was applied. Elution with 1% CH_3OH–CH_2Cl_2 gave the desired 5′-*O*-monotrityl material as a solid foam (390 mg, 88%) which was sufficiently pure for oligonucleotide coupling reactions. The p.m.r. spectrum showed signals (δ TMS) at 8.20 and 8.12 (2H, 2 singlets; 2 and 8 protons of adenine); 7.65 (2H, multiplet; *o*-benzoate protons); 7.15 (3H, multiplet; other benzoate protons); 6.90 (14H, multiplet; trityl aromatic protons); 5.95 (1H, doublet $J \sim 5$ Hz; 1′-anomeric proton); 4.80 (1H, triplet $J \sim 4$ Hz; 3′-sugar proton); 4.57 (1H, singlet; THP acetal proton); 4.41 and 4.11 (1H each, multiplets; 2′- and 4′-sugar protons); 3.62 (4H, multiplet; *O*-methylene of THP and 5′-sugar protons); 3.41 (3H, singlet; MeO of *p*-methoxytrityl); and 1.6 p.p.m. (6H, broad multiplet; *C*-methylenes of THP).

2′,3′-O-Methoxyethylidenecytidine (5)

This compound was prepared in 95% yield as described

Can. J. Chem. Downloaded from www.nrcresearchpress.com by 210.87.254.6 on 09/05/12
For personal use only.

(8) and was used in the next reaction without further purification.

*N^4-5′-O-Dibenzoyl-2′,3′-O-methoxyethylidenecytidine (**6**)*

Benzoyl chloride (2.5 ml, 0.021 mol) was added dropwise, with stirring to a cooled (ice) solution of 2′,3′-*O*-methoxyethylidenecytidine (**5**) (2.95 g, 0.01 mol) in anhydrous pyridine (30 ml). When the addition was completed, the reaction mixture was allowed to warm up to room temperature and stirred for a further 1 h. The t.l.c. indicated complete conversion into a product of R_F: 0.85 in 10% CH_3OH–CH_2Cl_2. Water was then added (1 ml) and stirring continued for a further 1 h. The reaction mixture was then concentrated *in vacuo* to *ca.* 10 ml, dilute triethylammonium bicarbonate buffer (p*H* 7.5) was added (25 ml), and the product extracted repeatedly with chloroform (3 × 25 ml). The combined organic extracts were washed, dried (Na_2SO_4), and evaporated to dryness *in vacuo*. The pale yellow glass (4.34 g, 86%, R_F: 0.85 in 10% CH_3OH–CH_2Cl_2) was used in the next reaction without further purification.

*3′-O-Acetyl-N^4-5′-O-dibenzoylcytidine (**7**)*

A mixture of N^4-5′-*O*-dibenzoyl-2′,3′-*O*-methoxyethylidenecytidine (**6**) (4.34 g, 0.0086 mol) and 5% acetic acid (50 ml) was stirred at room temperature. After 30 min t.l.c. indicated the presence of products of R_F: 0.89, 0.80, and 0.66 in 10% CH_3OH–CH_2Cl_2. The reaction mixture was then repeatedly extracted with methylene chloride (4 × 25 ml), the combined organic extracts were washed, dried (Na_2SO_4), and evaporated *in vacuo*. The colorless glass (4.08 g) was purified by chromatography on silica gel (60 g) in methylene chloride. Elution with 2% methanol – methylene chloride (400 ml) and 2.5% methanol – methylene chloride mixtures (400 ml) gave a mixture of **7** and **8** (1.85 g, 44% yield, R_F: 0.66 in 10% CH_3OH–CH_2Cl_2).

Pure 3′-*O*-acetyl-N^4-5′-*O*-dibenzoylcytidine (**7**), 1.48 g, 35% yield of m.p. 192–194°, was obtained by crystallization from absolute ethanol (50 ml). The p.m.r. spectrum showed signals (δ TMS) at 8.28–7.28 (12H, multiplet, two C_6H_5CO—, and 6-, 5-cytidine protons); 5.90 (1H, doublet, $J \sim 5$ Hz; 1′-anomeric proton); 5.12 (1H, triplet; 2′-sugar proton) and at 2.1 p.p.m. (3H, sharp singlet; —$COCH_3$ protons).

Anal. Calcd. for $C_{25}H_{23}N_3O_8$ (mol. wt. 492.46): C, 60.85; H, 4.70; N, 8.52. Found: C, 60.36; H, 4.71; N, 8.26.

Concentration of the mother liquor to a small volume yielded a *ca.* 1:1 mixture of N^4-benzoyl-2′(3′)-*O*-acetates **8** and **7** respectively of m.p. 177–185°. The p.m.r. spectrum showed signals (δ TMS) at 5.99 (1H, two doublets of the 1′-anomeric protons of **7** and **8** superimposed); 5.48 and 5.23 (1H, two triplets of 2′-proton of **7** and 3′-proton of **8** superimposed); and at 2.18 and 2.15 p.p.m. (3H, two sharp singlets; of 3′-$COCH_3$ protons of **7** and 2′-$COCH_3$ protons of **8** respectively).

*N^4-Benzoyl-2′-O-tetrahydropyranylcytidine (**11**)*

(*a*) A solution of *p*-toluenesulfonic acid monohydrate (0.86 g, 4.3 mmol) in dry dioxan (15 ml) containing molecular sieves (0.25 g) was cooled in ice until solidified. Dihydropyran (5.24 g, 6.0 ml; 0.062 mol) was then added dropwise with stirring, followed by a suspension of 3′-*O*-acetyl-N^4-5′-*O*-dibenzoylcytidine (3.0 g, m.p. 190–192°; 0.06 mol, R_F: 0.62 in 10% CH_3OH–CH_2Cl_2) in dry dioxan (15.0 ml). The reaction mixture was then allowed to warm up to room temperature (*ca.* 10 min) and kept at this temperature with continued stirring. After 2 h t.l.c. indicated complete conversion into products of R_F: 0.84 and 0.73 in 10% CH_3OH–CH_2Cl_2. The colorless solution was then cooled in ice and neutralized with concentrated ammonia. The precipitated ammonium tosylate was filtered off, washed well with methylene chloride, and the combined filtrate and washings evaporated *in vacuo*. The yellow oil (3.2 g) obtained was suspended in a mixture of ethanol (30 ml) and pyridine (15 ml), and 50% ethanolic sodium hydroxide (containing 15 ml 2 *N* NaOH and 15 ml absolute ethanol) was added with stirring, and the reaction mixture set aside at room temperature. After 5 min t.l.c. indicated two products of R_F: 0.69 and 0.61 in 10% CH_3OH–CH_2Cl_2 in about 1:1 proportion. The p*H* of the solution was then adjusted to 7.0 with Dowex 50W-X8 resin (pyridinium form). The resin was then filtered off, washed well with methylene chloride – ethanol, and the combined filtrate and washings evaporated *in vacuo*. The resulting mixture of diastereoisomers was separated on silica gel (40 g) in methylene chloride. Elution with 3% methanol – methylene chloride mixture (400 ml) yielded 0.88 g (34.1%) of the low m.p. diastereoisomer of R_F: 0.61 in 10% CH_3OH–CH_2Cl_2. Continued elution with 4% methanol – methylene chloride mixture (200 ml) gave 0.46 g (17.8%) of a mixture of the two diastereoisomers R_F: 0.61 and 0.54 in 10% CH_3OH–CH_2Cl_2. Finally, the high m.p. isomer of R_F: 0.54 (0.41 g, 15.5%) was obtained on elution with 4.0–4.5% methanol – methylene chloride mixtures (200 + 400 ml). The mixture of diastereoisomers (0.46 g; R_F: 0.61 and 0.54 in 10% CH_3OH–CH_2Cl_2) was rechromatographed on silica gel (15 g) to yield further 0.38 g (14.5%) of the high m.p. diastereoisomer of R_F: 0.54. An analytically pure sample of m.p. 162–164°, R_F: 0.61 was prepared by crystallization from methylene chloride – hexane. Its p.m.r. spectrum showed signals (δ TMS) at 8.05–7.25 (6H, multiplet, C_6H_5CO—, and 5-cytidine proton); 5.85 (1H, singlet, 1′-anomeric proton); 5.02 (1H, singlet, acetal proton of THP); 3.78 (4H, —O—CH_2— protons of THP and 5′-sugar protons); and a broad peak at 1.6 p.p.m. (6H, multiplet, THP protons).

Anal. Calcd. for $C_{21}H_{25}N_3O_7$ (mol. wt. 431.43): C, 58.46; H, 5.84; N, 9.74. Found: C, 58.33; H, 5.61; N, 9.27.

Crystallization from methylene chloride – hexane provided an analytical sample of m.p. 194–196° of the other isomer of R_F: 0.54 (Reese reported (11) m.p. 195–197°). Its p.m.r. spectrum showed signals (δ TMS) at 8.45 (1H, doublet, $J \sim 8$ Hz; 6-cytidine proton); 8.08–7.2 (6H, multiplet, C_6H_5CO—, and 5-cytidine proton); 6.03 (1H, doublet, $J \sim 4$ Hz; 1′-anomeric proton); 4.80 (1H, singlet, acetal proton of THP); and a broad peak at 1.58 p.p.m. (6H, multiplet, THP protons).

Anal. Calcd. for $C_{21}H_{25}N_3O_7$ (mol. wt. 431.43): C, 58.46; H, 5.84; N, 9.74. Found: C, 58.55; H, 5.82; N, 8.94.

(*b*) A solution of *p*-toluenesulfonic acid monohydrate (142 mg, 0.75 mmol) in dry dioxan (5 ml) containing molecular sieves (0.05 g) was cooled in ice till solidified.

Can. J. Chem. Downloaded from www.nrcresearchpress.com by 210.87.254.6 on 09/05/12
For personal use only.

Dihydropyran (0.92 g, 1 ml, 1.1 mmol) was then added dropwise with stirring, followed by a suspension of 3′-*O*-acetyl-N^4-benzoyl-5′-*O*-methoxyacetylcytidine (**15**) (0.461 g, 1.0 mmol; m.p. 95–97° R_F: 0.69 in 10% CH_3OH–CH_2Cl_2) in dry dioxan (2.5 ml). The reaction mixture was then allowed to warm up to ambient temperature (*ca.* 10 min) and maintained with continued stirring. After 3.5 h, t.l.c. indicated complete conversion into products of R_F: 0.93 and 0.86 in 10% CH_3OH–CH_2Cl_2. The colorless solution was then cooled in ice, neutralized with concentrated ammonia, the precipitated ammonium tosylate filtered off, and washed well with methylene chloride and the combined filtrate and washings evaporated *in vacuo*. The yellow oil obtained was suspended in a mixture of ethanol(5.0 ml) – pyridine(2.5 ml), 50% ethanolic sodium hydroxide (containing 2.5 ml 2 N NaOH and 2.5 ml absolute ethanol) was added with stirring, and the reaction mixture set aside at room temperature. After 5 min, t.l.c. indicated two products of R_F: 0.69 and 0.61 in 10% CH_3OH–CH_2Cl_2. The p*H* of the solution was then adjusted to 7.0 with Dowex 50W-X8 resin (pyridinium form). The resin was then filtered off, washed well with methylene chloride – ethanol, and the combined filtrate and washings evaporated *in vacuo*. The resulting colorless glass (0.4 g) was purified by chromatography on silica gel (15 g) in methylene chloride. Elution with 3% methanol – methylene chloride mixture (200 ml) first yielded pure N^4-benzoyl-2′-*O*-tetrahydropyranylcytidine (62 mg, 14%; R_F: 0.61); then some mixture (0.044 g, R_F: 0.69 and 0.61). The second diastereoisomer (0.161 g, 37%; R_F: 0.61) was obtained on further elution with 4% methanol – methylene chloride mixture (200 ml). An analytical sample of m.p. 193–195°, R_F: 0.61 was obtained by crystallization from methylene chloride – hexane. The p.m.r. spectrum was identical with that of a sample obtained from the N^4-5′-*O*-dibenzoyl-3′-*O*-acetylcytidine (**7**) prepared previously (*a*).

*N^4-Benzoyl-5′-O-p-methoxytrityl-2′-O-tetrahydropyranylcytidine (**12**)*

N^4-Benzoyl-2′-*O*-tetrahydropyranylcytidine (**11**) (107 mg, 0.25 mmol; m.p. 193–195°; R_F: 0.54 in 10% CH_3OH–CH_2Cl_2) was evaporated from anhydrous pyridine (2 × 10 ml) and finally its volume reduced to *ca.* 3 ml. *p*-Anisylchlorodiphenylmethane (90 mg, 0.27 mmol; 1.1 equiv) was added and the reaction mixture set aside at room temperature in the dark. After 16 h t.l.c. indicated the presence of a product of R_F: 0.73 and some starting material of R_F: 0.51 in 10% CH_3OH–CH_2Cl_2. Further amount of the reagent (45 mg, 0.13 mmol) was then added, and the reaction allowed to continue till completed (*ca.* 2–3 days). Absolute ethanol (5 ml) was then added, and the mixture evaporated *in vacuo*. The resulting oil was dissolved in methylene chloride, washed with water, and evaporated to dryness *in vacuo*. The last traces of pyridine were removed by co-distillation with toluene (2 × 5 ml). The colorless glass (280 mg) obtained was purified by chromatography on silica gel (12 g) in methylene chloride. Elution with 1–2% methanol – methylene chloride mixtures (200 + 200 ml) yielded N^4-benzoyl-5′-*O*-*p*-methoxytrityl-2′-*O*-tetrahydropyranylcytidine (**12**) (170 mg, 96%) (R_F: 0.73 in 10% CH_3OH–CH_2Cl_2). The p.m.r. spectrum showed signals (δ TMS) at 8.35–6.85 (21H, multiplet, C_6H_5CO—, 6-, and 5-cytidine protons; and *p*-methoxytrityl protons); 6.10 (1H, doublet $J \sim 2$ Hz; 1′-anomeric proton); 4.98 (1H, broad singlet, acetal proton of THP); 3.68 (3H, sharp singlet; OCH_3); and 1.62 p.p.m. (6H, broad multiplet; THP protons).

*Selective De-O-acylation of 3′-O-Acetyl-N^4-5′-O-dibenzoylcytidine (**7**)*

*(a) N^4-Benzoylcytidine (**10**)*

To a stirred suspension of 3′-*O*-acetyl-N^4-5′-*O*-dibenzoylcytidine (**7**) (200 mg, 0.4 mmol, m.p. 188–190°, R_F: 0.62 in 10% CH_3OH–CH_2Cl_2) in ethanol (1.0 ml) and pyridine (0.5 ml), 50% ethanolic sodium hydroxide (containing 0.5 ml of 2 *N* NaOH and 0.5 ml of absolute ethanol) was added at room temperature. The clear solution obtained was stirred for 5 min, when t.l.c. indicated complete conversion into a product of R_F: 0.16 in 10% CH_3OH–CH_2Cl_2. The p*H* of the solution was then adjusted to 7.0 with Dowex 50W-X8 resin (pyridinium form), the resin was filtered off, washed well with methanol – methylene chloride, and the combined filtrate and washings evaporated *in vacuo*. The white crystals of N^4-benzoylcytidine (**10**) (82 mg, 57%) had m.p. 220–222° (dec.) R_F: 0.16 in 10% CH_3OH–CH_2Cl_2; lit. m.p. 219–220° (12).

The p.m.r. spectrum showed signals (δ TMS) at 8.55 (1H, doublet, $J \sim 8$ Hz; 6-cytidine proton); 7.35 (1H, doublet, $J \sim 8$ Hz; 5-cytidine proton); 8.15–7.40 (5H, multiplet, C_6H_5CO—); and 5.90 p.p.m. (1H, doublet, $J \sim 3$ Hz; 1′-anomeric proton). N^4-Benzoylcytidine (**10**) was also prepared from cytidine by selective benzoylation.

A mixture of cytidine (5.0 g, 0.02 mol) in methanol (250 ml) and benzoic anhydride (1.0 g, 4.4 mmol) was heated under reflux. Further portions of benzoic anhydride (5 × 1 g, 0.022 mol) were added at *ca.* 1 h intervals. After the addition was completed (total added 6.0 g, 0.026 mol) the reaction mixture was cooled, and the precipitated N^4-benzoylcytidine (1.77 g, R_F: 0.16 in 10% CH_3OH–CH_2Cl_2) was filtered off. The t.l.c. indicated still some unreacted starting material (R_F: at origin in 10% CH_3OH–CH_2Cl_2), so the filtrate was concentrated *in vacuo* to *ca.* 150 ml, and was again heated under reflux with further portions of benzoic anhydride (3 × 1 g, 1.3 mmol). On cooling further 2.33 g of product (R_F: 0.16 in 10% CH_3OH–CH_2Cl_2) was filtered off. Total obtained: 4.1 g, m.p. 220–222° (dec.) 59%. The sample of N^4-benzoylcytidine (**10**) was identical with that obtained above (*a*) from (**7**) as confirmed by its p.m.r. spectrum.

*(b) N^4-5′-O-dibenzoylcytidine (**9**)*

3′-*O*-Acetyl-N^4-5′-*O*-dibenzoylcytidine (**7**) (200 mg, 0.4 mmol; m.p. 188–190°, R_F: 0.62 in 10% CH_3OH–CH_2Cl_2) was suspended in dilute methanolic ammonia (4 ml, prepared by diluting saturated (at 20°) methanolic ammonia with an equal volume of methanol) and stirred at room temperature. After 2.5 h t.l.c. indicated complete conversion into a product of R_F: 0.46 in 10% CH_3OH–CH_2Cl_2. The reaction mixture was then evaporated *in vacuo*, and the product crystallized from ethanol. N^4-5′-*O*-Dibenzoylcytidine was obtained (150 mg, 85%; m.p. 193–195°, R_F: 0.46 in 10% CH_3OH–CH_2Cl_2; lit. m.p. 186–190° (8)). Its p.m.r. spectrum showed signals (δ

Can. J. Chem. Downloaded from www.nrcresearchpress.com by 210.87.254.6 on 09/05/12
For personal use only.

TMS) at 8.3–7.25 (12H, multiplet, 6-, and 5-cytidine protons, and *two* C_6H_5CO— protons); 5.95 (1H, doublet, $J \sim 2$ Hz; 1′-anomeric proton); and 4.85 and 4.25 p.p.m. (5H, 2 multiplets, sugar protons).

(c) Cytidine (4)

3′-*O*-Acetyl-N^4-5′-*O*-dibenzoylcytidine (**7**) (100 mg, 0.2 mmol; m.p. 188–190°, R_F: 0.62 in 10% CH_3OH–CH_2Cl_2) was suspended in dilute methanolic ammonia (4 ml, prepared by diluting saturated (at 20°) methanolic ammonia with an equal volume of methanol) and stirred at room temperature. After 40 h t.l.c. indicated complete conversion into a product of R_F: at the origin in 10% CH_3OH–CH_2Cl_2. The reaction mixture was then evaporated to dryness *in vacuo* and triturated with ether (3 × 5 ml), and the residue crystallized from ethanol. The cytidine (**4**) obtained (33 mg, 69%; m.p. 210–212°, R_F, at origin in 10% CH_3OH–CH_2Cl_2) was identical with that of an authentic sample.

N^4-Benzoyl-2′,3′-O-methoxyethylidenecytidine (13)

A mixture of N^4-benzoylcytidine (5.2 g, 0.015 mol), *p*-toluenesulfonic acid monohydrate (0.70 g, 3.7 mmol; 0.25 equiv) and trimethyl orthoacetate (12.5 ml) was stirred at room temperature. After 2.5 h t.l.c. indicated complete conversion into a product of R_F: 0.72 in 10% CH_3OH–CH_2Cl_2. The reaction mixture was then cooled, and neutralized with concentrated ammonia solution, then chloroform was added (50 ml), and the precipitated ammonium tosylate filtered off. The precipitate was washed well with chloroform (3 × 25 ml), and the combined organic solutions evaporated *in vacuo*. The yellow glass obtained (5.0 g, 90%) had R_F: 0.70 in 10% and 0.48 in 5% CH_3OH–CH_2Cl_2. This material was used for the next reaction without any further purification.

3′-O-Acetyl-N^4-benzoyl-5′-O-methoxyacetylcytidine (15)

Methoxyacetic acid (1.15 g, 12.5 mmol) was evaporated from anhydrous pyridine (2 × 25 ml), and finally its volume reduced to *ca.* 10 ml. The solution was sealed under nitrogen, tri-isopropylbenzenesulfonyl chloride (3.5 g, 12.5 mmol) added, and the reaction mixture allowed to stand at room temperature for 1 h. N^4-Benzoyl-2′,3′-*O*-methoxyethylidenecytidine (**13**) (5.0 g, 12.5 mmol) was evaporated from anhydrous pyridine (2 × 25 ml), and finally its volume reduced to *ca.* 10 ml. This solution was added to the methoxyacetic acid – TPS complex (prepared above) and the reaction mixture set aside at room temperature. After 4 h t.l.c. indicated *ca.* 90% conversion into a product of R_F: 0.84 in 5% CH_3OH—CH_2Cl_2. A small piece of ice was then added to the mixture, and stirring continued for a further 1 h. The reaction mixture was then poured into ice-water (50 ml) and repeatedly extracted with methylene chloride (6 × 30 ml). The combined organic extracts were washed and evaporated *in vacuo* to give N^4-benzoyl-5′-*O*-methoxyacetyl-2′,3′-*O*-methoxyethylidenecytidine (**14**) as a cream colored glass (8.0 g). Crude (**14**) (8.0 g) was treated with 5% acetic acid (100 ml), and the mixture stirred at room temperature. After 16 h t.l.c. indicated complete conversion into products R_F: 0.59, and 0.48 in 5% CH_3OH—CH_2Cl_2. The reaction mixture was then repeatedly extracted with methylene chloride (6 × 40 ml). The combined organic extracts were washed, dried (Na_2SO_4), and evaporated *in vacuo*. The colorless glass obtained (8.5 g) was purified by chromatography on silica gel (100 g) in methylene chloride. Elution with 2% methanol – methylene chloride mixture (300 ml) yielded a mixture, (0.6 g, R_F: 0.59, and 0.48 in 5% CH_3OH–CH_2Cl_2). The required 2′(3′)-*O*-acetyl-N^4-benzoyl-5′-*O*-methoxyacetylcytidine (1.9 g, 33.0%, R_F: 0.48 in 5% CH_3OH–CH_2Cl_2) was obtained on elution with 2.5% methanol – methylene chloride mixture (600 ml). Further material (0.58 g, R_F: 0.25 in 5% CH_3OH–CH_2Cl_2) tentatively identified as N^4-benzoyl-2′(3′)-*O*-acetylcytidine by its p.m.r. spectrum, was obtained by washing the column with 3% methanol – methylene chloride (300 ml). The pure 3′-*O*-acetyl-N^4-benzoyl-5′-*O*-methoxyacetylcytidine (**15**) was obtained by repeated crystallization from absolute ethanol – small amount of methylene chloride. The pure 3′-acetate had m.p. 95–97° (lit. m.p. 99–100° (10)). The p.m.r. spectrum showed signals (δ TMS) at 8.2–7.25 (7H, multiplet; 6-, and 5-cytidine protons; and C_6H_5CO— protons); 5.90 (1H, doublet; $J \sim 4$ Hz, 1′-anomeric proton); 5.30 and 4.28 (3H, two multiplets, sugar protons); 3.25 (3H, sharp singlet, CH_3O— protons); and 2.08 p.p.m. (3H, sharp singlet, —$COCH_3$ protons).

Pure 2′-*O*-acetyl-N^4-benzoyl-5′-*O*-methoxyacetylcytidine of m.p. 146–148° (lit. m.p. 155–157° (10)) was also obtained by repeated crystallization from absolute ethanol – trace of methylene chloride.

Attempts to record the mass spectra of cytidine derivatives **10**, **7**, **15**, and the two diastereoisomers of **11** were unsuccessful. The high temperatures (above 280°, probe 3.5) required for volatilization of these compounds gave only decomposition products.

Financial assistance from the Medical Research Council of Canada is gratefully acknowledged.

1. T. Neilson. Chem. Commun. 1139 (1969).
2. R. Lohrmann, D. Soll, H. Hayatsu, E. Ohtsuka, and H. G. Khorana. J. Amer. Chem. Soc. **88**, 819 (1966).
3. F. Eckstein and I. Rizk. Angew. Chem. **79**, 684 and 939 (1967).
4. K. H. Scheit. Tetrahedron Lett. 3243 (1967).
5. R. L. Letsinger and K. K. Ogilvie. J. Amer. Chem. Soc. **89**, 4801 (1967).
6. B. E. Griffin, M. Jarman, and C. B. Reese. Tetrahedron, **24**, 639 (1968).
7. H. Schaller, G. Weiman, B. Lerch, and H. G. Khorana. J. Amer. Chem. Soc. **85**, 3821 (1963).
8. H. P. M. Fromageot, B. E. Griffin, C. B. Reese, and J. E. Sulston. Tetrahedron, **23**, 2315 (1967).
9. H. P. M. Fromageot, B. E. Griffin, C. B. Reese, J. E. Sulston, and D. R. Trentham. Tetrahedron, **22**, 705 (1966).
10. C. B. Reese and J. C. M. Stewart. Tetrahedron Lett. 4273 (1968).
11. C. B. Reese. ACS-CIC Joint Conference. Toronto, Ontario, 1970. Paper No. 16.
12. D. H. Rammler and H. G. Khorana. J. Amer. Chem. Soc. **84**, 3112 (1962).

Bicyclo[2.2.1]heptyl phosphonates. III.[1] Radical Addition of Dimethyl Phosphonate to Norbornadiene

HENRY J. CALLOT[2] AND CLAUDE BENEZRA
Department of Chemistry, University of Ottawa, Ottawa 2, Canada

Received August 26, 1970

Radical addition of dimethyl phosphonate to norbornadiene was found to give four main compounds **2**, **3**, **4**, and **5** whose structures have been demonstrated by chemical and spectroscopical methods. Particularly noteworthy is the formation of norbornene phosphonate derivatives in addition to the nortricyclene derivatives.

L'addition radicalaire du phosphonate de diméthyle sur le norbornadiène conduit à quatre produits principaux **2**, **3**, **4**, et **5** dont les structures ont été démontrées par spectroscopie et par voie chimique. Il est intéressant de noter la formation de dérivés du norbornène phosphonate à côté des dérivés nortricycliques.

Canadian Journal of Chemistry, 49, 500 (1971)

Can. J. Chem. Downloaded from www.nrcresearchpress.com by 210.87.254.6 on 09/05/12
For personal use only.

The course of radical addition to norbornadiene (**1**) depends on the nature of the attacking species (1, 2). Generally nortricyclene derivatives are obtained. Only sulfur (1, 2) or silicon (3) radicals lead to some norbornenyl compounds. Among several radicals (generated from aldehydes, CCl_4, RSH, $(EtO)_2PHO$, etc.), Trecker and Henry (2) found that only mercaptans were able to give norbornene adducts. Since phosphorus, as sulfur and silicon, is also a third-row element, we felt that phosphorus radicals might also give norbornene adducts. Trecker and Henry (2) have reported that addition of phosphorus radicals to norbornadiene gives only nortricyclene products. However these authors investigated only the volatile fraction. In order to test our hypothesis (possible formation of norbornene derivatives with phosphorus radicals) we decided to study in detail the addition of dimethylphosphonate to norbornadiene in the presence of benzoyl peroxide.

Results and Discussion

Addition of dimethylphosphonate to norbornadiene (**1**) affords four compounds **2**, **3**, **4**, and **5**, the latter two being obtained as an inseparable mixture.

The first product is assigned the nortricyclene structure **2** on the following grounds. The n.m.r. spectrum shows no olefinic protons. A doublet centered at 3.71 p.p.m.[3] is assignable to the methoxy groups and H-4 appears as a broad singlet at 2.21 p.p.m. The proton appearing at 2.06 p.p.m. as part of an AB quartet shows a large H–H coupling (11 Hz) compatible, in such a system, only with a geminal relationship. This proton is probably H-7 since among the protons of the nortricyclene only H-7 *syn* to the dimethyl phosphonate group is likely to be deshielded. The signal corresponding to H-3, α to phosphorus, is a broad doublet centered at 1.81 p.p.m. (J_{PCH} = 9 Hz) collapsing to a broad singlet by phosphorus decoupling.

The i.r. spectrum of compound **2** is consistent with a nortricyclyl structure since it shows absorptions at 807 and 3040 cm^{-1} (4, 5). The i.r. spectroscopy technique in this case is not useful since peaks at 807 and 3050 cm^{-1} are also found in the i.r. spectrum of dimethyl *exo*-5-norbornenyl-2-phosphonate (**6**) (6), a possible reaction product which is formed when an excess olefin is used (see below).

The mass spectrum of the nortricyclene phosphonate **2** which will be discussed in detail elsewhere (7) confirms the assigned structure: the base peak at *m/e* 92 and the strong parent ion at *m/e* 202 are typical of nortricyclene derivatives (8).

Chemical evidence for the proposed structure was gained from two cyclopropane ring opening reactions. The first one was the reaction of compound **2** with boiling concentrated HCl to give, after methylation, chloro-**7** and hydroxy-**8** derivatives. Compound **2** was unexpectedly resistant to the classical treatment with an HCl

[1]For Part II see ref. 6.
[2]Postdoctoral fellow 1969–1970.
[3]All p.p.m. values are given in δ units with tetramethylsilane as internal reference.

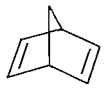

1

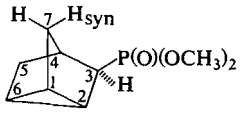

2

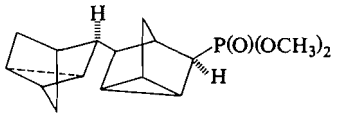

3

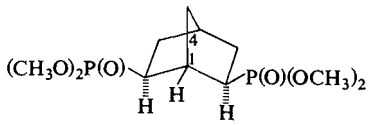

4

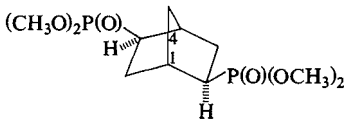

5

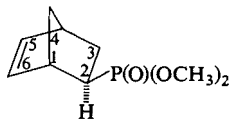

6

saturated solution in methylene chloride (9); starting material was recovered after 48 h.

The n.m.r. spectrum of **7** showed a double doublet centered at 3.89 p.p.m. assignable to H-5 on the carbon bearing the chlorine atom.

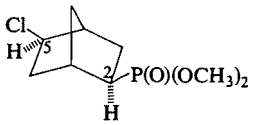

7

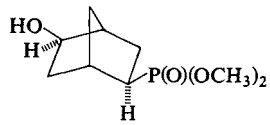

8

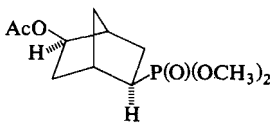

9

This pattern is characteristic of an *endo* proton in the bicyclo[2.2.1]heptane system (10), which leaves the *exo* configuration for Cl. *exo*-Configuration for the $(MeO)_2P(O)$ group stems from the existence of a *ca.* 6 Hz spin–spin coupling between ^{31}P and H-1 (11). The absence of coupling between phosphorus and the low field hydrogen (—C*H*Cl), as confirmed by phosphorus decoupling experiments, rules out the possibility of an attack of Cl^- at C-2 in compound **2**.

Structure **7** is confirmed by dehydrochlorination with tert-BuOK in DMSO, a reaction known to proceed without skeletal rearrangement (12), followed by an acidification of the reaction mixture and diazomethane treatment of the resulting phosphonic acid. This base treatment was incomplete and an inseparable mixture of the expected dimethyl *exo*-5-norbornenyl-2-phosphonate (**6**) and of the starting material was recovered. Nevertheless, it was possible to estimate the percentage of norbornene derivative by n.m.r. and a spectrum of a mixture prepared with the calculated proportions of **7** and **6** was superimposable to the n.m.r. of the products of base treatment.

The second product of the $HCl–H_2O$ treatment of the nortricyclene phosphonate followed by methylation is a hydroxyphosphonate, **8**, which was acetylated to **9**. The *exo* orientation for the OAc group (and therefore for OH) is apparent from the double doublet displayed by H-5 as discussed above; the phosphorus again has the same *exo* configuration as in **7**. The alcohol probably results from a direct attack by H_2O on the protonated cyclopropane. Compounds **8** and **9** could also be obtained on treatment of **2** with an acetic acid – sulfuric acid mixture, followed by esterification.

Three other compounds **3**, **4**, and **5** were isolated from the high-boiling fraction. Compound **3** was shown, by combustion analysis, to be a 2:1 adduct (diene:phosphonate). Structure **3** is tentatively assigned to this product. The n.m.r. spectrum shows one dimethylphosphonate

Can. J. Chem. Downloaded from www.nrcresearchpress.com by 210.87.254.6 on 09/05/12
For personal use only.

Can. J. Chem. Downloaded from www.nrcresearchpress.com by 210.87.254.6 on 09/05/12
For personal use only.

group for two bicyclo [2.2.1]heptyl moieties and *no* olefinic protons. The *exo,exo* junction of the two tricyclic moieties seems reasonable since radical additions to norbornenes generally give mainly *exo* derivatives (13) (except in the case of silicon radicals (3)). The part of the mass spectrum of compound **3** below *m/e* 110 is quite similar to that of the 1:1 adduct **2**. Particularly characteristic of the nortricyclene phosphonate system seem to be the *m/e* 92 and 91 peaks which probably correspond to a nortricyclyl cation (having or not having the nortricyclene skeleton) which has lost one or two hydrogens. The other peaks at *m/e* 79, 66, and 65 are often found in nortricyclene derivatives (8). Finally, as expected from a tricyclic structure, the parent ion [294] is very strong (73% of the base peak 91). The presence of a telomer compound such as **3** is not surprising (14) and their existence was suggested by Trecker and Henry (2) but no isolation was attempted.

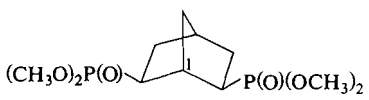

4

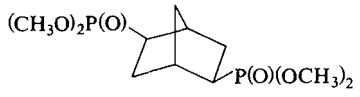

5

Compounds **4** and **5** are isolated as an inseparable mixture. The structures arise from the examination of their n.m.r. and mass spectra. On the basis of symmetry, it is possible to predict that the two bridgehead protons in structure **4** should be very different and that H-1 should appear as a broad triplet. In structure **5**, the two bridgehead hydrogens play the same role *vs.* the two phosphonate groups and should give a broad doublet, provided the two $(CH_3O)_2P(O)$ groups are *exo* (11). In agreement with the above, the n.m.r. spectrum of the mixture of **4** and **5** showed a doublet and a triplet at 2.57 and 2.97 p.p.m. respectively; these collapse to broad singlets on ^{31}P decoupling. The presence of the parent ion in the mass spectrum confirms the assigned structure.

The structure of diphosphonates **4** and **5** was further proven by their independent preparation through addition of dimethyl phosphonate to the *exo* norbornene derivative **6**. Exactly the same mixture of **4** and **5** is obtained.

Formation of compounds **4** and **5** is of significance and confirms the expectation that phosphorus radicals are able to give norbornene derivatives. Compounds **4** and **5** probably arise from a radical addition to the intermediate dimethyl *exo*-5-norbornenyl-2-phosphonate (**6**) (see Scheme 1). There is competition for the initially formed radical **10** between ring closure, to give the nortricyclyl radical **11** and hydrogen transfer to give the intermediate norbornene derivative **6** which leads to **4** + **5**. The 1:1 ratio of the two compounds is in favor of a statistical attack on the double bond of **6** by dimethyl phosphonate radical.

The intermediacy of dimethyl *exo*-5-norbornenyl-2-phosphonate (**6**) has been confirmed by a radical addition of dimethyl phosphonate to norbornene performed with an excess amount of olefin.[4] The n.m.r. spectrum of the product showed the presence of both **6** and **2**. A mixture of **6** and **2** prepared with authentic samples in the same proportions (3:7) showed n.m.r. and i.r. spectra superimposable to those of the reaction product.

The results of this study confirm that the major products of radical additions to norbornadiene (see Table 1 for product distribution) have a nortricyclene structure (2). It is however of interest to note that formation of norbornene phosphonate and norbornene derivatives does occur. Thus far only silicon and sulfur radicals have been shown to give such products.

Experimental

The n.m.r. spectra were run on a HA-100 Varian Spectrometer in deuterochloroform solutions, chemical shifts are given in δ p.p.m. values with TMS as internal

[4]A referee has pointed out that the decrease in the amount of dimethyl phosphonate used should result in the increase of the ratio nortricyclyl/norbornene adducts (or at least this ratio should remain constant) as was shown in a kinetic study by Cristol *et al.* (1) on radical addition of thiols to norbornadiene. However the isolation techniques of the two experiments are too different to be compared. In the first one (excess phosphonate) the norbornene derivatives are isolated from the high-boiling fraction followed by a chromatography; in the second one (excess olefin) the norbornene phosphonate **6** is isolated by distillation together with the nortricyclyl phosphonate **2**. In the first experiment the yield of diphosphonates **4** and **5** could well be higher than the one indicated in the experimental part and corresponding to the isolated product. In our opinion neither the isolation techniques nor the overall yields are comparable (52.5% total yield in the first experiment, 20% only in the second) and only allow *qualitative* conclusions to be drawn.

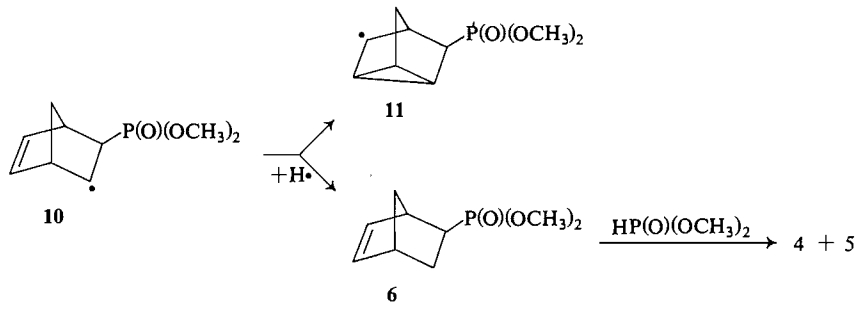

TABLE 1. Products distribution (radical addition to norbornadiene)

Ratio olefin: phosphonate	Overall yield (%)	2	3	4 + 5	6
1:2	52.5*	76†	10	14	—
2:1	20‡	70	—	—	30

*Calculated from norbornadiene for the isolated products.
†Calculated relative to the total mixture.
‡Calculated from the starting phosphonate.

reference. The i.r. spectra were all consistent with the proposed structure and showed P=O (1250 cm^{-1}) and P—O—C (1050 cm^{-1}) absorptions. Dimethyl phosphonate and norbornadiene were purchased from Aldrich Company. Mass spectra were recorded on a Hitachi–Perkin–Elmer RMU-6D spectrometer at 70 eV.

Addition of Dimethyl Phosphonate to Norbornadiene (1)

To a boiling solution of norbornadiene (37 g) in dimethyl phosphonate (88 g) was added benzoyl peroxide (2 g) over a 1.5 h period. The reaction mixture was distilled yielding (after a forerun containing both starting materials) two fractions, b.p. 100–150° and 150–225°/10 Torr, and leaving a dark residue (not investigated). The first fraction (35.4 g) was redistilled to give a colorless oil (30 g; 37% from norbornadiene), b.p. 120–123°/10 Torr: compound **2**.

Anal. Calcd. for $C_9H_{15}O_3P$: C, 53.47; H, 7.43; P, 15.35. Found: C, 53.33; H, 7.26; P, 15.40.

The n.m.r.: 3.71 (*d*, 6H, OCH_3, J_{PH} = 8 Hz); 2.21 (broad s, 1H, H-4); 2.06 (*d*, part of an AB quartet, 1H, H-7, J_{AB} = 11 Hz); 1.81 (*d*, 1H, H-3, J_{PH} = 9 Hz); *ca.* 1.25 (m, 6H).[5]

[5]Although most of these assignments agree with Trecker and Henry's (2) for the n.m.r. spectrum of the diethyl ester analog of **2** (within the experimental errors, and considering that their spectrum was taken in CCl_4), these authors describe *two* singlets (assigned to H-4 and -2) and *one* doublet (assigned to H-3) whereas there actually are *one* singlet (H-4) and *two* doublets (probably H-7 and -3, as shown by ^{31}P decoupling). A spectrum of compound **2** was taken in CCl_4 solution at 60 MHz (on a T-60 Varian Spectrometer) and the same pattern (one *s*, H-4, two *d*, H-7 and -3) was found. There is no reason why **2** and its diethyl ester analog (2) should show different absorptions for protons H-4, -7, and -3.

Mass Spectrum: *m/e* 202 (M^+; 53%); 137 (18%), 111 (37%), 110 (45%), 93 (29%), 92 (100%), 91 (70%), 79 (26%), 77 (20%), 65 (18%).

The higher boiling fraction (25 g) was chromatographed on silica gel. Elution with acetone gave successively an oily fraction (1.5 g) showing no P—O—CH_3 resonance (n.m.r.), followed by monophosphonates (9.1 g) and diphosphonates (9.5 g; 7.5% from norbornadiene). Rechromatography of the monophosphonates on silica gel (5 to 20% acetone in carbon tetrachloride) afforded compound **3** (5.1 g; 8.5% from norbornadiene) and some **2** (2.5 g; total yield of **2**: 40%). Compound **3** was purified by microdistillation (130°/0.4 Torr).

Anal. Calcd. for $C_{16}H_{23}O_3P$: C, 65.31; H, 7.82; P, 10.54. Found: C, 64.93; H, 7.66; P, 10.42.

The n.m.r.: 3.71 (*d*, 6H, OCH_3, J_{PH} = 10.5 Hz); complex multiplet 0.8–2.15 (17 H).

Mass Spectrum: *m/e*: 294 (M^+; 74%), 184 (47%), 137 (76%), 124 (66%), 110 (38%), 105 (52%), 92 (36%), 91 (100%), 79 (60%), 77 (48%).

The diphosphonates **4** and **5** were purified by microdistillation (145°/0.25 Torr) and analyzed as a mixture.

Anal. Calcd. for $C_{11}H_{22}O_6P_2$: C, 42.31; H, 7.05; P, 19.87. Found: C, 42.27; H, 7.28; P, 19.77.

Mass Spectrum: *m/e* 312 (M^+; 19%), 203 (19%), 176 (52%), 175 (100%), 174 (12%), 137 (52%), 110 (20%), 93 (15%), 91 (12%), 79 (15%).

Reaction of 2 with Acids

(a) Hydrochloric Acid

A mixture of **2** (1.6 g) and concentrated hydrochloric acid (25 ml) was refluxed for 4 h. The excess acid was evacuated under vacuum and the resulting colorless oil (1.5 g) crystallized slowly. Part of this crude phosphonic acid mixture (1 g) was dissolved in methanol (5 ml) and treated with excess diazomethane in ether. Distillation of solvent followed by chromatography on silica gel (eluent: acetone–CCl_4 mixtures) gave chloride **7** (620 mg, 53%), an oily mixture (30 mg; not further investigated) and alcohol **8** (110 mg, 10%). Compound **7** was purified by microdistillation (120°/15 Torr).

Anal. Calcd. for $C_9H_{16}ClO_3P$: C, 45.28; H, 6.75; P, 13.00; Cl, 14.88. Found: C, 44.99; H, 6.80; P, 12.71; Cl, 15.30.

The n.m.r.: 3.85 (*d* of *d*, 1H, C*H*Cl, J_{HH} 4 and 6.5 Hz); 3.73 and 3.71 (2*d*, 6H, unequivalent OCH_3, J_{PH} = 10.5 Hz); 2.61 (H-1, broad *m*, J_{PH} *ca.* 6 Hz); 2.53 (H-4, *s*).

Mass Spectrum: *m/e* 238 and 240 (M^+, 4 and 13%),

Can. J. Chem. Downloaded from www.nrcresearchpress.com by 210.87.254.6 on 09/05/12
For personal use only.

203 (61%), 175 (32%), 137 (100%), 110 (99%), 109 (36%), 93 (38%), 91 (29%), 80 (38%), 79 (69%).

Alcohol **8** (100 mg) was acetylated in acetic anhydride (0.5 ml)/pyridine (0.5 ml) at room temperature. After standing 5 h, the excess reagents were vacuum distilled (50°/0.2 Torr) yielding the acetate **9** as a colorless oil (105 mg), purified by microdistillation (90°/0.1 Torr).

Anal. Calcd. for $C_{11}H_{19}O_5P$: C, 50.38; H, 7.31; P, 11.83. Found: C, 50.29; H, 7.34; P, 12.01.

The n.m.r.: 4.62 (H-5, *d* of *d*, J_{HH} = 3.5 and 7.5 Hz); 3.74 and 3.72 (2*d*, unequivalent OCH_3, J_{PH} = 10.5 Hz); 2.57 (H-1, broad *s*, J_{PH} *ca.* 6 Hz); 2.40 (H-4); 1.99 (CH_3, *s*).

Mass Spectrum: *m/e* 262 (M^+, 7%), 220 (20%), 202 (19%), 179 (21%), 137 (100%), 124 (19%), 111 (27%), 110 (40%), 109 (61%), 79 (34%).

(b) Acetic acid/sulfuric acid

A solution of **2** (1 g) in acetic acid (20 ml) containing 5 drops of concentrated sulfuric acid, was refluxed for 19 h. Evacuation of acetic acid left a colorless oil, which was dissolved in methanol (50 ml) and left standing for 5 days. Treatment of the resulting solution with excess diazomethane in ether and chromatography on silica gel (carbon tetrachloride – acetone) gave successively acetate **9** (350 mg; 27%), a mixture (190 mg; not investigated), and alcohol **8** (300 mg; 27.5%). Compounds **8** and **9** were identified (i.r., n.m.r., t.l.c.) with the compounds described above.

Dehydrochlorination of Dimethyl exo-5-Chlorobicyclo-[2.2.1]-exo-2-phosphonate (7)

Chloride **7** (100 mg) in anhydrous DMSO (4 ml) was treated with potassium *t*-butoxide (300 mg) in a N_2 atmosphere for 24 h at room temperature. Water (5 ml) was added and the solvent removed (35°/0.05 Torr). The dry solid was dissolved in water (10 ml) treated with HCl and extracted with chloroform (3 × 10 ml). After drying on sodium sulfate and evacuating the solvent, the resulting oil was dissolved in methanol (5 ml) and treated with excess diazomethane. The residue (50 mg), after removal of the solvents, was found to be a mixture of starting material (60–65%) and unsaturated compound **6** (35–40%) by comparing i.r. and n.m.r. spectra of authentic samples.

Preparation of 4 + 5 from 6

A solution of **6** (0.5 g) in dimethyl phosphonate (1 g) was heated at 100° and benzoyl peroxide (40 mg) added over 10 min. Chromatography of the mixture (silica gel; ether–methanol) gave some unreacted dimethyl phosphonate followed by the diphosphonates (650 mg; 84%) as mixture, identified (i.r., n.m.r.) with the sample described above.

Reaction of Dimethyl Phosphonate with Excess Norbornadiene

To a boiling mixture of norbornadiene (46 g; 0.5 mol) and dimethyl phosphonate (27.5 g, 0.25 mol) was added benzoyl peroxide (1 g) during 0.5 h. The mixture was distilled under reduced pressure. After a forerun (10 ml) of dimethyl phosphonate, a fraction, b.p. 92–99°/0.15 Torr (10.5 g), was collected and identified as a mixture of **2** and **6** (7/3) by comparison with n.m.r. and i.r. spectra of authentic samples. The viscous residue left in the distillation flask was not further investigated.

Support of this work by the National Research Council of Canada is gratefully acknowledged.

1. S. J. Cristol, G. D. Brindell, and J. A. Reeder. J. Amer. Chem. Soc. **80**, 635 (1958).
2. D. J. Trecker and J. P. Henry. J. Amer. Chem. Soc. **85**, 3204 (1963).
3. H. G. Kuivila and C. R. Warner. J. Org. Chem. **29**, 2845 (1964).
4. J. D. Roberts, E. R. Trumbull, Jr., W. Bennett, and R. Armstrong. J. Amer. Chem. Soc. **72**, 3116 (1950).
5. G. E. Pollard. Spectrochim. Acta **18**, 837 (1962).
6. H. J. Callot and C. Benezra. Can. J. Chem. **48**, 3382 (1970).
7. C. Benezra and H. J. Callot. In preparation.
8. J. Holmes. Personal communication.
9. A. Nickon and J. H. Hammons. J. Amer. Chem. Soc., **86**, 3322 (1964).
10. P. Laszlo and P. von R. Schleyer. J. Amer. Chem. Soc. **86**, 1171 (1964).
11. C. Benezra. Tetrahedron Lett. 4471 (1969).
12. W. C. Baird, Jr. J. Org. Chem. **31**, 2411 (1966).
13. H. Stockmann. J. Org. Chem. **29**, 245 (1966) and references cited therein.
14. C. Walling and M. S. Pearson. *In* Topics in phosphorus chemistry. Vol. 3. E. J. Griffith and M. Grayson, *editors*, Interscience Publishers, New York, N.Y., 1966. p. 1.

Can. J. Chem. Downloaded from www.nrcresearchpress.com by 210.87.254.6 on 09/05/12
For personal use only.

Can. J. Chem. Downloaded from www.nrcresearchpress.com by 210.87.254.5 on 09/05/12
For personal use only.

Model Calculations on the Energy Levels of Diatomic Anharmonic Oscillators: Relation to Hydrogen Bonding[1]

A. FOLDES[2] AND C. SANDORFY
Département de Chimie, Université de Montréal, Montréal, Québec

Received September 14, 1970

Vibrational frequencies and anharmonicity constants for diatomic anharmonic oscillators are obtained by model calculations based on the conventional potential function

$$V = \tfrac{1}{2}k_2q^2 + k_3q^3 + k_4q^4 + \cdots$$

and assumed values of the potential constants. Values obtained from formulas derived from second order perturbation theory are compared with those obtained by diagonalization of a 20 by 20 perturbational matrix. Various sets of potential constants are studied and the range of validity of the second order approximations is determined. An attempt is made to correlate the observed anharmonic behavior of vibrations affected by hydrogen bonding with the results of these model calculations.

In cases of strong perturbations the inapplicability of second order perturbation theory precludes the calculation of the potential constants from the experimentally determined anharmonicity constants. These cannot be deduced from a simple series of overtone frequencies.

Canadian Journal of Chemistry, **49**, 505 (1971)

Introduction

In previous publications from this laboratory, the influence of hydrogen bonding and solvent effects on the anharmonicity of diatomic vibrators have been examined (1–6). It was found that hydrogen bonding has a profound influence on anharmonicity; and, furthermore, that different hydrogen bonds showed different, characteristic anharmonic behavior. Thus O—H···O bond formation in alcohols increased the anharmonicity constant obtained from the fundamental and first overtone frequencies of the OH stretching vibration by a factor of about two; but the same quantity decreased when deduced from the frequencies of the first and second overtones. On the other hand, N—H stretching vibrations in secondary amines showed first a decrease, and then an increase to about the same value as that found for free NH bonds.

Both cases involve a breakdown of second order (Morse curve) approximations, since in this approximation

$$[1]\quad X_{12} \equiv \nu_{01} - \nu_{02}/2 = \nu_{02}/2 - \nu_{03}/3 \equiv X_{23}$$

An alternative way of stating this is that if we use two anharmonicity constants but still within the framework of second order perturbation theory, then

$$[2]\quad X_{123} \equiv \nu_{01} - \tfrac{1}{2}\nu_{02} - 4.5\ Y_{123}$$

$$[3]\quad Y_{123} \equiv \frac{1}{2}\left(\nu_{02} - \nu_{01} - \frac{\nu_{03}}{3}\right)$$

the value of Y_{123} must be very much smaller than X_{123} for the approximation to be valid. (Here ν_{01}, ν_{02}, ν_{03}, $\cdots$ denote the frequencies of the fundamental and the first-, second-, $\cdots$ etc., overtones.) A large value of Y_{123} implies that $X_{12} \neq X_{23}$. (See refs. 3 and 6.)

It would be very useful to be able to compute potential constants from experimentally determined anharmonicity constants in order to gain an insight into the nature of the potential surface controlling the vibrations of hydrogen bonded systems. However, this is not, in general, possible. The dependence of the latter on the former is complex, and the degree of the complexity increases rapidly if we exceed approximations to the second order. We therefore decided to make some model calculations in the reverse order; *i.e.* values of potential constants were assumed and frequencies were calculated.

The aim of these calculations was to determine the approximate magnitudes of the various constants beyond which the second order perturbation method loses its validity; and if possible, to find sets of potential constants which reproduce the observed anharmonic behavior of hydrogen bonded systems.

[1]A more complete manuscript contains Tables 1, 3, 4 and the Appendix referred to in the text. Photo copies may be obtained free of charge, upon request, to the Depository of Unpublished Data, National Science Library, National Research Council of Canada, Ottawa, Canada.

[2]Present address: Delmar Chemicals Ltd., LaSalle, Québec.

Can. J. Chem. Downloaded from www.nrcresearchpress.com by 210.87.254.5 on 09/05/12
For personal use only.

Calculations

We take the conventional expression for the potential,

$$[4] \qquad V = \tfrac{1}{2}k_2q^2 + k_3q^3 + k_4q^4 + \cdots$$

where the harmonic, cubic, quartic, $\cdots$ potential constants are in cm^{-1}, and q is a dimensionless normal coordinate for a diatomic molecule or a group frequency which is supposed to be perfectly localized in a bond. The Hamiltonian of the system is then

$$[5] \qquad H \equiv \left[\tfrac{1}{2}k_2\left(\frac{p^2}{\hbar} + q^2\right)\right] + k_3q^3 + k_4q^4 + \cdots$$

where the expression in brackets is the energy of the unperturbed system, and the kinetic part is taken to be unaffected by the perturbation. In the perturbation calculation, the perturbed wave functions are, as usual, considered to be expanded in terms of the harmonic oscillator wave functions, and the matrix of the Hamiltonian is then computed. The non-zero terms of p^2, q^2, q^3, and q^4 have been tabulated by Barchewitz (7) and by Buckingham (8); those for q^5 and q^6 have been given by us in a previous publication (3). Using these we have constructed the matrix of the Hamiltonian as in Table 1[1] wherein $q_{vv'}{}^n$ denotes the matrix element of the nth power of the normal coordinate for two harmonic oscillator wave functions characterized by vibrational quantum numbers v and v'; and we have computed the matrix elements numerically for v and $v' = 0$ to 20 and $n = 3$ to 6. These are given in extenso in the Appendix,[1] since they are useful in actual calculations. We have effected the diagonalization of such 20×20 matrices with assumed values of the potential constants on a CDC-3400 Computer, using the subroutine "HDIAG" due to Corbato and Merwin (9) and given by Wiberg (10).

The results are presented in Tables 2, 3,[1] and 4.[1] Under the heading M.C. are the results obtained with the complete 20×20 matrices for the wave numbers of the fundamentals and the first, second, and third overtones. In column 1 are the results obtained by a conventional second order perturbation treatment.

$$[6] \qquad E_v = E_v{}^0 + H'_{vv'} - \sum_{v=v'} \frac{H'_{vv'}{}^2}{E_{v'}{}^0 - E_v{}^0}$$

where $E_v{}^0$ is the unperturbed energy and $H' = k_3q^3 + k_4q^4$, the perturbation. Only the diagonal term of q^4 contributes to the first order, and only the off-diagonal terms of q^3 contribute to the second order perturbation corrections.

Under column 2 are the results of a calculation in which second order perturbation formulas are used, but in which the off-diagonal terms of q^4 are also included; whilst column 3 lists the results obtained under the further inclusion of terms in q^5 and q^6. Approximations 2 and 3 do not correspond to a well defined order of perturbation, but we were interested to know the effect on the results of the additional terms. We also computed the anharmonicity constants X_{123} and Y_{123} from eqs. 2 and 3 using the frequencies obtained by the different approximations.

Results and Discussion

In Table 2 the assumed harmonic frequency was $\omega_e = k_2 = 3800\ cm^{-1}$, and the constants k_3, k_4, k_5, k_6 are related to each other by a factor f multiplying the preceding constant. f was varied from 0.01 to 0.15. In Tables 3[1] and 4[1] the values assumed for ω_e were 3600 and 2700 cm^{-1}, respectively.

These tables require little comment. The most interesting is the comparison between columns "1" and "M.C.", since these contain the frequencies and anharmonicity constants obtained from simple second order perturbation theory and the complete 20×20 matrices where the terms of the successive potential constants up to k_6 were included. It is immediately apparent that the results are almost identical until $f = 0.05$. Significant deviations occur for $f = 0.075$, and from $f = 0.10$ the results of the second order calculation are quite unreliable.

As a "rule of thumb" we might say that if $f \geqslant 0.075$, *i.e.*, if $k_3 \geqslant 0.075\,k_2$, then second order perturbation formulas lead to erroneous results.

The inclusion of the off-diagonal terms of q^4 (column "2") has little effect; but it may be useful since it enables us to introduce the anharmonicity constants W and Y into the expression of the vibrational term values

$$G_v = \omega_e(v + \tfrac{1}{2}) - (v + \tfrac{1}{2})W - (v + \tfrac{1}{2})^2X - (v + \tfrac{1}{2})^3Y - (v + \tfrac{1}{2})^4Z$$

As expected, the inclusion of quintic and sextic

Can. J. Chem. Downloaded from www.nrcresearchpress.com by 210.87.254.5 on 09/05/12
For personal use only.

TABLE 2. Frequencies and anharmonicity constants in cm^{-1} for $\omega_e = k_2 = 3800\ cm^{-1}$ in different approximations and for different choices of potential constants (see text)

Frequencies				X_{123}				Y_{123}				Z			
1	2	3	M.C.	1	2	3	M.C.	1	2	3	M.C.	1	2	3	M.C.
				$f = 0.01$ ($k_3 = 38.0$, $k_4 = 0.38$, $k_5 = 0.0038$, $k_6 = 0.0000$)											
3798.3	3798.3	3798.3	3798.3												
7594.9	7594.9	7594.8	7594.9												
11389.7	11389.7	11389.7	11389.7	0.86	0.86	0.86	0.86	0.00	0.00	0.00	0.00	0.0	0.0	0.0	0.00
15182.9	15182.9	15182.8	15182.9												
				$f = 0.02$ ($k_3 = 76.0$, $k_4 = 1.52$, $k_5 = 0.0304$, $k_6 = 0.0006$)											
3793.1	3793.1	3793.1	3793.1												
7579.5	7579.4	7579.3	7579.4												
11358.9	11358.8	11358.4	11358.8	3.42	3.42	3.42	3.42	0.00	0.00	0.00	0.00	0.0	0.0	0.0	0.00
15131.6	15131.3	15130.5	15131.2												
				$f = 0.05$ ($k_3 = 190.0$, $k_4 = 9.5$, $k_5 = 0.475$, $k_6 = 0.0237$)											
3757.2	3756.8	3755.4	3756.6												
7471.7	7469.9	7463.9	7469.0												
11143.5	11138.9	11122.6	11136.0	21.39	21.38	21.34	21.37	0.00	0.10	0.47	0.17	0.0	0.0	0.0	0.00
14772.5	14762.9	14728.6	14756.7												
				$f = 0.075$ ($k_3 = 285.0$, $k_4 = 21.275$, $k_5 = 1.5956$, $k_6 = 0.1216$)											
3703.5	3701.4	3694.2	3700.4												
7310.5	7301.7	7270.4	7296.5												
10821.1	10797.9	10713.4	10783.1	48.28	48.28	47.74	48.41	−0.01	0.50	2.51	0.84	0.0	0.0	0.03	0.04
14235.1	14187.1	14007.4	14156.4												
				$f = 0.10$ ($k_3 = 380.0$, $k_4 = 38.0$, $k_5 = 3.8$, $k_6 = 0.38$)											
3629.0	3622.1	3598.8	3619.7												
7087.0	7058.8	6955.6	7045.6												
10374.0	10300.2	10018.8	10271.3	85.56	85.56	82.47	92.12	−0.01	1.60	8.57	1.06	0.0	0.0	0.17	1.11
13490.0	13336.7	12732.9	13317.2												
				$f = 0.125$ ($k_3 = 465.0$, $k_4 = 58.125$, $k_5 = 7.2656$, $k_6 = 0.9082$)											
3547.6	3531.6	3475.2	3530.8												
6842.8	6776.8	6525.1	6782.6												
9885.7	9713.0	9018.8	9815.6	126.29	126.29	114.68	184.81	−0.02	3.76	21.78	−10.06	0.0	0.01	0.63	−4.23
12676.2	12317.5	10810.5	12791.7												
				$f = 0.15$ ($k_3 = 570.0$, $k_4 = 85.5$, $k_5 = 12.825$, $k_6 = 1.9237$)											
3415.2	3380.6	3252.9	3384.2												
6445.7	6302.9	5726.2	6404.4												
9091.5	8717.8	7107.4	9367.0	192.52	192.52	155.25	406.45	−0.03	8.15	52.11	−50.09	0.01	0.01	2.05	1.17
11352.6	10576.4	7034.6	12538.6												

Can. J. Chem. Downloaded from www.nrcresearchpress.com by 210.87.254.5 on 09/05/12
For personal use only.

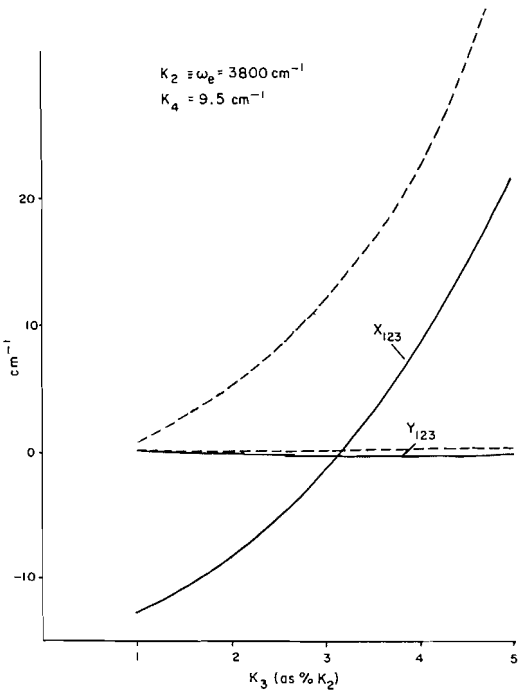

FIG. 1. Anharmonicity constants as functions of k_3. Solid lines, values obtained by diagonalizing the complete perturbation matrix; dashed lines, by second order perturbation formulas ($k_4 = 9.5\ \text{cm}^{-1}$).

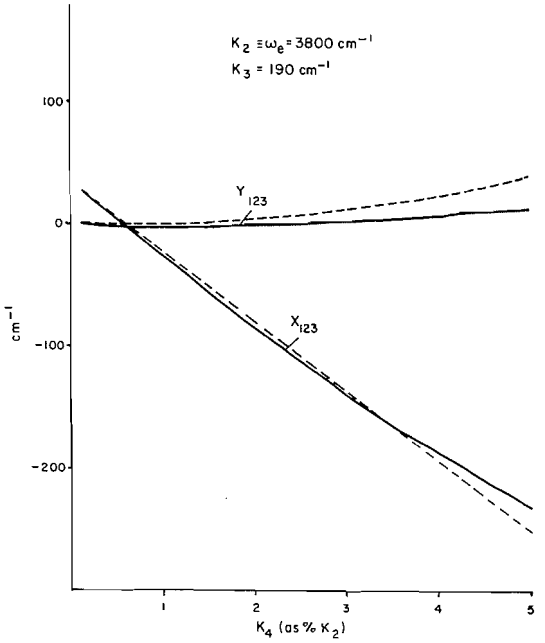

FIG. 2. Anharmonicity constants as functions of k_4. Solid lines, values obtained by diagonalizing the complete perturbation matrix; dashed lines, by second order perturbation formulas ($k_3 = 190\ \text{cm}^{-1}$).

terms into the second order formulas leads to obvious errors (column "3").

In order to observe the behavior of the anharmonicity constants for less regular sets of potential constants we examined four more cases. The results are shown in Figs. 1 to 4. In these figures the solid curves give X_{123} and Y_{123} values computed from the frequencies given by the complete secular determinant; whereas the dashed lines were obtained through approximation 2. The numerical values of X_{123} are different according to the approximation used; but the general trend is the same.

In Fig. 1, $k_2 \equiv \omega_e = 3800\ \text{cm}^{-1}$, k_4 is kept at the constant, small value $9.5\ \text{cm}^{-1}$ (0.25% of k_2) and k_3 is varied from 1 to 5% of k_2. It is seen that under these circumstances Y_{123} varies little but X_{123} increases gradually from about -12 to $+22\ \text{cm}^{-1}$.

In Fig. 2, k_2 is still $3800\ \text{cm}^{-1}$, k_3 is held at the large, constant value $190\ \text{cm}^{-1}$ (5% of k_2) and k_4 is varied from 0 to 5% of k_2. Y_{123} still shows little variation, but X_{123} decreases sharply (from about 30 to $-230\ \text{cm}^{-1}$) when k_4 increases. This is a particularly important diagram since it shows how a large k_4 can make the anharmonicity constants low or even negative while the vibration is actually very anharmonic (*cf.* the case of amines (1, 3, 6, 11)). In Fig. 3, $k_4 = 19\ \text{cm}^{-1}$ is fixed and k_3 varies between 0 and 10%. In this case X_{123} increases until k_3 reaches a value of about 8% of k_2 and then it starts to decrease. Y_{123} remains nearly unchanged until the same point; and from there it increases sharply. Figure 4 illustrates the case of an even higher k_3, $380\ \text{cm}^{-1}$ with k_4 varying between 0 and 10%. X_{123} diminishes with increasing k_4 whereas Y_{123} first decreases and then increases. We repeated these calculations including values of k_5 and k_6 up to $38\ \text{cm}^{-1}$. This produces changes in the numerical results, but does not affect the qualitative aspect of the problem.

We have also studied a few cases with $k_3 = k_5 = 0$ corresponding to symmetrical hydrogen bonds (Table 5). Negative values are obtained for X_{123}; and Y_{123} remains small except for very high values of k_4 (the last section of Table 5). The full secular equation gives lower values for Y_{123} than the simpler approximations. (A small value was given to k_6 in these calculations.) The

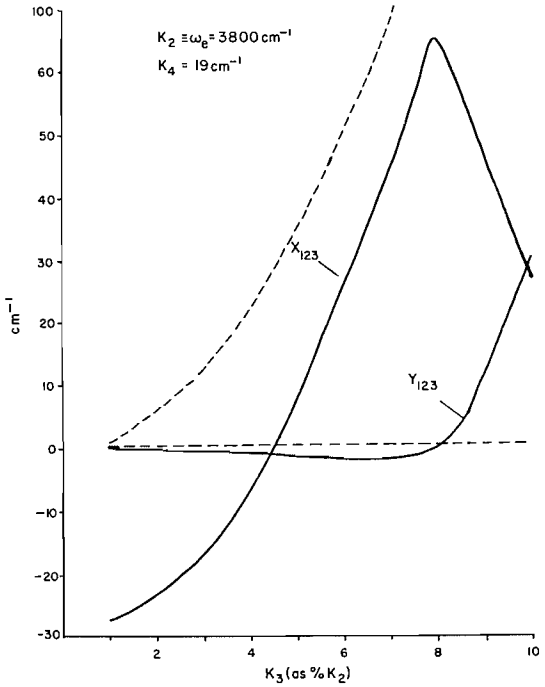

FIG. 3. Anharmonicity constants as functions of k_3. Solid lines, values obtained by diagonalizing the complete perturbation matrix; dashed lines, by second order perturbation formulas ($k_4 = 19\ cm^{-1}$).

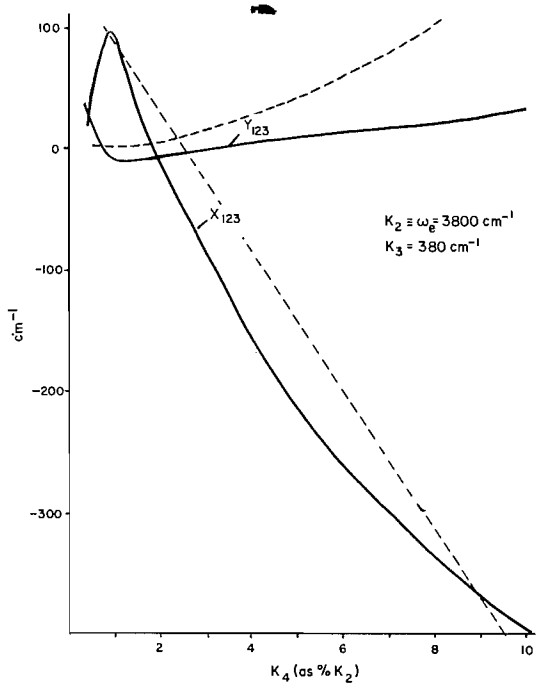

FIG. 4. Anharmonicity constants as functions of k_4. Solid lines, values obtained by diagonalizing the complete perturbation matrix; dashed lines, by second order perturbation formulas ($k_3 = 380\ cm^{-1}$).

first, third, $\cdots$ overtones are forbidden in this case, and the even order overtones diverge. This is substantiated by the frequencies of the fundamental and the second overtones of the antisymmetric stretching vibration of the $(FHF)^-$ ion determined by Coté and Thompson (12, 13).

Conclusion

It has been shown that vibrational frequencies and anharmonicity constants obtained from the usual potential function

$$V = \tfrac{1}{2}k_2q^2 + k_3q^3 + k_4q^4 + \cdots$$

using second order perturbation theory approximate reasonably closely those obtained by a diagonalization of the complete perturbational secular determinant in cases where k_3 does not exceed about 7.5% of k_2 (or Y_{123} no greater than about 5 cm^{-1}) and in which similar ratios apply between k_3, k_4 and the subsequent higher potential constants. Even this applies only when the k_3, k_4, $\cdots$ decrease regularly in this order. With less regular choices or larger values of the anharmonic potential constants the applicability of second order formulas becomes doubtful. In general, increasing k_3 values make X_{123} increase; while increasing k_4 values decrease X_{123} and increase Y_{123}. According to our previous work, the first corresponds to the case of the OH stretching vibrations of self-associated alcohols, and the second to the case of self-associated secondary amines and many other hydrogen bonded NH groups.

Externally unperturbed molecules or molecules only slightly perturbed by solvent effects usually constitute "regular" cases where second order perturbation theory can be considered reliable.

In cases of stronger perturbations, especially hydrogen bonding, the disappointing conclusion is that inapplicability of second-order perturbation theory precludes any simple calculation of the potential constants from the experimentally determined anharmonicity constants. On the other hand the changes observed in the values of the anharmonicity constants together with the model calculations presented in this paper provide an insight into the corresponding trends in the values of the potential constants.

Can. J. Chem. Downloaded from www.nrcresearchpress.com by 210.87.254.5 on 09/05/12
For personal use only.

TABLE 5. Frequencies and anharmonicity constants in cm^{-1} for $\omega_e \equiv k_2 = 3800\ cm^{-1}$, when the odd order potential constants ($k_3, k_5, \cdots$) are equal to zero

(*a*) $k_2 \equiv \omega_e = 3800$; $k_3 = 0$; $k_4 = 38.0$; ($k_5 = 0$, $k_6 = 0.38$) (all in cm^{-1})

Complete matrix			Approx. 2			Approx. 3		
n	ν_{on}		n	ν_{on}		n	ν_{on}	
1	3911.5	$X_{123} = -56.6$	1	3907.2	$X_{123} = -57.0$	1	3910.6	$X_{123} = -58.6$
2	7931.3	$Y_{123} = +0.55$	2	7913.8	$Y_{123} = +1.61$	2	7926.4	$Y_{123} = +1.34$
3	12056.0		3	12010.2		3	12039.4	
4	16282.3	$Z = 0$	4	16186.7	$Z = 0$	4	16239.3	$Z = +0.1$

(*b*) $k_2 \equiv \omega_e = 3800$; $k_3 = 0$; $k_4 = 58.125$; ($k_5 = 0$, $k_6 = 0.9082$) (all in cm^{-1})

Complete matrix			Approx. 2			Approx. 3		
n	ν_{on}		n	ν_{on}		n	ν_{on}	
1	3968.7	$X_{123} = -86.4$	1	3958.4	$X_{123} = -87.2$	1	3965.5	$X_{123} = -93.4$
2	8099.3	$Y_{123} = +1.23$	2	8057.1	$Y_{123} = +3.8$	2	8081.2	$Y_{123} = +4.0$
3	12384.3		3	12273.5		3	12322.9	
4	16817.1	$Z = -0.03$	4	16585.0	$Z = 0$	4	16657.7	$Z = +0.3$

(*c*) $k_2 \equiv \omega_e = 3800$; $k_3 = 0$; $k_4 = 85.5$; ($k_5 = 0$, $k_6 = 1.9237$) (all in cm^{-1})

Complete matrix			Approx. 2			Approx. 3		
n	ν_{on}		n	ν_{on}		n	ν_{on}	
1	4044.2	$X_{123} = -125.9$	1	4021.9	$X_{123} = -128.2$	1	4033.6	$X_{123} = -148.7$
2	8318.3	$Y_{123} = +2.44$	2	8226.7	$Y_{123} = +8.2$	2	8259.6	$Y_{123} = +11.6$
3	12807.7		3	12565.3		3	12608.1	
4	17499.9	$Z = 0.08$	4	16988.8	$Z = 0$	4	16980.6	$Z = +1.2$

(*d*) $k_2 \equiv \omega_e = 3800$; $k_3 = 0$; $k_4 = 152$; ($k_5 = 0$, $k_6 = 6.08$) (all in cm^{-1})

Complete matrix			Approx. 2			Approx. 3		
n	ν_{on}		n	ν_{on}		n	ν_{on}	
1	4219.1	$X_{123} = -217.5$	1	4146.6	$X_{123} = -228.0$	1	4156.3	$X_{123} = -358.2$
2	8818.3	$Y_{123} = +6.09$	2	8516.6	$Y_{123} = +25.8$	2	8469.5	$Y_{123} = +62.0$
3	13761.1		3	12955.0		3	12566.4	
4	19018.9	$Z = -2.0$	4	17306.7	$Z = 0$	4	15881.8	$Z = +8.0$

We acknowledge financial help from the National Research Council of Canada.

1. C. BERTHOMIEU and C. SANDORFY. J. Mol. Spectry, **15**, 15 (1965).
2. G. DUROCHER and C. SANDORFY. J. Mol. Spectry, **15**, 22 (1965).
3. A. FOLDES and C. SANDORFY. J. Mol. Spectry, **20**, 262 (1966).
4. G. DUROCHER and C. SANDORFY. J. Mol. Spectry, **22**, 347 (1967).
5. M. ASSELIN, G. BELANGER, and C. SANDORFY. J. Mol. Spectry, **30**, 96 (1969).
6. A. FOLDES and C. SANDORFY. Can. J. Chem. **48**, 2197 (1970).
7. P. BARCHEWITZ. Spectroscopie Infrarouge. Gauthier-Villars, Paris. 1961. p. 189.
8. A. D. BUCKINGHAM. Proc. Roy. Soc. London, Ser. A, **248**, 169 (1958).
9. F. J. CORBATO and M. MERWIN. Cited in ref. 10.
10. K. B. WIBERG. Computer Programming for Chemists. W. H. Benjamin, Inc., New York. 1965.
11. P. J. KRUEGER. Can. J. Chem. **41**, 363 (1963).
12. G. L. COTÉ and H. W. THOMPSON. Proc. Roy. Soc. London, Ser. A, **210**, 206 (1951).
13. R. BLINC. Nature, **182**, 1016 (1958).

Can. J. Chem. Downloaded from www.nrcresearchpress.com by 210.87.254.5 on 09/05/12
For personal use only.

Can. J. Chem. Downloaded from www.nrcresearchpress.com by 210.87.254.6 on 09/05/12
For personal use only.

Magnetic and Spectral Studies on Cobalt(II) Fluorosulfate

J. M. TAYLOR AND R. C. THOMPSON
Department of Chemistry, The University of British Columbia, Vancouver 8, British Columbia

Received September 2, 1970

The magnetic moment of cobalt(II) fluorosulfate has been measured over the temperature range 312 to 120 °K and the results agree with theory for cobalt(II) in a regular octahedral ligand environment with λ equal to the free-ion value and no reduction in the magnetic moment due to electron delocalization. From its electronic spectrum, values of the ligand-field parameters Dq and B are estimated to be 765 and 860 cm^{-1}, respectively. The infrared spectrum shows no distortion of the fluorosulfate groups from C_{3v} symmetry.

Canadian Journal of Chemistry, 49, 511 (1971)

Introduction

Several transition-metal fluorosulfates have been prepared previously by heterogeneous displacement reactions in fluorosulfuric acid (1, 2). Because of their insolubility in fluorosulfuric acid the compounds are obtained as microcrystalline powders and as yet no structural determinations by single crystal X-ray methods have been reported. In view of their lack of volatility and insolubility in fluorosulfuric acid it seems likely that these compounds are highly polymeric. On the basis, largely, of room-temperature magnetic moments Edwards *et al.* (3) suggested that the metal ions are in an octahedral environment of oxygen atoms; for the fluorosulfates of divalent transition metals this would require each anion to be three-coordinate. The most likely form of coordination by the fluorosulfate ion, FSO_3^-, would be via the three oxygen atoms and a plausible structure would be a layer type of structure (4) in which each fluorosulfate group acts as a tridentate bridge between three different metal ions.

In the work described here the magnetic and spectral properties of cobalt(II) fluorosulfate are examined in an attempt to obtain more information on bonding and on distortions from regular stereochemistry in this compound.

Experimental

Cobalt(II) fluorosulfate was prepared by the reaction of anhydrous cobalt(II) *m*-bromobenzoate with fluorosulfuric acid. The carboxylic acid salt was obtained by reacting sodium *m*-bromobenzoate with an excess of cobalt(II) chloride hexahydrate in water, followed by drying the precipitate under reduced pressure at about 70 °C (5). Fluorosulfuric acid was doubly distilled directly into a reaction flask equipped with a magnetic stirrer and containing finely powdered cobalt(II) *m*-bromobenzoate. The reaction was instantaneous and exothermic yielding a pale pink, insoluble product. The product was vacuum filtered, washed several times in the vacuum filtration apparatus with freshly distilled fluorosulfuric acid (to ensure removal of *m*-bromobenzoic acid), and finally pumped dry. During all these manipulations, care was taken to avoid hydrolysis by atmospheric moisture and the vacuum filtrations and washings were carried out in a manner analogous to that described previously for the preparation of anhydrous chlorosulfates (6). The product was stored in a vacuum desiccator over phosphoric oxide. Cobalt was determined by EDTA titration and fluorine and sulfur analyses were obtained in the A. Bernhardt microanalytical laboratories.

Anal. Calcd. for $CoS_2O_6F_2$: Co, 22.93; S, 24.95; F, 14.78. Found: Co, 22.6; S, 24.79; F, 14.53.

Magnetic susceptibilities were determined, at a field strength of approximately 4,500 G, using the Gouy apparatus described previously (7). A measurement of the magnetic susceptibility at room temperature and a field of approximately 7 000 G gave no evidence for dependence of the susceptibility on field strength. Calibration was achieved using $HgCo(CNS)_4$ (8). Diamagnetic corrections of 12.8×10^{-6} for Co^{2+} and 40.1×10^{-6} (c.g.s.u.) for SO_3F^- (this value obtained by assuming the correction for SO_3F^- will be the same as that for the isoelectronic SO_4^{2-} ion) were made (9).

Infrared spectra in Nujol were obtained using a Perkin–Elmer model 457 spectrophotometer with the sample contained between AgCl and KBr plates.

Electronic spectra were obtained on a powdered sample (diffuse reflectance) using a Bausch and Lomb Spectronic 600 spectrophotometer and on a sample mulled in hexachlorobutadiene using a Cary model 14 spectrophotometer.

Results and Discussion

Vibrational Spectrum

The infrared spectrum of cobalt(II) fluorosulfate shows six bands corresponding to the six

Can. J. Chem. Downloaded from www.nrcresearchpress.com by 210.87.254.6 on 09/05/12
For personal use only.

fundamental modes of vibration of a fluorosulfate group possessing C_{3v} symmetry. The frequencies (cm^{-1}) observed, with assignments according to Goubeau and Milne (2), are as follows: 1265, $\nu_4(E)$; 1109, $\nu_1(A_1)$; 850, $\nu_2(A_1)$; 610, $\nu_5(E)$; 568, $\nu_3(A_1)$; 420, $\nu_6(E)$. The strongest band is ν_4 and the remaining bands have medium intensities. Any significant reduction in the symmetry of the fluorosulfate group from C_{3v} would cause a splitting of the doubly degenerate E modes. Although ν_4 is a fairly broad band the other two E modes, ν_5 and ν_6 are sharp single bands with no evidence of splitting. Within the limitation of resolution of the instrument used ($\sim 3\ cm^{-1}$) there is no evidence for a lowering of symmetry below C_{3v}.

In its more ionic salts such as those of the larger alkali metals, where cation–anion interactions are relatively weak, the fluorosulfate ion retains C_{3v} symmetry (2, 10, 11). However, in compounds of the bivalent transition metals, interaction of the fluorosulfate ions with the metal ions would be expected to be sufficiently important to alter the vibrational frequencies of the fluorosulfate group. Indeed the frequencies observed for cobalt(II) fluorosulfate are significantly shifted from those in the alkali metal salts. In particular a shift in ν_2 to high frequencies has been shown to be a sensitive test of increased cation–anion interaction (11) and in the cobalt compound it is shifted by about 110 cm^{-1} from the value observed in the potassium salt. The maintenance of C_{3v} symmetry by the fluorosulfate ions in cobalt(II) fluorosulfate in the presence of significant cation–anion interaction indicates that all three oxygens are involved in coordination in an equivalent manner to cobalt ions. One can now assume, for the moment, octahedral coordination of the cobalt ions resulting in a CoO_6 skeleton, not significantly distorted from O_h symmetry. This situation is also indicated by the magnetic susceptibility data discussed below. Support for the arguments used here comes from the observation by Goubeau and Milne (2) that in copper(II) fluorosulfate, the fluorosulfate ions are reduced in symmetry from C_{3v} to C_s. As discussed by these authors, the CuO_6 octahedron is probably distorted with four short Cu—O distances in a square plane and two longer Cu—O distances. It follows then that two of the oxygen atoms in each fluorosulfate ion are closer to copper ions, and thus interact more with the metal ions than the other oxygen atom resulting in the observed reduction in symmetry.

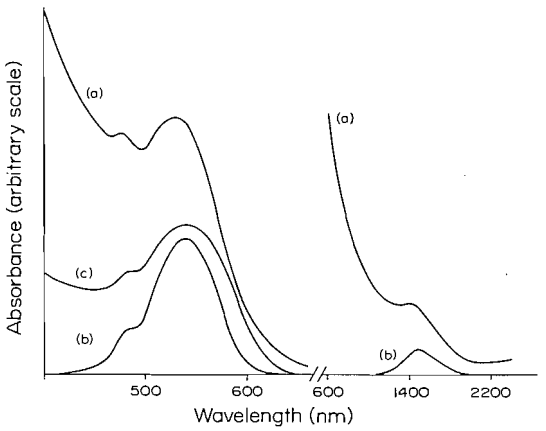

FIG. 1. Electronic spectrum of cobalt(II) fluorosulfate. *a*, hexachlorobutadiene mull; *b*, hexachlorobutadiene mull spectrum corrected for background; *c*, diffuse reflectance.

Electron Spectrum

The electronic spectrum of cobalt(II) fluorosulfate is shown in Fig. 1. The diffuse reflectance spectrum (curve *c*) agrees with that reported by Edwards *et al.* (3) with the exception that our instrument did not have the range required to observe the band at 13 500 cm^{-1} reported by the previous authors. The hexachlorobutadiene mull spectrum (curve *a*) gave a strong background, due presumably to light scattering from the sample, which increased with decreasing wavelength. Subtraction of this background from the spectrum yielded curve *b* in Fig. 1. In view of the excellent agreement between curve *b* and the diffuse reflectance spectrum in the visible region, we feel the procedure used of subtracting the background from the mull spectrum is valid.

Two principal bands are observed in the electronic spectrum at 1500 nm (6670 cm^{-1}) and 540 nm (18 500 cm^{-1}) with a shoulder on the latter band at approximately 480 nm (20 600 cm^{-1}). Assuming a ligand environment of O_h symmetry about Co^{2+} we assign the band ν_1 at 6670 cm^{-1} to the transition $^4T_{1g}(F) \rightarrow {}^4T_{2g}(F)$ and the band ν_3 at 18 500 cm^{-1} to the transition $^4T_{1g}(F) \rightarrow {}^4T_{1g}(P)$. The third ligand field band, ν_2, corresponding to the transition $^4T_{1g}(F) \rightarrow {}^4A_{2g}(F)$ is formally a two-electron transfer and is usually observed, if at all, as a weak band in the spectra of octahedral cobalt(II) complexes. This transition

probably occurs beyond the range of the instrument we used to obtain the diffuse reflectance spectrum and may correspond to the band observed by Edwards *et al.* at 13 500 cm^{-1}. The intense background of the mull spectrum would make observation of a weak band very difficult. The shoulder which appears at 20 600 cm^{-1} on the principal visible band is a common feature of the spectra of octahedral cobalt(II) complexes and its origin has been the subject of considerable discussion. It cannot be assigned to the ν_2 transition since, as discussed by Lever and Ogden (12) this transition should not occur at a frequency more than 2.2 times greater than the ν_1 frequency. It is also unlikely that it is a component of the ν_3 band arising through lowering of the symmetry from O_h, since the magnetic susceptibility results (to be discussed later) indicate that there is no significant distortion of the ligand environment about the cobalt ion. Following the previous work of Ferguson *et al.* (13), we therefore tentatively assign the shoulder to an enhanced spin-forbidden transition.

Initial estimates of the ligand field parameters Dq and B were obtained from the measured ν_3/ν_1 ratio using the appropriate transition energy ratio and Tanabe–Sugano diagrams as described by Lever (14). Final values of 765 cm^{-1} for Dq and 860 cm^{-1} for B were determined by an iterative fit to the expressions for the energies of the $^4T_{1g}(F)$, $^4T_{2g}(F)$, and $^4T_{1g}(P)$ levels given in p. 183 of ref. 14. Using these values the calculated frequency of ν_2 is 14 300 cm^{-1}, in approximate agreement with the band observed by Edwards *et al.* at 13 500 cm^{-1}.

It is instructive to compare the results obtained here for cobalt(II) fluorosulfate with those reported previously for cobalt(II) chloride. The overall spectra are very similar (13). The values of Dq and B for $CoCl_2$ are 764 and 775 cm^{-1} (p. 324 of ref. 14). This places the SO_3F^- ion at the same position as the Cl^- ion in the spectrochemical series for octahedral cobalt(II) but lower than the Cl^- ion (less reduction in the interelectron repulsion parameter B) in the nephelauxetic series.

Magnetic Properties

Magnetic susceptibility data for cobalt(II) fluorosulfate are given in Table 1. The theoretical expression for the magnetic moment of spin-free cobalt(II) complexes in a regular octahedral ligand field, ignoring the effects of electron delocalization, is (15),

$$[1]\quad \mu_{eff}^2 = \frac{3\left[\frac{7(3-A)^2}{5} + \frac{12(2+A)^2}{25Ax} + \left(\frac{2(11-2A)^2}{45} + \frac{176(2+A)^2}{675Ax}\right)\exp\left(\frac{-5Ax}{2}\right) + \left(\frac{(5+A)^2}{9} - \frac{20(2+A)^2}{27Ax}\right)\exp(-4Ax)\right]}{3 + 2\exp\left(\frac{-5Ax}{2}\right) + \exp(-4Ax)}$$

The quantity $x = \lambda/kT$ where λ is the spin–orbit coupling constant. The parameter A allows for the admixture of the higher lying $^4T_{1g}(P)$ into the ground $T_{1g}(F)$ term by the primary cubic field and may be obtained from a knowledge of the parameters Dq and B (16). From the values of Dq and B determined in the present work A is calculated to be 1.43 for cobalt(II) fluorosulfate. Using this value for A and the value -170 cm^{-1} for λ (the free ion spin–orbit coupling constant for Co^{2+} is -172 cm^{-1}), theoretical magnetic moments were calculated at each temperature studied and these are recorded in the last column of Table 1. Although there is some scatter in the experimental magnetic moments at the lower temperatures, in general the agreement between experimental and calculated values is good.

Figgis *et al.* have examined in some detail the effects of electron delocalization and low symmetry ligand fields on the magnetic properties of complexes with $^4T_{1g}$ ground terms (16). These authors tabulate theoretical magnetic moments calculated from expressions which involve two additional parameters: k, the orbital reduction factor, which allows for a reduction in the orbital contribution to the magnetic moment due to electron delocalization ($k = 1$ for no electron delocalization and is otherwise less than unity), and Δ, the axial ligand-field component, which is the magnitude of splitting of the ground term by

Can. J. Chem. Downloaded from www.nrcresearchpress.com by 210.87.254.6 on 09/05/12
For personal use only.

TABLE 1. Magnetic data for $Co(SO_3F)_2$

Temperature (°K)	$10^6\chi_{Co}$(c.g.s.u.)	μ_{eff} (B.M.)	
		Experimental	Calculated*
312.0	10 580	5.14	5.14
290.0	11 330	5.13	5.13
286.0	11 510	5.13	5.13
268.5	12 200	5.12	5.12
251.5	12 950	5.10	5.11
247.5	13 180	5.11	5.10
239.0	13 570	5.09	5.09
213.5	15 030	5.07	5.05
208.5	15 330	5.06	5.04
189.5	16 430	4.99	5.00
187.5	16 790	5.02	5.00
172.5	17 740	4.95	4.95
170.5	17 600	4.90	4.94
153.0	19 910	4.93	4.88
134.0	21 050	4.75	4.79
120.0	23 160	4.71	4.72

*Calculated from eq. 1.

fields of axial symmetry. Equation 1 corresponds to the situation where $k = 1$ and $\Delta = 0$. Attempts to fit our experimental magnetic moments with those tabulated by Figgis *et al.* for other values of k or Δ gave only poorer agreement with theory. The accuracy to which the parameters k, λ, and Δ may be determined by this method warrants some comment. Examining the effects of variations in these parameters on the calculated magnetic moments and considering an experimental uncertainty in the measured magnetic moments of about ± 0.03 at room temperature to about ± 0.05 at the lower temperatures, it is apparent that a reduction of either k or λ up to about 5% from the values 1.0 and -170 cm^{-1} respectively would be difficult to detect. Moreover, the calculated magnetic moments are relatively insensitive to small distortions from octahedral symmetry. The data do indicate, however, that a distortion giving rise to a splitting of the ground term by more than about 300 cm^{-1} is unlikely.

Since the fluorosulfate ion is the anion of a very strong acid (17, 18) it would be expected to exhibit a rather high degree of ionic character in its bonds to transition metals. Consistent with this is the relatively low position of the fluorosulfate ion in the nephelauxetic series as mentioned in the previous section. Values of the parameters k and λ as deduced here from magnetic susceptibility data should give some measure of the degree of metal–ligand covalent bonding, since strong covalent bonding should reduce k below unity and λ below the free-ion value (16). The values of these parameters for cobalt(II) fluorosulfate would appear to be consistent with relatively weak covalent interactions in this compound. It has been pointed out previously (16, 19), however, that a direct correlation between k and λ values and the degree of covalent bonding is not always possible and, indeed, values of these parameters do not as yet provide a sound basis on which to decide the degree of covalent bonding.

The financial support of the National Research Council of Canada is gratefully acknowledged. The authors also thank Mr. C. T. Wong for technical assistance.

1. A. A. WOOLF. J. Chem. Soc. A, 355 (1967).
2. J. GOUBEAU and J. B. MILNE. Can. J. Chem. **45**, 2321 (1967).
3. D. A. EDWARDS, M. J. STIFF, and A. A. WOOLF. Inorg. Nucl. Chem. Lett. **3**, 427 (1967).
4. A. F. WELLS. Structural Inorganic Chemistry. Claredon Press, Oxford, 1962. p. 77.
5. R. C. THOMPSON and C. T. WONG. Unpublished results.
6. J. A. CIRUNA and E. A. ROBINSON. Can. J. Chem. **46**, 1715 (1968).
7. H. C. CLARK and R. J. O'BRIEN. Can. J. Chem. **39**, 1030 (1961).
8. B. N. FIGGIS and R. S. NYHOLM. J. Chem. Soc. 4190 (1958).
9. B. N. FIGGIS and J. LEWIS. *In* Modern Coordination Chemistry. *Edited by* J. Lewis and R. G. Wilkins. Interscience Publ. Inc., New York. 1960. p. 403.
10. D. W. A. SHARP. J. Chem. Soc. 3761 (1957).
11. VON A. RUOFF, J. B. MILNE, G. KAUFMANN, and M. LEROY. Z. Anorg. Allg. Chem. **372**, 119 (1970).
12. A. B. P. LEVER and D. OGDEN. J. Chem. Soc. A, 2041 (1967).
13. J. FERGUSON, D. WOOD, and K. KNOX. J. Chem. Phys. **39**, 881 (1963).

Can. J. Chem. Downloaded from www.nrcresearchpress.com by 210.87.254.6 on 09/05/12
For personal use only.

14. A. B. P. LEVER. Inorganic Electronic Spectroscopy. Elsevier Publ. Co., Inc., Amsterdam. 1968.
15. B. N. FIGGIS. Introduction to Ligand Fields. Interscience Publ. New York. 1967. p. 339.
16. B. N. FIGGIS, M. GERLOCH, J. LEWIS, F. E. MABBS, and G. A. WEBB. J. Chem. Soc. A, 2086 (1968).
17. R. J. GILLESPIE. Accounts Chem. Res. **1**, 202 (1968).
18. R. C. THOMPSON. *In* Inorganic Sulphur Chemistry. *Edited by* G. Nickless. Elsevier Publ. Co., Inc., Amsterdam. 1968. p. 587.
19. M. GERLOCH and J. R. MILLER. Progress in Inorganic Chemistry. Vol. 10. *Edited by* F. A. Cotton. Interscience Publ. Inc., New York. 1968. p. 1.

Mobility of Phosphorescent Solutes in Polymethylmethacrylate

R. J. WOODS
Department of Chemistry and Chemical Engineering, University of Saskatchewan, Saskatoon, Saskatchewan
AND
J. F. MANVILLE
Forest Products Laboratory, 6620 North West Marine Drive, Vancouver 8, British Columbia

Received June 16, 1970

Nuclear magnetic resonance measurements upon polymerizing methyl methacrylate solutions show that a significant proportion of the solute molecules (naphthalene, phenanthrene) remain untrapped when the material becomes solid (60–30% residual unsaturation), complete rigid trapping of the solute occurring only as the unsaturation present is reduced to near zero.

Phosphorescence measurements show increasing phosphorescence from solid polymethylmethacrylate containing phenanthrene as the residual unsaturation in the polymer is reduced from about 4% to zero, which is attributed to the gradual immobilization of an increasing fraction of the solute molecules as the unsaturation is reduced. Methyl isobutyrate reduces the phosphorescence from solutions of phenanthrene in polymethylmethacrylate at room temperature, but polymer solutions containing methyl isobutyrate and those containing residual unsaturation phosphoresce strongly at 77 °K.

L'étude par r.m.n. de la polymérisation des solutions de méthacrylate de méthyle indique qu'une proportion significative des molecules solutées (naphthalène, phenanthrène) n'est pas capteé lorsque le matériel se solidifie (60–30% de monomère résiduel). Le soluté est complètement et rigidement capté seulement lorsque le montant de monomère résiduel approche le valeur de zéro.

L'intensité de la phosphorescence d'échantillons de polyméthacrylate de méthyle solide contenant de la phenanthrène augmente lorsque le monomère résiduel dans le polymère est réduit de 4% à 0%. Ceci est attribué à l'immobilisation graduel d'une plus grande fraction de molecules de soluté lorsque le degré de saturation est diminué. L'isobutyrate de méthyle diminue l'intensité de phosphorescence d'une échantillon de polyméthacrylate de méthyle à température ambiante. Mais, les échantillons contenant l'isobutyrate de méthyle aussi bien que ceux contenant le monomère résiduel sont fortement phosphorescents à la température 77 °K.

Canadian Journal of Chemistry, **49**, 515 (1971)

Triplet states of certain aromatic hydrocarbons and *N*-heterocyclic compounds show an initial, unexpected, non-exponential decay in thermally polymerized polymethylmethacrylate (PMMA) containing residual unsaturation (1–15% of the unsaturation originally present in the monomer); the decay becomes essentially exponential as the triplet population falls (1). The ratio of non-exponential to exponential decay is increased by warming the polymer or by incorporating methyl isobutyrate during polymerization but is reduced if the polymer is first annealed at 80–100 °C for periods up to about 48 h (further annealing has relatively little effect). The non-exponential decay was attributed to diffusion-controlled quenching reactions occurring in low-viscosity regions in the solid polymer; it was suggested that the viscosity in such regions would be reduced by incorporating a low-viscosity solvent (*e.g.* methyl isobutyrate) in the polymer or (temporarily) by warming the polymer, while thermal annealing would reduce the proportion of low-viscosity material present by leading to more complete polymerization. The present experiments were carried out to determine whether the solutes used were in fact mobile in "solid" polymethylmethacrylate containing residual unsaturation. They consist of two parts: an investigation of the simultaneous loss of monomer and of solute (naphthalene, phenanthrene) mobility in polymerizing methyl methacrylate by nuclear magnetic resonance

Can. J. Chem. Downloaded from www.nrcresearchpress.com by 210.87.254.6 on 09/05/12
For personal use only.

14. A. B. P. LEVER. Inorganic Electronic Spectroscopy. Elsevier Publ. Co., Inc., Amsterdam. 1968.
15. B. N. FIGGIS. Introduction to Ligand Fields. Interscience Publ. New York. 1967. p. 339.
16. B. N. FIGGIS, M. GERLOCH, J. LEWIS, F. E. MABBS, and G. A. WEBB. J. Chem. Soc. A, 2086 (1968).
17. R. J. GILLESPIE. Accounts Chem. Res. **1**, 202 (1968).
18. R. C. THOMPSON. *In* Inorganic Sulphur Chemistry. *Edited by* G. Nickless. Elsevier Publ. Co., Inc., Amsterdam. 1968. p. 587.
19. M. GERLOCH and J. R. MILLER. Progress in Inorganic Chemistry. Vol. 10. *Edited by* F. A. Cotton. Interscience Publ. Inc., New York. 1968. p. 1.

Mobility of Phosphorescent Solutes in Polymethylmethacrylate

R. J. WOODS
Department of Chemistry and Chemical Engineering, University of Saskatchewan, Saskatoon, Saskatchewan
AND
J. F. MANVILLE
Forest Products Laboratory, 6620 North West Marine Drive, Vancouver 8, British Columbia

Received June 16, 1970

Nuclear magnetic resonance measurements upon polymerizing methyl methacrylate solutions show that a significant proportion of the solute molecules (naphthalene, phenanthrene) remain untrapped when the material becomes solid (60–30% residual unsaturation), complete rigid trapping of the solute occurring only as the unsaturation present is reduced to near zero.

Phosphorescence measurements show increasing phosphorescence from solid polymethylmethacrylate containing phenanthrene as the residual unsaturation in the polymer is reduced from about 4% to zero, which is attributed to the gradual immobilization of an increasing fraction of the solute molecules as the unsaturation is reduced. Methyl isobutyrate reduces the phosphorescence from solutions of phenanthrene in polymethylmethacrylate at room temperature, but polymer solutions containing methyl isobutyrate and those containing residual unsaturation phosphoresce strongly at 77 °K.

L'étude par r.m.n. de la polymérisation des solutions de méthacrylate de méthyle indique qu'une proportion significative des molecules solutées (naphthalène, phenanthrène) n'est pas capteé lorsque le matériel se solidifie (60–30% de monomère résiduel). Le soluté est complètement et rigidement capté seulement lorsque le montant de monomère résiduel approche le valeur de zéro.

L'intensité de la phosphorescence d'échantillons de polyméthacrylate de méthyle solide contenant de la phenanthrène augmente lorsque le monomère résiduel dans le polymère est réduit de 4% à 0%. Ceci est attribué à l'immobilisation graduel d'une plus grande fraction de molecules de soluté lorsque le degré de saturation est diminué. L'isobutyrate de méthyle diminue l'intensité de phosphorescence d'une échantillon de polyméthacrylate de méthyle à température ambiante. Mais, les échantillons contenant l'isobutyrate de méthyle aussi bien que ceux contenant le monomère résiduel sont fortement phosphorescents à la température 77 °K.

Canadian Journal of Chemistry, **49**, 515 (1971)

Triplet states of certain aromatic hydrocarbons and *N*-heterocyclic compounds show an initial, unexpected, non-exponential decay in thermally polymerized polymethylmethacrylate (PMMA) containing residual unsaturation (1–15% of the unsaturation originally present in the monomer); the decay becomes essentially exponential as the triplet population falls (1). The ratio of non-exponential to exponential decay is increased by warming the polymer or by incorporating methyl isobutyrate during polymerization but is reduced if the polymer is first annealed at 80–100 °C for periods up to about 48 h (further annealing has relatively little effect). The non-exponential decay was attributed to diffusion-controlled quenching reactions occurring in low-viscosity regions in the solid polymer; it was suggested that the viscosity in such regions would be reduced by incorporating a low-viscosity solvent (*e.g.* methyl isobutyrate) in the polymer or (temporarily) by warming the polymer, while thermal annealing would reduce the proportion of low-viscosity material present by leading to more complete polymerization. The present experiments were carried out to determine whether the solutes used were in fact mobile in "solid" polymethylmethacrylate containing residual unsaturation. They consist of two parts: an investigation of the simultaneous loss of monomer and of solute (naphthalene, phenanthrene) mobility in polymerizing methyl methacrylate by nuclear magnetic resonance

Can. J. Chem. Downloaded from www.nrcresearchpress.com by 210.87.254.105 on 09/05/12
For personal use only.

Can. J. Chem. Downloaded from www.nrcresearchpress.com by 210.87.254.105 on 09/05/12
For personal use only.

spectroscopy (n.m.r.), and an investigation of the effect of thermal annealing upon the quenching of phenanthrene phosphorescence in PMMA glasses containing no added quencher and in glasses containing iodine or uranyl nitrate. In both studies the unsaturation present was monitored by the infrared absorption at 1621 nm.

Experimental

Methyl methacrylate (Eastman Organic Chemicals) was rapidly distilled twice immediately before use. The remaining materials were reagent grade and used as supplied.

Nuclear magnetic resonance spectra were recorded with a Varian T-60 n.m.r. spectrometer operating in the "auto" mode; integrals were measured without the sample spinning in order to eliminate spinning sidebands from overlapping regions of interest. All solutions studied were freshly prepared and sealed in 5 mm Pyrex n.m.r. tubes; air-free samples were sealed under vacuum but were not exhaustively degassed.

Phosphorescence measurements were made on right-angled prisms (approx. 12 × 12 × 50 mm) cut from material prepared by thermal polymerization of methyl methacrylate solutions at 80 °C for 12–20 h; solutions were not degassed since during polymerization any oxygen present is converted to a form that is not an efficient phosphorescence quencher (1), although completed samples were stored *in vacuo* to reduce oxygen diffusion into the polymer. Iodine added prior to polymerization was converted to (colorless) organic iodide during the polymerization. Total emission spectra (fluorescence, 300–450 nm; phosphorescence, 450–600 nm) were recorded at room temperature with an Aminco-Bowman spectrophotofluorometer (model 4-8202) using 340 nm exciting light. Polymer samples were annealed in baths at 80 or 100 °C for periods up to 20 h and then cooled to room temperature before making spectral measurements.

Unsaturation present in the samples was estimated from their absorption at 1621 nm (2), determined with a Cary 14 recording spectrophotometer, compared with that of a freshly distilled sample of methyl methacrylate of the same dimensions; no allowance was made for the reduction in volume (~21%) which occurs upon polymerization (concentrations referred to in this paper are those of the solutes in methyl methacrylate prior to polymerization).

Results

Figure 1 shows the effect of heating a 1 *M* solution of naphthalene in methyl methacrylate at 80 °C upon the methyl methacrylate concentration (determined from the $=CH_2$ n.m.r. absorption at *ca.* τ 4.6), the concentration of "mobile polymer" (determined from the CH_3 n.m.r. absorption at *ca.* τ 9.1 normalized to methyl methacrylate), the "mobile naphthalene" concentration (determined from the n.m.r. absorption at *ca.* τ 2.8), and the concentration of unsaturation (determined from the absorption at 1621 nm). During polymerization the liquid became progressively more viscous, gelled, and finally contracted sufficiently to pull away from the walls of the container. The points labelled "gel" and "solid" in Figs. 1 and 2 are approximations and correspond to the times at which the liquid became too viscous to flow in the 5 mm diameter tube and at which the material contracted from the walls of the tube, respectively. The fine structure of the n.m.r. spectra was lost only after the material had become solid and no significant n.m.r. absorption was observed with samples which had been heated longer than 20–25 h at 80 °C. Similar results were obtained

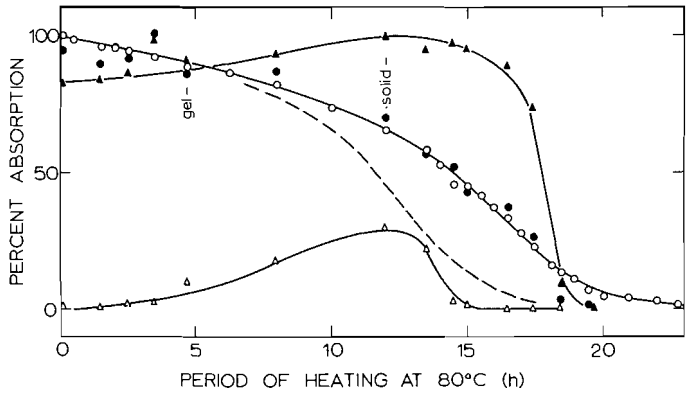

FIG. 1. Effect upon 1 *M* naphthalene in methyl methacrylate of heating at 80 °C *in vacuo*. ▲, naphthalene n.m.r. absorption; △, methyl methacrylate detected as polymer (n.m.r.); ●, methyl methacrylate remaining (n.m.r.); ○, unsaturation remaining (1621 nm absorption); ----, unsaturation remaining, air-saturated solution (1621 nm absorption).

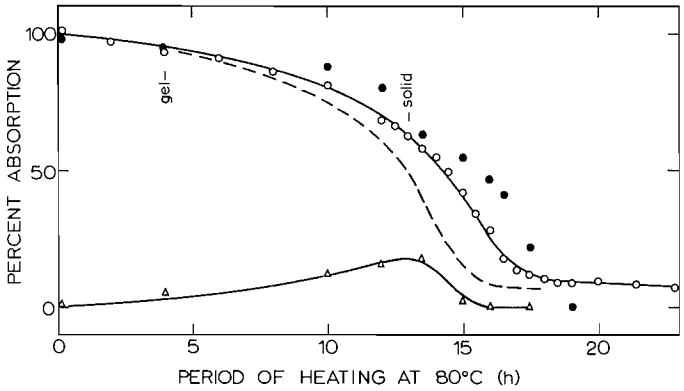

FIG. 2. Effect upon 10^{-3} *M* phenanthrene in methyl methacrylate of heating at 80 °C *in vacuo*. △, methyl methacrylate detected as polymer (n.m.r.); ●, methyl methacrylate remaining (n.m.r.); ○, unsaturation remaining (1621 nm absorption); ----, unsaturation remaining, air-saturated solution (1621 nm absorption).

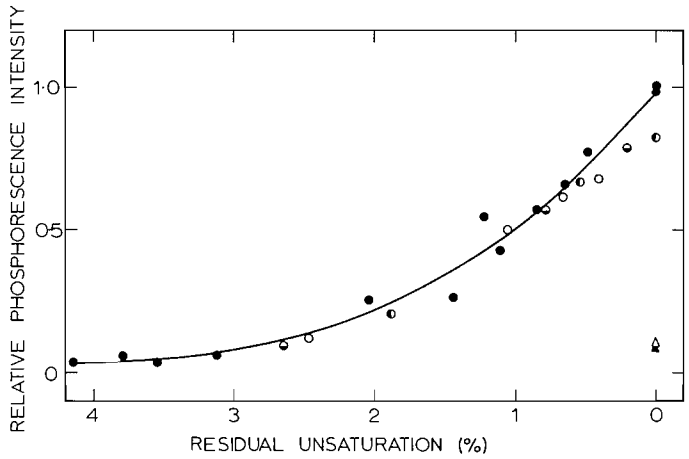

FIG. 3. Relative phosphorescence intensity of polymethylmethacrylate containing 10^{-3} *M* phenanthrene and the following additives: ●, none; ◐, 1.7×10^{-6} *M* iodine; ◒, 10^{-4} *M* iodine; ○, 3×10^{-4} *M* iodine; ▲, 10% methyl isobutyrate; △, 10% methyl isobutyrate + 10^{-4} *M* iodine.

with 10^{-3} *M* solutions of phenanthrene in methyl methacrylate (Fig. 2) although the concentration of phenanthrene was too low for useful measurements of "mobile solute" concentration to be made; the phenanthrene appeared to retard the loss of unsaturation (measured by the 1621 nm absorption) once the concentration of unsaturation had fallen below 10% of the initial value, this effect was very marked with *M* phenanthrene solutions but was not found with any of the other solutes examined. The broken curves in Figs. 1 and 2 show the effect upon the concentration of unsaturation of heating solutions in the presence of air. Infrared and n.m.r. measurements were also made on air-saturated methyl methacrylate solutions containing 1 *M* naphthalene, 1 *M* benzene, and 0.5 *M* benzene + 0.5 *M* methyl isobutyrate, respectively. No significant differences were observed between these experiments and the results depicted in Figs. 1 and 2; the n.m.r. absorption of the benzene and the methyl isobutyrate disappeared at approximately the same rate in the solution containing both of these solutes and the sample showed no measurable n.m.r. absorption after 20 h at 80 °C. An apparent increase in solute concentration, determined from the solute n.m.r. absorption, as the solutions solidify (*e.g.* Fig. 1) is attributed to the contraction that takes place at this point.

Figure 3 illustrates the effect upon phenanthrene phosphorescence intensity at 463 and

Can. J. Chem. Downloaded from www.nrcresearchpress.com by 210.87.254.105 on 09/05/12
For personal use only.

Can. J. Chem. Downloaded from www.nrcresearchpress.com by 210.87.254.105 on 09/05/12
For personal use only.

496 nm (the plotted points are averages of the intensities at these two wavelengths) of annealing polymethylmethacrylate containing 10^{-3} *M* phenanthrene alone and with organic iodide ($\sim 10^{-6}$ or $\sim 10^{-4}$ *M*) formed by the addition of iodine to the monomer prior to polymerization. The observed phosphorescence intensities are expressed relative to the intensity of a PMMA sample containing 10^{-3} *M* phenanthrene and essentially free of residual unsaturation used as a standard. Small differences ($\pm 4\%$) between individual samples have been allowed for by assuming that the intensity of the fluorescence (at 366 nm) from each sample should be the same (it is independent of the amount of unsaturation present) and normalizing the observed emission spectra to the fluorescence of the standard sample. Polymer samples containing 1 *M* (10% by weight) methyl isobutyrate and 10^{-3} *M* phenanthrene, alone or with the addition of 10^{-4} *M* iodide, had no residual unsaturation detectable by adsorption at 1621 nm after thermal polymerization at 80 °C for 18 h and showed relative phosphorescence intensities about 10% of that of the standard (Fig. 3). These samples and others containing several percent residual unsaturation, all of which showed relatively low phosphorescence intensities at room temperature, phosphoresced strongly when cooled to 77 °K. No quantitative measurements were made at 77 °K.

Discussion

The n.m.r. studies on polymerizing methyl methacrylate containing relatively large amounts of naphthalene (Fig. 1), benzene, and methyl isobutyrate show that polymerization proceeds with the build-up of polymer which becomes immobilized (the polymer-CH_3 n.m.r. absorption broadens and then disappears) as the gelled material contracts and solidifies. However, rigid trapping of the solute only occurs at a rather later stage in the polymerization, and samples containing 10–20% residual unsaturation still contain appreciable amounts of "mobile" solute which appears to be trapped in liquid regions between the polymer chains. Thus the suggestion (1) that PMMA with this degree of residual unsaturation may allow some solute mobility appears to be substantiated. The n.m.r. experiments indicate that some solute molecules have freedom of movement when the polymer contains less than 5% residual unsaturation, although broadening of the n.m.r. spectra make quantitative measurements difficult in this region. Phosphorescence studies were therefore used to investigate solute mobility at low concentrations of residual unsaturation and at low solute concentrations comparable to those used (10^{-6} to 10^{-2} *M*) in the original triplet decay experiments (1).

Triplet quenching occurs rapidly in liquid solutions and is generally attributed to diffusion controlled processes that are restricted in the solid state. Thus liquid solutions of phenanthrene in methyl methacrylate, with or without added quencher, do not phosphoresce although solid solutions of phenanthrene in PMMA do. The present experiments show that the phosphorescence intensity from solutions of phenanthrene in PMMA increases as the residual unsaturation is reduced from about 4% to zero, consistent with the postulates (1) that in this region some solute molecules are still mobile and quenching occurs as a consequence of this, and that solute mobility (and quenching) will be reduced as polymerization becomes more complete (as indicated by the reduction in residual unsaturation). The experiments give no indication of the nature of the quenching species, although it was shown earlier (1) that the unsaturated material present, by itself, does not produce any marked quenching. The addition of iodine, an efficient phosphorescence quencher, to the system has little effect (Fig. 3), suggesting that the availability of quenching species is not a decisive factor. Quenching experiments with uranyl nitrate (10^{-6} or 10^{-4} *M*), which would probably concentrate in the liquid regions of the polymer to a greater extent than iodine, gave results almost identical to those obtained using iodine (Fig. 3).

Polymer samples containing phenanthrene and methyl isobutyrate, but no residual unsaturation, show marked quenching (Fig. 3), consistent with the suggestion that methyl isobutyrate forms low viscosity regions in the polymer in which quenching can occur (however, absence of any n.m.r. absorption characteristic of methyl isobutyrate in PMMA containing this ester but no residual unsaturation indicates that any such regions are small and that movement within them is restricted). The marked increase in phosphorescence from samples containing methyl iso-

butyrate or residual unsaturation when the temperature is lowered to 77 °K is also consistent with solute motion within the solid polymer since any such motion would be reduced as the temperature is lowered.

The financial support of the National Research Council of Canada is gratefully acknowledged.

1. M. A. West, K. J. McCallum, R. J. Woods, and S. J. Formosinho. Trans. Faraday Soc. **66**, 2135 (1970).
2. R. G. J. Miller and H. A. Willis. J. Appl. Chem. **6**, 385 (1956).

Can. J. Chem. Downloaded from www.nrcresearchpress.com by 210.87.254.105 on 09/05/12
For personal use only.

On the Existence of Five-Coordinate Titanium(IV) Acetylacetonates

C. E. Holloway and A. E. Sentek
Department of Chemistry, York University, Downsview, Ontario

Received July 3, 1970

Monomeric trialkoxy(acetylacetonato)titanium(IV) compounds postulated as five coordinate complexes, are shown to be mixtures of well-established four and six coordinate derivatives. A structure is suggested for the dimeric species.

Canadian Journal of Chemistry, **49**, 519 (1971)

Introduction

The preparation of a number of compounds of the general formula $TiX_3(acac)$, where X is an alkoxy or halide group and acac is chelated acetylacetone, was described several years ago (1). Molecular weight determinations at the time, and also in a later study by other investigators (2) suggested an equilibrium between monomer and dimer dependent upon the bulk of the X group. In particular, when X is the highly branched *iso*-propoxy or *sec*-butoxy group the complexes were found to be monomeric. In less sterically hindered systems the metal atom would be expected to expand its coordination number to six by oligomer formation via bridging alkoxy groups (3). The monomeric derivatives, having a chelated acetylacetonato group (1) should afford examples of five-coordinated titanium(IV). As such they would provide convenient models for investigating ligand exchange processes which are believed to involve five-coordinated intermediates. However, attempts to isolate a monomeric species using highly branched alkoxy groups have failed, and the present results show that such compounds cannot be prepared by the literature methods. Instead, the so-called five coordinate complexes are actually 1:1 mixtures of the more familiar six- and four-coordinated derivatives already known. The former is the bis-acetylacetonato complex, $TiX_2(acac)_2$, and the latter unreacted starting material TiX_4.

Experimental

The *tert*-butoxy and *iso*-propoxy derivatives were prepared by the prescribed method (2) and after pumping under vacuum at room temperature for 24 h gave the correct metal analyses for the mono-acetylacetonato complexes. Metal analysis was carried out gravimetrically (2). The ratio of acetylacetone to alkoxide protons was determined by integration of the proton magnetic resonance (p.m.r.) spectra (5). Two types of alkoxy group were observed in the ratio 1:2 and one type of acetylacetone undergoing intramolecular exchange. The alkoxy to acetylacetone ratio was 3.0:1.0.

The trichloro derivative, $TiCl_3(acac)$, was prepared by the literature method (2) and also by the dropwise addition of $TiCl_4$ to $TiCl_2(acac)_2$ in a 1:1 mole ratio in benzene solution. The dark red crystals were filtered under dry nitrogen and dried *in vacuo*. Satisfactory metal and chloride analyses were carried out gravimetrically (2).

Infrared spectra were obtained on Perkin–Elmer 225 and a Beckmann IR-12 spectrometers using liquid films or mulls in KBr cells. Nuclear magnetic resonance data were obtained on a Varian A-60 instrument at normal operating temperature, using TMS as an internal reference.

Results and Discussion

The *tert*-butoxy and *iso*-propoxy derivatives are pale yellow liquids. Since previous preparations (2) yielded a compound of the correct stoichiometry, no further purification steps have been reported. The p.m.r. spectra of these complexes are shown in Table 1 together with spectra for the starting material, TiX_4 (4), and the bis-acetylacetonato derivative (5) under similar solvent conditions. The estimated rates of exchange

butyrate or residual unsaturation when the temperature is lowered to 77 °K is also consistent with solute motion within the solid polymer since any such motion would be reduced as the temperature is lowered.

The financial support of the National Research Council of Canada is gratefully acknowledged.

1. M. A. West, K. J. McCallum, R. J. Woods, and S. J. Formosinho. Trans. Faraday Soc. **66**, 2135 (1970).
2. R. G. J. Miller and H. A. Willis. J. Appl. Chem. **6**, 385 (1956).

Can. J. Chem. Downloaded from www.nrcresearchpress.com by 210.87.254.105 on 09/05/12
For personal use only.

On the Existence of Five-Coordinate Titanium(IV) Acetylacetonates

C. E. Holloway and A. E. Sentek
Department of Chemistry, York University, Downsview, Ontario

Received July 3, 1970

Monomeric trialkoxy(acetylacetonato)titanium(IV) compounds postulated as five coordinate complexes, are shown to be mixtures of well-established four and six coordinate derivatives. A structure is suggested for the dimeric species.

Canadian Journal of Chemistry, **49**, 519 (1971)

Introduction

The preparation of a number of compounds of the general formula $TiX_3(acac)$, where X is an alkoxy or halide group and acac is chelated acetylacetone, was described several years ago (1). Molecular weight determinations at the time, and also in a later study by other investigators (2) suggested an equilibrium between monomer and dimer dependent upon the bulk of the X group. In particular, when X is the highly branched *iso*-propoxy or *sec*-butoxy group the complexes were found to be monomeric. In less sterically hindered systems the metal atom would be expected to expand its coordination number to six by oligomer formation via bridging alkoxy groups (3). The monomeric derivatives, having a chelated acetylacetonato group (1) should afford examples of five-coordinated titanium(IV). As such they would provide convenient models for investigating ligand exchange processes which are believed to involve five-coordinated intermediates. However, attempts to isolate a monomeric species using highly branched alkoxy groups have failed, and the present results show that such compounds cannot be prepared by the literature methods. Instead, the so-called five coordinate complexes are actually 1:1 mixtures of the more familiar six- and four-coordinated derivatives already known. The former is the bis-acetylacetonato complex, $TiX_2(acac)_2$, and the latter unreacted starting material TiX_4.

Experimental

The *tert*-butoxy and *iso*-propoxy derivatives were prepared by the prescribed method (2) and after pumping under vacuum at room temperature for 24 h gave the correct metal analyses for the mono-acetylacetonato complexes. Metal analysis was carried out gravimetrically (2). The ratio of acetylacetone to alkoxide protons was determined by integration of the proton magnetic resonance (p.m.r.) spectra (5). Two types of alkoxy group were observed in the ratio 1:2 and one type of acetylacetone undergoing intramolecular exchange. The alkoxy to acetylacetone ratio was 3.0:1.0.

The trichloro derivative, $TiCl_3(acac)$, was prepared by the literature method (2) and also by the dropwise addition of $TiCl_4$ to $TiCl_2(acac)_2$ in a 1:1 mole ratio in benzene solution. The dark red crystals were filtered under dry nitrogen and dried *in vacuo*. Satisfactory metal and chloride analyses were carried out gravimetrically (2).

Infrared spectra were obtained on Perkin–Elmer 225 and a Beckmann IR-12 spectrometers using liquid films or mulls in KBr cells. Nuclear magnetic resonance data were obtained on a Varian A-60 instrument at normal operating temperature, using TMS as an internal reference.

Results and Discussion

The *tert*-butoxy and *iso*-propoxy derivatives are pale yellow liquids. Since previous preparations (2) yielded a compound of the correct stoichiometry, no further purification steps have been reported. The p.m.r. spectra of these complexes are shown in Table 1 together with spectra for the starting material, TiX_4 (4), and the bis-acetylacetonato derivative (5) under similar solvent conditions. The estimated rates of exchange

TABLE 1. Nuclear magnetic resonance spectra of $Ti(OR)_n(acac)_{4-n}$*

Resonance	*iso*-Propoxide in CS_2 solution			*tert*-Butoxide pure		
	$n = 4$	$n = 3$	$n = 2$	$n = 4$	$n = 3$	$n = 2$
Alkoxy CH_3	8.83	8.95 (3) 8.83 (6)	8.95	8.77	8.76 (9) 8.72(18)	8.76
Alkoxy —OCH	5.60	5.59 (2) 5.375(1)	5.37			
acac CH_3		8.125(6)	8.125		8.21 (3) 8.105(3)	8.205 8.105
acac —CH—		4.62 (1)	4.62		4.59 (1)	4.625
	Acetylacetone methyl group exchange					
Rate (s^{-1}) (38 °C)		6.18	5.95		13.4	14.1

*Chemical shifts in τ units, relative intensities in parentheses.

of acetylacetone methyl sites, based on line shape, are included for comparison. The unimolecular nature of the exchange process was shown by the concentration independence of the methyl line shape. In the case of the *tert*-butoxy derivative the two resonances of equal area indicate two methyl environments per acetylacetone. This is also true of the *iso*-propoxy derivative at low temperature. The close coincidence of the data suggested that the complexes might be mixtures of the bis-acetylacetonato complex and parent alkoxide. A striking difference in the α-proton shifts of alkoxy groups bonded to titanium in different coordination states has been documented elsewhere (6). The infrared spectra from 380 to 4000 cm^{-1} (Table 2) also show the same coincidence (5, 7) and support such an interpretation. Previously reported infrared data for the bis-acetylacetonato complexes (8) are incomplete due to interference from the solvent CS_2, which could not be eliminated by the use of balanced cells. The alternative explanation requires dimer formation with bridging alkoxy groups, which is contrary to the reported molecular weight data.

Careful fractionation of the materials *in vacuo* (0.001 mm Hg) yielded two distinct fractions, in each case with no residue. The first fraction, at a bath temperature between 65–70 °C, was readily identified by n.m.r. and metal analysis as the colorless monomeric tetraalkoxide. The second fraction, at 120–130 °C was the pale yellow bis-acetylacetonato complex. The boiling point of the first fraction is lower than the temperature (75–80 °C) at which the reactants are initially refluxed, hence any ligand scrambling due to heating can be assumed to have taken place during the first steps of the preparation. The similarity of the boiling points of the first fraction and that of the free tetraalkoxide suggests that any association between the two components of the mixture is very weak, consistent with previous molecular weight data. It therefore seems certain that the complexes $TiX_3(acac)$ have not yet been prepared, the primary products of the preparative reaction being the parent compound and its disubstituted derivative.

A feasible explanation for this is that substitution by acetylacetone is more rapid for the second alkoxy group than for the first.

$$[1] \quad TiX_4 + Hacac \xrightarrow{\text{slow}} TiX_3(acac) + HX$$

$$[2] \quad TiX_3(acac) + Hacac \xrightarrow{\text{fast}} TiX_2(acac)_2 + HX$$

This can be understood in terms of reduced steric hindrance to S_N2 attack by which the reaction most likely proceeds. The bis-acetylacetonato complex thus formed can then act as a Lewis base towards the unreacted TiX_4 via lone pairs of electrons of its alkoxy or halide groups. The structure of the dimeric species would be as shown in reaction 3, there being no need to postulate coordination numbers other than 4 and 6 for the titanium atoms in the resulting equilibrium.

With the present two alkoxy derivatives the equilibrium is expected to lie very much to the left. In less sterically hindered derivatives, such as methoxide and ethoxide, the equilibrium would lie more to the right. However, in these cases the parent alkoxide is itself polymerized (3) and a more complicated situation obtains. These cases are being studied further.

Support for the dimer structure (Fig. 1) is

Can. J. Chem. Downloaded from www.nrcresearchpress.com by 210.87.254.105 on 09/05/12
For personal use only.

[3] 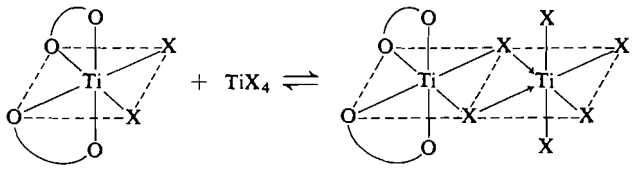

afforded by the nature and behavior of trichloro(acetylacetonato)titanium. During the preparation it is fairly evident from color changes that some $TiCl_2(acac)_2$ is initially formed. This is also evident from the alternative preparation in which the insoluble trichloro complex is immediately precipitated on mixing benzene solutions of $TiCl_4$ and $TiCl_2(acac)_2$ at room temperature. The infrared spectra of the Chloro complexes are given in Table 2. The spectra have several interesting differences in both the acetylacetonato and metal–chlorine regions. It is observed (8) that in the $TiX_2(acac)_2$ complexes the band associated with metal–oxygen stretching of the acetylacetonato group moves to higher energy as the X groups become more electro-

TABLE 2. Infrared spectra of $TiX_n(acac)_{4-n}$ (cm^{-1})*

iso-Propoxide (pure)			*tert*-Butoxide (pure)			Chloride (Nujol)		
$n = 4$	$n = 3$	$n = 2$	$n = 4$	$n = 3$	$n = 2$	$n = 3$	$n = 2$	Region
		3085w			3090w			ν(C—H) acac
2962s	2960s	2965s	2969s	2973s	2975s			
	2935s	2935s		2939sh	2941sh			
2920m	2920sh	2920sh	2921m	2927m	2926m			ν(C—H) acac
2859m	2866m	2862m	2893w	2901sh	2902sh			and (OR)
	2800w	2800w	2860w	2870sh	2870sh			
2620w	2620w	2620w						
	1608s	1608s		1614s	1613s	1560sb		ν(C—C) acac
	1586s	1586s		1592s	1593s	1500sb	1550s.vb	
	1525s	1525s		1524s	1524s			ν(C—O) acac
	1463w	1463w		1468w	1468w			
	1445m	1435w		1440w	1435m	1415mb	1420mb	Bending
	1388m	1378sb	1381w	1385sb	1384sb	1365w	1365w	and
1373m	1372m		1359m	1359s	1360s			skeletal
1360m	1365sh	1365sh				1330m	1325m	deformation
1330m	1328m	1329w						modes
	1278m	1278s	1232m	1231m	1231m	1265sb	1290sb	
				1200m	1200m			
(1182)	1185m	1190w	1179s	1182sb	1182sb			
1159w	1162w	1165w						ν(C—C)
1123s	1125s	1125s	1040m	1040m	1040m			Alkoxy
(1028)	1012sh	1012sh	(1030)	1025sh	1025sh	1030sb	1038s	and acac
1002s	992s	992s	1003s	1008sb	1008sb	1020sh	1020sh	bands
947m	939m	930m		930w	929w	955m	955m	(ref. 5)
			912w			940m	938m	plus ν(C—O)
851s	853s	853s						alkoxy
820w	820w	820w						
785w	785w		794m	800sh		815w	800w	
				790m	789m			
	772m	772s		765m	768m			
	665m	665m		667m	667m	695s	675s	
						680s		
618m	620mb	620mb		598m				
	590w	590w		580m	582m	555m	554m	ν(Ti—O)
(565)	565w	560w	(555)	550w	551w			Alkoxy
	550w	550w				545m	542m	and
473m	460m	465sh	478m	480m	486m	490sb	472sb	acac
		442m						
	410w	410w		405w	408w	412w	414w	
	360m	360m		375m	378m			
						405sb	378sb	ν(Ti—Cl)

*s = strong, m = medium, w = weak, sh = shoulder, b = broad, v = very. Parentheses indicate Raman-active band not seen in i.r.

Can. J. Chem. Downloaded from www.nrcresearchpress.com by 210.87.254.105 on 09/05/12
For personal use only.

Can. J. Chem. Downloaded from www.nrcresearchpress.com by 210.87.254.105 on 09/05/12
For personal use only.

negative. At the same time the bands in the C···C and C···O region (1500–1600 cm^{-1}) move to lower energy. This trend is also followed on going from $TiCl_2(acac)_2$ to the compound $TiCl_3(acac)$, with the exception that the higher frequency band (tentatively assigned to C···C) does not move significantly. Formation of halide bridges between the two titanium atoms would be expected to have such an effect proposed since the bridging chlorines will become more electronegative with respect to the $Ti(acac)_2$ fragment. Shifts to higher energy are also observed for the band assigned to π(C—H) of the acetylacetone. The band at 675 cm^{-1}, assigned to ring deformation and metal–oxygen stretch moves to higher energy and splits into a doublet. However, the general appearance of the spectra are otherwise very similar except for the ν(Ti—Cl) region, where the band at 378 cm^{-1} is no longer seen in the trichloro derivative. This is not unexpected since ν(Ti—Cl) for bridging halides has been found (9, 10) below 300 cm^{-1}. A new band, broad with almost a doublet appearance, centered at 405 cm^{-1} appears and can be assigned to the stretching modes of the terminal Ti—Cl bonds. Terminal ν(Ti—Cl) modes have been reported between 380 and 420 cm^{-1} in several cases (9–11). Also, the infrared (i.r.) spectra for $TiCl_4(L)$, where L is the keto form of a β-diketone, have been reported (12) unassigned. These spectra all have fairly strong bands in the region 370 to 430 cm^{-1}, which are probably associated with the titanium–chlorine bonds. From the i.r. spectra, the existence of a lattice of ions, such as $Ti(acac)_2^{2+}$ and $TiCl_6^{2-}$, can probably be ruled out (15).

Hydrolysis of the solid in the atmosphere yielded HCl, $TiCl_2(acac)_2$ which was isolated by extraction with benzene, and an unidentified residue containing titanium and chlorine. Treatment with ethanol yields a red oil (2) previously held to be $TiCl_2(OEt)(acac)EtOH$. This is almost certainly a mixture of two known compounds, $TiCl_2(acac)_2$ and $TiCl_2(OEt)_2(EtOH)_2$, since on pumping *in vacuo* for several days ethanol is lost and a yellow solid formed. This recrystallizes from benzene petroleum-ether to give two crops of crystals, the first being orange-red $TiCl_2(acac)_2$ and the second white needles of $TiCl_2(OEt)_2$, both compounds being readily identifiable by analysis and spectroscopy.

Recent studies (13) on titanium(IV) halide complexes of the 3-methyl-2,4-pentanedionate anion have suggested the existence of monomeric five coordinate structures for $X_3Ti(C_6H_9O_2)$, where X is chloride or bromide. However, the spectral data and solubilities reported are all consistent with an interpretation based on Fig. 1, in which the dimer structure dissociates to the two monomer species of 4 and 6 coordination number, respectively. The greater solubility of the bromide derivative would reflect a greater degree of dissociation due to weaker halide bridging between titanium atoms. A five coordinate structure has been proposed (14) for $[TiOCl(acac)]_2$, the preparation of which may suggest a feasible route to the five coordinate trialkoxy derivatives.

Financial support of the National Research Council of Canada is gratefully acknowledged.

1. A. YAMAMOTO and S. KAMBARA. J. Amer. Chem. Soc. **79**, 4344 (1957).
2. D. M. PURI and R. C. MEHROTRA. J. Less Common Metals, **3**, 253 (1961). D. M. PURI, K. C. PANDE, and R. C. MEHROTRA. J. Less Common Metals, **4**, 393, 481 (1962).
3. D. C. BRADLEY. Progr. Inorg. Chem. **2**, 303 (1960).
4. D. C. BRADLEY and C. E. HOLLOWAY. J. Chem. Soc. A, 1316 (1968).
5. D. C. BRADLEY and C. E. HOLLOWAY. J. Chem. Soc. A, 282 (1969).
6. D. C. BRADLEY and C. E. HOLLOWAY. Official Digest Fed. Soc. Paint Technol. **37**, 487 (1965).
7. A. H. WESTLAKE. Ph.D. Dissertation. University of Western Ontario, London, Ontario. 1964.
8. D. C. BRADLEY and C. E. HOLLOWAY. J. Chem. Soc. A, 282 (1969).
9. R. J. H. CLARK. Spectrochim. Acta, **21**, 955 (1965).
10. J. A. CREIGHTON and J. H. S. GREEN. J. Chem. Soc. A, 808 (1968).
11. M. J. FRAZER and B. RIMMER. J. Chem. Soc. A, 69 (1968).
12. A. L. ALLRED and D. W. THOMPSON. Inorg. Chem. **7**, 1196 (1968).
13. D. W. THOMPSON, W. A. SOMERS, and M. O. WORKMAN. Inorg. Chem. **9**, 1252 (1970).
14. R. E. COLLIS. J. Chem. Soc. A, 1895 (1969).
15. R. J. H. CLARK, L. MARESCA, and R. J. PUDDEPHATT. Inorg. Chem. **7**, 1603 (1968).

Thermochemistry of Silver Bromate[1]

L. M. GEDANSKY[2] AND L. G. HEPLER
Department of Chemistry, The University of Lethbridge, Lethbridge, Alberta

Received June 10, 1970

Calorimetric measurements of the heat of solution of $AgBrO_3$(c) in NH_3(aq) have been combined with earlier data on heats of solution of $AgNO_3$(c) in water and in NH_3(aq) to yield $\Delta H^0 = 11.78 \pm 0.11$ kcal mol^{-1} for $AgBrO_3$(c) = Ag^+(aq) + BrO_3^-(aq). Combination of this value with $\Delta G^0 = 5.83$ kcal mol^{-1} from the solubility product gives $\Delta S^0 = 19.96$ cal deg^{-1} mol^{-1} for the standard entropy of solution of $AgBrO_3$(c) at 298 °K.

Canadian Journal of Chemistry, 49, 523 (1971)

Can. J. Chem. Downloaded from www.nrcresearchpress.com by 210.87.254.42 on 09/05/12
For personal use only.

Introduction

Sillen and Martell (1) have cited four investigations of the solubility of $AgBrO_3$(c) in H_2O(liq) at 25 °C. Results of these investigations lead to K_{sp} values and thence to ΔG^0 values ranging from 5.79 to 5.84 kcal mol^{-1} for the reaction represented by

[1] $AgBrO_3(c) = Ag^+(aq) + BrO_3^-(aq)$

Weighting the work of Ramette and Dratz (2) most heavily, we adopt ${\Delta G_1}^0 = 5.83$ kcal mol^{-1}. Ramette and Dratz (2) have also calculated ${\Delta H_1}^0 = 11.7 \pm 0.3$ kcal mol^{-1} via the van't Hoff equation applied to their K_{sp} values at 14.7, 25.0, and 35.0 °C. They also measured the solubilities of $AgBrO_3$(c) in D_2O(liq) at these same temperatures and carried out similar calculations.

Because of interest in comparison of H_2O and D_2O as solvents (3) and the possibility of large errors in ΔH^0 and ΔS^0 values derived via the van't Hoff equation (4), we undertook calorimetric measurements leading to an independent value of ${\Delta H_1}^0$.

Experimental

The calorimetric apparatus has been described (5). All reported ΔH values refer to 25.00 ± 0.15 °C and are in terms of the defined calorie (1 cal = 4.1840 J).

Two samples of $AgBrO_3$(c) were prepared according to the method described by Ramette and Dratz (2). Iodometric analyses corresponded to each sample being 99.7 ± 0.2% $AgBrO_3$. Aqueous ammonia solution was prepared from Baker and Adamson reagent ammonium hydroxide and standardized against aqueous HCl.

Results

Heats of solution of $AgBrO_3$(c) in 0.16 M NH_3(aq) are given in Table 1 as ΔH_2 values corresponding to the reaction represented by

[2] $AgBrO_3(c) + 2\,NH_3(M = 0.16) \rightarrow Ag(NH_3)_2^+(M) + BrO_3^-(M)$

We take $\Delta H_2 = -1.72$ kcal mol^{-1} of $AgBrO_3$(c) for $M = 0.02$ for our calculations that follow.

Earlier calorimetric measurements (6) of heats of solution of $AgNO_3$(c) in 0.16 M NH_3(aq) and in water have led to $\Delta H_3 = -8.06$ kcal mol^{-1} and $\Delta H_4 = 5.46$ kcal mol^{-1} for reactions (both with $M = 0.02$) represented by

[3] $AgNO_3(c) + 2\,NH_3(M = 0.16) \rightarrow Ag(NH_3)_2^+(M) + NO_3^-(M)$

and

[4] $AgNO_3(c) \rightarrow Ag^+(M) + NO_3^-(M)$

We combine results cited above to obtain $\Delta H_1 = \Delta H_2 - \Delta H_3 + \Delta H_4 = 11.80$ kcal mol^{-1} for $M = 0.02$. Taking ϕ_L (the relative apparent molal enthalpy) for $AgBrO_3$($M = 0.02$) to be the same as tabulated (7) for $AgNO_3$ at the same concentration, we obtain ${\Delta H_1}^0 = 11.78$ kcal mol^{-1}. Total uncertainty due to sample composition, calorimetric errors in all the reactions, and estimated ϕ_L is about ±0.11 kcal mol^{-1}. There is excellent agreement between our calorimetric

TABLE 1. Heats of solution of $AgBrO_3$(c) in NH_3 ($M = 0.16$)

Moles $AgBrO_3$/ 950 ml solution	ΔH_2(kcal mol^{-1} of $AgBrO_3$)
0.01751	−1.70
0.01912	−1.72
0.01980	−1.73
0.02071	−1.74

[1]Calorimetric data reported in Table 1 were obtained at Carnegie Institute of Technology with the aid of a grant from the National Science Foundation.

[2]Present address: Scott Paper Co., Philadelphia, Pennsylvania.

$\Delta H_1^0 = 11.78 \pm 0.11$ kcal mol^{-1} and $\Delta H_1^0 = 11.7 \pm 0.3$ kcal mol^{-1} from Ramette and Dratz (2).

We have combined our ΔH_1^0 with the ΔG_1^0 cited above to obtain $\Delta S_1^0 = 19.96$ cal deg^{-1} mol^{-1}, compared to $\Delta S_1^0 = 19.7$ cal deg^{-1} mol^{-1} from Ramette and Dratz (2).

Combination of our ΔH^0 and ΔS^0 values with thermodynamic properties (8) of $Ag^+(aq)$ and $BrO_3^-(aq)$ leads to $\Delta H_f^0 = -6.55$ kcal mol^{-1} and $S_{298}^0 = 36.4$ cal deg^{-1} mol^{-1} for $AgBrO_3(c)$. These values are in excellent agreement with those cited recently by the National Bureau of Standards (8), apparently obtained on the basis of the results reported by Ramette and Dratz (2).

We are grateful to Dr. Gary Bertrand, now at the University of Missouri, Rolla, for his advice and help.

1. L. G. Sillen and A. E. Martell. Stability Constants of Metal–Ion Complexes. Special Publication No. 17, The Chemical Society, London. 1964.
2. R. W. Ramette and E. A. Dratz. J. Phys. Chem. **67**, 940 (1963).
3. L. G. Hepler. Aust. J. Chem. **17**, 587 (1964); J. Phys. Chem. **68**, 2645 (1964).
4. J. W. Larson and L. G. Hepler. Solute–Solvent Interactions. *Edited by* J. F. Coetzee and C. D. Ritchie. Marcel Dekker, New York. 1969. Chap. 1.
5. L. M. Gedansky and L. G. Hepler. Can. J. Chem. **47**, 699 (1969).
6. R. L. Graham and L. G. Hepler. J. Amer. Chem. Soc. **80**, 3538 (1958).
7. V. B. Parker. Thermal Properties of Aqueous Electrolytes. NSRDS-NBS 2, National Bureau of Standards, Washington, D.C. 1965.
8. D. D. Wagman, W. H. Evans, V. B. Parker, I. Halow, S. M. Bailey, and R. H. Schumm. Selected Values of Chemical Thermodynamic Properties. National Bureau of Standards Technical Notes 270-3 and 270-4, U.S. Government Printing Office, Washington, D.C. 1968 and 1969.

Can. J. Chem. Downloaded from www.nrcresearchpress.com by 210.87.254.42 on 09/05/12
For personal use only.

Alkaloids of *Lycopodium alopecuroides*. Part 4.[1] The Structure of Lycopecurine

William A. Ayer and Norio Masaki[2]
Department of Chemistry, University of Alberta, Edmonton, Alberta

Received August 31, 1970

Lycopecurine, an alkaloid of *Lycopodium alopecuroides* has been shown by an X-ray crystallographic study of the hydrobromide to possess structure **2**.

Canadian Journal of Chemistry 49, 524 (1971)

In Part 2 of this series (1), we described the isolation of a small quantity of a compound $C_{16}H_{25}ON$, m.p. 239–241°, which appears not to have been described previously and for which we suggested the name *lycopecurine*. We have succeeded in isolating this compound only once (2), and then in small quantity, and thus have been forced to rely almost exclusively on physical methods in the determination of the structure of this alkaloid. This paper summarizes the results of this investigation.

The molecular formula $C_{16}H_{25}ON$ for lycopecurine was established by high resolution mass spectrometry (h.r.m.s.). The mass spectrum, shown in Fig. 1, is characterized by an intense M^+-15 peak, a feature which is not predominant in the mass spectra of the common Lycopodium alkaloids (3).

The n.m.r. spectrum of lycopecurine, determined on a small amount of material, was not particularly revealing, but did show the presence of a secondary *C*-methyl group and the absence of olefinic protons.

The oxygen atom in lycopecurine is present as a secondary hydroxyl group as indicated by the i.r. spectrum (Fig. 2) and by the fact that oxidation with Jones' reagent furnished a ketone, *dehydrolycopecurine*, which absorbed at 1695

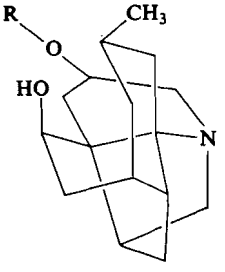

1

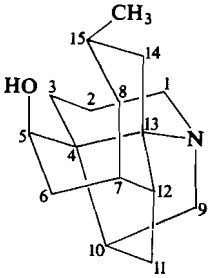

2

[1]Part 3. See ref. 7.
[2]Present address, Faculty of Pharmaceutical Sciences, Kyoto University, Kyoto, Japan.

$\Delta H_1^0 = 11.78 \pm 0.11$ kcal mol^{-1} and $\Delta H_1^0 = 11.7 \pm 0.3$ kcal mol^{-1} from Ramette and Dratz (2).

We have combined our ΔH_1^0 with the ΔG_1^0 cited above to obtain $\Delta S_1^0 = 19.96$ cal deg^{-1} mol^{-1}, compared to $\Delta S_1^0 = 19.7$ cal deg^{-1} mol^{-1} from Ramette and Dratz (2).

Combination of our ΔH^0 and ΔS^0 values with thermodynamic properties (8) of $Ag^+(aq)$ and $BrO_3^-(aq)$ leads to $\Delta H_f^0 = -6.55$ kcal mol^{-1} and $S_{298}^0 = 36.4$ cal deg^{-1} mol^{-1} for $AgBrO_3(c)$. These values are in excellent agreement with those cited recently by the National Bureau of Standards (8), apparently obtained on the basis of the results reported by Ramette and Dratz (2).

We are grateful to Dr. Gary Bertrand, now at the University of Missouri, Rolla, for his advice and help.

1. L. G. Sillen and A. E. Martell. Stability Constants of Metal–Ion Complexes. Special Publication No. 17, The Chemical Society, London. 1964.
2. R. W. Ramette and E. A. Dratz. J. Phys. Chem. **67**, 940 (1963).
3. L. G. Hepler. Aust. J. Chem. **17**, 587 (1964); J. Phys. Chem. **68**, 2645 (1964).
4. J. W. Larson and L. G. Hepler. Solute–Solvent Interactions. *Edited by* J. F. Coetzee and C. D. Ritchie. Marcel Dekker, New York. 1969. Chap. 1.
5. L. M. Gedansky and L. G. Hepler. Can. J. Chem. **47**, 699 (1969).
6. R. L. Graham and L. G. Hepler. J. Amer. Chem. Soc. **80**, 3538 (1958).
7. V. B. Parker. Thermal Properties of Aqueous Electrolytes. NSRDS-NBS 2, National Bureau of Standards, Washington, D.C. 1965.
8. D. D. Wagman, W. H. Evans, V. B. Parker, I. Halow, S. M. Bailey, and R. H. Schumm. Selected Values of Chemical Thermodynamic Properties. National Bureau of Standards Technical Notes 270-3 and 270-4, U.S. Government Printing Office, Washington, D.C. 1968 and 1969.

Can. J. Chem. Downloaded from www.nrcresearchpress.com by 210.87.254.105 on 09/05/12
For personal use only.

Alkaloids of *Lycopodium alopecuroides*. Part 4.[1] The Structure of Lycopecurine

William A. Ayer and Norio Masaki[2]
Department of Chemistry, University of Alberta, Edmonton, Alberta

Received August 31, 1970

Lycopecurine, an alkaloid of *Lycopodium alopecuroides* has been shown by an X-ray crystallographic study of the hydrobromide to possess structure **2**.

Canadian Journal of Chemistry 49, 524 (1971)

In Part 2 of this series (1), we described the isolation of a small quantity of a compound $C_{16}H_{25}ON$, m.p. 239–241°, which appears not to have been described previously and for which we suggested the name *lycopecurine*. We have succeeded in isolating this compound only once (2), and then in small quantity, and thus have been forced to rely almost exclusively on physical methods in the determination of the structure of this alkaloid. This paper summarizes the results of this investigation.

The molecular formula $C_{16}H_{25}ON$ for lycopecurine was established by high resolution mass spectrometry (h.r.m.s.). The mass spectrum, shown in Fig. 1, is characterized by an intense M^+-15 peak, a feature which is not predominant in the mass spectra of the common Lycopodium alkaloids (3).

The n.m.r. spectrum of lycopecurine, determined on a small amount of material, was not particularly revealing, but did show the presence of a secondary *C*-methyl group and the absence of olefinic protons.

The oxygen atom in lycopecurine is present as a secondary hydroxyl group as indicated by the i.r. spectrum (Fig. 2) and by the fact that oxidation with Jones' reagent furnished a ketone, *dehydrolycopecurine*, which absorbed at 1695

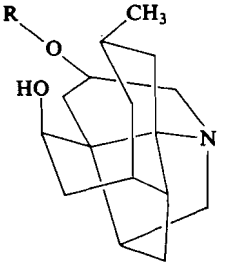

1

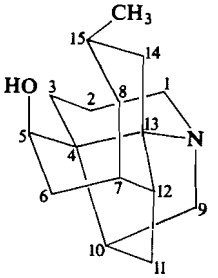

2

[1]Part 3. See ref. 7.
[2]Present address, Faculty of Pharmaceutical Sciences, Kyoto University, Kyoto, Japan.

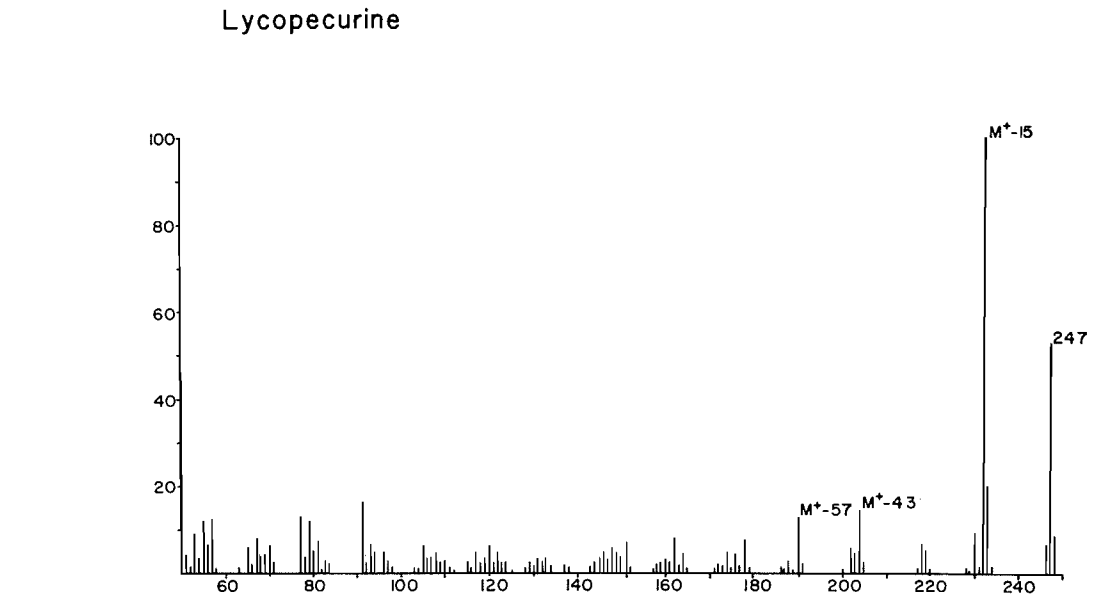

FIG. 1. Mass spectrum of lycopecurine.

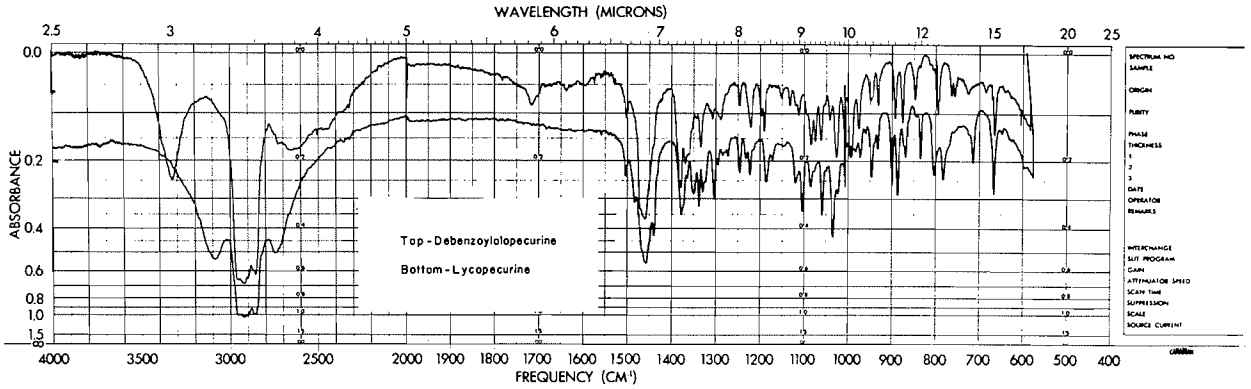

FIG. 2. The i.r. spectra (Nujol) of lycopecurine (bottom trace) and debenzoylalopecurine.

cm^{-1} in the i.r. The i.r. spectrum also showed no olefinic absorption, and it thus appeared that the alkaloid was pentacyclic. This view was strengthened by the fact that the i.r. spectrum showed an unusual absorption band at 1505 cm^{-1} (see Fig. 2). During our work on the pentacyclic alkaloid alopecurine (**1**, R = COC_6H_5) (1) we had noticed an absorption band in the 1490–1510 cm^{-1} region of the spectra of this alkaloid and its derivatives, *e.g.*, debenzoylalopecurine (**1**, R = H), shown in Fig. 2. It has previously been shown that high frequency methylene vibrations are frequently associated with tightly-bridged systems (4, 5), and since the tetracyclic *Lycopodium* alkaloids do not show this absorption band, this suggested that lycopecurine might have the alopecurine skeleton. Since the known lycopodium alkaloids are invariably oxygenated (or unsaturated) at C-5, structure **2** (without regard to stereochemistry at C-5) seemed worthy of consideration. However, attempts at a direct correlation of lycopecurine with alopecurine were precluded by a lack of material and we turned to X-ray methods for confirmation of the structure.

Lycopecurine hydrobromide crystallizes in two orthorhombic forms, the α-form from methanol–acetone and the β-form from methanol – ethyl acetate. The crystal data for these two modifica-

Can. J. Chem. Downloaded from www.nrcresearchpress.com by 210.87.254.105 on 09/05/12
For personal use only.

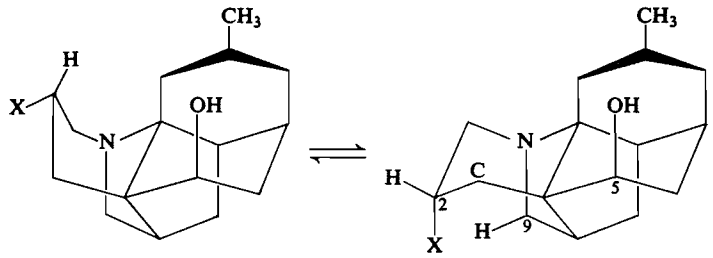

Alopecurine (X = OCOPh) Lycopecurine (X = H)

SCHEME 1

TABLE 1. Crystal data for the polymorphic forms of lycopecurine hydrobromide

Parameter	α-Form (m.p. 308–312°)	β-Form (m.p. 305–307°)
a	9.46 Å	11.64 Å
b	17.30 Å	14.33 Å
c	9.17 Å	8.81 Å
V	1501 Å^3	1470 Å^3
$d_{obs.}$ $^{26°}$	1.41 g/cm^3	1.43 g/cm^3
$d_{calcd.}$	1.46 g/cm^3	1.49 g/cm^3
Space group	$P2_12_12_1$	$P2_12_12_1$
Z	4	4

tions are shown in Table 1. The complete solution,[3] including absolute configuration, was obtained on the α-form and is shown in Fig. 3. Lycopecurine is thus represented by structure **2**. It is of interest to note that ring C is in the chair conformation. In alopecurine and debenzoylalopecurine ring C adopts the twist conformation (1). As summarized in Scheme 1, it appears that the non-bonded interaction between an oxygen substituent at C-2 and the hydrogen shown at C-9 is sufficient to tip the energy balance in favor of the twist conformation.

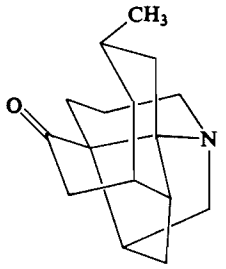

3

[3]Complete details of the X-ray analysis will be published separately.

[4]The general experimental details are the same as those given in Part 2 of this series (1).

Recently, dehydrolycopecurine (**3**) has been isolated from *L. inundatum* and has been correlated with lycopecurine (6).

Experimental[4]

Lycopecurine

Lycopecurine, m.p. 239–241°, was isolated as previously described (1). Mass spectrum: see Fig. 1. The i.r. spectrum: see Fig. 2.

Lycopecurine Hydrobromide

A solution of lycopecurine (8 mg) in acetone was acidified with two drops of concentrated hydrobromic acid. The crystalline material obtained on standing was recrystallized from methanol–acetone to give lycopecurine hydrobromide (α-form), m.p. 308–312° (dec). Crystallization from methanol – ethyl acetate provided the β-form, m.p. 305–307° (dec). The properties of the

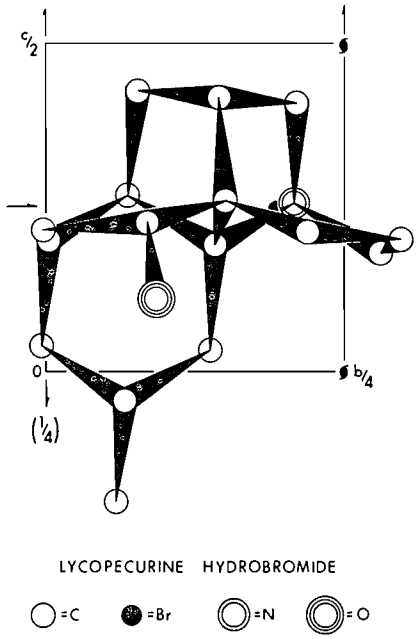

FIG. 3. Perspective drawing of a molecule of lycopecurine hydrobromide.

Can. J. Chem. Downloaded from www.nrcresearchpress.com by 210.87.254.105 on 09/05/12
For personal use only.

two forms are described in Table 1. Because of the limited amount of material available, combustion analyses were not performed. The i.r. spectrum (β-form): ν_{max}(Nujol) 3370 (OH), 2550–2750 ($^+$NH), 1505 cm^{-1}.

Dehydrolycopecurine

Lycopecurine (5 mg) was dissolved in acetone (2 ml) and Jones' reagent (2 drops) was added. Methanol (2 drops) was added after 5 min and the resulting solution evaporated to dryness. The residue was dissolved in chloroform and washed with dilute sodium bicarbonate. Evaporation of the chloroform left a low melting solid which was purified by sublimation, m.p. 55–56°. The i.r. spectrum: ν_{max}($CHCl_3$) 1695, 1500 cm^{-1}.

Mol. Wt. Calcd. for $C_{16}H_{23}NO$: 245.1780. Found (h.r.m.s.): 245.1785.

We wish to thank Drs. S. Valverde-Lopez and B. Altenkirk for their contributions to the early phases of this work, and the National Research Council of Canada for financial support.

1. W. A. Ayer, B. Altenkirk, N. Masaki, and S. Valverde-Lopez. Can. J. Chem. **47**, 2449 (1969).
2. S. Valverde-Lopez. Ph.D. Thesis. University of Alberta, Edmonton, Alberta. 1966.
3. D. B. MacLean. *In* The Alkaloids. Vol. 10. *Edited by* R. H. F. Manske. Academic Press, Inc., New York, N.Y., 1968. p. 377–379, and references quoted therein.
4. L. De Vries and P. R. Ryason. J. Org. Chem. **26**, 621 (1961).
5. G. Eglington, J. Martin, and W. Parker. J. Chem. Soc. 1243 (1965).
6. J. C. Braekman, C. Hootele, and W. A. Ayer. Bull. Soc. Chim. Belg. In press.
7. W. A. Ayer and B. Altenkirk. Can. J. Chem. **47**, 2457 (1969).

Structure of the Amino Sugar Component in Baker's Yeast Mannan[1]

P. A. J. Gorin

Prairie Regional Laboratory, National Research Council of Canada, Saskatoon, Saskatchewan

Received September 1, 1970

Baker's yeast mannan was methylated and the fully methylated polysaccharide hydrolyzed. The product contained a trace of 2-deoxy-3,6-di-*O*-methyl-2-methylamino-glucose which was characterized chromatographically. It likely arose from one or more 4-*O*-substituted 2-acetamido-2-deoxy-D-glucopyranose units (or the 5-*O*-substituted furanosyl isomer). One possibility is that it arose from a 4-*O*-substituted 2-acetamido-(1-L-β-aspartamido)-1,2-dideoxy-β-D-glucopyranose unit which is probably the bridge in one of the carbohydrate–peptide links in the glycoprotein of the cell wall.

Canadian Journal of Chemistry, 49, 527 (1971)

Ethylenediamine extraction of baker's yeast cell walls gives rise to two glycoproteins which are distinguishable on ultracentrifugation, but on prolonged extraction only the component with the lower sedimentation coefficient is formed (1). Sentandreu and Northcote have examined the glycoprotein in detail and shown that it contains two types of peptide–carbohydrate linkages. One linkage is probably represented by 2-acetamido-(1-L-β-aspartamido)-1,2-dideoxy-β-D-glucopyranose which connects a high molecular weight mannan moiety to a peptide (2). The other is mannose, or oligosaccharides consisting of mannose units, connected by glycosidic linkages to the hydroxyl groups of serine and threonine (3).

The glucosamine unit or units are *N*-acetylated and some, at least, are resistant to oxidation by periodate (2). From these data 3-*O*- and/or 4-*O*-substituted 2-acetamido-2-deoxy-D-glucopyranose units were considered to be the most likely (2) although 5-*O*-substitution of furanose units or the presence of more than one *O*-substituent per sugar unit is also possible. The present study describes a methylation–fragmentation study on yeast mannan derived from the glycoproteins and identification of a partially methylated glucosamine fragment.

The mannan was more amenable to methylation than the glycoprotein which is insoluble in *N*,*N*-dimethylformamide. The mannan was obtained by extraction of yeast cells with hot aqueous alkali and purified via the insoluble copper complex formed with Fehling solution (4). It contains, in addition to mannose, small amounts of amino acids, phosphate, and glucos-

[1]Issued as NRCC No. 11629.

Can. J. Chem. Downloaded from www.nrcresearchpress.com by 210.87.254.105 on 09/05/12
For personal use only.

two forms are described in Table 1. Because of the limited amount of material available, combustion analyses were not performed. The i.r. spectrum (β-form): ν_{max}(Nujol) 3370 (OH), 2550–2750 ($^+$NH), 1505 cm^{-1}.

Dehydrolycopecurine

Lycopecurine (5 mg) was dissolved in acetone (2 ml) and Jones' reagent (2 drops) was added. Methanol (2 drops) was added after 5 min and the resulting solution evaporated to dryness. The residue was dissolved in chloroform and washed with dilute sodium bicarbonate. Evaporation of the chloroform left a low melting solid which was purified by sublimation, m.p. 55–56°. The i.r. spectrum: ν_{max}($CHCl_3$) 1695, 1500 cm^{-1}.

Mol. Wt. Calcd. for $C_{16}H_{23}NO$: 245.1780. Found (h.r.m.s.): 245.1785.

We wish to thank Drs. S. Valverde-Lopez and B. Altenkirk for their contributions to the early phases of this work, and the National Research Council of Canada for financial support.

1. W. A. Ayer, B. Altenkirk, N. Masaki, and S. Valverde-Lopez. Can. J. Chem. **47**, 2449 (1969).
2. S. Valverde-Lopez. Ph.D. Thesis. University of Alberta, Edmonton, Alberta. 1966.
3. D. B. MacLean. *In* The Alkaloids. Vol. 10. *Edited by* R. H. F. Manske. Academic Press, Inc., New York, N.Y., 1968. p. 377–379, and references quoted therein.
4. L. De Vries and P. R. Ryason. J. Org. Chem. **26**, 621 (1961).
5. G. Eglington, J. Martin, and W. Parker. J. Chem. Soc. 1243 (1965).
6. J. C. Braekman, C. Hootele, and W. A. Ayer. Bull. Soc. Chim. Belg. In press.
7. W. A. Ayer and B. Altenkirk. Can. J. Chem. **47**, 2457 (1969).

Structure of the Amino Sugar Component in Baker's Yeast Mannan[1]

P. A. J. Gorin

Prairie Regional Laboratory, National Research Council of Canada, Saskatoon, Saskatchewan

Received September 1, 1970

Baker's yeast mannan was methylated and the fully methylated polysaccharide hydrolyzed. The product contained a trace of 2-deoxy-3,6-di-*O*-methyl-2-methylamino-glucose which was characterized chromatographically. It likely arose from one or more 4-*O*-substituted 2-acetamido-2-deoxy-D-glucopyranose units (or the 5-*O*-substituted furanosyl isomer). One possibility is that it arose from a 4-*O*-substituted 2-acetamido-(1-L-β-aspartamido)-1,2-dideoxy-β-D-glucopyranose unit which is probably the bridge in one of the carbohydrate–peptide links in the glycoprotein of the cell wall.

Canadian Journal of Chemistry, 49, 527 (1971)

Ethylenediamine extraction of baker's yeast cell walls gives rise to two glycoproteins which are distinguishable on ultracentrifugation, but on prolonged extraction only the component with the lower sedimentation coefficient is formed (1). Sentandreu and Northcote have examined the glycoprotein in detail and shown that it contains two types of peptide–carbohydrate linkages. One linkage is probably represented by 2-acetamido-(1-L-β-aspartamido)-1,2-dideoxy-β-D-glucopyranose which connects a high molecular weight mannan moiety to a peptide (2). The other is mannose, or oligosaccharides consisting of mannose units, connected by glycosidic linkages to the hydroxyl groups of serine and threonine (3).

The glucosamine unit or units are *N*-acetylated and some, at least, are resistant to oxidation by periodate (2). From these data 3-*O*- and/or 4-*O*-substituted 2-acetamido-2-deoxy-D-glucopyranose units were considered to be the most likely (2) although 5-*O*-substitution of furanose units or the presence of more than one *O*-substituent per sugar unit is also possible. The present study describes a methylation–fragmentation study on yeast mannan derived from the glycoproteins and identification of a partially methylated glucosamine fragment.

The mannan was more amenable to methylation than the glycoprotein which is insoluble in *N*,*N*-dimethylformamide. The mannan was obtained by extraction of yeast cells with hot aqueous alkali and purified via the insoluble copper complex formed with Fehling solution (4). It contains, in addition to mannose, small amounts of amino acids, phosphate, and glucos-

[1]Issued as NRCC No. 11629.

Can. J. Chem. Downloaded from www.nrcresearchpress.com by 210.87.254.42 on 09/05/12
For personal use only.

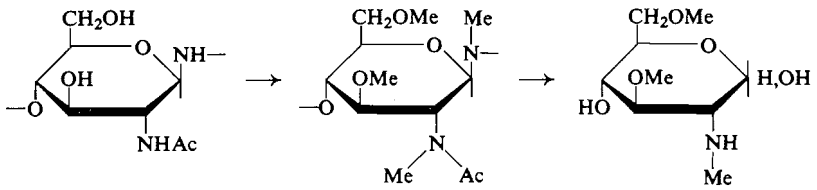

1 2 3

amine (2). An estimate of 1 mol of the latter per molecular weight of 73 000 was made, but this may be low if hydrolytic decomposition of glucosamine took place. Korn and Northcote (1) quote 59 000 as the molecular weight of baker's yeast mannan.

The mannan was partially *O*-methylated by the Haworth procedure (5) and methylation completed by the method of Kuhn *et al.* (6). During the latter procedure the nitrogen proton of the *N*-acetyl group (**1**) was replaced by a methyl group **2** (7, 8). Methanolysis of the methylated mannan by refluxing methanolic hydrogen chloride followed by hydrolysis with hydrochloric acid gave a mixture of sugars. These corresponded on a paper chromatogram to di-*O*-, tri-*O*-, and tetra-*O*-methyl mannoses and a faint ninhydrin-positive 2-deoxy-di-*O*-methyl-2-methylaminoglucose with R_{Rh} 1.00 (Table 1). The latter was concentrated by cellulose column chromatography. The resulting fraction, when examined on the Spinco amino acid analyzer, gave a peak with a retention time (r.t.) corresponding to the 3,6-di-*O*-methyl **3**, but not the 4,6-di-*O*-methyl derivative (9) (Table 1, Fig. 1). The peak was typically broader than that arising from an amino acid. The presence of the 3,6-di-*O*-isomer was confirmed by g.l.c. of its trimethylsilyl (t.m.s.) derivative (9), since a peak with typical r.t. (Table 1, Fig. 2) was obtained. A peak corresponding to the 4,6-di-*O*-isomer was absent. The structure of the *N*-methyl sugar is consistent with the presence of a 4-*O*-substituted 2-acetamido-2-deoxy-D-glucopyranosyl unit or units although the possibility of a 5-*O*-substituted furanosyl counterpart is not eliminated. The amino sugar could be part of a 2-acetamido-(1-L-β-aspartamido)-1,2-dideoxy-β-D-glucopyranosyl moiety.

Although 2-deoxy-3,6-di-*O*-methyl-2-methylamino-glucose could arise from chitin, the presence of such a contaminant is unlikely with the extraction procedure used. Furthermore, when the mannan was treated with a chitinase from *Streptomyces griseus*, no *N*-acetyl-D-glucosamine could be detected on paper chromatograms using the Elson–Morgan spray reagent.

The above results can be related to the methylation–fragmentation data obtained from the 2-acetamido-2-deoxy-D-gluco-D-mannans of *Pichia bovis* and *Saccharomyces phaseolosporus* (7). The hydrolysis products each contained 2-deoxy-3,4,6-tri-*O*-methyl-2-methylamino-glucose arising from amino sugar non-reducing end-units and small amounts of the 3,6-di-*O*-methyl isomer. This fragment could well also arise from *N*-acetyl glucosamine unit(s) associated with polysaccharide–protein linkages.

TABLE 1. Chromatographic characteristics of unknown fragment compared with those of *O*-methylated 2-deoxy-2-methylamino-D-glucoses (9)

O-Methyl derivative of 2-deoxy-2-methylamino-D-glucose	Rate relative to rhamnose on a paper chromatogram*	Retention time on amino acid analyzer, relative to phenylalanine (min)	Retention time of t.m.s. derivative on g.l.c. (main peak) (min)†
Unsubstituted	0.49	−6	14.4
3-*O*-	0.62	−31	10.9
4-*O*-	0.71	−18	8.5
6-*O*-	0.71	−11	16.0
3,4-Di-*O*-	1.00	+40	7.6
3,6-Di-*O*-	1.00	−40	12.1
4,6-Di-*O*-	1.00	+8	8.8
3,4,6-Tri-*O*-	1.33	+55	8.5
Unknown	1.00	−40	12.0

*Solvent: butyl alcohol – ethanol – pyridine – water, 40:11:2:19 v/v/v/v; spray: ninhydrin.
†Column: 3 ft × 1/8 in. i.d. glass column containing 10% neopentylglycol sebacate on Chromosorb W(80–100 mesh) at 140°.

Can. J. Chem. Downloaded from www.nrcresearchpress.com by 210.87.254.42 on 09/05/12
For personal use only.

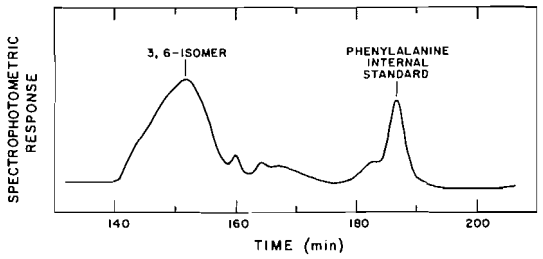

FIG. 1. Pattern obtained from the *O*-methyl 2-deoxy-2-methylamino-glucose fraction using the Spinco amino acid analyzer.

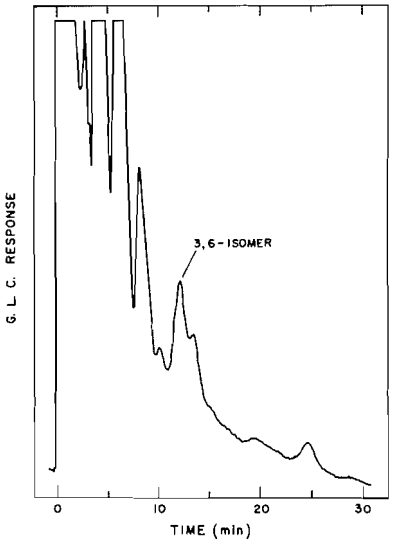

FIG. 2. The g.l.c. of t.m.s. derivatives of the *O*-methyl 2-deoxy-2-methylamino-glucose fraction.

Experimental

Methylation–Fragmentation Study on Baker's Yeast Mannan

Mannan (1.0 g) was extracted from Fleischmann's baker's yeast with hot aqueous alkali and purified via the insoluble copper complex formed with Fehling solution (4). A sample (1.0 g) was partially methylated with aqueous sodium hydroxide – dimethyl sulfate (5) and methylation was completed by the Kuhn procedure (6). The product did not show hydroxyl absorption at 3400–3650 cm^{-1} in the i.r. A portion (0.20 g) of the total product (0.95 g) was refluxed in 3% methanolic hydrogen chloride (20 ml) for 18 h, which was evaporated and hydrolysis completed with 3 *M* HCl (20 ml) at 100° for 3 h. Following evaporation the product was examined on a paper chromatogram (solvent: butyl alcohol – ethanol–water (40:11:19 v/v/v)) and with the *p*-anisidine hydrochloride spray spots were obtained with color reactions and R_f's corresponding to di-*O*-, tri-*O*-, and tetra-*O*-methylmannose. With the ninhydrin spray a faint blue spot was obtained running at the speed of rhamnose. This corresponded to a 2-deoxy-di-*O*-methyl-2-methylamino-glucose and was concentrated by chromatography of the mixture on a cellulose column (eluant: benzene–ethanol 5:1 v/v). A portion (10 mg) of the concentrate (29 mg) was examined on a Model 120C Spinco amino acid analyzer with the UR-30 type resin and a 250 min running time ((10) see Spinco Procedures Manual 120C-PM-1); a peak was obtained corresponding in r.t. to 2-deoxy-3,6-di-*O*-methyl-2-methylamino-glucose ((9) Table 1, Fig. 1). A portion (2 mg) of the concentrate was trimethylsilylated and examined by g.l.c. (9). The resulting chromatogram, depicted in Fig. 2, contained a peak with an r.t. (Table 1) corresponding to the 3,6-di-*O*-methyl derivative.

Treatment of Mannan with Chitinase from Streptomyces griseus

Samples of mannan (50 mg) were dissolved in 0.2 *M* phosphate buffers (2 ml) of p*H* 4, 5, 6, 7, and 8. Chitinase (10 mg), isolated from *Streptomyces griseus* and supplied by Calbiochem, was added to each solution. After 18 h, excess ethanol (10 ml) was added to precipitate the polysaccharides, and the supernatants were decanted. These were evaporated to residues which were deionized by aqueous slurries of mixed Amberlite IR120 (H^+ form) and Dowex 1-X8 (bicarbonate form). The filtered solutions were evaporated and examined on a paper chromatogram (solvent: as above, spray: the Elson–Morgan reagent as used by Partridge and Westall (11)). Mauve spots corresponding to *N*-acetyl-D-glucosamine were not detected. Identical attempted enzymolyses were carried out in the presence of *N*-acetyl-D-glucosamine (0.2 mg) which would be approximately the amount of amino sugar formed (2) if it were combined completely in the form of chitin. In these runs, strong mauve spots of typical R_f were detected on a paper chromatogram.

The author gratefully thanks Mr. R. J. Magus and Mr. C. M. Christ for technical assistance.

1. E. D. KORN and D. H. NORTHCOTE. Biochem. J. **75**, 12 (1960).
2. R. SENTANDREU and D. H. NORTHCOTE. Biochem. J. **109**, 419 (1968).
3. R. SENTANDREU and D. H. NORTHCOTE. Carbohyd. Res. **10**, 584 (1969).
4. W. N. HAWORTH, E. L. HIRST, and F. A. ISHERWOOD. J. Chem. Soc. 788 (1937).
5. W. N. HAWORTH. J. Chem. Soc. 8 (1915).
6. R. KUHN, H. TRISCHMANN, and I. LÖW. Angew. Chem. **67**, 32 (1955).
7. P. A. J. GORIN, J. F. T. SPENCER, and A. J. FINLAYSON. Carbohyd. Res. To be published.
8. R. U. LEMIEUX and R. J. CUSHLEY. Can. J. Chem. **41**, 858 (1963).
9. P. A. J. GORIN and A. J. FINLAYSON. Carbohyd. Res. Submitted for publication.
10. D. H. SPACKMAN, W. H. STEIN, and S. MOORE. Anal. Chem. **30**, 1190 (1958).
11. S. M. PARTRIDGE and R. G. WESTALL. Biochem. J. **42**, 238 (1948).

Can. J. Chem. Downloaded from www.nrcresearchpress.com by 210.87.254.42 on 09/05/12
For personal use only.

Can. J. Chem. Downloaded from www.nrcresearchpress.com by 210.87.254.105 on 09/05/12
For personal use only.

Benzo[*b*]phosphole[1] and Derivatives

T. H. CHAN AND L. T. L. WONG[2]
Department of Chemistry, McGill University, Montreal, Quebec

Received October 8, 1970

A potentially general synthesis of 1-heteroindene has been developed and applied to the preparation of 1-phenylbenzo[*b*]phosphole, a novel heterocyclic system.

Une synthèse qui peut s'avérer générale pour la synthèse d'hétéro-1 indène a été développée et appliquée à la préparation du phényl-1 benzo[*b*]phosphole, un nouveau système hétérocyclique.

Canadian Journal of Chemistry, **49**, 530 (1971)

Since the first isolation of 9-phenyl-9-phosphafluorene (**3**, R = C_6H_5) in 1953 (1), the chemistry of phosphole (**1**) derivatives has been extensively investigated (2, 3). Recent achievements are the synthesis of 1-methylphosphole (4) and 1-phenylphosphole (5). However, other than a brief report on the preparation of a highly substituted benzo[*b*]phosphole derivative (6), there is lacking a description on the chemistry of benzo[*b*]phosphole (**2**). This is somewhat surprising in view of the fact that the aromatic character involving delocalization of phosphorus electron pair has been a subject of much current interest (7). In this communication, we wish to report on a potentially general synthesis of 1-heteroindene; its application to the preparation of a simple benzo[*b*]phosphole derivative and the chemistry of the benzo[*b*]phosphole system.

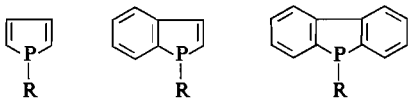

1 **2** **3**

A general synthesis of 1-heteroindene is developed according to Scheme 1. Thus, 2,3-dihydrothiophene-1,1-dioxide (**5***a*) reacted with *trans-trans*-1,4-diacetoxybutadiene (**4**) at 150° for 7 days to give 2,3-dihydrobenzothiophene-1,1-dioxide (**6***a*). The construction of benzene ring is based on the method developed by Hill and Carlson (8). Free radical bromination of **6***a* with *N*-bromosuccinimide (NBS) followed by dehydrobromination with triethylamine gave benzothiophene-1,1-dioxide, identical with authentic compound.

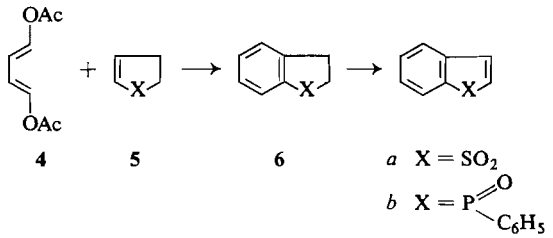

4 **5** **6** *a* X = SO_2 *b* X = $P(=O)C_6H_5$

SCHEME 1

1-Phenyl-2-phospholene 1-oxide (**5***b*), obtained from the reaction of butadiene with phenyldichlorophosphine (9) and basic hydrolysis (10), reacted with **4** at 150° for 10 days to give 50% yield (based on reacted **5***b*) of 1-phenyl-2,3-dihydrobenzo[*b*]phosphole 1-oxide (**6**),[3] m.p. 97–101°. The p.m.r. spectrum ($CDCl_3$) of **6***b* was in accord with structure [2H multiplet at 2.5, 2H multiplet at 3.3, and 9H multiplet at 7.5 p.p.m.]. Benzoyl peroxide-initiated NBS bromination of **6***b* in refluxing benzene for 3 h followed by triethylamine dehydrobromination gave 1-phenylbenzo[*b*]phosphole 1-oxide as the sole product, isolable by sublimation as a colorless hygroscopic solid, m.p. 84–88°.[3] Its p.m.r. spectrum showed only aromatic and vinylic hydrogens. It was reduced to 1-phenylbenzo[*b*]phosphole (**2**, R =

[1]Phosphindole is the trivial name for this compound according to Ring Index.

[2]Holder of an NRCC Studentship 1968–1970.

[3]All new compounds have satisfactory elemental analysis and spectroscopic data consistent with structures.

phenyl) by trichlorosilane (11) in refluxing benzene. Compound **2** could be purified by sublimation and had m.p. 66–68°.[3] The mass spectrum showed a strong molecular ion (exact mass; found: 210.0591; calcd: 210.0598).

The u.v. spectrum of **2** (R = phenyl) in ethanol showed λ_{max} (log ε) at 233 (4.39), 260 (4.05), 306 (3.56), 316 nm (3.56), a pattern common to most benzo-heteroaromatics, and resembled closely that of 1-phenylindole[4] [217(4.41), 258(4.26), 291(3.91), 297 nm (3.89)]. The phenyl and vinylic protons were well separated in the 220 MHz n.m.r. spectrum of **2**.[5] The vinylic protons could be considered as part of the AMX (X = phosphorus) system with the following spectral parameters: J_{AM} = 7.2, J_{AX} = 16, J_{MX} = 38 Hz; δ_M = 6.80 and δ_A = 7.49. The coupling constants are in close agreement with those deduced for 1-methylphosphole (4). The chemical shifts of the vinylic protons are in the region generally considered as aromatic. Compound **2** (R = phenyl) quaternized with benzyl bromide to the corresponding phosphonium salt. Compound **2** could also be oxidized readily by air to the oxide. In these respects, the chemistry of **2** (R = phenyl) differs somewhat from that of **1** (R = methyl or phenyl). The oxides of **1** dimerized spontaneously and have eluded isolation thus far.

This work was supported by a grant from the National Research Council of Canada for which grateful acknowledgement is made.

1. G. WITTIG and G. GEISSLER. Ann. **580**, 44 (1953).
2. A. N. HUGHES and C. SRIVANAVIT. J. Heterocycl. Chem. **7**, 1 (1970).
3. K. D. BERLIN and D. M. HELLWEGE. *In* Topics in phosphorus chemistry. Vol. 6. *Edited by* M. Grayson and E. J. Griffith. Interscience, New York, N.Y. 1969.
4. L. D. QUIN, J. G. BRYSON, and C. G. MORELAND. J. Amer. Chem. Soc. **91**, 3308 (1969).
5. G. MÄRKL and R. POTTHAST. Tetrahedron Lett. 1755 (1968).
6. M. D. RAUSCH and L. P. KLEMAN, J. Amer. Chem. Soc. **89**, 5732 (1967).
7. W. EGAN, R. TANG, G. ZON, and K. MISLOW. J. Amer. Chem. Soc. **92**, 1442 (1970) and references cited therein.
8. R. K. HILL and R. M. CARLSON. J. Org. Chem. **30**, 2414 (1965).
9. W. B. MCCORMACK. U.S. Pat. 2 663 736 and 2 663 737 (December 22, 1953), also Chem. Abstr. **49** 7601 (1955).
10. L. D. QUIN, J. P. GRATZ, and T. P. BARKET. J. Org. Chem. **33**, 1034 (1968).
11. H. FRITZSCHE, U. HASSERODT, and F. KORTE. Chem. Ber. **98**, 171 (1965).

[4]Sample kindly supplied by Dr. M. Kuehne, University of Vermont, Burlington, Vermont.
[5]Spectrum obtained from the 220 MHz laboratory, Sheridan Park, Ontario.

Synthesis of 2,3-Dihydrotriquinacen-2-one[1,2]

ROBERT RUSSO,[3] YVON LAMBERT, AND PIERRE DESLONGCHAMPS[4]
Laboratoire de synthèse organique, Département de chimie, Université de Sherbrooke, Sherbrooke, Québec

Received November 3, 1970

A synthesis of the title compound from Thiele's acid is reported.

La synthèse du dihydro-2,3 triquinacènone-2 a été effectuée à partir de l'acide de Thiele.

Canadian Journal of Chemistry, 49, 531 (1971)

The synthesis of triquinacene (tricyclo-[5.2.1.$0^{4,10}$]deca-2,5,8-triene) was first achieved by Woodward and his co-workers (1). Later, another synthesis has also appeared in the literature (2).

We wish to report a synthesis of 2,3-dihydrotriquinacen-2-one (**1**), a derivative of triquinacene, by a different approach.

The Thiele's acid, (**2**) (3) was transformed into the diketone **5** (m.p. 113–115 °C) via the acid chloride **3** (m.p. 61–12 °C, lit. m.p. 62 °C (4)) and the azide **4** (m.p. 75–77 °C dec.) in 55% over-

[1]Support for this work by the National Research Council of Canada, Ottawa and by the "Ministère de l'Education," Québec, is gratefully acknowledged.
[2]This work has been presented at The First Annual Symposium on Organic Synthesis, August 24–26, 1970, Santa Cruz, California.
[3]Holder of a "bourse du Ministère de l'Education," Québec, 1966–1970.
[4]A. P. Sloan Fellow, 1970–1972.

Can. J. Chem. Downloaded from www.nrcresearchpress.com by 210.87.254.105 on 09/05/12
For personal use only.

phenyl) by trichlorosilane (11) in refluxing benzene. Compound **2** could be purified by sublimation and had m.p. 66–68°.[3] The mass spectrum showed a strong molecular ion (exact mass; found: 210.0591; calcd: 210.0598).

The u.v. spectrum of **2** (R = phenyl) in ethanol showed λ_{max} (log ε) at 233 (4.39), 260 (4.05), 306 (3.56), 316 nm (3.56), a pattern common to most benzo-heteroaromatics, and resembled closely that of 1-phenylindole[4] [217(4.41), 258(4.26), 291(3.91), 297 nm (3.89)]. The phenyl and vinylic protons were well separated in the 220 MHz n.m.r. spectrum of **2**.[5] The vinylic protons could be considered as part of the AMX (X = phosphorus) system with the following spectral parameters: J_{AM} = 7.2, J_{AX} = 16, J_{MX} = 38 Hz; δ_M = 6.80 and δ_A = 7.49. The coupling constants are in close agreement with those deduced for 1-methylphosphole (4). The chemical shifts of the vinylic protons are in the region generally considered as aromatic. Compound **2** (R = phenyl) quaternized with benzyl bromide to the corresponding phosphonium salt. Compound **2** could also be oxidized readily by air to the oxide. In these respects, the chemistry of **2** (R = phenyl) differs somewhat from that of **1** (R = methyl or phenyl). The oxides of **1** dimerized spontaneously and have eluded isolation thus far.

This work was supported by a grant from the National Research Council of Canada for which grateful acknowledgement is made.

1. G. WITTIG and G. GEISSLER. Ann. **580**, 44 (1953).
2. A. N. HUGHES and C. SRIVANAVIT. J. Heterocycl. Chem. **7**, 1 (1970).
3. K. D. BERLIN and D. M. HELLWEGE. *In* Topics in phosphorus chemistry. Vol. 6. *Edited by* M. Grayson and E. J. Griffith. Interscience, New York, N.Y. 1969.
4. L. D. QUIN, J. G. BRYSON, and C. G. MORELAND. J. Amer. Chem. Soc. **91**, 3308 (1969).
5. G. MÄRKL and R. POTTHAST. Tetrahedron Lett. 1755 (1968).
6. M. D. RAUSCH and L. P. KLEMAN, J. Amer. Chem. Soc. **89**, 5732 (1967).
7. W. EGAN, R. TANG, G. ZON, and K. MISLOW. J. Amer. Chem. Soc. **92**, 1442 (1970) and references cited therein.
8. R. K. HILL and R. M. CARLSON. J. Org. Chem. **30**, 2414 (1965).
9. W. B. MCCORMACK. U.S. Pat. 2 663 736 and 2 663 737 (December 22, 1953), also Chem. Abstr. **49** 7601 (1955).
10. L. D. QUIN, J. P. GRATZ, and T. P. BARKET. J. Org. Chem. **33**, 1034 (1968).
11. H. FRITZSCHE, U. HASSERODT, and F. KORTE. Chem. Ber. **98**, 171 (1965).

[4]Sample kindly supplied by Dr. M. Kuehne, University of Vermont, Burlington, Vermont.
[5]Spectrum obtained from the 220 MHz laboratory, Sheridan Park, Ontario.

Synthesis of 2,3-Dihydrotriquinacen-2-one[1,2]

ROBERT RUSSO,[3] YVON LAMBERT, AND PIERRE DESLONGCHAMPS[4]
Laboratoire de synthèse organique, Département de chimie, Université de Sherbrooke, Sherbrooke, Québec

Received November 3, 1970

A synthesis of the title compound from Thiele's acid is reported.

La synthèse du dihydro-2,3 triquinacènone-2 a été effectuée à partir de l'acide de Thiele.

Canadian Journal of Chemistry, 49, 531 (1971)

The synthesis of triquinacene (tricyclo-[5.2.1.$0^{4,10}$]deca-2,5,8-triene) was first achieved by Woodward and his co-workers (1). Later, another synthesis has also appeared in the literature (2).

We wish to report a synthesis of 2,3-dihydrotriquinacen-2-one (**1**), a derivative of triquinacene, by a different approach.

The Thiele's acid, (**2**) (3) was transformed into the diketone **5** (m.p. 113–115 °C) via the acid chloride **3** (m.p. 61–12 °C, lit. m.p. 62 °C (4)) and the azide **4** (m.p. 75–77 °C dec.) in 55% over-

[1]Support for this work by the National Research Council of Canada, Ottawa and by the "Ministère de l'Education," Québec, is gratefully acknowledged.
[2]This work has been presented at The First Annual Symposium on Organic Synthesis, August 24–26, 1970, Santa Cruz, California.
[3]Holder of a "bourse du Ministère de l'Education," Québec, 1966–1970.
[4]A. P. Sloan Fellow, 1970–1972.

Can. J. Chem. Downloaded from www.nrcresearchpress.com by 210.87.254.5 on 09/05/12
For personal use only.

Can. J. Chem. Downloaded from www.nrcresearchpress.com by 210.87.254.5 on 09/05/12
For personal use only.

1

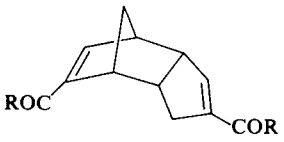

2 R = OH
3 R = Cl
4 R = N_3

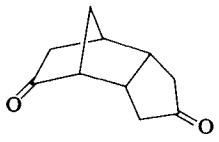

5

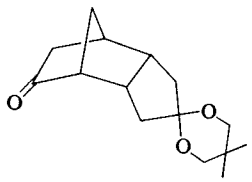

6

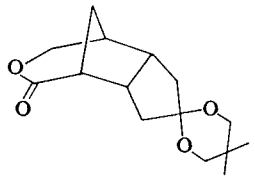

7

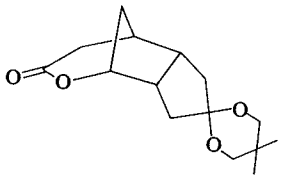

8

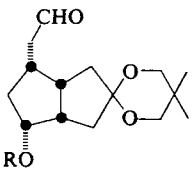

9 R = H
10 R = CH_3CO

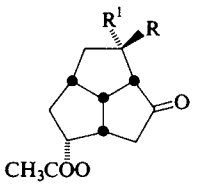

11 R = H; R^1 = OH
12 R = OH; R^1 = H

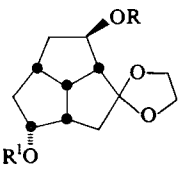

13 R = H; R^1 = CH_3CO
14 R = R^1 = H
15 R = R^1 = CH_3SO_2

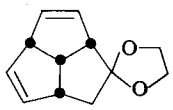

16

all yield. Monoketalization of diketone **5** with 1 equiv. of 2,2-dimethylpropane 1,3-diol in refluxing benzene containing *p*-toluenesulfonic acid gave **6**[5] (m.p. 125–126 °C, 70% yield). Baeyer–Villiger oxidation of **6** with *m*-chloroperbenzoic acid in refluxing dichloromethane gave the lactone mixture **7** and **8** (90% yield, ratio 1:3). The undesired lactone **7** was removed selectively by hydrolysis (*N* NaOH–DME, 25 °C).

Reduction of **8** (m.p. 158 °C) with diisobutylaluminum hydride furnished the hydroxy aldehyde **9** (75% yield). The corresponding acetate **10** was converted by acid treatment to a 1:1 mixture of **11** (m.p. 73–74 °C) and **12** (m.p. 141–142 °C) having the tricyclic skeleton.

Ketalization of either epimer gave the same ketal alcohol **13**[6] (m.p. 73–74 °C) which was then hydrolyzed (→ **14**, m.p. 148 °C) and mesylated (→ **15**, 111 °C). Treatment of **15** with potassium *t*-butoxide in dimethyl sulfoxide gave ketal **16** as the major product (50% yield) which, by

[5]Wolff–Kishner reduction of **6** followed by acid hydrolysis gave *endo*-tetrahydrodicyclopentadien-2-one identical with a sample synthesized by an unambiguous route.

[6]Isomer **11** must have been first converted into **12** (via retroaldolization–aldolization) before ketalization took place.

acid hydrolysis, afforded the dienone **1** (1) (DNP derivative m.p. 155 °C). The dienone **1** was shown to be identical (i.r., t.l.c. and DNP m.p. comparison) with an authentic sample.[7]

All new crystalline compounds reported in this communication gave satisfactory elemental analysis and spectroscopic data.

[7]Obtained by oxidation of 2-*endo*-2,3-dihydrotriquinacenol. We are grateful to Professor R. B. Woodward for his generous gift of this alcohol.

1. R. B. WOODWARD, T. FUKUNAGA, and R. C. KELLY. J. Amer. Chem. Soc. **86**, 3162 (1964); R. C. KELLY. Ph.D. Thesis. Harvard University, Cambridge, Massachusetts, 1965.
2. I. T. JACOBSON. Acta Chem. Scand. **21**, 2235 (1967).
3. G. L. DUNN and J. K. DONAHUE. Tetrahedron Lett. 3485 (1968) and references quoted therein.
4. D. PETERS. J. Chem. Soc. 1832 (1960).

Can. J. Chem. Downloaded from www.nrcresearchpress.com by 210.87.254.5 on 09/05/12
For personal use only.

Can. J. Chem. Downloaded from www.nrcresearchpress.com by 210.87.254.6 on 09/05/12
For personal use only.

Canadian Journal of Chemistry

Published by THE NATIONAL RESEARCH COUNCIL OF CANADA

VOLUME 49 FEBRUARY 15, 1971 NUMBER 4

Kinetics of the Mercury-Photosensitized Decomposition of Propane. Part I. The Overall Mechanism

M. M. PAPIC[1] AND K. J. LAIDLER

Department of Chemistry, University of Ottawa, Ottawa 2, Canada

Received April 22, 1970

The mercury-photosensitized decomposition of propane was investigated from 250 to 350 °C, and at pressures from 5 to 700 Torr. The following products were identified and their initial rates of formation measured: H_2, CH_4, C_2H_4, C_2H_6, $(CH_3)_2CHCH(CH_3)_2$, $(CH_3)_2CHCH_2CH_2CH_3$, and n-C_6H_{14}. The results lead to conclusions about the mechanism. The pressure dependence of the rates were determined and interpreted in terms of a simplified steady-state treatment based on the mechanism.

Canadian Journal of Chemistry, 49, 535 (1971)

Introduction

Recent investigations in this laboratory have been concerned with the mercury-photosensitized decompositions of ethane (1) and dimethyl ether (2–5), the object being to obtain more reliable kinetic parameters for the decompositions of the various radicals produced. In particular, an effort has been made to study the decompositions of these radicals over a range of pressure as well as temperature, in order to obtain the limiting behavior at high and low pressures. The present investigation is concerned with the mercury-photosensitized decomposition of propane, the object being to establish the mechanism and to study the decompositions of the *n*-propyl and *i*-propyl radicals in their high and low pressure regions. The work relates to a study by Lin and Laidler (6) of the decomposition of propane sensitized by azomethane. One matter of particular concern in the present investigation was the establishment of a reliable value for the activation energy for the decomposition of the *n*-propyl radical into $CH_3 + C_2H_4$, seven previous studies (6–12) having given values ranging from 20 to 35 kcal mol^{-1}.

There have been many previous investigations of the mercury-photosensitized decomposition of propane (7, 12–22). This earlier work, together with that on related systems (*cf.* Cvetanovic (23)) has established the main features of the mechanism. Initially the $Hg(^1S_0)$ is excited into $Hg^*(^3P_1)$ which has an excitation energy of 112.2 kcal mol^{-1}

$$Hg + h\nu \rightarrow Hg^*$$

This is followed by

$$Hg^* + C_3H_8 \rightarrow Hg + C_3H_7 + H$$

the radicals produced being either n-C_3H_7 or i-C_3H_7. Below 300 °C the main subsequent reactions are

$$H + C_3H_8 \rightarrow H_2 + C_3H_7 \ (n \text{ or } i)$$

$$2n\text{-}C_3H_7 \rightarrow n\text{-}C_6H_{14}$$

$$2i\text{-}C_3H_7 \rightarrow \text{2,3-dimethylbutane}$$

$$n\text{-}C_3H_7 + i\text{-}C_3H_7 \rightarrow \text{2-methylpentane}$$

$$2n\text{-}C_3H_7 \rightarrow C_3H_8 + C_3H_6$$

$$2i\text{-}C_3H_7 \rightarrow C_3H_8 + C_3H_6$$

$$n\text{-}C_3H_7 + i\text{-}C_3H_7 \rightarrow C_3H_8 + C_3H_6$$

Bywater and Steacie (7) and Back and Takamuku (12) suggested that above 300 °C, methane and additional hydrogen are produced by the following reactions

$$C_3H_7 \ (n \text{ or } i) \rightarrow H + C_3H_6$$

$$C_3H_7 \ (n \text{ or } i) \rightarrow CH_3 + C_2H_4$$

followed by abstractions by H and CH_3. In the present work measurements have been made of

[1]Present address: Department of Chemistry, University of British Columbia, Vancouver 8, British Columbia.

the initial rates of formation of more products than have been studied in previous investigations. All of the expected products have, in fact, been determined with the exception of propylene and the C_4 hydrocarbons, which presented special difficulties.

The present paper deals with the over-all mechanism; the following paper (Part II) analyzes the results for the decompositions and other reactions of the *n*-propyl and *i*-propyl radicals.

Experimental

Apparatus

The reaction was studied in a conventional static system. The reaction vessel was a quartz cylinder about 10 cm in length and about 5 cm in diameter, with plane windows at each end; its volume was 166 cm^3. It was wrapped in asbestos and placed inside a cylindrical iron collar 23 cm in length, 6 cm in diameter, with walls 0.5 cm thick to ensure even heating. The iron collar was well insulated and heated electrically, the heating being regulated by a Thermo Electronic Co. signalling controller potentiometer connected with the control relay. The controller was activated by means of a chromel–alumel thermocouple, and the temperature could be maintained constant within a degree. The temperature of the reaction vessel was measured at three positions by means of chromel–alumel thermocouples.

The concentration of mercury in the reaction zone was controlled by the temperature of a spiral trap in the lead to the reaction vessel. The temperature of the trap was kept constant at −33 °C by means of 1,3-dibromopropane slush.

A low-pressure mercury resonance lamp of low light intensity, operated at 9.0 mA, was supported at about 30 cm from the incident face of the reaction vessel. Between the lamp and the reaction vessel was placed a Corning glass ultraviolet (u.v.) color filter C.S. No 9-54, which was non-transparent for the light of wavelength shorter than 2000 Å; in this way the mercury 1849 Å line was eliminated.

Gas Chromatography

The reaction products were analyzed by a gas chromatograph assembled from commercially available units. As a detection unit the Gow-Mac Co. Model A-9283 thermal conductivity cell for gas chromatography was used, supplied by power from Trygon Electronics power supply Model HR 40-750. The output used was 12 V d.c., and the current through the filament in the detector was 250 mA. In order to obtain high sensitivity the signal from the detector was pre-amplified by means of a Leeds and Northrup stabilized d.c. microvolt amplifier, Model 9835-A. The amplified signal was put through a 10 mV Leeds and Northrup Co. Speedomax recorder, Model S. Edwards Vacuum Ltd. vacuum and pressure controllers, Model V. P. C. -1, were inserted in both the reference flow and the sample flow of the chromatograph, in order to eliminate the fluctuations of pressure between the helium source and the detector.

Materials

The propane used was obtained from Phillips Petroleum Company with stated research-grade purity of 99.99 mol%. It was subjected to several trap-to-trap distillations at −160°; gas-chromatographic analysis of such a sample showed no impurities. The purified propane was stored in a black-painted storage bulb and was degassed from time to time.

The hydrogen, methane, ethylene, ethane, 2,3-dimethylbutane, and 2-methylpentane used for calibrations of the chromatograph were obtained from the Phillips Petroleum Company; *n*-hexane was obtained from the Matheson Company. 2,3-Dimethylbutane, 2-methylpentane, and *n*-hexane were subjected to thorough degassing at −130 °C to eliminate air.

Procedure and Analysis

Before each experiment the system was evacuated to 10^{-5} Torr. Propane was allowed to pass over mercury at room temperature and then through the spiral trap at −33 °C, after which it was admitted to the reaction vessel. The mercury lamp was switched on about 30 min before use; the reaction was started by the removal of a shutter and was stopped by switching off the lamp. The residual propane and the reaction products were first condensed in a trap immersed in liquid nitrogen, and then separated into fractions by pumping them through a series of traps by a mercury diffusion pump and a Toepler pump; the fractions were: (*1*) non-condensables; (*2*) condensable at −210 and −196 °C (solid nitrogen and liquid nitrogen, respectively), and (*3*) condensable at −130 °C (*n*-pentane slush).

The non-condensable products, which comprised hydrogen and methane, were collected in a sample tube by a Toepler pump. They were analyzed on a 6.0 m long column filled with 80–100 mesh Porapak Q (Waters Assoc. Inc.) operating at 0 °C with a helium flow of 50 cc min^{-1}. On this column hydrogen could be separated from air; this is important since small quantities of air could cause big errors in the analysis. The traps at −210 and −190 °C retained ethylene and ethane (and C_3 and C_4 hydrocarbons which were not analyzed). Ethylene and ethane were analyzed on a 3.5 m long column filled with 80–100 mesh Porapak Q operating at 35 °C with a helium flow of 100 cc min^{-1}; the characteristics of this column have been described elsewhere (24). The traps at −130 °C (two in tandem) retained 2,3-dimethylbutane, 2-methylpentane, and *n*-hexane (and some of the C_4 hydrocarbons). 2,3-Dimethylbutane and 2-methylpentane were analyzed on a 7.0 m long column filled with 4% α-chloronaphthalene (Fisher Scientific Co.) on chromosorb P a.w. (Johns–Manville Co.), 45–60 mesh operating at 0 °C, with helium flow of 120 cc min^{-1}. The retention time of *n*-hexane on this column was too long (42 min) and the amounts of *n*-hexane were considerably smaller than those of the other two C_6 isomers. For this reason separate runs were made and *n*-hexane was analyzed on a 2.0 m long column filled with 20% di-2-ethylhexylsebacate (Chromatographic Specialities Ltd.) on Chromosorb P a.w., 45–60 mesh operating at 25 °C with helium flow of 150 cc min^{-1}. 2,3-Dimethylbutane could not be separated from 2-methylpentane on this column.

Peak-height measurements provided good calibration

Can. J. Chem. Downloaded from www.nrcresearchpress.com by 210.87.254.6 on 09/05/12
For personal use only.

curves for all products except for C_6 hydrocarbons, for which it was necessary to make area measurements.

All columns were made from copper tubing with an inner diameter of 4 mm, and helium was used as carrier gas.

In the experiments where the effect of CO_2 as a foreign gas was studied, CO_2 was first trapped together with ethylene and ethane at -210 and -196 °C and then removed from the product mixture by adsorbing it on ascarite.

Reaction Conditions

The work was done at five different temperatures, 252.0, 276.0, 301.0, 325.0, and 350.0 °C, and the propane pressure varied from 5 to 700 Torr; above 350 °C there is considerable thermal decomposition of propane. Mercury vapor in the reaction zone was at its equilibrium vapor pressure at -32 °C, which is about 3.5×10^{-6} Torr. The low concentration of mercury in the reaction zone was necessary in order to approach a homogeneous absorption of light throughout the reaction vessel. With the reaction vessel used the mercury saturator at -32 °C should give rise to a fairly homogeneous reaction, as shown by Loucks and Laidler (1); effects of inhomogeneous absorption will be very much less than in earlier work by Bywater and Steacie (7) and by Back and Takamuku (12) in which the mercury saturator was kept at room temperature and at 0 °C, respectively.

The low-pressure mercury resonance lamp of low light intensity was used so that the concentration of radicals produced was not too high. Under these conditions the reaction could be investigated at very low conversions of about 10^{-1}–10^{-2}%. This ensures that true initial rates are measured, the addition of hydrogen atoms and radicals to olefins produced being negligible.

Results and Interpretations

The reaction products analyzed were H_2, CH_4, C_2H_4, C_2H_6, 2,3-dimethylbutane (2,3-DMB), 2-methylpentane (2-MP), and *n*-hexane. The C_4-hydrocarbons could not be separated from propane by distillation, and the huge propane peak made gas-chromatographic analysis impossible. For all of the products the plots of yield against time were linear, so that reliable initial rates could be calculated from the slopes; as an example, Fig. 1 shows the yield of hydrogen as a function of time. All rates quoted in the present and following paper are initial rates. The initial rates of formation of the various products are shown plotted against propane pressure, at five different temperatures, in Figs. 2–8.

The rates of formation of all of the products are seen to be proportional to propane pressure at low pressures, and to become independent of propane pressure at higher pressures. The limiting propane pressure for H_2, 2,3-DMB, 2-MP, and n-C_6H_4 is about 150–160 Torr, and is hardly

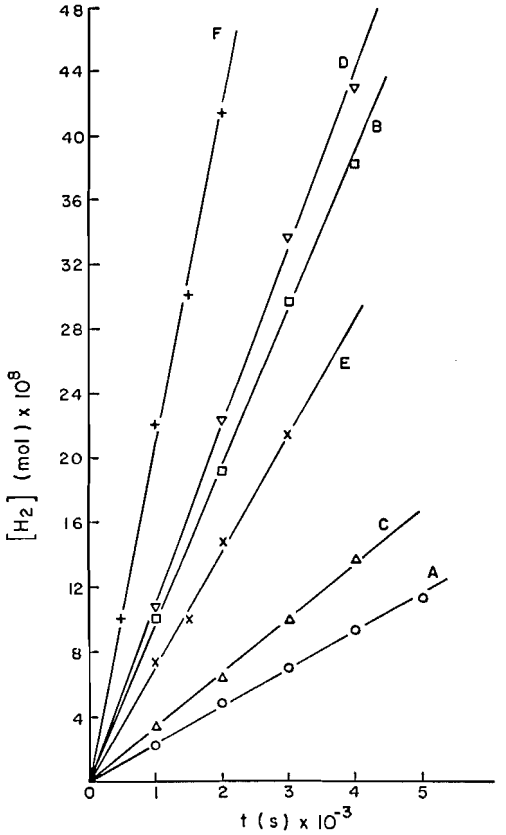

FIG. 1. Typical curves for hydrogen yield as a function of time under various conditions: *A*, 252 °C and 10 Torr; *B*, 252 °C and 382 Torr; *C*, 301 °C and 11 Torr; *D*, 301 °C and 394 Torr; E, 350 °C and 8 Torr; *F*, 350 °C and 386 Torr.

dependent on temperature. For CH_4, C_2H_4, and C_2H_6, on the other hand, the limiting pressure increases significantly with increasing temperature. This behavior can be explained as follows. At low propane pressures the rate of quenching of Hg* increases with increasing concentration of the C_3H_8 molecules. At a certain C_3H_8 pressure complete quenching of Hg* is achieved, and further increase in the C_3H_8 concentration does not affect the rates of formation of H and C_3H_7. At higher temperatures the C_3H_7 radicals also undergo decomposition into $H + C_3H_6$ and $CH_3 + C_2H_4$. The H atoms produced react with C_3H_8 much faster ($k = 6.3 \times 10^{13} \exp(-8.0/RT)$ cc mol^{-1} s^{-1}) than do the CH_3 radicals ($k = 8.1 \times 10^{11} \exp(-10.3/RT)$ cc $mol^{-1}s^{-1}$) (25). Consequently, the rate of H_2 production becomes pressure-independent at lower C_3H_8

Can. J. Chem. Downloaded from www.nrcresearchpress.com by 210.87.254.6 on 09/05/12
For personal use only.

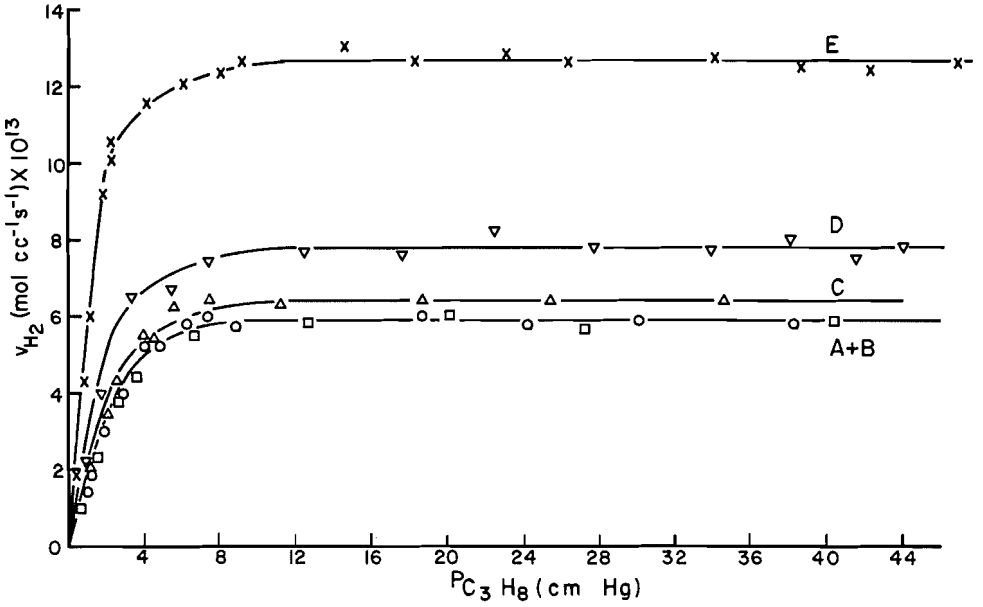

FIG. 2. Plots of initial rates of hydrogen production against propane pressure; *A*, 252.0 °C; *B*, 276.0 °C; *C*, 301.0 °C; *D*, 325.0 °C; *E*, 350.0 °C.

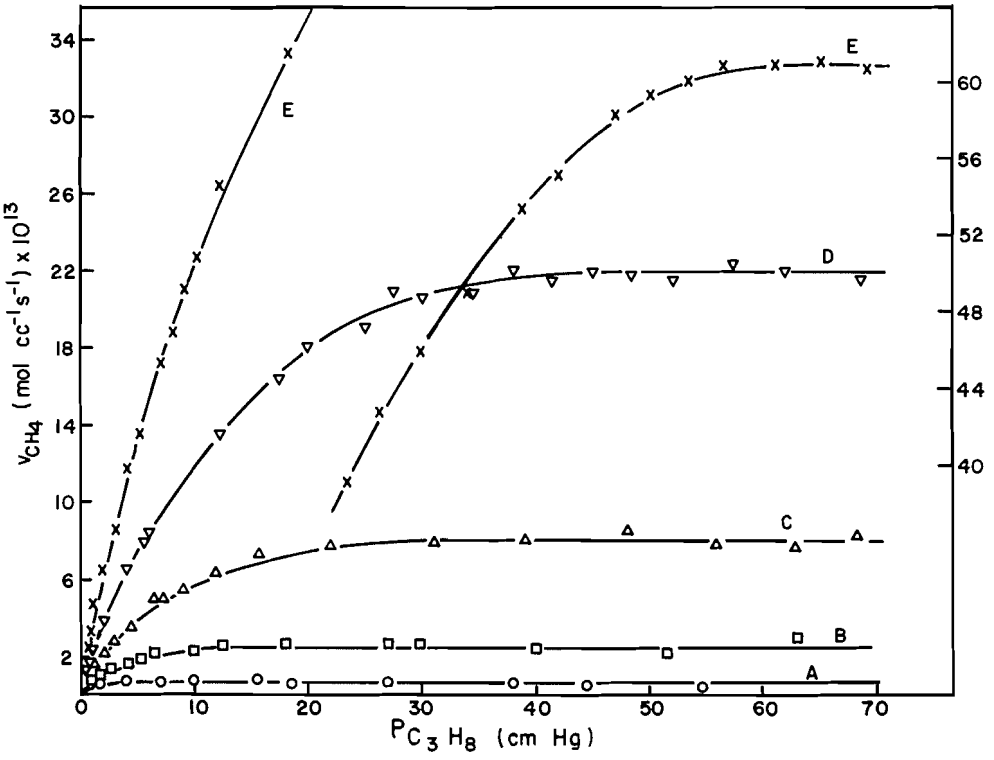

FIG. 3. Plots of initial rates of methane production against propane pressure; temperatures as in Fig. 2.

Can. J. Chem. Downloaded from www.nrcresearchpress.com by 210.87.254.6 on 09/05/12
For personal use only.

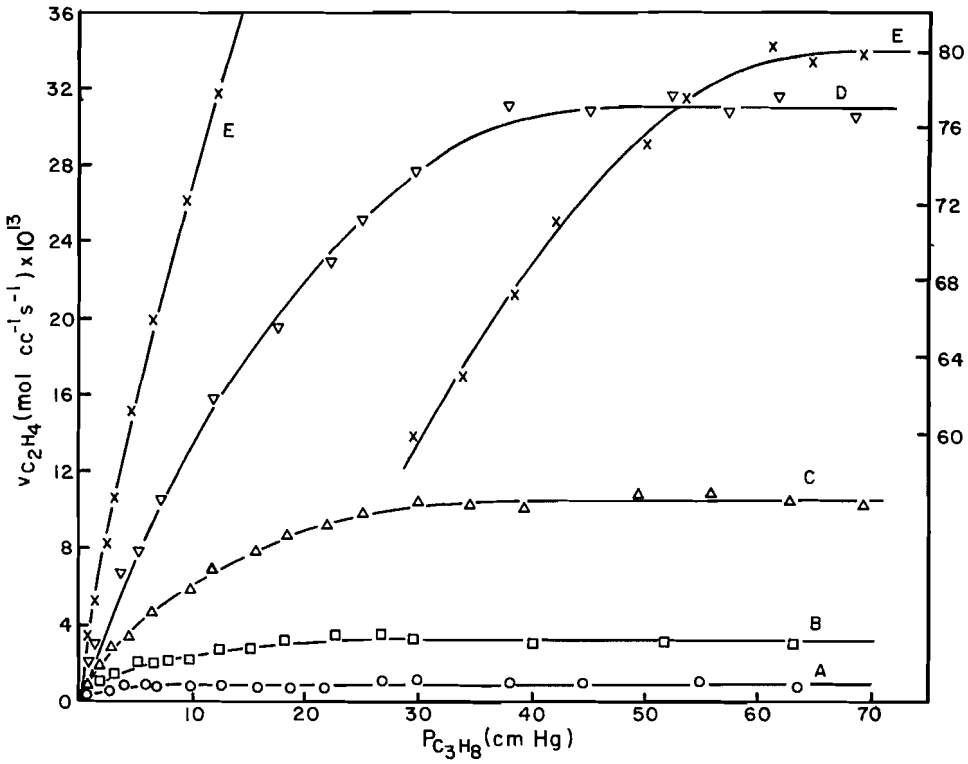

FIG. 4. Plots of initial rates of ethylene production against propane pressure; temperatures as in Fig. 2.

pressures, and the rate of CH_4 production at higher pressures. This matter is later discussed in more detail.

At the lower temperatures (252 and 276 °C) there is little decomposition of the C_3H_7 radical, so that the rate of H_2 production is independent of temperature and is greater than the rate of production of any other product. In the high-temperature region (including 301, 325, and 350 °C) C_3H_7 radicals do decompose to a considerable extent; the rate of H_2 production then becomes temperature-dependent, and the rate of CH_4 production becomes considerably greater than that of H_2 production.

Hydrogen Production

The yield–time curves for hydrogen shown in Fig. 1 indicate that the rates measured are truly initial rates. Reactions such as the scavenging of H atoms by C_3H_6 are therefore not playing an important role as far as the present results are concerned.

Double logarithmic plots of v_{H_2} against propane pressure are shown in Fig. 9. The orders are unity at the lower pressures and zero at the higher ones. Curve *A* in Fig. 10 shows a plot of the logarithm of the rate of hydrogen production against the reciprocal of the absolute temperature; in the low-temperature region the rate is independent of temperature, the H_2 then resulting only from the H atoms produced in the initial step. By subtraction of the low-temperature rate of H_2 production from the total rate one obtains the rate of H_2 production by the chain mechanism; the resulting plot is shown as curve *B* in Fig. 10. From this plot an activation energy of 38.7 ± 0.5 kcal mol^{-1} was obtained for the chain-hydrogen production of 300 Torr. The same procedure was applied at other propane pressures, and the resulting activation energies are shown plotted against propane pressure in Fig. 11.

Methane Production

The order plots for CH_4 production, at the five temperatures, led to orders of about 0.8 at lower propane pressures and of zero at higher pressures. Activation energies for methane production were

Can. J. Chem. Downloaded from www.nrcresearchpress.com by 210.87.254.6 on 09/05/12
For personal use only.

Can. J. Chem. Downloaded from www.nrcresearchpress.com by 210.87.254.6 on 09/05/12
For personal use only.

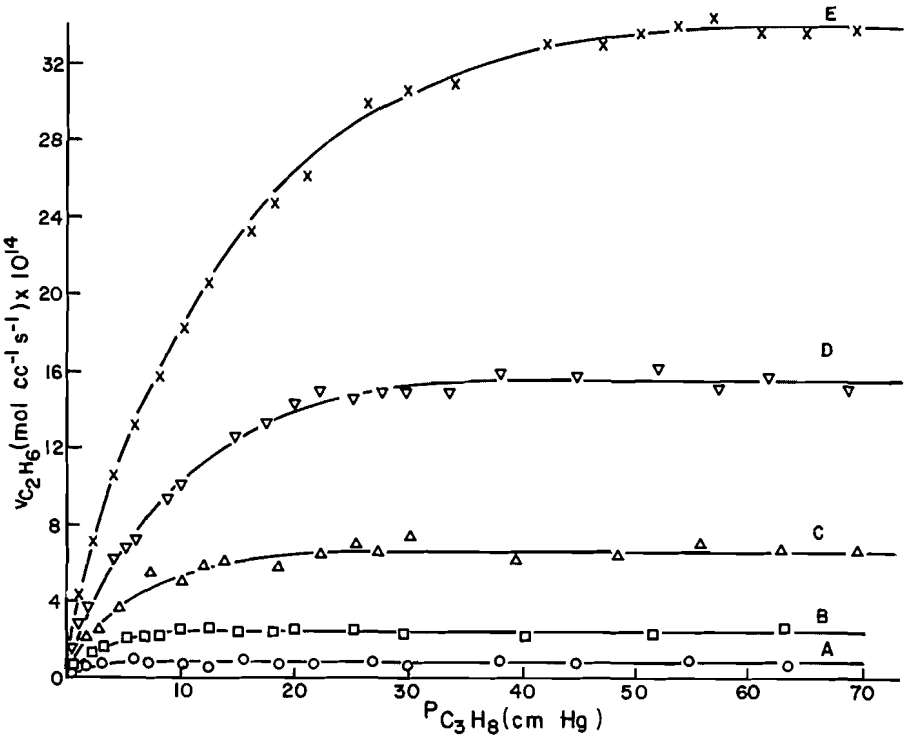

FIG. 5. Plots of initial rates of ethane production against propane pressure; temperatures as in Fig. 2.

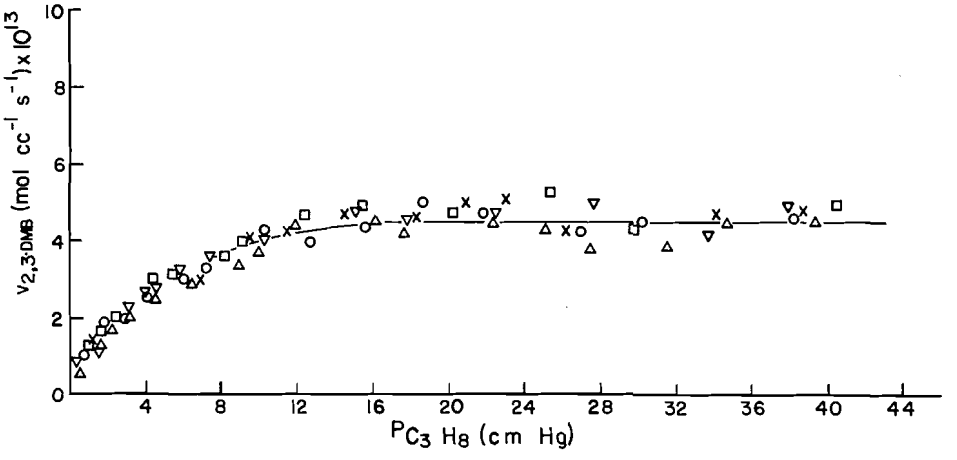

FIG. 6. Plots of initial rates of formation of 2,3-dimethylbutane against propane pressure; ○, 252.0 °C; □, 276.0 °C; △, 301.0 °C; ▽, 325.0 °C; ×, 350.0 °C.

obtained at a number of propane pressures, and are shown plotted against pressure in Fig. 12. The activation energy is seen to increase from an extrapolated value of 15 kcal mol^{-1} at zero propane pressure to a limiting value of 29.5 kcal mol^{-1} at high pressures of propane.

Formation of Other Products

The same procedure as for methane was applied to the rates of formation of ethylene, ethane, 2,3-dimethylbutane, 2-methylpentane, and *n*-hexane. Figures 13 to 16 show the variations of activation energy with propane pressure for these products

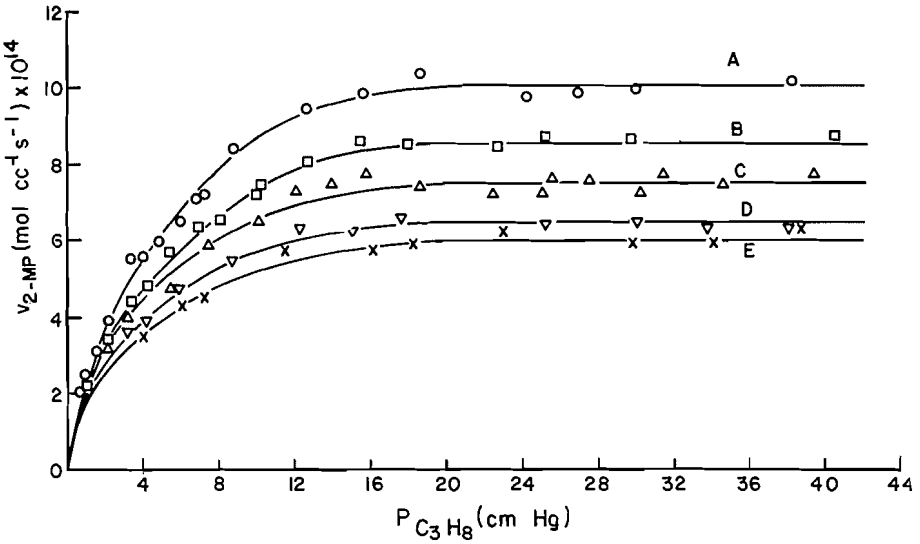

FIG. 7. Plots of initial rates of formation of 2-methylpentane against propane pressure; temperatures as in Fig. 2.

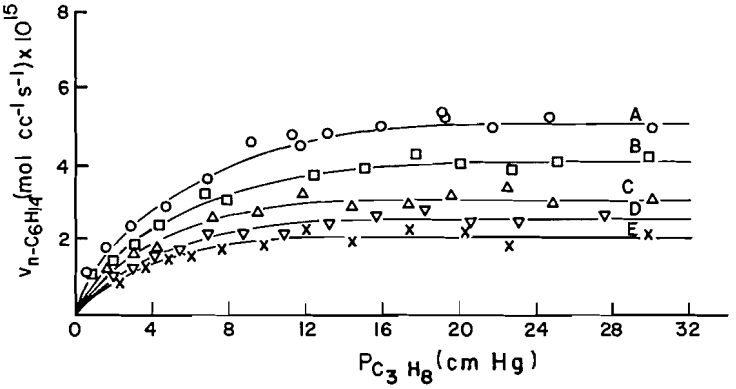

FIG. 8. Plots of the initial rates of formation of *n*-hexane against propane pressure; temperatures as in Fig. 2.

measured except 2,3-dimethylbutane, for which the activation energies were zero. Table 1 gives the low- and high-pressure orders of reaction, and the extrapolated low-pressure and limiting high-pressure activation energies.

Inert-Gas Effect

The overall dependence of the rates of product formation on the propane pressure, shown in Figs. 2 to 8, is attributed to the complete quenching of the excited mercury atoms at the higher pressures. If this is the case, introduction of some other gas of comparable quenching cross section would cause a decrease in the rates of product formation, and complete quenching would occur at lower propane pressures. A few experiments were carried out to test these conclusions.

The effects of carbon dioxide and helium on the rates of product formation were examined at 301 °C and at a propane pressure of 15 Torr. The results with carbon dioxide are shown in Fig. 17; helium showed very similar behavior. There is seen to be marked effect of inert gases, the rates falling to $\leqslant 20\%$ of their values in the absence of added gas. This behavior is atrributed to quenching of excited mercury by the CO_2 or He; the former has a quenching cross-section of about 3 Å, to be compared with 2 Å for propane (26).

Can. J. Chem. Downloaded from www.nrcresearchpress.com by 210.87.254.6 on 09/05/12
For personal use only.

TABLE 1. Summary of reaction orders and activation energies for the formation of the various products

Product	Order of reaction		Activation energy (kcal mol^{-1})	
	Low pressure	High pressure	Extrapolated low-pressure value	Limiting high-pressure value
Hydrogen	1	0	38.7±0.5	38.7±0.5
Methane	0.8	0	15.0±0.5	29.5±0.5
Ethylene	0.8	0	15.0±0.5	29.7±0.5
Ethane	0.8	0	15.0±0.5	24.0±0.5
2,3-Dimethylbutane	0.5	0	0	0
2-Methylpentane	0.5	0	−2.5±0.5	−3.4±0.5
n-Hexane	0.5	0	−5.5±0.5	−6.0±0.5

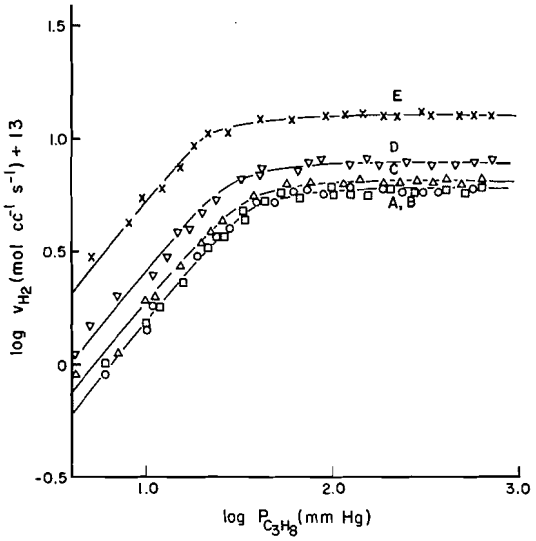

FIG. 9. Order plots for hydrogen production; temperatures as in Fig. 2.

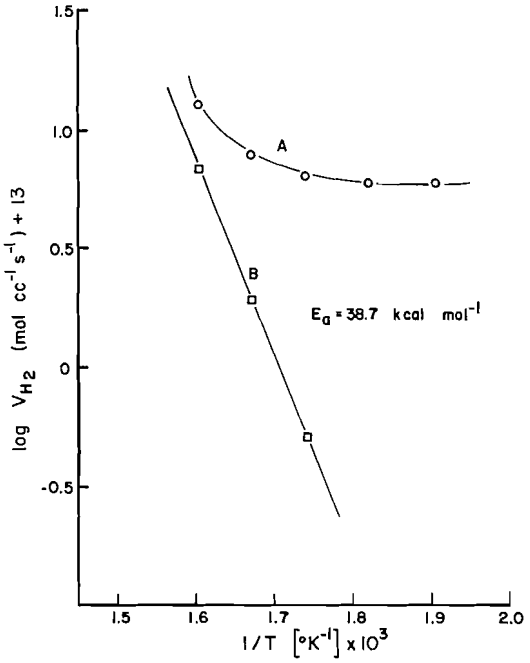

FIG. 10. Arrhenius plots for hydrogen production, at a propane pressure of 300 Torr; *A*, total hydrogen, *B*, hydrogen produced in chain processes.

Discussion

The subsequent discussion will be based on the following reaction scheme

[1] $Hg + h\nu \rightarrow Hg^*$

[2p] $Hg^* + C_3H_8 \rightarrow Hg + H + P$

[2s] $Hg^* + C_3H_8 \rightarrow Hg + H + S$

[3p] $H + C_3H_8 \rightarrow H_2 + P$

[3s] $H + C_3H_8 \rightarrow H_2 + S$

[4] $2P \rightarrow n\text{-}C_6H_{14}$

[5] $2S \rightarrow$ 2,3-DMB

[6] $P + S \rightarrow$ 2-MP

[7] $2P \rightarrow C_3H_8 + C_3H_6$

[8] $2S \rightarrow C_3H_8 + C_3H_6$

[9] $P + S \rightarrow C_3H_8 + C_3H_6$

[10p] $CH_3 + C_3H_8 \rightarrow CH_4 + P$

[10s] $CH_3 + C_3H_8 \rightarrow CH_4 + S$

[11*a*] $P \rightarrow H + C_3H_6$

[11*b*] $P \rightarrow CH_3 + C_2H_4$

[12*a*] $S \rightarrow H + C_3H_6$

[12*b*] $S \rightarrow CH_3 + C_2H_4$

In this scheme P represents the *n*-propyl radical, and S the *i*-propyl radical.

In addition to the above reactions the following processes may also play some part; they are un-

Can. J. Chem. Downloaded from www.nrcresearchpress.com by 210.87.254.6 on 09/05/12
For personal use only.

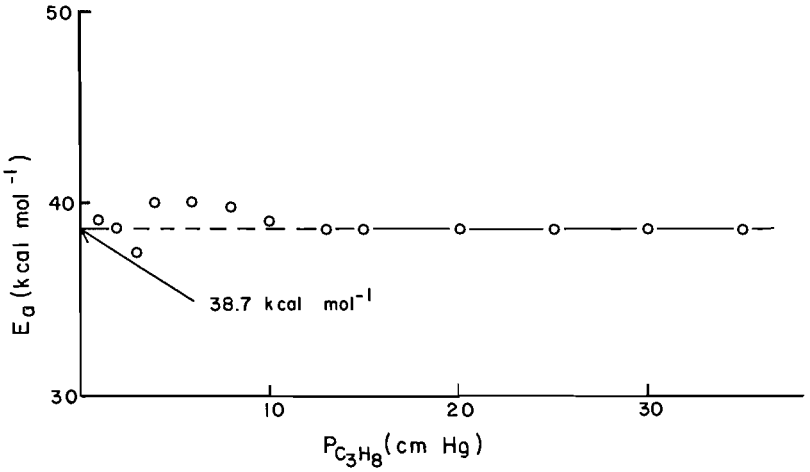

FIG. 11. Plot of the energy of activation for chain-hydrogen production against the pressure of propane.

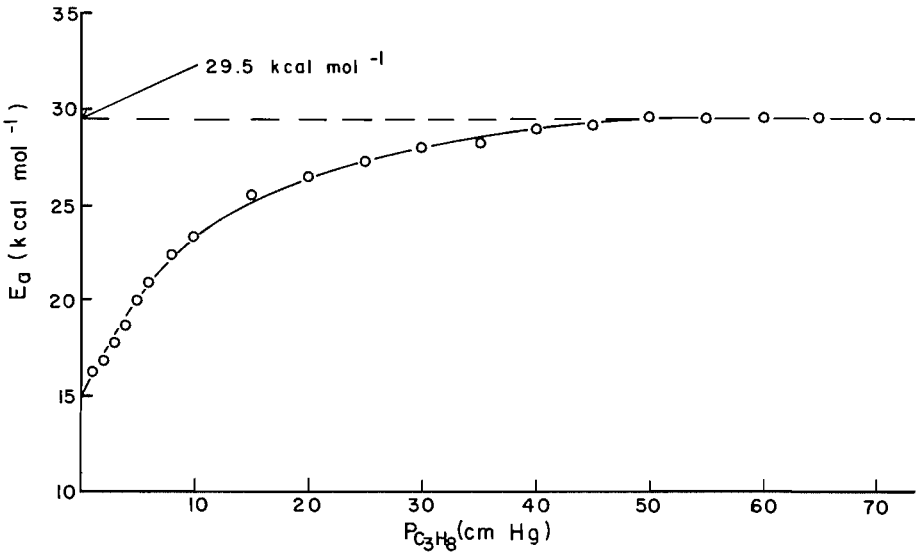

FIG. 12. Plot of the energy of activation for methane production against the pressure of propane.

important at higher propane pressures and become relatively more important at lower pressures

[13] $H + C_3H_6 \rightarrow C_3H_7^* \rightarrow (H_2 + C_3H_5)$

[14] $H + C_3H_7 \rightarrow CH_3 + C_2H_5$

[15] $H + C_3H_7 \rightarrow C_3H_8$

[16] $C_2H_5 + C_3H_8 \rightarrow C_2H_6 + C_3H_7$

[17] $CH_3 + C_3H_7 \rightarrow C_4H_{10}$

[18] $2CH_3 \rightarrow C_2H_6$

It may be noted that there is considerable doubt as to the importance of reaction 12*b*, which is included for completeness; the present results have no bearing on the occurrence of this reaction.

Besides the products studied, and propane itself, the above scheme is seen to lead to propylene and butane. These products could not be determined because of the interference of the propane, although butane was detected. The present results are entirely consistent with this scheme of reactions, and with the conclusion that the decomposition of the propyl radicals is important only at the higher temperatures studied.

Can. J. Chem. Downloaded from www.nrcresearchpress.com by 210.87.254.6 on 09/05/12
For personal use only.

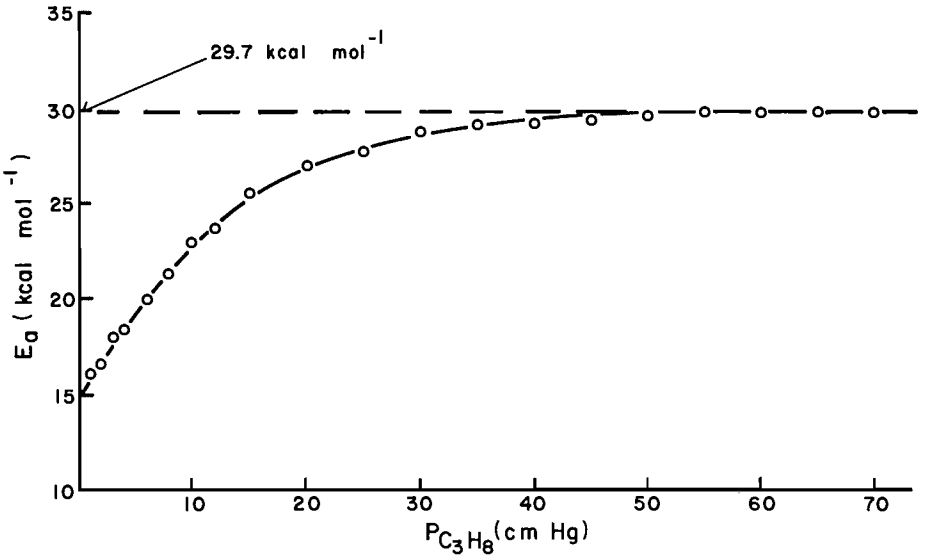

FIG. 13. Plot of the energy of activation for ethylene production against the pressure of propane.

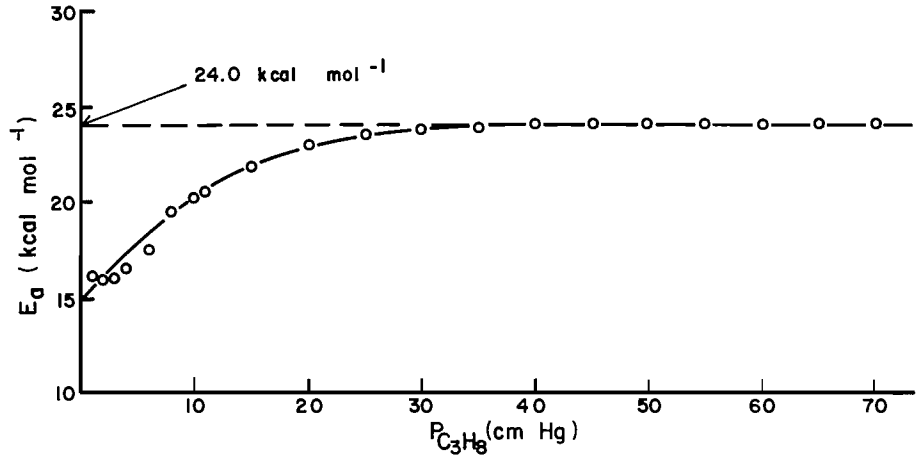

FIG. 14. Plot of the energy of activation for ethane production against the pressure of propane.

Arrhenius parameters for the various reactions, taken from various sources including the present results, are summarized in Table 2. On the basis of these values, and of the initial rates measured in the present investigation, it is possible to calculate the concentrations of free radicals. The results are shown in Table 3 for pressures of 10 and 700 Torr and at the five temperatures.

It is to be noted that the total concentration of free radicals in the system, $[R]_{total}$, is essentially independent of temperature. This is consistent with the fact that the total radical concentration depends only on the rate with which the excited mercury is quenched by propane, a process that is temperature-independent. Once complete quenching is achieved, *i.e.* at the higher propane pressures, the total radical concentration is also independent of propane pressure.

With increasing concentration of propane the concentrations of the n-C_3H_7 and i-C_3H_7 radicals are seen from Table 3 to increase slightly, whereas the concentrations of C_2H_5, CH_3, and H atoms decrease fairly strongly.

Simplified Steady-State Treatment; Kinetics of Product Formation

In view of the fact that five radicals (H, CH_3, C_2H_5, n-C_3H_7, and i-C_3H_7) are involved in the

Can. J. Chem. Downloaded from www.nrcresearchpress.com by 210.87.254.6 on 09/05/12
For personal use only.

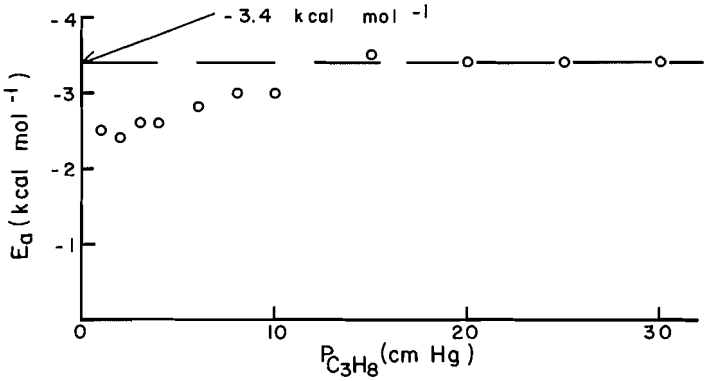

FIG. 15. Plot of the energy of activation for 2-methylpentane production against the pressure of propane.

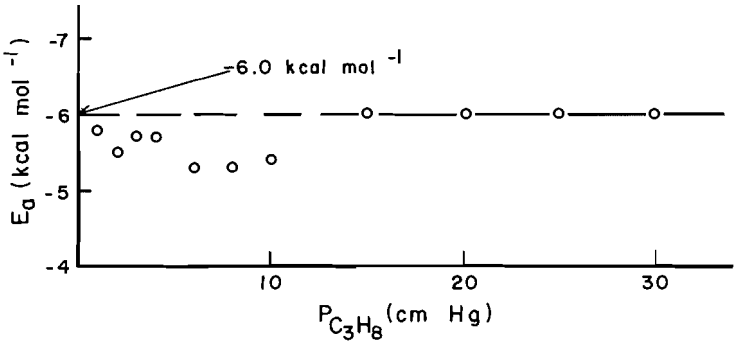

FIG. 16. Plot of the energy of activation for *n*-hexane production against the pressure of propane.

TABLE 2. Kinetic parameters for elementary reactions

Reaction	Log k‖	Reference
$H + C_3H_8 \rightarrow H_2 + C_3H_7$	13.8–8.0/2.3 RT	25
$H + C_3H_7 \rightarrow CH_3 + C_2H_5$ $H + C_3H_7 \rightarrow C_3H_8$	~ 15	*
$CH_3 + C_3H_8 \rightarrow CH_4 + C_3H_7$	11.9–10.3/2.3 RT	25
$CH_3 + C_3H_7 \rightarrow C_4H_{10}$	~ 13.7	27
$CH_3 + CH_3 \rightarrow C_2H_6$	13.6	28
$C_2H_5 + C_3H_8 \rightarrow C_2H_6 + C_3H_7$	11.3–10.4/2.3 RT	29
$P + P \rightarrow n\text{-}C_6H_{14}$	13.4	25
$S + S \rightarrow$ 2,3-DMB	13.4	30
$P + S \rightarrow$ 2-MP	13.7	†
$P + P \rightarrow C_3H_8 + C_3H_6$	12.6	9
$S + S \rightarrow C_3H_8 + C_3H_6$	13.2	31
$P + S \rightarrow C_3H_8 + C_3H_6$	13	‡
$P \rightarrow H + C_3H_6$	14.1–37.0/2.3 RT	11
$P \rightarrow CH_3 + C_2H_4$	14.4–32.6/2.3 RT	§
$S \rightarrow H + C_3H_6$	14.3–38.7/2.3 RT	§
$S \rightarrow CH_3 + C_2H_4$	12.0–34.5/2.3 RT	32
$H + C_3H_6 \rightarrow C_3H_7$	12.0–2.0/2.3 RT + 0.5 Log T	33

(P = CH_3—CH_2—CH_2, S = CH_3—CH—CH_3)

*These values are assumed to be approximately equal to the collision frequency at 500 °K. The rate constants of cracking and combination reactions are combined.
†Calculated from intercombination ratio.
‡Assumed value.
§This work, high-pressure value.
‖All A factors are in cc mol^{-1} s^{-1} or s^{-1}; E in kcal mol^{-1}.

Can. J. Chem. Downloaded from www.nrcresearchpress.com by 210.87.254.6 on 09/05/12
For personal use only.

Can. J. Chem. Downloaded from www.nrcresearchpress.com by 210.87.254.6 on 09/05/12
For personal use only.

TABLE 3. Approximate estimates of concentrations of reactive species in reaction cell*

$P_{C_3H_8}$ (mm Hg)	T (°C)	Concentration (mol cc^{-1})						
		$[C_3H_8]$	$[n\text{-}C_3H_7]$	$[i\text{-}C_3H_7]$	$[C_2H_5]$	$[CH_3]$	[H]	[R] total
10	252.0	3.0×10^{-7}	0.7×10^{-14}	0.7×10^{-13}	1.2×10^{-15}	2.8×10^{-15}	2.0×10^{-17}	0.81×10^{-13}
	276.0	2.9×10^{-7}	0.6×10^{-14}	0.7×10^{-13}	1.6×10^{-15}	3.8×10^{-15}	1.4×10^{-17}	0.81×10^{-13}
	301.0	2.8×10^{-7}	0.6×10^{-14}	0.7×10^{-13}	2.4×10^{-15}	4.6×10^{-15}	1.3×10^{-17}	0.83×10^{-13}
	325.0	2.7×10^{-7}	0.5×10^{-14}	0.7×10^{-13}	2.6×10^{-15}	6.6×10^{-15}	1.2×10^{-17}	0.84×10^{-13}
	350.0	2.6×10^{-7}	0.5×10^{-14}	0.7×10^{-13}	3.2×10^{-15}	8.0×10^{-15}	2.0×10^{-17}	0.86×10^{-13}
700	252.0	2.1×10^{-5}	1.4×10^{-14}	1.3×10^{-13}	0.5×10^{-16}	0.8×10^{-16}	1.1×10^{-18}	1.44×10^{-13}
	276.0	2.0×10^{-5}	1.3×10^{-14}	1.3×10^{-13}	0.9×10^{-16}	2.0×10^{-16}	0.7×10^{-18}	1.43×10^{-13}
	301.0	2.0×10^{-5}	1.1×10^{-14}	1.3×10^{-13}	1.7×10^{-16}	4.0×10^{-16}	0.6×10^{-18}	1.41×10^{-13}
	325.0	1.9×10^{-5}	1.0×10^{-14}	1.3×10^{-13}	2.6×10^{-16}	8.0×10^{-16}	0.5×10^{-18}	1.41×10^{-13}
	350.0	1.8×10^{-5}	0.9×10^{-14}	1.3×10^{-13}	4.2×10^{-16}	17×10^{-16}	0.7×10^{-18}	1.41×10^{-13}

*[R] total denotes total concentration of radicals and hydrogen atoms in the system. The following expressions were used for estimations: $[H] = v_{H_2}/k_3[C_3H_8]$; $[CH_3] = v_{CH_4}/k_{10}[C_3H_8]$; $[C_2H_5] = (v_{C_2H_2} - k_{18}[CH_3]^2)/k_{16}[C_3H_8]$; $[n\text{-}C_3H_7] = (v_{n\text{-}C_6H_{14}}/k_4)^{1/2}$; $[i\text{-}C_3H_7] = (v_{2,3\text{-}DMB}/k_5)^{1/2}$.

Can. J. Chem. Downloaded from www.nrcresearchpress.com by 210.87.254.6 on 09/05/12
For personal use only.

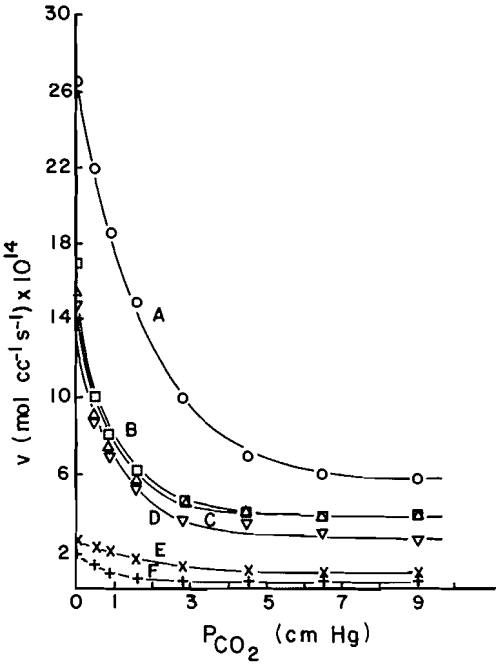

FIG. 17. The influence of carbon dioxide on the initial rates of formation of the various products: $T = 301.0$ °C; $P_{C_3H_8} = 15$ Torr; *A*, v_{H_2}; *B*, v_{CH_4}; *C*, $v_{C_2H_4}$; *D*, $v_{2,3\text{-DMB}}$; *E*, $v_{2\text{-MP}}$; *F*, $v_{C_2H_6}$.

mechanism, the steady-state analysis is complicated and does not lead to rate equations which are sufficiently simple to permit a useful analysis of the experimental results. As an alternative, the following simplified treatment is useful in leading to an understanding of the behavior.

For the rate of hydrogen production the steady-state equations lead to

$$[19] \qquad v_{H_2} = \frac{F_1}{1 + \dfrac{F_2}{k_3[C_3H_8]}}$$

where F_1 and F_2 are given by

$$[20] \qquad F_1 = \phi I_a + k_{11a}[P] + k_{12a}[S]$$

$$[21] \qquad F_2 = k_{14}[C_3H_7] + k_{15}[C_3H_7] + k_{13}[C_3H_6]$$

Reference to Table 3 shows that F_1 and F_2 vary only weakly with $[C_3H_8]$; at low pressures of C_3H_8 the rate should thus be proportional to $[C_3H_8]$, and independent of it at higher pressures. This is the behavior observed. The result is easy to understand at the lower temperatures, where the hydrogen arises only from the initial split of C_3H_8 by the Hg*; at the lower pressures the rate of quenching is proportional to $[C_3H_8]$, but at higher pressures there is complete chemical quenching by C_3H_8. At higher temperatures the situation is complicated by the chain reactions, involving reactions 11*a*, 12*a*, 3p, and 3s, but again there is a levelling-off due to complete quenching by C_3H_8.

According to the mechanism the rates of formation of CH_4 and C_2H_4 should be approximately equal, their main sources being reactions 11*b* and 12*b*, of which the latter is unimportant. The rates are in fact close to one another (Figs. 3 and 4). At lower propane pressures (< 40 Torr) v_{CH_4} is slightly higher, whereas at higher pressures $v_{C_2H_4}$ predominates. This may be due to the fact that at lower pressures reaction 14 is relatively more important, and gives rise to additional CH_4. At lower pressures, but not at the higher ones, it may more than compensate for the loss of CH_3 through reactions 17 and 18.

The steady-state treatment leads to

$$[22] \qquad v_{CH_4} = \frac{F_3}{1 + \dfrac{F_4}{k_{10}[C_3H_8]}}$$

where

$$[23] \qquad F_3 = k_{14}[H][C_3H_7] + k_{11b}[P] + k_{12b}[S]$$

$$[24] \qquad F_4 = k_{17}[C_3H_7]$$

Again (*cf.* Table 3) F_3 and F_4 vary only weakly with $[C_3H_8]$, so that the order is expected to vary from ~ 1 at low pressures to zero at high pressures; Table 1 shows that this is the case. The fact that the methane production becomes pressure independent at higher pressures than does the hydrogen production (compare Figs. 2 and 3) may be due to the fact that $k_3 \gg k_{10}$. The variation of the activation energy for methane production with the pressure is due to the pressure-dependence of the first-order rate coefficient for the decomposition of a propyl radical into CH_3 and C_2H_4; this is considered in detail in the following paper. Similar remarks apply to the rates of ethylene production.

The steady-state equations for the formation of ethane and the three hexanes are complicated, and are not helpful in explaining the orders at lower pressures; they do explain the zero-order dependence at higher pressures, however.

Chain Lengths

Chain length for this system, involving several radicals and chain processes, may be defined in

several ways. One definition is the number of H atoms released by the decomposition of propyl radicals divided by the number of propyl radicals formed; its order of magnitude is v_{H_2} (chain)/$v_{C_6H_{14}}$. This rough procedure leads to a magnitude of about unity at the lowest temperature. Alternatively, chain length may be defined as the number of ethylene molecules produced for each *n*-propyl radical formed, *i.e.* approximately $v_{C_2H_4}/(v_{n\text{-}C_6H_{14}} + v_{2\text{-MP}})$. This procedure leads to an order of magnitude of unity at 250 °C, increasing to 10^2 at 350 °C.

Thanks are due to Drs. M. H. Back and J. L. Holmes of the University of Ottawa and to Dr. R. A. Back of the National Research Council of Canada for their helpful suggestions.

1. L. F. Loucks and K. J. Laidler. Can. J. Chem. **45**, 2795 (1967).
2. L. F. Loucks and K. J. Laidler. Can. J. Chem. **45**, 2763 (1967).
3. L. F. Loucks and K. J. Laidler. Can. J. Chem. **45**, 2767 (1967).
4. L. F. Loucks. Can. J. Chem. **45**, 2775 (1967).
5. L. F. Loucks and K. J. Laidler. Can. J. Chem. **45**, 2785 (1967).
6. M. C. Lin and K. J. Laidler. Can. J. Chem. **44**, 2927 (1966).
7. S. Bywater and E. W. R. Steacie. J. Chem. Phys. **19**, 319 (1951).
8. J. G. Calvert and W. C. Sleppy. J. Amer. Chem. Soc. **81**, 1544 (1959).
9. J. A. Kerr and A. F. Trotman-Dickenson. Trans. Faraday Soc. **55**, 572 (1959).
10. J. A. Kerr and J. G. Calvert. J. Amer. Chem. Soc. **83**, 3391 (1961).
11. W. M. Jackson and J. R. McNesby. J. Amer. Chem. Soc. **83**, 4891 (1961).
12. R. A. Back and S. Takamuku. J. Amer. Chem. Soc. **86**, 2558 (1964).
13. E. W. R. Steacie and D. J. Dewar. J. Chem. Phys. **8**, 571 (1940).
14. B. deB. Darwent and E. W. R. Steacie. J. Chem. Phys. **13**, 563 (1945).
15. C. R. Masson and E. W. R. Steacie. J. Chem. Phys. **18**, 210 (1950).
16. R. A. Back. Can. J. Chem. **37**, 1834 (1959).
17. G. N. C. Woodall and H. E. Gunning. Bull. Soc. Chim. Belg. **71**, 725 (1962).
18. M. Avrahami and P. Kebarle. Can. J. Chem. **41**, 347 (1963).
19. E. Jakubowski, P. Kebarle, O. P. Strausz, and H. E. Gunning. Can. J. Chem. **45**, 2287 (1967).
20. R. A. Holroyd and G. W. Klein. J. Phys. Chem. **67**, 2273 (1963).
21. Y. Rousseau, G. N. C. Woodall, and H. E. Gunning. J. Chem. Phys. **37**, 2722 (1962).
22. Y. Rousseau and H. E. Gunning. Can. J. Chem. **41**, 465 (1963).
23. R. J. Cvetanovic. J. Chem. Phys. **23**, 1208 (1955).
24. M. Papic. J. Gas Chromatogr. **6**, 493 (1968).
25. A. F. Trotman-Dickenson and G. S. Milne. Tables of Bimolecular Gas Reactions. NSRDS-NBS 9, U.S. Department of Commerce, Washington, D.C. 1967.
26. R. J. Cvetanovic. *In* Progress in Reaction Kinetics. Vol. 2. *Edited by* G. Porter. Pergamon Press. 1964.
27. J. A. Kerr and A. F. Trotman-Dickenson. *In* Progress in Reaction Kinetics. Vol. 1. *Edited by* G. Porter. Pergamon Press. 1961.
28. A. F. Trotman-Dickenson. Ann. Rep. Chem. Soc. 36 (1968).
29. A. F. Trotman-Dickenson. Advan. Free Radical Chem. **1**, 1 (1965).
30. E. L. Metcalfe and A. F. Trotman-Dickenson. J. Chem. Soc. 4620 (1962).
31. J. A. Kerr and A. F. Trotman-Dickenson. Trans. Faraday Soc. **55**, 921 (1959).
32. J. A. Kerr and A. C. Lloyd. Quart. Rev. **22**, 549 (1968).
33. K. Yang. J. Amer. Chem. Soc. **84**, 719 (1962); **84**, 3795 (1962).

Can. J. Chem. Downloaded from www.nrcresearchpress.com by 210.87.254.6 on 09/05/12
For personal use only.

Can. J. Chem. Downloaded from www.nrcresearchpress.com by 210.87.254.5 on 09/05/12
For personal use only.

Kinetics of the Mercury-Photosensitized Decomposition of Propane. Part II. Reactions of the Propyl Radicals

M. M. PAPIC[1] AND K. J. LAIDLER
Department of Chemistry, University of Ottawa, Ottawa 2, Canada

Received April 22, 1970

The results of the previous paper are analyzed to yield information about the reactions of the *n*-propyl and *i*-propyl radicals. The various combination and disproportionation reactions are considered. The rate of decomposition of the *n*-propyl radical was determined as a function of temperature and pressure, and limiting high-pressure and low-pressure kinetic parameters were obtained. The high-pressure activation energy is 32.6 kcal mol^{-1}, and this leads to a value of 24.3 kcal mol^{-1} for the dissociation energy of the C—C bond in the *n*-propyl radical, to 22.2 kcal mol^{-1} for its heat of formation, and to 99.1 kcal mol^{-1} for the primary C—H dissociation energy in propane. Entropy changes are also calculated from the results.

For the decomposition of the *i*-propyl radical $E_\infty = 38.7$ kcal mol^{-1}, and this leads to 37.7 kcal mol^{-1} for the C—H bond dissocation energy in this radical and to 19.3 kcal mol^{-1} for its heat of formation. The secondary C—H dissociation energy in propane is calculated to be 96.2 kcal mol^{-1}. Corresponding entropy changes are calculated.

Canadian Journal of Chemistry, 49, 549 (1971)

Introduction

In the present paper the results of Part 1 are analyzed as far as the reactions of the *n*-propyl and *i*-propyl radicals are concerned. Particular attention is given to the unimolecular decompositions of these radicals at their high- and low-pressure limits, and to their thermochemistry.

Calculations, Results, and Discussion

Combination and Cross-combination of Propyl Radicals

According to either simple collision theory or activated-complex theory, the rate ratio

$$v_{2\text{-MP}}/(v_{2,3\text{-DMB}} \times v_{n\text{-}C_6H_{14}})^{1/2}$$

should have a statistical factor of 2. The effects of different masses and moments of inertia in the rate expressions will be fairly unimportant, and one might therefore expect that the above ratio of rates will also be 2. That this is so is confirmed by the results shown in Table 1. The mean value and standard deviation of our ratio of rate constants is

$$k_6/(k_4k_5)^{1/2} = 2.0 \pm 0.1$$

The same ratio is to be expected for the sum of the rate constants for combination and disproportionation

$$[1] \quad (k_6 + k_9)/(k_4 + k_7)^{1/2}(k_5 + k_8)^{1/2} = 2$$

From these two equations

$$[2] \quad \frac{k_9}{k_6} = \left(1 + \frac{k_7}{k_4}\right)^{1/2}\left(1 + \frac{k_8}{k_5}\right)^{1/2} - 1$$

The ratios $k_7/k_4 = 0.16$ and $k_8/k_5 = 0.63$ are reliably known (1), but k_9/k_6 is more difficult to measure; Terry and Futrell (2) have given a value of 0.41 ± 0.02. Insertion of the k_7/k_4 and k_8/k_5 ratios into eq. 2 leads to

$$k_9/k_6 = 0.38 \pm 0.04$$

which agrees very well with the value of Terry and Futrell (2).

Concentrations of Propyl Radicals

The *i*-propyl radical is more stable than the *n*-propyl radical, its energy being about 3.5 kcal/mol lower; if equilibrium were established in the reaction the concentration of *n*-C_3H_7 would be only a few percent of that of *i*-C_3H_7. From the mechanism (Part 1) it is to be seen that if $k_4 = k_5$,

$$[3] \quad \frac{[S]}{[P]} = \left(\frac{v_{2,3\text{-DMB}}}{v_{n\text{-}C_6H_{14}}}\right)^{1/2}$$

The ratios calculated from these rates range from 9.5 at 252 °C to 15.0 at 350 °C, so that there is much more *n*-C_3H_7 than the corresponding value at equilibrium. Figure 1 shows a plot of log [S]/[P] against $1/T$, from which it is deduced that

$$[4] \quad [S]/[P] = 1.7 \times 10^2 \exp(-3.1/RT)$$

Not only is the [S]/[P] ratio smaller than the cor-

[1]Present address: Department of Chemistry, University of British Columbia, Vancouver 8, British Columbia.

TABLE 1. Cross-combination of propyl radicals*

$P_{C_3H_8}$(mm Hg)	$V_{ab}/(V_{aa} \times V_{bb})^{1/2}$ at 252.0 °C	276.0 °C	301.0 °C	325.0 °C	350.0 °C
10	2.1	2.1	2.1	2.2	2.2
20	2.1	2.1	2.1	2.1	2.2
30	2.1	2.0	2.1	2.0	2.1
40	2.1	2.0	2.1	2.0	2.0
60	2.1	2.0	2.0	1.9	1.9
80	2.1	2.0	2.0	1.9	1.9
100	2.1	2.0	2.0	1.9	1.9
150	2.1	2.0	2.0	1.9	1.9
200	2.1	2.0	2.0	1.9	2.0
250	2.1	2.0	2.0	1.9	2.0
300	2.1	2.0	2.0	1.9	2.0

*$v_{aa} = v_{2,3\text{-DMB}}$, $v_{bb} = v_{n\text{-}C_6H_{14}}$, $v_{ab} = v_{2\text{-MP}}$.

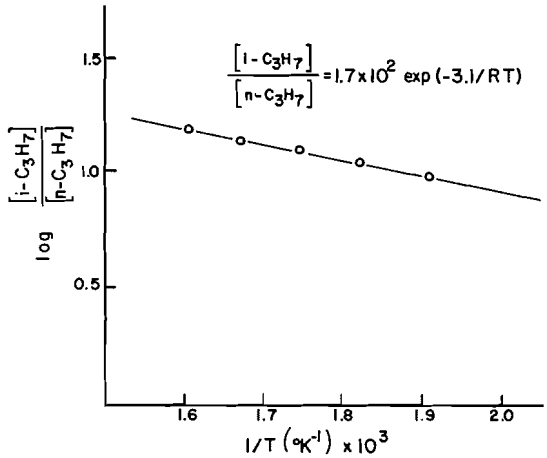

FIG. 1. Plot of the logarithms of the ratios of concentrations of *i*-propyl and *n*-propyl radicals against $1/T$; propane pressure = 300 Torr.

responding one at equilibrium, but the temperature dependence is in the opposite direction.

The result expressed in eq. 4 is qualitatively the same as that obtained by Lin and Laidler (4), but there is a considerable numerical difference, their result being

$$[5] \quad [S]/[P] = 5 \times 10^6 \exp(-17.0/RT)$$

Decomposition of n-Propyl Radicals

The decomposition of *n*-propyl radicals to ethylene and CH_3 is about 10^3 faster than the decomposition of *i*-C_3H_7 into the same products (5), and the rate of decomposition of *n*-C_3H_7 to C_3H_6 and H is lower than the rate of their decomposition to C_2H_4 and CH_3 by a factor of $\sim 10^3$. The ethylene can therefore be assumed to result entirely from reaction 11*b*, and the loss of *n*-C_3H_7 radicals by reaction 11*a* can be neglected in the present discussion. Therefore, from the reaction scheme

$$[6] \quad \frac{k_{11b}}{k_4^{1/2}} = \frac{v_{C_2H_4}}{(v_{n\text{-}C_6H_{14}})^{1/2}}$$

With k_4 taken as $10^{13.4}$ cc mol^{-1} s^{-1}(6), k_{11b} can therefore be evaluated from the rates of C_2H_4 and *n*-C_6H_{14} formation. The results are shown plotted in Fig. 2 at the five different temperatures. Figure 3 shows an Arrhenius plot for the limiting high-pressure rate constants; the line corresponds to the equation

$$k_{11b}^{\infty} = 2.5 \times 10^{14} \exp(-32.6 \pm 0.5/RT) \text{ s}^{-1}$$

The activation energy obtained from the rate of formation of ethylene at high propane pressures (*cf.* Fig. 13 of Part 1) was 29.7 kcal mol^{-1}, the difference being due to the temperature dependence of [P]. From the k_{11b}^{∞} value and the ethylene rates it can be deduced that

$$[7] \quad [P] \propto \exp(2.9/RT)$$

and in view of eq. 4

$$[8] \quad [S] \propto \exp(-0.2/RT)$$

This agrees with the result (Table 3 of Part 1) that [P] decreases with increasing temperature and [S] remains practically constant.

Values of k_{11b}^0, the limiting low-pressure rate constant, were obtained from plots of $1/k_{11b}$ against $1/[C_3H_8]$. The Arrhenius plot is shown in Fig. 4 and leads to

$$k_{11b}^0 = 2.5 \times 10^7 \exp(-17.0 \pm 0.5/RT) \text{ cc mol}^{-1} \text{ s}^{-1}$$

Can. J. Chem. Downloaded from www.nrcresearchpress.com by 210.87.254.5 on 09/05/12
For personal use only.

Can. J. Chem. Downloaded from www.nrcresearchpress.com by 210.87.254.5 on 09/05/12
For personal use only.

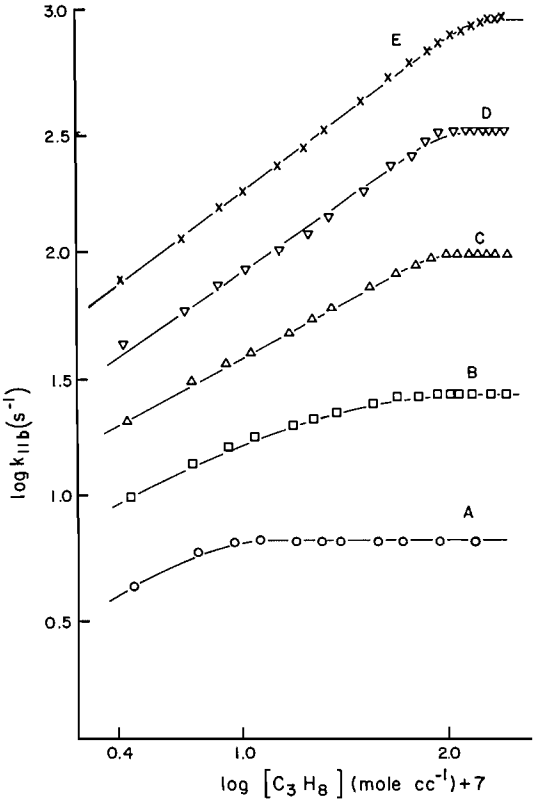

FIG. 2. Double logarithmic plots of the rate constant k_{11b} for the process n-$C_3H_7 \rightarrow CH_3 + C_2H_4$ against the propane concentration; A = 252.0 °C; B = 276.0 °C; C = 301.0 °C; D = 325.0 °C; E = 350.0 °C.

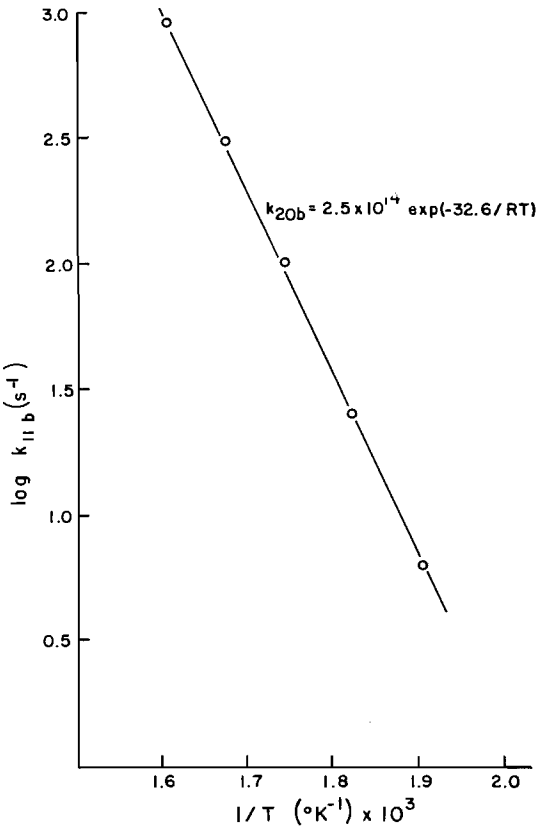

FIG. 3. Arrhenius plot of k_{11b}, at a pressure (700 Torr) at which the limiting rate has been attained.

The abnormally low value obtained for the frequency factor of this reaction might possibly be due to the formation of hot C_3H_7* radicals by the reaction H + C_3H_6.

On the basis of the Hinshelwood–Kassel–Rice–Ramsberger theories of unimolecular reactions

$$[9] \qquad E^{\infty} - E^{0} = (s - 1)\,RT$$

where s is the number of effective degrees of freedom for the decomposition. This equation leads to s = 15; the total number of vibrational degrees of freedom is 24, so that, as is common, s is roughly half the total number.

The various values which have been reported for the rate constant of this decomposition are summarized in Table 2; the activation energies quoted are seen to range from 20 to 35 kcal mol^{-1}. Our value is in reasonable agreement with those obtained by Kerr and Calvert (8), Calvert and Sleppy (9), Jackson and McNesby (10), and Lin and Laidler (4). The lower values obtained (7, 11, 12) are almost certainly due to the fact that the reaction was somewhat in its pressure-dependent region.

Thermochemistry

The activation energy E_{11b}^{∞} = 32.6 kcal mol^{-1} is related to the enthalpy change ΔH_{11b} by

$$[10] \qquad \Delta H_{11b} = E_{11b}^{\infty} - E_{-11b} + RT$$

$$[11] \qquad = \Delta H_{11b}^{0} + \int_0^T \Delta C_p \, dT$$

where ΔH_{11b}^{0} is the enthalpy change at 0 °K, equal to the dissociation energy D^0(n-CH_3—CH_2-CH_2—) at 0 °K. The enthalpy of n-C_3H_7 was assumed to be the same as that of C_3H_8 and with the use of the enthalpies of C_2H_4, C_3H_8, and CH_3 (13, 14) the value of the integral in eq. 11, with T = 600 °K, is 1.3 kcal mol^{-1}. With E_{-11b} = 8.6 kcal mol^{-1} (15) we obtain

TABLE 2. Kinetic parameters for the decomposition of n-C_3H_7 into $CH_3 + C_2H_4$

Method of investigation	log k (s^{-1})	Reference
Photolysis of n-C_3H_7CHO	11.7–25.2/2.3 RT	Kerr and Trotman-Dickenson (7)
Photolysis of n-$C_3H_7N_2C_3H_7$	15.4–34.5/2.3 RT	Kerr and Calvert (8)
Photolysis of $CH_3N_2CH_3$ in the presence of n-C_3H_7CHO	15.3–34.9/2.3 RT	Calvert and Sleppy (9)
Thermochemical estimate	13.9–31/2.3 RT	Jackson and McNesby (10)
$CH_3N_2CH_3$-sensitized decomposition of C_3H_8	13.5–31.4/2.3 RT	Lin and Laidler (4)
Hg-photosensitized decomposition of C_3H_8	9.2–20/2.3 RT	Bywater and Steacie (11)
Hg-photosensitized decomposition of C_3H_8	9.6–22/2.3 RT	Back and Takamuku (12)
Hg-photosensitized decomposition of C_3H_8	14.4–32.6/2.3 RT	This work; limiting high-pressure results
Hg-photosensitized decomposition of C_3H_8	7.4–17.0/2.3 RT	This work; limiting low-pressure results

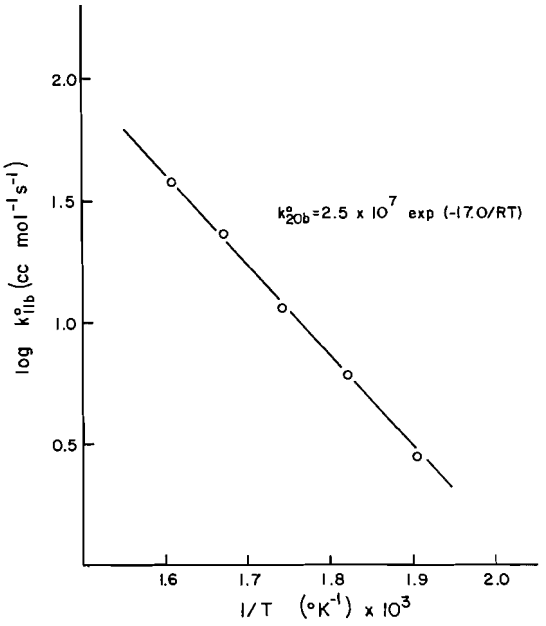

FIG. 4. Arrhenius plot of $k_{11b}{}^{0}$ obtained by extrapolation to the low-pressure limit.

$D^0(n\text{-}CH_3\text{—}CH_2CH_2\text{—}) =$ 23.9 kcal mol^{-1} at 0 °K

and

$D(n\text{-}CH_3\text{—}CH_2CH_2\text{—}) =$ 24.3 kcal mol^{-1} at 25 °C.

The latter value agrees satisfactorily with 23.0 kcal mol^{-1} listed by Lin and Laidler (4) and 25.5 obtained by Benson (3).

With the use of the following heats of formation: CH_3, 34.0 kcal mol^{-1} (3, 17); C_2H_4, 12.5 kcal mol^{-1} (16), the value for the n-propyl radical is found to be

$$\Delta H_f\,(n\text{-}C_3H_7) = 22.2 \text{ kcal mol}^{-1} \text{ at } 25\ ^\circ\text{C}$$

This is to be compared with the value of 20.9 listed by Calvert and Pitts (16) and with that of 21 ± 2 listed by Kerr (17).

The primary C—H bond dissociation energy in propane can be calculated from the following heats of formation: C_3H_8, −24.8 kcal mol^{-1}; H, 52.1 kcal mol^{-1} (16); n-C_3H_7, 22.2 kcal mol^{-1} (present work). The result is

$D\,(CH_3CH_2CH_2\text{—H}) =$ 99.1 kcal mol^{-1} at 25 °C

Kerr (17) listed a value of 98 ± 2 kcal mol^{-1}.

The entropy change for the reaction 11b can be calculated from the frequency factors in forward and reverse directions; the values used are $A_{11b} = 10^{14.4}$ s^{-1} (present work) and $A_{-11b} = 10^{12.1}$ cc mol^{-1} s^{-1} (15). The result is

$$\Delta S_{11b} = 10.6 \text{ cal deg}^{-1} \text{ mol}^{-1}$$

the standard state being 1 mol/cc. This value agrees satisfactorily with 12.0 cal deg^{-1} mol^{-1} calculated from entropies for C_2H_4, CH_3, and n-C_3H_7 listed by Calvert and Pitts (16). The entropy of activation for reaction 11b is calculated to be 4.1 cal deg^{-1} mol^{-1} at 600 °C, and estimated as 5.4 cal deg^{-1} mol^{-1} at 25 °C. These values indicate a fairly loose structure for the activated complex.

Decomposition of i-Propyl Radicals

There is some uncertainty about the relative rates of the processes

[12a] $\quad i\text{-}C_3H_7 \rightarrow C_3H_6 + H$

and

[12b] $\quad i\text{-}C_3H_7 \rightarrow C_2H_4 + CH_3$

If i-C_3H_7 does give rise to C_2H_4 it is not certain whether the process occurs directly or via isomerization into n-C_3H_7. There is no direct evidence

Can. J. Chem. Downloaded from www.nrcresearchpress.com by 210.87.254.5 on 09/05/12
For personal use only.

TABLE 3. Kinetic parameters for the decomposition of i-C_3H_7 into H + C_3H_6

Method of investigation	log k (s^{-1})	Reference
Photolysis of i-C_3H_7CHO	13.8–36.9/2.3 RT	Kerr and Trotman-Dickenson (21)
Photolysis of $(i$-$C_3H_6D)_2CO$	13.1–35/2.3 RT	Heller and Gordon (22)
Thermochemical estimate	15.0–42/2.3 RT	Leathard and Purnell (23)
Hg-photosensitized decomposition of C_3H_8	14.6–38/2.3 RT	Bywater and Steacie (11)
Hg-photosensitized decomposition of C_3H_8	14.0–37/2.3 RT	Back and Takamuku (12)
Hg-photosensitized decomposition of C_3H_8	14.3–38.7/2.3 RT	This work; limiting high-pressure results

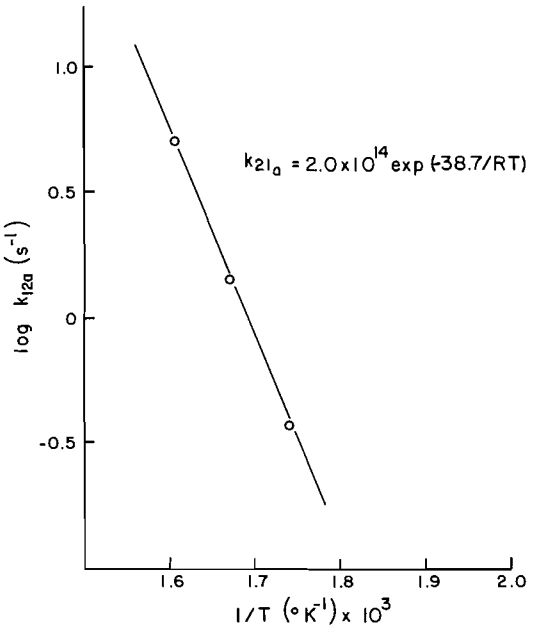

FIG. 5. Arrhenius plot of k_{12a}; the pressure is 300 Torr, and there was no pressure dependence over the entire pressure range.

for such isomerization; Billinge and Gowenlock (18) pyrolyzed separately di-n-propylmercury and di-i-propylmercury, but in neither case found evidence for isomerization.

Jackson and McNesby (19) found the ratio k_{12b}/k_{12a} to be about 0.04 at 500 °C, with little temperature dependence. They concluded that if the isomerization of i-C_3H_7 to n-C_3H_7 is simultaneous with, or occurs just before, decomposition, the ratio k_{12b}/k_{12a} is approximately 0.07. Falconer, Rabinovitch, and Cvetanovic (20) suggested that this value is an upper limit.

On the other hand, Kerr and Trotman-Dickenson (21) and Heller and Gordon (22), who studied the photolysis of i-C_3H_7CHO and $(i$-$C_3H_6D)_2CO$, respectively, have presented evidence that in the temperature range from 250 to 350 °C the ratio k_{12b}/k_{12a} is approximately unity. The percentage conversions in these experiments is not stated; it is possible that C_2H_4 is produced not directly but from the scavenging of H atoms by C_3H_6 with the formation of n-C_3H_7 which breaks down into CH_3 + C_2H_4.

From the point of view of hydrogen production, the eventual loss of i-propyl radicals via reaction 12b tends to be compensated for by the occurrence of reaction 11a. The present discussion will be based on the assumption that all chain hydrogen comes from the decomposition of i-C_3H_7, and that i-C_3H_7 radicals decompose entirely via reaction 12a. If this assumption proves to be incorrect, the derived kinetic parameters would correspond to some average value for n-C_3H_7 and i-C_3H_7. The kinetic parameters for the decomposition of n-C_3H_7 and i-C_3H_7 into C_3H_6 are close to one another (*cf.* Table 2 of Part 1) so that the error involved in the assumption will not be great.

The rate of hydrogen production by reaction 12a (chain hydrogen) is obtained by subtracting the low-temperature rate of H_2 production, v_3, from the total rate of H_2 production. The rate of 2,3-DMB production is

$$[13] \qquad v_{2,3\text{-DMB}} = k_5[S]^2$$

whence

$$[14] \qquad k_{12a} = k_5^{1/2} v_{H_2(\text{chain})}/(v_{2,3\text{-DMB}})^{1/2}$$

The value of k_5 was taken to be $10^{13.4}$ cc mol^{-1} s^{-1} and to be temperature-independent (6). The rate constants observed showed no fall off down to the lowest pressures, so that they must be limiting high-pressure values. An Arrhenius plot of the results obtained in this way is shown in Fig. 5. The resulting rate equation is

$$k_{12a}^{\infty} = 2.0 \times 10^{14} \exp(-38.7)RT)\, s^{-1}$$

A comparison with other values is shown in Table 3. The agreement is satisfactory except with the activation energy of Leathard and Purnell

Can. J. Chem. Downloaded from www.nrcresearchpress.com by 210.87.254.5 on 09/05/12
For personal use only.

(23), which was based on thermochemical estimates and may not be too reliable.

Thermochemistry

From the value of $E_{12a}^{\infty} = 38.7$ kcal mol^{-1} various energy values can be derived. Thus, by analogy with eq. 11

$$[15]\quad D^0(i\text{-}CH_3CHCH_2\text{—}H) = E_{12a} - E_{-12a} + RT - \int_0^T \Delta C_p \, dT$$

From the enthalpies the value of the integral at 600 °K is 1.5 kcal mol^{-1}. With $E_{-12a} = 2.0$ kcal mol^{-1} (24) we obtain

$$D^0(i\text{-}CH_3CHCH_2\text{—}H) = 36.4 \text{ kcal mol}^{-1} \text{ at } 0\,^{\circ}\text{K}$$

and

$$D\,(i\text{-}CH_3CHCH_2\text{—}H) = 37.7 \text{ kcal mol}^{-1} \text{ at } 25\,^{\circ}\text{C}$$

A value of 39 kcal mol^{-1} is listed by Kerr (17).

Use of the value of 37.7 together with $\Delta H_f(H) = 52.1$ kcal mol^{-1} and $\Delta H_f(C_3H_6) = 4.9$ kcal mol^{-1} (16) leads to

$$\Delta H_f(i\text{-}C_3H_7) = 19.3 \text{ kcal/mol}$$

Benson (3) listed a value of 17.6 kcal mol^{-1}.

The secondary C—H bond dissociation energy in C_3H_8 can be obtained using the above values together with $\Delta H_f(C_3H_8) = -24.8$ kcal mol^{-1} (16); the result is

$$D\,[(CH_3)_2CH\text{—}H] = 96.2 \text{ kcal mol}^{-1}$$

Kerr (17) listed the value of 94.5 kcal mol^{-1}.

The present results lead to the following entropies of activation for the decomposition of i-C_3H_7 into $C_3H_6 + H$

$$\Delta S_{12a}^{\ddagger} = 3.7 \text{ cal deg}^{-1} \text{ mol}^{-1} \text{ at } 600\,^{\circ}\text{K}$$

$$\Delta S_{12a}^{\ddagger} = 5.0 \text{ cal deg}^{-1} \text{ mol}^{-1} \text{ at } 25\,^{\circ}\text{C}$$

These values suggest a loose structure for the activated complex.

With Yang's (24) value of 10^{13} cc mol^{-1} s^{-1} for A_{-12a}, it is found that the overall entropy change is

$$\Delta S_{12a} = 6.0 \text{ cal deg}^{-1} \text{ mol}^{-1}$$

the standard state being 1 mol cc^{-1}. This value agrees satisfactorily with that of 5.2 cal deg^{-1} mol^{-1} calculated from listed entropies (16) for C_3H_6, H, and i-C_3H_7 at 25 °C.

Thanks are due to Drs. M. H. Back, R. A. Back, and J. L. Holmes for helpful suggestions.

1. J. A. Kerr and A. F. Trotman-Dickenson. Progr. React. Kinet. Vol. 1. *Edited by* G. Porter, Pergamon Press. 1961
2. J. O. Terry and J. H. Futrell. Can. J. Chem. **45**, 2327 (1967).
3. S. W. Benson. J. Chem. Educ. **42**, 502 (1965).
4. M. C. Lin and K. J. Laidler. Can. J. Chem. **44**, 2927 (1966).
5. J. A. Kerr and A. C. Lloyd. Quart. Rev. **22**, 549 (1968).
6. A. F. Trotman-Dickenson and G. S. Milne Tables of Bimolecular Gas Reactions. NSRDS-NBS 9, U.S. Dept. of Commerce, Washington, D.C. 1967.
7. J. A. Kerr and A. F. Trotman-Dickenson. Trans. Faraday Soc. **55**, 572 (1959).
8. J. A. Kerr and J. G. Calvert. J. Amer. Chem. Soc. **83**, 3391 (1961).
9. J. G. Calvert and W. C. Sleppy. J. Amer. Chem. Soc. **81**, 1544 (1959).
10. W. M. Jackson and J. R. McNesby. J. Amer. Chem. Soc. **83**, 4891 (1961).
11. S. Bywater and E. W. R. Steacie. J. Chem. Phys. **19**, 319 (1951).
12. R. A. Back and S. Takamuku. J. Amer. Chem. Soc. **86**, 2558 (1964).
13. F. D. Rossini *et al.* Selected Values of Physical and Thermodynamical Properties of Hydrocarbons and Related Compounds. American Petroleum Institute Research Project 44, Carnegie Press, Pittsburgh. 1953.
14. JANAF Interim Thermochemical Tables, Dow Chemical Co., Midland, Michigan.
15. R. K. Brinton. J. Chem. Phys. **29**, 781 (1958).
16. J. G. Calvert and J. N. Pitts. Photochemistry. Wiley, New York. 1966.
17. J. A. Kerr. Chem. Rev. **66**, 465 (1966).
18. B. H. M. Billinge and B. G. Gowenlock. J. Chem. Soc. 3252 (1962).
19. W. M. Jackson and J. R. McNesby. J. Chem. Phys. **36**, 2272 (1962).
20. W. E. Falconer, B. S. Rabinovitch, and R. J. Cvetanovic. J. Chem. Phys. **39**, 40 (1963).
21. J. A. Kerr and A. F. Trotman-Dickenson. Trans. Faraday Soc. **55**, 921 (1959).
22. C. A. Heller and A. S. Gordon. J. Phys. Chem. **62**, 709 (1958).
23. D. A. Leathard and J. H. Purnell. Proc. Roy. Soc. Ser. A. **306**, 553 (1968).
24. K. Yang. J. Amer. Chem. Soc. **84**, 719, 3795 (1962).

Can. J. Chem. Downloaded from www.nrcresearchpress.com by 210.87.254.5 on 09/05/12
For personal use only.

The Crystal and Molecular Structure of Bis-(2,4-pentanedionato)-4-aminopyridinecopper(II)

G. W. BUSHNELL
Department of Chemistry, University of Victoria, Victoria, British Columbia
Received June 29, 1970

The crystal structure of bis-(2,4-pentanedionato)4-aminopyridinecopper(II) has been refined to an R value of 0.070 from photometric Weissenberg film measurements. The cell is monoclinic with $a = 836 \pm 3$ pm, $b = 1475 \pm 3$ pm, $c = 1435 \pm 3$ pm, $\beta = 112.14 \pm 0.20°$. The space group is $P2_1/c$ (No. 14) with four molecules per cell. The density is 1.44 ± 0.01 g cm^{-3} (measured), 1.442 ± 0.013 g cm^{-3} (calculated). The geometry about each copper atom is approximately that of a tetragonal pyramid, with the copper atom 22 pm above the basal plane. The apex of the pyramid is occupied by an oxygen atom, the heterocyclic nitrogen is in the basal plane, and the 4-amino group is uncoordinated and hydrogen bonded to oxygen in a neighboring molecule.

Canadian Journal of Chemistry, 49, 555 (1971)

Can. J. Chem. Downloaded from www.nrcresearchpress.com by 210.87.254.42 on 09/05/12
For personal use only.

Introduction

A survey of known five coordinate copper(II) complexes (1) shows that the geometry about the central metal atom is usually based on that of a tetragonal pyramid. Trigonal bipyramidal structures are known but they are fewer in number, and sometimes the reason for their occurrence can be rationalized in terms of rigid ligand geometry (2), or adverse steric effects in the tetragonal pyramidal model (3).

A large fraction of the known five coordinate complexes contain two bidentate ligands and one unidentate. In this case, a central metal atom with tetragonal pyramidal geometry affords the possibility of two kinds of structure, Type 1 with the unidentate ligand at the apical position, and Type 2 with the unidentate ligand in the basal plane. There is no way of predicting which structure will arise in any particular reaction, but Type 1 has been found more often than Type 2.

The structure of bis-(2,4-pentanedionato)-copper(II) contains a square planar copper atom (4). Graddon (5) measured the formation constants of a number of pyridine adducts of bis-(2,4-pentanedionato)copper(II), which he claimed were five coordinate. Traill (6) pointed out that one side of a diketone ligand might become detached in the presence of pyridine or chloroform. Reference was made to the early work of Burgess and Lowry (7) on the catalytic action of pyridines on the mutarotation of bis-(benzoylcamphor)beryllium(II) in chloroform or carbon tetrachloride. Graddon and Watton (8) replied to the query and gave evidence for a five coordinate structure, rather than a four coordinate one. The pyridine was assumed to be in the apical position of a tetragonal pyramid. Walker and Li (9) investigated the equilibrium constant for the formation of bis-(2,4-pentanedionato)4-methylpyridinecopper(II) in solution.

Duckworth *et al.* (10) reported the crystal structure of bis-(*o*-hydroxyacetophenonato)4-methylpyridinecopper(II). The molecule contains a tetragonal pyramidal five coordinate copper atom with nitrogen at the apex and the two chelates at the base (Type 1). Ooi and Fernando (11) crystallized bis-(2,4-pentanedionato)quinolinecopper(II) from a solution of bis-(2,4-pentanedionato)copper(II) in quinoline. They report a molecular structure of Type 1. The diketone ligands are bent downwards away from the apex of the pyramid. The plane of the quinoline molecule lies between the two diketone ligands.

The crystal structure of bis-(2,4-pentanedionato)4-aminopyridinecopper(II) was undertaken when spectral results suggested five coordination, and the crystals were found to be markedly different and of better quality than those which could be obtained from the corresponding pyridine and 4-methylpyridine compounds. The electron donating amino group in the 4-position was expected to increase the stability of the pyridine coordination without adverse steric effects. The amino group also made prediction of the structure very uncertain; known structures of copper complexes showed such variety (1) that they were of little help for this purpose.

Experimental

The 4-aminopyridine used was recrystallized from acetone. Bis-(2,4-pentanedionato)copper(II) was prepared by the method of Jones (12), and allowed to react with

Can. J. Chem. Downloaded from www.nrcresearchpress.com by 210.87.254.42 on 09/05/12
For personal use only.

an equimolar quantity of 4-aminopyridine in chloroform under reflux for 5 min. The reaction mixture was filtered and allowed to crystallize by evaporation. Bis-(2,4-pentanedionato)4-aminopyridinecopper(II) appears as well formed green crystals.

Anal. Calcd. for $C_{15}H_{20}CuN_2O_4$: C, 50.63; H, 5.66; Cu, 17.85. Found: C, 50.77; H, 5.74; Cu, 18.0.

Crystallographic Measurements

The crystal habit and dimensions of the specimen used for the main data set are shown in Fig. 1. The acute angle shown was calculated from the cell dimensions to be 49.6°, microscopic observation gave 49.2, 49.4, and 49.9°. The crystal data are listed in Table 1. Systematic absences gave an unequivocal space group determination. Cell dimensions were measured from Weissenberg films, calibrated using pure copper wire. The density was measured by flotation in a trichloroethene/acetone solution.

Intensity measurements were obtained using CuKα radiation and the multiple film technique. Integrated equi-inclination Weissenberg photographs were taken of all accessible layers on the *a*-axis, and of the zero layer on the *b*-axis. The films were measured using a Hilger Model 1 photometer and processed using the expression $\ln I_0/I$. Of the 2319 reflections scanned, 1573 were found above background using this technique. No absorption corrections were made (μt(max) = 0.82, μt(min) = 0.14). Lorentz and polarization factors were applied and the

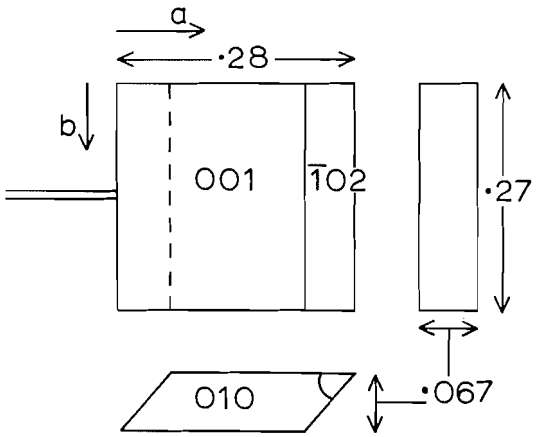

FIG. 1. Crystal habit and dimensions (in mm) of the specimen of $Cu(acac)_2$4-aminopyridine used.

TABLE 1. Crystal data for Cu $acac_2$.4-aminopyridine

System	Monoclinic
Space group	$P2_1/c$ (No. 14)
Molecular weight	355.9
Cell dimensions	$a = 836 \pm 3$ pm
	$b = 1475 \pm 3$ pm
	$c = 1435 \pm 3$ pm
	$\beta = 112.14 \pm 0.20$
Volume	1639×10^{-24} cm^3
Density (measured)	1.44 ± 0.01 g cm^{-3}
Molecules per cell (calcd.)	3.99
Absorption coeff. (CuKα)	20.8 cm^{-1}

h,0,*l* data were used to put the 0,*k*,*l* to 5,*k*,*l* data onto a common scale.

Structure Determination

Atomic scattering factor curves were obtained from the International Tables for X-Ray Crystallography (13). All atoms were assumed to be uncharged. A correction of -2.1 *e* was made for the real part of the anomalous dispersion of copper. Computations were done on an I.B.M. 360/44 computer using the programs of Ahmed *et al.* (14). The copper atom was located by using a three dimensional Patterson synthesis. A Fourier synthesis using phases calculated from the copper atom alone gave the complete structure. Structure factors were calculated for all reflections but only the observed reflections were used in the minimization of $\Sigma w(|F_o| - |F_c|)^2$ by the block diagonal least squares method. (3 × 3) and (6 × 6) blocks were used for each atom, and a 2 × 2 block was used for the scale and an overall thermal parameter. The weighting scheme was $\sqrt{w} = |F_o|/P_1$ if $|F_o| \leqslant P_1$ and $\sqrt{w} = P_1/|F_o|$ if $|F_o| > P_1$ with $P_1 = 30.0$. This scheme gives low weight to the very weak as well as to the very strong reflections, and was appropriate to the measurement technique used as shown by analysis of $w(|F_o| - |F_c|)^2$ for systematic variations. A partial shift of 0.8 was used in the refinement. The final *R*-values decreased in the sequence 0.076, 0.070, 0.070. When the refinement was terminated, no temperature factor shift was greater than one standard deviation, the atomic position parameter shifts were all less than 0.65 of a standard deviation, and generally much smaller than this. No systematic trends were to be found in the shifts.

The estimated standard deviations of the parameters were calculated according to the formula

$$\sigma(P_i) = [(a^{-1})_{ii}(\Sigma w\Delta^2)/(m - n)]^{\frac{1}{2}}$$

where $(a^{-1})_{ii}$ is a diagonal element in the inverse matrix, *m* is the number of reflections included in the least squares refinement, *n* is the number of variable parameters in the structure, and *w* is the relative weight. The final difference map showed a slight negative peak at the Cu atom position (−2.7% of the Fourier peak height). There was no indication of misplacement of any atom. The hydrogen atom peaks were visible at approximately twice the background variations. The methyl hydrogens were most poorly defined. The structure factor table is in the Depository for Unpublished Data.[1]

Results

The fractional atomic coordinates of bis-(2,4-pentanedionato)4-aminopyridinecopper(II) are given in Table 2. The molecular structure is shown in Fig. 2 and the complete unit cell in Fig. 3. The origin of the cell is at the lower left front, with *y* vertical, *z* left to right, and *x* approximately into the page. Atoms marked N1 in Fig. 3 belong to neighboring cells, and the thin

[1]Copies may be obtained free of charge, upon request, from the Depository of Unpublished Data, National Science Library, National Research Council of Canada, Ottawa, Canada.

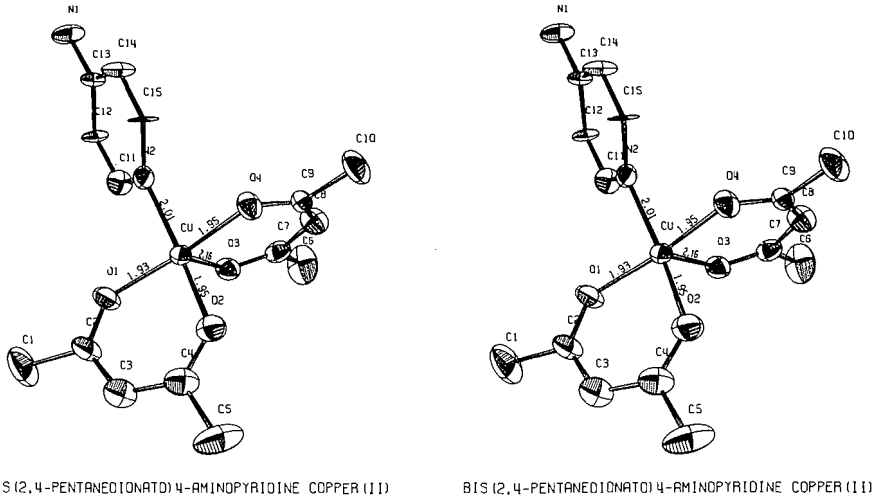

FIG. 2. Single molecule with labels.

TABLE 2. Fractional atomic coordinates*

Atom	X/A	Y/B	Z/C
Cu	1865(2)	2176(1)	2279(1)
O(1)	667(7)	1480(4)	1075(4)
O(2)	−66(8)	3012(4)	1978(4)
O(3)	1453(8)	1329(4)	3400(4)
O(4)	3152(8)	3071(3)	3279(4)
N(1)	8501(10)	62(5)	2623(6)
N(2)	4050(9)	1524(4)	2411(4)
C(1)	−1227(17)	1114(7)	−585(7)
C(2)	−693(12)	1700(6)	368(6)
C(3)	−1787(13)	2424(6)	389(6)
C(4)	−1437(12)	3018(6)	1193(6)
C(5)	−2761(15)	3746(7)	1136(10)
C(6)	1545(17)	948(7)	5028(7)
C(7)	1945(12)	1578(6)	4296(5)
C(8)	2814(12)	2394(5)	4690(6)
C(9)	3300(11)	3077(5)	4184(5)
C(10)	4123(13)	3928(6)	4779(6)
C(11)	4003(12)	601(5)	2343(6)
C(12)	5448(11)	103(5)	2418(6)
C(13)	7036(11)	534(5)	2577(5)
C(14)	7071(12)	1487(5)	2675(6)
C(15)	5596(10)	1937(5)	2594(6)

*All values have been multiplied by 10^4. Estimated standard deviations in parentheses.

TABLE 3. Intramolecular bonds*

(*a*) Coordinate bonds

Bond	Length	Bond	Length
Cu—O(1)	1934(5)	Cu—O(2)	1946(7)
Cu—O(3)	2165(6)	Cu—O(4)	1948(5)
Cu—N(2)	2010(8)		

(*b*) 2,4-Pentanedionato bonds

Bond	Length	Bond	Length
O(1)—C(2)	1248(11)	O(3)—C(7)	1249(9)
O(2)—C(4)	1268(11)	O(4)—C(9)	1258(9)
C(1)—C(2)	1536(13)	C(6)—C(7)	1531(14)
C(2)—C(3)	1413(14)	C(7)—C(8)	1409(12)
C(3)—C(4)	1390(12)	C(8)—C(9)	1388(11)
C(4)—C(5)	1523(16)	C(9)—C(10)	1529(11)

(*c*) 4-Aminopyridine bonds

Bond	Length	Bond	Length
N(2)—C(11)	1364(10)	N(2)—C(15)	1362(12)
C(11)—C(12)	1382(13)	C(15)—C(14)	1366(13)
C(12)—C(13)	1411(13)	C(14)—C(13)	1412(11)
N(1)—C(13)	1389(12)		

*Bond length × 10 is in pm, standard deviation in parentheses.

lines denote the three shortest intermolecular distances. It is evident that the copper atom is five coordinate and that there is no atom near the sixth coordination position. Table 3 gives the intramolecular bond lengths. Comparable measurements from the literature are given in Table 4. In the basal plane the copper to ligand bond lengths are normal. The apical Cu—O(3) length at 216.5 pm is greater than the basal Cu—O distances but, limited by the span of the chelate, it is shorter than any of its kind shown in Table 4.

The bond lengths within each 2,4-pentanedionato ligand agree well with the average values given by Lingafelter (22). In Table 4 $(C—C)_i$ and $(C—C)_x$ are bond lengths internal and external to the chelate ring, respectively. In Table 5, the O—O distance in each ligand is compared with the values cited by Lingafelter. The O(3)—O(4) distance is larger than usual; together with the short Cu—O(3) bond this may indicate an ener-

Can. J. Chem. Downloaded from www.nrcresearchpress.com by 210.87.254.42 on 09/05/12
For personal use only.

Can. J. Chem. Downloaded from www.nrcresearchpress.com by 210.87.254.42 on 09/05/12
For personal use only.

TABLE 4. Literature bond lengths for comparison with Table 3

(*a*) Coordinative bond lengths in tetragonal pyramidal Cu(II) complexes*

Cu — Basal O	Cu — Basal N	Cu — Apical O	Reference
1910, 1870	2010, 1990		(15)
1940, 1930, 1950		2400	(16)
1936, 1959, 1936	1913	2352	(17)
1925, 1935	1974, 1972	2830	(18)
	1940	2430	(19)
2050, 1850	1850, 1950	2290	(20)
1920, 1930	1930, 1990	2280	(21)
2000, 1900			(10)

(*b*) Average bond lengths in 2,4-pentanedionato ligands

$(C—C)_i$	$(C—C)_x$	(C—O)	Reference
1400	1520	1280	(22)

*Bond length × 10 is in pm.

The coordinative bond lengths were measured in the following compounds given in the same order as the tabulated data.

bis-(N-phenylsalicylaldiminato)pyridinecopper(II),
anhydrous cupric formate,
N-salicylideneglycinatoaquocopper(II),
bis-(8-hydroxyquinolinato)copper(II) dimer (β form),
bis-(dimethylglyoximato)copper(II) dimer,
NN'-ethylenebis-(acetylacetoneiminato)aquocopper(II),
pyridoxylidene(±)-valinecopper(II),
bis-(*o*-hydroxyacetophenonato)4-methylpyridinecopper(II).

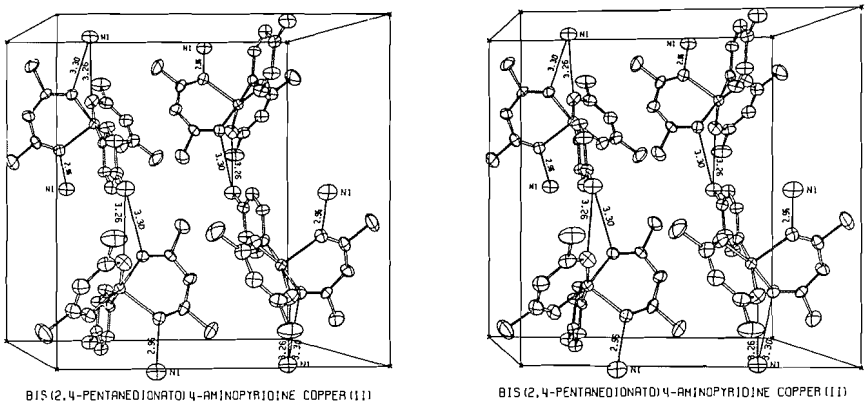

FIG. 3. Complete unit cell showing intermolecular contacts. (Atoms marked N1 belong to neighboring cells.)

getically unfavorable factor which had to be overcome in the formation of a Type 2 copper complex rather than a Type 1. The 1,1,1,5,5,5-hexafluoro-2,4-pentanedionato ligands in the six coordinate complex, $Cu(hfacac)_2$ bipyridine have been shown to have Cu—O distances of 196.7 and 229.6 pm (23). In this case the O—Cu—O angle is acute, the span of the chelate is normal, and accompanied by an alternation of bond lengths suggestive of the enol form of the ligand. There is no indication of a similar effect in the unfluorinated ligands of our five coordinate complex.

Table 6 gives the distribution into various ranges of intermolecular distances between 290 and 400 pm. Those below 360 pm have been specified and their lengths given owing to their probable role as structure determining factors. The three shortest distances are marked in Fig. 3 by thin lines. The shortest of them all (N(1)—O(3), 296 pm) may be attributed to a N—H---O hydrogen bond, for which a typical N—O distance is 290 pm (24). The difference map has a peak attributable to hydrogen at approximately the correct position. The N(1)—O(2) and N(1)—O(4) lengths are more difficult to interpret, being at the upper limit of those expected for a bifurcated hydrogen bond but still considerably shorter than average. If the atom N(1) were pressed wedge-like

TABLE 5. O—O Distances in 2,4-pentanedionato ligands

Compound	O—O (pm)	Compound	O—O (pm)
$Cu(acac)_2$4-aminopyr	299*	$Cu(acac)_2$4-aminopyr	280†
$Co(acac)_2 2H_2O$	296	$Cr(acac)_3$	279
$Ni(acac)_2 2H_2O$	291	$VO(acac)_2$	272
$Zn(acac)_2 H_2O$	282	$Be(acac)_2$	268
$Mn(acac)_3$	281	$Zr(acac)_4$	267
$Ce(acac)_4$	281		

*Apex–base.
†Base–base.

TABLE 6. Intermolecular distances

Range (pm)	No. in range	Intermolecular distance	
		Bond	Distance (pm)
290–300	1	N(1)—O(3)	296
300–310	0		
310–320	0		
320–330	2	N(1)—O(2)	326
		N(1)—O(4)	330
330–340	0		
340–350	3	C(14)—O(3)	342
		C(10)—C(10)	344
		C(12)—O(4)	350
350–360	1	C(8)—O(1)	355
360–370	6		
370–380	7		
380–390	16		
390–400	16		

between atoms O(2) and O(4), the O(2)—O(4) distance would be larger than normal. In fact this distance is remarkably short at 264 pm and subtends an angle of only 85.2° at the copper atom. Furthermore the angle Cu—N(2)—C(11), 118.1°, is less than Cu—N(2)—C(15), 124.5°, supporting the view that N(1) is weakly hydrogen bonded to O(2) and O(4). The difference map has a reasonably well shaped peak attributable to hydrogen lying in the N(1), O(2), O(4) triangle. The short C(14)—O(3) and C(12)—O(4) distances may be attributed to the proximity of C(12) and C(14) to N(1), and the pyridine ring position. The closest contact definitely not affected by hydrogen bonding is between two C(10) methyl groups. It is clearly visible across the center of Fig. 3, and may control the plane of the pyridine ring.

The bond angles are given in Table 7. The angles subtended by the copper atom deviate markedly from the 90, 180° values of a pure tetragonal pyramid but are best described in terms of this geometry. O(1) and O(2) are bent downwards away from the apex by 10.6 and 10.3°. This is similar to the effect observed by Ooi and Fernando (11). O(4) and N(2) are bent away from the apex by 2.4 and 2.7°, thus the symmetry of coordinated atoms about a plane defined by Cu, C(3), and O(3) is remarkably good.

The angles of the pentanedionato groups agree well with the following average values (22): $(O—C—C)_i = 125.3$, $(O—C—C)_x = 115.7$. Angles of the type $(C—C—C)_i$ are known (22) to be dependent on the (O—O) span; this is confirmed by the results.

The least squares planes for the three ligand molecules and the basal plane of the tetragonal pyramid (excluding Cu) are given in Table 8. The orthogonal axis system used has x along a, y in the (a,b) plane, and z along c^*. The quantity minimized was $R = \sum_i W_i P_i^2$, where the weight W_i for atom i is given by $3/(\sigma^2(x_i) + \sigma^2(y_i) + \sigma^2(z_i))$ and P_i is the perpendicular distance of atom i from the plane. The quantity $\chi^2 = \sum_i (P_i^2/\sigma^2(P_i))$ is calculated as an index of the planarity of the group.

We conclude that the 4-aminopyridine ligand and the basal group O(1), O(2), O(4), and N(2) are planar, the copper atom lying 0.22 Å above the basal plane. Deviations from planarity of the 2,4-pentanedionato groups are shown in Fig. 4.

The thermal vibration parameters are given in Table 9 and pictorially displayed in Figs. 2 and 3, of which the viewing lines are mutually perpendicular. Figure 2 shows the lower left hand molecule of Fig. 3 as seen from above. The terminal carbon atoms of the diketone ligands have large amplitudes of vibration. Atoms C(12) to C(15), and N(1) which constitute the far end of the 4-aminopyridine ligand, appear to be moving in a concerted fashion. This is consistent with the ring structure having a certain rigidity and the amine group being hydrogen bonded to a neighboring molecule. Relative motion of adjacent molecules might be expected to cause the 4-aminopyridine to wag.

Conclusion

The structure of bis-(2,4-pentanedionato)4-aminopyridinecopper(II) has been shown to be

Can. J. Chem. Downloaded from www.nrcresearchpress.com by 210.87.254.42 on 09/05/12
For personal use only.

TABLE 7. Bond angles in bis-(2,4-pentanedionato)4-aminopyridinecopper(II)

(*a*) Copper atom

Bonds	Angle (deg)	Bonds	Angle (deg)	Bonds	Angle (deg)
O(1)—Cu—O(2)	91.8±0.3	O(1)—Cu—O(3)	100.6±0.2	O(1)—Cu—O(4)	167.0±0.2
O(2)—Cu—O(4)	85.2±0.3	O(2)—Cu—O(3)	100.3±0.2	O(2)—Cu—N(2)	166.7±0.3
O(4)—Cu—N(2)	91.4±0.3	O(4)—Cu—O(3)	92.4±0.2		
N(2)—Cu—O(1)	88.6±0.3	N(2)—Cu—O(3)	92.7±0.3		

(*b*) 2,4-Pentanedionato ligands

Bonds	Angle (deg)	Bonds	Angle (deg)	Bonds	Angle (deg)
$(Cu—O—C)_1$		$(Cu—O—C)_1$		$(C—C—C)_1$	
Cu—O(1)—C(2)	126.5±0.6	Cu—O(3)—C(7)	120.8±0.5	C(2)—C(3)—C(4)	123.9±0.9
Cu—O(2)—C(4)	126.7±0.6	Cu—O(4)—C(9)	125.3±0.5	C(7)—C(8)—C(9)	128.2±0.8
$(O—C—C)_x$		$(O—C—C)_1$		$(C—C—C)_x$	
O(1)—C(2)—C(1)	116.6±0.8	O(1)—C(2)—C(3)	125.3±0.8	C(1)—C(2)—C(3)	118.1±0.8
O(2)—C(4)—C(5)	116.6±0.9	O(2)—C(4)—C(3)	124.8±0.9	C(3)—C(4)—C(5)	118.6±0.9
O(3)—C(7)—C(6)	117.1±0.8	O(3)—C(7)—C(8)	125.7±0.8	C(6)—C(7)—C(8)	117.2±0.8
O(4)—C(9)—C(10)	115.5±0.7	O(4)—C(9)—C(8)	126.9±0.8	C(8)—C(9)—C(10)	117.6±0.7

(*c*) 4-Aminopyridine ligands

Bonds	Angle (deg)	Bonds	Angle (deg)	Bonds	Angle (deg)
$(Cu—N—C)_x$		$(C—C—N)_1$		$(C—C—C)_1$	
Cu—N(2)—C(11)	118.1±0.6	C(12)—C(11)—N(2)	121.6±0.8	C(11)—C(12)—C(13)	120.9±0.8
Cu—N(2)—C(15)	124.5±0.5	C(14)—C(15)—N(2)	124.1±0.8	C(12)—C(13)—C(14)	116.6±0.8
$(C—C—N)_x$		$(C—N—C)_1$		C(13)—C(14)—C(15)	119.4±0.8
C(12)—C(13)—N(1)	122.7±0.8	C(11)—N(2)—C(15)	117.4±0.7		
C(14)—C(13)—N(1)	120.7±0.8				

TABLE 8. Least squares planes: $C_1x + C_2y + C_3z + C_4 = 0$

No.	Plane*	C_1	C_2	C_3	C_4	χ^2
1	O(1), O(2), O(4), N(2)	+0.5138	+0.5870	−0.6256	−0.3799	2.38
2	O(1), O(2), C(1)—C(5)	+0.6811	+0.6084	−0.4075	−0.7983	268.8
3	O(3), O(4), C(6)—C(10)	−0.8632	+0.4461	−0.2364	−0.2913	157.4
4	N(1), N(2), C(11)—C(15)	+0.1292	+0.0882	−0.9877	+2.7256	42.8

*Angles between normals of planes *1* and *2* = 15.8°; *1* and *3* = 91.9°; *1* and *4* = 42.6°.

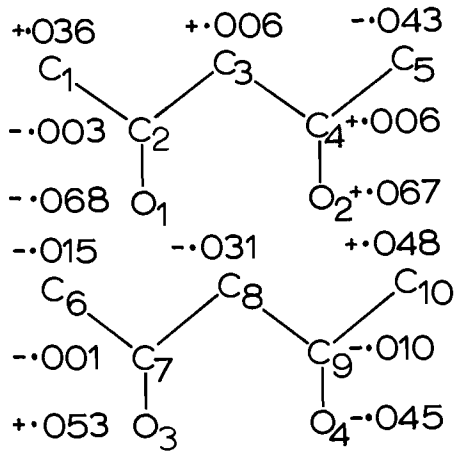

FIG. 4. Deviation from planarity (in Å) of each 2,4-pentanedionato ligand.

approximately tetragonal pyramidal and of Type 2 (see Introduction). The axial bond is longer than the basal bonds and in order to span from the apex to the base of the pyramid, one of the diketone chelates is strained open more than usual. Nevertheless, the axial bond is shorter than analogous bonds in many other tetragonal pyramidal copper complexes in which the compressive effect of chelation is absent. It is reasonable to suppose that energy has been expended in attaining this molecular structure and regained in the formation of a more stable crystal structure. Intermolecular hydrogen bonding is suggested as an important stabilizing factor. The difference between this structure and the Type 1 structure of bis-(2,4-pentanedionato)quinolinecopper(II) can also be rationalized in terms of the base strengths of the

Can. J. Chem. Downloaded from www.nrcresearchpress.com by 210.87.254.42 on 09/05/12
For personal use only.

TABLE 9. Anisotropic temperature parameters*

Atom	β_{11}	β_{22}	β_{33}	β_{23}	β_{13}	β_{12}
Cu	64(3)	24(1)	30(1)	−77(1)	34(2)	−17(2)
O(1)	86(15)	37(3)	36(3)	−11(5)	−11(9)	7(10)
O(2)	105(15)	43(3)	54(4)	−16(6)	42(11)	16(10)
O(3)	87(14)	33(3)	36(3)	0(5)	38(10)	−27(9)
O(4)	118(14)	29(3)	36(3)	−15(4)	45(10)	−47(9)
N(1)	56(19)	39(4)	75(5)	6(8)	45(14)	31(12)
N(2)	95(17)	27(3)	32(3)	−16(5)	52(11)	−28(11)
C(1)	257(31)	59(6)	47(6)	−49(10)	4(20)	−30(22)
C(2)	95(23)	40(5)	40(5)	−11(8)	−2(14)	−18(15)
C(3)	128(23)	38(4)	53(6)	−1(8)	32(17)	−5(15)
C(4)	107(23)	32(5)	58(6)	9(8)	36(17)	5(14)
C(5)	117(28)	41(5)	133(11)	8(12)	104(26)	38(18)
C(6)	306(35)	54(6)	57(6)	21(10)	158(23)	−63(23)
C(7)	85(21)	37(4)	35(4)	20(7)	54(14)	10(14)
C(8)	121(22)	29(4)	42(5)	2(7)	50(15)	−46(13)
C(9)	75(21)	25(4)	34(4)	−23(6)	31(13)	−17(12)
C(10)	171(26)	42(5)	49(6)	−45(8)	49(18)	−80(17)
C(11)	118(23)	21(4)	45(5)	−5(7)	45(16)	−5(13)
C(12)	32(22)	35(4)	49(5)	−2(7)	39(14)	−23(13)
C(13)	39(19)	27(3)	37(5)	−2(6)	18(14)	−23(13)
C(14)	36(20)	27(4)	67(6)	−2(8)	22(15)	−8(14)
C(15)	10(21)	26(4)	59(5)	−15(7)	30(15)	−27(11)

*Anisotropic values have been multiplied by 10^4. $T = \exp[-(h^2\beta_{11} + k^2\beta_{22} + l^2\beta_{33} + kl\beta_{23} + hl\beta_{13} + hk\beta_{12})]$. Estimated standard deviations in parentheses.

two heterocyclic molecules, provided that the diketone groups are assigned a non-dominant role, as is observed experimentally. We assume a C_{4v} ligand field for the d^9 Cu ion. The strongly basic 4-aminopyridine molecule ($pK_a = 9.114$) donates electrons toward the half filled $d_{x^2-y^2}$ orbital. The more weakly basic quinoline molecule ($pK_a = 4.81$) is better able to tolerate the electron density of the Cu atom at the apical position.

Operating funds were obtained from the National Research Council of Canada and the Committee for Research, Leave, and Travel of the University of Victoria. A major equipment grant and computing facilities were provided by the University of Victoria. Mr. R. D. Menhenett and Dr. A. Tweedale have generously given computing assistance. The author gratefully acknowledges all these contributions.

1. W. E. HATFIELD and R. WHYMAN. Transition Metal Chemistry. *Edited by* R. L. Carlin. Marcel Dekker, New York. **5**, 47 (1969).
2. M. CIAMPOLINI and N. NARDI. Inorg. Chem. **5**, 41 (1966).
3. H. ELLIOT, B. J. HATHAWAY, and R. C. SLADE. J. Chem. Soc. A, 1443 (1966).
4. T. S. PIPER and R. L. BELFORD. J. Mol. Phys. **5**, 169 (1962).
5. D. P. GRADDON. Nature, **183**, 1610 (1959).
6. R. C. TRAILL. Nature, **186**, 631 (1960).
7. H. BURGESS and T. M. LOWRY. J. Chem. Soc. **125**, 2081 (1924).
8. D. P. GRADDON and E. C. WATTON. Nature, **187**, 1021 (1960). J. Inorg. Nucl. Chem. **21**, 49 (1961).
9. W. R. WALKER and N. C. LI. J. Inorg. Nucl. Chem. **27**, 2255 (1965).
10. V. F. DUCKWORTH, D. P. GRADDON, G. M. MOCKLER, and N. C. STEPHENSON. Inorg. Nucl. Chem. Lett. **3**, 471 (1967).
11. S. OOI and Q. FERNANDO. Chem. Commun. 532 (1967).
12. M. M. JONES. J. Amer. Chem. Soc. **81**, 3188 (1959).
13. J. A. IBERS. International Tables for X-Ray Crystallography. I. U. Cr. by the Kynoch Press, Birmingham. Vol. III, Table 3.3.1A, 201 (1962).
14. F. R. AHMED, S. R. HALL, C. P. HUBER, and M. E. PIPPY. NRCC Crystallographic Programs for the I.B.M. 360 System. Division of Pure Physics and Pure Chemistry, National Research Council, Ottawa, Canada.
15. D. HALL, S. V. SHEAT, and T. N. WATERS. Chem. Ind. 1428 (1965).
16. G. A. BARCLAY and C. H. L. KENNARD. J. Chem. Soc. 3289 (1961).
17. T. UEKI, T. ASHIDA, Y. SASADA, and M. KAKUDO. Acta Cryst. **B25**, 328 (1969).
18. G. J. PALENIK. Acta Cryst. **17**, 687 (1964).
19. E. FRASSON, R. BARDI, and S. BEZZI. Acta Cryst. **12**, 201 (1959).
20. D. HALL, H. J. MORGAN, and T. N. WATERS. J. Chem. Soc. A, 677 (1966).
21. J. F. CUTFIELD, D. HALL, and T. N. WATERS. Chem. Commun. 785 (1967).
22. E. C. LINGAFELTER. Coord. Chem. Rev. **1**, 151 (1966).
23. M. V. VEIDIS, G. H. SCHREIBER, T. E. GOUGH, and G. J. PALENIK. J. Amer. Chem. Soc. **91**, 1859 (1969).
24. W. C. HAMILTON and J. A. IBERS. Hydrogen Bonding in Solids. W. A. Benjamin Inc., New York. 166 (1968).

Can. J. Chem. Downloaded from www.nrcresearchpress.com by 210.87.254.42 on 09/05/12
For personal use only.

Can. J. Chem. Downloaded from www.nrcresearchpress.com by 210.87.254.105 on 09/05/12
For personal use only.

Investigations of Paramagnetic Centers Produced by Tritium β-Particle Irradiation. I. The Cd(I) Cation in Single Crystals of Calcium Tetraacetato Cadmium (II) Hexahydrate

R. S. EACHUS AND F. G. HERRING
Chemistry Department, University of British Columbia, Vancouver 8, British Columbia

Received July 8, 1970

The Cd(I) center has been produced by both tritium β-particle irradiation and by γ-irradiation. The tritium was introduced as water of crystallization in calcium tetraacetato cadmium(II) hexahydrate in the form of THO. It is found that both forms of irradiation lead to the same center. The orientation of the hyperfine components of the Cd(I) center throws some light on the possible mechanism of its formation.

Canadian Journal of Chemistry, 49, 562 (1971)

Introduction

The primary interaction of high energy radiation with a solid is the ejection of electrons from the constituent molecules of the solid. When these high energy electrons become thermalized they can either recombine with the parent molecule to produce an excited state (which will often undergo homolytic fission to produce a radical fragment) or an electron may become trapped at an impurity center or at another molecule to produce an electron excess center. This last trapping may require either an intramolecular or an intermolecular configuration change (1).

The usual sources of high energy radiation are X-rays and γ-rays. However, an alternative procedure for producing electrons in a lattice, which may be subsequently trapped, is the β-particle decay of the tritium atom. Previous studies using this form of internal radiation are limited. One of the first studies appears to have been carried out by Spinks *et al.* (2) who used electron spin resonance (e.s.r.) to monitor the decay of tritium oxide in frozen water. Subsequently Lassmann (3) studied the self-radiolysis of tritium-labelled amino and dicarboxylic acids. This study showed that, in these systems, stable free radicals are formed by the conversion of primary unstable free radicals; the unstable precursors being detected at 77 °K. Lloyd, Magnotta, and Wood (4) studied the free radical reaction initiated by the radioactive decay in solid naphthalene-1-*t*. Very recently Hase and Kevan (5) undertook an e.s.r. study of the trapped species produced by tritium β-particles in alkaline and acid ices at 77 °K. They found that the yield of trapped species was always larger in γ-irradiated systems than in the corresponding β-irradiated systems.

In order to study the production of free radicals in the solid state the tritium is most conveniently incorporated into the lattice as water of crystallization as THO. The following decay is expected

$$HTO \rightarrow HHeO^+ + \beta^-$$

$$HHeO^+ \rightarrow HO^+ + He$$

The electron produced will cause some 200 ionizations or excitations in about 10^4 Å due to the high linear energy transfer of the β-particle radiation. The secondary electrons so produced will become thermalized and consequently can be trapped at, for example, a heavy metal ion whose inelastic scattering cross section is expected to be high due to the large number of electrons present on the ion (6).

This first study reports the formation of the Cd(I) center produced by β-particle decay in calcium tetraacetato cadmium(II) hexahydrate. These results are compared with the effects of γ-irradiation, previously described in a preliminary report (7).

Experimental

(i) Sample Preparation

All solid reagents used were AnalaR grade and tritium oxide, having a specific activity of 0.5 Ci g^{-1}, was obtained from the New England Nuclear Corporation. Calcium tetraacetato cadmium(II) hexahydrate was prepared according to the method described by Holden and Singer (8). Single crystals for irradiation by tritium β-particles were grown by slow cooling from a saturated solution in tritiated water. Samples for γ-irradiation were grown by slow evaporation from aqueous solution. Large, colorless crystals were readily obtained by both methods, the majority of which had the characteristic form

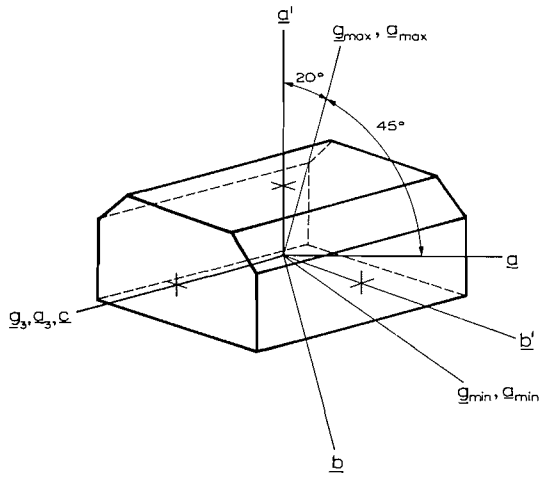

FIG. 1. Crystal morphology and axis systems. (g_{max}, a_{max}, g_{min}, a_{min} are the maximum and minimum values of the Cd(I) g- and hyperfine tensors in the a' b' plane.)

depicted in Fig. 1. Suitable "tritiated" crystals were mounted upon a quartz rod and maintained at 77 °K for approximately 14 days prior to the measurement of electron paramagnetic resonance (e.p.r.) spectra. γ-Irradiations were accomplished using a ^{60}Co γ-source whose effective dose rate was approximately 0.3 Mrads per hour. The crystal was mounted on a "spectrosil"-grade quartz sample holder and immersed in liquid nitrogen in a Dewar vessel designed to fit close to the radiation source. An approximate total dose of 1.2 Mrads was necessary to obtain e.p.r. spectra of sufficient intensity.

(ii) Electron Paramagnetic Resonance Measurements

Electron paramagnetic resonance measurements were made at 77 °K on a conventional X-band spectrometer, operating at approximately 9.3 GHz, incorporating a Varian variable-temperature accessory. This spectrometer and the method of field calibration have been described in detail elsewhere (9). With this assembly the sample temperature could be controlled within ±5° of 77 °K. A metal pointer attached to the exposed end of the quartz sample holder, coupled with a fixed protractor of large radius, enabled accurate orientations of the crystals to be made. Crystal alignments, with respect to the direction of the applied magnetic field, were accurate to within ±2.5°.

Results

(i) Single-Crystal Studies of $CaCd(CH_3COO)_4.6H_2O$ Grown from Water Containing Tritium Oxide

For e.p.r. measurements of a "tritiated" crystal of $CaCd(CH_3COO)_4.6H_2O$ rotations were performed about the well defined elongated c-axis and about orthogonal directions projecting from two well developed faces. The latter directions are labelled a' and b' in Fig. 1.

A typical e.s.r. spectrum was dominated by signals from two paramagnetic species. The less stable radical, which we tentatively identify as the methyl radical, was characterized by an isotropic 1:3:3:1 quartet.

A first derivative spectrum of the second center, measured with the applied magnetic field ($\boldsymbol{H}_0$) in the ac plane at $\theta = 40°$ (where θ is the angle between $\boldsymbol{H}_0$ and the c-axis), is shown in Fig. 2. For all orientations of the crystal resonant fields were disposed over approximately 5000 G. The multiplet spectrum is composed, essentially, of a five line hyperfine pattern with a superimposed doublet site splitting. Also, as is clear from Fig. 2, the free spin features and the resonances at highest field are accompanied by weaker pairs of satellite lines separated by approximately 10.6 G at $\mathbf{g} = 2$ and 17.0 G around $\boldsymbol{H}_0 = 4250$ G. The intensity of these weaker resonances increased, with respect to the associated hyperfine feature, as the incident microwave power was increased. Such behavior is characteristic of features arising from the sympathetic nuclear spin-inversion of neighboring protons (10, 11). Similar interactions were observed in the e.p.r. spectrum of Cu(II) ions doped substitutionally for Cd(II) in this lattice (12). The separation, $\Delta\boldsymbol{H}$ between the satellite lines and the corresponding central resonance has been shown to vary with the applied magnetic field strength. At approximately $\boldsymbol{H}_0 = 1000$ G, $\Delta\boldsymbol{H}$ would be less than 3 G and consequently the satellite features, which necessarily accompany the low field features in Fig. 2, would be hidden within, and contribute to, their excessive linewidths.

This complex spectrum has been interpreted in terms of the paramagnetic Cd(I) cation which has a $^2S_{1/2}$ ground state configuration and is isoelectronic with atomic silver. There are two magnetic isotopes of cadmium in natural abundance (^{111}Cd:I = 1/2, $\mu_n = -0.5912$ N.M.; 12.86% and ^{113}Cd:I = 1/2, $\mu_n = -0.6195$ N.M.; 12.34%). We assign the strong central resonances to the even isotopes of the Cd(I) ion and consider that the weaker features at low and high fields arise from the less abundant magnetic ^{111}Cd and ^{113}Cd isotopes.

A structural analysis of calcium tetraacetato cadmium(II) hexahydrate has recently been completed by Langs and Hare (13) at room temperature. Figure 3 shows the Cd(II) environment

Can. J. Chem. Downloaded from www.nrcresearchpress.com by 210.87.254.105 on 09/05/12
For personal use only.

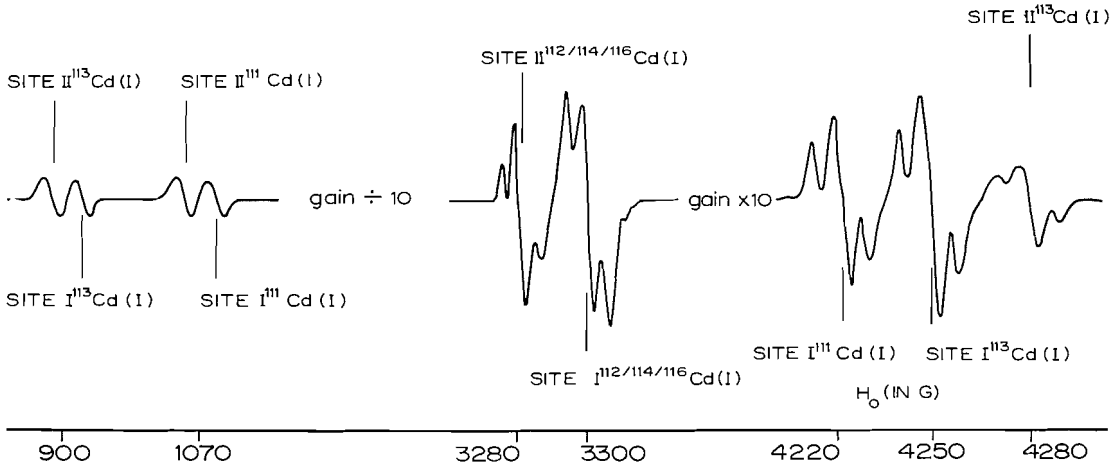

FIG. 2. Electron paramagnetic resonance spectrum of the Cd(I) center in the $a'c$ plane at $\theta = 40°$.

in the undamaged crystal. This crystal belongs to the tetragonal system with four molecules per unit cell at ambient temperature. When the crystal is cooled to 77 °K, however, it undergoes a distinct tetragonal–orthorhombic transition and four sites are now no longer equivalent at all orientations of the magnetic field (14).

When $\boldsymbol{H}_0$ was parallel to the crystal c-axis the multiplet spectrum coalesced completely into a five line pattern. This was not the case when $\boldsymbol{H}_0$ was parallel to a' or b'. We conclude from rotation studies in the plane perpendicular to c that the crystallographic a- and b-axis make angles of 65° to a' and b'. The orientation of the four Cd(I) sites relative to the a, b, and c crystallographic axes shown in Fig. 4. The principal axes of the **g**- and hyperfine tensors are seen to be spatially coincident. The angle θ is small, less than 5°. Consequently, since the hyperfine tensor is almost isotropic and linewidths approaching 5.0 G are common, rotation in the $a'c$- and $b'c$-plane revealed only two magnetically non-equivalent sites, instead of the four expected.

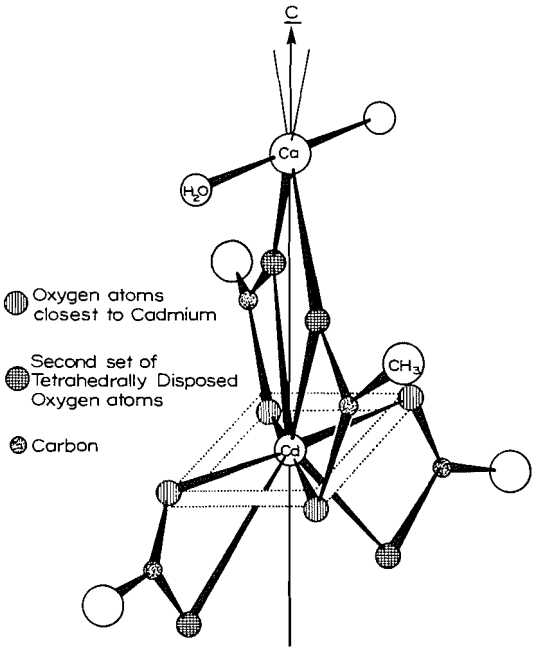

FIG. 3. The molecular structure of the undamaged system.

The angular variation in the $a'c$-plane of the hyperfine features arising from the two distinguishable Cd(I) sites is given in Fig. 5. The solid lines and dotted lines are the computer fit of the experimental data to the spin Hamiltonian.

$$\mathcal{H} = \boldsymbol{H}.\mathbf{g}.\boldsymbol{S} + \boldsymbol{S}.\mathbf{A}.\boldsymbol{I}. - \mathbf{g}_N\beta_N\boldsymbol{H}.\boldsymbol{I}$$

Computations were accomplished using a program written by J. A. Hebden based on the general method of Byfleet *et al.* (15) and the values collated in Table 1 yielded the best fit. The direction arbitrarily labelled x in the Table is parallel to the crystallographic c-axis whilst y and z make angles of 20° to a and b, respectively. It was also found that the Cd(I) centers are divided into two symmetry-related pairs whose principal z and y directions are interchanged. This result, together with the form of the hyperfine tensor, sheds some light on a possible mechanism for the formation of the Cd(I) center.

Can. J. Chem. Downloaded from www.nrcresearchpress.com by 210.87.254.105 on 09/05/12
For personal use only.

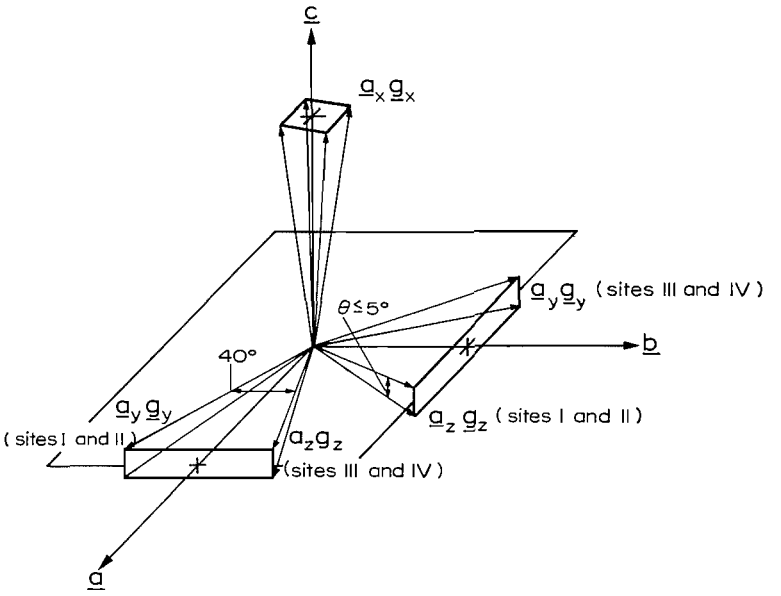

FIG. 4. Orientations of the four Cd(I) sites.

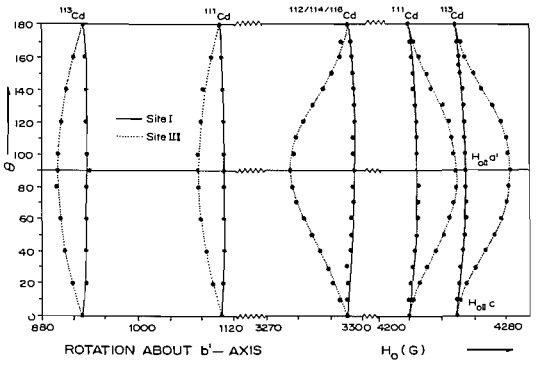

FIG. 5. Angular variation of the hyperfine lines in the *a'c* plane for the two distinguishable sites.

(ii) Single Crystal Investigations of Samples Exposed to γ-Rays

A typical e.p.r. spectrum revealed the existence of several distinguishable paramagnetic centers. By analogy to the results of Rogers and Kispert (16) for the effect of γ-rays on polycrystalline $Ca(CH_3CO_2)_2.H_2O$ we can offer tentative identifications for the centers arising from radiation damage of the acetate ligands. A strong isotropic quartet centered upon $\mathbf{g} = 2$ almost certainly arises from the methyl radical; a well-characterized product in inorganic acetates possessing a large number of molecules as water of crystallization. A second, weaker asymmetric spectrum underlying the quartet remains unidentified, although the electron-excess $CH_3CO_2^{2-}$ cannot be ruled out. Both centers were temperature sensitive and decayed rapidly when the host crystal was annealed at 120 °K. Their decomposition resulted in the formation of the stable $CH_2CO_2^-$; the product of radiation damage at ambient temperature.

Features from a third paramagnetic species, having a **g**-value lower than that of the free-electron, dominated the spectrum of a crystal which was irradiated at 77 °K, warmed to 120 °K for 5 min, and recooled to 77 °K for the measurement of spectra. All subsequent investigations of this latter center were carried out upon irradiated crystals which had undergone this annealing process prior to study.

The magnetic parameters of this relatively stable species were identical to those of the Cd(I) cation formed by β-electron capture in the "tritiated" crystal. Furthermore, careful orientation studies revealed that the principal axis system of the Cd(I) center produced by γ-irradiation was coincident with that produced by tritium β-irradiation.

Discussion

The Cd(I) center has been observed previously (17–19); Table 1 contains the results of these

Can. J. Chem. Downloaded from www.nrcresearchpress.com by 210.87.254.105 on 09/05/12
For personal use only.

TABLE 1. Magnetic data for the Cd(I) ion in a variety of matrices

Matrix	Nucleus	Hyperfine tensor (G) a_{xx}	a_{yy}	a_{zz}	g-tensor g_{xx}	g_{yy}	g_{zz}	Reference
Argon	^{111}Cd	$a_{iso} = -5137$			$g_{iso} = 2.0006$			17
	^{113}Cd	$a_{iso} = -5374$						
EtOH	^{111}Cd	-3280 ± 130*			1.9924	1.9896	1.9896	18
	^{113}Cd							
NaCl	^{111}Cd	-4270			$g_{iso} = 1.996$			19
$CaCd(CH_3CO_2)_4 6H_2O$	^{111}Cd	-2593	-2582	-2689	1.9877	1.9825	1.9996	This work
	^{113}Cd	-2716	-2706	-2818				

*Separate components corresponding to the ^{111}Cd and ^{113}Cd isotopes were not resolved.

observations. The large isotropic hyperfine coupling for Cd is ascribed to the large Fermi contact term of the 5s orbital in which the odd electron is thought to reside. The center observed in an argon lattice has the largest isotropic hyperfine component, the present center having the smallest.

The magnitude of the Fermi contact term depends mainly upon the spin density in the 5s orbital and to a smaller extent the polarization of inner s orbitals on the Cd(I) cation. The spin density in the 5s orbital can be reduced in two ways; firstly if the cation interacts with the lattice substantially the spin density may be distributed to neighboring atoms. Secondly the symmetry of the site in which the cation finds itself may allow the admixture of a cadmium 5p orbital into the odd electron orbital which again will decrease the probability of the odd electron being in the 5s orbital. In addition to these two main effects the polarization contribution to the Fermi contact term will also be reduced by increased covalent participation of the 5s orbital (20).

Thus the Cd(I) center produced in ethanol at 77 °K has a reduced isotropic hyperfine coupling, relative to Cd(I) produced in argon (17), due to solvation by the lattice (18) which causes a decrease in the spin density in the cadmium 5s orbital. In the present case it is expected that the original Cd(II) is covalently bound to the acetate ligands and that the Cd(I) center produced by radiation damage will be similarly bound. Further the center considered here also possesses an anisotropy (-68, $+34$, $+34$ for ^{111}Cd) in its hyperfine tensor which is larger than previously observed. This suggests that the ground state for this ion contains some 5p orbital admixture. Thus the substantially reduced Fermi contact term of the center produced in calcium tetraacetato cadmium(II) hexahydrate can be understood.

With regard to the anisotropy of the Cd(I) hyperfine coupling tensor it will be noticed that the largest component of the anisotropy does not lie parallel to the crystallographic *c*-axis. This indicates that some intramolecular rearrangement has taken place. Some evidence as to the nature of this rearrangement is found in the fact that the radiation induced Cd(I) centers are divided into two symmetry-related pairs whose principal *z* and *y* directions are interchanged.

These observations can be understood if we make the reasonable assumption that the primary process involved in both the γ- and β-irradiation of the acetate is the formation of the electron-excess $CH_3CO_2^{2-}$. The mechanism of radiation-damage in a variety of inorganic acetates has been discussed by Rogers and Kispert (16). At 77 °K, the principal product in hydrated salts was found to be CH_3, a highly reactive intermediate which was rapidly anihilated by a process involving hydrogen abstraction from the lattice. The paramagnetic $CH_2CO_2^-$ was the stabilized product from this reaction. The methyl radical itself was almost certainly formed as a result of the decomposition of the unstable $CH_3CO_2^{2-}$. If the reduction of Cd(II) in calcium tetraacetato cadmium(II) hexahydrate occurred through the reaction of this ion with the decomposition products of the primary center, $CH_3CO_2^{2-}$, the resultant Cd(I) molecular complexes would have the structures displayed in Fig. 6. We would then expect, as we indeed find, two pairs of equivalently oriented complexes in the unit cell related by a plane of reflection. If the remaining nearest oxygen atoms retain their essentially planar configuration, the molecule will have

Can. J. Chem. Downloaded from www.nrcresearchpress.com by 210.87.254.105 on 09/05/12
For personal use only.

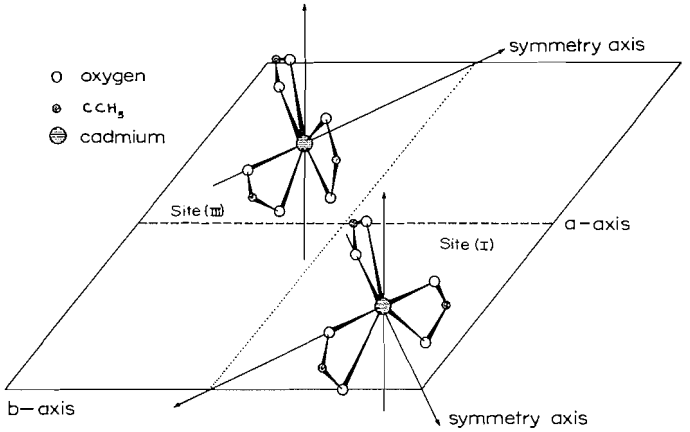

FIG. 6. Disposition of the symmetry axes for two radicals in the unit cell relative to *a* and *b*.

effectively C_{2v} symmetry, the unique axis lying in the plane perpendicular to *c*. This point group allows the $5p_z$ orbital to mix with the 5s orbital and this will lead to the observed anisotropy of the hyperfine tensor.

The authors wish to thank Professor McDowell for his interest in this work. The National Research Council of Canada is thanked for its financial support.

1. J. CUNNINGHAM. *In* Radical Ions. *Edited by* Kaiser and Kevan. John Wiley. 1968.
2. J. W. T. SPINKS, J. KROH, and B. C. GREEN. Nature, **189**, 655 (1961).
3. G. LASSMAN. Proc. of the Second Tihany. Symp. Rad. Chem. 1966. Akademiai Kiado, Budapest. 1967. p. 69.
4. R. V. LLOYD, F. MAGNOTTA, and D. E. WOOD. J. Amer. Chem. Soc. **90**, 7143 (1968).
5. H. HASE and L. KEVAN. J. Chem. Phys. **52**, 3183 (1970).
6. T. L. COTTRELL and I. C. WALKER. Quart. Rev. London, **20**, 153 (1966).
7. R. S. EACHUS and F. G. HERRING. Chem. Phys. Lett. **5**, 405 (1970).
8. A. HOLDEN and P. SINGER. Crystals and crystal growing. Anchor Books, Doubleday and Co., Inc., Garden City, New York. 1960.
9. M. HAMPTON, F. G. HERRING, W. C. LIN, and C. A. MCDOWELL. Mol. Phys. **10**, 565 (1966).
10. R. LIVINGSTON, H. ZELDES, and E. H. TAYLOR. Discuss. Faraday Soc. **19**, 166 (1955).
11. R. S. EACHUS and M. C. R. SYMONS. Chem. Commun. 285 (1969).
12. R. S. EACHUS and F. G. HERRING. J. Chem. Soc. In press.
13. D. A. LANGS and C. B. HARE. Chem. Commun. 890 (1967).
14. D. E. BILLING, B. J. HATHAWAY, and P. NICHOLLS. J. Chem. Soc. A, 1877 (1970).
15. C. R. BYFLEET, D. P. CHONG, J. A. HEBDEN, and C. A. MCDOWELL. J. Mag. Res. **2**, 69 (1970).
16. M. T. ROGERS and L. D. KISPERT. Radiation Chemistry. Advan. Chem. Ser. Amer. Chem. Soc. **2**, 327 (1968).
17. P. H. KASAI. Phys. Rev. Lett. **21**, 67 (1968).
18. R. S. EACHUS, M. C. R. SYMONS, and J. K. YANDELL. Chem. Commun. 979 (1969).
19. R. A. ZHITINKOV, N. I. MELNIKOV, and P. G. BARANOV. Physica Status Solidi, **85**, K81 (1969).
20. B. R. MCGARVEY. J. Phys. Chem. **71**, 51 (1967).

Can. J. Chem. Downloaded from www.nrcresearchpress.com by 210.87.254.105 on 09/05/12
For personal use only.

Can. J. Chem. Downloaded from www.nrcresearchpress.com by 210.87.254.42 on 09/05/12
For personal use only.

A New Approach to 3′-Amino-3′-deoxynucleosides. Synthesis of 9-(3-Amino-3-deoxy-α-L-ribofuranosyl)adenine[1]

HANS H. BAER AND MONIKA BAYER[2]

Department of Chemistry, University of Ottawa, Ottawa 2, Canada

Received August 28, 1970

Methyl 2,3,4-tri-*O*-acetyl-6-deoxy-6-nitro-α-D-glucopyranoside (**1**) was acetolyzed to give 1,2,3,4-tetra-*O*-acetyl-6-deoxy-6-nitro-α-D-glucopyranose (**2**). Compound **2** (or alternatively, 6-deoxy-1,2-*O*-isopropylidene-6-nitro-α-D-glucofuranose **4**) was converted into 2,3,4-tri-*O*-acetyl-6-deoxy-6-nitro-α-D-glucopyranosyl bromide (**3**) which was condensed with chloromercuri 6-benzamidopurine. De-*O*-acetylation of the condensation product **5** afforded 6-benzamido-9-(6-deoxy-6-nitro-β-D-glucopyranosyl)purine (**6**) which could be hydrogenated to the corresponding 6′-amino nucleoside **7**. Periodate oxidation of **6** followed by internal Henry cyclization and borohydride reduction gave 6-benzamido-9-(3-deoxy-3-nitro-α-L-ribofuranosyl)purine (**10**) which upon catalytic hydrogenation and subsequent de-*N*-benzoylation produced the title compound, **12**. The sensitivity of certain nitro intermediates towards alkali is commented upon.

Canadian Journal of Chemistry, 49, 568 (1971)

Amino nucleosides command great interest especially because of the biological activity of such natural products as puromycin, 3′-amino-3′-deoxyadenosine, and gougerotin (1–3), and because of the potential usefulness of synthetic analogs in biochemical and medicinal research. Among other methods for the synthesis of 3′-amino-3′-deoxy-hexopyranosyl nucleosides, the cyclization of sugar dialdehydes with nitromethane (4) has been applied (5, 6) with much success, and the related principle of adding nitromethane to oxo sugars (7–9) has been used in the synthesis of nucleosides that contain branched-chain amino sugars (9, 10). In our laboratory was recently accomplished (11) a novel furanoside synthesis which involves the conversion of methyl 6-deoxy-6-nitro-α-D-glucopyranoside into methyl 3-deoxy-3-nitro-β-L-ribo- and -arabinofuranosides and the corresponding amino sugars, and we now report an application of this reaction to a nucleoside. The work opens a new avenue into the hitherto comparatively little-investigated class of ribonucleosides having the L-configuration (12).

As key starting compound, a nucleoside bearing a nitro group at the terminal carbon of the sugar moiety was required. We attempted to prepare 5′-deoxy-5′-nitro-inosine and -uridine from the corresponding 2′,3′-*O*-isopropylidene-6-iodo derivatives (or 6-tosylates) by displacement with sodium nitrite, using a wide variety of solvents and reaction conditions. However, the desired nitro compounds could not be obtained. We therefore resorted to a nucleoside synthesis departing from a nitro sugar and a purine base. It was decided to prepare in this fashion 6-benzamido-9-(6-deoxy-6-nitro-β-D-glucopyranosyl)-purine (**6**) which would then serve as an intermediate for the synthesis of 9-(3-amino-3-deoxy-α-L-ribofuranosyl)purine (**12**) whose β-D isomer (3′-amino-3′-deoxyadenosine) has been reported to possess antitumor activity (13).

Acetolysis of known (11, 14) methyl 2,3,4-tri-*O*-acetyl-6-deoxy-6-nitro-α-D-glucopyranoside (**1**) afforded 1,2,3,4-tetra-*O*-acetyl-6-deoxy-6-nitro-α-D-glucopyranose (**2**) in 92% yield. The tetraacetate was then converted into 2,3,4-tri-*O*-acetyl-6-deoxy-6-nitro-α-D-glucopyranosyl bromide (**3**). Although one of the standard procedures for such a bromination, namely the use of hydrogen bromide in glacial acetic acid, was successfully applied (15) to the 3-nitro isomer of **2**, it did not prove satisfactory in this instance.[3] However, the modification of Scheurer and Smith (16) readily gave the desired bromide in 77% yield. Alternatively, the known (17) 6-deoxy-1,2-*O*-isopropylidene-6-nitro-α-D-glucofuranose (**4**) was deacetonated with 80% acetic acid and then brominated by the same method (16), giving **3** in about 50% yield. Analytical, spectral, and optical rotation data of **2** and **3** were in accord with the structures. Employing the general method of Davoll and Lowy (18) we then pro-

[1]Part XVIII in a series on the reactions of nitro sugars. For Part XVII see ref. 15.

[2]Postdoctoral Fellow 1968–1970. Present address: Syntex Institute of Molecular Biology, Palo Alto, California 94309.

[3]Only unchanged **2** could be isolated even after prolonged reaction times.

Can. J. Chem. Downloaded from www.nrcresearchpress.com by 210.87.254.42 on 09/05/12
For personal use only.

ceeded to couple **3** with chloromercuri 6-benzamidopurine (19) in refluxing toluene. A 36% yield of crystalline 6-benzamido-9-(2,3,4-tri-*O*-acetyl-6-deoxy-6-nitro-β-D-glucopyranosyl)-purine (**5**) was obtained. The β-D configuration was indicated by its levorotation ($[\alpha]_D$ −26° in $CHCl_3$), and definitely established by a large splitting observed in the n.m.r. signal assignable to H-1′ (doublet at τ 3.92, $J_{1',2}$ = 8.7 Hz, in $CDCl_3$). The t.l.c. of the mother liquor revealed the presence of unreacted **3**, 6-benzamidopurine, an unidentified sugar derivative,[4] and a second nucleoside. The latter possibly was the α-anomer of **5**; however, it could not be isolated.[5]

Next, removal of the acetyl blocking groups in **5** was necessary. Since the nucleosidic bond in this nitro derivative is extremely prone to cleavage in alkaline media as will be outlined further below, we first tried methanolytic deacetylation catalyzed by *p*-toluenesulfonic acid, which had served satisfactorily (11) in the de-*O*-acetylation of **1**. Unfortunately, in the present case, debenzoylation and salt formation at N-6 predominated, and deacetylation was extremely slow, remaining incomplete even after a reaction time of 2 weeks. However, the acetyl groups were selectively removed by cautious treatment of **5** with sodium methoxide in chloroform at −19°, which produced 6-benzamido-9-(6-deoxy-6-nitro-β-D-glucopyranosyl)purine (**6**) in yields of 72–90%. In order to buttress the structure of the product at this stage, a sample was converted by catalytic hydrogenation and subsequent debenzoylation into the known (21) 6′-amino-6′-deoxy-β-D-glucopyranosyladenine (**7**). The potential usefulness of nitro sugar bromides in conjunction with the chloromercuri procedure for the synthesis of amino nucleosides was thereby demonstrated.

Periodate oxidation of the nitro nucleoside **6** was carried out in aqueous suspension and, although proceeding sluggishly, it afforded the dialdehyde **8** in good yield. Without characterization other than by t.l.c., **8** was then cyclized in methanolic solution by the addition of sodium methoxide at −19°, and the 5′-aldo derivative **9** that arose was immediately reduced with sodium borohydride, at low temperature, to give crystalline 6-benzamido-9-(3-deoxy-3-nitro-α-L-ribofuranosyl)purine (**10**) in a yield of 50% (based on **8**). Catalytic hydrogenation in the presence of 1 equiv of hydrochloric acid converted **10** into the corresponding 3′-amino ribonucleoside hydrochloride (**11**) which, although crystalline

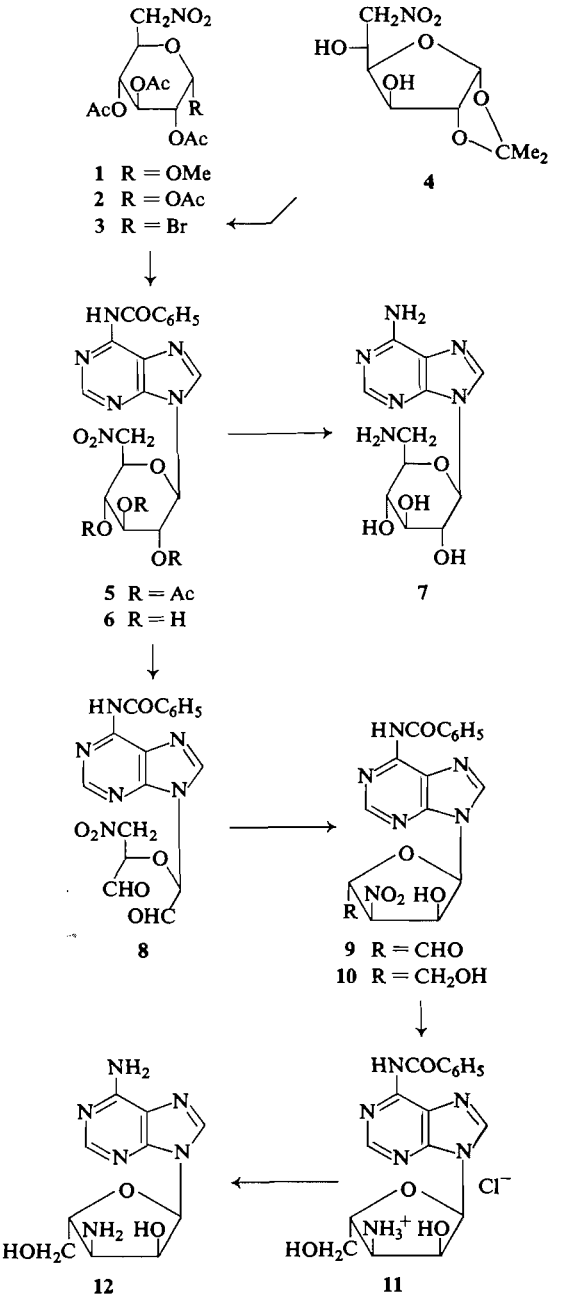

[4]Compare the formation of an unsaturated sugar in a similar nucleoside synthesis (19).

[5]Attempted separation of the mother liquor components by column or preparative t.l.c. resulted in extensive decomposition. Equally discouraging were pilot experiments to synthesize the α-anomer by the boron trichloride method recently described by Furukawa *et al.* (20).

Can. J. Chem. Downloaded from www.nrcresearchpress.com by 210.87.254.42 on 09/05/12
For personal use only.

and chromatographically homogeneous, was difficult to handle due to considerable hygroscopicity and was, therefore, not analyzed. Treatment of **11** with picric acid removed the *N*-benzoyl group and gave a crystalline dipicrate from which the title compound **12** was liberated, by anion exchange, in a yield of 37% based on **10**. The L-*ribo* configuration was proved by hydrochloric acid hydrolysis producing the known 3-amino-3-deoxy-L-ribose hydrochloride (22, 23). The anomeric center must possess the same absolute configuration as that of the precursor **6** and consequently receives the α designation. In agreement herewith, physical constants found for **12** are different from those expected[6] for the β-L anomer. The reaction sequence **6** → **8** → **9** → **10** is therefore seen to have taken a stereochemical course that was predictable on the basis of our previous work (11). That is to say, an α-L-ribofuranosyl derivative was generated from a β-D-glucopyranosyl derivative, in full harmony with the analogous, earlier synthesis of a β-L-ribofuranoside.[7]

The mother liquor of the nitro ribonucleoside **10** contained a small proportion of a compound that moved slightly faster in t.l.c. and was presumed to be an isomeric nucleoside. Complete separation from remnant **10** could not be effected, but a sample enriched in this by-product was hydrogenated and hydrolyzed with hydrochloric acid for inspection by paper chromatography. The major, ninhydrin-positive spot had the same mobility as an authentic sample of 3-amino-3-deoxy-L-arabinose hydrochloride (25), and a minor spot corresponded to the L-*ribo* isomer. Assignment of the α-L-arabinofuranosyl structure to the by-product must remain tentative but would be in line with previous results (11).

The nitro nucleosides **5**, **6**, and **10**, as well as the intermediates **8** and **9**, possess an acetal linkage activated by a nitro group in β-position, and such linkages are known to be prone to eliminative cleavage by alkali (4). For example, the primary nitro compound **5** suffered complete loss of the aglycon in a 1:1 mixture of acetone and 0.1 *M* sodium bicarbonate within 5 min at room temperature, and **6** was cleaved to about 50% after 35 min. The secondary nitro compound **10** was stable under these conditions but was cleaved to about 50% by *N* alcoholic potassium hydroxide within 50 min at room temperature. It was largely cleaved by 0.1 *N* aqueous sodium hydroxide within a few minutes at 98°. Further examples are given in the Experimental. It is obvious that, with compounds of this type, synthetic work in which alkaline reagents are indispensable must be conducted under most carefully controlled conditions.

[6]Compare the data published for the β-D enantiomer (24*a*, *b*). The α-D antipode of **12** has been encountered (24*a*), but no physical constants were given.

[7]These configurational inversions result from the interchange of positions, relative to each other in the sugar chain, that is incurred by C-4 and -6 of the pyranose structure when these carbon atoms become C-5 and -3, respectively, in the furanose structure. No chemical epimerization takes place at the configurationally determinant carbon atom, at least not as far as the products isolated under the reaction conditions are concerned (11).

Experimental

General Techniques

Melting points were determined in capillaries in an electric aluminum block apparatus equipped with a calibrated thermometer. Optical rotations were measured at about 25° in a Perkin–Elmer 141 automatic polarimeter. The i.r. spectra were obtained from Nujol mulls on Beckman IR-8 or IR-20 instruments, and significant bands only are reported as ν_{max} values. The u.v. data reported were obtained with a Jasco ORD/UV-5 spectrophotometer, whereas a Perkin–Elmer 202 instrument was used for routine monitoring. The n.m.r. spectra (100 MHz) were recorded on a Varian HA-100 spectrometer. The t.l.c. was performed on silica gel HT-254 according to Stahl, with the following solvent systems (v/v): *a*, chloroform–ether (2:1); *b*, chloroform–methanol (9:1); *c*, chloroform–methanol (4:1); *d*, 2-propanol – water (7:3); *e*, ethyl acetate – methanol (9:1). The t.l.c. plates were viewed under u.v. light and (or) sprayed with ceric sulfate – sulfuric acid and heated. For paper chromatography, the following systems were used: *f*, 1-propanol – water (8.5:1.5); *g*, ethyl acetate – pyridine – water – acetic acid (5:5:3:1); *h*, 1-butanol – ethanol – water (10:5:7). The spots were indicated by ammoniacal silver nitrate or ninhydrin.

1,2,3,4-Tetra-O-acetyl-6-deoxy-6-nitro-α-D-glucopyranose (2)

The nitro glucoside triacetate **1** (11) (26 g) was dissolved in a mixture of acetic acid (260 ml) and acetic anhydride (260 ml), and the solution was cooled to 0°. Concentrated sulfuric acid (26 ml) was added dropwise and with stirring which was maintained for 2 h at 0° and 5 days at room temperature, during which time some of the product crystallized. The reaction mixture was poured into ice–water (2.5 l) and the solid was collected and washed successively with water, ethanol, and ether. The dried product (23.5 g, 92%) consisted of white needles, m.p. 241°, which gave a single spot on t.l.c. (system *a*) and could be used without further purification. Samples were recrystallized from ethanol–chloroform, acetone, acetic acid, or dioxane: m.p. to 245°; $[\alpha]_D$ +99.3° (*c*, 0.5 in dimethylformamide); ν_{max} 1740 (acetyl C=O), 1545 (NO_2), 1230 with shoulder at 1260 cm^{-1} (acetyl C—O); n.m.r. data ($CDCl_3$), τ 3.70 (doublet, H-1, with $J_{1,2}$ = 4

Can. J. Chem. Downloaded from www.nrcresearchpress.com by 210.87.254.42 on 09/05/12
For personal use only.

Hz), 7.79 (singlet, axial acetyl), 7.93, 7.97, 7.98 (singlets, 3 equatorial acetyls); in DMSO-d_6, τ 3.89 (doublet, H-1, with $J_{1,2}$ = 4 Hz), 7.82 (singlet, axial acetyl), 8.00–8.02 (singlets, 3 equatorial acetyls).

Anal. Calcd. for $C_{14}H_{19}NO_{11}$ (377.3): C, 44.56; H, 5.08; N, 3.71. Found: C, 44.72; H, 5.20; H, 3.84.

2,3,4-Tri-O-acetyl-6-deoxy-6-nitro-α-D-glucopyranosyl Bromide (3)

(a) From 2

Bromine (48 ml) was added dropwise to a chilled suspension of red phosphorus (24 g) in glacial acetic acid (240 ml). When all the bromine had reacted, the mixture was filtered through glass wool and the filtrate was stored at 0° if it was not to be used immediately. The tetraacetate **2** (22 g) was introduced, and the mixture was stirred for 2 h at 60–70° (bath temperature) and then kept at room temperature overnight. The crystalline product **3** (16 g) was collected on a fritted funnel and washed thoroughly with ether. Additional **3** (2 g) was obtained from the mother liquor by aeration with nitrogen under diminished pressure; total yield, 77%. The product, which is only sparingly soluble in most common solvents except dimethylformamide (DMF) and dimethyl sulfoxide (DMSO), was recrystallized by dissolution in a large volume of boiling acetone and concentration of the solution at reduced pressure. It forms white needles that decompose at 212–215° and show $[\alpha]_D$ +148° (*c*, 1.6 in DMF). The mobility in t.l.c. (system *a*) is slightly greater that that of **2**. The i.r. data, ν_{max} 1740 (C=O), 1555 (NO_2), and 1220 with shoulder at 1250 cm^{-1} (C—O); n.m.r. data ($CDCl_3$), τ 3.48 (doublet, H-1, with $J_{1,2}$ = 4 Hz), 7.90, 7.92, 7.97 (singlets, 3 equatorial acetyls); in DMSO-d_6 the corresponding signals were at τ 3.17, 7.96, 7.99, and 8.01.

Anal. Calcd. for $C_{12}H_{16}NO_9Br$ (398.2): C, 36.19; H, 4.05; Br, 20.07. Found: C, 36.19; H, 3.96; Br, 19.97.

(b) From 4

The monoisopropylidene derivative **4** (14.3 g) (17) was hydrolyzed in 80% acetic acid (300 ml) for 6 h at 100–105°, with the progress of deacetonation being monitored by t.l.c. (system *d*). Evaporation followed by one co-evaporation with toluene gave a syrup which was treated with the brominating reagent (300 ml) as described in section (*a*). The product (11.5 g, 50%) was identical with **3** in every respect.

6-Benzamido-9-(2,3,4-tri-O-acetyl-6-deoxy-6-nitro-β-D-glucopyranosyl)purine (5)

A suspension of chloromercuri 6-benzamidopurine (6 g) (19) and Celite (8.5 g) in toluene (500 ml) was dried azeotropically by distilling off about 150 ml of the solvent. The bromide **3** (5 g) in dry toluene (100 ml) was added at about 70° and the bath temperature was then raised slowly to 130–135°. Reflux and vigorous stirring were maintained for 3 h. The reaction mixture was then filtered and the filtrate evaporated to dryness. The residue as well as the filter cake were extracted by stirring each with 150 ml of chloroform for 30 min. The filtered and combined extracts were washed successively with 30% aqueous potassium iodide solution (2 × 50 ml), and water (3 × 50 ml), dried over magnesium sulfate, and evaporated to give a partly oily residue (*ca.* 6 g). The material crystallized from 99% ethanol (60 ml) upon scratching of the flask. Recrystallization from ethanol furnished **5** (2.5 g, 36%) as colorless needles, m.p. 203° (dec.); $[\alpha]_D$ −26° (*c*, 1.4 in chloroform); homogeneous in t.l.c. (system *b*); ν_{max} 3650 (NH), 1755 (acetyl C=O), 1700 (*N*-benzoyl C=O), 1615, 1585 (purine C=N and C=C), 1555 (NO_2), 1255–1215 cm^{-1} (C—O); λ_{max} 277 nm (ε 20 900) and λ_{min} 242 nm (in methanol). The n.m.r. data ($CDCl_3$), τ 1.17, 1.78 (singlets, H-2 and -8), 1.94 and 2.40 (2- and 3-proton multiplets of benzoyl), 3.92 (doublet, H-1′, with $J_{1',2'}$ = 8.7 Hz), 4.24, 4.43, 4.74 (three triplets with spacings of 9–10 Hz assigned to H-2′, -3′, and -4′, but not necessarily in that order), 5.4 region (overlapping signals of H-5′, -6*a*′, -6*e*′), 7.89, 7.96, 8.24 (singlets, 3 acetyls). The high value τ 8.24 is noteworthy; it presumably represents the C-2′ acetoxy group which is strongly shielded by the purine ring.

Anal. Calcd. for $C_{24}H_{24}N_6O_{10}$ (556.5): C, 51.80; H, 4.35; N, 15.10. Found: C, 51.62; H, 4.46; N, 14.95.

In the above condensation, deviations from the 3-h reaction time on either side, or use of xylene as the solvent, were found to decrease the yield. Even though substantial quantities of unreacted **3** remained after 3 h, employment of a large excess of the purine component was of little effect, and yields generally ranged from 15–30%. Equimolar proportions of **3** and the chloromercuri derivative in DMF solution reacted at room temperature (4 days), but the isolation of **5** was difficult (yield, <20%).

Column chromatography of the mother liquor of **5** on silica gel or acid-washed alumina (Brockmann, activity grade 1) with chloroform and chloroform containing 5–10% of methanol resulted in extensive decomposition of the nucleoside components to give yellow substances that could not be eluted.

6-Benzamido-9-(6-deoxy-6-nitro-β-D-glucopyranosyl)-purine (6)

High-purity anhydrous solvents stored over molecular sieves were used, and moisture was excluded during the reaction. To a magnetically stirred solution of the acetate **5** (3.6 g) in chloroform (18 ml), which was kept at −19°, was added dropwise from a syringe a solution of sodium (360 mg) in methanol (18 ml). Stirring at −19° was continued for 1 h after which time the mixture was stirred for 5–10 min with added water (18 ml) and then acidified to p*H* 4–5 with methanolic hydrochloric acid under continued cooling. Removal of most of the organic solvents *in vacuo* (bath temperature 35°) caused sudden crystallization of white needles from the concentrated, largely aqueous solution. The product was collected at once, washed with water, and air-dried. Recrystallization from methanol gave **6** (2.0 g, 72%) showing a single spot in t.l.c. (system *c*) and decomposing at 194° (with gradual darkening above 175°). Yields up to 90% were obtained in smaller-scale runs. The compound exhibited $[\alpha]_D$ +4° (*c*, 1.2 in DMF), λ_{max} 278 nm (ε 21 800) and λ_{min} 242 nm (in methanol), ν_{max} 3600–3100 (broad, NH, OH), 1690 (*N*-benzoyl C=O), 1610, 1585 (C=C, C=N), 1550 cm^{-1} (NO_2).

Anal. Calcd. for $C_{18}H_{18}N_6O_7$ (430.4): C, 50.24; H, 4.22; N, 19.53. Found: C, 50.04; H, 4.12; N, 19.24.

9-(6-Amino-6-deoxy-β-D-glucopyranosyl)adenine (7)

A solution of the nitro nucleoside **6** (100 mg) in 95%

Can. J. Chem. Downloaded from www.nrcresearchpress.com by 210.87.254.42 on 09/05/12
For personal use only.

ethanol (15 ml) was hydrogenated using 10% palladium-on-charcoal (200 mg) at ordinary temperature and pressure (3 days). Paper chromatography (system *h*) then revealed a single ninhydrin-positive spot, R_f about 0.6. The filtered solution was concentrated to a small volume (*ca.* 1 ml), a solution of picric acid (140 mg) in ethanol (3 ml) and water (1 ml) was added, and the mixture was refluxed on a steam bath for 1 h. The crystalline picrate that separated on cooling was recrystallized once from water; decomposition point 217° (with sintering at 160–170°); lit. (21), dec. 215° with sintering from 168°. It was dissolved in a sufficiently large amount of water, and the solution was stirred with Dowex 1-X2 (carbonate form) until it was colorless. The ion exchange resin was filtered off and washed well with water. Evaporation of the combined filtrate and washing water gave a residue which by trituration with ethanol yielded **7** as a white powder that showed a single spot ($R_{adenine}$ 0.36) in paper chromatography (system *h*), decomposed at 210°, and exhibited λ_{max} 259 nm (in water), in agreement with the reported data (21).

*6-Benzamido-9-(3-deoxy-3-nitro-α-L-ribofuranosyl)-purine (**10**)*

A suspension of finely powdered nitro nucleoside **6** (1.5 g) in a solution of sodium metaperiodate (3 g) in water (60 ml) was stirred in the dark for 3 days. The t.l.c. of the reaction mixture (system *c*) indicated the conversion, in heterogeneous phase, of **6** into fast-moving dialdehyde **8** which was the only major reaction product that exhibited u.v. absorption. The product was collected by filtration, washed thoroughly with water, dried in a vacuum desiccator over P_2O_5, and stored below 0°. The yield was 1.0 g (72%).

A solution of **8** (500 mg) in absolute methanol (25 ml) was cooled to −19° in an ice–salt bath, and a chilled, 0.1 *N* sodium methoxide solution (15 ml) was added dropwise with magnetic stirring. The mixture was kept at −19° for 1 h after which time almost complete conversion of **8** into a slightly slower-migrating product **9** was indicated by t.l.c. (system *b*). With continued cooling, sodium borohydride (200 mg) suspended in chilled ethanol (10 ml) was added immediately, and the mixture was then allowed to stand at −15° for 24 h. Although the 5′-aldo nucleoside **9** and its reduction product **10** had identical R_f values in several t.l.c. and paper chromatographic systems tested, the course of the reduction could be conveniently monitored on short paper strips (ascending technique in system *f*), unreacted **9** being detectable by spraying with Tollens reagent. The reaction mixture was then acidified with acetic acid – methanol (1:1) and evaporated to dryness. Three portions of methanol were successively evaporated from the oily residue which was then triturated twice with small amounts of cold water to remove sodium acetate. The remaining, water-insoluble gum was dissolved in ethanol or methanol from which colorless crystals of **10** were deposited overnight at −15°. Recrystallization from methanol yielded **10** (250 mg, 50% based on **8**); m.p. 172°; $[\alpha]_D$ −61° (*c*, 1 in DMF); λ_{max} 277 nm (ε 20 300) and λ_{min} 245 nm (in methanol); ν_{max} 3600–3100 (broad, NH, OH), 1690 (*N*-benzoyl C=O), 1610, 1580 (C=N, C=C), and 1550 cm^{-1} (NO_2).

Anal. Calcd. for $C_{17}H_{16}N_6O_6$ (400.4): C, 51.00; H, 4.03; N, 20.99. Found: C, 50.90; H, 4.03; N, 20.98.

The mother liquor from which **10** had crystallized was shown by t.l.c. (system *e*) to contain, besides a large amount of additional **10**, a minor component of slightly greater mobility. Preparative t.l.c. (system *e*) provided a material in which this by-product was enriched but which contained some **10** (see Discussion).

*6-Benzamido-9-(3-amino-3-deoxy-α-L-ribofuranosyl)-purine Hydrochloride (**11**)*

Platinum dioxide catalyst (150 mg) was prehydrogenated in 36 ml of 0.01 *N* hydrochloric acid. The solid nitro nucleoside **10** (150 mg) was added, and it went slowly into solution as its hydrogenation proceeded. About 3 h of vigorous shaking under hydrogen at ordinary temperature and pressure was needed. The filtered solution was then concentrated to a volume of about 5 ml. A small sample was withdrawn and evaporated to dryness with several additions of absolute ethanol. Trituration of the residue with ethyl acetate gave hygroscopic needles of the hydrochloride **11** which decomposed above 160° and showed a single spot in paper chromatography (system *g*, ninhydrin spray).

*9-(3-Amino-3-deoxy-α-L-ribofuranosyl)adenine (**12**)*

The major part of the concentrated aqueous solution from the hydrogenation just described (estimated to contain about 130 mg of **11**) was mixed with a solution of picric acid (74 mg) in ethanol (2 ml). The mixture was refluxed on a steam bath for 1 h, and for another 30 min following the addition of a second, identical portion of alcoholic picric acid. The debenzoylation could be monitored by paper chromatography (system *g*). On cooling of the reaction mixture, the picrate of **12** (m.p. 185°) crystallized in part but was redissolved by dilution with ethanol. The solution was stirred with 20 ml of Dowex 1-X2 (OH^-), 50–100 mesh, and then applied to a column (2 × 15 cm) of the same ion exchange resin. The column was eluted with water, 15-ml fractions being collected and checked for u.v. absorption at 257 nm which appeared in fractions 17–65. These fractions were pooled and evaporated to dryness, with several portions of ethanol finally being evaporated from the residue which was then dried in a high vacuum. Compound **12** was thus obtained as a white powder (32 mg, 37% based on **10**), m.p. 162° with sintering from 150°, $[\alpha]_D$ +18° (*c*, 0.4 in water), λ_{max} 257 nm (ε 13 600) and λ_{min} 225 nm (in 0.1 *N* HCl). It appeared homogeneous in paper chromatography (system *g*) and t.l.c. (system *d*).

Anal. Calcd. for $C_{10}H_{14}N_6O_3$ (266.3): C, 45.11; H, 5.30; N, 31.57. Found: C, 44.88; H, 5.17; N, 31.32.

A sample of **12** (5.00 mg) was hydrolyzed in 3 *N* hydrochloric acid (1.00 ml) for 2 h at 98°. The hydrolysate had a rotation of α_D +0.067° (1 dm tube, 25 °C), corresponding to a specific rotation of $[\alpha]_D$ +19° calculated for the aminodeoxypentose hydrochloride produced. Reported for 3-amino-3-deoxy-L-ribose hydrochloride: +18.9° (11), +23° (23). The hydrolysate was evaporated with several additions of water, and paper chromatography (system *g*) of the residue indicated complete cleavage of **12** into adenine and a single amino sugar whose spot was indistinguishable from that of an authentic sample of 3-amino-3-deoxy-L-ribose hydrochloride.

Can. J. Chem. Downloaded from www.nrcresearchpress.com by 210.87.254.42 on 09/05/12
For personal use only.

Alkaline Degradations

The behavior of the nitro compounds **5**, **6**, **8**, **9**, and **10** in alkaline media was examined by t.l.c. Samples taken at intervals were acidified with dilute acetic acid before application. The chromatograms were viewed under u.v. light and spot intensities were estimated visually, with 6-benzamidopurine and adenine used as controls. The aglycons were readily distinguished from the nucleosides not only by the mobilities but also by spraying the plates with ceric sulfate – sulfuric acid followed by heating, dark spots being produced from carbohydrate-containing substances only.

(*a*) To compound **5** (2 mg) in acetone (0.4 ml) was added aqueous, 0.1 *M* sodium bicarbonate buffer (0.4 ml, p*H* 8.4). After 5 min at room temperature, 6-benzamidopurine was the only spot visible in the u.v., indicating complete cleavage of the nucleoside (system *b*).

(*b*) A similar experiment with compound **6** revealed 50% cleavage in 35 min (system *c*).

(*c*) A solution of the dialdehyde **8** (100 mg) in methanol (5 ml) was adjusted to p*H* 7.5 with alcoholic potassium hydroxide, at room temperature, and 50% cleavage was observed after 30 min (system *e*).

(*d*) To an ice-cooled solution of **8** (100 mg) in methanol (5 ml) was added 3 ml (1.2 equiv) of a 0.1 *N* sodium methoxide solution. After 1 h at 0°, about 30% of the aglycon was liberated (system *e*).

(*e*) When the sodium borohydride reduction of intermediate **9** (for the preparation of **10** as described above) was carried out at room temperature rather than at −19 to −15°, the *N*-glycosidic bond was cleaved to the extent of 30–50% depending on the amount of $NaBH_4$ employed (system *e*).

(*f*) A few milligrams of compound **10** were tested in 1 ml of each of the following media: *i*, 0.1 *M* sodium bicarbonate – acetone (1:1) at 25°; *ii*, 0.01 *N* sodium hydroxide – acetone (1:1) at 25°; *iii*, *N* potassium hydroxide, ethanolic, at 25°; *iv*, 0.1 *N* sodium hydroxide, aqueous, at 98°. Compound **10** appeared to be stable overnight in *i* and *ii*, but was 50% cleaved within 50 min in *iii* and still more extensively within 3 min in *iv* (system *e*).

Attempted Displacements with Nitrite

5′-Deoxy-5′-iodo-2′,3′-*O*-isopropylideneinosine (26) was treated with sodium nitrite (1–3 equiv) according to the general procedure of Kornblum (27). Solvents tried were DMF, DMSO, mixtures of the same, and hexamethylphosphoric triamide. Reaction times and temperatures ranged from 2–4 days and 5 to 25° respectively. Trials were made with and without addition of phloroglucinol or urea. The t.l.c. (system *b*) revealed the formation of several reaction products, but the desired 5′-nitro derivative could not be isolated.

Support of this work by the Life Insurance Medical Research Fund, Rosemont, Pennsylvania, and in part by the National Research Council of Canada is gratefully acknowledged.

1. J. D. Dutcher. Advan. Carbohyd. Chem. **18**, 259 (1963).
2. D. Horton. *In* The Amino Sugars, Vol. IA. *Edited by* R. W. Jeanloz. Academic Press Inc., New York, N.Y., 1969. pp. 173–176.
3. D. Gottlieb and P. D. Shaw, editors. Antibiotics. Vol. I. Springer-Verlag New York Inc., New York, N.Y., 1967.
4. H. H. Baer. Advan. Carbohyd. Chem. Biochem. **24**, 67 (1969).
5. H. A. Friedman, K. A. Watanabe, and J. J. Fox. J. Org. Chem. **32**, 3775 (1967), and earlier papers from that laboratory.
6. F. W. Lichtenthaler and H. P. Albrecht. Ber. **102**, 964 (1969), and earlier papers from that laboratory.
7. G. J. Lourens. Tetrahedron Lett. 3733 (1969).
8. A. Rosenthal and K.-S. Ong. Tetrahedron Lett. 3981 (1969); A. Rosenthal, K.-S. Ong, and D. Baker. Carbohyd. Res. **13**, 113 (1970).
9. H. P. Albrecht and J. G. Moffatt. Tetrahedron Lett. 1063 (1970).
10. A. Rosenthal, M. Sprinzl, K.-S. Ong, and D. Baker. Joint Conference, American Chemical Society and Canadian Institute of Chemistry, Toronto, Ontario, May 1970. Abstract of papers, CARBO, 1.
11. H. H. Baer and I. Furić. J. Org. Chem. **33**, 3731 (1968).
12. E. M. Acton, K. J. Ryan, and L. Goodman. J. Amer. Chem. Soc. **86**, 5352 (1964); J. Smejkal and F. Šorm, Collect. Czech. Chem. Commun. **29**, 2809 (1964); B. M. Chassy and R. J. Suhadolnik. J. Biol. Chem. **242**, 3655 (1967); M. J. Robins, T. A. Khwaja, and R. K. Robins. J. Org. Chem. **35**, 636 (1970).
13. N. N. Gerber and H. A. Lechevalier. J. Org. Chem. **27**, 1731 (1962).
14. J. M. Sugihara, W. J. Teerlink, R. MacLeod, S. M. Dorrence, and C. H. Springer. J. Org. Chem. **28**, 2079 (1963).
15. H. H. Baer, W. Rank, and F. Kienzle. Can. J. Chem. **48**, 1302 (1970).
16. P. G. Scheurer and F. Smith. J. Amer. Chem. Soc. **76**, 3224 (1954).
17. J. M. Grosheintz and H. O. L. Fischer. J. Amer. Chem. Soc. **70**, 1476 (1948).
18. J. Davoll and B. A. Lowy. J. Amer. Chem. Soc. **73**, 1650 (1951).
19. H. Paulsen, H. Köster, and K. Heyns. Ber. **100**, 2669 (1967).
20. Y. Furukawa, K. Imai, and M. Honjo. Tetrahedron Lett. 4655 (1968).
21. S. Fukatsu and S. Umezawa. Bull. Chem. Soc. Japan, **38**, 1443 (1965).
22. R. E. Schaub and M. J. Weiss. J. Amer. Chem. Soc. **80**, 4683 (1958).
23. H. H. Baer and H. O. L. Fischer. J. Amer. Chem. Soc. **81**, 5184 (1959).
24. (*a*) B. R. Baker, R. E. Schaub, and H. M. Kissman. J. Amer. Chem. Soc. **77**, 5911 (1955); (*b*) E. J. Reist and B. R. Baker. J. Org. Chem. **23**, 1083 (1958).
25. H. H. Baer and A. Ahammad. Can. J. Chem. **41**, 2931 (1963).
26. A. Hampton, M. Bayer, V. S. Gupta, and S. Y. Chu. J. Medicinal Chem. **11**, 1229 (1968).
27. N. Kornblum. Org. Reactions. **12**, 101 (1962).

Can. J. Chem. Downloaded from www.nrcresearchpress.com by 210.87.254.5 on 09/05/12
For personal use only.

Conversion of a 3-Oxaquadricyclane to a Substituted Cyclobutane.[1] Preparation and Proton Magnetic Resonance Spectra of Four Stereoisomeric 1,2-Diacetyl-3,4-dicarbomethoxycyclobutanes

J. LAING,[2] A. W. MCCULLOCH, D. G. SMITH, AND A. G. MCINNES
Atlantic Regional Laboratory, National Research Council of Canada, Halifax, Nova Scotia

Received August 11, 1969[3]

Reaction of 1,5-dicarbomethoxy-2,4-dimethyl-3-oxaquadricyclane with water gave a mixture of *cis,cis, cis*- and *cis,cis,trans*-1,2-diacetyl-3,4-dicarbomethoxycyclobutanes. The latter on treatment with acid epimerized to the corresponding *trans,trans,trans*-isomer, whereas the former yielded the *trans,trans,cis*-epimer together with 3,10-dimethyl-3,10-epoxy-5,8-dioxo-4,9-dioxatricyclo[5.3.0.$0^{2,6}$]decane which contains a new bridged ring system. The structure and stereochemistry of each compound was derived from symmetry considerations as reflected in its p.m.r. spectrum, and was facilitated by selective deuteration experiments. Vicinal and long-range spin–spin interactions between the cyclobutane ring hydrogens were deduced from pertinent p.m.r. sub-spectra using the NMRIT–NMREN computer program.

Canadian Journal of Chemistry, **49**, 574 (1971)

Classical methods of synthesis of cyclobutanes (1) have been largely superseded in recent years by the introduction of generally applicable photocycloaddition procedures (2), such as the photosensitized dimerization of olefins (3) or enones (4) or the photoaddition of enones to olefins (5). In this communication we show that in suitable cases (see section on generality) a cyclobutane ring may be formed by hydrolyzing a 3-oxaquadricyclane derivative of type **2**. This approach to the synthesis of substituted cyclobutanes is of more limited scope than the more general photochemical methods discussed above.

The Diels–Alder adduct **1** may be converted photochemically in very high yield to the known 3-oxaquadricyclane **2** (6). The latter reacts readily with water in acetone, methanol, or tetrahydrofuran, to give a mixture of isomers **3** and **4** (approximate ratio 1:2) in *ca.* 90% yield. Since **3** and **4** were recovered unchanged when heated in these aqueous solvents it follows that the reaction product from **2** was not an equilibrium mixture, and that the two isomeric products must have been formed by competitive reactions. Both **3** and **4** are isomerized if treated with sulfuric acid in CH_2Cl_2 at room temperature, **3** being converted to **6** (and **9**) and **4** to **7**.

Compounds **3**, **4**, **6**, and **7** each had a molecular formula of $C_{12}H_{16}O_6$ (mass spectra), and their p.m.r. spectra (Table 1) contained resonances indicating the presence of four cyclobutane ring hydrogens (7) as well as two acetyl and two carbomethoxy groups. Positive iodoform tests for acetyl, carbonyl absorptions in the i.r. for ester (1737–1743 cm^{-1}) and ketone (1710–1719 cm^{-1}) functions, as well as characteristic losses of 15 (CH_3), 31 (CH_3O), 42 ($CH_2{=}C{=}O$), and 43 (CH_3CO) mass units from the parent ions in the mass spectra further confirmed the presence of the two types of functional groups. From these data it could be deduced that these compounds contained a cyclobutane ring substituted with two acetyl and two carbomethoxy groups.

If D_2O was substituted for H_2O in the original reaction, **2** was converted to a mixture of **3**-d_2 and **4**-d_2. The molecular formula, $C_{12}H_{14}D_2O_6$, for each pure compound was confirmed by mass spectral analysis, and their i.r. spectra only differed from those of the corresponding undeuterated compounds in the regions associated with C—H or C—D vibrations. The only difference in the p.m.r. spectra (Table 1) of **3** and **3**-d_2 was the replacement of an AA'BB' multiplet for the cyclobutane ring hydrogens in the former by a singlet for two chemically equivalent ring hydrogens, $J = 9.3$ Hz (derived from the ^{13}C—H satellites), in the latter. Similarly, only the ABMX multiplet for the ring hydrogens in **4** was replaced by an AM quartet, $J = 9.0$ Hz, in **4**-d_2. Spin-decoupling experiments further established that each of the two ring hydrogens in **3**-d_2 and **4**-d_2 was coupled ($J \approx 0.3$ Hz) to the methyl hydrogens of an acetyl group; in **3**-d_2 the acetyl groups were chemically equivalent whereas in **4**-d_2 they

[1]Issued as NRCC No. 11639.
[2]National Research Council of Canada Summer Student, 1968.
[3]Revision received August 17, 1970.

Can. J. Chem. Downloaded from www.nrcresearchpress.com by 210.87.254.5 on 09/05/12
For personal use only.

TABLE 1. The p.m.r. data (100 MHz spectra) for cyclobutanes*

	Chemical shifts								Coupling constants (Hz)					
	τ				Hz‡				$J_{p,q}$					
Compound	—$COCH_3$	—CO_2CH_3	—CH_3	System†	ν_1	ν_2	ν_3	ν_4	1,2§	1,3	1,4	2,3	2,4	3,4
3	8.02	6.56		A(H-1)A′(H-2)B(H-3)B′(H-4) 7.06 τ		24.7		0.0	9.3	0.7	9.2	9.2	0.7	9.3
3-d_2‖	8.01	6.55		br. s¶, 7.17 τ					9.2					
4	7.97, 8.21	6.67, 6.74		A(H-2)B(H-3)M(H-1)X(H-4) H-4, 5.88 τ	131.0	88.0	92.0	0.0	8.9	−0.1	10.3	9.2	−0.9	9.6
4-d_2‖	7.99, 8.25	6.70, 6.76		A(H-2)M(H-1) 6.98 τ	43.0	0.0			9.0					
6	8.07, 8.37	6.66, 6.73		A(H-1)B(H-3)C(H-4)X(H-2) H-2, 5.81 τ	129.8	0.0	128.6	104.2	10.2	−0.4	9.2	9.9	−0.7	9.0
6-d_1	**	6.67, 6.73		A(H-1)B(H-3)C(H-4) 6.75–7.25 τ										
6-d_2	8.07, 8.38	6.66, 6.73		A(H-1)X(H-2) H1, 7.13 τ; H2, 5.83 τ										
6-d_3	**	6.67, 6.73		br. s, 7.12 τ										
7	7.84	6.30		A(H-1)A′(H-2)B(H-3)B′(H-4) 6.52 τ		0.0		9.9	9.5	−0.3	9.2	9.2	−0.3	9.5
7-d_1	**	6.30		A(H-1)B(H-3)B′(H-4)										
7-d_2	7.84	6.30		br. s, 6.48 τ					9.6					
7-d_3	**	6.30		br. s, 6.47 τ										
9			8.15	A(H-1)A′(H-2)B(H-3)B′(H-4) 6.15 τ		39.1		0.0	7.6	2.5	6.6	6.6	2.5	7.6
9-d_2			8.16	br. s, 6.33 τ					7.6					

*The spectra of 3, 4, 6 and their deuterated analogues were recorded in benzene-d_6 at a concentration of 10 mg/0.35 ml. The spectra of 7 and its analogues were recorded in acetone-d_6, also at 10 mg/0.35 ml. The spectra of 9 and 9-d_2 were measured in trifluoroacetic acid using 25 mg/0.35 ml.

†The chemical shifts reported in this column refer to the centroid of the AA′BB′ (3, 7, 9), AM (4-d_2), H-2 (6), or H-4 ( ) multiplet. In the case of the ABC (6-d_1) or ABB′ (7-d_1) systems the range of the multiplet is given.

‡For computer purposes the chemical shift of the lowest-field proton (or protons when chemically equivalent) was empirically given a value of 0.0 Hz and all others were measured relative to it.

§Values for $J_{1,2}$ were obtained either directly from the AM or AX spectra of 4-d_2 and 6-d_2, or from the ^{13}C—H satellite spectra in the case of 3-d_2, 7-d_2, and 9-d_2.

‖In 3-d_2 long-range coupling (J < 0.3 Hz) was observed between H-1 and -2 and the acetyl methyl protons. Similar coupling was observed in 4-d_2 between H-1 ($J \simeq 0.1$ Hz) and the protons of one acetyl methyl (8.25 τ) and between H-2 ($J \simeq 0.3$ Hz) and those of the second acetyl methyl group (7.99 τ).

¶br. s = broad singlet.

**The acetyl methyl protons underwent deuterium exchange in the presence of D_2SO_4 (conditions of preparation).

Can. J. Chem. Downloaded from www.nrcresearchpress.com by 210.87.254.5 on 09/05/12
For personal use only.

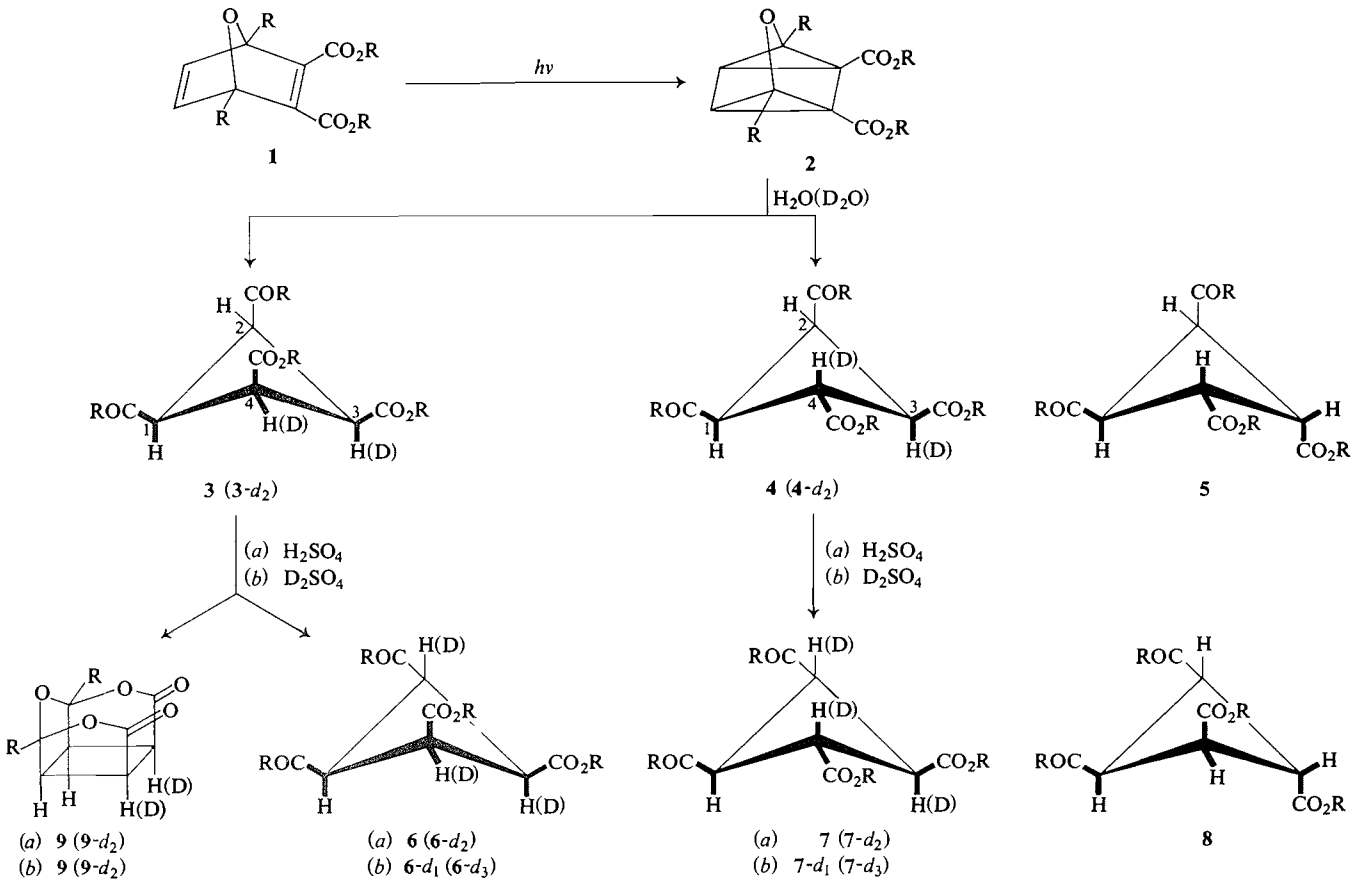

1 2 3 (3-d_2) 4 (4-d_2) 5

(a) 9 (9-d_2) (b) 9 (9-d_2) (a) 6 (6-d_2) (b) 6-d_1 (6-d_3) (a) 7 (7-d_2) (b) 7-d_1 (7-d_3) 8

SCHEME 1

Can. J. Chem. Downloaded from www.nrcresearchpress.com by 210.87.254.5 on 09/05/12
For personal use only.

were not. The above evidence requires that the two ring hydrogens in **3**-d_2 and **4**-d_2 be vicinal and that each of them is geminal to an acetyl group. Since no epimerization had occurred at the carbons bearing these hydrogens and acetyl groups during the conversion from **2** it follows that the acetyl groups (and therefore hydrogens) must have a *cis*-relationship. Each of the two deuterium atoms in **3**-d_2 and **4**-d_2, or the corresponding hydrogens in **3** and **4**, must therefore be geminal to a carbomethoxy group since there is no acceptable mechanism by which they could both be present on the same carbon atom. In any case **3**, in addition to the structural features discussed above, must possess at least C_2 symmetry (AA′BB′ system for the ring hydrogens and two chemically equivalent acetyl and carbomethoxy groups) clearly invalidating such a possibility, and analyses of the 4-spin systems in **3** and **4** (Table 1) established the presence of four vicinal but no geminal spin–spin coupling constants. Consequently, **3** and **4**, and therefore **6** and **7**, must be isomeric 1,2-diacetyl-3,4-dicarbomethoxycyclobutanes.

Structure of 4

The six possible stereoisomeric 1,2-diacetyl-3,4-dicarbomethoxycyclobutanes are depicted in Scheme 1. Of these only **3**, **4**, and **5** have the acetyl substituents in a *cis*-relationship; *a necessary requirement in the two reaction products* (**3** and **4**) *formed from* **2** (see above). Because of rapid interconversion between two equivalent conformations both **3** and **5** would behave as if they possessed at least C_2 symmetry and the ring hydrogens would be expected to give an AA′BB′ (or AA′XX′) multiplet in their p.m.r. spectra. Structure **4**, on the other hand, has no element of symmetry and all of the ring hydrogens would therefore be expected to be chemically nonequivalent. Since **4** contained an ABMX multiplet for the ring hydrogens in its p.m.r. spectrum as well as signals for pairs of chemically nonequivalent acetyl and carbomethoxy groups (Table 1), it follows that this compound must possess structure **4** with the substituents in a *cis,cis,trans*-orientation. Furthermore, the other reaction product must possess structure **3** or **5**.

Structures of 3 and 9

Both H_2SO_4 and D_2SO_4 converted **3** to **9**, or **3**-d_2 to **9**-d_2 (Scheme 1). The other products of reaction, **6** and **6**-d_1, or **6**-d_2 and **6**-d_3, are not pertinent to the discussion at this stage. From the above observations it was clear that **9** was formed from **3** *without epimerization* having occurred at any center in the latter.

Compound **9** had a molecular formula of $C_{10}H_{10}O_5$ (mass spectrum), and its i.r. spectrum contained no carbonyl absorptions for the two types of functional groups present in **3** but instead *contained a single band at 1790 cm^{-1} characteristic of a γ-lactone grouping*. Its p.m.r. spectrum (Table 1), moreover, contained no resonances for carbomethoxy methyl groups but did have a singlet for two chemically equivalent methyl groups whose chemical shift was consistent with their being attached to carbon atoms bearing two oxygen substituents. The molecular formula of **9** and the chemical shifts of the four remaining hydrogens required that the latter be attached to a cyclobutane ring. These hydrogens in addition appeared as a characteristic AA′BB′ multiplet in the p.m.r. spectrum establishing that **9** possessed at least C_2 symmetry. The molecular formula of **9**-d_2 as well as its i.r. and p.m.r. spectra only differed in a predictable fashion from those of **9** although from the latter it was possible to assign the hydrogens β to the lactone carbonyl group. The collective evidence is thus only compatible with **9** being 3,10-dimethyl-3,10-epoxy-5,8-dioxo-4,9-dioxatricyclo[5.3.0.0^{2,6}]decane, *i.e.* structure **9** in Scheme 1.

In **9** the substituents are *cis* to one another and it is formed from **3** without epimerization. Consequently, the latter must possess structure **3** of Scheme 1, in which the substituents have a *cis,cis,cis*-orientation, and not the alternative structure **5**, which has the substituents in a *cis,trans,cis*-relationship.

Structure of 6

Conversion of **3** to **6**, and **3**-d_2 to **6**-d_2, with H_2SO_4 and of **3** to **6**-d_1, and **3**-d_2 to **6**-d_3, with D_2SO_4 (Scheme 1; Table 1) established that the transformations were accompanied by epimerization only at C-1 or -2 of **3** or **3**-d_2. Consequently, the acetyl substituents in **6** must be *trans* since they were *cis* in **3**. Moreover, the product formed by epimerization at C-1 (equatorial acetyl) of **3** is simply the enantiomer of that produced by a corresponding change at C-2 (axial acetyl). In other words epimerization at either center in **3** leads to the same product (**6**) in which the substituents are in a *trans,trans,cis*-relationship. The

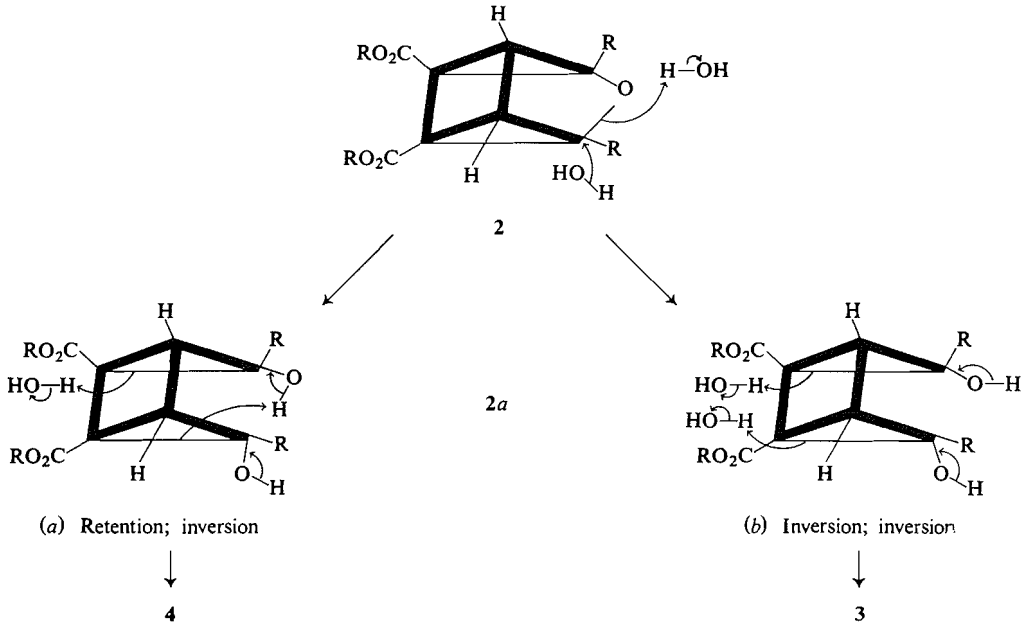

SCHEME 2

four ring hydrogens in **6** should therefore be chemically non-equivalent and it was observed experimentally that they appeared as an ABCX system (Table 1) in the p.m.r. spectrum of this compound. Furthermore, epimerization could only have occurred at the carbon atom in **3** bearing the axial acetyl substituent, otherwise it would be difficult to explain why further deuterium exchange did not occur in **6**-d_1 and **6**-d_3 which both contain two equatorial acetyl substituents. It should be borne in mind that **3** can exist in two equivalent conformations and that the substituents which are equatorial in one conformation are axial in the other. This of course results in **6** being produced as a racemic mixture. Previous work has shown that the cyclobutane ring is puckered and that substituents do in fact occupy positions analogous to the axial and equatorial positions of cyclohexane (8) and will prefer an equatorial orientation where possible.

Structure of 7

As in the above case the formation of **7** from **4**, and **7**-d_2 from **4**-d_2, with H_2SO_4, as well as of **7**-d_1 from **4**, and **7**-d_3 from **4**-d_2 with D_2SO_4 (Scheme 1; Table 1) established that epimerization had occurred at C-1 or -2 of **4**, or **4**-d_2, and that the acetyl groups in **7** must be *trans* to one another. Structure **5** (Scheme 1) is therefore eliminated as a possibility since in this compound the acetyl groups are *cis*. Furthermore, if **8** was produced from **4** we would anticipate further deuterium incorporation at the carbon atoms bearing acetyl substituents since one of the two possible conformations in which **8** could exist would have both acetyl groups in an axial orientation. The above evidence therefore requires that epimerization occur at C-2 of **4** to produce **7** in which the substituents are in a *trans,trans*, *trans*-relationship. The m.p. and i.r. spectrum of the latter were also identical to those reported for *trans,trans,trans*-1,2-diacetyl-3,4-dicarbomethoxycyclobutane (9) thereby confirming our structural assignment. As **7** contains a C_2 axis of symmetry its p.m.r. spectrum showed resonances for pairs of chemically equivalent acetyl and carbomethoxy methyl groups as well as an AA'BB' multiplet for the ring hydrogens as expected.

Mechanism of Formation of 3 and 4

Any mechanism must explain (*i*) the formation of isomers possessing two *cis* acetyl groups, (*ii*) the incorporation of two D atoms at the ester-bearing carbon atoms when D_2O is used, and (*iii*) the absence of the *cis,trans,cis*-isomer **5**. We believe that fission of the oxygen bridge prob-

Can. J. Chem. Downloaded from www.nrcresearchpress.com by 210.87.254.5 on 09/05/12
For personal use only.

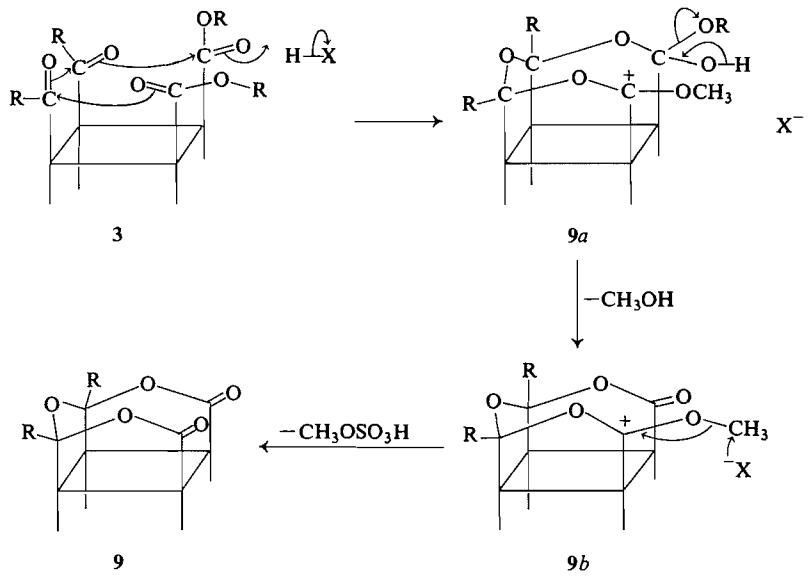

SCHEME 3

ably proceeds as shown in Scheme 2, to give the diol **2***a*. This can then react with water in two ways: either in the intramolecular pathway (*a*), with retention and inversion of configuration at C-3 and -4, to give **4**, or as in (*b*), with double inversion at these carbon atoms to give the all-*cis* isomer **3**. Isomer **4** is the major product, suggesting that (*a*) is favored. Formation of the *cis,trans,cis*-compound would necessitate retention of configuration at both ester-bearing centers, and such a transformation is not possible from **2***a*.

Mechanism of Formation of 9 from 3

Initial protonation at one of the ester carbonyl oxygen atoms in **3** would induce participation of the three remaining carbonyl groups as depicted in Scheme 3 to produce carbonium ion **9***a*. Loss of methanol from the latter followed by nucleophilic attack of $^-OSO_3H$ at the methoxyl methyl of carbonium ion **9***b* would then result in the production of **9**. Both carbonium ions would be stabilized by electron delocalization from adjacent oxygen atoms.

Proton Magnetic Resonance Analyses (see Table 1)

Chemical Shift Assignments

The chemical shifts of H-1 and -2 in **3** (behaves as if it possessed C_2 symmetry), **7** (C_2 symmetry), and **9** (C_s symmetry) could be assigned because they gave singlet resonances in the spectra of **3**-d_2, **7**-d_2, and **9**-d_2. These hydrogens occurred at higher field than H-3 and -4 in **3** and **9** whereas the reverse was true for **7**.

In **6** H-2 and the carbomethoxy group attached to C-4 are in a 1,3-diaxial relationship so it could be anticipated that the former would experience a paramagnetic shift due to magnetic anisotropy associated with the ester carbonyl group (10). The X part of the ABCX spectrum for the four ring hydrogens of **6** appeared at lowest field and was therefore provisionally assigned to H2. This could be confirmed since H-1 appeared as a broadened singlet in the spectrum of **6**-d_3 and this resonance had the same chemical shift as the high field A component of the AX spectrum for H-1 and -2 in **6**-d_2. Furthermore, the low field X part of the ABCX spectrum for the ring hydrogens of **6** was missing from the spectrum of **6**-d_1; the three ring hydrogens of the latter gave an ABC spectrum broadened by coupling with deuterium. Since only H-2 was replaced by deuterium in **6**-d_1 it follows once again that the low field X part of the ABCX spectrum for the ring hydrogens of **6** must have been due to this hydrogen. From these experiments it could also be deduced that H-1 resonated at higher field (lower frequency) than H-3 and -4. Double

Can. J. Chem. Downloaded from www.nrcresearchpress.com by 210.87.254.5 on 09/05/12
For personal use only.

Can. J. Chem. Downloaded from www.nrcresearchpress.com by 210.87.254.5 on 09/05/12
For personal use only.

irradiation experiments also established unambiguously that H-2 was vicinally coupled to the two ring hydrogens appearing at highest field thus enabling H-3, and therefore H-4, to be assigned.

The four ring hydrogens of **4** gave an ABMX spectrum, the X component occurring at lowest, and the M component at highest, field. The AB multiplet was always partially hidden beneath the signals for the two carbomethoxy methyl groups irrespective of the solvent used. Since H-4 was in a 1,3-diaxial relationship to the acetyl substituent at C-2, the low field X component of the above system was assigned to this hydrogen for the same reason as the low field X component of the ABCX spectrum of **6** was assigned to H-2. Decoupling experiments also established that H-4 was *vicinally coupled* to the hydrogen occurring at highest field (M component of ABMX spectrum). The latter was also present as the M doublet of an AM quartet for H-1 and -2 in the spectrum of **4**-d_2. This evidence, therefore, established that H-1 was at highest field, and since H-2 and -3 constitute the AB part of the ABMX system, the chemical shift of H-2 required that it occur at lower field than H-3.

Assignments of Spin–Spin Coupling Constants

Values for $J_{1,2}$ were measured directly from the spectra of **4**-d_2 and **6**-d_2, or from the ^{13}C—H satellite spectra of **3**-d_2, **7**-d_2, and **9**-d_2. The other spin–spin coupling constants for **3**, **7**, and **9** were first obtained from preliminary analyses of their AA′BB′ sub-spectra (11), and later the final values were determined with the NMRIT–NMREN programs of Swalen and Reilly (12).[4] Data obtained from **3** and **7**, or from other similarly substituted cyclobutanes reported in the literature (13–15), were then used as trial parameters in the computer analysis (12) of the sub-spectra of **4** (ABMX) and **6** (ABCX) taking due account of substituent effects and the steric relationships of relevant hydrogens. Only the non-iterative part of the NMRIT program was used in the case of **4** because the signals for H-2 and -3 were partially hidden by those for the carbomethoxy methyl groups. In this case chemical shift and spin–spin coupling values were adjusted by trial and error until the experimental and calculated sub-spectra for H-1 and -4, and for H-2 and -3 where visible, were in close agreement. In all cases experimental and calculated spectra agreed within the limits of experimental error. A similar analysis of other cyclobutanes has been reported recently (13). The spectra of **6**-d_1 and **7**-d_1 were not analyzed because many of the hydrogen resonances were excessively broadened due to hydrogen–deuterium coupling.

[4]Both the 60 and 100 MHz spectra of **3**, **7**, and **9** were analyzed, good agreement being obtained in all cases.

Conclusions from Proton Magnetic Resonance Data

(*1*) In **3**, **4**, **6**, and **7** vicinal hydrogens with a *trans* diaxial orientation have slightly larger spin–spin coupling constants than those in a *cis*-relationship, although in other cyclobutanes the reverse has been observed (14). (None of the above compounds have vicinal hydrogens which are diequatorial.)

(*2*) The sign and magnitude of the spin–spin coupling constants between hydrogens in a 1,3-relationship in **3**, **4**, **6**, and **7** depend on whether they are in a diequatorial ($J_{e,e}$), diaxial ($J_{a,a}$), or axial–equatorial ($J_{a,e}$) orientation. From the data obtained for **4**, **6**, and **7** it would appear that both $J_{a,a}$ and $J_{a,e}$ are negative with the latter being of slightly greater magnitude. Although $J_{e,e}$ could not be obtained directly it was known that $J_{1,3} = J_{2,4} = 1/2(J_{a,a} + J_{e,e}) = 0.7$ Hz in **3** and an average value of $J_{a,a} = -0.3$ Hz could be obtained from the data for **4**, **6**, and **7**. Substitution then gave a value for $J_{e,e} = 1.7$ Hz indicating that $J_{e,e}$ was probably of greater magnitude and opposite sign to $J_{a,a}$ and $J_{a,e}$.

(*3*) Vicinal *cis* spin–spin coupling constants in the more rigid molecule **9** are considerably lower than the corresponding value in **3**, but the 1,3-spin–spin interactions are somewhat greater.

Generality

Further experiments have established that hydrolysis of **2** (R = H, CH_3) yields one stereoisomeric form of 1-formyl-2-acetyl-3,4-dicarbomethoxycyclobutane. It is, therefore, possible that such conversions may be general for 3-oxaquadricyclanes bearing one or more alkyl substituents at the bridgehead, and that the conversions in some cases may take place with a high degree of stereospecificity. On the other hand, compounds of type **2** with aryl substituents at the bridgehead are not converted to cyclobutane derivatives but undergo spontaneous thermal rearrangement to oxepines in the presence of water. The results of these investigations will be published at a later date.

Can. J. Chem. Downloaded from www.nrcresearchpress.com by 210.87.254.5 on 09/05/12
For personal use only.

Experimental

The p.m.r. spectra were obtained on Varian HA-100 and Varian A-60A spectrometers with tetramethylsilane as internal standard. The spectra were analyzed with the aid of the NMRIT and NMREN programs (12) using the IBM 360 at Dalhousie University Computer Centre Halifax, Nova Scotia. The i.r. spectra were recorded on a Perkin–Elmer model 521 spectrometer, and mass spectra using a Consolidated Electrodynamics Corporation 21-110B mass spectrometer, with electrical detection being used for mass measurements. The deuterium oxide and deuteriosulfuric acid used were of minimum isotopic purity 99.7 and 98% D respectively.

The adduct **1** was prepared by thermal Diels–Alder reaction of 2,5-dimethylfuran and dimethylacetylenedicarboxylate (6).

Preparation of the Oxaquadricyclane 2 (cf. (6))

A solution of the adduct **1** (4.0 g) in anhydrous ether (450 ml) was irradiated for 12 h at room temperature in a Rayonet Photochemical reactor with light of wavelength 3100 Å, the reaction mixture being water-cooled by means of an internal jacket immersed in the solution. Evaporation of the solvent gave the oxaquadricyclane **2** as a yellow oil; p.m.r. analysis indicated essentially quantitative conversion. This material was used without further purification. It should be noted that **2** can cause a temporary but painful irritation of the eyes and skin.

Preparation of 3 and 4

A solution of **2** (10.0 g) in 50% aqueous acetone (100 ml) was refluxed for 6 h. It was then diluted with water (60 ml) and thoroughly extracted with chloroform. Evaporation of solvent from the dried (Na_2SO_4) extract gave a viscous red–brown oil (10.6 g), which on cooling slowly solidified. Trituration with cold ether gave a colorless solid (4.72 g, 44%).[5] Fractional crystallization from ether gave (*i*) isomer **3** as colorless needles (1.52 g, 14%); m.p. 130–132°; parent molecular ion (for $C_{12}H_{16}O_6$) at *m/e* 256 with prominent ions at *m/e* 241, 225, 214, and 213; ν_{max} (CCl_4): 1719, 1743 cm^{-1}; **3** can be recrystallized from ether or benzene; and (*ii*) colorless prisms and needles; m.p. 76–83°; shown by p.m.r. to be *ca.* 90% **4**, contaminated by **3**. Pure **4** (2.85 g, 26.5%) could be obtained by crystallization from water as colorless prisms, m.p. 83–84°; parent molecular ion (for $C_{12}H_{16}O_6$) at *m/e* 256 with prominent ions at *m/e* 241, 225, 214, and 213; ν_{max} (CCl_4): 1710, 1738 cm^{-1}.

Conversion of **2** to **3** and **4** also proceeded in refluxing 50% aqueous tetrahydrofuran, although more slowly (*ca.* 60% conversion in 6 h). The reaction was promoted (complete in 2 h) by a few drops of acetic acid, but the product obtained was somewhat less tractable.

Solutions of **3** and **4** in 50% aqueous acetone were each refluxed for 2 h. On dilution with water and extraction with chloroform quantitative recoveries of the starting compounds were made.

Preparation of 3-d_2 and 4-d_2

The conversion of **2** to **3**-d_2 and **4**-d_2 was accomplished as above, but using a 50% mixture of tetrahydrofuran and deuterium oxide and refluxing for 16 h. The yields of **3**-d_2 and **4**-d_2 were similar to those of **3** and **4**. The molecular formula $C_{12}H_{14}D_2O_6$ was confirmed by mass spectrometry [peaks at *m/e* 258, 243, 227, 216, and 215].

Conversion of 3 to 9

A stirred solution of **3** (300 mg) in CH_2Cl_2 (15 ml) was treated with an excess of concentrated sulfuric acid (900 mg). Stirring was continued at room temperature for 1 h, during which a reddish oil precipitated. The mixture was washed twice with water, dried, and evaporated to give a solid residue. Trituration of the latter with cold ethyl acetate gave **9** as a colorless solid (142 mg, 58%) m.p. 229–230°. The ethyl acetate - soluble portion afforded a gummy solid, shown by p.m.r. to be mainly **6** (see below).

The expected parent molecular ion for **9** (for $C_{10}H_{10}O_5$) at *m/e* 210 was absent. However mass measurements of ions at *m/e* 195 (measured 195.0297, $C_9H_7O_5$ requires 195.02935) and 166 (measured 166.0625, $C_9H_{10}O_3$ requires 166.0630) indicated losses of 15 (CH_3) and 44 (CO_2) mass units; ν_{max} (KBr): 1790 cm^{-1}. Compound **9** was only sparingly soluble in common organic solvents.

Conversion of **3** to **9** was promoted by D_2SO_4 and the conversion of **3**-d_2 to **9**-d_2 could also be carried out under similar conditions using either H_2SO_4 or D_2SO_4.

The ratio of **9** to **6** obtained by acid treatment of **3** increases with the concentration of acid present.

Conversion of 3 to 6

A stirred solution of **3** (100 mg) in CH_2Cl_2 (6 ml) was cooled to 0° and treated with concentrated sulfuric acid (90 mg) in CH_2Cl_2 (4 ml). After stirring at room temperature for 1 h the reaction mixture was washed with water, dried, and evaporated to give a colorless crystalline solid (97 mg). Analysis of the latter by p.m.r. indicated 70–75% **6**, with 20–25% **9**, and 5–10% unreacted **3**. The crude product was triturated with ethyl acetate to remove **9** (see above) and the ethyl acetate – soluble residue crystallized from a small amount of ether or water to give **6** as colorless prisms, m.p. 65–67°, parent molecular ion (for $C_{12}H_{16}O_6$) at *m/e* 256, with prominent ions at *m/e* 241, 225, 214, and 213; ν_{max} (CCl_4): 1710, 1743 cm^{-1}.

Conversion of **3**-d_2 to **6**-d_2 was carried out under identical conditions.

The conversions of **3** to **6**-d_1 and of **3**-d_2 to **6**-d_3 were brought about under similar conditions using D_2SO_4 in place of H_2SO_4. In each case D_2O was substituted for H_2O in the work-up. However, exchange of D with the acetyl methyl protons causes dilution and it is therefore necessary to employ an excess of D_2SO_4 to ensure complete exchange at the site of epimerization. Under such conditions (high acid concentration) the yields of **6**-d_1 and **6**-d_3 are limited by production of **9** and **9**-d_2 respectively.

Conversion of 4 to 7

A stirred solution of **4** (100 mg) in CH_2Cl_2 (6 ml) was cooled to 0° and treated with concentrated sulfuric acid

[5]A p.m.r. analysis of the crude product indicated a very high (*ca.* 90%) conversion to **3** and **4**. However attempted separations by column chromatography on silicic acid or neutral alumina or by preparative g.l.p.c. using 20% carbowax on chromosorb W at 200°, led to epimerization of the products. A better method for recovery of **3** and **4** is now being sought.

(90 mg) in CH_2Cl_2 (4 ml). Stirring was continued at room temperature for 1 h. After washing with H_2O, drying and evaporation gave a crystalline solid. This was crystallized from ether to give **7** as colorless needles (90 mg), m.p. 82–83° [lit. (10) 82°], parent molecular ion (for $C_{12}H_{16}O_6$) at *m/e* 256, with prominent ions at *m/e* 241, 225, 224, 214, and 213; ν_{max} (CCl_4): 1712, 1737 cm^{-1}.

Conversion of **4**-d_2 to **7**-d_2 was carried out under identical conditions.

The conversions of **4** to **7**-d_1 and of **4**-d_2 to **7**-d_3 were brought about in the presence of a 6 mole excess of D_2SO_4, to ensure complete exchange at the site of epimerization.

We thank J. van Ingen for measurement of some p.m.r. data and D. J. Embree and Dr. W. D. Jamieson for measurement of and assistance with the interpretation of the mass spectra.

1. J. D. ROBERTS and C. M. SHARTS. *In* Organic Reactions. Vol. 12. J. Wiley, New York, 1962. Chapt. 1. R. A. RAPHAEL. *In* Chemistry of carbon compounds. *Edited by* E. H. Rodd. Vol. II, Part A. Elsevier, 1953. Chapt. III. p. 46.
2. G. O. SCHENCK and R. STEINMETZ. Bull. Soc. Chim. Belg. **71**, 781 (1962). G. O. SCHENCK, W. HARTMANN, S.-P. MANNSFELD, W. METZNER, and C. H. KRAUCH. Chem. Ber. **95**, 1642 (1962).
3. W. METZNER and D. WENDISCH. Ann. **730**, 111 (1969). G. W. GRIFFIN, J. E. BASINSKI, and L. I. PETERSON. J. Amer. Chem. Soc. **84**, 1012 (1962). H. P. KAUFMANN and A. K. SEN GUPTA. Ann. **681**, 39 (1965).
4. P. E. EATON. J. Amer. Chem. Soc. **84**, 2344, 2454 (1964); Tetrahedron Letters, 3695 (1964). G. O. SCHENCK, I. VON WILUCKI, and C. H. KRAUCH. Chem. Ber. **95**, 1409 (1962).
5. E. J. COREY, J. D. BASS, R. LEMAHIEU, and R. B. MITRA. J. Amer. Chem. Soc. **86**, 5770 (1964).
6. H. PRINZBACH, P. VOGEL, and W. AUGE. Chimia (Aarau). **21**, 469 (1967).
7. H. WEITKAMP and F. KORTE. Tetrahedron Suppl. **7**, 75 (1966).
8. J. B. LAMBERT and J. D. ROBERTS. J. Amer. Chem. Soc. **85**, 3710 (1963). E. L. ELIEL, N. L. ALLINGER, S. J. ANGYAL, and G. A. MORRISON. Conformational analysis. Interscience, New York, 1965. Chapter 4. p. 199.
9. G. W. GRIFFIN and R. B. HAGER. Revue de Chimie, Acad. Rep. Populaire Roumaine. **7**, 901 (1962).
10. F. A. BOVEY. Nuclear magnetic resonance spectroscopy. Academic Press, New York, 1969. p. 75–77.
11. E. LUSTIG, E. P. RAGELIS, N. DUY, and J. A. FERRETTI. J. Amer. Chem. Soc. **89**, 3953 (1967). J. W. EMSLEY, J. FEENEY, and L. H. SUTCLIFFE. High resolution nuclear magnetic resonance spectroscopy. Vol. I. Pergamon Press, London, 1965. p. 347. D. M. GRANT, R. C. HIRST, and H. S. GUTOWSKY. J. Chem. Phys. **38**, 470 (1963).
12. J. D. SWALEN. *In* Computer programs for chemistry. *Edited by* Delos F. Detar. Vol. 1. W. A. Benjamin Inc., New York, 1968. Chapt. 4. p. 54–116. *cf.* J. D. SWALEN and C. A. REILLY. J. Chem. Phys. **37**, 21 (1962).
13. L. PAOLILLO, H. ZIFFER, and O. BUCHARDT. J. Org. Chem. **35**, 38 (1970).
14. I. FLEMING and D. H. WILLIAMS. Tetrahedron, **23**, 2747 (1967).
15. J. D. PARK, R. O. MICHAEL, and R. A. NEWMARK. J. Org. Chem. **34**, 2525 (1969).

Can. J. Chem. Downloaded from www.nrcresearchpress.com by 210.87.254.5 on 09/05/12
For personal use only.

Can. J. Chem. Downloaded from www.nrcresearchpress.com by 210.87.254.5 on 09/05/12
For personal use only.

Some Factors Affecting the Synthesis of Hindered Diphenyl Ethers[1]

W. D. CHANDLER, J. J. BERGMAN, AND G. H. HAAS
Department of Chemistry, University of Saskatchewan, Regina, Saskatchewan

Received July 16, 1970

A study is presented which shows how, in the Hems synthesis of two tri-ortho-substituted diphenyl ethers, the nature of the *leaving group* of the substrate is important in determining yield. The yield increases in the order: OTosyl (p-$OSO_2C_6H_4CH_3$) < Cl < F. As well, a synthetic method, involving reaction of an activated substrate with a sodium phenoxide in dimethyl sulfoxide, has been investigated in a similar way and a number of highly-hindered diphenyl ethers, which cannot be synthesized by the Hems synthesis, have been prepared.

Canadian Journal of Chemistry, 49, 583 (1971)

Introduction

In undertaking a conformational study of diphenyl ethers it was found necessary to synthesize a number of these compounds having one ring substituted at positions-2 and -4. Recently, Neville and Moir (1) have discussed the synthesis of some highly hindered diphenyl ethers by a modification of the Hems synthesis in which *N*-(4-carbomethoxy-2,6-dinitrophenyl)pyridinium chloride (**1***a*) was heated with various phenols in pyridine. Their modification allowed easier purification, and, in some cases, larger yields than had been the case previously (2–5).

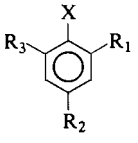

1

a $R_1 = R_3 = NO_2$; R_2 = COOMe; X = Py^+Cl^-
b $R_1 = NO_2$; R_2 = COOMe; R_3 = H; X = $Py^+OTosyl^-$
c R_1 = COOMe; $R_2 = NO_2$; R_3 = H; X = $Py^+OTosyl^-$
d $R_1 = NO_2$; R_2 = COOMe; R_3 = H; X = OTosyl
e R_1 = COOMe; $R_2 = NO_2$; R_3 = H; X = OTosyl

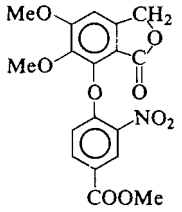

2

[1]Some of the material for this paper is taken from the Honors Thesis of G. H. Haas, University of Saskatchewan, Regina, Saskatchewan, April, 1969.

The use of *N*-(4-carbomethoxy-2-nitrophenyl)-pyridinium tosylate (**1***b*) has been reported with 7-hydroxymetameconine in the Hems synthesis of **2** (4–6) but no reaction occurred when the phenol was methyl salicylate (5).

Although we have succeeded in preparing 2-(4′-carbomethoxy-2′-nitrophenoxy)-1,3,5-trichlorobenzene (**3***a*) by reacting 2,4,6-trichlorophenol with **1***b* in pyridine using a method essentially that of Neville and Moir, the isomeric ether, **3***b*, could not be made in the same way since the corresponding *N*-phenylpyridinium tosylate (**1***c*) could not be synthesized by the usual method (4).

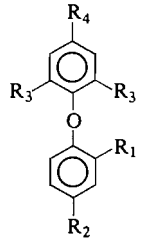

3

a $R_1 = NO_2$; R_2 = COOMe; $R_3 = R_4$ = Cl
b R_1 = COOMe; $R_2 = NO_2$; $R_3 = R_4$ = Cl
c $R_1 = NO_2$; R_2 = COOMe; $R_3 = R_4$ = Me
d $R_1 = R_2 = NO_2$; $R_3 = R_4$ = Me
e $R_1 = R_2 = NO_2$; $R_3 = R_4$ = *t*-Bu
f $R_1 = R_2 = NO_2$; R_3 = *i*-Pr; R_4 = H

In their original paper on the Hems synthesis, Borrows *et al.* (2) pointed out that, although the pyridinium salt was essential for the reaction, they had not found it necessary to isolate it from the reaction mixture prior to adding the phenol. In all of their reactions, Neville and Moir formed and reacted **1***a in situ*. On this basis, it seemed reasonable to expect that diphenyl ethers **3***a* and *b* would be formed directly from the action of 2,4,6-trichlorophenol on the appropriate tosylate

TABLE 1. Comparison of yields of diphenyl ethers prepared using 2,4,6-trichlorophenol with various substrates in the Hems synthesis and the method of Wright and Jorgenson

Substrate	Hems synthesis		Wright and Jorgenson method	
	Reaction time (h)	Yield of ether (%)	Reaction time (h)	Yield of ether (%)
1*d*	24	31	24	6
	48	48	—	—
	72	49	70	18
	96	50	—	—
1*a*	24	35	24	55
	48	52	—	—
Methyl 4-chloro-3-nitrobenzoate	24	61	24	75
	48	73	70	78
Methyl 4-fluoro-3-nitrobenzoate	24	77	—	—
	48	67	—	—
1*e*	24	0	24	0
	48	0	70	10
Methyl 2-chloro-5-nitrobenzoate	24	8	24	63
	48	23	—	—
	72	12	—	—
	96	8	—	—
Methyl 2-fluoro-5-nitrobenzoate	24	71	24	68
	48	57	—	—

esters (**1***d* and *e*) in pyridine without the necessity of isolating and purifying the salts, **1***b* and *c*.

As expected, when **1***d* was used with the *in situ* technique, **3***a* was formed in about 50% yield, nearly the same yield as for the reaction of **1***b* with the phenol under the same experimental conditions. However, 2,4,6-trichlorophenol and **1***e* would not react to give **3***b* even after 48 h in pyridine at 90°. Compound **3***b* was, however, synthesized in up to 20% yield when methyl 2-chloro-5-nitrobenzoate was used as the substrate in the Hems synthesis.

Since so little is known about the role of the leaving group in the Hems synthesis and since the practice has been to use tosylate esters in difficult syntheses and chloro compounds in easier ones (1, 4–6), it was decided that an investigation of the relation between leaving group and the yield of the two diphenyl ethers (**3***a* and *b*) would be undertaken. For this purpose, seven substrates were reacted with 2,4,6-trichlorophenol and pyridine at 90°. The yields of the ethers formed are given in Table 1.

Using a different approach to the synthesis of hindered diphenyl ethers, Wright and Jorgenson (7) showed that good yields of some ethers of type **4** could be obtained by reacting a phenol, sodium hydroxide and an activated chloro compound together in dimethyl sulfoxide. The reaction of a phenol with an activated halide and base or of a phenoxide with an activated halide to form a diphenyl ether is not novel as there are numerous examples in the literature (3, 8–11). However, the use of dimethyl sulfoxide as a solvent and the ease of product isolation are new and worthy of investigation.

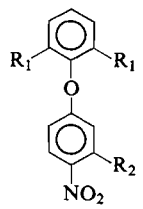

4

R_1 = Me, *i*-Pr, *sec*-Bu, *t*-Bu; R_2 = H, Me

By means of a procedure similar to that of Wright and Jorgenson, the effect of the leaving group on the yields of the two diphenyl ethers, **3***a* and *b*, was studied. The results are compared with the yields from the Hems synthesis in Table 1.

In addition, because Wright and Jorgenson were able to prepare alkyl-substituted diphenyl ethers, **4**, in good yield, we used their method to investigate some of the steric factors associated with the synthesis and we have prepared some additional hindered ethers (**3***c*, *d*, *e*, and *f*) for conformational studies. The yields, melting points, and elemental analyses are given in Table 2.

Can. J. Chem. Downloaded from www.nrcresearchpress.com by 210.87.254.5 on 09/05/12
For personal use only.

TABLE 2. Diphenyl ethers synthesized via the method of Wright and Jorgenson

Compound 3	Yield* (%)	Melting point (°C)	Formula	Calculated (%) C	H	N	Cl	Found (%) C	H	N	Cl
a	†	133–134	$C_{14}H_8Cl_3NO_5$	44.65	2.14	3.72	28.25	44.70	2.07	3.65	28.23
b	†	137–138	$C_{14}H_8Cl_3NO_5$	44.65	2.14	3.72	28.25	44.61	2.09	3.51	28.12
c	50	105–106	$C_{17}H_{17}NO_5$	64.75	5.44	4.42	—	64.35	5.17	4.64	—
d	70	153–154	$C_{15}H_{14}N_2O_5$	59.60	4.67	9.27	—	59.52	4.52	9.23	—
e	18	147–148	$C_{24}H_{32}N_2O_5$	67.26	7.53	6.54	—	67.34	7.46	6.54	—
f‡	13	88–89	$C_{18}H_{20}N_2O_5$	62.78	5.85	8.14	—	62.89	5.89	8.36	—

*Yields are the maximum obtained after optimum reaction time.
†See Table 1.
‡The crude reaction mixture was first distilled and the fraction, b.p. 205°/5 mm Hg, was collected and recrystallized.

Results and Discussion

Using the Hems synthesis, the yields of **3***a* are, for the most part, better than those of **3***b* where substrates having the same leaving group are compared. This observation is to be expected since a nitro group ortho to the leaving group should be better able to delocalize the negative charge formed during a nucleophilic substitution than would a para-nitro.

Where sufficient data are available, the yield of diphenyl ether appears to reach a maximum with time and then decrease; Constantin and L'Ecuyer (12) observed similar behavior in some Hems syntheses they studied. Undoubtedly, pyridine scission of the ether in competition with ether formation lowers the yield. With the two fluoro compounds the reaction is so fast that the formation of diphenyl ether must be essentially complete in less than 48 h while such cannot be the case with other substrates. It is clear that halogen-containing substrates are preferable to tosylate esters in the Hems synthesis. A fluoro compound would react faster but in some cases the more easily prepared chloro analogue would give satisfactory yields.

With one exception, the method of Wright and Jorgenson gives yields as good as or better than the Hems synthesis. For the more activated substrates, the yields by the two methods are very similar, and there does not appear to be any problem of by-product formation. The observation of poor yields with the tosylate esters agrees with the results of Borrows *et al.* (2) who noted that the lithium salt of phenol gave only a *trans*-tosylated product when treated with a tosylate ester but the expected diphenyl ether did form when the *N*-phenylpyridinium tosylate was used.

The synthetic advantage of the method of Wright and Jorgenson becomes obvious from the fact that 2,4,6-trimethylphenol and methyl 4-chloro-3-nitrobenzoate did not react to form **3***c* in a Hems synthesis after 24 h at 90°. Under the same conditions a 50% yield of **3***c* was obtained by the method of Wright and Jorgenson.

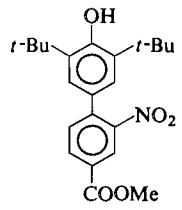

5

With methyl 4-chloro-3-nitrobenzoate, 2,6-di-*t*-butylphenol gave only the phenolbiphenyl, **5**, in complete agreement with previous results using *p*-chloronitrobenzene as substrate (7). Under the same conditions 2,4,6-tri-*t*-butylphenol and methyl 4-chloro-3-nitrobenzoate formed no diphenyl ether after 48 h. With the more activated substrate, 2,4-dinitrochlorobenzene, 12% of **3***e* was obtained after 48 h at 90°. Refluxing the reaction mixture in dimethyl sulfoxide for 76 h increased the yield to 17% but reaction for 7 days at 95–100° did not increase it further. By comparison, **3***d* was isolated in 70% yield when 2,4,6-trimethylphenol and 2,4-dinitrochlorobenzene were heated together at 90° for only 4.5 h and **3***f* was obtained in greater than 13% yield when 2,6-diisopropylphenol and 2,4-dinitrochlorobenzene were reacted together for 20 h at 85°.

When the yields noted in Table 2 are compared to those obtained by Wright and Jorgenson for some of the ethers in series **4** (R_2 = H, R_1 = Me (82%); R_2 = H, R_1 = *i*-Pr (75%); R_2 = H, R_1 = *sec*-Bu (70%)) it becomes clear that large alkyl groups ortho to the phenol oxygen severely hinder attack on the substrate. This is especially true in the case of a large substituent such as NO_2 in a position ortho to the leaving group of the

Can. J. Chem. Downloaded from www.nrcresearchpress.com by 210.87.254.5 on 09/05/12
For personal use only.

Can. J. Chem. Downloaded from www.nrcresearchpress.com by 210.87.254.5 on 09/05/12
For personal use only.

substrate. The steric crowding around the oxygen in 2,6-di-*t*-butylphenol is so large that the nucleophilic center becomes the carbon para to the oxygen rather than the oxygen itself. Diphenyl ethers with two *t*-butyl ortho to the oxygen can be prepared if a sufficiently activated substrate is used and if the para position of the phenol is blocked. It is interesting to note that Neville and Moir (1) were unable to prepare such an ether in their series using the Hems synthesis.

It appears that the method of Wright and Jorgenson is preferable to the older Hems synthesis for preparing tri-ortho-substituted diphenyl ethers. Work is continuing with attempts to prepare even more-highly hindered diphenyl ethers.

Experimental

All melting points were obtained on a Kofler, hot stage apparatus and are reported uncorrected. The structures of all the reported compounds were consistent with their n.m.r. and i.r. spectra.

Except as noted, all reagents (phenols and substrates) were purchased from chemical suppliers and were used without further purification.

The following compounds were prepared by methods described previously: 4-carbomethoxy-2-nitrophenyl *p*-toluenesulfonate (**1***d*) (6), m.p. 96–97°; *N*-(4-carbomethoxy-2-nitrophenyl)pyridinium *p*-toluenesulfonate (**1***b*) (4), m.p. 223–225°; methyl 4-fluoro-3-nitrobenzoate (13), m.p. 53–55°.

2-Carbomethoxy-4-nitrophenyl p-Toluenesulfonate (1e)

Salicylic acid (reagent) was nitrated according to the method of Epstein and Meyer (14) to obtain 5-nitrosalicylic acid, m.p. 233–235° (45%). The acid was methylated in methanol, dichloroethane, and sulfuric acid using the procedure of Clinton and Laskowski (15) and the ester was recrystallized twice from ethanol (95%) as long, yellow–white needles, m.p. 116–118° (lit. m.p. 116–117° (16)).

Methyl 5-nitrosalicylate (15 g), *p*-toluenesulfonyl chloride (15 g, technical), and pyridine (25 ml, reagent) were shaken in a stoppered flask for 1 h. The sludge that formed was poured into a mixture of ice-water (500 g) and concentrated HCl (26 ml, 12 *N*) and the solid was crushed to yield a nearly white product. This was collected and recrystallized from ethanol (95%) as large needles, m.p. 74–76°, yield, 23.5 g (88%). The analytical sample was obtained after two further recrystallizations from absolute ethanol, m.p. 75–76°.

Anal. Calcd. for $C_{15}H_{13}NSO_7$: C, 51.28; H, 3.73; N, 3.99. Found: C, 51.31; H, 3.63; N, 3.89.

Methyl 4-Chloro-3-nitrobenzoate and Methyl 2-Chloro-5-nitrobenzoate

The corresponding acids (Eastman white label) were methylated by the method of Clinton and Laskowski (15). The crude esters were recrystallized as needles from methanol, m.p. 82–83° and 69–70° respectively (lit. m.p. 83 and 73° respectively (17)).

Methyl 2-Fluoro-5-nitrobenzoate

Methyl 2-chloro-5-nitrobenzoate was heated with KF in dimethyl formamide at 155° for 4 h as described by Finger and Kruse (13) in their preparation of methyl 4-fluoro-3-nitrobenzoate. The impure product was distilled and the material boiling at 130–135°/5 mm Hg was collected (62%). Light, yellow needles were obtained after recrystallization from methanol, m.p. 44–45°.

Anal. Calcd. for $C_8H_6FNO_4$: C, 48.25; H, 3.04; N, 7.04. Found: C, 48.11; H, 3.18; N, 7.00.

Generalized Hems Synthesis

The results listed in Table 1 were obtained by the following procedure:

The appropriate substrate (0.02 mol) and 2,4,6-trichlorophenol (6.0 g, 0.03 mol, Eastman white label) were dissolved[2] in chloroform (20 ml, stock) and pyridine (45 ml, reagent). The solution was heated with magnetic stirring for the designated time at a temperature of 90 ± 1°.

At the end of the reaction time, the dark mixture[3] was poured into a beaker containing ice-water (400 g), concentrated HCl (75 ml, 12 *N*), and chloroform (40 ml, stock). The reaction flask was rinsed with chloroform (20 ml) and water (10 ml) which were also added to the beaker. After the two-phase mixture had been stirred vigorously for 5 min, the chloroform layer was drawn off and diluted with absolute ethanol (100 ml). If a solid formed at the water–chloroform interphase, it was removed by filtration prior to extracting the chloroform layer.

The volume of the chloroform–ethanol solution was reduced by boiling with stirring until the vapor temperature reached 74°. Any solid that formed when the solution was chilled in ice was collected, washed with cold absolute ethanol, and recrystallized from ethanol. The yield of once-recrystallized product is that reported in Table 1.

Generalized Method of Wright and Jorgenson

The results listed in Table 1 were obtained by the following procedure:

2,4,6-Trichlorophenol (5.0 g, 0.025 mol, Eastman white label) and NaOH (0.82 g, 0.02 mol, reagent) were heated with stirring in dimethyl sulfoxide (30 ml, reagent) at 90° until the base dissolved and a dark blue solution resulted. To this solution was added the substrate (0.02 mol) and heating was carried out for the designated time at 90 ± 1°.

At the end of the reaction time, the mixture[4] was poured into a beaker containing ice-water (300 g), concentrated HCl (25 ml, 12*N*), and chloroform (60 ml, stock). The flask was rinsed with water (10 ml) and chloroform (10 ml) which were also added to the beaker. The procedure of isolating and purifying the diphenyl ether product was the same as for the generalized Hems syn-

[2]The *N*-phenylpyridinium tosylate (**1***b*) did not dissolve.

[3]A solid formed from the solution when **1***d* and methyl 2-chloro-5-nitrobenzoate were substrates. This solid did not entirely disappear. The *N*-phenylpyridinium tosylate (**1***b*) did not entirely disappear either.

[4]If Cl or F were the leaving group a precipitate of NaCl or NaF formed.

thesis. The yield of once-recrystallized product is reported in Table 1.

For synthesis of the new ethers (*3c*, *d*, *e*, and *f*) the procedure was exactly that outlined above except the nature of the phenol was changed and, in some cases, temperatures other than 90° were used. The reactants were always in the ratio: NaOH (0.02 mol), phenol (0.025 mol), substrate (0.02 mol), and dimethyl sulfoxide (30 ml). Yields and elemental analyses of these ethers are given in Table 2 along with melting points.

2,6-Di-t-butyl-4-(4'-carbomethoxy-2'-nitrophenyl)phenol (5)

2,6-Di-*t*-butylphenol (Aldrich, m.p. 36°) and methyl 4-chloro-3-nitrobenzoate were reacted together for 41 h by the method of Wright and Jorgenson at 80–85° to give an orange solid, m.p. 144–147° (88%). A recrystallization from ethanol (absolute) gave a mixture of two types of needles: brown needles melting sharply at 247° and yellow-green needles melting at 152–153°. A separation of the two was achieved by washing the solid with methanol. The methanol was evaporated and the product recrystallized from ethanol (absolute) five times to give greenish cubes, m.p. 154–155°. The n.m.r. and i.r. spectra showed the presence of a hydroxyl group in the molecule.

Anal. Calcd. for $C_{22}H_{27}NO_5$: C, 68.55; H, 7.06; N, 3.64. Found: C, 68.27; H, 7.04; N, 3.89.

The brown needles have not been identified.

The authors wish to acknowledge the National Research Council of Canada for a grant in support of research and for a bursary to one of us (J. J. B.). The assistance of Mr. R. Lang in several syntheses is also acknowledged.

1. G. A. Neville and R. Y. Moir. Can. J. Chem. **47**, 2787 (1969).
2. E. T. Borrows, J. C. Clayton, B. A. Hems, and A. G. Long. J. Chem. Soc. S190 (1949).
3. J. H. Barnes, E. T. Borrows, J. Elks, B. A. Hems, and A. G. Long. J. Chem. Soc. 2824 (1950).
4. J. A. McRae, R. Y. Moir, J. J. Ursprung, and H. H. Gibbs. J. Org. Chem. **19**, 1500 (1954).
5. M. Allen and R. Y. Moir. Can. J. Chem. **37**, 1799 (1959).
6. W. D. Chandler, W. MacF. Smith, and R. Y. Moir. Can. J. Chem. **42**, 2549 (1964).
7. J. Wright and E. C. Jorgenson. J. Org. Chem. **33**, 1245 (1968).
8. L. C. Raiford and J. C. Colbert. J. Amer. Chem. Soc. **48**, 2652 (1926).
9. M. J. Rarick, R. Q. Brewster, and R. B. Dains. J. Amer. Chem. Soc. **55**, 1289 (1933).
10. R. W. Bost and F. Nicholson. J. Amer. Chem. Soc. **57**, 2368 (1935).
11. A. L. Beckwith and J. Miller. J. Org. Chem. **19**, 1416 (1954).
12. R. Constantin and P. L'Ecuyer. Can. J. Chem. **36**, 1627 (1958).
13. G. C. Finger and C. W. Kruse. J. Amer. Chem. Soc. **78**, 6034 (1956).
14. E. Epstein and M. Meyer. J. Amer. Chem. Soc. **77**, 4059 (1955).
15. R. O. Clinton and S. C. Laskowski. J. Amer. Chem. Soc. **70**, 3135 (1948).
16. H. Hoyer and R. Macdonald. Z. Electrochem. **66**, 269 (1962).
17. J. Miller and V. A. Williams. J. Chem. Soc. 1475 (1953).

Can. J. Chem. Downloaded from www.nrcresearchpress.com by 210.87.254.5 on 09/05/12
For personal use only.

Can. J. Chem. Downloaded from www.nrcresearchpress.com by 210.87.254.42 on 09/05/12
For personal use only.

Studies of Carbohydrate Derivatives by Nuclear Magnetic Double Resonance. Part VI. The Identification of ^{13}C Chemical Shifts of Methyl Resonances via the ^{1}H–$\{^{13}C\}$ INDOR Technique

R. BURTON, L. D. HALL, AND P. R. STEINER[1]

Department of Chemistry, The University of British Columbia, Vancouver 8, British Columbia

Received August 26, 1970

The ^{13}C chemical shifts of acetate- and methoxyl-methyl substituents of several pyranose carbohydrate derivatives have been measured by the ^{1}H–$\{^{13}C\}$ INDOR technique. The chemical shifts ($\delta^{13}C$) of anomeric methoxyl-methyl resonances fall into two groups: for α-anomers (axial substituent), $\delta^{13}C$ = 55.12–56.63 p.p.m.; for β-anomers (equatorial substituent), $\delta^{13}C$ = 56.63–58.69 p.p.m. *O*-Acetyl-methyl shifts fall between 20.54–20.72 p.p.m. and *N*-acetyl-methyl shifts were detected between 22.98–23.08 p.p.m.

Canadian Journal of Chemistry, 49, 588 (1971)

Introduction

Recent improvements in n.m.r. instrumentation have made possible the direct measurement of the "natural-abundance" ^{13}C n.m.r. spectra of complex organic derivatives such as carbohydrates (1) on a routine basis. However, in certain instances it is convenient, indeed advantageous, to obtain ^{13}C n.m.r. spectra via indirect methods and in the present discussion we describe measurements based on the ^{1}H–$\{^{13}C\}$ INDOR technique.[2] Although a number of other workers (3) have previously discussed such experiments the present paper describes the first measurements in the carbohydrate area. For a general discussion of the INDOR technique the reader is referred to three review articles (4); a simplified discussion was given in the previous paper of this series (5).

As part of another project (1*a*) we had previously measured *directly* the natural-abundance ^{13}C resonances of several pyranose derivatives and had shown that the chemical shifts of anomeric methoxyl resonances have a stereospecific dependence. This dependence has now been investigated further.

Experimental

The compounds used were synthesized by standard literature methods:

Methyl 2,3,4,6-tetra-*O*-acetyl-α-D-glucopyranoside (**1**), m.p. 102° (lit. (6), 101°); methyl 2,3,4,6-tetra-*O*-acetyl-β-D-glucopyranoside (**2**), m.p. 105° (lit. (6), 104°); methyl 2,3,4-tri-*O*-acetyl-α-D-xylopyranoside (**3**), m.p. 88–89°; methyl 2,3,4-tri-*O*-acetyl-β-D-xylopyranoside (**4**), m.p. 116–117°; 1,2,3,4,6-penta-*O*-acetyl-β-D-galactopyranose (**5**), m.p. 142–143° (lit. (7), 142°); methyl-α-D-glucopyranoside[3] (**6**), m.p. 160–161°; methyl-β-D-glucopyranoside[4] (**7**), m.p. 102–104°; methyl-α-D-xylopyranoside[5] (**8**), m.p. 93°; methyl-β-D-xylopyranoside[4] (**9**), m.p. 154–156°; 2-acetamido-2-deoxy-D-glucopyranose[4] (**10**), m.p. 215° (dec.); 2-acetamido-2-deoxy-D-mannopyranose[4] (**11**), m.p. 127–130°.

The n.m.r. spectra of derivatives **1–5** were measured using *ca.* 35% (w/v) solutions in chloroform-*d*, contained in a 5 mm o.d. sample tube; tetramethylsilane was used as the internal reference for the field–frequency lock.

The n.m.r. measurements on compounds **6–11** were made with samples prepared as follows: the derivative was lyophilized several times with deuterium oxide and then a solution (*ca.* 40% w/v) was made with deuterium oxide. The sample was contained in a 5 mm o.d. tube. Tetramethylsilane, contained in a capillary tube, was used as the lock signal for the spectrometer.

All n.m.r. measurements were made with an extensively modified Varian Associates HA-100 spectrometer, using components originally (8) purchased for heteronuclear spin-decoupling experiments. A block diagram of the accessories used is given in Fig. 1.

In order to obtain the required frequency–frequency lock, several standard frequencies {34, 34, and 32 MHz} were taken from a Hewlett Packard synthesizer driver (model 5110 B) and added together using Hewlett Packard double balanced mixers (model 10514 A). The resultant 100 MHz signal was then amplified to 6.5 V (r.m.s.). The oscillator tube (V-103) was removed from a 100 MHz V-4311 radiofrequency unit and the 6.5 V, 100 MHz signal was injected via a B.N.C. connector at J 108.

The ^{13}C frequency was obtained from a Hewlett Packard frequency synthesizer (model 5105 B). The output frequency was digitally programmed using a Barry Research[6] linear sweep control (model LSC-7B).

---

[1]Recipient of an NRCC Scholarship, 1969–1970.

[2]An acronym coined by Baker (2) for Inter Nuclear DOuble Resonance.

[3]From Eastman Organic Chemicals, Rochester, New York.

[4]From Pfanstiehl Laboratories, Wankegan, Illinois.

[5]From Koch-Light Laboratories, Colnbrook, Great Britain.

[6]Barry Research, 934 East Meadow Drive, Palo Alto, California.

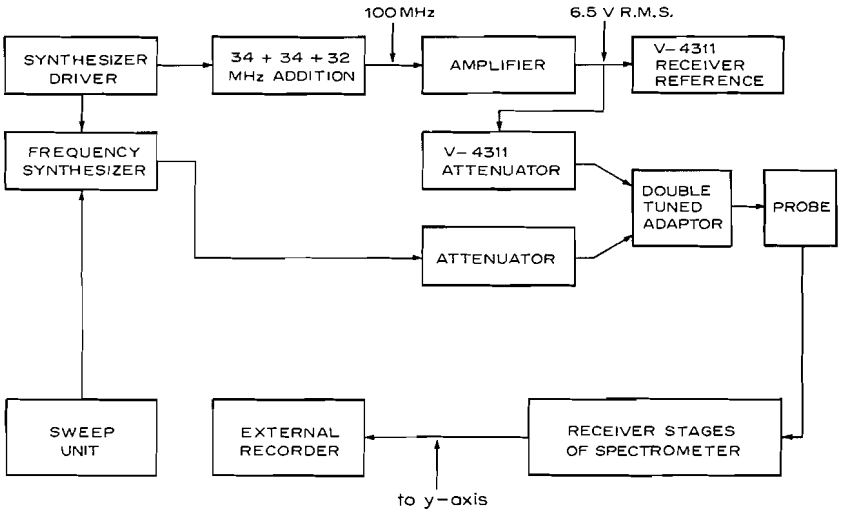

FIG. 1. Block diagram of the components used for ^1H–$\{^{13}C\}$ INDOR measurements.

The power output of the frequency synthesizer was suitably attenuated with a Telonic Industry[7] attenuator (model TG-9050).

The transmitter coil of a Varian V-4311 probe was double-tuned to 100 and 25.1 MHz following previously reported methods (8).

For convenience, the INDOR spectra were recorded on either a Varian Associates Strip Chart Recorder (model G-14) or a Hewlett Packard, Moseley Recorder (model 7005B). The *y*-axis drive was obtained from the EXTERNAL-RECORDER output of the V-4391 unit. The *x*-axis of the charts was calibrated directly using the time-base, event-marker output of the Barry Programmer. Repeated measurements made over a period of time showed that the reproducibility of the chemical shifts obtained directly from 1000 Hz sweep-width charts is better than ± 2 Hz (± 0.08 p.p.m. for ^{13}C shifts) which was adjudged to be adequate for most organo-chemical applications. Higher precision could be obtained by measuring, in turn, the resonance frequency of each transition using much narrower sweep-widths, or by direct calibration methods. The sole limitation in the accuracy of shifts obtained by either of these latter methods is then governed by the line-widths of the INDOR responses themselves.

The general procedure followed during these INDOR measurements was as follows. The frequency–frequency lock was set-up as described above and the field–frequency lock established in the usual fashion via a tetramethylsilane reference, with the instrument in the frequency-swept mode. The normal ^1H n.m.r. spectrum of the compound was measured under conventional conditions and then the "gain" settings increased to measure the ^{13}C-satellites of the appropriate resonance. The sweep-oscillator of the Varian recorder was set to the precise resonance frequency (± 0.1 Hz) of the satellite which was to be monitored and then the receiver output of the spectrometer was connected to the *y*-axis of the recorder. With the full power output of the synthesizer connected to the probe, the synthesizer was swept over the 10 000 Hz range at a rate of 100 Hz/s. The broad resonance initially detected in this way was subsequently measured on a narrower sweep-width (1000 Hz) and with a somewhat slower sweep rate (2 Hz/s).

Although the experimentally determined shifts may be quoted in "absolute" frequency units it is more convenient to compare them with the ^{13}C shift of tetramethylsilane. Several groups of workers have given formulae whereby the experimental frequency data may be converted to a basis where the ^{13}C shift is given in p.p.m. from that of tetramethylsilane and at a magnetic field such that the protons of tetramethylsilane resonate at precisely 100 MHz. We have followed the procedure of White and Olah (3*f*) which is based on the relationship formulated by Paul and Grant (3*g*), *i.e.* eq. 1.

$$[1] \qquad \delta^{13}C = \frac{\Gamma_i - \Gamma_{TMS}}{\Gamma_{TMS}} \times 10^6 + \delta_H$$

where $$\Gamma_i = \frac{\text{frequency at which a particular proton is measured}}{\text{frequency of the corresponding } ^{13}C \text{ resonance}}$$

and δ_H = proton chemical shift (in p.p.m.) of the lock proton from tetramethylsilane

[7]Telonic Industry Inc., Beech Grove, Indiana.

Can. J. Chem. Downloaded from www.nrcresearchpress.com by 210.87.254.42 on 09/05/12
For personal use only.

TABLE 1. Resonance frequencies for the ^1H and ^{13}C resonances of tetramethylsilane (TMS)

Solution	^1H-Frequency (ν_0 MHz)	^{13}C-Frequency (f_0 MHz)	$\Gamma = \nu_0/f_0$
Neat TMS	100.002505	25.145632	3.9769334
TMS:acetone (7:3)	100.002505	25.145628	3.9769341
TMS:chloroform (1:1)	100.002505	25.145639	3.9769323

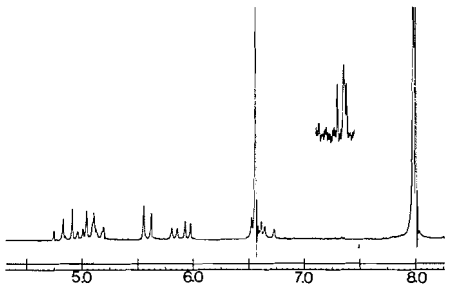

FIG. 2. The ^1H n.m.r. spectrum (100 MHz) of methyl 2,3,4-tri-*O*-acetyl-β-D-xylopyranoside (**4**) in $CDCl_3$ solution. The ^{13}C satellites of the methoxyl-methyl and acetate-methyl substituents, measured at higher gain, are shown as an insert.

We were concerned that our evaluation of Γ_{TMS} differed from the value (3.9769331) quoted both by White and Olah (3*f*) and by Paul and Grant (3*g*). Repeated evaluation of this parameter gave the value listed in Table 1. The difference between these values is noteworthy. The value for neat tetramethylsilane was used for the conversion of the data obtained for aqueous solutions and the value for chloroform solution was used for the data from chloroform solutions.

The values for $\delta^{13}C$ given in Tables 2 and 3 were also calculated using the formula given in reference 4*b*. Identical values were obtained.

Results and Discussion

The normal ^1H n.m.r. spectrum of methyl 2,3,4-tri-*O*-acetyl-β-D-xylopyranoside (**4**) is shown in Fig. 2. The high-field ^{13}C satellite of the methoxyl-methyl resonance, recorded at increased gain, is shown as an insert. The ^{13}C spectrum of the methoxyl-carbon, measured using the methods given in the Experimental section, is given in Fig. 3A. It will be noted that all of the peaks are negative-going; this indicates that the "spin-tickling" mechanism involving both population and energy level changes is the main process responsible for their occurrence (4). The ^{13}C spectrum of the methoxyl-carbon of methyl 2,3,4-tri-*O*-acetyl-α-D-xylopyranoside (**3**) is shown in Fig. 3B. It is obvious that this shift is significantly different from that of **4**.

The ^1H and ^{13}C parameters of the anomeric methoxyl resonances of derivatives **1**–**4** and **6**–**9** are summarized in Table 2. Although there is a systematic difference between the ^1H chemical shifts of the α- and β-anomeric pairs of derivatives, this is so small that it could not be used with confidence as the basis for a configurational assignment. The ^{13}C chemical shift difference is also systematic, with that of the β-anomer coming to *higher* frequency (*lower* field) in every instance. Furthermore, the shift difference is now sufficiently large for it to be used with confidence for structural assignments. Interestingly, the shift difference appears to be slightly larger for the methyl glycosides than it is for the methyl glycoside peracetates.

The ^{13}C–^1H couplings for the methoxyl-methyl substituents are also listed in Table 1. The values lie between 143 and 148 Hz and do not appear to have any diagnostic significance.

In contrast to the above findings, where ^{13}C shifts of methoxyl resonances appear to be more useful than ^1H shifts for structural assignments, it is evident that the converse is true for the acetate substituents. The data obtained for several acetylated pyranose derivatives are summarized in Table 3. The ^{13}C shifts of the acetate-methyl groups all fall within a rather narrow range, with no immediately obvious dependencies, beyond the trivial fact that they fall *ca.* 1 KHz (40 p.p.m.) to low frequency of those of methoxyl-methyl groups.

Had the acetate-methyl shifts had any diagnostic value, we had originally planned to exploit one of the advantages which INDOR spectroscopy has over the direct-measurement method. Horton and Lauterbach (9) had previously identified the ^1H resonances of the individual acetate-methyl resonances of several pyranose

Can. J. Chem. Downloaded from www.nrcresearchpress.com by 210.87.254.42 on 09/05/12
For personal use only.

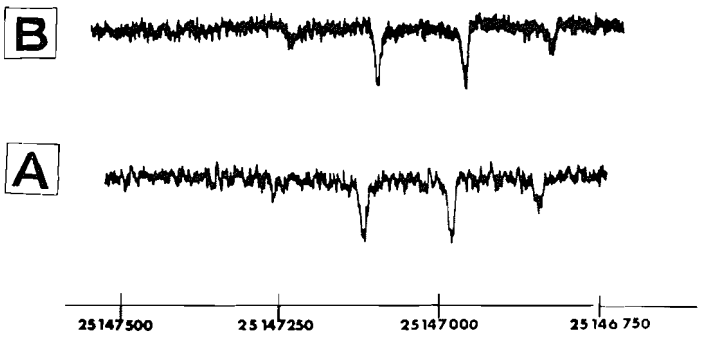

FIG. 3. Natural-abundance, ^{13}C resonances, measured by the ^{1}H-{^{13}C} INDOR technique; A, the methoxyl-methyl carbon of methyl 2,3,4-tri-*O*-acetyl-β-D-xylopyranoside (**4**); B, the methoxyl-methyl carbon of methyl 2,3,4-tri-*O*-acetyl-α-D-xylopyranoside (**3**).

TABLE 2. The ^{1}H and ^{13}C n.m.r. parameters for methoxy-methyl resonances of pyranose derivatives

Compound		^{1}H Shifts		^{13}C Shifts			$J_{^{13}C-^{1}H}$ (Hz)
		τ OMe	Δτ*	$\nu^{13}C$†	$\delta^{13}C$‡	Δδ§	
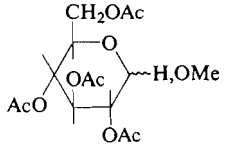	α-(**1**)‖	6.590	0.080	25.147025	55.12	1.58	148
	β-(**2**)‖	6.510		25.147065	56.70		143
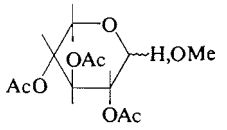	α-(**3**)‖	6.610	0.075	25.147029	55.27	1.36	147
	β-(**4**)‖	6.535		25.147063	56.63		145
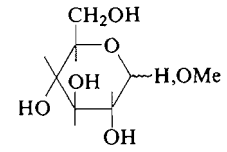	α-(**6**)¶	6.060	0.190	25.147051	56.43	2.26	144
	β-(**7**)¶	5.870		25.147108	58.69		145
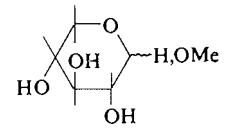	α-(**8**)¶	6.085	0.095	25.147056	56.63	1.98	145
	β-(**9**)¶	5.990		25.147106	58.61		148

*{τ OMe_{α} − τ OMe_{β}}.
†Chemical shift, in Hz, measured at a magnetic field such that the protons of tetramethylsilane resonate at 100.000000 MHz.
‡Chemical shift, in p.p.m. re ative to that of tetramethylsilane; see Experimental and Table 1. It should be noted that a higher resonance frequency corresponds to a lower field chemical shift.
§{$\delta^{13}C_{\beta} - \delta^{13}C_{\alpha}$}.
‖In $CDCl_3$ solution.
¶In D_2O solution.

peracetates via a study of a series of specifically trideuteroacetylated derivatives. Their study thus provided the assignment of the individual ^{13}C satellites of the acetate-methyl resonances which in turn, would have enabled the ^{13}C shifts of the acetate-methyl resonances to be assigned. To make a similar assignment of these ^{13}C resonances by the direct-measurement technique would have required us to repeat the original syntheses of the specifically trideuteroacetylated

Can. J. Chem. Downloaded from www.nrcresearchpress.com by 210.87.254.42 on 09/05/12
For personal use only.

TABLE 3. The ^{13}C n.m.r. parameters for the acetoxy-methyl resonances of pyranose sugars

Compound	Chemical shifts $\nu^{13}C$*	Chemical shifts $\delta^{13}C$†	$J_{^{13}C-^{1}H}$ (Hz)
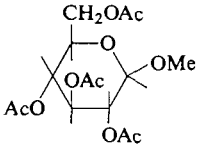 **2**‡	25.146157	20.59	130
	25.146157	20.59	131
	25.146160	20.72	130
	25.146156	20.54	130
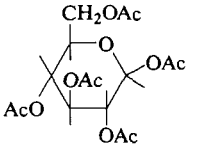 **5**‡	25.146159	20.67	131
	25.146157	20.59	131
	25.146157 (2 ×)	20.59 (2 ×)	130
	25.146156	20.54	131
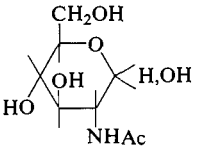 **10**§	25.146220	23.08	131
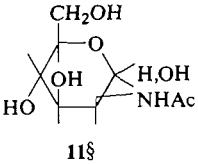 **11**§	25.146217	22.98	131

*Chemical shift, in Hz, measured at a magnetic field such that the protons of tetramethylsilane resonate at 100.000000 MHz. These data are given in the order for which the ^{13}C-satellites of the proton spectrum were monitored, which is from low- to high-field.

†Chemical shift, in p.p.m. relative to that of tetramethylsilane, see Experimental and Table 1. It should be noted that a higher resonance frequency corresponds to a lower field chemical shift.

‡In $CDCl_3$ solution.

§In D_2O solution.

compounds. Although this intention was frustrated in this instance, it remains that the assignment of ^{13}C resonances via the known assignment of a proton spectrum is a most useful technique.

We took this opportunity to measure the methyl ^{13}C shifts of two acetamido derivatives. These data are also reported in Table 3; again, these shifts appear to have no diagnostic value, even though they are *ca.* 50 Hz (2 p.p.m.) removed from the *O*-acetyl-methyl shifts.

In summary, the ^{13}C shifts of the methyl groups of *O*-methyl, *O*-acetyl, and *N*-acetyl substituents of carbohydrate derivatives can be readily measured by the INDOR method and the shifts of the methoxyl-methyl substituents have a pronounced stereospecific dependence which has some diagnostic potential. The INDOR method appears to have several important advantages over the direct measurement approach for obtaining the *natural-abundance*, ^{13}C spectra of methyl substituents. For example, spectra can be obtained on a rapid, *single-scan*, basis using moderate concentrations and 5 mm o.d. n.m.r. tubes. However, it is quite obvious that these advantages do not apply as directly to the measurement of the ^{13}C shifts of other substituents such as the ring-carbons of pyranose sugars. For such resonances, it is probably best

Can. J. Chem. Downloaded from www.nrcresearchpress.com by 210.87.254.42 on 09/05/12
For personal use only.

to use direct-measurement methods which are, mercifully, becoming less time consuming (1) than they were.

We have used the apparatus outlined in this paper to measure on a routine-basis the resonances of a number of other nuclear species, including ^{2}H, ^{19}F, ^{29}Si, ^{31}P, ^{117}Sn, ^{119}Sn, ^{199}Hg, and ^{207}Pb; we shall report on these studies elsewhere.

We thank the National Research Council of Canada for their generous financial support, especially for the equipment grant (E 1338) for the frequency synthesizer which forms the basis of our INDOR spectrometer. The digital programmer was purchased with funds from the President's Research Fund of the University of British Columbia. It is a pleasure to thank Professor C. A. McDowell for his continued interest.

1. (*a*) L. D. HALL and L. F. JOHNSON. Chem. Commun. 509 (1969). (*b*) D. E. DORMAN and J. D. ROBERTS. J. Amer. Chem. Soc., **92**, 1355 (1970). (*c*) A. S. PERLIN, B. CASU, and H. J. KOCH. Can. J. Chem. **48**, 2596 (1970).
2. E. B. BAKER. J. Chem. Phys. **37**, 911 (1962).
3. (*a*) R. FREEMAN and W. A. ANDERSON. J. Chem. Phys. **39**, 806, (1963); (*b*) R. FREEMAN. J. Chem. Phys. **40**, 3571 (1964); (*c*) J. H. ALLEN, J. K. BECCONSALL, and D. W. TURNER. J. Sci. Instrum. **41**, 673 (1964); (*d*) W. J. HORSELY and H. STERNLICHT. J. Amer. Chem. Soc. **90**, 3738 (1968); (*e*) F. W. WEHRLI and W. SIMON. Helv. Chim. Acta, **52**, 1749 (1969); (*f*) A. M. WHITE and G. A. OLAH. J. Amer. Chem. Soc. **91**, 2943 (1969), and references therein; (*g*) E. G. PAUL and D. M. GRANT. J. Amer. Chem. Soc. **86**, 2977 (1964).
4. (*a*) R. HOFFMAN and S. FORSEN. *In* Progress in n.m.r. spectroscopy. J. W. Emsley, J. Feeney, and L. H. Sutcliffe, *editors*. Pergamon Press, 1966; (*b*) W. MCFARLANE. *In* Annual reviews of n.m.r. spectroscopy. Vol. 1. E. F. Mooney, *editor*. Academic Press, 1968; (*c*) V. J. KOWALEWSKI. *In* Progress in n.m.r. spectroscopy. *Edited by* J. W. Emsley, J. Feeney, and L. H. Sutcliffe. Pergamon Press, 1969.
5. R. BURTON, L. D. HALL, and P. R. STEINER. Can. J. Chem. **48**, 2679 (1970).
6. J. S. BACON and D. J. BELL. J. Chem. Soc. 1869 (1939).
7. C. S. HUDSON and H. P. PARKER. J. Amer. Chem. Soc. **37**, 1589 (1915).
8. R. BURTON and L. D. HALL. Can. J. Chem. **48**, 59 (1970).
9. D. HORTON and H. LAUTERBACH. J. Org. Chem. **34**, 86 (1969).

Can. J. Chem. Downloaded from www.nrcresearchpress.com by 210.87.254.42 on 09/05/12
For personal use only.

Can. J. Chem. Downloaded from www.nrcresearchpress.com by 210.87.254.42 on 09/05/12
For personal use only.

Effect of an External Heavy Atom on the Photochemistry of Monofluorobenzene Vapor. II

M. E. MacBeath and I. Unger

Department of Chemistry, University of New Brunswick, Fredericton, New Brunswick

Received August 25, 1970

The effect of added Xe on the singlet and triplet yields of monofluorobenzene vapor excited at 2670, 2520, and 2470 Å has been reinvestigated. The fluorescent yields, and hence the singlet yields, were monitored directly while triplet yields were determined by both the sensitized emission of biacetyl technique and the isomerization of olefins technique. The data obtained confirm that Xe enhances intersystem crossing in monofluorobenzene (1). However, contrary to results previously published from this laboratory (1), Xe does not quench the triplet state of biacetyl.

Canadian Journal of Chemistry, 49, 594 (1971)

Introduction

It has been established that Xe enhances singlet–triplet transitions in all phases (2–5). The effect appears to be most marked in liquid phase and it was recently reported (6) that for benzene solutions irradiated at 254 nm, a [Xe] of 0.2 *M* completely converts all the benzene singlets to the triplet state. A communication (1) from this laboratory indicated that Xe promoted intersystem crossover in monofluorobenzene (FB) vapor excited at 2470, 2520, and 2670 Å. It was also suggested, in the previous report (1), that Xe could quench the phosphorescent emission of biacetyl (BiA) by the reaction

$$^3\text{BiA} + \text{Xe} \rightarrow \text{BiA} + \text{Xe}$$

Further work (7) on the photochemistry of BiA excited at various wavelengths and with a number of added inert gases including Xe showed that the above reaction did not occur. Consequently it was decided to reexamine the effect of Xe on FB and to monitor the triplet yield of FB by both the sensitized emission of BiA technique (8), as was the case previously (1), and by the isomerization of olefins technique (9).

Experimental

Materials

The monofluorobenzene used was obtained from the Aldrich Chemical Company and used without further purification after a vapor phase chromatographic (v.p.c.) check showed it to be 99.98% pure. The biacetyl, from the same company, was stored in a dark bulb and purified by bulb-to-bulb distillation in vacuo. The xenon was "Research Grade" from Matheson Company and was used without purification since the only impurity quoted was 10 p.p.m. of krypton. Similarly, Philips research grade *cis*-butene-2 having less than 0.1% impurity was used without further purification. The CO_2 was obtained from "Dry Ice" by bulb-to-bulb sublimation *in vacuo*, only the middle portion being retained for use. All materials were thoroughly out-gassed prior to use.

A modified Aminco-Bowman spectrophotofluorometer was used for all emission and absorption measurements. Experimental details concerning the light source, slit widths, band pass, method of obtaining absorption and emission measurements, and correction factors have been given previously (10) except that an R136 potted photomultiplier tube (Aminco: No. C156-62140) was used for viewing emission.

The vacuum system was exactly the same as that described in ref. 1.

For the isomerization experiments two quartz cylindrical cells were used, 10 cm long by 5 cm in diameter. The light source employed was a compact arc Hg–Xe 1000 W lamp from Hanovia (No. 1-5080-000). It was operated at 27 A and 26 V d.c., and cooled by air flow to 110–130 °C during operation. The beam from this lamp was focused on a 6.0 mm entrance slit of the first of two 0.25 m Ebert Monochromators operating as a double monochromator (Model 82-410 obtained from Jarrell-Ash Company). The exit slit from the second monochromator was 2 mm. This arrangement gave the following spectral distributions

Setting (Å)	Range (Å)	Maximum intensity (Å)	Half band width (Å)
2470	2390–2490	2445	52
2520	2495–2530	2523	10
2660	2600–2685	2657	28

The emerging light beam was made to strike a torroidal mirror placed at a 45° angle off axis and 3 cm from the exit slit of the second monochromator. This mirror, 7.5 cm in diameter, had a tangential radius of 41.19 cm and a sagittal radius of 20.60 cm. The reflected beam impinged on a diagonal beam splitting plate, 7 cm away. This plate of fused quartz and achromatic from 2000 Å to the visible was made by the Continental Optical Corporation (Farmington, New York). It was 3 in. in diameter, parellel to 2 in. with its two surfaces flat to 1/20 wave and had transmission approximately equal to reflection. The split beam then passed through the cells

Can. J. Chem. Downloaded from www.nrcresearchpress.com by 210.87.254.42 on 09/05/12
For personal use only.

(labelled A and B) containing the samples to be photolyzed. Cell B always contained 10 Torr FB and 100 Torr *cis*-butene-2 while cell A in control experiments contained exactly the same mixture. In those photolyses when the effect of Xe was being studied, both cells contained the same mixture as in control experiments except that a given pressure of Xe was put into cell A. A Hg- and grease-free high vacuum system equipped with Hoke metal valves was used for filling the cells and in obtaining samples from them.

Samples from the cells after photolysis were analyzed by v.p.c. on a Model 500 Linear Programmed Temperature Gas Chromatograph made by the F and M Scientific Corporation. A 25 ft column containing 15% dinonylphthalate on Chromosorb P was used at 35 °C with helium carrier gas and a flow rate of 45 cc/min. The retention time for *trans*-butene-2 was 13 min 40 s; for *cis*-butene-2, 14 min 10 s.

Results and Discussion

All emission yields reported in this paper are on a relative basis, they may be converted to absolute values by referring to absolute fluorescent yields given previously (11).

Addition of Xe to FB excited at 2470, 2520, and 2670 Å produces a decrease in the fluorescent emission yield and plots of $1/\Phi_f$ *vs.* Xe are linear, see Fig. 1. The above is also true when Xe is added to mixtures of FB and BiA, see Fig. 2. The fluorescent data substantiate those reported previously (1) and thus will not be discussed extensively here. However, it should be noted that other added gases (CO_2, $CHCl_3$) do not quench the fluorescent yield (10).

Addition of Xe to mixtures of FB and BiA produces an increase in the sensitized emission yield at all exciting wavelengths studied, see Fig. 3. While this behavior is completely contrary to that noted previously (1) for the Xe, FB, BiA system, it is consistent with the known photochemical behavior of BiA excited below 4000 Å (12).[1] Furthermore this sort of effect should be expected since the triplet of FB is estimated to lie at 80 kcal (13). Consequently energy transfer from FB triplets to BiA will result in BiA triplets whose energy would be more nearly equivalent to those formed from the direct excitation of BiA at about 3600 rather than 4358 Å. Such BiA triplets are vibrationally hot and will dissociate, without emitting, unless a vibrational quencher

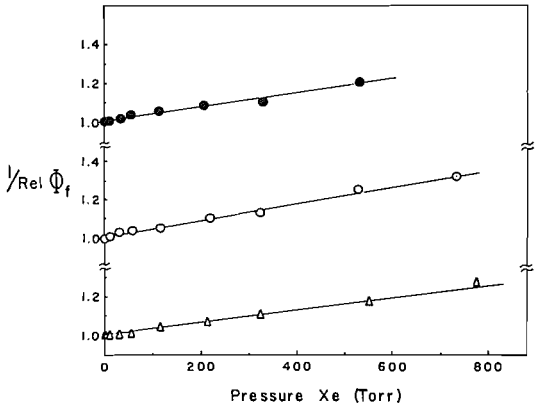

FIG. 1. The effect of Xe on the relative fluorescent yield of FB excited at 2470 Å, △; 2520 Å, ○; 2670 Å, ●. FB pressure constant at 10 Torr.

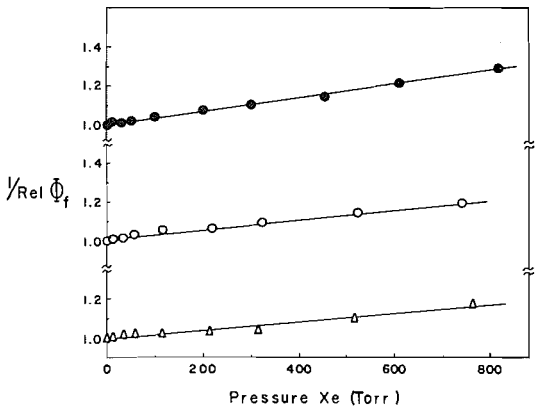

FIG. 2. The effect of Xe on the relative fluorescent yield of mixtures of FB and BiA, excited at 2470 Å, △; 2520 Å, ○; 2670 Å, ●. FB pressure = 10 Torr, BiA pressure = 5 Torr.

is present. We suggest therefore that in the system FB–BiA, the addition of Xe serves both to enhance intersystem crossover from the FB singlet to the triplet and to quench vibrationally hot triplet BiA molecules, thus causing an increase in the sensitized emission yield of BiA. Consequently the sensitized emission of BiA technique cannot be used to establish whether or not Xe enhances intersystem crossover in this system.

That the presence of Xe increases the triplet yield of FB, at all exciting wavelengths studied, is corroberated by the olefin isomerization experiments; the results are summarized in Table 1. The increase in triplet yield given in Table 1 should be fairly accurate in spite of the possibility

[1]A recent study done in this laboratory (7) indicates that when a sample of BiA vapor (at a pressure of 9 Torr) is irradiated at 3650 Å and Xe is added, the phosphorescent yield of BiA increases steadily, leveling off at around 400 Torr of Xe when the increase amounts to a little over 100% of the original quantum yield.

Can. J. Chem. Downloaded from www.nrcresearchpress.com by 210.87.254.42 on 09/05/12
For personal use only.

TABLE 1. Effect of various pressures of Xe and CO_2 on the quantum yield of triplet FB*

$\lambda_{excitation}$ (Å)	Xe pressure (Torr) cell A	CO_2 pressure (Torr) cell A	Ratio of *trans*-butene-2 cell A/cell B	% increase in triplet yield
2470	0	0	0.609±0.034†	0
2470	100	0	0.613±0.034	1.30
2470	300	0	0.665±0.017	18.2
2470	500	0	0.664±0.025	17.9
2470	0	300	0.648±0.022	12.7
2470	0	300	0.640±0.034	10.1
2520	0	0	0.585±0.003†	0
2520	100	0	0.602±0.033	5.7
2520	300	0	0.622±0.043	12.5
2520	300	0	0.619±0.020	11.5
2520	500	0	0.628±0.066	14.6
2520	0	300	0.589±0.027	1.4
2670	0	0	0.529±0.045	
2670	300	0	0.569±0.029	15.0

*FB pressure = 10 Torr, *c*-B-2 pressure = 100 Torr, in both cells. Cell B was used as a control containing no added CO_2 or Xe. Photolysis time = 9 h.
†Average value of 4 runs interspersed between runs with either CO_2 or Xe added in cell A.
‡The increase in the triplet yield was calculated, using recent values for the ratio of the rates of *cis–trans* isomerization (16, 17), i.e. (the difference in the amount of isomerization with and without added gas) × 1.98.

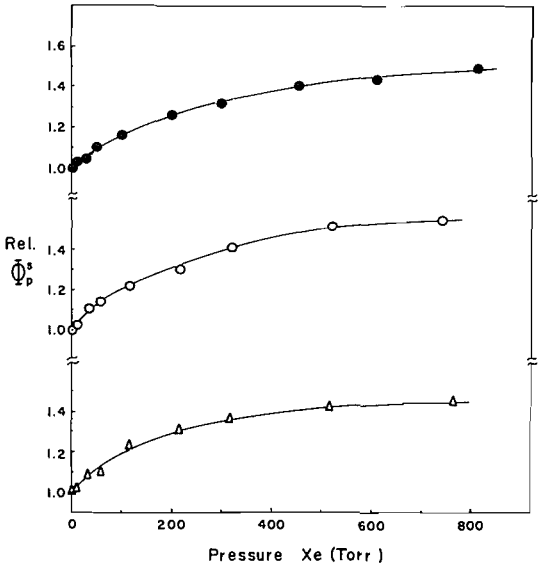

FIG. 3. The effect of Xe on the relative phosphorescent yield of BiA sensitized by FB excited at 2470 Å, △; 2520 Å, ○; 2670 Å, ●. FB pressure = 10 Torr, BiA pressure = 5 Torr.

of photo-adduct formation between FB and *cis*-butene-2 (*c*-B-2) since such reactions only occur in very small yield (14) and since the experimental set up was such that two identical cells containing identical mixtures of FB and *c*-B-2 were irradiated simultaneously by a beam of light originating from a single source, being split just prior to entering the cells. The only difference was that Xe was added to one of the cells. Finally, in order to be certain that the increase in triplet FB formation in the presence of Xe was not due to some sort of pressure effect, several experiments were carried out with added CO_2 in place of Xe. Addition of CO_2 does not markedly increase the triplet FB yield, except at 2470 Å. At 2470 Å, CO_2 prevents the dissociation of vibrationally hot singlet FB molecules, see Table 1.[2]

A kinetic scheme capable of explaining our experimental observations is given below

[1*a*] $FB + h\nu \rightarrow {}^1FB^I$

[1] ${}^1FB^I \rightarrow FB + h\nu_f$

[2] ${}^1FB^I \rightarrow {}^3FB^I$

[3] ${}^1FB^I + Xe \rightarrow {}^3FB^I + Xe$

[4] ${}^1FB^I + FB \rightarrow 2\ FB$

[5] ${}^3FB^I \rightarrow FB$

[2]The fluorescent yield of FB excited in the 2500 Å region has been given as 0.13 to 0.17 (10) depending on wavelength and the triplet yield in this region varies from 0.39 to 0.48 (10). Our fluorescence data indicate that the net decrease in the singlet yield at λ_{ex} 2470 Å and 500 Torr of Xe is 2%, at λ_{ex} 2520 Å and 500 Torr of Xe it is 3.5%, while at λ_{ex} 2670 Å and 300 Torr of Xe it is 2%. The isomerization studies show that the net increases in triplet yield at the same wavelengths and pressures are respectively ~ 3.2, 7.4, and 7.4%.

Can. J. Chem. Downloaded from www.nrcresearchpress.com by 210.87.254.42 on 09/05/12
For personal use only.

[6] $^1FB^I + BiA \rightarrow {}^1BiA^{II} + FB$

[7] $^3FB^I + BiA \rightarrow {}^3BiA_v^I + FB$

[8] $^1BiA^{II} \rightarrow$ Dissoc

[9] $^3BiA_v^I + M \rightarrow {}^3BiA_0^I + M$

[10] $^3BiA_0^I \rightarrow BiA + h\nu_p$

[11] $^3BiA_0^I \rightarrow BiA$

[12] $^3BiA_v^I \rightarrow$ Dissoc

In the above scheme arabic numerals denote spin multiplicity, roman numerals indicate 1st and 2nd excited states, the subscript 0 represents a molecule in its lowest vibrational level, the subscript v a molecule in a hot vibrational level, and M denotes any species capable of removing vibrational energy, or, in our case, the total pressure of FB, BiA, and Xe. This kinetic scheme differs only from the one suggested previously (1) in that it allows for the formation, dissociation, and vibrational deactivation of hot triplet BiA molecules. The scheme predicts (1) that plots of $1/\Phi_f$ *vs.* Xe pressure should be linear which is confirmed experimentally, see Figs. 1 and 2.

Application of the steady state treatment to this scheme gives for the phosphorescent emission yield of BiA

$$[13] \quad \Phi_p = \left(\frac{k_{10}k_9[M]}{k_{10} + k_{11}}\right)\left(\frac{k_7[BiA]}{k_4[M] + k_{12}}\right)\left(\frac{k_2 + k_3[Xe]}{k_5 + k_7[BiA]}\right) \times \left(\frac{1}{k_1 + k_2 + k_3[Xe] + k_4[FB] + k_6[BiA]}\right)$$

Our experimental observations indicate that k_3 is small, also it has been shown that k_2 is large (15); one may therefore neglect $k_3[Xe]$ with respect to k_2 and bearing in mind that in all the experiments the FB and BiA pressures were constant eq. 13 reduces to

$$[14] \quad 1/\Phi_p = K_1 + K_2/[M]$$

where K_1 and K_2 are collections of constants. Equation 14 predicts that a plot of $1/\Phi_p$ *vs.* 1/[M] should be linear. This prediction is confirmed experimentally at low pressures of Xe; at high pressures of Xe the assumption made above is not justified and the plots rapidly begin to deviate from linearity, see Fig. 4.

The only explanation that we can offer for the previous observation that Xe quenched the phosphorescent emission of BiA (1) is that trace quantities of O_2 must have been present in the previous study.

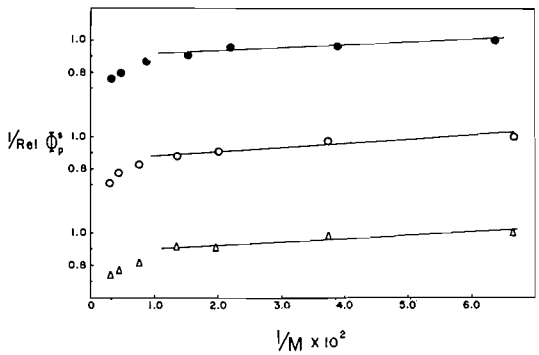

FIG. 4. Plots of $1/\Phi_p$ *vs.* 1/[M] excited at 2470 Å, △; 2520 Å, ○; 2670 Å, ●. FB pressure = 10 Torr, BiA pressure = 5 Torr, M = total pressure of FB + BiA = Xe.

The authors are grateful to the National Research Council of Canada for financial assistance and to Dr. G. P. Semeluk for many useful discussions.

1. A. COOK, G. P. SEMELUK, and I. UNGER. Can. J. Chem. **47**, 4527 (1969).
2. G. W. ROBINSON. J. Mol. Spectrosc. **6**, 58 (1961).
3. A. R. HORROCKS and F. WILKINSON. Proc. Roy. Soc. A**306**, 257 (1968).
4. R. B. CUNDALL and A. J. R. VOSS. Chem. Commun. 902 (1968).
5. C. S. BURTON and W. A. NOYES, JR. J. Chem. Phys. **49**, 1705 (1968).
6. R. B. CUNDALL and W. TIPPETT. Trans. Faraday Soc. **66**, 350 (1970).
7. S. H. NG, G. P. SEMELUK, and I. UNGER. To be published.
8. H. ISHIKAWA and W. A. NOYES, JR. J. Chem. Phys. **37**, 583 (1962).
9. R. B. CUNDALL and D. G. MILNE. J. Amer. Chem. Soc. **83**, 3902 (1961).
10. M. E. MACBEATH and I. UNGER. Can. J. Chem. **48**, 1607 (1970) and references therein.
11. M. MACBEATH, G. P. SEMELUK, and I. UNGER. J. Phys. Chem. **73**, 995 (1969).
12. J. G. CALVERT and J. N. PITTS, JR. Photochemistry. John Wiley and Sons, Inc., New York. 1966. p. 328ff.
13. D. F. EVANS. J. Chem. Soc. 2753 (1959).
14. A. MORIKAWA, S. BROWNSTEIN, and R. J. CVETANOVIC. J. Amer. Chem. Soc. **92**, 1471 (1970).
15. D. PHILLIPS. J. Phys. Chem. **71**, 1839 (1967).
16. S. SATO, K. KIKUCHI, and M. TANAKA. J. Chem. Phys. **39**, 239 (1963).
17. G. A. HARRINGER, JR. and E. K. C. LEE. J. Phys. Chem. **71**, 3104 (1967).

Can. J. Chem. Downloaded from www.nrcresearchpress.com by 210.87.254.42 on 09/05/12
For personal use only.

Chalkogenides of the Transition Elements. VIII. An X-Ray and Neutron Diffraction Study of the Spinel $CoNi_2S_4$[1]

CHUNG-HSI HUANG[2] AND OSVALD KNOP
Department of Chemistry, Dalhousie University, Halifax, Nova Scotia

Received August 26, 1970

The crystal structure of the spinel $CoNi_2S_4$ was refined from X-ray and neutron powder-diffractometer data. The lattice parameter at room temperature and the positional parameter of the sulfur atom were determined as 9.424(1) Å and 0.2591(3). The neutron intensities show clearly that $CoNi_2S_4$ is an inverse spinel, $Ni[CoNi]S_4$.

Canadian Journal of Chemistry, 49, 598 (1971)

In a previous investigation by X-ray and neutron diffraction (1) it was established that the spinel $NiCo_2S_4$ is normal or essentially normal, $Ni[Co_2]S_4$. The analogous spinel $CoNi_2S_4$ was prepared by Bouchard *et al.* (2), who reported its lattice parameter but did not refine its structure or determine the distribution of the Co and Ni atoms. This has now been done by X-ray and neutron powder diffraction.

Experimental

The sample (120 g) for neutron diffraction was prepared by direct synthesis from the elements *in vacuo* (sample I). Freshly reduced high-grade cobalt and nickel powders (Sherritt-Gordon Grade S) and sublimed sulfur were slowly reacted by raising the furnace temperature gradually to 500°. The product was ground to pass 100 mesh, thoroughly mixed by repeated screening, resealed under vacuum and kept at 550° for 3 days. The procedure was then repeated and the powder annealed successively at 600° for 2 days, 550° for 5 days, and 500° for 6 days; ground again and kept at 500° for one month; and finally at 500° for 20 days. In each annealing step the sample was cooled from 500° to room temperature at an average rate of 50°/day and the condition of the product was examined by powder diffraction.

For comparison, a 15 g sample was prepared in a similar manner from spectrographic-grade elements (sample II). After the final annealing both samples were homogeneous and their lattice parameters were practically the same (Table 1). Both were slightly larger than the a_0 reported in ref. 2.

Density of sample I was determined by weighing in air and in CCl_4 (for details of method *cf.* ref. 15). The mean of 4 determinations at 22.5(5)° was 4.756(8) g/cm³. This is 1.6(3)% lower than the density calculated from a_0 and $N = 6.0226 \times 10^{23}$, 4.829(3) g/cm³, which indicates that the intrinsic vacancy concentration could not have been unusually high.

Integrated X-ray diffraction intensities from sample I were obtained with a Philips powder diffractometer fitted with a focussing monochromator after the rotating specimen. This arrangement gave very low background counts. Copper K radiation ($\lambda_{\alpha_1} = 1.54056$ Å, $\lambda_{\alpha_2} = 1.54440$ Å) was used throughout. For details of specimen preparation (smear mounts), counting, etc., refs. 1 and 16 may be consulted.

The neutron-diffraction experiments were performed at the NRX reactor of Atomic Energy of Canada Limited at Chalk River, Ontario. The neutron beam was monochromatized by Bragg reflection from the (111) plane of

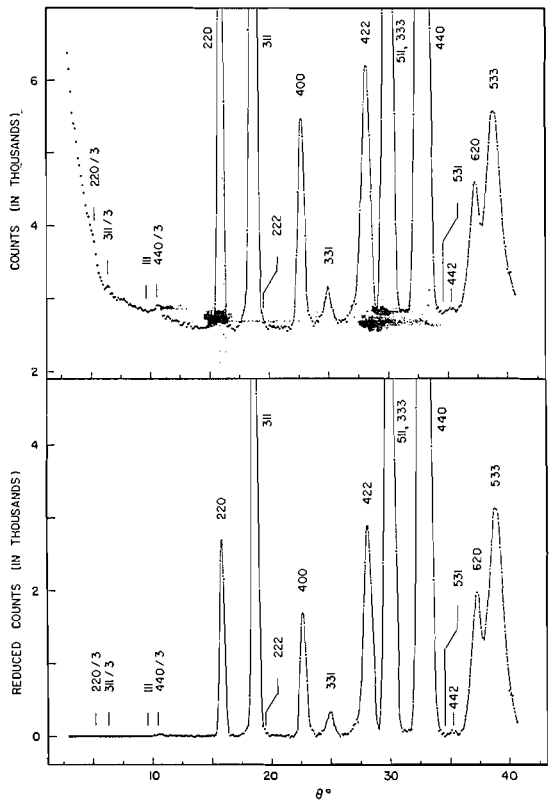

FIG. 1. Raw (*top*) and reduced (pF^2; *bottom*) neutron diffraction patterns of $CoNi_2S_4$ at room temperature. Monochromator, Ge(111); $\lambda = 1.801$ Å; average counting time per point, 8 min.

[1]For Part VII, see ref. 15.
[2]INCO Graduate Fellow, 1968–1970.

TABLE 1. Lattice parameters, positional parameters, and M—S distances in sulfospinels of Fe, Co, and Ni

Compound	a_0 (Å)*	x(S)	M^{IV}—S (Å)†	M^{VI}—S (Å)†	Reference
$Co[Co_2]S_4$	9.399(2)				2
	9.406(2)	0.2588(9)	2.179(46)	2.271(24)	1‡
$Ni[Co_2]S_4$	9.384(2)				2
	9.387(1)	0.2588(4)	2.174(20)	2.268(11)	1‡
$Ni[CoNi]S_4$	9.418(2)				2
	(I) 9.427(1)	0.2591(3)	2.190(15)	2.274(8)	This work
	(II) *9.424(1)*				This work
$Ni[Ni_2]S_4$	9.476§	0.260**			3
	9.477(1)§				4
	9.480(3)				5
	9.480(1)				6
$Cu[Co_2]S_4$¶	9.482‖				7
	9.461(2)				2
$FeNi_2S_4$	9.464§				8
	9.463(3)				5
Fe_3S_4 (synthetic)	9.870				9
(greigite)	*9.876(2)*	0.2505(38)	2.15(20)	2.46(10)	10
(synthetic)	9.90				11

*Values in italics are those used in calculating the interatomic distances and for comparing lattice parameters.
†The distances (not corrected for thermal motion) have been calculated from the listed x(S) and a_0 values using $3\sigma(x)$ and $2\sigma(a_0)$.
‡Re-refined from diffraction data of ref. 1.
§Converted from *k*X.
‖Contained traces of a second phase.
¶This spinel has been formulated as $Cu^+[Co_{1.5}^{3+}\ Co_{1.5}^{4+}]S_4$ (12–14).
**Converted from −0.135 using an alternative choice of origin.

a squeezed Ge crystal ($\lambda = 1.801$ Å, $2\theta_M = 32.0°$). This choice of wavelength and a single-crystal quartz filter 5 in. thick practically eliminated the third-order contamination of the incident beam. The raw diffraction pattern was reduced to a pF^2 pattern (Fig. 1) and the peaks were fitted (and resolved, where necessary) by Gaussian analysis.

The origin of the unit cell of the spinel structure (space group *Fd3m*) was taken at the center of symmetry. Cromer and Waber's X-ray scattering factors (17) and dispersion corrections (both parts; ref. 18) for Co and Ni, and neutron scattering amplitudes listed in ref. 19, were used in full-matrix least-squares refinements (*cf.* ref. 1 for other details). Weighting scheme W3 was normally employed in refinements from $|F_o|$, while in refinements from intensities the weights were defined as $w(hkl) = \varepsilon^{-1}(hkl)$ (*cf.* ref. 20).

Results and Discussion

Refinement from X-Ray Data

The 40 integrated powder intensities that were measured correspond to the 53 reflections possible in *Fd3m* up to and including 10.6.0 + 866. The refinements from intensities thus included all the information obtainable from a powder specimen of $CoNi_2S_4$ within this volume of the Cu K_α sphere of reflection. These refinements and *F*-refinements from the 28 single reflections in the measured set gave practically identical values of x(S), regardless of whether individual isotropic temperature factors or an overall temperature factor were employed (Table 2). There was no significant difference, at the 50 or 25% levels (21), between results which were obtained using neutral scattering factors, ionic scattering factors, and different cation distributions. However, it was found that *I*-refinements gave best results when the weighting scheme $\varepsilon^{-1}(hkl)$ was employed, while the *F*-refinements responded best to the weighting scheme W3.

The value of 0.2591(3) is considered to be the best estimate, from the present investigation, of

TABLE 2. Results of full-matrix refinements of $CoNi_2S_4$ from X-ray data (Cu K_α)*

Refinement	*A*	*E*
Input	28 $\|F_o\|$	40 I_o
Weighting scheme	W3	$\varepsilon^{-1}(hkl)$
After cycle	12	7
x(S)	0.2590(3)	0.2592(2)
$B(8a)$, Å²	0.37(7)	0.37(6)
$B(16d)$, Å²	0.64(6)	0.58(7)
B(S), Å²	0.28(6)	0.41(6)
R, %; R_w, %	1.88; 1.44	—
$D(\Delta I)$, %; $D(I)$	2.40; 994†	2.16; 1001‡
e.s.d.(w)	0.73	14 853

*Scattering factors for neutral atoms; inverse model. Estimated standard deviations are expressed in the form 0.2590(3) = 0.2590 ± 0.0003. Symbols: $R = \Sigma[\Delta|F|/\Sigma|F_o|$; $R_w = [\Sigma w(|F_o| - |F_c|)^2/\Sigma w|F_o|^2]^{\frac{1}{2}}$; $D(\Delta I) = \Sigma|\Delta I|/\Sigma I_o$; $D(I) = 1000\Sigma I_c/\Sigma I_o$; e.s.d.($w$) = e.s.d. × $(\Sigma w)^{-\frac{1}{2}}$.
†For reflections used in the refinement. For all possible reflections up to and including 10.6.0 + 866 the corresponding figures were 2.83% and 988.
‡For all possible reflections up to and including 10.6.0 + 866.

Can. J. Chem. Downloaded from www.nrcresearchpress.com by 210.87.254.42 on 09/05/12
For personal use only.

Can. J. Chem. Downloaded from www.nrcresearchpress.com by 210.87.254.42 on 09/05/12
For personal use only.

x(S) in $CoNi_2S_4$. The agreement of $|F_o|$ and F_c is shown in Table 3.

Refinement from Neutron-diffraction Data

The raw pattern was of a better quality than a similar pattern obtained previously for $NiCo_2S_4$ with an Al(111) monochromator (1). Twelve of the 14 peaks extracted from the reduced pattern corresponded to single reflections and were used in F-refinements (Table 4). In spite of uncertainties in the baseline correction the three-parameter refinement based on a completely inverse distribution, Ni[CoNi]S_4, gave very reasonable values of R and e.s.d.(w) (*cf.* the corresponding figures for $NiCo_2S_4$ in ref. 1). As might be expected, the scale factor was strongly correlated with the temperature factor (0.516), but the other two correlations were weak. The x(S) value was quite close to those obtained in the X-ray refinements.

TABLE 3. Observed and calculated intensities for X-ray and neutron diffraction

	X-Rays (refinement E)*			Neutrons†	
hkl	$10\,I_o$	$10\,I_c$	$10\,I_o'$	pF_o^2	pF_c^2
111	164	172	168	0.0	0.0
220	311	311	313	9.7	9.8
311	1000	1000	1000	31.9	30.8
222	20	17	20	0.0	0.0
400	592	592	583	8.3	8.5
331	2	0	2	1.5	1.5
422	108	107	104	18.4	18.4
511, 333	481	469	457	53.7	50.2
440	886	926	829	97.5	100
531	31	26	28	0.0	0.1
442	2	1	1	0.2	0.1
620	38	37	34	17.4	17.4
533	109	106	99	30.4	29.5
622	6	3	6		
444	113	111	101		
711, 551	32	30	29		
642	56	57	49		
731, 553	149	147	129		
800	130	128	112		
733	8	7	7		
644	0	0	0		
822, 660	28	28	24		
751, 555	106	104	91		
662	4	3	3		
840	140	141	120		
911, 753	16	15	14		
842	1	2	1		
664	6	5	5		
931	101	103	88		
844	289	286	254		
933, 771, 755	10	10	9		
10.2.0, 862	24	27	22		
951, 773	143	147	129		
10.2.2, 666	6	4	5		
953	24	22	22		
864	1	2	1		
10.4.2	10	11	10		
11.1.1, 775	17	16	16		
880	148	144	143		
10.6.0, 866	21	21	21		

*The intensities have been normalized to $I_c(311) = 100$. These monochromatized integrated intensities are converted to conventional integrated intensities I' by multiplication by the ratio of the polarization factors, $(1 + \cos^2 2\theta)/(1 + 0.66 \cos^2 2\theta)$.

†Inverse model. The pF_c^2 values are based on the F-refinement using individual isotropic temperature factors (see text). The reduced intensities have been normalized to $pF_c^2(440) = 100$.

The results of the refinements for random and normal distributions were very poor (Table 4). Compared with the inverse model they could be rejected at the 0.5% significance level. The drastic increase in R from the inverse to the random model shows unmistakeably that the inverse ordering is complete or very nearly so: R or e.s.d.(w) plotted against the ordering parameter s give straight lines.[3] A separate K,s,B-refinement based on x(S) = 0.2591 resulted in a value of s that corresponds clearly to an inverse arrangement, 0.00(2) (Table 4).

The observed and calculated pF^2 values for the inverse model are compared in Table 3, and a comparison of the reduced intensities is shown for all three models in Fig. 2. The trend, with increasing θ, toward low F_c values was removed by using individual temperature factors instead of B(overall), but $B(8a)$ tended to assume negative indefinite values, and the B's were strongly correlated among themselves and with the scale factor; an exception was $B(16d) - B$(S). Since the positional parameter refined to 0.2592(2), further attempts to improve on the pF^2 agreement were abandoned.

Interatomic Distances

These are compared in Table 1 with similar distances in a number of related sulfospinels. Since in Co_3S_4, $NiCo_2S_4$, and $CoNi_2S_4$ the numerical values of x(S) are very similar, the M—S distances are determined essentially by the lattice parameter a_0. The differences in a_0 being real (*i.e.*, well outside the standard deviations), the differences between the corresponding Co—S and Ni—S distances, though slight, should also be real. On the other hand, $\delta(M^{IV}—S) \simeq 17\,\delta x + 0.22\,\delta a_0$ and $\delta(M^{VI}—S) \simeq -9\,\delta x + 0.24\,\delta a_0$. For typical values of $\delta x = 3\sigma(x) = 0.001$ and $\delta a_0 = 2\sigma a_0 = 0.002$ Å one has $\delta(M^{IV}—S) = (0.017 + 0.0005)$ Å and $\delta(M^{VI}—S) = (-0.009 + 0.0005)$ Å. Hence the distances are much more sensitive to variations in x(S) than to variations in a_0. This must be taken into

[3] *Cf.* ref. 1 for definition of s.

TABLE 4. Results of full-matrix refinements of $CoNi_2S_4$ from neutron data

Nature of refinement	No. of cycles	x(S)	B(overall) (Å^2)	s	R (%)	R_w (%)	e.s.d.(w)
K,x,B							
Inverse, $s = 0$	8	0.2577(27)	1.24(22)	—	4.83	4.05	0.14
Random, $s = \frac{1}{3}$	6	0.2410(134)	0.89(124)	—	22.54	19.90	0.71
Normal, $s = 1$	15	0.2422(391)	−4.04(290)	—	60.36	45.99	1.90
K,s,B							
s (initial) $= \frac{1}{3}$	22	—	1.12(20)	0.000(21)	4.62	3.83	0.14

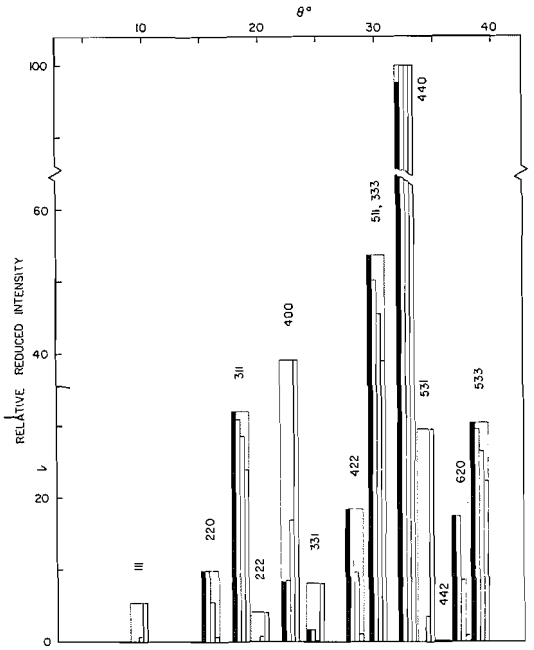

FIG. 2. Comparison of the reduced (pF^2) neutron diffraction pattern of $CoNi_2S_4$ with the pF^2 patterns calculated for the three assumed model structures. The individual peak heights in each composite column correspond, from left to right, to the observed pattern, to the completely inverse, to the random, and to the completely normal distributions, respectively. The relative reduced intensities have been normalized to pF_c^2(440).

account when considering the apparent constancy of x(S) in the three sulfides in the light of the respective $3\sigma(x)$ estimates. For example, while the independent estimates of Co^{VI}—S in Co_3S_4 and $NiCo_2S_4$ are very similar and appear to support the optimistic view of the accuracy of determination of this interatomic distance, the independent estimates of the Ni^{IV}—S distances in $NiCo_2S_4$ and $CoNi_2S_4$ differ by 0.016 Å, which in magnitude is almost three times the difference between Co^{IV}—S in Co_3S_4 and Ni^{IV}—S in $CoNi_2S_4$. All these differences are however within their respective error estimates.

The uncertainties in x(S) and the smallness of the differences in the lattice parameters and M—S distances render interpretations of the oxidation and spin states in the four $(Co,Ni)_3S_4$ spinels from dimensional arguments largely speculative. The Co^{VI}—S distance in Co_3S_4 and $Ni[Co_2]S_4$, 2.27 Å, is significantly smaller than similar distances in CoS_2 (*C*2) and Co_9S_8, 2.32 and 2.39 Å respectively (1). If cobalt is present in CoS_2 as Co_{LS}^{2+} (*cf.* ref. 1), then Co^{VI} in Co_3S_4 would appear to be at least partly Co^{3+} and probably Co_{LS}^{3+} (*cf.* ref. 7), so that Co_3S_4 could be formulated as $Co_{HS}^{2+}[Co_{LS}^{3+}\ Co_{LS}^{3+}]S_4$.[4] The analogous formulation of $Ni[Co_2]S_4$ as $Ni_{HS}^{2+}[Co_{LS}^{3+}\ Co_{LS}^{3+}]S_4$ would seem to account for the increase of 0.037(4) Å in a_0 from $Ni[Co_2]S_4$ to $Ni[CoNi]S_4 = Ni_{HS}^{2+}[Co_{LS}^{3+}\ Ni_{LS}^{3+}]S_4$, and for the further increase of 0.056(6) Å from $Ni[CoNi]S_4$ to $Ni_3S_4 = Ni_{HS}^{2+}[Ni_{LS}^{3+}Ni_{LS}^{3+}]S_4$, even though the observed increase in M^{VI}—S from $Ni[Co_2]S_4$ to $Ni[CoNi]S_4$ is very small, if any, 0.006(14) Å. However, substitution of the tetrahedrally-coordinated Co^{IV} atom in Co_3S_4 by Ni causes the lattice parameter to decrease by 0.019(4) Å (Table 1). This decrease implies a reduction instead of the expected increase in M^{IV}—S and consequently in a_0, unless there is compensation by a simultaneous decrease in x(S); the increase would be small for $Co_{HS}^{3+} \rightarrow Ni_{HS}^{3+}$. If compensation were present, the Co^{VI}—S distance would become greater, which is inconsistent with the assumption of Co^{VI} being in the Co_{LS}^{3+} state in both compounds.

The difficulty with this and alternative explanations based solely on size criteria is that they do not take account of the effect of possible differences in the degree of electron delocalization on the metal atoms in the four sulfospinels, nor of the possible existence of mixed oxidation states.

[4]It is appreciated that the formulae used here are not completely appropriate descriptions of these sulfides, which show metallic conduction (2).

Can. J. Chem. Downloaded from www.nrcresearchpress.com by 210.87.254.42 on 09/05/12
For personal use only.

Furthermore, a change in a_0 amounting to 0.01 Å will produce a variation of 0.005 Å in an M—S distance, but the same variation results in M^{IV}—S by changing x(S) by only 0.0003, and in M^{VI} by changing x(S) by only about 0.0006. To explain with confidence the reasons for an observed difference in the lattice parameters of any two of the four spinels the x(S) values would have to be known to within at least ± 0.0001 or better, an accuracy which cannot be achieved by powder diffractometry. This constitutes a strong plea for redetermination of the structures of these sulfospinels from accurate low-temperature single-crystal intensities, paying proper attention to the dependability of available scattering factors for Co and Ni.

We wish to express our gratitude to the staff of the Neutron Physics Branch, Atomic Energy of Canada Limited, for making available the neutron diffraction facilities and for assistance with the experiments. Award of an INCO graduate fellowship to one of the authors is gratefully acknowledged.

This work was supported by grants in aid of research from the National Research Council of Canada and the Geological Survey of Canada.

1. O. KNOP, K. I. G. REID, SUTARNO, and Y. NAKAGAWA. Can. J. Chem. **46**, 3463 (1968).
2. R. J. BOUCHARD, P. A. RUSSO, and A. WOLD. Inorg. Chem. **4**, 685 (1965).
3. D. LUNDQVIST. Arkiv. Kemi, Min. Geol. **24A**, No. 21 (1947).
4. V. G. KUZNETSOV, A. A. ELISEEV, Z. S. SHPAK, K. K. PALINA, M. A. SOKOLOVA, and A. V. DMITRIEV. Vopr. Met. Fiz. Poluprovod., Akad. Nauk SSSR, Trudy 4-go Soveshch., Moscow, 1961, p. 159; (Eng. transl.) Proc. 4th All-Union Conf. on Semicond. Materials. Consultants Bureau, New York. P. 128.
5. J. R. CRAIG. Carnegie Inst. Wash., Year Book, **66**, 434 (1967).
6. G. KULLERUD and R. A. YUND. J. Petrology, **3**, 126 (1962).
7. F. K. LOTGERING. Philips Res. Repts. **11**, 337 (1956).
8. D. LUNDQVIST. Arkiv Kemi. Min. Geol. **24A**, No. 22 (1947).
9. R. A. BERNER. J. Geol. **72**, 293 (1964).
10. B. J. SKINNER, R. C. ERD, and F. S. GRIMALDI. Amer. Mineral. **49**, 543 (1964).
11. M. UDA. Z. Anorg. Allgem. Chem. **350**, 105 (1967).
12. F. K. LOTGERING and R. P. VAN STAPELE. Solid State Commun. **5**, 143 (1967); Mat. Res. Bull. **3**, 507 (1968).
13. A. W. SLEIGHT. Mat. Res. Bull. **2**, 1107 (1967).
14. R. P. VAN STAPELE and F. K. LOTGERING. J. Phys. Chem. Solids, **31**, 1547 (1970).
15. O. KNOP, C. H. HUANG, and F. W. D. WOODHAMS. Amer. Mineral. **55**, 1115 (1970).
16. O. KNOP, F. BRISSE, L. CASTELLIZ, and SUTARNO. Can. J. Chem. **43**, 2812 (1965).
17. D. T. CROMER and J. T. WABER. Acta Cryst. **18**, 104 (1965).
18. D. T. CROMER. Acta Cryst. **18**, 17 (1965).
19. G. E. BACON. Neutron Diffraction. 2nd ed. Oxford University Press, 1962.
20. SUTARNO, O. KNOP, and K. I. G. REID. Can. J. Chem. **45**, 1391 (1967).
21. W. C. HAMILTON. Acta Cryst. **18**, 502 (1965).

Can. J. Chem. Downloaded from www.nrcresearchpress.com by 210.87.254.42 on 09/05/12
For personal use only.

Oxochloride Complexes of Rhenium[1]

A. GUEST[2] AND C. J. L. LOCK[3]

Department of Chemistry and Institute for Materials Research, McMaster University, Hamilton, Ontario

Received September 4, 1970

Attempts to prepare rhenium hexachloride by the method described by Colton (2) have been unsuccessful. The products of the reaction were always impure rhenium oxotetrachloride and rhenium pentachloride. A compound of rhenium(VI), $ReOCl_4OPCl_3$, is shown to have a structure analogous to that of rhenium(V) ions $[ReOX_4.L]^-$ in which the ligands are in a pseudooctahedral arrangement with L *trans* to the oxo-group (3). Reactions of $ReOCl_4$ and $ReOCl_4$-$OPCl_3$ with pyridine and 2,2′-dipyridyl are described, and a scheme is proposed for the reactions of the products. Two stable complexes of perrhenyl chloride with the above amines have been obtained.

Canadian Journal of Chemistry, **49**, 603 (1971)

Can. J. Chem. Downloaded from www.nrcresearchpress.com by 210.87.254.105 on 09/05/12
For personal use only.

Introduction

The highest chlorides of molybdenum and tungsten are $MoCl_6$ (4) and WCl_6 (5). The highest chlorides of ruthenium and osmium are $RuCl_3$ (5) and $OsCl_4$ (5). Thus, there is a decrease in the highest formal oxidation state which is stabilized by chlorine in going from the group VIA metals to the group VIII metals. The preparation of $TcCl_6$ (6) as the highest chloride of technetium was surprising therefore, particularly because both $MoCl_6$ and $ReCl_6$ were unknown at the time, the highest chloride of rhenium being the pentachloride (5).

Subsequently, the preparation of rhenium hexachloride was reported (2) by Colton. Colton noted that previous workers who prepared their own rhenium metal had observed "green vapors" in chlorination reactions (7), but these reports ceased when the metal became available commercially. Commercial metal gave only rhenium pentachloride on chlorination. Colton repeated the work of the early workers and was able to get small amounts of "green vapors". A much improved yield could be obtained if ammonium perrhenate was absorbed on porous pot, the salt reduced to rhenium metal with hydrogen and the resulting finely divided metal chlorinated. The product was "dark dichroic crystals which melt a few degrees above room temperature to give a black liquid and green vapors", and was claimed to be rhenium hexachloride (2). The observed magnetic moment of 2.07 B.M. was high for a d^1 system (9), particularly as ReF_6 has a reported effective magnetic moment of 0.25 B.M. at room temperature (10). The low moment of ReF_6 has been attributed to large spin–orbit coupling effects resulting from the postulated O_h symmetry of the molecule. Brown and Colton (9) postulate that this high symmetry was not present in $ReCl_6$, and thus a low magnetic moment was not observed. We were interested in studying the magnetic properties of $ReCl_6$ further but we have tried without success to prepare $ReCl_6$. Studies of $ReOCl_4$ suggest that "$ReCl_6$" might be impure $ReOCl_4$. Certain of the results of our studies on $ReOCl_4$ have been anticipated in another paper (11). As a continuation of our studies of this system we have investigated reactions of $ReOCl_4$ and also ReO_3Cl.

Experiments

Most analyses for carbon, hydrogen, chlorine, and phosphorus were performed by Galbraith Laboratories, Inc., Knoxville, Tennessee. Some carbon, hydrogen, nitrogen, and chlorine analyses were performed by A. B. Gygli, Toronto, Ontario and some phosphorus analyses were performed by A. Bernhardt, West Germany. Rhenium and chloride analyses and rhenium:chlorine ratios were determined by neutron activation using a method described by us previously (12).

Infrared spectra were recorded on Perkin–Elmer 337, 521, and 301 instruments. Solid samples were ground into a mull with dry Nujol and mounted between potassium bromide or polyethylene plates. The Nujol was dried by refluxing over phosphorus pentoxide and then vacuum distilled. Solution samples were prepared using carbon tetrachloride or titanium tetrachloride as solvents. The solutions were contained in standard solution cells with potassium bromide windows, or were injected into sealed polyethylene sacks using a syringe. Gas samples were contained in the special cell described by us previously (13) or in a glass cell with polyethylene windows fused directly to the glass under pressure. Magnetic susceptibilities were determined for solid samples from −180 to 25 °C using an apparatus described previously (1).

---

[1]Previous paper in this series is ref. 1.

[2]Present address: Department of Chemistry, University of the West Indies, Mona, Jamaica.

[3]Author to whom correspondence should be addressed.

Can. J. Chem. Downloaded from www.nrcresearchpress.com by 210.87.254.105 on 09/05/12
For personal use only.

Purification of Reagents and Solvents

Carbon Tetrachloride

Carbon tetrachloride was dried by distillation from phosphorus pentoxide, and stored in a dry-box[4] over freshly regenerated molecular sieve (type 4A).

Chlorine

Commercial chlorine (supplied by Matheson, Whitby, Ontario) was dried by passing through concentrated sulfuric acid and phosphorus pentoxide traps, then condensed in a trap cooled in liquid nitrogen. The solid chlorine was evacuated at 10^{-4} mm Hg. The chlorine was allowed to warm up, melt, and start to boil and was then refrozen in liquid nitrogen and again evacuated to 10^{-4} mm Hg. This process was repeated until no increase in pressure was observed when the trap containing solid chlorine was opened to the vacuum line. A steady stream of chlorine was obtained from the trap by allowing the liquid to boil off at −31.5 °C. This temperature was maintained by standing the chlorine container in a slush of "*m*"-toluidine.

Hydrogen

Commercial grade hydrogen (supplied by Canadian Liquid Air) was dried by passing through concentrated sulfuric acid and phosphorus pentoxide traps.

Nitrogen

Purified grade nitrogen (supplied by Canadian Liquid Air) was deoxygenated by hot activated copper in an apparatus described elsewhere (14), and then dried by passing through concentrated sulfuric acid and phosphorus pentoxide traps.

Oxygen

Commercial grade oxygen (supplied by Canadian Liquid Air) was dried by liquefication of the gas in a liquid nitrogen cooled trap in a similar manner to that described for chlorine. The oxygen was then allowed to evaporate slowly by controlled cooling with liquid nitrogen.

Pyridine

Reagent grade pyridine was dried by distillation from barium oxide as recommended by Leis and Currans (15).

Thionyl Chloride

Thionyl chloride was purified by the method of Friedman *et al.* (16) by distillation from triphenyl phosphite.

All other reagents and solvents used were of the normal reagent grade.

Preparation and Purification of Rhenium Compounds used as Starting Materials

Metallic Rhenium

Rhenium metal was obtained commercially in powdered form and purified by reduction with hydrogen where indicated in the text. In all other cases, the powder was vacuum dried at 120 °C for 24 h before use. Suppliers of rhenium were Johnson, Matthey and Mallory (Toronto, Ontario), The University of Tennessee, and Chase Brass and Copper Company, Rhenium Division, Solon, Ohio.

[4]Vacuum Atmospheres Corporation Dryboxes Models DRILAB HE-43 and HE-43-2.

Rhenium Heptoxide

Some rhenium heptoxide was purchased from the University of Tennessee and some from Koch-Light Laboratories, Colnbrook, Bucks., England, but most was prepared by burning rhenium in oxygen, in an apparatus of the type described by McLaren *et al.* (17).

Rhenium Trioxide

Rhenium trioxide was prepared by reduction of rhenium heptoxide by two different methods. (*i*) Rhenium heptoxide was reduced with dioxan as described by Nechamkin and Hiskey (18). This method was found to be messy and high yields of trioxide were difficult to obtain. (*ii*) A method (19) for producing ReO_3 by reducing Re_2O_7 with CO was modified and the reaction carried out at high pressure. Re_2O_7 was finely ground in a dry-box and transported to the autoclave in a stoppered bottle. The Re_2O_7 was placed in a glass liner and the autoclave sealed and flushed with carbon monoxide as rapidly as possible to minimize hydrolysis of the Re_2O_7 by atmospheric moisture. After reduction at 200 °C and 500 p.s.i.g. carbon monoxide pressure for 24 h, the product was washed with water to remove unreacted starting material and dried at 110 °C. Ninety percent yields of very pure rhenium trioxide were recorded.

Perrhenyl Chloride

Perrhenyl chloride was prepared according to the method of Wolf *et al.* (20) by direct chlorination of rhenium trioxide at 180 °C. The pale yellow product was isolated in break seals and purified by trap-to-trap distillation to give a colorless liquid product. Yields of pure compound were about 70%.

Rhenium Oxotetrachloride

(*a*) Rhenium oxotetrachloride was prepared by the method of Bagnall *et al.* (21) from rhenium heptoxide and thionyl chloride. The product of this reaction was invariably contaminated by sulfur dioxide, which proved very difficult to remove by vacuum distillation. The presence of sulfur dioxide was readily detected by its gas-phase ultraviolet spectrum (22). (*b*) Direct chlorination of rhenium metal gave low yields of rhenium oxotetrachloride if powdered rhenium was used, but gave high yields of rhenium oxotetrachloride if rhenium metal suspended on porous brick was used. The oxotetrachloride was separated from pentachloride which was also produced by pumping at reduced pressure, but separation from other volatile products was tedious. Thirty or forty trap-to-trap distillations were sometimes required to remove all impurities (see Discussion).

Rhenium Pentachloride

Some rhenium pentachloride was purchased from Alpha Inorganics, Beverley, Mass. and Shattuck Chemical Company, but was generally prepared either by a modification of the method of Hurd and Brimm (23) using distillation through U-tubes as the method of purification, or by the method of Knox *et al.* (24). The material obtained was usually in the form of small crystals. The best method of purifying the material was to seal rhenium pentachloride in a Carius tube with chlorine and distil it along the tube by applying a temperature gradient. Large plate-like crystals were obtained. Rhenium pentachloride so obtained is a black crystalline material which melts at 261 °C.

Can. J. Chem. Downloaded from www.nrcresearchpress.com by 210.87.254.105 on 09/05/12
For personal use only.

Anal. Calcd. for Cl_5Re: Cl, 48.8; Re, 51.2. Found: Cl, 49.7; Re, 51.6. Re:Cl ratio (average of twelve different samples) 1: 4.98 ± .02.

Rhenium pentachloride was refluxed with liquid chlorine for several hours in an evacuated system. In certain experiments the bulb was irradiated with ultraviolet light during the period of reflux. Rhenium pentachloride was obtained essentially unchanged; there was no sign of a higher chloride. This was confirmed by analysis and by a mixed melting point (261 °C) with a genuine sample.

New Rhenium Compounds and New Methods of Obtaining Known Rhenium Compounds

Rhenium Oxotetrachloride

Rhenium pentachloride and dry oxygen were sealed in a Carius tube which was fitted with a break-seal. The tube was heated to 180 °C in a furnace for a few hours. The break-seal was then attached to a vacuum line, which was evacuated and heated for at least 24 h before the seal was broken and the product distilled. This was the most convenient preparative method. Only two or three vacuum distillations were necessary to produce very pure oxotetrachloride in about 70% yield. The average Re:Cl ratio found for 18 independent neutron activation analyses on $ReOCl_4$ was 1:3.92 (±0.02).

Anal. Calcd. for Cl_4ORe: Cl, 41.4; Re, 54.1. Found[5]: Cl, 41.3, 41.1; Re, 54.1, 54.4.

Oxotrichlorobispyridinerhenium(V), [$ReOCl_3py_2$]

(*a*) Rhenium oxotetrachloride was sealed under vacuum in a tube fitted with a break-seal, and the tube above the break-seal filled with pyridine. The seal was broken with a glass rod, causing the pyridine to be sucked onto the $ReOCl_4$. The tube was shaken vigorously to dissolve the $ReOCl_4$ and form a red solution. Heat was evolved during dissolution. After 1/2 h a green precipitate was formed and continued to be formed until the red solution faded to a pale yellow. The green compound, which could also be obtained by a similar reaction using $ReOCl_4.OPCl_3$, was shown to be identical with the isomer of $ReOCl_3py_2$ described previously (25).

Anal. Found: C, 25.6; H, 2.3; Cl, 22.6; N, 5.9. Neutron activation analysis gave Cl, 22.9; Re, 40.0 (stoichiometry Re:Cl; 1:2.97(0.03)).

This was confirmed by converting our sample of $ReOCl_3.py_2$ to blue $ReOCl_2.OEtpy_2$ which had identical properties to an authentic sample (27).

Found: C, 30.2; H, 3.0; Cl, 14.7; N, 5.6. The residual yellow solution gave $[Re(py)_4O_2Cl]$ (26) on evaporation.

Oxotrichloro(2,2-Dipyridyl)Rhenium(V)

[$ReOCl_3$dipy] (28) was prepared by the reaction of α,α′-dipyridyl and rhenium oxotetrachloride.

Found: C, 25.3; H, 1.8; Cl, 22.4; N, 5.60. Neutron activation analysis gave Cl, 22.7; Re, 40.6.

μ-Oxobis[Oxodichloro(2,2-Dipyridyl)Rhenium(V)], [(dipy)$ReOCl_2$—O—Cl_2ORe (dipy)]

[$ReOCl_3$dipy] was refluxed with boiling absolute ethanol. Very slowly the solution changed to a pale orange color and a green compound was precipitated. The green compound was filtered, washed with ice-cold absolute ethanol and vacuum dried.

Anal. Calcd. for $C_{20}H_{16}Cl_4N_4O_3Re$: C, 27.5; H, 1.8; Cl, 16.3; N, 6.4. Found: C, 27.8; H, 2.1; Cl, 16.2; N, 6.3.

Yield of green, air-stable crystalline material, melting point > 300 °C was 60%.

Trioxochlorobispyridinerhenium(VII), [ReO_3Clpy_2]

Pyridine and perrhenyl chloride were dissolved separately in carefully dried carbon tetrachloride and the solutions mixed. A white precipitate was formed immediately. The precipitate was filtered, washed with carbon tetrachloride, and pumped on a vacuum-line at room temperature to remove volatile impurities. The compound was then sublimed at 100 °C in vacuum. The yield of pure, air-unstable very pale yellow compound, melting point 155 °C (decomp.) was approximately 40%.

Anal. Calcd. for $C_{10}H_{10}ClN_2O_3Re$: C, 28.1; H, 2.3; Cl, 8.3; N, 6.5; Re, 43.6. Found: C, 28.0; H, 2.9; Cl, 8.4; N, 6.3. Neutron activation analyses gave Cl, 7.9; Re, 43.4.

Trioxochloro-2,2′-Dipyridylrhenium(VII), [ReO_3Cldipy]

2,2′-Dipyridyl and perrhenyl chloride were dissolved separately in carefully dried carbon tetrachloride and the solutions mixed. The heavy white precipitate which formed immediately was filtered, washed with carbon tetrachloride, and pumped at room temperature for 24 h to remove volatile impurities. The yield of white, involatile, air-stable, compound melting point 280 °C (decomp.), was estimated at 60–70%.

Anal. Calcd. for $C_{10}H_8ClN_2O_3Re$: C, 28.2; H, 1.9; Cl, 8.3; N, 6.6; Re, 43.8. Found: C, 26.7; H, 1.7; Cl, 8.4; N, 6.1. Neutron activation analysis gave Cl, 8.0; Re, 43.1.

Oxotetrachloro(Oxotrichlorophosphorus(V)) Rhenium(VI), [$ReOCl_4(OPCl_3)$]

(*a*) A Pyrex tube was constructed with a constriction in the middle giving two sections A and B. A break-seal was fitted to A and an inlet tube to B. In a dry-box, powdered phosphorus pentachloride was weighed into section A and rhenium heptoxide into section B (mole ratio $5PCl_5$: $1Re_2O_7$). The tube was removed from the dry-box and the inlet tube sealed before the reactants were allowed to mix. The tube was then shaken until the solids reacted with evolution of heat to form a red-brown semi-liquid mass. The tube was attached to a vacuum line and after pumping and heating the line for at least 24 h, the seal was broken and the reaction products fractionated. Phosphoryl chloride and unreacted phosphorus pentachloride were volatile at room temperature. The $ReOCl_4.OPCl_3$ sublimed more slowly at room temperature and was freed from phosphorus chlorides after three or four trap-to-trap sublimations. The yield of $ReOCl_4.OPCl_3$ was about 50%.

(*b*) $ReOCl_4.OPCl_3$ was prepared in a manner analogous to (*a*) using ReO_3 instead of Re_2O_7 as starting material.

(*c*) $ReOCl_4$ and $POCl_3$ were sealed in glass apparatus fitted with a break-seal and allowed to mix. A red solution was formed and heat was evolved. The apparatus was attached to a vacuum-line, and after baking the glassware dry the seal was broken and excess $POCl_3$ pumped off at ice temperature. The $ReOCl_4.OPCl_3$ was purified by sublimation and isolated in break-seals.

[5]Analysis by conventional wet method; the sample was hydrolyzed with hydrogen peroxide. Chloride was determined gravimetrically as silver chloride, and perrhenate gravimetrically as tetraphenylarsonium perrhenate.

Yields of approximately 70% were recorded. $ReOCl_4$-$.OPCl_3$ forms long acicular crystals with a melting-point of 90.5 °C.

Anal. Calcd. for Cl_7O_2PRe: Cl, 49.9; P, 6.2; Re, 37.5. Found: Cl, 53.5; P, 5.8 (Galbraith), 6.2 (Bernhardt). Neutron activation analyses gave (mean of 12 analyses) Cl, 52.5; Re, 38.7 (Re:Cl = 1:7.08 ± 0.12).

Results and Discussion

Rhenium Hexachloride and Rhenium Oxotetrachloride

It was mentioned above that the reported thermal stability and high magnetic moment of rhenium hexachloride (9) were unexpected. Attempts were made to prepare rhenium hexachloride by Colton's method (2). The major product resembled the compound described by Colton, and a little rhenium pentachloride was also produced. In many early experiments the first test applied to the product was the measurement of the infrared spectrum of a carbon tetrachloride solution of the compound prepared in a dry-box. Invariably, absorption peaks were observed in the range 900–1050 cm^{-1}. This region of the spectrum is too high in energy for any metal–chloride vibrational frequency (29), but is the normal region for heavy metal–oxygen stretching frequencies (30). Therefore the absorptions appeared to be the result of oxygen contamination of the product.

In an effort to eliminate any contamination, increasingly rigorous conditions were applied to keep moisture and oxygen out of the reactants, solvents, and products. Vacuum systems used contained no greased taps, joints or seals and all handling was done using break-seals. A special high temperature vacuum infrared cell was designed (13) to enable the product to be examined in the gas phase and a neutron activation analysis method (12) was developed to enable accurate analyses to be performed without risk of contamination of the product.

Early analysis results by classical wet methods (31, 32) were not precise but indicated that the ratio of rhenium to chlorine atoms was about 1:4. After development of the neutron activation analysis technique, many analyses were performed. It was found possible to prepare a product having a chlorine-to-rhenium atom ratio of approximately six, but careful separation showed that more than one component was present (see later). Samples which were purified by many trap-to-trap sublimations (30 or 40 in some cases) formed large black crystals (appearing dichroic in smaller samples, being dark green by reflected light and dark red by transmitted light). The crystals had a very sharp melting point at 32 °C and had a chlorine–rhenium atom ratio of 4. On hydrolysis with ammonium hydroxide solution the compound gave a Re^{VIII}:Re^{IV} ratio of 2:1 which is typical of rhenium(VI) (33, 34).

Gaseous infrared spectra of the vapor of the compound in the special gas cell filled on a vacuum line, with no possibility of oxygen entering the system, showed a large peak with two distinct shoulders centered at 1040 cm^{-1}. The lower branch was 1033 cm^{-1} and the higher at 1047 cm^{-1} and we assign these to the P, Q, and R branches of an Re=O stretch of the compound. The absorption occurred at slightly lower energies in solution: 1033 cm^{-1} in CCl_4 and 1029 cm^{-1} in $TiCl_4$. From the above evidence, it was apparent that the chlorination product was rhenium oxotetrachloride. Subsequent investigations showed that it was possible to obtain classical wet analyses for rhenium and chlorine, and these analyses confirmed the formulation of the chlorination product as $ReOCl_4$. Another strong peak was observed in the gas-phase infrared spectrum at 368 cm^{-1}. A similar strong peak was observed at 372 cm^{-1} for carbon tetrachloride and titanium tetrachloride solutions. The peak is probably ν_{Re-Cl} for $ReOCl_4$ but some attack of the polythene windows occurred, so that we cannot be certain that this peak was not caused by an impurity.

Further support for this formulation is afforded by a study of the magnetic susceptibility of the compound. The susceptibilities of samples of $ReOCl_4$ prepared by direct chlorination and by the reaction of pentachloride with oxygen are recorded in Table 1, together with the results obtained by Klemm and Schuth (35).

The effective magnetic moments from the measurements of Klemm and Schuth and this work are not in agreement. This is understandable when one considers the method of filling the sample tube. Because of the low melting point of the compound, both others (9) and ourselves have found it impossible to grind solid $ReOCl_4$ and pack a tube in the normal manner. The method used by us was to seal the quartz sample tube through a graded seal onto Pyrex apparatus, which contained the $ReOCl_4$ under a break-seal. The apparatus was evacuated and heated to re-

Can. J. Chem. Downloaded from www.nrcresearchpress.com by 210.87.254.105 on 09/05/12
For personal use only.

TABLE 1. Magnetic susceptibilities of $ReOCl_4$, $ReOCl_4$, $OPCl_3$, $ReOCl_3$, and $ReCl_5$

$ReOCl_4$†		$ReOCl_4$‡	$ReOCl_4.OPCl_3$	$ReCl_5$		$ReOCl_4$§	
T(°K)	χ_m'*	χ'_m	χ'_m	T(°K)	χ'_m	T(°K)	χ'_m
80	3334	3292	3548			90	2540
100	2815	2780	3086	102	1812		
120	2432	2405	2689	128	1689		
140	2134	2113	2320	144	1639		
160	1906	1881	2087	168	1544		
180	1719	1701	1880				
200	1576	1556	1771	192	1473	199	1310
220	1450	1431	1620	218	1414		
240	1339	1293	1516	250	1345		
270	1209	1192	1315	264	1309		
293	1150	1117	1212	291	1261	293	928
μ_{eff} = 1.7		μ_{eff} = 1.7	μ_{eff} = 1.7	μ_{eff} = 2.31		μ_{eff} = 1.5	
θ = 24 °K		θ = 27 °K	θ = 23 °K	θ = 265 °K		θ = 25 °K	

*All magnetic data are ($\times 10^6$) c.g.s.u.; μ_{eff} in B.M.
†$ReCl_5 + O_2$.
‡Direct chlorination.
§Reference 35.

move surface moisture. The seal was then broken, and the compound melted, and poured into the tube as a liquid. Thaw–melt techniques were employed in an attempt to obtain a continuous 10 cm length of rod of solid compound, but as the solid has a smaller specific volume than the liquid some empty space was apparent in all cases.

If the disagreement in the results is caused only by packing, one would expect that the magnetic susceptibility (uncorrected for diamagnetism) of a given sample will have a constant ratio to that of another sample throughout the whole temperature range and give the same Curie–Weiss constant. Such is the case for our results and those of Klemm and Schuth. The Curie–Weiss constants are identical within experimental error and the ratio of the uncorrected magnetic susceptibilities is 1.20 ± 0.01. It is interesting to note that the values given by Brown and Colton (9) for $ReCl_6$ when compared to our values for $ReOCl_4$ also fulfil this condition. The ratio of magnetic susceptibilities is 1.52 ± 0.01 which is somewhat larger than the above ratio, but this can be reduced to 1.31 if Brown and Colton's gram susceptibilities are multiplied by the molecular weight for $ReOCl_4$ rather than $ReCl_6$. A more recent study of the magnetic properties of $ReCl_6$ prepared by another method (36) gives quite different results. The Curie–Weiss constant of 75° is much larger and a constant ratio is not obtained; the values ($ReCl_6/ReOCl_4$) vary from 1.07 at 294° to 1.21 at 105°.

It seemed strange that the major product of chlorination of rhenium should be altered so much, just by using metal with a higher specific surface area. The first conclusion drawn was that a higher chloride was formed which attacked the glass or ceramic to abstract oxygen. A small amount of volatile yellow material, from which it was difficult to separate the $ReOCl_4$, had often been observed during trap-to-trap sublimations, and it now seemed possible that this was a higher chloride. By many careful sublimations a few milligrams of this compound were isolated. Activation analysis gave a rhenium:chlorine ratio of 1:50 and the γ-ray spectrum of ^{24}Na was observed. An emission spectrographic analysis[6] of the compound showed that it contained several percent of Si and Al, about 1% of Na and Ti, and traces of Sn, Mg, Pb, Fe, Be, V, Cu, Ni, Co, and Cr. Obviously, the yellow "compound" was "ceramic chloride", and the oxygen in the major chlorination product was the result of attack on the porous brick.

Further experiments established that attack of the ceramic was essential to the production of $ReOCl_4$. Experiments using glass wool yielded mostly $ReCl_5$. It was also established that attack of the ceramic was not caused by chlorine, rhenium pentachloride, or rhenium trichloride.

The most reasonable explanation of this attack was offered by Chatt (37). He suggested that rather than a higher chloride being formed which then attacked the ceramic, the rhenium metal was acting as a reducing agent, and that the reduced

[6]Kindly performed by Professor D. Shaw, Geology Department, McMaster University.

Can. J. Chem. Downloaded from www.nrcresearchpress.com by 210.87.254.105 on 09/05/12
For personal use only.

TABLE 2. Infrared spectra of $ReOCl_4.OPCl_3$

$ReOCl_4.OPCl_3$				$POCl_3$	$ReOCl_4$	
CCl_4 soln.	Nujol mull	$TiCl_4$ soln.	Vapor	(48) Vapor	Vapor (This work)	Assignment
1300			1290	1290		ν_{P-O}
1248	1239	1258				
1210	1202	1214				
1028	1020	1021	1040		1040	$\nu_{Re=O}$
1021						
612	610	605				ν_{P-Cl}
584			584	581		
484				486		

ceramic and oxidized rhenium were then chlorinated.

We have been unable to make rhenium hexachloride by the method of Colton (2), obtaining, instead, rhenium oxotetrachloride. We feel that the material described by Colton as "rhenium hexachloride" may be impure rhenium oxotetrachloride rather than $ReCl_6$. We cannot be certain of this since the data given for "rhenium hexachloride" are of minimal value in identifying the material. Properties such as melting point, color, and magnetic properties are very like those of $ReOCl_4$, but no data useful for identification purposes, such as vibrational spectra or X-ray diffraction data, are given. The reported thermal stability of "rhenium hexachloride" is not that which would be expected on the basis of the chemistry of neighboring elements. Rhenium hexachloride should be decomposed quite easily to a lower chloride and chlorine. However, the reported thermal stability is consistent with that for rhenium oxotetrachloride.

Rhenium Pentachloride

The melting point of rhenium pentachloride is quoted in the standard texts as 220 °C (33, 34), but it should be noted that the melting point of rhenium pentachloride prepared throughout this work was much higher (261 °C), very close to the value of 260 °C quoted by Lebedev (38). Nevertheless, the magnetic results we obtained (given in Table 1) are in close agreement with those of previous workers (9, 35, 39).

$ReOCl_4.OPCl_3$

Attempts were made to prepare rhenium halides and oxohalides by using phosphorus halides as chlorinating agents, but the reaction of both ReO_3 and Re_2O_7 with PCl_5 yielded the volatile molecular complex oxotetrachloro(phosphoryl chloride)rhenium(VI). This compound was subsequently synthesized from $POCl_3$ and $ReOCl_4$. Cotton and Lippard (3) have shown that rhenium(V) ions of the type $[ReOX_4.L]^-$(X = Br, Cl, L = H_2O, CH_3CN) have a pseudo-C_{4v} structure with the oxo-group *trans* to the ligand, which is very weakly bonded to rhenium. We consider that $ReOCl_4.OPCl_3$ has a similar structure.

The infrared spectral data presented in Table 2 show that $POCl_3$ is bonded in the normal manner (40) through the oxygen atom. The P—O stretching frequency is lowered by $\sim$ 40 cm^{-1}, as the bond is weakened by donation of electron density from the oxygen atom to the rhenium atom and the phosphorus–chlorine stretching frequency is increased slightly. The infrared data show clearly that the compound, $ReOCl_4.OPCl_3$ exists in the solid state and in titanium tetrachloride solution, but in the gas phase it is completely dissociated into $ReOCl_4$ and $POCl_3$. In carbon tetrachloride an equilibrium is evident between $ReOCl_4$, $POCl_3$, and $ReOCl_4.OPCl_3$. This suggests that the Re—O bond between $ReOCl_4$ and $OPCl_3$ is relatively weak.

The magnetic susceptibility data for $ReOCl_4$-$.OPCl_3$ (Table 1) obey the Curie–Weiss Law with $\theta = 23\ ^\circ K$ and $\mu_{eff} = 1.71$ B.M. These results are similar to those for $ReOCl_4$ so the addition of $OPCl_3$ to $ReOCl_4$ has not significantly affected the magnetic properties. Spin–orbit coupling effects are again absent and the local symmetry cannot be higher than C_{4v}.

Rhenium(V) Amine Complexes

We attempted to prepare a series of $ReOCl_4.L$ compounds by ligand replacement reactions with $ReOCl_4.OPCl_3$. Ligands such as triphenyl phosphine and alkyl or aryl phosphites gave black tars on direct reaction with $ReOCl_4.OPCl_3$, and no

Can. J. Chem. Downloaded from www.nrcresearchpress.com by 210.87.254.105 on 09/05/12
For personal use only.

Can. J. Chem. Downloaded from www.nrcresearchpress.com by 210.87.254.105 on 09/05/12
For personal use only.

products were isolated. Pyridine and 2,2′-dipyridyl, which are more resistant to oxidation than the ligands mentioned above, underwent clean reactions forming easily isolated, stoichiometric compounds. None of the products was of the expected type, however; in all cases reduction had taken place to yield compounds of Re(V). The amine complexes isolated appeared to be the same isomeric forms as had been prepared in other reactions (25–27, 41). The preparation and reactions of the amines are summarized in Fig. 1 which is based on our results and those of Johnson *et al.* (27). One feature, worthy of note, is the significant difference in the reactivity of the bispyridine- and 2,2′-dipyridyl-rheniumoxotrichloride complexes with ethanol. $ReOCl_3dipy$ gives the oxo-bridged dimer molecule which does not react further whereas $ReOCl_3py_2$ gives the ethoxo-complex; in addition the oxo-bridged dimer containing pyridine is readily cleaved by ethanol. It is difficult to rationalize this marked difference in reactivity unless the two oxo bridged compounds have completely different structures, but our attempts to show structural differences by vibrational spectroscopy were unsuccessful.

Rhenium(VII) Amine Complexes

Re(VII) is a common, stable, formal oxidation state of rhenium found in the perrhenate ion and perrhenyl halides. Reports of coordination compounds are restricted to $Cs_2ReO_3Cl_3$ (42), $(ReO_3Cl)_2SO_2Cl_2$ (21), $ReO_3Cl[(CH_3)_2SO]_2$, and $ReO_3Cl[(CH_3)_2N.CO.H]_2$ (43), but all were obtained from Re_2O_7 or perrhenate ion. It appeared possible that direct interaction of ReO_3Cl and a ligand might also yield complexes. Since this work was started Ringel (49) has obtained amide complexes in this manner.

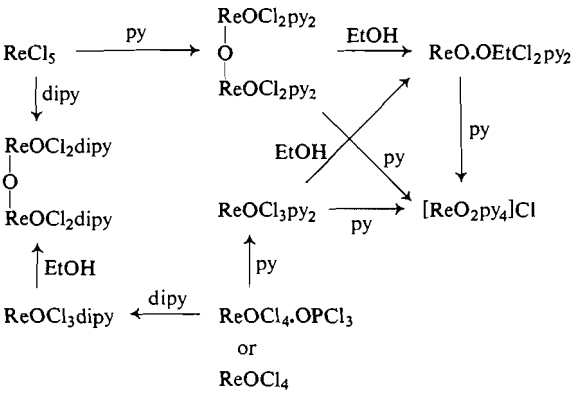

FIG. 1. Reactions of rhenium(V) amines.

Trioxochlorobispyridinerhenium(VII) (ReO_3Clpy_2) and trioxochloro-2,2′-dipyridylrhenium(VII) were obtained from the direct reaction of perrhenyl chloride and the corresponding ligand in carbon tetrachloride solution. The compounds were almost white and decomposed slowly in air, the pyridine complex being less stable. $ReO_3Cl.dipy$ was involatile at 100 °C, but the pyridine complex sublimed at this temperature. A small amount of residue was shown, by analysis and infrared spectroscopy to be pyridinium perrhenate. The compounds are interesting in that the central rhenium atom must have a co-ordination number of six. Rhenium(VII) normally has a coordination number of four, but it has been shown that in solid Re_2O_7 mixed six and four coordination is observed (44).

The infrared spectra of ReO_3Clpy_2 and $ReO_3Cldipy$ both showed the absorptions normally associated with the coordinated ligands (45, 46), and in addition showed several absorptions in the range 800–1000 cm^{-1} which may be assigned to rhenium–oxygen vibrations (26, 30). $ReOCl_3py_2$ showed absorptions at 858, medium, 901 and 914, very strong, 939, strong, and 946, shoulder, and $ReOCl_3dipy$ showed absorptions at 888 and 913, strong, 918, very strong, and 943, strong, all data having units of cm^{-1}. From the complexity of the spectra it appears the molecule is highly asymmetric. The spectra are very similar in appearance, suggesting the two compounds have similar structures. It is not possible to decide unambiguously whether the three oxygen atoms have the 1,2,3 or 1,2,6 arrangement, but Griffith's arguments (47) concerning the expected spectra for such arrangements suggest that the 1,2,6 arrangement is more probable.

We thank the National Research Council of Canada for financial support of this work and the award of a Graduate Scholarship to one of us (A.G.).

1. P. W. FRAIS, A. GUEST, and C. J. L. LOCK. Can. J. Chem. **47**, 1069 (1969).
2. R. COLTON. Nature, **194**, 374 (1962).
3. F. A. COTTON and S. J. LIPPARD. Inorg. Chem. **4**, 1621 (1965); **5**, 9, 416 (1966).
4. M. MERCER. Chem. Commun. 119 (1967).
5. F. A. COTTON and G. WILKINSON. Advanced Inorganic Chemistry. 2nd *ed.* Interscience Publ., New York. 1966.
6. R. COLTON. Nature, **193**, 872 (1962).
7. W. NODDACK. Z. Elektrochem. **34**, 627 (1928); Agnew. Chem. **44**, 215 (1931).

8. F. SCHACERAL. Chem. Listy. **23**, 632 (1929).
9. D. BROWN and R. COLTON. J. Chem. Soc. 714 (1964).
10. H. SELIG, F. A. COFASSO, D. N. GRUEN, and J. G. MALM. J. Chem. Phys. **36**, 3440 (1962).
11. B. J. BRISDON and D. A. EDWARDS. Inorg. Chem. **7**, 1898 (1968).
12. W. D. COURRIER, A. GUEST, C. J. L. LOCK, and R. H. TOMLINSON. Can. J. Chem. **46**, 2965 (1968).
13. A. GUEST and C. J. L. LOCK. Rev. Sci. Instrum. **39**, 780 (1968).
14. R. E. DODD and P. L. ROBINSON. Experimental Inorganic Chemistry. Elsevier Publ. Corp. Inc., Amsterdam. 1957. p. 66.
15. D. G. LEIS and B. C. CURRANS. J. Amer. Chem. Soc. **67**, 79 (1945).
16. L. FRIEDMAN and W. P. WETTER. J. Chem. Soc. A, 36 (1967).
17. A. D. MCLAREN, F. N. FOWLE, W. BRICKNELL, and C. F. HISKEY. Inorg. Syn. **3**, 188 (1950).
18. H. A. NECHAMKIN and C. F. HISKEY. Inorg. Syn. **3**, 186 (1950).
19. A. D. MCLAREN, J. N. FOINE, W. BRICKNELL, and C. F. HISKEY. Inorg. Syn. **3**, 187 (1950).
20. C. J. WOLF, A. F. CLIFFORD, and W. H. JOYNSON. J. Amer. Chem. Soc. **79**, 4257 (1957).
21. K. W. BAGNALL, D. BROWN, and R. COLTON. J. Chem. Soc. 3017 (1964).
22. G. HERZBERG. Molecular Spectra and Molecular Structure III. D. Van Nostrand Co., Inc., New York. 1966. p. 605.
23. L. C. HURD and E. BRUNNI. Inorg. Syn. **1**, 180 (1939). McGraw Hill Publ. Co., New York.
24. K. KNOX, S. Y. TYREE, R. D. SRIVASTA, V. NORMAN, J. Y. BASSETT, and J. H. HOLLOWAY. J. Amer. Chem. Soc. **79**, 3358 (1957).
25. M. C. CHAKRAVORTI. J. Indian Chem. Soc. **60**, 81 (1963).
26. N. P. JOHNSON, C. J. L. LOCK, and G. WILKINSON. J. Chem. Soc. 1054 (1964).
27. N. P. JOHNSON, F. I. M. TAHA, and G. WILKINSON. J. Chem. Soc. 2614 (1964).
28. M. C. CHAKRAVORTI. J. Indian Chem. Soc. **42**, 503 (1965).
29. R. J. H. CLARK. Spectrochim. Acta, **21**, 955 (1965) and references therein.
30. C. G. BARRACLOUGH, J. LEWIS, and R. S. NYHOLM. J. Chem. Soc. 3552 (1959).
31. H. H. WILLARD and C. C. SMITH. Ind. Eng. Chem. Anal. Ed. **11**, 305 (1939).
32. A. I. VOGEL. A Text Book of Quantitative Inorganic Analysis. 3rd *ed.* Longmans, Green and Co. Ltd., London. 1961. p. 460.
33. R. COLTON. The Chemistry of Rhenium and Technetium. Wiley, New York. 1965.
34. R. D. PEACOCK. The Chemistry of Technetium and Rhenium. Elsevier. 1966.
35. W. SCHUTH and W. KLEMM. Z. anorg. allgen. Chem. **220**, 193 (1934).
36. J. H. CANTERFORD. Private communication. 1970.
37. J. CHATT. Private communication. 1968.
38. K. B. LEBEDEV. The Chemistry of Rhenium. Butterworths, London. 1962. p. 22.
39. K. KNOX and C. E. COFFEY. J. Amer. Chem. Soc. **81**, 5 (1959).
40. N. L. PADDOCK. Roy. Inst. Chem. Lecture Series. 1962. No. 2, p. 35 and references therein.
41. F. A. COTTON, W. R. ROBINSON, and R. A. WALTON. Inorg. Chem. **6**, 223 (1967).
42. D. E. GROVE, N. P. JOHNSON, and G. WILKINSON. Inorg. Chem. **8**, 1196 (1969).
43. H. A. LEHMANN and C. RINGEL. German (East) Patent 54,680 Mar. 20, 1967 (Application Dec. 28, 1964).
44. B. KREBS, A. MULLER, and H. BEYER. Inorg. Chem. **8**, 436 (1969).
45. A. A. SCHILT and R. C. TAYLOR. J. Inorg. Nucl. Chem. **9**, 211 (1959).
46. N. S. GILL, R. H. NUTTALL, D. E. SCAIFE, and D. W. A. SHARP. J. Inorg. Nucl. Chem. **18**, 79 (1961).
47. W. P. GRIFFITH and T. D. WICKINS. J. Chem. Soc. A, 400 (1968).
48. K. NAKAMOTO. Infrared Spectra of Inorganic and Coordination Compounds. Wiley, New York. 1963. p. 86.
49. C. RINGEL. Z. Chem. **9**, 461 (1969).

Can. J. Chem. Downloaded from www.nrcresearchpress.com by 210.87.254.105 on 09/05/12
For personal use only.

Can. J. Chem. Downloaded from www.nrcresearchpress.com by 210.87.254.42 on 09/05/12
For personal use only.

The Thermal Pressure and Energy–Volume Coefficients of Dimethyl Sulfoxide – Water Mixtures

DIGBY D. MACDONALD[1] AND J. B. HYNE
Department of Chemistry, University of Calgary, Calgary, Alberta

Received August 10, 1970

Thermal pressure and energy–volume coefficients are reported for several DMSO–water mixtures over the temperature range 13–55 °C. The energy–volume coefficient at 25 °C is found to pass through a maximum at 0.3–0.4 mole fraction DMSO and this observation is rationalized in terms of maximization of intercomponent interactions. The relationship between the energy–volume coefficient and the cohesive energy density of the binary liquid system is examined. The temperature dependence of the thermal pressure coefficient is discussed in terms of the effect of temperature on the susceptibility of the entropy of DMSO–water mixtures to isothermal expansion.

Canadian Journal of Chemistry, 49, 611 (1971)

Introduction

Dimethylsulfoxide (DMSO) – water mixtures have been used extensively as solvent media for kinetic studies (1–4) including recent work reported by the authors concerning the effect of pressure on the solvolysis of benzyl chloride in several aqueous DMSO solvent systems (1). It was found in this study, and many others of the same type (5), that variation in solvent composition greatly influences the various psuedo-thermodynamic parameters of activation through differential effects on the properties of the initial and transition states. Since these properties are determined, at least in part, by the structural and molecular interaction properties of the solvent, it is necessary to possess detailed information on solvent structure and the extent of intercomponent interaction if the kinetic behavior is to be fully understood.

It is generally accepted that deviation of liquid mixtures from ideality is a consequence of intercomponent interaction. Many studies, both thermodynamic and non-thermodynamic, have been performed in an effort to characterize the type and extent of these interactions in a great variety of liquid mixtures. Surprisingly, however, few studies appear to have been made on the energy–volume coefficient of binary liquid mixtures. Since both the energy–volume coefficient and the cohesive energy density are closely related to the extent and strength of intermolecular interaction, it seems that these two parameters would be of particular value in investigating the structural properties and intercomponent interactions in liquid mixtures.

In this paper we report the energy–volume coefficients and cohesive energy densities of various DMSO–water mixtures. These data further illustrate the importance of intermolecular association in determining the properties of this system.

Experimental

Materials

DMSO was dried over freshly cut calcium hydride and distilled at reduced pressure (~ 0.1 mm Hg). The middle 70% cut was collected and stored in a tightly stoppered flask until use. The purity of the distilled liquid was determined by melting point (found, 19 °C; lit. (6), 18.55 °C) and refractive index (found, $n_D^{20} = 1.3590$; lit. (6), $n_D^{19.4} = 1.35886$).

Aqueous mixtures were prepared by weight from doubly distilled water and were degassed using the conventional freeze–pump–thaw technique.

Apparatus and Method

The apparatus used to determine the thermal pressure coefficient $\gamma_V = (\partial P/\partial T)_V$ of the liquid mixtures was similar in design to that employed by several other investigators (7, 8). The sample cell was constructed from Pyrex glass and had a volume of about 23 ml. The condition of constant volume was determined by a metal probe, mercury contact which activated a milliammeter in an external circuit. The metal probe was constructed from tungsten for rigidity and was tipped with a platinum spike for a cleaner contact with mercury. The sample cell was enclosed in a 316 stainless steel pressure vessel equipped with a heat exchanger constructed from a coil of 0.25 in. i.d. copper tubing. Pressure (0–20 atm) was generated by a Blackhawk Model P228 hand pump using transformer oil as the pressurizing medium. The pressure was measured with an Ashcroft–Bourdon tube gauge (0–20 atm). The gauge was checked periodically against a dead weight tester and was found to be accurate to ±0.03 atm. The apparatus was connected to the pressure line, and placed in an oil thermostat bath which was controlled to better than ±0.02 °C. The pressure was adjusted until the platinum–mercury contact was made. The temperature was then changed and the pressure readjusted to again make contact. Temperature changes

[1]Present address: Materials Science Branch, Atomic Energy of Canada Ltd., Pinawa, Manitoba.

Can. J. Chem. Downloaded from www.nrcresearchpress.com by 210.87.254.42 on 09/05/12
For personal use only.

were measured with a 6° Beckman thermometer which was calibrated to ±0.005 °C against a platinum resistance thermometer.

It is important to examine at this stage the effect of the heat of compression of the oil and sample liquid on the *P–T* data obtained as described above. When liquids are compressed adiabatically (*i.e.* rapidly), the temperature increases according to eq. 1.

$$[1] \qquad \left(\frac{\partial T}{\partial P}\right)_s = \frac{T\alpha V}{C_p}$$

where α is the coefficient of thermal expansion, V the volume, and C_p the heat capacity of the liquid. Over a small pressure range (*e.g.* 20 atm) the temperature change may be expressed as

$$[2] \qquad \Delta T = (T\alpha V/C_p).\Delta P$$

Equation 2 predicts a temperature increase on rapid compression at room temperature of ~ 0.04 and ~ 0.4 °C for water and a number of organic liquids (including oil), respectively. It is clear, therefore, that rapid compression of the system introduces serious errors into temperature measurement since the temperature intervals used in the measurement of γ_V varied between 0.8 and 2.5 °C. In order to alleviate this problem a thermistor was placed inside the pressure vessel to monitor the temperature of the contents. It was found that before a *P–T* reading could be taken the pressure had to be maintained to within ±0.5 atm of the contact pressure for 1 h so that the heat of compression could be fully dissipated to maintain isothermal conditions between the vessel contents and the thermostatting oil.

Results

Typical plots of applied pressure (P) *vs.* temperature (T) over the range of temperature employed in each determination (0.8 to 2.5 °C) showed that the data are adequately represented by the linear expression

$$[3] \qquad P = mT + C$$

where the gradient m is equal to the observed *thermal–pressure coefficient*, γ_{obs}. Each γ_{obs} value requires correction for the finite expansion and compression of glass. This correction is normally made (9) using eq. 4.

$$[4] \qquad \gamma_V = \gamma_{obs}\left(1 - \frac{\beta_g}{\beta_l}\right) + \frac{\alpha_g}{\beta_l}$$

where α_g and β_g are the coefficients of thermal expansion and compressibility of Pyrex glass and β_l is the coefficient of compressibility of the liquid under investigation. Insufficient data are available in the literature on the compressibility of aqueous DMSO as a function of composition and temperature to allow the correction to be made using eq. 4 directly. Instead, the necessary correction can be applied using the following equality derived from thermodynamics.

$$[5] \qquad \beta_l = \alpha_l/\gamma_V$$

Substitution of eq. 5 into eq. 4 results in the following expression for γ_V

$$[6] \qquad \gamma_V = \gamma_{obs} \cdot \left(\frac{\alpha_l}{\gamma_{obs}\beta_g + \alpha_l - \alpha_g}\right)$$

Numerical values for α_g and β_g were taken as 9.9×10^{-6} deg^{-1} (8) and 3.06×10^{-6} atm^{-1} (8) and were assumed to be independent of temperature over the range of temperature employed in this study. Coefficients of expansion of the mixtures were calculated using eq. 7 where ρ_T is the density of the liquid at temperature T.

$$[7] \qquad \alpha_l = -(\partial \ln \rho_T/\partial T)$$

Plots of ρ_T *vs.* T using data reported in the literature (10) revealed that for all the liquid systems studied except pure water, α_l could be considered temperature independent without significantly altering the magnitude of the correction to γ_{obs}. In the case of pure water, α_l was calculated for each temperature from density data tabulated in the literature (11).

The *energy–volume coefficient*, $(\partial U/\partial V)_T$, of a system can be related to the thermal pressure coefficient, $(\partial P/\partial T)_V$ or γ_V by eq. 8 which is often termed the "thermodynamic equation of state."

$$[8] \qquad \left(\frac{\partial U}{\partial V}\right)_T = T\left(\frac{\partial P}{\partial T}\right)_V - P$$

For most systems (including aqueous DMSO) $T\gamma_V$ is very much greater than the external pressure, P, and eq. 8 can be approximated to

$$[9] \qquad \left(\frac{\partial U}{\partial V}\right)_T = T\left(\frac{\partial P}{\partial T}\right)_V, \qquad P = 1 \text{ atm}$$

Thermal pressure and energy–volume coefficients calculated using eqs. 6 and 9, respectively, for various DMSO–water mixtures at several temperatures are listed in Table 1. In view of the probable errors in temperature (< 0.02 °C) and pressure (< 0.05 atm), both quantities are considered accurate to better than ±2%. Thermal pressure coefficients listed in parentheses were calculated from data given in the literature. In general the agreement between both sets of data is very satisfactory.

TABLE 1. Thermal pressure coefficients and internal pressure of DMSO–water mixtures at various temperatures

Mole fraction DMSO	T (°C)	γ_V (atm deg^{-1})	$\left(\frac{\partial U}{\partial V}\right)_T$ (atm)	Mole fraction DMSO	T (°C)	γ_V (atm deg^{-1})	$\left(\frac{\partial U}{\partial V}\right)_T$ (atm)
0.000	13.1	2.68 (2.70)*	767	0.100	21.1	12.93	3805
	21.2	4.86 (4.80)	1431		41.2	14.78	4646
	27.1	6.09 (6.10)	1829		51.3	15.66	5081
	33.5	7.50 (7.45)	2300				
	43.5	9.23 (9.20)	2923				
	57.4	11.63 (11.50)	3844				
0.200	23.1	18.45	5466	0.300	22.1	20.42	6029
	34.6	18.50	5694		40.0	19.45	6091
	52.6	18.62	6066		51.4	19.16	6219
0.400	23.4	20.52	6085	0.600	23.7	19.04	5652
	37.9	19.69	6125		38.2	17.95	5589
	51.9	18.74	6091		52.0	16.92	5502
0.800	24.5	17.74	5281	1.000	25.5	16.96(17.06)†	5065
	36.8	16.76	5195		37.8	16.59(16.05)	5159
	52.6	15.96	5199		51.8	15.45	5021

*Reference 23.
†Reference 8.

TABLE 2. Internal pressure and cohesive energy density parameters for DMSO–water mixtures at 25 °C

Mole fraction DMSO	γ_V (atm deg^{-1})	$\left(\frac{\partial U}{\partial V}\right)_T$ (atm)	$\left(\frac{\Delta U_V}{V}\right)$ (atm)	n	$\left(\frac{\partial \gamma_V}{\partial T}\right)$ (atm deg^{-2})
0.000	5.68	1694	22703	0.075	0.223
0.100	13.31	3969	18854	0.210	0.090
0.200	18.45	5501	16119	0.341	0.0075
0.300	20.25	6038	13872	0.435	−0.046
0.400	20.48	6106	12307	0.496	−0.064
0.600	18.95	5650	9755	0.579	−0.078
0.800	17.65	5263	8144	0.646	−0.068
1.000	17.10	5099	6955	0.733	−0.059

Numerical values for γ_V, $(\partial U/\partial V)_T$, and the temperature dependence of γ_V were calculated graphically at 25 °C and are listed in Table 2. The $d\gamma_V/dT$ values are considered accurate to ± 0.015 atm deg^{-2}. It is interesting to note that the value obtained in this work for pure DMSO is significantly less negative than that reported by Lau, Malcolm, and Fenby (8). However, the value measured in this work was found reproducible to within the error limits claimed.

In 1945 Frank (12) proposed that for small changes in volume the energy of the liquid, U, can be written as

$$[10] \qquad U = U_g - A/V^n$$

where U_g represents the energy of the perfect gas state. Differentiation of U with respect to volume at constant temperature results in eq. 11 for the energy–volume coefficient of the system.

$$[11] \qquad \left(\frac{\partial U}{\partial V}\right)_T = n\left(\frac{U_g - U}{V}\right)$$

This relationship is commonly expressed as eq. 12.

$$[12] \qquad \left(\frac{\partial U}{\partial V}\right)_T = n\left(\frac{\Delta U_V}{V}\right)$$

where ΔU_V is the energy of vaporization to the perfect gas state. The quantity $\Delta U_V/V$ is referred to as the *cohesive energy density* of the liquid.

The energy of vaporization of a real liquid mixture to the perfect gas state can be calculated using eq. 13, which was derived from simple thermodynamics.

$$[13] \qquad \Delta U_V = x_1\Delta H_{V,1} + x_2\Delta H_{V,2} - \Delta H_M - RT$$

The quantities $\Delta H_{V,1}$ and $\Delta H_{V,2}$ are enthalpies of vaporization to the perfect gas state for com-

Can. J. Chem. Downloaded from www.nrcresearchpress.com by 210.87.254.42 on 09/05/12
For personal use only.

Can. J. Chem. Downloaded from www.nrcresearchpress.com by 210.87.254.42 on 09/05/12
For personal use only.

ponents 1 and 2, respectively, and ΔH_M is the heat of mixing per mole of mixture. At 25 °C the enthalpies of vaporization of water and DMSO to the perfect gas states are 10.52 (13) and 12.60 kcal mol^{-1} (8, 13), respectively. Energies of vaporization for various DMSO–water mixtures were calculated using these data and heats of mixing taken from the literature (14). Division of each ΔU_V value calculated as described above by the molar volume of the mixture (14) results in the cohesive energy density. The cohesive energy densities are listed in Table 2 together with energy–volume coefficients interpolated at 25 °C from data listed in Table 1. Numerical values for n are also listed and were calculated using eq. 12.

Discussion

Energy–Volume Coefficients

The variation of the energy–volume coefficient, $(\partial U/\partial V)_T$, with solvent composition for the DMSO–water binary liquid system is illustrated in Fig. 1. The most significant feature of this plot is the rapid increase in $(\partial U/\partial V)_T$ on addition of DMSO to water culminating in a maximum in this parameter at 0.3–0.4 mole fraction cosolvent. Many other properties of this system, including the excess thermodynamic functions of mixing (14, 15) and various non-thermodynamic properties such as viscosity (10), exhibit extrema in this region of solvent composition. Various workers (10, 16) have attributed these extrema to maximization of DMSO–water interactions resulting in the formation of transient polymeric species of the type, $(DMSO.2H_2O)_n$, in the liquid mixture. This same hypothesis can be used to account for the maximum in the variation of $(\partial U/\partial V)_T$ with solvent composition.

Gibson and Loeffler (17, 18) and others (19) postulate that where classical mechanics are applicable, the total energy of a fluid may be regarded as the sum of three terms; (*a*) the mean kinetic energy of the molecules at their equilibrium positions including the energy associated with rotation or internal degrees of freedom, $U(T)$; (*b*) the potential energy due to attractive intermolecular forces, U_A; and (*c*) due to repulsive forces U_R.

$$[14] \qquad U = U(T) + U_A + U_R$$

Since $U(T)$ is dependent only on temperature then differentiation of the total energy, U, with respect to volume at constant temperature yields

$$[15] \qquad \left(\frac{\partial U}{\partial V}\right)_T = \left(\frac{\partial U_A}{\partial V}\right)_T + \left(\frac{\partial U_R}{\partial V}\right)_T$$

The variation of the experimentally measured energy–volume coefficient can now be discussed in terms of separate components for intermolecular attraction and repulsion. Before doing so, however, it is necessary to examine the properties of the two terms on the right hand side of eq. 15.

U_A and U_R are known to vary with intermolecular distance, and therefore volume, as illustrated in Fig. 2, $(\partial U_A/\partial V)_T$ and $(\partial U_R/\partial V)_T$ are clearly positive and negative, respectively; and since

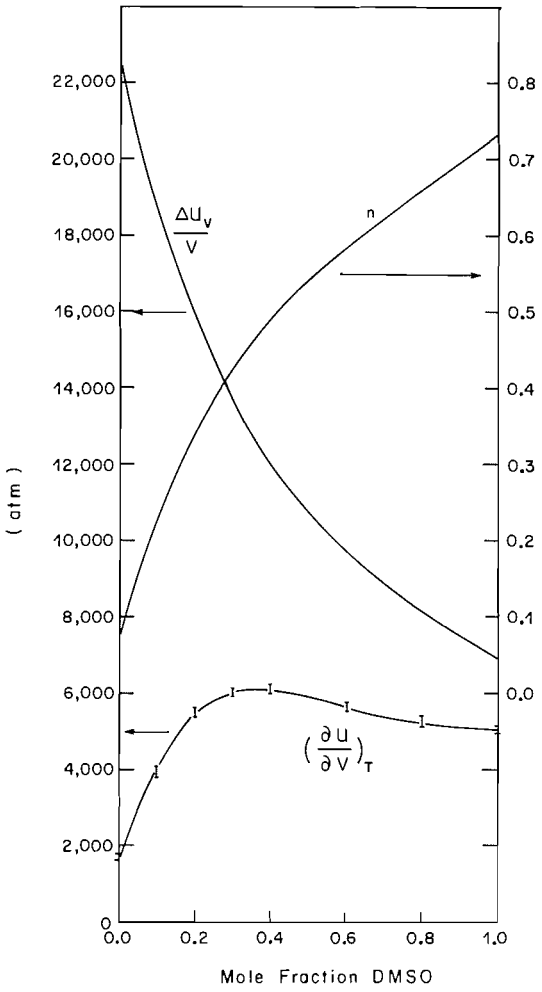

FIG. 1. Energy–volume coefficients and cohesive energy density parameters for DMSO–water mixtures at 25 °C.

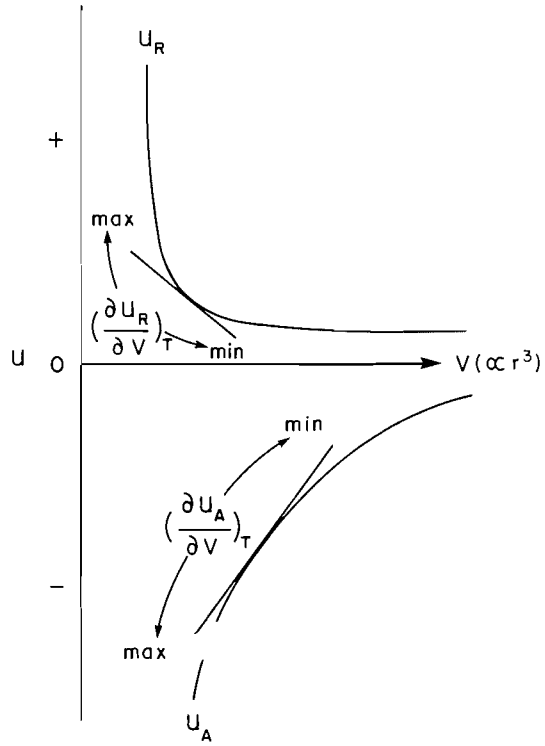

FIG. 2. Schematic representation of intermolecular interaction potential energy curves.

the sum of these terms, $(\partial U/\partial V)_T$, is observed to be positive the attractive term must always be numerically larger than the repulsive term. However, the excess volume of mixing of DMSO–water mixtures (14) passes through a minimum at 0.3 to 0.4 mole fraction DMSO and it is reasonable to expect that the average molecular separation passes through a minimum in the same region of solvent composition. Inspection of Fig. 2 shows that if the average intermolecular distance passes through a minimum $(\partial U_A/\partial V)_T$ and $(\partial U_R/\partial_V)_T$, the tangents to the curves in Fig. 2 will pass through positive and negative maxima, respectively. Since the observed $(\partial U/\partial V)_T$ passes through a positive maximum we conclude that the energy–volume coefficient behavior of the mixture results from the dominance of the attractive term $(\partial U_A/\partial V)_T$. Hence the observed maximum in the energy–volume coefficient at 0.3 to 0.4 mole fraction DMSO is consistent with the previously suggested (10, 16) maximization of attractive intercomponent (*i.e.* DMSO–water) interactions in this region of solvent composition. The low energy–volume coefficient observed for pure water probably reflects a large negative contribution from $(\partial U_R/\partial V)_T$ due to repulsive forces which attempt to arrange the molecules in the energetically favored open three-dimensional structure characteristic of ice.

The foregoing arguments permit the prediction that, for a system with a positive maximum in the excess volume of mixing, $(\partial U/\partial V)_T$ will exhibit either a minimum or at least negative deviations from ideal behavior, *i.e.* the reverse situation to that observed and rationalized above for the DMSO–water case. Very few systems have been examined in sufficient detail to permit a test of this prediction. Dunlap and Scott (20), however, have reported that the energy–volume coefficient for the perfluoro-*n*-hexane/*n*-hexane system shows negative deviations from ideality. Since this system exhibits a positive maximum in the excess volume of mixing the energy–volume coefficient behavior is in keeping with our prediction.

Cohesive Energy Densities

The dependence of $(\partial U/\partial V)_T$ on solvent composition can also be examined by considering the relationship between the energy–volume coefficient and the cohesive energy density $(\Delta U_V/V)$ of the system. This has been examined at length (21, 22) for one-component systems, but no equivalent analyses appear to have been performed for aqueous–organic binary mixtures. Such an analysis for the system under investigation in this work is shown in Fig. 1. Both the cohesive energy density and n vary monotonically with solvent composition although their product, $(\partial U/\partial V)_T$, does not. The initial rapid increase of $(\partial U/\partial V)_T$ with solvent composition is seen to be a consequence of a rapid increase in n which outweighs the simultaneous decrease in the cohesive energy density. On the other hand, at DMSO mole fractions greater than 0.4, $(\partial U/\partial V)_T$ decreases and this behavior is seen to result from the continued decrease of $(\Delta U_V/V)$ with solvent composition and a less pronounced increase in n.

While few conceptual difficulties exist in the interpretation of cohesive energy densities, the significance of n is less clear. Hildebrand (21) and Allen, Gee, and Wilson (22) report that for non-polar liquids, n is approximately equal to unity, and this provides a useful rule for esti-

Can. J. Chem. Downloaded from www.nrcresearchpress.com by 210.87.254.42 on 09/05/12
For personal use only.

Can. J. Chem. Downloaded from www.nrcresearchpress.com by 210.87.254.42 on 09/05/12
For personal use only.

mating energy–volume coefficients from cohesive energy densities for these liquids. However, the extensive compilation of n values reported by Allen, Gee, and Wilson (22) reveal that for strongly associated liquids, n is much less than unity and especially so for hydrogen bonded liquids. Thus, the monotonic increase in n from 0.075 for pure water to 0.733 for pure DMSO may reflect a general decrease in the overall hydrogen bonding in the system with increasing DMSO content. Despite the unidirectional trend of n from pure water to pure DMSO, it is worth remarking that there is a distinct change in the form of the dependence of n on solvent composition at or near the mole fraction commonly associated (10, 16) with the DMSO–water complex.

Entropy–Volume–Temperature Relationships

An important relationship, eq. 16, exists between the thermal pressure coefficient and the volume derivative of the entropy of a system at equilibrium.

$$[16] \qquad \gamma_V = (\partial S/\partial V)_T$$

The data reported in Table 2 reveals that γ_V passes through a maximum at 0.3–0.4 mole fraction DMSO. Equation 16 demands that at this composition the entropy (structure) of the system is most susceptible to isothermal expansion. Since expansion of the system should result in destruction of intermolecular interactions, these data indicate that the interactions present in a mixture of composition 0.3 to 0.4 mole fraction DMSO are more easily disrupted by isothermal expansion of the system than those present in either pure water or pure DMSO. It is reasonable to assume that the relatively specific intermolecular interactions that would be present in any transient complex of the form, $(DMSO.2H_2O)_n$, might be expected to show such susceptibility to isothermal expansion of the system.

The temperature dependence of γ_V as a function of solvent composition is illustrated in Fig. 3. This plot clearly shows that the sign of $(\partial\gamma_V/\partial T)$ changes from positive to negative on passing through 0.2 mole fraction DMSO. This observation is rationalized as follows. Ordered configurations in water are not favored at smaller volumes, *i.e.* entropy increases as volume decreases and hence for these configurations, $(\partial S/\partial V)_T$ is negative. With increasing temperature, this order is destroyed and the contribution to the total $(\partial S/\partial V)_T$ becomes less negative. Thus for pure water, $(\partial\gamma_V/\partial T) = \partial(\partial S/\partial V)_T/\partial T$ is positive as observed. Conversely, for a "normal" associated liquid such as DMSO, the ordered configurations are energetically favored at smaller V resulting in a positive $(\partial S/\partial V)_T$. With increasing temperature $(\partial S/\partial V)_T$ becomes less positive due to thermal agitation, resulting in the observed negative value for $(\partial\gamma_V/\partial T)$. It should also be noted that at DMSO mole fractions greater than 0.5, $(\partial\gamma_V/\partial T)$ is virtually independent of solvent composition. This observation is in keeping with the suggestion of Lindberg and Kenttämma (16) that between 0.5 mole fraction DMSO and pure DMSO the structure of this system varies little with composition.

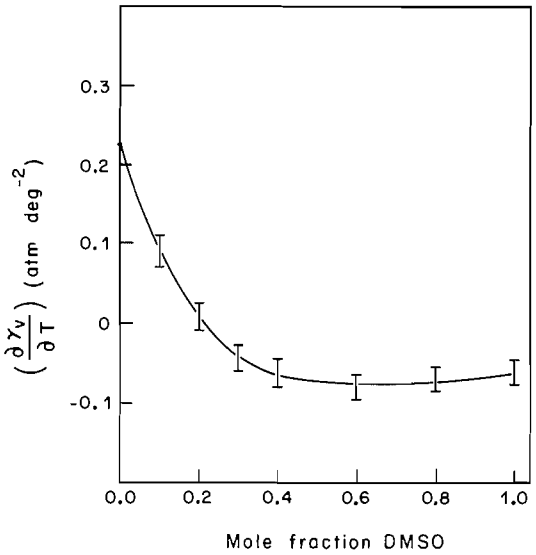

FIG. 3. Plot of the temperature dependence of the thermal pressure coefficient *vs.* solvent composition for DMSO–water mixtures at 25 °C.

Financial assistance for this work from the National Research Council of Canada is gratefully acknowledged.

1. D. D. MACDONALD and J. B. HYNE. Can. J. Chem. **48**, 2494 (1970).
2. E. TOMMILA. Acta Chem. Scand. **20**, 923 (1966).
3. E. TOMMILA and I. P. PITKÄNEU. Acta Chem. Scand. **20**, 937 (1966).
4. E. TOMMILA and M. SAVOLAINEN. Acta Chem. Scand. **20**, 946 (1966).
5. H. S. GOLINKIN, I. LEE, and J. B. HYNE. J. Amer. Chem. Soc. **89**, 1307 (1967).
6. D. MARTIN, A. WEISE, and H. J. NICLAS. Angew. Chem. Internat. Ed. 6, 318 (1967).

7. G. N. MALCOLM and G. L. D. RITCHIE. J. Phys. Chem. **66**, 852 (1962).
8. C. F. LAU, G. N. MALCOLM, and D. V. FENBY. Aust. J. Chem. **22**, 855 (1969).
9. W. WESTWATER, H. W. FRANTZ, and J. H. HILDEBRAND. Phys. Rev. **31**, 135 (1928).
10. J. M. G. COWIE and P. M. TOPOROWSKI. Can. J. Chem. **39**, 2240 (1961).
11. Handbook of Chemistry and Physics. The Chemical Rubber Publishing Co., Cleveland, Ohio, 40th Ed. (1959).
12. H. S. FRANK. J. Chem. Phys. **13**, 493 (1945).
13. D. R. STULL, E. F. WESTRUM JR., and G. C. SINKE. The Chemical Thermodynamics of Organic Compounds. Wiley, New York. 1969.
14. J. KENTTÄMAA and J. J. LINDBERG. Suomen Kemistilehti, B33, 32 (1960).
15. J. KENTTÄMAA and J. J. LINDBERG. Suomen Kemistilehti, B33, 98 (1960).
16. J. J. LINDBERG and J. KENTTÄMAA. Suomen Kemistilehti, B33, 104 (1960).
17. R. E. GIBSON and O. H. LOEFFLER. J. Amer. Chem. Soc. **61**, 2515 (1939).
18. R. E. GIBSON and O. H. LOEFFLER. J. Amer. Chem. Soc. **63**, 898 (1941).
19. W. A. ADAMS and K. J. LAIDLER. Can. J. Chem. **45**, 123 (1967).
20. R. D. DUNLAP and R. L. SCOTT. J. Phys. Chem. **66**, 631 (1962).
21. J. H. HILDEBRAND. Phys. Rev. **34**, 984 (1929).
22. G. ALLEN, G. GEE, and G. J. WILSON. Polymer, **1**, 456 (1960).
23. J. S. ROWLINSON. Liquids and Liquid Mixtures. Butterworths, London, 2nd Ed. 1969.

Can. J. Chem. Downloaded from www.nrcresearchpress.com by 210.87.254.42 on 09/05/12
For personal use only.

Can. J. Chem. Downloaded from www.nrcresearchpress.com by 210.87.254.5 on 09/05/12
For personal use only.

Sulfur Dioxide Insertion Reactions of some Compounds containing Sn—C and Fe—Sn—C Bonds[1]

R. C. EDMONDSON
Department of Chemistry, U.M.I.S.T., Sackville Street, Manchester M60 1QD, England

AND

D. S. FIELD AND M. J. NEWLANDS
Department of Chemistry, Memorial University of Newfoundland, St. John's, Newfoundland

Received September 9, 1970

The preparations of $[CpFe(CO)_2]_2Sn[OS(O)Ph]_2$, $CpFe(CO)_2SnPh[OS(O)Ph]_2$, $CpFe(CO)_2SnPh[OS(O)Ph]OH$, and $Ph_2Sn[OS(O)Ph]_2$ by sulfur dioxide insertion into the C—Sn bond and also by reaction of the sodium phenyl sulfinate with the corresponding chloro-compounds are reported. The infrared (i.r.) spectra and some reactions of these compounds are also discussed.

Canadian Journal of Chemistry, **49**, 618 (1971)

Introduction

Insertion reactions between sulfur dioxide and organometallic compounds have received much attention during the last few years (*e.g.*, refs. 1–6 and references therein). A wide variety of reactions and of types of insertion product has now been claimed. Thus, for a compound containing Fe—Sn—C bonds, insertion of sulfur dioxide between either the Fe—Sn and/or the Sn—C bonds might be expected. The product could also be an *S*-sulfinate

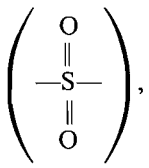

O-sulfinate

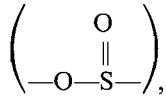

or a polymeric O-bonded sulfinate

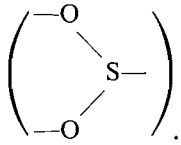

The first insertion of sulfur dioxide into a C—Sn bond was briefly reported earlier by two of us (7). We now discuss this reaction and others in more detail.

[1]Presented in brief at the C.I.C.–A.C.S. Joint Conference, Toronto, 24–29 May, 1970. Abstract No. 30.

Discussion

Bis(dicarbonyl-π-cyclopentadienyliron)diphenyltin(IV) reacts with sulfur dioxide, either in benzene solution or in liquid sulfur dioxide, giving $[CpFe(CO)_2]_2Sn[OS(O)Ph]_2$ in good yield (70 and 60%, respectively). The infrared spectrum shows no bands in the 1200–1300 and 1030–1150 cm^{-1} regions expected for the ν_{asym} S=O and ν_{sym} S=O of compounds containing the 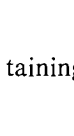 group (8, 9). Instead, a pattern is observed at 800–900 cm^{-1} (Fig. 1) which is assigned to $\nu_{S=O}$ and ν_{S-O} of an *O*-sulfinate and also the δ_{CH} of the cyclopentadienyl group. The same compound is also obtained using sodium phenylsulfinate

$$[CpFe(CO)_2]_2SnCl_2 + 2NaSO_2Ph \rightarrow [CpFe(CO)_2]_2Sn[OS(O)Ph]_2\ (60\%) + 2NaCl$$

This shows that the product is an *O*-sulfinate rather than an *S*-sulfinate or a sulfone. Ultimate proof of this structure has been obtained by X-ray analysis (10).

On heating at 180° for 48 h, $[CpFe(CO)_2]_2Sn[OS(O)Ph]_2$ decomposes to give diphenyldisulfide and a black non-volatile solid. Although organic sulfones and diphenyl-*O*-sulfinato-mercury evolve sulfur dioxide on thermal decomposition, no sulfur dioxide was detected in this case (11, 12), *cf.*

Can. J. Chem. Downloaded from www.nrcresearchpress.com by 210.87.254.5 on 09/05/12
For personal use only.

$$Hg(SO_2Ph)_2 \xrightarrow{\Delta} HgPh_2 + SO_2$$

$$R{-}\overset{\overset{O}{\|}}{\underset{\underset{O}{\|}}{S}}{-}R^1 \xrightarrow{\Delta} R{-}R^1 + SO_2$$

(R = alkyl, R^1 = alkyl or aryl)

Reaction with hydrogen chloride likewise evolved no sulfur dioxide. The products were $[CpFe(CO)_2]_2SnCl_2$ and diphenylthiolsulfonate (13, 14), *cf.*

$$Mn(CO)_5SO_2Me \xrightarrow{Cl_2} Mn(CO)_5Cl + SO_2$$

$$[CpFe(CO)_2]SnPh_3 \xrightarrow{HCl} [CpFe(CO)_2]SnCl_3$$

The diphenylthiosulfonate probably arises via decomposition of phenylsulfinic acid under acidic conditions (15) although no sulfonic acid was detected.

$$[CpFe(Co)]_2Sn[OS(O)Ph]_2 \xrightarrow{HCl} [CpFe(CO)_2]_2SnCl_2\ (79\%) + 2PhSO_2H$$

$$3\ PhSO_2H \xrightarrow{H^+} PhSO_2SPh\ (80\%) + PhSO_3H + H_2O$$

Treatment of (dicarbonyl-π-cyclopentadienyliron)triphenyltin(IV) with sulfur dioxide was expected to yield the analogous $[CpFe(CO)_2]Sn[OS(O)Ph]_3$. However, the initial yellow product was found to be $[CpFe(CO)_2]SnPh[OS(O)Ph]_2$ which decomposed on treatment with boiling ethanol to give orange crystals of $CpFe(CO)_2SnPh[OS(O)Ph]OH$.

$$CpFe(CO)_2SnPh_3 \xrightarrow{SO_2} CpFe(CO)_2Sn(Ph)(OS(O)Ph)(OS(O)Ph)$$

$$\xrightarrow{EtOH} CpFe(CO)_2Sn(Ph)(OS(O)Ph)(OH)\ (32\%)$$

Fong and Kitching (3) have very recently shown that the insertion of sulfur dioxide into a carbon–tin bond is very likely an electrophilic substitution. A consequence of this in the present system is that insertion of sulfur dioxide is more difficult into the second Sn—Ph bond than into the first, and no insertion occurs into the third Sn—Ph bond. A similar product is obtained in the reaction between $(CO)_5MnSnPh_3$ and sulfur dioxide (16). Confirmation of the identity of the two iron compounds was provided by the synthesis using sodium phenylsulfinate

$$CpFe(CO)_2SnPhCl_2 + NaSO_2Ph \rightarrow CpFe(CO)_2SnPh[OS(O)Ph]_2\ (18\%) + CpFe(CO)_2SnPh[OS(O)Ph]OH\ (18\%)$$

The nuclear magnetic resonance (n.m.r.) and infrared (i.r.) spectra are consistent with these formulations. The $\nu_{S=O}$ and ν_{S-O} occur in the same region as for $[CpFe(CO)_2]_2Sn[OS(O)Ph]_2$ where the *O*-sulfinate structure is confirmed by X-ray analysis (Fig. 1).

Thermal decomposition of $CpFe(CO)_2SnPh[OS(O)Ph]OH$ at 190° yields diphenyldisulfide; no sulfur dioxide was evolved. Treatment with hydrogen chloride yields $[CpFe(CO)_2]SnCl_3$ and diphenylthiolsulfinate, again no sulfur dioxide was evolved.

The only product which was isolated when $[CpFe(CO)_2]_2SnMe_2$ was treated with sulfur dioxide was $CpFe(CO)_2SO_2Me$ (8). This may be a decomposition product of $[CpFe(CO)_2]_2Sn[OS(O)Me]_2$ although the reaction between $CpFe(CO)_2SnMe_3$ and sulfur dioxide is said to yield a product containing $Fe{-}\overset{\overset{O}{\|}}{\underset{\underset{O}{\|}}{S}}{-}Sn$ (4). The lack of reactivity of $[CpFe(CO)_2]_2SnCl_2$ towards sulfur dioxide at 50° for 5 days clearly reflects the stability of this compound. No insertion of sulfur dioxide between the Fe—Sn bond or substitution of sulfur dioxide for carbonyl groups was detected. The starting material was completely recovered in 97% yield.

Although diphenyltin dichloride and tetraphenyltin are recovered unchanged after 24 h at 20° in liquid sulfur dioxide (the latter probably owing to its insolubility), triphenyltin chloride readily reacts under identical conditions yielding diphenyltin dichloride and a white insoluble compound, diphenylbis(phenyl *O*-sulfinato)tin(IV).

$$2Ph_3SnCl \xrightarrow{SO_2} Ph_2SnCl_2\ (80\%) + Ph_2Sn[OS(O)Ph]_2\ (84\%)$$

The same product was also obtained from the reaction between diphenyltin dichloride and sodium phenylsulfinate

$$Ph_2SnCl_2 + 2PhSO_2Na \rightarrow Ph_2Sn[OS(O)Ph]_2\ (99\%) + 2NaCl$$

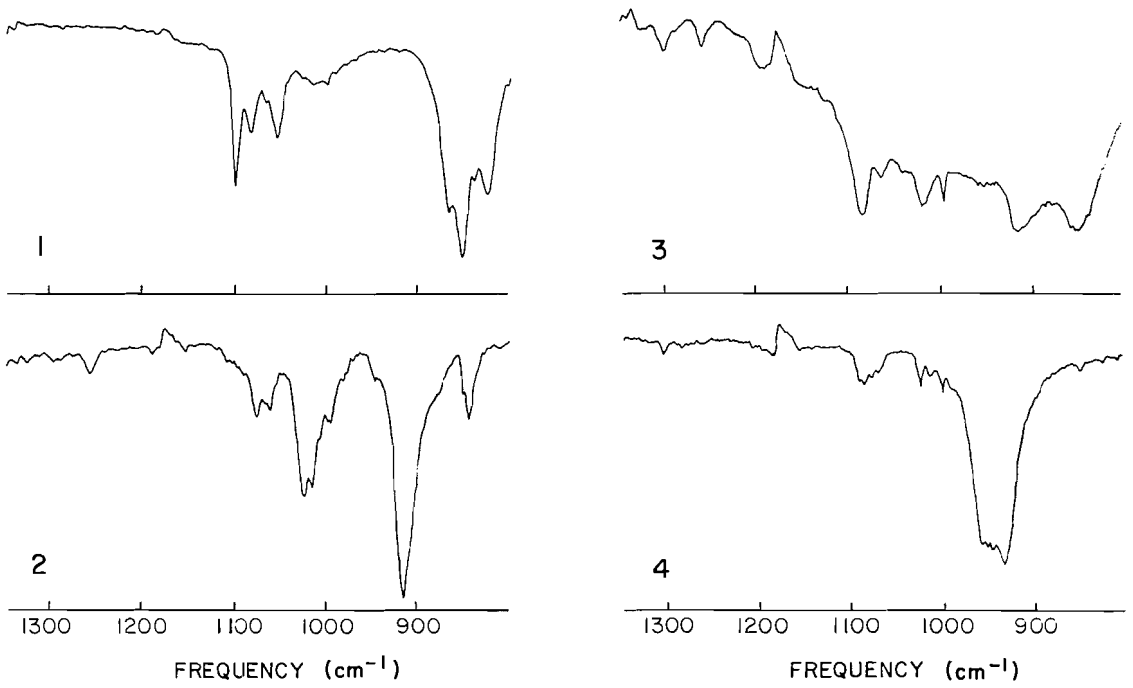

FIG. 1. Infrared spectra in the region 1350 to 800 cm^{-1}; (1), $[CpFe(CO)_2]_2Sn[OS(O)Ph]_2$; (2), $CpFe(CO)_2SnPh[OS(O)Ph]OH$; (3), $CpFe(CO)_2SnPh[OS(O)Ph]_2$; (4) $Ph_2Sn[OS(O)Ph]_2$.

Other workers have very recently reported similar results (5). The infrared spectrum of $Ph_2Sn[OS(O)Ph]_2$ showed ν_{SO} at 850 cm^{-1} which is consistent with the *O*-sulfinate linkage, probably in a hexacoordinate *O*-sulfinate-bridged polymer (*5b*) (Fig. 1).

It is possible that sulfur dioxide inserts into one Sn—Ph bond of triphenyltin chloride and that anion exchange then occurs between two such mono-substitution products

$$Ph_3SnCl + SO_2 \rightarrow Ph_2Sn\begin{matrix}OS(O)Ph\\Cl\end{matrix}$$

$$2Ph_2Sn\begin{matrix}OS(O)Ph\\Cl\end{matrix} \rightleftharpoons Ph_2Sn[OS(O)Ph]_2 + Ph_2SnCl_2$$

Further electrophilic substitution in either product is then probably unfavorable. An analogous reaction with sulfur trioxide has also been reported (17).

$$Me_3SnCl + SO_3 \rightarrow Me_2Sn(OSO_2Me)_2 + Me_2SnCl_2$$

Thermal decomposition of $Ph_2Sn[OS(O)Ph]_2$ at 225° yields diphenylsulfone; no sulfur dioxide is evolved. When $Ph_2Sn[OS(O)Ph]_2$ is treated with hydrogen chloride in methylene dichloride suspension, an oil is obtained which yields $Ph_2Sn[OS(O)Ph]_2$ on treatment with water. Presumably a hydrochloride is formed. Reaction with concentrated hydrochloric acid under reflux gives some diphenylthiolsulfonate and a hygroscopic oil, probably tin(IV) chloride.

Experimental

The starting materials were either purchased (Alfa Inorganics Ltd.) or prepared as reported in the literature. Anhydrous grade sulfur dioxide (*ex.* Matheson) was dried by passing through concentrated sulfuric acid and over phosphorus pentoxide/calcium chloride. All experiments were carried out under an atmosphere of nitrogen. Compounds containing iron and tin tended to be unstable in air especially when in solution. Infrared spectra were obtained as KBr discs using a Perkin–Elmer Model 457 spectrometer. Nuclear magnetic resonance spectra were recorded using a Varian A60 instrument operating at 60 Hz and for mass spectrometry a Perkin–Elmer Hitachi RMU6E spectrometer was employed. Element analyses were carried out by the A. Bernhardt Microanalytical Laboratory, West Germany, or the Schwarzkopf Microanalytical Laboratory, New York, except for the iron analyses which were performed in this laboratory using a Unicam S.P. 90 Atomic Absorption instrument.

Can. J. Chem. Downloaded from www.nrcresearchpress.com by 210.87.254.5 on 09/05/12
For personal use only.

Can. J. Chem. Downloaded from www.nrcresearchpress.com by 210.87.254.5 on 09/05/12
For personal use only.

Reaction of Sulfur Dioxide with Bis(dicarbonyl-π-cyclopentadienyliron)diphenyltin(IV)

(*a*) Sulfur dioxide (*ca.* 15 ml) was condensed into a 100 ml Pyrex ampoule containing bis(dicarbonyl-π-cyclopentadienyliron)diphenyltin(IV) (18) (2.02 g, 3.22 mmol). The ampoule was sealed *in vacuo* and left for 24 h at 22°. The volatile products were removed under reduced pressure leaving a reddish tar which yielded bis(dicarbonyl-π-cyclopentadienyliron)bis(phenyl-*O*-sulfinato)tin(IV) (1.47 g, 1.95 mmol, 60%) as yellow crystals on crystallization from ethanol.

(*b*) In a similar reaction sulfur dioxide was passed through a solution of bis(dicarbonyl-π-cyclopentadienyliron)diphenyltin(IV) (3.3 g, 5.3 mmol) in benzene (400 ml) during 48 h. The solvent was removed under reduced pressure leaving a yellow oil which crystallized from ether/petroleum ether (b.p. 60–80°). Recrystallization from methylene chloride/petroleum ether (b.p. 30–40°) yielded yellow crystals of bis(dicarbonyl-π-cyclopentadienyliron)bis(phenyl-*O*-sulfinato)tin(IV) (2.8 g, 3.7 mmol, 70%) m.p. 153–155°.

Anal. Calcd. for $C_{26}H_{20}O_8S_2Fe_2Sn$: C, 41.4; H, 2.7; S, 8.5; $Fe_2O_3SnO_2$, 41.1. Found: C, 41.7; H, 2.8; S, 8.2; residue 40.4.

λ_{max}(KBr): 3112 vw, 3084 vw, 3067 vw, 2008 vs, 1968 vs, 1966 vs, 1953 vs, 1926 w, 1475 vw, 1442 w, 1429 w, 1414 w, 1358 vw, 1100 m, 1084 w, 1055 w, 1016 vw, 1000 vw, 866 m, 852 s, 840 m, 825 m, 754 m, 699 m, 630 m, 600 w, 580 s, 573 s, 454 vw, 425 vw, 384 vw, 298 vw, 263 vw, 235 vw cm^{-1}. $^1H_{n.m.r.}$ $\delta_{(CDCl_3)}$ 5.09 (singlet, C_5H_5), 2.4 (multiplet, C_6H_5) τ. Intensity 1:1.

(*c*) Bis(dicarbonyl-π-cyclopentadienyliron)bis(phenyl-*O*-sulfinato)tin(IV) was also prepared when dichlorobis-(dicarbonyl-π-cyclopentadienyliron)tin(IV) (3.0 g, 5.5 mmol) and sodium phenylsulfinate dihydrate (1.86 g, 9.3 mmol) were heated under reflux (65°) in methanol (300 ml) during 22 h. The solvent was removed under reduced pressure leaving a yellow solid which recrystallized from methylene chloride/petroleum ether (b.p. 40–60°) to give bis(dicarbonyl-π-cyclopentadienyliron)bis(phenyl-*O*-sulfinato)tin(IV) (3.29 g, 4.4 mmol, 79% [based on $[CpFe(CO)_2]_2SnCl_2$]) m.p. 153–155°.

Anal. Calcd. for $C_{26}H_{20}O_8S_2Fe_2Sn$: C, 41.4; H, 2.7; S, 8.5; $Fe_2O_3.SnO_2$, 41.1. Found: C, 41.4; H, 3.0; S, 8.2; residue 41.0.

Reactions of Bis(dicarbonyl-π-cyclopentadienyliron)-bis(phenyl-O-sulfinato)tin(IV)

(a) Effect of Heat

Bis(dicarbonyl-π-cyclopentadienyliron)bis(phenyl-*O*-sulfinato)tin(IV) (0.29 g, 0.38 mmol) was placed in a sublimation apparatus fitted with a water-cooled finger and open to the atmosphere (fume hood) via a trap at −78° (solid CO_2/MeOH) and a calcium chloride tube. The sample was kept at 180° for 48 h. A white solid collected on the cold finger and was identified by i.r. (9) and mass spectrometry as diphenyldisulfide (0.026 g, 0.12 mmol, 31%) m.p. 58–60° (lit. (9) m.p. 61°). The non-volatile residue was a black solid (0.23 g) which contained no carbonyl groups (i.r.) and was not identified. No sulfur dioxide was detected (19).

(b) Effect of Hydrogen Chloride

Hydrogen chloride was passed through a stirred solution of bis(dicarbonyl-π-cyclopentadienyliron)bis(phenyl-*O*-sulfinato)tin(IV) (0.37 g, 0.49 mmol) in benzene (40 ml) during 1 h. The exit gases from the reaction vessel were passed through a trap cooled to −78°. No sulfur dioxide was detected in the trap after the reaction. The solvent was removed under reduced pressure leaving a reddish tar. Treatment with petroleum ether (b.p. 30–60°) afforded a white solid identified by its i.r. (9) and mass spectra as diphenylthiosulfonate (0.10 g, 0.40 mmol, 80%). The residual red tar which was insoluble in the petroleum ether was crystallized from ethanol to yield (i.r. and mass spectral analysis) dichlorobis(dicarbonyl-π-cyclopentadienyliron)tin(IV) (0.21 g, 0.39 mmol, 79%) m.p. 166–168% (lit. (20) m.p. 166–168°).

Reaction of Sulphur Dioxide with (Dicarbonyl-π-cyclopentadienyliron)triphenyltin(IV)

(Dicarbonyl-π-cyclopentadienyliron)triphenyltin(IV) (15) (10.24 g, 19.4 mmol) was stirred under reflux (−10°) in sulfur dioxide (*ca.* 30 ml) for 10 h. The sulfur dioxide was removed in a stream of nitrogen leaving a sticky yellow residue which slowly solidified *in vacuo*. The solid was treated with petroleum ether (b.p. 60–80°) in a Soxhlet apparatus which extracted a pale yellow solid, (dicarbonyl-π-cyclopentadienyliron)triphenyltin(IV) (1.50 g, 2.85 mmol, 15% recovery). The residue, insoluble in petroleum ether, was a yellow solid which was identified by i.r. spectroscopy (see later) as $CpFe(CO)_2SnPh[OS(O)Ph]_2$. However, recrystallization from boiling ethanol gave yellow needles of $CpFe(CO)_2SnPh[OS(O)Ph]OH$ (3.30 g, 6.22 mmol, 32%), m.p. 149–151°.

Anal. Calcd. for $C_{19}H_{16}SSnFeO_5$: C, 42.97; H, 3.04; S, 6.04; Fe, 10.52; $Fe_2O_3.SnO_2$, 43.41. Found: C, 42.98; H, 2.97; S, 5.82; Fe, 10.7; residue, 42.71.

λ_{max}(KBr) 3400–2800 bw, 3112 w, 3079 vw, 3056 vw, 2018 vs, 1995 w, 1970 vs, 1928 w, 1576 vw, 1479 w, 1473 vw, 1442 w, 1436 vw, 1429 m, 1414 w, 1358 vw, 1301 vw, 1261 vw, 1194 vw, 1157 vw, 1114 vw, 1080 vw, 1065 vw, 1027 m, 1020 m, 1000 w, 997 w, 920 vs, 847 w, 771 m, 732 m, 703 sh, 697 m, 691 sh, 626 m, 590 s, 578 s, 496 m, 451 m, 389 vw, 375 vw, 359 vw, 303 vw, 265 w, cm^{-1}. $^1H_{n.m.r.}$ $\delta_{(CDCl_3)}$ 5.53 (singlet, C_5H_5), 2.5 (multiplet, C_6H_5) τ. Intensity 1:2. Molecular weight (benzene) 1050 ± 2% (calcd. 531).

An identical sample was obtained from the reaction between dichloro(dicarbonyl-π-cyclopentadienyliron)-phenyltin(IV) and sodium phenylsulfinate:

Dichloro(dicarbonyl-π-cyclopentadienyliron)phenyltin-(IV) (0.986 g, 2.22 mmol) and sodium phenylsulfinate (2.43 g, 14.8 mmol) were stirred under reflux in absolute ethanol (50 ml) for 24 h. The solvent was removed under reduced pressure and the residue treated with methylene chloride and filtered through celite. The filtrate was evaporated to yield a reddish oil which on crystallization from absolute ethanol yielded yellow crystals of $CpFe(CO)_2SnPh[OS(O)Ph]OH$ (0.214 g, 0.403 mmol, 18% yield).

Anal. Calcd. for $C_{19}H_{16}SSnFeO_5$: C, 42.97; H, 3.04; S, 6.04; $Fe_2O_3.SnO_2$ 43.41. Found: C, 42.93; H, 2.94; S, 6.09; residue 43.25.

Evaporation of the ethanol filtrate yielded a reddish oil which gave $CpFe(CO)_2SnPh[OS(O)Ph]_2$ as a yellow powdery solid on washing with ether (0.265 g, 0.404 mmol, 18% yield).

Can. J. Chem. Downloaded from www.nrcresearchpress.com by 210.87.254.5 on 09/05/12
For personal use only.

Anal. Calcd. for $C_{25}H_{20}O_6S_2FeSn$: C, 45.83; H, 3.08; S, 9.79%. Found: C, 45.90; H, 3.24; S, 10.08.

λ_{max}(KBr) 3115 vw, 3053 w, 2018 vs, 1966 vs, 1575 vw, 1477 w, 1445 m, 1430 m, 1421 sh, 1303 vw, 1262 vw, 1089 m, 1067 vw, 1018 vw, 997 vw, 909 vw, 851 m, 753 m, 729 m, 694 m, 622 m, 584 s, 508 vw, 448 w, 308 vw, 263 vw cm^{-1}. $^1H_{n.m.r.}$ $\delta_{(CDCl_3)}$ 4.97 (singlet C_5H_5), 2.5 (multiplet C_6H_5) τ. Intensity 1:3.

Reactions of (Dicarbonyl-π-cyclopentadienyliron)-phenyl(phenyl-O-sulfinato)tin(IV)hydroxide

(a) Effect of Heat

$[C_5H_5Fe(CO)_2]SnPh[OS(O)Ph]OH$ (0.304 g, 0.572 mmol) was placed in a sublimation apparatus fitted with a water cooled finger and open to the atmosphere (fume hood) *via* a trap cooled to −78° and a calcium chloride tube. The sample was kept at 190° for 72 h. The apparatus was then evacuated and maintained at 190° for a further 6 h. No sulfur dioxide was detected. A white solid collected on the cold finger and was shown to be diphenyldisulfide (0.010 g, 0.046 mmol). The black tar-like residue contained no carbonyl groups (i.r.) and was not identified.

(b) Effect of Hydrogen Chloride

Hydrogen chloride was passed through a stirred solution of $[C_5H_5Fe(CO)_2]SnPh[OS(O)Ph]OH$ (0.597 g, 1.090 mmol) in benzene (40 ml) in 1 h. The exit gases from the reaction were passed through a trap cooled to −78°. No sulfur dioxide was detected. The solvent was removed under reduced pressure leaving a sticky yellow solid. Treatment with petroleum ether (b.p. 40–60°) and diethyl ether extracted a white solid identified by i.r. and mass spectroscopic analysis as diphenylthiosulfonate (0.116 g, 0.463 mmol). The yellow solid which was insoluble in the petroleum ether and diethyl ether was shown to be (i.r., mass spectroscopy) trichloro(dicarbonyl-π-cyclopentadienyliron)tin(IV) (14) (0.275 g, 0.684 mmol, 63%) m.p. 159–160° (from ethanol) (lit. (14) 150° decomp.).

Reaction of Sulfur Dioxide with Bis(dicarbonyl-π-cyclopentadienyliron)dimethyltin(IV)

Sulfur dioxide was passed through a stirred solution of bis(dicarbonyl-π-cyclopentadienyliron)dimethyltin(IV) (1.19 g 2.37 mmol) in diethylether (40 ml) in 3 h. The solvent was removed under reduced pressure leaving a dark red oily solid which proved difficult to crystallize. The oil was heated with methylene chloride (10 ml) and petroleum ether (b.p. 100–120°) (60 ml). The supernatant yellow solution was decanted and on cooling to 0° yielded pale yellow needles of dicarbonyl-π-cyclopentadienyl methyl-*S*-sulfinatoiron (8) (0.05 g, 0.20 mmol, 8%) m.p. 143–145° (lit. (8) 135°) identified by n.m.r., i.r. and mass spectrometry.

Reaction of Sulfur Dioxide with Dichlorobis(dicarbonyl-π-cyclopentadienyliron)tin(IV)

Sulfur dioxide (*ca.* 10 ml) was condensed into a 100 ml Pyrex ampoule containing dichlorobis(dicarbonyl-π-cyclopentadienyliron)tin(IV) (1.44 g 2.65 mmol). The ampoule was sealed *in vacuo* and left for 24 h at 22°. The reddish crystalline solid dissolved to give an orange red solution. The sulfur dioxide was removed under reduced pressure leaving a yellow solid, dichlorobis(dicarbonyl-π-cyclopentadienyliron)tin(IV) (1.37 g, 2.52 mmol, 95% recovery).

A similar experiment carried out at 50° for 5 days afforded only the dichlorobis(dicarbonyl-π-cyclopentadienyliron)tin(IV) (97% recovery).

Reaction of Sulfur Dioxide with Diphenyltin Dichloride

No reaction was observed between diphenyltin dichloride (5.79 g, 16.8 mmol) and sulfur dioxide (*ca.* 15 ml) after 24 h at 23°. On removal of the sulfur dioxide, a white solid was obtained, diphenyltin dichloride (5.56 g, 16.2 mmol, 96% recovery).

Reaction of Sulfur Dioxide with Triphenyltin Chloride

Sulfur dioxide (*ca.* 20 ml) was condensed into a 100 ml Pyrex ampoule containing triphenyltin chloride (2.27 g, 5.89 mmol). The ampoule was sealed *in vacuo* and left at 22° for 20 h. As the ampoule warmed up to 0° the colorless crystalline triphenyltin chloride dissolved to form a colorless solution. At 20° a white milky precipitate was formed and after 20 h at 22° the mixture was a stiff suspension. The sulfur dioxide was removed under reduced pressure and the white residue placed in a Soxhlet apparatus. Extraction with diethyl ether during 24 h afforded a colorless oily liquid which crystallized from petroleum ether (b.p. 30–60°) as a white crystalline solid identified by m.p. (41–42°) (lit (21) m.p. 40–41.5°), i.r., and mass spectroscopy as diphenyltin dichloride (0.81 g, 2.36 mmol, 80%). The white powdery residue which was insoluble in ether was $Ph_2Sn[OS(O)Ph]_2$ (1.38 g, 2.49 mmol, 84%) m.p. 218–219°.

Anal. Calcd. for $C_{24}H_{20}O_4S_2Sn$: C, 51.90; H, 3.64; S, 11.54; SnO_2, 27.14. Found: C, 52.00; H, 3.74; S, 11.46; residue, 26.89.

λ_{max}(KBr), 3082 vw, 3065 w, 1485 vw, 1475 w, 1442 w, 1429 m, 1083 w, 1079 w, 1060 sh, 1024 w, 1013 vw, 1001 w, 959 vs, 946 vs, 934 vs, 756 w, 741 sh, 737 m, 700 m, 691 m, 600 m, 590 m, 474 m, 459 m, 414 vw, 348 vw, 329 vw, 298 w cm^{-1}. $^1H_{n.m.r.}$ $\delta_{(dimethylsulfoxide)}$ 2.53 (broad singlet) τ.

An identical sample of diphenyldi[phenyl-*O*-sulfinato]-tin(IV) was obtained from the reaction of diphenyltin dichloride with sodium phenylsulfinate.

Diphenyltin dichloride (2.09 g, 6.09 mmol) in 95% ethanol (20 ml) was added to a stirred solution of sodium phenylsulfinate (3.15 g, 19.2 mmol) in 95% ethanol (50 ml). A copious white precipitate was immediately formed. The mixture was stirred under reflux for 1 h before the white product was filtered, washed with water, and dried over phosphorous pentoxide *in vacuo* to yield diphenyldi[phenyl-*O*-sulfinato]tin(IV) (3.34 g, 6.01 mmol, 98% yield) m.p. 218–220°.

Found; C, 51.96; H, 3.77; S, 11.46; Residue, 26.84%. $C_{24}H_{20}O_4S_2Sn$ requires; C, 51.90; H, 3.64; S, 11.54; SnO_2, 27.14%.

Reactions of Diphenyldi[phenyl-O-sulfinato]tin(IV)

(i) Effect of Heat

$Ph_2Sn[OS(O)Ph]_2$ (0.95 g, 1.71 mmol) was placed in a water-cooled sublimation apparatus open to the atmosphere (fume hood) via a cold trap (−78°) and a calcium chloride tube. A white solid sublimed during 18 h at 225° which was identified as diphenylsulfone (0.32 g,

1.47 mmol). The sublimation residue was a brownish solid (0.52 g). No sulfur dioxide was detected.

(ii) Effect of Hydrogen Chloride

Hydrogen chloride was passed through a stirred suspension of $Ph_2Sn[OS(O)Ph]_2$ (0.67 g, 1.21 mmol) in methylene chloride (40 ml) in 30 min. The exit gases from the reaction vessel were passed through a cold trap (−78°). After 10 min, the white suspension dissolved forming a colorless solution. The solvent was removed under reduced pressure yielding a colorless oil. On addition of water a white solid was formed. It was filtered, washed with water and diethylether to yield $Ph_2Sn[OS(O)Ph]_2$ (0.43 g, 0.77 mmol, 64% recovery), identical to the starting material (i.r.), m.p. 216–218°. No sulfur dioxide was detected.

(iii) Effect of Hydrochloric Acid

$Ph_2Sn[OS(O)Ph]_2$ (0.48 g, 0.86 mmol) and concentrated hydrochloric acid (40 ml) were heated under reflux during 20 h. A white oily solid was formed within 10 min, and became a white suspension in another 10 min. After 20 h a colorless solution was obtained containing a colorless oil ($d > 1$). Water (40 ml) was added and the mixture extracted with methylene chloride (3 × 40 ml) to yield a colorless oil (0.19 g), which was mostly diphenylthiolsulfonate containing probably some diphenyltin dichloride (i.r.). A foul odor was also detected. The aqueous solution was evaporated, yielding a white oily solid which, after 24 h *in vacuo* over phosphorus pentoxide and sodium hydroxide pellets, became an oily liquid. The liquid produced white fumes on contact with air with the formation of a white solid (0.13 g), probably $SnCl_4.nH_2O$.

Reaction of Sulfur Dioxide with Tetraphenyltin

No reaction was observed between tetraphenyltin (0.94 g, 2.20 mmol) and sulfur dioxide (*ca.* 15 ml) after 24 h at 22°. The tetraphenyltin appeared to be completely insoluble in the sulfur dioxide and was recovered after removal of the sulfur dioxide under reduced pressure (0.92 g, 2.15 mmol, 98% recovery).

We acknowledge the support of the National Research Council of Canada for the major part of this work and we thank Professor R. N. Haszeldine for his support of the initial part of this work at Manchester, England.

1. G. B. Deacon and P. G. Cookson. Inorg. Nucl. Chem. Lett. **5**, 607 (1969).
2. Y. Yamano, I. Masuda, and K. Shinra. Inorg. Nucl. Chem. Lett. **5**, 729 (1969).
3. C. W. Fong and W. Kitching. J. Organometal. Chem. **22**, 107 (1970).
4. R. E. J. Bichler and H. C. Clark. J. Organometal. Chem. **23**, 427 (1970).
5. (*a*) E. Lindner and U. Kunze. J. Organometal. Chem. **23**, C53 (1970). (*b*) E. Lindner, U. Kunze, G. Ritter, and A. Haag. J. Organometal. Chem. **24**, 119 (1970). (*c*) E. Lindner, U. Kunze, G. Vitzthum, G. Ritter, and A. Haag. J. Organometal. Chem. **24**, 131 (1970).
6. M. R. Churchill, J. Wormald, D. A. Ross, J. A. Thomasson, and A. Wojcicki. J. Amer. Chem. Soc. **92**, 1795 (1970).
7. R. C. Edmondson and M. J. Newlands. Chem. Commun. 1219 (1968).
8. J. P. Bibler and A. Wojcicki. J. Amer. Chem. Soc. **88**, 4862 (1966).
9. J. Cymerman and J. B. Willis. J. Chem. Soc. 1332 (1951).
10. R. F. Bryan and A. R. Manning. Chem. Commun. 1220 (1968).
11. G. B. Deacon. Aust. J. Chem. **20**, 1367 (1967).
12. J. L. Kice. Org. Sulfur Cpds. **2**, 115 (1966).
13. F. A. Hartman and A. Wojcicki. Inorg. Chem. **7**, 1504 (1968).
14. R. D. Gorsich. J. Amer. Chem. Soc. **84**, 2486 (1962).
15. J. L. Kice and K. W. Bowes. J. Amer. Chem. Soc. **84**, 605 (1962).
16. D. S. Field and M. J. Newlands. To be published.
17. H. Schmidbaur, L. Scohser, and M. Schmidt. J. Organometal. Chem. **15**, 77 (1968).
18. A. N. Nesmeyanov, K. N. Anisimov, N. E. Kolobova, and V. V. Skripkin. Izv. Akad. Nauk. SSSR, Ser. Khim. 1292 (1966).
19. A. E. Vogel. Practical Organic Chemistry. Longmans Press, 3rd Ed., 553 (1962).
20. F. Bonati and G. Wilkinson. J. Chem. Soc. 179 (1964).
21. R. C. Poller. J. Inorg. Nucl. Chem. **24**, 593 (1962).

Can. J. Chem. Downloaded from www.nrcresearchpress.com by 210.87.254.5 on 09/05/12
For personal use only.

Can. J. Chem. Downloaded from www.nrcresearchpress.com by 210.87.254.42 on 09/05/12
For personal use only.

Optical Activity of Symmetric Compounds in Chiral Media. I. Induced Circular Dichroism of Unbound Substrates

L. D. HAYWARD AND R. N. TOTTY
Department of Chemistry, University of British Columbia, Vancouver 8, British Columbia

Received August 5, 1970

In the presence of chiral environment compounds, C, optical rotation is induced in symmetric substrates, S, and may be detected as circular dichroism in the electronic spectra of the solutions. Thus the n–π^* transitions of symmetric and racemic carbonyl compounds, and of symmetric nitro and azo compounds, become optically active when these S are dissolved in chiral hydrocarbons, ketones, or carbinols, or in solutions of these C in achiral solvents. The rotational strengths of the induced circular dichroism bands of S are solvent, temperature, and concentration dependent. Only limited correlation of the sign and magnitude of the induced bands with the stereochemistry of C and S is evident on the data so far accumulated. Halogenated achiral solvents enhance the intensity, and, in some cases reverse the sign of the induced bands.

A new mechanism of asymmetric induction is proposed in which specific bonding of C with S is not prerequisite.

Canadian Journal of Chemistry, **49**, 624 (1971)

Introduction

The induced circular dichroism (i.c.d.) of the n–π^* transition of symmetric aromatic ketones (symmetric substrates, S) in chiral solvents (chiral environment compounds, C) was first observed by Bosnich (1). In a preliminary communication (2) we reported i.c.d. of symmetric and racemic aliphatic carbonyl compounds in the presence of chiral tetrahydrofuranols. Subsequent reports confirmed these results and indicated that circular dichroism may be induced in the lowest energy isotropic transitions of nitroalkanes (3) and thiones (4). Bolard, assuming that induction occurred *via* a hydrogen-bonded 1:1 ketone–alcohol complex, calculated the induced rotational strength (R_s) of acetone in the presence of (−)-menthol from the probable geometry of the complex but was unable to predict the sign of the i.c.d. band (5, 6). A similar 1:1 hydrogen-bonded complex was proposed by Noack on the basis of the concentration dependence of R_s of the n–π^* transition of cyclohexanone in (−)-menthol (3). However, Axelrod, Barth, and Bunnenberg have shown that hydrogen-bonding is not prerequisite to i.c.d. as circular dichroism is induced in the n–π^* transition of p,p′-dimethoxythiobenzophenone by a chiral ether or a chiral ketone (4).

We report here our investigations of the i.c.d. of symmetric and racemic carbonyl compounds, and of symmetric nitro and azo compounds in 2- and 3-component liquid systems. The plan of the work was to map on the largest practical scale the interactions of C of known configuration with S having accessible chromophores in ranges of solvent, temperature, and concentration in order to reveal the mechanism of induction of optical activity.

Experimental

Although the optical activity of a chiral compound is fully described by the signs and magnitudes of the rotational strengths, R, of each of its optically active electronic transitions, it is customary to report only the maximum differential molar absorption coefficient, $\Delta\varepsilon$, or the related quantity $[\theta] = 3300\,\Delta\varepsilon$ (deg mol^{-1} cm^2) of the experimentally accessible bands. Molar absorption coefficients are defined as molecular properties of solutes although it is well recognized that there are no truly "inert" solvents. Continuing these conventions $[\theta]_{max}$ values are quoted herein for the accessible i.c.d. bands of S in C + S systems as if they referred to S alone.

Circular dichroism spectra were measured on a JASCO ORD/UV/CD-5 spectrophotometer with a sensitivity of 1×10^{-4} with reference to a baseline of the chiral solution run at the same temperature. Racemic solvents gave no detectable circular dichroism (c.d.) signals. Measurements were repeated at intervals of up to 18 months using freshly prepared solutions of varying concentration. Low temperature measurements were made using 0.1 cm cells cooled in a quartz Dewar (J. F. Scanlon Co.) with the boil-off from liquid nitrogen (7); by controlling the flow rate a temperature stability of $\pm 2°$ was achieved. At the temperature of measurement solutions were either in the liquid state or formed stable glasses and the spectra were uncorrected for changes in density. All compounds, after purification, had infrared (i.r.), nuclear magnetic resonance (n.m.r.), and ultraviolet (u.v.) spectra and specific rotations in agreement with literature data.

Results

Carbonyl Compounds

In the presence of (+)-D-isosorbide ((+)-1,4;3,6-dianhydro-D-glucitol, (1R,4S,5R,8R)-

TABLE 1. Induced c.d. of symmetric and racemic carbonyl compounds (S)* in (+)-D-isosorbide (**1**) solution† at 25°

S	M	$\lambda_{max} \pm 2$ nm	$[\theta]_{max}$
Acetone	0.13	280	+14
Acetone-d_6	0.12	283	+17
2-Adamantanone	0.10	292	+26
Benzophenone	0.006	335	−58
Camphor	0.04	293	+25
Cyclohexanone	0.12	287	+21
2-Cyclohexylcyclohexanone	0.07	290	+16
Cyclopentanone	0.08	290	+16
2-Methylcyclohexanone	0.12	290	+11
3-Methylcyclohexanone	0.08	288	+18
3-Methylcyclopentanone	0.05	288	+16
Propanal	0.24	290	+8

*No i.c.d. was observed in solutions of acetophenone, anthrone, benzaldehyde, benzil, benzoin, 2,3-butanedione, *trans*-2-butenal, 9-fluorenone, or 2,4-pentanedione.
†1.37 M in acetonitrile.

4,8-dihydroxy-*cis*-2,6-dioxabicyclo[3.3.0]octane, **1**), in acetonitrile solution as C, symmetric and racemic carbonyl compounds (S) show a single positive or negative circular dichroic absorption band at or near the wavelength maximum characteristic of their lowest energy isotropic transition (Table 1). The i.c.d. band approximates the shape of the n–π^* absorption band and R_s of the ketones shows only slight dependence on their geometry, although Noack found that strongly sterically hindered ketones, such as hexamethylacetone, exhibit only very weak i.c.d. (3). Our failure to observe i.c.d. in several aromatic carbonyl compounds, including some that are relatively sterically unhindered, and in diketones, does not indicate that the induction of optical activity in these systems is not possible, but rather that it is too weak to be detected under our experimental conditions. Indeed, benzil and 9-fluorenone give rise to relatively strong i.c.d. bands in other C (1, 4).

Whilst the i.c.d. band of benzophenone in the presence of **1** is negative, the i.c.d. bands of the aliphatic ketones are all positive. To determine whether this behavior is general, the i.c.d. of benzophenone (S1) and 3-methylcyclohexanone (S2) were compared in the presence of a series of C of known absolute configuration (**1** to **14**, Table 2). It is at once apparent that the sign of the i.c.d. is a property of the C/S system and does not reflect the geometry of either C or S. There is no correlation between the sign of the $[\alpha]_D$ of C (or of the c.d. bands which determine $[\alpha]_D$) with the sign of the i.c.d. band of a particular S, nor between the signs of the i.c.d. bands of C/S1 and C/S2.

Although it may be taken as axiomatic that the enantiomers of C should give rise to i.c.d. bands of opposite sign with a particular S, this was verified with the enantiomers of 2-octanol, pantolactone, and diethyl tartrate; the observed bands are opposite in sign and equal in magnitude within experimental error.

The temperature dependence of the i.c.d. bands of aliphatic ketones has been reported (3, 6). We confirm these observations and note that the i.c.d. of benzophenone is also temperature dependent, $[\theta]_{max}$ in solvent **8** increasing from −130 at 25° to −330 at −40°. A similar increase is observed in solvent **11**.

A solution of benzophenone in (−)-*cis*-pinane (**13**) exhibits no detectable circular dichroism at 25° but at 10° a distinct negative i.c.d. band appears which increases in R_s when the temperature is further lowered to −45°. This observation confirms that hydrogen bonding is not essential for the induction of optical activity in achiral ketones, as has already been demonstrated for the thione chromophore (4).

Both benzophenone and 3-methylcyclohexanone show i.c.d. bands in solutions of **1** in a large molar excess of methanol (14:1) (Table **3**). In such 3-component systems competition between C and the achiral solvent for hydrogen-bonding sites would be expected, and the fact that the observed R_s are similar to those in non-hydroxylic "inert" solvents (Table 3) also indicates that hydrogen bonding between C and S is not prerequisite for i.c.d. Significantly in this context the use of 1,1,1-trifluoro-2-propanol as achiral solvent leads to an increase in R_s of the carbonyl i.c.d. band in comparison to a meth-

Can. J. Chem. Downloaded from www.nrcresearchpress.com by 210.87.254.42 on 09/05/12
For personal use only.

TABLE 2. Induced c.d. of benzophenone (S1) and of 3-methylcyclohexanone (S2) in chiral media (C)*

				Benzophenone (S1)		3-Methylcyclohexanone (S2)	
C	$[\alpha]_D$	M	Solvent	M	$[\theta]_{max}$†	M	$[\theta]_{max}$‡
Isosorbide (**1**)§	+45°	1.37	CH_3CN	0.09	−40	0.08	+18
Isomannide (**2**)	+90°	0.68	CH_3CN	0.09	−40	0.10	+14
Threitan (**3**)	−5°	0.96	CH_3CN	0.01	0	0.11	+13
Pantolactone (**4**)	−50°	1.53	CH_3CN	0.006	+68	0.08	+11
Diethyl tartrate (**5**)	−7.6°			0.08	+60‖	0.68	+20¶
Diethyl malate (**6**)	−10.0°			0.10	−141	0.58	−11
Ethyl lactate (7)	−11.7°			0.12	−138	0.62	−34
2,3-Butanediol (**8**)	−14.1°			0.09	−130	0.73	+3
1,2-Propanediol (**9**)	+11.2°			0.09	+60	0.50	−10
Menthol (**10**)	−49.7°	3.60	CH_3CN	0.08	−112	0.09	+6
2-Octanol (**11**)	−9.2°			0.05	+100	0.58	0
2-Methylbutanol (**12**)	−5.6°			0.09	0	0.72	0
cis-Pinane (**13**)	−24.5°			0.10	−285**	0.34	0**
Bornyl acetate (**14**)	−44°			1.00	0	0.10	0

*At 25 °.
†At 337 ± 3 nm.
‡At 288 ± 3 nm.
§No i.c.d. in solutions of the di-*O*-acetyl derivative.
‖At 358 ± 2 nm.
¶At 300 ± 2 nm.
**At −45 °; no i.c.d. at 25 °.

TABLE 3. Solvent effects on i.c.d. of carbonyl compounds in chiral solutions*

	Acetone		Benzophenone		3-Methylcyclohexanone	
Solvent	M	$[\theta]_{max}$	M	$[\theta]_{max}$	M	$[\theta]_{max}$
Water	0.9	+6				
Deuterium oxide	0.8	+5				
Methanol	0.8	+13†	0.11	−67	0.44	+11
Tetrahydrofuran			0.11	−46	0.45	+22
Trimethylphosphate			0.11	−61	0.45	+14
N,*N*-Dimethylformamide			0.11	−28	0.45	+10
1,1,1-Trifluoro-2-propanol			0.06	−114	0.31	+18
Acetic acid			0.10	−42	0.44	+15
Trifluoroacetic acid			0.11	0	0.45	0
Sulpholane			0.11	−59	0.45	+12
1,4-Dioxan			0.11	−58	0.44	+12
Formamide			0.11	0	0.45	0
Diethylene glycol			0.10	−68	0.45	+12
(−)-(R)-2,3-Butanediol (**8**)			0.06	−192	0.38	+23

*At 25 °, 1.37 *M* (+)-D-isosorbide (**1**).
†+19 at −65 °.

anolic solution; perfluoroalcohols are usually considered capable of forming stronger hydrogen bonds to carbonyl compounds than are the hydrocarbon analogues (8, 9). The absence of i.c.d. in trifluoroacetic acid is probably due to rapid chemical change in the system.

We find no correlation between the molar ellipticities of the i.c.d. bands of benzophenone and 3-methylcyclohexanone and the polarity of the "inert" solvent, as measured by dielectric constant or E_T values (10) with (+)-D-isosorbide as C. Solvents of low dielectric constant such as 1,4-dioxan or tetrahydrofuran lead to i.c.d. bands of the same strength as solvents of high dielectric constant, such as methanol or sulfolane, although formamide, with an exceptionally high dielectric constant, gives rise to no detectable i.c.d. No shifts in wavelength of the i.c.d. band maxima or multiple i.c.d. bands are occasioned by the use of any "inert" solvent.

The molar ellipticity of the i.c.d. band of S in the systems benzophenone/(+)-D-isosorbide (**1**)/methanol and 3-methylcyclohexanone/(+)-D-isosorbide (**1**)/methanol is directly proportional

Can. J. Chem. Downloaded from www.nrcresearchpress.com by 210.87.254.42 on 09/05/12
For personal use only.

Can. J. Chem. Downloaded from www.nrcresearchpress.com by 210.87.254.42 on 09/05/12
For personal use only.

to the molarity of C, at constant molarity of S. No saturation effect appears even at the highest concentration of C (Fig. 1). This difference from the nonlinear relationship of i.c.d. and [C] at constant [S] found by Noack (3) for the menthol/cyclohexanone/cyclohexane system may be due to the conformational rigidity of the C used here.

The inductive properties of (−)-diethyl tartrate (**5**) appear to be atypical of chiral environment compounds in general. The i.c.d. of benzophenone in this solvent shows distinct fine structure and is bathochromically shifted by *ca.* 30 nm from the maximum of the isotropic spectrum, and that of 3-methylcyclohexanone is similarly shifted by *ca.* 10 nm. Whilst such considerable shifts are usually deemed to be indicative of the presence of multiple circular dichroic absorption bands, attributed to asymmetric solvation (11) when observed for chiral ketones in achiral solvents (12), we propose that the formation of charge-transfer complexes between C and S in this solvent be considered (13, 14).

Alone of the C compounds so far examined,

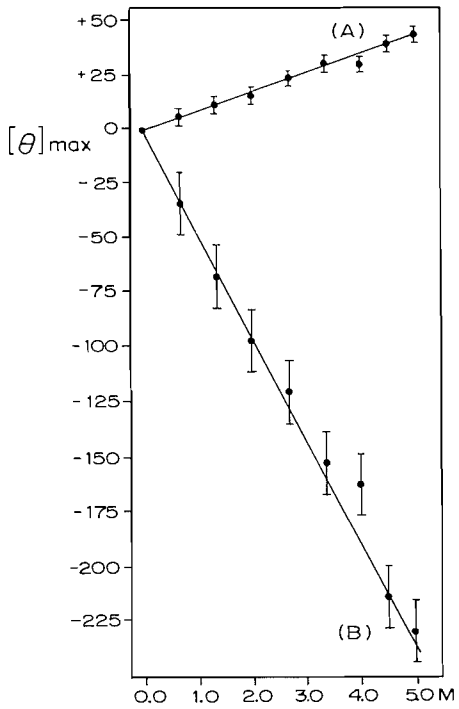

FIG. 1. Induced circular dichroism of S as a function of [C] in methanol at constant [S] and 25°. C = (+)-D-isosorbide, S = 3-methylcyclohexanone 0.45 *M* (*A*), S = benzophenone 0.10 *M* (*B*).

(−)-diethyl tartrate (**5**) gives rise to i.c.d. bands which show distinct fine structure or are shifted in wavelength from the isotropic absorption (4). The structurally related solvents **6** and **7** give rise to strong single i.c.d. bands, and 2-adamantanone (which shows two oppositely signed i.c.d. bands in solvent **5** (4)) shows a single positive i.c.d. band in the presence of (+)-D-isosorbide (**1**).

Since the stable conformation of benzophenone is itself chiral (15), in a chiral environment the equilibrium between the two enantiomers might be disturbed, leading to a higher population of one of them. Although i.c.d. of the rigid bicyclic ketones camphor and 2-adamantanone shows that any mechanism involving adoption of preferred chiral configurations is not of general applicability, there remains the possibility that induction of circular dichroism in benzophenone and in similar labile structures proceeds by this means.

Nitro Compounds

The lowest energy isotropic absorption band of nitroalkanes is at approximately 275 nm, at almost the same position as that of the carbonyl chromophore, and is similarly attributed to a n–π^* transition (16). For chiral nitro compounds the transition is optically active and its sign may be predicted by application of a sector rule (17). In the presence of C, symmetric nitroalkanes (S) show a single positive or negative i.c.d. band at, or near, 275 nm (Table 4). Primary, secondary, tertiary, and halogenated nitroalkanes give i.c.d. bands of the same sign and magnitude in the same C.

The i.c.d. band of these S is positive with (+)-diethyl-L-tartrate (**5**) as C, and does not change sign upon dilution with methanol, whereas when 1,1,1,3,3,3-hexafluoro-2-propanol (HFP) is used as diluant the i.c.d. band becomes negative and is shifted to shorter wavelengths by *ca.* 8 nm (Fig. 2). A similar shift has been reported for the isotropic n–π^* absorption of nitroalkanes in perfluoroalcohols (18). Although fluorinated solvents have large effects (9, 19) and fluorine substituents are "antioctant" (20, 21) in the c.d. of chiral carbonyl compounds, fluorine substitution in nitromethane does not affect either the sign or frequency of the i.c.d. band although the rotational strength is somewhat decreased (Table 4). A reversal of sign of an i.c.d. band upon addition of a halogenated solvent has been

TABLE 4. Induced c.d. of symmetric nitroalkanes (S) in chiral media (C) at 25°

S	Concentration (*M*)	Solvent†	(+)-Diethyl-L-tartrate (**5**)* $\lambda_{max} \pm 2$ nm	(+)-Diethyl-L-tartrate (**5**)* $[\theta]_{max}$	(+)-D-Isosorbide (**1**)* $\lambda_{max} \pm 2$ nm	(+)-D-Isosorbide (**1**)* $[\theta]_{max}$
CH_3NO_2	0.37		278	+21		
	0.51	HFP	270	−14	272	+28
	0.51	MeOH	278	+17		0
CH_2FNO_2	0.51	HFP	273	−11	274	+20
	0.54	MeOH	278	+5		0
CCl_3NO_2‡	0.14	HFP		0	283	*ca.* +20
	0.13	MeOH	280	*ca.* +30		0
$(CH_3)_2CHNO_2$	0.46		284	+22		
	0.50	HFP	274	−14	274	+22
	0.50	MeOH	284	+17		0
$CH_3C(CH_2OH)_2NO_2$	0.30	HFP	280	−40	280	+18
	0.30	MeOH	284	+10		0

*C, undiluted or 2.4 *M* solutions in solvents listed in column 3.
†HFP = 1,1,1,3,3,3-Hexafluoro-2-propanol.
‡Approximate only due to strong isotropic absorption.

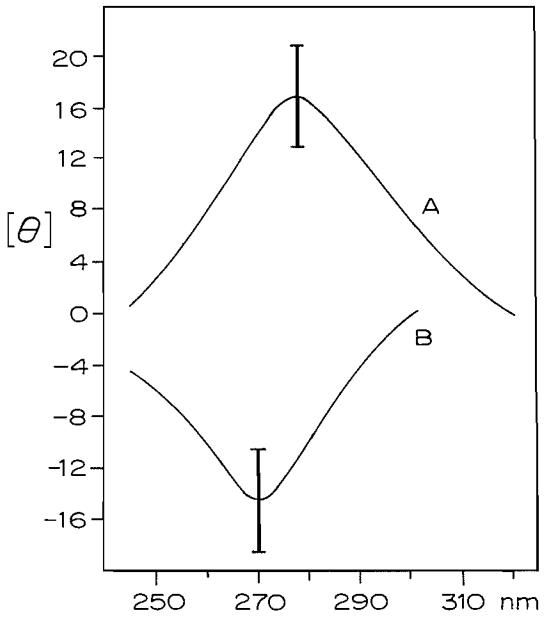

FIG. 2. Induced circular dichroism of nitromethane (0.51 *M*) and (+)-diethyl-L-tartrate (2.4 *M*) in methanol (*A*) and in 1,1,1,3,3,3-hexafluoro-2-propanol (*B*).

reported for the system diethyl tartrate/cyclohexanone (4).

In order to determine if the reversal of the sign of the i.c.d. band of the system RNO_2/**5** upon addition of HFP is due to a specific interaction between HFP and either C or S which may disturb the conformational or solvational equilibrium of C or S, we have examined the c.d. and optical rotatory dispersion (o.r.d.) spectra of **5** and the c.d. spectrum of a chiral primary nitrocompound (methyl 3-*O*-acetyl-4,6-*O*-benzylidene-2-deoxy-3-*C*-nitromethyl-α-D-*ribo*hexopyranoside, **15**) in both HFP and methanol. In both solvents **5** exhibits a single negative c.d. band, at 218 nm in methanol ($[\theta] = -1850$) and at 213 nm in HFP ($[\theta] = -1900$). The slight blue shift of the c.d. band is consistent with data for other hydroxyesters in perfluoroalcohols (22). The o.r.d. spectrum of **5** is consistent with the c.d. spectrum and previously reported o.r.d. data (23). The c.d. spectrum of **15** shows a single negative band at 282 nm in methanol ($[\theta] = -3900$) and at 274 nm in HFP ($[\theta] = -4600$). There is thus no factor evident from the chiroptical spectra of **5** or **15** to which the sign reversal of the i.c.d. band of the system RNO_2/**5** upon addition of HFP may be attributed, and we conclude that the action of HFP is upon the system C/S rather than on either C or S alone. That the strong hydrogen-bonding properties of HFP (9) are not *per se* the cause of the sign reversal is indicated by the strong positive i.c.d. of the system CH_3NO_2/**5** in aqueous solution (2.4 *M* **5**, $[\theta]_{max} = +25$).

It is generally agreed that the nitro group can act as a proton acceptor for hydrogen bonding from alcohols (18, 24, 25). As the efficiency of HFP for hydrogen-bonding to proton acceptors is greater than that of methanol (9), the appearance of i.c.d. in the system RNO_2/(+)-D-iso-

Can. J. Chem. Downloaded from www.nrcresearchpress.com by 210.87.254.42 on 09/05/12
For personal use only.

TABLE 5. Induced c.d. of symmetric diazenes (S) in chiral solvents (C)

Diazene (S)†	Concentration (*M*)	$[\theta]_{max}$ (+)-(S)-1,2-Propanediol (**9**)* 25°	(+)-(S)-1,2-Propanediol (**9**)* −85°	(−)-(R)-2,3-Butanediol (**8**)* 25°	(−)-(R)-2,3-Butanediol (**8**)* −85°	(−)-(1S,2R,5S)-*cis*-Pinane (**13**) 25°	(−)-(1S,2R,5S)-*cis*-Pinane (**13**) −48°	(−)-(R)-Carvone (**19**) 25°
16	0.12	+40	+230	−80	−290	+60	+60	—
17	0.012	+770	+5700	0	−4850	0	+2850	+870
18	0.024	0	+600	+400	+1300	0	+1300	0

*Solutions in the achiral compound showed no detectable c.d.
†2,3-Diazabicyclo[2.2.1]hept-2-ene (**16**), *cis*-(**17**)- and *trans*(**18**)-azobenzene.

sorbide (Table 4) in HFP, but not in methanol solution, is evidence against hydrogen-bonding of C and S as the cause of induced optical activity in nitroalkanes (*cf.* ref. 3).

We have attempted to observe i.c.d. of nitromethane in (−)-*cis*-pinane (**13**), however, experimental conditions are not favorable due to low solubility and at both 25 and −15° no i.c.d. is apparent in a 0.18 *M* nitromethane solution.

The 330 nm band in the isotropic spectrum of nitrobenzene is usually attributed to a n–π^* transition by analogy with nitroalkanes (16). This transition should therefore exhibit i.c.d. in a suitable C, and, although the band is partly obscured by higher energy transitions, we have observed i.c.d. in that part of the band experimentally accessible in both nitrobenzene ($[\theta]$ = *ca.* 80 at 330 nm, C = **5**, 2.4 *M* in methanol) and in *o*-nitrotoluene. The sign of the band is not reversed when methanol is replaced by HFP as solvent.

Azo Compounds

The diazenes ("azo" compounds (11)) were selected as S because they have conveniently isolated isotropic absorption bands, which have been assigned to the n_+–π^* transition (26, 27) and afford the possibility of observing i.c.d. in both alkyl (at ~340 nm) and aryl (at ~450 nm) substituted compounds with different degrees of conformational rigidity, and because of interest in the i.c.d. of this class of organic dyes in biopolymer–dye complexes (28, 29).

The R_s of the symmetric azobenzenes **17** and **18** at −48° in the chiral saturated hydrocarbon solvent, **13**, were comparable in magnitude with the rotational strengths of chiral diazenes at 25° in isooctane solution (11, 26, 30) (Table 5). These stereoisomeric diazenes differed in response to a given C in both sign and magnitude of R_s. The i.c.d. band of the conformationally rigid alicyclic diazene, 2,3-diazabicyclo[2.2.1]-hept-2-ene, (**16**) in the diol solvents (**8** and **9**) was non-Gaussian, its shape closely resembling that of its isotropic absorption band in ethanol solution (31), and the temperature coefficient of R_s for **16** in the hydrocarbon solvent (**13**) was zero within experimental error, whereas for the other C + diazene systems examined (Table 5, Fig. 3) it was significantly negative. It should be noted that Severn and Kosower (11) were unable to detect i.c.d. in 1-ethyl-2-methyldiazene in the presence of β-lactoglobulin.

For the three component systems C/S1/S2 (*e.g.* C = **1**, 2.4 *M* in methanol, S1 = 3-methylcyclohexanone, S2 = **16**) an i.c.d. band appeared for each S, and the spectrum was equivalent to superimposed spectra of the C/S1 and C/S2 systems. For three component systems C1/C2/S (*e.g.* C1 = (+)-**5**, C2 = (−)-**19**, S = **17**) where the R_s for C1/S and C2/S were of opposite sign and approximately equal magnitude, the net R_s was essentially zero, as it was also for the case where C1 and C2 were enantiomers.

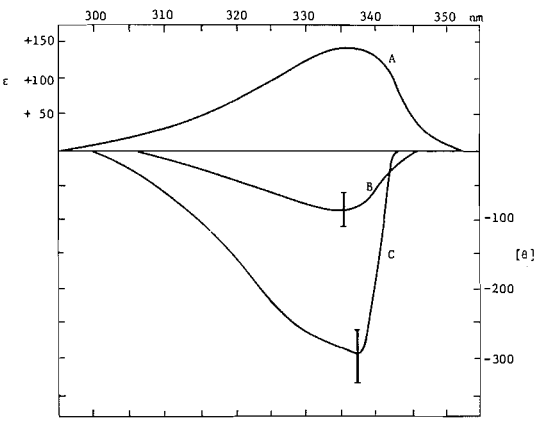

FIG. 3. Ultraviolet and i.c.d. spectra of 2,3-diazabicyclo[2.2.1]hept-2-ene (**16**) in (−)-(R)-2,3-butanediol (**8**). (*A*) u.v.; (*B*) i.c.d. at 25°; (*C*) i.c.d. at −85°.

Can. J. Chem. Downloaded from www.nrcresearchpress.com by 210.87.254.42 on 09/05/12
For personal use only.

Can. J. Chem. Downloaded from www.nrcresearchpress.com by 210.87.254.42 on 09/05/12
For personal use only.

As for the carbonyl and nitro compounds there was no apparent correlation in sign and magnitude between i.c.d. of S and $[\alpha]_D$ of C; the i.c.d. band of the diazenes was not significantly shifted in frequency or changed in shape when compared to the isotropic n–π^* absorption band.

Discussion

(*1*) Considering the signal enhancement that may be obtained by cooling, by the use of fluorinated achiral solvents, and by increasing [C]/[S] and dichrometer sensitivity, there is little doubt that all stable C/S solutions of the type described here will show i.c.d. under appropriate conditions; we conclude that the induction of optical rotation in n–π^* transitions by chiral media is completely general.

(*2*) Limited patterns of correlation of n–π^* i.c.d. with the structure of C and S are evident in Tables 1, 3, and 4; however, the data base is still too small (*e.g.* Table 5), and solvent effects insufficiently understood (*cf.* Table 4) to permit accurate prediction of sign or magnitude outside these patterns.

(*3*) We arrive at the conclusion that induction of optical activity does not require specific bonding between C and S by the following arguments: (*a*) The structural integrity of C and S is maintained in the C/S solutions as shown by their spectra. (*b*) Although hydrogen-bonding occurs between proton–donor C and X = Y chromophores in S, it is neither necessary nor sufficient for the appearance of i.c.d. (*c*) With the possible exception of the atypical system diethyl tartrate/S, the observed i.c.d. bands do not show the bathochromic shift, enhanced intensity, and band broadening characteristic of electronic absorption of charge-transfer complexes (13, 14). (*d*) If the equilibrium C + S $\rightleftarrows$ CS occurs in C/S systems the position of equilibrium should be revealed by methods used for organic charge-transfer complexes (13); however, application of the Foster–Hammick–Wardley equation (13) to the data in Fig. 1 gives equilibrium constants close to zero for both C/S systems. (*e*) It is difficult to envisage specific bonding of the saturated hydrocarbon *cis*-pinane (**13**) with benzophenone or with the diazenes **16**–**18**. (*f*) In 3-component systems C1/C2/S and C/S1/S2 each C/S pair appears to behave independently of the other.

(*4*) In the absence of specific bonding the origin of i.c.d. must lie in perturbation of the S chromophore by the dissymmetric field (33) of the chiral medium. The fact that the magnetic circular dichroism bands of acetone and 2-adamantanone are of opposite sign (32) and their i.c.d. bands have the same sign suggests that it is the electric rather than the magnetic field that is involved.

(*5*) This mechanism implies that in enzymic reactions (28) and chiroptical studies of biopolymer structure (29, 34) "binding" of small molecules at specific sites in the chiral macromolecules may not be prerequisite to induction of optical activity.

We thank Miss V. Gibb and Mr. D. F. Dong for technical assistance, Professors J. P. Lorand, L. Muenster, A. Rosenthal, and Drs. E. Klein, M. T. Leffler, W. E. Marsico, E. von Rudloff, G. Schollnhammer, and A. H. Somers for chemical samples, and the National Research Council of Canada for financial support.

1. B. Bosnich. J. Amer. Chem. Soc. **89**, 6143 (1967).
2. L. D. Hayward and R. N. Totty. Chem. Commun. 676 (1969).
3. K. Noack. Helv. Chim. Acta, **52** 2501 (1969).
4. E. Axelrod, G. Barth, and E. Bunnenberg. Tetrahedron Lett. 5031 (1969).
5. J. Bolard. J. Chim. Phys. Physicochim. Biol. **66**, 389 (1969).
6. J. Bolard. J. Chim. Phys. Physicochim. Biol. **67**, 550 (1970).
7. J. Horwitz, E. H. Strickland, and C. Billups. J. Amer. Chem. Soc. **91**, 184 (1969).
8. H. C. Eckstrom, J. E. Berger, and L. R. Dawson. J. Phys. Chem. **64**, 1458 (1960).
9. D. N. Kirk, W. Klyne, and S. R. Wallis. J. Chem. Soc. C, 350 (1970).
10. C. Reichardt. Angew. Chem. Int. Ed. Engl. **4**, 29 (1965).
11. D. J. Severn and E. M. Kosower. J. Amer. Chem. Soc. **91**, 1710 (1969).
12. A. Rassat. *In* Optical Rotatory Dispersion and Circular Dichroism in Organic Chemistry. *Edited by* G. Snatzke. Heyden and Son, Ltd., London. 1967. Chap. 16.
13. R. Foster. Organic Charge-Transfer Complexes. Academic Press, New York. N.Y. 1969.
14. G. Briegleb, H. G. Kuball, and K. Henschel. Z. Phys. Chem. Frankfurt am Main, **46**, 229 (1965).
15. R. Hoffmann and J. R. Swenson. J. Phys. Chem. **74**, 415 (1970).
16. J. N. Murrell. The Theory of the Electronic Spectra of Organic Molecules. Methuen and Co., London. 1963.
17. G. Snatzke. J. Chem. Soc. 5002 (1965).
18. H. E. Ungnade, E. M. Roberts, and L. W. Kissinger. J. Phys. Chem. **68**, 3225 (1964).
19. R. A. Smith. Ph.D. Thesis. State University of New York, Buffalo, New York. 1968.
20. C. Djerassi, J. Osiecki, R. Riniker, and B. Riniker. J. Amer. Chem. Soc. **80**, 1216 (1958).
21. J. Hudec. Papers presented at the C.I.C./A.C.S. meeting, Toronto, May 1970. Abstract no. ORGN 78.
22. I. Listowsky, G. Avigad, and S. Englard. J. Org. Chem. **35**, 1080 (1970).

23. Y. TSUZUKI, K. TANABE, K. OKAMOTO, and M. FUKUBAYASHI. Bull. Chem. Soc. Japan, **39**, 1387 (1966).
24. P. J. KRUEGER and H. D. METTEE. Can. J. Chem. **43**, 2888 (1965).
25. W. F. BAITINGER, P. VON R. SCHLEYER, T. S. S. R. MURTY, and L. ROBINSON. Tetrahedron, **20**, 1635 (1964).
26. E. HASELBACH and E. HEILBRONNER. Helv. Chim. Acta, **51**, 16 (1968).
27. E. HASELBACH and E. HEILBRONNER. Helv. Chim. Acta, **53**, 684 (1970).
28. J. E. COLEMAN. J. Amer. Chem. Soc. **89**, 6757 (1967).
29. K. SENSSE and F. CRAMER. Chem. Ber. **102**, 509 (1969).
30. C. G. OVERBERGER and D. A. LABIANCA. J. Org. Chem. **35**, 1762 (1970).
31. S. S. COHEN, R. ZAND, and C. STEEL. J. Amer. Chem. Soc. **83**, 2895 (1961).
32. G. BARTH, E. BUNNENBERG, and C. DJERASSI. Chem. Commun. 1246 (1969).
33. F. P. DWYER, E. C. GYARFAS, and M. F. O'DWYER. Nature, **167**, 1036 (1951).
34. J. H. PERRIN and P. A. HART. J. Pharm. Sci. **59** 431 (1970).

Can. J. Chem. Downloaded from www.nrcresearchpress.com by 210.87.254.42 on 09/05/12
For personal use only.

Competitive Reactions in the Thermal Decomposition of Cellulose

DONALD F. ARSENEAU
Department of Chemistry, Xavier College, St. Francis Xavier University, Sydney, Nova Scotia
Received September 11, 1970

Further evidence is presented to show that when cellulose is heated it undergoes two competitive reactions. The actual sequence of these is clarified, being different from that previously postulated. The natures of these reactions are studied, activation energies are determined, and their possible mechanisms are suggested. The thermogram for levoglucosan decomposition is given and briefly discussed.

Canadian Journal of Chemistry, **49**, 632 (1971)

Can. J. Chem. Downloaded from www.nrcresearchpress.com by 210.87.254.6 on 09/05/12
For personal use only.

Introduction

The combustion of cellulose has been studied quite frequently during recent years (1–7), and several reviews have appeared (8, 9). Much of the evidence strongly suggested that when the cellulose is heated, the following sequence of reactions occurs (1):

(*1*) Dehydration of the cellulose by an endothermic process to produce what Kilzer and Broido call a "dehydrocellulose". This reaction can be detected by differential thermal analysis techniques in the range 200–280 °C.

(*2*) At 280°, a depolymerization reaction competes for the residual cellulose by an endothermic process, and the product escapes as a tar. Work (10) has shown that levoglucosan (1,6-anhydro-β-D-glucopyranose) is an essential intermediate in this step.

(*3*) A decomposition of the "dehydrocellulose" formed in the first step via one or several exothermic reactions into a number of gaseous products and residual char.

More recently, MacKay using i.r. spectroscopy, g.l.c., and differential thermal analysis (2), gained further evidence that supported the fundamental ideas of sequential and competitive reactions. His review however (9) pointed out some interesting discrepancies that required clarification. This present work was undertaken to seek these clarifications.

Experimental

Most of the work was done on Whatman No. 1 filter paper having an ash content of about 0.1%. For differential scanning calorimetry (d.s.c.) small discs having an area of 0.33 cm^2 and a weight of about 3 mg were prepared using a simple paper punch, and dried in an oven at 110° for 1 h before use. The source of "ash-free" cellulose was Whatman No. 41 filter paper having an ash content of less than 0.01%. The cellulose powder was standard grade ashless Whatman Cellulose Powder. All were products of W. and R. Balston Limited of England.

Levoglucosan was prepared by heating 200 g of commercial corn starch in a 1-l pyrex round bottom flask which was connected directly to a condenser and a receiver. The receiver was placed in an ice bath, and was evacuated using a water aspirator. The reaction flask was rapidly heated with the flame from two Fischer burners. Vapors distilled at 250 to 300°. These were condensed, and the viscous brownish-black syrup was evaporated to dryness until there was no trace of moisture remaining. Dry acetone (50 ml) was added and the mixture warmed on a steam bath to the b.p. of acetone. The distillate dissolved and after seeding, was allowed to crystallize in a refrigerator for several days. The product was recrystallized from dry methanol, and showed a m.p. of 179° (16, 27).

Reduction Using Sodium Borohydride

The removal of carbonyl from heated cellulose was attempted using sodium borohydride and a modification of the method reported by Wolfrom and Wood (11). Preheated cellulose (40 mg) was added to 10 ml of water in which 8.0 mg of sodium borohydride had been dissolved. The p*H* was adjusted to 3–4 using *N* sulfuric acid. A nitrogen atmosphere was put over the solution, and the flask stoppered. It was periodically agitated. After 1 week, the solid was filtered off, washed with distilled water, and permitted to stand for 2 more days in a methanolic hydrogen chloride solution. The solid was once more filtered, washed with distilled water, and dried in a vacuum desiccator.

The i.r. spectra were obtained using the potassium bromide disc technique (12) and a Perkin–Elmer 237B Grating Infrared Spectrophotometer.

Thermograms

Thermograms were obtained using a Perkin–Elmer DSC-1 Differential Scanning Calorimeter with Effluent Analyser. In this instrument the sample is heated at a preselected rate in a controlled atmosphere. As the sample undergoes an endothermic transition, the extra power required to maintain the selected heating rate in the sample is plotted against its linearly increasing temperature. Should the sample undergo an exothermic change it is the amount of power withheld that is plotted. Thus the final graph records the energy of the transition and the temperature ranges in which these transitions occur.

During a run the sample chamber is continuously swept by a nitrogen flow. This nitrogen is passed through

Can. J. Chem. Downloaded from www.nrcresearchpress.com by 210.87.254.6 on 09/05/12
For personal use only.

a detector system which records the passage of any effluent from the sample decompositions.

The sample for this work, whether cellulose or levoglucosan, was placed in an aluminum pan and an aluminum cover was crimped on. To ensure rapid exit of volatile decomposition products, ten random holes were made in the cover using a pin. The nitrogen used had a maximum oxygen content of 20 p.p.m. To ensure removal of atmospheric oxygen the heating chamber was swept with nitrogen for at least 15 min prior to each run.

The signal from the DSC-1 was used to plot the thermogram on a Leeds and Northrup Speedomax W, with a 20 mV span and a 1 s response. Simultaneously the signal was led into a Cahn Time Derivative Computer which produces an output voltage proportional to the rate of change of the input voltage. This output became the input for a Brown Electronik, 1 mV span recorder, thereby giving the derivative of the original curve (Fig. 1*b*).

Thermogravimetry

For thermogravimetric analysis, a rectangular sample of filter paper weighing about 180 mg and measuring 4¼ in. by ¾ in. was coiled into a loose spiral and tucked into the porcelain crucible suspended from the balance spring in the pyrolysis chamber of American Instrument Company's ThermoGrav. Nitrogen (50 cc/min) was used to continuously sweep the reaction vessel. Heating began at room temperature and was programmed upwards at 1.5 °/min. The outputs from the instrument were recorded using a Plotomatic 690 X-Y recorder (Data Equipment Company) with the temperature being recorded along the abscissa (16 °/in.) and weight loss along the ordinate (25 mg/in.).

Results and Discussion

In Fig. 1, curve *a* is the thermogram for the decomposition of a thin (0.46 mm) layer of Whatman No. 1 filter paper at a heating rate of 10 °/min in a flowing nitrogen atmosphere. A very mild endotherm is discernible beginning at about 180°, followed by a mild exotherm at 220°. These phenomena are so gentle that they are easily lost in the baseline. Repeated experiments utilizing varying heating rates, sample sizes, and recorder chart speeds show that they are real. This portion of the curve presumably indicates the formation of the "anhydrocellulose" suggested by Kilzer and Broido (1). This rising exotherm gives way to a more rapid endotherm at a temperature of about 280°. It is apparent that this endotherm consists of a composite of at least two reactions. At 350° there is a gentle break in the curve, this being especially noticeable in the derivative curve *b* of Fig. 1. The endotherm recovers, peaks at about 370°, and then quickly returns to the baseline. Contrary to the results of other workers (13, 14) there is no exotherm evident beyond 350°. Apparently the two reactions contributing to this endotherm are, first, the depolymerization of the residual cellulose (1, 2), followed by the volatilization of most of the product, levoglucosan.

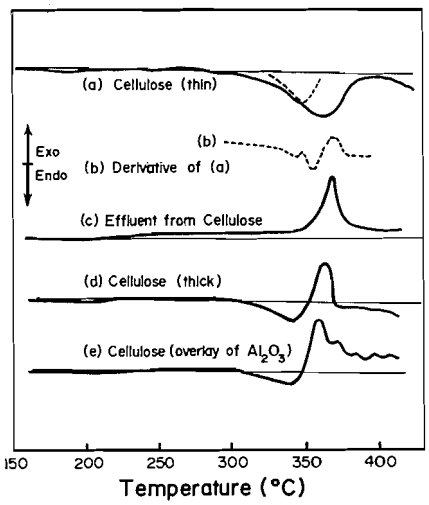

FIG. 1. The d.s.c. curves for cellulose in nitrogen and the gas effluent curve for the decomposition.

It has been demonstrated that the manner in which cellulose decomposes is modified by the presence of even low quantities of ash (1). Therefore similar runs were made using ashless (0.01%) filter paper and cellulose powder. No significant differences were found from the above.

To test this two-step possibility, conditions were modified to reduce the probability of loss of the volatile levoglucosan. Figure 1*d* shows the thermogram of Whatman No. 1 filter paper but this time using sufficient discs to give a sample thickness of 0.9 mm. Figure 1*e* is the thermogram of a thin layer of the same kind of paper over which 25 mg of dried alumina had been placed. These two runs were also made in a flowing nitrogen atmosphere at a heating rate of 10 °/min. They differ from Fig. 1*a* in the region above 350°. Whereas the thin layer of cellulose permits the easy loss of levoglucosan, both the alumina and the overlay of cellulose trap the levoglucosan, thereby eliminating the latter portion of the endotherm observed in Fig. 1*a*. Indeed, the hot surfaces of these overlays cause a thermal decomposition of the levoglucosan giving the exotherm so evident in *d* and *e* of Fig. 1, and reported by other workers (13,14). One must conclude that the exotherm appearing

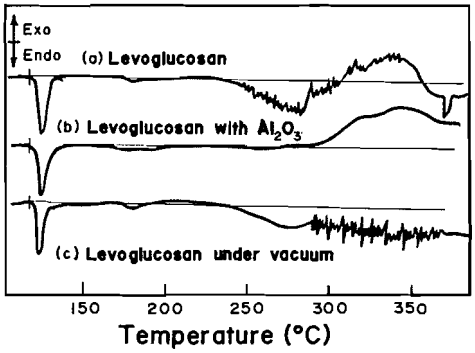

FIG. 2. The d.s.c. curves for levoglucosan (1,6-anhydro-β-D-glucopyranose) under various conditions.

in the thermograms of cellulose is not the result of the decomposition of the "anhydrocellulose" as suggested by Kilzer and Broido (1), but rather is the breakdown of the product of the depolymerization reaction, presumed to be levoglucosan.

Thermograms of Levoglucosan

The thermal decomposition of prepared levoglucosan was studied under conditions parallelling those used above. Figure 2*a* is the thermogram of a 5 mg sample that was heated at the rate of 10 °/min in a nitrogen atmosphere. The endotherm beginning at 117° apparently indicates a transition in the solid phase because no melting occurs at this point. The endotherm beginning at 175° represents the melting of the crystal, while the broad one commencing at 240° signals the onset of boiling. The jagged tracings seen in this region are often indicative of boiling or evaporation. Before all of the levoglucosan can escape, an exothermic reaction takes over, the product being a porous char. The rapid upturn occurs at 286°, and the exotherm continues upward until it peaks at 340°. This is the same temperature range in which the exotherm for thick cellulose and for cellulose overlaid with alumina occurs. When levoglucosan is overlaid with alumina, it is noted (Fig. 2*b*) that evidence of evaporation is clouded, while the thermal decomposition peaks persist. When levoglucosan was heated under reduced pressure (Fig. 2*c*), ready evaporation of the levoglucosan occurred, but no exotherm appeared.

Evidence gained from the thermograms of levoglucosan support the conclusion made earlier that the exotherm appearing in the thermograms of thick or overlaid cellulose marks the breakdown of the depolymerization product rather than of the "anhydrocellulose". A revision of the sequence of reactions proposed by Kilzer and Broido (1) must therefore be made. While steps *1* and *2* are left essentially unchanged, step *3* departs from that proposed by Kilzer and Broido.

(*1*) The dehydration of cellulose beginning at temperatures as low as 210°, resulting in the formation of "anhydrocellulose". The gas evolution curve shown in Fig. 1*c* suggests that reaction begins at this low temperature. This "anhydrocellulose" is quite reactive and soon undergoes further reactions that result in the formation of CO, CO_2, and H_2O, and most of the residual char.

(*2*) The depolymerization of non-reacted cellulose yielding the levoglucosan tar. This reaction becomes significant at about 270°, and builds up quite rapidly, becoming dominant over the one initiated earlier, but which is still going on.

(*3*) The final reaction observed by d.s.c. will vary depending upon the conditions of the experiment. It may be endothermic or exothermic, or indeed, neither. The levoglucosan formed in step *2* may volatilize giving an endotherm or it may be trapped by the overlay of cellulose and decomposed exothermally. Probably both of these are occurring simultaneously but to varying degrees depending upon heating rate, sample thickness, pressure, and so on. The amount of char left from the levoglucosan decomposition would therefore vary.

There is much in literature to support the above proposals:

(*a*) Kilzer and Broido (1) report that cellulose first held at 250° for a day forms about three times the amount of char at 400° as does a sample heated directly to 400°. Such preheats allow the early char-producing reaction to proceed to a greater extent. The sample directly heated to 400° rushes through the char-producing reaction, and on into levoglucosan-formation, some of which volatilizes before decomposition.

(*b*) Berkowitz (5) heated cellulose to about 200° for 20 min and then did a differential thermal analysis of the sample. The early exotherm observed in our work (at 220°) was greatly enhanced. When a similar sample was heated to

Can. J. Chem. Downloaded from www.nrcresearchpress.com by 210.87.254.6 on 09/05/12
For personal use only.

Can. J. Chem. Downloaded from www.nrcresearchpress.com by 210.87.254.6 on 09/05/12
For personal use only.

250° for 1–2 h, and then scanned, the endotherm beginning at 280° disappeared entirely. Very likely, the preheat to 200° for 20 min formed more-than-usual quantities of "anhydrocellulose" which enhanced the exotherm at 220° when it was analyzed. The same phenomenon occurred at 250° but to such an extent that the heat evolved exceeded the heat absorbed by the depolymerization reaction of step 2. Thus the endotherm is replaced by an exotherm. Work done in our laboratory duplicating Berkowitz's finding supports this conclusion.

(*c*) MacKay (2) reproduces thermograms of cellulose preheated in a nitrogen atmosphere to a temperature of 350° for 5, 10, 15, and 30 min. Although neither sample size nor density of packing were rigidly controlled, the traces suggest in some cases the lack of an exotherm in the region above 360° (his curves 2 and 3), as well as showing an exotherm prior to the major depolymerization endotherm (his curves 2, 3, and 4).

(*d*) MacKay (2) used i.r. spectrophotometry and found the absorption bands at 1700 and 1625 cm^{-1} were two of the few features remaining in the spectrum of the residue from cellulose heated at 325° for 1 h. Our work has shown that these bands appear after heating for only a few hours at 260°. This ready formation along with their persistence in the residue which contains only about 10% of the weight of the material in the original sample, strongly suggests that it is the product of the earliest reaction that contributes to the major portion of the char.

(*e*) Domansky and Rendos (15) report an exotherm at 230°, and a strong endotherm at 315–320°, but no exotherm above these. Their experimental set-up allowed the depolymerized product to escape.

(*f*) Morita and Rice (13) found no exotherm at 230° but an endotherm at 340° and a strong exotherm beginning at 400° and peaking at 655°. (Differences in positions of peaks can be attributed to furnace designs and heating rates.) In this work the sample was intimately mixed with alumina which probably adsorbed the depolymerized product and held it for further reactions.

(*g*) Browne and Tang (14), using samples weighing about 5 g obtained an exotherm peaking at about 450° as might be expected since chances of the volatile product being trapped are very great. Their results (their Fig. 5) also give a hint of the existence of the exotherm preceding depolymerization.

(*h*) Reported yields (3, 16) of levoglucosan are increased by the rapid heating of cellulose under vacuum to the temperature required for volatilization. Rapid heating quickly moves the sample through the regions of competitive reaction and into the range where depolymerization occurs rapidly. Vacuum draws the product out of the reaction zone quickly thereby minimizing further degradation.

(*i*) In their fine work, Chatterjee and Conrad (7) found that when their data were plotted, they obtained good straight lines in all cases, thereby supporting the theory which they had proposed. But they point out that the lines do not pass exactly through the origin as expected. They go on to say "This deviation could be due to some unavoidable decomposition before the desired temperature was reached, leading to small errors in the determination of the arbitrary origin". Their proposed decomposition could well be the exotherm observed in this work.

(*j*) Golova *et al.* (17) report that during the decomposition of the first 5–10% (which are the approximate limits of our earlier exotherm), the cellulose macromolecule yielded no levoglucosan.

(*k*) Glassner and Pierce (18) used gas chromatographic techniques to analyze the products from the controlled application of heat to paper and levoglucosan. Their results revealed that at 242° and above, the degradation products were essentially the same for the two substances. Data obtained at 190 and 215° did not correlate well. The explanation may be that cellulose degrades in this lower temperature range by a mechanism not involving levoglucosan as an intermediate, but by a route through the "anhydrocellulose".

The Nature of the "Anhydrocellulose"

The nature of the "anhydrocellulose" and of the reaction producing it were investigated. Figure 3 shows the i.r. spectra over the range 2000–650 cm^{-1} of cellulose and of cellulose heated at 260° for 5 h in a nitrogen atmosphere. Although several changes are noted, the one of particular interest here is the appearance of a strong absorption band at 1700 cm^{-1} and the intensifying of the band at 1625 cm^{-1} relative to other absorptions. These two bands have been attributed by Higgins *et al.* (19) and by

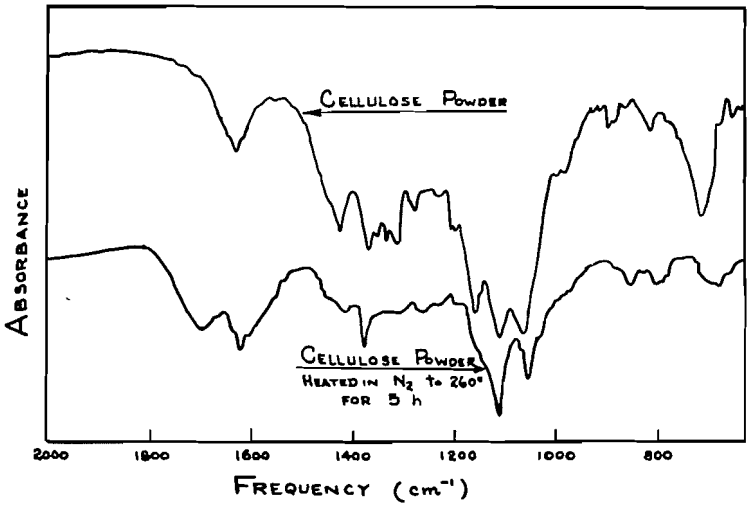

FIG. 3. The i.r. spectra for cellulose and cellulose heated in N_2 to 200° for 5 h.

[1]

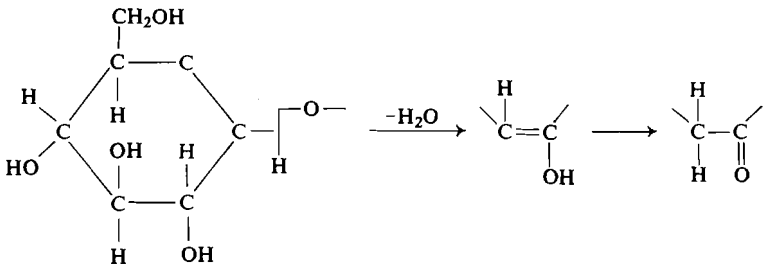

Tang and Bacon (20) to C=O and C=C. Attempts were made to reduce the C=O using sodium borohydride. The absorption at 1625 cm^{-1} was decreased slightly, but that at 1700 cm^{-1} did not change. This test might not have been too meaningful however because of difficulty in penetration of the preheated cellulose by the reducing reagents. Thus the unstable acidic sodium borohydride solution could have decomposed before reaching the interior reaction sites.

A possible explanation for the appearance of the absorption bands at 1625 and 1700 cm^{-1} is the dehydration and rearrangement shown in eq. 1. Theander (21) points out that the formation of oxo-groups, either aldehyde groups at C-6, or keto-groups at C-2 and -3, is of importance not only under controlled conditions known to produce reducing types of oxidized cellulose (chromate oxidation) but also under conditions considered specific for the introduction of carboxyl groups at C-6 (*e.g.* NO_2-oxidation). Further, he says, most of the very reactive keto-groups undergo further changes, these keto-groups probably being the starting points for the formation of dicarboxylate groups (carbonyl groups at C-2 and -3) which make the cellulose chain susceptible to depolymerization. Browne (8) says that such ketones may be produced before hydrolysis or pyrolytic scission begins. Hurd (22) points out that such ketones commonly decompose thermally to ketenes, compounds of the structure $\diagdown C{=}C{=}O$. Note that these contain both the C=C and C=O linkages suggested in the i.r. spectrum of heated cellulose (Fig. 3). Ketenes have been reported by Browne (8) among the pyrolysis products of cellulose but they are very reactive and can be expected to react further, possibly to the residual char.

Usually dehydration of alcohols proceeds by a carbonium ion mechanism. A polar or ionic environment would stabilize this carbonium ion

Can. J. Chem. Downloaded from www.nrcresearchpress.com by 210.87.254.6 on 09/05/12
For personal use only.

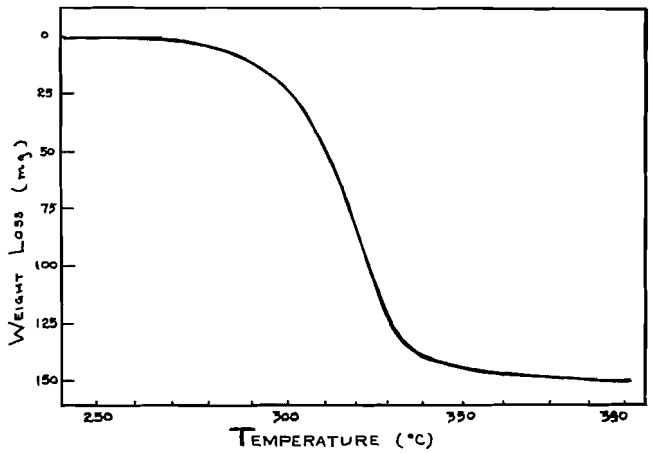

FIG. 4. Weight loss *vs.* temperature curve for cellulose heated in nitrogen at a rate of 1.5°/min.

intermediate and would favor this route to decomposition. Many workers (14, 23, 24) have reported that the presence of inorganic salts in cellulose influences its flammability by modifying the ability of the cellulose to produce the volatile tar (levoglucosan). It may be that the presence of salts favors the formation of "anhydrocellulose" and its subsequent decomposition, thereby diminishing the amount of levoglucosan that can be formed. Further, carbonium ions readily rearrange to produce more stable carbonium ions. This would account for the wide array of products obtained from the thermal decomposition of cellulose (25).

Determination of Activation Energies

Once aware of the temperature ranges wherein each of the two competing reactions is dominant, and of some of the variables (*e.g.* sample thickness) which might introduce errors into the determinations of true weight losses, the activation energies of the two reactions were found as outlined in the Experimental. The coiled paper permitted rapid escape of levoglucosan, and a heating rate of 1.5 °/min assured a slow passage through the earlier reaction thereby providing adequate data for meaningful calculations.

The data were treated according to the method outlined by Ingraham and Marier (26). Whereas their method yielded a linear relationship between weight loss and reciprocal temperature, all other methods attempted gave lines of continuously changing slopes. The method of Ingraham and Marier allows for changing surface area of the paper as decomposition progresses, by plotting $\log aw/T$ against $1/T$, where a is the weight loss per unit area, w is the heating rate, and T is the absolute temperature. A preliminary run had to be carried out to determine the paper's area loss with rising temperature. The activation energies of the reactions are calculated from the slopes, and equal $2.303 \times R \times$ Slope, where R is the gas constant. The weight loss *vs.* temperature curve is shown in Fig. 4 while the Arrhenius' graph for the determination of activation energies is shown in Fig. 5.

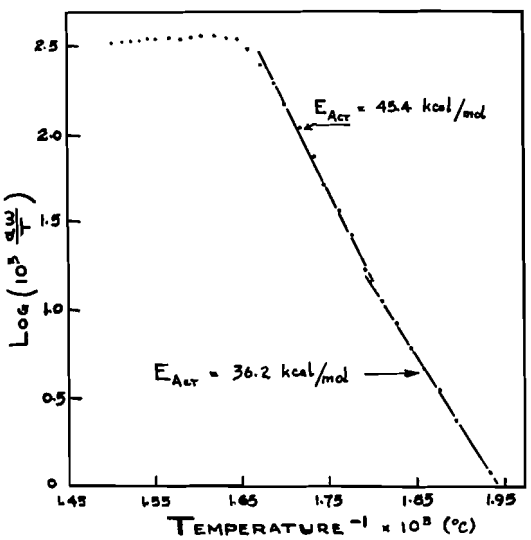

FIG. 5. Modified Arrhenius' graph for the determination of activation energy of the thermal decomposition of cellulose.

Can. J. Chem. Downloaded from www.nrcresearchpress.com by 210.87.254.6 on 09/05/12
For personal use only.

It is seen that two distinct straight lines result. The first runs from 250°, the point of first detectable weight loss, up to 280°, when only 5% of the toal weight loss has taken place. The second line runs from 285–320°, by which time about 60% of the total weight loss has occurred. The reaction at the lower temperature has an activation energy of 36.2 kcal/mol, while for the depolymerization reaction it is 45.4 kcal/mol. Murphy (4) who used the rate at which gas was evolved from heated cellulose to determine reaction rates, obtained results that suggested two reactions were present, and reported activation energies of 34.0 and 39.4 kcal/mol for these two. He proposed however that the former one was due to an impure substance in the cellulose, or perhaps end groups of the cellulose chains. The work of Chatterjee and Conrad (7) considered weight changes that occurred only after a temperature of 275° had been reached, thereby missing most of the reaction resulting in the formation of "anhydrocellulose".

The author wishes to gratefully acknowledge equipment grants from the National Research Council of Canada and the Defence Research Board, and financial assistance for technical help from the Council for Research of St. Francis Xavier University. He also wishes to thank Vincent Morrison for his help in the i.r. studies and Allan McIntyre for his work in thermogravimetry.

1. F. J. KILZER and A. BROIDO. Pyrodynamics, **2**, (1965).
2. G. D. M. MACKAY. Forest Prod. J. **18**, 71 (1968).
3. S. L. MADORSKY, V. E. HART, and S. STRAUS. J. Res. Nat. Bur. Stds. **56**, 343 (1956).
4. E. J. MURPHY. J. Polym. Sci. **58**, 649 (1962).
5. N. BERKOWITZ. Fuel, **36**, 355 (1957).
6. G. A. BYRNE, D. GARDINER, and F. H. HOLMES. J. Appl. Chem. **16**, 81 (1966).
7. P. K. CHATTERJEE and C. M. CONRAD. Text. Res. J. **36**, 487 (1966).
8. F. L. BROWNE. U. S. Dept. of Agr. Forest Prod. Lab. Report 2136 (1958).
9. G. D. M. MACKAY. Can. Dept. of Forest. and Rural Develop. Forest. Branch. Public. No. 1201 (1967).
10. R. F. SCHWENKER and E. PASCU. Ind. Eng. Chem. **50**, 91 (1958).
11. M. L. WOLFROM and H. B. WOOD. J. Amer. Chem. Soc. **73**, 2933 (1951).
12. R. G. ZHBANKOV. Infrared spectra of cellulose and its derivatives. Consultants Bureau, New York, N.Y., 1966.
13. H. MORITA and H. M. RICE. Anal. Chem. **27**, 336 (1955).
14. F. L. BROWNE and W. K. TANG. U.S. Dept. of Agr. Forest Ser. Report. No. TP-118 (1961).
15. H. DOMANSKY and F. RENDOS. Holz als Roh-u Werkstoff, **20**, 473 (1962).
16. A. PICTET and J. SARASIN. Helv. Chim. Acta, **1**, 87 (1918).
17. O. P. GOLOVA, R. G. KRYLOVA, and I. I. KIKOLAEVA. Vysokomolekul. Soedin, **1**, 9, 1295 (1959).
18. S. GLASSNER and A. R. PIERCE. Anal. Chem. **37**, 525 (1965).
19. H. G. HIGGINS, C. M. STEWART, and K. J. HARRINGTON. J. Polym. Sci. **51**, 59 (1961).
20. M. M. TANG and R. BACON. Carbon, **2**, 211 (1964).
21. O. THEANDER. Svensk Kem. Tidskr. **71**, 1 (1959).
22. C. O. HURD. The pyrolysis of carbon compounds. Chemical Catalogue Co. New York, N.Y., 1929.
23. K. TAMARU. Bull. Chem. Soc. Japan, **24**, 164 (1951).
24. W. K. TANG and W. K. NEILL. J. Polym. Sci. Part C, **6**, 65 (1964).
25. A. W. GOOS. Wood chemistry. *By* L. E. Wise and E. C. Jahn. 2nd Edition. Reinhold, New York, N.Y., 1952. Chapt. 20.
26. T. R. INGRAHAM and P. MARIER. Can. J. Chem. Eng. **42**, 161 (1964).
27. J. DA S. CARVALHO, W. PRINS, and C. SCHUERCH. J. Amer. Chem. Soc. **81**, 4054 (1959).

Can. J. Chem. Downloaded from www.nrcresearchpress.com by 210.87.254.6 on 09/05/12
For personal use only.

Can. J. Chem. Downloaded from www.nrcresearchpress.com by 210.87.254.105 on 09/05/12
For personal use only.

Proton Magnetic Resonance Study of the Conformational Equilibria in Some Substituted *N*-Acetylpyrrolidines

C. M. WONG, J. BUCCINI, R. SCHWENK, AND J. TE RAA
Department of Chemistry, University of Manitoba, Winnipeg, Manitoba

Received January 28, 1970[1]

In the p.m.r. spectra of eight *N*-acetyl-2-(*p*-methoxybenzyl)-pyrrolidines, the acetamido methyl group gives rise to two peaks in the range 7.7–8.5 τ. Compounds **9** and **10** also exhibit two peaks for the acetoxy methyl group in the same range. When the samples were heated, the pairs of peaks coalesced to give singlets. These results are interpreted as evidence for the existence of conformational equilibria.

Canadian Journal of Chemistry, **49**, 639 (1971)

Introduction

Recently, a communication (1) appeared which dealt, in part, with the n.m.r. spectra of *N*-acetylanisomycin (**2**) and diacetylanisomycin (**3**). The n.m.r. spectra of these compounds merited attention because the acetamido methyl group exhibited two different singlets in the range 8.0–8.5 τ. As an explanation for this phenomenon, Butler proposed that there existed in solution an equilibrium between **3** and **12** involving a four-centered mechanism as shown in eq. 1.

The main support for this proposal came from the following experimental evidence. In separate runs, labelled anisomycin (**1**, $R_1 = —^{14}COCH_3$) and labelled isoanisomycin (**5**, $R_2 = —^{14}COCH_3$) were refluxed with acetic anhydride and pyridine to give diacetylanisomycin (**3**), which gave the diol-amide **4** on alkaline hydrolysis. Liquid scintillation counting showed that the sample of **4** derived from anisomycin contained 27–30% of the label originally present in **1** while the sample of **4** derived from isoanisomycin contained only 7% of the original label. This transfer of the labelled acetyl group from oxygen to nitrogen was interpreted as evidence for the existence of an intermediate such as **11** or **12**. From the quantitative results, Butler concluded that **12** is more stable than **11**. It was also observed that when diacetylanisomycin (**3**) was subjected to t.l.c., two bands were observed which gave identical i.r. and n.m.r. spectra. When these two fractions were again subjected to t.l.c., each gave two bands.

During our recent synthetic study (2) of anisomycin (**1**), we observed that all the intermediates containing an *N*-acetylpyrrolidine ring showed two absorptions in the n.m.r. spectrum corresponding to the acetamido group. In two of the compounds, **9** and **10**, the acetoxy methyl also appeared as two singlets. Further n.m.r. studies of these compounds have led us to believe that the

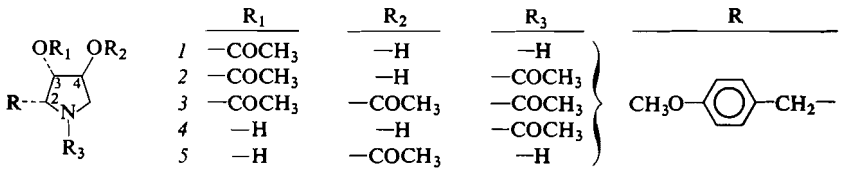

[1]

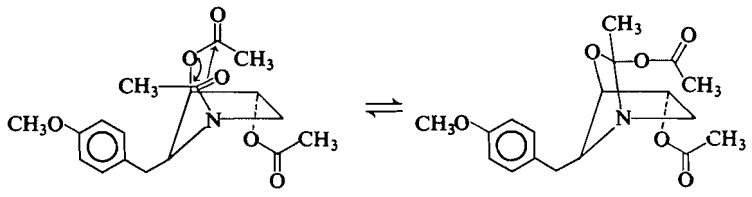

[1]Revision received August 17, 1970.

[2] 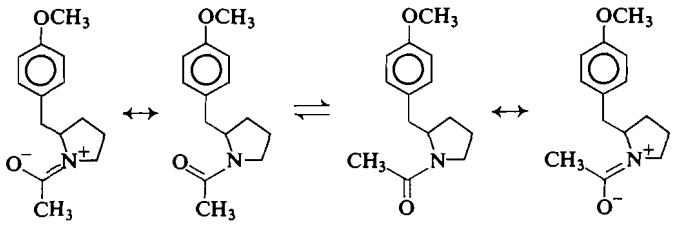

two absorptions of both the acetamido and the acetoxy methyl groups are due to restricted rotation about the C—N bond of —N—CO—CH_3 (3) and hydrogen bond formation between the hydroxy and the acetamido groups of **9** and **10**.

Experimental

The preparations of *N*-acetylanisomycin (**2**), diacetylanisomycin (**3**) and *N*-acetyldeacetylanisomycin (**4**) have been reported (5). Compounds **6–10** were reported in our synthesis o anisomycin (2). The n.m.r. samples were prepared with either $CDCl_3$ or DMSO-d_6, with TMS added as internal reference. The samples were degassed and sealed in thick-walled glass tubes. The spectra were recorded on a Varian A-56/60 A NMR Spectrometer which is equipped with a variable temperature apparatus.

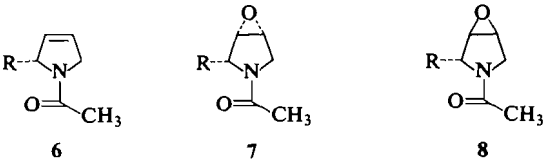

6 **7** **8**

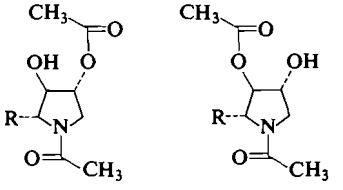

9 **10**

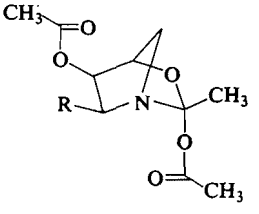

11

Results and Discussion

The acetamido methyl groups of compounds **2–4** and **6–10** appear as two singlets in their n.m.r. spectra at about 40 °C (Table 1). The acetoxy methyl group of **10** appears as two singlets at 39 °C while the acetoxy methyl group of **9** appears as a singlet at 39 °C, but at 20 °C, two peaks are observed. The magnitude of the separation between the pairs of peaks generally increased with cooling of the sample and decreased with heating until a coalescence temperature was reached. Such temperature behavior is typical of rate processes in which two conformers, appearing non-equivalent in the n.m.r. spectrum, are forced into a rapid rate of interconversion, thus becoming equivalent in the n.m.r. spectrum. We therefore postulate that the two acetamido methyl peaks arise from the type of equilibrium shown in eq. 2. The acetamido methyl group experiences a different environment due to the difference of anisotropic effect of the *p*-methoxybenzyl group in the two conformers. Using the Eyring equation and Nakagawa's method, we have estimated the free energy barrier to rotation to be about 17–21 kcal/mol.[2] These values agree with the values obtained for some 2,4,6-trialkylacetanilides (8, 9) where similar chemical shift differences were observed and a similar type of hindered rotation is implied.

A conformational equilibrium would explain the change in the magnitude of the chemical shift differences in the n.m.r. spectrum. If, as suggested

[2]Due to the unequal population of the two conformers, the estimated values of the free energy barrier to rotation (ΔF) obtained from coalescence temperatures, are not very accurate (7). Estimations obtained by Nakagawa's method (6) also would not be accurate because the formation of hydrogen bonded intermediates, eq. 4, makes the precise measurement of free energy barrier (ΔF) very difficult. Changes in internal shift of the exchanging proton sites arising from solvent effects were measured in the region of very slow exchange and extrapolated to temperatures where the exchange is relatively rapid. Unless such corrections are made, substantial errors in ΔF occur (10).

Can. J. Chem. Downloaded from www.nrcresearchpress.com by 210.87.254.105 on 09/05/12
For personal use only.

TABLE 1. Chemical shifts (τ) of the acetamido and acetoxy methyl groups

Compound	N—$COCH_3$	C_3—O—$COCH_3$	C_4—O—$COCH_3$	Temperature (°C)	Solvent
2	8.03, 8.39 8.16	8.00 8.03		38 97*	DMSO-d_6
3	7.97, 8.51 8.01	8.00 8.01	8.01 8.01	38 75*	$CDCl_3$
4	8.05, 8.17 8.12			38 95*	DMSO-d_6
6	7.80, 7.95 7.86, 7.97 8.02			−40 39 85*	$CDCl_3$
7	7.73, 7.91 7.85, 8.00 8.01			−40 38 95*	$CDCl_3$
8‡	7.90, 7.98 8.01, 8.03			−40 95	$CDCl_3$
9	8.15 8.03, 8.12 8.03, 8.18 8.03, 8.18 8.10		7.76, 7.90 7.73, 7.76 7.86, 7.90 7.87 7.94	−70 −40 20 39† 91*	$CDCl_3$
10	8.01 7.75, 8.02 7.90, 8.20 7.95, 8.22 8.12	7.75, 7.88 7.90, 8.00 8.02, 8.08 8.10 8.12		−70 −40 39 65† 91*	$CDCl_3$

*Coalescence temperatures of acetamido groups.
†Coalescence temperatures of acetoxy methyl groups.
‡Relative peak areas are 7.90/7.98 = 1/1; 8.01/8.03 = 1/3.

[3] 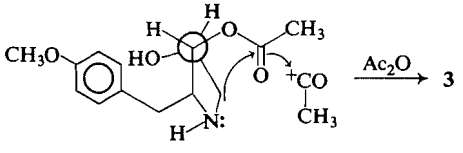

1

by Butler, the two peaks were due to an equilibrium between **3** and **11** or **12**, changing the temperature would shift the equilibrium and hence alter the peak intensities, but a coalescence of lines is not likely. The proposal of conformational equilibrium is further supported by the fact that n.m.r. spectra of compounds **4**, **6** (Fig. 1), **7**, and **8** all show two singlets for the acetamide methyl groups but these compounds cannot enter into the equilibrium suggested by Butler.

Based on a study of the ring proton absorptions in the n.m.r. spectra of anisomycin (**1**) and isoanisomycin (**5**), Butler concluded that **1** existed in the conformation shown in eq. 3 and that **5** existed in a similar but somewhat less stable conformation. In such a conformation, the transfer of a labelled acetyl group from oxygen to nitrogen could take place as shown in eq. 3. The fact that **1** transferred four times more label than **5** would indicate that Butler's conclusions

[4] 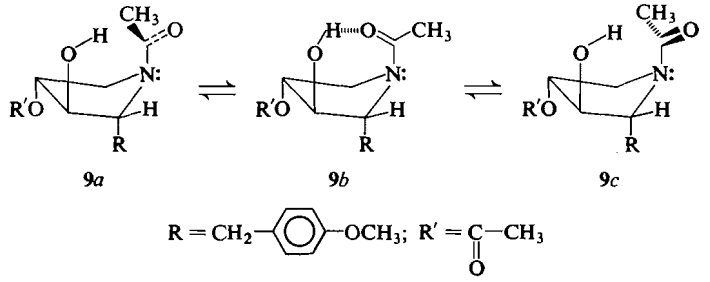

9a *9b* *9c*

Can. J. Chem. Downloaded from www.nrcresearchpress.com by 210.87.254.105 on 09/05/12
For personal use only.

Can. J. Chem. Downloaded from www.nrcresearchpress.com by 210.87.254.105 on 09/05/12
For personal use only.

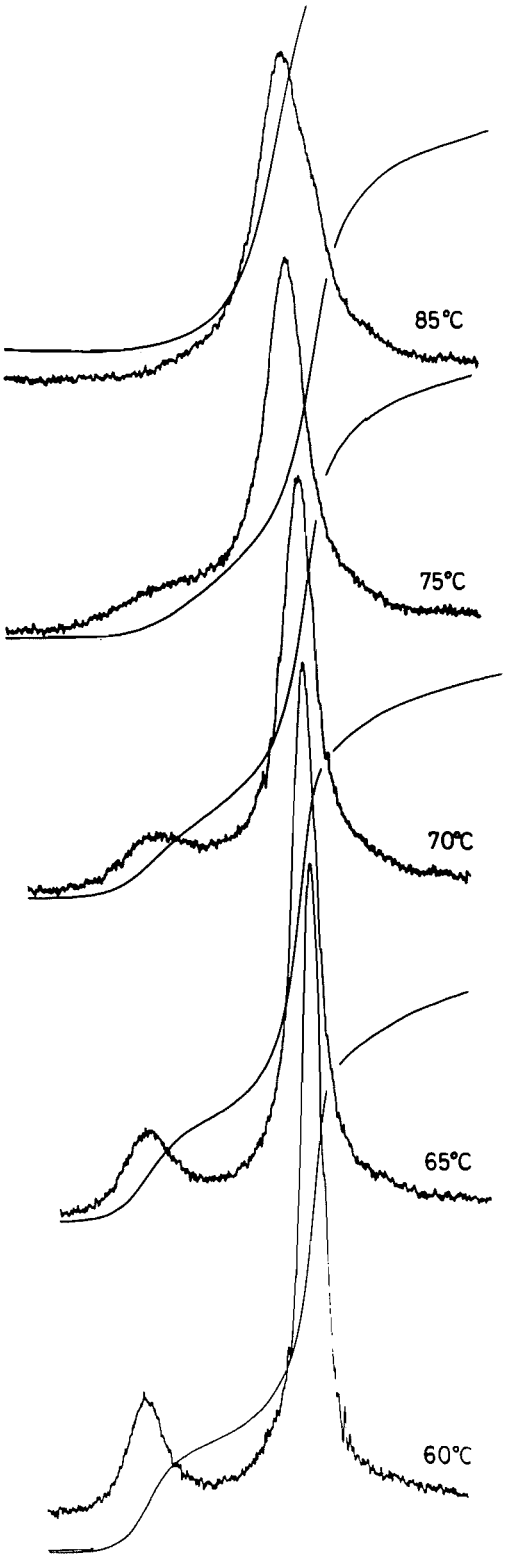

FIG. 1. Coalescence of the acetamido methyl group of **6**.

as to the conformations of the pyrrolidine ring are correct.

The t.l.c. separation of diacetylanisomycin (**3**) into two fractions which showed identical i.r. and n.m.r. spectra does not necessarily indicate the presence of an equilibrium between **3** and **12**; rather it could mean the separation of the two conformers as has been reported in the case of some 2,4,6-trialkylacetanilides (8).

In the case of simple formate and acetate esters, the presence of *s-cis* and *s-trans* rotamers has been detected by i.r. and ^{13}C n.m.r. studies (4). However, this is not the reason for the splitting of acetoxy groups of **9** and **10**, because such a conformational difference amounts to an energy difference of about 3 kcal/mol. Non-equivalence in anisotropy due to the difference in the relative positions of the acetamido group in the two conformers could be the reason. However, low temperature n.m.r. studies of **9** and **10** reveal an unusual phenomenon which can explain the splitting of the acetoxy methyl group more satisfactorily.

The interconversion of conformers **9***a* and *c* involves a transition state **9***b*, [4], which loses the partial double bond character of an amide. This transition state usually is unstable and thus cannot be detected by spectroscopic methods. However, due to the formation of a strong intramolecular hydrogen bond as shown in **9***b*, this otherwise unstable transition state becomes a stable conformer, [4]. Evidence came from the downfield shift of the hydroxy proton and simultaneously the collapse of the two peaks of the acetamide methyl group (Fig. 2). The broadening and resharpening of the hydroxy proton signal as the temperature lowered further substantiate the formation of **9***b*.

The formation of **9***b* at low temperature would bring the i.r. absorption of the acetamide group from 1650 cm^{-1} to that of a normal ketone. However, the i.r. spectrum at -70 °C showed the reverse effect. The acetamide group sharpened and moved down to 1640 cm^{-1}. Hydrogen bond formation is known to lower the carbonyl group absorption by 50 cm^{-1} (11) and the result here agrees with the formation of **9***b*. In the dilute solution i.r. spectrum the hydroxy stretching of **9** at room temperature shows quite a strong hydrogen bonding character at 3300 cm^{-1} while

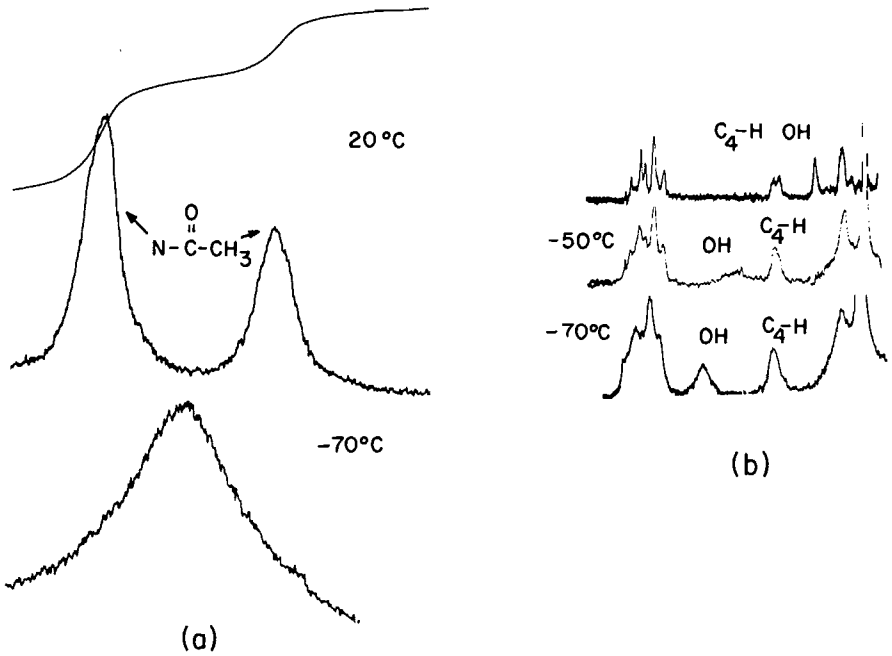

FIG. 2. (*a*) The two singlets of the acetamido methyl group of **9** at 20 °C and its coalescence at −70 °C. (*b*) Broadening and resharpening of the hydroxy proton of **9** at −50 and −70 °C.

the *N*-benzyl anisomycin shows only a sharp absorption at 3550 cm^{-1}.

The technique of n.m.r. has been used very extensively to study hindered rotation. However, the transition state has not been detected. The formation of conformer **9***b* would show the existence of the transition during a hindered rotation, although **9***b* in this case is more a conformer than a true transition state.

More work will be done on similar systems with emphasis on the accurate measurement of free energy barrier to rotation.

We thank Professor T. Schaefer of the Department of Chemistry, University of Manitoba, Winnipeg. Manitoba, for his very helpful discussions. We would also like to thank the National Research Council of Canada for financial support.

1. K. BUTLER. J. Org. Chem. **33**, 2136 (1968).
2. C. M. WONG, J. BUCCINI, I. CHANG, J. TE RAA, and R. SCHWENK. Can. J. Chem. **47**, 2421 (1969).
3. H. A. STAAB and D. LAUER. Tetrahedron Lett. 4593 (1966).
4. G. J. KARABATSOS, N. HSI, and C. E. ORGECH, JR. Tetrahedron Lett. 4639 (1966).
5. J. J. BEEREBOOM, K. BUTLER, F. C. PENNINGTON, and I. A. SOLOMONS. J. Org. Chem. **30**, 2334 (1965).
6. T. NAKAGAWA. Bull. Chem. Soc. Jap. **39**, No. 5, 1006–1008 (1966).
7. H. S. GUTOWSKY and C. H. HOLM. J. Chem. Phys. **25**, 1228 (1956).
8. H. KESSLER and A. RIEKER. Liebigs Ann. Chem. **708**, 57 (1967).
9. H. KESSLER. Angew. Chem. Int. Ed. **9**, No. 3 (1970).
10. B. J. FUHR, B. W. GOODWIN, H. M. HUTTON, and T. SCHAEFER. Can. J. Chem. **48**, 1558 (1970).
11. KOJI NAKANISHI. Infrared absorption spectroscopy. Holden–Day Inc., San Francisco, California. p. 42.

Can. J. Chem. Downloaded from www.nrcresearchpress.com by 210.87.254.105 on 09/05/12
For personal use only.

Can. J. Chem. Downloaded from www.nrcresearchpress.com by 210.87.254.42 on 09/05/12
For personal use only.

Preparation and Properties of some Non-Metallic Derivatives of Pentafluorothiophenol

M. E. PEACH AND H. G. SPINNEY
Department of Chemistry, Acadia University, Wolfville, Nova Scotia

Received June 12, 1970

Various non-metallic derivatives of pentafluorothiophenol, containing sulfur bonded to boron, carbon, silicon, germanium, phosphorus, arsenic, antimony, sulfur, and chlorine, have been prepared, mainly from the reaction of $Pb(SC_6F_5)_2$ with a non-metallic halide, and characterized. The ^{19}F n.m.r. spectra have been examined. The coordinating power of sulfur attached to a C_6F_5 group is minimal.

Divers dérivés non-métalliques du pentafluorothiophénol contenant du soufre lié au bore, au carbone, au silicium, au germanium, au phosphore, à l'arsenic, à l'antimoine, au soufre, et au chlore ont été préparés, principalement par réaction de $Pb(SC_6F_5)_2$ avec des halogénures non-métalliques et caractérisés. Les spectres r.m.n. de ^{19}F ont été examinés. Le pouvoir de coordination du soufre attaché à un groupe C_6F_5 est minimal.

Canadian Journal of Chemistry, **49**, 644 (1971)

The metallic derivatives of pentafluorothiophenol, $M(SC_6F_5)_x$ (1) and complex ions of the types $M(SC_6F_5)_x^{n-}$, where M is a metal, have been investigated (2, 3). Few non-metallic derivatives have been reported; this paper describes the preparation of some pentafluorophenylthio derivatives of B, C, Si, Ge, P, As, Sb, S, and Cl. The aims of this study were to examine the effects, if any, of the relatively electronegative C_6F_5 group, on the ease of preparation of these derivatives and its effect on the coordinating ability of the sulfur. The electronegativity of the C_6F_5 group depends on its interaction with the rest of the molecule, and has been estimated to be between that of chlorine and bromine to less than that of iodine in various organotin compounds (4). The C_6F_5 group could be classified as a pseudohalide group.

Non-metallic derivatives of thiols may be prepared by two general methods, starting with the non-metallic halide (5).

(*a*) The reaction of a thiol with the non-metallic halide in a suitable solvent; when the product is susceptible to attack by the hydrogen halide generated, a hydrogen halide acceptor, such as triethylamine is added. Similar products may be obtained from the reaction of a sulfenyl chloride with some non-metallic hydrides.

(*b*) The reaction of a thiol salt, such as a lead salt, with the non-metallic halide.

The compounds $C_6F_5SMR_3$, where MR_3 = $SiMe_3$, $SiPh_3$, $GeMe_3$, and $GePh_3$ (6), have been prepared using method *a*. Pentafluorothiophenol slowly polymerizes in air in the presence of a base (1), including triethylamine which was used as a hydrogen chloride acceptor in method *a*. Exclusion of air, either by working in a nitrogen atmosphere or using vacuum line techniques has enabled simple salts of pentafluorothiophenol with bases such as diethylamine, which would cause polymerization in air, to be prepared. Method *b*, which was used with the majority of compounds described in this paper, can be used in air without polymerization occurring.

The compounds $(C_6F_5S)_xY$, where Y = B, Me, CPh_3, CH_2, CH_2CH_2, MeCO, PhCO, C_6F_5CO, Me_3Si, Ph_3Ge, Ph_2Ge, Ge, P, PO, Ph_2P, As, PhAs, Sb, MeHg, and PhHg, were prepared from the corresponding chloride or iodide and bis(pentafluoro-phenylthio) lead, $Pb(SC_6F_5)_2$, subsequently referred to as the lead salt, in an inert solvent such as carbon tetrachloride or benzene. The products containing B—S, Si—S, and P—S bonds were somewhat hydrolytically sensitive.

No reaction was observed with $Me_{4-x}SiCl_x$, x = 2, 3, or 4, and the lead salt although this is a standard method for preparation of this type of mercapto silicon derivative (7). Trimethyl(pentafluorophenylthio) silane was also prepared from pentafluorothiophenol and hexamethyldisilazane in benzene, eq. 1. A similar reaction occurs with

[1] $(Me_3Si)_2NH + 2C_6F_5SH \rightarrow 2Me_3SiSC_6F_5 + NH_3\uparrow$

allylthiol(8). Phosphorus and arsenic trichlorides react with bis(trifluoromethylthio) mercury to give the compounds $(CF_3S)_xMCl_{3-x}$, x = 1, 2, or 3, depending on the stoichiometry of the reactants (9). No mixed pentafluorophenylthio chloro derivatives of phosphorus or arsenic,

TABLE 1. The ^{19}F chemical shifts relative to $CFCl_3$ as internal standard (p.p.m.) and coupling constants (Hz)

Compound	Solvent	$\delta_{2,6}$	δ_4	$\delta_{3,5}$	$\pm J_{3,4}$	$\pm J_{2,4}$
$(C_6F_5)_2S$	CCl_4	132.4	150.4	160.4	20.6	3.5
$(C_6F_5S)_2$	Acetone	134.1	151.3	162.9	19.8	4.0
$(C_6F_5S)_2$	CCl_4	131.6	148.4	160.1	—	—
$(C_6F_5SCH_2)_2$	CCl_4	132.7	152.2	161.0	20.0	2.0
C_6F_5SCl	CCl_4	128.0	145.6	160.1	20.0	5.9
$C_6F_5SCPh_3$	CCl_4	126.8	151.4	162.6	20.5	3.7
$(C_6F_5S)_3P$	CCl_4	130.2	149.2	163.1	~20	—
C_6F_5SCN*	CCl_4	130.2	146.3	158.8	20.4	5.1

*See ref. 18.

$(C_6F_5S)_xMCl_{3-x}$, $x = 1$ or 2, were obtained in the present work even if a considerable excess of the trichloride was present, the products being always the fully substituted derivative, $(C_6F_5S)_3M$, and the unreacted trichloride.

Bis(pentafluorophenyl) disulfide is readily obtained by oxidation of pentafluorothiophenol (1) and reacts with ammonia breaking the S—S bond according to eq. 2. Initial cleavage of the

[2] $2(C_6F_5S)_2 + 3NH_3 \rightarrow (C_6F_5S)_2NH + 2NH_4SC_6F_5$

S—S bond would form C_6F_5SH and $C_6F_5SNH_2$. The thiol forms the ammonium salt with excess ammonia, and the sulfenamide decomposes to the sulfenimide on purification by sublimation (10). A similar reaction of ammonia and $C_6F_5SSCF_3$ is observed, but the thiol formed, CF_3SH, reacts with the excess ammonia forming ammonium fluoride and thiocyanate (10). Attempted preparations of $(C_6F_5)_2S_x$, $x = 3$ or 4, from the lead salt and sulfur dichloride or sulfur monochloride, gave products whose mass spectra indicated that they were primarily mixtures of the disulfide and sulfur, although some of the desired product was present, but this may have been formed by recombination in the source. It was not possible to prepare $C_6F_5S—SO_x$ bonds. Thionyl and sulfuryl chlorides reacted with the lead salt yielding the disulfide, sulfur dioxide, and sulfur (thionyl chloride only) and benzene- and *p*-toluenesulfonyl chlorides did not react with the lead salt. The same types of reaction were observed with bis(trifluoromethylthio) mercury and thionyl and sulfuryl chlorides (11).

Attempts were made to prepare compounds containing S—Se—S and S—Te—S bridges. The compound $C_6F_5SSeC_6F_5$ has been prepared by heating bis(pentafluorophenyl) disulfide and bis(pentafluorophenyl) diselenide (12). Compounds of the type $(RS)_2M$, M = Se, Te, are known, but are relatively unstable (13), decomposing to the disulfide and selenium or tellurium; analogous results were obtained in the present work when R = C_6F_5. The reactions of R_2MCl_2 (R = Me, M = Se, Te: R = Ph, M = Se) with the lead salt yielded R_2M and the disulfide, the reaction probably proceeding through the formation of $R_2M(SC_6F_5)_2$ as an intermediate.

Sulfur compounds should theoretically be able to act as donors or acceptors. Sulfur acts as a donor in complexes such as $Me_2S.BCl_3$ (14), but examples where sulfur is an acceptor are rarer and usually occur with S(IV), as in liquid sulfur dioxide solution (15). The presence of the relatively electronegative C_6F_5 group attached to the sulfur would be expected to weaken its donor properties and enhance its acceptor properties, although the ^{19}F n.m.r. indicates π electron donation from the C_6F_5 ring to the sulfur. Sulfur complexes with the class B metals undoubtedly involve metal to ligand as well as ligand to metal bonding; the π electron donation from the C_6F_5 ring to the sulfur would impede the metal to ligand bonding, and complexes with the class B metals if formed, would not be expected to be particularly stable. Bis(pentafluorophenyl) sulfide formed no adducts with various donors or acceptors, such as the boron trihalides, various amines, metal ions, etc. The disulfide did not form complexes with Pd^{2+} or Ag^+ ions. The coordinating properties of both these potential ligands can be classified as minimal. The coordinating ability of the metal derivative, $Hg(SC_6F_5)_2$ has been studied; it formed an adduct with PPh_3, and an unstable adduct with $Ph_2P(SC_6F_5)$ but no adduct with triethylamine or ammonia.

The ^{19}F n.m.r. spectra of some of the products have been examined and the results are shown in Table 1. Similar spectra have been obtained for various other C_6F_5S derivatives (1). Using the derivations of Hogben *et al.* (16), it can be seen that the coupling constant $J_{2,4}$ varies regularly

Can. J. Chem. Downloaded from www.nrcresearchpress.com by 210.87.254.42 on 09/05/12
For personal use only.

Can. J. Chem. Downloaded from www.nrcresearchpress.com by 210.87.254.42 on 09/05/12
For personal use only.

TABLE 2. Product and analyses

Product (ref.)	Color	Melting point (°C)	n_D^{23}	Method: solvent: time: purification*	Found (%)			Calculated (%)		
					C	H	S	C	H	S
$B(SC_6F_5)_3$	White	135–139	—	D′: CCl_4: 1 day: 2	35.6	0.6	16.0	35.6	0.0	15.8
$C_6F_5SCPh_3$	Light yellow	120–122	—	A: acetone: 5 min: 2	68.1	3.4	7.2	67.9	3.4	7.3
$(C_6F_5S)_2CH_2$	White	65	—	A′: CH_2Br_2: 1 week: 2	37.8	0.7	16.2	37.9	0.5	15.6
$(C_6F_5SCH_2)_2$	White	139–140	—	A′: $(CH_2Br)_2$: 1h: 2	39.4	1.1	15.4	39.5	1.0	15.1
C_6F_5SCOMe	Colorless	b.p. 92/17 mm	1.4770	A: MeCOCl: 5 min: 1 B: CCl_4: 5 min: 1	39.7	1.8	—	39.7	1.3	—
C_6F_5SCOPh	Yellow	34–37 b.p. 76/0.02 mm	1.5578	A′: CCl_4: 1 h: 1	51.6	—	11.3	51.3	—	10.6
$C_6F_5SCOC_6F_5$	White	57–59	—	A′: CCl_4: 12 h: 2	39.6	0.0	8.2	39.6	0.0	8.1
$Me_3SiSC_6F_5$ (6)	Colorless	b.p. 76/15 mm	1.4676	A′: C_6H_6: 5 h: 1 B: C_6H_6: 3 day: 1 C′: C_6H_6: 3 day: 1	40.1	3.0	—	39.7	3.3	—
$Ph_3GeSC_6F_5$ (6)	White	87–90	—	A: Et_2O: 5 min: 2	57.9	3.1	6.1	57.3	3.0	6.4
$Ph_2Ge(SC_6F_5)_2$	White	62–66	—	A: Et_2O: 15 min: 3	46.9	0.9	10.5	46.1	1.6	10.3
$Ge(SC_6F_5)_4$	White	115	—	A′: Et_2O: 10 min: 3	32.6	0.0	—	33.2	0.0	—
$PO(SC_6F_5)_3$	White	145–146	—	A′: CCl_4: 12 h: 3	33.3	0.2	15.2	33.6	0.0	14.9
$P(SC_6F_5)_3$	White	63–64	—	A: C_6H_6: 5 min: 1	34.6	0.0	15.2	34.4	0.0	15.3
$Ph_2PSC_6F_5$	White	61–63	—	A: CCl_4: 1 h: 3	56.3	2.6	8.2	56.3	2.6	8.3
$PhP(SC_6F_5)_2$	White	63–65	—	A: C_6H_6: 10 min: 3	43.2	1.1	12.8	42.7	1.0	12.6
$As(SC_6F_5)_3$ (1)	White	76–77	—	A: Et_2O: 1 min: 2	32.5	0.0	14.3	32.2	0.0	14.3
$PhAs(SC_6F_5)_2$	White	74–76	—	A: Et_2O: 1 min: 3	38.9	0.6	12.1	39.3	0.9	11.7
$Sb(SC_6F_5)_3$	White	softens 80	—	A: C_6H_6: 1 h: 3	29.9	0.0	13.3	30.1	0.0	13.4
C_6F_5SCl†	Yellow	b.p. 89/0.1 mm	1.4993	D: — : 1 min: 1	31.0	0.0	13.3	30.7	0.0	13.7
$MeHgSC_6F_5$	White	95–97	—	A: Et_2O: 5 min: 2	20.7	0.7	7.6	20.3	0.7	7.7
$PhHgSC_6F_5$	White	148–149	—	A′: Et_2O: 40 h: 2	30.9	1.1	6.5	30.2	1.1	6.7
$Ph_3PHg(SC_6F_5)_2$	White	155–157	—	E: C_6H_6: 8 h: 4	42.3	2.0	7.4	41.8	1.8	7.5
$C_6F_5SH{\cdot}NH_3$	Yellow	296 dec.	—	D: — : 2 h: —	32.9	2.2	14.7	33.2	1.9	14.8
$C_6F_5SH{\cdot}HNEt_2$	White	>300	—	C: CCl_4: 1 h: 4	43.8	4.5	4.8‡	43.9	4.4	5.1‡
$(C_6F_5SH)_2{\cdot}(H_2NCH_2)_2$	White	170 dec.	—	C: CCl_4: 1 h: 4	36.6	2.3	6.0‡	36.5	2.5	6.1‡
$C_6F_5SH{\cdot}H_2NPh$	White	121–122	—	C: CCl_4: 20 min: 4	48.3	2.7	4.9‡	48.5	2.7	4.7‡

*Methods of purification: 1 = distillation; 2 = recrystallization; 3 = vacuum sublimation; 4 = precipitation from reaction solvent.
†Percentage Cl: Found, 14.9; Calcd., 15.1.
‡Percentage N.

Can. J. Chem. Downloaded from www.nrcresearchpress.com by 210.87.254.42 on 09/05/12
For personal use only.

with the chemical shift δ_4 in a particular solvent. The values of $J_{2,4}$ suggest π electron withdrawal from the C_6F_5 nucleus due to the vacant d orbitals on the sulfur, and the magnitude of the withdrawal increases $CH_2CH_2SC_6F_5 < C_6F_5 < CPh_3 < SCN < SCl$. The i.r. spectra are analogous to those expected for compounds containing the C_6F_5S group and the requisite functional group (17).

Experimental

Most reagents were available commercially. Microanalyses were performed by Mikroanalytisches Laboratorium Beller, Göttingen, Western Germany. The i.r. spectra were recorded on a Perkin–Elmer 457 spectrophotometer as mulls with Nujol or hexachlorobutadiene or as liquid films. The n.m.r. spectra were recorded on a Varian A60 instrument. The new, and some known, compounds prepared are shown in Table 2, together with some physical properties and analytical data. All experiments were performed using 1–2 mmol of reagents.

On refluxing a benzene solution of pentafluorothiophenol and triethylamine in air for 18 h a yellow precipitate formed; further precipitation occurred on standing at room temperature. Analysis showed it to be somewhat impure perfluoropoly(phenylene sulfide), and the reaction is similar to that of other nitrogenous bases with the thiol (1).

Methods A and B

The lead and silver salts of pentafluorothiophenol (used in methods A and B respectively) were prepared by literature methods (1). The requisite amount of a nonmetallic chloride or iodide was added to a suspension of the lead or silver salt in a suitable solvent and the mixture was stirred at room temperature (A or B) or refluxed (A′ lead salt only). The extent of the reaction was estimated qualitatively by the disappearance of the yellow lead salt and the appearance of white plumbous chloride, and quantitatively by weighing the plumbous halide formed; all reactions proceeded in greater than 80% yield. Products were purified by standard techniques, recrystallizations being from EtOH or CCl_4.

Known products were obtained with the following reagents (products shown after reagents): MeI - C_6F_5SMe (19); PCl_5 - $(C_6F_5S)_3P$ and $(C_6F_5S)_2$ (19); $SOCl_2$ - $(C_6F_5S)_2$, SO_2, and S; SO_2Cl_2 - $(C_6F_5S)_2$ and SO_2; Se_2Cl_2 - $(C_6F_5S)_2$ and Se; Me_2SeCl_2 (preparation (20)) - $MeSe_2$ and $(C_6F_5S)_2$; Ph_2SeCl_2 - Ph_2Se and $(C_6F_5S)_2$; $SeOCl_2$ - $(C_6F_5S)_2$, SeO_2, and Se; $TeCl_2$ - $(C_6F_5S)_2$ and Te; Me_2TeCl_2 (preparation (20)) - Me_2Te and $(C_6F_5S)_2$; Br_2 - $(C_6F_5S)_2$. The products were identified by standard techniques, including melting points, boiling points, i.r. spectra, and molecular weights (mass spectroscopically).

The lead salt did not react appreciably (less than 10%) with $SiCl_4$, $MeSiCl_3$, Me_2SiCl_2 (anhydrous CCl_4 as solvent) $PhSO_2Cl$ (CCl_4), or *p*-$TolSO_2Cl$ (toluene); the latter two did not react with the silver salt.

Method C

Stoichiometric amounts of C_6F_5SH were allowed to react in an N_2 atmosphere with the appropriate amine by shaking at room temperature in CCl_4. The product precipitated in high yield from solution. In method C′ C_6F_5SH was refluxed with $(Me_3Si)_2NH$ in C_6H_6.

Method D

Stoichiometric amounts of C_6F_5SH and NH_3 or Cl_2 were allowed to react in a sealed tube. Method D′ used the lead salt in place of C_6F_5SH. Quantitative yields were obtained.

Method E

Equimolar amounts of $Hg(SC_6F_5)_2$ (1) and PPh_3 or $Ph_2PSC_6F_5$ were refluxed in C_6H_6 and the product precipitated. No reactions were observed between $(C_6F_5)_2S$ (preparation (21)) and BCl_3 (sealed tube), BBr_3 (CCl_4), $BI_3(C_6H_6)$, NH_3 (sealed tube), $MeI(Et_2O)$, $Hg(SC_6F_5)_2(C_6H_6)$, $Et_3N(C_6H_6)$, $Hg^{2+}(H_2O,C_6H_6)$, Pd^{2+} $(2NHCl,C_6H_6)$, $Ag^+(H_2O,C_6H_6)$; $(C_6F_5S)_2$ and Pd^{2+} $(2NHCl, C_6H_6)$, $Ag^+(H_2O,C_6H_6)$; $(C_6F_5SCH_2)_2$ and $Hg^{2+}(H_2O,C_6H_6)$, $Pd^{2+}(2MHCl,C_6H_6)$; $Hg(SC_6F_5)_2$ and $Et_3N(C_6H_6)$, NH_3 (sealed tube); $PhHgSC_6F_5$ and $PPh_3(C_6H_6)$. The reactants were recovered unchanged after refluxing or allowing the sealed tube reactions to stand at room temperature for up to 5 days.

$(C_6F_5S)_2$ and NH_3

After allowing 10.0 mmol of $(C_6F_5S)_2$ and 30.0 mmol of NH_3 to stand at room temperature in a sealed tube for 6 days, 10.4 mmol of NH_3 were recovered on opening the tube. The increase in weight of the solid product recovered corresponded to 18.4 mmol of NH_3 having reacted. On vacuum sublimation of the solid product $(C_6F_5S)_2NH$, m.p. 80–82° (lit. 80–82° (10)) sublimed, which is formed by decomposition of $C_6F_5SNH_2$ on vacuum sublimation (10), leaving $C_6F_5SH.NH_3$, identified by its i.r. spectrum. The stoichiometry of the reaction is,

$$2(C_6F_5S)_2 + 4NH_3 \rightarrow 2C_6F_5SNH_2 + 2C_6F_5SH.NH_3$$
$$\downarrow \text{ Vacuum sublimation}$$
$$(C_6F_5S)_2NH + NH_3$$

The National Research Council of Canada is thanked for generous financial assistance.

1. M. E. Peach. Can. J. Chem. **46**, 2699 (1968).
2. W. Beck, K. H. Stetter, S. Tadros, and K. E. Schwarzhans. Chem. Ber. **100**, 3944 (1967).
3. R. S. Nyholm, J. F. Skinner, and M. H. B. Stiddard. J. Chem. Soc. A, 38 (1968).
4. J. A. J. Thompson and W. A. G. Graham. Inorg. Chem. **6**, 1875 (1967).
5. A. Haas. Angew. Chem. Int. Ed. **4**, 1014 (1965).
6. A. J. Oliver and W. A. G. Graham. J. Organometal. Chem. Amsterdam, **19**, 17 (1969).
7. M. Schmeisser and H. Mueller. Angew. Chem. **69**, 781 (1957).
8. J. L. Speier. U.S. Patent 2746 (1956): Chem. Abs. **51**, 1246 (1957).
9. H. J. Emeléus and H. Pugh. J. Chem. Soc. 1108 (1960).
10. M. E. Peach. Can. J. Chem. **45**, 429 (1967).
11. A. Haas and M. E. Peach. Z. Anorg. Allgem. Chem. **338**, 299 (1965).
12. E. Kostiner, M. L. N. Reddy, D. S. Urch, and A. G. Massey. J. Organometal. Chem. Amsterdam, **15**, 383 (1968).
13. H. Rheinboldt. Methoden der Organischen Chemie. Vol. IX. 4th ed. Georg Thieme Verlag, Stuttgart, 1955. p. 1114.

14. M. E. PEACH and T. C. WADDINGTON. J. Chem. Soc. 1238 (1961).
15. T. C. WADDINGTON. Non-aqueous solvent systems. Academic Press, London, 1965. p. 253.
16. M. G. HOGBEN, R. S. GAY, A. J. OLIVER, J. A. J. THOMPSON, and W. A. G. GRAHAM. J. Amer. Chem. Soc. **91**, 291 (1969).
17. M. E. PEACH. Can. J. Chem. **46**, 211 (1968).
18. R. J. NEIL, M. E. PEACH, and H. G. SPINNEY. Inorg. Nucl. Chem. Lett. **6**, 509 (1970).
19. P. ROBSON, M. STACEY, R. STEPHENS, and J. C. TATLOW. J. Chem. Soc. 4754 (1960).
20. M. E. PEACH. Can. J. Chem. **47**, 1675 (1969).
21. L. J. BELF, M. W. BUXTON, and G. FULLER. J. Chem. Soc. 3372 (1965).

Can. J. Chem. Downloaded from www.nrcresearchpress.com by 210.87.254.42 on 09/05/12
For personal use only.

Can. J. Chem. Downloaded from www.nrcresearchpress.com by 210.87.254.105 on 09/05/12
For personal use only.

Mechanism of Oxidative Decarboxylation of α-Hydroxy Acids by Bromine Water. Part I. Oxidation in Neutral and Alkaline Medium[1]

JUDITH M. PINK[2] AND ROSS STEWART
Department of Chemistry, University of British Columbia, Vancouver 8, British Columbia

Received September 2, 1970

A kinetic study of the oxidative decarboxylation of α-hydroxy acids by bromine water shows that above p*H* 6 Br_2 is a much more significant oxidant for these compounds than is HOBr, and that OBr^- is virtually inert. The rate law $-d[oxidant]/dt = k[oxidant][substrate]$ is observed and the oxidation pattern differs from that of alcohols in that the α-hydrogen is not involved in the reaction.

All the compounds studied (benzilic, mandelic, and 2-hydroxy-2-methylpropanoic acids) exhibit bell-shaped p*H*–rate profiles with maxima at about p*H* 8. A mechanism is proposed involving the attack of Br_2 (or HOBr) at the carboxylate site concurrently with base-catalyzed loss of the hydroxylic proton. A steady state treatment based on this mechanism yields calculated rates in good agreement with the observed values. Furthermore, the same parameters predict the rates observed at lower p*H* in the presence of added excess bromide. The Br_2 oxidation rate is greater than the HOBr rate by a factor of 60 for benzilic acid, 37 for 2-hydroxy-2-methylpropanoic acid, and 10 for mandelic acid.

Canadian Journal of Chemistry, 49, 649 (1971)

Introduction

α-Hydroxy acids possessing an α-hydrogen **1** may undergo oxidative decarboxylation by a number of routes (1) (Scheme 1). Reaction *B* is exemplified by the conversion of lactic acid

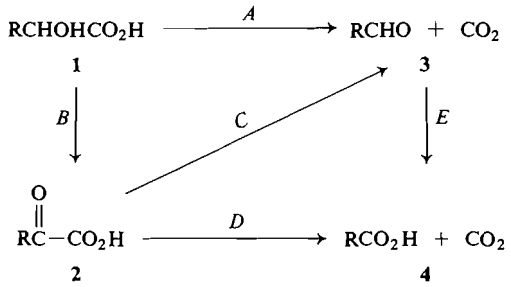

SCHEME 1

(**1**, R = CH_3) to pyruvic acid under the influence of lactic dehydrogenase. Other enzymic processes (*C*, *D*, *E*) can convert pyruvic acid to acetate (**4**, R = CH_3), either directly or via the aldehyde, **3**.

Many chemical oxidants, on the other hand, convert **1** to **4** by paths *A* and *E* in which the keto acid **2** is not an intermediate and the reaction can often be stopped at the aldehyde **3** stage. Reactions which appear to follow path *A* include the Hunsdiecker reaction (2), anodic oxidation (3), and oxidation by many, but by no means all, transition metal oxidants (4–10). For example, manganese(VII) oxidations follow *A* in acid solution but *B* in basic solution (10), and chromium(VI) is believed to react by path *B* (5, 9).

The present work is a study of the oxidative decarboxylation of three α-hydroxy acids, benzilic, mandelic, and 2-hydroxy-2-methylpropanoic acids, by bromine water in neutral and alkaline solution. The accompanying paper deals with the somewhat different situation that exists under acidic conditions (11).

A mechanistic study of α-hydroxy acid oxidation by bromine water is all the more interesting because of the different behavior of this oxidizing agent towards alcohols on the one hand and towards many carboxylic acids on the other. There is now considerable evidence (12–19) that alcohol oxidation occurs through a rate determining abstraction of a hydride ion from an α-position by Br_2 and that this step is assisted by the removal of the hydroxylic hydrogen as a proton. This interpretation is in agreement with the kinetic isotope effects (12–14), substituent effects (17, 18), and the presence of general base catalysis (17, 19), though it fails to explain the observations of Barker *et al.* (20) concerning the oxidation of cycloalkanols. The oxidation of formate is analogous to the alcoholic oxidation pattern (21) but that of oxalic acid is entirely different. In the latter case HOBr is a much more efficient oxidant than Br_2 and reaction takes place with oxalic acid or mono-oxalate but not with the dioxalate (19).

[1]Taken from the Ph.D. Thesis of Mrs. Judith M. Pink, University of British Columbia, Vancouver, British Columbia, 1970.

[2]Present address: St. Francis Xavier University, Antigonish, Nova Scotia.

Can. J. Chem. Downloaded from www.nrcresearchpress.com by 210.87.254.105 on 09/05/12
For personal use only.

Experimental

Analar grade inorganic reagents were used throughout. The highest grade organic reagents available were several times recrystallized or freshly distilled prior to use. Water was doubly distilled and cooled under a stream of nitrogen. All glassware was meticulously cleaned with chromic acid or with a 5% solution of hydrogen fluoride and rinsed several times with distilled water. The u.v. spectra were recorded on a Bausch and Lomb 502 or on a Cary Model 14 Spectrophotometer. The pH was determined by a Beckman Model G pH meter and, for most of the kinetic runs, by a Radiometer TTT1 Titrator. The computations were carried out with the aid of IBM 1620 and 1130 computers.

Product Analysis

The hydroxy acids gave nearly quantitative yields of the corresponding ketones or aldehydes. Yields were estimated on the basis of absorption in the u.v.; the identity of the ketones was also established by preparing their 2,4-dinitrophenylhydrazone derivatives.

Kinetics

The pH of the reaction medium was monitored by continuous titration with a Radiometer Model TTT1 Titrator. The reactions were carried out in a 150 ml darkened glass vessel having four necks with ground glass joints. Through the necks were fitted (*a*) a glass electrode; (*b*) a fritted glass salt bridge connecting the reaction vessel with a calomel electrode; (*c*) a syringe filled with 0.5 M KOH, its tip ending in a fine glass capillary under the surface of the reaction mixture; (*d*) a glass stopper. The vessel, containing a teflon coated magnetic stirring bar and a known volume (about 100 ml) of freshly prepared bromine water (10^{-4}–10^{-3} M), was equilibrated in a constant temperature bath at 25°. The pH of the stirred reaction mixture was brought to the desired value by adding acid from a pipette or base from the syringe. Three 5 ml aliquots were removed for analysis at 3–5 min intervals for determining the initial oxidant concentration. The substrate solution was made up to have a pH similar to that intended in the run in order to minimize pH changes caused by its addition to the reaction mixture. The reaction was started by adding a stoichiometrically equivalent amount of substrate (2–5 ml) by blowing from a specially calibrated pipette. Aliquots were withdrawn at appropriate time intervals, using a fast delivery pipette, and were quenched in acidified potassium iodide solution and titrated. The pH was controlled by the instrument to within 0.10 pH units and the volume of base added during the reaction never amounted to more than 0.4 ml. Most reactions were complete within 5 min, corrections for bromine loss due to evaporation were made for slower reactions. In calculations the concentration of all compounds were corrected according to the total volume of the reaction mixture after adding the substrate.

Results and Discussion

The oxidation of benzilic, mandelic, and 2-hydroxy-2-methylpropanoic acids by bromine water above pH 5.5 was found to follow second order kinetics; first order with respect to each

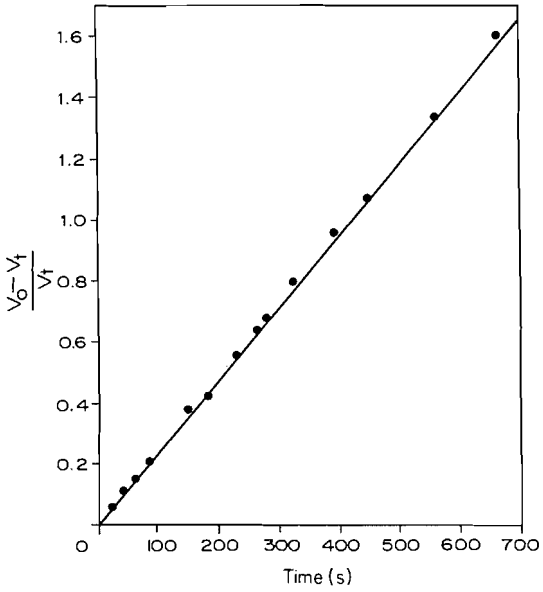

FIG. 1. A typical second-order rate plot for the oxidation of mandelic acid by bromine water, pH = 8.5, T = 25 °C. The initial concentration, C_0, of substrate and oxidant was 2.84×10^{-3} M; $k_2 = (V_0 - V_t)/V_t \cdot 1/tC_0 = 0.829$ 1 mol^{-1} s^{-1}; V = thiosulfate titre.

reagent (Fig. 1). The stoichiometry of the oxidation by molecular bromine shows that acid is released during the reaction (eq. 1). Furthermore,

[1] $$RR'COHCO_2^- + Br_2 \rightarrow RR'C{=}O + CO_2 + 2Br^- + H^+$$

both the composition of bromine water and the nature of the substrate are pH dependent and it was therefore necessary to maintain a constant pH during individual runs.

The reaction was found to be subject to general base catalysis, but not in a simple manner; *e.g.* the oxidation rate of benzilic acid was greatly enhanced by certain buffers (phosphate at pH 6 for example) but the Brønsted relation was not obeyed. Thus, in order to simplify the kinetics a constant pH was maintained by means of a pH-stat. In the absence of buffers the pH–rate profile of each substrate is bell-shaped and the rate maximum occurs at about pH 8 (see Figs. 2–4). This superficially corresponds to the HOBr content of these solutions[3] and suggests

[3]At a given bromide concentration the HOBr content is a function of the pH and can be calculated from the following equations:

$K_h = [Br^-][HOBr][H^+]/[Br_2] = 9.6 \times 10^{-9}$ (ref. 22)

and

$K_{HOBr} = [H^+][OBr^-] = 2.1 \times 10^{-9}$ (ref. 23)

Can. J. Chem. Downloaded from www.nrcresearchpress.com by 210.87.254.105 on 09/05/12
For personal use only.

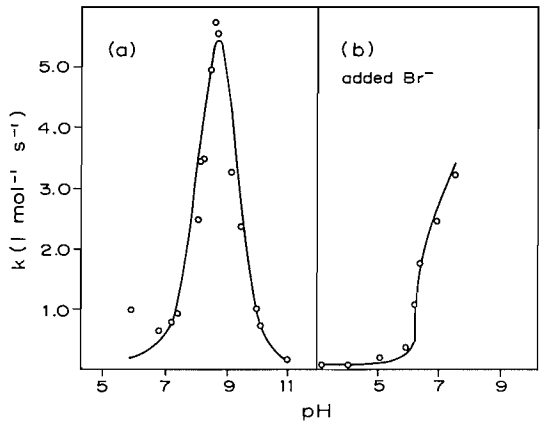

FIG. 2. The pH dependence of the rate of benzilic acid oxidation by bromine water in (*a*) the absence and (*b*) the presence of added bromide ion (0.0338 – 0.153 M). The curves in both cases were drawn using values calculated from eqs. 6 and 7 and the values $\kappa_{H_2O} = 4.5 \times 10^{-2}$, $\kappa_{OH} = 9 \times 10^3$, $\kappa_{HOBr} = 2 \times 10^5$, and $\kappa_{Br} = 1.2 \times 10^7$. The open circles represent experimental points.

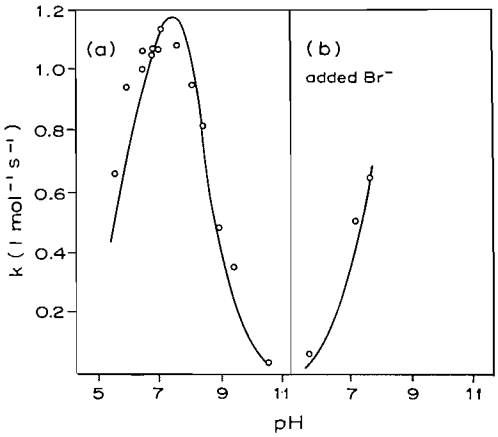

FIG. 3. The pH dependence of the rate of mandelic acid oxidation by bromine water in (*a*) the absence and (*b*) the presence of added bromide ion (0.0540 – 0.0763 M). The curves in both cases were drawn using values calculated from eqs. 6 and 7 and the values $\kappa_{H_2O} = 5 \times 10^{-5}$, $\kappa_{OH} = 6 \times 10^4$, $\kappa_{HOBr} = 8 \times 10^4$, $\kappa_{Br} = 8 \times 10^5$. The open circles represent experimental points.

that OBr^- is inert. However, when the HOBr concentration in reaction mixtures having a pH above 5 was reduced by adding bromide, the rate was found to increase. This shows Br_2 to be a better oxidant than HOBr under these conditions. (In more acidic solutions the reactivity order is reversed; see accompanying paper.) Above pH 5 all the substrates studied are completely dissociated and a likely possibility would

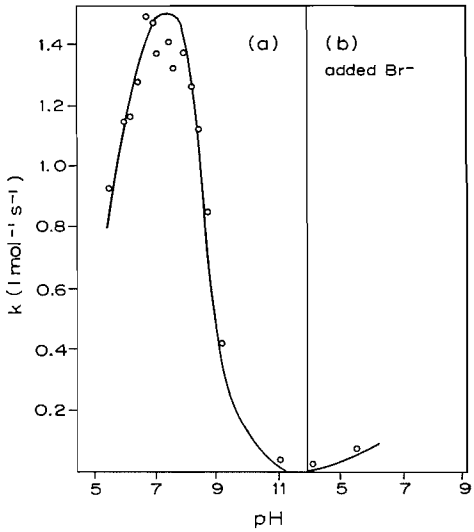

FIG. 4. The pH dependence of the rate of 2-hydroxy-2-methylpropanoic acid oxidation by bromine water in (*a*) the absence and (*b*) the presence of added bromide ion (0.054 – 0.055 M). The curves in both cases were drawn using values calculated from eqs. 6 and 7 and the values $\kappa_{H_2O} = 8 \times 10^{-4}$, $\kappa_{OH} = 3 \times 10^4$ $\kappa_{HOBr} = 5 \times 10^4$, $\kappa_{Br} = 1.87 \times 10^6$. The open circles represent experimental points.

be a base-catalyzed bromine–carboxylate reaction. The eventual rate decrease as the pH is increased beyond 8.6 is expected on the basis of the pH dependence of the composition of bromine water. Above this pH the concentration of Br_2 is negligible and the oxidant is all in the form of HOBr and OBr^-.

A possible mechanism is shown in eq. 2, where S^- is the dissociated form of the α-hydroxy acid

$$[2] \qquad S^- + Br_2 \overset{K_{Br}}{\rightleftharpoons} SBr + Br^- \qquad SBr + :B \longrightarrow \text{products}$$

and :B represents a base. (In the unbuffered systems the two strongest bases are OH^- and OBr^-.)

An attempt was made to measure K_{Br} for a closely related compound, α-methoxyphenylacetic acid, which is only slowly degraded by bromine water. Calculations based on the pH-drop, observed when solutions of this acid and of bromine water, both initially at the same pH, were mixed, showed that in this reaction the upper limit of the equilibrium constant, K_{Br}, is 0.1. By assuming an equilibrium constant of the same order of magnitude for the hydroxy acid – bromine water reaction, and estimating the catalytic rate coefficients for hypobromite and

Can. J. Chem. Downloaded from www.nrcresearchpress.com by 210.87.254.105 on 09/05/12
For personal use only.

hydroxide by comparing rate constants observed at constant pH and constant hypobromite concentration, respectively, it can be shown that if Br_2 were the only oxidant the rate maximum for benzilic acid would appear at a pH no higher than 7.5 instead of at the observed value of 8.6. This indicates the presence of an HOBr reaction path. Scheme 2 should then be considered.

$$S^- + HOBr \underset{k_{-1}}{\overset{k_1}{\rightleftharpoons}} SBr + OH^-$$

$$S^- + Br_2 \underset{k_{-2}}{\overset{k_2}{\rightleftharpoons}} SBr + Br^-$$

$$SBr + H_2O \xrightarrow{k_3} S^- + HOBr + H^+$$

$$SBr + OH^- \xrightarrow{k_P} \text{products}$$

$$SBr + OBr^- \xrightarrow{k_P'} \text{products}$$

SCHEME 2

In this case the SBr concentration is assumed to be low, so that a steady state approximation is applicable. The observed rate is given by eq. 3,

$$[3] \quad \text{rate} = k_P[SBr][OH^-] + k_P'[SBr][OBr^-]$$

where the second term can be neglected to a first approximation. Accordingly, the steady state concentration of SBr is eq. 4.

$$[4] \quad [SBr] = \frac{k_1[S^-][HOBr] + k_2[S^-][Br_2]}{k_{-1}[OH^-] + k_{-2}[Br^-] + k_3 + k_P[OH^-]}$$

Since good second order kinetics was observed above pH 6 when stoichiometrically equivalent amounts of substrate (S^-) and oxidant (Ox) were used, eq. 5 results.

$$[5] \quad \text{rate} = k_{obs}[S^-][Ox] = k_{obs}[S^-]^2 = k_P[SBr][OH^-]$$

The substitution of eq. 4 into 5 gives eq. 6.

$$[6] \quad k_{obs}k_{-2}[S^-][Br^-] + k_{obs}k_3[S^-] + k_{obs}(k_P + k_{-1})[S][OH^-] - k_Pk_1[HOBr][OH^-] - k_Pk_2[Br_2][OH^-] = 0$$

Equation 6 can be used, in principle, to calculate the composite rate constants if the variables

$$[7] \quad \kappa_{H_2O} = k_3/k_{-2} \qquad \kappa_{OH} = (k_{-1} + k_P)/k_{-2}$$
$$\kappa_{HOBr} = k_Pk_1/k_{-2} \qquad \kappa_{Br} = k_Pk_2/k_{-2}$$

k_{obs}, $[S^-]$, $[Br^-]$, [HOBr], $[Br_2]$, and $[OH^-]$ are known for four runs. However, the pH of the runs could be maintained only within $\pm.10$ pH units which is not sufficient precision to obtain accurate values for the partition of the oxidant between Br_2, HOBr, and OBr^-. Equation 6 is ill-conditioned and thus it is not possible to solve for the rate constants from experimental values. Therefore, values were chosen for the composite rate constants defined in eq. 7 and eq. 6 was solved for k_{obs} instead. The self-consistently calculated values of k_{obs} at different pH's showed fair agreement with the observed rate constants, as can be seen in Figs. 2–4.

If Scheme 2 is indeed valid then it must be applicable to all conditions when the $[Br_2]$/[HOBr] ratio is constant throughout the reaction. This is not the case for oxidation by bromine water below pH 6, for the bromide accumulating during the course of the reaction changes the oxidant composition considerably. If, however, the reaction is carried out in the presence of a fairly large excess of Br^-, the effect of Br^- formed will be negligible. Thus, the composite rate constants (κ), used in the calculations at high pH should also predict the observed rate constants for runs carried out at lower pH in the presence of excess Br^-. Figures 2*b*, 3*b*, and 4*b* show that this indeed is the case. This result is significant, for the concentration terms of these two sets of runs differ from each other by several powers of ten. Further refinement of the self-consistent calculations could bring the calculated rate constants even closer to the observed values but in the opinion of the authors the present numerical data are sufficient to support the proposed mechanism.

The apparently autocatalytic kinetics of mandelic acid oxidation at pH 6–7 in the presence of added bromide is explained by further reaction of the primary oxidation product, benzaldehyde. Rate studies carried out on pure benzaldehyde showed its rate of oxidation to be about a third of that of mandelic acid under these conditions. Our results also support earlier observations (24) that Br_2 is a much more important oxidant for benzaldehyde than HOBr and that the reaction is subject to general base catalysis (25).

The relative importance of the HOBr and Br_2 oxidation paths for the various α-hydroxy acids can be assessed by comparing the ratios of $\kappa_{HOBr}/\kappa_{OH}$ with those of κ_{Br}/κ_{OH}, listed in Table 1. The ratio of the HOBr/Br_2 routes is of the same

TABLE 1. Comparison of HOBr and Br_2 oxidation rates of α-hydroxy acids in alkaline medium*

α-Hydroxy acid	$\kappa_{HOBr}/\kappa_{OH} = \alpha k_1$	$\kappa_{Br_2}/\kappa_{OH} = \alpha k_2$	Br_2 rate/HOBr rate
Benzilic	22.2	1335	60
2-Hydroxy-2-methylpropanoic	1.66	62.3	37
Mandelic	1.33	13.3	10

*$\alpha = \frac{k_P}{k_P + k_{-1}}$

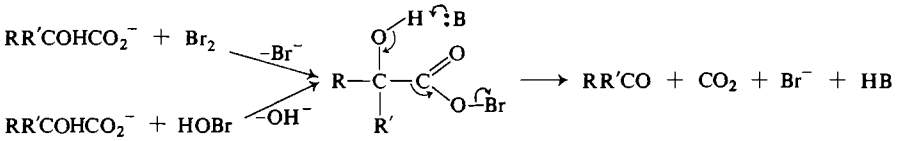

SCHEME 3

order of magnitude as was found for formate oxidation by Binoun and Perlmutter-Hayman (26). It is not surprising that the highly polarizable Br_2 is more reactive towards carboxylate than is HOBr, though it is puzzling why oxalate should be an exception. We have confirmed previous reports (19) that HOBr is much the more significant oxidant for oxalate throughout the p*H* range.

The results presented show that the presence of an α-hydrogen is not a requirement for oxidative decarboxylation indicating that path *A* (Scheme 1), rather than paths *B* and *C* convert mandelic acid to benzaldehyde. Isotopic studies reported in the accompanying paper (8) support this conclusion.

The most reasonable mechanism that is in agreement with the kinetic analysis is formation of an acyl-hypobromite type intermediate which can readily decompose if the hydroxylic proton is removed by base (Scheme 3). Thus the observed rate is determined by the Br_2 and HOBr concentrations (which decrease with increasing p*H*) and by the concentration of base.

It is interesting to note that the rate maximum for the oxidative decarboxylation of α-hydroxy acids by bromine water occurs under near-neutral conditions, unlike those prevailing in most other *in vitro* oxidations.

The financial support of the National Research Council of Canada is gratefully acknowledged. Some of the experimental work was done by J.M.P. in Mr. R. P. Bell's laboratory at the University of Oxford, Oxford, England, and we express our thanks for this and for his interest.

1. R. STEWART. Oxidation mechanisms. Application to organic chemistry. W. A. Benjamin, Inc., New York, N.Y., 1964.
2. R. G. JOHNSON and R. K. INGHAM. Chem. Rev. **56**, 219 (1956).
3. B. C. L. WEEDON. Quart. Rev. **6**, 380 (1952).
4. K. B. WIBERG, *Editor*. Oxidation in organic chemistry. Part A. Academic Press, New York, N.Y., 1965. pp. 65, 207, 265, 403.
5. T. J. KEMP and W. A. WATERS. J. Chem. Soc. 1192 (1964).
6. J. R. JONES, W. A. WATERS, and J. S. LITTLER. J. Chem. Soc. 630 (1961).
7. G. V. BAKORE and R. SHANKER. Can. J. Chem. **44**, 1717 (1966).
8. H. G. FLETCHER, JR., H. W. DIEHL, and C. S. HUDSON. J. Amer. Chem. Soc. **72**, 4546 (1950).
9. R. N. MEHROTRA. J. Chem. Soc. B, **1968**, 642.
10. J. M. PINK and R. STEWART. Unpublished results.
11. J. M. PINK and R. STEWART. This issue.
12. L. KAPLAN. J. Amer. Chem. Soc. **76**, 4645 (1954).
13. L. KAPLAN. J. Amer. Chem. Soc. **79**, 2639 (1957).
14. C. G. SWAIN, R. A. WILES, and R. F. W. BADER. J. Amer. Chem. Soc. **83**, 1945 (1961).
15. B. PERLMUTTER-HAYMAN and Y. WEISSMANN. J. Amer. Chem. Soc. **84**, 2323 (1962).
16. L. FARKAS, B. PERLMUTTER, and O. SCHACHTER. J. Amer. Chem. Soc. **71**, 2827 (1949).
17. P. ANKETT and I. R. L. BARKER. Chem. Ind. 193 (1967).
18. N. VENKATASUBRAMANIAN and V. THIAGARAJAN. Tetrahedron Lett. 1711 (1968).
19. B. PERLMUTTER-HAYMAN and Y. WEISSMANN. J. Amer. Chem. Soc. **91**, 668 (1969).
20. (*a*) I. R. L. BARKER, W. G. OVEREND, and C. W. REES. Chem. Ind. 558 (1961); (*b*) Chem. Ind. 463 (1962); (*c*) J. Chem. Soc. 3263 (1964).
21. I. R. L. BARKER. Chem. Ind. 1936 (1964).
22. J. M. PINK. Can. J. Chem. **48**, 1169 (1970).
23. I. E. FLIS, K. P. MISCHENKO, and G. I. PUSENOK. Khim. i Khim. Tekhnol, 7, 764 (1964).
24. P. T. MCTIGUE and J. M. SIME. J. Chem. Soc. 1303 (1963).
25. I. R. L. BARKER and R. H. DAHM. Chem. Commun. 194 (1965).
26. L. BINOUN and B. PERLMUTTER-HAYMAN. Bull. Res. Council Israel, **A5**, 52 (1955).

Can. J. Chem. Downloaded from www.nrcresearchpress.com by 210.87.254.105 on 09/05/12
For personal use only.

Can. J. Chem. Downloaded from www.nrcresearchpress.com by 210.87.254.40 on 09/05/12
For personal use only.

Mechanism of Oxidative Decarboxylation of α-Hydroxy Acids by Bromine Water. Part II. Oxidation in Acidic Medium. A Comparison with the HOBr – Oxalic Acid Reaction[1]

JUDITH M. PINK[2] AND ROSS STEWART
Department of Chemistry, University of British Columbia, Vancouver 8, British Columbia

Received September 2, 1970

The oxidative pattern of α-hydroxy acids by acidic bromine water is shown to be similar to the oxalic acid – bromine water reaction. In both cases HOBr is the oxidant and the undissociated form of the organic acid is required for reaction to occur. The rate law $-d[HOBr]/dt = k[HOBr][\text{hydroxy acid}]$ is observed for oxidations carried out in the presence of Ag^+ ion in the p*H* range 2–5. Below that p*H* bromination occurs. Bell-shaped p*H*–rate profiles are obtained for the oxidations of benzilic, mandelic, and 2-hydroxy-2-methylpropanoic acids. The calculated rates, based on a steady state treatment of a reaction path involving a hypobromite intermediate ($R_2COBrCO_2H$) are in agreement with the observed values and with the observation that the rates of oxidation of mandelic acid in D_2O and H_2O are the same.

Canadian Journal of Chemistry, 49, 654 (1971)

Introduction

In Part I it was shown that α-hydroxy acids undergo ready oxidative decarboxylation by the action of bromine water under neutral conditions (1). The reaction appears to take place via the carboxylate anion with Br_2 being a much more effective oxidant than HOBr. The reverse is true for the oxidation of oxalic acid by bromine water; in this case HOBr is the oxidant and only the mono-oxalate and the undissociated acid appear to react (2). Oxalic acid seems to be exceptional in this regard since all other compounds studied to date are preferentially oxidized by Br_2 (3). α-Hydroxy acids (**1**) are structurally related to oxalic acid (**2**), and it was hoped that their behavior might shed some light on this enigma.

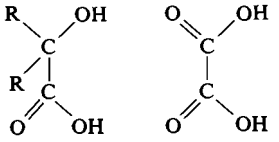

1 **2**

Experimental

Reagents

Most of the reagents and apparatus used were described in Part I. D_2SO_4 was prepared using Ingold's method (4). α-D-Mandelic acid was obtained by exchanging sodium mandelate in 99.87% D_2O in a sealed tube at 150° for 3 weeks. The α-hydrogen exchange was shown to be quantitative by n.m.r. spectroscopy.

The methods published for the preparation of α-methoxydiphenylacetic acid (5) failed to give satisfactory yields. The following synthetic method was therefore developed. A mixture of 12 g of benzilic acid and 15 ml of phosphorus tribromide was allowed to react for 12 h at 100° in a flask fitted with a condenser and drying tube containing silica gel. After standing overnight the solution was cooled in ice, the precipitate formed was filtered off, washed with ligroin, then added to anhydrous ice-cold methanol. The product thus obtained was hydrolyzed in alcoholic potassium hydroxide on a steam bath, then this solution was evaporated to dryness and the residue extracted with boiling water. The cooled acidified aqueous solution was extracted with ether. The amorphous acidic material obtained after evaporating the ether was dissolved in a 5% solution of sodium bicarbonate and this solution was then carefully acidified until it became cloudy. Upon standing, colorless needles separated. After two recrystallizations from benzene–ligroin, the compound had a m.p. of 109.5–110.0 (lit. 110.0–110.6 (6)).

Product Analysis

Reaction mixtures containing excess bromine and silver nitrate relative to the substrate, but otherwise similar to those employed in kinetic runs, were allowed to react. Then excess aqueous ammonia was added in order to dissolve the silver bromide and to react with the unused hypobromous acid. The mixture was then extracted with ether. The u.v. spectra were taken of the aqueous fraction and of an alcoholic solution of the solid obtained from the ether extract. Nearly quantitative yields of the appropriate ketones or aldehyde were obtained above p*H* 2.5.

Kinetics

The procedure described in Part I was followed. The iodometric determination of the oxidant in the presence of added silver ion involves a grey to yellow color change at the end point; it requires some experience to distinguish this transition reproducibly.

[1]Taken from the Ph.D. Thesis of Mrs. Judith M. Pink, University of British Columbia, Vancouver, British Columbia, 1970.

[2]Present address: St. Francis Xavier University, Antigonish, Nova Scotia.

Can. J. Chem. Downloaded from www.nrcresearchpress.com by 210.87.254.40 on 09/05/12
For personal use only.

Oxidation of triphenylacetic acid: Triphenylacetic acid (0.10 g) was dissolved in 10 ml glacial acetic acid and added to a 3×10^{-3} *M* bromine solution (100 ml) containing excess silver nitrate (1×10^{-2} *M*). This mixture was allowed to stand at room temperature for 1 month in the dark. Occasionally 5 ml aliquots were withdrawn for analysis. After 1 month the oxidizing power of the reaction mixture decreased to 41% relative to the control solution containing all the components except triphenylacetic acid. The reaction was terminated by quenching the oxidant with an equivalent amount of sodium bisulfite; then the silver was precipitated by adding potassium bromide. The mixture was centrifuged, the solid residue extracted with benzene, and the liquid analyzed by t.l.c. The spots developing in the chromatogram corresponded to those of a mixture of triphenylacetic acid and triphenylcarbinol, chromatogrammed concurrently. No triphenylcarbinol was formed when triphenylacetic acid was allowed to react with bromine water in the presence of added silver bromide.

The IBM 1620 and 1130 computers were used in carrying out the computations.

pK_a Determination of Mandelic Acid in 90% D_2O

A standard potentiometric technique (7) was employed, using Radiometer SBR2c/SUB1/TTA3 titration equipment in conjunction with a type PHA 630T Scale Expander. The pK_a of mandelic acid in water was determined to be 3.385 ± .007 (lit. 3.388, (8)) at 25°. The pK_a in 90% D_2O was found to be 3.472 ± .006 using activity corrections based on the equation given by Glasoe and Long (9).

Results and Discussion

The kinetics of α-hydroxy acid oxidation by bromine water below p*H* 5 is complex. When stoichiometrically equivalent amounts of oxidant and substrate are used autoretardation occurs. This is due to the accumulation of bromide, which inhibits the reaction greatly; Br^- forms Br_3^- with Br_2 (10), but the depletion of oxidant by tribromide formation can only account for a part of the observed rate decrease.

When the formation of bromide is suppressed by the addition of excess silver ion the reaction occurs at a much higher rate and obeys a second order rate law, first order with respect to oxidant and with respect to substrate (Fig. 1). At least 2 mol of Ag^+ are necessary per mol of bromine to obtain good second order kinetics, but increasing the $[Ag^+]$ beyond that point does not alter the rate (see Fig. 1). Hence the effect of silver ion on the rate can be attributed to its shifting the bromine hydrolysis equilibrium in favor of HOBr (eq. 1) rather than to its participation in the rate-controlling step.

[1] $Br_2 + H_2O + Ag^+ \rightarrow HOBr + H^+ + AgBr(s)$

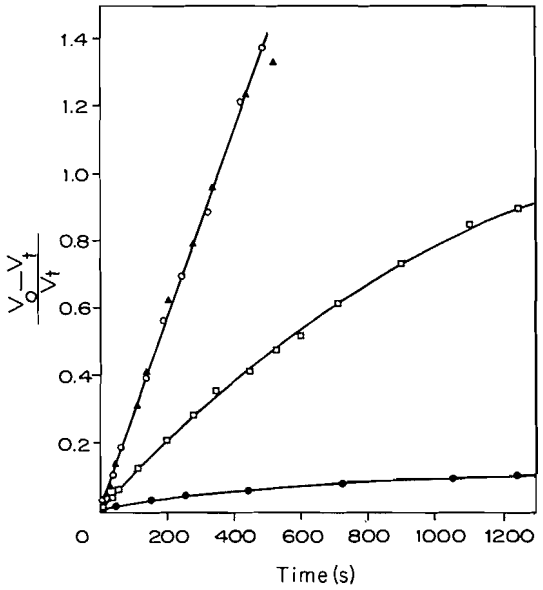

FIG. 1. The effect of silver ion concentration on the rate of oxidation of benzilic acid by bromine water at p*H* 1.77; $[Ag^+]_0/[\text{oxidant}]$ = 0.0 (●), 1.0 (□), 2.0 (▲), 13 (○); *V* = thiosulfate titre.

In strongly acidic media and in the presence of silver ion bromine water brominates aromatic α-hydroxy acids. The logarithm of the rate of benzilic acid bromination in this system shows a linear dependence on the H_0 function. Such a relation has also been observed previously for halogenation by positive agents (11). The rate of bromination becomes negligible above p*H* 1.5; hence the study of the oxidative decarboxylation process in the presence of silver ion was restricted to the p*H* range 2–5. Above p*H* 5 bromine water was found to be unstable in the presence of silver ion.

The oxidative decarboxylation of α-hydroxy acids by hypobromous acid is accompanied by the liberation of acid, eq. 2.

[2] $RR'COHCO_2H + HOBr \rightarrow RR'C{=}O + CO_2 + Br^- + H_2O + H^+$

Two methods of maintaining a constant p*H* during the reaction were employed. The first method, the use of buffers, increased the reaction rates appreciably relative to the values observed when the p*H* was kept constant by the second method, that of continuous titration. However, no simple relation could be established between buffer concentration and rate data. Changing the ionic strength had no effect on the reaction

Can. J. Chem. Downloaded from www.nrcresearchpress.com by 210.87.254.40 on 09/05/12
For personal use only.

rate. The rate increase due to increasing buffer concentration may be due either to base catalysis, or to the formation of species like acetyl hypobromite (12) or bromine–phosphate complexes (13). For this reason the discussion below is restricted to treatment of data obtained in unbuffered, p*H*-statted systems.

The p*H*–rate profiles for oxidations carried out in the presence of silver ion are bell-shaped for all the hydroxy acids studied in the p*H* region 2–5 (see Figs. 2–4). The only significant oxidant in these solutions is HOBr. The rate increase with increasing p*H* as the pK_a of the substrate is approached would suggest that the rate controlling step involves the carboxylate anion but does not explain the rate decrease on the high p*H* side of the bell-shaped curve. Scheme 1, in which HOBr reacts with the undissociated acid to form a hypobromite intermediate, HZ, satisfies

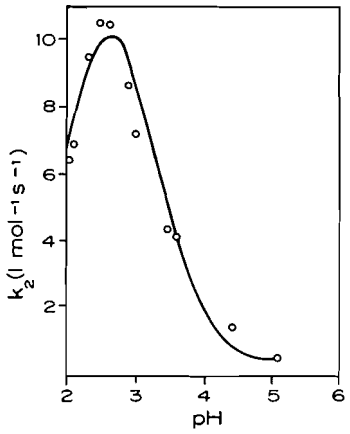

FIG. 2. The p*H*-dependence of the rate of oxidation of benzilic acid by bromine water in the presence of silver ion. Solid line is calculated using eq. 10, pH_{max} = 2.60, pK_s = 3.05.

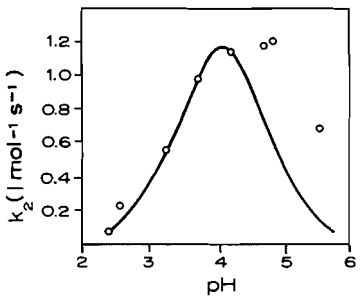

FIG. 3. The p*H*-dependence of the rate of oxidation of 2-hydroxy-2-methylpropanoic acid by bromine water in the presence of silver ion. Solid line is calculated using eq. 10, pH_{max} = 4.05, pK_s = 3.97.

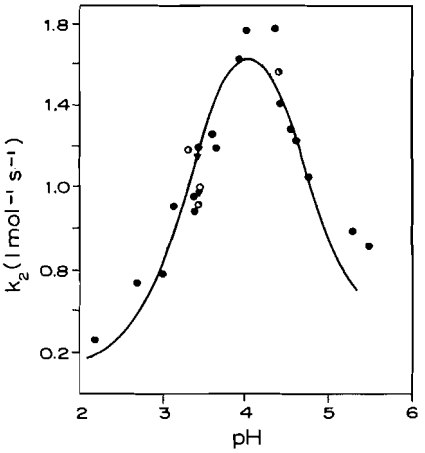

FIG. 4. The p*H*-dependence of the rate of oxidation of mandelic acid by bromine water in the presence of silver ion. Solid line is calculated using eq. 10, pH_{max} = 4.04, pK_s = 3.39. Legend: mandelic acid in H_2O (●), mandelic-α-*d* acid (○), mandelic acid in D_2O (p*H* corrected) (▼).

both requirements. This intermediate can decompose into oxidation products when it loses a proton. Scheme 1 requires that the hypobromite be formed at the hydroxyl site, not at the carboxyl site as in the oxidation at higher p*H* (1), because

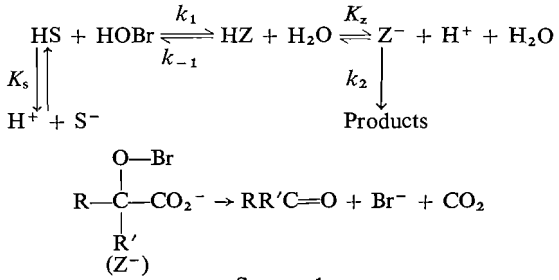

SCHEME 1

the intermediate HZ must be sufficiently acidic to ionize in acid solution. Furthermore, reaction of the neutral α-hydroxy acid with hypobromous acid should occur more readily at the hydroxyl than at the carboxyl group. The terms in Scheme 1 are defined as:

$$\mathrm{HS} = \mathrm{RR'COHCO_2H}$$

$$K_s = [\mathrm{H^+}][\mathrm{S^-}]/[\mathrm{HS}]$$

$$\mathrm{HZ} = \mathrm{RR'COBrCO_2H}$$

$$\left\{ \begin{array}{l} \mathrm{Z^-} = \mathrm{RR'COBrCO_2^-} \\ K_z = [\mathrm{H^+}][\mathrm{Z^-}]/[\mathrm{HZ}] \end{array} \right. \quad [3]$$

Can. J. Chem. Downloaded from www.nrcresearchpress.com by 210.87.254.40 on 09/05/12
For personal use only.

furthermore,

$$[4] \quad \begin{cases} [S_t] = [HS] + [S^-] \\ [Z_t] = [HZ] + [Z^-] \end{cases}$$

The rate of formation of the hypobromite intermediate $[Z_t]$ is eq. 5.

$$[5] \quad d[Z_t]/dt = k_1[HS][HOBr] - k_{-1}[HZ] - k_2[Z^-]$$

Assuming a steady state concentration of $[Z_t]$ and substituting the appropriate mole fractions according to [3] and [4] we get eq. 6.

$$[6] \quad [Z_t] = \frac{k_1 \dfrac{[HOBr][S_t][H^+]}{K_s + [H^+]}}{k_{-1}\dfrac{[H^+]}{K_z + [H^+]} + k_2 \dfrac{K_z}{K_z + [H^+]}}$$

The observed rate depends on the Z^- concentration (eq. 7) where k is the experimental second

$$[7] \quad \text{rate} = k[HOBr][S_t] = k_2[Z^-] = k_2 \frac{K_z[Z_t]}{K_z + [H^+]}$$

order rate constant. Combining eqs. 6 and 7 we get eq. 8. According to eq. 8 k vanishes as

$$[8] \quad k = \frac{k_1 k_2 \dfrac{[H^+]}{K_s + [H^+]} \dfrac{K_z}{K_z + [H^+]}}{\dfrac{k_{-1}[H^+] + k_2 K_z}{K_z + [H^+]}}$$

$[H^+] \to 0$ and as $[H^+] \to \infty$ and has a maximum at

$$[9] \quad [H^+]_{max} = \left(\frac{K_s K_z}{k_{-1}}\right)^{1/2}$$

A combination of eqs. 8 and 9 gives eq. 10. Thus

$$[10] \quad k = k_1 \frac{[H^+][H^+]^2_{max}}{(K_s + [H^+])(K_s[H^+] + [H^+]^2_{max})}$$

it is seen that the dissociation constant, K_s, of the hydroxy acid and the experimental pH value at the observed rate maximum uniquely determine k in terms of k_1. If we designate the coefficient of k_1 in eq. 10 as k_{calc} ($k = k_1 k_{calc}$), k_{calc} can be readily computed for any value of $[H^+]$. The comparison of k_{calc} with the experimentally observed rate constant gives $k_1 = k/k_{calc}$. The constancy of k_1 is indicative of the validity of Scheme 1.

In some cases better agreement between calculated and observed rates could be achieved throughout the pH range if a pH maximum slightly different from the observed value was assumed. If the observed rates are not solely due to the process described, but there is contribution from other processes (*e.g.* bromination at low pH, reaction with the carboxylate at high pH) then, even if the contribution from these is small, the true rate maximum may be masked.

The results of some computations are shown graphically in Figs. 2–4. The calculated rate constants show a reasonable agreement with the experimentally obtained values. Of course, the nature of the intermediate cannot be determined on the basis of kinetics alone. The above treatment is compatible not only with a low steady state concentration of a hypobromite intermediate, formed at the hydroxyl site, but also with a concerted reaction between undissociated carboxylic acid, hypobromous acid, and base. The data of Fig. 4 also show that the oxidation rate in water and in 90% D_2O are almost the same when rates are compared at pH values corresponding to the same degree of ionization of mandelic acid. This is in accordance with Scheme 1 if the steady state concentration of the intermediate Z^- is unaffected by isotopic substitution. A concerted reaction between neutral mandelic acid, HOBr, and base seems somewhat less likely since it is difficult to conceive of a concerted mechanism that does not involve O—H cleavage and a cancellation of isotope effects would be required. However, the solvent isotope experiments are not definitive; they were conducted at a single pH and the effect of D_2O on the various equilibria is hard to assess.

At this point it may be of interest to recall the parallel behavior of oxalic acid. In that case too, HOBr is the most important oxidant and while the mono-oxalate is the most reactive species, the dioxalate is inert. An unionized carboxyl group is thus required for the oxidation in both cases. The importance of the $—CO_2H$ group is further illustrated by the observation that neither methyl benzilate nor the carboxylate anion of α-methoxydiphenylacetic acid are oxidized by bromine water but the undissociated form of α-methoxydiphenylacetic acid reacts slowly. The presence of a reaction path for oxidative decarboxylation other than that shown in Scheme 1 is revealed by the slow but definite oxidation of

Can. J. Chem. Downloaded from www.nrcresearchpress.com by 210.87.254.40 on 09/05/12
For personal use only.

triphenylacetic acid by HOBr (again, no oxidation takes place with Br_2) and by the rapid degradation of α-amino acids by HOBr. Amino acids behave rather differently to hydroxy acids in basic solution; glycine is rapidly degraded by hypobromite ion whereas glycolic acid is inert.

In the case of mandelic acid it might be expected that the compound would be oxidized both as an alcohol and as a hydroxy acid. A comparison of rates for α-H and α-D mandelic acids (Fig. 4) shows that α-deuteriation has no effect on the rate. Thus the hydroxy acid route is energetically much more favorable and the α-proton is not involved in the reaction at all.

Comparison of Oxidation in Acidic and Basic Solution

The oxidative decarboxylation of α-hydroxy acids by bromine water exhibits bell-shaped curves both in acid solution (Figs. 2, 3, and 4) and in neutral or basic solution (1). If the two curves were combined a camel-like pH–rate profile would appear, with peaks at pH 2.8 and 8.6 for benzilic acid. However, the conditions for the two reactions are different; the acid reaction was conducted in the presence of silver ion to allow a satisfactory kinetic analysis to be made.

Combining the two reaction paths, one can derive a rate law describing the complex kinetics observed in acidic bromine water, in the absence of Ag^+.

Neglecting the less important contributions, we have eq. 11. Because of the accumulation of

$$[11] \quad \text{rate} = k_{HOBr}[HOBr][HS] + k_{Br_2}[Br_2][S^-][OH^-]$$

bromide during the course of the reaction, the $HOBr/Br_2$ ratio changes with time in accordance with the equilibria

$$K = [Br_2][Br^-]/[Br_3^-] = 0.0594 \text{ (ref. 10)}$$

$$K_h = [H^+][HOBr][Br^-]/[Br_2] = 9.6 \times 10^{-9} \text{ (ref. 14)}$$

When stoichiometrically equivalent oxidant and substrate are used,

$$[\text{total oxidant}] = [\text{total substrate}] = S$$

Assuming that the initial bromide concentration, due to hydrolysis of Br_2, is negligible, the bromide concentration at any time is expressed as

$$[Br^-] = 2(S_0 - S)$$

Thus eq. 11 yields eq. 12. where K_s and K_w are the dissociation constants of the substrate and

$$[12] \quad -\frac{dS}{dt} = \frac{S^2}{KK_h + 2[H^+](S_0 - S)[2(S_0 - S) + K]} \times \left\{k_{HOBr}KK_h + k_{Br_2}\frac{2K_sKK_w(S_0 - S)}{[H^+] + K_s}\right\}$$

water respectively. The integrated form of eq. 12 is not suitable for the separation of unknowns, but using the graphically determined value of $-dS/dt$ and assuming that the rate constants observed in the presence of Ag^+ are identical to k_{HOBr} at the given pH, one can determine k_{Br_2}. The value of k_{Br_2} was found to be acceptably constant for benzilic acid (see Tables 1 and 2). For the other substrates the approximation $k_{HOBr} \approx k_{Ag}$ is less valid because the oxidation of the carboxylate by HOBr is not negligible relative to Br_2 oxidation. However, since at high pH only the relative rates could be established,

TABLE 1. The kinetics of the oxidation of benzilic acid by bromine water in the presence of accumulating bromide.* A typical run

Time (s)	$k_{Br_2} \times 10^{-10}$
50	1.24
100	1.45
200	1.04
300	1.19
400	1.02
500	0.98
600	0.84
800	1.00
1000	1.05

*[Benzilic acid] = [oxidant] = 7.40 × 10^{-4} M; pH maintained by a pH-stat at 3.35; k_{Br_2} was calculated on the basis of eq. 12.

TABLE 2. Calculated rate constants for the oxidation of benzilic acid by bromine water in the presence of accumulating bromide*

pH	$k_{Br_2} \times 10^{-10}$
2.60	0.98±0.01
3.35	1.07±0.14
3.60	1.10±0.12
3.90	1.17±0.11

*[Benzilic acid] = [oxidant] = 7.40 × 10^{-4} M; pH maintained by a pH-stat; k_{Br_2} was calculated on the basis of eq. 12.

it is not possible to correct k_{Ag} numerically for contributions from carboxylate oxidation.

In summary, the principal oxidant in neutral or basic solution is molecular bromine and the substrate is the carboxylate anion of the α-hydroxy acid. In acid solution containing silver ion the oxidant is hypobromous acid and the substrate appears to be the neutral α-hydroxy acid.

This work was supported by the National Research Council of Canada. Valuable discussions with Professor R. P. Bell and with Dr. D. Dolman and the comments of Professor B. Perlmutter-Hayman are all gratefully acknowledged.

1. J. M. PINK and R. STEWART. This issue.
2. B. PERLMUTTER-HAYMAN and Y. WEISSMANN. J. Amer. Chem. Soc. **91**, 668 (1969); Y. KNOLLER and B. PERLMUTTER-HAYMAN. J. Amer. Chem. Soc. **77**, 3212 (1955).
3. I. R. L. BARKER. Chem. Ind. 1936 (1964).
4. R. H. HERBER. Inorganic isotopic syntheses. W. A. Benjamin, Inc., New York, N.Y., 1962. p. 45.
5. H. MEERWEIN. Ann. **396**, 261 (1913).
6. H. STAUNDINGER and S. BEREZA. Ann. **380**, 271 (1911).
7. A. ALBERT and E. P. SERJEANT. Ionization constants of acids and bases. Methuen, London, England, 1962.
8. L. J. EDWARDS. Trans. Faraday Soc. **46**, 725 (1950).
9. P. K. GLASOE and F. A. LONG. J. Phys. Chem. **64**, 188 (1960).
10. D. B. SCAIFE and H. J. V. TYRRELL. J. Chem. Soc. 386 (1958).
11. P. B. D. DE LA MARE, I. C. HILTON, and S. VARMA. J. Chem. Soc. 4044 (1960); S. J. BRANCH and B. JONES. J. Chem. Soc. 2317 (1954); see also E. BERLINER. J. Chem. Educ. **43**, 124 (1960).
12. R. JOSEPHSON, R. M. KEEFER, and L. J. ANDREWS. J. Amer. Chem. Soc. **83**, 3562 (1961).
13. A. LIFSHITZ and B. PERLMUTTER-HAYMAN. Bull. Res. Council of Israel, **8A**, 166 (1955).
14. J. M. PINK. Can. J. Chem. **48**, 1169 (1970).

Can. J. Chem. Downloaded from www.nrcresearchpress.com by 210.87.254.40 on 09/05/12
For personal use only.

Can. J. Chem. Downloaded from www.nrcresearchpress.com by 210.87.254.5 on 09/05/12
For personal use only.

Charge Localization in the Mass Spectra of Substituted Phenylbutyrophenones

D. A. LIGHTNER AND FRANK S. STEINBERG
Department of Chemistry,[1] *University of California, Los Angeles, California 90024*

Received August 18, 1970

A study of the McLafferty rearrangement of substituted phenylbutyrophenones relative to butyrophenones and 1-(4-butyrophenyl)-2-ethanes shows a peculiar non-linear relationship with the type of substituent and the distance of the substituent from the reaction site.

Canadian Journal of Chemistry, 49, 660 (1971)

Introduction

The role of electron-donating and -withdrawing substituents in localizing charge in unimolecular ion reactions observed in mass spectra has been investigated in substituted butyrophenones (1), valerophenones (2), nitro- and butyryldiphenyl ethers (3), and methyl butyrates (4). Among the conclusions reached for the McLafferty rearrangements of substituted butyrophenones are that the reaction is (*i*) enhanced by an increased positive charge at the reaction site (the ratio $[M\text{-}C_2H_4]/[M]$ is greater for an electron-withdrawing substituent than for an electron-donating substituent) (1*a*), and (*ii*) much slower when the substituent has been removed and "isolated" from the reaction site (1*b*, 2). The influence of a *remote but conjugated* substituent in the McLafferty rearrangement has been discussed only briefly in connection with the fragmentation of nitrodiphenylethers (3). In this note we discuss new information on remote substituent effects.

Experimental

All mass spectra were determined on an AEI MS-9 mass spectrometer at varied ionizing voltages using a 100 μA electron beam. The i.r. spectra were taken on a Perkin–Elmer Model 137 spectrophotometer and n.m.r. spectra were determined on a Varian Model A-60 instrument. All melting points (capillary) are uncorrected. Satisfactory micro analyses were performed on all compounds in this work.

In a typical experiment, the substituted (except amino and hydroxy) phenylbutyrophenones were obtained by acylation of the substituted biphenyl with butanoyl chloride and a molar excess of anhydrous aluminum chloride in gently refluxing carbon disulfide. The aminophenylbutyrophenones were prepared by stannous chloride reduction (5) of corresponding nitro compounds, and the hydroxy isomer via diazotization of the corresponding amino isomer. Most substituted butyrophenones may be obtained as indicated (6) or synthesized by modification (R. Nicoletti, this laboratory) of established procedures (7, 8).

Results and Discussion

In our work we have investigated the behavior of substituted phenylbutyrophenones (**1** and **2**) and have noted several new effects (see Table 1) which were not observed for the [M-28] fragmentation of substituted butyrophenones (**3**) (1*a*) or 1-(4-butyrophenyl)-2-phenylethanes (**4**) (1*b*). (*1*) Whereas electron-donating substituents have a very similar influence on the [M-28] rearrangement in **1**, **2**, and **3**, electron-withdrawing substituents do not, and (*2*) the influence of an electron-withdrawing substituent in enhancing the [M-28] fragmentation is an order of magnitude greater in **3** than in **1** and **2** but is smaller (by a factor of 2) in **1** ($Y = NO_2$) compared to **4** ($Y = NO_2$),[2] wherein the substituent is not only remote from but incapable of conjugation with the reaction site. The behavior mentioned under (2) may be contrasted with that of electron-donating substituents in **1**, **2**, and **3** in which the closeness of the [M-28] values suggests that fragmentation behavior here is relatively *insensitive* to the substituent's distance from the reaction center. Considering the very large difference shown by **1**, **2**, and **3** for electron-withdrawing groups, the behavior noted for

[1]Contribution no. 2566.

[2]At 75 eV, [M-28] in **4** ($Y = NO_2$) is 94 for M = 100%. See ref. 1*b*.

TABLE 1. Substituent effects* on the abundance of M-C_2H_4 ions from p-(Y-C_6H_4)-$C_6H_4COCH_2CH_2CH_3^{+\cdot}$

Y (M = 100.0)	[M-28], 20 eV† Phenylbutyrophenones	[M-28], 20 eV† Butyrophenones	Ionization potential of C_6H_5Y,‡ (eV)
H	20.0	27.2	9.24§
m-NH_2	8.0	5.5	7.70
p-NH_2	10.4	19.5	
p-OCH_3	12.8	27.6	8.22
p-OH	13.8	31.0	8.50
p-CH_3	18.5	25.6	8.82
p-Br	27.5	228	8.98
p-Cl	28.9	204	9.07
p-F	29.0	173	9.20
p-CN	44.2		9.71
p-NO_2	42.0	945	9.92
m-NO_2	50.0	733	

*The effect of these substituents on further fragmentations of the [M-28] ion is negligible.
†The values are essentially the same as those determined at 70 eV, and they closely parallel the percent ionization values.
‡See ref. 9.
§Value for biphenyl is 8.27 eV.

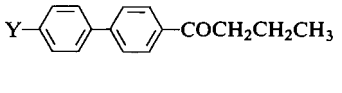

1

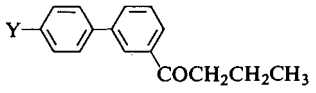

2

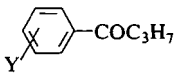

3

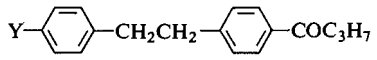

4

electron-donating groups is rather surprising. Also, judging from the usual behavior of an electron-donating substituent far removed from the reaction site, *e.g.*, **4** (Y = NH_2),[3] the [M-28] intensities of **1** and **2** are expected to be considerably smaller than those of **3**.

The peculiar non-linear effects in **1**, **2**, **3**, and **4** noted by varying distance from the reaction site and changing from electron-withdrawing to electron-donating substituents suggest that the qualitative arguments of charge localization (1–4) do not sufficiently explain certain types of fragmentation behavior. Conjugation of the substituent Y of **1** with the carbonyl group (presumed transfer site) by resonance appears to have no special influence on the [M-28] intensities which are very similar for the meta- and para-nitro or amino isomers.[4] Thus, canonical resonance structures such as **5** and **7** apparently contribute no more to the total picture than either **6** or **8**, although the rationalization (1) for the butyrophenone (**3**) behavior was interpreted using the concept of radical site *and* positive charge localization on the carbonyl oxygen.

Probably a more satisfying explanation of the data of Table 1 is lodged in the quasi-equilibrium treatment (4) and a knowledge of how given substituents perturb the energy profile for excited states leading to product. Even though a clear linear parallel is observed between the effect of a substituent on the [M-28] fragmentation of phenylbutyrophenones and the ionization poten-

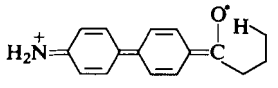

5

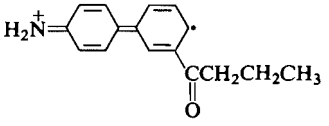

6

[3]At 75 eV, [M-28] in **4** (Y = NH_2) is < 1 for M = 100%. See ref. 1*b*.
[4]This behavior holds for the nitrobutyrophenones **3** (Y = NO_2) as well and suggests that biphenyl twisting is not responsible for the observed effects.

Can. J. Chem. Downloaded from www.nrcresearchpress.com by 210.87.254.5 on 09/05/12
For personal use only.

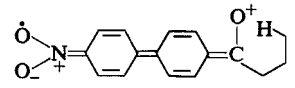

7

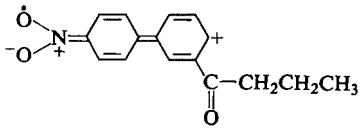

8

tial of the corresponding substituted benzene (9), no satisfactory explanation for the reported data is available.

Financial assistance from the Research Corporation is gratefully acknowledged. The AEI MS-9 mass spectrometer used in this work was purchased with funds made available by the National Science Foundation Grant GP3672. We thank Miss Elizabeth Irwin for assistance in obtaining the mass spectra.

1. (*a*) F. W. McLafferty and T. Wachs. J. Amer. Chem. Soc. **89**, 5043 (1967). (*b*) T. Wachs and F. W. McLafferty. J. Amer. Chem. Soc. **89**, 5044 (1967).
2. A. Mandelbaum and K. Biemann. J. Amer. Chem. Soc. **90**, 2975 (1968).
3. T. H. Kinstle and W. R. Oliver. J. Amer. Chem. Soc. **91**, 1864 (1969).
4. I. Howe and D. H. Williams. J. Amer. Chem. Soc. **90**, 5461 (1968).
5. L. C. King, M. McWhirter, and D. M. Barton. J. Amer. Chem. Soc. **67**, 2089 (1945).
6. J. K. S. Kan, R. N. McCormick, E. J. Braun, and J. N. Pitts, Jr. J. Amer. Chem. Soc. **87**, 4409 (1965).
7. H. Zimmer and J. P. Bercz. Ann. **686**, 107 (1965).
8. B. L. Zenitz and W. Hartung. J. Amer. Chem. Soc. **11**, 446 (1946).
9. R. W. Kiser. Introduction to mass spectrometry and its application. Prentice-Hall, Inc., Englewood Cliffs, N.J., 1965. Appendix IV.

Can. J. Chem. Downloaded from www.nrcresearchpress.com by 210.87.254.5 on 09/05/12
For personal use only.

X-Ray and Infrared Studies of Lead Apatites

Vijay Mohan Bhatnagar[1]

Chemistry Department, University of New Brunswick, Fredericton, New Brunswick

Received July 27, 1970

The cell constants and infrared spectra of lead apatites have been investigated. The lowering of the molecular symmetry T_d of the phosphate ion, and the nature and extent of changes in vibration frequencies of lead apatites with the ionic substitution of PO_4^{3-} by AsO_4^{3-} and VO_4^{3-} are discussed.

Canadian Journal of Chemistry, 49, 662 (1971)

We are investigating the infrared spectra of apatites in the light of detailed knowledge of atomic positions provided by X-ray studies. A previous study (1) was on the investigation of synthetic apatites and the present work is a report on the study of mineralogical apatites. The mineral specimens of this investigation were obtained from the United States National Museum. A description of them has been reported (2). The unit cell dimensions of these samples calculated from the X-ray powder diffraction patterns are given in Table 1. There seems to be no variation of X-ray data for phosphatian-mimetite of this work with the replacement of arsenic by phosphorus. In fact, the unit cell dimensions should have different values with the changing composition. Our observation is confirmed by the interesting work of Adler (3) who could not determine in his X-ray spectrogram the presence of phosphate in his phosphatian-mimetite sample.

Table 1. Unit cell dimensions of lead apatites

Apatite	*a*-Axis (Å)	*c*-Axis (Å)	*c*/*a*
$Pb_{10}(PO_4)_6Cl_2$	9.98	7.33	0.734
$Pb_{10}(AsO_4)_6Cl_2$	10.25	7.45	0.726
$Pb_{10}[(As,P)O_4]_6Cl_2$	10.25	7.45	0.726
$Pb_{10}(VO_4)_6Cl_2$	10.33	7.34	0.710

Although pyromorphite, mimetite, and vanadinite are isomorphous, their infrared spectra

[1]This work was carried out at Fisk University, Nashville, Tennessee, U.S.A., and Faculté des Sciences de Toulouse, Toulouse, France.

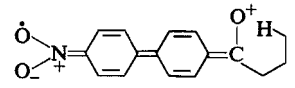

7

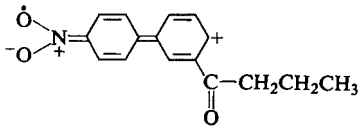

8

tial of the corresponding substituted benzene (9), no satisfactory explanation for the reported data is available.

Financial assistance from the Research Corporation is gratefully acknowledged. The AEI MS-9 mass spectrometer used in this work was purchased with funds made available by the National Science Foundation Grant GP3672. We thank Miss Elizabeth Irwin for assistance in obtaining the mass spectra.

1. (*a*) F. W. McLafferty and T. Wachs. J. Amer. Chem. Soc. **89**, 5043 (1967). (*b*) T. Wachs and F. W. McLafferty. J. Amer. Chem. Soc. **89**, 5044 (1967).
2. A. Mandelbaum and K. Biemann. J. Amer. Chem. Soc. **90**, 2975 (1968).
3. T. H. Kinstle and W. R. Oliver. J. Amer. Chem. Soc. **91**, 1864 (1969).
4. I. Howe and D. H. Williams. J. Amer. Chem. Soc. **90**, 5461 (1968).
5. L. C. King, M. McWhirter, and D. M. Barton. J. Amer. Chem. Soc. **67**, 2089 (1945).
6. J. K. S. Kan, R. N. McCormick, E. J. Braun, and J. N. Pitts, Jr. J. Amer. Chem. Soc. **87**, 4409 (1965).
7. H. Zimmer and J. P. Bercz. Ann. **686**, 107 (1965).
8. B. L. Zenitz and W. Hartung. J. Amer. Chem. Soc. **11**, 446 (1946).
9. R. W. Kiser. Introduction to mass spectrometry and its application. Prentice-Hall, Inc., Englewood Cliffs, N.J., 1965. Appendix IV.

Can. J. Chem. Downloaded from www.nrcresearchpress.com by 210.87.254.5 on 09/05/12
For personal use only.

X-Ray and Infrared Studies of Lead Apatites

Vijay Mohan Bhatnagar[1]

Chemistry Department, University of New Brunswick, Fredericton, New Brunswick

Received July 27, 1970

The cell constants and infrared spectra of lead apatites have been investigated. The lowering of the molecular symmetry T_d of the phosphate ion, and the nature and extent of changes in vibration frequencies of lead apatites with the ionic substitution of PO_4^{3-} by AsO_4^{3-} and VO_4^{3-} are discussed.

Canadian Journal of Chemistry, 49, 662 (1971)

We are investigating the infrared spectra of apatites in the light of detailed knowledge of atomic positions provided by X-ray studies. A previous study (1) was on the investigation of synthetic apatites and the present work is a report on the study of mineralogical apatites. The mineral specimens of this investigation were obtained from the United States National Museum. A description of them has been reported (2). The unit cell dimensions of these samples calculated from the X-ray powder diffraction patterns are given in Table 1. There seems to be no variation of X-ray data for phosphatian-mimetite of this work with the replacement of arsenic by phosphorus. In fact, the unit cell dimensions should have different values with the changing composition. Our observation is confirmed by the interesting work of Adler (3) who could not determine in his X-ray spectrogram the presence of phosphate in his phosphatian-mimetite sample.

Table 1. Unit cell dimensions of lead apatites

Apatite	*a*-Axis (Å)	*c*-Axis (Å)	*c*/*a*
$Pb_{10}(PO_4)_6Cl_2$	9.98	7.33	0.734
$Pb_{10}(AsO_4)_6Cl_2$	10.25	7.45	0.726
$Pb_{10}[(As,P)O_4]_6Cl_2$	10.25	7.45	0.726
$Pb_{10}(VO_4)_6Cl_2$	10.33	7.34	0.710

Although pyromorphite, mimetite, and vanadinite are isomorphous, their infrared spectra

[1]This work was carried out at Fisk University, Nashville, Tennessee, U.S.A., and Faculté des Sciences de Toulouse, Toulouse, France.

show certain basic differences. The free phosphate ion, PO_4^{3-}, belongs to the point group T_d. The normal modes of the tetrahedral phosphate ion are (4): ν_1, symmetric P—O stretching; ν_2, OPO bending; ν_3, P—O stretching, and ν_4, OPO bending. The observed frequencies are: ν_1, 980; ν_2, 363; ν_3, 1082; and ν_4, 515. In the undistorted state, only the absorptions corresponding to ν_3 and ν_4 vibrations are observed. The two remaining fundamentals ν_1 and ν_2 become infrared active when the configuration of the PO_4^{3-} ion is reduced to some lower symmetry. The degenerate modes are split by distortion of the phosphate groups through lack of symmetry in the lattice sites. The frequencies thus vary somewhat for different crystal structures.

The frequencies observed for PO_4^{3-}, AsO_4^{3-}, and VO_4^{3-} ions in pyromorphite, $Pb_{10}(PO_4)_6Cl_2$; phosphatian-mimetite, $Pb_{10}[(As,P)O_4]_6Cl_2$; and vanadinite, $Pb_{10}(VO_4)_6Cl_2$ in our present work are shown in Table 2.

The absorption frequencies of PO_4^{3-} in phosphatian-mimetite are given in Table 3. They are compared with those reported by Adler (5) in his phosphatian-mimetite specimens from Zacatecas, Mexico and Cumberland, England. Our data agree very well with the experimental results of Adler (5). As the number of allowable bands for each fundamental mode depends on the symmetry of the individual ion, a slight variation in frequencies is observed in pyromorphites. The symmetry of the three ions in lead apatites is expected to be C_s (2, 3, 5, 6). If this is the case, it appears that not all of the modes are being resolved completely. It is also possible that there is coincidence of ν_1 and ν_3 in some of these apatites. It is difficult to resolve

TABLE 2. Absorption frequencies of PO_4^{3-}, AsO_4^{3-}, and VO_4^{3-}

Ion	ν_1	ν_2	ν_3	ν_4
PO_4^{3-}	925	—	968, 1028	542, 572
AsO_4^{3-}	—	—	785, 805, 816	385, 415
VO_4^{3-}	—	—	740, 805	322, 380, 419

TABLE 3. Absorption frequencies of PO_4^{3-} in phosphatian-mimetite

Reference	ν_1	ν_2	ν_3	ν_4
This work	920	325	955, 985, 1000	538, 550, 565
Adler (5)	917	—	951, 982, 1000	537, 548, 564

TABLE 4. The number of infrared active vibrations for molecular point groups C_s and C_{3v}

Point group	ν_1	ν_2	ν_3	ν_4
C_s	1	2	3	3
C_{3v}	1	1	2	2

ν_1 for mimetite and vanadinite, although the vibration is allowed by structural considerations. According to Siebert (7), the Raman lines for ν_1 and ν_3 in AsO_4^{3-} show coincidence at 813 cm^{-1}; this may account for absence of ν_1 in the infrared spectrum of mimetite.

Considering the site group data for apatite (the P atom is on a C_s site) and the bond length data for the phosphate group in apatite by Posner *et al.* (8), C_s molecular symmetry appears reasonable for all apatites. However, the infrared data for pyromorphite conform to the vibrational requirements of C_{3v} symmetry for the PO_4^{3-} ion. The number of infrared active vibrations for molecular point groups C_s and C_{3v} are (3) given in Table 4.

Thus the one band of ν_3 and one band of ν_4 in the pyromorphite spectrum are not resolved. However, ν_3 and ν_4 of phosphate ion in phosphatian-mimetite show resolution of three ν_3 and ν_4 bands at 955, 985, and 1000 cm^{-1}, and at 538, 550, and 565 cm^{-1}, respectively. This supports the position that the PO_4^{3-} group in phosphatian-mimetite, which is isostructural with the apatite, has C_s symmetry rather than C_{3v} symmetry. It is still impossible, however, to identify the third bands in ν_3 and ν_4 for PO_4^{3-} in pyromorphite.

The apatite work was supported by research grants DE-02105 from the U.S. Department of Health, Education, and Welfare and Office National de l'Azote, France.

1. V. M. BHATNAGAR. Arch. Oral. Biol. **15**, 469 (1970).
2. V. M. BHATNAGAR. Bull. Soc. Fr. Miner. Crist. **91**, 479 (1968).
3. H. H. ADLER. Amer. Miner. **49**, 1002 (1964).
4. G. HERZBERG. Infrared and Raman Spectra of Polyatomic Molecules. D. Van Nostrand Co., New York. 1958.
5. H. H. ADLER. Amer. Miner. **53**, 1740 (1968).
6 V M. BHATNAGAR. Zeit. Anorg. Allgem. Chem. **367**, 289 (1969).
7. H. SIEBERT. Zeit. Anorg. Allgem. Chem. **275**, 225 (1954).
8. A. S. POSNER, A. PERLOFF, and A. F. DIORIO. Acta Cryst. **11**, 308 (1958).

Can. J. Chem. Downloaded from www.nrcresearchpress.com by 210.87.254.5 on 09/05/12
For personal use only.

A Facile Formation of Dibenzo[*a*,*d*]cycloheptenylium Ion by Decarbonylation. Color Reactions of the Cyheptamide Metabolites

K. SESTANJ

Department of Biochemistry, Ayerst Research Laboratories, Montreal, Quebec

Received August 17, 1970

Treatment with concentrated sulfuric acid of different 10-hydroxylated metabolites of the anticonvulsant cyheptamide results in intensely colored products. These have been identified as dibenzo-[*a*,*d*]cycloheptenylium ions.

Canadian Journal of Chemistry, 49, 664 (1971)

Can. J. Chem. Downloaded from www.nrcresearchpress.com by 210.87.254.6 on 09/05/12
For personal use only.

Studies (1) of the metabolic fate of the anticonvulsant cyheptamide (AY-8682) (**1**) have indicated that in laboratory animals and man the compound is mainly hydroxylated, preferably on the benzylic carbon, C-10. Of particular interest is the property of 10-hydroxylated metabolites of cyheptamide upon acid hydrolysis to undergo deamination followed by transannular lactone formation, to yield **2** (1). The fact that several of the compounds produced, *e.g.* **2**, **3**, **4**, on treatment with concentrated or 30 *N* H_2SO_4 give intense color reactions was used as the basis for a procedure for the quantitative determination of 10-hydroxylated metabolites of cyheptamide (2). The purpose of the present communication is to describe the chemical nature of this reaction, the products of which have been identified as tropylium ions.

Tropylium ions are remarkably stable organic cations. They are energetically favored even in the case of a two-fold fusion with benzene rings, **6**, where the coplanarity and electronic delocalization tend to be largely distorted (3–5). It has been known that 5*H*-dibenzo[*a*,*d*]cyclohepten-5-ol (**5**) gives an intense orange–red coloration in concentrated sulfuric acid, due to the formation of dibenzo[*a*,*d*]cycloheptenylium ion (**6**) (3). We have found that solutions of the lactone **2** and the acid **3** in concentrated sulfuric acid are spectroscopically undistinguishable from an equimolar solution of the alcohol **5** in sulfuric acid. On dilution with water an identical mixture of the alcohol **5** and the ether **7** is obtained from each of the three solutions.

The formation of dibenzo[*a*,*d*]cycloheptenylium ion **6** from **2** and **3** is initiated by dehydration followed by decarbonylation; the stability of the ion **6** which acts as driving force could also account for the cleanness of the reaction. Another example of tropylium ion formation by decarbonylation is the conversion of cyclohepta-2,4,6-triene carbonylchloride with silver perchlorate reported by Dewar and Ganellin (6). Pertinent examples of carbonium ion formation by decarbonylation are tritylium ion generation from triphenylacetic acid (7) and of cyclopropenium ion from cyclopropene carboxylic acid (8).

The 5-hydroxy lactone **4** in concentrated or 30 *N* sulfuric acid solution produces a deeper red color than compounds **2**, **3**, and **5**. The tropylium ion **8** is formed by opening of the transannular lactone bridge and loss of the benzylic hydroxyl by protonation. This reaction is analogous to the formation of the ion **6** from alcohol **5**. Conjugation of the carboxylic group and the tropylium ion causes a shift to longer wavelengths. The 5-hydroxy acid **9** (9) has been isolated on dilution with water and was characterized by i.r., u.v., and n.m.r. spectra as well as by lead tetraacetate oxidation to the dibenzotropone **10**.

Experimental

The u.v. and visible spectra were recorded on a Unicam SP-800 UV Spectrophotometer, i.r. spectra on a Perkin–Elmer 225, and n.m.r. spectra on a Varian A-60A instrument with tetramethylsilane as internal standard. Melting points were not corrected.

Reaction of Compounds 2, 3, and 5 with Concentrated Sulfuric Acid

The compounds **2** (11), **3** (10), and **5** (5–10 mg each) were dissolved in 10 ml of concentrated H_2SO_4 and heated for 2–3 min in a boiling water bath. After cooling to room temperature, the absorption spectra were measured. Identical absorption maxima and molecular extinction coefficients were obtained with all of the three compounds: λ_{max} (ε) 528 (2860); 500 (3170); 392 (7720); 376 (9035); 305 mμ, (115 840).

Reaction of the 5-Hydroxylactone 4 with Concentrated Sulfuric Acid

A solution of the lactone (11) in concentrated or

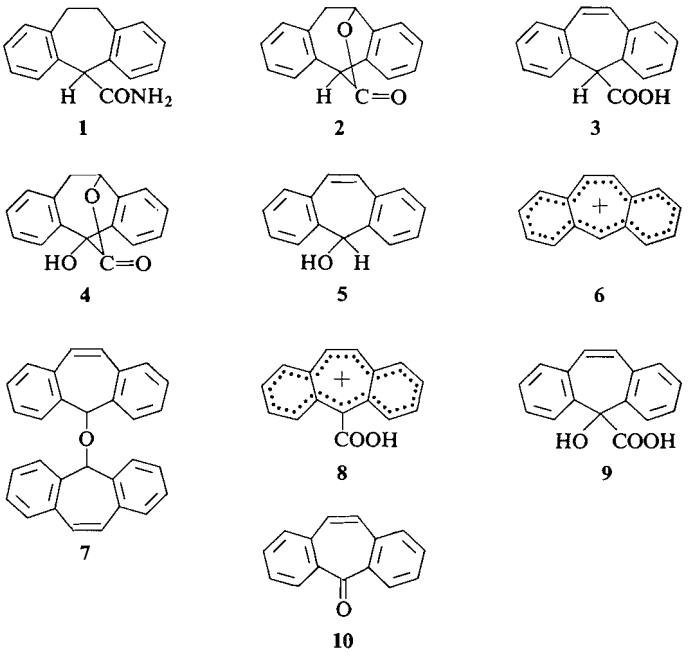

30 *N* H_2SO_4 had the following absorption maxima: λ_{max} (ε) 564 (2700); 528 (3010); 412 (7790); 392 (7060); 314 (103 820); 270 (8720); 242 mμ (15 780).

Formation of 5-Hydroxy Acid ***9*** *from 5-Hydroxylactone* ***4***

The 5-hydroxylactone **4** (233 mg, 0.025 mmol) was dissolved in 23 ml of 30 *N* H_2SO_4, the red solution stirred for 15 min at 50° and poured on ice; the mixture was extracted with ether, the extract dried over magnesium sulfate, and evaporated under reduced pressure. The residue crystallized from ether and carbon tetrachloride to give 138 mg (60%) of **9**, m.p. 166–168°. Purity was verified by t.l.c. in ethyl acetate/benzene (1:4) and spraying with concentrated H_2SO_4. The u.v. spectrum: λ_{max} (ε) 283 mμ (11 170); i.r. spectrum (Nujol): ν_{OH} 3550, ν_{COOH} 3000 (broad); $\nu_{C=O}$ 1730 and 1750 cm^{-1} (split); n.m.r. spectrum: multiplet between δ 8.0 and 7.0.

Anal. Calcd. for $C_{16}H_{12}O_3$: C, 76.18; H, 4.80. Found: C, 76.42; H, 4.99.

*Formation of Dibenzo[a,d]cyclohepten-5-one (****10****) from 5-Hydroxy Acid* ***9***

To 25.2 mg of the acid **9** (0.1 mmol) dissolved in 5 ml of benzene a solution of 56 mg of lead tetraacetate in 1 ml of benzene and one drop of acetic acid was added and stirred for 15 min at room temperature. Ten milliliters of hexane were added, the mixture filtered, and the filtrate washed repeatedly with an aqueous solution of $NaHCO_3$ and water, dried over magnesium sulfate, and evaporated under reduced pressure. The residue crystallized from hexane to give 14.8 mg of a product shown to be identical with an authentic sample of dibenzotropone **10** (commercial product, Aldrich Chem. Co.).

The author acknowledges with gratitude the skillful assistance of Mrs. Diane Watts, B.Sc. and wishes to thank Dr. D. Dvornik for his interest in this work, and Drs. M. A. Davis and T. A. Dobson for the authentic samples of the compounds used in the study.

1. M. Kraml, K. Sestanj, and D. Dvornik. Biochem. Pharmac. In press.
2. M. Kraml, D. Dvornik, and L. Cosyns. To be published.
3. G. Berti. J. Org. Chem. **22**, 230 (1957); Gazz. Chim. Ital. **87**, 293 (1957).
4. G. Naville, H. Strauss, and E. Heilbronner. Helv. Chim. Acta, **43**, 1221 (1960).
5. J. Michl and R. Zahradnik. Coll. Czech. Chem. Commun. **31**, 2311 (1966).
6. M. J. S. Dewar and C. R. Ganellin. J. Chem. Soc. 2438 (1959).
7. A. Bistrzycki and E. Reintke. Ber. **38**, 839 (1905).
8. D. G. Farnum, G. Mehta, and R. G. Silberman. J. Amer. Chem. Soc. **89**, 5048 (1967).
9. Neth. Appl. 6 513 732; C.A. **65**, 15352d (1966).
10. M. A. Davis, S. O. Winthrop, R. A. Thomas, F. Herr, M. P. Charest, and R. Gaudry. J. Med. Chem. **7**, 88 (1964).
11. T. A. Dobson, M. A. Davis, A. M. Hartung, and J. M. Manson. Can. J. Chem. **46**, 2843 (1968).

Can. J. Chem. Downloaded from www.nrcresearchpress.com by 210.87.254.6 on 09/05/12
For personal use only.

The Effects of Substituents on the Abstraction of Halogens by Fluoroalkyl Radicals

LEONARD O. MOORE

Research and Development Department, Chemicals and Plastics, Union Carbide Corporation, South Charleston, West Virginia 25303

Received September 1, 1970

The relative reactivities of halogens to abstraction by fluoroalkyl radicals at 125° have been found to be 58.0 for $-CF_2-I$, 4.9 for $-CF_2-Br$, 1.8 for $-CCl_2-Cl$, and 1.0 for $-CClF-Cl$. The nature of halogens on adjacent carbons does not appear to affect the reactivity significantly.

Canadian Journal of Chemistry, 49, 666 (1971)

Can. J. Chem. Downloaded from www.nrcresearchpress.com by 210.87.254.6 on 09/05/12
For personal use only.

The recent report by Tarrant and Tandon (1) on the reactions of chlorofluoroalkanes with unsaturated hydrocarbons prompts publication of some similar results involving tetrafluoroethylene. It was known that the abstraction of chlorine from compounds such as trichlorofluoromethane was difficult since the reaction of this compound with ethylene gave only very high molecular weight telomers (2). Tarrant and Tandon (1) have also noted that their attempts to utilize trichlorofluoromethane in radical addition reactions to olefins were unsuccessful.

There are, however, other reports in the patent literature of chain transfer using chlorofluoroalkanes to give telomeric products; for example, 1,1,1-trichloro-2,3,3,3-tetrafluoropropane with tetrafluoroethylene (3) and chlorotrifluoromethane (4), 1,1,2-trichloro-1,2,2-trifluoroethane (5, 6), and 1,2-dichloro-1,2,3,3,4,4-hexafluorocyclobutane (6) with chlorotrifluoroethylene. It was felt that telomer reactions could be used to obtain information on reactivity of halogen[1] in molecules variously substituted with chlorine and fluorine, which would shed additional light on the relative importance of resonance and polar effects in radical abstraction reactions.

Reactivities of several halofluoroalkanes were determined by treating them with tetrafluoroethylene catalyzed by benzoyl peroxide. The values for the reactivities were based on chain transfer constants, calculated using the method of Walling (7) based on the average chain length of the telomers. These values were then divided by the number of equivalent atoms to arrive at a relative reactivity for the individual atoms. The concentration of tetrafluoroethylene was estimated by calculating the amount in the vapor state ($P_{total} = P_{telogen} + P_{C_2F_4}$ and $PV = nRT$) and subtracting this from the total charged for an initial concentration and from the amount unreacted for a final concentration. The average concentration was used in calculating the chain transfer constant. It is assumed that the chain transfer constants are nearly independent of chain length, primarily since the radicals formed initially as well as the growing chain radicals are perhalogenated and the variation of chain transfer constant with chain length due to differing inductive effect noted by Lewis and Mayo (8) would not be expected. The results are presented in Table 1.

The possibility that the phenyl radicals from the benzoyl peroxide added to tetrafluoroethylene to initiate telomerization was considered, but analysis indicated little incorporation of phenyl groups into the telomeric product.

The ease of abstraction of the different halogens is in the same sequence as previous results (9) I > Br > Cl, but relative values can now be given, $-CF_2-I$, 58; $-CF_2-Br$, 4.9; $-CCl_2-Cl$, 1.8; and $-CClF-Cl$, 1.0.

The results reported here further allow the effects of substituted chlorine and fluorine to be evaluated. Chlorine is abstracted by fluoroalkyl radicals from a trichloromethyl group approximately twice as readily as from a dichlorofluoromethyl group. However, there is no difference in the reactivity of chlorine to radical abstraction with varying ratios of chlorine to fluorine on adjacent carbons.

In perhalocarbons, the influences of adjacent halogens on reactions are based mainly on two effects, the inductive effect and resonance interactions. Substituents on the same carbon as an atom being abstracted will exhibit both effects. The present study indicates that the transition state during the reaction, the radical being formed, or both, are stabilized more by chlorine

[1]Since this discussion considers the reactions of chlorine, bromine, and iodine in fluorine-containing compounds, the term *halogen* as used here excludes fluorine.

TABLE 1. Telomerization of chlorofluoroalkanes with tetrafluoroethylene (1 h at 125°)

Run No.	Telogen		Pressure (p.s.i.g.)	C_2F_4 recovered (g)	Telomer		Chain transfer constant	Constant per reactive atom
	Structure	Moles			(g)	$\bar{n}$		
1	CF_3CF_2I	0.325	275	5	17	5.72	0.213	0.213
2	$CBrF_2CBrF_2$	0.308	225	9	14	15.71	0.036	0.018
3	CCl_2FCCl_3	0.363	225	15	3	11.22	0.021	0.007
4	$CClF_2CCl_3$	0.392	205	12	9	20.90	0.018	0.006
5	CF_3CCl_3	0.427	250	17	6	19.52	0.020	0.007
6	CCl_2FCCl_2F	0.392	275	14	7	30.77	0.015	0.004
7	$CClF_2CCl_2F$	0.427	185	17	5	57.63	0.008	0.004
8	$CCl_2FCF_2CCl_2F$	0.315	225	9	8	23.39	0.013	0.003

on the same carbon atom than by fluorine (10) as seen by comparing experiments 3–5 with experiments 6–8. This result agrees with the apparent greater stability of the $—CCl_2\cdot$ radical over the $—CF_2\cdot$ radical in olefin cyclodimerization reactions (11) and the differences of bond energies in CCl_3—Cl, 68 kcal/mol, and CF_3—Cl, 83 kcal/mol (12).

Variation of the amount of chlorine relative to fluorine on an adjacent carbon will change only the inductive effect. The unchanged reactivity in experiments 3–5 and experiments 6–8 indicate that in perchlorofluorocarbons the differences of the inductive effects of chlorine and fluorine do *not* affect the ease of chlorine abstraction.

It is well to keep in mind that these values are applicable only to the present system. Other results might be observed if the attacking radicals were alkyl or aryl radicals, or if the molecule attacked were not a perhalofluorocarbon. For example, chlorine and fluorine influence the reactivity of hydrogen to abstraction by chlorine atoms in an entirely different way (13).

Experimental Section

Materials

The tetrafluoroethylene used for these reactions was purchased from Peninsular ChemResearch, Gainsville, Florida. It was found to be 99.9% pure with 1% *alpha*-pinene added as an inhibitor. The vaporization of tetrafluoroethylene from the cylinder effectively separated it from the inhibitor so no further purification was used. The saturated halofluorocarbons used were commercial grades which were carefully redistilled or were samples prepared in the laboratory. All were over 99.9% pure by gas chromatography.

General Procedure

To a 300 cc Parr Magnedash autoclave made of 316 stainless steel was charged 80 g of halofluoalkane and 1.6 g of benzoyl peroxide. The autoclave was cooled to −70° in a Dry Ice – acetone bath, evacuated, and 20 g (0.20 mol) of tetrafluoroethylene was added. The autoclave was heated to 125° and stirred at 300 oscillations per min for 1 h. Unreacted tetrafluoroethylene was bled from the reactor and the mixture of halofluorocarbon and telomer was poured out. The telomer was isolated as a residue from distillation of the halofluorocarbon. Analyses for chlorine, fluorine, and carbon were used to determine the molecular weight or chain length, $\bar{n}$, of the telomer and indicate whether there was incorporation of phenyl groups in the telomer. Table 1 shows the results obtained for the experiments.

1. P. TARRANT and J. P. TANDON. J. Org. Chem. **34**, 864 (1969).
2. W. E. HANFORD and R. M. JOYCE (to E. I. du Pont de Nemours and Co.). U.S. Patent 2,440,800, May 4, 1948.
3. W. E. HANFORD and R. M. JOYCE (to E. I. du Pont de Nemours and Co.). U.S. Patent 2,562,547, July 31, 1951.
4. R. L. EHRENFELD. U.S. Patent 2,788,275, April 9, 1957.
5. W. T. MILLER. U.S. Patent 2,700,661, January 25, 1955.
6. W. T. MILLER, JR., A. L. DITTMAN, R. L. EHRENFELD, and M. PROBER. Ind. Eng. Chem. **39**, 333 (1947).
7. C. WALLING. Free Radicals in Solution. John Wiley and Sons, Inc., New York, N.Y. 1957. pp. 150–153.
8. F. M. LEWIS and F. R. MAYO. J. Amer. Chem. Soc. **76**, 457 (1954).
9. R. N. HASZELDINE. J. Chem. Soc. 4291 (1955).
10. See also G. W. WHELAND. Resonance in Organic Chemistry. John Wiley and Sons, Inc., New York. N.Y. 1955. pp. 444–5.
11. P. D. BARTLETT, L. K. MONTGOMERY, and B. SEIDEL. J. Amer. Chem. Soc. **86**, 616 (1964).
12. J. B. FARMER, I. H. S. HENDERSON, F. P. LOSSING, and D. G. H. MARSDEN. J. Chem. Phys. **24**, 348 (1956).
13. J. M. TEDDER. Quart. Rev. London, **14**, 336 (1960).

Can. J. Chem. Downloaded from www.nrcresearchpress.com by 210.87.254.6 on 09/05/12
For personal use only.

Synthesis of 1-Substituted Derivatives of Anhydro(3-chloroacetyl-2-hydroxyimidazo[1,2-*a*]pyridinium Hydroxide)

WAYNE K. ANDERSON[1] AND ALAN E. FRIEDMAN

Department of Medicinal Chemistry, School of Pharmacy, State University of New York at Buffalo, Buffalo, New York 14214

Received September 14, 1970

The reaction of chloroacetic anhydride and chloroacetic acid with *N*-substituted 2-aminopyridine derivatives **3** produced 1-substituted derivatives of anhydro(3-chloroacetyl-2-hydroxyimidazo[1,2-*a*]-pyridinium hydroxide) (**4**). The isomeric anhydro(1-benzyl-2-chloroacetyl-3-hydroxyimidazo[1,2-*a*]-pyridinium hydroxide) (**10***a*) was prepared by a reported procedure and the spectral data of the two isomeric series of compounds were compared. The significant differences in the n.m.r. spectra of the two series were attributable to the deshielding influence of the exocyclic acyl moiety.

Canadian Journal of Chemistry, 49, 668 (1971)

Can. J. Chem. Downloaded from www.nrcresearchpress.com by 210.87.254.5 on 09/05/12
For personal use only.

During an investigation of the reaction of 1-azaphenothiazine with chloroacetic anhydride and chloroacetic acid it was found that acylation of the secondary amine did not proceed as expected. 10-Chloroacetyl-1-azaphenothiazine was not obtained and the mesoionic compounds, **1** and **2**, have been proposed as possible structures for the compound produced from this reaction.[2]

The present investigation was undertaken as a model study to explore further the utility of this reaction in the synthesis of ring-fused mesoionic systems and to examine the structure of the compounds prepared.

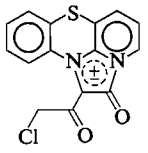

1

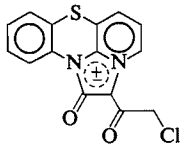

2

Reaction of chloroacetic anhydride (100 mmol) and chloroacetic acid (100 mmol) with 2-benzylaminopyridine (**3***a*; 50 mmol) for 1 h in refluxing dioxane gave anhydro(1-benzyl-3-chloroacetyl-2-hydroxyimidazo[1,2-*a*]pyridinium hydroxide) (1)[3] (**4***a*) in good yield. Similarly, reaction of **3***b*, *c*, *d*, and *e* with chloroacetic anhydride and chloroacetic acid yielded mesoionic compounds **4***b*, *c*, *d*, and *e* respectively. Melting points and microanalytical data for the compounds prepared are given in Table 1.

Scheme 1 outlines a possible mechanism for the formation of **4**. The first step involves chloroacetylation of **3** to give **5**. Acylation of the exocyclic nitrogen, in preference to the nuclear nitrogen, appears most probable based on the report by Jones and Katritzky (2*a*) that acylation of 2-amino- and 2-(methylamino)pyridine (with acetic anhydride–acetic acid) occurred exclusively on the exocyclic nitrogen.[4]

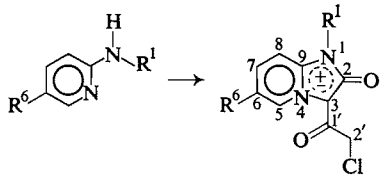

3 4

a $R^1 = -CH_2C_6H_5$; $R^6 = H$
b $R^1 = -C_6H_5$; $R^6 = H$
c $R^1 = -SO_2C_6H_5$; $R^6 = H$
d $R^1 = -CH_3$; $R^6 = H$
e $R^1 = -CH_3$; $R^6 = NO_2$

The situation for 2-benzenesulfonamidopyridine is less clear. It is known that 2-methanesulfonamido- and 2-benzenesulfonamido-pyridine exist in a tautomeric equilibria in which the imino forms predominate (2*b*). Thus acylation of **3***c* could have presumably occurred at the nuclear nitrogen, in which case compound **10***c* ($R^1 = SO_2C_6H_5$; R = Cl) would have been produced. The low field position of the C-5 proton in the n.m.r. spectra (see Table 2) is consistent with structure 4*c* and it was concluded that acylation

[1]To whom all inquiries should be addressed.
[2]J. W. Steele *et al.* (8).
[3]Katritzky's nomenclature has been adopted in this paper.
[4]Several attempts were made to isolate the intermediate chloroacetate **5**. In each instance only cyclized, acylated mesoionic compounds **4** were isolated. Moreover, no intermediate was formed in sufficient concentration to be detected by t.l.c.

TABLE 1. Melting points and microanalytical data for 1-substituted derivatives of 3-chloroacetyl-2-hydroxy- and 2-chloroacetyl-2-hydroxyimidazo[1,2-*a*]pyridinium hydroxide

Compound*	Melting point (°C)†	Calculated (%)				Found (%)‡			
		C	H	Cl	N	C	H	Cl	N
4*a*	154–155‖	63.88	4.36	11.81	9.32	64.01	4.39	11.78	9.49
4*b*	194–195¶	62.81	3.87	12.39	9.77	63.22	3.65	12.50	9.72
4*c*§	214–215‖	51.35	3.16	10.13	7.99	51.56	3.12	10.35	7.95
4*d*	233.5–234**	53.44	4.04	15.81	12.47	53.61	4.14	15.90	12.40
4*e*	232–233††	44.53	2.99	13.18	15.58	44.53	3.03	13.21	15.54
10*a*	154–154.5‡‡	63.88	4.36	11.81	9.32	63.85	4.35	11.60	9.16

*Yields of pure products ranged from 10 to 60%; no attempts were made to optimize the yields.
†Melting points were determined in a capillary on a Melt Temp apparatus and are uncorrected.
‡Microanalyses were performed by Galbraith Laboratories.
§Anal. Calcd. for S: 9.12. Found: 9.29.
‖Recrystallized from $CHCl_3$–benzene–hexane.
¶Recrystallized from $CHCl_3$–benzene.
**Recrystallized from acetone–ethanol.
††Recrystallized from CH_2Cl_2–hexane.
‡‡Recrystallized from benzene–hexane; mixture m.p. with **4***a* showed significant depression.

of the exocyclic nitrogen was preferred in this reaction.

Intramolecular cyclization (3) of **5** with concomitant proton abstraction from **6** would afford the mesoionic intermediate **7**. Acylation (*4a–j*) of **7** with subsequent proton abstraction would give **4**.

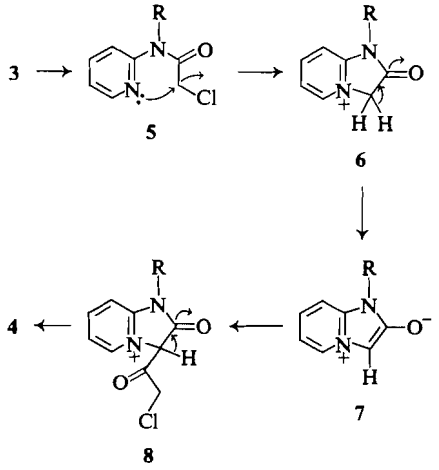

SCHEME 1

An alternative explanation for the formation of **4** involving initial nucleophilic attack by the nuclear atom to form an imino intermediate **9**, was considered unlikely since chloroacetonitrile, chloroacetic acid, and α-bromopropionic acid failed to react with **3***a* in refluxing dioxane.

If the initial acylation of **3** occurred at the nuclear nitrogen, rather than the exocyclic nitrogen, the resultant product would be **10**. Although

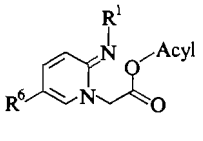

9

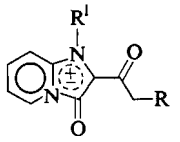

10

this seemed unlikely, the isomeric compound, **10***a*, was synthesized by an unambiguous route in order to effect a spectral comparison with **4***a*. Benzylation of *N*-2-pyridylaminoacetonitrile (prepared by treatment of 2-aminopyridine with formalin, sodium bisulfite, and sodium cyanide) followed by acid hydrolysis of the nitrile afforded *N*-benzyl-*N*-2-pyridylglycine, which was isolated as the sodium salt (*4i*, 5). Cyclization of sodium *N*-benzyl-*N*-2-pyridylglycine with chloroacetic anhydride and chloroacetic acid in refluxing dioxane gave anhydro(1-benzyl-2-chloroacetyl-3-hydroxyimidazo[1,2-*a*]pyridinium hydroxide (**10***a*: R^1 = —CH_2Ph; R = Cl). Cyclization with acetic anhydride afforded the known **10***b* (R^1 = —CH_2Ph; R = H) (*4i*).

The most significant differences between the n.m.r. spectra of the two isomeric series of compounds were the chemical shifts for the C-5 protons and the benzylic methylene protons of R^1 (see Table 2). The exocyclic acyl moiety strongly deshielded the C-5 aromatic proton in **4***a–e* while in the isomeric series (**10***a* and *b*) the benzylic methylene protons were shifted downfield by *ca.* τ 0.8.[5]

[5]*Cf.* the benzylic methylene protons of *N*-benzyl-2-aminopyridine acetamide which appeared as a 2-proton singlet at τ 4.87.

Can. J. Chem. Downloaded from www.nrcresearchpress.com by 210.87.254.5 on 09/05/12
For personal use only.

Can. J. Chem. Downloaded from www.nrcresearchpress.com by 210.87.254.5 on 09/05/12
For personal use only.

TABLE 2. Spectral data for 1-substituted derivatives of 3-chloroacetyl-2-hydroxy- and 2-acyl-3-hydroxyimidazo[1,2-*a*]pyridinium hydroxide

Compound	Infrared (KBr) μ*	λ_{max} (MeOH) nm (log ε)†	60 MHz n.m.r. data (τ, $CDCl_3$–TMS)‡			
			C-5	C-2′	R^1§	C-6, -7, -8, and aromatic protons of R^1
4*a*	5.95; 6.20	230 (4.225), 264 (4.363), 316 sh (4.003), and 344 (4.147).	−0.07 d	5.07	4.77 (2H)	2.62 m (8H)
4*b*	5.95; 6.12	232 (4.267), 265 (4.371), 320 sh (3.989), and 344 (4.129).	−0.12 d	5.12	—	2.42 s (7H) 2.75 m (1H)
4*c*‖	5.84; 6.20	220 (4.245), 257 (4.421), and 340 (4.168).	−0.05 d	5.33	—	1.80 d (3H) 2.25 m (5H)
4*d*	5.98; 6.31	230 (4.208), 264 (4.335), 318 sh (4.143), and 343 (4.193).	−0.13	5.13	6.45 (3H)	2.48 m (1H) 2.80 m (2H)
4*e*‖	5.91; 6.22	259 (4.382) and 300 (4.258)	−0.73 d (2.5)	5.18	6.45 (3H)	1.32 q (1H: 9.5; 2.5) 2.10 d (1H: 9.5)
10*a*	5.94; 6.22	261 (4.017) and 400 (4.041)	1.53 d	5.07	4.07 (2H)	2.68 s (8H)
10*b*¶	5.97; 6.27	262 (4.170)	1.53 d	7.31	4.06 (2H)	2.72 s (8H)

*The i.r. spectra were obtained on a Perkin–Elmer model 237 spectrophotometer.
†The u.v. data were obtained on a Beckman DB-G spectrophotometer.
‡The n.m.r. spectra were obtained on a Varian A60 spectrometer; coupling constants, in Hz, are given in parentheses.
§Excluding aromatic protons of R^1.
‖The n.m.r. solvent was d^6-DMSO–TMS.
¶The u.v. solvent was 95% ethanol.

The first reported example of this mesoionic 4-oxoimidazole system was the dye "Besthorn's red" (6). The only other fused ring system of this type has been prepared by Ohta and Sato (7). The monocyclic mesoionic ring system has been synthesized by Lawson and Mills (4*i*) and more recently by Roche and Stansloski (4*j*). The advantage of the method reported in this communication lies in the relatively simple synthesis for these ring systems. Furthermore, the reaction may have potential application in the synthesis of other mesoionic ring systems (*e.g.* thiaza and oxaza systems).

This investigation was supported by a training grant (5-T1-GM-555-08) from the Division of Medical Sciences, U.S. Public Health Services, Bethesda, Maryland. We thank Dr. R. A. Coburn for many helpful discussions and comments.

1. (*a*) A. R. KATRITZKY. Chem. Ind. (London), 521 (1955); (*b*) M. OHTA and H. KATO. *In* Nonbenzoid aromatics. Vol. I. J. P. Snyder, Editor. Academic Press, Inc., New York, N.Y. 1969. Chapt. 4.
2. (*a*) R. A. JONES and A. R. KATRITZKY. J. Chem. Soc. 1317 (1959); (*b*) J. Chem. Soc. 378 (1961).
3. (*a*) A. E. TSCHITSCHIBABIN. Chem. Ber. **57**, 2092 (1924); (*b*) G. B. CHHEDA and R. H. HALL. J. Org. Chem. **34**, 3492 (1969).
4. (*a*) K. T. POTTS and U. P. SINGH. Chem. Commun. 569 (1969); (*b*) G. V. BOYD and P. H. WRIGHT. Chem. Commun. 182 (1969); (*c*) G. V. BOYD. Chem. Commun. 1410 (1968); (*d*) C. V. GRECO, R. P. GRAY, and V. G. GROSSO. J. Org. Chem. **32**, 4101 (1967); (*e*) W. D. BURROWS. J. Org. Chem. **31**, 3435 (1966); (*f*) G. SINGH. Tetrahedron Lett., 3789 (1964); (*g*) A. LAWSON and D. H. MILES. Chem. Ind. (London), 461 (1958); (*h*) A. LAWSON and C. E. SEARLE. J. Chem. Soc. 1556 (1957); (*i*) A. LAWSON and D. H. MILES. J. Chem. Soc. 2865 (1959); (*j*) E. B. ROCHE and D. W. STANSLOSKI. J. Heterocycl. Chem. **7**, 139 (1970).
5. N. W. BRISTOW, P. T. CHARTON, D. A. PEAK, and W. F. SHORT. J. Chem. Soc. 616 (1954).
6. (*a*) E. BESTHORN and J. IBEL. Chem. Ber. **37**, 1236 (1904); (*b*) F. KNOLLPFEIFFER and K. SCHNEIDER. Ann. Chem. **530**, 34 (1937); (*c*) D. L. HAMMICK and A. M. ROE. Chem. Ind. (London), 900 (1953).
7. M. OHTA and S. SATO. Unpublished results; see ref. 1*b*, p. 198.
8. J. W. STEELE, W. K. ANDERSON, and W. F. TRAGER. In preparation.

Can. J. Chem. Downloaded from www.nrcresearchpress.com by 210.87.254.5 on 09/05/12
For personal use only.

Measurement of Depolarization Ratios in the Raman Spectra of Powdered Crystalline Solids

D. W. JOHNSON AND D. SUTTON
Department of Chemistry, Simon Fraser University, Burnaby 2, British Columbia

Received July 23, 1970

The change in apparent depolarization ratio as a function of the refractive index of the surrounding liquid medium has been measured for the Raman active vibrational modes of powdered crystalline barium nitrate and sodium sulfate. This method provides an accurate measurement of the refractive index and depolarization ratios for barium nitrate, but fails to do so for sodium sulfate due to birefringent effects. The general applications of this technique for determining depolarization ratios of powdered crystalline solids are discussed.

Canadian Journal of Chemistry, **49**, 671 (1971)

Introduction

The recent advances in instrumentation brought about by the introduction of continuous-wave laser excitation have made the recording of excellent Raman spectra from powdered crystalline samples almost a routine matter. Nowhere has this advantage been recognized more than in the study of solid inorganic compounds, for which the alternative and more usual technique of making measurements on solutions is frequently hindered by lack of an appropriate solvent or because of problems associated with complexing or dissociation. Where measurements on solutions are practicable, the additional information from depolarization measurements considerably aids assignment by enabling bands which arise from totally symmetric modes to be distinguished. Similar information may be obtained from the study of oriented single crystals. However, experience shows that the Raman emission from powdered crystalline solids is almost invariably depolarized as a result of the multiple reflections and refractions which both the polarized incident radiation and the Raman emitted light suffer at crystal surfaces within the sample. Two authors (1, 2) have recently de-

The first reported example of this mesoionic 4-oxoimidazole system was the dye "Besthorn's red" (6). The only other fused ring system of this type has been prepared by Ohta and Sato (7). The monocyclic mesoionic ring system has been synthesized by Lawson and Mills (4*i*) and more recently by Roche and Stansloski (4*j*). The advantage of the method reported in this communication lies in the relatively simple synthesis for these ring systems. Furthermore, the reaction may have potential application in the synthesis of other mesoionic ring systems (*e.g.* thiaza and oxaza systems).

This investigation was supported by a training grant (5-T1-GM-555-08) from the Division of Medical Sciences, U.S. Public Health Services, Bethesda, Maryland. We thank Dr. R. A. Coburn for many helpful discussions and comments.

1. (*a*) A. R. KATRITZKY. Chem. Ind. (London), 521 (1955); (*b*) M. OHTA and H. KATO. *In* Nonbenzoid aromatics. Vol. I. J. P. Snyder, Editor. Academic Press, Inc., New York, N.Y. 1969. Chapt. 4.
2. (*a*) R. A. JONES and A. R. KATRITZKY. J. Chem. Soc. 1317 (1959); (*b*) J. Chem. Soc. 378 (1961).
3. (*a*) A. E. TSCHITSCHIBABIN. Chem. Ber. **57**, 2092 (1924); (*b*) G. B. CHHEDA and R. H. HALL. J. Org. Chem. **34**, 3492 (1969).
4. (*a*) K. T. POTTS and U. P. SINGH. Chem. Commun. 569 (1969); (*b*) G. V. BOYD and P. H. WRIGHT. Chem. Commun. 182 (1969); (*c*) G. V. BOYD. Chem. Commun. 1410 (1968); (*d*) C. V. GRECO, R. P. GRAY, and V. G. GROSSO. J. Org. Chem. **32**, 4101 (1967); (*e*) W. D. BURROWS. J. Org. Chem. **31**, 3435 (1966); (*f*) G. SINGH. Tetrahedron Lett., 3789 (1964); (*g*) A. LAWSON and D. H. MILES. Chem. Ind. (London), 461 (1958); (*h*) A. LAWSON and C. E. SEARLE. J. Chem. Soc. 1556 (1957); (*i*) A. LAWSON and D. H. MILES. J. Chem. Soc. 2865 (1959); (*j*) E. B. ROCHE and D. W. STANSLOSKI. J. Heterocycl. Chem. **7**, 139 (1970).
5. N. W. BRISTOW, P. T. CHARTON, D. A. PEAK, and W. F. SHORT. J. Chem. Soc. 616 (1954).
6. (*a*) E. BESTHORN and J. IBEL. Chem. Ber. **37**, 1236 (1904); (*b*) F. KNOLLPFEIFFER and K. SCHNEIDER. Ann. Chem. **530**, 34 (1937); (*c*) D. L. HAMMICK and A. M. ROE. Chem. Ind. (London), 900 (1953).
7. M. OHTA and S. SATO. Unpublished results; see ref. 1*b*, p. 198.
8. J. W. STEELE, W. K. ANDERSON, and W. F. TRAGER. In preparation.

Can. J. Chem. Downloaded from www.nrcresearchpress.com by 210.87.254.6 on 09/05/12
For personal use only.

Measurement of Depolarization Ratios in the Raman Spectra of Powdered Crystalline Solids

D. W. JOHNSON AND D. SUTTON
Department of Chemistry, Simon Fraser University, Burnaby 2, British Columbia

Received July 23, 1970

The change in apparent depolarization ratio as a function of the refractive index of the surrounding liquid medium has been measured for the Raman active vibrational modes of powdered crystalline barium nitrate and sodium sulfate. This method provides an accurate measurement of the refractive index and depolarization ratios for barium nitrate, but fails to do so for sodium sulfate due to birefringent effects. The general applications of this technique for determining depolarization ratios of powdered crystalline solids are discussed.

Canadian Journal of Chemistry, **49**, 671 (1971)

Introduction

The recent advances in instrumentation brought about by the introduction of continuous-wave laser excitation have made the recording of excellent Raman spectra from powdered crystalline samples almost a routine matter. Nowhere has this advantage been recognized more than in the study of solid inorganic compounds, for which the alternative and more usual technique of making measurements on solutions is frequently hindered by lack of an appropriate solvent or because of problems associated with complexing or dissociation. Where measurements on solutions are practicable, the additional information from depolarization measurements considerably aids assignment by enabling bands which arise from totally symmetric modes to be distinguished. Similar information may be obtained from the study of oriented single crystals. However, experience shows that the Raman emission from powdered crystalline solids is almost invariably depolarized as a result of the multiple reflections and refractions which both the polarized incident radiation and the Raman emitted light suffer at crystal surfaces within the sample. Two authors (1, 2) have recently de-

Can. J. Chem. Downloaded from www.nrcresearchpress.com by 210.87.254.6 on 09/05/12
For personal use only.

scribed instances in which the measurement of depolarization ratios on powdered solids was made possible by immersing the solid in a liquid of similar refractive index. In the present study, we have applied a similar technique to a quantitative study of the variation of ρ with refractive index of the liquid phase to determine its suitability for obtaining accurate values of the refractive index of the solid and depolarization ratios for the Raman modes. In addition, we have been concerned with the adaptation of this method to the regular 180° coaxial sample arrangement of the Cary Model 81 Raman spectrometer.

Experimental

Spectra

Finely ground anhydrous samples of barium nitrate or sodium sulfate were contained in a 3 mm diameter borosilicate glass tube with smoothly rounded end to a depth of 2–3 mm. Sufficient liquid of known refractive index was added to yield a thick paste. Spectra were obtained for 180° coaxial viewing using the Cary Model 81 Raman spectrophotometer with 60 mW Spectra-Physics Model 125 He/Ne laser excitation. In some preliminary runs, the light scattered at 90° was analyzed, but these were abandoned in favor of the much higher Raman intensity collected in the 180° viewing mode. Polarization measurements were made by rotating the plane of polarization of the incident radiation relative to the fixed analyzer. The values obtained were in all cases corrected by reference to a depolarization ratio calibration curve obtained using a similar depth of liquid carbon tetrachloride in the same sample cell. The liquid was held in place by means of a tightly fitting glass piston. Methylene diiodide and diethyl ether were mixed in various proportions to provide a range of refractive index values measured using a standard Abbé refractometer.

Results

(a) Barium Nitrate

Crystalline barium nitrate exhibits a Raman spectrum which consists of the following three Raman active nitrate bands: 733 cm^{-1} (e'), 1048 cm^{-1} (a_1'), and 1367 cm^{-1} (e'). The totally symmetric mode (a_1') is expected to yield a polarized band with a depolarization ratio (ρ) close to zero, whilst the e' mode should be depolarized with $\rho = 0.75$ when plane polarized incident radiation is used. Spectra recorded using the powdered sample alone showed negligible difference in the intensities of the bands with respect to the orientation of the plane of polarization of the incident radiation. However, when the sample was immersed in either diethyl ether (refractive index $\eta = 1.349$), methylene diiodide ($\eta = 1.756$) or mixtures of the two liquids yielding intermediate η values, a close direct correlation of ρ with $(\eta_{solid} - \eta_{liquid})$ was observed. The results for the 733 and 1047 cm^{-1} bands are summarized in Table 1. The 1367 cm^{-1} band is close to a polarized solvent band in methylene diiodide (1353 cm^{-1}) so that the results are less reliable but follow a similar trend.

TABLE 1. Variation of apparent depolarization ratio (ρ) for $Ba(NO_3)_2$, with refractive index (η) of liquid phase

	ρ	
η	733 (cm^{-1})	1047 (cm^{-1})
1.349	0.84	0.835
1.486	0.82	0.343
1.499	0.79	0.305
1.505	0.82	0.235
1.519	0.82	0.208
1.540	0.81	0.180
1.548	0.78	0.087
1.561	0.78	0.045
1.572	0.75	0.023
1.583	0.76	0.025
1.605	0.77	0.073
1.639	—	0.230
1.647	0.77	0.285
1.675	0.79	0.325
1.707	0.82	0.360
1.756	0.84	0.390

The polarized 1047 cm^{-1} band showed the largest effect, as illustrated in Fig. 1, the apparent value of ρ dropping rapidly to a minimum of $\rho = 0.023$ at the true unique refractive index of the cubic solid, $\eta = 1.572$. The utility of the method for the qualitative identification of polarized bands is seen from the fact that the band appears significantly polarized ($\rho < 0.4$), even when $(\eta_{solid} - \eta_{liquid})$ is as large as 0.15. Again, the method provides the refractive index of a solid which exhibits strongly polarized Raman bands. The plot of ρ *vs.* η for the depolarized 733 cm^{-1} band (Fig. 2) is much more erratic and less symmetrical. Nevertheless, the same general trend is observed and the curve minimizes again at $\eta = 1.572$, at the expected value of $\rho = 0.75$. A similar plot for the 1367 cm^{-1} band gave a value of $\rho = 0.70$, the error being due to overlap with a polarized solvent band.

(b) Sodium Sulfate

The free sulfate ion has T_d symmetry and four Raman active frequencies: 451 cm^{-1}(e), 613

Can. J. Chem. Downloaded from www.nrcresearchpress.com by 210.87.254.6 on 09/05/12
For personal use only.

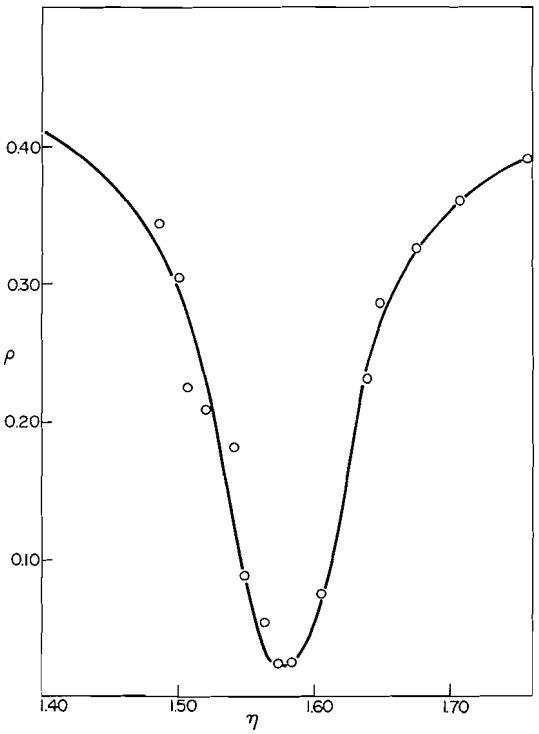

FIG. 1. Variation of apparent depolarization ratio (ρ) for the 1047 cm^{-1} band of $Ba(NO_3)_2$ with refractive index η of the liquid.

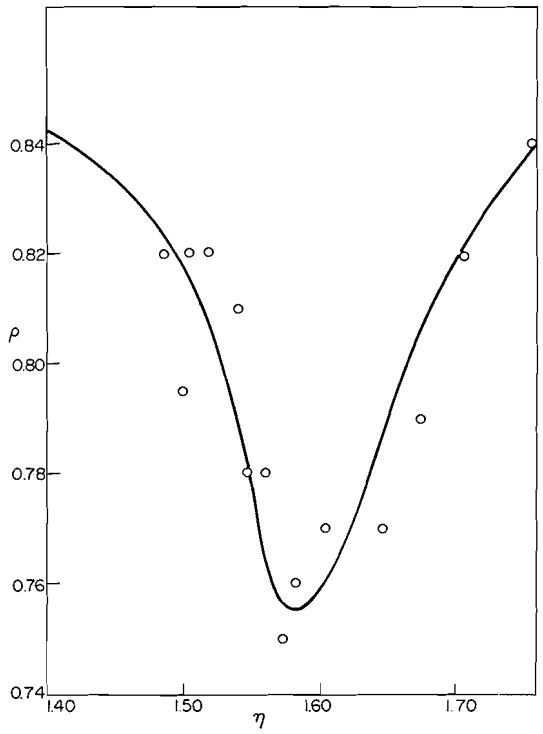

FIG. 2. Variation of apparent depolarization ratio (ρ) for the 733 cm^{-1} band of $Ba(NO_3)_2$ with refractive index η of the liquid.

$cm^{-1}(t_2)$, 981 $cm^{-1}(a_1)$, and 1104 $cm^{-1}(t_2)$. In orthorhombic anhydrous sodium sulfate the symmetry is lowered sufficiently to split all the modes into their non-degenerate components, so that the Raman spectrum of Na_2SO_4 consists of nine bands in the sulfate ion region. It was hoped that the symmetric components of the split modes could be identified in a similar manner as was used for $Ba(NO_3)_2$. The totally symmetric mode (a_1) is expected to be totally polarized with ρ close to zero, so we studied the variation of the apparent ρ value for this band as a function of the refractive index of the liquid to determine the most favorable η at which to examine the other bands (Table 2). The plot of ρ *vs.* η for this band, which occurred at 993 cm^{-1} in our sample (Fig. 3), displayed an effect which was quite different from that displayed by any of the nitrate bands in $Ba(NO_3)_2$. Rather than reaching a distinct minimum at any of the three refractive indices of Na_2SO_4 (1.464, 1.474, 1.485), only two minima were observed. Furthermore, the depolarization ratios at the minima

TABLE 2. Variation of apparent depolarization ratio for the a_1 mode of Na_2SO_4 with refractive index of the liquid phase

η	ρ
1.435	0.84
1.448	0.82
1.452	0.80
1.455	0.79
1.456	0.78
1.4565	0.76
1.459	0.68
1.460	0.69
1.461	0.75
1.462	0.82
1.463	0.85
1.466	0.85
1.469	0.82
1.4695	0.75
1.471	0.61
1.474	0.67
1.480	0.77
1.489	0.82
1.506	0.84

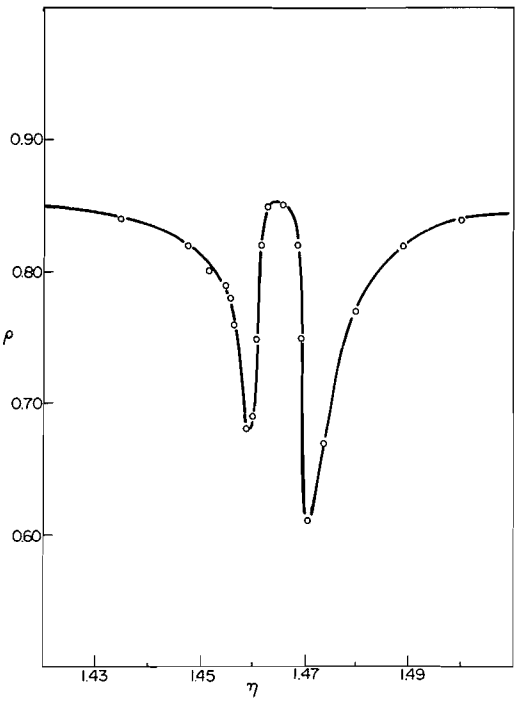

FIG. 3. Variation of apparent depolarization ratio (ρ) for the 993 cm^{-1} band of Na_2SO_4 with refractive index η of the liquid.

are not representative of a totally polarized band and an extremely sharp increase in ρ between the minima is observed. The band at no time appears to be strongly polarized, and it is evident that this is a result of birefringent effects in the anisotropic solid. A single crystal of anhydrous sodium sulfate in the form of a pyramidal plate (height 0.5 mm, base 2.2 mm × 2.2 mm) was viewed in the 180° mode with incident and scattered radiation propagated normal to the base. With the plane of polarization of the incident radiation parallel to the crystallographic axes, the 993 cm^{-1} band gave $\rho = 0.05$; the apparent ρ value increased steadily as the crystal was rotated about the incident beam to a maximum value of $\rho = 0.97$ corresponding to complete depolarization when the plane of polarization was 45° to the crystallographic axes. This is exactly the result expected as a result of birefringence splitting of the incident radiation into two components polarized at right angles (3, 4).

Discussion

The results described above indicate that there are severe limitations to this immersion technique as a method of obtaining accurate depolarization ratios for a powdered anisotropic solid. For the method to be effective, the sample should be isotropic (*cf.* $Ba(NO_3)_2$) with a single refractive index. In powdered anisotropic solids, birefringent effects will always operate to increase the apparent ρ value, and high values may be obtained even for totally symmetric modes, making it virtually impossible to distinguish reliably between polarized and depolarized Raman bands. For this reason we were not able to apply the powder method further to the study of site splitting in sodium sulfate. Problems may also arise with respect to the immersion liquid. Pairs of liquids which are miscible and yield mixtures which cover a sufficiently wide range of refractive index are difficult to find; if the solid is reactive this difficulty is increased. Thus we have found it a great problem to obtain suitable mixtures for the study of powdered nitrato-complexes. The most satisfactory liquid in our work has been methylene diiodide – diethyl ether, which is inert towards ionic nitrates and the majority of monodentate nitrato complexes; however it is unsuitable for use with many bidentate nitrato complexes (5) because of reaction.

The authors gratefully acknowledge support of this work by the National Research Council of Canada through operating grants, and Dr. E. J. Wells for discussion.

1. B. J. BULKIN. J. Opt. Soc. Amer. **59**, 1387 (1969).
2. D. G. SHRIVER. Appl. Spectrosc. **23**, 552 (1969).
3. S. P. S. PORTO, J. A. GIORDMAINE, and T. C. DAMEN. Phys. Rev. **147**, 608 (1966).
4. I. R. BEATTIE and T. R. GILSON. Proc. Royal Soc. Ser. A, **307**, 407 (1968).
5. C. C. ADDISON and D. SUTTON. Progr. Inorg. Chem. **8**, 195 (1967).

Can. J. Chem. Downloaded from www.nrcresearchpress.com by 210.87.254.6 on 09/05/12
For personal use only.

Erratum: Some Potentially Physiologically Active β,β-Diphenylethylamines Derived from Adrenaline

JANET E. FORREST, S. KASPAREK, AND R. A. HEACOCK
Atlantic Regional Laboratory, National Research Council of Canada, Halifax, Nova Scotia

AND

T. P. FORREST
Department of Chemistry, Dalhousie University, Halifax, Nova Scotia

Received October 23, 1970

(Ref.: Can. J. Chem. **48**, 1850 (1970))

Canadian Journal of Chemistry **49**, 675 (1971)

On page 1855, the legend for Fig. 5 names compound **11** as epinine. This should be corrected to read epepinine, *i.e.* "Fig. 5. The n.m.r. spectra of adrepine (**7**) hydrochloride and epepinine (**11**) hydrochloride, etc."

Can. J. Chem. Downloaded from www.nrcresearchpress.com by 210.87.254.42 on 09/05/12
For personal use only.

Can. J. Chem. Downloaded from www.nrcresearchpress.com by 210.87.254.6 on 09/05/12
For personal use only.

Photolysis of 2,4,6-Tri-*t*-butylnitrobenzene

L. R. C. BARCLAY AND I. T. MCMASTER
Department of Chemistry, Mount Allison University, Sackville, New Brunswick

Received October 21, 1970

Photolysis of 2,4,6-tri-*t*-butylnitrobenzene gave 5,7-di-*t*-butyl-3,3-dimethyloxindole. The latter was synthesized by an unambiguous route from 3,3-dimethyloxindole. The mechanism of this intramolecular photocyclization is discussed.

La photolyse du tri-*t*-butyl-2,4,6 nitrobenzène conduit au di-*t*-butyl-5,7 diméthyl-3,3 oxindole. Ce dernier composé a aussi été synthétisé par une méthode non ambiguë à partir du diméthyl-3,3 oxindole. Le mécanisme de cette photocyclisation intermoléculaire est discuté.

Canadian Journal of Chemistry, 49, 676 (1971)

Intramolecular cyclizations involving an aromatic nitro group in the ground or excited states ortho to a reactive function are well known (1); those involving an aromatic nitro group in an excited state ortho to a relatively unreactive group have not been reported. We now wish to report an example of a cyclization into an ortho-*t*-butyl group, which exhibits some unusual features.

Photolysis of 2,4,6-tri-*t*-butylnitrobenzene (**1**) in cyclohexane at ambient temperatures after 114 h gave, in addition to starting material (38% recovery) and unidentifiable tars, a new compound 5,7-di-*t*-butyl-3,3-dimethyloxindole (**2**) (20%), m.p. 237–238° ν_{max} (KBr) 3220, 1700 cm^{-1}, n.m.r. (CCl_4 with tetramethylsilane as internal standard) 8.68, 8.62, 8.56 (singlets, 24H), 2.98 (doublet, 1H), 2.82 (doublet, 1H), and −0.55 τ (singlet, 1H, exchanges with D_2O).[1–3] Photolysis of **1** in benzene after 67 h increased the yield of **2** to 36%; starting material was completely consumed in this reaction. That the carbon skeleton had not rearranged in the transformation of **1** into **2** was shown by an unambiguous synthesis of **2** in 65% yield from 3,3-di-methyloxindole (2) and *t*-butylchloride using aluminum chloride as catalyst. Lithium aluminum hydride reduced **2** to the amine **3** (64%), m.p. 105° ν_{max} (KBr) 3440 cm^{-1}, n.m.r. (CCl_4) 8.62, 8.55 (singlets, 24H), 6.62 (singlet, 2H), 6.27 (singlet, 1H), 3.03 (doublet, 1H), and 2.89 τ (doublet, 1H).[2]

Of the various possible mechanisms that may be considered for the conversion of **1** into **2**, the one outlined receives support from current literature. Electronically excited aromatic nitro compounds are reported to abstract hydrogen atoms from solvent molecules to produce a low stationary-state concentration of aromatic monohydronitro radicals (3). Due to the proximity of an ortho-*t*-butyl group to the nitro function in **1**, monohydronitro radicals may alternatively be formed during photolysis by hydrogen abstraction from an ortho-*t*-butyl group with the formation of an intermediate biradical **4**, which might be expected to spontaneously cyclize to **5** before the side-chain alkyl radical had time to rearrange (4). Elimination of water from **5** would yield the *N*-oxide **6**, which under photolytic conditions may be expected to rearrange to the oxaziridine **7** (5). This in turn might be expected to undergo photofragmentation to give the nitrene **8** (6). The latter species are well known to intramolecularily insert readily into carbon-hydrogen bonds which are sp^2 hybridized (7). Nitrenes are least reactive towards primary carbon-hydrogen bonds which are sp^3 hybridized (8). Alternatively, it is possible that **7** may rearrange directly to **2** (5). The decrease in yield of **2** from **1** in changing solvent from benzene to cyclohexane is expected since hydrogen abstraction from the secondary carbon of cyclohexane by the electronically-excited nitro group (**1** → **9**)

[1]An accurate mass determination by high resolution mass spectroscopy established the molecular formula to be $C_{18}H_{27}NO$.

[2]New compounds reported gave microanalyses in agreement with their formulae.

[3]Photolyses were performed using a quartz vessel in a Rayonet Photochemical Reactor and a 2537 Å u.v. light source.

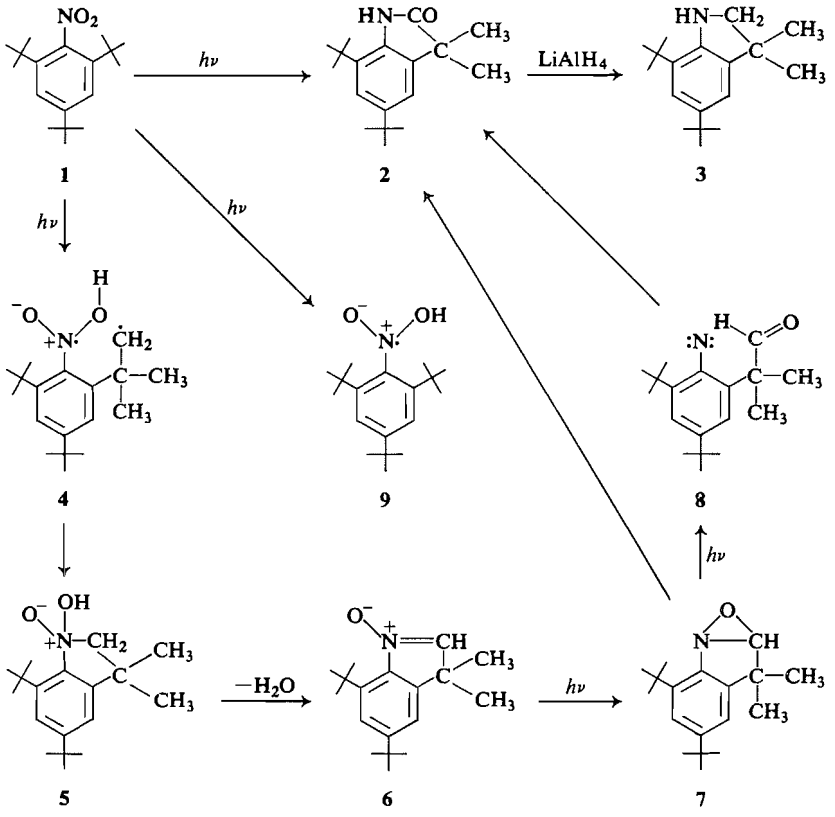

would compete with hydrogen abstraction from a primary carbon of adjacent *t*-butyl groups (**1** → **4**).[4]

There is no close analogy in the literature to this reaction, which apparently involves three photolytic steps and two intramolecular cyclization steps by electrophilic nitrogen, without rearrangement of any portion of the carbon skeleton. In this regard, a comparison may be made with the intramolecular alkylation of an ortho-*t*-butyl group observed recently in this laboratory (9).

This reaction is under further study to substantiate the proposed mechanism and to explore its synthetic significance.

[4]Hydrogen abstraction from an ortho methyl to a photochemical excited nitro group has been reported (Morrison and Migdalof, ref. 10.). We are not aware of such hydrogen abstraction from an *o*-*t*-butyl group.

This research was supported by a grant from the National Research Council of Canada. The mass spectroscopic analysis was performed by Dr. W. D. Jamieson of the National Research Council, Halifax, Nova Scotia.

1. J. D. Loudon and G. Tennant. Quart. Rev. **18**, 389 (1964). P. de Mayo and S. T. Reid. Quart. Rev. **15**, 393 (1961).
2. K. Brunner. Monatsh. **18**, 95 (1897).
3. D. J. Cowley and L. H. Sutcliffe. Trans. Faraday Soc. **65**, 2286 (1969).
4. L. Harvey, G. J. Gleicher, and W. D. Totherow. Tetrahedron, **25**, 5019 (1969).
5. G. G. Spence, E. C. Taylor and O. Buchardt. Chem. Rev. **10**, 231 (1970).
6. J. S. Splitter and M. Calvin. Tetrahedron Lett. 1445 (1968). P. L. Kumler and O. Buchardt. J. Chem. Soc. D, 1321 (1968).
7. R. J. Sundberg, L. Lin, and D. E. Blackburn. J. Heterocyclic Chem. **6**, 441 (1969).
8. M. F. Sloan, T. J. Prosser, N. R. Newberg, and D. S. Breslow. Tetrahedron Lett. 2945 (1964).
9. L. R. C. Barclay and M. C. MacDonald. Tetrahedron Lett. 881 (1968).
10. H. Morrison and B. H. Migdalof. J. Org. Chem. **30**, 3994 (1965).

Can. J. Chem. Downloaded from www.nrcresearchpress.com by 210.87.254.6 on 09/05/12
For personal use only.

Can. J. Chem. Downloaded from www.nrcresearchpress.com by 210.87.254.40 on 09/05/12
For personal use only.

Canadian Journal of Chemistry

Published by THE NATIONAL RESEARCH COUNCIL OF CANADA

VOLUME 49 MARCH 1, 1971 NUMBER 5

Sensitized Photolysis of Octacyanomolybdate(IV)[1]

R. D. WILSON, V. S. SASTRI, AND C. H. LANGFORD[2]

Department of Chemistry, Carleton University, Ottawa 1, Ontario

Received October 22, 1970

The photochemical loss of cyanide from $Mo(CN)_8^{4-}$ is shown to be sensitized by common organic triplet donors naphthalene, phenanthrene, anthraquinone, and benzophenone, but not by biacetyl. This suggests that the reactive state may be $^3B_1$, not the lower lying $^3A_2$. The quantum yields for sensitized photolysis (near 0.25) are larger than for the direct reaction (near 0.15). This is unlike the behavior of $Co(CN)_6^{3-}$ where the similarity of the two yields leads to the conclusion that higher excited states are efficiently converted to "the lowest triplet".

Naphthalene irradiated at 286 nm leads to a quantum yield of 0.4 which is, perhaps, associated with a new process involving sensitized production of a solvated electron.

Thermal solvolysis rates in several media are also reported. The medium dependence of solvolysis is small.

Il est démontré que la perte photochimique de cyanure par $Mo(CN)_8^{4-}$ est sensibilisée par les donneurs organiques de triplets tels que naphtalène, phénanthrène, anthraquinone et benzophénone mais pas par le diacétyle. Ceci suggère que l'état intermédiaire peut être $^3B_1$, mais pas l'état inférieur $^3A_2$. Les rendements quantiques de la photolyse sensibilisée (près de 0.25) sont plus grands que pour la réaction directe (près de 0.15). Ceci est contraire au comportement de $CO(CN)_6^{3-}$ où la similarité des deux rendements a conduit à la conclusion que les états excités les plus élevés sont efficacement amenés au niveau du "plus bas triplet".

Le naphtalène irradié à 286 nm conduit à un rendement quantique de 0.4 qui est peut être associé avec un nouveau processus impliquant la production sensibilisée d'un électron solvaté.

Les taux de solvolyse thermique dans plusieurs milieux sont aussi rapportés. La dépendance de la solvolyse sur le milieu est faible.

Canadian Journal of Chemistry, 49, 679 (1971)

Introduction

Sensitized photolysis has proved its value in attempts to understand organic photochemical pathways and has recently been applied to analysis of mechanisms of photo substitution reactions of complexes of Cr(III) (1), Co(III) (2), and Pt(II) (3). Photochemical substitution of $Mo(CN)_8^{4-}$ in basic aqueous buffers has been described (4), and it has been suggested that the wavelength independence of quantum yield in the ligand field bands implies a pathway involving efficient conversion of singlet excited states to the lowest triplet which then undergoes either relaxation to the $Mo(CN)_8^{4-}$ ground state or relaxation to an intermediate on the substitution pathway, with the ratio of efficiencies of these two processes determining the magnitude of the quantum yield. Such a pathway is entirely analogous to the mechanism proposed for reaction of $Co(CN)_6^{3-}$ and implies that sensitized quantum yields produced by energy transfer from efficient organic triplet donors should equal the direct yield.

Several well characterized organic triplet donors are discussed in this study. Their properties (5, 6) are collected in Table 1. E_T denotes the triplet energy (from emission spectroscopy). The variations of E_T are significant in comparison to the energy levels of the acceptor complex $Mo(CN)_8^{4-}$. Our spectrum of $Mo(CN)_8^{4-}$ complex is consistent with that described by Perumareddi *et al.* (7) and we follow their assignments which are based on an approximate D_{2d} symmetry for the ion. Figure 1 shows the energy

[1]We thank the National Research Council of Canada for financial support.

[2]Alfred P. Sloan Foundation research fellow 1968–1970.

TABLE 1. Spectral data on organic sensitizers (from refs. 5, 6)

Sensitizer	λ_{max} (nm)	ε_{max}	E_T (kcal/mol)
Naphthalene	311	256	60.8
Benzophenone	360	96	69.3
Phenanthrene	376	143	62
Anthraquinone	400	95	62
Biacetyl*	410	9.1	55.0

*This compound was examined in media used in the present study. The emission band energy quoted is for a biacetyl solution in C_2H_5OH/H_2O in the ratio of 50/50 by volume.

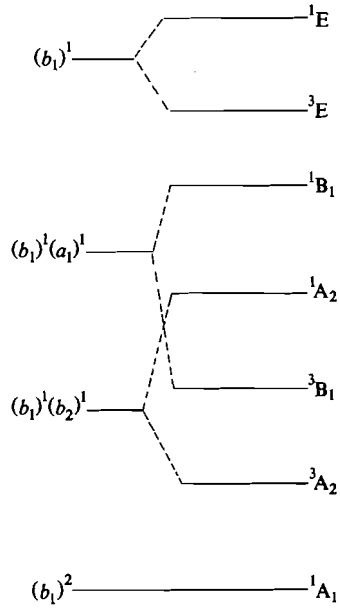

FIG. 1. Energy level scheme for $Mo(CN)_8^{4-}$ in D_{2d} symmetry after ref. 7 (not to scale).

level scheme with orbital configurations indicated. Table 2 lists the experimental absorption bands with band maxima quoted in both wavelength and energy (kcal) units.

Experimental

Preparation of Potassium Octacyanomolybdate(IV)

The complex was prepared using the method of Furman and Miller (8). The golden yellow crystals that were formed were dried at 110 °C and stored in the dark. The purity of the complex was checked by comparison with the spectrum in the literature (7). Periodic recrystallizations from ethanol–water mixtures were found to be necessary during the course of the investigation. The pure product was analyzed for total molybdenum by titration with standard permanganate.

TABLE 2. Spectral characteristics of the octacyanomolybdenum(IV) ion

λ_{max} (nm)	ε_{max}	Assignment (ref. 7)	E (kcal/mol)
510	2.9	$^3B_1 \leftarrow {}^1A_1$	56.3
431	72	$^1A_2 \leftarrow {}^1A_1$	66.4
368	169	$^1B_1 \leftarrow {}^1A_1$	77.7
308	260	$^1E_1 \leftarrow {}^1A_1$	93.0

Anal. Calcd. for $K_4Mo(CN)_8.2H_2O$: Mo, 19.35. Found: Mo, 19.6.

The infrared spectrum of the complex showed C≡N stretching frequencies at 2160, 2130, and 2090 cm^{-1}, and the presence of water of crystallization. The salt is extremely soluble in water and concentrated aqueous solutions turn green on exposure to light.

Cyanide Analysis

The *microquantities* of cyanide produced in the photolysis were determined by the method of Epstein (9). The method is based on the conversion of cyanide to cyanogen chloride with an aqueous solution of chloramine-T and the reaction of this cyanogen chloride with a mixture of pyridine containing 0.1% bis-pyrolazone and 1-phenyl-3-methyl-5-pyrolazone. The blue dye that develops is stable for several hours in the p*H* range 7–9, and measurements of optical density at 630 nm may be performed after 30 min. The calibration of the method was performed by making a stock solution from analytical grade KCN and taking aliquots in the 0.2–1.2 μg interval. The stock solution was analyzed by potentiometric titration, with standard 0.002 *M* $AgNO_3$, using a silver electrode. The analysis was found to be quantitatively unaffected by the presence of the sensitizers used, although color development required a longer period of time.

Actinometry

Irradiation equipment consisted of a 1000 W xenon–mercury source (Oriel Optics) and the beam collimated by lenses of 7.5 and 5 cm focal length passed through Jarrell-Ash monochromator (model 82-410) and then to 5 cm cell thermostatted at 25 ± 0.1 °C (13). The light source was calibrated using Ferrioxalate (10, 11) for wavelengths below 380 nm and reineckate system (12) for longer wavelengths. The quantum yields obtained were in good agreement with the values reported for these systems assuring that the band pass was comparable to interference filter system of ref. 12.

Sensitizers

Naphthalene, phenanthrene, and benzophenone were sensitizer grade chemicals as supplied by the J. T. Baker Chemical Co. These were recrystallized from ethanol and their purity was determined spectroscopically. Biacetyl was Fisher reagent grade which was distilled at 88 °C before use and stored in darkness, as degradation was observed on exposure to light. The anthraquinone was British Drug Houses reagent.

The spectra of all the sensitizers were recorded on a Cary-14 model recording spectrophotometer; the compounds being dissolved in the solvents which were used

Can. J. Chem. Downloaded from www.nrcresearchpress.com by 210.87.254.40 on 09/05/12
For personal use only.

Can. J. Chem. Downloaded from www.nrcresearchpress.com by 210.87.254.40 on 09/05/12
For personal use only.

in the photolysis. Spectral parameters were compared to those found in the literature (5).

Photolysis Solutions

Solutions of the octacyanomolybdate complex were prepared by dissolving the total amount of salt required in a minimum volume of water and adding this to the remainder of the solvent mixture, for the case of mixed solvents. For solutions containing the organic sensitizers the complex was dissolved in a minimum volume of the solvent mixture and the sensitizer dissolved, with heating, in the remainder. The sensitizer solution was then added slowly, with vigorous stirring, to the dissolved molybdenum cyanide complex. All operations were carried out in the presence of red "photographic" light to eliminate any predecomposition of the complex before photolysis.

Deaeration of solutions was accomplished by passing a vigorous stream of nitrogen through the solvent mixture for periods of 3 to 12 h. The solutions were then prepared as before, all operations including transfer to the reaction cell were carried out in a nitrogen atmosphere in red light.

Complex concentrations were chosen so that a minimum of 99% of the incident light was absorbed by the reacting solution. Concentration ratios in the sensitized reactions were chosen so as to have 95–98% of the light absorbed by the sensitizer, and the sensitized quantum yields were calculated on the basis of the number of moles of cyanide released and the quanta of light absorbed by the sensitizer.

Kinetics

The thermal reactions were slow enough to allow conventional manual analytical techniques to be used. Runs were carried out in darkened flasks with transfer being carried out in the presence of red "photographic" light. Aliquot portions of the reaction solution were diluted by a factor of 12.5 and the cyanide analyzed by the spectrophotometric method previously described. The analysis was calibrated for each of the mixed solvents used.

Results

In common with earlier workers (4), we lack satisfactorily detailed information on the Mo-containing product. It seems likely that it is initially $Mo(CN)_7OH^{4-}$ in aqueous basic buffers. What is clear is that the reaction is a substitution process which we study by initial *cyanide release* at quite low conversion. The quantum yields are for cyanide release in every case and the thermal rate constants are pseudo first order rate constants for cyanide release in the media in question. Table 3 contains thermal rate constants for CN^- formation in aqueous carbonate buffers, dimethylsulfoxide (DMSO) – water mixtures, and CH_3CN – water mixtures (also buffered to a glass electrode reading of "pH" = 10), the most interesting point is the low solvent sensitivity.

TABLE 3. Thermal solvolysis rate constants for $Mo(CN)_8^{4-}$ at 0.05 M, pH 10 (carbonate buffer)

Solvent	T(°C)	k(s^{-1})*	E_a (kcal/mol)
H_2O (pH=10.0)	22.0	8.5×10^{-8}	
H_2O (pH=10.0)	50.1	1.17×10^{-7}	13
DMSO/H_2O			
70/30 (V/V)	22.0	4.7×10^{-8}	
40/60 (V/V)	22.0	7.3×10^{-8}	
CH_3CN/H_2O			
70/30 (V/V)	22.0	4.0×10^{-8}	
40/60 (V/V)	22.0	7.0×10^{-8}	

*The rate constant describes the initial rate of CN^- release.

TABLE 4. Direct CN^- release quantum yields from irradiation of 0.05 M solutions of $Mo(CN)_8^{4-}$ in buffers of boric acid, KOH, and KCl

Solvent	Wavelength (nm)	Φ (24.8 °C)	Φ (37.3 °C)
pH 8.00 buffer	368	0.149	
pH 10.00 buffer	368	0.158	0.141
pH 12.00 buffer	368	0.155	
pH 10.00 buffer	431	0.155	
pH 10.00 buffer	308	0.152	
H_2O/C_2H_5OH			
50/50 (V/V)	368	0.135	0.115
70/30 (V/V)	368	0.141*	
H_2O/DMSO			
50/50 (V/V)	368	0.161	0.144
H_2O/CH_3CN			
50/50 (V/V)	368	0.141	0.123

*This result is the "control" for all the sensitization experiments reported in Table 5.

Table 4 collects quantum yields for direct photolysis of the complex in various media. The values which are comparable to earlier work (4) (aqueous buffers) are slightly higher and possibly within experimental error. But, the small increases reported may be real since our analytical system allowed study at much lower net cyanide release and product absorption may have been better avoided. These quantum yields are seen to be wavelength independent from 368 to 431 nm, relatively solvent insensitive, and apparently decreasing with increasing temperature.

Table 5 reports results of sensitization experiments. The solvent system was C_2H_5OH/H_2O in the ratio 70/30 (V/V) buffered to a pH meter reading of 10.0 (borate buffer). Only biacetyl was ineffective as a sensitizer. At basic pH biacetyl phosphorescence is quenched significantly, casting doubt on the significance of the biacetyl ineffectiveness.

TABLE 5. Quantum yields for sensitized photolysis of $Mo(CN)_8^{4-}$ at 24.8 °C in C_2H_5OH/H_2O mixtures (70/30, *V*/*V*), at p*H* 10 (boric acid, KCl, KOH)

Sensitizer*	Irradiation Wavelength (nm)	Sensitizer Conc. (*M*)	Complex Conc. (*M*)	Φ
Naphthalene	311	0.10	0.002	0.26
	286	0.10	0.002	0.42
Benzophenone	360	0.05	0.001	0.31
Phenanthrene	376	0.05	0.001	0.28
Anthraquinone	400	0.05	0.001	0.33
Biacetyl	410	0.05	0.001	Nil

*Solutions deaerated except naphthalene and phenanthrene.

In neutral solutions, phosphorescence of biacetyl was not quenched. However, 0.001 *M* $Mo(CN)_8^{4-}$ quenched the phosphorescence of 0.05 *M* biacetyl by 40% suggesting triplet energy transfer to the $^3A_2$ state of $Mo(CN)_8^{4-}$. In these neutral solutions, the direct yields for photolysis of $Mo(CN)_8^{4-}$ and 368 nm was $\phi = 0.151$. But, in the neutral solution, the biacetyl sensitized yield remained zero. These results support the idea that energy transfer from biacetyl can occur but that such energy transfer is *not* fruitful for solvolysis of $Mo(CN)_8^{4-}$

Discussion

The effectiveness of four well-known organic triplet donors in sensitizing the photosolvolysis of $Mo(CN)_8^{4-}$ implicates a low lying triplet in the reaction. The energy level diagram in Fig. 1 suggests the $^3B_1$ and $^3A_2$ as the most likely candidates. In conjunction with the triplet energies cited in Tables 1 and 2, the "unique" failure of biacetyl suggests that the $^3B_1$ might be the reactive state. This suggestion would require that radiationless deactivations from $^3B_1$ to the lower $^3A_2$ is not efficient in competition with reaction of the $^3B_1$ state. This could arise if the $^3B_1$ state were substantially structurally distorted which seems plausible but cannot be established in the absence of $Mo(CN)_8^{4-}$ phosphorescence data. (This suggestion deserves further research.)

We can make another point with more assurance. The quantum yields of the sensitized reactions are significantly larger than for direct reactions. This circumstance contrasts to that for $Co(CN)_6^{3-}$ (2). It implies that the direct reaction cannot proceed by highly efficient conversion of singlet excited states to the reactive triplet followed by a quantum yield determining competition between deactivation and reaction of that triplet. The wavelength independence of the direct quantum yield must be consistent with an intersystem crossing yield of significantly less than unity.

Flash photolysis studies on $Mo(CN)_8^{4-}$ in the ultraviolet (14) have suggested a high energy electron ejection mechanism. The high sensitized yield for naphthalene irradiated at 286 nm suggests that the electron ejection process may also be subject to sensitization.

Finally, it is interesting that the thermal and photochemical reactions both show low medium sensitivity. This suggests that there may be a resemblance between the photoreactive excited state and the transition state for thermal solvolysis.

1. A. W. ADAMSON, J. E. MARTIN, and F. D. CAMESSEI. J. Amer. Chem. Soc. **91**, 7530 (1969).
2. G. B. PORTER. J. Amer. Chem. Soc. **91**, 3980 (1969).
3. V. S. SASTRI and C. H. LANGFORD. J. Amer. Chem. Soc. **91**, 7533 (1969).
4. A. W. ADAMSON and J. PERUMAREDDI. Inorg. Chem. **4**, 247 (1965). V. CARASSITI and M. CLAUDI. Ann. Chim. Rome, **49**, 1697 (1959). V. CARASSITI and V. BALZANI. Ann. Chim. Rome, **50**, 630 (1960).
5. N. J. TURRO. Molecular Photochemistry. W. A. Benjamin, New York. 1965.
6. J. B. BIRKS and I. H. MUNRO. Progr. React. Kinet. **4**, 239 (1967).
7. J. R. PERUMAREDDI, A. D. LIEHR, and A. W. ADAMSON. J. Amer. Chem. Soc. **85**, 249 (1963).
8. N. J. FURMAN and C. O. MILLER. Inorg. Syn. **3**, 160 (1950).
9. J. EPSTEIN. Anal. Chem. **19**, 272 (1947).
10. C. G. HATCHARD and C. A. PARKER. Proc. Roy. Soc. Sec. A. **235**, 518 (1956).
11. H. H. SLAGER and J. LEE. J. Chem. Phys. **40**, 519 (1964).
12. E. E. WEGNER and A. W. ADAMSON. J. Amer. Chem. Soc. **88**, 394 (1966).
13. J. G. CALVERT and J. N. PITTS, Jr. Photochemistry. John Wiley and Sons, New York. 1966. p. 763.
14. W. L. WALTZ, A. W. ADAMSON, and P. D. FLEISCHAUER. J. Amer. Chem. Soc. **89**, 3923 (1967).

Can. J. Chem. Downloaded from www.nrcresearchpress.com by 210.87.254.40 on 09/05/12
For personal use only.

Activities and Ionic Distributions in Cobalt Silicate Melts[1]

I. B. SMITH AND C. R. MASSON
Atlantic Regional Laboratory, National Research Council of Canada, Halifax, Nova Scotia

Received October 13, 1970

Activities of CoO in $CoO–SiO_2$ melts were measured at 1450–1500 °C by equilibrating the melts, held in Pt–Rh containers, with atmospheres of known oxygen potential. Activities were calculated by the relationship

$$CoO_{(melt)} \rightleftarrows Co_{(in\ container)} + \tfrac{1}{2}O_2 \qquad K = a_{Co}p_{O_2}^{\frac{1}{2}}/a_{CoO}$$

where a_{Co}, the activity of cobalt in the container, was determined in separate experiments.

The results were compared with theoretical activity–composition curves based on the application of polymer theory to silicate melts. The results were in good agreement with theoretical curves calculated on the assumption of linear chains. In contrast, for all other binary silicate melts so far investigated the results are best represented in terms of theory in which all chain configurations are allowed. Ionic distributions and number average and weight average molecular weights were calculated as functions of the silica content from the experimental data. The calculated proportions of monomeric ion, SiO_4^{4-}, dimer $Si_2O_7^{6-}$, and trimer $Si_3O_{10}^{8-}$ were in reasonable agreement with experimental values based on trimethylsilylation and gas-chromatographic separation of the ionic constituents in quenched melts.

On a mesuré l'activité de CoO dans des mélanges fondus $CoO–SiO_2$ en équilibre avec des atmosphères d'oxygène de potentiel connu, dans des récipients de Pt-Rh, à 1450–1500 °C. Les activités ont été calculées à l'aide de la relation

$$CoO_{(mélange\ fondu)} \rightleftarrows Co_{(recipient)} + \tfrac{1}{2}O_2 \qquad K = a_{Co}p_{O_2}^{\frac{1}{2}}/a_{CoO}$$

où a_{Co}, l'activité du cobalt dans le récipient, a été déterminée à partir de mesures séparées.

Les résultats sont comparés aux courbes théoriques activité–composition établies en appliquant la théorie des polymères aux silicates fondus. Ils sont en bon accord avec les courbes théoriques établies en supposant que l'on a affaire à des chaînes linéaires. Par contre, les résultats obtenus pour tous les autres silicates binaires étudiés jusqu'à présent se montrent en meilleur accord avec les courbes théoriques établies en supposant toutes les configurations possibles pour les chaînes. La distribution des ions ainsi que les masses moléculaires moyennes en nombre et en poids ont été calculées en fonction de la teneur en silice. Les proportions calculées des monomères ioniques SiO_4^{4-}, dimères $Si_2O_7^{6-}$ et trimères $Si_3O_{10}^{8-}$ présentent un accord raisonnable avec les valeurs expérimentales obtenues de la triméthylsilylation et de la séparation par chromatographie en phase gazeuse des constituants ioniques dans les silicates trempés.

Canadian Journal of Chemistry, 49, 683 (1971)

Introduction

Recent work in this laboratory has been concerned with theoretical interpretations of the structure of simple binary silicate melts, regarding them as equilibrium distributions of polyanionic silicate units (1–4). Experimental activity–composition data upon which to test the theory are relatively scarce, being largely confined to systems of greatest practical or industrial importance, *e.g.* the systems 'FeO'–SiO_2 (5, 6) and PbO–SiO_2 (7–9). Comparison between theory and experiment has often had to be made indirectly by interpolation from ternary systems ($CaO–SiO_2$, (10)) or from phase diagrams ($CoO–SiO_2$, (11)). To obtain more direct evidence for comparison, a study of activity–composition relationships has been made on the system $CoO–SiO_2$ and forms the subject of the present paper. In addition to the further insight to be gained into the ionic structure of silicate melts from such a study, the work forms a logical extension to studies already carried out on $MnO–SiO_2$ (12) and 'FeO'–SiO_2 (5, 6), systems which also involve oxides of transition or group VIII metals with incompletely filled d-orbitals.

The technique used was to equilibrate $CoO–SiO_2$ melts of varying composition in 80% Pt – 20% Rh containers under known partial pressures of oxygen in the temperature range 1450–1500 °C. The equilibrium of interest is

$$[1] \qquad CoO_{melt} \rightleftarrows Co_{Pt-Rh} + \tfrac{1}{2}O_2$$

This equilibrium has already been studied with pure CoO (13), so that the cobalt oxide activities can be calculated from these results.

[1]NRCC No. 11 705.

Experimental

Materials

Cobalt Oxide

Pure CoO was prepared as described previously (13).

Silica

Mallinckrodt silicic acid (100 mesh powder) was fired at about 1000 °C and stored in a vacuum dessicator.

Batch slags were prepared by melting CoO–SiO_2 mixtures of the appropriate compositions in air in a Pt crucible. The melts were quenched between brass plates and crushed in a percussion mortar. This procedure was repeated several times to ensure a homogenous slag.

Containers

The 80% Pt – 20% Rh containers and strips were the same as described previously. The containers held about 1 g of silicate.

Gas Mixtures

A variety of methods was employed to obtain the required partial pressures of oxygen. These can be summarized as

(1) Ar–CO_2–H_2

(*a*) The three gases were purified, metered and mixed as described before.

(*b*) Premixed Ar–CO_2–H_2 gas mixtures were prepared in the laboratory. The mixtures were analyzed at room temperature by mass spectrometry and also at the temperature of interest by means of a lime-stabilized zirconia solid electolyte cell installed directly in the equilibrium furnace.

(2) CO_2

For several experiments CO_2 only was used to generate the required p_{O_2} value. Exact partial pressures of oxygen were determined using the solid electrolyte cell.

Apparatus

The apparatus used has been described previously (13).

Procedure

The Pt–Rh cups containing the coiled strips and charge of slag were supported on cradles of Pt–Rh wire mounted in turn on preshaped alumina trays. Four cups were used in each experiment.

To vary conditions as much as possible in any one experiment the slag compositions and initial cobalt content of the crucibles and strips were varied. Slag compositions were chosen to cover as wide a range as possible within the liquid region of the phase diagram. The initial cobalt content of the crucibles and strips varied from zero to values in excess of that required for equilibrium. Thus, by starting an experiment with slags of one composition and four cups and strips of widely differing cobalt content, equilibrium could be approached from both sides. Conversely, the same type of effect could be obtained by using four cups and strips of one cobalt content and slags of varying composition. This method also served as a useful check on the time required to establish equilibrium between the melt and the container and strip.

The furnace was brought to the required temperature and flushed with dried, purified argon. The slag samples were pushed slowly into the hot zone in the stream of argon, the furnace was closed and the carbon dioxide and hydrogen admitted. When premixed Ar–CO_2–H_2 gas mixtures or pure CO_2 were used the procedure was similar, except that the argon flow was turned off after the samples had been introduced.

Gas analyses were performed immediately before and after an experiment. Samples of the gas mixtures were collected at the inlet and exit of the furnace for analysis by mass spectrometry and a direct estimation of the partial pressure of oxygen at the temperature of interest was made using the lime-stabilized zirconia solid electrolyte cell.

At the end of an experiment the mixed gas flow, or CO_2, was turned off and argon reintroduced to the furnace. The samples were then quickly pulled into the water-cooled end of the equilibration tube in the stream of argon and quenched with a blast of helium.

The coiled strips were separated from the quenched melt and thoroughly cleaned as described previously.

Analysis

Each silicate sample was dissolved in concentrated HCl and the resulting solution evaporated to dryness. The material was then boiled in 50% HCl, filtered, and washed several times. The precipitated silica was determined by a conventional gravimetric method, being volatilized with HF. Occasionally, as a check, the filtrate was anlayzed spectrophotometrically to determine the CoO. The Co–Pt–Rh strips were analyzed using the technique described earlier.

Results

The results are presented in Table 1. Activities of CoO were calculated, relative to pure solid oxide as standard state, in a manner analogous to that described by Abraham *et al.* (12). Thus

$$[2] \qquad a_{CoO} = (p_{O_2}/p_{O_2}{}^0)^{1/2}$$

where p_{O_2} is the partial pressure of oxygen above the melt during equilibration and $p_{O_2}{}^0$ is the partial pressure of oxygen which would be in equilibrium with pure CoO and a Co–Pt–Rh alloy containing the same amount of cobalt as found in the slag experiment. In the range of temperatures and partial pressures used in the present work, solid CoO is virtually stoichiometric, so that the activity of solid CoO may be set at unity. Values of $p_{O_2}{}^0$ were derived from the data on the equilibrium between solid CoO and 80% Pt – 20% Rh (13). Figure 1 shows the activities, relative to the pure solid oxide, plotted as functions of composition.

Discussion

Activities of CoO were calculated with reference to pure liquid CoO as standard state by assuming a value of 9100 cal mol^{-1} for the heat of fusion of CoO (2). These values are plotted against the mole fraction of silica in Figs. 2 and 3. Included for comparison are activities cal-

TABLE 1. Experimental results

Time of equilibration (h)	Partial pressure of O_2 in gas phase (atm)	Mole fraction of Co in alloy after equilibration	Activity of Co in alloy after equilibration	Mole fraction of CoO in quenched melt	Activity of CoO relative to solid CoO as standard state
		(*a*) Temperature = 1450 °C			
23	8.375×10^{-5}	0.216	0.0318	0.625	0.740
70	7.379×01^{-7}	0.538	0.291	0.602	0.635
		0.511	0.254	0.575	0.556
24	5.571×10^{-7}	0.601	0.387	0.589	0.735
		0.610	0.403	0.606	0.765
23	1.849×10^{-6}	0.453	0.186	0.586	0.643
		0.477	0.212	0.614	0.733
		0.469	0.203	0.623	0.702
23	2.320×10^{-3}	0.0949	0.0072	0.645	0.877
		0.0823	0.0058	0.578	0.706
		0.0900	0.0066	0.608	0.808
		0.0873	0.0063	0.586	0.771
24	1.030×10^{-6}	0.460	0.193	0.568	0.499
		0.541	0.295	0.617	0.762
24	1.517×10^{-6}	0.532	0.283	0.665	0.887
		0.522	0.269	0.640	0.843
		0.492	0.230	0.593	0.722
		0.468	0.202	0.583	0.634
23	1.117×10^{-6}	0.429	0.161	0.561	0.433
		0.484	0.220	0.571	0.592
22	1.146×10^{-6}	0.481	0.217	0.570	0.591
		0.544	0.299	0.641	0.814
49	7.057×10^{-6}	0.409	0.142	0.695	0.962
		(*b*) Temperature = 1500 °C			
28	1.211×10^{-4}	0.264	0.0520	0.689	0.891
		0.220	0.0347	0.617	0.596
		0.235	0.0401	0.627	0.688
24	1.023×10^{-4}	0.231	0.0386	0.596	0.609
		0.219	0.0344	0.576	0.542
		0.266	0.0529	0.683	0.834
		0.274	0.0568	0.688	0.895
24	1.009×10^{-5}	0.423	0.167	0.650	0.826
		0.428	0.172	0.652	0.850
		0.385	0.131	0.593	0.647
		0.398	0.142	0.612	0.705
23	3.370×10^{-3}	0.086	0.0065	0.578	0.585
		0.097	0.0078	0.621	0.706
		0.089	0.0068	0.594	0.616
		0.107	0.0090	0.631	0.815
24	3.370×10^{-3}	0.086	0.0064	0.584	0.581
		0.088	0.0067	0.579	0.602
		0.095	0.0075	0.582	0.683
		0.090	0.0069	0.581	0.627
19	2.568×10^{-3}	0.085	0.0063	0.580	0.496
		0.098	0.0078	0.579	0.619
		0.090	0.0069	0.579	0.541
21	1.122×10^{-5}	0.430	0.174	0.666	0.909
		0.433	0.177	0.661	0.923
		0.416	0.159	0.657	0.832
		0.422	0.165	0.660	0.863
23	1.023×10^{-5}	0.380	0.126	0.576	0.629
		0.377	0.124	0.564	0.619
		0.388	0.133	0.599	0.662
25	3.670×10^{-6}	0.548	0.331	0.695	0.987

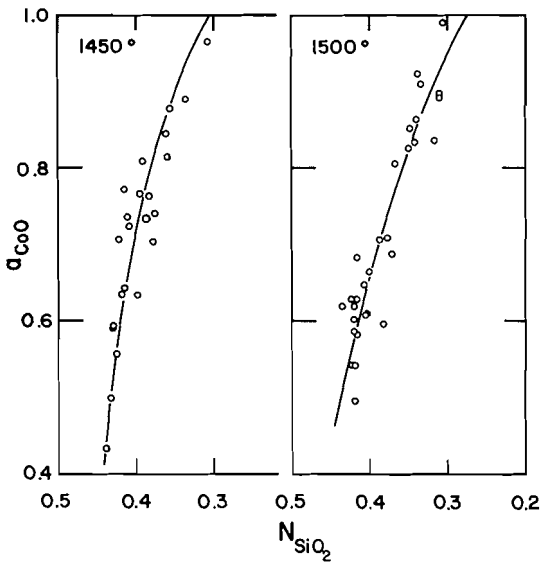

FIG. 1. Experimental activities of CoO, with respect to the solid oxide as standard state, plotted against mole fraction of silica for the two temperatures studied.

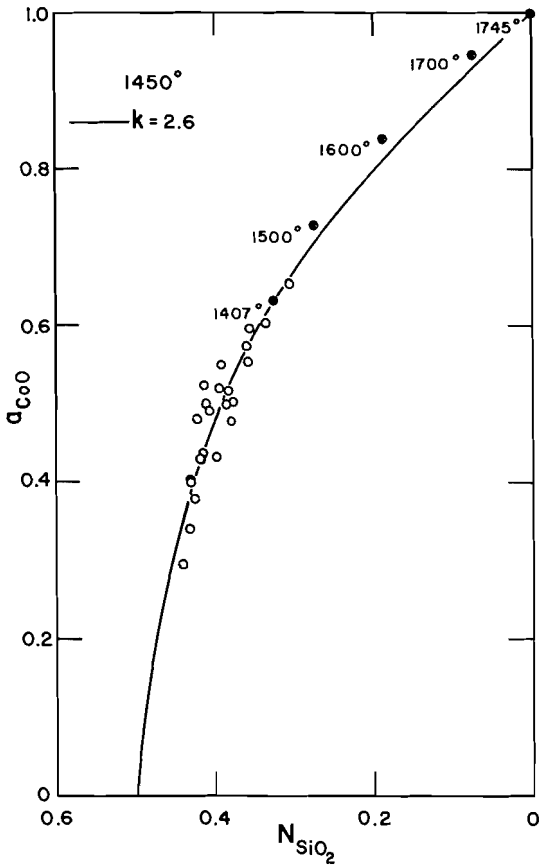

FIG. 2. Calculated activities of CoO, with respect to liquid oxide as standard state, plotted against mole fraction of silica at 1450 °C. The filled circles are points calculated from the phase diagram (11). The line is theoretical, corresponding to $k = 2.6$, calculated on the basis of a bifunctional condensation polymerization.

culated from the phase diagram of Masse and Muan (11). Experimental activities decrease steadily with increasing silica content of the melt. The line is a theoretical curve, the significance of which has been discussed previously (1, 2). The most striking result is the close fit between the experimental data and the theoretical treatment for linear chains. For all other binary silicate systems so far studied, the results are in better agreement with a theory (3, 4) in which all chain configurations are allowed, as might be expected for a condensation polymerization involving the tetrafunctional monomeric unit SiO_4^{4-}. The experimental evidence so far accumulated for the system $CoO–SiO_2$ indicates that the reactive unit SiO_4^{4-} is rendered pseudobifunctional in this system. Ionic distributions can therefore be calculated in a manner analogous to that used in ref. 1, or by reference to the more general polymer theory for the case of a multifunctional condensation (4, 14) by setting $f = 2$. In either case identical results are obtained, as ref. 1 deals with a particular case of the more general theory.

In the application of polymer theory to silicate melts, a particular ionic distribution for the anions present (O^{2-}, SiO_4^{4-}, $Si_2O_7^{6-}$, $Si_3O_{10}^{8-}$, etc.) can be calculated and activity–composition curves drawn on the basis that the distribution can be characterized by a constant k_{11}. This represents the equilibrium ratio for the reaction

$$[3] \quad SiO_4^{4-} + Si_nO_{3n+1}^{2(n+1)-} \rightleftarrows Si_{n+1}O_{3n+4}^{2(n+2)-} + O^{2-}$$

where $n = 1$. In the case where $f = 2$, all k_{1n} values for polycondensation reactions of this type become identical, and are referred to in the figures and text of this paper merely as k. As a consequence of the mathematics, values of activity become zero at $N_{SiO_2} = 0.5$, the limit of applicability of the theory. In practice, however, activities will remain finite beyond this region, due to the onset of intramolecular condensation. The observation that activities close to $N_{SiO_2} = 0.5$ were low lends further support to the linear chain model and indicates the virtual absence of

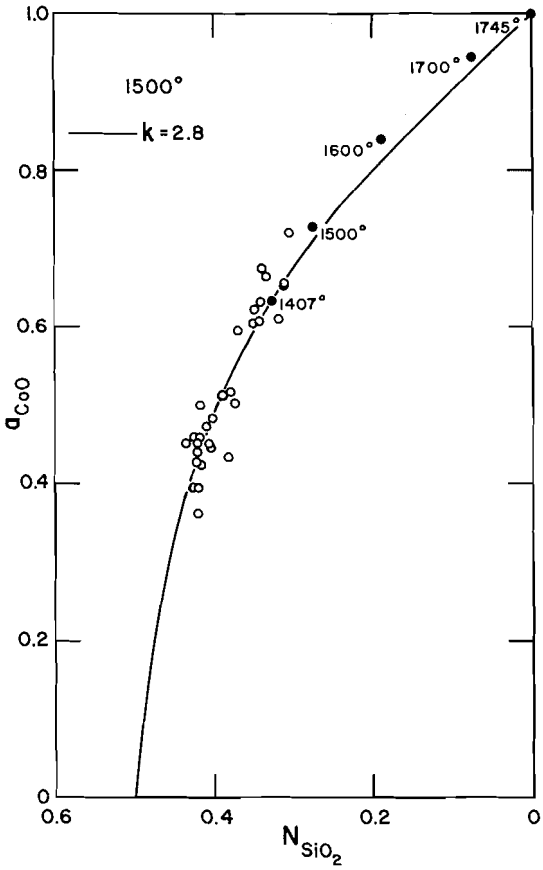

FIG. 3. As Fig. 2 but for 1450 °C read 1500 °C and for $k = 2.6$ read $k = 2.8$.

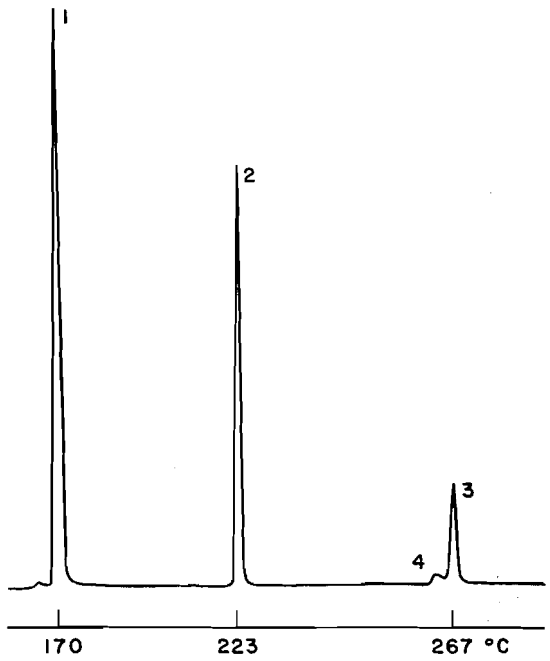

FIG. 4. Gas–liquid phase chromatographic trace of a cobalt silicate slag of overall composition $CoO/SiO_2 = 1.38$ (close to $Co_4Si_3O_{10}$), showing peaks due to monomer (*1*), dimer (*2*), trimeric chain (*3*), and tetrameric ring (*4*).

cross-linked or extensively branched structures. Activity–composition values beyond the metasilicate region (*i.e.* for $N_{SiO_2} > 0.5$) cannot be obtained at the present temperatures since the liquid region for $CoO–SiO_2$ does not extend into this range. Temperatures in excess of 1700 °C are required for studies at these compositions.

Further indirect evidence for lack of branching in the system $CoO–SiO_2$ comes from the observation that it proved impossible to quench any of the slags studied to glasses; there was always some crystalline material present. A highly branched slag would presumably be fairly viscous and be readily quenched to a glass. In spite of the failure to achieve a homogeneous glass, a sample of quenched cobalt silicate was analyzed by a gas–liquid partition chromatography technique (15, 16). The result is shown in Fig. 4. The quenched slag had a CoO/SiO_2 ratio of 1.38, *i.e.* representation by conventional formula would place it close to $Co_4Si_3O_{10}$ in composition. Although the gas–liquid phase chromatographic analysis is qualitative, it is evident that there is a distribution of silicate ions, with monomer the most abundant species, and including a small fraction of tetrameric ring species, $Si_4O_{12}^{8-}$.

Ion fractions of SiO_4^{4-}, $Si_2O_7^{6-}$, $Si_3O_{10}^{8-}$, etc., (based on all anions, including O^{2-}) were calculated as described previously (1, 2). Figure 5 shows ion fractions of monomer, dimer, trimer, tetramer, and decamer plotted against mole fraction of silica for the two temperatures. Since the theory cannot be applied to intramolecular condensations, ion fractions appear to approach zero at $N_{SiO_2} = 0.5$, although around and beyond this region rings and cross-linked structures will occur, resulting in finite ion fractions at these compositions. Figure 6 is a plot of ion fractions against chain size for the case when $N_{SiO_2} = 1/3$, the orthosilicate composition. This plot shows clearly that although the orthosilicate ion, SiO_4^{4-}, is the predominant species, there are also substantial amounts of

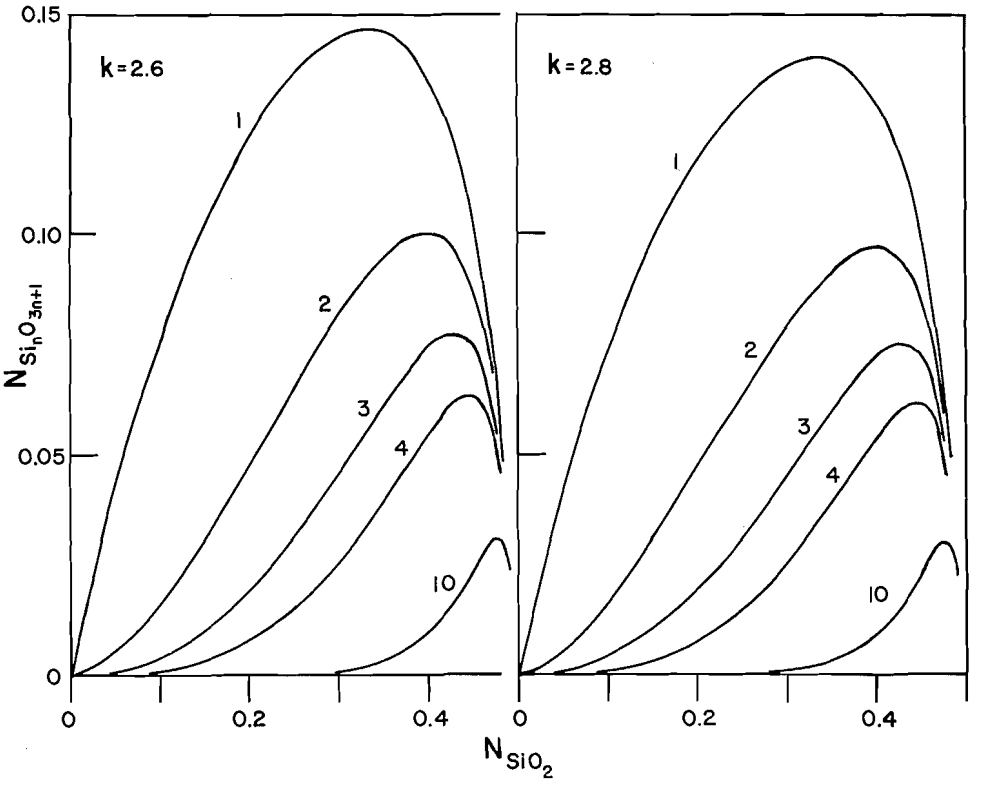

FIG. 5. Calculated ion fractions of SiO_4^{4-}, $Si_2O_7^{6-}$, $Si_3O_{10}^{8-}$, $Si_4O_{13}^{10-}$, and $Si_{10}O_{31}^{22-}$ plotted against mole fraction of silica for the two values of k corresponding to temperatures of 1450 and 1500 °C.

TABLE 2. Calculated weight % of silicate constituents for $N_{SiO_2} = 1/3$

x-mer	$CaO-SiO_2$ $k_{11} = 0.0016$	$SnO-SiO_2$ $k_{11} = 2.55$	$CoO-SiO_2$ $k = 2.6$
1	93.0386	13.6101	16.4123
2	6.4484	10.3717	18.4999
3	0.4739	8.3813	16.5845
4	0.0360	7.0075	13.4248
5	0.0028	5.9871	10.2541
6	0.0002	5.1921	7.5437
7		4.5517	5.4059
8		4.0233	3.7993
9		3.5794	2.6306
10		2.2012	1.8000
Total wt.% silicate up to decamer	99.9999	65.9054	96.3551

dimer, trimer, etc. In theory, monomeric ion is the most abundant species at all compositions. The broken curve for $k = 2.8$ crosses the value for $k = 2.6$ around $n = 4$ indicating that the distribution of anions becomes very slightly broader and larger anions become relatively more important as temperature increases. This effect also holds as the slag composition becomes more acid. These effects are displayed more clearly in Fig. 7 which shows the percentage by weight of the various silicate species (these calculations exclude O^{2-}) for the two compo-

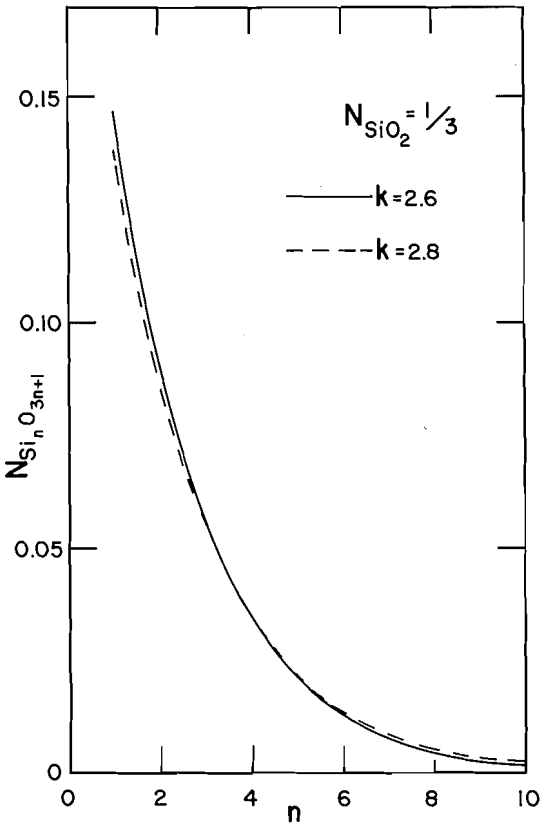

FIG. 6. Calculated ion fractions of silicate anions for the two values of k, when the overall composition is the orthosilicate, $N_{SiO_2} = 1/3$.

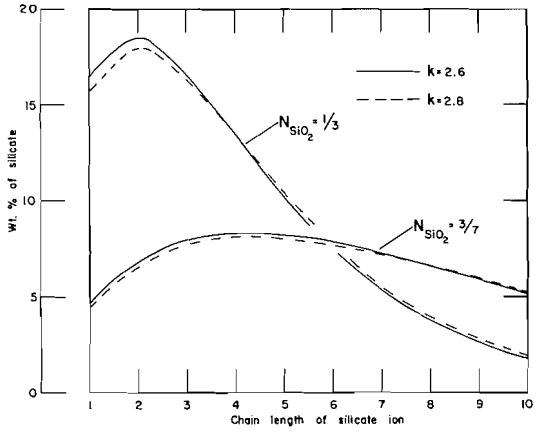

FIG. 7. Calculated weight % of silicate constituents plotted against chain length for both values of k, when the overall compositions are Co_2SiO_4($N_{SiO_2} = 1/3$) and $Co_4Si_3O_{10}$($N_{SiO_2} = 3/7$).

sitions Co_2SiO_4($N_{SiO_2} = 1/3$) and $Co_4Si_3O_{10}$ ($N_{SiO_2} = 3/7$). For purposes of comparison, calculated values of weight % of the silicate constituents for the orthosilicate composition are shown in Table 2 for three binary silicate systems, $CaO–SiO_2$, $SnO–SiO_2$, and $CoO–SiO_2$ (at 1450 °C). Values of k_{11} for $CaO–SiO_2$ and $SnO–SiO_2$ are taken from ref. 4 and weight % values calculated for x-mers from 1 to 10 on the basis of tetrafunctional condensation. Values for $CoO–SiO_2$ are calculated on the basis of bifunctional condensation, as outlined in this paper. The system $CaO–SiO_2$, with a low value of k_{11}, is highly depolymerized, and weight % values become negligible beyond trimer. The distribution of ions is very narrow, monomer being by far the dominant species. In contrast, for the system $SnO–SiO_2$, with a high value of k_{11}, the silicate is highly polymerized, even at the orthosilicate composition and the distribution is much broader. Although monomer is still the most abundant species weight % values are quite appreciable even up to the decamer. For the system $CoO–SiO_2$ the maximum weight % of silicates occurs around the dimer. This is a reflection of the fact that for linear chains, where

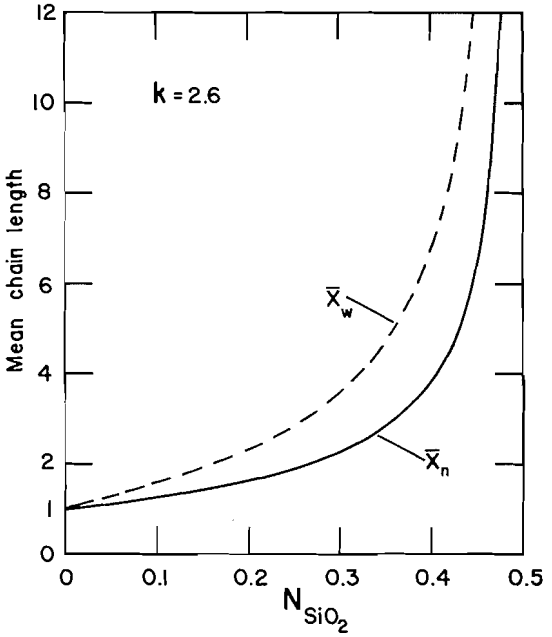

FIG. 8. Calculated number average ($\bar{x}_n$) and weight average ($\bar{x}_w$) chain lengths of silicate anions plotted against mole fraction of silica for the system $CoO–SiO_2$ at 1450 °C.

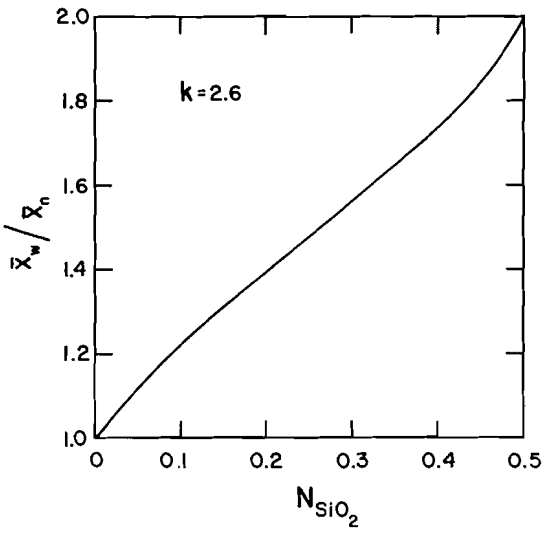

FIG. 9. Calculated ratio of $\bar{x}_w$ to $\bar{x}_n$ plotted against mole fraction of silica for $k = 2.6$.

only one configuration is possible for any x-mer, values of $N_{SiO_4}{}^{4-}$ are slightly lower at all compositions and values for the other species slightly higher, compared to those for systems where all configurations are allowed.

Number average chain lengths ($\bar{x}_n$) and weight average chain lengths ($\bar{x}_w$) of the silicate ions are shown in Fig. 8 as functions of the mole fraction of silica for one temperature, 1450 °C. At the orthosilicate composition the number average chain length is about three, *i.e.* the "average" silicate species corresponds closely to the formula $Co_4Si_3O_{10}$. The balance of the melt may be regarded as CoO, which accounts for the finite activity of CoO at this composition. Finally Fig. 9 shows a plot of $\bar{x}_w/\bar{x}_n$ against N_{SiO_2} up to the maximum applicable value of $N_{SiO_2} = 0.5$. At the maximum extent of reaction, neglecting intramolecular condensation, the ratio of $\bar{x}_w$ to $\bar{x}_n$ remains finite and equal to two, as for all linear condensation polymerizations.

We thank Mr. G. W. Caines for the chemical analyses, Mr. T. J. Uher for performing the mass spectrometric analysis of the gas mixtures and Dr. J. Götz for the chromatographic analysis of the quenched slag.

1. C. R. MASSON. Proc. Roy. Soc. A**287**, 201 (1965).
2. C. R. MASSON. J. Amer. Ceram. Soc. **51**, 134 (1968).
3. C. R. MASSON, I. B. SMITH, and S. G. WHITEWAY. Can. J. Chem. **48**, 201 (1970).
4. C. R. MASSON, I. B. SMITH, and S. G. WHITEWAY. Can. J. Chem. **48**, 1456 (1970).
5. R. SCHUHMANN, JR. and P. J. ENSIO. J. Metals, **3**, 401 (1951).
6. C. BODSWORTH. J.I.S.I. **193**, 13 (1959).
7. F. D. RICHARDSON and L. E. WEBB. Bull. Inst. Mining Met. **584**, 529 (1955).
8. R. SRIDHAR and J. H. E. JEFFES. Trans. Inst. Mining Met. C **76**, 44 (1967).
9. G. C. CHARETTE and S. N. FLENGAS. Can. Met. Quart. **7**, 191 (1968).
10. L. S. DARKEN and R. W. GURRY. Phys. Chem. of Metals, New York. McGraw-Hill. 1953.
11. D. P. MASSE and A. MUAN. Trans. A.I.M.E. **233**, 1448 (1965).
12. K. P. ABRAHAM, M. W. DAVIES, and F. D. RICHARDSON. J.I.S.I. **196**, 82 (1960).
13. I. B. SMITH and C. R. MASSON. Can. Met. Quart. **9**, 415 (1970).
14. S. G. WHITEWAY, I. B. SMITH, and C. R. MASSON. Can. J. Chem. **48**, 33 (1970).
15. F. F. H. WU, J. GÖTZ, W. D. JAMIESON, and C. R. MASSON. J. Chromatogr. **48**, 515 (1970).
16. J. GÖTZ and C. R. MASSON. J. Chem. Soc. A, 2683 (1970); In press (1971).

Can. J. Chem. Downloaded from www.nrcresearchpress.com by 210.87.254.5 on 09/05/12
For personal use only.

Aqueous Nonelectrolyte Solutions. Part VIII. Deuterium and Hydrogen Sulfides Solubilities in Deuterium Oxide and Water[1]

E. C. W. Clarke and D. N. Glew
Exploratory Research Laboratory, Dow Chemical of Canada, Limited, Sarnia, Ontario

Received September 30, 1970

A new apparatus is described in which the solubility of deuterium sulfide in deuterium oxide and of hydrogen sulfide in water have been determined with 0.1% accuracy between 0 and 50 °C. Solubility equations are derived and the solubility standard thermodynamic function changes, together with their standard errors, are tabluated. Equal solubilities would occur at −1 °C. The solubility of hydrogen sulfide in water is greater than for deuterium sulfide in deuterium oxide, the solubility difference increases to a maximum at 40 °C and thence decreases at higher temperatures.

Un nouvel appareil permettant la mesure de la solubilité du sulfure de deutérium dans l'oxyde de deutérium et celle du sulfure d'hydrogène dans l'eau entre 0 et 50 °C avec une précision de 0.1% est décrit. Les équations de solubilité sont dérivées et les changements des fonctions thermodynamiques standards de solubilité de même que leurs erreurs standards sont présentés sous forme de tableau. Les solubilités seraient égales à −1 °C. La solubitilé du sulfure d'hydrogène dans l'eau est plus grande que celle du sulfure de deutérium dans l'oxyde de deutérium, la différence de solubilité passe par un maximum à 40 °C et décroit par la suite aux températures plus élevées.

Canadian Journal of Chemistry, 49, 691 (1971)

Introduction

In the evaluation of thermodynamic functions for the formation of deuterium sulfide deuterate (1), we required values for the solubility of deuterium sulfide in deuterium oxide. It seemed that this solubility might be obtained by the application of isotope effect correction factors to the well-known solubility of hydrogen sulfide in water (2). A literature search was made to find the magnitude, direction, and temperature coefficient for these isotope effects.

Carbon dioxide at 25 °C is equally soluble in water and deuterium oxide (3). The methyl halides are more soluble in water at 30 °C, except for methyl fluoride which is more soluble in deuterium oxide (4). At higher temperatures all methyl halides showed an increasing preference for dissolution in deuterium oxide. The hydrocarbons *n*-heptane, cyclohexane, and toluene are more soluble in water than in deuterium oxide at 60 to 90 °C and also show an increasing preference for dissolution in deuterium oxide at higher temperatures (5). Argon, however, is more soluble in deuterium oxide than in water at 25 °C and shows a decreasing preference for dissolution in deuterium oxide at higher temperatures (6). Evidently no reliable estimate of aqueous solution isotope effects can be made at present.

To measure the small solubility differences between deuterium sulfide in deuterium oxide and hydrogen sulfide in water we have designed and constructed a new solubility apparatus capable of 0.1% accuracy in the 0–50 °C temperature range.

Experimental

Materials

Water was laboratory distilled. Deuterium oxide contained 0.25 weight% protium oxide as supplied by Atomic Energy of Canada, Limited. Hydrogen and deuterium sulfides were prepared as previously described (7).

A diagram of the solubility apparatus is shown in Fig. 1. All tubing, fittings, and diaphragm valves were made of type-316 stainless steel which was found to resist corrosion. Only vessels B, C, D, and E were made of Pyrex glass and these were fused to capillary tubing and attached to the apparatus via 1/4 in. Swagelok fittings using Teflon front and nylon back ferrules.

Apparatus Calibration

In preliminary experiments the volume of the precision variable piston, A (stainless steel volumetric micrometer, Volumetrics Incorporated), was calibrated by weighing water, using the density compilation of Dorsey (8). At 25 °C over its 200 cm^3 range the standard error on a single volume determination was 0.013 cm^3.

The 130-cm^3 solubility cell B, containing magnetic stirring bar, and the 55-cm^3 vessels C, D, and E were immersed in a thermostat bath controlled to ±0.0015 °C. The bath temperature adjacent to the solubility cell was measured with a precision of 0.001 °C by a platinum resistance thermometer in conjunction with a Mueller bridge, amplifier, and galvanometer. Pressure was measured with an accuracy of 0.02% by a 0–16 p.s.i. range Texas Instruments Incorporated fused quartz precision Bourdon

[1]Contribution No. 187.

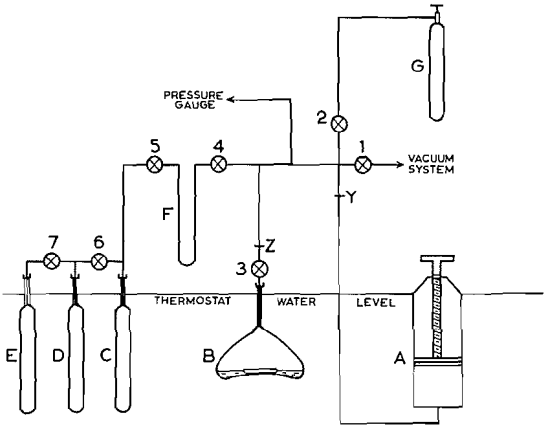

FIG. 1. Solubility apparatus.

gauge. The gauge was calibrated against a wide-bore mercury manometer, for which the column height difference was determined by cathetometer comparison against a meter standard. The apparatus not immersed in the thermostat bath was at room temperature (26 °C) for solubilities below 27 °C, or was heated by infrared lamps to about 60 °C for solubilities above 27 °C.

The volumes of B, C, D, and E at each experimental temperature were determined by isopiestic displacement of nitrogen from A. The variable piston A, set to maximum volume, was attached via capillary tubing to the apparatus at Y. The system was evacuated with valves *1*, *4*, *5*, *6*, and *7* open, and all others closed. After closing valves *7*, *6*, and *5* dry nitrogen was admitted through *1* until the pressure reached about atmospheric when *1* was closed and the pressure measured. Valve *5* was opened and A adjusted to restore the pressure to its original value. The volume difference of A was equal to the volume equivalent of C and its connections at thermostat temperature. Valve *6* was opened and A adjusted to restore the same pressure: this volume change of A gave the volume equivalent of D and its connections at thermostat temperature. Valve *7* was opened and the procedure repeated for the volume equivalent of E. At each experimental temperature the C, D, and E volumes were determined three times with a standard error of less than 0.010 cm^3. The volume equivalent of the solubility cell B below valve *3* was similarly determined with the same accuracy. The variable volume was then detached and the system plugged at Y. The volume between valves *1*, *2*, *3*, and *5*, including F and the pressure gauge, was calibrated with a standard error of 0.02 cm^3 by three separate nitrogen expansions into C.

The temperature scales are related by 0 °C ≡ 273.15 K, and the gas constant R is taken as 1.98717 thermochemical cal/mol deg (9). The International Practical Temperature Scale of 1948 defines the Celsius temperature.

Solubility Measurement

The evacuated solubility cell B with *3* closed was detached from the apparatus at Swagelok fitting Z and weighed. Approximately 23 cm^3 of water or deuterium oxide were sucked into B. The liquid was degassed at ambient temperature by evacuation for 10 min with vigorous stirring leaving about 21 cm^3 in B, which was reweighed and reattached at Z. Cylinder G containing hydrogen or deuterium sulfide was immersed in liquid nitrogen and the apparatus evacuated to 0.005 Torr with all valves open except *3*. After closing *1* the liquid nitrogen was removed from G and the vapor pressure rose to a predetermined value at which *2* and the cylinder valve were closed. The equilibrium pressure and temperature were measured The quantity of gas taken was such that the pressure ranged from ~ 720 Torr at 0 °C to ~ 530 Torr at 50 °C. The glass-covered stirring bar in B was activated by an air-driven magnetic stirrer (not shown). Valve *3* was opened and after about 20 min stirring the equilibrium pressure and temperature were measured, after which *4* was closed. U-tube F was immersed in liquid nitrogen for 10 min, *7* was closed and F was then heated to ambient temperature. Valve *4* was reopened and after about 20 min stirring the equilibrium pressure and temperature were measured. Valve *4* was closed, F immersed in liquid nitrogen for 10 min, *6* closed, F heated to ambient, *4* opened, and after 20 min stirring the equilibrium pressure and temperature were measured. Finally, *4* was closed, F cooled in liquid nitrogen for 10 min, *5* closed, F heated to ambient, *4* opened, and after 20 min stirring the equilibrium pressure and temperature were measured. In each experiment the known weight of water and volume of hydrogen sulfide were brought to pressure equilibrium four times, making successive transfers of dry hydrogen sulfide from E + D + C + F to D + C + F to C + F to F in such a manner to limit the water vapor to B below *3*.

Results and Discussion

Solubility is expressed as the Henry Law constant $H = f_2/a_2$ in which f_2 is the solute vapor fugacity in atm and a_2 its equilibrium solution activity. The activity is defined by $a_2 = x_2 \exp (P - 1)\bar{v}_2/RT$ in which x_2 is the mole fraction of unionized solute in solution, $\bar{v}_2$ its partial molar volume, and P the total pressure. The fugacities and volumetric properties of all components are evaluated from the Redlich–Kwong (10) equation of state

$$[1] \qquad (P + a/T^{1/2}V(V + b))(V - b) = RT$$

At our experimental pressures of 350–750 Torr these properties are relatively insensitive to the values taken for the covolume b. For hydrogen and deuterium sulfides b_{22} was taken as 35.91, and for water and deuterium oxide b_{11} was 18.02 cm^3/mol. The hydrogen sulfide a_{22} was 9.613×10^7 $(cm^2/mol)^2$ atm $(°K)^{1/2}$, derived from the least squares fit of the P–V–T data of Wright and Maass (11). The deuterium sulfide a_{22} was 9.592×10^7 obtained taking the same ratio to the hydrogen sulfide value as in our earlier

Can. J. Chem. Downloaded from www.nrcresearchpress.com by 210.87.254.5 on 09/05/12
For personal use only.

work (7). The water-vapor a_{11} was 54.39×10^7 $(cm^2/mol)^2$ atm $(°K)^{1/2}$, derived from a least-squares fit of P–V–T data supplied by Liley (12); the same a_{11} value was taken for deuterium oxide.

Values of the Redlich–Kwong constants for the binary vapor mixtures, hydrogen sulfide – water and deuterium sulfide – deuterium oxide were calculated from the pure-component values using the relations (13),

$$[2] \quad a_{12} = 0.875\,(a_{11}a_{22})^{1/2}$$

$$[3] \quad b_{12} = (b_{11}b_{22})^{1/2}$$

$$[4] \quad a_m = a_{11}y_1^2 + 2a_{12}y_1y_2 + a_{22}y_2^2$$

$$[5] \quad b_m = b_{11}y_1^2 + 2b_{12}y_1y_2 + b_{22}y_2^2$$

in which y_1 and y_2 are the component mole fractions and a_m and b_m are the constants for the vapor mixture. The factor of 0.875 in [2] was assessed for systems containing hydrogen sufide from the work of Spear, Robinson, and Chao (13). The component fugacities and molar volumes were evaluated by standard methods (10) from [1] using the mixing laws [2]–[5].

For the fugacity f_1 in a binary mixture we obtain

$$[6] \quad \ln f_1 = \ln\left(\frac{RTy_1}{(V-b_m)}\right) + \frac{b_{11} + (2b_{12} - b_{11} - b_{22})y_2^2}{(V-b_m)} - \frac{2(a_{11}y_1 + a_{12}y_2)}{b_mRT^{3/2}}\ln\left(\frac{V+b_m}{V}\right) + \frac{a_m(b_{11} + [2b_{12} - b_{11} - b_{22}]y_2^2)}{b_m^2RT^{3/2}}\left\{\ln\left(\frac{V+b_m}{V}\right) - \frac{b_m}{V+b_m}\right\}$$

with a similar expression for the second component.

Figure 2 illustrates the equilibria attained in cell B during solubility measurement. An iterative computer program was written which took the solubility total pressure P with the water vapor pressure to yield initial values for the water and hydrogen sulfide vapor mixture mole fractions y_1 and y_2, and fugacities f_1 and f_2. Taking this f_2 with a preselected value of H we obtained the unionized hydrogen sulfide solution

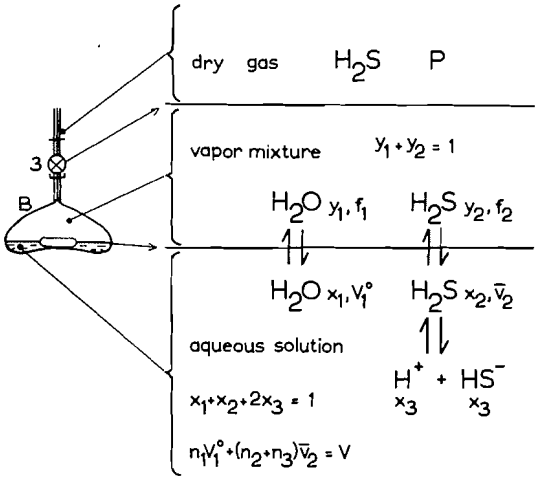

FIG. 2. Equilibria established in solubility cell.

mole fraction x_2, which was used to calculate the mole fraction of hydrosulfide ions x_3 (14), and thence obtained the water mole fraction x_1 from the relation $x_1 + x_2 + 2x_3 = 1$. Using x_1 with the pure water activity a new value was obtained for the water vapor fugacity f_1. The value of y_1 was iterated to obtain coincidence of the values of f_1 from the vapor and solution phases. In this manner we obtained values for the vapor and liquid phase compositions at total pressure P, consistent with the preselected value of H. The number of moles of hydrogen sulfide, dissolved in the water, contained in the mixed vapor phase in B, and in the dry state beyond *3* in F and etc., was compared with the known initial number of moles of hydrogen sulfide. The square of this difference of moles of hydrogen sulfide was minimized to zero by iteration of H. In this manner we obtained the unique value of H consistent with all experimental quantities for the solubility measurement at P. Similarly the three other solubility pressures each gave a value for H. To obtain the best H for the whole experiment the iteration was performed minimizing the sum of squares of the mole differences for the four solubility pressures.

The ionization of hydrogen sulfide in water was determined from the equation

$$[7] \quad \log_{10} K_{H_2S} = 55.06 - 3760/T - 20\log_{10} T$$

Can. J. Chem. Downloaded from www.nrcresearchpress.com by 210.87.254.5 on 09/05/12
For personal use only.

TABLE 1. Pressure, fugacity, and phase compositions for hydrogen sulfide solubility in water

t (°C)	P (atm)	f_2 (atm)	f_1 (atm)	y_2	$x_2 \times 10^3$	$x_3 \times 10^6$	H_{H_2S} (atm)
0.001	0.53985	0.53084	0.00601	0.98864	2.0189	1.14	263.18
0.001	0.64663	0.63635	0.00601	0.99048	2.4198	1.25	263.16
0.000	0.81496	0.80220	0.00601	0.99240	3.0497	1.40	263.01
4.956	0.49205	0.48108	0.00857	0.98228	1.5515	1.11	310.51
4.958	0.57457	0.56275	0.00857	0.98478	1.8146	1.20	310.21
4.955	0.69533	0.68202	0.00856	0.98738	2.1988	1.32	310.43
4.955	0.89032	0.87404	0.00856	0.99008	2.8171	1.50	310.11
10.019	0.46154	0.44737	0.01211	0.97334	1.2365	1.09	362.21
10.018	0.54041	0.52551	0.01211	0.97717	1.4522	1.18	362.01
10.019	0.65667	0.64048	0.01211	0.98115	1.7697	1.31	362.25
10.019	0.84654	0.82772	0.01210	0.98529	2.2864	1.49	361.94
15.008	0.57265	0.55280	0.01680	0.97010	1.3234	1.24	418.17
15.008	0.70044	0.67914	0.01680	0.97546	1.6255	1.37	418.11
15.006	0.91275	0.88843	0.01679	0.98105	2.1258	1.57	417.65
20.010	0.49456	0.46925	0.02304	0.95265	0.9847	1.16	477.44
20.011	0.58325	0.55711	0.02304	0.95975	1.1689	1.27	476.72
20.011	0.71673	0.68910	0.02304	0.96712	1.4456	1.41	477.10
20.009	0.94115	0.91036	0.02303	0.97479	1.9091	1.62	476.32
25.018	0.55244	0.51844	0.03122	0.94250	0.9616	1.25	540.07
25.016	0.66766	0.63249	0.03122	0.95227	1.1729	1.38	539.74
25.015	0.85319	0.81570	0.03121	0.96245	1.5122	1.56	538.73
25.018	0.58192	0.54764	0.03122	0.94536	1.0162	1.28	539.64
25.017	0.71834	0.68258	0.03122	0.95557	1.2663	1.43	539.79
25.017	0.95039	0.91146	0.03121	0.96620	1.6904	1.65	538.32
25.030	0.55377	0.51974	0.03124	0.94259	0.9645	1.25	539.12
25.029	0.68442	0.64903	0.03124	0.95338	1.2042	1.39	539.07
25.031	0.90833	0.87002	0.03123	0.96465	1.6137	1.61	539.49
29.995	0.56822	0.52353	0.04175	0.92521	0.8680	1.27	603.29
29.992	0.70403	0.65794	0.04175	0.93942	1.0907	1.43	604.07
29.995	0.93731	0.88816	0.04174	0.95421	1.4719	1.66	603.09
39.991	0.49072	0.41580	0.07250	0.84998	0.5616	1.17	741.34
39.991	0.61249	0.53649	0.07250	0.87943	0.7245	1.33	740.86
39.992	0.82651	0.74812	0.07249	0.91016	1.0100	1.57	740.57
49.987	0.54699	0.42269	0.12099	0.77499	0.4801	1.22	880.80
49.984	0.68605	0.56039	0.12099	0.82000	0.6364	1.40	882.07
49.985	0.93305	0.80438	0.12097	0.86687	0.9132	1.68	880.08

given by Ellis and Milestone (14) with K_{H_2S} in molarity units and T in degrees absolute. From the difference of ionization constants for the deuterium and protium acids (16) and assuming a constant ratio between H_2S and D_2S, we obtain the equation

$$[8]\quad \log_{10} K_{D_2S} = 54.50 - 3760/T - 20 \log_{10} T$$

for the ionization of deuterium sulfide in deuterium oxide. The effect of the second ionizations for hydrogen and deuterium sulfides is negligible.

The volume of the aqueous solution was taken as $n_1 V_1^0 + 34(n_2 + n_3)$, in which V_1^0 is the pure water molar volume in cm^3, 34 cm^3 is the partial molar volume, $\bar{v}_2$, assumed to be temperature-invariant for hydrogen sulfide in water (15), and n_1, n_2, and n_3 are the number of moles of water, unionized hydrogen sulfide, and hydrosulfide ion in solution. The value of n_1 is smaller than the total number of moles of water by the amount present as vapor in B. The partial molar volume of deuterium sulfide in deuterium oxide was taken as 34 cm^3, the same as for hydrogen sulfide.

Vapor pressures and volumetric properties of water were taken from Dorsey (8), those for deuterium oxide from the critical review by Whalley (17).

In Table 1 are presented the individual temperature and pressure measurements, the derived fugacities, phase compositions, and Henry's Law constants for the solubility of hydrogen sulfide in water. The individual solubility measurements for deuterium sulfide in deuterium oxide are presented in Table 2.

New solubility measurements for hydrogen sulfide in water between 0 and 50 °C are presented in Table 3, together with calculated values from the best (18) representative equation

Can. J. Chem. Downloaded from www.nrcresearchpress.com by 210.87.254.5 on 09/05/12
For personal use only.

TABLE 2. Pressure, fugacity, and phase compositions for deuterium sulfide solubility in deuterium oxide

t (°C)	P (atm)	f_2 (atm)	f_1 (atm)	y_2	$x_2 \times 10^3$	$x_3 \times 10^6$	H_{D_2S} (atm)
4.954	0.46205	0.45286	0.00709	0.98441	1.4489	0.56	313.07
4.953	0.53869	0.52876	0.00709	0.98659	1.6916	0.61	312.58
4.954	0.65058	0.63937	0.00709	0.98886	2.0451	0.67	312.84
4.953	0.83037	0.81661	0.00708	0.99122	2.6113	0.76	312.70
4.969	0.48660	0.47716	0.00711	0.98514	1.5266	0.58	312.86
4.969	0.56686	0.55661	0.00711	0.98721	1.7806	0.63	312.61
4.971	0.68365	0.67200	0.00711	0.98935	2.1493	0.69	312.96
4.970	0.87050	0.85607	0.00710	0.99159	2.7373	0.78	312.76
10.012	0.49623	0.48372	0.01016	0.97917	1.3152	0.59	368.17
10.011	0.58177	0.56841	0.01016	0.98219	1.5453	0.64	367.82
10.011	0.70846	0.69360	0.01016	0.98531	1.8853	0.71	368.35
10.011	0.91626	0.89831	0.01016	0.98857	2.4409	0.81	367.92
10.016	0.49103	0.47857	0.01016	0.97895	1.3017	0.59	368.13
10.017	0.57614	0.56285	0.01016	0.98201	1.5308	0.64	367.86
10.017	0.70225	0.68747	0.01016	0.98519	1.8694	0.71	368.07
10.015	0.90982	0.89199	0.01016	0.98849	2.4248	0.80	367.60
14.996	0.49292	0.47636	0.01430	0.97051	1.1202	0.60	425.51
14.995	0.58044	0.56305	0.01430	0.97489	1.3239	0.65	425.58
14.994	0.71133	0.69245	0.01430	0.97943	1.6278	0.72	425.82
14.992	0.92970	0.90768	0.01429	0.98416	2.1331	0.83	425.35
14.998	0.50118	0.48455	0.01430	0.97098	1.1375	0.60	426.70
14.999	0.58946	0.57197	0.01430	0.97526	1.3425	0.66	426.27
14.998	0.72127	0.70226	0.01430	0.97970	1.6480	0.73	426.45
14.997	0.94014	0.91795	0.01429	0.98433	2.1535	0.83	425.75
20.015	0.47451	0.45258	0.01987	0.95748	0.9288	0.59	488.06
20.017	0.56008	0.53739	0.01987	0.96388	1.1027	0.65	487.12
20.018	0.68930	0.66523	0.01987	0.97054	1.3647	0.72	487.94
20.017	0.90742	0.88041	0.01986	0.97748	1.8056	0.83	487.52
25.002	0.53870	0.50893	0.02718	0.94869	0.9207	0.64	552.92
25.001	0.65900	0.62804	0.02717	0.95792	1.1360	0.71	553.61
25.000	0.85875	0.82531	0.02717	0.96752	1.4924	0.82	552.78
25.003	0.55844	0.52849	0.02718	0.95048	0.9577	0.65	551.90
25.003	0.68292	0.65169	0.02717	0.95936	1.1807	0.73	552.79
25.003	0.88929	0.85541	0.02717	0.96861	1.5494	0.83	551.86
25.004	0.46306	0.43391	0.02719	0.94042	0.7867	0.59	552.79
25.005	0.54848	0.51861	0.02719	0.94958	0.9401	0.65	551.67
25.006	0.67873	0.64754	0.02718	0.95911	1.1736	0.72	552.34
25.005	0.90170	0.86763	0.02718	0.96902	1.5721	0.84	551.19
29.991	0.55882	0.51929	0.03676	0.93309	0.8361	0.66	621.27
29.991	0.69356	0.65267	0.03675	0.94589	1.0506	0.74	622.10
29.991	0.92605	0.88218	0.03674	0.95922	1.4196	0.86	621.08
29.998	0.62235	0.58221	0.03675	0.93982	0.9373	0.70	621.17
29.997	0.77226	0.73045	0.03675	0.95130	1.1757	0.78	622.14
29.996	1.03080	0.98533	0.03674	0.96326	1.5853	0.91	621.18
39.984	0.43164	0.36483	0.06494	0.84752	0.4797	0.57	761.39
39.982	0.51421	0.44676	0.06493	0.87173	0.5874	0.63	759.73
39.983	0.64240	0.57379	0.06493	0.89699	0.7543	0.71	761.57
39.983	0.86778	0.79658	0.06492	0.92331	1.0469	0.84	761.47
49.991	0.54232	0.42928	0.10994	0.79389	0.4746	0.64	905.21
49.991	0.68071	0.56635	0.10993	0.83525	0.6260	0.73	904.75
49.990	0.92773	0.81043	0.10992	0.87840	0.8956	0.87	905.12

[9] $$\log_{10} H_{H_2S}\ (\text{atm}) = 104.06904 - 4423.113/T - 36.62959 \log_{10} T + 0.0138700T$$

with H_{H_2S} in normal atmosphere (9) and T absolute. The percentage differences between observed and calculated Henry's Law constants, H_{H_2S}, lead to a standard error of 0.069% on a single determination. The percentage differences of the data from eq. 9 are plotted in Fig. 3. The final column of the table gives the percentage standard error on H_{H_2S} evaluated from eq. 9.

To check our experimental procedure three experiments were conducted at 25 °C under widely different conditions. The experiment at 25.030 °C was made with infrared heating of the

Can. J. Chem. Downloaded from www.nrcresearchpress.com by 210.87.254.5 on 09/05/12
For personal use only.

TABLE 3. Solubility of hydrogen sulfide in water

Temperature (°C)	Henry's law constant, H_{H_2S} Observed (atm)	Calculated (atm)	Difference (%)	Error on calculated H_{H_2S} (%)
0.001	263.12	263.19	−0.029	0.062
4.956	310.32	310.11	+0.065	0.038
10.019	362.10	362.33	−0.064	0.038
15.007	417.97	417.73	+0.059	0.036
20.010	476.89	476.88	+0.001	0.029
25.016	539.51	539.27	+0.044	0.028
25.017	539.24	539.28	−0.007	0.028
25.030	539.23	539.45	−0.041	0.028
29.994	603.48	604.02	−0.089	0.035
39.991	740.91	740.24	+0.090	0.045
49.985	880.96	881.20	−0.028	0.066

TABLE 4. Comparison of hydrogen sulfide solubility measurements

T (°C)	$x_2/p_2 \times 10^6$ (Torr^{-1}) Wright and Maass	This work
5	4.22	4.20
10	3.62	3.60
15	3.14	3.13
20	2.75	2.74
25	2.43	2.42
30	2.18	2.16
40	1.79	1.77
50	1.52	1.49

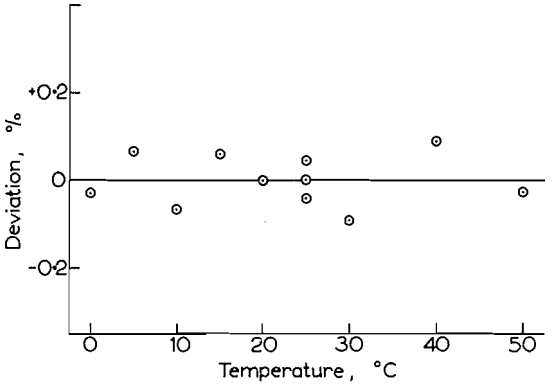

FIG. 3. Deviations from eq. 9 of Henry's law constants for hydrogen sulfide solubility in water.

unthermostatted parts of the apparatus, while that at 25.017 °C was made without heating. The experiment at 25.016 °C was made using 41 g water, double the usual amount. The correctness of our solubility method is demonstrated by the very good agreement of these experiments with each other and with eq. 9.

The hydrogen sulfide solubility work of Wright and Maass (2) provides insufficient data to calculate H_{H_2S} so that in Table 4 we compare our measurements with their x_2/p_2 values. Good agreement is found. The measurements of Selleck, Carmichael, and Sage (19) at 37.8 °C are unreliable and give H_{H_2S} values varying between 640 and 780 atm compared with our value of 709.5 ± 0.3 from eq. 9.

Unique solubility measurements for deuterium sulfide in deuterium oxide between 5 and 50 °C are presented in Table 5, together with calculated values from the best (18) representative equation

$$[10] \quad \log_{10} H_{D_2S}\,(\text{atm}) = 137.39155 - 5463.378/T - 49.56328 \log_{10} T + 0.0211857T$$

The percentage differences of the measurements from eq. 10, plotted in Fig. 4, lead to a standard error of 0.12% on a single solubility determination. We do not know why this error

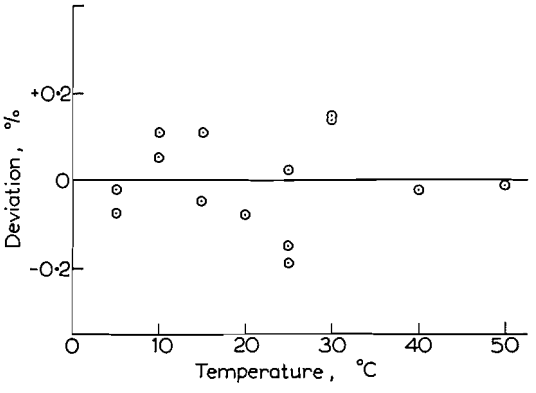

FIG. 4. Deviations from eq. 10 of Henry's law constants for deuterium sulfide solubility in deuterium oxide.

Can. J. Chem. Downloaded from www.nrcresearchpress.com by 210.87.254.5 on 09/05/12
For personal use only.

TABLE 5. Solubility of deuterium sulfide in deuterium oxide

Temperature (°C)	Henry's law constant H_{D_2S} Observed (atm)	Calculated (atm)	Difference (%)	Error on calculated H_{D_2S} (%)
4.954	312.80	312.86	−0.020	0.079
4.970	312.80	313.03	−0.073	0.078
10.011	368.06	367.65	+0.111	0.050
10.016	367.92	367.71	+0.055	0.050
14.994	425.56	425.77	−0.048	0.054
14.998	426.29	425.82	+0.111	0.054
20.017	487.66	488.04	−0.078	0.049
25.001	553.10	552.97	+0.024	0.044
25.003	552.18	553.00	−0.148	0.044
25.005	551.99	553.03	−0.188	0.044
29.991	621.48	620.56	+0.149	0.055
29.997	621.50	620.64	+0.138	0.055
39.983	761.05	761.22	−0.021	0.076
49.991	905.02	905.12	−0.010	0.115

is nearly twice that for the hydrogen sulfide measurements and conclude that the standard error for our solubility method is about 0.10%.

The H_{D_2S}/H_{H_2S} ratio is plotted against temperature in Fig. 5. Extrapolated solubilities are equal at about − 1 °C, above which hydrogen sulfide is more soluble in water than deuterium sulfide in deuterium oxide. A maximum ratio of 1.028_5 is attained near 40 °C.

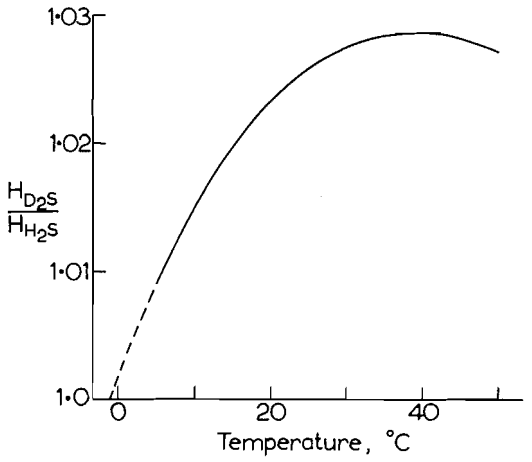

FIG. 5. Temperature effect on the Henry's law constant ratio H_{D_2S}/H_{H_2S}.

Standard Thermodynamic Functions for Solute Evolution

The solute evolution equilibrium constant H (atm) at total pressure P and T absolute is defined by the relation

$$[11] \quad \ln H = \Delta G^0/(-RT) = \ln f_2 - \ln x_2 - (P - 1)\bar{v}_2/RT$$

in which ΔG^0 is the standard free energy change for the transfer of 1 mol of solute from solution at unit mole fraction and 1 atm pressure to give vapor at 1 atm fugacity. The standard thermodynamic function changes, the enthalpy ΔH^0, entropy ΔS^0, heat capacity ΔC_p^0, and its temperature derivative $d\Delta C_p^0/dT$, together with their errors, are evaluated by treating the ln H values from eq. 11 according to the method of Clarke and Glew (18). Tables 6 and 7 present values for the standard thermodynamic function changes, together with their standard errors σ, between 0 and 50 °C for hydrogen sulfide evolution from water and for deuterium sulfide from deuterium oxide. Proper representation of our solubility measurements required use of the $d\Delta C_p^0/dT$ term, its value arising from chance alone with 16% probability for hydrogen sulfide in water, and with 28% probability for deuterium sulfide in deuterium oxide.

The values of $d\Delta C_p^0/dT$ agree in sign and magnitude with those found for the methane–water system (20) and with predictions from the Eley model. This model predicts that the value of ΔC_p^0 at 25 °C should be about 20% larger in deuterium oxide than in water and our experimental value is larger by 16 ± 2%. At 5 °C the enthalpy change for deuterium sulfide evolution from deuterium oxide is 4.1% larger than for hydrogen sulfide evolution from water, at 40 °C the enthalpies are equal, and at higher temperatures the deuterium sulfide evolution has the smaller value. Literature solubilities for the

Can. J. Chem. Downloaded from www.nrcresearchpress.com by 210.87.254.5 on 09/05/12
For personal use only.

TABLE 6. Standard thermodynamic function changes for hydrogen sulfide evolution from water*

Temperature (°C)	ΔG^0 (cal/mol)		ΔH^0 (cal/mol)		ΔS^0 (cal/deg mol)		$\Delta C_p{}^0$ (cal/deg mol)	
	Value	σ	Value	σ	Value	σ	Value	σ
0.0	−3024.91	0.34	5091.2	18.9	29.713	0.068	−38.12	1.97
5.0	−3171.75	0.21	4902.2	10.6	29.027	0.038	−37.48	1.58
10.0	−3315.23	0.22	4716.4	5.2	28.365	0.018	−36.85	1.19
15.0	−3455.44	0.21	4533.7	4.6	27.726	0.016	−36.21	0.81
20.0	−3592.52	0.17	4354.2	6.2	27.108	0.021	−35.58	0.46
25.0	−3726.56	0.17	4177.9	6.8	26.512	0.023	−34.95	0.32
30.0	−3857.67	0.21	4004.8	6.0	25.936	0.020	−34.31	0.56
35.0	−3985.95	0.26	3834.8	4.9	25.380	0.016	−33.68	0.92
40.0	−4111.50	0.28	3668.0	7.1	24.843	0.023	−33.04	1.31
45.0	−4234.41	0.29	3504.4	13.3	24.324	0.042	−32.41	1.70
50.0	−4354.77	0.43	3343.9	22.3	23.824	0.070	−31.77	2.09

*$d\Delta C_p{}^0/dT = 0.127 \pm 0.080$ cal/deg² mol.

TABLE 7. Standard thermodynamic function changes for deuterium sulfide evolution from deuterium oxide*

Temperature (°C)	ΔG^0 (cal/mol)		ΔH^0 (cal/mol)		ΔS^0 (cal/deg mol)		ΔCp^0 (cal/deg mol)	
	Value	σ	Value	σ	Value	σ	Value	σ
0.0	−3025.83	1.04	5328.3	49.3	30.584	0.177	−45.53	4.45
5.0	−3176.70	0.43	5103.0	29.7	29.767	0.106	−44.56	3.62
10.0	−3323.56	0.28	4882.6	14.9	28.982	0.053	−43.59	2.79
15.0	−3466.57	0.31	4667.1	7.2	28.227	0.025	−42.63	1.98
20.0	−3605.88	0.28	4456.4	9.2	27.502	0.031	−41.66	1.21
25.0	−3741.64	0.26	4250.5	11.6	26.806	0.039	−40.69	0.65
30.0	−3873.98	0.33	4049.5	11.2	26.137	0.037	−39.72	0.89
35.0	−4003.05	0.43	3853.3	9.1	25.495	0.030	−38.75	1.61
40.0	−4128.98	0.47	3662.0	11.9	24.879	0.038	−37.78	2.41
45.0	−4251.89	0.50	3475.6	23.3	24.289	0.074	−36.81	3.23
50.0	−4371.91	0.74	3293.9	40.4	23.722	0.127	−35.84	4.05

*$d\Delta C_p{}^0/dT = 0.194 \pm 0.168$ cal/deg² mol.

same solute in water and deuterium oxide (3–6) exhibit no consistent preference for either solvent and no consistent trend of isotope effect with temperature. The maximum of solubility isotope effect found in this work, analogous to that for the vaporization of the pure liquids (7), has not been reported previously.

1. E. C. W. CLARKE and D. N. GLEW. Unpublished data.
2. R. H. WRIGHT and O. MAASS. Can. J. Res. **6B**, 94 (1932).
3. J. CURRY and C. L. HAZELTON. J. Amer. Chem. Soc. **60**, 2771 (1938).
4. C. G. SWAIN and E. R. THORNTON. J. Amer. Chem. Soc. **84**, 822 (1962).
5. A. N. GUSEVA and E. I. PARNOV. Radiokhimiya. **5**, 507 (1963).
6. A. BEN-NAIM. J. Chem. Phys. **42**, 1512 (1965).
7. E. C. W. CLARKE and D. N. GLEW. Can. J. Chem. **48**, 764 (1970).
8. N. E. DORSEY. Properties of Ordinary Water-Substance. Reinhold Publishing Corp., New York. 1940.
9. Nat. Bur. Std. Tech. News Bull. **47**, 175 (1963).
10. O. REDLICH and J. N. S. KWONG. Chem. Rev. **44**, 233 (1949).
11. R. H. WRIGHT and O. MAASS. Can. J. Res. **5B**, 442 (1931).
12. P. E. LILEY. Private communication.
13. R. R. SPEAR, R. L. ROBINSON, Jr., and K. C. CHAO. Ind. Eng. Chem. Fund. **8**, 2 (1969).
14. A. J. ELLIS and N. B. MILESTONE. Geochem. Cosmochim. Acta, **31**, 615 (1967).
15. J. STALONY-DOBRZANSKI. Roczniki Chem. Polon. **17**, 353 (1937).
16. M. PAABO and R. G. BATES. J. Phys. Chem. **74**, 706 (1970).
17. E. WHALLEY. Proc. Conf. Thermodynamic and Transport Properties Fluids, London. 1957, 15 (Institution of Mechanical Engineers, London 1958).
18. E. C. W. CLARKE and D. N. GLEW. Trans. Faraday Soc. **62**, 539 (1966).
19. F. T. SELLECK, L. T. CARMICHAEL, and B. H. SAGE. Ind. Eng. Chem. **44**, 2219 (1952).
20. D. N. GLEW. J. Phys. Chem. **66**, 605 (1962).

Can. J. Chem. Downloaded from www.nrcresearchpress.com by 210.87.254.5 on 09/05/12
For personal use only.

The Reaction of Carbon Disulfide with Aziridine Complexes of Nickel(II)

B. JACK MCCORMICK, ROY I. KAPLAN, AND BENJAMIN P. STORMER
Department of Chemistry, West Virginia University, Morgantown, W.Va. 26506

Received August 31, 1970

Carbon disulfide has been shown to undergo insertion reactions with $[Ni(aziridine)_{4,6}]^{2+}$ and $[Ni(2\text{-methylaziridine})_4]^{2+}$. The diamagnetic products are formulated as planar dithiocarbamate complexes in which the heterocyclic ring remains intact. The complexes have properties which are atypical of all dithiocarbamate complexes heretofore reported, and infrared and optical spectral measurements suggest that the insertion products may be the first examples of N,S-bonded dithiocarbamate ligands. In methanol the products slowly rearrange to give S,S-bonded complexes in which the aziridine rings have been opened.

Canadian Journal of Chemistry, 49, 699 (1971)

Can. J. Chem. Downloaded from www.nrcresearchpress.com by 210.87.254.5 on 09/05/12
For personal use only.

Introduction

Most primary and secondary amines react smoothly with carbon disulfide to produce dithiocarbamic acids (1). In contrast the three-membered, heterocyclic amine aziridine (ethyleneimine) undergoes ring opening when treated with carbon disulfide to form 2-thiazolidinethione (2).

[1] 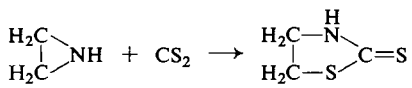

A similar reaction occurs with 2-methylaziridine (3, 4), although it has been reported in the patent literature that dithiocarbamate salts can be obtained from 2-methylaziridine, carbon disulfide, and base (5, 6). Since dithiocarbamate complexes

[2] 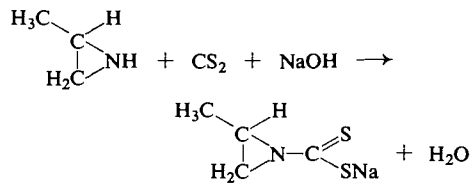

can be prepared directly from many amine complexes by carbon disulfide insertion reactions (7–10), it was of interest to investigate the reaction of carbon disulfide with aziridines coordinated to a metal ion. We report here the results of these investigations and some tentative conclusions concerning the structure of the unusual compounds formed.

Experimental

Materials

Aziridine (az) and 2-methylaziridine (meaz) were obtained from the Dow Chemical Corporation and from Matheson, Coleman and Bell, respectively. Both compounds were distilled before use. Reagent grade nickel(II) salts and carbon disulfide were used without further purification. The aziridine compounds, $Ni(az)_4SO_4$, $Ni(az)_6(NO_3)_2$, and $Ni(az)_4Cl_2$ were prepared according to Jackson and Edwards (11).

Preparation of $Ni(meaz)_4Cl_2$

To 1.0 g (0.0042 mol) of $NiCl_2 \cdot 6H_2O$ in 5 ml of ethanol was added slowly 0.92 g (0.018 mol) of 2-methylaziridine to give a blue solution of $Ni(meaz)_4Cl_2$. Cooling the solution to 0° with periodic scratching of the sides of the container resulted in the crystallization of a light blue powder which was dried and then recrystallized from absolute ethanol. The recrystallized product was dried in vacuum over P_4O_{10} for 24 h. The complex was soluble in water, methanol, and ethanol, slightly soluble in dimethyl sulfoxide and dimethyl formamide, and insoluble in acetone, ether, and methylene chloride.

Anal. Calcd. for $[Ni(C_3H_7N)_4]Cl_2$: C, 40.3; H, 7.88; N, 15.7. Found: C, 40.1; H, 7.65; N, 15.7.

Reaction of Aziridine and 2-Methylaziridine Complexes with Carbon Disulfide

The three aziridine complexes studied in this work, $Ni(az)_4SO_4$, $Ni(az)_6(NO_3)_2$, and $Ni(az)_4Cl_2$, all react with carbon disulfide to provide the same product; hence, only one such reaction will be described in detail.

A 3.3 g (0.010 mol) sample of $Ni(az)_4SO_4$ was dissolved in 50 ml of methanol to which was added 7.6 g (0.10 mol) of carbon disulfide in 10 ml of methanol. The solution rapidly went through a series of color changes from blue, through several shades of green, to brown. After about 1 min a red crystalline precipitate began to form, and after 5 min the red compound was collected on a filter, washed with 100 ml of cold methanol, and air dried for 20 min at room temperature.

Anal. Calcd. for $Ni(S_2NC_3H_4)_2$: C, 24.4; H, 2.73; N, 9.49; S, 43.5. Found: C, 24.0; H, 2.76; N, 9.30; S, 43.7.

A solution of 0.354 g (0.001 mol) of $Ni(meaz)_4Cl_2$ in 6 ml of methanol was treated with 0.315 g (0.004 mol) of carbon disulfide. Again a series of color changes was observed, the color being deep red after 5 min. This red solution was cooled in ice and the sides of the container were scratched with a glass rod, whereupon a reddish-brown, microcrystalline product formed. The analytical sample was recrystallized quickly from methanol and dried in vacuum over P_4O_{10} for 2 h.

Can. J. Chem. Downloaded from www.nrcresearchpress.com by 210.87.254.5 on 09/05/12
For personal use only.

Anal. Calcd. for $Ni(S_2NC_4H_6)_2$: C, 29.7; H, 3.74; N, 8.67; mol. wt., 323. Found: C, 28.9; H, 3.75; N, 8.62; mol. wt., 336.

Properties of Insertion Products

The compound prepared from $Ni(az)_{4,6}^{2+}$ is thermally unstable and at room temperature decomposes completely within a few hours; however, it can be stored at $-10°$ for several weeks without significant decomposition. On several occasions the compound decomposed somewhat violently upon grinding with a mortar and pestle. The complex is slightly soluble in numerous polar organic solvents, but it decomposes so rapidly as to preclude most types of solution study, *e.g.*, molecular weight determinations. Addition of the complex to pyridine at room temperature resulted in the formation of an emerald green solution, from which was deposited a brown powder after 1–2 min. The complex prepared from $Ni(meaz)_4^{2+}$ has properties very similar to those derived from $Ni(az)_{4,6}^{2+}$. In general, however, the former derivative is somewhat more stable and more soluble than the latter.

At $-15°$ dilute solutions of the compounds in methylene chloride containing pyridine (in excess) exhibit an absorption band at 8.83 kK. This band is absent in methylene chloride alone. It can be concluded that the compounds become six-coordinate and pseudo-octahedral in the presence of pyridine. Infrared studies indicate that neither compound contains N—H bonds, since bands assignable as NH stretching or deformation modes were not found.

Decomposition Reactions

In methanol, a suspension of the red aziridine derivative decomposes slowly to give a diamagnetic green material which is very slightly soluble in dimethyl sulfoxide.

Anal. Calcd. for $Ni(S_2NC_3H_5)_2$: C, 24.3; H, 3.39; N, 9.43. Found: C, 24.3; H, 3.49; N, 9.42.

A methanol solution of the 2-methylaziridine derivative behaves similarly.

Anal. Calcd. for $Ni(S_2NC_4H_7)_2$: C, 29.6; H, 4.34; N, 8.62. Found: C, 29.3; H, 4.04; N, 8.36.

Infrared spectroscopic studies clearly show the presence of NH bonds in these products; NH stretching and deformation bands were found at 3150–3200 and 1610–1620 cm^{-1}, respectively. Bands found at 1495 and 1520 cm^{-1} in the aziridine and 2-methylaziridine derivatives, respectively, are reasonably assigned as C···N stretching vibrations. This band is quite characteristic of the previously reported dithiocarbamate complexes that involve chelation through the two sulfur donors (1, 10). Electronic spectral studies also indicate that both of the decomposition products are the usual type of dithiocarbamate complex. The diffuse reflectance spectra of the samples were quite similar to that of bis(*N*,*N*-dimethyldithiocarbamato)nickel(II).

In the presence of solvents such as chloroform or carbon tetrachloride, or in the dry state, both of the red complexes decompose to black insoluble materials that have not been characterized. When the solids decompose in the dry state, there is no perceptible weight change.

Measurements

All measurements were made on freshly prepared samples, unless otherwise indicated.

Electronic spectra were measured with a Cary Model 14 spectrophotometer. Diffuse reflectance spectra were measured in conjunction with a Cary Model 1411 reflectance attachment. The reflectance standard was $MgCO_3$. The reflectance spectra of the red products were measured for samples which were held at *ca.* 0°. Solution spectra were measured as quickly as possible in order to minimize effects due to decomposition. Infrared spectra were measured with Beckman Models IR-8 and IR-12 spectrometers by using Nujol and perfluorokerosene mulls as well as KBr discs. Very concentrated samples were required to observe the carbon–hydrogen stretching frequencies in the red reaction products. Infrared and electronic spectra are shown in Figs. 1 and 2, respectively.

Magnetic susceptibility measurements were made with a Gouy balance of standard design. Both of the insertion products are diamagnetic.

The molecular weight determination was carried out with a vapor pressure osmometer using benzene as the solvent.

Elemental analyses were done by Galbraith Laboratories. In some cases the samples were packed in Dry Ice for shipment and were analyzed within a few hours of preparation.

Results and Discussion

When treated with carbon disulfide, solutions of $Ni(az)_{4,6}^{2+}$ and $Ni(meaz)_4^{2+}$ form the red complexes $Ni(S_2NC_3H_4)_2$ (**1**) and $Ni(S_2NC_4H_6)_2$ (**2**), respectively. Initially it was thought that the aziridine rings would be opened in the reactions to provide coordinated 2-thiazolidinethione groups. However, infrared studies indicate that the reaction products are not 2-thiazolidinethione complexes, since the infrared spectra of authentic samples of bis(2-thiazolidinethionato)nickel(II) (12, 13) are quite different from those of compounds **1** and **2**. Indeed, the infrared spectral studies indicate that the heterocyclic rings

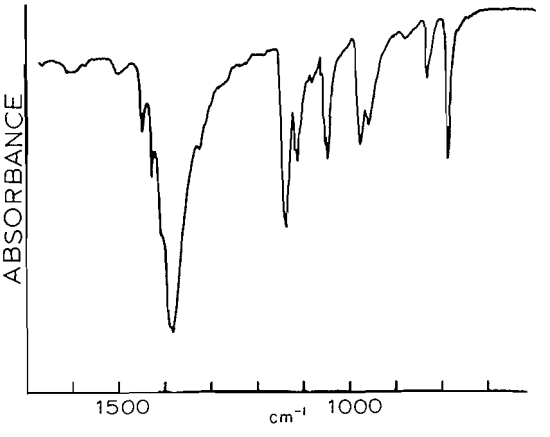

FIG. 1. Infrared spectrum of $Ni(S_2NC_3H_4)_2$ in KBr.

Can. J. Chem. Downloaded from www.nrcresearchpress.com by 210.87.254.5 on 09/05/12
For personal use only.

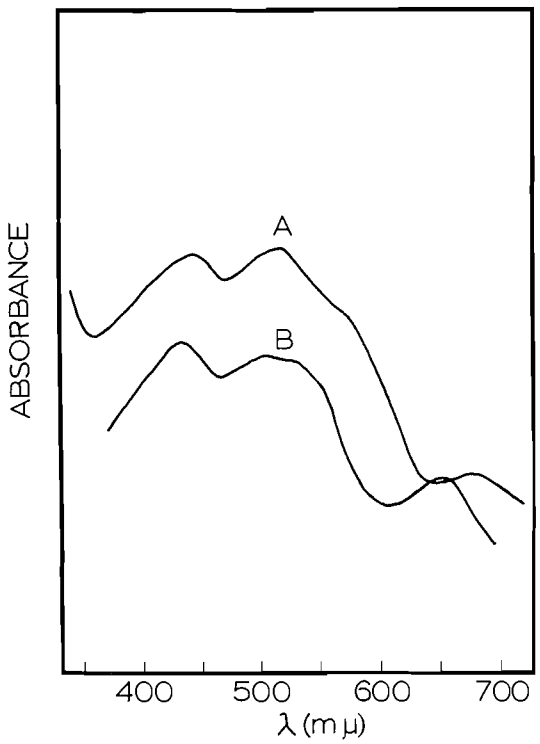

FIG. 2. Diffuse reflectance spectrum of $Ni(S_2NC_3H_4)_2$, *A*; and *B*, $Ni(S_2NC_4H_6)_2$.

remain intact in both insertion products. It has been established that C—H stretching frequencies are abnormally high in strained three membered ring systems (14). In aziridine and 2-methylaziridine C—H stretching frequencies have been assigned from 3079 to 2940 cm^{-1} (15, 16). In $Ni(az)_4SO_4$ and $Ni(meaz)_4Cl_2$ we have observed C—H stretching frequencies in the 2900–3015 cm^{-1} region. In compounds **1** and **2** corresponding weak bands are located at 2992 and 2970 cm^{-1}, respectively. Should the rings have been opened by carbon disulfide, the C—H stretching frequencies would be expected at lower energies. Since there are no N—H bonds in products **1** and **2**, as there are in the parent compounds and in 2-thiazolidinethione complexes, it is concluded that $Ni(az)_{4,6}^{2+}$ and $Ni(meaz)_4^{2+}$ undergo carbon disulfide insertion reactions [3] to provide dithiocarbamates as has been reported previously for other nickel(II)–amine complexes (10).

[3] 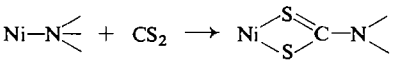

A particularly intriguing feature of compounds **1** and **2** is their red color (most nickel(II) dithiocarbamates have been described as green). Further, the infrared spectra (Fig. 1) of the insertion products suggest that they are not "normal" dithiocarbamate complexes. It is well known that canonical forms of type **A** play an important role in the description of the electronic structure of the usual type of S,S-bonded dithiocarbamate complexes (17, 18). The $(S_2)C—N$ bond order is

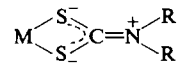

A

greater than one, and, consequently, a characteristic C⋯N stretching frequency is found as a generally broad and intense band near 1500 cm^{-1} in *N,N*-dialkyldithiocarbamate complexes (17). In product **1** there is no band near 1500 cm^{-1}, but there is a very strong broad band at 1383 cm^{-1} (Fig. 1) which is assigned as the $(S_2)C—N$ stretching frequency. The sharp weak bands at 1429 and 1450 cm^{-1} are reasonably assigned to CH_2 deformation modes (14). The infrared spectrum of product **2** is complicated in the 1300–1500 cm^{-1} region by CH_3 and CH_2 deformation modes, as well as by CH bending modes, but there is a strong band located at 1381 cm^{-1} that can be assigned as the $(S_2)C—N$ stretching frequency. Thus, the $(S_2)C—N$ bond order in the insertion products is significantly reduced from that normally observed in *N,N*-dialkyldithiocarbamate complexes. Such a significant reduction in the $(S_2)C—N$ bond order might arise in one of two ways. If the dithiocarbamate ligand should be N,S-bonded, the lone pair on the nitrogen atom would not be available for π-donation to the carbon atom. Consequently the $(S_2)C—N$ bond order would be reduced from that normally observed. If the ligands are S,S-bonded with a low contribution from canonical forms of type **A**, a low $(S_2)C—N$ bond order might also be expected. In this case the complexes would resemble those of xanthate ligands for which it is known that structures of type **B** are not of great significance (19).

In dithiocarbamate complexes that are coordinated through two sulfur atoms there nor-

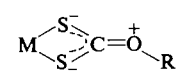

B

Can. J. Chem. Downloaded from www.nrcresearchpress.com by 210.87.254.5 on 09/05/12
For personal use only.

mally are observed three bands in the 1130–1290 cm^{-1} region which are associated with the NCS_2 group (20). This band structure is absent in compounds **1** and **2**, again suggesting that these compounds are not "normal" dithiocarbamates. It is particularly significant to point out, however, that in both compounds a band is found at 1045 cm^{-1}, which is in the region where C=S stretching frequencies are usually located (21). In a closely related complex, $Ni(CS_3)_2^{2-}$, the C=S stretch has been assigned at 1010 cm^{-1} (22). The presence of the 1045 cm^{-1} band in both complexes is strongly indicative of the presence of an uncoordinated C=S group and suggests that the complexes have structure **3** rather than **4**.

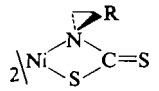

3

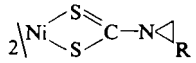

4

Sharp bands at 378 and 384 cm^{-1} in compounds **1** and **2**, respectively, can be assigned with confidence as nickel–sulfur stretching frequencies (19, 23). Compounds having structure **3** should also exhibit a nickel–nitrogen stretching frequency. Bands of moderate intensity are located in the 450–600 cm^{-1} region that can be assigned to the Ni—N stretch. However, because of the uncertainty usually associated with the assignment of metal–nitrogen frequencies (23), we are reluctant to attach any structural significance to the bands in this region.

Electronic spectral data are recorded in Fig. 2. The spectra are similar to those that have been observed previously for planar complexes such as xanthates and dithiocarbamates (24). These spectra do not provide a clear indication as to whether the complexes have structure **3** or structure **4**.

In the absence of X-ray crystallographic studies we cannot unequivocally make a choice between structures **3** and **4**. However, we believe that the data favor structure **3**, which is unique in dithiocarbamate complex chemistry. Such structures were alluded to as a "delicate problem" in 1931 by Cambi and Cagnasso (25), although all crystal structure determinations to date on dithiocarbamate complexes have revealed that coordination is through sulfur alone. There seems to be no fundamental reason for not observing simultaneous coordination through nitrogen and sulfur atoms, although N,S-bonded complexes are expected to be unstable owing to the loss in resonance stabilization energy involving canonical forms of type **A**. On the other hand, the Walsh model (26) of the bonding in aziridine, which has recently received additional experimental confirmation (27), suggests that dithiocarbamates derived from aziridines would not be expected to involve in a significant way canonical forms of type **A** because the lone-pair electrons on the nitrogen atom would be directed *away* from the carbon atom of the CS_2 moiety by 120°. In fact the expected orientation of the lone-pair renders it available for coordination, as judged from molecular models. We conclude that N,S-coordination is entirely possible because of the unique nature of the bonding in the three membered rings.

Decomposition Reactions

Suspensions of insertion products **1** and **2** in methanol slowly decompose to give green S,S-bonded dithiocarbamate complexes in which the heterocyclic rings have been opened, as judged by infrared and electronic spectral studies. These complexes appear to be polymeric and although we do not know the details of the structures, it seems plausible that the rings may open to give an unstable vinyl derivative (28) followed by polymerization, *viz.*

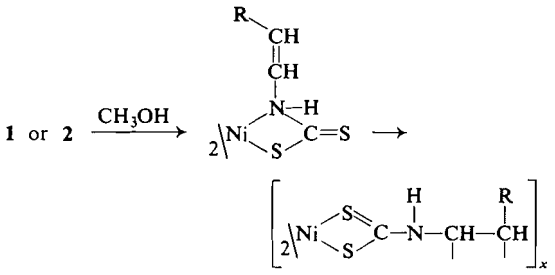

This work was supported by the National Science Foundation.

1. G. D. THORNE and R. A. LUDWIG. The Dithiocarbamates and Related Compounds. Elsevier Publ. Co., New York. 1962.
2. S. GABRIEL and C. F. VON HIRSH. Ber. **29**, 2747 (1896).
3. C. GOLUMBIC, J. S. FRUTON, and M. BERGMANN. J. Org. Chem. **11**, 518 (1946).
4. L. B. CLAPP and J. W. WATJEN. J. Amer. Chem. Soc. **75**, 1490 (1953).
5. I. WILLIAMS and B. M. STURGIS. U.S. Patent 2,290,262 (1942).
6. I. WILLIAMS and B. M. STURGIS. U.S. Patent 2,303,593 (1942).

7. D. C. BRADLEY and M. H. GITLITZ. Chem. Commun. 289 (1965).
8. D. C. BRADLEY and M. H. GITLITZ. J. Chem. Soc. A, 1152 (1969).
9. M F. LAPPERT. Advances in Organometallic Chemistry. *Edited by* F. G. A. Stone and R. West. Academic Press, Inc., New York. pp. 291–292.
10. B. J. MCCORMICK and R. I. KAPLAN. Can. J. Chem. **48**, 1876 (1970).
11. T. B. JACKSON and J. O. EDWARDS. J. Amer. Chem. Soc. **83**, 355 (1961).
12. P. P. SINGH and R. RIVEST. Can. J. Chem. **46**, 2361 (1968).
13. B. J. MCCORMICK and R. I. KAPLAN. Unpublished observations.
14. N. B. COLTHUP, L. H. DALY, and S. E. WIBERLEY. Introduction to Infrared and Raman Spectroscopy. Academic Press, Inc., New York. 1964. p. 198.
15. H. T. HOFFMAN, JR., G. E. EVANS, and G. GLOCKLER. J. Amer. Chem. Soc. **73**, 3028 (1951).
16. J. R. DURIG, S. F. BUSH, and W. C. HARRIS. J. Chem. Phys. **50**, 2851 (1969).
17. J. CHATT, L. A. DUNCANSON, and L. M. VENANZI. Suomen Kemistilehti, B**29**, 75 (1956).
18. D. COUCOUVANIS and J. P. FACKLER, JR. Inorg. Chem. **6**, 2047 (1967).
19. G. W. WATT and B. J. MCCORMICK. Spectrochim. Acta, **21**, 753 (1965).
20. M. L. SHANKARANARGANA and C. C. PATEL. Spectrochim. Acta, **21**, 95 (1965).
21. L. J. BELLAMY. Advances in Infrared Group Frequencies. Methuen and Co., Ltd., London. 1968.
22. J. P. FACKLER and D. COUCOUVANIS. J. Amer. Chem. Soc. **88**, 3913 (1966).
23. D. M. ADAMS. Metal–Ligand and Related Vibrations. St. Martin's Press, New York. 1968.
24. D. COUCOUVANIS. Progress in Inorganic Chemistry. Vol. 11. *Edited by* S. Lippard. Interscience Publishers, New York. 1970.
25. L. CAMBI and A. CAGNASSO. Alti. Accad. Linceri, **13**, 809 (1931).
26. A. D. WALSH. Trans. Faraday Soc. **45**, 179 (1949).
27. M. K. KEMP and W. H. FLYGARE. J. Amer. Chem. Soc. **90**, 6267 (1968).
28. J. D. BEHUN. Encyclopedia of Polymer Science and Technology. Vol. 1. Interscience Publishers, New York. p. 856.

Can. J. Chem. Downloaded from www.nrcresearchpress.com by 210.87.254.5 on 09/05/12
For personal use only.

Can. J. Chem. Downloaded from www.nrcresearchpress.com by 210.87.254.6 on 09/05/12
For personal use only.

The Gas Phase Raman Spectrum and Molecular Structure of Dichlorodibromotellurium(IV) $TeCl_2Br_2$. Novel Penta- and Hexa-co-ordinate Mixed Halide Anions of Tellurium(IV). Synthesis and infrared and Raman Spectra of $[Et_4N]TeCl_2Br_3$ and $[Et_4N]_2TeCl_2Br_4$

G. A. Ozin and A. Vander Voet
Department of Chemistry and Erindale College, University of Toronto, Toronto 181, Ontario

Received August 10, 1970

The Raman spectrum of gaseous $TeCl_2Br_2$ at 310 °C is reported for the first time. The gas phase data is consistent with the presence of a monomolecular species having C_1 symmetry. A synthetic route for the preparation of penta- and hexa-co-ordinate mixed halide anions of tellurium(IV), under anhydrous conditions, is described for the first time. The infrared and Raman spectra for solid $[Et_4N]TeCl_2Br_3$ and $[Et_4N]_2TeCl_2Br_4$ are reported. A stereochemistry based on a square pyramid, is favored for $[Et_4N]TeCl_2Br_3$. In the case of $[Et_4N]_2TeCl_2Br_4$ the vibrational data strongly suggests the presence of a *cis*-octahedral anion, having C_{2v} symmetry.

Le spectre Raman de $TeCl_2Br_2$ à l'état gazeux à 310 °C est décrit ici pour la première fois. Les résultats obtenus en phase gazeuse s'expliquent par la présence d'une espèce monomoléculaire de symétrie C_1. Pour la première fois, on décrit une méthode synthétique en milieu anhydre pour la préparation des anions penta- et hexacoordonnés d'halogénures mixtes de tellure(IV). Les spectres Raman et infrarouges des solides $[Et_4N]TeCl_2Br_3$ et $[Et_4N]_2TeCl_2Br_4$ sont aussi décrits. Pour $[Et_4N]TeCl_2Br_3$, la stéréochimie favorisée est une pyramide carrée. Dans le cas de $[Et_4N]_2TeCl_2Br_4$ les spectres suggèrent fortement la présence d'un anion cis-octaédrique ayant une symétrie C_{2v}.

Canadian Journal of Chemistry, 49, 704 (1971)

Dichlorodibromotellurium(IV)

Dichlorodibromotellurium(IV) $TeCl_2Br_2$ was first prepared and characterized by Aynsley (1) in 1953. Until 1968 the literature was devoid of structural information concerning this interesting mixed halide (2). $TeCl_2Br_2$ represents the only known example of a Group VI mixed tetrahalide which is sufficiently stable in the vapor phase to allow a structural investigation by gas phase laser Raman spectroscopy. By analogy with gaseous $TeCl_4$ (3–6), the species present in the vapor of $TeCl_2Br_2$ would also be expected to be molecular although suitable electron diffraction data is not available. As far as the authors can be certain, the only spectral data available for $TeCl_2Br_2$ is an infrared study of the solid and of a benzene and dimethylformamide solution (2).

The possible gas phase dissociations

$$[1] \qquad TeCl_2Br_2 \rightleftharpoons TeCl_2 + Br_2$$

$$[2] \qquad TeCl_2Br_2 \rightleftharpoons TeBr_2 + Cl_2$$

$$[3] \qquad 2TeCl_2 \rightleftharpoons Te_2 + 2Cl_2$$

$$[4] \qquad 2TeBr_2 \rightleftharpoons Te_2 + 2Br_2$$

at temperatures near and above the boiling point of $TeCl_2Br_2$ (415 °C) were found to be negligible at the temperature of our gas phase Raman experiment (310 °C). This was confirmed by the non-observation of the extremely intense and depolarized resonance fluorescence spectra of diatomic bromine, diatomic tellurium, and triatomic tellurium dibromide (7, 8) which would be expected to be observed using 4880 Å laser excitation, even for vapor pressures of Br_2, Te_2, or $TeBr_2$ of the order of less than 1 mm of Hg. Our Raman data for $TeCl_2Br_2$ (Tables 1 and 4 and Fig. 1) parallel that for $TeCl_4$ and show that the structure in the solid state differs from that in the vapor phase and in solution in C_6H_6 and MeCN in which a molecular form is probable. Let us consider the Raman data for $TeCl_2Br_2$ in the gaseous

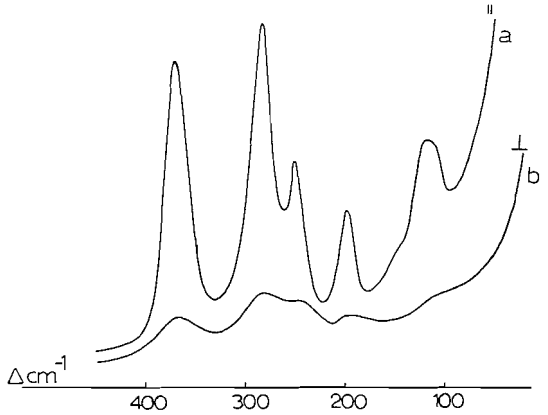

FIG. 1. The Raman spectrum of gaseous $TeCl_2Br_2$ at 310 °C: (*a*) parallel; (*b*) crossed polarization measurement.

TABLE 1. The vibrational spectrum of $TeCl_2Br_2$*

Assignment	Raman† (gas, 310 °C)	In C_6H_6 solution Raman†	In C_6H_6 solution Infrared (2)	Raman† (MeCN solution)	Infrared (2) (DMF solution)
$\nu_{TeCl_{equ}}$	370s (p)	373s (p)		¶	¶
$\nu_{TeCl_{ax}}$	285s (p)	286m (p)	279vs br	275ms (p)	¶
$\nu_{TeBr_{equ}}$	242m sh (p)	248ms (p)	255m 234m	249s (p)	246s
$\nu_{TeBr_{ax}}$	198m (p) ~ 150vw ~ 130m br (p)‡	~ 195m (p)§		194ms (p) 164ms br (p)	195s

*s = strong, m = medium, w = weak, v = very, br = broad, sh = shoulder.
†This study.
‡This band was very broad and probably consists of more than one line.
§Occurred on rising base line.
¶Region obscured by solvent.

TABLE 2. The vibrational spectrum of $(Et_4N)TeCl_2Br_3$*

Infrared (solid)	Raman (solid)	Assignment† C_s
*302*s	*304*m	a' ν_{TeCl}
*250*vs	*252*w	a'' ν_{TeCl}
~ 220m sh‡	222w sh‡	
*210*s	*204*s	a' ν_{TeBr}
*192*s		a'' ν_{TeBr}
	*163*vs	a' ν_{TeBr}
~ 144w	144w sh	
	87ms	

*Tellurium–halogen stretching modes in italics.
†The assignments to a' and a'' symmetry types are based purely on infrared and Raman band intensities.
‡Probably a Fermi doublet with 204 cm^{-1} in resonance with 87 + 144 = 231 cm^{-1} or 304 − 87 = 217 cm^{-1}.

TABLE 3. The vibrational spectrum of $(Et_4N)_2TeCl_2Br_4$*

Infrared† (solid)	Raman (solid)	Assignment C_{2v}
	330vw br	
300vw		Et_4N^+
	268vw‡	
	*243*s	ν_{TeCl}
*235*s br	~ *230*w sh	ν_{TeCl}
	*222*s	ν_{TeBr}
*185*s br	~ *185*w sh	ν_{TeBr}
	*173*s	ν_{TeBr}
	*155*s	ν_{TeBr}
	110m br	
	92s	
	70s	

*Tellurium–halogen stretching modes in italics.
†All bands below 185 cm^{-1} were very weak.
‡Probably a combination band 155 + 110 = 265.

and solution phases in terms of the most probable stereochemistries based (*a*) on a regular trigonal bipyramid with an equatorial lone pair **1**, **2**, and **3** and (*b*) similar to (*a*) but in a distorted form.

The gas and solution phase Raman data of the present study favors **3** for the following reasons.

TABLE 4. The vibrational spectrum of solid $TeCl_2Br_2$

Raman	Infrared
357mw sh	
338s	340vs
242vs	247vs
233m sh	230vs
226mw sh	
158w	
148w	146s
132w	131s
109w	
102w	
74s	
51s	

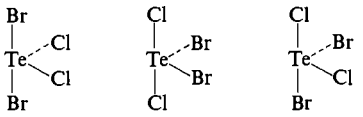

1 (C_{2v}) **2** (C_{2v}) **3** (C_1)

All of the observed Raman lines for $TeCl_2Br_2$ in the gaseous and solution phases were definitely polarized. Also, *four polarized* Raman active *stretching* modes were observed, the frequencies of which correspond very closely with those to be expected for equatorial and axial Te—Cl stretching modes (370 and 285 cm^{-1}), and equatorial and axial Te—Br stretching modes (242 and 198 cm^{-1}), respectively.

In the analysis of the gas phase data one should also consider the possibility that the axial bonds may be somewhat distorted from the 180° configuration as shown below.

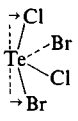

4 (C_1)

A distortion of structure **3** of the kind shown in **4**,

Can. J. Chem. Downloaded from www.nrcresearchpress.com by 210.87.254.6 on 09/05/12
For personal use only.

Can. J. Chem. Downloaded from www.nrcresearchpress.com by 210.87.254.6 on 09/05/12
For personal use only.

which is tending towards a *distorted* square pyramidal configuration about tellurium, would tend to reduce the lone pair-bonding pair interactions (9). Note that a similar distortion of structure **1** and **2** retain the symmetry C_{2v}. To summarize we can say that the Raman data for molecular $TeCl_2Br_2$ is consistent with either of the low symmery (C_1) structures **3** or **4** and not structure **2** which would have been predicted (10).

Penta- and Hexa-Co-ordinate Mixed Halide Ions of Tellurium(IV)

Five co-ordinate anionic species of Se(IV) and Te(IV) are rare and very little definitive structural data are available. X-Ray crystallographic data (11, 12) shows that $KTeF_5$ contains the discrete TeF_5^- anions and βMe_2TeI_2 exists as $[Me_3Te^+][MeTeI_4^-]$ where both anions can be considered to be based on an octahedral stereochemistry with an apical, non-bonding electron pair. The presence of $SeBr_5^-$ together with the $SeBr_6^{2-}$ anion has been inferred from the Raman spectra of SeO_2–HBr solutions (13). Infrared data is available (14) for solid $(Et_4N)TeCl_5$ and ultraviolet (u.v.) spectral data (15) provide evidence for the existence of $TeCl_5^-$ in methyl cyanide solution, in equilibrium with $TeCl_4$ and $TeCl_6^{2-}$. Square pyramidal, penta-co-ordinate Te(IV) has also been postulated (16) for the trimethylamine complex $Me_3N.TeF_4$ which is supposed to exist in the ionized form $(TeF_32NMe_3^+)(TeF_5^-)$.

It is important to note that infrared, Raman, Mossbauer, nuclear quadrupole resonance, and X-ray crystallographic data (17) all support a regular octahedral stereochemistry for TeX_6^{2-} (X = Cl, Br, or I) despite the presence of a 14 electron valency shell for Te(IV) in the complexes. The absence of hexa-co-ordinate fluoride anionic complexes of Te(IV) is also noteworthy.

The purpose of this paper is to (*a*) report a general synthetic route to five and six co-ordinate mixed halide anions of Te(IV) and (*b*) to investigate by means of infrared and Raman spectroscopy the structures of the various species and whether any trends in their stereochemistry and bonding are apparent.

Previous work on mixed halide anionic systems of tellurium(IV) is limited to an early report (18) on an aqueous type preparation of $(pyH)_2TeCl_4Br_2$ and $(pyH)_2TeCl_2Br_2I_2$. Spectral or structural data has not been reported for either of the above species and the synthetic route is itself restricted.

We discovered that two general approaches for the preparations of five and six co-ordinate mixed halide anions of Te(IV) were feasible. The first consisted of mixing (*in vacuo*) benzene – methylene dichloride solutions of Et_4NX (X = halide) with the appropriate tellurium tetrahalide in exact 1:1 and 1:2 molar ratios. The complexes immediately precipitated from solution. In the case of the 1:1 product, it was necessary to shake the mixture for at least 1 h to effect quantitative conversion to the desired 1:1 complex. The second approach consisted of directly triturating the tellurium tetrahalide with Et_4NX or CsX in exact 1:1 or 1:2 molar proportions. The second technique was less satisfactory for the 1:1 complexes from the point of view of successfully effecting a quantitative conversion to the pure 1:1 mixed halide salt. The analyses of the complexes precipitated from solution by the first method and the corresponding infrared and Raman spectra of the solids were satisfactory and characteristic of penta- and hexa-co-ordinate species (Tables 2 and 3).

Let us now formalize the evidence in favor of the formation of penta- and hexa-co-ordinate *mixed* complex anions of Te(IV)

$$[5]\quad TeCl_2Br_2 + Br^- \xrightarrow{C_6H_6/CH_2Cl_2} TeCl_2Br_3^-$$

$$[6]\quad TeCl_2Br_2 + 2Br^- \xrightarrow{C_6H_6/CH_2Cl_2} TeCl_2Br_4^{2-}$$

$$[7]\quad TeBr_4 + 2Cl^- \xrightarrow{C_6H_6/CH_2Cl_2} TeCl_2Br_4^{2-}$$

Different infrared and Raman spectra were obtained for the products of reactions 5 (Table 2) and 6 (Table 3) which were both different to the spectra of the starting material $TeCl_2Br_2$ (Table 4). The alternative synthetic route to $TeCl_2Br_4^{2-}$ (reaction 7) yielded a complex with identical spectra to the product of reaction 6. The spectra were not superpositions of the $TeCl_6^{2-}$ and $TeBr_6^{2-}$ species (13, 17). The products of reactions 5, 6, and 7 analyzed satisfactorily for the 1:1 and 1:2 complexes, respectively.

Thus we feel that the evidence is overwhelmingly in favor of the penta- and hexa-co-ordinate mixed halide anions $TeCl_2Br_3^-$ and $TeCl_2Br_4^{2-}$, respectively.

The possible stereochemistries for $TeCl_2Br_4^{2-}$ are shown below together with the respective vibrational representations.

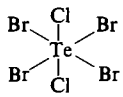

D_{4h}

$\nu_{TeCl}\ a_{1g} + a_{2u}$
$\nu_{TeBr}\ a_{1g} + b_{1g} + e_u$

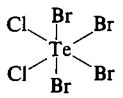

C_{2v}

$\nu_{TeCl}\ a_1 + b_2$
$\nu_{TeBr}\ 2a_1 + b_1 + b_2$

$$\Gamma_{vib}^{trans} = 2a_{1g}(R) + b_{1g}(R) + b_{2g}(R) + e_g(R) + 2a_{2u}(i.r.) + b_{2u}(i.r.) + 3e_u(i.r.)$$

$$\Gamma_{vib}^{cis} = 6a_1(i.r./R) + 2a_2(R) + 3b_1(i.r./R) + 4b_2(i.r./R)$$

The infrared and Raman spectra for $(Et_4N)_2TeCl_2Br_4$ are extremely informative (Table 3) and show a total of *six* tellurium–halogen stretching modes, all of which are Raman active. This is very strong evidence in favor of a *cis*-octahedral stereochemistry[1] for $TeCl_2Br_4^{2-}$ as the corresponding *trans*-octahedral species should display a total of five tellurium–halogen stretching modes of which only *three* are Raman active.

The vibrational spectrum of the $TeCl_2Br_3^-$ species is clearly not that to be expected for a D_{3h} trigonal bipyramidal species but rather like $TeCl_5^-$ and TeF_5^-, that is, based on a square pyramidal five co-ordinate stereochemistry. For a species $TeCl_2Br_3^{3-}$ with D_{3h} symmetry (*cf.* $CuCl_2Br_3^{3-}$) the metal–halogen stretching modes to be expected are $2a'$ (R) + a_2'' (i.r.) + e' (i.r./R). Consider now the three possible configurations shown below, which are based on a square pyramidal stereochemistry.

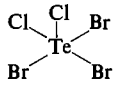

5 (C_s)

$\nu_{TeCl}\ 2a'$
$\nu_{TeBr}\ 2a' + a''$

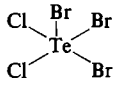

6 (C_{2v})

$a' + a''$
$2a' + a''$

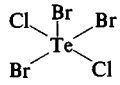

7 (C_s)

$a_1 + b_1$
$2a_1 + b_2$

Thus on the basis of the metal–halogen stretching modes we can immediately eliminate the D_{3h} structure on the basis of infrared and Raman activities.

For the three configurations **5**, **6**, and **7** all tellurium–halogen stretching modes are infrared and Raman active. Without additional data it is virtually impossible to distinguish these three configurations.

[1] $TiX_4Y_2^{2-}$ and $SnX_4Y_2^{2-}$ (X = Cl, Br, or I; Y = Cl; Br, or I) are reported to be *cis*-octahedral (18).

TABLE 5. Theoretical and experimental number of lines observed in spectroscopy

Symmetry	Infrared	R	Coincidences
D_{3h} Trigonal bipyramid	3	2	1
C_s or C_{2v} square pyramid	5	5	5
Observed (Table 2)	4	4	3

Experimental

$TeCl_2Br_2$ (m.p. 292 °C) and $TeBr_4$ were prepared by standard techniques (1) and were purified before use by sublimation in vacuo. The tetraethylammonium and cesium halides were dried by heating to 100° under vacuum. All solvents were dried by refluxing with CaH_2 followed by vacuum distillation. Preparations of the 1:1 and 1:2 complexes were carried out in either an all-glass vacuum system or in a glove box.

Analyses

The method employed consisted of the quantitative hydrolysis of the complex in acetic acid (0.1 *N*) or nitric acid. The resulting solutions were titrated potentiometrically against a standard solution of silver nitrate.

Anal. Calcd. for $[Et_4N]TeCl_2Br_3$: Cl, 12.5; Br, 42.2. Found: Cl, 11.2; Br, 40.8.

Anal. Calcd. for $[Et_4N]_2TeCl_2Br_4$: Cl, 9.1; Br, 41.0. Found: Cl, 9.2; Br, 39.5.

Spectra

Infrared spectra were recorded as Nujol mulls using a Beckmann IR-11. Raman spectra of powdered solids were recorded using a Carson argon ion or krypton ion laser coupled to a Spex Raman Spectrometer. Gas phase Raman spectra were recorded for $TeCl_2Br_2$ at 310 °C and a pressure of approximately 1 atm.

We wish to thank Dr. R. J. O'Brien for helpful discussion and the National Research Council of Canada for generous financial support.

1. E. A. AYNSLEY. J. Chem. Soc. 3016 (1953).
2. N. KATSAROS and J. W. GEORGE. Inorg. Chem. Acta, **3**, 165 (1968).
3. A. MICHAELIS. Ber. **20**, 1781 (1887).
4. J. H. SUNANS. J. Amer. Chem. Soc. **52**, 348 (1930).
5. D. P. STEVENSON and V. SCHOMAKER. J. Amer. Chem. Soc. **62**, 1267 (1940).
6. I. R. BEATTIE, J. R. HORDER, and P. J. JONES. J. Chem. Soc. A, 329 (1970).
7. G. A. OZIN and A. VANDER VOET. Unpublished work.
8. I. R. BEATTIE and G. A. OZIN. Unpublished work.
9. R. J. GILLESPIE. J. Amer. Chem. Soc. **82**, 5978 (1960); Can. J. Chem. **39**, 318 (1961).
10. E. L. MUETTERTIES, W. MAHLER, and R. SCHMUTZLER. Inorg. Chem. **2**, 613 (1963).
11. A. J. EDWARDS and M. A. MOUTY. J. Chem. Soc. A, 303 (1969).
12. E. EINSTEIN, J. TROTTER, and C. WILLISTON. J. Chem. Soc. 2018 (1967).
13. P. HENDRA and Z. JOVICH. J. Chem. Soc. A, 600 (1968).
14. J. A. CREIGHTON and J. H. S. GREEN. J. Chem. Soc. A, 808 (1968).

Can. J. Chem. Downloaded from www.nrcresearchpress.com by 210.87.254.6 on 09/05/12
For personal use only.

15. I. R. BEATTIE and H. CHUDZYNSKA. J. Chem. Soc. A, 1119 (1967).
16. N. N. GREENWOOD, A. C. SARMA, and B. P. STRAUGHAN. J. Chem. Soc. A, 1561 (1968).
17. D. M. ADAMS and D. M. MORRIS. J. Chem. Soc. A, 2067 (1967); N. N. GREENWOOD and B. P. STRAUGHAN. J. Chem. Soc. A, 962 (1966) (and references therein). V. A. BRYUKHANOV, B. Z. IOFA, A. A. OPALENKO, and V. S. SHPINEL. Russ. J. Inorg. Chem. **12**, 1044 (1967).
18. R. J. H. CLARK, L. MARESCA, and R. J. PUDDEPHATT. Inorg. Chem. **7**, 1603 (1968).

Can. J. Chem. Downloaded from www.nrcresearchpress.com by 210.87.254.6 on 09/05/12
For personal use only.

Osmotic and Activity Coefficients of Some Simple Borate Solutions at the Freezing Point

R. F. PLATFORD
Canada Center for Inland Waters, Burlington, Ontario
Received September 25, 1970

Activity coefficients for aqueous sodium and potassium tetraborate, sodium metaborate, sodium and potassium fluoroborate, and orthoboric acid were derived from their freezing points. The measurements confirmed in general the behavior of these salts at 25° except that the tetraborates showed different low concentration behavior from that predicted from isopiestic data. Because of this difference, the 25° activity coefficients reported earlier for sodium and potassium tetraborates have been revised. The new values for 0.15 *m* solutions of the tetraborates are 0.345 at 25° and 0.303 at the freezing point.

Canadian Journal of Chemistry, 49, 709 (1971)

Can. J. Chem. Downloaded from www.nrcresearchpress.com by 210.87.254.6 on 09/05/12
For personal use only.

Introduction

The osmotic properties of some borates of geochemical interest have been determined at 25° by means of the isopiestic vapor pressure method (1). In order to obtain more detailed information on the low concentration behavior of these borates, a series of freezing point measurements was made for concentrations 0.6 *m* and below. The mineral avogadrite (KBF_4) which was not soluble enough to be studied by the isopiestic method was investigated also.

Experimental

Potassium fluoroborate was precipitated by mixing aqueous sodium fluoroborate and aqueous potassium chloride and was recrystallized three times from water. The other chemicals were those used in the previous study (1). All solutions were made up by weight. It is worth noting the large solubility difference at 25° between KBF_4 (0.03 *m*) and $NaBF_4$ (9.8 *m*) and the solubility difference in the opposite sense between $K_2B_4O_7$ (0.65 *m*) and $Na_2B_4O_7$ (0.16 *m*).

All the freezing points were measured with an Advanced Instruments 3R osmometer. This comparative thermometer is used in the following way. A 2.5 ml sample of solution of known concentration is supercooled by 3° (a preliminary measurement may be needed if the freezing point is not known to better than about 0.02°). The sample is then thermally isolated and a 1-s period of violent stirring causes a small fixed fraction of solvent to be frozen out. This fraction is 3° times the ratio of the heat capacity of the solution to the heat of fusion of ice. The temperature of the solution in equilibrium with the ice is then measured with a thermistor. Good reproducibility depends on freezing out the same fraction of solvent each time (the fraction chosen is not critical as long as it is reproducible from one measurement to the next). Calibration with solutions of known freezing points is essential because the osmometer measures the freezing point of a solution about 4% more concentrated than the starting solution, and calibration very nearly compensates for this error. Compensation would be exact if all the solutions had the same heat capacity.

In this work, the osmometer was calibrated with solutions of both NaCl and KCl using the freezing points of Scatchard and Prentiss (2). The results were consistent with each other and reproducible to within 0.002° times the molality up to 0.6 *m*, the maximum concentration studied, and the calibration did not change over the six month period during which the measurements were made.

Results and Discussion

The results are reported in Table 1 as $1 - \phi$ values at rounded concentrations,[1] where ϕ, the osmotic coefficient at the freezing point ($-\theta$) is given by $(1/\nu m\lambda)(\theta + 4.9 \times 10^{-4}\theta^2)$ using a value for λ of 1.860 (3). At the concentrations referred to here the values of $1 - \phi$ differ by less than 0.001 from the *j* values which are often used in freezing point measurements. The imprecision in ϕ was not greater than 0.001 and the inaccuracy probably was not greater than 0.002. There was no detectable difference in behavior either between sodium and potassium tetraborate (see Fig. 1) or between sodium and potassium fluoroborate in the regions of common solubilities, and for this reason, the results for each pair of salts are combined in Table 1.

The fluoroborates hydrolyzed in solution (4) and the two sets of data in Table 1 refer firstly to solutions less than a few hours old and secondly to solutions which had been stored in polypropylene bottles until the freezing point depressions had reached constant values, thus

[1]Photo copies of the original data may be obtained free of charge, upon request, from the Depository for Unpublished Data, National Science Library, National Research Council of Canada, Ottawa, Canada.

TABLE 1. Values of $1 - \phi$ for borates at the freezing point

			$1 - \phi$			
	$1 - \phi$				$NaBF_4$	
m	($K_2B_4O_7$*)	m	H_3BO_3	$NaBO_2$	$t = 0$†	$t = \infty$
0.001	0.0065	0.01	0.001	0.025	0.028	−0.2
0.002	0.0130	0.02	—	0.035	0.038	−0.1
0.005	0.0355	0.05	0.002	0.060	0.060	—
0.01	0.0720	0.10	0.004	0.088	0.088	0.01
0.02	0.137	0.2	0.006	0.128	0.121	—
0.05	0.277	0.3	0.007	0.158	0.146	—
0.10	0.393	0.4	0.008	0.180	0.168	—
0.20	0.504	0.5	—	0.200	0.186	0.150
—	—	0.6	—	0.218	0.203	—

*These values also apply to $Na_2B_4O_7$ up to 0.05 m.
†These values also apply to KBF_4 up to 0.015 m.

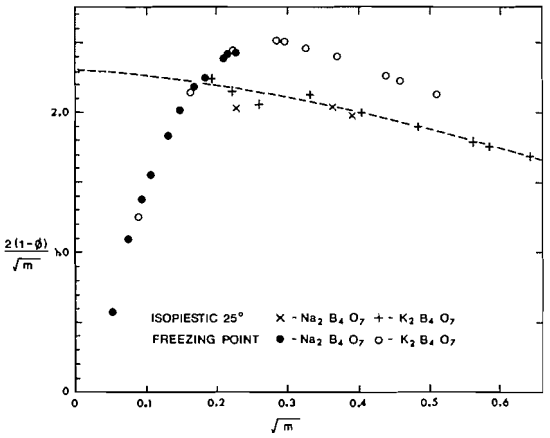

FIG. 1. Low concentration osmotic behavior of sodium and potassium tetraborates.

TABLE 2. Rates of hydrolysis of aqueous sodium fluoroborate

		$t_{\frac{1}{2}}$(h)	
m	θ_∞/θ_0	At 25°	At 0°
0.01*	1.25	250	—
0.02	1.15	150	1200
0.1	1.08	75	—
0.5	1.04	30	400

*Also applies to KBF_4.

indicating probable equilibrium between the fluoroborates and their hydrolysis products. The times for the initial freezing points to go halfway to their equilibrium values are given in Table 2 as an aid to those who wish to store such solutions.

One obvious way to use the freezing points is to apply them to correct low concentration isopiestic measurements, even though this may require some assumptions to be made regarding temperature coefficients of the osmotic data. The evaluation of activity coefficients from osmotic coefficients is complicated by the evaluation of an integral of the form $n\int(1 - \phi)/\sqrt[n]{m} \cdot d\sqrt[n]{m}$ and this quantity must usually be estimated graphically (3). The limit for $2(1 - \phi)/\sqrt{m}$ at $m = 0$ for 1–1 electrolytes is given by the Debye–Hückel theory (5); it is 0.77 ± 0.01 from 0–25° and this facilitates the extrapolation. The limit for non-electrolytes or mixtures cannot be calculated from theory although it is known to be finite (5) for non-electrolytes.

The tetraborates are equivalent to equimolal mixtures of boric acid and metaborate and their low concentration integral limit is not known. The uncertainty that can arise in evaluating the integral term is illustrated by Fig. 1, which combines 25° isopiestic data (1) with freezing point data. The limit given by the freezing points is near zero, whereas the isopiestic limit is very large. The difference may be due to different behavior at the two temperatures, but it seems unlikely that the limits could be so different. If it is assumed that the osmotic coefficients for concentrations of tetraborates below 0.04 m are more accurately represented by the freezing point data than the extrapolated isopiestic data of ref. 1, the values originally reported will be changed as shown in Table 3. The only osmotic coefficient change is that at 0.01 m which changes from 0.89 to 0.93. At concentrations above 0.04 m there are real differences between the freezing point results and the isopiestic results and these give rise to the results shown in Table 3.

Can. J. Chem. Downloaded from www.nrcresearchpress.com by 210.87.254.6 on 09/05/12
For personal use only.

TABLE 3. Revised activity data for sodium and potassium tetraborates

	25°		Freezing points	
m	Old $\gamma_\pm$	New $\gamma_\pm$	$\gamma_\pm$	ϕ
0.01	0.74	0.87	0.87	0.93
0.05	0.48	0.575	0.547*	0.725*
0.10	0.355	0.43	0.386	0.608
0.15	0.29*	0.345*	0.303	0.538
0.2	0.25	0.30	0.253	0.496
0.3	0.19	0.23	—	—
0.4	0.16	0.19	—	—
0.5	0.14	0.16	—	—
0.6	0.12	0.145	—	—
0.7	0.11	0.13	—	—
0.8	0.10	0.12	—	—
0.9	0.09	0.11	—	—
1.0	0.08	0.10	—	—
1.1	0.08	0.09	—	—
1.2	0.07	0.09	—	—

*Values apply only to $K_2B_4O_7$ above these concentrations.

TABLE 4. Mean activity coefficients of borates at the freezing point and at 25°

	0.1 m		0.5 m	
Borate	Freezing point	25°	Freezing point	25°
H_3BO_3	0.99	0.97	0.97	0.94
$NaBO_2$	0.77	0.80	0.55	0.61
$NaBF_4$	0.77	0.82	0.50	0.65

The freezing point data for boric acid indicated a limit for $2(1 - \phi)/\sqrt{m}$ of 0.032 compared with a limit of 0.066 at 25° (1) These gave values for γ at the two temperatures listed in Table 4.

Both the freezing point and the isopiestic measurements led to the same value for the limit for $NaBO_2$ of 0.50 ± 0.05 as opposed to the theoretical value of 0.77. The limit for $NaBF_4$ also was less than expected with a value of about 0.55 for freshly prepared solutions and a negative value for aged solutions. This difference and the difference at high concentrations was consistent with the hydrolysis constant reported (4) which indicates that the BF_4^- ion was hydrolyzed to less than 0.2% at above 1 m, and about 2% at 0.1 m. The activity coefficients calculated using limits of 0.50 for $NaBO_2$ and 0.55 for $NaBF_4$ are shown in Table 4. If the theoretical limits had been used instead, such as would apply for comparisons with e.m.f. measurements, the $\gamma_\pm$ values would have been 0.02–0.03 lower at both 0.1 and 0.5 m. The values for the fluoroborates in Table 4 refer to freshly prepared solutions. It should be realized that the osmotic coefficients reported here are sensitive to the total number of particles in solution including dissociation products, whereas e.m.f. measurements would respond to specific ions and for this reason, the two types of measurements may not be entirely consistent for metaborates and fluoroborates.

1. R. F. PLATFORD. Can. J. Chem. **47**, 2271 (1969).
2. G. SCATCHARD and S. S. PRENTISS. J. Amer. Chem. Soc. **55**, 4355 (1933).
3. R. A. ROBINSON and R. H. STOKES. Electrolyte Solutions. Revised 2nd ed. Butterworths, London. 1965. p. 180.
4. I. G. RYSS and D. B. DONSKAYA. Zh. Fiz. Khim. **33**, 107 (1959).
5. G. N. LEWIS and M. RANDALL. Thermodynamics. 2nd ed. Revised by K. S. Pitzer and L. Brewer. McGraw-Hill, New York. 1961. pp. 339, 264.

Can. J. Chem. Downloaded from www.nrcresearchpress.com by 210.87.254.6 on 09/05/12
For personal use only.

Dielectric Relaxation of the Butyl Alcohols in *p*-Xylene Solution

JOHN CROSSLEY
Chemistry Department, Lakehead University, Thunder Bay, Ontario
Received September 24, 1970

Dielectric constants and losses of the four butyl alcohols have been measured at concentrations of 0.02–0.12 mol fraction in *p*-xylene solution over the frequency range 1–35 GHz at 25 °C. The data for the most dilute solutions can be represented by a symmetrical distribution of relaxation times. For the more concentrated solutions the Cole–Cole plots indicate a separation into two absorption regions and the data can be analyzed in terms of two relaxation times both of which lengthen with increased alcohol concentration. The contribution from the long relaxation time and the apparent dipole moment for each butanol, is independent of alcohol concentration and decreases in the order *n*-butanol > iso-butanol > *sec*-butanol > *t*-butanol. The results are discussed in terms of previous dielectric relaxation studies of pure liquid aliphatic alcohols and their solutions in non-polar solvents.

Canadian Journal of Chemistry, 49, 712 (1971)

Can. J. Chem. Downloaded from www.nrcresearchpress.com by 210.87.254.5 on 09/05/12
For personal use only.

The dielectric absorption of pure liquid aliphatic alcohols, which has been extensively investigated over a wide range of frequency and temperature (1–4), is characterized by three discrete relaxation processes. A model capable of satisfactorily explaining the experimental results is as yet unavailable and even further experimental data are desirable if one is to be obtained. Dielectric constant and loss measurements of monohydric aliphatic alcohols in non-polar solvents at microwave frequencies offer an excellent means of examining the high frequency relaxation processes (5, 6) which are obscured in the pure liquids by the dominant Debye-like low frequency process whose contribution diminishes on dilution with a non-polar solvent (7). In addition, this type of study provides valuable information on inter- and intramolecular relaxations for simple aliphatic molecules (8, 9) which, if carefully selected, may provide suitable models for the more complex polymer systems.

In dilute benzene and *n*-heptane solutions, the dielectric absorption of primary aliphatic alcohols is characterized by two dielectric relaxation times which have been attributed to —OH group and whole molecule reorientations (5, 6). However, the dielectric absorption of the same alcohols in *p*-dioxane solution shows a symmetrical distribution of relaxation times with a short mean relaxation time (6). In this study *p*-xylene has been used as solvent since it is non-polar and a stronger base than *n*-heptane and benzene but weaker than *p*-dioxane. The four butyl alcohols were selected as solutes because of the variation in the steric environment of the hydroxyl group amongst these molecules, and *n*-butanol had been measured previously in *n*-heptane, benzene, and *p*-dioxane at 25 °C.

Experimental

The apparatus and procedure for determining the dielectric constant and loss at the frequencies employed in this study have been described previously (10, 11).

Materials

The butyl alcohols were all dried over calcium hydride and fractionally distilled using a spinning band column; *p*-xylene was dried over and distilled from sodium.

Experimental Results

Typical Cole–Cole plots obtained for the butyl alcohols in *p*-xylene solution at 25 °C are shown in Fig. 1. For the most dilute solutions it is possible to draw smooth semicircular arcs, with only slightly depressed centers, through the experimental points plotted in the complex plane. For this reason these data were analyzed using a computer programmed to solve the Cole–Cole equations (12) for the most probable or mean relaxation time, τ_0, the Cole–Cole distribution parameter, α, and the high frequency dielectric constant ε_∞. The Cole–Cole plots for the other solutions were either asymmetric or had significant distribution parameters (>0.1) and these data were analyzed, using an IBM 360 computer, for two relaxation times, τ_1 and τ_2, and their relative contributions, C_1 and C_2, using eqs. 1 and 2.

$$[1]\quad \varepsilon' - i\varepsilon'' = \varepsilon_0 + (\varepsilon_0 - \varepsilon_\infty) \times \left[\frac{C_1}{1 + i\omega\tau_1} + \frac{C_2}{1 + i\omega\tau_2}\right]$$

$$[2]\quad C_1 + C_2 = 1$$

Can. J. Chem. Downloaded from www.nrcresearchpress.com by 210.87.254.5 on 09/05/12
For personal use only.

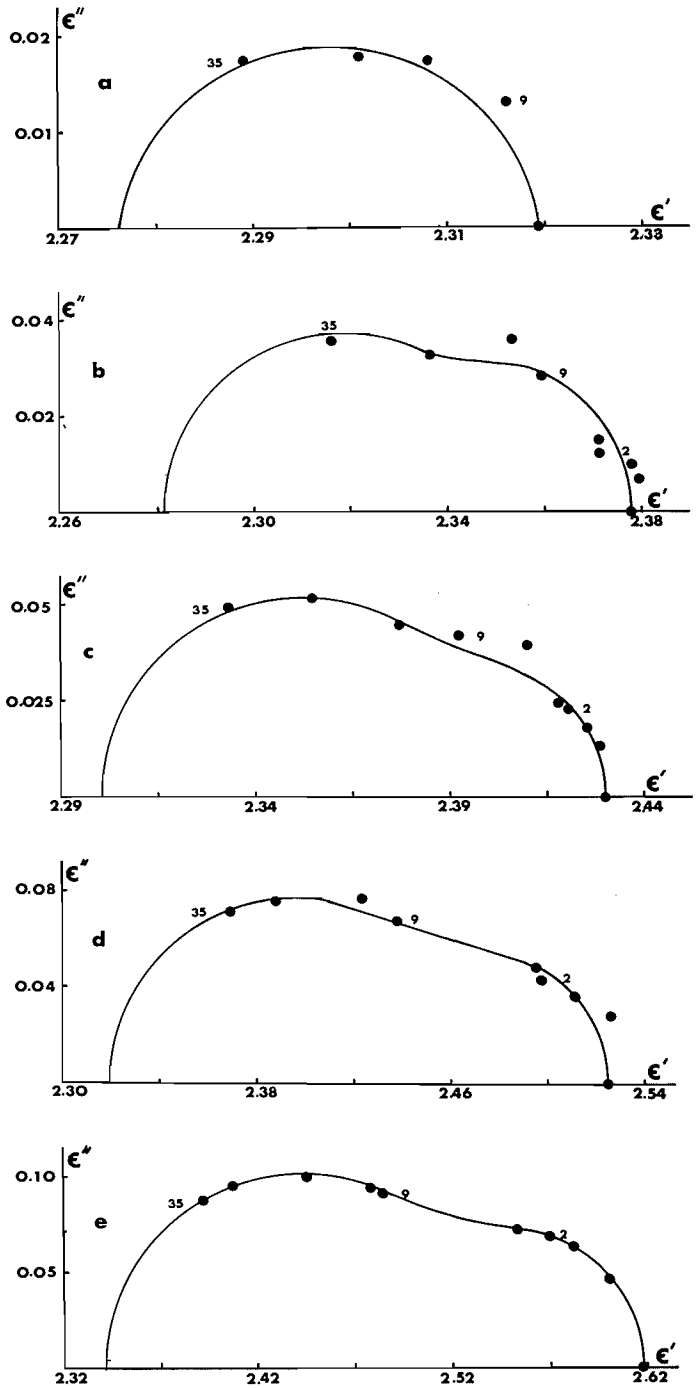

FIG. 1. Cole–Cole plots for *n*-butanol at (*a*) 0.02123, (*b*) 0.04205 (*c*) 0.06094, (*d*) 0.09152 (*e*) 0.1193 mol fraction in *p*-xylene solution at 25 °C.
The numbers alongside some points are the approximate frequencies in GHz.

Can. J. Chem. Downloaded from www.nrcresearchpress.com by 210.87.254.5 on 09/05/12
For personal use only.

The errors involved in the measured ε' and ε'' values and the accuracy of the relaxation data obtained as described here have been assessed previously (13).

Apparent dipole moments, μ, were calculated from eq. 3, in which kT is the thermal energy and

$$[3] \qquad \mu^2 = \frac{9kT}{4\pi N} \cdot \frac{(\varepsilon_0 - \varepsilon_\infty)(2\varepsilon_0 + \varepsilon_\infty)}{\varepsilon_0(\varepsilon_\infty + 2)^2}$$

N is the number of solute molecules per ml of solution.

The experimentally determined dielectric constant and dielectric loss data which have been corrected for the small absorption of *p*-xylene are given in Table 1. The values for τ_0, α, τ_1, τ_2, C_1, and ε_∞ obtained from the analytical procedures outlined above, the static dielectric constants measured at 2 MHz, and the apparent dipole moments calculated using eq. 1 are listed in Table 2.

Discussion

The Cole–Cole plots for all the butanols at 0.02 mol fraction in *p*-xylene solution are symmetrical with small distribution parameters, and their mean relaxation times are very similar. A separation of the data into two dispersion regions becomes increasingly evident with increased alcohol concentration, especially for *n*- and iso-butanol. The analyses, Table 2, indi-

TABLE 1. Dielectric constants and losses of butanols in *p*-xylene as a function of concentration at 25 °C

f_2	Frequency (GHz)	ε'	ε''	f_2	Frequency (GHz)	ε'	ε''
		n-Butanol				*iso-Butanol*	
0.02123	35.11	2.289	0.0177	0.02083	35.11	2.281	0.0175
	23.98	2.301	0.0180		23.98	2.303	0.0168
	16.20	2.308	0.0173		16.20	2.308	0.0168
	9.313	2.316	0.0131		9.313	2.312	0.0121
0.04205	35.11	2.316	0.0367		2.478	2.314	0.0059
	23.98	2.336	0.0333		1.505	2.314	0.0050
	16.20	2.353	0.0361	0.04156	35.11	2.312	0.0344
	9.313	2.359	0.0290		23.98	2.334	0.0340
	2.50	2.371	0.0144		16.20	2.342	0.0310
	2.017	2.371	0.0123		9.313	2.355	0.0275
	1.507	2.378	0.0103		2.485	2.369	0.0134
	1.001	2.382	0.0080		1.506	2.372	0.0097
0.06094	35.11	2.333	0.0500		1.003	2.374	0.0071
	23.98	2.355	0.0521	0.06083	35.11	2.337	0.0488
	16.20	2.377	0.0460		23.98	2.356	0.0503
	9.313	2.392	0.0432		16.20	2.374	0.0473
	6.700	2.409	0.0409		9.313	2.389	0.0429
	2.478	2.418	0.0243		2.485	2.417	0.0236
	2.014	2.420	0.0219		1.508	2.422	0.0169
	1.508	2.426	0.0186		1.001	2.429	0.0129
	1.001	2.433	0.0141	0.09398	35.11	2.377	0.0709
0.09152	35.11	2.369	0.0711		23.98	2.386	0.0760
	23.98	2.388	0.0761		16.20	2.417	0.0711
	16.20	2.424	0.0779		9.313	2.447	0.0704
	9.313	2.438	0.0691		6.700	2.455	0.0656
	2.500	2.495	0.0485		2.500	2.489	0.0459
	2.009	2.497	0.0436		2.012	2.499	0.0413
	1.506	2.512	0.0373		1.512	2.507	0.0364
	1.002	2.526	0.0283		1.005	2.513	0.0272
0.1193	35.11	2.392	0.0879	0.1155	35.11	2.380	0.0856
	23.98	2.408	0.0951		23.98	2.406	0.0911
	16.20	2.445	0.1001		16.20	2.445	0.0939
	9.313	2.477	0.0937		9.313	2.470	0.0884
	6.700	2.483	0.0912		6.700	2.479	0.0821
	2.500	2.553	0.0734		2.495	2.534	0.0640
	2.012	2.570	0.0680		2.017	2.548	0.0606
	1.510	2.581	0.0618		1.510	2.559	0.0532
	1.002	2.602	0.0478		1.005	2.574	0.0419

TABLE 1 (*Concluded*)

f_2	Frequency (GHz)	ε′	ε″	f_2	Frequency (GHe)	ε′	ε″
		Sec-Butanol				*t-Butanol*	
0.02013	35.11	2.290	0.0192	0.01905	35.11	2.284	0.0153
	23.98	2.302	0.0184		23.98	2.293	0.0166
	16.20	2.309	0.0174		16.20	2.299	0.0155
	9.313	2.312	0.0113		9.313	2.305	0.0095
0.03870	35.11	2.318	0.0340	0.03858	35.11	2.319	0.0323
	23.98	2.334	0.0335		23.98	2.329	0.0307
	16.20	2.343	0.0272		16.20	2.314	0.0256
	9.313	2.352	0.0237		9.313	2.345	0.0198
	2.440	2.361	0.0098		2.465	2.346	0.0086
0.06254	35.11	2.347	0.0548				
	23.98	2.365	0.0529	0.06105	35.11	2.340	0.0462
	16.20	2.384	0.0486		23.98	2.362	0.0441
	9.313	2.397	0.0413		16.20	2.370	0.0398
	6.700	2.405	0.0358		9.313	2.380	0.0319
	2.487	2.419	0.0187		2.465	2.396	0.0147
	2.012	2.419	0.0162		1.994	2.399	0.0127
	1.504	2.422	0.0128		1.508	2.402	0.0106
	1.001	2.429	0.0099				
0.09043	35.11	2.372	0.0700	0.08890	35.11	2.365	0.0602
	23.98	2.390	0.0721		23.98	2.383	0.0591
	16.20	2.420	0.0740		16.20	2.406	0.0621
	9.313	2.442	0.0635		9.313	2.420	0.0467
	6.700	2.452	0.0523		6.700	2.422	0.0426
	2.495	2.478	0.0333		2.440	2.446	0.0221
	2.013	2.483	0.0296		1.998	2.447	0.0188
	1.511	2.490	0.0238		1.498	2.451	0.0153
	1.002	2.498	0.0175		0.984	2.458	0.0128
0.1184	35.11	2.403	0.0901	0.1190	35.11	2.399	0.0784
	23.98	2.422	0.0905		23.98	2.407	0.0785
	16.20	2.459	0.0955		16.20	2.443	0.0769
	9.313	2.480	0.0843		9.313	2.456	0.0636
	6.700	2.493	0.0769		6.700	2.466	0.0547
	2.486	2.541	0.0508		2.488	2.484	0.0342
	2.012	2.544	0.0409		1.994	2.501	0.0293
	1.510	2.552	0.0383		1.510	2.509	0.0247
	1.002	2.570	0.0288		1.003	2.526	0.0185

cate that the separations are due more to increased τ_1/τ_2 ratios than increased C_1/C_2 ratios. The most significant difference between the results for the butanols is in the C_1 values which decrease *n*-butanol > iso-butanol > *sec*-butanol > *t*-butanol.

The results for *n*-butanol in *p*-xylene solution, Table 2, may be compared with previous relaxation data for this alcohol (5, 6), at similar concentrations in benzene, *p*-dioxane, and *n*-heptane solution also at 25 °C and as the pure liquid at 20 °C, in Table 3. Methanol and *n*-decanol show similar behavior to *n*-butanol in benzene solution (6); *n*-hexanol, *n*-heptanol, *n*-decanol, and six isomers of octanol show a similar behavior to *n*-butanol in *n*-heptane solution (5) at similar concentrations. The Cole–Cole plots for the benzene and *n*-heptane solutions separate into two dispersion regions; the low frequency process (τ_1) lengthens and the high frequency process (τ_2) remains almost constant with increased molecular size. For methanol, *n*-butanol, and *n*-decanol in *p*-dioxane solution the dielectric constant and loss data may be fitted to symmetrical depressed center Cole–Cole plots with short mean relaxation times which lengthen with increased molecular size (6).

The apparent dipole moment for *n*-butanol shows a significant solvent dependence and increases *n*-heptane < *p*-xylene < benzene < *p*-dioxane. For all the alcohols at concentrations less than 0.12 mol fraction in benzene, *n*-heptane, and *p*-xylene the apparent dipole moments are less than their vapor phase and pure liquid values, ~ 1.7 and ~ 2.8 D respectively, which

Can. J. Chem. Downloaded from www.nrcresearchpress.com by 210.87.254.5 on 09/05/12
For personal use only.

TABLE 2. Static dielectric constant, high frequency dielectric constant, relaxation time (ps) and apparent dipole moment (in D units) for the butanols at mole fraction f_2 in *p*-xylene solution at 25 °C

f_2	τ_0	α	τ_1	τ_2	C_1	ε_0	ε_∞	μ
					n-Butanol			
0.02123	6.1	0.10				2.3191	2.276	1.42
0.04205			22.3	3.7	0.36	2.3773	2.281	1.49
0.06094			34.9	5.6	0.32	2.4303	2.301	1.42
0.09152			54.5	6.8	0.33	2.5257	2.318	1.45
0.1193			65.5	8.2	0.38	2.6191	2.341	1.46
					iso-Butanol			
0.02083	6.6	0.02				2.3152	2.278	1.33
0.04156			26.7	4.5	0.30	2.3711	2.285	1.46
0.06083			37.0	5.9	0.28	2.4236	2.300	1.44
0.09398			45.7	6.7	0.36	2.5245	2.325	1.45
0.1155			66.1	7.5	0.35	2.5949	2.330	1.50
					sec-Butanol			
0.02013	5.8	0.03				2.3142	2.274	1.41
0.03870			22.4	4.3	0.21	2.3632	2.285	1.40
0.06254			28.1	5.3	0.23	2.4251	2.300	1.40
0.09043			48.9	7.0	0.22	2.4996	2.322	1.35
0.1184			46.0	7.1	0.29	2.5773	2.340	1.35
					t-Butanol			
0.01905	6.2	0.0				2.3083	2.275	1.31
0.03858			28.3	4.3	0.13	2.3535	2.282	1.36
0.06105			32.8	4.9	0.19	2.4025	2.297	1.29
0.08890			35.0	6.1	0.20	2.4579	2.315	1.22
0.1190			49.6	6.4	0.21	2.5198	2.331	1.26

TABLE 3. Relaxation and dipole moment data for *n*-butanol solutions at 25 °C obtained by Smyth and co-workers. The relaxation times are in ps and the dipole moments in D

Solvent	f_2	τ_0	α	τ_1	τ_2	C_1	μ
n-Heptane	0.039			31	1.5	0.19	1.23
	0.060			44	2.5	0.35	1.12
	0.092			69	2.8	0.37	1.18
Benzene	0.0235			18.6	2.9	0.23	1.46
	0.0353			22.9	2.9	0.23	1.55
	0.0524			22.2	2.9	0.25	1.60
p-Dioxane	0.0290	4.5	0.18				1.81
	0.0464	5.0	0.18				1.73
Pure liquid (20 °C)*	1.0			27	2.4	—	2.85

*The τ_1 and τ_2 values listed here are the τ_2 and τ_3 values respectively reported by Garg and Smyth (1). Pure liquid alcohols have an additional low frequency relaxation process (for *n*-butanol $\tau \sim 670 \times 10^{-12}$s at 25 °C) which dominates the absorption.

suggests the presence of weakly polar multimers in these solutions. In the pure liquid state at low temperatures several isomers of octanol have dipole moments very close to zero and association into non-polar closed dimers has been suggested as a reasonable explanation (14). The large dipole moments for pure liquid straight chain alcohols probably result from association into larger multimers, either linear chains (14) or cyclic tetramers (15) and pentamers (16).

The short relaxation time τ_2 for alcohols in benzene (6) has been interpreted in terms of —OH group rotation since it shows only a small increase with increased molecular size and is of a similar magnitude to the —OH group relaxation times found for phenols (17, 18). The τ_2 values for the butanols in *p*-xylene solution given in Table 2 are all longer than those for *n*-butanol in benzene and *n*-heptane solution at similar concentrations, Table 3. Magee

Can. J. Chem. Downloaded from www.nrcresearchpress.com by 210.87.254.5 on 09/05/12
For personal use only.

Can. J. Chem. Downloaded from www.nrcresearchpress.com by 210.87.254.5 on 09/05/12
For personal use only.

and Walker (19) observed that the —OH group relaxation time in cholesterol lengthened considerably with increased solvent basicity. Thus the fact that the τ_2 values in Table 2 are longer than obtained previously may be partially explained by increased solute–solvent interactions since *p*-xylene is a stronger electron donor than benzene and *n*-heptane (the even stronger electron donor solvent *p*-dioxane leads to a symmetrical arc plot with a short mean relaxation time). By analogy the considerable concentration dependence shown by τ_2 in *p*-xylene solution could be reasonably explained by solute–solute interactions. However, τ_2 is seemingly independent of concentration in *n*-heptane and benzene solution where solute–solute interactions should be stronger.

Electric polarization measurements over a wide range of temperatures (20) indicate that the degree of association amongst the butanols decreases *n*-butanol $\simeq$ iso-butanol > *sec*-butanol > *t*-butanol. The C_1 values for these alcohols in *p*-xylene solution also decrease in this order. In addition the C_2 values for both straight and branched chain alcohols appear to decrease with increased alcohol concentration in *n*-heptane solution. It would seem then that increased solute–solute interactions lead to a decrease in the contribution to the total absorption from —OH group rotation because of a decrease in the number of relaxing hydroxyl groups due to association. This effect is probably partly responsible for the corresponding decreases shown by the apparent dipole moments. However, the C_2 values for each butanol in *p*-xylene solution and for methanol, *n*-butanol, and *n*-decanol in benzene solution are, within the limit of error, almost independent of concentration and in *p*-xylene solution both τ_1 and τ_2 lengthen indicating increased association. In analyzing dielectric data by computer methods based on the Budó equations (13) a bias towards a fixed C_2 could possibly result in a varying τ_2 and vice versa. The experimental results for the alcohols in benzene and *n*-heptane solutions obtained by the Princeton workers (5, 6) were re-analyzed with the program used in this study to analyze the *p*-xylene solution data, and very probably quite different initial estimates of τ_1, τ_2, and C_2. The analyses were almost identical with those reported by the Princeton workers.

The τ_1 values for *n*-butanol, Table 2, compare well with those obtained in *n*-heptane and benzene solution, Table 3, and like τ_2, lengthen with increased alcohol concentration. The values for all the butanols in *p*-xylene solution are significantly longer than the molecular relaxation times for chloroethanes, which are of a similar size as the butanols, also in *p*-xylene solution (21). However, the alcohols are much stronger electron acceptors and τ_1, which increases with increased molecular size (5, 6), is probably due to a molecular rotation mechanism. The lengthening of τ_1 with increased alcohol concentration in *n*-heptane and *p*-xylene solution is probably due to increased solute–solute interactions. Although the experimental data for the *p*-xylene solutions reveal no evidence of the third lowest frequency process which is evident at slightly higher concentrations (5) and dominate the absorption of the pure liquids (1), the onset of highly polar multimer formation cannot be discounted and may be partially responsible for the lengthening of τ_1.

In benzene solution increased alcohol concentration, over a limited range, has virtually no effect on the relaxation data; increasing alcohol concentration in *n*-heptane solution has almost no effect on the τ_2 values but τ_1 lengthens and C_1 increases; increasing alcohol concentration in *p*-xylene solution gives rise to constant C_1 values and lengthening τ_1 and τ_2 values. These results, especially the solvent effect on τ_2 and C_1, are not readily explained and further work is in progress on a number of alcohols in a variety of non-polar solvents.

1. S. K. Garg and C. P. Smyth. J. Phys. Chem. **69**, 1294 (1965).
2. C. Brot and M. Magat. J. Chem. Phys **39**, 841 (1963).
3. R. H. Cole and co-workers. J. Chem. Phys. **19**, 1484 (1951); **20**, 1389 (1952); **23**, 1762 (1955); **23**, 1756 (1955).
4. W. Dannhauser and A. F. Flueckinger. Phys. and Chem. of Liquids. **2**, 37 (1970).
5. J. Crossley, L. Glasser, and C. P. Smyth. J. Chem. Phys. **52**, 6203 (1970); and unpublished results.
6. G. P. Johari and C. P. Smyth. J. Amer. Chem. Soc. **91**, 6215 (1969).
7. D. J. Denney and J. W. Ring. J. Chem. Phys. **39**, 1268 (1963).
8. J. Crossley and C. P. Smyth. J. Amer. Chem. Soc. **91**, 2482 (1969).
9. J. Crossley, G. P. Johari, and C. P. Smyth. J. Amer. Chem. Soc. **91**, 5197 (1969)

10 W. F. HASSELL, M. D. MAGEE, S. W. TUCKER and S. WALKER. Tetrahedron, **20**, 2137 (1964).
11. S. E. KEEFE and E. H. GRANT. Rev. Sci. Instrum. **39**, 800 (1968).
12. K. S. COLE and R. H. COLE. J. Chem. Phys. **9**, 341 (1941).
13. M. D. MAGEE and S. WALKER. Trans. Faraday Soc. **62**, 3093 (1966).
14. G. P. JOHARI and W. DANNHAUSER. J. Phys. Chem. **72**, 3273 (1968). W. DANNHAUSER. J. Chem. Phys. **48**, 1911, 1918 (1968).
15. P. BORDEWIJK, F. GRANSCH, and C. J. F. BOTTCHER. J. Phys. Chem. **73**, 3255 (1969).
16. J. MALECKI. J. Chem. Phys. **43**, 1351 (1965).
17. M. DAVIES and R. J. MEAKINS. J. Chem. Phys. **26**, 1584 (1957).
18. F. K. FONG and C. P. SMYTH. J. Amer. Chem. Soc. **85**, 1565 (1963).
19. M. D. MAGEE and S. WALKER. J. Phys. Chem. **74**, 2378 (1970).
20. W. DANNHAUSER and L. W. BAHE. J. Chem. Phys. **40**, 3058 (1964).
21. J. CROSSLEY and S. WALKER. J. Chem. Phys. **48**, 4742 (1968).

Can. J. Chem. Downloaded from www.nrcresearchpress.com by 210.87.254.5 on 09/05/12
For personal use only.

Synthesis and Properties of 5-Hydroxymethyl-2′-deoxyuridine and its α-Anomer[1]

V. S. GUPTA[2] AND G. L. BUBBAR

Department of Physiology, Western College of Veterinary Medicine, University of Saskatchewan, Saskatoon, Saskatchewan

Received September 4, 1970

The synthesis and properties of 5-hydroxymethyldeoxyuridine (**6**) and its α-anomer **7** are described. Treatment of 5-hydroxymethyluracil (**2**) with trimethylchlorosilane in the presence of triethylamine gave 2,4,5-tris(trimethylsilyl)-5-oxymethyluracil (**3**) in excellent yield (92%) which, upon condensation with 3,5-di-(*O*-*p*-toluoyl)-2-deoxy-D-ribofuranosyl chloride in acetonitrile at room temperature, furnished an anomeric mixture of substituted nucleosides β-anomer (**4**) and α-anomer (**5**) in high yield 90% (by a fusion method (12) yield of blocked nucleosides was 70%). Compound **4** was the major product formed by both methods and was recovered as a crystalline solid in high yield. However, condensation of **3** with chlorosugar in benezene with mercuric chloride as a catalyst at room temperature gave a mixture of protected nucleosides; the amount of **5** formed was appreciably higher (34%) and was isolated as a microcrystalline solid from mother liquors in low yield (without the catalyst nucleosides were formed in low yield 30%). Removal of the blocking groups by alcoholysis gave **6** and **7** in high yields. The structure was confirmed by n.m.r. studies, u.v. and i.r. absorption spectra, elemental analysis, and by conversion of **4** to β-thymidine (**8**).

Canadian Journal of Chemistry, 49, 719 (1971)

Can. J. Chem. Downloaded from www.nrcresearchpress.com by 210.87.254.5 on 09/05/12
For personal use only.

5-Hydroxymethyl-2′-deoxyuridylate replaces thymidylate of the DNA of a virulent group of *Bacillus subtilis* bacteriophages (1–4). Its biosynthesis from deoxyuridylate and 5,10-methylene tetrahydrofolate is catalyzed by the enzyme, hydroxymethylase (5, 6), which is analogous to the hydroxymethylation of deoxycytidylate of *Escherichia coli* T-even bacteriophages (7). The enzymic transformation of thymidine to 5-hydroxymethyldeoxyuridine (**6**), has been demonstrated in *Neurospora*, and 5-substituted pyrimidines may be intermediates in the transformation of thymine to RNA pyrimidines (8).

The synthesis of **6** from deoxyuridine under acidic conditions[3] was reported by Cline *et al.* (9), and the base-catalyzed hydroxymethylation[4] of deoxyuridine has been described by Baker *et al.* (10). Recently the chemical synthesis of **6** using a mercury procedure[5] has been reported (11); in this method the removal of the benzyl group by catalytic hydrogenation is a critical step for the synthesis of **6**. Although a quantitative yield of **4** from **9** has been reported (11), we were able to recover **4** in a yield of only 45–55% even after repeated experiments under similar conditions. Since none of these methods (9–11) was particularly suitable for the synthesis of **6** on a preparative scale (see also footnotes (3–5), we have therefore devised its synthesis by the following methods: (*a*) a fusion method developed by Nishimura and Schimizu (12); (*b*) a modified condensation method using mercuric chloride – benzene (13); and (*c*) by the interaction of silyl–pyrimidine with halogenose in organic solvents at room temperature,[6] all of which have several distinct advantages over the mercury procedure (11). They obviate the need for the synthesis of 5-benzyloxymethyluracil and debenzylation by catalytic hydrogenation. The desired natural β-anomer predominated in the reaction mixture in methods *a* and *c*.

5-Hydroxymethyluracil (**2**) on treatment with trimethylchlorosilane in the presence of triethylamine furnished tris(trimethylsilyl)-5-methoxyuracil (**3**) as an oil (92%). Condensation of **3** with 3,5-di-(*O*-*p*-toluoyl)-2-deoxy-D-ribofuranosyl chloride at 185–195° under anaerobic conditions (12) gave an anomeric mixture[7] of the

[1]This work was supported by the Medical Research Council of Canada (Grant MA-3136).

[2]To whom correspondence should be sent.

[3]From a mixture of products, **6** was isolated by ion exchange chromatography in poor yield (19%). Using the described conditions, Baker *et al.* (10) reported an even lower yield (< 10%).

[4]Although **6** was the main product under basic conditions, it could not be induced to crystallize and was difficult to isolate in the pure state.

[5]Mercury salt of 5-benzyloxymethyluracil was coupled with 3,5-di-(*O*-*p*-toluoyl)-D-ribofuranosylchloride, and from the reaction mixture, the blocked nucleoside 1-(2-deoxy-3,5-di-(*O*-*p*-toluoyl)-β-D-ribofuranosyl-5-benzyloxymethyluracil (**9**) was isolated in a yield of 57%. The removal of the benzyl group by catalytic hydrogenation yielded **4** which, upon deacylation gave **6**.

[6]Using this method we have also prepared 5-fluorodeoxyuridine, 5-iododeoxyuridine, and several other pyrimidine deoxyribonucleosides in excellent yields (14).

[7]Since the *trans* rule (15) is not obeyed during synthesis of the deoxyribonucleosides, both anomers are formed during the condensation reaction.

Can. J. Chem. Downloaded from www.nrcresearchpress.com by 210.87.254.5 on 09/05/12
For personal use only.

substituted nucleoside **4** and its corresponding α-anomer, **5**, in a ratio of *ca.* 8.5:1.5. After removal of the silyl groups by refluxing in aqueous acetone (60%), compound **4** was isolated from the reaction mixture as a crystalline solid in 44% yield. Chromatography of the filtrate on a silica gel column gave an additional 14% yield of **4**.

The β-configuration was assigned to **4** on the basis of a triplet for the anomeric proton at δ 6.33 with a coupling constant ($J_{1',2'} = J_{1',2''} = 6.95$ Hz). Catalytic hydrogenation of **4** with palladium oxide followed by alcoholysis resulted in almost complete conversion to β-thymidine (**8**) (16). This established the site of attachment of the deoxyribose and also its configuration. After deblocking with hot sodium methoxide in methanol, **6** was recovered as a microcrystalline solid in 80% yield. The structure and configuration of compound **6** and its corresponding α-anomer **7** was unequivocally established from the n.m.r. spectrum. In compound **6** the signal of the anomeric hydrogen (H-1′) appeared as a triplet at δ 6.18 and exhibited a coupling constant ($J_{1',2'} = J_{1',2''} = 7.0$ Hz). From mother liquors, 1-(2-deoxy-3,5-di-(*O*-*p*-toluoyl)-α-D-ribofuranosyl)-5-hydroxymethyluracil (**5**), was recovered in small yield (10%).[8] In compound **5**, the signal of the anomeric proton (H-1′) appeared as a quartet at δ 6.28. Deblocking by alcoholysis gave 1-(2-deoxy-α-D-ribofuranosyl)-5-hydroxymethyluracil (**7**) as a micro-crystalline solid in 62% yield. The α-configuration was assigned to **7** on the basis of a quartet at δ 6.12 for the anomeric proton and a coupling constant ($J_{1\ 2''} = 3.2$ and $J_{1',2'} = 7.8$ Hz). The signals of all other protons in compounds **6** and **7** appeared at the expected positions and the observed integration ratios were equal to the calculated values. The reactions are summarized in Scheme 1.

With the hope of improving further the yield of the deoxyribonucleosides and avoiding the formation of α-anomers, the synthesis of **6** was attempted under mild experimental conditions. Initially, the reactions were carried out using a recently published procedure (13).[9] The reaction mixture, consisting of **3**, halogenose, and the Lewis acid ($HgCl_2$) in benzene, was stirred at room temperature for 30 h. The total yield of the blocked nucleosides, **4** and **5**, as indicated by chromatography (t.l.c.) was higher (85–90%), but contrary to our expectations the amount of α-anomer formed was also appreciably increased (34%).

In order to obviate the formation of α-anomer, the synthesis of **6** in solvents (without catalyst) was studied. The reactions were carried out in benzene (nonpolar); and two polar solvents, dioxane and acetonitrile. The chlorosugar was allowed to react with **3** in the appropriate solvent for 30 h at room temperature. In benzene and dioxane, only relatively small amounts of the nucleosides were formed (yields 28 and 62% respectively) but in acetonitrile the blocked nucleosides were formed in excellent yields (90–95%). The yield of the β-anomer under these conditions was 80–85%. These results suggest that acetonitrile has a catalytic effect in the condensation reaction and its use provides a simple alternative procedure for the synthesis of **6** and other pyrimidine deoxyribonucleosides in high yields.

Experimental

Melting points were observed with a Gallenkamp apparatus and are uncorrected. Specific rotations were measured (1 dm tube) with a Perkin–Elmer model 141 automatic digital read out polarimeter. The n.m.r. spectra were recorded on a Varian Associate A-100 spectrometer using tetramethylsilane (TMS) as a standard (unless otherwise indicated). All compounds were dissolved in dimethylsulfoxide (DMSO-d_6). The i.r. spectra were recorded with a Perkin–Elmer Model 421 spectrophotometer. The Unicam spectrophotometer, Model SP800 was used to measure the complete u.v. absorption spectra. Microanalyses were performed by the microanalytical laboratories of the Prairie Regional Research Laboratory, Saskatoon, Saskatchewan. The t.l.c. was carried out on silica gel (HF_{254}) at room temperature. Ascending paper chromatography was carried out on Whatman No. 1 paper at room temperature using the following solvents (by volume): (*A*) *n*-butanol – glacial acetic acid – water (4:1:5), upper phase and (*B*) *i*-propanol–NH_4OH–water (7:1:2). The spots were detected by visual examination under u.v. illumination. The R_f values are ±0.05. Evaporations under diminished pressure were performed on rotary evaporators at 35°.

5-Hydroxymethyluracil (2)

The base-catalyzed hydroxymethylation of uracil was carried out by the method of Cline *et al.* (9) and the product was twice crystallized from aqueous ethanol to give **2** as a microcrystalline powder; n.m.r. spectrum was at δ 11.02 (1H,s,3-NH), 10.67 (1H,s,1-NH), 7.23 (1H,s, H-6), 4.81 (1H,t,J = 6.0 Hz, proton of the hydroxyl group 5-CH_2OH), 4.12 (2H,d,5-CH_2—) p.p.m. The

[8]The high specificity for β-configuration of the silyl condensation method has been observed previously (17 18).

[9]Besides mercury halides (see also 19–21), the use of several other catalysts in the synthesis of pyrimidine nucleosides has been discussed (20, 22–25).

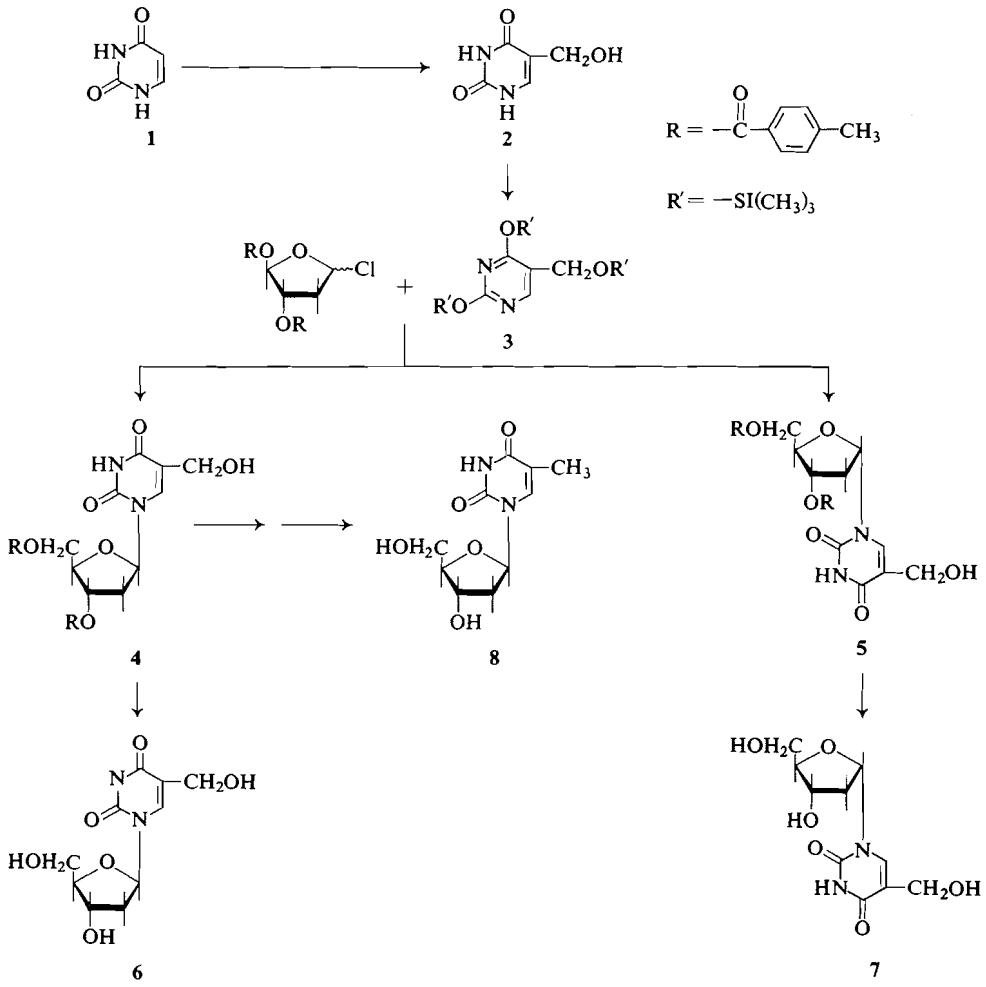

SCHEME 1

product showed a homogenous spot by t.l.c. on silica gel (R_f 0.53) using $CHCl_3$–MeOH (8:2) as the developer. The u.v. absorption spectrum and m.p. were the same as reported (9).

2,4,5-Tris(trimethylsilyl)-5-oxymethyluracil (3)

Trimethylchlorosilane (17.36 g, 160 mmol) was added to a stirring suspension of **2** (5.62 g, 40 mmol) in 100 ml of anhydrous benzene. After 5 min triethylamine (16.16 g, 160 mmol) was added dropwise over a period of 30 min, and the reaction mixture was stirred at room temperature for 20 h. Precipitated triethylamine hydrochloride was filtered and the residue was washed with benzene (3 × 20 ml). The filtrate and washings were combined and the solvent was removed *in vacuo* at 30° to yield a viscous, oily liquid of crude product. The oil was distilled at 124°/0.1 mm to yield **3** (13.20 g 92%); i.r. (26) ν_{max} (liquid film) cm^{-1} 1030 (Si—O—C), 830 and 1246 Si-$(CH_3)_3$, no absorption at 3500 (free OH).

The n.m.r. (solvent CCl_4; formic acid external to locate trimethylsilyl groups) at δ 2.59 (9H,s,2 or 4-Si$(CH_3)_3$), 2.55 (9H,s,2 or 4-Si$(CH_3)_3$), 2.34 (9H,s,5-*O*-Si$(CH_3)_3$), 6.69 (2H,s,5-CH_2—) p.p.m. to locate the 6 position proton of the pyrimidine ring (TMS lock) at δ 7.97 (1H,s,6-H) and 4.34 (2H,s,5-CH_2—) p.p.m. integration ratio 1:2:27.

1-[2-Deoxy-3,5-di-(O-p-toluoyl)-β-D-ribofuranosyl]-5-hydroxymethyluracil (4)

(a) Fusion Method (12)

A mixture of **3** (5.37 g, 15 mmol) and 3,5-di-(*O*-*p*-toluoyl)-2-deoxy-D-ribofuranosyl chloride (27) 5.83 g, 15 mmol) was placed in a preheated (to 170°) oil bath under anhydrous conditions. As soon as the halogenose melted, the mixture was flushed with nitrogen, the temperature of the bath was raised to 185–195°, and the reaction mixture was kept at this temperature for an additional 30 min under a continuous stream of nitrogen. The gummy residue was triturated with 75 ml of aqueous acetone (60%), and the resulting mixture was refluxed for 30 min and filtered hot through a bed of celite–charcoal under reduced pressure. The celite–charcoal mixture was washed with hot EtOH (3 × 25 ml) and examined by chromatography (t.l.c. $CHCl_3$–MeOH, 95:5). In addition to the blocked nucleosides (R_f 0.55) there were two

Can. J. Chem. Downloaded from www.nrcresearchpress.com by 210.87.254.5 on 09/05/12
For personal use only.

Can. J. Chem. Downloaded from www.nrcresearchpress.com by 210.87.254.5 on 09/05/12
For personal use only.

additional quenching spots (R_f 0.05, minor unreacted **2** and R_f 0.98, sugar by-products). The solvent was evaporated to dryness and the residue was shaken with chloroform (2 × 15 ml). The insoluble material was collected by filtration, the solvent was removed *in vacuo*, the residue was dissolved in hot EtOH (30 ml) and after standing overnight at room temperature, the crystals (2.83 g) were filtered. Recrystallization from MeOH gave white glistening needles of the β-anomer (1.87 g m.p. 167–168°). The combined mother liquors were concentrated to dryness and the residue (3.25 g) was dissolved in benzene (15 ml) and applied to a column (2 × 25 cm) of silica gel packed in benzene. Elution was begun with benzene (2 l) and followed with benzene containing increasing amounts of ether (10, 20, 30, and 40%, 200 ml of each). Fractions (25 ml) were collected and monitored by t.l.c. using $CHCl_3$–MeOH (9:1) as the developer. Only sugar by-products and other contaminants were eluted until fractions 27 and 28, in which a small amount of nucleosides (< 5%) along with sugar components appeared (as shown by t.l.c.). All these fractions were discarded. The mixture of nucleosides was finally desorbed from the column with ether (1200 ml) and the solvent was evaporated to dryness. The residue (2.135 g) containing both anomers of blocked nucleoside was dissolved in hot MeOH and on standing at room temperature gave an additional 0.53 g of **4**. The total yield of **4** was 2.403 g, 57.6%.

(b) Benzene – Mercuric Chloride (13)

The mixture of **3** (716 mg, 2 mmol), halogenose (855.1 mg, 2.1 mmol), and $HgCl_2$ (108.6 mg, 0.4 mmol) in anhydrous benzene (10 ml) was stirred at room temperature for 30 h. Two ml of water was added and after stirring for 30 min at room temperature the solvent was removed under reduced pressure. The gummy residue was taken up in $CHCl_3$ (15 ml) and the resulting mixture was refluxed for 30 min. The aqueous layer was separated and extracted with $CHCl_3$ (2 × 10 ml). The combined organic extract was washed with NaI (10 ml of 10% aqueous solution), water (3 × 20 ml), dried, and evaporated to yield an anomeric mixture of nucleosides as a white fluffy powder (975 mg). Crystallization from MeOH followed in EtOH gave **4** as a crystalline solid (410 mg, 41.5%). Mother liquors on standing gave an additional quantity (112 mg, 11.33%). Total yield of **4** was 52.83%.

(c) Using Acetonitrile

To a stirred suspension of chlorosugar (4.274 g, 11 mmol) in anhydrous acetonitrile (15 ml) was added **3** (3.58 g, 10 mmol). The reaction mixture was slightly warmed and then stored at room temperature for 30 h. Water (5 ml) was added, stirred for 30 min, solvent was removed, and the residue was extracted with $CHCl_3$ (3 × 20 ml). The chloroform layer was washed with water, dried, the solvent was removed *in vacuo*; the residue was dissolved in hot MeOH (30 ml) and after keeping overnight at room temperature the crystals (3.80 g, 67.9%) were collected by filtration; m.p. 167–168° (lit. (11), 167–169°); $[\alpha]_D^{25}$ −60.5° (*c*, 0.08 in $CHCl_3$); u.v. (EtOH 95%) λ_{max} 242.0 (ε 36.6 × 10^3 M^{-1} cm^{-1}) and broad sh. at 265–270 mμ; n.m.r. at δ 11.45 (1H,s,3-NH), 7.62 (1H,s,H-6), 4.93 (1H,t,J = 5.5 Hz, proton of the hydroxyl group of 5-CH_2OH), 4.12 (2H, d, 5-CH_2— with ring), 6.33 (1H,t,$J_{1',2'} = J_{1',2''}$ = 6.95 Hz H-1′ (lit. (11), 6.34, t, J = 6.7 Hz), 5.59 (1H,m,H-3′, 4.57 (2H,s,5′-CH_2—) 4.49–4.52 (1H,m,H-4′ overlapped by the hydroxy group of 5′-CH_2OH), 2.46–2.68 (2H,m, solvent and H-2′, -2′′), 7.87 and 7.95 (4H, d, 2 sets, two phenyl rings H-3 and -5), 7.29 and 7.37 (4H, d, 2 sets, two phenyl rings H-2 and -6), 2.40 p.p.m. (6H,s,two *p*-methyl groups of benzene rings).

Anal. calcd. for $C_{26}H_{26}N_2O_8$ (mol. wt. 494.5): C, 63.15; H, 5.30; N, 5.66. Found: C, 62.95; H, 5.35; N, 5.62.

From mother liquors an additional quantity (0.39 g, 7.89%) of **4** was recovered as a crystalline solid. Examination of the mother liquor by t.l.c. showed that it contained mostly α-anomer **5** along with a small amount of **4** (*ca.* 5%). This compound was homogeneous by t.l.c. on silica gel (R_f 0.56) using $CHCl_3$–MeOH (95:5) as the developer.

1-[2-Deoxy-3,5-di-(O-p-toluoyl)-α-D-ribofuranosyl]-5-hydroxymethyluracil (5)

(a) Fusion Method (12)

Mother liquors left after the removal of the β-anomer (**4**) were combined, concentrated (*ca.* 15 ml), and on standing at 4° after several days slowly gave a microcrystalline solid (555 mg, m.p. 148–151°). On recrystallization from MeOH–ether **5** was obtained as fine needles (255 mg). Examination of the mother liquors by t.l.c. showed a single spot corresponding to the nucleosides; but additional quantity of either nucleoside anomer was not obtained by crystallization. After deblocking, the corresponding free anomers **6** and **7** could be separated by preparative t.l.c. (*vide infra*).

(b) Benzene – Mercuric Chloride (13)

The solvent was evaporated from the mother liquors and the residue (480 mg) was dissolved in boiling ether (20 ml). On cooling the crystals (320 mg) separated and were collected by filtration. Crystallization from MeOH gave **5** as fine needles (187 mg, 18.92%). Mother liquors on keeping at room temperature gave an additional amount (34 mg) of the material. Total yield of **5** (221 mg, 22.36%); m.p. 154–155° (lit. (11), 151–152°); $[\alpha]_D^{25}$ −13.9° (*c*, 1.0 in $CHCl_3$); u.v. (EtOH 95%) λ_{max} 241.5 (ε 34.4 × 10^3 M^{-1} cm^{-1}) and broad sh. 265–270 mμ; n.m.r. at δ 11.38 (1H,s,3-NH), 7.76 (1H,s, H-6), 5.04 (1H,s,proton of the hydroxyl group of 5-CH_2OH overlapped with H-4′), 4.17 (2H,d,5-CH_2— with ring) 6.28 (1H, q, $J_{1'} = J_{2'} = 6.0$ Hz, $= J_{1'} = J_{2''} = 1.7$ Hz, H-1′), 4.93 (1H,t, H-4′ overlapped with the hydroxy group of 5-CH_2OH), 4.46 (2H,d,5′-CH_2—), 2.82–3.14 p.p.m. (2H,m, solvent and H-2′ and -2′′ and all other bands for protons given under **4**).

Anal. Calcd. for $C_{26}H_{26}N_2O_8$ (mol. wt. 494.5): C, 63.15; H, 5.30; N, 5.66. Found: C, 63.20; H 5.25; N, 5.57.

The compound showed a single quenching spot by t.l.c. on silica gel (R_f 0.56, $CHCl_3$–MeOH, 95:5).

1-(2-Deoxy-β-D-ribofuranosyl)-5-hydroxymethyluracil (6)

Compound **4** (300 mg) was dissolved in 4.0 ml of NaOH (2 *N*) containing EtOH (8.0 ml) and the solution was left overnight at room temperature or, alternatively, refluxed with MeONa (150 mg) in absolute MeOH (5 ml) for 30 min. Dowex 50 (H^+; X_8; 200–400 mesh) was added

Can. J. Chem. Downloaded from www.nrcresearchpress.com by 210.87.254.5 on 09/05/12
For personal use only.

and the solution (p*H* 4–5) was stirred for 30 min. The resin was removed by filtration and was repeatedly washed with water (2 × 4 ml). The acidic filtrate and washings were combined, the solvent was evaporated, and the syrup was triturated with water (30 ml). Precipitated toluic acid was filtered and the mother liquors were freed of residual toluic acid by extraction with ether (2 × 30 ml). The aqueous phase was concentrated and finally co-evaporated with absolute ethanol to remove the last traces of water. The residue was crystallized from absolute EtOH–EtOAc (95 mg, 61%); m.p. 182° (lit. (9) 176–179°, and (11) 180–182°); $[\alpha]_D^{25}$ +19.5° (*c*, 1.25 in water); u.v. at p*H* 1 λ_{max} 264 (ε 10.55 × 10^3 M^{-1} cm^{-1}), 208 mμ (ε 11.15 × 10^3 M^{-1} cm^{-1}) and λ_{min} 232 mμ (ε 2.73 × 10^3 M^{-1} cm^{-1}); n.m.r. at δ 11.29 (1H,s,3-NH), 7.73 (1H,s, H-6), 4.85 (1H,t, proton of the hydroxyl group of 5-CH_2OH overlapped with the proton of the hydroxyl group of 5′-CH_2OH), 4.12 (2H,d,5-CH_2 with ring), 6.18 [1H,t,$J_{1',2'} = J_{1',2''}$ = 7 Hz, H-1′, lit. (11) 6.20 (1H,t,$J_{1',2'} = J_{1',2''}$ = 6.6 Hz), 4.24 (1H,t, H-3′), 5.23 (1H,d,proton of the hydroxyl group of 3′-CHOH), 3.80 (1H,q, H-4′), 3.55 (2H,t,5′-CH_2—), 4.92 (1H,t,proton of the hydroxyl group of 5′-CH_2OH overlapped with the proton of the hydroxyl group of 5-CH_2OH), 2.10 p.p.m. (2H,q,*J* = 6 Hz, H-2′ and -2″).

Anal. Calcd. for $C_{10}H_{14}N_2O_6$ (mol. wt. 258.2): C, 46.50; H, 5.46; N, 10.85. Found: C, 46.24; H, 5.26; N, 10.55.

The compound moved as a homogeneous spot on paper (R_f 0.34, 0.48) in solvents *A* and *B* and on silica gel (R_f 0.28, $CHCl_3$–MeOH 8:2). Mother liquors gave an additional (30 mg) of product with a slightly lower m.p. (176–178°) but it was chromatographically homogeneous (R_f 0.31).

1-(2-Deoxy-α-D-ribofuranosyl)5-hydroxymethyluracil (7)

(a) Hydrolysis of 5

Compound **5** (300 mg) was added to 5 ml of absolute MeOH containing MeONa (150 mg), and refluxed for 30 min, deionized, and worked-up as described for **6** (above). The residue was twice crystallized from EtOAc–cyclohexane and **7** (85 mg) was recovered as a microcrystalline solid.

(b) By Preparative Thin-layer Chromatography of Mother Liquors (Fusion Method)

After removal of **4** and **5**, the mother liquors were combined, the solvent was removed *in vacuo*, and the residue (0.95 g) was hydrolyzed by refluxing with sodium methoxide (500 mg in 15 ml of anhydrous MeOH) and treated as above for **6**. The concentrated solution (*ca.* 6 ml) was spread on silica gel plates (8, 20 × 20 cm, 0.65 mm) and developed with $CHCl_3$–MeOH (80:20). The respective zones were marked under u.v. and nucleoside bands were separately extracted with hot MeOH. The solvent was removed and the residue (395 mg) was crystallized from ethylacetate–cyclohexane to yield **7** as a microcrystalline solid (137 mg, 62%); m.p. 171° (lit. (11) 169–170°; $[\alpha]_D^{25}$ + 5.8° (*c*, 1.35 in water); u.v. at p*H* 1, λ_{max} 264.5 (ε 10.4 × 10^3 M^{-1} cm^{-1}), 207 mμ (ε 11.05 × 10^3 M^{-1} cm^{-1}) and λ_{min} 231 mμ (ε 2.68 × 10^3 M^{-1} cm^{-1}); n.m.r. at δ 7.90 (1H,s, H-6), 6.12 (1H,q,$J_{1',2''}$ = 3 Hz, and $J_{1',2'}$ = 7.5 Hz H-1′), 2.44–2.78 (1H,m, partially buried under the solvent, H-2′), 1.82 and 1.96 (1H, two triplets, H-2″), 4.17–4.26 (2H,m, H-3′ and H-4′) p.p.m. and all other proton peaks as given under **6**.

Anal. calcd. for $C_{10}H_{14}N_2O_6$ (mol. wt. 258.2): C, 46.50; H, 5.46; N, 10.85. Found: C, 46.75; H, 5.46; N, 10.45.

The product was homogeneous on paper (R_f 0.51, 0.75 in solvents *A* and *B*) and t.l.c. (R_f 0.44, $CHCl_3$–MeOH, 8:2). Mother liquors showed a single quenching spot (R_f 0.5) but the nucleoside did not crystallize.

1-(2-Deoxy-β-D-ribofuranosyl)5-methyluracil (β-Thymidine) (8)

Compound **4** (200 mg) was added to glacial acetic acid (15 ml) containing palladium oxide (300 mg) and hydrogenated for 4 h at 2 lb pressure in Parr's apparatus. The catalyst was filtered, solvent removed *in vacuo*, and the residue was crystallized from EtOH to yield 1-[2-deoxy-3,5-di-(*O*-*p*-toluoyl)-β-D-ribofuranosyl]5-methyluracil, (130 mg, m.p. 198–199°, R_f 0.85, $CHCl_3$–MeOH, 95:5). Toluoyl groups were removed using sodium methoxide, and β-thymidine (7) was isolated from the reaction mixture in quantitative yield. Specific rotation, u.v. absorption and n.m.r. spectra were identical with the authentic sample.

The authors wish to thank Drs. J. C. MacDonald (P.R.L., Saskatoon) for allowing use of the polarimeter, and F. M. Loew (Veterinary College) for helpful suggestions in the preparation of this manuscript; Mr. T. Mazurek for measuring the n.m.r. spectra and Mr. B. Haid for recording the i.r. spectra and microanalyses.

1. R. G. KALLEN, M. SIMON, and J. MARMUR. J. Mol. Biol. **5**, 248 (1963).
2. S. OKUBO, B. STRAUSS, and M. STODOLSKY. Virology, **24**, 552 (1964).
3. J. J. PENE and J. MARMUR. Fed. Proc. **23**, 318 (1964).
4. D. H. ROSCOE, and R. G. TUCKER. Biochem. Biophys. Res. Commun. **16**, 106 (1964).
5. F. KAHAN, E. KAHAN, and B. RIDDLE. Fed. Proc. **23**, 318 (1964).
6. D. H. ROSCOE and R. G. TUCKER. Virology, **29**, 157 (1966).
7. J. G. FLAKS and S. S. COHEN. J. Biol. Chem. **234**, 1501 (1959).
8. M. T. ABBOT, R. J. KADNER, and R. M. FINK. J. Biol. Chem. **239**, 156 (1964).
9. R. E. CLINE, R. M. FINK, and K. FINK. J. Amer. Chem. Soc. **81**, 2521 (1959).
10. B. R. BAKER, T. J. SCHWAN, and D. V. SANTI. J. Med. Chem. **9**, 66 (1966).
11. R. BROSSMER and E. ROHM. Hoppe-Seyler's Z. Physiol. Chem. **348**, 1431 (1967).
12. T. NISHIMURA and B. SCHIMIZU. Agr. Biol. Chem. Tokyo, **28**, 224 (1964).
13. B. SCHIMIZU and A. SAITO. Agr. Biol. Chem. Tokyo, **33**, 119 (1969).
14. V. S. GUPTA and G. L. BUBBAR. Unpublished results.
15. B. R. BAKER. The chemistry and biology of purines. Ciba Foundation Symposium, 1957. p. 213.
16. A. M. MICHELSON and A. R. TODD. J. Chem. Soc. 816 (1955).
17. H. G. STOUT and R. K. ROBINS. J. Org. Chem. **33**, 1219 (1968).

18. G. L. BUBBAR and V. S. GUPTA. Can. J. Chem. **48**, 3147 (1970).
19. M. PRYSTAS and F. SÖRM. Coll. Czechoslov. Chem. Comm. **30**, 1900 (1965).
20. E. WITTENBERG. Chem. Ber. **101**, 1095 (1968).
21. G. T. ROGERS, R. S. SHADBOLT, and T. L. V. ULBRICHT. J. Chem. Soc. C, 203 (1969).
22. G. WAGNER. Z. Chem. **6**, 367 (1966).
23. D. THACKER and T. L. V. ULBRICHT. J. Chem. Soc. C, 333 (1968).
24. G. T. ROGERS, R. S. SHADBOLT, and T. L. V. ULBRICHT. J. Chem. Soc. C, 209 (1969).
25. U. NIEDBALLA and H. VORBRÜGGEN. Angew. Chem. Int. Ed. **9** (6), 461 (1970).
26. L. J. BELLAMY. The infrared spectra of complex molecules. 2nd Edition. John Wiley and Sons, Inc., New York, N.Y., 1958. p. 334.
27. M. HOFFER. Chem. Ber. **93**, 277 (1960).

Can. J. Chem. Downloaded from www.nrcresearchpress.com by 210.87.254.5 on 09/05/12
For personal use only.

Can. J. Chem. Downloaded from www.nrcresearchpress.com by 210.87.254.40 on 09/05/12
For personal use only.

γ-Radiolysis of Cysteine-Cysteamine Disulfide in Aqueous Solution[1]

J. W. PURDIE[2]
Division of Biology, National Research Council of Canada, Ottawa, Canada

Received September 21, 1970

γ-Radiolysis of a mixed disulfide, cysteine-cysteamine disulfide, in unbuffered aqueous solution (0.3 m*M*) was investigated in the presence and absence of oxygen. The principal products were the thiols (cysteine and cysteamine), the corresponding sulfinic and sulfonic acids, the symmetrical disulfides (cystine and cystamine) and ammonia. Cystine and cystamine were formed in very high yields in deaerated solution; (G(CySSCy) ~ 15) but addition of oxygen reduced the yield sharply and it was inversely proportional to the oxygen concentration except at very low oxygen levels. In aerated solution G(CySSCy) = 0.8. These observations were attributed to a chain reaction which was suppressed by oxygen:

$$RS\cdot + R'SSR \rightleftarrows RSSR + R'S\cdot$$

$$RS\cdot + O_2 \rightarrow RSOO\cdot$$

In the case of proteins, it was concluded that although chain reactions between RS· radicals and protein disulfide bonds were possible, they should be inhibited by oxygen.

On a exposé un disulfide asymétrique, cysteine-cysteamine disulfide, dans une solution aqueuse (0.3 m*M*), aux rayonnements gamma avec et sans la présence de l'oxygène. Les produits principaux étaient les thiols (cysteine et cysteamine), les acides sulfiniques et sulfoniques, les disulfides symétriques (cystine et cystamine) et l'ammoniaque. Les rendements de cystine étaient grands dans les solutions déaérées (G(CySSCy) ~ 15) mais ils ont diminué rapidement lorsqu'on a ajouté de l'oxygène et ils étaient en proportion inverse de la concentration de l'oxygène. Dans les solutions aérées G(CySSCy) = 0.8. Pour expliquer ces résultats on propose une réaction chaîneuse qui est supprimée par l'oxygène:

$$RS\cdot + R'SSR \rightleftarrows RSSR + R'S\cdot$$

$$RS\cdot + O_2 \rightarrow RSOO\cdot$$

Tant qu'aux protéines, on a conclu que des réactions entre les radicaux RS· et les disulfides du protéine sont possible mais ils doivent être inhibités par l'oxygène.

Canadian Journal of Chemistry, 49, 725 (1971)

In previous communications (1–3) we have reported results from the γ-radiolysis of cystine, penicillamine disulfide, and cysteine-penicillamine mixed disulfide. The study has now been extended to cysteine-cysteamine disulfide. This series of disulfides provides a direct comparison of cysteine in combination with a protective thiol (cysteamine) and a non-protective thiol (penicillamine). The radiation chemistry of these compounds is important to studies of the mechanism of radiation protection and the effects of ionizing radiation on protein disulfide bonds. Recent work in this field has been concentrated mainly on the radiation chemistry of cysteine and related thiols; Armstrong and co-workers (4), Packer and Winchester (5), Adams *et al.* (6), and Henglein and co-workers (7).

The abbreviation CySSCya is used to represent *L*-cysteine-cysteamine disulfide hydrochloride which was used in this study, *i.e.* (1,6-diamino-3,4-dithiahexane-1-carboxylic acid hydrochloride).

$$COO^-CH(NH_3^+)CH_2SSCH_2CH_2NH_3^+Cl^-$$

Experimental

Materials

Reference amino acids were obtained from Mann Research Laboratories or Calbiochem. Cystine and cystamine for irradiation were purchased from Mann Research Laboratories (M.A. grade) and were used without further purification. A sample of the cystamine hydrochloride was converted to the sulfate salt by passing a solution through a column of Dowex 1-X8 anion exchange resin in the sulfate form. The cystamine sulfate was crystallized from aqueous ethanol.

L-*Cysteine-cysteamine Disulfide Hydrochloride*

The material used for irradiation was prepared from cysteamine hydrochloride and cystine-*S*-monoxide (8). The monoxide was prepared by the method of Savige *et al.* (9) as described previously (3). Cystine-*S*-monoxide (3.2 g) in water (10 ml) was mixed with cysteamine hydrochloride (2.5 g) in water (10 ml) and shaken for 30 min. Sufficient ethanol was added to precipitate the product (about 100 ml) which was filtered off and dried.

---

[1]Issued as DREO Report No. 627.

[2]Attached staff from Defence Research Establishment Ottawa.

Can. J. Chem. Downloaded from www.nrcresearchpress.com by 210.87.254.40 on 09/05/12
For personal use only.

The material obtained (3.3 g) was dissolved in 0.1 *N* hydrochloric acid (15 ml) then the solution was filtered, adjusted to p*H* 5 with pyridine and again filtered. The product crystallized out at 5 °C after addition of ethanol (10 ml). A further fraction was obtained after addition of more ethanol to the filtrate. Total yield 2.5 g (50%), m.p. 181–182 °C.

Anal. Calcd. for $C_5H_{13}N_2O_2S_2Cl$: C, 25.81; H, 5.65; N, 12.04; S, 27.52; Cl. 15.26. Found: C, 25.74; H, 5.73; N, 11.92; S, 27.27; Cl, 15.10.

Examination with the amino acid analyzer showed only slight traces of cystine and cysteine sulfinic acid. The n.m.r. spectrum of the mixed disulfide in trifluoroacetic acid had peaks centered at $\tau = 2.28$ (NH_3^+ of Cy—), 2.90 (NH_3^+ of Cya—), 5.20 (CH), 6.42 ($2 \times CH_2$). and 6.74 (CH_2).

Irradiations and Analysis

Solutions of CySSCya for irradiation were unbuffered, 0.3 m*M* except where otherwise stated, and were prepared using triply distilled water with the usual precautions (1). The aerated solution had a p*H* close to 5. Preliminary irradiations were performed with a ^{60}Co source in a well as before but the work was completed using a "Gammacell" 220 (Atomic Energy Canada Ltd.) which provided approximately the same dose rate; 600 rad per min (ferrous sulfate dosimetry).

Most of the products were measured using a Technicon amino acid analyzer with columns of "Chromobeads" cation exchange resin and Dowex 1-X8 anion exchange resin (10). However, cystamine was too basic to be eluted successfully from the cation exchange resin and it could not be separated from the mixed disulfide on Dowex 1 resin since buffers of p*H* greater than 6 would have converted the mixed disulfide to a mixture of cystine and cystamine. Consequently, the yield of cystamine was determined by electrophoresis on strips of cellulose polyacetate "Sepraphore" III (Gelman Ltd.) (11). The disulfides separated well in 20 min at 200 V using a sodium acetate – acetic acid buffer at p*H* 5. The strips were developed with ninhydrin and the yields were estimated using a densitometer (Photovolt Ltd.) or a microdensitometer (Joyce Recording Microdensitometer, Model 12B Mark III).

Results

The products of the radiolysis of cysteine-cysteamine disulfide in aqueous solution consisted of those products which have been obtained by radiolysis of cystine (1, 12) and cystamine (13) together with the symmetrical disulfides cystine and cystamine. In aerated solution the yields were linear with dose up to at least 10 krad and the *G* values (molecules formed per 100 eV) of the products were determined from several experiments following exposure to 10 krad or less. In deaerated solution the yields of products were linear with dose in the same range with the exception of the symmetrical disulfides, CySSCy and CyaSSCya. The yields of the latter compounds were very high and *G* values were determined from the initial slopes of dose-yield plots.

Solutions of cystamine hydrochloride, 0.3 m*M*, were irradiated for comparison with the unsymmetrical disulfide under similar conditions. The sulfate of cystamine was also irradiated and it was found to give the same results as the hydrochloride. The p*H* of the unbuffered aerated solutions was close to 5. In solutions of low p*H* the chloride ion reacts with an ·OH radical to give a chlorine atom which can cause deamination (14) but this problem did not arise in the present work. Additional results were obtained by irradiating a mixture of cystine and cystamine hydrochloride and measuring the yield of products resulting, including the unsymmetrical disulfide. The solution contained equimolar amounts of cystine and cystamine and had a total disulfide concentration of 0.3 m*M*. The yields of the thiols were determined by adding sodium iodoacetate to the irradiated solution to produce the *S*-carboxymethyl derivatives and then analyzing with the amino acid analyzer. Table 1 contains the results of these experiments: *G* values are given for the major products from the mixed disulfide, from the mixture of cystine and cystamine, and from cystine and cystamine irradiated separately.

The yields of the products from CySSCya were reproducible to within ±5% with the exception of the thiols (±10%) and the disulfides in deaerated solution (±30%). The yields of disulfides in deaerated solution were very sensitive to traces of oxygen. The loss of unsymmetrical disulfide, *G*(—CySSCya), was 2.8 in aerated solution and hence the recovery of nitrogen in the products after 10 krad was about 90%. The recovery of nitrogen in deaerated solution, measured after exposure to 10 krad, was approximately 80%.

In contrast with cysteine-penicillamine disulfide (3), very little trisulfide was obtained from cysteine-cysteamine disulfide by radiolysis. No trisulfide of cystamine (*i.e.* CyaSSSCya) was observed and only trace amounts of ethylamine and ethanolamine were found. The latter compounds could be by-products resulting from splitting of the C—S bond of the cystamine half of the mixed disulfide. In the case of penicillamine disulfides significant yields of penicillamine trisulfide, valine, and hydroxyvaline were obtained.

TABLE 1. Radiolysis of CySSCya in 0.3 m*M* solution. The *G* values for principal products and comparison with CySSCy and CyaSSCya

Product	Aerated solutions			Deaerated solutions		
	CySSCya	Mixture	CySSCy or CyaSSCya	CySSCya	Mixture	CySSCy or CyaSSCya
$CySO_2H$	0.10	0.37	0.9	0.31	0.51	1.2
$CySO_3H$	0.54	0.53	1.2	0.01	Trace	Trace
$CyaSO_3H$	0.81	1.04	1.03	0.10	0.09	0.15
$CyaSO_2H$	Trace	0.13	0.14	0.13	0.22	0.44
Serine	0.04	0.04	0.05	0	0	0
CySH	Trace	0.10	0.7	1.0	0.7	2.5
Alanine	0	0	0	0	0.04	0.1
CySSCy	0.80	—	—	15	—	—
CySSCya	—	3.5	—	—	20	—
CyaSSCya	0.7	—	—	15	—	—
CySSSCy	Trace	Trace	0.15	0.06	0.01	0.25
CyaSH	0.05	Trace	0.10	0.66	1.20	2.0
NH_3	0.28	0.43	—	0.27	0.11	—
Ethylamine	Trace	0	0	Trace	Trace	Trace
Ethanolamine	Trace	0	0.1	Trace	0	Trace

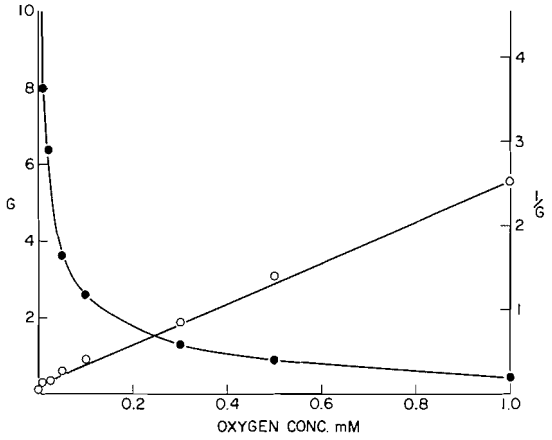

FIG. 1. Effect of oxygen concentration on the yield of cystine: ●, *G*(CySSCy), left-hand scale; ○, 1/*G*-(CySSCy), right-hand scale.

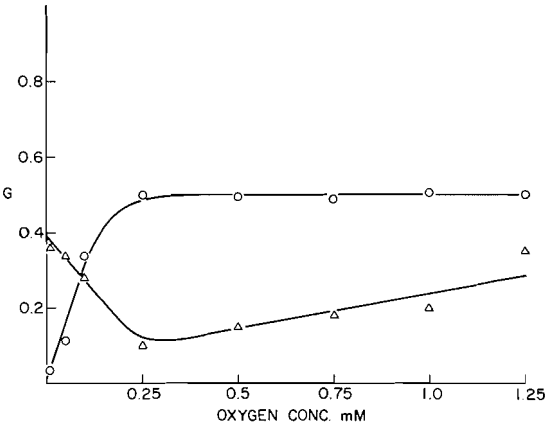

FIG. 2. Effect of oxygen concentration on $G(CySO_3H)$, ○, and $G(CySO_2H)$, △.

In view of the large difference in the yields of symmetrical disulfides between aerated and deaerated solutions, the effect of oxygen on the yield of cystine was investigated in more detail. Solutions were degassed in the usual way (four cycles of freezing, pumping, and thawing) and a measured amount of oxygen was added before sealing and irradiating the samples. The *G* values were determined for each oxygen concentration studied from the slope of the initial dose–yield plot. The results are illustrated in Fig. 1 which shows the variation of *G*(CySSCy) with oxygen concentrations. The reciprocal, 1/*G*(CySSCy), was approximately linear with oxygen concentration. The effect of oxygen on two other products was also interesting and Fig. 2 illustrates the changes in $G(CySO_3H)$ and $G(CySO_2H)$. The effect of changing the concentration of the solute on *G*(CySSCy) was investigated: two oxygen levels were chosen for this, aerated ($[O_2]$ = 0.25 m*M*) and oxygenated ($[O_2]$ = 1.2 m*M*), and the results are shown in Fig. 3. The yield of cystine was followed in these experiments as it could be measured more accurately than that of cystamine. Similarly, it was easier to measure the sulfinic and sulfonic acids of cysteine since they separated easily from all other products using the Dowex 1 column.

The effect of nitrous oxide on the yield of cystine was measured by degassing 25 ml samples then adding nitrous oxide. The concentration of

Can. J. Chem. Downloaded from www.nrcresearchpress.com by 210.87.254.40 on 09/05/12
For personal use only.

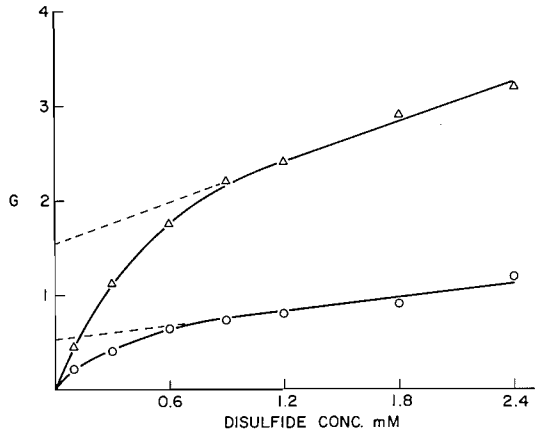

FIG 3. Effect of disulfide concentration on *G*-(CySSCy): △, aerated solution; ○, oxygenated solution.

nitrous oxide used was 20 m*M*. Found: *G*(CySSCy) = 8.0. A similar yield was obtained using a solution saturated with N_2O at atmospheric pressure.

Discussion

Radiolysis of cysteine-cysteamine disulfide was similar to radiolysis of cysteine-penicillamine disulfide in that the same products were obtained irrespective of whether the cysteine and cysteamine were combined in symmetrical or unsymmetrical disulfides. Also, as shown in Table 1, the mixed disulfide, the mixture of both symmetrical disulfides, and the pure symmetrical disulfides gave the same products and in the same relative yields. Hence it is concluded that the cysteine and cysteamine sulfur atoms react with the free radicals from water at approximately equal rates. Some variations in the yields were found between the mixed disulfide and the symmetrical disulfides, but these could have resulted from the secondary reactions rather than from the primary radical attack.

It has been reported that when a mixture of cystine and cystamine is irradiated in aqueous solution only the cystamine is attacked (15). This statement was not substantiated. Products from both cystine and cystamine were invariably produced when a mixture in aqueous solution was irradiated.

The principal reactions of solvated electrons (6, 7) and hydroxyl radicals (16) with disulfides appear to be as in reactions 1–3. From recent

[1] $\mathrm{RSSR + \cdot OH \rightarrow RSOH + RS\cdot}$

[2] $\mathrm{RSSR + e_{aq}^- \rightarrow (RSSR)^-}$

[3] $\mathrm{(RSSR)^- \rightarrow RS\cdot + RS^-}$

measurements of the yields of free radicals from water at low doses Bielski and Allen (17) obtained values of $G_{OH} = 2.74$ and $G_{red} = 3.3$. If all primary free radicals reacted to produce RS· radicals which combined to give symmetrical disulfides, *i.e.* eq. 4, the maximum possible yield

[4] $\mathrm{2\,RS\cdot \rightarrow RSSR}$

of both symmetrical disulfides from this reaction would be *G*(RSSR) = 3.0. Only a limited amount could be formed from reactions not involving RS· radicals. Thus the high yields of symmetrical disulfides from the mixed disulfide in deaerated solutions indicate that a chain reaction must be involved. The initial *G* values of cystine and cystamine were close to 15 which is too high to be attributed to any non-chain mechanism. The simplest explanation is that RS· radicals react with the solute causing extensive rearrangement of the disulfide bonds before they are eliminated by recombination, *e.g.* eqs. 5*a* and *b*. This chain

[5*a*] $\mathrm{RS\cdot + R'SSR \rightleftarrows RSSR + R'S\cdot}$

[5*b*] $\mathrm{R'S\cdot + R'SSR \rightleftarrows R'SSR' + RS\cdot}$

reaction was surprising in view of the low yields of symmetrical disulfides obtained from cysteine-penicillamine disulfide (CySSPen). In the latter case the yield of cystine was always higher than that of penicillamine disulfide. This may have been due to CyS· radicals reacting with mixed disulfide but it appears that PenS· radicals did not participate in a chain reaction.

As illustrated in Fig. 1, the presence of oxygen in solution during radiolysis reduced the yield of cystine very significantly. A small part of this may be due to competition between oxygen and the disulfide for the solvated electron: $k_{RSSR+e^-} = 1.3 \times 10^{10}\ M^{-1}\ s^{-1}$ for cystine; $k_{O_2+e^-} = 1.8 \times 10^{10}\ M^{-1}\ s^{-1}$ (18). However, oxygen must also be suppressing the chain reaction (see below),

[6] $\mathrm{RS\cdot + O_2 \rightarrow RSOO\cdot}$

probably by reacting with RS· radicals. This reaction has also been postulated to explain the radiolysis of cysteine in the presence of oxygen (5). Packer (19) estimated the rate of this reaction during pulse radiolysis studies and found it was fast: $k_{CyS\cdot + O_2} = 8 \times 10^9\ M^{-1}\ s^{-1}$. When the oxygen concentration was the same as the

Can. J. Chem. Downloaded from www.nrcresearchpress.com by 210.87.254.40 on 09/05/12
For personal use only.

Can. J. Chem. Downloaded from www.nrcresearchpress.com by 210.87.254.40 on 09/05/12
For personal use only.

disulfide concentration (0.3 mM) the yield of cystine was reduced approximately by an order of magnitude. Hence it appears that reaction 6 is much faster than reaction 5 and k_6/k_5 is probably about 10. The exact ratio could not be derived due to uncertain factors such as the fate of the RSOO· radical and the ultimate yield of cystine in oxygen-free solution.

The experiments with N_2O-saturated solutions were performed to distinguish between reactions of RS· radicals and the $(RSSR)^-$ anion-radical. Under these conditions most of the solvated electrons would be scavenged by the N_2O to yield mainly ·OH radicals: $k_{e^- + N_2O} = 5.6 \times 10^9\ M^{-1}\,s^{-1}$ (18). Hence $(RSSR)^-$ would not be produced directly by reaction 2. A chain reaction still occurred although the yield of cystine was lower than in degassed solution. It was concluded that the main chain reaction was reaction 5 rather than the alternative reaction 7.

[7] $\quad RSSR' + (RSSR')^- \rightleftarrows RSSR + (R'SSR')^-$

Reaction 7 could also be inhibited by oxygen; *i.e.* reaction 8. The solvated electron would be

[8] $\quad (RSSR')^- + O_2 \rightarrow RSSR' + O_2^-$

scavenged in solutions saturated with nitrous oxide or oxygen, preventing formation of $(RSSR)^-$. Hence, since the chain reaction occurred in the presence of nitrous oxide but not in oxygenated solution, reaction 6 must be the main chain-suppressing reaction.

The chain reaction was demonstrated by plotting G(CySSCy) *vs.* solute concentration for aerated solution, Fig. 3. The graph became linear at solute concentrations above 1 mM with an upward slope due to the effect of increasing RSSR′ concentration in reaction 5. Extrapolation back to zero solute concentration gave a value of 1.5 for G(CySSCy) in the absence of a chain reaction when all primary free radicals are scavenged. This value is still surprisingly high and suggests that the RSOO· radicals may have reacted to yield disulfide, *e.g.* reaction 9. In

[9] $\quad RSOO\cdot + RS\cdot \rightarrow RSSR + O_2$

oxygen-saturated solution the chain reaction was almost completely suppressed and the value of G(CySSCy) at zero chain reaction was reduced to 0.5. However another product, cystine-S,S-dioxide, was obtained in significant yield; $G(CyS(O_2)SCy) \sim 1$. This product probably comes from the RSOO· radical, reaction 10.

[10] $\quad RSOO\cdot + RSOO\cdot \rightarrow RS(O_2)SR + O_2$

This is analogous to reactions which have been observed in photochemistry.

The RSOO· radical is probably the precursor of sulfonic acid which is a major product from radiolysis of cystine or cystamine, in solutions containing oxygen. The relationship between $CySO_3H$, $CySO_2H$, and oxygen concentration is illustrated in Fig. 2. Only $CySO_2H$ was produced in deaerated solution. When oxygen was present $CySO_3H$ was formed and the yield increased with increasing oxygen concentration up to a value of $G(CySO_3H) = 0.5$ at oxygen levels above 0.25 mM. The value for $G(CySO_2H)$ reached a minimum at the same oxygen concentration indicating that $CySO_2H$ has a precursor in common with $CySO_3H$. Reactions 11–13 are consistent with these observations and with the dose-rate effect observed previously in the radiolysis of cystine (1).

[11] $\quad RSOO\cdot + RSOH \rightarrow RSO_3H + RS\cdot$[3]

[12] $\quad 2RSOH \rightarrow RSO_2H + RSH$

[13] $\quad RSOH + H_2O_2 \rightarrow RSO_2H + H_2O$

The sulfinic acid formed at the higher oxygen concentrations may come indirectly from the RSOO· radical, *e.g.* reaction 10 followed by [14].

[14] $\quad RS(O_2)SR + RSH \rightarrow RSO_2H + RSSR$

It is difficult to relate the present findings to the radioprotective ability of the respective thiols. The chain reaction between RS· radicals and disulfides is undesirable in a biological system as it could result in damage to sulfur-containing proteins. However, the observation that the chain reaction is suppressed by oxygen may explain the fact that radioprotective compounds are more effective in the presence of oxygen. There appears to be little difference between the reactivities of the different sulfur atoms of the disulfides towards the free radicals from water and this agrees with the rate constants for these reactions (16, 18). The reduced reactivity of the penicillamine radicals, as indicated from the low yield of penicillamine disulfide from a mixed

[3]Alternatively, RSOO· may react with an initial ·OH-disulfide complex (3)

$$RSOO\cdot + RS(OH)SR' \rightarrow RSO_3H + RSSR$$

disulfide, and the higher yield of products resulting from C—S bond splitting in penicillamine disulfides, suggest that penicillamine may be less efficient than cysteine or cysteamine in a hydrogen transfer process of radiation repair.

The tertiary structure of many proteins is maintained by disulfide bridges and hence destruction or rearrangement of these bridges by ionizing radiation would be harmful (20). The present results indicate that extensive rearrangement of disulfide bridges is unlikely to occur in an aerated environment although reactions could occur between favorably positioned groups. This may be the case with papain where a large part of the activity lost by irradiation can be regenerated by treatment with cysteine (21, 22). Chain reactions have been reported for the destruction of thioctic acid (α-lipoic acid) during photolysis (23) and radiolysis (24) and hence it was postulated that the main effect of ionizing radiation is rearrangement of protein disulfide bonds (24). However, in the case of thioctic acid the chain reaction was not affected by oxygen so it differs significantly from the disulfides of amino acids and does not provide a satisfactory model of protein disulfide bonds.

I wish to thank Dr. R. A. Back of the Division of Chemistry, National Research Council of Canada, for many valuable discussions. Thanks are also extended to Mrs. D. E. Hanafi for excellent technical assistance throughout this investigation.

1. J. W. PURDIE. J. Amer. Chem. Soc. **89**, 226 (1967).
2. J. W. PURDIE. Can. J. Chem. **47**, 1029 (1969).
3. J. W. PURDIE. Can. J. Chem. **47**, 1037 (1969).
4. (*a*) V. G. WILKENING, M. LAL, M. ARENDS, and D. A. ARMSTRONG. J. Phys. Chem. **72**, 185 (1968). (*b*) M. LAL, D. A. ARMSTRONG, and M. WIESER. Radiat. Res. **37**, 246 (1969).
5. (*a*) J. E. PACKER and R. V. WINCHESTER. Chem. Commun. 826 (1968). (*b*) J. E. PACKER and R. V. WINCHESTER. Can. J. Chem. **48**, 417 (1970).
6. (*a*) G. E. ADAMS, G. S. MCNAUGHTON, and B. D. MICHAEL. *In* The chemistry of ionization and excitation. *Edited by* G. R. A. Johnson and G. Scholes, Taylor and Francis, London, 1967. p. 281. (*b*) G. E. ADAMS, G. S. MCNAUGHTON, and B. D. MICHAEL. Trans. Faraday Soc. **64**, 902 (1968). (*c*) G. E. ADAMS, R. C. ARMSTRONG, A. CHARLESBY, B. D. MICHAEL, and R. L. WILLSON. Trans. Faraday Soc. **65**, 732 (1969).
7. W. KARMANN. A. GRANZOW, G. MEISSNER, and A. HENGLEIN. Int. J. Radiat. Phys. Chem. **1**, 395 (1969).
8. A. SCHÖBERL and H. GRÄFJE. Ann. **617**, 71 (1958).
9. W. E. SAVIGE, J. EAGER, J. A. MACLAREN, and C. M. ROXBURGH. Tetrahedron Lett. 3289 (1964).
10. (*a*) J. W. PURDIE, J. P. FARANT, and R. A. GRAVELLE. J. Chromatog. **23**, 242 (1966). (*b*) J. W. PURDIE, R. A. GRAVELLE, and D. E. HANAFI. J. Chromatog. **38**, 346 (1968).
11. G. A. SCHERR. Anal. Chem. **34**, 777 (1962).
12. D. W. GRANT, S. N. MASON, and M. A. LINK. Nature, **192**, 352 (1961).
13. (*a*) B. SHAPIRO and L. ELDJARN. Radiat. Res. **3**, 255 (1955). (*b*) G. G. JAYSON, T. C. OWEN, and A. C. WILBRAHAM. J. Chem. Soc. B, 944 (1967).
14. W. A. ARMSTRONG and D. W. GRANT. Can. J. Chem. **41**, 1882 (1963).
15. T. C. OWEN, M. RODRIGUEZ, B. G. JOHNSON, and J. A. G. ROACH. J. Amer. Chem. Soc. **90**, 196 (1968).
16. (*a*) W. A. ARMSTRONG and W. G. HUMPHREYS. Can. J. Chem. **45**, 2589 (1967). (*b*) W. A. ARMSTRONG. Can. J. Chem. **47**, 3737 (1969).
17. B. H. J. BIELSKI, and A. O. ALLEN. Int. J. Radiat. Phys. Chem. **1**, 153 (1969).
18. N. ANBAR and P. NETA. Int. J. Appl. Radiat. Isotop. **18**, 493 (1967).
19. J. E. PACKER. Private communication.
20. A. PIHL and L. ELDJARN. Pharmacol. Rev. **10**, 437 (1958).
21. A. PIHL and S. SANNER. Radiat. Res. **19**, 27 (1963).
22. D. A. ARMSTRONG. Private communication.
23. M. CALVIN. Fed. Proc. **13**, 697 (1954).
24. T. C. OWEN and A. C. WILBRAHAM. J. Amer. Chem. Soc. **91**, 3365 (1969).

Can. J. Chem. Downloaded from www.nrcresearchpress.com by 210.87.254.40 on 09/05/12
For personal use only.

Can. J. Chem. Downloaded from www.nrcresearchpress.com by 210.87.254.5 on 09/05/12
For personal use only.

Nuclear Magnetic Resonance Studies of Molecular Motion in a Number of Stearates and Oleates

J. A. RIPMEESTER[1,2] AND B. A. DUNELL

Department of Chemistry, University of British Columbia, Vancouver 8, British Columbia

Received September 1, 1970

The broad line p.m.r. spectra of the alkali metal oleates have been observed from 77 °K up to or beyond the crystalline to waxy phase transition. Lower phase transition temperatures are observed in the oleates than in the stearates. This fact is attributed to larger entropies of transition in the oleates than in the stearates. The n.m.r. second moments indicate that in the stearates the packing of chains is probably not closer than in the oleates and consequently that the barriers to chain reorientation are not significantly higher in the stearates than in the oleates. Sodium oleate and stearate both appear to behave irregularly in the series of alkali metal soaps. Spin-lattice relaxation times have been measured by adiabatic rapid passage methods for both alkali metal oleates and stearates. Values of T_1 and of the activation energy barrier for the reorientation of end methyl groups are compared with values obtained by other workers. No significant difference is seen between relaxation processes in stearates and oleates, at least in the lower temperature range. Soaps which seem to have some amorphous character have a second relaxation mechanism, in addition to end methyl group rotation, which is evidently important in the region of about 150–250 °K.

Canadian Journal of Chemistry, 49, 731 (1971)

Introduction

Interpretation of the nature of molecular motion in the various phases of the alkali metal salts of long chain fatty acids from a study of their p.m.r. absorption has been the subject of a number of papers that have appeared during the past ten years or so. Recently van Putte has investigated spin-lattice relaxation times of sodium and lithium salts of fatty acids of varying chain length (1, 2) and Lawson and Flautt have used line widths, shapes, and second moments to study various soaps (3–5). Earlier work from this laboratory has also been concerned with the use of line width and second moment to describe the behavior of fatty acids and their soaps (6–8).

It is the purpose of this paper to report the results of n.m.r. line width and second moment studies on the alkali metal oleates and also the results of spin-lattice relaxation studies by the adiabatic rapid passage technique on these oleates and the alkali metal stearates.

Experimental

Oleic acid was obtained from the Hormel Foundation, Austin, Minnesota. It was quoted to be better than 99% pure and was used without further treatment to prepare the alkali metal oleates. A hot aqueous ethanol solution of reagent grade metal hydroxide was used to neutralize a hot ethanol solution of the acid. On cooling, the solution generally deposited white flaky crystals, which were filtered, washed with cold ethanol and then acetone, and air dried. The soaps were dried at about 100 °C under vacuum for a day, powdered and packed into sample tubes, heated again under vacuum at 110 °C for another day and finally sealed off under vacuum. The stearates were prepared directly from Eastman Kodak white label grade stearic acid, but were then all recrystallized once from ethanol before being dried and treated as the oleates. We may note that not all the soaps precipitated as flaky white crystals. Sodium stearate normally came down as a gel, and to some extent the sodium oleate also. On drying, however, these soaps resembled the other fatty acid salts. Caesium oleate was a sticky white solid, and rather difficult to handle. These materials did not improve physically on reprecipitation from solvent.

The steady-state or continuous wave n.m.r. spectra were run at 16 or 30 MHz. The spectrometer and the techniques and precautions which were used have all been described elsewhere (9). The adiabatic rapid passage experiments were done at 8 MHz using the methods reported by Janzen *et al.* (10).

In all experiments an equilibration time of at least 1 h was allowed at each different temperature, and at least two spectra were obtained for each line width and second moment reported. Values of T_1 were generally obtained from the slopes of lines plotted from "π–$\pi/2$" sequences of rapid passages (10).

Results and Discussion

(1) Line Width and Second Moment

Line widths and second moments for the oleates are displayed as functions of temperature in Figs. 1–5, together with the spin lattice relaxation times derived from the adiabatic rapid passage experiments. Inspection of these curves allows

[1]Present address: Department of Chemistry and Chemical Engineering, University of Illinois, Urbana, Illinois 61801, U.S.A.

[2]National Research Council of Canada Scholarship holder 1967–1970.

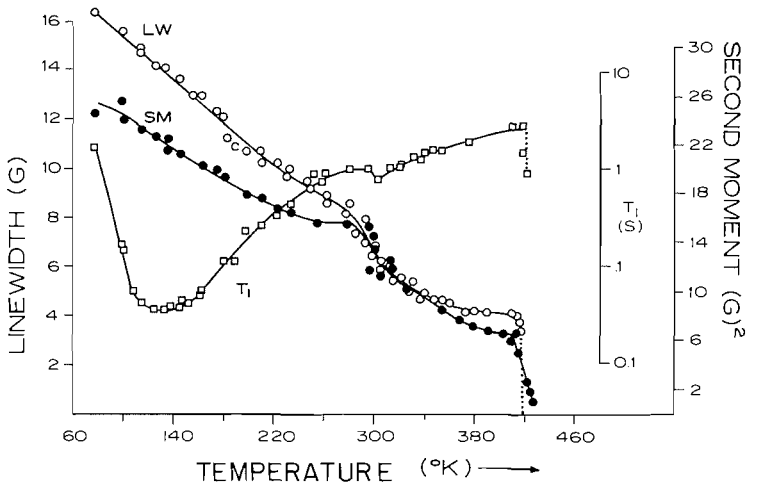

FIG. 1. Line width, second moment, and spin-lattice relaxation time plotted as functions of temperature for lithium oleate.

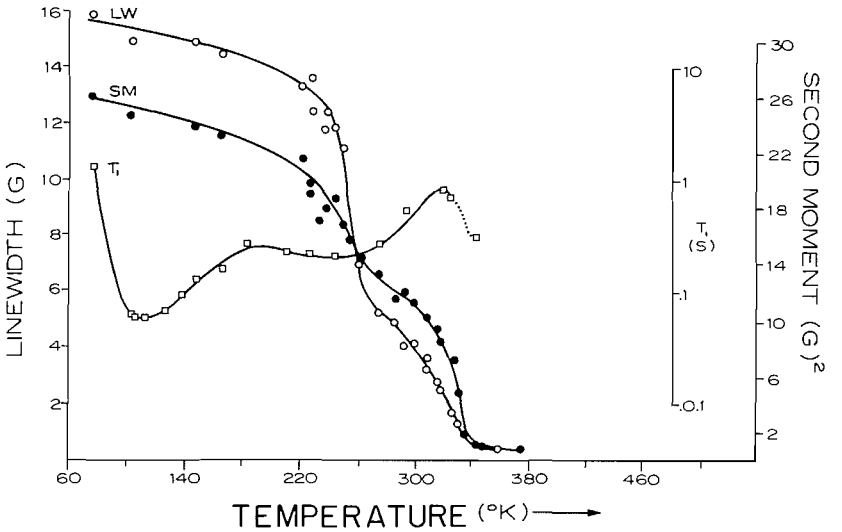

FIG. 2. Line width, second moment, and spin-lattice relaxation time plotted as functions of temperature for sodium oleate.

one to distinguish two transitions in all but caesium oleate (for which there is one observable transition) within the temperature range of the measurements. The higher temperature transition is the more abrupt one, leading at the high temperature side to second moments of about 1 G^2 and line widths which are determined by depth of modulation. In terms of n.m.r., the nature of this transition is very similar to the crystalline to waxy phase transitions of the alkali metal stearates (6, 11–13). The lower temperature transition, which is apparently absent in caesium oleate and not especially well defined in rubidium and sodium oleates, is a more gradual one in terms of the n.m.r. results. Second moments on the low temperature side of the transition are in the range of about 16–20 G^2, which is very similar to the values on the low temperature side of the crystal–crystal phase transitions of the alkali metal stearates, and on the high temperature side they have decreased to about 12 G^2. The lower temperature transitions in the stearates are quite

Can. J. Chem. Downloaded from www.nrcresearchpress.com by 210.87.254.5 on 09/05/12
For personal use only.

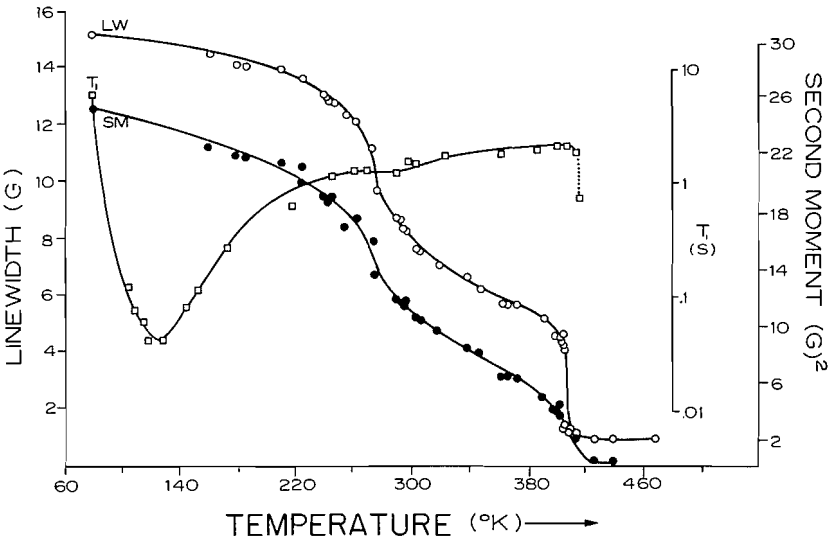

FIG. 3. Line width, second moment, and spin-lattice relaxation time plotted as functions of temperature for potassium oleate.

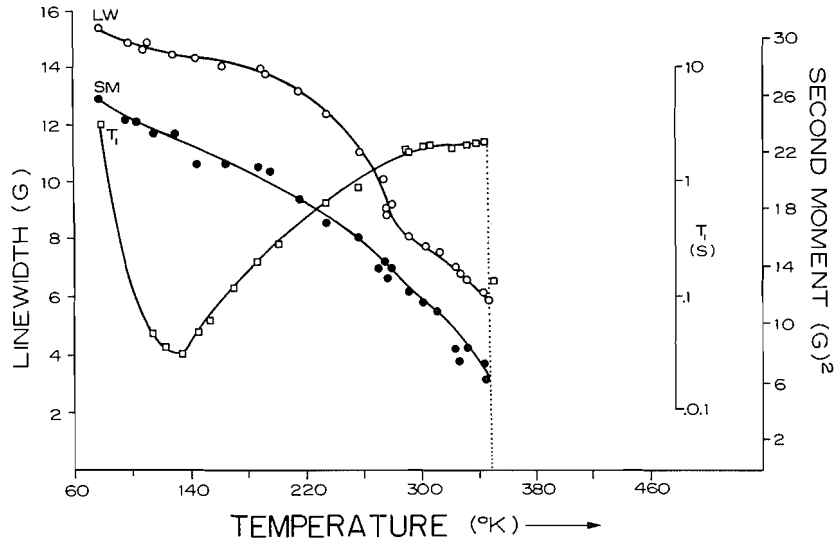

FIG. 4. Line width, second moment, and spin-lattice relaxation time plotted as functions of temperature for rubidium oleate.

abrupt, and correspond to a change in crystal structure (6, 11–13). Although the gradualness of this transition in the oleates makes one doubt that the transition involves a phase change, the motional changes in the hydrocarbon chain seem to be very similar to those of the hydrocarbon chains of the stearates in their low temperature crystal phase change. Further evidence that this low temperature transition in the oleates is not a crystal–crystal phase transition is the fact that we observed no peaks in the differential scanning calorimeter thermograms in the vicinity of this n.m.r. transition temperature for the oleates. Table 1 gives a summary of the transition temperatures of the oleates and stearates. One can see that the behavior of the sodium soaps is irregular in the alkali metal soap series. Apart from the sodium salts, there is a progressive

Can. J. Chem. Downloaded from www.nrcresearchpress.com by 210.87.254.5 on 09/05/12
For personal use only.

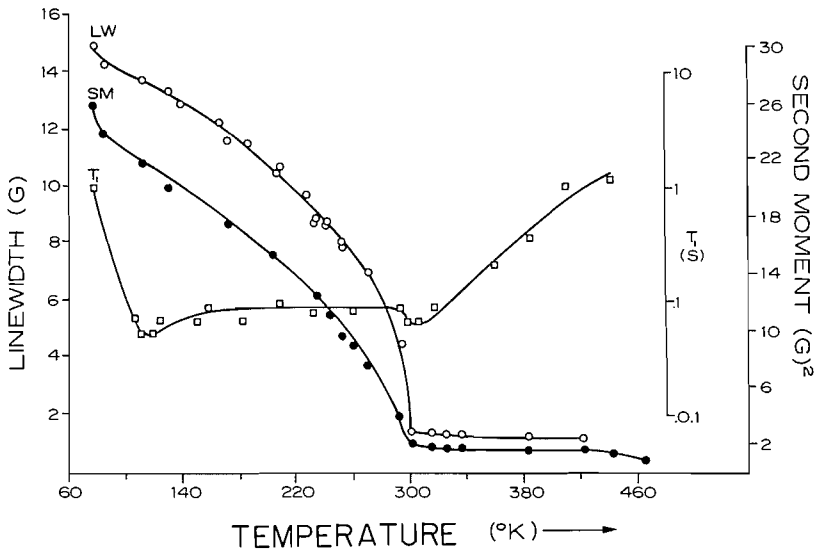

FIG. 5. Line width, second moment, and spin-lattice relaxation time plotted as functions of temperature for caesium oleate.

TABLE 1. The n.m.r. transition temperatures (°K) of alkali metal oleates and stearates

	Oleates		Stearates	
	Low temperature transition	High temperature transition	Crystal–crystal transition	Crystal–waxy transition
Li	295	418	387 (6)*	460 (6)
Na	260	337	358 (3, 13)	387 (3, 13)
K	280	407	333 (12)	443 (12)
Rb	280	348	348 (11)	416 (11)
Cs	—	297	343 (11)	373 (11)

*Numbers in parentheses are literature references.

decrease in the temperature of the crystal–waxy transition as the cation size increases from lithium to caesium. The low temperature transitions are more irregular and less sensitive to cation size. For each alkali metal oleate the transition temperatures are lower than the corresponding stearate transition temperatures.

At liquid nitrogen temperature, the experimental second moments of the oleates range from 25–26 G^2, which is effectively the same as the corresponding range of 25–28 G^2 for the stearates. The rigid lattice intramolecular contribution to the second moment of the oleate chain may reasonably be taken as 18.5 G^2 (8), and that of the stearate chain as the same value (12). One concludes that at liquid nitrogen temperature the intermolecular contribution to the second moment is about the same for the stearate and oleate soaps. Since both second moment and van der Waals interactions depend on the inverse sixth power of internuclear distances, we may assume (14) that interactions between chains are very similar at liquid nitrogen temperature in all the oleates and stearates studied. With the exception of caesium oleate, whose second moment decreases much more rapidly than that of the other oleates, the oleate second moments do not differ greatly one from another until one is somewhat above the low temperature transition. Between liquid nitrogen temperature and higher temperatures where the second moment is in the vicinity of 16–20 G^2, the second moments of all the alkali metal oleates decrease a little more rapidly with increasing temperature than do

Can. J. Chem. Downloaded from www.nrcresearchpress.com by 210.87.254.5 on 09/05/12
For personal use only.

Can. J. Chem. Downloaded from www.nrcresearchpress.com by 210.87.254.5 on 09/05/12
For personal use only.

those of the stearates. One could attribute this decrease in second moment from 25 or 26 G^2 at 77 °K to torsional oscillation of the chains. The oscillation is probably of somewhat greater amplitude in the oleate chain than in the stearate chain up to the low temperature side of the low temperature transition. Reorientation of the end methyl groups already takes place at sufficiently high frequency at liquid nitrogen temperature to provide the significant spin-lattice relaxation mechanism for the protons. This will be considered in the next section. Above the low temperature transition the second moment of the oleates is in the range of 11–14 G^2, corresponding to an increase in the amplitude of torsional oscillation of the hydrocarbon chains. The extent of this motion is not so great, or at least not greater than, the extent of motion in the stearates above their low temperature transitions. For the stearates, the second moments above the crystal–crystal transitions lie in the range of 4–12 G^2. One should presumably attribute, therefore, the lower value of the temperature of transition in the oleates to larger entropy effects due to chain disordering because of the influence of the double bond in the oleates more than to less dense packing of chains in the oleates than in the stearates at low temperature. If density of chain packing and energy barriers to oscillation are only slightly smaller in oleates than stearates, one can understand that the second moments of the oleates above the low temperature transition should be generally larger than those of the stearates above their higher temperatures of crystal–crystal transition.

Above the crystal–waxy phase transition (the higher temperature transition) the observed second moments of 0.5–2 G^2 indicate reorientation of the hydrocarbon chains about several axes for both oleates and stearates. Such motion requires space for the chains and one may understand the progressively lower transition temperature for increasing size of cation (except for the irregular sodium soaps) in terms of the lower energy required to separate larger diameter ions than smaller ones. Once again it is suggested that the oleates have a much lower crystal–waxy transition temperature than stearates because of an entropy effect; that is, because of greater disorder in the oleate chains than in the stearate chains on the high temperature side of the transition. It seems reasonable to associate the greater disorder of the oleate chains with the presence of the double bond with its cis configuration.

It is worth mentioning that for sodium stearate (15) and caesium oleate, and to a lesser extent for sodium oleate, a narrow component, whose linewidth was much less than 1 G, appeared in the spectra well below the first transition temperature. The intensity of this narrow component is dependent on the history and method of preparation of the sample. The existence of a narrow component in n.m.r. spectra of some polymers has been attributed to the presence of amorphous regions in the polymer (16). It is suggested that amorphous regions are present to a significant extent in sodium stearate and oleate and caesium oleate. This is consistent with the peculiar character of these soaps as they were precipitated from solution (see Experimental).

(2) Spin–Lattice Relaxation Time

The spin-lattice relaxation times of the alkali metal oleates, as determined by adiabatic rapid passage methods at 8 MHz, are displayed as a function of temperature in Figs. 1–5. They are also plotted as functions of reciprocal temperature for oleates in Fig. 6 and stearates in Fig. 7. The uncertainties in T_1 are greatest at liquid nitrogen temperature, where the adiabatic rapid passage signal is comparatively weak for these substances, and at temperatures near the T_1 minimum, where T_1 becomes rather too short for completely satisfactory measurement by this technique. We estimate the uncertainty in these two regions to be ± 15 to 20%. Elsewhere we estimate the T_1 values to be reliable to within ± 5 to 10%. Except for sodium and caesium oleate and sodium stearate, whose irregular behavior has already been mentioned, the plots of $\log T_1$ *vs.* T^{-1} are, up to about 250 °K, the V-shaped curves typical of a single relaxation process. The often used expression, developed by Bloembergen *et al.* (17), Kubo and Tomita (18) and others, and applied by, among others, Anderson and Slichter in their study of long chain hydrocarbons (19), relating spin–lattice relaxation time with the correlation time τ_c for reorientation of pairs of spins is eq. 1, where K is a constant that

$$[1] \quad \frac{1}{T_1} = K\left(\frac{\gamma^4\hbar^2}{\omega_0}\right)I(I+1)\sum_j r_{ij}^{-6} \times \left[\frac{\omega_0\tau_c}{1+\omega_0^2\tau_c^2} + \frac{4\omega_0\tau_c}{1+4\omega_0^2\tau_c^2}\right]$$

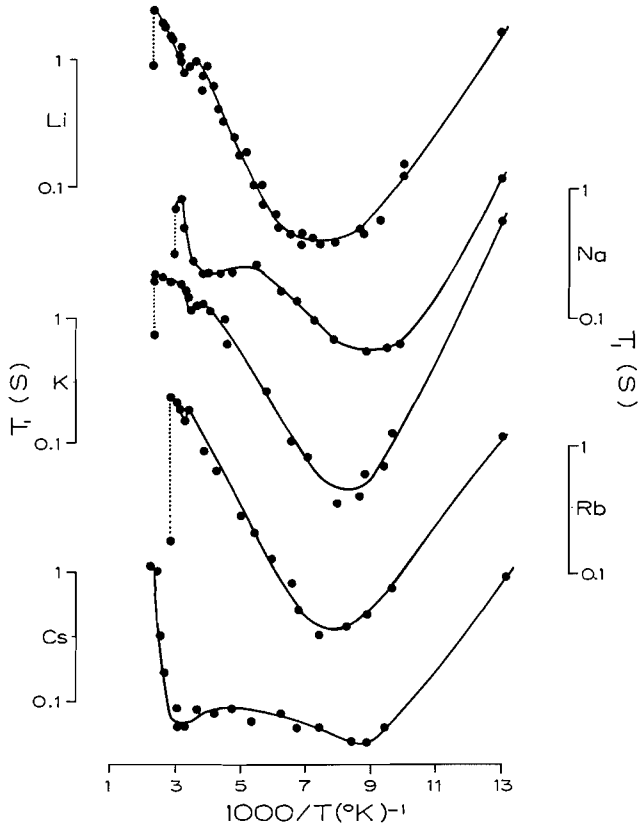

FIG. 6. Spin-lattice relaxation time on a logarithmic scale as a function of reciprocal temperature for the alkali metal oleates.

depends on the reorientation process, ω_0 is the Larmor frequency, and r_{ij} is the separation between spins in the pairs. There is a minimum in T_1 at $\omega_0\tau_c = 0.62$. If there exists a single τ_c which has a simple Arrhenius dependence on activation energy and temperature, $\tau_c = \tau_c^0 \exp(E_a/RT)$, it is easily seen that at low temperature, where $\omega_0\tau_c \gg 1$, $\ln T_1 = \text{constant} + E_a/RT$, and at high temperature, where $\omega_0\tau_c \ll 1$, $\ln T_1 = \text{constant} - E_a/RT$. One may note that Hubbard and his co-workers (20, 21) have predicted a more complex relaxation behavior for an isolated three spin system reorienting about a C_3 axis and have experimental evidence substantiating their analysis in the case of a methyl group which has been isolated by isotopic dilution. In the systems we are discussing here, however, the methyl groups are not isolated, and in the temperature range where we believe that methyl group reorientation provides the dominant relaxation mechanism, the decay of magnetization in the Z direction does not depart observably from the simple exponential decay predicted by eq. 1. The values of T_1 at the minimum in the curve, the temperature of the minimum, and the apparent activation energies determined from the slopes of the straight line portions of the curves on either side of the minimum are listed in Table 2.

The principal minimum in the T_1 curves, which lies between 110 and 132 °K may be attributed to relaxation through reorientation of the end methyl groups. Similar minima have been observed for *n*-alkanes (19), polymers (22–24), and other compounds containing methyl groups (25), and in previous studies on soaps (1). The studies on the *n*-alkanes (19) showed that the methyl group rotation provided a sink for the relaxation of the methylene protons by means of a spin diffusion process and that the minimum value of T_1 is directly proportional to the ratio of the total number of protons to the number of protons in reorienting methyl groups. According to Anderson and Slichter's results for *n*-alkanes, a ratio of total protons to methyl protons of 11.7,

Can. J. Chem. Downloaded from www.nrcresearchpress.com by 210.87.254.5 on 09/05/12
For personal use only.

TABLE 2. Summary of spin-lattice relaxation results for the alkali metal oleates and stearates

	Temperature at T_1 minimum (°K)	T_1 minimum (ms)	E_a (kcal/mol) Low temperature	E_a (kcal/mol) High temperature
Oleates				
Li	134	35	1.7	2.4
Na	110	56	1.7	
K	122	37	2.3	1.7
Rb	132	33	1.5	2.1
Cs	115	50	1.7	
Stearates				
Li	115	42	1.8	2.3
Na	118	58	1.7	
K	122	45	2.1	2.4
Rb	132	50	2.3	2.5
Cs	116	59	2.2	1.8

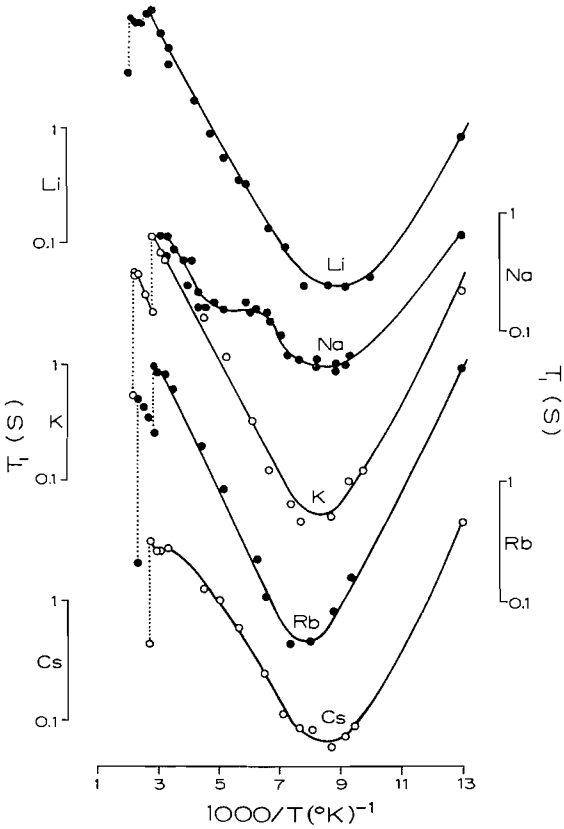

FIG. 7. Spin-lattice relaxation time on a logarithmic scale as a function of reciprocal temperature for the alkali metal stearates.

which is the appropriate value for stearate chains, corresponds to a T_1 minimum of 257 ms at 50 MHz. Equation 1 indicates that T_1 minimum is directly proportional to the Larmor frequency. Assuming that the activation energy for methyl group reorientation is the same in stearates and *n*-alkanes, one should then expect a T_1 minimum of 41 ms for the stearates observed at 8 MHz if they relax by spin diffusion to reorienting methyl groups which have a single relaxation time. As indicated in Table 2, our observed values of T_1 minimum range from 42–59 ms for the stearates and from 33–56 ms for the oleates, in reasonable agreement with predictions based on the work of Anderson and Slichter. Van Putte found a T_1 minimum, uncorrected for H-1 inhomogeneity, of 380 ms for sodium stearate at 60 MHz. Correction for H-1 inhomogeneity (1) gives a T_1 minimum of 475 ms. This value would reduce to 63 ms at 8 MHz, which corresponds reasonably well with our value of 58 ms at 8 MHz. The fact that we observe the T_1 minimum at a lower temperature than Anderson and Slichter (19) or van Putte (1) is consistent with the lower frequency at which our measurements were made. From eq. 1 and the Arrhenius expression for τ_c we can obtain eq. 2, a simple relation between the temperatures T and T' of T_1 minima measured at Larmor frequencies ν and ν'. If we may again assume that

$$[2] \qquad \log(\nu/\nu') = E_a(T - T')/2.3\,RTT'$$

the activation energy for methyl group reorientation is the same in stearates and *n*-alkanes, we can compare Anderson and Slichter's value of $T = 148$ °K for measurements on *n*-alkanes at 50 MHz with our average value of $T = 121$ °K for stearate soaps at 8 MHz and calculate $E_a = 2.4$ kcal/mol. Dispensing with the supposition that energy barriers to methyl group reorientation are the same in the different substances, one may compare van Putte's value of $T = 161$ °K for sodium stearate at 60 MHz with our value of

Can. J. Chem. Downloaded from www.nrcresearchpress.com by 210.87.254.5 on 09/05/12
For personal use only.

Can. J. Chem. Downloaded from www.nrcresearchpress.com by 210.87.254.5 on 09/05/12
For personal use only.

$T = 118$ °K for sodium stearate at 8 MHz and obtain $E_a = 1.8$ kcal/mol. These values are consistent with the values of the activation energy of the relaxation process obtained from the slopes of the straight line portions of the T_1 curve to either side of the minimum and listed in Table 2. It is estimated that the activation energies in Table 2 are reliable to within about ± 0.2 kcal/mol. The average of the values listed in Table 2 is 2.0 kcal/mol for the activation energy of the relaxation process. This may be compared with a value of 2.6 ± 0.2 kcal/mol found (19, 25) for reorientation of methyl groups in paraffins, and 2.1 kcal/mol, the average obtained by van Putte (1) for sodium soaps containing an even number of carbon atoms. Van Putte's average value for the even-numbered lithium soaps is 2.65 kcal/mol. The activation energies obtained from our results appear to be rather low. It seems unlikely that we should attribute this to the presence in the samples of residual molecular oxygen, which would be particularly effective in lowering the relaxation time at low temperatures and thereby would lead to a low activation energy on the low temperature side of the T_1 minimum. However, even though samples were pumped off at elevated temperature for a considerable length of time (see Experimental), one should not rule out this as a possible explanation. It is also possible, since only modest precautions were taken to ensure purity of sample, that residual impurities have broadened and raised the T_1 minimum sufficiently to give slightly low slopes on either side of the minimum. Although it is somewhat surprising that the activation energy obtained from the low temperature side of the T_1 minimum is smaller than that from the high temperature side, such a situation has been reported previously for polymers containing methyl groups attached to the main polymer chain (26). One might expect the apparent activation energy on the high temperature side to be lower because of possible contributions to the relaxation mechanism from motions other than methyl group reorientation lowering T_1 on the high temperature side of the T_1 minimum. One might attribute our observation to the presence of residual oxygen, as discussed above, or to an inadequate number of points between 77 °K and the T_1 minimum or to the somewhat larger uncertainty in the value of T_1 at 77 °K than in its value at temperatures appreciably above the T_1 minimum. None of these explanations seems to us at the moment to be totally convincing.

The average value of T_1 minimum found for oleates (42 ms) is lower than that for stearates (51 ms), but considering the range of deviation of individual values from the mean, they are very similar. It would seem reasonably clear, therefore, that the presence of the double bond in the middle of the oleate chain does not offer a bottleneck or rate limiting step in the spin diffusion process which is believed to serve as the main pathway for relaxation of the methylene hydrogens in the lower temperature range.

In the oleates the low temperature transition is accompanied by at most a small dip, or shallow minimum, in the T_1 *vs.* temperature curve; the higher temperature transition, however, involves a very rapid decrease, if not a discontinuity in T_1. It should be mentioned that for all the oleates, the higher temperature transition was preceded by the appearance, in the steady state spectra, of a narrower component which grew gradually at the expense of the broad component until only the narrow line remained at the transition point. This narrow component is much dependent on sample purity and thermal history. It may affect the observed T_1 to some extent since the narrow component must have a smaller T_1 than the broad component (there being a marked decrease in T_1 just at the transition temperature). This would explain the slight drop-off in T_1 observed somewhat below the higher temperature transition and the moderation of the decrease in T_1 at the transition.

Sodium and caesium oleates and sodium stearate are notable for showing low values of T_1 with either a plateau or a minimum in T_1 between about 160 °K (lower for caesium oleate) and the phase transition temperatures. In this temperature region, T_1 minima have been observed in polyethylene (22, 23) and other polymers (23, 27). Bergmann and Nawotky (22) found the value of this T_1 minimum to be proportional to the percent crystallinity of the sample and therefore the minimum has been associated with relaxation through chain motion in amorphous regions of the solid. Spin diffusion to relaxation sinks in the amorphous regions may operate in this case also, and lead to a dominant relaxation mechanism and single relaxation time. The irregular behavior of the two sodium soaps and of caesium oleate has already been mentioned.

These results for the spin–lattice relaxation time add support to the suggestion that these soaps have been obtained in a more amorphous state than the other soaps.

In lithium, potassium, and rubidium stearate there is an abrupt drop in T_1 at, or somewhat above, the crystal–crystal phase transition. In the lithium case, the drop is less abrupt than in the other cases. The question has been raised as to whether this drop in T_1 is related to the genotypical transition reported by Thiessen and Ehrlich (28). The genotypical transition in stearates should be at 343 °K. This corresponds to the drop in T_1 for potassium stearate at approximately 343 °K, but seems scarcely related to the drop in T_1 at approximately 385 °K for lithium stearate or 355 °K for rubidium stearate. For these three soaps there is better correlation of the T_1 drop with the crystal–crystal transition temperature than with the "genotypical transition". Values of T_1 for sodium stearate were not obtained above 360 °K because no part of the magnetization decays could be fitted by a single exponential. Between 150 and 360 °K, the magnetization decay was somewhat complex, but T_1 values could be found, and the shorter T_1 values are plotted. In the caesium case only a very small perturbation in T_1 occurs near the crystal–crystal transition. An abrupt drop in T_1 occurs at the crystal–waxy transition.

The authors gratefully acknowledge the financial support of the National Research Council of Canada in the form of a Grant-in-Aid awarded to B.A.D. and a Scholarship to J.A.R. We are also indebted to the Research Committee of the University of British Columbia for financial assistance.

1. K. P. A. M. VAN PUTTE. Trans. Faraday Soc. **66**, 523 (1970).
2. K. P. A. M. VAN PUTTE. J. Magn. Res. **2**, 23 (1970).
3. K. D. LAWSON and T. J. FLAUTT. J. Phys. Chem. **69**, 4256 (1965).
4. K. D. LAWSON and T. J. FLAUTT. Mol. Cryst. **1**, 214 (1966).
5. T. J. FLAUTT and K. D. LAWSON. Ordered fluids and liquid crystals. Advan. in Chem. Series No. 63. Amer. Chem. Soc. Washington, D.C., 1967, p. 26.
6. T. J. R. CYR, W. R. JANZEN, and B. A. DUNELL. Advan. in Chem. Series No. 63. Amer. Chem. Soc. Washington, D. C., 1967, p. 13.
7. W. R. JANZEN and B. A. DUNELL. Can. J. Chem. **47**, 2722 (1969).
8. D. R. WARE and B. A. DUNELL. Trans. Faraday Soc. **61**, 834 (1965).
9. B. A. DUNELL, C. A. FYFE, C. A. MCDOWELL, and J. RIPMEESTER. Trans. Faraday Soc. **65**, 1153 (1969).
10. W. R. JANZEN, T. J. R. CYR, and B. A. DUNELL. J. Chem. Phys. **48**, 1246 (1968).
11. D. J. SHAW and B. A. DUNELL. Trans. Faraday Soc. **58**, 132 (1962).
12. R. F. GRANT and B. A. DUNELL. Can. J. Chem. **38**, 1951 (1960).
13. R. F. GRANT and B. A. DUNELL. Can. J. Chem. **38**, 2395 (1960).
14. E. R. ANDREW and R. G. EADES. Proc. Roy. Soc. **A216**, 398 (1953).
15. R. F. GRANT. Ph.D. Thesis, The University of British Columbia, Vancouver, British Columbia, 1959.
16. C. W. WILSON, III and G. E. PAKE. J. Chem. Phys. **27**, 115 (1957).
17. N. BLOEMBERGEN, E. M. PURCELL, and R. V. POUND. Phys. Rev. **73**, 679 (1948).
18. R. KUBO and K. TOMITA. J. Phys. Soc. Jap. **9**, 888 (1954).
19. J. E. ANDERSON and W. P. SLICHTER. J. Phys. Chem. **69**, 3099 (1965).
20. R. L. HILT and P. S. HUBBARD. Phys. Rev. **134**, A 392 (1964).
21. M. F. BAUD and P. S. HUBBARD. Phys. Rev. **170**, 384 (1968).
22. K. BERGMANN and K. NAWOTKY, Kolloid Z, and Z. Polymere. **219**, 132 (1967).
23. N. J. TRAPPENIERS, C. J. GERRITSMA, and P. H. OOSTING. Phys. **30**, 997 (1964).
24. J. G. POWLES, Polym. **1**, 219 (1960).
25. D. C. DOUGLASS and G. P. JONES. J. Chem. Phys. **45**, 956 (1966).
26. T. M. CONNOR and D. J. BLEARS. Polym. **6**, 385 (1965).
27. T. M. CONNOR. Polym. **4**, 263 (1963).
28. P. A. THIESSEN and E. EHRLICH. Z. phys. Chem. **A165**, 453, 464 (1933).

Can. J. Chem. Downloaded from www.nrcresearchpress.com by 210.87.254.5 on 09/05/12
For personal use only.

Can. J. Chem. Downloaded from www.nrcresearchpress.com by 210.87.254.6 on 09/05/12
For personal use only.

Electrochemical Bifunctionalization of Olefins in the Presence of Halide Ions[1]

N. L. WEINBERG[2] AND A. KENTARO HOFFMAN
American Cyanamid Company, Central Research Division, Stamford, Connecticut 06904

Received August 25, 1970

An electrochemical procedure has been developed for halofunctionalization of olefins, which allows for introduction of both nitrogen and oxygen containing substituents. The method obviates the need for silver salts or chemical oxidants, presently employed in analogous chemical routes. Thus 1-phenyl-2-butene on electrolysis in acetonitrile solution containing Et_4NI, Et_4NBr, or Et_4NCl was converted to the corresponding haloamide derivative. In a related study, which extends the scope of electrochemical functionalization by nitrogen to negatively substituted olefins, dimorpholinization of *trans*-dibenzoylethylene was carried out by anodic oxidation of an acetonitrile solution of the olefin in presence of morpholine and Et_4NI.

Canadian Journal of Chemistry, **49**, 740 (1971)

Electrochemical oxidation has been previously employed for halofunctionalization of olefins. Indeed epoxidation of lower alkenes with electrochemically generated HOCl has become a commercially viable route to olefin oxides (1). Other examples in the literature describe the formation of the halohydrin ethers of cinnamic acid (2) and *trans*-stilbene (3) on electrolysis of these olefins in methanol containing chloride or bromide electrolytes. We were interested in extending the scope of electrochemical halofunctionalization to include introduction of other nucleophiles especially those containing nitrogen.

The use of halogens, especially iodine, and silver salts for functionalization of olefins is well-known (4–9). In general the method involves the reaction of a cyclic halonium ion intermediate (**1**) with a suitable nucleophile to give a halofunctionalized (**2**) or bifunctionalized derivative (**3**) (eqs. 1 and 2) of the olefin. Precipitation of insoluble silver halide serves to drive the reaction to completion. For X = I and R = OAc eqs. 1 and 2 represent the well-known Prévost reaction (4, 5) and **3** (R = OAc) the observed product. Hassner and co-workers (6–9) are largely responsible for developing the corresponding reactions allowing introduction of nitrogen substituents to give synthetically useful haloadducts (**2**; X = I, Cl, or Br, and R = NO_2, N_3, NCO, and $\overset{+}{N}{\equiv}CCH_3$).

[1] $\text{C=C} + X_2 \rightleftharpoons$ 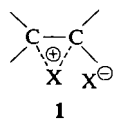

1

[2] 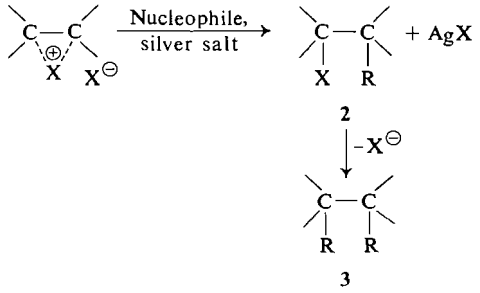

2 **3**

X = I, Br, Cl

R = OH, O–alkyl, OAc, NO_2, N_3, NCO, $\overset{\oplus}{N}{\equiv}CCH_3$, X

Halonium ion **1** can be partitioned between starting material and **2**. Since **1** may be regarded as an ion pair, electrochemical oxidative removal of halide ion from **1** suggested itself as a means of driving [1] and [2] to the right.

Results

A series of reactions have been carried out which demonstrate that not only oxygen but nitrogen functionalization of olefins may be carried out electrochemically. An electrolysis cell divided into compartments for anode, cathode and reference electrode was employed to minimize possible side reactions of the product with the cathode. Table 1 lists results of controlled potential electrolyses of cyclohexene and 1-phenyl-2-butene in 0.5 *M* $LiClO_4$ in acetonitrile with a variety of halogen sources. It is emphasized that no attempt was made to maximize yields by seeking the optimum reaction conditions. High anodic potentials were avoided since organic halides are known to undergo electrooxidation (10). It is noteworthy that soluble salts

[1]Paper VI in the series "Anodic oxidation of organic compounds". For Part V see ref. 16.

[2]Present address: Hooker Chemical Corporation, Grand Island Complex, MPO Box 8, Niagara Falls, New York 14302.

TABLE 1. Functionalization of olefins by halogen and nitrogen nucleophiles

Olefin	Source of halogen*	Controlled potential† (V)	Product(s) (current efficiency)‡
Cyclohexene	I_2	+0.3	*trans*-1-Iodo-2-acetamidocyclohexane (~ 100)
1-Phenyl-2-butene	Et_4NI	+0.3	$C_6H_5CH_2\underset{\displaystyle I}{\underset{\vert}{C}}H\underset{\displaystyle NHCOCH_3}{\underset{\vert}{C}}HCH_3$ (51)§
1-Phenyl-2-butene	Et_4NBr	+1.3	$C_6H_5CH_2\underset{\displaystyle OAc}{\underset{\vert}{C}}H—\underset{\displaystyle NH_2\cdot HBr}{\underset{\vert}{C}}HCH_3$ (12)§
			$C_6H_5CH_2\underset{\displaystyle Br}{\underset{\vert}{C}}H\underset{\displaystyle Br}{\underset{\vert}{C}}HCH_3$ (31)
1-Phenyl-2-butene	Et_4NCl	+1.3	$C_6H_5CH_2\underset{\displaystyle Cl}{\underset{\vert}{C}}H\underset{\displaystyle NHCOCH_3}{\underset{\vert}{C}}HCH_3$ (15)§
			$C_6H_5CH_2\underset{\displaystyle Cl}{\underset{\vert}{C}}H\underset{\displaystyle Cl}{\underset{\vert}{C}}HCH_3$ (10–20)‖

*Reaction medium: 0.5 *M* $LiClO_4$ in acetonitrile.
†Potential of the platinum anode *vs.* Ag, Ag^+ (0.01 *M*) reference.
‡Current efficiency for 2 F per mol.
§The structure of this product is assigned on the basis of n.m.r. analyses including spin decoupling experiments on **6**.
‖Estimated value.

of I^-, Br^-, and Cl^- can be used as a convenient source of halogen in these reactions and the need for handling reactive halogens is thereby conveniently avoided.

Haloamides are produced in acetonitrile solution, with solvent acting as the nucleophilic reagent. It is interesting that the product isolated on electrolysis of 1-phenyl-2-butene with Et_4NBr was not the bromoamide **4** but the acetoxy amine hydrobromide **6**. Strong evidence (i.r.) for the presence of **4** in the crude electrolysis product suggests that **6** arises as a result of an intramolecular nucleophilic displacement reaction to give an oxazoline intermediate **5** which is hydrolyzed to **6** (eq. 3). This type of displacement reaction has been studied previously (11).

In a related study, which extendes the scope of electrochemical functionalization by nitrogen to negatively substituted olefins, dimorpholinization of *trans*-dibenzoylethylene (**7**) was carried out. Electro-oxidation of **7** in acetonitrile in presence of Et_4NI and excess morpholine at +0.35 V *vs.* Ag, Ag^+ (0.01 *M*) gave the dimorpholino product (**9**) in 37% yield, and the previously unobserved iodomorpholino adduct **8** in 27% yield (12). An attempt to apply the morpholinization reaction to 1-phenyl-2-butene failed and almost all of the olefin was recovered

[3]

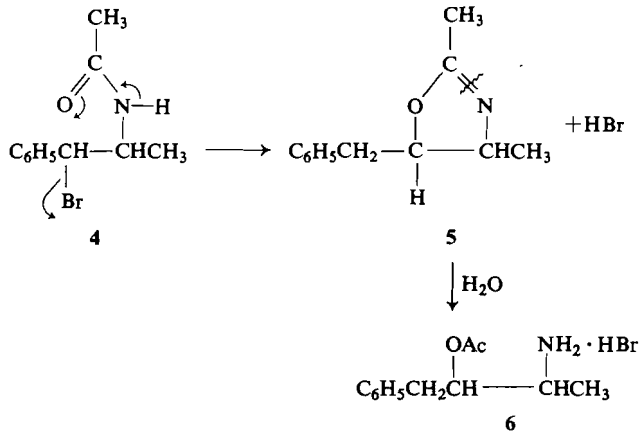

Can. J. Chem. Downloaded from www.nrcresearchpress.com by 210.87.254.6 on 09/05/12
For personal use only.

TABLE 2. Functionalization of olefins by halogen and oxygen nucleophiles

Olefin	Source of halogen	Controlled potential (V)	Product(s) (current efficiency)*
Cyclopentene	I_2†	+0.4‡	1,2-dihydroxycyclopentane monoacetate (26) 1,2-diacetoxycyclopentane (7.8) 1-iodo-2-acetoxycyclopentane (140)
Cyclohexene	I_2†	+0.4‡	1,2-dihydroxycyclohexane monoacetate (22) 1,2-diacetoxycyclohexane (2) 1-iodo-2-acetoxycyclohexane (85)
1-Phenyl-2-butene	Et_4NBr§	+0.9‖	$C_6H_5CH_2\underset{\displaystyle Br}{\underset{\vert}{C}}H\underset{\displaystyle Br}{\underset{\vert}{C}}HCH_3$ (35) $C_6H_5CH_2\underset{\displaystyle Br}{\underset{\vert}{C}}H\underset{\displaystyle OCH_3}{\underset{\vert}{C}}HCH_3$ (50) $C_6H_5CH_2\underset{\displaystyle H_3CO}{\underset{\vert}{C}}H\underset{\displaystyle OCH_3}{\underset{\vert}{C}}HCH_3$ (27)

*"Apparent" current efficiencies for 2 F per mol are given. Simultaneous air oxidation of iodide gives current efficiencies greater than 100%.
†In 3 *M* KOAc in HOAc with 3% Ac_2O.
‡Ag, AgOAc reference electrode.
§In 0.5 *M* $NaClO_4$ in CH_3OH.
‖SCE reference electrode.

[4]

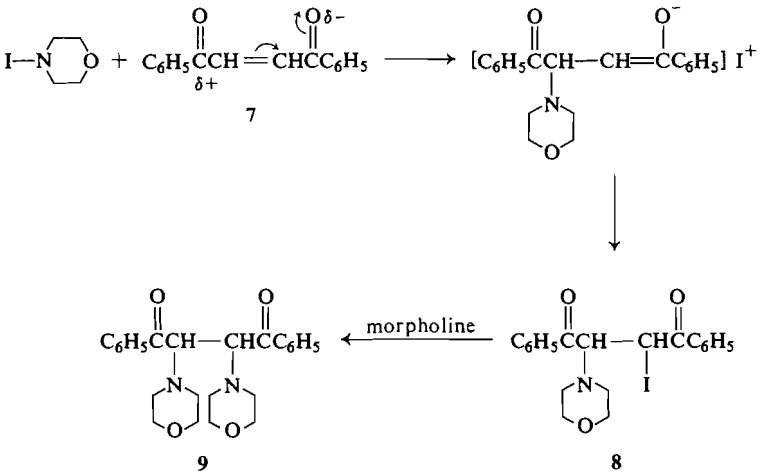

7 9 8

unchanged, in agreement with the unsuccessful analogous chemical reaction reported in the literature (12). The mechanism of this reaction probably involves addition of *N*-iodomorpholine to the olefin in a Michael-type reaction (eq. 4). This electrochemical procedure should prove applicable to other negatively substituted olefins as well as to primary amines.

Table 2 lists examples of oxygen functionalization reactions of olefins. Cyclopentene and cyclohexene undergo an electrochemical Prévost-type reaction in which the intermediate iodoacetate is isolated as the major product. The diacetate may be obtained as the major constituent by carrying out the electrolysis at elevated temperatures[3] for extended reaction times, thus facilitating the comparatively slow displacement of iodide. The electrolysis of 1-phenyl-2-butene in methanol containing Et_4NBr affords the expected products of reaction including a relatively sizable quantity of the glycol dimethyl ether. The latter observations agree with similar results previously reported (2, 3).

[3]Details of studies at elevated temperatures will be reported elsewhere.

Can. J. Chem. Downloaded from www.nrcresearchpress.com by 210.87.254.6 on 09/05/12
For personal use only.

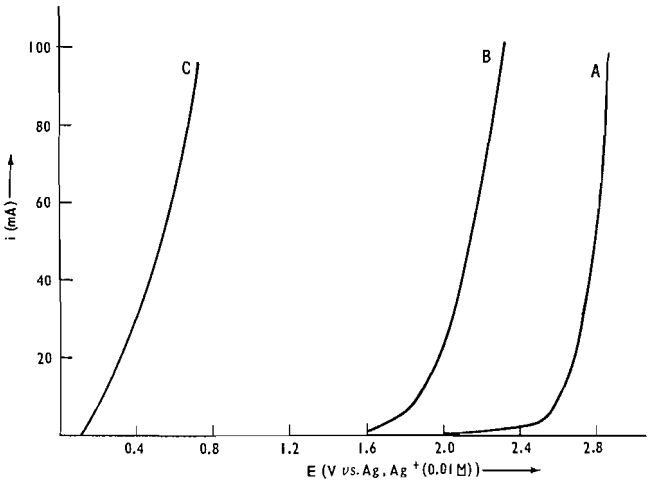

FIG. 1. Current voltage curves at smooth platinum (10 cm^2): (A) 0.5 *M* $LiClO_4$ in acetonitrile; (B) 0.10 *M* cyclohexene in solution *A*; (C) 0.10 *M* iodine in solution *B*.

Discussion

Electrochemical oxidation of iodine or of halide salts (I^-, Br^-, Cl^-) in the presence of an olefin and nucleophile has been found to be a promising method for halofunctionalization of olefins. Moreover, both oxygen and nitrogen functionalized products may be obtained under certain conditions, and negatively substituted olefins may be functionalized as well.

While bromide and chloride electrolytes are conveniently employed in the electrochemical method, vicinal dihalides are formed in appreciable amount. Iodide ion and I_2 do not possess this disadvantage because of the appreciable steric interaction present in vicinal diiodides. A number of additional properties of I^- and I_2 contribute to the unique success of electrochemical iodofunctionalization of olefins. Thus it is well recognized that I^-, besides being a very powerful nucleophile is a very effective leaving group (13). In addition, the low oxidation potentials of I^- and I_3^- compared to that of most olefins and nucleophiles allow for a conveniently wide range in which to control the electrolysis potential. While controlled potential methods have been employed in most of the examples in this report, constant current techniques should be applicable where iodide ion is used, providing it is present in excess. In this case discharge of iodide ion would keep the electrolysis potential at a low anodic value.

The anodic half-wave potential of I_2 ($E_{1/2} \approx$ 1.9 V *vs.* Ag, Ag^+ (0.01 *M*)(10)is comparable to that of olefins. Yet an acetonitrile solution of cyclohexene ($E_{1/2}$ = 2.05 V *vs.* Ag, Ag^+ (0.01 *M*) (14) containing I_2 is oxidized at +0.3 V *vs.* Ag, Ag^+ (0.01 *M*). Polarization curves for 0.5 *M* $LiClO_4$ in acetonitrile with added iodine and with added cyclohexene are shown in Fig. 1. To understand the large cathodic shift in the latter curve, a blank run was carried out using the same reaction conditions but with no current flowing. The product, *trans*-1-iodo-2-acetamidocyclohexane (**10**) was isolated in 70% yield. An explanation is that I_2 can compete effectively for I^- in the iodonium ion, forming I_3^-. In addition, traces of water could react with the resultant nitrilium ion giving the product **10** (eqs. 5 and 6) in an irreversible reaction. The large oxidation current observed at 0.3 V appears, therefore, to result from electro-oxidation of I_3^-, eventually converting all I_3^- in solution to organically bound iodoamide **10**.

Experimental[4]

Acetonitrile was purified as previously described (10). Sodium and lithium perchlorate were G. F. Smith Anhydrous Grade, dried over P_2O_5 *in vacuo*. Other chemicals used were reagent grade. A three compartment electrolysis cell divided for anode, cathode, and reference electrodes,

[4]Melting points are corrected. Microanalyses were performed by Mrs. P. Stehman and associates. The i.r. spectra were obtained with a Perkin–Elmer Infracord spectrometer. The n.m.r. spectra were carried out by Dr. J. Lancaster and Mrs. M. Neglia with a Varian Model A-60 instrument. The v.p.c. analyses on SE-30 and preparative separations using QF-1 on Gas Chrome CLA (60-80 mesh) were performed by Dr. R. Landowne and associates.

Can. J. Chem. Downloaded from www.nrcresearchpress.com by 210.87.254.6 on 09/05/12
For personal use only.

[5] 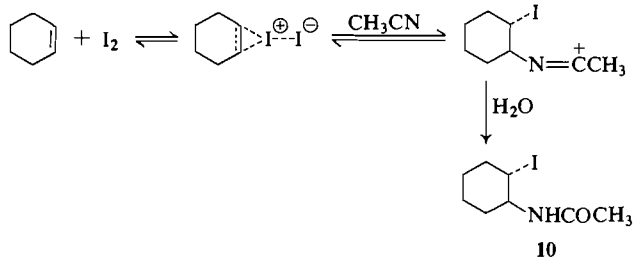

10

[6] $$I^- + I_2 \rightleftharpoons I_3^-$$

and separated by fine glass frits was employed throughout. The anode was smooth platinum (10 cm^2) and the cathode either platinum or a mercury pool. All reactions were carried out with magnetic stirring of the anode solution and under an atmosphere of dry nitrogen at 20° unless otherwise stated. The electronic equipment has been described (15).

Iodoamidation of Cyclohexene

(a) Electrochemical Preparation

A solution consisting of 3.2 g iodine, and 10 ml of cyclohexene in 100 ml of 0.5 *M* $NaClO_4$ in acetonitrile containing 3% water was electrolyzed at a smooth platinum anode (10 cm^2) at +0.32 V *vs.* Ag, Ag^+ (0.01 *M*). After 2106 C had been passed, during which the current dropped from 245 to 7 mA, the solution in the anode compartment was concentrated *in vacuo* at 35°, 10 mm. The residue was taken up in chloroform, washed with water, dilute aqueous sodium bisulfite solution, and the organic layer dried over anhydrous $MgSO_4$. On filtration and evaporation 6.6 g of solid m.p. 90–100 was obtained. This was identified as *trans*-1-iodo-2-acetamidocyclohexane by comparison of its i.r. spectrum with that of an authentic sample (6). After three recrystallizations from diethyl ether – acetone, the solid had m.p. 118–120.5°.

(b) Chemical Preparation

The above reaction was repeated using the same reaction conditions but without passage of current. After 16 h the solution was worked-up as above to give 2.0 g of crude *trans*-1-iodo-2-acetamidocyclohexane (i.r. mineral oil): 3250 (w), 1665 (w), 1640 (s), 1560 (s) cm^{-1}).

Electrochemical Iodoamidation of 1-Phenyl-2-butene

Using the above procedure, a solution of 1.3 g (0.010 mol) 1-phenyl-2-butene and 2.6 g (0.010 mol) Et_4NI in 0.5 *M* $LiClO_4$ in acetonitrile was electrolyzed at 0.5 V *vs.* Ag, Ag^+ (0.01 *M*). After 1800 C had been passed, work-up gave 1.9 g, m.p. 182–184°, of 1-phenyl-2-iodo-3-acetamidobutane on crystallization from acetone. The i.r. and n.m.r. analyses (the n.m.r. spectrum was similar to that described for the chloroamidation product) were in agreement with the structural designation, including one acetone of crystallization (i.r. (mineral oil): 3250 (w), 1745 (s), 1675 (s), 1520 (w) cm^{-1}).

Anal. Calcd. for $C_{12}H_{16}NIO \cdot C_3H_6O$: C, 48.00; H, 5.87; N, 3.70; I, 33.87. Found: C, 48.23; H, 6.00; N, 3.61; I, 33.82.

Electrochemical Bromoamidation of 1-Phenyl-2-butene

In a similar manner 0.01 mol of 1-phenyl-2-butene, and Et_4NBr in 0.5 *M* $LiClO_4$ in acetonitrile, electrolyzed at 1.3 V *vs.* Ag, Ag^+ (0.01 *M*) gave 2.26 g of a crude oily product. This material exhibited strong absorption bands at 3350 (w), 1645 (s) and 1560 (m) cm^{-1} in the i.r. (mineral oil). On standing a solid was slowly deposited. Crystallization of this from diethyl ether – acetone gave 0.35 g of 1-phenyl-2-acetoxy-3-aminobutane hydrobromide, m.p. 184–186.5° (i.r. (mineral oil): 1725 (s), 1560 (m) cm^{-1}). The n.m.r. spectrum in $CDCl_3$ exhibited a broad band at 1.6 (NH_2), aromatic at 2.6, a multiplet at 4.8 (O—C—H), a broad absorption at 6.5 (N—C—H), a double doublet at 6.9 ($ArCH_2$), a single peak at 7.8 ($OCOCH_3$), and a doublet at 8.4 τ (C—CH_3). The proton ratios were 2:5:1:1:2:3:3 respectively. Spin decoupling experiments demonstrated that the 8.4 doublet was coupled to the 6.5 proton and the 6.9 double doublet was coupled to the 4.8 proton.

Anal. Calcd. for $C_{12}H_{18}NBrO_2$: C, 49.85; H, 6.27; N, 4.67; Br, 27.70. Found: C, 50.00; H, 6.26; N, 4.86; Br, 27.70.

On distillation, the mother liquors provided 0.19 g of 1-phenyl-2,3-dibromobutane (b.p. 90°, 0.15 mm). This oil was identical (i.r.) to a sample of the olefin dibromide prepared by conventional methods.

Anal. Calcd. for $C_{10}H_{12}Br_2$: C, 41.27; H, 4.15; Br, 54.58. Found: C, 41.06; H, 4.12; Br, 54.54.

Electrochemical Chloroamidation of 1-Phenyl-2-butene

In the above manner, a solution of 0.02 mol of Et_4NCl and 0.01 mol of olefin in 100 ml of 0.5 *M* $LiClO_4$ in acetonitrile was electrolyzed at +1.2 to 1.3 V *vs.* Ag, Ag^+ (0.01 *M*) until 2000 C had been passed. Work-up gave 0.35 g of colorless solid identified by i.r. and n.m.r. analyses as 1-phenyl-2-chloro-3-acetamidobutane, m.p. 122–124°; (i.r. (mineral oil): 3350 (m), 1650 (s), 1545 (m) cm^{-1}). The proton integral in the n.m.r. spectrum was in agreement with the designated structure with ratios 5:1:2:2:3:3 for aromatics at 2.8, NH at 4.2, two C—H's at about 5.7, CH_2 at 7.0, CH_3CO at 8.0, and CH_3—CH at 8.8 τ respectively.

Anal. Calcd. for $C_{12}H_{16}NOCl$: C, 63.85; H, 7.08; N, 6.19; Cl, 15.71. Found: C, 63.88; H, 7.16; N, 6.24; Cl, 15.83.

The mother liquor provided a small amount of an oil whose i.r. spectrum suggested that it was 1-phenyl-2,3-dichlorobutane along with some 1-phenyl-2-butene. No attempt was made to separate this mixture.

Dimorpholinization of trans-1,2-Dibenzoylethylene

A solution of 2.4 g of *trans*-1,2-dibenzoylethylene,

Can. J. Chem. Downloaded from www.nrcresearchpress.com by 210.87.254.6 on 09/05/12
For personal use only.

1.3 g of Et_4NI, and 4 ml of morpholine in 100 ml of 0.5 *M* $LiClO_4$ in acetonitrile was electrolyzed at +0.35 V *vs.* Ag, Ag^+ at a smooth platinum anode (10 cm^2). After 1990 C, the solid which had precipitated during the course of the reaction was filtered off and crystallized from methanol to give 1.6 g, m.p. 180–183°, of 1,2-dibenzoyl-1,2-dimorpholinoethane. The i.r. spectrum of this solid was identical to a sample prepared according to the literature (12). A mixed m.p. was not depressed.

Anal. Calcd. for $C_{24}H_{28}O_4N_2$: C, 70.56; H, 6.91; N, 6.86. Found: C, 70.77; H, 6.89; N, 6.82.

From the mother liquor 1.2 g of a second product was isolated, m.p. 125–130° (dec.). Crystallization from ethanol–benzene gave 0.9 g, m.p. 132–134° (dec.), of pale yellow crystals, identified as the iodomorpholino adduct **8**.

Anal. Calcd. for $C_{20}H_{20}NO_3I$: C, 53.46; H, 4.49; N, 3.12; I, 28.25. Found: C, 53.89, 54.03; H, 4.54, 4.52; N, 3.16; I, 27.83.

The i.r. spectrum in mineral oil had characteristic bands at 1645 (s), 1580 (m), and 1560 (w) cm^{-1}. The n.m.r. spectrum in $CDCl_3$ exhibited a ratio of aromatic to all other protons of 10.0 to 10.4 respectively.

Electrochemical Iodoacetoxylation of Cyclopentene

Electro-oxidation of a solution consisting of 30 ml of cyclopentene and 3 g of iodine in 3 *M* KOAc in glacial acetic acid (containing 5% of acetic anhydride) was carried out at 50° (reflux temperature) under a $CaCl_2$ tube. A silver wire dipping into 3 *M* KOAc in glacial acetic acid containing AgOAc (saturated) served as the reference electrode.[5] A controlled potential electrolysis was conducted at +0.4 V *vs.* Ag, AgOAc until 2260 C had been passed. Removal of solvent and electrolyte gave 5.1 g of liquid product. The v.p.c. analysis showed the presence and yields of acetates listed in Table 2. The i.r. spectra of the three components separated by preparative v.p.c. techniques were identical to those of authentic samples.

Electrochemical Iodoacetoxylation of Cyclohexene

In a similar manner as that described in the preceding section, electrolysis at 80° of cyclohexene (10 ml) and 3 g iodine in 100 ml of 3.0 *M* KOAc – glacial acetic acid at +0.4 V *vs.* Ag, AgOAc gave 3.7 g of product after 2072 C had been passed. The products and yields are listed in Table 2.

[5]The Ag, AgOAc (saturated) reference electrode was +0.44 V *vs.* SCE at 20°.

Electrochemical Bromomethoxylation of 1-Phenyl-2-butene

A mixture of 4.2 g (0.020 mol) of Et_4NBr and 2.64 g (0.020 mol) of 1-phenyl-2-butene was electrochemically oxidized in 100 ml of 0.5 *M* $NaClO_4$ in methanol at +0.9 V *vs.* SCE. After 2650 C was passed the solution was concentrated *in vacuo*, the residue taken up in water, extracted with diethyl ether, and the ether extract dried over anhydrous $MgSO_4$. Filtration and evaporation of solvent gave 4.55 g of crude product. The v.p.c. analysis on a QF-1 column showed the presence of four compounds. Two were identified by retention times with authentic samples as 1-phenyl-2-butene (0.72 g) and 1-phenyl-2,3-dibromobutane (1.4 g). The other two, 1-phenyl-2,3-dimethoxybutane (0.74 g) and 1-phenyl-2-bromo-3-methoxybutane (1.7 g) were separated by preparative v.p.c. methods; i.r. and mass spectrometry were consistent with the designated structures.

1. N. L. WEINBERG and H. R. WEINBERG. Chem. Rev. **68**, 471 (1968) and references therein.
2. R. LEININGER and L. A. PASUIT. Trans. Electrochem. Soc. **88**, 73 (1945).
3. T. INOUE, K. KOYAMA, and S. TSUTSUMI. Bull. Chem. Soc. Jap. **40**, 162 (1967).
4. C. V. WILSON. Organic React. **9**, 332 (1957).
5. K. B. WIBERG and K. A. SAEGEBARTH. J. Amer. Chem. Soc. **79**, 6256 (1957).
6. A. HASSNER, L. A. LEVY, and R. GAULT. Tetrahedron Lett. 3119 (1966).
7. A. HASSNER and C. C. HEATHCOCK. Tetrahedron Lett. 1125 (1964).
8. A. HASSNER, M. E. LORBER, and C. C. HEATHCOCK. J. Org. Chem. **32**, 540 (1967).
9. A. HASSNER, J. E. KROPP, and G. J. KENT. J. Org. Chem. **34**, 2628 (1969).
10. L. L. MILLER and A. K. HOFFMANN. J. Amer. Chem. Soc. **89**, 593 (1967).
11. J. BEGER, K. GUENTHER, and J. VOGEL. J. Prakt. Chem. **311**, 15 (1969).
12. P. L. SOUTHWICK and D. R. CHRISTMAN. J. Amer. Chem. Soc. **75**, 629 (1953); *ibid* **74**, 1886 (1952).
13. E. S. GOULD. Mechanism and structure in organic chemistry. Henry Holt and Co., New York. N.Y. 1959. p. 262.
14. M. FLEISCHMANN and D. PLETCHER. Tetrahedron Lett. 6255 (1968).
15. N. L. WEINBERG and T. B. REDDY. J. Amer. Chem. Soc. **90**, 91 (1968); N. L. WEINBERG. J. Org. Chem. **33**, 4326 (1968).
16. N. L. WEINBERG. Can. J. Chem. **48**, 1533 (1970).

Can. J. Chem. Downloaded from www.nrcresearchpress.com by 210.87.254.6 on 09/05/12
For personal use only.

Can. J. Chem. Downloaded from www.nrcresearchpress.com by 210.87.254.40 on 09/05/12
For personal use only.

Derivatives of 1-Phenylphthalan, 2-Methyl-1-phenylisoindoline, and 5*H*-Dibenzo[*a*,*d*]cycloheptene Oxides; Synthesis and Conformational Aspects

ROBERT R. FRASER AND ROGER N. RENAUD[1]
Department of Chemistry, University of Ottawa, Ottawa, Canada

Received August 10, 1970

For the purpose of correlation of chemical shifts and geminal coupling constants with stereochemistry a number of compounds of fixed geometry have been synthesized. These include seven 6-substituted 1-phenylphthalans, five 6-substituted 2-methyl-1-phenylisoindolines, and six 2-substituted 5*H*-dibenzo-[*a*,*d*]cycloheptene oxides. The geometrical properties of the three ring systems are discussed and arguments in favor of a quasi-equatorial epoxide substituent in the latter series are supported by n.O.e. measurements.

Canadian Journal of Chemistry, 49, 746 (1971)

In an accompanying paper (1) we have investigated substituent effects on the geminal coupling constant between protons on a methylene carbon adjacent to a benzene ring. The chemical shifts of these protons have also been described (2). Three series of compounds were synthesized in which the substituent para to the benzylic methylene group was varied. In each series the substituent effects on the geminal coupling constant and on the shifts were determined and discussed in relation to the stereochemistry at the benzene—CH_2 bond. This paper describes the synthesis and conformational properties of each series of compounds; the 6-*X*-1-phenylphthalans, **1**, the 6-*X*-2-methyl-1-phenylisoindolines, **2**, and the 2-*X*-5*H*-dibenzo-[*a*,*d*]cycloheptene oxides, **3**.

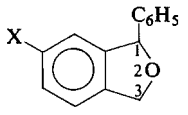

1
(*a*, *b*, *c*, *e*, *f*, *i*, *j*)

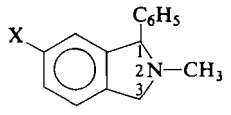

2
(*a*, *c*, *e*, *h*, *j*)

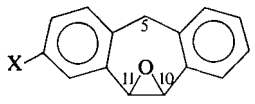

3
(*c*, *d*, *e*, *g*, *h*, *i*)

For *a*, X = NH_2; *b*, OH; *c*, OCH_3; *d*, CH_3; *e*, H; *f*, Cl; *g*, Br; *h*, $COOCH_3$; *i*, CN; *j*, NO_2.

[1]Present address: Division of Chemistry, National Research Council of Canada, Ottawa, Canada.

Synthesis of Substituted 1-Phenylphthalans

One method of synthesis of the parent compound 1-phenylphthalan (**1***e*) has been described by Vaulx *et al.* (3). Unfortunately, their method is unsuitable to the preparation of derivatives in the 6-position. A second method (4), involving cyclization of the appropriate diol, readily gave **1***e* and proved adaptable to the preparation of the series of 6-substituted 1-phenyl phthalans as shown in Scheme 1. 4-Nitro-2-benzoylbenzoic acid (**4***j*) prepared by Kliegl's method (5), was converted in two steps to 6-nitro-1-phenylphthalan (**1***j*). The yield in the cyclization was increased from 60 to 87% by use of potassium bisulfate rather than phosphoric acid (4). Reduction of **1***j* gave the amino derivative, **1***a*, which was easily converted to the hydroxyl, chloro, and cyano compounds, **1***b*, *f*, and *i* via the diazonium salt. Methylation of the hydroxyl function gave **1***c*.

Synthesis of Substituted 2-Methyl-1-phenylisoindolines

The parent compound, **2***e*, was originally prepared by Wittig *et al.* (6). We chose to use a more recently described route (7) which could utilize the available diols, **5***e* and *j*. Conversion of the diols to their corresponding dibromides, **7***e* and *j*, and subsequent treatment with methylamine gave **2***e* and *j* in good yields. Reduction of the nitro group in **2***j* with ferrous sulfate gave **2***a*. For the synthesis of the other members of this series we used the remaining available phthalans, **1***c* and *i*. Conversion of **1***c* to the isoindoline **2***c* was accomplished in good yield by treatment with HBr, followed by methylamine. The cyano derivative,

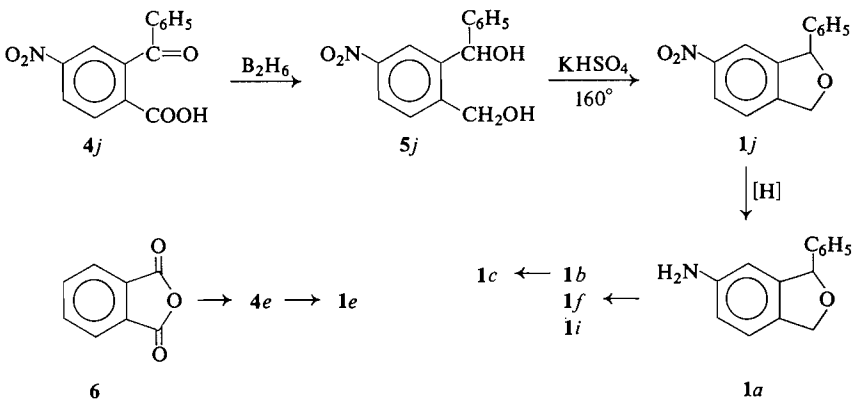

SCHEME 1

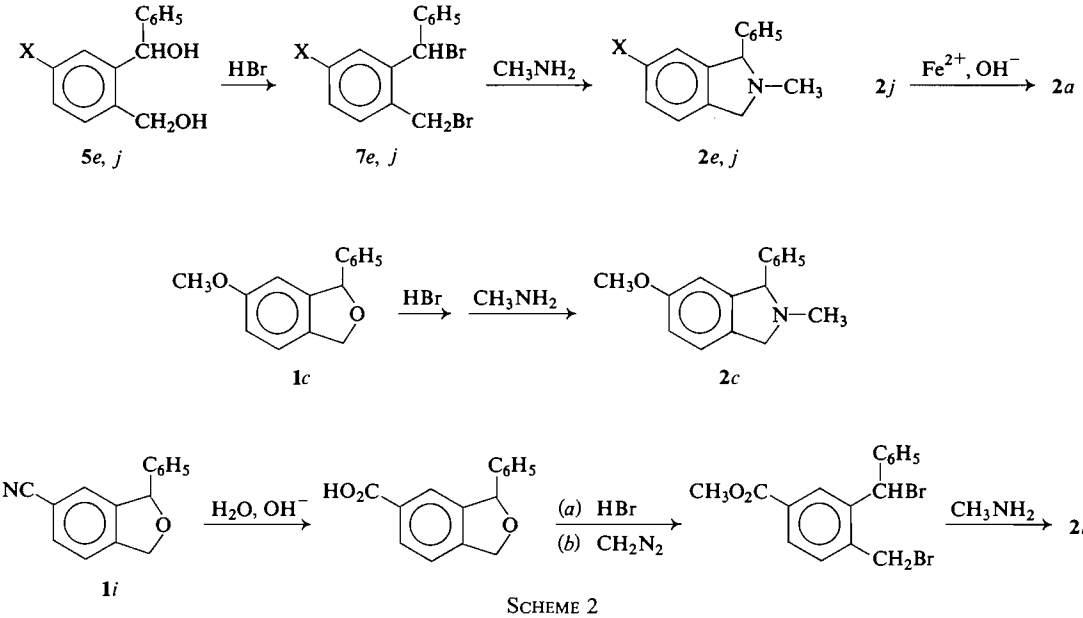

SCHEME 2

1*i*, was used to prepare the ester derivative, **2*h***. All these transformations are summarized in Scheme 2.

As can be seen in the Experimental, considerable difficulty was encountered in obtaining acceptable combustion analyses for derivatives in this series. All of these compounds became light green on exposure to air. Due to limited supplies of their precursors, the compounds were prepared, purified, and then immediately dissolved in deuterochloroform for recording of their n.m.r. spectra. The second crop of crystals from the preparation was recrystallized several times to produce an analytical sample. The nitro, amino, and methoxy derivatives gave combustion analyses close to the theoretical values but outside of the acceptable limits. Nevertheless the n.m.r. spectral properties of all members of this series strongly support the structural assignments and showed no identifiable impurities.

Synthesis of Substituted 10,11-Dihydro-10,11-epoxy-5H-dibenzo[a,d]cycloheptenes

For the preparation of the series of epoxides, **3**, we required the immediate precursors, the 5*H*-dibenzo[*a*,*d*]cycloheptenes, **9**. The parent mem-

Can. J. Chem. Downloaded from www.nrcresearchpress.com by 210.87.254.40 on 09/05/12
For personal use only.

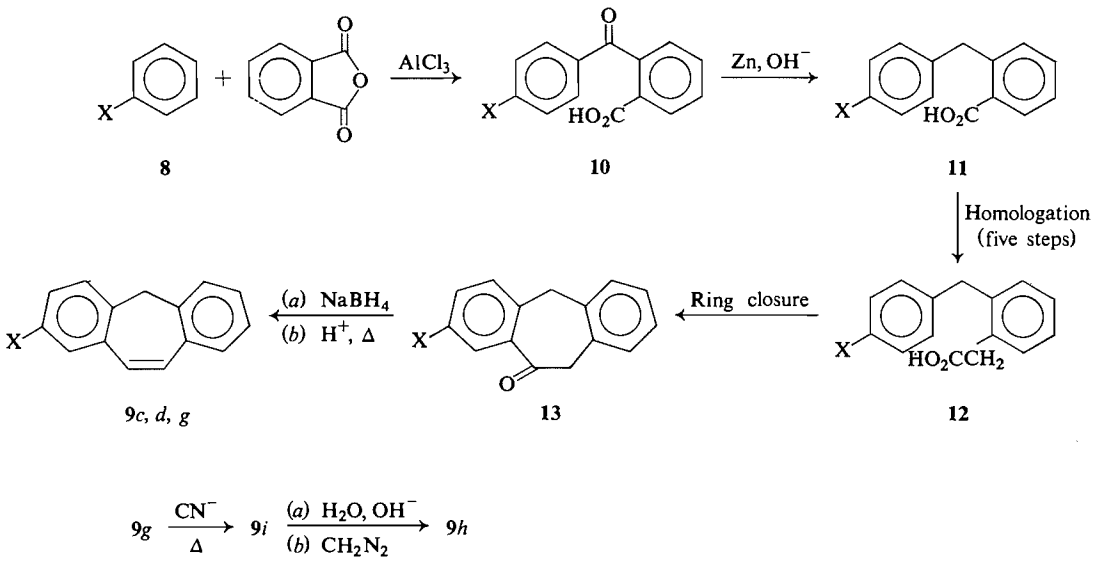

SCHEME 3

ber **9e** was prepared by methods described in the literature (8, 9). Several syntheses of related dibenzo[*a*,*d*]cycloheptane derivatives have been disclosed (10–13) from which we chose the approach of S. A. Rhone-Poulenc (13) as most suitable for obtaining derivatives at position 2. This patent describes the synthesis of several 11-keto derivatives, **13**, which we could easily convert to the desired olefins. This sequence of reactions is outlined in Scheme 3. Although lengthy, the route presented no difficulties in the preparation of **9***c*, *d*, and *g*. Since the first step in this route works only with electron-donating substituents, the bromo derivative **9***g* was used as the precursor of the remaining compounds in the series. For this purpose the bromine in **9***g* was displaced by cyanide in DMF, a solvent shown to be advantageous by Friedman and Shechter (14). This reaction gave **9***i* in good yield but in *N*-methylpyrrolidone (15) an improved yield of 79% was achieved. The cyano group was then hydrolyzed and esterified with diazomethane to give **9***h*.

Epoxidation of all members of series **9** by meta-chloroperbenzoic acid proceeded in yields of 50 to 60% to give series **3**.

Conformations of 1-Phenylphthalan and 2-Methyl-1-phenylisoindoline

To the extent that Dreiding models represent the geometrical features of a molecule, it can be said that 1-phenylphthalan has a planar five-membered ring. Although the molecule is quite rigid certain allowed torsional vibrations may be present. Also, the phenyl substituent gives asymmetry to the molecule, which may result in at least a slightly puckered preferred conformation. The best estimate of the amount of puckering can be made from crystallographic data (16) available for a related compound, 3-*p*-bromophenylphthalide (**14**). This compound, though not an ideal model, provides some basis of assessment. A detailed X-ray analysis revealed the five-membered ring to have its oxygen atom within 0.03 Å of the completely planar conformation. The molecule was found to possess a distortion of the C_3—phenyl bond in a direction bending away from both the adjacent oxygen and carbon atoms but exhibited little distortion elsewhere. It would seem reasonable that the structural features common to the phthalans and phthalides (a strained five-membered ring attached to a rigid *o*-disubstituted benzene) would confer similar

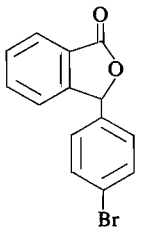

14

Can. J. Chem. Downloaded from www.nrcresearchpress.com by 210.87.254.40 on 09/05/12
For personal use only.

Can. J. Chem. Downloaded from www.nrcresearchpress.com by 210.87.254.40 on 09/05/12
For personal use only.

conformational properties to each. We would then expect the projected angle ϕ[2] in the 1-phenylphthalans, and in the 2-methyl-1-phenylisoindolines also, to be within 5° of zero, the value for a completely planar molecule.

Conformation of 3e

Although information regarding the exact geometry of the seven-membered ring in the epoxide **3e** is not available, an X-ray analysis of the related compound dibenzo[*b*,*f*]tropone has been reported (17). In this molecule the tropone ring is in a boat conformation and the two benzene rings are inclined by an angle of 40° from a planar arrangement. In a Dreiding model this angle is about 50°, the difference being due to molecular distortions in the crystal form but not in the liquid state and also to the fact that the Dreiding model is, in general, too rigid. With this in mind, one can examine a Dreiding model of **3e** and estimate the various bond angles of the molecule. The angle of particular interest to us is the projected angle ϕ at the benzene–methylene bond. In the model of **3e** this angle is 73°. Distortion which would decrease the angle between the benzene rings would also decrease the angle ϕ, but not by as many degrees. The above estimate of 73° should be accurate to within 5°.

Two other aspects of the conformation of **3e**, the barrier to inversion and the preferred conformation of the epoxide ring, merit consideration. Barriers to inversion have been measured on several compounds closely related to **3e**. The dibenzo[*a*,*d*]cycloheptene **9e** has been found to have a barrier of 9.2 kcal/mol (18, 19) while the 5,5-dimethoxy derivative is reported to have a barrier to inversion of 15 kcal/mol (20). It is likely that the barrier in **3e** is similar to that of **9e**, in which case the molecule should be inverting rapidly at room temperature on the n.m.r. time scale. An examination of the temperature dependence of the n.m.r. spectrum of **3e** over the temperature range of −90 to +140 °C failed to detect any significant spectral changes. Either the molecule has a very low or a very high barrier to inversion, or else it possesses one dominant conformation.

For a hydroxyl derivative of **3e**, 10,11-dihydro-

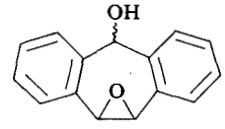

15

10,11-epoxy-5-hydroxy-5*H*-dibenzo[*a*,*d*]cycloheptene (**15**), a dominant conformation in which both the epoxide ring and the hydroxyl group occupy the quasi-axial positions (*cis* configuration) has been proposed by Bauld and Rim (21). The authors made this assignment to account for the presence of a bonded OH absorption in its i.r. spectrum (ν = 3440 cm^{-1}). Furthermore an H—C—O—H coupling of 12 Hz led them to propose a *trans* or *anti* orientation (22) for the OH proton relative to the proton at C-5.

From an examination of Dreiding models of **15** and **3e** it would appear that the above assignment is in error and that the epoxide ring is quasi-equatorial in both compounds. In a model of *cis*-**15** occupying the proposed conformation, the distance between the epoxide and hydroxyl oxygens is estimated as 1.5 Å and the distance between the O—H proton and the epoxide oxygen is less than 1 Å. In a model of **3e** the distance between a quasi-axial epoxide oxygen and the quasi-axial proton at C-5 is 1.8 Å. Since all these distances are much less than the sums of the Van der Waals' radii of the two atoms, the repulsive interactions would make these conformations much less stable than the ones with a quasi-equatorial epoxide ring in which no significant steric interactions are present. In all likelihood the 5-hydroxy derivative, **15**, has a *trans* configuration for the two substituents with the epoxide in the quasi-equatorial position. The unusual spectral properties (i.r. and n.m.r.) might be accounted for by hydrogen-bond formation between the quasi-axial O—H and the C_{10}—C_{11} bond of the epoxide ring. Such bonding to a three-membered ring has precedence in cyclopropane–OH interactions (23, 24) although these were not so strong ($\Delta\nu$ = 40 cm^{-1}). Perhaps the C_{10}—C_{11} bond is a better donor due to its large amount of strain and the fact that in **15** C-10 and -11 are benzylic.

We sought additional evidence for the quasi-equatorial orientation of the epoxide ring from a study of the n.O.e.'s in a degassed sample of **3c** in deuterochloroform. Figure 1 gives the spectrum, as well as a drawing of the boat form of **3c**, show-

[2]The angle ϕ is taken as zero when an imaginary line joining the benzylic methylene protons is parallel to the adjacent π orbitals of the benzene ring (1).

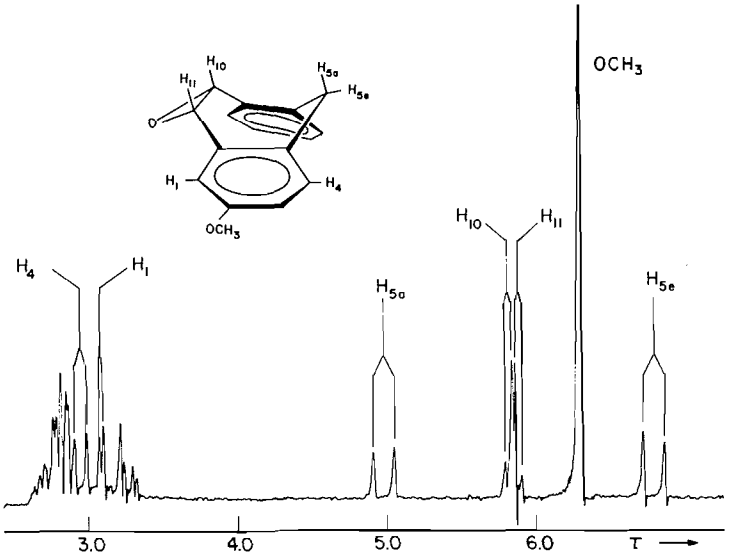

FIG. 1. The 100 MHz spectrum of compound 3*c* in deuterochloroform, with the assignment of protons as indicated in the formula.

TABLE 1. The n.O.e.'s in 3*c* (see inset, Fig. 1)

H-4	H-5$_e$	H-5$_a$	H$_{10}$–H$_{11}$	H-11	Internuclear distance (Å)*	
		[5]†		‡	3.1	(3.9)
		‡	[3]†		3.1	(3.9)
‡	[16]†				2.3	
‡		[5]†			3.6	

*The distance given without brackets represents that for the quasi-equatorial epoxide, the value in brackets being for the quasi-axial conformer.
†Value representing the % increase in integrated intensity on irradiation.
‡Indicates the proton being irradiated.

ing the numbering of the protons. The results of our n.O.e. experiments are listed in Table 1.

Interpretation of n.O.e.'s must be made with caution as many mechanisms of relaxation may contribute to the observed effects. Discussions of these problems in interpretation have been made in many papers, a few of which (25–27) are particularly helpful. The data in Table 1 provide some information on the preferred conformation for 3*c*. Observation of a 5% increase in intensity of the signal for the quasi-axial proton at C-5 on irradiation of H-11 is consistent with a quasi-equatorial epoxide ring (H_{11}–H_5 distance = 3.1 Å) but not with a quasi-axial ring (H_{11}–H_5 distance = 3.9 Å). The inverse experiment gives a similar result in that an n.O.e. of 3% for H-11 on irradiation of H-5 (quasi-axial) was seen. Assignments for the H-5 protons are made on the basis of the last two n.O.e.'s in Table 1. The small magnitude for all of the n.O.e.'s in Table 1 is expected since each proton investigated has either a geminal or a vicinal neighbor proton which also contributes to its relaxation. Nevertheless, since values of 3 and 5% are in the range of the experimental error in measurement (±3%), they can only be interpreted as mild support for a quasi-equatorial epoxide ring in 3*c*. A quasi-equatorial cyclopropane ring has been proposed in a similar case (35).

Experimental

All melting points are corrected. Unless specified, the drying agent used for solutions was magnesium sulfate. All i.r. spectra were recorded on a Perkin–Elmer Infracord spectrometer. Only the characteristic bands are reported (cm^{-1}). The n.m.r. spectra were measured in deuterochloroform and the chemical shifts are reported on the τ scale. The instrument used was a Varian HA-100 spectrometer. The technique used for determining the n.O.e.'s is the same as that described previously (27).

1-Phenylphthalan (1e)

o-Benzoylbenzoic acid was prepared from phthalic anhydride and converted to 1-phenylphthalan by the procedure of Pernot and Willemart (4). The crude oily product obtained was purified by bulb-to-bulb distillation and the fraction distilling at 155° (0.25 mm) collected.

Can. J. Chem. Downloaded from www.nrcresearchpress.com by 210.87.254.40 on 09/05/12
For personal use only.

Can. J. Chem. Downloaded from www.nrcresearchpress.com by 210.87.254.40 on 09/05/12
For personal use only.

The overall yield was 54%. The i.r. and n.m.r. spectra of this product were identical to those reported by Vaulx *et al.* (3).

(5-Nitro-2-hydroxymethylphenyl)phenyl Carbinol (5j)

Reduction of 3.2 g of 4-nitro-2-benzoylbenzoic acid (5) with diborane, generated as described by Schmitt and co-workers (28) gave an oil in 96% yield (3.3 g) which slowly crystallized to a light brown solid, m.p. 92–93°; i.r. (film): 3490 (OH), 1530, 1355 (NO_2); n.m.r. (DMSO): 1.80 (1H doublet, proton at C-6), 2.02 (1H quartet, proton at C-4), 2.54 (1H doublet, proton at C-3), 2.86 (5H singlet, aromatic), 3.82 (1H doublet, hydroxyl proton of CHOH), 4.04 (1H doublet, methine), 4.52 (1H triplet, hydroxyl proton of CH_2OH), 5.44 (2H octet, methylene).

Anal. Calcd. for $C_{14}H_{13}NO_4$: C, 64.86; H, 5.02; N, 5.21. Found: C, 64.68; H, 5.25; N, 5.24.

6-Nitro-1-phenylphthalan (1j)

To a solution of **5***j* (6.8 g) in ether (150 ml) was added 100 g of freshly powdered fused potassium bisulfate. The ether was distilled off and the residue heated at 160° for 1 h. The cooled residue was extracted with ether and the dark solution was passed through a column containing magnesium sulfate and aluminum oxide. Concentration of the eluent gave a solid, m.p. 55.5–56.5°, in a yield of 87% (5.8 g); i.r. (KBr): 1522 and 1350 (NO_2), 1048 (C—O—C); n.m.r.: 1.82 (1H quartet, proton at C-5), 2.14 (1H doublet, proton at C-7), 2.66 (6H multiplet, aromatic), 3.81 (1H multiplet, methine), 4.70 (2H octet, methylene).

Anal. Calcd. for $C_{14}H_{11}NO_3$: C, 69.70; H, 4.57; N, 5.81. Found: C, 69.67; H, 4.74; N, 5.65.

6-Amino-1-phenylphthalan (1a)

6-Nitro-1-phenylphthalan (2.7 g) dissolved in 25 ml methanol was reduced at room temperature in the presence of 0.2 g of 10% palladium-on-charcoal catalyst under hydrogen at a pressure of 4 atm. The theoretical volume of hydrogen was absorbed in 5 h. Removal of the catalyst by filtration followed by evaporation of the methanol gave a dark brown oil. This crude material was treated with excess of dilute hydrochloric acid and filtered. The filtrate on treatment with dilute sodium hydroxide solution gave 2.2 g (93%) of a light brown amorphous solid, m.p. 84–85°, which was recrystallized from water. Long colorless needles, m.p. 85.5–86°, were obtained; i.r. (KBr): 3475 and 3385 (NH_2), 1032 (C—O—C); n.m.r.: 2.73 (5H singlet, aromatic), 2.98 (1H at C-4), 3.44 (1H quartet at C-5), 3.72 (1H doublet at C-7), 3.96 (1H broad singlet, methine), 4.83 (2H octet, methylene), 7.05 (2H broad singlet, NH_2).

Anal. Calcd. for $C_{14}H_{13}NO$: C, 79.62; H, 6.16; N, 6.64. Found: C, 79.75; H, 6.35; N, 6.80.

6-Chloro-1-phenylphthalan (1f)

Conversion of the aminophthalan, **1***a*, by diazotization and reaction under standard conditions (29) gave a 35% yield of a yellow oil, **1***f*; i.r. (film): 1040 (C—O—C); n.m.r.: 2.69 (7H multiplet, aromatic), 3.00 (1H broad singlet at C-7), 3.88 (1H broad singlet, methine), 4.77 (2H octet, methylene).

Anal. Calcd. for $C_{14}H_{11}ClO$: C, 72.88; H, 4.77; Cl, 15.41. Found: C, 73.21; H, 5.01; Cl, 15.02.

6-Cyano-1-phenylphthalan (1i)

Diazotization of **1***a*, followed by reaction with cyanide (29) gave a 46% yield of a semi-solid, which, after sublimation and recrystallization from ethanol, melted at 104.5–105.5°; i.r. ($CHCl_3$): 2260 (C≡N); 1040 (C—O—C); n.m.r.: 2.70 (8H multiplet, aromatic), 3.86 (1H broad singlet, methine), 4.71 (2H octet, methylene).

Anal. Calcd. for $C_{15}H_{11}NO$: C, 81.49; H, 5.21; N, 6.33. Found: C, 81.56; H, 5.13; N, 6.04.

6-Hydroxy-1-phenylphthalan (1b)

Diazotization of **1***a* and decomposition in boiling water (29) gave, after work-up, an oily solid which was purified by sublimation and recrystallization from water to give 0.27 g (34.5%) of long colorless needles melting at 133–134°; i.r. ($CHCl_3$): 3225 (OH), 1020 (C—O—C); n.m.r.: 2.72 (5H multiplet, aromatic), 2.92 (1H doublet at C-4), 3.30 (1H quartet at C-5), 3.58 (1H doublet at C-7), 3.92 (1H broad singlet, methine), 4.82 (2H octet, methylene).

6-Methoxy-1-phenylphthalan (1c)

To a stirred solution of 6-hydroxy-1-phenylphthalan (0.13 g) in 5 ml of aqueous sodium hydroxide (10%) was added dropwise dimethyl sulfate (0.4 ml). Stirring was continued for 5 h. The product was extracted into ether and the slightly orange solid obtained after removal of the dried solvent was purified by sublimation to give 0.11 g (79%) of a colorless solid melting at 78.5–79.5°; i.r. (KBr): 1040 (C—O—C); n.m.r.: 2.70 (5H singlet, aromatic), 2.84 (1H doublet at C-4), 3.18 (1H quartet at C-5), 3.48 (1H doublet at C-7), 3.90 (1H broad singlet, methine), 4.79 (2H octet, methylene).

Anal. Calcd. for $C_{15}H_{14}O_2$: C, 79.60; H, 6.19. Found: C, 79.50; H, 6.39.

2-Methyl-1-phenylisoindoline (2e)

To 2 g of (2-hydroxymethylphenyl)phenyl carbinol dissolved in 2 ml of chloroform was added 50 ml of 48% hydrobromic acid. The mixture was kept at 70° for 6 h. During this time hydrogen bromide was passed into the reaction mixture. The reaction product was extracted with chloroform, dried, and concentrated *in vacuo* to give a red oil which was dissolved in 15 ml of benzene and added to a stirred saturated solution of methylamine in 25 ml of benzene. The mixture was kept at 40° for 3 h while methylamine was passed through the reaction mixture. The supernatant benzene solution was decanted and concentrated. The residue was dissolved in ether and extracted with dilute hydrochloric acid. The free base was then precipitated from the acid solution with NaOH solution, re-extracted into ether, and the ether solution dried and concentrated to dryness. The solid residue after crystallization from ethanol amounted to 1.4 g (71%) of a white solid, m.p. 59–59.5°, lit. m.p. 58.5–59° (6); n.m.r.: 2.64–2.84 (8H multiplet), 3.24 (1H doublet at C-7), 5.48 (1H quintet at C-1), 5.62 (1H quartet at C-3), 6.25 (1H quartet at C-3), 7.56 (3H singlet, *N*-methyl).

6-Nitro-2-methyl-1-phenylisoindoline (2j)

By use of the above procedure, 0.4 g of (5-nitro-2-hydroxymethylphenyl)phenyl carbinol (**5***j*) was converted to 0.26 g of 6-nitro-2-methyl-1-phenylisoindoline in 66% yield. The product was a yellow solid, m.p. 84.0–85°; i.r.

Can. J. Chem. Downloaded from www.nrcresearchpress.com by 210.87.254.40 on 09/05/12
For personal use only.

($CHCl_3$) 1348 and 1528 (NO_2); n.m.r.: 1.90 (1H doublet, aromatic), 2.41 (1H singlet, aromatic), 2.60 (6H singlet, aromatic), 5.43 (1H multiplet, methine), 5.56 (1H quartet, methylene), 6.20 (1H quartet, methylene), 7.55 (3H singlet, methyl).

Anal. Calcd. for $C_{15}H_{14}N_2O_2$: C, 70.03; H, 5.47; N, 11.02. Found: C, 70.42; H, 5.98; N, 10.87.

*6-Amino-2-methyl-1-phenylisoindoline (**2a**)*

Reduction of the nitro group of **2***j* with ferrous sulfate and ammonium hydroxide (30) followed by work-up and purification as described for **2***e* gave an 85% yield of light green solid, m.p. 87.5–89°. This material rapidly darkened on exposure to air. The i.r. ($CHCl_3$) 3400 and 3480 (NH_2); n.m.r.: 2.61 (6H broad singlet, aromatic), 3.02 (1H doublet, aromatic), 3.51 (1H doublet, aromatic), 5.57 (1H multiplet, methine), 5.73 (1H quartet, methylene), 6.36 (1H quartet, methylene), 7.57 (3H singlet, methyl).

Anal. Calcd. for $C_{15}H_{16}N_2$: C, 80.36; H, 7.14; N, 12.50. Found: C, 79.48; H, 7.53; N, 12.32.

*6-Methoxy-2-methyl-1-phenylisoindoline (**2c**)*

This compound was prepared from **1***c* using the procedure reported above for the preparation of **2***j* except that the reactions were done at room temperature. A 78% yield of a light green solid, m.p. 54.5–56.5°, was obtained; n.m.r. 2.61–3.02 (7H, aromatic), 3.35 (1H doublet, aromatic), 5.49 (1H multiplet, methine), 5.68 (1H quartet, methylene), 6.40 (1H quartet, methylene), 6.37 (3H methoxyl), 7.58 (3H singlet, N-methyl).

Anal. Calcd. for $C_{16}H_{17}NO$: C, 80.2; H, 7.1; N, 5.9. Found: C, 78.2; H, 6.6; N, 6.1.

*6-Carbomethoxy-2-methyl-1-phenylisoindoline (**2h**)*

A mixture of 6-cyano-1 phenylphthalan (82 mg) and 10 ml of 10% aqueous NaOH was heated at 100° for 5 h. Then the reaction mixture was cooled on ice and acidified with hydrochloric acid. The solid that separated was collected by filtration and treated with hydrobromic acid as described in the preparation of **2***e* above. The resulting dibromoacid was then esterified with diazomethane. The solution was concentrated *in vacuo* and the resulting oil in benzene was treated with methylamine at room temperature for 3 h. The light green solid obtained after evaporation of the solvent was purified by sublimation at reduced pressure (0.02 mm) to give a colorless solid (50 mg; 51%), m.p. 79–80.5°; i.r. ($CHCl_3$), 1728 (CO); n.m.r.: 2.10 (1H doublet, aromatic at C-5), 2.58–2.78 (7H, aromatic), 5.45 (1H multiplet, methine proton), 5.59 (1H quartet at C-3), 6.22 (1H quartet at C-3), 6.21 (3H singlet, methoxyl), 7.57 (3H singlet, *N*-methyl).

*5H-Dibenzo[a,d]cycloheptene (**9e**)*

This compound was prepared from commercially available 10,11-dihydro-5*H*-dibenzo[*a*,*d*]cycloheptene-5-one, by bromination and dehydrobromination (8) followed by reduction of the carbonyl group (9). Physical constants and spectral properties agreed with those previously reported (9).

*Reactions Leading to 2-Bromo-5H-dibenzo[a,d]cycloheptene (**9g**)*

Since the reactions of Scheme 3 up to and including the synthesis of **13***g* are documented in the literature, only a general description of the methods employed is given below. A Friedel–Crafts reaction of phthalic anhydride with bromobenzene gave 2-(4-bromobenzoyl)benzoic acid (31). This was reduced, via the phthalide (32), to 2(4-bromobenzyl)benzoic acid (32). Reduction to the alcohol with diborane (28), treatment with HBr, displacement by cyanide, and hydrolysis of the nitrile gave 2-(4-bromobenzyl)phenylacetic acid (11). Cyclization with polyphosphoric acid according to the industrial method (12) gave only trace amounts of the ketone, **13***g*. Different cyclization conditions were then sought.

A mixture of compound **12***g* (2 g) and thionyl chloride (6 ml) was heated under reflux for 3 h. Then the excess thionyl chloride was removed *in vacuo*. The oily residue was dissolved in carbon disulfide (25 ml) and added dropwise during 2 h to a stirred suspension of aluminum chloride (5 g) in carbon disulfide (100 ml) at room temperature. After 1 h of additional stirring, the mixture was poured onto ice containing hydrochloric acid. The organic layer was washed with 5% sodium bicarbonate, with water, and then dried. The brown solid obtained after evaporation of the solvent was sublimed as a light yellow solid (1.7 g; 90%) melting at 101–102°, (lit. m.p. 106°, (12)), i.r. ($CHCl_3$): 1675 (C=O); n.m.r.: 1.76 (1H doublet, aromatic proton at C-1), 2.70 (6H multiplet, aromatic), 5.79 and 5.82 (total of 4H, two singlets, $2CH_2$).

Anal. Calcd. for $C_{15}H_{11}BrO$: C, 62.72; H, 3.83; Br, 27.88. Found: C, 62.72; H, 3.93. Br, 27.99.

2-Bromo-10,11-dihydro-5H-dibenzo[a,d]cyclohepten-11-ol

To a solution of compound **13***g* (1 g) in absolute ethanol (25 ml) was added during a period of 10 min a solution of sodium borohydride (1.3 g) in absolute ethanol (20 ml). The mixture was stirred at room temperature for 20 h and then enough water was added to decompose the complex. The solvent was removed *in vacuo*. Water (5 ml) was added to the residue which was then extracted with ether. Drying and concentration of the solution gave 1 g (99%) of a colorless solid melting at 99–103°, lit. m.p. 106° (12). The crude alcohol was not purified further and was used as such in the next step.

*2-Bromo-5H-dibenzo[a,d]cycloheptene (**9g**)*

A mixture of the above alcohol (1 g) and *p*-toluenesulfonic acid (0.05 g) in toluene (40 ml) was heated to boiling and the azeotropic mixture was slowly collected for 3 h. Then the toluene solution was washed with a solution of sodium bicarbonate and dried. The solvent was evaporated to dryness and the residue recrystallized from ethanol to give 0.84 g (70%) of colorless plates melting at 117–118°; n.m.r.: 2.70 (7H multiplet, aromatic), 3.00 (2H quartet, CH=CH), 6.33 (2H singlet, CH_2).

Anal. Calcd. for $C_{15}H_{11}Br$: C, 66.42; H, 4.06; Br, 29.52. Found: C, 66.24; H, 4.01; Br, 29.35.

*2-Cyano-5H-dibenzo[a,d]cycloheptene (**9i**)*

A stirred mixture of **9***g* (0.6 g), freshly prepared cuprous cyanide (0.36 g) and *N*-methylpyrrolidone (23 ml) was refluxed for 3 h. To the resulting brown mixture was added a hot solution of 1.8 g of ferric chloride in 3.5 ml of 1.7 *N* hydrochloric acid. After heating the mixture at 60° for 20 min to decompose the complex, dilute hydrochloric acid was added and the organic material was extracted

TABLE 2. Analytical data for epoxides, 3

Compound	Melting point (°C)		Analyses C	H	N	Br
c	138.5–139.5	Calcd.	80.67	5.88		
		Found	80.47	6.09		
d	151–152	Calcd.	86.49	6.31		
		Found	86.45	6.24		
g	113.5–115	Calcd.	62.72	3.83		27.87
		Found	62.86	3.75		27.75
h	146–147.5	Calcd.	76.69	5.26		
		Found	76.69	5.20		
i	175–176	Calcd.	82.40	4.72	6.01	
		Found	82.25	4.75	5.84	

into four 25 ml portions of toluene. The extracts were washed with sodium hydroxide (10%), water, then dried and concentrated. The light brown solid residue obtained was purified by sublimation to give 0.38 g (79%) of light yellow crystals melting at 102.5–103.5°; i.r. ($CHCl_3$): 2250 (C≡N); n.m.r.: 2.60 (7H multiplet, aromatic), 2.92 (2H quartet, CH=CH), 6.25 (2H singlet, CH_2).

Anal. Calcd. for $C_{16}H_{11}N$; C, 88.48; H, 5.07; N, 6.45. Found: C, 88.40; H, 4.99; N, 6.27.

2-Carbomethoxy-5H-dibenzo[a,d]cycloheptene (9h)

To a solution of compound **9***i* (0.2 g) in ethylene glycol monoethyl ether (3 ml) was added a solution of potassium hydroxide (0.7 g) in water (0.5 ml). The resulting mixture was heated to 140° for 7 h with stirring. Then the solvent was removed, the residue dissolved in water, and the solution acidified with dilute sulfuric acid. The product was collected by filtration and dried in air. The yield was 0.2 g (92%) (m.p. 227–228°).

Into a solution of 0.1 g of this acid in ether was distilled an ethereal solution of diazomethane until the yellow color persisted. After evaporation of the solvent *in vacuo*, the residue was purified by sublimation to give 0.09 g (85%) of colorless crystals melting at 110–110.5°; i.r. ($CHCl_3$): 1700 (C=O); n.m.r.: 2.01 (1H singlet at C-1), 2.71 (6H multiplet, aromatic), 2.92 (2H singlet, CH=CH), 6.12 (3H singlet, CH_3), 6.23 (2H singlet, CH_2).

Anal. Calcd. for $C_{17}H_{14}O_2$: C, 81.60; H, 5.60. Found: C, 81.70; H, 5.56.

2-Methoxy-5H-dibenzo[a,d]cycloheptene (9c)

Most of the reactions used for the preparation of **9***g* were used to obtain the methoxy derivative, **9***c*. Differences were that **10***c* was reduced to **11***c* with zinc in alkali (33) and the carboxyl group **11***c* was reduced to the primary alcohol with lithium aluminum hydride. The overall yield of **9***c* for the ten steps was 23%. The final product was a colorless solid, m.p. 131–132°, i.r. ($CHCl_3$): 2850, 1260 (CH_3O); n.m.r.: 2.76 (5H multiplet, aromatic), 3.00 (2H singlet, CH=CH), 3.16 (2H multiplet, aromatic protons at C-1 and C-3), 6.25 (3H singlet, CH_3), 6.33 (2H singlet, CH_2).

Anal. Calcd. for $C_{16}H_{14}O$: C, 86.49; H, 6.31. Found: C, 86.64; H, 6.17.

2-Methyl-5H-dibenzo[a,d]cycloheptene (9d)

Compound **9***d* was prepared via the sequence of reactions used for the preparation of the 2-methoxy derivative starting with toluene instead of anisole. The yield was essentially the same at each step. Colorless plates melting at 137–138° were obtained from ethanol; n.m.r.: 2.80 (7H multiplet, aromatic), 3.00 (2H singlet, CH=CH), 6.31 (2H singlet, CH_2), 7.71 (3H singlet, CH_3).

Anal. Calcd. for $C_{16}H_{14}$: C, 93.20; H, 6.80. Found: C, 93.32; H, 6.97.

10,11-Dihydro-10,11-epoxy-5H-dibenzo[a,d]cycloheptene (3e)

5H-Dibenzo[*a*,*d*]cycloheptene (**9***e*) (1 g) was added to a solution of *m*-chloroperbenzoic acid (1.2 g) in chloroform (10 ml) and the mixture was stirred at room temperature for 20 h. The *m*-chlorobenzoic acid formed was removed by shaking with a 5% solution of sodium bicarbonate. The organic layer was dried, then evaporated to dryness *in vacuo*. The crude residue was recrystallized from ethanol to give 0.59 g (54%) of colorless plates melting at 144–145° (lit. m.p. 144–146°) (34); n.m.r.: 2.80 (8H multiplet, aromatic), 4.83 (1H doublet, axial proton of CH_2), 5.77 (2H singlet, epoxide protons), 6.69 (1H doublet, equatorial proton of CH_2).

Anal. Calcd. for $C_{15}H_{12}O$: C, 86.54; H, 5.77. Found: C, 86.42; H, 5.95.

2-Substituted 10,11-Dihydro-10,11-epoxy-5H-dibenzo-[a,d]cycloheptenes (3)

Five new 2-substituted 10,11-dihydro-10,11-epoxy-5H-dibenzo[*a*,*d*]cycloheptenes were obtained in yields of 50 to 60% from their olefinic derivatives as described for **3***e*. A list of the melting points and elemental analyses are given in Table 2. The n.m.r. spectra of all compounds were similar to that of **3***e* and completely consistent with structure.

1. R. R. FRASER and R. N. RENAUD. Can. J. Chem. This issue.
2. R. R. FRASER and R. N. RENAUD. Can. J. Chem. This issue.
3. R. L. VAULX, F. N. JONES, and C. R. HAUSER. J. Org. Chem. **29**, 505 (1964).
4. A. PERNOT and A. WILLEMART. Bull. Soc. Chim. Fr. **20**, 321 (1953).

Can. J. Chem. Downloaded from www.nrcresearchpress.com by 210.87.254.40 on 09/05/12
For personal use only.

5. A. KLIEGL. Chem. Ber. **38**, 284 (1905).
6. G. WITTIG, G. CLOSS, and F. MINDERMANN. Ann. **594**, 89 (1955).
7. W. METLESICS, T. ANTON, and L. H. STERNBACH. J. Org. Chem. **32**, 2185 (1967).
8. A. C. COPE and S. W. FENTON. J. Amer. Chem. Soc. **73**, 1673 (1951).
9. T. W. CAMPBELL, R. GINSIG, and H. SCHMID. Helv. Chim. Acta, **36**, 1489 (1953).
10. S. O. WINTHROP, M. A. DAVIS, G. S. MYERS, J. G. GAVIN, A. THOMAS, and R. BARBER. J. Org. Chem. **27**, 231 (1962).
11. S. A. RHONE-POULENC. Neth. Appl. 6 600 710. July 28, 1966. Chem. Abstr. **65**P-20066*c*.
12. S. A. RHONE-POULENC. Neth. Appl. 6 600 711. July 28, 1966. Chem. Abstr. **66**P-2586*m*.
13. S. A. RHONE-POULENC. Fr. M. 4395 October 10, 1966. Chem. Abstr. **68**P-68763*k*.
14. L. FRIEDMAN and H. SHECHTER. J. Org. Chem. **26**, 2522 (1961).
15. M. S. NEWMAN and H. BODEN. J. Org. Chem. **26**, 2525 (1961).
16. V. KALYANI and M. VIJAYAN. Acta Crystall. **B25**, 1281 (1969).
17. H. SHIMANOUCHI, T. HATA, and Y. SASADA. Tetrahedron Lett. 3573 (1968).
18. R. N. RENAUD. Ph.D. Thesis. University of Ottawa, Ottawa, Canada. May, 1970.
19. M. NOGRADI, W. W. OLLIS, and I. O. SUTHERLAND. Chem. Commun. 158 (1970).
20. W. TOCHTERMANN, U. WALTER, and A. MANNSCHRECK. Tetrahedron Lett. 2981 (1964).
21. N. L. BAULD and Y. S. RIM. J. Org. Chem. **33**, 1303 (1968).
22. R. R. FRASER, M. KAUFMAN, P. MORAND, and G. GOVIL. Can. J. Chem. **47**, 403 (1969).
23. L. JORIS, P. VON R. SCHLEYER, and R. GLEITER. J. Amer. Chem. Soc **90**, 327 (1968).
24 S. C. CLARKE, K. J. FRAYNE, and B. L. JOHNSON. Tetrahedron. **25**, 1265 (1969).
25. F. A. L. ANET and A. J. R. BOURN. J. Amer. Chem. Soc. **87**, 5250 (1965).
26. R. A. BELL and J. K. SAUNDERS. Can. J. Chem. **48**, 1114 (1970).
27. R. R. FRASER and F. J. SCHUBER. Can. J. Chem. **48**, 633 (1970).
28. J. SCHMITT, J. J. PANOUSE, A. HALLOT, H. PLUCKET, P. COMOY, and P. J. CORNU. Bull. Soc. Chim. Fr. 816 (1963).
29. A. I. VOGEL. Practical organic chemistry. 3rd Ed. Longmans, Green and Co. Inc., New York, N.Y., 1956.
30. L. I. SMITH and J. W. OPIE. Organic Synthesis. Coll. Vol. III. 56 (1955).
31. P. H. GROGGINS, A. J. STIRTON, and H. P. NEWTON. Ind. and Eng. Chem. **23**, 893 (1931).
32. E. D. BERGMANN and E. LOEWENTHAL. Bull. Soc. Chim. Fr. 66 (1952).
33. E. DE B. BARNETT, J. W. COOK, and I. G. NIXON. J. Chem. Soc. 504 (1927).
34. S. KIMOTO and S. OTA. Yakugaku Zasshi. **87**, 861 (1967). Chem. Abstr. **67**, 116752, (1967).
35. R. F. CHILDS and S. WINSTEIN. J. Amer. Chem. Soc. **89**, 6348 (1967).

Can. J. Chem. Downloaded from www.nrcresearchpress.com by 210.87.254.40 on 09/05/12
For personal use only.

Can. J. Chem. Downloaded from www.nrcresearchpress.com by 210.87.254.42 on 09/05/12
For personal use only.

The Effect of Substituents on Geminal Proton–Proton Coupling Constants; a Conformational Dependence. II

ROBERT R. FRASER AND ROGER N. RENAUD[1]
Department of Chemistry, University of Ottawa, Ottawa, Canada

Received August 10, 1970

The effect of para-substituents on the geminal coupling constants in benzylic methylene groups has been studied as a function of the conformation at the benzene—CH_2 bond. The slopes of Hammett plots of J_{gem} *vs.* σ are large (-1.6 to -1.9) when the geometry permits a hyperconjugative interaction between the benzene ring and the methylene group but negligible ($+0.2$) when this interaction is geometrically restricted. The effect of a change in electronegativity of the group attached to the methylene carbon has also been investigated. The change in the slope, ρ, from -1.7 to -1.6 on protonation of the nitrogen attached to the methylene group in a series of isoindolines shows this effect to be extremely small. Solvent effects on ρ are also very small. The potential of this J–σ relation for conformational analysis of benzyl groups is discussed in comparison with existing methods.

Canadian Journal of Chemistry, **49**, 755 (1971)

The influence of an aromatic ring on the magnitude of a geminal coupling constant between the methylene protons at an adjacent carbon has been the subject of theoretical treatments (1, 2) and extensive experimental measurements (3). Both valence bond (v.b.) (1) and molecular orbital (m.o.) (2) methods have predicted the ring to provide a negative increment to the geminal coupling constant, the magnitude of which will be conformationally dependent. This increment results from a hyperconjugative interaction and will be maximal when the H–H axis of the methylene group is aligned parallel to the adjacent π orbitals of the aromatic ring. For this conformation the projected angle ϕ is 0° (see Fig. 1). A 90° rotation about the Ar—CH_2 bond produces a conformation which was predicted to have a minimal interaction between the aromatic ring and the geminal methylene group. Direct evidence pertinent to these theoretical predictions was provided by the independent observations of two groups of workers (4, 5). Both reported that the geminal coupling constants in the benzylic methylene groups of a series of para-substituted 2-benzyloxytetrahydropyrans showed a linear correlation with the Hammett sigma values of the para-substituents. In a second series a strikingly different effect was noted (4) in that invariant geminal coupling constants were found for a series of para-substituted benzyl phenyl sulfoxides. This led to the proposal (4) that the slope ρ, in the J_{gem} *vs.* σ plot, was conformationally dependent and should be proportional to $\cos^2\phi$.

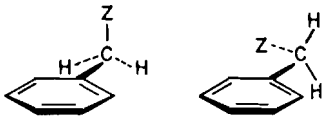

FIG. 1. The conformations in which maximal ($\phi = 0°$) and minimal ($\phi = 90°$) hyperconjugative enhancement of geminal coupling constants occur.

In order to continue an investigation of the angular dependence of ρ, we have undertaken the synthesis of three new series of para-substituted benzyl derivatives in which the benzylic methylene group is constrained in a definite orientation with respect to the adjacent benzene ring. The synthesis and conformational properties of the compounds studied herein will be described in an accompanying paper (6). In this article we wish to present the results of a determination of the coupling constants in each series of compounds which show that the sensitivity parameter ρ indeed appears to depend primarily on ϕ and only slightly on the electronegativity of the substituent attached to the benzylic methylene group.

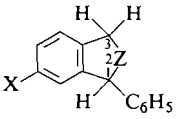

1 Z = O
2 Z = NCH_3
3 Z = $^+NHCH_3$

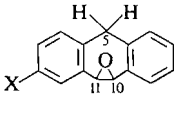

4

[1]Present address: Division of Chemistry, National Research Council, Ottawa, Canada.

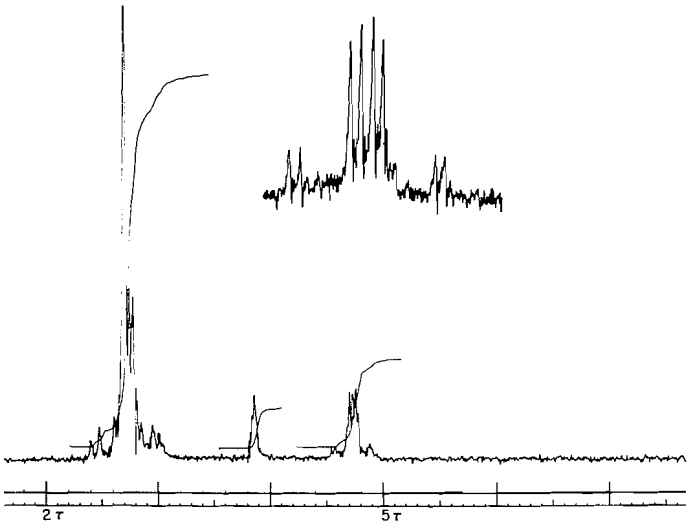

FIG. 2. The 100 MHz spectrum of 6-cyano-1-phenylphthalan (**1**, X = CN) (0.1 *M* in $CDCl_3$). The inset shows the absorption of the C-3 methylene protons during simultaneous irradiation at τ 2.7 (sweep-width 250 Hz).

Results

The systems chosen for study are the 1-phenylphthalans, **1**, the 2-methyl-1-phenylisoindolines, **2**, their conjugate acids, **3**, and the dibenzo[*a*,*d*]-cycloheptene-10,11-oxides, **4**. The n.m.r. spectra of series **1** and **2** were measured in deuterochloroform. For series **3** solutions of **2** in trifluoroacetic acid were studied. Series **4** was studied in two solvents, deuterochloroform and acetone-d_6. In series **1** and **2** the absorptions due to the methylene and methine protons in the five-membered ring comprised an ABX system because of the presence of appreciable cross-ring coupling. These long-range interactions have been noted previously in both systems (7–9). Other smaller long-range couplings between the aromatic and benzylic protons produce substantial line-broadening. These effects were adequately removed by double irradiation of the aromatic proton ortho to the methylene group. Figure 2 presents a typical spectrum of **1** (X = CN) in which the complete spectrum is shown, and, in the inset, the ABX portion appears on an expanded scale having been measured during double irradiation of the ortho aromatic proton at τ 2.7. In series **1** all ABX absorption patterns were analyzed using the LAOCN3 program of Castellano and Bothner-By (10). It was found that the differences between the spacings and the exact values for the long-range couplings were negligible (<0.1 Hz) and of course the geminal couplings[2] are directly obtainable from the experimental spectrum (11). For this reason first-order analysis was used for series **2** and **3**. In series **3** (**2** in trifluoroacetic acid) the spectra were remarkable in that the long-range cross-ring coupling constants were greatly reduced from those observed in **2**.[3] They were always less than 1.2 Hz and could not be accurately determined since several long-range couplings to the ring protons were also present, not all of which could be removed by multiple irradiation and, in addition, the spectrum consisted of absorptions due to two diastereomeric conjugate acids. In each diastereomer strong vicinal H—C—N—H coupling was present. The values for the geminal couplings were obtained by first-order analysis of the absorption due to the major diastereomer which always comprised 80% of the mixture. As a result of the above complications the parameters for series **3** are less accurate (±0.2 Hz). In series **4** the methylene group appears essentially as an AX pattern, the chemical shift difference between the diastereotopic methylene protons being 1.8 p.p.m. The large nonequivalence in shifts has precedence in observations on similarly

[2]The observation of a negative geminal coupling constant in 2,3-diphenylpropionic acid (31) supports the assumption that all geminal couplings reported herein are negative in sign.

[3]Similar effects due to increasing the effective electronegativity of the nitrogen atom have been reported by Gerig (8).

Can. J. Chem. Downloaded from www.nrcresearchpress.com by 210.87.254.42 on 09/05/12
For personal use only.

Can. J. Chem. Downloaded from www.nrcresearchpress.com by 210.87.254.42 on 09/05/12
For personal use only.

TABLE 1. The $-J_{gem}$ values for benzylic methylene protons

	Series				
X	1*	2*	3†	4*	4‡
NH_2	11.35	11.87			
OH	11.39				
OCH_3	11.43	12.00	13.45	13.96	13.73
CH_3				13.77	13.59
H	12.13	12.61	14.05	13.66	13.52
Cl	12.44				
Br				13.80	13.60
$COOCH_3$		13.48	14.84	13.71	13.50
CN	13.60			13.68	13.52
NO_2	13.79	14.10	15.07		
$^+NH_3$			14.50		

*In deuterochloroform.
†In trifluoroacetic acid.
‡In acetone.

constrained diarylmethane derivatives (12, 13). The geminal coupling constants obtained by analysis of all four series of compounds are presented in Table 1.

Discussion of Results

In order to determine directly a geminal H–H coupling constant in any molecule, the molecule must itself be chiral (on the n.m.r. time scale) or else possess a pseudoasymmetric center. In view of the considerable difficulties inherent in the synthesis of any such series it was felt at the outset that it would be wiser to survey several limited series to determine whether or not a geometrical dependence of ρ is encountered, rather than to concentrate efforts on synthesis of a large number of compounds in any one series. Should the initial survey prove encouraging, more complete studies might prove advantageous later. We chose five as the minimum number of compounds necessary for a series with the requirement that they cover at least a range of one unit of Hammett σ values.

The results from Table 1 have been analyzed by the least squares method and the results of these analyses are presented in Table 2. In series **1–3** it can be seen that a good linear relation is present, the correlation coefficient being 0.976 or greater. A plot of J_{gem} *vs.* sigma[4] for the data in series **1** is presented in Fig. 3. The data for series **4** in deuterochloroform is presented in Fig. 4. Even though the correlation coefficient for this series is much lower (0.619) the deviations (in Hz) of individual points from the best straight line are smaller than in **1–3** so this series shows at least as good a correlation of J_{gem} with σ. Others have commented previously about the significance of correlation coefficients, pointing out the fact that they decrease as ρ decreases (14).

The magnitudes of ρ are −1.9, −1.7, −1.6, and +0.2 for series **1** through **4** respectively. The slight decrease in the ρ value in series **2** is of the

[4]It has been suggested to us that a more rigorous treatment would require plotting $\Delta J/J$ *vs.* σ in order to plot one dimensionless quantity against another (ΔJ represents the difference between geminal couplings in the para-substituted and unsubstituted benzyl groups). However, the value for J depends on several factors besides the hyperconjugative effect (2) and for this reason its inclusion would weaken the correlation.

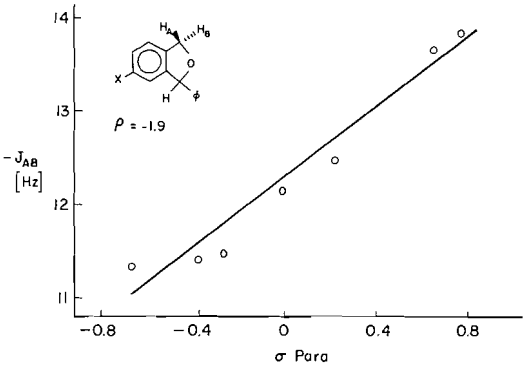

FIG. 3. The plot of J_{gem} *vs.* Hammett σ constants for series **1**.

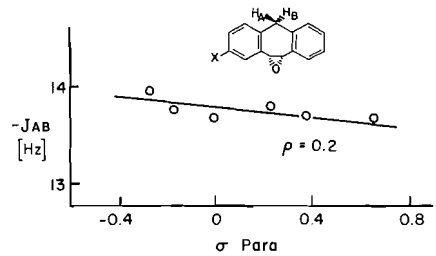

FIG. 4. The plot of J_{gem} *vs.* sigma for series **4**.

TABLE 2. Slopes of Hammett plots for series **1–4**

Series	ρ	r‖	s‖
1*	−1.9	0.976	0.25
2*	−1.7	0.979	0.23
3†	−1.6§	0.982	0.17
4*	+0.19	0.619	0.10
4‡	+0.17	0.698	0.07

*Deuterochloroform solvent.
†Trifluoroacetic acid solvent.
‡Acetone solvent.
§The value of J for the $^+NH_3$ group was not included in the plot as the σ value for this group is unknown.
‖r, Correlation coefficient; s, standard deviation.

Can. J. Chem. Downloaded from www.nrcresearchpress.com by 210.87.254.42 on 09/05/12
For personal use only.

order of accuracy of the correlations, and does not necessarily reflect a deviation from planarity in the isoindoline ring. If we assume that the projected angle ϕ in series **1–3** is zero,[5] then any variation in ρ for these series must be due to changes in internal bond angles or bond hybridizations resulting from a change in the electronegativity of the atom attached to the methylene group. The very slight difference in ρ's for series **2** relative to **3**, for which one of the largest possible changes in electronegativity has been made, indicates the electronegativity effect to be small. A point of concern in making this conclusion is what the effect of changing solvent might be. It has been widely recognized that solvent effects on J_{gem} are normally less than 0.2 Hz (15) and tend to make J_{gem} more negative as the dielectric constant of solvent is increased. The values in Tables 1 and 2 show that the changes in J_{gem} in series **4** using acetone solvent are small and that the solvent effect on ρ is negligible. One noteworthy point in comparing the data for series **4** in both solvents is that, in contrast to the findings of Smith and Cox (15), J_{gem} becomes more positive as the medium dielectric is increased.

The change in the value of J_{gem} for an individual member of series **2** relative to series **3** is of interest, the value becoming more negative by 1.2 ± 0.3 Hz on protonation. This change can be attributed to the dominant effect of removing the "lone pair" on the adjacent nitrogen atom (16) which overrides the effect of increasing the substituent electronegativity (2).

In contrast to the substantial negative slopes in series **1**, **2**, and **3**, series **4** shows a small positive slope of 0.2. The value of ϕ for the compounds in series **4** can be estimated from Dreiding models to be 72°. Thus the change in ρ is in qualitative agreement with a $\cos^2\phi$ relation. The experimental values can be compared with the existing theoretical predictions. Figure 5 shows the angular dependence of the increment to J_{gem} produced by a hyperconjugative interaction as calculated by (*a*) the $\cos^2\phi$ relation of Pople and Bothner-By (2), (*b*) a $\cos\phi \cdot \cos\phi'$ relation in which the angles describe the contributions from individual C—H bond m.o.'s, (*c*) the v.b. calculations of Barfield and Grant (1). It should be remembered that our ρ values

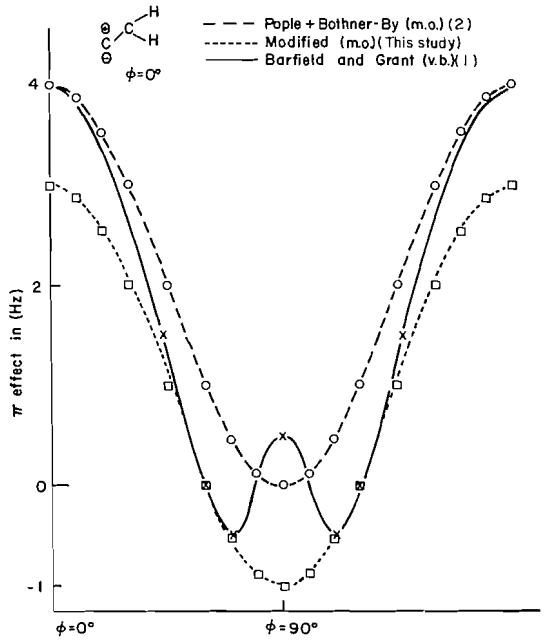

FIG. 5. A plot of the theoretical predictions for hyperconjugative enhancement of geminal coupling constants.

represent only a perturbation of the total hyperconjugative effect whose maximum magnitude has been estimated to be 4 Hz per π interaction (1, 3). The ρ values for series **1–4** are in good agreement with either relation (*b*) or (*c*). Data for a series in which $\phi = 90°$ will be of particular interest as it could distinguish between these alternatives.

In summary, the findings for series **1–4** provide support for the theoretical and experimental evidence that ρ is a conformationally dependent parameter. In spite of the limited scope of our investigations we feel the results are sufficiently promising to warrant further study, particularly in view of the scarcity of information regarding rotation about a benzene to carbon bond. Indeed, most examples of compounds in which conformational assignments to benzyl rotamers have been made, involved strong hindrance to rotation about the benzene—CH_2 bond. This allowed n.m.r. observation of individual rotamers. The compounds studied in this manner include 2,6-disubstituted benzyl halides (17), 2,6-dichlorobenzal chloride (18), 2,4,6-trimethylcumene (19), di-*t*-butylanisylcarbinol (20), and 1,2,3,4-tetramethyl-5,6-dineopentylbenzene (21). In addition,

[5]Justification for this assumption is presented in ref. 6.

Can. J. Chem. Downloaded from www.nrcresearchpress.com by 210.87.254.42 on 09/05/12
For personal use only.

conformational assignments have been made to ortho-substituted benzotrifluorides (22) and related fluorotoluenes (23) on the basis of the temperature dependence of F–F coupling constants. In compounds lacking hindrance the barrier to rotation is very much lower, that in toluene having been reported to be 14 cal/mol (24). In freely rotating systems ρ offers the potential ability to determine the time-average of all existing conformations and in this way will provide an indication of the dominant conformer. For instance, our present results support the original claims (4) that the tetrahydropyranyl ethers possess a dominant conformation having $\phi = 0°$ while the sulfoxides have $\phi = 90°$ as their dominant conformation. Closely related to this are Chow's recent observations on para-substituted benzyl 2-methylpiperidines (25). Chow observed a correlation between J_{gem} and σ in this series which had a slope of -1.4 in carbon tetrachloride and 0.0 in 1 *N* deuterium chloride solution. He proposed a dominant conformation of $\phi = 0°$ in the former solvent, and either a change to $\phi = 90°$ or a medium effect being responsible for the decrease in ρ. Our results eliminate the medium effect as an explanation.

One other study of substituent effects on J_{gem} has been reported since our initial paper (4). Ripka and Applequist (26) determined the geminal coupling constants in a series of para-substituted toluenes by measuring the H–D coupling constants. From their data we estimate ρ to be -0.6. From our data the value for ρ in a freely rotating methyl group can be estimated as $\frac{1}{2}\cos^2\phi_{max}$ or 0.95. This discrepancy for the toluenes is not beyond the limits of accuracy of the method since their precision in J_{gem} is reduced sixfold by measuring J_{H-D} and only those toluenes bearing an electron-withdrawing para-substituent were examined.

An additional feature in the spectra obtained from series **1** and **2** is the presence of appreciable long-range couplings between protons on C-1 and -3. These couplings, listed in Table 3, show a slight increase with increasing substituent electronegativity. In series **1** the low field absorption is assigned to the proton at C-3 and *cis* to the phenyl group at position 1, for reasons put forward previously by Roberts and co-workers (27). This means $|J_{trans}| > |J_{cis}|$ in series **1**. In series **2**, it is the high field absorption which shows the larger long-range splitting. It is not possible to make an assignment of chemical shifts to the protons at C-3 in this series since the effects of the *N*-methyl group and the lone pair on nitrogen will be conformationally dependent (28) and not readily estimated. To make an assignment on the basis of $|J_{trans}| > |J_{cis}|$ in analogy with series **1** would be unwise since the long-range couplings are likely a composite of two effects (29).

TABLE 3. Long-range coupling constants between protons on C-1 and -3 for series **1** and **2**

	Series **1**		Series **2**	
X_p	J_{cis}*	J_{trans}*	J_{BX}†	J_{AX}†
NH_2	1.88	2.53	1.56	3.10
OH	1.98	2.61	—	—
OCH_3	1.99	2.51	1.61	3.20
H	1.91	2.57	1.63	3.26
Cl	2.09	2.60	—	—
$COOCH_3$	—	—	1.62	3.28
CN	2.03	2.57	—	—
NO_2	2.02	2.71	1.66	3.28

*Refers to orientation of protons at C-1 and -3 relative to each other.
†Proton A appears at higher field than proton B.

Experimental

All spectra were recorded with a Varian HA 100 n.m.r. spectrometer using 0.3, 0.2, and 0.1 *M* solutions of each compound in series **1**. As no detectable difference in coupling constants was seen, 0.2 *M* solutions were used for series **2**, **3**, **4**. Spin-decoupling experiments were performed in the frequency-sweep mode. The spectral line positions were always determined from the average of at least ten measurements. Exact analyses of the ABX spectra in the 1-phenylphthalan series were performed using the LAOCN3 program (10) on an IBM 360 Model 65 computer. All slopes from the plotting of geminal coupling constants against Hammett substituent constants were obtained by a least squares analysis of the data using a program prepared by Dr. Gurudata. A paper describing the synthesis of all compounds studied herein appears in this issue (6). The chemical shifts and their substituent dependence will be described shortly (30).

The authors thank the National Research Council of Canada for financial support of this work. Discussions with Professor Bothner-By are greatly appreciated.

1. M. BARFIELD and D. M. GRANT. J. Amer. Chem. Soc. **85**, 1899 (1963).
2. J. A. POPLE and A. A. BOTHNER-BY. J. Chem. Phys. **42**, 1339 (1965); G. E. MACIEL, J. W. MCIVER, N. S. OSTLUND, and J. A. POPLE. J. Amer. Chem. Soc. **92**, 4151 (1970).
3. R. CAHILL, R. C. COOKSON, and T. A. CRABB. Tetrahedron, **25**, 4711 (1969).
4. R. R. FRASER, P. HANBURY, and C. REYES-ZAMORA. Can. J. Chem. **45**, 2481 (1967).
5. R. W. FRANCK and J. AUERBACH. Can. J. Chem. **45**, 2489 (1967).

6. R. R. FRASER and R. N. RENAUD. Can. J. Chem. This issue.
7. R. L. VAULX, F. N. JONES, and C. R. HAUSER. J. Org. Chem. **29**, 505 (1964).
8. J. T. GERIG. Tetrahedron Lett. 4625 (1967).
9. W. METLESICS, T. ANTON, and L. H. STERNBACH. J. Org. Chem. **32**, 2187 (1967).
10. S. CASTELLANO and A. A. BOTHNER-BY. J. Chem. Phys. **41**, 3863 (1964).
11. J. A. POPLE, W. G. SCHNEIDER, and H. J. BERNSTEIN. High-resolution nuclear magnetic resonance. McGraw-Hill Book Co., New York, N.Y., 1959. p. 132.
12. P. T. LANSBURY, J. F. BIERON, and A. J. LACHER. J. Amer. Chem. Soc. **88**, 1482 (1966).
13. R. F. CHILDS and S. WINSTEIN. J. Amer. Chem. Soc. **89**, 6348 (1967).
14. C. D. RITCHIE and W. F. SAGER. Prog. Phys. Org. Chem. **2**, 323 (1964).
15. S. L. SMITH and R. H. COX. J. Chem. Phys. **45**, 2848 (1966).
16. R. CAHILL, R. C. COOKSON, and T. A. CRABB. Tetrahedron, **25**, 4681 (1969).
17. C. CUPAS, J. M. BOLLINGER, and M. HASLANGER. J. Amer. Chem. Soc. **90**, 5502 (1968).
18. T. SCHAEFER, R. SCHWENK, C. J. MACDONALD, and W. J. REYNOLDS. Can. J. Chem. **46**, 2187 (1968).
19. A. MANNSCHRECK and L. ERNST. Tetrahedron Lett. 5939 (1968).
20. G. B. NEWSOROFF and S. STERNHELL. Tetrahedron Lett. 2539 (1967).
21. D. J. DIX, G. FRAENKEL, G. KARNES, and M. S. NEWMAN. Tetrahedron Lett. 517 (1966).
22. H. S. GUTOWSKY and V. D. MOCHEL. J. Chem. Phys. **39**, 1195 (1963).
23. J. JONAS, L. BOROWSKY, and H. S. GUTOWSKY. J. Chem. Phys. **47**, 2441 (1967).
24. H. D. RUDOLPH, H. DREIZLER, A. JAESCHKE, and P. WEUDLING. Z. Naturforsch. **22***a*, 940 (1967).
25. Y. L. CHOW, S. BLACK, J. E. BLIER, and M. M. TRACEY. Can. J. Chem. **48**, 2134 (1970).
26. W. C. RIPKA and D. E. APPLEQUIST. J. Amer. Chem. Soc. **89**, 4035 (1967).
27. F. J. PETRACEK, N. SUGISAKA, M. W. KLOHS, R. G. PARKER, J. BORDNER, and J. D. ROBERTS. Tetrahedron Lett. 707 (1970); R. A. SMITH, R. G. PARKER, and J. D. ROBERTS. Tetrahedron Lett. 1763 (1970).
28. J. B. LAMBERT, D. S. BAILEY, and B. F. MICHAEL. Tetrahedron Lett. 691 (1970).
29. S. STERNHELL. Quarterly Revs. **23**, 269 (1969).
30. R. R. FRASER and R. N. RENAUD. Can. J. Chem. This issue.
31. R. R. FRASER. Can. J. Chem. **40**, 1483 (1962).

Can. J. Chem. Downloaded from www.nrcresearchpress.com by 210.87.254.42 on 09/05/12
For personal use only.

Can. J. Chem. Downloaded from www.nrcresearchpress.com by 210.87.254.6 on 09/05/12
For personal use only.

Nitrato and Acetylacetonato Complexes of Copper(I)

W. A. ANDERSON, A. J. CARTY,[1] G. J. PALENIK, AND G. SCHREIBER
Department of Chemistry, University of Waterloo, Waterloo, Ontario

Received July 28, 1970

Copper(I) nitrate complexes of the types L_2CuNO_3, L_3CuNO_3, and L_4CuNO_3 (L = tertiary phosphine) have been synthesized by reduction of copper(II) nitrate with tertiary phosphines. Infrared spectra and single crystal X-ray measurements indicate the presence of bidentate nitrate in L_2CuNO_3, monodentate nitrate in L_3CuNO_3, and ionic nitrate in L_4CuNO_3. The single crystal X-ray structure of nitratobis(tricyclohexylphosphine)copper(I) is reported. $CuO_3N(PC_{18}H_{33})_2$ crystallizes in the monoclinic space group $C2/c$ with $a = 18.18(1)$ Å, $b = 9.240(6)$ Å, $c = 22.41(2)$ Å, and $\beta = 96.57(5)°$. The structure was solved by the heavy atom method and refined with isotropic thermal parameters to an R of 0.14. The copper atom is tetrahedrally coordinated by two phosphorus atoms and two oxygen atoms of a bidentate nitrate group. The P—Cu—P angle (140(1)°) and Cu—P bond lengths (2.29(1) Å) are the largest reported for tetrahedral copper complexes.

A facile synthetic route to acetylacetonatobis(phosphine)copper(I) complexes is also described.

La réduction du nitrate de cuivre (II) avec des phosphines tertiaires (L) a permis de synthétiser des complexes du cuivre(I) de formules L_2CuNO_3, L_3CuNO_3 et L_4CuNO_3. La spectroscopie infrarouge et l'étude de monocristaux par rayons X indiquent que le groupe nitrate est bicoordiné dans L_2CuNO_3, monocoordiné dans L_3CuNO_3 et ionique dans L_4CuNO_3. On a déterminé au moyen de la diffraction des rayons X par monocristaux la structure du nitratobis(tricyclohexylphosphine)cuivre(I). $CuO_3N(PC_{18}H_{33})_2$ cristallise dans le système monoclinique, groupe spatial $C2/c$: $a = 18.18$ (1) Å, $b = 9.240$ (6) Å, $c = 22.41$ (2) Å et $\beta = 96.57$ (5)°. On a appliqué la méthode de l'atome lourd et, utilisant des facteurs thermiques isotropes, on a obtenu après affinement un facteur R égale à 0.14. Deux atomes de phosphore et les deux atomes d'oxygène d'un groupe nitrate bicoordiné assurent à l'atome de cuivre une coordination tétraédrique. L'angle P—Cu—P (140(1)°) et la longueur de liaison Cu—P (2.29 (1) Å) sont les plus grandes qu'on ait rapportés pour des composés tétraédriques du cuivre.

On présente également une méthode commode pour la synthèse des complexes acétylacétonatobis-(phosphine)cuivre(I).

Canadian Journal of Chemistry, 49, 761 (1971)

Introduction

The synthesis and stereochemistry of copper(I) complexes of tertiary phosphines are of current interest (1–11) because of the wide variety of structural types that have been found. X-Ray structural studies have revealed tetrahedral (1–5), pseudo-tetrahedral (6), a tetrahedral–trigonal dimer (7), dimeric (3), tetrameric (3), and polymeric (8) molecules including compounds with halogen (5, 7) and azide (4) bridges. Although several of the above complexes can be synthesized by the reduction of the appropriate copper(II) salt with the tertiary phosphine, the scope of this preparative method has not been explored. We have now extended the reaction of copper(II) nitrate with triphenylphosphine (13) to include a variety of other tertiary phosphines. Several new types of phosphine–copper(I) nitrate complexes have been prepared and the crystal structure of nitratobis(tricyclohexylphosphine)-copper(I) has been determined. An extension of the reaction to copper(II) acetylacetonates has provided a more convenient route to substituted acetylacetonatobis (tertiaryphosphine) copper(I) complexes than that previously reported (11, 12).

Experimental

The copper(II) nitrate trihydrate and acetylacetone were British Drug Houses reagent grade and the substituted acetylacetones were obtained from Columbia Organic Chemicals, Columbia, South Carolina. The tertiary phosphines were supplied by Orgmet Inc., Hampstead, New Hampshire in sealed ampoules and were subsequently handled *in vacuo* or in a Vacuum Atmospheres Corporation Dri-Lab filled with a 10% hydrogen–nitrogen mixture. All solvents were spectral grade and were thoroughly degassed before use.

Microanalyses were performed by A. B. Gygli, Toronto, Ontario and/or Chemalytics Inc., Tempe, Arizona. Molecular weights were measured by an osmometric method using benzene or chloroform as solvents (14). Infrared spectra were taken on Beckman IR-9 and IR-12 spectrometers and the frequencies are accurate to ± 2 cm^{-1}.

[1]To whom all correspondence should be addressed.

Can. J. Chem. Downloaded from www.nrcresearchpress.com by 210.87.254.6 on 09/05/12
For personal use only.

Preparations

Nitratobis(tri-m-tolylphosphine)copper(I)

Cupric nitrate trihydrate (0.5 g) in hot ethanol (30 ml) was added carefully to tri-*m*-tolylphosphine (*m*-tol$_3$P) (2 g) in hot ethanol (60 ml). The color of the copper(II) solution was discharged immediately and colorless crystals precipitated. Colorless needles were obtained after recrystallization from chloroform–ethanol, m.p. 166–167°.

Anal. Calcd. for [(*m*-tol)$_3$P]$_2$CuNO$_3$: C, 68.70; H, 5.77; N, 1.92. Found: C, 68.06; H, 6.04; N, 1.88.

Nitrato[bis(diphenylphosphino)methane]copper(I)

[(DPPM)CuNO$_3$] (DPPM = bis(diphenylphosphino) methane) was prepared in a similar manner and gave colorless crystals, m.p. 228° decomp.

Anal. Calcd. for [(DPPM)CuNO$_3$]: C, 58.88; H, 4.35; N, 2.74. Found: C, 59.03; H, 4.69; N, 2.73.

Nitratobis(tricyclohexylphosphine)copper(I)

(Cy$_3$P)$_2$CuNO$_3$ (Cy$_3$P = tricyclohexylphosphine) was prepared in a similar manner to give colorless crystals; m.p. 225–227°.

Anal. Calcd. for (Cy$_3$P)$_2$CuNO$_3$: C, 62.98; H, 9.69; N, 2.04. Found: C, 62.85; H, 9.56; N, 1.96.

Nitratotris(ethyldiphenylphosphine)copper(I)

Ethyldiphenylphosphine (EtPh$_2$P) (1 ml) in warm ethanol was treated with cupric nitrate in ethanol until the blue color was no longer discharged and a pale green color persisted. The total volume of ethanol was approximately 30 ml. Addition of cyclohexane (10 ml) and chilling gave colorless crystals which were recrystallized from ethanol–cyclohexane; m.p. 128–129°.

Anal. Calcd. for (EtPh$_2$P)$_3$CuNO$_3$ (mol. wt., 768): C, 65.66; H, 6.24; N, 1.82. Found (mol. wt., 758, benzene): C, 65.44; H, 6.27; N, 1.69.

Nitratotris(dimethylphenylphosphine)copper(I)

The product was prepared by the same method used for (EtPh$_2$P)$_3$CuNO$_3$. Recrystallization from ethanol–diethylether gave colorless prisms; m.p. 84–85°.

Anal. Calcd. for (Me$_2$PhP)$_3$CuNO$_3$ (mol. wt., 540): C, 53.4; H, 6.16; N, 2.59. Found (mol. wt., 527, chloroform); C, 52.28; H, 6.24; N, 2.55.

Nitratotris(methyldiphenylphosphine)copper(I)

A solution of methyldiphenylphosphonium nitrate in hot methanol was added to Cu(NO$_3$)$_2$.3H$_2$O (0.7 g) in methanol (30 ml) until the blue color was discharged. Refrigeration at 0° for 30 h gave colorless crystals which were recrystallized from methanol; m.p. 158–160°.

Anal. Calcd. for (MePh$_2$P)$_3$CuNO$_3$: C, 64.49; H, 5.38; N, 1.93. Found: C, 65.17; H, 5.55; N, 1.88.

The same product was obtained from the direct reaction of MePh$_2$P with cupric nitrate in ethanol.

Reaction of 1,2-Bis(diphenylphosphino)ethane (DPPE) with Cu(NO$_3$)$_2$.3H$_2$O

Reduction of copper(II) nitrate by DPPE in hot ethanol followed by addition of *n*-hexane yielded colorless crystals; m.p. 131–135° decomp. These crystals were occasionally contaminated with a light green product which could be removed manually, with the aid of a microscope.

Anal. Calcd. for (DPPE)$_3$(CuNO$_3$)$_2$: C, 64.77; H, 5.02; N, 1.94. Found: C, 64.34; H, 5.11; N, 2.41.

This complex is very unstable in halogenated solvents, yielding dark green solutions and evolving nitrogen dioxide.

A second product was isolated from solutions of (DPPE)$_3$(CuNO$_3$)$_2$ by bubbling oxygen through a refluxing ethanolic solution for 3 h. Large crystals of (DPPE)$_2$CuNO$_3$ were obtained on slow evaporation; m.p. 213–215°.

Anal. Calcd. for (DPPE)$_2$CuNO$_3$: C, 67.6; H, 5.24; N, 1.52. Found: C, 66.82; H, 5.69; N, 1.49.

Tetrakis(diphenylphosphinopropyne)copper(I) Nitrate

Cupric nitrate in hot ethanol was added to diphenylphosphinopropyne (DPPP) (1 g) in hot ethanol (10 ml) until a pale yellow color persisted. The solution began turning red after several minutes and addition of diethyl ether yielded the crude product contaminated with red oil. Recrystallization from ethanol–pentane–ether (1:1:20) mixtures gave colorless crystals; m.p. 176–178°.

Anal. Calcd. for [Cu(DPPP)$_4$]NO$_3$: C, 70.4; H, 5.11; N, 1.37. Found: C, 70.59; H, 5.08; N, 1.26.

Oxidation of 1,2-Bis(diphenylphosphino)ethane Complexes of Copper(I) in Halogenated Solvents

Dinitrato[1,2-Bis(diphenylphosphinyl)ethane]-copper(II)

(DPPE)$_3$(CuNO$_3$)$_2$ (0.3 g) was dissolved in dichloromethane (7 ml) with evolution of brown fumes and production of a green solution. High boiling petroleum ether (6 ml) was added and the solution cooled for several weeks to yield bright green crystals; m.p. 225–226°.

Anal. Calcd. for (DPDO)$_2$Cu(NO$_3$)$_2$ (DPDO = 1,2-bis(diphenylphosphinyl)ethane): C, 58.6; H, 4.61. Found: C, 58.88; H, 4.61.

Dichlorobis[1,2-bis(diphenylphosphinyl)ethane]-copper(II)

The complex [CuCl(DPPE)]$_3$ (6) was dissolved in hot chloroform and allowed to stand in air for several days. The solution became green and deposited yellow-green crystals; m.p. 278–280°.

Anal. Calcd. for [CuCl$_2$(DPDO)]: C, 55.30; H, 4.29; Cl, 12.54. Found: C, 55.52; H, 4.55; Cl, 12.69.

Hexafluoroacetylacetonatobis(triphenylphosphine)-copper(I), Trifluoroacetylacetonatobis(triphenylphosphine)copper(I), and Thienyltrifluoroacetylacetonatobis(triphenylphosphine)copper(I)

The bis chelates Cu(hfac)$_2$, Cu(tfac)$_2$, and Cu(ttfac)$_2$, where hfac is hexafluoroacetylacetone, tfac is trifluoroacetylacetone, and ttfac is thienyltrifluoroacetylacetone, were prepared by published procedures (15–17). The chelates were purified by recrystallization from benzene (Cu(hfac)$_2$ and Cu(tfac)$_2$) or by soxhlet extraction with chloroform (Cu(ttfac)$_2$).

The copper(I) complexes were prepared by adding a stoichiometric quantity of triphenylphosphine in warm ethanol to 0.001 mol of copper(II) chelate in the same solvent. The color of the copper(II) solution gradually changed to the lighter color of the phosphine adduct. The complexes were recrystallized from ethanol.

(Ph$_3$P)$_2$Cu(hfac); yellow needles, m.p. 154°.

Anal. Calcd.: C, 61.93; H, 3.93. Found: C, 61.93; H, 3.88.

(Ph$_3$P)$_2$Cu(tfac); yellow-orange crystals, m.p. 121°.

Anal. Calcd.: C, 66.42; H, 4.13. Found: C, 66.32; H, 4.10.

TABLE 1. Infrared spectra (1500–1700 cm^{-1}) for acetylacetonate complexes

Complex	Frequency (cm^{-1})
$(Ph_3P)_2Cu(hfac)$	1649s, 1590vw, 1576vw, 1546w, 1518sh, 1505s
$(Ph_3P)_2Cu(tfac)$	1630s, 1589vw, 1542vw
$(Ph_3P)_2Cu(ttfac)$	1614s, 1588sh, 1528s, 1509m

$(Ph_3P)_2Cu(ttfac)$; orange-yellow needles, m.p. 123°. Mol. wt. calcd. (4 molecules per unit cell): 809.3. Found (X-ray): 807.3. The molecular structures of all three substituted acetylacetonato complexes have been determined by X-ray methods (18).

Attempts to reduce bis(acetylacetonato)copper(II) with triphenylphosphine under a variety of experimental conditions were unsuccessful. Addition of trimethyl and triethyl phosphines to copper(II) nitrate resulted in reduction to copper(I) as evidenced by complete removal of the blue color of copper(II). However, attempts to obtain crystalline complexes from these solutions yielded only sticky, colorless oils which could not be induced to crystallize. Infrared spectra of these oils revealed the presence of only ionic nitrate bands in addition to phosphine absorptions.

Results and Discussion

Acetylacetonate Complexes

Reduction of copper(II) acetylacetonates with triphenylphosphine in ethanolic solution yields complexes of formulae $(Ph_3P)_2Cu(B)$ (B = anion of hexafluoroacetylacetone, trifluoroacetylacetone, and thienyltrifluoroacetylacetone). Previous investigators have used either the metathetical reaction of $(Ph_3P)_2CuCl$ with thallium(I) acetylacetonate (11) or the reaction of $(Ph_3P)_2CuBH_4$ with acetylacetone (12) to obtain copper(I) acetylacetonato complexes. The method described herein is considerably more convenient than either of the above syntheses.

The failure of triphenylphosphine to reduce copper(II) acetylacetonate is rather surprising. However, the substituted acetylacetonate ligands are poorer donors than the acetylacetone anion and hence form weaker complexes with copper(II). Moreover, the ability of a tertiary phosphine to reduce copper(II) salts in solution will clearly be related not only to the R_3P/R_3PO oxidation–reduction potential but also to the stability to reduction of the original copper(II) salt.

The infrared spectra of the acetylacetonates between 1700–1500 cm^{-1} are shown in Table 1. Agreement is reasonable with frequencies previously reported (11) for the hexafluoro- and trifluoro derivatives. Strong absorptions in this region of the spectrum are due to coupled ν(C=O) and ν(C=C) modes. If the frequency of the highest absorption band is taken as a rough estimate of the strength of the donor–acceptor interaction between the anion and copper, the results suggest that the strongest C=O bonds (and weakest Cu—O interaction) occur in the hexafluoro complex. This is borne out by the X-ray data for $(Ph_3P)_2Cu(hfac)$ (18) where the C—O and Cu—O average bond lengths are 1.240 and 2.120 Å, respectively compared with $(Ph_3P)_2Cu(ttfac)$ (C—O, 1.247 Å; Cu—O, 2.102 Å) and $(Ph_3P)_2Cu(tfac)$ (C—O, 1.247 Å; Cu—O, 2.086 Å). Comparison of frequencies and bond lengths for $(Ph_3P)_2Cu(ttfac)$ and $(Ph_3P)_2Cu(tfac)$ shows no such correlation, however, thus pointing out the dangers of an oversimplified approach to the interpretation of frequency shifts.

Nitrate Complexes

Complexes of the formulae $L_2Cu(NO_3)$ (L = (*m*-tol)$_3$P, Cy_3P, ½DPPM), $L_3Cu(NO_3)$ (L = $EtPh_2P$, $MePh_2P$, Me_2PhP), $L_4Cu(NO_3)$ (L = ½DPPE, DPPP), $L_3(CuNO_3)_2$ (L = DPPE) have been synthesized by reaction of copper(II) nitrate trihydrate with tertiary phosphines in ethanolic solution. Since the simple copper(I) nitrate is unknown, this method provides the most facile route to nitrato complexes of copper(I). Although the majority of copper(I) halide – tertiary phosphine complexes have been prepared from copper(I) halides by prolonged reaction with phosphines (12), a recent paper (19) has also demonstrated that simple reduction of copper(II) halides is an alternative method of synthesis.

Compounds of the type $L_2Cu(NO_3)$ are analogous to $(Ph_3P)_2CuNO_3$ prepared earlier by Cotton and Goodgame (13). The crystal structure of $(Ph_3P)_2CuNO_3$ has recently been reported (2). The copper atom is approximately tetrahedrally coordinated by two phosphine molecules and a bidentate nitrate group. The infrared spectra of the new compounds $[(m\text{-tol})_3P]_2CuNO_3$, $(Cy_3P)_2CuNO_3$, and $(DPPM)CuNO_3$ are virtually identical with that of $(Ph_3P)_2CuNO_3$ in the regions of

Can. J. Chem. Downloaded from www.nrcresearchpress.com by 210.87.254.6 on 09/05/12
For personal use only.

Can. J. Chem. Downloaded from www.nrcresearchpress.com by 210.87.254.6 on 09/05/12
For personal use only.

TABLE 2. Assignment of nitrate absorptions in the infrared spectra of copper(I) complexes*

	Bidentate			
Complex	ν_1	ν_4	ν_2	ν_6
$(Ph_3P)_2CuNO_3$	1475	1275	1022	810
$[(m\text{-tol})_3P]_2CuNO_3$	1450	1258	†	812
$(DPPM)CuNO_3$	1445	1289	†	812
$(Cy_3P)_2CuNO_3$	1452	1288	1028	814
	Monodentate			
Complex	ν_4	ν_1	ν_2	ν_6
$(EtPh_2P)_3CuNO_3$	1409 1427	1305	†	822
$(MePh_2P)_3CuNO_3$	1418 1400	1304	†	812
$(Me_2PhP)_3CuNO_3$	1434 1420	1326	1029	830
$(DPPE)_3(CuNO_3)_2$	1412	†	†	802
	Ionic			
Complex	ν_3	ν_1	ν_2	
$[Cu(DPPE)_2]NO_3$	1379	1043	829	
$[Cu(DPPP)_4]NO_3$	1379 1348	1052	833	

*The ν formalism used is that for bidentate, monodentate, and ionic nitrate (20).
†Bands obscured by ligand absorption.

nitrate absorption (Table 2). This argues strongly in favor of similar bidentate behavior for nitrate in these compounds. In the case of (DPPM)-$CuNO_3$, a formulation involving bidentate nitrate and tetrahedral copper(I) presupposes either a chelating or bridging diphosphine molecule. We have now confirmed the bidentate coordination of nitrate ion in $(Cy_3P)_2CuNO_3$ by a single crystal X-ray diffraction study. Crystal data are

$C_{36}H_{66}P_2CuNO_3$ mol. wt. = 686.42

Monoclinic crystals, space group $C2/c$ (from intensity statistics), $a = 18.18(1)$ Å, $b = 9.240(6)$ Å, $c = 22.41(2)$ Å, $\beta = 96.57(5)$, $U = 3740.2$ Å^3, $D_m = 1.206$ g/cm^3, $D_c = 1.218$ g/cm^3, and $Z = 4$.

The positions of the copper and phosphorus atoms were determined by examining the sharpened three dimensional Patterson function. Successive Fourier syntheses were used to locate the remaining light atoms. The structure was refined by isotropic least-squares methods to an R of 0.14.[2]

[2]Due to instrumental problems this is the limit of refinement justified by the quality of our data.

The main features of interest are the copper–phosphorus bond distance of 2.29(1) Å, the P—Cu—P angle of 140(1)° and the bidentate nitrate group. The P—Cu—P angle is one of the largest observed to date for a presumably tetrahedral copper(I)–phosphine complex. Furthermore the Cu—P bond length is the longest found in a series of similar complexes (18). Since the tricyclohexylphosphine is very bulky, apparently steric factors have a strong influence on the dimensions of copper(I)–phosphine complexes. A detailed analysis of factors affecting bond angles and bond lengths in copper(I) complexes will be presented elsewhere.

The nitrate group is bonded symmetrically in bidentate fashion to the copper atom with the terminal N—O bond lying on a twofold axis of symmetry and a Cu—O distance of 2.34(2) Å. In view of the obvious similarity to the structure of $(Ph_3P)_2CuNO_3$ (2), further discussion is unwarranted.[3]

The trisphosphine complexes of the type L_3CuNO_3 have nitrate spectra which differ considerably from the spectra of the bis complexes containing bidentate nitrate (Table 2). In particular, the two highest frequency nitrate bands which arise from removal of the degeneracy of the ν_3 NO_3^- mode on coordination are separated by < 125 cm^{-1} whereas for the bis species, ν_1 and ν_4 of the bidentate nitrate differ in frequency by > 150 cm^{-1}. ν_6 for $(EtPh_2P)_3CuNO_3$ and $(Me_2PhP)_3CuNO_3$ is also at higher frequency than in L_2CuNO_3. These results suggest either monodentate or very weakly bonded bidentate nitrate in these complexes. While it is not possible from vibrational spectroscopy, without Raman polarization data, to establish positively the monodentate or bidentate coordination of nitrate, the known preference of copper(I) for tetrahedral coordination and the low polarizing power of a copper(I) ion attached to three phosphine molecules leads us to favor a unidentate formulation in the complexes L_3CuNO_3. Molecular weight measurements on $(Me_2PhP)_3CuNO_3$ and $(EtPh_2P)_3CuNO_3$ reveal that the compounds are monomeric and undissociated in solution. Single crystal X-ray measurements in this laboratory

[3]Photocopies of tables of atomic positional parameters and related data may be obtained free of charge, upon request, from the Depository of Unpublished Data, National Research Council Library, National Research Council of Canada, Ottawa, Canada.

Can. J. Chem. Downloaded from www.nrcresearchpress.com by 210.87.254.6 on 09/05/12
For personal use only.

have now confirmed the monodentate behavior of nitrate in $(MePh_2P)_3CuNO_3$. These complexes thus belong to a relatively small group of molecules in which the unidentate nature of coordinated nitrate has been definitely established by X-ray methods (21).[4]

The complex $(DPPE)_3(CuNO_3)_2$ has the same molecular formula as $(DPPA)_3(CuNO_3)_2$ (DPPA = bis(diphenylphosphino)acetylene) which has been shown to be a binuclear diphosphine bridged complex containing pseudo tetrahedral copper atoms (10). Since 1,2-bis(diphenylphosphino)-ethane can also behave as a bridging ligand (10), a similar structure seems likely for $(DPPE)_3$-$(CuNO_3)_2$.

The third class of compounds prepared are exemplified by $[(DPPE)_2Cu]NO_3$ and $[(DPPP)_4$-$Cu]NO_3$. Both compounds contain ionic nitrate only and in the latter, $\nu(C{\equiv}C)$ of the ligand appears at 2205 cm^{-1}, 5 cm^{-1} higher than in the free ligand, thus confirming the absence of coordination via the triple bond. Both complexes are clearly analogous to $[Cu(PPh_3)_4]ClO_4$ and $[Cu(PPh_3)_4]BrO_3$ prepared earlier by Cotton and Goodgame (13). These are nevertheless the first ionic copper(I) nitrate complexes prepared by direct reaction of a copper(II) salt with a tertiary phosphine and demonstrate that nitrate groups can be displaced from copper provided a suitable phosphorus donor is chosen.

Finally the compounds $(DPDO)CuCl_2$ and $(DPDO)_2Cu(NO_3)_2$, derived from $[(DPPE)$-$CuCl]_3$ and $(DPPE)_3(CuNO_3)_2$, respectively, by atmospheric oxidation in the presence of a halogenated solvent, are worth mentioning. All of the nitrate complexes described in this paper (with the possible exception of $(DPPM)(CuNO_3)$ which is rather insoluble in halogenated solvents) give blue-green solutions on standing for several days in $CHCl_3$ or CH_2Cl_2. Phosphine oxide complexes of copper(II) can be readily crystallized from these solutions on slow evaporation. However, we have only characterized the complexes of $Ph_2P(O)CH_2CH_2P(O)Ph_2$ since we were interested in the coordinating properties of this ligand and in the possibility of chelation involving a seven-membered ring. Both complexes show several strong bands in the infrared between 1050–1200 cm^{-1} due to P=O stretching. $(DPDO)CuCl_2$: 1195vs, 1171vs, 1160vs, 1140vs, 1125vs, 1085. $(DPDO)_2Cu(NO_3)_2$: 1140vs, 1122vs, 1086s. DPDO: 1182sh, 1170vs, 1120vs, 1100m, 1085m, 1070m. The spectra of the free ligand and complexes are so complex in the ν(P=O) region that little information, if any, can be gleaned concerning the magnitude of the shift in the P=O stretching frequency on complexing.

X-Ray studies on $(DPDO)CuCl_2$ have revealed a polymeric structure with a distorted tetrahedral configuration around copper and bridging $Ph_2P(O)CH_2CH_2P(O)Ph_2$ moieties (22). Nitrate absorptions for $(DPDO)_2Cu(NO_3)_2$ confirm the presence of coordinated nitrate in this compound (1496vs, 1290vs, 1015m, 802w). A polymeric structure based on octahedral copper(II) and monodentate nitrate groups therefore seems most likely for this species. Both of the above complexes are highly crystalline even though polymeric in the solid state. Although other workers (23) have usually formulated diphosphine dioxide complexes as monomeric species having chelating ligands, polymeric formulations now seem more reasonable.

The series of copper(I) nitrate complexes described would seem to indicate that the stoichiometry of a complex crystallizing from solution is not a simple function of the basicity of the ligand involved. The evidence suggests that replacement of electron withdrawing aryl groups on phosphorus by electron donating alkyl groups favors an increase in the number of molecules of phosphine coordinated.

Compare, for example, the pK_a values for Ph_3P (2.73), Ph_2EtP (4.49), and Me_2PhP (6.49) with the stoichiometry of the complexes formed. However, Cy_3P, a ligand of high basicity (pK_a = 9.70) but large size, gives only $(Cy_3P)_2CuNO_3$ and the electron withdrawing nature of the $-C{\equiv}CCH_3$ group does not prevent formation of $[(DPPP)_4Cu]NO_3$. Apparently, as in other systems (14), prediction of stoichiometry based on ligand properties alone can be misleading.

We acknowledge the support of the National Research Council of Canada.

[4]A recent paper (24) has suggested that X-ray crystallographic evidence for monodentate nitrate coordination is non-existent. This assumption is erroneous.

1. S. J. Lippard and K. M. Melmed. Inorg. Chem. **8**, 2755 (1969); **6**, 2223 (1967).
2. G. G. Messmer and G. J. Palenik. Inorg. Chem. **8**, 2750 (1969).

3. F. G. MANN, D. PURDIE, and A. F. WELLS. J. Chem. Soc. 1503 (1963).
4. R. F. ZIOLO, A. P. GAUGHAN, Z. DORI, C. G. PIERPONT, and R. EISENBERG. J. Amer. Chem. Soc. **92**, 738 (1970).
5. S. J. LIPPARD. Private communication.
6. (*a*) F. A. COTTON and J. TAKATS. J. Amer. Chem. Soc. **92**, 2353 (1970). (*b*) L. T. J. DELBAERE, D. W. MCBRIDE, and R. B. FERGUSON. Acta Cryst. B**26**, 515 (1970).
7. D. F. LEWIS, S. J. LIPPARD, and P. S. WELCKER. J. Amer. Chem. Soc. **92**, 3805 (1970).
8. P. W. R. CORFIELD and H. M. M. SHEARER. Acta Cryst. **21**, 957 (1966).
9. E. L. MUETTERTIES and C. W. ALEGRANTI. J. Amer. Chem. Soc. **92**, 4114 (1970).
10. A. J. CARTY and A. EFRATY. Inorg. Chem. **8**, 543 (1969).
11. D. GIBSON, B. F. G. JOHNSON, and J. LEWIS. J. Chem. Soc. A, 367 (1970).
12. F. CARIATI and L. NALDINI. Gazz. Chim. Ital. **95**, 3 (1965).
13. F. A. COTTON and D. M. L. GOODGAME. J. Chem. Soc. 5267 (1960).
14. A. J. CARTY, T. HINSPERGER, and P. M. BOORMAN. Can. J. Chem. **48**, 1959 (1970).
15. H. F. HOLTZCLAW, JR. and J. P. COUMAN. J. Amer. Chem. Soc. **79**, 3318 (1957).
16. N. C. LI, S. M. WANG, and W. R. WALKER. J. Inorg. Nucl. Chem. **27**, 2263 (1965).
17. W. R. WALKER and N. C. LI. J. Inorg. Nucl. Chem. **27**, 411 (1965).
18. M. BARTLETT. Ph.D. Thesis. University of Waterloo, Waterloo, Ontario, 1970.
19. F. H. JARDINE, L. RULE, and A. G. BOHRA. J. Chem. Soc., A, 238 (1970).
20. C. C. ADDISON and N. LOGAN. Advan. Inorg. Chem. Radiochem. **6**, 71 (1964).
21. (*a*) C. D. GARNER and C. S. WALLWORK. Chem. Commun. 108 (1969). (*b*) B. DUFFIN. Acta Cryst. B**24**, 396 (1968). (*c*) P. GALLEZOT, D. WEIGEL, and M. PRETTRE. Acta Cryst. **22**, 699 (1967). (*d*) D. A. LANGS, C. R. HARE, and R. G. LITTLE. Chem. Commun. 1080 (1967).
22. M. MATHEW and G. PALENIK. Can. J. Chem. **47**, 1093 (1969).
23. (*a*) N. P. CRAWFORD and G. A. MELSON. J. Chem. Soc. A, 141 (1970). (*b*) S. S. SANDHU and S. S. SANDHU. Chem. Ind. 626 (1970).
24. D. W. JAMES and G. M. KIMBER. Aust. J. Chem. **22**, 2287 (1969).

Can. J. Chem. Downloaded from www.nrcresearchpress.com by 210.87.254.6 on 09/05/12
For personal use only.

Can. J. Chem. Downloaded from www.nrcresearchpress.com by 210.87.254.105 on 09/05/12
For personal use only.

Peptide Conformations. I. Nuclear Magnetic Resonance Study of the Carbamate Reaction of Amino Acids and Peptides[1]

R. U. LEMIEUX AND M. A. BARTON[2]
University of Alberta, Department of Chemistry, Edmonton, Alberta

Received August 12, 1970

Nuclear magnetic resonance spectroscopy has been applied to the study of carbamate formation in solutions of amino acids and peptides in a carbonate–bicarbonate system. The possible conformations of these carbamates are discussed in terms of the n.m.r. data obtained. The n.m.r. parameters are reported for the diastereomers L-alanyl-L or D-phenylalanine and L-phenylalanyl-L or D-alanine and for the dipeptide glycyl-L-phenylalanine and their carbamates. The results are interpreted in terms of preferred rotamers about the C_α—C_β bond of the phenylalanine residue and a β-type conformation of the peptide chain, wherein the two α-protons lie in the plane of the amide bond. All observations are in agreement with a shorter end to end distance in L,D- compared with L,L-dipeptides.

Canadian Journal of Chemistry, 49, 767 (1971)

Introduction

Amines, amino acids and peptides enter into equilibrium with their carbamate derivatives ($RHNCO_2Na$) in weakly alkaline aqueous carbonate.

$$2NaHCO_3 \rightleftarrows Na_2CO_3 + H_2CO_3$$

$$H_2CO_3 \rightleftarrows CO_2 + H_2O$$

$$Na_2CO_3 + H_2O \rightleftarrows NaHCO_3 + NaOH$$

$$RHNH + CO_2 + NaOH \rightleftarrows RHNCO_2Na + H_2O$$

Mild alkalinity is required to maintain free amine and an adequate concentration of carbon dioxide. Caplow (1) has proposed a detailed reaction scheme. The reaction has also been studied by other workers (2–9). Carbamate formation occurs at the terminal amino groups of hemoglobin in the blood stream and thus is important for the physiological transport of carbon dioxide. A carbamate derivative, *N*-carboxybiotin, is also formed as an intermediate in some enzyme catalyzed carbon dioxide transfer reactions (10–12).

The studies of carbamate formation have generally depended on the physical separation of the reaction products. In the present work we report the observation of carbamate formation by p.m.r. spectroscopy. This method provides an experimentally simple means of distinguishing the reaction products in the intact equilibrium mixture. We have made use of the carbamate reaction in an investigation of dipeptide conformations.

[1]Presented in part at the Annual Meeting of the Canadian Federation of Biological Societies, Montreal, Quebec, June 12th, 1970.

[2]University of Alberta Postdoctorate Fellow, 1970–1971.

Experimental

The amino acids were recrystallized to high purity. The dipeptides were prepared by coupling of the benzyloxycarbonyl amino acid and amino acid methyl ester using dicyclohexylcarbodiimide according to conventional procedures (13). Saponification and hydrogenation yielded the free dipeptides having the following physical constants: glycyl-L-phenylalanine, $[\alpha]_D^{25}$ +40.0°, *c* 2, water (lit. value (14), $[\alpha]_D^{25}$ +41.5°, *c* 2, water); L-phenylalanyl-L-alanine, $[\alpha]_D^{20}$ +12.7°, *c* 2, water (lit. value (15), $[\alpha]_D^{20}$ +12.8°, *c* 2, water); L-phenylalanyl-D-alanine, Anal. Calcd. for $C_{12}H_{16}N_2O_3$: C, 61.00; H, 6.83; N, 11.86. Found: C, 61.04; H, 6.94; N, 11.81, $[\alpha]_D^{25}$ +119°, *c* 2, water; L-alanyl-L-phenylalanine, Found: C, 60.93; H, 6.53; N, 11.77, $[\alpha]_D^{25}$ +38.8°, *c* 2, water; L-alanyl-D-phenylalanine, Found: C, 60.92; H, 6.62; N, 11.93; $[\alpha]_D^{25}$ −16.4°, *c* 2, water.

Molar solutions of the sodium salts in deuterium oxide were prepared by adding equivalent amounts to NaOD in deuterium oxide (1.7 *M*) followed by dilution. In order to observe carbamate formation at various p*H*'s in the range 8–12, the p*H* of an aliquot of the *M* solution was adjusted, using DCl (6.4 *M*) in deuterium oxide, to that required. This solution was then mixed with a molar solution of sodium carbonate in deuterium oxide whose p*H* had been adjusted to that required in the same way. In all experiments 1 mol of the amino compound was present per mol of added carbonate and the solution was 0.5 *M* in the amino compound used. The p*H*'s recorded in Fig. 2 were determined at the temperature of the n.m.r. probe immediately before obtaining the spectrum. The solutions were kept a further 24 h and the spectra were redetermined to ensure that equilibrium conditions had been achieved. The peaks assigned to the carbamate derivative were not observed in control experiments wherein sodium carbonate had not been added.

The n.m.r. spectra were obtained using a Varian A56/60 spectrometer, operating at 40 °C with tetramethylsilane as external reference. The increased sensitivity of the Varian HA-100 spectrometer, operating at 33 °C, was required for the dipeptides. The chemical shifts and coupling constants were determined using pyrazine as internal standard. In order to avoid the possible effect of pyrazine on the equilibrium for the carbamate reaction, the equilibrium data at 100 MHz were obtained

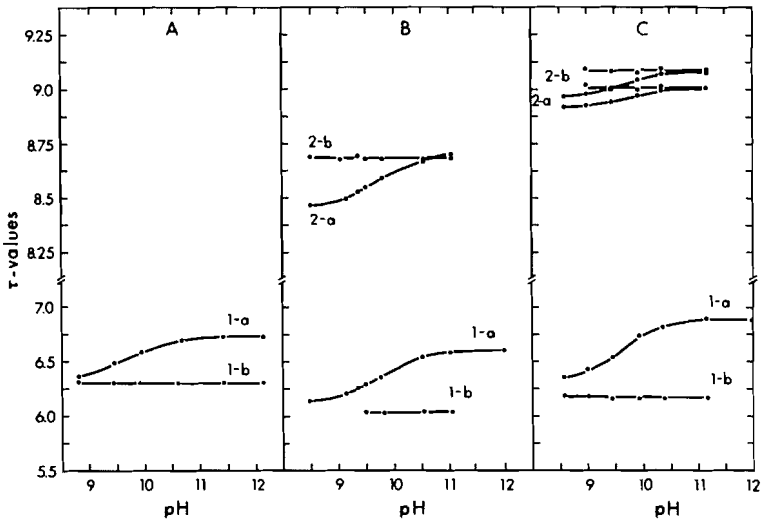

FIG. 1. Chemical shift as a function of p*H* in equilibrium mixtures of amino acid and carbamate, obtained from 0.5 *M* solution of amino acid in 0.5 *M* sodium carbonate – bicarbonate buffer in D_2O (A, glycine; B, alanine; C, valine): 1, α-protons; 2, methyl protons; a, amino acid; b, carbamate.

using hexamethyldisilane as external reference. The chemical shifts reported herein are all relative to tetramethylsilane as external reference at 60 MHz in the A56/60 spectrometer. These were calculated on the basis of the chemical shifts of pyrazine and 3-(trimethyl)-1-propane sulfonic acid sodium salt in both spectrometers relative to the external references mentioned above. In the p*H* range 2–12 the chemical shifts (τ) of the reference compounds were as follows: external tetramethylsilane, 10.00; external hexamethyldisilane, 10.11; 3-(trimethyl)-1-propane sulfonic acid sodium salt, 10.28; pyrazine, 1.55. A plot of chemical shift against p*H* showed the pyrazine resonance to move downfield in the range p*H* 0–2. At p*H* 0.5 the chemical shift of pyrazine was τ 1.14.

The three coupling constants characteristic of the ABX system of the phenylalanine residue in dipeptides were obtained from spectra recorded at a sweep width of 250 Hz. The geminal coupling constant of the glycyl residue in glycyl-L-phenylalanine was determined at the same sweep width.

Results and Discussion

We have studied the extent of carbamate formation in deuterium oxide solutions of the amino acids glycine, alanine, valine, α-amino-isobutyric acid, lysine and histidine over the p*H* range 7–12, in a carbonate–bicarbonate system. In this p*H* range, equilibria are established between the zwitterionic and anionic forms of the amino acid, and between the amino acid anion and carbamate derivative. The rapid exchange between zwitterion and anion leads to a time-averaged spectrum for these species. However, the rate of exchange between the carbamate derivative and the amino acid is sufficiently slow to give separate peaks for the carbamate and thus the extent of carbamate formation can be determined by integration. The carbamate peaks are readily identifiable since their positions are independent of p*H* under their conditions of formation. The time-averaged peaks of the zwitterion and anion move upfield with increase in p*H*, due to dissociation of the ammonium group. The assignment of the p*H*-independent spectrum to carbamate was confirmed by the use of ^{13}C-enriched (58%) carbon dioxide, since the α-proton of the amino acid in the presumed carbamate produced a signal which displayed the expected coupling with the ^{13}C-atom. The results obtained with ^{13}C-labelled carbamates, including the measurement of $^{13}C—N—C—H$ coupling constants, will be discussed in a subsequent paper.

The chemical shifts of the α-hydrogens of glycine, alanine and valine in the p*H* range 9–12 are plotted in Fig. 1. The decreased shielding observed as the α-amino group is liberated, is well known (16). In contrast, it is seen that the chemical shifts for these hydrogens in the carbamate derivative are p*H* independent.

Figure 2 reports the effect of p*H* on the equilibrium of the carbamate forming reaction for the three amino acids, glycine, valine, and

Can. J. Chem. Downloaded from www.nrcresearchpress.com by 210.87.254.105 on 09/05/12
For personal use only.

Can. J. Chem. Downloaded from www.nrcresearchpress.com by 210.87.254.105 on 09/05/12
For personal use only.

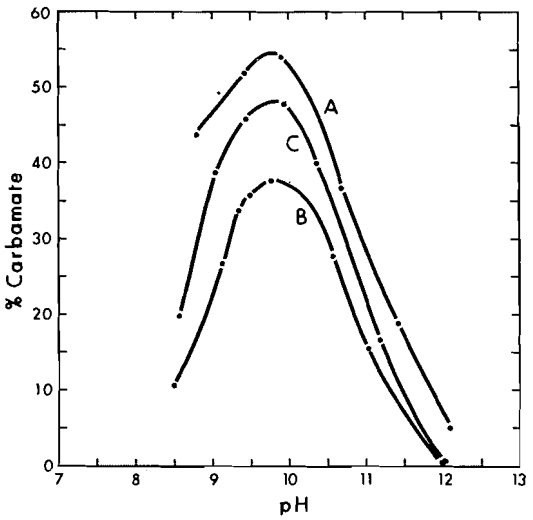

FIG. 2. Variation of percentage carbamate with change in p*H* in equilibrium mixtures obtained from 0.5 *M* solutions of amino acid in 0.5 *M* sodium carbonate – bicarbonate buffer in D_2O: (A, glycine; B, alanine; C, valine).

alanine. It is seen that the optimum p*H* is about p*H* 9.8 in all cases. The pK_a's of the amine group for these amino acids are 9.60, 9.62, and 9.69, respectively, in good agreement with the optimum p*H* for extent of carbamate formation. Increasing alkalinity is expected to depress the concentration of carbonic acid, which is considered to be the precursor in the rate controlling stage for carbamate formation. Strong support for this contention was found by Giustina *et al.* (17), who showed that the addition of carbonic anhydrase, an enzyme known to catalyze the dehydration of carbonic acid to carbon dioxide, caused carbamate formation to occur at an increased rate. Thus increased alkalinity not only depresses the extent of carbamate formation but also the rate of carbamate formation. In keeping with these known characteristics of carbamate formation, integrations of the signals obtained in the n.m.r. spectra of solutions of sodium glycinate with equimolar amounts of sodium carbonate after various reaction times showed the reaction to reach equilibrium in less than 1 h at p*H*'s below 9.8 but that increasingly longer reaction times were required at higher p*H*'s up to about 6 h at p*H* 11.6.

Carbamate formation was not observed at the imidazole group (pK_a 5.97) of histidine. However in the p*H* range 8.7–10.7, carbamate formation was clearly indicated at the α-amino group (Fig. 3). In the case of lysine, carbamate formation at the α-position clearly occurred in the p*H* range 9.4 to 10. At higher p*H*'s, carbamate formation was evident at both amino groups. The pK_a's of the amino groups of lysine are 8.90 and 10.28. In summary, n.m.r. spectroscopy can serve as a convenient tool to monitor carbamate formation in deuterium oxide solutions.

It was found that α-aminoisobutyric acid (**1**) did not form a detectable amount of carbamate under conditions where valine gave about 50% yield. Carbamate formation should have been detected by the presence of a p*H* independent peak due to the carbamate methyl group. In practice only the p*H* dependent signal of the methyl group of the free amino acid was obtained.

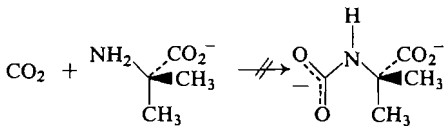

I

We consider this result to be important since it indicates that the general conformation of a carbamate contains the α-proton in non-bonded interaction with an oxygen atom of the carbamate group. In α-aminoisobutyric acid a methyl group is substituted for the α-hydrogen, a strongly unfavorable interaction is therefore introduced, and the carbamate is destabilized.

This conclusion appears supported by the strong deshielding observed for the α-hydrogen on carbamate formation. That is, strong electrostatic deshielding of the α-hydrogen can be expected should the carbamate exist largely in the conformation **2***a*. Although resonance stabilization of the negative charge of the carbamate group cannot be expected to involve the nitrogen atom, it seems likely that the grouping is planar in order to achieve coplanarity of a C—O and the N—H bond. Regardless of whether the nitrogen is trigonal or tetrahedral, clearly conformations which bring an oxygen in *syn*-axial-like relationship with the α-hydrogen seem energetically most favorable in view of the undoubtedly planar $-CO_2^-$ group. It is of interest to note in this regard the analogy between the deshielding effects observed for carbamates and amides depending on whether there are only one or two α-hydrogens. In the case of amides, as seen in

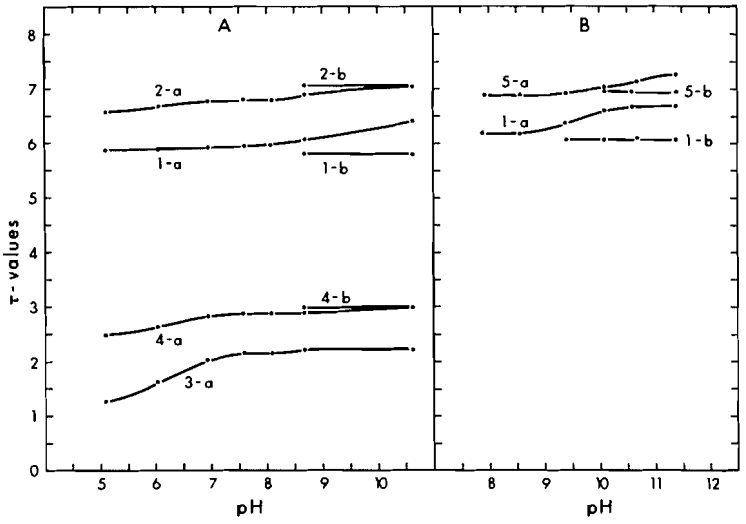

FIG. 3. Chemical shift as a function of p*H* in equilibrium mixtures of amino acid and carbamate, obtained from 0.5 *M* solution of amino acid in 0.5 *M* sodium carbonate – bicarbonate buffer in D_2O (A, histidine; B, lysine): 1, α-protons; 2, β-protons; 3, H-2 protons (imidazole); 4, H-4 protons (imidazole); 5, ε-protons; *a*, amino acid; *b*, carbamate.

Table 1, the chemical shifts for the *N*-acyl derivatives of glycine as compared to glycine are substantially less (about 0.4 τ-values) than when the amino acid has only one α-hydrogen. This difference can be ascribed to the carbonyl oxygen bisecting the H—C—H angle in the case of the *N*-acyl glycines (**3***b*) but in much closer non-bonded interaction with methine α-hydrogens, **3***a* (18). As seen from Table 1, the carbamates for glycine show differences in chemical shift that are about 0.2 τ-values less than those of the other amino acids which have only one α-hydrogen. For these reasons, it can be expected that the carbamates of glycine exist mainly in the conformation depicted in **2***b* rather than conformations corresponding to **2***a* with R = H.

It can be seen that the arrangement about the N—C_α bond in our proposed carbamate conformation, **2***a*, is identical to that in the β-type structure of a dipeptide, **3***a*. The β-structure, with both α-protons in the plane of the amide link has recently been proposed by Lande (19) as accounting for many of the observed properties of dipeptides and the analogy with the carbamates is a further indication of the importance of this conformation.

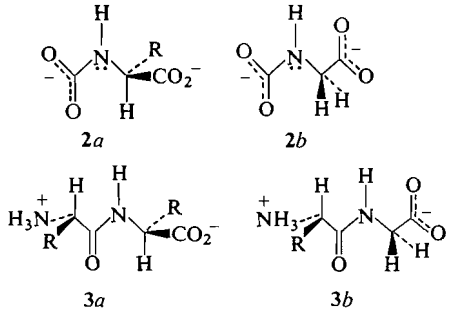

2*a* **2***b*

3*a* **3***b*

In the course of this study we obtained the n.m.r. parameters for two pairs of diastereomeric peptides L-phenylalanyl-L or D-alanine and L-alanyl-L or D-phenylalanine, and also for the dipeptide glycyl-L-phenylalanine. The peak positions obtained for each of these peptides, in acid, basic and neutral solution, are given in Tables 2–4. In general the —CH_2—CH— system of the phenylalanine residue gave a well resolved 12-line pattern of the ABX type and the three coupling constants could be obtained on this basis. In the case of L-phenylalanyl-D-alanine anion, the spectrum collapsed to a six-line pattern and only the average of the vicinal coupling constants was obtained. The coupling constants J_{AX} (*vic*), J_{BX} (*vic*), and J_{AB} (*gem*) and the chemical shifts of the A and B protons are included in Tables 2–4. The high field resonance is assigned to the B proton.

From Tables 2 and 3 it can be seen that the CH_3 resonance is always shifted upfield in the L,D-peptides compared to the corresponding L,L-isomers. This effect has been noted in many

Can. J. Chem. Downloaded from www.nrcresearchpress.com by 210.87.254.105 on 09/05/12
For personal use only.

TABLE 1. Chemical shifts of α-H in amines (NH_2—CH_α—), *N*-acyl amines (R—NH—CH_α—) and carbamate derivatives

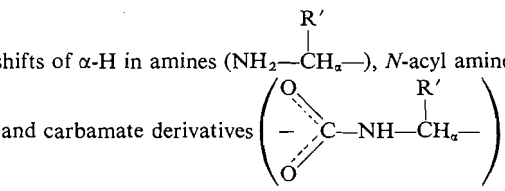

	Amine anion	Carbamate	Δ Amine anion – carbamate	Δ Amine anion – *N*-acyl amine anion
Glycine	6.74	6.31	0.43	0.48* 0.63† 0.59‡
Alanine	6.60	6.03	0.57	0.85§ 0.90‖ 0.89¶
Histidine	6.42	5.80	0.62	0.96** 1.00††
Valine	6.87	6.17	0.70	
Lysine	6.70	6.07	0.63	
Glycyl-L-phenylalanine	6.89	6.42	0.47	
L-Alanyl-L-phenylalanine	6.73	5.92	0.80	
L-Alanyl-D-phenylalanine	6.75	5.89	0.86	

*R = Glycyl (37).
†R = Glycyl (38).
‡R = Alanyl (38).
§R = Glycyl (37).
‖R = Glycyl (38).
¶R = Alanyl (38).
**R = Acetyl (28).
††R = Glycyl (28).

TABLE 2. Coupling constants* (Hz) for the ABX system of diastereoisomeric alanylphenylalanines and phenylalanylalanines

	L-Alanyl-L-phenylalanine (5)	L-Alanyl-D-phenylalanine (6)	L-Phenylalanyl-L-alanine (7)	L-Phenylalanyl-D-alanine (8)
p*H* 0.5				
J_{AX}	5.7	4.9	6.4	6.5
J_{BX}	8.9	9.7	7.7	8.6
$-J_{AB}$	14.0	14.0	14.4	13.7
p*H* 6				
J_{AX}	5.4	4.6	6.0	6.1
J_{BX}	8.7	9.7	7.9	8.8
$-J_{AB}$	13.9	14.0	14.2	13.7
p*H* 13				
J_{AX}	4.8	4.7	5.4	—
J_{BX}	8.8	8.9	7.6	—
$-J_{AB}$	13.8	13.9	13.8	—

*Precise to ± 0.2 Hz.

pairs of dipeptide diastereoisomers containing an aromatic function (20–22). It is known from the work of Kenner and co-workers (23–25) that peptides containing some D-amino acids show a shorter end-to-end distance than do all L-peptides. In the case of dipeptides these results find a ready explanation if the conformation of both L,L- and L,D-peptides is assumed to be of the β-type, ***4a*** and *b* (19).

In this conformation the charged groups exist

Can. J. Chem. Downloaded from www.nrcresearchpress.com by 210.87.254.105 on 09/05/12
For personal use only.

TABLE 3. Chemical shifts (τ-values) for diastereoisomeric alanylphenylalanines and phenylalanylalanines

	$CH_3CH_\alpha ND_2CONDCH_X(COOD)CH_AH_BC_6H_5$		$C_6H_5CH_ACH_BCH_XND_2CONDCH_\alpha(COOD)CH_3$	
	L-Alanyl-L-phenylalanine (5)	L-Alanyl-D-phenylalanine (6)	L-Phenylalanyl-L-alanine (7)	L-Phenylalanyl-D-alanine (8)
p*H* 0.5				
H_A	6.97	6.90	6.93	6.94
H_B	7.11	7.21	7.00	7.05
H_X	5.50	5.43	5.85	5.93
C_6H_5*	2.88	2.87	2.85	2.85
H_α	6.08	6.12	5.81	5.92
CH_3	8.64	8.89	8.79	9.00
p*H* 6				
H_A	6.95	6.88	6.81	6.92
H_B	7.16	7.25	6.95	7.00
H_X	5.66	5.60	5.82	5.90
C_6H_5*	2.86	2.88	2.80	2.81
H_α	6.10	6.11	5.94	6.04
CH_3	8.58	8.89	8.74	9.00
p*H* 13				
H_A	6.92	6.93	7.14	—
H_B	7.17	7.22	7.28	—
H_X	5.64	5.65	6.47	6.52
C_6H_5*	2.87	2.88	2.87	2.87
H_α	6.73	6.75	5.95	6.04
CH_3	8.98	9.10	8.81	9.00

*Broad singlet.

TABLE 4. Nuclear magnetic resonance parameters for glycyl-L-phenylalanine (ND_2—$CH_A{\cdot}H_{B'}$—COND—CH_X(COOD)—CH_AH_B—C_6H_5)

	p*H* 13	p*H* 6	p*H* 0.5
Chemical shifts (τ-values)			
H_A	6.95	6.93	6.82
H_B	7.19	7.20	6.99
H_X	5.64	5.58	5.27
$H_{A'}$	6.89 (single peak)	6.23	6.10
$H_{B'}$		6.35	6.18
C_6H_5	2.87	2.89	2.74
Coupling constants* (Hz)			
J_{AX}	4.3	4.6	5.1
J_{BX}	8.3	9.1	8.5
$-J_{AB}$	13.9	14.1	14.0
$-J_{A'B'}$	—	16.5	16.3

*Precise to ± 0.2 Hz.

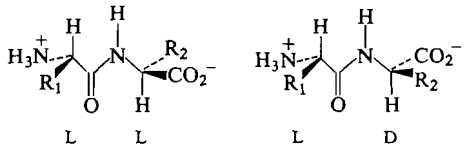

4*a* 4*b*

on opposite sides of the amide bond in the L,L-diastereomer, as also do the two side chains R_1 and R_2. In the L,D-form the charged groups both exist on the same side of the amide bond and R_1 and R_2 are both on the opposite side. Thus shielding of R_1 by R_2 is possible in the L,D-peptide but not in the L,L-case.

The rotational isomerism about the C_α—C_β bond of amino acids and peptides has been studied by several workers by the n.m.r. method (26–33). These studies have generally been based on the assumption of constant values for the vicinal couplings between hydrogen atoms in *gauche* (J_g) and *trans* (J_t) positions to each other. The validity of this approach is open to some doubt since it is known, for example (34), that the size of a *gauche* coupling can be significantly

Can. J. Chem. Downloaded from www.nrcresearchpress.com by 210.87.254.105 on 09/05/12
For personal use only.

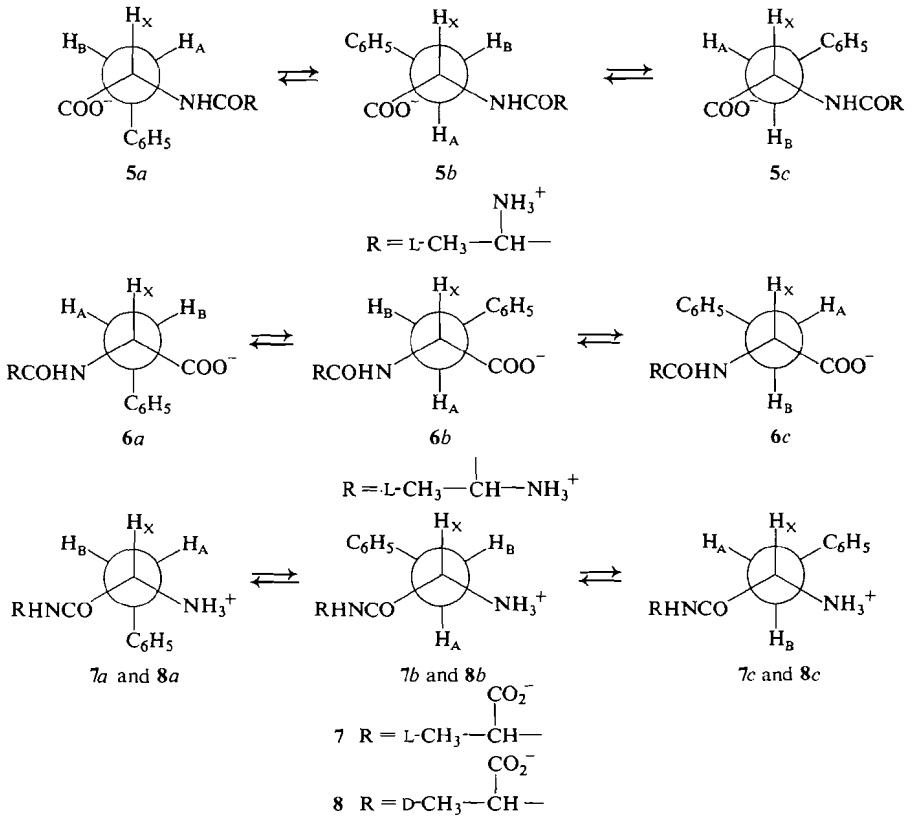

affected by substituents in a *trans* coplanar arrangement with either of the coupled protons. Also, there is no basis for assuming that torsional angles for *gauche* hydrogens are 60°; indeed, for open-chain compounds these angles, in the absence of evidence to the contrary, must be assumed in the range 45–75° and the coupling constant, therefore, in the range of *about* 1 to 5 Hz (35). This uncertainty obviously severely limits the utility of n.m.r. in establishing the relative population of rotamers for acyclic structures such as dipeptides since the dependence of coupling constant on torsional angle is very high in the range 45 to 75° (35). However, it is possible to make some deductions simply on the basis that J_t is very much larger than J_g.

A comparison of the coupling constants (Table 2) for diastereomeric L-alanyl derivatives of L-phenylalanine (**5**) and D-phenylalanine (**6**) shows that the change in configuration has little effect on the coupling constants for the $—CH_X—CH_AH_B—$ grouping of the phenylalanine residues. Also, the same situation is evident for the L-phenylalanyl derivatives, **7** and **8**, of L-alanine and D-alanine, respectively. However, it is seen that time averaged coupling constants labelled J_{AX} are substantially smaller for **5** and **6** than for **7** and **8** and those assigned J_{BX} are substantially larger for both **5** and **6** than for **7** and **8**. Obviously, therefore, compounds **5** and **6** are much richer in a conformer that has the B and X hydrogens in antiplanar relationship. A consideration of the staggered conformations for the $—CH—CH_2—$ groups of these compounds clearly requires conformations **5***a*, **6***a*, **7***a*, and **8***a* to be of little importance and this is substantiated for compounds **5** and **6** in view of the large values for J_{BX} (9.3 $\pm$ 0.5 Hz at p*H*'s 0.5, 6, and 13). Also, for all compounds, values for $(J_{AX} + J_{BX})/2$ are close (about 7 Hz) to the expected values (about 8 Hz) (31) for conformations involving H_X antiplanar to either H_A or H_B. The shift in conformational equilibria on passing from either compounds **5** and **6** to either of the positional isomers **7** and **8** must arise from the change of the vicinal carboxyl group in **5** and **6** to amino group in

Can. J. Chem. Downloaded from www.nrcresearchpress.com by 210.87.254.105 on 09/05/12
For personal use only.

Can. J. Chem. Downloaded from www.nrcresearchpress.com by 210.87.254.105 on 09/05/12
For personal use only.

7 and 8. One must expect a stronger non-bonded interaction between the large phenyl group and the large carboxyl group when in *gauche* relationship as seen in the conformers 5*b* and 6*b* than between the phenyl group and the *gauche* group in conformers 7*b* and 8*b*. Indeed, it is to be expected on well established conformational theory that 5*c* and 6*c* should be favored over 5*b* and 6*b*, respectively, whereas a smaller energy difference should exist both between 7*b* and *c* and between 8*b* and *c*; precisely as demanded by the n.m.r. data. Thus, there can be no doubt that conformers 5*c* and 6*c* are the largely favored conformers for compounds 5 and 6. There can be no such certainty as to which is the preferred conformer for compounds 7 and 8. However, it is likely that the amino rather than the amide grouping would tend to be *gauche* to the phenyl group. That is, conformations 7*c* and 8*c* seem preferred on steric grounds but, as will be seen below, solvation and dipole–dipole interactions also appear important in establishing these conformational preferences.

Assuming a basically β-form for the peptide linkage, projection formulae 9 and 10 for the conformers 5*c* and 6*c*, respectively, are implied. Of course, the ionic state will depend on the p*H*; the carboxylate group being protonated at p*H* 3, the zwitterionic stage largely prevailing at p*H* 6, and the unprotonated amine existing at p*H* 13.

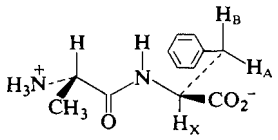

9 (5*c*)

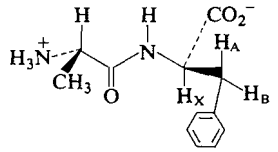

10 (6*c*)

Examination of molecular models for 6*c* suggests the methyl group should project toward the plane of the phenyl group at a distance of about 4.5 Å and perpendicular to the plane of the ring at about the edge of ring. The relationship derived by Johnson and Bovey (36) would predict for this situation (*z*-value = 3.2 and *p*-value = 1) a shielding from this origin of the methyl group in 6*c* of 0.46 p.p.m. For compound 5 in conformation 5*c* the methyl group and the phenyl group are separated by about 6 Å and the *p*-value is estimated to be about 3. On this basis, and by extrapolation of the Johnson–Bovey table, the phenyl group should shield the methyl group by about 0.06 p.p.m. Thus, assuming all other shielding effects on the methyl groups to be equal for the compounds in conformations 5*c* and 6*c*, it would be expected that the methyl group in 6*c* would produce its signal about 0.4 p.p.m. to higher field than that in 5*c*. However, other conformations are expected to be present all of which should experience smaller such shielding effects. Therefore, the observed difference in chemical shift should be less than that expected on the basis of conformations 5*c* and 6*c* only and probably about 0.3 p.p.m. Indeed, the observed difference (0.25 and 0.31) at p*H*'s 0.5 and 6, respectively (see Table 3), are of this order of magnitude and confirm well the assignments (based on vicinal coupling constants and conformational analysis) of conformations close to 5*c* and 6*c* as the predominant conformations for the dipeptides 5 and 6, respectively. It is noteworthy with regard to the relatively small difference, 0.12 p.p.m., observed at p*H* 13 that J_{BX} also is substantially smaller at this p*H* for compound 6 than at the lower p*H*'s (see Table 2). It is expected that conformation 6*c* will best accommodate the electrostatic attraction between the NH_3^+ and COO^- groups and thereby serve as a stabilizing influence for this conformation. Indeed, the methyl group is most strongly shielded for compound 6 relative to that for compound 5 at p*H* 6. As will be seen below, the fact that the hydrophobic phenyl group extends into close contact with the peptide portion of the molecule may be a further important stabilizing factor for conformations 5*c* and 6*c*.

In accord with the foregoing discussion of the conformational equilibria for compounds 7 and 8 and assuming the β-form for the peptide linkage, these compounds can be represented by the projection formulae 11*a* and *b* (in the case of 7) and 12*a* and *b* (in the case of 8). In view of the prevalence of 12*a*, it would be expected that the methyl group signal would be to somewhat higher field for compound 8 than for compound 7. Indeed, as has been already noted (Table 3), this

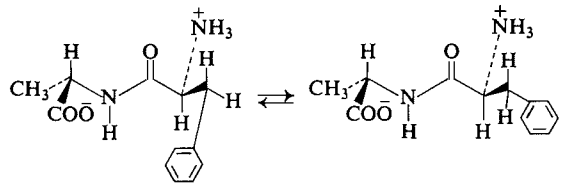

11*a* (7*b*) **11***b* (7*c*)

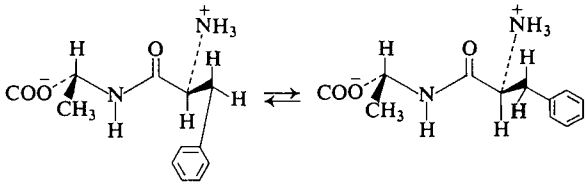

12*a* (8*b*) **12***b* (8*c*)

was found to be the case with the chemical shift difference being the greatest for the zwitterionic form. In fact, the large difference of 0.26 p.p.m. observed at p*H* 6 (Table 3) appears to favor conformation **12***a* substantially over **12***b*. If so, this situation likely results at least in part from a tendency for the hydrophobic phenyl group to minimize solvation by water (in other words, to maximize the water structure of the system).

The n.m.r. data for glycyl-L-phenylalanine reported in Table 4 confirm the stabilizing effect of the zwitterionic state for the dipeptide in the β-form. That is, the largest chemical shift for the methylenic hydrogens of the glycyl residue would be expected for conformation **13***b* which is also the conformer having most favorable spatial disposition of the NH_3^+ and COO^- groups. In fact we find a chemical shift difference of 0.15 in the zwitterion, 0.08 in the cation, and 0 in the anion.

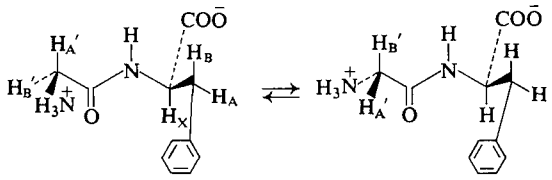

13*a* **13***b*

The coupling constants J_{AX} and J_{BX} for the ABX grouping of **13** (Table 4) have magnitudes similar to those observed for the alanylphenylalanines **5** and **6**, and **13** is assigned the conformation for the phenylalanine residue as shown in **13***a* and *b* for the same reasons as discussed earlier for **5** and **6**.

Carbamate formation in solutions of the four isomeric dipeptides was studied by n.m.r. in the p*H* range 7–11. In all cases the carbamate could be distinguished by the p*H*-independent resonances of the *N* terminal α-proton and of the alanyl methyl group. The remaining protons of the carbamate gave peaks superimposed on those of the free peptide. The peptides showed yields of carbamate comparable with those obtained for glycine (Table 5). However, carbamate formation occurred in solutions of lower p*H* in the case of the peptides, in keeping with the generally lower pK_a values of dipeptides compared with amino acids. The yields of carbamate obtained for the four dipeptides were identical within experimental error.

TABLE 5. Percent yields of carbamate

	Alanylphenyl-alanine		Phenylalanyl-alanine	
p*H*	L,L-	L,D-	L,L-	L,D-
10.4	40	38	35	34
8.6	50	50	55	50
7.3	0	0	0	0

It was noticed that for alanine, the chemical shift of the methyl group was nearly the same for the anion as for the carbamate (see Fig. 1B). For this reason, it was expected that the chemical shift of the methyl group for the alanyl residue would be unaffected on converting the L,L-dipeptide anion of **5** to carbamate. The same situation should apply for the L,L-dipeptide **7** in view of the distance between the methyl group and the carbamate group with the compound in the β-conformation. As seen in Table 6, this was the case within 0.02 p.p.m. However, for the corresponding L,D-isomers, carbamate formation introduces a negatively charged group on the same side of the β-structure as the negatively charged carboxylate group. As a consequence, a conformational change away from the β-conformation could result and, if so, this would likely be reflected by a substantial chemical shift

TABLE 6. Downfield shift of CH_3 hydrogens in dipeptide carbamate relative to dipeptide anion

	Δ Anion–carbamate (τ units)
L-Phenylalanyl-L-alanine	0.02
L-Phenylalanyl-D-alanine	0.08
L-Alanyl-L-phenylalanine	0.02
L-Alanyl-D-phenylalanine	0.09

Can. J. Chem. Downloaded from www.nrcresearchpress.com by 210.87.254.105 on 09/05/12
For personal use only.

difference between the methyl group of the L,D-dipeptides as anions and as carbamates. As seen in Table 6, a small but definite such change did occur inferring an increased distance between the phenyl group and the methyl group in the carbamate derivatives of compounds **6** and **8** as compared to the distances in the anionic forms.

In conclusion, all the data accumulated in the course of this research are in accord with a shorter end-to-end distance in L,D- compared with L,L-peptides. This evidence is compatible with a β-structure for dipeptides.

Thanks are expressed to D. Gifford for the determination of the 100 MHz n.m.r. spectra. The financial support of the National Research Council of Canada is gratefully acknowledged.

1. M. CAPLOW. J. Amer. Chem. Soc. **90**, 6795 (1968).
2. C. FAURHOLT. J. Chim. Phys. Physico chim. Biol. **22**, 1 (1925).
3. F. J. W. ROUGHTON and L. ROSSI-BERNARDI. Proc. Roy. Soc. London, B, **164**, 381 (1966).
4. J. R. CHIPPERFIELD. Proc. Roy. Soc. London, B, **164**, 401 (1966).
5. A. JENSEN and C. FAURHOLT. Acta Chem. Scand. **6**, 385 (1952).
6. M. B. JENSEN and C. FAURHOLT. Acta Chem. Scand. **18**, 377 (1964).
7. O. HENRIKSEN and M. B. JENSEN. Acta Chem. Scand. **21**, 2819 (1967).
8. M. CAPLOW and M. YAGER. J. Amer. Chem. Soc. **89**, 4513 (1967).
9. J. L. FRAHN and J. A. MILLS. Aust. J. Chem. **17**, 256 (1964).
10. F. LYNEN, J. KNAPPE, and E. LORCH. Proc. Int. Congr. Biochem. 5th, 1961, **4**, 225 (1963).
11. S. OCHOA and Y. KAZIRO. Compr. Biochem. **16**, 210 (1966).
12. H. G. WOOD and M. F. UTTER. Essays Biochem. **1**, 1 (1965).
13. M. WINITZ, L. BLOCH-FRANKENTHAL, N. IZUMIYA, S. M. BIRNBAUM, C. G. BAKER, and J. P. GREENSTEIN. J. Amer. Chem. Soc. **78**, 2423 (1956).
14. K. R. RAO, S. M. BIRNBAUM, R. B. KINGSLEY, and J. P. GREENSTEIN. J. Biol. Chem. **198**, 507 (1952).
15. W. GRASSMANN, E. WÜNSCH, and A. RIEDEL. Chem. Ber. **91**, 455 (1958).
16. M. SHEINBLATT. J. Amer. Chem. Soc. **88**, 2845 (1966).
17. G. GIUSTINA, E. MILLA, and R. MARGARIA. Bull. Soc. Ital. Biol. Sper. **28**, 691 (1952).
18. A. McL. MATHIESON. Tetrahedron Lett. 4137 (1965).
19. S. LANDE. Biopolymers, **7**, 879 (1969).
20. F. A. BOVEY and G. V. D. TIERS. J. Amer. Chem. Soc. **81**, 2870 (1959).
21. T. WIELAND and H. BENDE. Chem. Ber. **98**, 504 (1965).
22. B. HALPERN and D. E. NITECKI. Tetrahedron Lett. 3075 (1967).
23. G. W. KENNER, P. J. THOMSON, and J. M. TURNER. J. Chem. Soc. 4148 (1958).
24. P. M. HARDY, G. W. KENNER, and R. C. SHEPPARD. Tetrahedron, **19**, 95 (1963).
25. J. BEACHAM, V. T. IVANOV, G. W. KENNER, and R. C. SHEPPARD. Chem. Commun. 386 (1965).
26. K. G. R. PACHLER. Spectrochim. Acta, **20**, 581 (1964).
27. K. G. R. PACHLER. Z. Anal. Chem. **224**, 211 (1967).
28. R. B. MARTIN and R. MATHUR. J. Amer. Chem. Soc. **87**, 1065 (1965).
29. H. OGURA, Y. ARATA, and S. FUJIWARA. J. Mol. Spectrosc. **23**, 76 (1967).
30. J. R. CAVANAUGH. J. Amer. Chem. Soc. **92**, 1488 (1970).
31. J. R. CAVANAUGH. J. Amer. Chem. Soc. **90**, 4533 (1968).
32. J. R. CAVANAUGH. J. Amer. Chem. Soc. **89**, 1558 (1967).
33. V. F. BYSTROV, S. L. PORTNOVA, T. A. BALASHOVA, V. I. TSETLIN, V. T. IVANOV, P. V. KOSTETZKY, and Y. A. OVCHINNIKOV. Tetrahedron Lett. **59**, 5225 (1969).
34. H. BOOTH. Tetrahedron Lett. 411 (1965).
35. M. KARPLUS. J. Amer. Chem. Soc. **85**, 2870 (1963).
36. C. E. JOHNSON, JR. and F. A. BOVEY. J. Chem. Phys. **29**, 1012 (1958).
37. N. C. LI, R. L. SCHRUGGS, and E. D. BECKER. J. Amer. Chem. Soc. **84**, 4650 (1962).
38. M. VAN GORKOM. Tetrahedron Lett. 5433 (1966).

Can. J. Chem. Downloaded from www.nrcresearchpress.com by 210.87.254.105 on 09/05/12
For personal use only.

Can. J. Chem. Downloaded from www.nrcresearchpress.com by 210.87.254.42 on 09/05/12
For personal use only.

The Anomeric Effect: The Conformational Equilibria of Tetrahydro-1,3-oxazines and 1-Methyl-1,3-diazane

H. BOOTH[1] AND R. U. LEMIEUX
Department of Chemistry, University of Alberta, Edmonton, Alberta

Received August 14, 1970

By measurement of CH–NH coupling constants at low temperatures, the N—H axial conformation was shown to be the dominant, or sole, conformation for tetrahydro-1,3-oxazine, tetrahydro-2-methyl-1,3-oxazine, and 1-methyl-1,3-diazane. These results provide further experimental evidence for the generalized anomeric effect. Nuclear Overhauser experiments established the partial axial character of the *N*-methyl substituent in tetrahydro-3,4,4,6-tetramethyl-1,3-oxazine.

The n.m.r. spectral data for a number of tetrahydro-1,3-oxazines and derived salts are tabulated and discussed.

Canadian Journal of Chemistry, 49, 777 (1971)

The position of conformational equilibria (*e.g.* **1** ⇄ **2**) in saturated six-membered nitrogen-containing heterocycles is a problem which has provoked considerable effort, discussion, and controversy (1–15). The microwave spectrum of piperidine has been interpreted in terms of a mixture containing 60% N—H equatorial and 40% N—H axial conformations (12). Lines characteristic of the N—H equatorial conformation were recorded in the microwave spectrum of morpholine, but since the undetected lines for the N—H axial conformation were *expected* to be weak, no assessment of the position of equilibrium was possible (13).

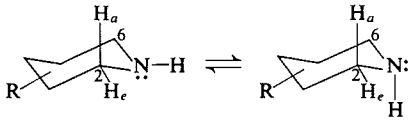

1 **2**

The position of equilibria (*e.g.* **3** ⇄ **4**) in cyclohexane compounds, corresponding to **1** ⇄ **2**, is thought to depend largely on the repulsive 1,3-interactions illustrated, and these in turn are a function of the size and polarizability of the group R, the bond length C—R and the nature of the solvent. In the case of a heterocycle (**1** ⇄ **2**) there is the further complication caused by the presence of unshared electron pair(s) on the heteroatom.

Allinger *et al.* (10) have maintained that the concept of size for a lone-pair has been an unfortunate one. Nevertheless, equilibria such as

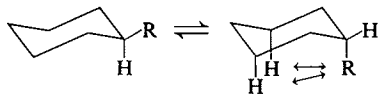

3 **4**

1 ⇄ **2** are undoubtedly influenced by 1,3-interactions involving lone-pair orbitals, and evaluation of such effects is, therefore, a study of some importance. Recent work on *N*-substituted aziridines has suggested that interactions between lone-pair orbitals on directly bonded atoms are also important in determining conformational equilibria (16).

However, according to the recent proposals regarding the stereochemical requirements of adjacent electron pairs and polar bonds (17), interactions between lone-pair orbitals are unimportant. Instead, the interactions of *bonded* electron pairs of polar bonds with each other are considered of importance. A non-directional behavior of lone electron pairs was concluded on the basis of *ab initio* quantum mechanical calculations.

The problem of assessing the position of conformational equilibria such as **1** ⇄ **2** has been approached by the use of n.m.r. techniques, but with some exceptions (18–20), these have all utilized chemical shift data for the protons on C-2 and -6, adjacent to the nitrogen atom. Comparisons of chemical shifts (τ_{2a}, τ_{2e}) (21), or chemical shift differences ($\tau_{2a} - \tau_{2e}$) (3), in the parent amines **1** ⇄ **2** with those in their *N*-methyl derivatives **5** ⇄ **6**, are not expected to yield reliable information on the position of equilibrium **1** ⇄ **2**, for the following reasons: (*a*) lack of standards, of known conformation about the nitrogen atom; (*b*) uncertainty as to the position

[1]University of Alberta Visiting Professor, 1968–1969. Present address: Department of Chemistry, University of Nottingham, England.

Can. J. Chem. Downloaded from www.nrcresearchpress.com by 210.87.254.42 on 09/05/12
For personal use only.

of conformational equilibrium **5** ⇄ **6** in the *N*-methyl derivatives themselves (6, 22, 23); (*c*) the problem, hitherto unsolved, of separating those effects on τ_a and τ_e due to the anisotropy of the *N*-alkyl substituent, from those effects on τ_a and τ_e due to the anisotropy of the nitrogen lone pair (4, 24).

Hutchins *et al.* (21) have recently made the statement: "It is known that the signal of an axial hydrogen on carbon next to an amino nitrogen undergoes an appreciable upfield shift when the nitrogen bears an axial electron pair and equatorial methyl group, as compared to the case when the electron pair is equatorial and the methyl group is axial or absent." Unfortunately, there is no convincing evidence in the literature to support the statement. It is *only* possible to state that the conversion of a cyclic amine **1** ⇄ **2** (position of equilibrium in dispute) into its *N*-methyl derivative **5** ⇄ **6** (position of equilibrium in dispute) causes a shielding of the axial

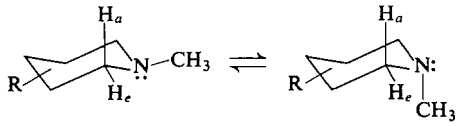

5 **6**

proton H_a which is usually much greater than the shielding of the equatorial proton H_e (*N.B.* tetrahydro-1,3-oxazine is an exception, *vide infra*).

The cyclic compounds studied in this investigation are derivatives of tetrahydro-1,3-oxazine **7** ⇄ **8**, a molecule which exhibits an effect not present, for example, in simple piperidines **1** ⇄ **2**.

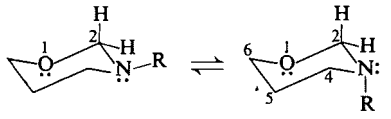

7 R = H **8** R = H
9 R = Me **10** R = Me

This is the generalized anomeric effect (25-27), a phenomenon first associated with the unexpectedly higher stability of glycosyl halides in that conformation bearing the halogen axial (28). Edward pointed out that the placing of the halogen axial avoided an interaction between the polar C—halogen bond and the axial orbital of the ring oxygen. Later Kabayama and Patterson (29) discussed the effect in terms of a destabilization of the equatorial conformation by repulsion between lone-pair orbitals on halogen and ring oxygen. This aspect of the "anomeric effect" was fully discussed by Lemieux (30) in 1964. Hutchins *et al.* (21) have recently introduced the term "rabbit-ear" effect to describe the generalized anomeric effect, *i.e.*, that aspect of the anomeric effect involving the disfavoring of conformations in which unshared electron pairs are *syn*-axial on non-adjacent atoms. Lemieux and Chü (25) showed that the anomeric effect was enhanced by the introduction of more electronegative groups at the 5-position of 1,2,3,4-tetra-*O*-acetyl-D-glucopyranoses. It was therefore suggested that the origin of the anomeric effect may reside at least in part from the relative orientations of the polar C—O bonds about the acetal linkage (30). Edward *et al.* (31) found confirmatory evidence in studies involving 3-alkoxy-4-oxa-5α-cholestanes. Indeed, as mentioned above, recent theoretical studies by Wolfe and co-workers (17) seem to favor this origin for the anomeric effect over that involving repulsions between *syn*-axial lone-pair orbitals. Thus, the presence of a *syn*-axial disposition of lone-pair orbitals may serve more for the identification of the anomeric effect than for its understanding.

Taking the bulk of evidence available at present, neither the *N*–H equatorial nor the *N*–H axial conformation is strongly preferred for piperidine and morpholine. However, the situation is different for tetrahydro-1,3-oxazine **7** ⇄ **8**, where **8** is expected to predominate, since here the polar *N*–H bond is more favorably disposed electrostatically to the O—C_2 bond. This situation is formally analogous to the conformational preference for fluoromethanol anticipated by calculation (17). It was hoped that additional information on these matters would be provided by an investigation of the positions of equilibria **7** ⇄ **8** and **9** ⇄ **10**.

Tetrahydro-1,3-oxazine **7** ⇄ **8** was readily prepared from 3-aminopropan-1-ol and formaldehyde, both by the method of Eden (32), involving azeotropic removal of water from the mixture in benzene, and by the method of Lehn *et al.* (33), in which the two components react smoothly in the presence of water. In principle, the most direct method of establishing the position of equilibrium **7** ⇄ **8** involves measurement of the proton–proton CH–NH coupling constant, on the reasonable assumptions that such coupling

Can. J. Chem. Downloaded from www.nrcresearchpress.com by 210.87.254.42 on 09/05/12
For personal use only.

constants will occur in the range 0 to 14 Hz (*cf.* the corresponding proton–proton CH–OH coupling constants (34)), and that such coupling constants show a dependence on torsional angle similar to that shown by the corresponding CH–CH coupling constants.

Hitherto, to our knowledge, observations of proton–proton CH–NH coupling constants in *amines* have not been made (see, especially, footnote on p. 3766 of ref. 3), owing to rapid proton exchange between amine and amine, and/or amine and solvent, and/or amine and water. Proton–proton CH–NH coupling constants are readily observed in protonated amines dissolved in strongly acidic solvents and in amides.

The n.m.r. spectrum of tetrahydro-1,3-oxazine **7** ⇄ **8** showed no evidence for CH–NH coupling at room temperature, even when the solvent was dimethyl sulfoxide. The spectrum in $CDCl_3$ showed features which are expected for a molecule which is undergoing rapid ring inversion, in addition, presumably, to rapid nitrogen inversion (**7** ⇄ **8**). Thus, we observed a singlet at τ 5.60 (protons at 2), a fairly broad singlet at 7.90 (N—H), a triplet at 6.97 (protons at 4), a triplet at 6.09 (protons at 6), and a quintet at 8.40 (protons at 5). The spectrum in $CFCl_3$ at +10° was similar. However, interesting changes were observed when the spectrum in $CFCl_3$ was recorded at reduced temperatures. At −10°, exchange of proton on nitrogen was already sufficiently slow for the 2-protons signal to appear as a *doublet*, separation about 7 Hz. At −30°, the 2-protons signal was a doublet, J = 8.5 Hz, due to CH–NH coupling; for the same reason the 4-protons signal now consisted of *two* triplets (separation of triplets ~8 Hz). The correctness of the explanation was evident from the observation that, at the same temperature, (−30°), the signal for the 6-protons remained a well resolved triplet; clearly, ring inversion was still relatively rapid at −30° and the process which had been slowed was that of proton exchange between nitrogen and other electronegative atoms (the possibility exists that nitrogen inversion had also been slowed at −30°, but this possibility could not be revealed by the n.m.r. methods owing to the bias of the equilibrium **7** ⇄ **8**).

At −50°, with the slowing of ring inversion, all signals were very broad, except, interestingly, the N—H resonance, which was a clearly defined quintet, separations ~8.5 Hz.

At −80°, ring inversion was slow, and a well resolved spectrum was obtained, from which the chemical shifts and coupling constants listed in Tables 1 and 2 were deduced. The signals for H_{2a} and H_{6e} overlapped, but assignments were proved by double irradiation. The protons at position 2 gave an octet (AB part of ABX), analysis of which yielded the following parameters: J_{AB} = 10.1, J_{AX} = 2.9, J_{BX} = 13.1 Hz; H_A at τ 5.62, H_B at 5.93, H_X at 7.5. That the small splittings in the A quartet were due to coupling with the N—H proton was confirmed by decoupling; irradiation at the N—H frequency caused these splittings to disappear. The values of the coupling constants J_{AX} and J_{BX} suggest strongly that conformation **8**, with N—H axial, makes the major or sole contribution to the conformational equilibrium **7** ⇄ **8**.

Tetrahydro-2-methyl-1,3-oxazine (**11** ⇄ **12**) was next studied. The ring inversion process is not important in this instance, since that ring conformation having the methyl equatorial is expected to predominate to the extent of about 95% (see later for evidence from spectra that the 2-methyl group is indeed equatorial). The spectrum of **11** ⇄ **12** at 40° in $CDCl_3$ permitted a

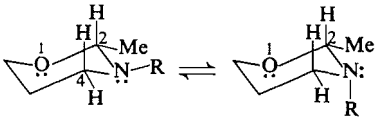

11 R = H **12** R = H
13 R = Me **14** R = Me

first-order interpretation (see Tables 1 and 2). At this temperature, the spectrum gave no evidence for CH–NH coupling, presumably due to rapid exchange of protons on nitrogen. However, at 0° this exchange was already relatively slow, since the signals for H_{2a}, H_{4e}, and H_{4a} were broadened, whilst the remaining signals maintained their sharpness.

At −50°, with very slow exchange, a well resolved spectrum was obtained (see Tables 1 and 2 for full details). In particular, the signal for H_{2a} consisted of *two* 1,3,3,1-quartets, with coupling constants of 12.6 Hz ($J_{2a,NH}$) and 5.8 Hz (J_{2a,CH_3}). It was concluded that the conformation with axial N—H made the major or sole contribution to the equilibrium **11** ⇄ **12**.

Can. J. Chem. Downloaded from www.nrcresearchpress.com by 210.87.254.42 on 09/05/12
For personal use only.

TABLE 1. Chemical shift data for tetrahydro-1,3-oxazines (τ-values)

Entry	Compound	Solvent	Temperature °C	H_{2e}	H_{2a}	H_{4e}	H_{4a}	H_{5e}	H_{5a}	H_{6e}	H_{6a}	N—CH_3	C—CH_3		Other
1	**7⇄ 8**	$CDCl_3$	40	5.60	5.60	6.97	6.97	8.40	8.40	6.09	6.09				
2	**7⇄ 8**	$CFCl_3$	10	5.75	5.75	7.10	7.10	8.50	8.50	6.21	6.21				
3	**7⇄ 8**	$CFCl_3$	−80	5.62	5.93	7.02*	7.20*	8.71	8.30	6.03	6.45				
4	**7⇄ 8**	DMSO-d_6	40	5.90	5.90	7.28	7.28	8.65	8.65	6.36	6.36				
5	**7⇄ 8**	C_6H_6	40	5.70	5.70	7.35	7.35	8.80	8.80	6.35	6.35				
6	**9⇄10**	$CDCl_3$	40	5.90	5.90	7.25	7.25	8.33	8.33	6.26	6.26	7.67			
7	**9⇄10**	$CFCl_3$	10	5.96	5.96	7.29	7.29	8.39	8.39	6.32	6.32	7.69			
8	**9⇄10**	$CFCl_3$	−90	5.82	6.14	7.17*	7.40*	8.79	7.92	6.05	6.57	7.68			
9	**9⇄10**	C_6H_6	40	5.90	5.90	7.75	7.75	8.62	8.62	6.45	6.45	7.85			
10	**11⇄12**	$CDCl_3$	40	—	5.80	6.91	7.12	8.66	8.32	5.95	6.29	—	8.75		
11	**11⇄12**	$CFCl_3$	−50	—	6.08	7.12*	7.33	8.87*	8.55*	6.16	6.51	—	9.00		
12	**13⇄14**	$CDCl_3$	40	—	6.11	7.01	7.35	8.72	7.95	5.97	6.42	7.71	8.74		
13	**13⇄14**	$CFCl_3$	0	—	6.25	7.16	7.45	8.90	8.04	6.12	6.56	7.83	8.89		
14	**13⇄14**	C_6D_6	40	—	6.25	7.30	7.63	9.18	8.35*	6.17	6.68	7.90	8.78		
15	**13⇄14**	CD_3CN	40	—	6.22	7.11	7.45	8.80	8.05*	6.10	6.50	7.80	8.85		
16	**21⇄22**	$CDCl_3$	40	5.83	5.55	—	—	8.80	8.47	—	6.25	7.68	8.87	8.88	8.88†
17	**21⇄22**	$CFCl_3$	0	6.00	5.65	—	—	8.95	8.54	—	6.39	7.73	8.96	8.90	8.96†
18	**21⇄22**	C_6D_6	40	5.86	5.64	—	—	9.11	8.58	—	6.45	7.80	8.91	9.02	9.04†
19	**21⇄22**	CD_3CN	40	5.79	5.65	—	—	8.7*	8.7*	—	6.30	7.75	8.93	8.90	8.92†
20	**17⇄18**	$CDCl_3$	40	5.75	5.75	7.17	7.17	8.35	8.35	6.20	6.20	—	—	6.23‡	
21	**19⇄20**	$CDCl_3$	40	—	5.72	7.09	7.38	8.86	8.02	5.96	6.35	—	8.69	6.16	6.34§

*Approximate.
†4,4-Dimethyl.
‡Benzylic (singlet).
§Benzylic (AB quartet, J = 13.8 Hz).

TABLE 2. Coupling constants for tetrahydro-1,3-oxazines (Hz)

Compound	Solvent	Temperature °C	$J_{2e,2a}$	$J_{4e,4a}$	$J_{5e,5a}$	$J_{6e,6a}$	$J_{2a,3a}$	$J_{4a,5a}$	$J_{5a,6a}$	$J_{2e,3a}$	$J_{4a,5e}$	$J_{4e,5a}$	$J_{5a,6e}$	$J_{5e,6a}$	$J_{4e,5e}$	$J_{5e,6e}$	$J_{4e,6e}$
7⇄ 8	$CFCl_3$	−80	10.1	—	12.5	—	13.1	—	—	2.9	—	—	—	—	—	—	—
9⇄10	$CFCl_3$	−90	9.5	—	13	11.5	—	—	—	—	—	—	—	—	—	—	—
11⇄12	$CDCl_3$	+40	—	14	—	11.5	—	11.2	12	—	3.5	5.2	4.8	2.8	2.1	1.8	1.8
11⇄12	$CFCl_3$	−50	—	—	—	—	12.6	—	—	—	3	—	—	2.5	—	—	—
13⇄14	$CDCl_3$	+40	—	12.3	13.8	11.5	—	12.2	11.8	—	3.2	4.6	5.0	2.7	2.2	1.8	1.8
13⇄14	$CFCl_3$	0	—	12.5	—	11.0	—	12.1	12.5	—	3	4.9	5	2.7	1.8	1.8	1.8
21⇄22	$CDCl_3$	+40	9.7	—	13	—	—	—	11	—	—	—	—	3.3	—	—	—
21⇄22	C_6D_6	+40	9.8	—	13	—	—	—	11.5	—	—	—	—	2.5	—	—	—
19⇄20	$CDCl_3$	+40	—	13	13.5	11.2	—	12	11.2	—	3	4	5.2	2.8	2.2	1.8	1.8

Can. J. Chem. Downloaded from www.nrcresearchpress.com by 210.87.254.42 on 09/05/12
For personal use only.

1-Methyl-1,3-diazane (**15** ⇄ **16**), readily prepared from *N*-methyl-1,3-diaminopropane and formaldehyde, is a molecule which, at room temperature, is expected to undergo rapid ring inversion in addition to rapid nitrogen inversion about both nitrogen atoms. However, it was of interest to discover whether spectra recorded at low temperatures would reveal the preferential orientation of the N—H bond.

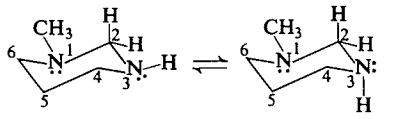

15 **16**

The following data were observed in the spectrum of **15** ⇄ **16** measured at room temperature in $CDCl_3$; a singlet at τ 6.70 (protons at 2), a multiplet at 7.22 (protons at 4), a multiplet at 7.46 (protons at 6), a multiplet at 8.50 (protons at 5), and a singlet at 7.85 (*N*-CH_3). The N–H resonance at τ 8.05 was relatively sharp. With $CFCl_3$ as solvent, and at reduced temperatures, broadening of signals commenced at about −5°, and at −70° ring inversion was slow. The protons at position-2 gave a doublet (H_{2e}), each component showing broadening due to a further coupling, and a quartet (H_{2a}) (AM portion of AMX system). Analysis gave the following parameters: $J_{2a,2e} = 11.3$, $J_{2a,NH} = 13.0$, $J_{2e,NH} \leqslant 3$ Hz; H_{2e} at τ 6.58, H_{2a} at 7.50. The *N*-H signal was not seen clearly. However, irradiation of H_{2e} caused the quartet for H_{2a} to collapse to a doublet, $J \sim 13$ Hz, thus confirming the assignments.

It is clear from the coupling constants obtained that the preferred conformation of 1-methyl-1,3-diazane (**15** ⇄ **16**) is conformation **16**, with the N—H bond in the axial orientation.

Attempts to extend the technique to the determination of the preferred orientation of the N—H bond in piperidine and morpholine were not successful. Thus, no evidence was obtained for CH–NH coupling from the spectrum of piperidine, recorded at temperatures down to −100° ($CFCl_3$), and from the spectrum of morpholine, recorded at temperatures down to −115° (CF_2Cl_2).

It is remarkable that a technique which enabled the $J_{2a,NH}$ coupling to be measured for **7** ⇄ **8** at −80°, failed to reveal this information for either piperidine (−100°) or morpholine (−115°). Only −50° was required for **11** ⇄ **12**. Likely, the relatively slow proton exchange for compounds **7**, **11**, and **15** is due to the presence of highly electronegative geminal heteroatom which reduces the basicity of the NH group and thereby inhibits proton exchange as is found for amides. According to Wolfe and co-workers (17) "Electron pair – electron pair, electron pair – polar bond or polar bond – polar bond interactions cause a significant increase in rotation–inversion barriers of atoms bearing these substituents." It is interesting to note in this regard that ring inversion was slow at −50° for compound **7** and that signal broadening commenced at about −5° for 1-methyl-1,3-diazane.

It is concluded that the equilibria **7** ⇄ **8**, **11** ⇄ **12**, and **15** ⇄ **16** are predominantly toward the conformation with N—H in axial orientation at the temperature where the CH–NH coupling could be observed. However, no information on the temperature effects on these equilibria was obtained. In view of the nature of the anomeric effect, it seems likely that these conformations also prevail at room temperature. It is possible that presumably quite polar N—H bonds in these compounds have established a substantial bond, akin to a hydrogen bond, through electrostatic attraction with the *syn*-axial lone-pair electrons as depicted below. Such an *added* driving force for maintaining the N—H axial

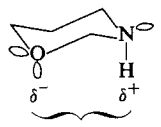

Attractive

orientation seems needed, should, as expected from the magnitudes of the CH–NH coupling constants, the compounds exist virtually entirely in the one conformation. Further information on these matters promises to be of importance in relation to solvation effects on the anomeric equilibria of sugars and on the orientation of axial aglycons of glycopyranosides (35).

It was considered of interest to examine further the conformational properties of tetrahydro-3-methyl-1,3-oxazine (**9** ⇄ **10**) in order to gain further insight into the generalized anomeric effect.

Riddell and Lehn (19), using chemical shift differences $\tau_{2e} - \tau_{2a}$, and the geminal coupling constant $J_{2e,2a}$, in comparison with those of conformationally rigid standards, deduced that the percentage of conformation **10** (axial N—CH_3)

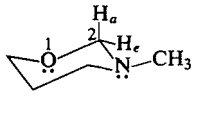

9

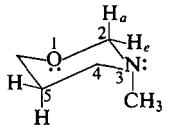

10

was 60 ± 10 (shifts) or 45 ± 10 (coupling constants). Allingham *et al.* (20) measured geminal coupling constants for ring protons in a series of 5-methyl-5-nitrotetrahydro-1,3-oxazines substituted on nitrogen by alkyl groups. The figures were interpreted in terms of a preference for *N*-alkyl *axial* when the alkyl substituent was methyl, ethyl, or propyl, and a preference for *N*-alkyl *equatorial* when the substituent was isopropyl, cyclohexyl, or *t*-butyl.

The determination of the position of equilibrium **9** ⇄ **10** by the application of nuclear Overhauser effects (n.O.e.) appeared promising. This effect, which has found increasing application to stereochemical problems during the past few years (36–53), involves saturation of the signal due to a nucleus H_A, whilst a second nucleus H_K is observed, usually by integration. If H_K lies close to H_A, then an enhancement of up to 30% (theoretical maximum 50%) may be observed in the intensity of the signal for H_K. Enhancements are not usually observed if H_A and H_K are separated by more than 3 Å, but become measurable at distances 2.5 to 3 Å. Distances of only 1.8 to 2.5 Å may lead to enhancements of up to 30%.

The experimental conditions necessary for the success of a nuclear Overhauser experiment have been clearly described (36, 48, 52). We carried out our experiments without degassing the sample, having obtained satisfactory enhancements (15%) on a control sample of dimethylformamide which had not been degassed. All experiments mentioned in the literature have employed instrumental integration to measure signal intensities. We obtained inconsistent results by this method. We attributed this to the fact that we were generally integrating signals covering 25 to 40 Hz, and phase alteration during the frequency sweep caused poor reproducibility of the integral. This difficulty was overcome by measurement of signal areas using a planimeter (see Experimental).

In the case of tetrahydro-3-methyl-1,3-oxazine (**9** ⇄ **10**), studied at temperatures low enough to cause a slowing of ring-inversion, the proximity of the axial N—CH_3 and H_{5a} in **10** should allow observation of a n.O.e. Since no effect will occur in conformation **9**, where the N—CH_3 bond is equatorial, the *magnitude* of n.O.e. experiments can be carried to the proportion of **10** in the mixture, *provided* an assessment can be made, from a model compound with the characteristics of **10**, of the expected n.O.e. for the isolated conformation **10**. As far as we are aware, n.O.e. effects have not been applied to rapidly interconverting mixtures of conformers such as **9** ⇄ **10**, presumably due to the difficulty of placing measurements on a quantitative basis.

Unfortunately, a n.O.e. study of **9** ⇄ **10** at −90° was frustrated by the closeness in shift of *N*-CH_3 and H_{5a} signals (see Table 1). An attempt to study the enhancement of the H_{5a} signal, on irradiation of the benzylic proton signal in the spectrum of 3-benzyltetrahydro-2-methyl-1,3-oxazine **19** ⇄ **20** also failed, because the benzylic proton resonance was an AB quartet ($J \sim 14$ Hz) needing a high power of irradiation to cause saturation.

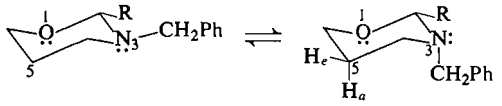

17 R = H **18** R = H
19 R = Me **20** R = Me

Finally, tetrahydro-3,4,4,6-tetramethyl-1,3-oxazine **21** ⇄ **22** was selected, as possessing features of advantage for an n.O.e. study. Thus the *N*-CH_3 signal (τ 7.80, benzene) and the H_{5a} signal (τ 8.58) are now well shifted, as a result of replacement of two adjacent equatorial hydrogens by methyl groups (54). Moreover, in both

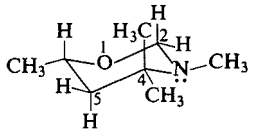

21

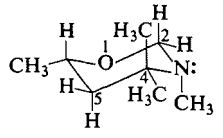

22

conformations **21** ⇄ **22**, the axial methyl group at position-4 is in a 1,3-diaxial relationship to the axial hydrogen at position-2. Therefore, the magnitude of a nuclear Overhauser enhancement for H_{2a} on irradiation of the axial CH_3 at position-4 is a convenient standard on which to base any quantitative treatment of the enhancement observed for H_{5a} on irradiation of the *N*-CH_3.

Can. J. Chem. Downloaded from www.nrcresearchpress.com by 210.87.254.42 on 09/05/12
For personal use only.

Can. J. Chem. Downloaded from www.nrcresearchpress.com by 210.87.254.42 on 09/05/12
For personal use only.

Indeed, measurements on Dreiding models gave the distance between H_{2a} and the closest hydrogen of the axial CH_3 at position-4 as almost the same as that between H_{5a} and the closest hydrogen of the *N*-CH_3 (1.95 to 2.00 Å, staggered conformations assumed). Therefore, it might be expected that the enhancement observed for H_{2a} (on saturation of the signal for axial CH_3 at position-4) would be the same as that observed for H_{5a} (on saturation of the *N*-CH_3 signal) in **22**, if the compound possessed this conformation only. However, even this is unlikely since nuclear Overhauser enhancements are proportional to the sixth power of the separation between the nuclei involved (55) and therefore highly sensitive to small differences in molecular dimensions. Furthermore, since relaxation of H_{5a} (for example) may occur by protons other than those of the N—Me group, it is clear that a quantitative treatment is not feasible.

The results obtained from nuclear Overhauser experiments on **21** ⇄ **22** are listed in Table 3. In view of the limitations mentioned above, the only conclusion possible is the qualitative one that the contribution made by conformation **22** in which the *N*-CH_3 group is in axial orientation is appreciable and may dominate. These results are equivalent to those of Riddell and Lehn (19) in that the evidence does not necessarily require a large preponderance of the conformer **10** which has the *N*-CH_3 group in axial orientation. Nevertheless, the indication is clear that the anomeric effect, as expected and whatever its origins, may well have an influence on these conformational equilibria.

In trifluoroacetic acid as solvent, the salts of *N*-alkyl tetrahydro-1,3-oxazines **27**, **28**, **30**, and **33** exist in the conformation which has the *N*-H in axial orientation as expected in view of the conformational preference of tetrahydro-1,3-oxazine. The reverse anomeric effect (56) is expected to strongly influence the conformational preferences of these salts, especially the quaternary salts **31**, **32**, and **34**.

TABLE 3. The n.O.e. results on **21** ⇄ **22**

Signal saturated	Signal observed	Increase in area (%)
CH_3 (4-axial)	H_{2e}	2.0
CH_3 (4-axial)	H_{2a}	8.8
N-CH_3	H_{5a}	6.0

The recorded values of the vicinal axial–axial coupling $J_{2a,\overset{+}{N}H}$ ($J_{2a,3a}$ of Table 5) lie in the range 7.5 to 9.6 Hz, in agreement with reported figures (19); these values are considerably less than the values of $J_{2a,\overset{+}{N}H}$ ($J_{2a,3a}$ of Table 2) in the free bases.

The spectrum of **30** in CF_3CO_2H was clearly that of a single conformation, and the value of 7.5 Hz for $J_{2a,\overset{+}{N}H}$ shows that this conformation possesses both methyl substituents in equatorial orientation. However, the spectrum in $CDCl_3$ indicated the presence of two species which are geometrical isomers, differing, most probably, only in the orientation of the $\overset{+}{N}—CH_3$ substituent. For one isomer, the 2-proton appeared as two 1,3,3,1-quartets, separated by 7.8 Hz ($J_{2a,\overset{+}{N}H}$); for the second isomer, the 2-proton appeared as two 1,3,3,1-quartets, separated by only 1.2 Hz ($J_{2a,\overset{+}{N}H}$). When spectra in $CDCl_3$ were recorded at different concentrations, there was not only a marked variation in chemical shifts, but also in the relative proportions of the two isomers. Similar observations have been made by Japanese workers (57) in the case of *cis*-1,2,6-trimethylpiperidine hydrochloride dissolved in organic solvents.

Finally, the fact that the geminal coupling constant $J_{5e,5a}$ is numerically larger than $J_{2e,2a}$, $J_{4e,4a}$, or $J_{6e,6a}$ is in agreement with theory (58) and with some previous observations (59).

The preparation of tetrahydro-3,4,4,6-tetramethyl-1,3-oxazine involved some points of interest. The reaction of mesityl oxide and methylamine was carried out by the published method (60), and was found to give mostly 4-methyl-4-methylaminopentan-2-one (**23**), contaminated with the derived *N*-methylimine **24**. Reduction

$CH_3—\underset{\underset{O}{\|}}{C}—CH_2—C(CH_3)_2—NH—CH_3$

23

$CH_3\ \ \underset{\underset{\overset{+}{N}—CH_3}{\|}}{C}—CH_2—C(CH_3)_2—NHCH_3$

24

of the crude product with sodium borohydride, or catalytically over PtO_2, gave the expected mixture of aminoalcohol and diamine, which were separable as hydrochlorides. The mixture was converted by aqueous formaldehyde to the required tetrahydro-1,3-oxazine **21** ⇄ **22**, contaminated with 1,3,4,4,6-pentamethyl-1,3-di-

Can. J. Chem. Downloaded from www.nrcresearchpress.com by 210.87.254.42 on 09/05/12
For personal use only.

TABLE 4. Chemical shift data for tetrahydro-1,3-oxazine salts (τ-values, 40°)

Compound	X	Solvent	H_{2e}	H_{2a}	H_{4e}	H_{4a}	H_{5e}	H_{5a}	H_{6e}	H_{6a}	$\overset{+}{N}CH_3(e)$	$\overset{+}{N}CH_3(a)$	C—CH_3	$\overset{+}{N}H$	Other	
26	Br	$CDCl_3$	5.03	5.03	6.42	6.42	7.85	7.85	6.02	6.02	—	—	—	0.92	—	—
26	Br	CF_3CO_2H	4.93	4.93	6.30	6.30	7.80	7.80	5.87	5.87	—	—	—	2–3.5	—	—
27	CF_3CO_2	CF_3CO_2H	4.85	5.48	6.16*	6.62	7.97	7.65	5.80	6.08	7.06†	—	—	—	—	—
28	CF_3CO_2	CF_3CO_2H	4.86	5.52	6.2*	6.8*	8.06	7.76	5.86	6.16	6.76‡	—	8.62	—	—	—
28	Br	CH_3CN	5.10	5.60	6.42	6.90	—	—	5.97	6.22	6.93‡	—	8.65	−0.7	—	—
29	Cl	CF_3CO_2H	—	5.14	6.21*	6.46*	8.11	7.70	5.69	6.07	—	—	8.34§	—	—	—
30	Cl	CF_3CO_2H	—	5.41	6.19	6.63	8.05	7.63	5.71	6.11	7.06†	—	8.29‖	—	—	—
33	Cl	CF_3CO_2H	5.00	5.29	—	—	8.0*	8.0*	—	5.76	7.17†	—	8.63§	—	8.39	8.43¶
31	I	CH_3CN	5.2	5.2	6.35	6.35	—	—	6.00	6.00	6.87	6.87	—	—	—	—
31	I	CF_3CO_2H	5.1	5.1	6.23	6.23	7.80	7.80	5.82	5.82	6.73	6.73	—	—	—	—
32	I	CD_3CN	—	4.95	6.25*	6.25*	8.25	7.74	5.92*	6.06*	6.95	7.03	8.6*	—	—	—
32	I	CF_3CO_2H	—	5.10	—	—	8.08	7.56	5.68	6.00	6.88	6.92	8.42‖	—	—	—
32	I	$CDCl_3$	—	4.47	—	—	8.11	7.7*	—	—	6.56	6.82	8.48†	—	—	—
34	I	DMSO-d_6	5.27	4.97	—	—	8.23	7.97	—	5.88	7.17	6.95	8.82§	—	8.46	8.65¶

*Approximate.
†Doublet, J = 5.5 Hz.
‡$\overset{+}{N}CH_2$.
§Doublet, J = 6.0 Hz.
‖Doublet, J = 5.7 Hz.
¶$C(CH_3)_2$.

TABLE 5. Coupling constants for tetrahydro-1,3-oxazine salts (Hz)

Compound	X	Solvent	$J_{2e,2a}$	$J_{4e,4a}$	$J_{5e,5a}$	$J_{6e,6a}$	$J_{2a,3a}$	$J_{4a,5a}$	$J_{5a,6a}$	$J_{2e,3a}$	$J_{4a,5e}$	$J_{4e,5a}$	$J_{5a,6e}$	$J_{5e,6a}$	$J_{4e,5e}$	$J_{5e,6e}$	Other
27	Br	CF_3CO_2H	9.0	—	15.0	12.0	7.7	—	10.5	⩽2	4.2	—	—	3.4	—	—	—
28	Br	CF_3CO_2H	9.2	—	—	—	8.0	—	—	⩽2	—	—	—	—	—	—	1.7*
28	Br	CH_3CN	9.1	11.5	—	11.5	7.5	11.0	9.3	—	3.5	—	4.0	3.5	—	4.0	3.6†, 6.5‡
29	Cl	CF_3CO_2H	9.3	—	—	12.0	—	—	—	—	—	—	5.0	2.7	—	—	<0.5§
30	Cl	CF_3CO_2H	—	—	15.0	12.0	7.5	—	12.0	—	—	—	5.0	2.6	—	—	—
33	Cl	CF_3CO_2H	9.4	—	—	—	9.6	—	—	2.5	—	—	—	—	—	—	—
32	I	CF_3CO_2H	—	—	14.5	12.0	—	—	12.3	—	—	—	5.2	3.0	—	—	—
34	I	DMSO-d_6	9.3	—	15.0	—	—	—	9.9	—	—	—	—	4.3	—	—	—

*$J_{2e,4e}$.
†$J_{2e,3a} + J_{2e,4e}$.
‡J_{4aNH}.
§$J_{2a,3e}$.

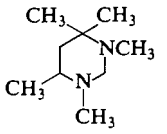

25

azane **25**. The two bases were easily separable as the hydrochlorides.

Tables 1 and 2 contain, respectively, chemical shift and coupling constant data for the tetrahydro-1,3-oxazines prepared during this work. The corresponding data for tetrahydro-1,3-oxazine salts **26–30**, **33**, and quaternary salts **31**, **32**, **34** are given in Tables 4 (shifts) and 5 (coupling constants). Spectral data for some *N*-alkyl

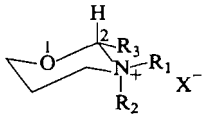

26 $R_1 = R_2 = R_3 = H$
27 $R_1 = CH_3$; $R_2 = R_3 = H$
28 $R_1 = CH_2CH_3$; $R_2 = R_3 = H$
29 $R_3 = CH_3$; $R_1 = R_2 = H$
30 $R_1 = R_3 = CH_3$; $R_2 = H$
31 $R_1 = R_2 = CH_3$; $R_3 = H$
32 $R_1 = R_2 = R_3 = CH_3$

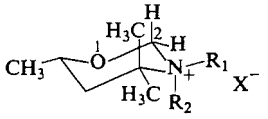

33 $R_1 = CH_3$; $R_2 = H$
34 $R_1 = R_2 = CH_3$

tetrahydro-1,3-oxazines and salts have previously been contributed by Gurne *et al.* (61), by Riddell *et al.* (19, 33), and by Allingham *et al.* (20). In general, our figures are in broad agreement with previous data.

Most spectra were obtained at both 60 and 100 MHz; the 100 MHz spectra were first order, or nearly first order, and chemical shifts were obtained directly, except for the ABX patterns mentioned below. Coupling constants were generally obtained by direct measurement and are, therefore, accurate to about ± 0.2 Hz. The following, obtained by ABX analyses, are accurate to ± 0.1 Hz:

$J_{2e,2a}$ $J_{2e,2a}$ $J_{2a,3a}$ in **7** ⇄ **8**

$J_{2e,2a}$ $J_{2e,3a}$ $J_{2a,3a}$ in **33**

$J_{5e,5a}$ $J_{5e,6a}$ $J_{5a,6a}$ in **34**

For all compounds examined, H_{5a} occurs at *lower* field than H_{5e}. A similar situation holds for the 5-position of 1,3-dioxans (62) and the 3-position of morpholines (63) and has been associated particularly with the presence of an oxygen atom in a 1,3-relationship to the carbon atom holding the protons (63, 64).

The proof that the 2-methyl substituent has the equatorial orientation in **11** ⇄ **12** and **13** ⇄ **14** rests on the observation that the chemical shifts of the 6-axial proton in **11** ⇄ **12** (entry 11, Table 1) and **13** ⇄ **14** (entry 13) are almost identical with the shifts of H_{6a} in **7** ⇄ **8** (entry 3) and **9** ⇄ **10** (entry 8). An axial methyl group would have caused a noticeable deshielding of the H_{6a} signal (54). A similar argument establishes the equatorial orientation of the 2-methyl group in tetrahydro-2,3-dimethyl-1,3-oxazine methiodide (**32**). Thus, the mean (τ 5.84) of the chemical shifts of H_{6e} and H_{6a} in **32** is almost identical to the chemical shift (τ 5.82) of the 6-protons in the spectrum of the rapidly inverting tetrahydro-3-methyl-1,3-oxazine methiodide (**31**).

The assignment of signals to H_{2a} and H_{2e} in **7** ⇄ **8**, **27**, **28**, and **33** is trustworthy, requiring only the usual assumption that $J_{a,a} > J_{e,a}$. On the other hand, it is likely, but not certain, that a correct assignment of signals to H_{2e} and H_{2a} in tetrahydro-3-methyl-1,3-oxazine **9** ⇄ **10** (entry 8) has been made (*cf.* ref. 19). In the tetramethyl compound **21** ⇄ **22**, the H_{2e} and H_{2a} protons give an AB quartet in the spectrum. The low field half of the quartet is due to H_{2a}, rather than H_{2e}, a result of one of the n.O.e. experiments described earlier. Interestingly, the lines of the high field doublet, due to H_{2e}, were significantly broader than those due to H_{2a}. That this was due to 5-bond coupling with the protons of one or both methyl groups at position-4 was demonstrated by double irradiation. It was not possible to irradiate separately the equatorial and axial 4-methyl signals, but stereochemical considerations (*cf.* ref. 59) suggest that the protons of the equatorial methyl group are responsible for this long-range coupling.

In the spectrum of **34**, it was possible to assign the *N*-methyl signals by decoupling experiments, with the usual assumption that a planar zig-zag arrangement of atoms produces an appreciable 4-bond coupling. Thus, irradiation of the low-field *N*-methyl signal (τ 6.95) caused the lines of the doublet at τ 4.97, due to *one* of the protons

Can. J. Chem. Downloaded from www.nrcresearchpress.com by 210.87.254.42 on 09/05/12
For personal use only.

Can. J. Chem. Downloaded from www.nrcresearchpress.com by 210.87.254.42 on 09/05/12
For personal use only.

at position-2, to be sharpened, the lines of the doublet at τ 5.27, due to the other proton at position-2 being affected only slightly. On the other hand, irradiation of the *N*-methyl signal at τ 7.17 produced no effect on the doublet at τ 4.97 and only a slight sharpening of the doublet at τ 5.27. It was concluded that the signal at τ 6.95 was due to the axial *N*-methyl group, and that the doublet at τ 4.97 (*J* 9.3 Hz) was due to the axial proton H_{2a}. However, a similar decoupling experiment, designed to confirm the assignment of *N*-methyl signals in the spectrum of **32**, was unsuccessful.

Experimental

Melting points were determined in capillary tubes. The n.m.r. spectra were recorded on Varian A60, A56/60, HA-100, and HA-100-15 spectrometers. Variable temperature n.m.r. measurements were recorded on Varian A56/60 and HA-100-15 spectrometers.

Tetrahydro-1,3-oxazine

Tetrahydro-1,3-oxazine, prepared by literature methods (32, 33), had b.p. 120–121° at 700 mm. The derived picrate, prepared in benzene and crystallized from methanol, had m.p. 138–139°.

Anal. Calcd. for $C_{10}H_{12}N_4O_8$: C, 37.98; H, 3.83; N, 17.72. Found: C, 37.8; H, 3.8; N, 17.4.

The hydrobromide, prepared in dry ether and crystallized from dry acetone, was extremely hygroscopic.

3-Ethyltetrahydro-1,3-oxazine

Tetrahydro-1,3-oxazine (9.5 g) was dissolved in benzene (20 ml) containing pellets of sodium hydroxide (4.5 g). Ethyl iodide (17 g) was added to the mixture, and the whole was warmed on the steam bath for 2 h. The benzene layer was decanted from solid material and dried (KOH). Distillation gave benzene and crude 3-ethyltetrahydro-1,3-oxazine (1.5 g, 12%), b.p. (bath temperature) 115–116° at 695 mm. The picrate, prepared in benzene and crystallized from methanol, had m.p. 190–192° but a satisfactory analysis could not be obtained.

Anal. Calcd. for $C_{12}H_{16}N_4O_8$: C, 41.86; H, 4.68; N, 16.28. Found: C, 43.13, 43.48; H, 5.11, 5.23; N, 15.31.

The hydrobromide, prepared in dry benzene and recrystallized from dry acetone, was hygroscopic. The n.m.r. spectra of free base and hydrochloride were satisfactory.

Tetrahydro-2-methyl-1,3-oxazine

(*i*) A solution of 3-aminopropan-1-ol (50 g) in benzene (100 ml) was distilled in a Dean–Starck apparatus until no more water was evolved. The mixture was cooled in iced water and acetaldehyde (32 g) was added, with stirring, during 50 min. The mixture was finally heated for 12 h, water (12 ml) being collected. Distillation of the residue gave benzene and crude tetrahydro-2-methyl-1,3-oxazine, b.p. 100–105° at 690 mm (15 g, 22%).

(*ii*) To a solution of 3-aminopropan-1-ol (7.5 g) in water (5 ml) was added, during 20 min, an ice cold mixture of acetaldehyde (6.5 ml) and water (5 ml). The solution was allowed to remain at room temperature for 60 min, and was then saturated with pellets of potassium hydroxide. The upper organic layer was removed, dried (KOH), and distilled, giving tetrahydro-2-methyl-1,3-oxazine, b.p. 100–105° at 700 mm (5.4 g, 53%).

Tetrahydro-2-methyl-1,3-oxazine hydrochloride, prepared in benzene and crystallized from acetone–methanol, had m.p. 133–135°.

Anal. Calcd. for $C_5H_{12}NOCl$: C, 44.0; H, 8.8; N, 10.2. Found: C, 43.7; H, 9.0; N, 10.1.

Tetrahydro-2,3-dimethyl-1,3-oxazine

To a mixture of 3-methylaminopropan-1-ol(33) (3.5 g) and water (5 ml) was added a solution of acetaldehyde (2.5 ml) in water (5 ml) during 20 min with cooling in ice. The mixture was allowed to remain at room temperature for 60 min, and then saturated with pellets of potassium hydroxide, when the product separated as an upper layer. The layer was removed, dried (KOH), and distilled, giving tetrahydro-2,3-dimethyl-1,3-oxazine as a colorless liquid, b.p. 97° at 700 mm (3.3 g, 73%).

The methiodide was produced rapidly from methyl iodide and a solution of the base in dry acetone at 30°. Recrystallization of the solid from acetone–methanol gave tetrahydro-2,3-dimethyl-1,3-oxazine methiodide, m.p. 223.5–224° (dec.).

Anal. Calcd. for $C_7H_{16}NIO$: C, 32.7; H, 6.3; N, 5.5. Found: C, 32.3; H, 6.2; N, 5.8.

3-Benzyltetrahydro-1,3-oxazine

To 3-benzylaminopropan-1-ol (4.12 g) in water (15 ml) was added, during 15 min, aqueous formaldehyde (2.5 ml, 37%). A white oil was precipitated. The mixture was allowed to remain at room temperature for 15 min and then extracted several times with ether. The combined ethereal extracts were dried (KOH) and distilled, giving 3-benzyltetrahydro-1,3-oxazine as a colorless liquid, b.p. 128° at 35 mm (4.0 g, 90%).

Anal. Calcd. for $C_{11}H_{15}NO$: C, 74.5; H, 8.5; N, 7.9. Found: C, 74.2; H, 8.5; N, 8.1.

3-Benzyltetrahydro-2-methyl-1,3-oxazine

The method was similar to that in the preceding experiment.

From 3-benzylaminopropan-1-ol (4.1 g) and acetaldehyde (1.5 g) was obtained 3-benzyltetrahydro-2-methyl-1,3-oxazine as a colorless liquid, b.p. 126° at 37 mm (4.0 g, 85%).

Anal. Calcd. for $C_{12}H_{17}NO$: C, 75.4; H, 9.0. Found: C, 74.9; H, 9.0.

4-Methyl-4-methylaminopentan-2-one (60)

Using the published method, freshly distilled mesityl oxide (19.6 g) was reacted with aqueous methylamine (25 ml, 33%). After the reaction, the mixture (mixture *A*) was allowed to remain at room temperature for 30 min, and then treated with anhydrous potassium carbonate (18 g). Extraction with ether, and distillation of the dried ($MgSO_4$) extracts gave 4-methyl-4-methylaminopentan-2-one, contaminated with 4-methyl-4-methylaminopentan-2-one *N*-methylimine, b.p. 59–61° at 20 mm (17.4 g).

Treatment of the crude ketone with picric acid in methanol, followed by crystallization of the product from

Can. J. Chem. Downloaded from www.nrcresearchpress.com by 210.87.254.42 on 09/05/12
For personal use only.

methanol, gave 4-methyl-4-methylaminopentanone-2-picrate, m.p. 150–153°.

Anal. Calcd. for $C_{13}H_{18}N_4O_8$: C, 43.6; H, 5.03; N, 15.64. Found: C, 43.5; H, 5.4; N, 15.6.

4-Methyl-4-methylaminopentanol-2 hydrochloride

(*i*) To mixture *A*, obtained as described in the preceding experiment, was added, with stirring, a solution of sodium borohydride (12 g) in water (50 ml). The temperature of the mixture rose initially to 50°, but was later maintained at 30° by external cooling. Finally, the solution was stirred at room temperature for 3 h, cooled in ice, and treated slowly with hydrochloric acid (80 ml, 18%). After 16 h, the solution was extracted with ether (2 × 100 ml), the ether extracts being discarded. The aqueous portion was evaporated under reduced pressure to a small volume, and then saturated with potassium hydroxide. The upper layer was extracted into ether, the ether extracts dried (KOH) and distilled, giving 4-methyl-4-methylaminopentan-2-ol, contaminated with 4-methyl-2,4-di(methylamino)pentane, b.p. 73–74° at 20 mm (18 g). This mixture (11.0 g) was dissolved in dry ether (200 ml) and treated with dry hydrogen chloride, with external cooling. The precipitated oil was separated by decantation and triturated with dry acetone containing 2% methanol. A solid (solid *B*, see below) was removed by filtration and evaporation of the filtrate to dryness gave 4-methyl-4-methylaminopentan-2-ol hydrochloride as a thick uncrystallizable oil (6.0 g). The n.m.r. spectrum proved the absence of the diamine.

(*ii*) To mixture *A* (see above) was added, with ice cooling, glacial acetic acid (40 ml). The solution was hydrogenated over platinum oxide (2.4 g) until the uptake of hydrogen ceased (72 h). The mixture was filtered, treated with hydrochloric acid (20 ml, 25%) and evaporated to dryness under reduced pressure. The mixture of hydrochlorides thus obtained was separated as described in section (*i*).

4-Methyl-2,4-di(methylamino)pentane Dihydrochloride

Solid *B*, from the previous experiment, was washed with dry acetone and crystallized from acetone–methanol, giving 4-methyl-2,4-di(methylamino)pentane dihydrochloride, m.p. 195–198° (1.08 g).

Anal. Calcd. for $C_8H_{22}N_2Cl_2$: C, 44.2; H, 10.2; N, 12.9. Found: C, 44.4; H, 10.3; N, 12.8.

Tetrahydro-3,4,4,6-tetramethyl-1,3-oxazine

4-Methyl-4-methylaminopentanol-2 hydrochloride (6.0 g) was dissolved in water (5 ml) and the solution was treated first with 40% potassium hydroxide (5 ml) and then with solid potassium hydroxide. The upper organic layer was separated and dissolved in water (5 ml). To the solution was added aqueous formaldehyde (3.5 ml, 37%) during 10 min. The mixture was allowed to remain at room temperature for 45 min and then saturated with potassium hydroxide. The organic phase was separated, dried (KOH), and distilled, giving tetrahydro-3,4,4,6-tetramethyl-1,3-oxazine (3.0 g), b.p. 105–110° at 704 mm. The derived hydrochloride crystallized from acetone, had m.p. 144–147°. The methiodide, prepared in acetone and crystallized from acetone – 2% methanol, had m.p. 252–253° (dec.).

Anal. Calcd. for $C_9H_{20}NI$: C, 37.9; H, 7.1; N, 4.9. Found: C, 37.8; H, 6.9; N, 5.1.

1,3,4,4,6-Pentamethyl-1,3-diazane Dihydrochloride

The mixture (6.5 g) of 4-methyl-4-methylaminopentan-2-ol and 4-methyl-2,4-di(methylamino)pentane, prepared as described above, was dissolved in water (5 ml) and to the solution, cooled in ice, was added aqueous formaldehyde (4.1 ml, 37%) during 20 min. The mixture was allowed to remain at room temperature for 60 min and then saturated with potassium hydroxide. The upper layer was separated, dried (KOH), and distilled, giving (*a*) a fraction, b.p. 100–121° at 700 mm (1.0 g), consisting of methanol and tetrahydro-3,4,4,6-tetramethyl-1,3-oxazine and (*b*) a fraction, b.p. 122–130°, consisting of tetrahydro-3,4,4,6-tetramethyl-1,3-oxazine and 1,3,4,4,6-pentamethyl-1,3-diazine. Fraction (*b*), dissolved in ether and treated with dry hydrogen chloride, gave a sticky precipitate which was separated from ether by decantation and crystallized from acetone–methanol. 1,3,4,4,6-Pentamethyl-1,3-diazane dihydrochloride (0.75 g) had m.p. 183–184° (dec.).

Anal. Calcd. for $C_9H_{22}N_2Cl_2$: C, 47.2; H, 9.7; N, 12.2. Found: C, 47.5; H, 9.8; N, 11.9.

1-Methyl-1,3-diazane

Using the method of Riddell (65), *N*-methyl-1,3-propanediamine (4.4 g) and formaldehyde (5.1 ml, 40% aqueous solution) yielded 1-methyl-1,3-diazane (4.0 g, 80%), b.p. (bath temperature) 150° at 705 mm. The derived dipicrate, crystallized from methanol, had m.p. 210–214°.

Anal. Calcd. for $C_{17}H_{18}N_8O_{14}$: C, 36.6; H, 3.3; N, 20.1. Found: C, 36.3; H, 3.6; N, 20.1.

Nuclear Overhauser Experiments

Nuclear Overhauser experiments were performed using a Varian HA-100-15 spectrometer. Samples were not specially prepared and were not degassed. The power of irradiation causing saturation was varied within the range 50 to 200 mV, but in all cases the optimum power level was at about 100 mV. Instrumental integration of the signals affected did not give reproducible results. Therefore, relatively large samples (20–40 mg) were employed, affected signals were amplified and expanded to a sweep width of 100 Hz, and areas were obtained by using a planimeter. A number of scans were made to check the reproducibility, both of "blank" spectra (irradiation in a signal-free region) and of spectra recorded with nuclear Overhauser enhancements. Area measurement figures were reproduced to better than 2%.

The authors are grateful to Glen Bigam, David Gifford, and Peter Bohlmann for helpful discussion, and considerable technical assistance during experiments involving n.m.r. measurements.

1. F. G. RIDDELL. Quart. Rev. **21**, 364 (1967).
2. T. MASAMUNE and M. TAKASUGI. Chem. Commun. 625 (1967); T. MASAMUNE. Chem. Commun. 244 (1968); T. MASAMUNE, M. TAKASUGI, and M. MATSUKI. Bull. Chem. Soc. Jap. **41**, 2466 (1968).
3. J. B. LAMBERT, R. G. KESKE, R. E. CARHART, and A. P. JAVANOVITCH. J. Amer. Chem. Soc. **89**, 3761 (1967); J. B. LAMBERT and R. G. KESKE. J. Amer. Chem. Soc. **88**, 620 (1966); J. B. LAMBERT, D. S. BAILEY and B. F. MICHEL. Tetrahedron Lett. 691 (1970).

Can. J. Chem. Downloaded from www.nrcresearchpress.com by 210.87.254.42 on 09/05/12
For personal use only.

4. M. J. T. ROBINSON. Tetrahedron Lett. 1153 (1968).
5. R. W. BALDOCK and A. R. KATRITZKY. Tetrahedron Lett. 1159 (1968); J. Chem. Soc. (B), 1470 (1968).
6. R. A. Y. JONES, A. R. KATRITZKY, A. C. RICHARDS, and R. J. WYATT. J. Chem. Soc. (B), 122 (1970).
7. R. A. Y. JONES, A. R. KATRITZKY, A. C. RICHARDS, R. J. WYATT, R. J. BISHOP, and L. E. SUTTON. J. Chem. Soc. (B), 127 (1970).
8. H. BOOTH. Chem. Commun. 802 (1968).
9. T. A. CLAXTON. Chem. Ind. 1713 (1964).
10. N. L. ALLINGER, T. A. HIRSCH, and M. A. MILLER. Tetrahedron Lett. 3729 (1967).
11. F. MOLL. Tetrahedron Lett. 5201 (1968).
12. P. J. BUCKLEY, C. C. COSTAIN, and J. E. PARKIN. Chem. Commun. 668 (1968).
13. J. J. SLOAN and R. KEWLEY. Can. J. Chem. **47**, 3453 (1968).
14. J. R. FLETCHER and I. O. SUTHERLAND. Chem. Commun. 1504 (1969).
15. W. L. F. ARMAREGO and T. KOBAYASHI. J. Chem. Soc. (C), 1635 (1969).
16. S. J. BROIS. J. Amer. Chem. Soc. **90**, 506, 508 (1968); Tetrahedron Lett. 5997 (1968).
17. S. WOLFE, A. RAUK, L. M. TEL, and I. G. CSIZMADIA. J. Chem. Soc. (B). In press.
18. T. A. CRABB and R. F. NEWTON. Tetrahedron, **26**, 701 (1970).
19. F. G. RIDDELL and J. M. LEHN. J. Chem. Soc. (B), 1224 (1968).
20. Y. ALLINGHAM, R. C. COOKSON, T. A. CRABB, and S. VANY. Tetrahedron, **24**, 4625 (1968).
21. R. O. HUTCHINS, L. D. KOPP, and E. L. ELIEL. J. Amer. Chem. Soc. **90**, 7174 (1968).
22. N. L. ALLINGER, J. G. D. CARPENTER, and F. M. KARKOWSKI. J. Amer. Chem. Soc. **87**, 1232 (1965).
23. R. J. BISHOP, L. E. SUTTON, D. DINEEN, R. A. Y. JONES, A. R. KATRITZKY, and R. J. WYATT. J. Chem. Soc. (B), 493 (1967).
24. H. BOOTH and J. H. LITTLE. Tetrahedron, **23**, 291 (1967).
25. R. U. LEMIEUX and N. J. CHÜ. Abstr. of Pap. Amer. Chem. Soc. 133, 31N (1958).
26. N. J. CHÜ. Ph.D. Thesis, Department of Chemistry, University of Ottawa, Ottawa, Canada, 1959.
27. R. U. LEMIEUX. Effects of unshared pairs of electrons and their solvation on conformational equilibria. International Symposium on Conformational Analysis, Brussels, Belgium, September, 1969.
28. J. T. EDWARD. Chem. Ind. 1102 (1955).
29. M. KABAYAMA and D. PATTERSON. Can. J. Chem. **36**, 563 (1958).
30. R. U. LEMIEUX. *In* Molecular rearrangements. P. de Mayo, editor. Interscience, New York, N.Y. **2**, 739 (1964).
31. J. T. EDWARD, P. E. MORAND, and J. PUSKAS. Can. J. Chem. **39**, 2069 (1961).
32. J. E. EDEN. U.S.Pat. 2 911 294. Chem. Abstr. **54**, 3842 (1960).
33. J. M. LEHN, P. LINSCHEID, and F. G. RIDDELL. Bull. Soc. Chim. Fr. 1175 (1968).
34. R. R. FRASER, M. KAUFMAN, P. MORAND, and G. GOVIL. Can. J. Chem. **47**, 403 (1969).
35. R. U. LEMIEUX, A. A. PAVIA, J. C. MARTIN, and K. A. WATANABE. Can. J. Chem. **47**, 4427 (1969).
36. F. A. L. ANET and A. T. R. BOURN. J. Amer. Chem. Soc. **87**, 5250 (1965).
37. M. C. WOODS, I. MIURA, Y. NAKADAIRA, A. TERAHARA, M. MARUYAMA, and R. NAKANISHI. Tetrahedron Lett. 321 (1967).
38. J. G. COLSON, P. T. LANSBURY, and F. D. SALVA. J. Amer. Chem. Soc. **89**, 4987 (1967).
39. N. ABE, R. ONODA, K. SHIRAGATA, J. KATO, M. C. WOODS, Y. KITAHARA, K. RO, and T. KURIHARA. Tetrahedron Lett. 1793 (1968).
40. M. C. WOODS, I. MIURA, A. OGISO, M. KURABAYASHI, and H. MISHIMA. Tetrahedron Lett. 2009 (1968).
41. M. C. WOODS, H. C. CHIANG, Y. NAKADAIRA, and K. NAKANISHI. J. Amer. Chem. Soc. **90**, 522 (1968).
42. R. W. FRANCK and K. YANAGI. J. Org. Chem. **33**, 811 (1968).
43. R. H. MARTIN and J. C. NOULS. Tetrahedron Lett. 2727 (1968).
44. J. C. NOULS, P. WOLLOST, J. C. BRAEKMAN, and G. VAN BINST. Tetrahedron Lett. 2731 (1968).
45. K. F. KUHLMANN and D. M. GRANT. J. Amer. Chem. Soc. **90**, 7355 (1968).
46. J. LUGTENBURG and E. HAVINGA. Tetrahedron Lett. 1505 (1969).
47. T. FUKUMI, Y. ARATA, and S. FUJIWARA. J. Mol. Spectrosc. **27**, 443 (1968).
48. J. K. SAUNDERS, R. A. BELL, C.-Y. CHEN, D. B. MACLEAN, and R. H. F. MANSKE. Can. J. Chem. **46**, 2876 (1968).
49. N. S. BHACCA and N. H. FISCHER. Chem. Commun. 68 (1969).
50. R. D. G. COOPER, P. V. DE MARCO, J. C. CHENY, and N. D. JONES. J. Amer. Chem. Soc. **91**, 1408 (1969).
51. R. A. ARCHER and P. V. DE MARCO. J. Amer. Chem. Soc. **91**, 1530 (1969).
52. R. A. BELL and E. N. C. OSAKWE. Chem. Commun. 1093 (1968).
53. P. A. HART and J. P. DAVIS. J. Amer. Chem. Soc. **91**, 512 (1969).
54. H. BOOTH. Tetrahedron, **22**, 615 (1966).
55. R. A. BELL and J. K. SAUNDERS. Can. J. Chem. **48**, 1114 (1970).
56. R. U. LEMIEUX and J. A. MORGAN. Can. J. Chem. **43**, 2205 (1965); R. U. LEMIEUX and S. S. SALUJA. Joint Conference CIC–ACS, Toronto, Ontario. Abstract of Papers, CARBO, 33 (1970).
57. Y. KAWAZOE, M. TSUDA, and M. OHNISHI. Chem. Pharm. Bull. **15** (1), 51 (1967).
58. J. A. POPLE and A. A. BOTHNER-BY. J. Chem. Phys. **42**, 1339 (1965).
59. S. STERNHELL. Quart. Rev. 236 (1969).
60. Organic Syntheses. Coll. Vol. III. 1955. p. 244.
61. D. GURNE, L. STEFANIAK, T. URBANSKI, and M. WITANOWSKI. Proc. Intern. Symp. on Nitro Compounds. Warsaw, Poland. 211 (1963); Chem. Abstr. **63**, 17855 (1965).
62. A. ANTEUNIS, D. TAVERNIER, and F. BORREMANS. Bull. Soc. Chim. Belges. **75**, 396 (1966).
63. R. A. SPRAGG. J. Chem. Soc. (B), 1128 (1968).
64. H. BOOTH. Applications of ^{1}H NMR spectroscopy to the conformational analysis of cyclic compounds. *In* Progress in NMR spectroscopy. Vol. 5. Pergamon Press, London, 1969.
65. F. G. RIDDELL. J. Chem. Soc. (B), 560 (1967).

Can. J. Chem. Downloaded from www.nrcresearchpress.com by 210.87.254.40 on 09/05/12
For personal use only.

Applications of Proton Magnetic Resonance to Rotational Isomerism in Halotoluene Derivatives. V. α,α,α′,α′,2,3,5,6-Octachloro-*p*-xylene, Semiempirical Barrier Calculations

B. H. BARBER[1] AND T. SCHAEFER
Chemistry Department, University of Manitoba, Winnipeg, Manitoba

Received August 25, 1970

In toluene-d_8 solution the p.m.r. spectrum of α,α,α′,α′,2,3,5,6-octachloro-*p*-xylene at temperatures below −25 °C consists of two sharp peaks corresponding to the two conformations in which the methine protons lie *cis* and *trans* to each other in the plane of the aromatic ring. The barrier to rotation of the dichloromethyl groups is derived from a line-shape analysis of the rate-dependent spectra using the computer program ABXFIT. The activation parameters are $E_A = 13.6 \pm 0.4$ kcal/mol, $\log A = 11.3 \pm 0.3$, $\Delta H‡ = 13.1 \pm 0.4$ kcal/mol, $\Delta S‡ = -7.3 \pm 1.3$ e.u., $\Delta G‡ = 15.4$ kcal/mol at 286 °K. The quoted errors are standard errors from least squares fits. These parameters are compared to the extensive data known for α,α,2,4,6-pentachlorotoluene. A series of barrier calculations, based on modified Buckingham and on van der Waals potential energy functions, are discussed with reference to various halotoluenes.

Canadian Journal of Chemistry, 49, 789 (1971)

Introduction

In previous studies (1–3) of the barrier to rotation about the sp^2–sp^3 carbon–carbon bond in α,α,2,4,6-pentachlorotoluene (PCT) and α,α-dichloro-2,4,6-tribromotoluene (DCTBT), various spectral types and line-shape analyses were used to establish the probably small and negative entropies of activation for the rotation as well as the conformations of the unactivated molecules. In this study, a similar investigation is carried out for α,α,α′,α′,2,3,5,6 - octachloro - *p* - xylene (POCX) and is briefly described. In addition, a moderately successful barrier calculation is carried out for PCT and similar molecules using the modified Buckingham and van der Waals potential energy functions (4–6).

Experimental

The POCX was prepared by chlorination of 2,3,5,6-tetrachloro-*p*-xylene and was also obtained from Aldrich Chemical Company. A 3 mol % solution of POCX in toluene-d_8 was degassed by the freeze–pump–thaw technique and tetramethylsilane (TMS) served as an internal reference and lock signal.

The p.m.r. measurements were made on an HA-100D spectrometer in the frequency sweep mode. Frequency calibrations were obtained by a period averaging technique. Variable temperature work involved the V4341/V6057 accessory and temperature calibrations were based on thermocouple measurements in a dummy toluene sample. All spectra were recorded at a sweep rate of 0.02 Hz/s.

[1]Holder of an NRCC Scholarship, 1969–1970.

Results and Discussion

(*1*) *Determination of Rate Constants*

(a) General Remarks

In the low temperature region the spectrum consists of two sharp peaks, of *equal* intensity within experimental error, which are attributed to **1** and **2**. The C—H bonds lie in the plane of the

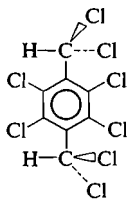

1

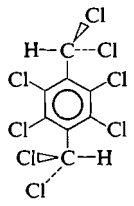

2

ring in **1** and **2** as expected on the basis of the behavior of PCT (1, 2) and on the basis of potential barrier calculations described below. At higher temperatures the peaks broaden and eventually collapse to a single sharp peak. The equal populations of **1** and **2** are somewhat surprising because **1** is expected to have a finite dipole moment[2] and therefore a higher stability

[2]A 3 mol % solution of POCX in the polar solvent CH_2ClBr (dielectric constant = 8.5) also displayed two peaks of equal intensity with an internal shift at −15 °C of 3.6 Hz. Solubility problems at lower temperatures did not allow a determination of the intrinsic temperature dependence of the shift. The small shift of 3.6 Hz made an accurate determination of other than $\Delta G‡$ very difficult (small temperature range).

Can. J. Chem. Downloaded from www.nrcresearchpress.com by 210.87.254.40 on 09/05/12
For personal use only.

in a solvent of dielectric constant greater than unity. On the other hand, it is likely that **1** is less stable than **2** because of steric strain arising from the dichloromethyl group orientation in **1**. It may be that the two opposing causes fortuitously cancel in POCX.

(b) Solvent Effects on the Internal Chemical Shift

The well-known solvent shifts induced by aromatic solvents vary with temperature (7) and, as described for PCT (1), must be accounted for before a proper line-shape fit can be made. Below −4 °C the exchange rate is slow enough to cause little shifting of the two peaks. An assumed linear decrease of the internal shift as the temperature increases between −39 and −4 °C gave the least squares eq. 1 ($r = 0.9863$). Rate-independent

$$[1]\quad \text{internal shift (Hz)} = 0.0438 \pm 0.002T(°C) + 7.118 \pm 0.075$$

shifts were calculated at higher temperatures using eq. 1 in a manner similar to that described for PCT (1). The internal shift in absence of exchange varies from 8.84 Hz at −39.3 °C to 4.21 Hz at 66.5 °C.

(c) Line-shape Fitting Procedure

Line-shapes were fitted as before (1) to theoretical spectra generated by the computer program ABXFIT (1), based on a proper density-matrix treatment of the exchange process. The effective T_2 values were determined from the width at half-height of a weak impurity peak arising from α,α,α′,α′,α′,2,3,5,6 - nonachloro - *p* - xylene. This width could be kept constant at 0.185 ± 0.02 Hz over the temperature range and yields T_2 = 1.72 s.

The rate constants k ranged from 185 s^{-1} at 52.3 °C to 0.0535 s^{-1} at −35 °C, a change of more than a factor of 10^3.

(2) Derivation of Activation Parameters

Plots of log k *vs.* $1/T$ ($r = 0.9964$) gave the activation energy and the frequency factor. A plot of log k/T *vs.* $1/T$ (8) is shown in Fig. 1 (r = 0.9961) from which the enthalpy of activation, $\Delta H‡$, and the entropy of activation, $\Delta S‡$, were derived. The parameters are $E_A = 13.6 \pm 0.4$ kcal/mol, log $A = 11.3 \pm 0.3$, $\Delta H‡ = 13.1 \pm 0.4$ kcal/mol, $\Delta S‡ = -7.3 \pm 1.3$ e.u., $\Delta G‡ = 15.4 \pm 0.1$ kcal/mol at 286 °K. The errors are

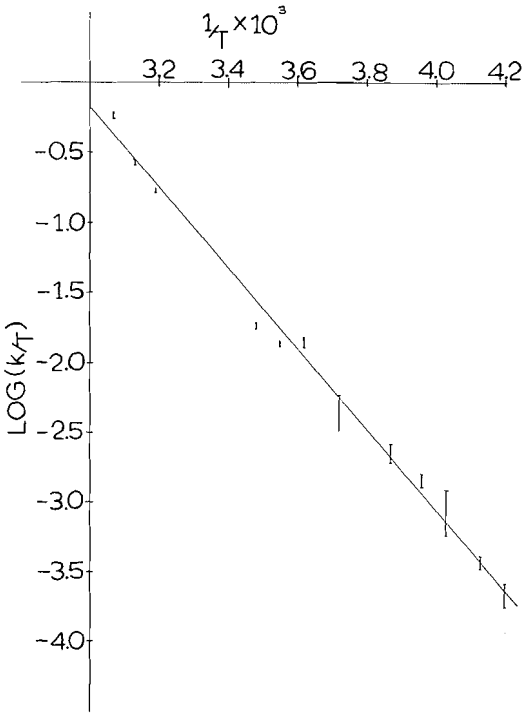

FIG. 1. A plot of log (k/T) *vs.* $1/T$ for the internal rotation in α,α,α′,α′,2,3,5,6-octachloro-*p*-xylene. The error bars reflect the estimated error in the rate constant derived from the line-shape analysis at various temperatures. The least squares line is drawn.

standard errors from the least squares fits. In CH_2ClBr we found $\Delta G‡ = 15.2 \pm 0.1$ kcal/mol at 286 °K. The values for PCT in methylcyclohexane, toluene-d_8, and carbon disulfide solutions (2) are $E_A = 14.2 \pm 0.3$ kcal/mol, log $A = 11.9_5 \pm 0.2$, $\Delta H‡ = 13.7 \pm 0.3$ kcal/mol, $\Delta S‡ = -4.4 \pm 1.0$ e.u., and $\Delta G‡$ 15.1 ± 0.1 kcal/mol at 286 °K.

(3) Discussion of Activation Parameters

Within experimental error the activation parameters are nearly equal for PCT and POCX. Yet the barrier calculations below indicate that if normal bond angles are maintained throughout the rotation of the dichloromethyl group in PCT, the barrier should be considerably greater than the experimental values. Consequently a certain degree of bond bending probably occurs in order to relieve the repulsive interactions and thereby lowers the barrier. In PCT the ring substituents in the ortho positions are relatively free to relieve

Can. J. Chem. Downloaded from www.nrcresearchpress.com by 210.87.254.40 on 09/05/12
For personal use only.

the strain but in POCX a further source of steric hindrance is met in the adjacent chlorine ring substituents.

Conformational calculations show that 2,3,5,6-tetrahalosubstitution of the benzene nucleus introduces considerable distortion of the bond angles in the plane of the ring (9). The calculated equilibrium conformation of 2,3,5,6-tetrachlorobenzene has an adjacent chlorine–chlorine internuclear distance of 3.18 Å whereas the equilibrium van der Waals distance for chlorine–chlorine is 3.60 Å (10). Steric interactions of this nature very likely raise the ground state of the tetrachloro structure relative to the 2,6-dichloro structure.

It would appear, therefore, that the ground state energy of POCX is raised by more than its transition state energy, leading to an equal or slightly lower energy barrier than in PCT. It is tempting to suggest that the transition state in POCX will be more crowded than in PCT, thus rationalizing a tendency towards a somewhat more negative $\Delta S\ddagger$ in POCX. The transition state in both molecules has eclipsed Cl–Cl interactions (see below).

In summary, the rate of rotation of the dichloromethyl group is not significantly different at any given temperature in POCX and PCT. Any "buttressing" effect of the ring chlorine atoms apparently does not dramatically alter the nature of the internal rotation.

(4) Semiempirical Barrier Calculations

(a) The Potential Functions

Molecular orbital methods are not at present suitable for the calculations of barriers to internal rotation in molecules containing halogens (11). Therefore, following Jonas *et al.* (6) and, on the assumption that the largest part of the rotational barrier arises from the pair-wise, nonbonded steric and electrostatic interactions between the dichloromethyl group and the ortho ring substituents (4), two separate potential energy functions were used. In eqs. 2 (modified Buckingham potential) and 3 (van der Waals function) each summation is over the jth pair of atoms and r_j is the internuclear distance.

$$[2] \quad V(\theta) = \sum_j A_j \exp(-B_j r_j) - C_j/r_j^6 + D_j/r_j$$

$$[3] \quad V(\theta) = \sum_j A_j \exp(-r_j/P_j)$$

Equation 2 was applied in the form developed by Scott and Scheraga (4). The parameters A, B, and C are the normal ones for the six-exponential potential (12–14). The constant D enters as the dipole moment contribution (15). Equation 3 was employed as described by Howlett (5) and the interaction constants A_j and P_j, including Br–Cl, F–Cl, and Br–F interactions as estimated by the geometric mean method (4, 15) are tabulated in ref. 16.

(b) Computational Method

The computation of the barrier involved the determination of six internuclear distances, *i.e.*, the distance of each ring substituent to each of the three methyl group substituents for each degree of the rotation, and applying these distances to the designated function. The bond lengths were taken from data available for analogous compounds (17).

Two programs were written in Fortran IV for use on an IBM 360/65 computer. One program, POTL1, was designed to handle asymmetric ring substitution and the other, POTL2, handles symmetric substitution. For example, for the compound, α,α,2,6-tetrachlorotoluene, the input parameters include the C—Cl bond length of the ring, the C—Cl bond length of the methyl group substituent, and the methyl C—H bond length in Å. Depending upon the choice of potential function, one requires the appropriate interaction constants for the Cl–Cl and Cl–H interactions. The value of the potential energy in kcal/mol is output for each degree of rotation about the sp^2–sp^3 carbon–carbon bond and can be had as data on the line printer and/or as a Calcomp plot. Both programs in their present form require that two of the methyl substituents be the same, although three different substituents on the methyl rotor could be accommodated by a modest modification.

In realization of the probable importance of bond bending in the rotation process, a rather naive approach (necessary to retain simplicity in the computing) consisted of repetition of the calculation after changing from normal bond angles[3] of all bonds to a geometry where all bonds

[3]Normal bond angles in this context refer to 109° 28′ at the sp^3 carbon, and 120° at sp^2 carbon, atoms.

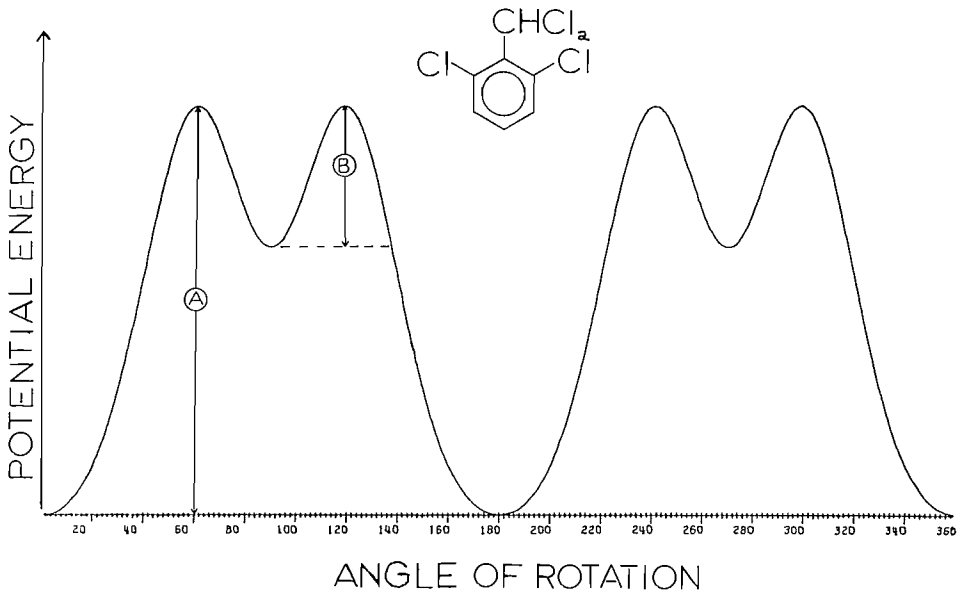

FIG. 2. The shape of the potential energy barrier to rotation as given by both the modified Buckingham and the van der Waals functions for α,α,2,6-tetrachlorotoluene. The values of the barriers *A* and *B* are collected in Table 1. The 0° angle of rotation has the C—H bond of the sidechain in the plane of the aromatic ring.

TABLE 1. Values of the energy barriers *A* and *B* to rotation for α,α,2,6-tetrachlorotoluene*

	van der Waals function		Modified Buckingham function	
Bend†	Barrier *A*‡	Barrier *B*	Barrier *A*	Barrier *B*
0	23.087§	7.575	58.748	20.246
1	18.437	5.837	46.189	15.451
2	5.643	1.427	15.061	3.569
3	4.560	1.128	11.996	2.808
4	3.689	0.896	9.542	2.220
5	2.987	0.713	7.576	1.764

*The compound has structure shown below with the following bond lengths: ring C—Cl, 1.71 Å; methyl C—Cl, 1.78 Å; methyl C—H, 1.11 Å.

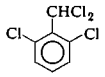

Comment on the barrier shape: the barrier shape appears in Fig. 2 and is unchanged for 5° of bending. Both potential energy functions indicate the same barrier shape.

†Note that bend = 0 refers to the normal bond angle case, bend = 1 to all five bonds involved in the rotational interactions bent back by 1°, etc.

‡All barrier values are in kcal mol^{-1}.

§All barrier values are recorded to three decimal places with the realization that the accuracy of the constants does not necessarily warrant this number of significant figures in the final barrier value.

were bent back by a specified number of degrees. Thus, the methyl substituent bonds were bent towards the sp^2–sp^3 bond axis while the ring substituent bonds were bent away from the rotational site but in the plane of the ring.

This treatment of bond bending is in no way rigorous. A more realistic mechanism is more likely that of bond-wagging at points of greatest strain in the rotation and the energy of bond bending, although relatively small, should be

Can. J. Chem. Downloaded from www.nrcresearchpress.com by 210.87.254.40 on 09/05/12
For personal use only.

TABLE 2. Values of the energy barriers to rotation for α,α-dichloro-α,2-difluorotoluene*

Bend	van der Waals function			Modified Buckingham function	
	Barrier A†	Barrier B	Barrier C	Barrier A	Barrier B
0	1.362	2.316	2.871	2.818	3.481
1	1.113	2.012	2.357	2.600	2.818
2	0.914	1.751	1.941	2.417	2.286
3	0.754	1.527	1.602	2.262	1.861

*The compound has structure shown below with the following bond lengths: ring C—F, 1.33 Å; ring C—H, 1.04 Å, methyl C—Cl, 1.78 Å; methyl C—F, 1.39 Å.

†All barrier values are in kcal mol^{-1}.

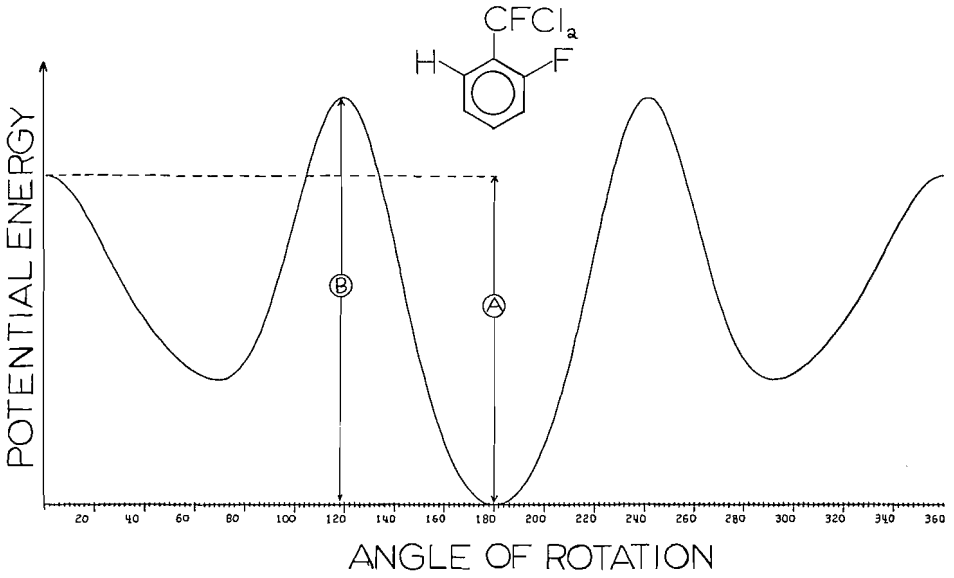

FIG. 3. The shape of the potential barrier to internal rotation as given by the modified Buckingham potential for α,α-dichloro-α,2-difluorotoluene. Barrier values at points *A* and *B* are given in Table 2. At 0° of rotation the C—F bond of the sidechain eclipses the C—F bond in the ring.

included at these points. Such a treatment would be comparable to one on a dynamic framework but would also require large amounts of computer time.

(c) An Example: PCT Barriers and Conformers

As an example of the computations, Fig. 2 reproduces the shape of the rotational potential energy barrier for the dichloromethyl group of α,α,2,6-tetrachlorotoluene. The zero angle of rotation has the C—H bond of the group in the plane of the ring. In this case both potential functions yield the same barrier shape. The magnitude of the barrier is different for the two functions and a set of values for different degrees of bond-bending is given in Table 1. The shape of the barrier does not change as the bond angles are bent back.

The two potential functions yield the same results whether or not a chlorine is substituted in position 4 so that the computation is also valid for PCT (and roughly also for POCX). The

Can. J. Chem. Downloaded from www.nrcresearchpress.com by 210.87.254.40 on 09/05/12
For personal use only.

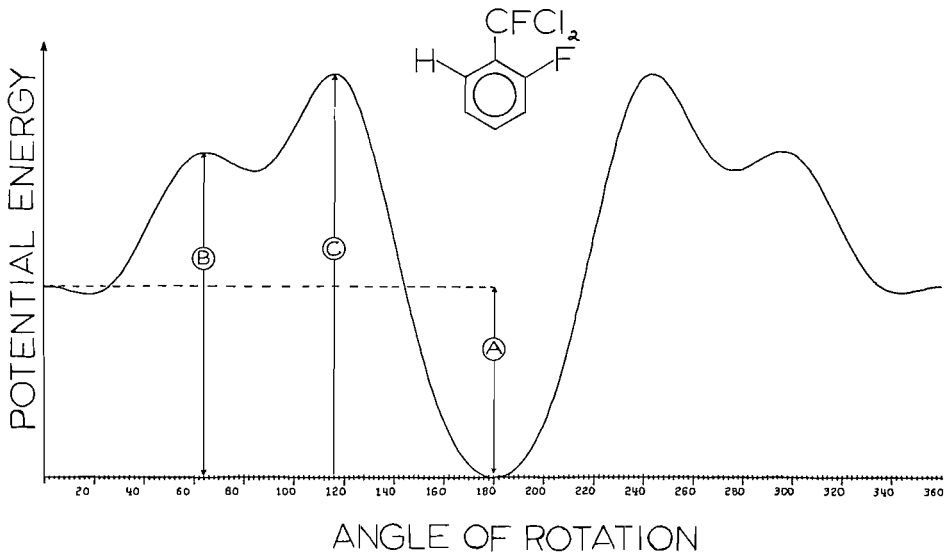

FIG. 4. As in Fig. 3 but for the van der Waals function. Barriers *A*, *B*, *C* are tabulated in Table 2.

experimental barrier of near 14 kcal/mol is reproduced by the van der Waals function for a bond-bend of just over 1° while the Buckingham function would "demand" a bend of just over 2°.

The qualitative result (1) that **3** is the ground state of the molecule and that **4** is not appreciably populated at any of the temperatures up to 400 °K, is well reproduced by the computation.

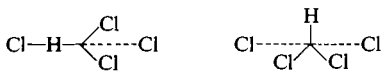

3 **4**

Experimentally (3) the barrier in α,α-dibromo-2,6-dichlorotoluene is about 1.5 kcal/mol higher than in PCT. For the bond-bend which reproduces the barrier in PCT, the van der Waals function predicts a barrier about 5 kcal/mol higher in the bromo compound while the Buckingham potential overestimates it by 10 kcal/mol. Of course, the amount of bond bending during the rotation could well be larger in the bromo compound than in PCT.

(d) The Usefulness of the Functions

Computations for a variety of halosubstitution patterns indicate that fluorine or hydrogen substituents lead to barriers which are too small to allow the detection of individual conformers by n.m.r. For example, in Table 2 results for some of the calculations on α,α-dichloro-α,2-difluorotoluene are given. The barriers correspond to those drawn in Figs. 3 and 4. Both potential energy functions predict the most stable conformation as one in which the C—F bond of the sidechain eclipses the ortho C—H bond of the ring for normal bond angles (0° bend) and that this conformation is the only one appreciably populated near room temperature. Again, both functions agree in predicting the highest energy for an eclipse of the ring C—F bond by the C—Cl bond in the sidechain. On the other hand, the functions predict different potential shapes in the region of a 20–100° twist of the sidechain C—F bond from its eclipsed position over the C—F bond in the ring.

By using the stereospecificity of the H–H and H–F coupling constants from the sidechain to the ring, it is probable that at least some of these predictions can be verified experimentally. Such experiments are in progress.

The extensive help of Mr. Bruce Goodwin with the computing problems is gratefully acknowledged. This work was supported by the National Research Council of Canada. We thank Dr. C. M. Wong and Mr. K. Chum for the synthesis of POCX.

1. B. J. FUHR, B. W. GOODWIN, H. M. HUTTON, and T. SCHAEFER. Can. J. Chem. **48**, 1558 (1970).
2. H. G. GYULAI, B. J. FUHR, H. M. HUTTON, and T. SCHAEFER. Can. J. Chem. **48**, 3877 (1970).

Can. J. Chem. Downloaded from www.nrcresearchpress.com by 210.87.254.40 on 09/05/12
For personal use only.

3. W. J. PEELING, T. SCHAEFER, and C. M. WONG. Can. J. Chem. **48**, 2839 (1970).
4. R. A. SCOTT and H. A. SCHERAGA. J. Chem. Phys. **42**, 2209 (1965).
5. K. E. HOWLETT. J. Chem. Soc. 1055 (1960).
6. J. JONAS, L. BOROWSKI, and H. S. GUTOWSKY. J. Chem. Phys. **47**, 2441 (1967).
7. P. LASZLO. *In* Progress in nuclear magnetic resonance spectroscopy. Vol. 3. *Edited by* J. Emsley, J. Feeney, and L. H. Sutcliffe. Pergamon Press, Oxford, 1967.
8. G. BINSCH. *In* Topics in stereochemistry. Vol. 3. *Edited by* E. Eliel and N. Allinger. Interscience Publishers, New York, N.Y., 1968.
9. A. KITAIGORODSKII and V. G. DASHEVSKII. Theor. and Exp. Chem. **3**, 22 (1967) (English translation).
10. L. PAULING. The nature of the chemical bond. Cornell University Press. Ithaca, New York, N.Y., 1960.
11. M. S. GORDON. J. Amer. Chem. Soc. **91**, 3122 (1969).
12. J. O. HIRSCHFELDER, C. F. CURTISS, and R. B. BIRD. Molecular theory of gases and liquids. John Wiley and Sons, Inc., New York, N.Y., 1954.
13. I. AMDUR and A. L. HARKNESS. J. Chem. Phys. **22**, 664 (1954).
14. I. AMDUR and E. A. MASON. J. Chem. Phys. **23**, 415 (1955).
15. E. A. MASON and M. M. KREEVOY. J. Amer. Chem. Soc. 77, 5808 (1955).
16. B. H. BARBER. M.Sc. Thesis. University of Manitoba, Winnipeg, Manitoba, 1970.
17. L. E. SUTTON, *editor*. Tables of interatomic distances and configurations in molecules and ions. The Chemical Society. London, 1958.

Can. J. Chem. Downloaded from www.nrcresearchpress.com by 210.87.254.40 on 09/05/12
For personal use only.

Synthesis of Paratose (3,6-Dideoxy-D-*ribo*-hexose) and Tyvelose (3,6-Dideoxy-D-*arabino*-hexose)[1]

E. H. WILLIAMS, W. A. SZAREK, AND J. K. N. JONES
Department of Chemistry, Queen's University, Kingston, Ontario

Received August 14, 1970

Convenient syntheses of the biologically important 3,6-dideoxyhexoses paratose (**12**) and tyvelose (**8**) from the readily available chlorodeoxy sugar methyl 4,6-*O*-benzylidene-3-chloro-3-deoxy-β-D-allopyranoside (**1**) are described.

Canadian Journal of Chemistry, 49, 796 (1971)

Can. J. Chem. Downloaded from www.nrcresearchpress.com by 210.87.254.40 on 09/05/12
For personal use only.

Introduction

Paratose (3,6-dideoxy-D-*ribo*-hexose) and tyvelose (3,6-dideoxy-D-*arabino*-hexose) have been isolated from lipopolysaccharides elaborated by Gram–negative bacteria (1–3). They, along with abequose (3,6-dideoxy-D-*xylo*-hexose) and colitose (3,6-dideoxy-L-*xylo*-hexose), were first recognized among the *Salmonella* and *E. coli* strains. When present, these 3,6-dideoxyhexoses occur at the nonreducing ends of chains and constitute immunodominant groups of their respective antigenic determinants (1–5). Syntheses of paratose (6, 7) and tyvelose (7–11) have been reported previously. In continuation of our studies on the synthesis and reactions of chlorodeoxy sugars (12–14), we now report convenient syntheses of both paratose (**12**) and tyvelose (**8**) from the same intermediate, methyl 4,6-*O*-benzylidene-3-chloro-3-deoxy-β-D-allopyranoside (**1**). This work demonstrates further the utility of the readily available chlorodeoxy sugars in the synthesis of biologically significant sugars.

Results and Discussion

Crystalline methyl 4,6-*O*-benzylidene-3-chloro-3-deoxy-β-D-allopyranoside (**1**) was prepared by reaction of methyl 4,6-*O*-benzylidene-β-D-glucopyranoside with sulfuryl chloride, and dechlorosulfation of the product using sodium iodide, as described previously (14, 15). Hydrogenation of compound **1**, in the presence of potassium hydroxide, over a W-4 Raney nickel catalyst (12), afforded methyl 4,6-*O*-benzylidene-3-deoxy-β-D-*ribo*-hexopyranoside (**2**) (16–18) (Scheme 1). Oxidation of the 3-deoxy sugar derivative **2** with ruthenium tetroxide, according to the improved procedure of Lawton *et al.* (19), gave methyl 4,6-*O*-benzylidene-3-deoxy-β-D-*erythro*-hexopyranosid-2-ulose (**3**) (16). Treatment of the 2-ketone **3** with sodium borohydride in methanol at reflux temperature yielded compound **2** and methyl 4,6-*O*-benzylidene-3-deoxy-β-D-*arabino*-hexopyranoside (**4**) (10), which were separated by column chromatography on silica gel. The remaining steps in the route for the synthesis of tyvelose were the same as those employed by Stirm *et al.* (10). Thus, acid-catalyzed de-*O*-benzylidenation of **4** gave methyl 3-deoxy-β-D-*arabino*-hexopyranoside (**5**), which yielded the 6-*O*-*p*-tolylsulfonyl derivative **6**. Desulfonyloxylation of **6** with lithium aluminum hydride in tetrahydrofuran afforded methyl 3,6-dideoxy-β-D-*arabino*-hexopyranoside (methyl β-D tyveloside) (**7**), which was converted into the crystalline free sugar **8** by acid-catalyzed hydrolysis.

The first route in the present work for the synthesis of paratose, with methyl 4,6-*O*-benzylidene-3-chloro-3-deoxy-β-D-allopyranoside (**1**) as an intermediate, involved a further reaction with sulfuryl chloride (Scheme 2). Acid-catalyzed de-*O*-benzylidenation of compound **1** gave the previously reported (15) methyl 3-chloro-3-deoxy-β-D-allopyranoside (**9**) as a syrup. Treatment of **9** with sulfuryl chloride yielded a syrup, which, on dechlorosulfation, gave crystalline methyl 3,6-dichloro-3,6-dideoxy-β-D-allopyranoside(**10**) (20). The lack of substitution by chloride ion of the intermediate chlorosulfonyloxy group at C-4 is attributed to the presence of the vicinal axial substituent at C-3; also, a chlorosulfonyloxy group at C-2 is deactivated to nucleophilic substitution by chloride ion (14, 15, 20, 21). Hydrogenation of **10**, in the presence of potassium hydroxide, over a W-4 Raney nickel catalyst (12), gave crystalline methyl 3,6-dideoxy-β-D-*ribo*-hexopyranoside (**11**).

The glycoside **11** was prepared also by an alternative procedure (Scheme 3). Treatment of methyl 4,6-*O*-benzylidene-3-deoxy-β-D-*ribo*-hex-

[1]Part IV in the series Synthesis and Reactions of Chlorodeoxy Sugars.

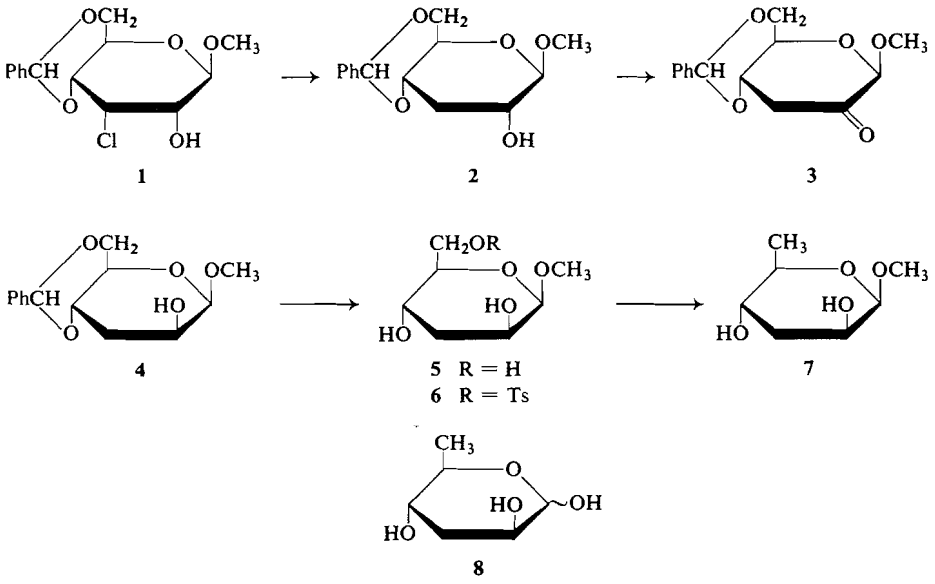

SCHEME 1

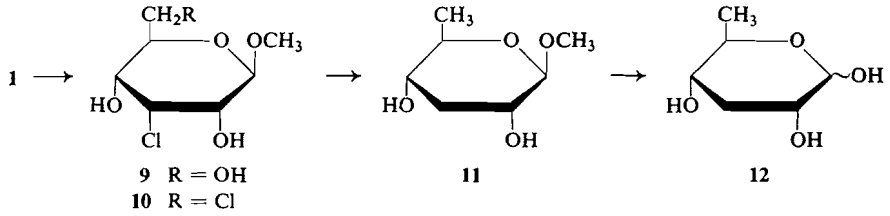

SCHEME 2

opyranoside (**2**) with *N*-bromosuccinimide (22) in boiling carbon tetrachloride, in the presence of barium carbonate, gave a high yield of methyl 4-*O*-benzoyl-6-bromo-3,6-dideoxy-β-D-*ribo*-hexopyranoside (**13**). When compound **13** was heated with lithium aluminum hydride in tetrahydrofuran at reflux temperature, debromination and debenzoylation occurred to give **11**. Acid-catalyzed hydrolysis of **11** afforded paratose (**12**).

A synthesis of abequose (3,6-dideoxy-D-*xylo*-hexose) was attempted also from methyl 4,6-*O*-benzylidene-3-chloro-3-deoxy-β-D-allopyranoside (**1**). It has been shown previously (14, 23) that heating the chlorodeoxy sugar (**1**) in *N*,*N*-dimethylformamide at reflux temperature with sodium benzoate gives a high yield of an unsaturated derivative, methyl 4,6-*O*-benzylidene-β-D-*erythro*-hex-3-enopyranoside. An effort was made to convert this unsaturated compound into methyl 4,6-*O*-benzylidene-3-deoxy-β-D-*xylo*-hexopyranoside, which would be a convenient precursor to abequose. Thus, when a solution of the unsaturated compound in ethanol containing palladium-on-carbon was subjected to a hydrogen pressure of 40 p.s.i.g., even after 3 days, only a 50% conversion to compound **2** was achieved; there was no evidence for the presence of the desired compound.

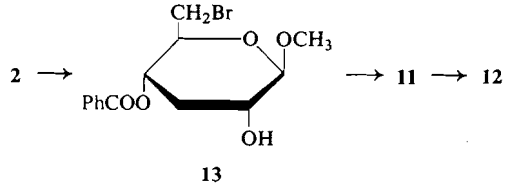

SCHEME 3

Experimental

Melting points were determined on a Fisher–Johns melting point apparatus and are uncorrected. Optical rotations were measured with a Perkin–Elmer model 141 automatic polarimeter at 23 ± 2°. The n.m.r. spectra were determined at 60 MHz in chloroform-*d* and using tetramethylsilane as internal standard. The t.l.c. was per-

Can. J. Chem. Downloaded from www.nrcresearchpress.com by 210.87.254.40 on 09/05/12
For personal use only.

Can. J. Chem. Downloaded from www.nrcresearchpress.com by 210.87.254.40 on 09/05/12
For personal use only.

formed with Silica Gel G as the adsorbent. The developed plates were air dried, sprayed with 5% ethanolic sulfuric acid, and heated at about 150°. The term "petroleum ether" refers to the fraction of b.p. 60–80°.

Methyl 4,6-O-Benzylidene-3-chloro-3-deoxy-β-D-allopyranoside (1)

This compound was prepared from methyl 4,6-*O*-benzylidene-β-D-glucopyranoside (15 g) as described previously (14, 15). The crystalline product was recrystallized from ether – petroleum ether to give colorless prisms (14.9 g, 93%) with the same physical constants as reported by Lawton *et al.* (14) for compound **1**.

Methyl 4,6-O-Benzylidene-3-deoxy-β-D-ribo-hexopyranoside (2)

A solution of compound **1** (5 g) in ethanol (300 ml) containing potassium hydroxide (2.5 g) and W-4 Raney nickel catalyst (12) (1 g) was shaken in an atmosphere of hydrogen for 2 h. A solid product was isolated in the usual manner; recrystallization from chloroform – petroleum ether gave compound **2** (3.85 g, 87%), m.p. 174°, $[\alpha]_D$ −61° (*c*, 1.0 in chloroform); lit., m.p. 174–175° (16), 165° (17), 168–169° (18), $[\alpha]_D^{18}$ 59.5° (*c*, 4.1 in chloroform) (17), $[\alpha]_D$ −60.5° (*c*, 1.05 in chloroform) (18).

Methyl 4,6-O-Benzylidene-3-deoxy-β-D-erythro-hexopyranosid-2-ulose (3)

This compound was prepared by oxidation of methyl 4,6-*O*-benzylidene-3-deoxy-β-D-*ribo*-hexopyranoside (**2**) (1 g) with a mixture of ruthenium dioxide and potassium metaperiodate in chloroform, in the presence of potassium carbonate, by the procedure described by Lawton *et al.* (19). The crystalline product was recrystallized from ethyl acetate – petroleum ether to give colorless needles (0.7 g, 70%), whose physical constants were the same as those obtained previously (16) for compound **3**, namely, m.p. 153–155°, $[\alpha]_D$ −30° (*c*, 0.5 in chloroform).

Reduction of Methyl 4,6-O-Benzylidene-3-deoxy-β-D-erythro-hexopyranosid-2-ulose (3) with Sodium Borohydride

To a solution of the 2-ketone **3** (650 mg) in methanol at reflux temperature was added dropwise a solution of sodium borohydride in methanol. The t.l.c. (1:4 ethyl acetate – chloroform) revealed after 3 h the presence of an approximately 1:1 mixture of methyl 4,6-*O*-benzylidene-3-deoxy-β-D-*ribo*-hexopyranoside (**2**) (R_F 0.7) and another component (R_F 0.55). The mixture of these two components was isolated in the usual manner, and chromatographed on silica gel, with 1:4 ethyl acetate – chloroform as eluent, to yield compound **2** and a second crystalline product. Recrystallization of the latter from chloroform – petroleum ether gave methyl 4,6-*O*-benzylidene-3-deoxy-β-D-*arabino*-hexopyranoside (**4**) (230 mg, 35%), m.p. 171–172°, $[\alpha]_D$ −66.3° (*c*, 1.0 in chloroform); n.m.r. data: τ 2.38–2.78 (5-proton multiplet, aromatic H's), 4.41 (1-proton singlet, benzylidene-methine H), 5.57 (1-proton doublet, $J_{1,2}$ 2Hz, H-1), 6.46 (3-proton singlet, OMe), 7.34–7.85 (2-proton multiplet, 2H-3's).

Anal. Calcd. for $C_{14}H_{18}O_5$: C, 63.2; H, 6.8. Found: C, 63.1; H, 6.7.

Stirm *et al.* (10) report m.p. 172–174° and $[\alpha]_{5461}^{25}$ −75 ± 2° (*c*, 0.7 in chloroform) for compound **4**.

Methyl 3-Deoxy-β-D-arabino-hexopyranoside (5)

A solution of methyl 4,6-*O*-benzylidene-3-deoxy-β-D-*arabino*-hexopyranoside (**4**) (200 mg) in acetone (6 ml) and 0.1 *N* hydrochloric acid (4 ml) was heated at reflux temperature for 1 h. The acetone was removed by distillation, and the aqueous solution was neutralized with Duolite A-4 (OH^-) ion-exchange resin and concentrated to yield a chromatographically homogeneous (t.l.c., 6:1 chloroform–methanol) syrup (100 mg, 91%), $[\alpha]_D$ −67.6° (*c*, 0.9 in methanol); n.m.r. data: τ 5.43 (1-proton doublet, $J_{1,2}$ 2 Hz, H-1), 6.46 (3-proton singlet, OMe), 7.49–8.35 (2-proton multiplet, 2H-3's).

Methyl 3-Deoxy-6-O-p-tolylsulfonyl-β-D-arabino-hexopyranoside (6)

Methyl 3-deoxy-β-D-*arabino*-hexopyranoside (**5**) (170 mg) was treated with *p*-toluenesulfonyl chloride (260 mg) in dry pyridine (5 ml) at 0°. The solution was kept at room temperature for 24 h, and then poured into water; the mixture was extracted several times with chloroform. Concentration of the combined extracts, after they had been washed with 2 *N* sulfuric acid and then water, yielded a syrup, which was chromatographed on silica gel, with 19:1 ethyl acetate – methanol as eluent. Compound **6** was obtained as a syrup (155 mg, 71%), $[\alpha]_{5461}$ −41° (*c*, 1.0 in chloroform); n.m.r. data: τ 2.04–2.74 (4 protons, aromatic H's), 5.59 (1-proton doublet, $J_{1,2}$ 2 Hz, H-1), 6.5 (3-proton singlet, OMe), 7.5 (3-proton singlet, aromatic Me). Stirm *et al.* (10) report $[\alpha]_{5461}^{25}$ −43 ± 2° (*c*, 1.3 in chloroform) for compound **6**.

Methyl 3,6-Dideoxy-β-D-arabino-hexopyranoside (7)

The 6-*O*-*p*-tolylsulfonyl derivative **6** (150 mg) was heated under reflux with lithium aluminum hydride in tetrahydrofuran for 1 h. Fractionation of the product on silica gel, with 9:1 ethyl acetate – methanol as eluent, gave the glycoside **7** as a homogeneous syrup (65 mg, 89%), $[\alpha]_{5461}$ −72° (*c*, 1.1 in methanol); R_F 0.4 (19:1 ethyl acetate – methanol); n.m.r. data: τ 5.62 (1-proton doublet, $J_{1,2}$ 2 Hz, H-1), 6.49 (3-proton singlet, OMe), 8.52 (3-proton doublet, *J* 6 Hz, C-5 Me). Stirm *et al.* (10) report $[\alpha]_{5461}^{25}$ −72 ± 2° (*c*, 0.9 in methanol) for compound **7**.

3,6-Dideoxy-D-arabino-hexose (Tyvelose) (8)

A solution of methyl 3,6-dideoxy-β-D-*arabino*-hexopyranoside (7) (57 mg) in 0.2 *N* sulfuric acid (5 ml) was heated at 90° for 3 h. The cooled solution was neutralized with Duolite A-4 (OH^-) ion-exchange resin and concentrated to a syrup (48 mg, 92%). Distillation of this material at 100–125° (bath)/0.01 Torr gave a homogeneous syrup, with R_F 0.33 (19:1 ethyl acetate – methanol), which crystallized spontaneously. Recrystallization from acetonitrile gave tyvelose (**8**), m.p. 95–99°, $[\alpha]_D$ +22° (*c*, 0.7 in water). These physical constants are in agreement with those reported previously (1, 7) for tyvelose.

Methyl 3-Chloro-3-deoxy-β-D-allopyranoside (9)

A solution of methyl 4,6-*O*-benzylidene-3-chloro-3-deoxy-β-D-allopyranoside (**1**) (2.45 g) in acetone (40 ml) and 0.2 *N* hydrochloric acid (13 ml) was heated at reflux temperature for 4h. The acetone was removed by distillation, and the aqueous solution was neutralized with Duolite A-4(OH^-) ion-exchange resin and concentrated

Can. J. Chem. Downloaded from www.nrcresearchpress.com by 210.87.254.40 on 09/05/12
For personal use only.

to yield a chromatographically homogeneous (t.l.c.) syrup (15) (1.56 g), R_F 0.5 (6:2:1 1-butanol–ethanol–water); $[\alpha]_D$ −49° (*c*, 1.0 in water).

*Methyl 3,6-Dichloro-3,6-dideoxy-β-D-allopyranoside (**10**)*

This compound was prepared from methyl 3-chloro-3-deoxy-β-D-allopyranoside (**9**) (1.39 g) by reaction with sulfuryl chloride and subsequent dechlorosulfation, as described by Cottrell *et al.* (20). The crystalline product was recrystallized from chloroform – petroleum ether to give **10** (0.5 g, 33%), m.p. 162–163°, $[\alpha]_D$ −43° (*c*, 0.6 in chloroform). Cottrell *et al.* (20) report m.p. 154–156° and $[\alpha]_D$ −45° (*c*, 1.0 in chloroform) for **10**.

*Methyl 3,6-Dideoxy-β-D-ribo-hexopyranoside (**11**)*

A solution of compound **10** (148 mg) in ethanol (50 ml) containing potassium hydroxide (70 mg) and W-4 Raney nickel catalyst (12) (40 mg) was shaken in an atmosphere of hydrogen for 2 days. A solid product was isolated in the usual manner; recrystallization from ethyl acetate – petroleum ether gave compound **11** (89 mg, 86%), m.p. 63–65°, $[\alpha]_D$ −60° (*c*, 1.5 in methanol); n.m.r. data: τ 5.89 (1-proton doublet, $J_{1,2}$ 8 Hz, H-1), 6.49 (3-proton singlet, OMe), 8.7 (3-proton doublet, *J* 6 Hz, C-5 Me). The molecular formula of the crystalline compound was confirmed as $C_7H_{14}O_4$ by mass spectrometry: M^+ 162.0862 (Calcd. for $C_7H_{14}O_4$: 162.0892).

*Methyl 4-O-Benzoyl-6-bromo-3,6-dideoxy-β-D-ribo-hexopyranoside (**13**)*

A solution of methyl 4,6-*O*-benzylidene-3-deoxy-β-D-*ribo*-hexopyranoside (**2**) (250 mg) and *N*-bromosuccinimide (190 mg) in carbon tetrachloride (15 ml) containing barium carbonate (91 mg) was heated at reflux temperature with vigorous stirring for 3 h. The reaction mixture was filtered, and the filtrate concentrated to a syrup, which was chromatographed on silica gel, with 1:2 ethyl acetate – chloroform as eluent. Compound **13** was obtained as a homogeneous (t.l.c.) syrup (489 mg, 84%), R_F 0.52 (1:2 ethyl acetate – chloroform); n.m.r. data: τ 1.86–2.74 (multiplets, 5 protons, aromatic H's), 4.71–5.24 (1-proton multiplet, H-4), 5.7 (1-proton doublet, $J_{1,2}$ 8 Hz, H-1), 6.4 (3-proton singlet, OMe).

Anal. Calcd. for $C_{14}H_{17}O_5Br$: C, 48.6; H, 4.9; Br, 23.2. Found: C, 48.3; H, 5.3; Br, 23.1.

A mixture of compound **13** (450 mg) and lithium aluminum hydride (250 mg) in tetrahydrofuran (10 ml) was heated at reflux temperature for 3 h. The product was isolated in the usual manner, and chromatographed on silica gel, with 19:1 ethyl acetate – methanol as eluent, to give a homogeneous (t.l.c.) syrup which crystallized spontaneously. Recrystallization from ether – petroleum ether gave pale yellow prisms (137 mg, 65%) with the same physical constants as obtained above for methyl 3,6-dideoxy-β-D-*ribo*-hexopyranoside (**11**).

*3,6-Dideoxy-D-ribo-hexose (Paratose) (**12**)*

A solution of methyl 3,6-dideoxy-β-D-*ribo*-hexopyranoside (**11**) (86 mg) in 1 *N* sulfuric acid (10 ml) was heated at 90° for 5 h. The cooled solution was neutralized with Duolite A-4 (OH^-) ion-exchange resin and concentrated to yield paratose (**12**) as a homogeneous (t.l.c.) syrup (61 mg, 78%), R_F 0.21 (6:1 chloroform – methanol); $[\alpha]_D$ +7° (*c*, 1.1 in water), in agreement with values reported previously (1, 7) for paratose.

The authors thank the National Research Council of Canada for financial support of this research. We also acknowledge the counsel of Dr. B. T. Lawton.

1. O. Westphal and O. Lüderitz. Angew. Chem. **72**, 881 (1960).
2. O. Lüderitz. Bull. Soc. Chim. Biol. **42**, 1355 (1960).
3. D. A. L. Davies. Advan. Carbohyd. Chem. **15**, 271 (1960).
4. D. A. L. Davies. Nature, **191**, 43 (1961).
5. O. Lüderitz, A. M. Staub, and O. Westphal. Bact. Rev. **30**, 193 (1966).
6. C. Fouquey, J. Polonsky, E. Lederer, O. Westphal, and O. Lüderitz. Nature, **182**, 944 (1958).
7. C. Fouquey, J. Polonsky, and E. Lederer. Bull. Soc. Chim. Fr. 803 (1959).
8. C. Fouquey, E. Lederer, O. Lüderitz, J. Polonsky, A. M. Staub, S. Stirm, R. Tinelli, and O. Westphal. Compt. Rend. **246**, 2417 (1958).
9. G. Rembarz. J. prakt. Chem. **19**, 319 (1963).
10. S. Stirm, O. Lüderitz, and O. Westphal. Ann. Chem. **696**, 180 (1966).
11. S. Svensson. Acta Chem. Scand. **22**, 2737 (1968).
12. B. T. Lawton, D. J. Ward, W. A. Szarek, and J. K. N. Jones. Can. J. Chem. **47**, 2899 (1969).
13. B. T. Lawton, W. A. Szarek, and J. K. N. Jones. Carbohyd. Res. **14**, 255 (1970).
14. B. T. Lawton, W. A. Szarek, and J. K. N. Jones. Carbohyd. Res. In press.
15. H. J. Jennings and J. K. N. Jones. Can. J. Chem. **43**, 2372 (1965).
16. B. T. Lawton. Ph.D. Thesis, Queen's University, Kingston, Ontario. 1969.
17. E. J. Hedgley, W. G. Overend, and R. A. C. Rennie. J. Chem. Soc. 4701 (1963).
18. S. Hanessian and N. R. Plessas. J. Org. Chem. **34**, 1045 (1969).
19. B. T. Lawton, W. A. Szarek, and J. K. N. Jones. Carbohyd. Res. **10**, 456 (1969).
20. A. G. Cottrell, E. Buncel, and J. K. N. Jones. Can. J. Chem. **44**, 1483 (1966).
21. A. C. Richardson. Carbohyd. Res. **10**, 395 (1969).
22. S. Hanessian. Carbohyd. Res. **2**, 86 (1966); S. Hanessian and N. R. Plessas. J. Org. Chem. **34**, 1053 (1969), and references therein.
23. E. H. Williams, W. A. Szarek, and J. K. N. Jones. Carbohyd. Res. In press.

Can. J. Chem. Downloaded from www.nrcresearchpress.com by 210.87.254.105 on 09/05/12
For personal use only.

Effect of Substituents on the Chemical Shift of Benzylic Protons. III

ROBERT R. FRASER AND ROGER N. RENAUD[1]
Department of Chemistry, University of Ottawa, Ottawa, Canada

Received September 21, 1970

The effects of para substituents on the chemical shifts of the diastereotopic benzylic protons in three series of chiral molecules have been determined from a study of the 100 MHz spectra of these molecules in deuterochloroform. The results show that the slope, ρ, obtained from a plot of τ *vs.* Hammett σ constant, is influenced by a number of factors and that the conformational disposition of the benzylic proton with respect to the aromatic ring is not a dominant factor.

Canadian Journal of Chemistry, 49, 800 (1971)

The effect of substituents on the chemical shift of benzylic protons is a subject of current controversy. Concurrent with the appearance of our complete paper (1) on this topic a comprehensive review and assessment of the same subject was published by Yokoyama *et al.* (2). These authors showed that several literature discrepancies regarding the substituent chemical shifts (s.c.s.) for the benzylic protons of benzyl chlorides and fluorides were caused by association effects (solute–solute interactions) of considerable magnitude. From an examination of their own data in conjunction with that already in the literature, Miller and co-workers expressed the opinion that at present "correlations of the Hammett type are of little value" mainly because there is an urgent need for isolating and identifying the factors which affect them. In a very recent paper, Bentley and Dewar report s.c.s. for several series of the type $ArCH_2Z$, in which Ar represents a variety of alternant aromatic nuclei including naphthyl, anthryl, and phenanthryl and Z = OH, Cl, Br, I, H, and OTs. They conclude that ring-current anisotropy rather than hyperconjugation is responsible for the s.c.s. resulting from changes in Ar. Both papers, then, are in conflict with the proposal (1) that the slope ρ of an s.c.s. *vs.* σ plot for the CH_2 protons in a series of the type $X—C_6H_4—CH_2Z$ is strongly conformationally dependent, possibly as a result of a hyperconjugative interaction between the benzene ring and the methylene protons.

Data herein will describe further investigations in this field and, in particular, a test of the proposal that ρ is a conformationally dependent parameter. Three new series of *p*-substituted benzyl derivatives have been studied and the chemical shifts of the benzylic protons measured as a function of the para substituent. The compounds examined include seven 6-X-1-phenylphthalans, **1**, five 6-X-2-methyl-1-phenylisoindolines, **2**, and five 2-X-5[*H*]dibenzo[*a*,*d*]cycloheptene oxides, **3**. In all three series, the disposition of the benzylic protons with respect to the adjacent benzene rings is fixed in a known geometry. A companion paper (4) on the synthesis and conformational properties of these three series provides an assessment of geometry for the molecules in each series. The assignment of absorption due to the diastereotopic protons in series **1** was made (5) in analogy with previous chemical shift arguments for similar 1-phenylphthalans (6), in series **3** on the basis of n.O.e. experiments (4). In series **2** unambiguous assignment was not possible.

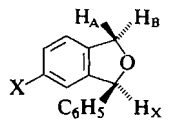

1

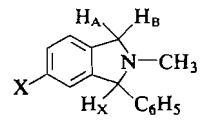

2

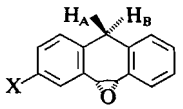

3

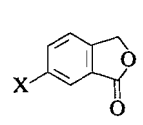

4

[1]Present address: Division of Chemistry, National Research Council, Ottawa, Canada.

TABLE 1. Chemical shifts (τ values) of the benzylic protons for series **1–3**

	1		**2**		**3** (In $CDCl_3$)		**3** (In acetone)	
X_p	H_A	H_B	H_A	H_B	H_A	H_B	H_A	H_B
NH_2	4.766	4.894	5.732	6.360				
OH	4.762	4.877						
OCH_3	4.732	4.861	5.681	6.298	4.960	6.734	5.023	6.658
CH_3					4.907	6.720	4.966	6.660
H	4.668	4.795	5.622	6.251	4.833	6.691	4.898	6.619
Cl	4.721	4.849						
$COOCH_3$			5.589	6.222	4.791	6.627	4.871	6.494
CN	4.647	4.773			4.788	6.638	4.869	6.451
NO_2	4.664	4.741	5.560	6.202				

TABLE 2. The ρ values of s.c.s.–Hammett σ plots

Series	Proton	$-\rho$ (p.p.m./σ)	r*	s†	n‡
1	H_A	0.08	0.865	0.027	7
	H_B	0.10	0.910	0.026	7
2	H_A	0.12	0.982	0.015	5
	H_B	0.11	0.970	0.018	5
3	H_A	0.17	0.899	0.038	5
(In $CDCl_3$)	H_B	0.12	0.924	0.022	5
3	H_A	0.15	0.866	0.039	5
(In acetone)	H_B	0.25	0.988	0.018	5

*r, Correlation coefficient.
†s, Standard deviation.
‡n, Number of compounds studied.

Results and Discussion

The data for the three series of compounds are presented in Table 1. In Fig. 1, a plot of the chemical shifts for each of the diastereotopic protons at C-3 in series **1** is shown. A least squares analysis of plots of chemical shifts *vs.* σ values leads to reasonable correlations in all three series, the results of which are presented in Table 2.[2] It can be seen that the diastereotopic protons in series **1** and **2** exhibit similar ρ values. Unequal ρ values are found for the two diastereotopic protons in the series **3** in which these protons differ significantly in their orientation with respect to the adjacent π orbitals of the benzene ring. The magnitudes of all ρ's differ from those expected if the chemical shifts of the benzylic protons were being altered solely by a hyperconjugative effect. For example in series **3**, a $\cos^2\phi$ relation would predict the ρ's for H_A (quasi-axial) and H_B (quasi-equatorial) ($\phi = 40$ and 80°) to be -0.23 and -0.02 respectively (assuming $\rho_{max} = -0.42$ or twice the value for the freely rotating methyl group of toluene). Nevertheless the larger value for the slope of H_A *vs.* H_B in **3** ($CDCl_3$ solvent) is in qualitative agreement with the conformational effect.

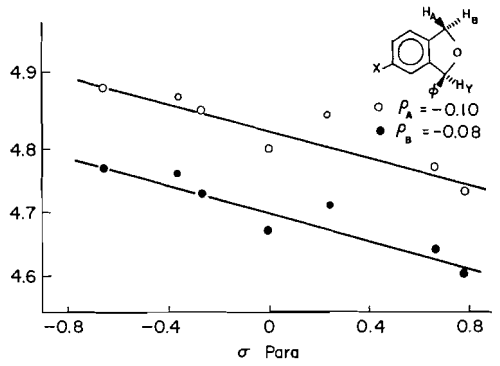

FIG. 1. A plot of the chemical shifts (τ values) of the diastereotopic protons at position 3 *vs.* the Hammett σ constant of the substituent at position 6 in a series of 6-X-1-phenylphthalans, **1**.

The effect of solvent on s.c.s. can be seen to be

[2]It has been suggested (2, 3) that a minimum of ten members of any series be required to provide a reliable assessment of any τ *vs.* σ correlation. While such a requirement is desirable, it was felt at the outset of the investigation, that its practical disadvantages could be offset by the advantages of studying a wider range of series containing fewer members. It seems highly unlikely that the conclusions reached in this paper would be altered by increasing the number of compounds studied in each series.

Can. J. Chem. Downloaded from www.nrcresearchpress.com by 210.87.254.105 on 09/05/12
For personal use only.

particularly influential from the data for series **3** in acetone. In this solvent the quasi-axial proton at C-5 shows a ρ similar to that for the $CDCl_3$ measurements, but the ρ for the quasi-equatorial proton at C-5 increases from -0.12 to -0.25.[3] It would appear then that the concern of Miller and co-workers regarding the influence of solvent on s.c.s. is forcefully justified. The dominance of solvent in completely reversing the relative magnitudes of ρ values for the fixed protons in **3** weakens our proposal that conformational effects determine the size of ρ. It remains possible that deuterochloroform, as solvent, does not exert a significant influence on ρ.

The cause of the pronounced effect of solvent can only be speculated upon. It has been shown previously (1) that, for the series **4**, variations in ρ with changing solvent failed to show any correlation with the dielectric constant of the medium, indicating the possibility of specific solute–solvent interactions or "complex formation". One way to account for the data in series **3** would be to invoke a substituent effect on the stability of the solute–solvent complex.[4] In this complex both aromatic rings may interact with the electron-deficient carbon of the acetone carbonyl group in such a way that the anisotropy of the carbonyl (9, 10) exerts a deshielding effect on the quasi-equatorial proton at C-5 while the quasi-axial proton may be situated in an insensitive region of the deshielding cone (10). Whether or not the above explanation is valid in its detail, it is obvious that a substituent effect on complex formation, or its orientation, will influence the s.c.s. and thus decrease the importance of conformational effects on ρ.

In view of the mounting evidence that solvent, association, conformation, ring-current, and substituent anisotropy all influence s.c.s. it would appear that Miller's rather pessimistic viewpoint (2) on the understanding of their causes is justified.

Experimental

All spectra were run on a Varian HA-100 spectrometer. The data reported herein were obtained by exact analysis of the AB patterns or by using the iterative computer program of Castellano and Bothner-By for the ABX patterns. Dilution effects were found to be negligible from a study of the spectra at concentrations of 0.3, 0.2, and 0.1 *M* solutions in deuterochloroform. The shifts are reported for 0.1 *M* solutions in series **1** and **3** and 0.2 *M* solutions in series **2**. All line positions were obtained from the average of five measured spectra. The least squares analyses were performed by computer calculation. The sigma constants employed in the calculation are taken from the compilation of McDaniel and Brown (11). The syntheses of the compounds and the other n.m.r. spectral parameters obtained by analyses are described in separate papers (4, 5).

The authors thank the National Research Council of Canada for generous financial support.

1. R. R. Fraser, Gurudata, R. N. Renaud, C. Reyes-Zamora, and R. B. Swingle. Can. J. Chem. **47**, 2767 (1969). See also R. R. Fraser, Gurudata, C. Reyes-Zamora, and R. B. Swingle. Can. J. Chem. **46**, 1595 (1968).
2. T. Yokoyama, G. R. Wiley, and S. I. Miller. J. Org. Chem. **34**, 1859 (1969).
3. M. D. Bentley and M. J. S. Dewar. J. Org. Chem. **35**, 2707 (1970).
4. R. R. Fraser and R. N. Renaud. Can. J. Chem. This issue.
5. R. R. Fraser and R. N. Renaud. Can. J. Chem. This issue.
6. R. A. Smith, R. G. Parker, and J. D. Roberts. Tetrahedron Lett. 1963 (1970).
7. T. Ledaal. Tetrahedron Lett. 1683 (1968).
8. P. Lazlo. *In* Progress in n.m.r. spectroscopy. Vol. 3. *Edited by* Emsley, Feeney, and Sutcliffe. Pergamon Press, London, 1967.
9. G. J. Karabatsos, G. C. Sonnichsen, N. Hsi, and D. J. Fenoglio. J. Amer. Chem. Soc. **89**, 5067 (1967).
10. J. W. ApSimon, W. G. Craig, P. V. Demarco, D. W. Mathieson, A. Karim, L. Saunders, and W. B. Whalley. Tetrahedron, **26**, 119 (1970).
11. D. H. McDaniel and H. C. Brown. J. Org. Chem. **23**, 420 (1958).

[3]The slight possibility that the assignments for H_A and H_B might be reversed in acetone was eliminated by examining the spectra for the methoxy derivative of **3** in mixtures of $CDCl_3$–acetone, wherein intermediate values of τ H_A and H_B showed that no reversal occurred.

[4]Formation of such "complexes" between aromatic solvents and ketone solutes are well-known (7). The exact nature of the "complex" is the subject of considerable controversy (8).

Can. J. Chem. Downloaded from www.nrcresearchpress.com by 210.87.254.105 on 09/05/12
For personal use only.

Reaction of Hydrogen Atoms with Carbon Suboxide

NICK DEMCHUK[1] AND H. D. GESSER
Chemistry Department, University of Manitoba, Winnipeg, Manitoba

Received April 11, 1969[2]

The gas phase reaction of hydrogen atoms with carbon suboxide was studied over the temperature range of −96 to 235 °C and was found to proceed via a chain reaction. The products found were CH_4, CO, CH_2CO, C_2H_6, $(CHO)_2$, and polymer. A mechanism is proposed and the chain reaction is explained by the intermediate formation of ketene and the formyl radical.

Canadian Journal of Chemistry, 49, 803 (1971)

Within the past decade a great deal of interest has been shown in the relatively unfamiliar compound C_3O_2 chiefly because of the formation of the suboxide or its polymer as a product in the radiolysis of CO and CO_2 (1–4) and in the photolysis of CO (5). The suboxide polymer is also formed during the pyrolysis, photolysis, and radiolysis of C_3O_2 (6–8). Comprehensive studies (9–11) on the photochemical decomposition of carbon suboxide have shown that the primary process is wavelength dependant and can be described by the sequence of reactions shown in eq. 1, where S refers to the singlet state, T the triplet state, and the asterisk indicates an energetic species. The CCO intermediate was found to be very reactive and its reaction has been studied in the presence of added gases such as C_2H_4, O_2 and NO (12–17).

[1] $$C_3O_2 + h\nu \rightarrow C_3O_2^* \begin{cases} \xrightarrow{(a)} CO + CCO(S) & 2000\,\text{Å} < \lambda < 2500\,\text{Å} \\ \xrightarrow{(b)} CO + CCO(T) & \lambda > 2900\,\text{Å} \end{cases}$$

Carbon suboxide has been recently photolyzed in the presence of H_2 (18) and the products found and analyzed were CO, CH_4, C_2H_6, and C_3H_8. Ketene was not found. Reaction 2 was proposed to account for the products.

[2] $$CCO(S) + H_2 \rightarrow CH_2(S) + CO$$

Carbon suboxide has been reacted with oxygen atoms (18–20) as well as N-atoms (20) but as yet no report has been published on its reaction with hydrogen atoms. We have previously reported on the reactions of H-atoms with ketene (21) and in view of the similarity between C_3O_2 and ketene it was desirable to examine this reaction.

Experimental

The apparatus was similar to that used previously (21) except for a few changes. (*1*) A D.C. condensed discharge system was connected across a Wood–Bonhoeffer tube (with aluminum electrodes) with the hope of obtaining a more constant hydrogen atom supply. However, spark gap difficulties were encountered. (*2*) The reaction vessel was altered to prevent back diffusion of reactants into the discharge zone and to prevent a direct light path from the discharge to the reaction region (22).

The hydrogen was purified by passage through a copper furnace at 450 °C and then through two silica gel traps maintained at 77 °K. The molecular hydrogen flow rate was about 2.7×10^3 μmol/min with 1.05 ± 0.01 Torr as the reaction pressure. The reaction vessel was not poisoned and the H atom concentration as determined from the HCl formed from reaction with C_2H_5Cl at 65 °C (23) was 45 μmol/min or about 1.7%.

The C_3O_2 was prepared by the dehydration of malonic acid (Matheson, Coleman and Bell), with P_2O_5 according to Stock and Stoltzenberg (24) and was fractionated by bulb-to-bulb distillation *in vacuo*. The final product contained less than 3 mol% of CO_2 and suitable corrections were made for this.

The non-condensable products, CO and CH_4, were trapped in a silica gel trap (25) pumped into the gas burette and quantitatively determined by gas chromatography.

Results and Discussion

The products identified and analyzed were CO, CH_4, C_2H_6, and ketene. Glyoxal was detected in experiments at 77 and −78 °C but no attempt was made to estimate it quantitatively. In all experiments a small amount of a dark residue was formed in the reaction vessel. This may have been carbon or polymer, or both, and probably accounts for the lack in material balance. This residue was not removed after each run. At

[1]Deceased, January 11, 1971.
[2]Revision received September 22, 1970.

Can. J. Chem. Downloaded from www.nrcresearchpress.com by 210.87.254.40 on 09/05/12
For personal use only.

TABLE 1. Yields of products in the reaction of H-atoms with carbon suboxide

Duration of experiment (min)	C_3O_2 Flow	C_3O_2 Reacted	Product (μmol/min)* CO	CH_4	CH_2CO	C_2H_6	Carbon balance†
Temperature: −96 ± 2 °C							
2.5	46	34	29	8.4	trace	trace	0.36
3.0	72	48	72	21	trace	trace	0.65
2.0	95			(120)			
2.5	108	26	24	5.4	trace	trace	0.43
2.0	170	44	49	4.0	trace	trace	0.40
1.0	203	50	47	15	trace	trace	0.43
Temperature: −78 ± 2 °C							
4.0	19	19	29	6.3	trace	trace	0.69
3.0	89	84	158	35	8.8	trace	0.65
2.0	126	93	137	25	7.2	trace	0.64
1.0	203	104	162	26	10	2.6	0.69
Temperature: 77 ± 2 °C							
5.0	33	21	38	7.0	trace	2.1	0.71
4.0	60	46	85	10	4.6	5.7	0.86
3.0	98	63	115	11	7.8	7.4	0.84
2.0	136	71	123	14	8.2	7.9	0.80
1.0	214	148	228	15	15	13	0.68
Temperature: 235 ± 2 °C							
6.0	45	15	36	2.0	3.8	trace	
3.0	77	30	43	2.3	6.1	2.0	
2.0	103	46	55	2.9	6.7	4.5	
1.0	203	58	88	4.6	14	7.5	
Temperature: −196 °C (ads.)							
5.0	139 adsorbed	27	13	trace	nil	nil	trace glyoxal

*A blank indicates that the product was not analyzed for. "Trace" indicates that the amount of product was less than 2 μmol/min.
†The "carbon balance" was determined by taking the ratio of the total carbon in the gaseous products to three times the C_3O_2 reacted.

235 °C large amounts of a dark brown polymer were formed within the reaction zone near the C_3O_2 inlet. Because of the predominant polymer formation at this temperature it is believed that a thermopolymerization of C_3O_2 took place in the presence of hydrogen, catalyzed by hydrogen atoms. These high temperature results will be discussed separately.

The results are tabulated in Table 1. In one experiment some C_3O_2 was condensed at −196 °C onto the inner walls of the reaction vessel where it was allowed to react with H atoms. Only CO and a trace of glyoxal were detected.

At −96 °C and high C_3O_2 flow rates the reaction follows "clean up" behavior with the yield of CO and the C_3O_2 consumed approaching the H-atom flow rate. At low flow rates of C_3O_2 the yield of CO is almost twice that of the H-atom and the C_3O_2 consumed almost equals the H-atom flow rate. The CH_4 similarly shows a maximum in yield as a function of the C_3O_2 flow rate.

Though similar trends are obtained at −78 and 77 °C, the yield of products far exceeds the H-atom flow rate and a chain reaction must be effective.

The primary reaction most consistent with the results would seem to be the addition of a hydrogen atom to the double bond (eq. 3). Displacement reactions must be rejected because of the endothermic nature of such reactions

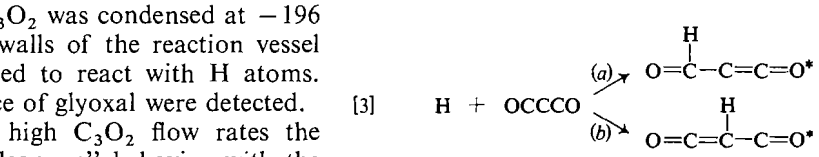

where reaction 3*a* is believed to be more likely in view of the presence of glyoxal as a product.

At low flow rates of C_3O_2 where H-atoms are in excess, reactions 4 and 5 occur, where OCC

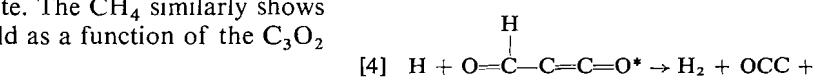

Can. J. Chem. Downloaded from www.nrcresearchpress.com by 210.87.254.40 on 09/05/12
For personal use only.

Can. J. Chem. Downloaded from www.nrcresearchpress.com by 210.87.254.40 on 09/05/12
For personal use only.

[5] $OCC + H_2 \rightarrow CH_2CO^* \xrightarrow{(a)\ wall} CH_2CO$
$\qquad\qquad\qquad

19. H. VON WEYSSENHOFF, S. DONDES, and P. HARTECK. J. Amer. Chem. Soc. **84**, 1526 (1962).
20. G. LIUTI, C. KUNZ, and S. DONDES. J. Amer. Chem. Soc. **89**, 5542 (1967).
21. N. DEMCHUK and H. GESSER. Can. J. Chem. **42**, 1 (1964).
22. H. GESSER and S. HUSSAIN. Nature, **201**, 290 (1964).
23. D. M. WILES and C. A. WINKLER. J. Phys. Chem. **61**, 620 (1957).
24. A. STOCK and H. STOLTZENBERG. Ber. **50**, 498 (1917).
25. N. DEMCHUK and H. GESSER. Can. J. Chem. **41**, 1645 (1963).
26. A. N. STRACHAN and D. E. THORTON. Can. J. Chem. **46**, 2353 (1968).
27. M. GROSSMAN, G. P. SEMELUK, and I. UNGER. Can. J. Chem. **47**, 3079 (1969).
28. R. N. SMITH, D. A. YOUNG, E. N. SMITH, and C. C. CARTER. Inorg. Chem. **2**, 829 (1963).
29. A. R. BLAKE, W. T. EELES, and P. P. JENNINGS. Trans. Faraday Soc. **60**, 691 (1964).

Can. J. Chem. Downloaded from www.nrcresearchpress.com by 210.87.254.40 on 09/05/12
For personal use only.

Conformation in Solution of 1,1,2,3,4,4-Hexachlorobutane

J. B. ROWBOTHAM,[1] H. M. HUTTON,[2] AND T. SCHAEFER
Chemistry Department, University of Manitoba, Winnipeg, Manitoba

Received September 16, 1970

Commercially available (Aldrich) 1,1,2,3,4,4-hexachlorobutane is as the meso isomer. On the basis of the values of the three distinct proton–proton coupling constants it is concluded that, with respect to the C—H bonds, the conformation is *gauche* about the C_1—C_2 bond and *trans* about the C_2—C_3 bond.

Canadian Journal of Chemistry, 49, 806 (1971)

In carbon disulfide (CS_2) and in dimethylsulfoxide (DMSO) solution the p.m.r. of **1** is an $[AX]_2$ spectrum. Analysis by LAOCN3 (1) yields $J_{1,2} = J_{3,4} = 1.80$ (1.86), $J_{2,3} = 10.14$ (10.08),

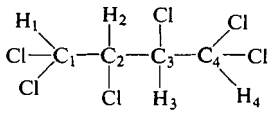

1

$J_{1,3} = J_{2,4} = -0.22$ (−0.16), and $J_{1,4} < 0.05$ Hz; the values in DMSO solution are given in brackets. The error in the coupling constants is very likely less than 0.05 Hz.

In ethane derivatives the vicinal *trans* proton–proton coupling, J_t, is much larger than the vicinal *gauche* coupling J_g (2). For example, in meso 2,3-dibromobutane $J_t = 10.3$ Hz while $J_g = 2.9 \pm 0.4$ Hz (3). In 2,3-dibromosuccinic acid $J_t = 10.7$ Hz (4), while $J_g < 2$ Hz in both sets of rotational isomers of 1-chloro-1,2-dibromo-2-iodoethane (2). Solvent effect studies (3) suggest $J_t = 6.3$ and $J_g = 2.0 \pm 0.6$ Hz in 1,1,2-trichloroethane.

Now, space-filling models indicate clearly that the meso form of **1** has minimum steric hindrance between groups when the C—H_2 and C—H_3 bonds are *trans* and that the destabilizing "parallel 1-3 interactions" between C—Cl bonds on C-1 and -3 (5) need not occur when the C—H_1 and C—H_2 bonds are *gauche*. On the other hand, the *dl*-isomer has the greatest steric freedom when C—H_1 and C—H_2 are *trans* while C—H_2 and C—H_3 are approximately *gauche*. The magnitudes of the coupling constants above, where $J_{1,2} \approx J_g$ and $J_{2,3} \approx J_t$, are therefore consistent with the meso form of **1**.

The preferred conformations of **1** about C_1—C_2 and C_2—C_3 are then as in **2** (or **2***a*) and **3**, respectively. Conformation **2** is preferred over **2***a* because $J_{1,3} = -0.2$ Hz. Thus, $J_g^{H,CH_3} \approx -0.3$ and $J_t^{H,CH_3} \approx 0.5$ Hz in propane derivatives (3, 6).

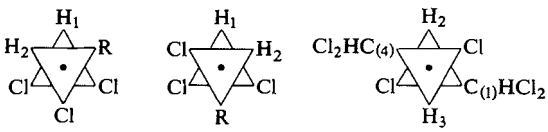

2 **2***a* **3**

R = $C_{(3)}H_{(3)}C_{(4)}H_{(4)}Cl_3$

Hence **2** is indicated as more stable than **2***a* if it is assumed that the two chlorine substituents on

[1]Postdoctoral fellow, 1970–1971.
[2]University of Winnipeg, Winnipeg, Manitoba.

19. H. VON WEYSSENHOFF, S. DONDES, and P. HARTECK. J. Amer. Chem. Soc. **84**, 1526 (1962).
20. G. LIUTI, C. KUNZ, and S. DONDES. J. Amer. Chem. Soc. **89**, 5542 (1967).
21. N. DEMCHUK and H. GESSER. Can. J. Chem. **42**, 1 (1964).
22. H. GESSER and S. HUSSAIN. Nature, **201**, 290 (1964).
23. D. M. WILES and C. A. WINKLER. J. Phys. Chem. **61**, 620 (1957).
24. A. STOCK and H. STOLTZENBERG. Ber. **50**, 498 (1917).
25. N. DEMCHUK and H. GESSER. Can. J. Chem. **41**, 1645 (1963).
26. A. N. STRACHAN and D. E. THORTON. Can. J. Chem. **46**, 2353 (1968).
27. M. GROSSMAN, G. P. SEMELUK, and I. UNGER. Can. J. Chem. **47**, 3079 (1969).
28. R. N. SMITH, D. A. YOUNG, E. N. SMITH, and C. C. CARTER. Inorg. Chem. **2**, 829 (1963).
29. A. R. BLAKE, W. T. EELES, and P. P. JENNINGS. Trans. Faraday Soc. **60**, 691 (1964).

Can. J. Chem. Downloaded from www.nrcresearchpress.com by 210.87.254.42 on 09/05/12
For personal use only.

Conformation in Solution of 1,1,2,3,4,4-Hexachlorobutane

J. B. ROWBOTHAM,[1] H. M. HUTTON,[2] AND T. SCHAEFER
Chemistry Department, University of Manitoba, Winnipeg, Manitoba

Received September 16, 1970

Commercially available (Aldrich) 1,1,2,3,4,4-hexachlorobutane is as the meso isomer. On the basis of the values of the three distinct proton–proton coupling constants it is concluded that, with respect to the C—H bonds, the conformation is *gauche* about the C_1—C_2 bond and *trans* about the C_2—C_3 bond.

Canadian Journal of Chemistry, 49, 806 (1971)

In carbon disulfide (CS_2) and in dimethylsulfoxide (DMSO) solution the p.m.r. of **1** is an $[AX]_2$ spectrum. Analysis by LAOCN3 (1) yields $J_{1,2} = J_{3,4} = 1.80$ (1.86), $J_{2,3} = 10.14$ (10.08),

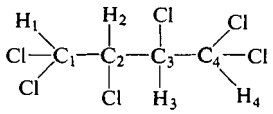

1

$J_{1,3} = J_{2,4} = -0.22$ (−0.16), and $J_{1,4} < 0.05$ Hz; the values in DMSO solution are given in brackets. The error in the coupling constants is very likely less than 0.05 Hz.

In ethane derivatives the vicinal *trans* proton–proton coupling, J_t, is much larger than the vicinal *gauche* coupling J_g (2). For example, in meso 2,3-dibromobutane $J_t = 10.3$ Hz while $J_g = 2.9 \pm 0.4$ Hz (3). In 2,3-dibromosuccinic acid $J_t = 10.7$ Hz (4), while $J_g < 2$ Hz in both sets of rotational isomers of 1-chloro-1,2-dibromo-2-iodoethane (2). Solvent effect studies (3) suggest $J_t = 6.3$ and $J_g = 2.0 \pm 0.6$ Hz in 1,1,2-trichloroethane.

Now, space-filling models indicate clearly that the meso form of **1** has minimum steric hindrance between groups when the C—H_2 and C—H_3 bonds are *trans* and that the destabilizing "parallel 1-3 interactions" between C—Cl bonds on C-1 and -3 (5) need not occur when the C—H_1 and C—H_2 bonds are *gauche*. On the other hand, the *dl*-isomer has the greatest steric freedom when C—H_1 and C—H_2 are *trans* while C—H_2 and C—H_3 are approximately *gauche*. The magnitudes of the coupling constants above, where $J_{1,2} \approx J_g$ and $J_{2,3} \approx J_t$, are therefore consistent with the meso form of **1**.

The preferred conformations of **1** about C_1—C_2 and C_2—C_3 are then as in **2** (or **2***a*) and **3**, respectively. Conformation **2** is preferred over **2***a* because $J_{1,3} = -0.2$ Hz. Thus, $J_g^{H,CH_3} \approx -0.3$ and $J_t^{H,CH_3} \approx 0.5$ Hz in propane derivatives (3, 6).

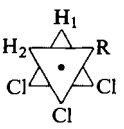

2

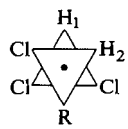

2*a*

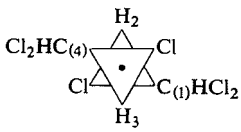

3

R = $C_{(3)}H_{(3)}C_{(4)}H_{(4)}Cl_3$

Hence **2** is indicated as more stable than **2***a* if it is assumed that the two chlorine substituents on

[1]Postdoctoral fellow, 1970–1971.
[2]University of Winnipeg, Winnipeg, Manitoba.

C-1 do not substantially affect $J_{1,3}$. The value of -0.2 Hz is, in fact, in agreement with the relationship (3, 7) ${}^4J = \cos^2\psi_1 + \cos^2\psi_2 - 0.7$ Hz where ψ_1 and ψ_2 are the dihedral (60°) angles of the fragments $H_1—C_1—C_2—C_3$ and $H_3—C_3—C_2—C_1$, respectively.

Of course, steric repulsions in the hexachlorobutane have probably altered the C—C—H angles somewhat and the dihedral angle of the fragment $H_2—C_2—C_3—H_3$ of **3** is almost certainly less than 180° while the dihedral angles of the *gauche* form **2***a* are probably also somewhat less than 60°. Furthermore, the electronegativities of bromine and chlorine are somewhat different so that a direct comparison of J_t in hexachlorobutane and meso-2,3-dibromobutane is difficult. Finally, the alternating electronegativity effect (8), as well as the steric dependence of the influence of the substituent electronegativity (9), introduces further complexities.[3] The alternating effect implies that the 1,1 and 4,4 chlorine atoms will compensate for the higher electronegativity of chlorine at positions 2 and 3. In spite of these second order effects it is felt that the conclusions above are valid.

Conformation **2** avoids the 1:3 interactions between C—Cl bonds and has a zero dipole moment. The invariance of the coupling constants to the dielectric constant of the solvent (2.6 for CS_2 and 48 for DMSO) suggests that **2** and **3** are by far the most stable of the possible conformations (3) and perhaps that their stability is determined mainly by intramolecular steric interactions as opposed to intermolecular dipole or quadrupole interactions with the dielectric medium.

[3]See ref. 10 for a full discussion of stereochemical and substituent effects on ${}^4J$.

Experimental

The proton resonance spectra of 1,1,2,3,4,4-hexachlorobutane as dilute (less than 10 mol %) degassed solutions in CS_2 and DMSO were taken on a DA60I spectrometer in the frequency sweep mode. The spectra were calibrated by period-averaging techniques. The r.m.s. error in the LAOCN3 analyses was 0.011 and the probable errors in the coupling parameters were 0.01 Hz or less.

We are grateful to the National Research Council of Canada for financial assistance.

1. S. Castellano and A. A. Bothner-By. J. Chem. Phys. **41**, 3863 (1964).
2. G. Govil and H. J. Bernstein. J. Chem. Phys. **49**, 911 (1968), and references therein.
3. R. J. Abraham. J. Phys. Chem. **73**, 1192 (1969).
4. R. Freeman and K. G. R. Pachler. Mol. Phys. **5**, 85 (1962).
5. A. B. Dempster, K. Price, and N. Sheppard. Spectrochim. Acta, **25A**, 1381 (1969).
6. H. Finegold. J. Chem. Phys. **41**, 1808 (1964).
7. M. Barfield. J. Chem. Phys. **41**, 3825 (1964).
8. A. D. Cohen and T. Schaefer. Mol. Phys. **10**, 209 (1966).
9. H. Booth. Tetrahedron Lett. 411 (1965).
10. M. Barfield and B. Chakrabarti. Chem. Rev. **69**, 757 (1969).

Potassium Methylamide: Preparation and Infrared Spectrum

R. C. Makhija and R. A. Stairs
Department of Chemistry, Trent University, Peterborough, Ontario

Received September 9, 1970

Potassium methylamide has been prepared by a convenient method using potassium hydride. The i.r. absorption spectrum is reported.

On a préparé la méthylamide de potassium par une méthode commode à partir de l'hydrure de potassium. Le spectre d'absorption i.r. est enregistré.

Canadian Journal of Chemistry, **49**, 807 (1971)

A survey of the literature yielded no satisfactory method for the preparation of potassium methylamide. Methods suitable for higher-boiling amines are known (1, 2), but methods described for alkali amides (3–5), when used with methylamine, yielded unstable mixtures. Juza and Hillenbrand (6) successfully prepared lithium methylamide by reaction of the amine with metal without catalyst in a sealed tube at 60 °C, but they state that with the heavier alkali metals this

Can. J. Chem. Downloaded from www.nrcresearchpress.com by 210.87.254.42 on 09/05/12
For personal use only.

C-1 do not substantially affect $J_{1,3}$. The value of -0.2 Hz is, in fact, in agreement with the relationship (3, 7) ${}^4J = \cos {}^2\psi_1 + \cos {}^2\psi_2 - 0.7$ Hz where ψ_1 and ψ_2 are the dihedral (60°) angles of the fragments $H_1—C_1—C_2—C_3$ and $H_3—C_3—C_2—C_1$, respectively.

Of course, steric repulsions in the hexachlorobutane have probably altered the C—C—H angles somewhat and the dihedral angle of the fragment $H_2—C_2—C_3—H_3$ of **3** is almost certainly less than 180° while the dihedral angles of the *gauche* form **2***a* are probably also somewhat less than 60°. Furthermore, the electronegativities of bromine and chlorine are somewhat different so that a direct comparison of J_t in hexachlorobutane and meso-2,3-dibromobutane is difficult. Finally, the alternating electronegativity effect (8), as well as the steric dependence of the influence of the substituent electronegativity (9), introduces further complexities.[3] The alternating effect implies that the 1,1 and 4,4 chlorine atoms will compensate for the higher electronegativity of chlorine at positions 2 and 3. In spite of these second order effects it is felt that the conclusions above are valid.

Conformation **2** avoids the 1:3 interactions between C—Cl bonds and has a zero dipole moment. The invariance of the coupling constants to the dielectric constant of the solvent (2.6 for CS_2 and 48 for DMSO) suggests that **2** and **3** are by far the most stable of the possible conformations (3) and perhaps that their stability is determined mainly by intramolecular steric interactions as opposed to intermolecular dipole or quadrupole interactions with the dielectric medium.

[3]See ref. 10 for a full discussion of stereochemical and substituent effects on ${}^4J$.

Experimental

The proton resonance spectra of 1,1,2,3,4,4-hexachlorobutane as dilute (less than 10 mol %) degassed solutions in CS_2 and DMSO were taken on a DA60I spectrometer in the frequency sweep mode. The spectra were calibrated by period-averaging techniques. The r.m.s. error in the LAOCN3 analyses was 0.011 and the probable errors in the coupling parameters were 0.01 Hz or less.

We are grateful to the National Research Council of Canada for financial assistance.

1. S. Castellano and A. A. Bothner-By. J. Chem. Phys. **41**, 3863 (1964).
2. G. Govil and H. J. Bernstein. J. Chem. Phys. **49**, 911 (1968), and references therein.
3. R. J. Abraham. J. Phys. Chem. **73**, 1192 (1969).
4. R. Freeman and K. G. R. Pachler. Mol. Phys. **5**, 85 (1962).
5. A. B. Dempster, K. Price, and N. Sheppard. Spectrochim. Acta, **25A**, 1381 (1969).
6. H. Finegold. J. Chem. Phys. **41**, 1808 (1964).
7. M. Barfield. J. Chem. Phys. **41**, 3825 (1964).
8. A. D. Cohen and T. Schaefer. Mol. Phys. **10**, 209 (1966).
9. H. Booth. Tetrahedron Lett. 411 (1965).
10. M. Barfield and B. Chakrabarti. Chem. Rev. **69**, 757 (1969).

Potassium Methylamide: Preparation and Infrared Spectrum

R. C. Makhija and R. A. Stairs
Department of Chemistry, Trent University, Peterborough, Ontario

Received September 9, 1970

Potassium methylamide has been prepared by a convenient method using potassium hydride. The i.r. absorption spectrum is reported.

On a préparé la méthylamide de potassium par une méthode commode à partir de l'hydrure de potassium. Le spectre d'absorption i.r. est enregistré.

Canadian Journal of Chemistry, **49**, 807 (1971)

A survey of the literature yielded no satisfactory method for the preparation of potassium methylamide. Methods suitable for higher-boiling amines are known (1, 2), but methods described for alkali amides (3–5), when used with methylamine, yielded unstable mixtures. Juza and Hillenbrand (6) successfully prepared lithium methylamide by reaction of the amine with metal without catalyst in a sealed tube at 60 °C, but they state that with the heavier alkali metals this

Can. J. Chem. Downloaded from www.nrcresearchpress.com by 210.87.254.6 on 09/05/12
For personal use only.

TABLE 1. Infrared bands of potassium methylamide and methylamine (7)*

KCH_3NH (CsI solid)	CH_3NH_2 (Gaseous)	Assignments
3490 m	3387	
—	3360	N—H stretching
2925 w	2962, 2842, 2822	C—H stretching
—	2630	
—	2565	
2410–2465 mw b	2425	
2280 vw	2234	
2165 m	—	
—	2072	2C—N stretching
1925 w	—	
1660 sh	1622	N—H deformation
1570 s	—	
1430 sh	1460	CH_3 bending
1405 vs	1410	
1330 m, 1315 m	—	
1265 m, 1210 w, 1120 w	1244, 1129	CH_3 rocking
1075 bw, 1052 w	1044	C—N stretching
8875	—	
768 w, 745 w	779	N—H rocking
682 m, 640 w, 630 w	600	N—H
525 w	515	
430–450 wb	470	

*s, Strong; m, medium; w, weak; b, broad; and sh, shoulder.

method led to the formation of cyanide. We have tried two methods: Juza and Hillenbrand's, but at room temperature, and reaction of methylamine with potassium hydride either at room temperature or at −20 °C. Both methods yielded products that could be handled, but the first was very slow. The method using hydride took 4–6 h at room temperature, or 24–36 h at −20 °C. This method only is described in detail in the Experimental.

An i.r. spectrum of potassium methylamide (CsI disc) was obtained. The bands observed are listed in Table 1 as well as those bands and assignments reported for gaseous methylamine by Barceló Matutano and Bellanato (7). It will be noted that most of the bands we observed can be related to methylamine bands by suitable shifts. The unassigned band at 2165 cm^{-1} is due to cyanide.

Caution

(*1*) The method described involves evolution of hydrogen (a mole for each mol of potassium hydride). The quantities used must not be so large that dangerous pressures are generated in the sealed tubes.

(*2*) Potassium methylamide is very hygroscopic and pyrophoric, and may explode on contact with air. It reacts very vigorously with water and alcohols. It must be stored in vials sealed *in vacuo* or under argon, and opened with proper precautions.

Experimental

Potassium hydride (50% in oil, Alfa) was washed several times with sodium-dried cyclohexane to free it from oil and fines. Small-scale preparations (~2 mmol) were carried out in break-seal ampoules of about 20 ml capacity. About 0.1 g of the cleaned potassium hydride was transferred to the ampoule along with some cyclohexane. (This operation was performed in a dry-box in argon.) The ampoule was attached to a vacuum line and the cyclohexane was removed by distillation. Methylamine (Matheson), about 5 ml, was distilled from the cylinder onto lithium metal, allowed to stand at Dry-Ice temperature for 8–10 h, then degassed and subjected to several bulb-to-bulb fractional distillations, before being distilled onto the potassium hydride in the ampoule. This was then sealed. After 4–6 h at room temperature the reaction was complete, and a clear yellow solution was obtained. This solution was transferred into another vessel through the break-seal and a sintered filter, on the vacuum line. The excess of methylamine was removed under vacuum, and white crystals of potassium methylamide remained. These were subjected to further evacuation, and then sealed *in vacuo*.

Somewhat larger scale (~20 mmol) preparations were carried out in a ground joint flask, which was fitted for attachment to the vacuum line, and which contained a syphon tube with a sintered-glass filter permitting transfer of the yellow amide solution to another flask, to separate the product from the potassium hydroxide that was always formed in small amount. Procedure was as before, except that the reaction was carried out at −20 to −15 °C rather than at room temperature. Since at this temperature the reaction took 24–36 h to complete, a cryostat was used to maintain the temperature.

Can. J. Chem. Downloaded from www.nrcresearchpress.com by 210.87.254.6 on 09/05/12
For personal use only.

The product was analyzed acidimetrically. The sealed tube containing potassium methylamide was opened in the dry box, and samples weighed into separate vials. An entire sample was then added quickly to excess standard hydrochloric acid and the excess acid titrated with standard base, with methyl orange as indicator. Equivalent weight required (for $KCH_3NH + 2HCl = KCl + CH_3NH_3Cl$) 34.50; found, 35.50, 35.30, 35.10; average, 35.30. This discrepancy, if KCN is the sole impurity, corresponds to an assay of 95.2% $KNHCH_3$.

The authors wish to thank Atomic Energy of Canada, Limited, for support, and also thank A. R. Bancroft for drawing their attention to certain of the references.

1. D. D. HUMPHREYS. U.S. Pat. 2 685 604 (Chem. Abstr. **49**, 10358*c*). British Pat. 755 373 (Chem. Abstr. **51**, 10569*c*).
2. Ethyl Corporation. British Pat. 742 790 (Chem. Abstr. **50**, 16826*c*).
3. H. H. SISLER. *In* Comprehensive inorganic chemistry. M. C. Sneed and R. C. Brasted, editors. Vol. 5. Van Nostrand, Princeton, N.J., 1956. p. 29.
4. W. L. JOLLY. Synthetic inorganic chemistry. Prentice-Hall, New York, N.Y., 1960. pp. 153–155.
5. K. BAR-ELI and F. S. KLEIN. J. Chem. Soc. 1378, 3083 (1962).
6. R. JUZA and E. HILLENBRAND. Z. anorg. allgem. Chem. **273**, 297 (1953).
7. J. R. BARCELÓ MATUTANO and J. BELLANATO. Spectrochim. Acta, **8**, 27 (1956).

Significance of Heterogeneous Catalysis of Certain Oxidation Reactions by Oxides in Relation to their Heats of Formation

ASHOK K. VIJH[1] AND P. LENFANT[2]
Hydro-Quebec Institute of Research, Varennes, Quebec

Received May 6, 1970

The significance of previous correlations observed by Morooka *et al.* between heats of formation per oxygen atom, ΔH_0, for oxides and their catalytic activity towards oxidation of some hydrocarbons has been discussed. It has been pointed out that ΔH_0 values do not represent metal–oxygen bond energies, as assumed by Morooka and co-workers, but instead signify band gap values for the oxides. The catalytic activity of these oxides must therefore be interpreted in terms of their electronic conductivity and not in relation to the stength of metal–oxygen bond involved.

La signification des corrélations antérieures, observées par Morooka *et coll.*, entre la chaleur de formation des oxydes par atome d'oxygène, ΔH_0, et leur activité catalytique dans l'oxydation de certains hydrocarbures a été discutée. Il a été montré que les valeurs de ΔH_0 ne représentent pas les énergies de liaison métal-oxygène, comme supposé par Morooka *et coll.*, mais signifient plutôt des valeurs de bande d'énergie interdite des oxydes. L'activité catalytique de ces oxydes doit donc être interprétée en termes de leur conductivité électronique et non pas en relation avec la force des liaisons métal–oxygène impliquées.

Canadian Journal of Chemistry, **49**, 809 (1971)

It has been shown in the literature that certain regularities exist in the catalytic behavior of some metal oxides towards oxidation of propylene (1), ethylene (2), propane (2), acetylene (2), and isobutene (2). Specifically, it was observed that with increasing (exothermic) heat of formation (standard state) per oxygen atom, ΔH_0, of an oxide, the rate of oxidation of a given hydrocarbon decreases. These experimental observations were interpreted by *assuming* that ΔH_0 signifies the strength of a metal–oxygen (MO) bond in an oxide; and, that since heterogeneous oxidation catalysis by oxides involves surface reactions in which loosening or breaking of MO bonds probably occurs, relation between ΔH_0 and the catalytic activity of the oxide must follow.

The purpose of the present note is to point out that: (*1*) the ΔH_0 values do *not* represent the strength of the MO bond; therefore the previous interpretations (1, 2) merit modifications; (*2*) in fact, there exists no correlation between MO bond energy of an oxide and its catalytic activity towards oxidation of hydrocarbons; (*3*) re-

[1]At present, also Visiting Professor in the Energy Centre of National Institute of Scientific Research, University of Quebec at Varennes, Quebec.
[2]At present, also Lecturer in Ecole Polytechnique de Montreal, Quebec.

Can. J. Chem. Downloaded from www.nrcresearchpress.com by 210.87.254.6 on 09/05/12
For personal use only.

The product was analyzed acidimetrically. The sealed tube containing potassium methylamide was opened in the dry box, and samples weighed into separate vials. An entire sample was then added quickly to excess standard hydrochloric acid and the excess acid titrated with standard base, with methyl orange as indicator. Equivalent weight required (for $KCH_3NH + 2HCl = KCl + CH_3NH_3Cl$) 34.50; found, 35.50, 35.30, 35.10; average, 35.30. This discrepancy, if KCN is the sole impurity, corresponds to an assay of 95.2% $KNHCH_3$.

The authors wish to thank Atomic Energy of Canada, Limited, for support, and also thank A. R. Bancroft for drawing their attention to certain of the references.

1. D. D. HUMPHREYS. U.S. Pat. 2 685 604 (Chem. Abstr. **49**, 10358*c*). British Pat. 755 373 (Chem. Abstr. **51**, 10569*c*).
2. Ethyl Corporation. British Pat. 742 790 (Chem. Abstr. **50**, 16826*c*).
3. H. H. SISLER. *In* Comprehensive inorganic chemistry. M. C. Sneed and R. C. Brasted, editors. Vol. 5. Van Nostrand, Princeton, N.J., 1956. p. 29.
4. W. L. JOLLY. Synthetic inorganic chemistry. Prentice-Hall, New York, N.Y., 1960. pp. 153–155.
5. K. BAR-ELI and F. S. KLEIN. J. Chem. Soc. 1378, 3083 (1962).
6. R. JUZA and E. HILLENBRAND. Z. anorg. allgem. Chem. **273**, 297 (1953).
7. J. R. BARCELÓ MATUTANO and J. BELLANATO. Spectrochim. Acta, **8**, 27 (1956).

Significance of Heterogeneous Catalysis of Certain Oxidation Reactions by Oxides in Relation to their Heats of Formation

ASHOK K. VIJH[1] AND P. LENFANT[2]
Hydro-Quebec Institute of Research, Varennes, Quebec

Received May 6, 1970

The significance of previous correlations observed by Morooka *et al.* between heats of formation per oxygen atom, ΔH_0, for oxides and their catalytic activity towards oxidation of some hydrocarbons has been discussed. It has been pointed out that ΔH_0 values do not represent metal–oxygen bond energies, as assumed by Morooka and co-workers, but instead signify band gap values for the oxides. The catalytic activity of these oxides must therefore be interpreted in terms of their electronic conductivity and not in relation to the stength of metal–oxygen bond involved.

La signification des corrélations antérieures, observées par Morooka *et coll.*, entre la chaleur de formation des oxydes par atome d'oxygène, ΔH_0, et leur activité catalytique dans l'oxydation de certains hydrocarbures a été discutée. Il a été montré que les valeurs de ΔH_0 ne représentent pas les énergies de liaison métal-oxygène, comme supposé par Morooka *et coll.*, mais signifient plutôt des valeurs de bande d'énergie interdite des oxydes. L'activité catalytique de ces oxydes doit donc être interprétée en termes de leur conductivité électronique et non pas en relation avec la force des liaisons métal–oxygène impliquées.

Canadian Journal of Chemistry, **49**, 809 (1971)

It has been shown in the literature that certain regularities exist in the catalytic behavior of some metal oxides towards oxidation of propylene (1), ethylene (2), propane (2), acetylene (2), and isobutene (2). Specifically, it was observed that with increasing (exothermic) heat of formation (standard state) per oxygen atom, ΔH_0, of an oxide, the rate of oxidation of a given hydrocarbon decreases. These experimental observations were interpreted by *assuming* that ΔH_0 signifies the strength of a metal–oxygen (MO) bond in an oxide; and, that since heterogeneous oxidation catalysis by oxides involves surface reactions in which loosening or breaking of MO bonds probably occurs, relation between ΔH_0 and the catalytic activity of the oxide must follow.

The purpose of the present note is to point out that: (*1*) the ΔH_0 values do *not* represent the strength of the MO bond; therefore the previous interpretations (1, 2) merit modifications; (*2*) in fact, there exists no correlation between MO bond energy of an oxide and its catalytic activity towards oxidation of hydrocarbons; (*3*) re-

[1]At present, also Visiting Professor in the Energy Centre of National Institute of Scientific Research, University of Quebec at Varennes, Quebec.
[2]At present, also Lecturer in Ecole Polytechnique de Montreal, Quebec.

Can. J. Chem. Downloaded from www.nrcresearchpress.com by 210.87.254.105 on 09/05/12
For personal use only.

Can. J. Chem. Downloaded from www.nrcresearchpress.com by 210.87.254.105 on 09/05/12
For personal use only.

lationship between ΔH_0 and the catalytic activity arises because ΔH_0 is the band gap and hence related to the electronic conductivity of the oxide.

Some Definitions and Related Matters

It may be shown by means of a Born–Haber cycle (3) that heat of formation per mol of a substance in its standard state, *e.g.*, of solid NiO, is given by

$$[1] \quad \Delta H_m = I_m + \Delta H_S + \tfrac{1}{2}\Delta H_D + A_X - U$$

where ΔH_m is the heat of formation (standard state) of NiO per *mol*; I_m is the sum of first and second ionization potentials of Ni; ΔH_S is the heat of sublimation of Ni metal to give Ni atoms; ΔH_D is the heat of dissociation of O_2 molecule to give O atoms; U is the lattice energy of NiO; A_X is the electron affinity of O atom to form O^{2-} ion.

All quantities refer to the heat absorbed by the system for the indicated process.

All the above quantities are per mol, which in the case of NiO is the same as per oxygen atom. However, in the case of, say, Ta_2O_5, ΔH_0, the heat of formation *per oxygen atom* (*i.e.* the quantity used in refs. 1 and 2) is 1/5 the heat of formation per *mol*. Here, we define another quantity, namely, heat of formation per equivalent, ΔH_e, which will be the heat of formation per mol of Ta_2O_5 divided by the number of valence electrons transferred (*viz.* 10) in the formation of 1 mol of Ta_2O_5. The foregoing definitions for a typical case, *e.g.*, Ta_2O_5 may be summarized by the equation

$$[2] \quad -(\Delta H_m)_{Ta_2O_5} = -(1/5)(\Delta H_0)_{Ta_2O_5} = -(1/10)(\Delta H_e)_{Ta_2O_5}$$

The negative signs in eq. 2 signify exothermicity. Neither ΔH_m, nor ΔH_0, nor ΔH_e, however, represents *bond* energy. The bond energy, after suitable corrections for some minor factors which may arise in certain cases (4), *e.g.*, NiO is essentially given by

$$[3] \quad b = (-\Delta H_m + \Delta H_S + \tfrac{1}{2}\Delta H_D)/2$$

where b is the MO bond energy; ΔH_m, ΔH_S, ΔH_D are defined as above, and 2 is the number of valence electrons transferred in the formation of the nickel oxide from the constituent elements in the standard state.

The b value thus obtained is the enthalpy change (see eq. 10) in the process MO(S) $\rightarrow$ O(g) + M(g). The $-\Delta H_0$ of Morooka *et al.* (1) is the enthalpy change (see eq. 11) in the process MO(S) $\rightarrow \frac{1}{2}O_2$ (g) + M (S). Further amplification of the significance of this matter is given in a subsequent section here.

The basic misconception in the interpretations of Morooka *et al.* has been to equate b of eq. 3 here with the ΔH_0 of eq. 2; the two quantities are, of course, quite different. The observation of Morooka *et al.* that ΔH_0 is related to the catalytic activity of the oxide is still correct; however, their assumption that ΔH_0 represents bond energy of the oxide is incorrect. An excellent discussion of these matters has been given by Howald (4).

What then is the significance of ΔH_0? It follows from eq. 2 that for any oxide

$$[4] \quad -(\Delta H_0) = -2(\Delta H_e)$$

It has been shown previously (5) that

$$[5] \quad E_g \simeq -2(\Delta H_e)$$

where E_g is the band gap of a material, oxide in the present context. Combination of eqs. 4 and 5 would give

$$[6] \quad E_g = -(\Delta H_0)$$

i.e., ΔH_0 does not represent the bond energy but it denotes the *band gap* of the oxide.

Relation to Catalysis of Hydrocarbon Oxidation

Results of Morooka *et al.* (1, 2) in which with decreasing (exothermic) ΔH_0 values of oxides, rate of hydrocarbon oxidation increases may now be interpreted in a somewhat different way. Since ΔH_0 is *not* the bond energy but a band gap value, the rate of hydrocarbon oxidation may be concluded to increase with increasing oxide conductivity, *i.e.*, with decreasing value of $-\Delta H_0$.

The fact that $-\Delta H_0$ ($= -2\Delta H_e$), is indeed related to the conductivity values of the oxides may also be seen in Fig. 1. For semiconducting materials, the intrinsic electronic conductivity, σ (6), is given by

$$[7] \quad \sigma = \sigma_0 \exp(-E_g/kT)$$

where k is the Boltzmann's constant, and, T, the absolute temperature; σ_0 is the limiting electronic conductivity when E_g approaches zero.

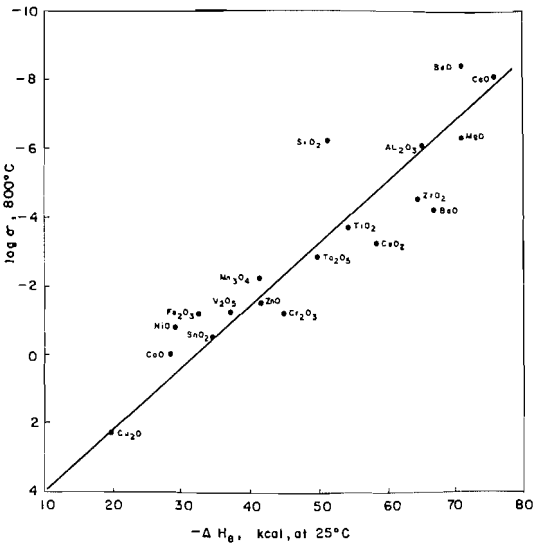

FIG. 1. Relationship between logarithm of "intrinsic" electronic conductivity and heats of formation per equivalent for several oxides. Data for this figure have been obtained from refs. 7 and 9.

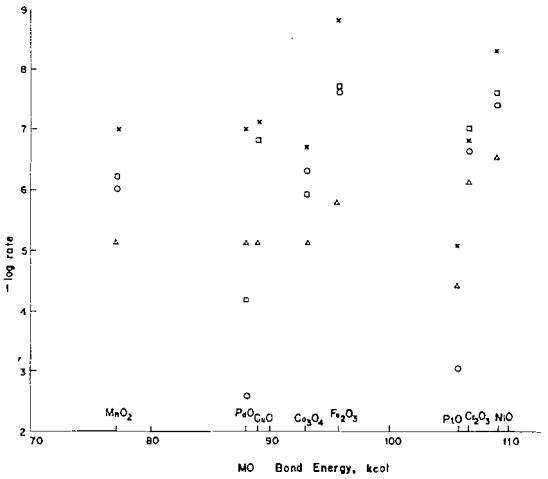

FIG. 2. A plot of heats of atomization per equivalent (*i.e.* approximate value of average bond energies as calculated from thermochemical data in ref. 8) for various oxide catalysts *vs.* their catalytic activity at 300 °C for the oxidation of isobutene (○), acetylene (△), ethylene (□), and propane (×). Reaction rate for acetylene oxidation refers to 220 °C. Rate data have been obtained from ref. 2. Thermochemical data for calculation of bond energies of CeO_2 and ThO_2 are not available. It may be noted that no correlation exists between catalytic activity and bond energies for the several oxides shown in this figure. The bond energies plotted here are, of course, the *b* values as obtained from eq. 3 of the paper.

Combination of eqs. 7 and 5 gives

$$[8] \qquad \sigma = \sigma_0 \exp - (\Delta H_e/kT)$$

or

$$[9] \qquad \log \sigma = \log \sigma_0 - \Delta H_e/2.303\, kT$$

Equation 9 predicts a linear relation between $\log \sigma$ and $1/T$ for a *given* oxide, with a slope equal to $\Delta H_e/2.303\ k$. If, however, $\log \sigma_0$ values for several oxides fall within a narrow range, an approximate correlation between $\log \sigma$ and $-\Delta H_e$ values for various oxides will be expected with the value of slope *roughly* equal to $1/2.303\, kT$, at a constant T.

This is what is indeed observed in practice and is depicted in Fig. 1. It is clear that Fig. 1 only arises, because, fortuitously, values of $\log \sigma_0$ for various oxides have a roughly constant value. In any case, the empirical significance of Fig. 1, namely, higher $-\Delta H_e$ $(= -\frac{1}{2}\Delta H_0)$ values for oxides are associated with lower electronic conductivity, is quite clear.

The fact that the catalytic activity for hydrocarbon oxidation is not related to the bond energy (as calculated, of course, by eq. 3 above) of the oxides, as implied in the foregoing analysis, is directly supported by Fig. 2. Here the bond energy values, *b*, for various oxides are taken from Sanderson (8) and plotted against the rate of catalytic oxidation of various oxides reported by Morooka *et al.* (2). No correlation is indeed observed.

The higher catalytic activity of the oxides associated with higher electronic conductivity, as concluded here, would seem to emphasize that the rate-determining step in these catalytic oxidations is probably limited by the availability of charge carriers in the oxides, namely, electrons and holes. This is not entirely unexpected since oxidation reactions must involve either injection of electrons into the oxide or consumption of holes extracted from the oxide at some stage during the overall oxidation reaction.

Even though there is no relationship between the catalytic activity of the oxides and their bond energies as usually defined (4), *i.e.*, as the enthalpy change in the reaction (*viz.* eq. 3 above)

$$[10] \qquad \mathrm{MO\ (S)} \rightarrow \mathrm{M\ (g)} + \mathrm{O\ (g)}$$

one could always write the rupture of metal oxide bond as represented by

$$[11] \qquad \mathrm{MO\ (S)} \rightarrow \mathrm{M(S)} + \mathrm{O\ (g)}$$

The enthalpy change in reaction 11, which is

Can. J. Chem. Downloaded from www.nrcresearchpress.com by 210.87.254.105 on 09/05/12
For personal use only.

not the bond energy of the oxide according to the accepted definition of the term (4), may then be denoted by $(\Delta H)_{11}$ and would be given by

[12] $$(\Delta H)_{11} = -\Delta H_m + \tfrac{1}{2}\Delta H_D$$

For a series of oxides, $\frac{1}{2}\Delta H_D$ is, of course, constant so that

[13] $$(\Delta H)_{11} = -\Delta H_m + \text{constant}$$

In other words, $(\Delta H)_{11}$ would be linearly related to $-\Delta H_m$; hence, any relationship between $-\Delta H_m$ (or $-\Delta H_0$) and catalytic activity, as indeed is observed by Morooka *et al.*, would signify that the catalytic activity is related to the enthalpy change in reaction 11, probably because of the involvement of a bond-breaking reaction of the type

[14] MO (S) + HyC (g) → M(S) + gaseous products

In this sense, therefore, one may speak of the relationship of catalytic activity to the enthalpy change in a bond-breaking reaction of types [11] and [14]. Even though this interpretation may be extended to the data of Morooka *et al.*, the alternative interpretation in terms of relationship to band gaps and hence electron–hole concentration, as suggested here, is not entirely excluded. Furthermore, even if the foregoing interpretation of the data of Morooka *et al.* in terms of bond rupture is accepted as valid, the catalytic activity is related to the enthalpy of reaction 11 and not to the bond energy (4), the latter being given by eq. 3.

Conclusions

For the particular data reported by Morooka *et al.* (1, 2) on the catalytic oxidation of several hydrocarbons by various oxides, it has been shown that Morooka's correlations between ΔH_0 and catalytic activity do not signify the dependence of latter on the bond energy; instead, they arise because ΔH_0 is equal to the band gap of the oxide and is thence related to its conductivity and therefore to its catalytic activity.

1. Y. Morooka and A. Ozaki. J. Catal. **5**, 116 (1966).
2. Y. Morooka, Y. Morikawa, and A. Ozaki. J. Catal. **7**, 23 (1967).
3. W. J. Moore. Seven Solid States. W. A. Benjamin, Inc., New York. 1967.
4. R. Howald. J. Chem. Ed. **45**, 163 (1968).
5. A. K. Vijh. J. Phys. Chem. Solids. **29**, 2233 (1968); J. Electrochem. Soc. **117**, 173C (1970); J. Matl. Sci. **5**, 379 (1970).
6. J. P. Suchet. Chimie Physique des Semiconducteurs, Dunod, Paris. 1962.
7. V. N. Eremenko. *In* The Role of Surface Phenomena in Metallurgy. *Edited by* V. N. Eremenko. Consultants Bureau, New York. 1963. English Translation.
8. R. T. Sanderson. Inorganic Chemistry. Reinhold, New York. 1969.
9. Handbook of Chemistry and Physics. The Chemical Rubber Co., Cleveland. 1966–1967.

Can. J. Chem. Downloaded from www.nrcresearchpress.com by 210.87.254.105 on 09/05/12
For personal use only.

Electron Spin Resonance Spectra of Radicals Produced in the Thermal Reaction of Benzophenone with Triphenylsilane

A. R. McIntosh[1] and J. K. S. Wan
Department of Chemistry, Queen's University, Kingston, Ontario

Received September 21, 1970

Thermal reaction of benzophenone with triphenylsilane at 400 °K produced an electron spin resonance (e.s.r.) spectrum which is interpreted due to the triphenylsiloxydiphenylmethyl radical, $Ph_2\dot{C}OSiPh_3$.

La réaction thermique de la benzophénone avec le triphénylsilane à 400 °K produit un spectre r.p.e. qui peut être interprété comme étant du au radical triphénylsiloxydiphenylméthyle, $Ph_2\dot{C}OSiPh_3$.

Canadian Journal of Chemistry, 49, 812 (1971)

Introduction

The question of d-orbital participation in π-bonding in simple organic radicals has recently been of great interest. Direct e.s.r. evidence has been reported for d–p π-bonding in a series of Group IV*B* substituted methyl radicals (1). A number of silyl radicals have also been reported (2). We have recently attempted to generate triphenylsilyl radicals in liquid solution by various methods for e.s.r. study, since such radicals

[1]National Research Council of Canada Postgraduate Scholar, 1968–1971.

not the bond energy of the oxide according to the accepted definition of the term (4), may then be denoted by $(\Delta H)_{11}$ and would be given by

[12] $$(\Delta H)_{11} = -\Delta H_m + \tfrac{1}{2}\Delta H_D$$

For a series of oxides, $\frac{1}{2}\Delta H_D$ is, of course, constant so that

[13] $$(\Delta H)_{11} = -\Delta H_m + \text{constant}$$

In other words, $(\Delta H)_{11}$ would be linearly related to $-\Delta H_m$; hence, any relationship between $-\Delta H_m$ (or $-\Delta H_0$) and catalytic activity, as indeed is observed by Morooka *et al.*, would signify that the catalytic activity is related to the enthalpy change in reaction 11, probably because of the involvement of a bond-breaking reaction of the type

[14] MO (S) + HyC (g) → M(S) + gaseous products

In this sense, therefore, one may speak of the relationship of catalytic activity to the enthalpy change in a bond-breaking reaction of types [11] and [14]. Even though this interpretation may be extended to the data of Morooka *et al.*, the alternative interpretation in terms of relationship to band gaps and hence electron–hole concentration, as suggested here, is not entirely excluded. Furthermore, even if the foregoing interpretation of the data of Morooka *et al.* in terms of bond rupture is accepted as valid, the catalytic activity is related to the enthalpy of reaction 11 and not to the bond energy (4), the latter being given by eq. 3.

Conclusions

For the particular data reported by Morooka *et al.* (1, 2) on the catalytic oxidation of several hydrocarbons by various oxides, it has been shown that Morooka's correlations between ΔH_0 and catalytic activity do not signify the dependence of latter on the bond energy; instead, they arise because ΔH_0 is equal to the band gap of the oxide and is thence related to its conductivity and therefore to its catalytic activity.

1. Y. Morooka and A. Ozaki. J. Catal. **5**, 116 (1966).
2. Y. Morooka, Y. Morikawa, and A. Ozaki. J. Catal. **7**, 23 (1967).
3. W. J. Moore. Seven Solid States. W. A. Benjamin, Inc., New York. 1967.
4. R. Howald. J. Chem. Ed. **45**, 163 (1968).
5. A. K. Vijh. J. Phys. Chem. Solids. **29**, 2233 (1968); J. Electrochem. Soc. **117**, 173C (1970); J. Matl. Sci. **5**, 379 (1970).
6. J. P. Suchet. Chimie Physique des Semiconducteurs, Dunod, Paris. 1962.
7. V. N. Eremenko. *In* The Role of Surface Phenomena in Metallurgy. *Edited by* V. N. Eremenko. Consultants Bureau, New York. 1963. English Translation.
8. R. T. Sanderson. Inorganic Chemistry. Reinhold, New York. 1969.
9. Handbook of Chemistry and Physics. The Chemical Rubber Co., Cleveland. 1966–1967.

Can. J. Chem. Downloaded from www.nrcresearchpress.com by 210.87.254.40 on 09/05/12
For personal use only.

Electron Spin Resonance Spectra of Radicals Produced in the Thermal Reaction of Benzophenone with Triphenylsilane

A. R. McIntosh[1] and J. K. S. Wan
Department of Chemistry, Queen's University, Kingston, Ontario

Received September 21, 1970

Thermal reaction of benzophenone with triphenylsilane at 400 °K produced an electron spin resonance (e.s.r.) spectrum which is interpreted due to the triphenylsiloxydiphenylmethyl radical, $Ph_2\dot{C}OSiPh_3$.

La réaction thermique de la benzophénone avec le triphénylsilane à 400 °K produit un spectre r.p.e. qui peut être interprété comme étant du au radical triphénylsiloxydiphenylméthyle, $Ph_2\dot{C}OSiPh_3$.

Canadian Journal of Chemistry, 49, 812 (1971)

Introduction

The question of d-orbital participation in π-bonding in simple organic radicals has recently been of great interest. Direct e.s.r. evidence has been reported for d–p π-bonding in a series of Group IV*B* substituted methyl radicals (1). A number of silyl radicals have also been reported (2). We have recently attempted to generate triphenylsilyl radicals in liquid solution by various methods for e.s.r. study, since such radicals

[1]National Research Council of Canada Postgraduate Scholar, 1968–1971.

Can. J. Chem. Downloaded from www.nrcresearchpress.com by 210.87.254.40 on 09/05/12
For personal use only.

should prove to be interesting for the study of d-orbital effect in π conjugation.

We have studied by e.s.r. the thermal reactions of *t*-butylperoxide and benzoylperoxide with triphenylsilane in solution at high temperature, the photolyses of *t*-butylperoxyperbenzoate with triphenylsilane in CF_3CCl_3 at low temperature, the photochemical reactions of benzophenone with triphenylsilane at a range of low temperatures. Unfortunately all our attempts to date to produce resolvable e.s.r. spectra from triphenylsilyl radicals in solution have failed. Other efforts to produce triphenylsilyl radical by γ-irradiation of polycrystalline triphenylsilane have resulted only in unresolvable broad line spectra. We have just learned that Geoffroy and Lucken (3) have analyzed the e.s.r. spectra of X-irradiated single crystal of triphenylsilane at room temperature and assigned the main radical species to triphenylsilyl radical, formed both as isolated and pair-wise trapped radicals. However, their value of the ^{29}Si coupling constant obtained from the analysis is much smaller than those reported for various silyl radicals in the fluid state (2). The authors (3) pointed out that although the crystal structure of triphenylsilane is not known, the trapped radical is presumably non-planar and thus the small value of the ^{29}Si coupling constant is not in accord with the simple valence theory. Furthermore, no proton hyperfine structures were observed.

In the present note, the study of the thermal reaction of benzophenone with triphenylsilane in the fluid state was undertaken as a possible means to generate the triphenylsilyl radical for e.s.r. observation, since benzophenone is known (4) to abstract an H atom from triphenylsilane at high temperatures. However, it was disappointing that the primary intermediate triphenylsilyl radical was not detected and instead an e.s.r. spectrum believed to be due to secondary triphenylsiloxydiphenylmethyl radical, $Ph_2\dot{C}OSiPh_3$ was observed. The results would cast some light on the mechanism of the thermal reaction.

Experimental

Benzophenone (Aldrich) and benzophenone-d_{10} (Merck Sharp and Dohme) were repeatedly recrystallized from ethanol–water until completely free from paramagnetic contaminants. Triphenylsilane (Alfa) was used without further purification, after it was established that samples using zone-refined triphenylsilane gave identical e.s.r. results.

Samples of mixtures of benzophenone and triphenylsilane (1:1 and 2:1 molar ratio) form supercooled liquid solutions at room temperature. They were placed in suprasil tubes sealed off after being degassed and evacuated to 10^{-5} Torr. The sample tube was then introduced into the microwave cavity equipped with a variable temperature controller which heated the sample up to 400 °K. In a few separate experiments samples were dissolved in *p*-dichlorobenzene (0.2 *M*) and they gave less resolved e.s.r. spectra under identical conditions.

Electron spin resonance spectra were recorded with a Varian 4500 X-band spectrometer with 100 kc modulation. The magnetic field was calibrated with a Varian F-8A fluxmeter by monitoring its transmitter frequency with a Hewlett–Packard 5245M frequency counter. The microwave frequency was measured using the same counter and a 5256A frequency converter.

Results and Discussion

A typical e.s.r. spectrum recorded when samples of benzophenone and triphenylsilane solution were heated within the microwave cavity to temperatures between 370–420 °K, is given in Fig. 1*a*. Below 370 °K no appreciable spectrum was dectected and above 420 °K the observed spectrum decayed rapidly. An optimum steady-state concentration of radicals was achieved at about 400 °K. During the recording of e.s.r. spectra, the originally colorless solution became slightly pink. The *g*-value of the e.s.r. spectrum was found to be 2.00305 $\pm$ 0.0001.

Previous reports of the thermal (4) and photochemical (5) reactions of benzophenone with triphenylsilane have suggested that the reactions proceed via free radical intermediates. Thus, Gilman and Wittenberg (4) obtained a 62% yield of $Ph_2HCOSiPh_3$ after heating an equimolar mixture of benzophenone and triphenylsilane at 510 °K for 3 h. Becker (5) found a major product of $Ph_3SiOCPh_2CPh_2OH$ in the photolysis of a benzene solution of benzophenone and the silane. Upon heating the product to 95 °C at 10 mm pressure, $Ph_3SiOCPh_2CPh_2OH$ was found to decompose into benzophenone and $Ph_2HCOSiPh_3$. Their results appear to be consistent with the following common mechanism

[1] $Ph_2CO + Ph_3SiH \xrightarrow{h\nu \text{ or heat}} Ph_2\dot{C}OH + Ph_3\dot{S}i$

[2] $Ph_3\dot{S}i + Ph_2CO \rightarrow Ph_2\dot{C}OSiPh_3$

[3] $Ph_2\dot{C}OH + Ph_2\dot{C}OSiPh_3 \rightarrow Ph_3SiOCPh_2CPh_2OH$

[4] $Ph_3SiOCPh_2CPh_2OH \xrightarrow{\text{heat}} Ph_2CO + Ph_2HCOSiPh_3$

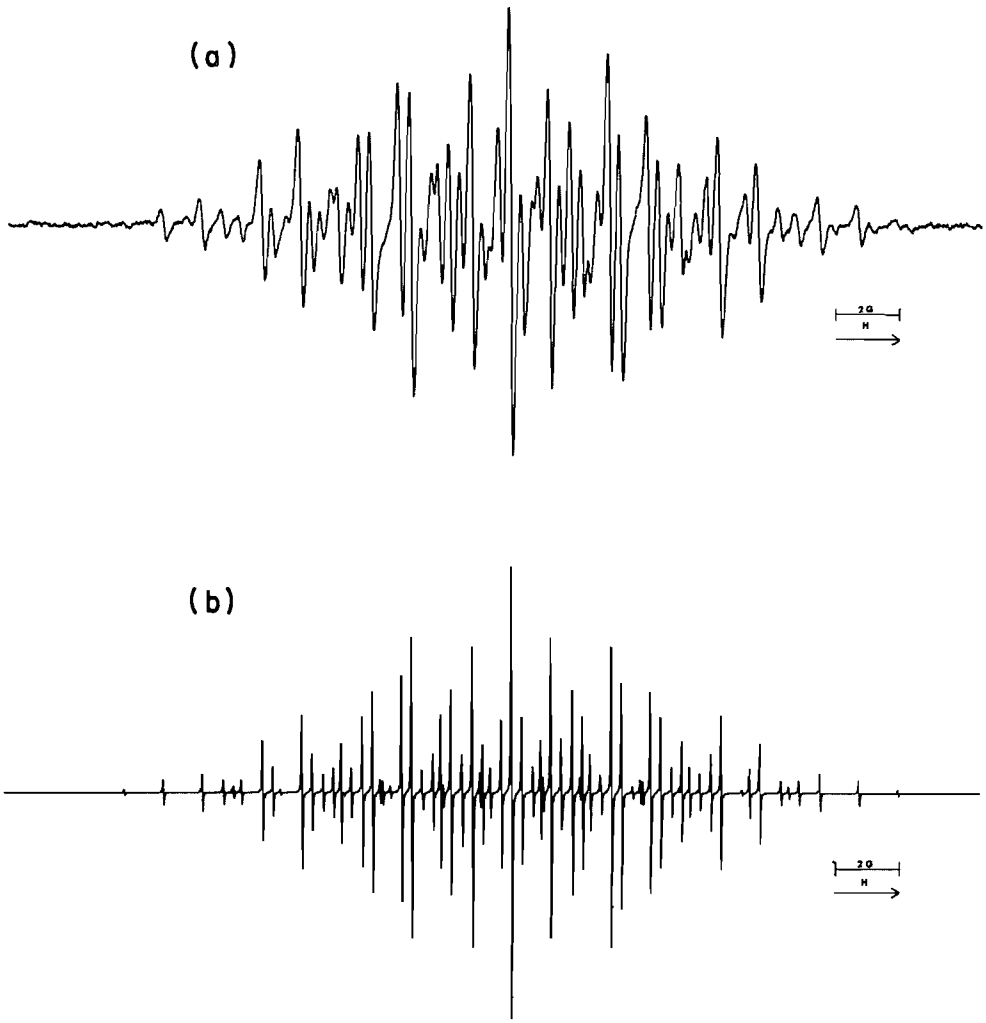

FIG. 1. The e.s.r. spectra at 400 °K of the thermal reaction of benzophenone with triphenylsilane: (*a*) experimental spectrum, (*b*) computer simulated spectrum.

Cage recombination of the primary radicals is considered to be less important at high temperatures. Moreover, Brook (6) has shown that the recombined product Ph_3SiCPh_2OH would be readily converted to $Ph_2HCOSiPh_3$. However, it should be emphasized that the exact nature of the thermal initiation leading to reaction 1 is not known and the overall reaction may proceed via a chain-mechanism as suggested by one of the referees

[2] $$Ph_3\dot{S}i + Ph_2CO \rightarrow Ph_2\dot{C}OSiPh_3$$

[5] $$Ph_2\dot{C}OSiPh_3 + Ph_3SiH \rightarrow Ph_3SiOCHPh_2 + Ph_3\dot{S}i$$

In an attempt to identify the radical responsible for the observed e.s.r. spectrum, all three radicals $Ph_3\dot{S}i$, $Ph_2\dot{C}OH$, and $Ph_2\dot{C}OSiPh_3$ were therefore considered. The possibility of the radical being $Ph_3\dot{S}i$ was eliminated, since the e.s.r. spectrum drastically changed its structure when benzophenone-d_{10} was used (Fig. 2*a*). The second possibility of a $Ph_2\dot{C}OH$ radical was also ruled out by comparing the observed spectrum with those of $Ph_2\dot{C}OH$ reported in the literature (7). Thus it is thought that the species responsible for the spectrum is the triphenylsiloxydiphenylmethyl radical, $Ph_2\dot{C}OSiPh_3$. Computer analysis of the experimental spectrum based on this radical yields the spectral param-

Can. J. Chem. Downloaded from www.nrcresearchpress.com by 210.87.254.40 on 09/05/12
For personal use only.

TABLE 1. Spectral parameters of $Ph_2\dot{C}OSiPh_3$ and related radicals

Radicals	g-Value	Proton splittings (G) Ortho	Meta	Para	Hydroxy	Reference
$Ph_2\dot{C}OSiPh_3$	2.00305	3.16±0.03	1.23	3.48	—	This work
$Ph_2\dot{C}OH$	2.0030	3.23	1.23	3.66	3.0	7
Ph_2CO^- free anion	—	2.52	0.82	3.50	—	10

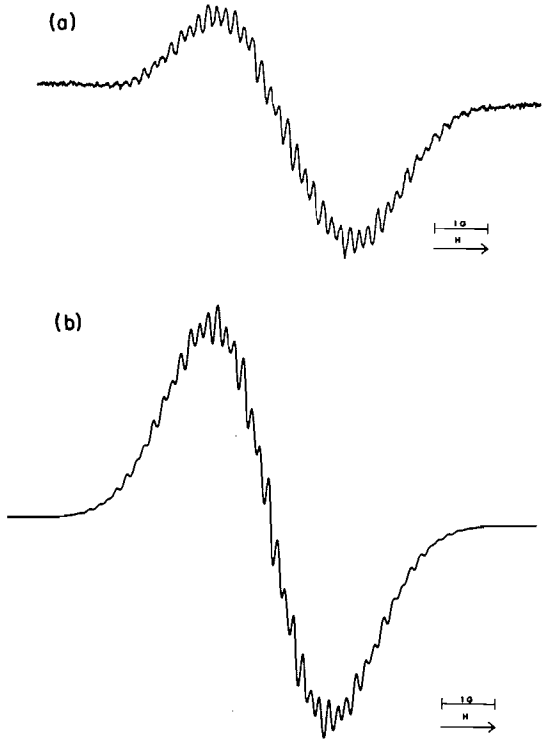

FIG. 2. The e.s.r. spectra at 400 °K of the thermal reaction of benzophenone-d_{10} with triphenylsilane: (*a*) experimental spectrum, (*b*) computer-predicted spectrum.

eters given in Table 1. The proton coupling constant assignments are supported by comparing the $(C_6D_5)_2\dot{C}OSiPh_3$ spectrum (Fig. 2*a*) with the theoretically predicted one (Fig. 2*b*). Using the familiar McConnell relationship, the proton hyperfine splitting can account for more than 90% of the unpaired spin. Thus, hyperfine splitting due to ^{29}Si would be very difficult to resolve, since the natural abundance of ^{29}Si having a nuclear spin of $\frac{1}{2}$ is only 4.7%.

Several authors (8, 9) have reported evidence for the relative ease of rotation of the phenyl rings in the ketyl radical $Ph_2\dot{C}OH$. Theoretical considerations also led to the conclusion (10) that in the ketyl radical the phenyl rings are not locked into a planar configuration for a time as long as a microsecond. In the present experiment, the spectra of $Ph_2\dot{C}OSiPh_3$ were obtained at 400 °K and it is conceivable that the phenyl rings of the radical are freely rotating and that the observed proton splittings are indeed time-averaged values.

While the observation of $Ph_2\dot{C}OSiPh_3$ radical during the thermal reaction appears to be consistent with the above mechanism, the failure of detecting the primary triphenylsilyl radical remains to be explained. Perhaps it is due to the great affinity of the silyl radicals for the oxygen atom of the benzophenone leading to a more stable $Ph_2\dot{C}OSiPh_3$ radical.

Present effort in producing triphenylsilyl radicals in solution for e.s.r. study involves electrolysis and pulsed electrolysis experiments.

This research is supported by the National Research Council of Canada.

1. J. H. MACKEY and D. E. WOOD. Mol. Phys. **18**, 783 (1970).
2. R. L. MOREHOUSE, J. J. CHRISTIANSEN, and W. GORDY. J. Chem. Phys. **45**, 1751 (1966); P. J. KRUSIC and J. K. KOCHI. J. Amer. Chem. Soc. **91**, 3938 (1969); S. W. BENNETT, C. EABORN, A. HUDSON, H. A. HUSSAIN, and R. A. JACKSON. J. Organometal. Chem. **16**, p36 (1969).
3. M. GEOFFROY and E. A. LUCKEN. Helv. Chim. Acta, **53**, 813 (1970).
4. H. GILMAN and D. WITTENBERG. J. Org. Chem. **23**, 501 (1958).
5. HANS-DIETER BECKER. J. Org. Chem. **34**, 2469 (1969).
6. A. G. BROOK. J. Amer. Chem. Soc. **80**, 1886 (1958).
7. R. WILSON. J. Chem. Soc. B, 84 (1968).
8. T. TAKESHITA and N. HIROTA. J. Chem. Phys. **51**, 2146 (1969).
9. F. C. ADAM and H. R. FALLE. Can. J. Chem. **44**, 1387, 1396 (1966).
10. P. H. RIEGER and G. K. FRAENKEL. J. Chem. Phys. **37**, 2811 (1962).

Can. J. Chem. Downloaded from www.nrcresearchpress.com by 210.87.254.40 on 09/05/12
For personal use only.

Valence Force Field Calculations for Octahedral Anions

A. M. QURESHI, A. H. HARDIN, AND F. AUBKE[1]

Department of Chemistry, University of British Columbia, Vancouver 8, British Columbia

Received September 23, 1970

Vibrational force constants for the octahedral anion AsF_6^-, SbF_6^-, SnF_6^{2-}, and $SnCl_6^{2-}$ in the corresponding potassium salts are calculated using a simple valence force field treatment, with the intention of obtaining better agreement with recently reassigned bending modes in these compounds and to arrive at improved values for the inactive mode $\nu_6[F_{2u}]$.

Canadian Journal of Chemistry, 49, 816 (1971)

Can. J. Chem. Downloaded from www.nrcresearchpress.com by 210.87.254.42 on 09/05/12
For personal use only.

Introduction

Whereas potential constants for many neutral octahedral molecules have been calculated by various authors (1–3), little attention has been given to the octahedral hexahalo anions formed by Group IV and Group V elements. In addition to an earlier report on force constants of some hexachloro anions (4), valence force field calculations on a number of hexafluoro anions were recently reported (5).

During recent studies (6, 7) on heterocation complexes with the anions $SnCl_6^{2-}$, SnF_6^{2-}, SbF_6^-, AsF_6^- it became apparent that infrared data for both force constant calculations (3, 4) did not extend below 250 cm^{-1}, so that $\nu_4[F_{1u}]$ was either not recorded (4) at all as for $SnCl_6^{2-}$ or had been wrongly assigned (5) as for SnF_6^{2-} and SbF_6^-. This of course renders the reported force constants somewhat unreliable, in particular, where the bending force constants are concerned. As a consequence, all calculations of the inactive mode $\nu_6[F_{2u}]$, which is generally not accessible experimentally for solids where only a small number of combination bands are observed, appear to be questionable.

The obtained set of new vibrational frequencies (6, 7) was taken as a basis for a normal coordinate analysis, using a simple valence force field treatment. The potassium salts were selected because the unit cell dimensions are known for all four compounds, thus permitting us to assess site symmetry effects on the vibrational spectra, and interatomic distances are reported for all but one of the salts. The intention of the calculation is to check the correctness of the new assignment via comparison of calculated values and to gain more accurate information regarding the position of ν_6. Anion–cation interaction has been found for a number of heterocation complexes with hexafluoro anions (6, 7) to reduce the symmetry of the anion, whereby ν_6 may now become partly infrared and/or Raman active.

Experimental

The far infrared spectrum of K_2SnCl_6 was recorded on a Perkin–Elmer 301 spectrophotometer for the range of 300–150 cm^{-1}. Polyethylene windows were employed and Nujol was used as a mulling agent.

The force constants were calculated by using a Fortran IV program written by Schachtschneider (10) and adjusted for an IBM 360/67 computer. The construction and orientation of the symmetry coordinates, the potential and kinetic energy matrices, and the secular equations giving the normal frequencies have been discussed previously by Pistorius (1) and Classen (11). The harmonic potential function in terms of the internal coordinates is given by the expression

$$\begin{aligned}2V = {} & k_r[(\Delta R_1)^2 + (\Delta R_2)^2 + (\Delta R_3)^2 + (\Delta R_4)^2 + (\Delta R_5)^2 + (\Delta R_6)^2] \\ & + 2k_{rr}\,[(\Delta R_4 + \Delta R_2)(\Delta R_6 + \Delta R_3 + \Delta R_7 + \Delta R_5) + (\Delta R_3 + \Delta R_5)(\Delta R_6 + \Delta R_7)] \\ & + 2k_{rr'}\,[(\Delta R_6)(\Delta R_7) + (\Delta R_3)(\Delta R_5) + (\Delta R_4)(\Delta R_2)] \\ & + 2d^2k_\delta\,[(\Delta\theta_{63})^2 + (\Delta\theta_{64})^2 + (\Delta\theta_{65})^2 + (\Delta\theta_{62})^2 + (\Delta\theta_{34})^2 + (\Delta\theta_{37})^2 + (\Delta\theta_{32})^2 \\ & + (\Delta\theta_{47})^2 + (\Delta\theta_{45})^2 + (\Delta\theta_{75})^2 + (\Delta\theta_{72})^2 + (\Delta\theta_{52})^2] \\ & + 2d^2k_{\delta\delta}\,[(\Delta\theta_{64} + \Delta\theta_{62})(\Delta\theta_{63} + \Delta\theta_{65}) + (\Delta\theta_{34})(\Delta\theta_{63} + \Delta\theta_{64} + \Delta\theta_{37}) \\ & + (\Delta\theta_{32})(\Delta\theta_{63} + \Delta\theta_{62} + \Delta\theta_{37}) + (\Delta\theta_{47})(\Delta\theta_{34} + \Delta\theta_{37} + \Delta\theta_{75}) \\ & + (\Delta\theta_{45})(\Delta\theta_{64} + \Delta\theta_{65} + \Delta\theta_{47} + \Delta\theta_{75}) + (\Delta\theta_{72})(\Delta\theta_{37} + \Delta\theta_{32} + \Delta\theta_{75}) \\ & + (\Delta\theta_{52})(\Delta\theta_{65} + \Delta\theta_{62} + \Delta\theta_{75} + \Delta\theta_{72})]\end{aligned}$$

[1]To whom correspondence should be addressed.

TABLE 1. Crystal symmetry data of potassium hexahalometallates

Compound	Space group	Group symmetry	Site symmetry	M–Hal distance (d) (Å)	Reference
$KAsF_6$	$R\bar{3}$	O_h	S_6	1.82	16
$KSbF_6$	$R\bar{3}$	O_h	S_6	1.877	17
K_2SnF_6	$P\bar{3}m1$	O_h	D_{3d}	1.90*	12, 18
K_2SnCl_6	$Fm3m$	O_h	O_h	2.45	19

*Denotes average bond distance from ref. 12.

TABLE 2. Values of force constants of some hexahalometallate ions (mdyn/Å)

Compound	k_r	k_{rr}	$k_{rr'}$	k_δ/d^2	$k_{\delta\delta}/d^2$	Reference
$KAsF_6$	3.780	0.260	0.530	0.407	0.057	This work
$KSbF_6$	3.850	0.190	0.240	0.224	0.028	"
K_2SnF_6	2.850	0.230	0.220	0.184	0.034	"
K_2SnCl_6	1.285	0.185	0.080	0.155	0.016	"
SeF_6	4.414	—	—	0.363	0.061	20
TeF_6	4.772	—	—	0.207	0.045	20

where ΔR_1, ΔR_2, etc. are the deviation from the element halogen bond lengths and $\Delta\theta$'s are the changes in the non-linear bond angles. The position of the halogen atoms is shown in the figure, which depicts the equilibrium geometry of the MX_6 species where the six halogen atoms are labelled from X_2 to X_7 and the central metal

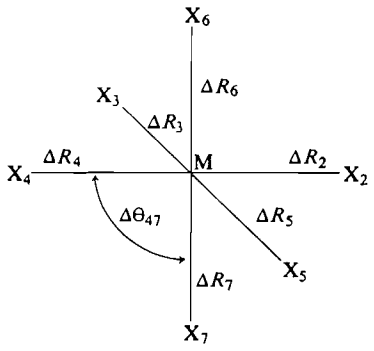

atom M is at the origin of the coordinate system. The angles are measured in radians and consequently the bending force constants are multiplied by the square of the bond lengths (d) in order to keep the units of the stretching and bending force constants consistent (mdyn/Å). The bond lengths (d) for each ion are shown in Table 1, together with other pertinent structural information. The Sn—F bond distance for K_2SnF_6 is not reported. The average values (12) for the distorted octahedral SnF_6^{2-} ion in Na_2SnF_6 is taken instead. The site symmetry of the anion is deduced according to Halford (13).

Results

The values of the force constants in mdyn/Å are given in Table 2 together with reported values for hexafluorides SeF_6, isoelectronic to AsF_6^- and TeF_6, isoelectronic to SbF_6^- and SnF_6^{2-}. In this table, k_r is the element–halogen stretching force constant, k_{rr} is the stretching interaction constant for M–Hal bonds perpendicular to each other, and $k_{rr'}$ is the corresponding constant for bonds opposite to each other; k_δ is the bending force constant of bonds with non-linear angles and $k_{\delta\delta}$ is the bending interaction constant for bonds with adjacent angles.

Other stretching–bending interactions have been ignored in this study because of the complexity of the problem.

Discussion

The vibrational frequency for $\nu_4[F_{1u}]$ in K_2SnCl_2 is found at 172 cm^{-1} in rather poor agreement with the previously predicted (4) value of 143 cm^{-1} but consistent with recent reports (21, 22). As pointed out previously, splittings due to site symmetry effects are found only for $\nu_3[F_{1u}]$ and $\nu_4[F_{1u}]$ in K_2SnF_6 (6) and for $\nu_5[F_{2g}]$ in $KSbF_6$ (7, 14) where doublets are found, suggesting a splitting into A_{2u} and E_u as well as A_{1g} and E_g modes. Assignment of the observed bands is made strictly on the basis of intensity differences and average frequencies are calculated according to Lehmann's rule (15).

As was expected, good agreement with previously reported stretching force constants exists (4, 5). The conclusions reached by those authors are identical with our point of view. The decrease in k_r from SeF_6 to AsF_6 and from TeF_6 over SbF_6^- to SnF_6^{2-} is expected but it should be pointed out that the most recent reference values

Can. J. Chem. Downloaded from www.nrcresearchpress.com by 210.87.254.42 on 09/05/12
For personal use only.

Can. J. Chem. Downloaded from www.nrcresearchpress.com by 210.87.254.42 on 09/05/12
For personal use only.

TABLE 3. Observed and calculated vibrational frequencies*

	Vibrational frequency (cm^{-1})											
	SeF_6		AsF_6^-		TeF_6		SbF_6^-		SnF_6^{2-}		$SnCl_6^{2-}$	
Vibrational Modes	Obsd. (refs. 8, 9)	Calcd. (ref. 20)	Obsd. (ref. 7)	Calcd.†	Obsd. (refs. 8, 9)	Calcd. (ref. 20)	Obsd. (ref. 7)	Calcd.‡	Obsd. (ref. 6)	Calcd.§	Obsd. (ref. 6)	Calcd.¶
$\nu_1(A_{1g})$	708	712	692	691.5	701	706	661	658.4	598	597.2	317	317.5
$\nu_2(E_g)$	662	659	580	582.1	674	670	575	575.9	478	483	218	218.3
$\nu_3(F_{1u})$	780	778	698	696.3	752	751	655	657.6	582 557 (565)	565.0	322	322.1
$\nu_4(F_{1u})$	437	424	382	381.7	327	321	270	269.4	258 254 (256)	256.0	172	172.3
$\nu_5(F_{2g})$	405	422	375	375.6	313	327	294 278 (283)	283.2	257	257.0	167	167.4
$\nu_6(F_{2u})$	260	260	—	228.8	197	194	—	173		143.7	—	107.4

*Values in parentheses are calculated average values.
†Average deviation, 0.18%.
‡Average deviation, 0.22%.
§Average deviation, 0.05%.
¶Average deviation, 0.15%.

(20) for SeF_6 and TeF_6 are obtained *via* a modified Urey–Bradley force field calculation.

The bending force constants show marked departure from the previous values and as a consequence the calculated values for the inactive mode $\nu_6[F_{2u}]$ are found considerably lower than reported. In particular, for the hexafluoro anions, differences of about 100 cm^{-1} are found. Doubt in the correctness of the previously (5) calculated values for ν_6 is centered around the value for SbF_6^-, which is reported to be higher than experimental values for ν_4 and ν_5 in departure from the observed trends. The ν_6 values reported in this paper compare favorably with experimental values for SeF_6 and TeF_6. Furthermore, good agreement with the observed frequencies is found: the average deviation does not exceed more than $\frac{1}{4}\%$ as shown in Table 3.

Financial support from the National Research Council of Canada is gratefully acknowledged.

1. C. W. F. T. Pistorius. J. Chem. Phys. **29**, 1328 (1958).
2. H. Kim, P. A. Sonder, and H. H. Classen. J. Mol. Spectrosc. **26**, 46 (1968).
3. J. W. Linnel and C. J. S. M. Simpson. Trans. Faraday Soc. **31**, 857 (1959).
4. J. Hiraishi, J. Nakagawa, and T. Shimanouchi. Spectrochim. Acta, **20**, 819 (1964).
5. G. M. Begun and A. C. Rutenberg. Inorg. Chem. **6**, 2212 (1967).
6. H. A. Carter, A. M. Qureshi, J. R. Sams, and F. Aubke. Can. J. Chem. **48**, 2853 (1970).
7. A. M. Qureshi and F. Aubke. Can. J. Chem. **48**, 3117 (1970).
8. J. Gaunt. Trans. Faraday Soc. **49**, 1122 (1953).
9. D. M. Yost, C. C. Steffens, and C. T. Gross. J. Chem. Phys. **2**, 311 (1934).
10. J. H. Schachtschneider. Vibrational Analysis of Polyatomic Molecules V and VI, Technical Report No. 231-64, Shell Development Company.
11. H. H. Classen. J. Chem. Phys. **30**, 968 (1959).
12. C. H. Hebecker, H. G. von Schnerig, and R. Hoppe. Naturwissenschaften, 154 (1966).
13. R. S. Halford. J. Chem. Phys. **14**, 8 (1946).
14. M. Azeem, M. Brownstein, and R. J. Gillespie. Can. J. Chem. **47**, 4159 (1969).
15. W. J. Lehmann. J. Mol. Spectrosc. **7**, 261 (1961).
16. R. B. Roff, Jr. Acta Cryst. **8**, 739 (1955).
17. H. Bode and E. Voss. Z. Anorg. Allg. Chem. **264**, 144 (1951).
18. W. Klemm, J. Krause, K. Wahl, E. Huss, R. Hoppe, E. Weise, and W. Brandt. Forschungsber. Wirtschafts u. Verkehrsministerium Nordrhein-Westfalen, **160**, 38 (1955).
19. J. A. Lerbscher and J. Trotter. Private communication.
20. S. N. Thakur and D. K. Rai. J. Mol. Spectrosc. **19**, 341 (1966).
21. N. N. Greenwood and B. P. Straughan. J. Chem. Soc. (A), 962 (1966).
22. D. M. Adams and D. M. Morris. J. Chem. Soc. (A), 1669 (1967).

Can. J. Chem. Downloaded from www.nrcresearchpress.com by 210.87.254.42 on 09/05/12
For personal use only.

Can. J. Chem. Downloaded from www.nrcresearchpress.com by 210.87.254.105 on 09/05/12
For personal use only.

Canadian Journal of Chemistry

Published by THE NATIONAL RESEARCH COUNCIL OF CANADA

VOLUME 49 MARCH 15, 1971 NUMBER 6

The Decomposition of Benzoyl Hypochlorite in the Presence of Metal Ions[1]

N. J. BUNCE[2] AND L. O. URBAN

Department of Chemistry, University of Guelph, Guelph, Ontario

Received August 5, 1970

The decomposition of benzoyl hypochlorite, the intermediate in the Hunsdiecker reaction between chlorine and silver benzoate, is accelerated by light and by azobisisobutyronitrile (AIBN), but not by transition metal ions. The molar yield of the chlorobenzene produced in the decomposition increases as the temperature of the reaction mixture is raised, but is independent of whether or not the reaction is promoted by light or AIBN. It is suggested that this variation in the yield is a result of the readier decarboxylation at higher temperatures of the benzoyloxy radicals which are believed to be intermediates in the decomposition process. No such pronounced effect of temperature on the yield of halides from aliphatic silver carboxylates has been observed, presumably because aliphatic acyloxy radicals decarboxylate readily even at low temperatures.

La décomposition de l'hypochlorite de benzoyle, l'intermédiaire dans la réaction de Hunsdiecker entre le chlore et le benzoate d'argent est accélérée par la lumière et l'azo bis isobutyronitrile mais non par les ions des métaux de transition. Le rendement molaire de chlorobenzène produit lors de la décomposition augmente proportionnellement avec la température du mélange réactionnel mais est indépendant des catalyseurs comme la lumière ou l'AIBN. Il est suggéré que ces variations dans le rendement sont le résultat d'une décomposition plus facile à haute température des radicaux benzoyloxy qui seraient les intermédiaires dans le processus de décomposition. Un effet aussi prononcé de la température sur les rendements de dérivés halogénés aliphatiques provenant des carboxylates d'argent correspondants n'a pas été observé probablement parce que les radicaux acyloxy aliphatiques se décarboxylent facilement même à basse température.

Canadian Journal of Chemistry, 49, 821 (1971)

The reaction between chloride ion and benzoyl peroxide has recently been investigated by several groups of workers (1–3). The first formed intermediate was found to display chemistry similar to that of the intermediate in the reaction between the halogens and silver carboxylates. The reactions compared included the decomposition to chlorobenzene and CO_2, addition to olefins, electrophilic chlorination of arenes, and free radical halogenation of alkanes. The reaction between halogens and silver carboxylates is the basis of the Hunsdiecker halodecarboxylation reaction (4, 5), which has been supposed to involve an acyl hypohalite as an intermediate. It was proposed therefore that the reaction of chloride ion with benzoyl peroxide also gives rise to such an intermediate, in this case benzoyl hypochlorite.

[1] $Cl^- + PhCO.OO.COPh \rightarrow PhCO_2Cl + PhCO_2^-$

[2] $Cl_2 + PhCO_2Ag \rightarrow PhCO_2Cl + AgCl$

In the Hunsdiecker reaction it is thought that the intermediate acyl hypohalite suffers homolytic fission (reaction 3) and that this initiates a free radical chain pathway for alkyl (or aryl) halide formation (reactions 4 and 5).

[3] $RCO_2X \rightarrow RCO_2^{\cdot} + X^{\cdot}$

[4] $RCO_2^{\cdot} \rightarrow R^{\cdot} + CO_2$

[5] $R^{\cdot} + RCO_2X \rightarrow RX + RCO_2^{\cdot}$

This homolytic fission of the O—X bond of the acyl hypohalite might be presumed to be a very facile process, for the Hunsdiecker reaction may often (5) be carried out successfully at temperatures below 0°. By contrast, however, the pre-

[1]Presented in part at the 160th National Meeting of the American Chemical Society, Chicago, Illinois, September 1970.

[2]To whom correspondence should be addressed.

Can. J. Chem. Downloaded from www.nrcresearchpress.com by 210.87.254.105 on 09/05/12
For personal use only.

sumed benzoyl hypochlorite of the previous work did not seem to suffer homolysis with great ease. For example (1, 2), at neither 60° nor 100° did it cause the polymerization of added styrene (addition is preferred), nor in the absence of excess benzoyl peroxide as a free radical initiator did it either cause free radical chlorination of an added alkane or decompose cleanly to chlorobenzene.

A possible cause of this apparently different behavior might be that the Hunsdiecker reaction is carried out with silver carboxylates, whereas no transition metal ions were present in the reaction mixtures of chloride ion with benzoyl peroxide. Since transition metal ions are well known to catalyze the homolytic decomposition of organic peroxides (6, 7), peresters (8), *N*-chloroamines (9), and alkyl hypochlorites (10), it is possible that a similar catalytic decomposition of the acyl hypohalite to free radicals could account for the apparent ease of reaction of Hunsdiecker reaction mixtures and the lack of reactivity of the chloride ion/benzoyl peroxide reagent. Such reasoning is consistent with the observation that the Hunsdiecker decarboxylation reaction proceeds more readily with heavy metal salts than with the salts of the alkali or alkaline earth metals.

This study was therefore initiated to discover whether silver (or copper) salts are effective catalysts for the decomposition of benzoyl hypochlorite, with a view to enlarging our knowledge of the Hunsdiecker reaction mechanism. During the work we had occasion to examine the effect of temperature on the reaction, and these results are also included.

Results and Discussion

The required metal-free solutions of benzoyl hypochlorite were prepared by filtration of silver benzoate – chlorine mixtures in carbon tetrachloride as solvent (11).[3,4] Aliquots of these solutions were allowed to decompose at different temperatures under identical conditions except for the presence or absence of various initiators or reagents; after 1 h the solutions were analyzed for the extent of benzoyl hypochlorite decomposition and for chlorobenzene formation (Tables 1–4).[5]

From an examination of these Tables, the following points may be noted. First, light (at all temperatures) and AIBN (at 60°) accelerated the decomposition of the acyl hypochlorite, as would be expected since the reaction is known to be a free radical chain process (4, 5).

Second, neither cuprous ions nor silver ions cause any increase in the rate of decomposition, indicating that neither is a catalyst for the reaction. This is in contrast to the previously mentioned findings for peroxides, chloroamines, etc., but is consistent with the observation by Kochi *et al.* (3) that in the reaction of benzoyl hypochlorite (from benzoyl peroxide/lithium chloride) with toluene, the free radical chlorination of the side chain is not catalyzed but rather is suppressed by the addition of cupric ions to the reaction mixture. In a related system Jennings and Ziebarth (12) have found that the decomposition to 1-bromobutane of the intermediate in the reaction between bromine monoxide and valeric acid (presumed to be valeryl hypobromite) is not

TABLE 1. Decomposition[a] of 0.303 *M* benzoyl hypochlorite after 1 h at 0°

Conditions[a]	$PhCO_2Cl$ remaining[b] in *M*	Chlorobenzene produced[c]	
		M	%[d]
Dark	0.259	0.013	29
hν	0.012	0.111	38
Dark, Ag^+	0.273	0.013	43
Dark, Cu^+	0.271	0.011	34

[a]For notes *a–d* see Table 3.

TABLE 2. Decomposition[a] of 0.255 *M* benzoyl hypochlorite after 1 h at 40°

Conditions[a]	$PhCO_2Cl$ remaining[b] in *M*	Chlorobenzene produced[c]	
		M	%[d]
Dark	0.197	0.031	54
hν	0.054	0.137	68
Dark, AIBN	0.194	0.026	42
Dark, Ag^+	0.181	0.025	34
Dark, Cu^+	0.194	0.028	46

[a]For notes *a–d* see Table 3.

[3]Other metal benzoates could not successfully be substituted for the silver salt, neither could acetonitrile be used as solvent instead of carbon tetrachloride. In acetonitrile there forms a red silver-containing substance whose chemistry is under investigation.

[4]The benzoyl peroxide – chloride ion route to benzoyl hypochlorite is inapplicable because reaction 1 is so slow that the hypochlorite decomposes at a rate comparable with its rate of production (2, 3).

[5]Tables 1 and 2 record the average of duplicate experiments; at 60° (Table 3) identical results were not obtained and both values are quoted.

TABLE 3. Decomposition of 0.245 *M* benzoyl hypochlorite after 1 h at 60°

Conditions[a]	$PhCO_2Cl$ remaining[b] in *M*	Chlorobenzene produced[c]	
		M	%[d]
Dark	0.142, 0.162	0.091, 0.074	88, 89
hν	0.018, 0.020	0.160, 0.170	71, 75
Dark, AIBN	0.033, 0.012	0.168, 0.214	79, 92
Dark, Ag^+	0.148, 0.063	0.067, 0.125	69, 69
Dark, Cu^+	0.120, 0.080	0.095, 0.134	76, 81

[a]All added substances were added in 2.0–10.0 mg quantities. Ag^+ was silver benzoate; Cu^+ was cuprous oxide.
[b]By iodometric titration.
[c]By vapor phase chromatography.
[d]Moles of chlorobenzene produced per mol of benzoyl hypochlorite decomposed.

TABLE 4. Average yield of chlorobenzene from benzoyl hypochlorite at different temperatures

Temperature (°C)	Chlorobenzene (%)[a]
0	36 ± 7
40	49 ± 19
60	79 ± 13

[a]Average values of the data in Tables 1–3.

catalyzed by mercuric salts. Furthermore, in the reaction of silver carboxylates with iodine (reaction 6), the Simonini complex (4, 13) of constitution (**1**) may often be isolated, whereas it might be anticipated that if silver ions were active catalysts for acyl hypohalite decomposition, the silver ions in the complex would cause its ready destruction.

[6] $2RCO_2Ag + I_2 \rightarrow AgI + RCO_2I.RCO_2Ag$

(1)

A third point to note from Tables 1–3 is the effect of temperature on the decomposition. Apart from the rate of reaction increasing at higher temperatures, the yield of chlorobenzene (per mol of hypochlorite destroyed) is markedly greater at higher temperatures (Table 4) and is virtually independent of whether photoinitiation is employed. Since photoinitiation must increase the rate of reaction 3, we conclude that the temperature dependence of the yield is *not* caused by there being some other reaction competing with free radical decomposition. If that had been so, photoinitiation would have increased the yield by promoting reaction 3, the initiation step of the free radical chain reaction.

The temperature dependence of the yield of chlorobenzene is consistent with step 4 or step 5 having a large activation energy. This is unlikely for step 5 because of its analogy with one of the steps in free radical chlorinations by alkyl hypochlorites, which proceed readily even at −80° (14, 15). An appreciable activation energy for step 4 is consistent with the well-known stability of benzoate radicals towards decarboxylation, in particular, their ability to survive long enough to be intercepted by a variety of other reagents (16–20) to give products retaining the benzoate moiety intact. Of interest in the present connection are occasional observations of variations with temperature of the ratio of carboxyl-retaining to decarboxylated products (17, 21). Correspondingly in our studies, the decomposition of benzoyl hypochlorite in carbon tetrachloride at 0° gave benzoic acid as a major product, even when moisture was excluded from the system. It is not clear from where the hydroxyl hydrogen in the acid arises. Small quantities of chlorinated benzoic acid were also formed, presumably by electrophilic chlorination, since the *meta* isomer was produced in the largest amount (*cf.* the production of *m*-bromobenzoic acid from bromine and silver benzoate (5, 22)).

An alternative fate of a benzoyloxy radical is free radical substitution of a suitable aromatic substrate to give the aryl benzoate (23). Because of this reaction, benzene has been noted to be a poor solvent for carrying out Hunsdiecker reactions (4, 24). In our studies we found that the decomposition of silver-free solutions of benzoyl hypochlorite in benzene gave virtually no phenyl benzoate, and that even at 0°, electrophilic chlorination of the solvent occurred almost exclusively. Benzoyl hypobromite was found to be a much less active halogenating agent, and on decomposition in benzene at 3° afforded a moderate yield of phenyl benzoate, though little

Can. J. Chem. Downloaded from www.nrcresearchpress.com by 210.87.254.105 on 09/05/12
For personal use only.

TABLE 5. Effects of silver salts as halogen carriers for the electrophilic chlorination of benzene at 0°

Chlorinating agent (*M*)	Silver salt (mmol/ml)	Time (h)	(Cl^+) remaining, (*M*)	PhCl	
				M	%[a]
Cl_2 (0.60)	None (—)	140	0.29	0.21	68
Cl_2 (0.60)	Ag_2O (0.11)	140	0.23	0.32	88
Cl_2 (0.60)	AgCl (0.35)	140	0.23	0.35	95
$PhCO_2Cl$ (0.31)	None (—)[b]	120	~0.01	0.22	71
$PhCO_2Cl$ (0.30)	AgCl (0.30)[c]	70	~0.01	0.25	85

[a]Estimated by v.p.c.; % yields based on the chlorinating agent destroyed.
[b]Hunsdiecker reaction mixture, filtered after 5 min at 0°.
[c]As *b*, only not filtered.

of this product was formed at reflux. It was noted that silver salts have a slight catalytic effect as halogen carriers for both benzoyl hypochlorite and elemental chlorine, and that benzoyl hypochlorite is the more reactive halogenating agent (Table 5). Acetyl hypohalites are likewise more reactive electrophilic reagents than the elemental halogens (25–27).

The dependence of the yield of aryl halide on the temperature of decomposition is not peculiar to benzoyl hypochlorite. Benzoyl hypobromite and substituted benzoyl hypobromites behave similarly. The polar solvent acetonitrile gave results similar to those obtained in the non-polar carbon tetrachloride (Table 6).

In Table 6 we have also collected literature values for the yields of aliphatic halides from Hunsdiecker reactions that have been conducted at different temperatures, for comparison with our own data. Aliphatic substrates do not exhibit the same marked depression of the yield on lowering the temperature; indeed halides derived from *secondary* alkyl groups R are produced in better yield at lower temperatures. On the limited data at hand we propose the following explanation. Aryl halides form with difficulty at low temperatures because of the less facile decarboxylation of the resonance-stabilized aroyloxy radicals; by contrast alkanoy oxy radicals decarboxylate readily even at low temperatures (28). There is thus less tendency for alkanoyloxy radicals to be diverted to other products before decarboxylation occurs. Readier formation of halide in aliphatic compared with aromatic systems has also been observed in diacyl peroxide/chloride ion systems (3, 29), again indicating the importance of the nature of the R group in decarboxylations. In the valeryl peroxide reaction (29), a faster reaction in the presence of copper salts was attributed to copper catalyzed decomposition of the peroxide rather than of an intermediate valeryl hypochlorite.

The increased yield of secondary halides at low temperatures probably results from less of the product being destroyed after formation: tertiary halides cannot be synthesized by the Hunsdiecker method (4, 5) because the silver salts present in solution destroy them as they are formed by assisted ionization (eq. 7).[6]

[7] $$RX + Ag^+ \rightarrow AgX + R^+ \rightarrow \text{products}$$

Silver salts attack secondary halides less rapidly, and this reaction may be suppressed by low temperature operation, so that a better yield of halide is obtained.

To conclude, these experiments show that neither silver nor cuprous ions are catalysts for the decomposition of benzoyl hypochlorite. The only reservation we have to this conclusion is that while we were unable to detect any silver salts in the carbon tetrachloride solutions used in our experiments, there remains the possibility that a small but undetected quantity was present and that this was sufficient to catalyze the decomposition even when no further quantity was added. To try to resolve this problem, we are currently trying to prepare acyl hypohalites by routes not involving metallic precursors. Concerning the effect of temperature on the yield of aryl halides from the Hunsdiecker reaction, we suggest that this is simply a reflection of the readier decomposition of benzoate radicals at elevated temperatures.

[6]In the case where R = cyclobutyl, products derived by rearrangement of R^+ are observed.

Can. J. Chem. Downloaded from www.nrcresearchpress.com by 210.87.254.105 on 09/05/12
For personal use only.

TABLE 6. Percentage yields of halides from several silver carboxylates at different temperatures[a]

R— of RCO_2Ag	Halogen	RX% (Upper temperature)	RX% (Lower temperature)
Aryl R[b]			
C_6H_5	Br[c]	46 (reflux)	5 (3°)
C_6H_5	Br[d]	53 (reflux)	16 (3°)
C_6H_5	Br[e]	36 (reflux)	22 (3°)
C_6H_5	Cl	65 (reflux)	3 (3°)
C_6H_5	Cl[d]	36 (reflux)	16 (0°)
p-$NO_2C_6H_4$	Br[f]	76 (reflux)	2 (3°)
p-ClC_6H_4	Br	31 (reflux)	8 (3°)
p-$CH_3C_6H_4$	Br	17[g] (reflux)	< 1 (3°)
Primary R			
n-C_5H_{11}—	Br	92 (reflux)[h]	67 (cold)[i]
$(CH_3)_3CCH_2$—	Br	83 (reflux)[h]	53 (cold)[i]
n-$C_{15}H_{31}$—	Cl	55 (reflux)[j]	31 (cold)[j]
—CH_2—CH_2—	Br	32 (reflux)[k]	37 (15°)[k]
$C_6H_5CH_2$—	Br	37 (reflux)[l]	20 (cold)[l]
Secondary R			
3-Heptyl-	Br	35, 29 (reflux)[m]	40–60 (cold)[i]
cyclo-C_4H_7—	Br	44 (12°)[n]	53 (−25°)[o]
cyclo-C_6H_{11}—	Br	58 (reflux)[h]	73–80 (cold)[p]
cis-4-*t*-Butyl-cyclo-C_6H_{11}—	Br	38 (reflux)[q]	62 (−15°)[q]
Tertiary R			
7,7-Dimethyl-bicyclo[2,2,1]-hept-1-yl	Br	58 (reflux)[r]	60 (−10°)[r]

[a]In CCl_4 except as noted otherwise.
[b]This work except as noted otherwise.
[c]For other values, see ref. 5.
[d]In acetonitrile.
[e]In benzene; includes electrophilic halogenation of the solvent; at 3° phenyl benzoate (28%) was also formed.
[f]Barnes and Prochaska, ref. 31, quote a 79% yield at reflux and no reaction at room temperature.
[g]Reference 31.
[h]Reference 34.
[i]Reference 35, quoted in ref. 5.
[j]Reference 36, quoted in ref. 5.
[k]Reference 37.
[l]Reference 38, quoted in ref. 5.
[m]Reference 39.
[n]Reference 40.
[o]Reference 41.
[p]Reference 42, quoted in ref. 5.
[q]Reference 43.
[r]Reference 44.

Experimental

Solvents were reagent grade materials, dried with activated molecular sieve. Silver benzoate was supplied by Eastman Organic Chemicals or alternatively by British Drug Houses Ltd. Substituted silver benzoates were prepared by the method of Dauben and Tilles (32). Lithium benzoate (m.p. > 360°) was prepared by the action of lithium hydroxide on benzoic acid. Cupric benzoate was prepared by reacting cupric sulfate solution with aqueous sodium benzoate; the product was recrystallized from acetonitrile. Lead benzoate (m.p. 90–95°) was prepared from lead acetate and hot aqueous benzoic acid; mercuric benzoate (dec. > 156°) from mercuric nitrate/nitric acid solution and hot aqueous benzoic acid. All the metal benzoates were dried at 70° (120° for the alkali metal salts) for several days before use.

Solutions of chlorine or of benzoyl hypochlorite were estimated iodometrically. The color of iodine was used as its own indicator.

Vapor phase chromatography (v.p.c.) analyses were carried out on a Varian Aerograph Model 90-P3 instrument using helium as the carrier gas. Where quantitative determinations were to be made a weighed quantity of a standard substance was added to the reaction mixture, and the product in question quantitated by measuring the area of the product relative to the area of the standard. All such analyses were carried out in triplicate, and the reported values are the average. In the present study, chlorocyclohexane or bromobenzene were used as standards for chlorobenzene, and chlorobenzene or chlorocyclohexane as standards for bromobenzene. The response of the gas chromatograph was shown to be approximately equal towards these three compounds.

Attempts to Prepare Benzoyl Hypochlorite

(i) Reaction of Chlorine with Silver Benzoate and Addition of the Product to Cyclohexene

A 0.37 *M* solution of chlorine in carbon tetrachloride (18 ml) cooled to 0° was allowed to react in the dark with dry silver benzoate (3.0 g, 13.1 mmol) for 5 min and then filtered. To the filtrate was added cyclohexene (5 ml), after which the solution was washed twice with 0.1 *M* sodium bicarbonate (50 ml), with water (50 ml), and dried over calcium chloride. The solvent was removed,

Can. J. Chem. Downloaded from www.nrcresearchpress.com by 210.87.254.105 on 09/05/12
For personal use only.

Can. J. Chem. Downloaded from www.nrcresearchpress.com by 210.87.254.105 on 09/05/12
For personal use only.

and the residue was redissolved in carbon tetrachloride and examined by nuclear magnetic resonance (n.m.r.) (τ 1.8–3.0, 5H; τ 4.8–5.3, 1H; τ 5.7–6.3, 1H; τ 7.0–9.1, 8H; all multiplets). The n.m.r. was identical to that previously reported for 2-chlorocyclohexyl benzoate (1) and the compound was essentially free of 1,2-dichlorocyclohexane, which would change the spectrum by increasing the relative intensities of the resonances at τ 5.7–6.3 and τ 7.0–9.1.

(ii) Reaction of the Halogens with Other Metal Benzoates

Chlorine (occasionally bromine) was allowed to interact with various metal benzoates in different solvents (carbon tetrachloride, acetonitrile, *N,N*-dimethylformamide (*cf.* ref. 2), and water (*cf.* ref. 33), at temperatures in the range 0–100°. There was no evident reaction when the lithium, sodium, cupric, or lead salts were used. Both the mercuric and silver salts reacted with the halogens, but only the latter was used because the reactions with the mercuric salt were very slow and, furthermore, did not subsequently yield any aryl halide (possibly because the mercuric salt is hydrated).

Decomposition of Benzoyl Hypochlorite at Different Temperatures

A solution (approximately 0.3 *M*) of chlorine in carbon tetrachloride was cooled to 0° and allowed to react at 0° with silver benzoate (5.0 g), so that the latter was in at least two fold excess. After 5 min the solution was filtered, and 2 ml portions of the solution were placed in Pyrex ampoules, some of which already contained added reagents. (At this point two 2 ml portions were allowed to react with acidified potassium iodide solution and shown by v.p.c. *not* to have decomposed to chlorobenzene in the procedure.) The ampoules were cooled to 77 °K and evacuated to a pressure of 1 mm, after which they were sealed and placed in a constant temperature bath. Those samples to be irradiated were placed a few inches from two 100 W tungsten lamps; the other samples were protected from the light by means of aluminum foil. After 1 h the reaction ampoules were cooled to 77 °K, opened, their contents poured into acidified potassium iodide solution, and the liberated iodine was estimated volumetrically. The carbon tetrachloride solution from each such analysis was recovered; to a 1 ml portion was added bromobenzene as a standard and the chlorobenzene produced was estimated by v.p.c. The results of this study are given in Tables 1–4.

Decomposition of Benzoyl Hypochlorite at 0°

To silver benzoate (2.5 g) was added 15 ml of a 0.33 *M* solution of chlorine in carbon tetrachloride. After 5 min the reaction mixture was filtered and the filtrate was stored at 3° in a corked ampoule for 16 days, at which time the "positive chlorine" content of the sample was 0.06 *M*. Vapor phase chromatographic analysis of the carbon tetrachloride phase gave an estimated yield of chlorobenzene at 0.116 *M* (34%). A 5 ml portion of the solution was extracted with aqueous sodium bicarbonate; the aqueous phase was acidified and after extraction into ether, drying and evaporation of the solvent, yielded 107 mg of a white solid, m.p. 105–109°. The solid was esterified with methanol/sulfuric acid and analyzed by v.p.c. (10% diisodecyl phthalate on acid-washed 60/80 Chromosorb W). The esters of benzoic acid and of *o*-, *m*-, and *p*-chlorobenzoic acids were present in the ratio of 80:1.2:6.1:1.0.

Reaction of Halogens with Silver Benzoate at 80 and 0°

(i) Bromine at 80°

The following procedure is typical: To duplicate samples of dry silver benzoate (5.8 g, 25 mmol) and dry acetonitrile (40 ml) in 100 ml flasks equipped with reflux condensers and calcium chloride drying tubes was added in small portions a mixture of bromine (4.0 g, 25 mmol) and acetonitrile (total volume 10 ml). After 9.5 (9.5) ml of this mixture had been added, the solution assumed the red color of molecular bromine, and this color was not discharged by refluxing for a further 0.5 h. Heating now continued for 3 h more, after which weighed quantities of chlorobenzene were added to two aliquots of each solution. The bromobenzene produced was estimated by v.p.c. (Carbowax 20 *M*, 130°) and a sample of bromobenzene was isolated and its identity checked by infrared (i.r.) (this was not done in subsequent experiments).

(ii) Bromine at 0°

To a solution of bromine in the appropriate solvent cooled to 0° was added an equimolar quantity of silver benzoate. The reaction mixture was stirred at 0° with a magnetic stirrer for 4 h, then analyzed by v.p.c. as described above.

(iii) Chlorine at 0°

A solution of chlorine in the appropriate solvent was cooled to 0° and estimated iodometrically. Sufficient of this solution to contain 12.5 mmol of chlorine was added to silver benzoate (12.5 mmol) and the mixture was stirred at 0° for 4 h, then analyzed by v.p.c. as described previously.

(iv) Chlorine at 80°

Silver benzoate (12.5 mmol) and the appropriate solvent (40 ml) were placed in a two-necked flask equipped with reflux condenser and the mixture was brought to reflux. Through the second neck of the flask was introduced a slow stream of chlorine gas, which was maintained for 0.5 h. The mixture was refluxed for 1 h more, then analyzed by v.p.c. as described above.

Reaction of Bromine with Substituted Silver Benzoates

The following procedure is typical. To duplicate reaction mixtures of silver *p*-nitrobenzoate (2.7 g, 10 mmol) and carbon tetrachloride (40 ml) at reflux was added bromine (1.6 g, 10 mmol) and the solution was refluxed for 2 h. After the reaction bromine (0.050, 0.052 *M*) was estimated by iodometric titration of aliquots of the solution. To other aliquots was added bromobenzene as a v.p.c. standard (SE30, 200°), when the *p*-bromonitrobenzene produced was estimated at 0.20, 0.18 *M*. The solutions remaining were combined and filtered, yielding 52 ml of filtrates. Evaporation of the solvent followed by chromatography of the residue on silica gel (50 g) eluted *p*-bromonitrobenzene (1.6 g, 61%) as pale yellow needles, m.p. 126–126½°, undepressed by admixture with authentic material made from *p*-nitroaniline by the Sandmeyer reaction.

The experiment at 3° was also carried out in duplicate as follows. To the mixture of carbon tetrachloride and

the silver salt cooled to 0° was added bromine, after which the mixture was allowed to stand in a refrigerator (3 ± 2°) for 140 h. Analysis of the solutions was as described above but there was too little product to be isolated.

The authors wish to express their thanks for financial support of this work by the National Research Council of Canada, the Research Advisory Board (University of Guelph) and the Department of Chemistry, University of Guelph.

1. N. J. Bunce and D. D. Tanner. J. Amer. Chem. Soc. **91**, 6096 (1969).
2. C. H. Bamford and E. F. T. White. J. Chem. Soc. 4490 (1960).
3. J. K. Kochi, B. M. Graybill, and M. Kurz. J. Amer. Chem. Soc. **86**, 5257 (1964).
4. C. V. Wilson. Org. React. **9**, 332 (1957).
5. R. G. Johnson and R. K. Ingham. Chem. Rev. **56**, 219 (1956).
6. J. K. Kochi. J. Amer. Chem. Soc. **85**, 1958 (1963).
7. J. K. Kochi. Record Chem. Progr. **27**, 207 (1966).
8. See G. Sosnovsky and S. Lawesson. Angew. Chem. Intern. Ed. **3**, 269 (1964).
9. F. Minisci, G. P. Gardini, and F. Bertini. Can. J. Chem. **48**, 544 (1970) and references cited therein.
10. M. Anbar and D. Ginsberg. Chem. Rev. **54**, 925 (1954).
11. W. Bockemüller and F. W. Hoffmann. Ann. **519**, 165 (1935).
12. P. W. Jennings and T. D. Ziebarth. J. Org. Chem. **34**, 3216 (1969).
13. I. R. Beattie and D. Bryce-Smith. Nature, **179**, 577 (1957).
14. C. Walling and B. B. Jacknow. J. Amer. Chem. Soc. **82**, 6108 (1960).
15. W. O. Haag and E. I. Heiba. Tetrahedron Lett. 3683 (1965).
16. B. Knauer and E. G. Janzen. Abstracts of the 158th meeting of the A.C.S. New York. 1969. Abstract ORGN 121.
17. C. Walling. Free Radicals in Solution. John Wiley and Sons Inc., New York. 1957. p. 474 ff.
18. J. C. Martin and J. H. Hargis. J. Amer. Chem. Soc. **91**, 5399 (1969).
19. G. S. Hammond and L. M. Soffer. J. Amer. Chem. Soc. **72**, 4711 (1950).
20. G. B. Gill and G. H. Williams. J. Chem. Soc. 5756 (1965).
21. J. C. Bevington and T. D. Lewis. Trans. Faraday Soc. **54**, 1340 (1958).
22. L. G. S. Brooker and S. Smiles. J. Chem. Soc. 1723 (1926).
23. M. E. Kurz and M. Pellegrini. J. Org. Chem. **35**, 990 (1970) and references cited therein.
24. C. Prévost and J. Weinmann. Compt. rend., **204**, 989 (1937).
25. P. B. D. de la Mare and J. H. Ridd. Aromatic Substitution, Nitration, and Halogenation. Butterworths, London. 1959. Chapt. 9.
26. Y. Hatanaka, R. M. Keefer, and L. J. Andrews. J. Amer. Chem. Soc. **87**, 4280 (1965).
27. Y. Ogata and K. Nakajima. Tetrahedron, **20**, 43, 2751 (1964).
28. J. W. Taylor and J. C. Martin. J. Amer. Chem. Soc. **89**, 6904 (1967) and references cited therein.
29. J. K. Kochi and R. V. Subramanian. J. Amer. Chem. Soc. **87**, 1508 (1965).
30. J. D. Roberts and H. E. Simmons. J. Amer. Chem. Soc. **73**, 5487 (1951).
31. R. A. Barnes and R. J. Prochaska. J. Amer. Chem. Soc. **72**, 3188 (1950).
32. W. G. Dauben and H. Tilles. J. Amer. Chem. Soc. **72**, 3185 (1950).
33. D. D. Tanner and E. Protz. Can. J. Chem. **44**, 1555 (1966).
34. J. W. H. Oldham. J. Chem. Soc. 100 (1950).
35. C. E. Berr. Ph.D. Thesis. University of California, Los Angeles. 1952.
36. T. N. Mehta, V. S. Mehta, and V. B. Thosar. J. Ind. Chem. Soc. (Indian Ed.) **3**, 137 (1940).
37. J. C. Conly. J. Amer. Chem. Soc. **75**, 1148 (1953).
38. M. Heintzeler. Ann. **569**, 102 (1950).
39. R. T. Arnold and P. Morgan. J. Amer. Chem. Soc. **70**, 4248 (1948).
40. E. R. Buchman and J. C. Conly. J. Amer. Chem. Soc. **75**, 1990 (1953).
41. J. Cason and R. L. Way. J. Org. Chem. **14**, 31 (1949).
42. C. Hunsdiecker, H. Hunsdiecker, and E. Vogt. German Patent 730,410 (1942).
43. F. R. Jensen, H. L. Gale, and J. E. Rodgers. J. Amer. Chem. Soc. **90**, 5793 (1968).
44. P. Wilder and A. Winston. J. Amer. Chem. Soc. **75**, 5370 (1953).

Can. J. Chem. Downloaded from www.nrcresearchpress.com by 210.87.254.105 on 09/05/12
For personal use only.

Hydrogen Abstraction from Methyl Formate by Methyl Radicals[1]

T. R. Donovan,[2] W. Dorko, and A. G. Harrison
Department of Chemistry, University of Toronto, Toronto 181, Ontario

Received March 13, 1970

The reactions of CH_3 radicals with methyl formate and CD_3 radicals with methyl formate and methyl formate-*d* have been studied. The CH_3 and CD_3 radicals were produced by the photolysis of acetone and acetone-*d*. The Arrhenius parameters (log *A*, *A* in l mol^{-1} s^{-1}; *E*, in kcal mol^{-1}) for hydrogen abstraction are as follows

$$CH_3 + HCO_2CH_3 \rightarrow CH_4 + C_2O_2H_3: \log A, 8.7_0; E, 10.3;$$

$$CD_3 + HCO_2CH_3 \rightarrow CD_3H + C_2O_2H_3: \log A, 8.6_4; E, 10.1;$$

$$CD_3 + DCO_2CH_3 \rightarrow CD_4 + CO_2CH_3: \log A, 8.4_8; E, 11.7;$$

$$CD_3 + DCO_2CH_3 \rightarrow CD_3H + DCO_2CH_2: \log A, 8.0_9; E, 10.8;$$

$$CD_3 + HCO_2CH_3 \rightarrow CD_3H + CO_2CH_3: \log A, 8.5_5; E, 10.0.$$

Les réactions du radical $CH_3\cdot$ avec le formiate de méthyle et du radical $CD_3\cdot$ avec le formiate de méthyle et $DCOOCH_3$ ont été étudiées. Les radicaux $CH_3\cdot$ et $CD_3\cdot$ ont été obtenus par photolyse de l'acétone et de l'acétone-d_6 respectivement. Les paramètres d'Arrhénius (log *A*, *A* en l mol^{-1} s^{-1}; *E*, in kcal mol^{-1}) pour l'abstraction d'hydrogène sont les suivants

$$CH_3 + HCO_2CH_3 \rightarrow CH_4 + C_2O_2H_3: \log A, 8.7_0; E, 10.3;$$

$$CD_3 + HCO_2CH_3 \rightarrow CD_3H + C_2O_2H_3: \log A, 8.6_4; E, 10.1;$$

$$CD_3 + DCO_2CH_3 \rightarrow CD_4 + CO_2CH_3: \log A, 8.4_8; E, 11.7;$$

$$CD_3 + DCO_2CH_3 \rightarrow CD_3H + DCO_2CH_2: \log A, 8.0_9; E, 10.8;$$

$$CD_3 + HCO_2CH_3 \rightarrow CD_3H + CO_2CH_3: \log A, 8.5_5; E. 10.0.$$

Canadian Journal of Chemistry, 49, 828 (1971)

Introduction

Arthur and Gray (1) recently have reported the results of a study of the hydrogen-abstraction reactions of methyl radicals attacking methyl formate. Using isotopically labelled formate ($DCOOCH_3$) they measured the Arrhenius parameters for abstraction of both the methyl and formyl hydrogens and showed that at 182 °C, approximately 15% of the hydrogen is abstracted from the methyl position. This result is in contrast with those of Thynne (2) who concluded that abstraction occurred only from the formyl position for several alkyl formates, including methyl formate.

Prior to the publication by Arthur and Gray (1), we had undertaken a study of the reaction of methyl radicals with $DCOOCH_3$ to determine the position of abstraction. It has been suggested (3) that abstraction of hydrogen from the alkyl group in formates could be followed by CO_2 elimination to yield an alkyl radical. This reaction sequence in $DCOOCH_3$ would give a CH_2D radical which, by subsequent reaction with the methyl radical source, acetone, would yield CH_3D. Such a reaction sequence if it occurred would make the determination of the rate of abstraction of D from $DCOOCH_3$ ambiguous. To eliminate such ambiguity we have studied the reactions of CD_3 with $DCOOCH_3$. For comparison with previous work we have also studied the reaction of CH_3 radicals with unlabelled methyl formate. The results obtained support, on the whole, the conclusions reached by Arthur and Gray (1) although we differ in some of the details and it therefore appeared worthwhile to present our results at this time.

Experimental

Methyl radicals were produced by photolysis of acetone and methyl-d_3 radicals by photolysis of acetone-d_6, in both cases the total decomposition being limited to

[1]This work constitutes part of the M.Sc. thesis of W. Dorko (University of Toronto, 1967) and T. R. Donovan (University of Toronto, 1969).

[2]Recipient of Province of Ontario Graduate Fellowship, 1968–1969.

Can. J. Chem. Downloaded from www.nrcresearchpress.com by 210.87.254.6 on 09/05/12
For personal use only.

Can. J. Chem. Downloaded from www.nrcresearchpress.com by 210.87.254.6 on 09/05/12
For personal use only.

2–3%. The apparatus and experimental techniques were essentially identical with those used in a previous study (4) with the exception that the product analysis was carried out using an AEI MS-10 mass spectrometer.

The acetone was Fisher Spectroanalyzed Grade, dried and distilled *in vacuo* before use. Eastman Spectro Grade methyl formate was distilled *in vacuo* before use and showed no detectable impurities in its mass spectrum. Acetone-d_6 and methyl formate-d were obtained from Merck, Sharp and Dohme, Montreal.

Mass spectrometric analyses at low electron energy showed that the acetone-d_6 contained 2.3_6 mol% acetone-d_5, while the methyl formate-d contained 1.0% unlabelled formate.

Results[3]

Photolysis of Acetone

Above 373 °K the production of methane and ethane in the photolysis of acetone can be described by the mechanism

[1] $(CH_3)_2CO + h\nu \rightarrow 2\,CH_3 + CO$

[2] $2\,CH_3 \rightarrow C_2H_6$

[3] $CH_3 + (CH_3)_2CO \rightarrow CH_4 + CH_2COCH_3$

leading to the expression

$$R_{CH_4}/R_{C_2D_6}^{1/2}[Ac] = k_3/k_2^{1/2}$$

In the present work acetone was photolyzed in the temperature range 400 to 513 °K. Least squares analysis of the results for $k_3/k_2^{1/2}$ led to the expression

$$\log k_3/k_2^{1/2}\ (l^{1/2}\ mol^{-1/2}\ s^{-1/2}) = 3.26\ (\pm 0.15) - 2.07_1\ (\pm\ 0.067)\ 10^3/T$$

In combination with $k_2 = 2.2 \times 10^{10}$ l mol^{-1} s^{-1} and $E_2 = 0$ (5), this result leads to $E_3 = 9.4_8 \pm 0.3$ kcal/mol and log A_3 (l mol^{-1} s^{-1}) = $8.4_3 \pm 0.15$, in good agreement with the previous values of E and log A, respectively, of 9.3 and 8.3_5 (4), 9.43 and 8.42 (6), 9.63 and 8.53 (1), and 9.53 and 8.2 (7).

Photolysis of Acetone-d_6

The main products can be accounted for by the following mechanism, similar to that for the unlabelled acetone

[1′] $(CD_3)_2CO + h\nu \rightarrow 2CD_3 + CO$

[1″] $CD_3COCD_2H + h\nu \rightarrow CD_3 + CD_2H + CO$

[2′] $2CD_3 \rightarrow C_2D_6$

[3′] $CD_3 + (CD_3)_2CO \rightarrow CD_4 + CD_2COCD_3$

[3″] $CD_2H + (CD_3)_2CO \rightarrow CD_3H + CD_2COCD_3$

[5] $CD_3 + HCD_2COCD_3 \rightarrow CD_3H + CD_2COCD_3$

Reactions 1″, 3″, and 5 must be included because of the presence of 2.3_6 mol% acetone-d_5. Letting $[CD_2H]/[CD_3] = K_1$ and $[\text{Ac-}d_6]/[\text{Ac-}d_5] = K_2$, we may derive expressions 6 and 7 from the above mechanism

[6] $$\frac{R_{CD_4}}{R_{C_2D_6}^{1/2}[\text{Ac-}d_6]} = \frac{k_3'}{k_2'^{1/2}}$$

[7] $$\frac{R_{CD_3H}}{R_{C_2D_6}^{1/2}[\text{Ac-}d_5]} = \frac{k_5 + k_3''K_1K_2}{k_2'^{1/2}}$$

Experimental results were obtained over the temperature range 385 to 499 °K. Analysis of the experimental results by eq. 6 led by least squares treatment to the expression

$$\log k_3'/k_2'^{1/2}\ (l^{1/2}\ mol^{-1/2}\ s^{-1/2}) = 3.77\ (\pm\ 0.086) - 2.605\ (\pm\ 0.038)\ 10^3/T$$

Assuming $k_2' = k_2$ and $E_2' = 0$, we obtain log A_3' (l mol^{-1} s^{-1}) = 8.94 (± 0.09) and $E_3' = 11.9 \pm 0.2$ kcal mol^{-1}. These results are in reasonable agreement with earlier determinations of log A_3' and E_3', respectively, of 8.6_2 and 11.5_4 (8), 8.7 and 11.4 (9), 9.1 and 11.5 (10), and 8.7 and 11.5 (11).

The rate of formation of CD_3H is required primarily to correct the results in the photolysis of mixtures for the CD_3H arising from the acetone alone. Since the same sample was used for all experiments, K_1 and K_2 should remain essentially constant and we have evaluated only the expression

$$(k_5 + k_3''K_1K_2)/k_2'^{1/2}$$

as a function of temperature by treating the experimental results of eq. 7. Least squares treatment of the results led to the expression

$$\log (k_5 + k_3''K_1K_2/k_2'^{1/2}) = 3.25\ (\pm\ 0.15) - 2.28_5\ (\pm\ 0.066)\ 10^3/T$$

This expression was then used in the following to correct for CD_3H formation from the labelled acetone itself when mixtures with the labelled acetone were photolyzed.

Photolysis of Acetone – Methyl Formate Mixtures

When acetone is photolyzed in the presence of

[3] Photo copies of the complete tables of data upon which the present conclusions are based may be obtained free of charge, upon request, from the Depository of Unpublished Data, National Science Library, National Research Council of Canada, Ottawa, Canada.

Can. J. Chem. Downloaded from www.nrcresearchpress.com by 210.87.254.6 on 09/05/12
For personal use only.

methyl formate, reaction 8 must be added to reaction 3 as a source of CH_4.

[8] $CH_3 + HCO_2CH_3 \rightarrow CH_4 + C_2O_2H_3$

The following equation may be derived

$$[9] \quad \left[\frac{R_{CH_4}}{R_{C_2H_6}^{1/2}[Ac]} - \frac{k_3}{k_2^{1/2}}\right]\frac{[Ac]}{[Form]} = \frac{k_8}{k_2^{1/2}}$$

Results obtained in the photolysis of acetone–formate mixtures ([Ac]/[Form] = 1.17 to 1.69) over the temperature range 405 to 519 °K are shown in Fig. 1 as an Arrhenius plot of log $(k_8/k_2^{1/2})$ *vs.* $10^3/T$. Least squares analysis yields the expression

$$\log k_8/k_2^{1/2}\ (l^{1/2}\ mol^{-1/2}\ s^{-1/2}) = 3.53\ (\pm 0.10) - 2.25_3\ (\pm 0.044)\ 10^3/T$$

leading to $\log A_8\ (l\ mol^{-1}\ s^{-1}) = 8.70 \pm 0.10$ and $E_8 = 10.3 \pm 0.20$ kcal mol^{-1}.

Photolysis of Acetone-d_6 – Methyl Formate Mixtures

In the photolysis of these mixtures reaction 10 must be considered in addition to reactions 3'' and 5 as a source of CD_3H.

[10] $CD_3 + HCO_2CH_3 \rightarrow CD_3H + C_2O_2H_3$

The ratio $k_{10}/k_2'^{1/2}$ may be evaluated from the relation

$$[11] \quad \left[\frac{R_{CD_3H}}{R_{C_2D_6}^{1/2}[Ac\text{-}d_5]} - \frac{k_5 + k_3''K_1K_2}{k_2'^{1/2}}\right] \times \frac{[Ac\text{-}d_5]}{[Form]} = \frac{k_{10}}{k_2'^{1/2}}$$

Results obtained over the temperature range 408 to 494 °K are shown as an Arrhenius plot in Fig. 1 and lead, on least squares analysis, to the relation

$$\log k_{10}/k_2'^{1/2}\ (l^{1/2}\ mol^{-1/2}\ s^{-1/2}) = 3.47\ (\pm 0.14) - 2.207\ (\pm 0.064)\ 10^3/T$$

yielding $\log A_{10} = 8.64 \pm 0.14$ and $E_{10} = 10.1 \pm 0.3$ kcal/mol.

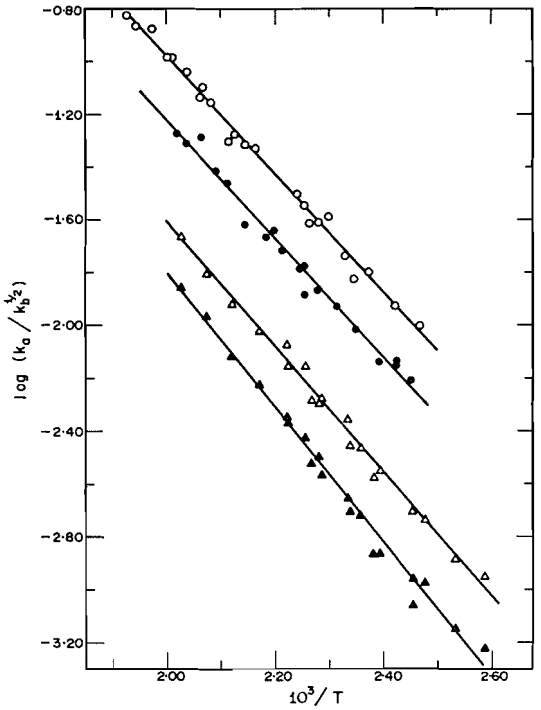

FIG. 1. Arrhenius plots for methyl radical reactions ○, log $(k_8/k_2^{1/2})$ *vs.* $10^3/T$; ●, log $(k_{10}/k_2'^{1/2})$ *vs.* $10^3/T$, curve displaced downwards by 0.3 units; △, log $(k_{14}/k_2'^{1/2})$ *vs.* $10^3/T$, curve displaced upwards by 0.2 units; ▲, log $(k_{12}/k_2'^{1/2})$ *vs.* $10^3/T$.

Photolysis of Acetone-d_6 – Methyl Formate-d Mixtures

In the photolysis of these mixtures CD_4 is formed by reaction 12 in addition to reaction 3'

[12] $CD_3 + DCD_2CH_3 \rightarrow CD_4 + CO_2CH_3$

The reaction scheme leads to the expression

$$[13] \quad \left[\frac{R_{CD_4}}{R_{C_2D_6}^{1/2}[Ac\text{-}d_6]} - \frac{k_3'}{k_2'^{1/2}}\right] \times \frac{[Ac\text{-}d_6]}{[Form\text{-}d]} = \frac{k_{12}}{k_2'^{1/2}}$$

Acetone-d_6 — methyl formate-d_1 mixtures were photolyzed over the temperature range 387 to 493 °K with the values of $k_{12}/k_2'^{1/2}$ being evaluated from eq. 13. The results are plotted as a function of temperature in Fig. 1 and treatment of the data by the method of least squares leads to the result

$$\log k_{12}/k_2'^{1/2}\ (l^{1/2}\ mol^{-1/2}\ s^{-1/2}) = 3.31\ (\pm 0.16) - 2.55_4\ (\pm 0.070)\ 10^3/T$$

from which one obtains $\log A_{12} = 8.48 \pm 0.16$ and $E_{12} = 11.7 \pm 0.3$ kcal mol^{-1}.

In the photolysis of these mixtures CD_3H may be formed by the following reactions, where reaction 10 is included to allow for the 1.0% HCO_2CH_3 impurity in the labelled formate.

[3''] $CD_2H + (CD_3)_2CO \rightarrow CD_3H + CD_2COCD_3$

TABLE 1. Reactions of methyl radicals with methyl formates

Reaction	E (kcal mol^{-1})	log A*	log k* (182 °C)	Reference
Total H abstraction				
$CH_3+HCO_2CH_3 \rightarrow CH_4+C_2O_2H_3$	10.3±0.2	8.70±0.10	3.7_5	This Work
$CD_3+HCO_2CH_3 \rightarrow CD_3H+C_2O_2H_3$	10.1±0.3	8.64±0.14	3.7_9	This Work
$CH_3+HCO_2CH_3 \rightarrow CH_4+C_2O_2H_3$	9.4_7±0.13	8.24±0.06	3.5_6	1
$CH_3+HCO_2CH_3 \rightarrow CH_4+C_2O_2H_3$	9.0	7.9	3.5_7	2*a*
$CH_3+HCO_2CH_3 \rightarrow CH_4+C_2O_2H_3$	9.8	8.3	3.6_0	12
Abstraction from formyl position				
$CD_3+DCO_2CH_3 \rightarrow CD_4+CO_2CH_3$	11.7±0.3	8.48±0.16	2.8_4	This Work
$CH_3+DCO_2CH_3 \rightarrow CH_3D+CO_2CH_3$	11.66±0.14	8.29±0.07	2.6_9	1
$CD_3+HCO_2CH_3 \rightarrow CD_3H+CO_2CH_3$	10.0±0.5	8.55±0.24	3.7_2	This Work
$CH_3+HCO_2CH_3 \rightarrow CH_4+CO_2CH_3$	9.89±0.20	8.23±0.09	3.4_8	1
Abstraction from methyl position				
$CD_3+DCO_2CH_3 \rightarrow CD_3H+DCO_2CH_2$	10.8±0.2	8.09±0.11	2.8_8	This Work
$CH_3+DCO_2CH_3 \rightarrow CH_4+DCO_2CH_3$	8.95±0.38	7.01±0.19	2.7_1	1

*Units of A and k l mol^{-1} s^{-1}.

[5] $CD_3 + CD_2HCOCD_3 \rightarrow CD_3H + CD_2COCD_3$

[10] $CD_3 + HCO_2CH_3 \rightarrow CD_3H + C_2O_2H_3$

[12′] $CD_2H + DCO_2CH_3 \rightarrow CD_3H + CO_2CH_3$

[14] $CD_3 + DCO_2CH_3 \rightarrow CD_3H + DCO_2CH_2$

Letting $[HCO_2CH_3]/[DCO_2CH_3] = K_3$ we obtain the following expression for the rate of formation of CD_3H

$$[15]\quad R_{CD_3H} = (k_5 + k_{3''}K_1K_2)[CD_3][\text{Ac-}d_5] + (k_{14} + k_{10}K_3 + k_{12'}K_1)[CD_3][\text{Form-}d]$$

where K_1 and K_2 are as defined in the section of photolysis of acetone-d_6 alone. From eq. 15 we may derive

$$[16]\quad \left[\frac{R_{CD_3H}}{R_{C_2D_6}^{1/2}[\text{Ac-}d_5]} - \frac{k_5 + K_1K_2k_{3''}}{k_{2'}^{1/2}}\right] \times \frac{[\text{Ac-}d_5]}{[\text{Form-}d]} - \frac{k_{10}K_3}{k_{2'}^{1/2}} - \frac{k_{12'}K_1}{k_{2'}^{1/2}} = \frac{k_{14}}{k_{2'}^{1/2}}$$

The expression within the brackets on the left hand side of eq. 16 may be evaluated from the experimental results for photolysis of the mixture and the results from photolysis of acetone-d_6 alone. The expression $k_{10}K_3/k_{2'}^{1/2}$ corrects for the CD_3H formed by reaction 10 and may be evaluated from the results for $k_{10}/k_{2'}^{1/2}$ obtained above taking $K_3 = 0.010$. The expression $k_{12'}K_1/k_{2'}^{1/2}$ corrects for the CD_3H formed by reaction 12′. Assuming $k_{12'} = k_{12}$, this correction can be estimated from the measured value of $k_{12}/k_{2'}^{1/2}$ taking $K_1 = 0.012$. These two corrections amounted to approximately 8% of the first term. The values of $k_{14}/k_{2'}^{1/2}$ obtained after these corrections are shown in the form of an Arrhenius plot in Fig. 1 and lead on least squares analysis to the expression

$$\log k_{14}/k_{2'}^{1/2}\ (l^{1/2}\ mol^{-1/2}\ s^{-1/2}) = 2.92\ (\pm 0.11) - 2.36_6\ (\pm 0.044)\ 10^3/T$$

From this expression one derives log A_{14} (l mol^{-1} s^{-1}) = 8.09 ± 0.11 and E_{14} = 10.8 ± 0.2 kcal mol^{-1}.

Neglecting secondary isotope effects, as is customary, the rate coefficient for the reaction

[17] $CD_3 + HCO_2CH_3 \rightarrow CD_3H + CO_2CH_3$

may be obtained from the relation

$$[18]\quad \frac{k_{17}}{k_{2'}^{1/2}} = \frac{k_{10}}{k_{2'}^{1/2}} - \frac{k_{14}}{k_{2'}^{1/2}}$$

Using the relevant experimental data we obtain

$$\log k_{17}/k_{2'}^{1/2}\ (l^{1/2}\ mol^{-1/2}\ s^{-1/2}) = 3.38\ (\pm 0.24) - 2.19_2\ (\pm 0.107)\ 10^3/T$$

leading to log A_{17} (l mol^{-1} s^{-1}) = 8.5_5 ± 0.24 and E_{16} = 10.0 ± 0.5 kcal mol^{-1}.

Discussion

Table 1 summarizes the data available concerning hydrogen abstraction from methyl formate by methyl radicals. Although the rate constants at 182 °C for the overall hydrogen abstraction from the unlabelled formate are in reasonable agreement, our activation energies both for CH_3 and CD_3 are considerably higher

Can. J. Chem. Downloaded from www.nrcresearchpress.com by 210.87.254.6 on 09/05/12
For personal use only.

Can. J. Chem. Downloaded from www.nrcresearchpress.com by 210.87.254.6 on 09/05/12
For personal use only.

than obtained by Arthur and Gray (1) and by Thynne (2*a*), although they are in agreement, within experimental error, with the results of Kutschke (12). There are no readily apparent reasons for this spread in Arrhenius parameters.

The present results for abstraction of D from DCO_2CH_3 are in excellent agreement with the results of Arthur and Gray (1); however, the results for abstraction of the methyl hydrogen, while agreeing in the rate constant at 182 °C disagree significantly in the activation energy and A factor. Arthur and Gray point out that the accuracy of their Arrhenius parameters for abstraction from the methyl position is limited, presumably because the amount of CH_4 produced by this reaction is small compared to the CH_4 produced by abstraction from the radical source, acetone. In our experiments the product resulting from abstraction from the methyl group is CD_3H and, at a maximum, only 3% of the total CD_3H arises from reaction involving the acetone-d_5 isotopic impurity. Thus for experimental reasons we would suggest that the present results are to be preferred.

Some support for our data comes from the following observations. The activation energy for abstraction from the methyl group of methyl formate, $E = 10.8 \pm 0.2$ kcal/mol, is in reasonable agreement with the activation energy, $E = 10.0 \pm 0.2$ kcal/mol, for hydrogen abstraction from dimethyl ether. Our Arrhenius parameters when compared to Arthur and Gray's results for abstraction of a methyl hydrogen from methyl formate by CF_3 radicals leads to $E_{CD_3} - E_{CF_3} = 2.0$ kcal/mol and a ratio of A factors of $A_{CF_3}/A_{CD_3} = 1.2_3$ while Arthur and Gray's data lead to $E_{CH_3} - E_{CF_3} = 0.14$ kcal/mol and $A_{CF_3}/A_{CH_3} \approx 10$. As Arthur and Gray point out, abstraction by CF_3 is usually faster than abstraction by CH_3 and this rate difference usually arises from a lower activation energy rather than a higher frequency factor. Our results thus appear more in line with previous experience assuming their kinetic data for the CF_3 reaction is correct.

The difference between the present work and that of Arthur and Gray for attack on the methyl position of methyl formate is counterbalanced by the difference in the parameters for the total hydrogen abstraction reaction, with the result that we obtain essentially the same Arrhenius parameters for abstraction of hydrogen from the formyl position of the unlabelled formate. Our experimental results for k_{14} and k_{17} lead to the conclusion that at 182 °C, approximately 10% of the total hydrogen is abstracted from the methyl position, in agreement with the conclusion of Arthur and Gray.

The authors are indebted to the National Research Council of Canada for financial support and to Dr. A. Herod for helpful discussions.

1. N. L. Arthur and P. Gray. Trans. Faraday Soc. **65**, 424 (1969).
2. (*a*) J. C. J. Thynne. Trans. Faraday Soc. **58**, 676 (1962). (*b*) J. C. J. Thynne. Trans. Faraday Soc. **58**, 1394, 1533 (1962).
3. J. Grotewold and J. A. Kerr. J. Chem. Soc. 442 (1963).
4. T. W. Shannon and A. G. Harrison. Can. J. Chem. **41**, 2455 (1963).
5. A. Shepp. J. Chem. Phys. **24**, 939 (1956).
6. L. Endrenyi and D. J. Le Roy. J. Phys. Chem. **71**, 1334 (1967).
7. J. C. J. Thynne and P. Gray. Trans. Faraday Soc. **58**, 2403 (1962).
8. P. Gray and A. A. Herod. Trans. Faraday Soc. **64**, 1568 (1968).
9. R. Shaw and J. C. J. Thynne. Trans. Faraday Soc. **62**, 104 (1966).
10. W. M. Jackson, J. R. McNesby, and B. DeB. Darwent. J. Chem. Phys. **37**, 1610 (1962).
11. E. Whittle and E. W. R. Steacie. J. Chem. Phys. **21**, 993 (1953).
12. K. O. Kutschke. Unpublished results, quoted in ref. 2*a*.
13. N. L. Arthur, P. Gray, and A. A. Herod. Can. J. Chem. **47**, 1347 (1969).

Influence of p*H* on the Kinetics of Hydration of Tricalcium Silicate

K. G. McCURDY AND B. P. ERNO
Department of Chemistry, University of Lethbridge, Lethbridge, Alberta

Received September 1, 1970

An investigation has been made of the influence of p*H* on the kinetics of hydration of tricalcium silicate in a large excess of water. The rate constants increase with increasing hydrogen ion activity $(a_{H^+})_{aq}$ in the liquid phase when the $(a_{H^+})_{aq}$ is low; however, as the $(a_{H^+})_{aq}$ is increased further the rate constants become independent of the $(a_{H^+})_{aq}$. The results have been interpreted by proposing that the rate constants are proportional to the hydrogen ion activity adsorbed, $(a_{H^+})_{ads.}$, on the solid surface. The Langmuir adsorption isotherm was used to correlate the hydrogen ion activity on the surface to the hydrogen ion activity in the liquid phase.

Several particle sizes of tricalcium silicate were investigated and a surface area effect is indicated.

Canadian Journal of Chemistry, 49, 833 (1971)

Can. J. Chem. Downloaded from www.nrcresearchpress.com by 210.87.254.6 on 09/05/12
For personal use only.

Introduction

Tricalcium silicate, Ca_3SiO_5, contains calcium (Ca^{2+}), oxide (O^{2-}), and silicate (SiO_4^{4-}) ions (1). When tricalcium silicate is dissolved in basic aqueous solutions, the reaction products are calcium hydroxide and calcium silicate hydrates of various compositions (2). When a large excess of water, 1000:1 weight liquid to weight solid ratio, is used the dissolution reaction is complete and may be represented as in eq. 1 with no precipitation of calcium silicate hydrate

[1] $3Ca^{2+}(c) + O^{2-}(c) + SiO_4^{4-}(c) + nH_2O(l) \rightarrow$

$$3Ca^{2+}(aq) + 6OH^-(aq) + SiO_2(aq)$$

The silicate species is denoted by $SiO_2(aq)$, realizing that it is distributed among the species H_4SiO_4, $H_3SiO_4^-$, and $H_2SiO_4^{2-}$ as a function of the p*K*'s of silicic acid and the p*H* of the medium. The reaction generates hydroxide ions and the p*H* increases as the reaction proceeds. In a previous publication (3) from this laboratory, a p*H* stat technique was described for following the progress of the reaction. The following mechanism was proposed for the overall chemical reaction in reaction 1

[2] $3CaO.SiO_2(s) + nH_2O(l) \xrightarrow{k_1} 1.5Ca^{2+}(aq) + 3OH^-(aq) + 1.5CaO.SiO_2(s)$

[3] $1.5CaO.SiO_2(s) + nH_2O(l) \xrightarrow{k_2} 1.5Ca^{2+}(aq) + 3OH^-(aq) + SiO_2(aq)$

[4] $1.5CaO.SiO_2(s) + SiO_2(aq) \overset{K_3}{\rightleftharpoons} 1.5CaO.SiO_2.SiO_2(s)$

[5] $1.5CaO.SiO_2.SiO_2(s) + nH_2O(l) \xrightarrow{k_4} 1.5Ca^{2+}(aq) + 3OH^-(aq) + 2SiO_2(aq)$

This mechanism successfully accounted for the amount of hydroxide produced at various times (3).

No other investigations using the constant p*H* technique of hydration of tricalcium silicate have been reported. Recent reviews (4, 5) report experiments that have been conducted in systems which rapidly reach lime saturation and therefore do proceed at a constant p*H* corresponding to lime saturation. Since calcium silicate hydrates are precipitated during this reaction, these results are not directly comparable with the present results.

Lerch and Bogue (6) hydrated tricalcium silicate in a medium in which the supernatant, containing the soluble products of the hydration, was intermittently replaced by water. This technique is only remotely comparable to the present continuously controlled p*H* method. They reported that the rate of production of $Ca(OH)_2$ was faster when the supernatant was replaced intermittently than when the supernatant was not replaced.

The heterogenous reaction kinetics of the dissolution of hydrated metal silicates by aqueous acid solutions have been studied by several investigators (7–9). It has been suggested that the rate of dissolution of a crystalline powder by excess acid (or alkali) should depend on the surface area of the solid and on the mean ionic activity of the liquid phase (10, 11).

In the present study, tricalcium silicate was hydrated in a large excess of water at several

Can. J. Chem. Downloaded from www.nrcresearchpress.com by 210.87.254.6 on 09/05/12
For personal use only.

different but constant pH's in order to determine the pH dependence of the various steps in the mechanism described by reactions 2 to 5.

Experimental

Materials

The tricalcium silicate studied was synthesized from Baker analyzed low alkali calcium carbonate and Baker analyzed reagent silica with a 3:1 molar ratio, lime to silica, in platinum crucibles in a high temperature furnace. The mixture was put into the cold furnace and the temperature slowly raised to 950 °C and then rapidly raised to 1510 °C. The sample was removed from the furnace, ground to pass a 200 mesh sieve and reignited at 1510 °C until tests for free lime (12) were less than 0.5%. Chemical analysis of the product indicated 73.2% lime and 26.3% silica, and 0.4% free lime. Calculations of the composition of the product from the above data indicated 96.0% tricalcium silicate and 3.1% dicalcium silicate.

The particle size ranges used in the present study were obtained by sieving the tricalcium silicate for 30 min with a stack of Endicott N.B.S. sieves. Sieve openings for U.S.B.S. sieve numbers 400, 325, 270, 230, 100, and 50 are 0.037, 0.044, 0.053, 0.062, 0.149, and 0.297 mm, respectively. Samples *A*, *B*, *C*, *D*, and *E* were obtained with the following characteristics

Sample	Passed through N.B.S. sieve number	Did not pass through N.B.S. sieve number
A	400	—
B	325	400
C	270	325
D	230	270
E	50	100

All solutions were prepared using doubly distilled water.

Lime solutions were prepared by igniting low alkali Baker analyzed calcium carbonate to lime and dissolving in water. Calcium ion was determined by EDTA titration (13).

All reactions were initiated in 0.2 mM calcium hydroxide solution. The various experimental pH's were obtained by adjusting the calcium hydroxide with concentrated solutions of HCl or NaOH.

Equipment and Procedure

The experimental apparatus and the kinetic analysis procedure have been previously described (3). All reactions were again treated as first order with respect to the weight of solid.

All experiments involved 10 mg of tricalcium silicate in 10 ml of solution at 25 °C.

Results

Experimental conditions of the series and results of the kinetic analysis are given in Table 1. All series are results of at least duplicate investigations.

Series 41 to 61 were with Sample *A* of tricalcium silicate. Series 62 to 64 were with Sample *B* of tricalcium silicate. Series 65 to 69 were with Sample *D* of tricalcium silicate. Series 70 to 74 were with Sample *E* of tricalcium silicate. Series 75 to 84 were with Sample *C* of tricalcium silicate.

Discussion

Influence of pH on the Rate Constants k_1, k_2, and k_4

The results reported in Table 1 indicate that the first order rate constants k_1, k_2, and k_4 are affected by varying the pH of the reaction medium. The rate constants increase with increasing hydrogen ion activity in liquid phase, $(a_{H^+})_{aq}$, up to a certain hydrogen ion activity and then remain constant with further increases in the activity of the hydrogen ion in the liquid phase. A typical graph is given in Fig. 1, a_{H^+} is plotted as pH to compress the scale.

It has been suggested (10, 11) that dissolution reaction rates should depend on the surface area of the solid and on the mean ionic activity of the liquid phase.

The rate constants in this investigation are for a reaction that is first order with respect to the weight of solid. A first order mechanism suggests a two dimensional attack with adsorption on the solid surface.

The fraction of the total surface covered at any time by hydrogen ions is (14)

$$\theta = \alpha\mu/(\alpha\mu + \nu)$$

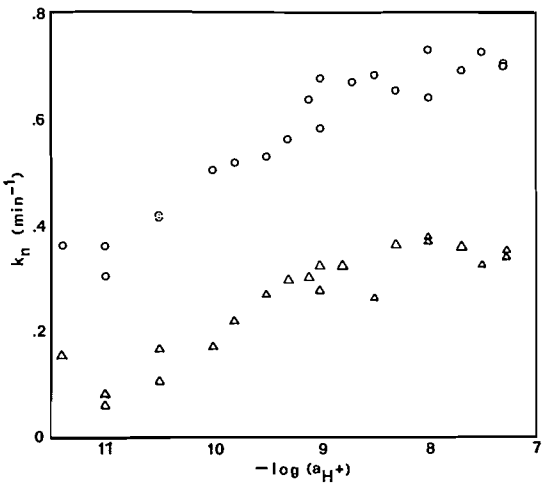

FIG. 1. Plots of log k_1, ○, and log k_2, △, *vs.* −log $(a_{H^+})_{aq}$ for sample *A* at 25 °C.

TABLE 1. Experimental conditions and kinetic parameters for the hydration of tricalcium silicate at 25 °C

Series	pH	Tricalcium silicate reacted (μmol)	k_1 (min^{-1})	k_2 (min^{-1})	K_3 (l/mol)	k_4 (min^{-1})
41	7.5	40.31	0.724	0.321	506	0.375
42	9.0	41.32	0.580	0.271	1280	0.323
43	9.8	42.20	0.517	0.220	903	0.158
44	10.5	39.81	0.420	0.106	1069	0.125
45	11.0	32.19	0.361	0.062	1674	0.080
46	11.4	19.04	0.362	0.151	537	0.125
47	8.0	41.60	0.639	0.377	2771	0.400
48	8.5	39.78	0.683	0.260	685	0.425
49	9.1	40.64	0.638	0.300	680	0.380
50	9.5	38.56	0.528	0.266	809	0.290
51	10.0	35.13	0.505	0.169	1257	0.190
52	10.5	33.74	0.416	0.167	568	0.130
53	11.0	27.57	0.302	0.081	1281	0.091
54	7.3	40.50	0.699	0.346	814	0.410
55	7.3	40.05	0.698	0.341	585	0.420
56	7.7	39.55	0.690	0.358	709	0.405
57	8.0	40.42	0.731	0.376	801	0.400
58	8.3	39.99	0.651	0.362	1081	0.400
59	8.7	39.57	0.667	0.323	970	0.380
60	9.0	39.46	0.675	0.323	745	0.350
61	9.3	39.53	0.563	0.296	831	0.330
62	8.3	41.96	0.697	0.345	917	0.458
63	9.4	41.26	0.641	0.206	831	0.315
64	10.1	36.83	0.553	0.123	1073	0.170
65	7.5	39.79	0.288	0.103	757	0.151
66	8.5	41.09	0.266	0.093	1346	0.156
67	9.0	40.45	0.270	0.074	1716	0.140
68	9.5	39.48	0.226	0.067	1530	0.119
69	10.5	37.36	0.233	0.042	1104	0.067
70	7.5	43.04	0.230	0.080	1196	0.117
71	8.5	42.86	0.205	0.072	1101	0.118
72	9.0	40.90	0.181	0.061	897	0.107
73	9.5	32.21	0.150	0.054	987	0.084
74	10.5	34.97	0.141	0.041	1314	0.048
75	7.5	40.63	0.310	0.105	950	0.165
76	8.3	41.89	0.310	0.107	811	0.160
77	8.6	39.77	0.286	0.091	1071	0.160
78	8.9	39.19	0.274	0.093	1585	0.155
79	9.2	40.37	0.235	0.089	1279	0.135
80	9.5	36.75	0.262	0.057	1769	0.115
81	9.8	36.97	0.225	0.055	1836	0.097
82	10.3	35.48	0.213	0.042	1057	0.070
83	10.3	35.22	0.181	0.051	2240	0.080
84	11.0	29.41	0.270	0.048	1993	0.056

where α is the fraction of molecules striking the surface which adhere, μ is the number striking 1 cm^2 per unit of time, and ν is a constant for adsorption of hydrogen ions on the surface. The rate constants reported in Table 1, k_n, (n = 1, 2, or 4) are proportional to the fraction of the total surface covered by hydrogen ions, therefore since μ is proportional to $(a_{H^+})_{aq}$

$$[6] \qquad k_n = k_n^1 \frac{\alpha[a_{H^+}]_{aq}}{\alpha[a_{H^+}]_{aq} + \nu}$$

where $k_n = k_n^1$ when θ = 1 and is the pH independent rate constant for the dissolution of solid in excess water. Rearranging eq. 6 gives

$$[7] \qquad \frac{(a_{H^+})_{aq}}{k_n} = \frac{(a_{H^+})_{aq}}{k_n^1} + \frac{\nu}{\alpha k_n^1}$$

Plots of $(a_{H^+})_{aq}/k_n$ *vs.* $(a_{H^+})_{aq}$ should be linear with a slope of $1/k_n^1$ and intercept $\nu/\alpha k_n^1$.

Figure 2 gives a typical plot for sample *A*. The reciprocal of the slope is k_n^1. The results, in terms of k_n^1, of the plots for the samples investigated are given in Table 2.

The results of Table 2 suggest a surface area dependence of the rate constants k_n^1. The values of k_n^1 for sample *B* may have a considerable

Can. J. Chem. Downloaded from www.nrcresearchpress.com by 210.87.254.6 on 09/05/12
For personal use only.

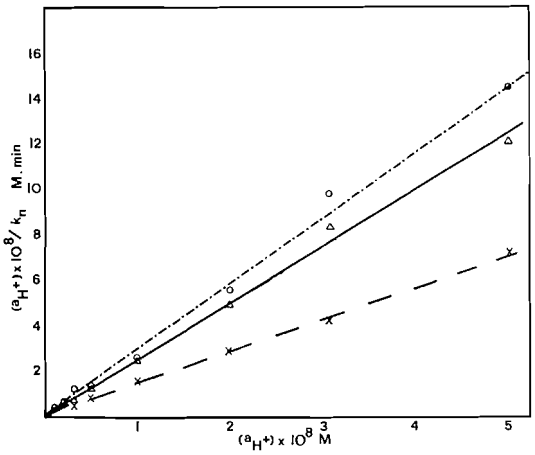

FIG. 2. Plots of a_{H+}/k_n *vs.* a_{H+} for sample *A*. k_1 ----, k_2 —, and k_4 ·–·– at 25 °C.

TABLE 2. p*H* independent rate constants for the hydration of tricalcium silicate at 25 °C

Sample	k_1^1 (min^{-1})	k_2^1 (min^{-1})	k_4^1 (min^{-1})
A	0.719	0.342	0.400
B	0.699	0.359	0.471
C	0.319	0.104	0.165
D	0.288	0.104	0.151
E	0.232	0.080	0.117

error. They were determined from only three p*H* investigations, and the apparently larger values for k_n^1 for *A* and *B* compared to *C* and *D* may be due to the values for *B* being too high. The effect of surface on the kinetics of the various steps in the proposed mechanism is under further investigation in this laboratory with a larger number of samples with various particle sizes.

Influence of pH on K_3

The influence of p*H* on the value of K_3 is small over the p*H* range investigated. If the equilibrium represented by reaction 4 depended on a particular species of silica, H_4SiO_4, $H_3SiO_4^-$, or $H_2SiO_4^{2-}$, the equilibrium constant should show a considerable variation over the range of p*H*'s investigated. The amounts of each silicic acid species present can be calculated from a knowledge of the p*H* and the ionization constants of silicic acid $pK_1 = 9.77$ and $pK_2 = 11.8$ (15, 16). Over the p*H* range of investigation the relative amounts of each species changes many fold. This is not reflected in the change of K_3 with p*H*, thus the association of $1.5CaO.SiO_2$ with silica is independent of the species of silica involved.

We are indebted to the National Research Council of Canada for financial support. The continuing financial support of the Uhiversity of Lethbridge Research Committee is greatly appreciated. The authors wish to thank the Departments of Physics and Mathematics for use of their computing facilities.

1. J. D. BERNAL, J. W. JEFFERY, and H. F. W. TAYLOR. Mag. Concrete Res. **11**, 49 (1952).
2. S. BRUNAUER, L. E. COPELAND, and R. H. BRAGG. J. Phys. Chem. **60**, 112 (1956).
3. K. G. MCCURDY and B. P. ERNO. Can. J. Chem. In press.
4. L. E. COPELAND and D. L. KANTRO. Proceedings of the Fifth International Symposium on the Chemistry of Cement, Tokyo. 1968.
5. R. KONDO and S. UEDA. Proceedings of the Fifth International Symposium on the Chemistry of Cement, Tokyo. 1968.
6. WM. LERCH and R. H. BOGUE. J. Phys. Chem. **31**, 1627 (1927).
7. A. PACKTER. Chem. and Ind. 1384 (1955).
8. W. T. GRANDQUIST. Proc. 6th Natl. Conf. Clay Minerals. 292 (1959).
9. B. SEMMENS. J. Appl. Chem. **16**, 125 (1966).
10. E. A. MOELYWN-HUGHES. Physical Chemistry. Pergamon Press, Oxford. 1961.
11. A. PACKTER and H. S. DHILLON. J. Chem. Soc. A, 2588 (1969).
12. WM. LERCH and R. H. BOGUE. Ind. Eng. Chem. Anal. Ed. **2**, 296 (1930).
13. A. I. VOGEL. A Text-book of Quantitative Inorganic Analysis Including Elementary Instrumental Analysis. 3rd ed. Longmans. p. 436.
14. S. GLASSTONE. Textbook of Physical Chemistry. 2nd ed. D. Van Nostrand Company, Inc., New Jersey. 1946. Chap. XIII.
15. S. A. GREENBERG and E. W. PRICE. J. Phys. Chem. **61**, 1539 (1957).
16. S. A. GREENBERG. J. Amer. Chem. Soc. **80**, 6508 (1958).

Can. J. Chem. Downloaded from www.nrcresearchpress.com by 210.87.254.6 on 09/05/12
For personal use only.

Can. J. Chem. Downloaded from www.nrcresearchpress.com by 210.87.254.6 on 09/05/12
For personal use only.

H_2O, HDO, and CH_3OH Infrared Spectra and Correlation with Solvent Basicity and Hydrogen Bonding[1]

D. N. GLEW AND N. S. RATH[2]

Exploratory Research Laboratory, Dow Chemical of Canada, Limited, Sarnia, Ontario

Received August 4, 1970

A study has been made of the infrared O—H bands for CH_3OH, DOH, and H_2O in solution and of their correlation with hydrogen bonding and solvent basicity. Infrared bands for the three fundamentals and the first bending overtone of H_2O and for the O—H stretching fundamentals of DOH and CH_3OH have been measured between 30 and -40 °C in a solvent range extending from weakly interacting fluorocarbons to strongly hydrogen-bonding organic amines. The O—H stretching bands for the weakly acidic solutes CH_3OH, DOH, and H_2O are mostly Lorentzian in shape and move to lower frequencies with higher extinctions in the more basic solvents. Many correlations are found between the stretching frequencies and band areas, and between the frequencies and solvent basicity. Monofunctional CH_3OH is found to be a stronger acid and forms stronger hydrogen-bonds with a given base than do the doubly bonded DOH and HOH which show equal dibasic acid strengths.

The wide, overlapped, fundamental stretching bands for H_2O strongly hydrogen-bonded to the tertiary amines and for ice have been partially resolved and unequivocally assigned, showing that there is no cross-over of the ν_3 and ν_1 bands despite the strong hydrogen-bonding.

At higher temperatures in solvents containing both hydrophobic and strongly basic groups water was found with the lower C_s type symmetry, in which unbonded O—H groups gave sharp bands in the 3680–3650 cm^{-1} region in addition to the wide hydrogen-bonded bands at lower frequencies.

Une étude infrarouge des bandes O—H des molécules CH_3OH, DOH et H_2O en solution et de leur corrélation avec la liaison hydrogène et la basicité du solvant a été effectuée. Les bandes infrarouges des trois fondamentales et de la première harmonique de déformation de H_2O ainsi que les fondamentales de valence de DOH et CH_3OH ont été mesurées entre 30 et -40 °C dans une série de solvants connus pour leurs interactions faibles: fluorocarbures et également connus pour leurs interactions spécifiques par liaison hydrogène comme les amines aromatiques. Les bandes de valence OH des solutés faiblement acides CH_3OH, DOH et H_2O sont de forme quasi-Lorentzienne et se déplacent vers les basses fréquences avec des extinctions supérieures dans les solvants davantage basiques. Plusieurs corrélations sont trouvées entre les fréquences de valence et les surfaces de bande et entre les fréquences et la basicité du solvant. La molécule monofonctionnelle CH_3OH est un acide plus fort et forme des liaisons hydrogènes plus fortes avec une base donnée que les molécules doublement liées DOH et HOH qui montrent des forces acides égales aux différents protons.

Les bandes fondamentales de valence, larges et recouvertes, de H_2O fortement lié par la liaison hydrogène aux amines tertiaires et pour la glace ont été partiellement résolues et attribuées sans ambiguité, montrant qu'il n'existe aucun croisement des bandes ν_3 et ν_1 en dépit de la liaison hydrogène forte.

Aux températures supérieures dans les solvants contenant des groupes hydrophobes et fortement basiques l'eau possède la symétrie inférieure de type C_s suivant laquelle des groupes O—H non-liés procurent des bandes fines dans la région 3680–3650 cm^{-1} en plus des bandes larges causées par les liaisons hydrogènes aux fréquences inférieures.

Canadian Journal of Chemistry, 49, 837 (1971)

Introduction

The bent, triatomic H_2O molecule exhibits three, nondegenerate, fundamental vibrations (1), of which two are high frequency, O—H valence-stretching modes absorbing in the 3756–3200 cm^{-1} region, while the remaining vibration is a lower frequency angular-deformation or bending mode absorbing at 1595–1670 cm^{-1}. When both protons of H_2O are subject to nearly equivalent force fields, both unbonded or both H-bonded (hydrogen-bonded) equally, so that the H_2O molecule retains its normal C_{2v} type symmetry (1, 2), the two O—H stretching modes are coupled and split to yield an upper-frequency, antisymmetric-stretch, molecular vibration, ν_3, and a lower-frequency, symmetric-stretch, molecular vibration, ν_1, which is isosymmetric with the low-frequency bending vibration ν_2. However, when the H_2O molecule in its force field has the lower C_s type symmetry, as for the asymmetrically bonded HOH molecule in which one proton forms an H-bond but the second proton does not, or for the mass-asymmetric DOH species, the two stretching modes remain uncoupled and behave as independent group vibrations.

Early infrared studies of dissolved H_2O (3)

[1]Contribution No. 185.

[2]Present address: Lambton College, Sarnia, Ontario.

Can. J. Chem. Downloaded from www.nrcresearchpress.com by 210.87.254.6 on 09/05/12
For personal use only.

showed displacements to lower frequencies of the stretching bands with increased H-bonding to the solvent. Later studies have been made on higher-dispersion instruments. Greinacher, Lüttke, and Mecke (4) measured the H_2O fundamentals and overtones in a solvent range extending from weakly interacting CCl_4 in which the ν_3 and ν_1 bands at 3705 and 3614 cm^{-1} (5, 6) were narrow and well-resolved, to the strongly H-bonding pyridine in which the bands were both wide and unresolved with a peak at 3412 cm^{-1}. Saumagne and Josien (7) measured the stretching fundamentals for H_2O, HDO, and D_2O in the same solvent range: in inert CCl_4 similar narrow O—H and O—D stretching bands were shown, whereas in pyridine wide bands at lower frequency attested strong H-bonding. Those authors demonstrated the decoupling of the two stretching modes for H_2O in CCl_4–pyridine mixtures, where the unbonded stretching mode, O—H u, gave a narrow band at 3678 cm^{-1} and the H-bonded mode, O—H b, gave a wide band at 3400 cm^{-1}: the similarly uncoupled O—H b mode for DOH H-bonded to pyridine gave a wide band with peak at 3415 cm^{-1}. More recently Mohr, Wilk, and Barrow (8) measured the H_2O stretching bands in CCl_4 solutions containing a series of organic bases and in solutions containing the halide ions as bases. The spectra again showed the decoupled bands for singly H-bonded H_2O molecules with C_s type symmetry, and the coupled molecular bands for doubly H-bonded H_2O molecules with C_{2v} type symmetry.

In our recent measurements of both the thermodynamic properties and the proton magnetic resonance chemical shifts of the water solvent (9–11), it was shown that the addition to water of small quantities of the solutes, ethylene oxide, propylene oxide, 1,4-dioxane, acetone, tetrahydrofuran, and *t*-butyl alcohol (2-methyl-2-propanol) gave solutions exhibiting both water stabilization and enhanced H-bonding. Since this group of solutes was known from other studies (9, 11–14) to form only relatively weak H-bonds with water protons, the water stabilization probably arose from stronger H-bonding between the oriented water molecules adjacent to the solute. To confirm the relative strengths of water H-bonding to these hydrophilic solutes in the absence of cooperative water structural effects, we have used the same organic liquids as solvents for measurement of the dilute H_2O infrared spectra.

It was our purpose to resolve and to assign the wide H-bonded stretching bands of H_2O in strongly interacting solvents such as pyridine to provide a better basis for the band assignments in the liquid water and ice spectra. We further wanted to establish an experimental infrared scale for H_2O proton H-bonding acceptance by a range of the more common hydrophilic groups.

To provide additional cross checks on our water band assignments we have measured the O—H stretching bands for dilute DOH and CH_3OH in many of the same solvents. The present study thus may be regarded as defining three infrared scales for the "basicity" (15) of various organic solvents using the H-bonded infrared shifts from the gas phase for the three weakly acidic proton donors HOH, DOH, and CH_3OH. In this sense our measurements are complementary to earlier studies using the deuteron donors DOD and CH_3OD (16).

Experimental

All composition percentages are given on a mole basis unless denoted otherwise.

Materials

Laboratory distilled water, 99.75 wt.% deuterium oxide from Atomic Energy of Canada, Limited, and 99.998% ethylene oxide from Dow Chemical of Canada, Limited were used without further purification.

Other solvents were the best grades available from the listed suppliers and all were purified immediately before use. Eastman Organic Chemicals supplied spectro-grade 1,2-dichloroethane and nitromethane; white label grade 2,4,6-collidine, 3-ethyl-3-pentanol, 2,6-lutidine, pentachloroethane, and 4-picoline; and practical grade hexachloro-1,3-butadiene and 2-picoline. Fisher Scientific Company supplied certified A.C.S. grade chloroform, dimethyl sulfoxide, 1,4-dioxane, methanol, 2-propanol, and pyridine; certified grade acetone, *t*-butanol (2-methyl-2-propanol), and tetrahydrofuran; and reagent grade *t*-amyl alcohol (2-methyl-2-butanol) and 1,1,2,2-tetrachloroethane. Pierce Chemical Company supplied 1,2-dibromotetrafluoroethane, hexafluorobenzene, perfluoro-*n*-heptyl iodide, perfluoro-*n*-propyl iodide, and perfluoromethylcyclohexane. City Chemical Company supplied triethylamine, Canadian Industrial Alcohols and Chemicals Limited supplied U.S.P. absolute ethyl alcohol, and Merck, Sharp and Dohme of Canada, Limited supplied the methyl alcohol-*d* of 99 at.% isotopic purity. CCl_4 (carbon tetrachloride), methylene chloride, tetrachloroethylene, and 1,1,1-trichloroethane of better than 99.8% purity were supplied by Dow Chemical of Canada, Limited.

Method

The water-immiscible solvents, shown above nitromethane in Tables 1, 2, and 4, were washed with water to remove acidic impurities, separated and dried by passing

TABLE 1. Fundamental O—H stretching bands for CH_3OH

Solvent/phase	Temperature (°C)	ν_{MeOH} (cm^{-1})	w (cm^{-1})	ε ($l\ mol^{-1}\ cm^{-1}$)
Vapor	—	3687*	—	—
Perfluoro-methylcyclohexane	30	3676	44	—
Hexafluorobenzene	30	3661	22	110
Carbon tetrachloride	30	3643	23	116
Tetrachloroethylene	30	3643	24	113
Hexachloro-1,3-butadiene	30	3643	23	110
1,1,1-Trichloroethane	30	3638	24	96
Pentachloroethane	30	3632	26	102
1,1,2,2-Tetrachloroethane	30	3616	23	136
Nitromethane	30	3605	65	136
" "	0	3592	70	139
Acetonitrile	30	3542†	—	—
Ethylene oxide	0	3513	122	121
" "	−38	3487	130	128
Tetrahydrofuran	30	3478	98	211
" "	0	3464	91	212
" "	−42	3452	86	241
Dimethyl sulfoxide	30	3369	153	178
Methyl alcohol-*d*	30	3344	216	—
Pyridine	30	3305	194	182
2-Picoline	30	3302	180	214
4-Picoline	30	3300	188	219
2,6-Lutidine	30	3287	170	236
2,4,6-Collidine	30	3277	158	271
Pyridine	−20	3277	158	233
2-Picoline	−44	3254	143	293
2,4,6-Collidine	−20	3253	147	287
Triethylamine	30	3247	178	187
Methyl alcohol-*d* solid	−150	3222	57	—
Triethylamine	−44	3212	126	257

*Reference 18.
†Reference 19.

through a 15-cm column containing Woelm neutral activated alumina. In these solvents spectra were measured at 30 °C, first for the dry solvent and then for the dilute solution of water, in a Research and Industrial Instruments Company (R.I.I.C.) P-E.I. variable-path cell with Irtran-2 windows set at 0.1–0.5 cm path length, compensated in the reference beam by a similar cell containing dry solvent. The water content in hexafluorobenzene, CCl_4, and in 1,2-dichloroethane solutions was determined by Karl Fischer titration.

The water-soluble solvents, including and below nitromethane in Tables 1, 2, and 4, were both dried and purified by passing twice (or more times if required) through fresh 15-cm columns of Woelm neutral activated alumina. Tetrahydrofuran was distilled under nitrogen from a still-pot containing lithium aluminum hydride and then was passed through a fresh activated alumina column. All water solutions (0.05–0.4 mol/l) in these solvents were prepared by weight. Infrared spectra, first for the dry solvent and then for the solution of water, were measured at set temperatures in a R.I.I.C. VLT-2 variable-temperature cell with Irtran-2 windows at 0.0105 cm path length, compensated in the reference beam by a R.I.I.C. AT-04 attenuator. Sample cell temperatures between −45 and 30 °C were kept constant to ±1 °C by manual addition of Dry Ice to acetone in the central reservoir, and were measured by a copper–constantan thermojunction cemented to the front Irtran-2 window just out of the infrared beam path.

The DOH spectra in water-soluble solvents were obtained in the same way as the H_2O spectra, replacing each 2 mol H_2O by 1 mol H_2O + 5 mol D_2O. For example, the H_2O extinction in pyridine was determined from the transmittance ratio for a dry pyridine blank divided by that for a pyridine solution containing 0.250 mol H_2O/l. The DOH spectrum in the O—H stretch region similarly was determined from the transmittance ratio for a pyridine blank containing 0.625 mol D_2O/l divided by that for a pyridine solution containing 0.125 mol H_2O/l and 0.625 mol D_2O/l.

The molar extinction coefficient ε_{H_2O} for water was evaluated from the solution absorbance A using the equation

$$A = \log T_b/T_s = d\,[\varepsilon_{H_2O}C_{H_2O} - \varepsilon_s(V_{H_2O}/V_s)C_{H_2O}]$$

in which T_b/T_s is the transmittance ratio of the blank relative to the solution containing C_{H_2O} mol H_2O/l and d is the cell path length in cm. ε_s is the known molar extinction coefficient for the solvent and V_{H_2O} and V_s are the molar volumes for the water and solvent, respectively. The molar extinction coefficient ε_{DOH} for DOH was evaluated similarly from the deuterium oxide – water solution absorbance using

$$A = d\,[\varepsilon_{DOH}C_{DOH} + \varepsilon_{H_2O}C_{H_2O} - \tfrac{1}{2}\varepsilon_{D_2O}C_{DOH} - \varepsilon_s(V_{H_2O}/V_s)(C_{H_2O} + \tfrac{1}{2}C_{DOH})]$$

in which ε_{H_2O}, ε_{D_2O}, and ε_s are known and the concen-

Can. J. Chem. Downloaded from www.nrcresearchpress.com by 210.87.254.6 on 09/05/12
For personal use only.

TABLE 2. Fundamental O—H stretching bands for DOH

Solvent/phase	Temperature (°C)	Ratio D_2O/H_2O	DO—H u, unbonded ν (cm^{-1})	w* (cm^{-1})	ε ($l\,mol^{-1}\,cm^{-1}$)	DO—H b, H-bonded ν (cm^{-1})	w (cm^{-1})	ε ($l\,mol^{-1}\,cm^{-1}$)
Vapor	—	—	3707†	—	—	3707†	—	—
Hexafluorobenzene	30	1–4				3676	25	51
Carbon tetrachloride	30	1				3662	42	28
Tetrachloroethylene	30	1				3662		
Hexachloro-1,3-butadiene	30	1–2				3657		
1,1,1-Trichloroethane	30	3				3654	28	
Pentachloroethane	30	4				3652		
1,1,2,2-Tetrachloroethane	30	1–8				3646		
1,2-Dichloroethane	30	—				3635‡		
Nitromethane	30	5				3622	55	72
Acetonitrile	30	—				3575§		
Ethylene oxide	0	5				3542	169	69
Tetrahydrofuran	30	5				3524	147	83
" "	0	5				3514	146	95
Dimethyl sulfoxide	30	5	3680	n	2	3452	141	96
4-Picoline	30	5	3655	n, sh	5	3413	229	83
2,6-Lutidine	30	5	3655	n, sh	5	3413	223	91
Deuterium oxide	30	200	3628‖	sh		3407	260	73
Pyridine	30	5	3660	n, sh	6	3405	232	89
2-Picoline	30	5	3655	n, sh	7	3402	224	87
2,4,6-Collidine	30	5	3655	n, sh	6	3393	230	94
Pyridine	−20	5				3380	205	117
2,4,6-Collidine	−20	5				3380	172	124
2-Picoline	−44	5				3375	190	139
Triethylamine	30	5	3678	n	5	3374	316	59
" "	−44	5				3358	261	88
Deuterium oxide ice	−10	400				3300	62	

*n, narrow band with w less than 50 cm^{-1}, sh, shoulder on edge of H-bonded band.
†Reference 31.
‡Reference 35.
§Reference 34.
‖Reference 37.

trations C_{H_2O}, C_{DOH}, and C_{D_2O} were obtained from the equation

$$(C_{DOH})^2 = 4\,C_{H_2O}C_{D_2O}$$

using the initial weights of H_2O and D_2O. At frequencies above 3200 cm^{-1} the term containing ε_{D_2O} was always negligible, while the term containing ε_s was small and decreased rapidly with increasing frequency.

All methanol solutions (0.05–0.2 mol/l) were prepared by weight and their spectra measured in the R.I.I.C. VLT-2 cell as for the water solutions.

The spectra for solid CH_3OH in methyl alcohol-*d* at −150 °C and for solid DOH in deuterium oxide at −10 °C were measured in the VLT-2 cell cooled respectively with liquid nitrogen and cold acetone in the central chamber. The ice spectra at −50 °C were obtained from condensed films on the windows of the VLT-2 cell cooled using Dry Ice – acetone.

Infrared spectra were all measured on a Perkin–Elmer 221G double-beam spectrophotometer in the grating region 4000–1450 cm^{-1}, using the water vapor and polystyrene bands for wavenumber calibration (17). In a typical run the sample-cell initially containing pure solvent was arranged to give transmittances above 90% and the spectrum was scanned very slowly giving the pure solvent baseline. The spectrum for the dilute solution of water was measured and typically was arranged to give a minimum transmittance between 40 and 70%. Wavenumber calibration bands were superposed and finally the 0% transmittance line was traced with the sample shutter closed. All spectra were scanned at the lowest speed of about 10 cm^{-1}/m, using maximum amplification short of oscillation with no suppression. During the 3-h period required to complete a run covering the 3800–3100 cm^{-1} region, the instrument drift was normally less than 1% at 90% transmittance, as shown by replicate experiments and by the usually exact superposition of the solution spectra on the pure solvent baseline outside the regions of the water extinction. For the sharp stretching bands above 3600 cm^{-1} and for the bending bands near 1600 cm^{-1} the uncertainty of the band peak positions was ±3 cm^{-1}, while for the wide H-bonded stretching bands between 3500 and 3200 cm^{-1} the uncertainty was increased to ±10 cm^{-1}.

All correlation lines shown in the figures and regression coefficients in all equations have been evaluated by the method of least squares. All errors quoted are standard errors.

Results and Discussion

Fundamental O—H Stretching Bands of Methanol

Table 1 presents new measurements between 3800 and 3100 cm^{-1} for the fundamental O—H

Can. J. Chem. Downloaded from www.nrcresearchpress.com by 210.87.254.6 on 09/05/12
For personal use only.

Can. J. Chem. Downloaded from www.nrcresearchpress.com by 210.87.254.6 on 09/05/12
For personal use only.

stretching band of monomeric methanol in a solvent range from weakly interacting perfluoromethylcyclohexane at 30 °C to strongly H-bonding triethylamine at −44 °C. Following the vapor phase value (18), the solvents are listed in order of decreasing band frequency, ν_{MeOH} (cm^{-1}), which order generally corresponds with both increasing band width at half-extinction, w (cm^{-1}), and increasing peak extinction coefficient, ε (l mol^{-1} cm^{-1}, decadic logarithms).

Good agreement is found between our bands at 3643 cm^{-1} in CCl_4 and tetrachloroethylene and earlier values between 3642 and 3644 cm^{-1} (20–24), between our highest frequency band at 3676 cm^{-1} in perfluoro-methylcyclohexane and 3675 cm^{-1} in the similarly inert perfluoro-octane (22), and between our wide band at 3247 cm^{-1} in triethylamine and the earlier value of 3243 cm^{-1} (21).

The observed band shapes were similar to those illustrated elsewhere (21, 22, 24), but, because our measurements were made at methanol concentrations of up to 0.20 mol/l, the spectra showed weak dimer bands, so that the monomer extinctions recorded in Table 1 are slightly low. For a few monomer bands the extinction coefficient dependence on frequency was fitted numerically by skewed Lorentz–Gauss product functions (25), using a least-squares technique similar to Pitha and Jones' method V (26). Our monomer band contours showed an approximate fraction 0.7 Lorentzian to 0.3 Gaussian character. The bands were slightly skewed with larger extinctions on the low-frequency side of the peaks, due only in part to the weak dimer bands (24).

Results in Table 1 show that at lower temperatures the peaks move to lower frequencies and most bands become sharper, with higher extinctions and smaller half-widths. In tetrahydrofuran and the tertiary amines the band areas change little with temperature, so that at low temperatures the increased extinctions are almost exactly compensated by the decreased band-widths.

For the methanol monomer bands, which are of similar shape, the integrated band area is proportional to the $\varepsilon \cdot w$ product. Figure 1 presents the correlation of $\varepsilon \cdot w$ with frequency ν_{MeOH} represented numerically by the one-constant equation

$$[1] \qquad \varepsilon \cdot w = 91.0\,(3687 - \nu_{MeOH})$$

The regression coefficient 91.0 has a standard error of 2.5. The band area enhancement at lower frequencies is characteristic of more strongly H-bonded stretching modes (3), and here the O—H stretching band area is increased by a factor of 15 on changing from the chlorinated hydrocarbon solvents to pyridine and its homologs.

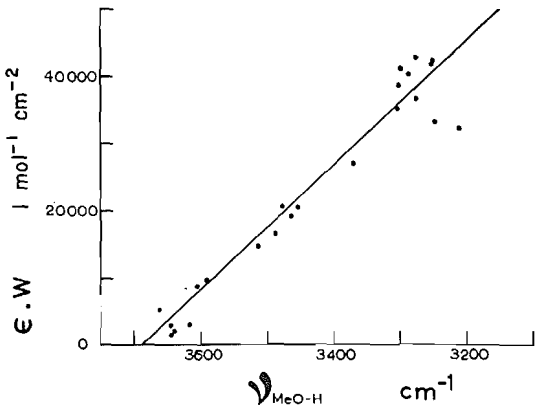

FIG. 1. Correlation of band area with frequency for the O—H stretch vibration of CH_3OH in various basic solvents at 30 °C.

In all solvents below nitromethane a search was made for extra bands in the 3687–3560 cm^{-1} region, in addition to those in Table 1, which might arise from non-bonded O—H stretching modes. None was observed. It is therefore certain that in these dilute solutions all methanol O—H groups form H-bonds and that the concentration of non-bonded methanol is below our limit of detection.

Measurements at 30 °C for methanol in solutions with more extensive H-bonding, for example dilute methanol in methyl alcohol-*d* and concentrated methanol in inert solvents, showed absorption in the three distinct O—H stretching band regions 3680–3600, 3560–3450, and 3360–3344 cm^{-1}. Similar bands in these regions have been reported previously for benzyl alcohol by Fox and Martin (27) and for 1-dodecanol and *t*-butyl alcohol by Smith and Creitz (28). Following the Bellamy and Pace proof (24) of the open-chain dimers for methanol, which is consistent with the measurements of Fox and Martin, we assign the three groups of bands to the H-bonded methanol species as follows.

(*i*) The sharp monomer band at 3643 cm^{-1} is pre-eminent for 0.5% methanol in CCl_4. For 55% methanol diluted with 45% CCl_4 we found the sharp band moved to 3635 cm^{-1}, occurring as a narrow, weak band superposed on the high fre-

Can. J. Chem. Downloaded from www.nrcresearchpress.com by 210.87.254.6 on 09/05/12
For personal use only.

quency edge of intense lower frequency bands. For liquid methanol in the absence of CCl_4 we could detect no sharp band near to 3635 cm^{-1}. Since the sharp band at 3643–3635 cm^{-1} occurs only in methanol solutions containing CCl_4, this band must arise from the direct, weakly H-bonding interaction of the O—H group with the covalent chlorine atoms of the "inert" CCl_4. The monomer band at 3643 cm^{-1} is thus assigned to the methanol species *A*, O—H---Cl, with un-
|
CH_3
bonded oxygen and the hydroxyl proton interacting with CCl_4. The band at 3635 cm^{-1} for 55% methanol is then assigned to the methanol species *B*, ---O—H---Cl, in which the oxygen is H-
|
CH_3
bonded by other methanol and the hydroxyl proton interacts with CCl_4. Our band at 3635 cm^{-1} is in very good agreement with similar bands at 3637 and 3633 cm^{-1} reported (24) for the methanol dimer and the methanol–phenol adduct respectively in CCl_4, which bands again are assigned to the methanol species *B*. Species *B* is one half of the methanol dimer and also occurs at the end of the open polymer chains with the hydroxyl group adjacent to the CCl_4.

(*ii*) A wide, weak shoulder centered around 3450–3480 cm^{-1} for 2% methanol in methyl alcohol-*d* causes the main band at 3344 cm^{-1} to appear asymmetric. This weak shoulder is assigned to the methanol species *C*, O—H---O, on
|
CH_3
which oxygen is unbonded and the hydroxyl proton is H-bonded to oxygen of adjacent methanol. The same band is calculated (vide infra) to occur at 3446 cm^{-1} using the methanol pK_a of -2.2 (15) in the correlation [31] for methanol H-bonded to aprotic solvents with no bonding to the methanol oxygen. Similar bands were reported at 3488 cm^{-1} for the benzyl alcohol dimer (27), at 3484 and 3490 cm^{-1}, respectively, for the 1-dodecanol and *t*-butyl alcohol dimers (28), and within the range 3565–3482 cm^{-1} depending on solvent for the methanol dimer (22). Species *C* is the other half of the methanol dimer and occurs as the second type of polymer chain-terminating group.

(*iii*) The main, intense and wide band at 3344 cm^{-1} found for 2% methanol in methyl alcohol-*d* is assigned to the methanol species *D*, ---O—H---O, in which both the oxygen and hy-
|
CH_3
droxyl proton are involved in H-bonds with methanol neighbors. Similar intense wide bands were reported at 3348 and 3323 cm^{-1}, respectively, for polymeric benzyl alcohol in CCl_4 and in the pure liquid (27), and at 3322 and 3356 cm^{-1} for polymeric 1-dodecanol and *t*-butyl alcohol in CCl_4 (28). The methanol species *D*, predominant in the liquid and in concentrated solutions at room and lower temperatures, is the species forming the unbranched polymer chains, which may be cyclic or open-ended terminated by species *B* and *C*. The methanol polymer chains are presumably zigzag with approximately tetrahedral angles along their O—H---O—H---O—H length,
| | |
R R R
being the dynamic liquid phase analogs of the stronger infinite zigzag chains (29) in the solid, which exhibits the 3222 cm^{-1} band for 1% methanol in methyl alcohol-*d* at -150 °C. The same band has been reported (18) at 3225 cm^{-1} and -180 °C.

The almost constant O—H frequency for the polymer chain H-bonds of methanol and of the substituted methanols, benzyl alcohol, 1-dodecanol, and *t*-butyl alcohol, attests the maximum strength of these intra-chain H-bonds, which is evidently insensitive to the very different steric and inductive effects of the various substituent groups.

The greater stability of the methanol species *D* relative to species *C* is best interpreted by the specific dipolar association model suggested by Bellamy, Morgan, and Pace (30). On this model the 241 cm^{-1} frequency shift from the gas phase to the singly bonded species *C* is enhanced further to 343 cm^{-1} for the doubly bonded species *D*. This 102 cm^{-1} shift between methanol species *C* and *D* is entirely comparable with the 71 cm^{-1} shift to lower frequency of the methanol dimer band in CCl_4 on addition of H-bonding chloroform (30). Since the weakest methanol H-bonds occur at the chain ends, whereas the strongest are intra-chain H-bonds, there will be a tendency in the liquid and in concentrated solutions to form rings and long chains with few unbonded ends and fewer of the less stable trimers and dimers. This is why the high frequency bands of the rela-

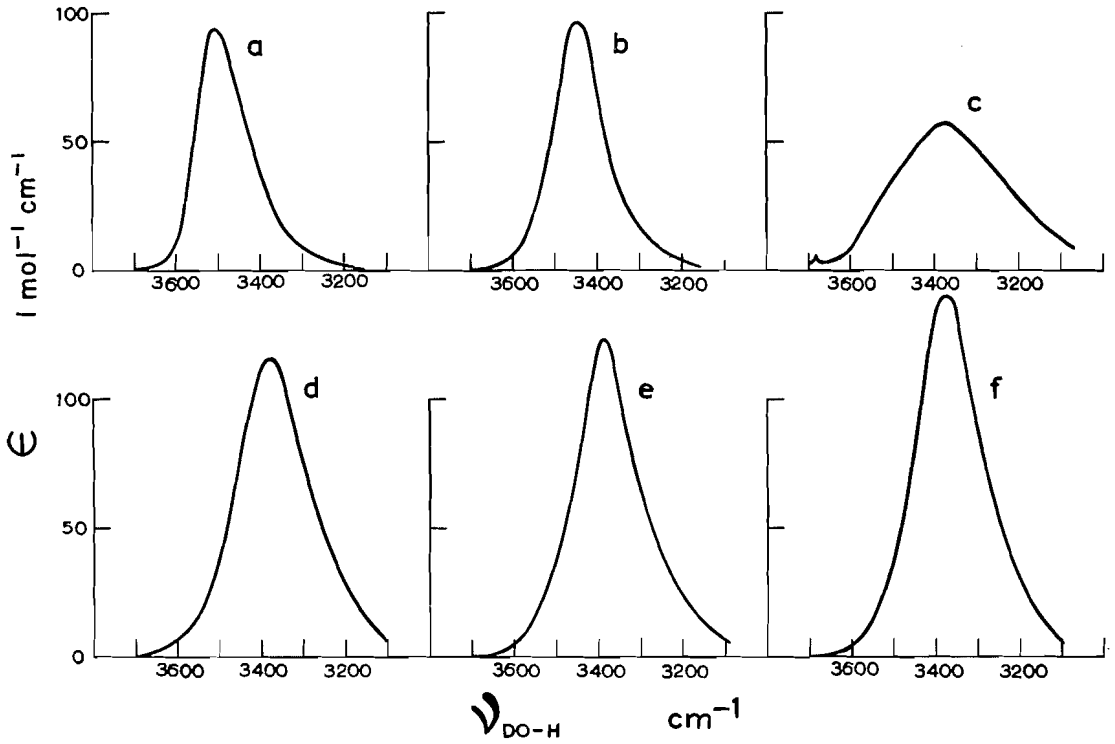

FIG. 2. The O—H stretch bands for DOH, (*a*) in tetrahydrofuran at 0 °C, (*b*) in dimethyl sulfoxide at 30 °C, (*c*) in triethylamine at 30 °C, (*d*) in pyridine at −20 °C, (*e*) in 2,4,6-collidine at −20 °C, and (*f*) in 2-picoline at −44 °C.

tively unstable dimers, readily found at high dilutions, are not found in liquid methanol at room and lower temperatures.

Fundamental O—H Stretching Bands of Hydrogen Deuterium Oxide

New measurements are presented in Table 2 for the fundamental O—H stretching bands of monomeric DOH in solvents of widely differing basicities. The D_2O/H_2O mole ratio used for the DOH solute is listed in the third column. Extinction coefficients for DOH have been corrected for the presence of equilibrium water. Figure 2 illustrates the characteristic Lorentzian shapes of the DO—H stretching bands in H-bonding solvents.

Below the vapor phase band origin at 3707 cm^{-1} (31), solvents are listed in order of decreasing frequency for the most intense band, ν_{DO-H} b, which is also the order of increasing H-bonding to the solvent and correlates with both band width at half-extinction and peak extinction coefficient.

The narrow bands at 3662 cm^{-1} in CCl_4 and tetrachloroethylene are 3 cm^{-1} above the earliest value (5), agree well with more recent values 3660 and 3662 cm^{-1} (7, 34) and show that the value of 3670 cm^{-1} (32) is too high. At 30 °C in pyridine the wide H-bonded band, denoted DO—H b, at 3405 cm^{-1} is just within experimental error of the earlier determination at 3415 cm^{-1} (7); its position agrees better with the similar wide H-bonded band at 3400 cm^{-1} (7) for singly bonded HOH with C_s type symmetry in the mixed CCl_4–pyridine solvent. Our band parameters for DOH in liquid deuterium oxide at 30 °C and for the sharp Lorentzian band in deuterium oxide ice at −10 °C are in general agreement with earlier measurements (32, 33).

New weak and narrow bands have been found in the 3680–3650 cm^{-1} region at 30 °C in solvents more basic than tetrahydrofuran, in addition to the main H-bonded bands reported under DO—H b. The new bands are assigned to low concentrations of weakly bonded or unbonded O—H u stretching vibrations and are listed in Table 2

Can. J. Chem. Downloaded from www.nrcresearchpress.com by 210.87.254.6 on 09/05/12
For personal use only.

Can. J. Chem. Downloaded from www.nrcresearchpress.com by 210.87.254.6 on 09/05/12
For personal use only.

under DO—H u, where the u for unbonded refers to the O—H groups not being bonded to the most basic group of the solvent molecule. The O—H u groups are probably adjacent to the hydrophobic alkyl-group protons in dimethyl sulfoxide and triethylamine, and near and weakly bonded to the aromatic ring of the substituted pyridines. In liquid deuterium oxide the DO—H u band is difficult to locate in the infrared (32, 33, 36), so we have included the better resolved Raman band at 3628 cm^{-1} (37).

At lower temperatures the weak DO—H u bands disappear below the limit of detection, indicating that substantially all DOH molecules then form two H-bonds (strictly one H-bond and one D-bond) to the basic groups of the solvent giving the bent, double-bonded, b D—O—H b, di-solvent complexes,

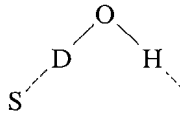

, already suggested for dissolved water (7, 8, 38).

The DO—H b bands, which are invariably uncoupled from the O—D stretching mode, at lower temperatures move to lower frequencies and become more Lorentzian in shape with smaller half-widths and higher peak extinctions, indicating fewer and more specific configurations for the di-solvent complexes. The DO—H b bands in all organic solvents at lower temperatures and in deuterium oxide ice exhibit predominantly Lorentzian band shapes despite the strong H-bonding, whereas only in liquid deuterium oxide is the band shape more nearly Gaussian. These results are in complete accord with recent measurements (39) on the similar HO—D b stretching band which exhibited a narrow Lorentzian contour in ice at −8 °C and which was replaced on melting by a much wider Gaussian contour in liquid water at 4 °C.

The intensification of the DO—H b band area with stronger H-bonding to the solvent is illustrated in Fig. 3, and represented by the one-constant equation

$$[2] \qquad \varepsilon \cdot w = 66.3\,(3707 - \nu_{DOH})$$

The regression coefficient 66.3 has a standard error of 1.7. The band area is smaller by a factor of 18 in the inert solvents hexafluorobenzene and CCl_4 than in the strongly H-bonding pyridines and triethylamine.

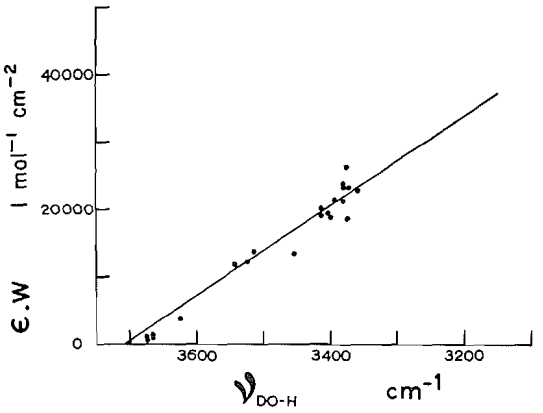

FIG. 3. Correlation of band area with frequency for the O—H stretch vibration of DOH in various basic solvents at 30 °C.

The uncoupled DO—H b stretching band in liquid deuterium oxide, despite its more Gaussian shape, falls properly within the correlation of [2] and does not exhibit any special intensification due to the extensive bonding to both the HDO lone pairs and the O—D group by the deuterium oxide solvent. Since it is clear from the earlier (39) and the present work that strongly H-bonded DOH normally gives Lorentzian-shaped fundamental-stretch band contours, we ascribe the more Gaussian contour in liquid deuterium oxide to a Gaussian distribution of Lorentzian DOH oscillators arising from the thermally induced multiplicity of radial and orientational configurations of the bonded nearest neighbors. Suggestions similar to this have been made elsewhere (32, 33, 40, 54). Thus for the hydroxyl stretching vibration of DOH the main perturbation leading to Gaussian band shape derives from the motions of the oxygen nearest-neighbor bonded directly to the O—H group. Additional smaller inductive and dynamic perturbations arise indirectly from the effect of the nearest neighbors bonded to the lone pairs and to the O—D group.

Fundamental O—H Stretching Bands for Water with C_s Type Symmetry

In this section we consider bands for the decoupled O—H stretching modes of HOH molecules with C_s type symmetry arising from unequal H-bonding of the two protons with the solvent. In Table 3 we report new bands from C_s-symmetric water molecules, denoted u H—O—H b, in which the O—H u stretching mode is weakly bonded or unbonded while the O—H b is strongly

TABLE 3. Fundamental O—H stretching bands for water with C_s type symmetry

Solvent/phase	Temperature (°C)	Water mol%	HO—H u, unbonded ν (cm^{-1})	*w** (cm^{-1})	ε ($l\,mol^{-1}\,cm^{-1}$)	HO—H b, H-bonded ν (cm^{-1})	*w* (cm^{-1})	ε ($l\,mol^{-1}\,cm^{-1}$)
Vapor	—	—	3707†	—		3707†	—	—
Carbon tetrachloride 67 1,4-Dioxane 33 vol%	30		3684	40				
Carbon tetrachloride 67 Tetrahydrofuran 33 vol%	30		3683	27	60	3500		
Carbon tetrachloride 67 Tetrahydrofuran 33 vol%	0		3680	26	36	3490		
Carbon tetrachloride 67 Dimethyl sulfoxide 33 vol%	30		3678	28				
Carbon tetrachloride 91 Methyl alcohol 9 vol%	30		3676	30				
Carbon tetrachloride 50 *t*-Butyl alcohol 50 vol%	30		3679	40				
Carbon tetrachloride 67 Pyridine 33 vol%	30		3674	24	35	3400	265	80
1,2-Dichloroethane 67 Pyridine 33 vol%	30		3657	40	50	3400	265	80
Dimethyl sulfoxide	30	2	3680	sh	3			
Methyl alcohol	30	5–40	3679	sh	8			
Ethyl alcohol	30	5–40	3681	sh	8			
iso-Propyl alcohol	30	2–40	3678	40	17–11			
iso-Propyl alcohol	0	4–40	3681	40	10–7			
t-Butyl alcohol	30	5–40	3683	26	19–13			
t-Amyl alcohol	30	2–10	3678	28	27			
t-Amyl alcohol	0	2	3677	28	16			
3-Ethyl-3-pentanol	30	2	3678	19	29			
" "	0	2	3678	22	18			
4-Picoline	30	2	3660	32	23			
2,6-Lutidine	30	2	3660	27	21			
Water	35	100	3625‡					
2-Picoline	30	2	3660	25	22			
Pyridine	30	2–20	3657	27	28–17			
2,4,6-Collidine	30	2	3657	33	18			
2,6-Lutidine	10	2	3658	sh	11			
4-Picoline	0	2	3655	sh	12			
2-Picoline	0	2	3655	sh	12			
Pyridine	0	2	3660	sh	14			
2,4,6-Collidine	0	2	3657	sh	8			
Triethylamine	30	2–16	3680	24	38–16			

*sh, shoulder on edge of H-bonded band.
†Reference 31.
‡Reference 45.

H-bonded to a basic group of the solvent. In the first row the vapor phase band origins for the decoupled vibrations are shown at 3707 cm^{-1}, the mean of ν_3 and ν_1 (31), notably the same as for the uncoupled O—H stretching vibration of DOH. The mixed solvents are listed with their component volume percentages and are followed by the single-component solvents ordered for comparison with Table 4. Approximate values for the extinctions are included in Table 3 to show trends, these values being obtained from the total water concentration without allowance for the fraction of C_{2v}-symmetric species.

In mixed solvents containing CCl_4 with 1,4-dioxane and pyridine our results are in agreement with earlier measurements and assignments (7, 8) which we follow here. Replacement of nonpolar CCl_4 by dipolar 1,2-dichloroethane in admixture with pyridine enhances the extinction and shifts the sharp O—H u band from 3674 to 3657 cm^{-1}, but leaves the wide O—H b band H-bonded to the nitrogen of pyridine unaffected. The decoupled HO—H b band assignment is confirmed by the similarity of its 3400 cm^{-1} frequency and 265 cm^{-1} half-width in CCl_4–pyridine to 3405 and 232 cm^{-1} for the uncoupled DO—H b in pyridine.

The wide HO—H b bands are not reported in the single-component solvents since they are overlapped by the strong ν_3 and ν_1 water bands

Can. J. Chem. Downloaded from www.nrcresearchpress.com by 210.87.254.6 on 09/05/12
For personal use only.

Can. J. Chem. Downloaded from www.nrcresearchpress.com by 210.87.254.6 on 09/05/12
For personal use only.

TABLE 4. Infrared bands for dissolved water with C_{2v} type symmetry

Solvent/phase	Temperature (°C)	ν_3	w_3*	ε_3	ν_1	w_1*	ε_1	w_{13}	$2\nu_2$	ν_2	w_2	ε_2
Vapor†	—	3756	—	—	3657	—	—		3152	1595	—	—
Hexafluorobenzene	30	3720	27	50	3630	24	18					
Perfluoro-*n*-heptyl iodide	30	3716	54		3622							
1,2-Dibromotetrafluoroethane	30	3715	44		3621	40						
Perfluoro-*n*-propyl iodide	30	3712	42		3622	41						
Carbon tetrachloride	30	3705	42	34	3613	38	13					
Tetrachloroethylene	30	3705	43	34	3613	39	13					
Hexachloro-1,3-butadiene	30	3703	38		3613	25						
1,1,1-Trichloroethane	30	3698	32	69	3609	23	30					
Pentachloroethane	30	3691	30		3608	27						
Chloroform	30	3690	38		3607	30						
1,1,2,2-Tetrachloroethane	30	3680	33		3603	24						
Methylene chloride	30	3676	50		3601	47						
1,2-Dichloroethane	30	3671	41	88	3592	38	37			1603	26	90
Nitromethane	30	3663	50	133	3579	48	64					
" "	0	3658	50	152	3576	52	74					
Ethylene oxide	0	3606		130	3526	sh	100	166	3270	1640	40	57
" "	−40	3584		149	3519	sh	113	158	3274			
1,4-Dioxane	20	3580		143	3509		123	138		1639	53	42
Tetrahydrofuran	30	3572		128	3499		111	161	3250			
" "	0	3562		168	3496		126	140	3275			
" "	−40	3552		198	3489		150	128	3280	1655	38	53
Dimethyl sulfoxide	30	3490		173	3450		171	174	3280*	1663	54	38
4-Picoline	30	3440	sh	120	3409		132	280				
2,6-Lutidine	30	3446		138	3405		144	280	3280			
2-Picoline	30	3446	sh	132	3405		147	270				
Pyridine	30	3450	sh	128	3405		143	283				
2,4,6-Collidine	30	3444		143	3400		148	280	3280			
2,6-Lutidine	10	3445		156	3396		163	253	3280			
4-Picoline	0	3445	sh	164	3395		184	252	3280			
2-Picoline	0	3442	sh	168	3395		185	251	3274			
Pyridine	−20	3440	sh	173	3395		203	261	3280			
2,4,6-Collidine	0	3442		173	3392		181	240	3275			
" "	−20	3440		189	3387		201	214	3275			
2-Picoline	−40	3440	sh	182	3380		220	233	3280			
Triethylamine	30	3410	sh	88	3368		100	394	3270			
" "	−20	3422	sh	133	3365		148	332	3230			
" "	−40	3408	sh	172	3356		194	286	3235	1663	60	19
Ice	−50	3300	sh	154	3220		228	350	3150			

*sh, shoulder. Except in the cyclic ethers all $2\nu_2$ bands occur as shoulders.
†References 31, 46.

Can. J. Chem. Downloaded from www.nrcresearchpress.com by 210.87.254.6 on 09/05/12
For personal use only.

in dimethyl sulfoxide and in the tertiary amines, and by the strong H-bonded bands in the alcohols.

Sharp HO—H u bands with 25–30 cm^{-1} half-widths are found over the 3684–3655 cm^{-1} frequency range. In the saturated aliphatics and in the mixed solvents with CCl_4 the sharp bands occur near 3680 cm^{-1}, characteristic of decoupled modes with O—H u groups adjacent to and interacting with non-bonding alkyl groups or weakly bonding chlorine. In the pyridines, alone and with 1,2-dichloroethane, the frequency is decreased to about 3657 cm^{-1} through the stronger interaction of the O—H u groups with the pyridines' aromatic rings and the dipolar $—CH_2Cl$ groups. In the more intense dipolar fields of liquid water between 20 and 35 °C, in which an 80 cm^{-1} KBM shift was expected (40), the well-known, weak Raman (41–44) and weak infrared (45) bands at about 3625 cm^{-1} undoubtedly arise from the decoupled, unbonded O—H u stretching mode of C_s-symmetric water molecules, for which the second protons and presumably the lone pairs remain H-bonded. This assignment properly corresponds with that for the weak Raman band at 3628 cm^{-1} for dilute DOH in liquid deuterium oxide (37), which band derives from the uncoupled, unbonded O—H u stretching mode of invariably C_s-symmetric DOH molecules, for which the deuterons and presumably the lone pairs remain D-bonded. These assignments are strongly supported by the reduction of the 3625 cm^{-1} band extinction at lower temperatures where liquid water H-bonding is stronger and more complete, and by the total absence of any similar unbonded band for completely H-bonded ice.

In the alcohol solvents at 30 °C the HO—H u extinctions increase roughly with the number of alkyl group protons per solvent molecule, which suggests that the O—H u groups are mostly adjacent to the non-bonding alkyl groups. In triethylamine, which is structurally similar to 3-ethyl-3-pentanol, the HO—H u band frequency, half-width, extinction, and shape are all similar to those found in the alcohol. At the other end of the alcohol series, the low extinction for O—H u in water (45) is consistent with water as the first alcoholic solvent having only covalent hydrogen as the nonbonding alkyl group.

When the temperature is reduced the O—H u bands (*i*) invariably decrease in extinction, indicating reduced fractions of singly unbonded b H—O—H u species, as shown in Fig. 4(*a*, *b*, *d*) for isopropyl and tertiary-amyl alcohols, (*ii*) further decrease in extinction to give shoulders, as found in the substituted pyridines at 0 °C reported in Table 3, and (*iii*) finally disappear below the detection limits, as found for pyridine and 2,4,6-collidine at −20 °C and for 2-picoline at −45 °C and shown in Fig. 5(*c*, *d*, *e*). Under these low temperature conditions essentially all the C_s-symmetric, singly unbonded b H—O—H u molecules are converted to C_{2v}-symmetric, doubly bonded b H—O—H b species forming two H-bonds to the most basic groups of the solvent molecules (7, 8, 38).

When the water solute percentage is increased in the single-component solvents the O—H u extinction falls continuously whereas the H-bonded extinction at lower frequencies increases, as shown for iso-propyl and *t*-butyl alcohols, pyridine and triethylamine in Fig. 4(*a*, *b*, *c*, *e*, *f*). This behavior indicates an invariably decreasing fraction of singly unbonded b H—O—H u species relative to the doubly bonded b H—O—H b species at higher water concentrations.

The helium–neon gas laser excited Raman spectra of 10, 20, 40, and 60% water in *t*-butyl alcohol at 30 °C, determined for us by Dr. J. C. Evans, exhibited the same sharp band at 3680 cm^{-1} which evidences a decreasing fraction of unbonded O—H u groups with increasing water concentration. In a solution containing 80% water the sharp band was not detected.

Infrared Bands for Water with C_{2v} Type Symmetry

The main infrared bands for monomeric water in a range of basic solvents are presented in Table 4. In the first row of the table are shown the water vapor band origins assigned (31, 46) to the fundamental antisymmetric stretch ν_3 at 3756 cm^{-1} and symmetric stretch ν_1 at 3657 cm^{-1}, the first bending overtone $2\nu_2$ at 3152 cm^{-1} and its fundamental ν_2 at 1595 cm^{-1}. The solvents are listed in order of decreasing frequency for the ν_3 and ν_1 bands, which order generally corresponds with increasing water H-bonding to the solvent, as in Tables 1 and 2.

Our measurements are in good general agreement with earlier determinations (3–8) and show sharp, well-resolved ν_3 and ν_1 bands with low extinctions in the inert solvents. In CCl_4 our ν_3 and ν_1 bands are 3 and 2 cm^{-1}, respectively,

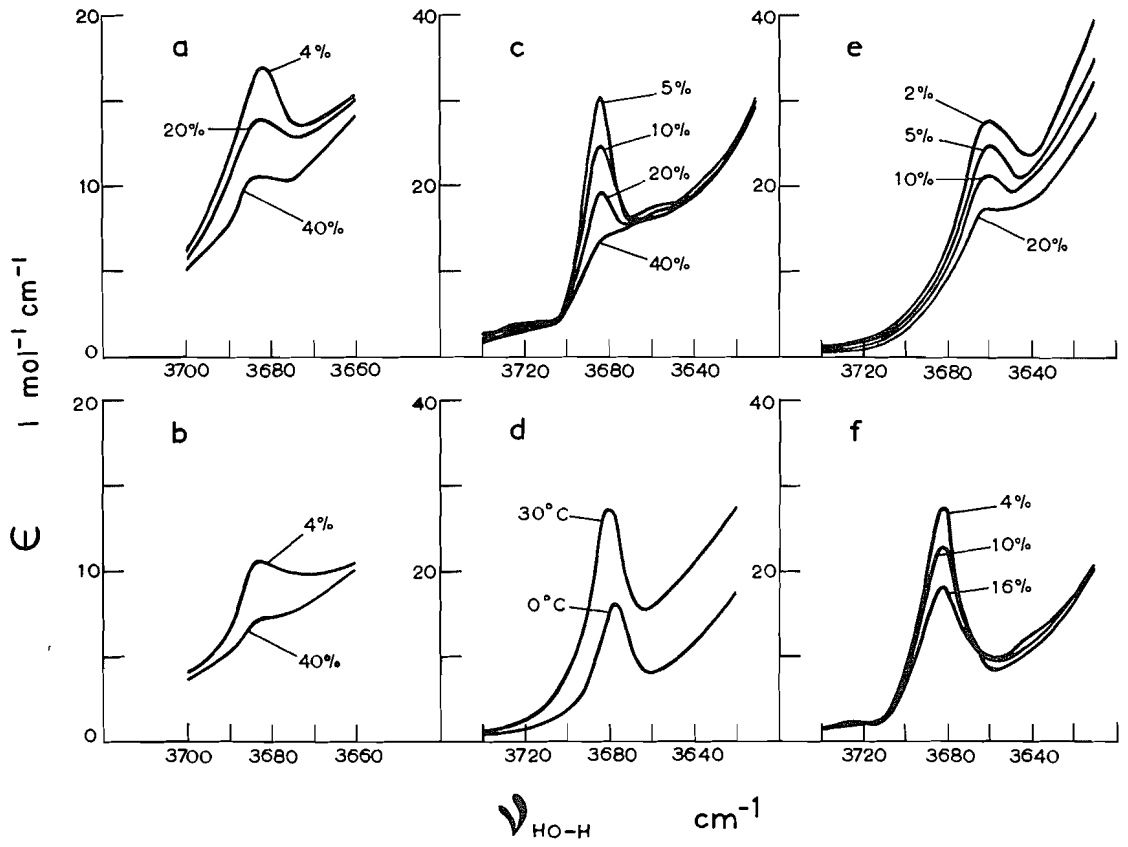

FIG. 4. Fundamental stretch bands for unbonded, decoupled O—H groups of H_2O, (*a*) in iso-propyl alcohol at 30 °C, (*b*) in iso-propyl alcohol at 0 °C, (*c*) in tertiary-butyl alcohol at 30 °C, (*d*) for 5% H_2O in tertiary-amyl alcohol at 0 and 30 °C, (*e*) in pyridine at 30 °C, and (*f*) in triethylamine at 30 °C. H_2O mol% are indicated.

higher in frequency than the earliest measurements (5), agree well with the values 3705 and 3614 cm^{-1} (4, 6) and 3706 and 3614 cm^{-1} (8), and indicate that of the values 3708 and 3613 cm^{-1} (7) that for ν_3 is too high. Our extinction coefficient ε_3 of 34 ($l\ mol^{-1}\ cm^{-1}$) in CCl_4 agrees with the earlier value of 37 determined (6, 47) on instruments of different design.

Results for the solvent series, inert fluorocarbons, nonpolar chlorocarbons, dipolar chlorohydrocarbons, and weakly H-bonding nitromethane, show well-separated ν_3 and ν_1 bands, illustrated elsewhere (4, 6, 7), for which we report the increasing extinctions ε_3 and ε_1 and the increasing half-widths w_3 and w_1. However, with slightly stronger H-bonding to ethylene oxide and tetrahydrofuran, the further increased half-widths lead to overlapped ν_3 and ν_1 contours, shown in Fig. 5*a* for ethylene oxide and elsewhere (4, 7) for dioxane and diethyl ether (8). For the more strongly H-bonding dimethyl sulfoxide, tertiary amines, and ice we show in Fig. 5(*b–f*) the progressively more strongly overlapped contours of the three water bands, ν_3, ν_1, and $2\nu_2$, resolved for the first time (4, 6–8, 14). The ice extinctions are in arbitrary units since the film thickness was unknown. For these strongly overlapped contours, in Table 4 we report (*i*) ν_3 and ν_1 for the frequencies of the observed peaks or shoulders, although these are displaced towards each other from their true positions, (*ii*) ε_3 and ε_1 for the extinctions observed at ν_3 and ν_1, recognizing that these values contain significant contributions from both bands, and (*iii*) w_{13} for the width of the overall band contour at half-extinction.

The ν_3 and ν_1 band frequencies for 54 water

Can. J. Chem. Downloaded from www.nrcresearchpress.com by 210.87.254.6 on 09/05/12
For personal use only.

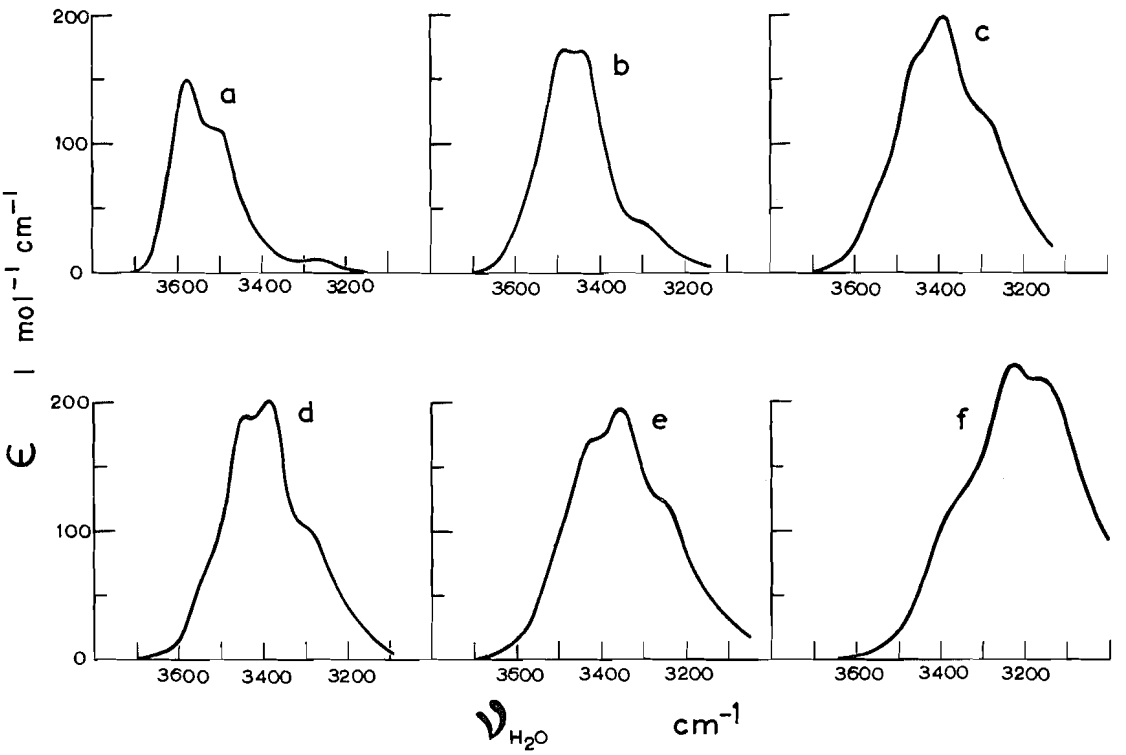

FIG. 5. Antisymmetric and symmetric stretch and bending overtone bands for H_2O, (*a*) in ethylene oxide at 0 °C, (*b*) in dimethyl sulfoxide at 30 °C, (*c*) in pyridine at −20 °C, (*d*) in 2,4,6-collidine at −20 °C, (*e*) in triethylamine at −44 °C, and (*f*) for ice at −50 °C.

solutions in the 24 solvents of Table 4 are seen to be linearly correlated in Fig. 6, and are properly represented by the one-constant equation

$$[3] \qquad 3657 - \nu_1 = 0.8285(3756 - \nu_3)$$

giving an assessed standard error of 6.7 cm^{-1} on a single determination of ν_1. The regression coefficient 0.8285 has a standard error of 0.0044. This eq. 3 for dissolved water is in good agreement with the earlier eq. 11 given by Schiffer and Hornig (54) for undistorted water molecules in crystalline hydrates and organic solvents.

In solvents down to and including dimethyl sulfoxide in Table 4 the highest extinction of the overlapped band contour, ε_{13}, invariably obtains near ν_3, whereas in the more strongly H-bonding amines and ice the maxima occur near the narrower ν_1 band, as shown in Fig. 5. The monotonous and approximately linear correlation of $\varepsilon_1/\varepsilon_3$ with ν_3, shown in Fig. 7, is represented by the empirical equation

$$[4] \qquad \varepsilon_1/\varepsilon_3 = 0.276 + 0.00263(3756 - \nu_3)$$

which gives a standard error of 0.055 on a single $\varepsilon_1/\varepsilon_3$ determination.

The correlation of the sum $\varepsilon_3 \cdot w_3 + \varepsilon_1 \cdot w_1$ for resolved bands or of $\varepsilon_{13} \cdot w_{13}$ for overlapped bands with ν_3 is shown in Fig. 8 together with the representative one-constant equation

$$[5] \qquad \varepsilon_{13} \cdot w_{13} = 131.3(3756 - \nu_3)$$

The regression coefficient 131.3 has a standard error of 2.6. As expected, the band area increases with stronger H-bonding (3, 4) and the regression coefficient for H_2O in [5] is almost exactly double that in [2] for DOH containing half as many O—H stretching modes per molecule.

The systematics and continuity of our data in [3], [4], and [5], from the gas phase and for all solvents examined, positively establish our assignments of the wide, overlapped bands in the strongly basic solvents to the ν_3 and ν_1 modes of

Can. J. Chem. Downloaded from www.nrcresearchpress.com by 210.87.254.6 on 09/05/12
For personal use only.

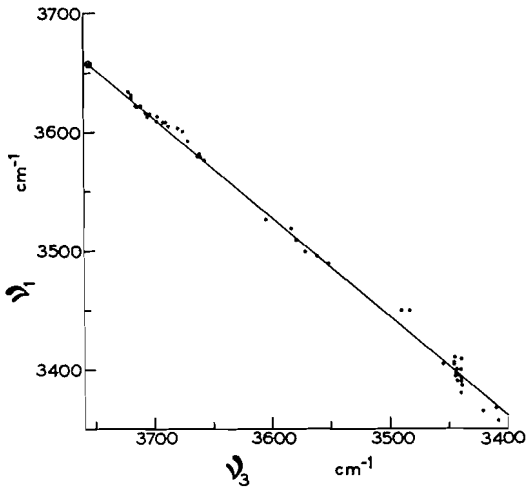

FIG. 6. Correlation of the symmetric ν_1 and antisymmetric ν_3 stretch frequencies for H_2O in various basic solvents.

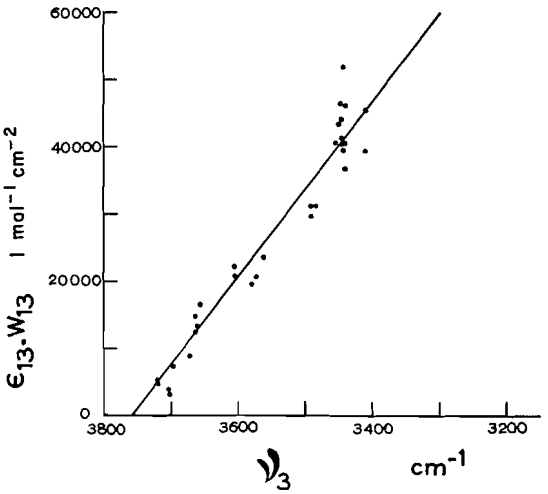

FIG. 8. Correlation of band area with antisymmetric stretch frequency ν_3 for H_2O in various basic solvents at 30 °C.

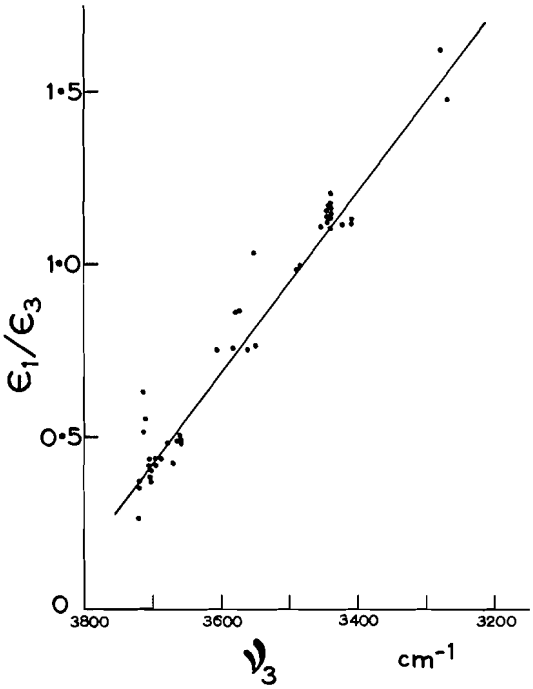

FIG. 7. Correlation of the extinction ratio $\varepsilon_1/\varepsilon_3$ with antisymmetric stretch frequency ν_3 for H_2O in various basic solvents.

doubly H-bonded H_2O molecules with nearly C_{2v} type symmetry. Our water stretching bands in ethylene oxide, dimethyl sulfoxide, and the amines, similar to those for DOH, all exhibit predominantly Lorentzian shapes, showing again that strong H-bond formation does not of itself lead to Gaussian band shapes.

Results for the bending fundamental ν_2 band in Table 4 show that stronger water H-bonding leads to (*i*) the well-known shift (3, 4) of the ν_2 band to higher frequencies, (*ii*) an increase of w_2, (*iii*) a decrease of ε_2, and (*iv*) a decrease of the $\varepsilon_2 \cdot w_2$ product.

In solvents below nitromethane we report the frequency of the first bending overtone $2\nu_2$, which occurs as a weak band (extinction $\varepsilon \sim 3.5$ l mol^{-1} cm^{-1}) in ethylene oxide at 0 °C, and which increases in intensity due to Fermi resonance (1, 43, 48) with the isosymmetric ν_1 to yield a moderate shoulder (extinction $\varepsilon \sim 50$ l mol^{-1} cm^{-1}) in pyridine at −20 °C. The progressive enhancement of the $2\nu_2$ band extinctions is shown in Fig. 5.

Assignment of the ice bands using eqs. 3 and 4 favors the wider ν_3 at the higher frequency and the sharper ν_1 at 3220 cm^{-1} in Fermi resonance with an enhanced $2\nu_2$ at 3150 cm^{-1}.

Comparison of O—H Stretching Bands for CH_3OH, DOH, and H_2O

(a) Correlation of Frequencies

In Table 5 are presented the 12 equations for the best linear regressions between the O—H stretching frequencies of the weak acids CH_3OH, DOH, and H_2O in our range of basic solvents.

Can. J. Chem. Downloaded from www.nrcresearchpress.com by 210.87.254.6 on 09/05/12
For personal use only.

TABLE 5. Correlation between O—H stretching frequencies of CH_3OH, DOH, and H_2O

Equation	Y	= $B1$	X	$\sigma(Y)$ (cm^{-1})	$\sigma(B1)$ (%)	ϕ	Correlation coefficient
[6]	$3756-\nu_3$	= 1.2053	$(3657-\nu_1)$	8.0	0.53	53	0.9985
[3]	$3657-\nu_1$	= 0.8285	$(3756-\nu_3)$	6.7			
[7]	$3707-\nu_{DOH}$	= 1.1935	$(3657-\nu_1)$	6.7	0.62	22	0.9992
[8]	$3657-\nu_1$	= 0.8372	$(3707-\nu_{DOH})$	5.6			
[9]	$3756-\nu_3$	= 1.0073	$(3707-\nu_{DOH})$	10.1	0.92	22	0.9981
[10]	$3707-\nu_{DOH}$	= 0.9910	$(3756-\nu_3)$	10.0			
[11]	$3687-\nu_{MeOH}$	= 1.2634	$(3756-\nu_3)$	22.3	1.55	25	0.9940
[12]	$3756-\nu_3$	= 0.7868	$(3687-\nu_{MeOH})$	17.6			
[13]	$3687-\nu_{MeOH}$	= 1.2835	$(3707-\nu_{DOH})$	18.0	1.28	22	0.9964
[14]	$3707-\nu_{DOH}$	= 0.7763	$(3687-\nu_{MeOH})$	14.0			
[15]	$3687-\nu_{MeOH}$	= 1.5235	$(3657-\nu_1)$	19.5	1.35	25	0.9955
[16]	$3657-\nu_1$	= 0.6534	$(3687-\nu_{MeOH})$	12.8			

TABLE 6. Regression of O—H stretch frequencies for CH_3OH with DOH and H_2O*

Equation	Variate Y	Variate X	$B1$	$B2$	$\sigma(Y)$ (cm^{-1})	ϕ
[17]	$3687-\nu_{MeOH}$	$3756-\nu_3$	0.8679	0.001351	11.8	24
[18]	$3756-\nu_3$	$3687-\nu_{MeOH}$	1.0447	−0.000665	8.3	24
[19]	$3687-\nu_{MeOH}$	$3707-\nu_{DOH}$	0.9155	0.001227	9.0	21
[20]	$3707-\nu_{DOH}$	$3687-\nu_{MeOH}$	1.0082	−0.000584	6.3	21
[21]	$3687-\nu_{MeOH}$	$3657-\nu_1$	1.1148	0.001673	9.9	24
[22]	$3657-\nu_1$	$3687-\nu_{MeOH}$	0.8304	−0.000457	7.0	24

*Regression $Y = B1 \cdot X + B2 \cdot X^2$.

The equations are written for evaluation of the best Y at specified X, where $B1$ is the regression coefficient Y on X. Also shown are $\sigma(Y)$ the assessment from the regression of the standard error on a single determination of Y with X assumed to be error-free, $\sigma(B1)$ the standard error on $B1$ expressed as a percentage, and ϕ the number of degrees of freedom (in this case the number of data pairs minus one) used to evaluate $\sigma(Y)$. The final column shows the correlation coefficient between the X and Y variates.

All correlation coefficients are seen to be 0.9940 or larger evidencing high degrees of correlation between the stretching frequency shifts for CH_3OH, DOH, and H_2O in the same solvents. Excellent correlations are shown between the frequencies ν_3, ν_1, and ν_{DOH} for H_2O and DOH, represented by eqs. 3, 6 to 10 for which the $\sigma(Y)$ values of 6–10 cm^{-1} are of the correct magnitude for the known experimental error. Regressions [9] and [10] prove that within experimental error the frequency shift for the ν_3 molecular vibration of H_2O in a particular solvent is identical with the ν_{DOH} for the O—H group vibration of DOH. Fifer and Schiffer (55) have given a theoretical explanation for the smaller shifts to lower frequency of ν_1.

Uniformly poorer correlations are found between the methanol frequency shifts and those for H_2O and DOH as represented by eqs. 11 to 16 for which the $\sigma(Y)$ assessments of 13–22 cm^{-1} are larger than experimental error by a factor of about two. Thus to adequately represent the experimental relationships between the frequencies of methanol and of the water, we use the quadratic function $Y = B1 \cdot X + B2 \cdot X^2$, for which Table 6 presents the Y and X variates together with values for the regression coefficients $B1$ and $B2$. The values of $\sigma(Y)$, the error assessment from the quadratic equation based on error-free X measurements, are now of the correct magnitude for the known experimental error.

The assessments for $\sigma(Y)$ from eqs. 3, 6 to 10 and eqs. 17 to 22 only provide proper estimates for the true standard error on Y when the X variate measurements are error-free. But since X and Y are infrared band frequency measurements and are both subject to comparable errors of measurement, the $\sigma(Y)$ assessments presented in Tables 5 and 6 are too large and must be divided by the

Can. J. Chem. Downloaded from www.nrcresearchpress.com by 210.87.254.6 on 09/05/12
For personal use only.

TABLE 7. Correlation of O—H stretch band areas for CH_3OH, DOH, and H_2O

Equation	Y = $B1$	X	$\sigma(Y)$	$\sigma(B1)$ (%)	ϕ	Correlation coefficient
[23]	$(\varepsilon.w)_{H_2O}$ = 2.0361	$(\varepsilon.w)_{DOH}$	3000*	2.01	17	0.9932
[24]	$(\varepsilon.w)_{DOH}$ = 0.4878	$(\varepsilon.w)_{H_2O}$	1500			
[25]	$(\varepsilon.w)_{MeOH}$ = 1.7562	$(\varepsilon.w)_{DOH}$	4400	3.45	17	0.9802
[26]	$(\varepsilon.w)_{DOH}$ = 0.5581	$(\varepsilon.w)_{MeOH}$	2500			
[27]	$(\varepsilon.w)_{MeOH}$ = 0.8543	$(\varepsilon.w)_{H_2O}$	5100	3.88	21	0.9693
[28]	$(\varepsilon.w)_{H_2O}$ = 1.1347	$(\varepsilon.w)_{MeOH}$	5800			
[29]	w_{13} = 1.2347	w_{DOH}	4.5*	0.52	9	0.9998
[30]	w_{DOH} = 0.8097	w_{13}	3.6			

*Units for $\varepsilon.w$, l mol^{-1} cm^{-2} for w, cm^{-1}.

term, $(1 + B1^2)^{\frac{1}{2}}$, which then gives an estimate of the standard error on a single Y measurement when X and Y are equally in error. The standard error on a single frequency determination then becomes 6.0 cm^{-1} for methanol, 5.7 for hydrogen deuterium oxide, 6.1 for the antisymmetric, and 5.1 for the symmetric stretching bands of water.

The average frequency shifts for singly H-bonded methanol in eqs. 11 and 13 are seen to be 26–28% larger than those for the doubly bonded water and hydrogen deuterium oxide; in the more basic amine solvents the methanol shifts are some 50% larger. Since more acidic phenol forms stronger H-bonds and exhibits even larger frequency shifts than methanol in these same solvents (3, 15, 49), our frequency shifts indicate that (*i*) with a given base, singly bonded methanol forms stronger H-bonds than doubly bonded water and hydrogen deuterium oxide, and (*ii*) monobasic methanol is more acidic than the dibasic water and hydrogen deuterium oxide, which are about equally acidic.

(b) Correlation of Areas

The six best linear equations relating the band area products $\varepsilon \cdot w$ for the hydroxyl stretching bands of CH_3OH, DOH, and H_2O are presented in Table 7. The best correlation is shown between the water bands of DOH and H_2O, with correspondingly poorer correlations for each of these with the methanol bands. The slopes in eqs. 23 and 24 are within experimental error equal to the theoretical values 2.00 and 0.50, respectively, confirming identical transition dipole derivatives (1, 2) and equally strong H-bonding for the group stretching vibration of DOH and for the molecular stretching vibrations of H_2O. The singly H-bonded methanol in eq. 25 shows a 76% greater band area and 33% larger transition dipole moment derivative than doubly bonded DOH. Thus again the singly bonded methanol is indicated to form significantly stronger H-bonds than the doubly bonded hydrogen deuterium oxide and water, which form essentially equivalent H-bonds.

The complete absence of non-bonded, sharp O—H u bands for methanol in dimethyl sulfoxide, the pyridines and in triethylamine, together with the occurrence of such sharp bands for both the DOH and HOH solutes, is consistent and supports the view that in these aprotic, basic solvents the singly H-bonded methanol forms stronger H-bonds with the solvent than do the doubly H-bonded hydrogen deuterium oxide and water. Similarly, weaker H-bonding by water is indicated in protonic liquid methanol at 0 °C, in which the proton magnetic resonance chemical shift for the protons of dilute water is 0.3 p.p.m. to higher field than that for the hydroxyl proton of methanol (unpublished work).

In addition to the band area correlations we include in Table 7 the band-width relations [29] and [30], valid in dimethyl sulfoxide and in more basic solvents, between w_{13} for the overlapped water bands and w_{DOH} for hydrogen deuterium oxide.

The transition dipole moment derivatives (2), $d\mu/dr$, for the O—H stretching modes of CH_3OH, DOH, and H_2O are given in Table 8. These are derived from the band area products $\varepsilon \cdot w$ (l mol^{-1} cm^{-2}, decadic logarithms) using the relations $d\mu/dr = 2.27 \times 10^{-12} \sqrt{\varepsilon \cdot w}$ for CH_3OH and DOH, and $1.61 \times 10^{-12} \sqrt{\varepsilon \cdot w}$ for H_2O.

At the head of the table good agreement is seen for $d\mu/dr$ of water vapor (50) and water dissolved in weakly interacting solvents. It is remarkable that these band areas are equal, despite the very

Can. J. Chem. Downloaded from www.nrcresearchpress.com by 210.87.254.6 on 09/05/12
For personal use only.

TABLE 8. Transition moment derivative for O—H stretching modes of CH_3OH, DOH, and H_2O

Solvent/phase	Temperature (°C)	$d\mu/dr$ (e.s.u.) $\times 10^{10}$		
		CH_3OH	DOH	H_2O
Vapor	—	—	—	0.74*
Hexafluorobenzene	30	1.12	0.81	0.68
Carbon tetrachloride	30	1.17	0.78	0.73
Tetrachloroethylene	30	1.17	—	0.72
1,1,1-Trichloroethane	30	1.09	—	0.72
Pentachloroethane	30	1.17	—	—
1,1,2,2-Tetrachloroethane	30	1.27	—	—
1,2-Dichloroethane	30	—	—	1.14
Nitromethane	30	2.14	1.43	1.58
" "	0	2.24	—	1.72
1,4-Dioxane	20	—	—	2.26
Ethylene oxide	0	2.76	2.45	2.39
" "	−40	2.93	—	2.47
Tetrahydrofuran	30	3.27	2.51	2.31
" "	0	3.16	2.68	2.46
" "	−40	3.27	—	2.56
Dimethyl sulfoxide	30	3.75	2.64	2.80
Deuterium oxide	30	—	3.13	—
Triethylamine	30	4.15	3.10	3.19
Pyridine	30	4.27	3.27	3.23
2-Picoline	30	4.46	3.17	3.10
4-Picoline	30	4.61	3.13	3.09
2,6-Lutidine	30	4.55	3.24	3.23
2,4,6-Collidine	30	4.70	3.34	3.28
Triethylamine	−44	4.09	3.44	3.79
2,4,6-Collidine	−20	4.67	3.32	3.33
Pyridine	−20	4.36	3.52	3.59
2-Picoline	−44	4.65	3.69	3.64
Ice	−100	—	—	4.01†

*Reference 50.
†Reference 51.

different extinction ratios and rotational structures of the ν_3 and ν_1 bands in the gas and liquid solvent phases. In a given solvent DOH and H_2O show essentially equal $d\mu/dr$ values which are invariably smaller than for CH_3OH.

The solvent order in Table 8 is that of increasing $d\mu/dr$ and thus of generally increasing H-bonding between the solute O—H group and the solvent base. This order is similar to those in Tables 1, 2, and 4, except for the position of triethylamine which differs significantly. The small $d\mu/dr$ values indicate that triethylamine forms either fewer or weaker H-bonds with CH_3OH, DOH, and HOH than do the substituted pyridines, whereas the frequency shifts indicate that triethylamine H-bonds are stronger than those of the pyridines. We consider that the low $d\mu/dr$ values for CH_3OH at both 30 and −44 °C in triethylamine reflect steric repulsions due to the librations of the ethyl groups. The DOH and HOH bands in triethylamine exhibit low peak extinctions with larger half-widths and more Gaussian shape (see Fig. 2*c*) than in the pyridines, which we interpret by the wider thermal distribution of O—H---N configurations arising from the three relaxing ethyl groups of triethylamine, absent in the rigid pyridines.

Recent absolute intensity measurements (51) for the stretching bands of the H_2O, DOH, and D_2O ices at −100 °C show overlapped ν_3, ν_1, and ν_2 contours similar to those in Fig. 5*f* and yield a $d\mu/dr$ of 4.01×10^{-10} e.s.u. for the water molecule in ice. This attests stronger H-bonding of water in ice than in the liquid tertiary amines, consistent with the frequency-shift orders in Tables 2 and 4. The proper sign for $d\mu/dr$ is almost certainly positive as given in Table 8, in the same sense that the gas phase water molecule has the positive dipole moment, +1.85 D, with an excess positive charge at the protons when the O—H internuclear separation r is 0.958 Å (1). This means that the extension of r to 1.01 Å (52) by the H-bonding in ice leads to a further increase of positive charge at the protons giving an en-

Can. J. Chem. Downloaded from www.nrcresearchpress.com by 210.87.254.6 on 09/05/12
For personal use only.

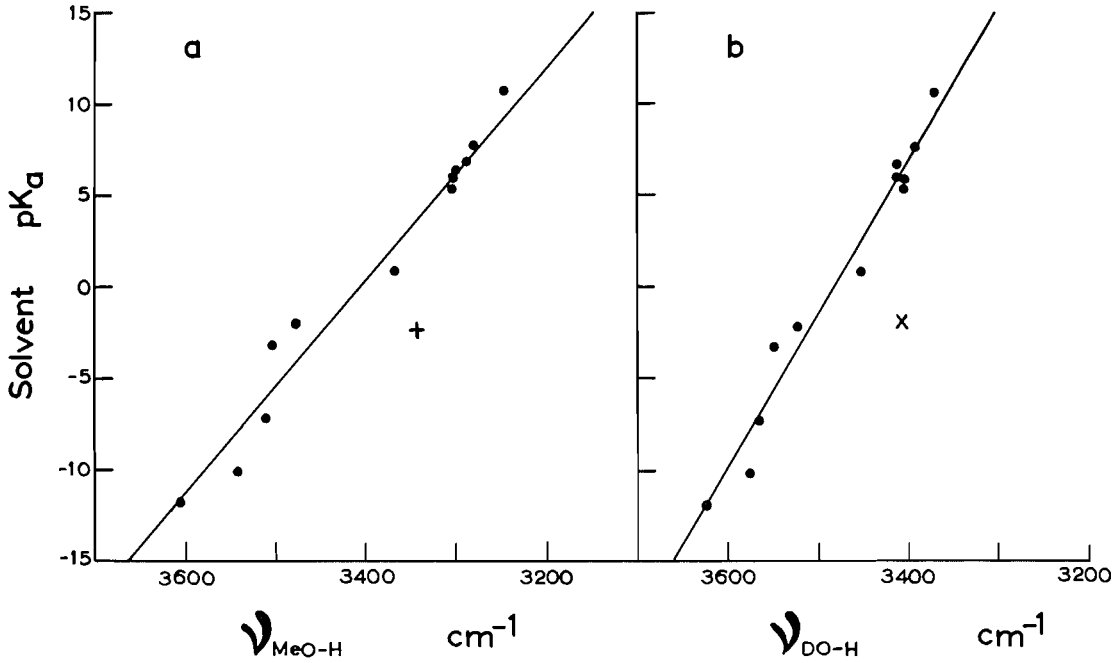

FIG. 9. Correlation of basicity pK_a values for aprotic solvents with O—H stretch frequency for two weakly acidic solutes at 30 °C. (*a*) The solute CH_3OH, showing its deviation at + in methyl alcohol-*d*. (*b*) The solute DOH, showing its deviation at × in deuterium oxide.

hanced dipole moment of about 1.99 D for the water molecule in ice, as evaluated assuming a constant $d^2\mu/dr^2$ over the range of r.

Solvent Basicity

The solvents in Tables 1, 2, and 4 are ordered according to the frequency value for the solute O—H stretch bands. These orders are very similar for each of the weakly acidic solutes, CH_3OH, DOH, and H_2O, and this common spectral order corresponds closely with the basicity order defined by the solvent pK_a values (15). Arnett has shown an impressive correlation of solvent pK_a values with the O—D stretching frequencies of dissolved methyl alcohol-*d*, while Gordy and Stanford (16) earlier showed a good correlation between the O—D stretching band wavelengths for D_2O and CH_3OD in a wide range of basic solvents.

Correlations between the solvent pK_a values (15, 53) and our O—H stretching frequencies for CH_3OH and DOH in aprotic solvents are presented in Fig. 9. Representative linear equations, including one for H_2O, are

$$[31]\quad pK_a = -16.11 + 0.0577(3687 - \nu_{MeOH})$$

$$[32]\quad pK_a = -19.10 + 0.0847(3707 - \nu_{DOH})$$

$$[33]\quad pK_a = -19.09 + 0.0821(3756 - \nu_3)$$

with standard errors on single pK_a values of 1.61, 1.62, and 1.40 for eqs. 31 to 33, respectively, and with standard errors on the regression coefficients of 0.0038, 0.0056, and 0.0047. These empirical equations are recommended and give equivalent results for interpolation of aprotic solvent pK_a values within the range −11.9 for nitromethane and +10.7 for triethylamine. They should not be used for extrapolation since the lack of linearity of the CH_3OH and DOH frequency scales leads to significantly different predicted pK_a values.

A large deviation for the D-bonded solvent methyl alcohol-*d* from the correlation line, eq. 31, for methanol in aprotic solvents is shown in Fig. 9*a*. If we calculate the oxygen basicity for methyl alcohol-*d* using the methanol frequency 3344 cm^{-1} in eq. 31 we obtain a pK_a value of 3.7 ± 0.5, which is 5.9 units higher and more strongly basic than the −2.2 reported for methanol (15). Alternately, if the −2.2 value for methanol is accepted, substitution into eq. 31 gives an O—H frequency of 3446 cm^{-1}, similar to that for methanol in tetrahydrofuran, but 102 cm^{-1}

Can. J. Chem. Downloaded from www.nrcresearchpress.com by 210.87.254.6 on 09/05/12
For personal use only.

higher than for the main band at 3344 cm^{-1}. This deviation exceeds possible experimental error and is most readily understood in terms of a specific dipolar association model for methanol H-bonding (30), represented by

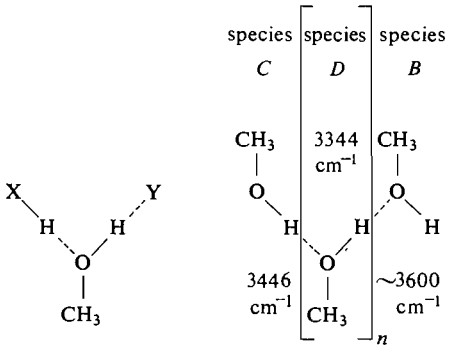

in which electronic charge displacements at the methanol oxygen atoms arise (*i*) from the H-bonding of Y by the hydroxyl proton which makes the oxygen atom more basic, and (*ii*) from the X—H bonding of the oxygen atom which makes the hydroxyl proton more acidic. This is an induction–polarization effect in which the field of the hydroxyl proton attracts the regions of high electronic charge on Y. The electrons of Y attract the proton but repel its bonding electrons so that the O—H bond length is increased and electronic charge is returned to the oxygen atom, making it more basic. In the same sense the H-bond formation by X—H attracts electronic charge onto the oxygen atom and withdraws some of this charge from the O—H bond, thereby reducing the shielding of the proton and making it more acidic. For each of these H-bonds the charge polarization at the oxygen atom is in the same direction, so that simultaneous formation of both bonds leads to their mutual stabilization and strengthening. Thus, we expect strongest H-bonds between doubly bonded methanol species *D* within the alcohol polymer chains and rings, with weaker H-bonds to the terminal species *B* and *C*, and with weakest H-bonds in the dimer between species *C* and *B*.

The D-bonded solvent deuterium oxide in Fig. 9*b* shows a similar large deviation from the correlation line, eq. 32, for DOH in aprotic solvents. Evaluation of the deuterium oxide oxygen basicity using the frequency 3407 cm^{-1} in eq. 32 gives a pK_a of 6.3 $\pm$ 0.6, which is 8.1 units more basic than the -1.8 reported for water (15). If we take the -1.8 for the oxygen basicity in deuterium oxide, substitution into eq. 32 gives 3503 cm^{-1} for the O—H frequency of the double bonded species

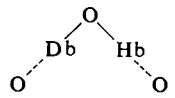

denoted b D—O—H b, with no bonds to the oxygen lone pairs: this frequency is 96 cm^{-1} higher than for the main band at 3407 cm^{-1}. This large discrepancy for DOH in liquid deuterium oxide is again beyond possible experimental error and is interpreted in terms of tetrahedrally induced polarization and charge redistribution on each central oxygen atom caused by the bonding of four nearest neighbors. The formation of D-bonds by X—D with the central oxygen atom

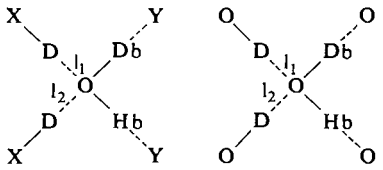

enhances the electronic charge density within the lone pair orbitals l_1 and l_2 oriented towards the D—X groups. This shift of charge on the central oxygen withdraws some charge within the O—D and O—H orbitals and reduces the electronic shielding of the deuteron and proton, making them become more acidic and form stronger D- and H-bonds. Similarly the electrons of the basic Y atoms attract the deuteron and proton but repel their orbital electrons so that the O—D and O—H bond lengths are increased while electronic charge is displaced back to the central oxygen atom, making it more basic and able to form stronger bonds. The formation of both the O—D b and O—H b donor and the l_1 and l_2 acceptor bonds leads to charge polarization of the central oxygen atom in the same sense and corresponds to increasing dipole moments for unbonded gaseous DOH, through two-bonded b D—O—H b in aprotic tetrahydrofuran, to four-bonded l_1l_2b D—O—H b in deuterium oxide liquid and ice.

In the contrary sense and opposing the four bond-stabilizing interactions (l_1 – O—D b, l_1 – O—H b, l_2 – O—D b, l_2 – O—H b) between the acceptor and donor bonds of four-bonded hydrogen deuterium oxide, the formation of the

Can. J. Chem. Downloaded from www.nrcresearchpress.com by 210.87.254.6 on 09/05/12
For personal use only.

second acceptor bond at lone pair l_2 inductively opposes and weakens the first acceptor bond at l_1, while similarly the formation of the second donor bond O—H b weakens the first donor bond O—D b. Thus, each of the four bonds to dibasic hydrogen deuterium oxide in liquid deuterium oxide is weaker than each of the two bonds to monobasic methanol within its liquid polymer chains.

We are indebted to A. L. Baker and J. C. Evans for technical discussions and to D. M. Young for editorial advice.

1. G. Herzberg. Infrared and Raman Spectra of Polyatomic Molecules. D. Van Nostrand Company, Princeton, N.J. 1945.
2. G. M. Barrow. Introduction to Molecular Spectroscopy. McGraw-Hill Book Company, Inc., New York. 1962.
3. G. C. Pimentel and A. L. McClellan. The Hydrogen Bond. W. H. Freeman and Company, San Francisco. 1960.
4. E. Greinacher, W. Lüttke, and R. Mecke. Z. Elektrochem. **59**, 23 (1955).
5. L. B. Borst, A. M. Buswell, and W. H. Rodebush. J. Chem. Phys. **6**, 61 (1938).
6. J. J. Fox and A. E. Martin. Proc. Roy. Soc. Ser. A. **174**, 234 (1940).
7. P. Saumagne and M-L. Josien. Bull. Soc. Chim. 813 (1958).
8. S. C. Mohr, W. D. Wilk, and G. M. Barrow. J. Amer. Chem. Soc. **87**, 3048 (1965).
9. D. N. Glew, H. D. Mak, and N. S. Rath. Can. J. Chem. **45**, 3059 (1967).
10. D. N. Glew, H. D. Mak, and N. S. Rath. Chem. Commun. 264 (1968).
11. D. N. Glew, H. D. Mak, and N. S. Rath. *In* Hydrogen-bonded Solvent Systems. *Edited by* A. K. Covington and P. Jones. Taylor and Francis Limited, London. 1968.
12. G. Mavel. Compt. rend. **248**, 1505 (1959).
13. G. Mavel. Compt. rend. **250**, 1477 (1960).
14. J. R. Holmes, D. Kivelson, and W. C. Drinkard. J. Amer. Chem. Soc. **84**, 4677 (1962).
15. E. M. Arnett. *In* Progress in Physical Organic Chemistry. Vol. 1. Interscience Publ., New York. 1963.
16. W. Gordy and S. C. Stanford. J. Chem. Phys. **9**, 204, (1941).
17. I.U.P.A.C. Commission on Molecular Structure and Spectroscopy. Tables of Wavenumbers for the Calibration of Infrared Spectrometers. Butterworths, London. 1961.
18. M. Falk and E. Whalley. J. Chem. Phys. **34**, 1554 (1961).
19. R. T. Iwamasa. Ph.D. Thesis. California Institute of Technology. 1967.
20. L. P. Kuhn. J. Amer. Chem. Soc. **74**, 2492 (1952).
21. G. M. Barrow. J. Phys. Chem. **59**, 1129 (1955).
22. A. Allerhand and P. von R. Schleyer. J. Amer. Chem. Soc. **85**, 371 (1963).
23. G. Durocher and C. Sandorfy. J. Mol Spectry. **15**, 22 (1965).
24. L. J. Bellamy and R. J. Pace. Spectrochim. Acta, **22**, 525 (1966).
25. S. Abramowitz and R. P. Bauman. J. Chem. Phys. **39**, 2757 (1963).
26. J. Pitha and R. N. Jones. Can. J. Chem. **44**, 3031 (1966).
27. J. J. Fox and A. E. Martin. Trans. Faraday Soc. **36**, 897 (1940).
28. F. A. Smith and E. C. Creitz. J. Res. Nat. Bur. Standards, **46**, 145 (1951).
29. K. J. Tauer and W. N. Lipscomb. Acta Cryst. **5**, 606 (1952).
30. L. J. Bellamy, K. J. Morgan, and R. J. Pace. Spectrochim. Acta, **22**, 535 (1966).
31. W. S. Benedict, N. Gailar, and E. K. Plyler. J. Chem. Phys. **24**, 1139 (1956).
32. M. Falk and T. A. Ford. Can. J. Chem. **44**, 1699 (1966).
33. H. R. Wyss and M. Falk. Can. J. Chem. **48**, 607 (1970).
34. I. S. Perelygin and N. R. Safiullina. J. Struct. Chem. **8**, 178 (1967).
35. C. Jolicoeur and A. Cabana. Can. J. Chem. **46**, 567 (1968).
36. W. A. Senior. *In* Hydrogen-bonded Solvent Systems. *Edited by* A. K. Covington and P. Jones. Taylor and Francis Limited, London. 1968.
37. G. E. Walrafen. J. Chem. Phys. **50**, 560 (1969).
38. G. V. Yukhnevich, A. V. Karyakin, and A. V. Petrov. Zh. Prikl. Spektrosk. **3**(2), 142 (1965).
39. W. Yellin and W. L. Courchene. Nature, **219**, 852 (1968).
40. T. T. Wall and D. F. Hornig. J. Chem. Phys. **43**, 2079 (1965).
41. G. Bolla. Nuovo cimento, **9**, 290 (1932).
42. J. Cabannes and J. de Riols. Compt. rend. **198**, 30 (1934).
43. J. W. Schultz and D. F. Hornig. J. Phys. Chem. **65**, 2131 (1961).
44. G. E. Walrafen. J. Chem. Phys. **47**, 114 (1967).
45. W. K. Thompson, W. A. Senior, and B. A. Pethica. Nature, **211**, 1086 (1966).
46. D. M. Gates, R. F. Calfee, D. W. Hansen, and W. S. Benedict. Line Parameters and Computed Spectra for Water Vapor Bands at 2.7μ. Nat. Bur. Standards Monograph 71. 1964.
47. J. W. Forbes. Anal. Chem. **34**, 1125 (1962).
48. R. E. Weston. Spectrochim. Acta, **18**, 1257 (1962).
49. D. P. Eyman and R. S. Drago. J. Amer. Chem. Soc. **88**, 1617 (1966).
50. C. C. Ferriso and C. B. Ludwig. J. Quant. Spectry. Radiative Transfer, **4**, 215 (1964).
51. S-I. Ikawa and S. Maeda. Spectrochim. Acta, **24A**, 655 (1968).
52. S. W. Peterson and H. A. Levy. Acta Cryst. **10**, 70 (1957).
53. H. C. Brown, D. H. McDaniel, and O. Haflinger. *In* Determination of Organic Structures by Physical Methods. *Edited by* E. A. Braude and F. C. Nachod. Academic Press, New York. 1955.
54. J. Schiffer and D. F. Hornig. J. Chem. Phys. **49**, 4150 (1968).
55. R. A. Fifer and J. Schiffer. J. Chem. Phys. **52**, 2664 (1970).

Can. J. Chem. Downloaded from www.nrcresearchpress.com by 210.87.254.6 on 09/05/12
For personal use only.

Synthesis of 1*H*-Benzo[*d*,*e*-1,7]naphthyridines, a Novel Heterocyclic Ring System

L. G. HUMBER
Ayerst Research Laboratories, Montreal, Quebec

Received August 31, 1970

A simple six-step synthesis, from homoveratrylamine, of 5,6-dimethoxy-2,3,7,8,9,9*a*-hexahydro-1-(*p*-toluenesulfonyl)-1*H*-benzo[*d*,*e*-1,7]naphthyridine, the first representative of a novel heterocyclic ring system, is described. Various transformation products and derivatives of the ring-system are also recorded.

Une synthèse simple, en six étapes à partir de l'homovératrylamine de la diméthoxy-5,6 hexahydro-2,3,7,8,9,9*a* *p*-toluènesulfonyl-1 1*H*-benzo[*d*,*e*-1,7]naphthyridine, le premier représentant d'un nouveau système hétérocyclique, est décrite. Divers produits de transformation et dérivés de ce système cyclique sont aussi rapportés.

Canadian Journal of Chemistry, 49, 857 (1971)

Can. J. Chem. Downloaded from www.nrcresearchpress.com by 210.87.254.105 on 09/05/12
For personal use only.

Compounds containing the benzo[*d*,*e*-1,7]-naphthyridine ring system, *e.g.* **17**, have hitherto been undescribed. As part of a program aimed at the syntheses of novel heterocyclic systems for the study of their chemical and biological properties, a synthetic route to this ring-system has been developed and is described in this report.

The general approach selected required the use of a 1-aminomethyl-1,2,3,4-tetrahydroisoquinoline (*e.g.*, **8**–**13**, **15**, **16**) which should give rise to the desired tricyclic system on application of either the Bischler–Napieralski, the Pictet–Spengler, or the Friedel–Crafts reaction to the appropriate derivative.

Initially, the Bischler–Napieralski reaction on the 1-formamidomethyl-2-methyltetrahydroisoquinoline **11** was investigated. Compound **11** was obtained via the methylation of **3** with formic acid and formaldehyde to afford **5** which was treated with hydrazine to remove the phthalyl blocking group. The resultant 1-aminomethyl-2-methyl derivative **8** was converted to **11** with formic acetic anhydride. Ring closure of **11** was investigated using conventional Bischler–Napieralski reagents such as phosphorous oxychloride, phosphorous pentoxide, and phosphorous pentachloride (2), as well as the use of polyphosphoric acid (3), polyphosphoric ester (4), phosphorous oxychloride and tin dust (5), the mixture of phosphorous pentoxide and phosphorous oxychloride in pyridine (6), and the action of aluminum chloride on the imidochloride formed from **11** with phosphorous pentachloride in ether (7). In no instance was any of the benzonaphthyridine of type **14** observed. Either starting material **11**, its hydrolysis product **8**, or intractable tars were obtained.

The non-basic 2-(*p*-toluenesulfonyl)-1-formamidomethyl derivative **12** was next investigated in the Bischler-Napieralski reaction. Compound **12** was obtained from **3** through intermediates **6** and **9** by the sequence of tosylation, hydrazinolysis, and formylation. Using variants of the Bischler–Napieralski reaction as described above, no cyclization products could be detected. Cyclizations were also attempted without success on **13**, (obtained from **2** as shown in Scheme 1), the 5,6-dimethoxy analog of compound **12**, which does not bear a methoxyl group ortho to the intended site of ring closure, while retaining activation by methoxyl at that site. Attempted cyclization of the 2-(*p*-toluenesulfonyl)-isocyanates in both the 6,7-dimethoxy- and the 5,6-dimethoxy- series, **15** and **16** respectively, with aluminum chloride in toluene, and with *p*-toluenesulfonic acid in toluene failed to yield any tricyclic lactam.

The next variant of the general approach to be investigated was the application of the Pictet–Spengler reaction to a suitable substrate. Thus, the 1-aminomethyl-5,6-dimethoxy-2-(*p*-toluenesulfonyl) derivative **10**, obtained through intermediate **7**, was employed. When the hydrochloride salt of this compound, in water, was treated with one molar equivalent of aqueous formaldehyde for 45 min on the steam bath, then allowed to remain at room temperature for 12 h, there was obtained by filtration, a 90.5% yield of the hydrochloride of the desired benzo[*d*,*e*-1,7]-naphthyridine **17**. That ring-closure had occurred was readily confirmed by the n.m.r. spectrum of the product. The distinguishing feature of the spectrum is the aromatic region, which shows the four protons of the toluenesulfonyl group as two

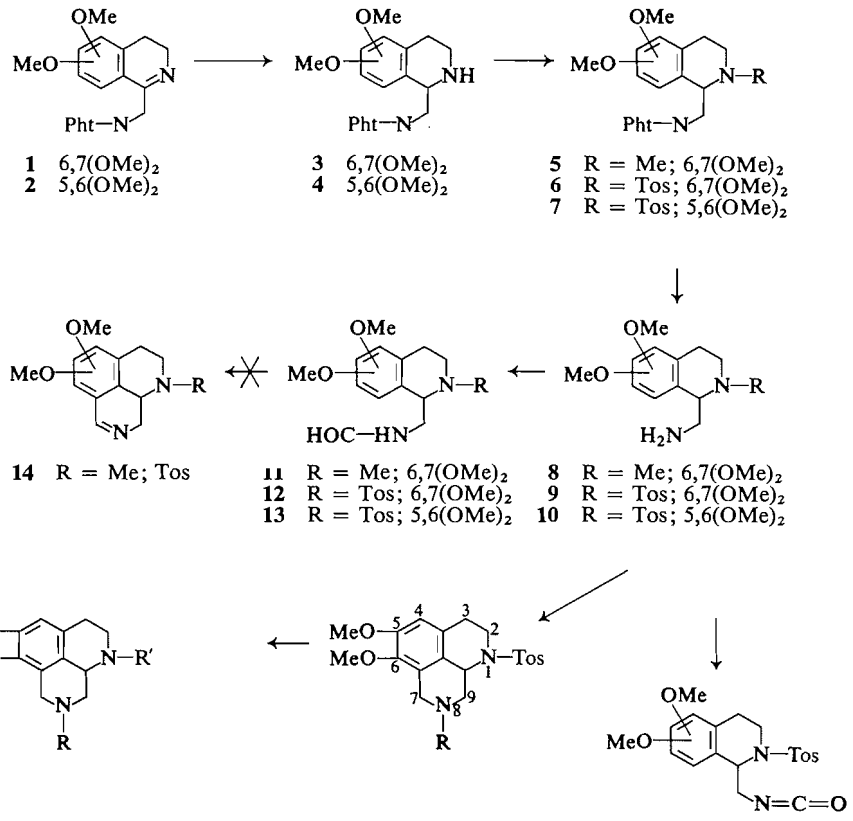

1 6,7(OMe)$_2$
2 5,6(OMe)$_2$

3 6,7(OMe)$_2$
4 5,6(OMe)$_2$

5 R = Me; 6,7(OMe)$_2$
6 R = Tos; 6,7(OMe)$_2$
7 R = Tos; 5,6(OMe)$_2$

14 R = Me; Tos

11 R = Me; 6,7(OMe)$_2$
12 R = Tos; 6,7(OMe)$_2$
13 R = Tos; 5,6(OMe)$_2$

8 R = Me; 6,7(OMe)$_2$
9 R = Tos; 6,7(OMe)$_2$
10 R = Tos; 5,6(OMe)$_2$

24 R = H; R′ = H
25 R = Me; R′ = H
26 R = Me; R′ = Ac
27 R = Ac; R′ = H
28 R = Et; R′ = H
29 R = $(CH_2)_3NMe_2$; R′ = H
30 R = Me; R′ = 3,4-dimethoxy-β-phenethyl

17 R = H[4,5(OMe)$_2$]
18 R = H
19 R = Me
20 R = Ac
21 R = $CO(CH_2)_2Cl$
22 R = $CO(CH_2)_2NMe_2$
23 R = CH_2COOEt

15 6,7(OMe)$_2$
16 5,6(OMe)$_2$

SCHEME 1. Pht = Phthalyl; Tos = *p*-toluenesulfonyl

doublets centered at 7.28 and 7.88 δ (J = 8 Hz), the one aromatic proton on the benzo[*d*,*e*-1,7]-naphthyridine nucleus as a singlet at 6.79 δ, and the two hydrogens at C-7 as a sharp singlet at 3.97 δ. A similar ring closure on the 6,7-dimethoxy analog **9** affords a 65% yield of the benzo[*d*,*e*-1,7]-naphthyridine **18**, reflecting a steric effect of the methoxyl group adjacent to the site of closure.

The former facile cyclization, in high yield under almost "physiologic" conditions, is striking when viewed in contrast to the various unsuccessful attempts, described above, to obtain the tricyclic ring system. Application of the Pictet–Spengler reaction using the conditions described above with the intermediate **8** which bears a basic center apart from the primary amino group that is expected to react, fails to give any cyclization product.

With the benzo[*d*,*e*-1,7]naphthyridine derivative **18** readily available by a six-step synthesis from commercially available homoveratrylamine, various transformations were studied. The *p*-toluenesulfonyl blocking group of **18** was removed in 61% yield with sodium–ammonia to give **24**, or alternatively, compound **18** was converted to the methylated derivative **19** followed by lithium–ammonia reduction to afford **25**, in which the two nitrogens are differentiated. Lithium–ammonia reduction of the acetyl derivative **20** allows the preparation of the corresponding detosylated

Can. J. Chem. Downloaded from www.nrcresearchpress.com by 210.87.254.105 on 09/05/12
For personal use only.

Can. J. Chem. Downloaded from www.nrcresearchpress.com by 210.87.254.105 on 09/05/12
For personal use only.

derivative **27**, while detosylation and simultaneous reduction of the 8-acetyl group of **20** occurs, to afford the 8-ethyl derivative **28** in 61% yield. Analogously, the treatment of the 1-tosyl-8-dimethylaminopropionyl derivative **22**, obtained through the chloropropionyl derivative **21**, afforded **29** bearing the dimethylaminopropyl group in the 8-position. Alkylation of **18** with ethyl bromoacetate yielded the ethoxycarbonyl derivative **23**, while an acylation of **25** followed by reduction with lithium aluminum hydride afforded the 1-(3,4-dimethoxy-β-phenethyl)-substituted benzo[*d*,*e*-1,7]naphthyridine **30**.

Experimental

Melting points were taken on a Thomas-Hoover apparatus. Analyses were done by Mr. W. Turnbull and staff of the Ayerst Research Laboratories. The n.m.r. spectra were recorded on a Varian A-60-A instrument. All new compounds gave i.r. and n.m.r. spectra consistent with their respective structures. Unless stated otherwise, reported yields are for materials homogeneous by t.l.c. and further identified by i.r. and/or n.m.r. spectroscopy.

N-Phthalimidoacetyl-2,3-dimethoxy-β-phenethylamine

To a vigorously stirred mixture of 2,3-dimethoxy-β-phenethylamine (1) (47.7 g, 0.263 mol), dichloromethane (200 ml), sodium carbonate (13.25 g, 0.125 mol), and water (200 ml) was added during 45 min at 5°, a solution of phthalylglycyl chloride (58.9 g, 0.263 mol) dissolved in dichloromethane (200 ml). The mixture was stirred at 22° for 1 h and the insoluble product was filtered off, dissolved in warm chloroform, washed with 3 × 150 ml of saturated sodium chloride solution, dried over sodium carbonate, and the solvent evaporated *in vacuo* to give 65.0 g of product (67%) as a solid, m.p. 196–198° from ethanol.

Anal. Calcd. for $C_{20}H_{20}N_2O_5$: C, 65.20; H, 5.47. Found: C, 64.98; H, 5.61.

N-Phthalimidoacetyl-3,4-dimethoxy-β-phenethylamine

Using the procedure described above but substituting 3,4-dimethoxy-β-phenethylamine for 2,3-dimethoxy-β-phenethylamine, the title compound is obtained in 78% yield. It has m.p. 188–189° (ethanol). This compound has been described previously (8), but no m.p. is given.

3,4-Dihydro-5,6-dimethoxy-1-phthalimidomethyl-isoquinoline (2)

N-Phthalimidoacetyl-2,3-dimethoxy-β-phenethylamine (65.0 g, 0.176 mol) was dissolved in 1 l of benzene and 500 ml of phosphorous oxychloride was added. The mixture was refluxed for 16 h, cooled, and diluted with 4 l of petroleum ether (b.p. 60–80°). The supernatant was decanted and the residual red oily phosphate salt of the title compound was dissolved in chloroform (500 ml) and shaken vigorously with 4 × 200 ml of 5% aqueous sodium carbonate solution. The chloroform solution was dried over sodium sulfate, concentrated to 150 ml, and passed through a column of alumina (650 g of activity II, neutral). Elution with chloroform gave 36.0 g of the product (58.2%) m.p. 204–206° (chloroform–methanol).

Anal. Calcd. for $C_{20}H_{18}N_2O_4$: C, 68.55; H, 5.18. Found: C, 69.02; H, 5.37.

3,4-Dihydro-6,7-dimethoxy-1-phthalimidomethyl-isoquinoline (1)

Using the procedure described above with *N*-phthalimidoacetyl-3,4-dimethoxy-β-phenethylamine affords a 71% yield of the title compound, m.p. 204–204.5° (chloroform–hexane). This compound has been described previously (8) but without a m.p.

5,6-Dimethoxy-1-phthalimidomethyl-1,2,3,4-tetrahydroisoquinoline (4)

Compound **2** (29.8 g, 0.085 mol) was dissolved in a mixture of 2 *N* hydrochloric acid (42.4 ml, 0.085 mol) and 200 ml of glacial acetic acid. Platinum oxide catalyst (1.0 g) was added and the mixture was hydrogenated at 22° and at an initial pressure of 50 p.s.i. After 2 min the reduction was complete. Filtration and dilution with ether gave a solid which was distributed between chloroform and aqueous sodium carbonate solution. The chloroform phase afforded 22.5 g (75.7%) of the product, m.p. 186–188° (benzene).

Anal. Calcd. for $C_{20}H_{20}N_2O_4$: C, 68.20; H, 5.68; N, 7.95. Found: C, 68.48; H, 5.81; N, 7.78.

The *2-(p-toluenesulfonyl)-derivative 7* was prepared in pyridine in 65% yield. Analytically pure material had m.p. 181–182° (acetonitrile).

Anal. Calcd. for $C_{27}H_{26}N_2O_6S$: C, 64.02; H, 5.17; N, 5.53; S, 6.32. Found: C, 64.24; H, 5.15; N, 5.47; S, 6.61.

6,7-Dimethoxy-1-phthalimidomethyl-1,2,3,4-tetrahydroisoquinoline (3)

Using the procedure described above with **1** affords a 65% yield of the title compound, m.p. 132–133° (acetone–hexane). This compound has been described previously as the hydrochloride (8) but no m.p. is given.

Anal. Calcd. for $C_{20}H_{20}N_2O_4$: C, 68.20; H, 5.68; N, 7.95. Found: C, 68.19; H, 5.75; N, 7.72.

6,7-Dimethoxy-2-methyl-1-phthalimidomethyl-1,2,3,4-tetrahydroisoquinoline (5)

Compound **3** (183 g, 0.519 mol) was dissolved in a mixture of 97% formic acid (183 ml), water (183 ml), and 37% aqueous formaldehyde (183 ml). The mixture was heated on the steam bath for 3 h, then poured into 4 l of water. The p*H* of the mixture was adjusted to 7 with sodium carbonate and it was extracted with benzene to afford 112 g (59%) of product, m.p. 146–148° (benzene–hexane).

Anal. Calcd. for $C_{21}H_{22}N_2O_4$: C, 68.83; H, 6.05; N, 7.65. Found: C, 68.93; H, 6.23; N, 7.66.

1-Aminomethyl-6,7-dimethoxy-2-methyl-1,2,3,4-tetrahydroisoquinoline (8)

To a solution of **5** (89.6 g, 0.245 mol) in 1.61 of ethanol at 50° was added 1.35 l of 1 *M* hydrazine in ethanol. The mixture was heated on the steam bath for 1.5 h, concentrated to a thick paste *in vacuo*, then heated for 30 min on a steam bath with 2 l of 2 *N* hydrochloric acid. After

Can. J. Chem. Downloaded from www.nrcresearchpress.com by 210.87.254.105 on 09/05/12
For personal use only.

filtration, the filtrate was made alkaline with potassium hydroxide and extracted with chloroform to afford the product, (49.6 g, 86%) b.p. 140° (0.03 mm.).

Anal. Calcd. for $C_{13}H_{20}N_2O_2$: C, 66.10; H, 8.52; N, 11.86. Found: C, 65.88; H, 8.41; N, 11.77.

The corresponding *2-(p-toluenesulfonyl)-derivative*, **6** was prepared in pyridine in 84% yield. It had m.p. 146–147° (ethanol).

Anal. Calcd. for $C_{27}H_{26}N_2O_6S$: C, 64.02; H, 5.17; N, 5.53; S, 6.32. Found: C, 63.75; H, 5.36; N, 5.56; S, 6.50.

*6,7-Dimethoxy-1-formamidomethyl-2-methyl-1,2,3,4-tetrahydroisoquinoline (**11**)*

Compound **8** (11.5 g, 0.049 mol) was added to formic acetic anhydride prepared by heating at 60° for 2 h, a mixture of 97% formic acid (53 ml) and acetic anhydride (125 ml). The mixture was kept at 22° for 18 h, poured into iced water, and extracted with chloroform to afford the product (12.4 g, 90%) b.p. 200° (0.3 mm). An analytical sample had m.p. 109–111° (acetone).

Anal. Calcd. for $C_{14}H_{20}N_2O_3$: C, 63.61; H, 7.63; N, 10.60. Found: C, 63.81; H, 7.55; N, 10.70.

*1-Aminomethyl-6,7-dimethoxy-1,2,3,4-tetrahydro-2-(p-toluenesulfonyl)-isoquinoline (**9**)*

Using the hydrazinolysis procedure described in the preparation of **8** with compound **6** affords an 84% yield of the title compound, m.p. 138–139° (benzene).

Anal. Calcd. for $C_{19}H_{24}N_2O_4S$: C, 60.62; H, 6.43; N, 7.44. Found: C, 61.03; H, 6.59; N, 7.37.

The hydrochloride salt had m.p. 225–226° (2-propanol–ether).

Anal. Calcd. for $C_{19}H_{25}ClN_2O_4S$: C, 55.28; H, 6.10; Cl, 8.59; N, 6.79. Found: C, 55.05; H, 6.17; Cl, 8.79; N, 6.66.

*1-Aminomethyl-5,6-dimethoxy-1,2,3,4-tetrahydro-2-(p-toluenesulfonyl)-isoquinoline (**10**)*

Using the hydrazinolysis procedure described above with **7** affords a 98% yield of the product as an oil. The hydrochloride salt had m.p. 235–238° (methanol–ether).

Anal. Calcd. for $C_{19}H_{25}ClN_2O_4S$: C, 55.28; H, 6.10; Cl, 8.59; N, 6.79. Found: C, 55.26; H, 6.12; Cl, 8.61; N, 6.59.

*6,7-Dimethoxy-1-formamidomethyl-1,2,3,4-tetrahydro-2-(p-toluenesulfonyl)-isoquinoline (**12**)*

Using the formylation procedure described above for the preparation of **11** with compound **9** affords a 62% yield of the product, m.p. 115–116° (chloroform–hexane).

Anal. Calcd. for $C_{20}H_{24}N_2O_5S$: C, 59.40; H, 5.98; N, 6.93. Found: C, 59.47; H, 6.20; N, 6.93.

*5,6-Dimethoxy-1-formamidomethyl-1,2,3,4-tetrahydro-2-(p-toluenesulfonyl)-isoquinoline (**13**)*

Using the formylation procedure described above with **10** affords a 90% yield of the title compound as a gum which could not be obtained crystalline. It was homogeneous by t.l.c. and the i.r. spectrum in chloroform had bands at 1675 (CONH) and 3400 cm^{-1} (NH). Good analyses could not be obtained with this gum.

*6,7-Dimethoxy-1-isocyanatomethyl-1,2,3,4-tetrahydro-2-(p-toluenesulfonyl)-isoquinoline (**15**)*

Phosgene was bubbled for 1 h into a refluxing mixture of **9** (7.53 g, 0.02 mol) in toluene (100 ml) which had been saturated with hydrogen chloride. The homogeneous solution was cooled and the solvent evaporated *in vacuo* to give an oily residue. Crystallization from benzene gave the product (6.02 g, 75%) m.p. 125–126°.

Anal. Calcd. for $C_{20}H_{22}N_2O_5S$: C, 59.69; H, 5.51; N, 6.96. Found: C, 59.88; H, 5.66; N, 6.90.

*5,6-Dimethoxy-1-isocyanatomethyl-1,2,3,4-tetrahydro-2-(p-toluenesulfonyl)-isoquinoline (**16**)*

Using the procedure described above, phosgene was reacted with **10** to afford the product in 54% yield, m.p. 116–119° (benzene–hexane).

Anal. Calcd. for $C_{20}H_{22}N_2O_5S$: C, 59.69; H, 5.51; N, 6.96. Found: C, 59.80; H, 5.74; N, 7.04.

*5,6-Dimethoxy-2,3,7,8,9,9a-hexahydro-1-(p-toluenesulfonyl)-1H-benzo[d,e-1,7]naphthyridine (**18**)*

Compound **9** (1.0 g, 0.00266 mol) was dissolved in 2 *N* hydrochloric acid (13.3 ml, 0.00266 mol) with gentle warming. Aqueous 37% formaldehyde (2.5 ml, 0.00266 mol) was added all at once and the mixture heated on the steam bath for 45 min. The solution was kept at 22° for 12 h and the resulting crystals isolated by filtration. They were washed with water then acetone and dried to give the product (730 mg, 65%), homogeneous by t.l.c. The analytical sample had m.p. 238–239° (methanol–ether) and the free base obtained from the hydrochloride had m.p. 90–92° (isopropanol); λ_{max} (EtOH) 225 (ε 22 080), 275 (ε 2680), 284 mμ (ε 2800). The n.m.r. spectrum of the hydrochloride in dimethylsulfoxide showed the lone aromatic proton of the benzonaphthyridine nucleus as a singlet at 6.42 δ.

Anal. Calcd. for $C_{20}H_{25}ClN_2O_4S$: C, 56.54; H, 5.93; Cl, 8.34. Found: C, 56.72; H, 6.10; Cl, 8.47.

*4,5-Dimethoxy-2,3,7,8,9,9a-hexahydro-1-(p-toluenesulfonyl)-1H-benzo[d,e-1,7]naphthyridine (**17**)*

Using the procedure described above with **10** a 90.5% yield of the hydrochloride salt of the title compound was obtained. It had m.p. 224–226° (acetonitrile); λ_{max} (EtOH) 231 (ε 15 450), 264 (ε 1525), 275 (ε 1746), 292 mμ (ε 1455). The n.m.r. spectrum showed characteristic bands, *viz.* two doublets centered at 7.28 (J = 8 Hz) and 7.88 δ (J = 8 Hz) (4 tosyl aromatic protons), a singlet at 6.79 (benzonaphthyridine aromatic proton), and the two hydrogens at C-7 as a sharp singlet at 3.97 δ. The free base obtained from the hydrochloride had m.p. 103–109° (benzene–hexane).

Anal. Calcd. for $C_{20}H_{25}ClN_2O_4S$: C, 56.54; H, 5.93; Cl, 8.34; N, 6.59. Found: C, 56.26; H, 5.95; Cl, 8.73; N, 6.71.

*5,6-Dimethoxy-2,3,7,8,9,9a-hexahydro-8-methyl-1-(p-toluenesulfonyl)-1H-benzo[d,e-1,7]naphthyridine (**19**)*

A mixture of **18** (5.0 g, 0.013 mol) 37% aqueous formaldehyde (5 ml), formic acid (5 ml), and water (5 ml) was heated on the steam bath for 2 h. Water (200 ml) was added, the mixture was made basic with ammonium hydroxide, and extracted with chloroform to afford the product (5.0 g, 95%) as an amorphous solid. The hydrochloride salt had m.p. 208–209° (methanol–ether).

Anal. Calcd. for $C_{21}H_{27}ClN_2O_4S$: C, 57.45; H, 6.20; Cl, 8.08; N, 6.38. Found: C, 57.16; H, 6.23; Cl, 7.99; N, 6.40.

Can. J. Chem. Downloaded from www.nrcresearchpress.com by 210.87.254.105 on 09/05/12
For personal use only.

5,6-Dimethoxy-2,3,7,8,9,9a-hexahydro-8-methyl-1H-benzo[d,e-1,7]naphthyridine (25)

A solution of **19** (1.0 g, 0.0025 mol) in 25 ml of tetrahydrofuran was added to 200 ml of anhydrous ammonia, followed by 2-propanol (1.0 ml). Lithium wire (0.043 g/cm) was added in small pieces until the resulting blue color persisted for 3 min (4.0 cm of lithium wire was required). The ammonia was evaporated and benzene (50 ml) and saturated sodium chloride solution (75 ml) were added. The benzene phase afforded the product as an oil (600 mg). It was chromatographed on neutral alumina (activity II). Elution with chloroform gave the pure product (520 mg, 76%) as an oil. It could be obtained crystalline from benzene–hexane and had m.p. 40–43°. The n.m.r. spectrum in chloroform shows a 3-proton peak at 2.5 (N—CH_3) and a one-proton peak at 6.52 δ (aromatic proton). The dihydrochloride salt had m.p. 257° (methanol–ether).

Anal. Calcd. for $C_{14}H_{22}Cl_2N_2O_2$: C, 53.33; H, 6.91. Found: C, 53.02; H, 7.14.

The *1-acetyl derivative* **26** was prepared with acetic anhydride and pyridine. It had m.p. 116–117° (ethyl acetate – hexane).

Anal. Calcd. for $C_{16}H_{22}N_2O_3$: C, 66.31; H, 7.76; N, 9.44. Found: C, 66.18; H, 7.64; N, 9.65.

5,6-Dimethoxy-2,3,7,8,9,9a-hexahydro-1H-benzo-[d,e-1,7]naphthyridine (24)

Compound **18** (1.0 g, 0.0035 mol) was dissolved in 10 ml of tetrahydrofuran and 100 ml of anhydrous ammonia. Sodium was added in small pieces until the blue color persisted for 10 min, then the ammonia was allowed to evaporate. The residue was distributed between chloroform and water. The organic phase afforded the product (500 mg, 61%), m.p. 134–135° (2-propanol – ether). The dihydrochloride salt had m.p. 295–297° (methanol).

Anal. Calcd. for $C_{13}H_{18}N_2O_2$: C, 66.64; H, 7.74; N, 11.96. Found: C, 66.95; H, 7.71; N, 11.91.

The *8-acetyl derivative* **20** was prepared with acetic anhydride in pyridine at 75°. It had m.p. 134–136° (benzene–hexane).

Anal. Calcd. for $C_{22}H_{26}N_2O_5S$: C, 61.11; H, 5.98; N, 6.33. Found: C, 61.38; H, 6.09; N, 6.51.

5,6-Dimethoxy-8-ethyl-2,3,7,8,9,9a-hexahydro-1H-benzo[d,e-1,7]naphthyridine (28)

Compound **20** (2.1 g, 0.005 mol) was refluxed for 16 h with 2.0 g of lithium aluminum hydride in 30 ml of tetrahydrofuran to afford, after a conventional work-up procedure, 800 mg of the product (61%). The dihydrochloride salt had m.p. 239–240° (methanol–ether).

Anal. Calcd. for $C_{15}H_{24}Cl_2N_2O_2$: C, 53.72; H, 7.22; Cl, 21.15. Found: C, 53.96; H, 7.38; Cl, 20.84.

8-Acetyl-5,6-dimethoxy-2,3,7,8,9,9a-hexahydro-1H-benzo[d,e-1,7]naphthyridine (27)

To a solution of **20** (1.0 g, 0.0025 mol) in ammonia (300 ml) was added lithium wire (0.035 g, 0.0025 mol) during 5 min. The ammonia was allowed to evaporate overnight and the residue was distributed between water and chloroform. The chloroform phase afforded the product (560 mg, 81.5%), m.p. 115–117° (ethyl acetate – hexane). The hydrochloride salt had m.p. 235–240° (ethanol–ether).

Anal. Calcd. for $C_{15}H_{21}ClN_2O_3$: Cl, 11.33; N, 8.96. Found: Cl, 11.61; N, 9.15.

8-(3′-Chloropropionyl)-5,6-dimethoxy-2,3,7,8,9,9a-hexahydro-1-(p-toluenesulfonyl-1H-benzo[d,e-1,7]-naphthyridine (21)

To a refluxing solution of **18** (10.0 g) in 120 ml of benzene was added 3-chloropropionyl chloride (3.5 ml). After refluxing for 2 h, the solvent was evaporated *in vacuo* to give a semi-solid residue. Crystallization from methanol gave the product (7.7 g, 64%), m.p. 125–127°.

Anal. Calcd. for $C_{23}H_{27}ClN_2O_5S$: C, 57.53; H, 5.84; Cl, 7.47; N, 5.56. Found: C, 57.68; H, 5.69; Cl, 7.40; N, 5.85.

5,6-Dimethoxy-8-(3′-dimethylaminopropionyl)-2,3,7,8,9,9a-hexahydro-1-(p-toluenesulfonyl)-1H-benzo[d,e-1,7]naphthyridine (22)

Compound **21** (11.4 g) and dimethylamine (15 ml) were combined in 70 ml of ethanol and heated in a pressure bottle at 95° for 16 h. The alcohol was evaporated *in vacuo* and the residue was distributed between chloroform and dilute ammonium hydroxide. The organic phase afforded the product (10.0 g, 79%), m.p. 129–131° (ethyl acetate – hexane).

Anal. Calcd. for $C_{25}H_{33}N_3O_5S$: C, 61.49; H, 6.73; N, 8.52. Found: C, 61.58; H, 6.82; N, 8.62.

The hydrochloride salt had m.p. 190–192° (2-propanol).

Anal. Calcd. for $C_{25}H_{34}ClN_3O_5S$: Cl, 6.57; N, 7.69. Found: Cl, 6.77; N, 8.02.

5,6-Dimethoxy-8-(3′-dimethylaminopropyl)-2,3,7,8,9,9a-hexahydro-1H-benzo[d,e-1,7]naphthyridine (29)

Compound **22** (6.0 g) and lithium aluminum hydride (6.0 g) were combined in tetrahydrofuran (100 ml) and refluxed for 16 h. A conventional work-up procedure afforded the product (2.4 g, 56%) as a gum. It was converted to the trihydrochloride salt which was obtained as a monohydrate. It had m.p. 247–249°.

Anal. Calcd. for $C_{18}H_{34}Cl_3N_3O_3$: C, 48.46; H, 7.67; Cl, 23.80; N, 9.40. Found: C, 48.82; H, 7.66; Cl, 23.92; N, 9.39.

5,6-Dimethoxy-8-ethoxycarbonylmethyl-2,3,7,8,9,9a-hexahydro-1-(p-toluenesulfonyl)-1H-benzo-[d,e-1,7]naphthyridine (23)

A mixture of **18** (970 mg), ethyl bromoacetate (417.5 mg), potassium carbonate (1.0 g), and benzene (40 ml) were stirred vigorously and heated at 100° for 3 h. The mixture was filtered and the benzene evaporated *in vacuo* to leave an oil. Trituration with hexane gave the product (850 mg, 72%). It had m.p. 133–134° on crystallization from an ethyl acetate – hexane mixture.

Anal. Calcd. for $C_{24}H_{30}N_2O_6S$: C, 60.75; H, 6.37; N, 5.90. Found: C, 60.91; H, 6.12; N, 6.02.

5,6-Dimethoxy-1-(3,4-dimethoxy-β-phenethyl)-2,3,7,8,9,9a-hexahydro-8-methyl-1H-benzo-[d,e-1,7]naphthyridine (30)

Compound **25** (5.86 g), ethylene dichloride (40 ml), and aqueous sodium hydroxide (23.67 ml of 1 *N*) were combined and stirred vigorously while a solution of 3,4-dimethoxyphenylacetyl chloride (5.04 g) was added. The mixture was stirred at 22° for 2 h then the organic phase was separated, washed, dried, and evaporated to

afford *5,6-dimethoxy-1-(3,4-dimethoxyphenylacetyl)-2,3,7,8,9,9a-hexahydro-8-methyl-1H-benzo[d,e-1,7]naphthyridine* as a foam (10.0 g). It was homogeneous by t.l.c. but could not be obtained crystalline. It was reduced directly by refluxing with lithium aluminum hydride (9.0 g) in tetrahydrofuran (200 ml) for 16 h. A conventional work-up procedure afforded the product (6.3 g) as a semi-solid. The dihydrochloride salt was prepared and crystallized from a methanol–ether mixture. It had a m.p. in excess of 275°.

Anal. Calcd. for $C_{24}H_{34}Cl_2N_2O_4$: C, 59.39; H, 7.06; Cl, 14.61. Found: C, 59.69; H, 6.92; Cl, 14.88.

The author wishes to acknowledge the technical assistance of Messrs. R. Otson, P. Berchtold, and R. Thomas. Thanks are also due to Mrs. J. Jachner for i.r. and u.v. spectra.

1. R. D. HAWORTH. J. Chem. Soc. 2281 (1927).
2. W. M. WHALEY and T. R. GOVINDACHARI. *In* Organic reactions. Vol. 6. Wiley and Sons, New York, N.Y., 1951. p. 74.
3. H. R. SNYDER and F. X. WERBER. J. Amer. Chem. Soc. **72**, 2962 (1950).
4. Y. KANAOKA, E. SATO, O. YONEMITSU, and Y. BAN. Tetrahedron Lett. 2419 (1964).
5. O. HROMATKA, W. GRAF, and M. KNOCKMULLER. Monatsh. Chem. **97**, 28 (1966).
6. N. ITOH and S. SUGASAWA. Tetrahedron, **1**, 45 (1957).
7. D. H. HEY and J. M. WILLIAMS. J. Chem. Soc., 1527 (1951).
8. H. J. HARWOOD and T. B. JOHNSON. J. Amer. Chem. Soc. **55**, 4178 (1933).

Can. J. Chem. Downloaded from www.nrcresearchpress.com by 210.87.254.105 on 09/05/12
For personal use only.

Can. J. Chem. Downloaded from www.nrcresearchpress.com by 210.87.254.105 on 09/05/12
For personal use only.

Reaction of 9-Acetyl-2,3,4,4*a*-tetrahydrocarbazoles with Ozone: a Novel Oxidative Rearrangement[1]

STEWART MCLEAN AND U. O. TROTZ
Department of Chemistry, University of Toronto, Toronto 181, Ontario

Received August 11, 1970

When 4*a*-ethyl-2,3,4,4*a*-tetrahydrocarbazole or its 4*a*-bromoethyl analog reacted with ozone, only a small amount of material that corresponded to the anticipated ozonolysis product was obtained, the principal reaction pathway leading to a 4*a*-substituted 1-acetoxytetrahydrocarbazolenine, the product of an oxidative rearrangement.

La réaction de l'éthyl-4*a* (ou bromoéthyl-4*a*) tétrahydro-2,3,4,4*a* carbazole avec l'ozone fournit seulement des faibles quantités du produit d'ozonolyse attendu; la réaction principale conduit à un produit de réarrangement oxydant, l'acétoxy-1 tétrahydrocarbazolénine substitué en position 4*a*.

Canadian Journal of Chemistry, **49**, 863 (1971)

In connection with our studies of synthetic pathways to compounds containing the indole nucleus, we converted the tetrahydrocarbazolenines, **1***a* and *b* (1), to the 4*a*-substituted 9-acetyl-2,3,4,4*a*-tetrahydrocarbazoles, **2***a* and *b*, by treatment with acetic anhydride. These crystalline products were characterized by elemental analysis and spectroscopy, critical features of the latter being the appearance of an amide carbonyl (5.99 μ) in the i.r. and the signals for one vinyl proton and an aromatic proton adjacent to the *N*-acetyl group (2) in the n.m.r. spectra; the methyl signal of the 4*a*-substituent in **2***a* appeared at τ 9.38, providing evidence that it still experienced some shielding from the π system, but that this effect was not as pronounced as in the parent tetrahydrocarbazolenine, **1***a* (1).

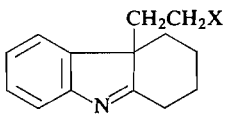

1

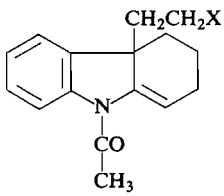

2

a X = H
b X = Br

It was our intention to convert the compounds of formula **2** to oxindoles of type **3** by ozonolysis, but in neither case was an oxindole the principal product of treatment of the tetrahydrocarbazole with ozone under a variety of conditions. When a solution of **2***a* or *b* in methanol at −78° was treated with ozonized oxygen under standard conditions followed by treatment of the reaction mixture with sodium iodide in acetic acid, t.l.c. of the product obtained showed that two components, one major and one minor, were present. In the case of **2***a*, the minor component was separated by chromatography and obtained as a white powder which melted in the range 88–92°. That this was the product, **3** (X = Y = Z = H), of ozonolysis and solvolysis of **2***a* is suggested on the following grounds: the molecular formula (from the high resolution mass spectrum) was $C_{14}H_{17}NO_2$, the i.r. spectrum included peaks at 2.90, 3.64, and 5.84 μ (broad and very strong suggesting that the two carbonyl peaks were superimposed), and the n.m.r. spectrum had signals at τ 0.70 and 0.90 (removed by D_2O) that could be associated with the CHO and NH protons, respectively. However, the spectra were not entirely characteristic of a single pure substance, and since the material resisted purification and conversion to useful derivatives, this component was not studied further. In the case of the reaction of ozone with **2***b*, there was some indication in the spectra of the crude product that the corresponding minor component was present, but it was not isolated in that series.

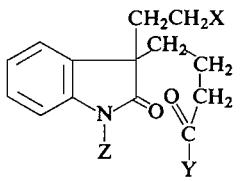

3

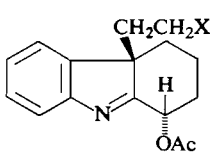

4

a X = H
b X = Br

[1] Taken from the Ph.D. Thesis of U. O. Trotz, University of Toronto, Toronto, Ontario, 1970.

Can. J. Chem. Downloaded from www.nrcresearchpress.com by 210.87.254.105 on 09/05/12
For personal use only.

The major component in both cases was an oxidative rearrangement product to which a structure corresponding to **4** has been assigned. Compound **2***a* afforded an 80% yield of **4***a*, m.p. 75–77°, $C_{16}H_{19}NO_2$, the u.v. spectrum of which was compatible with the presence in the molecule of the proposed tetrahydrocarbazolenine chromophore, and its i.r. spectrum showed an ester carbonyl absorption at 5.72 μ in place of the amide carbonyl of **2***a*, and a peak at 6.32 μ, indicative of the presence of ArN=C in the molecule (1). The n.m.r. spectrum was particularly informative, showing the signals for the four aromatic protons in the range τ 2.4–3.0, the methyl triplet of the 4*a*-substituent at τ 9.62, a position that has been found to be characteristic of 4*a*-ethyltetrahydrocarbazolenines (1), the acetyl methyl at τ 7.86, and the C*H*OAc proton as a four-line pattern centered at τ 4.50, the appearance of which was consistent with its being the X part of an ABX system with $|J_{AX} + J_{BX}| \sim 18$ Hz. The low τ value for this proton can be attributed to the presence of the adjacent C=N moiety and its multiplicity indicates that it is axial with one axial–axial and one axial–equatorial coupling to an adjacent CH_2 group. These observations consequently lead us to conclude that the compound has the structure and stereochemistry depicted by **4***a*. Hydrolysis converted **4***a* to the corresponding alcohol, the spectroscopic characteristics of which showed the presence of an OH group in place of the OAc group in the precursor, but were otherwise very similar to those of **4***a*. Catalytic hydrogenation of **4***a* in the presence of acetic anhydride converted it to an uncrystallizable viscous oil to which structure **5***a* is assigned. The u.v. spectrum is that of an *N*-acetylhexahydrocarbazole; the i.r. spectrum shows both carbonyl peaks, the ester at 5.74 μ and the amide at 6.01 μ, and the absence of the 6.3 μ band; the n.m.r. spectrum now has the methyl triplet of the 4*a* side chain at τ 9.26, the OAc singlet is at τ 7.80, and a three-proton singlet at τ 8.52 assigned, despite its high value indicative of unusual shielding, to the NAc protons. Two one-proton signals, a multiplet at τ 4.62 assigned to the C-1 proton, and a doublet with $J = 5$ Hz at τ 5.90 assigned to the C-9*a* proton, which could be decoupled by double irradiation, provide strong support for the structural assignments in **5***a*, and the value of the coupling constant is indicative of an axial–equatorial relationship between the protons and is in accord with the stereochemistry shown in **5***a*. This evidence provides confirmation for stereostructure **4***a* assigned to the ozonization product, and suggests that the catalytic hydrogenation has followed a path leading to the *cis*-fused hexahydrocarbazole, a stereochemical outcome we have recently demonstrated for certain other 4*a*-substituted tetrahydrocarbazolenines (1, 3).

In a completely analogous manner, **2***b* reacted with ozone to afford in 85% yield a product, m.p. 148–149°, $C_{16}H_{18}NO_2Br$, to which the structure **4***b* is assigned. The spectroscopic characteristics of **4***b* corresponded closely to those of **4***a*, all differences being just those expected on the basis of the difference in chemical constitution. Although attempted hydrolysis led only to an intractable oil, catalytic hydrogenation of **4***b* in acetic anhydride smoothly converted it to **5***b*, which bore the expected spectroscopic relationship to **5***a* except that the n.m.r. signal of the C-9*a* proton was very much broader, indicative of a difference in conformational mobility of **5***a* and *b*. One further feature of the n.m.r. spectrum of **5***b* was that the signal for the CH_2Br protons appeared at τ 6.88, while for its precursor **4***b*, in which the shielding effect already noted is expected, the corresponding signal was probably buried in the envelope of absorption at higher field.

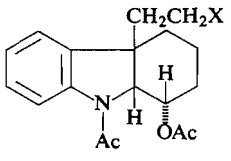

5

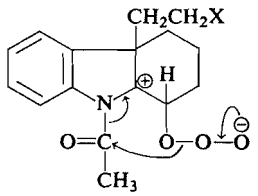

6

a X = H
b X = Br

The conversion of compounds **2** to **4** by ozone is an unusual reaction for which we can find no direct precedent. Although the details of the mechanism of the reaction of ozone with carbon–carbon double bonds are still a subject of some controversy and it is probable that no single mechanism is followed in all reactions (4), there is general agreement that an adduct, or molozonide, in which a carbon–carbon linkage is still intact is formed first, followed by a rearrangement to form an ozonide in which the two carbon atoms are no

Can. J. Chem. Downloaded from www.nrcresearchpress.com by 210.87.254.105 on 09/05/12
For personal use only.

longer directly bonded to each other. It is clear in the cases described here that the major product, **4**, is formed by a reaction that diverts the process before the ozonide is reached, and this is supported by the observations that much less than an equivalent of iodine was liberated in the reductive work-up of the reaction mixture and that **4** was also obtained in exploratory runs in which the work-up employed oxidative conditions. On the other hand, the minor product, **3**, appears to result from a process which incorporates the cleavage of the carbon–carbon linkage and the formation of an ozonide. (However, since there is no evidence bearing on the timing of the solvolysis that also occurs, it is still possible that this reaction does not follow the "ordinary" ozonolysis pathway.) Although a number of possible mechanisms can be suggested to account for the formation of **4**, the most economical description of the process in terms of present theories of the ozonization reaction is given in **6**.

NOTE ADDED IN PROOF

Professor S. Fliszár, to whom we extend our thanks for his interest and courtesy, has kindly pointed out to us that **2** represents a special case of a heavily substituted (and rigid) *cis* olefin, a class of compounds that he has demonstrated (5) follows an "abnormal" ozonolysis pathway, and he feels that an "abnormal" route (related to that which leads to epoxide formation) seems plausible in this case. A referee has pointed out that the reported rearrangement of the epoxide of an enamide to an α-acycloxyketone under hydrolytic conditions (6) may be a related reaction. (It may be noted, however, that the enamide underwent a normal ozonolysis.)

Experimental

Melting points were determined on a Thomas–Kofler micro hot stage. The i.r. spectra were obtained on a Perkin–Elmer 237B spectrometer, u.v. spectra on a Perkin–Elmer 350 or Unicam SP800 spectrometer with solutions in Fisher "Certified" methanol, and n.m.r. spectra on a Varian A60, T60, or HA100 spectrometer with tetramethylsilane as the internal standard in the solvent indicated. Only certain significant i.r. data are reported; n.m.r. chemical shifts are reported, followed in parentheses by an indication of the multiplicity and number of protons associated with each signal or group of signals. Mass spectrometric molecular weights were determined on an AEI MS-902 mass spectrometer.

9-Acetyl-4a-ethyl-2,3,4,4a-tetrahydrocarbazole (2a)

A solution of 4*a*-ethyltetrahydrocarbazolenine (**1***a*) (1) (2.90 g; 14.5 mmol) in 10 ml acetic anhydride under a nitrogen atmosphere was stirred at 100° for 2.5 h and then at room temperature for 14 h. The acetic anhydride was removed under reduced pressure and the residue was stirred with water and extracted with methylene chloride. The extract afforded an oil (2.97 g; 12.3 mmol), which was obtained as white crystals, m.p. 68–69°, on recrystallization from hexane.

Anal. Calcd. for $C_{16}H_{19}NO$: C, 79.63; H, 7.94; N, 5.80. Found: C, 79.61; H, 7.97; N, 6.11.

The i.r (CCl_4) 5.99, 6.21 μ; u.v. max (strong absorption < 220 mμ) 257 (ε 7600), 276 (infl.), 284 mμ (infl.); n.m.r. (τ, CCl_4, 60 MHz) 2.02 (d, J = 7 Hz, with further splitting, 1), 2.7–3.2 (m, 3), 4.65 (three peaks, splitting 3 Hz, 1), 7.70 (s, 3), 7.7–8.8 (complex, 8), 9.38 (t, J = 7.5 Hz, 3).

9-Acetyl-4a-(2'-bromoethyl)-2,3,4,4a-tetrahydrocarbazole (2b)

In a manner corresponding to that used for the preparation of **2***a*, **1***b* (630 mg; 2.3 mmol) was converted to **2***b* (712 mg; 2.2 mmol). The product, after recrystallization from a hexane–acetone mixture, was obtained as white crystals, m.p. 119–120°.

Anal. Calcd. for $C_{16}H_{18}NOBr$: C, 60.02; H, 5.66; N, 4.37; Br, 24.96. Found: C, 60.25; H, 5.66; N, 4.60; Br, 24.94.

The i.r. (CCl_4) 5.99, 6.23 μ; u.v. max (strong absorption < 220 mμ), 261 (ε 6500), 275 (infl.), 283 mμ (infl.); n.m.r. (τ, CCl_4, 60 MHz) 1.98 (d, J = 7.5 Hz with further splitting, 1), 2.7–3.2 (m, 3), 4.52 (three peaks, splitting 4 Hz, 1), 6.8–7.3 (m, 2), 7.68 (s, 3), 7.7–9.0 (complex, 8).

Ozonization of 2a

Ozonized oxygen (3–5% ozone) was passed through a solution of **2***a* (0.80 g; 3.3 mmol) in 75 ml methanol at −78° until the solution turned blue. After excess ozone had been removed by a stream of nitrogen, the reaction mixture was poured into a solution of sodium iodide (20 g) in 12.5 ml acetic acid and 38 ml methanol, shaken thoroughly, and allowed to reach room temperature. The iodine liberated was discharged by titration with sodium thiosulfate (the amount corresponded to 1.2 mmol), and the solution was diluted with a large volume of water and thoroughly extracted with methylene chloride. The extract afforded a yellow oil (1.05 g) which, after its behavior on t.l.c. had been checked, was chromatographed on a column of neutral alumina. The major fraction (**4***a*), eluted with 1:1 chloroform–ether, was obtained as crystals (665 mg; 2.6 mmol) which, after recrystallization from ether–hexane, had m.p. 75–77°.

Anal. Calcd. for $C_{16}H_{19}NO_2$: C, 74.68; H, 7.44; N, 5.44. Found: C, 74.89; H, 7.61; N, 5.51.

The i.r. (CCl_4) 5.72, 6.32 μ; u.v. max (strong absorption < 220 mμ), 225 (infl.), 258 mμ (ε 7700); n.m.r. (τ, $CDCl_3$, 100 MHz) 2.4–3.0 (complex, 4), 4.50 (four lines, X part of ABX with $|J_{AX} + J_{BX}| \sim 18$ Hz, 1), 7.5–9.2 (complex, 8), 7.86 (s, 3), 9.62 (t, J = 7.5 Hz, 3).

The minor fraction, a pale yellow oil (127 mg; 0.55 mmol) eluted by 4:1 chloroform–methanol, precipitated from hexane–chloroform as a white powder which melted in the range 88–92°, but could not be recrystallized; most of the data reported here are therefore only approximate. The mol. wt. determined from mass spectrum, 231.1265;

calcd. for $C_{14}H_{17}NO_2$, 231.1259; i.r. ($CHCl_3$) 2.90, 3.64, 5.84 (vs), 6.16 μ; u.v. max (strong absorption < 220 mμ), 250 (ε 8200), 278 mμ (ε 1800); n.m.r. (τ, CCl_4, 60 MHz) 0.70 (narrow m, 1), 0.90 (broad, removed by D_2O, 1), 2.8–3.2 (m, 4), 7.4–9.0 (complex, 8), 9.40 (t, J = 7 Hz, 3).

Ozonization of 2b

A methanolic solution of **2b** (1.5 g; 4.7 mmol) was ozonized in the manner just described. The crude product was a solid which showed t.l.c. evidence for the presence of a major component and a very small amount of a second component. Recrystallization from ether–hexane yielded the principal product (**4b**) (1.35 g; 4.0 mmol) as white needles, m.p. 148–149°.

Anal. Calcd. for $C_{16}H_{18}NO_2Br$: C, 57.16; H, 5.35; N, 4.17; Br, 23.79. Found: C, 56.92; H, 5.45; N, 4.15; Br, 23.91.

The i.r. (CCl_4) 5.72, 6.30 μ; u.v. max (strong absorption < 220 mμ), 225 (infl.), 258 mμ (ε 5400); n.m.r. (τ, $CDCl_3$, 100 MHz) 2.3–2.9 (complex, 4), 4.34 (four lines, X part of ABX with $|J_{AX} + J_{BX}| \sim 18$ Hz, 1), 7.0–9.0 (complex, 10), 7.80 (s, 3).

1-Hydroxy-4a-ethyltetrahydrocarbazolenine

A solution of **4a** (42 mg; 0.16 mmol) in 6 ml methanol containing 1 ml 2 *N* aqueous sodium hydroxide was stirred under nitrogen for 10 h. The reaction afforded a colorless oil (33 mg; 0.15 mmol) from which crystals, m.p. 84–88°, that were very sensitive to air or light were obtained. The mol. wt. determined from mass spectrum, 215.1306; calcd. for $C_{14}H_{17}NO$, 215.1310; i.r. ($CHCl_3$) 2.82, 6.30 μ; u.v. max (strong absorption < 220 mμ), 225 (infl.), 253 mμ (ε 7400); n.m.r. (τ, CCl_4, 60 MHz) 2.2–2.8 (complex, 4), 5.32 (four lines, X part of ABX with $|J_{AX} + J_{BX}| \sim 18$ Hz, 1), 5.71 (broad, removed by D_2O, 1), 7.2–9.1 (complex, 8), 9.63 (t, J = 8 Hz, 3).

1-Acetoxy-4a-ethyl-9-acetyl-1,2,3,4,4a,9a-hexahydrocarbazole (5a)

A solution of **4a** (24.5 mg; 0.095 mmol) in 1 ml acetic anhydride was hydrogenated at room temperature and atmospheric pressure in the presence of pre-reduced platinum oxide. After 10 h the reaction was complete and the solution afforded a colorless oil (27 mg; 0.09 mmol). The mol. wt. determined from mass spectrum, 301.1686; calcd. for $C_{18}H_{23}NO_3$, 301.1678; i.r. (CCl_4) 5.74, 6.01 μ; u.v. max (strong absorption < 220 mμ), 254 (ε 11 900), 278 (ε 3300), 286 mμ (ε 2900); n.m.r. (τ, CCl_4, 60 MHz) 2.3 (broad, 1), 2.8–3.2 (m, 3), 4.62 (m, 1), 5.90 (d, J = 5 Hz, 1) (τ 4.62 and 5.90 signals decoupled by double irradiation), 7.80 (s, 3), 7.8–8.8 (complex, 8), 8.52 (s, 3), 9.26 (t, J = 7 Hz, 3).

1-Acetoxy-4a-(2'-bromoethyl)-1,2,3,4,4a,9a-hexahydrocarbazole (5b)

A solution of **4b** (82 mg; 0.24 mmol) in acetic anhydride was hydrogenated in the manner just described. The product was isolated as a colorless oil (87 mg; 0.23 mmol). The mol. wt. determined from mass spectrum, 379.0765; calcd. for $C_{18}H_{22}NO_3Br$, 379.0784; i.r. (CCl_4) 5.74, 6.00 μ; u.v. max (strong absorption < 220 mμ), 254 (ε 12 700), 280 (ε 3000), 287 mμ (ε 2900); n.m.r. (τ, $CDCl_3$, 100 MHz) 2.2 (broad, 1), 2.6–3.0 (m, 3), 4.46 (m, 1), 5.6–6.3 (broad, 1), 6.88 (three lines, 8.5 Hz spacing, with further fine splitting, 2) 7.67 (s, 3), 7.7–8.8 (complex, 8), 8.48 (s, 3).

We thank the National Research Council of Canada for financial support of this research, and the Canadian Commonwealth Scholarship and Fellowship Committee for a Fellowship awarded to U.O.T.

1. S. McLean, A. L. Fallas, U. O. Trotz, and W. F. Reynolds. Can. J. Chem. **47**, 3647 (1969).
2. S. McLean. Can. J. Chem. **38**, 2278 (1960).
3. S. McLean, U. O. Trotz, J. K. Fawcett, K. S. Dichmann, and S. C. Nyburg. Tetrahedron Lett. 2645 (1970).
4. R. W. Murray. Accounts Chem. Res. **1**, 313 (1968).
5. S. Fliszár and J. Renard. Can. J. Chem. **48**, 3002 (1970).
6. J. Schmidt-Thomé and W. Fritsch. Ann. **662**, 27 (1963).

Can. J. Chem. Downloaded from www.nrcresearchpress.com by 210.87.254.105 on 09/05/12
For personal use only.

Can. J. Chem. Downloaded from www.nrcresearchpress.com by 210.87.254.105 on 09/05/12
For personal use only.

Reaction of *trans*-Chlorocarbonylbis(triphenylphosphine) Iridium(I) and its Analogues with Oxidizing Metal Salts

D. N. CASH AND R. O. HARRIS[1]

Scarborough College Chemical Laboratories, Department of Chemistry, University of Toronto, 1265 Military Trail, West Hill, Ontario

Received September 2, 1970

The effect of several oxidizing metal salts on the square planar iridium(I) complexes *trans*-$[Ir^{I}(CO)(PPh_3)_2X]$ (where $X^- = Cl^-$, Br^-, I^-, N_3^-, NCO^-, NCS^-, and NO_2^-) has been investigated. With nitrate salts of Ce(IV), Fe(III), and Cu(II), several of the reactions gave products characterized by analysis and i.r. spectroscopy as $[Ir^{III}(CO)(PPh_3)_2X(NO_3)_2]$. With $CuCl_2 \cdot 2H_2O$ and $CuBr_2$ several of the same starting materials gave products, $[Ir^{III}(CO)(PPh_3)_2XY_2]$ (where $X^- = NCO^-$, NCS^-, NO_2^- and $Y^- = Cl^-$; and $X^- = NCO^-$, NCS^-, Br^-, NO_2^- and $Y^- = Br^-$). These have been similarly characterized. An iridium(III) complex, $[Ir^{III}(PPh_3)_2(NO_3)_2H]$ has also been characterized.

L'effet de plusieurs sels métalliques oxydants sur les complexes plan carré $[Ir^{I}(CO)(PPh_3)_2X]$ *trans* (ou $X^- = Cl^-$, Br^-, I^-, N_3^-, NCO^-, NCS^-, et NO_2^-) a été étudié. Avec les nitrates de Ce(IV), Fe(III), et Cu(II), plusieurs de ces réactions ont conduit à des produits caractérisés par analyse et spectroscopie i.r. comme étant $[Ir^{III}(CO)(PPh_3)_2X(NO_3)_2]$. Avec le $CuCl_2 \cdot 2H_2O$ et $CuBr_2$ plusieurs des mêmes composés de départ ont fourni $[Ir^{III}(CO)(PPh_3)_2XY_2]$ (où $X^- = NCO^-$, NCS^-, NO_2^- et $Y^- = Cl^-$; et $X^- = NCO^-$, NCS^-, Br^-, NO_2^- et $Y^- = Br^-$). Ces derniers ont été caractérisés de la même manière. Un complexe d'iridium(III), $[Ir^{III}(PPh_3)_2(NO_3)_2H]$ a aussi été caractérisé.

Canadian Journal of Chemistry, 49, 867 (1971)

Introduction

Reactions of *trans*-chlorobis(triphenylphosphine) carbonyliridium(I) and its analogues have been discussed in some detail (*1*, *2a*). The reactions described here are very much like the oxidative addition reaction (eq. 1) which is characteristic of iridium(I) d^8-square planar compounds. However, in this case (eq. 2), oxidation is carried out by an oxidizing metal cation, with the ligand which is to enter the co-ordination sphere of the iridium already present in its ionic form.

Oxidative addition:

[1] $$[Ir^{I}(CO)P_2X] + Y_2 \rightarrow [Ir^{III}(CO)P_2XY_2]$$

Reaction under discussion:

[2] $$[Ir^{I}(CO)P_2X] + 2M^{n+}(Y)_n \rightarrow [Ir^{III}(CO)P_2XY_2] + 2M^{(n-1)+}(Y)_{n-1}$$

($P = PPh_3$ in all complexes)

In some cases, as when chlorine is the oxidizing agent, use of reaction 1 can lead to the decomposition or replacement of other ligands in the complex (*2b*); use of method 2 can avoid such complications. Also, as will be described, use of the latter method can introduce unusual ligands such as nitrate into the co-ordination sphere (eq. 3).

[3] $$[Ir^{I}(CO)P_2X] \xrightarrow[\text{acetone}]{M(NO_3)_n} [Ir^{III}(CO)P_2X(NO_3)_2]$$

These dinitrato species are not stable indefinitely in solution and, under some conditions, the decomposition products can be characterized. When the complex $[Ir^{III}(CO)P_2(NCO)(NO_3)_2]$ is left standing, in the open air and light, in a solution mixture of chloroform and ethanol, reaction 4 occurs.

[4] $$[Ir^{III}(CO)P_2(NCO)(NO_3)_2] \xrightarrow[\text{Several days}]{CHCl_3/EtOH} [Ir^{III}P_2(NO_3)_2H]$$

Results and Discussion

Infrared Spectroscopy

The compounds reported have been characterized mainly by analysis and i.r. spectroscopy. The latter can be discussed, for the purposes required here, in four sections.

(i) Co-ordinated Nitrato Ligand

The vibrational absorptions characteristic of a co-ordinated nitrate ion are understood on the basis of a lowering of the D_{3h} symmetry of the free ion to C_{2v} (or lower) symmetry when co-ordination through one or more of the oxygen

[1]Author to whom communications should be directed.

TABLE 1. Reaction of $[Ir(CO)(PPh_3)_2X]$ with metal nitrate salts, in acetone at room temperature*

Compound X^- in $[Ir(CO)(PPh_3)_2X]$	Nitrate salt		
	$(NH_4)_2Ce^{IV}(NO_3)_6$	$Fe^{III}(NO_3)_3 \cdot 9H_2O$	$Cu^{II}(NO_3)_2 \cdot 3H_2O$
Cl^-	CO lost	CO retained	CO retained
Br^-	CO lost	CO retained	CO retained
I^-	CO lost	CO retained	CO retained
NCO^-	CO, NCO^- retained	CO, NCO^- retained	CO, NCO^- retained
N_3^-	CO, N_3^- retained	CO, N_3^- retained	CO, N_3^- retained
NCS^-	CO, NCS^- retained	CO, NCS^- retained	CO, NCS^- retained
NO_2^-	No product obtained	Some CO retained, NO_2^- lost	Some CO retained, NO_2^- lost

*Notes:
(*i*) Absorptions due to triphenylphosphine indicated that this ligand was retained in each reaction (6).
(*ii*) In each case that it was observed, the position of ν_{CO}, the carbonyl stretching mode, indicated that oxidation to Ir(III) had occurred.
(*iii*) In each case, modes due to coordinated nitrato ligand were observed (3).

atoms occurs (3). Absorption in the regions ~1500, ~1250, ~950, and ~800 cm^{-1} indicates a co-ordinated rather than an ionic nitrate group. However, it is impossible, without reference compounds, to deduce the mode of co-ordination from the band positions (4). Moreover, since the observed spectra are all those of solid state mulls, correlation coupling effects may be observed (5). For this reason, no deductions about *cis* or *trans* stereochemistry for the nitrato ligands can be made. This restriction also applies to the dichloro and dibromo complexes described below.

(ii) Carbonyl Ligand

Co-ordinated carbon monoxide exhibits well known i.r. absorptions, in both the C—O stretching region, and the M—C—O bending and M—C stretching region. The C—O stretch is often taken as being characteristic of the oxidation state of the iridium in a given compound ranging from ~1950 cm^{-1} in iridium(I) to ~2080 cm^{-1} in iridium(III) complexes.

(iii) Triphenylphosphine Ligand

The vibrational spectrum of this ligand, both free and complexed, has been assigned (6), and can be separated from the absorptions due to other ligands in these complexes.

(iv) Other Ligands

The ligands isocyanate (NCO^-) (7), azide (N_3^-) (8), thiocyanate (NCS^-) (9), and nitrite (NO_2^-) (10) all exhibit characteristic frequencies in the i.r., depending on whether, and in what manner, they are co-ordinated to a metal. In each case, an asymmetric and symmetric stretching mode, and a bending mode may be observed, along with a metal-ligand mode. In the case of halide as ligand, only the latter metal-halide mode is expected.

Reactions with Nitrate Salts

The products obtained when $[Ir^I(CO)P_2X]$ (where $X^- = Cl^-$, Br^-, I^-, NCO^-, N_3^-, NCS^-, and NO_2^-) was reacted with the nitrate salts of several oxidizing metal cations are described in Table 1. In each case, the solid complex was added to a solution or slurry of excess salt in acetone at room temperature. The product was obtained by adding several volumes of water, filtering off, and drying with ethanol and ether, and then examined by running a Nujol mull i.r. spectrum of the solid. The position of the carbonyl absorption was taken (if present) as an indication of the oxidation state of the metal. Similarly the modes due to triphenylphosphine, nitrato, and other ligands could also be observed.

Some features of the results deserve comment. None of the products recovered when X^- was NO_2^- contained any nitro modes in the i.r. spectrum; in the case of Ce(IV) ion oxidation, no product could be recovered because of the formation of an emulsion. In Ce(IV) oxidation, when $X^- = Cl^-$, Br^-, or I^-, carbon monoxide was clearly absent from the products. This was true even when these reactions were repeated at acetone/carbon dioxide bath temperatures. In the case of $X^- = I^-$, although an apparently satisfactory product was obtained by reaction with Fe(III) or Cu(II) nitrates, in fact it proved impossible to reprecipitate an analytically acceptable sample of the desired $[Ir(CO)(PPh_3)_2I(NO_3)_2]$ from these reactions. Whether some loss of carbon monoxide or some other side

Can. J. Chem. Downloaded from www.nrcresearchpress.com by 210.87.254.105 on 09/05/12
For personal use only.

TABLE 2. Analysis results

Compound	Color	Elemental composition									
		Calculated (%)					Found (%)				
		C	H	N	Cl	Br	C	H	N	Cl	Br
$[Ir(CO)(PPh_3)_2Cl(NO_3)_2]\cdot 1\frac{1}{2}(CHCl_3)$	White	42.6	2.9	2.6	18.0		42.1	3.1	2.5	17.3	
$[Ir(CO)(PPh_3)_2Br(NO_3)_2]$	Yellow	46.8	3.2	3.0		8.4	46.9	3.2	2.7		7.6
$[Ir(CO)(PPh_3)_2(NCO)(NO_3)_2]\cdot(CH_2Cl_2)$	White	47.0	3.2	4.2			47.2	3.2	4.1		
$[Ir(CO)(PPh_3)_2(NCS)(NO_3)_2]$	White	49.2	3.2	4.5			50.3	3.4	4.5		
$[Ir(CO)(PPh_3)_2N_3(NO_3)_2]$	Brown	48.8	3.3	7.7			49.0	3.6	7.9		
$[Ir(CO)(PPh_3)_2(NCO)Cl_2]$	Yellow	53.2	3.5	1.6	8.3		52.6	3.8	1.2	9.0	
$[Ir(CO)(PPh_3)_2(NCO)Br_2]$	Yellow	48.2	3.2	1.5		16.9	48.1	3.3	1.3		17.4
$[Ir(CO)(PPh_3)_2(NCS)Cl_2]$	Yellow	52.2	3.4	1.6	8.1		51.4	3.5	1.6	9.0	
$[Ir(CO)(PPh_3)_2(NCS)Br_2]$	Yellow	47.4	3.1	1.5		16.6	46.5	3.3	1.3		15.8
$[Ir(CO)(PPh_3)_2(NO_2)Cl_2]$	Yellow	51.5	3.5	1.6	8.2		51.0	3.8	1.3	9.3	
$[Ir(CO)(PPh_3)_2(NO_2)Br_2]$	Yellow	46.7	3.2	1.5		16.8	46.4	3.4	1.3		17.0
$[Ir(CO)(PPh_3)_2Br_3]$	Yellow	45.1	3.1			24.4	44.4	3.1			23.1
$[Ir(PPh_3)_2(NO_3)_2H]$	Yellow	51.4	3.7	3.3			51.5	3.8	3.6		
$[Ir(CO)(PPh_3)_2(NO_2)]$	Yellow	56.2	3.8	1.8			55.7	4.0	1.7		

reaction occurs during the oxidation, or the desired product is unstable in solution, is not known.

The products, $[Ir^{(III)}(CO)P_2X(NO_3)_2]$ (where $X^- = Cl^-$, Br^-, NCO^-, N_3^-, NCS^-) are all sparingly soluble in solvents such as benzene, chloroform, or dichloromethane, and insoluble in ethanol, ether, or pentane. They can be reprecipitated from suitable solvent combinations, with the solids so formed giving the analytical results shown in Table 2. The solid state Nujol mull i.r. spectra are described in Table 3. None of these compounds is sufficiently soluble in chloroform ($<0.005\ M$) to give a reliable molecular weight.

From Table 3 it will be seen that all these compounds exhibit the i.r. absorptions characteristic of co-ordinated nitrato-ligand. In these compounds bands are seen at ~1520 (strong to very strong), ~1280 (strong to very strong), ~970 (medium), and ~780 cm^{-1} (weak). The relative intensities of these bands to each other are essentially the same in all the compounds, but the splitting patterns do vary; the weak but sharp absorption at ~780 cm^{-1} is unsplit in each.

A compound of formula $[Ir^{III}(CO)P_2Cl(NO_3)_2]$ has been reported (11) as the product of reacting $[Ir^{I}(CO)P_2Cl]$ with nitric acid in tetrahydrofuran. This material, however, has a reported i.r. spectrum which is not the same as that reported here. This difference is not due to the fact that the compound reported here is a chloroform solvate, since a recrystallization from benzene solution with ether gave a non-solvated product in extremely low yield, which gave satisfactory analysis, and showed virtually identical i.r. absorptions as the solvated product, including the sharp mode at ~780 cm^{-1}.

Reactions with Cu(II) Halides

To demonstrate the general use of this reaction, the dichloro and dibromo adducts of several iridium(I) species were prepared (eq. 5).

$$[5]\qquad [Ir^{I}(CO)P_2X] \xrightarrow[\text{acetone}]{CuY_2} [Ir^{III}(CO)P_2XY_2]$$

$$X^- = NCO^-, NCS^-, NO_2^-;\ Y^- = Cl^-, Br^-$$

In addition, since it has been reported that the addition of bromine to $[Ir^{I}(CO)P_2Br]$ does not proceed simply in chloroform (12), an addition was carried out using $CuBr_2$ in acetone (eq. 6)

$$[6]\qquad [Ir^{I}(CO)P_2Br] \xrightarrow[\text{acetone}]{CuBr_2} [Ir^{III}(CO)P_2Br_3]$$

The products of all these reactions are described in Tables 2 and 3.

The carbonyl stretching frequency of the complex $[Ir^{III}(CO)(PPh_3)_2Br_3]$ observed here (2076 cm^{-1}, very strong, sharp) is in agreement with that previously reported (12), but in this case no absorptions due to impurities or by-products are observed.

Hydridodinitratobis(triphenylphosphine)-iridium(III)

This compound, of formula $[Ir^{III}(PPh_3)_2(NO_3)_2H]$, was first prepared accidentally. A sample of the compound $[Ir^{III}(CO)(PPh_3)_2$-

Can. J. Chem. Downloaded from www.nrcresearchpress.com by 210.87.254.105 on 09/05/12
For personal use only.

Can. J. Chem. Downloaded from www.nrcresearchpress.com by 210.87.254.105 on 09/05/12
For personal use only.

$(NCO)(NO_3)_2$] had been prepared by precipitation from dichloromethane with ether and the solid was found to contain a molecule of solvent (dichloromethane) in the crystal. In order to carry out a proposed molecular weight in chloroform, a reprecipitation from chloroform with ethanol was attempted. The solution stood at room temperature for several days, during which time it became progressively more yellow in color, and pale yellow crystals began to deposit. This solid was found to have quite different properties from the starting material, which is white. The analytical details and i.r. spectrum are given in Tables 2 and 3. The compound is diamagnetic (Gouy Method), and a molecular weight (M) determination in chloroform ($\sim$0.01 M) gave $M = 840 \pm 20$.

The analytical results suggest an empirical formula $[Ir(PPh_3)_2(NO_3)_2]$ ($M = 840$), and this is confirmed by the molecular weight results. However, since the material is diamagnetic, and exhibits a weak but definite i.r. absorption at $\sim$2270 cm^{-1}, the formula $[Ir^{III}(PPh_3)_2(NO_3)_2H]$ has been assigned. The position of the Ir—H stretching mode is in agreement with the previously reported complexes of formulae $[Ir^{III}(PPh_3)_2Br_2H]$ (13) and $[Ir^{III}(PPh_3)_2Cl_2H]$ (14) which are at 2250 and 2242 cm^{-1} respectively. Unfortunately, the solubility of this compound ($\sim$0.02 M in $CDCl_3$) is insufficient to allow the observation of a high-field metal hydride resonance in the n.m.r. (attempted on a Varian T60).

The absence of any carbonyl or isocyanate modes in the i.r., where they would normally be very intense, is indicative that both these ligands have been lost during the reaction. The nature of the reaction route is unclear, though it has been shown that the same procedure without ethanol (or methanol) present gives other, less easily characterized products.

TABLE 3. The i.r. spectra. Observed absorptions of Nujol mulls (cm^{-1})*

Compound	Nitrato modes	Carbonyl modes	Other modes[a]
$[Ir(CO)(PPh_3)_2Cl(NO_3)_2]\cdot 1\frac{1}{2}(CHCl_3)$	1524 vvs, sp 1280, 1263 vs, sp 964 (sh 978) s, sp 783 w, sp	2079 vs, sp[b] 2041 w, sp* 571 m, sp[c]	345 m, m br[d]
$[Ir(CO)(PPh_3)_2Br(NO_3)_2]$	1526 vs, m br 1280, 1262 vs, m br 975, 961 s, sp 782 w, sp	2076 vs, sp[b] 2052, 2042, 2028 w, sp* 570 m, 568 m w, 547 w, sp*,[c]	328 vw, br[e]
$[Ir(CO)(PPh_3)_2(NCO)(NO_3)_2]\cdot(CH_2Cl_2)$	1522, 1505 vs, sp 1272, 1258 vs, sp 975, 959 s, sp 787 w, sp	2075 vs, sp[b] 559 m, 568 mw, sp*,[c]	2273 vvs, br[f] 1361 m, sp[g] 596, 587 w, sp[e] 307 m, br[e]
$[Ir(CO)(PPh_3)_2(NCS)(NO_3)_2]$	1523 (sh 1515) vs, sp 1276, 1261 vs, sp 973, 964 s, sp 786 w, sp	2083 vvs, sp[b] 566, 556 m, sp*,[c]	2110 vvs, sp[h] 873 w, sp[c] 310 w, m br[e]
$[Ir(CO)(PPh_3)_2N_3(NO_3)_2]$	1523, 1508 vs, sp 1280, 1260 vs, sp 990 (sh 983) s, sp 785 w, sp	2075[j] 555 m, 585 vw, sp*,[c]	2060–2075 vvs, br[j] 306 m, br[e]
$[Ir(CO)(PPh_3)_2(NCO)Cl_2]$		2053 vvs, sp[b] 586 m, 578 m, 564 w, sp*,[c]	2265 vvs, sp[f] 1365 m, sp[g] 331 ms, sp[d]
$[Ir(CO)(PPh_3)_2(NCO)Br_2]$		2086 s, 2078 s, 2051 vs, sp*,[b] 590 m, 573 m, 560 w, sp*,[c]	2263, 2249 vvs, sp*,[f] 1364, 1352 m, sp*,[g] 252 w, sp[e]
$[Ir(CO)(PPh_3)_2(NCS)Cl_2]$		2052 vvs, sp[b] 575 m, sp[c]	2110 vvs, sp[h] 871 w, sp[i] 332 ms, sp[d]
$[Ir(CO)(PPh_3)_2(NCS)Br_2]$		2090 vs, br[k] 571, 559 m, sp*,[c]	2090 vs, br[k] 858 m, sp[i] 254 w, sp[e]

TABLE 3. (*Concluded*)

Compound	Nitrato modes	Carbonyl modes	Other modes[a]
$[Ir(CO)(PPh_3)_2(NO_2)Cl_2]$		2074 vs, 2064 s, 2052 ms, 2028 w, sp*,[b] 568 w, 559 w, 549 w, sp*,[c]	1413 s, sp[f] 1338, 1323 ms, sp[f] 826 m, sp[f] 615 m, br[e] 342 (sh 329)*,[d]
$[Ir(CO)(PPh_3)_2(NO_2)Br_2]$		2089 vs, 2084 s, 2073 s, 2059 m, sp*,[b] 546 m, br[c]	1402 ms, sp[f] 1336 m, 1311 ms, sp[f] 823 m, sp[f] 605 w, br[e]
$[Ir(CO)(PPh_3)_2Br_3]$		2076 vs, sp 2020 w, sp*,[b] 555 m, 540 m, sp*,[c]	243 w, sp[e]
$[Ir(PPh_3)_2(NO_3)_2H]$	1554 s, sp 1527 vvs, sp 1276 vs, sp 973 m, 955 m, sp 777 w, 769 w, sp		2274 w, 2259 w, m sp[m] 346 w, sp[e]
$[Ir(CO)(PPh_3)_2(NO_2)]$		1980 vvs, sp[b] 1957 m, sp*,[b] 1932 w, sp*,[b] 630 m, sp[c]	1375 vs, sp[f] 1338 s, sp[f] 815 m, sp[f]

*Indicates that observed splittings may be due to the presence of more than one isomer and/or solid state effects. Notes:
(*i*) v, very; w, weak; m, medium; s, strong; br, broad; sp, sharp; sh, shoulder.
(*ii*) All spectra were recorded as Nujol mulls of the solids, employing polyethylene, KBr, or KRS-5 plates, or some combination to obtain the range 200–2500 cm^{-1}.
[a]Absorptions due to ligand triphenylphosphine are present in each compound, and are omitted from this table (6).
[b]Carbonyl stretching modes, νCO.
[c]Carbonyl bending modes, δMCO (17).
[d]Iridium–chlorine stretching modes, νIr–Cl.
[e]Unassigned modes.
[f]Asymmetric isocyanate stretching modes, ν_3NCO.
[g]Symmetric isocyanate stretching modes, ν_1NCO.
[h]Asymmetric thiocyanate stretching modes, ν_3NCS.
[i]Symmetric thiocyanate stretching modes, ν_1NCS; the observed absorptions are characteristic of N-bonded thiocyanate (9).
[j]The absorption is an overlapping of νCO and the asymmetric stretching mode, ν_3N_3, of the azido ligand (8).
[k]The absorption is an overlapping of νCO and the asymmetric stretching mode, ν_3NCS, of the thiocyanate.
[l]These are modes due to N-bonded nitrite ligand (10).
[m]Iridium–hydride stretching modes, νIr–H.

The pattern of the nitrato modes, and the splitting of the mode at 770 cm^{-1} suggest that there may be more than one type of nitrate co-ordination with one mono- and one bidentate nitrate group. However, based only on a solid mull spectrum, this is speculation. It will be noted that this compound is much less reactive than $[Ir^{III}(PPh_3)_2Cl_2H]$ (14), and this might be rationalized if the molecule was indeed six co-ordinate, since the co-ordinately saturated iridium would then be much less reactive. In fact, $[Ir^{III}(PPh_3)_2(NO_3)_2H]$ is not reactive to $CHCl_3$, EtOH, CCl_4, or PPh_3; it does interact with CO, to give an as yet uncharacterized product.

Experimental

All reagents and solvents were reagent or solvent grade used as supplied. The i.r. spectra were recorded on a Beckman I.R. 12 spectrophotometer. The molecular weight measurement was made with a Hewlett-Packard Mechrolab 302 osmometer, in chloroform solution. Analyses were by A. Gygli of Toronto, and Huffman Laboratories of Colorado.

trans-[Ir^I(CO)(PPh$_3$)$_2$Cl]

This material was prepared by a standard method (15) from a variety of chloroiridium complexes. The material was then used without recrystallization.

trans-[Ir^I(CO)(PPh$_3$)$_2$Br]

This was prepared by a standard route (15), from $K_2[Ir^{IV}Br_6]$.

trans-[Ir^I(CO)(PPh$_3$)$_2$X] (X$^-$ = NCO$^-$, N$_3^-$, NCS$^-$)

These were all prepared from *trans*-$[Ir^I(CO)(PPh_3)_2Cl]$ through exchange of the chloride ligand with the ligand X^-. The $[Ir^I(CO)(PPh_3)_2Cl]$ and a 100-fold excess of the sodium or potassium salt of the ligand X^- were refluxed in acetone (10 ml per 0.1 g of Ir(I) complex). After 15 min, the solution was cooled by diluting with several volumes of water. A yellow solid product rapidly separated, was filtered off, washed well with water, ethanol, and ether, and dried under vacuum, yield: up to 100%. The products have i.r. spectra in agreement with those from previously reported preparations.[2]

[2]For X = NCO and NCS see ref. 16*a*; for X = NCS, N_3, and I see ref. 16*b*.

Can. J. Chem. Downloaded from www.nrcresearchpress.com by 210.87.254.105 on 09/05/12
For personal use only.

Can. J. Chem. Downloaded from www.nrcresearchpress.com by 210.87.254.105 on 09/05/12
For personal use only.

trans-[Ir^{I}(CO)(PPh$_3$)$_2$I]

This was prepared exactly as above, from [Ir^{I}(CO)(PPh$_3$)$_2$Cl] and KI, but the procedure was carried out under nitrogen until the product had separated out. The solid is air stable, and has i.r. absorption in agreement with those from previous preparations.[2]

trans-[Ir(CO)(PPh$_3$)$_2$NO$_2$]

This was prepared by the reaction of [Ir^{I}(CO)(PPh$_3$)$_2$Cl] (0.3 g) and KNO_2 (5 g) in acetone (600 ml). The acetone was degassed by boiling under nitrogen prior to adding the solid reagents. The solids were then added and the solution was refluxed under nitrogen for 1 h, when water (1200 ml) was added to precipitate the product. The water had previously been degassed by boiling under nitrogen. The yellow solid is stable in air, but is extremely oxygen sensitive in solution. The bright yellow product was washed with water, ethanol and ether, and dried under vacuum, yield ~95%.

The analytical and i.r. spectral details for the compound are given in Tables 2 and 3. The absorptions at 1375, 1338, and 815 cm^{-1} indicate an *N*-bonded nitrite (nitro) group (10).

[Ir^{III}(CO)(PPh$_3$)$_2$Cl(NO$_3$)$_2$] · 1½(CHCl$_3$)

The [Ir^{I}(CO)(PPh$_3$)$_2$Cl] (0.25 g) was added with excess solid $Cu(NO_3)_2 \cdot 3H_2O$ (0.5 g) to acetone (20 ml) at room temperature, and the resulting green slurry was stirred for 5 min, during which time it became blue. The solvent was removed under vacuum. The product was extracted with three portions of chloroform (8 ml each), and the resulting solution filtered several times. This pale yellow solution was then slowly diluted with several volumes of *n*-pentane, giving fine white fibrous crystals over several days, which were filtered off and dried under vacuum, yield 0.20 g.

[Ir^{III}(CO)(PPh$_3$)$_2$Br(NO$_3$)$_2$]

The [Ir^{I}(CO)(PPh$_3$)$_2$Br] (0.21 g) was added with excess $Cu(NO_3)_2 \cdot 3H_2O$ (0.5 g) to acetone (20 ml) at room temperature and the initially green slurry stirred for several minutes, during which time it became blue. This slurry was then diluted to 115 ml with water, and after some minutes the resulting yellow solid was filtered from the pale blue solution, and washed with water, ethanol, and ether. The solid was then dissolved in chloroform, and the resulting solution (bright yellow, 10 ml) filtered. This solution was diluted to 200 ml with ether, and after several hours the resulting pale yellow powder was filtered off, washed with ether, and dried under vacuum, yield 0.069 g.

[Ir^{III}(CO)(PPh$_3$)$_2$(NCO)(NO$_3$)$_2$] · (CH$_2$Cl$_2$)

The [Ir^{I}(CO)(PPh$_3$)$_2$NCO] (0.30 g) was added to a stirring solution of $(NH_4)_2Ce^{IV}(NO_3)_6$ (0.8 g) in acetone (20 ml) at room temperature. The solid rapidly dissolved in the orange solution, and addition of water (80 ml) gave a white product. The solid was filtered off, washed with water, ethanol, and ether, and dried. The crude product was reprecipitated by dissolving in a minimum of dichloromethane, in which it is sparingly soluble, filtering, and adding several volumes of ether. The solid rapidly separated as white needles, which were filtered off and washed with ether, and dried in vacuum, yield ~0.15 g.

[Ir^{III}(CO)(PPh$_3$)$_2$(NCS)(NO$_3$)$_2$]

This is prepared exactly as the isocyanate complex above, but crystallizes as a white solid with no CH_2Cl_2 in the crystal, yield ~40%.

[Ir^{III}(CO)(PPh$_3$)$_2$N$_3$(NO$_3$)$_2$]

The [Ir^{I}(CO)(PPh$_3$)$_2$N$_3$] (0.39 g) was stirred with $Fe^{III}(NO_3)_3 \cdot 9H_2O$ (0.5 g) in acetone (20 ml) at room temperature for several minutes. Then the slurry was diluted to 100 ml with water. A brownish solid was filtered off and washed with water, ethanol, and ether. The crude solid was reprecipitated after dissolving in a minimum of dichloromethane, filtering, and adding several volumes of ether. The product, a silky, pale brown solid, separated rapidly and was collected and washed with ether, and dried in vacuum, yield 0.22 g.

[Ir^{III}(CO)(PPh$_3$)$_2$(NCO)Cl$_2$]

The [Ir^{I}(CO)(PPh$_3$)$_2$NCO] (0.11 g) was added as a solid to $CuCl_2 \cdot 2H_2O$ (0.3 g) stirring in acetone (15 ml) at room temperature. After some 10 min, the slurry was diluted to 40 ml with water. The resulting white solid was filtered from the blue solution and washed with water, ethanol, and ether. This crude product was reprecipitated from chloroform (10 ml) after filtration of the solution and addition of methanol (30 ml). The product, a yellow powder, separated over several hours at −5 °C, yield 0.050 g.

[Ir^{III}(CO)(PPh$_3$)$_2$(NCO)Br$_2$]

The [Ir^{I}(CO)(PPh$_3$)$_2$NCO] (0.11 g) was reacted with $CuBr_2$ (0.3 g) exactly as in the preceding preparation. The crude product was reprecipitated from chloroform (10 ml) by filtration of the bright yellow solution, followed by addition of methanol (35 ml). The bright yellow solid separated rapidly, yield 0.080 g.

[Ir^{III}(CO)(PPh$_3$)$_2$(NCS)Cl$_2$]

The [Ir^{I}(CO)(PPh$_3$)$_2$NCS] (0.15 g) was reacted with $CuCl_2 \cdot 2H_2O$ (0.4 g) as above. The crude product was reprecipitated from chloroform (8 ml) by filtration of the pale yellow–green solution, followed by addition of methanol (35 ml). The product pale yellow solid separated over several hours at −5 °C, yield 0.11 g.

[Ir^{III}(CO)(PPh$_3$)$_2$(NCS)Br$_2$]

The [Ir^{I}(CO)(PPh$_3$)$_2$NCS] (0.11 g) was reacted with $CuBr_2$ (0.3 g) as above. The crude product was reprecipitated from chloroform (10 ml) by filtration of the bright yellow solution and addition of methanol (35 ml). The product, a bright yellow solid, separated rapidly, yield 0.10 g.

[Ir^{III}(CO)(PPh$_3$)$_2$(NO$_2$)Cl$_2$]

The [Ir^{I}(CO)(PPh$_3$)$_2$(NO$_2$)] (0.128 g) was reacted with $CuCl_2 \cdot 2H_2O$ (0.3 g) as above. The product was reprecipitated from dichloromethane solution (20 ml, brownish yellow) with methanol (80 ml). The product, a pale yellow solid, separated rapidly, yield 0.070 g.

[Ir^{III}(CO)(PPh$_3$)$_2$(NO$_2$)Br$_2$]

The [Ir^{I}(CO)(PPh$_3$)$_2$(NO$_2$)] (0.156 g) was reacted with $CuBr_2$ (0.3 g) exactly as above. The product was repre-

cipitated from chloroform (35 ml, bright yellow solution) with methanol (85 ml). The product, a bright yellow solid, separated within minutes, yield 0.065 g.

[$Ir^{III}(CO)(PPh_3)_2Br_3$]

The [$Ir^{I}(CO)(PPh_3)_2Br$] (0.13 g) was reacted with $CuBr_2$ (0.3 g) as above. The crude product is very sparingly soluble in chloroform (100 ml), from which it was reprecipitated after filtration by the addition of ether (300 ml). The product, a bright yellow solid, was collected after several hours at −5 °C, yield 0.052 g.

[$Ir^{III}(PPh_3)_2(NO_3)_2H$]

The [$Ir^{III}(CO)(PPh_3)_2NCO(NO_3)_2$] · ($CH_2Cl_2$) (0.3 g, prepared as above) was dissolved in chloroform (20 ml) and the pale yellow solution was filtered. Ethanol (25 ml) was added, and the resulting solution left at room temperature in a stoppered flask, in air and light. After 2 days, the solution became more brightly yellow and yellow crystals were deposited. When no further solid was formed, the solution was diluted with ethanol, to 150 ml total volume. After another day, the product yellow solid, mostly powder, was filtered off, yield 0.125 g.

The authors wish to thank the National Research Council of Canada for support of this work, and for a bursary to D. N. C. in 1968–1969. Thanks are also due the Province of Ontario for fellowships to D. N. C. in 1967–1968, 1969–1971.

1. L. Malatesta. Some recent aspects of iridium chemistry. Alfred Werner Commemorative Volume. Helv. Chim. Acta, 1967.
2. (*a*) J. P. Collman and W. R. Roper. Advances in organometallic Chemistry. *Edited by* F. G. A. Stone and R. West. Vol. 7. Academic Press, New York, N.Y., 1968. Chapt. 2; (*b*) p. 60.
3. K. Nakamoto. Infra-red spectra of inorganic and co-ordination compounds. John Wiley and Sons, New York, N.Y., 1963. p. 161.
4. G. Topping. Spectrochim Acta, **21**, 1965, 1743. N. G. Curtis and Y. M. Curtis. Inorg. Chem. **4**, 804 (1965).
5. R. S. Halford. J. Chem. Phys. **14**, 8 (1946). I. R. Beattie and T. R. Gilson. Proc. Roy. Soc. (London), Ser. A, **307**, 407 (1968).
6. G. B. Deacon and J. H. S. Green, Spectrochim Acta, **24A**, 845 (1968).
7. J. S. Thayer and R. West. Advances in organometallic chemistry. *Edited by* F. G. A. Stone and R. West. Academic Press, New York, N.Y., 1967. Chapt. 4.
8. A. D. Joffe. Advances in inorganic nitrogen chemistry. *Edited by* C. B. Colburn, Elsevier, Amsterdam, 1966. Chapt. 2.
9. L. Nakamoto. Infra-red spectra of inorganic and co-ordination compounds. John Wiley and Sons, New York, N.Y., 1963. p. 173.
10. L. Nakamoto. Infra-red spectra of inorganic and co-ordination compounds. John Wiley and Sons, New York, N.Y., 1963. p. 151. F. Basolo and G. S. Hammaker. J. Amer. Chem. Soc. **82**, 1001 (1960); Inorg. Chem. **1**, 1 (1962).
11. H. Singer and G. Wilkinson. J. Chem. Soc. A. 2516 (1968).
12. M. A. Bennett, R. J. H. Clark, and D. L. Milner. Inorg. Chem. **6**, 1967, 1647.
13. A. P. Ginsberg. Transition metal chemistry. Vol. 1. *Edited by* R. L. Carlin. Marcel Dekker, New York, N.Y., 1965, Chapt. 3. p. 136, and references therein.
14. J. Chatt, R. L. Richards, J. R. Sanders, and J. E. Fergusson. Nature, **221**, 551 (1969). D. M. Blake and M. Kubota. J. Amer. Chem. Soc. **92**, 2578 (1970).
15. Inorganic syntheses. Vol. XI. McGraw-Hill, New York, N.Y., 1968. p. 101.
16. (*a*) W. H. Baddley. J. Amer. Chem. Soc. **90**, 3705 (1968). (*b*) J. Chatt, D. P. Melville, and R. L. Richards. J. Chem. Soc. A, 2841 (1969).
17. D. M. Adam. Metal-ligand and related vibrations. Edward Arnold, London, 1967. pp. 94 ff.

Can. J. Chem. Downloaded from www.nrcresearchpress.com by 210.87.254.105 on 09/05/12
For personal use only.

Can. J. Chem. Downloaded from www.nrcresearchpress.com by 210.87.254.40 on 09/05/12
For personal use only.

Thermal and Photochemical Ring Expansion of Some Phosphole Derivatives

A. N. HUGHES AND CHIT SRIVANAVIT
Department of Chemistry, Lakehead University, Thunder Bay, Ontario

Received August 28, 1970

Pyrolysis and photolysis of 3,4,5-triphenyl-4-phosphabicyclo[3.1.0]hex-2-ene-4-oxide and the 1:1 adduct of diazomethane with 1,2,5-triphenylphosphole oxide lead to the formation of compounds of formula $C_{46}H_{36}O_2P_2$ and $C_{46}H_{34}O_2P_2$, respectively. These compounds are shown to be derivatives of the 4,4′-diphosphabi(cyclohexa-1,5-dienyl) and 4,4′-diphosphabi(cyclohexa-2,5-dienylidene) systems, respectively, and possible mechanisms for the formation of these systems are briefly discussed.

La pyrolyse et la photolyse du triphényl-3,4,5 phospha-4 bicyclo[3.1.0]hexène-2 oxyde-4 et du produit d'addition 1:1 du diazométhane avec l'oxyde du triphényl-1,2,5 phosphole conduisent respectivement à la formation de composés de formule $C_{46}H_{36}O_2P_2$ et $C_{46}H_{34}O_2P_2$. Il est démontré que ces composés sont respectivement des dérivés des systèmes du diphospha-4,4′ bis(cyclohexadienyl-2,5) et du diphospha-4,4′ bis(cyclohexadienylydène-2,5). Les mécanismes possibles pour la formation de ces systèmes sont discutés brièvement.

Canadian Journal of Chemistry, 49, 874 (1971)

Unsaturated six-membered ring phosphorus heterocycles, particularly the phosphorins, have received considerable attention recently, and several synthetic routes to these systems have been developed (1). It is well known that pyrrole derivatives will undergo ring expansion reactions to give pyridine derivatives, sometimes in good yield. For example, pyrrole on treatment with methylene chloride and methyl lithium gives pyridine in 32% yield (2). In principle then, phosphole (**1**) derivatives should also undergo ring expansion reactions although not necessarily by the same mechanistic path as for pyrrole derivatives. Indeed, certain 9-phosphafluorene (dibenzophosphole) derivatives have already been shown to undergo ring expansion on treatment with methyl propiolate in the presence of water (3) or with methylene iodide followed by alkaline hydrolysis (4). There is, however, only one report of the ring expansion of a simple phosphole derivative (5). In this reaction, treatment of 1,2,5-triphenylphosphole oxide (**2**) with methyl diazoacetate in boiling dioxan leads to the formation of the phosphacyclohexa-2,5-diene derivative **3** (R = Me). The same workers showed that reaction of the phosphole oxide **2** with diazomethane followed by treatment of the intermediate pyrazolino derivative **4** with copper in boiling diglyme leads to the formation of 3,4,5-triphenyl-4-phosphabicyclo[3.1.0]hex-2-ene-4-oxide (**5**) which could possibly be a convenient starting material for ring expansion reactions of the phosphole system. Moreover, it was observed (5) that this compound resolidifies above its m.p. to give a dark red compound which was not further investigated. The following is therefore an account of the thermal and photochemical ring expansion reactions of **4** and **5**.

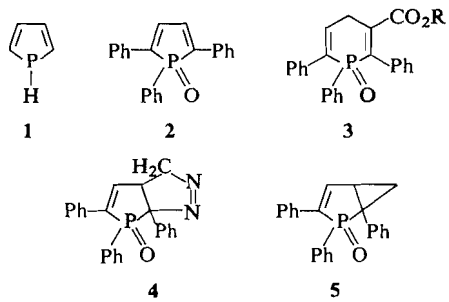

1 **2** **3** **4** **5**

The cyclopropano derivative **5** was carefully pyrolyzed in a Woods metal bath at 238° until gas evolution ceased and the material turned dark brown and resolidified. The crude product was recrystallized from a chloroform/ethanol mixture and a good yield of a deep orange compound, m.p. 386–387°, was obtained. Pyrolysis of **5** under vacuum gives a slightly higher yield of the same compound. The high m.p. and very low solubility of the pyrolysis product indicate a higher molecular weight than the starting material. Elemental analyses are consistent with a formula of $C_{46}H_{38}O_2P_2$, $C_{46}H_{36}O_2P_2$, or $C_{46}H_{34}O_2P_2$, *i.e.* a dimer of the starting material, a dimer minus H_2, or a dimer minus $2H_2$, although trimeric structures cannot be entirely ruled out. Because of the highly involatile nature of the product, its mol. wt. could not be determined by mass spectrometry. However, pyrolysis of **5** under high vacuum ($< 4 \times 10^{-7}$ Torr) followed by mass spectrometric analysis of the gas evolved showed

Can. J. Chem. Downloaded from www.nrcresearchpress.com by 210.87.254.40 on 09/05/12
For personal use only.

that hydrogen is given off in substantial amounts during the reaction and that water is not a significant product. This suggests that thermal dimerization of **5** occurs with elimination of hydrogen and, therefore, the molecular formula $C_{46}H_{38}O_2P_2$ can be tentatively ruled out.

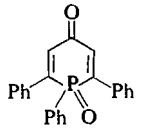

6

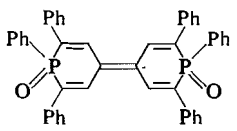

7

A compound of molecular formula $C_{46}H_{34}O_2P_2$ having two unsaturated phosphorus-containing six-membered rings has previously been prepared (6) by treatment of 1,2,6-triphenyl-1-phosphacyclohexa-2,5-diene-4-one-1-oxide (**6**) with triethylphosphite to give 3,3′,4,4′,5,5′-hexaphenyl-4,4′-diphosphabi(cyclohexa-2,5-dienylidene)-4,4′-dioxide (**7**). This compound melts at 425–428° and shows λ_{max} at 324.5 and 437 mμ. It is therefore not identical with the pyrolysis product of **5** which shows in ethanol λ_{max} (log ε) at 315 (483) and 408 mμ (4.87). Furthermore, the i.r. spectrum (Nujol) of the pyrolysis product shows a typical P=O stretching band at 1180 cm^{-1} and the n.m.r. spectrum (in trifluoroacetic acid) shows a ratio of 17 aromatic and olefinic protons (complex multiplet at τ 2.01–3.13) to one tertiary proton (very broad unresolved hump at τ 6.11). The n.m.r. evidence then is consistent with the formula $C_{46}H_{36}O_2P_2$.

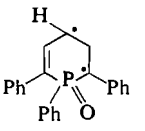

8

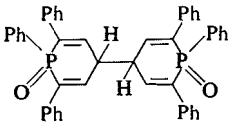

9

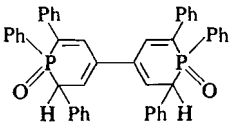

10

A number of modes of reaction are open to the cyclopropane **5** on pyrolysis. For example, the vinylcyclopropane → cyclopentene type of rearrangement (7) could possibly occur although this seems unlikely in this case since the products would contain little conjugation. A more likely mode of reaction is one in which one of the three bonds of the cyclopropane ring (probably the bond forming the ring junction) is cleaved to give a diradical such as **8** which dimerizes and eliminates molecular hydrogen to give **9** or **10**. However, since mechanistic studies were not undertaken, a dipolar mechanism cannot be ruled out. Clearly structure **9** may be discarded because there would be insufficient conjugation to account for the u.v. spectrum although this structure is consistent with the n.m.r. spectrum. Moreover, the related structure **3** is colorless (5). Cleavage of the other bonds of the cyclopropane ring followed by dimerization and elimination of hydrogen would again give products containing too little conjugation to account for the u.v. spectrum. Thus, it seems that structure **10** is the most likely structure for the pyrolysis product since it fits all the evidence available at this point.

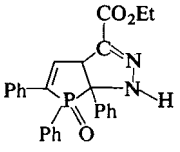

11

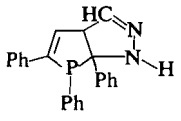

12

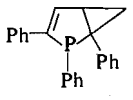

13

The same compound is obtained in good yield (60%) by pyrolysis of **4** under vacuum at 238° although pyrolysis of the related compound **11** yields only the phosphacyclohexadiene **3** (R = Et) in excellent yield (75%). Reduction of **4** and **5** with trichlorosilane in dry benzene (8) gives the corresponding tertiary phosphines **12** and **13** respectively in good yield (60 and 73% respectively) but pyrolysis of these phosphines only gives general decomposition and no ring expanded products could be isolated. It should also be noted that in the reduction of **4** to **12**, a prototropic shift occurs to give the 2-pyrazoline structure rather than the 1-pyrazoline structure which is present in **4**. Evidence for this comes from the fact that in the i.r. spectrum of **12** there is a strong N—H stretching absorption at 3280 cm^{-1} which is not present in the i.r. spectrum of **4**. The prototropic shift is not unexpected since the reduction of **4** is carried out under acidic conditions and it is known (9) that 1-pyrazolines isomerize under these conditions to give the corresponding 2-pyrazolines.

Irradiation of the cyclopropane **5** in dry, peroxide-free tetrahydrofuran under dry, oxygen-free nitrogen with a medium pressure mercury

Can. J. Chem. Downloaded from www.nrcresearchpress.com by 210.87.254.40 on 09/05/12
For personal use only.

lamp (100 W) through pyrex for 8 days gives a 44% yield of a deep orange compound (m.p. 439–440°) similar, but not identical, to the pyrolysis product. Irradiation of the pyrazoline **4** under similar conditions gives a 14% yield of the same compound.

Elemental analyses of the photolysis product are in excellent agreement with the formula $C_{46}H_{34}O_2P_2$. The u.v. spectrum shows λ_{max}(log ε) at 325 (4.53) and 438 mμ (4.91) which confirms extensive conjugation in the molecule. The i.r. spectrum shows a typical P=O stretching vibration at 1169 cm^{-1} and the n.m.r. spectrum (in trifluoroacetic acid) shows only aromatic and olefinic protons as a complex multiplet at τ 2.22–2.96. The m.p. of the photolysis product is very similar to that of Märkl's compound **7** (6) and the n.m.r. spectrum is in good agreement with this structure. The u.v. spectrum is virtually identical with that of compound **7** (although Märkl does not quote values for the extinction coefficients) and it therefore appears that the photolysis product has structure **7**.

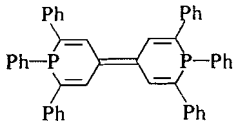

14

Confirmation of this structure is provided by the fact that it may be reduced to the corresponding phosphine **14** by treatment first with phosphorus pentachloride to give an unisolated deep red *P,P,P',P'*-tetrachloro compound which is reduced smoothly to **14** with lithium aluminum hydride as briefly outlined by Märkl (6). The sample of **14** isolated is identical (m.p. and u.v. spectrum) with that described by Märkl (6) and the molecular weight was confirmed as 648 by mass spectrometry.

The mechanism of formation of the photolysis product **7** is again uncertain although it is probable that an intermediate such as **8** is involved. However, both further pyrolysis at 380° under vacuum of the initial pyrolysis product **10** and irradiation of the same compound in dry, peroxide-free tetrahydrofuran under nitrogen for several days leave the material unchanged and it therefore seems likely that **10** is not an intermediate in the formation of **7**. Since the irradiation of **5** occurs over a very long period of time, ring enlargement to a phosphacyclohexadiene of type **3** (without the CO_2R group) followed by photo-oxidation by trace amounts of oxygen to give **6** which condenses with unoxidized material to give **7** cannot be excluded. However, both pyrolysis and irradiation of the phosphacyclohexadiene **3** (R = Et) under conditions very similar to those used for **5** for extended periods result in virtually complete recovery of the starting material and the intermediacy of **6** and its phosphacyclohexadiene precursor in the photolysis of **5** therefore seems unlikely.

Irradiation of **12** and **13** under similar conditions gives only some general decomposition and recovery of some starting material.

Turning again to the pyrolysis product tentatively assumed to be **10**, treatment of this compound with a large excess of phosphorus pentachloride followed by reduction of the intermediate deep-red *P,P,P',P'*-tetrachloro compound with lithium aluminum hydride gives the 4,4'-diphosphabi(cyclohexa-2,5-dienylidene) system **14** identical in all respects with an authentic sample. This, then, confirms the basic skeleton of the pyrolysis product. Final confirmation of the ring structure of the compound assigned structure **10** comes from the fact that on treatment with ethereal lithium aluminum hydride alone, it is transformed into the photolysis product **7** in good yield. A similar reaction occurs between the pyrolysis product and sodium hydride in benzene. The mechanisms of these last two reactions are obscure but, in view of all the foregoing evidence, the structures of the pyrolysis and photolysis products of **4** and **5** are established as **10** and **7** respectively.

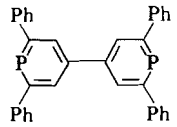

15

Compounds of type **14** (with the P—Ph grouping replaced by the P—CH_2Ph grouping) have recently been found (10) to be converted into the previously unknown biphosphorinyl system **15** on heating and it is possible that pyrolysis or irradiation of compounds such as **12** or **13**, in which the P—Ph grouping is similarly replaced by the P—CH_2Ph grouping, could lead directly to the biphosphorinyl system.

Attempts to prepare other compounds of type

Can. J. Chem. Downloaded from www.nrcresearchpress.com by 210.87.254.40 on 09/05/12
For personal use only.

5 by addition of dichlorocarbene or dibromocarbene to **2** were unsuccessful.

Experimental

The i.r. spectra were recorded in Nujol mulls using a Beckman IR12 spectrophotometer while u.v. spectra were obtained on dilute ethanol or chloroform solutions using a Unicam SP800 spectrophotometer. The n.m.r. measurements were made with a Varian Associates model A60-A spectrometer using deuteriochloroform or trifluoroacetic acid solutions with tetramethylsilane as internal reference. Mass spectra were determined using an Hitachi–Perkin–Elmer model RMU-7 double focussing mass spectrometer fitted with a direct heated inlet system. Melting points are uncorrected and were recorded using a Mel-Temp high-temperature m.p. apparatus.

Ether was dried by distillation from sodium or lithium aluminum hydride while tetrahydrofuran and benzene were dried by distillation from calcium hydride.

1,2,5 - Triphenylphosphole, 1,2,5 - triphenylphosphole oxide (**2**), the phosphacyclohexadiene **3** (R = Et), 3,4,5-triphenyl-4-phosphabicyclo[3.1.0]hex-2-ene-4-oxide (**5**), and the pyrazolines **4** and **11** were prepared by the method of Campbell (5).

*Reduction of **4** and **5** with Trichlorosilane*

A solution of the pyrazoline **4** (4.0 g, 10.82 mmol) in dry benzene (200 ml) was treated with a large excess of trichlorosilane (15 g, 110.5 mmol) and the mixture was heated under reflux in a slow stream of dry nitrogen for 48 h. With ice-bath cooling and vigorous stirring, the reaction mixture was then treated slowly with water (100 ml) until evolution of hydrogen chloride ceased. The mixture was filtered and the benzene layer was separated and washed with water (3 × 50 ml) as was the residue in the funnel. All of the washings were added to the acidic aqueous layer. The aqueous solution was neutralized with dilute aqueous sodium hydroxide, saturated with sodium chloride, and extracted with chloroform (3 × 50 ml). The chloroform extracts were combined, dried over anhydrous sodium sulfate, and evaporated to dryness under reduced pressure. The crude solid was recrystallized from hot ethanol to give long colorless needles (2.3 g, 60%) of the pyrazoline **12**, m.p. 211–212° (dec.).

Anal. Calcd. for $C_{23}H_{19}N_2P$: C, 77.95; H, 5.36; N, 7.91; P, 8.77. Found: C, 77.67; H, 5.46; N, 8.04; P, 8.54.

The i.r. spectrum shows ν_{max} at 3280, 1596, 1490, 1443, 1431, 1329, 1300, 1201, 1119, 1084, 1065, 1040, 1024, 1019, 998, 946, 910, 899, 880, 850, 814, 758, 740, and 690 cm^{-1}. The u.v. spectrum in absolute ethanol shows λ_{max} at 224 and 250 mμ and the n.m.r. spectrum ($CDCl_3$) shows 16 aromatic and olefinic protons at τ 2.32–3.06, one amino proton at 3.39, and two methine protons at 4.47. The mass spectrum shows a strong molecular ion peak at *m/e* 354.

3,4,5-Triphenyl-4-phosphabicyclo[3.1.0]hex-2-ene-4-oxide (**5**) (5.0 g, 14.62 mmol) was reduced in a similar manner with trichlorosilane (20 g, 147.7 mmol) to give the bicyclic phosphine **13** (3.5 g, 73%) as colorless needles, m.p. 134–135° (dec.).

Anal. Calcd. for $C_{23}H_{19}P$: C, 84.63; H, 5.84; P, 9.53. Found: C, 84.71; H, 5.94; P, 9.38.

The i.r. spectrum shows ν_{max} at 1601, 1580, 1495, 1445, 1432, 1304, 1269, 1095, 1088, 1072, 1022, 1000, 935, 911, 902, 871, 851, 828, 760, 751, 698, and 688 cm^{-1}. The u.v. spectrum in absolute ethanol shows λ_{max} (log ε) at 214.5 (4.50) and 267 mμ (4.24). The n.m.r. spectrum ($CDCl_3$) shows a ratio of 16 aromatic and olefinic protons (complex multiplet at τ 2.43–3.12) to one methine proton (multiplet centered at τ 7.32) to two methylene protons (multiplet centered at τ 8.82). The mass spectrum shows a very strong molecular ion peak at *m/e* 326.

Pyrolysis of 3,4,5-Triphenyl-4-phosphabicyclo[3.1.0]hex-2-ene-4-oxide (5)

A pure sample of the cyclopropane **5** (1 g, 2.92 mmol) was carefully pyrolyzed in a Woods metal bath at 238° until gas evolution ceased and the material turned dark brown and resolidified. The crude product was washed with ether followed by ethanol and the reddish-yellow solid left was recrystallized from a hot chloroform/ethanol mixture to give orange crystals (0.47 g, 47%) of 3,3′,4,4′,5,5′-hexaphenyl-4-4′-diphosphabi(cyclohexa-1,5-dienyl)-4,4′-dioxide (**10**), m.p. 386–387° (dec.).

Anal. Calcd. for $C_{46}H_{36}O_2P_2$: C, 80.91; H, 5.28; P, 9.08. Found: C, 80.46; H, 5.33; P, 9.34.

The i.r. spectrum shows ν_{max} at 3062, 2862, 1606, 1500, 1465, 1442, 1352, 1180, 1117, 1079, 1041, 900, 770, 754, 703, 670 cm^{-1}. The u.v. spectrum in chloroform shows λ_{max} (log ε) at 315 (4.83) and 408 mμ (4.87) and the n.m.r. spectrum in trifluoroacetic acid shows a ratio of 17 aromatic and olefinic protons (complex multiplet at τ 2.01–3.13) to one tertiary proton (very broad unresolved hump centered at τ 6.11).

The experiment was repeated on the same quantity of material at the same temperature in an evacuated (< 4 × 10^{-7} Torr) small cylindrical tube fitted with a high vacuum tap to which was attached a 10/30 ℧ glass cone such that the reaction tube could be connected directly to the liquid inlet of the mass spectrometer. A yield of 51% of **10** was obtained and mass spectral analysis of the gas evolved showed a ten-fold increase in the intensity of the H_2 peak over the background but no significant increase in the water peak.

*Pyrolysis of the Pyrazoline **4***

The pyrazoline (1 g, 2.7 mmol) was carefully pyrolyzed under vacuum (*ca.* 1 Torr) in a Woods metal bath at 238° until gas evolution ceased and the dark brown material resolidified. The crude product was worked-up as before to give orange crystals of the pyrolysis product **10** (0.55 g, 60%).

*Pyrolysis of the Pyrazoline Ester **11***

The pyrazoline ester (2.0 g, 4.53 mmol) in an evacuated (*ca.* 1 Torr) tube was pyrolyzed at 220–225° in a Woods metal bath for 20 min. The crude product was washed with a little ether and the off-white solid left was recrystallized from a benzene/light petroleum (60°–80°) mixture to give colorless needles (1.4 g, 75%) of ethyl 1,2,6-triphenyl-1-phosphacyclohexa-2,5-diene-3-carboxylate-1-oxide (**3**, R = Et), m.p. 217–218°, identical in all respects (m.p., i.r., n.m.r., mass spectrum) with a sample prepared by Campbell's method (5).

Photolysis of 3,4,5-Triphenyl-4-phosphabicyclo[3.1.0]hex-2-ene-4-oxide (5)

A solution of the cyclopropane **5** (3 g, 8.76 mmol) in

Can. J. Chem. Downloaded from www.nrcresearchpress.com by 210.87.254.40 on 09/05/12
For personal use only.

dry, peroxide-free tetrahydrofuran (1000 ml) was irradiated under dry, oxygen-free nitrogen with a medium pressure mercury lamp (100 Watt) through pyrex for 8 days. After evaporation of the mixture to dryness, the crude solid was digested with ethanol to remove starting material and the residue was recrystallized from a hot chloroform/ethanol mixture to give orange crystals (1.3 g, 44%) of 3,3′,4,4′,5,5′-hexaphenyl-4,4′-diphosphabi(cyclohexa-2,5-dienylidene)-4,4′-dioxide (**7**), m.p. 436–438° (lit. (6) m.p. 425–428°).

Anal. Calcd. for $C_{46}H_{34}O_2P_2$: C, 80.90; H, 4.98; P, 9.06. Found: C, 80.64; H, 4.90; P, 9.45.

The i.r. spectrum shows ν_{max} at 1604, 1490, 1463, 1443, 1336, 1245, 1169, 1106, 1075, 1066, 1031, 937, 887, 771, 750, 698 cm^{-1}. The u.v. spectrum in chloroform shows λ_{max} (log ε) at 325 (4.53) and 438 mμ (4.91) and the n.m.r. spectrum in trifluoroacetic acid shows only aromatic and olefinic protons as a complex multiplet at τ 2.22–2.86.

Irradiation of the pyrazoline **4** (8 g, 21.65 mmol) under very similar conditions gave the same product (1.0 g, 14%).

*Reduction of the Photolysis (**7**) and Pyrolysis (**10**) Products with Phosphorus Pentachloride and Lithium Aluminum Hydride*

The photolysis product **7** (0.1 g, 0.15 mmol) was fused with a large excess of phosphorus pentachloride (3 g, 14.51 mmol) at 120–130° until the mixture turned deep red (1 h). The excess of phosphorus pentachloride was removed by sublimation at 100° under vacuum. With Dry Ice/acetone cooling, the resulting deep red powder was treated dropwise with saturated ethereal lithium aluminum hydride under dry nitrogen until gas evolution ceased and the mixture was allowed to warm slowly to room temperature. The excess of hydride was decomposed with water-saturated ether, water (100 ml) was then added, and the ether removed under vacuum. The resulting aqueous suspension was extracted with chloroform (3 × 10 ml) and the chloroform extracts were combined and dried over anhydrous sodium sulfate. The chloroform solution was then evaporated to dryness and the crude solid was washed with ethanol and recrystallized from a hot chloroform/ethanol mixture to give red crystals (0.07 g, 74%) of 3,3′,4,4′,5,5′-hexaphenyl-4,4′-diphosphabi(cyclohexa-2,5-dienylidene) (**14**), m.p. 338–340° (lit. (6) m.p. 335–337°).

Anal. Calcd. for $C_{46}H_{34}P_2$: C, 85.18; H, 5.24; P, 9.57. Found: C, 84.37; H, 5.32; P, 9.50.

Good analyses are difficult to obtain since the compound crystallizes with up to 4% occluded chloroform which is very difficult to remove. Pumping the compound at 180–200° under high vacuum leads to slow loss of the chloroform but, even under vacuum, oxygen scavenging also takes place and slow oxidation of **14** occurs.

The i.r. spectrum shows ν_{max} at 3075, 1618, 1500, 1446, 1438, 1369, 1350, 1250, 1100, 1041, 941, 922, 889, 861, 776, 767, 749, 718, 700, and 694 cm^{-1}, *i.e.* the P=O bond present in the spectrum of **7** at 1169 cm^{-1} has vanished. The u.v. spectrum in chloroform shows λ_{max} (log ε) at 339 (3.88) and 468 mμ (4.64) (lit.(6) λ_{max} 337 and 467 mμ). The n.m.r. spectrum in trifluoroacetic acid shows only aromatic and olefinic protons as a complex multiplet at τ 2.18–2.87. The mass spectrum shows a molecular weight of 648.

Reduction of the pyrolysis product **10** (0.5 g, 0.73 mmol) with phosphorus pentachloride (15 g, 72.55 mmol) and lithium aluminum hydride under very similar conditions also gave **14** (0.4 g, 84%).

As stated by Märkl (6) the phosphine **14** is air stable but with traces of acid it oxidizes back to **7** very rapidly.

*Treatment of the Pyrolysis Product **10** with Lithium Aluminum Hydride*

With cooling (Dry Ice/acetone) and vigorous stirring, a suspension of the pyrolysis product **10** (0.6 g, 0.88 mmol) in dry ether (60 ml) was treated dropwise with a solution of lithium aluminum hydride (0.34 g, 8.82 mmol) in dry ether under dry nitrogen. The temperature of the reaction mixture was allowed to rise to room temperature and the mixture was maintained at this temperature for a further 15 min. Destruction of the excess hydride was carried out with water saturated ether. Water (60 ml) was added and the mixture was evaporated until ether-free. The resulting aqueous suspension was extracted with chloroform (3 × 60 ml). The chloroform extracts were combined, dried over anhydrous sodium sulfate, and evaporated to dryness. The crude solid was washed with ethanol and recrystallized from a hot chloroform/ethanol mixture to give orange crystals (0.55 g, 92%) of 3,3′,4,4′,5,5′-hexaphenyl-4,4′-diphosphabi(cyclohexa-2,5-dienylidene)-4,4′-dioxide (the photolysis product **7**) identical in all respects with an authentic sample.

The same reaction occurs with sodium hydride.

We thank the National Research Council of Canada and the Ontario Department of University Affairs for generous financial support.

1. See for example the review by K. D. Berlin and D. M. Hellwege. Topics in Phosphorus Chemistry, **6**, 1 (1969).
2. G. L. Closs and G. M. Schwarz. J. Org. Chem. **26**, 2609 (1961).
3. E. M. Richards and J. C. Tebby. Chem. Commun. 957 (1967).
4. D. W. Allen and I. T. Millar. Chem. and Ind. 2178 (1967); J. Chem. Soc. (C), 252 (1969).
5. I. G. M. Campbell, R. C. Cookson, M. B. Hocking, and A. N. Hughes. J. Chem. Soc. 2184 (1965).
6. G. Märkl and H. Olbrich. Angew. Chem. Intern. Ed. **5**, 589 (1966).
7. C. G. Overberger and A. E. Borchert. J. Amer. Chem. Soc. **82**, 4896 (1960).
8. L. D. Quin, J. G. Bryson, and C. G. Moreland. J. Amer. Chem. Soc. **91**, 3308 (1969).
9. C. G. Overberger and J. P. Anselme. J. Amer. Chem. Soc. **84**, 869 (1962).
10. G. Märkl, D. E. Fischer, and H. Olbrich. Tetrahedron Lett. 645 (1970).

Can. J. Chem. Downloaded from www.nrcresearchpress.com by 210.87.254.6 on 09/05/12
For personal use only.

Alkaline Hydrolysis of 1-Iodomethyl-1,2,5-triphenylphospholium Iodide, a New Route to the 4-Phosphabicyclo[3.1.0]hex-2-ene System

A. N. Hughes and Chit Srivanavit
Department of Chemistry, Lakehead University, Thunder Bay, Ontario

Received September 25, 1970

Alkaline hydrolysis of 1-iodomethyl-1,2,5-triphenylphospholium iodide gives 3,4,5-triphenyl-4-phosphabicyclo[3.1.0]hex-2-ene-4-oxide in very high yield. Three possible mechanisms are discussed and isolation of a key intermediate allows one of these mechanisms to be discarded. Alkaline hydrolysis of 1-allyl-1,2,5-triphenylphospholium bromide in methanol gives 1,2,5-triphenylphosphole and small quantities of a compound $C_{26}H_{27}O_2P$ which is an adduct of the original phospholium ion, hydroxide ion, and methanol.

L'hydrolyse alcaline de l'iodure de l'iodométhyl-1 triphényl-1,2,5 phospholium donne le triphényl-3,4,5 phospha-4 bicyclo[3.1.0]hexène-2 oxyde-4 avec un excellent rendement. Trois mécanismes possibles sont discutés; un de ceux-ci peut toutefois être rejeté en se basant sur le fait qu'un intermédiaire important a pu être isolé. L'hydrolyse alcaline du bromure d'allyl-1 triphényl-1,2,5 phospholium dans le méthanol donne le triphényl-1,2,5 phosphole et de petites quantités d'un composé en $C_{26}H_{27}O_2P$ qui est un produit d'addition de l'ion phospholium original avec l'ion hydroxyle et le méthanol.

Canadian Journal of Chemistry, 49, 879 (1971)

Ring expansion reactions of the phosphole system have been comparatively little explored as possible routes to six-membered unsaturated phosphorus heterocycles (1–4). One approach, due to Millar (3), involves the reaction of 9-phenyl-9-phosphafluorene (the dibenzophosphole **1**) with methylene iodide to give the salt **2** which on treatment with hydroxide ion gives **3** (in very good yield) by cleavage of the phosphole ring in the manner observed by Bergesen (5) followed by attack of the resulting carbanion (which migrates from the apical position of a trigonal bipyramidal intermediate (3)) upon the methylene group and displacement of iodide ion. This type of 1,2-migration has been shown to be fairly general in the hydrolysis of suitably substituted phosphonium compounds and similar ring expansions occur in the phosphetan system (6).

Simple phospholes are now relatively easily available (7) and the above reaction applied to simple phospholes could prove to be a convenient route to phosphorins, particularly those with unsymmetrical substitution patterns. In order to explore this possibility, 1,2,5-triphenylphosphole (**4**) was treated with methylene iodide in a pressure bottle for $4\frac{1}{2}$ days to give an excellent yield of the corresponding phospholium iodide **5**. Alkaline hydrolysis of **5** was expected to give the phosphacyclohexa-2,4-diene **6** since the five-membered ring should occupy an apical–equatorial arrangement in the expected trigonal bipyramidal intermediate (6) but, rather surprisingly, a 74% yield of 3,4,5-triphenyl-4-phosphabicyclo[3.1.0]hex-2-ene-4-oxide (**7**) (identical with an authentic sample (1)) was obtained when **5** was treated with aqueous methanolic sodium hydroxide for 24 h under reflux followed by acidification of the reaction mixture. This bicyclic compound has recently been shown (4) to be of value in the synthesis of six-membered ring phosphorus heterocycles.

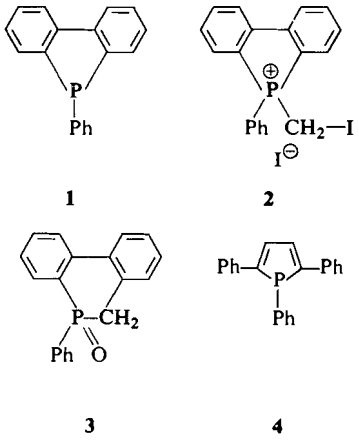

1 **2** **3** **4**

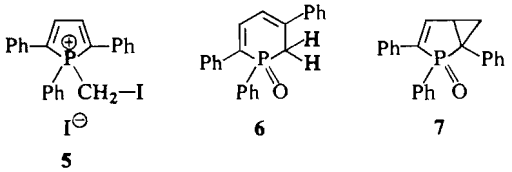

5 **6** **7**

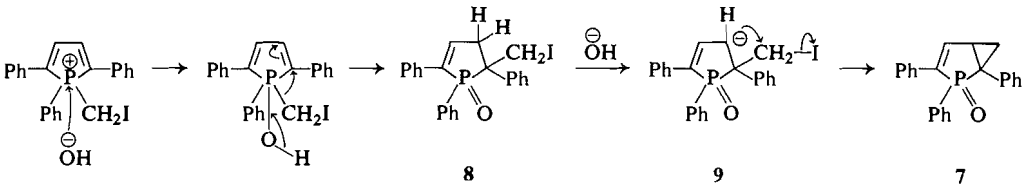

8 9 7

SCHEME 1

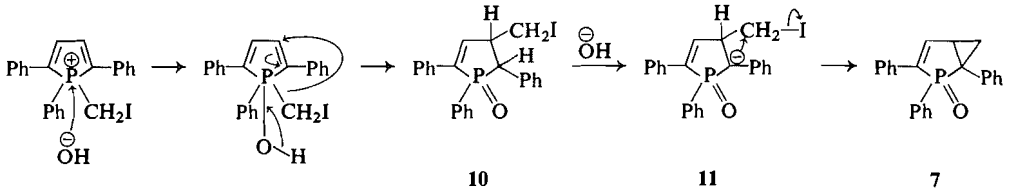

10 11 7

SCHEME 2

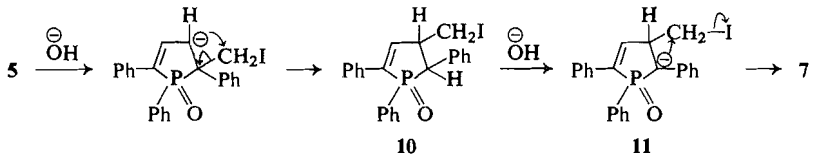

10 11

SCHEME 3

There are several possible mechanisms for the formation of **7** from **5**. At first sight perhaps the most likely of these is a 1,2-migration of the iodomethyl group followed by proton abstraction by hydroxide ion and ring closure involving expulsion of iodide ion as shown in Scheme 1. However, hydroxide ion abstraction of the allylic protons would seem unlikely. This reaction would parallel the 1,2-migrations observed (6) in other phosphonium salt hydrolyses but it would imply that, in this case, the five-membered ring does not occupy an apical–equatorial arrangement in the intermediate or that in the case of **2**, a $-CH_2I$ migration of the type outlined in Scheme 1 is inhibited by the fused nature of the ring system.

A second possible mechanism is illustrated in Scheme 2. In this case a 1,3-migration of the iodomethyl group occurs and the intermediate carbanion **11** could be to some extent stabilized by overlap with the d-orbitals of the neighboring phosphorus atom. However, this would be a most unusual type of rearrangement which would be difficult to account for except that it involves attack at the β-position of a vinylphosphonium type of system.

A third possibility[1] (Scheme 3) is that the intermediate **10** is formed by two consecutive 1,2-shifts of the iodomethyl group rather than a single 1,3-shift. The driving force for the second of these migrations would presumably come from the conversion of an allylic carbanion type of intermediate into the protonated α-phosphoryl benzylic carbanion **10**.

If any of these reaction schemes operates and if the predicted intermediate **8** or **10** has a significant lifetime it could possibly be isolated. Therefore, in an attempt to isolate the predicted intermediate, the reaction was carried out under much milder conditions at room temperature for 2 h. The product (obtained in good yield) was not **7** but analyzed well for $C_{23}H_{20}OPI$ and the mass spectrum confirmed the molecular weight as 470. The i.r. spectrum shows a typical P=O stretching vibration at 1180 cm^{-1} and the u.v. spectrum (ethanol) shows λ_{max}(log ε) at 220 (4.33) and 261 mμ (4.07), indicating considerable loss of conjugation relative to **5**. The n.m.r. spectrum shows a ratio of 16 aromatic and olefinic protons

[1]We are indebted to one of the referees for this suggestion.

Can. J. Chem. Downloaded from www.nrcresearchpress.com by 210.87.254.6 on 09/05/12
For personal use only.

Can. J. Chem. Downloaded from www.nrcresearchpress.com by 210.87.254.6 on 09/05/12
For personal use only.

(complex multiplet at τ 2.19–3.16) to two methylene or methine protons (multiplet at τ 5.52–6.08) to two methylene protons (multiplet at τ 6.65–7.02). That the compound is not a mixture of **8** and **10** was shown by a detailed t.l.c. examination on both alumina and silica of various activities using several solvent systems.

In our opinion, this evidence fits structure **10** considerably better than it fits structure **8**. Thus, structure **8** contains two allylic methylene protons which could possibly account for the multiplet in the n.m.r. spectrum at τ 6.65–7.02, although a signal at somewhat higher field would be expected. However, this would mean that the methylene protons of the iodomethyl group would be responsible for the signal at τ 5.52–6.08 which is clearly at too low field for such protons even bearing in mind the probable deshielding effect of the P=O grouping. Indeed, even in **5**, where the deshielding effect of the neighboring phosphonium grouping (8) is at a maximum, the methylene protons appear only as low as τ 5.68.

Equally, if the n.m.r. signal assignments for **8** are reversed, the signal at τ 6.65–7.02 would agree well with that expected for the methylene protons of the iodomethyl group (*cf.* ethyl iodide (9)) but the signal at τ 5.52–6.08 is again at too low field for the allylic methylene group which is relatively remote from the P=O grouping and attached to only a mildly electron-withdrawing group. Such a signal would be unlikely to occur below τ 7 unless some additional strong deshielding effect were present. For example, even in allyl bromide, where deshielding is very strong, the allylic methylene protons still resonate at τ 6.07 (10). The additional deshielding effect could conceivably be provided by the neighboring phenyl group but, if this were the case, it seems unlikely that both of the non-equivalent protons would be deshielded to the same extent bearing in mind the probable stereochemistry of the system.

On the other hand, in structure **10**, the signal at τ 6.65–7.02 agrees well with that expected for the iodomethyl group as in ethyl iodide (9) and the signal at τ 5.52–6.08 could be generated by the two tertiary protons both of which are allylic (or benzylic) and adjacent to electron-withdrawing groups. Furthermore, the benzylic protons in **12** have been shown to resonate in the same region at τ 6.11 (4).

It is worth noting that the side-chain methylene

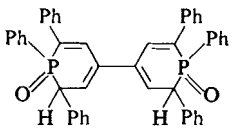

12

group of **10** appears as a multiplet of at least five peaks rather than a doublet in the n.m.r. spectrum. This is almost certainly because the two methylene protons are non-equivalent due to the adjacent asymmetric center since long-range coupling with the phosphorus atom would be very small. Such a case is similar to that of the diastereomeric methylene protons of 1,2-dichloropropane (11). The methine protons appear as a multiplet because of coupling with each other, the non-equivalent methylene protons and the phosphorus atom. In structure **8**, the protons in both methylene groups would be non-equivalent due to the neighboring asymmetric center so that the multiplicities of the signals are of little value in distinguishing between **8** and **10**. Also, the fact that both **8** and **10** could be mixtures of the various possible stereoisomers cannot be ignored.

Further treatment of **10** with sodium hydroxide in aqueous methanol under reflux for 24 h gives an almost quantitative yield of the cyclopropane **7**. This supports our tentative conclusion that **10** (and not **8**) is the intermediate isolated since it is unlikely that the protons of the allylic methylene group in **8** would be sufficiently acidic to be abstracted by hydroxide ion whereas benzylic protons of the type present in **10** and **12** are known to be abstractable by strong base (4). The compound assumed to be **10** is also converted very rapidly into **7** on treatment with sodium hydride in rigorously dried (molecular sieves) dimethylformamide. This, then, strongly suggests that **10** is formed as an intermediate in the alkaline hydrolysis of **5** and that the reaction proceeds via Schemes 2 or 3. Attempts to reduce the side-chain iodomethyl group of **10** with lithium aluminum hydride gave only resinous materials.

In a final attempt to confirm the identity of **10**, deuterium exchange studies were undertaken. Thus, it was observed that a solution of the compound assigned structure **10** in perdeuteroacetone containing NaOD and D_2O showed no exchange (n.m.r. studies) at room temperature over a period of 2 days. Treatment of the same compound in rigorously dried (molecular sieves) di-

Can. J. Chem. Downloaded from www.nrcresearchpress.com by 210.87.254.6 on 09/05/12
For personal use only.

methylsulfoxide with NaOD and D_2O resulted in the formation of **7**. The reaction was complete in little over a minute and n.m.r. measurements showed no incorporation of deuterium into the product. A solution of the compound assigned structure **10** in perdeuteroacetone containing NaOD and D_2O was heated under reflux until about 75% conversion into **7** had occurred (approximately 30 min). The n.m.r. studies of the mixture of the product and starting material showed that no deuterium exchange had occurred in the starting material (the peaks at τ 6.65–7.02 and 5.52–6.08 remained of equal area) and that no deuterium had been incorporated into **7**. These studies are inconclusive in that they do not favor either structure **10** or structure **8**. They show only that the proton abstraction steps **8** → **9** (Scheme 1) or **10** → **11** (Schemes 2 and 3) are not reversible under the conditions used and that intramolecular cyclization occurs before reprotonation can occur. However, in our opinion, all the evidence available strongly favors structure **10** in preference to structure **8** for the hydrolysis intermediate $C_{23}H_{20}OPI$.

Similar experiments were carried out with 1-allyl-1,2,5-triphenylphospholium bromide (**13**) in order to see if any corresponding migration of the allyl group occurs.

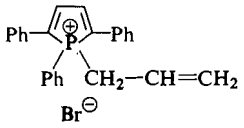

13

The quaternary salt **13** is readily prepared in very high yield by heating the phosphole **4** with allyl bromide in dry benzene under reflux for several days. Treatment of the quaternary salt with aqueous methanolic sodium hydroxide at room temperature gives at least two products together with large amounts of oily material. The first of these is the phosphole **4**, *not* its oxide as would be expected from normal attack (5) of hydroxide ion at the phosphorus atom, and it therefore appears that attack occurs at the terminal carbon atom of the allyl group with displacement of the neutral phosphole **4** as shown in Scheme 4.

The second product, obtained in very small quantities, is a colorless material analyzing for $C_{26}H_{27}O_2P$ and which is therefore an adduct of

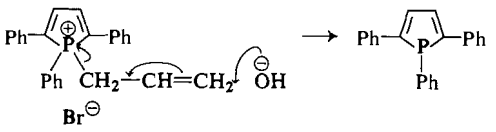

13 **4**

SCHEME 4

the phospholium ion **13**, hydroxide ion, and methanol. The mass spectrum confirms the molecular weight as 402 and elemental analyses show the presence of one methoxy group. The u.v. spectrum shows λ_{max}(log ε) at 219.5 (4.27) and 258 mμ (4.01) indicating that the diphenylbutadiene portion of the molecule is no longer intact and that the molecule contains little unsaturation. The i.r. spectrum shows P=O and ether-type C—O stretching vibrations at 1170 and 1105 cm^{-1} respectively. The n.m.r. spectrum shows 16 aromatic and olefinic protons as a complex multiplet at τ 2.15–3.14, three methoxy protons as a sharp singlet at 6.97, five methylene and/or methine protons as a complex multiplet at 5.81–7.99, and three methyl protons as a doublet (J = 6 Hz) at 9.0. Since the methoxy protons appear as a sharp singlet in the n.m.r. spectrum, the methoxy group is not attached to the phosphorus atom because this would give a doublet due to ^{31}P coupling (12).

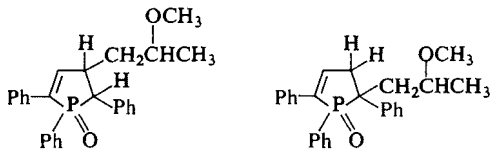

14 **15**

It therefore seems likely that migration of the allyl group has occurred and that some kind of addition of methanol to the unsaturated portion of the allyl group has also occurred to give a methyl group adjacent to a tertiary proton. Since only very small quantities of the product were available, the structure determination was not completed. However, structures **14** and **15** are consistent with all the evidence (with **14** preferred by analogy with **10**) but, apart from migration of the allyl group to the 2- or 3-position of the phosphole ring, it is difficult to visualize the reaction sequence which could lead to these structures. Some further evidence for the proposed structures **14** and **15** is given by the u.v. spectrum which is almost identical with that of **10**

Can. J. Chem. Downloaded from www.nrcresearchpress.com by 210.87.254.6 on 09/05/12
For personal use only.

and by the mass spectrum which shows a very intense peak at *m/e* 329 corresponding to loss of the allylic or tertiary $-CH_2CH(OMe)CH_3$ group and another strong peak at *m/e* 328 which suggests that the oxide of the phosphole **4** is regenerated on electron impact. The peak at *m/e* 329 is also present in the spectrum of the product tentatively assigned structure **10** but is much weaker. This is presumably due to the easy loss of the iodine atom which would lead to a different major fragmentation pattern. The structure of this adduct must, however, remain in doubt pending a complete structure determination.

Experimental

The i.r. spectra were recorded in Nujol mulls using a Beckman IR12 spectrophotometer while u.v. spectra were obtained on dilute ethanol solutions using a Unicam SP800 spectrophotometer. The n.m.r. measurements were made with a Varian Associates model A60-A spectrometer using trifluoroacetic acid or deuteriochloroform solutions with tetramethylsilane as internal reference. Mass spectra were determined using an Hitachi–Perkin–Elmer model RMU-7 double focussing mass spectrometer.

1,2,5-Triphenylphosphole was prepared by the method of Campbell (1).

1-Iodomethyl-1,2,5-triphenylphospholium Iodide (5)

A well-mixed paste of 1,2,5-triphenylphosphole (10 g, 32.05 mmol) and methylene iodide (26 g, 96.95 mmol) in a pressure bottle under dry nitrogen was kept with constant stirring at 80–85° for 4½ days. When cooled, the reaction mixture turned to a dark brown solid which was broken up and washed thoroughly with acetone. The yellow residue (17 g, 91%) was found to be almost pure 1-iodomethyl-1,2,5-triphenylphospholium iodide, m.p. 174–175° (dec.).

Anal Calcd. for $C_{23}H_{19}I_2P$: C, 47.59; H, 3.28; I, 43.79; P, 5.34. Found: C, 47.74; H, 3.45; I, 43.82; P, 5.37.

Attempts to recrystallize the yellow powder from a number of solvents such as benzene, chloroform, acetone, ethanol, methanol, water, acetic acid, dimethylformamide, and mixed solvents were unsuccessful and the material was therefore used directly for further investigation.

The i.r. spectrum of **5** shows ν_{max} at 1579, 1538, 1491, 1472, 1447, 1441, 1384, 1371, 1318, 1302, 1259, 1233, 1168, 1161, 1110, 1080, 1031, 1000, 946, 923, 860, 800, 766, 750, 740, 730, 700, 690 cm^{-1}. The u.v. spectrum in absolute ethanol shows λ_{max}(log ε) at 225 (4.58), 275 (3.71), and 411 mμ (4.19). The n.m.r. spectrum in trifluoroacetic acid shows a ratio of 17 aromatic and olefinic protons (complex multiplet at τ 1.75–2.76) to two methylene protons (doublet centered at τ 5.68 with J_{HP} = 8 Hz).

Complete Alkaline Hydrolysis of 1-Iodomethyl-1,2,5-triphenylphospholium Iodide (5)

To a suspension of the quaternary salt **5** (8 g, 13.79 mmol) in methanol (800 ml) was added slowly a 10% aqueous solution of sodium hydroxide (55 ml, 137.6 mmol) at room temperature with vigorous stirring. After the addition was complete, the reaction mixture was heated under reflux for 24 h. The cooled solution was then treated dropwise with dilute aqueous hydrochloric acid until it was just acidic to litmus paper. Water (200 ml) was added and the mixture was evaporated under reduced pressure to remove most of the methanol. The aqueous suspension was then extracted with chloroform (3 × 100 ml). The extracts were combined, dried over anhydrous sodium sulfate, reduced to a volume of 50 ml, and chromatographed on a silica gel column using chloroform as the eluent. Evaporation of the eluate to dryness yielded a pale yellow solid which was recrystallized from hot ethanol to give very pale yellow crystals (3.5 g, 74%) of 3,4,5-triphenyl-4-phosphabicyclo[3.1.0]hex-2-ene-4-oxide (7), m.p. 234–235° (dec.), identical in all respects with an authentic sample (1).

Incomplete Alkaline Hydrolysis of 1-Iodomethyl-1,2,5-triphenylphospholium Iodide (5)

To a suspension of the quaternary salt **5** (12 g, 20.68 mmol) in methanol (1200 ml) was added slowly a 10% aqueous solution of sodium hydroxide (83 ml, 207.1 mmol) at room temperature followed by vigorous stirring for 2 h. The solution was then treated dropwise with dilute aqueous hydrochloric acid until it was just acidic to litmus paper. Water (300 ml) was added and the mixture was evaporated under reduced pressure to remove most of the methanol. The aqueous suspension was extracted with chloroform (3 × 50 ml) and the extracts were combined, dried over anhydrous sodium sulfate, and evaporated to dryness. The dark brown residue was dissolved in the minimum amount of benzene and chromatographed on a column of silica gel using successively benzene and chloroform as eluents. The benzene fraction, upon evaporation, yielded a colorless solid which was recrystallized from a hot benzene/cyclohexane mixture to give long colorless needles (5.6 g, 58%) of 4-iodomethyl-1,2,5-triphenyl-2-phospholene-1-oxide (**10**), m.p. 199–200° (dec.).

Anal. Calcd. for $C_{23}H_{20}OPI$: C, 58.71; H, 4.26; I, 27.08; P, 6.60. Found: C, 59.01; H, 4.25; I, 27.09; P, 6.60.

The i.r. spectrum shows ν_{max} at 3058, 1601, 1587, 1499, 1438, 1422, 1304, 1268, 1180, 1159, 1148, 1104, 1068, 1025, 1000, 918, 881, 824, 792, 760, 748, 719, 699, 691 cm^{-1}. The u.v. spectrum in absolute ethanol shows λ_{max}(log ε) at 220 (4.33) and 261 mμ (4.07). The n.m.r. spectrum in deuterated chloroform shows a ratio of 16 aromatic and olefinic protons (complex multiplet at τ 2.19–3.16) to two tertiary protons (multiplet at τ 5.52–6.08) to two methylene protons (multiplet of at least five peaks at τ 6.65–7.02). The mass spectrum shows a good molecular ion peak at *m/e* = 470.

The chloroform fraction, upon evaporation to dryness yielded pale yellow crystals of 7 (0.7 g, 10%) identical in all respects with an authentic sample.

Alkaline Hydrolysis of 4-Iodomethyl-1,2,5-triphenyl-2-phospholene-1-oxide (10)

To a solution of the 2-phospholene oxide **10** (1 g, 2.13 mmol) in methanol (100 ml), was added slowly a 10% aqueous solution of sodium hydroxide (8.5 ml, 21.28 mmol) at room temperature with vigorous stirring. After

the addition was complete, the mixture was heated under reflux for 24 h. The cooled solution was treated dropwise with dilute hydrochloric acid until it was acidic to litmus paper and the mixture was worked-up and chromatographed in chloroform solution as before. The eluate from the silica column yielded a pale yellow solid which was crystallized from hot ethanol to give very pale yellow crystals (0.65 g, 90%) of the cyclopropane **7** identical in all respects with an authentic sample.

*1-Allyl-1,2,5-triphenylphospholium Bromide (**13**)*

The phosphole **4** (15 g, 48.09 mmol) and allyl bromide (29 g, 240 mmol) in dry benzene (500 ml) were heated under reflux in a dry nitrogen atmosphere for 5 days. The yellow solid which separated was collected and recrystallized from hot water or a hot methanol/benzene mixture to give yellow crystals (19 g, 91%) of 1-allyl-1,2,5-triphenylphospholium bromide (**13**), m.p. 202–203° (dec.).

Anal. Calcd. for $C_{25}H_{22}BrP$: C, 69.26; H, 5.07; Br, 18.52; P, 7.15. Found: C, 68.97; H, 5.01; Br, 19.05; P, 7.10.

The i.r. spectrum shows ν_{max} at 3038, 1635, 1610, 1579, 1490, 1443, 1344, 1313, 1259, 1190, 1154, 1108, 1078, 1030, 998, 981, 939, 906, 878, 813, 761, 748, 726, 685 cm^{-1}. The u.v. spectrum in absolute ethanol shows λ_{max} (log ε) at 212 (4.52), 227 (4.58), and 410 mμ (4.12). The n.m.r. spectrum in deuterated chloroform shows a ratio of 20 aromatic and olefinic protons (complex multiplet at τ 1.26–2.96) to two methylene protons (poorly defined quartet centered at τ 5.27).

*Alkaline Hydrolysis of 1-Allyl-1,2,5-triphenylphospholium Bromide (**13**)*

A solution of the quaternary salt **13** (1.4 g, 3.24 mmol) in methanol (70 ml) was treated dropwise with a 10% aqueous solution of sodium hydroxide (6.5 ml, 16.25 mmol) at room temperature with constant stirring for 10 min. Water (50 ml) was added and the mixture was evaporated to remove most of the methanol. The aqueous suspension was extracted with chloroform (3 × 50 ml) and the chloroform extracts were combined, dried, and evaporated as before. The residue was chromatographed on a neutral alumina column using successively benzene and chloroform as eluents.

The benzene fraction, upon evaporation to dryness, yielded an oily solid which, on recrystallization from hot ethanol gave the phosphole **4** (0.12 g, 12%) identical with an authentic sample.

Evaporation of the chloroform fraction also yielded an oily solid which was sublimed under vacuum (*ca.* 1 Torr) at 165° to give a colorless compound (0.16 g, 12%), m.p. 171–172°.

Anal. Calcd. for $C_{26}H_{27}O_2P$: C, 77.71; H, 6.72; P, 7.71; OCH_3, 7.71. Found: C, 77.4; H, 6.73; P, 7.60; OCH_3, 6.83.

The i.r. spectrum shows ν_{max} at 3051, 1610, 1600, 1578, 1494, 1431, 1368, 1299, 1262, 1220, 1170, 1105, 996, 955, 920, 878, 826, 791, 774, 752, 743, 718, 688 cm^{-1}. The u.v. spectrum in absolute ethanol shows λ_{max}(log ε) at 219.5 (4.27) and 258 mμ (4.01). The n.m.r. spectrum shows 16 aromatic and olefinic protons as a complex multiplet at τ 2.15–3.14, three methoxy protons as a sharp singlet at 6.97, five methylene and methine protons as a complex multiplet at 5.81–7.99, and three methyl protons as a doublet (J = 6 Hz) at 9.0. The mass spectrum shows a strong molecular ion peak at m/e = 402.

Alkaline hydrolysis using only water as solvent gave a mixture of uncrystallizable oils together with traces of the phosphole **4** and *p*-terphenyl.

We thank the National Research Council of Canada and the Ontario Department of University Affairs for generous financial support.

1. I. G. M. Campbell, R. C. Cookson, M. B. Hocking, and A. N. Hughes. J. Chem. Soc. 2184 (1965).
2. E. M. Richards and J. C. Tebby. Chem. Commun. 957 (1967).
3. D. W. Allen and I. T. Millar. Chem. and Ind. 2178 (1967); J. Chem. Soc. (C), 252 (1969).
4. A. N. Hughes and C. Srivanavit. Can. J. Chem. This issue.
5. K. Bergesen. Acta. Chem. Scand. **20**, 899 (1966).
6. S. Trippett. *In* Organophosphorus chemistry. Vol. 1. *Editor*, S. Trippett. The Chemical Society, London, 1970. pp. 24–28.
7. A. N. Hughes and C. Srivanavit. J. Heterocycl. Chem. **7**, 1 (1970).
8. G. Gaudiano, R. Mondelli, P. P. Ponti, C. Ticozzi, and A. Umani-Ronchi. J. Org. Chem. **33**, 4431 (1968).
9. Varian. High resolution n.m.r. spectra catalog. **1**, Spectrum No. 13 (1962).
10. Varian. High resolution n.m.r. spectra catalog. **1**, Spectrum No. 24 (1962).
11. Varian. High resolution n.m.r. spectra catalog. **1**, Spectrum No. 30 (1962).
12. J. W. Emsley, J. Feeney, and L. H. Sutcliffe. High resolution nuclear magnetic resonance spectroscopy. Vol. 2. Pergamon Press, 1966. p. 1063.

Can. J. Chem. Downloaded from www.nrcresearchpress.com by 210.87.254.6 on 09/05/12
For personal use only.

Bromination of Norbornene: the Question of Bromonium Ions *vs.* 6,1-Hydride Shift

D. R. MARSHALL, P. REYNOLDS-WARNHOFF, AND E. W. WARNHOFF
Department of Chemistry, University of Western Ontario, London, Ontario

AND

J. R. ROBINSON
Agricultural Research Institute, London, Ontario

Received October 1, 1970

The reaction of norbornene (**1**) with bromine has been re-investigated and found to give in addition to bromonortricyclene (**2**) and 2-*exo*-bromonorbornane (**20**) a complex mixture of dibromides of which five (**15–19**) have been isolated and identified. These dibromides have been found to be kinetically controlled products of ionic addition. Apparently dibromide **15** is also formed to some extent in carbon tetrachloride by a radical mechanism. The product composition from the bromine addition has been compared with that of the analogous chlorination and bromofluorination reactions. Degradation of the 2-*exo*,3-*endo*-dibromonorbornane from bromination of 5,6-^{14}C-norbornene has shown that this dibromide is formed by two ionic routes: (*a*) from a bromonium ion **14** (or its equivalent), and (*b*) from the cation **12** formed by 6,1-hydride shift. Improvements have been made in the first and final steps of the standard norbornene degradation method.

La réaction du norbornène (**1**) avec le brome a été réexaminée et s'est avérée donner, en plus du bromonortricyclène (**2**) et de l'*exo* bromo-2 norbornane (**20**), un mélange complexe de composés dibromés dont cinq (**15–19**) ont été isolés et identifiés. Il a été montré que ces composés dibromés sont des produits cinétiquement contrôlés résultant d'une addition ionique. Il semble que le dibromo **15** se forme également de façon appréciable dans le tétrachlorure de carbone par un mécanisme radicalaire. La composition des produits de la réaction d'addition du brome a été comparée aux réactions analogues de chloration et de bromofluoration. Par dégradation du dibromo *exo*-2,*endo*-3 norbornane obtenu par bromation du ^{14}C-norbornène-5,6, il a été montré que ce dibromure est formé par deux voies ioniques: (*a*) à partir d'un ion bromonium **14** (ou ses équivalents), et (*b*) à partir du cation **12** formé par une migration-1,6 d'hydrure. Des améliorations ont été apportées à la première et dernière étapes de la méthode standard de dégradation du norbornène.

Canadian Journal of Chemistry, 49, 885 (1971)

Can. J. Chem. Downloaded from www.nrcresearchpress.com by 210.87.254.6 on 09/05/12
For personal use only.

Introduction

In the course of a study of the reaction of "bromine fluoride" (*N*-bromoacetamide + hydrogen fluoride) with norbornene (**1**), it was found that the major dihalo products were 7-*syn*-bromo-2-*exo*-fluoronorbornane (**3**) and 7-*anti*-bromo-2-*exo*-fluoronorbornane (**4**), (Scheme 1) (1, 2). Since the ionic reaction of either "bromine fluoride" or bromine with norbornene would presumably lead to the same first intermediate, the 7-*anti*-isomer **4** was unexpected on the basis of the reported bromination of norbornene (3–5), from which the only dibromo products identified were 7-*syn*,2-*exo*-dibromonorbornane (**19**) and 2-*exo*,3-*endo*-dibromonorbornane (**15**). Most of the earlier investigation of this bromination reaction was done before g.l.p.c. and n.m.r. spectroscopy were available, and although some of the conclusions reached earlier (3, 4) have since been revised (5) (the bromination product was found to contain other dibromides), no further report has been published. To clarify the situation a re-investigation of the bromination reaction was undertaken. After the present work was undertaken, three other studies of halogenation of norbornene were reported which further underlined the desirability of reconciling the various reaction products. In one case (6) *N*,*N*-dibromobenzenesulfonamide was the halogenating agent, and the products **2**, **5**, and **6** were analogous to those from the "bromine fluoride" reaction, while in the other studies describing the chlorination of norbornene (7, 8), three of the four products, **7–10**, of the ionic reaction were analogous to the compounds reported from the bromination (Scheme 1).

Structural and Stereochemical Assignment of the Dibromides

When the bromination of norbornene in carbon tetrachloride at 0° was repeated according to the directions of Kwart and Kaplan (3, 4) and

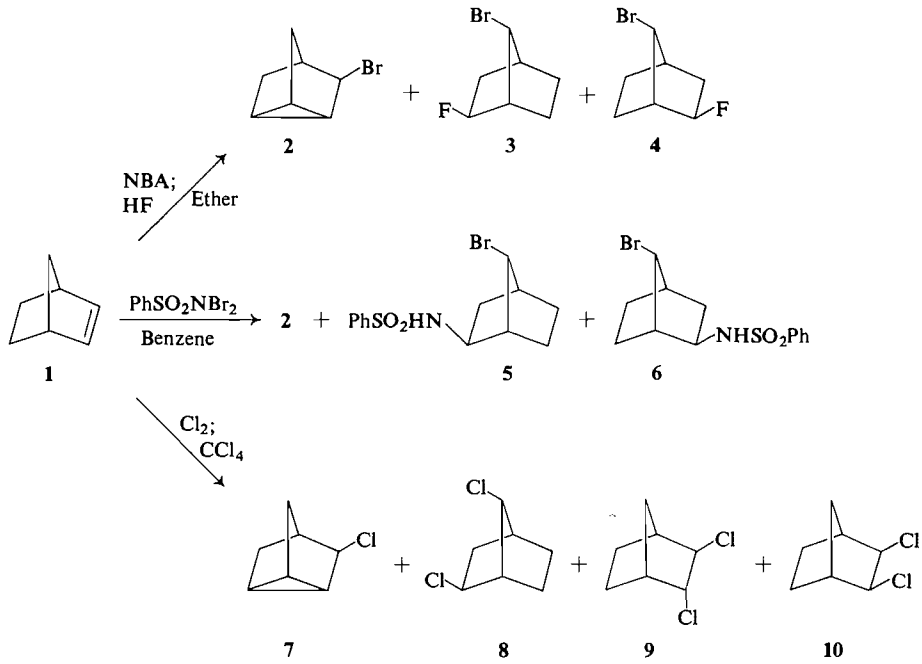

SCHEME 1

the crude product was examined by g.l.p.c.,[1] there were present eight peaks with retention times expected for dibromonorbornanes (Fig. 1). Five of these peaks corresponded to compounds present in greater than 1% yield, and they were isolated by preparative g.l.p.c.[1] From the clean n.m.r. spectra (Fig. 2) of four of the five g.l.p.c. fractions there is no reason to suspect the presence of more than one compound per peak. The five dibromonorbornanes[2] were assigned structure and stereochemistry on the basis of their n.m.r. spectra (including double irradiation spectra), dipole moments, g.l.p.c. retention times, and stability relationships.

Integration of the n.m.r. spectrum of each dibromide shows that every bromine atom is on a carbon atom bearing a hydrogen atom, thereby restricting the number of possible structures to 13 (Table 1). The three 2,3-dibromides have been synthesized previously and their stereochemistry determined unambiguously (10, 11). The *exo-cis*-2,3- and *endo-cis*-2,3-isomers were not identical with any of the five bromination products isolated. However, the first eluted (g.l.p.c.) di-

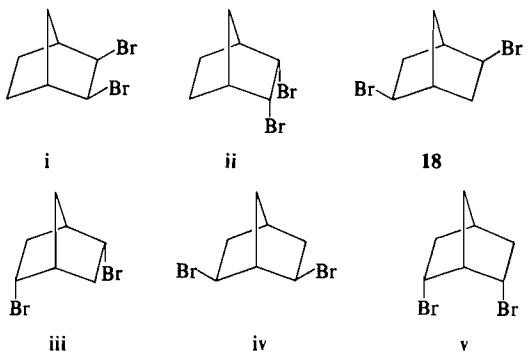

[1]When g.l.p.c. equipment with metal columns (copper or stainless steel) and a metal injection block was used, the dibromides were partially decomposed. For this reason a gas chromatograph with a glass column and injection chamber was used both for analytical and preparative g.l.p.c. For preparative work a stainless steel splitter was attached to the exit of the glass column, but little or no decomposition occurred during the short contact time in the metal splitter as tested by re-injection of the eluate.

[2]There appears to be no reason to doubt that all five compounds have the norbornane skeleton. For two of the isomers this has been proved: **19** has been reduced to norbornane by sodium and *t*-butyl alcohol, and **15** has been degraded to *cis*-1,3-cyclopentane dicarboxylic acid. Moreover, **19** is readily isomerized to the other four dibromides by hydrogen bromide, and the bicyclo[2.2.1] system would not be expected to be equilibrated with a more strained, less stable bicyclo[3.2.0], [3.1.1], or [4.1.0] system. For example, the bicyclo[3.2.0] system rearranges to the bicyclo[2.2.1] skeleton (9). The n.m.r. spectra exclude the presence of methyl groups and olefinic hydrogens.

Can. J. Chem. Downloaded from www.nrcresearchpress.com by 210.87.254.6 on 09/05/12
For personal use only.

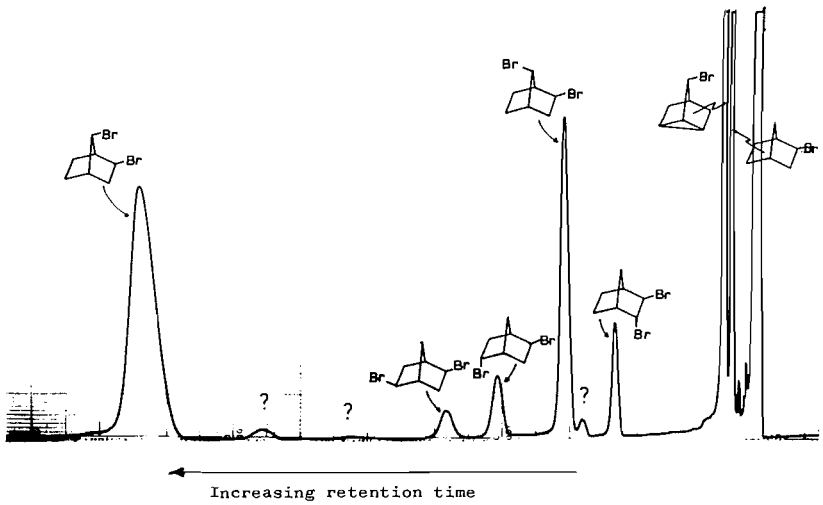

FIG. 1. The g.l.p.c. chart of the norbornene bromination product.

bromide was identical with 2-*exo*,3-*endo*-dibromonorbornane (**15**), one of the two compounds identified by Kwart and Nyce (5). The n.m.r. spectrum (Fig. 2*a*) is in agreement with that reported (10). Double irradiation of *exo* H-3 at 4.42 p.p.m. caused the three line pattern from *endo* H-2 at 3.83 p.p.m. to collapse to a doublet ($J_{endo}H_2$-*anti* H-7 ~3 Hz), and double irradiation of the bridgehead H-1 and -4 peaks at 2.46 p.p.m. caused the *exo* H-3 signal to collapse to a doublet ($J_{endo}H_2$-*exo* H-3 ~ 2.9 Hz) while the *endo* H-2 signal at 3.83 p.p.m. was undisturbed.[3,4] Therefore the two low field protons are on adjacent carbon atoms. Also in agreement with a vicinal structure is the fact that this dibromide is the most easily dehydrobrominated of the five. The final proof of structure was the degradation of this isomer to *cis*-1,3-cyclopentane dicarboxylic acid (5) (see below).

The second dibromide to be eluted (g.l.p.c.) was assigned the 7-*anti*,2-*exo* dibromo structure **16**. In its n.m.r. spectrum (Fig. 2*b*) the narrow absorption at 4.43 p.p.m. ($w_{1/2}$ ~ 4 Hz) is characteristic of a proton on C-7 bearing bromine. (2). The position and three line pattern of the peak at 3.93 p.p.m. is typical of a 2-*endo* proton on a carbon atom bearing bromine and coupled to the adjacent methylene group. The absence of additional observable splitting from long range coupling with an *anti* H-7 suggests that the C-7 bromine occupies this position. The *anti* orientation of the C-7 bromine atom is confirmed by the dipole moment of 2.4 D (calcd. (12): 2.07 D), a value much too small for the *syn*-isomer (calcd. (12): 3.92 D) which has been found to be the fifth dibromide. As expected for **16**, double irradiation of the bridgehead H-1 (2.56 p.p.m.) had no apparent effect on the *endo* H-2 peaks but caused H-7 to collapse to a doublet ($J_{H\text{-}7}$-*endo* H-6 < 1 Hz).[3]

The fourth dibromide eluted (g.l.p.c.) was crystalline, m.p. 94–95.5°, which property together with very simple i.r. and n.m.r. spectra (Fig. 2*d*) indicated the presence of a high degree of symmetry in the molecule. Both CHBr protons absorb at the same place (3.77 p.p.m.) with the same pattern and are therefore in identical environments. Of the six possible structures, **i** and **ii** have already been excluded. Of the remaining four isomers only **18** and **iv** have *endo* protons on carbon bearing bromine as required by the fact that double irradiation of both bridgehead methine hydrogens (2.55 p.p.m.) had no effect on the CHBr pattern. Moreover, double irradiation of the methylene protons (2.08 p.p.m.) caused the CHBr pattern to collapse to a singlet.[3] Structure **18** is preferred to **iv** since both bridgehead methine protons are in identical environments. The low value (0.66 D) of the observed dipole moment is also consistent with structure **18** which would have the lowest moment of any of the 13 isomers (Table 1).

The last dibromide to be eluted (g.l.p.c.) had

[3]For further details and double irradiation spectra see ref. 1.

[4]LeBel and co-workers (10, 11) have proved the stereostructure of **15** by double irradiation measurements on 2-*exo*,3-*endo*-dibromonorborn-5-ene which on hydrogenation gives **15**.

Can. J. Chem. Downloaded from www.nrcresearchpress.com by 210.87.254.6 on 09/05/12
For personal use only.

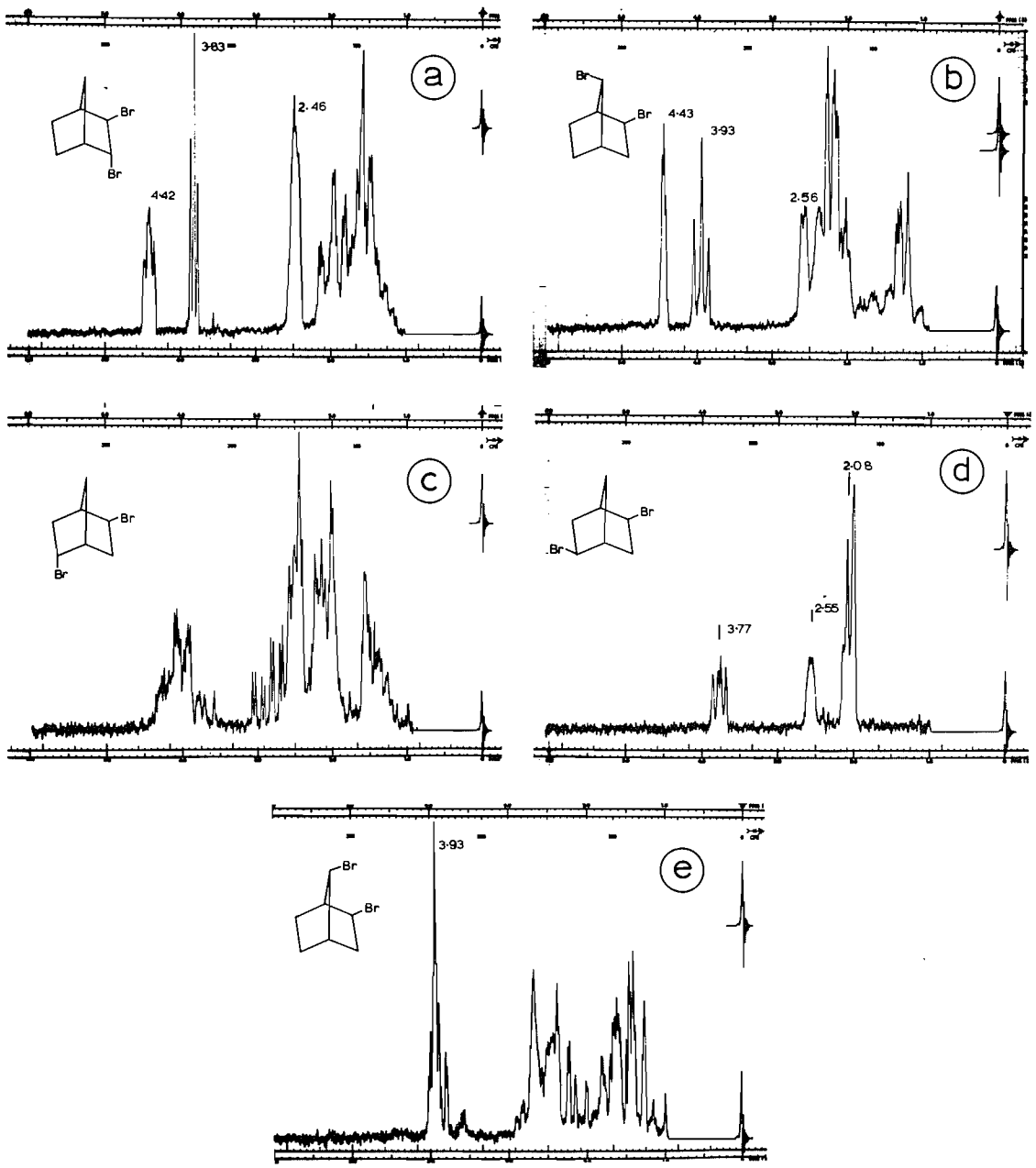

FIG. 2. The n.m.r. spectra of dibromonorbornanes in CCl_4 solution at 60 MHz.

an i.r. spectrum identical with that of the 7-*syn*-2-*exo*-dibromonorbornane isolated by Kwart and Kaplan (3, 4) and converted by them into norbornane-7-carboxylic acid. The dipole moment of this dibromo isomer (3.30 D) excludes all but five of the possible stereoisomers **19**, **i**, **ii**, **iii**, and **v** (see Table 1 for calculated dipole moments), and of these five, the four having both CHBr groups in identical environments can be excluded to leave only **19**. The two —CHBr protons of this isomer are clearly different in the n.m.r. spectrum (Fig. 2*e*) although they overlap.

Can. J. Chem. Downloaded from www.nrcresearchpress.com by 210.87.254.6 on 09/05/12
For personal use only.

Can. J. Chem. Downloaded from www.nrcresearchpress.com by 210.87.254.6 on 09/05/12
For personal use only.

TABLE 1. Permissible dibromonorbornanes and their calculated dipole moments

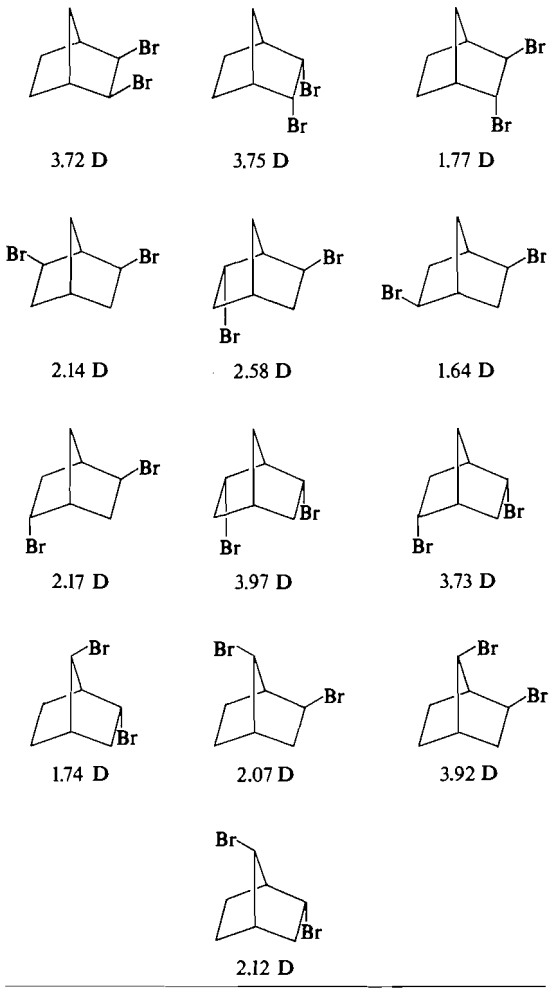

The chemical shift (~3.90 p.p.m.) is that expected for an *endo* CHBr proton on which is superimposed the "broadened singlet" of C_7HBr proton (3.93 p.p.m.). Comparison with the CHBr n.m.r. region of the 7-*anti*-bromo isomer **16** (Fig. 2*b*) clearly shows that the 2-*endo*-proton of the last eluted dibromide has an additional long range coupling (*endo* H-2 – *anti* H-7) which is missing in the 7-*anti*-bromo isomer **16** which has no 7-*anti* proton.[3] Additional chemical evidence for assigning the 7-*syn*-2-*exo* stereochemistry to this isomer is its facile isomerization to a mixture of the other four dibromides upon treatment with hydrogen bromide. The instability of this isomer relative to the others is explicable in terms of repulsive non-bonded interaction between the two bromine atoms which is diminished or absent in the other four isomers found.

The third dibromide eluted has not been assigned a unique structure on spectroscopic grounds alone; however, the number of possible structures may be limited to two, and a choice made on the basis of mechanistic arguments. The n.m.r. spectrum (Fig. 2*c*) reveals that the two CHBr protons are not in the same environment, nor is either CHBr proton on C-7 since the characteristic narrow peak is not present. Therefore only **17** and **vi** remain as possibilities.

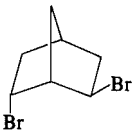

vi

Structure **vi** would arise from a more circuitous path than **17**, and moreover a path requiring a 3,2-hydride shift. There is abundant evidence that 3,2-hydride shift in norbornyl cations is much slower than 6,1- and 6,2-hydride shift and becomes appreciable only under equilibrating conditions (13). However, the bromination reaction is kinetically controlled (see below), and furthermore no other products attributable to 3,2-hydride shift were found unless the three very minor unidentified components (Fig. 1) arise in this way. For these reasons structure **17** is assigned to the third dibromide.[3]

Results and Discussion

Fortunately, it was possible to show that the products of bromination of norbornene at 0° in carbon tetrachloride are those of the kinetically controlled addition reaction. Both bromonortricyclene (**2**) and dibromide **19** can react with hydrogen bromide to give a mixture of the five dibromides, but *under the conditions of the addition* these reactions are undetectable.[5] In control experiments in the present work it was found that treatment of bromonortricyclene (**2**) or

[5]Kwart and Kaplan (3) reported that bromonortricyclene reacts with anhydrous hydrogen bromide at 0° in carbon tetrachloride. However, in their reaction, hydrogen bromide was passed through the solution for 12 h, much more drastic treatment than in the addition reaction which was worked-up after 5–20 min and in which the hydrogen bromide concentration was much lower.

Can. J. Chem. Downloaded from www.nrcresearchpress.com by 210.87.254.6 on 09/05/12
For personal use only.

TABLE 2. Effects of variables on the addition of bromine to norbornene in solvent CH_2Cl_2

Experiment type	**1** mg/ml	Special conditions	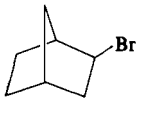 **20**	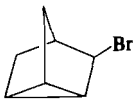 **2**	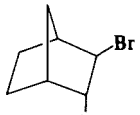 **15**	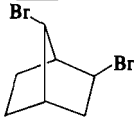 **16**	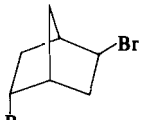 **17**	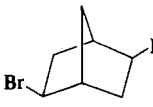 **18**	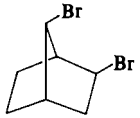 **19**
(*1*) Dilution	498/100	0°	16.7	34.4	3.0	12.4	3.1	1.9	27.3
(*2*) Dilution	481/2	0°	23.9	20.9	2.7	10.9	2.2	1.5	31.5
(*3*) Low temperature	510/100	−78°	10.2	45.5	1.1	9.7	1.7	0.6	30.7
(*4*) Radical scavenger	518/100	O_2 passed in	11.4	36.0	3.1	12.1	3.0	1.3	31.8
(*5*) HBr scavenger	543/100	0°, $CaCO_3$ (5 g)	7.2	41.8	3.2	12.2	3.0	1.6	30.6
(*6*) HBr scavenger	531/100	0°, $CaCO_3$ (25 g)	2.4	42.2	3.6	13.5	3.2	1.5	33.8
(*7*) Trapping	68.8/10	−5–0°, saturated with $Et_4\overset{+}{N}Br^-$	4.7	34.8	46.0	0.9	—	—	7.5

Can. J. Chem. Downloaded from www.nrcresearchpress.com by 210.87.254.6 on 09/05/12
For personal use only.

dibromide **19** at 0° in methylene chloride (in which hydrogen bromide is more soluble than in carbon tetrachloride) with more than 1 mol equiv of anhydrous hydrogen bromide gave no reaction over periods longer than the time required for bromine addition to norbornene (see Experimental).[6] The other four dibromides were also shown to be inert to hydrogen bromide under the addition reaction conditions. Brominations of norbornene carried out in the presence of suspended powdered calcium carbonate gave the same proportional yields of the five dibromides as were obtained in the absence of calcium carbonate within experimental error, although the yield of 2-*exo*-bromonorbornane was drastically reduced with a corresponding increase in **2** (Table 2). In bromination reactions in which the crude product was not washed to remove hydrogen bromide, the product composition was insensitive to the time that elapsed between reaction and g.l.p.c. analysis. Therefore, the dibromide isomers found are kinetically controlled addition products and do not result from secondary reactions or isomerizations.[7]

In view of Kwart and Kaplan's earlier suggestion that a radical chain reaction might be involved in the formation of one of the dibromides, and since Poutsma's recent work (7) revealed both ionic and free radical components in the chlorination of norbornene in carbon tetrachloride solution, it was necessary to establish the nature of the processes involved in the bromination reaction. The choice of solvent is apparently critical. The bromination in methylene chloride was found to be insensitive to concentration differences and to the radical scavenger oxygen (Tables 2 and 3). If some of the dibromides had been partially or wholly formed by radical processes, a change in product ratios would have been expected, but within experimental variation none was observed. In carbon tetrachloride on the other hand, although the dibromide distribution did not change in the presence of oxygen (7), the amount of 2-*exo*,3-*endo* dibromide **15** increased with increasing concentration of norbornene or bromine while the amount of 2-*exo*,7-*syn* dibromide **19** decreased. Furthermore, when a radical, diphenylpicrylhydrazyl, was present in the bromination of high concentrations of norbornene in carbon tetrachloride, the amount of **15** was reduced by half compared to bromination in the absence of the radical, and the dibromide distribution was essentially that obtained in methylene chloride solution. This evidence points to a radical component leading mainly to **15** in the formation of dibromonorbornanes in carbon tetrachloride; if radical intermediates are formed in methylene chloride, they are apparently scavenged by the solvent before they can give rise to dibromonorbornanes.[8]

A mechanistic interpretation of the *ionically* formed products and product ratios can now be made. The origin of the five dibromonorbornane isomers is consistent with *exo*-addition of a cationic bromine species to norbornene followed by 6,1- or 6,2-hydride shift in the resulting nonclassical ion (or Wagner–Meerwein related classical cations **21**) and reaction with bromine or bromide ion. The three non-classical ions, **11**, **12**, and **13**, can give rise to three pairs of dibromides (Fig. 3) of which the only one not formed was the

[6]Actually, the maximum amount of hydrogen bromide that would have been present at 0° was much less than 0.2–0.36 of the molar amount of norbornene used since some of the hydrogen bromide produced in the formation of bromonortricyclene then reacted with norbornene to give 2-*exo*-bromonorbornane (**20**). This latter reaction was fast since the amounts of **2** and **20** were always approximately equal.

[7]The formal possibility that some or all of these kinetically controlled products might have arisen from initially formed *exo-cis*-2,3-dibromonorbornane (**i**) in a fast reaction is excluded both by LeBel's finding (10) that **i** is a major product of the radical addition of hydrogen bromide to 2-bromonorbornene, and also by our finding that **i** is unchanged by hydrogen bromide in methylene chloride at 0°.

[8]The unlikely possibility that all of the dibromides are being formed by free radical mechanisms in carbon tetrachloride can be excluded by two observations. Firstly, addition of diphenylpicrylhydrazyl changed the distribution of dibromonorbornanes contrary to what would be expected for an all radical path. Secondly, the bromination of a mixture of norbornene and toluene gave less than 0.5% of benzyl bromide. From bond dissociation energies (14) the addition of a bromine atom to a double bond is approximately thermally neutral. However, if the difference (~6 kcal/mol) in heat of hydrogenation of cyclohexene or cyclopentene and norbornene (15) is taken as a measure of the relief of strain in the latter on breaking the π-bond, then the addition of a bromine atom to norbornene should be exothermic by ~6 kcal/mol. Since the rate of benzylic hydrogen abstraction by bromine atoms from toluene is 290 times greater than from the methylene group of propane and is exothermic to the extent of ~10 kcal/mol from bond dissociation energies (14), benzyl bromide should have been formed in quantity if the bromination of norbornene were exclusively a radical process, provided that the activation energies for the two reactions being considered here paralleled the energy differences between starting materials and intermediates.

TABLE 3. Variation in composition of dibromide fraction from addition of bromine to norbornene at 0°

Concentration of norbornene (mg/ml)	Solvent	Number of reactions	Normalized % of dibromides*					Other variables
			15	**16**	**17**	**18**	**19**	
1.0	$CCl_4(\varepsilon = 2.24)$	3	2.0–2.5	13–15	0.8	1.0	78–84	
10.		2	7–9	15–17	1.6–2.3	1.6–2.0	66–71	
430.		3	18–19	15–17	5.3–5.4	3.8–4.1	46–47	
430.		1	17	17	5.5	3.6	51.5	Toluene added
430.		2	9.8–11	19–21	4.6–5.0	3.2–3.5	60–61	DPPH (100 mg) added
10.		1	13	19	4	1.3	61	Norbornene added to 10 × excess Br_2
1.0	$CH_2Cl_2(\varepsilon = 9.08)$	1	5.2	23.7	6.2	2.8	62.4	
10.0		3	6.2–7.0	21–22	6.7–7.1	3.0–3.6	56–59	
215.		2	5.8–8.5	19–20	4–6.8	2.7–4.1	57	
240.								
430.		1	7.3	20	6.2	3.9	61.7	
1.0	$CH_3CN(\varepsilon = 37.50)$	1	1.8	11.9	<0.2	<0.2	86.3	
5.6		1	3.1	16.2	<0.2	<0.2	80.5	
10.0		2	2.3–3.0	13–17	0.6	2.0	77–82	
215.		1	3.6	18	<0.5	<0.5	78.5	10° instead of 0°

*The difference between 100% and the horizontal sum of % for a reaction is due to small amounts of other unidentified compounds, presumably dibromides because of their g.l.p.c. retention times, see Fig. 1 for example.

cis-exo-2,3-dibromonorbornane (**i**). An authentic sample of **i** was synthesized (10) and shown by mixed g.l.p.c. not to be identical with any peak from the bromination product. The absence of this isomer may be attributed to steric shielding by the bromine atom already present in cation **11**.[9]

As has been pointed out by Berson (16), one of the dibromides, the 2-*exo*,3-*endo* compound **15**, may arise by two routes: normal *trans* addition of bromine to norbornene via bromonium ion **14** as suggested by Kwart and Kaplan (3), or else by 6,1-hydride shift[10] in the initially formed cation **11** with subsequent attachment of bromide at C-2 of **12**. In the present work it has been found that both processes occur simultaneously. Evidence for two ionic paths to **15** comes from bromination in methylene chloride in the presence of a large amount of bromide anion (Table 2, entry 7). The dibromo product was almost entirely the 2-*exo*,3-*endo* isomer **15** with no detectable amount of **17** or **18** and a marked decrease in **16**. The increased formation of the 2-*exo*,3-*endo* dibromide **15** in this experiment requires a mechanism allowing capture of an intermediate cation by bromide before much hydride shift has taken place. Still, the fact that *some* 2-*exo*,7-*anti* dibromide **16** from 6,1-hydride shift cation **12** is formed in all of the brominations suggests that some of the 2-*exo*,3-*endo* dibromide must also result from bromide attack on the 6,1-hydride shift cation **12**.

To settle the point, an experiment with labelled norbornene was carried out. Bromination of 5,6-^{14}C-norbornene in carbon tetrachloride at 0° gave the previously described mixture of mono- and dibromo products. Rather than separate the small amount of labelled 2-*exo*,3-*endo* dibromide, advantage was taken of its greater reactivity toward dehydrobromination compared to the other four dibromides. After removal of the 2-*exo*-bromonorbornane and most of the bromonortricyclene by fractional distillation, the remaining mixture was treated with phenyllithium at 0° for 30 min, which conditions had been found to dehydrobrominate the 2-*exo*,3-*endo* dibromide cleanly without affecting bromonortricyclene, 2-*exo*-bromonorbornane, or the other dibromides. The crude product was distilled with added decalin to remove the lower boiling 2-bromonorbornene. Ozonization of the distillate gave *cis*-1,3-cyclopentane dicarboxylic acid which was degraded

[9] *Cf.* the corresponding methylnorbornyl cation in ref. 17.

[10] In this paper for convenience the carbon atoms of cations **11–13** and **24–26** as well as bromonortricyclene **2** have been numbered to retain the generally used terms for referring to hydride shifts in the unsubstituted norbornyl cation.

Can. J. Chem. Downloaded from www.nrcresearchpress.com by 210.87.254.6 on 09/05/12
For personal use only.

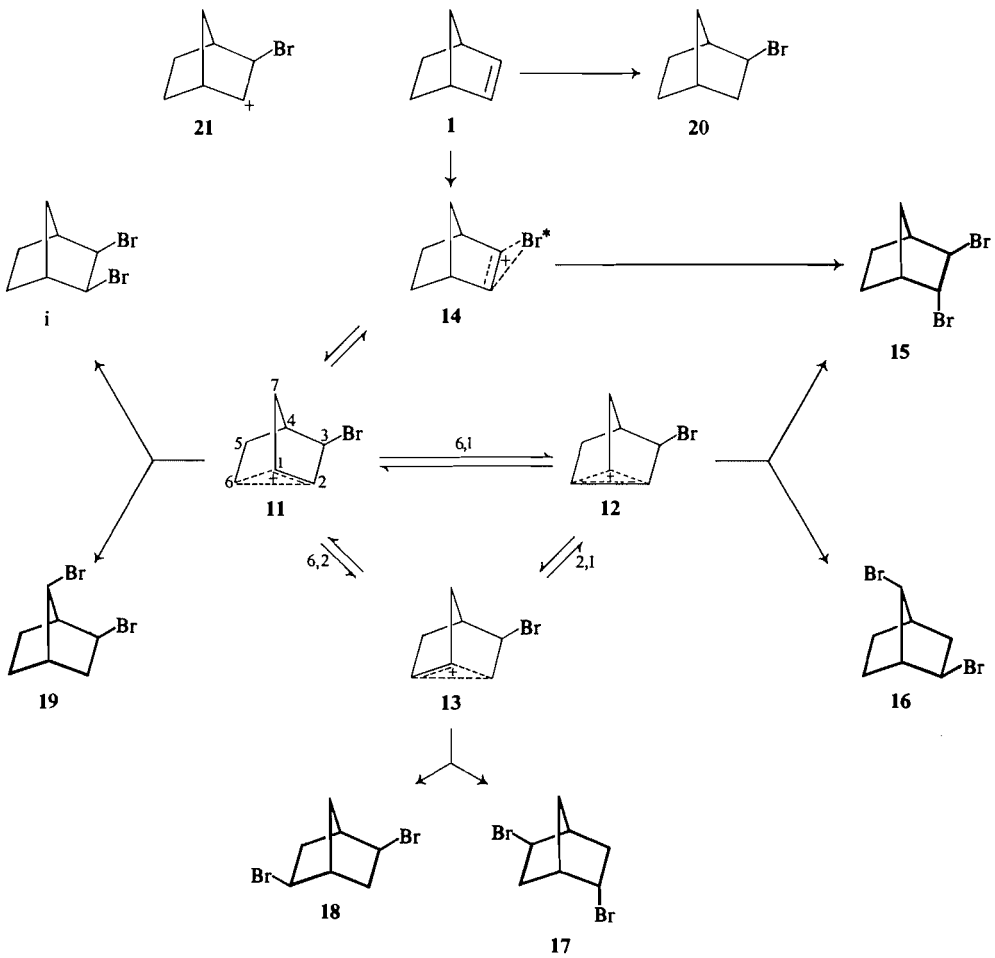

FIG. 3. Formation of norbornene bromination products.
*The structure drawn is not intended to exclude the possibility of other atoms being bonded to the bromine atom.

by a modification (see below) of the customary procedure (18). The degradation results are shown in Fig. 4. If **15** arose entirely from bromonium ion **14** or from the radical process in which rearrangement would not occur, the radioactive carbon would appear exclusively in the ethylenediamine, whereas if 6,1-hydride shift occurred, label would also appear in C-2 of the cyclopentanediamine and in a carboxyl group of the derived succinic acid. The carbon dioxide from degradation of the succinic acid was radioactive but the figure given is probably the least reliable of the five,[11] and the value given is a minimum figure (see Experimental). If this figure is disregarded, the amount of 2-*exo*,3-*endo* dibromide which arises from 6,1-hydride shift is 19–27%, depending on the way in which it is calculated (see Experimental) with the rest of the dibromide **15** arising from the bromonium ion **14** and from the radical pathway. Since the radical scavenger experiments indicate that at least half of the 2-*exo*,3-*endo* dibromide is formed by a radical path in carbon tetrachloride at the high concentrations used (3–5), and since about one quarter of the **15** arises by 6,1-hydride shift, the remaining quarter is all that results from bromonium ion **14** under these conditions.

A comparison of the products isolated from

[11]It was not certain that all carbon dioxide had been swept into the absorption solution for counting.

Can. J. Chem. Downloaded from www.nrcresearchpress.com by 210.87.254.6 on 09/05/12
For personal use only.

Can. J. Chem. Downloaded from www.nrcresearchpress.com by 210.87.254.6 on 09/05/12
For personal use only.

TABLE 4. Comparison of norbornene ionic addition reactions

Reagent	Solvent	Temperature (°C)	Products and % composition of crude product						
Br_2	CH_2Cl_2	0	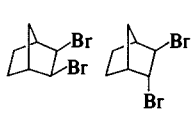 0.0	3.6	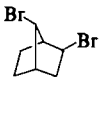 14.9	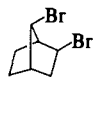 33.0	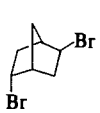 3.7	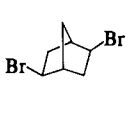 2.3	41.5
BrNHCOMe HF	Et_2O/HF	−78	Three unidentified minor products	38.0	22.0	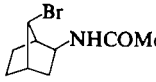 [11.0]*	—	37.0	
Cl_2	CCl_4	25	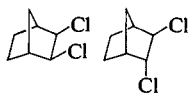 3.5	6	—	25.5	—	—	65
$Br_2NSO_2C_6H_5$	C_6H_5	25	Two unidentified dibromides ~8	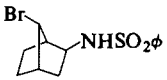 ~13	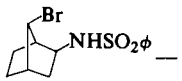 ~29	—	—	~46	

*Isolated from a separate run.

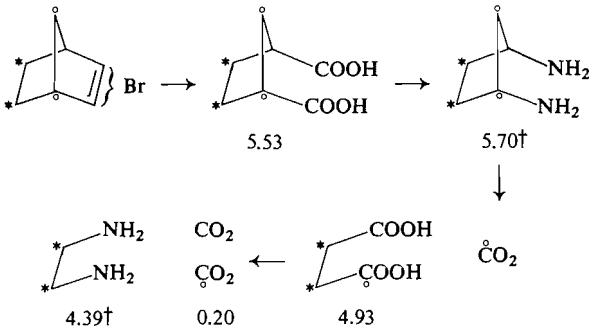

*Position of ^{14}C in **15** from bromonium ion **14**.
°Position of ^{14}C in **15** from 6,1-hydride shift cation **12**.
†Counted as the dibenzamide derivative.
The figures are counts per mmol per min × 10^{-5}

FIG. 4. Degradation of ^{14}C-labelled 2-bromonorbornene.

various halogenations of norbornene is given in Table 4. In comparing the chlorination and bromination reactions, which have been examined in greatest detail, the greater yield of chloronortricyclene relative to bromonortricyclene is perhaps a reflection of the greater basicity of chloride ion than bromide ion in aprotic solvents. The absence of hydride shift products in the chlorination reaction is explicable on the basis of a less stabilized (chlorine being more electronegative and less efficient at bridging than bromine) (20), and hence more reactive, initial cation reacting with the more nucleophilic (in aprotic solvents) chloride ion (however, see ref. 19).

As mentioned in a previous publication (2), two probably related points of difference between the bromination and bromofluorination reactions deserve comment. These are the absence of 2-*exo*,3-*endo* isomers as major products[12] and the much larger proportion of the 6,1-hydride shift product 7-*anti*-bromo,2-*exo*-fluoronorbornane in the latter reaction. Any initially formed bromonium ion in the bromofluorination reaction would presumably have a longer lifetime to undergo hydride shift since associated fluoride–hydrogen fluoride species in ether should be poorer nucleophiles than bromide anion in aprotic medium. If so, it would not be surprising to find much less product of attack on a bromonium ion and an increase in 6,1-hydride shift products. As an approximation, the proportion of 2-*exo*-fluoro-3-*endo*-bromo isomer to be expected from the 6,1-hydride shift cation **12** can be estimated to be the same (~10% of the 7-*anti* isomer) as for the bromination, or only about 4% of the total product and could be present as one of the minor components.[12] The observed product yields are not likely to be the result of prior formation of a 2-*exo*,3-*endo* compound followed by rearrangement; loss of bromide from such a product would eventually lead to 7-fluoro derivatives which are not observed.

A comparison of the relative rates of anion capture at each pair of Wagner–Meerwein related sites in the three substituent-bearing nonclassical ions is presented in Table 5. Although the reactions were not all run under the same conditions, the variation in the product ratios can be accounted for by a combination of steric and inductive effects. The preponderance of 7-*syn* isomer from reaction of cation **24** is favored by the steric bulk of the substituent X, which would hinder formation of the more crowded 2-*exo*,3-*exo* isomer. The difference in ratio for X = methyl *vs.* bromine is expected both from the electron withdrawing effect of bromine rendering C-1 relatively more positive than C-2 (compared to the reverse situation for the methyl substituted cation) and from the smaller size of the entering acetate oxygen atom (relative to bromide) when X = methyl.

In the capture of cation **25**, there is no steric interaction of entering nucleophile and substituent. However, a preference for attack at C-6 when X = bromine is consistent with the expected inductive effect of bromine rendering C-6

[12]There were three unidentified minor (< 3% of total) products detected during g.l.p.c. examination of the bromofluorination product. One or two of these may have been 2-*exo*,3-*endo* isomers.

Can. J. Chem. Downloaded from www.nrcresearchpress.com by 210.87.254.6 on 09/05/12
For personal use only.

TABLE 5. Ratios of attack at Wagner–Meerwein related sites

Non-classical ion	Wagner-Meerwein product pair	Ratios of products				
		X = Y = Br	X = Br Y = F	X = Y = Cl	X = Br Y = $NHSO_2C_6H_5$	X = Me Y = OAc
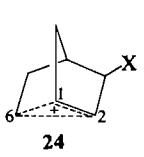 **24**	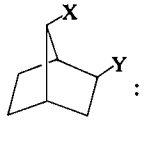	>66:1*	>22:1*	7.3:1	>29:1*	5:1
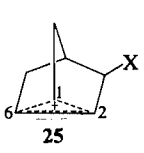 **25**	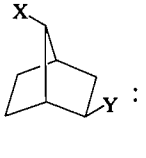	8:1†	>38:1§	—	>13:1§	1.08:1
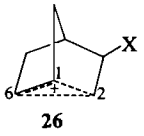 **26**	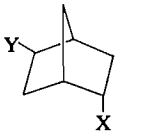	1.6:1‡	—	—	—	1.23:1‡

*2,3-*exo,exo* was not detected.
†Based on amount of **15** formed by hydride shift only.
‡Insensitive to solvent.
§No 2-*exo*,3-*endo* detected.

more electron deficient and therefore relatively more reactive than C-2. To harmonize this rationale with the result (approximately equal attack at both sites) for the same cation when X = methyl requires the introduction of some factor (torsional effect of the methyl with C-2 hydrogen being pushed up?) to explain why there is not more attack at C-2 in this case.

For cation **26**, in which not only is direct interaction of entering nucleophile and substituent X not possible, but also the inductive effect through bonds (not through space, however) would be the same for both C-1 and -6, the distinction between the two positions is almost negligible and the ratio of capture for X = bromine and methyl approaches unity.[13]

The effect of solvent on the bromination reaction was examined because of the previous reports[3,4,5] of the effect of added pyridine. In the present work it was found that the effect of pyridine and pyridine derivatives is much too complex to be accounted for by a simple solvent effect (1). However, when the solvent was changed from carbon tetrachloride to the more polar methylene chloride and acetonitrile, the relative constancy of the dibromide product composition was consistent with purely ionic bromination.

With the bromination of norbornene rationalized, a related reaction, the bromination of *exo*-trimethylene-2-norbornene (**22**), was also reexamined. In agreement with the previous report (21) we find that in carbon tetrachloride the major product (80%) is the 2-*exo*,3-*endo* dibromide **23** accompanied by minor amounts of at least seven other compounds. This same product was formed in the same 80% yield when the bromination was conducted in pyridine, but the proportions of the minor products changed (see Experimental). The minor products were not further investigated.

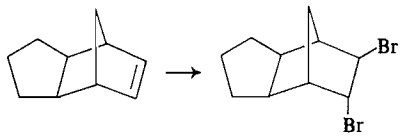

22 **23**

Improvement in Norbornene Degradation

The standard four-step procedure (18) for degradation of norbornene involving alternating

[13]We refrain from speculating here on reasons for the small but real difference from unity, but see ref. 1.

Can. J. Chem. Downloaded from www.nrcresearchpress.com by 210.87.254.6 on 09/05/12
For personal use only.

TABLE 6. Properties of norbornene dibromides*

Peak	Compound	% Purity (g.l.p.c.)	$\mu^{25}_{cyclohexane}$	Analysis found(%) C (Calcd. 33.09)	H (Calcd. 3.97)	Br (Calcd. 62.89)
1	2-*exo*,3-*endo*-Dibromonorbornane (**15**)	99	2.60	33.29	3.91	62.76
2	7-*anti*,2-*exo*-Dibromonorbornane (**16**)	97	2.42	32.89	4.09	63.25
3	2-*exo*,5-*endo*-Dibromonorbornane (**17**)	91	1.10	33.22	4.05	62.72
4	2-*exo*,5-*exo*-Dibromonorbornane (**18**)	>99	0.66	33.05	3.94	62.60
5	7-*syn*,2-*exo*-Dibromonorbornane (**19**)	98	3.30	33.43	4.03	62.65

*For the i.r. spectra see ref. 1.

oxidation and Schmidt reactions suffers from low yields. In the present work the yields and convenience of the first and last steps have been improved. In the first step, when ozone instead of permanganate was used as the oxidizing agent in ethyl acetate at $\sim -70°$, 87–99% yields of 1,3-cyclopentane dicarboxylic acid were obtained in agreement with previous work (22). The acid was a mixture of 92% of the *cis* isomer and 8% of an impurity which was not the *trans* isomer, but which was removed by recrystallization. Ethyl acetate was used as the ozonization solvent to avoid the formation of some monomethyl ester which occurred in methanol.

The second step, the Schmidt reaction on the diacid, proceeds well as described in the literature (18), but the third step, the oxidation of the cyclopentane-1,3-diamine to succinic acid has always been troublesome. Since succinic acid is stable to aqueous Cr^6 (23), this oxidizing agent was tried, but the reaction was capricious and the isolated yields were never more than 27%. On the possibility that initially formed succinic acid (or the diamine) was being oxidized further by Cr^5 or Cr^4 (24), oxidations were tried with Cr^6 in the presence of Mn^2 as scavenger for Cr^5 and Cr^4 (25), but the yield of succinic acid was still only 26%, which is about the yield obtained from oxidation by permanganate. In control experiments it was shown that succinic acid was recovered in over 90% yield from the Cr^6–Mn^2 reagent, and therefore the cyclopentane-1,3-diamine is oxidized by Cr^6 mainly to products not degraded to succinic acid.

The final step in the degradation sequence, the Schmidt reaction on succinic acid has been reported to go in only 8% yield (26), and for this reason the alternative Curtius degradation via the azide and urethane has been employed (27). This procedure, although a big improvement, is tedious and gives only 50% of the diamine. Since in succinic acid each carboxyl group may be considered as an electronegative substituent in close proximity to the other, it seemed that the Stothers–McNamara modification (28) of the Schmidt reaction might give better results. These workers found that the use of 20% oleum in the reaction with electronegatively substituted aromatic acids gave much better yields of carbon dioxide. When this procedure was applied to succinic acid, yields of 41–83% of barium carbonate and 30–51% of the dibenzamide derivative of ethylenediamine were realized. Although the yield of diamine from the modified Schmidt reaction is no better than from the Curtius procedure, the Schmidt procedure is more economical.

Experimental

General

Experimental details are the same as in ref. 2 with the following additions. For gas chromatography a Glowall Model 400 instrument equipped with a heated exit port and a hydrogen flame detector was employed. Its all glass column and injection chamber was a 1.8 m length of coiled 3.4 mm i.d. (analytical) or else 10 mm i.d. (preparative) tubing. Helium or argon was used as the carrier gas. For preparative work a 50:1 stainless steel splitter was used in conjunction with the 10 mm column. FFAP refers to Wilkens free fatty acid phase and DEGS to diethylene glycol succinate. The response of the hydrogen flame detector to the five dibromides and **2** and **20** was determined by analysis of synthetic mixtures of known weight percent (see ref. 1 for details). No correction factor was necessary for the dibromides to convert peak areas to weight percent, but an average factor of 0.81 was required for 2-*exo*-bromonorbornane.

For integration of the g.l.p.c. charts, the amount of **2** and **20** relative to the total dibromide area was determined by the cut-and-weigh technique or by planimeter from a trace in which all peaks were on scale. Dibromide ratios were obtained from a second trace in which the height of the dibromide peaks was optimized.

Melting points were taken on a Reichert Kofler microscope hotstage unless otherwise specified. Refractive

Can. J. Chem. Downloaded from www.nrcresearchpress.com by 210.87.254.6 on 09/05/12
For personal use only.

Can. J. Chem. Downloaded from www.nrcresearchpress.com by 210.87.254.6 on 09/05/12
For personal use only.

indices were measured on a Bausch and Lomb refractometer. Microanalyses were performed in the laboratories of A. Bernhardt, Mülheim, Germany, and A. B. Gygli, Toronto.

The ^{14}C counting was carried out with a Nuclear Chicago MK1 liquid scintillation counter. The "TFC" scintillation solution (29) used for counting was prepared by diluting 5 volumes of toluene containing 0.4% PPO (2,5-diphenyloxazole) and 0.005% bis-MSB [*p*-bis(*o*-methylstyryl)-benzene] with 4 volumes of methyl cellosolve (ethylene glycol monomethyl ether); samples were weighed (see Table 10) into scintillation vials and counted in 15 ml of TFC. Barium carbonate was counted by trapping the acid-liberated $^{14}CO_2$ in a scintillation vial containing 1.0 ml of NCS (a quaternary ammonium base, 0.6 *N* in toluene, supplied by Nuclear–Chicago Corp.) and then adding 15 ml of TFC for counting. Samples were counted at balance point in a 0.5–9.9 V window, using a channels ratio method to ensure that counting efficiency did not change from sample to sample. As there was no variation in counting efficiency, counts per min data were adequate for comparison.

In view of the fatalities which have occurred in work with closely related dibromo compounds (30), all operations with the dibromonorbornanes, including g.l.p.c., were conducted in a fume cupboard.

Dibromonorbornanes

The procedure of Kwart and Kaplan (3) was used. Norbornene[14] (20 g, 0.21 mol) in 40 ml of carbon tetrachloride was cooled to −10° with an ice–salt bath. A solution of 29 g (0.18 mol) of bromine in 20 ml of carbon tetrachloride was added with stirring at a rate such that the temperature remained at or just below 0°. After 30 ml of the bromine solution had been added, the persistence of red color and lack of exothermicity indicated that the olefin had been consumed. Evaporation of solvent left 40.4 g of crude product whose g.l.p.c. (Fig. 1) at 130° on a column of 5% DEGS on 60–80 mesh Chromasorb P indicated the presence of at least seven major components and three minor ones.

Bromonortricyclene and 2-*exo*-bromonorbornane, two of the major products, were separated as the lowest boiling (b.p. 60° at 11 mm) materials by fractional distillation on a 45 cm Nester and Faust platinum spinning band column. The mixture of higher boiling dibromides (b.p. 30–75° at 0.06 mm) was separated by preparative g.l.p.c. on a column of 10% FFAP on non acid-washed 60–80 mesh Chromasorb P. Operating conditions: injector temperature 270°, column temperature 170°, exit port temperature 200°, argon carrier gas flow rate ~80 ml/min, 40–50 μl of dibromide mixture per injection. Fractions collected were re-injected and the other five major products (numbered in order of elution) were obtained in the purity indicated in Table 6. Peak 4 (2-*exo*,5-*exo*-dibromonorbornane) was obtained as a crystalline solid, m.p. 94–95.5°, after recrystallization from petroleum ether (b.p. 30–60°).

[14]Norbornene (Aldrich Chemical Co.) was purified by distillation. It gave a single g.l.p.c. peak on a column of 5% DEGS on Chromasorb P. The purity must be checked regularly because even purified norbornene gives rise to higher boiling material on long standing.

Isomerization of Dibromonorbornanes

(a) A mixture of 418 mg of 7-*syn*,2-*exo*-dibromonorbornane (**19**) and 1 ml of 47% aqueous hydrobromic acid was refluxed for 3.25 h (*cf.* refs. 3 and 4). The resulting dark-colored mixture was cooled and extracted with 10 ml of ether and analyzed by g.l.p.c. to yield the following composition: **15**, 15.2%; **16**, 34.5%; **17**, 22.8%; **18**, 21.3%; **19**, 0.5%; 3 minor products (one in the starting material), total 6.0%. On shorter reflux times (1.5–2 h) the amount of **16** was greater at the expense of **17** and **18**.

(b) Hydrogen bromide gas was passed continuously at room temperature into a solution of 67 mg of the 7-*syn*,2-*exo* isomer **19** in 3 ml of carbon tetrachloride. Samples were withdrawn at intervals and analyzed by g.l.p.c. for the ratios of **15**:**16**:**17**:**18** (see Table 7).

(c) Each of the purified dibromides was treated with 5 ml of a standardized solution of hydrogen bromide in methylene chloride[15] at 0°. After the allotted time, the reaction was quenched with 2 ml of 10% aqueous sodium bicarbonate solution. The separated and dried organic layer was analyzed by g.l.p.c. and the results are summarized in Table 8.

Reaction of Bromonortricyclene with Hydrogen Bromide

Bromonortricyclene was treated with standardized solutions of hydrogen bromide in methylene chloride.[15] After the allotted time the reaction was quenched with aqueous sodium bicarbonate solution. The separated and dried organic layer was analyzed by g.l.p.c., and the results are summarized in Table 9. The kinetically controlled product from the 58% reaction entry had the following composition: **15**, 3.3%; **16**, 29.3%; **17**, 33.1%; **18**, 18.4%; **19**, 15.9%.

Brominations under Other Conditions

(a) With Calcium Carbonate

A solution of 543 mg (5.8 mmol) of norbornene in 100 ml of methylene chloride[15] was cooled to 0° and stirred vigorously (magnetic bar) with 5.0 g of suspended powdered calcium carbonate. A solution of 1.0 g (6.25 mmol) of bromine in 5 ml of methylene chloride was added during 20 min. Then 5 ml of 10% sodium bicarbonate solution was added, followed by 25 ml of water. Suspended solid was removed by filtration, and the organic layer was filtered and dried. After removal of solvent, the crude product was analyzed by g.l.p.c. (entry 5, Table 2). In an attempt to diminish further the amount of 2-*exo*-bromonorbornane the reaction was repeated with 25.0 g

TABLE 7. Products of reaction of **19** with HBr

Compound	3 h	20 h	25 h
15	12.7	14.3	16.8
16	54.9	49.8	39.8
17	17.8	19.3	24.0
18	14.6	16.5	19.2

[15]Except where carbon tetrachloride was used to reproduce exactly the conditions of Kwart and Kaplan (3), methylene chloride was generally substituted because of its lower freezing point and because of the greater solubility of hydrogen bromide and salts in this solvent.

TABLE 8. Reaction of dibromides with HBr

Compound	Weight (mg)	mg HBr/5 ml	Time (h)	The g.l.p.c. result
15	25.0	31	17	No isomerization
16	25.0	31	17	No isomerization
17	14.0	31	17	No isomerization
18	18.0	31	17	No isomerization
19	19.6	31	5	No isomerization or at most a trace (<4%)
19	7.4	42/1 ml	14.5 (25°)	No isomerization
i	15.0	13.4/2 ml	1	No isomerization

TABLE 9. Reaction of bromonortricyclene with HBr

mg of **2**	Time (h)	Temperature (°C)	mg HBr	Volume (ml)	The g.l.p.c. result
76.4	73	0	43.5	25	No reaction
5 μl	0.33	25	6.6	1	No reaction
6.5	1.0	25	20.2	1	Slight reaction
5	14.5	25	42	1	58% reaction
7.4 of **19**	14.5	25	42	1	No isomerization

of calcium carbonate to give 1.17 g (98%) of crude products (entry 6, Table 2).

(b) Dilution

The above experiment (*a*) was repeated without calcium carbonate on two different solutions of norbornene in methylene chloride,[15] one containing 498 mg in 100 ml and the other containing 481 mg in 2 ml. The reactions were quenched with aqueous sodium bicarbonate solution, and the organic layers were separated and dried over magnesium sulfate. The g.l.p.c. analyses of the crude products are entries 1 and 2 in Table 2.

(c) With Oxygen Scavenger

Oxygen was passed through a sintered glass bubbler into a vigorously stirred (magnetic bar) solution of 518 mg of norbornene in 100 ml of methylene chloride[15] maintained at 0°. A solution of 1.0 g of bromine in 2 ml of methylene chloride was added during 20 min. The reaction was worked up as in (*b*). The g.l.p.c. analyses gave the figures in entry 4 in Table 2.

(d) With Toluene

To a stirred (magnetic bar) solution of 526 mg (5.6 mmol) of norbornene and 2.415 g (26.2 mmol) of toluene in 100 ml of methylene chloride[15] maintained at 0.5–1.5° was added during 20 min a solution of 350 mg (2.19 mmol) of bromine in 2 ml of methylene chloride. The g.l.p.c. analysis showed that the dibromide products were formed in the same ratios as in the absence of toluene and that the small peak corresponding in retention time to benzyl bromide constituted less than 0.5% of the total products. The experiment was repeated with carbon tetrachloride solutions (see Table 3).

(e) With Other Solvents

Small scale brominations were run in carbon tetrachloride and acetonitrile as well as in methylene chloride. The general procedure was to add the bromine diluted with a little of the solvent to a stirred (magnetic bar) solution of norbornene in the solvent. The reaction mixture was washed with aqueous bicarbonate and analyzed by g.l.p.c. The total area under peaks in the dibromide region was equated to 100%, and the normalized percents of compounds **15–19** were calculated on this basis. The results are summarized in Table 3. Reactions in acetonitrile and in the more concentrated carbon tetrachloride solutions gave rise to variable amounts of a g.l.p.c. peak (different for the two solvents) suspected to arise from involvement of solvent in the reaction.

(f) With Diphenylpicrylhydrazyl

To a solution of 430 mg of norbornene in 1 ml of carbon tetrachloride was added 100 mg of diphenylpicrylhydrazyl. The radical was only partially soluble. Neat bromine (20 μl) was added dropwise at 0° with vigorous stirring by a magnetic bar. The reaction mixture was analyzed by g.l.p.c. Control experiments showed that diphenylpicrylhydrazyl had no effect on the dibromides, and also that the preformed product of bromine plus the radical acting on norbornene gave the same proportion of dibromides as bromine alone acting on norbornene at a given concentration (see Table 3).

(g) At −78°

To a solution of 510 mg (5.4 mmol) of norbornene in 100 ml of methylene chloride[15] cooled to −78° by a Dry-Ice – acetone bath was added with stirring (magnetic bar) during 20 min 1.0 g (6.2 mmol) of bromine dissolved in 2 ml of methylene chloride. The reaction was quenched with 5 ml of 10% aqueous sodium bicarbonate, and the separated organic layer analyzed by g.l.p.c. (entry 3, Table 2).

(h) With Tetraethylammonium Bromide

A solution of 68.8 mg (0.73 mmol) of norbornene in 10 ml of methylene chloride[15] was saturated with tetraethylammonium bromide (1.271 g, 6.05 mmol) at 0°. Bromine (0.20 g, 1.2 mmol) was added with stirring (magnetic bar) during 3 min at −5 to −3°. The mixture was allowed to stir at 0° for 17 min more. Work-up gave 157 mg of crude product whose g.l.p.c. analysis is entry 7, in Table 2.

Can. J. Chem. Downloaded from www.nrcresearchpress.com by 210.87.254.6 on 09/05/12
For personal use only.

TABLE 10. Counting results from degradation of ^{14}C-labelled norbornene and dibromonorbornane*

Compound	Weight (mg) counted		Counts ($min^{-1} \times 10^{-3}$)		Counts (min^{-1} $mmol^{-1} \times 10^{-5}$)	
	A	B	A	B	A	B
1,3-Cyclopentane dicarboxylic acid	2.89	5.72	21.3	20.0	11.6	5.53
1,3-Cyclopentanediamine dibenzamide	3.18	3.21	11.3	5.93	10.9	5.70
Succinic acid	1.34	2.30	12.2	9.59	10.7	4.93
Barium carbonate	6.75	1.70	0.0	0.172	0.0	0.20
Ethylenediamine dibenzamide		2.38		3.91		4.39

*All samples were counted to 10^5 total counts. A, Norbornene control degradation; B, degradation of 2-*exo*,3-*endo* dibromide **15** from norbornene.

Hydrogenolysis of 7-syn,2-exo-Dibromonorbornane (19)

Tetrahydrofuran (10 ml), *t*-butyl alcohol (2.1 ml, 22 mmol), and finely chopped sodium (1.5 g, 63 mga) were heated to reflux with stirring. 7-*syn*,2-*exo*-Dibromonorbornane (**19**) (1.01 g, 4.0 mmol) was added and the resulting dark solution was refluxed for 45 h. After dilution with water and extraction with ether, the organic solution was slowly distilled until the distillation temperature reached 40° when norbornane just began to sublime. The residual 1.00 g of liquid, containing some solvent, on analysis by g.l.p.c., was shown to contain 110 mg (30%) of norbornane. A sample was isolated by preparative g.l.p.c. and shown to be identical (i.r. spectrum, g.l.p.c. retention time) with an authentic specimen.

cis-1,3-Cyclopentanedicarboxylic Acid

A solution of 5.86 g (62 mmol) of norbornene in 150 ml of ethyl acetate was cooled to $\sim -78°$ in a Dry-Ice – acetone bath, and ozone was passed in until a blue color persisted. The solution was allowed to warm to room temperature, and the solvent was evaporated at reduced pressure on a rotating evaporator. The residual viscous oil was warmed with a mixture of 50 ml of 98% formic acid and 30 ml of 30% aqueous hydrogen peroxide solution, whereupon a vigorous exothermic reaction occurred at ~60° which caused the solution to reflux. Reflux was maintained for 1 h before the solution was evaporated to leave 9.53 g (97%) of a viscous oil which slowly solidified, m.p. 87–107°. The g.l.p.c. analysis of the methyl ester gave two peaks showing this material to be 92% of *cis*-diacid and 8% of an impurity. The impurity was not the *trans*-diacid since methoxide-catalyzed epimerization of the methyl ester of pure *cis*-diacid gave two isomers of g.l.p.c. retention times: 6.0 min (*trans*-dimethyl ester) and 7.5 min (*cis*-dimethyl ester) neither of which was identical with the impurity of retention time 4.5 min. However, the impurity was removed by recrystallization from ether – petroleum ether (b.p. 30–60°). Four such recrystallizations gave colorless diacid, m.p. 118–120° (lit. (22*b*): 121.5–122.5°).

Dehydrobromination of 2-exo,3-endo-Dibromonorbornane (15)

Pure (97%) **15** (101 mg) was treated under nitrogen at ice bath temperature with 0.75 ml of a 1.5 *M* solution of phenyllithium in benzene–ether (Alfa Inorganics). Samples withdrawn for g.l.p.c. showed complete reaction after 15 min. The n.m.r. spectrum of the solution had a vinyl proton doublet at 5.81 p.p.m. different from the vinyl proton absorption of added norbornene at 5.92 p.p.m. (dd).

In separate experiments it was demonstrated that **2** and **16–20** did not react with phenyllithium under the conditions used for **15** (see ref. 1).

Degradation of Radioactive 2-exo,3-endo-Dibromonorbornane (15)

(a) 1,3-Cyclopentanedicarboxylic Acid

Norbornene-5,6-^{14}C (752 mg, 1 mCi) supplied by Mallinckrodt Nuclear, Orlando, Florida, and synthesized by the Diels–Alder addition of ethylene-1,2-^{14}C to cyclopentadiene (31) was dissolved in 100 ml of carbon tetrachloride. A 1 ml aliquot was diluted with inactive norbornene and degraded to prove that the ^{14}C was entirely at C-5 and -6. See Table 10.

An aliquot of this radioactive norbornene solution (20 ml, ~200 μCi) was diluted with inactive norbornene (20.24 g, 0.22 mol) in 20 ml of carbon tetrachloride and cooled in an ice–salt bath. A solution of 34 g (0.21 mol) of bromine in 23 ml of carbon tetrachloride was added with stirring (magnetic bar) at a rate which kept the temperature between -2 and $+2°$. After ~1.25 h when the reaction solution retained the bromine color, addition of bromine was stopped and the solvent was removed at reduced pressure and room temperature. Most of the monobromides **20** and **2** were distilled at 72° (16 mm) to leave 38.23 g of dibromides containing some **2** and **20**. The g.l.p.c. analysis calculations gave 2.64 g (6.9%) of 2-*exo*,3-*endo*-dibromide **15** in this mixture. The normalized percents of the dibromonorbornanes were **15** (9.8%), **16** (20.5%), **17** (4.1%), **18** (3.6%), and **19** (62%); the difference between these figures and those for the 430 mg/ml reaction in Table 3 may be due to differences in instantaneous bromine/norbornene ratio for the large *vs.* small scale reaction. To this mixture, which was cooled under nitrogen in an ice bath, was added 75 ml of 1.9 *M* phenyllithium solution through a rubber septum. After 30 min the solution was cautiously quenched with 10 ml of aqueous sodium hydroxide. The g.l.p.c. of the organic layer showed **15** to have been completely destroyed, but the ratios of **16**:**17**:**18**:**19** remained the same. The aqueous layer was separated and the benzene–ether solvent removed under reduced pressure at room temperature. Decalin (20 ml) was added and distillation (a Bunsen burner was used to limit frothing) was carried out until a temperature of 80° (16 mm) was reached. A further 30 ml of decalin was added and the distillation continued until approximately 30 ml of distillate (receiver cooled in

Can. J. Chem. Downloaded from www.nrcresearchpress.com by 210.87.254.6 on 09/05/12
For personal use only.

Can. J. Chem. Downloaded from www.nrcresearchpress.com by 210.87.254.6 on 09/05/12
For personal use only.

an ice bath) had been collected. The distillate was diluted with 25 ml of ethyl acetate, and the solution cooled in a Dry-Ice – acetone bath. Ozone was passed into the stirred (magnetic bar) solution for 90 min by which time the solution was pale green. After evaporation of the solvent, 25 ml of 98% formic acid and 15 ml of 30% aqueous hydrogen peroxide was added, and the mixture *gently* warmed until reaction was initiated as indicated by gas evolution. When the exothermic reaction subsided, the mixture was heated on a steam bath for 30 min. After evaporation of most of the formic acid the solution was cooled and extracted with 10% aqueous sodium hydroxide. Acidification with 20% hydrochloric acid, saturation with sodium chloride, and extraction with six 30 ml portions of ether afforded 865 mg (57%) of a pale brown oil which slowly solidified. A sample recrystallized from ethyl acetate had m.p. 121–122° (lit. (22*b*): 121.5–122.5°).

(b) 1,3-Cyclopentanediamine Hydrochloride

The 865 mg of crude active diacid was diluted with 720 mg of inactive acid by solution in ethyl acetate and evaporation. A portion (1.43 g, 9.05 mmol) of the resulting acid was dissolved in 15 ml of 100% sulfuric acid in a 50 ml flask. The flask was equipped with a gas outlet attached to a wash bottle containing dilute aqueous chromic acid, a side arm for addition of solid sodium azide, and a nitrogen inlet projecting below the surface of the solution. After the system was flushed with dry nitrogen, the chromic acid wash bottle was attached to a wash bottle containing carbon dioxide free sodium hydroxide solution. Sodium azide (2.5 g, 38.5 mmol) was added as the solution was stirred (magnetic bar) and heated to 40–45°. After the addition (~0.75 h) a slow stream of nitrogen was passed through the system for a further 30 min. The carbon dioxide absorbed in the sodium hydroxide solution was precipitated as barium carbonate by treatment with 25 ml of a solution of barium chloride and ammonium chloride (0.33 *M* in each). The yield of barium carbonate after filtration and drying at 120° for 6 h was 2.114 g (59%).

The sulfuric acid solution was carefully neutralized with ~30 ml of 50% aqueous sodium hydroxide and the resulting solution distilled to dryness into 20 ml of 15% hydrochloric acid. Water (30 ml) was added to the residue and the resulting mixture again distilled to dryness; this procedure was repeated six times. Failure to distill almost to complete dryness results in very low yields. The aqueous distillate after evaporation afforded 819 mg (53%) of 1,3-cyclopentanediamine hydrochloride as a buff powder. Yields in other experiments ranged between 40 and 92%.

The *dibenzamide* derivative used for counting was obtained by vigorously shaking a solution of 51 mg (0.29 mmol) of the diamine hydrochloride in 3 ml of 10% aqueous sodium hydroxide with 0.15 ml of benzoyl chloride. The white precipitate was filtered, and the filtrate extracted with two portions of ether. The material (87.7 mg, 97%) from the combined precipitate and ethereal extracts was recrystallized thrice from ethanol to give colorless needles, m.p. 213.5–215° (lit. (18): 213–215°).

(c) Succinic Acid

Potassium permanganate (6.21 g) was added to a solution of 770 mg (4.45 mmol) of the diamine hydrochloride prepared in (*b*) in 60 ml of water. The reaction was heated in an oil bath (130–140°) for 15 min, cooled, and acidified with 5 ml of 10% hydrochloric acid. Sulfur dioxide was passed in until the solution was clear and colorless. Continuous ether extraction for 42 h afforded 146 mg (28%) of pale yellow solid succinic acid. The g.l.p.c. of the dimethyl ester of the crude acid indicated the absence of other components. Five recrystallizations from ethyl acetate gave colorless needles, m.p. 175–185°.

(d) Ethylenediamine Dibenzamide

Several variations in reaction procedure were tried, and it was found that failure to follow exactly the procedure described below frequently resulted in very low or no yield of the dibenzamide.

The same apparatus was used as described in (*b*) for the preparation of 1,3-cyclopentanediamine. A solution of 20 mg (0.17 mmol) of recrystallized succinic acid from (*c*) in 1 ml of 20% oleum was prepared in the 50 ml flask and warmed to 40°. The apparatus was flushed with dry nitrogen before attachment of the wash bottle containing sodium hydroxide. Sodium azide (104 mg, 1.6 mmol) was added *rapidly* (~1 min addition time) to the stirred solution (magnetic bar) at 40°. After the vigorous reaction was over, the flow of nitrogen was maintained for 60 min. The carbon dioxide was precipitated as barium carbonate from 10 ml of ammonium chloride – barium chloride solution (0.33 *M* in each). The yield of barium carbonate after filtration and drying was 27.3 mg. (41%).

The sulfuric acid solution was chilled in an ice bath, diluted with 6 ml of water, and carefully basified with 3 ml of 50% aqueous sodium hydroxide. The solution was allowed to warm to room temperature and water was added to dissolve any precipitated salts. Benzoyl chloride (0.10 ml) was added and the mixture shaken vigorously until a white precipitate formed. Filtration, water washing, and solution in ethanol gave 23.0 mg (51%) of crude dibenzamide after evaporation of the ethanol. Recrystallization from ethanol–water gave 10 mg of white needles, m.p. 259–260° (capillary) (lit. (32): 249°), undepressed on admixture with an authentic specimen.

Calculation of the Amount of 2-exo,3-endo-Dibromonorbornane (15) Formed by 6,1-Hydride Shift

$$\frac{2(\text{act. cyclopent. diacid} - \text{act. succinic}) \times 100}{\text{act. cyclopent. diacid}} = 22\%$$

$$\frac{2(\text{act. diamine} - \text{act. succinic}) \times 100}{\text{act. diamine}} = 27\%$$

$$\frac{(\text{act. cyclopent. diacid} - \text{act. ethylenediamine}) \times 100}{\text{act. cyclopent. diacid}} = 21\%$$

$$\frac{(\text{act. diamine} - \text{act. ethylenediamine}) \times 100}{\text{act. diamine}} = 23\%$$

$$\frac{2(\text{act. succinic} - \text{act. ethylenediamine}) \times 100}{\text{act. cyclopent. diacid}} = 20\%$$

$$\frac{2(\text{act. succinic} - \text{act. ethylenediamine}) \times 100}{\text{act. diamine}} = 19\%$$

Chromic Acid Oxidation of 1,3-Cyclopentanediamine

(a) To show that succinic acid could be recovered in good yield from chromic acid oxidation, 121 mg of pure succinic acid was dissolved in 7.5 ml of the oxidation reagent prepared by dissolving 33.6 g of chromium trioxide in 200 ml of water and 50 ml of concentrated sulfuric acid. The control mixture was diluted with water

Can. J. Chem. Downloaded from www.nrcresearchpress.com by 210.87.254.6 on 09/05/12
For personal use only.

and continuously extracted with ether for 46 h. The ether solution was dried over sodium sulfate and evaporated to leave 111 mg (93% recovery) of succinic acid which was found to be pure by g.l.p.c. of its methyl ester. From another control reaction refluxed for 1.5 h the recovery was 89%.

(b) 1,3-Cyclopentanediamine hydrochloride (379 mg, 2.19 mmol) was dissolved in 25 ml (33 mmol) of the chromic acid solution prepared in (*a*), and the resulting mixture was refluxed for 1.5 h. The oxidation mixture was then cooled, diluted with 120 ml of water, and extracted continuously with ether for 41 h. Evaporation of the dried ethereal solution left 70 mg (27%) of white crystalline succinic acid, m.p. 185–188°.

(c) 1,3-Cyclopentanediamine hydrochloride (250 mg, 1.45 mmol) was dissolved in 16.5 ml (22 mmol) of the chromic acid solution prepared in (*a*) to which had been added 4.0 g (23 mmol) of manganous sulfate. The reaction mixture was refluxed for 1.5 h, cooled, and the excess chromic acid destroyed with sodium sulfite. Continuous ether extraction for 40 h yielded 46 mg (26%) of crystalline succinic acid.

Bromination of exo-Trimethylenenorbornene

exo-Trimethylenenorbornene was prepared from dicyclopentadiene by the procedure of Cristol *et al.* (33). The purity of the crystalline precursor, 2-*exo*-benzoyloxy-5,6-*exo*-trimethylenenorbornane, was carefully checked by n.m.r. spectroscopy and had m.p. 71–72° (lit. (33): m.p. 71.5–72°). The liquid olefin obtained on pyrolysis had n_D^{25} 1.4940 (lit. (33): n_D^{25} 1.4943) and gave a single g.l.p.c. peak (>98%) on a column of 5% DEGS/Chromasorb P. The i.r. spectrum of a liquid film showed no discernible peaks at 6.08, 7.42, 8.06, or 8.74 μ from the *endo* isomer. The phenyltriazole derivative melted at 137–143° indicating <5% *endo*-trimethylene derivative present (33).

(a) In Carbon Tetrachloride

A solution of the olefin (4.31 g, 32 mmol) in 50 ml of carbon tetrachloride was cooled in an ice–salt bath, and a solution of 5.0 g (31 mmol) of bromine in 10 ml of carbon tetrachloride was added during 45 min with stirring (magnetic bar) at such a rate that the reaction temperature remained between −3 and 0°. The crude product (11.33 g) was analyzed by g.l.p.c. on a 5% DEGS/Chromasorb P column after removal of solvent and found to contain 80% of **23** and a total of 20% of seven other components. For spectra and further details see ref. 1.

(b) In Pyridine

To a cooled solution of the olefin (3.84 g, 28.6 mmol) in 50 ml of reagent grade pyridine (dried over potassium hydroxide) was added with stirring (magnetic bar) during 15 min a solution of 5 g (31 mmol) of bromine at a rate which kept the temperature between −5 and −1°. The solution was stirred at 0° for a further 45 min. The reaction mixture was diluted with 100 ml of ether and extracted with eight 100 ml portions of water. Evaporation of the dried solution left 4.58 g of liquid product which was analyzed by g.l.p.c. on a 5% DEGS/Chromasorb P column and found to contain 80% of **23** and a total of 20% of six other compounds which were not all identical in retention times with the products formed in carbon tetrachloride. For further details see ref. 1.

A pure (>98% by g.l.p.c.) sample of the major product, 2-*exo*,3-*endo*-dibromo-5,6-*exo*-trimethylenenorbornane, was obtained by vacuum distillation of the product from a larger scale pyridine reaction.

Control Comparison with exo,cis-2,3-Dibromonorbornane (i)

A specimen of authentic *exo,cis*-2,3-dibromide **i** was prepared by the Diels–Alder procedure of LeBel (10) and had m.p. 60.5–60.8° (lit. (10): 60.4–61.3°). The g.l.p.c. comparison (admixture) showed that the compound was not identical with any of the components of the bromination mixture. On a 5% DEGS/Chromasorb P column at 150° the following retention times (min) were observed: **15** (4.0), minor component (4.6), **16** (4.9), **17** (6.15), **18** (7.1), minor components (8.75 and 9.5), **i** (10.2), and **19** (12.0).

A sample of 15 mg of *exo,cis*-2,3-dibromide **i** was dissolved in 2 ml of a solution of hydrogen bromide in methylene chloride (6.7 mg/ml) previously cooled to 0°. The reaction mixture was allowed to stand for 1 h at 0°, and was then diluted with methylene chloride, washed with aqueous sodium bicarbonate, and dried over magnesium sulfate. Evaporation of the solvent left 13 mg of residual **i** whose g.l.p.c. trace was identical with starting material; there was no additional peak present.

The authors would like to thank Professor W. A. Ayer, Edmonton, Alberta, through whose courtesy the 100 MHz n.m.r. spectra and decoupling data were obtained, Professor R. K. Chan for help with the dipole moment measurements, Professor J. A. Berson for helpful discussions, and the National Research Council of Canada for financial support.

1. D. R. MARSHALL. Ph.D. Thesis. University of Western Ontario, London, Ontario, 1968.
2. F. H. DEAN, D. R. MARSHALL, E. W. WARNHOFF, and F. L. M. PATTISON. Can. J. Chem. **45**, 2279 (1967).
3. H. KWART and L. A. KAPLAN. J. Amer. Chem. Soc. **76**, 4072 (1954).
4. L. A. KAPLAN. Ph.D. Dissertation. University of Delaware, Newark, Delaware, 1955.
5. J. L. NYCE. Ph.D. Dissertation. University of Delaware, Newark, Delaware, 1960.
6. A. C. OEHLSCHLAGER, C. D. KENNEDY, and L. H. ZALKOW. J. Org. Chem. **31**, 1682 (1966).
7. M. L. POUTSMA. J. Amer. Chem. Soc. **87**, 4293 (1965).
8. D. D. TANNER and G. C. GIDLEY. J. Org. Chem. **33**, 38 (1968).
9. S. WINSTEIN, F. GADIENT, E. T. STAFFORD, and P. E. KLINEDINST. J. Amer. Chem. Soc. **80**, 5895 (1958).
10. N. A. LEBEL. J. Amer. Chem. Soc. **82**, 623 (1960).
11. P. M. SUBRAMANIAN, M. T. EMERSON, and N. A. LEBEL. J. Org. Chem. **30**, 2624 (1965).
12. C. F WILCOX. J. Amer. Chem. Soc. **82**, 414 (1960).
13. (*a*) C. J. COLLINS and C. E. HARDING. J. Amer. Chem. Soc. 91, 7194 (1969); (*b*) F. R. JENSEN and B. H. BECK. Tetrahedron Lett. No. 36, 4287 (1966); (*c*) J. A. BERSON, R. G. BERGMAN, J. H. HAMMONS, and A. W. MCROWE. J. Amer. Chem. Soc. **89**, 2581 (1967).
14. T. L. COTTRELL. The strengths of chemical bonds. 2nd ed. Butterworths, London, 1958. pp. 270–289.
15. R. B. TURNER, W. R. MEADOR, and R. E. WINKLER. J. Amer. Chem. Soc. **79**, 4116 (1957).

16. J. A. BERSON. *In* Molecular rearrangements. *Edited by* P. de Mayo. Part I, Interscience-Wiley, New York, N.Y., 1963. pp. 162–163.
17. J. A. BERSON, A. W. MCROWE, and R. G. BERGMAN. J. Amer. Chem. Soc. **89**, 2573 (1967).
18. J. D. ROBERTS, C. C. LEE, and W. H. SAUNDERS. J. Amer. Chem. Soc. **76**, 4501 (1954).
19. G. D. SARGENT. Quart. Rev. (London), **20**, 316 (1966).
20. G. A. OLAH and J. M. BOLLINGER. J. Amer. Chem. Soc. **90**, 947 (1968).
21. L. KAPLAN, H. KWART, and P. VON R. SCHLEYER. J. Amer. Chem. Soc. **82**, 2341 (1960).
22. (*a*) R. H. PERRY. J. Org. Chem. **24**, 829 (1959); (*b*) S. C. TEMIN and M. E. BAUM. Can. J. Chem. **43**, 705 (1965).
23. E. J. EISENBRAUN, S. M. MCELVAIN, and B. F. AYCOCK. J. Amer. Chem. Soc. **76**, 607 (1954).
24. J. ROČEK and A. RIEHL. Tetrahedron Lett. #14, 1437 (1966).
25. F. H. WESTHEIMER. Chem. Rev. **45**, 419 (1949).
26. H. WOLFF. Org. Reactions, **3**, 307 (1946).
27. H. KWART and W. G. VOSBURGH. J. Amer. Chem. Soc. **76**, 5400 (1954).
28. A. J. MCNAMARA and J. B. STOTHERS. Can. J. Chem. **42**, 2354 (1964).
29. J. R. ROBINSON. Int. J. Appl. Radiat. Isotopes, **20**, 536 (1969).
30. S. WINSTEIN. J. Amer. Chem. Soc. **83**, 1516 (1961).
31. J. MEINWALD and N. J. HUDAK. Org. Syn. **37**, 65 (1957).
32. A. LADENBURG. Ber. **28**, 3068 (1895).
33. S. J. CRISTOL, W. K. SIEFERT, and S. B. SOLOWAY. J. Amer. Chem. Soc. **82**, 2351 (1960).

Can. J. Chem. Downloaded from www.nrcresearchpress.com by 210.87.254.6 on 09/05/12
For personal use only.

Can. J. Chem. Downloaded from www.nrcresearchpress.com by 210.87.254.40 on 09/05/12
For personal use only.

Description de l'effet Overhauser dans les systèmes en échange: application à l'analyse conformationnelle d'aldéhydes hétérocycliques

S. COMBRISSON
Laboratoire de Chimie Organique, Ecole de Physique et Chimie, 10, rue Vauquelin, 75–Paris 5ème

B. ROQUES ET P. RIGNY
Département de Chimie, Ecole Polytechnique, 17, rue Descartes, 75–Paris 5ème

ET

J. J. BASSELIER
Laboratoire de Chimie Organique, Ecole de Physique et Chimie, 10, rue Vauquelin, 75–Paris 5ème

Reçu le 30 juillet 1970

Les relations décrivant l'effet Overhauser dans des systèmes en échange font apparaître dans le domaine où les temps de vie sont du même ordre que les temps de relaxation des augmentations relatives des signaux des protons concernés ce qui peut donner des informations sur leur environnement. Pour des températures suffisamment inférieures à la température de coalescence cette méthode permet donc de mettre en évidence des conformations préférentielles par examen du rapport des accroissements en fonction des dispositions spatiales des sites d'échange. Nous avons ainsi déterminé la conformation des formyl-2 bromo-4 thiophène et acétyl-2 dibromo-4,5 thiophène qui présentent à température ordinaire un seul rotamère de structure OS-*cis*. Dans le cas du formyl-2 bromo-4 furanne qui existe à -90 °C en équilibre entre les formes OO-*cis* et OO-*trans*, les résultats des différentes irradiations indiquent une conformation OO-*cis* pour le rotamère préférentiel. Cette méthode, dont une évaluation des limites est donnée, est, en outre, susceptible de fournir une estimation des temps de vie de chacun des sites.

The equations of the nuclear Overhauser effect (n.O.e.) in exchanging systems predict relative increases for proton signals where the life times for exchange are of the same order of magnitude as the relaxation times. This method allows one to obtain structural informations. Hence, for a temperature sufficiently below that of the coalescence, it allows one to infer a conformational preference by an examination of the relative increase in intensity with respect to spatial position of exchange sites. We have hereby determined the conformations of formyl-2 bromo-4 thiophene and acetyl-2 dibromo-4,5 thiophene. The compounds show at ambient temperature a single rotamer OS-*cis*. Formyl-2 bromo-4 furan exists at -90 °C in an equilibrium between the rotamers OO-*cis* and OO-*trans*. In this case, the results of different irradiations show OO-*cis* to be the preferred rotamer. Moreover, this method is able to give indications of the life time on different sites. We also give an evaluation of the limits of the method.

Canadian Journal of Chemistry, 49, 904 (1971)

L'effet Overhauser (n.O.e.) repose sur le phénomène de relaxation dipolaire de spins nucléaires et fournit des informations sur leurs voisinages. Depuis son observation en 1965 par Kaiser (1), Anet et Bourn (2) l'effet Overhauser a été utilisé pour résoudre un grand nombre de problèmes structuraux ou conformationnels en chimie organique (3). On peut citer parmi ceux-ci les échanges chimiques qui ont été étudiés par Forsen et Hoffman (4). L'application de l'effet Overhauser à des molécules en échange conformationnel n'a généralement été utilisé que dans les systèmes où l'échange est suffisamment lent pour que les temps de relaxation des protons concernés soient petits devant leur temps de vie sur chaque site (réf. 2 par exemple). Toutefois, dans une récente publication (23) Saunders et Bell font état, dans le cas de la *N*,*N*-diméthylformamide, des modifications de l'effet Overhauser en fonction de la température.

Par contre, il était admis que l'observation d'un effet Overhauser n'avait pas de signification dans le cas des échanges où les temps de vie et les temps de relaxation des protons irradiés étaient du même ordre. Dans un premier temps, nous avons étudié ce dernier système et établi les relations des rapports d'accroissement à partir des équations générales de l'effet Overhauser. Il ressort de ces relations que les transferts d'aimantation entre sites ne sont pas complets ce qui, a priori, autorise des conclusions structurales à partir d'expériences Overhauser. Dans un deuxième temps, nous avons cherché à vérifier expérimentalement ces résultats théoriques. Les systèmes hétérocycliques à cinq sommets (thiophène, furanne, pyrrole) se prêtent particulière-

Can. J. Chem. Downloaded from www.nrcresearchpress.com by 210.87.254.40 on 09/05/12
For personal use only.

ment bien à des recherches en r.m.n. du fait de la relative simplicité de leurs spectres. Nous avons donc choisi d'examiner la conformation des formyl-2 bromo-4 thiophène et furanne qui du fait de la forte conjugaison du groupement formyle peuvent exister sous deux conformations planes OX-*cis* ou OX-*trans* (X = S, O).

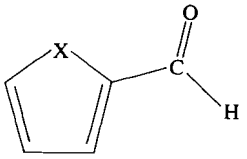

OX-*cis*

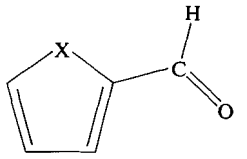

OX-*trans*

Le choix de la structure des rotamères par r.m.n. était basé jusque là sur deux critères: variation de l'influence du carbonyle selon le conformère au niveau du proton ortho (5); existence d'une stéréospécificité des couplages entre le proton aldéhydique et les protons du cycle (6) (disposition *trans–trans*). Les résultats déduits de ces deux critères n'étant apparemment pas toujours concordants (7) nous avons étudié dans un mémoire précédent (8) le problème controversé de la stéréospécificité des couplages dans les aldéhydes α thiophéniques et furanniques par r.m.n. et RX.

Dans le présent mémoire nous avons donc recherché une confirmation des précédentes conclusions dans une application de l'effet Overhauser à des systèmes en échange conformationnels. Ceci nous a amené à établir les relations décrivant les rapports des accroissements Overhauser dans le cas général des systèmes en échange. Le bon accord entre les résultats expérimentaux et les équations nous permet de proposer une nouvelle méthode d'analyse des systèmes en échange par irradiation sélective des sites d'échange pour des températures inférieures à la température de coalescence. Les augmentations Overhauser observées dans certains exemples permettent une estimation des temps de vie dans chacun des sites.

Calcul relatif à l'effet Overhauser dans un système soumis à un échange conformationnel

(A) Rappel des équations générales de l'effet Overhauser

Le traitement quantitatif de l'effet Overhauser peut se faire au moyen des équations de Bloch (9) modifiées par Solomon (10). Ainsi si l'on considère deux protons I et S relaxés par leur interaction mutuelle, les variations de leurs aimantations sont couplées et peuvent se décrire par le système, eqs. 1 et 2.

$$\left.\begin{aligned}[1]\quad \frac{dI_Z}{dt} &= -\alpha_I(I_Z - I_0) \\ &\quad -\beta_I(S_Z - S_0) \\ [2]\quad \frac{dS_Z}{dt} &= -\alpha_S(S_Z - S_0) \\ &\quad -\beta_S(I_Z - I_0)\end{aligned}\right\} \text{système A}$$

I_Z et S_Z sont les aimantations longitudinales instantanées et I_0 et S_0 leurs valeurs à l'équilibre. Si on impose $S_Z = 0$ par une irradiation prolongée de la résonance du proton S, on obtient pour l'aimantation I_Z une valeur d'équilibre supérieure à I_0, éq. 3.

$$[3]\qquad \frac{I_Z}{I_0} = 1 + \frac{\beta_I}{\alpha_I}$$

Dans cette présentation, nous ne tenons pas compte du couplage scalaire éventuel entre I et S. Si la seule interaction efficace pour la relaxation est l'interaction dipolaire entre I et S, on calcule $\beta_I/\alpha_I = 0.5$, et l'accroissement du signal des protons I dû à l'irradiation du signal des protons S est de 50%. En général d'autres interactions sont efficaces pour relaxer les spins I et l'on a, éqs. 4, 5

$$[4]\qquad \alpha_I = \alpha_I^0 + \alpha_I' = Kr_{IS}^{-6} + \alpha_I'$$

$$[5]\qquad \beta_I = 0.5\,\alpha_I^0$$

K est un coefficient dans lequel intervient le temps de correlation de la rotation moléculaire (10); r_{IS} est la distance entre I et S, α_I' est la vitesse de relaxation du spin I qui n'est pas due au couplage dipolaire entre I et S. L'accroissement Overhauser est alors, éq. 6

$$[6]\qquad \eta = \frac{0.5Kr_{IS}^{-6}}{Kr_{IS}^{-6} + \alpha_I'}$$

L'existence du terme α_I' explique que les valeurs expérimentales de l'accroissement η soient inférieures à 50% et permet des mesures relatives des distances r_{IS} (11).

(B) Equations relatives à l'effet Overhauser pour un système en échange

Si les spins I et S peuvent occuper plusieurs sites d'équilibre, la description de l'effet Overhauser est compliquée par l'existence d'un échange éventuel entre les différents sites. Qualitativement on peut distinguer les domaines suivants:

(*a*) Si le temps de vie d'un spin dans un site est long devant le temps de relaxation dans ce site, l'équilibre thermique est atteint séparément pour chaque site et l'on peut dire que l'échange n'a aucune influence sur les accroissements Overhauser.

(*b*) Si au contraire les temps de vie sont très courts devant les temps de relaxation (sans toutefois que les raies du spectre soient coalescées) les aimantations se transmettront d'un site à l'autre et le même accroissement Overhauser sera observé sur toutes les raies. L'effet Overhauser est alors non sélectif et ne peut plus être appliqué à l'étude des conformations correspondant à chaque site.

(*c*) Dans le domaine intermédiaire cependant, où les temps de vie sont du même ordre que les temps de relaxation, les transferts d'aimantation entre sites ne sont pas complets et des conclusions peuvent être déduites des expériences Overhauser.

Pour étudier quantitativement ce dernier cas, il faut remplacer les éqs. 1 et 2 du système A par des éqs. 7, 8, 9 et 10 qui tiennent compte de l'échange. Dans le cas où les spins I et S peuvent occuper deux sites d'indice 1 et 2, on écrit (système B)

$$\left.\begin{aligned}
[7]\quad & \frac{dI_{Z1}}{dt} = -\alpha_{I1}(I_{Z1} - I_{01}) - \beta_{I1}(S_{Z1} - S_{01}) + \frac{I_{Z2}}{\tau_2} - \frac{I_{Z1}}{\tau_1} \\
[8]\quad & \frac{dI_{Z2}}{dt} = -\alpha_{I2}(I_{Z2} - I_{02}) - \beta_{I2}(S_{Z2} - S_{02}) + \frac{I_{Z1}}{\tau_1} - \frac{I_{Z2}}{\tau_2} \\
[9]\quad & \frac{dS_{Z1}}{dt} = -\alpha_{S1}(S_{Z1} - S_{01}) - \beta_{S1}(I_{Z1} - I_{01}) + \frac{S_{Z2}}{\tau_2} - \frac{S_{Z1}}{\tau_1} \\
[10]\quad & \frac{dS_{Z2}}{dt} = -\alpha_{S2}(S_{Z2} - S_{02}) - \beta_{S2}(I_{Z2} - I_{02}) + \frac{S_{Z1}}{\tau_1} - \frac{S_{Z2}}{\tau_2}
\end{aligned}\right\} \text{ système B}$$

Entre[1] I_{01}, I_{02}, S_{01}, S_{02}, τ_1 et τ_2 existent les relations 11

$$[11]\quad \frac{\tau_1}{\tau_2} = \frac{I_{01}}{I_{02}} = \frac{S_{01}}{S_{02}} \text{ avec } I_{01} = S_{01} \text{ et } I_{02} = S_{02}$$

En tenant compte des relations 11 et en supposant l'équilibre atteint, le système d'équation B peut être écrit sous la forme d'un système linéaire homogène, éqs. 12, 13, 14 et 15.

$$\left.\begin{aligned}
[12]\quad & A_{I1}I_1 - \frac{1}{\tau_1} I_2 + \beta_{I1}S_1 + = 0 \\
[13]\quad & -\frac{1}{\tau_2} I_1 + A_{I2}I_2 + + \beta_{I2}S_2 = 0 \\
[14]\quad & \beta_{S1}I_1 + + A_{S1}S_1 - \frac{1}{\tau_1} S_2 = 0 \\
[15]\quad & + \beta_{S2}I_2 - \frac{1}{\tau_2} S_1 + A_{S2}S_2 = 0
\end{aligned}\right\} \text{ système C}$$

En posant

$$A_{Ij} = \alpha_{Ij} + \frac{1}{\tau_j} \qquad A_{Sj} = \alpha_{Sj} + \frac{1}{\tau_j}$$

$$I_j = \frac{I_{Zj} - I_{0j}}{I_{0j}} \qquad S_j = \frac{S_{Zj} - S_{0j}}{S_{0j}}$$

$$j = 1 \text{ (site 1)} \qquad j = 2 \text{ (site 2)}$$

[1] τ_1 et τ_2 sont les temps de vie dans les sites 1 et 2.

Can. J. Chem. Downloaded from www.nrcresearchpress.com by 210.87.254.40 on 09/05/12
For personal use only.

En l'absence de toute perturbation, ce système n'admet pas d'autres solutions que la solution banale où les I_j et S_j sont nuls, c'est-à-dire où $I_{Zj} = I_{0j}$ et $S_{Zj} = S_{0j}$.

Par contre, la dégénérescence est levée quand, à une température inférieure à la température de coalescence, on procède, par irradiation prolongée, à une saturation de la résonance des protons S dans le site j ce qui se traduit par $S_{Zj} = 0$ (soit $S_j = -1$). Le système d'équations C est ramené, suivant qu'est irradié le site 1 ou le site 2, aux deux systèmes d'équations D_1 (éqs. 16, 17, 18) et D_2 (éqs. 19, 20, 21).

$$\left.\begin{aligned}
[16]\quad & A_{I1}I_1 - \frac{1}{\tau_2}I_2 = +\beta_{I1} \\
[17]\quad & -\frac{1}{\tau_2}I_1 + A_{I2}I_2 + \beta_{I2}S_2 = 0 \\
[18]\quad & \beta_{S2}I_2 + A_{S2}S_2 = -\frac{1}{\tau_2}
\end{aligned}\right\} \text{système } D_1$$

$$\left.\begin{aligned}
[19]\quad & A_{I1}I_1 - \frac{1}{\tau_2}I_2 + \beta_{I1}S_1 = 0 \\
[20]\quad & -\frac{1}{\tau_2}I_1 + A_{I2}I_2 = \beta_{I2} \\
[21]\quad & \beta_{S1}I_1 + A_{S1}S_1 = -\frac{1}{\tau_1}
\end{aligned}\right\} \text{système } D_2$$

Les résultats de la résolution des systèmes D_1 et D_2 sont donnés dans les tableaux 1 et 2. Outre les expressions générales de I_{Zj} et S_{Zj} figurent dans ces tableaux les solutions correspondant à quelques cas limites.

(C) Discussion des résultats des tableaux 1 et 2

(*a*) Cas général. Il est facile de déterminer, compte tenu de ce que les termes β sont toujours inférieurs aux termes α correspondants, que les fractions figurant dans les expressions des I_{Zj}/I_{0j} et S_{Zj}/S_{0j} sont toujours positives. Par suite, dans le cas général, la saturation de S_{Z1} (tableau 1) entraîne celle de S_{Z2} à un degré plus ou moins grand selon les valeurs de τ (4). En outre, un transfert d'aimantation se produit de I_{Z1} sur I_{Z2}, I_{Z2} subissant lui aussi un accroissement.

La saturation de S_{Z2} (tableau 2) entraîne partiellement celle de S_{Z1}. Il se produit encore un transfert d'aimantation entre I_{Z2} et I_{Z1} qui est responsable de leurs accroissements respectifs.

(*b*) Lorsque l'échange est très lent ($\tau_j \to \infty$) on retrouve évidemment les expressions classiques de l'effet Overhauser, mais appliquées à un mélange de deux isomères.

L'irradiation de S_{Z1} (tableau 1) provoque un effet Overhauser β_{I1}/α_{I1} sur I_{Z1} et laisse I_{Z2} inchangé.

L'irradiation de S_{Z2} (tableau 2) ne modifie pas I_{Z1} et produit un effet Overhauser β_{I2}/α_{I2} sur I_{Z2}. Remarquons que cet effet disparaît lorsque β_{I2} est nul.

(*c*) Par ailleurs, le cas particulier du bromo-4 formyl-2 furanne, examiné à une température légèrement inférieure à la température de coalescence, nous a amené à considérer la situation où $\beta_{I2} = \beta_{S2} = 0$ et où l'échange est suffisamment rapide ($\tau \to \tau_c$) pour que les termes $\alpha\tau$ deviennent négligeables devant 1. On constate alors (*cf.* tableaux) que la saturation de S_{Z1} comme celle de S_{Z2} entraîne des augmentations égales pour I_{Z1} et I_{Z2}.

(*d*) Un cas d'intérêt plus général est celui où $\beta_{I2} = \beta_{S2} = 0$ (dernière colonne des tableaux 1 et 2). Il correspond à une situation telle que dans le site 1, les protons I et S sont proches et sont relaxés par leur interaction mutuelle ($\beta_{I1} \neq 0$, $\beta_{S1} \neq 0$) alors que dans le site 2 ces deux protons sont suffisamment éloignés pour que leur relaxation mutuelle ne soit plus efficace ($\beta_{I2} = \beta_{S2} = 0$).

Il est à remarquer que pour $\beta_{I2} = \beta_{S2} = 0$, la relation 13 (*cf.* système d'équations C) peut se mettre sous la forme éq. 22.

$$[22]\qquad I_1 = [1 + \alpha_{I2}\tau_2]I_2$$

Cette dernière relation qui implique que I_1 est toujours supérieure à I_2, reste vérifiée lorsque l'indétermination inhérente au système C est

Can. J. Chem. Downloaded from www.nrcresearchpress.com by 210.87.254.40 on 09/05/12
For personal use only.

TABLEAU 1. Expression de l'effet Overhauser dans un système en équilibre pour une irradiation prolongée de S_{Z1} ($S_{Z1} = 0$)*

Rapports	Solutions générales	$\tau \to \infty$	$\beta_{I2} = \beta_{S2} = 0$ $\alpha\tau \ll 1$	$\beta_{I2} = \beta_{S2} = 0$
$\frac{I_{Z1}}{I_{01}}$	$1 + \frac{\beta_{I1}(A_{I2}A_{S2} - \beta_{I2}\beta_{S2}) + \frac{\beta_{I2}}{\tau_1\tau_2}}{\Delta_1}$	$1 + \frac{\beta_{I1}}{\alpha_{I1}}$	$1 + \frac{\beta_{I1}}{\alpha_{I1}\left(1 + \frac{\alpha_{I2}\tau_2}{\alpha_{I1}\tau_1}\right)}$	$1 + \frac{\beta_{I1}(1 + \alpha_{I2}\tau_2)}{\alpha_{I1}\left(1 + \frac{\alpha_{I2}\tau_2}{\alpha_{I1}\tau_1} + \alpha_{I2}\tau_2\right)}$
$\frac{I_{Z2}}{I_{02}}$	$1 + \frac{\beta_{I2}\frac{A_{S2}}{\tau_2} + \beta_{I2}\frac{A_{I1}}{\tau_2}}{\Delta_1}$	1	$1 + \frac{\beta_{I1}}{\alpha_{I1}\left(1 + \frac{\alpha_{I2}\tau_2}{\alpha_{I1}\tau_1}\right)}$	$1 + \frac{\beta_{I1}}{\alpha_{I1}\left(1 + \frac{\alpha_{I2}\tau_2}{\alpha_{I1}\tau_1} + \alpha_{I2}\tau_2\right)}$
$\frac{S_{Z2}}{S_{02}}$	$1 - \frac{\frac{A_{I1}A_{I2}}{\tau_2} - \frac{1}{\tau_1\tau_2^2} + \frac{\beta_{I1}\beta_{S2}}{\tau_2}}{\Delta_1}$	1	0	$1 - \frac{1}{1 + \alpha_{S2}\tau_2}$

*$A_{Ij} = \alpha_{Ij} + \frac{1}{\tau_j}$; $A_{Sj} = \alpha_{Sj} + \frac{1}{\tau_j}$; $\Delta_1 = A_{I1}(A_{I2}A_{S2} - \beta_{I2}\beta_{S2}) - \frac{A_{S2}}{\tau_1\tau_2}$.

TABLEAU 2. Expression de l'effet Overhauser dans un système en équilibre pour une irradiation prolongée de S_{Z2} ($S_{Z2} = 0$)*

Rapports	Solutions générales	$\tau \to \infty$	$\beta_{I2} = \beta_{S2} = 0$ $\alpha\tau \ll 1$	$\beta_{I2} = \beta_{S2} = 0$
$\frac{I_{Z1}}{I_{01}}$	$1 + \frac{\beta_{I1}\frac{A_{I2}}{\tau_1} + \beta_{I2}\frac{A_{S1}}{\tau_1}}{\Delta_2}$	1	$1 + \frac{\beta_{I1}}{\alpha_{I1}\left(1 + \frac{\alpha_{I2}\tau_2}{\alpha_{I1}\tau_1}\right)}$	$1 + \frac{\beta_{I1}(1 + \alpha_{I2}\tau_2)}{\Delta_2\tau_1\tau_2}$
$\frac{I_{Z2}}{I_{02}}$	$1 + \frac{\frac{\beta_{I1}}{\tau_1\tau_2} + \beta_{I2}(A_{I1}A_{S1} - \beta_{S1}\beta_{I1})}{\Delta_2}$	$1 + \frac{\beta_{I2}}{\alpha_{I2}}$	$1 + \frac{\beta_{I1}}{\alpha_{I1}\left(1 + \frac{\alpha_{I2}\tau_2}{\alpha_{I1}\tau_1}\right)}$	$1 + \frac{\beta_{I1}}{\Delta_2\tau_1\tau_2}$
$\frac{S_{Z1}}{S_{01}}$	$1 - \frac{\frac{A_{I1}A_{I2}}{\tau_1} - \frac{1}{\tau_2\tau_1^2} + \frac{\beta_{S1}\beta_{I2}}{\tau_1}}{\Delta_2}$	1	0	$1 - \frac{\alpha_{I1}\left(1 + \alpha_{I2}\tau_2 + \frac{\alpha_{I2}\tau_2}{\alpha_{I1}\tau_1}\right)}{\Delta_2\tau_1\tau_2}$

*$A_{Ij} = \alpha_{Ij} + \frac{1}{\tau_j}$; $A_{Sj} = \alpha_{Sj} + \frac{1}{\tau_j}$; $\Delta_2 = A_{I2}(A_{I1}A_{S1} - \beta_{I1}\beta_{S1}) - \frac{A_{S1}}{\tau_1\tau_2}$.

levée par irradiation des protons S, soit dans le site 1, soit dans le site 2.

C'est donc sur le signal des protons I dans le site 1 qui est celui où I et S sont spatialement proches, que les effets Overhauser les plus importants se manifesteront et ceci indépendamment de la population relative des sites 1 ou 2 ainsi que de la nature du site S irradié.

Une application de ces considérations est présentée dans le cas d'aldéhydes thiophéniques et furanniques.

Etude de la conformation du formyl-2 bromo-4 thiophène et du formyl-2 bromo-4 furanne

(A) Formyl-2 bromo-4 thiophène

L'analyse aux RX du formyl-2 bromo-4 thiophène révèle qu'il existe à l'état solide sous la conformation plane OS-*cis* (8). Les distances entre le proton aldéhydique et le proton H_3 dans les deux conformères déterminée grâce aux résultats de l'étude cristalline sont de $r(cis) = 2.66$ Å, $r(trans) = 3.98$ Å (fig. 1).

En solution dans le chloroforme deutérié ou le THF-d_8 le spectre r.m.n. de ce composé à

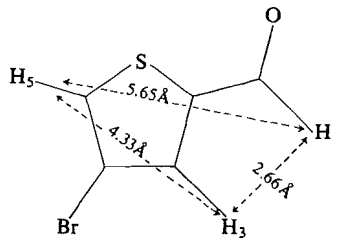

OS-*cis*

FIG. 1. La structure de OS-*cis* ($r_{trans} = 3.98$ Å).

Can. J. Chem. Downloaded from www.nrcresearchpress.com by 210.87.254.40 on 09/05/12
For personal use only.

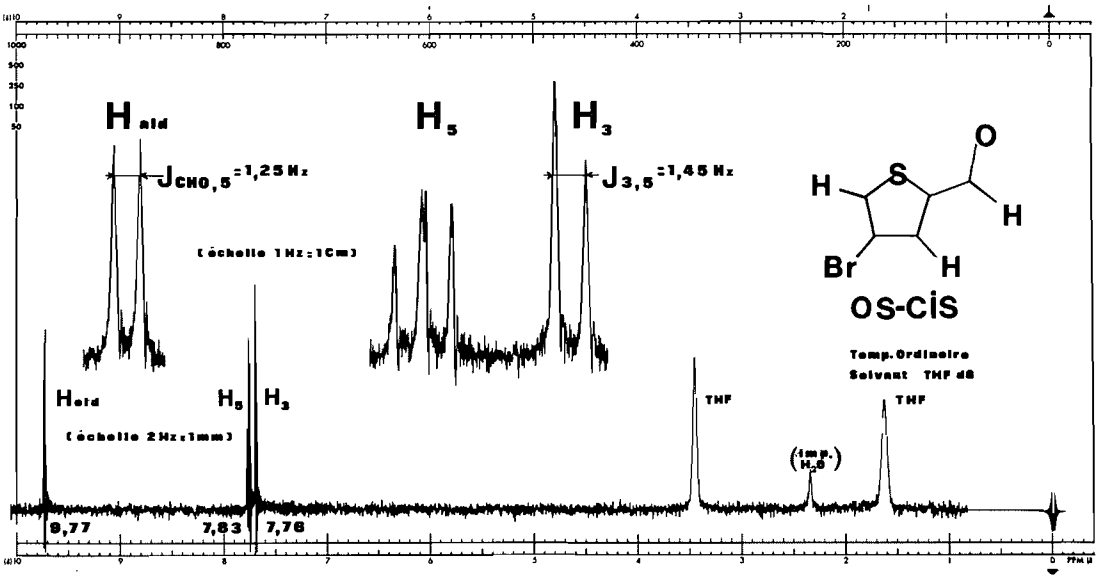

FIG. 2. Spectre r.m.n. du formyl-2 bromo-4 thiophène dans le THF-d_8 à température ordinaire.

température ordinaire présente un ensemble de signaux analysable au premier ordre (fig. 2, tableau 3).

Le signal du proton aldéhydique qui est un doublet par couplage avec le proton H_5(J_{CHO-5} = 1.25 Hz) ne subit aucune modification ni dans son intensité, ni dans sa largeur pour des températures allant de 25 à −75 °C. Dans ces conditions on peut considérer que le formyl-2 bromo-4 thiophène existe en solution sous une seule conformation au moins dans cet intervalle de température.[2] Cette hypothèse est du reste en accord avec des mesures de moment dipolaire de formylthiophènes (12). A température ordinaire et en termes de r.m.n. la conformation de ce dérivé apparaît donc comme bloquée c'est-à-dire que le temps de vie du spin du proton aldéhydique dans le rotamère préférentiel est infiniment long devant son temps de relaxation. On pourra donc étudier la structure de ce conformère par effet Overhauser en irradiant successivement le proton aldéhydique et le proton H_3 et en notant les modifications de l'intensité des signaux sur H_3 dans le premier cas et sur le proton aldéhydique dans le deuxième cas. Les augmentations (mesurées en %) du signal initial sont rassemblées dans le tableau 4.

La forte augmentation du signal de H_3 prouve

TABLEAU 3. Déplacements chimiques* et constantes de couplages† du formyl-2 bromo-4 thiophène (T = 27 °C)

δ_{Hald}	δ_{H5}	δ_{H3}	J_{CHO-5}	J_{3-5}	Solvant
9.87	7.64	7.68	1.25	1.45	$CDCl_3$
9.77	7.83	7.76	1.25	1.45	THF-d_8

*δ en p.p.m. par rapport au HMDS utilisé en référence interne.
†J en Hz.

[2]Les barrières de rotation des formyl-2 thiophène et furanne sont du même ordre (≈ 10.5 kcal/mol) (13). La température de décoalescence du furfural étant voisine de −60 °C, ceci entraînerait dans le cas d'un mélange de rotamères pour le formyl-2 bromo-4 thiophène une modification des signaux du spectre r.m.n. pour une température supérieure à −75 °C. Les effets sur la barrière de rotation produits par un atome de brome en série hétérocyclique sont considérés comme négligeables.

TABLEAU 4. Effet Overhauser observé dans le formyl-2 bromo-4 thiophène*

Proton irradié	Effet (%)			
	Hald	H_3	H_5	Solvant
Hald		35	0	$CDCl_3$
		30	0	THF-d_8
H_3	16		†	$CDCl_3$
	22		†	THF-d_8
H_5	0	†		$CDCl_3$
	0	†		THF-d_8

*Exprimé en % d'augmentation du signal initial.
†L'intégration de H_3 ne peut être effectuée lors de l'irradiation de H_5 et réciproquement du fait de la faible différence de déplacement chimique entre ces protons.

Can. J. Chem. Downloaded from www.nrcresearchpress.com by 210.87.254.40 on 09/05/12
For personal use only.

Can. J. Chem. Downloaded from www.nrcresearchpress.com by 210.87.254.40 on 09/05/12
For personal use only.

la proximité de ce proton avec le proton aldéhydique irradié. La conformation du bromo-4 formyl-2 thiophène en solution est donc OS-*cis* ce qui est en accord avec notre étude précédente (8).

Il est intéressant de remarquer que si l'irradiation du proton aldéhydique entraîne une augmentation de l'ordre de 30% du signal de H_3, l'irradiation de H_3 par contre ne produit qu'une augmentation de 16% du proton aldéhydique dans $CDCl_3$ et 22% dans le THF-d_8. Cette différence pourrait tenir à des vitesses de relaxation différentes pour le proton H_3 et le proton aldéhydique.

(B) Dibromo-4,5 acétyl-2 thiophène

Nous avons effectué une expérience similaire dans le cas du dibromo-4,5 acétyl-2 thiophène. On sait que la conformation dans le cristal de l'acétyl-2 bromo-5 thiophène est OS-*cis* (14). D'autre part, des études préliminaires ont montré qu'en r.m.n. l'absence de modification des signaux de l'acétyl-2 thiophène à basse température était en faveur d'une conformation bloquée, vraisemblablement OS-*cis*. Au cours de nos mesures nous avons observé une augmentation de 37% du signal du proton H_3 par irradiation du pic méthyle. Il se confirme donc que la conformation préférentielle du groupement acétylé α thiophénique est bien OS-*cis*.

(C) Formyl-2 bromo-4 furanne

L'étude aux RX (15) du formyl-2 bromo-4 furanne a montré que ce composé existe à l'état cristallisé dans la conformation OO-*cis*, comme son correspondant thiophénique. Les angles et distances dans les conformations OO-*cis* et OO-*trans*, calculées d'après cette étude se trouvent dans les schémas de la fig. 3.

En revanche le spectre de r.m.n. (fig. 4) du formyl-2 bromo-4 furanne enregistré à basse température (−90 °C) montre l'existence en solution des deux conformères OO-*cis* et OO-*trans*. Les déplacements chimiques du conformère majoritaire (80%) et du conformère minoritaire (20%) sont rassemblés dans le tableau 5.

En augmentant la température, l'échange s'accélère. La coalescence des signaux est observée vers −72 °C, l'échange étant très rapide à la température ordinaire. Le spectre de la fig. 4 met en évidence la présence d'un couplage $J_{CHO\text{-}5}$ de 1 Hz pour le rotamère majoritaire.

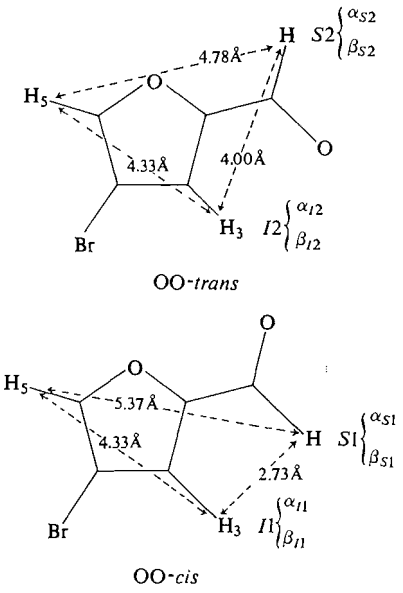

FIG. 3. La structure de OO-*trans* et OO-*cis*.

Nous avons effectué les expériences Overhauser à une température de −90 °C, inférieure à la température de décoalescence (t_C = −72 °C), en irradiant successivement chacun des signaux correspondant au proton aldéhydique et en mesurant dans chaque cas la surface des signaux de H_3 par intégration (figs. 5 et 6), les résultats expérimentaux étant regroupés dans le tableau 6.

Quel que soit le site irradié on constate une augmentation des signaux du proton H_3, l'augmentation relative la plus importante étant toujours observée dans le cas du rotamère majoritaire (30 et 13% pour, respectivement, 18 et 7%). Or, d'après la fig. 3, dans le conformère OO-*cis* (site 1), la distance entre le proton H_3 (proton *I*) et le proton aldéhydique (proton *S*) est assez faible (2.73 Å) pour qu'ils se relaxent mutuellement. Mais en revanche, dans le conformère OO-*trans*, (site 2) la distance entre *I* et *S* est assez grande (4 Å) pour que l'interaction soit pratiquement nulle.

On peut donc considérer que l'on se trouve dans le cas précédemment envisagé (tableaux 1 et 2) où $\beta_{I2} = \beta_{S2} = 0$. L'application de la relation 22 amène alors à conclure que le conformère pour lequel l'effet Overhauser est le plus marqué est le conformère OO-*cis*, et qu'il s'agit ici du conformère majoritaire.

Can. J. Chem. Downloaded from www.nrcresearchpress.com by 210.87.254.40 on 09/05/12
For personal use only.

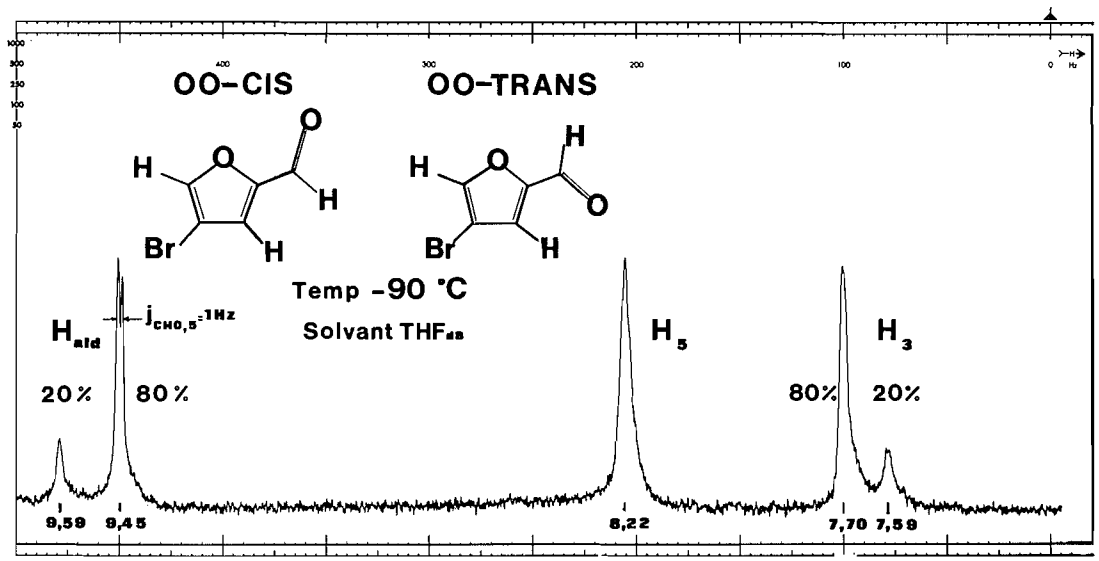

FIG. 4. Spectre r.m.n. du formyl-2 bromo-4 furanne dans le THF-d_8 à −90 °C.

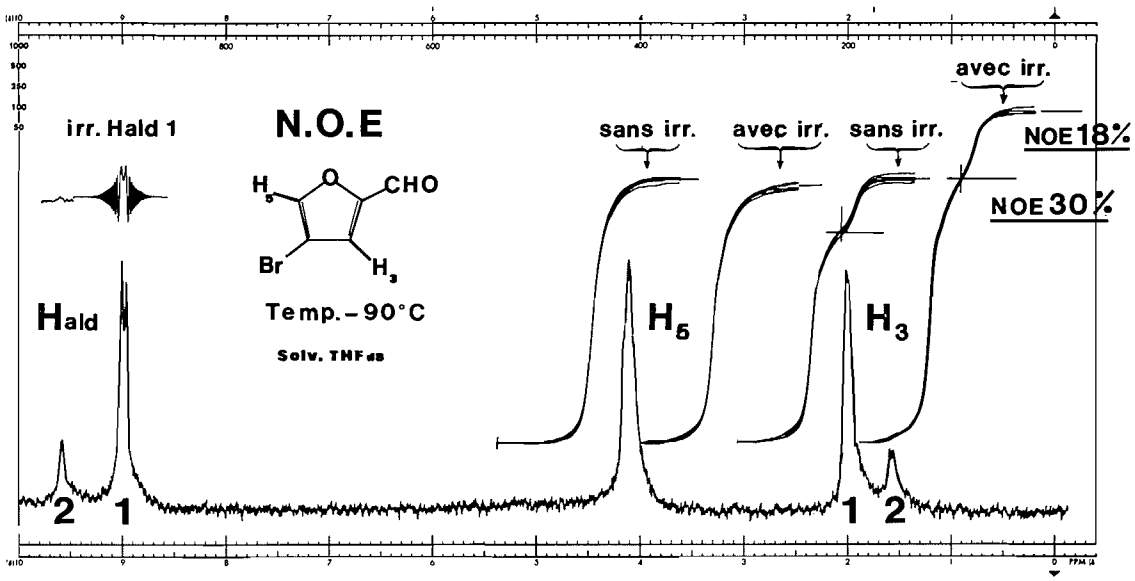

FIG. 5. Effets Overhauser observés dans le formyl-2 bromo-4 furanne en solution dans le THF-d_8 à −90 °C. Irradiation sur le pic aldéhydique 1.

TABLEAU 5. Déplacements chimiques* et constantes de couplage† des protons du formyl-2 bromo-4 furanne dans le THF-d_8

Proportions du mélange	T (°C)	δ_{Hald}	δ_{H_5}	δ_{H_3}	J_{CHO-5}	r_{H_3-CHO} (Å)
20%	−90	9.59	8.22	7.59	< 0.2	4.00
80%	−90	9.45	8.22	7.70	1	2.73

*δ en p.p.m. par rapport au HMDS utilisé en référence interne.
†J en Hz.

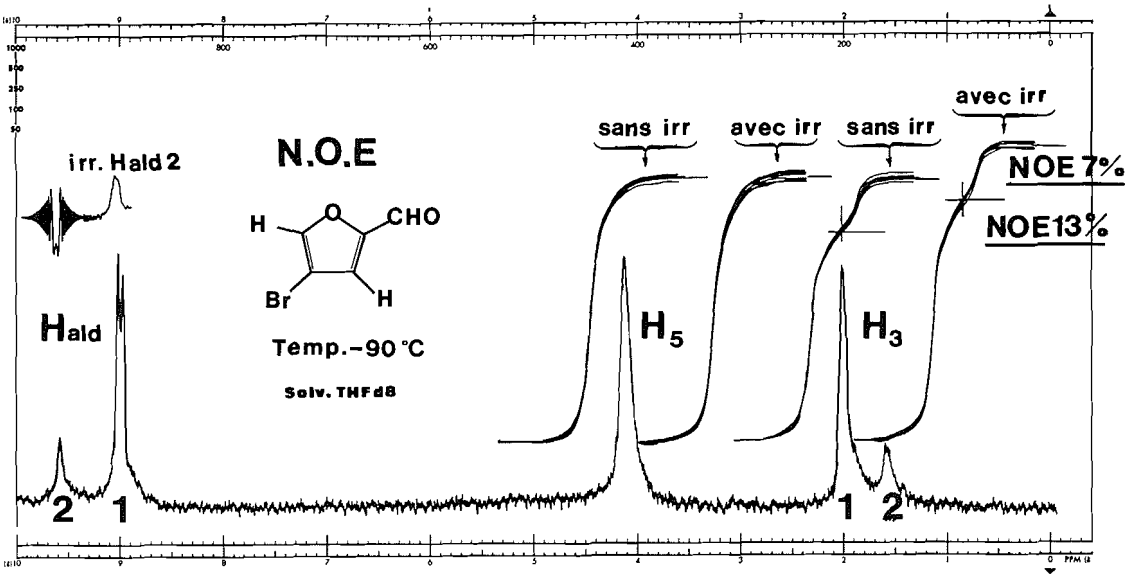

FIG. 6. Effets Overhauser observés dans le formyl-2 bromo-4 furanne en solution dans le THF-d_8 à −90 °C. Irradiation sur le pic aldéhydique 2.

TABLEAU 6. Effet Overhauser observé dans le formyl-2 bromo-4 furanne*

Site irradié	H_3 $\delta = 7.59$ (conformère minoritaire)	H_3 $\delta = 7.70$ (Conformère majoritaire)	H_5 $\delta = 8.22$ (signal non découplé)
Hald $\delta = 9.59$ (conformère minoritaire)	7%	13%	0%
Hald $\delta = 9.45$ (conformère majoritaire)	18%	30%	0%

*Exprimé en % d'augmentation du signal initial.

Ce résultat est en accord avec une étude (8) précédente de deux d'entre nous. Il faut toutefois noter à cet égard que cette étude avait été faite par r.m.n. à basse température et rayons X. Or, l'emploi simultané de ces techniques présente deux inconvénients

(*a*) il exige des composés cristallisés possédant de préférence un substituant lourd.

(*b*) il repose sur l'existence d'une identité entre la structure du conformère le plus stable en solution et dans le cristal. Bien que très largement vérifiée (16) cette analogie peut sans doute présenter des exceptions (17).

Remarques

(*a*) L'effet Overhauser sur des systèmes en échange permet en outre d'obtenir dans le cas particulier où $\beta_{I2} = \beta_{S2} = 0$ une valeur approchée du terme $\alpha_{I2}\tau_2$. En effet le rapport des accroissements relatifs I_1 de I_{Z1} et I_2 de I_{Z2} s'exprime très simplement en $\alpha\tau$ (éq. 22).

$$[22] \qquad \frac{I_1}{I_2} = (1 + \alpha_{I2}\tau_2)$$

Les valeurs expérimentalement déterminées sont

$$\left(\frac{I_1}{I_2}\right)_{S_{Z1}=0} \approx \frac{30}{18} = 1.7;$$

$$\left(\frac{I_1}{I_2}\right)_{S_{Z2}=0} \approx \frac{13}{7} = 1.9$$

ce qui compte tenu des incertitudes de mesure conduit à

$$1.5 < \left(\frac{I_1}{I_2}\right) = 1 + \alpha_{I2}\tau_2 < 2$$

La valeur correspondante de $\alpha_{I2}\tau_2$ est donc comprise dans le domaine

Can. J. Chem. Downloaded from www.nrcresearchpress.com by 210.87.254.40 on 09/05/12
For personal use only.

$$0.5 < \alpha_{I2}\tau_2 < 1$$

Si l'on admet un temps de relaxation de l'ordre de 50 s (18) la valeur de τ_2 est comprise dans l'intervalle

$$20\text{ s} < \tau_2 < 50\text{ s}$$

la valeur de τ_1 correspondante étant comprise dans l'intervalle

$$80\text{ s} < \tau_1 < 200\text{ s}$$

(*b*) Le précédent calcul n'est évidemment pas significatif si le terme $\alpha_{I2}\tau_2$ est négligeable devant 1. Dans ce cas (échange rapide notamment) les augmentations relatives I_1 et I_2 tendent vers une même limite (*cf.* tableaux 1 et 2).

Conclusion

L'établissement des relations décrivant les rapports des accroissements Overhauser dans les systèmes en échange fait apparaître pour des températures suffisamment inférieures à la température de coalescence, des augmentations relatives des signaux de *I* et *S* caractéristiques de leur environnement.

Dans ces conditions, l'utilisation de ces effets est applicable en particulier à l'analyse conformationnelle. Nous l'avons mis en évidence dans l'étude de la conformation des formyl-2 bromo-4 thiophène, acétyl-2 dibromo-4,5 thiophène et formyl-2 bromo-4 furanne. Les deux premiers composés possèdent à température ordinaire une conformation unique OS-*cis*. Le dérivé furannique qui existe en équilibre entre les formes OO-*cis* et OO-*trans* dans l'intervalle de température étudié, possède à $-90\,^{\circ}C$ une prépondérance du rotamère OO-*cis*.

Les valeurs des accroissements Overhauser observés permettent en outre une estimation des temps de vie de chacun des sites.

Cette méthode d'analyse structurale de systèmes en échange semble devoir s'appliquer à l'étude d'autres problèmes. Nous poursuivons actuellement l'étude de la conformation d'aldéhydes hétérocycliques substitués, à l'aide de cette technique.

Partie expérimentale

Les composés utilisés dans cette étude ont été préparés selon les méthodes décrites dans la littérature: formyl-2 bromo-4 thiophène (19), formyl-2 bromo-4 furanne (20), acétyl-2 dibromo-4,5 thiophène (21). Leur pureté a été contrôlée par chromatographie en phase gazeuse.

Les spectres ont été enregistrés en balayage de fréquence sur un appareil Varian HA 100. Le second champ de radio-fréquence nécessaire aux expériences de double irradiation est fourni par un générateur basse fréquence Hewlett–Packard modèle 200 AB.

L'intensité du champ est mesurée à l'aide de l'oscilloscope incorporé dans l'appareil. Les déplacements chimiques ainsi que les différentes fréquences sont obtenus par la lecture directe sur le fréquencemètre de l'appareil.

Les solutions soigneusement filtrées ont été dégazées sous vide à très basse température. La concentration est en moyenne de 10% dans le chloroforme ou le THF deutériés et la stabilisation interne est faite sur le signal du HMDS (hexaméthyldisiloxanne) dont le déplacement chimique par rapport au TMS est de 0.06 p.p.m. Pour la mesure des effets Overhauser nous avons procédé selon la méthode décrite par Bell et Saunders (11).

Nous tenons à exprimer nos très vifs remerciements au Dr. Scheidegger (Varian Ass. Zürich) pour l'aide qu'il nous a apportée dans les expériences Overhauser et aux rapporteurs du Can. J. Chem. pour leurs conseils et leurs suggestions.

1. R. KAISER. J. Chem. Phys. **42**, 1838 (1965).
2. F. A. L. ANET et A. J. R. BOURN. J. Amer. Chem. Soc. **87**, 5250 (1965).
3. G. MOREAU. Bull. Soc. Chim. France, 1770 (1969).
4. S. FORSEN et R. A. HOFFMAN. J. Chem. Phys. **45**, 2059 (1966).
5. L. M. JACKMAN. Applications of Nuclear Magnetic Resonance in Organic Chemistry, Pergamon Press, Oxford. 1962. p. 129.
6. G. J. KARABATSOS et F. M. VANE. J. Amer. Chem. Soc. **85**, 3886 (1963).
7. K. I. DAHLQUIST et S. FORSEN. J. Phys. Chem. **69**, 1760, (1965); **69**, 4062 (1965).
8. B. ROQUES, S. COMBRISSON, C. RICHE et C. PASCARD-BILLY. Tetrahedron, **26**, 3555 (1970).
9. F. BLOCH. Phys. Rev. **93**, 944 (1954).
10. I. SOLOMON. Phys. Rev. **99**, 559 (1955).
11. R. A. BELL et J. K. SAUNDERS. Can. J. Chem. **48**, 1114 (1970).
12. H. LUMBROSO, D. M. BERTIN, M. ROBBA et B. ROQUES. Compt. Rend. Acad. Sci. France, série C, **262**, 36 (1966).
13. R. A. PETRICK et E. WYN-JONES. J. Chem. Soc. A, 713 (1969).
14. H. J. STREURMAN et H. SCHENK. Rec. Trac. Chim. Pays-Bas, **89**, 392 (1970).
15. C. RICHE. D.E.S. Sciences Paris (1969).
16. S. MIZUSHIMA. Structure of Molecules and Internal Rotation. Academic Press, New York, 1954.
17. J. DANIELSEN. Acta. Chem. Scand. **23**, 2031 (1969).
18. S. FORSEN, B. O. GESTBLOM, S. GRONOWITZ et R. A. HOFFMAN. Acta. Chem. Scand. **18**, 313 (1964).
19. YA. L. GOLDFARB, YU. B. VOL'KENSTEIN et B. V. LOPATIN. Zh. Obshch. Khim. **34**, 969 (1964).
20. M. ROBBA et M. C. ZALUSKI. C. R. Acad. Sci. France, série C, **268**, 1884 (1969).
21. YU. B. VOL'KENSTEIN et YA. L. GOLDFARB. Doklady. Akad. Nauk. S.S.S.R., **138**, 161 (1961).
22. J. K. SAUNDERS et R. A. BELL. Can. J. Chem. **48**, 512 (1970).

Can. J. Chem. Downloaded from www.nrcresearchpress.com by 210.87.254.40 on 09/05/12
For personal use only.

Can. J. Chem. Downloaded from www.nrcresearchpress.com by 210.87.254.40 on 09/05/12
For personal use only.

Preparation of Substituted Anisylic Phenyl Ethers

J. M. PROKIPCAK AND T. H. BRECKLES
Department of Chemistry, University of Guelph, Guelph, Ontario

Received October 14, 1970

It is shown that anisylic phenyl carbonates thermally decompose to yield the corresponding anisylic phenyl ethers. The method involves heating the carbonates to their decomposition temperatures using hexamethylphosphoramide or toluene as a solvent. Thirteen anisylic phenyl ethers were prepared in good to excellent yields by this apparently general and simple procedure.

Il est démontré que les carbonates doubles de phényle et d'anisyles se décomposent thermiquement pour fournir les phénoxy anisoles correspondants. La méthode implique le chauffage des carbonates jusqu'à leur température de décomposition dans l'hexaméthylphosphoramide ou le toluène comme solvants. Treize éthers ont été préparés, avec des rendements variant de bons à excellents, par cette méthode simple et apparemment générale.

Canadian Journal of Chemistry, 49, 914 (1971)

In the process of preparing some substituted benzyl phenyl carbonates for study in our laboratory, unexpected difficulty was encountered in purifying anisyl phenyl carbonate (*p*-methoxybenzyl phenyl carbonate) by distillation. Instead of obtaining the desired carbonate, a white solid was recovered which was tentatively assigned the structure of anisyl phenyl ether. Attempts to prepare the ether by conventional methods *i.e.* by reacting anisyl bromide with sodium phenoxide failed. This is in accordance with the difficulty encountered by Russell and Williamson (1) who found that using the aforementioned method, *p*-methoxy-*p'*-hydroxydiphenylmethane (**1**) was the major product formed (Scheme 1). Product **1** might be anticipated as the phenoxide ion could readily undergo electrophilic substitution by a very stable anisyl carbonium ion which could form from the anisyl bromide (2). A further survey of the literature revealed that very few anisylic phenyl ethers had been reported and thus it became of interest whether the pyrolysis reaction encountered in our laboratory could be used as a general synthetic route to the title compounds.

All the carbonates were prepared by well-documented conventional methods. Substituted phenols were treated with phosgene to give the substituted phenyl chloroformates which were then reacted with the anisylic alcohols yielding the desired carbonates. The overall reaction scheme for the preparation of anisyl *p*-chlorophenyl carbonate and its subsequent thermal breakdown is shown in Scheme 2. Table 1 of the Experimental section lists the carbonates prepared in this study.

When the pyrolyses of the carbonates were first attempted without the use of solvent, the decomposition temperatures ranged from 100–170° and the crude ether yields were 30–60%. Starting phenols were identified as the major side product along with other unidentified materials (possibly multi-substituted phenols). Use of dimethylsulfoxide (DMSO) and hexamethylphosphoramide (HMP) as solvent media lowered reaction temperatures by 10–25°. However HMP had an additional advantage in that most of the carbonates which were decomposed using it as a solvent yielded ethers which crystallized after the pyrolysis was complete. In the case of *p*-methoxybenzhydryl phenyl carbonate, use of toluene as a solvent gave the most satisfactory results. In all the cases examined, the ether yields were good to excellent (see Table 2) and

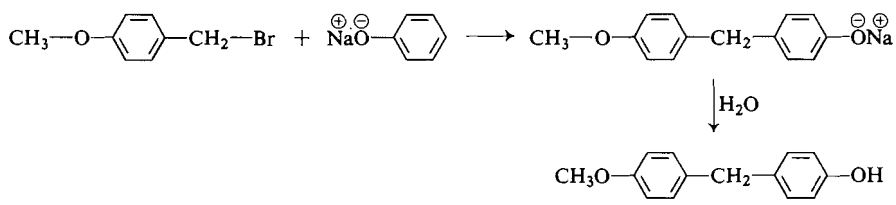

SCHEME 1

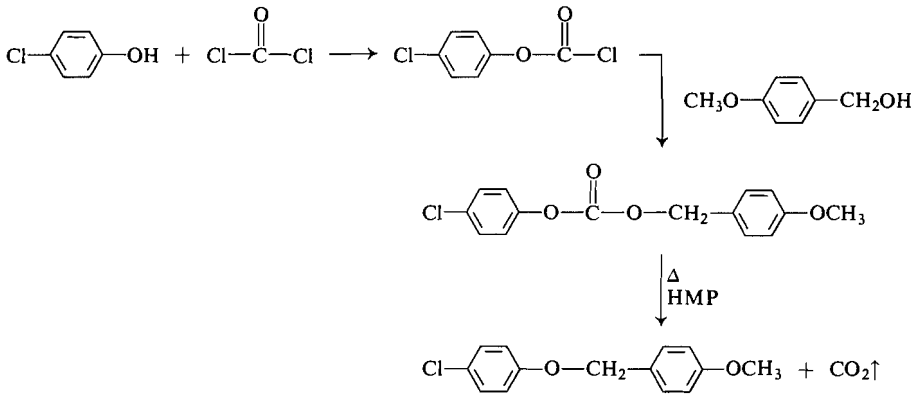

SCHEME 2

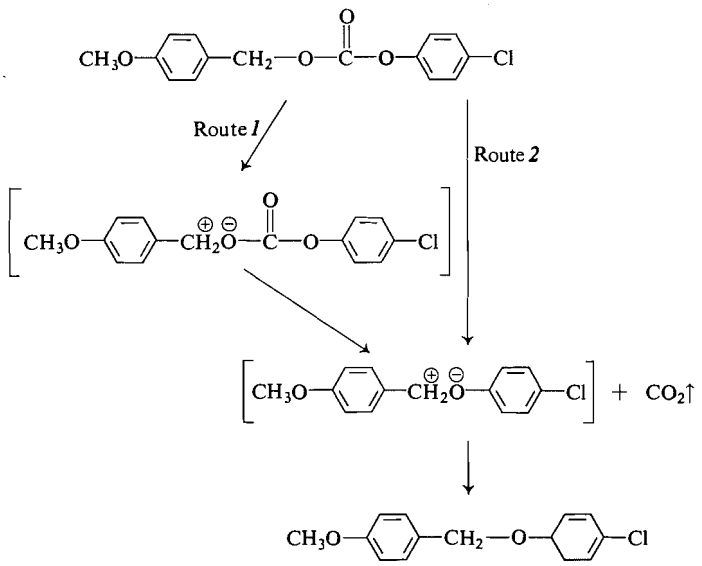

SCHEME 3

the amount of work required to obtain pure anisylic phenyl ethers from the corresponding carbonates was minimal.

The thermal decomposition of these aralkyl carbonates could well follow the SNi mechanism established for the decomposition of alkyl chlorocarbonates (3) and more recently to that proposed for the decomposition of aralkyl thiocarbonates (4) (Scheme 3). The question of the timing of the different bond scissions cannot be commented on at this time *i.e.* whether the heterolysis of the aralkyl-oxygen bond and the carbonyl-phenoxy bond occurs simultaneously (route *2*) or in two successive steps (route *1*). Extensive work has been carried out on the kinetics of the decomposition along with some stereochemistry which will help elucidate the mechanism involved. This will be reported in a later paper.

Experimental

All melting points were determined on the Fisher–Johns m.p. apparatus and are uncorrected. Analyses were performed by Organic Microanalyses, 5757 Decelles Avenue, Montreal, Quebec. The n.m.r. spectra were measured on a Varian A60A instrument using tetramethylsilane as a standard and the i.r. spectra on a Beckman IR 5A.

Preparation of Anisylic Alcohols

Anisyl alcohol and 3,4-dimethoxybenzyl alcohol were available commercially and used without further purification. *p*-Methoxybenzhydrol was prepared using a normal Grignard reaction. Phenyl magnesium bromide was

Can. J. Chem. Downloaded from www.nrcresearchpress.com by 210.87.254.40 on 09/05/12
For personal use only.

Can. J. Chem. Downloaded from www.nrcresearchpress.com by 210.87.254.40 on 09/05/12
For personal use only.

TABLE 1. The preparation of anisylic phenyl carbonates*

Carbonate R	Carbonate R^1	Melting point (°C)	Yield (%)	Decomposition temperature (°C)	Analysis (%) Calculated C	H	N	Cl	Found C	H	N	Cl
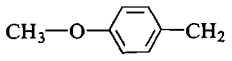	*p*-Methoxyphenyl	61.0–62.0	85	139	66.66	5.59	—	—	66.97	5.51	—	—
	p-Methylphenyl	56.5–57.5	75	138	70.57	5.92	—	—	70.66	5.78	—	—
	Phenyl	26.0–27.0§	76	130	69.76	5.46	—	—	69.92	5.64	—	—
	p-Chlorophenyl	69.5–70.5	75	105	61.55	4.48	—	12.11	61.60	4.49	—	12.31
	p-Cyanophenyl	89.0–90.0	70	89	67.84	4.63	4.94	—	68.05	4.54	4.84	—
	p-Nitrophenyl	104.5–106.0‖	35†	70	59.41	4.32	4.62	—	59.32	4.37	4.42	—
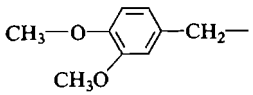	*p*-Methoxyphenyl	70.5–71.5	85	139	64.14	5.70	—	—	64.39	5.65	—	—
	p-Methylphenyl	62.0–63.0	80	138	67.54	6.00	—	—	67.47	5.92	—	—
	Phenyl	57.0–58.0	85	126	66.66	5.59	—	—	66.74	5.46	—	—
	p-Chlorophenyl	77.5–78.5	70	101	59.54	4.68	—	10.98	59.81	4.55	—	11.07
	p-Cyanophenyl	104.0–105.5	75	85	65.17	4.83	4.47	—	65.44	4.92	4.27	—
	p-Nitrophenyl	123.0–124.0	35†	83	57.66	4.54	4.20	—	57.45	4.36	4.44	—
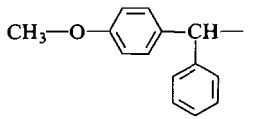	Phenyl	86.0–87.5	70	89‡	75.43	5.43	—	—	75.29	5.24	—	—

*The general structure was $R-O-\overset{O}{\overset{\|}{C}}-O-R^1$.
†Yield was low due to difficulty in purifying the chloroformates.
‡Toluene was used as the solvent for decomposition.
§Literature (7), m.p. 28–29°.
‖Literature (7), m.p. 96–97°.

Can. J. Chem. Downloaded from www.nrcresearchpress.com by 210.87.254.40 on 09/05/12
For personal use only.

TABLE 2. The preparation of anisylic phenyl ethers*

Ether		Melting point	Yield	Analysis (%)							
				Calculated				Found			
R	R¹	(°C)	(%)	C	H	N	Cl	C	H	N	Cl
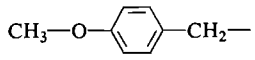	*p*-Methoxyphenyl	123.0–124.5	88	73.75	6.60	—	—	73.86	6.57	—	—
	p-Methylphenyl	88.0– 89.0	92	78.92	7.06	—	—	78.98	7.09	—	—
	Phenyl	91.0– 92.0†	96	78.48	6.59	—	—	78.34	6.53	—	—
	p-Chlorophenyl	103.5–104.5	97	67.61	5.27	—	14.25	67.60	5.42	—	14.47
	p-Cyanophenyl	127.0–128.0	92	75.29	5.48	5.85	—	75.24	5.40	6.07	—
	p-Nitrophenyl	106.0–108.0	60	64.86	5.05	5.40	—	64.70	4.97	5.58	—
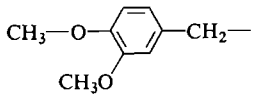	*p*-Methoxyphenyl	88.0– 89.0	93	70.06	6.61	—	—	70.25	6.59	—	—
	p-Methylphenyl	71.5– 72.5	93	74.40	7.02	—	—	74.10	6.85	—	—
	Phenyl	76.5– 77.5	94	73.75	6.60	—	—	74.02	6.51	—	—
	p-Chlorophenyl	89.0– 90.0	94	64.64	5.42	—	12.72	64.67	5.60	—	12.93
	p-Cyanophenyl	118.0–119.0	65	71.36	5.61	5.20	—	71.36	5.46	5.37	—
	p-Nitrophenyl	142.5–144.0	58	62.28	5.23	4.84	—	62.34	5.40	4.64	—
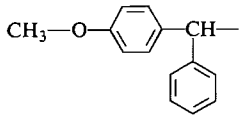	Phenyl	81.5– 82.5	84	82.73	6.24	—	—	82.83	6.27	—	—

*General structure is R—O—R¹.
†Literature (8), m.p. 92–92.5°.

Can. J. Chem. Downloaded from www.nrcresearchpress.com by 210.87.254.40 on 09/05/12
For personal use only.

reacted with *p*-anisylaldehyde to yield *p*-methoxybenzhydrol, m.p. 65–66° (lit. (5) m.p. 66–67°) in a 70% yield.

Preparation of Chloroformates

Commercial grade phenyl chloroformate was used without further purification. The substituted phenyl chloroformates were prepared by reacting the properly substituted phenol with phosgene according to the method of Zabik and Schuetz (6) who had previously prepared all the chloroformates used in this study. Yields for the chloroformates were in general 70% or greater.

Preparation of 3,4-Dimethoxybenzyl p-Methoxyphenyl Carbonate

The general method used in the preparation of the carbonates will be given. To a stirring solution of 40.0 g (0.238 mol) of 3,4-dimethoxybenzyl alcohol in 200 ml of anhydrous pyridine cooled to 0°, was added dropwise 49.0 g (0.262 mol) of *p*-methoxyphenyl chloroformate. The mixture was then stirred at room temperature for 12 h. Methylene chloride (200 ml) was added and the mixture was extracted twice with 200 ml of 5% HCl. The organic layer was then washed with 200 ml of 5% NaOH to remove any phenolic materials, washed with water, and dried over sodium sulfate. The solvent was removed *in vacuo* to give a white solid which was recrystallized from chloroform–petroleum ether (b.p. 30–60°) to give 66.3 g (88%) of pure carbonate, m.p. 70–71°. The carbonate had the following spectral data: n.m.r. ($CDCl_3$) δ (p.p.m.) 6.80–7.32 (7H multiplet, aromatic), 5.20 (2H singlet, methylene), 3.83 (6H singlet, benzyl CH_3O—), 3.77 (3H singlet, phenyl CH_3O—); i.r. (CCl_4) 1754 (C=O stretch), 1265–1200 (ester C—O stretch), and 1033 cm^{-1} (R—O—R^1 stretch).

Anal. Calcd. for $C_{17}H_{18}O_6$: C, 64.14; H, 5.70. Found: C, 64.39; H, 5.65.

The remainder of the carbonates were prepared in a similar manner and the details are shown in Table 1. The only variation in the method was in the case of the benzhydryl system where better results were obtained by reducing the amount of pyridine used by four-fifths. The spectral data for the carbonates prepared were consistent with the assigned structures.

Pyrolysis of 3,4-Dimethoxybenzyl p-Methoxyphenyl Carbonate

In a typical experiment, 5.0 g (0.016 mol) of 3,4-dimethoxybenzyl *p*-methoxyphenyl carbonate was placed in 3 ml of hexamethylphosphoramide (HMP) and the solution was heated. When CO_2 began to evolve at a steady rate (limewater trap was used), the temperature (140°) was kept constant. After 1 h an i.r. spectrum of the reaction mixture showed no starting material remained and the heating was stopped. Upon cooling, a solid formed in the reaction flask. Water (about 4 ml) was added dropwise to cause further precipitation and the solid formed was recovered by filtration; washed with water, and dried. Recrystallization from chloroform–petroleum ether (b.p. 30–60°) yielded 4.0 g (93%) of pure 3,4-dimethoxybenzyl *p*-methoxyphenyl ether (m.p. 86–87°). The ether had the following spectral data: n.m.r. ($CDCl_3$) δ (p.p.m.) 6.92 (7H unresolved aromatic multiplet centered at 6.92), 4.92 (2H singlet, methylene), 3.84 (9H singlet, CH_3O—), 3.76 (3H singlet, phenyl CH_3O—); i.r. (CCl_4) 1230 cm^{-1} (C—O—C stretch).

Anal. Calcd. for $C_{16}H_{18}O_4$: C, 70.06; H, 6.61. Found: C, 70.25; H, 6.59.

All the thermal decompositions were carried out in a similar manner with use of toluene as a solvent being the only variation. Details are shown in Table 2. The assigned structures for the ethers prepared were supported by spectral data.

The authors wish to thank the National Research Council of Canada for financial support of this research and the Department of University Affairs for the award of an Ontario Graduate Fellowship to T. H. Breckles. We also wish to thank Dow Chemical of Canada Ltd. for a generous supply of HMP.

1. G. A. Russell and R. C. Williamson, Jr. J. Amer. Chem. Soc. **86**, 2357 (1964).
2. B. G. Ramsey and J. Cook. Tetrahedron Lett. **7**, 535 (1969).
3. K. B. Wiberg and T. M. Shryne. J. Amer. Chem. Soc. **77**, 2774 (1955).
4. J. L. Kice, R. A. Bartsch, M. A. Dankleff, and S. L. Schwartz. J. Amer. Chem. Soc. **87**, 1734 (1965).
5. M. P. Balfe, M. A. Doughty, J. Kenyon, and R. Poplett. J. Chem. Soc. 605 (1942).
6. M. J. Zabik and R. D. Schuetz. J. Org. Chem. **32**, 300 (1967).
7. F. Weygand and K. Hunger. Chem. Ber. **95**, 1 (1961).
8. H. B. Henbest, J. A. W. Reid, and C. J. M. Stirling. J. Chem. Soc. 5239 (1961).

Can. J. Chem. Downloaded from www.nrcresearchpress.com by 210.87.254.5 on 09/05/12
For personal use only.

The Chlorination of Pyrroles. Part II[1]

G. R. BIRCHALL AND A. H. REES
Department of Chemistry, Trent University, Peterborough, Ontario

Received August 27, 1970

We report the chlorination of pyrryl-2-glyoxylic acid and derivatives and hence a synthesis of *O,O'*-dimethylpyoluteorin and 5-dechloro-*O,O'*-dimethylpyoluteorin. The different behavior of these compounds on demethylation is described and explained.

La chloruration de l'acide pyrolleglyoxylique-2 et quelques-uns de ses dérivés est rapportée; ces réactions constituent une synthèse de l'*O,O'*-diméthylpyolutéorine et du dechloro-5 *O,O'*-diméthylpyolutéorine. Le comportement différent de ces composés vis-à-vis de la réaction de déméthylation est décrit et expliqué.

Canadian Journal of Chemistry, 49, 919 (1971)

We found during the synthesis of pyoluteorin (2, 3) that the preparation (4) of pure 4,5-dichloropyrrole-2-carboxylate was troublesome. We therefore prepared pyrryl-2-glyoxylyl chloride (**1**, X = Y = Z = H; R = Cl) (5) and hence the acid (**1**, X = Y = Z = H; R = OH) and its isobutylamide **2**. We anticipated that chlorination at the 3-position would be blocked. This expectation was not fully met but we found that the products were more easily separated. We thus obtained the chloroamides **3**, **4**, and **5** and hence some of the corresponding ketoacids.

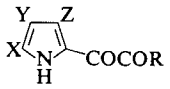

1

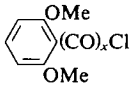

6

R = $NHCH_2CHMe$	
X = Y = Z = H	**2**
X = Y = Cl; Z = H	**3**
X = Z = Cl; Y = H	**4**
X = Z = H; Y = Cl	**5**

Before oxidation to the carboxylic acids, we used the salts of the ketoacids in reaction with **6** ($x = 1$) (2, 3). This went in poor yield when X = Y = Z = H. There was no improvement when we used 2,6-dimethoxyphenylglyoxylyl chloride (**6**, $x = 2$).

By reaction of **1** (X = Y = Cl; Z = H; R = Na) with **6** ($x = 1$) we obtained a pure sample of **8** (3) and hence of pyoluteorin.

Hydrolysis of **5** and oxidation gave 4-chloropyrrole-2-carboxylic acid. From this acid or the parent ketoacid we made 5-dechloro-*O,O'*-dimethylpyoluteorin **9** (6), identical with the compound obtained by partial hydrogenation of **8**. Demethylation with boron trichloride stopped at **10** in contrast to the complete demethylation of **8** under the same mild conditions. This resembled our earlier demethylation of **7** with this reagent which gave **11**. Complete demethylation to **12** (6) was done with aluminum bromide. The latter reagent converted **9** to 5-dechloropyoluteorin (**13**) (7).

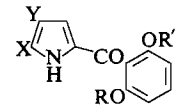

7 X = Y = H; R = R′ = Me
8 X = Y = Cl; R = R′ = Me
9 X = H; Y = Cl; R = R′ = Me
10 X = H; Y = Cl; R = Me; R′ = H
11 X = Y = R = H; R′ = Me
12 X = Y = R = R′ = H
13 X = R = R′ = H; Y = Cl

This difference is attributed to the acidity of the pyrrole NH whose anion can donate to the boron atom and promote a second mild demethylation in cases where there are sufficient electronegative groups in the heterocyclic ring or where the Lewis acid is sufficiently polar.

We prepared the ester **14** but neither it nor chloro-derivatives **15**, **16**, and **17** underwent thermal decarbonylation, probably because of NH to carbonyl bonding.

1 R = OCH_2CHMe_2	
X = Y = Z = H	**14**
X = Z = H; Y = Cl	**15**
X = Z = Cl; Y = H	**16**
X = Y = Cl; Z = H	**17**

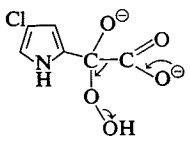

18

[1]For Part I, see ref. 1.

TABLE 1. The n.m.r. spectra ($CDCl_3$) of 2-pyrryl glyoxylic acid derivatives

Compound	1H	3H	4H	5H	CH_2CHMe_2	$—CHMe_2$	$—CHMe_2$	Amide H
2	−1.6m	2.81m	3.6m	2.48m	6.77t	8.1m	9.05d	2.3
3	−1.6m	2.55d			6.75t	8.1m	9.05d	2.5
4	−1.6d		3.81d		6.84t	8.2m	9.05d	2.5
	←———	$J_{1,4}$ 1.8Hz	———→					
5	−1.6m	2.92m		2.65m	6.78t	8.2m	9.05d	2.4
		←———	After D_2O J 1.6Hz	———→				
15	−0.5	2.8m		2.7m	5.83d	7.9m	8.94d	—

Finally we investigated the dichlorination in acetic acid of pyrryl-2-glyoxylic acid **1** (R = OH; X = Y = Z = H) to the 4,5-dichloro-derivative (plus minor amounts of 4-chloro-derivative). We attribute the absence of any other isomers to strong solvation of the ketoacid function, effectively blocking the 3-position. Taking advantage of the different NH acidities, we were able to selectively oxidize the monochloroketoacid to the easily separable monochloroacid with alkaline peroxide. We attribute the stability of the dichloroketoacid to the formation of an O,N-dianion, not attacked by HOO^- whereas in the monochloro-analogue there must be appreciable quantities of mono-anion present so that attack by HOO^- gives **18** which breaks down as indicated (8). This affords a convenient route to pure dichloroketoacid and hence by further oxidation to 4,5-dichloropyrrole-2-carboxylic acid.

Experimental

2-Pyrrylglyoxylic Acid and Isobutylamide

Pyrrole, 10.7 g in 50 ml dry ether was added dropwise with stirring to 16 ml oxalyl chloride in 200 ml ether at −70° over 3 h. The mixture was poured slowly into a vigorously stirred solution of 24 g sodium hydroxide in 240 ml ice-water and the aqueous layer was separated and acidified, giving ketoacid **1** (X = Y = Z = H; R = OH). This crude acid, in ether solution, was washed with water to remove oxalic acid and the solution dried ($MgSO_4$) and evaporated at 20° giving 15.4 g, 70% ketoacid, m.p. 112° crystallized from benzene (lit. m.p. 113° (9)).

When the ketoacid chloride, prepared as above, was poured into a stirred solution of 50 ml isobutylamine in 200 ml ether at −70° and the system allowed to warm up, the residue after filtration was crude amide. It was taken up in dichloromethane, filtered, dried ($MgSO_4$), and evaporated giving 28 g crystalline amide. This was chromatographed on 750 g neutral alumina. Elution with light petroleum/ether 4:1 gave 5 g di-isobutyloxamide, m.p. 168° (18%). Further elution, solvent ratio 20:7, gave *N*-isobutyl-2-pyrrylglyoxylamide, 20 g (70%), m.p. 90°, crystallized from aqueous ethanol; i.r. (Nujol) 3480 (NH), 1672, 1630 (CO bands) cm^{-1}.

Anal. Calcd. for $C_{10}H_{14}N_2O_2$: C, 61.8; H, 7.3; N, 14.4. Found: C, 61.65; H, 7.3; N, 14.5.

Chlorination of 2

Amide **2** (2% in acetic acid) was treated with 2.1 mol chlorine and left overnight at room temperature. Evaporation of the solvent and chromatography of the residue on silica, eluting with light petroleum/ether (increasing ratio), gave (*a*) 3,5-dichloro-derivative **4**, 6%, m.p. 118–119° crystallized from benzene/light petroleum; mass spectrum *m/e* 264 (20), 262 (40), 164 (64), 162 (100).

Anal. Calcd. for $C_{10}H_{12}Cl_2N_2O_2$: C, 45.6; H, 4.6; Cl, 26.9; N, 10.6. Found: C, 45.3; H, 4.2; Cl, 26.7; N, 10.6.

(*b*) 4,5-Dichloro-derivative **3**, 50%, m.p. 132°; mass spectrum *m/e* 264 (20), 262 (32), 57 (100).

Anal. Calcd. for $C_{10}H_{12}Cl_2N_2O_2$: C, 45.6; H, 4.6; Cl, 26.9; N, 10.6. Found: C, 45.7; H, 4.6; Cl, 27.2; N, 10.8.

(*c*) 4-Chloro-derivative **5**, 20%, m.p. 134°; mass spectrum *m/e* 230 (12), 228 (38), 130 (34), 128 (100), 57 (100).

Anal. Calcd. for $C_{10}H_{13}ClN_2O_3$: Cl, 15.5. Found: Cl, 15.1.

A mixture of products (12%), was also obtained, containing the trichloroderivative, *m/e* 296 (M^+).

Chlorination (1.2 mol) under the same conditions, gave as above 5% **4**, 22% **3**, and 50% **5** after chromatography.

The orientations of the chlorinated amides (and esters) follow from their n.m.r. spectra, Table 1.

4,5-Dichloro-2-pyrrylglyoxylic Acid

Amide **3**, 1.8 g, and potassium hydroxide, 2.3 g in 10 ml ethanol and 50 ml water, were refluxed 2 h. After evaporation of the solvent, water was added and the alkaline solution extracted with ether and acidified giving 1.2 g (90%) of the acid m.p. 177°, yellow needles crystallized from benzene/light petroleum, i.r. (Nujol) 1710, 1643 (CO bands); mass spectrum *m/e* 209 (24), 207 (40), 164 (40), 162 (100).

Anal. Calcd. for $C_6H_3Cl_2NO_3$: N, 6.75. Found: N, 7.0.

Can. J. Chem. Downloaded from www.nrcresearchpress.com by 210.87.254.5 on 09/05/12
For personal use only.

Can. J. Chem. Downloaded from www.nrcresearchpress.com by 210.87.254.5 on 09/05/12
For personal use only.

4-Chloro-2-pyrrylglyoxylic Acid

Amide **5**, by the method above, gave the acid (90%), m.p. 160° crystallized from benzene/light petroleum; mass spectrum *m/e* 175 (16), 173 (48), 130 (34), 128 (100).

Anal. Calcd. for $C_5H_4ClNO_3$: Cl, 20.4. Found, Cl, 20.4.

2,6-Dimethoxybenzoyl Cyanide

Compound **6** ($x = 1$) (10), 20 g, was refluxed 20 h in 100 ml dry benzene with 10.3 g cuprous cyanide. After filtration, the organic layer was washed with sodium bicarbonate solution, then with water, dried ($MgSO_4$), and evaporated. The residue was crystallized from benzene/light petroleum to give 11 g (60%) of ketonitrile, light yellow needles m.p. 69–70°, i.r. (Nujol) 2300 cm^{-1} (CN); mass spectrum *m/e* 191 (100%, M^+).

Anal. Calcd. for $C_{10}H_9NO_3$: C, 62.8; H, 4.75; N, 7.3. Found: C, 62.9; H, 4.8; N, 7.4.

2,6-Dimethoxyphenylglyoxylamide

The above cyanide (9 g) was left for 5 days at 20° in 100 ml concentrated hydrochloric acid solution. Dilution with water gave the amide, 7.5 g (80%) m.p. 148–150°, crystallized from benzene/light petroleum, i.r. 3500, 3320, 1690, 1643 cm^{-1}; mass spectrum *m/e* 209 (4), 165 (100).

Anal. Calcd. for $C_{10}H_{11}NO_4$: C, 57.4; H, 5.3; N, 6.7. Found: C, 56.8; H, 5.2; N, 6.3.

New Synthesis of 2,6-Dimethoxyphenylglyoxylic Acid

The above amide (7.5 g) was refluxed 1 h with 300 ml 5% potassium hydroxide solution. The cold solution was extracted with methylene chloride then acidified giving the acid, 5 g (66%), as an oil which slowly crystallized, m.p. 92–95° from benzene/petroleum ether (lit. m.p. 98° (11)); i.r. (Nujol) 1705, 1665 cm^{-1}; mass spectrum *m/e* 210 (14), 165 (100).

Monodechloro-O,O'-dimethylpyoluteorin (9)

Table 2 summarizes the syntheses of **9**. It formed colorless needles m.p. 150° from benzene/light petroleum, i.r. (Nujol) 3300, 1625, 1600 cm^{-1}; u.v. max (ethanol) 295 mμ.

Anal. Calcd. for $C_{13}H_{12}ClNO_3$: C, 58.6; H, 4.6; Cl, 13.4; N, 5.3. Found: C, 59.0; H, 4.6; Cl, 13.3; N, 5.1.

O,O'-Dimethylpyoluteorin (8)

The method of Table 2, after preparative t.l.c. and crystallization from benzene/light petroleum, gave 4% pure **8**, m.p. 193–196°; u.v. max (ethanol) 305 mμ; i.r. 1630, 1603 cm^{-1}.

Anal. Calcd. for $C_{13}H_{11}Cl_2NO_3$: C, 52.0; H, 3.7; Cl, 23.7; N, 4.7. Found: C, 52.4; H, 3.8; Cl, 23.4; N, 4.5.

Hydrogenation of O,O'-Dimethylpyoluteorin (8)

Compound **8**, 480 mg in 40 ml acetic acid containing 650 mg sodium acetate, was shaken in hydrogen with 1 g 5% palladium-on-charcoal. One molar equivalent was taken up in 1.5 h. After filtration and evaporation of the solvent, the residue was resolved by t.l.c. giving **8**, 180 mg and monodechloro-*O,O'*-dimethylpyoluteorin, **9**, 200 mg, identical with the material synthesized above.

5-Dechloro-O-monomethylpyoluteorin (10)

Compound **9** (80 mg) was demethylated with boron trichloride (3). The product, from the n.m.r. and mass spectrum was the monomethyl ether **10**, m.p. 148°, crystallized from benzene/light petroleum, 60 mg (80%), i.r. (Nujol) 3400, 3200, 1615, 1598 cm^{-1}.

Anal. Calcd. for $C_{12}H_{10}ClNO_3$: Cl, 14.1. Found: Cl, 13.9.

TABLE 2. Reactions of pyrrole acid salts with acid chlorides **6**

Pyrrole salt	Acid Chloride **6** x	Product	Yield (%)
2-COCOONa	1	**7**	5
2-COONa	2	**7**	5
4-Cl-2-COONa	1	9	5
4-Cl-2-COCOONa	1	**9**	2
4-Cl-2-COCOONa	2	**9**	1
4,5-di-Cl-2-COCOONa	1	**8**	4

Didechloro-O-monomethylpyoluteorin (11)

Didechloro-*O,O'*-dimethylpyoluteorin, 80 mg, was treated with boron trichloride as described (3). The product, after crystallization from benzene/light petroleum, had m.p. 129°, 60 mg (80%); i.r. (Nujol) 1613 cm^{-1}.

Anal. Calcd. for $C_{12}H_{11}NO_3$: C, 66.35; H, 5.1; N, 6.45. Found: C, 66.1; H, 4.8; N, 6.3.

The same product was obtained using aluminum chloride under mild conditions. Aluminum bromide effected removal of both methyl groups. So did boron tribromide (12).

5-Dechloropyoluteorin (13)

The dimethyl ether **9**, 135 mg, in 20 ml dry benzene, was treated with 400 mg anhydrous aluminum bromide, After stirring for 2 h at 20°, water was added and the organic layer separated and dried ($MgSO_4$). After evaporation of the solvent, the residue was recrystallized from benzene giving 110 mg (90%) 5-dechloropyoluteorin, m.p. 197°; i.r. 3500–3400, 1633, 1598, 1560 cm^{-1}; u.v. max (ethanol) 330 mμ, log ε = 4.25; n.m.r. see Table 3.

Isobutyl Pyrryl-2-glyoxylate (1, X = Y = Z = H; R = i-Bu)

Pyrrole, 10.7 g was converted to the glyoxylyl chloride as above. The mixture, at −70° was poured slowly into a solution of sodium, 3.4 g, in excess isobutanol. The system was allowed to warm up with stirring and left for 24 h. Evaporation of the solvent left a residue which was absorbed onto 600 g silica and eluted with light petroleum/ether, 10:1, giving 25 g, 75% of ester **14**, i.r. 1740, 1655 cm^{-1}.

Chlorination of the Above Ester

The ester, 12.5 g, was treated with 1.2 mol chlorine in acetic acid. Work-up, as above, gave after column chromatography on silica, 7.5 g (50%) isobutyl 4-chloropyrryl-2-glyoxylate as colorless needles, m.p. 75°; mass spectrum *m/e* 231 (8), 229 (24), 130 (33), 128 (100).

Anal. Calcd. for $C_{10}H_{12}ClNO_3$: C, 52.7; H, 5.3; Cl, 15.4; N, 6.1. Found: C, 52.3; H, 5.3; Cl, 15.3; N, 6.3.

Hydrolysis with 40% potassium hydroxide solution gave pure 4-chloropyrryl-2-glyoxylic acid in quantitative yield.

TABLE 3. The n.m.r. spectra of pyoluteorins

Compound	Solvent	1H	3H	4H	5H	3′	4′	5′	Me	OH
9*	$CDCl_3$	0.0	3.54m	—	3.0 m	3.43d†	2.66m	3.43d	6.25	—
10	DMSO-d_6	−2.0	3.8 m		2.9 m	3.58d	2.9 m	3.58d	6.4	0.4
11*	$CDCl_3$	0.1	3.14m	3.75m	2.98m	3.4 d	2.7 m	3.14d	6.3	0.2
			After D_2O $J = 3.6$ Hz		$J = 2.4$ Hz					
					$J_{3,5} = 1.2$ Hz					
13*	DMSO-d_6	−2.0	3.8 m	—	2.97m	3.75d	3.12m	3.75d	—	0.63

*After D_2O, $J_{3,5} = 1.6$ Hz.
†The 3′,4′,5′ protons form an AB_2 system, $J_{A,B} = 7$–7.5 Hz (K. Bailey, personal communication; compare J. R. Dyer, ref. 13).

A mixture of isobutyl 3,5- and 4,5-dichloropyrryl-2-glyoxylates, 5.0 g (30%) was also obtained, shown by n.m.r. to be in the ratio of 1:3.

4-Chloropyrrole-2-carboxylic Acid

4-Chloropyrryl-2-glyoxylic acid, 3.2 g in 60 ml 2 *N* sodium hydroxide solution, was treated dropwise with 18 ml 3% hydrogen peroxide solution at 5°. The stirred solution was allowed to warm to room temperature over 20 h then acidified and extracted with ether. The ether solution was extracted with sodium bicarbonate solution and the latter acidified giving a precipitate of 2.2 g (83%) of 4-chloropyrrole-2-carboxylic acid; m.p. 195° not sharp; i.r. (Nujol) 1700 cm^{-1} (CO); mass spectrum *m/e* 147 (20), 145 (60), 129 (35), 127 (100).

Anal. Calcd. for $C_5H_4ClNO_2$: C, 41.3; H, 2.8; Cl, 24.4; N, 9.6. Found: C, 41.4; H, 2.8; Cl, 24.2; N, 9.5.

The mass spectra of pyrrole acids, ketoacids, and their derivatives show cleavage to the pyrrol cation, loss of carbon monoxide to a pyrryl ion and then loss of HCN to give a cyclopropenyl ion (1).

Chlorination of Pyrryl-2-glyoxylic Acid

The above acid, 1 g, in 5 ml acetic acid was treated dropwise with 2.2 mol chlorine in 25 ml acetic acid. The system was stirred 20 h at 20° and the solvent taken off under vacuum. The residue, crystallized from benzene/light petroleum gave a 0.7 g cocrystalline mixture of 4- and 4,5-dichloroketoacids, analyzed by n.m.r. in NaOD solution as being in the ratio 1:4. There was no signal above 3 τ, indicating a total lack of 4-H protons.

Oxidation of the Mixture of Chloroketoacids

The acid mixture above, 240 mg, was oxidized with excess alkaline peroxide as described previously. Preparative t.l.c. on silica, chloroform/methanol/acetic acid (50:5:1) then gave bands at R_f 0.4 and 0.1 due to the chloropyrrole-2-carboxylic acid, 20 mg and the dichloropyrroleketoacid, 150 mg, respectively, after recrystallization, identical with pure authentic specimens obtained earlier, above.

Oxidation of 4,5-Dichloropyrryl-2-glyoxylic Acid (1, X = Y = Cl; Z = H; R = OH)

The dichloroketoacid, 20 mg, in 4 ml 50% aqueous acetic acid was treated with 45 mg lead tetraacetate at 20°. After 1 h the solvent was removed and the residue was shaken with ether and dilute sulfuric acid. The ether extract was dried ($MgSO_4$) and evaporated and the residue purified by t.l.c. giving, after recrystallization from benzene/light petroleum, 8 mg 4,5-dichloropyrrole-2-carboxylic acid.

We thank the National Research Council of Canada for financial support.

1. D. G. DURHAM and A. H. REES. Can. J. Chem. **49**, 136 (1971).
2. K. BAILEY and A. H. REES. J. Chem. Soc. D 1284 (1969).
3. K. BAILEY and A. H. REES. Can. J. Chem. **48**, 2257 (1970).
4. P. HODGE and R. W. RICKARDS. J. Chem. Soc. 459 (1965).
5. Y. G. PERRON. U.S. Pat. 3 202 654. C.A. **63**, 18093 (1965). Also J. L. ARCHIBALD and M. E. FREED. J. Hetero. Chem. **4**, 335 (1967).
6. G. R. BIRCHALL, C. G. HUGHES, and A. H. REES. Tetrahedron Lett. 4879 (1970).
7. R. TAKEDA. Bull. Agr. Chem. Soc. Jap. **23**, 126 (1959).
8. W. A. WATERS. Mechanism of oxidation of organic compounds. 2nd Edn. Methuen & Co. Ltd., London, 1965. p. 47.
9. B. ODDO. Gazz. Chim. Ital. **50**, 258 (1920).
10. J. F. NORRIS and V. W. WARE. J. Amer. Chem. Soc. **61**, 1418 (1939).
11. D. B. LIMAYE and D. D. GANGAL. Rasayanam. **1**, 64 (1936). C. A. **31**, 2128 (1937).
12. C. G. HUGHES and A. H. REES. Unpublished result.
13. J. R. DYER. Applications of absorption spectroscopy of organic compounds. Prentice Hall, 1965. pp. 104–105.

Can. J. Chem. Downloaded from www.nrcresearchpress.com by 210.87.254.5 on 09/05/12
For personal use only.

Can. J. Chem. Downloaded from www.nrcresearchpress.com by 210.87.254.40 on 09/05/12
For personal use only.

Electronic Excited States of the Cyclic 1,4-Diaza-1,3-diene (Cyclic α-Diimine) System. Photochemical Reactions of 2*H*-Isoimidazole, 5,6-Dihydropyrazine, and 1,4-Diazepine Derivatives[1]

D. R. ARNOLD,[2] V. Y. ABRAITYS, AND D. MCLEOD, JR.
Union Carbide Research Institute, P.O. Box 278, Tarrytown, New York 10591

Received September 17, 1970

The five-, six-, and seven-membered cyclic 1,4-diaza-1,3-dienes have been irradiated under a variety of conditions. The six-membered ring (dihydropyrazine) opens in a 6π e valence isomerization reaction. The resulting enediimine is stable at low temperatures and has been characterized (i.r.). Irradiation of 2,3,5,5-tetramethyl-5,6-dihydropyrazine (**1***b*) results in formation of the enediimine **2***b* which reacts further to give the rearranged monomer **12** and/or dimers **13** depending upon the temperature. The five- and seven-membered systems are stable to irradiation in inert solvents. However, irradiation of 2,2-dimethyl-4,5-diphenylisoimidazole (**10***h*) in isopropyl alcohol gives the dihydroderivative **19** and in tetramethylethylene the one-to-one adduct **25**.

The u.v. spectrum of the six-membered ring (5,6-dihydropyrazine) is very different from that of the five- and seven-membered rings. The long wavelength maximum (*ca.* 350 nm) of the six-membered ring is attributed to a transition directly into an excited state common to the enediimine **2** (*i.e.*, the excited state has a node between C-5 and -6 of the dihydropyrazine).

Les diaza-1,4 dienes-1,3 cycliques à cinq, six, et sept chaînons ont été irradiés sous plusieurs conditions. Le cycle à six chaînons (la dihydropyrazine) s'ouvre par une réaction impliquant une isomérisation de valence de 6π e. L'ènediimine résultante est stable à basse température et a été caractérisée (i.r.). L'irradiation de la tétraméthyl-2,3,5,5 dihydro-5,6-pyrazine (**1***b*) conduit à l'ènediimine **2***b* qui, selon la température, réagit pour donner le monomère réarrangé **12** et/ou le dimère **13**. Les systèmes à cinq et sept chaînons sont stables vis-à-vis de l'irradiation dans des solvants inertes. Cependant, l'irradiation du diméthyl-2,2 diphényl-4,5 isoimidazole (**10***h*) dans l'alcool isopropylique conduit au dérivé dihydro **19** et à un produit d'addition 1:1 **25** dans le tétraméthyléthylène.

Le spectre u.v. du cycle à six chaînons (dihydro-5,6 pyrazine) est très différent de celui des cycles à cinq et sept chaînons. L'importance de la longueur d'onde maximum (*ca.* 350 nm) du cycle à six chaînons est attribuée à une transition directement vers un état excité commun à l'ènediimine **2** (*i.e.*, l'état excité a un noeud entre les C-5 et -6 de la dihydropyrazine).

Canadian Journal of Chemistry, 49, 923 (1971)

Introduction

Photo- and thermal valence isomerization has proven to be a useful reaction for the synthesis of a variety of carbocyclic and heterocyclic systems (1). Scheme 1 illustrates some of the possible valence isomerizations of the 1,4-diazadiene system. The reactions shown with dark arrows have been observed.

The first report of a reaction in this series, starting with **1**, was by Beak and Miesel (2). It was found that several derivatives of **1** rearranged upon irradiation either to the imidazoles **9** (if R_4 was hydrogen) or to the isoimidazoles **10** (if neither R_3 nor R_4 were hydrogen) (see Scheme 2). These results were explained on the basis of the involvement of the intermediates **2** and **8**. While the intermediates were not detected, these products and the minor products, which were those expected from the addition of alcohol to **8**, made this mechanism plausible.

We report here details of our studies with **1** where the final products are consistent with the proposed mechanism. Furthermore, we have detected an intermediate, stable at low temperatures,[3] to which we assign structure **2**. Padwa *et al.*, have recently shown that some derivatives of **2**, which are stable at room temperature, can also be prepared in this way (4).

This system has also been approached from **3**. Heine and co-workers found that derivatives of **3** were photochromic and behaved like **8** toward dipolarophiles upon heating (5). The irradiation of derivatives of **3** has recently been reinvestigated, and both **2** and **8** were detected among the

[1]This paper was presented at the combined American Chemical Society/Chemical Institute of Canada Meeting, Toronto, Ontario, May 1970, Abstract, Orga, 61.

[2]Address correspondence to this author: Photochemistry Unit, Department of Chemistry, University of Western Ontario, London 72, Ontario.

[3]The characterization of intermediates in a photochemical reaction by irradiation at low temperatures is a powerful technique for understanding the mechanism (3).

Can. J. Chem. Downloaded from www.nrcresearchpress.com by 210.87.254.40 on 09/05/12
For personal use only.

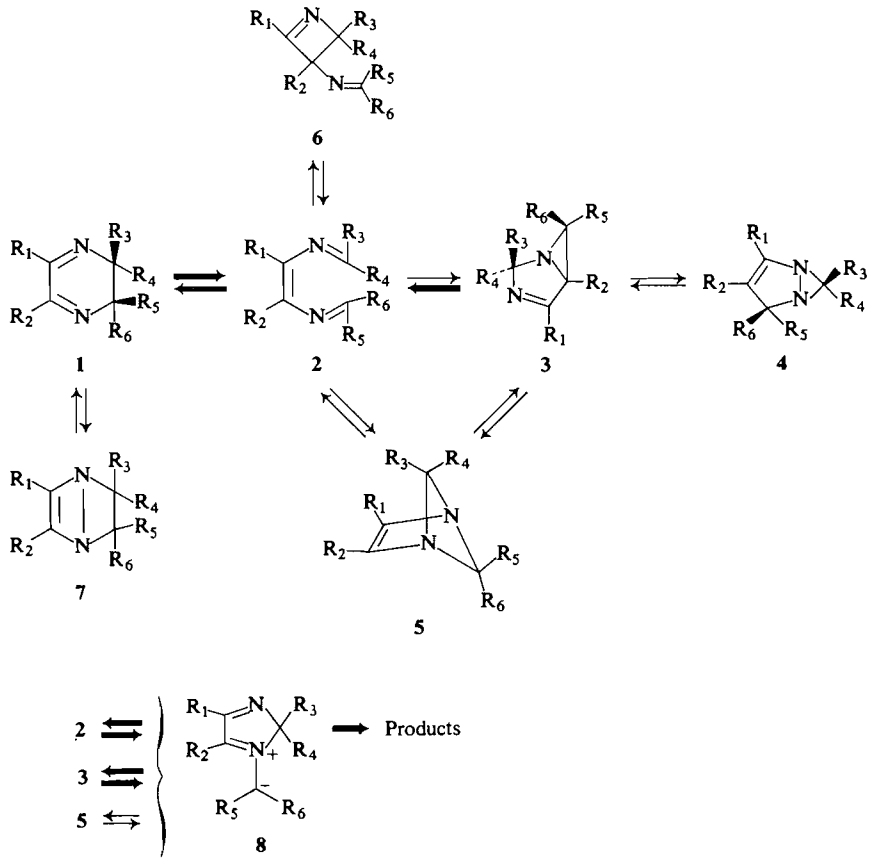

SCHEME 1

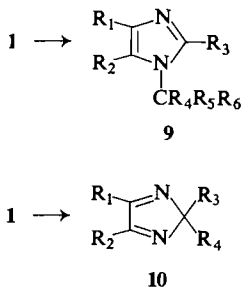

SCHEME 2

intermediates (4, 6). Table 1 summarizes the reported results of irradiations of this system.

There are no reported examples of the 4πe ring closure reaction (**7** from **1**) with a 1,4-diazadiene system. This reaction is of particular interest since the unknown 1,2-diazacyclobutene is predicted to have some aromatic character due to the presence of six electrons in a planar conjugated system (7). In a quest for an example of this reaction we have irradiated the isoimidazole **10***h* and the 1,4-diazepine **11** where the 6πe ring-opening reaction is prevented. The 4πe ring closure does occur in 1,3-cycloheptadiene (8) and cyclopentadiene (9) and in fact with some similar heterocyclic systems (10).

In the course of this work we were struck by the differences in the u.v. absorption spectrum of the seemingly identical chromophores contained in the five-, six-, and seven-membered ring. While some difference is expected due to strain and planarity variations through this series, the long wavelength (*ca.* 350 nm) absorption of the six-membered ring seems anomalous.[4] We interpret this absorption as a transition which involves the σ electrons of the 5,6-bond of **1**.

[4]The variation of absorption in the α-diketone series as a function of planarity has been studied in detail by N. J. Leonard and co-workers (11).

Can. J. Chem. Downloaded from www.nrcresearchpress.com by 210.87.254.40 on 09/05/12
For personal use only.

Results

The cyclic 1,4-diaza-1,3-dienes used in this study were readily prepared by condensation of the α-diketone with the appropriate amine. The syntheses of isoimidazoles (2, 12) and 5,6-dihydropyrazines (2, 13) are well known. The diazepine **11** was prepared in like manner from benzil and 1,3-propanediamine with little of the difficulty experienced by others (14). The analytical and spectral data for these compounds are given in

TABLE 1. Examples of reactions illustrated in Scheme 1

Reaction	Starting material	Intermediates	Products (%)	Footnotes
1	**1***a* $R_1 = R_2 = CH_3$; R_3–R_6 = H	$\xrightarrow{\Delta}$ **2***a* → **8***a*	**9***a* (71)	a, b, c, d
2	**1***b* R_1–$R_4 = CH_3$; $R_5 = R_6$ = H	$\xrightarrow{\Delta}$ **2***b* → **8***b*	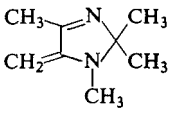 **12** (80)	a, e, f, 20°
			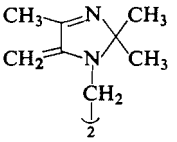 **13** (**12**:**13**, 6:1)	
3	**1***b*		**2***b*	a, e, f, −180°
4	**1***b*		**2***b*	a, f, g
5	**2***b*		**13**	e, f, h, −80°
6	**1***d* $R_1 = R_2 = C_6H_5$; R_3–R_6 = H		**2***d*	a, f, i
7	**1***d*	$\xrightarrow{\Delta}$ **2***d* → **8***d*	**9***d* (75)	a, b, c, d
			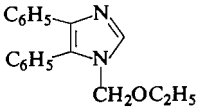 **14** (10)	
8	**1***d*	$\xrightarrow{\Delta}$ **2***d* → **8***d*	**9***d* (4) **14** (8)	a, c, d, j
			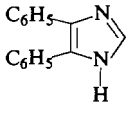 **15** (33)	
9	**1***d*	$\xrightarrow{\Delta}$ **2***d* → **8***d*	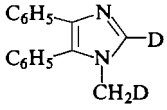	a, c, d, k

TABLE 1 (*Continued*)

Reaction		Starting material	Intermediates	Products (%)	Footnotes
10	**1***e*	$R_1 = R_2 = C_6H_5$; $R_3 = CH_3$ R_4–$R_6 = H$	$\xrightarrow{\Delta}$ **2***e* → **8***e*	**9***e* (42)	a, b, c, d
				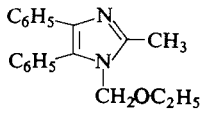 **16**	
				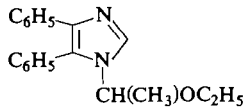 **17** (**16** + **17** = 20)	
11	**1***f*	$R_1 = R_2 = C_6H_5$; $R_3 = R_4 = CH_3$; $R_5 = R_6 = H$		**2***f*	a, f, g
12	**1***f*		$\xrightarrow{\Delta}$ **2***f* → **8***f*	**10***f* (35)	a, b, c, d
13	**1***g*	$R_1 = R_2 = C_6H_5$; $R_3 = R_5 = CH_3$; $R_4 = R_6 = H$	$\xrightarrow{\Delta}$ **2***g* → **8***g*	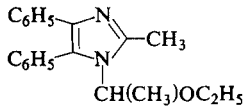 **18** (55)	a, b, c, d, l, m
14	**1***h*	$R_1 = R_2 = C_6H_5$; R_3–$R_6 = CH_3$	$\xrightarrow{\Delta}$ **2***h* → **8***h*	**10***h* (9)	a, b, c, d
				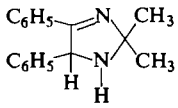 **19** (60)	
15	**1***i*	$R_1 = R_2 = C_6H_5$; $R_3 = CH_2CH(CH_3)_2$; R_4–$R_6 = H$	$\xrightarrow{\Delta}$ **2***i* → **8***i*	**9***i* (50)	a, b, c, d, l
				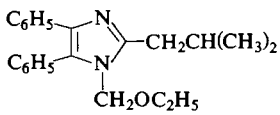 **20** (6)	
				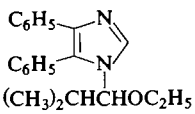 **21** (20)	

Can. J. Chem. Downloaded from www.nrcresearchpress.com by 210.87.254.40 on 09/05/12
For personal use only.

TABLE 1 (*Concluded*)

Reaction	Starting material	Intermediates	Products (%)	Footnotes
16 **1*i***		$\xrightarrow{\Delta}$ **2*i*** → **8*i***	**9*i*** (26)	a, c, d, n
			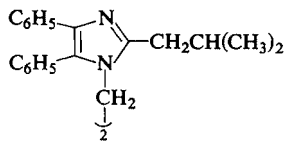 **22**	
17 **1*j***	$R_1 = R_2 = C_6H_5$; $R_3, R_6 =$ $-(CH_2)_4$-*trans*; $R_4 = R_5 = H$	$\xrightarrow{\Delta}$ **2*j*** → **8*j***	**9*j*** (9)	a, b, c, d
			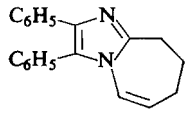 **23** (19)	
			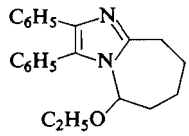 **14** (20)	
18 **1*j***		$\xrightarrow{\Delta}$ **2*j*** → **8*j***	**9*j*** (8) **23** (19)	a, c, d, n
19 **3*k***	$R_1 = R_4 = R_5 = C_6H_5$; $R_2 = R_3 = R_6 = H$	$\xrightarrow{\Delta}$ **2*k*** → **2*l***	**1*l*** (Exclusive)	a, o, p, 50°
20 **1*k***		**2*l***	**1*l***	a, o, p, 15°
21 **3*l***	$R_1 = R_3 = R_5 = C_6H_5$; $R_2 = R_4 = R_6 = H$	**2*l***	**1*l*** (94)	a, o, p, 50°
22 **3*l***			**2*l***	a, o, p, 15°
23 **2*l***			**1*l***	h, o, p, 50°
24 **1*l***		$\xrightarrow{\Delta}$ **2*k*** → **2*l***	**1*l***	a, o, p, 15°
25 **3**			**8**	q

a. The u.v. irradiation (usually a 450 W, Hanovia medium-pressure mercury vapor lamp through a Pyrex filter).
b. Ethanol (absolute) solution.
c. Temperature not specified (20–25° (2*c*)).
d. Reference 2.
e. Methylcyclohexane : isopentane (4:1), MCIP.
f. This work.
g. Xenon matrix at 63 °K.
h. Thermal.
i. Neon matrix 4 °K.
j. Ethanol (95%) solution.
k. Ethanol-*O*-*d*.
l. No isomerization or racemization was observed in recovered starting material.
m. A mixture of the *cis* and *trans* compounds gave similar results.
n. Cyclohexane solution.
o. Benzene solution.
p. Reference 4.
q. A variety of substituted 3 were found to be photochromic.[5] The photochromic species may well be derivatives of 8.[6] Derivatives of 3 react thermally with dipolarophiles as if 8 were an intermediate.[5,6]

Can. J. Chem. Downloaded from www.nrcresearchpress.com by 210.87.254.40 on 09/05/12
For personal use only.

Can. J. Chem. Downloaded from www.nrcresearchpress.com by 210.87.254.40 on 09/05/12
For personal use only.

detail in the Experimental and, with the exception of the u.v. spectrum to be discussed later, were in accord with the structures.

Irradiation of a benzene or methylcyclohexane: isopentane, (4:1), solution of 2,3,5,5-tetramethyl-5,6-dihydropyrazine (**1***b*) at room temperature (reaction 2, Table 1) gave a good yield of a rearranged product, to which we have assigned structure **12**, along with a mixture of less volatile products, presumably dimeric in nature. A major component of the less volatile mixture has been obtained pure and assigned structure **13**. The structural assignment of **12** rests primarily on spectral data and on deuterium exchange studies in acid solution. The i.r. spectrum of **12** shows strong absorption at 876 (hydrogen out-of-plane deformation of terminal methylene) and 1635 cm^{-1} (C=N stretching). The u.v. spectrum (λ_{max} 301 nm, ε 6000) reflects the conjugation in the system (14). The n.m.r. spectrum (C_6D_6) has absorption at δ 1.19 (the equivalent methyls), 1.99 (methyl on C=N), 2.39 (methyl on nitrogen), and a pair of doublets (J = 1.5 Hz) at 3.53 and 3.95 (the methylene group) consistent with the assigned structure. When the n.m.r. spectrum is taken in trifluoroacetic acid the spectrum of **12** protonated at the methylene group is obtained; δ 0.91 (the equivalent methyls), 1.34 (methyl on C=N), 1.41 (the methyl which was the methylene), and 1.94 (methyl on nitrogen). Deuterotrifluoroacetic acid exchanges the protons at δ 1.41 rapidly and those at δ 1.34 more slowly. The exchange of the hydrogens of the methyl C=N undoubtedly involves a diprotonated species which deprotonates from the methyl.

The molecular weight (mass spectrum and osmometric) requires a dimeric composition for **13**. The similarity in the i.r. and n.m.r. spectrum with that of **12** led to the assigned structure.

When the irradiation of **1***b* is carried out at low temperatures (reactions 3 and 4, Table 1), a different product is obtained which is stable at $-180°$ but which reacts when allowed to warm to $-80°$ (reaction 5). Little or no **12** is obtained in this way; instead the reaction mixture consists of the dimeric products (containing **13**) which were obtained in minor amounts in the room temperature irradiation.

The i.r. spectrum of the initial product (stable $< -180°$), and the subsequent reactions it undergoes upon warming, led to the tentative assignment of structure **2***b*. The i.r. absorption at 1677 cm^{-1} (C=N stretching) for **2***b* is consistent with the reported value for **2***l* (1625 cm^{-1}) where the imine is conjugated with the phenyl ring (4). The irradiation of **1***d* and *f* at low temperatures also forms the corresponding intermediates **2***d* and *f* with imine stretching frequencies of 1656 and 1675 cm^{-1} respectively.

The isoimidazole **10***h* and diazepine **11** were irradiated in inert solvents (hexane at 20°, neon at 4 °K, Scheme 3) under conditions which brought about isomerization of 1; however, no reaction was observed.

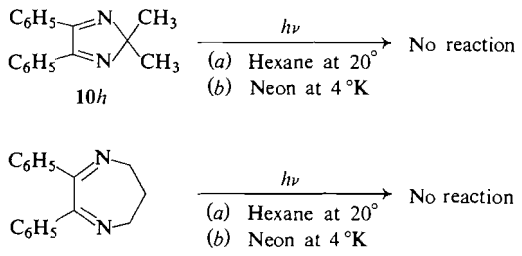

SCHEME 3

When the irradiation of **10***h* was carried out in isopropyl alcohol, the dihydroisoimidazole **19** was obtained in high yield. Compound **19** is reported as a direct irradiation product of **1***h* in ethanol, with **10***h* as a secondary product resulting from air oxidation of **19** upon work-up (reaction 14, Table 1) (2). The ease with which **10***h* is reduced in this solvent suggests the possibility of **10***h* being the precursor of **19**.

The diazepine **11** is also reduced upon irradiation in isopropyl alcohol although the reaction appears to be less efficient, and the product has not been fully characterized. Both of these photochemical reductions stop at the mono imine stage.

Irradiation of **10***h* in tetramethylethylene solution (Scheme 4) affords a one-to-one adduct in high yield. The structure **25** is assigned to the adduct on the basis of the analytical and spectral data reported in detail in the Experimental. The i.r. spectrum has absorption at 1630 (C=N stretch) and 3360 cm^{-1} (N—H stretch). The n.m.r. is consistent with the assigned structure with five nonequivalent methyl groups, a doublet attributed to the nonequivalent hydrogens of the methylene group, and a broad peak (δ 2.01) for the hydrogen attached to nitrogen. The hydrogen on nitrogen in the dihydroisoimidazole **19** appears in the same region (δ 2.08).

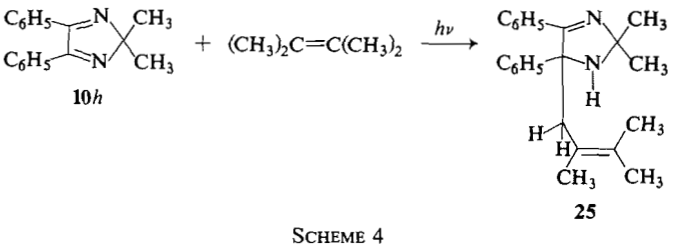

SCHEME 4

Discussion

The photo-valence isomerization of **1** to **2** appears to be a general reaction. The ultimate fate of the enediimine **2** depends upon substitution and temperature. This suggests competing reactions with low activation energies. For example, the formation of **12** upon irradiation of **1** at 20° can be explained by hydrogen migration within the intermediate **8***b*. If the irradiation is carried out at low temperatures, the enediimine **2***b* or the imine ylide **8***b* can react with each other or dimerize in competition with hydrogen migration.

The dimerization is a thermal reaction of the intermediate **2***b* and/or **8***b* since **2***b* is stable to the irradiation at low temperatures and yields dimers only, upon warming even in the dark. A photochemical dimerization of the enediimine **2***l* to give **22** (reaction 16, Table 1) has been suggested (2), and the reported formation of 4,4′-dimethylaminostilbene and azobenzene upon irradiation of 4-dimethylaminobenzaldehydeanil was given as an analogy (15). We have been unable to reproduce this reaction, however, and find the anil rather stable to irradiation.[5]

The ring closure of the enediimine **2***l* back to the dihydropyrazine **1***l* occurs to the exclusion of products derived from **8***l* (reaction 23, Table 1). In other cases studied where this reaction might have been observed, (reactions 5, 13, 15, Table 1) formation of **1** was, at most, a minor reaction. This may be the result of the decreased electrophilicity of the imine carbon when the imine moiety bears a phenyl group.

In the carbocyclic series, when the 6πe photovalence isomerization of cyclohexadiene to hexatriene is prevented, the 4πe reaction has been observed. Thus, irradiation of cyclopentadiene yields bicyclo[2.1.0]pentene, and 1,3-cycloheptadiene yields bicyclo[3.2.0]hept-6-ene (8, 9). The formally analogous reactions do not occur in the case of the 1,4-diaza-1,3-diene systems studied. Even at low temperatures, where thermal reversal of the bicyclic products would be prevented, no such product was detected.[6]

The u.v. absorption spectrum of the 1,4-diaza-1,3-diene chromophore is very different for the 5,6-dihydropyrazine **1**, and the isoimidazole **10***h* and diazepine **11**. Typical spectra are shown in Fig. 1. The long wavelength absorption maxima for several 5,6-dihydropyrazines are tabulated in Table 2. This maximum has been assigned to an $n \rightarrow \pi^*$ band (2). While it is certainly true that the geometry of the chromophore is dependent upon ring size and that the absorption spectrum is effected by the extent of planarity through the whole chromophore (11), it seemed desirable to look for another explanation for a difference as pronounced as this.

The first possibility which must be considered is that small concentrations of the enediimine **2** are present in the sample of **1**. This may seem reasonable since the enediimine **2** does have absorption in this region [**2***l* λ_{max} (cyclohexane) 360 nm, ε 12 000 (4*b*)]. However, it seems unlikely that even small concentrations of **2** are present since **2** is, in most cases, quite unstable, giving products in a thermal reaction, and no such products are obtained even upon heating **1**.[7]

Another possibility is that small amounts of a tautomeric structure, the 2,5-dihydroisomer, causes the anomalous absorption. This can easily be ruled out since **1***c* and *h*, which cannot tautomerize, have the long wavelength maximum.

The explanation that we favor attributes this long wavelength absorption to a transition between the ground state 5,6-dihydropyrazine and

[5]Azobenzene is produced if oxygen is not excluded.

[6]The 2,3-diaza-1,3-diene system is similarly reluctant to close to the azo compound. For example, 1,4-diphenyl-5,5-dimethylisopyrazole and 1,4-diphenyl-2,3-diazepine are stable to irradiation in inert solvents. In this case, even the 6πe reaction is not observed; 1,4-diphenyl-5,5,6,6-tetramethyl pyridizine is stable to irradiation (16).

[7]For example, **1***d* is stable in refluxing benzene for many hours. When heated to 200°, **1***d* apparently isomerizes to the 1,4-dihydropyrazine (17).

Can. J. Chem. Downloaded from www.nrcresearchpress.com by 210.87.254.40 on 09/05/12
For personal use only.

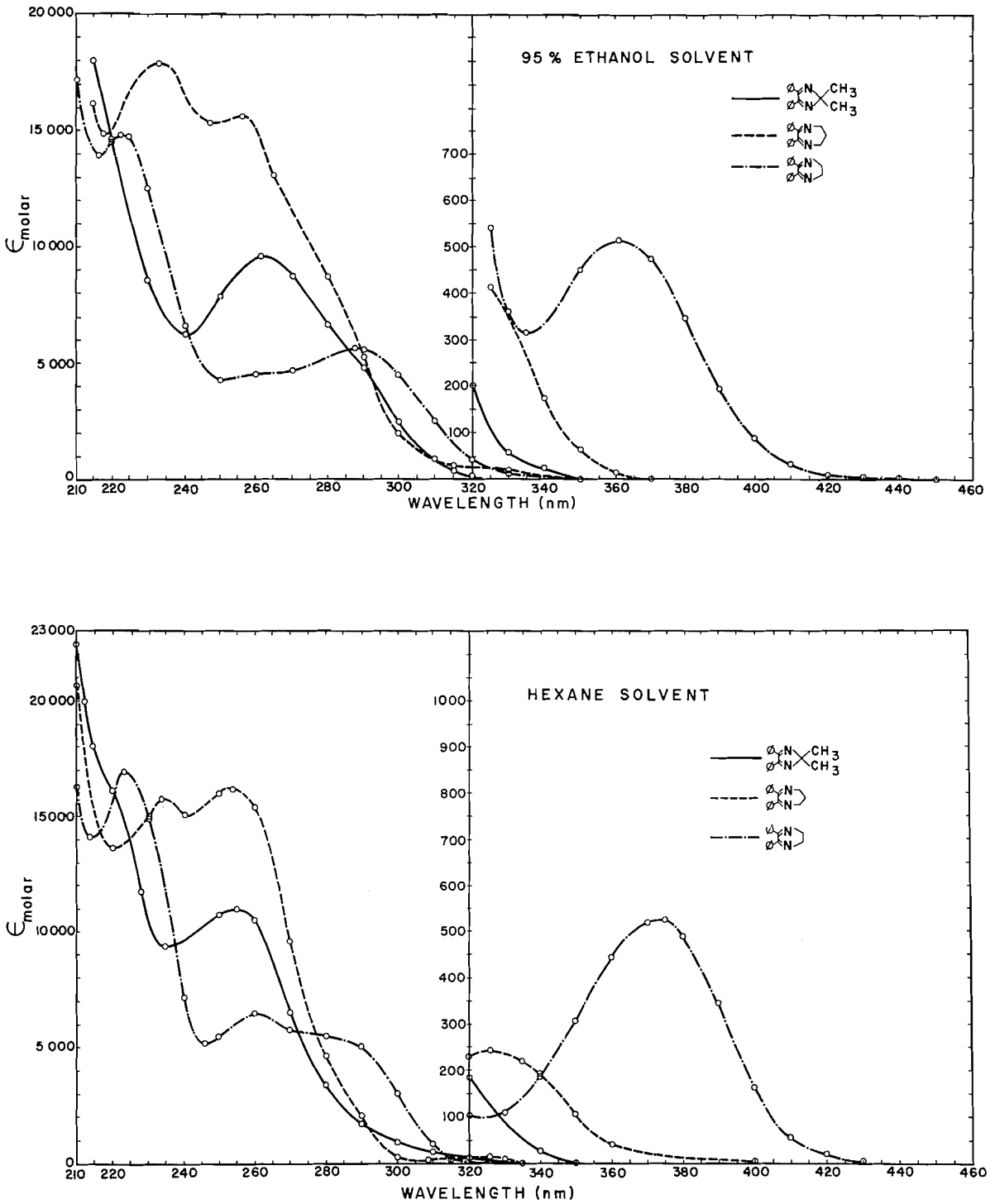

FIG. 1. The u.v. absorption spectra of 2,2-dimethyl-4,5-diphenylisoimidazole (**10***h*), 2,3-diphenyl-5,6-dihydropyrazine (**1***d*), and 2,3-diphenyl-1,4-diazepine (**11**).

Can. J. Chem. Downloaded from www.nrcresearchpress.com by 210.87.254.40 on 09/05/12
For personal use only.

TABLE 2. The long wavelength absorption maximum of some dihydropyrazines

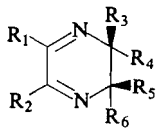

Compound 1	λ_{max}	ε	Solvent	Footnote
a $R_1 = R_2 = CH_3$; R_3–R_6 = H	337	200	Ethanol	a
	352	215	Cyclohexane	a
	349	240	Methylene chloride	a
	350	180	Hexane	b
	335	220	Ethanol	b
b R_1–$R_4 = CH_3$; $R_5 = R_6$ = H	354	187	Hexane	b
	340	200	Ethanol	b
c R_1–$R_6 = CH_3$	358	(1200)	Hexane	c
d $R_1 = R_2 = C_6H_5$; R_3–R_6 = H	377	315	Hexane	d
	364	440	Ethanol	a
	371	425	Methylene chloride	a
	373	440	Hexane	b
	362	510	Ethanol	b
	378	315	Cyclohexane	a
g $R_1 = R_2 = C_6H_5$; $R_3 = R_5 = CH_3$; $R_4 = R_6$ = H	375	350	Ethanol	a
h $R_1 = R_2 = C_6H_5$; R_3–$R_6 = CH_3$	365	420	Ethanol	a
i $R_1 = R_2 = C_6H_5$; $R_3 = CH_2CH(CH_3)_2$; R_4–R_6 = H	369	440	Ethanol	a
j $R_1 = R_2 = C_6H_5$; R_3–$R_6 = -(CH_2)_4-$; $R_4 = R_5$ = H	369	450	Ethanol	a
k $R_1 = R_4 = R_5 = C_6H_5$; $R_2 = R_3 = R_6$ = H	367	302	Ethanol	e
l $R_1 = R_3 = R_5 = C_6H_5$; $R_2 = R_4 = R_6$ = H	365	513	Ethanol	e

a. Reference 2*a*.
b. This work.
c. The reported extension coefficient is undoubtedly in error, see ref. 26.
d. Reference 2*b*.
e. Reference 4*b*.

an electronic excited state of the enediimine. That is, the electronic excited state has a node between C-5 and -6 of the 5,6-dihydropyrazine.

Of course the geometry of the initially formed excited state is the same as that of the ground state dihydropyrazine (Franck–Condon principle). In this geometry the nonbonding electrons on C-5 and -6 can interact with the nonbonding pair of electrons on the adjacent nitrogens. This is, thus, undoubtedly a less energetic structure than the initial state which would result from excitation of a planar enediimine and may, in fact, be the 0-vibrational, rotational structure of the excited state of the enediimine.[8]

[8]The 0-vibrational, rotational structure for the excited state of the analogous 1,3,5-hexatriene has one terminal methylene twisted out of the plane (18).

The suggestion that the σ-electrons of the 5,6-carbon–carbon bond are involved in this transition receives some support from the study of the anomalous absorption of triethylenediamine and from the study of the interaction of nonconjugated chromophores in general (19). Triethylenediamine has an absorption band at long wavelengths (λ_{max} 251 nm, ε 1000) (20) which has been assigned to the interaction of the nonbonding pairs of electrons on the nitrogens through the carbon–carbon σ-bonds (19). Calculations show that the carbon–carbon σ-bond in triethylenediamine is weakened in the low-lying excited state (19*a*).

The electronic transition from the ground state of one valence isomer to the electronic excited state of another valence isomer, described here

Can. J. Chem. Downloaded from www.nrcresearchpress.com by 210.87.254.40 on 09/05/12
For personal use only.

Can. J. Chem. Downloaded from www.nrcresearchpress.com by 210.87.254.40 on 09/05/12
For personal use only.

for the special case of 5,6-dihydropyrazine is undoubtedly a more general phenomena.[9] Indeed, the suggestion that the electrons of the 5,6-single bond are involved in the anomalously long wavelength absorption of 1,3-cyclohexadiene was made long ago (22) but abandoned in favor of an interpretation based on steric and hyperconjugative effects (23).

Experimental

The i.r. spectra (crystalline compounds, KBr; liquids, neat) were taken on a Beckman IR 5A spectrometer unless otherwise noted. The u.v. spectra were taken in spectral grade hexane or 95% ethanol using 10 mm cells on a Cary spectrophotometer model 14.

The n.m.r. spectra were determined on *ca.* 10% solutions with tetramethylsilane as internal standard on a Varian A 60 instrument.

The mol. wt. determinations (osmometric using benzene solution) and combustion analysis were by Schwarzkopf Microanalytical Laboratories, New York. Mass spectral analyses were by Morgan Schaffer Corp., Quebec City, Quebec, and utilized an ionization voltage of 70 eV. Melting points were taken on a Nalge apparatus and are not corrected.

*Preparation of 2,3,5,5-Tetramethyl-5,6-dihydropyrazine (**1b**)*

A solution of 8.8 g (0.1 mol) 1,2-diamino-2-methylpropane in 10 ml benzene was cooled in an ice bath and treated dropwise with 8.6 g (0.1 mol) biacetyl in 10 ml benzene. The reaction mixture became warm and homogeneous during the addition. This solution was refluxed for 30 min and then 3.6 ml of water was removed by a Dean–Stark trap. The benzene was removed on a rotary evaporator, and the oily residue was chromatographed on aluminia. The first fractions eluted with benzene contained 8.7 g (0.06 mol) 2,3,5,5-tetramethyl-5,6-dihydropyrazine (b.p. 60–61°/29 mm). This compound rapidly air oxidizes (turns purple) and was stored under nitrogen in a refrigerator. Pertinent analytical and spectral data for **1***b* are: n.m.r. (C_6D_6): δ 1.07 (6H, s), 1.82 (3H, s), 1.88 (3H, t, J = 1.5 Hz), 3.33 (2H, quartet, J = 1.5 Hz); (neat): δ 0.72 (6H, s), 1.42 (3H, s), 1.47 (3H, t, J = 2 Hz), 2.98 (2H, q, J = 2 Hz). The u.v. (hexane): 225 (ε 8900), 354 nm (190); (ethanol): 340 nm (200). The i.r. spectrum of a neat sample coincided with the spectrum taken in a xenon matrix which is reported in detail below.

Anal. Calcd. for $C_8H_{14}N_2$ (mol. wt. 138): C, 69.52; H, 10.21; N, 20.27. Found: (156 (osmetric)): C, 69.74; H, 10.23; N, 19.99.

*2,2-Dimethyl-4,5-diphenylisoimidazole (**10h**)*

This compound was prepared by a procedure similar to that reported (12). A solution of 10.5 g (0.05 mol) benzil, 40 g ammonium acetate, and 5 ml acetone in 100 ml glacial acetic acid was refluxed for 2 h. The solution was cooled, poured into 150 ml of ice–water, and then extracted with ether. The ether extract was washed with water until the washings were neutral, dried over magnesium sulfate, and evaporated to dryness. The resulting crude product was chromatographed on alumina with hexane eluent followed by short-path distillation (sublimation apparatus; 100°/10–15 mm) to afford 10 g (80%) of colorless crystals (m.p. 76–76.5°). The reported m.p. was 79–80° (12).

Pertinent spectral characteristics are: u.v. (hexane) 254 (ε 11 720), 215–220 (sh); (ethanol): 262 nm (ε 9700); n.m.r. (CCl_4) δ 7.20–7.62 (10H, m), 1.57 (6H, s); (acetic acid - d_4): δ 7.15–7.70 (10H, m), 1.70 (6H, s). No fluorescence or phosphorescence emission (methanol: ethanol, 4:1, 77°K) was observed from material purified in this way. Less pure samples showed emission believed due to trace amounts of triphenyloxazole and benzil. The i.r. spectrum taken in KBr coincided with the spectrum taken in a neon matrix which is reported in detail below.

*Preparation of 2,3-Diphenyl-1,4-diazepine (**11**)*

An equimolar benzene solution (3000 ml) of benzil (21 g) and 1,3-diaminopropane (7.4 g) and a trace of *p*-toluenesulfonic acid (0.5 g) was refluxed 3 days. Water (2.6 ml) was azeotroped out using a Dean–Stark trap and the benzene evaporated on a rotary evaporator. The oily residue (28.4 g) was crystallized from ethanol to obtain a crude solid (25 g, m.p. 111–115°) which was then chromatographed on alumina. The product (20.37 g) was eluted with 25% benzene in hexane. Further purification by recrystallization from hexane–ether gave **11** (m.p. 115–116.5°).

The following spectral and analytical data were obtained for **11**: u.v. (hexane); 234 (ε 15 824), 254 (16 213), shoulder 326 nm (240); (EtOH): 233 (17 890), 257 nm (16 720). The n.m.r. (CCl_4): δ 2.26 (pentet, 2H, J = 6.5 Hz), 3.49 (t, 4H, J = 6.5 Hz), 7.15–7.20 (m, 10H); ($CDCl_3$): δ 2.30 (pentet, 2H, J = 6.5 Hz), 3.53 (t, 4H, J = 6.5 Hz), and 7.15–7.75 (m, 10H). The i.r. spectrum taken in KBr coincides with the spectrum taken in a neon matrix which is reported in detail below.

Anal. Calcd. for $C_{17}H_{16}N_2$ (mol. wt. 248.3): C, 82.22; H, 6.50; N, 11.28. Found (251 (osmetric)): C, 82.24, 82.18; H, 6.60, 6.62; N, 11.30, 11.37.

*Irradiation of 2,3,5,5-Tetramethyl-5,6-dihydropyrazine (**1b**) at 20°*

A benzene (250 ml) solution of 2,3,5,5-tetramethyl-5,6-dihydropyrazine (3.4 g, 0.02 mol) was purged with nitrogen and irradiated with a 450 W Hanovia medium-pressure mercury vapor lamp through a Pyrex filter in an immersion well. The temperature of the solution was maintained at 20° by means of a water bath. After 1 day the benzene was removed on a rotary evaporatory at room temperature. The residue (3.7 g) was distilled on a spinning band column, and the fraction boiling 53–54° at 25 mm, $n_D^{18°}$ 1.4916 (2.7 g, 80%) was shown to be **12** on the basis of the following spectral and analytical data.

The i.r.: 2955 (s), 2920 (s), 1635 (s), 1430 (m), 1403 (s), 1363 (s), 1281 (s), 1266 (s), 1190 (s), 1160 (m), 1107 (m) 1030 (w), 1015 (w), 983 (w), 940 (m), 876 (s), 802 (w), 738–746 (s), and 694 (m) cm^{-1}. The u.v. (hexane): 301 nm (ε 6000); (ethanol): 312 nm (5400). The n.m.r. (neat): δ 1.10 (s, 6H), 1.91 (s, 3H), 2.47 (s, 3H), 3.34 (d, 1H, J = 1.5 Hz), 3.72 (d, 1H, J = 1.5 Hz); (C_6D_6): δ 1.19 (s, 3H), 1.99 (s, 3H), 2.39 (s, 3H), 3.53 (d, 1H, J = 1.5 Hz), 3.95 (d, 1H,

[9]For example, the long wavelength absorption of 2*H*-chromenes and 2*H*-pyrans may involve a transition into the excited states of the α,β, and γ,δ unsaturated carbonyl compound (21).

Can. J. Chem. Downloaded from www.nrcresearchpress.com by 210.87.254.40 on 09/05/12
For personal use only.

J = 1.5 Hz). The n.m.r. was also taken in trifluoroacetic acid (H and D) with internal standard (DDS). The tube containing the acid was purged with nitrogen and cooled prior to the addition of **12**. These spectra are described in the Results.

Anal. Calcd. for $C_8H_{14}N_2$ (mol. wt. 138): C, 69.52; H, 10.21; N, 20.27. Found (167 (osmetric)): C, 69.78; H, 10.19; N, 20.07.

The residue (0.3 g) from the above distillation of **12** was distilled under higher vacuum. The fraction boiling 96–98°/0.1 mm, n_D^{18} 1.50 (0.3 g, 19%) was shown to be a mixture of dimers with **13** as a major component, assigned on the basis of spectral and analytical data. This mixture was unstable toward air (turns purple), and **13** was not obtained free of the other isomers. One sample of the mixture was observed to partially crystallize, and the i.r. and n.m.r. reported below were taken on this sample.

The i.r.: 2960 (s), 2920 (m), 2855 (w), 2760 (w), 1690 (w), 1650 (w, shoulder), 1645 (m, shoulder), 1627 (C=N) (s), 1615 (s), 1450 (w), 1373 ($C(CH_3)_2$) (s), 1300 (w), 1280 (s), 1260 (w), 1220 (w), 1188 (m), 1162 (w), 1120 (w), 1036 (w), 878 (=C^H_H) (m), 820 (w), 737 (s), 696 (w), and 657 (w) cm^{-1}. The n.m.r. (C_6D_6): δ 1.28 (s, 12H), 1.99 (s, 6H), 3.24 (s, 4H), 3.78 (broad s, 2H), 3.95 (broad s, 2H).

The mass spectrum had a parent peak at 276 and peaks at 274 and 272. The ratio of these peaks varied with the temperature of the inlet. This is taken as evidence for loss of hydrogen (one and two molecules) in the inlet.

Anal. Calcd. for $C_{16}H_{28}N_4$ (mol. wt. 276): C, 69.52; H, 10.21; N, 20.27. Found (246 (osmetric)): C, 69.78; N, 10.30; N, 20.12.

The irradiation of neat **1***b* was carried out in a Pyrex n.m.r. tube kept at 20° by means of a water bath. The irradiation source was the 450 W Hanovia medium-pressure mercury vapor lamp 2 in. away. After 1 day of irradiation the n.m.r. indicated essentially complete conversion to monomer **12**. No dimers were detected.

Irradiation of 2,3,5,5-Tetramethyl-5,6-dihydropyrazine (1b) at Low Temperatures

A 1.0 g sample of the dihydropyrazine dissolved in 10 ml of methylcyclohexane:isopentane, 4:1, in a Pyrex tube, was purged with nitrogen, sealed, and cooled in liquid nitrogen in a Pyrex dewar to form a glass. This sample was irradiated at liquid nitrogen temperatures with a 1 kW high-pressure, mercury vapor lamp (General Electric AH6). After 6 h irradiation the tube was allowed to warm to room temperature, and the solvent was removed on a rotary evaporator. The n.m.r. and i.r. of the crude reaction mixture showed starting material and the mixture of dimeric material obtained in minor amounts from the irradiation at room temperature mentioned previously.

When the irradiation was carried out as above except at −50°, the rearranged monomer **12** was the major product (rearranged monomer: dimer mixture, *ca.* 6:1). Irradiation at room temperature for 19 h gave essentially complete conversion to the rearrangement monomer **12**.

Irradiation of 2,3-Diphenyl-1,4-diazepine (11) in Hexane at 20°

2,3-Diphenyl-1,4-diazepine (**11**) (3 g) was dissolved in hexane (275 ml), purged with nitrogen, and irradiated with a 450 W Hanovia medium-pressure mercury vapor lamp through a quartz immersion well. The temperature of the irradiation was maintained at 20° by means of a water bath. After 15 days irradiation, the solvent was removed on a rotary evaporator, and the residue (3 g) was found to be essentially pure starting material (t.l.c., i.r., n.m.r.).

Irradiation of 2,2-Dimethyl-4,5-diphenylisoimidazole (10h) in Hexane

A solution of 0.5 g of **10***h* in 5 ml of hexane in a quartz tube (9″ × 3/8″ i.d.) was purged with nitrogen, sealed, and irradiated with a 450 W Hanovia medium-pressure lamp *ca.* 2 in. away for 2 weeks. During the irradiation the temperature of the solution was maintained at 15° using a water bath. The solvent was evaporated leaving a crystalline residue which was shown by n.m.r. and i.r. to be essentially pure starting material.

A 4×10^{-5} *M* solution of **10***h* in hexane was irradiated in a 10 mm quartz tube through a Pyrex filter using the above conditions. No change in the u.v. absorption spectrum was observed after 16 h.

Procedure for Irradiation of Cyclic 1,4-Diazadienes in Inert Matrices at Low Temperatures

Inert gas matrices of 2,3,5,5-tetramethyl-5,6-dihydropyrazine (**1***b*), 2,3-diphenyl-5,5-dimethyl-5,6-dihydropyrazine (**1***f*), 2,3-diphenyl-5,6-dihydropyrazine (**1***d*), 2,3-diphenyl-1,4-diazepine (**11**), and 2,3-diphenyl-5,5-dimethylisoimidazole (**10***h*) were prepared by deposition of the vapors on a cesium bromide window in an apparatus described previously (24). The temperature of the sample was 4°K (liquid helium) for neon and 63°K (solidified nitrogen) for the xenon matrix. The i.r. spectrum was recorded on a Perkin–Elmer 225 spectrometer before and after irradiation with a General Electric AH-6 1 kW high-pressure, mercury vapor lamp through a Corning 7-54 filter (transmission 2300–4200 Å) and quartz focusing lenses. The reaction was complete after *ca.* 30 min irradiation of **1***b*, *f*, and *d*; while no reaction was observed after 1 h with **11** and **10***h*.

In one experiment a matrix of 2,3,5,5-tetramethyl-5,6-dihydropyrazine (**1***b*) in methylcyclohexane:isopentane, 4:1, was irradiated at 77 °K (liquid nitrogen) using a more conventional variable-temperature apparatus (Beckman VLT-2). This solvent is essentially transparent between 1500–1700 cm^{-1}, and the progress of the irradiation could be followed by scanning this region.

2,3,5,5-Tetramethyl-5,6-dihydropyrazine (1b) in Xenon

Starting material: 1657 (w), 1606 (m), 1595 (s), 1460 (m), 1440 (s), 1422 (m), 1377 (m), 1372 (w), 1365 (m), 1358 (m), 1330 (w), 1275 (m), 1260 (m), 1235 (m), 1213 (s), 1157 (m), 1145 (s), 1074 (s), 950 (s), 895 (s), 885 (s), 800 (s), 780 (w), 775 (w), 698 (s), 630 (w), 535 (m), and 478 (s) cm^{-1}. After irradiation: 1677 (s), 1628 (m), 1580 (m), 1455 (w), 1439 (s), 1429 (s), 1375 (w), 1367 (m), 1361 (m), 1358 (s), 1237 (s), 1208 (s), 1145 (m), 1108 (m), 1070 (w), 1065 (w), 1059 (w), 972 (s), 900 (w), 791 (w), 745 (w), 707 (m), 609 (w), and 588 (w) cm^{-1}.

2,3-Diphenyl-5,5-dimethyl-5,6-dihydropyrazine (1f) in Xenon

Starting material: 1560 (s), 1491 (w), 1444 (s), 1378 (w), 1360 (m), 1330 (m), 1315 (w), 1295 (w), 1275 (s), 1253 (m), 1185 (s), 1175 (w), 1152 (w), 1148 (w), 1085 (m), 1070 (w), 1062 (w), 1027 (m), 1018 (w), 1007 (w), 988 (s), 950 (w),

Can. J. Chem. Downloaded from www.nrcresearchpress.com by 210.87.254.40 on 09/05/12
For personal use only.

915 (w), 905 (w), 791 (s), 785 (w), 755 (s), 729 (s), 690 (s), 584 (w), 568 (s), and 551 (s) cm^{-1}. After irradiation: 1675 (b, s), 1495 (w), 1485 (w), 1443 (s), 1430 (m), 1368 (s), 1360 (s), 1227 (s), 1074 (w), 1030 (w), 990 (w), 971 (s), 888 (m), 769 (s), 755 (m), 699 (s), 690 (s), 661 (w), and 650 (m) cm^{-1}.

*2,3-Diphenyl-5,6-dihydropyrazine (**1d**) in Neon*

Starting material: 1560 (s), 1496 (m), 1440 (w), 1340 (w), 1330 (w), 1320 (b, m), 1300 (w), 1270 (s), 1234 (w), 1230 (w), 1175 (m), 1150 (w), 1090 (m), 1070 (w), 1035 (w), 1027 (m), 985 (s), 912 (w), 890 (w), 787 (s), 758 (s), 721 (s), 689 (s), 681 (w), 670 (w), 569 (s), and 550 (s) cm^{-1}. After irradiation: 1656 (m), 1601 (w), 1462 (m), 1458 (m), 1221 (s), 1195 (s), 1067 (w), 1029 (m), 1000 (s), 969 (s), 920 (w), 898 (m), 829 (w), 765 (s), 740 (w), 709 (w), 695 (s), 690 (s), 660 (w), and 589 (w) cm^{-1}.

*2,3,5,5-Tetramethyl-5,6-dihydropyrazine (**1b**) in MCIP*

Starting material: 1658 (w), 1610 (m, shoulder), and 1598 (s) cm^{-1}. After irradiation: 1675 (s), 1630 (m), and 1581 (m) cm^{-1}. Further irradiation had no effect. The initial irradiation product disappeared upon warming to 195 °K to give the product with i.r. absorption listed below: 1675 (w, shoulder), 1660 (m), 1640 (m), 1620 (s), and 1660 (w, shoulder) cm^{-1}.

*2,2-Dimethyl-4,5-diphenylisoimidazole **10h** in Neon*

Starting material: 1610 (w), 1561 (w), 1551 (s), 1495 (w), 1491 (s), 1480 (w), 1464 (w), 1446 (s), 1355 (w), 1338 (w), 1313 (w), 1300 (w), 1288 (m), 1271 (s), 1218 (s), 1182 (m), 1175 (m), 1169 (m), 1080 (m), 1071 (m), 1021 (m), 969 (s), 918 (w), 890 (w), 881 (m), 840 (w), 791 (s), 759 (s), 738 (s), 690 (s), 661 (m), 581 (s), 579 (s), and 534 (m) cm^{-1}. The spectrum was not affected by 1.5 h irradiation.

*2,3-Diphenyl-1,4-diazepine **11** in Neon*

Starting material: 1615 (w), 1609 (s), 1600 (m), 1581 (s), 1495 (m), 1479 (m), 1449 (s), 1340 (m), 1338 (w), 1333 (w), 1320 (s), 1315 (w), 1303 (m), 1291 (m), 1272 (s), 1260 (m), 1200 (m), 1175 (m), 1101 (w), 1090 (m), 1084 (m), 1071 (m), 1050 (w), 1029 (m), 951 (w), 945 (s), 920 (w), 791 (s), 767 (s), 760 (w), 731 (s), 690 (s), 689 (s), 672 (w), and 586 (s) cm^{-1}. No change in the spectrum was observed following 1.5 h irradiation.

*Irradiation of 2,2-Dimethyl-4,5-diphenylisoimidazole (**10h**) in Isopropyl Alcohol*

2,2-Dimethyl-4,5-diphenylisoimidazole (3.2 g) in isopropyl alcohol (275 ml) was purged with argon and irradiated with a 450 W Hanovia medium-pressure mercury vapor lamp in a quartz immersion well. After 1 day the n.m.r. spectrum of an aliquot indicated that only a small amount of the starting isoimidazole remained, the major signals being attributed to the dihydroisoimidazole **19**. The extent of reaction could also be determined by v.p.c. using a silicon oil column (SE 30/Chromsorb W, 1/2″ × 5′, 180°, 75 ml He/min, retention time **10*h***, 17; **19** 21 min). The solvent was removed to give an oil (3.4 g) which was dihydroisoimidazole (90% pure) contaminated with the isoimidazole (i.r. and n.m.r.). An attempt was made to purify this mixture by chromatography on alumina; however, even though manipulations were carried out under argon, the amount of isoimidazole increased.

This reaction may involve the hydrogen atom transfer mechanism shown to occur with ordinary imines (25).

*Irradiation of 2,3-Diphenyl-1,4-diazepine (**11**) in Isopropyl Alcohol*

The diazepine is not very soluble in isopropyl alcohol so dilute solutions were used. An isopropyl alcohol solution (2 ml) of the diazepine (**11**) (0.01 g) was irradiated in a quartz tube for 2 days with a 450 W Hanovia medium-pressure, mercury vapor lamp held 2 in. away. The temperature of the irradiated mixture was kept at 20°. The irradiation solution was light yellow; however, the color was discharged upon exposure to air. Evaporation of the solvent on a rotary evaporator gave a crystalline residue (0.01 g, m.p. 105–113°) shown (i.r.) to be essentially pure starting material.

More concentrated solution could be made if the mixed solvent isopropyl alcohol – dioxane was used. Then the progress of the reaction could be followed by n.m.r. Even when the solution was yellow, no change was observed in the aromatic region of the spectrum (the spectrum of **19** is very different from **10*h*** in this region); again, exposure to air led to a rapid loss of color.

Catalytic Hydrogenation of 2,2-Dimethyl-4,5-diphenylisoimidazole

A solution of **10*h*** (1 g) in 95% ethanol (100 ml) with 0.5 g of Pd/C (5%) was reduced in a Parr hydrogenation apparatus. After 1 day under a hydrogen pressure of 50 lb the solution was filtered rapidly and the solvent evaporated under vacuum to a yellow oil. The oil was taken up in methylcyclohexane, and crystalline (m.p. 90–92°) dihydroisoimidazole was deposited upon cooling. The reported m.p. of this compound is 85–88.5° (2). Pertinent spectral data for **19** are: i.r. 3300 (w), 3000 (w), 2950 (s), 2920 (w), 2830 (w), 1630 (s), 1570 (m), 1490 (s), 1450 (s), 1435 (m), 1370 (w), 1355 (m), 1320 (m), 1300 (w), 1245 (w), 1210 (s), 1195 (s), 1175 (s), 1150 (w), 1068 (s), 1050 (w), 1025 (w), 1015 (m), 922 (w), 875 (w), 845 (s), 760 (s), 720 (w), 696 (s), 694 (s), 672 (w), and 654 (w) cm^{-1}; u.v. (hexane): 230 (ε 15 400), 286 nm (Sh, ε = 720); n.m.r. ($CDCl_3$): δ 7.0–7.7 (m 10H), 544 (s, 1H), 2.08 (broad s, 1H), 1.60 (s, 3H), and 1.47 (s, 3H). The broad singlet at δ 2.08 is assigned to N–H since it disappears upon addition of 10% acetic acid - *d*; the singlet at δ 5.44, assigned to the benzylic hydrogen, shifts down field to δ 6.30.

Anal. Calcd: ($C_{17}H_{18}N_2$): C, 81.56; H, 7.25; N, 11.19. Found: C, 81.76; H, 7.45; N, 11.03.

*Catalytic Hydrogenation of 2,3-Diphenyl-1,4-diazepine (**11**)*

The diazepine (1.2 g) in ethanol (200 ml) was shaken under hydrogen (45 lb) with Pd/C (5%, 0.5 g) in a Parr hydrogenation apparatus. After 18 h the solution had turned yellow and after 64 h was colorless. The solution was filtered and concentrated to colorless crystals (1.2 g, m.p. 100–109°) which were recrystallized from hexane–ethanol giving the tetrahydro derivative (m.p. 109–110°). The gross structure of this compound was assigned on the basis of the following analytical and spectral evidence. The n.m.r. spectrum is consistent with formation of only one of the two possible stereoisomers.

The n.m.r. ($CDCl_3$): δ 7.0 (aromatic, 10H), 4.2 (ben-

Can. J. Chem. Downloaded from www.nrcresearchpress.com by 210.87.254.40 on 09/05/12
For personal use only.

zylic, sharp s, 2H), 1.7–2.1 (N–H, broad s, 2H), 3.3–3.8 (m, not symmetrical, 6H); (CCl_4): δ 6.97 (10H), 4.11 (benzylic, sharp s, 2H), 2.5–3.5 (m, 4H), 1.65–2.07 (m, 2H), and 1.57 (s, N–H, 2H). The i.r. 3320 (w), 3020 (w), 2920 (s), 2845 (m), 1600 (w), 1580 (w), 1460 (s), 1445 (s), 1420 (m), 1370 (m), 1279 (w), 1163 (s), 1155 (m), 1113 (m), 1072 (w), 1026 (w), 963 (w), 909 (w), 770 (s), 747 (s), 735 (w), 720 (w), 708 (s), 698 (s), 680 (m), and 670 (m) cm^{-1}.

Anal. Calcd. for $C_{17}H_{20}N_2$ (mol. wt. 252.35): C, 80.91; H, 7.99; N, 11.10. Found (242 (osmetric)): C, 81.04; H, 8.09; N, 10.97.

Several attempts were made to isolate the dihydroderivative from the reaction mixture before complete reduction; however, the yellow color was rapidly discharged upon exposure to air and the crude reaction mixture contained only diazepine and the tetrahydroderivative (i.r. and n.m.r.).

*Irradiation of 2,2-Dimethyl-4,5-diphenylisoimidazole (**10h**) in Tetramethylethylene*

A solution of 1.5 g of the isoimidazole **10*h*** in 10 ml of tetramethylethylene in a Pyrex tube (5/8″ o.d. × 9 1/2″) was irradiated 2 in. from a 450 W Hanovia medium-pressure mercury vapor lamp. The temperature of the solution was maintained at 20° by means of a water bath. After 2 days irradiation the excess tetramethylethylene was evaporated leaving 1.9 g of oil shown by n.m.r. to be *ca.* 70% adduct and 30% unreacted isoimidazole.

This mixture was difficult to separate by column chromatography; however, an analytical sample of the adduct (m.p. 92–96°) was obtained from the first fractions eluting with hexane and increasing amounts of benzene. The adduct could also be obtained by evaporating the unreacted isoimidazole (sublimation apparatus, 135°/11 mm) leaving 1.3 g (m.p. 85–95°) of adduct. We were unable to find a good solvent for recrystallization of the adduct. The following analytical and spectral properties led to the assigned structure **25**.

Anal. Calcd. for $C_{23}H_{28}N_2$ (mol. wt. 332): C, 83.08; H, 8.49; N, 8.43. Found (305 (osmetric)): C, 82.98; H, 8.29; N, 8.73.

The n.m.r. (CCl_4): δ 1.13 (s, 3H), 1.18 (m, 3H), 1.26 (s, 3H), 1.57 (s, 3H), 1.68 (bd, s, 3H), 2.01 (bd, s, 1H), 2.75 (d, J = 14 Hz, 1H), 3.26 (d, J = 14 Hz, 1H), 6.97–7.72 (m, 10H).

The i.r.: 3050 (w), 2970 (s), 2930 (s), 2870 (w), 1620 (s), 1570 (m), 1496 (m), 1448 (s), 1412 (m), 1375 (m), 1358 (m), 1330 (w), 1310 (w), 1278 (w), 1220 (s), 1180 (w), 1156 (w), 1075 (m), 1032 (w), 984 (w), 972 (w), 905 (w), 880 (w), 840 (w), 777 (s), 764 (s), 728 (w), 694 (s), 685 (m), and 652 (m) cm^{-1}.

The parent peak (*m/e* 332) is detected, but smaller than 331 and 333 (the P–H and P + H peaks). The base peak is 249, which can arrive through loss of the tetramethylethylene radical. Other prominent fragments are 145 ($C_{10}H_{11}N$) and 104 (C_7H_6N).

1. For recent reviews on the photochemistry of heterocyclic systems see: S. T. Reid. Advances in heterocyclic chemistry. Vol. 11. *Edited by* A. R. Katritzky and A. J. Boulton. Academic Press, New York, N.Y. 1970. Chapt. 1; P. Beak and W. R. Messer. Organic photochemistry. Vol. 2. *Edited by* O. L. Chapman. Marcel Dekker. New York, N.Y. 1969. pp. 117–167.
2. (*a*) P. Beak and J. L. Miesel. J. Amer. Chem. Soc. **89**, 2375 (1967); (*b*) J. L. Miesel. Ph.D. Thesis, University of Illinois, Urbana, Illinois. Diss. Abs., B**27** (11), 3860 (1967); (*c*) P. Beak. Private communication.
3. (*a*) G. Quinkert. Photochem. and Photobio. **7**, 783 (1968). (*b*) O. L. Chapman, and J. D. Lassila. J. Amer. Chem. Soc. **90**, 2449 (1968).
4. (*a*) A. Padwa, S. Clough, and E. Glazer. J. Amer. Chem. Soc. **92**, 1778 (1970). (*b*) A. Padwa. Private communication.
5. H. W. Heine, R. H. Weese, R. A. Cooper, and A. J. Durbetaki. J. Org. Chem. **32**, 2708 (1967). H. W. Heine, A. B. Smith, III, and J. D. Bower. J. Org. Chem. **33**, 1097 (1968).
6. A. M. Trozzolo and T. DoMinh. Abstract CIC/ACS Meeting, May, 1970. Orga. 62, and J. Amer. Chem. Soc. **92**, 6997 (1970).
7. J. A. Moore. Heterocyclic compounds with three and four-membered rings. Part 2. Interscience Publishers, New York, N.Y. 1964.
8. W. G. Dauben and R. L. Cargill. Tetrahedron. **12**, 186 (1961).
9. J. I. Brauman, L. E. Ellis, and E. E. van Tamelen. J. Amer. Chem. Soc. **88**, 846 (1966).
10. (*a*) W. J. Theuer and J. A. Moore. Chem. Commun. 468 (1965). (*b*) G. L. Closs, W. A. Böll, H. Heyn, and V. Dev. J. Amer. Chem. Soc. **90**, 173 (1968).
11. N. J. Leonard and P. M. Mader. J. Amer. Chem. Soc. **72**, 5388 (1950). N. J. Leonard, R. T. Rapala, H. L. Herzog, and E. R. Blout. J. Amer. Chem. Soc. **71**, 2997 (1949). N. J. Leonard and E. R. Blout. J. Amer. Chem. Soc. **72**, 484 (1950). N. J. Leonard, A. J. Kresge, and M. Oki. J. Amer. Chem. Soc. **77**, 5078 (1955).
12. M. Weiss. J. Amer. Chem. Soc. **73**, 5193 (1952).
13. T. Ishiguree and M. Matsummura. Yakugaku Zasshi, **78**, 229 (1958); Chem. Abs. **52**, 11862 (1958).
14. R. H. McDougall and S. H. Malik. J. Chem. Soc. C, 2044 (1969).
15. S. Searles, Jr. and R. A. Clasen. Tetrahedron Lett. 1627 (1965).
16. D. R. Arnold and V. Y. Abraitys. Unpublished results.
17. Mason and Dryfoos. J. Chem. Soc. **63**, 1293 (1893).
18. N. C. Baird. Mol. Photochem. **2**, 53 (1970) and references therein.
19. (*a*) R. Hoffmann, A. Imamura, and W. J. Hehre. J. Amer. Chem. Soc. **90**, 1499 (1968). (*b*) R. C. Cookson, J. Henstock, and J. Hudec. J. Amer. Chem. Soc. **88**, 1060 (1966).
20. T. M. McKinney and D. H. Geske. J. Amer. Chem. Soc. **87**, 3013 (1965).
21. R. S. Becker and J. Michl. J. Amer. Chem. Soc. **88**, 5931 (1966).
22. R. B. Woodward. J. Amer. Chem. Soc. **64**, 72 (1942).
23. Jaffé and Orchin. Theory and applications of ultraviolet spectroscopy. John Wiley and Sons, New York, N.Y. 1964. pp. 199–204.
24. W. Weltner, Jr. and J. R. W. Warn. J. Chem. Phys. **37**, 292 (1962).
25. A. Padwa, W. Bergmark, and D. Pashayan. J. Amer. Chem. Soc. **91**, 2653 (1969).
26. M. Lamchem and T. W. Mittay. J. Chem. Soc. C, 2300 (1966).

Can. J. Chem. Downloaded from www.nrcresearchpress.com by 210.87.254.5 on 09/05/12
For personal use only.

Synthesis and Thermolysis of 2*H*-1,2,3-Benzothiadiazine 1,1-Dioxide and 2,1-Benzoxathiin-3-one 1,1-Dioxide[1,2]

J. F. KING, B. L. HUSTON, ANNE HAWSON, J. KOMERY, DONNA M. DEAKEN, AND D. R. K. HARDING
Department of Chemistry, University of Western Ontario, London 72, Ontario

Received September 14, 1970

2*H*-1,2,3-Benzothiadiazine 1,1-dioxide (**6**) and 2,1-benzoxathiin-3-one 1,1-dioxide (**5**), representatives of little-known heterocyclic systems, have been synthesized from sodium *o*-formylbenzenesulfonate (**7**). Thermolysis of **5** and **6** was investigated in the hope of finding evidence for the formation of a sulfene. No characterized product was obtained from **5**, but **6** gave the sultine 3*H*-2,1-benzoxathiole 1-oxide (**21**), the compound expected from the sulfene **20**.

La 2*H*-benzothiadiazine-1,2,3 dioxyde-1,1 (**6**) et la benzoxathiin-2,1 one-3 dioxyde-1,1 (**5**), des représentants de systèmes hétérocycliques peu connus, ont été synthétisés à partir de l'*o*-formylbenzènesulfonate de sodium (**7**). La thermolyse de **5** et **6** a été examinée dans l'espoir de trouver des indications concernant la formation d'un sulfène. Aucun produit caractérisé ne fut obtenu à partir de **5**, mais **6** a donné la sultine 3*H*-benzoxathiole-2,1 oxyde-1 (**21**), le composé prévu du sulfène **20**.

Canadian Journal of Chemistry, 49, 936 (1971)

Introduction

Sulfenes ($RR'C{=}SO_2$) may now be regarded as established and respectable intermediates,[3] in certain reactions at least, even though they have thus far eluded all of the numerous attempts at their isolation and characterization. As a possible route leading to new information on sulfenes, and possibly even their isolation, we contemplated the synthesis of compounds which by the action of heat or light might fragment to give sulfenes. One tested recipe for the frangibility required to form high energy species requires the construction of a molecule so arranged that the other fragment of the reaction is a particularly stable species, *e.g.* molecular nitrogen, carbon dioxide, sulfur dioxide, and so on.[4] Among the possible ways of applying this notion to the formation of sulfenes is the synthesis of species of the general formula **1** which could undergo cycloreversion of the reverse Diels–Alder type to give vinylsulfene (**2**) and a stable fragment **3**. For reasons of synthetic convenience we focussed our attention on benz–fused analogues of **1**, the specific objectives in the work reported herein being 4*H*-1,2,3-benzothiadiazine 1,1-dioxide (**4**) and 2,1-benzoxathiin-3-one 1,1-dioxide (**5**), alias "*o*-sulfophenylacetic anhydride".

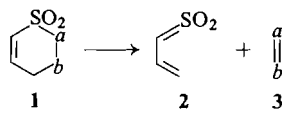

1 **2** **3**

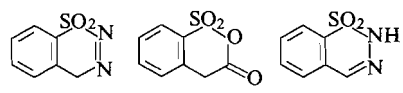

4 **5** **6**

The cyclic anhydride **5** was synthesized without difficulty but gave none of the hoped for fragmentation. The cyclic azo compound **4** was not obtained but its isomer **6** was prepared and found to extrude nitrogen on thermolysis with formation of a sultine (cyclic sulfinic ester); **6** is the parent of a heterocyclic system previously known only in the form of some 4-hydrazino-derivatives (3 and references cited) and the very recently reported 4-phenyl compounds (4). In the course of this work it was found that reaction of **6** with chlorine led to an interesting transformation possibly involving a sulfene; this is described in detail in the accompanying paper. Part of the substance of these two papers has already been reported in preliminary form (5).

[1]Organic Sulfur Mechanisms. Part 8. For part 7 see ref. 1.

[2]Some of the work recorded in this and the following paper is taken from the following theses (University of Western Ontario): D. M. Deaken (Honors B.Sc., 1964), A. Hawson (M.Sc. 1968), J. Komery (M.Sc. 1969).

[3]For a summary of the chemistry of sulfenes up to 1967 see Opitz' review (2); access to more recent work may be obtained from ref. 1 and papers cited therein.

[4]Thermolysis of four-membered rings, with and without fragmentation, has also been explored and appears to lead to sulfenes (1).

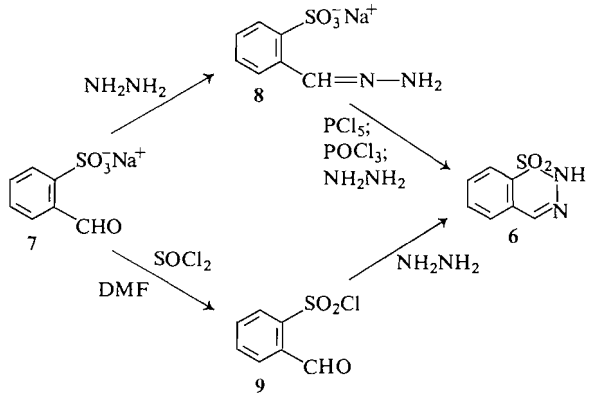

SCHEME 1

Results and Discussion

Synthesis of 2H-1,2,3-Benzothiadiazine 1,1-Dioxide (6)

The starting material for all of the syntheses described in this paper is sodium *o*-formylbenzenesulfonate (**7**), a material which is commercially available in a "practical" grade apparently as the monohydrate (*cf.* ref. 6). Reaction of **7** with hydrazine hydrate gave the hydrazone **8**, which when treated without purification with a mixture of phosphorus oxychloride and phosphorus pentachloride, gave **6** in about 5–10% yield (see Scheme 1). Attempts to improve the yield led to the observation that recrystallization of the hydrazone led to an even poorer yield of **6**. Acting on the inference that residual hydrazine was responsible for the difference, hydrazine was added to the reaction of **8** with $POCl_3$–PCl_5. The yields of **6** were much improved, though erratic; the best yield in a number of such experiments was 80% (based on **8**) but repetition of the procedure as recorded gave only low yields. Further study led to a procedure which incorporated minor changes in conditions and which gave yields of 30–50% with some consistency (see Experimental).

The structure **6** for the material thus obtained follows from elemental analysis and the following spectroscopic features: (*a*) bands at 3.1 (1H, N*H*), 7.9 (m, four aromatic hydrogens), and 8.2 p.p.m. (s, 1H, —C*H*=N—) in the n.m.r. spectrum, (*b*) i.r. peaks at 3280 (NH), 1657 (w, C=N—), 1345 (vs) and 1165 cm^{-1} (vs) (—SO_2—). Final confirmation of the structure (**6**) is provided by its synthesis from *o*-formylbenzenesulfonyl chloride (**9**) as described below.

Because of the erratic yields of **6** from **7** on treatment with the phosphorus chloride – hydrazine mixture, the *p*-toluidine anil **10** and the tosylhydrazone **13** (prepared from **7** via **12**) were investigated as possible precursors of **6** (see Scheme 2). The anil **10** apparently gave **11**, whereas the tosylhydrazone **13** gave a 3% yield of **6**. No attempt was made to improve the tosylhydrazone route because of the discovery of another, and evidently better, way of making **6**.

An obvious precursor of **6** is *o*-formylbenzenesulfonyl chloride (**9**), a compound which, prior

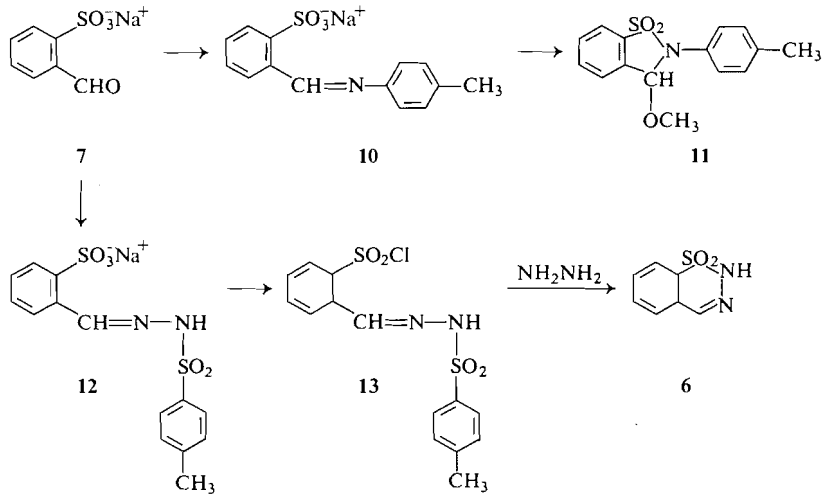

SCHEME 2

Can. J. Chem. Downloaded from www.nrcresearchpress.com by 210.87.254.5 on 09/05/12
For personal use only.

Can. J. Chem. Downloaded from www.nrcresearchpress.com by 210.87.254.5 on 09/05/12
For personal use only.

to this study, was unknown. The reaction of **7** with PCl_5–$POCl_3$ has been known for many years (6, 7) to lead, not to **9**, but to its cyclic isomer **14**, which does not give **6** on reaction with hydrazine hydrate. As is described in detail in the following paper we have found that chlorination of **6** in the presence of water gives **9**. As a route for the synthesis of **6**, this procedure is, of course, valueless, but it did lead to the characterization of **9** so that it could be readily recognized when made in other ways, even when mixed with other materials. In addition, by treating a sample of **9** prepared from **6** with hydrazine, it was possible to get **6** back in very good yield; this, as has been mentioned above, confirmed the structure of **6**.

Treatment of **7** with thionyl chloride gave no reaction, and conversion of **7** to *o*-formylbenzenesulfonic acid followed by reaction with thionyl chloride gave the cyclic chloride **14**. When **7** was allowed to react with thionyl chloride in the presence of a catalytic amount of dimethylformamide, however, the product was evidently mainly *o*-formylbenzenesulfonyl chloride (**9**) mixed with a little of the cyclic isomer (**14**) (Scheme 3). Reaction of this mixture with hydrazine hydrate led to the isolation of **6** in an overall yield of about 50% from **7**. The crude product also contains **14**, but this is readily separated by taking advantage of the acidity of **6**. This procedure is simple and gives reasonably consistent yields, and became our method of choice for the synthesis of **6**. It was found that only a short reaction time was required to convert **7** to **9**, longer times (or treatment of **9** with thionyl chloride) led to the benzal chloride **15**, which did not yield **6** under the conditions used to convert **9** to **6**.

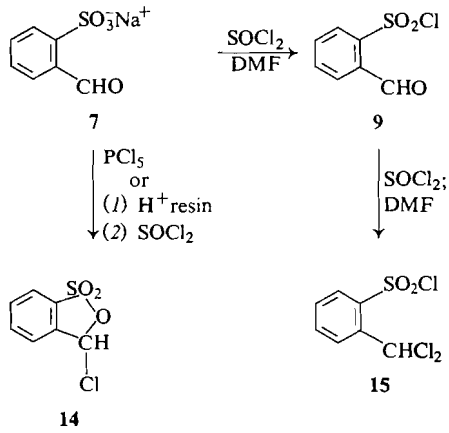

SCHEME 3

Synthesis of 2,1-Benzoxathiin-3-one 1,1-Dioxide (5) ("o-Sulfophenylacetic Anhydride")

The synthesis of **5** is straightforward and is summarized in Scheme 4. The starting material (**16**) was obtained from **7** via **14**, following the method of List and Stein (7) as described in detail by Helberger *et al.* (8). The structure of **5** follows from its mode of synthesis and is confirmed by elemental analysis and spectra; a conspicuous feature in the i.r. is a strong band at 1818 cm^{-1}. As would be expected of a mixed carboxylic–sulfonic anhydride, **5** is very easily hydrolyzed, for example, by atmospheric moisture, to *o*-sulfophenylacetic acid (**18**), and reacts very readily with aniline to give **19**.

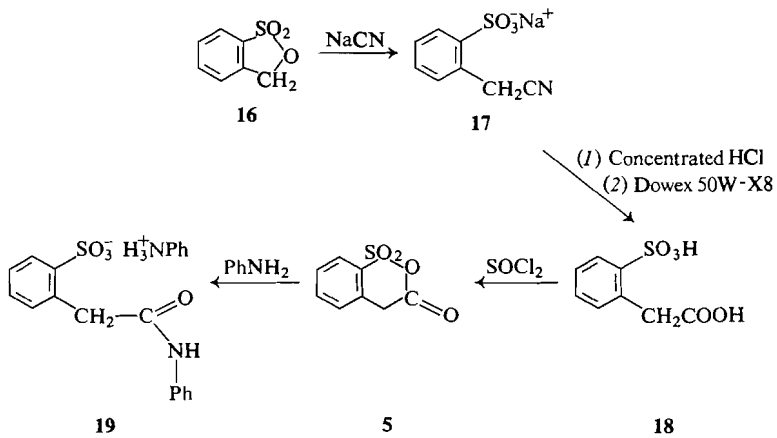

SCHEME 4

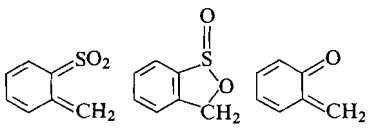

20 21 22

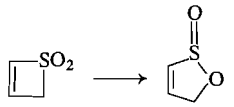

23 24

Thermolysis of 5 and 6

All attempts at thermal fragmentation of **5** to give **20** or materials evidently derived from **20** were without avail. On the basis of the results (1, 9) with thermolysis of thiete 1,1-dioxide (**23**), which appears to rearrange via vinylsulfene (CH_2=CH—CH=SO_2), we might have expected that **20** below 700–800° would have given the "sultine" (cyclic sulfinic ester) **21**, and at higher temperatures the "desulfinylation" (1) product, *o*-quinone methide (**22**). An authentic specimen of **21** was available from work connected with the chlorinolysis of **6** (see the following paper), and **22** and its trimerization product have been described (10) and should have been readily recognizable, if present. In either the simple quartz tube at 380–550° and pressures of 5–7 μ, or the flash thermolysis apparatus (1) at 600°, **5** was recovered substantially unchanged. In the flash apparatus at 1000°, only general decomposition was observed.

Thermolysis of the thiadiazine (**6**) at 600–620° in the flash apparatus gave back starting material and at 750° yielded only an uncharacterized gum. In a quartz tube at 500° and about 1 mm, **6** gave a roughly 25% yield of the sultine **21**; the yields appeared to be improved by the presence of a plug of glass wool in the tube. It has also been noted by Dr. L. J. Danks in these laboratories (private communication) that **21** is formed (in addition to black tar) in an estimated 10% yield on heating **6** in the melt at 180°. The sultine (**21**) is the product expected at these temperatures from **20** if, in fact, it were formed. When taken with our evidence (1) for the intermediacy of vinylsulfene in the rearrangement of **23** to **24**, and also the formation of the 4-chloro analogue of **21** on chlorinolysis of **6** as described in the following paper, this result would suggest that the simplest route to **21** from **6** is via **20**, though the present evidence does not exclude other pathways. Formation of **20** from **6** formally requires migration of a hydrogen from nitrogen to carbon; this could perhaps take place via **4**, followed by fragmentation as originally visualized, or conceivably by cleavage of one of the ring bonds in **6**, with formation of the diazene (diimide), followed by hydrogen migration accompanying loss of nitrogen. With either of these processes it is not surprising that the quartz tube apparatus and the melt, with their much greater likelihood of collisions with the walls and other molecules, would be more favorable conditions for a two (or more) step process than the flash apparatus.

Experimental

Sodium *o*-formylbenzenesulfonate (**7**) was obtained from Koch-Light Laboratories Limited, Colnbrook, England, under the designation "*o*-sulfobenzaldehyde Na salt" and indicated as "75–89%" or "practical" grade. No attempt was made either to assay or to purify the **7** before use; the yields given are based on the assumption that it is the pure mono-hydrate and would presumably be somewhat higher if pure **7** were used. All other reagents and solvents were of commercial reagent grade unless otherwise indicated.

Unless otherwise specified melting points were determined on a Kofler hot stage and are uncorrected. The i.r. spectra were obtained with Beckman IR-7 or IR-10 instruments using sodium chloride cells. The n.m.r. values given were determined on a Varian A60 instrument using tetramethylsilane as internal standard; a Varian T60 spectrometer was used in some instances to ascertain product composition. The t.l.c. was carried out using Camag Kieselgel DF5 or "GF-254 (acc. to Stahl)" silica gel supplied by E. Merck, Darmstadt, Germany. Petroleum ether refers to the fraction of boiling range 35–60°. Unless otherwise stated magnesium sulfate was used to dry the organic phase following extraction in a separatory funnel.

Preparation of 2H-1,2,3-Benzothiadiazine 1,1-Dioxide (6) from Sodium o-Formylbenzenesulfonate (7) via the Hydrazone (8)

Sodium *o*-formylbenzenesulfonate (**7**) (40.0 g) and hydrazine hydrate (99%) (50 ml) were refluxed together for 2 h. The hydrazine hydrate was then evaporated off under reduced pressure and the crude product was dissolved in methanol. The methanol insoluble material was removed by filtration and the methanol soluble material recrystallized from methanol–ether giving 24.0 g (56%) of white crystals.

The crude hydrazone **8** (10 g) obtained as above, was placed in a three-necked round-bottomed flask fitted with a condenser, mechanical stirrer, and dropping funnel. Hydrazine hydrate (99%, 5 ml) was added and the mixture stirred and cooled to 0° in an ice bath. Phosphorus oxychloride (50 ml) was added dropwise over a period of 45 min, followed by phosphorus pentachloride (10 g), and the mixture warmed to 60° and stirred until the mixture became smooth (about 4.5 h). The mixture

Can. J. Chem. Downloaded from www.nrcresearchpress.com by 210.87.254.5 on 09/05/12
For personal use only.

Can. J. Chem. Downloaded from www.nrcresearchpress.com by 210.87.254.5 on 09/05/12
For personal use only.

was poured onto crushed ice and allowed to stand until the phosphorus oxychloride appeared to have hydrolyzed completely, and extracted with chloroform. The extracts were washed with water, dried with anhydrous sodium sulfate, and the solvent evaporated leaving a pale yellow solid 2.4 g (30%). Recrystallization from chloroform gave crystals of **3** (1.35 g, 17%) melting at 142–143°.

A number of repetitions of this procedure with varying quantities of **8** gave erratic results with crude yields sometimes as low as 5–10% and on one occasion as high as 80%. The use of benzene or dimethylformamide as solvent led to little or no **6**. In one experiment with this general method, starting with a smaller quantity (3.9 g) of **8** and appropriately reduced amounts of the other reagents, further hydrazine hydrate (5 ml) was added after the addition of the phosphorus oxychloride was complete; this led to a 50% yield of crude product (25% after recrystallization).

The i.r. spectrum of **6** (Nujol mull) showed the following bands: 3280, 1657 (w), 1598 (w), 1565 (m), 1479 (w), 1448 (m), 1360 (sh), 1345 (vs), 1268 (m), 1225 (m), a very strong band with peaks at 1183, 1165, and 1145, 1080 (m), 993 (s), 970 (m), 915 (s), 883 (m), 858 (m), 780 (w), 785 (s), 735 (m), 690 (w), 640 (s). The n.m.r. spectrum (in acetone-d_6) showed a broad hump at 3.1 which disappeared on addition of D_2O, a singlet at 8.1, and a complex band from 7.8–8.0 p.p.m.

Anal. Calcd. for $C_7H_6SO_2N_2$: C, 46.14; H, 3.32; N, 15.38; S, 17.59. Found: C, 46.19; H, 3.29; N, 15.24; S, 17.42.

The pK_a of **6** was determined in 50% ethanol–water (by weight) by titration with 0.1 *N* sodium hydroxide measuring the p*H* with a Radiometer 25 p*H* meter with glass and calomel electrodes standardized with aqueous buffer solution, p*H* 7.00; to obtain the hydrogen ion activity in the aqueous alcohol medium 0.18 was subtracted from meter readings of the p*H* (*cf.* Bates *et al.* (11)). By this technique the following pK_a values were obtained: **6**, 7.2; benzaldehyde tosylhydrazone, 8.6; benzenesulfon-*p*-toluidide, 10.1. Dauphin *et al.* (12) report a pK_a value of 10.17 for benzenesulfon-*p*-toluidide in the same medium.

Preparation of 2H-1,2,3-Benzothiadiazine 1,1-Dioxide (6) via o-Formylbenzenesulfonyl Chloride (9)

Sodium *o*-formylbenzenesulfonate (**7**) (5 g, 0.24 mol) was suspended in thionyl chloride (20 ml) and dimethylformamide (12 drops) added. The mixture was refluxed for 1 h and then evaporated to dryness. The residue was extracted with methylene chloride and filtered. The filtrate was concentrated to about 25 ml and hydrazine hydrate (99%) (3 ml) cautiously added dropwise with stirring. The mixture was stirred at room temperature for 10 min, then diluted with water, cooled in an ice bath and acidified with concentrated HCl. The aqueous mixture was extracted with chloroform, the chloroform extract was extracted with 5% NaOH. The chloroform layer was dried, and the solvent evaporated, leaving a pale yellow solid (0.59 g) which melted at 113–115° and had the same i.r. spectrum as a sample of the "pseudo acid chloride" (**14**) prepared by the method of Helberger *et al.* (10). The sodium hydroxide extracts were acidified and extracted with chloroform; the chloroform extracts were dried and the solvent removed to give a crude 2*H*-1,2,3-benzothiadiazine 1,1-dioxide (**6**) (2.08 g, 50%), which after one recrystallization from chloroform melted at 141–142°.

It was found that best conversion of **4** to *o*-formylbenzenesulfonyl chloride (**9**) was obtained using only a very brief reaction time with thionyl chloride (*e.g.* 3 min reflux). Under such conditions using 7 (5 g), thionyl chloride (20 ml) and dimethylformamide (25 drops) and taking the product up in pentane and washing with water, **9** was obtained as a pale yellow oil (3.7 g, 76%), identified by i.r. and n.m.r. spectra. With longer reaction times **9** was further transformed to **15** (see below).

Attempted Synthesis of 2H-1,2,3-Benzothiadiazine 1,1-Dioxide (6) via the Anil 10. Formation of the Carbinolamine Ether 11

Sodium *o*-formylbenzenesulfonate (**7**) (10.4 g, 0.05 mol) and *p*-toluidine (5.4 g, 0.05 mol) were partially dissolved in absolute ethanol (50 ml) and gently refluxed for 20 min. The hot solution was filtered and the filtrate evaporated to dryness. Ether was added to the oily residue and the colorless crystals, presumed to be **10** (11 g 74%), collected by filtration. The i.r. spectrum (Nujol) showed bands at 1620 (w), 1565 (w), 1500 (w), 1190 (vs), 1140 (m), 1090 (m), 1045 (w), 1025 (s), 970 (w), 880 (w), 820 (m), 760 (m), 716 (s).

The anil (**10**) (5 g) was mixed with phosphorus pentachloride (5 g) and ground in a mortar for 5 min, and then left at room temperature for 0.5 h. The mixture was poured into ice–water and extracted with methylene chloride. The extracts were dried over anhydrous sodium sulfate and the solvent evaporated to give a yellow solid (4.3 g). Extensive recrystallization from methylene chloride – petroleum ether and methanol gave crystals melting at 129–130°, for which structure **11** is assigned. The i.r. spectrum showed peaks at 3000 (w), 1510 (m), 1450 (w), 1310 (s), 1270 (m), 1170 (s), 1130 (m), 1090 (m), 1040 (s), 970 (m), 600 (m), 580 (m) and the n.m.r. spectrum showed complex aromatic absorption from 7.1–8.0 (8H), and singlets at 6.40 (1H), 3.12 (3H) and 2.37 p.p.m. (3H).

Anal. Calcd. for $C_{15}H_{15}NO_3S$: C, 62.27; H, 5.23; N, 4.84; S, 11.06. Found: C, 62.46; H, 5.34; N, 4.91; S, 11.06.

Synthesis of 2H-1,2,3-Benzothiadiazine 1,1-Dioxide (6) via the Tosylhydrazones 12 and 13

p-Toluenesulfonylhydrazine (tosylhydrazine) (4.7 g) and sodium *o*-formylbenzenesulfonate (**7**) were partially dissolved in methanol (25 ml) and refluxed for 1 h. The hot solution was filtered and the filtrate treated with ether to give a white, crystalline solid (**12**) (6.1 g) which showed the following peaks in the i.r. (Nujol); 3350 (m), 1600 (w), 1320 (m), 1205 and 1170 (vs), 1140 (sh), 1090 (m), 1065 and 1045 (m), 1025 (m), 965 (m), 835 (m), 810 (m), 787 and 780 (w), 760 (w), 730 and 720 (m), and 700 (w).

The tosylhydrazone **12** was mixed with phosphorus pentachloride (2 g) and ground in a mortar. The resultant yellow paste was left at room temperature for 10 min whereupon it was mixed with water (50 ml) and the mixture extracted with ether. The extracts were dried over anhydrous sodium sulfate and the solvent removed leaving a colorless oil (1.2 g, 61%) which solidified on standing. The i.r. spectrum showed characteristic bands at

Can. J. Chem. Downloaded from www.nrcresearchpress.com by 210.87.254.5 on 09/05/12
For personal use only.

1375 and 1325 and 1174 ascribable to the SO_2Cl and $-SO_2N$ functions. Recrystallization from methylene chloride – petroleum ether gave colorless crystals (presumed to be **13**) (768 mg), m.p. 136–140° (dec) which were not further characterized.

The sulfonyl chloride – hydrazone (**13**) (3 g) was mixed with hydrazine hydrate (99%, 10 ml) and warmed at 60° for 1.5 h. The pale yellow solution was cooled, diluted with water, and acidified with concentrated hydrochloric acid. The mixture was extracted with chloroform and the extracts dried over anhydrous sodium sulfate. Removal of the solvent gave an orange oil (1.25 g), which on trituration with chloroform gave a small amount (105 mg) of colorless crystals, m.p. 137–410°, which gave no depression of m.p. on admixture with authentic **6**. The remaining products were not investigated further.

*Preparation of o-Dichloromethylbenzenesulfonyl Chloride (**15**)*

Sodium *o*-formylbenzenesulfonate (**7**) (5 g, 0.024 mol) was suspended in thionyl chloride (20 ml) and dimethylformamide (25 drops) added. The mixture was refluxed for 0.5 h. The excess thionyl chloride was then removed under reduced pressure, the residue was taken up in methylene chloride and the mixture filtered. Removal of the methylene chloride gave an oily residue which partially dissolved in pentane. The pentane solution was washed with water and dried; removal of the solvent gave a yellow oil (4.2 g) which crystallized on cooling in a Dry Ice – acetone mixture. Recrystallization from carbon tetrachloride – pentane at −60° gave colorless crystals (3.4 g, 55%) melting at 50–52°; recrystallization gave the analytical specimen, m.p. 54–55°. The i.r. spectrum showed bands at 3000 (w), 1570 (w), 1470 (w), 1445 (m), 1380 (vs), 1320 (w), 1285 (w), 1180 (vs), 1120 (m), 1060 (w), 980 (w), 840 (s), and 680 cm^{-1} (m). The n.m.r. spectrum showed only complex absorption from 7.4–8.4 with a prominent peak at 7.86 p.p.m.; the mass spectrum indicated a molecular weight of 258 with another peak at 260 of the same intensity.

Anal. Calcd. for $C_7H_5Cl_3O_2S$: C, 32.39; H, 1.94; Cl, 40.98; S, 12.35. Found: C, 32.58; H, 1.95; Cl, 41.18; S, 12.45.

o-Formylbenzenesulfonyl chloride (**9**) (1.01 g), thionyl chloride (5 ml), and dimethylformamide (5 drops) were refluxed for 0.5 h. The excess thionyl chloride was removed under reduced pressure and water and pentane added to the residue. The pentane extract was dried and the solvent evaporated leaving colorless crystals; the i.r. spectrum was virtually identical with that of **15** prepared as above except for a rather small peak at 1700 cm^{-1}, presumably due to a small amount of **9**. Recrystallization from carbon tetrachloride – pentane gave crystals melting at 49–52°.

*Reaction of 3H-2,1-Benzoxathiole 1,1-Dioxide (**16**) with Sodium Cyanide*

3*H*-2,1-Benzoxathiole 1,1-dioxide (**16**) (10) (5 g, 0.029 mol) was dissolved in absolute alcohol (150 ml) and was added slowly with stirring over a period of 30 min to a solution of sodium cyanide (1.48 g, 0.03 mol) in water (15 ml). The reaction mixture was refluxed for 4 h. Evaporation of solvent yielded sodium *o*-cyanomethylbenzenesulfonate (**17**) (6.4 g, 100%). The product was recrystallized three times from methanol, m.p. 298–301°.

Anal. Calcd. for $C_8H_6NaNO_3S$: C, 43.84; H, 2.76; N, 6.39; S, 14.63. Found: C, 43.95; H, 2.70; N, 6.41; S, 14.32.

The i.r. spectrum (Nujol) showed absorption bands at 3060 (w), 2240 (w), 1408 (w), 1235 (s), 1215 (s), 1195 (s), 1180 (s), 1145 (m), 1095 (m), 1050 (w), 1030 (m), 955 (w), 755 (m), 725 (m), 705 (m), 625 cm^{-1} (m). The n.m.r. spectrum (dimethyl sulfoxide-d_6) showed absorption bands at 4.43 (s, 2H) and 7.25–8.0 p.p.m. (aromatic hydrogen absorption, 4H).

*Hydrolysis of Sodium o-Cyanomethylbenzenesulfonate (**17**)*

Sodium *o*-cyanomethylbenzenesulfonate (**17**) (2 g, 9.1 mmol) was dissolved in water (20 ml). Concentrated hydrochloric acid (20 ml) was added dropwise with stirring. The reaction mixture was refluxed for 45 min and then evaporated to dryness. The material (2.2 g) obtained was not characterized but was dissolved in water and passed through a column of Dowex 50W-X8 ion exchange resin in the acid form. The aqueous solution was immediately evaporated under reduced pressure (0.1 mm) without heating, to yield *o*-sulfophenylacetic acid (**18**) (2.2 g, 94%, assuming one molecule of water of crystallization). The product was recrystallized three times from methanol, m.p. 215–219°.

Anal. Calcd. for $C_8H_8O_5S \cdot CH_3OH$: C, 43.51; H, 4.87; S, 12.91. Found: C, 43.55; H, 5.17; S, 12.95.

The i.r. spectrum (Nujol) showed bands at 3200 (s), 1705 (s), 1680 (s), 1315 (w), 1285 (m), 1270 (s), 1210 (s), 1195 (s), 1145 (m), 1085 (m), 1020 (s), 970 (w), 925 (w), 880 (w), 830 (w), 780 (m), 755 (m), 715 (m), 670 (w), 625 (m), 605 (m), 585 (m), and 575 cm^{-1} (m). The n.m.r. (dimethyl sulfoxide-d_6) bands were at 3.57 (s, 3H), 4.13 (s, 2H) 6.30 (s, 1H) 7.06–7.45 (complex aromatic hydrogen absorption and a hydroxyl group, 4H), 7.7–7.95 (complex aromatic absorption, 1H), and 8.01 p.p.m. (s, 1H); on addition of D_2O, peaks at 6.30, 7.15, and 8.01 p.p.m. disappeared.

*Reaction of o-Sulfophenylacetic Acid (**18**) with Thionyl Chloride*

Freshly distilled thionyl chloride (15 ml) was added to *o*-sulfophenylacetic acid (**18**) (0.3 g, 1.39 mmol). The reaction mixture was heated under reflux for 1 h under anhydrous conditions. The thionyl chloride was decanted from a sludge of 50 mg and was evaporated under reduced pressure without heating. The yield of crude solid material was 250 mg. Recrystallization from dried methylene chloride and pentane in a water-free atmosphere, yielded 2,1-benzoxathiin-3-one 1,1-dioxide ("*o*-sulfophenylacetic anhydride") (**5**) (160 mg, 60%), m.p. 107.5–108.5° (vacuum capillary). The product (**5**) had to be dried and stored over phosphorus pentoxide to prevent hydrolysis.

Anal. Calcd. for $C_8H_6O_4S$: C, 48.48; H, 3.05; S, 16.17. Found: C, 48.15; H, 3.24; S, 16.04.

The i.r. spectrum (CH_2Cl_2) showed absorption bands at 2900 (w), 1818 (s), 1600 (w), 1585 (w), 1480 (m), 1455 (w), 1385 (w), 1205 (s), 1195 (s), 1150 (w), 1085 (m), 1070 (m), 1015 (w), 965 (w), 940 (w), 845 (s), 790 (m), and 655 cm^{-1} (w). The n.m.r. spectrum ($CDCl_3$) showed bands at 4.28 (s, 2H) and 7.25–8.15 p.p.m. (aromatic absorption, 4H).

A similar yield of 2,1-benzoxathiin-3-one 1,1-dioxide (**5**) was obtained when the reaction was carried out at room temperature.

Reaction of 2,1-Benzoxathiin-3-one 1,1-Dioxide (5) with Aniline in Methylene Chloride

In a water–free atmosphere, 2,1-benzoxathiin-3-one 1,1-dioxide (5) (0.1 g, 0.51 mmol) was dissolved in dried methylene chloride (1 ml). Distilled aniline (0.096 g, 1.03 mmol) was added. The reaction mixture was left for 30 min at 5°, after which the methylene chloride was evaporated. The product was recrystallized from methanol to yield the anilinium derivative (19) (153 mg, 78%), m.p. 229–231°.

Anal. Calcd. for $C_{20}H_{20}N_2O_4S$: C, 62.48; H, 5.25; N, 7.29; S, 8.34. Found: C, 62.48; H, 4.99; N, 7.38; S, 8.42.

The i.r. spectrum (Nujol) showed absorption bands at 3270 (m), 2600 (w), 1650 (s), 1600 (s), 1560 (s), 1520 (m), 1500 (s), 1355 (m), 1320 (w), 1290 (w), 1260 (w), 1220 (s), 1185 (s), 1160 (s), 1140 (s), 1080 (m), 1050 (w), 1030 (w), 1020 (s), 970 (w), 910 (w), 855 (w), 845 (w), 820 (w), 800 (w), 780 (w), 760 (s), 745 (m), 720 (m), 710 (m), 700 (m), 660 (m), and 620 cm^{-1} (s). The n.m.r. spectrum (dimethyl sulfoxide-d_6) showed bands at 4.6 (s, 2H), 6.8–8.9 (aromatic absorption plus ammonium protons, 17H), 10.53–10.71 p.p.m. (broad band, 1H).

Quartz Tube Thermolysis of 2H-1,2,3-Benzothiadiazine 1,1-Dioxide (6)

The thermolyses were carried out in a tubulated quartz tube essentially as previously described (1) except that a 1–2 in. plug of glass wool was placed roughly in the center of the heated zone of the tube. The tube was heated for 12″ of its length by a Lindberg/Hevi-Duty oven (made by Hevi-Duty Heating Equipment Co., Watertown, Wisconsin). A sample of **6** was placed in one end of the tube and sublimed into the hot zone of the apparatus using a microburner and an i.r. heating lamp. In one run 106 mg of **6** gave 69 mg of crude product which on t.l.c. gave a fraction (22 mg, 25%) which appeared spectroscopically to be almost entirely the sultine **21**. A second run with 103 mg of **6** gave 60 mg of crude product which afforded 24 mg (27%) of the t.l.c. fraction. Combination of these two t.l.c.-purified specimens of **21**, followed by treatment with decolorizing charcoal and crystallization, gave **21** (21 mg) melting at 39–40°; mixed m.p. with an authentic specimen of **21** prepared as described in the following paper 39–42°. The i.r. and n.m.r. spectra were identical with those of the authentic material.

We gratefully acknowledge the support of the National Research Council of Canada, the Petroleum Research Fund (administered by the American Chemical Society), and the Alfred P. Sloan Foundation.

1. J. F. KING, P. DE MAYO, C. L. MCINTOSH, K. PIERS, and D. J. H. SMITH. Can. J. Chem. **48**, 3704 (1970).
2. G. OPITZ. Angew. Chem. Inter. Ed. **6**, 107 (1967).
3. P. SCHMIDT, K. EICHENBERGER, and M. WILHELM. Helv. Chim. Acta, **45**, 996 (1962).
4. J. B. WRIGHT. J. Heterocycl. Chem. **5**, 453 (1968).
5. J. F. KING, A. HAWSON, D. M. DEAKEN, and J. KOMERY. Chem. Commun. 33 (1969).
6. I. GOLDBERGER. Monatsh. **37**, 125 (1916).
7. R. LIST and M. STEIN. Ber. **31**, 1648 (1898).
8. J. H. HELBERGER, G. MANECKE, and R. HEYDEN. Ann. **565**, 22 (1949).
9. C. L. MCINTOSH and P. DE MAYO. Chem. Commun. 32 (1969).
10. S. B. CAVITT, H. SARRAFIZADEH R., and P. D. GARDNER. J. Org. Chem. **27**, 1211 (1962) and earlier references cited.
11. R. G. BATES, M. PAABO, and R. A. ROBINSON. J. Phys. Chem. **67**, 1833 (1963).
12. G. DAUPHIN, A. KERGOMARD, and H. VESCHAMBRE. Bull. Soc. Chim. France. 3395 (1967).

Can. J. Chem. Downloaded from www.nrcresearchpress.com by 210.87.254.5 on 09/05/12
For personal use only.

Can. J. Chem. Downloaded from www.nrcresearchpress.com by 210.87.254.42 on 09/05/12
For personal use only.

Chlorination of Heterocyclic and Acyclic Sulfonhydrazones[1]

J. F. KING, ANNE HAWSON, B. L. HUSTON, L. J. DANKS, AND J. KOMERY
Department of Chemistry, University of Western Ontario, London 72, Ontario

Received September 14, 1970

Chlorination of 2*H*-1,2,3-benzothiadiazine 1,1-dioxide (**1**) in wet methylene chloride gives *o*-formylbenzenesulfonyl chloride (**4**), but in dry methylene chloride at 0° yields the chlorosultine 3-chloro-3*H*-2,1-benzoxathiole 1-oxide (**2**); the latter is readily hydrolyzed to the "pseudo-acid" 3*H*-2,1-benzoxathiol-3-ol 1-oxide (**3**) which on further chlorination forms **4**. In 1,2-dichloroethane at −20° chlorination of **1** gave the "coupled product" **14**, whereas in dimethylformamide at room temperature the cyclic acyl chloride hydrazone 4-chloro-2*H*-1,2,3-benzothiadiazine was isolated in poor yield. The acyl chloride hydrazones (**16**) were the products obtained following chlorination of some representative aromatic acyclic tosylhydrazones (**15**). 3*H*-2,3,4-Benzothiadiazepine 2,2-dioxide (**19**), a previously unknown heterocyclic system, was synthesized in two steps from 1,3-dihydrobenzo[*c*]thiophene (**17**). Chlorinolysis of **19** gave *o*-chloromethylbenzal chloride (**21**). These reactions are believed to involve formation of the α-chloroazo compound (*e.g.* **22**) as the first step. The formation of **2** from **1** is discussed in terms of three possible routes, two which involve the sulfene **23**.

La chloration de la 2*H*-benzothiadiazine-1,2,3 dioxyde-1,1 (**1**) dans du chlorure de méthylène humide conduit au chlorure de l'*o*-formylbenzènesulfonyle (**4**), mais donne dans le chlorure de méthylène sec à 0 °C une chlorosultine à savoir la chloro-3 3*H*-benzoxathiole-1,2 oxyde-1 (**2**); celle-ci est rapidement hydrolysée en "pseudo acide" 3*H*-benzoxathiol-1,2 ol-3 oxyde-1 (**3**) qui est transformé en **4** par chloration ultérieure. La chloration de **1** à −20° dans le dichloro-1,2 éthane donne un "produit couplé" **14** alors que dans la diméthylformamide à la température de la pièce, l'hydrazone cyclique du chlorure d'acyle, la chloro-4 2*H*-benzothiadiazine-1,2,3 est obtenue avec un faible rendement. Les hydrazones (**16**) des chlorures d'acyle sont les produits obtenus par chloration de tosylhydrazones (**15**) aromatiques et acycliques caractéristiques. Un système hétérocyclique inconnu jusqu'à présent, la 3*H*-benzothiadiazépine-2,3,4 dioxyde-2,2 (**19**) a été synthétisé en deux étapes à partir du dihydro-1,3 benzo[*c*]thiophène (**17**).

L'ouverture de **19** par le chlore conduit au chlorure de l'*o*-chlorométhylbenzal (**21**). Il est supposé que ces réactions procèdent dans la première étape, par la formation de composés α-chloroazo (*e.g.* **22**). La formation de **2** à partir de **1** est discutée en considérant trois voies possibles, dont deux impliquant le sulfène **23**.

Canadian Journal of Chemistry, 49, 943 (1971)

As described in the preceding paper (1), our interest in the generation of sulfenes led us to synthesize 2*H*-1,2,3-benzothiadiazine 1,1-dioxide (**1**). Some observations made in the course of attempting to improve our early synthetic procedure led us to examine the effect of chlorine on **1**. Once we had determined the general features of this reaction, it appeared that one of the more likely mechanisms involved a sulfene. This prompted us to carry out a comparatively detailed investigation of the course of this transformation and also a study of the chlorination of other sulfonhydrazones, to find out whether the reaction of **1** was typical or exceptional. Some of the earlier results in this study have been described in a preliminary communication (2).

Results and Discussion

The Products of the Chlorinolysis and Subsequent Interconversions (Scheme 1)

When chlorine was bubbled into a solution of **1** in chloroform (reagent grade, containing 0.75% ethanol) or wet methylene chloride at room temperature, we observed effervescence (presumably due to nitrogen) and isolated a white crystalline solid melting at 33–35°. Structure **4** for the product readily follows from elemental analysis and spectra, the latter showing a singlet (1*H*) at 10.9 p.p.m. in addition to aromatic proton signals (4*H*) around 7.9 p.p.m. in the n.m.r., and bands at 1700 and 2900 due to the aldehyde group and at 1385, 1192, and 366 cm^{-1} characteristic (3, 4) of the $—SO_2Cl$ function. The peak at 2900 cm^{-1}, though at the high end of the range for such absorption was confirmed as due to the formyl group by observation of the combination band (5, 6) at 4600 cm^{-1} in the near i.r.

On adding a solution of **1** to a solution of chlorine in methylene chloride with careful exclusion of water, we again observed effervescence but the product obtained on evaporating the solvent showed only a small carbonyl maximum in the i.r., no significant bands attributable to a sulfonyl group, but absorption at 1140 and 960 cm^{-1} suggestive of a sulfinic ester (3). After shaking this material with a mixture of water and methylene chloride and evaporating the

[1]Organic Sulfur Mechanisms. Part 9. For part 8 see the accompanying paper (1).

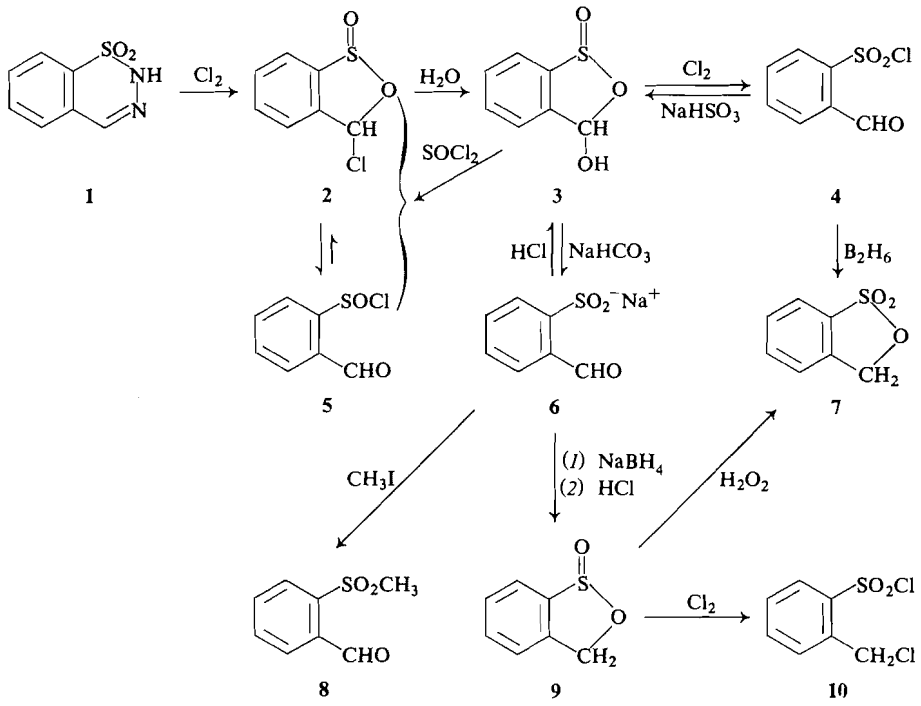

SCHEME 1

organic phase, we obtained a good yield of a crystalline solid, m.p. 98–102°, shown as described below to be 3*H*-2,1-benzoxathiol-3-ol 1-oxide (**3**). This structure is the cyclic tautomer of *o*-formylbenzenesulfinic acid, and because of the complexity of the systematic name **3** is referred to here as the "pseudo-acid".

The pseudo-acid character of this material is shown by titration with base, which gave an equivalent weight of 171 (theoretical for **3** is 170); this taken with the elemental analysis establishes the empirical formula $C_7H_6O_3S$. The i.r. spectrum of the sodium salt (**6**) shows bands at 2750, 1706, and 1686, and a very strong complex absorption centered around 1020 cm^{-1}, as expected for the aldehyde and sulfinate (3) functions. Structure **6** is confirmed by conversion of the sodium salt to *o*-methylsulfonylbenzaldehyde (**8**) by reaction with methyl iodide; **8** had previously been made (7) by oxidation of the sulfide. The pseudo-acid (**3**) itself is not very soluble in the usual solvents for i.r. spectroscopy. A Nujol mull spectrum showed strong bands at 3180, 1137 (sh), 1125, and 1085 and no absorption around 1700 cm^{-1}, whereas the spectrum of a dilute (but saturated) solution in methylene chloride showed absorption at 3540 and 3300, a strong band centered around 1140, and a rather weak peak at 1705 cm^{-1}. This last peak is presumably due to a small amount of aldehyde in the methylene chloride solution, though whether this means the presence of *o*-formylbenzenesulfinic acid itself or the conjugate base is not certain. The very strong absorption around 1140 cm^{-1} is in agreement with the cyclic sulfinate formulation (**3**) (3); the differences between the solid and liquid phase spectra could merely be a reflection of the differences in phase, but ring–chain tautomerism (acid $\rightleftharpoons$ pseudo-acid), ionization, and *cis–trans* isomerism in **3** may well contribute also.

The n.m.r. spectrum of the pseudo-acid (**3**) in D_2O showed complex aromatic absorption from 7.7–8.0 (4H) and an apparent singlet at 8.11 p.p.m. (1H). Addition of 1 equiv of sodium bicarbonate resulted in a broadening of the four-hydrogen aromatic absorption, complete removal of the singlet at 8.11, and its replacement by a sharp singlet at 10.60 p.p.m. (1H); with 0.5 equiv of $NaHCO_3$ the one-hydrogen peak is a broadened singlet at 9.33 p.p.m. Addition of perchloric acid caused a small upfield shift of the 8.11 p.p.m. peak so that it became superimposed

Can. J. Chem. Downloaded from www.nrcresearchpress.com by 210.87.254.42 on 09/05/12
For personal use only.

Can. J. Chem. Downloaded from www.nrcresearchpress.com by 210.87.254.42 on 09/05/12
For personal use only.

on the aromatic absorption. In acetone-d_6 **3** showed absorption in the aromatic region (5H) as well as a signal at 5.7 p.p.m. (1H) which disappeared on adding D_2O. The above results indicate that the pseudo-acid (**3**) and the conjugate base (and perhaps the "true" acid) are in rapid equilibrium with **3** predominating in the absence of added base. Phthalaldehydic acid shows comparable behavior (8).

Reduction of a solution of **3** in sodium hydroxide (*i.e.* **6**) with sodium borohydride, followed by acidification with hydrochloric acid led to **9**, a cyclic sulfinic ester or "sultine" (*cf.* refs. 9 and 10). Sultine **9** is also produced on thermolysis of **1**, as described in the accompanying paper (1), and its formation and n.m.r. spectrum were of interest in connection with the formation of sultines by thermal rearrangement of thiete 1,1-dioxide and derivatives (10). The anisotropy of the sulfinyl group is such that in a group of these sultines (10) the chemical shifts of the two methylene protons were found to differ by as much as 0.67 p.p.m. Confirmation of the sultine formulation (**9**) was obtained by oxidation to the sultone (**7**), identical to a specimen prepared from the cyclic chloride **11** by the procedure of Helberger *et al.* (11), and also from **4** by reduction with diborane.

It seemed from the results already described that **3** was probably the precursor of **4** in the chlorination of **1** in wet methylene chloride and that chlorination of **3** should yield **4**; this was found to be so. In addition, reduction of **4** with sodium bisulfite gave back **3**. Chlorination of the sultine **9** led to **10**, a previously unknown material which would appear to have potential as a synthetic intermediate. Chlorinolysis of a sulfinic ester has been observed before in the formation of methyl chloride from methyl methanesulfinate (12), and would also appear to have analogy in the cleavage of sulfite esters (13). *o*-Chloromethylbenzenesulfonyl chloride (**10**) is more conveniently prepared from sodium *o*-formylbenzenesulfonate by reduction with sodium borohydride followed by treatment with $POCl_3$–PCl_5.

Remaining to be discussed are the transformations involving **2** and **5**. The material obtained on chlorination of **1** in dry methylene chloride at room temperature proved intractable but when the reaction was carried out at 0–2°, again with exclusion of moisture, careful removal of solvent left a crystalline product melting at 64–66°. Structure **2** for this material follows from elemental analysis and spectra, the latter showing strong bands at 1150 and 970 cm^{-1} in the i.r., characteristic of sulfinic esters (3), while in addition to the aromatic absorption (4H) in the n.m.r. there was a sharp singlet (1H) at 7.08 p.p.m. appropriate to the methine hydrogen. When the n.m.r. sample was allowed to stand for a time, the singlet at 7.08 diminished and one at 9.88 p.p.m. grew. The latter peak is due (as is shown below) to presence of some of the ring–chain isomer **5**. On further standing (and addition of HCl) the 7.08 peak diminished further and the 9.88 grew until an equilibrium mixture consisting of about 17% of **2** and 83% of **5** was obtained. The equilibration was evidently catalyzed by hydrogen chloride and since the absence of HCl was difficult to ensure (or its concentration difficult to control) owing to the ease with which **2** and **5** may be hydrolyzed, no attempt was made to determine the rate of spontaneous equilibration.

The same equilibrium mixture of **2** and **5** is obtained by treatment of the pseudo-acid (**3**) with thionyl chloride. From the mixture so obtained we isolated a sample of **5** (m.p. 103–105°); the structure again follows from elemental analysis and spectra (see Experimental). A solution of **5**, showing initially no sign of **2** in the n.m.r., was found gradually to develop a small peak due to **2** at 7.08 p.p.m., eventually giving the spectrum of the equilibrium mixture. It should perhaps be mentioned that the purest specimen of **2** obtained showed no sign of the 9.88 peak in the n.m.r. but did show a very small carbonyl absorption at 1700 cm^{-1}; the i.r. sample at least would appear to have been contaminated with a small amount of **5**.

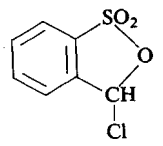

11

The ring–chain isomerism (**2** ⇌ **5**) observed here offers an interesting contrast with related systems. The analogous sulfonyl compounds **4** and **11** are reasonably stable species which show no sign of equilibrating under any circumstances in which we have observed them. With the carbonyl system on the other hand the only form that has been observed (see for example ref. 14)

Can. J. Chem. Downloaded from www.nrcresearchpress.com by 210.87.254.42 on 09/05/12
For personal use only.

has the cyclic (phthalide) structure; the failure to observe the open form ("normal" acid chloride) is assumed to be due to rapid conversion to the ring tautomer.

It is of interest to consider the variation in relative stabilities of "ring" *vs.* "chain" isomers in the light of Pearson's "hard–soft–acid–base" (HSAB) theory (15). If we symbolize the general situation by the equilibrium **12** ⇌ **13** and focus

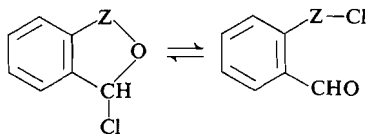

12 **13**

attention initially only on bond energies, it is evident that any change in equilibrium constant accompanying changing from one Z to another, reflects as a first approximation a change in the bond energy difference, $E_{Z-Cl} - E_{Z-O}$. Kice and Guaraldi have shown (16) that the sulfinyl group is a distinctly "softer" Lewis acid than the sulfonyl and carbonyl groups, which are "hard" (15, 17). Since Cl^- is "softer" than RO^- (15), we would expect the difference $(E_{Z-Cl} - E_{Z-O})$ to be larger for the sulfinyl compounds than for the sulfonyl or carbonyl analogues. With the sulfinyl *vs.* the carbonyl compounds this is evidently so, the equilibrium proportion of the open form **13** being much higher for the former than the latter. This would in turn suggest that the equilibrium mixture of **4** and **11** would be almost entirely **11**, but the point has not been tested. Another factor which could influence the position of the equilibrium **12** ⇌ **13** is variation in ring strain associated with change from one Z group to another, but the ring strain in these compounds is probably not large and its variation would not seem to us to be the most important influence.

A similar comparison of the isomerization **2** ⇌ **5** with the ring–chain tautomerization "pseudo-acid" (**3**) ⇌ *o*-formylbenzenesulfinic acid is also explicable in HSAB terms. The change in equilibrium constant in this case is a direct function of the change in the quantity $E_{S-X} - E_{C-X}$, where X may be Cl or OH. By the same reasoning as before the equilibrium proportion of the open-chain isomer is predicted to be greater with the acid chlorides than the acids; the same conclusion is drawn from experiment. Steric effects would be expected to be of even less significance in this case, since the cyclic compounds are derived from the same ring system.

Finally, mention should be made of two further variations in the course of the chlorination of the benzothiadiazine (**1**) accompanying change in reaction conditions. In 1,2-dichloroethane at −20°, a product melting at 198–200° was obtained; the yield of this high-melting material was improved (to 82%) by adding the chlorine to **1**, rather than the other way around. This material analyzed for $C_{14}H_{10}S_2O_4N_2$ and showed i.r. bands characteristic of both sulfinyl and sulfonyl groups, but no sign of N–H absorption. These points suggested that the material arose from reaction of **2** (or **5**) with unreacted **1**. In confirmation of this the mixture of **2** and **5** obtained by reaction of **3** with thionyl chloride, gave, when treated with an equimolar quantity of **1**, a 90% yield of the compound melting at 198–200°. Also, alkaline hydrolysis of the high-melting material gave back **3** and **1** in good yield. The simplest formulation for this "coupled product" that fits the above data is **14**, though the zwitterionic structure with the "sultinyl" residue attached to the other nitrogen is not excluded.

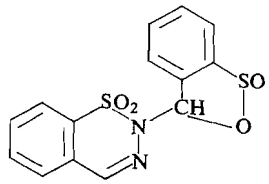

14

Use of cold dimethylformamide as the solvent in the chlorination of **1** led to another result. Part of the material suffered loss of nitrogen and, presumably via solvolysis, led to *o*-formylbenzenesulfonic acid, which was characterized by conversion to **11**. Some of the material, however, retained the nitrogen to give a material which, on the basis of analytical, i.r., n.m.r., and mass spectrometric data is evidently 4-chloro-2*H*-1,2,3-benzothiadiazine 1,1-dioxide, *i.e.* the cyclic acyl chloride hydrazone. As is described immediately below, the formation of acyl chloride hydrazones is the reaction found with acyclic sulfonhydrazones in both methylene chloride or dimethylformamide, though the yield is higher with the latter solvent. The properties of the 4-chloro-derivative of **1** are such that if it had been formed

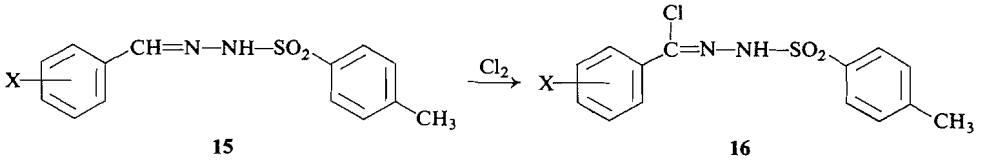

15 16

a X = H
b X = *p*-OCH_3
c X = *o*-SO_2CH_3

SCHEME 2

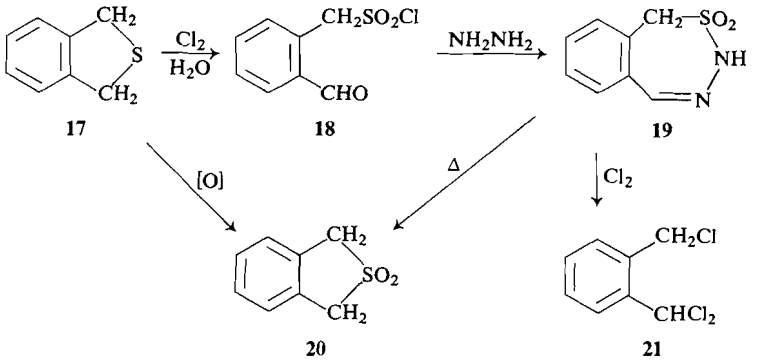

17 18 19 20 21

SCHEME 3

in significant amount in the chlorinations in the other solvents then it would probably have been readily detected.

Chlorination of Acyclic Sulfonhydrazones (Scheme 2)

It appeared that the reaction of aromatic sulfonhydrazones with chlorine had not been studied before, and that information on this reaction might be of use in helping to understand the nature of the chlorinolysis of the thiadiazine (**1**). Accordingly the sulfonhydrazones **15***a–c* were treated with chlorine at room temperature. The principal product in each case was the acyl chloride hydrazone (hydrazonoyl chloride) (**16***a–c*); this is the expected result on the basis of previous workers' findings on the halogenation of other hydrazones (18). In addition, small amounts of the aldehyde and *p*-toluenesulfonyl chloride were also formed.

Synthesis and Chlorinolysis of 3H-2,3,4-Benzothiadiazepine 2,2-Dioxide (19) (Scheme 3)

For reasons described more fully in the discussion of the mechanism (below) we decided to synthesize the previously unknown heterocycle 3*H*-2,3,4-benzothiadiazepine 2,2-dioxide (**19**) and to treat it with chlorine. The thiadiazepine **19** was readily obtained from the dihydrothiophene **17** via the sulfonyl chloride (**18**) produced by treatment of an aqueous suspension of **17** with chlorine. The thiadiazepine (**19**) was obtained as a white solid melting (with evolution of gas) at 169–170°, the mode of synthesis and its analytical and spectroscopic properties of which (see Experimental) support the thiadiazepine formulation (**19**). On heating just above its melting point for a few minutes the evolution of gas ceases and the sulfone (**20**) is obtained in good yield. The latter compound (**20**) on further heating (at 280°) has been previously shown (19) to undergo loss of sulfur dioxide to give products derivable from *o*-quinodimethane.

3*H*-2,3,4-Benzothiadiazepine 2,2-dioxide (**19**) reacts readily with chlorine at 0° with loss of both nitrogen and sulfur dioxide to give *o*-chloromethylbenzal chloride (**21**).

The Mechanism of the Chlorinolysis of 2H-1,2,3-Benzothiadiazine 1,1-Dioxide (1)

Three possible routes from **1** to the chlorosultine (**2**) are summarized in Scheme 4. The first step is common to the three mechanisms and

Can. J. Chem. Downloaded from www.nrcresearchpress.com by 210.87.254.42 on 09/05/12
For personal use only.

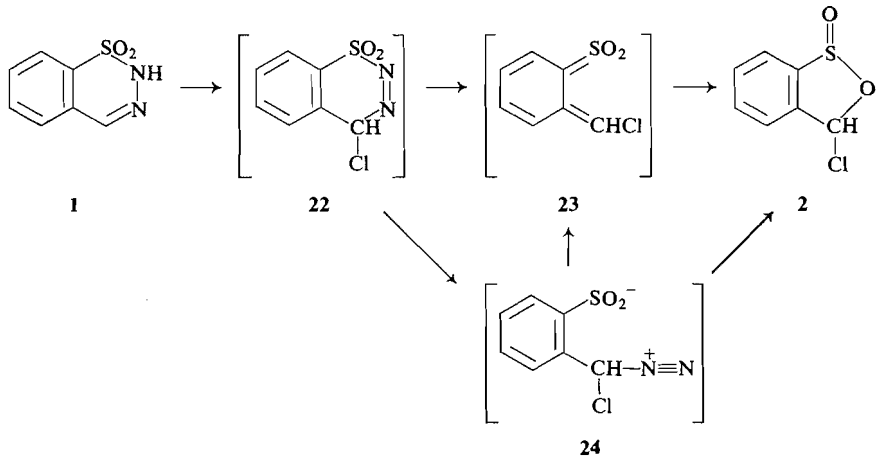

SCHEME 4

involves attack of chlorine at the α-carbon with formation of the α-chloroazosulfone (**22**), a reaction for which there is precedent from different quarters. As has been mentioned above halogenation of aldehyde hydrazones, including sulfonhydrazones, gives the acyl chloride hydrazone, most probably via the α-chloroazo compound. In agreement with such a formulation is the actual isolation of the azo compound on chlorination of ketazines (20, 21).

The cyclic α-chloroazo compound **22**, once formed, is well set up to undergo cycloreversion to the sulfene (**23**), which, following the route proposed for the formation of the sultines (1, 10), would be expected to give the chlorosultine **2**. Reverse Diels–Alder reactions with extrusion of nitrogen can be estimated to be strongly exothermic (by about 45 kcal/mol), and, though apparently not very frequently observed, would appear to be facile reactions taking place readily below room temperature (for examples see reference 22). A particularly close analogy to the present case is the formation of *o*-quinodimethane dimer by mercuric oxide oxidation of 1,2,3,4-tetrahydrophthalazine observed by Carpino (23). This reaction is believed to involve oxidation to the cyclic azo compound followed by extrusion of nitrogen to give *o*-quinodimethane.

Though the formulation **22** → **23** → **2** is attractive to us, it is not the only imaginable route from **22** to **2**. To judge from the work of Overberger and co-workers (24, 25) and more recently by Kice and Gabrielsen (26), azosulfones react by free radical processes under certain circumstances, but heating is normally required to induce the homolysis even in apparent free radical chain processes; such reaction would seem unlikely under the conditions of the chlorinolysis of **1**. Ionic cleavage of azosulfones to form the diazonium sulfinate is well-known; from **22** this would lead to **24** which could go to the chlorosultine (**2**), either directly or via the sulfene (**23**). Lewis and co-workers (27) have estimated that the half-life for the formation of benzenediazonium benzenesulfinate ($PhN^{+}{\equiv}N\ {}^{-}SO_2{-}Ph$) from the azosulfone ($PhN{=}NSO_2Ph$) in methanol is about 5 min at 29°. The formation of an aliphatic diazonium ion would not be expected to be much faster and at first glance such a process (*i.e.* via **24**) would seem a little slow to account for the rapid formation of **2** from **22** in non-polar solvents even at 0° and lower. These observations are also consistent with the formation of the hydrazonoyl chlorides (**16**), the prototropic shift in the presumed intermediate α-chloroazo compound taking place faster than the heterolysis to the *p*-toluenesulfinate and benzylic diazonium ions. In these chlorinations, however, small amounts of both *p*-toluenesulfonyl chloride and the aromatic aldehyde are, in fact, observed, suggesting that the decomposition to the diazonium sulfinate does compete to some extent. However, substituents on the azo group in **22** are held in a *cis* configuration whereas it is likely that in the azo compound from **15** they are *trans*, and it is by no means impossible that a *cis*-azosulfone (*e.g.* **22**) because of the favorable *anti* arrangement of the sulfonyl group and the free electron

Can. J. Chem. Downloaded from www.nrcresearchpress.com by 210.87.254.42 on 09/05/12
For personal use only.

Can. J. Chem. Downloaded from www.nrcresearchpress.com by 210.87.254.42 on 09/05/12
For personal use only.

pair, could undergo heterolysis a good deal more quickly than the *trans* analogues. Unfortunately, unlike a number of other azo compounds (including the closely related diazosulfonates), there is comparatively little information on geometrical isomerism in azosulfones, and in no instance has a pair of *cis–trans* isomers been isolated, or even been unambiguously shown to exist (27, 28); a study of the dipole moments of a number of azosulfones led to the conclusion that each of these compounds had the *trans* configuration (28).

It was hoped that the chlorination of 2*H*-2,3,4-benzothiadiazepine 2,2-dioxide (**19**) might be instructive, since the α-chloroazosulfone presumably formed initially would have a *cis* azo double bond but at the same time be less favorably arranged for cycloreversion than **22**. The result shows that the six-membered ring arrangement as in **22** is not *required* for easy loss of nitrogen, though, at the same time, it does not exclude the reverse Diels–Alder mechanism when the molecule is well set up for it. It would appear that it is not possible to determine at this stage which reaction path the reaction is actually proceeding by, and further discussion should await further information.

Experimental

Experimental procedures, materials, and apparatus are the same as in the accompanying paper. The i.r. spectra below 600 cm^{-1} were determined on a Beckman IR-5A spectrometer equipped with CsBr optics and using KBr cells; the near i.r. determination was made on a Cary 14 spectrophotometer.

Chlorinolysis of 2H-1,2,3-Benzothiadiazine 1,1-Dioxide (1)

(i) In Hydroxylic Media

2*H*-1,2,3-Benzothiadiazine 1,1-dioxide (**1**) (1) (1.005 g) was dissolved in chloroform (55 ml; Fisher Spectranalyzed, containing 0.75% ethanol), and dry chlorine gas was bubbled through. When the solution began to effervesce the passage of chlorine was stopped and when no more gas was given off (about 5 min) the solvent was evaporated under reduced pressure. The product, 1.265 g of a colorless oil, was recrystallized four times from carbon tetrachloride – petroleum ether (35–60°) cooled in an acetone – Dry Ice mixture, giving **4** as fine white crystals melting at 33–35°. The i.r. spectrum showed peaks at: 2900 (w), 2770 (vw), 1700 (s), 1585 (m), 1570 (m), 1445 (w), 1400 (sh), 1380 (vs), 1300 (w), 1265 (m), 1180 (vs), 1120 (m), 1060 (m), 1035 (w), 995 (w), 965 (vw), 820 (m), 700 (m), 640 (w), 570 (s), 505 (w), 470 (m), 435 (vw), and 370 (m) cm^{-1}. The n.m.r. spectrum (CCl_4) showed multiplets in the aromatic region at 7.9 p.p.m. (4H) and a singlet (1H) at 10.9 p.p.m.

Anal. Calcd. for $C_7H_5SO_3Cl$: C, 41.08; H, 2.46; S, 15.67; Cl, 17.23. Found: C, 41.05; H, 2.76; S, 15.47; Cl, 17.16.

In another experiment chlorine (~ 0.5 g) was dissolved in methylene chloride (50 ml) and water (0.1 ml) was added. To this mixture a solution of 2*H*-1,2,3-benzothiadiazine 1,1-dioxide (**1**) (387 mg) in methylene chloride (20 ml) was added dropwise over a period of about 10 min. When the strong effervescence, which accompanied addition of **1**, had subsided, a portion of the reaction mixture was examined by i.r. spectroscopy which showed the presence of unreacted **1**. The mixture was then left overnight, dried, and the solvent evaporated giving a colorless oil (251 mg, 52%) shown by its i.r. spectrum to be *o*-formylbenzenesulfonyl chloride (**4**). Recrystallization from cold petroleum ether–carbon tetrachloride gave crystals melting at 31–35°.

(ii) In Dry Methylene Chloride Followed by Aqueous Work-up

A solution of 2*H*-1,2,3-benzothiadiazine 1,1-dioxide (**1**) (1.02 g) in methylene chloride previously dried by distillation from lithium aluminum hydride, was added dropwise over a period of 20 min to a solution of chlorine (about 2.0 g) in dry methylene chloride (50 ml). Within a few minutes the mixture began to bubble and when the effervescence had stopped (1 h) the solvent was evaporated leaving a colorless oil showing bands at 1710, 1140, and 960 cm^{-1} in the i.r. Water (10 ml) was added to the product and the mixture warmed on the water bath (10 min) before being extracted with methylene chloride. The methylene chloride extract was dried and the solvent evaporated giving crude **3** as white crystals (75%), which after recrystallization from methylene chloride melted at 98–102°. The i.r. spectrum of a Nujol mull of **3** showed bands at 3180 (s), 1598 (w), 1585 (w), 1337 (m), 1325 (w), 1295 (s), 1253 (s), 1213 (s), 1137 and 1125 (vs), 1085 (vs), 1055 (s), 1020 (w), 957 (w), 888 (m), 840 (vs), 770 (s), 725 and 713 (vs), and 678 (m) with no absorption around 1700 ± 25 cm^{-1}, whereas a dilute (saturated) solution in methylene chloride showed bands at 3540 and 3300 (w), 3080 (w), 1705 (w), 1452 (w), 1425 and 1420 (w), 1305 (w), 1280 (w), 1220 (m), 1140 and 1125 (s and broad), 1055 (w), 883 (m), 850 (w), and 790 (m) cm^{-1}.

Anal. Calcd. for $C_7H_6SO_3$: C, 49.34; H, 3.55; S, 18.89. Found: C, 49.46; H, 3.78; S, 18.83.

The n.m.r. spectrum of **3** in acetone-d_6 showed complex absorption from 7.2 to 7.9 and a broad singlet at 5.7; the latter band disappeared in addition of D_2O. In D_2O solution, using external tetramethylsilane as the standard, **3** showed aromatic absorption as a relatively narrow band from 7.8 to 8.0 (4H) and a slightly broadened singlet (1H) due to the methine hydrogen at 8.11 p.p.m. Upon addition of 1 equiv of $NaHCO_3$ the aromatic absorption broadened 7.6–8.2 (4H) and a new sharp singlet appeared at 10.60 p.p.m. With only 0.5 equiv of $NaHCO_3$ there was aromatic absorption at 7.7–8.2 (4H) and a broadened singlet at 9.33 p.p.m. (1H). After addition of a few drops of 30% perchloric acid to the solution of **3** in D_2O, the n.m.r. spectrum showed only a relatively narrow band between 7.7 and 8.0 p.p.m. The integrated intensity of the 7.8–8.3 region (5H) in the spectrum of **3**, relative to that of a small amount of acetone added to the D_2O to serve as an integration standard, was found to be about the same as the relative

Can. J. Chem. Downloaded from www.nrcresearchpress.com by 210.87.254.42 on 09/05/12
For personal use only.

integrated intensity of the 7.7–8.0 band found after addition of perchloric acid; this was interpreted as showing that the band at 8.11 in **3** had moved upfield upon addition of perchloric acid and was obscured by the aromatic hydrogens.

Titration of **3** (18.9 mg) with 0.01 *N* sodium hydroxide led to consumption of 11.05 ml, corresponding to an equivalent weight of 171; theoretical equivalent weight, 170. On evaporation of the water sodium *o*-formylbenzenesulfinate (**6**) was left as a crystalline solid. The i.r. spectrum of this material (Nujol mull) showed peaks at 3060 (w), 2750 (w), 1710 and 1686 (vs), 1586 (s), 1567 (m), 1304 (m), 1255 (m), 1200 (s), 1162 (w), 1133 (w), 1118 (w), a very strong complex absorption with the following peaks, 1063, 1045, 1018, 1000, 987 and 972, 888 (w), 837 (m), 825 (m), 763 (s), 725 (m), 695 (m), and 682 (m) cm^{-1}.

When sodium *o*-formylbenzenesulfinate (**6**) (31 mg) was suspended in methylene chloride and hydrogen chloride bubbled through the mixture, the yellow salt disappeared and a white precipitate formed. After 15 min when there were no traces of **6** remaining, the solution was filtered and the solvent removed from the filtrate under reduced pressure without heating leaving a colorless oil (24 mg) the i.r. spectrum of which showed it to be the pseudo-acid (**3**). After crystallization from methylene chloride, the product melted at 92–96°.

(iii) In Dry Methylene Chloride at 1 ± 1°

A solution of 2*H*-1,2,3-benzothiadiazine 1,1-dioxide (**1**) (589 mg) in a mixture of dry methylene chloride (25 ml) and dry chloroform (5 ml) was added slowly to a stirred solution of chlorine (636 mg) in methylene chloride (15 ml), maintained at 0–2° by means of an ice-bath, over a period of 1 h. After addition was complete, the mixture was stirred for a further 1/2 h and then the solution was evaporated to about 5 ml under reduced pressure at room temperature. The concentrated solution was transferred to a Craig tube and solvent removed in a stream of dry nitrogen until crystallization took place. The white crystals of **2** (269 mg) were collected. The n.m.r. spectrum showed a singlet (1H) at 7.25 p.p.m. and a multiplet (4H) at 7.7 p.p.m. The i.r. spectrum (CH_2Cl_2) showed the following peaks: 3040 (w), 1700 (w), 1585 (w), 1465 (w), 1450 (m), 1300 (w), 1235 (w), 1200 (m), 1145 (vs), 1060 (m), 1020 (w), 970 (vs), 880 (w), 865 (s), 640 (s); the peak at 1700 cm^{-1} (and perhaps also that at 1200 cm^{-1}) is probably due to the aldehyde – sulfinyl chloride (**5**) present as impurity.

The analytical sample, prepared by recrystallization (twice) from methylene chloride, melted at 64–66°.

Anal. Calcd. for $C_7H_5SO_2Cl$: C, 44.57; H, 2.67; S, 16.99. Found: C, 44.49; H, 2.87; S, 17.11.

In some preparations the crude crystalline product showed a small peak at 9.88 p.p.m. in the n.m.r. due to the presence of **5**. One such sample, in which integration of the 7.08 and 9.88 peaks indicated a ratio of **2** to **5** of 94:6 was let stand at room temperature for 80 min. The n.m.r. showed a change in the intensities of the 7.08 and 9.88 peaks corresponding to a change in composition to 74% **2** and 26% **5**; the aromatic region also became broader. Dry hydrogen chloride was then bubbled into the sample and the mixture let stand for 10 min; the ratio of **2** to **5** was judged from the n.m.r. spectrum to be 49:51, and after a further 15 min to be 35:65. After standing overnight the above ratio was estimated as 17:83.

(iv) In 1,2-Dichloroethane at −20°

A solution of 2*H*-1,2,3-benzothiadiazine 1,1-dioxide (**1**) 364 mg, 2 mmol in dichloroethane (55 ml) was added dropwise with stirring to a solution of chlorine (168 mg) in dichloroethane (14 ml) cooled to −20°. The mixture was stirred for 1 h at −20°, and the solvent removed under reduced pressure at room temperature to give a sticky, colorless solid (317 mg). Recrystallization from methylene chloride gave crystals (177 mg) melting at 194–196° (dec.); further recrystallization from methylene chloride – acetone gave an analytical sample of the coupled product (**14**) melting at 198–200° (dec.). The i.r. spectrum of a dilute (saturated) solution in $CHCl_3$ showed prominent bands at 1350, 1185, and 1130 with weaker bands at 3000, 1440, 905, 890, and 655 cm^{-1}.

Anal. Calcd. for $C_{14}H_{10}N_2O_4S_2$: C, 50.28; H, 3.01; N, 8.38; S, 19.17. Found: C, 50.15; H, 2.89; N, 8.34; S, 19.35.

In another experiment in which chlorine (1 mmol) in dichloroethane (14 ml) was added to **1** (366 mg, 2 mmol) in dichloroethane at −20° as above, a higher yield (82%) of recrystallized **14** was obtained.

(v) In Dimethylformamide

2*H*-1,2,3-Benzothiadiazine 1,1-dioxide (**1**) (1.31 g) was dissolved in a mixture of dimethylformamide (18 ml) and water (3 ml) and the solution was cooled to 0°. Chlorine was passed into the solution until the yellow color persisted and after a further 2 min the reaction mixture was evacuated on a water aspirator to remove much of the excess chlorine. It was then poured into water (300 ml) and the product extracted with methylene chloride (4 × 100 ml, 2 × 50 ml). The combined extracts were dried and evaporated to give an oil which on standing overnight *in vacuo* partly solidified. Crystallization from methylene chloride gave 4-chloro-2*H*-1,2,3-benzothiadiazine 1,1-dioxide (327 mg, 21%), melting at 143–144°. The i.r. spectrum (CH_2Cl_2) showed absorption at 3310 (m), 1585 (w), 1560 (w), 1370 (m), 1345 (s), 1245 (w), 1185 (s), 1145 (m), 1040 (m), 990 (m), 865 (m), and 630 (m) cm^{-1}. The n.m.r. spectrum (CD_2Cl_2) exhibited a multiplet (4H) at 7.8–8.2 and a broad signal (1H) at 8.3–9.2 p.p.m. removed by addition of D_2O. In the mass spectrum the molecular ion was principally a doublet at 216 (Cl^{35}) and 218 mu (Cl^{37}), relative abundance 29:12.

Anal. Calcd. for $C_7H_5ClN_2O_2S$: C, 38.81; H, 2.33; Cl, 16.36; N, 12.93; S, 14.80. Found: C, 38.72; H, 2.23; Cl, 16.53; N, 12.93; S, 14.74.

In another experiment 2*H*-1,2,3-benzothiadiazine 1,1-dioxide (**1**) (239 mg) was dissolved in dimethylformamide (4.6 g) and solid calcium carbonate (480 mg) was added to the solution. The mixture was then cooled to 0° and added to a cooled, freshly prepared solution of chlorine (460 mg) in dimethylformamide (4.4 g). After 5 min the reaction mixture was filtered and the filtrate evaporated to give an oil which was partitioned between chloroform and water in three stages. The organic phase on evaporation gave an oil (104 mg) which was crystallized from chloroform–pentane to give needles of 4-chloro-2*H*-

Can. J. Chem. Downloaded from www.nrcresearchpress.com by 210.87.254.42 on 09/05/12
For personal use only.

1,2,3-benzothiadiazine 1,1-dioxide (52 mg, 18%), identified by direct comparison (i.r., mixed m.p., t.l.c.) with a specimen prepared as described above. Evaporation of the aqueous phase also gave an oil (456 mg) which was dissolved in water (5 ml) and passed through Dowex 50W-X8 ion exchange resin. Evaporation of the eluate gave an acidic oil (195 mg) whose i.r. absorption at 1020 (s) and 1240 (s) cm^{-1} suggested the presence of some sulfonic acid. It was treated with thionyl chloride (5 ml) on the steam bath for 15 min and evaporated to dryness under reduced pressure; crystallization of the resultant oil from chloroform gave **11** (55 mg, 22%), m.p. 111–114°, identified by direct comparison (mixed m.p., i.r.) with an authentic specimen (29).

Preparation of o-Formylbenzenesulfinyl Chloride (5) from the Pseudo-acid (3)

The pseudo-acid (**3**) (522 mg) was dissolved in thionyl chloride (5 ml) and left at room temperature for 0.5 h. The excess thionyl chloride was removed under reduced pressure leaving a pale yellow crystalline product (530 mg), which on recrystallization five times from methylene chloride containing a few drops of thionyl chloride and evaporating the excess solvent under a stream of dry nitrogen, gave *o*-formylbenzenesulfinyl chloride (**5**), m.p. 103–105° (vacuum capillary). The i.r. spectrum (CH_2Cl_2) showed bands at 3060 (w), 2850 (m), 2750 (w), 1700 (vs), and 1680 (sh), 1585 (m), 1575 (m), 1390 (w), 1305 (m), 1205 (s), 1145 (vs), 1050 (w), 1030 (w), 845 (s), and 650 cm^{-1} (s). The n.m.r. spectrum (CD_2Cl_2) showed complex aromatic absorption in the range 7.5–8.3 (4H) and a sharp singlet at 9.88 p.p.m. (1H).

Anal. Calcd. for $C_7H_5ClO_2S$: C, 44.57; H, 2.67; S, 16.99. Found: C, 44.54; H, 2.93; S, 17.04.

In other experiments the n.m.r. spectrum of the material obtained by dissolving **3** in thionyl chloride showed in addition to the peaks characteristic of **5**, a singlet at 7.08 p.p.m. and a prominent peak around 7.5 p.p.m. ascribable to the presence of about 20% of **2**.

Chlorination of 3H-2,1-Benzoxathiol-3-ol 1-Oxide (3) (the "Pseudo-acid")

The "pseudo-acid" **3** (84 mg) was dissolved in methylene chloride (25 ml) and a solution of chlorine (about 0.2 g) in methylene chloride (8 ml) was added. The mixture was shaken for 5 min and then allowed to stand for 1 h. When the solvent was evaporated 85 mg (83%) of a colorless oil was obtained. An i.r. spectrum (CCl_4) of the product was identical to that of *o*-formylbenzenesulfonyl chloride (**4**) prepared as above. The product was crystallized from carbon tetrachloride – petroleum ether cooled in an acetone – Dry Ice mixture; m.p. 31–35°.

Reduction of o-Formylbenzenesulfonyl Chloride (4) to the "Pseudo-acid" 3

o-Formylbenzenesulfonyl chloride (1.94 g, 9.5 mmol), sodium sulfite (2.5 g), and water (20 ml) were stirred at room temperature for 4.5 h. The solution was acidified with concentrated sulfuric acid and heated to 90–100° on the steam bath for 1 h. The solution was cooled and extracted with methylene chloride. The extracts were dried and the solvent evaporated under reduced pressure giving a colorless solid (1.01 g, 63%), melting at 97–98°. After recrystallization, it melted at 97–100°; mixed m.p. with a specimen of **3** prepared from **1**, 97–100°. The i.r. was also identical with that of authentic **3**.

Formation of o-Methylsulfonylbenzaldehyde (8) from the "Pseudo-acid" 3

A solution of sodium bicarbonate (504 mg, 6 mmol) in water (8 ml) was added to a solution of the "pseudo-acid" **3** (1.02 g, 6 mmol) in ethanol (10 ml) and the mixture let stand for 5 min. The mixture was then evaporated to dryness, benzene was added and the mixture evaporated again to dryness (3 ×); the last traces of volatile material were removed by means of an oil pump. The pale yellow solid (**6**) was then dissolved in absolute ethanol and methyl iodide (1 ml) added. The mixture was refluxed for 4.5 h, whereupon the dark red mixture was allowed to cool and was poured into water and extracted with methylene chloride. The extracts were washed with 0.1 *N* sodium thiosulfate (10 ml) and then with saturated potassium chloride solution. Evaporation of the solvent gave a colorless oil (1.39 g), the spectrum of which indicated the major portion of the material to be the diethyl acetal of **8**. The oil was suspended in 5% hydrochloric acid (10 ml) and warmed on the steam bath for 0.5 h. The mixture was then cooled in an ice-bath and the crystals of **8** (832 mg; 75%) removed by filtration. The crystals melted at 97–99°; reported for **8**, 97–98° (7). The i.r. spectrum ($CHCl_3$) showed peaks at 3000 (m), 1695 (s), 1585 (m), 1570 (w), 1395 (m), 1315 (vs), 1260 (w), 1185 (m), 1150 (vs), 1115 (w), 1060 (w), and 955 (m); the n.m.r. spectrum showed a singlet at 3.25 (3H), a complex multiplet around 7.6–8.2 (4H), and a singlet at 10.52 p.p.m. (1H).

Reduction of the "Pseudo-acid" 3 with Sodium Borohydride

3*H*-2,1-Benzoxathiol-3-ol 1-oxide (**3**) (1.76 g, 0.010 mol) was dissolved in 1.0 *N* sodium hydroxide (10.3 ml) and water (70 ml). Sodium borohydride (4 g, 0.106 mol) was added and the reaction mixture was left stirring overnight at room temperature. Concentrated hydrochloric acid (120 ml) was added slowly. The reaction mixture was extracted with methylene chloride which in turn was dried and evaporated under reduced pressure to yield 3*H*-2,1-benzoxathiole 1-oxide (**9**) (1.4 g, 88%). The crude product was distilled, b.p. 165°/0.005 mm. The distillate when cooled to −30° crystallized; recrystallization from ether and pentane yielded crystals of **9** melting at 40–41°.

Anal. Calcd. for $C_7H_6O_2S$: C, 54.52; H, 3.92; S, 20.80. Found: C, 54.60; H, 3.96; S, 20.78.

The i.r. spectrum (CCl_4) showed absorption bands at 3070 (w), 2930 (w), 2870 (w), 1580 (w), 1468 (m), 1450 (m), 1340 (w), 1298 (w), 1255 (w), 1210 (m), 1185 (w), 1130 (s), 1060 (m), 1020 (w), 1005 (w), 950 (s), 710 (s), 705 (s), 690 (s), 645 (s), and 560 cm^{-1} (m). The n.m.r. spectrum (CCl_4) showed an AB quartet, $\delta_A = 5.42$ and $\delta_B = 5.78$ p.p.m., $J_{AB} = 13.5$ Hz., and aromatic hydrogen absorption between 7.3–7.75 p.p.m., relative areas 1:2.

Oxidation of 3H-2,1-Benzoxathiole 1-Oxide (9) with Hydrogen Peroxide in Acetic Acid

A 2.1 ml aliquot of a solution made by mixing glacial

Can. J. Chem. Downloaded from www.nrcresearchpress.com by 210.87.254.42 on 09/05/12
For personal use only.

acetic acid (3 ml) with hydrogen peroxide (30%) (0.8 ml), was added to **9** (0.10 g, 0.65 mmol). The reaction mixture was heated under reflux for 1½ h, and was then poured into water (4 ml) and extracted three times with methylene chloride. The methylene chloride solution was washed with sodium carbonate solution, dried, and the solvent evaporated to yield 3*H*-2,1-benzoxathiole 1,1-dioxide (**7**) (0.06 g, 55%). Recrystallization from benzene gave white crystals, m.p. 113–114°, identified by mixed m.p. and comparison of i.r. and n.m.r. spectra with an authentic specimen prepared as described by Helberger *et al.* (11); reported m.p. 112.5° (11).

*Reduction of o-Formylbenzenesulfonyl Chloride (**4**) with Diborane*

o-Formylbenzenesulfonyl chloride (**4**) (0.14 g, 0.72 mol) was dissolved in diglyme (15 ml) which had been dried by distilling from calcium hydride. Diborane (13 mmol), generated by mixing sodium borohydride and boron trifluoride etherate in diglyme, was bubbled slowly into the diglyme solution under anhydrous conditions. The reaction mixture was poured into water (150 ml) to destroy unreacted diborane, and the water was evaporated from the diglyme under reduced pressure. Methylene chloride (30 ml) was added and then the solution was washed five times with water (25 ml portions). The methylene chloride was dried and evaporated to yield crude 3*H*-2,1-benzoxathiole 1,1-dioxide (**7**) (0.042 g, 35%). Recrystallization from methylene chloride and petroleum ether yielded crystals melting at 110–113°, and with an i.r. spectrum identical to that of an authentic specimen prepared by the method of Helberger *et al.* (11); reported m.p. 112.5° (11).

*Chlorination of 3H-2,1-Benzoxathiole 1-Oxide (**9**)*

3*H*-2,1-Benzoxathiole 1-oxide (**9**) (2.2 g, 14 mmol) was dissolved in methylene chloride which had been dried by distillation from lithium aluminum hydride. Chlorine was dissolved in methylene chloride (0°) until the solution was 0.6 *N*, as determined by titration with sodium thiosulfate. An aliquot of 48 ml (14.4 mmol of chlorine) was added dropwise under anhydrous conditions to the magnetically stirred solution of **9**. The reaction mixture was stirred for 3 h at room temperature. The methylene chloride was evaporated under reduced pressure without heating, to yield *o*-chloromethylbenzenesulfonyl chloride (**10**) (3.15 g, 98%). Recrystallization from methylene chloride and petroleum ether yielded short thin crystals (2.56 g, 80%), m.p. 46–47°.

Anal. Calcd. for $C_7H_6Cl_2O_2S$: C, 37.36; H, 2.69; Cl, 31.50; S, 14.24. Found: C, 37.25; H, 2.83; Cl, 31.16; S, 14.41.

The i.r. absorption bands (CH_2Cl_2) were found at 3060 (w), 1590 (w), 1570 (w), 1470 (m), 1442 (m), 1372 (s), 1305 (m), 1180 (s), 1115 (w), 1060 (m), 1040 (w), 962 (w), 820 (m), 675 (m), 585 (s), 570 (s), 547 (s), 490 (m), 445 (w), 373 cm^{-1} (w); n.m.r. spectrum (CCl_4) showed absorption bands at 5.10 (s, 2H) and 7.35–8.2 p.p.m. (4 aromatic hydrogens).

*Preparation of o-Chloromethylbenzenesulfonyl Chloride (**10**) from Sodium o-Formylbenzenesulfonate*

Sodium *o*-formylbenzenesulfonate (practical grade) (1 g, 0.048 mol) was dissolved in water (60 ml). Sodium borohydride (0.18 g, 4.74 mmol) was added. The reaction was stirred for 20 h at room temperature. Hydrochloric acid was added until the solution was slightly acidic. The water was evaporated under reduced pressure with heating. The white residue was leached with hot ethanol (70 ml) and the ethanol evaporated to yield crude sodium *o*-hydroxymethylbenzenesulfonate (0.75 g, 75%); i.r. bands (Nujol) at 3560 (w), 3490 (w), 3280 (m), 3060 (w), 1300 (w), 1240–1140 (s), (partially resolved), 1095 (m), 1058 (w), 1035 (s), 1010 (s), 955 (w), 890 (w), 835 (w), 760 (s), 710 (s), and 625 cm^{-1} (s).

The crude sodium *o*-hydroxymethylbenzenesulfonate as prepared above (12.2 g, 58 mmol) was cooled in ice. Phosphorus oxychloride (60 ml, 0.66 mol) was added slowly with stirring. Phosphorus pentachloride (12.2 g, 59 mmol) was added. The reaction was stirred at 50° for 3 days and then poured slowly with stirring onto ice. After the evolution of heat had subsided (3 h), the aqueous mixture was extracted with methylene chloride (400 ml). The methylene chloride solution was washed with water, dried, and the solvent evaporated under reduced pressure without heating. The crude yield of yellow viscous liquid was 12.7 g. Crystallization from methylene chloride and petroleum ether at −60° yielded *o*-chloromethylbenzenesulfonyl chloride (**10**) (6.1 g, 46%). Recrystallization from the same solvents gave 2.81 g, m.p. 46–47°. The i.r. spectrum and m.p. were identical to the sample of *o*-chloromethylbenzenesulfonyl chloride (**10**) prepared from **9**.

*Formation of the "Coupled Product" **14** by Reaction of **1** with the Chlorosultine – Sulfinyl Chloride (**2** ⇌ **5**) Mixture*

The pseudo-acid **3** (73 mg, 0.43 mmol) was added to thionyl chloride (5 ml) and left at room temperature for 15 min. The pale yellow solution was evaporated to dryness. The residual pale yellow solid (a mixture of **2** and **5**) was dissolved in dry methylene chloride and a solution of 2*H*-1,2,3-benzothiadiazine 1,1-dioxide (**1**) (78 mg, 0.43 mmol) in dry methylene chloride (5 ml) added. The mixture was left at room temperature for 1 h. Evaporation of the solvent gave colorless crystals which on recrystallization from methylene chloride – pentane melted at 197–198°; yield 122 mg (90%). The i.r. spectrum was identical to that of the "coupled product" **14** prepared by chlorination of **1** in dichloroethane at −20°.

*Hydrolysis of the "Coupled Product" **14***

The coupled product **14** (100 mg) was suspended in 5% sodium hydroxide solution (5 ml) and swirled for 10 min, whereupon most of the solid had dissolved to give a pale yellow solution. The mixture was left at room temperature for 1 h, and then acidified with 20% hydrochloric acid to give a white precipitate (41 mg, m.p. 135–140°). Recrystallization from chloroform gave **1**, m.p. 139–140°, mixed m.p. with a specimen of **1** prepared as described above 138–141°.

The filtrate was extracted with methylene chloride; removal of the solvent from the extracts gave a colorless oil (45 mg), which on recrystallization from methylene chloride gave crystals identified as the pseudo-acid **3** by

Can. J. Chem. Downloaded from www.nrcresearchpress.com by 210.87.254.42 on 09/05/12
For personal use only.

m.p. (97–100°) and mixed m.p. with an authentic specimen (98–101°).

Preparation of the Tosylhydrazones ***15***

Approximately equimolar amounts of the aldehyde and *p*-toluenesulfonylhydrazine were refluxed in absolute ethanol. The crude product was obtained either by cooling the reaction mixture and filtering off the crystalline product or by evaporating the solvent. Recrystallization from the indicated solvent gave the following samples with the indicated melting points: benzaldehyde tosylhydrazone (**15***a*) (ethanol), m.p. 128–129°, reported m.p. 127–128° (30); anisaldehyde tosylhydrazone (**15***b*) (methylene chloride – pentane), m.p. 109–111°, reported m.p. 112–114° (30); *o*-methylsulfonylbenzaldehyde tosylhydrazone (**15***c*) (ethanol), m.p. 209.5–211°, with the following elemental analysis.

Anal. Calcd. for $C_{15}H_{16}N_2O_4S_2$: C, 51.11; H, 4.57; N, 7.95; S, 18.19. Found: C, 50.96; H, 4.53; N, 7.85; S, 18.05.

Chlorination of the Tosylhydrazones ***15****: Formation of the Acyl Chloride Hydrazones*

*(a) Benzoyl Chloride Tosylhydrazone (**16a**)*

(*i*) A solution of benzaldehyde tosylhydrazone (**15***a*) (549 mg, 2.0 mmol) in dry methylene chloride (25 ml) was cooled to −20° and added dropwise to a stirred solution of chlorine (154 mg, 2.2 mmol) in dry methylene chloride (19 ml) maintained at −20°. The mixture was stirred for 1 h and the solvent then removed at reduced pressure and room temperature. The dark yellow oily residue was dissolved in methylene chloride and filtered from a trace of insoluble residue. Removal of the solvent gave a dark brown oil (342 mg) which was dissolved in benzene and filtered through a column of silica gel (B.D.H. Reagent). Removal of the solvent gave a colorless solid which was recrystallized from methylene chloride – pentane to give colorless crystals of **16***a* (163 mg, 26%), m.p. 112–114°, mixture m.p. with authentic **16***a* (prepared as described below) 112–114°; the i.r. spectra were indistinguishable.

(*ii*) To a solution of benzaldehyde tosylhydrazone (**15***a*) (367 mg, 1.34 mmol) in dimethylformamide (DMF) (3.0 ml, dried over Linde 4A molecular sieves) at 0° was added a solution of chlorine in DMF (0.23 *M*) to a permanent end point. After 5 min, the reaction mixture was evaporated to dryness to give a colorless oil (469 mg). Crystallization from methylene chloride gave **16***a* (295 mg, 71%), m.p. 112–114°, identical to an authentic sample (i.r., mixed m.p.).

*(b) Anisoyl Chloride Tosylhydrazone (**16b**)*

A solution of anisaldehyde tosylhydrazone (**15***b*) (238 mg, 0.78 mmol) in the minimum quantity of DMF was titrated to a permanent end point with a solution of chlorine (0.63 *M*) in the same solvent. When t.l.c. showed that all the starting material had been consumed, the reaction mixture was evaporated to dryness to give a yellow oil, which crystallized from methylene chloride to give **16***b* (143 mg, 54%), m.p. 146–149°. The i.r. ($CHCl_3$) showed peaks at 3245 (w), 1610 (s), 1510 (m), 1410 (m), 1310 (m), 1255 (s), 1175 (s), 1075 (m), 1040 (m), 975 (m), 910 (m), 865 (m), 840 (m), 815 (m), 705 (w), 675 (m), and 660 (m) cm^{-1}. The n.m.r. ($CDCl_3$) comprised a singlet (3H) at 2.4, a singlet (3H) at 3.8, an apparent AB quartet (4H), $\delta_A = 6.9$, $\delta_B = 7.75$, $J_{AB} = 10$ Hz, another apparent AB quartet (4H), $\delta_A = 7.3$, $\delta_B = 7.9$, $J_{AB} = 8$ Hz, and a broad singlet (1H), removed by addition of D_2O, at 8.2 p.p.m.

Anal. Calcd. for $C_{15}H_{15}ClN_2O_3$: C, 53.17; H, 4.46; Cl, 10.47; N, 8.27; S, 9.46. Found: C, 53.22; H, 4.40; Cl, 10.66; N, 8.24; S, 9.63.

*(c) o-Methylsulfonylbenzoyl Chloride Tosylhydrazone (**16c**)*

A solution of *o*-methylsulfonylbenzaldehyde tosylhydrazone (**15***c*) (352 mg, 1.0 mmol) in dichloroethane (65 ml) was added dropwise to a stirred solution of chlorine (75 mg, 1.05 mmol) in dichloroethane (7.5 ml), cooled to −20°. The solution was stirred for 1 h and the solvent then removed at room temperature and reduced pressure to give a pale yellow oil (369 mg). Trituration with methylene chloride gave some colorless solid (81.8 mg, m.p. 209–211°) which was removed by filtration. Addition of pentane to the filtrate afforded pale yellow crystals, recrystallized from acetone to give colorless crystals of **16***c* (108 mg, 28%), melting at 166.5–168° (dec.). Absorption in the i.r. (Nujol) occurred at 3200 (w), 1590 (w), 1295 (s), 1240 (m), 1170 (s), 1150 (s), 1125 (m), 1070 (m), 955 (m), 850 (m), 820 (w), 765 (m), 705 (w), 665 (m), 630 (w) cm^{-1}.

Anal. Calcd. for $C_{15}H_{15}ClN_2O_4S_2$: C, 46.56; H, 3.91; Cl, 9.16; N, 7.24; S, 16.57. Found: C, 46.68; H, 3.84; Cl, 9.23; N, 7.18; S, 16.64.

*Benzoyl Chloride Tosylhydrazone (**16a**)*

1-Benzoyl-2-(*p*-tolylsulfonyl)-hydrazine (31) (100 mg) was dissolved in thionyl chloride (5 ml) and the solution was refluxed for 2 h. The excess thionyl chloride was evaporated at reduced pressure and the residue was pumped *in vacuo*. The solid product was recrystallized from methylene chloride – pentane to give colorless needles of **16***a* (68 mg, 64%), m.p. 113–115°. The i.r. spectrum ($CHCl_3$) showed bands at 3280 (m), 1605 (m), 1500 (w), 1455 (w), 1400 (s), 1360 (s), 1265 (m), 1180 (s), 1090 (s), 1075 (s), 980 (m), 870 (s), 630 (m), 620 (m), 545 (m) cm^{-1}. The n.m.r. spectrum ($CDCl_3$) showed a singlet (3H) at 2.4, a multiplet (5H) at 7.35, a multiplet (4H) at 7.8, and a broad singlet (1H) at 8.3 p.p.m.

Anal. Calcd. for $C_{14}H_{13}ClN_2O_2S$: C, 54.45; H, 4.24; Cl, 11.48; N, 9.07; S, 10.38. Found: C, 54.26; H, 4.31; Cl, 11.62; N, 9.08; S, 10.22.

*Preparation of 1,3-Dihydrobenzo[c]thiophene (**17**)*

Sodium sulfide nonahydrate (51 g, 0.21 mol) was partially dissolved in a mixture of alcohol (500 ml) and water (100 ml) in a 1 l round-bottomed flask. The flask was fitted with a Soxhlet extraction apparatus (sintered disc type) charged with α,α′-dichloro-*o*-xylene (Aldrich 25 g, 0.14 mmol). The solution was heated to reflux and the α,α′-dichloro-*o*-xylene extracted into the solution. The mixture was refluxed for a further 0.75 h and then steam distilled until the distillate was clear. The distillate was extracted with ether and the extracts washed with water and dried. Evaporation of the solvent gave a colorless oil (16.49 g, 87%) showing i.r. and n.m.r. absorption

Can. J. Chem. Downloaded from www.nrcresearchpress.com by 210.87.254.42 on 09/05/12
For personal use only.

appropriate to 1,3-dihydrobenzo[*c*]thiophene (**17**). The oil solidified on cooling in the refrigerator, the solid melting at 23–24.5°; reported m.p. 22.5–23.5° (32).

*o-Formylphenylmethanesulfonyl Chloride (**18**)*

Ice water (2 l) was saturated with chlorine gas. The solution was rapidly stirred and a suspension of 1,3-dihydrobenzo[*c*]thiophene (**17**) (5.50 g) in water (50 ml) was injected below the surface over a period of 15 min. The reaction was stirred for a further 45 min with slow passage of chlorine and addition of more ice as necessary. The white crystalline solid (mixed with a little black tar) was collected, washed with water, and dissolved in methylene chloride. The solution was dried (Na_2SO_4), treated with animal charcoal, and the solvent evaporated to leave a dark solid (7.22 g). Crystallization from benzene–pentane gave a material (5.7 g, 70%) melting at 72–76°. To obtain the analytical specimen a methylene chloride solution was filtered through silica gel and the material recrystallized twice from carbon tetrachloride to give **18** m.p. 76.5–78°. The i.r. spectrum ($CHCl_3$) showed peaks at 2840 (w), 2750 (w), 1705 (s), 1600 (w), 1585 (m), 1380 (s), 1170 (s), 865 (m), and 625 (m) cm^{-1}. The n.m.r. spectrum ($CDCl_3$) showed a singlet (2H) at 5.6, a multiplet (4H) at 7.5–8.0, and a singlet (1H) at 10.1 p.p.m.

Anal. Calcd. for $C_8H_7ClO_3S$: C, 43.94; H, 3.22; Cl, 16.21; S, 14.66. Found: C, 43.84; H, 3.32; Cl, 15.99; S, 14.52.

*3H-2,3,4-Benzothiadiazepine 2,2-Dioxide (**19**)*

o-Formylphenylmethanesulfonyl chloride (**18**) (2.0 g, 9.2 mmol) was dissolved in methylene chloride (20 ml) and added dropwise at room temperature to a stirred solution of hydrazine hydrate (5.0 g, 100 mmol) in methylene chloride (50 ml) over a period of 20 min. After a further 10 min, the reaction mixture was poured into aqueous sodium hydroxide (2.0 g NaOH, 150 ml H_2O), shaken, and the brown organic phase discarded. The aqueous phase was added to methylene chloride (300 ml) and the rapidly stirred mixture treated dropwise with 8% hydrochloric acid until it was distinctly acidic. The layers were then separated, the aqueous phase re-extracted with methylene chloride (100 ml), and the combined extracts washed once with water (100 ml), dried, and concentrated to *ca.* 5 ml. The crystalline **19** (1.36 g, 76%) was collected by filtration; m.p. 163–167° (dec.). Repeated crystallization from ethanol gave material melting at 169–170° (dec.). The i.r. spectrum (Nujol) showed peaks at 3250 (m), 1325 (s), 1310 (s), 1170 (s), 1135 (s), 1005 (m), 885 (m), and 770 cm^{-1}.

Anal. Calcd. for $C_8H_8N_2O_2S$: C, 48.91; H, 4.11; N, 14.32; S, 16.33. Found: C, 48.76; H, 4.09; N, 14.09; S, 16.18.

*Thermolysis of 3H-2,3,4-Benzothiadiazepine 2,2-Dioxide (**19**)*

The benzothiadiazepine **19** (250 mg) was heated at 175–180° under slightly reduced pressure to remove evolving gases. After 5 min, gas evolution had ceased and the reaction product was cooled to room temperature, dissolved in methylene chloride (40 ml), and filtered through silica to remove colored impurities. Evaporation of the eluate gave a colorless solid (181 mg) whose i.r. and n.m.r. spectra were identical to those of an authentic sample of 1,3-dihydrobenzo[*c*]thiophene 2,2-dioxide (**20**) obtained by oxidation of **17** (19); yield 85%. On recrystallization from methylene chloride – hexane it melted at 151–151.5°; mixed m.p. with authentic **20**, 148–150.5°.

*Chlorinolysis of 3H-2,3,4-Benzothiadiazepine 2,2-Dioxide (**19**)*

The benzothiadiazepine **19** (250 mg) was stirred in dry methylene chloride (25 ml) and the suspension was cooled in an ice-bath. Chlorine gas was passed through the mixture until all the material had dissolved, and the solution was then diluted with methylene chloride (50 ml) and washed with sodium thiosulfate solution (50 ml, 10%) and water (2 × 50 ml). The organic phase was dried and evaporated to give a liquid (280 mg) whose n.m.r. spectrum indicated that it was essentially pure α,α,α′-trichloro-*o*-xylene (**21**) (100% yield). A redistilled sample (73°/0.05 mm) had n_D^{29} 1.5695 (reported (33) n_D^{18} 1.5740). In the i.r. ($CHCl_3$) it showed bands at 1490 (w), 1460 (m), 1270 (s), 1210 (w), 1185 (m), 860 (s), 695 (vs), and 680 (vs) cm^{-1}. The n.m.r. spectrum ($CDCl_3$) showed a singlet (2H) at 4.7, a singlet (1H) at 7.1, a multiplet (3H) at 7.3–7.5, and a further multiplet (1H) at 7.8–8.0 p.p.m.

Anal. Calcd. for $C_8H_7Cl_3$: C, 45.85; H, 3.37; Cl, 50.77. Found: C, 45.83; H, 3.48; Cl, 50.89.

Reaction of **19** with only 1 equiv of Cl_2 under similar conditions to the above, afforded a mixture of starting material and α,α,α′-trichloro-*o*-xylene (**21**).

We gratefully acknowledge the support of the National Research Council of Canada, the Petroleum Research Fund (administered by the American Chemical Society), and the Alfred P. Sloan Foundation.

1. J. F. KING, B. L. HUSTON, A. HAWSON, J. KOMERY, D. M. DEAKEN, and D. R. K. HARDING. Can. J. Chem. This issue.
2. J. F. KING, A. HAWSON, D. M. DEAKEN, and J. KOMERY. Chem. Commun. 33 (1969).
3. L. J. BELLAMY. *In* Organic sulfur compounds. *Edited by* N. Kharasch. Vol. 1. Pergamon Press, Oxford, 1961. p. 47.
4. J. F. KING and D. J. H. SMITH. Can. J. Chem. **43**, 1870 (1965).
5. R. M. POWERS, J. L. HARPER, and HAN TAI. Anal. Chem. **32**, 1287 (1960).
6. J. F. KING and B. VIG. Can. J. Chem. **40**, 1023 (1962).
7. B. EISTERT, W. SCHADE, and H. SELTZER. Ber. **97**, 1470 (1964).
8. J. KAGAN. J. Org. Chem. **32**, 4060 (1967).
9. D. C. DITTMER, R. S. HENION, and N. TAKASHINA. J. Org. Chem. **34**, 1310 (1969).
10. J. F. KING, P. DE MAYO, C. L. MCINTOSH, K. PIERS, and D. J. H. SMITH. Can. J. Chem. **48**, 3704 (1970).
11. J. H. HELBERGER, G. MANECKE, and R. HEYDEN. Ann. **565**, 22 (1949).
12. I. B. DOUGLASS. J. Org. Chem. **30**, 633 (1965).
13. A. H. J. CROSS and W. GERRARD. J. Chem. Soc. 2686 (1949).
14. M. RENSON. Bull. Soc. Chim. Belg. 70, 77 (1961).
15. R. G. PEARSON. *In* Survey of progress in chemistry. *Edited by* A. F. Scott. Vol. 5. Academic Press, New York, 1969. p. 1 and references cited.
16. J. L. KICE and G. GUARALDI. J. Amer. Chem. Soc. **90**, 4076 (1968).

17. J. L. KICE, G. J. KASPEREK, and D. PATTERSON. J. Amer. Chem. Soc. **91**, 5516 (1969).
18. P. A. S. SMITH. The chemistry of open-chain organic nitrogen compounds. Vol. II. W. A. Benjamin Inc., New York, N.Y., 1966. p. 165 and references cited.
19. M. P. CAVA and A. A. DEANA. J. Amer. Chem. Soc. **81**, 4266 (1959).
20. S. GOLDSCHMIDT and B. ACKSTEINER. Ber. **91**, 502 (1958).
21. E. BENZING. Ann. **631**, 1 (1960).
22. B. P. STARK and A. J. DUKE. Extrusion reactions. Pergamon Press, Oxford, 1967. pp. 152–156.
23. L. A. CARPINO. J. Amer. Chem. Soc. **85**, 2144 (1963).
24. C. G. OVERBERGER and I. TASHLICK. J. Amer. Chem. Soc. **81**, 217 (1959).
25. A. J. ROSENTHAL and C. G. OVERBERGER. J. Amer. Chem. Soc. **82**, 108, (1960); C. G. OVERBERGER and A. J. ROSENTHAL. J. Amer. Chem. Soc. **82**, 117 (1960).
26. J. L. KICE and R. S. GABRIELSEN. J. Org. Chem. **35**, 1004, 1010 (1970).
27. C. D. RITCHIE, J. D. SALTIEL, and E. S. LEWIS. J. Amer. Chem. Soc. **83**, 4601 (1961).
28. H. C. FREEMAN, R. J. W. LE FÈVRE, J. NORTHCOTT, and I. YOUHOTSKY. J. Chem. Soc. 3381 (1952).
29. R. LIST and M. STEIN. Ber. **31**, 1648 (1898).
30. D. G. FARNUM. J. Org. Chem. **28**, 870 (1963).
31. G. P. SCHIEMENZ and H. ENGELHARD. Ber. **92**, 1336 (1959).
32. J. A. OLIVER and P. A. ONGLEY. Chem. and Ind. (London), 1024 (1965).
33. G. ARDITTI. Comptes rendues, **223**, 635 (1946).

Can. J. Chem. Downloaded from www.nrcresearchpress.com by 210.87.254.42 on 09/05/12
For personal use only.

Can. J. Chem. Downloaded from www.nrcresearchpress.com by 210.87.254.42 on 09/05/12
For personal use only.

Etude des spectres de vibration du benzothiazole et des oscillations des liaisons CH de quelques uns de ses dérivés

JEAN-CLAUDE PANIZZI,[1] GISÈLE DAVIDOVICS,[1] ROBERT GUGLIELMETTI,[2] GILBERT MILLE,[1] JACQUES METZGER,[2] ET JACQUES CHOUTEAU[1]

Département de Chimie Organique, Faculté des Sciences de Marseille, Marseille, France

Reçu le 13 juillet, 1970

Les spectres i.r. du benzothiazole et de 29 de ses dérivés mono, di, et trisubstitués ont été analysés. Dans chaque série, un composé au moins a été examiné à l'état vapeur, à l'exception des hétérocycles ayant un substituant en position 7. Trois spectres Raman, dont celui du benzothiazole, ont aussi été étudiés. Les vibrations de valence ν(CH) et de déformation hors du plan γ(CH) ont été attribuées, ainsi que la plupart des autres oscillations fondamentales du benzothiazole.

Quatre dérivés dichlorés et un dérivé trichloré ont été spécialement synthétisés pour faciliter l'interprétation des vibrations γ(CH).

The i.r. spectra of benzothiazole and those of 29 of its derivatives, mono, di, and trisubstituted have been analyzed. In each series, at least one compound has been studied in the vapor state, except the heterocycles having a substituent in position 7. Three Raman spectra, one of which is the benzothiazole, have also been examined. The ν(CH) stretching and γ(CH) out-of-plane deformation vibrations have been assigned, as well as the majority of the other fundamentals of benzothiazole.

Four dichloro and one trichloro derivatives have been synthetized, in order to make easy the interpretation of the γ(CH) vibrations.

Canadian Journal of Chemistry, 49, 956 (1971)

Introduction

Dans les travaux spectroscopiques relatifs au benzothiazole et à ses dérivés, publiés jusqu'ici (1–16), il n'existe aucune analyse détaillée des

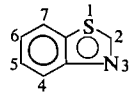

spectres de vibration de ces molécules pour lesquelles les attributions antérieures concernent quelques fréquences seulement (2–16) et sont très souvent imprécises.

Dans le cadre de recherches en série hétérocyclique, il nous a paru intéressant d'étudier les spectres i.r. sous différents états physiques, gazeux en particulier, ainsi que le spectre Raman à l'état liquide, du benzothiazole.

Afin d'identifier les vibrations des liaisons CH, nous avons comparé les spectres i.r. du benzothiazole et de 29 de ses dérivés substitués en position 2, disubstitués en -2,4, -2,5, -2,6, et -2,7 et trisubstitués en -2,6,7 et -2,4,6. Un certain nombre de ces composés ont également été examinés à l'état vapeur. Les spectres Raman de quelques dérivés monosubstitués ont aussi été enregistrés.

L'exposé des conditions expérimentales sera suivi d'un court chapitre consacré à la géométrie du benzothiazole. Après avoir indiqué nos résultats expérimentaux, nous discuterons l'interprétation des vibrations des liaisons CH du benzothiazole et de ses dérivés, puis celle des oscillations de noyau du benzothiazole.

[1]Laboratoire de spectroscopie infrarouge.
[2]Laboratoire de chimie organique A.

Conditions expérimentales

Préparation des composés benzothiazoliques

Les alcoyl-2 et benzyl-2 benzothiazoles, ainsi que la série des éthyl-2 benzothiazoles substitués, principalement en position 6, par divers groupements fonctionnels, ont été synthétisés au Laboratoire de Chimie Organique (17, 18) en vue de la préparation de composés spiropyranniques du type benzothiazolique (17, 19). En outre, nous avons entrepris la synthèse des dichloro -2,4, -2,5, -2,6, et -2,7 benzothiazoles et du trichloro-2,4,6 benzothiazole qui est un produit nouveau.

Nous indiquons succinctement les schémas réactionnels choisis et les références bibliographiques correspondantes. Pour certains composés déjà connus, nous avons amélioré les méthodes de synthèse et les rendements.

(1) Dichloro-2,4 benzothiazole (20–22)

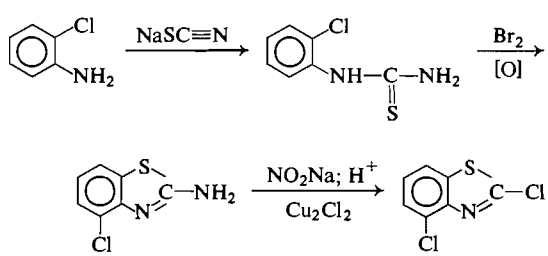

Solvant de recristallisation: éther de pétrole
F = 97° (litt. F = 97–98° (23))

Can. J. Chem. Downloaded from www.nrcresearchpress.com by 210.87.254.42 on 09/05/12
For personal use only.

(2) Dichloro-2,6 benzothiazole (22, 24)

Nous avons utilisé une méthode assez générale de thiocyanation spécifique des amines aromatiques substituées en position para (24).

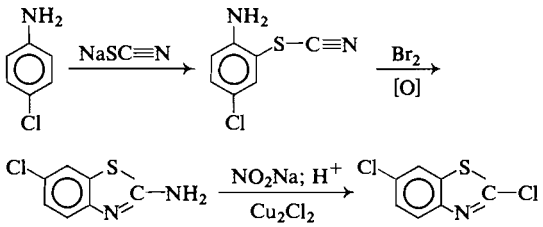

Solvant de recristallisation: éther de pétrole
F = 98° (litt. F = 98–99° (25))

(3) Dichloro-2,5 benzothiazole (25–27)

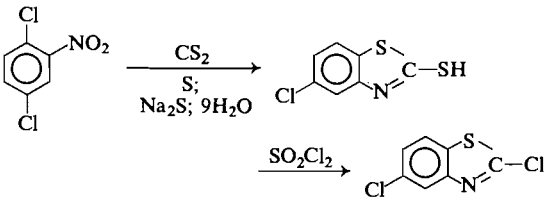

Solvant de recristallisation : méthanol en présence de charbon actif
F = 68° (litt. F = 70–71° (25))

Ce processus de synthèse, lorsqu'il peut être appliqué, donne de bien meilleurs résultats que celui faisant intervenir un dérivé aminé en position 2.

(4) Dichloro-2,7 benzothiazole (25, 28, 29)

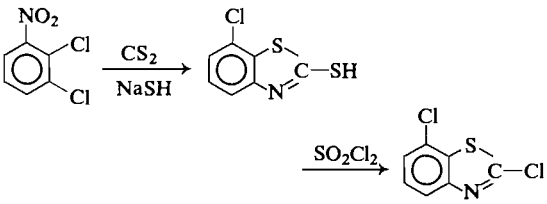

Solvant de recristallisation: éther de pétrole en présence de charbon actif et d'alumine
F = 53–54° (litt. F = 53–54° (29))

(5) Trichloro-2,4,6 benzothiazole (22, 30)

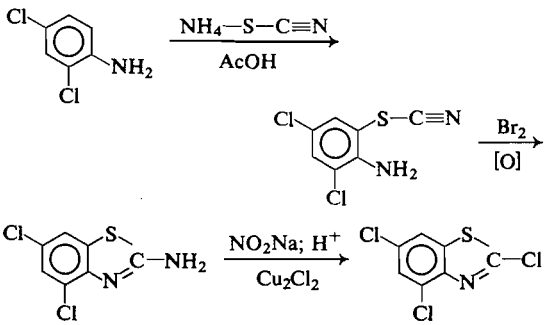

Nous avons utilisé la méthode de thiocyanation de Brewster (29) applicable aux amines aromatiques polysubstituées et possédant au moins une position disponible en ortho du groupement amine. Le rendement de cette séquence de synthèse a été amélioré en opérant en milieu moins dilué (rendement en amino-2 dichloro-4,6 benzothiazole: 61%, F = 268°; litt.: 45%, F = 260° (30)).

Solvant de recristallisation: éther de pétrole, le composé se présente sous forme de cristaux blancs de F = 108°.

Anal. calc. pour $C_7H_2NSCl_3$ (238.5 g): C, 33.22; H, 0.84; N, 5.87; S, 13.41; Cl, 44.65. Trouvé: C, 33.51; H, 0.82; N, 5.97; S, 13.25; Cl, 44.10.

La structure du composé est confirmée par r.m.n. Les déplacements chimiques observés pour les protons H-5 et -7 sont, respectivement, de 7.38 et 7.55 p.p.m. La constante de couplage $J_{H_5-H_7} = 2.2$ Hz, est caractéristique d'un couplage de type méta.

Spectres infrarouges

Les spectres i.r. des composés gazeux ont été mesurés à l'aide d'une cellule à gaz chauffante Perkin–Elmer de 5 cm d'épaisseur à fenêtres de KBr ou d'ICs.

Les concentrations des solutions, pour les spectres i.r. à l'état dissous étaient voisines de 0.2 mol/l. Le tétrachlorure de carbone a été utilisé dans les régions de 3000 et de 1500 à 1250 cm^{-1}, le tétrachlorure d'éthylène entre 1800 et 1500 et de 400 à 200 cm^{-1}, le sulfure de carbone entre 1250 et 400 cm^{-1}. Les coefficients d'extinction molaire apparents ont été mesurés au maximum des bandes d'absorption.

Les spectres i.r. des composés solides à la température ordinaire ont été réalisés, à l'état fondu, dans une cellule chauffante Perkin–Elmer, à des températures voisines de leurs points de fusion.

Les spectres i.r. ont été enregistrés sur spectrographes Perkin–Elmer, modèles 125 ou 225, double faisceau, équipés de deux réseaux et d'un prémonochromateur en KBr.

Spectres Raman

Le tube utilisé pour réaliser les spectres Raman du benzothiazole, du chloro-2, et du méthyl-2 benzothiazole à l'état liquide avait 22 cm de long et 9 mm de diamètre intérieur.

Les spectres ont été effectués avec un spectrographe Hilger et Watts, type E 612 et enregistrés à l'aide d'un microphotomètre Hilger L 470. La raie excitatrice 4358 Å du mercure a été sélectionnée avec un filtre de nitrite de sodium.

Les facteurs de dépolarisation ont été mesurés par la technique d'Edsall et Wilson (31) et corrigés d'après la méthode de Rank et Kagarise (32).

Structure géométrique du benzothiazole

La structure déterminée pour l'anhydrobase du diméthyl -2,3 benzothiazole (33) apporte un argument en faveur de la planéité du benzothiazole. Dans l'hypothèse de la symétrie maximale Cs, les 36 vibrations normales de cette molécule se décomposent en 25 mouvements de classe A′, devant donner lieu à des raies Raman plutôt fortes et polarisées et 11 oscillations de

TABLEAU 1. Fréquences i.r. des vibrations γ(CH) du benzothiazole et de ses dérivés*

Substituants										
2	4	5	6	7		γ(CH)	γ(CH)	γ(CH)	γ(C_2H)	γ(CH)
H	H	H	H	H	α	977	941m	~860e	827m	757FF
					σ	973 (8)	936 (28)	853 (65)	821 (140)	754 (530)
					ϕ		940 (C)	857 (C?)	825 (C)	754 (C)
Cl					α	970f	938f	850f		751FF
					σ	967 (27)	933 (27)	849 (5)		753 (730)
					ϕ		935 (C)			754 (C)
CH_3					α	~970e	937f	~861e		758FF
					ϕ	969 (C?)	935 (C?)	861 (C?)		757 (C)
C_2H_5					α	~960e	947F	861m		758FF
					ϕ			860		758 (C)
Pr					α	970ff	935m	855m		758FF
i-Bu					α	975ff	935ff	852f		757FF
t-Bu					α	~975e	936m	853m		762FF
neo-P					α	981ff	933f	853m		757FF
Benzyle					α	965ff	937f	857m		768FF
p-Cl Benzyle					α		936f	859ff		757FF
p-NO_2 Benzyle					α		937f	855F		761F
Benzothiazolyle					α	970ff	935F	853F		752FF
NH_2					α	965ff	927f	850ff		753FF
Cl	Cl				α		957ff	892ff		767FF
					σ					766 (280)
					ϕ					767 (C)
Cl	OCH_3				α		963f	883ff		768FF
NH_2	OCH_3				α		941ff	886m		768F
Cl		Cl			α		938ff	868F		799FF
					σ		937 (11)	870 (190)		799 (360)
					ϕ			875 (C)		799 (C)
Cl			Cl		α		943ff	854F		815FF
					σ		943 (9)	854 (135)		815 (362)
					ϕ			856 (C?)		818 (C)
C_2H_5			Cl		α		951F	875ff		817FF
C_2H_5			Br		α		947F	~867e		811FF
C_2H_5			CN		α		953m	875m		826F
C_2H_5			NO_2		α		~969e	887F		839F
C_2H_5			NH_2		α		~955e			819F
C_2H_5			OCH_3		α		~962e	899F?		825FF
C_2H_5			SCH_3		α		967ff	875ff		814FF
C_2H_5			OH		α		960F			807F
C_2H_5			COOH		α		956f	892f		807F
C_2H_5			OCH_3	NO_2	α					820FF
Cl				Cl	α		964f	892f		783FF
					σ		961 (12)	892 (9)		783 (526)
Cl	Cl		Cl		α			851F		762F
					σ			848 (230)		761 (252)
					ϕ			850 (C)		766 (C)

*Fréquences observées: α, à l'état liquide; σ, à l'état dissous, suivies entre parenthèses du coefficient d'extinction molaire apparent; ϕ, à l'état gazeux, (C) indique une structure de vibration rotation de type C.
Pr, propyle; *i*-Bu, isobutyle; *t*-Bu, tertiobutyle; P, pentyle.
FF, très forte; F, forte; m, moyenne; f, faible; ff, très faible; e, épaulement.

mode A'', caractérisées par des raies de diffusion généralement faibles et dépolarisées.

Les moments principaux d'inertie petit, moyen et grand du benzothiazole, calculés avec des paramètres choisis par comparaison avec le thiazole, pour l'hétérocycle pentagonal (34) et avec les dérivés benzéniques (35) et la *N*-méthyl benzothiazoline (33), ont les valeurs respectives 152, 367, et 519 u.m.a. $Å^2$. Le grand axe d'inertie étant perpendiculaire au plan de l'hétérocycle, aux vibrations de symétrie A'' doivent correspondre, dans le spectre i.r. du composé à l'état vapeur, des enveloppes de type C et à celles de symétrie A', des bandes de vibration rotation de type A, B ou hybride A + B (36).

Les séparations approximatives $\Delta\nu_{PR}$ cm^{-1} des branches P et R des bandes de vibration rotation, déterminées à l'aide des formules proposées par Seth-Paul et de Meyer (37), sont de 12 cm^{-1} pour les bandes A, de 7 cm^{-1} pour celles de type B, et de 19 cm^{-1} pour les enveloppes de type C.

Can. J. Chem. Downloaded from www.nrcresearchpress.com by 210.87.254.42 on 09/05/12
For personal use only.

TABLEAU 2. Spectres i.r. et Raman du benzothiazole*

Infrarouge				Raman				
Vapeur		Solution		Liquide				
ν cm^{-1}	Structure rotationnelle	ν cm^{-1}	ε	ν cm^{-1}	I	ρ	Attributions	
~3120		3116	4				$2\nu_2$ §	
~3098e		~3080e					νCH	A′
3081	P							
3075	Q	3068	25	3060	9	0.26	νCH	A′
3070	R							
~3040		3032	8				νCH?	A′
		3003	3				$\nu_1+\nu_5$ §	
		2994	3				$\nu_2+\nu_5$ §	
		2925	2				$\nu_3+\nu_4$ §	
		*2873*ff					$\nu_2+\nu_6$ §	
		*1958*f					$2\gamma_1$ §	
		*1912*f					$\gamma_1+\gamma_2$ §	
		*1878*f					$2\gamma_2$ §	
		*1820*f					$\gamma_1+\gamma_3$ §	
		*1796*f					$\gamma_1+\gamma_4$ §	
		~*1725*e					$\gamma_1+\gamma_5$ §	
		1693	5				$2\gamma_3$ §	
		1665	4				$\gamma_3+\gamma_4$ §	
1648	P							
1643	Q	1644	10				$2\gamma_4$ §	A′
1640	R							
		1612	5				$\gamma_4+\nu_{15}$ §	
1605	P?							
1595	R	1595	6	1591	2	0.44	ν_1	A′
1585		1580	7				$\gamma_4+\gamma_5$ §	
~1557	P?							
~1545	R?	1557	12	1557	7	0.58	ν_2	A′
1482	P							
1470	R	1474	130	1472	9	0.25	ν_3	A′
~1465e	P?							
1455	R	1457	150				ν_4	A′
		1440	20				$2\Gamma_1$ §	
1434	P							
1429	Q	1427	120				ν_5	A′
1424	R							
		~1405e		~1408e			$2\nu_{16}$ §	
1317	P							
1308	R	1315	85	1317	9	0.25	ν_6	A′
1297	P							
1292	Q	1290	86	1295	9	0.31	ν_7	A′
~1285e	R							
~1272	P	1275	14				$\gamma_3+\Gamma_5$ §	
1266	Q	1265	31	1269	2		ν_8(δCH?)	A′
1260	R							
1205	P							
1200	Q	1198	13	1200	8	0.23	ν_9(δCH?)	A′
1195	R							
1162	P							
1152	R	1155	13	1161	2	0.11	ν_{10}(δCH?)	A′
1128	P							
1123	Q	1122	30	1128	7	0.25	ν_{11}(δCH?)	A′
1117	R							
1076	P							
1071	Q	1069	30	1072	4	0.11	ν_{12}(δCH?)	A′
1065	R							
		1059	13	~1060e			$\nu_{16}+\nu_{20}$ §	
		1053	10				$2\nu_{18}$ §	
1018	P							
1012	Q	1013	54	1017	9	0.05	ν_{13}	A′
~1007	R							

Can. J. Chem. Downloaded from www.nrcresearchpress.com by 210.87.254.42 on 09/05/12
For personal use only.

TABLEAU 2. (*Conclu*)

Infrarouge				Raman				
Vapeur		Solution		Liquide				
ν cm^{-1}	Structure rotationnelle	ν cm^{-1}	ε	ν cm^{-1}	I	ρ	Attributions	
976	P	973	8				γ_1CH?	A''
966	Q							
950	P			959	1			
938	Q	937	28				γ_2CH	A''
~942	R							
		907	7				$2\Gamma_4$	§
876	P	869	310	875	1		ν_{14}	A'
867	R							
856	Q	852	65				γ_3CH	A''
~848	R							
832	P	821	140				γ_4CH	A''
824	Q							
806	P	797	165	801	10	0.05	ν_{15}	A'
796	R							
764	P							
756	Q	754	530	764	3/2	D	γ_5CH	A''
746	R							
728	Q	724	290				Γ_1	A''
718	R							
		710	15	709	8	0.04	ν_{16}	A'
		700	14				$2\nu_{20}$	§
		*~671*e		671	2	0.44	Γ_2?	A''
671	P							
667	Q	664	36				ν_{17}	A'
660	R							
		*587*ff		584	3/4	D	Γ_3?	A''
536	P							
530	Q	528	14	533	5	0.38	ν_{18}	A'
525	R							
		502	5	505	9	0.19	ν_{19}	A'
				452	3/4		Γ_4?	A''
430	P							
420	Q	422	84	427	1		Γ_5	A''
410	R							
354	P	352	33	355	5	0.36	ν_{20}	A'
345	R							
		220	11	~220e			$\gamma_1-\gamma_5$	§
~214	P	202	14	205	3	0.57	Γ_6	A''
206	Q							

*ε, Coefficient d'extinction molaire apparent; I, intensité relative; ρ, facteur de dépolarisation; D, dépolarisée. Les fréquences en italiques ont été observées à l'état liquide: e, épaulement; f, faible; ff, très faible. §, Attribution suggerée.

Pour les dérivés du benzothiazole, on peut s'attendre à ce que les vibrations entraînant une variation de moment électrique perpendiculaire au noyau benzothiazolique soient de type C, avec des séparations $\Delta\nu_{PR}$ cm^{-1} différentes suivant les composés.

Résultats expérimentaux

L'ensemble des résultats expérimentaux sur le benzothiazole est résumé dans le tableau 2. Les séparations $\Delta\nu_{PR}$ cm^{-1} observées dans le spectre i.r. du benzothiazole à l'état vapeur, représenté sur la fig. 1, sont respectivement, de 12, 9, et 19 cm^{-1}, en moyenne, pour les bandes de type A, B et C, en bon accord avec les valeurs calculées. Dans les spectres des dérivés du benzothiazole, lorsque le contour des bandes de vibration rotation de type C a pu être déterminé, leur structure, ainsi que la fréquence de la branche Q correspondante ont été mentionnées dans le tableau 1.

Analyse des spectres

A. Vibrations mettant en jeu les liaisons CH dans le benzothiazole et ses dérivés

Dans l'approximation des vibrations de

Can. J. Chem. Downloaded from www.nrcresearchpress.com by 210.87.254.42 on 09/05/12
For personal use only.

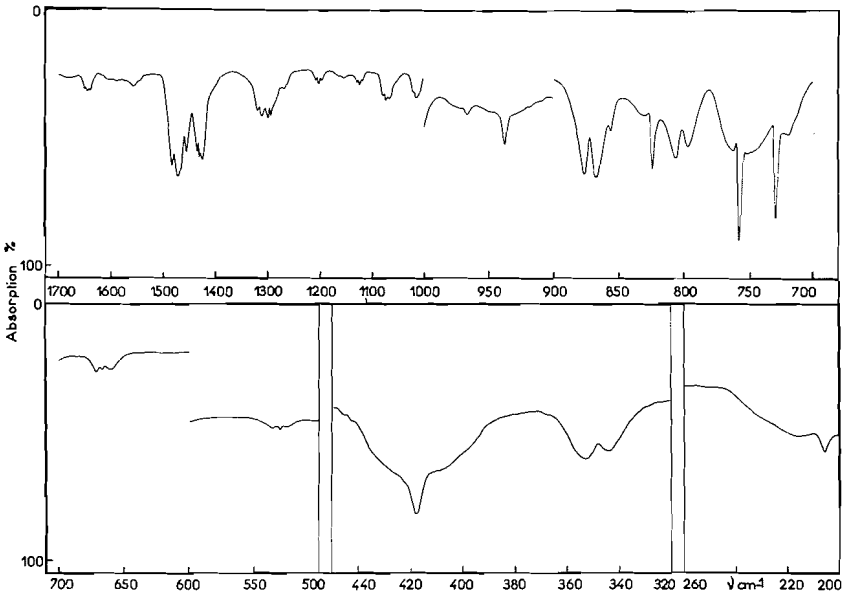

FIG. 1. Spectre i.r. entre 1700 et 200 cm^{-1} du benzothiazole à l'état vapeur.

groupe, on peut distinguer, pour le benzothiazole, 15 oscillations des liaisons CH, dont dix de symétrie A′ (5 ν(CH) + 5 δ(CH)) et cinq de symétrie A″ (5 γ(CH)).

(1) Vibrations de valence ν(CH)

La liaison CH en position 2 du benzothiazole n'étant pas adjacente aux liaisons CH de l'homocycle, l'interaction entre les oscillations de valence ν(CH) respectives du cycle benzénique et de l'hétérocycle pourrait être faible. La comparaison des spectres i.r. du benzothiazole et de ses dérivés substitués en position 2 ne permet pas, cependant, d'assigner une fréquence particulière à la vibration $\nu(C_2H)$ qui est observée vers 3080 cm^{-1} dans les spectres des composés thiazoliques (38).

Les vibrations des CH benzéniques du benzothiazole qui peuvent également être, soit couplées mécaniquement, soit à peu près indépendantes, doivent, dans les deux cas, donner naissance à quatre mouvements de valence ν(CH) distincts. Les oscillations ν(CH) aromatiques sont prévues par Scherer et Evans (39), entre 3086 et 3093 cm^{-1}, dans l'orthodichlorobenzène. Lebas (40) leur rattache, dans les dérivés orthodisubstitués du benzène, trois fréquences assez variables, entre 3111 et 3018 cm^{-1}. On peut, en outre, attendre dans la région de 3160 à 3000 cm^{-1}, des bandes harmoniques et de combinaison des vibrations fondamentales de noyau du benzothiazole. Quatre suites de fréquences, dont trois à 3129 ± 15, 3008 ± 11, 2991 ± 4 cm^{-1} se rapportant à de faibles bandes d'absorption du spectre du benzothiazole (*cf.* tableau 2) et une autre suite, plus élevée, vers 3163 ± 23 cm^{-1}, observée seulement pour certains dérivés, peuvent, effectivement, être reliées à des combinaisons binaires de mouvements de noyau (41).

En dehors des précédents, le spectre i.r. du benzothiazole dissous dans un solvant neutre ne montre, au dessus de 3000 cm^{-1}, que trois autres maximums à 3080, 3068, et 3032 cm^{-1} dont le deuxième, qui seul est assez intense, est aussi le seul qui soit vu dans le spectre Raman du benzothiazole. Aux deux premières de ces fréquences correspondent, dans les spectres des dérivés du benzothiazole, deux suites à 3078 ± 15 et 3064 ± 13 cm^{-1}, composées uniquement de bandes i.r., pour la plus élevée, et également de raies Raman, lorsque les spectres de diffusion ont été réalisés, dans le cas de la plus basse. Par analogie avec les benzènes orthodisubstitués (39, 40), ces deux suites doivent pouvoir être reliées à des vibrations de valence ν(CH). L'attribution à un mouvement ν(CH) de l'absorption à 3032 cm^{-1}, à laquelle on peut aussi rattacher une suite de bandes i.r. à 3027 ± 13

Can. J. Chem. Downloaded from www.nrcresearchpress.com by 210.87.254.42 on 09/05/12
For personal use only.

Can. J. Chem. Downloaded from www.nrcresearchpress.com by 210.87.254.42 on 09/05/12
For personal use only.

cm^{-1}, est moins sûre, plusieurs bandes de combinaison de vibrations de noyau étant prévues au voisinage de cette fréquence.

Un épaulement observé à 3065 cm^{-1}, dans les spectres i.r. des chloro-2 et dichloro-2,5 benzothiazoles, pourrait peut-être, appartenir aussi à une oscillation ν(CH).

(2) Vibrations de déformation dans le plan δ(CH)

On attend, pour le benzothiazole, cinq vibrations de déformation dans le plan δ(CH).

Dans les spectres des dérivés thiazoliques disubstitués en positions 4 et 5, la vibration $\delta(C_2H)$ est attribuée vers 1200 cm^{-1} (38), tandis que dans ceux des dérivés orthodisubstitués du benzène, les vibrations δ(CH) se situent vers 1200, 1150, 1130, et 1040 cm^{-1} (42–46).

Les spectres i.r. et Raman du benzothiazole présentent, vers 1200 cm^{-1}, une bande d'absorption faible et une forte raie de diffusion qui, du fait qu'elles n'apparaissent pas dans les spectres des dérivés benzothiazoliques substitués en position 2 (41, 47) pourraient être dues à la vibration $\delta(C_2H)$ notée ν_9 (tableau 2). Dans la région de 1260 à 1040 cm^{-1}, on relève encore, dans les spectres i.r. et Raman du benzothiazole quatre maximums: ν_8, ν_{10}, ν_{11}, et ν_{12} (*cf.* tableau 2) susceptibles d'appartenir à des mouvements δ(CH). Il semble, en effet, que certains d'entr'eux ne soient pas observés dans les spectres des benzothiazoles di ou trisubstitués (41, 47). Toutefois, un seul dérivé substitué sur les carbones en -2,5, -2,7, -2,4,6, et -2,6,7 ayant été étudié, il ne peut s'agir d'une interprétation définitive. C'est pourquoi nous n'avons pas établi, dans ce travail, de suites δ(CH) pour les dérivés du benzothiazole. Nous ferons cependant remarquer, à propos des bandes i.r. à 1267 (ν_8) et 1072 cm^{-1} (ν_{12}) qui ont été reliées précédemment, la première, à un mouvement ν(C–N), la deuxième, à une vibration propre à l'hétérocycle thiazolique du benzothiazole (13), qu'aucune des vibrations de noyau du thiazole ne possédant de telles fréquences (38, 48), ces attributions ne paraissent pas très convaincantes.

(3) Vibrations de déformation hors du plan γ(CH) (tableau 1)

Le benzothiazole doit donner lieu à cinq vibrations γ(CH) de type A''. En l'absence de couplage important entre les vibrateurs CH de l'hétérocycle et de l'homocycle, leurs oscillations respectives pourraient être attendues vers 810 cm^{-1} comme dans les dérivés thiazoliques (38) et vers 977, 934, 865 et 750 cm^{-1} (42, 44), puisque d'après O'Sullivan (49) et Derkosch et Specht (50) les fréquences des mouvements γ(CH) varient peu dans un cycle benzénique orthodisubstitué, même s'il est adjacent à un noyau pentagonal aromatique ou hétérocyclique. Dans la région de 1000 à 750 cm^{-1}, le spectre i.r. du benzothiazole à l'état vapeur (fig. 1) présente trois enveloppes de vibration rotation de type C à 938, 824, et 756 cm^{-1}, ainsi que deux autres bandes à 966 et 856 cm^{-1} dont la structure, bien que plus difficile à préciser, paraît cependant être également de type C. On note, qu'à l'exception de celle vers 760 cm^{-1}, à laquelle correspond une raie Raman faible, ces diverses fréquences ne sont pas observées dans le spectre de diffusion.

Le maximum vers 825 cm^{-1}, qui disparaît lors d'une monosubstitution en position 2 (41), semblant dû, en première approximation, à la vibration $\gamma(C_2H)$, les oscillations γ(CH) de l'homocycle doivent être responsables des quatre autres, à 966, 938, 856, et 756 cm^{-1}.

Dans les spectres i.r. des dérivés benzothiazoliques monosubstitués en position 2, quatre suites de fréquences pouvant être rapprochées des vibrations γ(CH) du benzothiazole à 966, 938, 856, et 756 cm^{-1} peuvent être constituées. Les structures de vibration rotation observées, dans les spectres i.r. des chloro-2, méthyl-2 et éthyl-2 benzothiazoles à l'état vapeur, confirment l'attribution des absorptions de la suite vers 760 cm^{-1}, déjà envisagée antérieurement (9, 11), ainsi que celle du sommet vers 940 cm^{-1}, dans le cas du chloro-2 benzothiazole (*cf.* tableau 1)

La faible influence de l'hétérocycle sur les mouvements de déformation γ(CH) de l'homocycle, dans le benzothiazole, étant vérifiée, nous avons cru pouvoir affecter (*cf.* tableau 1) aux oscillations γ(CH) des dérivés benzothiazoliques disubstitués en -2,4, -2,5, -2,6, et -2,7, des suites de bandes i.r. ayant des positions voisines de celles des vibrations homologues des benzènes trisubstitués correspondants (42). Cette interprétation, conforme en ce qui concerne la suite vers 800 cm^{-1}, à celle de Bassignana *et al.* dans les diméthyl-2,5 et -2,6 benzothiazoles (9) est en partie justifiée par les structures de vibration

Can. J. Chem. Downloaded from www.nrcresearchpress.com by 210.87.254.42 on 09/05/12
For personal use only.

rotation de type C de certaines des bandes d'absorption composant les deux suites vers 870 et 803 ± 36 cm^{-1} (*cf.* tableau 1).

L'étude du spectre i.r. du trichloro-2,4,6 benzothiazole à l'état vapeur, permet d'assigner les deux vibrations γ(CH) de cet hétérocycle à 850 et 766 cm^{-1} ce qui, pour la plus élevée, est en accord avec les résultats de Randle et Whiffen qui, pour les dérivés benzéniques tétrasubstitués en -1,2,3,5 ne proposent qu'une seule fréquence γ(CH) à 851 cm^{-1} (42). Ces auteurs (42) ayant également affecté un sommet i.r. ou Raman seulement, aux oscillations γ(CH) des benzènes tétrasubstitués en -1,2,3,4, nous n'avons, dans le spectre i.r. de l'éthyl-2, méthoxy-6, nitro-7 benzothiazole, qui n'a pas été examiné à l'état gazeux, retenu qu'un seul maximum γ(CH) à 820 cm^{-1} (*cf.* tableau 1).

B. Vibrations de noyau du benzothiazole

On attend, pour le benzothiazole, 15 vibrations de squelette dans le plan et six oscillations de noyau hors du plan, qui seront respectivement notées ν_1 à ν_7 et ν_{13} à ν_{20} d'une part et Γ_1 à Γ_6 d'autre part; nous les analyserons successivement. Nos attributions, ainsi que celles que nous suggérons pour les fréquences ne pouvant être considérées comme appartenant à des modes fondamentaux, sont indiquées dans le tableau 2.

(1) Vibrations de symétrie A'

Dans les travaux précédents consacrés au benzothiazole, Chambonnet (6) ainsi que Larivé *et al.* (8) pensent que l'on peut affecter entre 1588 et 1015 cm^{-1} dix absorptions aux vibrations de noyau ou de déformation δ(CH) de l'hétérocycle benzothiazolique. Les deux plus hautes, à 1588 et 1555 cm^{-1}, dénommées bandes thiazole I et II par Randall *et al.* (3), ont déjà été reliées, par ces auteurs, à des mouvements de noyau, celle à 1555 cm^{-1} étant, par ailleurs, rattachée simultanément à une oscillation ν(C=C) par Bassignana *et al.* (10) et à une vibration ν(C=N) par Chambonnet (6). Par ailleurs, outre ceux à 1065 et 1260 cm^{-1} qui ont déjà été discutés dans ce travail, Bonnier *et al.* (13) considèrent comme étant dus respectivement à une vibration du cycle thiazolique et à des mouvements ν(C=N) et ν(C—S) trois maximums à 1420, 1470, et 660 cm^{-1}.

Le spectre i.r. de vibration rotation du benzothiazole à l'état vapeur montre treize bandes de type A ou hybride A + B vers 1551, 1476, 1460, 1429, 1313, 1292, 1266, 1200, 1123, 1071, 1012, 667, et 530 cm^{-1} et cinq bandes de type B vers 1600, 1157, 872, 801 et 350 cm^{-1}. Ces fréquences, sauf celles vers 1460 et 1429 cm^{-1} sont également observées dans le spectre de diffusion, la plupart appartiennent à des raies Raman fortes et polarisées (*cf.* tableau 2). Le spectre Raman comporte encore deux autres raies intenses et polarisées à 709 et 505 cm^{-1}, auxquelles ne correspondent que des bandes i.r. faibles (tableau 2).

Ainsi que les 18 suivants, les deux maximums à 1595 et 1557 cm^{-1} sont, en accord avec les travaux précédents (3, 6, 8, 10) et bien qu'ils apparaissent dans une région où l'on observe des combinaisons des oscillations γ(CH), certainement attribuables à des vibrations fondamentales. S'il s'agissait de combinaisons, en effet, on les attendrait très faibles ou inactives dans le spectre de diffusion, ce qui n'est pas le cas (*cf.* tableau 2). De plus, il est à noter que ces deux fréquences sont très voisines de celles des deux vibrations de noyau de symétrie A' les plus élevées du benzothiophène (51, 52). Dans la mesure où les cinq fréquences 1266, 1200, 1157, 1123, et 1071 cm^{-1} appartiennent bien aux oscillations de déformation δ(CH), les quinze autres doivent être dues aux mouvements de noyau dans le plan ν_1 à ν_7 et ν_{13} à ν_{20}. On peut souligner, en faveur de cette interprétation, l'excellente concordance existant entre les positions de toutes les vibrations de noyau de symétrie A' du benzothiazole et du benzothiophène (51, 52).

(2) Vibrations de symétrie A''

En dehors de celles attribuées à des oscillations γ(CH), le spectre i.r. à l'état vapeur du benzothiazole montre trois autres bandes de vibration rotation de type C, à 728, 420, et 206 cm^{-1} (*cf.* tableau 2, fig. 1), qui peuvent être affectées à des mouvements de noyau hors du plan Γ_1, Γ_5, et Γ_6. En outre, les spectres Raman et i.r. du benzothiazole comportent, respectivement, une raie faible et partiellement dépolarisée et un épaulement vers 671 cm^{-1}, susceptibles d'appartenir à une vibration de noyau hors du plan, que nous désignerons par Γ_2. En effet, les spectres i.r. à l'état vapeur des dichloro-2,5, -2,6, et -2,7 benzothiazoles montrent, vers cette fréquence, une bande de vibration rotation de type C (41, 47). Les oscillations de noyau Γ_3 et Γ_4 pourraient peut-être, par analogie avec le benzothiophène qui possède deux vibrations de

noyau hors du plan à 558 et 471 cm^{-1} (51, 52) donner lieu aux faibles raies Raman à 584 et 452 cm^{-1}.

1. K. W. F. KOHLRAUSCH et R. SEKA. Chem. Ber. **71**, 1563 (1938).
2. J. METZGER et C. CHERRIER. C. R. Acad. Sci. **226**, 71 (1948) et **228**, 239 (1949).
3. H. M. RANDALL, N. FUSON, R. G. FOWLER, et J. R. DANGL. Infrared determination of organic structures. D. Van Nostrand Inc., New York, N.Y. 1949.
4. D. G. O'SULLIVAN. J. Chem. Soc. 3278 (1960).
5. K. S. SURESH, J. RAMACHANDRAN, et C. N. R. RAO. J. Sci. Ind. Res. **20B**, 203 (1961).
6. A. CHAMBONNET. Thèse Ing. Docteur, Marseille, Faculté des Sciences de Marseille, France, 1962.
7. M. AZZARO. Thèse Sciences, Faculté des Sciences de Marseille, Marseille, France, 1962.
8. H. LARIVE, A. CHAMBONNET, et J. METZGER. Bull. Soc. Chim. 1675 (1963).
9. P. BASSIGNANA, C. COGROSSI, et M. GANDINO. Chim. Ind. **90**, 370 (1963).
10. P. BASSIGNANA, C. COGROSSI, et M. GANDINO. Spectrochim. Acta. **19**, 1885 (1963).
11. C. N. R. RAO et R. VENKATARAGHAVAN. Can. J. Chem. **42**, 43 (1964).
12. A. LEIFER, D. BONIS, M. COLLINS, P. DOUGHERTY, A. J. FUSCO, M. KORAL, et J. E. LU VALLE. Spectrochim. Acta, **25**, 909 (1964).
13. J. M. BONNIER, M. GELUS, et B. PAPOZ. Bull. Soc. Chim. 2485 (1965).
14. A. LEIFER, D. BONIS, M. BOEDNER, P. DOUGHERTY, M. KORAL, et J. E. LU VALLE. Appl. Spectr. **20**, 289 (1966).
15. M. CONTE, R. GUGLIELMETTI, et J. METZGER. Bull. Soc. Chim. 2384 (1967).
16. R. JOECKLE, E. LEMPERLE, et R. MECKE. Zeit. Naturforsch. **22a**, 755 (1967).
17. R. GUGLIELMETTI. Thèse Sciences, Faculté des Sciences de Marseille, Marseille, France, 1967.
18. R. GUGLIELMETTI, E. PRETELLI, et J. METZGER. Bull. Soc. Chim. 2812 (1967).
19. R. GUGLIELMETTI et J. METZGER. Bull. Soc. Chim. 2824 (1967).
20. F. KURZER. Org. Syn. **31**, 21 (1951).
21. R. C. ELDERFIELD et F. W. SHORT. J. Org. Chem. **18**, 1098 (1953).
22. J. METZGER et H. PLANK. Bull. Soc. Chim. 1701 (1956).
23. P. E. TODESCO et P. VIVARELLI. Gazz. Chim. Ital. **94**, 372 (1964).
24. R. Q. BREWSTER et F. B. DAINS. J. Amer. Chem. Soc. **58**, 1364 (1936).
25. C. B. TODESCO et P. VIVARELLI. Gazz. Chim. Ital. **92**, 1221 (1962).
26. A. I. KIPRIANOV et P. I. MIKHAILENKO. Ukr. Khim. Zhur. 5 tech. pt. 225 (1930).
27. W. LOGEMANN, S. GALIMBERTI, G. TOSOLINI, I. de CARNERI, et G. COPPI. Il Farm. **12**, 796 (1961).
28. C. B. KREMER et A. BENDICH. J. Amer. Chem. Soc. **61**, 2658 (1939).
29. A. RICCI, P. TODESCO et P. VIVARELLI. Gazz. Chim. Ital. **95**, 490 (1965).
30. R. Q. BREWSTER et L. M. WHITE. Trans. Kansas Acad. Sci. **42**, 241 (1939).
31. J. T EDSALL et E. B. WILSON. J. Chem. Phys. **6**, 124 (1938).
32. D. H. RANK et R. E. KAGARISE. J. Opt. Soc. Amer. **40**, 89 (1950).
33. E. MILER SRENGER. Bull. Soc. Chim. 3970 (1969).
34. E. J. VINCENT. Thèse Sciences, Faculté des Sciences de Marseille, Marseille, France, 1966.
35. Tables of interatomic distances. The Chem. Soc. Londres, Public. No. 11 (1958).
36. R. M. BADGER et L. R. ZUMWALT. J. Chem. Phys. **6**, 711 (1938).
37. W. A. SETH-PAUL et H. de MEYER. Spectrochim. Acta, **25A**, 1671 (1969).
38. G. DAVIDOVICS, C. GARRIGOU-LAGRANGE, J. CHOUTEAU, et J. METZGER. Spectrochim. Acta, **23A**, 1477 (1967).
39. J. R. SCHERER et J. C. EVANS. Spectrochim. Acta, **19**, 1739 (1963).
40. J. M. LEBAS, Thèse Sciences, Faculté des Sciences de Bordeaux, Bordeaux, France, 1958.
41. J. C. PANIZZI. Doctorat de Spécialité, Faculté des Sciences de Marseille, Marseille, France, 1967.
42. R. R. RANDLE et D. H. WHIFFEN. J. Mol. Spectrosc. 111 (1955).
43. A. R. KATRITZKY et R. A. JONES. J. Chem. Phys. 3670 (1965).
44. M. BRIGODIOT et J. M. LEBAS. J. Chim. Phys. **62**, 347 (1965).
45. D. H. WHIFFEN. Phil. Trans. **248**, 131 (1955).
46. A. R. KATRITZKY. Quart. Rev. **13**, 353 (1959).
47. J. C. PANIZZI, G. DAVIDOVICS, R. GUGLIELMETTI, J. CHOUTEAU, et J. METZGER. A paraître.
48. G. SBRANA, E. CASTELLUCCI, et M. GINANNESCHI. Spectrochim. Acta, **23A**, 751 (1967).
49. D. G. O'SULLIVAN. Spectrochim. Acta, **16**, 762 (1960).
50. J. DERKOSCH et I. SPECHT. Mikrochim. Acta, 55 (1962).
51. G. MILLE. D.E.S., Marseille, France, 1968.
52. G. MILLE, G. DAVIDOVICS, et J. CHOUTEAU. A paraître.

Can. J. Chem. Downloaded from www.nrcresearchpress.com by 210.87.254.42 on 09/05/12
For personal use only.

Can. J. Chem. Downloaded from www.nrcresearchpress.com by 210.87.254.42 on 09/05/12
For personal use only.

The Spontaneous Resolution of Oxalatobis(ethylenediamine)cobalt(III) Chloride

D. G. BREWER AND K. T. KAN
Department of Chemistry, University of New Brunswick, Fredericton, New Brunswick

Received October 6, 1970

The spontaneous partial resolution of oxalatobis(ethylenediamine)cobalt(III) chloride was affected by the crystallization of the complex compound from a supersaturated aqueous solution (1 g/25 ml) at 20 °C without the influence of any dissymmetric agent. Crystals exhibiting in some cases dextro-rotatory properties, and in the others levo-rotatory were obtained with up to 25% optical purity.

La résolution spontanée partielle du chlorure d'oxalatobis(éthylènediamine)cobalt a été effectuée par cristallisation du complexe sans l'influence d'aucun agent dissymétrique, d'une solution aqueuse sursaturée (1 g/25 ml à 20 °C). Suivant les cas, des cristaux droits et des cristaux gauches ont été obtenus avec des rendements optiques allant jusqu'à 25%.

Canadian Journal of Chemistry, 49, 965 (1971)

Introduction

Since Pasteur's first resolution of optical isomers, various methods such as hand-picking, preferential crystallization, diastereoisomer formation, and chromatography have been utilized for the resolution of enantiomers. Detailed reviews of this subject have been given by Eliel (1), Secord (2), and Buss and Vermeulen (3).

Most of the methods for the resolution of racemic modifications require the presence of optically active environments, achieved by the use of other optically active substances, or polarized radiation. For a closed system not influenced by any dissymmetric agent, the probability of its becoming optically active will always be very low. However, there have been a couple of reports on the spontaneous resolution of organic isomers (4, 5).

In this work, we were able to effect a spontaneous resolution of the oxalatobis(ethylenediamine)cobalt(III) chloride from a supersaturated aqueous solution by a crystallization method without any dissymmetric influence.

Experimental

Oxalatobis(ethylenediamine)cobalt(III) chloride was prepared by two different methods. The first method involved the substitution of an oxalate ion with the chloride ions in a *cis*-dichlorobis(ethylenediamine)cobalt chloride molecule reported by Werner (6). The second method was a direct synthesis described by Dwyer *et al.* (7). Both methods yielded clear red crystals of oxalatobis(ethylenediamine)cobalt chloride with four hydrated waters at the time of their separation from the mother liquors (8). The compound lost part of its water of crystallization and the transparency of the crystals disappeared gradually when it was air dried. Dwyer *et al.* reported that this compound had only one hydrated water (7). The resolution of $[Co(en)_2(C_2O_4)]^+$ ion was affected by using the method described in ref. 7. The optical active isomers of $[Co(en)_2(C_2O_4)]I$ thus obtained was transformed into chloride form by shaking the iodide salt with freshly prepared silver chloride. The specific rotation of $[Co(en)_2(C_2O_4)]Cl.H_2O$ was found to be $[\alpha]_D = +920°$, which is close to the value reported by Dwyer *et al.*, *viz.*, $[\alpha]_D = +930°$ (7).

Optical rotations were determined on a Rudolph Model 200A photoelectric polarimeter equipped with a high intensity mercury lamp. A Honeywell Electronik 19 recorder was used to help obtain the polarimeter reading. The optical rotatory dispersion curves were measured with a Durum-Jasco ORD/UV-5 recording spectropolarimeter.

$[Co(en)_2(C_2O_4)]Cl.H_2O$ (1.00 g) dissolved in warm water (25 ml) was introduced into a clean test tube, which was then properly sealed. The temperature of the solution was kept at 25 ± 0.5 °C for 2 h by putting the test tube in a thermostated water bath, and it was lowered manually at a rate of 1 °C per 2 h until a temperature of 20 °C was reached. At this final temperature, the solution became barely supersaturated and initially a few clear red crystals of $[Co(en)_2(C_2O_4)]Cl$ slowly appeared. The solution was then allowed to stay at 20 °C for 12 h before the crystals were removed from the solution by quick filtration. The crystals were washed with 80% methanol, absolute methanol, and then air dried. The optical activity of the crystals, as well as the mother liquor, was then checked with the Rudolph spectropolarimeter at the wavelengths of 404.7 and 577.0 mμ using a high intensity mercury lamp. At these two wavelengths, $[Co(en)_2(C_2O_4)]Cl$ showed opposite rotation. By comparing the optical

TABLE 1. Experimental results of the spontaneous resolution of $[Co(en)_2(C_2O_4)]Cl$. (The optical rotation was determined at 23 °C, in a 1 dm cell, with a concentration close to 0.2%)

Expt. No.*	Specific rotation [α] of the crystals		Specific rotation [α]† of the mother liquors at 404.7 mμ	Approx. yield of crystals (g)
	577 mμ	404.7 mμ		
D-1	−54.0°	+59.1°	0°	0.05
D-2	−219°	+268°	−12°	0.03
D-3	+197°	−238°	+16°	0.05
D-4	+92.5°	−111°	+14°	0.10
W-5	−32°	+36°	0°	0.20
W-6	−63.6°	+71.5°	−8°	0.20
W-7	0°	0°	0°	0.20
D-8	−73.8°	+84.1°	−10°	0.12
D-9	−41°	+46°	0°	0.12
W-10	−121°	+140°	−25°	0.15
W-11	+165°	−193°	+35°	0.18
D-12	0°	0°	0°	0.22
W-13	−5.5°	+6.4°	0°	0.19
D-14	+62.4°	−74.1°	+16°	0.22

*W, compounds prepared by Werner's method (6); D, compounds prepared by Dwyer's method (7).
†The concentration of the diluted mother liquor was evaluated by a colorimetric method using standard $[Co(en)_2(C_2O_4)]Cl$ solutions at 500 mμ.

activities measured at these two wavelengths, it is possible to detect and confirm small rotations exhibited by the crystals. To avoid accidentally picking up a fraction of the crystals containing an unequal amount of enantiomers, the whole crop of crystals was ground and mixed completely in a motar before the examination of optical activity.

Results

The results of several consecutive experiments were tabulated in Table 1. The optical rotatory dispersion (o.r.d.) of the crystals from these experiments were identical with that of the optically pure complex resolved conventionally (Fig. 1). The mother liquors always showed a rotation opposite to that of the crystals, although when the resolutions were poor, the optical activities of the mother liquors could not be detected with our instrument. To ascertain that the observed optical activity did not come from the original complex, the compound was prepared in two entirely different ways, as described in the Experimental section, and it was found that in both cases the same compound obtained was optically inactive.

The same experiment was repeated more than 50 times, and no consistency was observed in the optical activities of the crystals. Sometimes the dextro-rotatory crystals were obtained, sometimes the levo ones, and, in the remainder, racemic mixtures. The yield of the crystals from 1 g starting material ranged from 0.2–0.05 g, with a trend towards better resolution at lower yields. The best resolution was about 25% optically pure. The largest crystal obtained

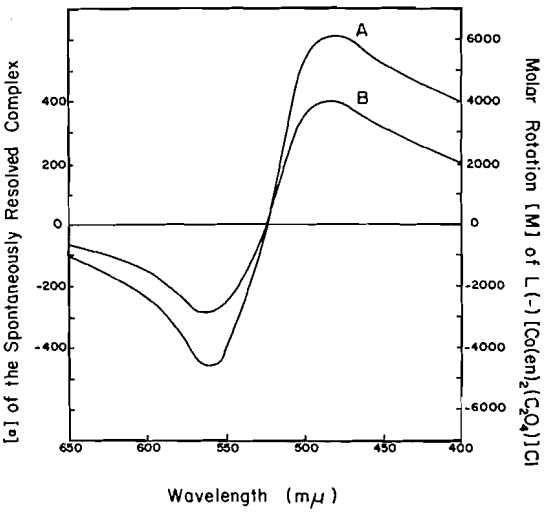

FIG. 1. The optical rotatory dispersion curves of the conventionally resolved (*A*), and the spontaneously resolved (*B*) $[Co(en)_2(C_2O_4)]Cl.H_2O$.

weighed 0.5 m and hence the minimum number of crystals in the larger batches is approximately 400.

There have been reports (9, 10) that optically active atmospheric dust would induce resolution. Special cares have therefore been taken to clean and seal the reaction tubes. An independent experiment by one of our colleagues in another part of the Chemistry Building, using separate facilities never exposed to any optically active substances, produced similar results.

All these experimental facts indicated that a

Can. J. Chem. Downloaded from www.nrcresearchpress.com by 210.87.254.42 on 09/05/12
For personal use only.

Can. J. Chem. Downloaded from www.nrcresearchpress.com by 210.87.254.42 on 09/05/12
For personal use only.

spontaneous resolution of the oxalatobis(ethylenediamine)cobalt ion had occurred.

Discussion

The mechanism for the spontaneous resolution of oxalatobis(ethylenediamine)cobalt chloride is not the same as that described by Havinga (4). For one thing, the methyl-ethyl-allyl-anilinium iodide is optically labile, and $[Co(en)_2(C_2O_4)]Cl$ is not. It was found that $[Co(en)_2(C_2O_4)]Cl$ did not racemize or undergo photoracemization in aqueous solution at room temperature (11, 12).

Yamasaki *et al.* (8) reported that $[Co(en)_2(C_2O_4)]Cl$ when crystallized from water formed a racemic mixture with crystals without distinguishable facets between 15–25 °C. Like that of any typical mixture, the solubility of a racemic mixture is higher than that of the pure components (1, 2). This is also true for $[Co(en)_2(C_2O_4)]Br$. Werner (6) observed that the solubility of the optically active bromide (1.05 g/100 ml at 17 °C) was much lower than that of the inactive form (1.85 g/100 ml at 17 °C). This difference in solubility is also expected to exist between the optical active and inactive chloride form of the same cation. If a supersaturated solution of oxalatobis(ethylenediamine)cobalt chloride is allowed to crystallize very slowly in solutions, the first nucleus, or the few nuclei formed will consist of one enantiomer only, or will be composed of an unequal amount of the two enantiomers. This nucleus or these nuclei will grow by the addition of molecules of its own configuration to form crystals, which, in turn, will act as seeds to induce an asymmetric separation of crystals from the solution in favor of their own kind, until the solution is sufficiently supersaturated with the other form for it to commence to separate. The mechanism for this asymmetric separation of crystals, we believe, is analogous to the partial resolution of $[Co(en)_2(C_2O_4)]Br$ by Werner (6) by the seeding of a supersaturated solution of this complex with an optically active crystal of one of the isomers. The chance for either one of the enantiomers to deposit first is the same and explains why the resolutions sometimes yielded crystals enriched in one of the forms. The spontaneous crystallization process is always very delicate. Any slight fluctuation in the system, such as temperature variation, vibration, dust, etc., will affect the process tremendously. It is understandable then that reproducible results were not obtained and also why no resolution was observed in some experiments. Some experiments were performed involving the rapid crystallization of the complex from a supersaturated solution by lowering the temperature quickly, and no optical activity was found in the products. On the other hand, in some experiments, the temperature was allowed to drop below 20 to 18 °C, and a large amount of crystals (0.4–0.5 g) showing very small rotations, or no rotation at all, was obtained. Thus, the process of crystallization is all important in the spontaneous resolution of oxalatobis(ethylenediamine)cobalt chloride.

The basic requirements for the spontaneous resolution of $[Co(en)_2(C_2O_4)]Cl$ appear to be: (*i*) the compound form a racemic mixture; (*ii*) the solubility of the pure enantiomers is lower than that of the racemic mixture; (*iii*) the crystallization process is very slow, and without, preferably, perturbation of any kind, so that only one of a few nuclei will form and grow at the early stage of the crystallization process; and (*iv*) last but not least, the compound should respond readily to a dissymmetric influence, such as those described by Werner(6), Schweitzer and Talbott (13), and Broomhead (14).

The authors wish to thank Dr. D. Idler and Mr. D. Ellis of the Fisheries Research Board in Halifax for the use of their Durum-Jasco Spectropolarimeter, and the National Research Council of Canada for financial support.

1. E. L. Eliel. Stereochemistry of Carbon Compounds. McGraw-Hill, New York. 1962.
2. R. M. Secord. Chem. Rev. **63**, 297 (1963).
3. D. S. Buss and T. Vermeulen. Ind. Eng. Chem. **60** (8), 12 (1968).
4. E. Havinga. Biochim. Biophys. Acta, **13**, 171 (1954).
5. R. C. Ferreira. Nature, **171**, 39 (1953).
6. A. Werner. Ber. **47**, 2171 (1914).
7. F. P. Dwyer, I. K. Reid, and F. L. Garvan. J. Amer. Chem. Soc. **83**, 1285 (1961).
8. Y. Yamasaki, H. Igarashi, Y. Yoshikawa, and H. Kuroya. Inorg. Nucl. Chem. Lett. **4**, 491 (1968).
9. F. S. Kipping and W. J. Pope. Proc. Chem. Soc. **14**, 113 (1898).
10. F. S. Kipping and W. J. Pope. J. Chem. Soc. **95**, 103 (1909).
11. E. Bushra and C. H. Johnson. J. Chem. Soc. 1937 (1939).
12. S. T. Spees and A. R. Adamson. Inorg. Chem. **1**, 531 (1962).
13. G. K. Schweitzer and C. K. Talbott. J. Tenn. Acad. Sci. **25**, 143 (1950).
14. J. A. Broomhead. Nature, **211**, 741 (1966).

Synthesis and Stereochemical Assignments of Some Trifluoromethylphenylcyclopropanes

L. J. ALTMAN, M. R. BRAMWELL, AND J. C. VEDERAS
Department of Chemistry, Stanford University, Stanford, California 94305

Received September 28, 1970

Stereochemical assignments of a series of substituted *cis*- and *trans*-1-trifluoromethyl-2-phenylcyclopropanes (unsubstituted, bromide, carbonitrile, and carboxamide) based on a detailed analysis of the n.m.r. spectra and on the ten-fold difference in rates in the reaction of *cis*- and *trans*-1-trifluoromethyl-2-phenylcyclopropyl carbonitrile with basic hydrogen peroxide are presented.

Des attributions de stéréochimie pour une série de trifluorométhyl-1 phényl-2 cyclopropanes substitués (non-substitué, bromo, carbonitrile, et carboxamide) *cis* et *trans* sont présentées; les conclusions sont basées sur analyse détaillée des spectres r.m.n. et sur le fait que le rapport des vitesses de réaction des trifluorométhyl-1 phényl-1 cyclopropylcarbonitriles *cis* et *trans* avec le peroxyde d'hydrogène en milieu basique est de 10/1.

Canadian Journal of Chemistry, 49, 968 (1971)

Can. J. Chem. Downloaded from www.nrcresearchpress.com by 210.87.254.6 on 09/05/12
For personal use only.

In connection with our work on the configurational stability of the α-trifluoromethylcyclopropyl radical (1), it was necessary to synthesize and assign the stereochemistry of a number of trifluoromethylphenylcyclopropanes. The stereochemical assignments are based to a large part on analysis of the n.m.r. spectra of these compounds. We present here the results of the analyses.

The synthesis of the compounds **1***a–c* and **2***a–c* was accomplished through a 1,3-dipolar addition (2) of phenyldiazomethane to an electron deficient olefin followed by pyrolysis of the resulting pyrazoline (Scheme 1). The isomers were separated by v.p.c. The amides **1***d* and **2***d* were prepared from the corresponding nitriles, **1***c* and **2***c*, by treatment with basic hydrogen peroxide (3).

The analyses of the 100 MHz n.m.r. spectra were accomplished with the LAOCN 3 computer program (4). In order to resolve the coupling between the fluorine nuclei and the benzylic protons in **1***a–d* it was found necessary to decouple the aromatic protons. The analysis of **2***c* was verified by obtaining a satisfactory agreement between the derived parameters from both the 60 and 100 MHz spectra. The relative sign of the geminal coupling constant was confirmed in **1***b* and **2***b* by means of a spin tickling experiment (5). The refined spectral parameters are presented in Tables 1 and 2.

The assignment of the relative stereochemistry in **1***a* and **2***a* is based on the well verified assumption (6) that in cyclopropanes the *cis* vicinal coupling is larger than the *trans* vicinal coupling. The comparison of the derived coupling constants between the hydrogen α to the trifluoromethyl group (X = H) and H-2 and -3 in **1***a* and **2***a* places H-2 *cis* to the α-proton in **1***a* and H-3 *cis* to the α-proton in **2***a*. Since H-2 is *cis* to the benzylic proton in both **1***a* and **2***a*, this allows the assignment of **1***a* as *cis*-trifluoromethylphenyl cyclopropane[1] and **2***a* as *trans*-trifluoromethylphenylcyclopropane. This assignment is confirmed by a comparison of the derived coupling constants between the α-proton and H-1 in **1***a* (8.97 Hz) and **2***a* (4.63 Hz).

The stereochemical assignments of the nitriles **1***c* and **2***c* come from a competition experiment in which the nitriles were converted to amides by the action of basic hydrogen peroxide. It was expected that the rate of reaction of the compound with the nitrile *cis* to the phenyl would be slower than the unhindered isomer with the nitrile *trans* to the phenyl based on experiments with the model compounds *cis*- and *trans*-1-methyl-2-phenylcyclopropyl carbonitrile. A rate difference of approximately 10 was found between the two isomers and therefore allows the assignment of nitriles (**1***c* as *cis*- and **2***c* as *trans*-1-trifluoromethyl-2-phenylcyclopropyl carbonitrile) as well as the corresponding amides **1***d* and **2***d*. This assignment is also corroborated by the relative v.p.c. retention times of the nitriles (**1***c* = 31 min, **2***c* = 25 min) and the t.l.c. R_f's of the amides (ether eluant, **1***d* = 0.5, **2***d* = 0.7).

[1]All compounds are named as derivatives of cyclopropane for convenience in following the stereochemical assignments; *cis* and *trans* refer to the relative orientation of the trifluoromethyl and phenyl substituents.

TABLE 1. Refined spectral parameters*

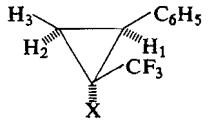

Parameter	**1***a* (X = H)	**1***b* (X = Br)	**1***c* (X = CN)	**1***d* (X = $CONH_2$)
ω(F)	17.26	12.96	15.74	19.23
ω(1)	2.386	3.016	3.176	3.102
ω(2)	1.169	1.707	1.948	1.976
ω(3)	1.369	1.964	2.049	1.832
ω(X)	1.774	—	—	—
J(F1)	0.99	0.93	1.33	1.24
J(F2)	1.36	1.62	1.68	1.94
J(F3)	0.27	−0.03	−0.15	−0.06
J(FX)	7.49	—	—	—
J(12)	9.21	10.49	9.89	9.63
J(13)	7.24	8.57	8.83	8.25
J(1X)	8.97	—	—	—
J(23)	−5.84	−7.36	−6.94	−5.25
J(2X)	8.92	—	—	—
J(3X)	5.92	—	—	—

*Proton chemical shifts are reported in p.p.m. downfield from internal TMS; fluorine chemical shifts are reported in p.p.m. downfield from external trifluoroacetic acid. The maximum probable error for any parameter obtained from the LAOCN3 program is 0.022 Hz. We believe that an error limit of ±0.09 Hz should be placed on any reported parameter.

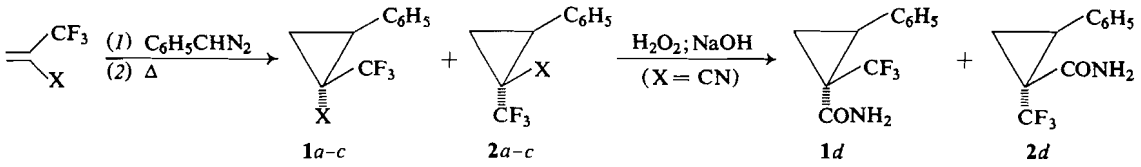

1*a–c* **2***a–c* **1***d* **2***d*

a X = H
b X = Br
c X = CN

SCHEME 1

With this series of six compounds in hand it was now possible to assign the bromides **1***b* and **2***b* on the basis of the four–bond fluorine proton coupling constants (J_{F2} and J_{F3}). It is observed that this four bond coupling is larger when the CF_3 and proton are *trans* to each other. Indeed, in the nitriles the spectra could only be fitted with a negative value of the *cis* coupling constant. Thus it was possible to assign **1***b* as *cis*- and **2***b* as *trans*-1-trifluoromethyl-2-phenylcyclopropyl bromide. This assignment is also consistent with the empirical observation that the fluorines on a CF_3 *cis* to a phenyl are deshielded by approximately 6 p.p.m. relative to those on a CF_3 *trans* to the phenyl.

Experimental

The n.m.r. spectra were taken of $CDCl_3$ solutions (≈20%) on a Varian HA-100 spectrometer. Peak positions were obtained to 0.1 Hz by means of charts calibrated by a Hewlett Packard 5512A frequency counter. The v.p.c.'s were run on an F&M model 700 with a 20 ft by 1/4 in. column of 20% carbowax 20 M on Chromosorb W with a gas flow of 100 ml/min at 145°.

1-Trifluoromethyl-2-phenylcyclopropane

A mixture of phenyldiazomethane (7) and excess trifluoropropene[2] at reflux was irradiated with two 300 W unfrosted incandescent lamps until all the phenyldiazomethane had reacted. The resulting crude pyrazoline was pyrolyzed directly in the v.p.c. injection port (200°) to give *cis*- and *trans*-1-trifluoromethyl-2-phenylcyclopropane. The v.p.c. retention times: *cis* 20 min, *trans* 13 min.

Anal. Calcd. for $C_{10}H_9F_3$: C, 64.52; H, 4.84; F, 30.64. Found: (*trans*): C, 64.66; H, 4.88; F, 30.32; (*cis*): C, 64.74; H, 4.91; F, 30.85.

1-Trifluoromethyl-2-phenylcyclopropyl Bromide

A solution of phenyldiazomethane in petroleum ether

[2]We thank E. I. du Pont de Nemours and Co. for a generous gift of this compound.

Can. J. Chem. Downloaded from www.nrcresearchpress.com by 210.87.254.6 on 09/05/12
For personal use only.

TABLE 2. Refined spectral parameters*

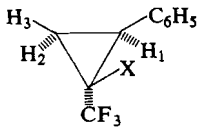

Parameter	2*a* (X = H)	2*b* (X = Br)	2*c* (X = CN)†	2*d* (X = $CONH_2$)
ω(F)	11.33	7.24	9.64	12.56
ω(1)	2.277	2.696	2.796	2.75
ω(2)	1.293	1.912	1.686	1.568
ω(3)	1.069	1.645	1.727	2.100
ω(X)	1.718	—	—	—
J(F1)	0.51	—‡	0.50	—‡
J(F2)	0.43	−0.03	−0.34	−0.01
J(F3)	1.09	1.35	1.39	1.90
J(FX)	6.59	—	—	—
J(12)	9.50	10.50	9.61	9.97
J(13)	6.31	8.31	8.15	7.85
J(1X)	4.63	—	—	—
J(23)	−5.65	−7.21	−6.50	−5.93
J(2X)	5.53	—	—	—
J(3X)	8.99	—	—	—

*Proton chemical shifts are reported in p.p.m. downfield from internal TMS; fluorine chemical shifts are reported in p.p.m. downfield from external trifluoroacetic acid. The maximum probable error for any parameter obtained from the LAOCN3 program was 0.027 Hz. We believe that an error limit of ±0.11 Hz should be placed on any reported parameter.

†In order to better resolve the second order spectrum approximately 5% C_6D_6 was added to the $CDCl_3$ solution.

‡The benzylic proton could not be effectively decoupled from the aromatic protons and thus sufficient resolution was not obtained to calculate this coupling constant.

was added to a refluxing solution of 2-bromo-3,3,3-trifluoropropene (8) in petroleum ether. The solvent was removed under reduced pressure when a pink color persisted and the crude pyrazoline was pyrolyzed directly in the v.p.c. injection port (injector temperature, 200°) to give *cis*- and *trans*-1-trifluoromethyl-2-phenylcyclopropyl bromide. The v.p.c. retention times: *cis* 36 min, *trans* 32 min.

Anal. Calcd. for $C_{10}H_8BrF_3$: C, 45.28; H, 3.01; Br, 30.14; F, 21.51. Found (*trans*): C, 45.38; H, 3.07; Br, 30.24; F, 21.23; (*cis*): C, 45.49; H, 3.12; Br, 30.27; F, 21.49.

1-Trifluoromethyl-2-phenylcyclopropanecarbonitrile

A crude mixture of *cis*- and *trans*-1-trifluoromethyl-2-phenylcyclopropanecarbonitrile, prepared by the addition of a solution of phenyldiazomethane in petroleum ether to a solution of α-trifluoromethylacrylonitrile[3] in petroleum ether at 0° followed by evaporation of the solvent under reduced pressure, was separated by preparative v.p.c. (retention times: *trans* 25 min, *cis* 31 min).

Anal. Calcd. for $C_{11}H_8F_3N$: C, 62.56; H, 3.82; N, 6.63. Found (*trans*): C, 62.67, H, 3.85; N, 6.55; (*cis*): C, 62.58; H, 3.89; N, 6.58.

1-Trifluoromethyl-2-phenylcyclopropanecarboxamide

cis-1-Trifluoromethyl-2-phenylcyclopropanecarboxamide was prepared from the reaction of *cis*-1-trifluoromethyl-2-phenylcyclopropanecarbonitrile (30 mg) in NaOH (0.3 ml) and 30% H_2O_2 (0.3 ml) in acetone (1 ml) at room temperature for 16 h followed by partitioning of the crude product between methylene chloride and water, preparative t.l.c. (silica gel HF; ether as eluant), and sublimation (80° at 10^{-3} mm Hg).

The *trans*-isomer was analogously prepared except for a longer reaction time (40 h). A mixture of the two amides could be separated by preparative t.l.c. (ether as eluant) with the *trans*-isomer having the highest R_f (0.5, 0.7).

Anal. Calcd. for $C_{11}H_{10}F_3NO$: C, 57.64; H, 4.40; N, 6.11. Found (*cis*): C, 57.44; H, 4.44; N, 6.04; (*trans*): C, 57.60; H, 4.44; N, 6.00.

Competition Experiment

To a stirred mixture of *cis*- (20.5 mg) and *trans*-1-trifluoromethyl-2-phenylcyclopropanecarbonitrile (20.5 mg) acetone (0.4 ml), 1.0 *N* NaOH (0.1 ml), and *o*-dichlorobenzene (15.9 mg) at 20° was added in one portion 30% H_2O_2 (0.80 ml). Aliquots were withdrawn and analyzed directly by v.p.c. by comparing the areas of the nitrile peaks and that of *o*-dichlorobenzene. After 1 h 4.8% of the *trans*-isomer had reacted whereas 53% of the *cis*-isomer had reacted.

We thank the donors of the Petroleum Research Fund, administered by the American Chemical Society, Eli Lilly and Company, and the Rohm and Haas Company for partial support of this research.

[3]Prepared from trifluoroacetone by the method of Buxton *et al.* (9).

1. L. J. ALTMAN and J. C. VEDERAS. Chem. Commun. 895 (1969).

Can. J. Chem. Downloaded from www.nrcresearchpress.com by 210.87.254.6 on 09/05/12
For personal use only.

2. R. HUISGEN. Helv. Chim. Acta, **50**, 2421 (1967) and references cited therein.
3. G. B. PAYNE, P. H. DEMING, and P. H. WILLIAMS. J. Org. Chem. **26**, 659 (1961); C. M. ATKINSON and C. J. SHARPE. J. Chem. Soc. 2858 (1959).
4. S. CASTELLANO and A. A. BOTHNER-BY. J. Chem. Phys. **41**, 3863 (1964). A copy of this program was obtained from the Quantum Chemistry Program Exchange, Indiana University, Bloomington, Indiana.
5. R. FREEMAN and W. A. ANDERSON. J. Chem. Phys. **37**, 2053 (1962).
6. L. M. JACKMAN and S. STERNHELL. Applications of nuclear magnetic resonance spectroscopy in organic chemistry. 2nd Edition. Pergamon Press, London, 1969. pp. 280–289 and references cited therein.
7. C. G. OVERBERGER and J. P. ANSELME. J. Amer. Chem. Soc. **86**, 658 (1964).
8. A. L. HENNE and M. NAGER. J. Amer. Chem. Soc. **73**, 1042 (1951).
9. M. W. BUXTON, M. STACEY, and J. C. TATLOW J. Chem. Soc. 366 (1959).

Can. J. Chem. Downloaded from www.nrcresearchpress.com by 210.87.254.6 on 09/05/12
For personal use only.

2-Arylimino-1,3-thiaazacycloalkanes

D. L. GARMAISE, G. Y. PARIS, AND G. EFTHYMIADIS
Abbott Laboratories Limited, Montreal, Quebec

Received October 14, 1970

The reaction of ω-bromoalkyl isothiocyanates with aromatic amines served as a general preparative method for homologous 2-arylimino-1,3-thiaazacycloalkanes. Rings containing seven to thirteen members were prepared in this way. The isothiocyanates and some of the thiaazacycloalkanes had anthelmintic activity.

La réaction d'isothiocyanates d'ω-bromoalkyles avec les amines aromatiques s'avère une méthode générale de préparation d'arylimino-2 thiaaza-1,3 cycloalcanes. Des cycles contenant de sept à treize atomes ont été préparés de cette manière. Les isothiocyanates et quelques-un des thiaazacycloalcanes possèdent une activité anthelmintique.

Canadian Journal of Chemistry, 49, 971 (1971)

Five- and six-membered ring compounds having the general structures **A** and **B** have been extensively studied; the thiazine derivatives have

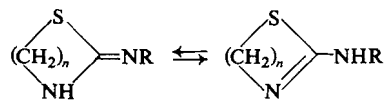

A **B**

shown potentially useful pharmacological properties (1) and the thiazolidines have anthelmintic action (2). Compounds in which $n > 3$ have not been previously reported; the preparation and some biological properties of compounds of general structure **A** where $n = 4$, 5, 6, 8, and 10 are described in this paper.

The methods commonly used for the preparation of 2-aryliminotetrahydro-1,3-thiazines were examined for possible applicability to the synthesis of larger rings. The most common procedure for preparing the six-membered rings is the acid-catalyzed cyclization of ω-hydroxyalkylthioureas (eq. 1). The reaction proceeded smoothly when $n = 3$ (or 2) but when $n = 4$, no cyclization occurred. Of the other methods which have been reported (1, 3, 4) for the synthesis of the six-membered rings, the reaction of 3-bromopropyl isothiocyanate with aromatic amines (1, 4) was the most readily adaptable to the synthesis of larger rings. The reaction of ω-bromopropylalkyl isothiocyanates with aromatic amines (eq. 2) was found to be a convenient general method.

[1] $$RNH\,C(=S)\,NH(CH_2)_nOH \xrightarrow[\text{HCl}]{\text{concentrated}} A$$

[2] $$Br(CH_2)nNCS + ArNH_2 \rightarrow A$$

(n = 4, 5, 6, 8, and 10)

The ω-bromoalkyl isothiocyanates (listed in Table 1) were obtained by the reaction of thiophosgene with ω-bromoalkylamine hydrobromides. In the case of the preparation of 4-bromopropyl isothiocyanate, it was observed that a variable amount (10–25%) of 4-chloropropyl isothiocyanate was also obtained, apparently by halogen exchange with thiophosgene. The ω-bromoalkylamines were obtained by standard methods from α,ω-dibromoalkanes via the monophthalimido derivatives.

Recent work by Toldy *et al.* (5), Cherbuliez

2. R. HUISGEN. Helv. Chim. Acta, **50**, 2421 (1967) and references cited therein.
3. G. B. PAYNE, P. H. DEMING, and P. H. WILLIAMS. J. Org. Chem. **26**, 659 (1961); C. M. ATKINSON and C. J. SHARPE. J. Chem. Soc. 2858 (1959).
4. S. CASTELLANO and A. A. BOTHNER-BY. J. Chem. Phys. **41**, 3863 (1964). A copy of this program was obtained from the Quantum Chemistry Program Exchange, Indiana University, Bloomington, Indiana.
5. R. FREEMAN and W. A. ANDERSON. J. Chem. Phys. **37**, 2053 (1962).
6. L. M. JACKMAN and S. STERNHELL. Applications of nuclear magnetic resonance spectroscopy in organic chemistry. 2nd Edition. Pergamon Press, London, 1969. pp. 280–289 and references cited therein.
7. C. G. OVERBERGER and J. P. ANSELME. J. Amer. Chem. Soc. **86**, 658 (1964).
8. A. L. HENNE and M. NAGER. J. Amer. Chem. Soc. **73**, 1042 (1951).
9. M. W. BUXTON, M. STACEY, and J. C. TATLOW J. Chem. Soc. 366 (1959).

Can. J. Chem. Downloaded from www.nrcresearchpress.com by 210.87.254.105 on 09/05/12
For personal use only.

2-Arylimino-1,3-thiaazacycloalkanes

D. L. GARMAISE, G. Y. PARIS, AND G. EFTHYMIADIS
Abbott Laboratories Limited, Montreal, Quebec

Received October 14, 1970

The reaction of ω-bromoalkyl isothiocyanates with aromatic amines served as a general preparative method for homologous 2-arylimino-1,3-thiaazacycloalkanes. Rings containing seven to thirteen members were prepared in this way. The isothiocyanates and some of the thiaazacycloalkanes had anthelmintic activity.

La réaction d'isothiocyanates d'ω-bromoalkyles avec les amines aromatiques s'avère une méthode générale de préparation d'arylimino-2 thiaaza-1,3 cycloalcanes. Des cycles contenant de sept à treize atomes ont été préparés de cette manière. Les isothiocyanates et quelques-un des thiaazacycloalcanes possèdent une activité anthelmintique.

Canadian Journal of Chemistry, 49, 971 (1971)

Five- and six-membered ring compounds having the general structures **A** and **B** have been extensively studied; the thiazine derivatives have

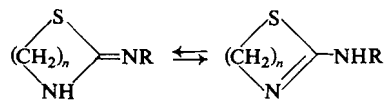

A **B**

shown potentially useful pharmacological properties (1) and the thiazolidines have anthelmintic action (2). Compounds in which $n > 3$ have not been previously reported; the preparation and some biological properties of compounds of general structure **A** where $n = 4$, 5, 6, 8, and 10 are described in this paper.

The methods commonly used for the preparation of 2-aryliminotetrahydro-1,3-thiazines were examined for possible applicability to the synthesis of larger rings. The most common procedure for preparing the six-membered rings is the acid-catalyzed cyclization of ω-hydroxyalkylthioureas (eq. 1). The reaction proceeded smoothly when $n = 3$ (or 2) but when $n = 4$, no cyclization occurred. Of the other methods which have been reported (1, 3, 4) for the synthesis of the six-membered rings, the reaction of 3-bromopropyl isothiocyanate with aromatic amines (1, 4) was the most readily adaptable to the synthesis of larger rings. The reaction of ω-bromopropylalkyl isothiocyanates with aromatic amines (eq. 2) was found to be a convenient general method.

[1] $$RNH\,C(=S)\,NH(CH_2)_nOH \xrightarrow[\text{HCl}]{\text{concentrated}} A$$

[2] $$Br(CH_2)nNCS + ArNH_2 \rightarrow A$$

(n = 4, 5, 6, 8, and 10)

The ω-bromoalkyl isothiocyanates (listed in Table 1) were obtained by the reaction of thiophosgene with ω-bromoalkylamine hydrobromides. In the case of the preparation of 4-bromopropyl isothiocyanate, it was observed that a variable amount (10–25%) of 4-chloropropyl isothiocyanate was also obtained, apparently by halogen exchange with thiophosgene. The ω-bromoalkylamines were obtained by standard methods from α,ω-dibromoalkanes via the monophthalimido derivatives.

Recent work by Toldy *et al.* (5), Cherbuliez

TABLE 1. ω-Bromoalkyl isothiocyanates
$Br(CH_2)_nNCS$

Compound	n	Yield (%)	Boiling point (°C)(mm Hg)	Formula	Analysis C Calcd.	C Found	H Calcd.	H Found	N Calcd.	N Found
1	4	65	91–94(0.2)	C_5H_8BrNS*	30.94	31.0	4.15	4.1	7.22	7.2
2	5	68	107(0.6)	$C_6H_{10}BrNS$	34.62	34.46	4.84	5.00	6.73	6.86
3	6	65	116(0.5)	$C_7H_{12}BrNS$	37.84	38.09	5.45	5.69	6.31	6.82
4	8	45	117(0.2)	$C_9H_{16}BrNS$	43.20	43.44	6.45	6.52	5.60	5.41
5	10	45	150(0.3)	$C_{11}H_{20}BrNS$	47.48	47.77	7.25	7.23	5.03	5.48

*Anal. Calcd.: Br, 41.17; S, 16.52. Found: Br, 41.2; S, 16.5.

et al. (6, 7), and Rabinowitz (8) on the use of n.m.r. spectra to distinguish between the tautomeric forms **A** and **B** in the thiazine series has cleared up the confusion resulting from earlier attempts to make this distinction on the basis of i.r. (3) and u.v. (9) spectra. Using model compounds of unequivocal structure, it has been shown that for given substituents on the aromatic ring, δ N—CH_2 is higher when the double bond is endocyclic. The presence of strongly electron-withdrawing substituents, such as the nitro group, on the aromatic ring tends to lower the value of δ N—CH_2; in general, however, tautomers of structure **A** have δ N—CH_2 ~ 3.32 and those of structure **B** have δ N—CH_2 ~ 3.57. Since the larger ring compounds prepared in this program had δ N—CH_2 = 3.30–3.35, it is assumed that the products are best represented by structure **A** and are named accordingly. In the absence of model compounds, however, this evidence can not be regarded as conclusive.

Biological Results

The ω-bromoalkyl isothiocyanates showed the anthelmintic activity characteristic of many isothiocyanates. 6-Bromohexyl isothiocyanate was particularly effective; at 400 mg/k, it eliminated 99% of the burden of *Nematospiroides dubius* from mice; at 250 mg/k, it reduced the number of larvae of *Ascaris suum* in mice by 81%, and at 100 mg/k, it reduced the number of eggs of gastro-intestinal nematodes of sheep by 76%. The other isothiocyanates listed in Table 1 also showed activity against the helminths tested and some fungistatic and bacteriostatic activity was also shown. None of them, however, was effective in doses low enough to warrant further interest.

Of the thiaazaalkanes, compounds **6**, **7**, **9**, and **16** showed activity against *N. dubius* and against the nematodes of sheep, but at too high dosages to warrant further interest.

Experimental

All melting points are uncorrected. Microanalyses were performed by the Microanalytical Department, Abbott Laboratories, North Chicago, Illinois.

4-Bromobutyl Isothiocyanate

Triethylamine (66 g, 0.66 mol) was added over a period of 2 h to a stirred solution of 4-bromobutylamine hydrobromide (70.0 g, 0.30 mol) and thiophosgene (35.8 g, 0.30 mol) in 500 ml chloroform at 5 °C. The reaction mixture was stirred at 25 °C for 2 h, and was then washed with 4% NaOH (2 × 500 ml), 5% HCl (2 × 500 ml), and water (2 × 500 ml).

The chloroform layer was dried and evaporated, and the residue was fractionated to yield 38.1 g (65%) of a mixture of 4-chlorobutyl isothiocyanate (20%) and 4-bromobutyl isothiocyanate (80%), b.p. 91–94°/0.2 mm. Pure samples of the two products could be obtained by preparative g.l.c. However, the unresolved mixture was adequate for the preparation of the 2-aryliminohexahydro-1,3-thiazepines.

The other isothiocyanates listed in Table 1 were prepared in the same way; with the longer-chain compounds, the presence of the chloro isomer was not detected.

2-Phenyliminohexahydro-1,3-thiazepine (6)

A solution of 4-bromobutyl isothiocyanate (4.81 g) and aniline (1.86 g) in ethanol (20 ml) was refluxed for 30 min. The solution was evaporated and the residue was dissolved in water (30 ml). The aqueous solution was washed with ether and was then neutralized with NaOH, giving the product m.p. 122–125°, yield 3.5 g (85%). Recrystallization from ether raised the melting point to 125–127°.

The other thiazepines listed in Table 2 were prepared in the same way; in most cases, the products were isolated as the hydrobromide salts. The course of the reaction was followed by the disappearance of the characteristic i.r. peak of the isothiocyanate (2150 cm^{-1}).

The thiazocine, thiazonine, thiaazacycloundecane, and thiaazacyclotridecane derivatives (compounds **16–27**) were also prepared in the same way. The reaction times were from 8–12 h for the larger rings; in several cases, some of the starting isothiocyanate remained unreacted.

Can. J. Chem. Downloaded from www.nrcresearchpress.com by 210.87.254.105 on 09/05/12
For personal use only.

Can. J. Chem. Downloaded from www.nrcresearchpress.com by 210.87.254.105 on 09/05/12
For personal use only.

TABLE 2. 2-Arylimino-1,3-thiaazacycloalkanes

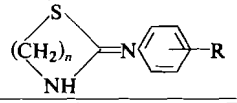

Compound	n	R	Yield (%)	Melting point (°C)	Formula	Analysis					
						C		H		N	
						Calcd.	Found	Calcd.	Found	Calcd.	Found
6	4	H	98	128–130	$C_{11}H_{14}N_2S$	64.04	64.12	6.84	6.63	13.58	13.72
7	4	3-Cl	89	150–151	$C_{11}H_{13}ClN_2S{\cdot}HBr$	41.07	40.94	4.39	4.46	8.71	8.66
8	4	4-Cl	90	194–195	$C_{11}H_{13}ClN_2S{\cdot}HBr$	41.07	41.17	4.39	4.40	8.71	8.51
9	4	3-F	57	152–153	$C_{11}H_{13}FN_2S{\cdot}HBr$	43.28	43.17	4.62	4.73	9.18	9.27
10	4	4-CH_3	63	141–143	$C_{12}H_{16}N_2S$	65.41	65.30	7.32	7.46	12.72	12.85
11	4	4-C_2H_5	78	122–123	$C_{13}H_{18}N_2S$	66.62	66.84	7.74	7.58	11.96	11.81
12	4	4-n-C_4H_9	56	95–97	$C_{15}H_{22}N_2S$	68.65	68.63	8.45	8.65	10.68	10.68
13	4	3-Cl-4-CH_3	48	140–141	$C_{12}H_{15}ClN_2S{\cdot}HBr$	42.93	43.05	4.80	4.98	8.35	8.22
14	4	3,4-$(Cl)_2$	68	179–180	$C_{11}H_{12}Cl_2N_2S$	48.00	47.94	4.40	4.28	10.18	9.79
15	4	2,3,4,5-$(F)_4$	50	194–196	$C_{11}H_{10}F_4N_2S{\cdot}HBr$	36.78	36.49	3.09	3.02	7.80	7.72
16	5	H	75	119–120	$C_{12}H_{16}N_2S{\cdot}HBr$	47.84	48.06	5.69	5.75	9.30	9.29
17	5	2-Cl	96	94–96	$C_{12}H_{15}ClN_2S{\cdot}HBr$	42.93	43.75	4.80	5.19	8.35	8.21
18	5	4-Cl	100	118–119	$C_{13}H_{17}ClN_2S{\cdot}HBr$	42.93	43.03	4.80	5.06	8.35	8.15
19	5	4-F	85	133–136	$C_{12}H_{15}FN_2S{\cdot}HBr$	45.14	44.91	5.05	4.94	8.78	8.62
20	5	4-CH_3	95	129–131	$C_{13}H_{18}N_2S{\cdot}HBr$	49.52	49.60	6.07	6.16	8.89	8.73
21	5	4-C_2H_5	100	157–159	$C_{14}H_{20}N_2S{\cdot}HBr$	51.06	57.06	6.43	6.76	8.51	8.31
22	5	3-Cl-4-CH_3	100	118–119	$C_{13}H_{17}ClN_2S{\cdot}HBr$	44.64	44.94	5.19	5.49	8.01	8.11
23	6	H	86	99–103	$C_{13}H_{18}N_2S{\cdot}HBr$	49.52	49.85	6.07	6.14	8.89	8.77
24	6	4-F	96	94–97	$C_{13}H_{17}FN_2S{\cdot}HBr$	46.85	47.01	5.44	5.54	8.41	8.26
25	6	4-CH_3	88	91–95	$C_{14}H_{20}N_2S{\cdot}HBr$	57.06	57.02	6.43	7.05	8.51	8.30
26	8	4-CH_3	50	93–95	$C_{16}H_{24}N_2S{\cdot}HBr$	53.77	53.58	7.05	7.16	7.84	7.84
27	10	4-CH_3	48	65–68	$C_{18}H_{28}N_2S{\cdot}HBr$	56.09	55.94	7.58	7.63	7.27	7.08

The 11- and 13-membered compounds were obtained as hygroscopic, non-crystalline hydrobromides which, nevertheless, gave good analyses and correct spectral data.

1. O. BEHNER, H. HENECKA, F. HOFFMEISTER, H. KREISKOTT, W. MEISER, H. W. SCHUBERT, and W. WIRTH. U.S. Pat. 3 227 713. January 4, 1966; 3 228 935. January 11, 1966; and 3 235 550. February 15, 1966.
2. M. GARBER and B. MILLER. U.S. Pat. 3 297 708. October 6, 1965.
3. M. TISLER. Tetrahedron Lett. **12**, 12 (1959).
4. P. FRIIS. Acta Chem. Scand. **19**, 766 (1965).
5. L. TOLDY, P. SOHAR, K. FARAGO, I. TOTH, and L. BARTALITS. Tetrahedron Lett. **25**, 2167 (1970).
6. E. CHERBULIEZ, B. BAEHLER, O. ESPEJO, H. JINDRA, B. WILLHALM, and J. RABINOWITZ. Helv. Chim. Acta, **50**, 331 (1967).
7. E. CHERBULIEZ, B. WILLHALM, O. ESPEJO, S. JACCARD, and J. RABINOWITZ. Helv. Chim. Acta, **50**, 1440 (1967).
8. J. RABINOWITZ. Helv. Chim. Acta, **52**, 255 (1969).
9. H. NAJER, R. GIUDICELLI, and S. MENIN. Bull. Soc. Chim. Fr. 2120 (1965).

Can. J. Chem. Downloaded from www.nrcresearchpress.com by 210.87.254.105 on 09/05/12
For personal use only.

Can. J. Chem. Downloaded from www.nrcresearchpress.com by 210.87.254.5 on 09/05/12
For personal use only.

The Mechanism of Oxygenation Reactions Catalyzed by Rhodium(I) Complexes in Solution

B. R. JAMES AND E. OCHIAI
Department of Chemistry, University of British Columbia, Vancouver 8, British Columbia

Received December 17, 1970

The mechanism of oxygenation reactions catalyzed by a rhodium complex which forms a 1:1 molecular oxygen adduct has been elucidated by infrared spectroscopy. Hydrogen abstraction from the substrate by the coordinated oxygen is involved, and the data give the first direct evidence for hydroperoxide intermediates in such reactions of d^8 metal complexes.

On a déterminé, par spectroscopie infrarouge, le mécanisme des réactions d'oxygénation catalysées par des complexes de rhodium pouvant donner des composés d'addition 1:1 avec l'oxygène. Un processus qui intervient, implique l'enlèvement, par de l'oxygène coordonné, d'un hydrogène du substrat; les résultats obtenus fournissent la première preuve directe que des hydroperoxydes se forment au cours de réactions de complexes métalliques d^8.

Canadian Journal of Chemistry, 49, 975 (1971)

Considerable interest has been aroused in the mechanism of oxidation catalyzed by molecular oxygen complexes since the discovery of Vaska's oxygen complex (1). Mechanisms involving oxygen–oxygen bond splitting and subsequent transfer to accepting ligand (2, 3) or free radical intermediates (4) have been proposed for square planar d^8 metal systems. A report by Stern (5) on the autoxidation of cumene catalyzed by palladium(0) phosphine complexes and other platinum metal complexes suggested that a free radical reaction might be initiated by hydrogen abstraction by the molecular oxygen complex with formation of a hydroperoxide complex. We have obtained direct evidence for a hydroperoxide intermediate in such oxidations involving a rhodium(I) cyclooctene complex.

Previous work from this laboratory (6) reported on the formation of a 1:1 molecular oxygen complex for $[RhCl(C_8H_{14})_2]_2$ in *N*,*N*-dimethylacetamide (DMA) containing lithium chloride (one O_2 per Rh atom) and its catalytic activity for oxidation of the solvent at 80°. We now find that this complex when dissolved in benzene, toluene, dichloromethane, or 1,2-dichloroethane rapidly absorbs oxygen to the same 1:1 mole ratio at 35°; a further uptake occurs very slowly for the toluene system. A brown precipitate, which forms at the completion of the rapid uptake, shows bands at 1690 and 1550 cm^{-1}, attributed to carbonyl and coordinated water,

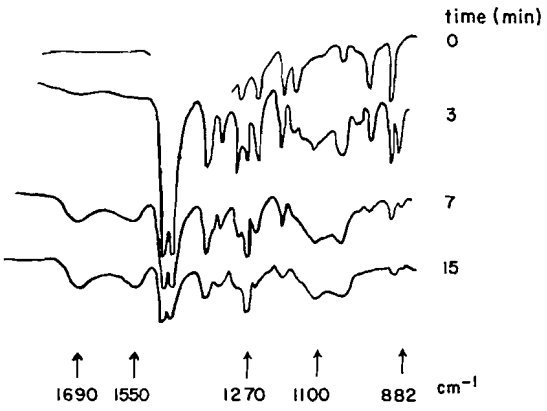

FIG. 1. Reaction of rhodium complex with oxygen in 1,2-dichloroethane as followed by infrared spectroscopy.

respectively, and around 3400 cm^{-1}, attributed to hydroxide. Oxidation of the cyclooctene seemed likely and some cyclooctenone was detected in the filtrate.

The reaction of the complex itself with oxygen in 1,2-dichloroethane was followed at room temperature (23°) using infrared spectroscopy by sampling onto a sodium chloride plate followed by rapid evaporation (see Fig. 1). A solution prepared under vacuum was exposed to air. At *ca.* 3 min, there appear the broad band centered at 3400 cm^{-1} and small peaks at 1270, 1100, and 882 cm^{-1}; at *ca.* 7 min, the peaks at 3400, 1270, and 1100 cm^{-1} intensify while the peak at 882 cm^{-1}

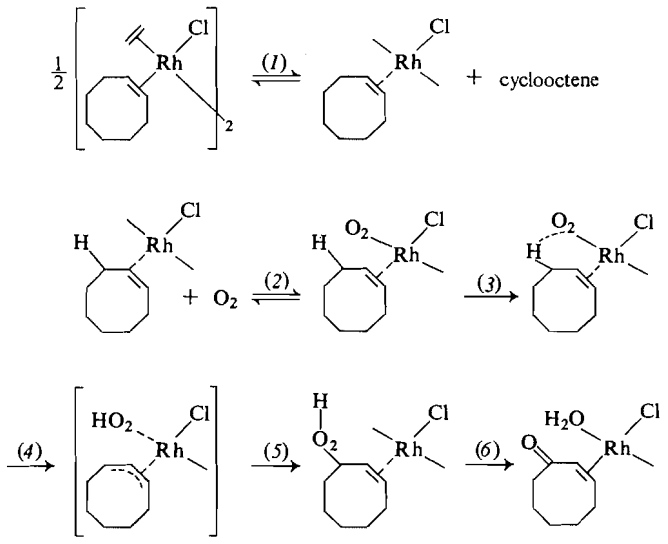

SCHEME 1

diminishes and weak peaks show up at 1690 and 1550 cm^{-1}; at *ca.* 15 min the same overall trend continues while the brown solid starts to precipitate. On assignment of the peaks: ν_{OH} at 3400 cm^{-1}, δ_{OH} (of hydroperoxide) at 1270 cm^{-1} (7), coordinated water at 1550 cm^{-1}, $\nu_{C=O}$ at 1690 cm^{-1}, ν_{C-O} at 1100 cm^{-1}, and ν_{O-O} at 882 cm^{-1} (coordinated), the observations could fit the reaction scheme shown, although it should be emphasized that neither the hydroperoxide moiety nor the cyclooctene substrate need remain coordinated to the rhodium (designated by broken lines to the rhodium atom). Indeed, cumene is also readily oxidized by this system with no induction period at 50 cm oxygen and 35° suggesting that coordination of the substrate is not essential for these oxidation processes. All that is necessary is hydrogen abstraction from the substrate by the coordinated oxygen (*cf.* step 4).

The mechanism shown readily explains the formation of cyclohexen-3-one from the catalyzed oxidation of cyclohexene with $RhCl(PPh_3)_3$ (8).

In the presence of a large excess of cyclooctene, no oxygen uptake is observed due to repression of the initial dissociation, which could involve loss of one or two cyclooctene ligands. The brown solid obtained from the cyclooctene system has not yet been obtained in a pure state and has not been identified but elemental analysis shows that it contains one coordinated C_8 unit per rhodium.

The formation of the allylic hydroperoxide intermediate suggested here is characteristic of the photochemical reaction by singlet oxygen ($^1\Delta_g$) (9). However, cyclohexadiene and anthracene, which are known to be good acceptors of singlet oxygen, are not oxidized by this catalyst system, and it is not clear at this stage how far the analogy between coordinated oxygen and singlet oxygen (10) in these systems can be drawn.

We thank the National Research Council of Canada for support of this research and Johnson Matthey Ltd. for loan of the rhodium.

1. L. VASKA. Sci. **140**, 809 (1963).
2. J. P. COLLMAN. Accounts Chem. Res. **1**, 136 (1968).
3. For example; B. W. GRAHAM, K. R. LAING, C. O'CONNOR, and W. R. ROPER. Chem. Commun. 1272 (1970).
4. For example; L. W. FINE, M. GRAYSON, and V. H. LUGGS. J. Organometal. Chem. **22**, 219 (1970).
5. E. STERN. Chem. Commun. 736 (1970).
6. B. R. JAMES and F. T. T. NG. Chem. Commun. **908** (1970).
7. J. A. CONNOR and E. A. V. EBSWORTH. Advan. Inorg. Radiochem. **6**, 279 (1964); H. L. ROBERTS and W. R. SYMES. J. Chem. Soc. A, 1450 (1968).
8. J. P. COLLMAN, M. KUBOTA, and J. W. HOSKING. J. Amer. Chem. Soc. **89**, 4809 (1967).
9. K. GOLLNICK. Advan. Photochem. **6**, 1 (1968); C. S. FOOTE. Accounts Chem. Res. **1**, 104 (1968).
10. R. MASON. Nature, **217**, 543 (1168).

Can. J. Chem. Downloaded from www.nrcresearchpress.com by 210.87.254.5 on 09/05/12
For personal use only.

Potential Energy- Sheets for the $n\pi^*$ and $\pi\pi^*$ Triplet States of Acrolein

Dedicated to Professor Paul de Mayo

A. DEVAQUET[1] AND L. SALEM

Laboratoire de Chimie Théorique,[2] Faculté des Sciences 91-Orsay, France

Received November 13, 1970

The energy of the $n\pi^*$ and $\pi\pi^*$ triplet states of acrolein as a function of the twist of the CH_2 terminal groups and relaxation of the three skeletal σ bonds has been investigated in an "*ab initio*" self-consistent field formalism. The potential energy sheets of these triplets show that the *cis* photoadducts of cyclic enones may arise from "planar, relaxed" triplet states whereas the *trans* photoadducts are given by "twisted, unrelaxed" triplet states.

Utilisant un formalisme SCF "ab initio" on étudie les niveaux énergétiques des états triplets $n\pi^*$ et $\pi\pi^*$ de l'acroleine en fonction de l'angle de torsion des groupes CH_2 terminaux et des temps de relaxation des trois liens σ de la chaîne. D'après les potentiels d'énergie de ces triplets, la formation de produits *cis* de photoaddition de cétones cycliques insaturées proviendrait d'états triplets "plan et relaxed" alors que les produits *trans* seraient obtenus à partir d'état triplets "tordus et unrelaxed".

Canadian Journal of Chemistry, 49, 977 (1971)

Can. J. Chem. Downloaded from www.nrcresearchpress.com by 210.87.254.105 on 09/05/12
For personal use only.

The photochemical reactions of 2-cyclohexenone are characterized by the occurrence of marked orientational specificity. The photocycloaddition reaction sometimes leads to products in which the six- and four-membered rings are fused *trans* as well as to the thermodynamically more stable *cis* fused adducts (1). The problem of identifying the excited state(s) of the enone responsible for such photoadditions is a matter of fundamental importance. There is, however, every reason to believe that most photocycloaddition reactions of simple enones are brought about by a triplet state (2).

In the present communication the potential energy surfaces of the $n\pi^*$ and $\pi\pi^*$ triplet states of s-*trans* acrolein are briefly described. This conformation which is 4.96 kcal/mol more stable than the s-*cis* conformation (the barrier of internal rotation around the single bond being 7.02 kcal/mol (3)) may be considered as a model for the enone systems. The geometries of these two triplet states have been investigated by the open-shell s.c.f. method of Nesbet (4) using a program developed by Stevens (5). Two internal motions have been considered: the twist of the CH_2 terminal group (θ_1) and the relaxation of the three skeletal σ bonds ($R_1R_2R_3$) (Fig. 1). These motions cause severe orbital changes.

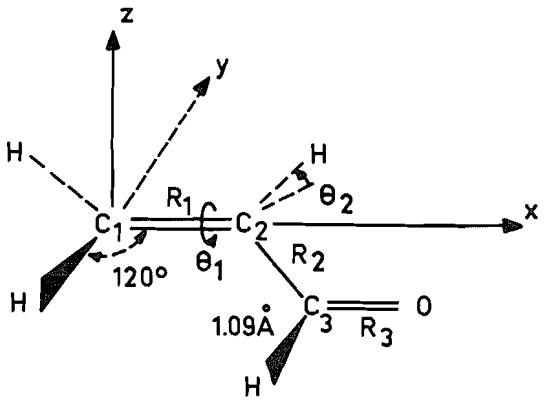

FIG. 1. Skeletal structure of acrolein.

In the 90° twisted acrolein, the $n\sigma$-type molecular orbital (m.o.) is a nearly pure $2p_y$ atomic orbital on the oxygen atom with little bonding character. There are also two non-bonding m.o.'s. The first one, namely y, is a nearly pure $2p_y$ atomic orbital on the C_1 carbon atom whereas the second one, which is the third π m.o., namely π_3, is of allylic type with a nodal plane passing near the C_3 carbon atom (Fig. 2).

Table 1 gives the various sets of values of the CC bond relaxations for which the total energy was calculated as a function of varying angle of twist θ_1. Figure 3 shows the resulting potential energy sheets for the two triplet states of acrolein (5). These sheets intersect along some curve passing points A and B. The true surfaces, of course, do not intersect even though they come

[1]Present address: Department of Chemistry, Cornell University, Ithaca, N.Y. 14850, U.S.A.

[2]The Laboratoire de Chimie Théorique is also part of the Laboratoire Associé de Physico-Chimie des Rayonnements supported by the CNRS.

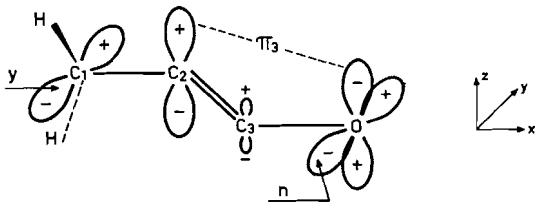

FIG. 2. "Frontier" orbitals in the 90° twisted acrolein.

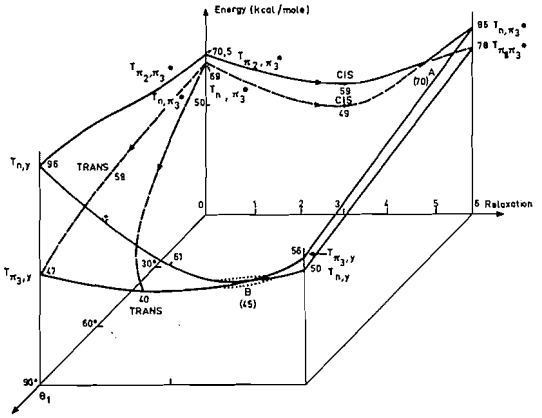

FIG. 3. Potential energy sheets of the two triplet states of acrolein (the origin of the vertical axis is the energy of the acrolein molecule in its ground state, geometry number zero of Table 1).

TABLE 1. Selected sets of bond lengths for R_1, R_2, and R_3

Geometry*	R_1(Å)	R_2(Å)	R_3(Å)
0	1.36	1.46	1.22
1	1.37	1.42	1.25
2	1.42	1.39	1.29
3	1.45	1.35	1.32
4	1.48	1.32	1.34
5	1.51	1.30	1.36
6	1.54	1.28	1.38

*These refer to positions on the "Relaxation" axis of Fig. 3.

very close: configuration interaction ultimately splits the states along the AB line as shown in the figure. Hence, whereas for instance the unrelaxed triplet π_2,π_3^* belongs to the *upper* sheet, the relaxed triplet belongs to the *lower* sheet.

A careful examination of these surfaces shows that it is not possible to distinguish any more between $n\pi^*$ and $\pi\pi^*$ states, only between highest and lowest triplet states. The "orbital" nature of these triplets is given by the detailed exploration of the sheet. For example, the highest relaxed and twisted triplet $T_{\pi_3,y}$, with energy 56 kcal/mol, has two paired electrons in the n oxygen orbital and one in each of the y and π_3 molecular orbitals. Because of the weak splitting throughout nearly the entire surface, the ordering of the potential energy sheets may be easily reversed by substitution with different electron donating or attracting groups, by use of different solvents, or by strain in cyclic compounds.

From a photochemical point of view these calculations lead to some hypotheses which may be useful in understanding the *cis* and *trans* cycloadditions of cyclic enones.

(*1*) the *cis* adduct may be found in either of the planar relaxed $n\pi^*$ and $\pi\pi^*$ triplet states with energies of 49 and 59 kcal/mol above the equilibrium ground state. These relaxed states need not twist immediately to decay respectively to the 90° twisted relaxed $T_{\pi_3,y}$ state (40 kcal/mol) and to point B (45 kcal/mol) because there appears to be small barriers for this motion. In the $n\pi^*$ state of acrolein there exists a 3 kcal/mol barrier to rotation about the double bond that can be explained in terms of a configuration interaction between the two triplets whereas the small rotational barrier in the $\pi\pi^*$ state should be increased in cyclic enones due to the strain energy associated with a twisted geometry. Therefore the molecule may remain in the relaxed (untwisted) triplet states for enough time to react.

(*2*) The *trans* adducts may arise from the 90° twisted and relaxed $T_{\pi_3,y}$ triplet state, whose energy is 40 kcal/mol. However, this state is nearly degenerate with the ground state at that particular nuclear configuration[3] and therefore intersystem crossing to this ground state should be very rapid.

(*3*) Alternatively the *trans* adduct may be formed near the 45° twisted but unrelaxed triplet state (58 kcal/mol). Indeed, an out-of-plane motion (θ_2) of the hydrogen atom adjacent to C_2 (Fig. 1) for this configuration provides an additional stabilization of 5 kcal/mol ($\theta_2 = -45°$ (5)). The C_1 and C_2 p orbital axes of the resulting triplet state are nearly perpendicular, and this should facilitate *trans* addition. Again in the cyclic case the strain energy arising from a twisted geometry can contribute to a "secondary minimum" in this region.

[3]Details will be published elsewhere.

Can. J. Chem. Downloaded from www.nrcresearchpress.com by 210.87.254.105 on 09/05/12
For personal use only.

All these possibilities are obviously strongly dependent on the ordering of the initial $n\pi^*$ and $\pi\pi^*$ triplet states and on their energetic separation in the specific cyclic enone.

The authors are grateful to the French National Research Center (CNRS) for generous access to its computing facilities.

1. E. J. COREY, J. D. BASS, R. LE MAHIEU, and R. B. MITRA. J. Amer. Chem. Soc. **86**, 5570 (1964).
2. P. E. EATON. Acc. Chem. Res. **1**, 50 (1968); O. L. CHAPMAN, T. H. KOCH, F. KLEIN, P. J. NELSON, and E. L. BROWN. J. Amer. Chem. Soc. **90**, 1657 (1968); P. DE MAYO, A. A. NICHOLSON, and M. F. TCHIR. Can. J. Chem. **48**, 225 (1970); J. L. RUHLER and P. A. LEERMAKERS. J. Amer. Chem. Soc. **89**, 4944 (1967).
3. M. S. DE GROOT and J. LAMB. Proc. Roy. Soc. London, Ser. A. **242**, 36 (1957).
4. R. K. NESBET. Rev. Mod. Phys. **33**, 28 (1961); **35**, 582 (1963).
5. R. M. STEVENS. J. Chem. Phys. **52**, 1397 (1970).

The Gas-Phase Acidity Order of Some Inorganic Acids

L. BREWSTER YOUNG
Mobil Chemical Company, Edison, New Jersey 08817

AND

E. LEE-RUFF AND D. K. BOHME[1]
Department of Chemistry, York University, Toronto, Ontario

Received December 29, 1970

The gas-phase acidity order at 300 °K of the inorganic acids, water, ammonia, and hydrogen has been directly determined using the flowing afterglow technique. The order established is $H_2O > H_2 > NH_3$, water being the strongest acid in this series. This result is inconsistent with recent calculations, current available thermochemical data, and the order found in solution.

Utilisant une technique continue de luminescence retardée, on détermine directement l'ordre de l'acidité en phase gazeuse à 300 °K d'acides inorganiques, de l'eau, de l'ammoniac et de l'hydrogène. On trouve que l'eau est le produit le plus acide et que l'ordre décroissant est $H_2O > H_2 > NH_3$. Ce résultat n'est pas consistant avec les calculs théoriques récents, les données thermodynamiques disponibles actuellement et l'ordre trouvée en solution.

Canadian Journal of Chemistry, 49, 979 (1971)

As part of a program directed towards the determination of relative acidities of organic acids in the gas phase, experiments were recently performed to determine the gas-phase acidities of some simple inorganic acids. The flowing afterglow technique was employed to investigate the kinetics at 300 °K of proton transfer reactions of the type

$$[1] \qquad X^- + YH \rightleftharpoons Y^- + XH$$

The determination of the preferred direction of proton transfer at thermal energies identifies the sign of the free energy change of reaction 1 which, in turn, provides a measure of the relative gas-phase acidity of the acids YH and XH. Such information is valuable in formulating intrinsic reactivity functions, which should have an important bearing on reactivity functions measured in solution. Proton transfer reactions proceeding in the gas phase represent a limiting behavior that can be employed as a standard against which the performance of proton transfer reactions proceeding in the condensed phase may be related.

The experiments were performed in one of the flowing afterglow systems of the Environmental Science Services Administration Research Laboratories in Boulder, Colorado. Details of the method of operation and data analysis have been thoroughly described elsewhere (1, 2). Helium was again used as the buffer gas. The helium pressure in the tube was typically *ca.* 0.4 Torr. The NH_2^- and H^- ions were generated by 100

[1]Author to whom correspondence should be addressed.

Can. J. Chem. Downloaded from www.nrcresearchpress.com by 210.87.254.105 on 09/05/12
For personal use only.

All these possibilities are obviously strongly dependent on the ordering of the initial $n\pi^*$ and $\pi\pi^*$ triplet states and on their energetic separation in the specific cyclic enone.

The authors are grateful to the French National Research Center (CNRS) for generous access to its computing facilities.

1. E. J. COREY, J. D. BASS, R. LE MAHIEU, and R. B. MITRA. J. Amer. Chem. Soc. **86**, 5570 (1964).
2. P. E. EATON. Acc. Chem. Res. **1**, 50 (1968); O. L. CHAPMAN, T. H. KOCH, F. KLEIN, P. J. NELSON, and E. L. BROWN. J. Amer. Chem. Soc. **90**, 1657 (1968); P. DE MAYO, A. A. NICHOLSON, and M. F. TCHIR. Can. J. Chem. **48**, 225 (1970); J. L. RUHLER and P. A. LEERMAKERS. J. Amer. Chem. Soc. **89**, 4944 (1967).
3. M. S. DE GROOT and J. LAMB. Proc. Roy. Soc. London, Ser. A. **242**, 36 (1957).
4. R. K. NESBET. Rev. Mod. Phys. **33**, 28 (1961); **35**, 582 (1963).
5. R. M. STEVENS. J. Chem. Phys. **52**, 1397 (1970).

Can. J. Chem. Downloaded from www.nrcresearchpress.com by 210.87.254.42 on 09/05/12
For personal use only.

The Gas-Phase Acidity Order of Some Inorganic Acids

L. BREWSTER YOUNG
Mobil Chemical Company, Edison, New Jersey 08817

AND

E. LEE-RUFF AND D. K. BOHME[1]
Department of Chemistry, York University, Toronto, Ontario

Received December 29, 1970

The gas-phase acidity order at 300 °K of the inorganic acids, water, ammonia, and hydrogen has been directly determined using the flowing afterglow technique. The order established is $H_2O > H_2 > NH_3$, water being the strongest acid in this series. This result is inconsistent with recent calculations, current available thermochemical data, and the order found in solution.

Utilisant une technique continue de luminescence retardée, on détermine directement l'ordre de l'acidité en phase gazeuse à 300 °K d'acides inorganiques, de l'eau, de l'ammoniac et de l'hydrogène. On trouve que l'eau est le produit le plus acide et que l'ordre décroissant est $H_2O > H_2 > NH_3$. Ce résultat n'est pas consistant avec les calculs théoriques récents, les données thermodynamiques disponibles actuellement et l'ordre trouvée en solution.

Canadian Journal of Chemistry, 49, 979 (1971)

As part of a program directed towards the determination of relative acidities of organic acids in the gas phase, experiments were recently performed to determine the gas-phase acidities of some simple inorganic acids. The flowing afterglow technique was employed to investigate the kinetics at 300 °K of proton transfer reactions of the type

$$[1] \qquad X^- + YH \rightleftharpoons Y^- + XH$$

The determination of the preferred direction of proton transfer at thermal energies identifies the sign of the free energy change of reaction 1 which, in turn, provides a measure of the relative gas-phase acidity of the acids YH and XH. Such information is valuable in formulating intrinsic reactivity functions, which should have an important bearing on reactivity functions measured in solution. Proton transfer reactions proceeding in the gas phase represent a limiting behavior that can be employed as a standard against which the performance of proton transfer reactions proceeding in the condensed phase may be related.

The experiments were performed in one of the flowing afterglow systems of the Environmental Science Services Administration Research Laboratories in Boulder, Colorado. Details of the method of operation and data analysis have been thoroughly described elsewhere (1, 2). Helium was again used as the buffer gas. The helium pressure in the tube was typically *ca.* 0.4 Torr. The NH_2^- and H^- ions were generated by 100

[1]Author to whom correspondence should be addressed.

TABLE 1. Summary of acid–base reactions investigated in the gas phase at 300 °K

Acid–base reaction	k_f*	k_r*	K	$-\Delta G_{300}^{\circ}$ (kcal mol^{-1})
$H^- + H_2O \rightleftharpoons OH^- + H_2$	$\gtrsim 5(-11)$	$< 5(-12)$	> 10	> 1.4
$NH_2^- + H_2O \rightleftharpoons OH^- + NH_3$	$\gtrsim 5(-11)$	$< 5(-12)$	> 10	> 1.4
$NH_2^- + H_2 \rightleftharpoons H^- + NH_3$	$\geqslant 3.7(-11)$	$\sim 4(-12)$	$\gtrsim 10$	$\gtrsim 1.4$

*Units in cm^3 molecule^{-1} s^{-1}, (-11) denotes 10^{-11}.

and 25 eV electron impact on NH_3, respectively. The production of OH^- has been described previously (2). The reactant, H_2O, concentration could not be measured by metering it into the flow tube through calibrated flow elements, which is our conventional technique for measuring neutral concentration. The H_2O concentration was therefore measured by monitoring the increase in the total pressure in the reaction region as the vapor was bled into it. This method of measuring H_2O concentration is, however, both insensitive (the smallest partial pressure measurable with capacitance manometer with a 10 Torr sensing head was at best 0.1 microns) and inaccurate. Consequently, the rate constants for the fast reactions involving H_2O are necessarily limits and are considered reliable only to within a factor of 2.

A summary of the kinetic data obtained for this series of experiments is given in Table 1. The measured equilibrium constant, which was taken to be equal to the ratio of the forward and reverse reaction rate constants, will be equal to the thermodynamic equilibrium constant only if the energy distributions of the respective reactants of the forward and backward proton transfer reactions investigated follow Boltzmann energy distributions. We expect that this is the case in this series of experiments since the ionic species are allowed to undergo many thousand collisions with helium atoms before entering the reaction region where the neutral reactant species are added in thermodynamic equilibrium at room temperature. Thus the data shown in Table 1 clearly indicate the gas-phase acidity order $H_2O > H_2 > NH_3$, water being the strongest acid in this series. Whereas the observation that water is a stronger acid than ammonia in the gas phase has already been reported (3, 4), the position of hydrogen in this sequence has not, to our knowledge, been previously determined.

The gas-phase acidity order determined in this series of experiments is inconsistent with the recent theoretical studies of Ritchie and King who, on the basis of their computations of the potential energy surfaces of proton transfer reactions, predicted both NH_3 and H_2O to be stronger acids than H_2 (5, 6). The position of H_2 in our acidity scale is also inconsistent with the thermochemical data presently available. The value of 4.38 eV for $D(NH_2—H)$ (7) and 1.21 eV for the electron affinity of NH_2 (8) are probably least reliable and may be low or high, respectively, by as much as 0.5 eV.[2] Finally, the solution acidity order of this series is $H_2O > NH_3 > H_2$ since metal hydrides undergo facile proton transfer reactions with both water and ammonia to liberate hydrogen in solution (9, 10). Although the exchange reaction between amide and D_2 proceeds quite readily in solution, it has been found that the hydride ion is not involved in this exchange process. The reversal of the acidity order of NH_3 and H_2 in the gas phase suggests that solvation effects favor the right-hand side of the equilibrium

$$[2] \qquad NH_3 + H^- \rightleftharpoons NH_2^- + H_2$$

Similar acidity order reversals have been shown in the gas phase for alcohols and substituted amines (3, 11).

1. E. E. FERGUSON, F. C. FEHSENFELD, and A. L. SCHMELTEKOPF. Advances in Atomic and Molecular Physics. Vol. 5. Academic Press, Inc., New York. 1969.
2. D. K. BOHME and L. B. YOUNG. J. Amer. Chem. Soc. **92**, 3301 (1970).
3. J. I. BRAUMAN and L. K. BLAIR. J. Amer. Chem. Soc. **91**, 2126 (1969).
4. D. K. BOHME and F. C. FEHSENFELD. Can. J. Chem. **47**, 2715 (1969).
5. C. D. RITCHIE and H. F. KING. J. Amer. Chem. Soc. **90**, 833 (1968).
6. C. D. RITCHIE and H. F. KING. J. Amer. Chem. Soc. **90**, 838 (1968).

[2]Indeed, in the course of this work the authors have become aware of a very recent redetermination of $D(NH_2—H)$ by S. W. Benson, who suggests a value of 4.73 ± 0.04 eV, which is considerably higher than the older value.

Can. J. Chem. Downloaded from www.nrcresearchpress.com by 210.87.254.42 on 09/05/12
For personal use only.

7. G. HERZBERG. Molecular Spectra and Molecular-Structure. Vol. III. Electronic Spectra and Electronic Structure of Polyatomic Molecules. D. Van Nostrand Co., Inc., New York, N.Y. 1966.
8. F. M. PAGE and G. C. GOODE. Negative Ions and the Magnetron. Wiley-Interscience, New York, N.Y. 1969.
9. A. E. FINHOLT, C. HELLING, L. NIELSON, V. INHOF, and E. JACOBSON. Inorg. Chem. **2**, 504 (1963).
10. G. B. SMITH, D. J. MCDANIEL, E. BIEHL, and C. A. HOLLINGSWORTH. J. Amer. Chem. Soc. **82**, 3560 (1960).
11. J. I. BRAUMAN and L. K. BLAIR. J. Amer. Chem. Soc. **90**, 6561 (1968).

Can. J. Chem. Downloaded from www.nrcresearchpress.com by 210.87.254.42 on 09/05/12
For personal use only.

Utility of Shift Reagents in Nuclear Magnetic Resonance Studies of Polyfunctional Compounds: *N*- and *O*-Acetylated Carbohydrates and Nucleosides

R. F. BUTTERWORTH[1], A. G. PERNET[2], AND S. HANESSIAN[3]
Department of Chemistry, University of Montreal, Montreal, Quebec

Received December 30, 1970

The utility of n.m.r. shift reagents, $Eu(DPM)_3$ and $Pr(DPM)_3$, can be extended to polyfunctional molecules containing acetate and amide groups with significant spectral simplification and definitive peak assignments based on "signal crossover" phenomena.

On démontre que l'utilité des réactifs $Eu(DPM)_3$ et $Pr(DPM)_3$ qui induisent des déplacements en r.m.n. peut être étendue aux molécules polyfonctionnelles contenant des groupes acétate et amides; il en résulte que les spectres sont simplifiés d'une façon remarquable et que des attributions définitives de pics peuvent être faites.

Canadian Journal of Chemistry, 49, 981 (1971)

Recent work has demonstrated the ability of europium (1, 2) and praseodymium (3) chelates of dipivaloylmethane to produce remarkable shifts in the ^1H n.m.r. spectra of monofunctional compounds possessing simple and relatively complex structures (4). We report herein the effects of shift reagents on the n.m.r. spectra (at 100 and 60 MHz) of various classes of *polyfunctional* compounds, in which, *a priori*, multiple sites of complexation would be anticipated. We demonstrate the application of $Eu(DPM)_3$ and $Pr(DPM)_3$ chelates in the assignment of *O*-acetyl and *N*-acetyl resonance signals in polyacetylated carbohydrates as well as in the spectral simplification of various polyfunctional derivatives, including *nucleosides*.

Model studies[4] on the mechanism and preferential sites of complexation of Eu chelates with polyfunctional molecules were performed on methyl 2,3-*O*-isopropylidene-β-D-ribofuranoside (6), the corresponding 5-*O*-acetate, and 5-deoxy (7) analogs. The induced shifts decreased as expected in the order $\Delta Eu{:}OH > H_{5,5'} > H_4$, $H_3 > H_1$ in accordance with the generalization that protons remote from the site of complexation suffer smaller induced shifts than those of closer proximity (8). The 5-*O*-acetate and 5-deoxy analogs were found to complex to the extent of approximately 40–50% and 10–20% respectively, compared to the parent compound. Upfield shifts of approximately the same relative magnitudes were observed using $Pr(DPM)_3$ in CCl_4.

The significant interaction with the 5-*O*-acetate derivative cited above, prompted us to study substrates containing more than one acetyl group. In the case of α- and β-D-glucose pentaacetates, in which the relative chemical shifts of the respective acetyl signals are known by inference with other model compounds (9, 10) and in the case of β-D-galactose pentaacetate, the signal of the *primary* acetoxy group was in each case, shifted substantially more than secondary acetoxy signals. Incremental additions of $Eu(DPM)_3$ in minute portions to a solution of α-D-glucose pentaacetate

[1]Postdoctoral fellow, 1969–1971.
[2]France–Quebec predoctoral fellow, 1969–1970.
[3]To whom correspondence should be addressed.
[4]Our initial studies with diacetone glucose revealed that at a defined concentration of $Eu(DPM)_3$ the order of chemical shifts increasing to higher field were $H_5 > H_3 > H_1 > H_4 > H_2 > H_{6,6'}$. Similar results have been reported on this compound while this work was in progress (5). We also note that the presence of two hydroxyl groups in a molecule as in 5-deoxy-1,2-*O*-isopropylidene-D-*xylo*-hexofuranose causes increased broadening of bands and presents some limitation on the method.

7. G. HERZBERG. Molecular Spectra and Molecular-Structure. Vol. III. Electronic Spectra and Electronic Structure of Polyatomic Molecules. D. Van Nostrand Co., Inc., New York, N.Y. 1966.
8. F. M. PAGE and G. C. GOODE. Negative Ions and the Magnetron. Wiley-Interscience, New York, N.Y. 1969.
9. A. E. FINHOLT, C. HELLING, L. NIELSON, V. INHOF, and E. JACOBSON. Inorg. Chem. **2**, 504 (1963).
10. G. B. SMITH, D. J. MCDANIEL, E. BIEHL, and C. A. HOLLINGSWORTH. J. Amer. Chem. Soc. **82**, 3560 (1960).
11. J. I. BRAUMAN and L. K. BLAIR. J. Amer. Chem. Soc. **90**, 6561 (1968).

Utility of Shift Reagents in Nuclear Magnetic Resonance Studies of Polyfunctional Compounds: *N*- and *O*-Acetylated Carbohydrates and Nucleosides

R. F. BUTTERWORTH[1], A. G. PERNET[2], AND S. HANESSIAN[3]
Department of Chemistry, University of Montreal, Montreal, Quebec

Received December 30, 1970

The utility of n.m.r. shift reagents, $Eu(DPM)_3$ and $Pr(DPM)_3$, can be extended to polyfunctional molecules containing acetate and amide groups with significant spectral simplification and definitive peak assignments based on "signal crossover" phenomena.

On démontre que l'utilité des réactifs $Eu(DPM)_3$ et $Pr(DPM)_3$ qui induisent des déplacements en r.m.n. peut être étendue aux molécules polyfonctionnelles contenant des groupes acétate et amides; il en résulte que les spectres sont simplifiés d'une façon remarquable et que des attributions définitives de pics peuvent être faites.

Canadian Journal of Chemistry, 49, 981 (1971)

Recent work has demonstrated the ability of europium (1, 2) and praseodymium (3) chelates of dipivaloylmethane to produce remarkable shifts in the ^1H n.m.r. spectra of monofunctional compounds possessing simple and relatively complex structures (4). We report herein the effects of shift reagents on the n.m.r. spectra (at 100 and 60 MHz) of various classes of *polyfunctional* compounds, in which, *a priori*, multiple sites of complexation would be anticipated. We demonstrate the application of $Eu(DPM)_3$ and $Pr(DPM)_3$ chelates in the assignment of *O*-acetyl and *N*-acetyl resonance signals in polyacetylated carbohydrates as well as in the spectral simplification of various polyfunctional derivatives, including *nucleosides*.

Model studies[4] on the mechanism and preferential sites of complexation of Eu chelates with polyfunctional molecules were performed on methyl 2,3-*O*-isopropylidene-β-D-ribofuranoside (6), the corresponding 5-*O*-acetate, and 5-deoxy (7) analogs. The induced shifts decreased as expected in the order $\Delta Eu{:}OH > H_{5,5'} > H_4$, $H_3 > H_1$ in accordance with the generalization that protons remote from the site of complexation suffer smaller induced shifts than those of closer proximity (8). The 5-*O*-acetate and 5-deoxy analogs were found to complex to the extent of approximately 40–50% and 10–20% respectively, compared to the parent compound. Upfield shifts of approximately the same relative magnitudes were observed using $Pr(DPM)_3$ in CCl_4.

The significant interaction with the 5-*O*-acetate derivative cited above, prompted us to study substrates containing more than one acetyl group. In the case of α- and β-D-glucose pentaacetates, in which the relative chemical shifts of the respective acetyl signals are known by inference with other model compounds (9, 10) and in the case of β-D-galactose pentaacetate, the signal of the *primary* acetoxy group was in each case, shifted substantially more than secondary acetoxy signals. Incremental additions of $Eu(DPM)_3$ in minute portions to a solution of α-D-glucose pentaacetate

[1]Postdoctoral fellow, 1969–1971.
[2]France–Quebec predoctoral fellow, 1969–1970.
[3]To whom correspondence should be addressed.
[4]Our initial studies with diacetone glucose revealed that at a defined concentration of $Eu(DPM)_3$ the order of chemical shifts increasing to higher field were $H_5 > H_3 > H_1 > H_4 > H_2 > H_{6,6'}$. Similar results have been reported on this compound while this work was in progress (5). We also note that the presence of two hydroxyl groups in a molecule as in 5-deoxy-1,2-*O*-isopropylidene-D-*xylo*-hexofuranose causes increased broadening of bands and presents some limitation on the method.

Can. J. Chem. Downloaded from www.nrcresearchpress.com by 84.22.46.98 on 09/08/12
For personal use only.

Can. J. Chem. Downloaded from www.nrcresearchpress.com by 84.22.46.98 on 09/08/12
For personal use only.

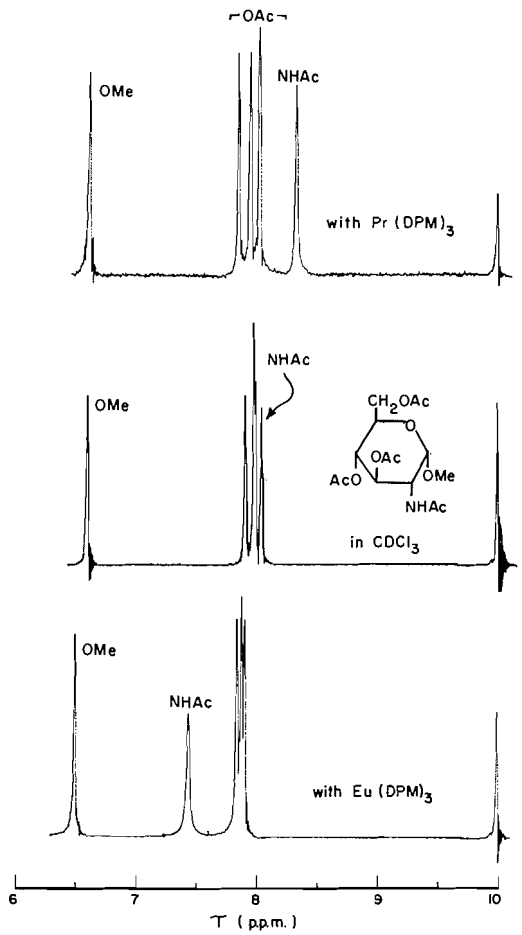

FIG. 1. The n.m.r. spectra (60 MHz) of methyl 2-acetamido-3,4,6-tri-*O*-acetyl-2-deoxy-α-D-glucopyranoside in $CDCl_3$ solution (0.065 g in 0.6 ml). Normal spectrum (middle); after addition of 15 mg of $Pr(DPM)_3$ (upper); after addition of 15 mg of $Eu(DPM)_3$ (lower).

in $CDCl_3$ causes the net expansion of the acetyl signals region and the observation of a "signal crossover" phenomenon; that is the gradual shift of the signal due to the most affected acetyl group (at C-6) passing through a coalescence point (with the C-1 OAc signal) and emerging on the low field portion of the spectrum. Such increment-induced shifts provide a useful technique[5] to eventually assign all acetyl resonances in acetylated carbohydrates, based on their relative dispositions and their respective interaction with the shift reagents. We also point out that, in such derivatives, ΔEu is largest for the $H_{6,6'}$ protons compared to other ring protons which is a confirmatory tool for the identity of the corresponding shifting acetyl group.

Complexation of amide functions seems to be favored over esters by a factor of 4-5, as evidenced by our studies with α- and β-D-glucosamine pentaacetate and related compounds. In all cases, the *N*-acetyl resonance suffers a very large paramagnetic induced shift which is also reflected in the proportional shift of the NH doublet to lower field. The assignment of *N*-acetyl signals in the presence of acetoxy groups in carbohydrates has been resolved only recently by specific *N*- and *O*-deuterioacetylation and solvent-induced shift techniques (9, 11, 12). As can be clearly seen in Fig. 1 the characteristic downfield and upfield shifts of the *N*-acetyl signal can serve as a diagnostic tool in such assignments, utilizing $Eu(DPM)_3$ and $Pr(DPM)_3$ respectively. This preferential complexation with amide groups and their shift patterns was observed with other derivatives containing axial and equatorial amide and acetoxy functions.

Finally, application of the utility of $Eu(DPM)_3$ in the spectral simplification of certain nucleosides is demonstrated using *N*-acetyl cytidine triacetate and adenosine triacetate. Figure 2 shows the partial n.m.r. spectra of the former nucleoside derivative, in which the unresolved multiplet corresponding to the C-2′ and -3′ protons (lower spectrum) is clearly resolved into two triplets, $J_{2',3'} = 5$ Hz[6] (upper spectrum). The relatively large shift observed for the anomeric proton is reflective of the site of complexation and could aid in the assignment of anomeric configuration in such nucleosides, which is otherwise a difficult problem (13). The n.m.r. spectrum of adenosine triacetate in the presence of $Eu(DPM)_3$ also undergoes considerable simplification and expansion in the $C_{1'}$–$C_{3'}$ proton region. Progressive addition of reagent caused a rapid shift of the NH_2 signal indicating a preferential complexation and resulted in some broadening and exten-

[5]The general applicability of the incremental addition technique and the significance of the "signal crossover phenomenon" has been demonstrated with a variety of acetylated sugars and glycosides in this laboratory.

[6]Considerably higher resolution was observed when the spectra were run at slightly elevated temperatures (45–55° in $CDCl_3$) in tightly stoppered tubes. This effect which could be due to the viscosity of the solution at higher reagent concentration is under study.

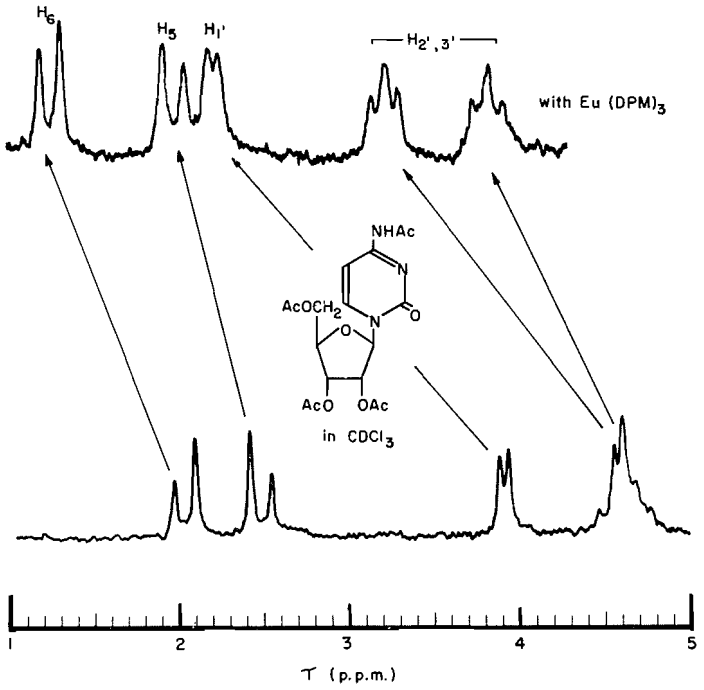

FIG. 2. Partial n.m.r. spectra (60 MHz) of *N*-acetyl cytidine triacetate in $CDCl_3$ solution before and after addition of $Eu(DPM)_3$.

sive downfield shift of the purine ring protons (C-2, -8). The anomeric and C-2′ protons were shifted considerably more than the C-3′ proton which, once again will have important implications in configurational assignments when further models are studied. Details concerning these and extended studies on the utility of shift reagents will be reported in this journal at a later date.[7]

The generous financial assistance of the National Research Council of Canada is gratefully acknowledged.

1. C. C. HINCKLEY. J. Amer. Chem. Soc. **91**, 5160 (1960).
2. J. K. M. SANDERS and D. H. WILLIAMS. Chem. Commun. 422 (1970).
3. J. BRIGGS, G. H. FROST, F. A. HART, G. P. MOSS, and M. L. STANIFORTH. Chem. Commun. 749 (1970).
4. P. V. DEMARCO, T. K. ELZEY, R. B. LEWIS, and E. WENKERT. J. Amer. Chem. Soc. **92**, 5734, 5739 (1970).
5. I. ARMITAGE and L. D. HALL. Chem. Ind. (London), 1537 (1970).
6. N. J. LEONARD and K. L. CARRAWAY. J. Heterocycl. Chem. **3**, 485 (1966).
7. C. H. SHUNK, J. B. LAVIGNE, and K. FOLKERS. J. Amer. Chem. Soc. **77**, 2210 (1955).
8. G. H. WAHL, JR. and M. R. PETERSON, JR. Chem. Commun. 1167 (1970).
9. D. HORTON, J. B. HUGHES, J. S. JEWELL, K. D. PHILLIPS, and W. N. TURNER. J. Org. Chem. **32**, 1073 (1967).
10. R. U. LEMIEUX and J. D. STEVENS. Can. J. Chem. **43**, 2059 (1965).
11. D. HORTON, W. E. MAST, and K. D. PHILLIPS. J. Org. Chem. **32**, 1471 (1967).
12. F. W. LICHTENTHALER and H. P. ALBRECHT. Chem. Ber. **99**, 575 (1966); F. W. LICHTENTHALER, G. BAMBACH, and P. EMIG. Chem. Ber. **102**, 994 (1969).
13. R. J. CUSHLEY, K. A. WATANABE, and J. J. FOX. J. Amer. Chem. Soc. **89**, 394 (1967).

[7]The n.m.r. spectra were obtained using JEOL 60 MHz and JEOL 4H-100 MHz instruments. Solutions containing the shift reagents were filtered or centrifuged prior to measurement.

Can. J. Chem. Downloaded from www.nrcresearchpress.com by 84.22.46.98 on 09/08/12
For personal use only.

Behavior of Extra Electrons in the Liquids Methane, Ethane, and Propane

M. G. ROBINSON, P. G. FUOCHI, AND G. R. FREEMAN
Chemistry Department, University of Alberta, Edmonton 7, Alberta

Received January 4, 1971

The radiation induced electrical conductances of liquids methane, ethane, and propane have been measured. At a field strength of 5 kV/cm the number of ion pairs collected at the electrodes per 100 eV absorbed by the liquid was 1.5 in methane (−160°), 0.20 in ethane (−90°), and 0.14 in propane (−90°). The short-lived conductance transient (k/u overshoot) observed at low field strengths in methane was 40% as large as that in argon. No transient was observable in ethane or propane. The freeness of motion of electrons in liquid methane is nearly as great as that in liquid argon and much greater than that in ethane or propane.

Les conductivités électriques provoquées sous irradiation ont été mesurées pour le méthane, l'éthane et le propane liquides. Pour une énergie de 100 eV absorbés par le liquide, le nombre de paires ioniques récoltées aux électrodes sous l'influence d'un champ électrique de 5 kV/cm est 1.5 pour le méthane à −160°, 0.20 pour l'éthane à −90° et 0.14 pour le propane à −90°. La conductivité tres éphémère (k/u overshoot) observée pour le méthane sous l'influence de champs peu élevés est 40% de celle de l'argon. Aucune conductivité éphémère semblable n'a été observée pour l'éthane ni le propane. La liberté de mouvement des électrons dans l'éthane ou le propane liquide est de beaucoup inférieure à celle qu'ils ont dans le méthane. Cette dernière est pratiquement aussi grande que la liberté de mouvement des électrons dans l'argon liquide.

Canadian Journal of Chemistry, 49, 984 (1971)

Can. J. Chem. Downloaded from www.nrcresearchpress.com by 210.87.254.6 on 09/05/12
For personal use only.

The study of the behavior of extra electrons in liquids contributes to the understanding of low energy electron–molecule interactions, electronic states of liquids, radiation-induced electrical conductance, and radiation chemistry (1–3).

Electrons are quasifree in liquid argon (1). They also tend to be quasifree in liquid neopentane, though they are less free in neopentane than in argon (2). There is some question about whether electrons remain quasifree or form a localized state in liquid *n*-hexane, but the motion of electrons in *n*-hexane is much less free than that in neopentane (2–4).

There appears to be a correlation between the freeness of motion of an electron in a hydrocarbon liquid and the shape of the molecules: the more sphere-like the molecules the greater the freeness of the electron motion. To test this suggestion we have studied the radiation induced electrical conductance of the liquids methane, ethane, and propane. The induced conductance of liquid argon has been remeasured and used as a standard for comparison, since all of the generated ions become "free ions" in that liquid.

The experimental techniques were the same as those reported earlier (2). Microsecond pulses of X-rays from a 2 MeV Van de Graaff accelerator were used.

The 100 eV yields of ions of each sign collected at electrodes in the liquids are plotted against applied voltage in Fig. 1. The free ion yield in methane is about one third that in argon; that in ethane is one seventh that in methane; that in propane is 70% of that in ethane. Thus the greatest change in behavior occurs between methane and ethane.

The fraction ϕ_{fi} of the total ionization yield that becomes free ions is given by eq. 1 (5).

$$[1] \qquad \phi_{fi} = \frac{\int N(y) \exp(-\xi^2/\varepsilon y k T)\, dy}{\int N(y)\, dy}$$

where $N(y)$ is the relative number of secondary electrons that attain a separation distance y from their parent ions during the slowing down process, ξ is the charge on an electron, ε is the dielectric constant of the liquid, k is Boltzmann's constant, and T is the absolute temperature. The exact form of the $N(y)$ distribution function is not known, but a frequently used form that lends itself readily to calculations is the single parameter, three dimensional Gaussian [2] (6–8).

$$[2] \qquad N(y)/N_0 = (4y^2/\pi^{1/2}b^3) \exp(-y^2/b^2)$$

where $N(y)/N_0$ is the fraction of the ion–electron pairs that have a given value of y, and b is the dispersion parameter. In the simple function [2], b is also the most probable value of y.

Approximate values of b in the different liquids are: argon, ∞; methane, 700 Å; ethane, 140 Å; propane, 120 Å. The values in propane and ethane are similar to each other, but are much smaller than that in methane. This indicates that

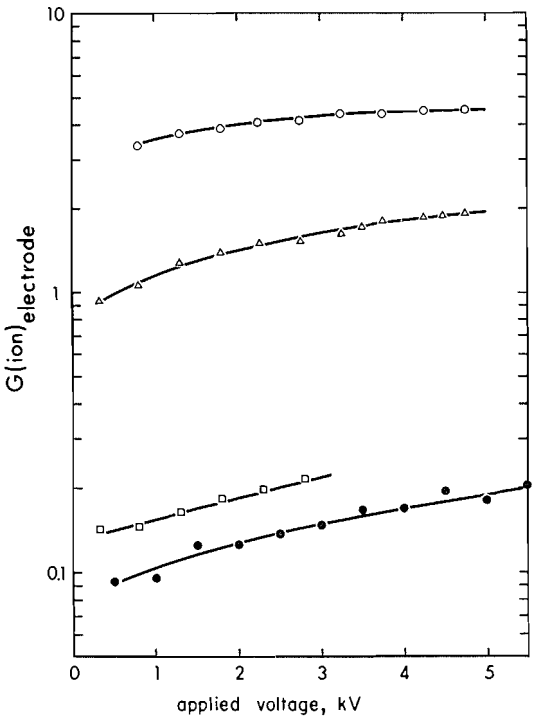

FIG. 1. G values of ions of each sign collected at the electrodes, as functions of the applied voltage. ○, argon, −186°; △, methane, −160°; □, ethane, −90°; ●, propane, −90°. Electrode spacing = 5 mm.

electron motion in liquid methane is much freer than that in ethane or propane.

The observation of a short-lived electrical conductance transient, previously called a k/u overshoot (2), after a pulse of radiation indicates the presence of quasifree electrons in the liquid. The transient in methane was 40% as large as that in argon, but was not observable in ethane or propane. This is further evidence that the freeness of motion of electrons is much greater in methane than in ethane or propane.

Thus the correlation between the molecular shape and the freeness of electron motion in the hydrocarbon liquid is substantiated. The contrast between the methane and ethane systems is striking.

This work is continuing and will be reported in detail at a later date.

1. B. E. SPRINGETT, J. JORTNER, and M. H. COHEN. J. Chem. Phys. **48**, 2720 (1968).
2. P. H. TEWARI and G. R. FREEMAN. J. Chem. Phys. **51**, 1276 (1969).
3. W. F. SCHMIDT and A. O. ALLEN. J. Chem. Phys. **52**, 4788 (1970).
4. R. M. MINDAY, L. D. SCHMIDT, and H. T. DAVIS. J. Chem. Phys. **50**, 1473 (1969).
5. G. R. FREEMAN and J. M. FAYADH. J. Chem. Phys. **43**, 86 (1965).
6. A. MOZUMDER. J. Chem. Phys. **48**, 1659 (1968).
7. P. K. LUDWIG. J. Chem. Phys. **50**, 1787 (1969).
8. J.-P. DODELET and G. R. FREEMAN. To be published.

Can. J. Chem. Downloaded from www.nrcresearchpress.com by 210.87.254.6 on 09/05/12
For personal use only.

49
p.987-2182
1971

Canadian Journal of Chemistry

Published by THE NATIONAL RESEARCH COUNCIL OF CANADA

VOLUME 49 APRIL 1, 1971 NUMBER 7

Radiation and Radiationless Processes in 2,3-Pentanedione; Phosphorescence Lifetime in the Gas Phase

A. W. JACKSON AND A. J. YARWOOD

Department of Chemistry, McMaster University, Hamilton, Ontario

Received October 21, 1970

Fluorescence and phosphorescence are observed when 2,3-pentanedione in the gaseous state is excited at 365, 405, and 436 nm. The phosphorescence lifetime has been investigated as a function of temperature (298 to 363 °K) and concentration of the diketone (0.5 to 90 × 10^{-4} M). A mechanism that explains the experimental data is proposed. Apart from the radiative process and an intersystem crossing to the ground state, the triplet state 2,3-pentanedione molecules are removed by two other processes. One is a unimolecular reaction with a rate constant of $1 \times 10^{11} \exp(-11.0/RT)\,s^{-1}$ (consistent with an intramolecular hydrogen atom abstraction), and the other is an interaction with ground state molecules. The photochemistry of the triplet state of 2,3-pentanedione is compared with that of biacetyl to consider the effect of substitution of a hydrogen atom by the methyl group on the radiationless processes in diketones.

De la fluorescence et de la phosphorescence sont observées quand la pentanedione-2,3 est excitée à l'état gazeux à 365, 405 et 436 nm. Il a été déterminé que le temps de vie de phosphorescence est fonction de la température (298 à 363 °K) et de la concentration en dicétone (0.5 à 90 × 10^{-4} M). Un mécanisme permettant d'expliquer les données expérimentales est proposé. En plus du procédé radiatif et d'un passage intercistant vers l'état fondamental, la désactivation des états triplets des molécules de pentanedione-2,3 se fait par deux autres procédés. L'un par une réaction unimoléculaire avec une constante de vitesse de $1 \times 10^{11} \exp(-11.0/RT)\,s^{-1}$ (en accord avec une abstraction intramoléculaire d'atome d'hydrogène) et l'autre par une interaction avec des molécules à l'état fondamental. La photochimie de l'état triplet des pentanediones-2,3 est comparée à celle des biacétyles afin d'examiner l'effet de la substitution d'un atome d'hydrogène par un groupe méthyle sur le procédé radiatif dans les dicétones.

Canadian Journal of Chemistry, 49, 987 (1971)

Many molecules that are of great photochemical interest do not phosphoresce in the gaseous phase, and the presence of triplet states in the system must be deduced in an indirect manner. Two methods that are widely used are the triplet sensitized isomerization of *cis*-butene-2 introduced by Cundall *et al.* (1, 2), and the triplet sensitized phosphorescence of biacetyl, first demonstrated by Ishikawa and Noyes (3).

The advantages and disadvantages of the techniques have been considered by Noyes and Unger (4). One of the difficulties with biacetyl is the large ratio for emission from the triplet state as compared with that from the singlet state; about 60:1 (5) in the direct photolysis at long wavelengths. This implies that the possibility of singlet–singlet energy transfer (with subsequent phosphorescence) must be carefully considered in the system. A further complexity in the biacetyl photolysis is a product which can quench the triplet states very efficiently (6, 7); *e.g.* in the time required to scan the emission from biacetyl as a function of wavelength (excitation source a 1000 W Hg/Xe lamp with a 0.25 m monochromator), an appreciable decrease can occur in the intensity of the phosphorescence and in the lifetime of the triplet biacetyl.

The research of Richtol and Klappmeier (8) on 2,3-pentanedione in a matrix at 77 °K and in solution at 298 °K suggests that in the gaseous phase the ratio of phosphorescence to fluorescence would be smaller than for biacetyl. 2,3-Pentanedione might also be less sensitive to the quenching product and it could be an appropriate alternative to biacetyl in energy transfer studies. We have investigated the photochemistry of 2,3-pentanedione at temperatures between 298 and 363 °K and the pre-exponential factors and

Can. J. Chem. Downloaded from www.nrcresearchpress.com by 210.87.254.105 on 09/05/12
For personal use only.

activation energies associated with some of the radiationless processes can be derived from the data. Also, a comparison with the rate constants for biacetyl photolysis shows the effect of substitution of a hydrogen atom by a methyl group on the rate processes in diketones in the gaseous phase.

Experimental

2,3-Pentanedione (Eastman Kodak, and Eastern Chemical Company) was purified (99.98%) by gas–liquid chromatography (on a 6 m 30% SE-30 on Chromosorb W column at 70 °C) and stored in a blackened bulb under vacuum at 77 °K. Mass spectral analysis showed no species with $m/e > 100$, and all fragments could be derived from 2,3-pentanedione. Only very pure diketone gave reproducible experimental results. The quinine sulfate (N. F. grade) was supplied by Fisher.

The luminescence spectrum of 2,3-pentanedione in the gas phase at 25 °C was obtained using a grating monochromator (Bausch and Lomb 0.25 m, 1200 lines/mm) to select the required incident wavelengths. The wavelength span of the exciting radiation was about 8 nm but a 1000 W Hg/Xe lamp (Hanovia) was used and a major portion of the radiation is that from the excited mecury. The emitted light was analyzed by a scanning Ebert monochromator (0.5 m Jarrell-Ash) and detected by a cooled photomultiplier (RCA 8575).

The corrected fluorescence and phosphorescence spectra as a function of wavelength were obtained using quinine sulfate to calibrate the monochromator–photomultiplier arrangement (9). The quantum yields were determined using quinine sulfate ($\phi_f = 0.55$) as a standard (10). The incident light intensities at 313, 405, and 436 nm were determined using potassium ferrioxalate actinometry (11).

The T shaped quartz cell (10 cm long) for the lifetime study was fitted with a Suprasil side window for viewing the emitted light. Gases were circulated through the cell by a teflon paddle which was rotated by an external magnet. The cell-stirrer arrangement was housed in an insulated air furnace which could be heated to greater than 100 °C. The temperature was measured using thermocouples attached to the cell and is precise to ±0.1 °C. The cell was isolated from the mercury-free gas handling line by a teflon O-ring stopcock (Delmar). The pentanedione was transferred from the chromatographic purification line through a trap held at −35° to minimize the mercury contamination of the system. Pressures were measured using a Bourdon spoon guage as a null-meter against a mercury manometer. Many experiments at the higher temperatures were performed at pressures which were greater than the saturated vapor pressure of the 2,3-pentanedione at 25 °C. In these cases, to attain the required concentration, the cell was filled the appropriate number of times at room temperature and then heated to a temperature at least 5 °C above the temperature at which the liquid and vapor were in equilibrium.

The excitation source for the lifetime study was a xenon discharge lamp (Strobotac Type 1531-AB, 0.018 J per flash) which had a decay time of 3.8×10^{-6} s. The lamp was triggered at about 2 Hz from the time base of an oscilloscope. The incident light was restricted to the region 360 to 520 nm by a glass filter (Corning CS5-60). The emitted light passed through a glass filter (Corning CS3-71) and was detected by a photomultiplier (1P28) with a response time of about 2×10^{-6} s. The output of the photomultiplier was displayed on an oscilloscope and photographed. (About 100 flashes per photograph were required.) No lifetimes shorter than 2×10^{-5} s are reported. In separate experiments, the effect of incident light intensity (100 to 15%) on the lifetime was determined using neutral density glass filters (Baird-Atomic).

For a particular concentration of pentanedione in the cell, the lifetime was measured at temperatures between 20 and 90 °C in about 10° intervals. (At the higher concentrations measurements were possible only at the higher temperature.) To ensure that quenching by decomposition products did not interfere, the lifetimes were occasionally remeasured at a low temperature after the usual sequence of experiments was complete. No attempt was made to reproduce the same temperatures for the different concentrations. The lifetimes at the experimental temperatures were calculated, and a cubic polynomial was fitted, using a least-squares technique, to the experimental data in the form $\log(1/\tau)$ *vs.* $1000/T$. From the polynomial that fitted the smoothly varying experimental data the lifetimes at 25, 30, 40, . . . 90° were calculated. There was no evidence of problems associated with liquid diketone using this procedure. The concentration of diketone in the cell was checked using the transmitted light intensity, which was essentially independent of temperature. If condensation were a problem, the amount of light absorbed might be expected to change at the higher temperature.

Results

In the region above 300 nm the absorption spectrum of 2,3-pentanedione extended from about 323 nm to about 480 nm with a maximum absorption in the range 415 to 433 nm. There was some structure in the absorption spectrum and bands were discernible at 442, 433, 423, 416, and possibly 410 nm.

The emission spectrum of 2,3-pentanedione (18.1 Torr) in the gas phase at 24 °C has been determined for excitation wavelengths of 405 and 436 nm. The emission spectrum was also recorded for a pentanedione (18.1 Torr)–oxygen (21 Torr) mixture. When oxygen was present the structureless emission extended from 426 nm to greater than 550 nm and had a maximum at 466 nm (the wavelengths quoted refer to the corrected emission spectrum). Through the use of quinine sulfate as a reference compound $\phi_r = 0.55$ (10) the quantum yield of the emission in the presence of oxygen was determined as $0.001 \pm 20\%$ for both 405 and 436 nm excitation. The emission which was quenched by oxygen was obtained as the difference between the total emission of pure

Can. J. Chem. Downloaded from www.nrcresearchpress.com by 210.87.254.105 on 09/05/12
For personal use only.

Can. J. Chem. Downloaded from www.nrcresearchpress.com by 210.87.254.105 on 09/05/12
For personal use only.

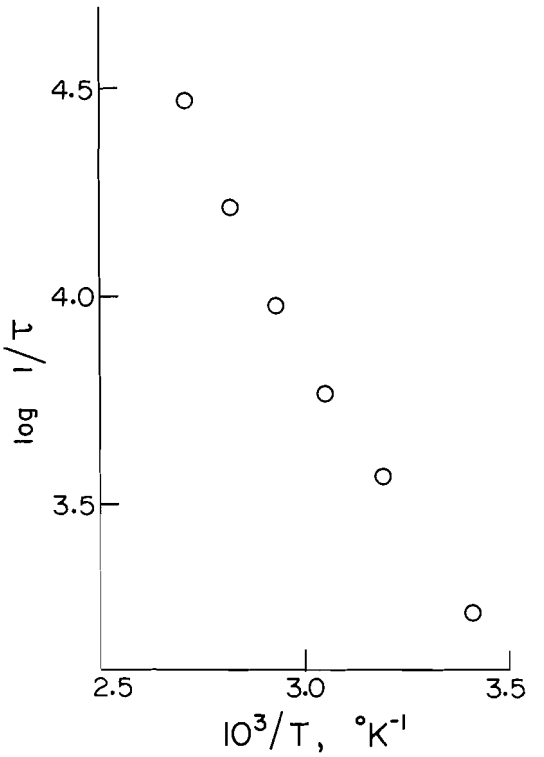

FIG. 1. Logarithm of the reciprocal of the lifetime of 2,3-pentanedione *vs.* the reciprocal of the temperature: pentanedione concentration, 0.66×10^{-4} *M*.

2,3-pentanedione (18.1 Torr) and the emission remaining when oxygen (21 Torr) was also present. It extended from 476 nm to greater than 610 nm (maxima at 520 and 568 nm) and at 24 °C had a quantum yield of 0.020 ± 20% for both 405 and 436 nm excitation. In all experiments the decays of the phosphorescence were well described by an exponential form, at times when the scattered light from the exciting flash was negligible. An example of the experimental results is shown in Fig. 1, where the lifetime data for a pentanedione concentration of 6.6×10^{-5} *M* are displayed at various temperatures. Data were obtained in separate experiments for concentrations in the range 6.6 to about 900×10^{-5} *M*. For some concentrations the lifetime was remeasured at low temperature after completing the sequence of lifetime measurements at increasing temperatures. In each case, the remeasured lifetime was in good agreement with the data obtained in the initial sequence, so that problems associated with the formation of a quenching product were not encountered. At each concentration the cubic equation was calculated which best fitted the experimental data, such as Fig. 1, and the lifetimes at 25, 30, 40, 50, 60, 70, 80, and 90 °C were derived. Figures 2 and 3 show how the reciprocals of the lifetimes obtained in this manner vary with concentration at each temperature.

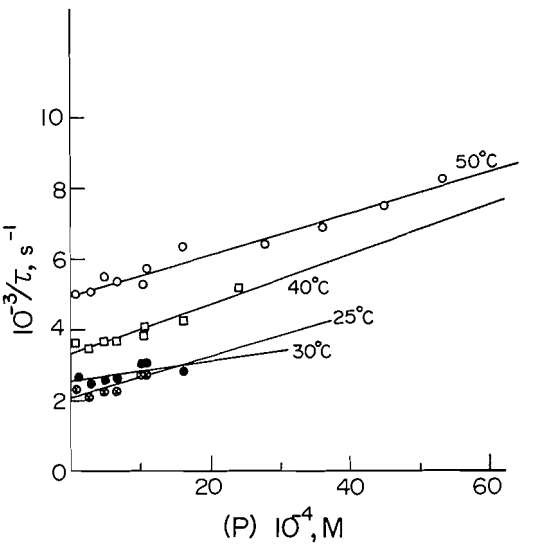

FIG. 2. Reciprocal of the lifetime of pentanedione *vs.* pentanedione concentration at temperatures between 25 and 50 °C.

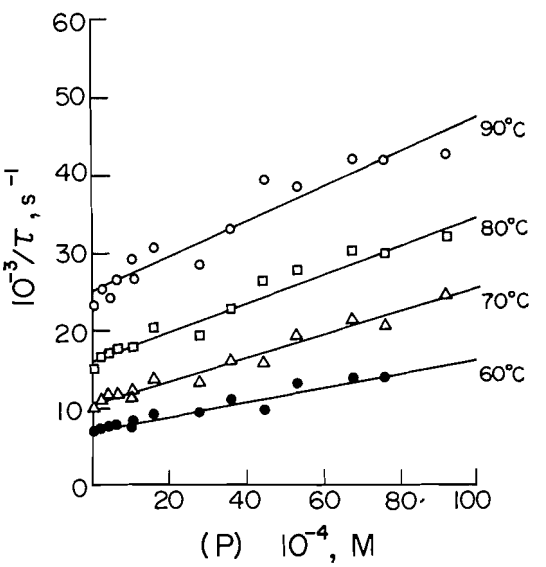

FIG. 3. Reciprocal of the lifetime of pentanedione *vs.* pentanedione concentration at temperatures between 60 and 90 °C.

Can. J. Chem. Downloaded from www.nrcresearchpress.com by 210.87.254.105 on 09/05/12
For personal use only.

The effect of an inert gas on the triplet lifetime was studied by adding sulfur hexafluoride to pentanedione at a concentration of 1.0×10^{-3} M. Addition of 1.1 and 2.0×10^{-2} M of sulfur hexafluoride did not change the triplet lifetime from that of the pure pentanedione over the temperature range 25 to 90 °C.

The effect of incident light intensity on the lifetime was checked using a pentanedione concentration of 6.8×10^{-3} M. At relative incident intensities of 1.0, 0.50, 0.30, and 0.15 the lifetimes at 63.9 °C were 59.7, 61.4, 60.9, and 62.4×10^{-6} s, respectively. Since the lifetimes show no trend with incident intensity, and within experimental error are the same, there is no dependence of lifetime on intensity under these conditions.

Discussion

The electronic absorption spectra of the diketones biacetyl and glyoxal show that the longest wavelength spin allowed transitions lie at about 420 nm. The next region of absorption is usually at about 320–230 nm and there are other transitions at 200–185 nm and at about 170 nm. There is general agreement that the longest wavelength spin allowed transition in glyoxal and biacetyl corresponds to π^*,n excitation, and the excited state molecular configuration proposed (12, 13) is

$$\sigma_{core}\,(a_u)^2(b_g)^2(b_u)^2(a_g)^1(a_u)^1\ {}^1A_u\ (\pi^*,n)$$

The electronic absorption spectrum in the 480–320 nm region of 2,3-pentanedione is very similar in wavelength and intensity to that of biacetyl and excitation populates a π^*,n excited state.

On excitation in the π^*,n absorption band pentanedione emits in the blue and green regions of the spectrum. As usual, the emission in the blue which is still observed in the presence of oxygen is classed as fluorescence. The phosphorescence is the difference between the total emission and the fluorescence. The gaseous phase phosphorescence is shifted with respect to the spectrum observed in the condensed phase. Richtol and Klappmeier (8) report the maximum of the phosphorescence in hexane solution at 25 °C as 532 nm and in mixed alcohol glass at −196 °C as 508 nm, whereas the maximum in gaseous phase is at 520 nm. Apart from changes in the position of the wavelength of maximum phosphorescence with changes in phase and solvent, there are also significant differences in the ratio of the quantum yields of fluorescence and phosphorescene. For pentanedione in the gaseous phase at 24 °C excited at 405 and 436 nm the ratio ϕ_f/ϕ_p is about 0.05 for a concentration of 10^{-3} M, whereas Richtol and Klappmeier report that in hexane solution at 25 °C and a similar concentration, the ratio is about 0.6.

From the overlap of the absorption and fluorescence spectra in the gaseous phase the energy of the first excited singlet state can be estimated as about 63 kcal. The triplet–singlet splitting can be estimated as about 9 kcal from the onset of the fluorescence and the phosphorescence so the triplet state energy is about 54 kcal. The energy of the singlet state of biacetyl is at 64 kcal and of the triplet state at 55 to 57 kcal (14, 15).

The general character of the absorption and emission spectra, and energetics of the singlet and triplet states of 2,3-pentanedione is very similar to that of biacetyl. The photochemistry of pentanedione can be considered in terms of a mechanism which is a modification of that used to describe the photochemistry of biacetyl (16).

[1]	$P + h\nu \rightarrow {}^1P_v \rightarrow {}^3P_0$	
[2]	${}^3P_0 \rightarrow P + h\nu_p$	k_2
[3]	${}^3P_0 \rightarrow P_n$	k_3
[4]	${}^3P_0 \rightarrow$ Product?	k_4
[5]	${}^3P_0 + P \rightarrow$ Removal	k_5

The subscripts n, v, and 0 indicate degree of vibrational excitation, while the superscripts 1 and 3 are the multiplicities of the electronic states, and the ground electronic state of pentanedione is indicated by P. The lowest concentration of diketone studied was about 6×10^{-5} M and the shortest triplet lifetime measured was about 2×10^{-5} s, so the relaxation can be assumed to be complete in the vibrational levels of the triplet before phosphorescence occurs. Accordingly, in this paper we are concerned with the kinetics of the triplet state in its lowest vibrational level. In the mechanism process 1 encompasses all photophysical processes prior to attainment of that level (*i.e.* light absorption, subsequent vibrational deactivation, intersystem crossing to the triplet and vibrational deactivation in the triplet state). Reaction 4 is added to the mechanism to account for the photochemical behavior in the gaseous phase and is in agreement with the rearrangement in solution (17) of 2,3-pentanedione to 1-hydroxy-1-methyl cyclobutanone.

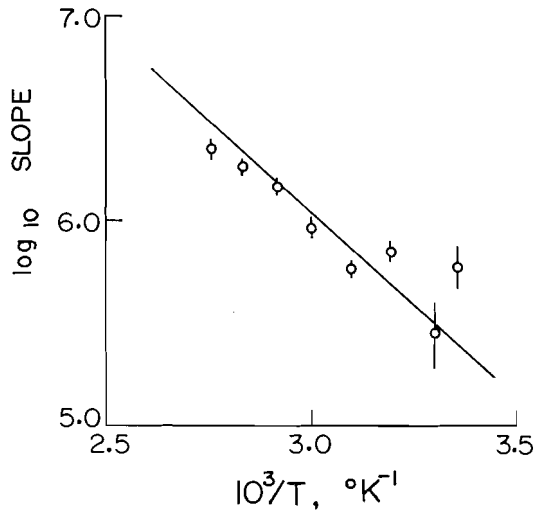

FIG. 4. Logarithm of the rate constants evaluated from the slopes of Figs. 2 and 3 *vs.* the reciprocal of the temperature.

A steady state treatment of this mechanism leads to the expression for the actual lifetime, τ, of the triplet state as $1/\tau = (k_2 + k_3 + k_4 + k_5P)$. Figures 2 and 3 show plots of the reciprocals of the triplet lifetimes *vs.* diketone concentration for temperatures between 25 and 90 °C. Clearly, the mechanism is consistent with the data. High concentrations of added sulfur hexafluoride do not change the triplet lifetime of the diketone. This shows that the photochemistry of pentanedione is quite unlike that of acetone (18), and does not involve a unimolecular reaction in its low pressure or fall-off region.

The slopes of the lines in Figs. 2 and 3 increase as the temperature increases, *i.e.* k_5 increases with temperature. A plot of the logarithm of the slopes from Figs. 2 and 3 *vs.* the reciprocal of the temperature is shown in Fig. 4, and the pre-exponential factor can be evaluated as 9×10^{10} M^{-1} s^{-1} and the activation energy as 7.5 kcal mol^{-1}. The value of the pre-exponential factor is larger than might be expected for the reaction of a polyatomic molecule with an activation energy of 7.5 kcal (20). However, a lower value of the pre-exponential factor is possible. The values derived from Fig. 4 depend significantly on the precision of the data at the lower temperatures. In that region, however, the precision of the data decreases rapidly. This is due to the low value of the rate constant for the bimolecular reaction at the lower temperature and to the concentration range investigated being severely limited by the low vapor pressure of the diketone at the low temperatures. (The error bars shown in Fig. 4 are the standard deviations of the slopes derived from Figs. 2 and 3.) This rate constant for the removal of triplet pentanedione by collision with a ground electronic state pentanedione molecule may be compared with the analogous rate constant in biacetyl photochemistry. At 25 °C the rate constant for 2,3-pentanedione is 3×10^5 M^{-1} s^{-1} and Garabedian and Dows report 7×10^4 M^{-1} s^{-1} for biacetyl (19). No studies have been made of the decomposition products of the system so the rate constant k_5 cannot at present be associated with product formation.

Another important aspect of Figs. 2 and 3 concerns the values of the intercepts of the lines corresponding to the various temperatures. The lowest concentration investigated in this research is about 6×10^{-5} M, however, Parmenter and Poland (21) found that the triplet emission of biacetyl at 25 °C excited at 436 nm is independent of pressure to at least 5×10^{-6} M. It is likely that the experimental data of Figs. 2 and 3 can be extrapolated to lower concentrations and intercepts evaluated that correspond to zero concentration of diketone. According to the steady state treatment of the mechanism, the intercepts on Figs. 2 and 3 are $(k_2 + k_3 + k_4)$ at the appropriate temperatures. From these data other interesting features of the system can be distinguished. It is usually assumed that the natural radiative rate constant does not depend on temperature. The rate constant for intersystem crossing from the triplet state to the ground electronic state can also be assumed to be independent of temperature. Although the temperature dependence of intersystem crossing rate constants has not been investigated extensively, there is theoretical and experimental evidence to validate the assumption. The theory of Siebrand (22) suggests a very small temperature effect on the intersystem crossing rate constants in molecules with a large energy gap between the states. This is corroborated by the experiments of Jones and Siegel (23) on aromatic compounds in a polymethylmethacrylate matrix. Also, the research of Kutschke and co-workers (24) on the triplet state of hexafluoroacetone in the gas phase has shown in that system a temperature independent k_{isc} can explain the experimental data. This leaves only the rate constant k_4 as a function of temperature, and the mechanism thus requires that a plot

Can. J. Chem. Downloaded from www.nrcresearchpress.com by 210.87.254.105 on 09/05/12
For personal use only.

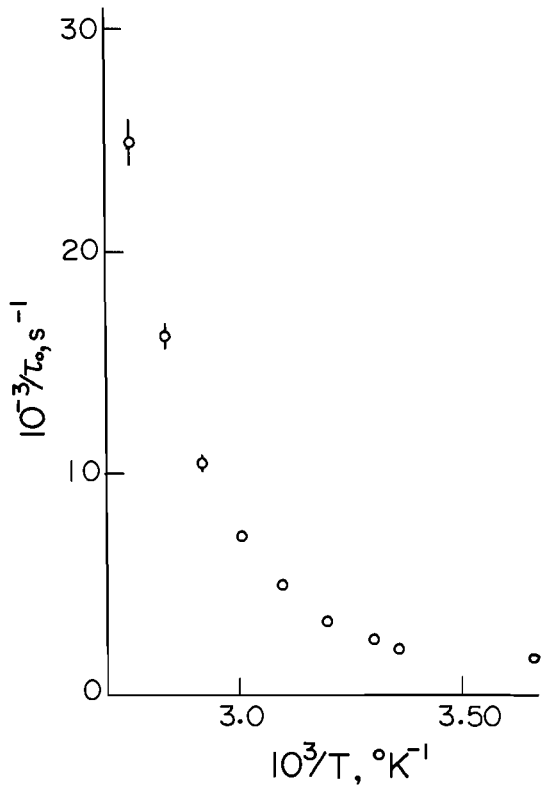

FIG. 5. Reciprocal of the rate constants evaluated from the intercepts of Figs. 2 and 3 *vs.* the reciprocal of the temperature.

of the intercepts of the lines of Figs. 2 and 3 *vs.* the reciprocal of the temperature be non-linear. Figure 5 shows that the experimental data do indeed behave in this manner. The data of Fig. 5 were fitted, using a weighted least-squares technique, to the form $a + b \exp(-C/RT)$; where "*a*" is the sum of the rate-constants k_2 and k_3 ($= 1.40 \times 10^3$ s^{-1}) and "*b*" and "*c*" are the pre-exponential factor and activation energy corresponding to rate constant k_4 (1.0×10^{11} s^{-1} and 11.0 kcal mol^{-1}). An explicit value for k_3 can be deduced if k_2 is derived from the quantum yield and lifetime data, $\phi_p = \phi_{isc}\tau_p k_2$ where ϕ_{isc} is the quantum yield of crossing from the first excited singlet state to the triplet state. Since the fluorescence yield is low ($\phi_f = 0.001$) and decomposition and internal conversion can be assumed to be small from the singlet formed on absorption at 405 and 436 nm, then ϕ_{isc} is approximately unity, k_2 about 47 s^{-1} and k_3, 1.3×10^3 s^{-1}. In a study of pentanedione in solution Richtol and Klappmeier (8) deduced a value for the total rate of removal of triplet molecules by unimolecular radiationless processes, *i.e.* $(k_3 + k_4)$. The data presented above yield individual values for k_3 and k_4 for pentanedione, and allow a comparison of the rate constants for intersystem crossing, k_3, from the triplet to the ground state in biacetyl and pentanedione. From the phosphorescence quantum yield determined by Gandini and Kutschke (25) and the triplet lifetime data of Kaskan and Duncan (26), $k_2 = 100$ s^{-1} and $k_3 = 460$ s^{-1} for biacetyl. So this work suggests that intersystem crossing increases with substitution of a hydrogen atom at an α-carbon by a methyl group in diketones. This effect in diketones is opposite to the trend noted in alkyl ketones (27) at low temperatures in a matrix. Apart from increasing the rate constant for intersystem crossing from the triplet to the ground state, an additional effect of substitution by the methyl group is to introduce another process (reaction 4) capable of removing the triplet state. Turro and Lee (17) have shown that photolysis of 2,3-pentanedione in solution at 25 °C forms 1-hydroxy-1-methyl cyclobutanone with a quantum yield of about 0.06. It is reasonable to associate the intramolecular photoreduction with the rate constant k_4, since the pre-exponential factor and activation energy are compatible with an internal hydrogen abstraction reaction.

In conclusion, the effect on the kinetics of the triplet state of substitution of a hydrogen atom in biacetyl by a methyl group is to decrease the radiative rate constant, increase the intersystem crossing rate constant, retain a bimolecular reaction for removal of the triplet state, and introduce an intramolecular reaction which is probably a photoreduction.

We thank the National Research Council of Canada for financial support.

1. R. B. CUNDALL, F. J. FLETCHER, and D. G. MILNE. Trans. Faraday Soc. **60**, 1146 (1964).
2. R. B. CUNDALL and A. S. DAVIE. Trans. Faraday Soc. **62**, 1151 (1966).
3. H. ISHIKAWA and W. A. NOYES, JR. J. Chem. Phys. **37**, 583 (1962).
4. W. A. NOYES, JR. and I. UNGER. Advan. Photochem. **4**, 49 (1966).
5. H. OKABE and W. A. NOYES, JR. J. Amer. Chem. Soc. **79**, 801 (1957).
6. D. S. WEIR. J. Chem. Phys. **36**, 1113 (1962).

Can. J. Chem. Downloaded from www.nrcresearchpress.com by 210.87.254.105 on 09/05/12
For personal use only.

7. J. LEMAIRE. J. Phys. Chem. **71**, 2653 (1967).
8. H. H. RICHTOL and F. H. KLAPPMEIER. J. Chem. Phys. **44**, 1519 (1966).
9. W. H. MELHUISH. J. Phys. Chem. **64**, 762 (1960).
10. W. H. MELHUISH. J. Opt. Soc. Amer. **54**, 183 (1964).
11. C. A. PARKER. Photoluminescence of Solutions. Elsevier, New York. 1968.
12. H. M. MCMURRY. J. Chem. Phys. **9**, 241 (1942).
13. A. D. WALSH. Trans. Faraday Soc. **42**, 66 (1946).
14. N. J. TURRO. Molecular Photochemistry. Benjamin, New York. 1967.
15. J. W. SIDMAN and D. S. MCCLURE. J. Amer. Chem. Soc. **77**, 6461 (1955).
16. W. A. NOYES, JR., G. B. PORTER, and J. E. JOLLEY. Chem. Rev. **56**, 49 (1956).
17. N. J. TURRO and T. J. LEE. J. Amer. Chem. Soc. **91**, 5651 (1969).
18. H. E. O'NEAL and C. W. LARSON. J. Phys. Chem. **73**, 1011 (1969).
19. M. E. GARABEDIAN and D. A. DOWS. J. Amer. Chem. Soc. **90**, 2468 (1968).
20. S. W. BENSON. The Foundations of Chemical Kinetics. McGraw-Hill, New York. 1960.
21. C. S. PARMENTER and H. E. POLAND. J. Chem. Phys. **51**, 1551 (1969).
22. W. SIEBRAND. J. Chem. Phys. **47**, 2411 (1967).
23. P. F. JONES and S. SIEGEL. *In* Molecular Luminescence, *Edited by* E. C. Lim. Benjamin, New York. 1969.
24. A. GANDINI, D. A. WHYTOCK, and K. O. KUTSCHKE. Proc. Roy. Soc. Ser. A, **306**, 541 (1968).
25. A. GANDINI and K. O. KUTSCHKE. Proc. Roy. Soc. Ser. A, **306**, 511 (1968).
26. W. E. KASKAN and A. B. F. DUNCAN. J. Chem. Phys. **18**, 427 (1950).
27. M. O'SULLIVAN and A. C. TESTA. J. Amer. Chem. Soc. **92**, 258 (1970).

Can. J. Chem. Downloaded from www.nrcresearchpress.com by 210.87.254.105 on 09/05/12
For personal use only.

Can. J. Chem. Downloaded from www.nrcresearchpress.com by 210.87.254.6 on 09/05/12
For personal use only.

The Flash Photolysis of Tetraphenyldiphosphine, Triphenylphosphine, and Diphenylphosphine in Alcohols

S. K. WONG[1], W. SYTNYK, AND J. K. S. WAN
Department of Chemistry, Queen's University, Kingston, Ontario

Received November 3, 1970

The photochemical reactions of tetraphenyldiphosphine, triphenylphosphine, and diphenylphosphine in alcohol were studied by flash photolysis and product analysis. The primary photochemical process of all three phosphines studied appeared to be the formation of diphenylphosphinyl radicals which subsequently abstract α-H atoms from the solvent alcohol. The relationship between the rate constants of the abstraction and the α-H bond energies of various alcohols was examined.

Les réactions photochimiques de la tétraphényldiphosphine et des di- et triphénylphosphines ont été étudiées, dans l'alcool, par photolyse "flash" et par analyse des produits. Le processus photochimique primaire pour les trois phosphines semble être la formation de radicaux diphénylphosphinyles qui arrachent subséquemment des atomes d'hydrogéne-α de l'alcool utilisé comme solvant. Une relation entre les constantes de vitesse d'abstraction et les énergies de liaison des hydrogènes-α de divers alcools a été examinée.

Canadian Journal of Chemistry, 49, 994 (1971)

The diphenylphosphinyl radical has been postulated as an intermediate in many organophosphorus reactions, such as in the photolysis of triphenylphosphine (1, 2), and in the reaction of tetraphenyldiphosphine with alcohols induced by light or heat (3). Some direct evidence of the existence of the radical has been obtained from an e.s.r. study of a combined effect of heat and light on tetraphenyldiphosphine and diphenylphosphine (4). More recently a better resolved e.s.r. spectrum was obtained from the u.v.-irradiation of a benzene solution of tetraphenyldiphosphine at liquid nitrogen temperature (5). We now wish to report the flash photolysis study of tetraphenyldiphosphine (TPDP), triphenylphosphine (TPP), and diphenylphosphine (DPP) in alcohols, presenting the electronic spectrum assigned to the diphenylphosphinyl radical and the kinetics of its reaction with alcohols.

Results and Discussion

The Electronic Spectrum of the Diphenylphosphinyl Radical

When a methanol solution of tetraphenyldiphosphine (TPDP) was flash photolyzed, a transient absorption spectrum of life-time about 160 μs was detected as shown in Fig. 1. Replacing TPDP by triphenylphosphine (TPP) or diphenylphosphine (DPP) gave identical transient spectra. The spectrum has its maximum around 3300 Å. The spectrum decayed when monitored at wavelengths between 3130 to 4350 Å with a similar time constant (Table 1). This suggests it arises from a single species. All three different substrates gave the same transient spectrum of similar life-time. With the complementary e.s.r. results (5) and the product analysis discussed below, the spectrum is assigned to the diphenylphosphinyl radical.

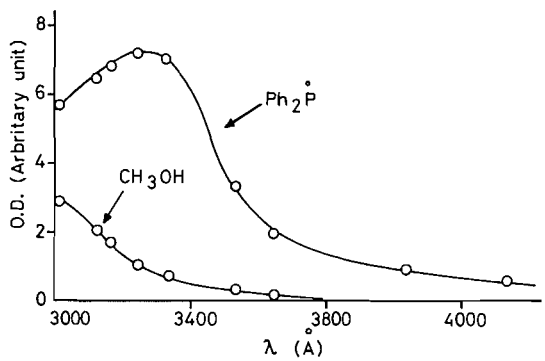

FIG. 1. The electronic absorption spectrum of diphenylphosphinyl radicals in methanol.

It should, however, be noted that methanol alone gave a transient spectrum under the same flash conditions. R. W. Yip has observed a similar transient spectrum by flashing methanol (private communication). The origin of this spectrum has not been investigated. The observation of some transients should not be too surprising when compared to the reported e.s.r. study of u.v.-irradiation of methanol (6). However, this methanol spectrum was much weaker

[1]Postdoctorate Fellow, 1969–1971.

TABLE 1. Rate constants for decay of transient spectrum in methanol

Substrate	$k_1 \times 10^{-3}$ (s^{-1})*				
	3130 Å	3330 Å	3650 Å	4050 Å	4350 Å
Tetraphenyldiphosphine	3.98	4.10	4.0	4.12	4.04
Triphenylphosphine	4.57	4.74	4.45	4.37	4.55
Diphenylphosphine	4.32	4.37	4.38	—	—

*Average values of 3 to 10 separate runs.

than that of diphenylphosphinyl radicals, and the shapes of the spectra are also different (Fig. 1).

The Reaction of Diphenylphosphinyl Radicals with Alcohols

Before we present and discuss the kinetic results of diphenylphosphinyl radicals with alcohols by flash photolysis, we first discuss the reaction mechanism based on reaction product analysis. In 1965 Horner and Dörges (1), and Kaufman and Griffin (2) simultaneously studied the photolysis of TPP. Methanol, 2-propanol, and dioxane were used as solvents by the former workers and benzene and benzene–ethanol mixtures by the latter workers. Both studies were in agreement regarding the primary photochemical process being the cleavage of the phosphorus–phenyl bond to produce a diphenylphosphinyl radical and a phenyl radical from a TPP molecule. Horner and Dörges isolated tetraphenylphosphonium salts (Ph_4P^+) and diphenylphosphinic acid ($Ph_2P(OH)O$) as major products by oxidizing the photolyzed methanol solution of 0.06 *M* TPP. They proposed the following mechanism

[1] $Ph_3P \xrightarrow{h\nu} Ph_2P\cdot + Ph\cdot$

[2] $Ph\cdot + Ph_3P \rightarrow Ph_4P\cdot$

[3] $Ph_4P\cdot + Ph_2P\cdot \rightarrow Ph_4P^+Ph_2P^-$

[4] $Ph_4P^+Ph_2P^- \xrightarrow{MeOH} Ph_4P^+OMe^- + Ph_2PH$

In more dilute methanol solution (0.03 *M*), or in 2-propanol, or in dioxane, the oxidation of the photolyzed TPP gave none or only traces of tetraphenylphosphonium salts. The major products in these cases were diphenylphosphinic acid and phenylphosphonic acid $PhP(OH)_2O$, which were presumably the oxidation products from diphenylphosphine and phenylphosphine. Horner and Dörges did not discuss in their note how these phosphines could be formed. On the other hand Kaufman and Griffin (2) observed diphenylphosphine and biphenyl as major products in benzene solution, and diphenylphosphine and ethyldiphenylphosphine were formed in benzene–ethanol mixture. They rationalized the results by proposing the following reactions

[1] $Ph_3P \xrightarrow{h\nu} Ph_2P\cdot + Ph\cdot$

[5] $Ph_2P\cdot + PhH \rightarrow Ph_2PH + Ph\cdot$

[6] $Ph\cdot + PhH \rightarrow Ph_2 + \frac{1}{2}H_2$

[7] $EtO\cdot + Ph_3P \rightarrow Ph_3\dot{P}OEt \rightarrow Ph_3PO + Et\cdot$

[8] $Et\cdot + Ph_3P \rightleftharpoons Ph_3\dot{P}Et \rightleftharpoons Ph_2PEt + Ph\cdot$

In 1966 Davidson, Sheldon, and Trippett (3) reported that diphenylphosphinyl radicals produced by u.v.-irradiation or thermal decomposition (>180 °C) of TPDP react with primary and secondary alcohols to give diphenylphosphine and alkyl phosphinites, the latter of which then either rearrange to give alkyl diphenylphosphine oxides or partially oxidize to the phosphinates according to conditions and substituents. Because they could not detect any products expected from the radical $R_2\dot{C}OH$, it was suggested that the apparent hydrogen abstraction of the O—H is initiated by the attack of the diphenylphosphinyl radical on the oxygen atom of the alcohol

[9] $Ph_2P—PPh_2 \xrightarrow[\text{or heat}]{h\nu} 2Ph_2P\cdot$

[10] $Ph_2P\cdot + R_2CHOH \rightarrow Ph_2\dot{P}^-—\overset{+}{O}(H)—CHR_2$

Thus, it appears that despite various reported studies, the reaction mechanism of diphenylphosphinyl radicals with alcohols is still uncertain and to some extent the experimental results are in disagreement. In order to provide a definite meaning to our kinetics study we undertook some product analysis experiments, with particular attention on the production of DPP, *i.e.* the hydrogen abstraction mechanism of diphenylphosphinyl radicals. We analyzed the products

Can. J. Chem. Downloaded from www.nrcresearchpress.com by 210.87.254.6 on 09/05/12
For personal use only.

TABLE 2. Mass balance experiments for photolysis of triphenylphosphine in methanol

Concentration and number of mmol	Irradiation time (h)	Products in mmol					
		C_6H_6	$PhPH_2$	Ph_2PH	$Ph_2P(O)H$	PH_3P	Ph_3PO
0.06 *M* 30 mmol	12	12.6	0.4	5.2	7.0	7.1	6.5
0.03 *M* 15 mmol	12	7.8	0.4	2.5	4.0	2.2	3.3
0.06 *M* 30 mmol	6	8.5	Trace	4.2	2.5	16.7	5.2

immediately after the photolysis without any further chemical complication by oxidation (1) or by removal of the excess alcohols with other chemicals added (3). The major technique of analysis in these experiments was ^{31}P n.m.r., the experiments covering the range from +70 to −80 p.p.m. with respect to H_3PO_4. By ^{31}P n.m.r., diphenylphosphine, diphenylphosphine oxide, and triphenylphosphine oxide were the only detectable organophosphorus products in the photolysis of TPP in methanol, whereas diphenylphosphine and diphenylphosphine oxide were observed in the photolysis of TPDP in methanol. In the case of the photolysis of DPP in methanol, diphenylphosphine oxide was the only observable organophosphorus product. It should, however, be emphasized that because of the low sensitivity of ^{31}P n.m.r. compared with the proton magnetic resonance and the limited solubility of the reactants in methanol, it was not practical in our n.m.r. experiments to detect minor organophosphorus products (*e.g.* phenylphosphine was detected by g.l.c. as a minor product, but not by ^{31}P n.m.r.) and to perform mass balance calculations. Thus, methyldiphenylphosphine, tetraphenylphosphonium salt, methyldiphenylphosphinite, and methyldiphenylphosphinate, could escape n.m.r. detection if they were formed in minor amounts. Gas–liquid chromatographic analysis, however, confirmed all the products identified by ^{31}P n.m.r. and further showed that phenylphosphine was also present in minute amounts in the products. Benzene was shown by g.l.c. to be the major product in the photolysis of TPP but a minor product in the photolysis of TPDP or DPP. When 2-propanol was used as solvent, acetone was shown to be a product of the photolysis in agreement with Horner and Dörges' work (1) but in contrast to Davidson, Sheldon, and Trippett's results (3). Further mass balance experiments were performed on the photolysis of TPP in methanol followed by g.l.c. The results are shown in Table 2. Mass spectrometric analysis of the gaseous products of the photolysis of TPP in methanol showed the presence of H_2, CO, and CH_4. The above analysis is consistent with the postulate that the formation of diphenylphosphine is initiated by the generation of diphenylphosphinyl radicals via a photolytic cleavage of P—P, Ph—P, and P—H bonds of TPDP, TPP, and DPP respectively, and then followed by hydrogen abstraction from the solvent alcohols. Thus a generalized reaction scheme would be

$$[11]\quad \left.\begin{array}{l} Ph_2P{-}PPh_2 \xrightarrow{-Ph_2P\cdot} \\ Ph_3P \xrightarrow{-Ph\cdot} \\ Ph_2PH \xrightarrow{-H\cdot} \end{array}\right\} Ph_2P\cdot \underset{h\nu(-H\cdot)}{\overset{R_2CHOH}{\rightleftharpoons}} Ph_2PH \xrightarrow[-Ph\cdot]{h\nu} Ph\dot{P}H \underset{h\nu(-H\cdot)}{\overset{R_2CHOH}{\rightleftharpoons}} PhPH_2$$

In addition there were some oxidation reactions

$$[12]\quad Ph_3P \rightarrow Ph_3PO$$

$$[13]\quad Ph_2PH \rightarrow Ph_2P(O)H$$

or

$$[14]\quad Ph_3PO \xrightarrow[(-Ph\cdot)]{h\nu} Ph_2\dot{P}(O) \xrightarrow{R_2CHOH} Ph_2P(O)H$$

However, it remains to be determined whether the α-H or O—H hydrogen atom is abstracted by diphenylphosphinyl radicals. It was thought that if the photolysis was carried out in the solvent CH_3OD, the production of Ph_2PH would be an indication of α-H abstraction, and the production of Ph_2PD would indicate O—H abstraction. The best method to distinguish between Ph_2PH and

Can. J. Chem. Downloaded from www.nrcresearchpress.com by 210.87.254.6 on 09/05/12
For personal use only.

Can. J. Chem. Downloaded from www.nrcresearchpress.com by 210.87.254.6 on 09/05/12
For personal use only.

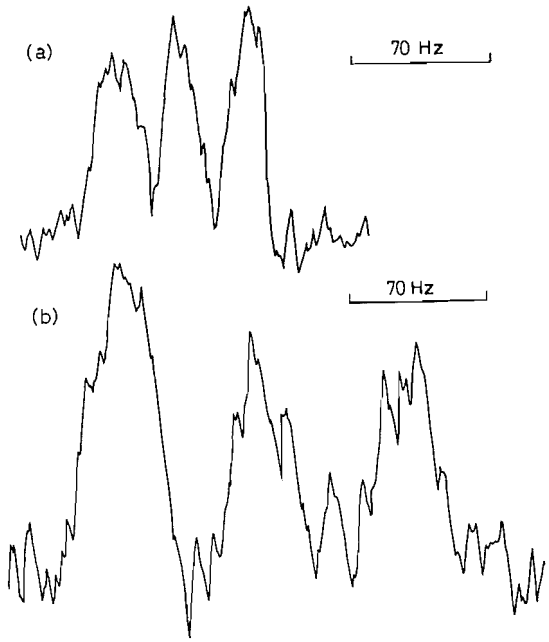

FIG. 2. The ^{31}P n.m.r. spectra of (*a*) Ph_2PD and (*b*) $Ph_2P(O)D$.

Ph_2PD, is probably ^{31}P n.m.r. (7, 8). The ^{31}P n.m.r. spectrum of Ph_2PH consists mainly of two lines separated by about 220 Hz, and that of Ph_2PD three lines separated by about 34 Hz (Fig. 2). However, we found that the hydrogen atom of Ph_2PH exchanged with the deuterium atom of CH_3OD. Thus the ^{31}P n.m.r. spectrum of Ph_2PH in CH_3OD with u.v.-irradiation gave three lines due to Ph_2PD by the exchange reaction

[15] $Ph_2PH + CH_3OD \rightleftharpoons Ph_2PD + CH_3OH$

When the proton magnetic resonance spectra of Ph_2PH in CH_3OD were carefully examined, it was found that O—H absorption of CH_3OH was increased by an observable amount. (There was about 1% CH_3OH in CH_3OD.) If TPDP or TPP is photolyzed in CH_3OD solution and the O—H absorption is increased, it may be concluded that the hydrogen abstraction occurs at α-H via the following schemes:

(*a*) If only α-H abstracted

[16] $Ph_2P\cdot + CH_3OD \rightarrow Ph_2PH + \dot{C}H_2OD$

[17] $Ph_2PH + CH_3OD \rightarrow Ph_2PD + \mathit{CH_3OH}$ (production of CH_3OH)

(*b*) If only O—D abstracted

[18] $Ph_2P\cdot + CH_3OD \rightarrow Ph_2PD + CH_3\dot{O}$

[19] $Ph_2PD + CH_3OD \rightarrow Ph_2PD + CH_3OD$ (no production of CH_3OH)

The experimental results are the following. When TPDP or TPP was irradiated in CH_3OD, ^{31}P n.m.r. indeed gave three lines due to Ph_2PD as well as another triplet due to $Ph_2P(O)D$. Most significantly ^1H n.m.r. spectra gave a large increase of CH_3OH signal (Fig. 3). The estimate of the amount of CH_3OH produced compared with the amounts of the substrates used and Ph_2PD and $Ph_2P(O)D$ formed might provide information about the relative importance of the two abstraction mechanisms. In fact, the amount of CH_3OH produced under the photolysis conditions was about 300 times as much as the number of moles of the substrates used. It is therefore concluded that diphenylphosphinyl radicals preferentially abstract α-H's of the alcohols. However, it must be pointed out that the labelling experiments do not exclude the possibility of minor O—H abstraction.

Kinetics Results

With the above conclusion, the kinetics data of the reaction involving diphenylphosphinyl

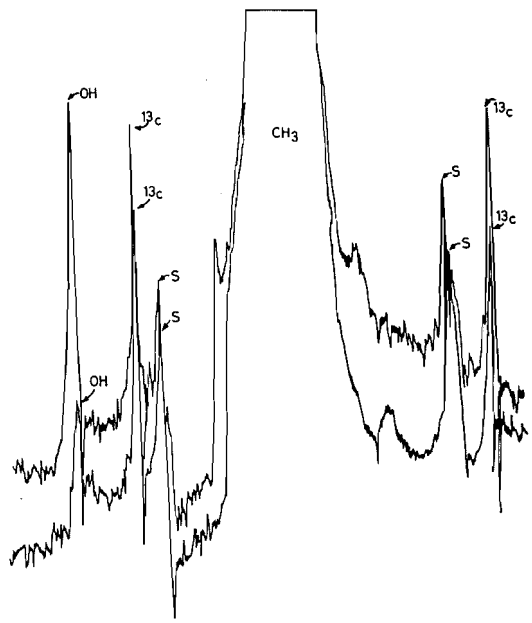

FIG. 3. The p.m.r. spectra of CH_3OH and CH_3OD. Upper trace: Photolyzed solutions of triphenylphosphine and tetraphenyldiphosphine in CH_3OD. Lower trace: Solvent spectrum (CH_3OD). "S" indicates side bands and "^{13}C" indicates splittings due to ^{13}C.

TABLE 3. Apparent first order rate constants for the decay of diphenylphosphinyl radicals

Solvent	$k_1 \times 10^{-3}$ (s^{-1})*			
	TPDP	TPP	DPP	Average
Methanol	4.02±0.20	4.46±0.30	4.37±0.20	4.25±0.30
Ethanol	15.4±2.0	13.0±1.8	1.33±2.0	13.9±2.0
Propanol	40.5±7.0	31.8±6.0	31.2±6.0	34.6±7.0

*Average value of 6 to 25 separate runs.

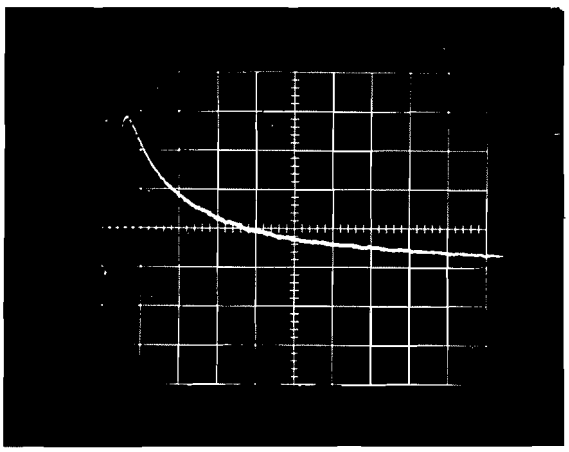

FIG. 4. Oscilloscope trace of decay of diphenylphosphinyl radicals in ethanol, monitored at 3650 Å. Time base is 50 μs/division.

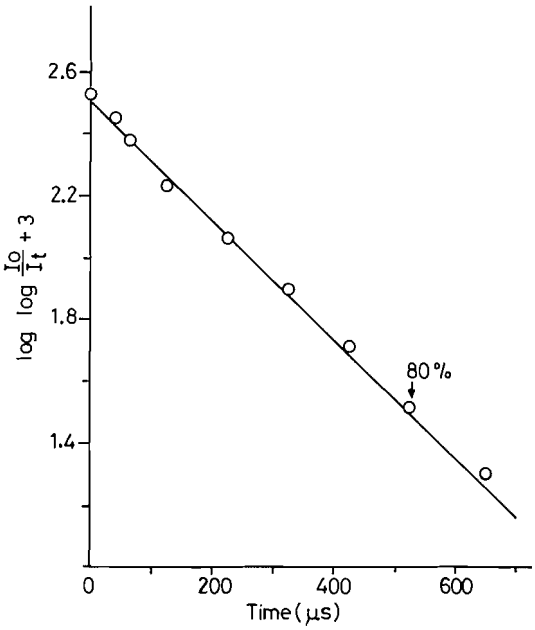

FIG. 5. The first order plot for the decay of diphenylphosphinyl radicals produced from flash photolysis of tetraphenyldiphosphine in methanol.

radicals can be presented to support the α-H abstraction mechanism.

A typical oscilloscope trace of the decay of the radicals in ethanol is shown in Fig. 4. Detailed analysis of the traces in methanol of all three substrates showed that the decay follows first order kinetics with respect to the radical concentration as seen in the log plot (Fig. 5) from which the rate constants were calculated. The first order kinetics was further confirmed by the fact that the rate constants are independent of the various initial concentrations over a 6-fold range. Since the life-times of the radicals are shorter in ethanol and in 2-propanol and are comparable to the duration of the flash, the rate constants involved a larger error and were determined by the half-life method (Table 3).

The first order kinetics with respect to diphenylphosphinyl radicals is consistent with the following expression

$$[20] \quad \text{Rate} = k_2[Ph_2P\cdot][\text{Alcohol}] = k_1[Ph_2P\cdot]$$

Alcohol was in excess amount and was considered to be practically constant. The results shown in Table 2 reveal an increase of apparent first order rate constant going from methanol, ethanol, to 2-propanol. This may be expected for the α-H abstraction since the bond dissociation energies of these α-H's decrease in that order. Whittle and co-workers (9, 10) determined the bond dissociation energies D(H—CH_2OH) and D[H—$CH(CH_3)OH$] by photobromination to be 92 and 90 kcal/mol, respectively. Benson and co-workers (11, 12) by the study of gas phase iodine-atom reactions estimated D(H—CH_2OH) and D[H—$C(CH_3)_2OH$] to be 95.9 ± 1.5 and 90.2 ± 1.1 kcal/mol, respectively. A relative difference of about 2–2.5 kcal/mol between D(H—CH_2OH)

Can. J. Chem. Downloaded from www.nrcresearchpress.com by 210.87.254.6 on 09/05/12
For personal use only.

TABLE 4. Relationship between rate constants and bond energies

Solvent	$k_1 \times 10^3$ (s^{-1})	k_2 (l mol^{-1} s^{-1})	k_2/n* (l mol^{-1} s^{-1})	E_a* (kcal/mol)	D(H—CR_1R_2OH)† (kcal/mol)
Methanol	4.25	17.7	5.9	11.5	94±2
Ethanol	13.9	81.4	40.7	10.4	92±2
2-Propanol	34.6	264	264	9.3	90±2

*n = Numbers of α-(C)—H in the alcohol molecules.
†See text.

and D[H—$C(CH_3)OH$], and between D[H—$C(CH_3)OH$] and D[H—$C(CH_3)_2OH$] may be deduced from these two studies. In order to correlate more precisely the relation between the bond dissociation energies and the rate constants, we should consider the second order rate constants k_2 rather than k_1, *i.e.* making the correction for the different alcohol concentrations. In addition we should also correct for the statistical number of abstractable hydrogen atoms. If only the α-H's are considered, there are three in methanol, two in ethanol, and one in 2-propanol. The relationship between rate constants and bond energies of the C—H bond being abstracted is given in Table 4. This selectivity of radicals attacking primary, secondary, and tertiary C—H bonds is well established (13) and has been described in terms of the Polanyi equation which relates the activation energies of radical reactions to the strengths of the bond broken, and hence to the heats of reaction

$$[21] \qquad E = \alpha\{D(\text{C—H}) - \beta\}$$

where α, β are constants for the particular reactions. For example, α = 0.49, β = 74.3 kcal/mol for methyl radical abstracting reactions (14), and α = 0.86 and β = 82.5 kcal/mol for bromine atom attack on alkanes (14). In our case, if the frequency factor in the Arrhenius equation for abstraction per hydrogen is assumed to be 10^9 l mol^{-1} s^{-1}, the activation energies calculated are 11.5 kcal/mol for methanol, 10.4 kcal/mol for ethanol, and 9.3 kcal/mol for 2-propanol. Hence the α and β values in the Polanyi relation can be estimated to be 0.55 and 73 kcal/mol, respectively for diphenylphosphinyl radicals abstracting from alcohols.

Experimental

Triphenylphosphine (Aldrich) was recrystallized three times from ethanol. Tetraphenyldiphosphine (K & K) and diphenylphosphine (Alfa) were used without further purification. Methanol and 2-propanol were spectroscopic grade. Ethanol was absolute grade. Methanol-d_1 (99% D) was purchased from Stohler Isotope Chemicals. Diphenylphosphine oxide was prepared by autooxidation of diphenylphosphine (15).

The flash apparatus is of conventional design. The photolysis flash system consisted of two xenon-filled flash tubes, with input energies ranging from 100–5000 J and the corresponding flash durations (1/3 peak) ranging from 20–80 μs. A Garton-type flash tube of 200 J energy with a duration of 2.2 μs manufactured by Chelsea Instruments Limited, London, England, was coupled with a Spex (Model 1700-III) 3/4 m Czerny-Turner spectrometer/spectrograph in the flash spectroscopy. In the case of kinetic spectrophotometry, a Jarrell-Ash 17-721E photomultiplier with a quartz envelope fitted with a cathode follower was placed at the exit of the spectrometer and the spectro-flash was replaced by a 200 W high pressure mercury lamp. A Tektronic Type 564 B storage oscilloscope with plug-in accessories was used for trace recording. The detecting system has been tested for time response and linearity. The flash cells made of quartz had the following dimensions: 43 cm long, 1.3 cm in diameter; 28 cm long, 2.5 cm in diameter; and 15 cm long, 2.5 cm in diameter. Solutions for the flash experiments were extensively degassed by repetitive freeze–pump–thaw cycles under vacuum. The concentrations of the solutions ranged from 1×10^{-4} to 1×10^{-6} M. The flash study was carried out at room temperature (20° ± 2°).

In the analyses of the decay curves, and the construction of the diphenylphosphinyl radical spectrum, correction was made for the transients from the pure alcohol solvents. The correction was based on Beer's law. For simplicity, assume the transient from the solvent has concentration C_1 and extinction coefficient at the wavelength studied ε_1, and C_2 and ε_2 are the respective terms for diphenylphosphinyl radicals, then we have

$$[22] \qquad \log I_0/I = \varepsilon_1 C_1 l + \varepsilon_2 C_2 l$$

where l is the length of the cell, I_0 the light intensity with no absorption and I the light intensity with absorption. If one of the species is present, we have

$$[23] \qquad \log I_0/I_1 = \varepsilon_1 C_1 l$$

$$[24] \qquad \log I_0/I_2 = \varepsilon_2 C_2 l$$

where I_1, I_2 have usual meanings.

Solving these equations, we obtain

$$[25] \qquad \varepsilon_2 C_2 l = \log I_0/I_2 = \log I_1/I$$

In the product analysis experiments, solutions were thoroughly degassed and irradiated by a 200 W high

Can. J. Chem. Downloaded from www.nrcresearchpress.com by 210.87.254.6 on 09/05/12
For personal use only.

TABLE 5. ^{31}P n.m.r. data for the phosphines and phosphine oxides

Compound	Chemical shift (p.p.m. from H_3PO_4) This work	Chemical shift (p.p.m. from H_3PO_4) Literature value	Coupling constant (Hz) This work	Coupling constant (Hz) Literature value	Reference
Ph_2PH	41.2±0.2	41.0 41.1 43.8	217±2	214 218 239	7, 8, 16
Ph_2PD	43.2±0.2	42.4	34±0.5	34	7
$Ph_2P(O)H$	−22.4±0.2	−22.9 −18	482±2	490	15, 16
$Ph_2P(O)D$	−22.4±0.2		74±2		
Ph_3P	6.0±0.2				
$Ph_3P{=}O$	−31.7±0.5				
$Ph_2{-}P{-}P{-}Ph_2$	16.0±0.2	15.2			16

pressure mercury lamp. A Bruker n.m.r. spectrometer was used for ^1H n.m.r. (60 MHz, with 3 mm tubes) and ^{31}P n.m.r. (24.3 MHz, with 15 mm o.d. tubes) spectra. The chemical shifts and the coupling constants of the organophosphorus compounds determined in this study are represented in Table 5.

Gas–liquid chromatography was performed by means of a Sargent flame-ionization unit. Nitrogen was used as carrier gas. An 8 ft 5% silicone gum rubber S.E. 30 column was used for analysis of the phosphorus compounds and a 10 ft 20% diisodecyl phthalate column for benzene and acetone. For quantitative g.l.c. analysis triphenylamine was used as internal standard for the phosphorus compounds, and toluene as internal standard for benzene.

The authors are indebted to Mrs. Penny Atkins and Mr. David Groves for some technical assistance. Financial support from the National Research Council of Canada and the Department of Energy, Mines, and Resources, is gratefully acknowledged.

1. L. HORNER and J. DÖRGES. Tetrahedron Lett. 763 (1965).
2. M. L. KAUFMAN and C. E. GRIFFIN. Tetrahedron Lett. 769 (1965).
3. R. S. DAVIDSON, R. A. SHELDON, and S. TRIPPETT. J. Chem. Soc. C, 722 (1966); Chem. Commun. 99 (1966).
4. U. Schmidt, F. GEIGER, A. MÜLLER, and K. MARKAU. Angew. Chem. Internat. Ed. **2**, 400 (1963); U. SCHMIDT, K. KABITZKE, K. MARKAU, and A. MÜLLER. Chem. Ber. **99**, 1497 (1966).
5. S. K. WONG and J. K. S. WAN. Spectrosc. Lett. **3**, 135 (1970).
6. P. J. SULLIVAN and W. S. KOSKI. J. Amer. Chem. Soc. **84**, 1 (1962).
7. E. FLUCK and H. BINDER. Z. Naturfursch. **22B**, 1001 (1967).
8. J. W. AKITT, R. H. CRAGG, and N. N. GREENWOOD. Chem. Commun. 134 (1966).
9. E. BUCKLEY and E. WHITTLE. Trans. Faraday Soc. **58**, 536 (1962).
10. A. M. TARR and E. WHITTLE. Trans. Faraday Soc. **60**, 2039 (1964).
11. R. WALSH and S. W. BENSON. J. Amer. Chem. Soc. **88**, 3480 (1966).
12. F. R. CRUICKSHANK and S. W. BENSON. J. Phys. Chem. **73**, 733 (1969).
13. A. F. TROTMAN-DICKENSON. *In* Advances in Free-Radical Chemistry. Vol. 1. *Edited by* G. H. Williams. Logos Press, London. 1965 Chap. 1.
14. A. F. TROTMAN-DICKENSON. Chem. Ind. 379 (1965).
15. M. M. RAUHUT and H. A. CURRIER. J. Org. Chem. **26**, 4626 (1961).
16. V. MARK, C. H. DUNGAN, M. CRUTCHFIELD, and J. VAN WAZER. *In* Topics in Phosphorus Chemistry. Vol. 5. *Edited by* M. Grayson and E. J. Griffin. John Wiley and Sons, New York. 1967. pp. 227–457.

Can. J. Chem. Downloaded from www.nrcresearchpress.com by 210.87.254.6 on 09/05/12
For personal use only.

Can. J. Chem. Downloaded from www.nrcresearchpress.com by 210.87.254.42 on 09/05/12
For personal use only.

Nonequilibrium Thermodynamics in Chemical Kinetics

M. L. ANDERSON[1] AND R. K. BOYD
Department of Chemistry, University of Guelph, Guelph, Ontario

Received October 7, 1970

The description of chemical reaction rates, in terms of the language of nonequilibrium thermodynamics, is compared with the conventional language of chemical kinetics. It is concluded that the formalism of nonequilibrium thermodynamics possesses considerable disadvantages, even in the regime where the rate is a linear function of affinity; this conclusion also holds for cases where chemical rates are coupled to diffusion processes. Some of the difficulties involved are illustrated using the experimental data of Nebeker and Pings (28).

La description de la vitesse de réaction en termes du langage de la thermodynamique irréversible est comparée avec le langage conventionnel de la cinétique chimique. Il est conclu que le formalisme de la thermodynamique irréversible a des désavantages considérables et ceci même quand la vitesse est une fonction linéaire de l'affinité; cette conclusion est aussi valable dans les cas où la vitesse des réactions est liée aux processus de diffusion. Certaines des difficultés impliquées sont illustrées à l'aide des résultats expérimentaux de Nebeker et Pings (28).

Canadian Journal of Chemistry, 49, 1001 (1971)

I. Introduction

A large number of texts on nonequilibrium thermodynamics (n.t.) has appeared, particularly in the last ten years (1–7); the advantage of this formalism is that it treats all rate processes from a common point of view. This feature of n.t. has formed the basis of the claim that n.t. offers the ideal language for the description of systems in which different irreversible processes are occurring simultaneously; in particular, the claims of n.t. in the realm of biological systems have been strongly urged (5). In this case, at least, chemical change is one of the more important irreversible processes involved. Despite these compelling features, almost no experimental investigation of the rate of a chemical reaction has been interpreted in terms of the language of n.t.; to the knowledge of the present authors, the only exceptions (8, 9) were cases where the specific aim of the experiments was to test the n.t. formalism, rather than to investigate the kinetic behavior of the reaction systems.

It is clear that the great empirical success of the conventional chemical kinetic language, together with its persuasive theoretical rationale, provides a considerable barrier to the adoption of an alternative description; indeed, it does not seem unreasonable to insist that any such alternative must be consistent with the kinetic description. In the present work, the relationship between the two descriptions is investigated, and, where possible, the advantages and disadvantages of each are evaluated.

[1]Summer student, summer 1970.

II. Rate of a Single Chemical Reaction

In its present state of development, n.t. is essentially limited to processes whose rate is a linear function of a suitably defined thermodynamic force; however, second-order terms will also be included here. Scalar processes only will be considered

$$[1] \qquad J = LX + MX^2$$

where J and X are the conjugate thermodynamic flux and force, respectively, and L and M are phenomenological coefficients.

For the case of a chemical reaction, denoted by the stoichiometric equation

$$[2] \qquad \sum_i \nu_i M_i = 0$$

the usual definition of rate $= 1/\nu_i(dc_i/dt)$, satisfies the requirements for the thermodynamic flux, while the affinity $A = -\sum_i \nu_i \mu_i$ is the corresponding force (11). Here, ν_i is the stoichiometric coefficient of species M_i, conventionally defined as negative for reactants, positive for products; μ_i is the chemical potential of M_i.

The conditions, under which the usual chemical kinetic equations reduce to the form [1], have frequently (1–11) been deduced for special cases where the kinetic equation takes the form

$$[3] \quad v = 1/\nu_i(dc_i/dt) = k\beta \prod_{r=1}^{n_r} (a_r)^{-\nu_r} - k'\beta \prod_{p=1}^{n_p} (a_p)^{+\nu_p}$$

Here, a_i is the activity of M_i; n_r and n_p are the

Can. J. Chem. Downloaded from www.nrcresearchpress.com by 210.87.254.42 on 09/05/12
For personal use only.

number of reactant and product species, respectively. The rate constants k and k′ are functions of temperature only, while β is a function of all thermodynamic variables; in terms of transition-state theory, β is the reciprocal of the activity coefficient of the transition complex (12). Equation 3 is a special case of a rate equation found to be satisfactory for a large number of systems (12); in general, however, the reaction orders α_i are not necessarily given by $\alpha_i = |\nu_i|$, as in eq. 3. A more general rate equation is

$$[4] \qquad v = k\beta \prod_{i=1}^{m} (a_i)^{\alpha_i} - k'\beta \prod_{i=1}^{m} (a_i)^{\alpha_i'}$$

when m is the total number of species whose activity affects the rate, other than via β. Now, the first term may contain the activities of species other than reactants, (*e.g.* products, catalysts), and the second term those of species other than products. It does not appear to have been demonstrated previously that empirically successful (12) rate expressions like [4] may be reduced to the form of eq. 1, suitable for treatment by n.t. In order to do this, it is necessary to discover the restrictions imposed upon the form of [4] by the requirement that *all* sets of equilibrium activities $\{a_i^{eq}\}$, which correspond to zero affinity, also make v vanish. All catalytic species, which do not affect the affinity, must have $\alpha_i = \alpha_i'$; for reactants and products, it may be shown (13–15) that a necessary and sufficient condition for A and v (given by eq. 4) to vanish together, is

$$[5] \qquad (\alpha_i' - \alpha_i)/\nu_i = n > 0, \text{ for all } i$$

It is readily shown, by considering [4] at equilibrium, that [5] implies;

$$[6] \qquad k/k' = K^n$$

where K is the thermodynamic equilibrium constant for reaction 2, given by

$$[7] \qquad K(T) = \prod_{i=1}^{N} (a_i^{eq})^{\nu_i}$$

In addition, the affinity may be expressed as

$$[8] \quad A = -\sum_{i=1}^{N} \nu_i \mu_i = RT \ln \prod_{i=1}^{N} (a_i^{eq}/a_i)^{\nu_i} = RT \ln \left[K \prod_{i=1}^{N} (1/a_i)^{\nu_i} \right]$$

where $N = n_r + n_p$ is the total number of species involved in reaction 2. Combination of eqs. 4–8 gives

$$[9] \quad v = \left[k\beta \prod_{i=1}^{m} (a_i)^{\alpha_i} \right] \times [1 - \exp(-nA/RT)]$$

recalling that $\alpha_i = \alpha_i'$ for species not appearing in [7] and [8]. In order to reduce [9] to the form of [1], the two factors in [9] may be expanded in Taylor Series in (A/RT). The second factor yields a series which converges for all real (nA/RT); the first factor may be written

$$[10] \quad k\beta \prod_{i=1}^{m} (a_i^{eq})^{\alpha_i} [1 + d_1(A/RT) + \cdots] = k\beta \prod_{i=1}^{m} (a_i)^{\alpha_i}$$

where

$$d_1 = \partial \left[\prod_{i=1}^{m} (a_i/a_i^{eq})^{\alpha_i} \right] \Big/ \partial [A/RT]_{A=0}$$

etc. It is not possible to give a general mathematical discussion of the region of convergence of [10]; however, on physical grounds, [10] must also converge for all real (A/RT), since even at the limit of infinite affinity, reactions are known to proceed with a finite velocity. Then

$$[11] \quad v = \left[k\beta \prod_{i=1}^{m} (a_i^{eq})^{\alpha_i} \right] \times [n(A/RT) + n(d_1 - n/2)(A/RT)^2 + \cdots]$$

Previous derivations (1–11) have involved the special case of [11] with $n = 1$. It may be pointed out that the common practice of identifying $[k\beta \prod_{i=1}^{m} (a_i^{eq})^{\alpha_i}]$ with v_{eq}, the one-way reactive flux at equilibrium, is not necessarily valid (16).

While eq. 4 is a very common rate equation (12), it does not include all known cases; a more general expression for v is

$$[12] \quad v = r(\{a_i\},T,x,y,\cdots) - r'(\{a_i\},T,x,y,\cdots)$$

where $\{a_i\}$ represents the set of activities defining the affinity of the reaction, and $x,y,\cdots$ are non-thermodynamic variables, such as catalyst concentration, area of active surface, etc. Hollingsworth (17) has elucidated necessary and sufficient conditions under which [12] shall vanish for all $\{a_i^{eq}\}$ which cause A to vanish. If f and

Can. J. Chem. Downloaded from www.nrcresearchpress.com by 210.87.254.42 on 09/05/12
For personal use only.

θ are defined by

$$f(\{a_i\}, T,x,y, \cdots) \equiv r'/r$$

$$\theta \equiv \exp(-A/RT) = \prod_{i=1}^{N} (a_i/a_i^{eq})^{\nu_i}$$

then the function f must be (17) such that

$$[13] \qquad f-1 = (\theta-1)[(\partial f^*/\partial\theta)_{\theta=1} + \tfrac{1}{2}(\partial^2 f^*/\partial\theta^2)_{\theta=1}(\theta-1) + \cdots]$$

where $f^* = (r'/r)$ is the function obtained from f by eliminating any *one* a_i from the defining equations for f and θ. If $g \equiv (r/r_{eq})$ may be expanded in a Taylor Series, [13] becomes

$$[14] \qquad v = r_{eq}[(f^*)'(A/RT) + \{\tfrac{1}{2}(f^{*\prime\prime} - f^{*\prime}) + g'f^{*\prime}\}(A/RT)^2 + \cdots]$$

where

$$f^{*\prime} \equiv (\partial f^*/\partial\theta)_{\theta=1}$$

and

$$g' \equiv [\partial g/\partial(A/RT)]_{A=0}$$

etc. It is readily shown that [14] reduces to [11] if [12] has the special form [4].

Thus, even for very general kinetic descriptions, it is possible to show that the rate of a single chemical reaction, occurring in isolation, may be described by a power series in the affinity. This conclusion follows from thermodynamic constraints upon the form of the kinetic rate expression; if the latter is known, the phenomenological coefficients of the n.t. description may be identified kinetically. An assumption implicit in all the above concerns the existence of a unique degree of advancement, and thus of a reaction velocity, for reaction 2; this is not necessarily a trivial problem (18, 19).

III. Thermodynamic Coupling of Chemical Reactions

Thermodynamic coupling of macroscopically distinguishable processes represents the field in which n.t. is highly successful. If two such processes are occurring in the same system, the two rates are given by

$$[15] \qquad J_1 = L_{11}X_1 + L_{12}X_2 + M_{111}X_1^2 + M_{122}X_2^2 + M_{112}X_1X_2 + \cdots$$

$$J_2 = L_{21}X_1 + L_{22}X_2 + M_{211}X_1^2 + M_{222}X_2^2 + M_{212}X_1X_2 + \cdots$$

If the coupling coefficients $L_{12}, L_{21}, M_{122}, M_{211}, M_{112}$ and M_{212} are nonzero, the two processes are said to be thermodynamically coupled; the Onsager Reciprocity Theorem (O.r.t.) then predicts $L_{12} = L_{21}$ (10). A glaring omission in the generally satisfactory experimental verification of O.r.t. (20) is the lack of any direct test for the chemical case. Previous work in this area has concentrated (1–11) on demonstrating the equivalence, for this case, of O.r.t. and the Principle of Detailed Balance (p.d.b.); these treatments have been restricted to triangular reaction schemes, in which the individual reaction steps follow simple mass-action expressions like [3]. To avoid the complexity of notation required for a completely general development, the particular reaction system, for which experimental data are available, will be treated here.

In an isothermal system, whose thermodynamic state is adequately represented in terms of the concentrations of five species NO, NOCl, Cl_2, ICl, and I_2, it is readily shown (ref. 12, pp. 169–171) that only *two* linearly independent stoichiometric equations may be written. This system may be written as a triangular scheme

[16]

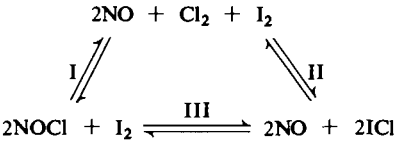

Any two of the three stoichiometric reactions in [16] may be chosen for the thermodynamic description, say I and II. Unambiguous experimental measures of the independent thermodynamic fluxes J_1 and J_2, will then be given by $(+\frac{1}{2}dc_{NO}/dt)$ and $(-dc_{I_2}/dt)$, respectively, if the forward directions are arbitrarily chosen to correspond to the clockwise direction in [16], as written. Assuming that no problems exist concerning definitions of degrees of advancement (18, 19), the n.t. description of the rate of relaxation of [16] is given by eq. 15, with the fluxes defined as above, and the forces given by the affinities of reactions I and II.

If each individual step in [16] is considered independently of the others, the considerations of Section II above apply, so that

$$[17] \qquad v_1 = l_1A_1 + m_1A_1^2$$

$$v_2 = l_2A_2 + m_2A_2^2$$

$$v_3 = l_3A_3 + m_3A_3^2$$

Can. J. Chem. Downloaded from www.nrcresearchpress.com by 210.87.254.42 on 09/05/12
For personal use only.

where v_1, v_2, and v_3 are the velocities of the individual steps, as distinct from the thermodynamic fluxes J_1 and J_2. As emphasized above, eqs. 17 are a consequence of thermodynamic constraints upon the form of the "true" rate equations at equilibrium. Equations 17 may thus be applied to the complex reaction mixture, in which all three reactions are occurring simultaneously, only if it is assumed that, when the whole system is at equilibrium, each mechanistic step in [16] is independently at equilibrium; this assumption is the Principle of Detailed Balance (p.d.b.).

For mechanism [16], assuming p.d.b., and noting that

$$A_3 = -(A_1 + A_2)$$

and

$$J_1 \equiv \tfrac{1}{2}\mathrm{d}c_{\mathrm{NO}}/\mathrm{d}t = v_1 - v_3$$
$$J_2 \equiv -\mathrm{d}c_{\mathrm{I}_2}/\mathrm{d}t = v_2 - v_3$$

eqs. 15 and 17 give

$$[18]\quad J_1 = (l_1 + l_3)A_1 + (l_3)A_2 + (m_1 - m_3)A_1^2 + (-m_3)A_2^2 + (2m_3)A_1A_2$$
$$J_2 = (l_3)A_1 + (l_2 + l_3)A_2 + (-m_3)A_1^2 + (m_2 - m_3)A_2^2 + (2m_3)A_1A_2$$

whence $L_{12} = L_{21}$, as has been demonstrated previously (1–11). However, extension of this widely-accepted treatment, to second order, shows that higher-order reciprocities are also predicted; should this be true, it would greatly extend the usefulness of n.t. for chemical kinetics. More general derivations of higher-order reciprocities have been given (21–23), independently of any particular mechanism.

It now seems certain that no such simple higher-order reciprocities exist, in general; Andrews (24) has elucidated the often subtle errors in these derivations (21–23), which are macroscopic arguments taking no account of the Principle of Microscopic Reversibility (p.m.r.), which underlies both O.r.t. (10) and p.d.b. (25). In addition, by extending Onsager's original treatment (10), Holmes and Mortimer (26) derived the rather complicated relationship between the higher-order coefficients and those of lower order. For the case of mechanism [16], the present authors have been unable to reduce this relationship (26) to any simple form. It appears, therefore, that the higher-order reciprocities evident in eq. 18 are incorrect, even though the derivation is an apparently trivial extension of standard treatments (1–11), which use p.d.b. explicitly. By considering a very special case, in which the exact kinetic equations could be unambiguously rearranged to the form of [15], Rastogi *et al.* (27) were able to confirm this general conclusion.

The source of error is an ambiguity in the term "independently", as used in justifying eqs. 17. As emphasized in Section II, such rate equations are consistent with the "correct" kinetic equations as a result of thermodynamic constraints upon the latter, considered at the equilibrium state; but the equilibrium state involved is the infinite time-limit for the single reaction concerned, proceeding in isolation. In the complex system, on the other hand, the time variation of the affinity of a given reaction is due not only to the rate of that reaction, as was assumed in deriving [17], but to the rates of the other reactions also. The three reactions are still proceeding "independently", in the sense demanded by p.d.b.; it is the description of these "independent" rates, in terms of the simple eqs. 17, which breaks down. Equation 18 is valid to first order only, as a *consequence* of O.r.t.

As a practical example of some of the difficulties involved, experimental data obtained by Nebeker and Pings (9, 28) for reaction system [16] were reinterpreted; true thermodynamic coupling, as distinct from interference (29), was demonstrated to exist in this system. Reactions I and III were chosen (9) as the independent processes, and the rate data were fitted to second-order equations [15]; in the experiment considered by the original authors (9, 28) to be their best case, the linear coupling coefficients differed by a factor of about -200. As a first attempt to improve upon this result, the raw data (9) were reanalyzed in terms of reactions I and II, since the original treatment of the reverse of reaction III, as a fourth-order reaction, seemed unlikely to be valid. Table 1 shows the results obtained for this best case (270 to 500 s reaction time, run 16 (9)); all other runs (9) gave better fits when second-order terms were included, but this example happened to give the best fit using only linear terms, even though $A > 10RT$. In this case, $L_{21}/L_{12} \simeq -5$, well outside the standard errors; examination of the computed residuals showed alternating sequences of positive deviations and negative deviations, an indication of a poor fitting function (30) (see also Fig. 25, ref. 9).

TABLE 1. Phenomenological coefficients derived for run 16, ref. 11 (Velocities in mol l^{-1} s^{-1}; affinities in calories)

Parameter	Value	
L_{11}	$(7.4\pm1.3) \times 10^{-11}$	$-(32\pm26) \times 10^{-11}$
L_{22}	$-(24.9\pm1.8) \times 10^{-11}$	$(13\pm32) \times 10^{-11}$
L_{12}	$-(5.3\pm1.4) \times 10^{-11}$	$(23\pm23) \times 10^{-11}$
L_{21}	$(25.9\pm1.8) \times 10^{-11}$	$-(16\pm37) \times 10^{-11}$
M_{111}		$(1\pm2) \times 10^{-14}$
M_{222}		$(0.4\pm2) \times 10^{-14}$
M_{122}		$(2.3\pm1.8) \times 10^{-14}$
M_{211}		$(2.6\pm3.2) \times 10^{-14}$
M_{112}		$(1.7\pm2.9) \times 10^{-14}$
M_{212}		$(1.5\pm4.1) \times 10^{-14}$

It is clear that inclusion of only low-order terms in [15] is inadequate, and the first-order coefficients derived from such least squares treatments bear no resemblance to those governing the relaxation near equilibrium (10). Even if sufficient terms were included for [15] to converge, there is no guarantee that the least-squares criterion will yield the correct first-order coefficients, unless data are available well into the linear regime. Another feature of the statistical analysis was the uniformly high level of correlation coefficients between the affinities (0.93 to 0.99). This is merely a quantitative confirmation of Andrews' criticism (24) of treatments which consider affinities to be independent variables; for a given system evolving naturally towards equilibrium, time is the only independent variable.

Although the experimental data obtained by Nebeker and Pings (9) thus appear unsuitable for testing O.r.t., they do, in principle, offer an opportunity for a direct test of p.d.b. However, to do so requires that the rate laws for the reactions involved are either known, or can be reasonably estimated. Reaction I, at room temperature, although not an elementary reaction, does appear (31) to proceed according to the appropriate form of [3]. Reaction II is predicted (32) to proceed by a second-order, bimolecular mechanism, but unfortunately appears to be surface-catalyzed; it was here assumed to proceed according to the appropriate form of [3], with the heterogeneous contribution kinetically indistinguishable. The following mechanism was assumed for reaction III

$$2NO + I_2 \underset{k_{3a}}{\overset{K_{3a}}{\rightleftharpoons}} 2NOI$$

$$NOI + ICl \underset{k_{3b}'}{\overset{k_{3b}}{\rightleftharpoons}} NOCl + I_2$$

This assumed mechanism, with step (3*a*) essentially at equilibrium is an example of one of Hollingsworth's cases (19) where a unique degree of advancement exists for the overall reaction. The mechanism was proposed by analogy with that for the $NO–Cl_2–Br_2$ system (33), and leads to an overall rate law of the form of [6], with $n = 1/2$

$$v_3 = k_2 C_{NO} C_{ICl} C_{I_2}^{\frac{1}{2}} - k_2' C_{NOCl} C_{I_2}$$

assuming ideal gas behavior.

In order to express these assumed rate equations in a form suitable for testing p.d.b. eq. 6 is rewritten

$$[19]\quad v = \left[k\beta \prod_{i=1}^{N} (a_i^{eq})^{\alpha_i}\right]\left[\prod_{i=1}^{N} (a_i/a_i^{eq})^{\alpha_i}\right] - \left[k'\beta \prod_{i=1}^{N} (a_i^{eq})^{\alpha_i'}\right]\left[\prod_{i=1}^{N} (a_i/a_i^{eq})^{\alpha_i'}\right]$$

$$= C \exp(A_f/RT) + C' \exp(A_r/RT)$$

where A_f and A_r are the respective affinities for the process

$$\sum_i \alpha_i M_i(a_i) \rightarrow \sum_i \alpha_i M_i(a_i^{eq})$$

$$\sum_i \alpha_i' M_i(a_i) \rightarrow \sum_i \alpha_i' M_i(a_i^{eq})$$

Here, $M_i(a_i)$ denotes the ith. constituent in a state with activity a_i; also, $A_f - A_r = nA$. Applying [19] to the assumed rate laws for scheme [16], gives

$$[20]\quad J_1 \equiv -\tfrac{1}{2} dc_{NO}/dt = C_{11}\exp(A_{f1}/RT) + C_{11}'\exp(A_{r1}/RT) + C_{13}\exp(A_{f3}/RT) + C_{13}'\exp(A_{r3}/RT)$$

$$J_2 \equiv -dc_{I2}/dt = C_{22}\exp(A_{f2}/RT) + C_{22}'\exp(A_{r2}/RT) + C_{23}\exp(A_{f3}/RT) + C_{23}'\exp(A_{r3}/RT)$$

Although eqs. 20 are expressed in language similar to that of n.t., they are simply re-ex-

Can. J. Chem. Downloaded from www.nrcresearchpress.com by 210.87.254.42 on 09/05/12
For personal use only.

TABLE 2. Coefficients for run 13, ref. 11, fitted to eq. 20

Parameter	Value
C_{11}	$(1.3\pm0.1) \times 10^{-12}$
C_{11}'	$-(5.2\pm2.1) \times 10^{-8}$
C_{13}	$-(0.02\pm0.01) \times 10^{-12}$
C_{13}'	$(0.08\pm0.03) \times 10^{-12}$
C_{23}	$(0.019\pm0.005) \times 10^{-12}$
C_{23}'	$-(0.014\pm0.025) \times 10^{-12}$
C_{22}	$(0.002\pm0.001) \times 10^{-12}$
C_{22}'	$-(1.5\pm2.1) \times 10^{-8}$

pressions of the kinetic rate laws. If p.b.d. is obeyed, then

$$[21] \quad C_{11} = -C_{11}'; \; C_{22}' = -C_{22}'; \; C_{13}' = -C_{13}' = -C_{23}' = C_{23}'$$

As shown in the typical result given in Table 2, this analysis also yielded negative results. This was doubtless due to erroneous assumptions made in writing the appropriate rate laws.

IV. Discussion

It is clear that there are no shortcuts in chemical kinetics; regardless of the language chosen to describe the rate, there is no substitute for an experimental determination of the rate equation. The only partial exception to this conclusion is expected to involve systems sufficiently close to equilibrium that rates are linear functions of affinities. In practical terms, this is probably limited to electrode reactions, where affinities are precisely controllable and measurable electrically (34). The importance of the linear regime lies in the validity of O.r.t. only at first-order; for the conventional kinetic description, on the other hand, p.d.b. offers a simplification over the entire range of affinities.

Even in the linear regime, a fundamental disadvantage of the n.t. description arises from the fact, apparent from a comparison of eqs. 1 and 14, that the coefficients are functions of the equilibrium state of the system. This implies that phenomenological coefficients, measured in one reaction mixture, cannot be applied directly to another. The necessary transformation can be made, but, as shown in Section II above, this requires knowledge of the relevant *kinetic* rate laws. In the latter case, only correction factors, such as β in eq. 4, vary in this way.

It is possible that these disadvantages of the n.t. description could be outweighed, for example, if thermodynamic coupling should be important. For the case of coupled chemical reactions, examination of eq. 18 shows that the coupling coefficients vanish if $l_3 = 0 = m_3$. Such coupling is thus simply a consequence of the thermodynamically redundant, but mechanistically significant, reaction III, and is thus well within the realm of conventional chemical kinetics. However, it has been suggested that n.t. offers an ideal language for a description of systems in which chemical rates are coupled to other processes, such as diffusion. However, direct coupling coefficients between forces of different tensorial orders, are identically zero, according to the Curie–Prigogine Principle (ref. 5, pp. 88–89). In the present case, this simply implies that a local chemical rate is independent of the local composition gradient; proposed mechanisms for "indirect" coupling of chemical rates to diffusion processes, although expressed in the n.t. formalism, (ref. 5, Chap. 14), appear equally valid if the chemical rate is described differently.

The present work has thus resulted in generally negative conclusions concerning the suitability of the n.t. language for chemical kinetics. Similar opinions have been expressed previously (11, 35), although the treatment of the principal points, discussed above, was considerably less detailed. However, O.r.t. is a fundamental theorem, offering the possibility of a macroscopic test of p.m.r.; we are presently attempting to test O.r.t. for the chemical case, using a relaxation technique with phase-sensitive detection to aid in obtaining precise data in the linear regime.

Financial support by the National Research Council of Canada is gratefully acknowledged. The Institute of Computer Studies, University of Guelph, provided valuable assistance with the statistical analysis.

1. I. PRIGOGINE. Introduction to Thermodynamics of Irreversible Processes. 3rd ed. John Wiley, New York. 1967.
2. S. R. DEGROOT and P. MAZUR. Non-equilibrium Thermodynamics. North-Holland Publishing Company, Amsterdam. 1962.
3. K. G. DENBIGH. Thermodynamics of the Steady State. Methuen, London. 1950.
4. D. D. FITTS. Non-equilibrium Thermodynamics. McGraw-Hill, New York. 1962.
5. A. KATCHALSKY and P. F. CURRAN. Non-equilibrium Thermodynamics in Biophysics. Harvard University Press, Cambridge, Mass. 1967.

Can. J. Chem. Downloaded from www.nrcresearchpress.com by 210.87.254.42 on 09/05/12
For personal use only.

6. W. YOURGRAU, A. VAN DER MERWE, and G. RAW. Treatise on Irreversible and Statistical Thermophysics. MacMillan, New York. 1966.
7. P. VAN RYSSELBERGHE. Thermodynamics of Irreversible Processes. Blaisdell Publishing Company, New York. 1963.
8. I. PRIGOGINE, P. OUTER, and C. HERBO. J. Phys. Colloid Chem. **52**, 321 (1948).
9. E. B. NEBEKER. Ph.D. Thesis. California Institute of Technology. 1965.
10. L. ONSAGER. Phys. Rev. **37**, 405 (1931); **38**, 2265 (1931).
11. T. A. BAK. Advan. Chem. Phys. **3**, 33 (1961).
12. K. G. DENBIGH. Principles of Chemical Equilibrium. Cambridge University Press, Cambridge. 1955. pp. 445–448.
13. M. MANES, L. J. E. HOFER, and S. WELLER. J. Chem. Phys. **18**, 1355 (1950).
14. Reference 12, pp. 444–445.
15. E. H. BLUM and R. LUUS. Chem. Eng. Sci. **19**, 322 (1964).
16. B. WIDOM. Science, **148**, 1555 (1965).
17. C. A. HOLLINGSWORTH. J. Chem. Phys. **20**, 1649 (1952).
18. S. H. BAUER. J. Chem. Phys. **21**, 1888 (1953).
19. C. A. HOLLINGSWORTH. J. Chem. Phys. **27**, 1346 (1957).
20. D. G. MILLER. Chem. Revs. **60**, 15 (1960).
21. J. C. M. LI. J. Chem. Phys. **29**, 747 (1958); J. Appl. Phys. **33**, 616 (1962).
22. P. VAN RYSSELBERGHE. J. Chem. Phys. **36**, 1329 (1962); Ind. Eng. Chem. Fundam. **5**, 151 (1966).
23. C. M. SLIEPCEVICH and D. FINN. Ind. Eng. Chem. Fundam. **2**, 249 (1963).
24. F. C. ANDREWS. Ind. Eng. Chem. Fundam. **6**, 48 (1967); J. Chem. Phys. **47**, 3170 (1967).
25. J. S. THOMSEN. Phys. Rev. **91**, 1263 (1953).
26. C. F. HOLMES and R. G. MORTIMER. Ind. Eng. Chem. Fundam. **6**, 321 (1967).
27. R. P. RASTOGI, R. C. SRIVASTAVA, and K. SINGH. Trans Faraday Soc. **61**, 854 (1964).
28. E. B. NEBEKER and C. J. PINGS. Ind. Eng. Chem. Fundam. **5**, 310 (1966).
29. E. B. NEBEKER and C. J. PINGS. Ind. Eng. Chem. Fundam. **4**, 376 (1965).
30. W. E. WENTWORTH. J. Chem. Ed. **42**, 96 (1965).
31. J. HEICKLEN and N. COHEN. Advan. Photochem. **5**, 157 (1968).
32. R. M. NOYES. J. Amer. Chem. Soc. **88**, 4311 (1966); **88**, 4318 (1966); **88**, 4324 (1966).
33. I. C. HISATSUNE and L. ZAFONTE. J. Phys. Chem. **73**, 2980 (1969).
34. R. PARSONS. J. Chem. Ed. **45**, 390 (1968).
35. J. WEI. *In* Applied Thermodynamics. Chap. 3. (American Chemical Society Publications, Washington, D.C. 1968).

Can. J. Chem. Downloaded from www.nrcresearchpress.com by 210.87.254.42 on 09/05/12
For personal use only.

Can. J. Chem. Downloaded from www.nrcresearchpress.com by 210.87.254.6 on 09/05/12
For personal use only.

Use of a Gettering Material to obtain Oxygen-free Liquid Samples for Nuclear Spin Relaxation Studies

H. S. SANDHU
Physics Department, University of Victoria, Victoria, British Columbia

Received November 3, 1970

An investigation into the gettering powers of aluminum, barium, magnesium, and misch metal for removing oxygen from liquid samples has been carried out. The liquids treated with each getter are: H_2O, CH_2Br_2, CH_2Cl_2, CH_2I_2, and CH_3OH. The results show that aluminum is more suitable for all these liquids even though the other getters are also effective. It appears that as long as there is no strong reaction, any of these getters can be used to remove oxygen from any liquid.

Une étude a été faite de la valeur de l'aluminum, du barium, du magnésium et du métal Misch® comme getters pour l'élimination de l'oxygène d'échantillons liquides. Les liquides traités avec chaque getter sont: H_2O, CH_2Br_2, CH_2Cl_2, CH_2I_2 et CH_3OH. Les résultats montrent que l'aluminum est le plus approprié pour tous ces liquides quoique tous les autres métaux étaient aussi effectifs. Il apparaît qu'en autant qu'il n'y a pas de réaction violente, n'importe lequel de ces getters peut être utilisé pour l'élimination de l'oxygène de tout liquide.

Canadian Journal of Chemistry, 49, 1008 (1971)

It is well known that the nuclear spin – lattice relaxation time T_1 in liquids is extremely sensitive to small amounts of dissolved oxygen. It is, therefore, necessary to remove oxygen from the liquid sample in order to study T_1 of the pure liquid. In addition to methods involving bubbling of helium, distillation under vacuum, or freeze–pump–thaw techniques (1–5), misch metal (6) and barium (7) have been used for removing oxygen from liquid samples so that T_1 could be measured in pure liquids. Magnesium (1) has also been used to degas in certain instances but its use as a getter has not been investigated in any detail.

It is the purpose of this paper to report an investigation into the use of aluminum and magnesium as getters. A simple and reliable technique has been developed for preparing the samples and a detailed comparison of the gettering powers of aluminum, magnesium, misch metal, and barium for obtaining oxygen-free samples has been carried out.

Experimental Procedure

A $\frac{1}{2}$-liter flask has two tungsten electrodes E of 0.04 in. diameter sealed through one end of the ground glass joint G and a small tube B on one side as shown in Fig. 1. A tungsten wire of 0.015 in. diameter wound in the form of a coil of about $\frac{5}{16}$ in. i.d. and containing the metal to be used as a getter is connected to the electrodes by stainless steel clamps C. M_1, M_2, and M_3 are metal valves.

The system is evacuated to a pressure of about 10^{-6} mm and baked several times to remove oxygen adsorbed on the walls. After boiling the tube S for about 30 min in distilled water, it is filled with a small amount of liquid and connected to the system by the demountable vacuum union D. The sample is frozen in a liquid nitrogen bath and the air above the sample pumped out by opening M_1. When a pressure of about 10^{-6} mm has been attained again, M_1 is closed and the flask is filled with argon[1] to a pressure of $\frac{1}{2}$–1 mm. The metal is then evaporated by passing a current through the tungsten coil using a variac. After the metal has been deposited properly, the argon is pumped out and valve M_2 is closed.

The sample is now transferred to the tube B by immersing the tube in a liquid nitrogen bath. Once transfer is completed, the liquid nitrogen bath is removed in order to allow the getter to degas the sample. The sample is then transferred to the trap above the tube A by pumping on the liquid and freezing the vapors in the trap. The tube A is finally sealed off from the system after collecting the sample in it.

It may be pointed out that the variac is set at such a value so as to provide just enough current to cause evaporation of the metal. The current is passed intermittently to prevent the joint G and coil T from overheating. The joint G is also kept cool by wrapping it with a wet cloth. Since the depositing of each getter requires slightly different procedures, each getter will be discussed in turn.

Aluminum

Aluminum was tried both in the form of a wire of 5 mil diameter and foil of 1 mil thickness. Foil was found to be easier to heat. The 1 in. × 1 in. foil was rolled into a cylinder and inserted inside the coil of 12–13 turns in $\frac{3}{4}$ in. length. The ends of the foil were pushed over the coil edges to prevent it from slipping. Since aluminum reacts with tungsten, it was found necessary to heat the foil rather quickly. A dark grey deposit was obtained.

[1]Reagent Assayed Grade Argon supplied by Matheson Company of Canada, P. O. Box 322, Whitby, Ontario.

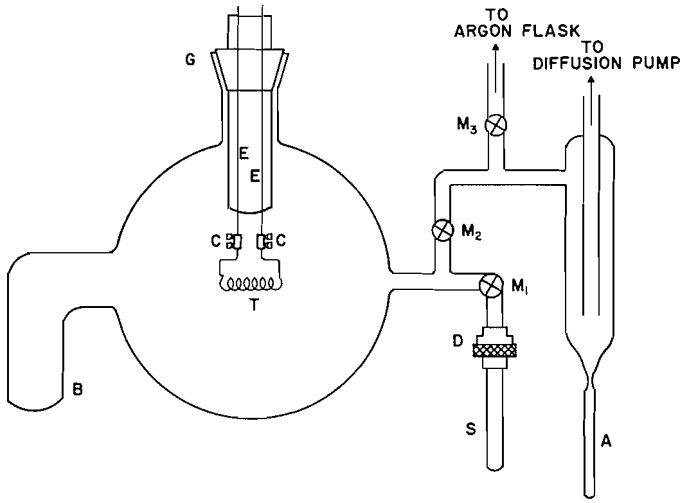

FIG. 1. Schematic diagram of the system for obtaining oxygen-free liquid samples.

TABLE 1. Nuclear spin – lattice relaxation time T_1 of oxygen-free liquids at 30 °C

	T_1 (s) with getter				
Liquid	Aluminum	Magnesium	Barium	Misch metal	Reported values
H_2O	3.91	3.89	3.79	3.93	3.96*
CH_2Br_2	14.40	14.50	14.20	14.20	14.70†
CH_2Cl_2	30.25	30.67	30.72	29.90	31.25‡
CH_2I_2	6.18	5.87	6.02	6.20	6.21†
CH_3OH	8.10	5.45	8.18	8.50	8.95§

*See ref. 10.
†See ref. 5.
‡See ref. 11.
§The sample was prepared using the technique described in ref. 5.

Barium

Barium was used in small pieces cut from a rod of 0.85 in. diameter. It was always kept immersed in paraffin oil to prevent oxidation. It was found necessary to place the metal pieces inside the flask as quickly as possible in order to minimize its contact with air. A tungsten coil of 20–22 turns in 1 in. length and containing closely packed barium pieces produced a good deposit of a dark grey-black color.

Magnesium

Small pieces of magnesium were closely packed in a tungsten coil of 12–14 turns in 1 in. length. Since magnesium has a lower melting point than the other getters, it was easy to produce a good diffused deposit of light grey color.

Misch Metal

Misch metal[2] was in rod form of diameter 0.165 in. Four to five small pieces in a tungsten coil of about 12 turns in 1 in. length generally produced a good deposit of dark black color. It was found easier to evaporate the metal by holding each piece between turns instead of placing the pieces inside the coil.

It may be pointed out that the getter was always deposited in the presence of argon because the gettering power of the diffused deposited layer is much higher (8) than the bright shiny deposit obtained without the presence of argon. Samples were taken after keeping the liquid in contact with the getter for (*i*) 2–4 h, (*ii*) 6–7 h, and (*iii*) 24 h.

[2]Misch metal (Ceralloy 100X) supplied by Ronson Metal Corporation, 45–65 Manufacturers Place, Newark, New Jersey 07105, U.S.A.

Results and Discussion

The liquids investigated with each getter were H_2O, CH_3OH, CH_2Br_2, CH_2Cl_2, and CH_2I_2. The measurements of nuclear spin – lattice relaxation time T_1 were made at 30 °C using pulse techniques (9) and have an accuracy of $\pm 5\%$. The results are summarized in Table 1. These

Can. J. Chem. Downloaded from www.nrcresearchpress.com by 210.87.254.6 on 09/05/12
For personal use only.

results show that all getters are equally effective in removing oxygen except for those liquids which react strongly with the getter. It was found that the samples taken after 2–4 h gave the same T_1 values as the others taken after longer intervals. It was also observed that heating the getter did not improve its gettering power noticeably.

Lees *et al.* (6) expressed uncertainty in the applicability of their technique to the degassing of water. The technique mentioned in this paper does work effectively for water. Aluminum appears to be more suitable for water as well as the other liquids because no change in the color of the deposit was observed. Barium, magnesium, and misch metal deposits did change in color in the presence of water but T_1 values in each case agree with the previously reported values. Furthermore, no deterioration of any sample was observed even after several weeks.

All getters are equally effective for CH_2I_2, CH_2Cl_2, and CH_2Br_2 even though barium deposit showed some change in color for these liquids.

CH_3OH appears to react strongly with all getters except aluminum.

It may be pointed out that the technique described is quite different from that used by Moniz *et al.* (7) and is a considerable improvement over the one described by Lees *et al.* (6). Some of the features of this technique are: (*1*) The joint *G* (Fig. 1) simplifies the assembly of the gettering material; (*2*) the same flask can be reused after removing the deposit with chromic acid; and (*3*) since the sample is sealed from the system, it prevents any deterioration of the sample by the getter.

Aluminum appears to be a more suitable getter for these liquids. However, other getters are also equally effective except for those liquids which react strongly with the getter. It would, therefore, appear that any of these getters can be used for removing oxygen from any liquid as long as there is no strong reaction between the liquid and the getter.

This work was supported in part by a grant from the National Research Council of Canada and in part by a grant from the University of Victoria. I am indebted to M. J. Bulinckx for his assistance in this work. I also thank A. Eisenberg and D. Searle for their assistance in glass blowing.

1. A. W. NOLLE and P. P. MAHENDROO. J. Chem. Phys. **33**, 863 (1960).
2. R. J. C. BROWN, H. S. GUTOWSKY, and K. SHIMOMURA. J. Chem. Phys. **38**, 76 (1963).
3. J. H. SIMPSON and H. Y. CARR. Phys. Rev. **111**, 1201 (1958).
4. G. BONERA and A. RIGAMONTI. J. Chem. Phys. **42**, 171 (1965).
5. H. S. SANDHU. J. Chem. Phys. **51**, 2452 (1969).
6. J. LEES, B. H. MULLER, and J. D. NOBLE. J. Chem. Phys. **34**, 341 (1961).
7. W. B. MONIZ, W. A. STEELE, and J. A. DIXON. J. Chem. Phys. **32**, 2418 (1963).
8. L. F. EHRKE and C. M. SLACK. J. Appl. Phys. **11**, 129 (1940).
9. E. L. HAHN. Phys. Rev. **80**, 580 (1950).
10. J. G. POWLES and D. W. G. SMITH. Phys. Lett. **9**, 239 (1964).
11. J. BLICHARSKI, J. W. HENNEL, K. KRYNICKI, J. MIKULSKI, T. WALUGA, and G. ZAPALSKI. Arch. Sci. Geneva, **13**, 452 (1960).

Can. J. Chem. Downloaded from www.nrcresearchpress.com by 210.87.254.6 on 09/05/12
For personal use only.

Can. J. Chem. Downloaded from www.nrcresearchpress.com by 210.87.254.40 on 09/05/12
For personal use only.

Cyclic Imides. Preparation of Silylphthalimides and Characterization by Infrared and Mass Spectrometry

A. F. JANZEN AND E. A. KRAMER
Department of Chemistry, University of Manitoba, Winnipeg, Manitoba

Received September 15, 1970

A series of silylphthalimides containing silicon substituents —H, —CH_3, —C_2H_5, —$CH_2CH{=}CH_2$, and —C_6H_5 have been prepared and characterized. The compounds are *N*-silylated and found to be monomeric in the liquid and gas phase. The i.r. spectroscopic studies in dilute (10^{-1} *M*) chloroform solution showed a decrease (approximately 40 cm^{-1}) in the carbonyl stretching frequency on silylation, but relatively small changes (± 7 cm^{-1}) on changing silicon substituents. The major effect appears to be electron donation by silyl groups. The N^{15} isotopomers were prepared and C—N and Si—N vibrations identified.

Mass spectrometric studies of methyl- and phenylsilylphthalimides, including N^{15} substitution, are reported. A possible mechanism of formation of methyl- and phenylbiphenylene silicon ions, involving loss of methyl or phenyl, carbon dioxide, and hydrogen cyanide, is suggested.

Une série de phtalimides sililés contenant des substituants liés au silicium —H, —CH_3, —C_2H_5, —$CH_2CH{=}CH_2$, et —C_6H_5 ont été préparés et caractérisés. Les composés sont *N*-sililés et se trouvent sous forme de monomères en phase liquide et gazeuse. Les études par spectroscopie i.r. en solution diluée dans le chloroforme indiquent une diminution (approximativement 40 cm^{-1}) de la fréquence de vibration du carbonyl, suite à la sililation, mais relativement peu de variation (± 7 cm^{-1}) si les substituants liés au silicium sont changés. L'effet principal apparaît comme étant l'effet donneur d'électrons des groupes sililés. Les isomères isotopiques N^{15} ont été préparés et les vibrations C—N et Si—N identifiés.

L'étude par spectrométrie de masse des méthyl et phényl phtalimides sililés, incluant les dérivés N^{15} substitués, est rapportée. Un mécanisme possible de la formation des ions méthyl- et phényl-biphénylène siliconium est suggéré et implique la perte de méthyle ou phényle, de dioxyde de carbone et de cyanure d'hydrogène.

Canadian Journal of Chemistry, 49, 1011 (1971)

Silicon–nitrogen compounds are useful synthetic intermediates in organic and organometallic chemistry (1). We have prepared a variety of silylphthalimides, including N^{15} isotopomers, and studied their i.r. and mass spectra. Although a number of silylphthalimides have been prepared previously (2) few details of their spectral properties or synthetic applications have been reported.

Table 1 lists compounds **1** to **7** prepared for this study. All are *N*-silylated and no evidence was found for *O*-silylation, although *O*-silylation may occur in cyclic imides if resonance stabilization is possible (3).

The compounds are monomeric in gas phase as determined by mass spectrometry, and monomeric in solution as confirmed by molecular weight measurements for **1** and **5**. The extent of association in the solid phase has not been established.

The silylphthalimides are relatively stable and may be handled in air, with the exception of **4** and **5**, where the presence of silicon–hydrogen bonds may account for more rapid hydrolysis.

Infrared Spectra

The i.r. spectra were examined in the region 4000–400 cm^{-1} with emphasis on those regions where C═O, Si—H, and Si—N vibrations normally occur.

In 10^{-1} *M* $CHCl_3$ solution, two bands were found in the carbonyl region, separated by 50 ± 7 cm^{-1}. These bands are generally assigned to the vibrationally coupled symmetric (higher frequency, weak intensity) and anti-symmetric (lower frequency, strong) modes of vibration (4). Values of C═O(asymmetric) for compounds **1** to **7** were found in the range 1700 ± 7 cm^{-1} as recorded in Table 1.

These C═O(asymmetric) values are lower than in phthalimide (1738 cm^{-1}, $CHCl_3$ solvent) or in phthalimide derivatives *e.g.N*-methylphthalimide (1720 cm^{-1}, CCl_4), 4-amino-*N*-methylphthalimide (1760 cm^{-1}, CCl_4 and 1766 cm^{-1}, $CHCl_3$) and 3,6-diamino-*N*-methylphthalimide (1748 cm^{-1}, CCl_4 and 1740 cm^{-1}, $CHCl_3$) (5).

The lowering in frequency on silylation may be ascribed to electron donation by the silyl group.

Can. J. Chem. Downloaded from www.nrcresearchpress.com by 210.87.254.40 on 09/05/12
For personal use only.

TABLE 1. Elemental analyses, molecular weights, melting points, and i.r. data

Compound	Elemental analyses (%) Calculated C H	Elemental analyses (%) Found C H	Molecular weight Calculated	Molecular weight Found	Melting point (boiling point) (°C)	Infrared (cm^{-1})* C=O (asymmetric)	Infrared (cm^{-1})* Si—H	Infrared (cm^{-1})* Si—N
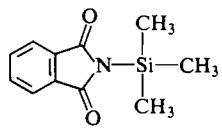 **1**	60.24 5.98	60.41 6.01	219	209	65–67	1700		1071
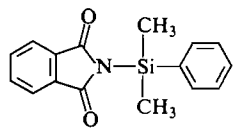 **2**	68.30 5.37	68.47 5.59			87–89	1695		1072
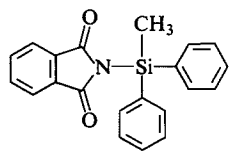 **3**	72.48 5.17	72.70 4.79			109–111	1703		1065
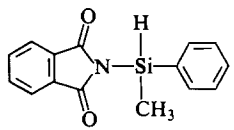 **4**	67.39 4.90	67.65 4.67			226–229	1700	2194	1077

Can. J. Chem. Downloaded from www.nrcresearchpress.com by 210.87.254.40 on 09/05/12
For personal use only.

TABLE 1 (*Concluded*)

Compound	Elemental analyses (%) Calculated C H	Elemental analyses (%) Found C H	Molecular weight Calculated	Molecular weight Found	Melting point (boiling point) (°C)	Infrared (cm^{-1})* C=O (asymmetric)	Infrared (cm^{-1})* Si—H	Infrared (cm^{-1})* Si—N
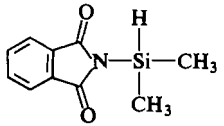 **5**	58.51 5.40	58.71 5.03	205	199	63–65	1706	2188	1083
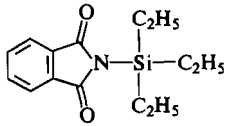 **6**	64.32 7.34	64.06 7.35			(112 at 10^{-2} mm)	1707		1069
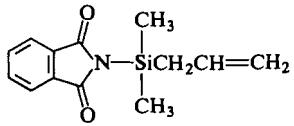 **7**	63.65 6.16	63.86 6.20			29–30	1694		1073

*Band positions are accurate to ±2 cm^{-1}.

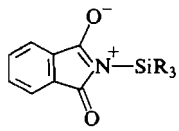

I

Polarization of the carbonyl bond, as in **I**, will be increased by electron donation resulting in a reduced bond order.[1] Metal complexing via the phthalimido carbonyl should result in a similar lowering as has been observed by Jain and Rivest (6). Analogous contributing structures such as **II** are considered important in describing the

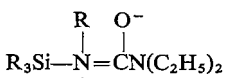

II

reactivity of silyl ureas (7).

Changing substituents on silicon has a relatively small effect on carbonyl absorptions (see Table 1). These effects could be accounted for by minor changes in molecular geometry, Si—N d_π—p_π bonding or intermolecular association.

Compounds **4** and **5** showed strong Si—H absorptions at 2194 and 2188 cm^{-1}, respectively, in the region expected for Si—H stretching frequencies (9).

Vibrations characteristic of the Si—N bond may vary considerably. A band at 899 cm^{-1} has been assigned to the Si—N stretching frequency in trimethylsilylaniline (10) whereas a band at 945 cm^{-1} was found in bis-trimethylsilylacetamide (7) and the region 1170–1180 cm^{-1} was found characteristic of the Si—N bond in *N*-silyl-heterocycles (11).

Silylphthalimides prepared for this study showed a strong band at 1074 ± 9 cm^{-1}, as recorded in Table 1, which we assign to a Si—N vibration. This assignment is supported by the i.r. spectra of N^{15} isotopomers **8** and **9**.

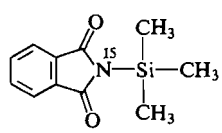

8

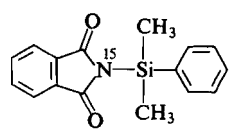

9

Only two bands shift significantly on N^{15} substitution as shown in Table 2. The bands at

[1]The lowering of C=O(asymmetric) in platinum phthalimides has been explained in opposite terms *i.e.* electron withdrawal (8).

TABLE 2. The i.r. bands which shift on N^{15} substitution

Compound	C—N (cm^{-1})	Si—N (cm^{-1})
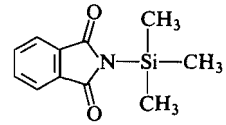 8	N^{14} 1295 N^{15} 1285	N^{14} 1071 N^{15} 1047
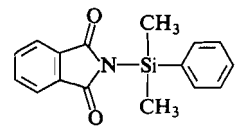 9	N^{14} 1295 N^{15} 1284	N^{14} 1072 N^{15} 1048

higher frequency, around 1290 cm^{-1}, are probably C—N vibrations or more complex mixed vibrations (12). Very similar bands were found for phthalimide-N^{15} and potassium phthalimide-N^{15}.

The band in the 1070 cm^{-1} region is then assigned to a Si—N stretching vibration. The N^{15} substitution shifts this band about 24 cm^{-1} to lower frequencies.[2] The Si—N band is generally broad, and in some cases additional bands are resolved. For example two bands are found in the 1070 cm^{-1} region of N^{14}-dimethylphenylsilylphthalimide, as shown in Fig. 1*a*. On N^{15} substitution, as shown in Fig. 1*b*, the more intense band at 1070 cm^{-1} shifts and therefore it is assigned to the Si—N stretching vibration.

Mass Spectra

There has been considerable interest recently in the mass spectra of organic phthalimides especially regarding the loss of CO_2 and the possibility of an imide–isoimide interconversion due to electron impact (13–15). We find that silylphthalimides also lose CO_2 but important differences are evident in their overall fragmentation schemes. Only methyl- and phenyl-silylphthalimides **1**, **2**, **3**, and the N^{15} isotopomer **9** will be discussed at this time since the remaining silylphthalimides showed more complex behavior not yet analyzed.

The mass spectra of compounds **1**, **2**, **3**, and **9** are shown in Fig. 2. Transitions supported by metastable peaks are indicated by an asterisk in

[2]The calculated frequency shift using the expression $\nu_i = \nu[\mu/\mu^1]$ is 25 cm^{-1}; if i = isotope, ν = 1070 cm^{-1}, μ = reduced mass.

Can. J. Chem. Downloaded from www.nrcresearchpress.com by 210.87.254.40 on 09/05/12
For personal use only.

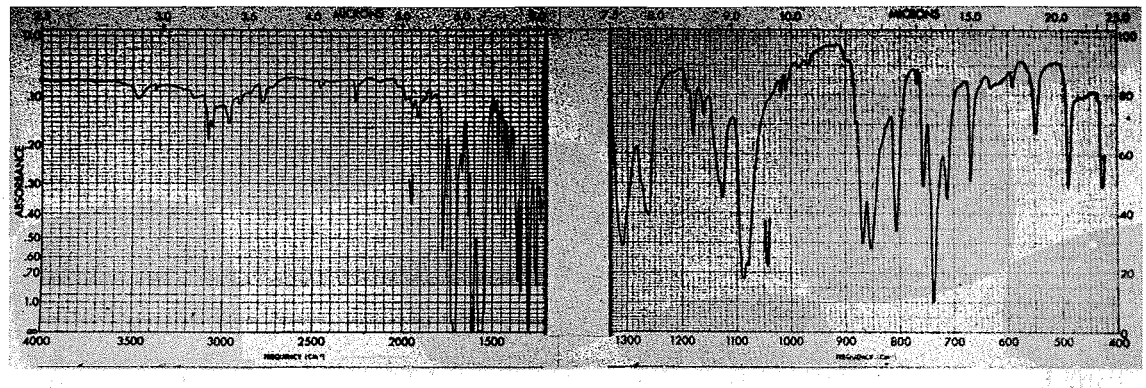

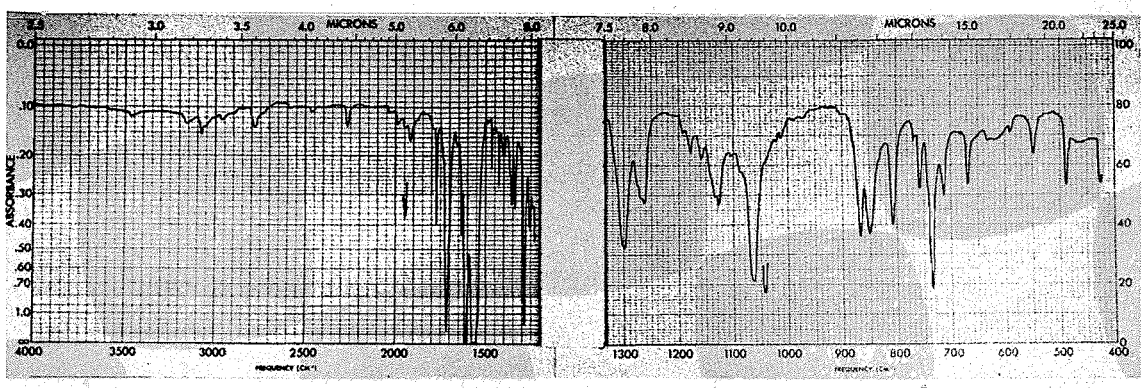

FIG. 1. The i.r. spectra of (*a*) *N*-(dimethylphenylsilyl)phthalimide (**2**) and (*b*) N^{15}-(dimethylphenylsilyl)phthalimide (**9**) recorded as mulls in hexachlorobutadiene (4000–1200 cm^{-1}) and Nujol (1330–400 cm^{-1}). Bands in region 1630–1550 cm^{-1} due to solvent.

TABLE 3. Some metastable peaks observed in the fragmentation of methyl- and phenyl-silylphthalimides

Compound	Observed	Calculated	Transitions
2	251.9	251.8	$281 \rightarrow 266 + CH_3$
9	253.0	252.8	$282 \rightarrow 267 + CH_3$
1	125.5	125.5	$204 \rightarrow 160 + CO_2$
9	126.5	126.4	$205 \rightarrow 161 + CO_2$
2	185.7	185.3	$266 \rightarrow 222 + CO_2$
9	186.5	186.3	$267 \rightarrow 223 + CO_2$
3	245.9	245.9	$328 \rightarrow 284 + CO_2$
2	171.1	171.3	$222 \rightarrow 195 + HCN$
9	170.8	170.5	$223 \rightarrow 195 + HCN^{15}$
2	80.1	80.0	$130 \rightarrow 102 + CO$
9	81.0	81.0	$131 \rightarrow 103 + CO$
9	55.0	56.1	$103 \rightarrow 76 + CN^{15}$

Fig. 2 and some metastable ions are listed in Table 3. These experimental results may be rationalized in terms of an overall fragmentation scheme shown in Fig. 3.

As seen in Fig. 3 the simplest fragmentation pattern is found for compound **1**. Molecular ion **a** loses CH_3 to give **b**. Ion **b** is analogous to **q** which has been suggested for *N*-*t*-butylphthalimide (14). Now **b** loses CO_2 to give **c** whereas **q** loses $CH_2{=}C{=}CH_2$.

Can. J. Chem. Downloaded from www.nrcresearchpress.com by 210.87.254.40 on 09/05/12
For personal use only.

Can. J. Chem. Downloaded from www.nrcresearchpress.com by 210.87.254.40 on 09/05/12
For personal use only.

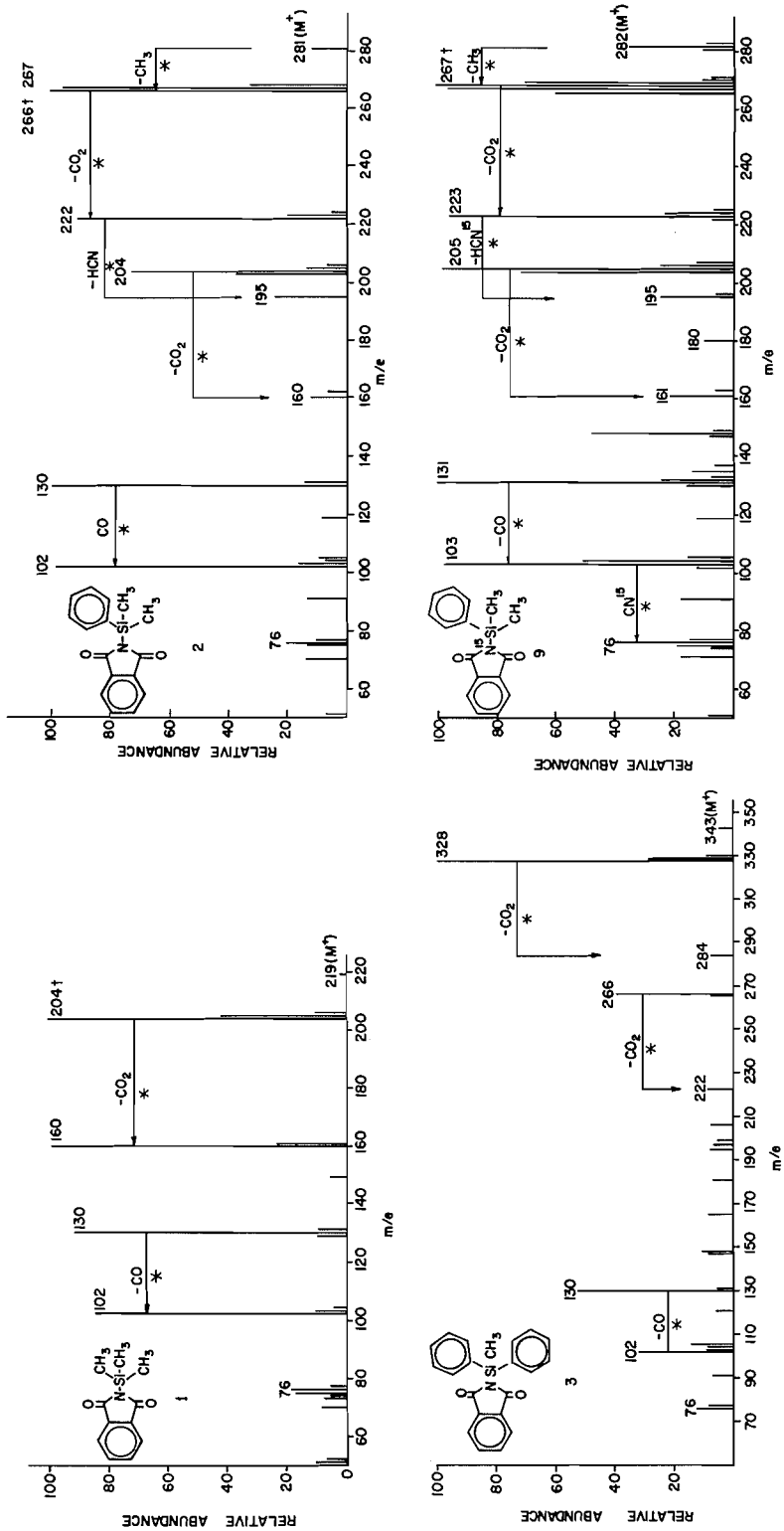

FIG. 2. Mass spectra of *N*-(trimethylsilyl)phthalimide (**1**), *N*-(dimethylphenylsilyl)phthalimide (**2**), N^{15}-(dimethylphenylsilyl)phthalimide (**9**), and *N*-(methyldiphenylsilyl)phthalimide (**3**) at 50 eV. An asterisk (*) denotes transitions supported by metastable peaks. Only peaks above 3% relative abundance are included. A dagger (†) denotes a peak off scale.

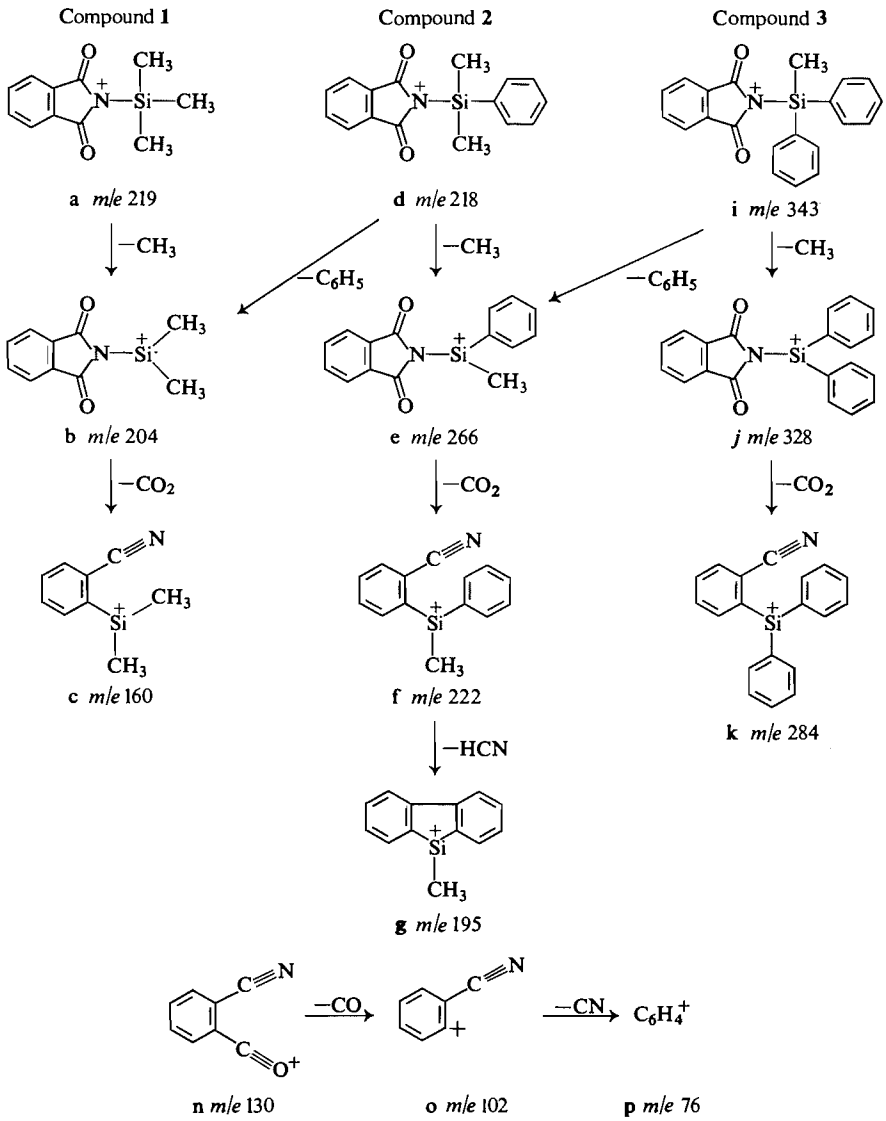

FIG 3. Fragmentation scheme for compounds **1**, **2**, and **3**. See Fig. 2 for relative abundance of peaks, transitions supported by metastable peaks, and N^{15} isotopomer **9**.

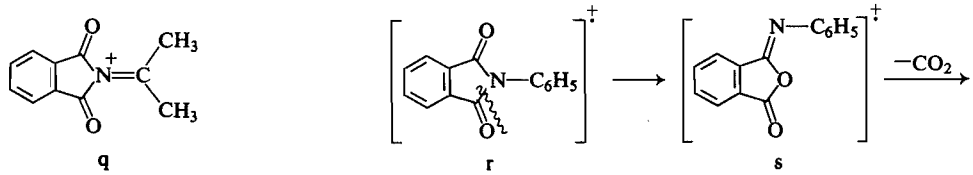

q **r** **s**

Loss of CO_2 may be preceded by electron impact induced isomerization. Anderson *et al.* suggested an imide–isoimide interconversion to explain the identical fragmentation patterns and loss of CO_2 for *N*-phenylphthalimide **r** and *N*-phenylisophthalimide **s** (15). Anderson *et al.* suggested the rearrangement occurs via an intermediate related to a spirolactam. For our purposes, however, their process could be described as breakage of a carbon–nitrogen bond followed by rotation and formation of oxygen–carbon bond.

Can. J. Chem. Downloaded from www.nrcresearchpress.com by 210.87.254.40 on 09/05/12
For personal use only.

Silylphthalimides could then lose CO_2 if a carbon–phenylene bond is broken, followed by rotation and formation of a phenylene–silicon bond.

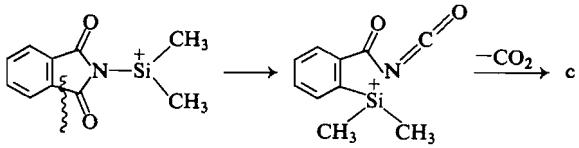

b b′

At some stage rearrangement could result in a benzoyl isocyanate derivative **b′** since benzoyl isocyanate is known to lose CO_2 in the ground state under mild conditions (16).

Extension of the above scheme accounts adequately for the mass spectra of **2** and **3**. In particular, the process resulting in a biphenylene silicon

$$\mathbf{f} \xrightarrow{-HCN} \mathbf{g}$$

derivative, **g**, is readily explained. A peak at *m/e* 97.5, assigned to doubly-charged ion $(\mathbf{g})^{++}$, supports the highly aromatic structure suggested for **g**.

Additional ions **n**, **o**, and **p** were found in all silylphthalimides and these ions are also characteristic of organic phthalimides.

Experimental

General

All compounds were manipulated in a conventional vacuum system or under dry nitrogen atmosphere. Organochlorosilanes were purchased from Peninsular Chemresearch, phthalimide from Aldrich Chemical Co., and potassium phthalimide-N^{15} from Merck, Sharp and Dohme of Canada Ltd. All solvents were dried and distilled prior to use. Elemental analyses and molecular weights (Rast method) were carried out by Dr. A. Bernhardt, West Germany.

The i.r. spectra were determined on a Perkin–Elmer 337 spectrophotometer using KBr windows and calibrated against polystyrene film. Mass spectra were obtained on a Hitachi Perkin–Elmer RMU-6D mass spectrometer at 50 eV. Samples were introduced directly into ion source. The chamber temperature was approximately 230°.

Preparation of N-(Dimethylphenylsilyl)phthalimide

Potassium phthalimide (5.72 g, 30.9 mmol), made from potassium pentoxide and phthalimide according to the method of Hammick and Locket (17) (commercial potassium phthalimide gave impure final products) was added to 50 ml dry tetrahydrofuran in 150 ml flask with reflux condenser under nitrogen atmosphere. Dimethylphenylchlorosilane (5.72 g, 33.6 mmol) was added slowly with stirring. Reaction mixture was heated to 60° for 15 min then cooled to 0° and potassium chloride filtered off. Solvent and volatile components were pumped off leaving a white solid. By dissolving the latter in dry benzene the unreacted insoluble phthalimide was filtered off leaving product in solution. Recrystallization from benzene gave *N*-(dimethylphenylsilyl)phthalimide (5.1 g, 27.6 mmol).

N^{15}-(Dimethylphenylsilyl)phthalimide was prepared from potassium phthalimide-N^{15} (0.401 g, 2.16 mmol) and dimethylphenylchlorosilane (0.375 g, 2.20 mmol) according to the procedure above.

The typical procedure outlined for *N*-(dimethylphenylsilyl)phthalimide was repeated for each silylphthalimide. Products were recrystallized from benzene in yields of at least 50%. *N*-(Triethylsilyl)phthalimide was purified by vacuum distillation (b.p. 112° at 10^{-2} mm).

The ^1H n.m.r. spectra at 60 MHz were obtained for all compounds. Chemical shifts, coupling constants, and proton integrations were all consistent with structures shown in Table 1.

We wish to thank the National Research Council of Canada for financial support. We also wish to thank the University of Manitoba for a Manitoba Graduate Fellowship (to E.A.K.).

1. For reviews see *e.g.* (*a*) R. Fessenden and J. S. Fessenden. Chem. Rev. **61**, 361 (1961). (*b*) U. Wannagat. Advan. Inorg. Chem. Radiochem. **6**, 225 (1964). (*c*) M. F. Lappert and B. Prokai. Advan. Organomet. Chem. **5**, 225 (1967).
2. L. H. Sommer and J. Rochckett. J. Amer. Chem. Soc. **73**, 5130 (1951); E. Frainnet, R. Caras, and C. Esclamadon. Bull. Soc. Chim. Fr. 886 (1961); J. F. Klebe. J. Amer. Chem. Soc. **86**, 3399 (1964); E. A. Sceckeev, V. M. Sheraleev, and Y. F. Askerov. Zh. Obsch. Khim. **8**, 1299 (1968).
3. A. E. Pierce. Silylation of organic compounds. Pierce Chemical Co., Rockford, Illinois, 1968. p. 63.
4. L. J. Bellamy. Advances in infrared group frequencies. Methuen, London, 1968. p. 129.
5. N. A. Borisevich and N. N. Khoratovitch. Opt. and Spectrosc. **10**, 309 (1961).
6. S. C. Jain and R. Rivest. J. Inorg. Nucl. Chem. **31**, 399 (1969).
7. W. Fink. Chem. Ber. **97**, 1433 (1964).
8. D. M. Roundhill. Inorg. Chem. **9**, 254 (1970).
9. B. J. Aylett. Advan. Inorg. Chem. Radiochem. **11**, 249 (1968).
10. E. W. Randall and J. J. Zuckerman. J. Amer. Chem. Soc. **90**, 3167 (1968).
11. U. Wallwitz, H. Schmidt, and W. Gosda. J. Prakt. Chem. **32**, 274 (1966).
12. L. J. Bellamy. The infra-red spectra of complex molecules. Methuen, London, 1957. p. 220.
13. H. Budzikiewicz, C. Djerassi, and D. H. Williams. Mass spectrometry of organic compounds. Holden-Day, San Francisco, California, 1967. p. 364; R. A. W. Johnstone, B. J. Millard, and D. S. Millington. Chem. Commun. 600 (1966); C. Nolde, S. O. Lawesson, J. H. Bowie, and R. G. Cooks. Tetrahedron, **24**, 1051 (1968); J. H. Bowie, M. T. W. Hearn, and A. D. Ward. Aust. J. Chem. **22**, 175 (1969).
14 R. T. Aplin and J. H. Jones. J. Chem. Soc. C 1770 (1968).
15. C. M. Anderson, R. N. Warrener, and C. S. Barnes. Chem. Commun. 166 (1968).
16. O. C. Billeter. Ber. **36**, 3213, 3218 (1903); A. J. Hill and W. M. Degnan. J. Amer. Chem. Soc. **62**, 1595 (1940).
17. D. L. Hammick and G. H. Locket. J. Chem. Soc. **121**, 2362 (1922).

Can. J. Chem. Downloaded from www.nrcresearchpress.com by 210.87.254.40 on 09/05/12
For personal use only.

Can. J. Chem. Downloaded from www.nrcresearchpress.com by 210.87.254.6 on 09/05/12
For personal use only.

Polysaccharides of Soybeans. VI. Neutral Polysaccharides from Cotyledon Meal

G. O. Aspinall and I. W. Cottrell
Department of Chemistry, Trent University, Peterborough, Ontario

Received September 11, 1970

An arabinan and the previously characterized arabinogalactan and acidic polysaccharide complex have been isolated by extraction of defatted and deproteinized soybean cotyledon meal with water. Methylation analysis involving gas chromatography – mass spectrometry of methylated alditol acetates formed from the methylated arabinan has shown that the parent polysaccharide is highly branched and of the same structural type as other arabinans associated with pectins. Methylated derivatives of mustard seed and lemon-peel arabinans and of soybean arabinogalactan have been similarly analyzed.

Un arabinane ainsi qu'un arabinogalactane et un polysaccharide acide déjà connus ont été isolés par extraction à l'eau de fèves soya cotylédon dont on a préalablement éliminé les matières grasses et les protéines. L'analyse des alditols partiellement méthylés et acétylés obtenus à partir de l'arabinane méthylé par la technique de chromatographie en phase gazeuse et spectrométrie de masse, montre que le polysaccharide est hautement branché et qu'il a le même type de structure que d'autres arabinanes qui se trouvent dans les pectines. On a analysé de la même façon les dérivés méthylés des arabinanes obtenus de graines de moutarde, de pelures de citron et de l'arabinogalactane provenant des fèves soya.

Canadian Journal of Chemistry, 49, 1019 (1971)

In previous studies (1, 2) an arabinogalactan and an acidic polysaccharide complex have been isolated from soybean cotyledon meal and the main structural features of these polysaccharides have been established. In parallel investigations Morita and co-workers (3–5) have obtained similar evidence for the structure of the arabinogalactan. Morita also reported (3) that this polysaccharide, which was isolated by extraction of the meal with hot water after removal of the protein with cold dilute alkali, was accompanied by an arabinan whose structure was not examined. Arabinans of the type which are associated with pectins may be of genuine natural occurrence, *e.g.* in white mustard seeds (6–8), but polysaccharides containing a high proportion of arabinose residues in similar types of linkage, *e.g.* from sugar beet (9, 10) can also result from degradation during alkaline conditions of extraction. We have therefore re-examined the more readily soluble polysaccharides from soybean cotyledons isolated under the mildest possible conditions.

Defatted soybean cotyledon meal was extracted with (*i*) phenol – acetic acid – water (1:1:1) (11) to remove protein and (*ii*) water at 85° to remove the more soluble polysaccharides. Further removal of protein from the aqueous extract followed by fractional precipitation and chromatography on diethylaminoethylcellulose afforded an arabinan, an arabinogalactan, which contained arabinose and galactose residues in the proportions of 1:2.8, and an acidic polysaccharide complex. Paper chromatography of the neutral and acidic oligosaccharides formed on partial acid hydrolysis and acetolysis of the acidic polysaccharide complex showed that this preparation was at least qualitatively similar to the previously studied sample (1, 2) which had been extracted under harsher conditions. Likewise gas chromatography of the methyl glycosides formed on methanolysis of the methylated arabinogalactan showed that the parent polysaccharide was qualitatively similar to that studied previously by Morita and co-workers (3–5) and by ourselves (1, 2).

Evidence for the structure of the arabinan was obtained by methylation analysis. Methanolysis of the methylated arabinan gave components with the retention times of methyl glycosides of 2,3,5-tri- and 2,3-di-*O*-methylarabinose. Although no methyl glycosides of a mono-*O*-methylarabinose were detected by g.l.c., paper chromatography of the hydrolysate of the methylated polysaccharide showed the presence of 2,3,5-tri- , 2,3,-di-, and 2-*O*-methylarabinose in approximately equimolar proportions together with traces of 3-*O*-methylarabinose and the unsubstituted sugar. These results therefore indicate that the arabinan is a highly branched polysaccharide containing $1 \rightarrow 3$- and $1 \rightarrow 5$-linked arabinofuranose residues. Assuming that the constituent sugar is the L-enantiomer commonly found in plant polysaccharides, the highly negative specific optical rotations of the parent polysaccharide ($[\alpha]_D - 108°$) and the

TABLE 1. The g.l.c. of methylated alditol acetates from methylated polysaccharides

Acetate of	Retention time (T_E)*	Percentages of components from methylated derivatives of: Soybean arabinan	Soybean arabinogalactan	Lemon-peel arabinan	Mustard seed arabinan
2,3,5-Me_3 Arabinitol	0.57	39.2	6.1	30.0	39.6
2,3,4-Me_3 Arabinitol	0.74		1.0		
2,3-Me_2 Arabinitol	1.52	30.0	13.2†	38.4	25.4
2-Me Arabinitol	2.60	14.2		15.0	28.6
3-Me Arabinitol	2.89	6.0		4.6	tr
Arabinitol	3.62	10.5		12.0	6.3
2,3,6-Me_3 Galactitol	3.45		70.1		
2,6-Me_2 Galactitol	4.27		9.5		

*Relative to erythritol tetraacetate.
†Estimated as a single component. The presence of some 2,3,4,6-Me_4 galactitol acetate (with similar retention time on column *c*) as a minor component (< 20%) of the fraction was indicated by the appearance of a primary peak *m/e* 145 in the mass spectrum.

methylated derivative ($[\alpha]_D - 130°$) suggest that the majority, at least, of the sugar residues are those of α-L-arabinofuranose.

In view of our failure to detect methyl glycosides of 2-*O*-methylarabinose in the methanolysate from the methylated arabinan (presumably because of irreversible adsorption on the column) additional evidence for the identities of the sugars formed on hydrolysis of the methylated polysaccharide was obtained by examination of the products of reduction with sodium borohydride and subsequent acetylation. The identities of the major components of the mixture of methylated alditol acetates were established by combined g.l.c. – mass spectrometry (12) and by comparison with the components in a similar mixture derived from the previously characterized methylated mustard seed arabinan (6, 7). The presence of 3-*O*-methylarabinitol tetraacetate as a minor component of the mixture derived from the soybean arabinan was indicated by the appearance of a primary fragment *m/e* 189 in the mass spectrum (12). The cleavage products from methylated lemon-peel arabinan (13) were also examined by this procedure. The quantitative results are summarized in Table 1. The soybean arabinan is clearly of the same general type as other arabinans associated with pectins. The degree of branching in the soybean arabinan through *ca.* 30% of arabinose residues as indicated by the methylation data is in agreement with the observation that oxidation of the polysaccharide with periodate resulted in the consumption of 0.69 mol of reagent per sugar residue.

Previously examined samples of soybean arabinogalactan (1, 4) were shown to contain L-arabinofuranose residues as sidechains with every fourth or fifth β-D-galactopyranose residue carrying on the average two such residues in disaccharide units. The present arabinogalactan preparation contained a slightly lower ratio (1:2.8) of arabinose to galactose residues. The absence of mono-*O*-methylarabinose as a cleavage product from the methylated polysaccharide indicated the absence of branching through arabinose residues. The evidence on this point has now been re-assessed by examination by combined g.l.c. – mass spectrometry of the mixture of methylated alditol acetates formed from the methylated arabinogalactan (see Table 1). The rather lower ratio (1:4) of arabinose to galactose residues in the methylated polysaccharide than in the parent polysaccharide (1:2.8) may be explained if some contaminating arabinose in the original preparation had been lost during the methylation. Insofar as the present results again failed to provide any indication for branching through arabinose residues in the polysaccharide, the evidence requires that the main component of the polysaccharide preparation is a true arabinogalactan.

Experimental

Paper chromatography was carried out in the following solvent systems (v/v): (A) ethyl acetate – pyridine – water (10:4:3); (B) ethyl acetate – acetic acid – formic acid – water (18:3:1:4); (C) ethyl acetate – acetic acid – formic acid – water (18:8:3:9); and (D) butanone–water–ammonia (200:17:1). The g.l.c. was performed with a Hewlett–Packard model 5750 chromatograph using columns of (*a*) 5% by weight of neopentylglycol adipate polyester at 165°; (*b*) 10% by weight of Carbowax 20M at 190°; and (*c*) 3% by weight of silicone gum XE-60 at 170° on dichlorodimethylsilane treated Celite. For mass spectrometry mixtures of alditol acetates in chloroform

Can. J. Chem. Downloaded from www.nrcresearchpress.com by 210.87.254.6 on 09/05/12
For personal use only.

Can. J. Chem. Downloaded from www.nrcresearchpress.com by 210.87.254.6 on 09/05/12
For personal use only.

were injected into column *c* in a Pye 104 chromatograph attached to an A.E.I. MS 12 mass spectrometer. The mass spectra were recorded at an inlet temperature of 200°, ionization potential of 70 eV, and a temperature of the ion source of *ca.* 150°. Electrophoresis of polysaccharide solutions (1%) were performed in 0.05 *M* sodium tetraborate buffer at p*H* 9.25, using a Tiselius type, Spinco Model H apparatus with Schlieren optics, and currents of 13 mA were maintained. Galacturonic acid contents were determined by a modified carbazole – sulfuric acid procedure (14). Protein was determined with the Folin phenol reagent (15). Optical rotations were measured on a Perkin–Elmer model 141 polarimeter at *ca.* 22° and, unless otherwise stated, were for aqueous solutions.

Extraction of Soybean Cotyledons and Fractionation of Polysaccharides

Soybean cotyledons (Lindarin variety, 1.5 kg) were extracted with boiling light petroleum (b.p. 60–80°) for 2 days, dried, and ground to a flour, and the flour was further extracted with boiling light petroleum for 2 days and then with boiling ethanol–water (4:1) for 2 days to remove coloring matter and soluble sugars (glucose, fructose, sucrose, raffinose, and higher oligosaccharides). Cotyledon meal (1 kg) was stirred for 2 days in phenol (6 kg), acetic acid (6 l), and water (6 l). The swollen meal was separated from the viscous supernatant liquid by high-speed centrifugation, and extraction of the resulting meal was repeated three times. The swollen residue was suspended in ethanol for several hours, the operation was repeated, and the deproteinized meal (440 g) was dried after further washing with ether. The combined extracts were dialyzed to remove phenol and acetic acid, and a portion of the resulting solution was hydrolyzed to give only traces of galactose and mannose.

Deproteinized meal (440 g) was stirred vigorously in water (4 l) for 3 h at 85°. Residual meal was removed by centrifugation and the extraction was repeated. The combined aqueous extracts were concentrated and freeze-dried to give crude polysaccharide extract (25 g) (found: total carbohydrate (as galactan by the phenol – sulfuric acid method (16)), 50; uronic acid residues, 12; protein, 25%), which gave on hydrolysis galacturonic acid, galactose, arabinose, and traces of glucose, xylose, fucose, and rhamnose. The crude polysaccharide extract in water (1300 ml) was shaken for 1 h with chloroform (325 ml) and amyl alcohol (65 ml). The chloroform layer and the emulsion which formed at the interface were separated, and the aqueous layer was poured into ethanol (1.5 volume) to give fraction 1 (11.8 g), $[\alpha]_D$ + 49.4° (*c*, 0.26) (found: uronic acid residues, 15; protein, 2%), which gave on hydrolysis galacturonic acid, galactose, arabinose, xylose, fucose, and rhamnose. The supernatant liquid was then concentrated and poured into ethanol (5 volumes) to give a precipitate which was dissolved in water and freeze-dried to give fraction 2 (arabinan, 4.9 g), $[\alpha]_D$ − 108° (*c*, 0.33), which gave on hydrolysis arabinose as the main sugar with small amounts (< 5%) of galactose and rhamnose, and traces of 2-*O*-methylxylose and 2-*O*-methylfucose. Electrophoresis showed the presence of a single component of mobility $\mu = 2.3 \times 10^{-5}$ cm^2 V^{-1} s^{-1}.

Polysaccharide fraction 1 (11 g) was chromatographed on diethylaminoethylcellulose (acetate form, 150 g) and elution with 0.04 *M* potassium acetate (10 l) and a gradient of 0.04–0.30 *M* potassium acetate (8 l) gave polysaccharide fractions 1*a* and *b*. Fraction 1*a* was brought to p*H* 5 by the addition of acetic acid, concentrated (to 600 ml) and poured into ethanol (2 volumes). The precipitate was washed with ethanol–water (4:1), dissolved in water, and freeze-dried to give arabinogalactan (4.1 g), $[\alpha]_D$ + 51° (*c*, 0.84), hydrolysis of which gave galactose, arabinose, and traces of glucose, xylose, fucose, and rhamnose. Quantitative analysis (17) of the hydrolysate showed the presence of arabinose and galactose in the proportions of 1:2.8. Electrophoresis showed the presence of a major component of mobility $\mu = 2.0 \times 10^{-5}$ cm^2 V^{-1} s^{-1} with only traces of a faster-moving component. Fraction 1*b* was treated similarly and afforded acidic polysaccharide complex (4 g), $[\alpha]_D$ + 57° (found: uronic acid residues, 24; OMe, 2%), hydrolysis of which gave galacturonic acid, galactose, arabinose, xylose, fucose, and rhamnose. Electrophoresis showed the presence of two components of mobility μ = 3.0 and 5.0 $\times 10^{-5}$ cm^2 V^{-1} s^{-1}.

Arabinan

Arabinan (290 mg) was methylated with methyl iodide and sodium hydride in dimethylsulfoxide as described by Sandford and Conrad (18), and gave methylated arabinan (240 mg), $[\alpha]_D$ − 130° (*c*, 1.69 $CHCl_3$) (found: OMe, 37.9%). A sample of the methylated polysaccharide was methanolyzed and g.l.c. on columns *a* and *b* showed components with the retention times of methyl glycosides of 2,3,5-tri- and 2,3-di-*O*-methylarabinose as major components. Although no methyl glycosides of 2-*O*-methylarabinose were detected, paper chromatography of the hydrolysate from the methylated arabinan showed the presence of 2,3,5-tri-, 2,3-di-, and 2-*O*-methylarabinose as major components, with smaller amounts of arabinose and 3-*O*-methylarabinose. Arabinan (20 mg) was oxidized in aqueous 1% sodium metaperiodate (3 ml) and aliquot portions (40 µl) were withdrawn every 2 h, diluted (× 500), and examined spectrophotometrically (19). The results indicated that oxidation was complete after 12 h with the consumption of 0.69 mol of reagent per sugar residue. Excess of periodate was destroyed by the addition of ethylene glycol, and the solution was dialyzed, and sodium borohydride was added. After 18 h, the solution was treated with Amberlite resin IR-120(H) to remove sodium ions and repeated distillations with methanol removed boric acid as methyl borate leaving a residue which gave arabinose on hydrolysis.

Arabinogalactan

Arabinogalactan (240 mg) was methylated with methyl iodide and sodium hydride in dimethylsulfoxide (18) to give methylated arabinogalactan (160 mg), $[\alpha]_D$ − 17° (*c*, 0.69 $CHCl_3$) (found: OMe, 41.1%). A sample of the methylated polysaccharide was methanolyzed and g.l.c. showed the presence of components with the retention times of methyl glycosides of 2,3,4- and 2,3,5-tri-, and 2,3-di-*O*-methylarabinose, and 2,3,4,6-tetra-, 2,3,6-tri-, and 2,6-di-*O*-methylgalactose. No accurate quantitative estimation could be made due to incomplete resolution of all peaks; however, in connection with the data recorded in Table 1, the relative peak heights indicated that methyl glycosides of 2,3,4,6-tetra-*O*-methylgalactose and

2,3-di-*O*-methylarabinose were present in the approximate proportion of 1:4. Paper chromatography of the hydrolysate from the methylated polysaccharide showed the presence of the above-mentioned but no additional sugars.

Gas-liquid Chromatography – Mass Spectrometry of Methylated Alditol Acetates from Methylated Polysaccharides

Samples of the following methylated polysaccharides were examined: methylated soybean arabinan, methylated soybean arabinogalactan, methylated lemon-peel arabinan (13), and methylated mustard seed arabinan. The latter methylated polysaccharide was prepared as described by Hirst *et al.* (6). Methylated polysaccharide (10 mg) was hydrolyzed by heating overnight on a boiling-water bath in aqueous 45% formic acid. The cooled hydrolysate was neutralized to p*H* 8 by the addition of concentrated ammonia. Sodium borohydride (75 mg) was added, the solution was kept at room temperature for 4 h, and a further quantity of sodium borohydride was added. The solution was left for 16 h, checked for completeness of reduction with the phenol sulfuric acid reagent (16), and passed through a column of Amberlite resin IR-120(H). The eluate and washings were concentrated to dryness, boric acid was removed by repeated evaporation with methanol, and the residue was acetylated with acetic anhydride (1 ml) and pyridine (1 ml) overnight. Water was added to the reaction mixture which was then concentrated to small volume and co-distilled several times with chloroform. The residue was dissolved in chloroform for g.l.c. – mass spectrometry. The proportions of methylated alditol acetates were estimated from the peak areas on the gas chromatograms and the results are summarized in Table 1.

The identities of most of the acetylated alditol acetates were established by (*i*) comparison of their retention times with those of the previously characterized products from methylated mustard seed arabinan (6, 7) or of known standards, and (*ii*) the appearance in the mass spectra of fragment ions having intensities of more than 10% of the base peak as reported by Björndal *et al.* (12). In all cases primary fragment ions, which were characteristic of the various substitution patterns, were detected. Although no standard for 3-*O*-methylarabinitol tetraacetate was available, the appearance of a primary fragment ion *m/e* 189 left little doubt as to the identity of this component. In examining the partially methylated alditol acetates from methylated soybean arabinogalactan some tailing of the g.l.c. peak of the major component, 2,3,6-tri-*O*-methylgalactitol triacetate, was observed. Since the following component, 2,6-di-*O*-methylgalactitol tetraacetate, may have been contaminated by the trimethyl ether and gives no unique additional fragment ions in the mass spectrum, the assignment of structure to this component is also based on the absence of primary fragments which could have arisen from isomeric dimethyl ethers.

We acknowledge generous financial support from the National Research Council of Canada. We thank Mr. J. M. Cashmore for assistance in the mass spectrometry and Dr. D. A. Rees for a sample of mustard seed arabinan.

1. G. O. Aspinall, R. Begbie, A. Hamilton, and J. N. C. Whyte. J. Chem. Soc. (C), 1065 (1967).
2. G. O. Aspinall, I. W. Cottrell, S. V. Egan, I. M. Morrison, and J. N. C. Whyte. J. Chem. Soc. (C), 1071 (1967).
3. M. Morita. Agric. Biol. Chem. Jap. **29**, 564 (1965).
4. M. Morita. Agric. Biol. Chem. Jap. **29**, 626 (1965).
5. M. Morita, M. Okuhara, T. Kikuchi, and Y. Saurai. Agric. Biol. Chem. Jap. **31**, 314 (1967).
6. E. L. Hirst, D. A. Rees, and N. G. Richardson. Biochem. J. **95**, 453 (1965).
7. D. A. Rees and N. G. Richardson. Biochem. **5**, 3099 (1966).
8. D. A. Rees and I. W. Steele. Biochem. **5**, 3108 (1966).
9. L. Hough and D. B. Powell. J. Chem. Soc. 16 (1960).
10. T. L. Hullar. Dissertation Abstr. **26**, 671 (1965).
11. M. Bagdasaran, N. A. Matheson, R. L. M. Synge, and M. A. Youngson. Biochem. J. **91**, 91 (1964).
12. H. Björndal, B. Lindberg, and S. Svensson. Carbohyd. Res. **5**, 433 (1967).
13. G. O. Aspinall and I. W. Cottrell. Can. J. Chem. **48**, 1283 (1970).
14. T. Bitter and H. M. Muir. Anal. Biochem. **4**, 330 (1962).
15. G. L. Millar. Anal. Chem. **31**, 964 (1959).
16. M. Dubois, K. A. Gilles, J. K. Hamilton, P. A. Rebers, and F. Smith. Anal. Chem. **28**, 350 (1956).
17. C. M. Wilson. Anal. Chem. **31**, 1199 (1959).
18. P. A. Sandford and H. E. Conrad. Biochem. **5**, 1508 (1966).
19. G. O. Aspinall and R. J. Ferrier. Chem. and Ind. 1216 (1957).

Can. J. Chem. Downloaded from www.nrcresearchpress.com by 210.87.254.6 on 09/05/12
For personal use only.

Kinetics of the Reaction of Atomic Hydrogen with Vinyl Chloride

J. S. TANNER AND J. W. S. JAMIESON
Department of Chemistry, Dalhousie University, Halifax, Nova Scotia

Received June 29, 1970

The reaction of hydrogen atoms, produced by electric discharge, with vinyl chloride vapor has been studied at four widely different temperatures. Since the maximum yields of HCl at both 328 and 494 °C exceeded the flow rates of atomic hydrogen, the reaction was observed to have limited chain characteristics. The products were hydrogen chloride, ethylene, methane, and ethane. The specific reaction rate for HCl production was found to be about $6 \times 10^{-13} e^{-2.75 \times 10^3/RT}$ and that for production of ethylene plus ethane was found to be about $3 \times 10^{-13} e^{-2.80 \times 10^3/RT}$.

La réaction d'atomes d'hydrogène, produits par une décharge électrique, avec le chlorure de vinyle en phase a été étudiée à quatre températures différentes. A cause du fait que les rendements maxima d'HCl à 328 et 494 °C étaient plus grands que les taux de diffusion des atomes d'hydrogène, les caractéristiques d'une réaction en chaîne étaient limitées. Les produits formés sont: l'acide chlorhydrique, l'éthylène, le méthane, et l'éthane. La vitesse spécifique de réaction pour la production d'HCl est approximativement $6 \times 10^{-13} e^{-2.75 \times 10^3/RT}$ et celle pour la production d'éthylène plus éthane est d'environ $3 \times 10^{-13} e^{-2.80 \times 10^3/RT}$.

Canadian Journal of Chemistry, 49, 1023 (1971)

Can. J. Chem. Downloaded from www.nrcresearchpress.com by 210.87.254.6 on 09/05/12
For personal use only.

Introduction

A study of the reaction of vinyl chloride with atomic hydrogen was undertaken since it was thought that this reaction might be suitable for measurement of the hydrogen atoms available for reaction, particularly at ambient temperature. Although this possibility was eliminated after it became apparent that a chain mechanism was involved, other interesting results have been obtained.

Experimental

Materials

Hydrogen was purchased from the Linde Gases Division, Union Carbide Canada Limited and vinyl chloride was supplied by Matheson of Canada Limited.

Apparatus and Methods

The apparatus, which was a fast-flow system of the conventional Wood–Bonhöffer type, has recently been described (1). At least twice during the course of the investigation the walls of the discharge tube and the reaction vessel were coated with Na_2HPO_4 to retard the combination of hydrogen atoms. Unreacted vinyl chloride and all the condensable products except methane were collected at liquid nitrogen temperature in large traps immediately below the reaction vessel, while methane was collected according to the method of Demchuk and Gesser (2) in a further trap containing silica gel. The HCl, which was the main product of the reaction, was distilled into a removable trap containing either water or standard base so that the acid could be determined by titration with either standard base or standard acid. Methane was transferred laboriously with the use of a Töpler pump to a gas burette for measurement of the quantity of gas before verifying its purity by gas chromatography. After measurement in a gas burette all the gaseous products of the reaction (except HCl) were analyzed by gas chromatography, using helium as carrier gas, a Gow–Mac thermal conductivity cell Model 9193, TE-II, a Leeds and Northrup Speedomax Type G, Model "S" 1 s recorder, and a 9 ft Porasil B column (for ethane, ethylene, and vinyl chloride) or a 4 ft molecular sieve 5A column (for methane). In some of the early experiments a 6 ft Porapak Q column was used. Since it did not give a very good separation of ethane and ethylene it was soon replaced by the Porasil B column.

Flow rates of vinyl chloride were estimated in experiments with the hydrogen discharge off. The vinyl chloride was trapped at liquid nitrogen temperature and distilled into a known volume connected to a manometer which was used to measure the pressure of the vapor at ambient temperature. No impurities were detected in the vinyl chloride since each sample analyzed by gas chromatography gave a single peak, even at 494 °C. Thus there was no evidence of thermal decomposition under the experimental conditions used.

In all experiments the flow rate of molecular hydrogen was 92.3 μmol/s, which gave a pressure of 1.10 mm in the reaction system. The atomic hydrogen flow rates at the various reaction temperatures were estimated from the maximum extent of the reactions of ethyl chloride (3) and formamide (3) with hydrogen atoms.

Results and Discussion

The flow rates of atomic hydrogen estimated at the various reaction temperatures are given in Table 1. The only products detected were HCl, ethylene, methane, and ethane. Acetylene was specifically sought but not found. No polymer formation was observed.

Since HCl was the only chlorine-containing product found it has been assumed that the

Can. J. Chem. Downloaded from www.nrcresearchpress.com by 210.87.254.6 on 09/05/12
For personal use only.

TABLE 1. Atomic hydrogen flow rates

Temperature (°C)	H Atoms flowed μmol/s
32	1.3
141	2.1
328	1.7
494	1.4

amounts of HCl produced are equal to the amounts of vinyl chloride reacted. Alternative estimates of the amounts of vinyl chloride reacted, obtained by subtraction of the amounts of vinyl chloride recovered (estimated from gas chromatography peaks) from the amounts of vinyl chloride flowed, were more erratic.

The amounts of ethane produced were never greater than one-third of the ethylene formed. Ethane production was highest at low reactant flow rates in experiments at the lower temperatures; it decreased to negligible amounts at higher reactant flow rates, particularly at the higher temperatures. The ethane results have not been shown separately.

The results obtained from ambient temperature to 494 °C are given in Figs. 1 and 2 which show that the maximum yields of HCl at both 328 and 494° and the maximum yield of ethylene plus ethane at 494° were substantially higher than the flow rates of hydrogen atoms at these temperatures. Thus it is obvious that a chain mechanism is involved, but only to a limited extent. The results which indicate a maximum extent of reaction ("clean-up" or "plateau" values) appear to be due to the fact that the total concentration of hydrogen atoms per unit time available for reaction, although augmented by occurrence of the chain mechanism, would still be limited by the occurrence of chain termination steps.

Specific reaction rates have been calculated with an IBM 360/50 computer from the usual second-order expressions (1) for conditions of both streamline and turbulent flow. The Arrhenius plots of Figs. 3 and 4 are essentially linear (within the limits of experimental error); hence no change of mechanism is implied. Figure 3 shows that the production of HCl was very rapid ($A = 2.7 \times 10^{-13}$, $E = 2.6$ kcal, for streamline flow; $A = 8.5 \times 10^{-13}$, $E = 2.9$ kcal, for turbulent flow).

It appears unlikely, however, that the HCl could have been formed in the primary step, since the only feasible chain carrier in this reaction would be atomic chlorine. Thus the initial reaction is probably [1]. Enthalpy changes for this and subsequent reactions have been calculated from recently published standard heats of formation at 298 °K (4–6).

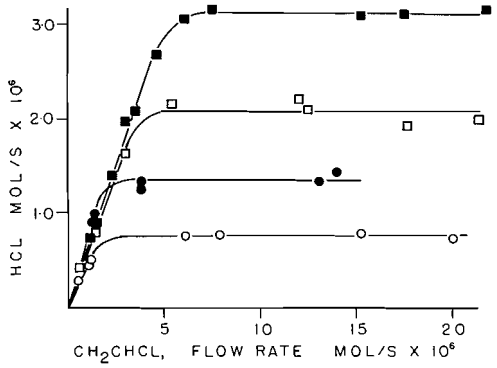

FIG. 1. HCl produced at 32 (○), 141 (●), 328 (□), and 494 °C (■).

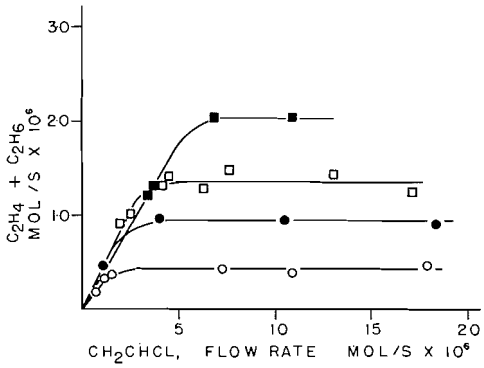

FIG. 2. Ethylene plus ethane produced at 32 (○), 141 (●), 328 (□), and 494 °C (■).

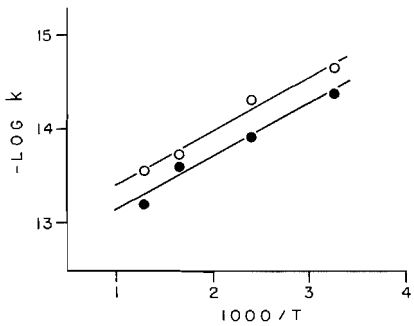

FIG. 3. Arrhenius plots for streamline flow: HCl production (●), production of ethylene plus ethane (○).

[1] $H + CH_2{=}CH{-}Cl \rightarrow CH_2{=}CH_2 + Cl$ $\quad \Delta H = -18.0$ kcal

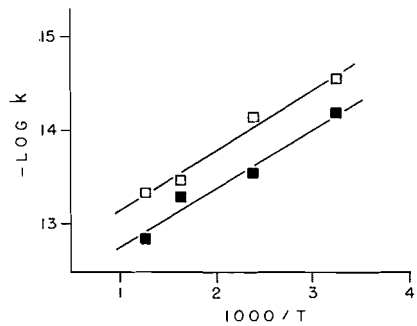

FIG. 4. Arrhenius plots for turbulent flow: HCl production (■), production of ethylene plus ethane (□).

The transition state for reaction 1 would resemble the radical C_2H_4Cl and there is some probability that this entity could exist for an appreciable time so that the reaction could take place in two steps, [2] and [3]. If so, the radical

[2] $H + CH_2{=}CH{-}Cl \rightarrow C_2H_4Cl \quad \Delta H = -40.0$ kcal

[3] $C_2H_4Cl \rightarrow CH_2{=}CH_2 + Cl \quad \Delta H = +22.0$ kcal

C_2H_4Cl might also decompose according to reaction 4, although no butadiene has been found

[4] $C_2H_4Cl \rightarrow CH_2{=}CH + HCl \quad \Delta H = +22.0$ kcal

among the products of the over-all reaction of atomic hydrogen with vinyl chloride.

Reactions 3 and 4 would probably not occur unless the radical C_2H_4Cl retained some or all of the energy released in reaction 2 so that the decomposition reactions would be exothermic, [3′] and [4′]. If the vibrationally excited radical

[3′] $C_2H_4Cl^* \rightarrow CH_2{=}CH_2 + Cl \quad \max \Delta H = -18.0$ kcal

[4′] $C_2H_4Cl^* \rightarrow CH_2{=}CH + HCl \quad \max \Delta H = -18$ kcal

$C_2H_4Cl^*$ had a sufficiently long lifetime it might also react with atomic hydrogen, [5] and [6].

[5] $H + C_2H_4Cl^* \rightarrow CH_3{-}CH_2 + Cl \quad \max \Delta H = -56.9$ kcal

[6] $H + C_2H_4Cl^* \rightarrow CH_2{=}CH + HCl \quad \max \Delta H = -121.3$ kcal

Since HCl was rapidly formed and no other chlorine-containing products, such as might have been formed by combination and other reactions of C_2H_4Cl or $C_2H_4Cl^*$, were detected, it is very likely that reaction 1 is the main primary reaction.

The chain characteristics would then be due to reaction 7, which is known (7) to be very fast. This

[7] $Cl + H_2 \rightarrow HCl + H \quad \Delta H = +0.951$ kcal

reaction not only regenerates atomic hydrogen but also can account for the rapid production of HCl.

The fact that only small quantities of ethane were found except at low flow rates of vinyl chloride might seem to imply that ethane is formed solely by the addition of excess hydrogen atoms to ethylene, [8] and [9].

[8] $H + CH_2{=}CH_2 \rightarrow CH_3{-}CH_2 \quad \Delta H = -38.9$ kcal

[9] $H + CH_3{-}CH_2 \rightarrow CH_3{-}CH_3 \quad \Delta H = -98.0$ kcal

The rate of production of ethylene plus ethane was found to be slightly slower ($A = 1.5 \times 10^{-13}$, $E = 2.6$ kcal, for streamline flow; $A = 3.6 \times 10^{-13}$, $E = 3.0$ kcal, for turbulent flow) than the rate of production of HCl, although the activation energies were virtually identical. Perhaps the most striking feature of the present investigation is that the reaction of atomic hydrogen with vinyl chloride seems to be essentially independent of flow conditions, since the measured rates of HCl production and of production of ethylene plus ethane agreed reasonably well when calculated for conditions of both streamline and turbulent flow.

Differences in these rates were probably due to the fact that some of the ethylene formed in reaction 1 reacted further to form methane. Due to the difficulty of accurately measuring the pressure of a small quantity of gas in a large volume and also the difficulty of completely transferring a small amount of a non-condensable gas with a Töpler pump into a small volume of a gas burette, quantitative results for methane were not obtained at all temperatures. At 141 °C, however, the results given in Table 2 were obtained. These data and those of Figs. 1 and 2 show that there was a reasonable carbon balance for experiments at this temperature. At the other temperatures the quantities of methane collected

TABLE 2. Methane produced at 141 °C

Vinyl chloride flowed μmol/s	Methane produced μmol/s
3.98	0.64
10.5	0.62
18.4	0.52

Can. J. Chem. Downloaded from www.nrcresearchpress.com by 210.87.254.6 on 09/05/12
For personal use only.

and measured in several experiments were of the magnitude to indicate the probability of a material balance for the overall reaction.

It appears that methane and ethane might have a common precursor, which could be either ethyl radical or methyl radical, since the formation of both methane and ethane would involve successive hydrogen atom reactions, but practically no ethane was produced at high vinyl chloride flow rates, particularly at high temperatures. Thus reaction 9 might be in competition with reactions 10 and 11. Methyl radicals formed in reaction 10

[10] $H + CH_3—CH_2 \rightarrow 2CH_3 \quad \Delta H = -11.4$ kcal

[11] $H + CH_3—CH_2 \rightarrow CH_4 + CH_2 \quad \Delta H = -2.0$ kcal

might then combine, [12], or react further with

[12] $2CH_3 \rightarrow CH_3—CH_3 \quad \Delta H = -86.6$ kcal

atomic hydrogen to form methane, [13], or react

[13] $H + CH_3 \rightarrow CH_4 \quad \Delta H = -103.2$ kcal

with HCl, [14], since it has been reported (8–10)

[14] $CH_3 + HCl \rightarrow CH_4 + Cl \quad \Delta H = +0.1$ kcal

that reaction 14 has an activation energy of less than 5 or 6 kcal.

If methylene radicals were formed in reaction 11 they could probably react readily with molecular hydrogen to form methane, reaction 15.

[15] $CH_2 + H_2 \rightarrow CH_4 \quad \Delta H = -111.6$ kcal

Termination of the chain mechanism would seem to be due to the occurrence of reactions which consume hydrogen atoms, such as reactions 8–11, 13, and 16 which would take place at the reaction vessel wall or in the first cold trap. Even at high vinyl chloride flow rates reactions 10 and 16, as well as reactions 11 and 13 which form methane, could be chain termination steps.

[16] $2H(+M) \rightarrow H_2(+M) \quad \Delta H = -104.190$ kcal

Financial assistance from the National Research Council of Canada is gratefully acknowledged. The authors are also grateful to Mr. D. W. Lemon for his assistance in the early stages of the experimental investigation.

1. J. W. S. Jamieson and G. R. Brown. Can. J. Chem. **42**, 1638 (1964).
2. N. Demchuk and H. Gesser. Can. J. Chem. **41**, 1645 (1963).
3. J. W. S. Jamieson. Can. J. Chem. **41**, 1568 (1963).
4. Frederick D. Rossini, Donald D. Wagman, William H. Evans, Samuel Levine, and Irving Jaffe. Nat. Bur. Stand. (U.S.) Circ. No. 500. 1952.
5. D. D. Wagman, W. H. Evans, I. Halow, V. B. Parker, S. M. Bailey, and R. H. Schumm. Nat. Bur. Stand. (U.S.) Technical note 270-1. 1965.
6. Robert C. Weast. Handbook of chemistry and physics. 50th edition. The Chemical Rubber Company, Cleveland. 1969–1970. p. F-164.
7. S. W. Benson, F. R. Cruickshank, and R. Shaw. Int. J. of Chem. Kinetics. **1**, 29 (1969).
8. E. W. R. Steacie. Atomic and free radical reactions. American Chemical Society Monograph 125. Reinhold, New York, 1954. p. 426 ff.
9. R. Cvetanovic and E. W. R. Steacie. Can. J. Chem. **31**, 158 (1953).
10. R. Cvetanovic and E. W. R. Steacie. Can. J. Chem. **31**, 171 (1953).

Can. J. Chem. Downloaded from www.nrcresearchpress.com by 210.87.254.6 on 09/05/12
For personal use only.

Can. J. Chem. Downloaded from www.nrcresearchpress.com by 210.87.254.42 on 09/05/12
For personal use only.

Transannular Reactions in the Dibenzo[*a*,*d*]cycloheptene Series. V. Preparation of 10,11-Dihydro-5,10-(iminomethano)-5*H*-dibenzo[*a*,*d*]cycloheptenes

T. A. Dobson and M. A. Davis
Ayerst Research Laboratories, Montreal, Quebec

Received August 25, 1970

Treatment of the ketonitrile **2***a* with sodium borohydride gave the lactone **3***a* which underwent ammonolysis to give 10,11-dihydro-5,10-(iminomethano)-5*H*-dibenzo[*a*,*d*]cyclohepten-13-one (**5***a*). This compound was used to prepare a number of 12- and 11,12-disubstituted derivatives of the ring system.

La réduction du céto-nitrile **2***a* par le borohydrure de sodium conduit à la lactone **3***a* qui, par ammonolyse, donne la dihydro-10,11 iminométhano-5,10 5*H*-dibenzo[*a*,*d*]cycloheptène-13 one (**5***a*). Ce composé a été utilisé pour préparer un certain nombre de dérivés substitués en -12 et -11,12 de ce système cyclique.

Canadian Journal of Chemistry, **49**, 1027 (1971)

We have previously (1) described the preparation of 10,11-dihydro-10,5-(iminomethano)-5*H*-dibenzo[*a*,*d*]cycloheptene derivatives. The pharmacological properties of these compounds were of sufficient interest to prompt us to prepare derivatives of the isomeric ring system **1**. Since previous work (2–4) has shown that suitably oriented substituents at positions 5 and 10 of the dibenzo[*a*,*d*]cycloheptene nucleus readily interact to form bridged systems, the same principle was adopted in the present case.

Treatment of the ketonitrile **2***a* with sodium borohydride followed by acid treatment resulted not only in reduction of the carbonyl group but also reduction of the 10,11- double bond and formation of the lactone **3***a*. A small amount of **3***a* was also obtained when the acid treatment was omitted. Nauta and his co-workers have recently reported that borohydride treatment of **2***a* gave a tetracyclic product (5). The reduction of the 10,11- double bond accords with the similar reduction of cinnamic acid esters (6). It is not clear whether the lactone **3***a* is formed via an iminolactone generated by an intramolecular Pinner reaction (7) or by prior hydration or hydrolysis of the nitrile function.

Support for the iminolactone pathway was obtained by converting **2***a* to the formamide **2***b* by the Leuckart reaction (8) and treating this product with sodium borohydride. The major product was the amidine **4**, precluding hydration or hydrolysis of the nitrile in this instance. A small amount of the lactam **5***a* was also obtained. On the other hand, treatment of the ketal **2***c* with sodium borohydride gave moderate amounts of the amide **6***a* and the acid **6***b* as well as the nitrile **6***c*. This ready hydration and hydrolysis of the 10-nitrile function contrasts markedly with the resistance of 10,11-dihydro-5*H*-dibenzo[*a*,*d*]cycloheptene-5-nitrile to similar reaction conditions (9).

Ammonolysis of the lactone **3***a* proceeded normally, as with the structurally related 4-phenylisochromanone (10), giving a better route to the lactam **5***a*. In marked contrast, the isomeric lactone **7** decarboxylates under similar conditions (1). The substituted lactams **5***b*, *c* were prepared by using methylamine and ethylamine respectively in place of ammonium hydroxide. Reduction of **5***a–c* with lithium aluminum hydride gave the amines **1***a–c*. Similar reduction of the phenylacetyl derivative of **1***a* gave **1***d*.

Several attempts were made to prepare 11-substituted derivatives of **1**. Despite the ready addition of hydride ion to **2***a*, attempts to add secondary amines were unsuccessful. Substituted acrylonitriles are known to be less reactive than acrylonitrile in cyanoethylation reactions (11). Bromination of **3***a* with *N*-bromosuccinimide gave the bromolactone **3***b*. Unfortunately this compound did not serve as a source for other 11-substituted lactones since treating it with dimethylamine gave the amide **2***d*. Similar bromination of the lactam **5***b* gave a mixture of two epimeric bromolactams **5***d*. They[1] were formed in approximately equal amounts but only one

[1]A referee has pointed out that the difference in chemical shifts of the C-11 protons in the isomers of A and B of **5***d* (see Experimental) is most probably due to the shielding effect of the amide carbonyl group. Isomer A will therefore be the *syn*-11-bromo compound (with respect to the amide bridge) and isomer B will be the *anti*-11-bromo compound.

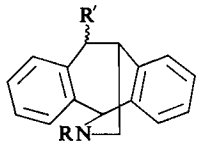

1

a R = R′ = H
b R = CH_3; R′ = H
c R = C_2H_5; R′ = H
d R = $CH_2CH_2C_6H_5$; R′ = H
e R = CH_3; R′ = $N(CH_2)_4$
f R = CH_3; R′ = OCH_3

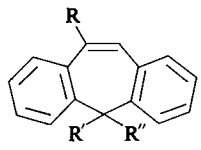

2

a R = CN; R′ + R″ = O=
b R = CN; R′ = NHCHO; R″ = H
c R = CN; R′ + R″ = $O(CH_2)_2O$
d R = $CON(CH_3)_2$; R′ = OH; R″ = H

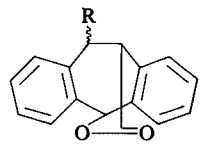

3

a R = H
b R = Br

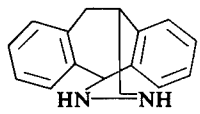

4

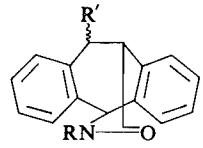

5

a R = R′ = H
b R = CH_3; R′ = H
c R = C_2H_5; R′ = H
d R = CH_3; R′ = Br
e R = CH_3; R′ = $N(CH_2)_4$
f R = CH_3; R′ = OCH_3

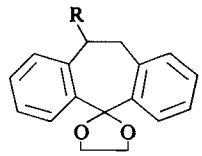

6

a R = $CONH_2$
b R = CO_2H
c R = CN

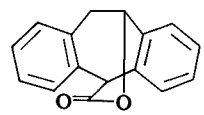

7

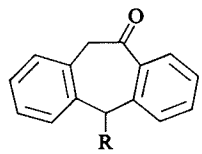

8

a R = $CONH_2$
b R = CH_2NH_2

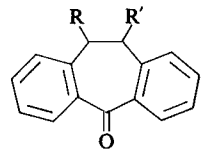

9

a R = $CONH_2$; R′ = H
b R = CH_2NH_2; R′ = H
c R = CN; R′ = H
d R = $CH_2N(CH_3)_2$; R′ = H
e R = R′ = OH

epimer was readily isolated in a pure state. This compound readily underwent displacement reactions when it was treated with pyrrolidine and with sodium methoxide to give **5***e*, *f* respectively. Reduction of **5***e*, *f* with lithium aluminum hydride gave the amines **1***e*, *f*.

Since **8***a*, *b* are known to exist in the carbinolamine and carbinolamide forms (4), it was of interest to determine whether or not the isomeric **9***a*, *b* exhibited the same behavior. Deketalization of **6***a* gave the ketocarboxamide **9***a* and catalytic hydrogenation of **6***c* followed by deketalization gave the amino-ketone **9***b*. Methylation of **9***b* with formic acid – formaldehyde gave **9***d*. Spectral data indicated that **9***a*, *b*, *d* existed in the open form in neutral, acidic and basic media. In contrast, **9***e* is known to exist in the hemiketal form in alkaline media (2, 3), demonstrating that the 5-keto function is able to interact with bridge substituents in certain cases.

Experimental

The n.m.r. spectra in the indicated solvents were determined using a Varian A-60A instrument; melting points were recorded on a Thomas-Hoover Uni-melt apparatus.

5-Oxo-5H-Dibenzo[a,d]cycloheptene-10-carbonitrile (2a)

This material was prepared as described by Nauta and co-workers (5) except that dimethyl formamide was used as the reaction medium. The yield was 90%.

The ethylene ketal **2***c* was prepared by heating under

Can. J. Chem. Downloaded from www.nrcresearchpress.com by 210.87.254.42 on 09/05/12
For personal use only.

Can. J. Chem. Downloaded from www.nrcresearchpress.com by 210.87.254.42 on 09/05/12
For personal use only.

reflux a mixture of **2***a* (3.0 g), ethylene glycol (4.0 ml), benzene (50 ml), and *p*-toluenesulfonic acid (250 mg) for 2 days. The product (2.9 g) had m.p. 118–120° (from ethanol).

Anal. Calcd. for $C_{18}H_{13}NO_2$: C, 78.53; H, 4.76; N, 5.09. Found: C, 78.31; H, 4.67; N, 5.28.

10,11-Dihydro-5,10-(epoxymethano)-5H-dibenzo[a,d]-cyclohepten-13-one (3a)

A mixture of **2***a* (70.0 g) and sodium borohydride (25 g) in ethanol (800 ml) was stirred and heated under reflux for 16 h. The reaction mixture was evaporated and the residue was dissolved in water. The solution was acidified and extracted with chloroform. Evaporation of the extracts and crystallization of the residue gave 56.5 g (80%) of the lactone, m.p. 148–150°; n.m.r. ($CDCl_3$), τ: 6.92 (1H at C-11, q, J = 5, 17 Hz); 6.33 (1H at C-11, q, J = 5, 17 Hz); 5.91 (1H at C-10, t, J = 5 Hz); 4.03 (1H at C-5, s); 2.69 (8-H aromatic, m).

Anal. Calcd. for $C_{16}H_{12}O_2$: C, 81.34; H, 5.12. Found: C, 81.49; H, 4.83.

5-Formamido-5H-dibenzo[a,d]cycloheptene-10-carbonitrile (2b)

A mixture of **2***a* (3.3 g), formamide (16 ml), and acetic acid (1.6 ml) was heated under reflux for 1 h. The mixture was poured into water and the precipitate was crystallized from ethanol (charcoal) to give 2.7 g of the formamide (73%), m.p. 204–206°; γ_{max} (Nujol) 3300, 2215, and 1660 cm^{-1}.

Anal. Calcd. for $C_{17}H_{12}NO$: C, 78.44; H, 4.65; N, 10.76. Found: C, 78.29; H, 4.86; N, 10.91.

10,11-Dihydro-5,10-(iminomethano)-5H-dibenzo[a,d]-cyclohepten-13-imine (4)

A mixture of **2***b* (15.0 g), sodium borohydride (15.0 g), and ethanol (300 ml) was heated under reflux for 8 h. The mixture was concentrated and then diluted with water. The precipitate was crystallized from ethanol to give 6.5 g of the title product, m.p. 241–243°.

The mother liquors were evaporated and the residue was chromatographed on a neutral alumina column to give 1.07 g of the lactam **5***a*, m.p. 227–229°, and a further 2.5 g of the title product (total yield 67%); n.m.r. ($CDCl_3$), τ: 7.42 (1H at C-11, q, J = 4, 18 Hz); 6.91 (1H at C-11, q, J = 4, 18 Hz); 6.33 (1H at C-10, t, J = 4 Hz); 4.93 (1H at C-5, s); 4.57 (2H at HN—C—NH, unresolved multiplet); 3.18, 2.93 (8H aromatic, m).

Anal. Calcd. for $C_{16}H_{14}N_2$; C, 82.02; H, 6.02; N, 11.96. Found: C, 82.22; H, 5.99; N, 11.73.

10,11-Dihydro-5,10-(iminomethano)-5H-dibenzo[a,d]-cyclohepten-13-one (5a)

A mixture of **3***a* (35.0 g) and ammonium hydroxide (500 ml, d 0.88) was heated in an autoclave for 10 h at 175°. The solid product was collected and crystallized from ethanol to give 30.0 g (88%) of the lactam, m.p. 227–229°; n.m.r. (DMSO), τ: 7.00 (1H at C-11, q, J = 4, 16 Hz); 6.42 (1H at q, J = 4, 16 Hz); 6.18 (1H at C-10, t, J = 4 Hz); 4.98 (1H at C-5, d; singlet after D_2O exchange); 2.75 (8H aromatic, m); 1.6 (NH, m).

Anal. Calcd. for $C_{16}H_{13}NO$: C, 81.68; H, 5.57; N, 5.85. Found: C, 81.39; H, 5.40; N, 5.82.

Reaction of 2c with Sodium Borohydride

A mixture of **2***c* (5.0 g), sodium borohydride (5.0 g), and ethanol (100 ml) was heated under reflux for 2 h. The mixture was evaporated, diluted with water and extracted with chloroform. Evaporation of the extracts and crystallization of the residue from chloroform–hexane gave 3.5 g of the ketal **6***c*, m.p. 113–115°; n.m.r. ($CDCl_3$), τ: 6.24 (3H at C-10 and -11, m); 5.88 (4H, ketal, m); 2.78 (8H aromatic, m).

Anal. Calcd. for $C_{18}H_{15}NO_2$: N, 5.05. Found: N, 5.12.

Fractional crystallization of the mother liquors from **6***c* gave 0.9 g of the amide **6***a*, m.p. 172–174° (from isopropanol); λ_{max} (EtOH) 265 (ε 680), 272 mμ (ε 502).

Anal. Calcd. for $C_{18}H_{17}NO_3$: C, 73.20; H, 5.80; N, 4.74. Found: C, 73.16; H, 5.92; N, 4.83.

The original aqueous solution was acidified to give 0.2 g of the acid **6***b*, m.p. 182–184° (from isopropanol); λ_{max} (EtOH) 264 mμ (ε 640).

Anal. Calcd. for $C_{18}H_{16}O_4$: C, 72.96; H, 5.44. Found: C, 73.16; H, 5.55.

Treatment of **6***c* with aqueous sodium hydroxide gave more **6***a* and *b*.

Deketalization of **6***c* (1.9 g) with a mixture of ethanol (25 ml) and 3 *N* HCl (25 ml) at room temperature gave the ketonitrile **9***c* (1.3 g), m.p. 108–110° (from isopropanol); λ_{max} (EtOH) 271 mμ (ε 16 050) (unchanged on addition of either 0.1 *N* HCl or 0.1 *N* NaOH).

Anal. Calcd. for $C_{16}H_{11}NO$: C, 82.38; H, 4.75; N, 6.01. Found: C, 82.19; H, 4.52; N, 6.10.

Similar treatment of **6***a* gave the ketoamide **9***a*, m.p. 178–180° (from isopropanol); λ_{max} (EtOH) 271 mμ (ε 15 880).

Anal. Calcd. for $C_{16}H_{13}NO_2$: C, 76.47; H, 5.22; N, 5.57. Found: C, 76.63; H, 5.08; N, 5.43.

10,11-Dihydro-12-methyl-5,10-(iminomethano)-5H-dibenzo[a,d]cyclohepten-13-one (5b)

A suspension of **3***a* (10.0 g) in 40% aqueous methylamine was heated in an autoclave for 8 h at 180°. The solids were crystallized from ethanol to give 9.0 g (87%) of the lactam, m.p. 244–246°.

Anal. Calcd. for $C_{17}H_{15}NO$: C, 81.9; H, 6.06; N, 5.62. Found: C, 81.56; H, 5.88; N, 5.33.

The same product (4.8 g) was obtained when **5***a* (5.0 g) was methylated with sodium hydride and methyl iodide in anhydrous benzene.

10,11-Dihydro-12-ethyl-5,10-(iminomethano)-5H-dibenzo[a,d]cyclohepten-13-one (5c)

A mixture of **3***a* (7.0 g), ethylamine (15.0 g), and water (50 ml) was kept at 175° for 10 h. The mixture was extracted with methylene chloride and the extracts were washed with 2 *N* HCl and evaporated. The residue was recrystallized from methanol to give 5.68 g (68%) of the lactam, m.p. 250–252°.

Anal. Calcd. for $C_{18}H_{17}NO$: C, 82.40; H, 6.46; N, 5.32. Found: C, 82.20; H, 6.51; N, 5.32.

10,11-Dihydro-5,10-(iminomethano)-5H-dibenzo[a,d]-cycloheptene Hydrochloride (1a)

Lithium aluminum hydride (5.0 g) was added portionwise to a stirred suspension of **5***a* (15.0 g) in anhydrous tetrahydrofuran (300 ml). The mixture was heated under reflux for 6 h and then cooled and cautiously

Can. J. Chem. Downloaded from www.nrcresearchpress.com by 210.87.254.42 on 09/05/12
For personal use only.

treated with water. The mixture was filtered and the filtrate was evaporated to dryness to leave the oily free base. The hydrochloride salt was crystallized from ethanol–ether to m.p. > 270°; n.m.r. ($CDCl_3$) (free base). τ: 7.72 (NH, s); 6.75 (CH_2—CH—CH_2, m); 5.27 (1H at C-5); 2.87 (8H aromatic, m).

Anal. Calcd. for $C_{16}H_{16}ClN$: C, 74.56; H, 6.22; Cl, 13.76; N, 5.44. Found: C, 74.54; H, 6.16; Cl, 14.29; N, 5.39.

The *N*-acetyl derivative was prepared by heating the free amine with an excess of acetic anhydride for 2 h on the steam bath. It showed m.p. 210–212° (from isopropanol).

Anal. Calcd. for $C_{18}H_{17}NO$: C, 82.14; H, 6.46; N, 5.32. Found: C, 81.87; H, 6.38; N, 5.26.

The *N*-phenylacetyl derivative was prepared from the free amine, phenylacetyl chloride, and anhydrous pyridine. It had m.p. 122–124° (from isopropanol).

Anal. Calcd. for $C_{24}H_{21}NO$: C, 84.92; H, 6.24; N, 4.13. Found: C, 84.65; H, 6.24; N, 4.01.

The *N*-methyl derivative, **1***b*, was prepared from the amine, formaldehyde, and formic acid. The hydrochloride salt had m.p. 244–247° (from isopropanol); n.m.r. ($CDCl_3$) (free base), τ: 7.61 (NCH_3, s); 6.82 (CH_2—CH—CH_2, m); 5.63 (1H at C-5, s); 2.80 (8H aromatic, m).

Anal. Calcd. for $C_{17}H_{18}ClN$: C, 75.10; H, 6.67; Cl, 13.08; N, 5.15. Found: C, 74.94; H, 6.67, Cl, 12.91, N, 5.37.

*10,11-Dihydro-12-ethyl-5,10-(iminomethano)-5H-dibenzo[a,d]cycloheptene (**1***c*)

A mixture of **5***c* (5.5 g), anhydrous tetrahydrofuran (100 ml), and lithium aluminum hydride (3.0 g) was stirred and heated over reflux for 5 h. The mixture was treated with water, filtered, and the filtrate was evaporated. The residue was converted to the hydrochloride salt (4.1 g) which had m.p. 231–234° (from isopropanol).

Anal. Calcd. for $C_{18}H_{19}ClN$: C, 75.90; H, 6.68; Cl, 12.47; N, 4.92. Found: C, 76.20; H, 6.87; Cl, 12.39; H, 4.68.

*10,11-Dihydro-12-phenethyl-5,10-(iminomethano)-5H-dibenzo[a,d]cycloheptene Hydrochloride (**1***d*)

A mixture of the *N*-phenylacetyl derivative of **1***a* (5.0 g), lithium aluminum hydride (3.0 g), and anhydrous tetrahydrofuran (50 ml) was stirred and heated under reflux for 5 h. The basic product was isolated as described above. The hydrochloride (3.0 g) had m.p. 225–228° (from methanol); n.m.r. ($CDCl_3$) (free base), τ: 7.15 (m); 6.75 (m); 5.38 (1H at C-5, s); 2.80 (13H aromatic, m).

Anal. Calcd. for $C_{24}H_{23}N.HCl.0.5H_2O$: C, 77.71; H, 6.79; Cl, 9.56; N, 3.78. Found: C, 77.71; H, 6.76; Cl, 9.29; N, 3.49.

*11-Bromo-10,11-dihydro-5,10-(epoxymethano)-5H-dibenzo[a,d]cyclohepten-13-one (**3***b*)

A suspension of **3***a* and *N*-bromosuccinimide (1.8 g) in carbon tetrachloride (30 ml) containing a trace of benzoyl peroxide was heated under reflux for 2 h. The mixture was filtered and evaporated and the residue was crystallized from ethanol to give the bromolactone (2.0 g), m.p. 167–169°; n.m.r. ($CDCl_3$), τ: 5.53 (1H at C-10, d, J = 5 Hz); 4.95 (1H at C-11, d, J = 5 Hz); 4.94 (1H at C-5, s); 2.52 (8H aromatic, m).

Anal. Calcd. for $C_{16}H_{11}BrO_2$: C, 60.96; H, 3.72; Br, 25.35. Found: C, 61.24; H, 3.71; Br, 25.08.

*5-Hydroxy-N,N-dimethyl-5H-dibenzo[a,d]cycloheptene-10-carboxamide (**2***d*)

A suspension of **3***b* (0.5 g) in ethanol (20 ml) and dimethylamine (0.5 ml) was kept at room temperature for 18 h and then evaporated. The residue was washed with water and crystallized from methanol to give 0.3 g of the amide, m.p. 230–232°; λ_{max} (EtOH) 285 mμ (ε 15 800); n.m.r. (DMSO), τ: 7.08, 6.95 (6H at $CON(CH_3)_2$, s); 4.78 (1H at C-5, s); 2.68, 2.18 (8H aromatic, m).

Anal. Calcd. for $C_{18}H_{17}NO_2$: C, 77.39; H, 6.13; N, 5.01. Found: C, 77.45; H, 6.13; N, 4.91.

*11-Bromo-10,11-dihydro-12-methyl-5,10-iminomethano-5H-dibenzo[a,d]cyclohepten-13-one (**5***d*)

A suspension of **5***b* (15.11 g), *N*-bromosuccinimide (11.4 g), and benzoyl peroxide (50 mg) in carbon tetrachloride (300 ml) was heated under reflux for 1.25 h. The mixture was filtered, the filtrate was evaporated and the residue was crystallized from ethyl acetate to give isomer A of **5***d* (8.0 g), m.p. 205–207°; γ_{max} ($CHCl_3$) 1670 cm^{-1}; n.m.r. ($CDCl_3$), τ: 2.79 (8H aromatic, m); 4.07 (1H at C-11, d); 5.19 (1H at C-5, s); 5.77 (1H at C-10, d); 7.02 (N—CH_3, s).

Anal. Calcd. for $C_{16}H_{14}BrNO$: C, 62.2; H, 4.27; Br, 24.4; N, 4.27. Found: C, 62.41; H, 4.28; Br, 24.66; N, 4.19.

Chromatography of the mother liquors on silica gel, eluting with benzene–chloroform mixture gave a further 0.5 g of isomer A and 7.0 g of almost pure isomer B of **5***d*. This material was repeatedly crystallized from benzene to give the analytical sample of isomer B, m.p. 183–186°; γ_{max} ($CHCl_3$) 1670 cm^{-1}; n.m.r. ($CDCl_3$), τ: 2.82 (8H aromatic, m); 4.52 (1H at C-11, d); 5.15 (1H at C-5, s); 5.77 (1H at C-10, d), 6.85 (N—CH_3, s.)

Anal. Found: C, 62.07; H, 4.21; Br, 24.50; N, 4.23.

*10,11-Dihydro-11-methoxy-12-methyl-5,10-(iminomethano)-5H-dibenzo[a,d]cyclohepten-13-one (**5***f*) (Isomer A)*

A suspension of **5***d* (6.7 g, isomer A) in a solution of sodium (470 mg) in anhydrous methanol was heated under reflux for 18 h. The solution was evaporated and the residue was washed with water and then crystallized from isopropanol to give 4.0 g of **5***f*, m.p. 190–193°; γ_{max} ($CHCl_3$) 1660 cm^{-1}; n.m.r. ($CDCl_3$), τ: 2.80 (8H aromatic, m); 5.17 (1H at C-5, s, 5.63 (2H at C-10 and -11, 2d, J = 4 Hz); 6.23 (O—CH_3, s); 6.92 (N—CH_3, s).

*10,11-Dihydro-11-methoxy-12-methyl-5,10-(iminomethano)-5H-dibenzo[a,d]cycloheptene (**1***f*) Hydrochloride (Isomer A)*

Lithium aluminum hydride (1.2 g) was added to a suspension of **5***f* (3.5 g) in anhydrous tetrahydrofuran (60 ml). The mixture was heated under reflux for 5 h and then treated with water. The mixture was filtered and evaporated and the residue was converted to the hydrochloride salt which was crystallized from methanol to give 2.5 g of product, m.p. 245–248°; n.m.r. ($CDCl_3$) (free base), τ: 7.60 (NCH_3, s); 6.84 (NCH_3, d, J = 3

Hz); 6.5; (1H at C-10, m); 6.35 (OCH_3, s); 5.58 (1H at C-5 and 1H at C-11, s); 2.80 (8H aromatic, m).

Anal. Calcd. for $C_{18}H_{20}ClNO$: C, 71.64; H, 6.64; N, 4.64; Cl, 11.78. Found: C, 71.84; H, 6.59; N, 4.90; Cl, 11.63.

*10,11-Dihydro-11-pyrrolidino-12-methyl-5,10-(imino-methano)-5H-dibenzo[a,d]cyclohepten-13-one (**5e**) (Isomer A)*

A mixture of **5d** (4.7 g) (isomer A) and pyrrolidine (20 ml) was heated under reflux for 3 h and then evaporated. The residue was dissolved in chloroform, washed with water, and evaporated. The residue was crystallized from ethanol to give 3.5 g of **5e**, m.p. 190–192°.

Anal. Calcd. for $C_{21}H_{22}N_2O$: C, 79.21; H, 6.96; N, 8.80. Found: C, 78.91; H, 6.96; N, 8.57.

*10,11-Dihydro-11-pyrrolidino-12-methyl-5,10-(imino-methano)-5H-dibenzo[a,d]cycloheptene (**1e**) (Isomer A)*

Lithium aluminum hydride (3.0 g) was added to a solution of **5e** (3.3 g) (isomer A) in anhydrous tetrahydrofuran (30 ml). The mixture was heated under reflux for 3 h and then worked-up in the usual manner to give the product (2.0 g), m.p. 106–107° (from ethanol).

Anal. Calcd. for $C_{21}H_{24}N_2$: N, 9.17. Found: N, 8.93.

*10-Aminomethyl-10,11-dihydro-5H-dibenzo[a,d]cyclo-hepten-5-one (**9b**) Hydrochloride*

A solution of **6c** (3.0 g) in ethanol (20 ml) and liquid ammonia (15 ml) was hydrogenated at 100 atm and 100° in the presence of Raney nickel catalyst (0.5 g) for 7 h. The crude basic product was dissolved in a mixture of ethanol (20 ml) and 3 *N* HCl (20 ml) and kept overnight. The solution was evaporated and the residue was crystallized from ethanol to give 1.3 g of the hydrochloride, m.p. 265–268°; λ_{max} (EtOH) 271 mμ (ε 16 050) (unchanged on addition of 0.1 *N* NaOH solution).

Anal. Calcd. for $C_{16}H_{16}ClNO$: C, 70.20; H, 5.88; Cl, 12.90; N, 5.12. Found: C, 69.98; H, 5.85; Cl, 12.94; N, 5.02.

*10,11-Dihydro-11-dimethylaminomethyl-5H-dibenzo[a,d]-cyclohepten-5-one (**9d**) Hydrochloride*

A mixture of **9b** (5.0 g), formic acid (25 ml), and 37% formaldehyde solution was heated on the steam bath for 2 h and then evaporated and basified. The basic material was converted to the hydrochloride salt which was crystallized from isopropanol, m.p. 242–244°; λ_{max} 271 mμ (ε 14 900) (unchanged on addition of either 0.1 *N* HCl or 0.1 *N* NaOH).

Anal. Calcd. for $C_{18}H_{20}ClNO$: C, 71.70; H, 6.66; Cl, 11.75; N, 4.64. Found: C, 71.64; H, 6.80; Cl, 11.69; N, 4.77.

We wish to thank Dr. G. S. Myers and his staff for furnishing the tricyclic compounds in quantity. Thanks are also due to Mrs. A.-M. Hartung for technical assistance, and to Dr. G. Schilling and his staff for spectral and analytical data.

1. T. A. Dobson, M. A. Davis, and A.-M. Hartung. Can. J. Chem. **46**, 3391 (1968).
2. J. Rigaudy and L. Nédélec. Bull. Soc. Chim. Fr. **643**, 648 (1959).
3. G. L. Buchanan and D. B. Jhaveri. J. Org. Chem. **26**, 4295 (1961).
4. M. A. Davis, T. A. Dobson, and J. M. Jordan. Can. J. Chem. **47**, 2827 (1969).
5. J. Gootjes, A. B. H. Funcke, and W. Th. Nauta. Arz. Forsch. **19**, 1936 (1969).
6. N. G. Gaylord. Reduction with complex metal hydrides. Interscience Publishers Inc., New York. N.Y., 1956. p. 931.
7. R. Roger and D. Nielson. Chem. Revs. **61**, 179 (1961).
8. M. L. Moore. Organic reactions. John Wiley and Sons Inc., New York, N.Y. **5**, 301 (1949).
9. M. A. Davis, S. O. Winthrop, R. A. Thomas, F. Herr, M.-P. Charest, and R. Gaudry. J. Med. Chem. **7**, 88 (1964).
10. J. Gardent and M. Hamon. Bull. Soc. Chim. Fr. 556 (1966).
11. H. A. Bruson. Organic reactions. John Wiley and Sons Inc., New York, N.Y. **5**, 106 (1949).

Can. J. Chem. Downloaded from www.nrcresearchpress.com by 210.87.254.42 on 09/05/12
For personal use only.

Can. J. Chem. Downloaded from www.nrcresearchpress.com by 210.87.254.40 on 09/05/12
For personal use only.

Kinetics and Mechanism of the Decarboxylation of Pyrrole-2-carboxylic Acid in Aqueous Solution

G. E. DUNN AND GORDON K. J. LEE
Department of Chemistry, University of Manitoba, Winnipeg, Manitoba

Received August 14, 1970

The decarboxylation of pyrrole-2-carboxylic acid in aqueous buffers at 50° and ionic strength 1.0 has been found to be first order with respect to substrate at a fixed p*H*. As the p*H* is decreased, the rate constant increases slightly in the p*H* range 3–1, then rises rapidly from p*H* 1 to 10 *M* HCl. The ^{13}C-carboxyl kinetic isotope effect is 2.8% in 4 *M* $HClO_4$ and negligible at p*H* ~ 3. These observations can be accounted for by a mechanism, previously proposed for the decarboxylation of anthranilic acid, in which the species undergoing decarboxylation is the carboxylate ion protonated at the 2-position of the pyrrole ring. This intermediate can be formed both by ring-protonation of the carboxylate anion and by ionization of the ring-protonated acid. At low acidities ring-protonation is rate determining, but at higher acidities the rate of protonation exceeds that of decarboxylation.

Il a été trouvé, qu'à p*H* donné dans des solutions tampons aqueuses à 50 °C et une force ionique de 1.0, la décarboxylation de l'acide pyrrole-2 carboxylique est du premier ordre en substrat. Quand le p*H* est diminué, la constante de vitesse augmente légèrement entre p*H* 3 et 1 puis augmente rapidement du p*H* 1 à HCl 10 *M*. L'effet isotopique cinétique du carboxyle ^{13}C est de 2.8% dans $HClO_4$ 4 *M* et négligeable à p*H* ~ 3. Il est possible de rationaliser ces observations à l'aide d'un mécanisme, proposé précédemment pour la décarboxylation de l'acide anthranilique, dans lequel l'espèce qui subit la décarboxylation est l'ion carboxylate protoné à la position 2 du noyau du pyrrole. Cet intermédiaire peut être formé soit par la protonation du noyau portant l'anion carboxylate soit par ionisation de l'acide protoné sur le noyau. A basses acidités, la protonation du cycle est l'étape déterminante mais à des acidités plus élevées la vitesse de protonation est plus grande que la décarboxylation.

Canadian Journal of Chemistry, **49**, 1032 (1971)

Pyrrolecarboxylic acids have long been known to decarboxylate much more readily than most aromatic acids. In this they resemble the amino and hydroxybenzoic acids, and the resemblance may be taken as an example of the general concept which leads to the term "π-excessive" for pyrroles because of the similarity of their properties to those of benzenes with electron-releasing substituents (1). Although the mechanism of decarboxylation of pyrrolecarboxylic acids has not been investigated, Corwin and Straughn have pointed out that the decarboxylation of pyrrolecarboxylic and hydroxybenzoic acids occur under similar conditions and are subject to similar substituent effects (2). Since the mechanism of decarboxylation of hydroxybenzoic acids (3, 4) is very similar to that of the anthranilic acids previously studied in this laboratory (5–7), the present investigation of the decarboxylation of pyrrole-2-carboxylic acid uses the approach previously applied to anthranilic aicds.

Experimental

Commercial pyrrole-2-carboxylic acid was recrystallized twice from benzene and sublimed under vacuum. It had a m.p. of 204–205°.

All p*H* measurements were made with a Radiometer Model 4C p*H* meter in cells thermostatted to 50.0 ± 0.1°. The meter was calibrated against National Bureau of Standards tetroxalate and hydrogen phthalate buffers at 50°. Measurements were reproducible to 0.003 p*H* unit.

Rates were measured spectrophotometrically by following the decrease in concentration of pyrrole-2-carboxylic acid using a Beckman DU spectrophotometer. Aliquots (2 ml) of a 2×10^{-3} *M* solution of pyrrole-2-carboxylic acid in the appropriate buffer were withdrawn from the thermostat and diluted to 25 ml with 1 *M* sodium hydroxide solution. Absorbance measurements were made at 25° and at 250 nm, where pyrrole does not absorb.

Kinetic isotope effects were obtained as described previously (7).

Results and Discussion

Pyrrole-2-carboxylic acid was decarboxylated in buffered aqueous solutions of ionic strength 1.0 at 50 ± 0.01°. For each p*H* the data gave excellent first-order plots to more than 90% conversion and rate constants reproducible to within ±2%. The results at various p*H*'s are shown in Table 1. It is seen that the rate increases only slightly as p*H* decreases from 3 to 1, but then increases very rapidly with increasing acidity until it appears to begin levelling off at hydrochloric acid concentrations around 10 *M*.

Clearly the rate of decarboxylation varies with the degree of protonation of the substrate. The

[1]

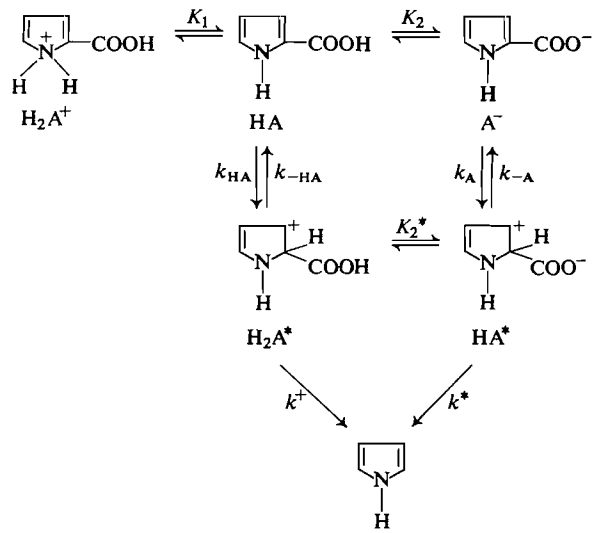

TABLE 1. Rates of decarboxylation of pyrrole-2-carboxylic acid at 50°, $\mu = 1.0$

Buffer*	pH at 50°	$k \times 10^4$ s^{-1}
HCl–NaH_2PO_4	3.41	0.280
HCl–NaH_2PO_4	2.93	0.321
HCl–NaH_2PO_4	2.66	0.345
HCl–NaH_2PO_4	2.19	0.422
HCl	1.82	0.601
HCl	1.51	0.913
HCl	1.32	1.23
HCl	0.992	2.42
HCl	0.795	3.48
HCl	0.603	4.90
HCl	0.443	6.99
HCl	0.399	7.20
HCl	0.332	8.41
HCl	0.181	10.5
HCl	0.079	12.6
HCl	(1.45 M)	16.8
HCl	(2.49 M)	20.8
HCl	(6.64 M)	31.8
HCl	(10.3 M)	35.7

*Adjusted to constant ionic strength with KCl.

acid–base equilibria of pyrrole-2-carboxylic acid are shown in the first line of eq. 1. The value of K_1 is unknown, and attempts to determine it spectrophotometrically showed no change in the u.v. spectrum from pH 3 to 10 M HCl. This is in agreement with the expectation that pK_1 should be more negative than the corresponding pK of pyrrole itself, which is −3.80 (8). The pK_2 is reported to be 4.39 (9). From these facts it is evident that the rapid increase in rate of decarboxylation as pH falls below 1 is not simply the result of a change of substrate from one protonated form to another at that pH. Clearly the decarboxylation must involve intermediates other than those related by K_1 and K_2.

The pH dependence of pyrrole-2-carboxylic acid decarboxylation recalls that of anthranilic acid (7), so the mechanism derived for anthranilic acid is applied to pyrrole-2-carboxylic acid in eq. 1. The rate equation derived by assuming a steady state for the sum of the concentrations of H_2A^* and HA^* is given by eq. 2.

$$[2] \quad k = \frac{k_A K_2 + k_{HA}[H^+]}{\frac{[H^+]}{K_1} + 1 + \frac{K_2}{[H^+]}} \times \frac{k^* K_2^* + k^+[H^+]}{(k^* + k_{-A})K_2^* + (k^+ + k_{-HA})[H^+]}$$

Since pK_1 is very negative and pK_2 is 4.39, the denominator of the first fraction in eq. 2 is very close to unity at all pH's for which rates are reported in Table 1. The general rate equation therefore reduces to eq. 3.

$$[3] \quad k = (k_A K_2 + k_{HA}[H^+]) \times \frac{k^* K_2^* + k^+[H^+]}{(k^* + k_{-A})K_2^* + (k^+ + k_{-HA})[H^+]}$$

The second factor in eq. 3 contains all the rate constants for carbon–carbon bond breaking, so this factor determines the magnitude of any kinetic isotope effect arising from isotopic substitution in the carboxyl carbon. Table 2 shows the experimental ^{13}C-carboxyl kinetic isotope effect obtained at high and low acidities. At

Can. J. Chem. Downloaded from www.nrcresearchpress.com by 210.87.254.40 on 09/05/12
For personal use only.

TABLE 2. ^{13}C-Carboxyl kinetic isotope effect in the decarboxylation of pyrrole-2-carboxylic acid at 50°, $\mu = 1.0$

Buffer*	pH at 50°	% Reaction	$^{13}CO_2/^{12}CO_2$	$100\left(\frac{k_{12}}{k_{13}} - 1\right)$
$HClO_4$	0.102	100	0.010301	
$HClO_4$	0.102	100	0.010301	
$HClO_4$	0.102	100	0.010300	
$HClO_4$–NaH_2PO_4	2.63	10.05	0.010296	0.043
$HClO_4$–NaH_2PO_4	2.63	9.945	0.010292	0.088
$HClO_4$–NaH_2PO_4	2.63	13.33	0.010300	0.016
$HClO_4$	(4.00 M)	23.31	0.010052	2.83
$HClO_4$	(4.00 M)	22.96	0.010056	2.79
$HClO_4$	(4.00 M)	22.74	0.010053	2.81

*Adjusted to constant ionic strength with KCl.

pH 2.63 the isotope effect is negligible, but in 4 M perchloric acid it amounts to 2.8%. This shows that carbon–carbon bond breaking is rate determining at high acidities but not at low ones, so that the second factor of eq. 3 must approach unity at low acidities. That is, eq. 3 reduces to eq. 4 at low acidities.

$$[4] \qquad k = k_A K_2 + k_{HA}[H^+]$$

Figure 1 shows a plot of the rate data from pH 3.4 to 1.5 according to eq. 4, the slope and intercept of which give $k_{HA} = 2.1 \times 10^{-3}\ s^{-1}$ and $k_A K_2 = 2.9 \times 10^{-5}\ s^{-1}$. Although K_2 is not known at 50° and ionic strength 1.0, its thermodynamic value at 20° is 2.45×10^{-5} (9), so it may be concluded that k_A is of the order of 1 and, consequently, that ring protonation is about 500 times faster for the pyrrole-2-carboxylate ion than for the acid itself.

From the fact that the second factor of eq. 3 approaches unity at low acidity, k_{-A} must be small compared to k^*; but since it is not unity at high acidities, k_{-HA} must be large compared to k^+. Consequently, at high acidities eq. 3 can be approximated by eq. 5. For anthranilic acid

$$[5] \qquad k = k_{HA}[H^+]\frac{k^*K_2^* + k^+[H^+]}{k^*K_2^* + k_{-HA}[H^+]}$$

it was possible to show that $k^+[H^+]$ is negligible up to very high acidities, so that the rate expression becomes eq. 6. That $k^+[H^+]$ is also

$$[6] \qquad \frac{1}{k} = \frac{1}{k_{HA}[H^+]} + \frac{k_{-HA}}{k_{HA}k^*K_2^*}$$

negligible for pyrrole-2-carboxylic acid is shown by Fig. 2, where a plot of the data from the pH range 0.8 to 0.08 fits eq. 6, giving $k_{HA} = 2.3 \times 10^{-3}\ s^{-1}$ and $k_{-HA}/k^*K_2^* = 5.8 \times 10^{-1}$. The two values of k_{HA} obtained from eqs. 4 and 6 are

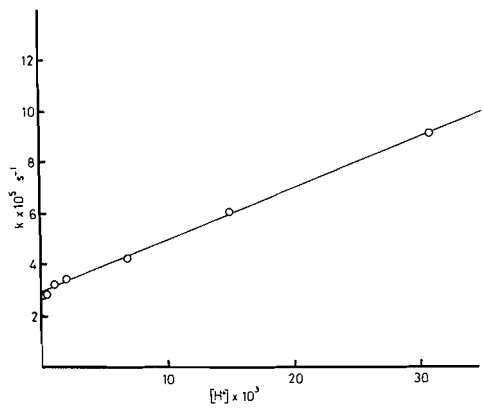

FIG. 1. A plot of rate constant *vs.* hydrogen ion concentration according to eq. 4.

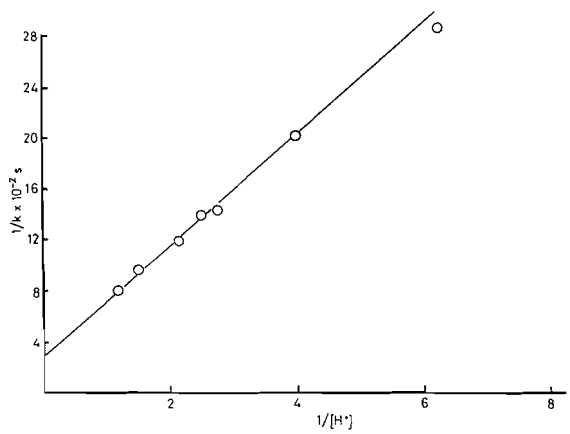

FIG. 2. A plot of rate constant *vs.* hydrogen ion concentration according to eq. 6.

Can. J. Chem. Downloaded from www.nrcresearchpress.com by 210.87.254.40 on 09/05/12
For personal use only.

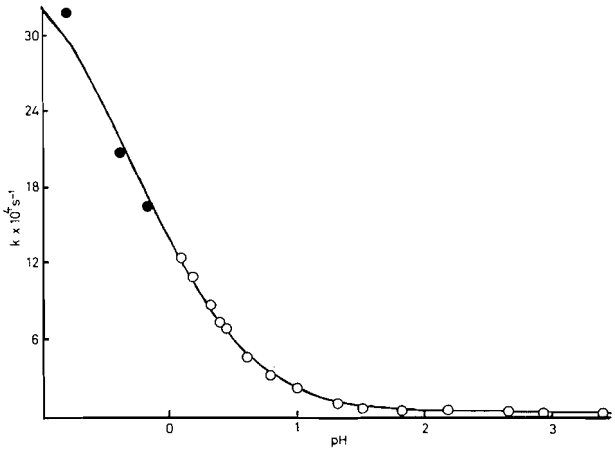

FIG. 3. A plot of rate constant *vs.* hydrogen ion concentration according to eq. 7. The line is calculated from eq. 7 and the circles are experimental points. The solid circles represent rate constants obtained at ionic strengths greater than 1.0, and are therefore not strictly comparable with the others. The p*H* values for these three points were obtained from $-\log$ [HCl].

in satisfactory agreement and have an average value of $2.2 \times 10^{-3}\ s^{-1}$. Therefore all the data obtained at ionic strength 1.0 can be accommodated by the rate expression, eq. 7. Figure 3 shows the experimental rate constants superimposed on a plot of eq. 7.

$$[7] \quad k = \frac{k_A K_2 + k_{HA}[H^+]}{1 + \frac{k_{-HA}}{k^* K_2^*}[H^+]} = \frac{(2.9 \times 10^{-5}) + (2.2 \times 10^{-3})[H^+]}{1 + 0.58[H^+]}$$

It is clear from Fig. 3 that the data obtained at constant ionic strength can be accounted for by omitting the term $k^+[H^+]$ in eq. 2; that is, by assuming that only the ionized carboxyl group decarboxylates. The data obtained at higher acidities where the ionic strength is greater than 1.0 are difficult to interpret quantitatively because for such solutions $[H^+]$ should presumably be replaced by h_0^n, and n is an additional unknown (7). However, it may be noted that if $k^+[H^+]$ is retained in eq. 5 the rate constant should increase continuously with $[H^+]$ (or h_0^n) at high acidities. On the other hand, if it is omitted, as in eq. 7, the rate constant should level off at about $3.8 \times 10^{-3}\ s^{-1}$. It will be seen from Table 1 that the rate, in fact, does not exceed this figure even in 10.3 *M* hydrochloric acid. There is, therefore, no necessity to postulate that the unionized carboxyl group decarboxylates.

It may be concluded then that pyrrole-2-carboxylic acid decarboxylates by a mechanism very similar to that of anthranilic acid. The species which decarboxylates (HA*) is an intermediate composed of the carboxylate anion protonated on the ring carbon to which the carboxylate group is attached. The intermediate can be formed both by ring-protonation of the anion (A^-) and by ionization of the ring-protonated acid (H_2A^*). At low acidities protonation is the slow step; at higher acidities the rate of protonation exceeds that of decarboxylation.

The authors are grateful to the National Research Council of Canada for financial support, to the Faculty of Graduate Studies for a fellowship, and to Mr. W. D. Buchannon for the mass-spectrometric measurements.

1. A. ALBERT. Heterocyclic chemistry. 2nd. Ed. Athlone Press, London, 1968. p. 57.
2. A. H. CORWIN and J. L. STRAUGHN. J. Amer. Chem. Soc. **69**, 2987 (1947).
3. A. V. WILLI. Trans. Faraday Soc. **55**, 433 (1959). A. V. WILLI and J. F. STOCKER. Helv. Chim. Acta, **37**, 1113 (1954).
4. K. R. LYNN and A. N. BOURNS. Chem. and Ind. London, 782 (1963).
5. G. E. DUNN, P. LEGGATE, and I. E. SCHEFFLER. Can. J. Chem. **43**, 3080 (1965).
6. G. E. DUNN and J. A. BUCCINI. Can. J. Chem. **46**, 563 (1968).
7. G. E. DUNN and S. K. DAYAL. Can. J. Chem. **48**, 3349 (1970).
8. Y. CHIANG and E. B. WHIPPLE. J. Amer. Chem. Soc. **85**, 2763 (1963).
9. M. K. A. KHAN and K. S. MORGAN. Tetrahedron, **21**, 2197 (1965).

Can. J. Chem. Downloaded from www.nrcresearchpress.com by 210.87.254.40 on 09/05/12
For personal use only.

Can. J. Chem. Downloaded from www.nrcresearchpress.com by 210.87.254.5 on 09/05/12
For personal use only.

Crystal Structure of $Ca_3(AsO_4)_2$ [1]

R. GOPAL AND C. CALVO

Institute for Materials Research and Department of Chemistry, McMaster University, Hamilton, Ontario

Received September 17, 1970

$Ca_3(AsO_4)_2$ crystallizes in the rhombohedral space group $R3c$ with unit cell parameters $a = 14.05(1)$ Å, $\alpha = 45.05(2)°$, and $Z_R = 7$. The equivalent hexagonal axes are $a = 10.77(1)$ and $c = 37.81(3)$ Å with $Z_H = 21$. The structure was refined, using 769 symmetry independent reflections and a full matrix least squares program from a trial structure obtained from Patterson functions, to a final R value of 0.063. The structure consists of interconnected chains of CaO_n polyhedra and AsO_4 tetrahedra paralleling the c axis. The six chains surrounding the three-fold axes are each much like those in $Ba_3(PO_4)_2$ with 3Ca followed by two AsO_4 groups per half cell. The chain on the three-fold axis has only one AsO_4 per half cell with one and half cations between adjacent arsenic atoms. The mean As—O bond lengths are 1.69, 1.65, and 1.69 Å for the three independent tetrahedra. The cation sites show coordination to 6, 7, or 8 oxygen atoms in contrast to the 10 or 6 + 6 found in $Ba_3(PO_4)_2$. These structural differences arise primarily from the shorter cation – oxygen atom bond lengths in this compound. This structure is the same as that of $Ca_3(VO_4)_2$ and although closely related to that of Whitlockite differs from it because of the need to accommodate hydrogen atoms in the latter compound.

$Ca_3(AsO_4)_2$ cristallise dans le groupe spatial rhomboédrique $R3c$: $a = 14.05(1)$ Å, $\alpha = 45.05(2)°$, and $Z_R = 7$. La maille hexagonale correspondante est: $a = 10.77(1)$, $c = 37.81(3)$ Å et $Z_H = 21$. D'une structure de départ obtenue à partir d'une synthèse de Patterson et utilisant 769 réflexions indépendantes, on a obtenu, par une matrice complète de moindres carrés, une structure affinée pour laquelle le facteur $R = 0.063$. La structure est formée de chaînes de polyèdres CaO_n et de chaînes de tétraèdres AsO_4, parallèles à l'axe c et reliées entre elles. Les six chaînes disposées autour de l'axe d'ordre trois, ressemblent à celles du $Ba_3(PO_4)_2$, 3 atomes de Ca alternant avec deux groupes AsO_4 par demi-maille. La chaîne située sur l'axe d'ordre trois ne comporte qu'un seul AsO_4 par demi-maille et un cation et demi entre atomes d'arsenic voisins. Pour les trois tétraèdres indépendants, les longueurs moyennes des liaisons As—O sont 1.69, 1.65, 1.69 Å. Le cation est coordiné à 6, 7 ou 8 atomes d'oxygène, alors qu'on trouve une coordination de 10 ou 6 + 6 dans le $Ba_3(PO_4)_2$. Ces différences de structure se rattachent principalement à une distance cation–oxygène plus courte dans le présent composé. Cette structure est la même que celle du $Ca_3(VO_4)_2$, mais elle diffère de celle de la Whitlockite par la présence d'hydrogènes dans cette dernière.

Canadian Journal of Chemistry, 49, 1036 (1971)

Introduction

In nMO.X_2O_5 systems where $n = 2$ or 3, M is a divalent cation and X = P, V, or As, a transitional structure type occurs near an ionic radius for the cation corresponding to about 1 Å. For orthocompounds, $M_3(XO_4)_2$, the ideal oxygen atom packing has octahedral and tetrahedral holes consistent with M—O and X—O bond lengths near 2.0 and 1.7 Å, respectively. Thus the structures of the orthovanadates of Mg(1), Zn(2), Co(3), and Ni(4) and the orthoarsenates of Ni(5) and Co(6) are based upon close packed arrays of oxygen atoms with the divalent metal ion in an octahedrally coordinated interstice while the pentavalent ion lies in a tetrahedral one. Here the radii of the M ion is less than 0.9 Å. Those orthocompounds with large cations show structures where the cations and the oxygen atoms both pack as hard spheres to the degree consistent with the constraints imposed by the tetrahedral shape of the anion. Such a structure is shared by the phosphates, arsenates, and vanadates of Sr, Ba, and Pb (7–11) with $R\bar{3}m$ for the space group and hexagonal cell parameters near $a = 5.5$ and $c = 20$ Å. In this case one-third of the cations show the twelve-fold coordination expected for packing of hard spheres but with the two unique bond lengths separated by about 0.5 Å. The existence of polymorphs among compounds containing Ca^{2+} (12), Pb^{2+} (9), and Cd^{2+} (13, 14), is a manifestation of the intermediate size of these ions. The orthocompounds containing Ca^{2+} for these three anions have had largely unknown structures except for the structure of $Ca_7Mg_9(Ca,Mg)_2(PO_4)_{12}$ which has recently been reported (15). A close relationship between the structure of $\beta Ca_3(PO_4)_2$ and the mineral Whitlockite has long been suspected (16). Since their space group and unit cell dimensions are similar to those of $Ca_3(AsO_4)$ and $Ca_3(VO_4)_2$ (17), these structures should also be related. Further, a structural analogy has been postulated

[1]This research is supported by the Defence Research Board of Canada under Grant No. 9510-44.

TABLE 1. Index powder pattern of $Ca_3(AsO_4)_2$*

Index h k l	Angle(°) θ_{cal}	θ_{obs}	Index h k l	Angle(°) θ_{cal}	θ_{obs}	Index h k l	Angle(°) θ_{cal}	θ_{obs}
0 1 2	5.290		0 4 2	19.460	19.588	2 3 11	25.110	
1 0 4	6.670	6.80	1 0 16	19.665		3 3 0	25.435	25.365
0 0 6	7.540		1 1 15	19.735		3 3 3	25.710	
1 1 0	8.230	8.240	3 1 8	19.860		0 4 14	25.900	
1 1 3	8.965	9.000	2 2 9	19.880		2 4 1	25.965	25.940
2 0 2	9.805	9.690	4 0 4	19.910		4 2 2	26.055	
0 1 8	10.535	10.640	2 1 13	20.095		2 0 20	*26.105*	*26.175*
0 2 4	10.620		0 3 12	*20.385*	*20.325*	1 3 16	26.220	
1 1 6	10.855		1 2 14	21.075		3 0 18	26.290	
2 1 1	12.685		3 2 1	21.130		5 0 8	26.375	26.330
1 0 10	*12.710*	*12.763*	1 3 10	21.165	21.165	2 1 19	26.415	
1 2 2	12.855		2 3 2	21.260		2 4 4	26.415	
2 0 8	13.430	13.425	0 2 16	21.450		3 3 6	26.520	
1 1 9	13.460		0 4 8	21.630		3 2 13	26.570	
2 1 4	13.495		3 2 4	21.675	21.690	4 2 5	26.685	
1 2 5	13.960		3 1 11	21.900		1 4 12	26.800	
0 0 12	14.160	14.025	2 3 5	21.990		1 1 21	26.835	
0 3 0	14.355	14.315	2 2 12	22.125		1 0 22	*27.135*	*27.087*
2 1 7	15.133		4 1 0	22.255		3 1 17	27.200	
2 1 10	15.215	15.290	4 1 3	22.560		2 3 14	27.365	27.415
1 2 8	*15.830*	*15.750*	3 2 7	22.800		2 4 7	27.390	
3 0 6	*16.050*	*16.013*	4 0 10	22.855	22.725	5 1 1	27.430	
1 1 12	16.465		2 1 16	23.125		0 5 10	27.440	
2 2 0	16.635	16.613	1 1 18	23.200		1 5 2	27.515	
2 2 3	17.025		2 3 8	23.295		1 2 20	27.560	
0 1 14	17.285		1 4 6	23.455	23.425	4 0 16	27.675	27.690
1 3 1	17.380	17.300	1 3 13	23.505		2 2 18	27.740	
2 1 10	17.395		1 2 17	24.195		4 2 8	27.825	27.827
3 1 2	17.505		3 1 14	24.370	24.290	3 3 9	27.840	
1 3 4	17.995		3 2 10	24.455		5 1 4	27.860	
2 2 6	18.143	18.113	5 0 2	24.535	24.540	0 2 22	28.555	28.505
1 2 11	18.255		0 1 20	24.585		5 1 7	28.850	
3 1 5	18.360	18.663	2 2 15	24.765		*2 4 10*	*28.850*	*28.900*
2 0 14	19.260	19.213	1 4 9	24.890		3 2 16	29.080	29.050
1 3 7	19.295		0 5 4	24.910	25.015	1 4 13	29.130	

*θ_{cal} were determined using $a = 10.767$ and $c = 37.81$ Å and the lines are indexed on the basis of a hexagonal cell. Values in italics were used in the least squares refinement to determine a and c. CuKα radiation was used.

between Whitlockite and $\beta Ca_3(PO_4)_2$ and $Ba_3(PO_4)_2$ (18, 19) since their space group is a subgroup of the latter's space group and their lattice parameters are nearly twice as long. However, the cells contain only seven formula units rather than the eight predicted by analogy. This discrepancy in the mineral has been discussed by Keppler (20).

Experimental

Single crystal of $Ca_3(AsO_4)_2$ were obtained from stoichiometric quantities of either $CaCO_3$ or $Ca(OH)_2$ with As_2O_5 reacted at high temperatures, melted in a platinum crucible and slowly cooled to room temperature. These crystals gave a diffraction pattern nearly the same as that of $Ca_3(VO_4)_2$[2] which has been shown to be rhombohedral with seven formula units per cell here and by Reden and Buerger (21). The extinctions of $Ca_3(AsO_4)_2$ are all reflections such that $-h + k + l \neq 3n$ and for $h0l$, $l \neq 2n$. Therefore the space group must be either $R3c$ or $R\bar{3}c$ with the former preferred. The latter space group with $Z_R = 7$ would require that an As ion lie at a point of $\bar{3}$ symmetry and thus probably have an octahedral environment of oxygen atoms. Although this feature is not unknown for As or V it is not likely for P.

Accurate unit cell parameters, $a = 10.77(1)$ and $c = 37.81(3)$ Å for the hexagonal cell, were obtained from a Debye–Scherrer pattern taken with CuKα radiation ($\lambda_{\alpha_1} = 1.5405$ Å) and refined by least squares. The indexed powder pattern is contained in Table 1. Z_R was taken to be seven by analogy with $Ca_3(VO_4)_2$ since the $Ca_3(AsO_4)_2$ preparations did not yield uniform samples.

Data were recorded relative to a monoclinic set of axes with the monoclinic A, B, and C equal to the hexagonal $a + 2b$, a, $\frac{1}{3}(c - a - b)$ axes, respectively. MoKα radiation was used throughout these measurements. Data of the type hkn with $n = 0$, 1, 2, or 3, $0kl$ and $1kl$ were recorded with an integrating precession camera and the intensities of these reflections measured with a Joyce–Lobel microdensitometer. In addition, the data hnl, $n = 1$, 2 were measured with a scintillation counter manually set to the proper 2θ while the crystal was

[2]The crystals were grown by C. D. Cox at the Defence Telecommunication Laboratories of Canada.

Can. J. Chem. Downloaded from www.nrcresearchpress.com by 210.87.254.5 on 09/05/12
For personal use only.

Can. J. Chem. Downloaded from www.nrcresearchpress.com by 210.87.254.5 on 09/05/12
For personal use only.

rocked through an ω angle of 2°. The intensities of the *h0l* reflections were determined by visual comparison with calibrated films. The intensities were corrected for background and Lorentz and polarization effects and transformed to the hexagonal cell. A total of 1253 reflections were examined and reduced to 769 symmetry independent reflections of which 553 were observable. Since the crystal used measured 0.08 × 0.11 × 0.15 mm^3 ignoring absorption corrections, with an average μR of 0.65 for a pseudo-sphere, leads to average errors of the order 10% in the intensity, absorption corrections were ignored.

A trial structure was obtained from slices in the three dimensional Patterson functions calculated perpendicular to the *c* axis. These were interpreted in terms of chains of Ca and As atoms distributed near x, y = (0,0)(1/6,1/3)-(1/3,1/6), and (1/2,1/2). Detailed deviations from these values were determined by a comparison of the Patterson functions of $Ca_3(AsO_4)_2$ and $Ca_3(VO_4)_2$. The nature of these chains are very much like those in $Ba_3(PO_4)_2$ (7) and $Ba_3(VO_4)_2$ (10) except for those on the three fold axis which had only half the normal number of formula units. On these axes only one As ion and its *c* glide plane related mate were placed in the trial model. This model was refined using data from both $Ca_3(AsO_4)_2$ and $Ca_3(VO_4)_2$ and subsequently calculated electron density maps used to distinguish Ca^{2+} from As^{5+}. Scattering curves for Ca^{2+} and O^- were obtained from the International Tables for X-Ray Diffraction (22) while that of As^{3+} was taken from Cromer and Waber (23). Next the oxygen atoms about the As ions on the three fold axes were found, followed by those about the remaining arsenic ions. These latter oxygen atoms were located as in $Ba_3(VO_4)_2$ with one AsO bond of the tetrahedron parallel to the *c* axis and the remaining ones nearly paralleling the glide planes of $Ca_3(AsO_4)_2$. The *R* value now stood at 0.17 with 1.5 Ca ions per rhombohedral cell remaining unaccounted for. Three Ca ions were placed on the three-fold axes between the AsO_4 groups displaced by nearly a half a rhombohedral translation from the cations already located. The central site was fully occupied and had an acceptable octahedral environment. The others were 1/4 occupied and had three of their six nearest oxygen atoms displaced by about 3 Å. When the populations of the cation sites were varied by least squares only the central one remained unchanged. At this point the chemical formulation corresponded to $Ca_{20}(AsO_4)_{14}$. The temperature factors for all atoms were varied first isotropically and then anisotropically using a full matrix least squares procedure. The program used was written by J. S. Stephens for the CDC6400. The weights, ω, were set equal to $(240 + 0.64F_o + 0.0023F_o^2)^{-1}$ with the coefficients of the observed structure factors chosen such that the difference in magnitude between the observed and calculated structure factors would be independent of $|F_o|$. The weights of unobserved reflections were set equal to zero if $|F_c| < |F_{min}|$, where F_{min} is the minimum observable value in that area of reciprocal space. Three strong reflections which seemed to be seriously affected by extinction were left out of the refinement. Multiply and symmetry related reflections were averaged and assigned randomly to one of the batches from which they arose. The refinement with this model was terminated when changes were less than one-third of the estimated standard deviations. The value of *R* and R_W ($= [\Sigma\omega|F_o| - |F_c|/\Sigma\omega F_o^2]^{1/2}$) were 0.063 and 0.085. Electron density and difference maps were prepared with particular attention given to the region near the *c* axis in quest of the remaining Ca^{2+}. No peak greater than about 1/3 of an oxygen atom could be located. On the other hand only O(1) and O(9) amongst all the oxygen atoms have near neighbor environments with only 2 calcium ions in addition to an arsenic. Further, the sum of the bond angles at O(1) deviated by 15° from the value expected if the three neighbors were coplanar suggesting that the missing cation lies in a site such as to complete a nearly tetrahedral environment about this oxygen atom. This site turned out to be one of the originally one-quarter occupied sites. A cycle of least squares refinement varying the isotropic temperature factor and the *z* coordinate of a site with the population fixed at one-half did not yield a significant improvement in *R*. In $\beta(Ca_{0.9}Mg_{0.1})_3(PO_4)_2$, however, Dickens has found this site to contain the extra Ca^{2+} (24). Thus the final cycles of refinement were preformed with this model and resulted in an *R* value of 0.063 and R_W = 0.079 when the calculated shifts ceased to be significant. The final atomic parameters are to be found in Table 2 while the magnitude of the observed and calculated structure factors are compared in Table 3.

Description of the Structure

The structure of $Ca_3(AsO_4)_2$ is most easily discussed by comparison with that of $Ba_3(VO_4)_2$ (10)[3] a recently refined isostructure of $Ba_3(PO_4)_2$. These latter structures have the rhombohedral space group $R\bar{3}m$ with the unit cell axes nearly half that of $Ca_3(AsO_4)_2$ and Z_R = 1. The structure consists of parallel chains, coincident with the three fold axis, with a sequence of $3BaO_n$, followed by two PO_4 tetrahedra, as seen in Fig. 1*a*. The central Ba ion of the triplet, Ba(I), lies at a site of $\bar{3}m$ symmetry and is strongly coordinated to six oxygen atoms which lie 2.76 Å away and weakly coordinated to a further six displaced by 3.33 Å. The first six form an octahedral environment about Ba(I) distorted by elongation along the three-fold axis while the remaining six are nearly coplanar and nearly at the same *z* level as Ba(I). The remaining Ba ions, Ba(II), are coordinated ten oxygen atoms. Three oxygen atoms are shared with Ba(I), six are coplanar and form a hexagon about Ba(II) and arise from three edges of three separate PO_4 groups lying on neighboring three fold axes. The remaining oxygen atom of this environment lies on the same three fold axis as Ba(II).

In $Ca_3(AsO_4)_2$, because of the doubled cell edges, only one quarter of the chains coincide with three fold axes. These will be called *A* chains

[3]Roman numerals will be substituted for the arabic ones in this reference.

Can. J. Chem. Downloaded from www.nrcresearchpress.com by 210.87.254.5 on 09/05/12
For personal use only.

TABLE 2. Positional and thermal parameters of $Ca_3(AsO_4)_2$*

Atom	Site symmetry	x	y	z	U_{11}†	U_{22}	U_{33}	U_{12}	U_{13}	U_{23}
As(1)	3	0	0	0	0.015(3)	U_{11}	0.016(3)	$\frac{1}{2}U_{11}$	—	—
As(2)	1	0.3096(5)	0.1382(6)	0.1325(2)	0.018(2)	0.017(2)	0.012(2)	0.012(2)	0.008(2)	0.003(2)
As(3)	1	0.3478(5)	0.1518(5)	0.2349(2)	0.015(2)	0.010(2)	0.012(2)	0.007(2)	−0.002(2)	−0.002(2)
Ca(1)	1	0.2740(8)	0.1391(13)	−0.1642(3)	0.011(4)	0.011(4)	0.017(5)	0.003(4)	−0.006(3)	−0.001(4)
Ca(2)	1	0.3827(10)	0.1753(10)	0.0345(3)	0.015(4)	0.019(6)	0.013(4)	0.010(3)	−0.004(3)	−0.003(4)
Ca(3)	1	0.2702(9)	0.1501(10)	−0.0589(3)	0.035(4)	0.032(5)	0.029(4)	0.023(4)	−0.012(4)	−0.017(4)
Ca(4)	3	0	0	0.2670(6)	0.022(5)	U_{11}	0.012(5)	$\frac{1}{2}U_{11}$	—	—
O(1)	1	0.270(6)	0.077(5)	0.092(1)	0.11(4)	0.08(3)	0.06(3)	0.08(3)	0.01(3)	−0.02(3)
O(2)	1	0.227(5)	0.219(4)	0.146(1)	0.08(3)	0.06(3)	0.03(2)	0.06(2)	0.01(2)	0.00(2)
O(3)	1	0.278(3)	−0.005(3)	0.155(1)	0.03(2)	0.01(2)	0.00(1)	0.01(1)	0.00(1)	0.01(1)
O(4)	1	0.487(3)	0.244(5)	0.140(1)	0.03(2)	0.07(3)	0.03(1)	0.04(2)	0.02(1)	−0.01(2)
O(5)	1	0.406(3)	0.038(3)	0.225(1)	0.03(2)	0.03(2)	0.04(2)	0.03(1)	0.01(2)	0.02(2)
O(6)	1	0.430(5)	0.315(4)	0.215(1)	0.06(2)	0.03(2)	0.04(2)	0.00(2)	0.01(2)	0.03(2)
O(7)	1	0.174(3)	0.077(4)	0.222(1)	0.03(2)	0.03(2)	0.04(2)	0.01(2)	−0.03(1)	−0.03(2)
O(8)	1	0.384(3)	0.188(3)	0.279(1)	0.02(2)	0.02(2)	0.01(1)	0.02(2)	0.01(1)	−0.01(1)
O(9)	1	−0.003(5)	0.148(2)	0.015(2)	0.05(2)	0.06(3)	0.09(3)	0.06(2)	0.03(2)	0.05(2)
O(10)	3	0	0	−0.043(1)	0.04(1)	U_{11}	0.01(2)	$\frac{1}{2}U_{11}$	—	—
Ca(5)	3	0	0	0.083(1)	0.05(1)‡					

*Estimated standard deviations in parentheses.
†The U_{ij}, in Å^2, are computed from $\beta_{ij} = 2\pi^2 b_i b_j U_{ij}$ where $T = \exp[-(\beta_{11}h^2 + 2\beta_{12}hk + \cdots)]$ appears in the structure factor expression and b_j are reciprocal lattice vectors.
‡Isotropic temperature factors in Å^2.

Can. J. Chem. Downloaded from www.nrcresearchpress.com by 210.87.254.5 on 09/05/12
For personal use only.

TABLE OF OBSERVED REFLECTIONS OF Ca_3ASO_6Cl. UNOBSERVED REFLECTIONS MARKED WITH * AND INCLUDED WITH A

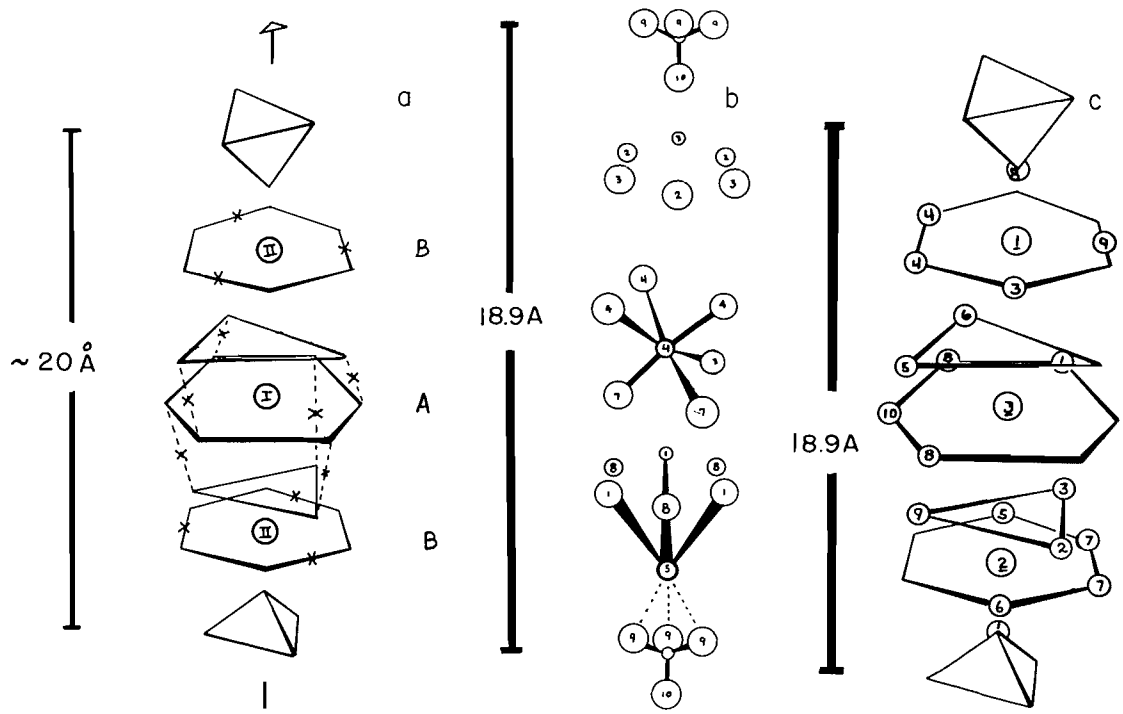

FIG. 1. (*a*) The BaO_n polyhedra and PO_4 tetrahedra in the $Ba_3(PO_4)_2$ structure are shown. The Ba ions lie at the center of the hexagonal planes (*B*,*A*,*B*) with at the corners of the outlined hexagons and triangles. The edges shared between the BaO_n polyhedra and the PO_4 groups are marked with crosses. (*b*) The *A* chain, coincident with the three fold axis, in the $Ca_3(AsO_4)_2$ structure is shown. The atoms are labelled as in Table 2 with the Ca ions at the center of the polyhedra. The strong cation–oxygen bonds are shown as filled bonds while the weak Ca(5)—O(9) bonds are shown dotted. (*c*) An idealized view of the *B* chain in the $Ca_3(AsO_4)_2$ structure is depicted. The oxygen atoms, shown as circles, around the perimeter of the hexagons and triangles are numbered as in Table 2. The cations are shown as circles with underlined numerals. The corners of the hexagons and triangles without circles correspond to broken cations oxygen bonds except for O(9) in the upper portion of the diagram which lies displaced by 30° from the comparable position in $Ba_3(VO_4)_2$. O(9) in the lower portion of the diagram is bonded only to Ca(2).

despite the fact that they contain only half as many formula units per unit length as those in $Ba_3(VO_4)_2$. The remaining chains, the *B* chains, are qualitatively much the same as those in $Ba_3(VO_4)_2$ with the polyhedral sequence $As(2)O_4$, $Ca(2)O_8$, $Ca(3)O_8$, $Ca(1)O_7$, and $As(3)O_4$. In contrast the *A* chains contain only one full cation, Ca(4), and one arsenic ion, As(1), and their glide plane related partners per cell. O(10) on the three-fold axis and O(1) bonded to As(2) and O(8) bonded to As(3) are related to O(I), the oxygen atom on the three-fold axis in $Ba_3(VO_4)_2$. Ca(4) is a cation of type *I*, when compared to this latter structure, since it lies half a rhombohedral lattice translation from the central cation, Ca(3), on the *B* chain. Ca(4) is coordinated to six oxygen atoms, as is shown in Fig. 1*b*, which lies either 2.24(4) or 2.34(4) Å from this cation. These oxygen atoms correspond to those of type *II*, those lying on the mirror planes only, in $Ba_3(VO_4)_2$. The equatorial bond angles indicate an elongation of the octahedron along the three fold axis. The bond lengths and angles for $Ca_3(AsO_4)_2$ are tabulated in Table 4. All the cation oxygen bond lengths less than 3.0 Å are given.

The half-filled cation site on the three fold axis contains Ca(5) which is bonded to three O(1)s and three O(9)s. The Ca(5)—O(1) bond length is 2.61 Å and the Ca(5)—O(9) bond length is 3.04 Å. The Ca(5)—O_6 group shares a face with the AsO_4 group involving O(9)s. The short Ca(5)—As(1) separation of 3.13 Å suggests a rather strong repulsion between these positively charged ions. The remaining cations lie in general positions and deviate substantially from being colinear with the *c* axis. The reduction in Z_R from 8 to 7 should result in the loss of two oxygen atoms from the environments of each of Ca(2)

Can. J. Chem. Downloaded from www.nrcresearchpress.com by 210.87.254.5 on 09/05/12
For personal use only.

TABLE 4. Bonding geometry in $Ca_3(AsO_4)_2$

Bond	Length (Å)	Bonds	Angle (deg)	Bonds	Angle (deg)
As(1)—O_4 Group					
As(1)—O(9) 3×	1.71(5)	O(9)—As(1)—O(9)	110(3)		
—O(10)	1.63(5)	—O(10)	109(2)		
As(2)—O_4 Group					
As(2)—O(1)	1.65(5)	O(1)—As(2)—O(2)	115(3)	O(2)—As(2)—O(3)	115(2)
—O(2)	1.61(6)	—O(3)	103(2)	—O(4)	109(2)
—O(3)	1.65(3)	—O(4)	114(2)	O(3)—As(2)—O(4)	100(2)
—O(4)	1.69(3)				
As(3)—O_4 Group					
As(3)—O(5)	1.67(5)	O(5)—As(3)—O(6)	118(3)	O(6)—As(3)—O(7)	104(3)
—O(6)	1.70(5)	—O(7)	109(2)	—O(8)	105(2)
—O(7)	1.70(4)	—O(8)	105(2)	O(7)—As(3)—O(9)	117(2)
—O(8)	1.70(4)				
Ca(1)—O_7 Group					
Ca(1)—O(3*b*′)	2.51(4)	O(3*b*′)—Ca(1)—O(4*b*′)	61(1)	O(4*b*′)—Ca(1)—O(5*b*′)	98(1)
—O(4*b*′)	2.52(2)	—O(5*b*′)	71(2)	—O(4*c*′)	71(1)
—O(5*b*′)	2.46(4)	—O(4*c*′)	128(1)	—O(6*c*′)	122(2)
—O(4*c*′)	2.49(5)	—O(6*c*′)	141(2)	—O(8*e*′)	84(1)
—O(6*c*′)	2.26(6)	—O(8*e*′)	74(1)	—O(9*d*″)	155(2)
—O(8*e*′)	2.39(4)	—O(9*d*″)	98(2)	O(5*b*′)—Ca(1)—O(4*c*′)	136(1)
—O(9*d*″)	2.46(4)	O(6*c*′)—Ca(1)—O(8*e*′)	142(2)	—O(6*c*′)	70(1)
Ca(1)—O_7 Group					
		O(6*c*′)—Ca(1)—O(9*d*″)	82(2)	O(5*b*′)—Ca(1)—O(8*e*)	138(2)
		—O(4*c*′)	81(2)	—O(9*d*″)	86(1)
		O(8*e*)—Ca(1)—O(9*d*″)	80(2)	O(4*c*′)—Ca(1)—O(9*d*″)	122(2)
		—O(4*c*′)	84(1)		
Ca(2)—O_8 Group					
Ca(2)—O(2*d*″)	2.42(4)	O(2*d*″)—Ca(2)—O(3*f*″)	72(2)	O(3*f*″)—Ca(2)—O(7*d*″)	127(1)
—O(3*f*″)	2.39(3)	—O(7*d*″)	81(2)	—O(7*f*)	79(1)
—O(5*f*″)	2.83(4)	—O(7*f*)	113(1)	—O(1*a*)	140(2)
—O(6*d*″)	2.82(5)	—O(1*a*)	141(2)	—O(9*c*)	87(2)
—O(7*d*″)	2.45(4)	—O(9*c*)	81(2)	—O(5*f*″)	67(1)
—O(7*f*)	2.45(5)	—O(5*f*″)	139(2)	—O(6*d*″)	144(2)
—O(1*a*)	2.45(5)	—O(6*d*″)	75(2)	O(5*f*″)—Ca(2)—O(6*d*″)	143(1)
—O(9*c*)	2.36(4)	O(6*d*″)—Ca(2)—O(7*d*″)	61(2)	—O(7*d*″)	126(1)
		—O(7*f*)	128(2)	—O(7*f*)	62(1)
		—O(1*a*)	67(2)	—O(1*a*)	77(2)
		—O(9*c*)	73(2)	—O(9*c*)	95(2)
		O(7*d*″)—Ca(2)—O(7*f*)	70(1)	O(7*d*″)—Ca(2)—O(1*a*)	96(1)
		—O(1*a*)	87(2)	—O(9*c*)	156(2)
		—O(9*c*)	133(2)	O(1*a*)—Ca(2)—O(9*c*)	81(2)
Ca(3)—O_8 Group					
Ca(3)—O(5*b*′)	2.33(4)	O(5*b*′)—Ca(3)—O(8*b*′)	64(1)	O(8*b*″)—Ca(3)—O(1*f*″)	156(2)
—O(8*b*′)	2.69(3)	—O(1*f*″)	97(1)	—O(2*e*″)	76(1)
—O(1*f*″)	2.62(4)	—O(2*e*″)	94(2)	—O(3*f*″)	128(1)
—O(2*e*″)	2.63(5)	—O(3*f*″)	149(2)	—O(6*c*′)	113(1)
—O(3*f*″)	2.46(3)	—O(6*c*′)	66(1)	—O(8*c*′)	124(1)
—O(6*c*′)	2.60(5)	—O(8*c*′)	128(2)	—O(10*a*)	61(1)
—O(8*c*′)	2.48(4)	—O(10*a*)	104(1)	O(1*f*″)—Ca(3)—O(2*e*″)	92(1)
—O(10*a*)	2.59(1)	O(2*e*″)—Ca(3)—O(3*f*″)	67(1)	—O(3*f*″)	61(1)
Ca(3)—O_8 Group					
		O(2*e*″)—Ca(3)—O(6*c*′)	148(2)	O(1*f*″)—Ca(3)—O(6*c*′)	68(1)
		—O(8*c*′)	138(2)	—O(8*c*′)	79(2)
		—O(10*a*)	117(1)	—O(10*a*)	143(2)
		O(3*f*″)—Ca(3)—O(6*c*′)	118(2)	O(6*c*′)—Ca(3)—O(8*c*′)	64(1)
		—O(8*c*′)	73(1)	—O(10*a*)	93(1)
		—O(10*a*)	106(1)	O(8*c*′)—Ca(3)—O(10*a*)	63(1)
Ca(4)—O_6 Group					
Ca(4)—O(4*e*′) 3×	2.24(5)	O(4*e*′)—Ca(4)—O(4*d*′)	81(2)	O(7*a*)—Ca(4)—O(7*b*)	74(2)
—O(7*a*) 3×	2.34(5)	—O(7*a*)	175(2)	O(4*e*′)—Ca(4)—O(7*c*)	101(1)
		—O(7*b*)	105(1)		

Can. J. Chem. Downloaded from www.nrcresearchpress.com by 210.87.254.5 on 09/05/12
For personal use only.

TABLE 4 (*Concluded*)

Bond		Length (Å)	Bonds	Angle (deg)	Bonds	Angle (deg)
Ca(5)—O_6 Group						
Ca(5)—O(1)	3×	2.61(7)	O(*e*)—Ca(5)—O(1*b*)	118(2)	O(9)—Ca(5)—O(9*b*)	55(2)
—O(9)	3×	3.04(7)	—O(9*a*)	104(2)	—O(1*c*)	66(2)
			—O(9*b*)	119(2)		

*Estimated standard deviations in parentheses. *O(nt)* represent atoms derived from those listed on Table 2 by the symmetry operations of the cell except for unit cell translations. $t = a$ or blank represent x, y, z; $b = -y, x - y, z$; $c = -x + y, -x, z$; $d = -y, -x, z + 1/2$; $e = x, x - y, z + 1/2$; $f = -x + y, y, z + 1/2$. One prime corresponds to an additional rhombohedral centering by 1/2, 2/3, 2/3 and two primes designated the added translation of 2/3, 1/3, 1/3.

and Ca(3) and one oxygen atom from Ca(1). The actual coordination numbers found are 7, 8, and 8 for Ca(1), Ca(2), and Ca(3), respectively. In addition to the cation – oxygen atom bonds lost because of the reduction in Z, Ca(1) has lost bonds to O(2) and O(9) and Ca(3) has lost bonds to O(1) and O(9)′ as is indicated in Fig. 1*c*. The range of the Ca(3)—O bond lengths extend from 2.33 to 2.69 Å, while for Ca(1) this range is from 2.26 to 2.52 Å and for Ca(2) these bond lengths range from 2.36 to 2.83 Å. The mean Ca—O bond lengths are 2.44, 2.52, 2.55, and 2.29 Å for Ca(1), Ca(2), Ca(3), and Ca(4), respectively.

The structure of $Ca_3(AsO_4)_2$ is shown in projection down the *c* axis in Fig. 2*a*, *b* and compared with the analogous projection in $Ba_3(VO_4)_2$ in Fig. 2*c*. The As(1)—O_4 tetrahedron contains a crystallographic three-fold axis with the As(1)—O(10) bond length parallel to the axis of 1.63(5) Å and the As(1)—O(9) bond length of 1.71(5) Å. This tetrahedron shows no significant angular deviation from ideality. The remaining As ions have one of their triad axes nearly parallel to the *c* axis. The As(2)—O(1) vector deviates by about 20° while the As(3)—O(8) vector shows a 13° deviation. The As(2)—O bond lengths range from 1.61 to 1.69 Å while those about As(3) range from 1.67 to 1.70 Å. Since the average estimated standard deviation on these bond lengths is 0.04 Å, these lengths do not deviate significantly from their mean values of 1.65 and 1.69 Å, respectively. The O—As—O deviates by as much as 5σ from regularity, however.

The polyhedra of oxygen atoms about the central cation of the *B* chain, Ca(3), shares an edge with each of the neighboring CaO_n polyhedra. The O(5)—O(6) edge is shared between Ca(1) and Ca(3), as seen in Fig. 3, while the O(2)—O(3) edge is common to Ca(2) and Ca(3). The bond angles subtended by these edges range from 66 to 72° and, as such, suggest some repulsion between neighboring cations. Each of these short chains is terminated by an AsO_4 group with O(8) shared between As(3) and Ca(1), and O(1) shared between As(2) and Ca(2). These *B* chains form a hexagonal array about the triad axes such that each chain participates in two hexagonal prism sharing oxygen atoms with cations in four neighboring chains. The hexagonal prisms share edges rather than faces and therefore the structure has triangular prisms devoid of cations. Adjacent chains in the hexagonal prisms are shifted by about 1/6*c*, with one As—O bond about each tetrahedron directed towards a three fold axis and two more along the edges of the hexagonal prism. Four AsO_4 groups share edges with a Ca(3)—O_8 group and one further AsO_4 group shares a single oxygen atom. In $Ba_3(VO_4)_2$ Ba(I), considered as bonded to 12 oxygen atoms, share edges with $6VO_4$ groups. The Ca(1)—O_7 group shares only one edge with an AsO_4 group while the Ca(2)—O_8 group has two such edges with two AsO_4 groups. Each such cation in $Ba_3(VO_4)_2$ shares three edges with three adjacent VO_4 tetrahedra. Thus the bonding about the hexagonal prism has become substantially more disordered compared with the $Ba_3(VO_4)_2$ structure with only seven edges shared with tetrahedra rather than twelve.

Discussion

The cations of the *B* chain are displaced from a line midway between the triad axes. The magnitude of the deviations from this line are about 1/4, 1/7, 1/2, 1/2, and 2/3 Å for As(2), As(3), Ca(1), Ca(2), and Ca(3), respectively and are related to the decrease in Z. This in turn results from the requirement for a shorter mean cation–oxygen atom bond length than in Ba or Sr orthophosphate. O(10) on the three fold axis is bonded to three Ca(3) ions which move towards this oxygen atom. As a result the bond between

Can. J. Chem. Downloaded from www.nrcresearchpress.com by 210.87.254.5 on 09/05/12
For personal use only.

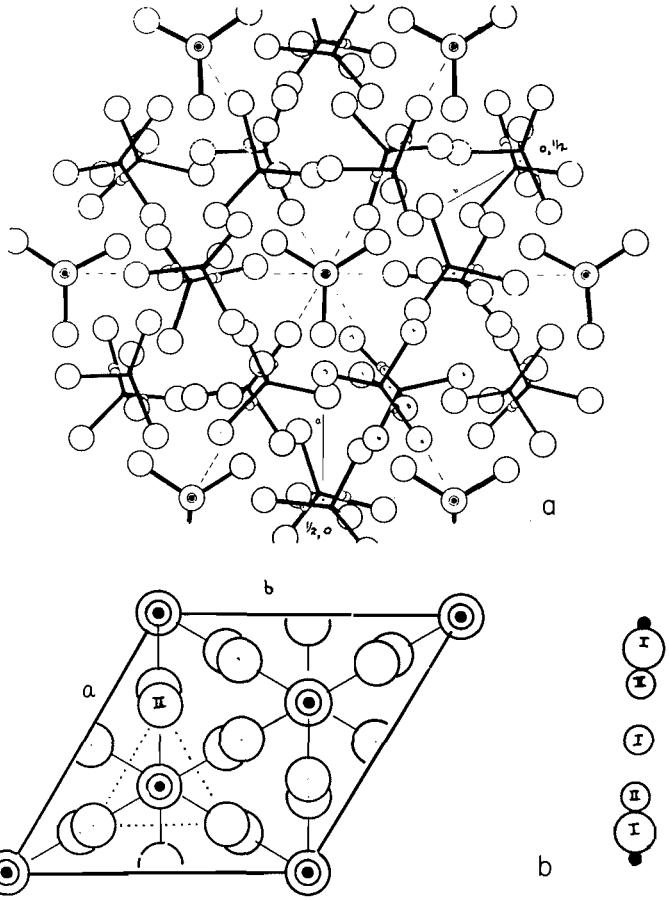

FIG. 2. (*a*) The structure of $Ca_3(AsO_4)_2$ projected another *a b* plane. A volume $\frac{1}{2}c$ thick is shown. The large open circles are oxygen atoms, the filled circles are As ions while the small open circles are cations. The three fold axis are seen as superpositions of O(10), As(1) and Q. The glide planes are represented with broken lines. (*b*) The structure of $Ba_3(VO_4)_2$ is schematic, projected down the *c* axis. The superpositions of three Ba, 2V, and 2 oxygen atoms are depicted by three concentric circles with the inner one filled and the insert shows their mutual arrangement. The type *II* oxygen atoms are shown as large circles. The mirror planes are represented by light lines in the figure. An example of the VO_4 edges shared with Ba(II) is shown dotted.

Ca(3) and the oxygen atom that would be related to O(10), if Ca(3) were at a center of symmetry, is broken and the AsO_4 group containing this oxygen atom is lost from the structure. O(8) and O(1) also move towards Ca(3) in order to achieve suitable Ca—O bond lengths. The former oxygen atom, bonded to the *B* chain at Ca(1), maintains two strong bonds to Ca(3) but O(1) is pulled by Ca(2) to such an extent that only one strong Ca(3)—O(1) bond remains in the environment of Ca(3).

As(1) lies nearly half way between any two Ca(4) ions on the same *A* chain and therefore does not lie in a position analogous with the As ions on the *B* chains. As(1) deviates slightly from being halfway between the two glide planes related Ca(4) ions on the same *A* chain. This deviation allows us to identify As(1) and O(10) with As(2) and O(1) and to assert that the former ions have been translated by about 1.3 Å from positions corresponding to half a rhombohedral lattice translation from those on the *B* chain. In addition, the As(1)—O(9) vector has been rotated so as to be displaced by 30° from the glide plane as is indicated in Fig. 1*c*.

Since the oxygen atoms of type *I* are pulled from the environment of Ca(4) the remaining oxygen atoms of that environment, three Ca(4)'s

Can. J. Chem. Downloaded from www.nrcresearchpress.com by 210.87.254.5 on 09/05/12
For personal use only.

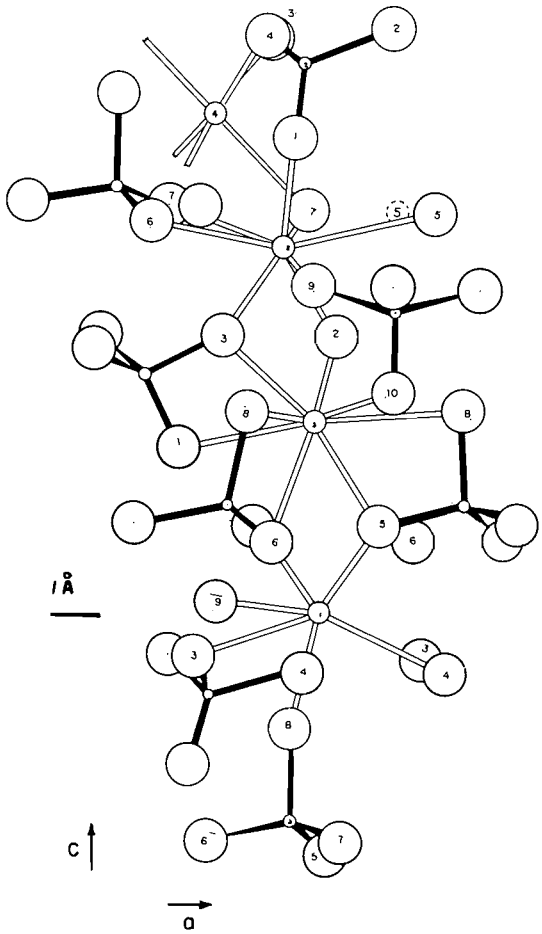

FIG. 3. One chain in the structure of $Ca_3(AsO_4)_2$ projected onto the *ac* plane. The open bonds connect Ca ions, represented by smaller open circles, and the oxygen atoms are represented by the larger open circles. The AsO_4 tetrahedra are shown with filled AsO bonds with the As represented by the smallest circles. The dotted circle represents Ca(5), the ion in the half filled site.

and three O(7)'s, reduce their *z* displacements relative to that of Ca(4) and enlarge their separations in the *ab* plane. The elongation of this octahedron along the three-fold axis, which Süsse and Buerger (10) attribute to the Ba(I)–Ba(II) repulsion, must in fact contain some contribution from other sources since Ca(5) lies about 7 Å from the Ca(4) on the same triad axis. The pertinent angle monitoring this elongation (O(II*d*)—Ba(I)—O(II*d*′)) is reduced from 114.6° in the Ba compound (10) to 105 and 101° in $Ca_3(AsO_4)_2$ and $Ca_3(VO_4)_2$. Even in Whitlockite, devoid of an extra cation, this angle is about 5° greater than the ideal value of 90° (25). The regularity of these octahedra are limited by the O(4)—O(4) and O(7)—O(7) repulsive interactions for a given separation between chains. The loss of the AsO_4 group from the structure results in a missing shared edge in the environment of Ca(2) and because an AsO_4 related by the rhombohedral centering is missing from the environment of Ca(3), these cations displace in opposite directions in the *ab* plane. The displacement of Ca(2) from the glide plane seems to be governed by O(9) which is displaced by the rotation of the As(1)—O(9) bond.

The structures of $Ca_3(AsO_4)_2$, and by analogy that of $Ca_3(VO_4)_2$, have a number of curious features. These relate to the large thermal parameter for all the atoms and particularly the exceptionally large value shown by some ions. The thermal parameters for $Ca_3(VO_4)_2$, as can be seen in Table 5, are qualitatively similar to those in $Ca_3(AsO_4)_2$ particularly so for the larger components. Thus, even considering differences between VO_4 and AsO_4 groups, it is apparent that these anomalies must be inherent in the structure. Leaving Ca(5) aside, the thermal parameters of Ca(3) are about twice as large as for the remaining calcium ions. In the arsenate the disorder of the As ions are qualitatively the same while in the vanadate it is substantially larger for V(2). O(1) shows uniformly large values for all its components, while O(2), O(6), O(9), and O(10) show at least one large component. Since the As(1)O_4 tetrahedron and Ca(5) share a face composed of three O(9) atoms, in half the cases, it is not unexpected that O(9) and probably O(10) will show anomalous effects because of positional disorder. The relatively small U_{33} component of O(10) suggests that this atom is disordered on a circle centered on the three fold axis. It is interesting to note that O(I) in $Ba_3(VO_4)_2$, which also lies on a three fold axis, could be considered to lie in an orbit with a radius of 0.18 Å (10). However, in $Ca_3(AsO_4)_2$ the magnitude of this effect should be relatively small since the Ca(5)—O(9) interaction is over 3 Å. On the other hand, the Ca(5)—O(1) bond in reasonably strong and therefore this oxygen atom would be expected to manifest a large positional disorder. The magnitude of the coefficients for O(1) are very large suggesting that the position O(1) occupies when Ca(5) is filled as compared to when it is empty differ by about 0.2 Å. Since O(1) is bonded to a Ca(3) at nearly the same

Can. J. Chem. Downloaded from www.nrcresearchpress.com by 210.87.254.5 on 09/05/12
For personal use only.

TABLE 5. Anisotropic thermal parameters of $Ca_3(VO_4)_2$*

Atom	U_{11}†(Å²)	U_{22}(Å²)	U_{33}(Å²)	U_{12}(Å²)	U_{13}(Å²)	U_{23}(Å²)
V(1)	0.011(1)	U_{11}	0.012(1)	$\frac{1}{2}U_{11}$	—	—
V(2)	0.023(1)	0.018(1)	0.013(1)	0.014(1)	0.010(1)	0.07(1)
V(3)	0.008(1)	0.009(1)	0.009(1)	0.001(1)	−0.001(1)	0.002(1)
Ca(1)	0.017(1)	0.018(1)	0.015(1)	0.010(1)	−0.003(1)	−0.005(1)
Ca(2)	0.016(1)	0.018(1)	0.015(1)	0.007(1)	−0.005(1)	−0.001(1)
Ca(3)	0.032(1)	0.024(1)	0.026(1)	0.020(1)	−0.011(1)	−0.013(1)
Ca(4)	0.025(2)	U_{11}	0.011(1)	$\frac{1}{2}U_{11}$	—	—
O(1)	0.137(16)	0.073(11)	0.013(4)	0.074(12)	−0.002(7)	0.004(6)
O(2)	0.048(7)	0.050(7)	0.036(6)	0.043(6)	0.030(5)	0.023(5)
O(3)	0.011(4)	0.015(4)	0.016(4)	0.004(3)	−0.002(3)	−0.006(3)
O(4)	0.038(7)	0.015(5)	0.084(10)	0.000(5)	0.024(7)	−0.002(6)
O(5)	0.045(6)	0.051(7)	0.023(5)	0.040(6)	−0.015(5)	−0.018(5)
O(6)	0.061(9)	0.031(7)	0.061(9)	−0.001(7)	−0.022(8)	0.026(7)
O(7)	0.017(4)	0.016(4)	0.021(4)	0.009(3)	−0.005(3)	−0.003(3)
O(8)	0.052(7)	0.044(6)	0 006(3)	0.034(6)	−0.008(4)	−0.007(4)
O(9)	0.022(5)	0.022(5)	0.060(7)	0.013(4)	0.008(5)	−0.007(5)
O(10)	0.084(20)	U_{11}	0.020(8)	$\frac{1}{2}U_{11}$		
Ca(5)	0.080(4)‡					

*Estimated standard deviations in parentheses.
†The U_{ij}, in Å², are computed from $\beta_{ij} = 2\pi^2 b_i b_j U_{ij}$ where $T = \exp[-(\beta_{11}h^2 + 2\beta_{12}hk + \cdots)]$ appears × in the structure factor expression and b_j are reciprocal lattice vectors.
‡Isotropic temperature factors in Å².

z level, some of the enhanced disorder at this cation may be due to this cation displacement. The large U_{11} component for O(6) may be associated with a weak Ca(2)—O(6) bond in both $Ca_3(AsO_4)_2$ and $Ca_3(VO_4)_2$. The analogous bond in Whitlockite is 2.60 Å long (25). The structural reason for this difference between the phosphate and the other calcium compounds is not clear.

In addition the disorder implies that the apparent bond lengths deviate from their true values. Until the details of the disorder are known corrections for these effects can not be made. Since the $Ca_3(VO_4)_2$ data has been measured both from films and by diffractometer[4] models with positional disorder will be tested with these data.

This research has been supported by grants from the Defence Research Board and National Research Council of Canada.

1. N. KRISHNAMACHARI and C. CALVO. Can. J. Chem. In press.
2. R. GOPAL and C. CALVO. Can. J. Chem. To be published.
3. C. BRISI. Ric. Sci. **30**, 1339 (1960).

[4]Data were kindly provided by J. Rowland and E. Gabe of the Department of Energy, Mines and Resources of Canada.

4. A. DURIF and E. F. BERTAUT. J. Phys. et de radium, **20**, S45 (1959).
5. R. J. DAVIS, M. H. HEY, and A. W. G. KINGSBURY. Mineral Mag. **35**, 72 (1965).
6. N. KRISHNAMACHARI and C. CALVO. Can. J. Chem. **48**, 881 (1970).
7. W. H. ZACHARIASEN. Acta Cryst. **1**, 263 (1948).
8. A. DURIF. Acta Cryst. **12**, 420 (1959).
9. R. F. HOODENBERG. Ber. Dtsch. Keran. Geo. **39**, 69 (1962).
10. P. SÜSSE and M. J. BUERGER. Zeits. für Kristallog. **131**, 161 (1970).
11. J. J. BROWN and F. A. HUMMEL. J. Electrochem. Soc. **110**, 1218 (1963).
12. A. L. MACKAY. Acta Cryst. **6**, 743 (1953).
13. J. S. STEPHENS. Ph.D. Thesis. McMaster University, Hamilton, Ontario. 1966.
14. J. J. BROWN and F. A. HUMMEL. J. Electrochem. Soc. **110**, 1218 (1963).
15. B. DICKENS and W. E. BROWN. American Crystallographic Association Winter Meeting, 74 (1970).
16. C. FRONDEL. Amer. Mineralog. **28**, 215 (1943).
17. C. CALVO and R. GOPAL. American Crystallographic Association Summer Meeting, 1970.
18. U. KEPPLER. Bull. de la Soc. Chim. de France, 1774 (1968).
19. A. L. MCKAY. Ph.D. Thesis, London University, London, England. 1952.
20. U. KEPPLER. N. Jb. Miner Mh. **6**, 171 (1965).
21. M. REDDEN and M. J. BUERGER. Zeits für Kristallog. **129**, 459 (1969).
22. International Tables for X-ray Diffraction. Vol. II. Kynock Press, Birmingham. 1952.
23. D. J. CROMER and J. T. WABER. Acta Cryst. **18**, 104 (1965).
24. B. DICKENS. Private communication.
25. R. GOPAL and C. CALVO. Acta Cryst. To be published.

Can. J. Chem. Downloaded from www.nrcresearchpress.com by 210.87.254.5 on 09/05/12
For personal use only.

Can. J. Chem. Downloaded from www.nrcresearchpress.com by 210.87.254.5 on 09/05/12
For personal use only.

Virial Scaling and Diatomic Force Constants

D. P. CHONG, P. J. GAGNON, AND J. THORHALLSSON[1]

Department of Chemistry, University of British Columbia, Vancouver 8, British Columbia

Received September 28, 1970

The application of virial scaling to calculation of diatomic force constants is studied. The ground states of H_2, LiH, BH, and Li_2 are used as test cases. We find that three-point calculations with fair-to-good wavefunctions lead to excellent k_2, fairly good k_3, but poor k_4. A wide variety of models for interpolating raw data is also investigated.

L'application de l'échelle variale au calcul des constantes de force diatomique est étudiée. Les états fondamentaux de H_2, LiH, BH et Li_2 sont utilisés comme prototypes. Il est trouvé que des calculs à trois points avec des fonctions d'ondes de passables a bonnes conduisent à des valeurs excellentes pour k_2, passablement bonnes pour k_3, mais mauvaises pour k_4. Une variété très grande de modèles pour l'interpolation des données brutes est aussi examinée.

Canadian Journal of Chemistry, 49, 1047 (1971)

Introduction

Ab initio calculations of spectroscopic constants for diatomic molecules have been a subject of considerable interest.[2] In this work, we are primarily concerned with the determination of the equilibrium internuclear separation R_e, the quadratic force constant k_2, and the cubic force constant k_3. These quantities appear in the usual Taylor's series expansion of the energy of a diatomic molecule in the Born–Oppenheimer approximation

$$[1] \quad E(R) = E(R_e) + \sum_{n=2}^{\infty} k_n(R - R_e)^n/(n!)$$

or

$$[2] \quad E(R) = E(R_e) + \tfrac{1}{2}k_2R_e^2\xi^2\left(1 + \sum_{m=1}^{\infty} a_m\xi^m\right)$$

In our notation,[3] $k_n = (d^nE/dR^n)_{R=R_e}$, $\xi = (R - R_e)/R_e$, and $(n!)a_{n-2}k_2 = 2R_e^{n-2}k_n$. Atomic units are used throughout: $e^2a_0^{-3}$ for k_2, for example.

Basically, there are three approaches. The most common practice is to determine k_n from $E(R)$ calculated at a number of values of R. Besides the errors in the computed values of $E(R)$, there are also difficulties in the numerical analysis (6, 7). To obtain force constants which reflect the behavior of the computed $E(R)$ faithfully, one must use many values of R.

At the other extreme, k_2 can be computed directly in a one-point calculation[4] at $R = R_e$. However, the results (8–11) obtained so far are not encouraging.[5] An interesting alternative was recently proposed by Parr and White (13), who considered a perturbation by the kinetic energy operator. Unfortunately, two test cases indicate that their method is extremely sensitive to how well the basis set can represent the first-order wavefunction. For example, the observed value of $\frac{1}{2}k_2R_e^2 = w_2 - w_1$, in their notation, for LiH is $-7.7647 + 8.0705 = 0.3058$; the corresponding value for the wavefunction of Browne and Matsen (14), recalculated at $R = 3.046\ a_0$ (15), is $-7.1506 + 8.0558 = 0.9052$.[6] A second test with a poorer wavefunction for BH gave much worse results.[7]

The third alternative, between these two extremes, is to calculate the force. Goodisman (16) computed the electrostatic force for H_2 and obtained a better value of k_2 than from the energy curve. However, electrostatic forces rarely give reliable values for dE/dR (9–11, 17–20). In a recent paper, Pulay (19) derived an expression for the correction to the electrostatic force in the Hartree–Fock approximation. In his actual computation (20), however, Pulay used the same basis sets for all geometrical configurations and therefore left out all the terms arising from the variation of orbital exponents. To include such terms would involve considerable additional effort, as indicated by Benston and Kirtman (9). On the other hand, the virial force can be readily calculated. In this work, we define the attractive virial force by

[1]Present address: Department of Physics, Red Deer College, Red Deer, Alberta.

[2]Numerous references can be found in refs. 1–4.

[3]The a_n coefficients (for $n \geq 1$) are those in the Dunham potential (5). However, we reserve the symbol a_0 for the Bohr.

[4]Calculations at N values of R are termed N-point calculations in this paper.

[5]An exception is the calculation of k_2 for H_2^+ by Bishop and Macias (12).

[6]D. P. Chong, unpublished result.

[7]P. J. Gagnon, M.Sc. thesis, University of British Columbia, 1970.

TABLE 1. Unscaled wavefunctions at three values of R

Molecule	No. of atomic orbitals	No. of configurations	R_1	R_2	R_3	E_e Model B	E_e H.F.R.	E_e Accurate
H_2	6+6	5	1.38	1.40	1.42	−1.166966	−1.133629*	−1.174475§
LiH	9+9	10	2.75	3.00	3.25	−8.022201	−7.987315†	−8.0705†
BH	6+1	13	2.329	2.433688	2.548230	−25.14959	−25.13147†	−25.290†
Li_2	5+5	8	4.92388	5.12388	5.32388	−14.86367	−14.8718‡	−14.9944‡

*Reference 27.
†Reference 28.
‡Reference 29.
§Reference 30.

[3] $$F(R) = -(2T + V)/R$$

where T and V are the kinetic and potential energies, respectively. Fortunately, the method of scaling (21, 22) is available to make any approximate wavefunction satisfy the diatomic virial theorem (23): $F(R) = dE/dR$. Consequently, one can compute dE/dR faithfully.

With virial forces from scaled wavefunctions, one hopes to encounter less severe difficulties with the numerical analysis than in the energy approach and to be able to calculate good force constants with fewer values of R. In our preliminary investigation (24), we found that three-point calculations gave excellent results for k_2 and k_3 of LiH. The object of this paper is to report on similar calculations for the ground states of H_2, BH, and Li_2.

In the earlier study (24), the correct scaling factor η was determined by the method given by Löwdin (21). In his notation,

[4] $$\eta = -[V(1,\rho) + \rho V_\rho(1,\rho)]/[2T(1,\rho) + \rho T_\rho(1,\rho)]$$

The derivatives V_ρ and T_ρ presented some difficulties. In this work we use another method of finding η at which $(\partial E/\partial\eta)_R = 0$. The scaling on LiH has therefore been repeated.

Calculations and Results

First, we give a brief description of the unscaled wavefunctions used in this work. All of them are valence-bond (v.b.) configuration–interaction (c.i.) functions constructed with Slater-type atomic orbitals. The wavefunction for H_2 is equivalent to the symmetry–orbital c.i. Function IX of McLean, Weiss, and Yoshimine (25). The LiH function has already been published (18). The wavefunction for BH is the only new one, for which further details are given in the Appendix. Finally, the Li_2 function is that used by Kockel and Grün (26). Of the four wavefunctions, the Li_2 function is the only one for which the same set of orbital exponents is used for all three values of R. The orbital exponents for the other three wavefunctions had been partially optimized at each R: less and less completely as one goes from H_2 to LiH to BH.

The energy at the calculated R_e according to Model B (see below) of each of these unscaled wavefunctions is shown on Table 1, along with other relevant specifications. For comparison, the Hartree–Fock–Roothaan (H.F.R.) and accurate energies (27–30) are also included. Thus one sees that our H_2 wavefunction is quite good, but the Li_2 function is not even of H.F.R. quality.

The wavefunctions were then scaled so that $(\partial E/\partial\eta)_R = 0$. At each value of R, the v.b.c.i. energy was computed with all orbital exponents multiplied by a factor of 1.0 ± 0.01. Interpolation of the energy by a parabola in η then led to the optimum scale factor at each R. The calculated energies and virial forces[8] for the unscaled and scaled functions are summarized in Table 2. Although the scaling is now performed at constant R instead of constant ηR (24), the same three features appear: (*a*) The scaling factor η is close to unity. (*b*) The energy is only slightly affected. (*c*) The virial force $F(R)$ is changed considerably by the scaling. It should be noted that $F(R)$, as defined by eq. 3, from an unscaled wavefunction is not dE/dR. Examine the results for BH in Table 2, for example.

Before going into the various methods of interpolating the raw data in Table 2, we have converted the experimental spectroscopic con-

[8]All computations were performed in double precision on an IBM 360/67 computer. Extra insignificant figures were carried to reduce round-off errors.

Can. J. Chem. Downloaded from www.nrcresearchpress.com by 210.87.254.5 on 09/05/12
For personal use only.

TABLE 2. Results of virial scaling*

Molecule	R	$\eta(R)$	$E(R)$	$F(R)$
H_2	R_1	(1)	−1.1668750	−0.0093228
		0.999335	−1.1668756	−0.0083059
	R_2	(1)	−1.1669630	+0.0011058
		1.001182	−1.1669650	−0.0006561
	R_3	(1)	−1.1668945	+0.0108657
		1.003005	−1.1669071	+0.0064961
LiH	R_1	(1)	−8.018264	−0.031791
		0.999830	−8.018275	−0.025448
	R_2	(1)	−8.022050	−0.010101
		0.999649	−8.022063	−0.003416
	R_3	(1)	−8.021277	+0.001362
		0.997984	−8.021308	+0.010627
BH	R_1	(1)	−25.147692	−0.020936
		1.000432	−25.147697	−0.030166
	R_2	(1)	−25.149526	−0.034830
		0.998778	−25.149563	−0.005485
	R_3	(1)	−25.148820	−0.024664
		0.997941	−25.148928	+0.015603
Li_2	R_1	(1)	−14.863020	−0.000879
		1.000645	−14.863026	−0.004720
	R_2	(1)	−14.863610	+0.002013
		1.000576	−14.863615	−0.001282
	R_3	(1)	−14.863582	+0.004250
		1.000504	−14.863586	+0.001472

*The entries with $\eta = 1$ correspond to results for the unscaled wavefunctions.

TABLE 3. Parameters calculated from observed spectroscopic constants

Molecule	a_1	a_2	$\frac{R_e}{a_0}$	$\frac{k_2}{e^2a_0^{-3}}$	$\frac{k_3}{e^2a_0^{-4}}$	$\frac{k_4}{e^2a_0^{-5}}$
H_2*	−1.60906	1.9130	1.4006	0.36925	−1.2726	4.321
LiH†	−1.885	2.382	3.015	0.06589	−0.1236	0.2072
BH‡	−2.115	2.9	2.336	0.19584	−0.5319	1.2
Li_2†	−1.911	1.997	5.050	0.01640	−0.01861	0.01540

*Reference 31.
†Reference 32.
‡Mulliken and Ramsey, unpublished results, quoted by Cade and Huo (28).

stants (31, 32) into parameters of interest and collected them in Table 3. The percentage errors given below are based on the entries in Table 3.

Interpolation

In our earlier study (24), we used a parabolic fit on the energy (Model *A* below) and on the virial force (Model *C* below). In this work, we have examined a wide variety of simple models. The input and basic assumption in each model are specified in Table 4. Thus, Model *A* is the simple harmonic oscillator, Model *B* is the Fues oscillator (33, 34), and Models *E*, *F*, and *G* represent three different six-parameter functions. Since $F(R)$ from the unscaled wavefunctions is not dE/dR, we have tested only Models *A* and *B* on them. The results for the unscaled wavefunctions are very similar but slightly inferior to the corresponding results (Models *A* and *B*) for the scaled wavefunctions. In Tables 5 and 6, we present the results from some of the better models, and percentage errors for the scaled wavefunctions from the various models are summarized in Table 7.

When we examine the results from various models, we should bear in mind two points: the quality of the wavefunctions and the spacing $\Delta(R)$ used. As mentioned earlier, our H_2 function is quite good, but the wavefunction for Li_2 is rather poor. Consequently, we obtain very good values for R_e, k_2, and k_3 for H_2 from several models, but k_2 for Li_2 is poor regardless of which model one uses. The spacing $\Delta(R)$ is small for H_2, and for Li_2 (relative to R_e); thus the effect of using R^{-1}, instead of R, as the argument in the various polynomials is also

Can. J. Chem. Downloaded from www.nrcresearchpress.com by 210.87.254.5 on 09/05/12
For personal use only.

Can. J. Chem. Downloaded from www.nrcresearchpress.com by 210.87.254.5 on 09/05/12
For personal use only.

TABLE 4. Basic assumption in various models

Model	Input*	Basic assumption†
A	3*E*	$E(R) = P_2(R)$
B	3*E*	$E(R) = P_2(R^{-1})$
C	3*F*	$F(R) = P_2(R)$
D	3*F*	$F(R) = P_2(R^{-1})$
E	3*E*+3*F*	$E(R) = P_5(R)$
F	3*E*+3*F*	$E(R) = P_5(R^{-1})$
G	3*E*+3*F*	$E(R) = P_2(R)/P_3(R)$‡
H	3*E*+3*F*	$E(R) = P_3(R)$, least-squares
I	3*E*+3*F*	$E(R) = P_3(R^{-1})$, least-squares
J	3*E*+3*F*	$E(R) = P_4(R)$, least-squares
K	2*E*+2*F*§	$E(R) = P_3(R)$

*3*E* means $E(R_1)$, $E(R_2)$, and $E(R_3)$; 3*F* means $F(R_1)$, $F(R_2)$, and $F(R_3)$.
†$P_N(u)$ = *N*-th order polynomial in *u*.
‡A Padé approximant.
§*E* and *F* at R_1 and R_3 are used. This model is a two-point calculation. See Discussion.

small, in contrast to LiH, for which $\Delta(R)$ is the largest. Another point which may be relevant is that $\Delta(R^{-1})$ for BH was chosen to be constant; the improvement in k_2 for BH in going from Model *C* to *D*, *E* to *F*, and from *H* to *I* may be related to this factor.

Turning now to the various models, we first compare Models *A* and *B*. Borkman and Parr (34) have shown some of the merits of the Fues potential (33). Our results indicate that, although Model *B* gives better force constants than *A* on the whole, k_3 from the Fues potential should be regarded with caution, since it is based on the assumption that $a_1 = -2$. Similarly, one should not place too much faith in k_4 from Model *D*, since it is based on $2a_2 = -3a_1 - 1$. In any event, Models *A* and *B* are inferior to *C* and *D*, both of which are simple to use. Model *C* appears to give the best overall results; Model *D* may be superior for k_2 when the spacing $\Delta(R^{-1})$ is constant. The disappointing performance of the two quintic polynomials in Models *E* and *F* seems surprising at first sight. However, it can be understood in terms of the presence of wiggles in the force curves for H_2 and LiH. On the other hand, the failure of Model *G* on H_2 is related to the fact that the fitted parameters are nearly linearly dependent. In short, all three six-parameter functions do not appear to have general applicability. Finally, the least-squares models give interesting results. The results from Model *H* are almost identical to those from Model *C*, as expected; those from Model *I* are similar to the ones from Model *D*. On the other hand, Model *J* does not appear to be superior. An attempt to fit $E(R)$ to a quartic in R^{-1} fails because of linear dependence.

From our results, we make the following observations: (*1*) The value of R_e is not particularly sensitive to the model, especially when

TABLE 5. Interpolation of $F(R)$ by Models *C* and *D*

Model	Molecule	R_e	k_2	k_3	k_4
C	H_2	1.4018	0.36784	−1.2438	0
	LiH	3.0495	0.06582	−0.1278	0
	BH	2.4605	0.19847	−0.4712	0
	Li_2	5.2109	0.01399	−0.0171	0
D	H_2	1.4018	0.36756	−1.2358	4.167
	LiH	3.0511	0.06382	−0.1158	0.187
	BH	2.4607	0.19677	−0.4472	0.895
	Li_2	5.2114	0.01394	−0.0157	0.015

TABLE 6. Least-squares models

Model	Molecule	R_e	k_2	k_3	k_4
H	H_2	1.4018	0.36784	−1.2438	0
	LiH	3.0497	0.06581	−0.1275	0
	BH	2.4605	0.19847	−0.4711	0
	Li_2	5.2109	0.01399	−0.0171	0
I	H_2	1.4018	0.36759	−1.2365	3.8508
	LiH	3.0514	0.06363	−0.1142	0.2031
	BH	2.4608	0.19657	−0.4441	0.9968
	Li_2	5.2115	0.01393	−0.0155	0.0171
J	H_2	1.4018	0.36798	−1.2470	−1.793
	LiH	3.0489	0.06688	−0.1327	−0.105
	BH	2.4600	0.20208	−0.5158	−1.943
	Li_2	5.2112	0.01396	−0.0163	0.0094

TABLE 7. Percentage errors in R_e, k_2, and k_3 for the scaled wavefunctions

	% error in R_e				% error in k_2				% error in k_3			
Model	H_2	LiH	BH	Li_2	H_2	LiH	BH	Li_2	H_2	LiH	BH	Li_2
A	0.1	2.4	5.5	3.2	−0.3	10.3	8.9	−5.8	*	*	*	*
B	0.1	1.8	5.3	3.2	−1.1	−5.1	2.1	−15.2	23	−2	−8	−14
C	0.1	1.1	5.3	3.2	−0.4	−0.1	1.3	−14.7	−2	3	−11	−8
D	0.1	1.2	5.3	3.2	−0.5	−3.1	0.5	−15.0	−3	−6	−15	−16
E	0.1	1.4	5.3	3.2	−2.2	−24.0	1.4	−15.4	*	*	48	−13
F	0.1	1.5	5.3	3.2	−2.3	−29.3	1.1	−15.3	*	68	37	−15
G	0.1	2.1	5.3	3.2	24.4	−0.6	0.8	−15.1	*	−81	−9	−18
H	0.1	1.2	5.3	3.2	−0.4	−0.1	1.3	−14.7	−2	3	−11	−8
I	0.1	1.2	5.3	3.2	−0.4	−3.4	0.4	−15.0	−3	−8	−17	−17
J	0.1	1.1	5.3	3.2	−0.4	−1.5	3.2	−14.9	−2	7	−3	−12

*Absolute error ≥ 100%.

TABLE 8. Two-point calculation: Model *K**

Molecule	R_e	k_2	k_3	k_4
H_2	1.4020(+0.1)	0.36831(−0.3)	−0.8805(−31)	0(−100)
LiH	3.0774(+2.1)	0.06715(+1.9)	−0.0645(−48)	0(−100)
BH	2.4621(+5.4)	0.19901(+1.6)	−0.4161(−22)	0(−100)
Li_2	5.2112(+3.2)	0.01401(−14.5)	−0.0168(+9)	0(−100)

*Percentage errors are given in parentheses.

$\Delta(R)$ is not large. (*2*) Poor wavefunctions cannot lead to reliable k_2. (*3*) The best models for k_2 are *C* and *H*, or *D* and *I* for constant $\Delta(R^{-1})$. (*4*) The best models for k_3 are *C*, *H*, and *J*. (*5*) None of the models tested give accurate k_4 from three-point calculations.

Discussion

Although the results on Li_2 are mainly negative, we do learn from them that we need better wavefunctions than the one used for Li_2 in order to determine good k_2 from three-point calculations.

Since we have not discovered a method of extracting reliable k_4 from three-point calculations, we tend to believe that computations at more than three values of R are required. As Models *C* and *H* appear to perform the best on the whole, they are the ones that should be extended.

Both Models *C* and *H* are based on a cubic polynomial in R for the energy. One may wonder how well a two-point calculation performs. In Model *K*, we use the energies and forces at only R_1 and R_3. The results are presented in Table 8. The reasonable values for R_e and k_2 are deceptively encouraging. However, if we use the data at R_2 and R_3 for LiH, we get a value of 0.050 for k_2. This points out the danger of drawing definite conclusions on a few results. Hence, we must regard our conclusions as tentative and encourage other workers to test Models *C* and *H* on similar calculations.

In the present study, we obtain excellent k_2, fairly good k_3, and unreliable k_4 for H_2, LiH, and BH. The wavefunctions used for these molecules are better than R.H.F. quality. Whether or not similar results can be obtained from scaled R.H.F. wavefunctions is still an open question.

In any event, we believe that virial scaling is important and may save considerable computer time.

The authors are grateful to the National Research Council of Canada for financial support and to one of the referees for valuable comments.

Appendix

The unscaled wavefunction used for BH resembles the one used by Ohno (35).[7] As indicated in Table 1, it is a 13-term v.b.c.i. function using seven Slater-type atomic orbitals. Instead of Ohno's closed-shell configuration for the two 1s electrons, we use a split core. The orbital exponents of the 1s and 1s′ orbitals have been partly optimized at each value of R. On the other hand, the orbital exponents for the valence electrons were optimized only at R_1, since we

Can. J. Chem. Downloaded from www.nrcresearchpress.com by 210.87.254.5 on 09/05/12
For personal use only.

TABLE 9. Orbital exponents in the unscaled wavefunction for BH

Orbital	Center	Orbital exponents		
1s	*B*	5.465763	5.479920	5.479919
1s′	*B*	3.865785	3.860518	3.860635
2s	*B*	1.30378		
$2p_0$	*B*	1.33424		
$2p_+$	*B*	1.32475		
$2p_-$	*B*	1.32475		
1s	*H*	1.21170		

hope that the full c.i. on the valence orbitals would compensate for most of the effects of a small change in *R*. All the orbital exponents are listed in Table 9.

1. R. K. NESBET. Advan. Quant. Chem. **3**, 1 (1967).
2. M. KRAUSS. Compendium of *ab initio* Calculations of Molecular Energies and Properties. National Bureau of Standards, Washington, D.C. 1967. Tech. Note 438.
3. A. C. WAHL, P. J. BERTONCINI, G. DAS, and T. GILBERT. Intern. J. Quant. Chem. **1S**, 123 (1967).
4. R. G. CLARK and E. T. STEWART. Quart. Rev. **24**, 95 (1970).
5. J. L. DUNHAM. Phys. Rev. **41**, 721 (1932).
6. R. H. SCHWENDEMAN. J. Chem. Phys. **44**, 2115 (1966).
7. J. GERRATT and I. M. MILLS. J. Chem. Phys. **49**, 1719 (1968).
8. I. M. MILLS. Mol. Phys. **1**, 107 (1957).
9. M. L. BENSTON and B. KIRTMAN. J. Chem. Phys. **44**, 119 (1966).
10. J. GERRATT and I. M. MILLS. J. Chem. Phys. **49**, 1730 (1968).
11. R. F. W. BADER and J. L. GINSBERG. Can. J. Chem. **47**, 3061 (1969).
12. D. M. BISHOP and A. MACIAS. J. Chem. Phys. **51**, 4997 (1969).
13. R. G. PARR and R. J. WHITE. J. Chem. Phys. **49**, 1059 (1968).
14. J. C. BROWNE and F. A. MATSEN. Phys. Rev. **135**, A1227 (1964).
15. D. P. CHONG and W. BYERS BROWN. J. Chem. Phys. **45**, 392 (1966).
16. J. GOODISMAN. J. Chem. Phys. **39**, 2397 (1963).
17. J. THORHALLSSON. Z. Naturforsch. **22a**, 1222 (1966).
18. J. THORHALLSSON, J. F. LARCHER, and D. P. CHONG. Theoret. Chim. Acta, Berlin, **16**, 51 (1970).
19. P. PULAY. Mol. Phys. **17**, 197 (1969).
20. P. PULAY. Mol. Phys. **18**, 473 (1970).
21. P. O. LÖWDIN. Mol. Spectrosc. **3**, 46 (1959).
22. A. D. MCLEAN. J. Chem. Phys. **40**, 2774 (1964).
23. J. C. SLATER. J. Chem. Phys. **1**, 687 (1933).
24. J. THORHALLSSON and D. P. CHONG. Chem. Phys. Lett. **4**, 405 (1969).
25. A. D. MCLEAN, A. WEISS, and M. YOSHIMINE. Rev. Mod. Phys. **32**, 211 (1960).
26. B. KOCKEL and N. GRÜN. Z. NATURFORSCH, **24a**, 731 (1969).
27. W. KOŁOS and C. C. J. ROOTHAAN. Rev. Mod. Phys. **32**, 219 (1960).
28. P. E. CADE and W. M. HUO. J. Chem. Phys. **47**, 614 (1967).
29. G. DAS. J. Chem. Phys. **46**, 1568 (1967).
30. W. KOŁOS and L. WOLNIEWICZ. J. Chem. Phys. **41**, 3663 (1964).
31. G. HERZBERG and L. L. HOWE. Can. J. Phys. **37**, 636 (1959).
32. G. HERZBERG. Spectra of Diatomic Molecules. 2nd ed. D. VanNostrand Co., Inc., Princeton, N.J., 1965.
33. E. FUES. Ann. Phys. **80**, 367 (1926).
34. R. F. BORKMAN and R. G. PARR. J. Chem. Phys. **48**, 1116 (1968).
35. K. OHNO. J. Phys. Soc. Japan, **12**, 938 (1957).

Can. J. Chem. Downloaded from www.nrcresearchpress.com by 210.87.254.5 on 09/05/12
For personal use only.

Can. J. Chem. Downloaded from www.nrcresearchpress.com by 210.87.254.42 on 09/05/12
For personal use only.

Chemistry of Fulvic Acid, a Soil Humic Fraction, and its Relation to Lignin[1]

G. OGNER[2] AND M. SCHNITZER
Soil Research Institute, Canada Department of Agriculture, Ottawa, Canada

Received October 21, 1970

Fulvic acid, a water-soluble soil humic fraction, was extracted from a Podzol soil and exhaustively methylated so as to make it soluble in benzene. The resulting material was separated repeatedly by column, thin layer, and preparative gas chromatography until relatively pure components were obtained. The latter were then identified by comparing their mass and micro-i.r. spectra and their gas chromatographic retention times with those of standards of known structures.

Twenty-one phenolic and benzene-carboxylic acids were identified as methyl ethers and esters. In addition, a number of polymethoxy-benzene polycarboxylic acids of as yet unknown identity were isolated.

A number of the compounds isolated have been reported to arise from the alkaline $KMnO_4$ oxidation of lignin. Since we did not oxidize the fulvic acid in the laboratory, it is likely that it originated from products resulting from the chemical and/or biological oxidation of lignin in the soil. Methylation of the fulvic acid was necessary to make the compounds extractable by organic solvents. Since methylation reduces hydrogen-bonding in the fulvic acid, it is suggested that in fulvic acid phenolic and benzenecarboxylic acids are joined by hydrogen-bonds to form a polymeric structure of yet unknown conformation. Any weakening of hydrogen-bonding will lead to a break-up of this structure.

L'acide fulvique, une fraction humique hydrosoluble d'un terroir, a été extrait d'une terre de Podzol et méthylé d'une façon exhaustive pour le rendre soluble dans le bènzène. Les produits résultants ont été séparés successivement par chromatographie sur colonne en couche mince et en phase gazeuse préparative jusqu'à ce que des composés relativement purs soient obtenus. Ces derniers ont été identifiés en comparant leurs spectres de masse et micro-i.r. ainsi que les temps de rétention en chromatographie en phase gazeuse, avec ceux de produits standards de structure connue.

Vingt et un acides carboxyliques phénoliques et benzéniques ont été identifiés comme étant des éthers méthylés et des esters. De plus, un certain nombre d'acides polycarboxyliques polyméthoxy-benzéniques, non identifiés jusqu'à présent, ont été isolés.

Un certain nombre de composés isolés ont été rapportés comme provenant de l'oxydation alcaline par $KMnO_4$ de la lignine. Puisque nous n'avons pas oxydé l'acide fulvique en laboratoire il semble que ceux-ci proviennent de produits résultant d'une oxydation chimique et/ou biologique de la lignine dans le sol. La méthylation de l'acide fulvique est nécessaire pour l'extraction des composés par les solvants organiques. Puisque la méthylation réduit les liaisons hydrogène dans l'acide fulvique, il semble que dans l'acide fulvique, les acides carboxyliques benzéniques et phénoliques soient unis par liaisons hydrogène pour former une structure polymérique de conformation encore inconnue. Toute faiblesse de la liaison hydrogène provoque une cassure de cette structure.

Canadian Journal of Chemistry, 49, 1053 (1971)

Introduction

Humic substances are among the most widely distributed natural products on the earth's surface, occurring in soils, lakes (1), rivers (2), and in the sea (3). In spite of their extensive distribution, little is known about their chemical structure, origin, synthesis, degradation, and reactions. Of special interest are fulvic acids which are water-soluble relatively low molecular weight humic materials that account for between 25 and 75% of the organic matter in soils and also for a substantial part of the organic matter in natural waters. Fulvic acids can form stable water-soluble and water-insoluble complexes with metal ions and hydrous oxides (4), interact with clay minerals (5), combine with hydrophobic organic compounds such as alkanes, fatty acids, and dialkyl phthalates and make them soluble in water (6–8). Fulvic acids can also exert considerable physiological activity in the areas of cell division and cell elongation (9). All of these properties point to a significant role of fulvic acids in reactions occurring in soils and waters, including those associated with pollution.

A fulvic acid extracted from the Bh horizon of a Podzol soil in Prince Edward Island has been under continuous investigation in this laboratory for more than a decade. Briefly, the fulvic acid is a chemically and biologically relatively stable polyelectrolyte with a number-average molecular weight of 951 (measured by vapor pressure osmometry) and contains 9.1 mequiv COOH, 3.3 mequiv phenolic OH, 3.6 mequiv alcoholic OH, and 3.1 mequiv C=O per g (4). Elemental

[1]Contribution No. 346, Soil Research Institute.
[2]Visiting scientist from the Norwegian Forest Research Institute, Vollebekk, Norway.

Can. J. Chem. Downloaded from www.nrcresearchpress.com by 210.87.254.42 on 09/05/12
For personal use only.

analysis (%) shows 50.90, C; 3.35, H; 0.75, N; 0.25, S; and 44.75, O (4). The molecular formula calculated from these data is $C_{28}H_{16}(COOH)_9(OH)_7(CO)_3$. The oxidative degradation of fulvic acid with alkaline permanganate produces 1.5% aliphatic monocarboxylic acids (ranging from acetic to caprylic acids), 3.0% oxalic acid, and 1.7% benzenecarboxylic acids (ranging from phthalic to mellitic acids) (10). Oxidation with 7.5 *N* NHO_3 yields 0.7% aliphatic dicarboxylic acids (succinic, glutaric, adipic, and pimelic acids), 5.5% nitrophenols (mainly picric acid), and 1.5% benzene-polycarboxylic acids (10). Reductive degradation such as zinc dust distillation and fusion yields polycyclic aromatic compounds the most prominent of which are naphthalene (0.1%), phenanthrene (0.1%), anthracene (0.2%), pyrene (0.1%), and perylene (0.2%) (11). X-Ray analysis indicates that the carbon skeleton of fulvic acid consists of a broken network of poorly condensed rings with appreciable numbers of disordered aliphatic chains or alicyclic structures around the edges of the aromatic layers (12).

In 1963 Barton and Schnitzer (13) proposed a new approach to unravelling the chemical structure of fulvic acid. The fulvic acid was first exhaustively methylated in order to make it soluble in benzene. The benzene-soluble methyl esters and ethers were then separated over Al_2O_3 with the aid of solvents of increasing polarity into chromatographically homogeneous fractions that differed in molecular weights, oxygen-containing functional group contents, and spectroscopic properties. The present investigation is a modification and extension of this approach. The fulvic acid was first extracted with a number of solvents of increasing polarity, then methylated and the benzene-soluble methyl esters and ethers were separated repeatedly by column, thin layer, and preparative gas chromatography until relatively pure components were obtained. The latter were then analyzed by mass spectrometry and micro-i.r. spectrophotometry. A comparison of the mass and i.r. spectra and gas chromatographic retention times of the major components isolated from the fulvic acid with those of authentic specimen led to their identification. In view of the increasing interest in humic substances in conncetion with environmental problems, we felt that the results of this investigation might be of interest to chemists.

Experimental

Fulvic Acid

Methods of extraction and purification were analogous to those reported previously (10). The purified fulvic acid accounted for approximately 75.0% of the organic matter in the original soil sample; its ash content was 1.0%.

Fractionation of the Fulvic Acid

Air-dry fulvic acid (100 g) was extracted for 24 h in a Soxhlet apparatus first with 1 l of *n*-hexane, then with 1 l of benzene, and finally with 1 l of ethyl acetate. The *n*-hexane soluble material was viscous yellowish oil (0.02 g) and contained mainly alkanes (6). The benzene and ethyl acetate extracts weighed 0.02 and 0.41 g, respectively. Both extracts were methylated with diazomethane and then separated by t.l.c. on silica gel. The benzene extract was found to consist mainly of fatty acid methyl esters (7).

The remaining 99.5 g of fulvic acid was then methylated with silver oxide-methyl iodide (13). Four successive methylations increased the methoxyl content from 0.2% for the unmethylated fulvic acid to 28.2%. The methylated fulvic acid (75.0 g) was refluxed for 24 h with 1 l of *n*-hexane. The hexane extract (0.71 g) was separated over Al_2O_3 (35.0 g) with hexane, benzene, and ethyl acetate to yield fractions weighing 0.02, 0.002, and 0.14 g, respectively. The fraction eluted with hexane contained mainly alkanes while the fraction eluted with benzene consisted chiefly of fatty acid methyl esters; the ethyl acetate extract was a complex mixture of fatty acid methyl esters and of aromatic compounds (7).

The methylated fulvic acid was then dissolved in benzene. The benzene-soluble material (41.3 g) was chromatographed over neutral Al_2O_3 (activity I, 2 kg) and eluted successively with 3 l of *n*-hexane (fraction A), benzene (fraction B), benzene – ethyl acetate (9:1)(fraction C), benzene – ethyl acetate (1:1)(fraction D), and an additional 3 l of benzene – ethyl acetate (1:1)(fraction E) to yield five fractions weighing 0.07, 0.02, 0.04, 0.51, and 0.60 g, respectively. All fractions were yellowish viscous oils. Fraction A contained only alkanes (6), whereas fractions B and C were found to contain both alkanes and fatty acid methyl esters (7). In addition, small amounts of dialkyl phthalates were isolated from fraction C (8). In total, normal plus branched-cyclic alkanes accounted for 0.16% of the ash-free weight of the fulvic acid, normal fatty acid methyl esters for 0.10%, and dialkyl phthalates for 0.03% (6–8). The alkanes and fatty acid esters ranged from C_{14} to C_{36} (6, 7). The dialkyl phthalates consisted of bis(2-ethylhexyl)-phthalate, dibutyl-phthalate, dicyclohexyl-phthalate, and benzyl-butyl-phthalate (8).

This paper deals primarily with the separation of fractions D and E, which were quantitatively the major fractions that we have isolated so far.

Analytical Techniques

Following chromatography over the Al_2O_3 column, each fraction was further separated by preparative t.l.c. on Al_2O_3 (activated at 150° for 18 h, thickness of sorbent coating: 0.5 mm). Three solvent systems were used: (*1*), toluene – ethyl acetate (3:1); (*2*), toluene – ethyl acetate (9:1), and (*3*), toluene – ethyl acetate (2:1).

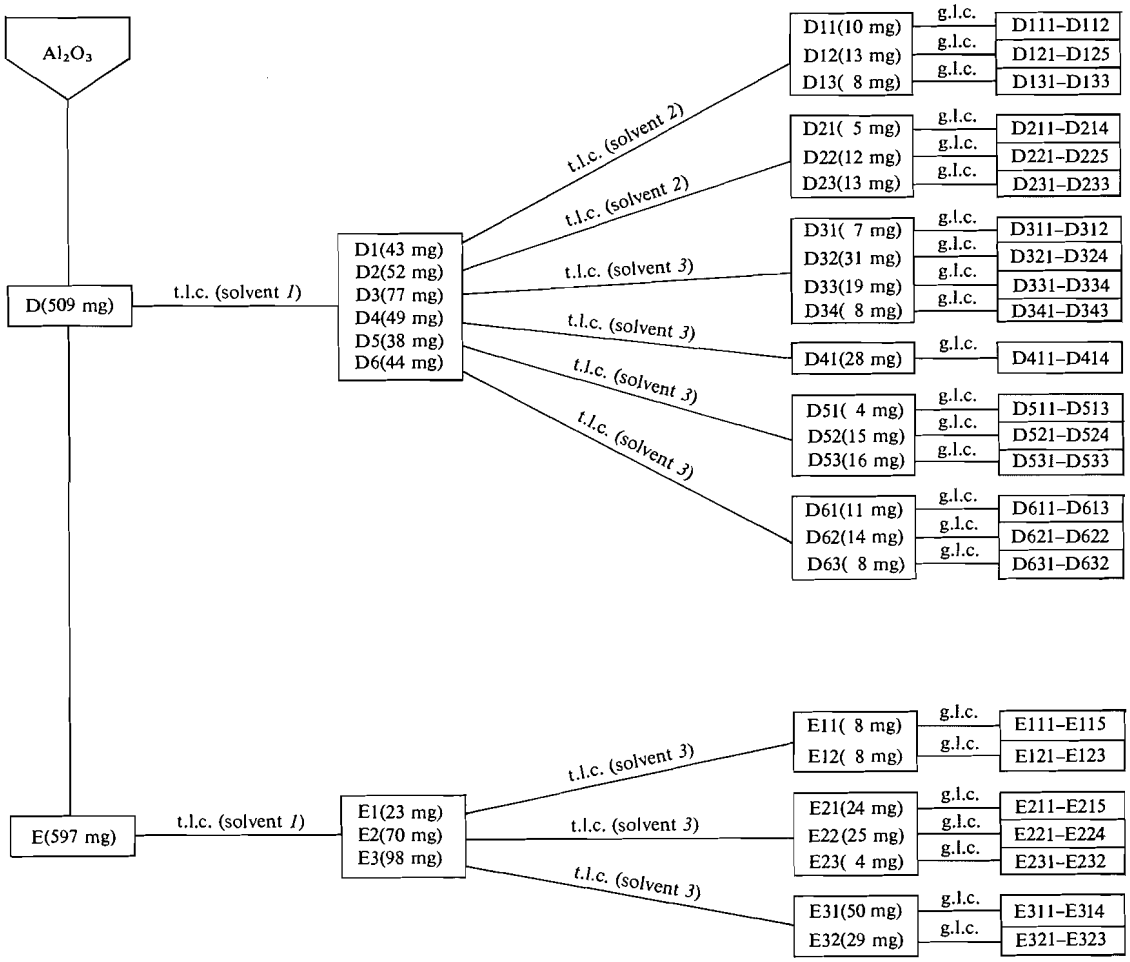

FIG. 1. Fractionation scheme.

After each t.l.c. separation, the plate was inspected under a u.v. lamp and a number of fractions were marked out, scraped off the plate, and extracted with ethyl acetate. Each fraction was subjected to at least two successive t.l.c. separations and then further separated by preparative gas chromatography (Hewlett-Packard model 402, flame ionization detector, 1800 × 4 mm glass column packed with 3% OV-17 on Chromosorb W HMDS, 60–80 mesh, programmed from 200–300° at a rate of 7.5 °C per min). Materials representing the major peaks were eluted from the gas chromatographic column, collected in capillary tubes, and analyzed by i.r. (as micro-KBr-pellets on a Beckman IR 12 spectrophotometer equipped with a beam condenser) and by mass spectrometric analysis on a CEC model 21–490 mass spectrometer using a heated direct inlet probe. The fractionation scheme is summarized in Fig. 1. The R_f values for the main fractions separated by t.l.c. are given in Table 1. The gas chromatographic separation of fraction D-51 is illustrated in Fig. 2.

Quantitative estimates of each major component were made by measuring peak areas on the gas chromatograms by triangulation. To obtain weight percentages each peak area was multiplied by its corresponding "substance-specific correction factor". The corrected area for each component was then expressed as a percentage of the sum of the corrected areas for all components (14).

All solvents used were purified by distillation through high-efficiency columns.

Origin and Preparation of Standards

When available, the known compounds used as standards were purchased as phenolic acids and benzenecarboxylic acids from commercial sources and purified by crystallization from suitable solvents. In the case of most compounds, phenolic OH groups were methylated with dimethyl sulfate (15), while COOH groups were esterified in methanol with an ether solution of diazomethane generated from diazald.

Compounds **1** and **2** (see Fig. 3 and Table 2) were pre-

Can. J. Chem. Downloaded from www.nrcresearchpress.com by 210.87.254.42 on 09/05/12
For personal use only.

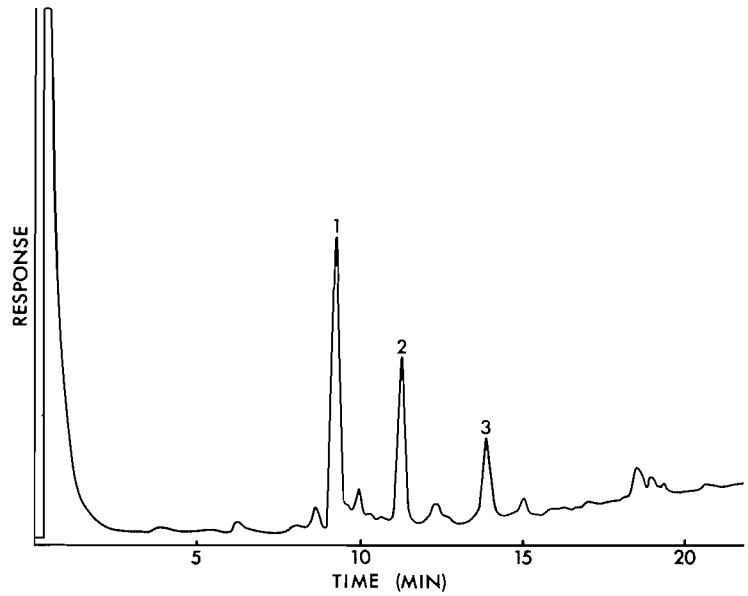

FIG. 2. Gas chromatographic separation of fraction D51: peak 1, 1,2,3,4-benzenetetracarboxylic acid tetramethyl ester; peak 2, 5-methoxy-1,2,3,4-benzenetetracarboxylic acid tetramethyl ester; peak 3, benzenepentacarboxylic acid pentamethyl ester.

TABLE 1. The R_f values of main fractions D_1 to E_3 separated by t.l.c. on Al_2O_3 with toluene – ethyl acetate (3:1)

Fraction	D_1	D_2	D_3	D_4	D_5	D_6	E_1	E_2	E_3
R_f value	0.53	0.43	0.32	0.24	0.17	0.11	0.53	0.46	0.33

pared by methylation and esterification of 3,4-dihydroxybenzoic acid and gallic acid, respectively. Compounds **5** and **15** were kindly supplied as acids by J. C. Pew of the Forest Products Laboratory, United States Department of Agriculture, Madison, Wisconsin and esterified with diazomethane. We thank H. Nimz of the University of Karlsruhe, Karlsruhe, West Germany, for sending us small samples of **6** and **7** as acids which we esterified. Compounds **3**, **4**, **8**, **9**, **10**, and **11** were prepared from 2,3-dimethylphenol, 2,4-dimethylphenol, 2,3,6-trimethylphenol, 2,4,6-trimethylphenol, 2,4,5-trimethylphenol, and 2,3,4-trimethylphenol, respectively, by the following procedure: 1.0 g samples were first dissolved in 5 ml of 2 *N* NaOH solution and methylated with dimethyl sulfate (15). The ethers were separated and oxidized with $KMnO_4$ (16). The resulting acids were then esterified with diazomethane. For the preparation of 12–14 it was found convenient to methylate phenolic OH groups in 2,3,4,5-tetramethylphenol, 2,3,4,6-tetramethylphenol, and pentamethylphenol with diazomethane prior to oxidation and esterification.

Compounds **16** to **21** were prepared by the esterification of the corresponding benzenecarboxylic acids which were obtained commercially.

Each compound was further purified by recrystallization and in some instances by preparative gas chromatography. The identity of each compound was verified by determining its mass and i.r. spectrum, m.p. or b.p., and by ultimate analysis. The analytical data so obtained were then compared with those published in the literature for the same compound.

Results and Discussion

Table 2 lists the yield, i.r. bands, mass spectrometric molecular ion and base peak, gas chromatographic retention time, and the identity of each compound isolated. Only for those compounds for which both mass and i.r. spectra and gas chromatographic retention times were identical with those of corresponding standards is the substitution given. Those isomers for which we were unable to obtain or prepare appropriate standards are listed without detailed substitution patterns. The base peaks for all compounds shown in Table 2 were at M-31 (OCH_3). The benzene – carboxylic acid methyl esters showed additional prominent peaks at M-59 (CO_2CH_3).

Can. J. Chem. Downloaded from www.nrcresearchpress.com by 210.87.254.42 on 09/05/12
For personal use only.

Can. J. Chem. Downloaded from www.nrcresearchpress.com by 210.87.254.42 on 09/05/12
For personal use only.

TABLE 2. Analytical characteristics and identification of compounds isolated

Component	Yield (%)	Infrared bands (cm^{-1}) (sh, shoulder; w, weak; m, medium; s, strong)	*m/e* Molecular ion and base peak	Gas chromatographic retention time (min)	Identification
D-111 D-121	2.5 3.5	750(m), 820(w), 960(m), 1040(w), 1080(m), 1130(m), 1195(w), 1290(s), 1440(m), 1450(sh), 1480(w), 1575(w), 1605(w), 1735(s), 2850(w), 2950(w), 3010(w)	194, 163	1.8	1,2-Benzenedicarboxylic acid dimethyl ester (16)*
D-112	7.5	770(s), 820(w), 830(w), 875(m), 890(w), 995(m), 1025(s), 1040(m), 1110(s), 1140(m), 1175(m), 1190(w), 1240(m), 1280(m), 1305(m), 1355(sh), 1420(m), 1440(w), 1470(m), 1530(m), 1605(m), 1730(s), 2870(s), 2960(m), 3010(w)	196, 165	2.4	3,4-Dimethoxy-benzoic acid methyl ester (1)
D-122	3.2	740(m), 765(s), 770(s), 800(w), 850(w), 870(s), 900(m), 930(w), 1000(s), 1010(s), 1045(w), 1120(sh), 1140(s), 1190(m), 1235(s), 1265(m), 1345(s), 1420(s), 1440(m), 1460(m), 1470(m), 1515(s), 1600(s), 1725(s), 2850(m), 2960(m), 2980(w), 3030(w)	226, 195	5.1	3,4,5-Trimethoxy-benzoic acid methyl ester (2)
D-123 D-132 D-214 D-224	2.4 1.2 1.4 1.2	740(m), 760(m), 790(w), 800(w), 885(m), 905(w), 915(w), 940(w), 1000(s), 1065(s), 1115(m), 1170(w), 1190(w), 1205(w), 1240(m), 1265(w), 1280(w), 1300(w), 1355(m), 1415(w), 1435(m), 1470(w), 1490(m), 1590(w), 1600(w), 1730(s), 2920(w), 2950(m), 3000(w)	254, 223	5.3	4,5-Dimethoxy-1,3-benzenedicarboxylic (isohemipinic) acid dimethyl ester (5)
D-124	2.9	770(m), 825(w), 870(w), 905(w), 930(w), 935(w), 965(w), 1000(m), 1050(w), 1090(m), 1135(s), 1195(w), 1280(w), 1340(s), 1415(m), 1440(m), 1470(m), 1500(sh), 1595(s), 1745(s), 2860(w), 2940(m), 2960(m), 3005(w)	254, 223	6.0	Mixture of dimethoxy-benzenedicarboxylic dimethyl esters
D-125	1.1	715(w), 765(m), 785(w), 795(w), 865(w), 885(w), 900(w), 940(w), 1000(m), 1050(m), 1090(w), 1110(m), 1170(m), 1190(w), 1235(m), 1290(s), 1365(m), 1410(m), 1435(w), 1455(m), 1490(w), 1510(w), 1590(m), 1725(s), 2850(w), 2920(m), 3000(w)	390, 359	18.7	Dehydrodiveratric acid dimethyl ester (15)
D-131 D-211 D-221	0.6 0.8 3.2	700(w), 760(s), 785(m), 820(w), 840(m), 880(m), 965(m), 1070(s), 1115(m), 1160(m), 1200(m), 1280(s), 1435(m), 1470(m), 1595(m), 1745(s), 2850(m), 2950(m), 3010(w)	224, 193	3.7	3-Methoxy-1,2-benzenedicarboxylic acid dimethyl ester (3)
D-133	2.5	740(m), 760(m), 790(w), 800(w), 885(m), 905(w), 915(w), 940(w), 1000(s), 1065(s), 1115(m), 1170(w), 1190(w), 1205(w), 1240(m), 1265(w), 1280(w), 1300(w), 1355(m), 1415(w), 1435(m), 1470(w), 1490(m), 1590(w), 1600(w), 1730(s), 2920(w), 2950(m), 3000(w)	254, 223	5.4	Dimethoxy-benzenedicarboxylic acid dimethyl ester
D-212 D-222	1.0 2.1	700(w), 710(w), 765(m), 785(w), 825(w), 885(w), 930(w), 940(w), 960(w), 990(m), 1070(s), 1120(s), 1195(m), 1250(s), 1290(s), 1315(m), 1405(w), 1435(s), 1495(m), 1575(w), 1615(w), 1735(s), 2850(w), 2900(w), 2950(m), 3000(w)	224, 193	4.3	4-Methoxy-1,3-benzenedicarboxylic acid dimethyl ester (4)

Can. J. Chem. Downloaded from www.nrcresearchpress.com by 210.87.254.42 on 09/05/12
For personal use only.

TABLE 2.—(*Continued*)

Component	Yield (%)	Infrared bands (cm^{-1}) (sh, shoulder; w, weak; m, medium; s, strong)	*m/e* Molecular ion and base peak	Gas chromatographic retention time (min)	Identification
D-213 D-223 E-111	0.7 1.6 0.2	700(w), 725(w), 755(m), 795(w), 810(w), 820(m), 865(w), 925(w), 960(m), 990(m), 1070(s), 1120(s), 1195(m), 1250(s), 1290(s), 1315(m), 1405(w), 1435(s), 1495(m), 1575(w), 1615(w), 1735(s), 2850(w), 2900(w), 2950(m), 3000(w)	252, 221	4.9	1,2,4-Benzenetricarboxylic acid trimethyl ester (17)
D-225 D-233	3.8 2.4	735(w), 760(m), 785(w), 800(w), 825(w), 860(w), 890(m), 920(w), 960(w), 975(w), 1000(m), 1065(s), 1090(m), 1130(m), 1145(m), 1200(w), 1215(w), 1250(m), 1280(m), 1340(m), 1410(m), 1445(m), 1460(m), 1485(w), 1585(w), 1610(m), 1735(s), 2860(w), 2960(m), 3010(w)	312, 281	8.1	Dimethoxy-benzenetricarboxylic acid trimethyl ester
D-231	2.0	710(w), 740(w), 755(m), 790(m), 835(w), 870(w), 910(w), 935(w), 990(w), 1040(m), 1060(s), 1145(w), 1160(w), 1195(w), 1225(w), 1280(s), 1320(w), 1420(w), 1435(w), 1460(m), 1500(w), 1580(w), 1600(m), 1725(s), 1745(s), 2860(w), 2960(m), 3000(w)	254, 223	5.2	3,4-Dimethoxy-1,2-benzenedicarboxylic (hemipinic) acid dimethyl ester (6)
D-232 D-311 D-321 E-112	8.5 3.5 8.5 2.7	715(w), 745(w), 760(s), 790(w), 815(w), 860(w), 890(w), 965(w), 970(w), 1000(m), 1045(s), 1120(m), 1165(m), 1200(m), 1255(m), 1280(s), 1295(s), 1400(m), 1435(m), 1450(m), 1480(w), 1575(w), 1600(w), 1735(s), 1740(s), 2950(w), 3030(w)	282, 251	6.5	3-Methoxy-1,2,4-benzenetricarboxylic acid trimethyl ester (8)
D-312	1.9	715(m), 725(w), 765(m), 820(m), 890(w), 930(w), 955(w), 990(s), 1000(s), 1010(s), 1035(w), 1100(m), 1145(m), 1185(w), 1200(s), 1235(s), 1255(m), 1280(s), 1305(m), 1340(m), 1425(w), 1440(m), 1475(m), 1585(w), 1610(m), 1715(sh), 1730(s), 1740(s), 1755(sh), 2860(w), 2940(w), 2960(m), 3010(w)	282, 251	7.0	2-Methoxy-1,3,5-benzenetricarboxylic acid trimethyl ester (9)
D-322 D-412 D-522 E-113 E-122 E-212	5.4 5.3 1.2 1.0 1.0 6.1	720(m), 735(w), 760(m), 770(m), 780(w), 810(m), 825(w), 890(m), 935(w), 960(w), 985(w), 1010(m), 1075(m), 1130(m), 1215(w), 1250(s), 1280(sh), 1305(w), 1350(w), 1435(m), 1450(m), 1470(m), 1580(w), 1735(m), 1740(s), 1750(sh), 2980(m), 3020(w)	310, 279	9.7	1,2,3,5-Benzenetetracarboxylic acid tetramethyl ester (18)
D-323 D-333 D-413 D-512 E-114 E-123 E-213	5.3 1.7 10.8 0.9 1.6 3.7 4.4	725(m), 765(w), 800(w), 820(w), 860(w), 885(w), 920(w), 975(w), 1005(m), 1055(m), 1090(sh), 1110(sh), 1130(m), 1165(m), 1250(s), 1340(w), 1400(m), 1450(s), 1575(m), 1600(w), 1740(s), 2960(m), 3010(sh)	340, 309	10.8	5-Methoxy-1,2,3,4-benzenetetracarboxylic acid tetramethyl ester (12)

Can. J. Chem. Downloaded from www.nrcresearchpress.com by 210.87.254.42 on 09/05/12
For personal use only.

TABLE 2.—(*Continued*)

Component	Yield (%)	Infrared bands (cm^{-1}) (sh, shoulder; w, weak; m, medium; s, strong)	*m/e* Molecular ion and base peak	Gas chromatographic retention time (min)	Identification
D-324 D-334 D-414 E-115	2.7 1.1 2.6 1.2	720(w), 740(w), 775(w), 790(w), 820(w), 850(m), 870(w), 910(w), 925(m), 965(m), 995(m), 1010(m), 1045(m), 1065(m), 1130(sh), 1155(w), 1250(s), 1325(w), 1345(m), 1415(m), 1445(s), 1460(sh), 1580(m), 1745(s), 2860(w), 2960(m), 3010(w)	370, 339	12.0	Dimethoxy-benzenetetracarboxylic acid tetramethyl ester
D-331	9.5	730(w), 770(m), 800(w), 890(w), 970(w), 1000(m), 1035(w), 1060(w), 1130(m), 1175(m), 1215(s), 1295(s), 1355(s), 1400(w), 1435(m), 1465(w), 1525(m), 1600(m), 1715(s), 1725(sh), 2850(w), 2950(m), 3010(w)	254, 223	6.2	4,5-Dimethoxy-1,2-benzenedicarboxylic (metahemipinic) acid dimethyl ester (7)
D-332 E-121	2.0 1.0	770(w), 785(m), 800(m), 815(sh), 845(w), 875(w), 920(w), 975(m), 1015(m), 1055(m), 1105(s), 1135(m), 1195(m), 1250(s), 1315(s), 1400(m), 1440(m), 1460(sh), 1510(w), 1575(m), 1615(m), 1735(s), 2860(w), 2960(m), 3010(w)	282, 251	8.2	5-Methoxy 1,2,4-benzenetricarboxylic acid trimethyl ester (10)
D-341	1.2	750(w), 770(w), 805(w), 825(w), 880(w), 900(w), 940(w), 950(w), 1000(m), 1060(m), 1100(m), 1140(m), 1190(m), 1235(s), 1305(w), 1340(m), 1440(m), 1460(w), 1495(w), 1600(m), 1725(s), 1745(m), 1765(m), 2850(w), 2960(m), 3010(w)	326, 295	9.1	Methyl-dimethoxy-benzenetricarboxylic acid trimethyl ester
D-342	2.7	720(w), 750(sh), 760(w), 770(sh), 790(w), 805(w), 815(w), 855(w), 885(w), 935(w), 960(w), 980(w), 1010(w), 1045(m), 1075(m), 1115(m), 1160(m), 1200(m), 1250(w), 1295(s), 1405(m), 1440(m), 1460(m), 1470(sh), 1580(w), 1740(s), 1765(w), 2860(w), 2960(m), 3010(w)	326, 295	10.0	Methyl-dimethoxy-benzenetricarboxylic acid trimethyl ester
D-343	0.7	725(w), 730(w), 740(w), 750(w), 775(w), 790(w), 810(w), 820(w), 1000(w), 1010(w), 1050(w), 1080(m), 1105(m), 1130(m), 1180(m), 1200(w), 1240(s), 1265(s), 1335(m), 1440(m), 1475(w), 1590(w), 1610(w), 1735(s), 1765(w), 2850(w), 2960(m), 3010(w)	326, 295	10.8	Methyl-dimethoxy-benzenetricarboxylic acid trimethyl ester
D-411 D-511	4.2 1.7	730(w), 755(m), 810(w), 820(w), 860(w), 870(m), 900(w), 945(w), 955(w), 985(m), 1000(m), 1110(m), 1150(m), 1175(m), 1200(m), 1255(w), 1275(s), 1315(m), 1600(w), 1735(s), 2960(w), 3020(w)	310, 279	9.2	1,2,3,4-Benzenetetracarboxylic acid tetramethyl ester (19)
D-513 D-523 D-611 E-214 E-222 E-312	0.5 1.2 3.2 3.6 5.4 8.8	710(w), 725(w), 750(w), 770(w), 790(w), 810(w), 825(w), 855(w), 875(w), 900(m), 1000(m), 1100(m), 1155(m), 1200(w), 1255(s), 1295(w), 1305(w), 1350(m), 1400(w), 1445(m), 1474(w), 1635(w), 1730(s), 1750(s), 1755(w), 2960(w), 3010(w)	368, 337	14.7	Benzenepentacarboxylic acid pentamethyl ester (20)

Can. J. Chem. Downloaded from www.nrcresearchpress.com by 210.87.254.42 on 09/05/12
For personal use only.

TABLE 2.—(*Concluded*)

Component	Yield (%)	Infrared bands (cm^{-1}) (sh, shoulder; w, weak; m, medium; s, strong)	*m/e* Molecular ion and base peak	Gas chromatographic retention time (min)	Identification
D-521 E-211 E-221	2.5 1.3 2.3	700(w), 720(w), 765(w), 770(w), 795(w), 805(w), 815(w), 835(w), 840(w), 870(w), 900(w), 960(w), 1010(m), 1060(s), 1110(m), 1165(m), 1200(m), 1250(s), 1290(s), 1435(m), 1450(m), 1490(m), 1510(w), 1525(w), 1540(w), 1560(w), 1595(m), 1735(s), 2860(w), 2960(w), 3010(w)	282, 251	9.2	4-Methoxy 1,2,3-benzenetricarboxylic acid trimethyl ester (11)
D-524 D-531 D-612 E-215 E-223 E-313	6.6 4.7 3.8 5.8 7.6 6.1	740(w), 760(w), 785(w), 790(w), 805(w), 835(w), 850(m), 860(m), 875(w), 905(w), 925(w), 965(m), 995(m), 1020(w), 1060(m), 1130(m), 1200(sh), 1230(s), 1255(s), 1330(s), 1350(sh), 1405(m), 1450(s), 1575(m), 1740(s), 2960(m), 3020(w)	398, 367	15.9	Methoxy-benzenepentacarboxylic acid pentamethyl ester (14)
D-532 E-231	3.5 0.9	725(m), 775(w), 785(w), 805(m), 875(w), 905(w), 925(w), 975(w), 1000(m), 1030(w), 1060(m), 1085(m), 1120(m), 1170(m), 1176(m), 1200(sh), 1215(sh), 1250(s), 1290(w), 1330(w), 1405(m), 1445(s), 1510(w), 1525(w), 1540(w), 1560(w), 1570(w), 1585(w), 1740(s), 1765(sh), 2850(w), 2960(m), 3010(w)	384, 353	16.3	
D-533	4.2	715(w), 730(w), 755(w), 770(w), 785(w), 805(m), 850(m), 860(m), 870(sh), 900(w), 960(w), 990(s), 1010(w), 1060(w), 1085(m), 1115(m), 1130(m), 1160(m), 1185(w), 1250(s), 1235(m), 1260(w), 1315(w), 1445(s), 1460(sh), 1490(w), 1500(w), 1510(w), 1525(w), 1545(w), 1575(w), 1600(w), 1625(w), 1640(w), 1650(w), 1745(s), 2850(w), 2960(m), 3010(w)	416, 398 385, 355	18.0	
D-613 D-622 D-632 E-224 E-232 E-314 E-322	4.1 11.5 6.2 6.6 2.5 24.2 16.0	715(w), 740(w), 755(m), 785(w), 805(w), 830(m), 850(m), 860(m), 875(m), 905(w), 985(s), 1020(w), 1125(w), 1160(w), 1185(w), 1235(s), 1330(m), 1360(m), 1415(m), 1445(s), 1575(w), 1740(s), 2850(w), 2900(w), 2950(m), 3010(w)	426, 395	17.6	Benzenehexacarboxylic acid hexamethyl ester (21)
D-621 D-631 E-311 E-321	2.6 1.3 10.8 8.9	730(w), 750(w), 785(w), 810(m), 860(w), 885(w), 925(w), 995(m), 1020(m), 1075(m), 1110(m), 1160(m), 1200(w), 1250(s), 1300(w), 1340(m), 1410(w), 1435(sh), 1450(m), 1595(m), 1735(s), 2860(w), 2960(m), 3010(w)	340, 309	13.2	2-Methoxy-1,3,4,5-benzenetetracarboxylic acid tetramethyl ester (13)

*Numerals refer to chemical structures shown in Fig. 3.

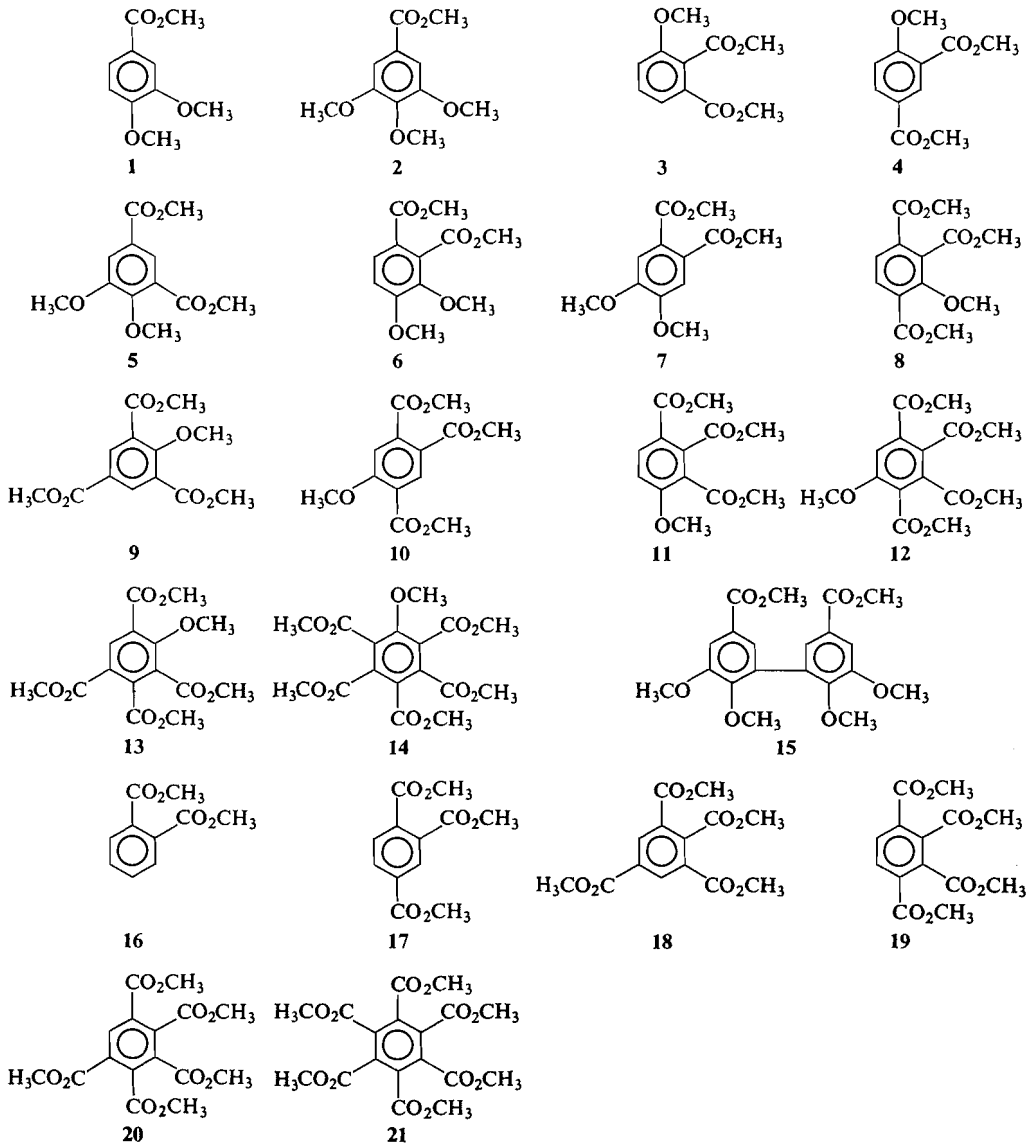

FIG. 3. Chemical structures of compounds isolated.

The results are summarized in Table 3. The most prominent methoxy-benzenecarboxylic methyl esters were fully methylated dimethoxy-benzenedicarboxylic acids, methoxy-benzenetricarboxylic acids, methoxy-benzenetetracarboxylic acids, and methoxy-benzenepentacarboxylic acid. Benzene-tetra-, -penta-, and -hexa-carboxylic acid methyl esters were the most abundant benzene-polycarboxylic acids; the latter constituted almost 25% of the total yield of products, which accounted for about 0.3% of the untreated fulvic acid. It is likely that our yield estimates are low because preliminary experiments with known benzenecarboxylic acid methyl esters showed that at least 50% of the starting material was lost during the fractionation and purification procedure. Assuming that similar losses occurred in the case of the compounds isolated from the fulvic acid, the compounds listed in Tables 2 and 3 may account for up to 0.6% of the weight of the fulvic acid.

The unmethylated fulvic acid contained only

Can. J. Chem. Downloaded from www.nrcresearchpress.com by 210.87.254.42 on 09/05/12
For personal use only.

TABLE 3. Summary of compounds isolated from fractions D and E

Compound	Weight (mg)
Dimethoxy-benzoic acid methyl esters	7.5
Trimethoxy-benzoic acid methyl esters	3.2
Methoxy-benzenedicarboxylic acid dimethyl esters	7.7
Dimethoxy-benzenedicarboxylic acid dimethyl esters	23.1
Methoxy-benzenetricarboxylic acid trimethyl esters	34.2
Dimethoxy-benzenetricarboxylic acid trimethyl esters	6.2
Methyl-dimethoxy-benzenetricarboxylic acid trimethyl esters	4.6
Methoxy-benzenetetracarboxylic acid tetramethyl esters	52.0
Dimethoxy-benzenetetracarboxylic acid tetramethyl esters	7.6
Methoxy-benzenepentacarboxylic acid pentamethyl esters	34.6
Dehydrodiveratric acid dimethyl esters	1.1
Benzenedicarboxylic acid dimethyl esters	6.0
Benzenetricarboxylic acid trimethyl esters	2.5
Benzenetetracarboxylic acid tetramethyl esters	25.9
Benzenepentacarboxylic acid pentamethyl esters	22.7
Benzenehexacarboxylic acid hexamethyl esters	71.1
Total	310.0

0.2% or 0.07 mequiv OCH_3 per g. Since the phenolic OH and COOH content of the fulvic acid is 3.3 and 9.1 mequiv per g, respectively (4) only a maximum of about 1 in 50 phenolic OH or 1 in 130 COOH groups can occur as OCH_3 or CO_2CH_3. Thus, in the soil, practically all of the phenolic hydroxyls and carboxyls in the fulvic acid are present as OH and COOH groups.

Origin of Compounds Isolated

Compounds **1** to **11** and **15** shown in Fig. 3 have been reported to result from the oxidative degradation in the laboratory, usually with alkaline $KMnO_4$, of lignin (17). While in the present investigation the fulvic acid was not oxidized in the laboratory, it is likely that these compounds were produced by chemical and/or biological oxidation in the soil and that they originated from lignin.

The origin of benzenecarboxylic acids, however, is more difficult to assess. Two types of precursors are worthy of consideration: (*a*) polycyclic aromatic compounds, and (*b*) saturated or hydroaromatic rings that become aromatic during oxidation.

With regard to (*a*) it is noteworthy that zinc dust distillation and fusion of fulvic acid produced small amounts of aromatic polycyclics, ranging from naphthalene to perylene (11). We suggested that these products originated from the polycyclic aromatic "core" of the fulvic acid or from structures giving rise to such systems under the experimental conditions of zinc dust distillation and fusion (11). Concerning point (*b*), Reed and Purves (18), have proposed that aromatic monomeric units of lignin underwent increasing degrees of nuclear condensation as the conditions of isolation from the wood became more drastic and that the benzenecarboxylic acids produced by the alkaline $KMnO_4$ oxidation of such materials resulted from the degradation of aromatic rings attached to cycloaliphatic rings formed by the condensation. It is therefore possible that the benzenecarboxylic acids shown in Table 2 and Fig. 3 originated from the oxidative degradation in the soil of condensed lignin structures.

The data in Table 2 thus indicate a lignin origin for the fulvic acid. It is noteworthy that only traces of the components listed in Table 2 could be extracted by organic solvents from unmethylated fulvic acid. Extraction of the bulk of these compounds was possible only after methylation of the fulvic acid, a process that reduces hydrogen-bonding in the fulvic acid (6). Similarly, we found earlier (6, 7) that methylation released alkanes, fatty acids, and dialkyl phthalates from the fulvic acid and facilitated their extraction by organic solvents. While the nature of the molecular forces that hold the fulvic acid components together, and the hydrophobic organic compounds to the fulvic acid, is still a matter for conjecture, one can visualize the fulvic acid as a hydrophilic polymeric structure that can absorb hydrophobic compounds. This structure consists of lignin degradation products, that is, aromatic hydroxycarboxylic and carboxylic acids (see Table 2) which are held together by hydrogen-bonding. Any weakening of these bonds will destroy the structure.

Fractions eluted from the Al_2O_3 column with

Can. J. Chem. Downloaded from www.nrcresearchpress.com by 210.87.254.42 on 09/05/12
For personal use only.

ethyl acetate and ethyl acetate – methanol mixtures, that is, fractions of greater molecular complexity, are presently being separated in an attempt to find out how far the approach described in this paper can be extended.

We thank J. G. Desjardins, S. I. M. Skinner, G. F. Morris, and M. Kalapurackal for technical assistance.

1. R. ISHIWATARI. Soil Sci. **107**, 53 (1969).
2. W. L. LAMAR. Geol. Survey Prof. Paper **600-D**, D24 (1968).
3. M. RASHID and L. H. KING. Geochim. et Cosmochim. Acta, **33**, 147 (1969).
4. M. SCHNITZER. Soil Sci. Soc. Amer. Proc. **33**, 75 (1969).
5. M. SCHNITZER and H. KODAMA. Sci. **153**, 70 (1966).
6. G. OGNER and M. SCHNITZER. Geochim. et Cosmochim. Acta, **34**, 921 (1970).
7. M. SCHNITZER and G. OGNER. Israel J. Chem. **8**, 505 (1970).
8. G. OGNER and M. SCHNITZER. Sci. **170**, 317 (1970).
9. M. SCHNITZER and P. A. POAPST. Nature, **213**, 598 (1967).
10. (*a*) M. SCHNITZER and J. R. WRIGHT. Proc. 7th Intern. Congr. Soil Sci. **2**, 112 (1960); (*b*) M. SCHNITZER and J. G. DESJARDINS. Can. J. Soil Sci. **44**, 272 (1964); (*c*) M. SCHNITZER and J. G. DESJARDINS. Soil Sci. Soc. Amer. Proc. **34**, 77 (1970).
11. E. H. HANSEN and M. SCHNITZER. Soil Sci. Soc. Amer. Proc. **33**, 29 (1969).
12. H. KODAMA and M. SCHNITZER. Fuel, **46**, 87 (1967).
13. D. H. R. BARTON and M. SCHNITZER. Nature, **198**, 217 (1963).
14. R. KAISER. Gas phase chromatography. Vol. 3. Butterworths, London, 1963. p. 100.
15. A. I. VOGEL. Practical organic chemistry. 3rd edition. Longmans, London, 1961. p. 669.
16. K. FREUDENBERG, CHEN-LOUNG CHEN, and G. CARDINALE. Chem. Ber. **95**, 2814 (1962).
17. K. FREUDENBERG and A. C. NEISH. Constitution and biosynthesis of lignin. Springer Verlag, New York, N.Y., 1968. p. 79.
18. D. E. READ and C. B. PURVES. J. Amer. Chem. Soc. **74**, 120 (1952).

Can. J. Chem. Downloaded from www.nrcresearchpress.com by 210.87.254.42 on 09/05/12
For personal use only.

Pyrrole Chemistry. Part XII. The Mechanism of the Reaction Between the Pyrrole Grignard Reagent and Acylating Agents[1]

C. E. LOADER AND HUGH J. ANDERSON
Department of Chemistry, Memorial University, St. John's, Newfoundland

Received October 5, 1970

Deuterium labeling experiments have shown that, in the reaction between the pyrrole Grignard reagent and methyl 1-pyrrolecarboxylate to form 1,2′-dipyrrolyl ketone, direct acylation occurs at the 2-position of the pyrrole Grignard reagent, rather than initial substitution onto the 1-position, followed by rearrangement to the 2-position. At an intermediate stage in the formation of the ketone, ring interchange takes place between the 1-substituted pyrrole rings in the intermediate and unused Grignard reagent, and as a result both pyrrole rings in the final product may originate from the Grignard reagent.

Des expériences de marquage par le deutérium ont montré que, dans la réaction entre le réactif de Grignard du pyrrole et du pyrrolecarboxylate-1 de méthyle pour former la dipyrrolyle-1,2′ cétone, l'acylation directe se fait en position 2 sur le réactif de Grignard, plutôt qu'une substitution initiale en position 1, suivie d'un réarrangement en position 2. Au cours d'une étape intermédiaire de la formation de la cétone, il se produit un échange de cycles entre le réactif de Grignard substitué en position 1 du pyrrole intermédiaire et le réactif de Grignard non utilisé; il en résulte donc que les deux cycles pyrroles du produit final peuvent provenir du réactif de Grignard.

Canadian Journal of Chemistry, 49, 1064 (1971)

In most of its reactions with acylating agents, the pyrrole Grignard reagent **1** gives products resulting from substitution at the 2-position of the pyrrole ring (1).

It was noted in the previous paper in this series (2) that the pyrrole Grignard reagent reacted with alkyl carbonates to give alkyl 1-pyrrolecarboxylates rather than the alkyl 2-pyrrolecarboxylates that might have been expected from the reaction. No reason for the selectivity of the acylation in this reaction is known. In this paper some work on the mechanism of the acylation reaction of the pyrrole Grignard reagent with esters is reported.

The intermediate in the reaction of methyl carbonate with the pyrrole Grignard reagent is probably a salt similar to **2**. The salt is hydrolyzed in the work-up of the reaction to give methyl 1-pyrrolecarboxylate (**3**), the main reaction product (Scheme 1). Although the same kind of intermediate seems likely from the reaction of ethyl acetate with pyrrole Grignard reagent the main product isolated from that reaction is not 1-acetylpyrrole but 2-acetylpyrrole (**4**) (Scheme 2) (3).

A possible reaction mechanism for the formation of 2-substituted pyrroles in the Grignard reaction is that substitution onto the 1-position of the pyrrole ring occurs first and is followed by rearrangement to give 2- or 3-substituted products. Some evidence against this mechanism in the alkylation of the pyrrole Grignard reagent has already been reported (4). If this mechanism does, however, prevail, the formation of 1-substituted products may simply be explained as being cases in which the rearrangement to the 2-position of the pyrrole ring does not occur. Alternatively, initial substitution might take place onto the 2-position with migration onto the 1-position of the pyrrole ring being possible in some cases. This latter possibility seems unlikely as a carbon–carbon bond must be broken if 1-substituted products are to be formed. Finally, direct substitution onto both the 1- and the 2-positions may occur.

A convenient method of studying the mechanism of acylation of the pyrrole Grignard reagent is offered in the case of the acylation of the reagent with methyl 1-pyrrole carboxylate. Here, if the initial attack is at the 1-position of the pyrrole ring, the intermediate **5** may be formed which then rearranges to finally give 1,2′-dipyrrolyl ketone (**6**). In the intermediate **5** the two pyrrole rings are indistinguishable, one of the rings being from the Grignard reagent and the other from the ester. Thus, if the intermediate **5** exists, both of the pyrrole rings should appear as the 2-substituted ring in the final product, 1,2′-dipyrrolyl ketone, with equal frequency. If the intermediate **5** does not exist and direct substitution onto the 2-position of the pyrrole ring in the Grignard reagent occurs, the pyrrole

[1]For Part XI see ref. 2.

Can. J. Chem. Downloaded from www.nrcresearchpress.com by 210.87.254.105 on 09/05/12
For personal use only.

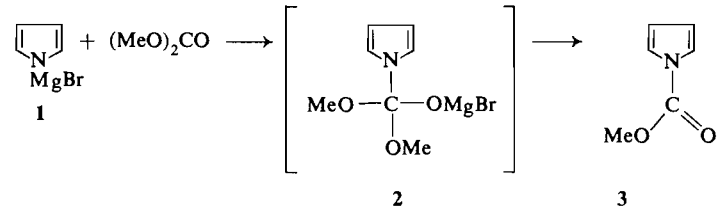

SCHEME 1

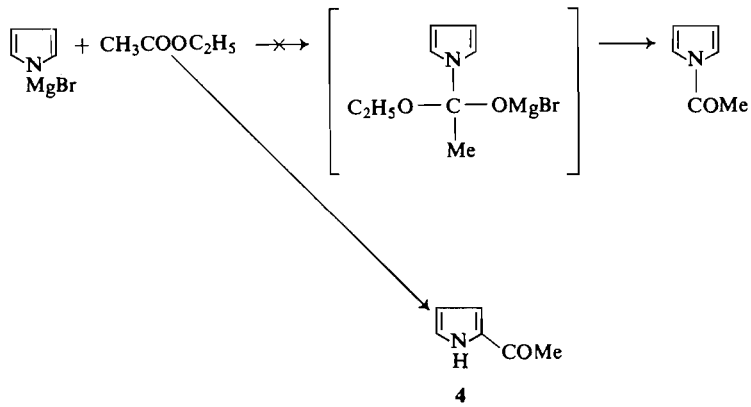

SCHEME 2

rings do not become indistinguishable. Thus, the 2-substituted pyrrole ring in the final product will originate from the Grignard reagent and the 1-substituted from the ester. In the latter case the probable intermediate involved in the reaction is the salt **7**.

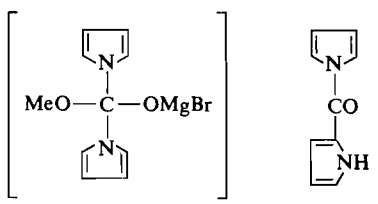

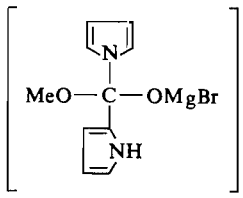

In order to investigate the path of the reaction of the pyrrole Grignard reagent with methyl 1-pyrrolecarboxylate, pyrrole-d_5 was prepared (4) and converted to the pyrrole-d_4 Grignard reagent. The d_4 Grignard reagent was allowed to react with the 1-pyrrolecarboxylate in the usual way and the 1,2′-dipyrrolyl ketone was isolated by careful fractional distillation of the reaction products. Also isolated in the distillations were pyrrole, methyl 1-pyrrolecarboxylate and traces of 2,2′-dipyrrolyl ketone.

The recovered pyrrole was a mixture of deuterated pyrroles as shown by mass spectrometry, but the recovered methyl 1-pyrrolecarboxylate was almost completely free of deuteration.

The 1,2′-dipyrrolyl ketone was found to be a mixture of the d_3, d_7 and undeuterated ketones (**8**, **9**, and **6** respectively), the d_3 product predominating.

The mass spectrum (Table 1) of the mixture

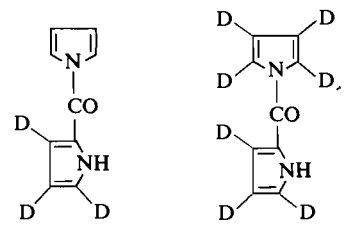

Can. J. Chem. Downloaded from www.nrcresearchpress.com by 210.87.254.105 on 09/05/12
For personal use only.

Can. J. Chem. Downloaded from www.nrcresearchpress.com by 210.87.254.105 on 09/05/12
For personal use only.

TABLE 1. Mass spectra of deuterium labeled 1,2′-dipyrrolyl ketone*

	Ketone			
m/e	A	B	C	D
167				18
165		5		
164		31		10
163		18		67
162		7	7	
161	6	5	62	
160	42	18	15	16
141		5		
140		7		
98				9
97		7		100
96			6	7
95	7	12	100	
94	100	100	25	24
71		32		13
70		19		
69		7		17
68	5	7	66	7
67	80	26	52	45
66	44	33	11	7
65	5			
43		6		
42		6	6	9
41	12	6	6	
40	10		14	
39	44	16	42	5
38	12		11	
29			5	
28	34		8	
27	7			

*A, 1,2′-Dipyrrolyl ketone; B, from methyl 1-pyrrole-d_4-carboxylate and the pyrrole Grignard reagent; C, 1,2′-dipyrrolyl-1′-*d* ketone; D, from methyl 1-pyrrolecarboxylate and pyrrole-d_4 Grignard reagent.

of ketones showed that about 12% of the undeuterated product **6** was formed and about 19% of the d_7 compound **9** (any *N*-deuterium on the 2-substituted ring having been equilibrated to natural abundance with water in the work-up). The remaining 70% of the product was the d_3 compound **8**. Clearly some form of 'ring interchange' takes place during the reaction.

Because no tri- or tetradeuterio methyl 1-pyrrolecarboxylate is formed in the reaction, the possibility of ring interchange between the pyrrole rings of the ester and the Grignard reagent can be excluded. That the isomerization takes place in the mass spectrometer can be excluded for two reasons. The proton resonances of 1,2′-dipyrrolyl ketone could clearly be seen in the p.m.r. spectrum of the reaction product and it is difficult to devise a mechanism for the formation of the d_7 ketone **9** in the mass spectrometer by rearrangement or by pyrolysis in the inlet system. In the latter case the most likely product is a d_6 ketone, which is not found, or the undeuterated product **6**, which is present, but it is unlikely that any is formed in this way (see below). The results discussed above suggest that the exchange between the pyrrole rings takes place at some intermediate stage in the chemical reaction.

The possibility that the ring interchange may involve the 1,2′-dipyrrolyl ketone was considered. However, it was found that interchange neither took place between the ketone and the pyrrole-d_4 Grignard reagent nor was there any between the ketone and pyrrole-d_4 under the reaction conditions used.

The d_4 ketone peak (*m/e* 164) is very small compared with the d_3 ketone peak (*m/e* 163) and can be attributed almost entirely to natural abundance of isotopes in the d_3 product. The presence of the d_7 ketone **6** and the undeuterated ketone **9** can be readily explained on the basis of the intermediate **7**, their formation arising from ring interchange between the molecules of intermediate and the pyrrole Grignard reagent.

If the intermediate **7** is important, since little if any d_4 ketone is formed in the reaction, we must conclude that the deuterated ring does not interchange with the undeuterated ring although it might interchange with the Grignard reagent. A more likely possibility is that ring interchange occurs between the undeuterated ring and the Grignard reagent or with free d_5 pyrrole (present due to the incomplete formation of the Grignard reagent). In this way the formation of the d_7 ketone and undeuterated pyrrole can be explained. The ring interchange will, at the same time as giving the d_7 intermediate (and thus the d_7 ketone **9**), give undeuterated pyrrole Grignard reagent which can react with unused methyl 1-pyrrolecarboxylate to give the deuterium free ketone **6** in the product. Because 1,2′-dipyrrolyl-d_4 ketone is not formed in the reaction in an amount equal to that of the 1,2′-dipyrrolyl-d_3 ketone, for the reasons given above the most likely intermediate in the reaction is similar to **7**. Thus, direct attack at the 2-position of the pyrrole Grignard reagent by the methyl 1-pyrrolecarboxylate predominates over attack at the 1-position followed by migration to the 2-position.

For further confirmation of this mechanism a sample of methyl 1-pyrrole-(2,3,4,5-d_4)-carboxylate was prepared and allowed to react with the pyrrole Grignard reagent to give a

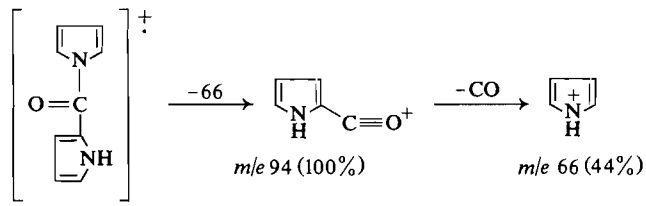

SCHEME 3

deuterated 1,2′-dipyrrolyl ketone with the deuteration having been introduced via the ester rather than via the pyrrole Grignard reagent as in the earlier case. The mass spectrum of the ketone showed deuterated parent ions at *m/e* 164, 163, and 160. The most abundant of these was the ion at *m/e* 164 (31%) and is clearly due to the d_4 ketone **10** and the product to be expected if no ring interchange takes place. However, the ion *m/e* 160 must be due to the undeuterated ketone **6** and indicates that ring interchange does occur. (The ion *m/e* 163 is almost exclusively due to the presence of about 30% trideuterated methyl 1-pyrrolecarboxylate in the 1-pyrrole-d_4-carboxylate used to prepare the ketone.) In this case the formation of d_7 ketone in the product requires not only ring interchange but reaction of the exchanged pyrrole Grignard reagent to give the d_7 product. The abundance of the ions due to the ketone formed by this mechanism showed wide variations from reaction to reaction as might be expected. In contrast, the abundance of the ions due to the ketone resulting from ring interchange only, remained almost constant.

There was no evidence to indicate that ring interchange involving the 2-substituted pyrrole ring in the intermediate took place. Once formed the carbon–carbon bond between the 2-substituted pyrrole ring and the rest of the intermediate is not broken.

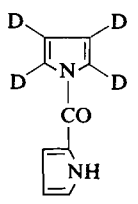

10

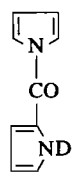

11

Mass Spectra (Table 1)

The mass spectrum of 1,2′-dipyrrolyl ketone **6** shows that the parent ion (*m/e* 160) fragments to give the ions *m/e* 94 and 66. The ion *m/e* 94 is the base peak and is only a little more abundant than the ion *m/e* 67. The fragmentation of the monodeuterio ketone **11** is dominated by the ions *m/e* 95, 68, and 67. Since these ions are the same as those from the undeuterated compound +1 we can assume that the fragments still contain the deuterium atom and thus that the fragmentation is dominated by the cleavage of the bond between the nitrogen of the 1-substituted pyrrole ring and the carbonyl group. The main fragmentation paths for 1,2′-dipyrrolyl ketone are shown in Schemes 3 and 4.

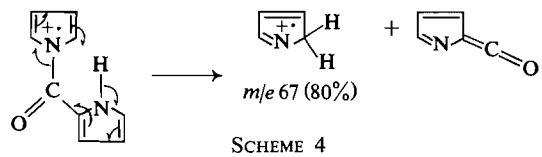

SCHEME 4

The deuterated 1,2′-dipyrrolyl ketone from the Grignard reaction of methyl 1-pyrrolecarboxylate with the d_4 pyrrole Grignard reagent showed parent ions at *m/e* 160, 163, 164, and 167. The most abundant ion was at *m/e* 97 and corresponds to the ion at *m/e* 94 in the nondeuterated compound. It is a deuterated ion arising from the d_3 and d_7 ketones **8** and **9**. Accurate mass measurements of the ions *m/e* 160, 163, and 167 showed them to correspond to the deuterated ketones of formulae $C_9H_8N_2O$, $C_9H_5D_3N_2O$, and $C_9HD_7N_2O$ respectively and confirms the nature of the reaction products, as shown in Table 2.

The cyclic mechanism (Scheme 4) for the

TABLE 2. High resolution mass measurement data for the deuterated 1,2′-dipyrrolyl ketone from methyl 1-pyrrolecarboxylate and pyrrole-d_4 Grignard reagent

Ion *m/e*	Found *m/e*	Calculated *m/e*	Formula
160	160.0640	160.06366	$C_9H_8N_2O$
163	163.0826	163.0825	$C_9H_5D_3N_2O$
167	167.1080	167.1076	$C_9HD_7N_2O$

Can. J. Chem. Downloaded from www.nrcresearchpress.com by 210.87.254.105 on 09/05/12
For personal use only.

Can. J. Chem. Downloaded from www.nrcresearchpress.com by 210.87.254.105 on 09/05/12
For personal use only.

formation of the *m/e* 67 ion in the mass spectrum of 1,2′-dipyrrolyl ketone is supported by the mass spectra of the deuterated ketones. The d_1 ketone **11** shows an ion at *m/e* 68 which replaces the *m/e* 67 ion in the mass spectrum of the undeuterated ketone and indicates that the 1′-proton (deuteron) is present in these ions. Thus, the abundant *m/e* 71 ion in the mass spectrum of the mixture of ketones from methyl 1-pyrrole-d_4-carboxylate and the pyrrole Grignard reagent arises from the 1′-substituted pyrrole-d_4 ring in the ketone mixture along with the 1-proton from the 2-substituted pyrrole ring in the same molecule. By applying this mechanism to the fragmentation of the deuterated ketones it is possible to explain the presence in the mass spectra of all the ions corresponding to the *m/e* 67 ion found in the mass spectrum of 1,2′-dipyrrolyl ketone.

This work has shown that the acylation of the pyrrole Grignard reagent with methyl 1-pyrrolecarboxylate proceeds by direct attack at the 2-position of the pyrrole ring in the Grignard reagent rather than by initial attack at the 1-position followed by rearrangement to the 2-position. This is also likely to be true for the acylation of the pyrrole Grignard reagent by other esters excluding the alkyl carbonates and a few other acylating agents (5) where a different mechanism or combination of mechanisms must operate to allow for the formation of the 1-substituted pyrroles found as the main reaction products. We are continuing our study of the pyrrole Grignard reagent with particular interest in the ring interchange reaction and its mechanism.

Experimental

High resolution mass spectra were recorded on a C. E. C. 21-110B spectrometer using a direct inlet system. Gas chromatography was carried out on a Beckman GC-2A chromatograph equipped with a 13-1/2 in. column packed with Apiezon L on firebrick. The remainder of the equipment used has already been described (2).

1,2′-Dipyrrolyl Ketone

Pyrrole Grignard reagent was prepared under nitrogen from magnesium (0.6 g), bromoethane (3.0 g), and pyrrole (1.67 g) in ether (20 ml) (2). The solution was cooled to room temperature and methyl 1-pyrrolecarboxylate (3.15 g) was added in ether (10 ml) with mechanical stirring. The stirred mixture was then heated under a reflux condenser for 2 h. It was then cooled and dilute HCl (1 *M*) was added until all of the precipitated solid dissolved. The aqueous layer was separated from the organic layer and extracted several times with ether. The organic layer and the ether extracts were combined, washed with water, sodium bicarbonate solution, water, and finally dried ($MgSO_4$). The ether was removed and the residue was fractionally distilled under vacuum. The distillate consisted of pyrrole, methyl 1-pyrrolecarboxylate (1.2 g) and 1,2′-dipyrrolyl ketone (1.1 g, 27%). The dipyrrolyl ketone was recrystallized from petroleum, m.p. 61–62°, lit. (6) m.p. 58.5–60°. Full details of the physical properties of these products have already been reported (6).

Reaction of Methyl 1-Pyrrolecarboxylate with Pyrrole-d_4 Grignard Reagent

The pyrrole-d_4 Grignard reagent was prepared from pyrrole-d_5 (7) as in the preparation of pyrrole Grignard reagent above. The reagent was then used in the reaction with methyl 1-pyrrolecarboxylate as in the previous experiment. The deuterated 1,2′-dipyrrolyl ketone was repeatedly recrystallized from petroleum, m.p. 60–61°. The low boiling fractions contained pyrrole and methyl 1-pyrrolecarboxylate and were purified by gas chromatography at a column temperature of 103°. The mass spectrum of the recovered methyl 1-pyrrolecarboxylate was almost identical to that of the methyl 1-pyrrolecarboxylate used as starting material and showed no indication of deuteration. The recovered pyrrole was extensively deuterated and showed parent ions for all stages of deuteration up to pyrrole-d_5. Accurate mass measurements on the main deuterated parent ions in the mass spectrum from the deuterated 1,2′-dipyrrolyl ketone are summarized in Table 2.

Reaction of the Pyrrole-d_4 Grignard Reagent with 1,2′-Dipyrrolyl Ketone

Pyrrole-d_4 Grignard reagent was allowed to react with 1,2′-dipyrrolyl ketone under conditions similar to those used in the preparation of 1,2′-dipyrrolyl ketone above. During the addition of the ether solution of 1,2′-dipyrrolyl ketone to the Grignard reagent the ether boiled and some solid was precipitated. However, on hydrolysis and work-up, the only product isolated was 1,2′-dipyrrolyl ketone which showed no deuteration in its mass spectrum. No ring interchange could be detected when 1,2′-dipyrrolyl ketone was refluxed in ether with pyrrole-d_4 for several hours.

Methyl 1-Pyrrole-d_4-carboxylate

The ester was prepared by the method reported earlier (2) using pyrrole-d_4 Grignard reagent in the place of pyrrole Grignard reagent. The product consisted of a mixture of methyl 1-pyrrole-d_3-carboxylate (30%) and methyl 1-pyrrole-d_4-carboxylate (70%) as shown by mass spectrometry. The reasons for the formation of the large amount of the d_3 ester have not yet been investigated.

Reaction of Methyl 1-Pyrrole-d_4-carboxylate with the Pyrrole Grignard Reagent

Pyrrole Grignard reagent was allowed to react with methyl 1-pyrrole-d_4-carboxylate as for the preparation of 1,2′-dipyrrolyl ketone described above. A deuterated 1,2′-dipyrrolyl ketone was obtained from the reaction products, m.p. 60–61°. The mass spectrum of this product is recorded in Table 1.

1,2′-Dipyrrolyl-1′-d Ketone

The ketone was prepared by repeated deuterium exchange between 1,2′-dipyrrolyl ketone (500 mg) and mix-

tures of deuterium oxide (1 ml) and acetone (2 ml) (8). After four exchanges the product was about 75% deuterated as shown by the mass spectrum and was suitable for the comparison spectrum used in this work.

We are pleased to acknowledge the financial support of the National Research Council of Canada. We wish to thank Dr. W. D. Jamieson of the Atlantic Regional Laboratory, N.R.C.C. for accurate mass measurements.

1. R. M. ACHESON. An introduction to the chemistry of heterocyclic compounds. Interscience, London, 1967. p. 71.
2. C. E. LOADER and H. J. ANDERSON. Can. J. Chem. **49**, 45 (1971).
3. G. P. BEAN. J. Heterocycl. Chem. **2**, 473 (1965).
4. P. S. SKELL and G. P. BEAN. J. Amer. Chem. Soc. **84**, 4660 (1962).
5. E. P. PAPADOPOULOS and H. S. HABIBY. J. Org. Chem. **31**, 327 (1966). E. P. PAPADOPOULOS. J. Org. Chem. **31**, 3060 (1966).
6. H. J. ANDERSON and C. W. HUANG. Can. J. Chem. **45**, 897 (1967).
7. B. BAK, D. CHRISTENSEN, L. HANSEN, and J. RASTRUP-ANDERSEN. J. Chem. Phys. **24**, 720 (1956).
8. E. FETZ and CH. TAMM. Helv. Chim. Acta, **49**, 349 (1966).

Can. J. Chem. Downloaded from www.nrcresearchpress.com by 210.87.254.105 on 09/05/12
For personal use only.

Can. J. Chem. Downloaded from www.nrcresearchpress.com by 210.87.254.6 on 09/05/12
For personal use only.

A Synthesis of *d,l*-Prostaglandin E_2 Methyl Ester and Related Compounds[1]

E. S. FERDINANDI[2] AND G. JUST
Department of Chemistry, McGill University, Montreal, Quebec

Received October 21, 1970

A synthesis of *d,l*-prostaglandin E_2 (PGE_2) methyl ester is described. Two new acetylenic prostaglandins, methyl 11α,15-dihydroxy-9-oxo-prost-5-yn-13-enoate and its C_{15} epimer, were obtained as intermediates in this synthesis. A solvolytic rearrangement of a bicyclo[2.1.0]hexane to a cyclopentane vinyl system is discussed.

Une synthèse de l'ester méthylique de la *d,l*-prostaglandine E_2 (PGE_2) est décrite. Deux nouvelles prostaglandines acétylèniques, le dihydroxy-11α,15 oxo-9 prostyn-5 èn-13-oate de méthyle et son épimère en C_{15}, furent obtenus comme intermédiaires dans cette synthèse. Un réarrangement solvolytique d'un bicyclo[2.1.0] hexane en un vinylcyclopentane est discuté.

Canadian Journal of Chemistry, 49, 1070 (1971)

Introduction

There have been a number of syntheses reported of biologically potent prostaglandins (1) and their analogs (2) in the recent literature. We wish to report a synthesis *d,l*-5-dehydro PGE_2 and *d,l*-PGE_2 methyl esters which follow the general principle published (1*a*) using the modification introduced by Schneider *et al.* (1*b*, *c*). A similar synthesis was described in a recent communication by Schneider (1*g*). In this paper we wish to describe (Scheme 1): (*1*) the synthesis of the iodo ester **6***b* which constitutes the C_1—C_7 side chain of PGE_2; (*2*) the alkylation of the bicyclic ketone **7** with the iodo ester **6***b* which gave the keto ester **9**; (*3*) a study of the solvolytic transformation of the bicyclo[3.1.0]hexanone **9** to the acetylenic prostaglandin analog **11** which showed high biological activity; and (*4*) the final reduction and isomerization of **11** to *d,l*-PGE_2 methyl ester **17**.

The best synthesis of the seven carbon sidechain **6***b* was achieved by the condensation of propargyl alcohol with a C_4 unit, 4-tetrahydropyranyloxybutyl bromide (**3***b*) (Scheme 2).

The bromide **3***b* was synthesized in four steps starting with γ-butyrolactone (**1**). Treatment of the lactone with saturated aqueous hydrogen bromide at reflux for 15 h gave 4-bromobutyric acid (**2***a*) (4). This was esterified with diazomethane (5), and the resulting ester **2***b* was reduced with excess lithium aluminum hydride in diethyl ether at −50° to give 4-bromobutanol (**3***a*). Finally, treatment of the bromo alcohol **3***a* with dihydropyran and a trace of phosphorus oxychloride (6) gave **3***b*. Yields of better than 90% were realized for each step in this sequence.

Reaction of **3***b* with propargyl alcohol by the method of D'Engenieres *et al.* (3) gave 7-tetrahydropyranyloxyhept-2-yn-1-ol (**4***a*) in 50–60% yield. Only moderate yields were realized because of the formation of the two by-products **4***b* (2.5%) and **4***c* (25%) which resulted from *O*-alkylation of propargyl alcohol and **4***b*, respectively.

The iodo ester **6***b* was obtained from **4***a* by the following sequence. The hydroxy group of **4***a* was mesylated by first forming the lithium alcoholate with butyl lithium followed by slow addition of mesyl chloride in diethyl ether at 0°. The mesylate **5***a* was then treated with sodium iodide in dry acetone for 1.5 h (7) to give the corresponding iodide **5***c*. The bromide **5***b* was similarly prepared by refluxing the mesylate **5***a* with anhydrous lithium bromide in acetone for 24 h (8). Cleavage of the tetrahydropyranyl ether with dilute methanolic hydrochloric acid gave 7-iodohept-5-yn-1-ol (**5***d*) which was oxidized with excess Jones reagent (17) at 0° to the carboxylic acid **6***a* in 20% overall yield starting from **4***a*. Methylation with diazomethane gave the acetylenic iodo ester **6***b*: i.r. (film) 2240, 1740, 1163 cm^{-1}; δ 3.64 (3H, OCH_3) and 3.70 (3H, J = 2 Hz, $-CH_2I$); M^+ 266, M^+-I 139.

Alkylation of Exo-6-(1'-heptenyl)-bicyclo-[3.1.0]hexan-3-one (7)

The reaction conditions for the alkylation of bicyclic ketone **7** with the iodo ester **6** were found to be extremely critical. Best results were obtained when freshly prepared potassium *t*-butoxide dissolved in tetrahydrofuran (THF) was added slowly to a THF solution of the ketone and iodo ester at 0–5° (9, 1*c*). It was also necessary to have

[1]Abstracted from the Ph.D. dissertation of E.S.F., McGill University, Montreal, Quebec, 1969.
[2]Holder of a Canadian Industries Ltd., Fellowship, 1966–1967.

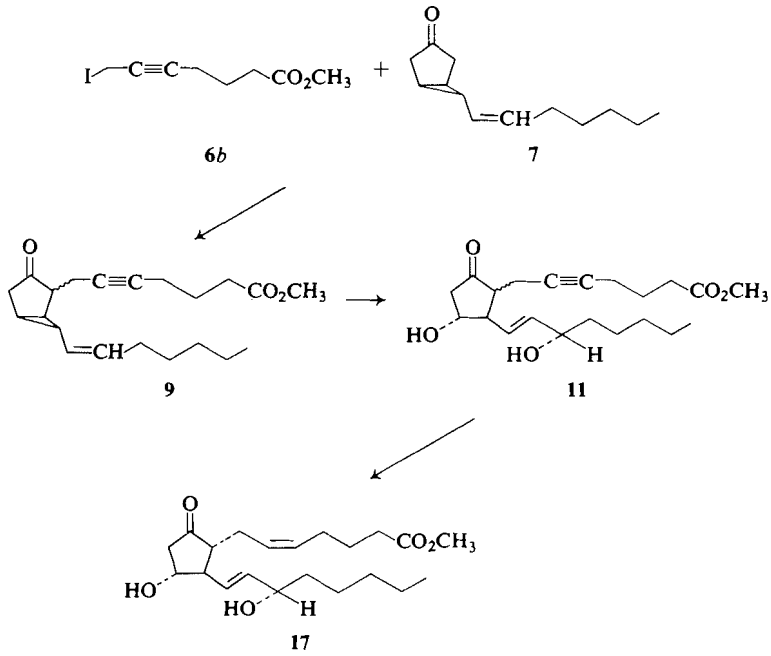

SCHEME 1

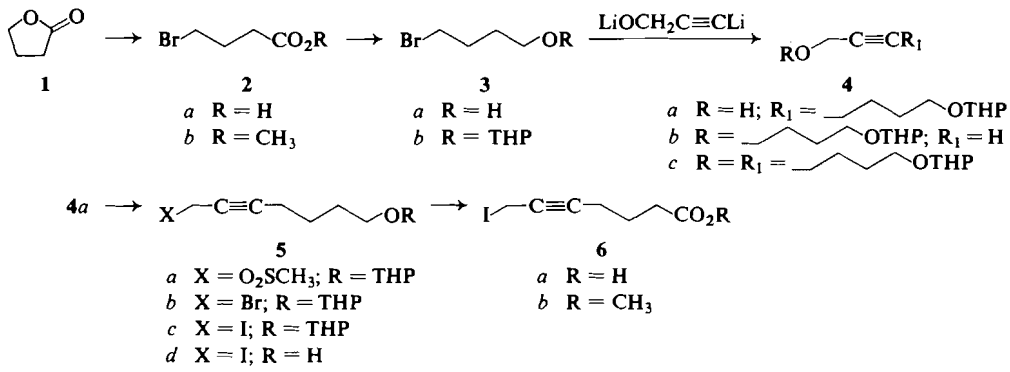

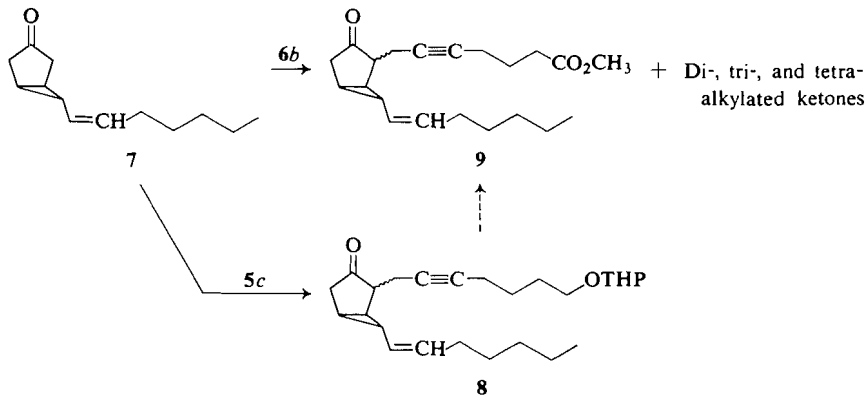

SCHEME 2

Can. J. Chem. Downloaded from www.nrcresearchpress.com by 210.87.254.6 on 09/05/12
For personal use only.

Can. J. Chem. Downloaded from www.nrcresearchpress.com by 210.87.254.6 on 09/05/12
For personal use only.

the iodo ester in a large excess relative to the ketone and rigorously dried THF in order to obtain maximum yields of the monoalkylated product. Alkylation was only achieved when iodide was the leaving group.

Alkylation of the ketone **7** with a three-fold excess of the iodo ester gave four alkylated products which were separated from the unreacted starting material by column chromatography on silica gel, and then from each other by preparative t.l.c. on silica gel (benzene–ether, 9:1). The major product was the monoalkylated compound **9**, obtained as a mixture of *cis* and *trans* (β and α) isomers in 23% yield: i.r. (film) 1740, 1165 cm^{-1}; n.m.r. ($CDCl_3$) δ 5.6–4.6 (2H, m, HC=CH), 3.62 (3H, s, OCH_3); M^+ 330. The other three products were the di- (M^+ 468), tri- (M^+ 606), and tetra- (M^+ 744) alkylated compounds obtained in 8, 11, and <5% yields respectively.

The g.l.c. of the monoalkylated product (6′ 3% SE30 on chromosorb W, 200°) indicated that there were two compounds present (R_t = 2.90 and 4.75 min) in the ratio 3:7. In the PGE_1 series, the analogous alkylation products **i***a* and *b* obtained in the ratio 28:72 (1*c*) had retention times of 3.05 and 4.67 min on the same g.l.c. column.[3]

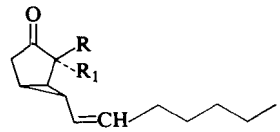

i

a R = H; R_1 = CO_2CH_3

b R = CO_2CH_3; R_1 = H

The minor component (R_t = 3.05 min) had been assigned the *trans* configuration, since it had been converted to $PGF_{1\alpha}$ (1*c*). Based on the close parallelism of the two sets of reactions, the minor and major components must be the *trans* (α) and *cis* (β) isomers of **9**. These isomers were carried through the final sequence of reactions without separation, since it has been found (29) that 8-iso-PGE_1 methyl ester isomerizes to the PGE_1 methyl ester in 5% methanolic sodium acetate.

The g.l.c. of the dialkylated product (6′, 3% SE30 on chromosorb W, 248°) showed two peaks (R_t = 3.50 and 5.25 min) in the ratio 1:5. Too little was known to make a structural assignment for the two dialkylated products. However, it has been shown (25) that the second condensation reaction occurs predominantly at the more substituted carbon.

The tri- and tetra-alkylated products were not eluted off the column at temperatures up to 250°.

An alternative route to the keto ester **9** involved alkylation of the bicyclic ketone **7** with an excess of the iodide **5***c* which gave the monoalkylated product **8** in 19% yield. The subsequent acid hydrolysis of the tetrahydropyranyl ether, Jones oxidation of the resulting alcohol to the carboxylic acid, and final esterification with diazomethane, gave a complicated mixture of products from which the keto ester **9** could not be isolated.

The Final Steps in the Synthesis of d,l-PGE_2 Methyl Ester

The crucial step in this prostaglandin synthesis was the solvolytic transformation of the cyclopropyl ring in **9** to the open chain diol or prostaglandin skeleton (**11** and **12**) (Scheme 3).

The acetylenic keto ester **9** was converted by the method of Swern *et al.* (26) to the diol **10***a* in 87% yield (i.r. (film) 3435 cm^{-1}; mass spectrum *m/e* 364 (M^+)). The diol **10***a* was then treated with an excess of methanesulfonyl chloride in anhydrous pyridine at −10°. The reaction was worked-up in the cold and gave the corresponding dimesylate **10***b* in 78–85% yields (i.r. (film) 1350, 1180 cm^{-1} (SO_2)).

The solvolysis of the dimesylate was carried out in acetone–water (2:1) at room temperature (22–25°) for 36 h in a nitrogen atmosphere. The reaction was followed by t.l.c. on silica gel (benzene – ethyl acetate 1:1) and was found to be more than 95% complete after this time. The solvolysis mixture consisted of five components which could be easily separated by preparative t.l.c. on silica gel using ethyl acetate as the solvent system.

The major products (R_f 0.62 and 0.48) were the isomeric hydroxy mesylates **13**, obtained in 70–80% yield (i.r. (film) 3475, 1355, 1180 cm^{-1}). A minor product (R_f 0.37) was also a hydroxymesylate but was never obtained pure for proper characterization. The other two components, R_f 0.29 and 0.19, were obtained in 11–16% yield and consisted of 5-dehydro PGE_2 methyl ester and its 8-isomer **11**, and the corresponding 15-epimers **12** (i.r. (film) 3440, 1740 cm^{-1}; n.m.r. ($CDCl_3$) δ 5.9–5.2 (*HC=CH*); *m/e* 346 (M^+-H_2O)).

Treatment of a mixture of **11** and **12** with 0.5 *M*

[3]Samples of **i***a* and *b* for g.l.c. analysis were supplied by Dr. J. E. Pike of the Upjohn Company, Kalamazoo, Michigan.

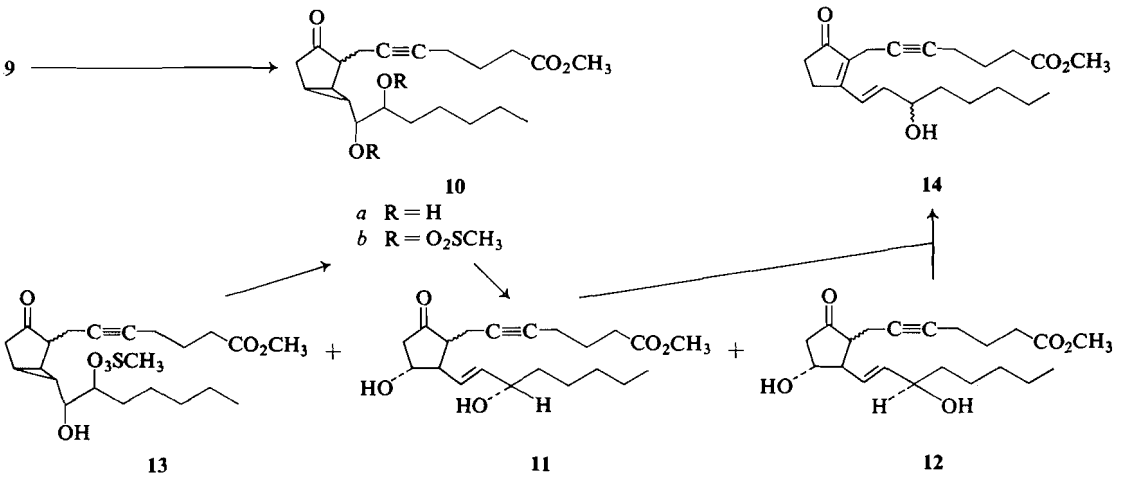

SCHEME 3

TABLE 1. Results of the bioassay of: A, the synthetic 5-dehydro PGE_2 methyl esters **11** and **12** for smooth muscle stimulating activity using the rat stomach fundus;* B, the synthetic PGE_2 methyl esters **16** and **17** for smooth muscle stimulating activity using gerbil colon†

	Compounds	Weight ($\times 10^{-9}$g) of material required for equivalent contraction	Potency
A.	Natural PGE_1	20	1.0
	8α and β-15-epi-5-Dehydro PGE_2 methyl ester **12**	720	0.028
	8α and β-5-Dehydro methyl ester **11**	192	0.10
	Epimerized **11**	160	0.13
	Mixture of **11** and **12**	256	0.078
B.	8α and β-15-epi PGE_2 Methyl ester **16**		0.21
	8α PGE_2 Methyl ester **17**		3.38

*Bioassay carried out by Dr. L. Wolfe, Montreal Neurological Institute, Montreal, Quebec.
†Bioassay carried out by Dr. J. R. Weeks, The Upjohn Company, Kalamazoo, Michigan.

sodium hydroxide in methanol at 38–48° for 1.5 h gave 5-dehydro-PGB_2 methyl ester **14** (ε_{275} 28 300)(27). Prolonged heating or heating at reflux temperatures for short times caused the chromophore to disappear. Presumably **14** decomposed under these more vigorous conditions.

The configuration at C-15 of the products **11** and **12** were assigned on the basis of their bioassay for smooth muscle stimulating activity. This assignment was subsequently confirmed when **11** and **12** were independently converted to the PGE_2 and 8-iso PGE_2 methyl esters **15** and **16** respectively, which in turn showed the predicted activity for smooth muscle stimulation (28). The bioassay on rat stomach fundus for smooth muscle stimulating activity of the prostaglandin-type products obtained from the solvolysis showed that the slower moving compound (R_f 0.19) had higher activity than the faster moving one (R_f 0.29) (Table 1).

Since it is known[4] that PG's with the natural α-configuration at C-15 are more active than the ones having the unnatural β-configuration, the slower moving isomer (R_f 0.19) was assigned the

[4]J. R. Weeks, private communication.

Can. J. Chem. Downloaded from www.nrcresearchpress.com by 210.87.254.6 on 09/05/12
For personal use only.

Can. J. Chem. Downloaded from www.nrcresearchpress.com by 210.87.254.6 on 09/05/12
For personal use only.

α-configuration shown in **11** while the faster moving isomer (R_f 0.29) was assigned the β-configuration **12**. The comparison of t.l.c. R_f values of the PGE_2 methyl ester, synthesized in the subsequent steps, with that of the natural PGE_2 methyl ester supported this assignment.

Treatment of **11**, a mixture of 8α and β isomers, with 5% methanolic sodium acetate for seven days at room temperature (29) gave a product with increased biological activity (Table 1). This result was consistent with the formation of more of the 8α isomer since PG's having the natural, 8α configuration are known to be more active than those having the 8β configuration.[4]

Attempts were made to improve the yields of the rearranged product by varying the leaving group, the solvolysis condition, and the type of carbonium ion generated. Because of the difficulty in synthesizing the alkylated bicyclic ketone **9** and since the side chain should not greatly affect the yields of rearranged products, the unalkylated ketone **7** was used as a model in these solvolysis studies. By analogy to the results of Wiberg and Ashe (10) where the exo isomer was found to give a cleaner reaction and more ring opened product than the endo isomer, only the exo isomer was considered in this study.

It was known that the rearrangement of the cyclopropyl carbinyl system gave, under kinetic control, the cyclopropyl carbinol as the major product (12), but that under thermodynamically controlled conditions, the homoallylic system was favored (13). In principle, thermodynamic control would be achieved by treating the glycol **20** (Scheme 4) with mineral acid. However, one competing reaction, a pinacol rearrangement (9), and, in the E-series, the known acid instability of the PG which is dehydrated to the PGA compounds (27), made this route unsuitable. The ditrichloroacetate **21** was, therefore, prepared by treating the diol **20** with excess trichloroacetylchloride in pyridine and solvolyzed in trichloroacetic acid. Under these conditions, any regenerated ditrichloroacetate would be resolvolyzed, giving effectively thermodynamic control.

The solvolysis of the ditrichloroacetate was carried out at various temperatures in trichloroacetic acid, trichloroacetic acid – dioxane 1:1, and trichloroacetic acid containing some *p*-toluenesulfonic acid. Pyrolysis of the ditrichloroacetate was also attempted. In order to determine if rearrangement had taken place, the reaction mixture was taken up in ether and washed with 5% sodium bicarbonate and water to remove all the acid solvent. Some of the resulting material was then treated with 0.5% sodium hydroxide in methanol at 50–60° for 10 min. If rearrangement took place, the resulting β-hydroxy ketone **22** would be converted to the conjugated ketone **29** in the same way the PGE_{1-3} were converted to PGB_{1-3} (27). This compound is easily identified by its u.v. spectrum (λ_{max}(MeOH) 268 mμ, ε 26 000). There was no detectable rearrangement in any of the solvolysis reactions carried out in trichloroacetic acid. The t.l.c. of the products on silica gel (benzene–ether, 7:3) showed only recovered ditrichloroacetate. Pyrolysis at 230° gave a small amount of rearrangement along with considerable charring. At 120–140°, no reaction took place.

Solvolysis of the ditrichloroacetate **21** in refluxing aqueous acetone, analogous to the reaction carried out by Lumb and Whitham (14), gave, after 4 days, the starting ditrichloroacetate (65%), the glycol **20** (30%), and the rearranged diol **22** (2%). Because of the long reaction time and poor yield of the rearranged product **22**, this reaction was not further studied.

A similar solvolysis of the dibromide **23**, prepared by treating the ketone **7** with pyridinium hydrobromide perbromide (15) in anhydrous chloroform,[5] was carried out in aqueous acetone. The solvolysis was carried out at room temperature for 112 h. After separation of the components by t.l.c. (benzene–ether 7:3), the reaction mixture was found to consist of the dibromide **23** (63%), the unrearranged bromohydrin **26***a* (15%) (M^+ 289, 291; *m/e* 210, M^+-^{79}Br, ^{81}Br), and a slow moving fraction (5%) which was still a mixture of four compounds. The components of this slow moving fraction had a low R_f value which

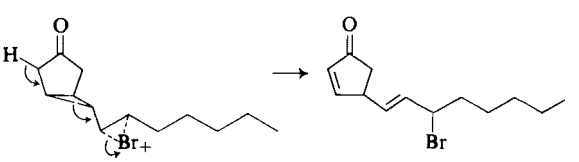

ii iii

[5]Two products were obtained from this reaction. The desired dibromide **21** (55%) was the major product but could only be separated with much difficulty from a minor product. This minor product was not obtained pure. However bands at 1720 and 1630 cm^{-1} in the i.r. spectrum of the mixture suggested that it was an α,β-unsaturated, five-membered ring ketone such as **iii**. Such a compound would be formed if, during the bromination reaction in a slightly acidic, aprotic solvent, rearrangement of **ii** to **iii** occurred as well.

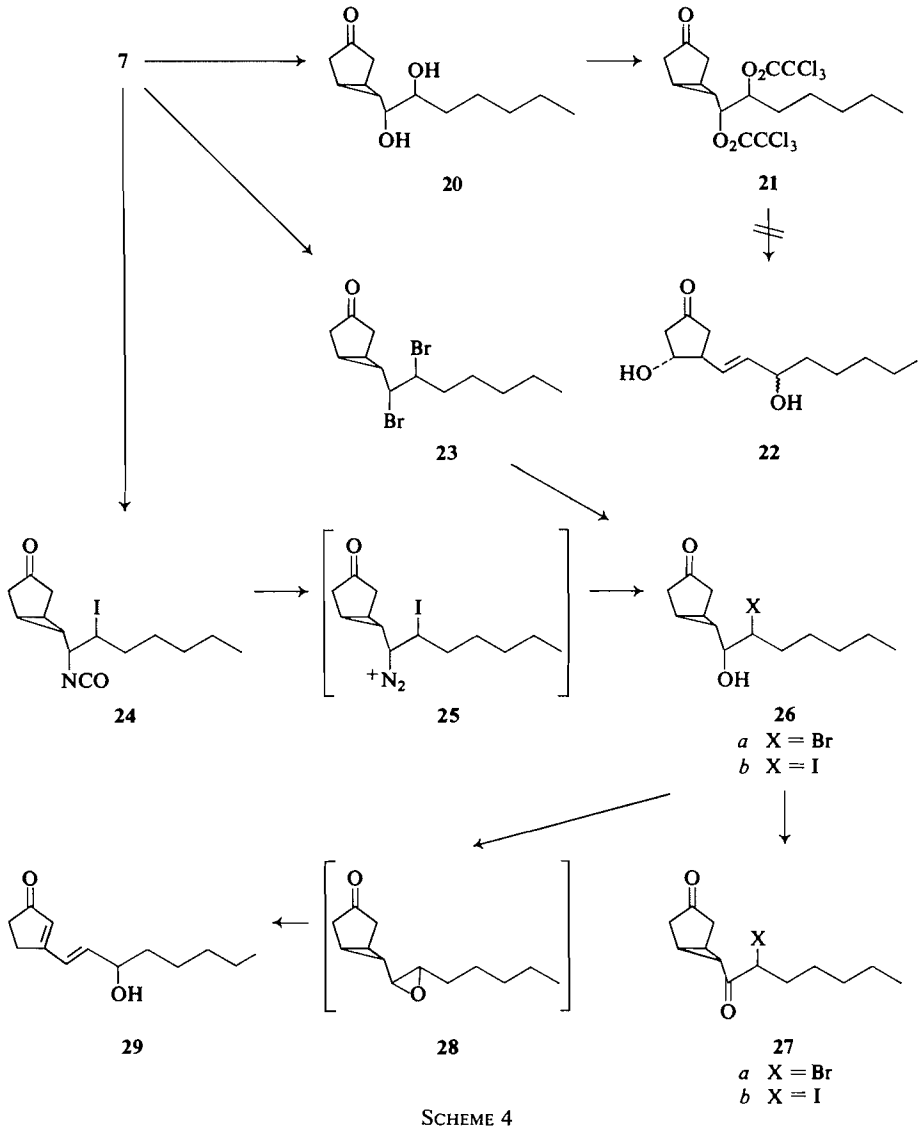

SCHEME 4

suggested that they were diols. This mixture probably contained some rearranged product, but there was not enough material available for proper characterization of its components.

The bromohydrin **26***a* was independently synthesized by treating the ketone **7** with *N*-bromosuccinimide (16). Oxidation of **26***a* with Jones reagent (17) at 0° gave the bromodiketone **27***a* in good yield (i.r. (CCl_4) 1748, 1700 cm^{-1}, n.m.r. (CCl_4) δ 4.27(t, 1H, J = 6.5 Hz, C*H*Br)).

When the bromohydrin **26***a* was treated with 0.5% methanolic sodium hydroxide at 50°, the conjugated hydroxy ketone **29** was obtained in about 30% yield (crude product ε_{268} 8500). This compound was probably formed via the epoxide **28** which is known to rearrange to the conjugated ketone under basic conditions (11).

Since the generation of a 'normal' carbonium ion gave products of rearrangement in less than 20% yield, it was decided to try to generate a 'hot' carbonium ion (19) (Scheme 4).

Addition of iodine isocyanate (20) to the olefin **7** gave the iodo isocyanate **24** in good yield: (i.r. (CCl_4) 2245 cm^{-1}). The mode of addition follows from subsequent reactions. The isocyanate was hydrolyzed to the corresponding amine in aqueous acetone. The amine was not isolated but treated, *in situ*, with formic acid and sodium ni-

Can. J. Chem. Downloaded from www.nrcresearchpress.com by 210.87.254.6 on 09/05/12
For personal use only.

Can. J. Chem. Downloaded from www.nrcresearchpress.com by 210.87.254.6 on 09/05/12
For personal use only.

trite at −4°. After 1 h at this temperature and 3.5 h at 25°, the only compound isolated was the unrearranged iodohydrin **26***b* (M^+ 336; *m/e* 209, M^+-I). If any rearrangement did occur, it was to an extent of less than 10%, and certainly no higher than in the dimesylate solvolysis. Oxidation of the iodohydrin **26***b* with Jones reagent gave the iodo diketone **27***b* (i.r. (CCl_4) 1745, 1695 cm^{-1}; n.m.r. (CCl_4), 100 Hz) δ 4.48(t, 1H, J = 4.0 Hz, C*H*I)).

Considerable work has been done to study the cyclopropylcarbinyl solvolysis and to understand the nature of the carbonium ion which was involved (21). Although rate enhancement of the solvolysis due to the participation of the cyclopropyl group adjacent to the leaving group has been widely demonstrated (10, 12*a–d*)[6] the exact nature of the carbonium ion is controversial (21, 12*e,f*, 13*a*) and the extent of rearrangement in various cyclopropylcarbinyl systems under similar solvolytic conditions is quite unpredictable (10, 14, 22).

The reason for the limited rearrangement in the bicyclo[3.1.0]hexanone system discussed above was not clear. A number of factors could influence the amount of rearrangement product. The stereochemical arrangement of the leaving groups to the migrating bond (18, 30) and the amount of ring strain in the transition state caused by bond breaking and rearranging (12*g,h*, 22, 23) have been found to greatly influence the type of products obtained in a solvolysis. Recently it was shown (24) in a modified PGE_1 synthesis that the *endo* isomer gives about twice as much rearranged product as the *exo* isomer under the same reaction conditions. In the case of the ditrichloroacetate **21**, where no reaction took place at all, the reaction might be very slow. Indeed, it was found that the dibromide solvolysis was much slower than that of the dimesylate but faster than that of the ditrichloroacetate. This order of reactivity of the leaving groups is the expected one (18). No extensive data on the reactivity of trichloroacetates, or the solvolyzing ability of trichloroacetic acid, have been reported. Another factor which may limit the amount of rearrangement is that the neighboring group participates in the formation of the cyclopropylcarbinyl carbonium ion, minimizing the effect of the cyclopropyl group, although the latter also participates in the ion formation.[6]

The final step in the synthesis of PGE_2 methyl ester was the reduction of the acetylenic bond to a *cis* double bond. Catalytic hydrogenation of the mixture of 5-dehydro PGE_2 methyl ester and its 8-isomer **11** using Lindlar catalyst poisoned with 1–3% quinoline (32) gave a mixture of PGE_2 and 8-iso PGE_2 methyl esters **15** in 63% yield. The corresponding mixture of 15-epi-5-dehydro PGE_2 methyl ester and its 8-isomer was hydrogenated in the same way to a mixture of 15-epi-PGE_2 methyl ester and its 8-isomer **16** (Scheme 5).

The mixture 8α- and β-PGE_2 methyl ester **15** was treated with 3% ethanolic potassium acetate solution for 94 h at 22° (28). The resulting reaction mixture consisted of one major and two minor components. The major product, isolated in 80% yield from the other two by preparative t.l.c. on silica gel (using ethyl acetate as the solvent system), was characterized as 8α-PGE_2 methyl ester **17** (i.r. (film) 3440, 1740 cm^{-1}; n.m.r. ($CDCl_3$) δ 5.6(m, 2H, *trans* *H*C=C*H*), 5.3 (m, 2H, *cis* *H*C≡C*H*); mass spectrum *m/e* 348 (M^+-H_2O)). The i.r. and mass spectra were identical with the corresponding spectra of the PGE_2 methyl ester obtained from natural PGE_2. The two minor products were identified as PGA_2 methyl ester **18** (18%) (ε_{217} 9000; mass spectrum *m/e* 348(M^+)) which was contaminated by a small amount of the second compound, PGB_2 methyl ester **19** (2%) (λ_{max} 277 mμ).

The 15-epi-PGE_2 methyl ester **16** was characterized from its mass spectrum. The fragmentation was the same as that obtained for PGE_2 methyl ester **17**. Exact mass measurement of the fragment *m/e* 348 was correct for $C_{21}H_{32}O_4$ or M^+-H_2O (calcd., 348.230045; found, 348.229694). The fragment *m/e* 190, one of the most abundant fragments in the mass spectrum of PGE_2 methyl ester (29), was correct for an empirical formula $C_{13}H_{20}O_2$ (calcd., 190.135758; found, 190.135990). Such an ion probably arises from $C_{21}H_{32}O_4$ by fragmentation of the ester side chain with hydrogen transfer to the ion fragment *m/e* 208, followed by loss of H_2O.

The R_f values of synthetic PGE_2 methyl ester obtained from natural PGE_2 were compared by t.l.c. on silica gel and 10% silver nitrate impreg-

[6]It was found that the leaving group adjacent to the cyclopropyl ring was the only one solvolyzed in all the reactions that were carried out. Indeed, in the case of the iodohydrin **26***b*, the iodide could not be solvolyzed when it was refluxed in aqueous acetone for 24 h. Therefore the cyclopropyl ring does participate in the initial solvolysis reaction.

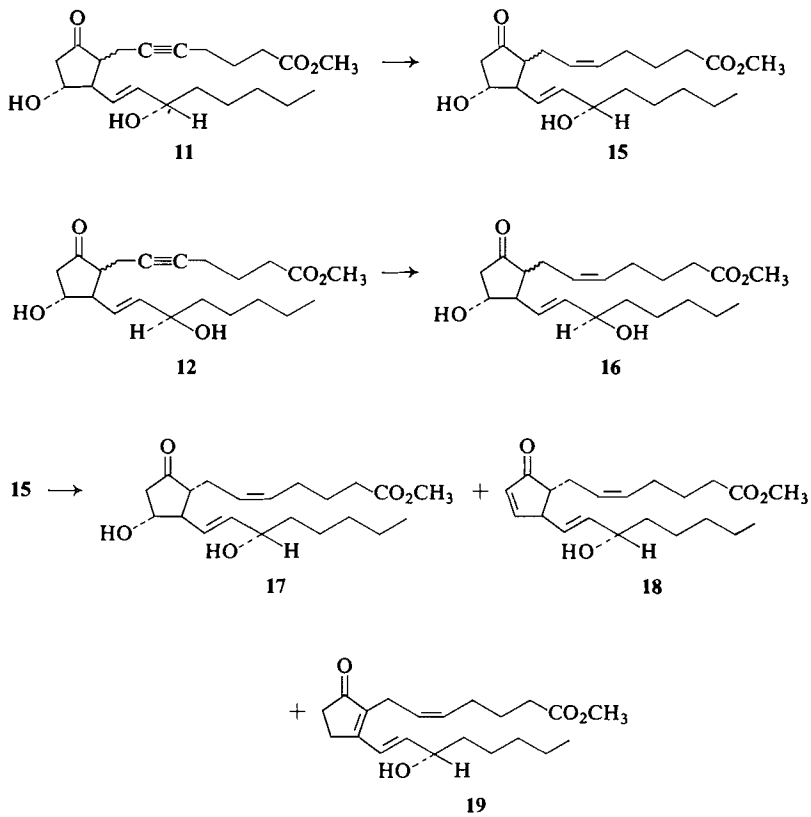

SCHEME 5

TABLE 2. The R_f values on silica gel

Compound	10% $AgNO_3$/MIII*	Ethyl acetate
PGE_2 Methyl ester from natural PGE_2	0.31	0.27
PGE_2 Methyl ester **17**	0.31	0.27
15-epi-PGE_2 Methyl ester **16**	0.32	0.35
5-Dehydro-PGE_2 methyl ester **11**	0.39	0.27

*MIII, Ethyl acetate – methanol – water (16:2.5:10).

nated silica gel. The R_f values are listed in Table 2. The PGE_2 methyl ester **17** had the same R_f value as that of the PGE_2 methyl ester derived from natural PGE_2, confirming the stereochemical assignment at C-15 made with the 5-dehydro-PGE_2 methyl esters. The 15-epi-PGE_2 methyl ester **16** had a higher R_f value in both systems.

The bioassay (30) on the isomerized product **17**, carried out on the gerbil colon smooth muscle showed that it had very high biological activity, and in the expected order of potency[4] (Table 1). Although PGE_1 and PGE_2 activity has not been compared on gerbil colon, it was estimated[4] that PGE_2 would be several-fold more potent. On the rabbit duodenum, the activity of PGE_2 was about three-fold PGE_1 and they were equal on guinea-pig ileum (31). Further, in tests on other prostaglandins, it has not been found that esterification with methyl has any great effect on activity in isolated baths.[4] The increased activity after

Can. J. Chem. Downloaded from www.nrcresearchpress.com by 210.87.254.6 on 09/05/12
For personal use only.

Can. J. Chem. Downloaded from www.nrcresearchpress.com by 210.87.254.6 on 09/05/12
For personal use only.

epimerization indicated that isomerization had taken place, and the 8α isomer **17** (*d,l*-PGE_2 methyl ester) had been obtained.

Experimental

The instruments used in this work to characterize the compounds were: Perkin–Elmer 257 and 357 i.r. spectrometers, Varian A60 and 100 Hz n.m.r. spectrometers, MS9 high resolution mass spectrometer, Unicam u.v. spectrometer, and F&M 700 gas chromatograph. Elemental analyses were carried out by Beller, Microanalytical Laboratory, West Germany and Dr. Franz Pascher Microanalytical Laboratory, Bonn, West Germany.

Unless otherwise mentioned, the term "worked-up as usual" means extracting with a specified solvent, washing the combined extracts with water and saturated aqueous sodium chloride, drying over anhydrous sodium sulfate or magnesium sulfate, filtering, and finally evaporating the solvent *in vacuo*.

4-Bromobutyric Acid (2a)

Compound **2***a* was prepared according to the procedure of Avison *et al.* (4).

Methyl 4-Bromobutyrate (2b)

The crude 4-bromobutyric acid (**2***a*) was treated with ethereal diazomethane (5) at 0°. The ether was then removed *in vacuo* and the product was distilled at 77°/15 mm: i.r. (CCl_4) 1778, 1740 cm^{-1} (C=O); n.m.r. (CCl_4) δ 3.59 (s, 3H, OCH_3), 3.38 (t, 2H, J = 6.0 Hz, CH_2Br), 2.63–1.96(m, 4H, CH_2CH_2CO).

Anal. Calcd. on $C_5H_9O_2Br$: C, 33.15; H, 4.97; Br, 44.19. Found: C, 33.42; H, 5.06; Br, 43.98.

4-Bromobutanol (3a)

A slurry of lithium aluminum hydride (3.05 g) in anhydrous ether (250 ml) in a 1 l, three-necked flask was cooled to −60°. The bromo ester **2***b* (23.8 g), dissolved in anhydrous ether (200 ml), was added at such a rate that the temperature did not go above −50°. Following the addition, the reaction was kept below −60° for 1.5 h, then slowly allowed to warm to −10°. The reaction was then quenched with 200 ml of 2 *N* sulfuric acid at 0° and worked-up as usual with ether. The resulting alcohol **3***a* was obtained in 95% yield (b.p. 48–49°/3 mm): i.r.(CCl_4) 3630, 3300 (OH), 1060 cm^{-1} (C—O); n.m.r. (CCl_4) δ 3.68(t, 3H, J = 6.5 Hz, CH_2O), 3.46(t, 3H, J = 6.0 Hz, CH_2Br), 2.25–1.50(m, 4H, CH_2CH_2), 4.62(s, 1H, exchangeable, O*H*).

Anal. Calcd. for C_4H_9OBr: C, 31.37; H, 5.88; Br, 52.22. Found: C, 31.49; H, 5.83; Br, 51.98.

4-Tetrahydropyranyloxybutyl Bromide (3b)

One equivalent of the bromo alcohol **3***a* was treated (neat) with a slight molar excess of 3,4-dihydropyran and three drops of phosphorous oxychloride. A vigorous exothermic reaction started almost immediately after the phosphorous oxychloride had been added (in one instance, the reaction started without addition of catalyst, probably because the mixture was contaminated with some mineral acid). The reaction temperature was controlled with an ice-water bath. After the exothermic reaction had subsided, the reaction mixture was stirred at room temperature for 3 h. The mixture was then taken up in ether and washed twice with 5% aqueous potassium hydroxide, followed by usual work-up procedure. The resulting tetrahydropyranyl ether could be distilled at 82–84°/2 mm as long as the distillation apparatus was acid free, otherwise the tetrahydropyranyl ether would cleave. Purification was also achieved by column chromatography on silica gel using hexane, then hexane–benzene mixtures (2.5 to 20%) as the solvent system. The yield of **3***b* was better than 95%: i.r. (CCl_4) 1143, 1130, 1038, 1028 (C—O—C), 914, 872 cm^{-1}; n.m.r. (CCl_4) δ 4.53 (m, 1H, *H*C ketal), 4.05–3.18 (m, 6H, 2(OCH_2), CH_2Br), 2.25–1.35 (m, 10H, CH_2).

Anal. Calcd. for $C_9H_{17}O_2Br$: C, 45.59; H, 7.17; Br, 33.75. Found: C, 45.33; H, 7.38; Br, 33.93.

7-Tetrahydropyranyloxy-2-heptyn-1-ol (4a)

A 500 ml, three-necked, round-bottom flask was fitted with a Claisen adapter on the middle neck, and a stopcock adapter (nitrogen inlet), and dropping funnel on the other two necks. A mechanical stirrer was passed through the middle neck and Dry Ice condenser was placed on the other arm of the Claisen adapter. The system was flushed with nitrogen gas and flame dried. The reaction flask was charged with 0.22 mol lithium amide, the flask and condenser were then cooled to −80° (isopropyl alcohol – Dry–Ice), and 200 ml ammonia was distilled through the condenser into the flask. It was not found necessary to redistill the ammonia from sodium metal. After the distillation, the system was again flushed with nitrogen and the dropping funnel was charged with 0.10 mol propargyl alcohol in 30 ml of anhydrous ether. The alcohol was added dropwise with stirring. The coolant from the flask was then removed and the solution was stirred for 2 h. After this time, the dropping funnel was charged with 0.09 mol of the bromide **3***b* in 20 ml of anhydrous ether under a positive nitrogen pressure. The bromide was added dropwise and then the reaction mixture was stirred for 6 h at −33° (refluxing ammonia). After this time the reaction was quenched by the addition of 0.05 mol of ammonium chloride and the ammonia was allowed to evaporate overnight. The resulting solid mass was then taken up in water and ether. The ether was separated and the aqueous phase was further extracted (six times) with ether. The work-up was then continued in the usual way. The crude reaction product was chromatographed on a silica gel column (30 g silica gel to 1 g mixture). The column was eluted with hexane containing increasing amounts of ethyl acetate (2.5%–20%).

The compounds that were isolated from the reaction mixture are given below in the order that they were eluted off the column.

(1) 4-Tetrahydropyranyloxybutyl Propargyl Ether (4b)

This compound was eluted with 2.5–5% ethyl acetate in hexane and obtained in 2.5–5% yield: i.r. (CCl_4) 3310 (≡CH), 2120 (C≡C, terminal), 1124, 1105, 1079, 1038, 1023 cm^{-1} (C—O—C); n.m.r. (CCl_4) δ 4.53(m, 1H, *H*C ketal) 4.09(d, 2H, J = 2.5 Hz, $OCH_2C{\equiv}$), 3.9–3.1(m, 6H, OCH_2), 2.57(t, 1H, J = 2.5 Hz, ≡C*H*), 1.8–1.4(m, 10H, CH_2).

Anal. Calcd. for $C_{12}H_{20}O_3$: C, 67.89; H, 9.50. Found: C, 68.10; H, 9.66.

Can. J. Chem. Downloaded from www.nrcresearchpress.com by 210.87.254.6 on 09/05/12
For personal use only.

(2) 4-Tetrahydropyranyloxybutyl-7-tetrahydropyranyloxy-2-heptynyl Ether (4c)

Compound **4c** was eluted with 5–10% ethyl acetate in hexane and obtained in 20–25% yield: i.r. (CCl_4) 2230 (C≡C), 1145, 1130, 1085, 1075, 1045, 1030 cm^{-1} (C—O—C); n.m.r. (CCl_4) δ 4.59(m, 2H, *H*C ketals), 4.09 (t, 2H, J = 2.0 Hz, ≡CCH_2O), 4.0–3.2(m, 10H, CH_2O), 2.2(m, 2H, CH_2C≡), 1.9–1.3(m, 20H, CH_2).

Anal. Calcd. for $C_{21}H_{36}O_5$: C, 68.44; H, 9.85. Found: C, 68.04; H, 9.74.

(3) 7-Tetrahydropyranyloxy-2-heptyn-1-ol (4a)

This compound was eluted off the column with 20% ethyl acetate in hexane and obtained in 50–60% yield. Distillation of this compound was unsatisfactory because of tetrahydropyranyl ether cleavage: i.r. (CCl_4) 3610, 3450 (OH), 2220 (C≡C), 1140, 1123, 1039, 1025 cm^{-1} (C—O—C); n.m.r. (CCl_4) δ 4.60(m, 1H, *H*C ketal), 4.17 (t, 1H, J = 2.0 Hz, OCH_2C≡), 4.0–3.2(m, 4H, CH_2O), 2.5–2.1(m, 2H, CH_2C≡), 2.0–1.4(m, 10H, CH_2), 2.91 (s, 1H, exchangeable, O*H*).

Anal. Calcd. for $C_{12}H_{20}O_3$: C, 67.89; H, 9.50. Found: C, 68.09; H, 9.63.

7-Tetrahydropyranyloxy-2-heptynyl Mesylate (5a)

A solution of *n*-butyl lithium (Alfa Inorganics) in hexane (66 g of 22.6% by weight) was transferred under nitrogen in a "glove bag" into a 1 l, three-necked flask. The flask was then fitted with a nitrogen inlet stopcock, mechanical stirrer, dropping funnel, and nitrogen outlet. Under a stream of nitrogen, the solution was cooled to 0° (ice-water bath) and the dropping funnel was charged with 45 g (0.212 mol) of the alcohol **4a** in 100 ml of anhydrous ether. The ethereal solution of alcohol was slowly added with stirring over a period of 1 h, then stirred at 0° for an additional hour to ensure complete salt formation. Mesyl chloride (24.3 g) in 70 ml anhydrous ether was placed into the dropping funnel and slowly added at 0°. A precipitate formed immediately. After addition (about 1 h) the solution was allowed to stand an additional 3 h. The reaction was then quenched with ice water and worked-up as usual in ether. The yields of the crude mesylate were better than 95% and were used as such for conversion to the iodide **10c**. The mesylate was purified by column chromatography on silica gel and elution with 2.5–10% ethyl acetate – hexane. This purified material was used for the alkylation: i.r. (CCl_4) 2245 (C≡C), 1390, 1188 (SO_2), 1145-1025 cm^{-1} (C—O—C).

1-Iodo-7-tetrahydropyranyloxy-2-heptyne (5c)

Sodium iodide (75 g), which had been heated in the oven at 120° for 2 h, was placed in a 2 l, three-necked flask fitted with a nitrogen gas inlet and outlet and mechanical stirrer. The sodium iodide was dissolved in 500 ml anhydrous acetone and the resulting solution was cooled to 0° under nitrogen. The crude mesylate **5a** (113 g) dissolved in 500 ml anhydrous acetone was added at once with stirring. The solution became cloudy, and finally turned into a thick, light brown slurry. This was stirred at 0–20° for 1.5 h, then diluted with ether, and worked-up the usual way. The crude iodide **5c**, obtained in 85–90% yields, was purified by column chromatography on silica gel using 2.5–10% ethyl acetate in hexane as the solvent system: i.r. (CCl_4) 2240 (C≡C), 1155–1032 cm^{-1} (C—O—C); n.m.r. (CCl_4) δ 4.60(m, 1H, *H*C ketal), 3.76(t, 2H, J = 2.0 Hz, CH_2I), 3.9–3.2(m, 4H, CH_2O), 2.30(m, 2H, CH_2C≡), 1.9–1.4(m, 10H, CH_2).

1-Bromo-7-tetrahydropyranyloxy-2-heptyne (5b)

The mesylate **5a** (1.55 g) was dissolved in anhydrous acetone under nitrogen. A slight molar excess of anhydrous lithium bromide was added and the solution was heated at 80° for 1 h. After cooling, the solution was concentrated *in vacuo*, taken up in ether, and worked-up as usual. The bromide **5b**, obtained in 85% yield, was purified by column chromatography on alumina III–IV using hexane as the solvent system; i.r. (CCl_4) 2245 (C≡C), 1142–1025 cm^{-1} (C—O—C); n.m.r. (CCl_4) δ 4.43(m, 1H, *H*C ketal), 3.79(t, 2H, J = 2.0 Hz, BrCH_2C≡), 3.7–3.1 (m, 4H, CH_2O), 2.21(m, 2H, CH_2C≡), 1.8–1.3(m, 10H, CH_2).

Anal. Calcd. for $C_{12}H_{19}O_2Br$: C, 52.36; H, 6.91; Br, 29.09. Found: C, 52.13; H, 7.10; Br, 28.89.

1-Iodo-2-heptyn-7-ol (5d)

The iodide **5c** (0.39 mol) was dissolved in 500 ml of methanol in a 1 l, three-necked flask containing a magnetic stirrer. Under a stream of nitrogen, 1 ml of concentrated hydrochloric acid was added and the solution was stirred at room temperature for 4 h. Most of the methanol was then removed *in vacuo* at room temperature, and the residue was diluted with ether, and washed with 5% sodium carbonate. The aqueous fraction was extracted with ether in the usual manner. The crude hydroxy iodide **5d** was not purified but oxidized directly with Jones reagent: i.r. (CCl_4) 3635, 3460 (OH), 2240 (C≡C), 1063 cm^{-1} (C—O); n.m.r. (CCl_4) δ 3.73(t, J = 2.0 Hz, ICH_2C≡), 3.9–3.4(m, CH_2O), 2.23(m,CH_2C≡), 1.8–1.2(m, CH_2), 3.99(s, exchangeable, O*H*).

Methyl 7-Iodo-5-heptynoate (6b)

The crude hydroxy iodide **5d**, dissolved in 1 l acetone, was placed in a 2 l three-necked flask fitted with a mechanical stirrer, dropping funnel, and thermometer.The solution was cooled to 5° and stirred while molar excess Jones reagent was added at such a rate that the temperature did not go above 10° (the addition took about 2.5 h). After the addition, isopropyl alcohol was added to destroy excess chromic acid, and the reaction mixture was diluted with water and ether. The aqueous phase separated and was extracted five times with ether. The combined ether fraction was then extracted with 5% sodium bicarbonate. This basic fraction was reacidified with 6 *N* hydrochloric acid and back extracted with ether. The ethereal solution was washed with brine, dried over sodium sulfate, filtered, and concentrated. The crude acid was then again dissolved in anhydrous ether, cooled to 0°, and treated with an ethereal solution of diazomethane. Concentration of this solution gave a brown oil which was chromatographed on a silica gel column using 10% ethyl acetate in hexane as the solvent system. The pure iodo ester **6b** was obtained as a colorless liquid in 20% overall yield from **4a**: i.r. (CCl_4) 2240 (C≡C), 1740 (C=O), 1163 cm^{-1} (C—O—C); n.m.r. (CCl_4) δ 3.70(t, J = 2.0 Hz, ICH_2-C≡), 3.64(s, OCH_3), these peaks overlap but integrate together to 5H, 2.5–2.1(m, 4H, CH_2C≡), 1.83(m, 2H, CH_2); mass spectrum: M^+ 266; *m/e* 235, M^+-OCH_3; 207, M^+-CO_2CH_3; 179, M^+-$CH_2CH_2CO_2CH_3$; 139, M^+-1; 193, M^+-$CH_2CO_2CH_3$.

Can. J. Chem. Downloaded from www.nrcresearchpress.com by 210.87.254.6 on 09/05/12
For personal use only.

6-Exo-(1'-heptenyl)-2-α and β-(6''-Carbomethoxy-2-hexynyl-bicyclo[3.1.0]hexan-3-one (9)

Iodo ester **6b** (0.0752 mol) and the bicyclic ketone **7**[7] (0.026 mol) were dissolved in 400 ml anhydrous freshly distilled tetrahydrofuran (THF).

Freshly prepared potassium *t*-butoxide (0.0395 mol) in 900 ml THF was slowly added to the stirred solution of the ketone **7** and iodide **6b** in a dry nitrogen atmosphere over a period of 6 h with the temperature being maintained between 0–5°. After about 30 min of addition, the solution became cloudy and assumed a beige color which did not change throughout the addition although the solution became thicker. This was probably due to potassium iodide precipitating out. After the base had been added, the reaction was quenched with 50 ml of 5% hydrochloric acid. The solution was then concentrated on an aspirator to about 300 ml, diluted with water, and extracted with ethyl acetate (five times, 100 ml). The combined dark organic fraction was then washed with 5% sodium thiosulfate to remove iodine, and with brine, and finally dried over sodium sulfate. The solution was then filtered and concentrated. A brown oil (19.1 g) was obtained.

Attempts to strip off unreacted ester and ketone failed at 100°/5 μ. A more efficient vacuum was required but was not available. The material was then chromatographed on a 1 kg silica gel column, eluted with hexane followed by 2.5–40% ethyl acetate in hexane. The components of the mixture were eluted in the order given below.

(1) Unreacted 7 and 6b (5% Ethyl Acetate (EtOAc))

These compounds were identified by t.l.c. comparison with the pure compounds.

(2) Monoalkylated Ketone 9 (5–10% EtOAc)

This ketone was obtained in 23% yield: i.r. (film) 1740 (C=O) ketone and ester, 1165 cm^{-1} (C—O—C); n.m.r. ($CDCl_3$) δ 5.6–4.6(m, 2H, *HC*=*CH*), 3.62(s, 3H, OCH_3). Mass spectrum: M^+ 330; *m/e* 299, M^+-OCH_3; 271, M^+-CO_2CH_3; 302, M^+-CO; 243, M^+-$(CH_2)_2CO_2CH_3$; 191, M^+-$CH_2C{\equiv}C(CH_2)_3CO_2CH_3$; 273, M^+-C_4H_9.

(3) Dialkylated Ketone (10–20% EtOAc)

This ketone was obtained in 8% yield; i.r. (film) 1740 (C=O) ketone and ester, 1168 cm^{-1} (C—O—C); n.m.r. ($CDCl_3$) δ 5.6–4.7(m, 2H, HC=CH), 3.66(s, 6H, OCH_3). Mass spectrum: M^+ 468; *m/e* 437, M^+-OCH_3; 409, M^+-CO_2CH_3; 440, M^+-CO; 329, M^+-$CH_2C{\equiv}C(CH_2)_3CO_2CH_3$; 425, M^+-C_3H_7; 411, M^+-C_4H_9.

(4) Trialkylated Ketone (20–40% EtOAc)

This ketone was isolated in 11% yield: i.r. (film) 1740 (C=O) ester and ketone, 1168 cm^{-1} (C—O—C); n.m.r. ($CDCl_3$) δ 5.6–4.6(m, 2H, *HC*=*CH*), 3.68(s, 9H, OCH_3). Mass spectrum: M^+ 606; *m/e* 575, M^+-OCH_3; 547, M^+-CO_2CH_3; 578, M^+-CO; 549, M^+-C_4H_9; 467, M^+-$CH_2C{\equiv}C(CH_2)_3CO_2CH_3$.

(5) Tetraalkylated Ketone (20–40% EtOAc)

This ketone was isolated in 5% yield: i.r. (film) 1740 (C=O) ester and ketone, 1168 cm^{-1} (C—O—C); n.m.r. ($CDCl_3$) δ 5.6–4.6(m, 2H, *HC*=*CH*), 3.79(s, 12H, OCH_3). Mass spectrum: M^+ 744; *m/e* 713, M^+-OCH_3; 685, M^+-CO_2CH_3; 716, M^+-CO; 699, M^+-C_4H_9; 605, M^+-$CH_2C{\equiv}C(CH_2)_3CO_2CH_3$. The four alkylated products were purified by preparative t.l.c. on silica gel HF 254 using benzene–ether 9:1 as the solvent system. The yields were calculated on the total amount of **12** used in the reaction.

The g.l.c. of the monoalkylated product (6', 3% SE30 on chromosorb W, 200°) showed two peaks (R_t 2.9 and 4.75 min) in the ratio 3:7. On the same column the retention times of the analogous compounds *ia* and *b*[3] were 3.05 and 4.67 min, respectively. Also on the same column (248°) the dialkylated ketone showed two peaks (R_t 3.50, 5.25) in the ratio 1:5. The tri- and tetraalkylated products did not come off the column at this temperature.

Alkylation of the Ketone 7 with 1-Iodo-7-tetrahydropyranyloxy-2-hexyne (5c)

(*a*) The procedure was used as described above except that the molar ratio of ketone to iodide was 1:1. Column chromatography of the product on silica gel (hexane and ethyl acetate solvent system) gave only one alkylated product in 30% yield. Spectral and elemental analysis showed this to be dialkylated: i.r. (CCl_4) 1750 (C=O), 1145–1025 cm^{-1} (C—O—C) tetrahydropyranyl group; n.m.r. (CCl_4) δ 5.6–4.6(m, 2H, *HC*=*CH*), 4.52 (m, 2H, *HC* ketals), 4.1–3.1(m, 8H, CH_2O).

(*b*) The procedure was the same as described above except that the molar ratio of ketone to iodide was 1:2. Column chromatography on silica gel using hexane and hexane – ethyl acetate mixtures as eluants gave the monoalkylated ketone **8** in 19% yield: i.r. (CCl_4) 1775 (C=O); 1138–1025 cm^{-1} (C—O—C) tetrahydropyranyl ether; n.m.r. (CCl_4) δ 5.5–4.6(m, 2H, *HC*=*CH*), 4.50(m, 1H, *HC* ketal), 4.0–3.0(m, 4H, CH_2O). Mass spectrum: *m/e* 302, M^+-dihydropyran (33); 84, $C_5H_8O^+$ (dihydropyran); 274, 302-CO; 245, 302-C_4H_9; 243, 302-C_3H_7O; 272, 302-CH_2O; 191, 302-side chain. No serious attempt was made to isolate polyalkylated materials.

Exo-6-(1',2'dihydroxyheptyl)-bicyclo[3.1.0]-hexan-3-one (20)

Exo-6-(1'-heptenyl)-bicyclo[3.1.0]hexan-3-one **7** (5.0 mmol) was dissolved in 25 ml ice cold 97–98% formic acid buffered with 25 mmol sodium carbonate (26) in a 100 ml three-necked flask fitted with a magnetic stirrer. The solution was cooled to 0° in an ice water bath and 5 mmol hydrogen peroxide as a 30% solution was added with stirring. The solution was brought to room temperature and stirred for 30 to 40 min under a stream of nitrogen. The formic acid was then stripped off *in vacuo* and the residue was dissolved in 80 ml of methanol. To this was added with stirring 18 g sodium carbonate dissolved in 50 ml water and the suspension was stirred at room temperature for three hours. The mixture was then acidified with 3 *N* hydrochloric acid, diluted with water, and extracted with methylene chloride in the usual manner. The yield of the diol **20** was 85%: i.r. (CCl_4) 3620, 3590 (OH), 3030 (CH, cyclopropyl), 1745 (C=O), 1060 cm^{-1} (C—O).

Exo-6-(1',2'ditrichloroacetoxyheptyl)-bicyclo[3.1.0]-hexan-3-one (21)

Anhydrous pyridine (20 ml) was placed into a 50 ml three-necked flask fitted with a magnetic stirrer, gas inlet and outlet, and a thermometer. The pyridine was cooled to 0° in an ice-water bath and trichloroacetyl chloride (20 mmol) was added. The diol **20** (4 mmol), dissolved in

[7]This compound was generously supplied by the Upjohn Company, Kalamazoo, Michigan.

Can. J. Chem. Downloaded from www.nrcresearchpress.com by 210.87.254.6 on 09/05/12
For personal use only.

5 ml pyridine, was added at such a rate that the temperature did not go above 10°. The mixture was stirred at 0° for 2 h. The reaction mixture was then poured onto crushed ice and extracted with methylene chloride in the usual way. The pyridine was stripped off *in vacuo* and the ditrichloroacetate **21** was obtained in 95% yield: i.r. (CCl_4) 1768 (C=O, acetate), 1748 (C=O, ketone), 3035 (CH, cyclopropyl), 1223 cm^{-1} (C—O—C); n.m.r. (CCl_4) δ 5.31(m, 1H, C_7H—O), 4.77(m, 1H, C_6H—O).

Anal. Calcd. for $C_{17}H_{20}O_5Cl_6$: C, 39.45; H, 3.87; Cl, 41.00. Found: C, 39.83; H, 3.80; Cl, 40.09.

*Example of a Solvolysis of Ditrichloroacetate (**21**) in Trichloroacetic Acid*

A 25 ml three-necked flask was fitted with a magnetic stirrer, stopcock adapter (nitrogen inlet), and condenser. The system was flushed with nitrogen and 1.5 g anhydrous trichloroacetic acid was added. The acid was heated to 60–65° and the ditrichloroacetate (6.0 mg), dissolved in a few drops of THF, was added. After 5 min the reaction mixture was cooled, diluted with ether, and poured onto crushed ice. The ether was separated and the aqueous layer was extracted with ether. The combined ether fractions were washed with 5% sodium bicarbonate, water, and dried over magnesium sulfate. The ether was then filtered and concentrated. The product was spotted on a silica gel t.l.c. plate along with the starting material and eluted with benzene–ether 7:3. The rest of the product was diluted with methanol and a portion heated in 0.5% sodium hydroxide in methanol at 50° for 10 min and a u.v. spectrum was taken of the sample before and after the base treatment.

*Exo-6-(1'2'dibromoheptyl)-bicyclo[3.1.0]hexan-3-one (**23**)*

The bicyclic ketone **7** (3.1 mmol) was dissolved in 40 ml anhydrous chloroform in a 100 ml three-necked flask. Under a stream of nitrogen 1 equiv of pyridinium hydrobromide perbromide (15) was added to the magnetically stirred solution at room temperature over a period of 20 min. The pyridinium salt gradually disappeared leaving a yellow solution. The chloroform solution was then washed with water, dried over magnesium sulfate, filtered, and concentrated. The crude product was chromatographed on a silica gel column (30 g) eluting with hexane – ethyl acetate mixtures.

The dibromide **23** was obtained in 55% yield: i.r. (CCl_4) 3040 (CH, cyclopropyl), 1748 (C=O) 1140 cm^{-1} (C—C—C, ketone); n.m.r. (CCl_4) δ 4.18(m, 1H, C_7H), 3.72(m, 1H, C_6H).

*Solvolysis of the Dibromide **23***

The dibromide **23** (200 mg) was placed in a 50 ml flask with 30 ml of acetone–water 2:1 mixture. The solution was stirred at room temperature for 112 h. After this time the solution was diluted with water and extracted with chloroform in the usual manner. The crude products were then separated by preparative t.l.c. using benzene–ether 7:3 as solvent system. The mixture consisted of the following components:

(*1*) Starting dibromide **23** (R_f 0.86), recovered as the major component (63%), was identified by t.l.c. (benzene–ether 7:3): i.r. (CCl_4) 3040 (CH, cyclopropyl), 1748 (C=O), 1140 cm^{-1} (C—C—C, ketone).

(*2*) Bromohydrin (**26***a*) (R_f 0.39), isolated in 15% yield: i.r. (CCl_4) 3620, 3565, 3480 (OH), 3040 (CH, cyclopropyl), 1748 (C=O), 1140, 1060 cm^{-1} (C—O). Mass spectrum: M^+ 291, 289 for ^{81}Br and ^{79}Br respectively; *m/e* 271, 273, M^+-H_2O; 260, 262, M^+-HCO; 210, M^+-Br; 209, M^+-HBr; 191, 271-^{79}Br, 273-^{81}Br; 181, 260-^{79}Br, 262-^{81}Br; 81, ^{81}Br; 79, ^{79}Br.

(*3*) Mixtures of four components (R_f 0.02–0.05) obtained in 5% yield could not be characterized because of lack of material.

*Exo-6-(1'-bromo-2'-hydroxyheptyl)-bicyclo[3.1.0]-hexan-3-one (**26***a*)*

This compound was prepared according to the procedure of Guss and Rosenthal (16). The bicyclic ketone **7** (5.21 mmol) was mixed with 95% *N*-bromosuccinimide (5.25 mmol) in 25 ml water at room temperature. The reaction was stirred until all the solid *N*-bromosuccinimide had disappeared (4 h). The usual work-up in chloroform followed by column chromatography on silica gel (30 g, benzene–ether mixture elutions) gave the bromohydrin **26***a* in 60% yield.

Anal. Calcd. for $C_{13}H_{21}O_2Br$: C, 53.97; H, 7.26; Br, 27.28. Found: C, 53.90; H, 7.40; Br. 27.50.

*6-(2'-Bromo-1-oxoheptanyl)-bicyclo[3.1.0]hexan-3-one (**27***a*)*

The bromohydrin **26***a* (200 mg) was dissolved in 20 ml acetone in a 50 ml flask. The solution was cooled in an ice-water bath and stirred magnetically. A slight molar excess of Jones reagent was added dropwise and the solution was stirred for 20 min at 0°. After this time, the mixture was diluted in water and extracted with ether in the usual way. The diketo bromide **27***a* was obtained in 80% yield: i.r. (CCl_4) 3045 (CH, cyclopropyl), 1748 (C=O, ring ketone), 1700 cm^{-1} (C=O, ketone α to cyclopropyl ring); n.m.r. (CCl_4) δ 4.27(t, 1H, J = 6.5 Hz, CHBr adjacent to CH_2).

*Exo-6-(1'-iodo-2'-isocyanoheptyl)-bicyclo[3.1.0]hexan-3-one (**24**)*

This compound was prepared according to the procedure of Hassner *et al.* (20). The silver isocyanate was freshly prepared before the reaction (20, 34). The bicyclic ketone **7** (5.21 mmol) was dissolved in 25 ml anhydrous ether in a 100 ml three-necked flask fitted with a nitrogen inlet, thermometer, gas outlet, and magnetic stirrer. The flask was cooled in an ice-salt bath to −10° and silver isocyanate (15.6 mmol) was added with stirring. The reaction mixture was then cooled to −14° and iodine (5.3 mmol) was added. The solution became dark purple. It was then stirred 2 h in the cold and another 6 h at room temperature. By this time the color of the solution was canary yellow. The silver salts were then filtered through celite and the ether was removed in the cold *in vacuo*. The yield of the iodo isocyanate was 75%: i.r. (CCl_4) 3030 (CH, cyclopropyl), 2245 (NCO, v. strong), 1748 cm^{-1} (C=O).

*Hydrolysis and Nitrous Acid Deamination of Iodoisocyanate (**24**)*

The iodoisocyanate (**24**) (75 mg) was placed in a 50 ml three-necked flask fitted with a magnetic stirrer, nitrogen inlet and outlet, and thermometer. The flask was cooled to −10° in an ice-salt bath and 10 ml of aqueous acetone

Can. J. Chem. Downloaded from www.nrcresearchpress.com by 210.87.254.6 on 09/05/12
For personal use only.

(30% water) was added to hydrolyze the isocyanate. The solution was then cooled to −8° and sodium nitrite (4.7 mmol) was added in 1 ml water followed by formic acid (4.7 mmol). The solution was stirred at 0° for 1 h and then 3.5 h at room temperature. The reaction mixture was then diluted with water and extracted with ether in the usual way. Purification by preparative t.l.c. (benzene–ether 7:3) gave the iodohydrin **27***b* in approximately 60% yield: i.r. (CCl_4) 3545, 3520, 3460 (OH), 3035 (CH, cyclopropyl), 1743 (C=O), 1137 (C—C—C, ketone), 1060 cm^{-1} (C—O); n.m.r. (CCl_4) 100 MHz δ 4.19(m, 1H, C*H*—O), 3.22(m, 1H, C*H*I), 0.59(m, C*H*, cyclopropyl). Mass spectrum: M^+ 336; *m/e* 318, M^+-H_2O); 308, M^+-CO; 209, M^+-I; 191, 318-I; 181, 308-I.

Exo-6-(2′-iodo-1′-oxoheptanyl)-bicyclo[3.1.0]hexan-3-one (27b)

The iodohydrin **26***b* (60 mg), obtained from the hydrolysis and deamination of the iodoisocyanate **24**, was oxidized with Jones reagent by the same procedure as described for the oxidation of the bromohydrin (**26***a*). The resulting diketoiodide **27***b* was obtained in 80% yield: i.r. (CCl_4) 3030 (CH, cyclopropyl), 1745 (C=O, ring ketone), 1695 cm^{-1} (C=O, ketone α to cyclopropyl group); n.m.r. (CCl_4) 100 MHz δ 4.48(t, 1H, J = 4.0 Hz, C*H*I adjacent to CH_2).

Exo-6-(1′,2′-dihydroxyheptyl)-2α and β-(6″-Carbomethoxy-2″-hexynyl)-bicyclo[3.1.0]-hexan-3-one (10a)

The bicyclic keto ester **9** was treated with performic acid in buffered formic acid (26) in the same way as the unalkylated ketone **7**. The diol **10***a* was obtained in 87% yield: i.r. (film) 3440 (OH); 3035 (CH, cyclopropyl), 1740 (C=O, ketone and ester), 1165 (C—O—C, ester) 1065 cm^{-1} (C—O, alcohol); n.m.r. ($CDCl_3$) δ 3.69(s, 3H, O*CH*$_3$), 3.7–2.7(m, 4H, C*H*—O and O*H*). Mass spectrum: M^+ 364; *m/e* 333, M^+-OCH_3; 305, M^+-CO_2CH_3; 225, M^+-$CH_2C{\equiv}C(CH_2)_3CO_2CH_3$; 263, M^+-C_5H_{11}-OH; 293, M^+-C_5H_{11}; 289, M^+-C_4H_8; 346, M^+-H_2O; 315, 346-OCH_3.

Exo-6-(1′,2′-dimesyloxyheptyl)-2α and β-(6″-Carbomethoxy-2″-hexynyl)-bicyclo[3.1.0]-hexan-3-one (10b)

A 50 ml round bottom flask was fitted with a stopcock adapter, thermometer, gas outlet, and a magnetic stirrer. Anhydrous pyridine (10 ml) was added to the flask and it was cooled to −15° in an ice-salt bath. A molar excess of methanesulfonyl chloride (3.26 mmol) was added to the stirred solution under nitrogen. After the temperature was again −15°, the diol **10***a* (1.20 mmol) in 5 ml pyridine was added. The reaction was stirred in the cold for 3 h and then kept at −10° overnight. The cold reaction mixture was then poured onto crushed ice, saturated with sodium chloride, and extracted with ethyl acetate in the usual way. The ethyl acetate was evaporated *in vacuo* at room temperature and traces of pyridine were removed on a vacuum pump. The yield of the dimesylate **10***a* was 78–85%: i.r. (film) 3030 (CH, cyclopropyl), 1740 (C=O, ketone and ester), 1350, 1180 cm^{-1} (SO_2); n.m.r. ($CDCl_3$) δ 4.83(m, 1H, C_7H), 4.30(m, 1H, C_6H), 3.65 (s, 3H, O*CH*$_3$), four singlets: 189.8, 189.1, 188.0, 187.2 Hz (6H, SO_2CH_3).

Solvolysis of the Dimesylate (10b)

A solution of the dimesylate **10***b* (380 mg) in 20 ml acetone–water (2:1) was stirred in a nitrogen atmosphere at room temperature for 36 h.[8] The mixture was then diluted with water and extracted with methylene chloride. The methylene chloride extract was dried over anhydrous sodium sulfate, filtered, and concentrated. The reaction products were separated by preparative t.l.c. on silica gel using ethyl acetate as the solvent system. The components of the mixture were detected on the t.l.c. plates in the following manner: silica gel HF 254 (E. Merck) was used which enabled the detection of the hydroxy mesylate bands on the plates by means of short wavelength u.v. light. The prostaglandin bands could be detected only by spraying with 10% phosphomolybdic acid in ethanol, a destructive process. In order to recover the prostaglandins, a small part of the mixture was sacrificed for detection purposes and applied on a 4 × 10 cm plate. The remainder was spread on 20 × 20 cm plates and separated by measuring the R_f obtained from the small plate. This made the separation difficult since the bands did not travel uniformly.

The silica gel was extracted a few times with methanol. The methanol was then evaporated and the residue was taken up in methylene chloride, dried over sodium sulfate, and filtered through celite. The recovery by this procedure was better than 95%.

The components of the reaction mixture separated on the t.l.c. plates are listed below.

(1) Exo-6-(1′-hydroxy-2′-mesyloxyheptyl)-2-(6′-carbomethoxy-2″-hexynyl)-bicyclo[3.1.0]-hexan-3-one (13)

This compound was obtained in 70–80% yield from the starting dimesylate **10***b*. Three hydroxymesylates were obtained (R_f 0.62, 0.48, 0.37). The latter (R_f 0.37) was obtained only in small amounts and could not be obtained pure for proper characterization. The first two (R_f 0.62, 0.48) had identical i.r. and n.m.r. spectra. Both gave the same prostaglandin mixture on recyclizing, therefore no stereochemical assignment could be made: i.r (film) 3475 (OH), 3030 (CH, cyclopropyl), 1740 (C=O, ketone and ester), 1355, 1180 (SO_2), 1070 cm^{-1} (C—O); n.m.r. ($CDCl_3$) 100 MHz δ 4.72(m, 1H, C*H*, mesylate), 3.68(s, 3H, O*CH*$_2$), 3.34(m, 1H, C*H*, alcohol), 3.09, 3.07(s, 3H, SO_2CH_3), 0.64(m, C*H*, cyclopropyl).

(2) 8α and 8β-5-Dehydro-15-epi-PGE$_2$ Methyl Ester 12 (R_f 0.29)

This was obtained in 5–8% yield from the starting dimesylate **10***b*: i.r. (film) 3440 (OH). 1740 (C=O, ester and ketone), 1170 (C—O—C, ester), 1070 cm^{-1} (C—O); n.m.r. ($CDCl_3$) 100 MHz δ 5.9–5.2(m, 2H, *HC*=C*H*), 4.1(m, 2H, C*H*—O), 3.66(s, 3H, O*CH*$_3$). Mass spectrum: *m/e* 346, M^+-H_2O; 328, M^+-$2H_2O$; 315, M^+-H_2O, OCH_3; 297, M^+-$2H_2O$, OCH_3; 317, M^+-H_2O, HCO; 293, M^+-C_5H_{11}; 285, M^+-$2H_2O$, C_3H_7; 275, M^+-H_2O, C_5H_{11}; 207, M^+-H_2O, $C_8H_{11}O_2$ (ester side chain).

(3) 8α and 8β-5-Dehydro-PGE$_2$ Methyl Ester 11 (R_f 0.19)

This was obtained in 5–8% yield from the starting dimesylate **10***b*: i.r. (film) 3400 (OH), 1740 (C=O ketone,

[8]In another run lasting 24 h, similar results were obtained.

Can. J. Chem. Downloaded from www.nrcresearchpress.com by 210.87.254.6 on 09/05/12
For personal use only.

ester), 1163 (C—O—C, ester), 1080 cm^{-1} (C—O); n.m.r. ($CDCl_3$) 100 MHz δ 5.9–5.2(m, 2H, *HC*=C*H*), 4.1 (m, 2H, C*H*—O), 3.68(s, 3H, OCH_3). Mass spectrum: *m/e* 346, M^+-H_2O. The fragmentation was identical with that of the 15-epi-5-dehydro PGE_2 methyl ester **12**.

Anal. Calcd. for $C_{21}H_{32}O_5$: C, 69.12; H, 8.79. Found: 69.02; H, 8.83.

*PGE_2 and 8-iso PGE_2 Methyl Ester **15***

5-Dehydro PGE_2 and 8-iso PGE_2 methyl ester **11** (10.3 mg) was placed in a sample cup with a small amount of ethyl acetate. Lindlar catalyst (32) (75 mg) was placed in a micro-hydrogenation flask and connected to a low pressure hydrogenation apparatus (35). Ethyl acetate (3 ml), containing 1 mg quinoline,[9] was added to the flask, and the mixture was hydrogenated for 4 h. The solution was filtered through celite and the solvent was evaporated *in vacuo*. The crude products were chromatographed on silica gel (t.l.c.) using ethyl acetate solvent system. The PG band was detected and extracted as was previously described. The isomeric mixture of **15** was obtained in 63% yield: n.m.r. ($CDCl_3$) 100 MHz δ 5.62 (m, 2H, *trans HC*=C*H*), 5.38(m, 2H, *cis HC*=C*H*), 4.1 (m, 2H, C*H*—O), 3.70(s, 3H, OCH_3).

Mass spectrum: *m/e* 348, M^+-H_2O; 330, M^+-$2H_2O$; 317, M^+-H_2O, OCH_3; 316, M^+-$3H_2O$, CH_3OH; 299, M^+-$2H_2O$, OCH_3; 298, M^+-$2H_2O$, CH_3OH; 299, M^+-C_5H_{11}; 277, M^+-H_2O, C_5H_{11}; 208, M^+-H_2O, $C_8H_{12}O_2$ (ester side chain with hydrogen transfer); 190, M^+-$2H_2O$, $C_8H_{12}O_2$.

*15-Epi-PGE_2 and 15-Epi-8-iso PGE_2 Methyl Ester **16***

The hydrogenation on 15-epi-5-dehydro PGE_2 and 15-epi-8-iso-5-dehydro PGE_2 methyl ester **12** was carried out in the same way as described for **11**. Because of lack of material, an n.m.r. spectrum could not be taken. Mass spectrum: *m/e* 348, M^+-H_2O. Mass measurement found: 348.229694; calcd. for $C_{21}H_{32}O_4$: 348.230045; other possible empirical formulae for this mass are: $C_{16}H_{32}N_2O_6$, $C_{19}H_{30}N_3O_3$, and $C_{24}H_{30}NO$. These are ruled out because **16** could not contain any nitrogen. Mass measurement of *m/e* 190: 190.135990; calcd. for $C_{13}H_{18}O$, 190.135758; another possible empirical formula for this mass is $C_{11}H_{16}N_3$ which is again ruled out because **16** contains no nitrogen.

Anal. Calcd. for $C_{21}H_{34}O_5$: C, 68.85; H, 9.23. Found: C, 70.12; H, 9.94.

*Epimerization of the Isomeric Mixture of **15***

The PGE_2 and 8-iso PGE_2 methyl ester mixture **15** (6.3 g) was dissolved in 3 ml of a 3% ethanolic potassium acetate solution and stirred at room temperature for 94 h. The reaction mixture was then diluted with water and extracted with pure methylene chloride. The organic layer was dried over anhydrous magnesium sulfate, filtered, and concentrated *in vacuo*. Preparative t.l.c. separation of the crude mixture on silica gel, using ethyl acetate as the solvent system, gave two compounds:

(*1*) PGA_2 methyl ester **18** made up 18% (0.7 mg) of the reaction mixture: u.v. (MeOH) 217 mμ, ε 9000; mass spectrum: M^+ 348, *m/e* 330, M^+-H_2O; 317, M^+-OCH_3; 299, 330-OCH_3; 298, 330-CH_3OH; 287, 330-C_3H_7; 190, 330-$C_7H_{10}CO_2CH_3$ + H-transfer); 207, M^+-$C_7H_{10}CO_2$-CH_3; 141, $[C_7H_{10}CO_2CH_3]^+$. The PGA_2 methyl ester was contaminated with about 2% PGB_2 methyl ester **19**: u.v. (MeOH) 277 mμ, ε 2200.

(*2*) PGE_2 methyl ester **17** made up 80% (2.9 mg) of the reaction mixture: 100 MHz n.m.r. ($CDCl_3$) using 109 scans which were analyzed with a computer of average transients (c.a.t.): δ 5.6(m, 2H, *trans HC*=C*H*), 5.3(m, 2H, *cis HC*=C*H*), 4.1(m, 2H, C*H*—O) 3.6(s, 3H, OCH_3). Accurate chemical shifts were not obtained because of drifting in the spectrometer. Mass spectrum: *m/e* 348, M^+-H_2O; the spectrum was identical to the PGE_2 methyl ester spectrum taken before epimerization. Because of the small amount of material, a good elemental analysis could not be obtained. However, from the spectral data and bioassay results, there was no doubt that this compound was *d,l*-PGE_2 methyl ester.

[9]More than 3% quinoline, by weight, to the amount of catalyst makes the reaction very slow. Best results were obtained using 1–2% quinoline.

We wish to thank the Upjohn Company, Kalamazoo, Michigan for generous samples of 6-exo-(1′-heptenyl)-bicyclo[3.1.0]hexan-3-one (7) and comparison samples of α- and β-isomers of 6-exo-(1′-heptenyl)-2-(6″-carbomethoxyhexyl)-bicyclo[3.1.0]hexan-3-one (**iii***a* and *b*) and natural PGE_2.

We wish to thank Dr. L. Wolfe of the Montreal Neurological Institute and Dr. J. R. Weeks of the Upjohn Company for carrying out the bioassays.

Financial assistance by the National Research Council of Canada and the Upjohn Co. is gratefully acknowledged.

1. (*a*) G. Just and Ch. Simonovitch. Tetrahedron Lett. 2093 (1967); (*b*) W. P. Schneider, U. Axen, F. H. Lincoln, J. E. Pike, and J. L. Thompson. J. Amer. Chem. Soc. **90**, 5095 (1968); (*c*) G. Just, Ch. Simonovitch, F. H. Lincoln, W. P. Schneider, U. Axen, J. B. Spero, and J. E. Pike. J. Amer. Chem. Soc. **91**, 5364 (1969); (*d*) E. J. Corey, N. H. Anderson, R. M. Carlson, J. Paust, E. Vedejs, I. Vlattas, and R. E. K. Winter. J. Amer. Chem. Soc. **90**, 3245 (1968); (*e*) E. J. Corey, I. Vlattas, N. H. Anderson, and K. Harding. J. Amer. Chem. Soc. **90**, 3247 (1968); (*f*) E. J. Corey, I. Vlattas, and K. Harding. J. Amer. Chem. Soc. **91**, 535 (1969); (*g*) W. P. Schneider. Chem. Commun. 304 (1969); (*h*) E. J. Corey, N. M. Weinshenker, T. K. Schaat, and W. Huber. J. Amer. Chem. Soc. **91**, 5675 (1969); (*i*) E. J. Corey, T. K. Schaaf, W. Huber, U. Koelliker, and N. M. Weinshenker. J. Amer. Chem. Soc. **92**, 397 (1970); (*j*) E. J. Corey, Z. Arnold, and J. Hutton. Tetrahedron Lett. 307 (1970); (*k*) E. J. Corey and R. Noyori. Tetrahedron Lett. 311 (1970); (*l*) U. Axen, J. L. Thompson, and J. E. Pike. Chem. Commun. 602 (1970).
2. (*a*) J. F. Bagli, T. Bogri, R. Dehenghi, and K. Wiesner. Tetrahedron Lett. 465 (1966); (*b*) J. F. Bagli and T. Bogri. Tetrahedron Lett. 5 (1967); (*c*) P. F. Beal, III, J. C. Babcock, and F. H. Lincoln. J. Amer. Chem. Soc. **88**, 3131 (1966); (*d*) E. Hardegger, H. P. Schenk, and E. Broger. Helv. Chim. Acta, **50**, 2501 (1967); (*e*) J. Fried, S. Heim, S. J. Etheredge, P. Sunder-Plassmann, T. S. Santahana Krishanan, J. I. Himizer, and C. H. Lin. Chem. Commun. 634 (1968); (*f*) J. F. Bagli and T. Bogri. Tetrahedron Lett. 1639 (1969).

3. M. D. D'ENGENIERES, M. MIOCQUE, and J.-A. GAUTIER. Bull. Soc. Chim. Fr. 1370, 2477 (1964).
4. A. W. D. AVISON and A. L. MORRISON. J. Chem. Soc. 1473 (1950).
5. A. I. VOGEL. Practical organic chemistry. 3rd Edition. Longmans.
6. L. CROMBIE and A. J. JACKLIN. J. Chem. Soc. 1622 (1957).
7. D. ROSENTHAL, P. GRABOWICH, E. M. F. SABO, and J. FRIED. J. Amer. Chem. Soc. **85**, 3971 (1963).
8. P. R. BIRD and J. S. CHADHA. Tetrahedron Lett. 4541 (1966).
9. CH. SIMONOVITCH. Ph.D. Thesis, McGill University, Montreal, Quebec, 1967.
10. (*a*) K. B. WIBERG and A. J. ASHE, III. Tetrahedron Lett. 1553 (1965); (*b*) K. B. WIBERG and A. J. ASHE, III. J. Amer. Chem. Soc. **90**, 63 (1968).
11. K. G. HOLDEN, B. HWANG, K. R. WILLIAMS, J. WEINSTOCK, M. HARMAN, and J. A. WEISBACH. Tetrahedron Lett. 1569 (1968).
12. (*a*) D. D. ROBERTS. J. Org. Chem. **30**, 23 (1965); (*b*) W. D. CLOSSEN and G. T. KWAITKOWSKI. Tetrahedron, **21**, 2779 (1965); (*c*) E. F. COX, M. C. CASERIO, M. S. SILVER, and J. D. ROBERTS. J. Amer. Chem. Soc. **83**, 2719 (1961); (*d*) H. HART and J. M. SANDRI. J. Amer. Chem. Soc. **81**, 320 (1959); J. Amer. Chem. Soc. **84**, 2462 (1962); (*e*) K. L. SERVICE and J. D. ROBERTS. J. Amer. Chem. Soc. **86**, 3773 (1964); (*f*) M. HANACK and H.-J. SCHNEIDER. Tetrahedron, **20**, 1863 (1964); (*g*) M. HANACK and H.-J. SCHNEIDER. Angew. Chem. Int. Ed. **3**, 698 (1964); (*h*) M. HANACK and H.-J. SCHNEIDER. Ann. **686**, 8 (1965).
13. (*a*) M. HANACK and H.-J. SCHNEIDER. Angew. Chem. Int. Ed. **6**, 666 (1967); (*b*) H. M. WALBORSKY and L. PLONSHER. J. Amer. Chem. Soc. **83**, 2138 (1961).
14. J. T. LUMB and G. H. WHITHAM. J. Chem. Soc. (C), 216 (1967).
15. L. F. FIESER and M. FIESER. Reagents for organic synthesis. John Wiley and Sons, Inc., New York, N.Y., 1967. p. 967.
16. C. O. GUSS and R. ROSENTHAL. J. Amer. Chem. Soc. **77**, 2549 (1955).
17. K. BOWDEN, I. M. HEILBRON, E. R. H. JONES, and B. C. L. WEEDON. J. Chem. Soc. 39 (1946).
18. E. S. GOULD. Mechanism and structure in organic chemistry. Holt, Rinehart, and Winston, New York, N. Y. 1959. p. 261.
19. R. H. MAZUR, W. N. WHITE, D. A. SEMENOW, C. C. LEE, M. S. SILVER, and J. D. ROBERTS. J. Amer. Chem. Soc. **81**, 4390 (1959).
20. A. HASSNER and C. HEATHCOCK. J. Org. Chem. **30**, 1748 (1965).
21. P. V. R. SCHLEYER and G. W. VAN DINE. J. Amer. Chem. Soc. **88**, 2321 (1966) and references therein.
22. S. WINSTEIN and M. KOSOWER. J. Amer. Chem. Soc. **81**, 4399 (1959).
23. K. B. WIBERG and J. G. PFEIFFER. J. Amer. Chem. Soc. **90**, 5324 (1968).
24. U. AXEN, F. H. LINCOLN, and J. L. THOMPSON. Chem. Commun. 303 (1969).
25. E. J. COREY, M. OHNO, R. B. MITRA, and P. A. VATAKENCHERRY. J. Amer. Chem. Soc. **86**, 478 (1964).
26. D. SWERN, G. N. BILLEN, T. W. FINDLEY, and J. T. SCANLAN. J. Amer. Chem. Soc. **67**, 1786 (1945).
27. J. W. HINMAN. Biol. Sci. **17**, 779 (1967).
28. E. G. DANIELS, W. C. KRUGER, F. P. KUPIECKI, J. E. PIKE, and W. P. SCHNEIDER. J. Amer. Chem. Soc. **90**, 5894 (1968).
29. S. BERGSTROM, F. DRESSLER, R. RYHAGE, B. SAMUELSSON, and J. SJOVALL. Arkiv. Kemi, **19**, 563 (1962).
30. J. R. WEEKS, J. R. SCHULTZ, and W. E. BROWN. J. Appl. Physiol. **25**, 783 (1968).
31. J. R. WEEKS, N. C. SEKHAR, and D. W. DUCHARME. J. Pharm. Pharmac. **21**, 103 (1969).
32. (*a*) H. LINDLAR. Helv. Chim. Acta, **35**, 446 (1952); (*b*) H. LINDLAR and R. DUBUIS. Org. Syn. **46**, 89 (1966).
33. H. BUDZIKIEWICZ, C. DJERASSI, and D. H. WILLIAMS. Mass spectrometry of organic compounds. Holden-Day, Inc., San Francisco, California, 1967. p. 479.
34. R. G. NEVILLE and J. J. MCGEE. Inorg. Syn., VIII, 23.
35. C. L. OGG and F. J. COOPER. Anal. Chem. **21**, 1400 (1949).

Can. J. Chem. Downloaded from www.nrcresearchpress.com by 210.87.254.6 on 09/05/12
For personal use only.

Can. J. Chem. Downloaded from www.nrcresearchpress.com by 210.87.254.42 on 09/05/12
For personal use only.

Proton Magnetic Resonance Studies of Rotational Isomerism in Halotoluene Derivatives. VI. Rotational Barrier and Conformational Energy Differences in α,α,2,3,6-Pentachlorotoluene

M. A. H. STEWART, T. SCHAEFER, H. M. HUTTON, AND C. M. WONG
Chemistry Department, University of Manitoba, Winnipeg, Manitoba

Received November 12, 1970

Rotation by π radians about the sp^2–sp^3 carbon–carbon bond of the dichloromethyl group in α,α,2,3,6-pentachlorotoluene interconverts the two conformations which are characterized by coplanarity of the aromatic ring with the C—H bond of the sidechain. The ring protons undergo effective nonmutual exchange during this rotation. The rate of rotation as a function of temperature is extracted by line-shape fitting of the ring p.m.r. spectra. The rotation is characterized by a negative entropy of activation. The free energy difference between the two conformations is 50 ± 20 cal/mol at 240 °K.

Une rotation de π radians autour de la liaison carbone–carbone sp^2–sp^3 du groupe dichlorométhyle du pentachloro-α,α,2,3,6 toluène interconvertit les deux conformations qui sont caractérisés par une disposition coplanaire du noyau aromatique et de la liaison C—H du substituant. Les protons du noyau changent leur environnement magnétique durant cette rotation et on peut obtenir la vitesse de rotation en fonction de la température par une simulation de la forme de raie du spectre de résonance magnétique. Cette rotation est caractérisée par une entropie d'activation négative. La différence d'énergie libre entre les deux conformations est 50 ± 20 cal/mol à 240 °K.

Canadian Journal of Chemistry, 49, 1085 (1971)

Introduction

Barriers to rotation about the sp^2–sp^3 carbon–carbon bond in α,α,2,4,6-pentachlorotoluene (PCT), α,α-dichloro-2,4,6-tribromotoluene (DCTBT), and α,α,α′,α′,2,3,5,6-octachloro-*p*-xylene (POCX) are known from line-shape analyses of rate dependent p.m.r. spectra (1–4). In all these molecules, rotation of the dichloromethyl group(s) causes effective mutual exchange of either the ring or methine protons. Semiempirical barrier calculations are also documented for model compounds of this series (4, 5). When the dichloromethyl group rotates through 180° in α,α,2,3,6-pentachlorotoluene (3PCT), conformation **1** is converted to **2** but, in contrast to PCT for example, nonmutual exchange of ring proton shifts

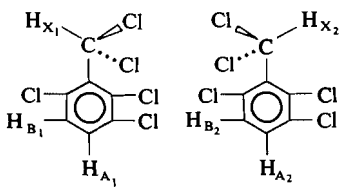

1 **2**

occurs. Thus B_1 exchanges with B_2, A_1 with A_2 so that at fast rates the ring proton spectrum becomes the AB part of an ABX spectrum. The shifts of the methine proton in **1** and **2** are not equal, in contrast to the corresponding conformations of PCT (1), nor are the populations of **1** and **2** the same.

By means of the computer program DNMR2 (6, 7) the rate-dependent p.m.r. spectra of 3PCT can be fitted to the rate constants for the hindered rotation of the dichloromethyl group. The spectral behavior is different than for the compounds above, providing a relatively independent check on the barriers obtained for the latter. In addition any buttressing effect of the chlorine atom at position 3 should become apparent. The solvent toluene-d_8 is used in this study because it causes sufficiently large solvent shifts of the ring proton resonances allowing an unambiguous assignment of resonance peaks to the four effectively different ring protons.

Experimental

The 3PCT was prepared by free radical chlorination of 2,3,6-trichlorotoluene in a manner similar to that described for PCT (1). It was dissolved as a 20 mol % solution in toluene-d_8, containing internal tetramethylsilane (TMS) as reference and lock signal. After careful degassing, p.m.r. spectra were taken at different temperatures on a DA60I spectrometer by the procedure described for PCT (1). More dilute solutions presented intolerable signal to noise problems while more concentrated solutions precipitated 3PCT at unacceptably high temperatures. Proton assignments could not be made in those other solvents which presented no solubility problems at temperatures necessary to the experiment. The temperatures were accurate to at least 1 °K and relative temperatures to better than 0.5 °K (3).

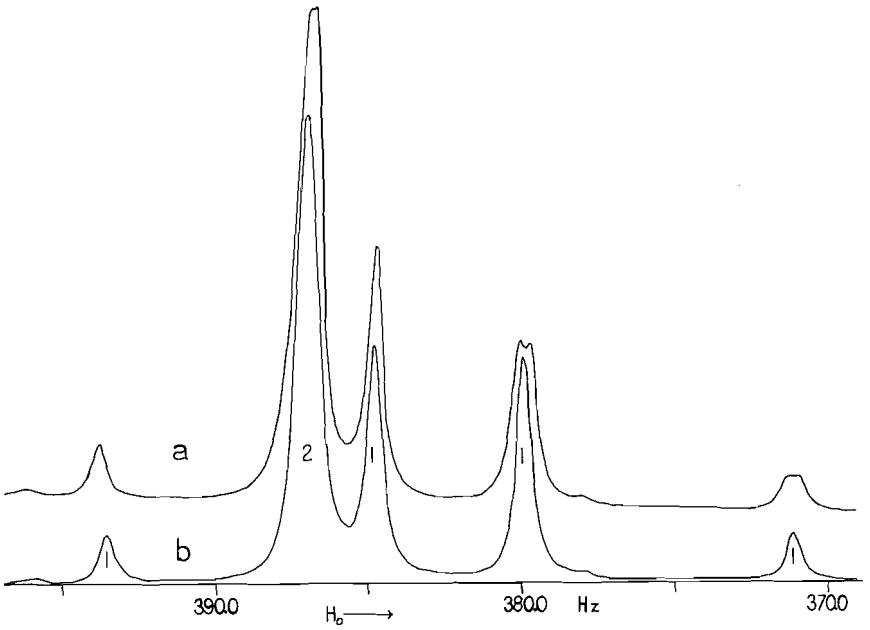

FIG. 1. In the upper part, *a*, the ring proton resonance spectrum of α,α,2,3,6-pentachlorotoluene at 255 °K is calculated on the assumption that conformation **2** of the text corresponds to the well defined quartet centered at high field and marked 1. In the lower part, *b*, it is assumed that this quartet corresponds to conformation **1** of the text. The latter agrees with the experimental spectrum in Fig. 3A.

Results and Discussion

(1) Assignment of the AB Quartets at Low Temperatures

At 255 °K, rotation of the dichloromethyl group is slow and the ring proton spectrum consists of two AB quartets, weakly coupled to the methine proton (see Fig. 3A). The quartet with an internal shift of 10.4 Hz (J = 8.7 Hz) is assigned to the ring protons of **1**, the quartet with an internal shift of 2.5 Hz (J = 8.9 Hz) to the ring protons of **2**. The assignment rests on the known stereospecificity of the long-range coupling constants between the methine and ring protons in such compounds (1, 8). Thus, in **1** and **2** the coupling over six bonds to H_A is less than −0.1 Hz in magnitude. The coupling over five bonds to H_B in **1** is less than 0.1 Hz but is 0.5 Hz in **2**. Now the proton system in **2** is tightly coupled so that the phenomenon of deceptive simplicity (9) or virtual coupling (10) leads to an effective coupling of roughly [0.5 + (−0.1)]/2 Hz between the ring protons and the methine proton. On the other hand, the ring protons in **1** are not tightly coupled and their resonance should display existing long-range couplings as large as 0.5 Hz. In Figs. 1*a* and *b* the theoretical spectra for the incorrect and correct assignments are displayed (compare with experimental spectrum in Fig. 3A).

(2) Assignment of Peaks at High Temperature

Of course, at this stage the assignment of the individual protons in **2** is still in question. Thus, does the resonance of B_2 lie to high or to low field of A_2? The clue to this question lies in the shape of the collapsed AB spectrum at temperatures where the rotation of dichloromethyl group is rapid. In Fig. 3F the two peaks at high field are broader than the other two at low field. Since the six-bond coupling between the methine proton and proton 4 is unobservable in both conformations (8), while the coupling between the methine proton and proton 5 is 0.5 Hz in **2** and less than 0.1 Hz in **1**, the resonance of the B protons should be 0.2 to 0.3 Hz broader than the resonance of the A protons. The pair of peaks at high field in Fig. 3F is therefore assigned to H_B in the averaged spectrum of **1** and **2**.

(3) Intrinsic Temperature Dependence of the Chemical Shifts

The chemical shifts of the coalesced and of the

Can. J. Chem. Downloaded from www.nrcresearchpress.com by 210.87.254.42 on 09/05/12
For personal use only.

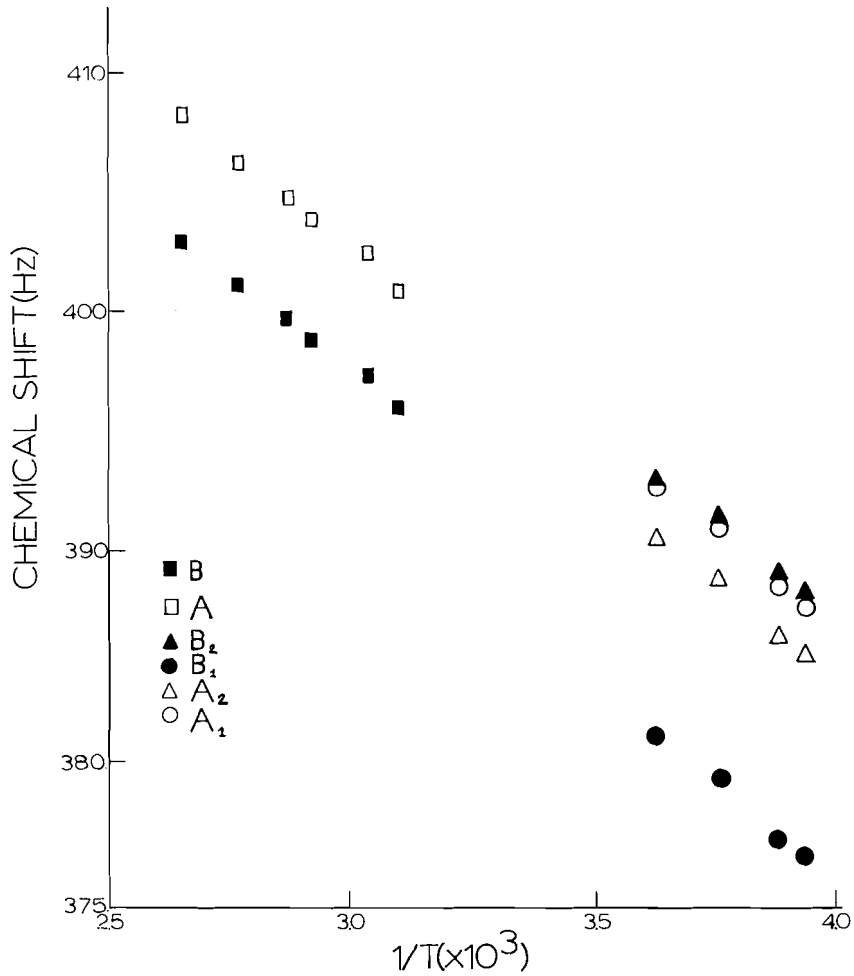

FIG. 2. The observed ring proton chemical shifts of α,α,2,3,6-pentachlorotoluene are plotted *vs.* $1/T$. At low temperatures there are four observable shifts corresponding to protons A_1, A_2, B_1, B_2 of the conformation **1** and **2** of the text. At high temperatures the shifts of A_1 and A_2 and of B_1 and B_2 are averaged by the exchange process to give the shifts marked A and B, respectively. The latter shifts are defined by eqs. 1 and 2 of the text.

uncoalesced spectra of 3PCT in toluene-d_8 are a linear function of $1/T$. In Fig. 2 the two ring proton shifts above coalescence temperatures are plotted *vs.* $1/T$ over a temperature range of 55 °C. The averaged shifts of H_A and H_B relative to internal TMS are given by eqs. 1 and 2 (r = correlation coefficient, T in °K). From eqs. 1 and 2

[1] Shift of H_A in Hz = 453.26 − 16 950 $(1/T)$

$(r = 0.9997)$

[2] Shift of H_B in Hz = 444.75 − 15 760 $(1/T)$

$(r = 0.9997)$.

the internal shift between H_B and H_A can be calculated at a given temperature.

Now at 255 °K, where the four chemical shifts are observed[1] to be 385.7, 387.5, 388.2, and 377.1 Hz, one has four possible assignments of the shifts to the four individual protons, given

[1]The internal shift of the proton resonance in the tightly coupled quartet is not easily obtainable from the spectrum at 60 MHz. However, after the spectral work was complete a 100 MHz instrument became available. At this frequency the internal shift of the quartet was easily measured. This value could then be used together with the position of the intense central peak of the quartet to calculate the chemical shift of the A_2 and B_2 protons.

Can. J. Chem. Downloaded from www.nrcresearchpress.com by 210.87.254.42 on 09/05/12
For personal use only.

Can. J. Chem. Downloaded from www.nrcresearchpress.com by 210.87.254.42 on 09/05/12
For personal use only.

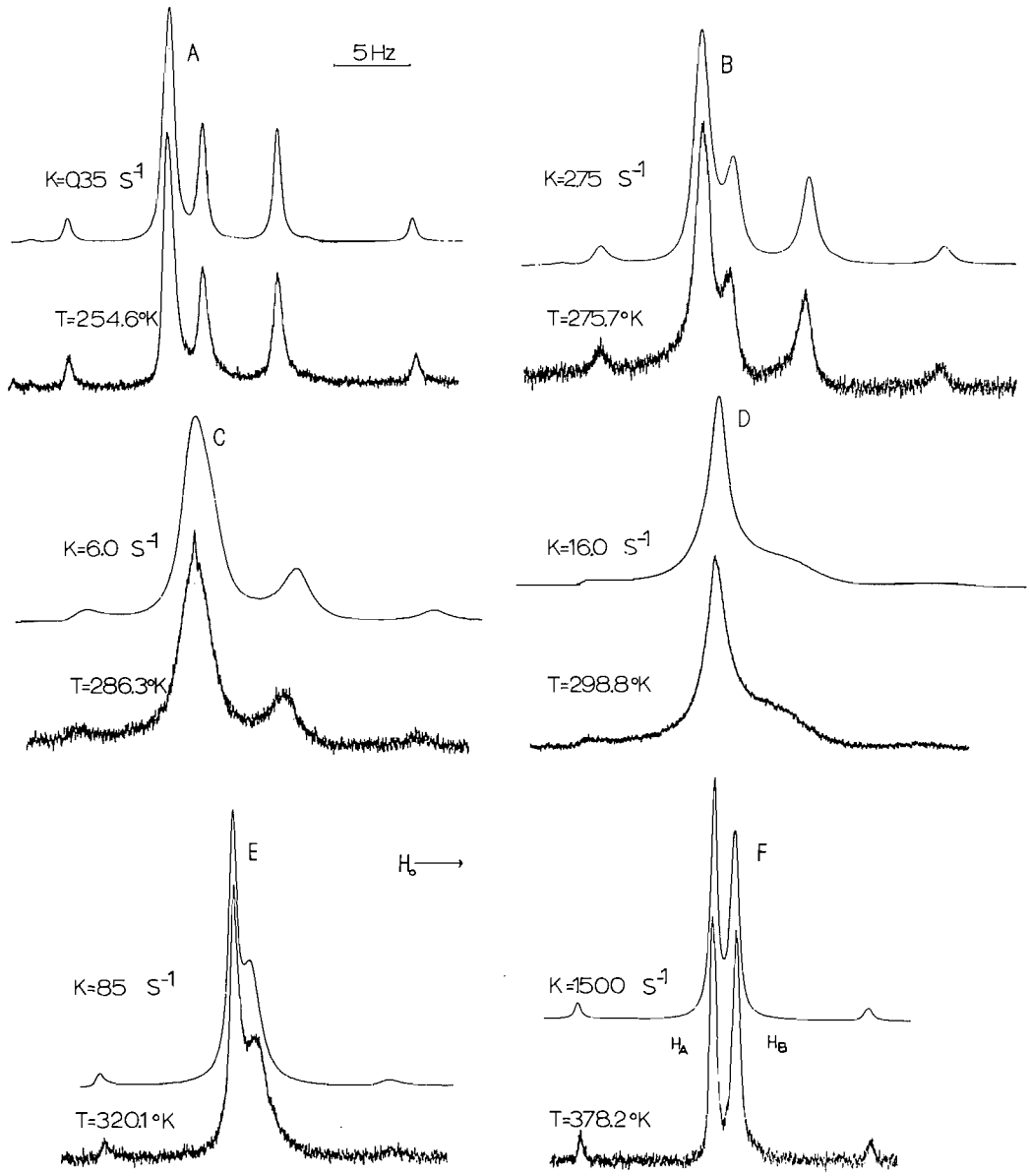

FIG. 3. The observed and calculated ring proton resonance spectra of α,α,2,3,6-pentachlorotoluene are shown at six representative temperatures and rate constants, k, for rotation of the dichloromethyl group.

that the original assignment of the quartets to **1** and **2** is correct. The four observed shifts predict different, averaged internal shifts between H_B and H_A. When population differences are taken into account (see below) the four assignments correspond to averaged internal shifts of $\pm 6.3 \pm 0.3$ and of $\pm 3.7 \pm 0.3$ Hz. Equations 1 and 2 predict this shift to be $+4.1$ Hz and therefore the correct assignment[2] is A_1(387.5 Hz), B_1(377.1 Hz), A_2(385.7 Hz), and B_2(388.2 Hz) at 255 °K.

In Fig. 2 the chemical shifts at temperatures where the exchange rate is slow are also plotted

[2]A detailed rationalization of this assignment in terms of substituent and solvent effects is given in ref. 11.

TABLE 1. Observed and calculated chemical shifts* of the ring protons of α,α,2,3,6-pentachlorotoluene in toluene-d_8 as a function of temperature in the absence of exchange. Rate constants for the conversion of **1** and **2**

Temperature(°K)	$\nu_A(1)$	$\nu_B(1)$	$\nu_A(2)$	$\nu_B(2)$	$k(s^{-1})$
254.6†	387.54	377.14	385.7	388.2	0.35‖
258.0†	388.45	378.01	386.5	389.0	0.80‖
266.7†	390.97	380.47	388.9	391.4	1.5 ±0.25‖
275.7†	392.72	382.15	390.5	393.0	2.75±0.25
281.7‡	394.00	383.39	392.20	394.19	4.25±0.25
284.5	394.59	383.96	392.79	394.72	5.25±0.25
286.3	394.96	384.32	393.16	395.08	6.00±0.25
289.8	395.67	385.00	393.87	395.72	8.7_5±0.5
291.0	395.92	385.22	394.12	395.94	8.7_5±0.5
298.0	397.28	386.53	395.48	397.19	16.0±1.5
301.0	397.85	387.06	395.05	397.70	24.0±2.5
304.5	398.50	387.68	396.70	398.30	31.0±3.0
306.3	398.82	387.98	397.02	398.58	32.5±3.0
309.3	399.36	388.50	397.56	399.08	36.5±4.0
315.5	400.44	389.52	398.64	400.06	56.0±5.0
320.1	401.21	390.26	399.41	400.76	85.0±10
323.5§	401.77	390.78	399.97	401.26	110±15
333.0	403.47	392.16	401.27	403.60	350‖
343.7	404.80	393.60	402.98	404.00	
349.2	405.70	394.50	403.90	404.86	
361.5	407.16	395.91	405.36	406.21	

*In Hz at 60 MHz to low field of internal TMS. The absolute shifts are accurate to about 0.1 Hz but the internal shifts are more accurate.
†Observed from experimental spectra.
‡At this and higher temperatures the shifts are calculated from eqs. 1–3, as explained in the text.
§At this and higher temperatures the means of the two sets of shifts reproduce the observed shift of the A and B protons in the coalesced spectrum to within experimental error.
‖These rate constants were extracted from spectra in which the effective T_2 values contribute substantially to the observed line-shapes and were therefore disregarded when computing activation parameters.

as a function of $1/T$. Between 255 and 276 °K the internal shift between B_1 and B_2 is given by eq. 3. Thus the solvent effect on the shift between these two protons changes by only 0.15 Hz over this temperature range and only by a further 0.3 Hz between 282 and 323 °K. Because the shift between A_1 and A_2 is only about 2 Hz, less than 20% of the shift between B_1 and B_2, the corresponding peaks are relatively insensitive to changes in the exchange rate and hence it is unimportant to correct for its temperature variation. The fitting procedure below concentrated on the line-shape changes observed in the B portion of the spectra.

[3] Internal shift in Hz = $8.43 + 667\,(1/T)\,(r = 0.993)$.

In Table 1 the calculated values of the chemical shifts of the four distinct protons are given. These are the shifts which would be observed as a function of temperature in the absence of exchange and include the temperature-dependent solvent effects. Note that experimental values are given between 255 and 276 °K. Between 323.5° and 361 °K the appropriate means of the shifts in Table 1 reproduce the measured shifts of the quartet observed at high temperatures.

(4) Relative Populations of the Two Conformations

At temperatures below 243 °K the two methine peaks of **1** and **2** are separated sufficiently to allow the determination by weighing of the areas of the two peaks. At 233 °K the substrate crystallizes from solution. At four temperatures in this 10° interval the ratio of the areas was 0.91 ± 06. A similar estimation of the relative intensities of the two AB quartets gave 0.91 ± 0.06 with **2** more abundant than **1** (a determination made when a 100 MHz spectrometer became available gave 0.90 ± 0.06). Extensive overlap of peaks made a more accurate estimation at these and other temperatures impossible.

It seems reasonable that steric interactions among chlorine atoms in **1** will destabilize **1** relative to **2**. The original assignment above is further supported by the fact that the resonance of the methine proton in **2** lies to low field of its resonance in **1**. Steric crowding involving the chlorine substituents at positions 2 and 3 is expected to

Can. J. Chem. Downloaded from www.nrcresearchpress.com by 210.87.254.42 on 09/05/12
For personal use only.

TABLE 2. Activation parameters[a] for the hindered rotation of the dichloromethyl group in 3PCT, POCX, and PCT dissolved in toluene-d_8

Parameter	3PCT[b]	POCX[c]	PCT[d]
E_a (kcal/mol)	13.9±0.2	13.6±0.4	15.2±0.2
log A	11.4±0.2	11.3±0.3	12.7±0.2
ΔH^*(kcal/mol)	13.3±0.3	13.1±0.4	14.6±0.3
ΔS^*(cal/mol deg)	−7.0±0.7	−7.3±1.3	−1.1±0.7
ΔG^*(kcal/mol)	15.4±0.1(298 °K)	15.4±0.1(286 °K)	14.9±0.1(304 °K)

[a]Quoted errors are standard deviations from least square plots.
[b]α,α,2,3,6-Pentachlorotoluene.
[c]α,α,α′,α′,2,3,5,6-Octachloro-*p*-xylene.
[d]α,α,2,4,6-Pentachlorotoluene.

deshield the methine proton more in **2** than in **1** (12).

The free energy difference between **1** and **2** is 50 ± 20 cal/mol at 240 °K. The normalized populations are $P_1 = 0.48$ and $P_2 = 0.52$. For line-shape fitting purposes the normalized populations must be known as a function of temperature. Direct trials showed assumption $P_1 = P_2 = 0.50$ to be indistinguishable from $P_1 = 0.48$ when computing line-shapes in the region of interest between 276 and 323 °C. Therefore $P_1 = 0.48$ was assumed throughout.

A rough calculation (13) of the entropy difference between **1** and **2** was performed as follows. The translational contribution to this difference is zero. The low-frequency vibrations of **1** and **2** are probably very nearly equal and therefore the vibrational contribution is taken as zero. The rotational contribution can be calculated from the products of the principal moments of inertia of **1** and **2**. These turn out to be 4.010×10^{17} amu^{3}Å^6 for **1** and 4.015×10^{17} amu^{3}Å^6 for **2**. The rotational contribution is therefore effectively zero. Hence the free energy difference between **1** and **2** is indicated to be independent of temperature. On this basis, $P_1/P_2 = 0.93$ at 375 °K, well within experimental error of the ratio at 243 °K.

(5) Extraction of Rate Constants and Activation Parameters

Line-shapes were generated by the computer program DNMR2 (7) adapted to an IBM 360/65 computer and were compared visually with the experimental spectra. Input data were $P_1 = 0.48$, $J_{AB} = 8.8$ Hz for both **1** and **2**, $J_{AX} = -0.1$ Hz for both **1** and **2**, $J_{BX} = 0.5$ Hz for **2** and $J_{BX} = 0.1$ Hz for **1**. The four chemical shifts for each rate constant k, were taken from Table 1. Best fits at high and low temperature extremes (narrow peaks) were obtained for an effective T_2 of 0.80 s, this value also being used at intermediate temperatures. Because a wrong T_2 can cause relatively large errors in the extracted rate constants, only those rate constants obtained for rather large line widths were employed in the extraction of activation parameters. Thus in Table 1 only the rate constants between 275.7 and 323.5 °K were so employed.

In Fig. 3 some representative observed and calculated spectra are displayed as an indication of the agreement obtainable between observation and theory. The spectral quality is only fair, a consequence of the relatively low solubility and the high molecular weight of the substrate. Some

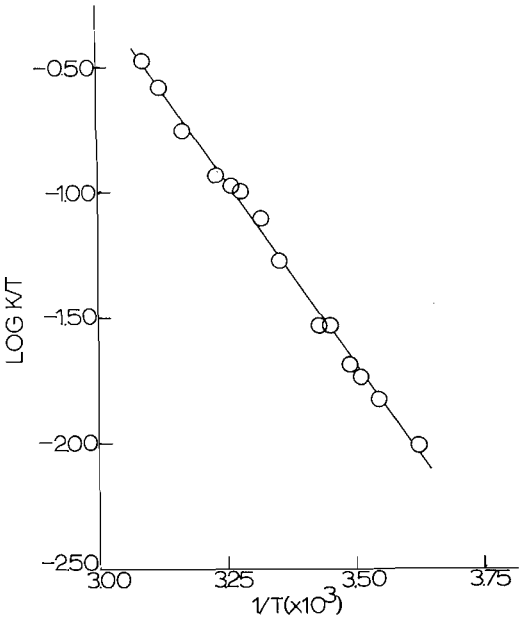

FIG. 4. A plot of log (k/T) *vs.* $1/T$ for the activated rotation of the dichloromethyl group in α,α,2,3,6-pentachlorotoluene. The least squares line for the temperature range from 276 to 324 °K as shown has a correlation coefficient of 0.998.

Can. J. Chem. Downloaded from www.nrcresearchpress.com by 210.87.254.42 on 09/05/12
For personal use only.

of the methine resonances were also fitted but were relatively insensitive to k. In Table 1 the error indicated for k refers to the value which, when added or subtracted to the quoted value of k, yields a computed spectrum clearly incompatible with the observed spectrum.

Activation parameters were derived from least squares plots of $\log k$ and $\log k/T$ *vs.* $1/T$. Figure 4 shows a plot of $\log k/T$ *vs.* $1/T$, $r = 0.997$. Table 2 gives the parameters for 3PCT and also for POCX and PCT. The quoted errors are standard errors. A transmission coefficient of 1/2 was assumed (1, 14).

(6) Discussion of Activation Parameters

The conformations of the dichloromethyl group in 3PCT can be represented as in **3** to **7** (**1** and **2** above correspond to **3** and **7**, respectively). The subscript 2 in these diagrams refers to the two chlorine substituents at ring positions 2 and 3.

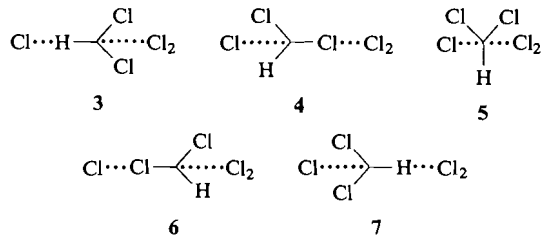

As discussed previously (1, 4) for PCT, **4** and **6** are the high energy (transition state) conformations and **5** lies at least 7 or 8 kcal/mol above the ground state conformations **3** and **7**. Therefore the measured barrier for 3PCT corresponds to the higher [3] of **4** and **6**. Now **3** is a little less stable than **7** because of the enhanced steric interaction or buttressing effect of the chlorine substituents at position 2 and 3 of the ring. It would therefore be sensible to assume that the transition state **4** is of higher free energy than **6**. The measured ΔG^* is 15.4 kcal/mol for both POCX and 3PCT, in agreement with this assumption. $\Delta G^* = 14.9$ kcal/mol for PCT, suggesting $\Delta G_4^* - \Delta G_6^* = 0.5 \pm 0.2$ kcal/mol for 3PCT. This difference evidently arises from increased steric hindrance in **4** causing a more negative ΔS^* than in **6**. If the data in Table 2 can be believed, ΔH^* is somewhat smaller in 3PCT than in PCT. The implication that increased steric hindrance in the transition state can markedly lower the entropy relative to the ground state while somewhat decreasing the internal energy ($\Delta E = \Delta H + P\Delta V$, ΔV very small), is intriguing but speculative. Replacement of the chlorine substituent at position 3 by much bulkier groups is indicated as a test.

[3] A molecule sufficiently activated to pass the lower of **4** or **6** will not be able to pass the higher of **4** or **6** and hence will not cause an effective exchange of the ring protons.

We are grateful to the National Research Council of Canada for financial assistance.

1. B. J. FUHR, B. W. GOODWIN, H. M. HUTTON, and T. SCHAEFER. Can. J. Chem. **48**, 1558 (1970).
2. H. GYULAI, B. J. FUHR, H. M. HUTTON, and T. SCHAEFER. Can. J. Chem. **48**, 3877 (1970).
3. J. PEELING, T. SCHAEFER, and C. M. WONG. Can. J. Chem. **48**, 2839 (1970).
4. B. H. BARBER and T. SCHAEFER. Can. J. Chem. **49**, 789, 1971.
5. B. H. BARBER. M.Sc. Thesis. University of Manitoba, Winnipeg, Manitoba, 1970.
6. G. BINSCH. J. Amer. Chem. Soc. **91**, 1304 (1969).
7. G. BINSCH and D. A. KLEIER. Computer program No. 140. QCPE. Chemistry Department, Indiana University, Bloomington, Indiana.
8. T. SCHAEFER, R. SCHWENK, C. J. MACDONALD, and W. F. REYNOLDS. Can. J. Chem. **46**, 2187 (1968).
9. R. J. ABRAHAM and H. J. BERNSTEIN. Can. J. Chem. **39**, 216 (1961).
10. J. I. MUSHER and E. J. COREY. Tetrahedron, **18**, 791 (1962).
11. M. A. H. STEWART. M.Sc. Thesis, University of Manitoba, Winnipeg, Manitoba, 1970.
12. B. RICHARDSON and T. SCHAEFER. Can. J. Chem. **46**, 2195 (1968).
13. G. GOVIL and H. J. BERNSTEIN. J. Chem. Phys. **47**, 2818 (1967); **49**, 911 (1968).
14. D. HOUALLA, R. WOLF, D. GAGNAIRE, and J. B. ROBERT. Chem. Commun. 433 (1969).

Can. J. Chem. Downloaded from www.nrcresearchpress.com by 210.87.254.42 on 09/05/12
For personal use only.

Can. J. Chem. Downloaded from www.nrcresearchpress.com by 210.87.254.42 on 09/05/12
For personal use only.

The Total Synthesis of a Thebaine Analogue and of the Corresponding "Bentley Adduct"

K. WIESNER, J. G. MCCLUSKEY, J. K. CHANG, AND V. ŠMŮLA
Natural Products Research Center, University of New Brunswick, Fredericton, New Brunswick

Received October 22, 1970

We are reporting the synthesis of the thebaine analogue **6** in which the nitrogen atom has been translocated within the ethanamino bridge from position 17 to 16. This compound has been further transformed by successive Diels–Alder and Grignard reactions into the derivative **3**.

Nous rapportons la synthèse d'un analogue de thébaine **6** dans laquelle l'atome d'azote a été transposé, à l'intérieur du pont éthanamino, de la fonction 17 à 16. En effectuant successivement des réactions de Diels–Alder et de Grignard, ce composé a été transformé en **3**.

Canadian Journal of Chemistry, 49, 1092 (1971)

Introduction

Some time ago we synthesized (1, 2) various 1,5-methanobenzazocines as typified for example by **1** (see Formula Scheme 1). These compounds were found[1] to have some analgesic properties to a certain extent free of the deleterious pharmacodynamic side effects hitherto associated with the use of morphine and its congeners. This possibly novel type of activity may be attributed to the location of the nitrogen atom since the benzomorphans, as typified by **2**, are known (3) to have morphine-like analgesic activity. Unfortunately, the compounds with the translocated nitrogen atom generally lacked potency. Despite this lack of potency it was hoped that compound **3** might be very much more active since, while lacking only the ether bridge and still featuring the translocated nitrogen atom, it otherwise resembles compound **4** reported by Bentley and co-workers (4) as an analgesic 500 times more potent than morphine itself.

The preparation of Bentley's compound **4**, which involved successive Diels–Alder and Grignard reactions upon thebaine **5**, is clearly adaptable to our preparation of **3** provided that a thebaine analogue **6**, having the translocated nitrogen atom, is available. However, this, or a similar compound, does not occur naturally and it cannot be prepared by simply relocating the nitrogen atom within the ethanamino bridge of thebaine. Consequently, we have devised a very efficient total synthesis of the thebaine analogue **6** which we have converted by Bentley's method into the desired product **3**. Since we believe that the synthesis of **3** has some novel and interesting features, we are reporting the synthesis in detail in the present paper.

Discussion

The pyrrolidine enamine (5) of 7-methoxy-2-tetralone **7** (see Formula Scheme 2) (6) was alkylated with ethyl bromoacetate to obtain the 1-monosubstituted 7-methoxy-2-tetralone **8** in high yield.[2] The subsequent alkylation of the sodium enolate of **8** with the ketal tosylate **9** (7) afforded the 1,1-disubstituted 7-methoxy-2-tetralone **10***a* in a very high yield also. This alkylation is a novel procedure which, in the present case, affords far superior yields of the diketo lactam **12** than can be obtained by the use of the methyl vinyl ketone equivalents recently listed (8).

The ester group of the 1,1-disubstituted tetralone **10***a* was saponified thus permitting a convenient removal of neutral impurities and the concomitant isolation of the acid **10***b*. This was sufficiently pure to permit its direct conversion into the acid azide **10***c* which was heated in dry toluene for 1 h at 80° to afford the isocyanate **10***d*. Refluxing this solution with an excess of sodium hydride for 6 h gave the sodium salt of the secondary lactam **11***a* which could be converted into the *N*-methyl lactam **11***b* *in situ* by adding methyl iodide. In practice, the secondary lactam **11***a* was first crystallized from ethanol and then *N*-methylated with sodium hydride and methyl iodide. The deketalization of the *N*-methyl

[1]The pharmacological properties of these and other compounds were determined by Ayerst Laboratories, Montreal, Quebec.

[2]The i.r., n.m.r., and mass spectra were recorded and were in agreement with the structures assigned to this and the other compounds reported here. Such data are recorded in the Experimental.

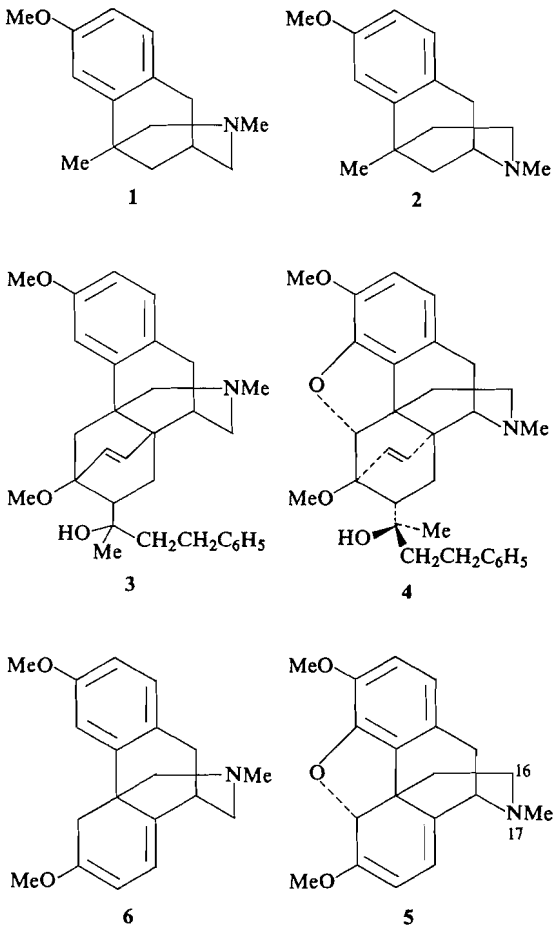

FORMULA SCHEME 1

lactam **11***b* to the diketo lactam **12** in acetone containing *p*-toluenesulfonic acid was followed by an acid-catalyzed aldol cyclization in benzene. The resulting α,β-unsaturated lactam **13** was obtained, after crystallization from ethanol, in *an overall yield of 21% from 7.*

The next phase of the synthesis involved the conversion of this α,β-unsaturated keto lactam into the thebaine analogue **6**. This operation requires the shift of the oxygen functional group from C-7 to -6 and it was accomplished via the endoperoxide as outlined in Formula Scheme 3.

The C-7 carbonyl group of the α,β-unsaturated keto lactam **13** was reduced with sodium borohydride and the resulting hydroxyl group of the product **14***a* was eliminated by pyrolysis of the corresponding benzoate **14***b*. This afforded the diene lactam **15** which, in ethanol containing eosin as photosensitizer, readily added oxygen on exposure to direct sunshine, presumably to form the endoperoxide **16** (9). This adduct, being unstable, was not isolated and the reaction mixture was hydrogenated over Adam's catalyst to give the diol **17**. The C-6 hydroxyl group of this compound was oxidized with Jones' reagent and the C-14 hydroxyl group of the resulting γ-hydroxy keto lactam **18** was eliminated using thionyl chloride in benzene containing pyridine. The product, the β,γ-unsaturated keto lactam **19**, on treatment with methyl orthoformate in methanol containing *p*-toluenesulfonic acid, gave the ketal lactam **20** which readily eliminated one molecule of methanol on pyrolysis in refluxing xylene to afford the methoxydiene lactam **21**. The lactam carbonyl group of this compound was reduced with lithium aluminum hydride to give the non-crystalline dienol ether amine **6**, the desired thebaine analogue, in 16% yield from **13**.

The Diels–Alder adduct **22** was prepared by refluxing the dienol ether **6** with methyl vinyl ketone. A subsequent Grignard reaction with phenethyl magnesium bromide afforded the non-crystalline tertiary alcohol **3** in 30% yield from **6**. This, the final compound of the series, was characterized as its sharply melting crystalline picrate. It is assumed to have the stereochemistry depicted in **3**, Formula Scheme 4, which is the same as the corresponding Bentley adduct (3), since the steric outcome of the Diels–Alder and Grignard reactions is unlikely to differ despite the missing ether bridge and the translocated nitrogen atom.

The overall yield of the Bentley adduct **3** from the tetralone **7** is 1%. This is mitigated by the mass increase by which 2.7 g of **3** are obtained from every 100 g of the starting material **7** and by the convenience of the route which is best evaluated by the fact that we have prepared several batches of several grams of **3** for pharmacological tests.

Experimental

All melting points were determined with a Gallenkamp melting point apparatus. The i.r. spectra were recorded on a Perkin–Elmer 237B spectrophotometer as chloroform solutions in sodium chloride (0.5 mm) cells. Pertinent maxima are cited in reciprocal cm. The u.v. spectra were taken on a Beckman DK-2, in absolute ethanol. Absorption maxima are given in nm with extinction coefficients in parentheses. The n.m.r. spectra were recorded on

Can. J. Chem. Downloaded from www.nrcresearchpress.com by 210.87.254.42 on 09/05/12
For personal use only.

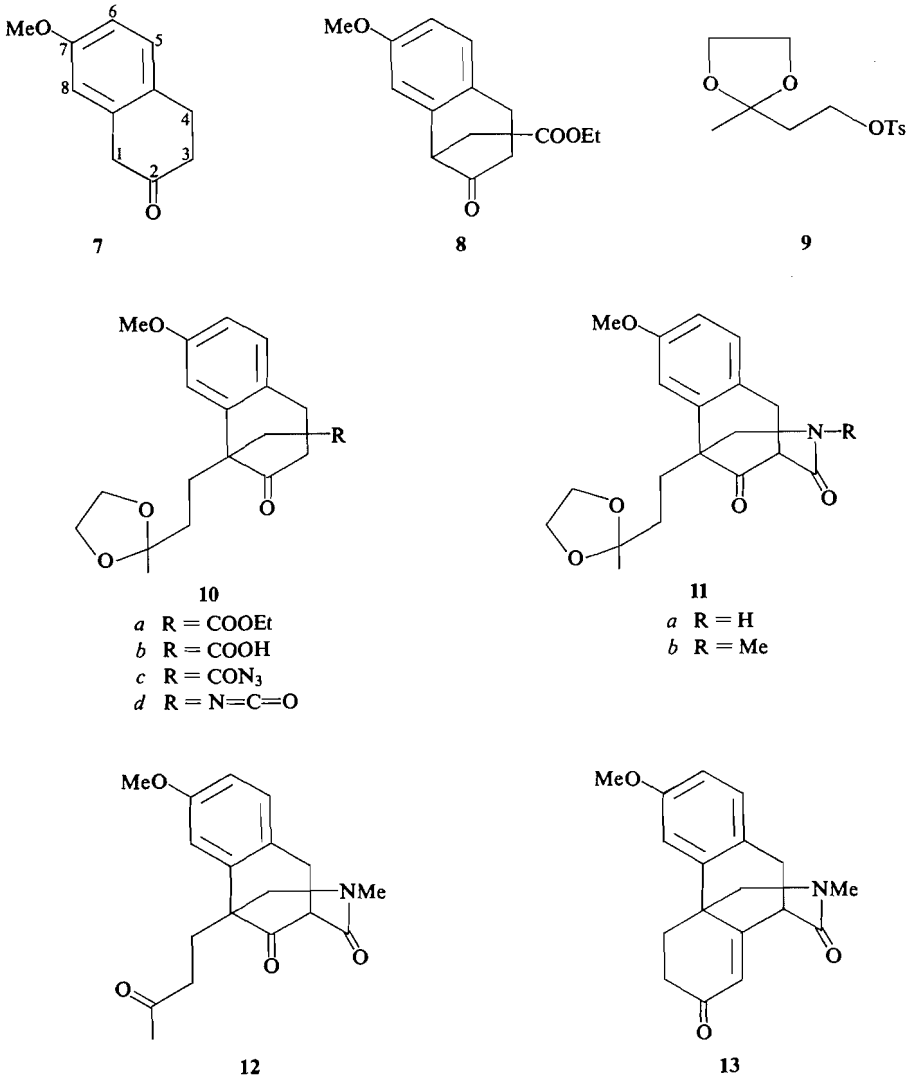

7 8 9

10
a R = COOEt
b R = COOH
c R = CON_3
d R = N=C=O

11
a R = H
b R = Me

12 13

FORMULA SCHEME 2

Varian Associates' 56.4 mHz or T-60 spectrometers using 10–15% solutions in $CDCl_3$ with tetramethylsilane as internal reference. The chemical shifts are expressed in τ values and coupling constants, *J*, in Hz. The low resolution mass spectra were taken on a Hitachi Perkin–Elmer RMU-6D while high resolution mass spectra were taken at the Mass Spectroscopy Laboratory, Chemistry Department, University of Alberta, Edmonton, Alberta. All elemental analyses were performed by Dr. F. Pascher, Mikroanalytisches Laboratorium, Bonn, Federal Republic of Germany.

1-Monosubstituted-7-methoxy-2-tetralone (8)

7-Methoxy-2-tetralone (7) (500 g) in benzene (1.3 l) containing pyrrolidine (300 ml) was refluxed under nitrogen for 4 h with continuous removal of a water azeotrope using a Dean–Stark trap. The mixture was cooled in an ice bath, ethyl bromoacetate (780 ml) was added in small portions and then heating to reflux was resumed. After 24 h, water (1.7 l) was added and the heating was maintained a further 5 h. The organic phase was then separated, rinsed with cold water (1.0 l), dried ($MgSO_4$), and distilled to afford the 1-monosubstituted-7-methoxy-2-tetralone **8** (500 g), b.p. 160–170° (90 μ); i.r., 1720 cm^{-1} (unresolved ketone and ester C=O); n.m.r., τ 2.7–3.3 (3H, m, Ar *H*), 5.84 (2H, q, *J* = 7.5 Hz, $CO_2CH_2CH_3$), 6.21 (3H, s, OCH_3), 8.76 (3H, t, *J* = 7.5 Hz, $CO_2CH_2CH_3$); mass spectrum, M^+ calculated 262, observed 262.

1,1-Disubstituted-7-methoxy-2-tetralone (10a)

The 1-monosubstituted tetralone **8** (200 g) was refluxed in dry benzene (1.5 l) containing sodium hydride (38.5 g of 55% dispersion in oil) under dry nitrogen. After 1 h, a

Can. J. Chem. Downloaded from www.nrcresearchpress.com by 210.87.254.42 on 09/05/12
For personal use only.

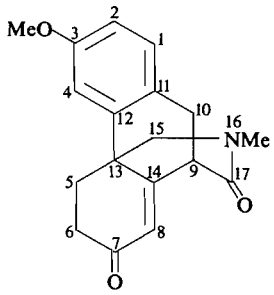

13

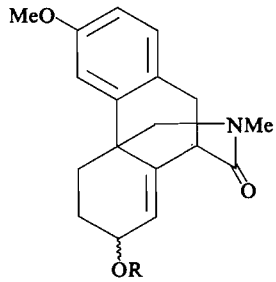

14

a R = H
b R = COC_6H_5

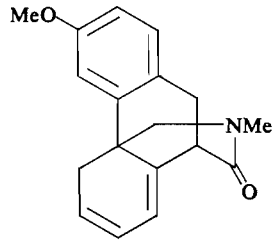

15

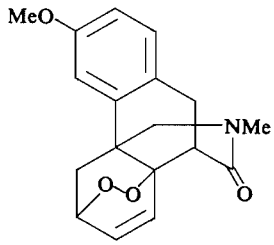

16

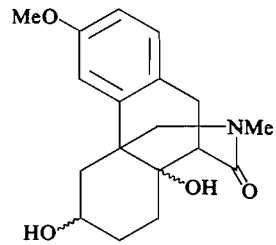

17

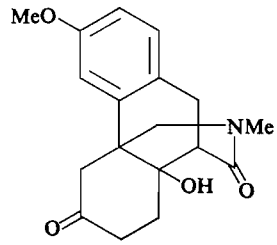

18

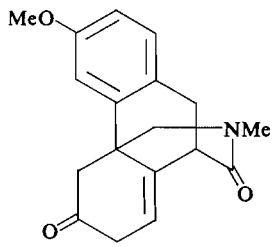

19

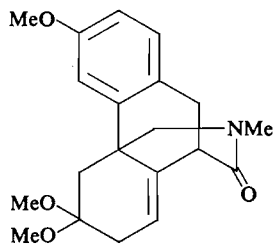

20

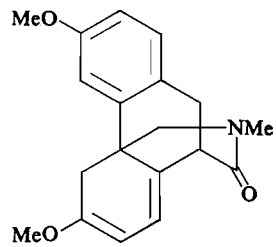

21

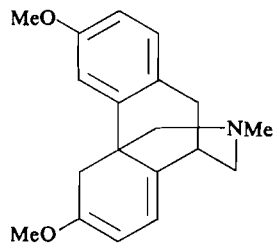

6

FORMULA SCHEME 3

dry solution of the ketal tosylate **9** (250 g) in benzene (500 ml) was added and reflux was maintained a further 16 h. The mixture was then rinsed with ice water (3 × 1.0 l), dried ($MgSO_4$), and evaporated to the crude 1,1-disubstituted tetralone **10***a* (313 g). A small portion was purified by preparative layer chromatography (silica gel), i.r., 1725, 1705 (ester and ketone C=O), 1600, 1570, 1500 (aromatic), 1055, 1040, 945 cm^{-1} (ketal); n.m.r., τ 3.25 (3H, m, Ar *H*), 6.05 (2H, q, *J* = 7 Hz, $CO_2CH_2CH_3$), 6.2 (7H, s, OCH_2CH_2O and

Can. J. Chem. Downloaded from www.nrcresearchpress.com by 210.87.254.42 on 09/05/12
For personal use only.

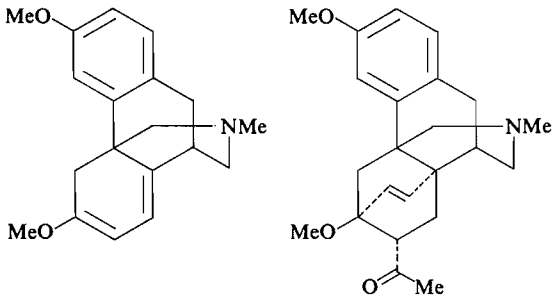

6 22

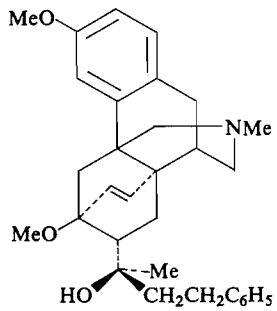

3

FORMULA SCHEME 4

Ar OCH_3), 8.8 (3H, s, CCH_3), 8.95 (3H, t, J = 7 Hz, $CO_2CH_2CH_3$); mass spectrum, M^+ calculated 376, observed 376.

Ketal Acid (10b)

The crude disubstituted tetralone **10***a* (313 g) was vigorously stirred with aqueous sodium hydroxide (5.5 l of 5% w/v) at 100° for 90 min. After being cooled, the aqueous phase was decanted, extracted with chloroform (3 × 300 ml), and then carefully neutralized with acetic acid. The resulting precipitate was extracted into chloroform (3 × 300 ml) which was rinsed with brine, dried ($MgSO_4$), and evaporated to the crude ketal acid **10***b* (170 g), i.r., 3600–3000 (—COOH), 1770 and 1710 (carboxyl and ketone C=O), 1060, 1045, 950 cm^{-1} (ketal); n.m.r., τ 2.3 (1H, diffuse s, CO_2H), 6.2 (7H, s, OCH_2CH_2O and Ar OCH_3), 8.8 (3H, s, CCH_3).

Secondary Lactam 11a

To the ketal acid **10***b* (70 g), in dry tetrahydrofuran (800 ml) at −5°, were added successively triethylamine (31.9 ml), ethyl chloroformate (21 ml), and, after 2 h, sodium azide (36 g) in distilled water (85 ml). After a further 1 h, the reaction mixture was decanted, evaporated to a reduced volume (*ca.* 150 ml), and partitioned between dichloromethane (350 ml) and aqueous sodium bicarbonate (100 ml of 10% w/v). The organic phase was further rinsed with ice water (2 × 100 ml), then dried ($MgSO_4$) and evaporated *in vacuo* to the oily acid azide **10***c* (70.6 g); i.r., 2145 (CON_3), 1710 cm^{-1} (ketone C=O). This, in dry toluene (1.2 l), was heated at an oil bath temperature of 80° for 1 h. The resulting solution of the isocyanate **10***d* (i.r., 2255 —NCO, 1710 cm^{-1} ketone C=O) was cooled, was treated with *fresh* sodium hydride (20.0 g of 55% dispersion in oil), and was then heated to reflux. After 6 h, the mixture was cooled, rinsed with water (1.2 l), then dried ($MgSO_4$), and evaporated. The solid residue was rinsed with ether and crystallized from ethanol to afford the pure secondary lactam **11***a* (35 g), m.p. 211–213°; i.r., 3400 (N—H), 1735 (keto C=O), 1670 (sec-lactam C=O), 1605, 1570, 1500 (aromatic), 1055, 1040, 945 cm^{-1} (ketal); n.m.r., τ 6.1 (3H, s, $ArOCH_3$), 6.25 (4H, s, OCH_2CH_2O), 8.7 (3H, s, CCH_3); mass spectrum, M^+ calculated 345, observed 345.

Anal. Calcd. for $C_{19}H_{23}NO_5$: C, 66.10; H, 6.67; N, 4.06. Found: C, 65.93; H, 6.64; N, 4.07.

N-Methyl Lactam (11b)

The secondary lactam **11***a* (76.5 g), in dry benzene (2.2 l) containing fresh sodium hydride (15 g of 55% dispersion in oil), was heated to reflux for 1 h. Methyl iodide (42 ml) was added and a gentle reflux was maintained. After 20 h, the mixture was cooled, extracted with water (1.7 l), dried ($MgSO_4$), and evaporated to the crude *N*-methyl lactam (**11***b*) (90 g) a portion of which was crystallized from ethanol for analysis, m.p. 90–110° (EtOH solvate); i.r., 1735 (ketone C=O), 1645 (*tert*-lactam C=O), 1605, 1570, 1500 (aromatic), 1055, 1040, 945 cm^{-1} (ketal); n.m.r., τ 6.05 (3H, s, Ar OCH_3), 6.19 (4H, s, OCH_2CH_2O), 7.2 (3H, s, NCH_3), 8.65 (3H, s, CCH_3); mass spectrum, M^+ calculated 359.1733, observed 359.1732.

Anal. Calcd. for $C_{20}H_{25}NO_5 \cdot 1/2C_2H_5OH$: C, 66.00; H, 7.33; N, 3.67. Found: C, 65.69; H, 7.21; N, 3.69.

Diketo Lactam (12)

The crude *N*-methyl lactam (**11***b*) (80.3 g), in acetone (600 ml) containing *p*-toluenesulfonic acid (3g), was heated to reflux for 2.5 h. The solvent (300 ml) was distilled, aqueous sodium bicarbonate (500 ml of 2% w/v) was added, and the mixture was then extracted with dichloromethane (3 × 100 ml) which was dried ($MgSO_4$) and evaporated to the diketo lactam **12** (68 g). A portion of this was purified by preparative layer chromatography (silica gel) and then crystallized from ethanol, m.p. 149–151°; i.r., 1740, 1720 (ketone C=O), 1650 (*tert*-lactam C=O), 1605, 1570, 1500 cm^{-1} (aromatic); n.m.r., τ 6.2 (3H, s, Ar OCH_3), 7.16 (3H, s, NCH_3), 7.87 (3H, s, CH_3CO); mass spectrum, M^+ calculated 315.1471, observed 315.1472.

Anal. Calcd. for $C_{18}H_{21}NO_4$: C, 68.57; H, 6.67. Found: C, 68.25; H, 6.67.

α,β-Unsaturated Keto Lactam (13)

The crude diketo lactam **12** (68 g), in dry benzene (4.0 l) containing *p*-toluenesulfonic acid (22 g), was refluxed with continuous removal of a benzene water azeotrope with a Dean–Stark trap. After 22 h, the mixture was rinsed with water (2.0 l) and saturated aqueous sodium bicarbonate (500 ml), then dried ($MgSO_4$), and evaporated. The residue was rinsed with hexane then crystallized from ethanol to afford the α,β-unsaturated keto lactam **13** (55 g), m.p. 156–158°; i.r., 1680, 1635 (α,β-unsaturated ketone), 1650 (*tert*-lactam C=O), 1605, 1570, 1500 cm^{-1} (aromatic); u.v., 230 mμ (ε 12 100); n.m.r., τ 4.0 (1H, s, conjugated C=C*H*), 6.2 (3H, s,

Can. J. Chem. Downloaded from www.nrcresearchpress.com by 210.87.254.42 on 09/05/12
For personal use only.

Can. J. Chem. Downloaded from www.nrcresearchpress.com by 210.87.254.42 on 09/05/12
For personal use only.

Ar OCH_3), 7.22 (3H, s, NCH_3); mass spectrum, M^+ calculated 297, observed 297.

Anal. Calcd. for $C_{18}H_{19}NO_3$: C, 72.60; H, 6.40; N, 4.72. Found: C, 72.30; H, 6.38; N, 4.63.

α,β-Unsaturated Hydroxy Lactam (14a)

The α,β-unsaturated keto lactam **13** (60 g) was stirred in methanol (600 ml) containing water (5 ml) and sodium borohydride (21 g) for 30 min at 0°. The solvent was then partly distilled (300 ml) *in vacuo* and the residue was partitioned between water (600 ml) and chloroform (3 × 200 ml) which was subsequently rinsed with brine, dried ($MgSO_4$), and evaporated to the crude α,β-unsaturated hydroxy lactam **14***a* (70 g); i.r., 3590, 3400 (hydroxyl), 1635 cm^{-1} (*tert*-lactam C=O); n.m.r., τ 4.38 (1H, s, C=C*H*), 6.25 (3H, s, Ar OCH_3), 7.30 (3H, s, NCH_3); mass spectrum, M^+ calculated 299, observed 299.

Diene Lactam (15)

The crude hydroxy lactam **14***a* (70 g), in dry tetrahydrofuran (500 ml) containing dry pyridine (27 ml), was treated dropwise with benzoyl chloride (36 ml) at 0°. After 20 h, the mixture was filtered then evaporated *in vacuo* to 200 ml. This was partitioned between water (500 ml) and chloroform (3 × 100 ml) which was subsequently rinsed with saturated aqueous sodium bicarbonate, then dried ($MgSO_4$), and evaporated to the crude non-crystalline benzoate **14***b* (90 g); i.r., 1710 (benzoate C=O), 1635 (*tert*-lactam C=O), 1605, 1600, 1580, 1570, 1500 (aromatic), 1270, 1120 cm^{-1} (benzoate C—O). This was then pyrolyzed (3 × 30 g portions) in an evacuated tube heated at one end to 200°. After 20 h a sublimate was dissolved in chloroform (50 ml) which was rinsed with saturated aqueous sodium bicarbonate (100 ml) and water (50 ml), and was then dried ($MgSO_4$), and evaporated. The residue crystallized from ether to afford the pure diene lactam **15** (3 × 10 g), m.p. 142–145° (dec.); i.r., 1635 (*tert*-lactam C=O), 1605, 1570, 1500 cm^{-1}; u.v., 279 nm (ε 5500); n.m.r., τ 4.26 (3H, s, C=C*H*—C*H*=C*H*—), 6.25 (3H, s, Ar OCH_3), 7.30 (3H, s, NCH_3); mass spectrum, M^+ calculated 281, observed 281.

Anal. Calcd. for $C_{18}H_{19}NO_2$: C, 76.87; H, 6.76; N, 4.98. Found: C, 76.90; H, 6.91; N, 4.80.

Diol Lactam (17)

The diene lactam **15** (11.7 g), in ethanol (675 ml of 95%) containing eosin (30 mg), was exposed to sunlight while oxygen was bubbled through the solution. After 7 h, platinum oxide (2 g) was added and the mixture was shaken under hydrogen for 20 h, at room temperature and pressure. The mixture was then filtered and evaporated to the crude diol lactam **17** (13.4 g) a portion of which was purified by crystallization from methanol, m.p. 286–288°; i.r., 3375, 3255 (2 × hydroxyl O—H), 1620 (*tert*-lactam C=O), 1600, 1570, 1500 cm^{-1} (aromatic); mass spectrum, M^+ calculated 317.1624, observed 317.1627.

γ-Hydroxy Keto Lactam (18)

The crude diol lactam **17** (13.4 g) was stirred for 2 h at room temperature in glacial acetic acid (150 ml) containing sodium dichromate·dihydrate (7 g). The solvent was then evaporated *in vacuo* and the residue was partitioned between aqueous sodium bicarbonate (500 ml of 5% w/v) and chloroform (3 × 200 ml); the chloroform layer was dried ($MgSO_4$) and evaporated. The residue was crystallized from ethanol to afford the γ-hydroxy keto lactam **18** (6.67 g), m.p. 274–276° (dec.); i.r., 3580, 3200 (hydroxyl O—H), 1705 (ketone C=O), 1635 (*tert*-lactam C=O), 1605, 1570, 1500 cm^{-1} (aromatic); u.v., 220 nm (ε 1250); n.m.r., τ 6.24 (3H, s, Ar OCH_3), 7.26 (3H, s, NCH_3); mass spectrum, M^+ calculated 315, observed 315.

Anal. Calcd. for $C_{18}H_{21}NO_4$: C, 68.57; H, 6.67; N, 4.44. Found: C, 68.17; H, 6.58; N, 4.44.

β,γ-Unsaturated Keto Lactam (19)

The γ-hydroxy keto lactam **18** (2.42 g), in dry benzene (40 ml) containing dry pyridine (2.8 ml), was treated with thionyl chloride (1.09 ml) then stirred in an ice bath. After 1 h, the mixture was extracted with saturated aqueous sodium bicarbonate (40 ml), then dried ($MgSO_4$), and evaporated to the crude β,γ-unsaturated keto lactam **19** (2.35 g) which was crystallized from ethanol, m.p. 166–168°; i.r., 1720 (unconjugated ketone C=O), 1640 (*tert*-lactam C=O), 1605, 1570, 1500 cm^{-1} (aromatic); u.v., 220 nm (ε 3000); n.m.r., τ 4.44 (1H, broad singlet, C=C*H*), 6.25 (3H, s, Ar OCH_3). 7.25 (3H, s, NCH_3); mass spectrum, M^+ calculated 297.3570, observed 297.3571.

Methoxydiene Lactam (21)

The β,γ-unsaturated keto lactam **19** (298 mg), in absolute methanol (9 ml) containing *p*-toluenesulfonic acid (60 mg) and methyl orthoformate (3.6 ml), was heated to reflux for 45 min. The mixture was then partitioned between dilute aqueous sodium bicarbonate (50 ml) and chloroform (3 × 15 ml). This was rinsed with brine (15 ml), then dried ($MgSO_4$), and evaporated to afford the oily β,γ-unsaturated ketal lactam **20** (400 mg); i.r., 1630 cm^{-1} (*tert*-lactam C=O); n.m.r., τ 4.55 (1H, broad singlet, C=C*H*), 6.2 (3H, s, Ar OCH_3), 6.77 (3H, s, OCH_3), 6.78 (3H, s, OCH_3), 7.25 (3H, s, NCH_3). This, in dry xylene (20 ml), was heated to reflux for 1 h. The solvent was evaporated and the residue was purified by preparative layer chromatography (alumina) to obtain the methoxydiene lactam **21** (180 mg) as crystals from benzene, m.p. 172–174°; i.r., 1630 cm^{-1} (*tert*-lactam C=O); u.v., 281 nm (ε 9700); n.m.r., τ 4.32 (1H, d, J = 6 Hz, =C*H*—C*H*=), 5.11 (1H, d, J = 6 Hz, =C*H*—C*H*=), 6.21 (3H, s, Ar OCH_3), 6.39 (3H, s, OCH_3), 7.27 (3H, s, NCH_3); mass spectrum, M^+ calculated 311, observed 311.

Anal. Calcd. for $C_{19}H_{21}NO_3$: C, 73.30; H, 6.75; N, 4.50. Found: C, 73.19; H, 6.70; N, 4.40.

Methoxydiene Amine (6)

The methoxydiene lactam **21** (956 mg), in dry tetrahydrofuran (17 ml) containing lithium aluminum hydride (310 mg), was heated to reflux for 1.5 h. Saturated aqueous sodium potassium tartrate (100 ml) was then added and the mixture was extracted with chloroform (3 × 30 ml) which was dried ($MgSO_4$) and evaporated to the oily methoxydiene amine **6** (916 mg); i.r., 2780 (Baumann), 1660 (C=C), 1605, 1575, 1500 (aromatic); n.m.r., τ 4.35 (1H, d, J = 6 Hz, =C*H*—C*H*=), 5.18 (1H, d, J = 6 Hz, =C*H*—C*H*=), 6.20 (3H, s, Ar OCH_3), 6.43 (3H, s, OCH_3), 7.90 (3H, s, NCH_3); mass spectrum, M^+ calculated 297, observed 297.

Diels–Alder Adduct (22)

The methoxydiene amine **6** (916 mg) was heated in methyl vinyl ketone (6 ml) to reflux for 20 h. The solvent was evaporated and the residue, in dichloromethane (15 ml), was extracted into sulfuric acid (30 ml of 3%). This was rinsed with chloroform (2 × 15 ml) and was then basified with ammonium hydroxide. The mixture was then extracted with chloroform (3 × 25 ml) which was dried ($MgSO_4$) and evaporated to the oily Diels–Alder adduct **22** (950 mg) which afforded a crystalline hydrochloride from ethanol–ether, m.p. 232–234°.

Anal. Calcd. for $C_{23}H_{29}NO_3 \cdot HCl \cdot 2H_2O$: C, 62.80; H, 7.75; Cl, 8.10; N, 3.19. Found: C, 62.03; H, 7.31; Cl, 8.27; N, 3.18.

A portion of the hydrochloride was converted into the free base, i.r., 1710 cm^{-1} (ketone C=O); n.m.r., τ 3.76 (2H, s, —C*H*=C*H*—), 6.18 (3H, s, Ar OCH_3), 6.6 (3H, s, OCH_3), 7.9 (3H, s, NCH_3), 7.98 (3H, s, CCH_3); mass spectrum, M^+ calculated 367, observed 367.

Tertiary Carbinol (3)

The Diels–Alder adduct **22** (950 mg), in dry ether (400 ml), was treated with the Grignard reagent from magnesium (600 mg) and phenethyl bromide (3 ml) in ether (20 ml). After 3 h at reflux, the mixture was treated with saturated aqueous ammonium chloride (100 ml). The ether phase was separated, dried ($MgSO_4$), and evaporated. The resulting residue was purified by chromatography (alumina: activity III–IV: eluent petroleum ether and benzene) to afford the oily tertiary alcohol **3** (420 mg) which gave a picrate as crystals from ethanol, m.p. 222°.

Anal. Calcd. for $C_{21}H_{39}NO_3 \cdot C_6H_3N_3O_7$: C, 63.30; H, 5.98; N, 7.98. Found: C, 63.24; H, 6.14; N, 8.05.

A portion of the picrate was converted into the free base, i.r., 3460 (hydroxyl O—H), 1675 (C=C), 1605, 1570, 1500 cm^{-1} (aromatic); n.m.r., τ 2.75–3.25 (8H, m, Ar *H*), 3.78 (2H, J_{A-B} = 9 Hz, $\Delta\nu_{A-B}$ = 42 Hz, —C*H*=C*H*—), 5.27 (1H, s, O*H*), 6.2 (3H, s, Ar OCH_3), 6.5 (3H, s, OCH_3), 7.98 (3H, s, NCH_3), 8.98 (3H, s, CCH_3); mass spectrum, M^+ calculated 473, observed 455 ($M^+ - H_2O$).

We wish to thank the Ayerst Laboratories, Montreal, for a grant which enabled us to carry out this entire investigation.

1. K. Wiesner, J. G. McCluskey, J. Šantroch, M. Georgiadis, M. A. Davis, and R. Deghenghi. In preparation.
2. (*a*) J. K. Chang. Ph.D. Thesis. University of New Brunswick, Fredericton, New Brunswick, 1969; (*b*) V. Šmůla. Ph.D. Thesis. University of New Brunswick, Fredericton, New Brunswick, 1970.
3. N. B. Eddy. Chem. Ind. (London), 1462 (1959).
4. K. W. Bentley, D. G. Hardy, and B. Meek, J. Amer. Chem. Soc. **89**, 3267, 3273 (1967).
5. G. Stork, A. Brizzolara, H. Landesmann, J. Szmuszkovicz, and R. Terrell. J. Amer. Chem. Soc. **85**, 207 (1963).
6. (*a*) M. D. Soffer, J. C. Cavanaugh, and H. E. Gellerson. J. Amer. Chem. Soc. **71**, 3857 (1949); (*b*) J. W. Cornforth, R. H. Cornforth, and Sir Robert Robinson. J. Chem. Soc. 689 (1942).
7. J. P. Yardley, R. W. Rees, and H. Smith. J. Med. Chem. **10**, 1088 (1967).
8. S. Danishefsky and R. Cavanaugh. J. Amer. Chem. Soc. **90**, 520 (1968).
9. A. Windhaus and J. Brunken. Ann. **460**, 225 (1928).

Can. J. Chem. Downloaded from www.nrcresearchpress.com by 210.87.254.42 on 09/05/12
For personal use only.

N-Bromosuccinimide-Induced Dimethyl Sulfoxide Oxidation of Acetylenes[1]

SAUL WOLFE, W. R. PILGRIM, T. F. GARRARD, AND P. CHAMBERLAIN
Department of Chemistry, Queen's University, Kingston, Ontario

Received October 22, 1970

The addition of less than 2 mol equiv. of *N*-bromosuccinimide (NBS) to a solution of diphenylacetylene in anhydrous dimethylsulfoxide (DMSO) leads to the formation of benzil in near-quantitative yield at room temperature. Under the same conditions stilbene gives the dibromo adduct. The conditions for this novel oxidation *of an acetylene* have been examined in some detail and it has been established that *anhydrous DMSO* must be employed as the *solvent* and that NBS is uniquely able to induce the oxidation. Preliminary studies indicate that alkyl aryl, dialkyl, and terminal acetylenes are converted to the corresponding α-dicarbonyl compounds, and that diphenylbutadiyne is oxidized to diphenyltetraketone. Optimum conditions for these latter oxidations have not yet been established.

L'addition à la température ordinaire de *N*-bromosuccinimide (NBS), moins de 2 équivalents, à une solution de diphénylacétylène dans du diméthylsulfoxyde (DMSO) conduit à la formation de benzil avec un rendement presque quantitatif. Dans les mêmes conditions, le stilbène conduit au dérivé dibromé. Les conditions conduisant à cette nouvelle oxydation *d'un acétylène* ont été examinées en détail et il a été établi que du *DMSO anhydre* doit être utilisé comme *solvant* et que seul le NBS peut induire l'oxydation. Des études préliminaires indiquent que les arylalkylacétylènes, dialkylacétylènes, et acétylènes vrais sont transformés en composés carbonylés-α correspondants et que le diphénylbutadiyne est oxydé en diphényltetracétone. Les conditions optimales pour ces dernières oxydations n'ont pas encore été établies.

Canadian Journal of Chemistry, 49, 1099 (1971)

The combination of an *N*-haloamide or imide and an aqueous medium is often employed to convert an alcohol into a ketone or an olefin into a halohydrin (1). Hypohalous acid, formed *in situ* by hydrolysis of the halogen source, is thought to be the oxidizing agent in most of these reactions (2). However, recent work by van Tamelen and Sharpless (3) and by Dalton and co-workers (4) indicates that the intervention of HOX is not obligatory. In aqueous glyme, *N*-bromosuccinimide (NBS) appears to effect direct transfer of positive bromine to a double bond (3); and, in the reaction of NBS with an olefin in moist dimethyl sulfoxide (DMSO), attack on the brominated cation or bromocarbonium ion is at least 95% by the DMSO (4). The bromohydrin is then produced by hydrolysis of the oxysulfonium intermediate **1**.

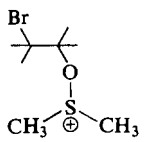

1

Acetylenes resemble olefins in a number of respects in their behavior towards these halogenating agents. With hypobromous acid, dibromoketones are produced (5) and, with *N*-chlorosuccinimide or NBS in alcoholic solvents, the products are dichloro (6) or dibromoketals (7). In aqueous glyme, NBS effects direct transfer of bromine to a triple bond (7). This similar behavior of olefins and of acetylenes suggested that, in DMSO, a brominated *vinyl* cation might, like its dihydro analog, be trapped by the solvent to give **2**, an unsaturated oxysulfonium cation. In the case of **2**, however, competition may now occur between hydrolysis and either unimolecular (**2** → **3**; eq. 1) or bimolecular (**2** + DMSO → **4**; eq. 2) elimination of dimethyl sulfide. Loss of $Br^{\oplus}$ and dimethyl sulfide from **4**, formed by the reactions of **2** or **3** with DMSO, would then lead, as indicated in eq. 3, to **5**, an α-diketone, in what might be described as NBS-induced DMSO oxidation.

[1] 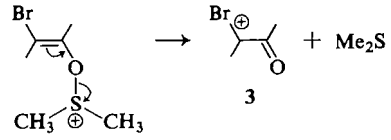

2 **3**

[2] 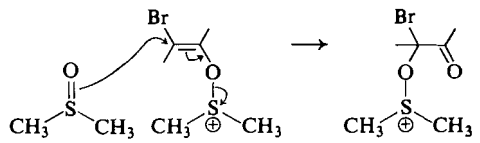

4

[1]Part II in the series "Aspects of Acetylene Chemistry". For Part I see ref. 34.

TABLE 1. Effect of reaction conditions on the oxidation of diphenylacetylene (tolan)

Reactant (mmol)						Recovery of products (%)	
Tolan	Halogen source	DMSO	Solvent*	Time (h)	Temperature (°C)	Benzil	Other
1.5	NBS (3.0)		DMSO	24	22	98	
1.5	NBS (3.0)		DMSO	0.5	80	92	
1.5	NBS (1.5)		DMSO	24	22	93	
1.5	NBS (0.75)		DMSO	24	22	42	58†
1.5	NBS (0.38)		DMSO	24	22	20	69†
1.5	NBS (3.0)	6.0	CH_2Cl_2	308	Reflux	<1	90–95†
1.5	NBS (3.0)	3.0	Benzene	21	Reflux	<1	98†,‡
1.5	NBS (3.0)	3.0	Dioxane	26	Reflux	1–5	56†
1.5	NBS (3.0)	20.0	Dioxane	69	Reflux	5	94†
1.5	NBS (3.0)	3.0	CCl_4	30	Reflux	0	
1.5	NBS (3.0)		DMSO-H_2O§	150	22	0	15‖
1.5	PHT¶ (3.0)		DMSO	72	22	<2	
1.5	NBA** (3.0)		DMSO	100	22	19	
1.5	Br_2 (3.0)		DMSO	48	22	0	

*Ten ml of solvent were used in each case.
†Unreacted tolan.
‡Tolan dibromide was detected in trace amounts.
§DMSO, 99.5%; H_2O, 0.5%.
‖Tolan dibromide.
¶Pyrrolidone hydrotribromide.
**N-bromoacetamide.

[3] 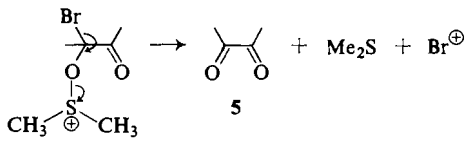

5

Although the scheme just depicted is intended to represent a working hypothesis rather than a mechanistic proposal, it will be noted that there are formal precedents for it in the well-known Kornblum (8) and Pfitzner–Moffatt (9) oxidations, and in the conversion of benzylamines to benzaldehydes upon diazotization in anhydrous DMSO (10). It may also be noted that oxidation of acetylenes to α-diketones has been observed previously: stearolic acid is converted to 9,10-diketostearic acid by neutral aqueous permanganate (11); and the highly strained acetylenes 3,3,6,6-tetramethyl-1-thiacycloheptyne and cyclooctyne undergo air oxidation to α-diketones (12).

Addition of NBS (0.5 g, 2.8 mmol) at room temperature to a solution of diphenylacetylene (**6**) (0.25 g, 1.4 mmol) in anhydrous DMSO (10 ml) afforded a bright yellow solution which was allowed to stand for 24 h at room temperature and then diluted with water. Chloroform extraction of the strongly acidic aqueous solution and work-up of this extract afforded benzil (**7**) *in 98% yield* (eq. 4). Repetition of the experiment for 30 min at 80° led to the formation of benzil *in 92% yield*. In contrast to these results, stilbene (**8**) reacted at room temperature with NBS in anhydrous DMSO to give the adduct meso-stilbene dibromide (**9**) (eq. 5).

Table 1 summarizes a number of experiments performed to define the conditions for the oxidation of diphenylacetylene, and the following main conclusions may be drawn: (*a*) DMSO must be utilized as the solvent since its presence in stoichiometric quantities in refluxing methylene chloride, benzene, carbon tetrachloride, or dioxane leads to only traces of benzil (*cf.* ref. 13); (*b*) NBS may function as a catalyst for the oxi-

[4] 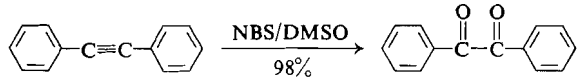

6 7

[5] 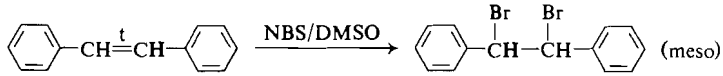

8 9

TABLE 2. Effect of reaction conditions on the oxidation of 1-phenylpropyne (**11**) in anhydrous DMSO

Reactant (mmol)		DMSO	Temperature		Composition of the reaction mixture (%)*			
11	Catalyst	(ml)	Time (h)	(°C)	**11**	**12**	**13**	**14**
4.41	A† (8.82)	20	52	20	5	21	20	21
4.43	A (4.46)	25	93	20	27	15	11	8
4.41	A (4.46)	10	45	90	14	40	22	8
4.41	A (4.46)	10	21	150	—	30	19	—
4.53‡	A (8.95)	10	49	20	Trace	12	19	17
4.74§	A (9.48)	10	70	20	0	0	0	0
4.44	B‖ (4.47)	30	701	20	27	16	—	—
4.41	B (4.52)	30	26	60	32	16	8	8
4.27	C¶ (8.70)	10	143	20	100	0	0	0

*Determined by n.m.r.
†NBS, dried but not recrystallized.
‡Calcium carbonate, 4.53 mmol, were added to the reaction mixture.
§Cyclohexene, 9.49 mmol, was added to the reaction mixture.
‖NBS, recrystallized and dried.
¶Acetic anhydride, 8.70 mmol, was substituted for the NBS. The product consisted of unreacted **11** and CH_3SCH_2OAc, the product of a Pummerer reaction of the anhydride with the solvent.

dation as implied by the above scheme; based on acetylene consumed, the ratio (mmol of diketone)/(mmol of NBS) is always greater than unity. However, because NBS is itself slowly consumed by DMSO (4), high conversions to benzil require 1–2 mol equiv of NBS per mol of acetylene; (*c*) NBS is unique in its ability to catalyze the reaction; with molecular bromine and pyrrolidone hydrotribromide (14), no diketone is produced, and with *N*-bromoacetamide the yield of benzil is only 19% after 100 h at room temperature. These findings are compatible with an initiation step for the reaction which involves direct transfer of bromine from NBS to the triple bond; (*d*) the reaction is inhibited by water; the only product formed (in a very slow reaction) in moist DMSO is diphenylacetylene dibromide (**10**).

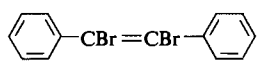

10

A preliminary study of the scope of the oxidation indicates that the conversion of acetylenes to α-diketones with NBS in DMSO may be a general reaction, but the optimum conditions for different types of substrates will differ from those established for **6**. The experiments summarized in Table 2 refer to the oxidation of 1-phenylpropyne (**11**) to 1-phenylpropanedione (**12**). For the conditions examined, the optimum conversion (47%) was realized with 0.4 *M* solutions containing 1 mol equiv of NBS per mol of substrate at 90°. In contrast to the oxidation of **6**, a diarylacetylene, the oxidation of **11**, an alkyl arylacetylene, produced significant quantities of bromine-containing side-products (eq. 6). These products, the dibromide **13** and the

[6]

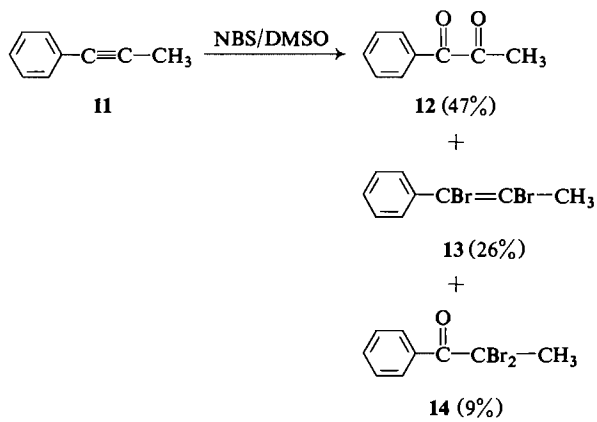

11 → **12** (47%) + **13** (26%) + **14** (9%)

dibromoketone **14**, may be considered to result from a competition for the intermediates **15** and **16**[2] between a bromine source in the medium (Br_2, HBr, NBS) (4) and the DMSO solvent. It is not at present clear why the bromine sources compete successfully for these cations when one of the substituents is an alkyl group and not when two aryl substituents are present. Oxidation of **9** in the presence of calcium carbonate (to remove HBr) did not reduce the yields of the side-products; and addition of cyclohexene to an oxidation mixture (to remove Br_2) caused the oxidation to be quenched. Replacement of the NBS by acetic anhydride led only to a Pummerer reaction of the anhydride with the solvent (15), the acetylene being recovered unchanged. We are presently examining alternatives to DMSO for the oxygen transfer step.

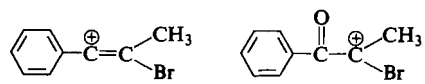

15 **16**

Oxidations of 2-butyne (**17**) and phenylacetylene (**18**) with NBS in anhydrous DMSO were performed at room temperature. In each case the total product was then treated with a derivatizing agent to yield biacetyl (**19**) (as the dihydrazone, see eq. 7) and phenylglyoxal (**20**) (as the di-*p*-nitrophenylhydrazone; see eq. 8), respectively. The derivatives were recovered in 20–25% yields. For these two oxidations, detailed examination of the reaction mixtures, and variation of the experimental conditions, were not performed.

It was of interest to examine the oxidation of a compound containing more than one triple bond. Polyacetylenes are readily available synthetic (16) and naturally occurring (17) compounds, and the polyketones potentially available from these substrates would be useful in several ways: base-catalyzed cyclization of the polyketone derived from a non-conjugated polyacetylene could be compared with the analogous treatment of a poly-β-ketone (18); and examination of molecular models suggests that a conjugated polyketone derived from a conjugated polyacetylene might adopt a chiral and, in favorable cases, a helical conformation (19).

[2]It has been established (5, 7) that electrophilic addition of halogen to **9** affords the vinyl cation $PhC^{\oplus}{=}CXCH_3$ preferentially.

Diphenylbutadiyne (**21**) was selected as the substrate for the preliminary study since the potential oxidation product, diphenyltetraketone (**22**) is a known compound (19, 20). Oxidation of **21**, at room temperature for 48 h or at 100° for 2 h, in DMSO containing 2 mol equiv of NBS appeared to proceed smoothly to give **22** (eq. 9). The compound was identified by its reversible color reaction with water (20, 21): red(anhydrous) ⇄ yellow(hydrate), by acid-catalyzed decarbonylation to benzil (22), and by formation of the known dioxime (20). However, although the reaction evidently proceeded smoothly, and no other product could be detected after extended reaction periods, we have been unable to crystallize the compound in either of its two forms. Both forms have been crystallized (19, 20). Consequently, although the reaction shows promise as a route to polyketones, more work is needed and is in progress.

Experimental

Melting points were determined on Fisher–Johns or Kofler hot stage m.p. apparati, and are uncorrected. The i.r. spectra were recorded on a Beckman IR 5A instrument, and calibrated against the 6.238 μ peak of polystyrene. The n.m.r. spectra were obtained on Varian A60 or T60 spectrometers as 10% solutions in chloroform-*d* or carbon tetrachloride. Tetramethylsilane was employed as an internal standard.

All solvents were dried before use by standard procedures. Dimethyl sulfoxide was refluxed over calcium hydride and then distilled under reduced pressure. It was stored in sealed bottles over 4A molecular sieves. *If the calcium hydride treatment was omitted, no oxidation took place.*

N-Bromosuccinimide was Fisher reagent grade material and was dried under reduced pressure over phosphorus pentoxide before use. Some samples, as indicated in Tables 1 and 2, were recrystallized prior to the drying procedure (23).

Diphenylacetylene was prepared from benzil by the method of ref. 24; it was purified by distillation under reduced pressure, followed by crystallization from 95% ethanol.

1-Phenylpropyne was prepared by methylation of lithium phenylacetylide in liquid ammonia (25). In the n.m.r. spectrum the methyl group of this compound appears at τ 8.02.

Diphenylbutadiyne was prepared by oxidative coupling of lithium phenylacetylide with potassium permanganate (26).

1,2-Dibromo-1,2-diphenylethylene (**10**) was prepared by bromination of diphenylacetylene. Diphenylacetylene (0.5 g, 2.8 mmol) was dissolved in chloroform (10 ml). A solution of bromine (2.8 mmol) in carbon tetrachloride was then added all at once. The color of the red solution slowly faded during a 4 h period at room temperature. Removal of the solvent then afforded a

[7] 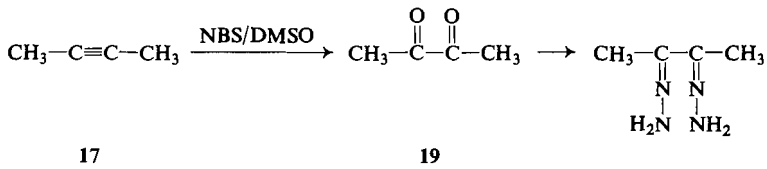

17 19

[8] 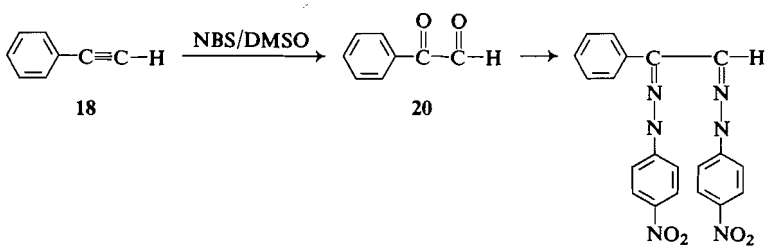

18 20

[9] 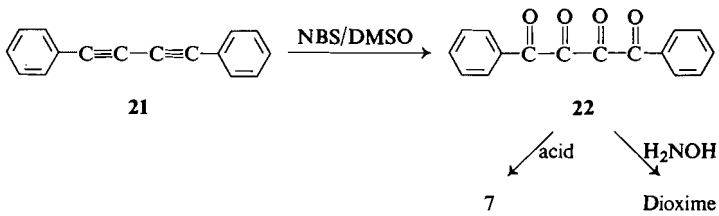

21 22

7 Dioxime

white solid, m.p. 65–173°. This was recrystallized from absolute ethanol to give 0.6 g of **10**, m.p. 211–212° (lit. (27) m.p. 211°).

1,2-Dibromo-1-phenylpropene (**13**) was prepared by bromination of 1-phenylpropyne. The acetylene (1.1 g, 9.5 mmol) in chloroform (10 ml) was cooled in an ice-bath and a solution of bromine (1.52 g, 9.5 mmol) in chloroform (20 ml) was added dropwise with stirring. When the addition was complete the solvent was removed from the colorless solution and the residual oil distilled.

Anal. Calcd. for $C_9H_8Br_2$: C, 39.17; H, 2.90. Found: C, 39.51; H, 2.97.

In the n.m.r. spectrum, the methyl peak of this compound appears at τ 7.42.

1-Phenyl-2,2-dibromopropane-1-one (**14**) was prepared from propiophenone. The ketone (1.0 g, 7.45 mmol) and NBS (2.6 g, 14.9 mmol) were refluxed in carbon tetrachloride (20 ml) containing 2 mg of benzoyl peroxide over a 100 W Photoflood No. 2 bulb. After 10 min an orange coloration appeared in the mixture and, after an additional 8 min, the color disappeared and the reaction was complete. Filtration followed by evaporation of the solvent yielded **14** as a pale yellow oil. This oil was found to be homogeneous by t.l.c. and by n.m.r. In the n.m.r. spectrum the methyl group appears at τ 7.30. Distillation of a portion of the oil gave crystalline material, m.p. 30–31° (lit. (28) 31°). This material gave a yellow 2,4-dinitrophenylhydrazone, m.p. 266–267°.

1-Phenylpropanedione (**12**) was prepared from propiophenone by oxidation with selenium dioxide (29). In the n.m.r. spectrum the methyl group of this compound appears at τ 7.72.

Oxidation of Diphenylacetylene

Diphenylacetylene (0.25 g, 1.4 mmol) was dissolved in anhydrous DMSO. The solution was stirred and NBS (0.5 g, 2.8 mmol) was added in one portion. The solid dissolved immediately to give a bright yellow solution. There was no temperature change. After 24 h at room temperature the solution was diluted with water (60 ml), and a pale yellow solid precipitated. The solid was isolated by extraction into chloroform (the aqueous phase was found to have p*H* 2). The chloroform extract was washed successively with water and saturated sodium chloride, and was then dried ($MgSO_4$) and evaporated. The pale yellow oil (280 mg) crystallized on standing. Its i.r. spectrum was identical with that of benzil. Recrystallization from methylene chloride – petroleum ether (30–60°) afforded light yellow needles, m.p. 94.5–95.5°, undepressed on admixture with benzil.

Anal. Calcd. for $C_{14}H_{10}O_2$: C, 79.98; H, 4.79. Found: C, 79.38; H, 4.75.

The compound gave a pale orange 2,4-dinitrophenylhydrazone (2,4-DNP) derivative, m.p. 190–191°, undepressed on admixture with the 2,4-DNP derivative of benzil.

Attempted Oxidation of trans-Stilbene

trans-Stilbene (0.253 g, 1.4 mmol) and NBS (0.25 g, 1.4 mmol) were dissolved in anhydrous DMSO (5 ml). There was no temperature change, but the solution gradually developed a pale yellow color. After 24 h at room temperature the solution was diluted with water (30 ml) and extracted with three 10 ml portions of chloroform. The combined chloroform extracts were washed

with water, dried, and evaporated to give 210 mg of a white solid, m.p. 124–214°. Recrystallization from xylene afforded 180 mg of fine white crystals, m.p. 241–242°. A mixture m.p. with meso-stilbene dibromide (30) was not depressed and the i.r. spectra of the two compounds were identical.

Oxidation of 1-Phenylpropyne

1-Phenylpropyne (512 mg, 4.41 mmol, freshly distilled) was dissolved in anhydrous DMSO (10 ml), the solution was stirred, and NBS (798 mg, 4.46 mmol) was added in one portion. A yellowish-orange color formed immediately and the reaction mixture became warm. The flask was fitted to a reflux condenser equipped with a calcium chloride drying tube and the contents were stirred at 90° for 45 h. By this time the solution was deep yellow. The solution was cooled, poured into 30 ml of a 1:1 mixture of petroleum ether (30–60°) and benzene, and water (10 ml) was added. When this mixture was shaken the yellow color diminished in intensity but the organic layer remained pale yellow. It was washed with nine 10 ml portions of water. The combined aqueous extracts were then back extracted with 20 ml of petroleum ether (30–60°) and the combined organic extracts, after drying over magnesium sulfate, were evaporated to give 993 mg of an orange oil. Integration of the methyl region of the n.m.r. spectrum of this oil and comparison with the spectra of standard mixtures revealed the oil to contain **12** (40%), **13** (22%), **14** (8%), and unreacted 1-phenylpropyne (14%). Based on acetylene consumed, the conversion to **12** is 47%.

The oil obtained from an oxidation conducted at room temperature with 2 mol equiv of NBS per mol of 1-phenylpropyne was heated under reflux for 0.5 h with *p*-nitrophenylhydrazine (0.5 g), ethanol (15 ml), and acetic acid (2 drops). The precipitated solid was collected by filtration and, after recrystallization from ethanol, melted at 254–255°. The reported m.p. of 1-phenylpropanedione di-*p*-nitrophenylhydrazone is 256–257° (31).

Oxidation of 2-Butyne

A solution of 2-butyne (0.2 ml) and NBS (712 mg, 4 mmol) in anhydrous DMSO (10 ml) was stirred at room temperature for 26 h. The yellow reaction mixture was then diluted with water (50 ml) and extracted with four 25 ml portions of ether. The yellow color remained in the organic layer. This layer was dried over magnesium sulfate and concentrated under reduced pressure at 20°. The residue was treated with water (10 ml) and 85% hydrazine hydrate (1 ml) and the resulting mixture stirred at room temperature for 2 h. The oil which separated during this period was extracted into chloroform. The chloroform extract was dried over anhydrous magnesium sulfate and evaporated. The semi-solid product was recrystallized from ethanol to give biacetyldihydrazone, m.p. 155–157° (lit. (32) 158°).

Oxidation of Phenylacetylene

A solution of phenylacetylene (306 mg, 3 mmol) and NBS (534 mg, 3 mmol) in anhydrous DMSO (10 ml) was stirred at room temperature for 20 h. The yellow mixture was then diluted with water (50 ml) and extracted with three 40 ml portions of ether. The ether extract was dried and evaporated. The i.r. spectrum of the resulting yellow oil showed a single strong carbonyl peak at 5.85 μ. The oil was treated with a solution of *p*-nitrophenylhydrazine (0.6 g) and glacial acetic acid (2 drops) in ethanol (15 ml). The resulting solution was refluxed for 0.5 h; during this period a deep red solid precipitated. This was collected and recrystallized from ethanol. It melted at 309–311° (phenylglyoxal di-*p*-nitrophenylhydrazone melts at 310–311.5° (33)).

In a second experiment, conducted with the same quantities of materials, the total reaction mixture was treated after 20 h with *p*-nitrophenylhydrazine (2.0 g), and stirring was continued for an additional 2.5 h. Addition of water precipitated a dark solid which was collected, washed with ethanol, and dried *in vacuo*. The di-*p*-nitrophenylhydrazone weighed 317 mg (corresponding to a 25% recovery, based on starting acetylene) and melted at 308–310°.

Oxidation of Diphenylbutadiyne

(*a*) Diphenylbutadiyne (116.3 mg, 0.58 mmol) was stirred in anhydrous DMSO (3 ml) at room temperature, and NBS (414 mg, 2.32 mmol, 4 mol equiv) was added in portions during a 10 min period. After 2 h the solution, now orange and strongly acidic, was diluted with water (10 ml) and extracted with methylene chloride. This extract was washed with water until the washings were neutral, and then dried over anhydrous magnesium sulfate and evaporated to dryness. The resulting yellow oil showed i.r. absorption at 3.0, 3.3, 4.56 (w), 5.8–6.05 (s), 6.3, 6.7, 6.9, 7.65, and 8.9 μ. The presence of both carbonyl and acetylenic stretching bands suggests that the initial stage of the reaction affords **23** rather than **24**. The t.l.c. analysis of the oil showed it to consist mainly of unreacted diphenylbutadiyne. Therefore, the yellow

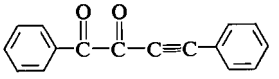

23

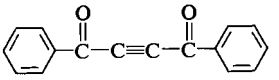

24

oil was redissolved in DMSO (3 ml) and the solution treated with NBS (0.4 g, 2.3 mmol). After 48 h the now bright red solution was diluted with water and extracted with methylene chloride to give, after drying and evaporation of the solvent, a red oil. The t.l.c. analysis showed this oil to contain only a trace of diphenylbutadiyne; its i.r. spectrum showed broad carbonyl absorption at 5.8–6.0 μ. Attempts to crystallize the oil from a variety of solvents were unsuccessful. The oil turned yellow when placed on a column of alumina (Woelm, grade IV), but no material could be eluted.

(*b*) Diphenylbutadiyne (202 mg, 1.0 mmol) and NBS (356 mg, 2 mmol) were dissolved in anhydrous DMSO (10 ml) and the solution was stirred at room temperature for 3 days. The deep red solution was then evaporated to dryness under high vacuum. When the red residue was treated with water (0.4 ml) it immediately turned yellow. Sulfuric acid (0.6 ml) and nitric acid (0.3 ml) were then added and the mixture was refluxed for 1 h. Then glacial acetic acid (1 ml) was added and the mixture was re-

fluxed for a further 2 h (22). Addition of water (10 ml) followed by extraction with petroleum ether, drying of the organic extract and evaporation, afforded a yellow solid. After two recrystallizations from petroleum ether (30–60°) this yellow solid melted at 93–94°. A mixture m.p. with benzil was not depressed.

(*c*) The above experiment was repeated and, after evaporation of the DMSO and addition of water (red → yellow), the mixture was extracted with carbon tetrachloride. The yellow carbon tetrachloride extract was dried and concentrated; after the residue had been maintained at 0.1 mm for 0.5 h it turned red. When this residue was exposed to air the yellow color reappeared instantly. The residue was dissolved in benzene and the yellow solution subjected to slow distillation. After a part of the benzene (and the trace of water) had been removed, the red color reappeared,

(*d*) Diphenylbutadiyne (1.0 g, 5 mmol) was dissolved in anhydrous DMSO (10 ml), and NBS (1.80 g, 10 mmol) was added in four portions at 3 h intervals. When the addition was complete the solution was stirred for 30 h and then extracted with three 100 ml portions of petroleum ether (30–60°) to remove the traces of unreacted diphenylbutadiyne. The red DMSO phase was then diluted with water (50 ml) (red → yellow) and extracted with three 50 ml portions of ether. The ether extract was washed thoroughly with water, dried, and evaporated to a residue which weighed 1.5 g. This residue was dissolved in ethanol (20 ml), hydroxylamine hydrochloride (690 mg, 10 mmol) was added, and this solution was refluxed briefly and then allowed to stand overnight. Water was added, the mixture extracted with chloroform, and the dried chloroform extract evaporated. The resulting product was purified by column chromatography on silica gel (25 g) with graded mixtures of petroleum ether (30–60°) and ether. Recrystallization from benzene–petroleum ether gave the dioxime of diphenyltetraketone, m.p. 173–175° dec. (lit. (20) 176°).

We thank the National Research Council of Canada for support of this work.

1. L. F. Fieser and M. Fieser. Reagents for organic synthesis. John Wiley and Sons, Inc., New York, N.Y., 1967. pp. 74, 79.
2. H. Reich and T. Reichstein. Helv. Chim. Acta, **26**, 562 (1943); L. F. Fieser and S. Rajagopalan. J. Amer. Chem. Soc. **71**, 3938 (1949); B. A. Koechlin, T. Kritchevsky, and T. F. Gallagher. J. Biol. Chem. **184**, 393 (1950); J. Fried and E. F. Sabo. J. Amer. Chem. Soc. **75**, 2273 (1953); C. O. Guss and R. Rosenthal. J. Amer. Chem. Soc. **77**, 2549 (1955); R. A. B. Bannard and L. R. Hawkins. Can. J. Chem. **36**, 1241 (1958); E. J. Langstaff, E. Hamanaka, G. A. Neville, and R. Y. Moir. Can. J. Chem. **45**, 1907 (1967).
3. E. E. van Tamelen and K. B. Sharpless. Tetrahedron Lett. 2655 (1967).
4. D. R. Dalton and D. G. Jones. Tetrahedron Lett. 2875 (1967); D. R. Dalton, V. P. Dutta, and D. C. Jones. J. Amer. Chem. Soc. **90**, 5498 (1968).
5. S. Wolfe and W. R. Pilgrim. Abstracts of the 49th Canadian Chemical Conference. Saskatoon, Saskatchewan, 1966. p. 78.
6. S. F. Reed. J. Org. Chem. **30**, 2195 (1965).
7. W. R. Pilgrim. Ph.D. Thesis. Queen's University, Kingston, Ontario, 1969.
8. N. Kornblum, J. W. Powers, G. J. Anderson, W. J. Jones, H. O. Larsen, O. Levand, and W. M. Weaver. J. Amer. Chem. Soc. **79**, 6562 (1957); R. T. Major and H. J. Hess. J. Org. Chem. **23**, 1563 (1958); I. M. Hunsberger and J. M. Tien. Chem. and Ind. 88 (1959).
9. K. E. Pfitzner and J. G. Moffatt. J. Amer. Chem. Soc. **85**, 3027 (1963); J. Amer. Chem. Soc. **87**, 5661, 5670 (1965).
10. K. H. Scheit and W. Kampe. Angew. Chem. Int. Ed. Engl. **4**, 787 (1965).
11. N. A. Khan and M. S. Newman. J. Org. Chem. **17**, 1063 (1952).
12. A. Krebs and H. Kimling. Tetrahedron Lett. 761 (1970).
13. E. Schipper, M. Cinnamon, L. Rascher, Y. H. Chiang, and W. Oroshnik. Tetrahedron Lett. 6201 (1968).
14. D. V. C. Awang and S. Wolfe. Can. J. Chem. **47**, 706 (1969).
15. C. R. Johnson and W. G. Phillips. J. Amer. Chem. Soc. **91**, 682 (1969).
16. E. R. H. Jones. Proc. Chem. Soc. 199 (1960).
17. J. D. Bu'Lock. *In* Progress in organic chemistry. Vol. 6. *Edited by* J. W. Cook and W. Carruthers, Butterworths, London, 1964. p. 86.
18. T. Money, I. L. Qureshi, G. B. Webster, and A. I. Scott. J. Amer. Chem. Soc. **87**, 3004 (1965); T. Money, J. L. Douglas, and A. I. Scott. J. Amer. Chem. Soc. **88**, 624 (1966).
19. L. Horner and F. Maurer. Ber. **101**, 1783 (1968).
20. P. W. Abenius and H. G. Söderbaum. Ber. **24**, 3034 (1891); Ber. **25**, 3468 (1892); *cf.* A. R. Gray and R. C. Fuson. J. Amer. Chem. Soc. **56**, 1367 (1934).
21. P. Ruggli, H. Dahn, and P. Fries. Helv. Chim. Acta, **29**, 302 (1946); A. H. Blatt. J. Amer. Chem. Soc. **58**, 1894 (1936).
22. A. Schönberg and R. C. Azzam. J. Org. Chem. **23**, 286 (1958).
23. A. I. Vogel. A textbook of practical organic chemistry. Longmans, Green and Co. Ltd., London, 1967. p. 927.
24. Organic Syntheses. Coll. Vol. IV. *Edited by* N. Rabjohn. John Wiley and Sons Inc., New York, N.Y., 1963. p. 377.
25. R. N. Renaud and L. C. Leitch. Can. J. Chem. **42**, 2089 (1964).
26. O. M. Behr, G. Eglinton, I. Lardy, W. McCrae, and R. A. Raphael. *In* Advances in organic chemistry. Vol. 4. *Edited by* R. A. Raphael, E. C. Taylor, and H. Wynberg, Interscience, New York, N.Y., 1963. p. 320.
27. Beilstein's Handbuch der Organischen Chemie. Vol. V. Suppl. II. Julius Springer Verlag, Berlin, 1943. p. 540.
28. F. Kröhnke and H. Timmler. Ber. **69**, 614 (1936).
29. H. L. Riley, J. F. Morley and N. A. C. Friend. J. Chem. Soc. 1875 (1932).
30. Dictionary of organic compounds, Vol. 2. Eyre and Spottiswoode Publishers Ltd., London, 1965. p. 923.
31. Dictionary of organic compounds. Vol. 4. Eyre and Spottiswoode Publishers Ltd., London, 1965. p. 2714.
32. Beilstein's Handbuch der Organischen Chemie. Vol. I. Suppl. I. Julius Springer Verlag, Berlin, 1928. p. 399.
33. Z. Rappoport. Handbook of tables for organic compound identification. Third edition. The Chemical Rubber Co., Cleveland, Ohio, 1964. p. 151.
34. S. Safe, W. D. Jamieson, W. R. Pilgrim, and S. Wolfe. Can. J. Chem. **48**, 1171 (1970).

Can. J. Chem. Downloaded from www.nrcresearchpress.com by 210.87.254.105 on 09/05/12
For personal use only.

Dielectric Studies. Part XXXI. Analysis of the Dielectric Data of Phenol and its Polymerized Forms

M. D. MAGEE
Department of Chemistry, University of Bradford, Yorkshire, England
AND
S. WALKER
Department of Chemistry, Lakehead University, Thunder Bay, Ontario

Received November 4, 1970

The dielectric absorption and dispersions of several solutions of phenol in *p*-xylene have been measured at four microwave frequencies and at 2 MHz at a temperature of 25 °C. The data have been analyzed in terms of a mean relaxation time, a distribution parameter, and an apparent dipole moment which are useful empirical parameters for assessing the state of aggregation of the phenol molecules. The relaxation time at the lowest practicable concentration (0.02 mole fraction) is long for a molecule expected to relax predominantly by an intramolecular process. This and the behavior of the relaxation time and apparent dipole moment with increasing concentration are considered in terms of a model based on progressive association into an extended series of multimers, the trimer having a zero (or low) dipole moment and higher multimers becoming increasingly flexible.

On a mesuré l'absorption et la dispersion diélectrique de solutions de phénol dans le *para*-xylène à quatre fréquences microonde ainsi qu'à 2 MHz, à 25 °C. Les résultats ont été analysés en termes d'un temps de relaxation moyen, d'un paramètre de distribution ainsi que d'un moment dipolaire apparent qui sont des paramètres empiriques utiles pour caractériser l'état d'aggrégation des molécules de phénol. Le temps de relaxation à la concentration la plus faible à laquelle il a été possible de le mesurer (0.02 en fraction molaire), est grand pour une molécule dont le processus de relaxation serait à prédominance intramoléculaire. Ce fait ainsi que la variation du temps de relaxation et du moment dipolaire apparent avec la concentration ont été interprétés en termes d'un modèle basé sur une association progressive en un nombre de plus en plus grand de multimères, le trimère possédant un moment dipolaire nul (ou faible) et les multimères d'ordre supérieur étant progressivement de plus en plus flexibles.

Canadian Journal of Chemistry, 49, 1106 (1971)

Introduction

Association of phenol in solutions has been studied by several physical methods (1) notable among which are infrared, nuclear magnetic resonance (n.m.r.), and polarization measurements. Fischer (2) has employed radiofrequency measurements to study the relationship between dielectric relaxation and self-association of phenols in carbon tetrachloride, while Aihara and Mansel Davies (3) considered some aspects of association in a more general study. More recently Garg and Smyth (4) have studied alcohols at microwave and lower frequencies. Malecki and Doperala (5) have also shown how dielectric polarization yields much information on the association of alcohols. However, detailed microwave investigations of the dielectric relaxation of phenol in solution with a view to obtaining more data on self-association seem to be lacking although this technique yields relaxation times, distribution coefficients, and dipole moments, each of which might be sensitive to the interactions. Our publications (6, 7) on dilute solutions of phenols have not been primarily concerned with association.

The initial intent in the present study was to examine phenol, a molecule well known to associate in dilute solution at different concentrations, in an attempt to determine how sensitive the relaxation parameters are to changes in the nature of the associated species, and how they correlate with dipole moment alteration.

Experimental

Apparatus

The apparatus and procedure for determining the dielectric constant (ε') and loss factor (ε'') have been described previously (8) and sources of error have been assessed (9). Measurements were made at four microwave frequencies ($\omega/2\pi$); 9.313, 16.20, 23.98, and 34.86 GHz. In addition the dielectric constant (ε_0) was determined at a frequency (2 MHz), very low compared with the microwave measurements, using a "Dipolmeter" DM 01. The viscosity (η) of each solution was measured using an Ubbelohde viscometer with the pure solvent as a standard. The solutions were made up in *p*-xylene and all measurements were made at 25 ± 0.01 °C.

Evaluation of Data

The Cole–Cole (10) equation

$$[1] \qquad \varepsilon' - i\varepsilon'' = \varepsilon_\infty + \frac{\varepsilon_0 - \varepsilon_\infty}{1 + (i\omega\tau_0)^{(1-\alpha)}}$$

TABLE 1. Experimental and calculated dielectric constants and losses for solutions of phenol in *p*-xylene at 25 °C

Mole fraction	Frequency (GHz)	ε_{obs}'	ε_{calcd}'	ε_{obs}''	ε_{calcd}''
0.0221	34.86	2.26_7	2.27_6	0.015_1	0.016_9
	23.98	2.27_1	2.28_2	0.020_2	0.021_4
	16.20	2.30_1	2.29_0	0.028_2	0.024_6
	9.313	2.30_3	2.30_3	0.020_5	0.023_2
0.0510	34.86	2.30_2	2.30_2	0.037_2	0.036_8
	23.98	2.30_7	2.31_3	0.043_4	0.044_8
	16.20	2.33_5	2.32_9	0.053_2	0.051_2
	9.313	2.35_1	2.35_5	0.051_0	0.052_4
0.0800	34.86	2.30_2	2.32_1	0.049_7	0.050_0
	23.98	2.32_2	2.33_4	0.065_0	0.066_5
	16.20	2.37_5	2.35_8	0.085_0	0.083_6
	9.313	2.40_8	2.40_5	0.092_9	0.094_8
0.1674	34.86	2.35_8	2.37_6	0.094_5	0.095_7
	23.98	2.38_8	2.39_9	0.122_9	0.123_3
	16.20	2.46_3	2.43_4	0.156_8	0.155_3
	9.313	2.51_3	2.50_9	0.194_0	0.195_5
0.2751	34.86	2.42_5	2.44_4	0.143_4	0.151_0
	23.98	2.47_2	2.47_6	0.199_5	0.197_0
	16.20	2.55_4	2.52_6	0.264_5	0.254_4
	9.313	2.63_4	2.63_9	0.334_3	0.341_3

was fitted to the data by an iterative method using an Elliott 803 computer. The disposable parameters of eq. 1 are a mean relaxation time (τ_0), a distribution coefficient (α), and the high frequency dielectric constant (ε_∞). From the dispersion of the dielectric constant ($\varepsilon_0 - \varepsilon_\infty$) the apparent dipole moment of phenol can be found from Debye's equation (11)

$$[2] \quad \mu = \left[\frac{9k}{4\pi N} \cdot \frac{(\varepsilon_0 - \varepsilon_\infty)}{f_2} \cdot \frac{M_1 T}{(\varepsilon_1 + 2)^2 d_1}\right]^{\frac{1}{2}}$$

where k is Boltzmann's constant, N is Avogadro's number, f_2 is the mole fraction of the solute, M_1 is the molecular weight of the solvent, d_1 is the density of the solvent of dielectric constant ε_1, and T is the absolute temperature.

The procedure used previously (6, 7, 9) of analyzing the data into two discrete relaxation times is assumed to be vitiated for the phenol solution owing to the multiplicity of dipolar hydrogen bonded species likely to be present.

Purification of Materials

The phenol was distilled from a spinning band column of 30 theoretical plates and a small central fraction selected. It was stored in a dark stoppered bottle in a darkened dry cupboard until needed. The *p*-xylene was dried and distilled over sodium and stored in amber winchesters over sodium wire.

Results

The accuracy of the loss factor and dielectric constant results for each waveband have been discussed previously (9) and the experimental results are given in Table 1 together with values of the dielectric constant and loss factor calculated by the Cole–Cole equation from the parameters giving the best fit. In Table 2 the mean relaxation time, distribution coefficient, static and high frequency dielectric constants, and apparent dipole moments of each solution are listed. Since the viscosities of the more concentrated solutions are appreciably greater than those of the dilute solutions, the reduced relaxation times (τ') are listed also, where

$$[3] \quad \tau' = \tau_0 \eta_1 / \eta$$

and η_1 is the viscosity of the solvent and η that of the solution. The relevant parameters τ_0, τ', and μ_{app} are plotted against concentration expressed as mole fraction in Figs. 1 and 2.

Discussion

From the plot of the mean and reduced relaxation times against concentration in Fig. 1, the limiting value at infinite dilution obtained by extrapolation is about 10×10^{-12} s. Of the values in Fig. 1 this would be the nearest to the relaxation time of an isolated phenol molecule in *p*-xylene. The value is surprisingly similar to the relaxation times obtained for rigid molecules of similar size and shape in similar environments *e.g.* bromobenzene in cyclohexane (8) at 20 °C ($\tau_0 = 12 \times 10^{-12}$ s) and nitrobenzene in *p*-xylene (12) at 25 °C ($\tau_0 = 13.1 \times 10^{-12}$ s). However, an important factor expected to shorten the mean relaxation time of an isolated phenol molecule is a contribution from OH group relaxation with a con-

Can. J. Chem. Downloaded from www.nrcresearchpress.com by 210.87.254.105 on 09/05/12
For personal use only.

TABLE 2. Mean (τ_0) and reduced (τ^1) relaxation times, distribution coefficients (α), static (ε_0) and high frequency (ε_∞) dielectric constants, and apparent dipole moments (μ_{app}) of the solutions listed in Table 1 (relaxation times are in ps and dipole moments in Debyes)

Concentration (mole fraction)	τ_0	τ^1	α	ε_0	ε_∞	μ_{app}
0.0221	11.7	10.6	0	2.319_3	2.26_9	1.51
0.0510	13.8	12.1	0.11	2.408_4	2.28_1	1.55
0.0800	16.7	14.1	0.02	2.501_1	2.30_5	1.57
0.1674	28.5	21.1	0.15	2.866_9	2.33_2	1.81
0.2751	41.4	26.5	0.17	3.468_6	2.37_9	1.99

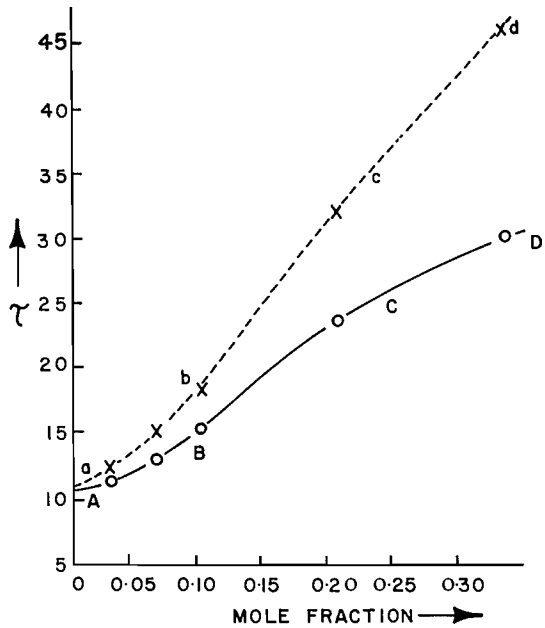

FIG. 1. Variation of mean (curve *abcd*) and reduced (curve *ABCD*) relaxation times of phenol with concentration at 25 °C. Relaxation times are in ps. The continuous curve is a calculated one and is to be compared with the data in Table 2.

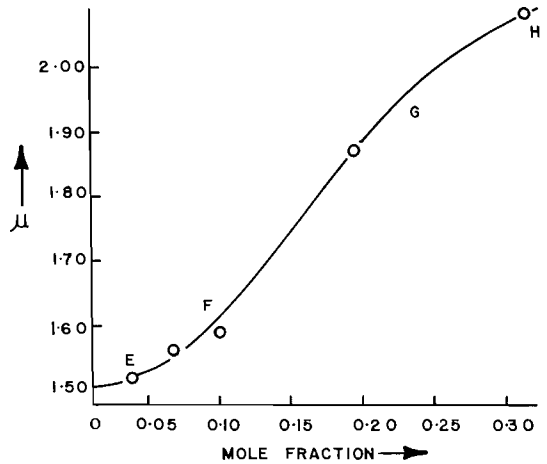

FIG. 2. Variation of apparent dipole moment (in D) of phenol with concentration in *p*-xylene at 25 °C. The continuous curve is a calculated one and is to be compared with the data in Table 2.

siderably shorter relaxation time. Hydroxyl group relaxation has been noted in previous communications (6, 7) on a variety of phenols in some of which the double bond character and therefore the rotational energy barrier of the C—O bond is greater than that of the phenol itself. Hydroxyl group relaxation has also been demonstrated by other workers (3, 13) in a number of phenols, and from this work it seems reasonable to expect OH group rotation in phenol to have a relaxation time of about 3.5×10^{-12} s (13).

There is a number of ways of estimating the mean relaxation time from the contributing group and molecular relaxation times (14) and it is enlightening to carry this out for phenol. The linear relationship

$$[4] \qquad \tau_0' = C_1\tau_1' + C_2\tau_2'$$

where τ_1' is the overall molecular relaxation time and τ_2' the group relaxation time will yield rather too long an estimate for τ_0', providing that the weight factor C_1 is less than about 0.6 and τ_1' and τ_2' are not too dissimilar (14). The weight factors C_1 and C_2 can be obtained by bond or group dipole moment considerations:

(*a*) Group moments: the hydroxyl group moment of 1.54 D (15) acts at 76° (16) from the direction of the O—C bond, so that the component (μ_1') along the bond responsible for molecular relaxation is (1.54 (15) cos 76°) D, while the component (μ_2') perpendicular to the bond responsible for group relaxation is (1.54 sin 76°) D. The weight factors for the molecular process (C_1) and the group process (C_2) are, respectively,

Can. J. Chem. Downloaded from www.nrcresearchpress.com by 210.87.254.105 on 09/05/12
For personal use only.

Can. J. Chem. Downloaded from www.nrcresearchpress.com by 210.87.254.105 on 09/05/12
For personal use only.

$\mu_1'^2/(\mu_1'^2 + \mu_2'^2) = 0.06$ and $\mu_2'^2/(\mu_1'^2 + \mu_2'^2) = 0.94$.

(*b*) Bond moments: the moment along the H—O bond is taken to be 1.5 D and that along the C—O bond is 1.0 D (16), the angle between the bonds (17) being 115°. There is also a component along the C—O axis due to the *p*-CH bond. This is taken to be 0.4 D acting into the benzene ring (16). Resolving as in (*a*), the component (μ_1') along O—C is (1.4–1.5 cos 65°) D and (μ_2') perpendicular to the O—C bond (1.5 sin 65°) D. The weight factors are obtained as before as $C_1 = 0.20$ and $C_2 = 0.80$.

The difference in C values for the two methods may perhaps be attributed to the neglect of mesomeric moments in (*b*) whereas this is allowed for in the group moments in (*a*). The calculations do show, however, that the contribution from group relaxation should be dominant. Inserting these values in eq. 4 and taking τ_2' to be 3.4×10^{-12} s, and τ_1' to be that already quoted for bromobenzene (12×10^{-12} s), owing to its similar size and shape to phenol, we obtain the estimated values for τ_0' of 3.9×10^{-12} s (group moments) and 5.1×10^{-12} s (bond moments). These values are less than a half of the observed value in Table 2, and it will be recalled that the estimate will tend to be too long (14).

More direct comparison can be made with the mean relaxation time of anisole, a molecule which primarily differs from phenol only in having a larger rotating group, OCH_3 instead of OH. Since both the group and molecular relaxation times (18) of this molecule should be longer than those of phenol, the mean relaxation time should also be longer. In fact, the value obtained is only 8.2×10^{-12} s at 25 °C in cyclohexane. 2,6-Di-*tert*-butylphenol is also a useful molecule for assessing the expected influence of the OH group. Although this is a much bigger molecule than phenol, its mean relaxation time is only 8.6×10^{-12} s in *p*-xylene at 25 °C, and this, of course, can be due only to a predominant contribution of OH relaxation with a short relaxation time, since the molecular relaxation time must be longer than that of benzotrichloride which in *p*-xylene at 25 °C has a value of 20×10^{-12} s (19). Clearly therefore, 10×10^{-12} s is anomalously long for the dilute solution relaxation time of phenol, and it seems that even at our lowest concentrations the mean relaxation time of phenol might be substantially lengthened by intermolecular association, due either to solute–solute interactions or to hydrogen bonding of the phenol to the π-electron cloud of the solvent.

Association by hydrogen bonding would lengthen the mean relaxation time (*i*) by introducing bigger species into solution, (*ii*) by lengthening the group relaxation time, and (*iii*) possibly by creating a longer relaxation time associated with the formation and disruption of the complexes. Dimers and higher multimers are, in fact, present in phenol solution at low concentrations as is shown by infrared data (20). Thus, in carbon tetrachloride, about 40% of the phenol is polymerized even at a concentration of 0.02 mole fraction, and although this fraction would be expected to be lower in a more interactive solvent such as *p*-xylene, it must still be considerable. It seems likely, therefore, that self-association is an important influence upon the mean relaxation time at our lowest concentration, but it is possible that solvent–solute interactions may also lengthen τ_0.

If the enhanced relaxation time of phenol at this concentration is primarily due to self-association, then at lower concentrations than those accessible by this technique, the mean relaxation time should fall rapidly. Radio-frequency measurements (21) have revealed behavior of this sort for solutions of eugenol in carbon tetrachloride. At eugenol concentrations below 0.01 mole fraction the mean relaxation time shortens so rapidly that it is impossible to extrapolate reliably to the infinite dilution value.

The plots of mean and reduced relaxation time against concentration in Fig. 1 may be compared with the behavior of apparent dipole moment against concentration in Fig. 2. There is closer correspondence in shape and variation in gradient between the dipole moment plot (*EFGH*) and the reduced relaxation time plot (*ABCD*) than with the mean relaxation time plot (*abcd*). In fact the regions *AB* and *EF* in the respective plots covering mole fractions between 0.02 and 0.08 indicate much less variation in these parameters than between *BC* and *FG* covering the range 0.08–0.20. Between 0.20 and 0.25 the reduced relaxation time and the apparent dipole moment plots begin to level off, and this is to be contrasted with the mean relaxation time plot which is virtually linear between mole fractions 0.08 and 0.25. It is inter-

Can. J. Chem. Downloaded from www.nrcresearchpress.com by 210.87.254.105 on 09/05/12
For personal use only.

esting to note that the reduced relaxation time which is mainly reflecting the increasing sizes of the complexes with rising concentration parallels the behavior of the increasing dipole moment which reflects alignment of the dipoles due to association. This suggests that it might be possible to construct a model system based on such data from which some insight into the phenol behavior can be obtained.

Theoretical Treatment

Let us consider that the phenol associates into a whole series of multimers. We shall denote the monomer, dimer etc. by A_1, A_2 etc. and corresponding concentrations by a_1, a_2 etc. Activities will be taken as equivalent to concentrations

$$[5]\quad \begin{aligned} 2A_1 &\rightleftarrows A_2 & K_2 &= a_2/a_1^2 \\ A_1 + A_2 &\rightleftarrows A_3 & K_3 &= a_3/a_1a_2 \\ &\vdots & &\vdots \\ A_1 + A_{n-1} &\rightleftarrows A_n & K_n &= a_n/a_1a_{n-1} \end{aligned}$$

Provided that solutions are not too strong the total concentration of phenol is

$$[6]\quad a = a_1 + 2a_2 + 3a_3 + \cdots + na_n$$

From eq. 5 this becomes

$$[7]\quad a = a_1 + 2K_2a_1^2 + 3K_3K_2a_1^3 + \cdots + nK_nK_{n-1}\cdots K_2a_1^n$$

Each step in the formation of the multimers is the creation of a hydrogen bond between hydroxyl groups. The successive reactions are therefore chemically very similar, the size of the reacting species being the major difference; therefore let us consider the case where

$$K_2 = K_3 = K_4 = \cdots = K_n = K$$

This assumption should hold more closely for higher multimers than for the dimer and trimer (and there is some evidence (22), which we shall discuss later, that K_3 is somewhat greater than K_2); thus this assumption becomes more justifiable with increasing concentration. Thus we have from [7]

$$[8]\quad a = a_1 + 2Ka_1^2 + 3K^2a_1^3 + \cdots + nK^{n-1}a_1^n$$

The degree of association of the phenol is conveniently expressed in terms of a parameter α_1, the proportion of phenol remaining in the monomeric form

$$[9]\quad \alpha_1 = a_1/a$$

$$[10]\quad (1/\alpha_1) = 1 + 2Ka_1 + 3K^2a_1^2 + \cdots + nK^{n-1}a_1^{n-1}$$

Provided that Ka_1 $(= Ka\alpha_1) < 1$ (which is the case for the solutions examined here) this sums to

$$[11]\quad \frac{1}{\alpha_1} = \frac{1}{(1 - Ka_1)^2} = \frac{1}{(1 - Ka\alpha_1)^2}$$

Equation 11 enables α_1 to be determined as a function of "a" (the initial phenol concentration) for any chosen value of K. Let us now apply a similar type of treatment to the dipole moments.

We may write

$$[12]\quad a\mu^2 = a_1\mu_1^2 + a_2\mu_2^2 + a_3\mu_3^2 + \cdots + a_n\mu_n^2$$

$$[13]\quad = a_1\mu_1^2 + Ka_1^2\mu_2^2 + K^2a_1^3\mu_3^2 + \cdots + K^{n-1}a_1n_{\mu_n}^2$$

$$[14]\quad (\mu^2/\alpha_1) = \mu_1^2 + Ka_1\mu_2^2 + K^2a_1^2\mu_3^2 + \cdots + K^{n-1}a_1^{n-1}\mu_n^2$$

For a cyclic trimer, μ_3 is close to zero so let $\mu_3 = 0$. The dipole moment of the higher multimers might be expected to tend to a limiting value since eventually curling and folding will occur (16). Hence the model consists of the formation of a series of multimers, initially approximately linear, with the exception of A_3, for which the non-polar cyclic structure is assumed to be preferred, but the higher multimers becoming increasingly folded so that their dipole moments do not increase linearly but reach a limiting value of μ_m.

Utilizing these ideas in eq. 14, extracting μ_m^2 from the series and performing the summation yields

$$[15]\quad \left[\frac{\mu^2}{\alpha_1} - \mu_1^2\right]\frac{1}{Ka_1} = \mu_2^2 + \frac{(Ka_1)^2}{1 - Ka_1}\mu_m^2$$

Whereas the additivity of μ^2 is well known, there is no precise additivity for relaxation times. In a previous paper we considered various relationships between the observed mean relaxation time (τ_0') and component relaxation times (τ_1', τ_2') and their weight factors (C_1, C_2) for systems having two contributory relaxation times. The simplest relationships are (*i*) a linear approximation eq. 4, which is true for the mean relaxation

Can. J. Chem. Downloaded from www.nrcresearchpress.com by 210.87.254.105 on 09/05/12
For personal use only.

time obtained from low frequency measurements but generally a poor approximation for the mean relaxation time obtained from microwave measurements, and (*ii*) a logarithmic approximation

$$[16] \quad \log \tau_0' = C_1 \log \tau_1' + C_2 \log \tau_2'$$

which in general is likely to give better agreement with the results of microwave measurements than is eq. 4.

In the more general case of several contributory relaxation times, these equations can be extended to

$$[17] \quad \tau_0 = \sum_{i=1}^{n} C_i \tau_i$$

$$[18] \quad \log \tau_0 = \sum_{i=1}^{n} C_i \log \tau_i$$

Now C_i is related to the concentration (a_i) and dipole moment (μ_i) of the ith relaxing species by the following equation

$$[19] \quad C_i = \frac{a_i \mu_i^2}{\sum_{i=1}^{n} a_i \mu_i^2}$$

a special case of which we have already used in the calculation of the weight factors expected for group and overall relaxation in phenol monomer. Using eq. 19 in eqs. 17 and 18 and simplifying via eq. 12 yields

$$[20] \quad a\mu^2 \tau_0 = \sum_{i=1}^{n} a_i \mu_i^2 \tau_i$$

in the linear approximation, and

$$[21] \quad a\mu^2 \log \tau_0 = \sum_{i=1}^{n} a_i \mu_i^2 \log \tau_i$$

in the logarithmic approximation. For phenol association the subscripts i refer to the ith multimer. We are assuming that $\mu_3 = 0$ and therefore the term in $a_3\mu_3^2 \log \tau_3$ or $a_3\mu_3^2\tau_3$ is eliminated. The overall relaxation time of complexes should increase as the number of included monomer units increases, but this would be counteracted by the increasing flexibility of the chains leading to a rising number of intramolecular relaxation modes of shorter relaxation time. Thus it would not seem unreasonable to suppose that the relaxation time of the higher multimers approached a constant value τ_m. This supposition permits a treatment of eqs. 20 and 21 analogous to the treatment of dipole moments and giving, in the linear approximation

$$[22] \quad \left[\frac{\mu^2\tau_0}{\alpha_1} - \mu_1^2\tau_1\right]\frac{1}{Ka_1} = \mu_2^2\tau_2 + \frac{(Ka_1)^2}{1 - Ka_1}\mu_m^2\tau_m$$

and in the logarithmic approximation

$$[23] \quad \left[\left(\frac{\mu^2 \log \tau_0}{\alpha_1} - \mu_1^2 \log \tau_1\right)\right]\frac{1}{Ka_1} = \mu_2^2 \log \tau_2 + \frac{(Ka_1)^2}{1 - Ka_1}\mu_m^2 \log \tau_m$$

It may be considered that the supposition of τ_i approaching the constant value τ_m overemphasizes the influence of flexibility. An alternative approximation would be that the relaxation times of the multimers increase directly in proportion to their size *i.e.* that $\tau_n = n\tau_{unit}$ where τ_{unit} might be expected approximately to equal τ_1, the overall relaxation time of a monomeric phenol molecule. Internal modes of relaxation, however, would have the effect of shortening τ_{unit}. Utilizing this approximation in the linear approximation gives

$$[24] \quad \left(\frac{\mu^2\tau_0}{\alpha_1} - \mu_1^2\tau_1\right) = Ka_1\mu_2^2\tau_2 + [4(Ka_1)^3 + 5(Ka_1)^4 + \ldots (n+1)(Ka_1)^n + \ldots]\mu_m^2\tau_{unit}$$

The portion of eq. 24 in brackets is part of a series of the form

$$1 + ax + (a + b)x^2 + (a + 2b)x^3 + \cdots$$

where $a = 2$ and $b = 1$ in our case. This series has a finite sum and subtraction of the missing terms $(1 + 2x + 3x^2)$ gives $x^3(4 - 3x)/(1 - x)^2$ where x is Ka_1. Hence we obtain

$$[25] \quad \left(\frac{\mu^2\tau_0}{\alpha_1} - \mu_1^2\tau_1\right)\frac{1}{Ka_1} = \mu_2^2\tau_2 + \frac{(Ka_1)^2}{(1 - Ka_1)^2}(4 - 3Ka_1)\cdot\mu_m^2\tau_{unit}$$

The treatment has yielded a series of equations by which the data can be plotted in the form of a straight line from a knowledge of μ, μ_1, τ_0, τ_1, and K. Figures 3, 4, 5, and 6 show the results plotted according to eqs. 15, 22, 23, and 25, respectively, where concentrations are expressed in mole fractions using 5 mf^{-1} (see later) for the

TABLE 3. Dipole moment and relaxation time data for phenol–*p*-xylene solutions expressed in terms of the functions yielded by eqs. 15, 22, 23, and 25. The equilibrium constant for multimer formation is taken to be 5 mf^{-1} and infinite dilution values of the phenol dipole moment and relaxation time are 1.50 D (*i.e.* μ_1) and 10 ps (*i.e.* τ_1), respectively

a	*b*	*c*	*d*	*e*	*f*	*g*	*h*	*i*	*j*	*k*
0.000	1.000	—	—	—	0.000	0.000	1.500	1.50	10.0	10.0
0.0221	0.826	5.58	74	0.755	0.009	0.038	1.508	1.51	10.6	10.6
0.0510	0.680	7.51	109	1.69	0.036	0.153	1.535	1.55	12.1	12.1
0.0800	0.586	8.35	157	2.68	0.072	0.313	1.596	1.57	14.5	14.1
0.1674	0.422	15.60	401	7.30	0.192	0.874	1.809	1.81	20.9	21.1
0.2751	0.316	23.62	713	12.20	0.337	1.608	1.987	1.99	26.1	26.6

[a]Initial phenol concentration in mole fraction.
[b]Proportion of phenol monomer (α_1).
[c]$(\mu^2/\alpha_1 - \mu_1^2)\ (1/Ka\alpha_1)$.
[d]$(\mu^2\tau_0/\alpha_1 - \mu_1^2\tau_1)\ (1/Ka\alpha_1)$.
[e]$(\mu^2 \log \tau_0/\alpha_1 - \mu_1^2 \log \tau_1)\ (1/Ka\alpha_1)$, relaxation times in units of 10^{-11} s.
[f]$(Ka\alpha_1)^2/(1 - Ka\alpha_1)$.
[g]$(Ka\alpha_1)^2(4 - 3Ka\alpha_1)/(1 - Ka\alpha_1)^2$.
[h]Observed dipole moment.
[i]Moment calculated with $\mu_2 = 2.24$ D and $\mu_m = 7.41$ D from eq. 15.
[j]Observed reduced relaxation time.
[k]Reduced relaxation time calculated with $\tau_2 = 12$ ps and $\tau_m = 42$ ps from eq. 23.

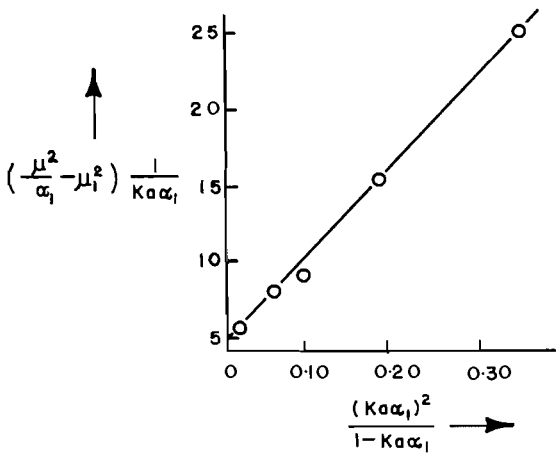

FIG. 3. Plot of dipole moment data according to eq. 15.

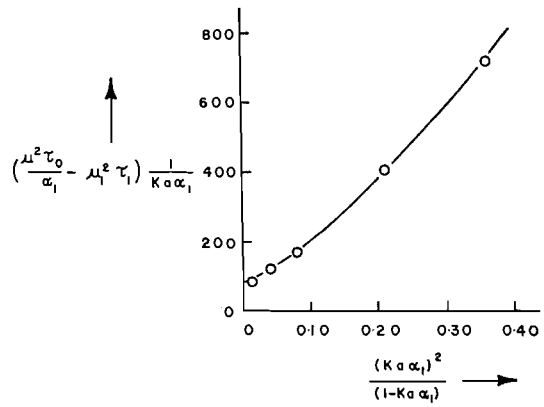

FIG. 4. Plot of dipole moment and relaxation data according to eq. 22. This plot is not linear over its full range possibly owing to the faulty assumption of linear additivity of relaxation times.

value of the association constant. The relevant variables are tabulated in Table 3.

Further Discussion of Results

The dipole moment data plotted in Fig. 3 according to eq. 15 give a good linear plot. From the slope μ_m is obtained as 7.41 D, and the intercept gives μ_2 as 2.24 D. Similarly the reduced relaxation time data plotted according to eq. 23 (see Fig. 5) in the logarithmic approximation, yields an excellent straight line, but the two equations based on the linear approximation yield gentle curves (see Fig. 4). Thus logarithmic additivity of relaxation times would again seem the better approximation for microwave data.

From the straight line in Fig. 5 and the values of μ_2 and μ_m derived from Fig. 3, τ_2 is found to be 12×10^{-12} s and $\tau_m = 42 \times 10^{-12}$ s corresponding to a mean relaxation time for the higher multimers of 65×10^{-12} s in the 0.275 *mf* solution.

In Fig. 6 the plot differs only slightly from linearity and permits τ_{unit} to be estimated as about 8×10^{-12} s in reasonable agreement with the extrapolated relaxation time for phenol monomer of 10×10^{-12} s (and in good agreement with the mean relaxation time of anisole of 8.2×10^{-12} s). The τ_2 estimate is again 12×10^{-12} s.

Since the treatment of the data requires a prior knowledge of *K*, some discussion of the choice of 5 mf^{-1} is required. Pimentel and McClellan (1) quote several values for phenol in systems similar

Can. J. Chem. Downloaded from www.nrcresearchpress.com by 210.87.254.105 on 09/05/12
For personal use only.

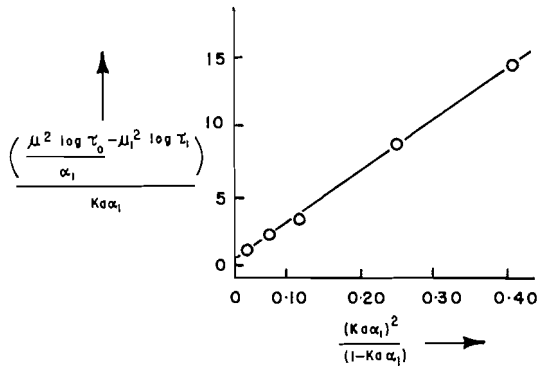

FIG. 5. Plot of dipole moment and relaxation time data according to eq. 23. In this case, for simplicity, τ_1 is expressed in units of 10^{-11} s.

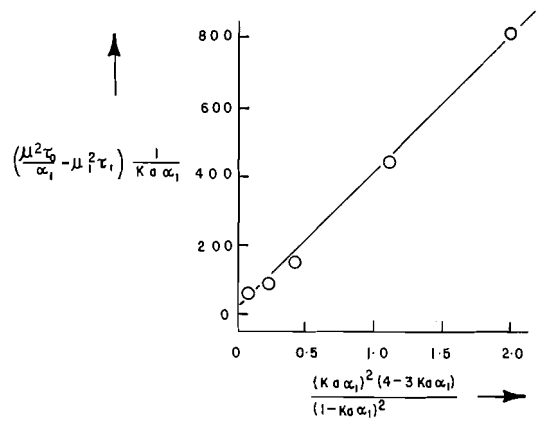

FIG. 6. Plot of dipole moment and relaxation time data according to eq. 25. Like Fig. 4 this graph is not exactly linear because of the faulty assumption for relaxation time addition.

to ours: 0.57 l mole^{-1} for phenol in benzene by vapor pressure and infrared measurements and 0.843 l mole^{-1} for phenol in toluene by a distribution method, while Mecke (20) gives data obtained from infrared measurements on the basis of a model identical to ours from which association constants of 0.24 and 3 l mol^{-1} can be calculated for phenol in benzene and carbon tetrachloride, respectively. The conversion of 1 mol^{-1} to mf^{-1} involves a factor of $1000d/M$ (where d is density of the solution and M is the molecular weight of the solute) which for $d \sim 1$ and $M \sim 100$ is close to 10. Hence the values quoted above are close to $5\,mf^{-1}$ in aromatic solvents.

It is relevant to ask how credible is the model assumed. Workers on n.m.r. interpreted their data (22) on the basis of a far simpler model consisting of a single equilibrium between monomer and multimer, all other multimers being neglected. The change in chemical shift was calculated for a monomer–dimer equilibrium, then monomer–trimer, and finally monomer–tetramer. For phenol in carbon tetrachloride the monomer–trimer equilibrium gave the closest data fit, and therefore the trimer was assumed to be the dominant species over the concentration range employed. However, for methanol a monomer–tetramer model gave the best fit.

While there is further evidence (5) that the trimer has the greatest formation constant for hydroxyl compounds in fairly inert solvents, such as carbon tetrachloride and cyclohexane, it seems that a model which excludes all except one multimer is unlikely to be valid in more interacting solvents such as benzene and *p*-xylene. In our case exclusion of all multimers except the cyclic trimer would lead to a marked fall in apparent dipole moment because three polar species are removed in the formation of each trimer of low dipolarity. Hence other polymers exist or the trimer could not be cyclic; a series of multimers seems most probable. The most likely explanation for the higher formation constant of the trimer is that it possesses some special structural stabilization such as cyclization, and if this is disregarded we must again fall back upon the model of an extended series of multimers. Of course, we are mindful of the possibility and even probability that K_3 is somewhat greater than the other equilibrium constants, but the equating of K_3 with the remaining constants may be a better approximation for this system than the neglect of all equilibrium constants except K_3.

The data appertaining to the curves are tabulated in Table 3 and the values of μ and τ for the various solutions calculated from these parameters are included for comparison. The continuous lines in Figs. 1 and 2 are also calculated. It is interesting that τ_m is about five times greater than τ_{unit} and μ_m is also about five times greater than μ_1. This suggests that folding and curling of the multimer chains dominate over straight chain formation when the multimer length is somewhat more than five monomer units. Beyond this complexity, internal relaxation mechanisms may become dominant and the model with τ_m approach-

Can. J. Chem. Downloaded from www.nrcresearchpress.com by 210.87.254.105 on 09/05/12
For personal use only.

ing a limiting value may have some validity. This agrees with n.m.r. work which indicates formation of molecular "clusters" which lose their rigidity above about 0.2 mole fraction (23). Both dipole moment and the relaxation time of the dimer seem low, possibly illustrating flexibility in the dimer.

In conclusion, it seems likely that none of the methods applied to the phenol systems has provided an unambiguous insight as to the various polymers present in the phenol solutions; the success of the model is judged by the ability of the species invoked to fit the experimental data but it still remains a possibility that another model, probably more complex, would give an equally good fit to the data. The procedure we have adopted leads to reasonable values for the various parameters, although it does not then necessarily follow that our model is the correct one. Treatments such as that given here, while limited by the complexity of the system and the nature of simplifying approximations, can nevertheless be illuminating. It would seem at present, however, that no one physical technique yields a complete picture of the behavior of phenols in solution, and by bringing together several techniques more confidence can be gained as to whether the species postulated from the results of one technique are tenable in the light of others or whether more than one model will fit the experimental data. In this treatment an independent accurate determination of K would be invaluable since at the moment we are fitting three parameters K, μ_2, and μ_m to the dipole moment data and two more to the relaxation time data, τ_2 and τ_m. Here we have obtained the order of magnitude of K from the compilation of Pimentel and McClellan (1) and varied it slightly to obtain the best plots and an internally self-consistent set of parameters.

We may conclude that the dielectric absorption approach is of value in that information may be gained on the changing size of the complexed species in solution with increasing concentration, while the dipole moment values may reflect the geometry of the polymerized species.

We wish to thank Mr. B. K. Morgan for his technical assistance. One of us (M.D.M.) thanks Professor D. A. Long for providing the opportunity to complete parts of this work.

1. G. C. PIMENTEL and A. L. MCCLELLAN. The Hydrogen Bond. Freeman and Co., San Francisco and London. 1960.
2. E. FISCHER. Z. Naturforsch. **8a**, 168 (1953).
3. A. AIHARA and M. DAVIES. J. Colloid Sci. **11**, 671 (1956).
4. S. K. GARG and C. P. SMYTH. J. Phys. Chem. **69**, 1294 (1965).
5. J. MALECKI and Z. DOPERALA. Acta Physica Polinica, **36**, 385 (1969).
6. M. D. MAGEE and S. WALKER. Molecular Relaxation Processes. *Edited by* M. Davies. Chem. Soc. and Academic Press, 88 (1966).
7. M. D. MAGEE and S. WALKER. Trans. Faraday Soc. **62**, 1748 (1966).
8. W. F. HASSELL, M. D. MAGEE, S. W. TUCKER, and S. WALKER. Tetrahedron, **20**, 2137 (1964).
9. M. D. MAGEE and S. WALKER. Trans. Faraday Soc. **62**, 3093 (1966).
10. K. S. COLE and R. H. COLE. J. Chem. Phys. **9**, 341 (1941).
11. P. DEBYE. Polar Molecules. Chemical Catalog Co., New York. 1929.
12. M. D. MAGEE and S. WALKER. Unpublished work.
13. F. K. FONG and C. P. SMYTH. J. Amer. Chem. Soc. **85**, 1565 (1963).
14. M. D. MAGEE and S. WALKER. J. Chem. Phys. **50**, 2580 (1969).
15. J. H. RICHARDS and S. WALKER. Trans. Faraday Soc. **57**, 406 (1961).
16. J. W. SMITH. Electric Dipole Moments. Butterworths, London. 1955.
17. C. P. SMYTH. Dielectric Behavior and Structure. McGraw-Hill, New York and London. 1955.
18. D. B. FARMER, A. HOLT, and S. WALKER. J. Chem. Phys. **44**, 4116 (1966).
19. J. CROSSLEY and S. WALKER. Can. J. Chem. **46**, 841 (1967).
20. R. MECKE. Discuss. Faraday Soc. **9**, 161 (1950).
21. E. FISCHER. Z. Naturforsch. **9a**, 360 (1954).
22. M. SAUNDERS and J. B. HYNE. J. Chem. Phys. **29**, 253, 1319 (1958).
23. L. GUILLOTTO, G. LANZI, and L. TOSCA. J. Chem. Phys. **24**, 632 (1956).

Can. J. Chem. Downloaded from www.nrcresearchpress.com by 210.87.254.105 on 09/05/12
For personal use only.

Can. J. Chem. Downloaded from www.nrcresearchpress.com by 210.87.254.5 on 09/05/12
For personal use only.

Ellipsometric Determination of the Spectra of Adsorbed Molecules

M. J. DIGNAM,[1] B. RAO, M. MOSKOVITS,[2] AND R. W. STOBIE
Department of Chemistry, University of Toronto, Toronto 181, Ontario

Received October 29, 1970

This paper presents a detailed analysis of the application of ellipsometry to obtaining the optical spectra (principally infrared (i.r.)) of molecules adsorbed on reflecting surfaces. Both external and total internal reflections are considered and the conditions for optimum sensitivity examined. A new empirical quantity, the relative complex optical density, is defined which exhibits thin film properties well, particularly in the case of multiple reflection measurements. An explicit expression is derived for this density function (relating it to the optical constants of the media and other system parameters), which is both reasonably simple and correct to second order terms in the film thickness. It is shown that for thin films, no higher order terms need be included, but that in general the second order term must be retained. Various limiting cases are examined to gain insight into the optical behavior of thin films, and to the same end, model calculations performed for CCl_4 physically adsorbed on Ag, Ni, Sb, and Ge. In relation to conventional reflection spectroscopy, ellipsometric spectroscopy is shown to have three major advantages: (*1*) in general, higher sensitivity to adsorbate properties; (*2*) very much lower sensitivity to absorption of radiation by the adjacent gas phase; (*3*) more information, permitting the optical constants and film thickness to be determined. Finally, the practicability of the technique is demonstrated by presenting preliminary results for CH_3OH reversibly adsorbed on Ag, showing clearly the C—H stretching bands.

Cette publication présente une analyse détaillée de l'application de l'ellipsométrie pour obtenir le spectre optique (principalement i.r.) de molécules absorbées sur des surfaces réfléchissantes. Les réflexions externes ainsi que les réflexions totales internes sont considérées et les conditions de sensibilité optimum sont examinées. Une nouvelle quantité empirique, la densité optique complexe relative, est définie, elle montre bien les propriétés des films minces, particulièrement dans le cas des mesures de réflexions multiples. Une expression explicite est dérivée pour cette fonction de densité (la reliant à des constantes optiques du milieu et d'autres paramètres du système), qui est raisonnablement simple et correcte jusqu'aux termes du second ordre pour l'épaisseur du film. Il est démontré que pour les films minces, des termes d'ordres supérieurs ne sont pas nécessaires, mais qu'en général, le terme du second ordre doit être retenu. Plusieurs cas limites sont examinés afin de mieux comprendre le comportement optique des films minces et dans le même but, des calculs modèles ont été effectués pour CCl_4 physiquement absorbé sur Ag, Ni, Sb et Ge. Par rapport à la spectroscopie de réflexion conventionnelle, la spectroscopie ellipsométrique possède trois avantages majeurs: (*1*) en général, une sensibilité supérieure aux propriétés d'un adsorbate; (*2*) beaucoup moins de sensibilité à l'absorption de radiation par la phase de gaz adjacent; (*3*) plus d'information, permettant de déterminer les constantes optiques et l'épaisseur du film. Finalement, la practicabilité de la technique est démontrée en présentant les résultats préliminaires pour CH_3OH absorbé réversiblement sur Ag, montrant clairement les bandes C—H de valence.

Canadian Journal of Chemistry, 49, 1115 (1971)

Introduction

Infrared spectroscopy has been applied extensively for the study of adsorption processes on solid surfaces, both to obtain information on adsorbate states as well as on catalytic surface properties (1). Adsorption phenomena frequently are limited to films of monolayer thickness, that is, of thickness about 10 Å or less. The usual method for obtaining the i.r. spectrum of adsorbed species is to employ a standard transmission spectrometer and an absorption cell filled with a porous or powdered material. A more recent technique (2) uses a stack of evaporated metal films, again in conjunction with a standard spectrometer. This technique is restricted to very thin metal films, since metals absorb strongly in the infrared. Thus, for both these techniques, it is extremely doubtful, that the substrate properties correspond to those for the material in bulk. For this reason alone, there is a distinct advantage in studying adsorption processes on bulk metallic surfaces using specular reflectance spectrometry. Lack of sensitivity employing a single reflection has prompted the use of multiple reflections between parallel surfaces (3). Such studies have been carried out on evaporated nickel (4), aluminum (5), silver (6, 7), copper (8), and on germanium by attenuated total internal reflection (9). Even for these studies, quantitative interpretation of the reflected intensity data is difficult, as the intensity is influenced by the refractive index of the film and the substrate optical constants in addition to the film absorption coefficient. Apart from the above problems, conventional i.r.

[1]To whom correspondence should be addressed.
[2]Present address: Aluminum Laboratories Ltd., Kingston, Ontario.

Can. J. Chem. Downloaded from www.nrcresearchpress.com by 210.87.254.5 on 09/05/12
For personal use only.

reflection and transmission techniques suffer from the fact that corrections have to be applied to take into account absorption of radiation by the gas phase whenever reversible adsorption is studied. For reflection studies in particular, such a correction could be so large as to obscure the absorption due to the surface species.

The use of polarized radiation (ellipsometry) for obtaining the spectrum of thin films has to date only been attempted by Bartell and Churchill (10), who used the technique successfully in the u.v.–visible for various films, including organic dyes dispersed in collodion, chelates, and Lewis bases on chromium and nickel; and by Bashara and Peterson (11) who calculated the optical properties of thin layers of polybutadiene evaporated onto Cr and Au films. Such a technique has certain major advantages for obtaining the spectrum of the optical constants of adsorbed molecules in general, and in the i.r. region in particular. A polarization state is uniquely characterized by the amplitude and phase relation between its parallel and perpendicular components. In the gas phase, the two components of the polarized radiation are attenuated to the same extent; thus, the gas phase exerts little influence on the results. In a sense one has an "ideal reference signal" in the use of polarized radiation. Furthermore, the analysis of reflected polarized radiation, both with respect to its phase and amplitude factors, provides information from which the thickness, the refractive index, as well as the chemical extinction coefficient of adsorbed films can be determined.

This paper consists of a detailed study of the application of ellipsometry to obtain the spectra of the optical constants of thin films, followed by model calculations relating to the i.r. spectra of monolayer films. The potential of this technique for monolayer films is then discussed and compared with that for conventional specular reflectance spectrometry.

When plane polarized light is incident on a reflecting surface, amplitude and phase changes are established between the components of the electric vector which lie parallel (p-component) and perpendicular (s-component) to the plane of incidence; the reflected light, is, therefore, in general elliptically polarized. The theory, both for semi-infinite reflecting substrates, and substrates covered by one or more uniform films, is well known (12). We begin by presenting the relevant equations in terms of which we define a quantity called the relative complex optical density D. For thin films and for either single or multiple reflections, D is shown to be proportional to the film thickness and to be nearly independent of substrate optical constants for substrates of good reflectivity. It is, therefore, a very convenient function for exhibiting the properties of thin films. The case of attenuated total internal reflection is also considered.

Reflection Equations

General Relations

Vasicek (13) gives the following expressions for the complex reflection coefficient, r_{jk}, for polarized light incident on medium k from the incident medium j.

$$r_{jk}^{p} = \frac{\hat{n}_k \cos \phi_j - \hat{n}_j \cos \phi_k}{\hat{n}_k \cos \phi_j + \hat{n}_j \cos \phi_k} \quad [1]$$

$$r_{jk}^{s} = \frac{\hat{n}_j \cos \phi_j - \hat{n}_k \cos \phi_k}{\hat{n}_j \cos \phi_j + \hat{n}_k \cos \phi_k} \quad [2]$$

where the superscripts p and s identify the polarization state of the incident light, n_j, is the complex refractive index of medium j, and ϕ_j is the complex angle of propagation in medium j measured from the normal to the interface. The angles ϕ_j and ϕ_k are related through Snell's law

$$\hat{n}_j \sin \phi_j = \hat{n}_k \sin \phi_k \quad [3]$$

The complex reflection coefficients for a film (medium 2) of uniform thickness d, separating the incident phase (medium 1) from a semi-infinite third phase (medium 3) can be expressed as follows

$$R_v = \frac{r_{12}^{v} + r_{23}^{v} \exp(-ix)}{1 + r_{12}^{v} r_{23}^{v} \exp(-ix)} \quad [4]$$

where

$$x = 4\pi(d/\lambda_0)\hat{n}_2 \cos \phi_2 \quad [5]$$

v = s or p, and λ_0 is the wavelength of the light in vacuo.

By analogy with transmission spectroscopy, we define the optical density function for a single reflection, D_v, as follows

$$D_v = \log_e (\bar{R}_v/R_v) \quad [6]$$

where $\bar{R}_v$ is the value of the complex reflection coefficient for the bare substrate. Thus in the case of external reflection from a metal surface, say, $\bar{R}_v$ is the value of R_v for $d = 0$ and $\hat{n}_1 = \bar{\hat{n}}_1$. The distinction between the value of $\hat{n}_1$ for the bare substrate case and for the film covered substrate case must be made since film formation results from adsorption of molecular species from phase 1; the composition of phase 1 therefore differs in general in the two cases. In the case of attenuated total internal reflection, the phase of variable composition is phase 3 so that $\bar{R}_v = R_v\,(d = 0, \hat{n}_3 = \bar{\hat{n}}_3)$.

To distinguish D_v from the conventional optical density function (which is defined in terms of intensities, not amplitudes), it will be referred to as the complex optical density for v polarized light. It is in general a function of the optical constants of all three phases. Finally, we define the relative complex optical density for a single reflection

$$D = D_p - D_s \quad [7]$$

The relationship between D and the conventional empirical ellipsometric quantities is obtained immediately on making the substitution $R_v = \rho_v \exp(i\delta_v)$ to obtain

$$D = \log_e (\tan \bar{\Psi}/\tan \Psi) + i(\bar{\Delta} - \Delta) \quad [8]$$

Thus the real part of D, $\mathscr{R}(D)$, is simply related to the relative amplitude attenuation, $\rho_p/\rho_s = \tan \psi$, while the imaginary part of D, $\mathscr{I}(D)$, is simply related to the relative phase retardation, $\Delta = \delta_p - \delta_s$, with $\bar{\Psi}$ and $\bar{\Delta}$ referring to the bare substrate condition. Accordingly, D can be readily calculated from conventional ellipsometric data.

In a precisely analogous manner, we define the relative complex optical density function for N identical reflections, D_N, in terms of the complex reflection coefficients for such multiple reflections, $R_{vN} = R_v^N$, to obtain

$$D_N = ND = \log_e (\tan \bar{\Psi}_N/\tan \Psi_N) + i(\bar{\Delta}_N - \Delta_N) \quad [9]$$

where the meaning of Ψ_N, Δ_N etc. is clear from the context. The relative complex optical density is seen to be related to the empirical ellipsometric parameters, Ψ and Δ, in exactly the same way for multiple reflection as it is for a single reflection.

Contribution to D from the Change in $\hat{n}_1$ (or $\hat{n}_3$)

For purposes of analysis, it is convenient to divide D into two parts, $D = D^{(g)} + D^{(f)}$, where $D^{(g)}$ is the contribution to D resulting from changing $\bar{\hat{n}}_1$ to $\hat{n}_1$ (or $\bar{\hat{n}}_3$ to $\hat{n}_3$) while maintaining $d = 0$ (*i.e.* no film formation), whereas $D^{(f)}$ is the contribution to D resulting from the formation of the film. Substituting the values of R_v and $\bar{R}_v$ given by [4] into [6], noting that $r_{13}^v = (r_{12}^v + r_{23}^v)/(1 + r_{12}^v r_{23}^v)$, we obtain

$$D_v = D_v^{(g)} + D_v^{(f)} \quad [10]$$

$$D_v^{(g)} = \log_e (\bar{r}_{13}^v/r_{13}^v) \quad [11]$$

$$D_v^{(f)} = \log_e \left[\left(\frac{1 + r_{12}^v r_{23}^v \exp(-ix)}{r_{12}^v + r_{23}^v \exp(-ix)} \right) \left(\frac{r_{12}^v + r_{23}^v}{1 + r_{12}^v r_{23}^v} \right) \right] \quad [12]$$

where $\bar{r}_{13}^v$ is the value of r_{13}^v for $\hat{n}_1 = \bar{\hat{n}}_1$ (or $\hat{n}_3 = \bar{\hat{n}}_3$). On substituting for r_{jk}^v from [1] and [2], and for ϕ_j from [3], the following expression for $D^{(g)}$ is obtained in terms of the optical constants and angle of incidence

Can. J. Chem. Downloaded from www.nrcresearchpress.com by 210.87.254.5 on 09/05/12
For personal use only.

Can. J. Chem. Downloaded from www.nrcresearchpress.com by 210.87.254.5 on 09/05/12
For personal use only.

$$D^{(g)} = \log_e [(1 + a/2)/(1 - a/2)] \quad [13]$$

where

$$a = \frac{i2(\bar{y} - y) \sin \phi_1 \tan \phi_1}{y\bar{y} + \sin^2 \phi_1 \tan^2 \phi_1} \quad [14]$$

$$y = (\sin^2 \phi_1 - \varepsilon_3/\varepsilon_1)^{1/2} \quad [15]$$

$\varepsilon_j = \hat{n}_j^2$ is the complex dielectric constant of medium j, and $\bar{y}$ is the value of y for $\varepsilon_1 = \bar{\varepsilon}_1 = \bar{\hat{n}}_1^2$ (or $\varepsilon_3 = \bar{\varepsilon}_3 = \bar{\hat{n}}_3^2$).

For the case of external reflection and $|\bar{\varepsilon}_1 - \varepsilon_1| \ll 1$, $D^{(g)} = a[1 + a^2/12 + \cdots] \simeq a$; also $y\bar{y} + \sin^2 \phi_1 \tan^2 \phi_1 \simeq y^2 + \sin^2 \phi_1 \tan^2 \phi_1 = \tan^2 \phi_1 - \varepsilon_3/\varepsilon_1$, and $\bar{y} = y\,[1 + \varepsilon_3(\bar{\varepsilon}_1 - \varepsilon_1)/\bar{\varepsilon}_1\varepsilon_1 y^2]^{1/2} \simeq y + \frac{1}{2}\varepsilon_3(\bar{\varepsilon}_1 - \varepsilon_1)/\bar{\varepsilon}_1\varepsilon_1 y$, which lead to the result

$$D^{(g)} \doteqdot i\left[\frac{\sigma - 1}{(\varepsilon_1 \sin^2 \phi_1 - \varepsilon_3)^{\frac{1}{2}}}\right]\left[\frac{\sin \phi_1 \tan \phi_1 \varepsilon_1^{\frac{1}{2}}(-\varepsilon_3)}{\varepsilon_1 \tan^2 \phi_1 - \varepsilon_3}\right] \quad [16]$$

where $\sigma = \varepsilon_1/\bar{\varepsilon}_1$. For studies in the infrared in which phase 1 is either a vacuum or a gas, typically $|\bar{\varepsilon}_1 - \varepsilon_1| \leqslant 10^{-3}$; the approximations employed in obtaining [16] will therefore introduce a negligible error. In the case of total internal reflection and an angle of incidence not too close to the critical angle (*i.e.* for $|\bar{\varepsilon}_3 - \varepsilon_3| \ll |\varepsilon_1 \sin^2 \phi_1 - \varepsilon_3|$) we may proceed as before, except that we now have $\bar{y} = y[1 + (\varepsilon_3 - \bar{\varepsilon}_3)/\varepsilon_1 y^2]^{1/2} \simeq y + \frac{1}{2}(\varepsilon_3 - \bar{\varepsilon}_3)/\varepsilon_1 y$. Once again this leads to [16], however, in this case $\sigma = \bar{\varepsilon}_3/\varepsilon_3$. Precisely at the critical angle, defined by $\varepsilon_1 \sin^2 \phi_1 = \bar{\varepsilon}_3$, $D^{(g)} \doteqdot -2i(1 - \varepsilon_3/\bar{\varepsilon}_3)^{1/2}(\varepsilon_1/\bar{\varepsilon}_3 - 1)^{1/2}$. This approximation is only valid for $|\varepsilon_1 \sin^2 \phi_1 - \bar{\varepsilon}_3| \ll |\bar{\varepsilon}_3 - \varepsilon_3|$, a condition virtually impossible to achieve. It is clear, however, that $|D^{(g)}|$ will increase very rapidly as the critical angle is approached.

Thin Films

Equation 12 may be written in the form

$$D_v^{(f)} = \log_e \left[\frac{1 - ixf(x)r_{12}{}^v r_{23}{}^v/(1 + r_{12}{}^v r_{23}{}^v)}{1 - ixf(x)r_{23}{}^v/(r_{12}{}^v + r_{23}{}^v)}\right] \quad [17]$$

where

$$f(x) = \frac{1 - \exp(-ix)}{ix} = 1 - \frac{ix}{2!} - \frac{x^2}{3!} + \cdots$$

For thin films (and certainly for monolayer films observed in the infrared), $|x| \ll 1$ so that $D_v^{(f)}$ may be expanded first in powers of $xf(x)$ and then on substituting for $f(x)$, in powers of x, to give on simplifying

$$D_v^{(f)} = ix\left[\frac{1/r_{13}{}^v - r_{13}{}^v}{1/r_{23}{}^v - r_{23}{}^v}\right]\left[1 - \frac{ix}{2}\left(\frac{1/r_{13}{}^v - r_{13}{}^v}{1/r_{12}{}^v - r_{12}{}^v}\right) + \cdots\right] \quad [18]$$

On substituting for $r_{jk}{}^v$ from [1] and [2], for x from [5], and for ϕ_j from [3], we obtain, after considerable algebra, the following expression for $D^{(f)} = D_p^{(f)} - D_s^{(f)}$

$$D^{(f)} = i\frac{4\pi d}{\lambda_0} \sin \phi_1 \tan \phi_1 \varepsilon_1^{\frac{1}{2}}\left(\frac{\varepsilon_2 - \varepsilon_1}{\varepsilon_2}\right)\left[\frac{\varepsilon_2 - \varepsilon_3}{\beta}\right][1 - T_2 + \cdots] \quad [19]$$

where

$$T_2 = \frac{2\pi d}{\lambda_0}\frac{(\varepsilon' \tan^2 \phi_1 - \varepsilon'')(\varepsilon_1 \sin^2 \phi_1 - \varepsilon_3)^{\frac{1}{2}}}{\beta}$$

$$\beta = -(\varepsilon_1 - \varepsilon_3)(\varepsilon_1 \tan^2 \phi_1 - \varepsilon_3)/\varepsilon_3$$

$$\varepsilon' = \varepsilon_1(1 - \varepsilon_1/\varepsilon_2 - \varepsilon_1/\varepsilon_3 + \varepsilon_2\varepsilon_1/\varepsilon_3^2)$$

$$\varepsilon'' = \varepsilon_2 - 2\varepsilon_1 + \varepsilon_2\varepsilon_1/\varepsilon_3$$

Can. J. Chem. Downloaded from www.nrcresearchpress.com by 210.87.254.5 on 09/05/12
For personal use only.

At first glance it would appear that for sufficiently thin films, both the real and imaginary parts of $D^{(f)}$, $\mathscr{R}(D^{(f)})$, and $\mathscr{I}(D^{(f)})$ respectively, are proportional to the film thickness. Although this is generally true, in the particular case of external reflection involving a dielectric film and dielectric substrate, it is not. For such a case, $\varepsilon_1, \varepsilon_2$, and ε_3 are all real valued and positive; furthermore, for external reflection $\varepsilon_1 \sin^2 \phi_1 - \varepsilon_3$ is negative, making T_2 totally imaginary. The first non-vanishing contribution to $\mathscr{R}(D^{(f)})$ arises, therefore, from the second order term, T_2, so that in the thin film limit, $\mathscr{R}(D^{(f)})$ is proportional to d^2, not d. (This situation has been noted previously by Saxena (14) although the present approach to the problem differs somewhat from his.) To cover all possible thin film cases, it is therefore necessary to include the second order term; in the majority of cases, however, and in particular those involving total internal reflection, or external reflection from a metallic substrate, the term T_2 and higher order terms can generally be neglected for sufficiently thin films. Thus for total internal reflection, and a non-absorbing film and substrate, $\varepsilon_1, \varepsilon_2$, and ε_3 will again be real valued with, however, in this case, $\varepsilon_1 \sin^2 \phi_1 - \varepsilon_3$ either zero or positive. The second order term, T_2, will accordingly be real valued (zero at the critical angle defined by $\sin^2 \phi_1 = \varepsilon_3/\varepsilon_1$) and hence negligible compared with 1 for small d. Again for external reflection from a metallic substrate and a nonabsorbing film, ε_1 and ε_2 will be real valued with $|\varepsilon_3| \gg \varepsilon_1$ and ε_2, $\mathscr{R}(\varepsilon_3)$ large and negative (~ -100) and $|\mathscr{R}(\varepsilon_3)| > |\mathscr{I}(\varepsilon_3)|$. It follows, therefore, that $|\mathscr{R}(T_2)| > |\mathscr{I}(T_2)|$ and hence that T_2 may usually be neglected for thin films since the dominant contribution to $\mathscr{R}(D^{(f)})$ will come from the leading term. In the limit of a perfectly reflecting metal, $\varepsilon_3 \to -\infty$ so that $T_2 \to 0$ and $(\varepsilon_2 - \varepsilon_3)/\beta \to 1$.

Before discussing further the consequences of [16] and [19], we note here that since

$$\frac{\tan \psi}{\tan \bar{\psi}} = \frac{1 - \tan(\bar{\psi} - \psi)/\tan \bar{\psi}}{1 + \tan(\bar{\psi} - \psi)/\tan \bar{\psi}} \simeq 1 - \left[\frac{1}{\tan \bar{\psi}} + \tan \bar{\psi}\right](\bar{\psi} - \psi)$$

$$\text{for } |\bar{\psi} - \psi| \ll \pi/4$$

$$\mathscr{R}(D^{(f)}) \simeq [\cot \bar{\psi} + \tan \bar{\psi}](\bar{\psi} - \psi)$$

For thin films, therefore, $\mathscr{R}(D^{(f)})$ is seen to be to a good approximation proportional to the change in ψ brought about by adsorption, so that usually $\bar{\psi} - \psi$, as well as $\bar{\Delta} - \Delta$, will be proportional to film thickness. For N identical reflections $D_N{}^{(f)} = ND^{(f)}$ remains proportional to film thickness for all N. As no such proportionality relationship exists between $(\bar{\psi}_N - \psi_N)$ and $(\bar{\psi} - \psi)$, in general $(\bar{\psi}_N - \psi_N)$ will not be linear in thickness, although $(\bar{\Delta}_N - \Delta_N) = \mathscr{I}(D_N) = N\mathscr{I}(D) = N(\bar{\Delta} - \Delta)$ will.

We turn now to an evaluation of the influence of the change in composition of phase 1 (phase 3 for total internal reflection), resulting from the addition to phase 1 (phase 3) of the adsorbate, on the determination of the film optical constants. A convenient measure of this will be given by the ratio $D^{(g)}/D^{(f)}$ which, from [16] and [19], takes the form

$$[20] \qquad \frac{D^{(g)}}{D^{(f)}} = \left[\frac{(\sigma - 1)/4\pi(d/\lambda)}{(\varepsilon_1 \sin^2 \phi_1 - \varepsilon_3)^{\frac{1}{2}}}\right]\left(\frac{\varepsilon_2}{\varepsilon_2 - \varepsilon_1}\right)\left[\frac{\varepsilon_1 - \varepsilon_3}{\varepsilon_2 - \varepsilon_3}\right][1 - T_2 + \cdots]^{-1}$$

For the case of a thin dielectric film on a metallic substrate of good reflectivity, making the substitutions $\varepsilon_j = \hat{n}_j{}^2 = (n_j - ik_j)^2$, and $\bar{\varepsilon}_1 = 1$ leads to the following approximations

$$(\varepsilon_1 - \varepsilon_3)/(\varepsilon_2 - \varepsilon_3) \simeq 1$$

$$(\varepsilon_1 \sin^2 \phi_1 - \varepsilon_3)^{1/2} \simeq k_3$$

$$(\sigma - 1) = \varepsilon_1 - 1 \simeq 2(n_1 - 1) - 2ik_1$$

$$\varepsilon_2/(\varepsilon_2 - \varepsilon_1) \simeq \varepsilon_2/(\varepsilon_2 - 1)$$

$$[1 - T_2 + \cdots]^{-1} \simeq 1$$

so that

$$[21] \qquad \frac{D^{(g)}}{D^{(f)}} \simeq \frac{(n_1 - 1) - ik_1}{2\pi k_3(d/\lambda_0)}\left(\frac{\varepsilon_2}{\varepsilon_2 - 1}\right)$$

In arriving at [21], the inequalities $K_3 \gg n_3, |\hat{n}_1|, |\hat{n}_2|$, and $1 \gg (n_1 - 1), K_1$, have been used. Since $|\varepsilon_2|$ will typically be of the order of 2 or larger, the condition that $D^{(f)}$ be the dominant term in D may be stated as follows

$$d/\lambda_0 \gtrsim (n_1 - 1)/K_3, \quad K_1/K_3 \qquad [22]$$

For a monolayer film and observation in the infrared, $d/\lambda_0 \sim 10^{-4}$ whereas typically K_3 will be greater than 10 (at 10μ, $K_3 = 69$ for Ag, 5.6 for Sb) so that [22] requires that $(n_1 - 1)$ and K_1 be less than 10^{-3}, a condition which will virtually always be satisfied for phase 1, a gas phase at reasonable pressures. Under certain conditions, however, even though $D^{(f)}$ will dominate, $D^{(g)}$ will make a significant contribution to D which should be taken into account in the calculations.

The effect on D arising from the change of composition of phase 1, is not completely accounted for by $D^{(g)}$, since $D^{(f)}$ is also a function of ε_1. For $|\bar{\varepsilon}_1 - \varepsilon_1| \ll 1$, however, the contribution arising in this way will always be very small.

For the case of a thin dielectric film and total internal reflection, upon setting $\bar{\varepsilon}_3 = 1$, $(\varepsilon_1 - \varepsilon_3)/(\varepsilon_2 - \varepsilon_1) \simeq -1$, $\varepsilon_2/(\varepsilon_2 - \varepsilon_3) \simeq \varepsilon_2/(\varepsilon_2 - 1)$, $(\sigma - 1) = 1/\varepsilon_3 - 1 \simeq -2(n_3 - 1) + 2ik_3$ and $\varepsilon_1 = {n_1}^2$, we obtain

$$\frac{D^{(g)}}{D^{(f)}} \simeq \frac{(n_3 - 1) - ik_3}{2\pi({n_1}^2 \sin^2 \phi_1 - 1)^{\frac{1}{2}}(d/\lambda_0)} \left(\frac{\varepsilon_2}{\varepsilon_2 - 1}\right) \qquad [23]$$

where the inequalities ${n_1}^2 \gg |\varepsilon_2|, |\varepsilon_3|$ have been employed. The condition that $D^{(f)}$ be the dominant term in D in this case becomes

$$\frac{d}{\lambda_0} \gtrsim \frac{(n_3 - 1)}{({n_1}^2 \sin^2 \phi_1 - 1)^{\frac{1}{2}}}, \frac{K_3}{({n_1}^2 \sin^2 \phi_1 - 1)^{\frac{1}{2}}} \qquad [24]$$

Unlike the case of a metallic reflector, the above condition is sensitive to the angle of incidence, particularly so close to the critical angle. Taking as an example germanium ($n_1 = 4$) and $\phi_1 = \pi/4$, $({n_1}^2 \cdot \sin^2\phi_1 - 1)^{1/2} = \sqrt{7} \simeq 2.6$. On comparing the case of total internal reflection with that of reflection from a metallic substrate involving the same film material and adsorbing gas, we have $[D^{(g)}/D^{(f)}$ for total internal reflection$]/[D^{(g)}/D^{(f)}$ for reflection from a metal$] \simeq K_{metal}/({n^2}_{dielectric} \sin^2 \phi_1 - 1)^{1/2} \gtrsim 10$. Thus contributions to D from the gas phase will in general be much more important in the case of total internal reflection. To minimize such contributions, the angle of incidence should be chosen well removed from the critical angle.

Highly Reflecting Metallic Substrate

As noted earlier, in the limit of a perfectly reflecting metallic substrate, $T_2 = 0$ and $(\varepsilon_2 - \varepsilon_3)/\beta = 1$ so that [19] reduces to the following, high reflectivity, thin film, approximation

$$D^{(f)} = i(4\pi d/\lambda_0) \sin \phi_1 \tan \phi_1 {\varepsilon_1}^{1/2}(1 - \varepsilon_1/\varepsilon_2) \qquad [25]$$

Expanding $(\varepsilon_2 - \varepsilon_3)/\beta$ in powers of $1/\varepsilon_3$ gives $1 + (\varepsilon_1/\cos^2 \phi_1 - \varepsilon_2)/\varepsilon_3 +$ higher order terms, so that for real systems and an angle of incidence not too large, the error incurred in using [25] will be of the order of $|\varepsilon_2|/|\varepsilon_3|$ compared with unity, or since $\varepsilon_3 \simeq -{K_3}^2$ for a metal, whereas for a dielectric film, $\varepsilon_2 \simeq {n_2}^2$, the error will be of the order of $(n_2/K_3)^2$ compared with unity. Even for a very good metallic reflector, however, the approximation will break down for a sufficiently large angle of incidence. It is interesting to note that for an angle of incidence defined by $\cos \phi_1 = n_2/n_1$, the error introduced in using [20] is greatly reduced, being now only of the order of $(n_2/K_3)^4$ which will nearly always be negligible compared with unity. Thus for angles of incidence which are not too large, and particularly for $\cos \phi_1 \simeq n_2/n_1$, $D^{(f)}$ is seen to be very nearly independent of substrate optical constants where the substrate is a good metallic reflector. No equivalent approximation exists in the case of total internal reflection.

Since $\tan \bar{\psi}$ is 1 to first order for a good metallic reflector ($\tan \bar{\psi} = 1 - \gamma$ say), then $\cot \bar{\psi} + \tan \bar{\psi}$ will be 2 to second order (*i.e.* $\cot \bar{\psi} + \tan \bar{\psi} = 2 + \gamma^2 + \gamma^3 + \cdots$) so that $\mathscr{R}(D^{(f)}) \doteqdot 2(\bar{\psi} - \psi)$ under these conditions. Thus $2(\bar{\psi} - \psi)$ will show essentially the same dependence on substrate optical con-

Can. J. Chem. Downloaded from www.nrcresearchpress.com by 210.87.254.5 on 09/05/12
For personal use only.

stants, or lack of it, as does $\mathscr{R}(D^{(f)})$. Once again, however, for multiple reflection $2(\bar{\psi}_N - \psi_N)$ may show a pronounced dependence on substrate optical constants even though $(\bar{\psi} - \psi)$ does not, since $\tan \bar{\psi}_N$ will not be close to unity, even for a highly reflecting substrate, for N sufficiently large. This point will be illustrated by numerical calculations in Section 3.

Finally, on setting $\varepsilon_1 = 1$ and $\varepsilon_2 = (n_2 - ik_2)^2$, we obtain from [25]

$$\mathscr{R}(D^{(f)}) = \alpha \sin \phi_1 \tan \phi_1 [n_2/(n_2^2 + k_2^2)^2] \quad [26]$$

$$\mathscr{I}(D^{(f)}) = (4\pi d/\lambda_0) \sin \phi_1 \tan \phi_1 \left[1 - \frac{n_2^2 - k_2^2}{(n_2^2 + k_2^2)^2}\right] \quad [27]$$

where $\alpha = 4\pi k_2(2d)/\lambda_0$ and is the conventional base e optical density of a film of thickness $2d$ and absorption coefficient $\chi = 4\pi k_2/\lambda_0$. A plot of $\mathscr{R}(D^{(f)})$ *vs.* λ_0 will therefore be a good representation of the absorption spectrum of the film (α *vs.* λ_0) provided that $n_2/(n_2^2 + k_2^2)^2$ does not change too rapidly across any given absorption band. This condition will frequently not be met, so that in general a complete analysis of data for D *vs.* λ_0 must be carried out to yield, amongst other things, α *vs.* λ_0. In this connection it is worth pointing out that conventional specular reflectance spectrometry, performed on thin films for the case $\varepsilon_1 = \bar{\varepsilon}_1 = 1$ and using the bare substrate as the reference system, will yield an optical density for p-polarized light very nearly equal to $2\mathscr{R}(D)$ (since $|R_s| \simeq |\bar{R}_s|$ for thin films (6)). Such spectra cannot be regarded, therefore, as true absorption spectra, and may in fact frequently be misleading if so interpreted.

Multiple Reflections and Optimum Conditions

We consider next the consequence, with regard to signal sensitivity, of employing parallel plate multiple reflection cells, or multiple reflection prisms in the case of total internal reflection. We begin by applying the constraint that the cell or prism geometry must be such as to pass the entire incident light beam, apart from absorption losses. In the case of the total internal reflection prism, we apply the further constraint that the entrance and exit faces of the prism be normal to the incident and exiting beam, respectively. This is to avoid problems that would otherwise arise due to changes in the angle of refraction with wave length.

A light beam, incident on the entrance aperture of a parallel plate reflection cell, and of width w in the plane of incidence, can be made to enter the cell in its entirety only if the separation between the plates is equal to or greater than t where t is given by

$$t = w/2 \sin \phi_1 \quad [28]$$

The situation corresponding to [28] is illustrated in Fig. 1 *A* for $\phi_1 > \pi/4$. The corresponding optimum geometry for a total internal reflection cell and $\phi_1 > \pi/4$ is shown by the broken line in Fig. 1*A*. If the shape of the internal reflection cell is limited to a rectangular parallelepiped, the optimum geometry for $\phi_1 > \pi/4$ is illustrated in Fig. 1*B*, and represented by the equation

$$t = w \sin \phi_1 \quad [29]$$

For $\phi_1 < \pi/4$, the geometry which minimizes the separation between the reflecting surfaces is the same for reflection cell and reflection prism, as illustrated in Fig. 1*C*, and is represented by [28]. For reflecting surfaces of length L and separation, t, the number of reflections, N, suffered by the light beam is given by

$$N = L/t \tan \phi_1 \quad [30]$$

so that the maximum number of reflections which can be achieved with a parallel plate reflection cell at all angles of incidence, and for a simple prism at $\phi_1 \leqslant \pi/4$ is given by

$$N = 2(L/w) \cos \phi_1 \quad [31]$$

whereas for a simple prism and $\phi_1 \geqslant \pi/4$

$$N = (L/w)/\sin \phi_1 \tan \phi_1 \quad [32]$$

Can. J. Chem. Downloaded from www.nrcresearchpress.com by 210.87.254.5 on 09/05/12
For personal use only.

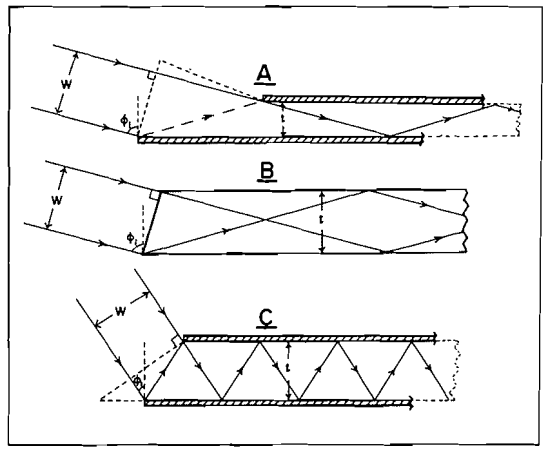

FIG. 1. Optimum geometry for: *A*, parallel plate reflection cell, $\phi_1 > \pi/4$; *B*, total internal reflection prism, $\phi_1 > \pi/4$; *C*, both reflection cell and reflection prism, $\phi_1 < \pi/4$.

As the relative complex optical density for N identical reflections, D_N, is simply ND, combining [19] with [31] and [32] in turn leads to the result

$$[33] \qquad D_N^{(f)} = i\left(\frac{4\pi d}{\lambda_0}\right)\left(\frac{L}{w}\right)F_N(\phi_1)\left(\frac{\varepsilon_2 - \varepsilon_1}{\varepsilon_2}\right)\left(\frac{\varepsilon_2 - \varepsilon_3}{\varepsilon_1 - \varepsilon_3}\right)\left(\frac{-\varepsilon_3}{\varepsilon_1^{\frac{1}{2}}}\right)[1 - T_2 + \cdots]$$

where $F_N(\phi_1) = 1/(\tan^2\phi_1 - \varepsilon_3/\varepsilon_1)$ for a simple prism and $\phi_1 \geqslant \pi/4$, otherwise $F_N(\phi_1) = 2\sin^2\phi_1/(\tan^2\phi_1 - \varepsilon_3/\varepsilon_1)$. Similarly from [16], [31], and [32]

$$[34] \qquad D_N^{(g)} = i\left(\frac{L}{w}\right)F_N(\phi_1)\left[\frac{\sigma - 1}{(\varepsilon_1\sin^2\phi_1 - \varepsilon_3)^{\frac{1}{2}}}\right]\left(\frac{-\varepsilon_3}{\varepsilon_1^{\frac{1}{2}}}\right)$$

We seek now the angle of incidence which maximizes $|D_N^{(f)}|$. If measurement precision is not intensity limited, this same condition will provide optimum sensitivity. If it is intensity limited, then for optimum sensitivity, to a good approximation $|r_{13}^{p}|^{2N}|D_N^{f}|$ must be a maximum, where $|r_{13}^{p}|^{2N}$ is proportional to the intensity of the p-component following N reflections, this intensity always being less than or equal to that of the s-component. For a good metallic reflector in the infrared, we may set $\varepsilon_1 \simeq 1$ and $|\tan^2\phi_1 - \varepsilon_3/\varepsilon_1| \simeq (\tan^2\phi_1 + K_3^2 + n_3^2) \simeq (\tan^2\phi_1 + K_3^2)$. Then, on setting $\partial|D_N^{f}|/\partial\phi_1 = 0 = \partial|F_N(\phi_1)|/\partial\phi_1$, we obtain $\tan^2\phi_1 = K_3$, with the corresponding value of $D_N^{(f)}$ given by setting $F_N(\phi_1) \simeq 2/(1 + K_3)^2$. Making this substitution into [33] and neglecting terms of order $1/K_3$ with respect to unity, the following expressions for $D_N^{(f)}$ at the angle which maximizes $(D_N^{(f)})$ is obtained

$$[35] \qquad (D_N^{(f)})_{max} \simeq i(4\pi d/\lambda_0)(L/w)2[1 - 1/\varepsilon_2]$$

The exact choice of angle is not critical, however, since $|F_N(\phi_1)|$ (and hence $D_N^{(f)}$) varies by less than a factor of 2 over the range of angles defined by $\tan\phi_1 = 1$ to K_3. (For $\tan\phi_1 = 1$ or K_3, $F_N(\phi_1) \simeq 1/(1 + K_3^2) > 1/(1 + K_3)^2 \simeq \frac{1}{2}(F_N(\phi_1))_{max}$.) Equation 35 represents conditions for optimum sensitivity at fixed (L/w) only if measurement precision is not intensity limited, as mentioned previously. Under such conditions, however, the restriction placed on the reflection cell geometry becomes unnecessary, a more convenient geometry being one of fixed separation for all incident angles. For such a cell, $D_N^{(f)}$ will be given by [33] with w replaced by t and $F_N(\phi_1)$ by $\sin\phi_1/(\tan^2\phi_1 - \varepsilon_3/\varepsilon_1)$. Employing the same approximation as before (*i.e.* setting $-\varepsilon_3/\varepsilon_1 \simeq K_3^2$) a maximum for this function is found at a slightly smaller angle given by $\tan^2\phi_1 = (K_3/\sqrt{2})[(1 + 1/8K_3^2)^{1/2} - 1/2\sqrt{K_3}] \simeq K_3/\sqrt{2}$, and the function is found to vary by about a factor of $\sqrt{2}$ in the angular range defined by $\tan\phi_1 = 1$ to K_3. The situation is therefore not greatly altered on going to this geometry.

For total internal reflection, $|r_{13}^{p}|^{2N} = 1$ independent of ϕ_1 and N, so that the angle which maximizes $|D_N^{(f)}|$ for fixed (L/w), also maximizes $|r_{13}^{p}|^{2N}|D_N^{f}|$ for the same conditions. As $|F_N(\phi_1)|$

Can. J. Chem. Downloaded from www.nrcresearchpress.com by 210.87.254.5 on 09/05/12
For personal use only.

increases monotonically as ϕ_1 decreases from $\pi/2$ towards the critical angle ($\sin \phi_1 = n_3/n_1$), its maximum permissible value occurs at the critical angle, and is given by $(F_N(\phi_1))_{crit} = 2(n_1^2/n_3^2 - 1)$. Making this substitution into [33] and setting $\varepsilon_3 \simeq 1, \varepsilon_1 = n_1^2$ we obtain

$$[36] \qquad (D_N^{(f)})_{max} = i(4\pi d/\lambda_0)(L/w)2n_1(1 - \varepsilon_2/n_1^2)[1 - 1/\varepsilon_2]$$

Unlike the case of multiple reflection from a metal, for multiple internal reflection, $(D_N^{(f)})_{max}$ decreases rapidly as the angle of incidence is increased. Taking germanium as an example, $F(\phi_1) = 30$ at the critical angle, 14.7°, whereas at 20°, $F_N(\phi_1) = 3.34$ and at 45°, 1.07. For the study of monolayers, it would therefore seem desirable to operate close to the critical angle. A serious practical difficulty arises in attempting to do so, however, in that the angular distribution of light in a collimated beam generally covers several degrees, except in the case of a laser source.

To treat the case of multiple reflection from a metal substrate under conditions in which measurement precision is light intensity limited, we look for conditions which maximize $|r_{13}^p|^{2N}|D_N^{(f)}|$ simultaneously with respect to L/w and ϕ_1. For a given value of ϕ_1, the optimum value of L/w, $(L/w)_{opt}$, is that which maximizes $|r_{13}^p|^{2N}(L/w)$ where N is given by [31]. Substituting for N and equating the derivative with respect to L/w to zero leads to the result that when $(L/w) = (L/w)_{opt}$, $\log_e |r_{13}^p|^{2N} = -1$. Thus for any given angle of incidence, the optimum number of reflections is that which leads to a reduction in the intensity of the p-component of a factor of $1/e$. For a metal in the infrared, $\cos \phi_3 \simeq 1$ to a good approximation. Making this substitution into [1] and setting $\hat{n}_1 = 1$ gives $|r_{13}^p|^2 \simeq (1 - b)/(1 + b)$ where $b = 2n_3 \cos \phi_1/[1 + (K_3^2 + n_3^2)\cos^2 \phi_1] \simeq 2n_3 \cos \phi_1/(1 + K_3^2 \cos^2 \phi_1)$. We then have for the case of optimum number of reflections, $-1 = \log_e |r_{13}^p|^{2N} \simeq -N.2b$ since $b \ll 1$, which on substituting for b from above and for N from [31] gives

$$[37] \qquad (L/w)_{opt} \simeq (1 + K_3^2 \cos^2 \phi_1)/8n_3 \cos^2 \phi_1$$

The optimum angle of incidence is now obtained by maximizing $(L/w)_{opt} \cdot |F_N(\phi_1)| \simeq \tan^2 \phi_1(1 + K_3^2 \cos^2 \phi_1)/4n_3(\tan^2 \phi_1 + K_3^2)$. This function possesses no maximum in the interval $[0,\pi/2]$, but rather increases monotonically with ϕ_1 from 0 at $\phi_1 = 0$ to $1/4n_3$ at $\phi_1 = \pi/2$. This curious result is the consequence of two competing effects, the decrease of $D^{(f)}$ for a single reflection towards zero as ϕ_1 approaches $\pi/2$, and the increase of $|r_{13}^p|^2$ towards unity as ϕ_1 approaches $\pi/2$, the latter effect allowing more reflections, approaching in fact an infinite number as ϕ_1 approaches $\pi/2$. The two effects battle to a standoff, and finite sensitivity is maintained to the limit. The result is, of course, strictly a mathematical curiosity since to achieve this result at $\phi_1 = \pi/2$, an infinitely long reflection cell would be required (see [31]). Furthermore, close to $\phi_1 = \pi/2$, the relationship for $(L/w)_{opt} \cdot F_N(\phi_1)$ would no longer be a good approximation due to imperfections (scattering centers) in the reflecting surfaces. Fortunately, once again the choice of angle of incidence is not very critical since $(L/w)_{opt} \cdot |F_N(\phi_1)|$ varies by less than a factor of 2 over the interval $[\pi/4,\pi/2]$. (At $\phi_1 = \pi/4$, $(L/w)_{opt} \cdot F_N(\phi_1) \simeq \frac{1}{2}[(1 + 2/K_3^2)/(1 + 1/K_3^2)]/4n_3 > \frac{1}{2}(1/4n_3)$). Values for $(L/w)_{opt} \cdot F_N(\phi_1)$ approaching $1/4n_3$ are therefore readily achievable. Substituting this value into [33], and making the usual approximations leads to the following expression for the optimum value of $D_N^{(f)}$

$$[38] \qquad (D_N^{(f)})_{opt} \simeq i(4\pi d/\lambda_0)(K_3^2/4n_3)[1 - 1/\varepsilon_2]$$

It is apparent that for intensity limited conditions, the feasibility of achieving useful results for monolayer films would depend critically on the optical constants of the metal, *i.e.* on the ratio K_3^2/n_3. If a laser source were used, however, this limitation would be removed.

Since $D_N^{(f)}$ varies only slowly with ϕ_1 where $(L/w) = (L/w)_{opt}$, a more practical solution to the optimization problem and one which leads to nearly as good a result as [38], is to fix (L/w) from practical considerations and then determine the value of ϕ_1 which maximizes $|r_{13}^p|^{2N}|F_N(\phi_1)|$. This problem involves the solution of a quartic equation. For $(L/w) \gtrsim K_3(K_3 + 3)/8n_3$, however, the optimum conditions are to a good approximation still given by [37], which on solving for $\tan^2 \phi_1$ becomes

$$[39] \qquad (\tan^2 \phi_1)_{opt} \simeq 8n_3(L/w) - K_3^2 - 1$$

Can. J. Chem. Downloaded from www.nrcresearchpress.com by 210.87.254.5 on 09/05/12
For personal use only.

Even for (L/w) smaller than $K_3(K_3 + 3)/8n_3$, however, [39] will give a value for $|r_{13}{}^p|^{2N}|F_N(\phi_1)|$ which is greater than half the optimum value, provided only that the calculated angle, ϕ_1, is $\pi/4$ or greater (*i.e.* provided that $(L/w) \gtrsim (K_3{}^2 + 2)/8n_3$).

We compare now the relative sensitivities to thin film detection of total internal reflection measurements and reflection measurements from a metallic substrate, first for multiple reflection with L/w the same for the two cases, then for single reflections, the angle of incidence in each case being chosen to maximize $D_N{}^{(f)}$. The ratio for the multiple reflection case is obtained directly from equations [35] and [36], the sensitivity for internal reflection being the greater by a factor of $n(1 - \varepsilon_2/n^2)$ where n is the refractive index of the internal reflectance prism. Thus operating precisely at the critical angle, multiple total internal reflection has a significant sensitivity advantage over multiple reflection from metal surfaces (a factor of nearly 4 for Ge). The situation is reversed, however, if one must operate at an angle of incidence only a few degrees greater than the critical angle, which will generally be the case, or if one is dealing with a case in which $|n^2 - \varepsilon_2| < n$. This analysis takes no account of loss of sensitivity due to intensity loss. Whenever sensitivity is intensity limited, multiple total internal reflection will clearly be potentially much more sensitive.

Repeating the above analysis, but this time for single reflection measurements, the following approximate relations are obtained. For the case of the metal substrate, setting $T_2 = 0$, $-\varepsilon_3 \simeq K_3{}^2 \gg 1$, and $\varepsilon_1 = 1$ as before, we find that the optimum angle of incidence is given by $\tan^2 \phi_1 = \frac{1}{2}K_3{}^2[1 + (1 + 8/K_3{}^2)^{1/2}] \simeq K_3{}^2$ and that at this angle

$$[40] \qquad (D^{(f)})_{max} \simeq i\left(\frac{4\pi d}{\lambda_0}\right)\left(\frac{K_3}{2}\right)[1 - 1/\varepsilon_2]$$

For total internal reflection, the optimum angle of incidence is still the critical angle, leading to a value for $D^{(f)}$ at this angle given by

$$[41] \qquad (D^{(f)})_{max} \simeq i\left(\frac{4\pi d}{\lambda_0}\right) n_1 \left[\frac{(1 - \varepsilon_2/n_1{}^2)}{(1 - 1/n_1{}^2)^{\frac{1}{2}}}\right][1 - 1/\varepsilon_2]$$

In the infrared, and for most metals, the condition $(K_{metal}/2) > n_{dielectric}$ will apply so that even operating at the critical angle in the total internal reflection case, the sensitivity is about the same or greater for reflection from a metal substrate. This advantage will be retained even when measurement sensitivity is intensity limited, since the intensity loss on single reflection will be small.

The analysis in this section has been based on the implicit assumption that the incident beam of light is perfectly parallel. Except where lasers are used, angular spreads of several degrees must normally be tolerated in the interest of maintaining reasonable intensity levels. This in turn will mean that different portions of the incident beam will undergo different numbers of reflections (cell design can guarantee that the various components of the beam differ in their number of reflections by an even integer, so that the light emerges from the cell as a single beam). We have shown that for a metal reflection cell of fixed length and spacing, $D_N{}^{(f)}$ varies only slowly with the angle of incidence in the interval $\tan \phi_1 = 1$ to K_3 so that the error involved in not taking explicit account of the angular spread will be very small for mean angles of incidence within this range. The situation for total internal reflection near the critical angle is, however, an entirely different one as $D_N{}^{(f)}$ varies rapidly with angle of incidence for such conditions.

Numerical Calculations

A computer program was written to calculate D, given the optical constants for the incident medium, the film, and the substrate, as well as values for the system parameters, λ_0, d, and ϕ_1. The calculations were based on the exact equations [1] to [12] and involved no mathematical approximations. To facilitate comparison of the calculated results for different angles of incidence, both with each other and with those based on the thin film, high reflectivity approximation [25], we have in the case of metal substrates plotted the results in the form $100\ D/\sin \phi_1 \tan \phi_1$, which we subsequently refer to as D_N. For angles of incidence, $\phi_1 \geqslant \pi/4$, these results correspond, therefore, to values of D_N which would be achieved using a simple prismatic multiple reflection cell (Fig. 1*B*) of shape factor $L/w = 100$. In the case of total internal reflection, the results are plotted in the form $200\ D \cos \phi_1$ and again

Can. J. Chem. Downloaded from www.nrcresearchpress.com by 210.87.254.5 on 09/05/12
For personal use only.

Can. J. Chem. Downloaded from www.nrcresearchpress.com by 210.87.254.5 on 09/05/12
For personal use only.

are referred to as D_N. These results correspond to values of D_N which would be obtained using a cell of optimum geometry (Fig. 1, *A* and *C*) and a shape factor $L/w = 100$.

The above calculations have been carried out for external reflection from adsorbed films of CCl_4, CH_3OH, H_2O, and cyclohexane on Ag, Ni, and Sb, Ag representing a very good, Ni a good, and Sb a poor reflecting substrate, and for internal reflection for the Ge/CCl_4 system. In all cases, the film optical constants have been taken to be those for the bulk liquid state, with the thickness, corresponding to one monolayer, calculated from the bulk liquid density. The calculations do not reflect, therefore, the specific nature of the interactions between the adsorbate and adsorbent and are intended only to test the equations developed herein and to gain insight into the optical behavior of such systems. The optical constants for the metals were obtained by interpolation from the tables of ref. 15. Their normal incidence reflectivities have been plotted in Fig. 2 for purposes of comparison.

To check the accuracy of eqs. 16 and 19 for $D^{(g)}$ and $D^{(f)}$ these quantities were calculated from [16] and [19] as well as from the exact equations [1] to [12]. In no case did the results for $|D_N{}^{(f)}|$, $(L/w) = 100$, differ by more than about 10^{-5} absolute. For $D_N{}^{(g)}$, the difference was also less than 10^{-5}. Omitting the second order term, T_2, led in some cases to a 10^3 fold increase in the discrepancy. Thus at $\lambda = 14.79\ \mu$, $\phi_1 = 85°$, on neglecting the term T_2, the error in $\mathcal{R}(D_N{}^{(f)})$ is 1.4×10^{-7} and is reduced to 8.0×10^{-10} on including T_2.

The results for CCl_4 adsorbed on Ag, assuming

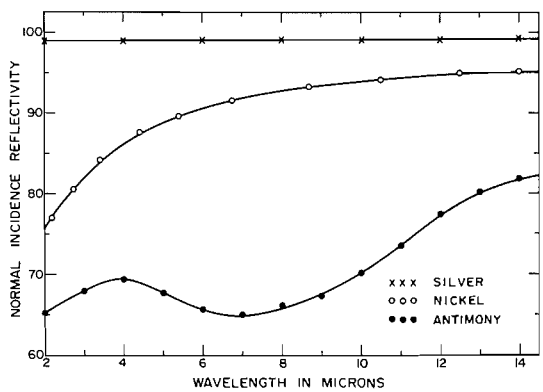

FIG. 2. Wavelength dependence of the normal incidence reflectivity for Ag, Ni, and Sb.

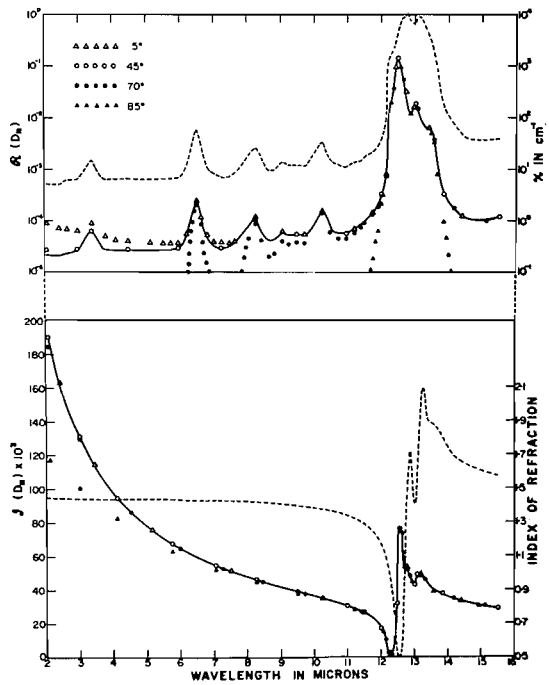

FIG. 3. Influence of angle of incidence on D_N for a monolayer film of CCl_4 (liquid state) on Ag. The solid lines were calculated using the approximate equation, [25]. The absorption coefficient χ and refractive index for liquid CCl_4 are shown as broken lines for comparison.

$\varepsilon_1 = \bar{\varepsilon}_1 = 1$, are presented graphically in Fig. 3, along with the values for the film optical constants (16) and curves calculated using the high reflectivity approximation, [25]. For values of $\mathcal{R}(D_N)$ which are large enough to measure (*i.e.*, $\mathcal{R}(D_N) > 10^{-3}$), it is effectively independent of angle of incidence from 5 to 85°, as predicted (*cf.* eq. 25 and related discussion). The accurately calculated values for $\mathcal{R}(D_N)$ at 45° angle of incidence are virtually indistinguishable from those calculated using the high reflectivity approximation over the entire wavelength range investigated, again an anticipated result, since at this angle the condition $\cos\phi_1 = n_2/n_1$ is very nearly met. Proceeding to larger angles of incidence, the discrepancy becomes progressively worse. The similarity of $\mathcal{R}(D_N)$ *vs.* wavelength to the adsorption spectrum, while close, is as expected by no means exact, a fact most clearly illustrated over the absorption band at 13 μ.

Again from Fig. 3 we see that the $\mathcal{I}(D_N)$ curves are virtually indistinguishable from each other and from that calculated using the high reflectivity

Can. J. Chem. Downloaded from www.nrcresearchpress.com by 210.87.254.5 on 09/05/12
For personal use only.

TABLE 1. Comparison of D_N and $\frac{1}{2}\mathscr{D}_N$ for a monolayer of CCl_4 (liquid state) adsorbed on Ag, both in vacuo and in contact with 100 Torr CCl_4 gas (angle of incidence, 45°)

K_1, gas absorption index	K_2, film absorption index	Wavelength (μ)	$\mathscr{R}(D_N) \times 10^4$		$\mathscr{I}(D_N) \times 10^4$		$\frac{1}{2}\mathscr{D}_N \times 10^4$	
			Vacuum	CCl_4 gas	Vacuum	CCl_4 gas	Vacuum	CCl_4 gas
0.0033	1.0454	12.796	165.5	243.6	528.0	512.3	165.7	1825
0.0026	0.8863	13.175	98.90	157.5	488.8	477.3	99.18	1329
0.0029	0.5909	12.578	986.3	1046	764.8	747.1	986.3	2196
0.00032	0.2045	13.577	36.91	43.94	393.6	392.2	37.02	184.0
0.00056	0.1136	12.225	136.5	142.7	23.37	22.10	136.5	279.5
0.00021	0.0175	13.850	3.286	7.654	376.6	375.7	3.349	93.34
0.0001	0.0027	11.890	1.936	4.285	199.5	199.1	1.952	52.95
0.00008	0.00097	10.970	0.550	2.632	304.5	304.1	0.582	45.61
0.0000	0.00024	4.510	0.277	0.277	865.61	865.6	0.527	0.527

TABLE 2. Comparison of the substrate dependence of $\mathscr{R}(D_N)$ with that of $2(\overline{\psi}_N - \psi_N)$ for a monolayer film of CCl_4 (liquid state) and 45° angle of incidence

K_2, film absorption index	Wavelength (μ)	$2(\overline{\psi}_N - \psi_N)$			$\mathscr{R}(D_N)$		
		Silver	Nickel	Antimony	Silver	Nickel	Antimony
1.0454	12.796	1.5195×10^{-2}	2.5926×10^{-3}	1.0165×10^{-6}	1.6551×10^{-2}	1.6594×10^{-2}	1.6706×10^{-2}
0.6681	13.020	1.6926×10^{-2}	3.0168×10^{-3}	2.3011×10^{-6}	1.8443×10^{-2}	1.8457×10^{-2}	1.8488×10^{-2}
0.500	12.500	1.2662×10^{-1}	1.9927×10^{-2}	3.3383×10^{-6}	1.4164×10^{-1}	1.4133×10^{-1}	1.3840×10^{-1}
0.00835	14.170	1.6702×10^{-4}	4.0003×10^{-5}	1.0049×10^{-6}	1.8340×10^{-4}	2.0362×10^{-4}	3.8544×10^{-4}
0.00475	15.520	1.0851×10^{-4}	2.9639×10^{-5}	3.5890×10^{-6}	1.1968×10^{-4}	1.2724×10^{-4}	1.7514×10^{-4}
0.0041	12.000	2.9499×10^{-4}	4.2335×10^{-5}	1.2325×10^{-9}	3.2195×10^{-4}	3.1251×10^{-4}	1.8157×10^{-4}
0.00265	10.250	1.3555×10^{-4}	1.3395×10^{-5}	6.4030×10^{-12}	1.4849×10^{-4}	1.4462×10^{-4}	9.4042×10^{-5}
0.0017	8.270	9.7950×10^{-5}	5.7544×10^{-6}	3.4063×10^{-13}	1.0813×10^{-4}	1.0950×10^{-4}	1.2624×10^{-4}
0.0004	7.250	2.6380×10^{-5}	1.0661×10^{-6}	1.2295×10^{-13}	2.8828×10^{-5}	3.1855×10^{-5}	6.1002×10^{-5}
0.00024	4.510	2.5047×10^{-5}	1.6774×10^{-7}	1.4300×10^{-12}	2.7706×10^{-5}	5.3747×10^{-5}	1.0487×10^{-4}

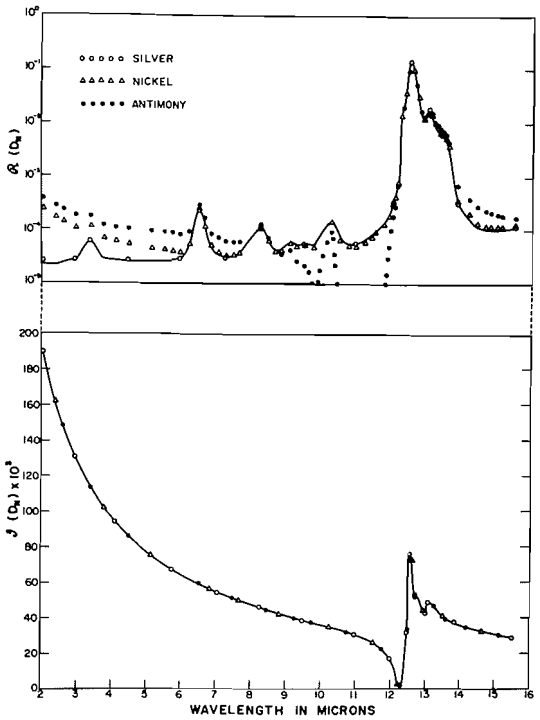

FIG. 4. Influence of substrate properties on D_N for a monolayer film of CCl_4 (liquid state) and an angle of incidence of 45°. The solid lines were calculated using the approximate equation, [25].

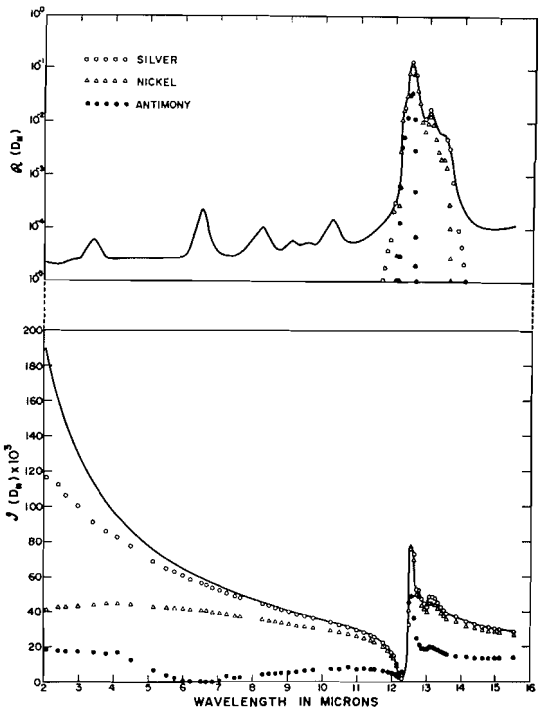

FIG. 5. Influence of substrate properties on D_N for a monolayer film of CCl_4 (liquid state) and an angle of incidence of 85°. The solid lines were calculated using the approximate equation, [25].

approximation for angles of incidence of 5 to 70° with a small discrepancy appearing at 85°.

In Fig. 4, the results for CCl_4 adsorbed on Ag, Ni, and Sb are compared for an angle of incidence of 45°, whereas in Fig. 5 the same comparison is made for an angle of incidence of 85°. The agreement between the exact calculations and the high reflectivity approximation is seen to decrease with decreasing substrate reflectivity and increasing angle of incidence. Although not reported here, similar results were obtained for CH_3OH, H_2O, and cyclohexane films.

The results calculated for total internal reflection employing a Ge prism are graphed in Fig. 6. The rapid fall-off in sensitivity as the angle of incidence is increased from the critical angle is clearly apparent.

To examine quantitatively the effects arising from absorption of light by the gas phase, D_N for CCl_4 adsorbed on Ag was calculated first for $\varepsilon_1 = \bar{\varepsilon}_1 = 1$, then for ε_1 given by that for CCl_4 gas at 100 Torr. In Table 1 these results are compared for an angle of incidence of 45°. The difference between the two results is always small in the case of $\mathscr{I}(D_N)$ and is small in the case of $\mathscr{R}(D_N)$ except near the absorption peak for the gas phase, when $K_1 \sim 10^{-3}$. Even here, the film contribution to D_N dominates, a result which can be deduced from [21]. This is in contrast with conventional absorption spectroscopy where absorption due to the gas phase can completely swamp the absorption due to the surface film. To show this, the conventional base e optical density for N identical reflections and for p-polarized light, $\mathscr{D}_N$, was calculated both for the vacuum case and for the case in which CCl_4 gas is present at 100 Torr. It is easily shown that

$$[42] \quad \mathscr{D}_N = 2N \log_e [|\bar{R}_p|/|R_p|] + 4\pi k_1 S/\lambda_0$$

where S is the path length of the light in the gas phase. The results using [42] and setting $S = 10^{-2}$ cm are presented in Table 2 and illustrate clearly the much greater dependence on gas phase absorption of $\mathscr{D}_N$ than of $\mathscr{R}(D_N)$. They also illustrate that for the vacuum case, and for K_2 not too small, $\frac{1}{2}\mathscr{D}_N \simeq \mathscr{R}(D_N)$, a point noted earlier. The

Can. J. Chem. Downloaded from www.nrcresearchpress.com by 210.87.254.5 on 09/05/12
For personal use only.

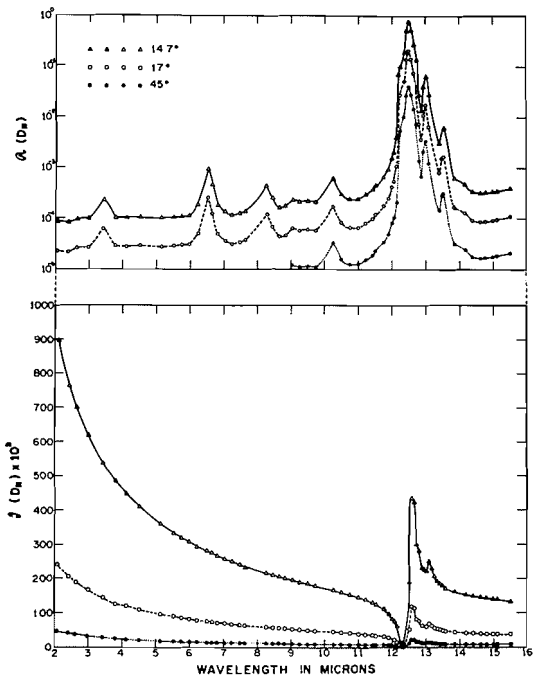

FIG. 6. Influence of angle of incidence on D_N (total internal reflection) for a monolayer film of CCl_4 (liquid state) on Ge, calculated at the critical angle, 14.7° and two larger angles.

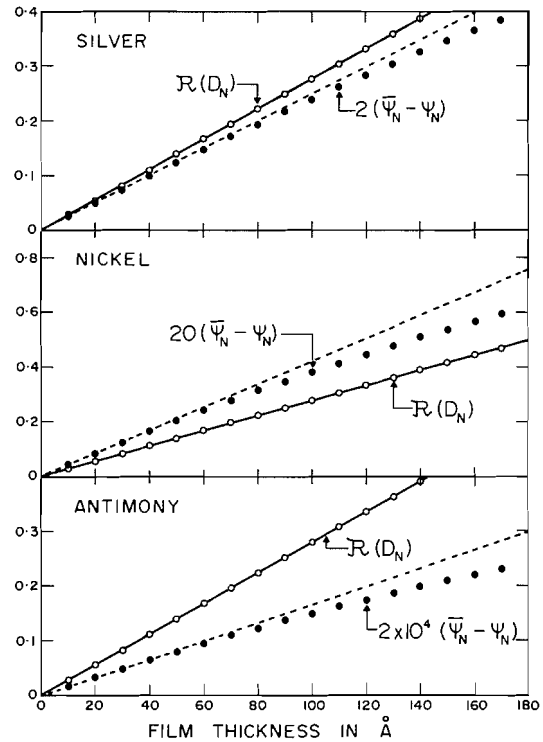

FIG. 7. Comparison of the extent to which $\mathscr{R}(D_N)$ and $(\bar{\psi}_N - \psi_N)$ are proportionally related to the film thickness for CCl_4 adsorption on Ag, Ni, and Sb, respectively. (Wavelength 12.8 μ, 45° angle of incidence.)

value $S = 10^{-2}$ cm is of course unrealistically small, but compensation to about this degree could possibly be achieved using a dual beam spectrophotometer to measure $\mathscr{D}_N$ and placing a compensating gas absorption cell in the reference beam. Because of difficulties arising due to multiple reflections between cell windows, etc., it is very unlikely that compensation to within 10^{-2} cm could in fact be achieved. The case chosen is, of course, extreme in that pressures as high as 100 Torr could usually be avoided. For substantially lower pressures, D_N will be virtually independent of the gas concentration, with significant effects still remaining in the case of $\mathscr{D}_N$.

Ellipsometric measurements cannot be made, usefully, close to or at normal incidence, but neither can conventional absorption measurements since the sensitivity is extremely poor under these conditions (6).

We show next the advantage of the function $\mathscr{R}(D_N)$ over $\bar{\psi}_N - \psi_N$ in relation to thin films and multiple reflection experiments. In Fig. 7, $\mathscr{R}(D_N)$ and $(\bar{\psi}_N - \psi_N)$ are plotted against film thickness for CCl_4 adsorbed on Ag, Ni, and Sb for an angle of incidence of 45° and at 12.8 μ. The lack of linearity of the graphs of $(\bar{\psi}_N - \psi_N)$ is apparent. Again in Table 2, $\mathscr{R}(D_N)$ and $2(\bar{\psi}_N - \psi_N)$ are tabulated for a monolayer of CCl_4 adsorbed on Ag, Ni, and Sb and at a number of wavelengths (*i.e.* a number of values for K_2). The pronounced dependence of $2(\bar{\psi}_N - \psi_N)$ on substrate properties compared with $\mathscr{R}(D_N)$ is dramatically illustrated. For single reflection measurements (*i.e.* $N = 1$), $\mathscr{R}(D)$ and $2(\bar{\psi} - \psi)$ are virtually indistinguishable. Of course, $\mathscr{R}(D_N)$ contains neither more nor less information than $(\bar{\psi}_N - \psi_N)$, given that the substrate optical constants are known, since one can be calculated from the other.

Finally, the need for retaining second order terms in film thickness for the case of external reflection from a weakly absorbing substrate is demonstrated in Fig. 8, where $\mathscr{R}(D_N)$ and $\mathscr{I}(D_N)$ ($L/w = 100$, $\phi_1 = 70°$, $\lambda_0 = 5461$ Å) for a non-absorbing film of refractive index 1.5 on silicon

Can. J. Chem. Downloaded from www.nrcresearchpress.com by 210.87.254.5 on 09/05/12
For personal use only.

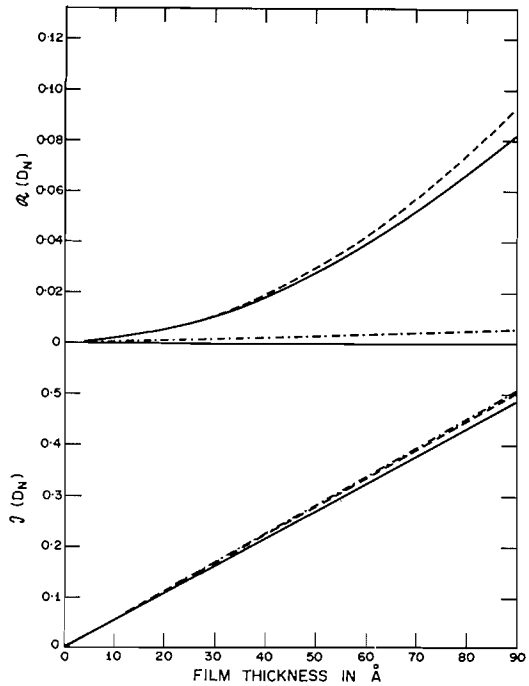

FIG. 8. D_N *vs.* film thickness for a non-absorbing film of refractive index 1.5 on Si, the calculations being performed using the exact equations (—) and using eq. 19 both including the terms T_2 (- - -) and excluding it (-·-·-) ($\phi_1 = 70°$, $\lambda_0 = 0.5461\ \mu$, $L/W = 100$).

are plotted against film thickness. D_N was calculated using the "exact" equations, and using [19] both with $T_2 = 0$ (*i.e.* ignoring second order terms in thickness) and including T_2.

Discussion

It has been shown in the previous sections, both from theory and from sample calculations, that $2\mathscr{R}(D_N)$ is very nearly the same as the conventional base e optical density $\mathscr{D}_N$ which would be obtained using standard specular reflectance spectrometry and p-polarized light. The connection between these can be easily seen, since $2\mathscr{R}(D_N) = N \log_e (\bar{I}_p/\bar{I}_s)/(I_p/I_s)$ whereas $\mathscr{D}_N = N \log_e (\bar{I}_p/\bar{I}_r)/(I_p/I_r)$, where I stands for intensity and the subscripts p, s, r, refer to p-component, s-component, and reference beam, respectively. Thus in ellipsometric spectrometry the s-component takes the place of the reference beam of conventional spectrometry and since I_s is in general much less dependent on the presence of a film than is I_p (*i.e.* $\bar{I}_s \simeq I_s$), the two density functions measure virtually the same thing. Furthermore, if measurement precision is intensity limited, there will be little to choose between them in this regard. If on the other hand precision is not intensity limited, then $\mathscr{R}(D_N)$ should be measurable with considerably greater precision than is possible for $\frac{1}{2}\mathscr{D}_N$, since the ellipsometric quantities required to calculate $\mathscr{R}(D_N)$ do not depend on intensity measurements for their evaluation, whereas $\mathscr{D}_N$ does. Drift in light intensity and photodetector–amplifier gain will therefore effect the measurement of $\mathscr{D}_N$, but not that of $\mathscr{R}(D_N)$.

In addition to the question of precision, however, there is another major advantage to be gained in measuring $\mathscr{R}(D_N)$ by ellipsometry rather than $\frac{1}{2}\mathscr{D}_N$ by conventional spectrometry, and that concerns the relative effectiveness of the "reference" beam in the two cases. Since the s- and p-components of the light beam used in ellipsometry travel exactly the same path, have exactly the same spatial intensity distributions, and are effected identically on transmission through both isotropic media and phase boundaries normal to the propagation direction, the s-component represents in a sense an ideal "reference" beam which cannot be matched by conventional reflection spectrometry. Thus the settling of dust or fogging of windows will effect directly the measured value of $\frac{1}{2}\mathscr{D}_N$, but will have no effect on the measured value of $\mathscr{R}(D_N)$. Again, compensation for light absorption in the gas phase is extremely difficult to achieve with accuracy in the case of conventional reflection spectrometry, whereas it is automatically achieved in ellipsometry as illustrated in the previous sections.

Although the above advantages of ellipsometry over conventional spectrometry are substantial, perhaps the most important advantage derives from the fact that in addition to providing the spectrum of $\mathscr{R}(D_N) \simeq \frac{1}{2}\mathscr{D}_N$, ellipsometry simultaneously provides the spectrum of the phase shift, $\mathscr{S}(D_N) = \bar{\Delta}_N - \Delta_N$. Thus, if the film thickness is measured by an independent technique, the complex refractive index spectrum of the film can be calculated from the measured spectrum of D_N and the optical constants of the substrate using [1] to [12] or [33] and [34] and one of the many equation solving procedures. It is clear that for a metallic substrate, the substrate

Can. J. Chem. Downloaded from www.nrcresearchpress.com by 210.87.254.5 on 09/05/12
For personal use only.

Can. J. Chem. Downloaded from www.nrcresearchpress.com by 210.87.254.5 on 09/05/12
For personal use only.

optical constants need not be known very accurately since D_N is only weakly dependent on these. In fact, to the extent that [25] is a satisfactory approximation, they need not be known at all. It is, however, quite unnecessary to make this approximation, the main value served by it being the insight it provides into the optical behavior of such systems. If a gas phase is present in contact with the reflecting surface, its optical constants will likewise not be required very accurately.

The question now arises as to whether or not the film thickness as well as the spectrum of $\hat{n}_2$ can be determined from an ellipsometric spectrum alone. At first glance the answer would appear to be no since at any given wavelength there are two data (ψ_N, Δ_N, or D_N etc.) and three unknowns, $\hat{n}_2$ and d. Bartell and Churchill (10), working in the u.v.–visible region of the spectrum, overcame this problem in the following way. If $K_2 = 0$, then the experimental values of $\mathscr{R}(D_N)$ and $\mathscr{I}(D_N)$ (or $\bar{\Delta}_N - \Delta_N$, $\bar{\psi}_N - \psi_N$) provide 2 independent data from which the two unknowns, n_2 and d, can be evaluated. The only problem remaining, therefore, is that of locating one or more spectral regions where $K_2 \simeq 0$, a problem which Bartell and Churchill solved without difficulty. That the above technique for calculating d will not always work can be seen from the following analysis. It has been shown that over a fairly wide range of conditions, the high reflectivity approximation, [25] or [26] and [27], represents the optical behavior of such systems very well. However, from these equations we see that for $K_2 = 0$, $\mathscr{R}(D) = 0$ so that the two data are reduced to one and n_2 and d may not be independently evaluated. The same situation arises without approximation in the case of total internal reflection. That Bartell and Churchill did not encounter this difficulty is due to the fact that [25] is a poor approximation in the u.v., since $|\varepsilon_3|$ is not very much larger than $|\varepsilon_1|$ and $|\varepsilon_2|$ in this spectral region. This problem cannot be resolved for the case of reflection from a metal in which $|\varepsilon_3| \gg |\varepsilon_1|$ and ε_2 simply by operating at large angles of incidence where [25] is no longer valid, since the angular dependent factor in $D_N^{(f)}$ is independent of ε_2 for $T_2 \simeq 0$.

A solution to this problem lies in an entirely different direction. It involves using simultaneously all of the ellipsometric data covering a spectral region which spans one or more absorption bands for the film. Since d is presumed to be independent of wavelength, such a set of data will be, numerically, only one less than that required to calculate all the unknowns. An additional relationship is available, however, in that the wavelength dependence of the real and imaginary part of ε_2 are related. One equation based on this relationship is the Kramers–Kronig integral equation (17) used to resolve normal incidence reflectance data for a semi-infinite reflector into the spectrum of n and K for the reflecting medium. Two approaches to this problem based on this principle, but differing substantially from each other in detail, are being investigated now and will be reported upon shortly. At present one of the methods has been successful in reducing synthetic ellipsometric spectra generated via [25] (and hence satisfying precisely the condition $\mathscr{R}(D_N) = 0$ when $K_2 = 0$).

One question that remains concerns the feasibility of making ellipsometric measurements in the infrared region of the spectrum and with sufficient precision to evaluate the spectrum of n_2 and K_2. Bartell and Churchill demonstrated the feasibility of the technique for the ultraviolet spectrum, but abandoned it apparently because of the extremely tedious nature of the data collecting process. Automated ellipsometers now exist, however, with a capability of 1 measurement per second at 0.01° angular precision (18). We are in the process of perfecting an automatic, wavelength scanning, ellipsometer for operation in the wavelength interval 0.5 to 5μ. Its present capabilities are one measurement per second at better than 0.05° angular precision and a wavelength resolution of 0.002μ, the data being directly stored on paper tape in digital form. The collecting of data is therefore no longer a serious problem, nor is data processing. The question of sensitivity is now examined.

An angular precision of 0.05° corresponds to a precision of about 10^{-3} in $\mathscr{R}(D_N)$ and $\mathscr{I}(D_N)$. This is a hundred times the precision required to just detect the absorption and dispersion effects in Figs. 2 to 5 caused by the principle absorption peaks at about 13 μ. A more general statement about precision may be obtained, however, on combining [26] with [32] to give: $\mathscr{R}(D_N) \simeq \alpha(L/w)[n_2/(n_2^2 + K_2^2)^2]$ or since in general for dielectric films, $n_2^2 \gg K_2^2$ and $n_2 \sim 1$, we have $\mathscr{R}(D_N) \sim \alpha(L/w)$, so that to be detectable, the absorption coefficient, χ, must satisfy the inequality

TABLE 3. Typical values for the absorption coefficient, χ, for various stretching and bending modes

Vibration mode	Liquid	Wavelength (μ)	χ (cm^{-1})	Reference
OH Stretching	Water	2.85	1.3×10^4	19
	Methanol	3.00	1.8×10^3	20
C—Cl Stretching	Chloroform	13.10	1.14×10^4	21
	Carbontetrachloride	13.10	1.50×10^4	21
C—H Asymmetric stretching	Methanol	3.40	1.3×10^3	20
C—H Symmetric stretching	Methanol	3.54	1.2×10^3	20
C—O Stretching	Methanol	9.71	1.85×10^3	20
C—H Bending	Methanol	6.75	6.90×10^2	20
C=C Breathing	Benzene	6.75	3.90×10^2	23
C—N Stretching	Nitromethane	10.89	4.78×10^2	22
NO_2 Symmetric bending	Nitromethane	15.20	3.30×10^3	22

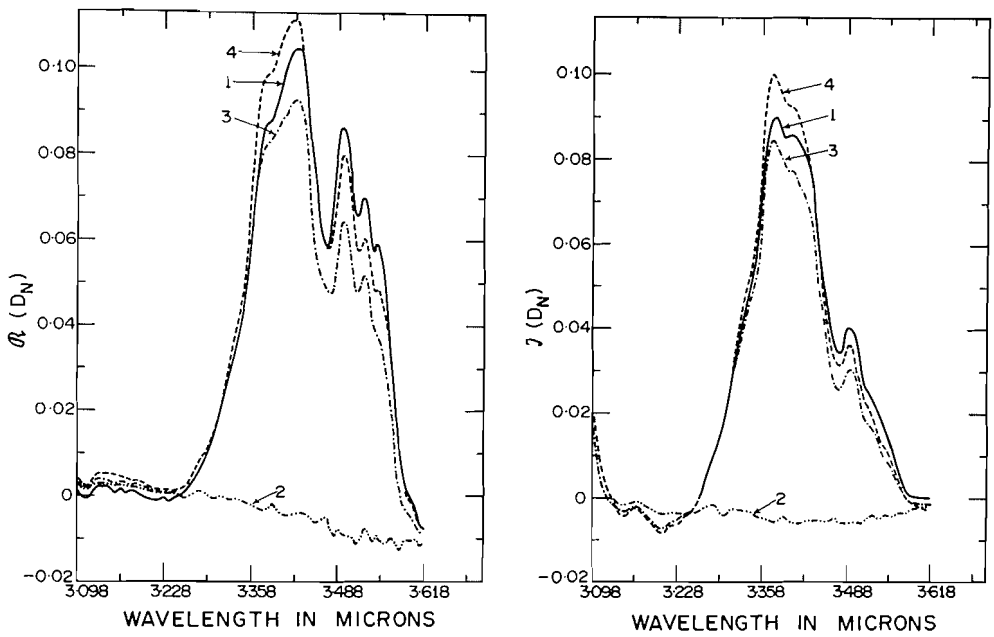

FIG. 9. Experimentally determined spectrum of D_N for CH_3OH adsorbed on Ag, 80° angle of incidence, 16 reflections, 5 Torr CH_3OH at 25 °C. Curves *1*, first adsorption scan; curves *2*, following desorption; curves *3* and *4*, second and third adsorption scans.

$$[43] \qquad \chi \gtrsim \delta[\mathscr{R}(D_N)]/(L/w)d$$

where $\delta[\mathscr{R}(D_N)]$ is the precision of the measurement of $\mathscr{R}(D_N)$. Setting the precision to 10^{-3}, L/w to 100, and d to 10 Å $= 10^{-7}$ cm, the condition becomes $\chi \gtrsim 10^2$ cm^{-1}. For liquid CCl_4 in the vicinity of the 13 μ absorption peaks, $\chi \sim 10^4$ cm^{-1}, which is 100 times above the threshold for detection, the same result obtained by direct inspection of Figs. 2 to 5.

In Table 3, values for χ for a number of common stretching and bending modes are listed along with references. They are typically of the order of 10^3 cm^{-1} or larger and hence readily detectable under the above conditions.

As final evidence of the practicability of the technique, we present in Fig. 9 our first, and preliminary, data obtained for CH_3OH adsorbed on vacuum deposited silver mirrors, 5 in. in length and spaced 1/16 in. apart. Measurements were made at 80° angle of incidence, which with the above geometry gives 16 reflections and $L/w = 46$. A flow system was employed with hydrogen as the carrier gas. The plates were first subjected to a flow of pure hydrogen gas for 3 h at 250 °C. Upon cooling to 25°, the bare substrate

Can. J. Chem. Downloaded from www.nrcresearchpress.com by 210.87.254.5 on 09/05/12
For personal use only.

TABLE 4. Comparison of frequencies for the peaks of $\mathscr{R}(D_N)$ for CH_3OH reversibly adsorbed on Ag with those for the absorption peaks for CH_3OH irreversibly adsorbed on Fe (24)

Present bands for CH_3OH on Ag		Bands for CH_3OH on Fe	
In μ	In cm^{-1}	cm^{-1}	Assignment
3.38	2960	2960	Asymmetric C—H stretch for CH_3
3.42	2924	2934	Asymmetric C—H stretch for CH_3
3.50	2860	2860	Symmetric C—H stretch for CH_3
3.52	2840	—	
3.55	2818	2820	Symmetric C—H stretch for CH_3O

measurements were made at a scan rate of 2 μ/h, then CH_3OH introduced into the flow stream at a partial pressure of 5 Torr (relative pressure of 0.05) and a second scan made. Pure hydrogen was once again passed through the cell until no detectable rate of change of optical properties was observed (this took about 10 min) and a third scan made. The procedures leading to scans 2 and 3 were repeated twice more, leading to a total of three "adsorption scans". The complex optical density function was calculated using runs 1 and 2, 1 and 3, 1 and 5, and 1 and 7, the results appearing in Fig. 9.

As the spectrum virtually disappears upon flushing the cell with pure hydrogen, CH_3OH is apparently reversibly adsorbed. All three adsorption scans show five peaks in the spectrum of $\mathscr{R}(D_N)$ in the vicinity of C—H stretching frequencies. The frequencies of the peaks are given in Table 4 and compared with those determined by Byholder and Wyatt (24) for CH_3OH adsorbed on silica supported iron, using transmission spectroscopy.

It is clear from Fig. 9 that a much weaker absorption band could be detected with our present instrument. Bearing in mind that this instrument is the first working model, and uses a conventional globar light source, further instrument improvement coupled with the probable development of tuneable lasers should provide virtually unlimited sensitivity. The present instrument, which will be described in detail in a subsequent publication, provides ample sensitivity for most purposes. Extension of the technique to the far infrared, while challenging, presents no serious obstacles.

The authors are grateful to the National Research Council of Canada for supporting this research and for a scholarship (M.M.), and to the Province of Ontario for a Fellowship award (R.W.S.). They would also like to express their appreciation to Mr. J. Roth for his invaluable assistance in the programming involved in reducing the raw ellipsometric data to spectra of $\mathscr{R}(D_N)$ and $\mathscr{I}(D_N)$.

1. L. H. LITTLE. Infrared Spectra of Adsorbed Species. Academic Press, New York. 1966.
2. J. F. HARROD, E. F. RISSAMANN, and R. W. ROBERTS. General Electric Report No. 66-C-280, 1966.
3. J. R. BEATTIE. Phila. Mag. **55**, 235 (1955).
4. H. L. PICKERING and H. C. ECKSTROM. J. Phys. Chem. **63**, 512 (1958).
5. S. A. FRANCIS and A. H. ELLISON. J. Opt. Soc. Amer. **49**, 131 (1959).
6. R. GREENLER. J. Chem. Phys. **44**, 310 (1966).
7. R. GREENLER. J. Chem. Phys. **50**, 1963 (1969).
8. J. PRITCHARD and M. L. SIMS. Trans. Faraday Soc. **66**, 427 (1970).
9. N. J. HARRICK. J. Phys. Chem. **64**, 1110 (1960).
10. L. S. BARTELL and D. CHURCHILL. J. Phys. Chem. **65**^{2}, 2242 (1961); **67**^{2}, 2518 (1963).
11. N. M. BASHARA and D. W. PETERSON. J. Opt. Soc. Amer. **56**, 1320 (1966).
12. A. B. WINTERBOTTOM. Det. Kong. Nosske Videnskarkers Selskabs. Skrifter No. 1, 1955.
13. A. VASICEK. Optics of Thin Films. North-Holland Publishing Co., Amsterdam. 1960.
14. A. N. SAXENA. J. Opt. Soc. Amer. **55**, 1061 (1965).
15. D. E. GRAY. Coordinating Editor. American Institute of Physics Handbook, McGraw-Hill, New York. 1963.
16. R. E. KAGARISE. J. Opt. Soc. Amer. **50**, 36 (1960). J. S. ARD and J. D. FONTAINE. Anal. Chem. **23**, 305 (1951). W. H. BEERMER and G. J. ATCHISON. Anal. Chem. **22**, 305 (1950). V. S. LIBOV and N. G. BAKHSHIEV. Opt. Spectrosc. 122 (1964).
17. H. J. BOWLDEN and K. K. WILMSHURST. J. Opt. Soc. Amer. **53**, 1073 (1963).
18. J. L. ORD and B. L. WILLS. Appl. Opt. **6**, 1673 (1967).
19. L. D. KISLOVSKII. Opt. Spectrosc. **7**, 201 (1959).
20. M. FALK and E. WHALLEY. J. Chem. Phys. **34**, 1554 (1961).
21. V. S. LIBOV and N. G. BAKHSHIEV. Opt. Spectrosc. **16**, 122 (1964).
22. D. C. SMITH, CHI-YUAN PAN, and J. R. NIELSEN. J. Chem. Phys. **18**, 706 (1950).
23. H. A. SZYMANSKI. Interpreted Infrared Spectra. Vol. 1. Plenum Press, New York. 102 (1964).
24. G. BYHOLDER and W. V. WYATT. J. Phys. Chem. **70**, 1745 (1966).

Can. J. Chem. Downloaded from www.nrcresearchpress.com by 210.87.254.5 on 09/05/12
For personal use only.

Can. J. Chem. Downloaded from www.nrcresearchpress.com by 210.87.254.6 on 09/05/12
For personal use only.

NOTES

Circular Dichroism of the Copper(II) *N,N'*-Bis(alanyl)stilbenediamine Complexes

M. PARRIS AND A. E. HODGES
Chemistry Department, Carleton University, Ottawa, Canada

Received September 29, 1970

The preparations of the three diamides, RR(or RS or SS)-*N,N'*-bis(*S*-alanyl)stilbenediamine are described. The circular dichroism spectra of the 1:1 copper(II) complexes are compared to those of similar compounds previously described.

La préparation des trois diamides, RR (ou RS ou SS)-*N,N'*-bis(*S*-alanyl)stilbènediamine est décrite. Le spectre de dichroïsme circulaire de leurs complexes 1:1 avec le cuivre (II) est comparé avec ceux de composés similaires décrits prédécemment.

Canadian Journal of Chemistry, **49**, 1133 (1971)

The interaction between metal ions and peptide-like compounds has been reviewed (1). Peptides readily coordinate to copper(II) ion with the loss of the amide protons, two per molecule in the case of *N,N'* diamides (2), to form complexes only slightly distorted from planarity. Dissymmetric complexes of this type will exhibit Cotton effects in the visible region which are expected to be characteristic of the particular coordination environment (3). Accordingly, we present here the circular dichroism (c.d.) spectra for copper(II) complexes of some dissymmetric diamides of known absolute configurations, comparable to those previously described (8, 12).

Experimental

Materials

Established procedures were used for the preparation of *meso*-stilbenediamine (4), m.p. 120–121°, and for the preparation and resolution of *rac*-stilbenediamine (5), m.p. 80–82°, $(-)_D$ stien d tartrate, $|\alpha|_D$ −11.2° (0.10 g, 5 ml H_2O), $(-)_D$ stien, m.p. 82–83°, $|\alpha|_D$ −88° (0.048 g, 5 ml ether), $(+)_D$ stien d tartrate $|\alpha|_D$ +42° (0.041 g, 5 ml H_2O), $(+)_D$ stien, m.p. 81–83°, $|\alpha|_D$ +87° (0.049 g, 5 ml ether). L-alanine was obtained from Nutritional Biochemicals Corp., $|\alpha|_D$ +14.25° (2 *M*, 2 *N* HCl), and converted to phthaloyl L alanine by standard methods (6).

Preparation of Ligands

The procedure was adapted from that of Sheehan and Hess (7) and has been previously described (8).

RS-N,N'-bis(S-alanyl)stilbenediamine (1)

Using *meso*-stilbenediamine the intermediate RS-*N,N'*-bis(phthaloyl-*S*-alanyl)stilbenediamine was prepared, m.p. > 300°, $|\alpha|_D$ +58° (0.3%, DMF). Treatment with aqueous base converted the dihydrochloride from the hydrazinolysis into free amide, which was crystallized from aqueous methanol m.p. 258–259°, $|\alpha|_D$ +11° (0.7%, methanol).

Anal. Calcd. for $C_{20}H_{26}N_4O_2$, $2\frac{1}{2}$ H_2O: C, 60.2; H, 7.77; N, 14.0. Found: C, 60.5; H, 7.61; N, 13.9.

SS-N,N'-bis(S-alanyl)stilbenediamine (2)

$(-)_D$ Stilbenediamine was converted to SS-*N,N'*-bis-(phthaloyl-*S*-alanyl)stilbenediamine, m.p. > 300°, $|\alpha|_D$ +104° (0.35%, DMF), which was hydrazinolyzed. The amide dihydrochloride was recrystallized from aqueous HCl, m.p. 277–278° (decomp.), $|\alpha|_D$ +31.6° (1%, H_2O).

Anal. Calcd. for $C_{20}H_{26}N_4O_2.2$ HCl: C, 56.2; H, 6.60; N, 13.1. Found: C, 56.7; H, 6.04; N, 13.3.

RR-N,N'-bis(S-alanyl)stilbenediamine (3)

$(+)_D$ Stilbenediamine was converted to RR-*N,N'*-bis-(phthaloyl-*S*-alanyl)stilbenediamine, m.p. 155–156°, $|\alpha|_D$ −27.3° (1%, DMF) which was hydrazinolyzed. The amide dihydrochloride was recrystallized from aqueous HCl, m.p. 286–287° (decomp.), $|\alpha|_D$ +0.78° (1.3%, H_2O).

Anal. Found: C, 55.9; H, 6.87; N, 13.1.

Cupric Complexes

Aqueous solutions were prepared as previously described (8).

Discussion

Although the absolute configuration of stilbenediamine has not been determined crystallographically or chemically, a configurational relation has been established (9) between $(+)_D$ propanediamine, $(+)_D$ cyclohexanediamine, $(+)_D$ cyclopentanediamine, and $(-)_D$ stilbenediamine using the long wavelength absorption band of the *trans*-dichlorobis(diamine)cobalt(III) ions (10). The absolute configurations of the first three diamines are known from crystallographic studies (11) so that $(-)_D$ stilbenediamine is assigned the absolute configuration SS.

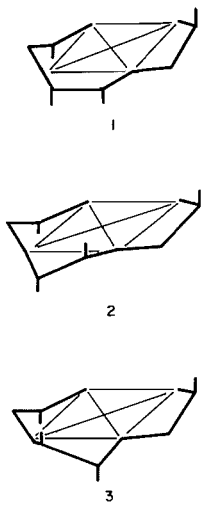

FIG. 1. Absolute configurations of compounds **1**, **2**, and **3** (see text).

The three 1:1 cupric complexes will have the structures indicated schematically in Fig. 1. Their visible absorption and c.d. spectra are shown in Fig. 2. If these spectra are compared to those previously described (8, 12), it seems evident that there are the expected three contributory bands beneath the total absorption envelope. The central band at about 500 nm has a negative c.d. related to λ chirality of the terminal rings (carbons 1 and 2) which is related to the ligand's absolute configuration in two ways. Firstly, SS-cyclohexanediamine always imposes δ chirality on the bridging ring (carbons 3 and 4) independently of the rest of the structure. This is, not unexpectedly, the strongest effect and overrides all other conformational preferences. A δ chirality is then transmitted to the terminal rings via the planar C—N—CO system (1). This effect is observed in RR-*N*,*N*′-bisglycylcyclohexanediamine, in RR-*N*,*N*′-bis(*S*-alanyl)cyclohexanediamine and in SS-*N*,*N*′-bis(*S*-alanyl)cyclohexanediamine (8, 12). Secondly, the terminal rings will tend to be non-planar in order to minimize any carbonyl–methyl interaction (13). A λ chirality here relates to S substitution, that is, the substituent becomes axial. This effect is seen in *N*,*N*′-bis(*S*-alanyl)ethanediamine, in **1**, in RS-*N*,*N*′-bis(*S*-alanyl)cyclohexanediamine, and in *N*,*N*′-bis(*S*-alanyl)butanediamine (8, 12).

Optical activity in two bands lying at about 450 and 550 nm appears to arise only upon dissymmetric substitution at the bridging ring.

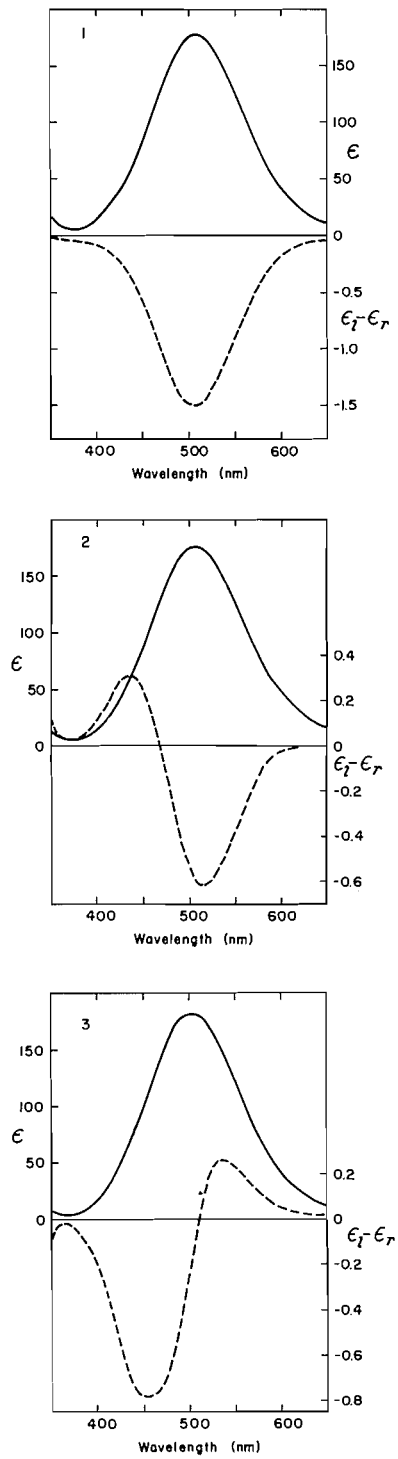

FIG. 2. Absorption spectra (—) and associated circular dichroism (---) for compounds **1**, **2**, and **3** (see text).

Can. J. Chem. Downloaded from www.nrcresearchpress.com by 210.87.254.6 on 09/05/12
For personal use only.

In this case positive c.d. at 450 nm and negative at 550 nm is associated with S substitution and the magnitude of the effect varies according to the bulk of the substituent. This is seen in **2** and **3**, in S-*N*,*N*′-bisglycylpropanediamine, in SS-*N*,*N*′-bisglycylbutanediamine (8, 12) and in SS-*N*,*N*′-bis(*S*-alanyl)butanediamine and RR-*N*,*N*′-bis-(*S*-alanyl)butanediamine (14). In these cases, *i.e.*, in other than fused ring systems, there appears to be no significant preference transmitted to the terminal rings (*e.g.*, terminal λ for R bridge substitution), as judged by the absence of any marked optical activity in the 500 nm region.

We would like to thank both Dr. C. Benezra of The University of Ottawa and Dr. D. H. Busch of The Ohio State University for affording c.d. facilities.

1. H. C. Freeman. Advan. Protein Chem. **22**, 257 (1967).
2. A. K. Chakraburtty, N. N. Ghosh, and P. Ray. J. Ind. Chem. Soc. **30**, 185 (1959).
3. G. F. Bryce, R. W. Roeske, and F. R. N. Gurd. J. Biol. Chem. **241**, 1072 (1966).
4. H. M. N. Irving and R. M. Parkins. J. Inorg. Nucl. Chem. **27**, 270 (1965).
5. I. Lifschitz and J. G. Bos. Rec. Trav. Chim. **59**, 173 (1940).
6. R. G. Asperger and C. F. Liu. Inorg. Chem. **4**, 1395 (1965).
7. J. C. Sheehan and G. P. Hess. J. Amer. Chem. Soc. **77**, 1067 (1955).
8. M. Parris and A. E. Hodges. Can. J. Chem. **48**, 7166 (1970).
9. R. D. Gillard. Tetrahedron, **21**, 503 (1965).
10. R. D. Gillard and G. Wilkinson. J. Chem. Soc. 1398 (1964). R. S. Treptow. Inorg. Chem. **5**, 1593 (1966). F. M. Jaeger and H. B. Blumendal. Zeit. anorg. allgem. Chem. **175**, 189 (1928).
11. Y. Saito, H. Iwasaki, and H. Ota. Bull. Chem. Soc. Japan, **36**, 1543 (1963). J. W. Turley, F. P. Boer, and F. van Remoortere. J. Chem. Soc. D, 720 (1970). M. Ito, F. Maruma, and Y. Saito. Inorg. Nucl. Chem. Lett. **6**, 519 (1970).
12. M. Parris and A. E. Hodges. J. Amer. Chem. Soc. **90**, 1909 (1968).
13. G. F. Bryce and F. R. N. Gurd. J. Biol. Chem. **241**, 1439 (1966).
14. M. Parris and A. E. Hodges. Unpublished results.

Electronic Levels of Methyl Amines by Photoelectron Spectroscopy and an i.n.d.o. Calculation

A. B. Cornford, D. C. Frost, F. G. Herring, and C. A. McDowell
The Department of Chemistry, The University of British Columbia, Vancouver 8, British Columbia

Received October 5, 1970

The ionization potentials of the methyl amines down to 20 eV binding energy, have been determined by photoelectron spectroscopy, and are compared with those predicted by i.n.d.o.-l.c.a.o.-s.c.f. theory. The first ionization potential for each compound refers to the removal of an electron from the lone pair, and is shown to be the one most affected by the inclusion of one center repulsion integrals in the i.n.d.o. calculations.

Les potentiels d'ionisation des méthylamines, en descendant jusqu'au niveau de 20 eV d'énergie de liaison, ont été déterminés par spectroscopie photoélectronique et comparés avec les valeurs prédites par la théorie i.n.d.o.-l.c.a.o.-s.c.f. Le premier potentiel d'ionisation de chaque composé se rapporte à l'enlèvement d'un électron du doublet libre et il est démontré que c'est celui qui est le plus affecté par l'inclusion, dans les calculs i.n.d.o., d'intégrales correspondant à une répulsion d'un centre.

Canadian Journal of Chemistry, **49**, 1135 (1971)

The first ionization potentials (i.p.'s) of the methyl amines have been measured by photoionization (1) and by photoelectron spectroscopy (2). We have obtained the 584 Å high resolution spectra of these compounds using a spectrometer with a hemispherical analyzer (3), and our adiabatic values for the first i.p.'s agree with those of ref. 1, which are all rather lower than those reported by Al-Joboury and Turner (2). Our actual values are 8.99 eV for the mono- , 8.25 eV for the di- , and 7.80 eV for the tri-substituted compounds. Our samples were C.P. grade, obtained from Matheson of Canada, and were found to contain no significant amount of impurities.

As far as inner i.p.'s are concerned, those re-

Can. J. Chem. Downloaded from www.nrcresearchpress.com by 210.87.254.6 on 09/05/12
For personal use only.

In this case positive c.d. at 450 nm and negative at 550 nm is associated with S substitution and the magnitude of the effect varies according to the bulk of the substituent. This is seen in **2** and **3**, in S-*N*,*N*′-bisglycylpropanediamine, in SS-*N*,*N*′-bisglycylbutanediamine (8, 12) and in SS-*N*,*N*′-bis(*S*-alanyl)butanediamine and RR-*N*,*N*′-bis-(*S*-alanyl)butanediamine (14). In these cases, *i.e.*, in other than fused ring systems, there appears to be no significant preference transmitted to the terminal rings (*e.g.*, terminal λ for R bridge substitution), as judged by the absence of any marked optical activity in the 500 nm region.

We would like to thank both Dr. C. Benezra of The University of Ottawa and Dr. D. H. Busch of The Ohio State University for affording c.d. facilities.

1. H. C. Freeman. Advan. Protein Chem. **22**, 257 (1967).
2. A. K. Chakraburtty, N. N. Ghosh, and P. Ray. J. Ind. Chem. Soc. **30**, 185 (1959).
3. G. F. Bryce, R. W. Roeske, and F. R. N. Gurd. J. Biol. Chem. **241**, 1072 (1966).
4. H. M. N. Irving and R. M. Parkins. J. Inorg. Nucl. Chem. **27**, 270 (1965).
5. I. Lifschitz and J. G. Bos. Rec. Trav. Chim. **59**, 173 (1940).
6. R. G. Asperger and C. F. Liu. Inorg. Chem. **4**, 1395 (1965).
7. J. C. Sheehan and G. P. Hess. J. Amer. Chem. Soc. **77**, 1067 (1955).
8. M. Parris and A. E. Hodges. Can. J. Chem. **48**, 7166 (1970).
9. R. D. Gillard. Tetrahedron, **21**, 503 (1965).
10. R. D. Gillard and G. Wilkinson. J. Chem. Soc. 1398 (1964). R. S. Treptow. Inorg. Chem. **5**, 1593 (1966). F. M. Jaeger and H. B. Blumendal. Zeit. anorg. allgem. Chem. **175**, 189 (1928).
11. Y. Saito, H. Iwasaki, and H. Ota. Bull. Chem. Soc. Japan, **36**, 1543 (1963). J. W. Turley, F. P. Boer, and F. van Remoortere. J. Chem. Soc. D, 720 (1970). M. Ito, F. Maruma, and Y. Saito. Inorg. Nucl. Chem. Lett. **6**, 519 (1970).
12. M. Parris and A. E. Hodges. J. Amer. Chem. Soc. **90**, 1909 (1968).
13. G. F. Bryce and F. R. N. Gurd. J. Biol. Chem. **241**, 1439 (1966).
14. M. Parris and A. E. Hodges. Unpublished results.

Electronic Levels of Methyl Amines by Photoelectron Spectroscopy and an i.n.d.o. Calculation

A. B. Cornford, D. C. Frost, F. G. Herring, and C. A. McDowell
The Department of Chemistry, The University of British Columbia, Vancouver 8, British Columbia

Received October 5, 1970

The ionization potentials of the methyl amines down to 20 eV binding energy, have been determined by photoelectron spectroscopy, and are compared with those predicted by i.n.d.o.-l.c.a.o.-s.c.f. theory. The first ionization potential for each compound refers to the removal of an electron from the lone pair, and is shown to be the one most affected by the inclusion of one center repulsion integrals in the i.n.d.o. calculations.

Les potentiels d'ionisation des méthylamines, en descendant jusqu'au niveau de 20 eV d'énergie de liaison, ont été déterminés par spectroscopie photoélectronique et comparés avec les valeurs prédites par la théorie i.n.d.o.-l.c.a.o.-s.c.f. Le premier potentiel d'ionisation de chaque composé se rapporte à l'enlèvement d'un électron du doublet libre et il est démontré que c'est celui qui est le plus affecté par l'inclusion, dans les calculs i.n.d.o., d'intégrales correspondant à une répulsion d'un centre.

Canadian Journal of Chemistry, **49**, 1135 (1971)

The first ionization potentials (i.p.'s) of the methyl amines have been measured by photoionization (1) and by photoelectron spectroscopy (2). We have obtained the 584 Å high resolution spectra of these compounds using a spectrometer with a hemispherical analyzer (3), and our adiabatic values for the first i.p.'s agree with those of ref. 1, which are all rather lower than those reported by Al-Joboury and Turner (2). Our actual values are 8.99 eV for the mono- , 8.25 eV for the di- , and 7.80 eV for the tri-substituted compounds. Our samples were C.P. grade, obtained from Matheson of Canada, and were found to contain no significant amount of impurities.

As far as inner i.p.'s are concerned, those re-

Can. J. Chem. Downloaded from www.nrcresearchpress.com by 210.87.254.42 on 09/05/12
For personal use only.

TABLE 1. Vertical ionization potentials for the methylamines (eV)

Methylamine			Dimethylamine			Trimethylamine*		
c.n.d.o./2	i.n.d.o.	Exp.	c.n.d.o./2	i.n.d.o.	Exp.	c.n.d.o./2	i.n.d.o.	Exp.
10.2	8.7	9.7	9.4	8.1	8.9	9.0	7.7	8.5
12.7	12.6	13.2	11.6	11.4	12.6	11.3	11.1	12.4
15.0	14.6	14.5	12.7	12.5	13.3	12.4	12.3	12.9
18.2	17.6	15.6	15.3	15.2	13.8	15.8	15.6	14.0
19.7	19.4	17.1	16.4	16.1	15.2	19.1	18.9	16.0
25.9	26.2		19.6	19.2	16.8	20.9	20.5	
			20.6	20.2		23.9	23.8	
			25.4	25.4				

*This molecule having C_{3v} symmetry the orbitals may be classified accordingly A_1, E, A_2, E, E, A_1, A_1 in order of increasing energy.

ported by Al-Joboury and Turner are probably somewhere between adiabatic and vertical values, and so strictly speaking cannot be compared with results which are the vertical i.p.'s corresponding to the maxima in the vibrational bands. These are the values required for comparison with the i.n.d.o. calculations.

As in previous studies (4–7) we have carried out both c.n.d.o./2 and i.n.d.o.-l.c.a.o.-s.c.f. calculations (8). This type of calculation has proved useful in the identification of the molecular orbital from which the photoelectron is removed. The results are given in Table 1. A consideration of the data in this Table shows that the inclusion of one center exchange integrals, on going from the c.n.d.o./2 to the i.n.d.o. scheme, most markedly affects the calculated values for first i.p.'s of the molecules. The values of the first i.p.'s from the i.n.d.o./2 method are uniformly lower whereas the remaining ones are essentially the same, in all cases for both types of calculation. The first i.p.'s for all three molecules are associated with the removal of an electron from an orbital with electron density localized on the nitrogen atom, which closely approximates a lone pair orbital. It is, therefore, not unreasonable that this energy level will be the most affected by the inclusion of the one center repulsion integrals in the i.n.d.o. calculations. It should also be pointed out that both computational schemes lead to the same ordering of the molecular energy levels.

The calculations satisfactorily reproduce the trend in the first i.p.'s found on going from ammonia (5) through to trimethylamine, with the i.n.d.o. method being superior since it more correctly predicts the first i.p. of ammonia. The observed and calculated trends are of a decrease in the ionization potentials on going from ammonia to trimethylamine, which parallels the decrease in the dipole moment for the same series. It is tempting to suggest that this is because of changes in the overall hybridization of the nitrogen atom as more methyl groups are attached to it, *i.e.* a change of the lone pair orbital groups from an sp^3 hybrid towards a pure p orbital. The magnitude of the change in bond angle, however, on going from ammonia (107.1°) to trimethylamine (108.7°) does not seem to be sufficient to account for the trend in the first i.p.'s or the dipole moments (8). It is possible, however, that the trend in first i.p. reflects a progressive stabilization of the positive ion by hyperconjugation due to the increasing number of methyl groups.

The i.p.'s of the methyl-substituted amines, other than the first i.p., all arise from the removal of electrons in orbitals associated with the nitrogen–carbon bonding framework, and exhibit a similar decrease on successive methylation.

This work was supported by generous financial grants from the National Research Council of Canada. We wish to thank Mr. J. P. Louwerens for assistance with the computations.

1. K. WATANABE and J. R. MOTTL. J. Chem. Phys. **26**, 1773 (1957).
2. M. I. AL-JOBOURY and D. W. TURNER. J. Chem. Soc. 4434 (1964).
3. G. R. BRANTON, D. C. FROST, T. MAKITA, C. A. MCDOWELL, and I. A. STENHOUSE. J. Chem. Phys. **52**, 802 (1970).
4. D. C. FROST, F. G. HERRING, C. A. MCDOWELL, M. R. MUSTAFA, and J. S. SANDHU. Chem. Phys. Lett. **2**, 63 (1968).
5. G. R. BRANTON, D. C. FROST, F. G. HERRING, C. A. MCDOWELL, and I. A. STENHOUSE. Chem. Phys. Lett. **3**, 581 (1969).
6. D. C. FROST, F. G. HERRING, C. A. MCDOWELL, and I. A. STENHOUSE. Chem. Phys. Lett. **4**, 533 (1970).
7. D. C. FROST, F. G. HERRING, C. A. MCDOWELL, and I. A. STENHOUSE. Chem. Phys. Lett. **5**, 291 (1970).
8. J. A. POPLE and D. L. BEVERIDGE. Approximate Molecular Orbital Theory. McGraw-Hill. 1970.

Can. J. Chem. Downloaded from www.nrcresearchpress.com by 210.87.254.42 on 09/05/12
For personal use only.

Infrared Spectrum and Hydrogen Bonding in Solid and Liquid Trimethylamine Hydrate $(CH_3)_3N.10\frac{1}{4}H_2O$[1]

MICHAEL FALK
Atlantic Regional Laboratory, National Research Council of Canada, Halifax, Nova Scotia

Received November 6, 1970

The OD band profiles of dilute HDO in liquid TMA.$10\frac{1}{4}H_2O$ differ only slightly from those in liquid water, showing that the distribution of hydrogen-bond strengths has the same general form in the two media. Absence of shoulders at frequencies corresponding to the OD stretching frequencies of HDO in ice and in crystalline TMA hydrate points to the absence of structurally well-defined ice-like or clathrate-like regions above the melting point of the crystalline TMA hydrate.

Les profiles des bandes OD et HDO dilué de la TMA.$10\frac{1}{4}H_2O$ liquide diffèrent seulement un peu de ceux dans l'eau liquide, montrant que la distribution des forces des liaisons hydrogènes a la même forme générale dans les deux milieux. L'absence des épaulements aux fréquences correspondant aux fréquences de valence du OD de HDO, dans la glace et dans l'hydrate TMA cristallin indique l'absence de régions de structure bien définies comme dans la glace ou un clathrate, ceci au-dessus du point de fusion de l'hydrate TMA cristallin.

Canadian Journal of Chemistry, 49, 1137 (1971)

Interactions between water and non-polar parts of solute molecules have often been described in terms of ordered regions which possess the structure of one of the ices or clathrate hydrates (1). The purpose of the present study has been to determine whether the hydrogen bonding scheme characteristic of a crystalline clathrate persists above the melting point.

The shape of the distribution of hydrogen bonds may be deduced from the infrared band profiles of the OD stretching fundamental of isotopically dilute HDO (2–6). Such band profiles were obtained above and below the melting point of the crystalline hydrate of trimethylamine (abbreviated TMA), of ideal composition $4TMA.41H_2O$. The crystal structure of this hydrate is known from the work of Panke (7), and important structural evidence on the aqueous solution has been provided by the recent X-ray diffraction study of Folzer, Hendricks, and Narten (8).

Experimental

Infrared spectra in the region of 2500 cm^{-1} were recorded on a Perkin–Elmer spectrophotometer model 521. A low-temperature infrared cell of the Wagner–Hornig type was used. TMA was obtained as 25 weight% aqueous solution from Anachemia Chemicals Co., Montreal, and was used without further purification. D_2O of 99.85% isotopic purity was from Merck, Sharp, and Dohme Co., Montreal. Stock solutions of TMA in H_2O, and in H_2O to which 2 to 4 mol% of D_2O was added, were prepared by weight to give the TMA–water ratio of 1:10.25, which corresponds to the stoichiometry of the hydrate. The liquid samples were studied as films of 28 μm thickness in sealed CaF_2 cells; spectra of pure H_2O and of H_2O containing a few percent D_2O were recorded for comparison under identical conditions.

Upon cooling in sealed CaF_2 cells, the films of TMA solution froze to a polycrystalline solid, which had a melting point of 5.2 ± 0.2°, recorded spectroscopically as in ref. 9. The melting point confirms that the solid was essentially pure TMA.$10\frac{1}{4}H_2O$, which has the reported melting point of 5.0° (7). Unfortunately, the films obtained with sealed cells were too thick for a spectral study, the transmittance of crystalline samples in the 2500 cm^{-1} region being much lower than that of the liquid samples. To obtain sufficiently thin films we had to resort to rapid cooling of capillary films of TMA solution held between AgCl or CaF_2 plates. The thickness of these films was not accurately known. Another disadvantage was the possibility of some volatilization of TMA during the preparation of the films. This would raise the water content in excess of the desired stoichiometry, TMA.$10\frac{1}{4}$-H_2O, which upon cooling would lead to an admixture of ice. However, the constancy of the relative intensities of the bands due to H_2O and TMA in the spectra of the capillary films gave us confidence that we were dealing with nearly stoichiometric hydrate.

Results and Discussion

Figure 1 shows the OD stretching profiles of isotopically dilute HDO in the four media: water, TMA solution, ice, and TMA hydrate. These profiles were obtained by subtracting the absorbances of the undeuterated films from those of the partly deuterated films, and normalizing to unit height.[2]

The half-width of the OD stretching band of

[1]NRCC No. 11 777.

[2]The peak absorptivity of the OD band in TMA solution was a few percent higher than that in water; that of the OD band in ice and the crystalline hydrate could not be determined because of uncertain film thickness.

Can. J. Chem. Downloaded from www.nrcresearchpress.com by 210.87.254.42 on 09/05/12
For personal use only.

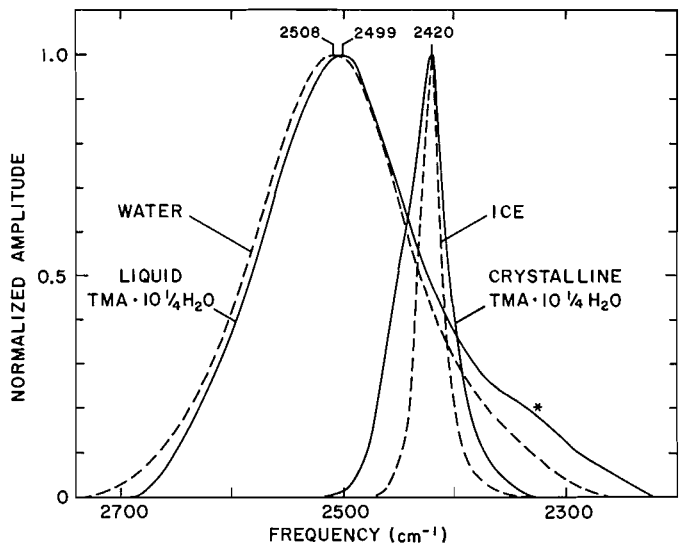

FIG. 1. Normalized OD stretching profiles of HDO in water (27°), TMA solution (27°), ice (−147°), and TMA hydrate (−149°). The shoulder marked with an asterisk is an artifact caused by the absorption of atmospheric CO_2.

isotopically dilute HDO in solid TMA.$10\frac{1}{4}H_2O$ is 50 to 60 cm^{-1}, compared to the values of 25 to 35 cm^{-1} for HDO in ice in the same temperature interval of −160 to −65°. Hydrates which contain fully ordered water molecules have OD half-widths of a few cm^{-1} (3, 5, 10, 11). The reason for the breadth of the band in ice I is its configurational disorder, which leads to a distribution of surroundings of individual OH groups (12). The two crystallographically distinct OH groups in ice ("axial" OH, pointing along the *c*-axis, and "equatorial" OH, forming an angle of about 109° with the *c*-axis) form hydrogen bonds of almost identical length (13), hence the corresponding two OH bands are too closely overlapped to be resolved. The much larger breadth of the band in TMA hydrate is due to the presence of twelve crystallographically distinct OH groups which form OH · · · O bonds with lengths from 2.740 to 2.850 Å and OH · · · N bonds with lengths of 2.668 and 2.705 Å (7). The bands due to the OD stretching frequencies of the individual hydroxyl groups must be broadened by hydrogen disorder as in ice, hence we cannot expect to resolve the resulting broad envelope. The envelope is highly asymmetric, in contrast to that of ice, which is symmetric and approximately Lorentzian (14). The half-width of this envelope is only slightly temperature-dependent, as the wide variety of hydrogen-bond lengths which correspond to the twelve distinct OH groups persists at all temperatures. As the widths of the individual subbands diminish at low temperatures, the band envelope begins to show some structure. Although the peak frequency is practically the same for the TMA hydrate and ice, the center of gravity of the band is about 10 cm^{-1} higher for TMA hydrate. This indicates that the *average* strength of hydrogen bonding in the hydrate is slightly lower than that of ice, in qualitative agreement with the average hydrogen-bond distance being about 2.80 Å in the hydrate (7) compared to about 2.76 Å in ice (13).

The OD band profile of isotopically dilute HDO in TMA.$10\frac{1}{4}H_2O$ above the melting point differs relatively little from that of HDO in water, showing that the distributions of hydrogen-bond strengths in the two media have the same general form. A closer inspection shows that the TMA solution has an increased absorbance on the low-frequency side of the band, a decreased absorbance on the high frequency side, and a downward shift of the peak frequency of about 9 cm^{-1} with respect to pure water. This indicates a small overall shift toward stronger hydrogen bonding when TMA is dissolved in water. However, at least a part of that shift must be due to the water–trimethylamine OH · · · N bonds, which are stronger than the water–water OH · · · O bonds. In crystalline TMA.$10\frac{1}{4}H_2O$ the OH · · · N bond distances

Can. J. Chem. Downloaded from www.nrcresearchpress.com by 210.87.254.42 on 09/05/12
For personal use only.

are 2.668 and 2.705 Å, much shorter than the OH · · · O bonds, which vary in length from 2.74 to 2.85 Å (7). Thus the distribution of water–water hydrogen-bond strengths in TMA solution must be nearly the same as that in pure water. The same conclusion has been reached earlier for aqueous solutions of dimethyl sulfoxide (15).

The OD band profile of HDO in water has appreciable intensity near 2440 cm^{-1}, corresponding to the peak frequency of HDO in ice and in crystalline TMA.$10\frac{1}{4}H_2O$ near the melting point. In the corresponding band profile in liquid TMA.$10\frac{1}{4}H_2O$ the relative intensity at 2440 cm^{-1} is slightly increased. However, there is no detectable shoulder near this frequency. This shows that while hydrogen bonding similar in strength to that occurring in crystalline ice or TMA hydrate does occur in water and, increasingly so, in aqueous solution of TMA, structurally well-defined regions do not persist above the melting point. Any "iceberg" regions are ill-defined and their OD stretching spectrum merges with that of the remainder of water.

The present observations and their interpretation are in full agreement with the findings of Folzer, Hendricks, and Narten (8) that the radial distribution function of the TMA solution is very similar to that of pure water and with their conclusion that long-range order (beyond 8 Å) is absent in the solution as well as in water.

I wish to thank Mr. P. F. Seto for technical assistance, Prof. G. A. Jeffrey for suggesting this investigation, and Drs. A. H. Narten and Cynthia Folzer for sending me a preprint of ref. 8 prior to its publication and for several discussions.

1. J. L. Kavanau. Water and Solute–Water Interactions. Holden-Day, Inc., San Francisco. 1964. pp. 22–28.
2. R. D. Waldron. J. Chem. Phys. **26**, 809 (1957).
3. J. Schiffer. Ph.D. Thesis. Princeton University, Princeton, N.J. 1964; Dissertation Abstr., **25**, 2786 (1964).
4. T. T. Wall and D. F. Hornig. J. Chem. Phys. **43**, 2079 (1965).
5. M. Falk and T. A. Ford. Can. J. Chem. **44**, 1699 (1966).
6. J. Schiffer and D. F. Hornig. J. Chem. Phys. **49**, 4150 (1969).
7. D. Panke. J. Chem. Phys. **48**, 2990 (1968).
8. C. Folzer, R. W. Hendricks, and A. H. Narten. J. Chem. Phys. In press.
9. T. A. Ford, P. F. Seto, and M. Falk. Spectrochim. Acta, **25A**, 1650 (1969).
10. T. A. Ford and M. Falk. J. Mol. Struct. **3**, 445 (1969).
11. G. Brink and M. Falk. Can. J. Chem. **48**, 2096 (1970).
12. T. A. Ford and M. Falk. Can. J. Chem. **46**, 3579 (1968).
13. K. Lonsdale. Proc. Roy. Soc. London, Ser. A. **247**, 424 (1958).
14. W. Yellin and W. L. Courchene. Nature, **219**, 852 (1968).
15. G. Brink and M. Falk. J. Mol. Struct. **5**, 27 (1970).

Comment: On the Decomposition of Aqueous Sodium Dithionite

L. Burlamacchi, G. Guarini, and E. Tiezzi
Institute of Physical Chemistry, The University of Florence, Via Gino Capponi, 9, 50121 Florence, Italy

Received November 3, 1970

The mechanism proposed by M. Wayman and W. J. Lem for the decomposition of dithionite ion in aqueous solution is reconsidered in the light of previous work done by the authors.

A la lumière de travaux effectués antérieurement par les auteurs, le mécanisme propose par M. Wayman et W. J. Lem pour la décomposition de l'ion dithionite est reconsidéré.

Canadian Journal of Chemistry, 49, 1139 (1971)

Lem and Wayman (1–3) have recently reported a polarographic study on the thermal decomposition of sodium dithionite in aqueous solution. They propose a rate expression which accounts for a rapid autocatalytic decomposition following an induction period. Their decomposition curve is identical in shape to the one obtained by us following the intensity of the e.s.r. signal which is due to the $\cdot SO_2^-$ radical-ion in equilibrium with its dimer (4). This work and the preceding one by Spencer (5) have not been cited by Lem and Wayman.

For their rate equation to hold, the dithionite concentration must fall towards zero following a

Can. J. Chem. Downloaded from www.nrcresearchpress.com by 210.87.254.42 on 09/05/12
For personal use only.

are 2.668 and 2.705 Å, much shorter than the OH · · · O bonds, which vary in length from 2.74 to 2.85 Å (7). Thus the distribution of water–water hydrogen-bond strengths in TMA solution must be nearly the same as that in pure water. The same conclusion has been reached earlier for aqueous solutions of dimethyl sulfoxide (15).

The OD band profile of HDO in water has appreciable intensity near 2440 cm^{-1}, corresponding to the peak frequency of HDO in ice and in crystalline TMA.$10\frac{1}{4}H_2O$ near the melting point. In the corresponding band profile in liquid TMA.$10\frac{1}{4}H_2O$ the relative intensity at 2440 cm^{-1} is slightly increased. However, there is no detectable shoulder near this frequency. This shows that while hydrogen bonding similar in strength to that occurring in crystalline ice or TMA hydrate does occur in water and, increasingly so, in aqueous solution of TMA, structurally well-defined regions do not persist above the melting point. Any "iceberg" regions are ill-defined and their OD stretching spectrum merges with that of the remainder of water.

The present observations and their interpretation are in full agreement with the findings of Folzer, Hendricks, and Narten (8) that the radial distribution function of the TMA solution is very similar to that of pure water and with their conclusion that long-range order (beyond 8 Å) is absent in the solution as well as in water.

I wish to thank Mr. P. F. Seto for technical assistance, Prof. G. A. Jeffrey for suggesting this investigation, and Drs. A. H. Narten and Cynthia Folzer for sending me a preprint of ref. 8 prior to its publication and for several discussions.

1. J. L. Kavanau. Water and Solute–Water Interactions. Holden-Day, Inc., San Francisco. 1964. pp. 22–28.
2. R. D. Waldron. J. Chem. Phys. **26**, 809 (1957).
3. J. Schiffer. Ph.D. Thesis. Princeton University, Princeton, N.J. 1964; Dissertation Abstr., **25**, 2786 (1964).
4. T. T. Wall and D. F. Hornig. J. Chem. Phys. **43**, 2079 (1965).
5. M. Falk and T. A. Ford. Can. J. Chem. **44**, 1699 (1966).
6. J. Schiffer and D. F. Hornig. J. Chem. Phys. **49**, 4150 (1969).
7. D. Panke. J. Chem. Phys. **48**, 2990 (1968).
8. C. Folzer, R. W. Hendricks, and A. H. Narten. J. Chem. Phys. In press.
9. T. A. Ford, P. F. Seto, and M. Falk. Spectrochim. Acta, **25A**, 1650 (1969).
10. T. A. Ford and M. Falk. J. Mol. Struct. **3**, 445 (1969).
11. G. Brink and M. Falk. Can. J. Chem. **48**, 2096 (1970).
12. T. A. Ford and M. Falk. Can. J. Chem. **46**, 3579 (1968).
13. K. Lonsdale. Proc. Roy. Soc. London, Ser. A. **247**, 424 (1958).
14. W. Yellin and W. L. Courchene. Nature, **219**, 852 (1968).
15. G. Brink and M. Falk. J. Mol. Struct. **5**, 27 (1970).

Comment: On the Decomposition of Aqueous Sodium Dithionite

L. Burlamacchi, G. Guarini, and E. Tiezzi
Institute of Physical Chemistry, The University of Florence, Via Gino Capponi, 9, 50121 Florence, Italy

Received November 3, 1970

The mechanism proposed by M. Wayman and W. J. Lem for the decomposition of dithionite ion in aqueous solution is reconsidered in the light of previous work done by the authors.

A la lumière de travaux effectués antérieurement par les auteurs, le mécanisme propose par M. Wayman et W. J. Lem pour la décomposition de l'ion dithionite est reconsidéré.

Canadian Journal of Chemistry, 49, 1139 (1971)

Lem and Wayman (1–3) have recently reported a polarographic study on the thermal decomposition of sodium dithionite in aqueous solution. They propose a rate expression which accounts for a rapid autocatalytic decomposition following an induction period. Their decomposition curve is identical in shape to the one obtained by us following the intensity of the e.s.r. signal which is due to the $\cdot SO_2^-$ radical-ion in equilibrium with its dimer (4). This work and the preceding one by Spencer (5) have not been cited by Lem and Wayman.

For their rate equation to hold, the dithionite concentration must fall towards zero following a

Can. J. Chem. Downloaded from www.nrcresearchpress.com by 210.87.254.42 on 09/05/12
For personal use only.

Can. J. Chem. Downloaded from www.nrcresearchpress.com by 210.87.254.42 on 09/05/12
For personal use only.

sigmoid curve. This may seem to be the case at initial dithionite concentration below 5×10^{-2} *M*. However, by increasing initial $S_2O_4^{-2}$ concentration or by adding HSO_3^- above 10^{-2} *M*, the rapid decomposition suddenly stops, sometimes leaving a relatively high dithionite concentration, as shown in Fig. 5 of ref. 4. In other words, what should be the curvature of the low portion of the S shaped curve is actually a sharp step, due to the sudden breakdown of the fast reaction. This is also evident in Figs. 4 and 5 of ref. 1, in which the agreement between theory and experiment appears rather poor. Thus, the rapid reaction cannot be simply autocatalytic and attempts to fit the overall decomposition curve to only a rate equation with two terms (the induction period and the autocatalytic term) may lead to erroneous results.

The results by Spencer, by Wayman and Lem, and by us, obtained under differing conditions, underline a rather unsatisfactory understanding of the decomposition mechanism. The p*H* variation recorded by Wayman and Lem (2) seems to confirm that initial and final stages of the reaction (p*H* decreasing) are distinct from the rapid reaction (p*H* increasing) in agreement with ref. 4. A thorough interpretation would require a complete knowledge of all the side reaction products formed in the various stages of the reaction. However, the curves show a rapid decrease of $[H^+]$ at the onset of the rapid reaction, probably related with the catalyst formation.

The rate-determining step of the overall slow reaction, as proposed by Spencer and by us (4, 5), is

$$\cdot HSO_2 + \cdot SO_2^- + HSO_3^- \rightarrow \text{Intermediate products}$$

Among the intermediate products, the sulfoxylate ion may be responsible for the formation of sulfur and/or sulfide ion (4) according, for instance, to reactions 6, 7, and 8 of ref. 2. The increased reaction rate (it is unclear whether the induction period or the fast reaction) by addition of Na_2S suggests that sulfide ion may be the catalyst. The presence of polythionates among the end products (5), the non-stoichiometric amount of bisulfite with respect to thiosulfate ion (2), and the disappearance of the catalyst by addition of bisulfite ion (4) are all in agreement with this suggestion. Moreover the absence of any fast reaction in the decomposition of ZnS_2O_4 (Fig. 1 of ref. 3), which gives only the S shaped slow reaction, is probably related to the low solubility of ZnS, as pointed out by Lem and Wayman.

1. W. J. Lem and M. Wayman. Can. J. Chem. **48**, 776 (1970).
2. M. Wayman and W. J. Lem. Can. J. Chem. **48**, 782 (1970).
3. W. J. Lem and M. Wayman. Can. J. Chem. **48**, 2778 (1970).
4. L. Burlamacchi, G. Guarini, and E. Tiezzi. Trans. Faraday Soc. **65**, 496 (1969).
5. M. S. Spencer. Trans. Faraday Soc. **63**, 2510 (1967).

Comment: On the Decomposition of Aqueous Sodium Dithionite

M. Wayman and W. J. Lem[1]

Department of Chemical Engineering and Applied Chemistry, University of Toronto, Toronto 181, Ontario

Received November 23, 1970

In response to a comment by L. Burlamacchi, G. Guarini, and E. Tiezzi, kinetic equations for the decomposition of aqueous sodium dithionite are compared, and the mode of action of catalysts and anti-catalysts for the decomposition is discussed.

En réponse à un commentaire de Burlamacchi, Guarini et Tiezzi, on compare les équations cinétiques proposées pour la décomposition de solutions aqueuses de dithionite de sodium; on discute aussi le mode d'action sur cette décomposition des catalyseurs positifs et négatifs.

Canadian Journal of Chemistry, 49, 1140 (1971)

The comment by L. Burlamacchi *et al.* (1) demonstrates a widespread current interest in the mechanism of decomposition of dithionite, and we welcome their contribution. In terms of experimental results, the decomposition curves measured in the two laboratories generally agree in shape even though they have been determined by widely different methods (polarography and

[1]Present address: Imperial Oil Enterprises Limited, Sarnia, Ontario.

Can. J. Chem. Downloaded from www.nrcresearchpress.com by 210.87.254.40 on 09/05/12
For personal use only.

sigmoid curve. This may seem to be the case at initial dithionite concentration below 5×10^{-2} *M*. However, by increasing initial $S_2O_4^{-2}$ concentration or by adding HSO_3^- above 10^{-2} *M*, the rapid decomposition suddenly stops, sometimes leaving a relatively high dithionite concentration, as shown in Fig. 5 of ref. 4. In other words, what should be the curvature of the low portion of the S shaped curve is actually a sharp step, due to the sudden breakdown of the fast reaction. This is also evident in Figs. 4 and 5 of ref. 1, in which the agreement between theory and experiment appears rather poor. Thus, the rapid reaction cannot be simply autocatalytic and attempts to fit the overall decomposition curve to only a rate equation with two terms (the induction period and the autocatalytic term) may lead to erroneous results.

The results by Spencer, by Wayman and Lem, and by us, obtained under differing conditions, underline a rather unsatisfactory understanding of the decomposition mechanism. The p*H* variation recorded by Wayman and Lem (2) seems to confirm that initial and final stages of the reaction (p*H* decreasing) are distinct from the rapid reaction (p*H* increasing) in agreement with ref. 4. A thorough interpretation would require a complete knowledge of all the side reaction products formed in the various stages of the reaction. However, the curves show a rapid decrease of $[H^+]$ at the onset of the rapid reaction, probably related with the catalyst formation.

The rate-determining step of the overall slow reaction, as proposed by Spencer and by us (4, 5), is

$$\cdot HSO_2 + \cdot SO_2^- + HSO_3^- \rightarrow \text{Intermediate products}$$

Among the intermediate products, the sulfoxylate ion may be responsible for the formation of sulfur and/or sulfide ion (4) according, for instance, to reactions 6, 7, and 8 of ref. 2. The increased reaction rate (it is unclear whether the induction period or the fast reaction) by addition of Na_2S suggests that sulfide ion may be the catalyst. The presence of polythionates among the end products (5), the non-stoichiometric amount of bisulfite with respect to thiosulfate ion (2), and the disappearance of the catalyst by addition of bisulfite ion (4) are all in agreement with this suggestion. Moreover the absence of any fast reaction in the decomposition of ZnS_2O_4 (Fig. 1 of ref. 3), which gives only the S shaped slow reaction, is probably related to the low solubility of ZnS, as pointed out by Lem and Wayman.

1. W. J. Lem and M. Wayman. Can. J. Chem. **48**, 776 (1970).
2. M. Wayman and W. J. Lem. Can. J. Chem. **48**, 782 (1970).
3. W. J. Lem and M. Wayman. Can. J. Chem. **48**, 2778 (1970).
4. L. Burlamacchi, G. Guarini, and E. Tiezzi. Trans. Faraday Soc. **65**, 496 (1969).
5. M. S. Spencer. Trans. Faraday Soc. **63**, 2510 (1967).

Comment: On the Decomposition of Aqueous Sodium Dithionite

M. Wayman and W. J. Lem[1]

Department of Chemical Engineering and Applied Chemistry, University of Toronto, Toronto 181, Ontario

Received November 23, 1970

In response to a comment by L. Burlamacchi, G. Guarini, and E. Tiezzi, kinetic equations for the decomposition of aqueous sodium dithionite are compared, and the mode of action of catalysts and anti-catalysts for the decomposition is discussed.

En réponse à un commentaire de Burlamacchi, Guarini et Tiezzi, on compare les équations cinétiques proposées pour la décomposition de solutions aqueuses de dithionite de sodium; on discute aussi le mode d'action sur cette décomposition des catalyseurs positifs et négatifs.

Canadian Journal of Chemistry, 49, 1140 (1971)

The comment by L. Burlamacchi *et al.* (1) demonstrates a widespread current interest in the mechanism of decomposition of dithionite, and we welcome their contribution. In terms of experimental results, the decomposition curves measured in the two laboratories generally agree in shape even though they have been determined by widely different methods (polarography and

[1]Present address: Imperial Oil Enterprises Limited, Sarnia, Ontario.

Can. J. Chem. Downloaded from www.nrcresearchpress.com by 210.87.254.40 on 09/05/12
For personal use only.

e.p.r.), both laboratories showing an initial slow reaction (the "induction" period) followed by a fast decomposition reaction; but Burlamacchi and co-workers have shown (2) that under some conditions the rapid reaction may be interrupted, and the concentration of dithionite may level off at some value well above zero. This was not observed by us (3, 4): Figs. 3–5 of ref. 3 show a sharp discontinuity at the conclusion of the rapid reaction, at which time more than 90% of the dithionite was decomposed and the remaining concentration was less than 0.5 m*M* in all cases. Nor was it observed by Burlamacchi and co-workers when they worked at our low initial concentrations, but only at much higher concentrations. They attribute the slowing up of the fast reaction to the removal of the catalyst by chemical reaction. We would not disagree with this interpretation, and we stated that the fast reaction is slow in the absence of a catalyst (4). In a later publication (5) we described experiments in which certain ions Zn^{2+}, Cd^{2+}, and In^{3+} slowed up the decomposition reaction, and we attributed this to anti-catalytic activity.

There are two questions raised by Burlamacchi and co-workers related to the mechanism of the reaction which require comment. They have to do with the rate limiting reaction for the slow initial reaction and the nature and mode of action of the catalyst. We have proposed that the rate limiting reaction for the slow initial reaction is

[1] $HS_2O_4^- + H_2O \rightarrow HSO_2^- + HSO_3^- + H^+$

while Burlamacchi and co-workers (1, 2) and Spencer (6) have proposed as the rate-determining step for the decomposition reaction

[2] $\cdot HSO_2 + \cdot SO_2^- + HSO_3^- \rightarrow$ Intermediate products

Reaction 2 depends upon the presence initially of a reaction product HSO_3^-; it does not account for the fall in p*H* which we observed during the initial slow reaction; and it cannot lead to an overall kinetic equation which fits the measured rates of reaction. We find it much easier to accept a two-body reaction of an ion and a neutral body, reaction 1, than a three-body reaction involving two negative ions and a neutral body, reaction 2.

Burlamacchi and co-workers complain of the poor fit of the calculated and observed decomposition curves in two Figs. of ref. 3, but since ours is the first proposal of an overall kinetic equation that predicts accurately the length of the induction period (Figs. 3–5 and 11 of ref. 3) and reasonably well the shape of the rest of the decomposition curve, we consider the fit remarkably good. We specifically stated that a two-term equation could not fully reflect all the influences on the rate of decomposition, and that "a better equation would have at least two more terms", the purposes of which were described (3).

We have proposed (4) that the fast reaction may be written as

[3] $HSO_2 + HS_2O_4^- \rightarrow S_2O_3^{2-} + HSO_3 + H^+$

a reaction very similar to that proposed by Rinker and co-workers (7). The reaction, according to our view, takes place rapidly in a solution of HSO_2^- and $HS_2O_4^-$ in the presence of an electron sink which can accept an electron from one of the reactants, allowing a fast reaction to occur between the resulting radical and the remaining ion. We have suggested that colloidal sulfur, sometimes observed to be present, sulfides and polysulfides may behave as such catalysts, and we have shown that sulfide does in fact act as a catalyst for the fast reaction (4). We regard it as probable that any sufficiently powerful electron acceptor will perform this role, and equally probable that any reaction which removes such electron acceptors from solution will retard the rate of the fast reaction. This explains, to a first approximation, the nature of the catalyst.

1. L. Burlamacchi, G. Guarini, and E. Tiezzi. This issue.
2. L. Burlamacchi, G. Guarini, and E. Tiezzi Trans. Faraday Soc. **65**, 496 (1969).
3. W. J. Lem and M. Wayman. Can. J. Chem. **48**, 776 (1970).
4. M. Wayman and W. J. Lem. Can. J. Chem. **48**, 782 (1970).
5. W. J. Lem and M. Wayman. Can. J. Chem. **48**, 2778 (1970).
6. M. S. Spencer. Trans. Faraday Soc. **63**, 2510 (1967).
7. R. G. Rinker, S. Lynn, D. M. Mason, and W. H. Corcoran. Ind. Eng. Chem. Fundam. **4**, 282 (1965)

Electrophilic Additions to Ethylidenenorbornene and Vinylnorbornene

T. C. SHIELDS

Union Carbide Corporation, Chemicals and Plastics, Research and Development Department, South Charleston, West Virginia 25303

Received October 5, 1970

Electrophilic and free radical additions to 5-ethylidenebicyclo[2.2.1]hept-2-ene and 5-vinylbicyclo-[2.2.1]hept-2-ene have been carried out with peracetic acid, hydrogen chloride, and methanol. In contrast to chlorosulfonyl isocyanate, peracetic acid primarily attacks the exocyclic double bond in 5-ethylidene-bicyclo[2.2.1]hept-2-ene. Several other electrophilic additions are discussed which demonstrate the unpredictable reactivity of the norbornyl system.

Des additions électrophiles et radicaliques de l'acide peracétique, de l'acide chlorhydrique, et du méthanol ont été faites sur l'éthylidène-5 bicyclo[2.2.1]heptène-2 et sur le vinyl-5 bicyclo[2.2.1]heptène-2. La réaction de l'acide peracétique qui attaque principalement la double liaison exocyclique de l'éthylidène-5 bicyclo[2.2.1]heptène-2 contraste avec celle de l'isocyanate de chlorosulfonyle. Plusieurs autres additions électrophiles qui démontrent la réactivité imprévisible du système norbonyle sont discutées.

Canadian Journal of Chemistry, 49, 1142 (1971)

Additions to norbornenyl olefins have resulted in some unusual rearrangements; the homoconjugated molecule 5-ethylidenebicyclo[2.2.1]hept-2-ene (1) (also called ethylidenenorbornene or EN) however has received relatively little attention. Recent work by Moriconi reports the puzzling fact that chlorosulfonyl isocyanate (CSI) adds exclusively to the norbornenyl ring double bond in dicyclopentadiene (2) and exclusively to the exocyclic double bond in EN (3). This impels us to report our findings with electrophilic additions to norbornenes.

In contrast to the behavior with CSI, peracetic acid treatment of EN results in products of epoxidation (83% yield) of both the ring double bond, **1**, and the exocyclic double bond, **2**, in a 1:6 ratio, respectively (Scheme 1). The *bis* epoxide **3** could be prepared with persistent peracid exposure.

Hydrochlorination of VN requires stannic chloride catalysis. Sodium–ammonia reduction of the products obtained afforded only the anticipated vinylnorbornane. An n.m.r. examination of the mixed hydrochlorides conforms with that of a mixture of *exo*-2-chloro-5 (and -6) vinylbicyclo[2.2.1]heptane (**4**). Three products arise from the reduction of EN hydrochlorides, 1-ethyltricyclo[2.2.1.$0^{2,6}$]heptane (**5**), *endo*-5-ethylbicyclo[2.2.1]hept-2-ene (**6**), and 2-ethylidenebicyclo[2.2.1]heptane (**7**) in a ratio of 3:4:13, respectively.

Three main products arise from hydrochlorination of EN (Scheme 2). Only one, the major product, which was retained longest by g.l.c., was isolated and characterized. Its n.m.r. spectrum agrees with the structure of *exo*-2-chloro-6-ethylidenebicyclo[2.2.1]heptane (**8**). On the basis of their hydrocarbon derivatives the other products are presumed to be *exo*-5-chloro-2-ethyltricyclo[2.2.1.$0^{2,6}$]heptane (**9**) and *exo*-2-chloro-2-ethylbicyclo[2.2.1]hept-5-ene (10); no dichlorides were found. In another experiment using chloroform as solvent the amount of **8** increased to over 80% of the mixture. The predominance of **8** is surprising in light of the earlier findings of Schleyer and O'Connor (4) with hydrochlorination of 5-methylenebicyclo[2.2.1]hept-2-ene in ether in which the tertiary chloride predominated.

Sulfuric acid catalyzed methanolations were then carried out on EN and VN as well as dicyclopentadiene (5). The products generated were identified easily by n.m.r. and are shown in Scheme 3.

The nortricyclene (**12**) is observed as the main methanolation product from EN. No tertiary ether was isolated; this may be caused by the fact that a second methanolation is possible on the remaining norbornenyl ring double bond of the methoxy analog of **10**. A very small amount of high boiling material (~5%), possible dimethoxy products, were observed by g.l.c.

In order to examine the free radical chlorination of EN and VN, treatment with *t*-butylhypochlorite was employed along with irradiation in a paraffin solvent (Scheme 4). The g.l.c. examination of the mixture from VN indicated a complex mixture of at least seven components.

Can. J. Chem. Downloaded from www.nrcresearchpress.com by 210.87.254.40 on 09/05/12
For personal use only.

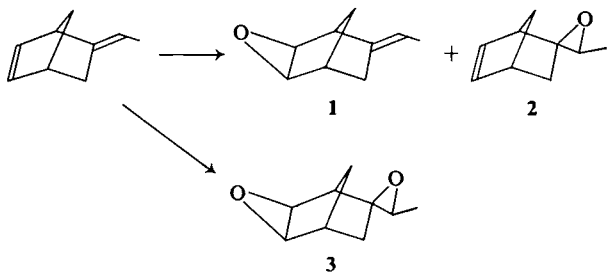

SCHEME 1

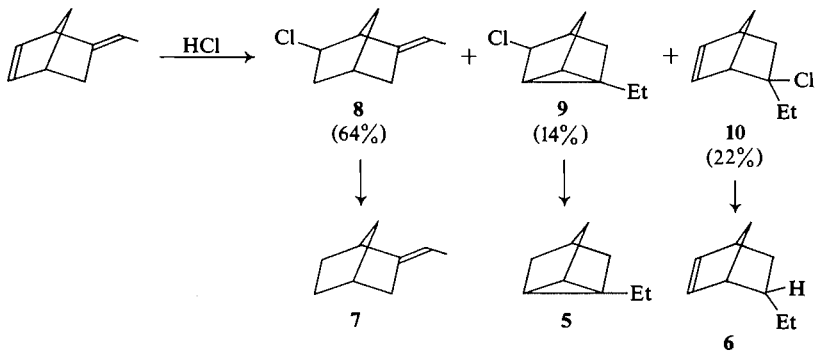

SCHEME 2

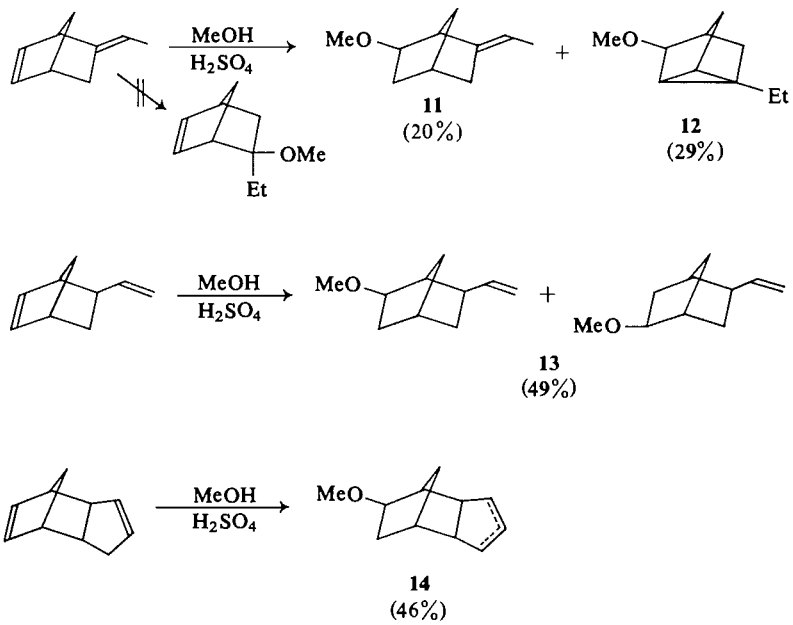

SCHEME 3

Can. J. Chem. Downloaded from www.nrcresearchpress.com by 210.87.254.40 on 09/05/12
For personal use only.

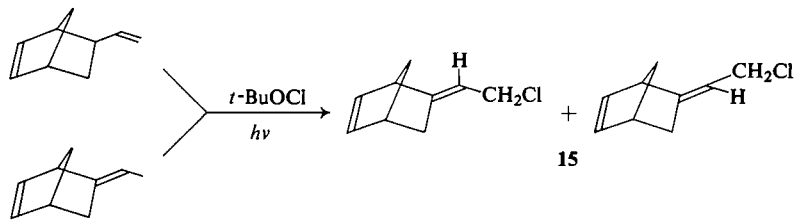

SCHEME 4

One component of shorter retention time was isolated by preparative g.l.c. It possesses an n.m.r. spectrum with a narrow multiplet at δ 6.10 (2H, norbornyl olefinic), a multiplet at 5.45 (1H, ethylidene olefinic), a pair of doublets (J = 7.8 Hz) at 4.10 and 3.92 (2H, chlorine geminal), and a complex pattern between 3.60 and 1.10 (6H, alkyl). The ratio of the doublets was variable with different experiments and varied with examination of different distillation crops. These data suggest a mixture of *cis*- and *trans*-2(2′-chloro)ethylidenetricyclo[2.2.1]hept-5-ene (**15**).

The unpredictability of electrophilic additions to norbornyl systems is readily apprehended here. One might expect epoxidation of EN to result in 2-ethylidene-5-formylbicyclo[2.1.1]hexane from a rearrangement analogous to that observed by Meinwald *et al.* (6) with norbornadiene. Instead expoxidation takes place in the normal manner but not exclusively on one double bond.

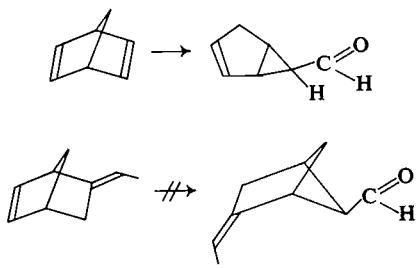

As previously noted CSI adds exclusively to the exocyclic double bond in EN (2) and the norbornenyl ring double bond in dicyclopentadiene (1). In the case of CSI, mechanistic changes can range from the concerted ($\pi^2s + \pi^2a$) to stepwise electrophilic. In addition dichlorocarbene (a generally accepted electrophilic reagent) adds to the five-membered ring double bond in dicyclopentadiene (7).

The secondary chloride **8** is the main product from EN hydrochlorination; on the other hand treatment of 5-methylene-2-norbornene by hydrochloric acid in ether prepares the tertiary chloride as the main product (4). In contrast to this, methanolation of EN in strong acid results mainly in the nortricyclyl ether **12**. It should also be mentioned that hydrochlorination of EN is quite rapid and spontaneous, presumably because of homoconjugation; however norbornadiene, also homoconjugated, undergoes hydrochlorination far more slowly.[1]

On the basis of these observations one can only say that these electrophilic additions are quite sensitive to reaction environment and subtle changes in substrate; until such time as a consistent, systematic clarification of these phenomena appears, hasty mechanistic supposition in this area should probably be avoided.

Experimental

Materials

Peracetic acid (25% in ethyl acetate), EN (UCC Plant Grade), VN (UCC Plant Grade), hydrogen chloride (Matheson Company CP. 99%), stannic chloride (analyzed reagent), sodium metal, redistilled ammonia, and freshly prepared *t*-butyl hypochlorite were used in the following experiments.

Procedure

General

Boiling points are uncorrected and distillations were performed on a short path column under non-equilibrium conditions. The n.m.r. spectra were taken in CCl_4 unless otherwise noted. Products were quenched with ice water, extracted with pentane, and dried over anhydrous sodium sulfate. Vacuum fractional distillation was employed and the products were isolated on an 8′ silicone gum rubber 10% SE 30 60-80S column between 110–150°. Unless otherwise noted all reactions were carried out in a mechanically stirred, three-neck, round-bottom pyrex flask equipped with nitrogen purge and reflux condenser.

Epoxidations

The EN (50.0 g, 0.417 mol) was dissolved in 100 ml pentane. Peracetic acid (80.2 g, 0.334 mol) was added dropwise at 0° for 3.5 h. The mixture was stirred 1 h longer, quenched, made alkaline with aqueous KOH, and extracted with pentane. Vacuum fractional distillation afforded two cuts; cut A (30–31°/0.8 mm) 34.4 g

[1]Unpublished results.

Can. J. Chem. Downloaded from www.nrcresearchpress.com by 210.87.254.40 on 09/05/12
For personal use only.

Can. J. Chem. Downloaded from www.nrcresearchpress.com by 210.87.254.40 on 09/05/12
For personal use only.

and cut B (33°/0.8 mm) 3.5 g, total yield 37.9 g, 0.278 mol, 83% based on peracid. Isolation of the main constituent, 2,2-methyloxirane-bicyclo[2.2.1]hept-5-ene (**2**) of cut A was accomplished by preparative g.l.c.: n.m.r. δ 6.18 (m, 2H, olefinic), 2.90 (q superimposed on a m, $J = 4.3$ Hz, 2H), a complex pattern 2.50–1.30 [containing prominences 2.20 (1H), 1.80 (2H), 1.43 (2H)], and 1.15 (d, $J = 4.30$, 3H, methyl). The i.r. bands appear at 3060, 1265, and 910 cm^{-1}.

Anal. Calcd. for $C_9H_{12}O$: C, 79.36; H, 8.88. Found: C, 79.42; H, 8.57.

The n.m.r. spectrum of cut B shows it contains a 50:50 mixture of epoxides **1** and **2**. This is revealed by the appearance of characteristic olefin patterns at 6.2 (norbornenyl) and 5.3 (ethylidene) in a 2:1 ratio. By the relationships of integrated areas of the two types of olefinic protons in **1** and **2** appearing in cuts A and B a product ratio of 14% **1** and 86% **2** was calculated.

The EN (75.0 g, 0.625 mol) was dissolved in 100 ml pentane at 25° and 75 g peracetic acid added over a period of 1.5 h. The pentane mixture was washed with ice water and made alkaline with a second wash of aqueous base before reintroduction into the reaction flask. Peracetic acid (125 g) was added over a period of 3 h at 45°. After quenching and washing with aqueous base, vacuum fractional distillation afforded cut A (45–56°/0.5–0.3 mm) 12.1 g containing 31% epoxides and 37% *bis*-epoxide and cut B (68°/0.3 mm) 39.7 g *bis*-epoxide. Yields based on EN, 46.4%, *bis*-epoxide, 4.4% epoxides.

Anal. Calcd. for $C_9H_{12}O_2$: C, 71.03; H, 7.95. Found: C, 71.34; H, 8.18.

Hydrochlorinations

The EN (48.0 g, 0.40 mol) was exposed to a stream of hydrogen chloride gas at 25° for 1 h. The product was washed with aqueous base and extracted with pentane. Vacuum fractional distillation afforded a mixture (42°/1.5 mm) consisting of 14% (7.6 g) *exo*-5-chloro-2-ethyltricyclo[2.2.1.$0^{2,6}$]heptane (**9**), 22% (14.1 g) *exo*-2-chloro-2-ethylbicyclo[2.2.1]hept-5-ene (**10**) and 64% (34.9 g) *exo*-2-chloro-6-ethylidenebicyclo[2.2.1]heptane (**8**). Isolation of **8** was accomplished by preparative g.l.c.: n.m.r. δ 5.40 (m, 1H, olefinic), 3.80 (m, 1H, chlorine geminal), 3.20–1.10 (complex pattern 11H, alkyl).

Anal. Calcd. for $C_{10}H_{13}Cl$: C, 69.02; H, 8.31; Cl, 22.67. Found: C, 69.20; H, 8.49; Cl, 22.41.

In a separate reaction employing the same procedure except that 8.0 g EN in 70 ml chloroform was exposed to HCl gas for 2 h, the product ratio changed to 8.5% **9**, 10% **10**, and 81.5% **8**.

Stannic chloride (0.25 ml) was dissolved in VN (38.4 g, 0.32 mol) and hydrogen chloride gas bubbled into the mixture for 10 min. The product was washed with aqueous base and extracted with pentane. Vacuum distillation (37°/1.0 mm) afforded 16.1 g (0.10 mol) of *exo*-2-chloro-5 (and -6) -vinylbicyclo[2.2.1]heptane (**4**): n.m.r. δ 6.20–4.70 (m, 3H, characteristic vinyl pattern), 3.80 (m, 1H, chlorine geminal), 2.60–0.70 (m, 9H, alkyl).

Anal. Calcd. for $C_9H_{13}Cl$: C, 69.02; H, 8.31; Cl, 22.67. Found: C, 69.31; H, 8.13; Cl, 22.53.

Metal–Ammonia Reductions

A mixture of 25.4 g (0.163 mol) EN hydrochlorides was mixed with 20 ml pentane and added dropwise to a solution of 9.0 g sodium in liquid ammonia (177 g). After quenching the mixture excess sodium with NH_4Cl, adding water and extracting with pentane, vacuum fractional distillation (34°/2 mm) of the extract resulted in 18.5 g (0.152 mol, 93% yield) of a mixture of 3 hydrocarbons **4**, **5**, and **6**, in a ratio of 3:4:13 which were all isolated by preparative g.l.c. They were identified as 1-ethyltricyclo[2.2.1.$0^{2,6}$]heptane (**5**): n.m.r. δ 2.10–0.70 complex pattern with prominences at 1.93, 1.26, 1.10, and 0.85, *endo*-5-ethylbicyclo[2.2.1]hept-2-ene (**6**): n.m.r. δ 6.00 (m, 2H, olefinic), 2.75 (m, 2H, norbornyl bridgehead), 2.10–0.40 (m, 10H, alkyl), and 2-ethylidenebicyclo[2.2.1]heptane (**7**): n.m.r. δ 5.20 (m, 1H, olefinic), 2.60 and 2.45 (m, 2H, norbornyl bridgehead), 2.15–1.0 (m, 11H, alkyl). Elemental analysis was performed on the mixed hydrocarbons.

Anal. Calcd. for C_9H_{14}: C, 88.46; H, 11 56. Found: C, 88.38; H, 11.34.

Similar treatment of VN hydrochlorides (18.0 g, 0.115 mol) rendered 12.1 g (0.10 mol, 89% yield) of one hydrocarbon product which possesses an n.m.r. superimposable on that of 2-vinylbicyclo[2.2.1]heptane.

Methanolations

Hydrocarbon (9.0 g) was dissolved in 50 ml methanol and stirred at 5° while 50 ml 96% sulfuric acid was added from a buret over a period of 20 min. The material was stirred 20 min longer, quenched, and neutralized with aqueous KOH. Pentane extraction and distillation resulted in the following.

(*a*) From EN two major products (**11** and **12**) (31°/3 mm) arise which were isolated by preparative g.l.c., 5-ethylidene-2-methoxybicyclo[2.2.1]heptane (**11**) (2.26 g, 0.015 mol, 20% yield): n.m.r. δ 5.30 (m, 1H, olefinic), 3.20 (s on m, 4H, oxygen geminal, 2.80–0.80 (m, 11H, alkyl) and 2-ethyl-5-methoxytricyclo[2.2.1.$0^{2,6}$]heptane (**12**) (3.24 g, 0.021 mol, 29% yield): n.m.r. δ 3.37 (m, 1H, oxygen geminal), 3.20 (s, 3H, methoxy), 2.00–0.70 (m, 13H, alkyl with prominences at 1.90, 1.65, 1.20, 0.98, and 0.88). Elemental analysis was performed on the mixture.

Anal. Calcd. for $C_{10}H_{16}O$: C, 78.14; H, 10.59. Found: C, 78.30; H, 10.48.

Two products of longer g.l.c. retention time comprising ~5% of the total product were not identified.

(*b*) Treatment of VN rendered upon distillation (29–30°/3.0 mm) 5.5 g, 0.036 mol, 49% yield, of 2-methoxy-5 (and -6) -vinylbicyclo[2.2.1]heptane (**13**); n.m.r. δ 5.90–4.70 (m, 3H, characteristic vinyl pattern), 3.21 (s on m, 4H, oxygen geminal), 2.40–0.80 (m, 9H, alkyl).

Anal. Calcd. for $C_{10}H_{16}O$: C, 78.14; H, 10.59. Found: C, 78.07; H, 10.43.

(*c*) Treatment of dicyclopentadiene afforded (48°/1.3 mm) 5.15 (0.031 mol, 46% yield) of *exo*-9-methoxy-*exo*-tricyclo[5.2.1.$0^{2,6}$]dec-3 (and -4) ene (**14**): n.m.r. δ 5.54 (m, 2H, olefin), 3.19 (s on m, 4H, oxygen geminal), 2.60–1.10 (m, 10H, alkyl). Material has the odor of anise (5).

Anal. Calcd. for $C_{11}H_{16}O$: C, 80.46; H, 9.83. Found: C, 80.26; H, 9.61.

Reaction with t-Butylhypochlorite

The VN (50.0 g, 0.417 mol) in 100 ml pentane was magnetically stirred and the dropwise addition of 21.5 g (0.2 mol) of *t*-butylhypochlorite was carried out over a period of 2 h with a 100 W tungsten lamp irradiating the mixture. Distillation afforded 9.2 g of mixed products. EN (50.0 g, 0.417 mol) treated in a like manner for

2.33 h resulted in 34.9 g of mixed products. Both reaction mixtures contained one product, **15**, in less than 15% yield. Isolation of **15** by preparative g.l.c. was performed. Its n.m.r. spectrum (see Discussion) suggested it to be a mixture of *cis*- and *trans*- 2(2′-chloro)ethylidenebicyclo-[2.2.1]hept-5-ene (**15**).

1. H. E. FRITZ, K. E. ATKINS, G. L. O'CONNOR. U.S. Pat. No. 3 347 944, October 17, 1967.
2. E. J. MORICONI and W. C. CRAWFORD. J. Org. Chem. **33**, 370 (1968).
3. E. J. MORICONI and C. JALANDONI. J. Org. Chem. **33**, 2073 (1970).
4. P. VON R. SCHLEYER and R. E. O'CONNOR. 134th Meeting, A.C.S. Chicago Illinois, September, 1958. Abstr. p. 39P.
5. L. A. KHEIFITS and S. I. VIREZUB. Zh. Obshch, Khim. **34** (6), 2081 (1964).
6. J. MEINWALD, S. S. LABANA, and M. S. CHADHA. J. Amer. Chem. Soc. **85**, 582 (1963).
7. L. GHOSEZ, P. LAROCHE, and L. BASTENS. Tetrahedron Lett. **49**, 3745 (1964).

The ^{19}F and ^{1}H Nuclear Magnetic Resonance Spectra of 2-Thienylcarbonyl Fluoride and 2-Thiazolylcarbonyl Fluoride

KJELD SCHAUMBURG
Chemical Laboratory V, H. C. Ørsted Institute, DK-2100 Copenhagen Ø, Denmark

Received April 21, 1970[1]

The preparation of 2-thienylcarbonyl and 2-thiazolylcarbonyl fluorides from the corresponding carboxylic acids is described. The n.m.r. spectroscopic parameters are determined and compared with experimental data for similar systems. Theoretical values for the coupling constants have been obtained in the CNDO/2 approximation and they are compared with the experimental data.

Les fluorures des acides thiophènecarboxylique-2 et thiazolecarboxylique-2 ont été préparés à partir des acides correspondants. Les paramètres spectroscopiques (r.m.n.) sont déterminés et comparés avec des valeurs expérimentales trouvées pour des systèmes similaires. Les valeurs théoriques des constantes de couplage obtenues en utilisant l'approximation CNDO/2 sont comparées avec les données expérimentales.

Canadian Journal of Chemistry **49**, 1146 (1971)

Introduction

In a growing number of publications, long-range coupling constants in substituted aromatic aldehydes have been cited (1). The carbonyl fluorides constitute a series of molecules with structures closely related to the aldehydes. Recently a correlation between long-range H–H and H–F coupling constants in benzaldehyde and benzoyl fluoride was reported (2). It is our primary aim to investigate if this can be extended to other aromatic systems.

In most cases long-range coupling constants in the aromatic aldehydes have been interpreted in terms of σ–π polarization assuming the σ-contribution to be negligible.

In our calculation of coupling constants we have used the CNDO/2 approximation (3, 4) which only permits calculation of the σ-contribution to the coupling constants. This was done in order to perform calculations of sulfur containing heterocycles on the same level of approximation as for the oxygen and nitrogen containing rings. The present version of the CNDO/2 approximation includes coulomb integrals between occupied and vacant orbitals. Hereby the major part of the correction to the coupling constants obtained by configuration interaction is included. For small molecules of known geometry the coupling constants obtained in this type of CNDO/2 calculation are in better agreement with experimental data than results from simple CNDO/2 calculation. On this basis we have found it of interest to apply the method to the calculation of coupling constants in aromatic carbonyl fluorides.

Experimental Methods and Results

2-Thienylcarbonyl fluoride was prepared according to the method of Yarowenko and Raksha (5) from the corresponding acid. Diethylenglycoldiethylether was used as solvent in the preparation. The yield was approximately 70%. The carbonyl fluoride was distilled into an n.m.r. tube containing diethylenglycoldiethylether as solvent

[1]Revision received December 7, 1970.

Can. J. Chem. Downloaded from www.nrcresearchpress.com by 210.87.254.40 on 09/05/12
For personal use only.

2.33 h resulted in 34.9 g of mixed products. Both reaction mixtures contained one product, **15**, in less than 15% yield. Isolation of **15** by preparative g.l.c. was performed. Its n.m.r. spectrum (see Discussion) suggested it to be a mixture of *cis*- and *trans*- 2(2′-chloro)ethylidenebicyclo-[2.2.1]hept-5-ene (**15**).

1. H. E. FRITZ, K. E. ATKINS, G. L. O'CONNOR. U.S. Pat. No. 3 347 944, October 17, 1967.
2. E. J. MORICONI and W. C. CRAWFORD. J. Org. Chem. **33**, 370 (1968).
3. E. J. MORICONI and C. JALANDONI. J. Org. Chem. **33**, 2073 (1970).
4. P. VON R. SCHLEYER and R. E. O'CONNOR. 134th Meeting, A.C.S. Chicago Illinois, September, 1958. Abstr. p. 39P.
5. L. A. KHEIFITS and S. I. VIREZUB. Zh. Obshch, Khim. **34** (6), 2081 (1964).
6. J. MEINWALD, S. S. LABANA, and M. S. CHADHA. J. Amer. Chem. Soc. **85**, 582 (1963).
7. L. GHOSEZ, P. LAROCHE, and L. BASTENS. Tetrahedron Lett. **49**, 3745 (1964).

The ^{19}F and ^{1}H Nuclear Magnetic Resonance Spectra of 2-Thienylcarbonyl Fluoride and 2-Thiazolylcarbonyl Fluoride

KJELD SCHAUMBURG
Chemical Laboratory V, H. C. Ørsted Institute, DK-2100 Copenhagen Ø, Denmark

Received April 21, 1970[1]

The preparation of 2-thienylcarbonyl and 2-thiazolylcarbonyl fluorides from the corresponding carboxylic acids is described. The n.m.r. spectroscopic parameters are determined and compared with experimental data for similar systems. Theoretical values for the coupling constants have been obtained in the CNDO/2 approximation and they are compared with the experimental data.

Les fluorures des acides thiophènecarboxylique-2 et thiazolecarboxylique-2 ont été préparés à partir des acides correspondants. Les paramètres spectroscopiques (r.m.n.) sont déterminés et comparés avec des valeurs expérimentales trouvées pour des systèmes similaires. Les valeurs théoriques des constantes de couplage obtenues en utilisant l'approximation CNDO/2 sont comparées avec les données expérimentales.

Canadian Journal of Chemistry **49**, 1146 (1971)

Introduction

In a growing number of publications, long-range coupling constants in substituted aromatic aldehydes have been cited (1). The carbonyl fluorides constitute a series of molecules with structures closely related to the aldehydes. Recently a correlation between long-range H–H and H–F coupling constants in benzaldehyde and benzoyl fluoride was reported (2). It is our primary aim to investigate if this can be extended to other aromatic systems.

In most cases long-range coupling constants in the aromatic aldehydes have been interpreted in terms of σ–π polarization assuming the σ-contribution to be negligible.

In our calculation of coupling constants we have used the CNDO/2 approximation (3, 4) which only permits calculation of the σ-contribution to the coupling constants. This was done in order to perform calculations of sulfur containing heterocycles on the same level of approximation as for the oxygen and nitrogen containing rings. The present version of the CNDO/2 approximation includes coulomb integrals between occupied and vacant orbitals. Hereby the major part of the correction to the coupling constants obtained by configuration interaction is included. For small molecules of known geometry the coupling constants obtained in this type of CNDO/2 calculation are in better agreement with experimental data than results from simple CNDO/2 calculation. On this basis we have found it of interest to apply the method to the calculation of coupling constants in aromatic carbonyl fluorides.

Experimental Methods and Results

2-Thienylcarbonyl fluoride was prepared according to the method of Yarowenko and Raksha (5) from the corresponding acid. Diethylenglycoldiethylether was used as solvent in the preparation. The yield was approximately 70%. The carbonyl fluoride was distilled into an n.m.r. tube containing diethylenglycoldiethylether as solvent

[1]Revision received December 7, 1970.

Can. J. Chem. Downloaded from www.nrcresearchpress.com by 210.87.254.42 on 09/05/12
For personal use only.

Can. J. Chem. Downloaded from www.nrcresearchpress.com by 210.87.254.42 on 09/05/12
For personal use only.

TABLE 1. Chemical shift and coupling constants (p.p.m.) for aldehyde and carbonyl fluoride derivatives of 2-substituted thiophene and thiazole

			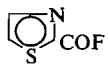	
δ(3)	7.97_3*	7.62§	—	‖
δ(4)	7.38_7	7.07	8.12*	7.75
δ(5)	8.06_4	7.62	7.95	7.32
δ(F)	23.28_2†	—	†	—
$J_{3,4}$	3.88‡±0.05	3.8		—
$J_{3,5}$	1.22 ±0.05			—
$J_{4,5}$	4.88 ±0.05	5.0	3.30‡±0.05	3.1
$J_{3,X}$	<0.2			—
$J_{4,X}$¶	1.99	~0	0.80 ±0.05	~0
$J_{5,X}$	2.44	0.9	2.15 ±0.05	1.3

*Measured relative to internal TMS.
†Measured relative to internal $CFCl_3$.
‡Error represents the necessary change in one parameter leading to a doubling of the r.m.s. error.
§Reference 12.
‖Reference 14.
¶The X indicates hydrogen or fluorine in the substituent.

(10% v/v). The TMS and $CFCl_3$ were added as internal standard and the tube sealed in vacuum.

2-Thiazolylcarbonyl fluoride was prepared according to the same procedure from 2-thiazolecarboxylic acid.

Spectra were recorded on a Varian HA-100 spectrometer at 32° using expanded sweep (6). Chemical shift and coupling constants were obtained using the LAOCOON iterative procedure on all lines observed. The experimental data are listed in Table 1.

The relative signs of the coupling constants were obtained from tickling experiments for 2-thienylcarbonyl fluoride. The three H–H coupling constants were found to have the same sign (positive) (7).

The long-range H–F coupling constants $J_{F,H(4)}$ and $J_{F,H(5)}$ were shown to have the same sign, which, in accordance with calculation, is taken to be positive. The coupling constant $J_{F,H(3)}$ is less than 0.2 Hz. The structure of the observed ^{19}F spectrum was in agreement with the data obtained from the ^1H spectrum.

For thiazolylcarbonyl fluoride, homonuclear INDOR (8) experiments showed the two long-range H–F coupling constants to be of the same sign. In accordance with the calculations they are taken to be positive. The ^{19}F spectrum was in agreement with the parameters obtained from the ^1H spectrum.

To carry out the CNDO/2 calculations the geometries of the molecules are required. In the carbonyl fluorides, as in the corresponding aldehydes, two planar conformations **1** and **2** exist.

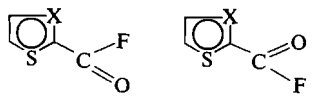

1 **2**

X = CH, N

The geometry of 2-thienylcarbonyl fluoride is unknown. However, it was assumed that it can be composed of the unperturbed thiophene ring (9) and the CCOF fragment of acetylfluoride (10). Similarly, the geometry of 2-thiazolylcarbonyl fluoride was assumed to be composed of CCOF fragment (10) and the unperturbed thiazole ring (11). In the calculation an sp basis set was used. The resulting coupling constants are listed in Table 2. The calculations yielded the total molecular energy for each conformation. For 2-thienylcarbonyl fluoride **2** is stable by 565 cal/mol relative to **1** whilst for 2-thiazolylcarbonyl fluoride, **1** was found to be stable by 188 cal/mol relative to **2**. To obtain the weighted mean coupling constant (see Table 2) which can be compared to the experimental data these energy differences were used.

Discussion

The H–H coupling constants observed in the two carbonyl fluorides are close to the data observed for the corresponding aldehydes given in Table 1. The long-range H–F coupling constants decrease in the order $J_{F,H(5)} > J_{F,H(4)} > J_{F,H(3)}$ in both compounds. The $J_{F,H(5)}$ coupling constant representing the coupling via sulfur is almost unchanged going from thiophene to thiazole. The $J_{F,H(4)}$ constant is reduced to about one-third going from thiophene to thiazole reflecting a coupling path involving the nitrogen atom.

In accordance with the results obtained for benzaldehyde and benzoylfluoride (2) we should expect the same sign for long-range coupling constants in aldehydes and carbonyl fluorides, the magnitude of the H–F coupling constants being two to six times the value of the H–H coupling constants. For 2-thiophenealdehyde only $J_{CHO,H(5)}$ has been reported (12) and the sign is not known. From data obtained for 3 bromo-2-thiophenealdehyde (13) $J_{CHO,H(5)}$ can be assumed to be positive. The ratio between $J_{H,F}$ and $J_{H,H}$ is within the range mentioned above. For thiazole again $J_{CHO,H(5)}$ has been observed (14) while $J_{CHO,H(4)}$ is very small. The results parallel the data observed for the carbonyl fluoride, and the ratio $J_{H,F}/J_{H,H}$ is again within the range given above.

The theoretical calculation of coupling constants yields results which are significantly different for the two configurations **1** and **2** and the weighted mean values are in considerably better agreement with experiment than any single conformation.

The $^3J_{H,H}$ coupling constants are relatively insensitive to conformational changes between **1** and **2** and the values are of the right order of magnitude. The $^4J_{H,H}$ constant is calculated much larger than the experimental value. This is a

TABLE 2. The CNDO/2 calculation of coupling constants in thiophene- and thiazole-2-carbonyl fluorides. The mean value is obtained assuming a Boltzmann distribution between two planar conformations for which energies are calculated in the CNDO/2 approximation

	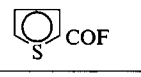			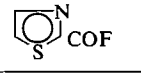		
Constant (p.p.m.)	**1**	**2**	Mean value	**1**	**2**	Mean value
$J_{3,4}$	1.983	3.500	+3.090	—	—	—
$J_{3,5}$	1.397	3.173	+2.693	—	—	—
$J_{4,5}$	3.078	2.847	+2.909	1.932	2.274	+2.076
$J_{3,F}$	0.158	−3.602	−2.586	—	—	—
$J_{4,F}$	3.050	−0.245	+0.645	2.570	0.799	+1.827
$J_{5,F}$	0.006	2.034	+1.485	0.618	4.427	+2.217

general feature observed in all the heterocycles studied (15).

The $J_{F,H(5)}$ and $J_{F,H(4)}$ coupling constants are calculated to be positive in both thienyl- and thiazolylcarbonyl fluorides and the relation $J_{F,H(5)} > J_{F,H(4)}$ is found for both systems in accordance with experiment. The $J_{F,H(3)}$ constant is calculated to be negative in thiophene. The very small value observed for this coupling constant does not permit a definite sign determination.

When the CNDO/2 data presented are judged it should be emphasized that for planar aromatic systems we have essentially calculated the σ-contribution to the long-range coupling constants. The procedure used does not allow for a σ–π polarization as used in the rationalization of the coupling constant for aromatic aldehydes (1). Since both mechanisms undoubtedly are of importance our data present only one of the two contributions. The present data demonstrate that a semiquantitative agreement can be obtained from the σ-contribution only.

In the present study considerable interest was focused on the possibility of freezing out the conformations **1** and/or **2** for the carbonyl fluorides thus establishing a more direct correlation between experimental and calculated data. However, the reactivity of carbonyl fluorides restricts the possible choice of solvents considerably. The 2-thienylcarbonyl fluoride sample investigated here shows a considerable broadening of the ^{19}F signal already at 0° C and at −40° the signal was about 100 Hz broad. At lower temperature no suitable solvent has been found.

The author expresses his gratitude to Northern Europe University Computing Centre for computational facilities, and to Dr. H. J. Jakobsen for helpful discussions.

1. T. SCHAEFER and S. S. DANYLUK. Can. J. Chem. **47**, 4289 (1969) and references given here.
2. R. J. KOSTELNIK, M. P. WILLIAMSON, D. E. WISNOSKY, and S. M. CASTELLANO. Can. J. Chem. **47**, 3313 (1969).
3. D. P. SANTRY and G. A. SEGAL. J. Chem. Phys. **47**, 158 (1967).
4. J. A. POPLE, J. W. MCIVER, JR., and W. S. OSTLUND. J. Chem. Phys. **49**, 2465 (1968).
5. N. N. YAROWENKO and M. A. RAKSHA. J. Gen. Chem. **29**, 2125 (1959).
6. D. GILLIES and K. SCHAUMBURG. J. Sci. Instr. **39**, 262 (1968).
7. B. GESTBLOM, S. GRONOWITZ, R. A. HOFFMAN, and B. MATHIASSON. Arkiv Kemi, **23**, 517 (1965).
8. V. D. KOWALEWSKI. Progress in n.m.r. spectroscopy Vol. **5**. Pergamon Press, 1969. p. 1.
9. B. BAK, D. CHRISTENSEN, L. HANSEN-NYGAARD, and J. RASTRUP ANDERSEN. J. Mol. Spectrosc. **7**, 58 (1961).
10. L. PIERCE and L. C. KRISHER. J. Chem. Phys. **31**, 875 (1959).
11. Unpublished results from this laboratory.
12. R. A. HOFFMAN and S. GRONOWITZ. Arkiv Kemi **16**, 515 (1961).
13. S. FORSÉN, B. GESTBLOM, S. GRONOWITZ, and R. A. HOFFMAN. Acta Chem. Scand. **18**, 313 (1964).
14. G. BORGEN, S. GRONOWITZ, R. DAHLBOM, and B. HOLMBERG. Acta Chem. Scand. **20**, 2593 (1968).
15. K. SCHAUMBURG. J. Mag. Res. **3**, 360 (1970).

Can. J. Chem. Downloaded from www.nrcresearchpress.com by 210.87.254.42 on 09/05/12
For personal use only.

Erratum: Photoconductivity of γ-Irradiated Methyltetrahydrofuran Glass at 77 °K

K. F. BAVERSTOCK AND P. J. DYNE

Materials Science Branch, Whiteshell Nuclear Research Establishment, Atomic Energy of Canada Limited, Pinawa, Manitoba

Received December 8, 1970

(Ref. Can. J. Chem. **48**, 2182 (1970))

Canadian Journal of Chemistry, **49**, 1149 (1971)

On p. 2188, vol. 48, the second sentence in the second paragraph of the Discussion should read as: "A single bound state lies 1 eV above the ground state, 0.4 eV below the conduction band." The level T′ in Fig. 13 should be adjusted accordingly.

Can. J. Chem. Downloaded from www.nrcresearchpress.com by 210.87.254.6 on 09/05/12
For personal use only.

Can. J. Chem. Downloaded from www.nrcresearchpress.com by 210.87.254.105 on 09/05/12
For personal use only.

Canadian Journal of Chemistry

Published by THE NATIONAL RESEARCH COUNCIL OF CANADA

VOLUME 49 APRIL 15, 1971 NUMBER 8

Reactions of Sodium *N,N*-Diethyldithiocarbamate with the Chlorides and Bromides of Niobium(V), Tantalum(V), and Protactinium(V)

P. R. HECKLEY AND D. G. HOLAH

Department of Chemistry, Lakehead University, Thunder Bay, Ontario

AND

D. BROWN

Chemistry Division, A. E. R. E. Harwell, England

Received October 23, 1970

Reactions between niobium(V), tantalum(V), and protactinium(V) chlorides and bromides and sodium *N,N*-diethyldithiocarbamate (Nadtc) have been examined in non-aqueous, non-oxygenated organic solvents. Complexes obtained are of the types $Mdtc_4X$, $Mdtc_3X_2$, $Mdtc_3S$, $Mdtc_2X_3$, and $Mdtc_2X_3.nC_6H_6$ (n = 0.7–1.0); not all complexes have been isolated for each metal. Within each group the niobium(V) and tantalum(V) complexes are isostructural; possible structures are discussed in the light of results from infrared (i.r.) and nuclear magnetic resonance (n.m.r.) spectra, molecular weight, and electrical conductivity measurements.

Des réactions entre, d'une part des chlorides (et bromures) de niobium(V), de tantale(V) et de protactinium(V) et d'autre part de *N,N*-diethydithiocarbamate de sodium (Nadtc) ont été examinées dans des solvants non-aqueux et ne contenant pas d'oxygène. Des complexes des types $Mdtc_4X$, $Mdtc_3X_2$, $Mdtc_3S$, $Mdtc_2X_3$ et $Mdtc_2X_3.nC_6H_6$ (n = 0.7 à 1.0) ont été obtenus; tous les complexes n'ont pas été isolés pour chaque métal. A l'intérieur de chaque groupe, les complexes du niobium(V) et du tantale(V) sont isostructuraux; les structures possibles sont discutées à la lumière des spectres i.r. et r.m.n., des masses moléculaires et des conductivités électriques mesurés.

Canadian Journal of Chemistry, 49, 1151 (1971)

Introduction

As part of our studies (1) on reactions between sodium *N,N*-diethyldithiocarbamate (Nadtc) and anhydrous metal halides in non-aqueous solvents, we have studied reactions (which have been the subject of a preliminary communication (2)), involving the niobium(V), tantalum(V), and protactinium(V) halides. Almost all of the work on dithiocarbamate complexes of these elements has been reported only recently (3). For example, it has been shown (4) that carbon disulfide can be inserted into the niobium(V) and tantalum(V) pentamides forming, in the latter case $Tadtc_5$ (dimethyl derivative) while the niobium(V) pentamide is reduced, $Nbdtc_4$ being the final product. The reduction is thought to occur because of the steric strain imposed on an intermediate complex, $Nbdtc_5$, which liberates a dithiocarbamate radical; the latter subsequently forms tetramethyl thiuram disulfide. This is one of the relatively rare examples of a major difference in the chemistry of niobium and tantalum. The complex $Tadtc_5$ has also been reported (5) to form in the reaction between stoichiometric quantities of tantalum(V) chloride and Nadtc in acetonitrile solution. The compound $Nbdtc_4$ is also formed (5, 6) from reactions of Nadtc with niobium(IV) chloride, while with niobium(V) bromide the product (6) is the more complex species $Nb_2Br_3dtc_5$. Salts of disubstituted dithiocarbamates also react (7) with niobium(V) and tantalum(V) halides in alcohol solutions producing monomeric compounds of the type $Mdtc_2(OR)_2X$ (X = Cl, Br).

It was noted (8), in work concerning the actinide(IV)–dithiocarbamate complexes, that protactinium(V) chloride reacts with Nadtc in both ethanol and methylene chloride solutions, but the metal(V) complexes were not identified.

Reaction conditions, particularly regarding

Can. J. Chem. Downloaded from www.nrcresearchpress.com by 210.87.254.105 on 09/05/12
For personal use only.

the choice of organic solvent, are extremely important in determining the nature of the products from reactions between Nadtc and high valent metal halides. The latter readily react with alcohols, and we have recently shown (9) that Nadtc reacts with several non-oxygenated solvents including methylene chloride, acetonitrile, and chloroform. This paper reports in detail the results of studies between the above mentioned halides and Nadtc in both methylene chloride and benzene.

Results and Discussion

Reactions between niobium(V) and tantalum(V) chlorides and bromides and Nadtc, have been examined in both methylene chloride and benzene solutions under dry, oxygen-free conditions. The protactinium(V) chlorides and bromides have been investigated only in methylene chloride solution using 1:5 stoichiometries.

In this latter solvent all the reactions are vigorously exothermic and produce the organic product dtc_2CH_2 (9) in addition to the desired metal complexes. This organic species is formed in negligible yields from the reaction between Nadtc and methylene chloride at room temperature even after prolonged standing but yields increase to over 90% when the mixture is refluxed. The strongly exothermic nature of the MX_5–Nadtc reactions in methylene chloride (sufficient to boil the solutions in some cases) means that yields of the organic product of up to 40% can occur, thus contaminating the metal complexes. When making up a reaction mixture of a given stoichiometry, the amount of Nadtc is therefore correspondingly increased to compensate for the formation of the organic material. Production of this species can be eliminated by carrying out reactions between the metal halides and Nadtc in benzene although the mixtures must be heated under reflux to obtain an appreciable reaction rate. However, these reactions result in the formation of additional species not observed in the reactions carried out in methylene chloride. Thus the nature and number of products is dependent on the stoichiometry of the reacting species, the solvent, and the temperature. The complexes which have been isolated are listed below: $Mdtc_4X$, M = Nb, Ta, Pa; X = Cl, Br; $Mdtc_3X_2$, M = Nb, X = Cl (X = Br in trace amounts); $Mdtc_3S$, M = Nb, Ta; $Mdtc_2X_3$ and $Mdtc_2X_3.nC_6H_6$, M = Nb, Ta; X = Cl, Br; n = 0.7–1.0.

It is significant to note that the complexes $Mdtc_5$ have not been observed in this work, although $Tadtc_5$ is reported to be produced (5) when the reaction between $TaCl_5$ and Nadtc in 1 to 5 stoichiometry is carried out in acetonitrile. Also, in all reactions between NbX_5 and Nadtc in benzene, the deep violet complex $Nbdtc_4$ is produced in yields up to 50%, consistent with the previous observation (4) that Nb(V) is reduced in the presence of dithiocarbamate.

Figures 1 and 2 summarize the results of the MX_5–Nadtc reactions (M = Nb, Ta, X = Cl, Br) with the differences in the behavior of $TaCl_5$ noted in Fig. 2. These figures illustrate how the various complexes, $Mdtc_4X$, $Mdtc_2X_3$, and $Mdtc_2X_3.(0.7–1.0\ C_6H_6)$ are formed and interconverted. $Nbdtc_3Cl_2$ is the only example of a compound of this particular stoichiometry isolated in a pure state, and is formed only in the reaction between $NbCl_5$ and Nadtc (1:3 ratio) in benzene. In the corresponding reaction involving $NbBr_5$, trace amounts of $Nbdtc_3Br_2$ have been observed (X-ray powder patterns), but this complex has not been isolated in a pure state. It is likely that excessive production of $Nbdtc_4$ ($\sim$ 60%) from the $NbBr_5$ reaction (compared to $\sim$ 20% from the $NbCl_5$ reaction) is seriously upsetting the Nb(V) to Nadtc stoichiometry and inhibiting the formation of the tris(dithiocarbamato) complex.

All these complexes, including the $Padtc_4X$ species are air sensitive, but are stable in anhydrous oxygen-free media. They are soluble in ethanol, but further reactions occur, possibly resulting in the formation of alkoxide species. For example, pale yellow solids isolated from solutions of $Padtc_4Cl$ in ethanol show bands characteristic of ethoxy groups in the 1000–1100 cm^{-1} region of their infrared spectra. The products, which appear to contain no halide, have not been fully characterized.

The green benzene soluble $Mdtc_3S$ complexes are the only air stable complexes isolated during this work. They form only in benzene solutions when there is a ratio of MX_5 to Nadtc of at least 1:4 and are readily separated from the benzene insoluble $Mdtc_4X$ complexes which are also formed in such reactions.

Properties and Possible Structures of the Complexes

Extensive use has been made of X-ray powder diffraction photographs in the identification of

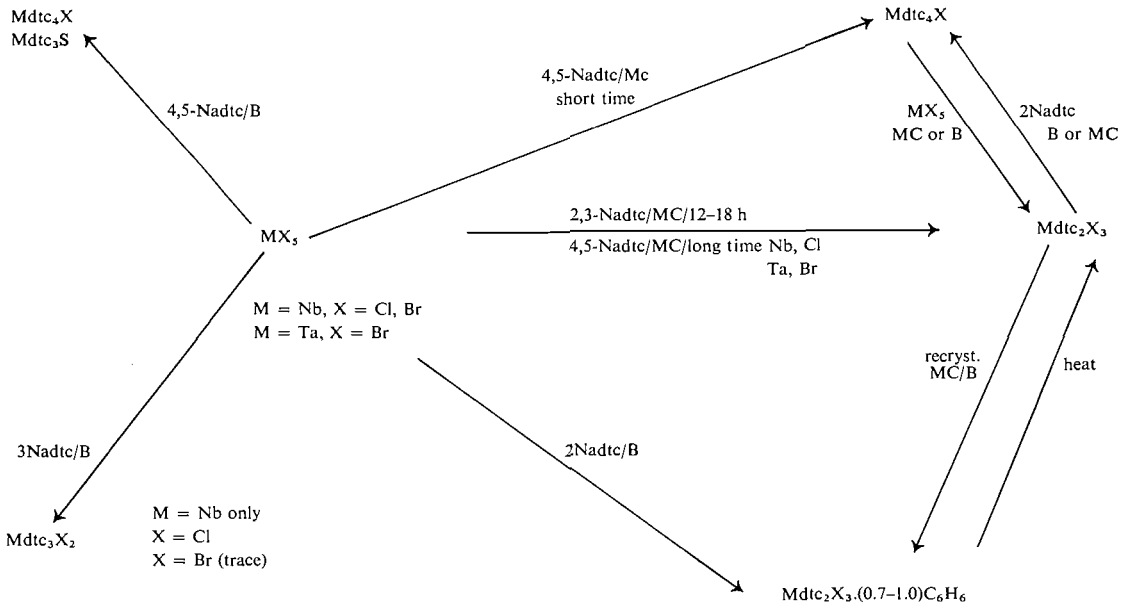

FIG. 1. Summary of reactions between $NbCl_5$, $NbBr_5$, and $TaBr_5$ and Nadtc. B = Benzene, MC = methylene chloride; all NbX_5/Nadtc/B reactions also produce $Nbdtc_4$ (not shown above), all MX_5/Nadtc/MC reactions also produce dtc_2CH_2 (not shown above).

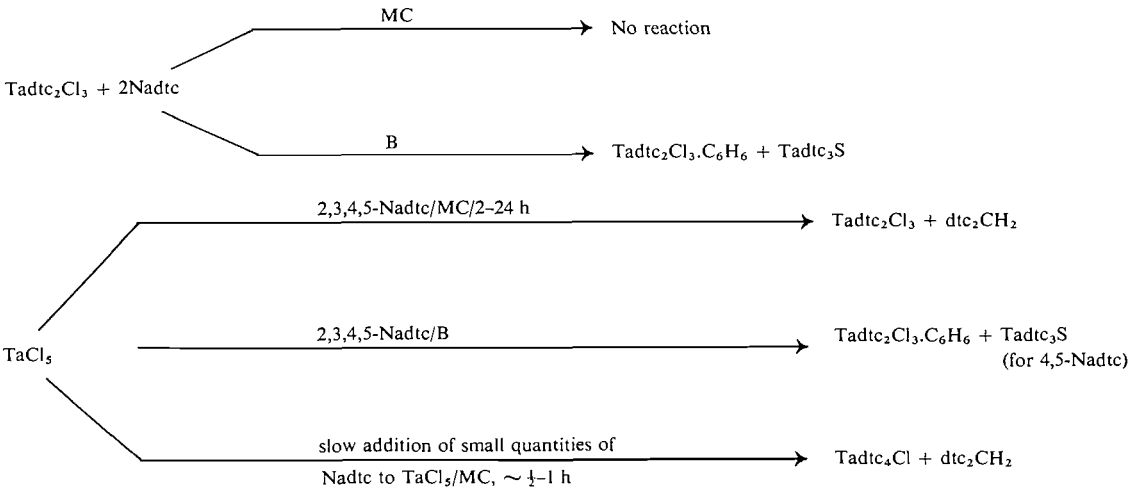

FIG. 2. Summary of major differences in behavior of $TaCl_5$.

the various products from the reactions. For niobium and tantalum the members of each group of complexes have identical powder patterns and it is therefore probable that they have a very similar orientation of ligands about the metal ion. Values of $\sin^2\theta$ for one member of each isostructural series are listed in Table 1. The protactinium compounds gave relatively poor X-ray powder diffraction patterns.

The n.m.r. spectra of concentrated methylene chloride solutions of the niobium and tantalum complexes all show a well resolved triplet in the region 8.6–8.7 τ (J = 7 Hz) and a quartet around 6.2–6.3 τ (J = 7 Hz) due to the ethyl protons, integrating in the ratio 3:2. The benzene adducts also show a singlet at 2.7 τ, with the integration indicating between 0.7 and 1.0 molecule of benzene per metal atom. The chemical shifts are

Can. J. Chem. Downloaded from www.nrcresearchpress.com by 210.87.254.105 on 09/05/12
For personal use only.

TABLE 1. Partial X-ray powder diffraction patterns of the complexes*

$Mdtc_3S$ (Ta)		$Mdtc_4X$ (Nb, Br)		$Mdtc_3X_2$ (Nb, Cl)		$Mdtc_2X_3$ (Ta, Cl)		$Mdtc_2X_3.nC_6H_6$ (Ta, Cl, n = 0.9)	
$\sin^2\theta$	I	$\sin^2\theta$	I	$\sin^2\theta$	I	$\sin^2\theta$	I	$\sin^2\theta$	I
0.0044	1	0.0030	4	0.0046	10	0.0029	2	0.0044	½
0.0064	2	0.0059	4	0.0054	8	0.0050	1	0.0067	10
0.0083	5	0.0078	10	0.0094	8	0.0067	½	0.0127	4
0.0104	10	0.0101	6	0.0102	5	0.0093	9	0.0147	8
0.0122	2	0.0111	6	0.0119	½	0.0109	8	0.0199	3½
0.0146	1½	0.0120	8	0.0145	7	0.0126	10	0.0271	6
0.0164	½	0.0122	3	0.0176	2	0.0171	½	0.0288	5
0.0183	½	0.0134	3	0.0212	4	0.0184	1	0.0322	1
0.0203	2	0.0163	3	0.0246	8	0.0194	5	0.0351	1
0.0245	5	0.0191	3	0.0260	¼	0.0228	1	0.0404	2½
0.0260	2	0.0212	3	0.0331	½	0.0263	5	0.0432	½
0.0287	3	0.0220	1	0.0372	1	0.0304	3	0.0551	1
0.0324	1	0.0233	1	0.0414	1	0.0334	3	0.0599	1
0.0344	1	0.0255	1	0.0475	1	0.0370	1	0.0630	½
0.0366	1	0.0274	1	0.0516	1	0.0385	1	0.0661	½

*First 15 lines only are recorded. The patterns of each member of the different groups are identical. I is intensity based on the arbitrary scale of 0–10.

almost invariant with the compound under study.

Signals arising from inequivalent ethyl groups have not been observed in spectra recorded at 42 °C, although certain other dithiocarbamate complexes (7, 10, 11) do show such effects. In one complex, $Tadtc_3S$, the n.m.r. spectrum has been recorded down to −60 °C and although there is some slight loss of resolution and general broadening of the peaks, there is no evidence of inequivalences. We interpret these data to mean that, in solution, the complexes contain equivalently bonded dithiocarbamate groups. This does not necessarily imply that the alkyl groups are in totally equivalent positions with respect to the metal ion in the solid, indeed on the basis of recent structural data on dithiocarbamate complexes (1, 12, 13) they almost certainly are not. Different signals arising from alkyl protons having small site inequivalences may not be detected, either because of a rapid exchange mechanism (4), or because of small conformational changes within the molecules in solution.

The infrared absorption spectra of all the complexes correspond rather closely to the complex spectrum of Nadtc. Each niobium and tantalum compound in the various groups has an identical infrared spectrum except for small differences in the region of the metal–halogen stretching frequencies. The absence of a strong absorption in the 850–950 cm^{-1} region ruled out the existence of M=O species and the absence of water was immediately apparent.

While no attempt has been made to make peak assignments for all the absorptions in the highly complex spectra, some of the major bands have been assigned in Table 2. Almost all the complexes have the C···N stretching frequency (14) between 1500 and 1525 cm^{-1}, implying considerable double bond character. This must confer a substantial degree of rigidity to the dithiocarbamate structure, suggesting that free rotation about this bond is absent (15), or at least hindered. There is little change in the band positions when the spectra are recorded in solution (except for the $Mdtc_3S$ species) and this, together with the above n.m.r. data suggests that the dithiocarbamate groups are chelated to the metal by the two sulfur atoms. The C···N frequencies for the niobium and tantalum complexes are considerably higher than those of the protactinium complexes (Table 2) and than those recorded (1) for the 8-coordinated actinide(IV) and lanthanide(III) dithiocarbamate complexes $Mdtc_4$ and $Mdtc_4^-$, respectively. If the niobium and tantalum complexes $Mdtc_4X$ and $Mdtc_2X_3$ are formulated as $[Mdtc_4]^+X^-$ and $[Mdtc_4]^+[MX_6]^-$ (see later) then the positive charge on the cation would facilitate the electron movement from the NR_2 group towards the metal thus increasing the strength of the C···N bond. These formulations are further discussed below.

The $Mdtc_3S$ complexes show two C···N frequencies in the solid state, like the somewhat analogous compound $Rudtc_3NO$ (16). In solution the former complexes have only one C···N stretching frequency and equivalent dithiocar-

Can. J. Chem. Downloaded from www.nrcresearchpress.com by 210.87.254.105 on 09/05/12
For personal use only.

TABLE 2. Infrared peak assignment (Nujol mulls)*

Compound	C···N	C···S	M—S	M—X (Assignment)
$Tadtc_2Cl_3$	1527 vs	1000, 1016 m	367 m	320 s (Ta—Cl)
$Tadtc_2Br_3$	1522 vs	1003, 1017 m	365 m	225 s (Ta—Br)
$Nbdtc_2Cl_3$	1520 vs	995, 1007 m	367 m	335 s (Nb—Cl)
$Nbdtc_2Br_3$	1522 vs	1000, 1010 m	366 m	260 s (Nb—Br)
$Nbdtc_3Cl_2$	1523 vs	1000, 1010 m	367 m	—
$Tadtc_4Cl$	1525 vs	1004, 1015 m	362 m	—
$Tadtc_4Br$	1522 vs	998, 1016 m	364 m	—
$Padtc_4Cl$	1485 vs	1000 m	357 m	317 M (Pa—Cl)
$Padtc_4Br$	1485 vs	1000 m	358 m	—
$Nbdtc_4Cl$	1520 vs	998, 1012 m	362 m	—
$Nbdtc_4Br$	1520 vs	998, 1012 m	362 m	—
$Tadtc_3S$	1515, 1500 vs	1002, 1010 m	361 m	483 s (Ta = S)
$Nbdtc_3S$	1515, 1500 vs 1508 vs†	1001, 1009 m 1008 (broad) m	363 m —	502 s (Nb = S) —
Nadtc	1475 s	990 s	—	—

*vs, very strong; s, strong; m, moderate; —, not observed. The complexes $Mdtc_2X_3 \cdot nC_6H_6$ show the following peaks *in addition* to those for $Mdtc_2X_3$, 772 vs, 788 s, 1036 m, 1480 m. These extra peaks are consistent with liquid benzene.

†Recorded in methylene chloride solution.

bamates in the n.m.r. spectrum, unlike the ruthenium compound which has both monodentate and bidentate dithiocarbamate groups. It appears, therefore, that the $Mdtc_3S$ complexes undergo a structural change when dissolved. It is possible that in the solid state the complexes $Mdtc_3S$ involve 6 coordinate metal species with two bidentate and one monodentate dithiocarbamate, and a crystal structure determination is now being carried out on $Nbdtc_3S$ in an attempt to confirm this. It is not clear what occurs when these species are dissolved, although in methylene chloride the tantalum compound is monomeric and could be seven coordinated.

The spectra of the complexes in the region of the C···S frequency are quite similar and all, apart from those of protactinium, show two bands in the 995–1015 cm^{-1} region. It is somewhat surprising that the $Mdtc_3S$ complexes do not show additional features in this region which has been mentioned as being particularly useful in providing structural information on dithiocarbamate complexes (4, 17).

The metal–sulfur vibration is assigned (Table 2) to the strong peak in the 360–370 cm^{-1} region (4). In addition, the $Mdtc_3S$ complexes have very strong bands at 483 (Ta) and 502 cm^{-1} (Nb), assigned to the M═S stretching frequencies.

In the infrared spectra of the $[Mdtc_4]^+X^-$ (M = Nb, Ta) complexes, there are no observed peaks that can be assigned to the metal–halogen stretching frequency, and this is entirely consistent with the formulation of the complexes as above. Furthermore for $[Tadtc_4]^+Cl^-$ the observed molecular weight of 424 is in good agreement with the expected value of 404 for the ionic species, compared to an expected value of 808 for a monomeric, non ionic unit $[Tadtc_4Cl]$. The complexes appear to be 1:1 electrolytes in 10^{-3} *M* solutions of both acetonitrile and methylene chloride. For example, $[Nbdtc_4]^+Br^-$ has a conductance of 120 $ohm^{-1}\,cm^2\,mol^{-1}$ in the former solvent, and $[Tadtc_4]^+Br$ has a value of 60 $ohm^{-1}\,cm^2\,mol^{-1}$ in the methylene chloride, in good agreement with other conductance data (18) in the latter solvent. In the cation the metal is probably eight coordinated by sulfur atoms from four bidentate dithiocarbamate groups (1, 12, 13).

The complexes $Padtc_4X$, X = Cl, Br, are significantly different from the above niobium and tantalum compounds. A medium intensity band at 317 cm^{-1} in the infrared spectrum of $Padtc_4Cl$ may be associated with a metal–chlorine stretching vibration. This observation contrasts with the apparent ionic nature of the protactinium(V) tropolone halides, PaT_4Cl and PaT_4Br (19). In addition these latter complexes are remarkably stable towards aqueous solution, behavior which contrasts markedly with the rapid hydrolysis of the dithiocarbamate complexes on exposure to moist air.

The infrared spectra of the $Mdtc_2X_3$ complexes are identical in the 200–650 cm^{-1} region except for the strong metal–halogen absorptions listed in Table 2. These bands are very close to those observed (20) in the complexes $[R_4N]^+[MX_6]^-$ (R = alkyl, M = Ta, Nb; X = Cl, Br).

Can. J. Chem. Downloaded from www.nrcresearchpress.com by 210.87.254.105 on 09/05/12
For personal use only.

Can. J. Chem. Downloaded from www.nrcresearchpress.com by 210.87.254.105 on 09/05/12
For personal use only.

Also, the complexes $Mdtc_2X_3$ can be synthesized by reactions of the following type

$$[Tadtc_4]^+Br^- + [R_4N]^+[TaBr_6]^- \xrightarrow[18\text{ h at room temperature}]{\text{methylene chloride}} Tadtc_2Br_3 + [R_4N]^+Br^-$$

It therefore appears highly likely that the complexes are indeed of the type $[Mdtc_4]^+[MX_6]^-$. They appear to be 1:1 electrolytes in both 10^{-3} *M* solutions of acetonitrile and methylene chloride as illustrated by $Tadtc_2Cl_3$ for which the conductance is 150 $ohm^{-1}\,cm^2\,mol^{-1}$ in acetonitrile and 50 $ohm^{-1}\,cm^2\,mol^{-1}$ in methylene chloride. The molecular weights of $Mdtc_2Cl_3$ (M = Nb and Ta) in methylene chloride are 757 and 870, respectively, suggesting a formulation $[Mdtc_2Cl_3]_n$ where $n = 1.5$ or a multiple thereof. These high values may be due to the existence of ion-pairs in solution and if this is so, then as the concentration of the complexes in solution is reduced, the molecular weights should approach the values of 495 (Nb) and 583 (Ta) for the $[Mdtc_4]^+[MCl_6]^-$ species. Over the range of concentrations studied (~ 1–4×10^{-2} *M*), the values obtained are almost constant, and below about 10^{-2} *M* the sensitivity of the instrument decreases rapidly making accurate measurements impossible.

On the other hand, a possible trimeric structure, such as

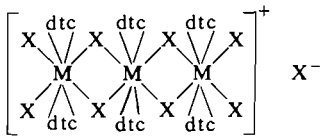

would satisfy the observed molecular weight data, but it is difficult to see how such complexes would arise from the above mentioned reactions between $[Mdtc_4]^+X^-$ and $[R_4N]^+[MX_6]^-$.

It seems unlikely that in the series $Mdtc_2X_3 \cdot nC_6H_6$ the benzene is chemically bonded to the transition metal since the infrared bands associated with benzene (Table 2) are virtually identical with those of liquid benzene. It is therefore assumed that the benzene is simply trapped in cavities in the lattice although these cavities do not appear to be large enough to accommodate molecules such as toluene or *p*-xylene.

The infrared spectrum of $Nbdtc_3Cl_2$ appears to have no peak above 200 cm^{-1} which can be assigned to an Nb—Cl stretching mode, although this does not rule out the possibility of bridging halides, the vibrations of which may be below 200 cm^{-1} (21). The complex is an electrolyte with an equivalent conductance in 10^{-3} *M* acetonitrile solution of 135 $ohm^{-1}\,cm^2\,mol^{-1}$ and the molecular weight (677) approximates to the value required for a monomer (607) or multiple thereof. A possible structure therefore would be

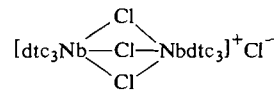

It is interesting to speculate on the mechanism of formulation of the $Mdtc_3S$ complexes, since the formation of these clearly involve decomposition of the dithiocarbamate ligand. Since the $[Mdtc_4]^+X^-$ complexes are the initially isolated species in the present study, it appears that the reactions involving the successive replacement of four halides by dithiocarbamate groups are fast. These replacements probably account for the observed rapid color changes in several of the reactions in methylene chloride. The existence of an activated complex

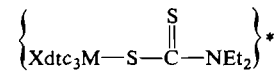

(dtc implies bidentate ligands) is postulated in an attempt to explain the formation of the $Mdtc_3S$ complexes. The presence of a monodentate ligand could arise from steric considerations (note that it has already been suggested (4) that $Nbdtc_5$ is unstable for steric reasons), although these should not be too severe in the light of the ability of the relatively small Ti^{4+} ion to accommodate eight sulfur atoms (12). However, this activated complex would be susceptible to several modes of decomposition as indicated below, although it is recognized that the reactions may be considerably more complicated.

The oils isolated in small yields from all reactions where the $Mdtc_3S$ complexes are formed could correspond to the organic fragments (or products from their further reactions) in (*b*) and (*c*). At room temperature in methylene chloride, reaction (*a*) occurs exclusively while at higher temperatures (boiling benzene) reactions (*b*) or (*c*) have significant rates and the net result is a mixture of $[Mdtc_4]^+X^-$, $Mdtc_3S$, and oils. However, it should be noted that while the isolation of $[Mdtc_4]^+X^-$ is consistent with the existence of the activated complex, the latter is not a prerequisite to the production of the former. In the

(*a*) intramolecular displacement

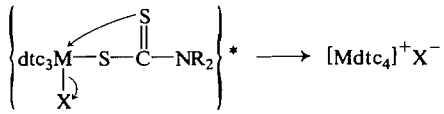

(*b*) nucleophilic attack

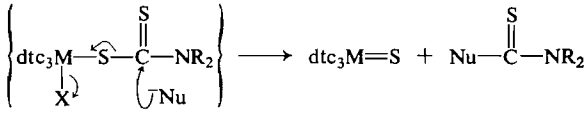

(Nu^- could be dtc^- or X^-)

(*c*) electron migration

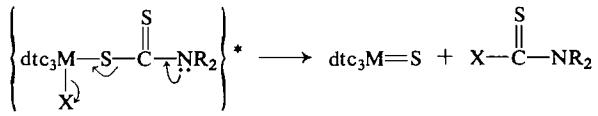

room temperature reactions in methylene chloride, the initially formed $[Mdtc_4]^+X^-$ species react further with equilibrium amounts of unreacted MX_5 with the result that reactions carried out over a long period of time produce the $[Mdtc_4]^+[MX_6]^-$ complexes. In no case has the $Mdtc_3S$ species been observed in reactions (between MX_5 and Nadtc in the 1:2 or 1:3 ratios in benzene) which produce $[Mdtc_4]^+[MX_6]^-$ and the reason for this is not clear. However, it should be noted that the reaction

$$[Mdtc_4]^+[MX_6]^- + [R_4N]^+X^- \rightarrow [Mdtc_4]^+X^- + [R_4N]^+[MX_6]$$

does not occur, at least under the conditions employed for the reverse reaction. It is therefore possible that, in reactions producing $[Mdtc_4]^+$-$[MX_6]^-$, the activated complex reacts only to give $[Mdtc_4]^+$ because of some stabilizing influence of the $[MX_6]^-$ ion, and not by routes (*b*) or (*c*)

The position of the compound $Tadtc_5$ in this proposed scheme is not clear, nor indeed is it obvious why we have not observed its formation in this work. A formulation such as $[Tadtc_4]^+$-dtc^- would appear to be ruled out from i.r. and n.m.r. spectral data (4) and clearly further work is needed on this extremely interesting molecule.

Experimental

All compounds were prepared in dry nitrogen filled glove boxes with the usual precautions being taken against the radioactive hazards associated with protactinium 231.

Materials

Niobium and tantalum pentachlorides were purchased from Alfa Inorganics and the bromides were prepared by direct reaction between the appropriate elements. Protactinium pentachloride (22) and pentabromide (23) were prepared as described previously. All halides were purified by vacuum sublimation prior to use. Commercial $Nadtc.3H_2O$ was dehydrated under high vacuum (10^{-6} Torr) at 80 °C and used without further purification. All solvents were deoxygenated by flushing with nitrogen and stored over fresh molecular sieves (4A) under nitrogen. Alumina was deactivated with ethyl acetate and dried under vacuum (10^{-6} Torr); silica gel was also dried under high vacuum.

Physical Measurements

All samples were suitably protected from the atmosphere during physical measurements. Infrared studies were carried out on a Beckman I.R. 12 Infrared spectrometer with samples mounted as Nujol mulls between KBr plates, in the region 400–4000 cm^{-1}, and between polythene plates in the region 200–650 cm^{-1}. The instrument was periodically calibrated using polystyrene.

X-Ray diffraction and proton n.m.r. studies were carried out as previously described (9). Concentrated methylene chloride solutions of the compounds at 40–42 °C were used for the latter work and the methylene protons of the solvent were used as the reference peak (4.73 τ) and checked periodically using TMS.

Molar conductivities were measured on a YSI model 31 conductivity bridge at 1 kHz, at room temperature (24 °C).

Molecular weights were determined ebullioscopically using a Gallenkamp semi-micro ebulliometer. The instrument was calibrated using the organic compound dtc_2CH_2, and all samples were run in methylene chloride (10 ml).

Analyses

For the niobium and tantalum compounds, microanalyses for carbon, hydrogen, nitrogen, sulfur, and constant weight ash (M_2O_5) were carried out by F.

Can. J. Chem. Downloaded from www.nrcresearchpress.com by 210.87.254.105 on 09/05/12
For personal use only.

Can. J. Chem. Downloaded from www.nrcresearchpress.com by 210.87.254.105 on 09/05/12
For personal use only.

TABLE 3. Chemical analyses

Complex	Yield %	Analysis											
		Found						Calculated					
		M	X	C	H	N	S	M	X	C	H	N	S
$Nbdtc_4Cl$(brown)	70	12.6	4.3	33.9	5.6	7.5		12.9	4.9	33.4	5.6	7.8	
$Nbdtc_4Br$(brown)	70	12.5	10.1					12.2	10.5				
$Tadtc_4Br$(yellow)	80	21.5	9.2	27.2	4.8	6.5		21.2	9.4	28.1	4.7	6.6	
$Tadtc_4Cl$(yellow)	70	22.2	4.2					22.4	4.4				
$Padtc_4Cl$(dark red)	60	26.7	3.9	26.9				26.9	4.1	28.0			
$Nbdtc_2Cl_3$(brown)	70	18.9	20.8					18.8	21.4				
$Nbdtc_2Br_3$(brown)	60	14.7	36.9					14.6	37.6				
$Tadtc_2Cl_3$(yellow)	80	31.4	17.9	20.9	3.5	4.9	22.0	31.0	18.2	20.6	3.4	4.8	22.0
$Tadtc_2Br_3$(yellow)	70	25.0	33.0					25.2	33.5				
$Tadtc_2Cl_3.0.9C_6H_6$(yellow)	80	27.4		27.8	4.1	4.5	18.4	27.7		28.2	4.0	4.3	19.6
$Nbdtc_3Cl_2$(brown)	60	15.2	11.2	30.2	5.2	7.0	31.2	15.3	11.1	29.6	4.9	6.9	31.6
$Nbdtc_3S$(green)	20	16.6	—					16.4	—				
$Tadtc_3S$(green)	50	28.0	—	27.4	4.6	6.0	32.6	27.6	—	27.4	4.6	6.4	34.0

Can. J. Chem. Downloaded from www.nrcresearchpress.com by 210.87.254.105 on 09/05/12
For personal use only.

Pascher, Bonn, West Germany; carbon assays on the protactinium compounds were done in the Analytical Services Division, A.E.R.E. Harwell. Metals were determined gravimetrically as M_2O_5 after overnight hydrolysis of methylene chloride solutions of the complexes with concentrated ammonia, filtration and ignition. Halides were determined gravimetrically as silver salts. Results of the analyses are listed in Table 3.

Syntheses of the Complexes

(1) $Mdtc_4X$ ($M = Nb, X = Cl, Br; M = Ta, X = Br$)

(*a*) To a suspension of the metal(V) halide (~ 1.0 g) in methylene chloride (10 ml) an excess, or a 4 or 5 molar ratio of Nadtc was added slowly with constant mixing. After the reaction subsided and cooled the mixture was stoppered and allowed to stand overnight. The brightly colored methylene chloride solution was separated by centrifugation, the solvent removed under vacuum (10^{-3} Torr), and the residue washed (5–10 ml aliquots) with benzene (~ 50 ml) to remove the organic material dtc_2CH_2. The remaining solid was dissolved in the minimum amount of methylene chloride and crystals of pure $Mdtc_4X$ obtained by the slow addition of benzene or diethylether.

(*b*) The metal pentahalides (~ 1 g) and Nadtc (1:4 stoichiometry) were refluxed in benzene (30 ml) for 4 h. The benzene solution was removed by centrifugation, and the solid residue, after washing (5–10 ml aliquots) with benzene (~ 50 ml), was dissolved in methylene chloride. This solution was centrifuged, concentrated, and yielded crystals of the $Mdtc_4X$ complexes on addition of benzene or diethyl ether.

(2) $Tadtc_4Cl$

$TaCl_5$ (1 g) and methylene chloride (20 ml) were placed in a 50 ml flask equipped with a magnetic stirrer. Nadtc in small portions (30 mg) was added with rapid mixing, and the solution was allowed to cool between each addition. When no further reaction occurred, a small excess of Nadtc (150 mg) was added, the stirring stopped and the solution stoppered for 1 h. The $Tadtc_4Cl$ was isolated as in *1(a)*. This reaction is extremely sensitive to the conditions employed and $Tadtc_2Cl_3$, instead of the above complex, has been isolated in very high yields on several occasions.

(3) $Padtc_4$ X($X = Cl, Br$)

These complexes were prepared as under *1(a)* except that the products were recrystallized from benzene–ether or methylene chloride – isopentane mixtures. Each preparation involved 0.08–0.10 g of the appropriate pentahalide in 1 ml of methylene chloride.

(4) $Mdtc_2X_3$ and $Mdtc_2X_3.C_6H_6$ ($M = Nb, Ta; X = Cl, Br$)

(*a*) The procedure in *1(a)* was followed except that the stoichiometry of MX_5:Nadtc was between 1:2 and 1:3.5. The complexes $Mdtc_2X_3$ were isolated by crystallization from concentrated methylene chloride solutions using diethylether, pentane, or *p*-xylene as the precipitating solvent. Using benzene as the precipitating agent, crystals of the $Mdtc_2X_3.(0.7–1.0)C_6H_6$ complexes were obtained. The benzene can be removed by prolonged pumping (10^{-3}–10^{-6} Torr) at 50–60 °C.

The number of benzene molecules on the latter type of complex was estimated by integrations of n.m.r. signals: *i.e.* the ratio of methyl to methylene to benzene protons gave *n*, the number of moles of benzene.

Complex	Ratio of methyl to methylene to benzene	*n*
$Nbdtc_2Cl_3.nC_6H_6$	12.0:8.0:5.0	0.83
$Nbdtc_2Br_3.nC_6H_6$	12.0:8.0:4.2	0.70
$Tadtc_2Cl_3.nC_6H_6$	12.0:8.0:5.8	0.97
$Tadtc_2Br_3.nC_6H_6$	12.0:8.0:5.0	0.83

(*b*) The benzene adducts were also isolated, using the procedure outlined in *1(b)*, from reactions between MX_5 and Nadtc in 1:2 or 1:3 ratios in benzene under reflux for 4 h (except for $NbCl_5$ and Nadtc in the 1:3 ratio).

(5) $Nbdtc_3Cl_2$

The reaction between $NbCl_5$ (~ 1 g) and Nadtc (1:3 stoichiometry) in benzene under reflux for 4 h gave a deep violet solution ($Nbdtc_4$) and a dark brown insoluble residue which was separated by centrifugation and washed (5–10 ml aliquots) with benzene (50 ml). The remaining brown solid was dissolved in methylene chloride, the solution centrifuged, concentrated, and a red-brown solid precipitated by slow addition of diethylether. Final purification of the complex was achieved by chromatography on a deactivated alumina column using a 75–25 *v/v* methylene chloride – benzene mixture as the eluting solvent. The rapidly moving brown fraction was evaporated to dryness and recrystallized from methylene chloride, pure $Nbdtc_3Cl_2$ being obtained on addition of diethylether.

(6) $Mdtc_3S$ ($M = Nb, Ta$)

The crude products were obtained by concentration of, and addition of diethylether to, the benzene solutions, obtained after the reactions described in *1(b)*. The complexes were purified by chromatography on a deactivated alumina column using benzene (or a 50–50 benzene – methylene chloride mixture) as the eluting solvent. The rapidly moving green phase was collected, concentrated, and produced the $Mdtc_3S$ complexes on addition of diethylether or pentane.

(7) $Nbdtc_4$

The resulting benzene solutions from reactions *4(b)* and *5* and between NbX_5 and Nadtc with stoichiometries of less than 1:4 gave the known compound (4) $Nbdtc_4$ (satisfactory chemical analysis has been obtained). The benzene solutions from reactions *1(b)* between NbX_5 and Nadtc with ratios greater than 1:4 also contained $Nbdtc_3S$. In these cases, the solutions were chromatographed on a silica gel column using methylene chloride or a methylene chloride benzene (50–50 *v/v*) mixture as eluting solvent. The $Nbdtc_4$ was left as an immobile phase on the column while $Nbdtc_3S$ was rapidly eluted.

(8) Other Products

In all reactions involving the formation of the $Mdtc_3S$ complexes, there also occurred, in small yields, various colored oils. These were generally immiscible with benzene and were either removed from the benzene by decantation or were left on the column during subsequent purification of the sulfide complexes. They were not investigated further.

(9) Interconversion Reactions $Mdtc_4X \rightleftharpoons Mdtc_2X_3$ (M = Nb, Ta)

The complexes $Mdtc_4X$ were heated under reflux in benzene or methylene chloride for 2 h with 1:1 molar ratios of MX_5. The reactions yielded $Mdtc_2X_3.nC_6H_6$ and $Mdtc_2X_3$, respectively

$$Mdtc_4X + MX_5 \rightarrow 2Mdtc_2X_3$$

The complexes $Mdtc_2X_3$ (or the benzene adducts) reacted with Nadtc (1:2 molar ratios) in benzene under reflux or methylene chloride after 2 h to produce $Mdtc_4X$ (except M = Ta, X = Cl) together with dtc_2CH_2 from methylene chloride and $Mdtc_3S$ from benzene. These were isolated as previously described.

The methylene chloride solutions immediately after the reactions *1(a)* between MX_5 and Nadtc (1:4) contain $Mdtc_4X$ which can be isolated as described. However, when these solutions were left at room temperature for various periods of time, the $Mdtc_2X_3$ complexes were isolated. The times involved were, M = Ta, X = Cl, 1 h; M = Nb, X = Cl, 7 days; M = Ta, X = Br, 14 days; M = Nb, X = Br, no conversion observed up to 28 days.

The $Mdtc_4X$ complexes (M = Nb, Ta) reacted with $[(C_2H_5)_4N][MX_6]$, prepared as previously described (20), in 1:1 ratios at room temperature in methylene chloride solution to produce the $Mdtc_2X_3$ complexes. Reactions were usually complete within 18–24 h.

We thank the Senate Research Committee of Lakehead University, the National Research Council of Canada, and the Ontario Department of University Affairs for generous financial support of this work. We also acknowledge stimulating discussions with Dr. A. N. Hughes and Professor K. W. Bagnall.

1. D. Brown, D. G. Holah, and C. E. F. Rickard. J. Chem. Soc. A, 786 (1970).
2. P. R. Heckley and D. G. Holah. Inorg. Nucl. Chem. Lett. **6**, 865 (1970). (Part of this work was also presented at the Second International Conference on Non Aqueous Solvents, Manchester, July 1970.)
3. Early literature references are contained in the review: D. Coucouvanis. Progr. Inorg. Chem. **11**, 233 (1970).
4. D. C. Bradley and M. H. Gitlitz. J. Chem. Soc. A, 1152 (1969).
5. J. N. Smith and T. M. Brown. Inorg. Nucl. Chem. Lett. **6**, 44 (1970).
6. D. J. Machin and J. F. Sullivan. J. Less. Common. Metals, **19**, 413 (1970).
7. D. C. Pantalco and R. C. Johnson. Inorg. Chem. **9**, 1248 (1970).
8. D. Brown and D. G. Holah. J. Chem. Soc. A, 1149 (1968).
9. P. R. Heckley, D. G. Holah, A. N. Hughes, and F. Leh. Can. J. Chem. **48**, 3827 (1970).
10. C. O'Connor, J. D. Gilbert, and G. Wilkinson. J. Chem. Soc. A, 84 (1969).
11. B. F. G. Johnson, K. H. Al-Obaidi, and J. A. McCleverty. J. Chem. Soc. A, 1668 (1969).
12. M. Colapietro, A. Vaciago, D. C. Bradley, M. B. Hursthouse, and I. F. Rendall. Chem. Commun. 743 (1970).
13. D. Brown, D. G. Holah, and C. E. F. Rickard. J. Chem. Soc. A, 423 (1970).
14. J. Chatt, L. A. Duncanson, and L. M. Venanzi. Suom. Kem. B**29**, 75 (1956).
15. C. E. Holloway and M. H. Gitlitz. Can. J. Chem. **45**, 2659 (1967).
16. A. Domenicano, A. Vaciago, C. Zambonelli, P. L. Loader, and L. M. Venanzi. Chem. Commun. 476 (1966).
17. F. Bonati and R. Ugo. J. Organomet. Chem. **10**, 257 (1967).
18. R. C. Fay and R. N. Lowry. Inorg. Chem. **9**, 2048 (1970).
19. D. Brown and C. E. F. Rickard. J. Chem. Soc. A, 3373 (1970).
20. K. W. Bagnall and D. Brown. J. Chem. Soc. 3021 (1964); D. Brown and P. J. Jones. J. Chem. Soc. A, 247 (1967).
21. M. Goldstein and W. D. Unsworth. Inorg. Nucl. Chem. Lett. **6**, 25 (1970).
22. D. Brown and P. J. Jones. J. Chem. Soc. A, 874 (1966).
23. D. Brown and P. J. Jones. J. Chem. Soc. A, 262 (1966).

Can. J. Chem. Downloaded from www.nrcresearchpress.com by 210.87.254.105 on 09/05/12
For personal use only.

Can. J. Chem. Downloaded from www.nrcresearchpress.com by 210.87.254.6 on 09/05/12
For personal use only.

Metastable Peak Analysis; a Method for Elucidating Fragmentation Mechanisms and Ion Structures in Mass Spectrometry. Part II.[1] Water Loss from the Molecular Ion of 1,2-Cyclohexanediol

F. BENOIT AND J. L. HOLMES
Chemistry Department, University of Ottawa, Ottawa, Canada

Received October 22, 1970

Defocussed metastable peaks have been used to elucidate the hitherto apparently complex fragmentation of the molecular ion of 1,2-cyclohexanediol. It was shown that the predominant mode of water loss from the molecular ion involved "scrambling" of six hydrogen atoms, those in the 4- and 5-methylene groups and the hydroxyl pair. A minor water elimination involves simple hydroxyl–hydroxyl interaction.

Les pics dus aux ions métastables obtenus par la technique de défocalisation ont été utilisés pour élucider la fragmentation jusqu'alors considérée complexe de l'ion moléculaire du cyclohexanediol-1,2. On a pu montrer que le mode principal d'élimination d'eau de l'ion moléculaire implique un processus selon lequel six atomes d'hydrogène (ceux des groupes méthylènes 4 et 5 ainsi que ceux des deux groupes OH) sont indiscernables. Un processus moins important d'élimination d'eau implique une interaction hydroxyle–hydroxyle.

Canadian Journal of Chemistry, 49, 1161 (1971)

Introduction

The use of deuterium labeling is an established procedure to aid the determination of ion fragmentation mechanisms in mass spectrometry. It is a successful technique particularly where there is no loss of positional identity of hydrogen/deuterium atoms in the molecular or fragment ions; in such cases (for example the elucidation of the fragmentation mechanism of ethyl butyrate (1)) the results usually allow unequivocal determination of the fragmentation mechanism and also permit reasonable speculation as to ion structures. However, where hydrogen "scrambling" is involved, results are often obtained which are ambiguous or uninterpretable, solely on the basis of peak shifts or relative peak heights. An early example was the loss of both OH and OD from the molecular ion of the carboxyl deuterated derivative (2, 3) of benzoic acid. The problem was elegantly solved (2) by the use of relative heights of the *metastable peaks* for the above processes. It was concluded that the molecular ion existed in two forms, one unrearranged which only lost OD and one in which the carboxyl and the two ortho ring hydrogen atoms had become indistinguishable. Various molecular ion structures have been proposed to account for these and similar observations (2–4). Such use of the relative heights of metastable peaks in conjunction with isotopic labeling is developing as a useful tool in the investigation of hydrogen "scrambling" and ion structures (5–7). It is assumed in such experiments that the relative intensities of a group of metastable peaks arising from a particular fragmentation are directly proportional to the relative abundances of their isomeric labeled precursor ions.

In this paper we report on the use of separately defocussed metastables to yield new information about a particularly difficult problem, namely the mode of water loss in the dissociation of the molecular ion of 1,2-cyclohexanediol. The mass spectrum of this molecule and deuterium labeled analogs have been recently thoroughly investigated by Buchs (8) and by Strong and Djerassi (9). Buchs was unable to formulate a fragmentation mechanism consistent with all his results; he stated that "even though we possessed a very complete series (thirteen) of deuterated derivatives of *cis* and *trans* 1,2-cyclohexanediols we think that it would be hazardous to attempt to establish a detailed fragmentation scheme by assigning a definite structure to each ion". He did, however, conclude that water loss occurred via three mechanisms: (*i*) by interaction between the two hydroxyl groups; (*ii*) by interaction between a hydroxyl group and a hydrogen atom in the 4 or 5 position; (*iii*) without participation of the hydroxyl hydrogen atoms. Strong and Djerassi (9) likewise suggested that at least four processes (distinguishing (*ii*) above as two) were involved in

[1]Part I: J. L. Holmes, D. McGillivray, and N. S. Isaacs. Can. J. Chem. **48**, 2791 (1970).

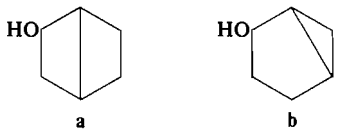

a b

the loss of water from the molecular ion. They proposed the specific ion structures (**a**, **b**) shown below as resulting from (*ii*); and that (*i*) produced the molecular ion of cyclohexene oxide. It was suggested that (*iii*) possibly involved the intermediate formation of an aldehydic ion.

To obtain the results described below we have used a modification of Jennings' (10) method of metastable defocussing. We have scanned magnetically at a series of constant electrostatic sector voltages varied by 0.1 V intervals, such that each metastable was examined in narrow sections thus enabling virtually complete resolution of metastables which otherwise would have overlapped each other. Provided that the energy profile of the ion beam exiting the ion source is both narrow and uniform, graphical summation of the sections produces the total metastable and the results of such summations are presented in the figures described below.

Results and Discussion

Our results for loss of H_2O, HDO, and D_2O obtained by comparing fragment peak heights in the mass spectrum of *cis*-1,2-cyclohexanediol-O-d_2 (**1**) agree closely with those of Strong and Djerassi (9). We also observe that the *cis* and *trans* isomers yield identical spectra. The separated, defocussed metastable peaks for water loss from **1** and *cis*-1,2-cyclohexanediol-3,3,5,5-d_4 (**2**) were of identical shape and those for **2** are shown in Fig. 1. Their heights are in the approximate ratio 6:8:1 for loss of H_2O, HDO, and D_2O, respectively. Figure 2 shows the metastable peaks for water loss (HDO and H_2O) from *trans*-1,2-cyclohexanediol-4-d_1 (**3**); these are in the ratio 2:1 for H_2O and HDO, respectively. In our experience, such sets of metastable peaks for the loss of labeled neutral fragments have the same width at half height and thus their heights may be taken as a proper measure of their relative abundances (given an energetically homogeneous ion beam).

Although it is formally possible that the observed metastables are unrelated and/or overlapping sets, it is probable that a single process gives rise to the above-mentioned metastables and that the mechanism involves "equilibration" or loss of distinguishability of four hydrogen and

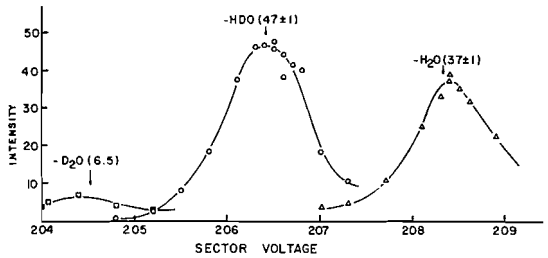

FIG. 1. Defocussed metastables for water loss from the molecular ion of *cis*-1,2-cyclohexanediol-3,3,5,5-d_4.

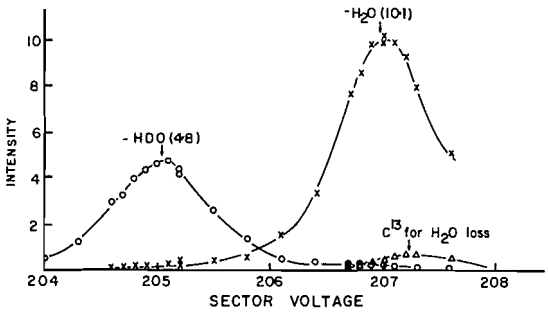

FIG. 2. Defocussed metastables for water loss from the molecular ion of *trans*-1,2-cyclohexanediol-4d_1.

two deuterium atoms in **1** and **2** and 5 hydrogen and 1 deuterium atoms in **3**. From the previous work (8, 9), hydrogen atoms at the 4 and 5 ring positions have been shown to be involved in water loss while those in the 3 position are not. We suggest that this equilibration may take place via a symmetrical species **c** such as that shown below in which the 1–2 carbon bond is broken

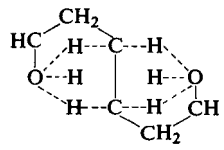

c

thus allowing independent interaction of the hydroxyl groups with the 4 and 5 ring methylenes. The dotted lines are used to indicate possible and not partial bonding. In a structure such as **c**, any of the six hydrogen atoms may be bonded to either a C-4 or C-5 carbon or oxygen atom and thus have become indistinguishable. The location of the oxygen atoms is indeterminate but positioning them directly above and below the 4–5 carbon bond would allow their interaction with any of the six hydrogen atoms. Such a structural representation is compatible with the experimental observations. Since structural repre-

Can. J. Chem. Downloaded from www.nrcresearchpress.com by 210.87.254.6 on 09/05/12
For personal use only.

TABLE 1.
(All peak heights normalized to 100 units)

M	$M - H_2O$			$M - HDO$			$M - D_2O$		
	Peak heights		Meta-	Peak heights		Meta-	Peak heights		Meta-
	Found*	Calcd.†	stables	Found*	Calcd.†	stables	Found*	Calcd†	stables
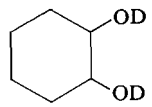	35	40	40	49	53	53.3	16	7	6.7
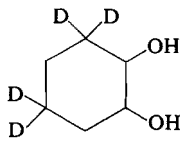	49	42	40	45	51	53.3	6	7	6.7
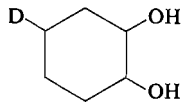	71	67	66.6	29	33	33.3	—	—	—

*Peaks are corrected for ^{13}C and M-H_2O-H (*m/e* 97) in 1,2-cyclohexanediol ~ 20%.
†Corrected for 12% water loss by mechanisms other than equilibrating one.

sentation of such ions must be highly speculative, we propose that in fragmentation schemes, atoms which have become indistinguishable and are randomly lost in a neutral or charged fragment be appropriately identified. As an example the present system is illustrated below. Further analysis of the metastables for dissociations of the $(M - H_2O)^+$ ion is in progress and will be reported in a future publication. This may yield more information concerning the structure of **c**.

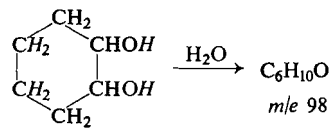

The above results indicate that some of the water lost from the molecular ion contains randomly selected hydrogen atoms; if this were the *only* mode of water loss then the fragment ion peaks will be in the same ratio as the metastables, provided that those ions which fragment in the source with loss of water, are, *before dissociation*, as "scrambled" as those which dissociate in the first field-free region. This is not observed; for example, the relative peak heights corrected for ^{13}C natural abundance and $[M - H_2O - H]$ for water loss from **1** are in the ratio 35:49:16 for loss of H_2O, HDO, and D_2O, respectively, in good agreement with the previous work (9). If it is assumed that H_2O loss (35 units) from **1** can only occur via a "scrambling" mechanism then, on the basis of the relative heights of the metastables, 88% of the total water loss occurs via this mechanism. The residual water loss is D_2O (10 units) and it could arise from the simple hydroxyl–hydroxyl interaction noted previously (8, 9). This discrepancy is not due to partial "scrambling" in those ions giving rise to the normal spectrum because such an effect would be expected to yield an excess of (M − HDO) fragment ions. Thus 98% of the water loss can be accounted for by the above two mechanisms. Using this result and a similar calculation it should be possible also to correlate the relative peak and metastable heights for **2** and **3**. The results of the calculations are presented in Table 1. They show that when correction is made for the simple mechanism (10%), the relative peak heights are in good accord with the relative metastable heights. It should be stressed that these calculations do not allow evaluation of the relative abundances of the molecular ions which are dissociating by the two mechanistically distinguishable pathways.

Whereas previous workers needed to invoke three (8) or four (9) mechanisms adequately to

Can. J. Chem. Downloaded from www.nrcresearchpress.com by 210.87.254.6 on 09/05/12
For personal use only.

account for the water loss from 1,2-cyclohexanediol, our investigation reveals that this fragmentation can better be explained by *two* mechanisms, one involving a direct interaction between hydroxyl groups, the other a complex interaction resulting in the loss of distinguishability of six hydrogen atoms (the four C-4 and C-5 methylene hydrogens and the two hydroxyl hydrogens) which are then randomly lost in the eliminated water molecule.

It is probable that other fragmentation mechanisms, hitherto presented as involving many complex parallel routes, will similarly be simplified (11, 12) and shown to involve one or several "scrambling" processes. At present the events which lead to random losses of hydrogen atoms in ion fragmentations are poorly understood but the frequent appearance of the appropriate metastable peaks indicates that the necessary rearrangements require an appreciable time to take place. It is still uncertain as to whether "scrambling" is a time and/or energy dependent effect or whether it is always complete *before* the ion dissociates. Some recent evidence (13, 14) indicates that the former is the case, particularly at low electron energies, but other results are equivocal (15).

Apart from energy considerations, it may well be found that structural features, present in the ground-state geometry of a molecule, may be important in atom scrambling. Further studies are in preparation for publication.

Experimental

Trans-1,2-cyclohexanediol was obtained commercially from Aldrich; the *cis* isomer was prepared from cyclohexene (16). The O-d_2 diol was prepared by recrystallizing the compound from successive quantities of D_2O. Compounds **2** and **3** were gifts from Dr. G. Singy. The mass spectra were obtained using a Hitachi–Perkin–Elmer RMU6D and metastable defocussing was achieved using a modified Hitachi–Perkin–Elmer RMU7.

The authors wish to thank T. Blackburn and A. Philpot for invaluable experimental assistance. One of us (F.B.) is grateful to the Province of Ontario for financial support. This work was supported by a National Research Council of Canada grant. The authors wish to thank Dr. G Singy for compounds **2** and **3** and Dr. R. Rye for use of the Hitachi RMU7 Mass Spectrometer.

1. K. Biemann. Mass spectrometry. McGraw-Hill, New York. 1962. p. 121.
2. J. H. Beynon, B. E. Job, and A. E. Williams. Z. Naturforsch. **20**a, 883 (1965).
3. S. Meyerson and J. L. Corbin. J. Amer. Chem. Soc. **87**, 3045 (1965).
4. J. L. Holmes and F. Benoit. Org. Mass Spectrom. **4**, 97 (1970).
5. D. H. Williams, S. W. Tam, and R. G. Cooks. J. Amer. Chem. Soc. **90**, 2150 (1968).
6. A. N. H. Yeo and D. H. Williams. J. Amer. Chem. Soc. **91**, 3582 (1969).
7. J. L. Holmes and D. McGillivray. Can. J. Chem. **48**, 2791 (1970).
8. A. Buchs. Helv. Chim. Acta, **51**, 688 (1968).
9. M. K. Strong and C. Djerassi. Org. Mass Spectrom. **2**, 631 (1969).
10. K. R. Jennings. *In* (R. Bonnett and J. G. Davis (eds)) Some newer physical methods in structural chemistry. United Trade Press Ltd., London. 1967. p. 105.
11. R. S. Ward and D. H. Williams. J. Org. Chem. **34**, 3373 (1969).
12. G. A. Smith and D. H. Williams. J. Amer. Chem. Soc. **91**, 5254 (1969).
13. I. Howe and F. W. McLafferty. J. Amer. Chem. Soc. **92**, 3797 (1970).
14. R. G. Cooks, R. S. Ward, and D. H. Williams. Chem. Commun. 850 (1967).
15. A. Venema, N. M. M. Nibbering, and Th. J. de Boer. Org. Mass Spectrom. **3**, 583 (1970).
16. M. F. Clarke and L. N. Owen. J. Chem. Soc. 315 (1949).

Can. J. Chem. Downloaded from www.nrcresearchpress.com by 210.87.254.6 on 09/05/12
For personal use only.

Can. J. Chem. Downloaded from www.nrcresearchpress.com by 210.87.254.105 on 09/05/12
For personal use only.

Reaction of Cyclopropenones with Heteroaromatic Nitrogen Compounds

J. W. LOWN AND K. MATSUMOTO[1]
Department of Chemistry, University of Alberta, Edmonton, Alberta

Received November 19, 1970

Diphenylcyclopropenone reacts with a variety of heteroaromatic nitrogen compounds to give in good yield either (*a*) 1,2-diphenyl-3-indolizinyl *cis*-1,2-diphenyl acrylates and aza analogs, (*b*) 5,6-diphenyl-7-hydroxypyrrolo[1,2-*b*]pyridazines and similar structures, or (*c*) adducts in which cycloaddition takes place to an N=N bond. Proof of structure of the new heterocycles is based on deuterium labelling experiments, hydrogenolysis to known compounds, and the preparation of chloro and iminoether derivatives. Cycloheptenocyclopropenones in the examples studied form heterocycles of type *b*.

La diphénylcyclopropénone réagit avec une variété de composés hétéroaromatiques contenant de l'azote et conduit avec de bons rendements soit (*a*) aux *cis*-diphényl-1,2 acrylates (et leurs analogues azotés) de diphényl-1,2 indolizinyle-3, (*b*) aux diphényl-5,6 hydroxy-7 pyrrolo[1,2-*b*]pyridazines et structures similaires, ou (*c*) des composés d'addition dans lesquels la cycloaddition se fait sur le lien —N=N—. Les preuves de structure de ces composés sont basées sur des expériences impliquant des marquages par le deutérium, des hydrogénolyses conduisant à des composés connus et la préparation de dérivés chlorés et iminoéthers. Dans les cas examinés, les cyclohepténocyclopropénones conduisent à des hétérocycles du type *b*.

Canadian Journal of Chemistry, **49**, 1165 (1971)

Indolizine (**1**) is one of the fundamental nitrogen heterocyclic systems which has been neglected in comparison to its isomer indole (*1*). Recently interest has been generated in this system since Boekelheide and co-workers have shown indolizine adds to activated acetylenes

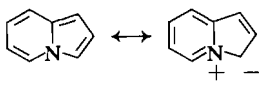

1

under dehydrogenating conditions to form the theoretically important class of cyclazines (2) in a reaction in which the indolizine reacts as an azomethine ylide, 1,3-dipole (3). Convenient synthetic routes to indolizines are few in number. There are also no synthetic routes which are readily adaptable to the preparation of aza-analogs of indolizine. An interest in the chemistry of cyclopropenones (4) led us to reinvestigate the suggested reaction of pyridine with diphenylcyclopropenone to form diphenylindolizinol derivatives (5) and to extend this reaction to include cycloheptenocyclopropenone and a variety of heteroaromatic nitrogen compounds. Breslow reports pyridine reacts with diphenylcyclopropenone in refluxing methanol to give a compound $C_{35}H_{25}NO_2$ tentatively assigned the indolizinol ester structure **2** or **3**. The product shows a prominent ester carbonyl absorption at 1730 cm^{-1} in the i.r. spectrum (5) like other similar adducts described below. We confirmed the implied cyclization step to the pyridine 2 position by examining the corresponding product obtained from pyridine-d_5. Accurate mass spectral peak measurement confirmed the incorporation of only four deuterons in the product.

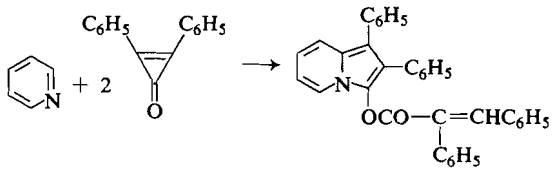

2

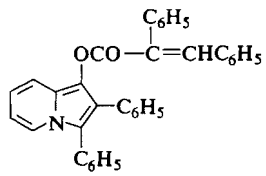

3

The adduct yields 1 mol of *cis*-1,2-diphenylacrylic acid on mild alkaline hydrolysis. More vigorous basic hydrolysis leads to extensive decomposition which is not unexpected in view of the reported similar behavior of indolizine **4** (6). Hydrogenolysis of the pyridine adduct with an equimolar mixture of lithium aluminum hydride and aluminum chloride afforded the known 1,2-diphenylindolizine (**5**) isolated at the picrate

[1]NRCC Postdoctorate Fellow, 1969 to present.

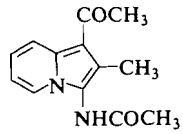

4

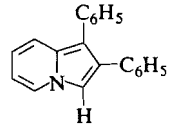

5

derivative thus proving the structure of the adduct as **2** unambiguously. Compound **5** was not isolated directly since the instability of indolizines unsubstituted in the 1 position has been noted previously (13).

Pyridazine reacts readily with diphenylcyclopropenone to give a different type of product $C_{19}H_{14}N_2O$ as a green crystalline solid *i.e.* corresponding to the incorporation of only 1 equiv of the cyclopropenone and is assigned the 5,6-diphenyl-7-hydroxypyrrolo[1,2-*b*]pyridazine structure **6** which, like similar compounds

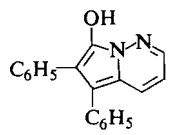

6

formed in this work, gave a positive color reaction for phenolic hydroxyl with ferric chloride and showed strong i.r. absorption at 3570 cm^{-1} typical of phenolic type hydroxyl shifted approximately 100 cm^{-1} by interaction with the chloroform solvent (7). Indolizinols and similar structures are reported to give a color reaction with ferric chloride (8). Structure **6**, which is an analog of a plausible intermediate in the formation of **2** and similar structures, receives support by its smooth conversion to the chloro compound **7***a*, $C_{19}H_{13}ClN_2$, by treatment with phosphorus oxychloride. Such reactions are

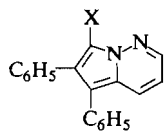

7

a X = Cl

b X = OCH_2CH_3

typical of amidic groups in heterocyclic systems, *e.g.* the conversion of α-pyridone to 2-chloropyridine (9). Compound **6** was also converted smoothly to the iminoether **7***b* in 87% yield with triethoxonium fluoroborate (*vide infra*). Nitrogen-1 in compound **6** would not be expected to react with a further equivalent of diphenylcyclopropenone since pyrrolopyridazines have been shown to be inert to quaternization (10).

Reaction of diphenylcyclopropenone in methanol with a first group of heteroaromatic nitrogen compounds resulted in the clean formation of either of the two types of adducts exemplified by **2** and **6**. In no case was a mixture of products obtained (see Tables 1 and 2). 3-Methylpyridazine reacted to give the pyrrolo[1,2-*b*]pyridazine (**8**), $C_{20}H_{16}N_2O$, in good yield which like **6** showed a strong phenolic hydroxyl absorption

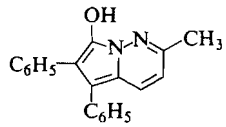

8

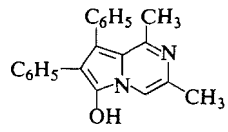

9

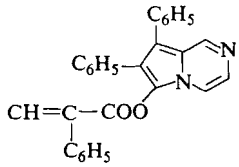

10

in the i.r. The position of quaternization of pyridazines is dictated by the position of ring substituents (11). The expected initial attack by N-1 of 3-methylpyridazine on diphenylcyclopropenone is in accordance with the formation of **8**. Investigation of a series of alpha methyl substituted pyridines and isoquinolines revealed that no reaction took place with cyclopropenones presumably for similar reasons of steric hindrance.

2,6-Dimethylpyrazine gave 1,3-dimethyl-7,8-diphenyl-6-hydroxypyrrolo[1,2-*a*]pyrazine (**9**), $C_{21}H_{18}N_2O$, in contrast to the behavior of pyrazine itself which gave 7,8-diphenyl-6-pyrrolo[1,2-*a*]pyrazinyl *cis*-1,2-diphenylacrylate (**10**), $C_{34}H_{24}N_2O_2$, which like **2** shows a prominent ester absorption at 1730 cm^{-1} in the i.r. spectrum. Compounds **2** and **10** and similar structures all show a sharp singlet at 7.78 δ characteristic of the vinyl proton in the 1,2-diphenylacrylic acid moiety (4*b*, *c*). The difference in reactivity of 2,6-dimethylpyrazine and pyrazine cannot be accounted for at this time since repeated attempts to acylate **9** by reaction with *cis*-1,2-diphenylacryloyl chloride or excess diphenylcyclopropenone regenerated **9** unchanged. Paquette similarly reports that normal

Can. J. Chem. Downloaded from www.nrcresearchpress.com by 210.87.254.105 on 09/05/12
For personal use only.

Can. J. Chem. Downloaded from www.nrcresearchpress.com by 210.87.254.105 on 09/05/12
For personal use only.

TABLE 1. Reaction products of diphenylcyclopropenone with heteroaromatic compounds

Number	Reactant	Product type*	Melting point (°C)	Yield (%)	Observed (%) C	H	N	Molecular ion (mass spectrum)	Calculated (%) C	H	N	Molecular ion (mass spectrum)
2	Pyridine	B	178	50	85.47	5.23	2.77	491.1880	85.52	5.13	2.85	491.1885
34	3-Picoline	B	169	19	85.20	5.17	2.72	505.2043	85.52	5.37	2.77	505.2042
6	Pyridazine	A	158	83	79.82	4.86	9.69	286.1100	79.70	4.93	9.78	286.1106
8	3-Methylpyridazine	A	120	65	79.87	5.55	8.95	300.1257	79.98	5.37	9.33	300.1263
10	Pyrazine	B	173	31	82.23	4.96	5.15	492.1840	82.91	4.91	5.69	492.1838
14	2-Methylpyrazine	A	263	45	80.17	5.36	9.41	300.1255	79.98	5.37	9.33	300.1263
9	2,3-Dimethylpyrazine	A	216	80	80.04	5.63	8.86	314.1418	80.23	5.77	8.91	314.1419
35	Quinoxaline	A	285	26	81.52	4.68	8.10	336.1260	82.12	4.79	8.33	336.1263
16	Isoquinoline	B	178	25	—	—	2.75	541.2032	—	—	2.59	541.2042
17	Phthalazine	A	187	61	82.15	4.62	8.34	336.1258	82.12	4.79	8.33	336.1263
19	Quinazoline	A	248	65	82.16	4.70	8.11	336.1258	82.12	4.79	8.33	336.1263
18	2-Methylquinoxaline	A	240	63	82.27	5.26	7.59	350.1415	82.26	5.18	7.99	350.1419
24	Cinnoline	C	174	77	81.90	4.69	8.39	336.1261	82.12	4.79	8.33	336.1263
23	3,4-Benzocinnoline	C	264	74	83.48	4.52	7.17	386.1422	83.92	4.69	7.25	386.1419
36	4-Phenylpyrimidine	A	151	64	—	—	7.89	362.1415	—	—	7.73	362.1419

*A, 1:1 Adduct exemplified by pyridazine product 6; B, 1:2 adduct exemplified by pyridine product 2; C, 1:1 adduct exemplified by cinnoline product 24.

TABLE 2. Spectroscopic data on indolizines and aza analogs

Number	Infrared spectrum (Nujol)	Nuclear magnetic resonance spectrum (δ) Solvent*	Indolizine ring, aryl and vinyl H	Methyl protons	Absorption spectrum (CH_3CN) λ_{max}	log ε
2	1728	$CDCl_3$	7.93(1H)s, 7.78(1H)bs, 7.0–7.5(21H)m, 6.1–6.7(2H)m		249 268(sh) 330(sh)	5.50 5.41 4.76
34	1733	$CDCl_3$	7.88(1H)s, 7.63(1H)bs, 6.9–7.5(21H)m, 6.3–6.6(1H)m	2.15(3H)s	250 267(sh) 320(sh)	5.52 5.44 4.94
6	3200(br) 1617	TFA	8.0–9.0(3H)m, 7.2–7.7(10H)m, 6.66(1H)s keto-form		253 276(sh) 430	5.18 5.07 4.54
8	3430(br) 1610	$CDCl_3$	6.5–8.2(13H)m	3.38(3H)s	250(sh) 290(sh) 333(sh) 465	5.13 4.93 4.68 4.25

Can. J. Chem. Downloaded from www.nrcresearchpress.com by 210.87.254.105 on 09/05/12
For personal use only.

TABLE 2. (*Concluded*)

Number	Infrared spectrum (Nujol)	Nuclear magnetic resonance spectrum (δ)			Absorption spectrum (CH_3CN)	
		Solvent*	Indolizine ring, aryl and vinyl H	Methyl protons	λ_{max}	log ε
10	1729	TFA	8.26(1H)s, 7.0–7.8(23H)m		286 417	5.44 4.48
14	2500(br) 1623	TFA	8.63(1H)d, 6.9–7.8(11H)m J = 7 Hz	2.40(3H)s	271(sh) 318 390	5.07 5.00 4.87
9	2500(br) 1623	TFA	10.15(1H)br, 6.7–8.0(10H)m	2.35(3H)bs 3.05(3H)bs	280(sh 325 388	5.00 5.04 4.85
35	2500(br) 1615	TFA	8.82(1H)d, 7.0–7.8(14H)m J = 7.5 Hz		362 480(sh)	4.82 3.72
16	1729	$CDCl_3$	7.86(1H)s, 6.61 and 7.75(2H)ABq, 7.0–7.6(24H)m J = 7.5 Hz		268 313(sh) 395(sh)	5.75 5.55 4.08
17	3540 2700 1620	TFA	9.33(1H)s, 8.2–8.6(3H)m, 7.2–7.8(11H)m, 6.83(1H)s keto-form		259 296 328(sh) 395(sh)	5.29 5.41 5.05 4.13
19	2600(br)	TFA	9.12(1H)s, 8.45(1H)bs, 7.0–8.0(14H)m		269 330 364	5.61 5.01 4.48
18	1640	TFA	7.0–8.3(14H)	3.16(3H)s	255 271 310(sh) 352 466	5.38 5.36 4.96 4.77 4.24
24	1641	$CDCl_3$	7.0–7.7(14H)m, 5.93 and 6.86(2H)ABq 9.4(1H)d J = 7.5 Hz J = 8 Hz		255 297(sh) 378	5.37 4.91 5.12
23	1655	$CDCl_3$	8.94(1H)q, 6.1–7.9(17H)m J = 7.5, 2.5 Hz		252(sh) 285(sh) 290 350	5.54 5.19 5.21 5.22
36	3100(br)	TFA	8.03 and 8.62(2H)ABq, 6.8–7.9(14H)m, 6.61(1H)s J = 7 Hz 8.2–8.5(1H)m, keto-form		266 281 295(sh) 340 404 450	5.32 5.32 5.31 4.93 4.59 4.39

*TF = Trifluoroacetic acid.

Can. J. Chem. Downloaded from www.nrcresearchpress.com by 210.87.254.105 on 09/05/12
For personal use only.

acylating reagents (*e.g.* dimethyl sulfate and benzene sulfonyl chloride) are ineffective in the conversion of the amide function in **11** to an imino derivative but that the Meerwein reagent triethoxonium fluoroborate was immediately effective (12). Treatment of compound **9** with

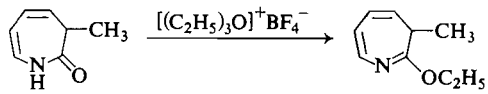

11 **12**

triethoxonium fluoroborate gave the imino ether **13** in good yield. The iminoethers **14** and **15** were similarly prepared quite smoothly from the parent enol compounds in good yield (see Tables 3 and 4).

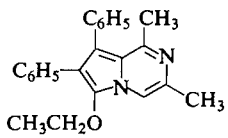

13

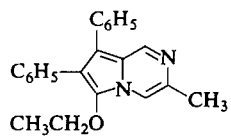

14

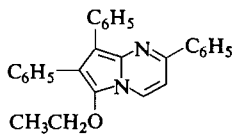

15

A difference in the reactivity of aza groups in nitrogen heterocycles towards cyclopropenones is exemplified by the ready reaction of isoquinoline to form 1,2-diphenyl-3-pyrrolo[1,2-*a*]-isoquinolinyl *cis*-1,2-diphenylacrylate (**16**), $C_{39}H_{27}NO_2$, in contrast to the complete lack of reactivity of quinoline under similar conditions. In compound **16** cyclization of the first diphenylcyclopropenone moiety to the quinoline 1-position is confirmed by the observation of a 7.5 Hz AB quartet due to protons-5 and -6 centered at 7.75 and 6.61 δ. The chemical shift of proton-5 relative to that in the corresponding adduct **24** obtained from cinnoline favors the orientation shown.

Phthalazine and 2-methylquinoxaline in contrast reacted readily with diphenylcyclopropenone but with the formation of the 1:1 adducts **17**, 1,2-diphenyl-3-hydroxypyrrolo-[1,2-*a*]-phthalazine, $C_{23}H_{16}N_2O$, and **18**, 4-methyl-2,3-diphenyl-1-hydroxypyrrolo[1,2-*a*]quinoxaline, $C_{24}H_{18}N_2O$, both of which showed prominent

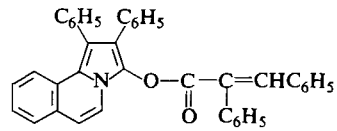

16

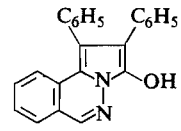

17

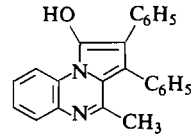

18

hydroxyl absorption in the i.r. spectrum. The latter evidence together with the correct integration of the aromatic region of the n.m.r. spectrum precludes addition across the N=N bond of phthalazine as occurred in the case of benzocinnoline and cinnoline (*vide infra*). In these additions as in the case of pyridazine there was no tendency for reaction of diphenylcyclopropenone with the second nitrogen.

The corresponding third product, isomeric with **17**, obtained from quinazoline is assigned the 1,2-diphenyl-3-hydroxypyrrolo[1,2-*c*]quinazoline structure **19** because of the susceptibility

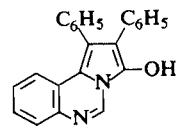

19

of N-3 of quinazoline to quaternize readily and the general reactivity of the 3,4-bond towards addition (14). Also there have been no cases reported of alkylation of the N-1 position in quinazoline (15). Structures **17**–**19** receive support by their conversion into the corresponding iminoethers **20**–**22** with triethoxonium fluoroborate.

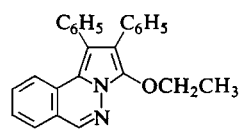

20

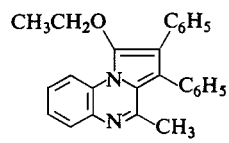

21

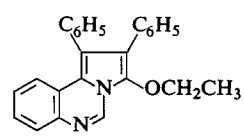

22

Can. J. Chem. Downloaded from www.nrcresearchpress.com by 210.87.254.105 on 09/05/12
For personal use only.

TABLE 3. Iminoethers of indolizines and aza analogs

Number	Original *N*-compound	Melting point (°C)	Yield (%)	Observed (%)				Calculated (%)			
				C	H	N	Molecular ion (mass spectrum)	C	H	N	Molecular ion (mass spectrum)
7*b*	Pyridazine	303	87	79.50	5.55	8.21	314.1409	80.25	5.79	8.92	314.1419
14	2-Methylpyrazine	157	91	79.68	5.96	8.59	328.1574	80.46	6.14	8.53	328.1578
13	2,6-Dimethylpyrazine	62	97	80.70	6.20	8.09	342.1727	80.67	6.48	8.18	342.1732
20	Phthalazine	130	83	—	—	7.78	364.1574	—	—	7.69	364.1575
22	Quinazoline	121	90	—	—	7.81	364.1579	—	—	7.69	364.1575
21	2-Methylquinoxaline	152	93	82.46	5.86	7.36	378.1727	82.51	5.86	7.40	378.1732
37	4-Phenylpyrimidine	120	70	83.30	5.28	6.90	390.1728	83.05	5.08	7.17	390.1732

TABLE 4. Spectroscopic data on iminoethers of indolizines and aza analogs

Number	Nuclear magnetic resonance spectra ($CDCl_3$) δ					Absorption spectra (CH_3CN)	
	Aryl protons		OCH_2	CH_3	CH_3 Aromatic	λ_{max}	log ε
7b		7.0–7.6(13H)m	3.75(2H) 7 Hz	1.25(3H)t 7 Hz		256 314 455	5.43 5.33 4.96
14		7.0–7.6(12H)m	3.94(2H)q 7 Hz	1.26(3H)t 7 Hz	2.29(3H)s	252 282(sh) 325(sh) 360(sh)	5.50 5.37 4.56 4.47
13		7.0–7.5(11H)m	3.73(2H)q 6.5 Hz	1.22(3H)t 6.5 Hz	2.27(3H)s, 2.81(3H)s	252 270(sh) 329	5.51 5.39 4.63
20	8.32(1H)d 8.10(1H)s 4 Hz	7.0–7.8(13H)m	3.81(2H)q	1.27(3H)t 7 Hz		261 292 320(sh) 387	5.40 5.61 5.18 4.02
22	8.46(1H)s	7.0–8.4(14H)m	3.81(2H)q 7 Hz	1.28(3H)t 7 Hz		271 308(sh) 327 355(sh)	5.64 5.05 5.02 4.46
21		6.8–8.0(14H)m	3.77(2H)q 7 Hz	1.23(3H)t 7 Hz	2.89(3H)s	254 346	5.55 4.95
37		6.7–8.3(17H)m	3.90(2H)q 7 Hz	1.25(3H)t 7 Hz		281 340 390(sh)	5.50 5.12 4.66

In all cases examined so far reaction has involved initial attack by an aza nitrogen on the carbonyl group of the cyclopropenone (which is supported by the observed lack of reactivity of all alpha substituted nitrogen heterocycles) followed by cyclization to an adjacent carbon (confirmed in the case of pyridine by the deuterium labelling experiment). Reaction of diphenylcyclopropenone with 3,4-benzocinnoline which lacks a free carbon alpha to the aza nitrogen resulted in the formation of a third type of adduct **23** formulated as the 2,3-diphenyl-1-ketopyrazolo[1,2-*a*]cinnoline, $C_{27}H_{18}N_2O$, in which addition occurs across the N=N double bond. The n.m.r. spectrum of **23** shows all the aromatic protons are intact and the i.r. spectrum shows a strong tertiary amidic carbonyl absorption at 1660 cm^{-1} but no hydroxyl group. The absence of any enolizable hydrogen is confirmed by the recovery of **23** unchanged after treatment with phosphorus oxychloride (contrast **5** and **7**). Similarly **23** is unaffected by treatment with trifluoroacetic acid unlike adducts of types **6**, **8**, **9**, **17**, and **18**, all of which undergo keto-enol displacements as the p*H* is altered. Observation of an 8 Hz doublet at 8.94 δ in the n.m.r. spectrum

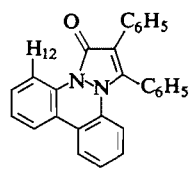

23

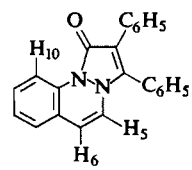

24

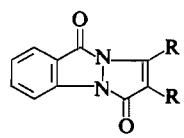

25

of **23** assigned to H-12 (the paramagnetic shift of which *ca.* −1.4 p.p.m. is in accordance with the *peri* effect exemplified by model compounds **26** and **27** (16)) allows an unambiguous assignment of structure **24** to the analogous cinnoline adduct. The n.m.r. spectrum of **24** shows H-10

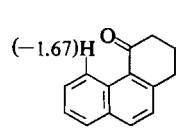

26

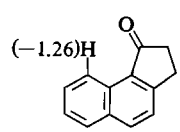

27

Can. J. Chem. Downloaded from www.nrcresearchpress.com by 210.87.254.105 on 09/05/12
For personal use only.

Can. J. Chem. Downloaded from www.nrcresearchpress.com by 210.87.254.105 on 09/05/12
For personal use only.

TABLE 5. Reaction products of cycloheptenocyclopropenone with heteroaromatic nitrogen compounds

Number	Reactant	Product type*	Melting point (°C)	Yield (%)	Observed (%)				Calculated (%)			
					C	H	N	Molecular ion (mass spectrum)	C	H	N	Molecular ion (mass spectrum)
32	2-Methylpyrazine	A	170	49	72.23	7.39	12.37	216.1267	72.19	7.46	12.95	216.1263
31	2-Dimethylpyrazine	A	217	50	—	—	11.73	230.1415	—	—	12.16	230.1419
33	3-Methylpyridazine	A	145	81	—	—	12.66	216.1267	—	—	12.95	216.1263

*See footnote to Table 1.

Can. J. Chem. Downloaded from www.nrcresearchpress.com by 210.87.254.105 on 09/05/12
For personal use only.

as an 8 Hz doublet at 9.4 δ (corresponding to a paramagnetic *peri* shift of *ca.* −1.6 p.p.m.) and a clear 8 Hz AB quartet due to H-5 and -6 centered at 5.93 and 6.86 δ thus defining the orientation of addition of the diphenylcyclopropenone moiety (contrast structure **16**). This is in accordance with expectation since cinnolines without exception quaternize at N-1 (17) and also indicates that in the reaction of nitrogen heterocycles with cyclopropenones attack by the nitrogen occurs at the carbonyl carbon, a result which is consistent with the formation of **2** from pyridine. Compound **24** shows a strong amide carbonyl at 1640 cm^{-1} in the i.r. spectrum and shows no hydroxyl or evidence of an enolizable proton.

Structures containing a fused pyrazolone ring are well documented, *e.g.* **25** (18).

It has been remarked elsewhere that diphenylcyclopropenone in certain of its reactions behaves like a more reactive form of diphenylacetylene (4*a*). The analogy is useful here since pyridine, pyridazine, and a pyrazinium ylide react with activated acetylenes to afford indolizine structures and aza analogs of the indolizine skeleton *e.g.* **28–30** respectively (19, 10, 20).

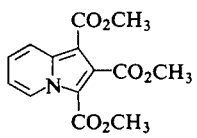

28

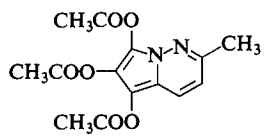

29

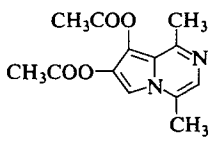

30

Cycloheptenocyclopropenone (5) reacts readily with 2,6-dimethylpyrazine to give a 1:1 adduct which shows a strong hydroxyl band at 3570 cm^{-1} and is similar in properties to those of adducts **6**, **8**, **9**, and **17–19** and is assigned structure **31**. Similarly adducts **32** and **33** are obtained from 2-methylpyrazine and 3-methylpyridazine respectively (see Table 5).

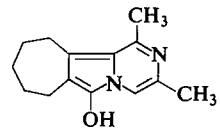

31

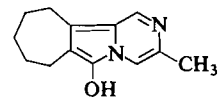

32

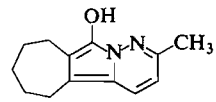

33

Experimental

Melting points were determined on a Fisher–Johns apparatus and are uncorrected. The i.r. spectra were recorded on a Perkin–Elmer model 421 spectrophotometer, and only the principal, sharply defined peaks are reported. The n.m.r. spectra were recorded on Varian A-60 and A-100 analytical spectrometers. The spectra were measured on approximately 10–15% (w/v) solutions in $CDCl_3$, with tetramethylsilane as a standard. Line positions are reported in p.p.m. from the reference. Absorption spectra were recorded in 'spectro'-grade solvents on a Beckman DB recording spectrophotometer. Mass spectra were determined on an Associated Electrical Industries MS-9 double focusing high resolution mass spectrometer. The ionization energy, in general, was 70 eV. Peak measurements were made by comparison with perfluorotributylamine at a resolving power of 15000. Kieselgel DF-5 (Camag, Switzerland) and Eastman Kodak precoated sheets were used for t.l.c. Microanalyses were carried out by Dr. C. Daesslé, Organic Microanalysis Ltd., Montreal, Quebec and by Mrs. D. Mahlow of this department.

Reaction of Diphenylcyclopropenone with Heteroaromatic Nitrogen Compounds

The reaction conditions and purification procedures are illustrated by the following examples. The analytical and spectroscopic properties of other compounds similarly prepared are summarized in Tables 1 and 2.

(a) Reaction of Diphenylcyclopropenone with Pyridine

A solution of 4.12 g (0.02 mol) of diphenylcyclopropenone (5) and 1.6 g (0.02 mol) of pyridine in 50 ml of methanol was heated under reflux for 2 h during which time the solution became dark yellow and a green precipitate formed. After cooling, 2.01 g of a 1,2-diphenyl-3-indolizinyl *cis*-1,2-diphenylacrylate were collected (40% yield) and purified by recrystallization from chloroform–ethanol.

Anal. Calcd. for $C_{35}H_{25}NO_2$ (mol. wt. 491.1885): C, 85.52; H, 5.13; N, 2.85. Found (491.1880 (mass spectrum)): C, 85.47; H, 5.23; N, 2.77.

The i.r. spectrum $\nu_{max}(CHCl_3)$: 1728 cm^{-1} (ester C=O). The n.m.r. $\delta_{TMS}(CDCl_3)$: 7.0–7.5 (21H, multiplet, aromatic and indolizine ring protons) 7.93 (1H, singlet, vinyl proton). The absorption spectrum $\lambda_{max}(CH_3CN)$: 249 (log ε 5.50); 268 (sh) (log ε 5.41); 330 mμ (sh) (log ε 4.76).

(b) Control Reaction of Diphenylcyclopropenone with Pyridine-d_5

A solution of 3.0 g (0.015 mol) of diphenylcyclopropenone and 1.2 g (0.015 mol) of pyridine-d_5 (99%, Merck, Sharpe and Dohme of Canada Ltd.) in 50 ml of methanol was heated under reflux for 1.5 h. After cooling the green solid was collected and purified by recrys-

Can. J. Chem. Downloaded from www.nrcresearchpress.com by 210.87.254.105 on 09/05/12
For personal use only.

tallization from chloroform–ethanol, 1.55 g (43% yield) m.p. 188°.

Mol. Wt. Calcd. for $C_{35}H_{21}D_4NO_4$: 495.2198. Found: 495.2192.

(c) Reaction of Diphenylcyclopropenone with Pyridazine

A solution of 2.06 g (0.01 mol) of diphenylcyclopropenone and 0.8 g (0.01 mol) of pyridazine in 40 ml of methanol was heated under reflux for 2 h. Upon cooling and setting aside for 24 h, a mass of green crystals precipitated and was collected and purified by recrystallization from methanol affording 5,6-diphenyl-7-hydroxypyrrolo[1,2-*b*]pyridazine, 2.37 g (83% yield), m.p. 158° (dec.).

Anal. Calcd. for $C_{19}H_{14}N_2O$ (mol. wt. 286.1106): C, 79.70; H, 4.93; N, 9.78. Found (286.1100 (mass spectrum)): C, 79.82; H, 4.86; N, 9.69.

The i.r. spectrum ν_{max}(Nujol): 3200 cm^{-1} (br) (OH). The n.m.r. spectrum $\delta_{TMS}(CF_3COOH)$: 6.66 (1H, singlet enolizable proton); 7.2–7.7 (10H, multiplet, aromatic protons); 8.0–9.0 (3H, multiplet, indolizine ring protons). The absorption spectrum $\lambda_{max}(CH_3CN)$: 253 (log ε 5.18); 276 (sh) (log ε 5.07); 430 mμ (log ε 4.54).

(d) Reaction of Diphenylcyclopropenone with 2,6-Dimethylpyrazine

A solution of 2.06 g (0.01 mol) of diphenylcyclopropenone and 1.08 g (0.01 mol) of 2,6-dimethylpyrazine in 40 ml of methanol was allowed to stand at room temperature for 3 days. The initially orange solution gradually turned dark red and a yellow solid which had precipitated was collected and purified by recrystallization from methanol giving 1,3-dimethyl-7,8-diphenyl-6-hydroxypyrrolo-[1,2-*a*]-pyrazine, 2.52 g (80% yield), m.p. 216° (dec.). This material shows only one spot on silica t.l.c. in 1:4 methanol–benzene which moved to a different position in acidic eluants. When exposed to air the yellow solid turned orange and finally red, but when the latter red material was recrystallized from methanol, the yellow form, m.p. 216°, was recovered unchanged. The sensitivity of this product to p*H* like others of similar structure described in this paper is attributed to facile keto–enol tautomerizations.

Anal. Calcd. for $C_{21}H_{18}N_2O$ (mol. wt. 314.1419): C, 80.23; H, 5.77; N, 8.91. Found (314.1418 (mass spectrum)): C, 80.04; H, 5.63; N, 8.86.

The i.r. spectrum ν_{max}(Nujol), 3500 br (OH), 1623 cm^{-1} (C=O). The n.m.r. spectrum $\delta_{TMS}(CF_3COOH)$ 2.35 (3H, broad singlet, CH_3), 3.05 (3H, broad singlet, CH_3); 6.7–8.0 (10H, aromatic protons), 10.15 (1H, broad singlet, 4-indolizine ring proton). The absorption spectrum $\lambda_{max}(CH_3CN)$ 280 (sh) (log ε 5.00); 325 (log ε 5.04); 388 mμ (log ε 4.84).

(e) Reaction of Cycloheptenocyclopropenone with 2-Methylpyrazine

A solution of 2.44 g (0.02 mol) of cycloheptenocyclopropenone (5) and 1.88 g (0.02 mol) of 2-methylpyrazine in 50 ml of methanol was heated under reflux for 2 h and set aside at room temperature overnight. A green crystalline solid precipitated and was collected and purified by recrystallization from methanol–dimethoxyethane giving 7,8-cyclohepteno-3-methyl-6-hydroxypyrrolo[1,2-*a*]pyrazine, 2.15 g (49% yield), m.p. 170° (dec.).

Anal. Calcd. for $C_{13}H_{16}N_2O$ (mol. wt. 216.1263): C, 72.19; H, 7.46; N, 12.95. Found (216.1267 (mass spectrum)): C, 72.23; H, 7.39; N, 12.37.

The i.r. spectrum ν_{max}(Nujol): 3500 (br) OH, 1619 cm^{-1} (C=O). The n.m.r. spectrum $\delta_{TMS}((CD_3)_2SO)$ 0.8–2.0 (10H, multiplet, cycloheptено protons), 3.07 (3H, singlet, CH_3), 6.5–8.5 (3H, multiplet, aromatic protons). The absorption spectrum $\lambda_{max}(CH_3CN)$: 303 (log ε 4.93); 365 mμ (log ε 4.65).

Hydrogenolysis of 1,2-Diphenyl-3-indolizinyl cis-1,2-Diphenylacrylate with Lithium Aluminum Hydride and Aluminum Chloride (21)

To a suspension of 1.23 g (2.5 mmol) of 1,2-diphenyl-3-indolizinyl *cis*-1,2-diphenylacrylate and 1.17 g (12 mmol) of aluminum chloride in 200 ml of dry ether was added with stirring a solution of 0.17 g (4.4 mmol) of lithium aluminum hydride in 50 ml of dry ether. The mixture was heated under reflux for 24 h with continued stirring. The excess lithium aluminum hydride was decomposed cautiously with methanol and a slight excess of 20% aqueous sodium carbonate was added with cooling. The ether layer was washed with water and dried ($MgSO_4$). The filtered ether solution was concentrated to *ca.* 50 ml, a saturated solution of picric acid in ethanol was added, and the mixture set aside for 2 days during which time a green solid precipitated. The collected 1,2-diphenylindolizine picrate, 0.15 g (12% yield), had m.p. 149–150° (ethanol) (lit. m.p. 146–148° (22)). The mass spectrum showed a base peak at *m/e* 269 corresponding to $C_{20}H_{15}N$ for diphenylindolizine.

Preparation of Iminoethers from Indolizinol Analogs with Triethoxonium Fluoroborate

Reaction conditions and purification procedures are exemplified for the preparation of the iminoether from the phthalazine adduct (see also Tables 3 and 4).

To a dried solution of 0.168 g (0.5 mmol) of 1,2-diphenyl-3-hydroxypyrrolo[1,2-*a*]phthalazine in 10 ml of chloroform was added with stirring at room temperature a freshly prepared solution of 2 mmol triethoxonium fluoroborate (23) in 10 ml of methylene chloride. After the addition was completed, stirring was continued for 2 h and the solution was set aside overnight. The mixture was treated with 50% aqueous potassium carbonate solution and filtered. The filtrate was washed with water and dried ($MgSO_4$). Evaporation of the solvent and trituration of the residual oil with 60% aqueous methanol afforded 1,2-diphenyl-3-methoxypyrrolo[1,2-*a*]phthalazine, 0.15 g (83% yield), m.p. 129–130° (aqueous methanol).

Anal. Calcd. for $C_{25}H_{20}N_2O$ (mol. wt. 364.1575): N, 7.69; Found: (364.1574 (mass spectrum)): N, 7.78%.

The n.m.r. spectrum $\delta_{TMS}(CDCl_3)$: 1.27 (3H, triplet CH_3); 3.81 (2H, quartet, J = 7 Hz CH_2CH_3); 7.0–7.8 (12H, multiplet, aromatic protons), 8.10 (1H, singlet, 6 proton); 8.32 (1H, doublet, J = 8 Hz, 10 proton). Absorption spectrum $\lambda_{max}(CH_3CN)$: 261 (log ε 5.40); 292 (sh) (log ε 5.61); 320 (sh) (log ε 5.18); 387 mμ (log ε 4.02).

Preparation of 7-Chloro-5,6-diphenylpyrrolo[1,2-b]-pyridazine

A mixture of 1.43 g (5 mmol) of 5,6-diphenyl-7-hydroxypyrrolo[1,2-*b*]pyridazine and 20 ml of phosphorus oxychloride was heated under reflux for 2 h and the

excess phosphorus oxychloride was removed *in vacuo*. Trituration of the residual oil with ethyl acetate gave a brown solid which was recrystallized from chloroform and ethanol giving 7-chloro-5,6-diphenylpyrrolo[1,2-*b*]-pyridazine, 1.03 g (68% yield), m.p. 164°.

Mol. Wt. Calcd. for $C_{19}H_{13}N_2Cl$: 304.0767. Found (mass spectrum): 304.0760.

1. E. T. Borrows and D. O. Holland. Chem. Rev. **42**, 611 (1948).
2. (*a*) A. Galbraith, T. Small, and V. Boekelheide. J. Org. Chem. **24**, 582 (1959); (*b*) V. Boekelheide and A. Miller. J. Org. Chem. **26**, 431 (1961); (*c*) V. Boekelheide and R. J. Windgassen. J. Amer. Chem. Soc. **81**, 1456 (1959); (*d*) R. J. Windgassen, W. H. Saunders, and V. Boekelheide. J. Amer. Chem. Soc. **81**, 1459 (1959).
3. R. Huisgen. Angew. Chem. Int. Ed. Engl. **2**, 581 (1963).
4. (*a*) J. W. Lown, T. W. Maloney, and G. Dallas. Can. J. Chem. **48**, 584 (1970); (*b*) J. W. Lown, R. K. Smalley, G. Dallas, and T. W. Maloney. Can. J. Chem. **48**, 89 (1970); (*c*) J. W. Lown, R. K. Smalley, G. Dallas, and T. W. Maloney. Can. J. Chem. **48**, 103 (1970); (*d*) J. W. Lown, R. Westwood, and J. P. Moser. Can. J. Chem. **48**, 1682 (1970); (*e*) J. W. Lown, R. K. Smalley, and G. Dallas. Chem. Commun. 1543 (1968); (*f*) J. W. Lown and R. K. Smalley. Tetrahedron Lett. 169 (1969); (*g*) J. W. Lown and T. W. Maloney. Chem. and Ind. (London), 870 (1970); (*h*) J. W. Lown and T. W. Maloney. J. Org. Chem. **35**, 1716 (1970); (*i*) J. W. Lown. J. Chem. Soc. C, 1338 (1969).
5. R. Breslow, T. Eicher, A. Krebs, R. A. Peterson, and J. Posner. J. Amer. Chem. Soc. **87**, 1320 (1965).
6. D. O. Holland and J. H. C. Nayler. J. Chem. Soc. 1504 (1955).
7. L. J. Bellamy. The infra-red spectra of complex molecules. Methuen, London, 1958. p. 96.
8. J. Hurst, T. Melton, and D. G. Wibberley. J. Chem. Soc. 2948 (1965).
9. H. E. Mertel. *In* Pyridine and its derivatives Part 2. *Edited by* E. Klinsberg. Interscience, New York, N.Y., 1961. Chapt. 6.
10. R. L. Letsinger and R. Lasco. J. Org. Chem. **21**, 764 (1956).
11. G. F. Duffin. Advan. Heterocycl. Chem. **3**, 19 (1964).
12. L. A. Paquette. J. Amer. Chem. Soc. **86**, 4096 (1964).
13. (*a*) R. J. Windgassen, W. H. Saunders, and V. Boekelheide. J. Amer. Chem. Soc. **81**, 1459 (1959); (*b*) D. R. Bragg and D. G. Wibberley. J. Chem. Soc. 2627 (1962); (*c*) E. D. Rossiter and J. E. Saxton. J. Chem. Soc. 3654 (1953).
14. (*a*) S. Gabriel and J. Colman. Ber. Deut. Chem. Ges. **37**, 3643 (1904); (*b*) A. Albert, W. L. F. Armarego, and E. Spinner. J. Chem. Soc. 5267 (1961); (*c*) A. Albert, W. L. F. Armarego, and E. Spinner. J. Chem. Soc. 2689 (1961); (*d*) T. Higashino. Yakagaku Zasshi **80**, 245 (1960), Chem. Abstr. **54**, 13125 (1960).
15. W. L. F. Armarego. Advan. Heterocycl. Chem. **1**, 253 (1963).
16. L. M. Jackman and S. Sternhell. Applications of nuclear magnetic resonance spectroscopy in organic chemistry. Second Ed. Pergamon Press, London, 1969. p. 207.
17. J. C. E. Simpson. Condensed pyridazine and pyrazine rings. *In* The chemistry of heterocyclic compounds. *Edited by* A. Weissberger. Interscience, New York, N.Y., 1953. p. 39.
18. W. L. Mosby. Chem. and Ind. (London), 1524 (1956).
19. O. Diels and R. Meyer. Ann. **513**, 129 (1934).
20. V. Boekelheide and K. Fahrenholtz. J. Amer. Chem. Soc. **83**, 458 (1961).
21. (*a*) R. F. Nystrom and C. R. A. Berger. J. Amer. Chem. Soc. **80**, 2896 (1958); (*b*) B. R. Brown and A. M. S. White. J. Chem. Soc. 3755 (1957); (*c*) J. Blackwell and W. H. Hickinbottom. J. Chem. Soc. 1405 (1961).
22. F. Krohnke and W. Weis. Ann. Chem. **679**, 136 (1964).
23. (*a*) H. Meerwein, E. Bettenberg, H. Gold, E. Pfeil, and G. Willfang. J. prakt. Chim. [2], **154**, 83 (1940); (*b*) H. Meerwein. Org. Syn. **46**, 113 (1966).

Can. J. Chem. Downloaded from www.nrcresearchpress.com by 210.87.254.105 on 09/05/12
For personal use only.

Can. J. Chem. Downloaded from www.nrcresearchpress.com by 210.87.254.40 on 09/05/12
For personal use only.

Synthesis of D-Idurone

WALTER SOWA
Department of Organic Chemistry, Ontario Research Foundation, Sheridan Park, Ontario
Received November 27, 1970

D-Idurone was prepared by periodate oxidation of D-*glycero*-D-*ido*-heptonolactone.

On rapporte la préparation de la D-idurone par oxydation périodique de la D-*glycero*-D-*ido*-heptonolactone.
Canadian Journal of Chemistry, 49, 1176 (1971)

L-Iduronic acid is a major constituent of the anticoagulant heparin according to recent evidence obtained from chemical degradation studies (1) and by 220 MHz p.m.r. spectroscopy (2). Contrary to earlier work (3–6), D-glucuronic acid appears to be a minor rather than a major component of the mucopolysaccharide. The p.m.r. data at 220 MHz confirm that L-idosyluronic acid residues occur also in dermatan (chondroitin sulfate B) and possibly heparitin (2).

Synthetic L-iduronic acid is not readily available. It has been prepared by application of the cyanohydrin synthesis to 1,2-*O*-isopropylidene-α-D-*xylo*-pentodialdo-1,4-furanose, the product of periodate oxidation of 1,2-*O*-isopropylidene-α-D-glucofuranose (7). In this procedure 1,2-*O*-isopropylidene-β-L-idofuranurono-6,3-lactone is separated from the co-product, 1,2-*O*-isopropylidene-α-D-glucofuranurono-6,3-lactone, by column chromatography on clay. Reported recently is an alternative synthesis also based on chain extension of 1,2-*O*-isopropylidene-α-D-*xylo*-pentodialdo-1,4-furanose (8). The *xylo* derivative, or its 3-benzyl ether, is ethynylated to yield a mixture of 5-epimeric, 7-carbon acetylenic sugars. The epimeric heptynes are separated by fractional distillation or by silica gel chromatography and converted by ozonolysis into derivatives of D-glucuronic and L-iduronic acids.

For many purposes in investigations of natural polymers containing L-iduronic acid, the enantiomer would serve as a reference compound. The first synthesis of a D-iduronic acid derivative appears to be that of Perlin and associates who recently reported the preparation of the α- and β-anomers of methyl D-iduronopyranoside by catalytic oxidation of the corresponding D-idopyranosides (footnote 5 in ref. 2). The present note describes a simple synthesis of D-iduronic acid, in the form of its lactone, by oxidation of D-*glycero*-D-*ido*-heptonolactone with periodic acid. Also reported is a modified procedure for the isolation of L-idurone synthesized by the cyanohydrin route.

The synthetic method employed for D-idurone is analogous to that for L-glucurone derived from D-*glycero*-D-*gulo*-heptonolactone (9). Oxidative (periodate) removal of the primary alcohol of a heptonolactone results in inversion of the molecule with the penultimate carbon atom of the heptonolactone becoming C-1 of the hexuronic acid lactone. On treatment of D-*glycero*-D-*ido*-heptonolactone with a molar equivalent of periodic acid, there was obtained a mixture of starting material, D-idurone and D-arabinose. The pentose arises from glycol cleavage of the heptonolactone at C_2—C_3, as in the preparation of L-glucurone (9). D-Idurone was isolated by preparative paper chromatography. On a millimolar scale, the yield was around 50%. A useful crystalline derivative is the dibenzyl dithioacetal. To minimize degradation of the uronic acid, it was advantageous to use trifluoroacetic acid instead of hydrochloric acid as a catalyst for thioacetalation.

The preparation of D-idurone was further simplified by oxidizing a mixture of D-*glycero*-D-*ido*-heptonolactone and D-*glycero*-D-*gulo*-heptonolactone, thus avoiding isolation of pure *ido* starting material. The mixture of heptonolactones was easily obtainable either from D-glucose by the cyanohydrin synthesis (10) or by epimerization of commercially-available D-*glycero*-D-*gulo*-heptonolactone with pyridine. After periodate oxidation of the mixed lactones, both D-idurone and L-glucurone were isolated by paper chromatography in butanol–ethanol–water (5:2:1 v/v), a solvent system in which they are widely-separated.

The straightforward resolution of D-idurone

Can. J. Chem. Downloaded from www.nrcresearchpress.com by 210.87.254.40 on 09/05/12
For personal use only.

and L-glucurone suggested a modified isolation procedure for obtaining L-idurone from the reaction of 1,2-*O*-isopropylidene-α-D-*xylo*-pentodialdo-1,4-furanose and cyanide. Instead of separating the 5-epimeric 1,2-*O*-isopropylidene hexuronolactones on clay (7), the mixture was first hydrolyzed to remove the acetal groups and then chromatographed on paper. L-Idurone and D-glucurone were readily isolated.

Experimental

Melting points were determined on a Fisher–Johns m.p. apparatus and are uncorrected. Optical rotations were done on a Carl Zeiss photoelectric polarimeter 0.005° using a sodium spectral light source. Preparative paper chromatography was on Whatman 3MM sheets with (*a*) *n*-butanol–pyridine–water (6:4:3 v/v) and (*b*) *n*-butanol–ethanol–water (5:2:1 v/v) as developing solvents. Qualitative paper chromatography was on Whatman No. 4 paper. Spray reagents for visualization of compounds were alkaline silver nitrate (11) and *p*-anisidine hydrochloride (12). Solutions were concentrated under reduced pressure using a rotary evaporator and a water bath at a temperature of 50° or less.

D-Idurone from D-Glycero-D-ido-heptonolactone

D-*Glycero*-D-*ido*-heptonolactone, m.p. 151–152°, was obtained by paper chromatographic separation of the mixture of epimeric heptonolactones resulting from treatment of D-glucose with sodium cyanide (10). As an alternative to the cyanohydrin procedure, the same mixture of heptonolactones was obtained by refluxing commercial D-*glycero*-D-*gulo*-heptonolactone (10 g) in pyridine (100 ml) for 24 h. The pyridine was removed *in vacuo* and the resulting syrup was redissolved in 80% ethanol in order to crystallize some of the unepimerized D-*glycero*-D-*gulo*-heptonolactone. The mother liquor was treated with activated carbon and evaporated to a syrup which contained an approximately 1:1 ratio of D-*glycero*-D-*gulo*- and D-*glycero*-D-*ido*-heptonolactones. The two lactones were resolved well by solvent (*a*). On a small scale it was more convenient to isolate D-*glycero*-D-*ido*-heptonolactone chromatographically rather than through the cadmium salt cadmium bromide double salt (13).

A solution of periodic acid (H_5IO_6, 228 mg) in water (5 ml) was added to a solution of D-*glycero*-D-*ido*-heptonolactone (208 mg) in water (5 ml). The reaction mixture was left for 15 min at room temperature and barium carbonate (150 mg) was added. The mixture was filtered and the filtrate evaporated to a syrup. This was evaporated with acetic acid to fully lactonize the sugar acids. Paper chromatography indicated that the syrup consisted of D-*glycero*-D-*ido*-heptonolactone, D-idurone, and a small amount of D-arabinose. Preparative paper chromatography of the mixture (200 mg) in solvent (*b*) provided D-idurone (95 mg) having $[\alpha]_D^{21}$ −30° (*c*, 1.5 in water). Yields were generally around 50%. The specific rotation reported for L-idurone is $[\alpha]_D^{25}$ +30° (*c*, 1 in water) (14).

A mixture of syrupy D-idurone (50 mg), trifluoroacetic acid (0.5 ml), and toluenethiol (0.07 ml) was left for 2 h at 5° and then evaporated to dryness. The product was recrystallized twice from ethyl acetate and dried at 40° over phosphorus pentoxide *in vacuo* to obtain D-idurone dibenzyl dithioacetal (47 mg) having m.p. 165–166° and $[\alpha]_D^{21}$ −9.7° (*c*, 1.1 in pyridine).

Anal. Calcd. for $C_{20}H_{22}O_5S_2$: C, 59.09; H, 5.46; S, 15.77. Found: C, 59.42; H, 5.72; S, 15.99.

The preparation was also carried out by oxidation of the 1:1 mixture of heptonolactones obtained above from pyridine epimerization of D-*glycero*-D-*gulo*-heptonolactone. In a typical run, the mixture (208 mg) was oxidized, worked-up as described previously, and chromatographed in solvent (*b*) to yield D-idurone (56 mg) and L-glucurone (45 mg), $[\alpha]_D^{23}$ −16.4° (*c*, 2.2 in water). On Whatman No. 4 paper, the rates of movement of D-idurone and L-glucurone (and their enantiomers) relative to rhamnose (R_{Rh}) were 1.25 and 0.90 respectively. The solvent system is based on that of Masamune and Satake (15) who reported R_{Rh} 1.24 and 0.92 for L-idurone and D-glucurone in *n*-butanol–methanol–water (5:2:1 v/v).

Paper Chromatographic Isolation of Synthetic L-Idurone

To 1,2-*O*-isopropylidene-α-D-*xylo*-pentodialdo-1,4-furanose and sodium bicarbonate (1.2 g) in water (40 ml) containing several lumps of Dry Ice and cooled in an ice bath was added a cold solution of sodium cyanide (0.8 g) in water (30 ml) (7). The reaction mixture was kept at 5° for 36 h, at room temperature for the same period and then heated at 60° for 5 h with aeration by a stream of air. The solution was evaporated to dryness and the residue redissolved in water (20 ml). The more concentrated solution, with its p*H* maintained at 2 with 10% hydrochloric acid, was extracted with ethyl acetate (10 × 50 ml). The extract was dried (Na_2SO_4), filtered, and evaporated to dryness. The syrupy mixture at this point was not lactonized by heating in toluene followed by dilution with petroleum ether to precipitate the lactones (7). Instead, the residue was hydrolyzed in 90% trifluoroacetic acid (30 ml) for 15 min at room temperature (16). The solution was evaporated to dryness and the residue lactonized by evaporation with acetic acid. The resulting mixture (2.3 g) of L-idurone and D-glucurone was separated by chromatography in solvent (*b*). From 1.00 g of syrup on two sheets (46 × 57 cm) of 3 MM paper, the yields of L-idurone, $[\alpha]_D^{21}$ +30° (*c*, 1.9 in water) and D-glucurone, m.p. 175–177°, were 0.43 and 0.37 g, respectively. The L-idurone was converted to the dibenzyl dithioacetal, m.p. 166–167°, $[\alpha]_D^{22}$ +9.6° (*c*, 1.2 in pyridine).

Anal. Calcd. for $C_{20}H_{22}O_5S_2$: C, 59.09; H, 5.46; S, 15.77. Found: C, 59.60; H, 5.47; S, 15.28.

The valuable technical assistance of Mrs. Brigitte Licht is gratefully acknowledged. This work was made possible by funds received from the Province of Ontario through the Department of Trade and Development.

1. A. S. PERLIN and G. R. SANDERSON. Carbohyd. Res. **12**, 183 (1970).
2. A. S. PERLIN, B. CASU, and G. R. SANDERSON. Can. J. Chem. **48**, 2260 (1970).
3. A. S. PERLIN, M. MAZUREK, L. B. JAQUES, and L. W. KAVANAGH. Carbohyd. Res. 7, 369 (1968).

4. M. L. WOLFROM and F. A. H. RICE. J. Amer. Chem. Soc. **68**, 532 (1946).
5. A. B. FOSTER, A. H. OLAVESEN, M. STACEY, and J. M. WEBBER. Chem. Ind. London, 143 (1961).
6. M. L. WOLFROM, J. R. VERCELLOTTI, and G. H. S. THOMAS. J. Org. Chem. **26**, 2160 (1961); **29**, 536 (1964).
7. F. SHAFIZADEH and M. L. WOLFROM. J. Amer. Chem. Soc. **77**, 2568 (1955); M. L. WOLFROM and G. H. S. THOMAS. *In* Methods in carbohydrate chemistry. Vol. II. Academic Press, Inc., New York, N.Y., 1963. p. 32.
8. D. HORTON and F. O. SWANSON. Carbohyd. Res. **14**, 159 (1970).
9. W. SOWA. Can. J. Chem. **47**, 3931 (1969).
10. H. KILIANI. Ber. **19**, 767 (1886); N. K. RICHTMYER. *In* Methods in carbohydrate chemistry. Vol. I. Academic Press, Inc., New York, N.Y., 1962. p. 160.
11. W. E. TREVELYAN, D. P. PROCTER, and J. S. HARRISON. Nature, **166**, 444 (1950).
12. L. HOUGH, J. K. N. JONES, and W. H. WADMAN. J. Chem. Soc. 1702 (1950).
13. E. M. MONTGOMERY, N. K. RICHTMYER, and C. S. HUDSON. J. Amer. Chem. Soc. **65**, 1848, footnote 17 (1943).
14. J. A. CIFONELLI, J. LUDOWIEG, and A. DORFMAN. J. Biol. Chem. **233**, 541 (1958).
15. H. MASAMUNE and M. SATAKE. Tohoku J. Exptl. Med. **69**, 167 (1959).
16. J. E. CHRISTENSEN and L. GOODMAN. Carbohyd. Res. **7**, 510 (1968).

Can. J. Chem. Downloaded from www.nrcresearchpress.com by 210.87.254.40 on 09/05/12
For personal use only.

Can. J. Chem. Downloaded from www.nrcresearchpress.com by 210.87.254.105 on 09/05/12
For personal use only.

Total Synthesis of α,β-DL-Allose and α,β-DL-Galactose. Stereoselective *cis*-Hydroxylation by Osmium Tetroxide

U. P. SINGH[1] AND R. K. BROWN
Department of Chemistry, University of Alberta, Edmonton, Alberta

Received October 30, 1970

The reaction of osmic acid with 1,6-anhydro-3,4-dideoxy-β-DL-*erythro*-hex-3-enopyranose and its 2-*O*-methyl and 2-*O*-acetyl derivatives in either pyridine or dioxane solution has produced 1,6-anhydro-β-DL-allopyranose and 1,6-anhydro-β-DL-galactopyranose and the corresponding 2-*O*-methyl and 2-*O*-acetyl derivatives. These or their fully acetylated derivatives could be hydrolyzed to α,β-DL-allose and α,β-DL-galactose and the 2-*O*-methyl derivatives. The proportion of *allo* to *galacto* product obtained varies widely with the solvent used in hydroxylation, showing that attack by osmic acid is subject to steric control.

La réaction de l'acide osmique avec le DL-anhydro-1,6 didéoxy-3,4 β-hexèno-3 pyranose et ses dérivés *O*-méthyl-2 ou *O*-acétyl-2 soit en solution dans la pyridine ou le dioxanne conduit aux DL-anhydro-1,6 β-allopyranose et DL-anhydro-1,6 β-galactopyranose et les dérivés correspondants *O*-méthyl-2 ou *O*-acétyl-2. Ces produits ou leurs dérivés complètement acétylés peuvent être hydrolysés en α,β-DL-allose et α,β-DL-galactose et les dérivés *O*-méthyl-2. Les proportions des produits *allo* et *galacto* obtenus varient grandement avec le solvant utilisé pour l'hydroxylation montrant ainsi que l'attaque par l'acide osmique est sujette au contrôle stérique.

Canadian Journal of Chemistry, 49, 1179 (1971)

Introduction

A recent communication (1) from this laboratory has reported the preparation of α,β-DL-glucose from 1,6-anhydro-3,4-dideoxy-β-DL-*erythro*-hex-3-enopyranose, (**1**, R = H), obtained by the reaction of *n*-butyllithium with 1,6:2,3-dianhydro-4-deoxy-β-DL-*ribo*-hexopyranose, a compound in turn obtained from acrolein dimer (2). The present paper describes the stereoselective reaction of osmic acid with **1** (R = H, CH_3— or CH_3CO—) to produce α,β-DL-allose and α,β-DL-galactose and their 2-*O*-methyl derivatives (Scheme 1).

Results and Discussion

The 100 MHz p.m.r. spectra were obtained for all of the compounds isolated and are in full agreement with the structures and conformations proposed and shown in Scheme 1. Signals for most of the protons could be determined by spin decoupling and these provided observed proton couplings which clearly supported these structures and conformations. Details are described in the Experimental.

Two methods were employed for the *cis* hydroxylation of olefin **1** with osmic acid. The first involved reaction in pyridine (3) while the second employed dioxane as the solvent (4). Reaction of **1** (R = H) with osmic acid in pyridine gave a mixture from which the products **2** (R = R′ = H) and **3** (R = R′ = H) together or separately could not be isolated. When the crude reaction mixture was treated with pyridine and acetic anhydride, the acetylated derivatives **2** (R = R′ = CH_3CO) and **3** (R = R′ = CH_3CO) could be isolated and separated by repeated chromatography in yields of 36 and 30% respectively. Osmic acid in dioxane gave a much cleaner reaction with **1** (R = H) and provided an 85% yield of an isolable solid whose elemental analysis and p.m.r. spectrum showed it to be a 2:1 mixture of **2** and **3** (R = R′ = H). Repeated attempts to separate these two isomers were unsuccessful. Accordingly the mixture was first converted to the triacetate and then separated by chromatography as above to provide excellent yields of the pure triacetates **2** and **3** (R = R′ = CH_3CO).

The reaction of **1** with osmic acid in either pyridine or dioxane was quite satisfactory when R was methyl or acetyl, and gave a mixture of the corresponding dihydroxy compounds **2** and **3** (R′ = H, R = CH_3, or CH_3CO) in crude yields that were practically quantitative.

Hydrolysis of **2** (R = R′ = CH_3CO) with a mixture of 1 *N* hydrochloric acid with dioxane (2:1 by volume) gave solid α,β-DL-allose in 91% yield based on the triacetate precursor. The 100 MHz p.m.r. spectrum in D_2O showed that this

[1]Postdoctoral Fellow 1969–1971.

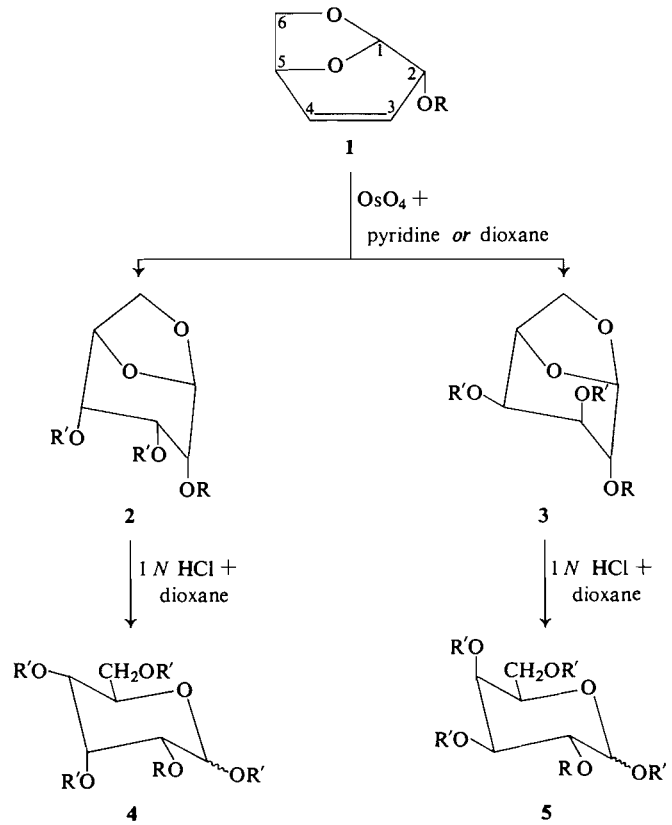

SCHEME 1

α,β-DL-allose existed as an equilibrium mixture of α- and β-furanose and α- and β-pyranose structures, with the β-pyranose isomer in great predominance. Similar isomeric distributions have been reported for aqueous solutions of several D-monosaccharides (5). This spectrum was identical with the p.m.r. spectrum (in D_2O) of authentic α,β-D-allose,[2] thus providing final proof of the structure of **4** (R = R′ = H). Treatment with acetic anhydride and pyridine converted the α,β-DL-allose to the solid pentaacetate **4** (R = R′ = CH_3CO) which, from the integrated areas of the C-1 proton signals in its p.m.r. spectrum, was shown to be a mixture of the α and β anomers in the approximate ratio of 1.0:3.6.

Hydrolysis of **3** (R = R′ = CH_3CO) under the same conditions as employed for the hydrolysis of **2** (R = R′ = CH_3CO), gave α,β-DL-galactose **5** (R = R′ = H) as a crystalline solid in 92% yield. The 100 MHz spectrum in D_2O showed two anomeric proton signals in the approximate area ratio of 1:1 corresponding to the α- and β-pyranose structures. No evidence was noted indicating the presence of the α- and/or β-furanose isomer. The p.m.r. spectrum of the viscous, syrupy DL-galactose pentaacetate **5** (R = R′ = CH_3CO) showed that this substance was a 1.0:2.7 mixture of the α and β anomers. An identical p.m.r. spectrum was obtained from the pentaacetate of authentic D-galactose.

cis-Hydroxylation of the oily 2-*O*-acetyl-1,6-anhydro-3,4-dideoxy-β-DL-*erythro*-hex-3-enopyranose (**1**, R = CH_3CO) in pyridine gave a product which showed only two spots on a thin layer chromatogram. A combination of column chromatography and fractional crystallization provided in good yield a 65:35 mixture of what was at first considered to be the two isomers 2-*O*-acetyl-1,6-anhydro-β-DL-allopyranose (**2**, R′ = H, R = CH_3CO), an oil, and 2-*O*-acetyl-

[2]The p.m.r. spectrum of α,β-D-allose in D_2O was kindly provided by Professor S. J. Angyal, University of New South Wales, Kensington, N.S.W., Australia.

Can. J. Chem. Downloaded from www.nrcresearchpress.com by 210.87.254.105 on 09/05/12
For personal use only.

TABLE 1. Ratio of *allo* to *galacto* isomer obtained by reaction of OsO_4 with **1***

Compound **1** R	In pyridine	In dioxane
H	36:30 (As triacetate) (66)	51:27 (As triacetate) (78) 2:1 (Unacetylated) (85)
CH_3CO	65:35 (96)	9:1 88:7.5 (As triacetate) (96)
CH_3	1:3 (~100)	4:3 (98)

*The overall yields (%) are in parentheses.

1,6-anhydro-β-DL-galactopyranose (**3**, R′ = H, R = CH_3CO), a solid. Separation was facilitated by the fact that the *allo* but not the *galacto* isomer is soluble in methylene chloride. Both substances showed only one spot on a thin layer chromatogram. The 100 MHz p.m.r. spectrum of the *galacto* isomer agreed completely with the assigned structure. However, that of the "*allo*" isomer, the major product, showed the presence of *three* singlets in the region where the acetyl methyl proton signals normally occur. The integrated area of these three signals was equivalent to three of the 12 protons. It is thus quite apparent that the advantageous orientation of the hydroxyl groups has permitted acetyl migration during the procedure of isolation of the *allo* monoacetate. We were unable to avoid this migration and also could not separate the three isomeric *allo* monoacetates. *cis*-Hydroxylation in dioxane solution resulted in similar unavoidable acetyl migration. Complete acylation of the *allo* or the *galacto* monoacetates gave the triacetates identical to those described above. Acid-catalyzed hydrolysis of the *allo* and *galacto* monoacetates gave respectively α,β-DL-allose and α,β-DL-galactose in excellent yield.

cis-Hydroxylation of **1** (R = CH_3) with osmic acid in pyridine gave a syrup which showed two spots on a thin layer chromatogram. The p.m.r. spectrum indicated two anomeric proton signals in the relative area ratio of 1:3. The two substances were separated by column chromatography and their 100 MHz p.m.r. spectra clearly identified the minor product, a solid, as 2-*O*-methyl-1,6-anhydro-β-DL-allopyranose, (**2**, R′ = H, R = CH_3) and the major product, also a solid, as the *galacto* isomer **3** (R′ = H, R = CH_3). Osmic acid in dioxane also produced both **2** and **3** (R′ = H, R = CH_3) but in the ratio of 4:3 respectively. Acylation of the mixture of isomers **2** and **3** (R′ = H, R = CH_3) provided the corresponding diacetates **2** and **3** (R′ = CH_3CO, R = CH_3) which could be separated as solids by column chromatography. Acid-catalyzed hydrolysis of the *allo* diacetate **2** (R′ = CH_3CO, R = CH_3) gave crystalline 2-*O*-methyl-α,β-DL-allose (**4**, R′ = H, R = CH_3). Its p.m.r. spectrum in D_2O showed the presence of α- and β-furanose along with the α- and β-pyranose structures, again with the β-pyranose isomer in large predominance. Acetylation of 2-*O*-methyl-α,β-DL-allose gave the corresponding tetraacetate **4** (R′ = CH_3CO, R = CH_3). The 100 MHz p.m.r. spectrum of this compound indicated that it was a single compound possessing the β-anomeric structure.

Acid-catalyzed hydrolysis of 1,6-anhydro-2-*O*-methyl-β-DL-galactopyranose (**3**, R′ = H, R = CH_3) provided 2-*O*-methyl-α,β-DL-galactopyranose (**5**, R′ = H, R = CH_3) whose 100 MHz p.m.r. spectrum in D_2O showed the presence of only the α- and β-pyranose structures and was identical to the p.m.r. spectrum of authentic 2-*O*-methyl-α,β-D-galactose.[3]

Table 1 shows the ratio of the *allo* to *galacto* isomers obtained by the osmic acid oxidation of **1** when R = H, CH_3CO, or CH_3.

Except for the reaction of osmic acid with **1** (R = H) in pyridine where product isolation was difficult, it is clear that *cis* hydroxylation with osmic acid is susceptible to steric approach control. For the compounds where R = H or CH_3CO in **1**, for both pyridine and dioxane, the oxymethylene group of the 1,6-anhydro ring offers greater resistance to approach of the osmic acid to the double bond than does either the hydroxy or the acetoxy group. Such steric hindrance to the reaction of osmic acid with a

[3]A sample of 2-*O*-methyl-α,β-D-galactose was kindly supplied by Professor R. U. Lemieux and Dr. T. L. Nagabhushan of the Department of Chemistry at the University of Alberta, Edmonton, Alberta.

Can. J. Chem. Downloaded from www.nrcresearchpress.com by 210.87.254.105 on 09/05/12
For personal use only.

Can. J. Chem. Downloaded from www.nrcresearchpress.com by 210.87.254.105 on 09/05/12
For personal use only.

double bond has already been noted (3, 6), and is reminiscent of the steric control exerted by alkyl, alkoxy, or acetoxy substituents, situated α or β to the double bond in the cyclohexene ring system, to reaction of peroxy acids with the double bond (7). Contrary to the observation that an α hydroxy group, probably by hydrogen bonding, directs the peroxy acid to the double bond on the side of the ring on which the hydroxyl group is located (7), no clear evidence of such an effect has been observed for the osmic acid reaction in this work. A methoxy group appears to provide a definitely greater steric resistance to approach to the double bond by osmic acid than does the oxymethylene group when hydroxylation is carried out in pyridine, whereas in dioxane, the methoxy group has *slightly less* hindrance than does the oxymethylene group. It is not clear why such a marked difference occurs in the behavior of osmic acid in the two solvents employed. It is known that an isolable complex is formed between one molecule of osmic acid and two molecules of pyridine (8), thus suggesting that the species attacking the double bond during *cis* hydroxylation in pyridine is the 1:2 complex.

Experimental

Melting points and boiling points are uncorrected.

Elemental analyses were made by Mrs. Darlene Mahlow and Mrs. A. Dunn of our microanalytical laboratory. The i.r. absorption spectra were obtained by Mr. R. Swindlehurst with a Perkin–Elmer Model 421 spectrophotometer. The 60 MHz p.m.r. spectra were made by Mr. Swindlehurst using a Varian A-60 instrument. The 100 MHz spectra and spin decoupling experiments were carried out by Mr. G. Bigham and his associates. Tetramethylsilane was the internal reference. Signal assignments were made with the aid of double irradiation spin decoupling. Coupling constants reported were estimated from the signal spacings where this was possible and are therefore approximate values.

Column and thin layer chromatography were carried out using silica gel G (E. Merck and Co.) as adsorbant. Solvents were usually removed by rotary evaporator under vacuum unless otherwise stated.

*Reaction of 1,6-Anhydro-3,4-dideoxy-*β*-*DL*-erythro-hex-3-enopyranose (**1**, R = H) with Osmic Acid*

(a) In Pyridine

Compound **1** (R = H) in pyridine was treated with osmic acid according to published directions (3) but at room temperature for 20 h. The orange solution obtained after the addition of sodium bisulfite was evaporated at 40° under vacuum to dryness rather than extracted with chloroform, and the product freeze-dried under vacuum. The crude product was treated with excess acetic anhydride in pyridine at 60° for 0.5 h, then stirred overnight at room temperature. The mixture was poured into ice water and extracted with chloroform (5 × 20 ml). The extract was dried (magnesium sulfate) and then freed from solvent. The crude viscous semi-solid showed two spots on a thin layer chromatogram (solvent, ethyl acetate – chloroform, 1:1). Repeated column chromatography using a 1:1 mixture of ethyl acetate – chloroform as eluent gave in the *first fraction*, solid 1,6-anhydro-2,3,4-tri-*O*-acetyl-β-DL-galactopyranose (**3**, R = R′ = CH_3CO) which crystallized from dichloromethane as colorless needles melting at 114–115°; yield, 30%. The i.r. spectrum in chloroform showed strong absorption at 1745 cm^{-1} (C=O).

Anal. Calcd. for $C_{12}H_{16}O_8$: C, 50.00; H, 5.59. Found: C, 50.27; H, 5.45.

The 100 MHz p.m.r. spectrum in deuteriochloroform showed signals at τ 4.58 for H-1 (doublet, $J_{1,2} \sim 1.5$ Hz); 5.26 for H-2 (narrow quartet, $J_{2,3} \sim 1.0$, $J_{1,2} \sim 1.5$ Hz); 4.75 for H-3 and -4 (multiplet, $J_{3,4} \sim 2.5$, $J_{4,5} \approx 2.5$ Hz); 5.56 for H-5 (multiplet, $J_{5,6exo} \sim 5.0$, $J_{4,5} \sim 2.5$, $J_{3,5} \sim$ 2.5 Hz, long range); 5.68 for H-6*endo* (quartet, $J_{5,6endo} \sim$ 0.5, $J_{6endo,6exo} \sim 7.5$ Hz); 6.30 for H-6*exo* (quartet, $J_{4,6exo} \sim 1.5$ Hz); 7.90 for two CH_3 (singlet); 8.00 for one CH_3 (singlet).

The *second fraction* gave *1,6-anhydro-2,3,4-tri-O-acetyl-*β*-DL-allopyranose* (**2**, R = R′ = CH_3CO), which produced colorless prisms from dichloromethane–pentane, melting at 128–129°; yield, 36%. The i.r. spectrum in chloroform showed strong absorption at 1745 cm^{-1} (C=O).

Anal. Calcd. for $C_{12}H_{16}O_8$: C, 50.00; H, 5.59. Found: C, 50.23; H, 5.34.

The 100 MHz p.m.r. spectrum in deuteriochloroform showed signals at τ 4.49 for H-1 (doublet, $J_{1,2} \sim 2.5$ Hz); 4.80–4.95 for H-2 and -4 (multiplet); 4.75 for H-3 (triplet, $J_{2,3} \approx J_{3,4} \sim 5.0$ Hz); 5.33 for H-5 (complicated doublet, $J_{4,5} \sim 2.5$, $J_{5,6endo} \sim 1.5$, $J_{5,6exo} \sim 5.0$ Hz); 6.07 for H-6*endo* (quartet, $J_{5,6endo} \sim 1.5$, $J_{6exo,6endo} \sim 8.5$ Hz); 6.22 for H-6*exo* (quartet, $J_{5,6exo} \sim 5.0$ Hz); 7.85 for CH_3 (singlet); 7.87 for CH_3 (singlet); and 8.03 for CH_3 (singlet).

(b) In Dioxane

A mixture of compound **1** (R = H) (0.43 g) and 1.0 g of osmic acid in 10 ml of dry dioxane was stirred at room temperature for 24 h, following published directions (6). The thick syrup obtained after treatment with hydrogen sulfide and removal of solvent (6) solidified on standing. The crude material (0.46 g, 85%) was shown by its p.m.r. spectrum in deuteriomethanol to be a 2:1 mixture of **2** (R = R′ = H) and **3** (R = R′ = H). The mixture was treated with acetic anhydride in pyridine and the triacetates separated by column chromatography as in section *a* above, to give *1,6-anhydro-2,3,4-tri-O-acetyl-*β*-DL-allopyranose* as colorless prisms melting at 128–129°. Mixed m.p. with sample from section *a*, 127–129°; yield, 0.49 g (51% based on **1**, R = R′ = H), and *1,6-anhydro-2,3,4-tri-O-acetyl-*β*-DL-galactopyranose* as fine needles melting at 114–115°. Mixed m.p. with sample from section *a*, 114–115°; yield, 0.265 g (27% based on **1**, R = R′ = H).

α,β-DL-*Allose* (**4**, *R = R′ = H*)

A solution of 288 mg of **2** (R = R′ = CH_3CO) in 10 ml of 1 *N* aqueous hydrochloric acid containing 5 ml of dioxane was heated for 5 h in an oil bath at ~100°. The mixture was cooled and then neutralized with Amberlite

Can. J. Chem. Downloaded from www.nrcresearchpress.com by 210.87.254.105 on 09/05/12
For personal use only.

IRA 400 (OH^-) and filtered. The solvent was removed and the residue freeze-dried. The colorless powder was crystallized from water–methanol, producing fine needles melting at 181–183°; yield, 165 mg (91%). Reported m.p. of an equimolar mixture of D- and L-allose, 180° (9).

Anal. Calcd. for $C_6H_{12}O_6$: C, 40.00; H, 6.71. Found: C, 39.81; H, 6.64.

The 100 MHz p.m.r. spectrum obtained in deuterium oxide after a 72 h period required for completion of mutarotation agreed fully with that of authentic α,β-D-allose, and showed signals for the anomeric proton at τ 4.23 (doublet, $J_{1,2} \sim 4.0$ Hz for the α-furanose isomer); 4.36 (doublet, $J_{1,2} \sim 2.4$ Hz for β-furanose isomer); 4.45 (doublet, $J_{1,2} \sim 4.0$ Hz for α-pyranose isomer); and 4.72 (doublet, $J_{1,2} \sim 8.0$ Hz for β-pyranose isomer, the major species). The 100 MHz p.m.r. spectrum of **4** (R = R′ = H) taken from a freshly prepared solution in deuterium oxide showed only the anomeric proton signals for the α- and β-pyranose isomers in the approximate ratio of 1.0:2.5.

α,β-DL-Allose Pentaacetate (4, R = R′ = CH_3CO)

Treatment of 90 mg of **4** (R = R′ = H) with 5 ml of acetic anhydride and 5 ml of pyridine at room temperature for 24 h, gave solid α,β-DL-*allose pentaacetate* (**4**, R = R′ = CH_3CO) which provided colorless needles from ether–pentane; m.p. 132–133°; yield, 190 mg (98%).

Anal. Calcd. for $C_{16}H_{22}O_{11}$: C, 49.24; H, 5.64. Found: C, 49.19; H, 5.45.

The i.r. spectrum in Nujol showed carbonyl absorption at 1760 cm^{-1}.

The 100 MHz p.m.r. spectrum in deuteriochloroform showed signals at τ 3.82 (doublet, $J_{1,2} \sim 4.0$ Hz for H-1 of the α-isomer) and at 4.06 (doublet, $J_{1,2} \sim 8.5$ Hz for H-1 of the β-isomer) with signal area ratio α:β = 1.0:3.6. Other signals were found at τ 4.90–5.20 for H-2 and -4 (multiplet); 4.34 for H-3 (triplet, $J_{2,3} \approx J_{3,4} \sim 3.0$ Hz); 5.8–6.0 for H-5, -6*exo*, and -6*endo* (multiplet); 7.40, 7.90, and 8.02 (three singlets for each of three methyl groups).

α,β-DL-Galactose (5, R = R′ = H)

Hydrolysis of 288 mg of **3** (R = R′ = CH_3CO) by the same method used to hydrolyze **2** (R = R′ = CH_3CO) gave crude α,β-DL-*galactose* as a glassy solid which crystallized from methanol–ether as colorless needles melting at 144–147°; yield, 178 mg (93%). Reported m.p. of an equimolar mixture of D- and L-galactose, 143–144° (10), 163° (11).

Anal. Calcd. for $C_6H_{12}O_6$: C, 40.00; H, 6.71. Found: C, 40.10; H, 6.68.

The 100 MHz p.m.r. spectrum in deuterium oxide, taken after the compound had been in solution 1 h, was completely superimposable on a 100 MHz p.m.r. spectrum of authentic α,β-D-galactose in deuterium oxide. No change was observed in the spectrum taken after either substance had been kept in solution for a period of 5 days.

α,β-DL-Galactose Pentaacetate (5, R = R′ = CH_3CO)

Acetylation of 90 mg of **5** (R = R′ = H) with acetic anhydride and pyridine (5 ml of each) for 24 h at room temperature gave crude pentaacetate as a viscous liquid which was purified by distillation to give a colorless syrup boiling at 155–160° at 0.1 mm; yield, 192 mg (98%).

Anal. Calcd. for $C_{16}H_{22}O_{11}$; C, 49.24; H, 5.64. Found: C, 48.94; H, 5.55.

The 100 MHz p.m.r. spectrum in deuteriochloroform was identical to that of authentic α,β-D-galactose pentaacetate in deuteriochloroform and showed by the integrated area of the two signals for the anomeric proton, that the α and β anomers were present in the approximate ratio of 1.0:2.7.

2-O-Acetyl-1,6-anhydro-3,4-dideoxy-β-DL-erythro-hex-3-enopyranose (1, R = CH_3CO)

A solution of **1** (R = H) (1.28 g, 0.001 mol) in a mixture of 5 ml of acetic anhydride and 5 ml of dry pyridine, first heated for 0.5 h at 60° then stirred overnight at room temperature, was poured into an ice–water mixture. The chloroform extract (5 × 20 ml) was dried (magnesium sulfate) and freed from solvent. The residual yellow liquid was twice distilled under vacuum to give **1** (R = CH_3CO) as a colorless liquid boiling at 93–95° at 0.5 mm; yield, 1.68 g (99%).

Anal. Calcd. for $C_8H_{10}O_4$: C, 56.47; H, 5.92. Found: C, 56.70; H, 6.05.

The 100 MHz p.m.r. spectrum in deuteriochloroform showed signals at τ 4.50 for H-1 (triplet, $J_{1,2} \sim 2.0$, $J_{1,3} \sim 1.5$ Hz); 5.28 for H-2 (quartet, $J_{1,2} \sim 2.0$, $J_{2,3} \sim 4.0$ Hz); 4.25 H-3 (doublet of quartets, $J_{3,4} \sim 10$, $J_{2,3} \sim 4$, $J_{1,3} \sim 1.5$ Hz); 3.70 for H-4 (doublet of quartets, $J_{3,4} \sim 10$, $J_{4,5} \sim 5$, $J_{2,4} \sim 1.5$ Hz); 5.25–5.35 for H-5 (multiplet); 6.25–6.40 for H-6*exo* and -6*endo* (multiplet); and 6.34 for CH_3 (singlet).

The i.r. spectrum (neat) showed strong absorption at 1735 cm^{-1} (C=O).

Reaction of 2-O-Acetyl-1,6-anhydro-3,4-dideoxy-β-DL-erythro-hex-3-enopyranose (1, R = CH_3CO) with Osmic Acid

(a) In Pyridine

Compound **1** (R = CH_3CO) was treated with osmic acid by the procedure employed for the similar oxidation of **1** (R = H) except that the solution obtained after addition of sodium bisulfite was continuously extracted with chloroform for 48 h. The extract was dried (magnesium sulfate) and freed from solvent at 45° under vacuum. The syrupy residue (crude yield, 96%) showed two closely situated spots on a thin layer chromatogram (solvent, 3% methanol in dichloromethane). The 60 MHz p.m.r. spectrum in deuteriochloroform showed two anomeric proton signals in the area ratio 65:35.

This syrup was separated into its two components by column chromatography using 3% methanol in dichloromethane as eluent. The first fraction (15 ml) was discarded (a gum). The second fraction (50 ml) gave a solid later identified as **3** (R = CH_3CO, R′ = H). The last fraction (200 ml) gave a mixture of **2** and **3** (R = CH_3CO, R′ = H) as a syrup (640 mg). A solution of this syrup in 15 ml of dichloromethane, seeded with the solid obtained from the second fraction, deposited all of the *2-O-acetyl-1,6-anhydro-β-DL-galactopyranose* (**3**, R = CH_3CO, R′ = H). Total yield, 31.5%; m.p. after sublimation at 130–135° at 0.1 mm, 144–145°.

Anal. Calcd. for $C_8H_{12}O_6$: C, 47.06; H, 5.92. Found: C, 46.93; H, 5.55.

The i.r. spectrum (KBr pellet) showed bands at 3470 and 3390 (OH) and at 1715 cm^{-1} (C=O).

The 100 MHz p.m.r. spectrum in trifluoroacetic acid (a solvent required to effect solution and which had no deleterious effect on the solute) showed signals at τ 4.25

Can. J. Chem. Downloaded from www.nrcresearchpress.com by 210.87.254.105 on 09/05/12
For personal use only.

for H-1 (singlet, $w/2 \sim 3.5$ Hz); 4.85 for H-2 (singlet, $w/2 \sim 4$ Hz); 5.50–5.80 for H-3 and -4 (multiplet); 5.10–5.30 for H-5 (multiplet, $J_{5,6exo} \sim 4$ Hz); 5.39 for H-6*endo* (doublet, $J_{6exo,6endo} \sim 8.0$ Hz); 6.08 for H-6*exo* (quartet showing long range coupling with H-1 and -4*exo*); and 7.76 for CH_3 (singlet).

Acetylation of **3** (R = CH_3CO, R′ = H) gave the triacetate **3** (R = R′ = CH_3CO) as a crystalline solid (needles from dichloromethane–pentane) melting at 114–115° and completely identical with the triacetate obtained above. Hydrolysis of this triacetate gave α,β-DL-galactose, also identical with the α,β-DL-galactose obtained above.

The dichloromethane mother liquor obtained after removal of the 2-*O*-acetyl-1,6-anhydro-β-DL-galactopyranose, was freed from solvent to provide a syrup (crude yield 60%) which gave only one spot on a thin layer chromatogram (solvent, 3% methanol in dichloromethane). Attempts to crystallize this failed, hence it was purified by distillation; b.p. 134–135° at 0.5 mm. Analysis agreed with the substance being a mixture of *2-*, *3-*, and *4-O-acetyl-1,6-anhydro*-β-DL-*allopyranose* (**2**).

Anal. Calcd. for $C_8H_{12}O_6$: C, 47.06; H, 5.92. Found: C, 47.09; H, 6.07.

The i.r. spectrum in carbon tetrachloride showed absorption at 3565 and 3605 (shoulder) (OH) and at 1752 cm^{-1} (C=O).

The 100 MHz p.m.r. spectrum in deuteriochloroform possessed signals at τ 4.54 for H-1 (poorly resolved narrow multiplet, $w/2 \sim 6$ Hz); 5.10–5.40 for H-2, -3, and -4 (complex multiplets); 5.40–5.60 for H-5 (multiplet); 6.15–6.50 for H-6*exo* and -6*endo* (multiplets); 7.98–8.02 (three singlets for CH_3).

Acetylation of a portion of this syrupy mixture gave crystalline (from dichloromethane–pentane) *1,6-anhydro-2,3,4-tri-O-acetyl*-β-DL-*allopyranose* (**2**, R = R′ = CH_3CO) melting at 128–129° and identical with the 1,6-anhydro-DL-*allo* triacetate obtained above.

Hydrolysis of the remainder of the syrupy mixture of monoacetates gave α,β-DL-*allose* (**4**, R = R′ = H) identical with that obtained above.

(b) In Dioxane

Compound **1** (R = CH_3CO) (0.67 g) was treated for 48 h with osmic acid according to the procedure used for the oxidation of **1** (R = H) above. The 60 MHz p.m.r. spectrum in deuteriochloroform of the syrup obtained (crude yield, 0.8 g, 99%) showed it to be a mixture of **2** (R = CH_3CO, R′ = H) and **3** (R = CH_3CO, R′ = H) in the ratio 9:1. This crude mixture was acetylated as usual and the two triacetates separated by column chromatography as described for the mixture of triacetates obtained following the osmic acid reaction with **1** (R = H) in pyridine. The products **2** (R = R′ = CH_3CO) and **3** (R = R′ = CH_3CO), obtained in yields of 88 and 7.5% respectively, were identical to those obtained above from the acetylation of the products obtained from the osmic acid reaction with **1** (R = H) in pyridine.

1,6-Anhydro-2-O-methyl-3,4-dideoxy-β-DL-*erythro-hex-3-enopyranose* (**1**, *R = CH_3*)

The general procedure for methylation (12) was modified as follows. A solution of **1** (R = H) (2.65 g, 0.02 mol) in 50 ml of dry 1,2-dimethoxyethane (DME) was added dropwise over a 1 h period to a well-stirred mixture of 0.8 g (0.04 mol) of sodium hydride and 5.68 g (0.04 mol) of methyl iodide in 50 ml of dry DME. The reaction flask was kept in a water bath at 20° to avoid temperature rise. The mixture was stirred for 3 h at 20°, then stirred and heated under reflux for an additional hour. The bulk of the solvent (75 ml) was removed by fractional distillation and the cooled residue was diluted with ether to precipitate the sodium iodide. Filtration and subsequent removal of solvent from the filtrate by fractional distillation gave a residue which was purified by distillation and afforded 2.20 (77.5%) of colorless liquid **1** (R = CH_3) boiling at 53–55° at 0.1 mm.

Anal. Calcd. for $C_7H_{10}O_3$: C, 59.14; H, 7.09. Found: C, 59.08; H, 7.02.

The 100 MHz p.m.r. spectrum in deuteriochloroform showed signals at τ 4.47 for H-1 (narrow triplet, $w/2 \sim 4.5$, $J_{1,2} \sim 1.0$ Hz); 6.74 for H-2 (doublet of triplets, $J_{2,3} \sim 3.5$; $J_{2,4} \sim 1.0$ Hz); 4.25 for H-3 (doublet of quartets, $J_{3,4} \sim 10$, $J_{1,3} \sim 1.0$ Hz); 3.81 for H-4 (quartet of doublets, $J_{4,5} \sim 4.7$ Hz); 5.30–5.42 for H-5 (multiplet); 6.35–6.45 for H-6*exo* and -6*endo* (narrow multiplet, $w/2 \sim 4$ Hz); 6.61 for OCH_3 (singlet).

Reaction of 1,6-Anhydro-2-O-methyl-3,4-dideoxy-β-DL-*erythro-hex-3-enopyranose (**1**, R = CH_3) with Osmic Acid*

(a) In Pyridine

Compound **1** (R = CH_3) (3.0 g, 0.0118 mol) was oxidized with osmic acid in pyridine as described for the oxidation of **1** (R = CH_3CO). The syrup obtained (crude yield 2.08 g, ~100%) showed two closely situated spots on a thin layer chromatogram (solvent, 10% methanol in dichloromethane). The 60 MHz p.m.r. spectrum of this crude syrup showed two anomeric proton signals in the area ratio of 3:1.

The two components were separated by column chromatography using 10% methanol in dichloromethane as eluent. From the *first fraction* was obtained a solid which, after sublimation at 135–140° at 0.1 mm, formed needles which melted at 124–125°; yield of *1,6-anhydro-2-O-methyl*-β-DL-*galactopyranose* (**3**, R = CH_3, R′ = H) was 1.20 g, 58%.

Anal. Calcd. for $C_7H_{12}O_5$: C, 47.74; H, 6.87. Found: C, 47.98; H, 6.80.

The 100 MHz p.m.r. spectrum in trifluoroacetic acid showed signals at τ 4.21 for H-1 (broad singlet, $w/2 \sim 4$, $J_{1,2} \sim 1.5$ Hz); 6.16 for H-2 (narrow multiplet, $w/2 \sim 3.5$ Hz); 5.52–5.65 for H-3 and -4 (multiplet); 5.20–5.35 for H-5 (multiplet); 5.45 for H-6*endo* (doublet, $J_{6exo,6endo} \sim 8.5$ Hz); 6.14 for H-6*exo* (quartet, $J_{5,6exo} \sim 5.0$ Hz); 6.37 for CH_3 (singlet).

The i.r. spectrum in Nujol had a broad band at 3350 cm^{-1} (OH).

Acetylation of **3** (R = CH_3, R′ = H) as usual gave *1,6-anhydro-2-O-methyl-3,4-di-O-acetyl*-β-DL-*galactopyranose* (**3**, R = CH_3, R′ = CH_3CO) which from ether–pentane formed colorless needles melting at 102–103°; yield, 98%.

Anal. Calcd. for $C_{11}H_{16}O_7$: C, 50.77; H, 6.20. Found: C, 50.78; H, 6.00.

The 100 MHz p.m.r. spectrum in deuteriochloroform showed signals at τ 4.57 for H-1 (triplet, $J_{1,2} \sim 1.5$, $J_{1,3} \sim 1.2$ Hz); 6.77 for H-2 (triplet, $J_{2,3} \sim 1.5$ Hz); 4.73–4.90 for H-3 (multiplet); 4.60–4.73 for H-4 (multiplet, $J_{4,5} \sim 4.5$, $J_{4,6exo} \sim 1.5$ Hz); 5.50–5.65 for H-5

Can. J. Chem. Downloaded from www.nrcresearchpress.com by 210.87.254.105 on 09/05/12
For personal use only.

(multiplet, $J_{5,6exo} \sim 5.0$ Hz); 5.70 for H-6*endo* (doublet, $J_{6endo,6exo} \sim 7.0$ Hz); 6.31 for H-6*exo* (complicated quartet); 6.60 for OCH_3 (singlet); 8.00 and 8.06 each a singlet for CH_3).

The i.r. spectrum in chloroform showed bands at 1765 (shoulder) and 1745 cm^{-1} for C=O.

The *second fraction* from the chromatographic separation above provided 400 mg of syrup which was a mixture of **2** and **3** (R = CH_3, R′ = H) as shown by the p.m.r. spectrum and by t.l.c. This was acetylated as usual and gave a solid which showed two spots on a thin layer chromatogram (solvent, ethyl acetate). Column chromatography, with ethyl acetate as eluent, provided from the first fraction the compound *1,6-anhydro-2-O-methyl-3,4-di-O-acetyl*-β-DL-*galactopyranose* (**3**, R = CH_3, R′ = CH_3CO) whose colorless needles from ether–pentane melted at 102–103°; yield, 74%. This was identical with the product obtained from the acetylation of pure **3** (R = CH_3, R′ = H) above. The second fraction from the chromatography of this acetylated mixture was *1,6-anhydro-2-O-methyl-3,4-di-O-acetyl*-β-DL-*allopyranose* (**2**, R = CH_3, R′ = CH_3CO) whose fine needles from ether–pentane melted at 133–134°, yield, 23%.

Anal. Calcd. for $C_{11}H_{16}O_7$: C, 50.77; H, 6.20. Found: C, 50.78; H, 6.00.

The i.r. spectrum in chloroform showed a band at 1750 cm^{-1} (C=O).

The 100 MHz p.m.r. spectrum in deuteriochloroform had signals at τ 4.45 for H-1 (doublet, $J_{1,2} \sim 2.5$ Hz); 6.45–6.57 for H-2 masked by the signal for OCH_3 (narrow multiplet); 4.82–4.92 for H-3 and -4 (multiplet, $J_{2,3} \sim 3$, $J_{4,5} \sim 1.0$ Hz); 5.33–5.45 for H-5 (multiplet); 6.05–5.35 for H-6*exo* and -6*endo* (multiplet, $J_{6exo,\ 6endo} \sim$ 8.5 Hz); 6.48 for OCH_3 (singlet); 7.94 and 8.06, each a singlet for CH_3.

The *third fraction* from the chromatographic separation of the products of osmic acid oxidation of **1** (R = CH_3) in pyridine gave a viscous oil (crude yield, 16.3%) which was distilled in a sublimation apparatus to provide *1,6-anhydro-2-O-methyl*-β-DL-*allopyranose* (**2**, R = CH_3, R′ = H) as a colorless solid, m.p. 99–100°.

Anal. Calcd. for $C_7H_{12}O_5$: C, 47.73; H, 6.87. Found: C, 47.97; H, 6.79.

The i.r. spectrum (film) showed a broad band at 3400 cm^{-1} (OH).

The 100 MHz p.m.r. spectrum in trifluoroacetic acid had signals at τ 4.09 for H-1 (doublet, $J_{1,2} \sim 2.5$ Hz); 6.20–6.33 for H-2 (multiplet, $J_{2,3} \sim 4.0$ Hz); 5.72–5.80 for H-3 and -4 (multiplet, $J_{4,5} \sim 1.2$ Hz); 5.02–5.15 for H-5 (multiplet); 5.95–6.05 for H-6*exo* and -6*endo* (multiplet, $J_{6exo,6endo} \sim 3.0$ Hz); 6.40 for OCH_3 (singlet).

(b) In Dioxane

Compound **1** (R = CH_3) (1.68 g) was treated with osmic acid for 24 h according to the procedure described for the oxidation of **1** (R = H) above. The crude product was a colorless syrup (2.04 g, 98%). The p.m.r. spectrum in deuteriochloroform showed it to be a mixture of **2** (R = CH_3, R′ = H) and **3** (R = CH_3, R′ = H) in the approximate ratio of 4:3. Separation of these compounds was accomplished by column chromatography as for the case of the products of the osmic acid reaction with **1** (R = CH_3) in pyridine above. Overall yield of **2** (R = CH_3, R′ = H), 1.01 g, 49%, and of **3** (R = CH_3, R′ = H) 0.95 g, 46%.

2-O-Methyl-α,β-DL-*allose* (**4**, R = CH_3, R′ = H)

Hydrolysis of 0.8 g of **2** (R = CH_3, R′ = H) by the method used to hydrolyze **2** (R = R′ = CH_3CO) above gave a syrup (crude yield, 0.85 g, 96%) which was purified by column chromatography using chloroform methanol (1:1) as eluent. The resulting viscous oil gave *2-O-methyl*-α,β-DL-*allose* (**4**, R = CH_3, R′ = H) as colorless needles from methanol–ether melting at 111–113°.

Anal. Calcd. for $C_7H_{14}O_6$: C, 43.30; H, 7.27. Found: C, 43.18; H, 7.24.

The 100 MHz p.m.r. spectrum in deuterium oxide, obtained after **4** (R = CH_3, R′ = H) had been in solution for 48 h, showed four anomeric proton signals which indicated the presence in solution of α-furanose and -pyranose as well as the β-furanose and -pyranose structures in the approximate area ratio, at equilibrium, of 1.0:2.6:1.0:11.0 respectively. The spectrum showed signals at τ 4.11 for H-1 (α-furanose isomer, doublet, $J_{1,2} \sim 2.5$ Hz); 4.30 for H-1 (β-furanose isomer, doublet, $J_{1,2} \sim 4.0$ Hz); 4.56 for H-1 (α-pyranose isomer, doublet, $J_{1,2} \sim 4.0$ Hz); 4.87 for H-1 (β-pyranose isomer, doublet, $J_{1,2} \sim 8.0$ Hz); 6.74 for H-2 (β-pyranose, doublet of doublets, $J_{2,3} \sim 3.0$, $J_{1,2} \sim 8.0$ Hz); 5.38 for H-3 (β-pyranose, triplet, $J_{3,4} \sim 3.0$ Hz); 5.16 for OH (broad singlet); 6.42 for OCH_3 (singlet); 5.90–6.20 (complex multiplet for remaining protons).

2-O-Methyl-α,β-DL-*allose Tetraacetate* (**4**, R = CH_3, R′ = CH_3CO)

Acetylation of **4** (R = CH_3, R′ = H) (0.36 g) with acetic anhydride and pyridine as usual gave 0.63 g (98% crude yield) of solid *2-O-methyl*-α,β-DL-*allose tetraacetate* (**4**, R = CH_3, R′ = CH_3CO) which formed colorless needles from dichloromethane–pentane, melting at 125–126°.

Anal. Calcd. for $C_{15}H_{22}O_{10}$: C, 49.72; H, 6.12. Found: C, 49.62; H, 6.08.

The i.r. spectrum in chloroform showed strong absorption at 1755 cm^{-1} (C=O).

The 100 MHz p.m.r. spectrum in deuteriochloroform indicated that the tetraacetate was a single compound, the β-pyranose isomer. The t.l.c. also indicated only one compound. The p.m.r. signals occurred at τ 4.12 for H-1 (doublet, $J_{1,2} \sim 8.0$ Hz); 6.65 for H-2 (quartet, $J_{1,2} \sim 8.0$, $J_{2,3} \sim 3.0$ Hz); 4.18 for H-3 (triplet, $J_{3,4} \sim 3.0$ Hz); 5.00–5.20 for H-4 (multiplet, $J_{4,5} \sim 10$ Hz); 5.60–6.00 for —CH_2— and H-5 (multiplet); 6.61 for OCH_3 (singlet); 8.15 and 8.20 each a singlet for CH_3; 8.07 a singlet for two CH_3.

2-O-Methyl-α,β-DL-*galactose* (**5**, R = CH_3, R′ = H)

Hydrolysis of 0.8 g of **3** (R = CH_3, R′ = H) with 15 ml of 1 *N* hydrochloric acid containing 5 ml of dioxane according to the procedure for the hydrolysis of **2** (R = R′ = CH_3CO) gave *2-O-methyl*-α,β-DL-*galactopyranose* (**5**, R = CH_3, R′ = H) as a syrup. Purification by column chromatography, using methanol–chloroform (1:2) as eluent, produced a solid which crystallized from ethanol–ether as colorless prisms melting at 140–141°; yield, 695 mg, 80%.

Anal. Calcd. for $C_7H_{14}O_6$: C, 43.30; H, 7.27. Found: C, 43.27; H, 7.04.

The 100 MHz p.m.r. spectrum in deuterium oxide was identical to that of an authentic sample of 2-*O*-methyl-α,β-D-galactopyranose in the same solvent.

We are grateful to the National Research Council of Canada for financial support which assisted us in the pursuit of this work. We thank Professor S. J. Angyal of the University of New South Wales, Kensington, N.S.W., Australia for the p.m.r. spectrum of α,β-D-allose and Professor R. U. Lemieux and Dr. T. L. Nagabhushan of this Department for a sample of 2-*O*-methyl-α,β-D-galactose.

1. U. P. SINGH and R. K. BROWN. Can. J. Chem. **48**, 1791 (1970).
2. F. SWEET and R. K. BROWN. Can. J. Chem. **46**, 2289 (1968).
3. J. S. BARAN. J. Org. Chem. **25**, 257 (1960).
4. D. H. R. BARTON and DOV ELAD. J. Chem. Soc. 2085 (1955).
5. S. J. ANGYAL and V. A. PICKLES. Carbohyd. Res. **4**, 269 (1967).
6. V. SRINIVASAN. Ph.D. Thesis. University of Western Ontario, London, Ontario, 1968.
7. H. B. HENBEST. Proc. Chem. Soc. 159, (1963).
8. R. CRIEGEE, B. MARCHAND, and H. WANNOWIUS. Ann. Chem. **550**, 99 (1942).
9. M. L. WOLFROM, J. N. SCHUMACHER, H. S. ISBELL, and F. L. HUMOLLER. J. Amer. Chem. Soc. **76**, 5816 (1956).
10. D. J. BELL and E. BALDWIN. Nature, **146**, 559 (1940).
11. E. O. LIPPMANN. Ber. **55**, 3038 (1922).
12. U. E. DINER, F. SWEET, and R. K. BROWN. Can. J. Chem. **44**, 1591 (1966).

Can. J. Chem. Downloaded from www.nrcresearchpress.com by 210.87.254.105 on 09/05/12
For personal use only.

Can. J. Chem. Downloaded from www.nrcresearchpress.com by 210.87.254.5 on 09/05/12
For personal use only.

Radiation Effects with a Model Lipid Membrane[1]

A. PETKAU

Medical Biophysics Section, Whiteshell Nuclear Research Establishment, Atomic Energy of Canada Limited, Pinawa, Manitoba

Received November 16, 1970

A cell is described that permits a model phospholipid membrane and the two adjacent aqueous compartments to be irradiated with a collimated beam of X-rays. During a 2 h irradiation a marked increase in $[H^+]$ in the aqueous phases is observed. A protonmotive force, given by the H^+ Nernst potential, is generated when one compartment only is irradiated or when both compartments separated by a membrane made structurally asymmetric by the adsorption of alamethicin, are irradiated equally.

The results of irradiations in N_2O, N_2, and O_2 indicate that the membrane scavenges the superoxide O_2^-. The effect is discussed in terms of a clearing field that is derived from the potential at the membrane interfaces.

La cellule décrite permet d'irradier une membrane phospholipidique modèle et ses deux compartiments aqueux par un faisceau de rayons-x munie d'un collimateur. Durant les deux heures d'irradiation, une augmentation marquée en $[H^+]$ a été observée dans les phases aqueuses. Une force protomotrice, obtenue par le H^+ du potentiel de Nernst, est générée quand un compartiment seulement est irradié ou lorsque les deux compartiments, séparés par une membrane structurellement a symétrique constituée d'alaméthicine, sont également irradiés.

Les résultats des irradiations dans le N_2O, N_2, et O_2 indiquent que la membrane élimine le superoxyde O_2^-. L'effet est discuté en terme de l'éclaircissement du champ obtenu par la différence de potentiel aux interfaces de la membrane.

Canadian Journal of Chemistry, 49, 1187 (1971)

Introduction

The response of irradiated membrane systems has been of interest over a considerable number of years (1–4) but the properties examined are few. Among the functional properties studied, radiation-induced permeability changes to ions have received much attention (3–8). They have been mimicked with agents known to react with sulfhydryl groups (9, 10) or largely prevented by the radioprotective action of cystamine, a compound known to react with the hydrogen atom (H•), hydroxyl radical (•OH), and possibly with the superoxide radical (O_2^-) at near neutral p*H* (11). Significantly, the radioprotective effect of cystamine was observed even if it were largely unbound to the irradiated membranes. This suggests that the compound reacts with the radicals, formed in the radiolysis of the extracellular water, before they reach the membrane surface to react with it.

The ability to scavenge radicals from a distance raises the interesting possibility that the membrane may influence which radicals reach it preferentially. The derivative force associated with the potential of membrane interfaces may exert an effect in this regard as far as any charged radicals are concerned. Of the radicals generated during the radiolysis of aerated water that are known to react with sulfhydryl groups, namely H•, •OH, the hydrated electron (e_{aq}^-), and O_2^- (12), only the latter two might conceivably be influenced in this manner. Since the potential of the interface nearest the bulk aqueous phase is positive (13) these radical anions may be accelerated toward the membrane, thus overcoming a limitation of diffusion-controlled reactions. By virtue of its property of acting over a distance, the membrane-associated electric field may be expected to produce an amplified effect not seen otherwise. In this communication irradiation experiments at near neutral p*H* on a model phospholipid membrane – water system are described and the observed p*H* changes are explained in terms of electric field effects on the charged free radicals produced during the radiolysis of water.

[1]A.E.C.L. Contribution No. 233/70.

Experimental Procedure

Irradiation Cell

The cell in which the membrane was irradiated is shown in Fig. 1. It consisted of two square compartments, each 1 cm deep and containing approximately 10 ml of double distilled water, separated by a 0.16 cm thick Teflon septum. At a level of 0.6 cm from the surface of the water a 0.2 cm diameter aperture for membrane location was milled in a portion of the septum thinned to a thickness of 0.013 cm. Each compartment was fitted with a combination p*H* electrode in a position that was well removed from the collimated direct X-ray beam. LiF

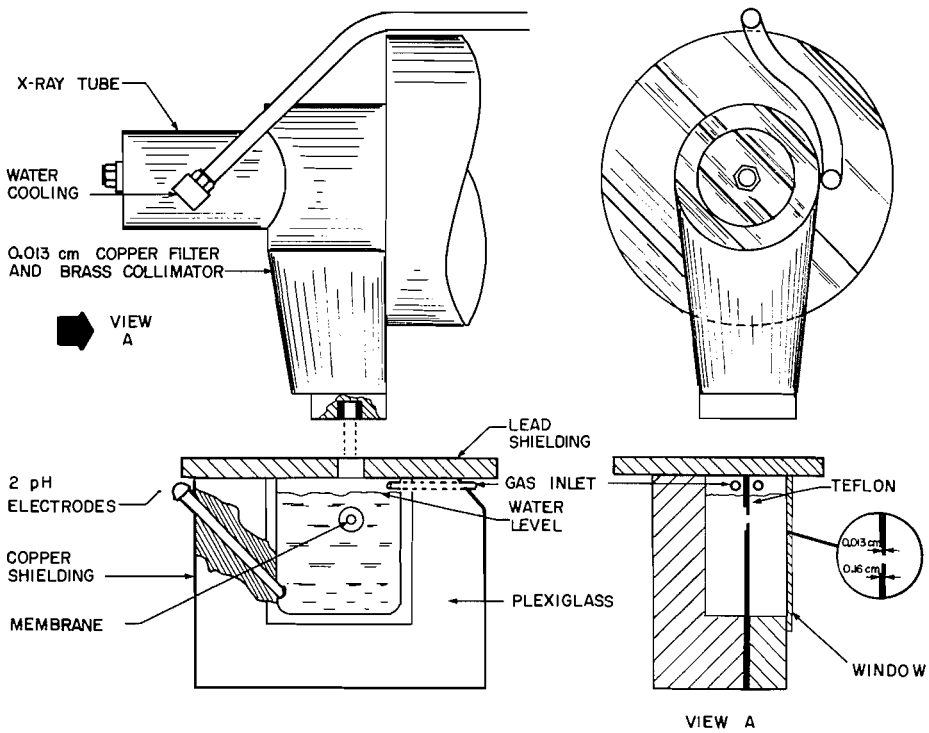

FIG. 1. Apparatus for irradiating a model phospholipid membrane.

dosimetry at the position of the p*H* bulbs indicated that a dose rate of 0.7 rad/min occurred at the electrodes from scattered radiation. Calibration measurements made with standard p*H* solutions before and after a 2 h irradiation showed that the performance of the electrodes was not measurably affected. The cell and the electrodes were fitted into a copper case that was grounded electrically. The copper case had two small rectangular openings, one over the window, so that the membrane could be observed through a low power microscope (not shown), and the other over that part of the top where the X-ray beam entered the cell through a suitable hole in a 0.63 cm thick lead shield. The cell was aligned with the X-ray tube in a position that ensured that the membrane aperture lay in the path of the collimated beam. The temperature of the water in the cell was kept at 37 °C by means of the heating stage (not shown) that supported it. A large, light-tight lead box was built around the X-ray tube and irradiation cell.

Membrane Formation

The composition of the phospholipid extract has been described previously (14). The reactivity of chloroform and methanol with the primary radicals produced in the radiolysis of water can be substantial (15) and for this reason the use of a chloroform–methanol solvent system was avoided. Instead, 15–19 mg of the phospholipid extract was dissolved in the apolar hydrocarbon, tetradecane, to form the membrane solution. The solution was applied under water to the aperture with a fine sable-hair brush as previously described (16). The black, bimolecular phospholipid membrane then developed in due course by a thinning process (16).

Membrane Irradiation

As shown in Fig. 1 radiation was obtained from a water-cooled X-ray tube (100 KVP, 9.5 mA, 0.013 Cu filter, half-value layer 0.38 cm water, and brass collimator) positioned directly above the membrane. The dose rate at the surface of the water for a source-target distance of 8.4 cm was 500 rad/min and corresponded to a dose rate of about 130 rad/min in the water at a level opposite the center of the membrane. The thin membrane (~100 Å) was partially protected from the direct beam by an intervening portion of the much thicker Teflon septum for which an attenuation factor of 19.5 was calculated. Therefore, the estimated dose rate at the geometric center of the membrane from the direct beam was reduced to about 26 rad/min. The actual dose rate would be somewhat higher because of scattered radiation distributed in and about the membrane. Nevertheless, the difference by a factor of 5 in the dose rates to the water at the level of the geometric center of the membrane and the membrane itself would be maintained to a first approximation since it is due to the attenuation of the direct beam in the Teflon septum. The difference was desirable because it permitted the production of primary radicals from the radiolysis of water in numbers adequate for an effect to be observed and spared the membrane to a certain degree from the direct effects of radiation.

Can. J. Chem. Downloaded from www.nrcresearchpress.com by 210.87.254.5 on 09/05/12
For personal use only.

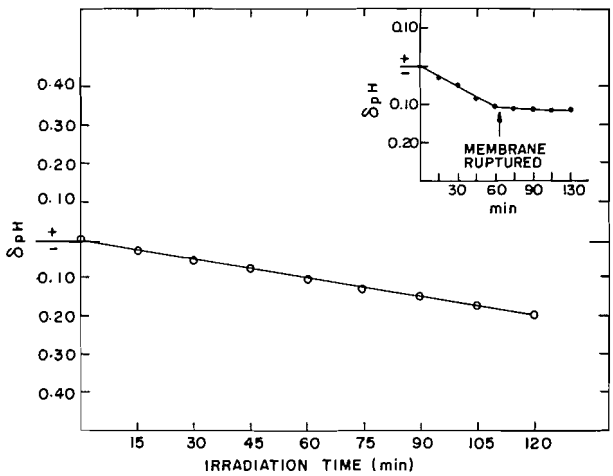

FIG. 2. Decrease in p*H* of aerated water in either compartment during a 2 h irradiation in the presence of a phospholipid membrane. Both compartments irradiated equally. *Inset*: Decrease in p*H* of aerated water in either compartment during a 2 h irradiation. The membrane ruptured at the 63 min mark.

In addition, collimation of the beam directed much of the radiation energy into a column of water nearest the membrane. Distribution of the H^+ by diffusion throughout the aqueous phase was permitted and may have produced a dilution effect. The absence of stirring was intentional in order to avoid interference with diffusion patterns set up naturally in the presence and absence of the membrane.

pH Measurement

During an irradiation the p*H* measurements were made every 15 min to a precision of 0.001 p*H*. The high resistance of the membrane ($\sim 10^{10}$ ohms) largely isolated the two aqueous compartments electrically and permitted the use of the two reference electrodes for the detection of any transmembrane potentials. A multi-pole switching arrangement was used to connect the two reference electrodes as desired to an electrometer amplifier (input resistance 10^{14} ohms) for the voltage measurements.

Results

Most of the irradiations were carried out on membranes formed by the first application of the lipid solution. In some duplicate runs the membrane formed after the second or third application was used but the change in p*H* was the same. As Fig. 2 shows, irradiation of the phospholipid membrane – water system produced in either aqueous compartment a linear decrease in p*H* with dose. Since the p*H* of both compartments was constant prior to irradiation the change is significant and indicates a first order reaction. It is equivalent to a net production of approximately 10^{15} H^+ and is about an order of magnitude greater than the total number of phospholipid and cholesterol molecules in the membrane. It seemed unlikely, therefore, that the change in p*H* was caused by radiation effects within the membrane.

An alternative explanation that the excess lipid material, left on the Teflon septum or in the aqueous phases, produced the change in p*H* was discounted for the following reasons. When a membrane was formed in the usual way and then ruptured prior to irradiation a different result was obtained. In this situation, as well as others, where two, three, or more dozens of membranes were formed and ruptured, the p*H* decreased at first and then increased, Fig. 3, in a manner that closely paralleled the p*H* response of aerated water, irradiated at the same dose rate.

Additional support was obtained by shielding about half the thickness of the septum and all of one aqueous compartment from the direct beam. In this situation the membrane and the shielded compartment received scattered radiation only and as Fig. 4 shows, the p*H* change in the two compartments was quite different. In the compartment exposed to the direct beam the p*H* change was similar to the result shown in Fig. 2 and was much more marked than in the other compartment which received scattered radiation only. The H^+ concentration gradient ΔpH generated across the membrane by the unequal radiation field gave rise to a trans-

Can. J. Chem. Downloaded from www.nrcresearchpress.com by 210.87.254.5 on 09/05/12
For personal use only.

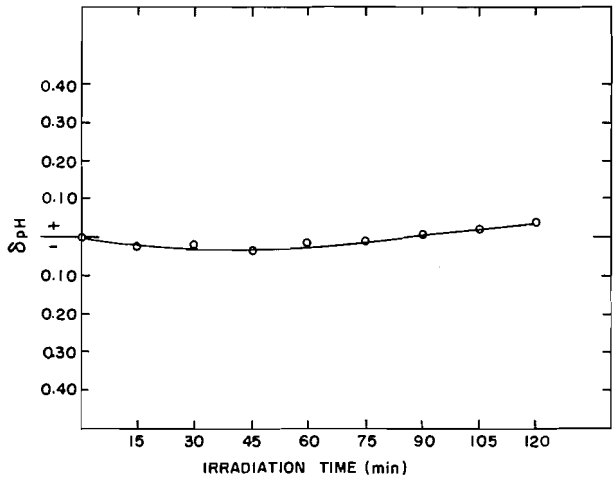

FIG. 3. Change in pH of aerated water in either compartment during a 2 h irradiation in the presence of phospholipid material left from rupturing one or more membranes prior to irradiation.

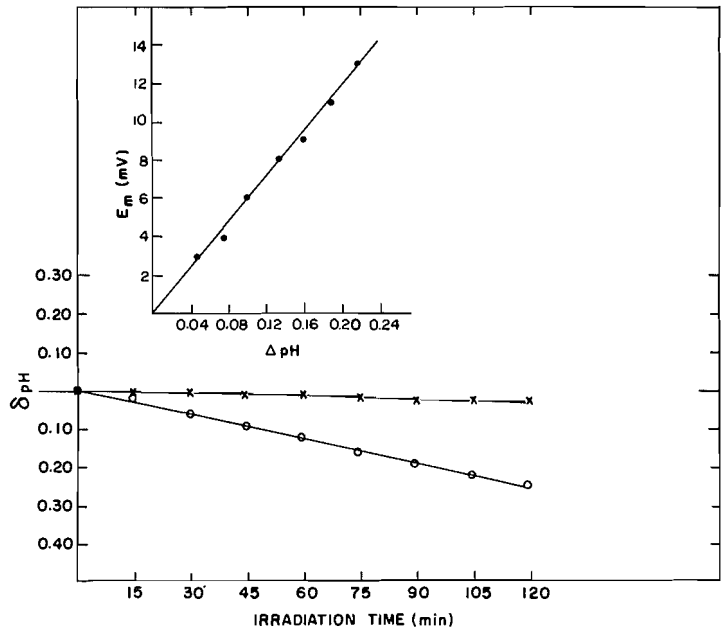

FIG. 4. Change in pH of aerated water in the irradiated (o--o) and shielded (x--x) compartments in the presence of a phospholipid membrane. *Inset*: Nernst potential (E_m) *vs.* the H^+ concentration gradient (ΔpH) that developed across the membrane during the unequal irradiation of the two aqueous compartments. E_m/pH unit = 60 mV.

membrane potential, E_m, as shown in the inset of Fig. 4. From the slope of the line, E_m/pH unit = 60 mV, a value for the H^+ Nernst potential that is satisfactorily close to the expected at 37 °C.

Finally, some membranes ruptured in the course of a 2 h irradiation. It was found that the decrease in pH changed abruptly once the membrane collapsed (Fig. 2, inset). The result confirms that the decrease in pH is due to the presence of the membrane and that it does not depend on any lipid material, sorbed to the Teflon septum or dispersed in the aqueous phases.

The composition of the phospholipid membrane may readily be altered by the adsorption

Can. J. Chem. Downloaded from www.nrcresearchpress.com by 210.87.254.5 on 09/05/12
For personal use only.

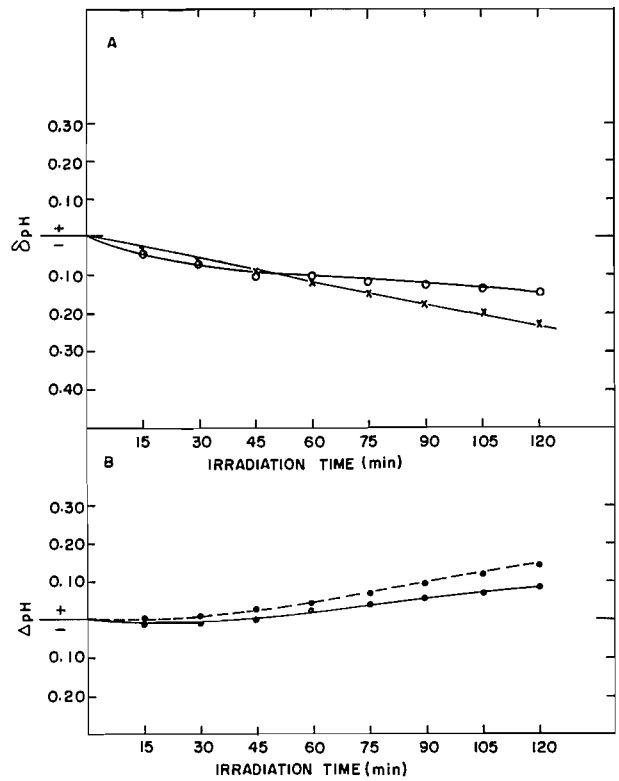

FIG. 5. (A) Change in pH of aerated water on the modified (o--o) and unmodified (x--x) side of a phospholipid membrane. The membrane was modified on one side with alamethicin (2×10^{-8} g/ml) and both sides were irradiated equally.

(B) The ΔpH (solid line) across the membrane obtained by plotting the difference between the two graphs of Fig. 5A. Positive values of ΔpH indicate δpH (modified side) < δpH (unmodified side). The ΔpH (broken line) corrected for effect on δpH of unbound alamethicin.

of a water-soluble cyclopeptide. If it is added to one aqueous compartment only, a structurally asymmetric membrane may be formed. Equal irradiation of both aqueous phases may then show up a differential effect on pH. Figure 5A shows the result of such an experiment. It is seen that the change in pH of the water on the side modified with alamethicin[2] is quite different from that on the unmodified side. The resultant pH gradient across the membrane is shown in Fig. 5B, solid line, where (+) values of ΔpH indicate the decrease in pH on the modified side was smaller than that on the other. It may be adjusted for the effect on pH of unavoidably irradiating the residual unbound alamethicin in solution. The corrected ΔpH, shown in Fig. 5B, broken line, is substantial and further emphasizes a role for the membrane interfaces in mediating the radiation-induced reactions.

Taken together the results of Figs. 2–5 suggest that the radiation-induced reactions in the aqueous phase were influenced in some way by the organization of the phospholipid material into a membrane. Following the initial ionization by radiation, the major radiochemical reactions in aerated water involve $\cdot OH$, H_3O^+, and e_{aq}^- (18). H_2O_2 and O_2^- are subsequently produced by reactions 1 and 2, respectively (15, 19). In addition, the hydrated electron may react with itself or with $\cdot OH$, $H\cdot$, H_2O_2, and H_2O to produce OH^- (15, 19). Except for the case of H_2O, the rate constants of these reactions are

[1] $$\cdot OH + \cdot OH \rightarrow H_2O_2$$

[2] $$e_{aq}^- + O_2 \rightarrow O_2^-$$

[2]Alamethicin, a cyclopeptide antibiotic derived from Trichoderma viride, was kindly made available by the UpJohn Company of Canada. Its amino acid composition has been given (17) as $(GluN)_2(Glu)_1(Pro)_2(Gly)_1$-$(Ala)_2(Dimethyl\ ala)_8(Val)_2(Leu)_1$. The amount added was 2×10^{-8} g/ml.

Can. J. Chem. Downloaded from www.nrcresearchpress.com by 210.87.254.5 on 09/05/12
For personal use only.

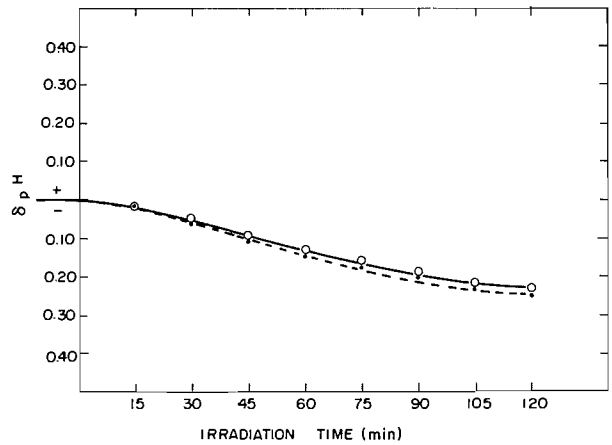

FIG. 6. The radiation-induced pH change in N_2-saturated water in the presence (solid line) and absence (broken line) of a phospholipid membrane.

within the diffusion-controlled range (15, 20). To account for the observed net production of H^+ in the presence of the membrane one might consider that a large number of OH^- was sorbed to the membrane or that the H_2O_2, generated by reaction 1, was responsible. The first possibility requires the membrane to sorb an inordinate number of OH^- (to a concentration of about 50 M) and may therefore be discounted. The second alternative can also be excluded because the addition of H_2O_2 to the aqueous phase in an amount 10^3 times that generated over the course of a 2 h irradiation decreased the pH by only 0.03 of a unit. Therefore, another explanation appears to be required, namely that the membrane affects the production of OH^- in the aqueous phase.

The results shown in Figs. 2–5 were obtained in aerated water and may be complicated by reactions involving O_2 and CO_2. These difficulties are obviated by saturating the water at 1 atm with nitrogen or nitrous oxide. The irradiation data are shown in graphical form in Figs. 6 and 7, respectively. They represent well-known results from the radiation chemistry of water (19, 21) and demonstrate the absence of a membrane effect if no oxygen is present.

In oxygen saturated water the e_{aq}^- reacts rapidly with O_2 by reaction 2 to form the superoxide radical anion O_2^-. Figure 8 shows the result obtained in this situation both with and without the membrane. The decrease in pH is significantly less in the absence of the membrane than in its presence. For instance, the probability that the difference between the two points, corresponding to an irradiation time of 75 min, might have occurred by chance is less than 0.001. The greater decrease in pH in the presence of the membrane may be accounted for if it is considered that the O_2^- is scavenged by the membrane. On this basis reaction 3 (22) would

$$[3] \qquad O_2^- + \cdot OH \rightarrow OH^- + O_2$$

be competitively inhibited, resulting in a decrease in the relative number of OH^- produced. Reaction 3 is fairly fast ($8.0 \times 10^9\ M^{-1}\ s^{-1}$) suggesting that the O_2^- scavenging activity of the membrane must also be quite fast to be competitive.

Discussion

Diffusion of the O_2^- radical to the phospholipid membrane must be one of the first factors to be considered as a basis for the effect of the membrane on the pH during irradiation. The distance over which the radical will diffuse by random walk is determined by its half-life and its diffusion constant. For the case of O_2^- in oxygenated water at near neutral pH (6.65) its half-life may be estimated to be 28 ms (23). The

TABLE 1. Root mean square diffusion distance (χ) within one half-life by random walk

Radical	Half-life (ms)	Diffusion constant (cm^2/s)	χ (μm)
O_2^-	28*	1.59×10^{-5}†	4.5

*In oxygenated water at pH 6.65 (ref. 23).
†Calculated for 21 °C from the mobility given in ref. 22.

Can. J. Chem. Downloaded from www.nrcresearchpress.com by 210.87.254.5 on 09/05/12
For personal use only.

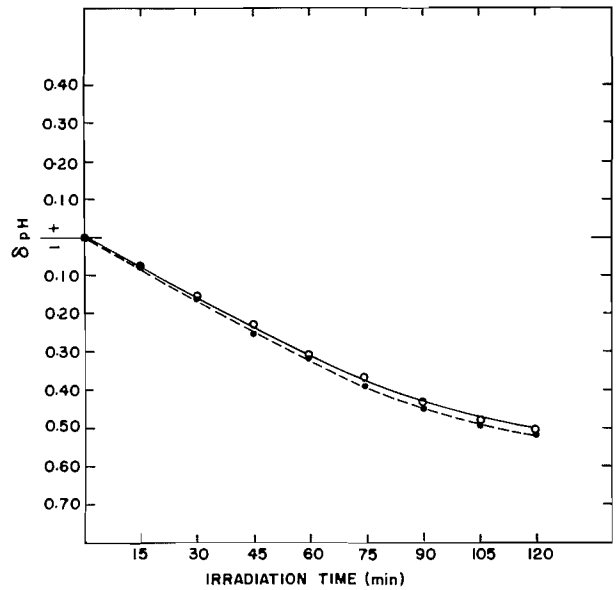

FIG. 7. The radiation-induced pH change in N_2O-saturated water in the presence (solid line) and absence (broken line) of a phospholipid membrane.

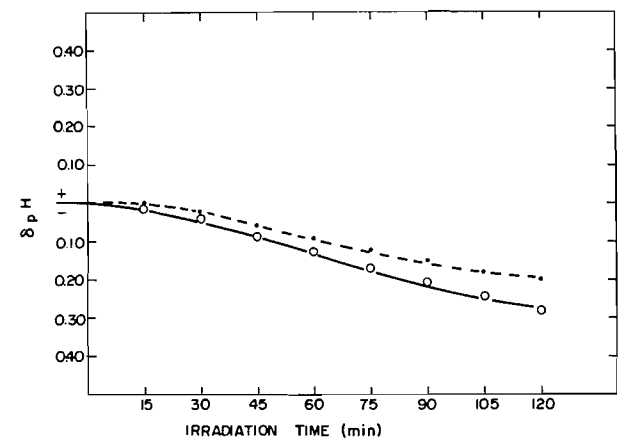

FIG. 8. The radiation-induced pH change in O_2-saturated water in the presence (solid line) and absence (broken line) of a phospholipid membrane.

diffusion constant of O_2^- may be calculated from its known mobility (22) and is equal to 1.59×10^{-5} cm^2/s at 21 °C. The root mean square diffusion distance of O_2^- by random walk for $P(t) \geqslant 0.99$, where $P(t)$ is the probability that the particular O_2^- still exists after one half-life, is then 4.5 μm, Table 1. If the diffusion distance is measured in a direction perpendicular to the plane of the membrane then it signifies the depth of the layer of water, adjacent to the membrane, from which the radicals may reach it within one half-life by diffusion. Although the calculated diffusion distance is substantial, it appears to be insufficient to account for the net production of H^+, indicated by the decrease in pH in Figs. 2 and 8. This is true if all the O_2^- generated within this distance of the membrane, diffused to it and reacted with it in a manner that produced neither H^+ or OH^-. From geometric and statistical considerations, however, it is clear that not all the radicals within the layer will reach the mem-

Can. J. Chem. Downloaded from www.nrcresearchpress.com by 210.87.254.5 on 09/05/12
For personal use only.

Can. J. Chem. Downloaded from www.nrcresearchpress.com by 210.87.254.5 on 09/05/12
For personal use only.

brane since at least an equal number must be expected to diffuse in the opposite direction under the experimental conditions. The thickness of the water layer can, of course, be readily increased at the expense of decreasing the value of $P(t)$.

The number of charged radicals, such as O_2^-, that reach the membrane from a given distance may be increased by introducing a clearing field. The derivative force of the potential associated with phospholipid membrane interfaces may serve in this capacity. The interface potential for an idealized phospholipid membrane has been described (13) and it was shown to be strongly positive in a plane near the aqueous phase and in fact extended into it for a considerable distance, especially in distilled water when ionic screening is minimal. From the equation $v = E\mu$, where v = velocity of the charged species in an electric field (cm/s), E = electric field (V/cm), and μ = mobility of the charged species ($cm^2/V\ s$), the range of the charged species within one half-life may be calculated if the potential, from which the electric field is derived, is known as a function of distance into the aqueous phase. In Table 2 the results of these calculations are tabulated for O_2^-, assuming that the potential to a first approximation falls off exponentially at rates given by the halving distances in the first column. A half-life of 28 ms for O_2^- was taken as being appropriate for the experimental conditions (23) and its mobility at 21 °C has been given as $65^{\pm 8}$ cm^2 $ohms^{-1}$ (22), which converts to a value of 0.67×10^{-3} $cm^2/V\ s$.

Although the maximum range as given in Table 2 is larger than the diffusion distance over the same period of time (Table 1) the most important difference is that the range defines the thickness of the water layer nearest the membrane within which most of the O_2^- generated are collected at the membrane. The collection efficiency is therefore much improved over the diffusion case, considered earlier, where at least half of the number generated will diffuse away from the membrane. The range may be extended by increasing the number of half-lives considered in the calculation.

TABLE 2. Effect of membrane interface potential on the range of the superoxide radical (O_2^-) within one half-life

Halving distance for interface potential (cm)	Electric field $E = d\psi/dx$* (V/cm)	Range (μm) O_2^-
10^{-6}	2.1×10^4	0.20
10^{-5}	2.1×10^3	1.24
10^{-4}	2.1×10^2	5.78
10^{-3}	21	6.25
10^{-2}	2.1	0.77

*The interface potential $\psi = \psi_0 e^{-x/a}$, where $\psi_0 = 60$ mV, the potential at the membrane interface ($x = 0$), x = perpendicular distance from the membrane and a = attenuation constant.

As shown in Table 2 the electric field within a short range of the membrane is large enough to act effectively as a clearing field (24) for O_2^-. It suggests an explanation for the membrane effect on pH when the irradiation occurs in oxygen-saturated water.

In O_2, reactions 2, 3, and 4 are important.

$$[4] \quad O_2^- + O_2^- \xrightarrow{2H_2O} H_2O_2 + O_2 + 2OH^-$$

Reaction 2 is fast (19) ensuring that virtually all the e_{aq}^- are converted to O_2^-. Inhibition of reaction 3 ($k_3 = 8.0 \times 10^9\ M^{-1}\ s^{-1}$ (22)) in the aqueous phase by virtue of the clearing field concentrating O_2^- near the membrane might favor reaction 4. However, reaction 4 is fairly slow ($k_4 = 1.7 \times 10^7\ M^{-1}\ s^{-1}$ (22, 25)) and might conceivably be inhibited by a suitably fast reaction of O_2^- with the membrane, *e.g.* electron transfer. The overall production of OH^- would then be reduced and, in principle, account for the membrane effect on pH observed in Fig. 8. The mechanism suggested is relevant to the pH change observed in aerated water (Figs. 2 and 3) although the presence of carbon dioxide adds to the number of reactions to be considered.

The ion clearing effect of the membrane electric field is suggested by data obtained during the irradiation of a black phospholipid membrane in a dilute aqueous solution of silver nitrate (work in progress). Following a short period of irradiation the membrane developed a speckled appearance due to the deposition of particles that possessed the lustre and reflectance of silver. The heaviest deposit was obtained in N_2-saturated water while in aerated or O_2-saturated water the deposit was about equal. The result is of interest for several reasons. In N_2-saturated water Ag^+ was reduced by the hydrated electron (26) which, as it can be shown, was not generated in sufficient numbers within the membrane to lead to a visible deposit of silver. Therefore, either the Ag^+ was reduced in the aqueous phase and then sorbed to the mem-

Can. J. Chem. Downloaded from www.nrcresearchpress.com by 210.87.254.5 on 09/05/12
For personal use only.

brane by a non-electrostatic process or the Ag^+, sorbed to the membrane as an ion (13), was reduced *in situ*. The second alternative seems favored but implies that the e_{aq}^- was collected at the membrane. In O_2-saturated water the situation is similar except that the reduction of Ag^+ would involve the redox couple,

$$\begin{aligned} Ag &\rightarrow Ag^+ + e & E_{Ag,Ag^+} &= -0.799\ V \\ O_2^- &\rightarrow O_2 + e & E_{O_2^-,O_2} &= +0.56\ V \\ Ag^+ + O_2^- &\rightarrow Ag + O_2 & E_{cell} &= 0.239\ V \end{aligned}$$

which has a favorable total cell emf of 0.239 V (27, 28).

The clearing effect of the membrane electric field is operative only under conditions where there exists a non-equilibrium distribution of ions or a varying electric field derived from a changing interface potential or from a variable degree of ionic screening. The p*H* measurements indicate that a non-equilibrium distribution of ions was established during the irradiation and because of the collection and possible sorption to the membrane of some of them the electric field may have varied as well (13). In this respect, reactions of the collected ions, such as O_2^- and the e_{aq}^-, with components of the membrane is of much interest but no experimental information on this point is available for model phospholipid membranes. Potential energy field calculations have shown that ethanolamine interacts more strongly with anions than does choline (29) suggesting that the phospholipid, phosphatidylethanolamine, may be one of the more reactive components.

The miniscule size of the membrane ($\sim 10^{-8}$ g), relative to the volume of water affected ($\sim$10 ml on either side), implies an amplification factor in the mediation effect that one might associate with a physical force, such as an electric field, acting over a distance. Inasmuch as the electric field arises from the structural organization within the membrane it is not a property of the constituent molecules *per se* and emphasizes the need to heed structure in evaluating the radiation effects observed. An interesting illustration, relevant to the phospholipid membrane considered here, is the large increase in the rate of radiolysis of sodium linoleate at critical micelle concentrations (30).

In a biological cell, ionic screening and other factors would reduce the interface potential halving distances considered in Table 2 and limit the effective electric field to perhaps a few hundred ångströms from the membrane (13). The range for O_2^-, as calculated in Table 2, would be correspondingly reduced. However, the collection of the radical anions at membranes may, nevertheless, be significant in a cell of normal size because of their general distribution within the cytoplasmic space. Important reactions with membrane constituents may then ensue. Notable in this regard is the change in the erythrocyte membrane, affecting monovalent cation permeability, following the alteration of sulfhydryl groups (31). A short chain reaction has been described to account for the high rate of disappearance of sulfhydryl groups in oxygenated aqueous solutions at neutral p*H* (12). The fact that both O_2^- and O_2 are used up in the proposed reaction scheme is of additional interest because it suggests a basis for the oxygen depletion effect on survival of irradiated bacteria (32). Furthermore, the estimated lifetime of 10 ms for the oxygen-sensitive species suspected to be induced within the irradiated cell (32) is not inconsistent with O_2^- being that oxygen-sensitive species. The obvious implications for radiation effects on the DNA replication system, associated with the bacterial cell membrane (33, 34), appear not to have been investigated. Indeed, the general lack of information on reactions involving O_2^- and biological components is surprising, particularly in view of the widespread radiosensitizing effect of oxygen.

The technical assistance of W. S. Chelack is acknowledged. Appreciation is also expressed to Dr. Alberta B. Ross, Radiation Chemistry Data Center, University of Notre Dame, Notre Dame, Indiana, for information on reactions with O_2^-; to Dr. Klaus Schmidt, Argonne National Laboratory, Argonne, Illinois, for information on O_2^- mobility; and to Mrs. H. G. Hamel, Information Services, A.E.C.L., for locating reference material. The helpful discussions with Drs. R. S. Dixon, J. A. Raleigh, and A. Sawatzky are gratefully acknowledged.

1. F. Lehmann and P. Wels. Pflügers Arch. Ges. Physiol. **213**, 628 (1926).
2. T. P. Ting and P. Zirkle. J. Cellular Comp. Physiol. **16**, 197 (1940).
3. C. W. Sheppard and M. Stewart. J. Cell. Comp. Physiol. **39**, Suppl. **2**, 189 (1952).
4. B. D. Stuart and J. N. Stannard. Radiat. Res. **34**, 459 (1968).
5. C. W. Sheppard and G. E. Beyl. J. Gen. Physiol. **34**, 691 (1951).
6. G. Cividalli. Radiat. Res. **20**, 564 (1963).
7. B. Shapiro, G. Kollmann, and J. Asnen. Radiat. Res. **27**, 139 (1966).
8. F. Bresciani, F. Auricchio, and C. Fiore. Biochem. Biophys. Res. Commun. **8**, 492 (1962).

9. R. M. SUTHERLAND, J. N. STANNARD, and R. I. WEED. Int. J. Radiat. Biol. **12**, 551 (1967).
10. G. KOLLMANN, B. SHAPIRO, and D. MARTIN. Radiat. Res. **37**, 551 (1969).
11. G. G. JAYSON, T. C. OWEN, and A. C. WILBRAHAM. J. Chem. Soc. (B), 944 (1967).
12. J. E. PACKER and R. V. WINCHESTER. Can. J. Chem. **48**, 417 (1970).
13. C. J. GILLESPIE. Biochim. Biophys. Acta **203**, 47 (1970).
14. A. PETKAU and W. S. CHELACK. Biochim. Biophys. Acta, **135**, 812 (1967).
15. M. ANBAR and P. NETA. Intern. J. App. Radiat. and Isotopes, **18**, 493 (1967).
16. P. MUELLER, D. O. RUDIN, H. T. TIEN, and W. C. WESCOTT. Circulation, **26**, 1167 (1962).
17. C. E. MEYER and F. REUSSER. Experientia **23**, 85 (1967).
18. J. K. THOMAS. *In* Radiation research. *Edited by* G. Silini. North-Holland Publishing Company, 1967. p. 180.
19. A. KUPPERMAN. *In* Radiation research. *Edited by* G. Silini. North-Holland Publishing Company, 1967. p. 220.
20. E. J. HART. Ann. Rev. Nucl. Sci. 125 (1965).
21. K. H. SCHMIDT and S. M. ANDER. J. Phys. Chem. **73**, 2846 (1969).
22. G. BECK. Int. J. Radiat. Phys. Chem. **1**, 361 (1969).
23. J. RABINI and S. O. NIELSEN. J. Phys. Chem. **73**, 3736 (1969).
24. W. F. SCHMIDT and A. O. ALLEN. Sci. **160**, 301 (1968).
25. G. CZAPSKI and L. M. DORFMAN. J. Phys. Chem. **68**, 1169 (1964).
26. J. H. BAXENDALE, E. M. FIELDEN, and J. P. KEENE. *In* Pulse radiolysis. *Edited by* M. Ebert, J. P. Keene, A. J. Swallow, and J. H. Baxendale. Academic Press, New York, N.Y., 1965. p. 207.
27. J. V. PETROCELLI. *In* The Encyclopaedia of electrochemistry. Vol. 1. *Edited by* C. A. Hampel. Reinhold, New York, N.Y., 1964. p. 511.
28. W. M. LATIMER. The oxidation states of the elements and their potentials in aqueous solutions. 2nd Edition, Prentice-Hall, Inc., Englewood Cliffs, N.J. 1952. p. 339.
29. J. E. ZULL and A. J. HOPFINGER. Sci. **165**, 512 (1969).
30. J. M. GERBICKI and A. O. ALLEN. J. Phys. Chem. **73**, 2443 (1969).
31. B. SHAPIRO and G. KOLLMANN. Radiat. Res. **34**, 335 (1968).
32. E. R. EPP, H. WEISS, and A. SANTOMASSO. Radiat. Res. **34**, 320 (1968).
33. R. KNIPPERS and W. STRÄTLING. Nature, **226**, 713 (1970).
34. D. W. SMITH, H. E. SCHALLER, and F. J. BONHOEFFER. Nature, **226**, 711 (1970).

Can. J. Chem. Downloaded from www.nrcresearchpress.com by 210.87.254.5 on 09/05/12
For personal use only.

New Synthesis of Columbianetin and Related Coumarins[1]

WARREN STECK
National Research Council of Canada, Prairie Regional Laboratory, Saskatoon, Saskatchewan
Received September 17, 1970

2,4-Dihydroxy-3-(3-methyl-2-butenyl)benzaldehyde was obtained from 2,4-dihydroxybenzaldehyde with either 3-hydroxy-3-methyl-1-butene or 1-bromo-3-methyl-2-butene. Oxidation of the product in neutral medium with *m*-chloroperoxybenzoic acid gave (±)-2,3-dihydro-2-(1-hydroxy-1-methylethyl)-4-hydroxybenzofuran-5-aldehyde, whose condensation product with malonic acid was (±)-3-carboxycolumbianetin. Oxidation in acidic medium gave (±)-2,2-dimethyl-3,5-dihydroxybenzopyran-6-aldehyde, whose condensation product with malonic acid was (±)-3-carboxylomatin. (±)-Columbianetin and (±)-lomatin were obtained by decarboxylation.

Le dihydroxy-2,4 (méthyl-3 butènyl-2)-3 benzaldéhyde est obtenu par réaction du dihydroxy-2,4 benzaldéhyde avec soit l'hydroxy-3 méthyl-3 butène-1 ou le bromo-1 méthyl-3 butène-2. L'oxydation de ce produit par l'acide *m*-chloroperbenzoique en milieu neutre conduit au (±)-dihydro-2,3 (hydroxy-1 méthyl-1 éthyl)-2 hydroxy-4 benzofuraldéhyde-5 qui par condensation avec l'acide malonique fournit la (±)-carboxy-3 columbianétine. L'oxydation en milieu acide donne le (±)-diméthyl-2,2 dihydroxy-3,5 benzopyrannealdéhyde-6 qui par condensation avec l'acide malonique conduit à la (±)-carboxy-3 lomatine. La (±)-columbianétine et la (±)-lomatine sont obtenues par décarboxylation.

Canadian Journal of Chemistry, 49, 1197 (1971)

Can. J. Chem. Downloaded from www.nrcresearchpress.com by 210.87.254.40 on 09/05/12
For personal use only.

Introduction

Columbianetin (**4***b*) is a natural plant coumarin (1) which has been shown (2) to be a biogenetic precursor of angular furanocoumarins. It is apparently identical with the lactone zosimol (3) and is isomeric with the angular pyranocoumarin lomatin (4). The synthesis of racemic columbianetin has been reported recently by Shipchandler, *et al.* (5) who employed a ten-step route starting from 2,6-dihydroxybenzoic acid; the overall yield of product was about 2%. An alternative four-step synthesis starting from β-resorcylaldehyde (**1***a*) is described below. Lomatin (**3***a*) and dihydroseselin (**3***c*) were also synthesized similarly.

Results and Discussion

2,4-Dihydroxybenzaldehyde (**1***a*) was treated with 3-hydroxy-3-methyl-1-butene in the presence of boron trifluoride etherate (6) to obtain the 3-methyl-2-butenyl derivatives **1***b*, *c*, and *d*, which were separated by column chromatography on silicic acid. The conversion of starting material was always low, about 20–30%, so that yields in this step were poor. However, residual starting material could be recovered easily and recycled several times. Austin and Seshadri (6) reported **1***b* and *d* as the products of this reaction but their m.p. and n.m.r. data for the former compound were different from those obtained in this study. For example, my compound **1***b* melted abruptly at 140.5–141.0°, not at the reported 113–116°, and showed no broad peak (δ 9.0–9.8) in its n.m.r. spectrum. The t.l.c. and g.l.c. indicated it was pure. To ensure its identity it was cyclized in dilute acid to 2,2-dimethyl-7-hydroxychroman-6-aldehyde (**6***a*), a known compound (7); the cyclization product agreed with the literature report in m.p., had appropriate u.v. and n.m.r. spectra, and gave dihydroxanthyletin (**7***a*) on construction of a coumarin pyrone ring by usual methods (7).

Compound **1***c* has not been described previously as a product of the reaction, but was isolated in reasonable quantities in this study. Its structure follows not only from its u.v. and n.m.r. spectra in conjunction with elemental analysis, but also from its alternate preparation from the disodium salt of **1***a* and 1-bromo-3-methyl-2-butene, in which it was the major product. The structure **1***c* was confirmed by treating the product with phenyldiazomethane (8) to form **1***f*, which was the same compound as that obtained by boiling the sodium salt of **1***e* with 1-chloro-3-methyl-2-butene in toluene.

Oxidation of **1***c* in chloroform with 1 equiv of *m*-chloroperoxybenzoic acid gave a product which n.m.r. and u.v. spectra indicated was **5**. It could not be crystallized. The n.m.r. signals ($DCCl_3$) included a sharp methylene doublet (J = 8.5 Hz), an equally sharp methine triplet (J = 8.5 Hz) at low field (δ 4.76), and a rather

[1]Issued as NRCC No. 11762.

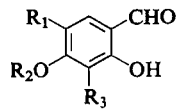

1

a $R_1 = H$; $R_2 = H$; $R_3 = H$
b $R_1 = -CH_2CH=C(CH_3)_2$; $R_2 = R_3 = H$
c $R_1 = R_2 = H$; $R_3 = -CH_2CH=C(CH_3)_2$
d $R_1 = R_3 = -CH_2CH=C(CH_3)_2$; $R_2 = H$
e $R_1 = H$; $R_2 = C_6H_5CH_2-$; $R_3 = H$
f $R_1 = H$; $R_2 = C_6H_5CH_2-$; $R_3 = -CH_2CH=C(CH_3)_2$
g $R_1 = -CH_2CH=C(CH_3)_2$; $R_3 = C_6H_5CH_2-$; $R_3 = H$

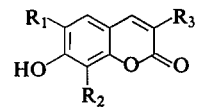

2

a $R_1 = H$; $R_2 = -CH_2CH=C(CH_3)_2$; $R_3 = COOH$
b $R_1 = H$; $R_2 = -CH_2CH=C(CH_3)_2$; $R_3 = H$ (osthenol)
c $R_1 = -CH_2CH=C(CH_3)_2$; $R_2 = R_3 = H$ (7-demethylsuberosin)

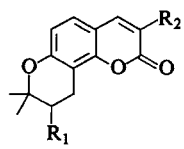

3

a $R_1 = OH$; $R_2 = H$ (lomatin)
b $R_1 = OH$; $R_2 = COOH$
c $R_1 = R_2 = H$ (dihydroseselin)

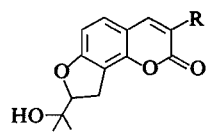

4

a R = COOH
b R = H (columbianetin)

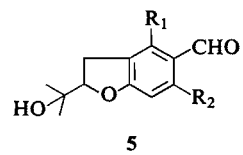

5

$R_1 = OH$; $R_2 = H$

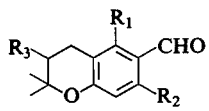

6

a $R_1 = H$; $R_2 = OH$; $R_3 = H$
b $R_1 = OH$; $R_2 = H$; $R_3 = OH$

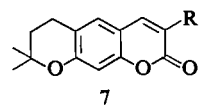

7

a R = H (dihydroxanthyletin)
b R = COOH

sharp hydroxyl singlet not coupled to this triplet. This suggested a five-membered ring and showed that no secondary hydroxyl was present, pointing to **5** as the only plausible structure. Oxidation of **1***c* similarly but with a trace of *p*-toluenesulfonic acid added to the reaction medium gave a different non-crystallized product, identified as **6***b*. The n.m.r. spectrum ($DCCl_3$) of this compound showed multiple signals for the methylene group, and a vague methine resonance (δ 3.84) strongly coupled also to a hydroxyl proton. When the secondary hydroxyl signal was removed with D_2O, the CH_2CH signals formed a clear ABX pattern. This was interpreted as indicating a six-membered ring.

These results are in accord with mechanistic considerations of the reactions involved. The peracid must attack the olefinic bond of the C_5 side chain of **1***c*, transforming it into an epoxide. Subsequent cyclization in neutral or basic medium would be expected to proceed by S_N2 mechanism, and take place at the less sterically hindered carbon of the epoxide bridge, giving **5**. An acid-catalyzed epoxide ring fission should, on the other hand, produce a carbonium ion which would be most favorably located at the tertiary carbon, so that ring closure in this case would produce a six-membered heterocycle.

Condensation of **5** with malonic acid in pyridine–aniline gave a carboxylic acid, m.p. 220–221°, which fluoresced a brilliant blue in u.v. light and had n.m.r. and u.v. spectra consistent with 3-carboxycolumbianetin (**4***a*). Decarboxylation of this acid in boiling quinoline, in presence of copper powder, yielded (±)-columbianetin (**4***b*), m.p. 168–169° [lit. 170–171° (5)], identical in its u.v. and n.m.r. spectra, and also in its chromatographic behavior, with natural (+)-columbianetin obtained by hydrolysis of columbianetin angelate isolated from roots of *Lomatium columbianum* (1).

Condensation of **6***b* similarly gave a carboxylic acid, m.p. 223–223.5°, with brilliant blue fluorescence. Its u.v. and n.m.r. spectra were consistent with 3-carboxylomatin (**3***b*). Decarboxylation of this compound in copper/quinoline afforded

Can. J. Chem. Downloaded from www.nrcresearchpress.com by 210.87.254.40 on 09/05/12
For personal use only.

Can. J. Chem. Downloaded from www.nrcresearchpress.com by 210.87.254.40 on 09/05/12
For personal use only.

(±)-lomatin (**3***a*), m.p. 163–165.5° [lit. 165.5–7.0° (9)], with spectral properties identical with those described for (+)-lomatin (4). This is the first total synthesis of lomatin.

The advantages of these synthetic routes are three: first, the sequences are short and the overall yields reasonably high; second, the method permits optical resolution at all stages, particularly at the carboxylic acid stage; third, and of particular interest to this laboratory, carbon-14 can be conveniently introduced in the malonic acid condensation.

A synthesis of osthenol (**2***b*) from **1***c* also seemed feasible, either by reaction with sodium acetate and acetic anhydride, or via the carboxylic acid **2***a*. This last compound was obtained without difficulty with malonic acid in pyridine–aniline, but its decarboxylation was attended by ring closure, yielding dihydroseselin (**3***c*) (6). Reaction of **1***c* with sodium acetate and acetic anhydride under the conditions described (6) for the synthesis of 7-demethylsuberosin (**2***c*) gave none of the expected osthenol acetate. The synthesis of osthenol reported (10, 11) while this work was in progress would seem to be an effective alternative.

Experimental

All melting points are uncorrected. The n.m.r. spectra were measured with a Varian model HA-100 Spectrometer. All proton assignments below are supported by signal integration. Tetramethylsilane was the reference standard. *2,4-Dihydroxybenzaldehyde (**1***a*)* was purchased from Eastman Organic Chemicals, and *3-hydroxy-3-methyl-1-butene* and *m-chloroperoxybenzoic acid* from Aldrich Chemical Co.

*Compounds **1***b, c, and d*

Compound **1***a* (50 g) in 300 ml dioxan was added to a stirred fresh solution of 40 g 3-hydroxy-3-methyl-1-butene and 25 ml BF_3 etherate in 200 ml dioxan, and stirring was continued for 2.5 h at room temperature. Ether (2500 ml) was added and the resulting solution extracted with water (3 × 1000 ml). The remaining organic layer was dried (Na_2SO_4) before evaporation to dryness. The crystalline residue was extracted with six 100-ml portions of pentane or hexane, which dissolved the reaction products and left behind most unchanged starting material. After removal of the solvent, the mixed products were adsorbed upon 50 g silicic acid (Mallinckrodt 100 mesh, used as received) and chromatographed on a column of 450 g more silicic acid prepared either in ether–hexane (1:1) or in ethyl acetate – hexane (1:9). Fractions of 20 ml were continuously collected. In development with ether–hexane, fractions 30–40 contained mostly **1***d*, 41–50 mostly **1***b*, and 53–66 **1***c*. Later fractions gave a little **1***a*. All products crystallized on standing in the collection tubes. In development with ethyl acetate – hexane, fractions 12–23 contained **1***d*; 68–117 **1***b* (development with 15% EtOAc after fraction 80, 20% after 92, 25% after 120, 100% after 145); 118–128 mixed **1***b* and *c*; 129–165, **1***c*. Higher fractions held unchanged **1***a*.

Each compound was recrystallized once from benzene–hexane.

Compound **1***b*, (yield 6–9 g), colorless rods, m.p. 140.5–141.0° [lit. 113–116° (6)].

Anal. Calcd. for $C_{12}H_{14}O_3$: C, 69.9; H, 6.8. Found: C, 69.9; H, 6.8.

λ_{max}(EtOH) 237, 281, and 324 nm; λ_{max}(EtOH/KOH) 255 and 343 nm. The n.m.r. signals ($DCCl_3$) at δ 1.76–1.80 (singlets, 2 vinyl methyls); 3.28 (doublet, J = 7 Hz, CH_2); 5.26 (triplet, J = 7 Hz, =CH); 6.19 (singlet, 4-OH). This peak and one at 11.23 (2-OH) disappeared on shaking the sample with D_2O; 6.34 (singlet, H-3); 7.20 (singlet, H-6); 9.66 (singlet, CHO).

Compound **1***c*, (yield 2–4 g), colorless rods, m.p. 117–120°.

Anal. Calcd. for $C_{12}H_{14}O_3$: C, 69.9; H, 6.8. Found: C, 69.6; H, 6.8.

λ_{max}(EtOH) 235, 287, and 320 (sh) nm. The n.m.r. signals ($DCCl_3$): δ 1.76 (singlet, vinyl CH_3); 1.82 (singlet, vinyl CH_3); 3.42 (doublet, J = 7 Hz, CH_2); 5.25 (triplet, J = 7 Hz, =CH); 6.15 (singlet, 4-OH); 6.45 (doublet, J = 8 Hz, H-5); 7.28 (doublet, J = 8 Hz, H-6); 9.66 (singlet, CHO); 11.74 (singlet, 2-OH). Shaking with D_2O eliminated the hydroxylic signals. Irradiation at the frequency of the δ 5.25 proton collapsed also the CH_2 signal and the methyl signals to sharp singlets; irradiation at δ 7.28 collapsed the doublet at 6.45.

Compound **1***d*, (yield 6–8 g), along colorless needles, m.p. 113–117° [lit. 120–121° (6)].

Anal. Calcd. for $C_{17}H_{22}O_3$: C, 74.3; H, 8.1. Found: C, 73.8; H, 8.0.

λ_{max}(EtOH) 228, 236 sh, 278, and 327 (sh). The n.m.r. signals at δ 1.75–1.85 (12H, 4 methyls): 3.26 and 3.40 (doublets, J = 7 Hz, 2 methylenes); 5.23 and 5.27 (triplets, J = 7 Hz, 2 =CH); 6.30 (singlet, 4-OH); 7.09 (singlet, H-6); 9.64 (singlet, CHO); 11.60 (singlet, 2-OH).

*Alternate Methods for **1***c and d*

To a solution of 2,4-dihydroxybenzaldehyde (13.8 g) in 100 ml dry methanol was added 100 ml methanol containing dissolved sodium metal (4.6 g). The solvent was evaporated at once at reduced pressure and the residual light-tan disodium salt was dried, first by evaporation from ethanol–benzene and then by standing 1 h at 120°. Yield 18.2 g (100%).

This salt (9.0 g) and 1-bromo-3-methyl-2-butene (12.5 g) (13) were put into 250 ml benzene and heated under reflux for 4 h, then cooled and shaken with a mixture of ether and cold dilute acid. The organic layer was washed with water, dried and freed of solvent, leaving a dark semi-solid mass. This was chromatographed on silicic acid as described above to yield 1.1 g (10.6%) **1***c* and 1.0 g (7.4%) **1***d*, along with a larger quantity of unchanged starting aldehyde.

*Derivatives of **1***b*

*(a) Compound **6***a*

Compound **1***b* (1 g) was boiled 30 min in 50 ml 30% alcohol containing 2 ml H_2SO_4. The alcohol was evaporated and the aqueous suspension remaining was extrac-

Can. J. Chem. Downloaded from www.nrcresearchpress.com by 210.87.254.40 on 09/05/12
For personal use only.

ted with 100 ml ether. After washing with water, the ether solution was dried (Na_2SO_4), treated with 10 ml hexane, and allowed to evaporate overnight. The deposited crystals of 2,2-dimethyl-7-hydroxychroman-6-aldehyde (**6***a*) (0.9 g), m.p. 103–104° from benzene [lit. 104° (7)], gave n.m.r. signals ($DCCl_3$) at δ 1.35 (singlet, 2 methyls); 1.80 (triplet, J = 6.5 Hz, CH_2); 2.72 (triplet, J = 6.5 Hz, benzylic CH_2); 6.28 and 7.16 (singlets, H-3 and -6); 9.63 (singlet, CHO); 11.53 (singlet, 2-OH).

(b) Dihydroxanthyletin

The above aldehyde (0.3 g) was kept for 16 h with 0.6 g malonic acid in 0.7 ml pyridine and 0.1 ml aniline, with occasional warming. The mixture was poured into ice/3 *N* HCl and the yellow precipitate filtered, giving 0.35 g crude 3-carboxydihydroxanthyletin (**7***b*), m.p. 140–158°; recrystallization from alcohol gave crystals, m.p. 158–159° [lit. 158–159° (7)].

λ_{max}(EtOH) 252, 262, and 356 nm. The n.m.r. signals (d_6-DMSO) at δ 1.72 (singlet, 2 methyls); 2.18 and 3.16 (triplets, J = 6.5 Hz, 2 adjacent CH_2's); 6.07 and 6.98 (singlets, H's of central ring); and 8.97 (singlet, H-4 of pyrone ring). The carboxyl proton was very broad, *ca.* δ 12–13.

The acid (0.15 g) was decarboxylated as described below for the preparation of columbianetin, giving 0.09 g dihydroxanthyletin (**7***a*), m.p. 122–123° from aqueous alcohol [lit. 124–125° (6)]. The mixed m.p. with authentic material, prepared by acid treatment of 7-demethylsuberosin (12), was undepressed, and the spectra were indistinguishable.

λ_{max}(EtOH) 249, 258, and 326 nm. The n.m.r. signals ($DCCl_3$) at δ 1.36 (singlet, 2 methyls); 1.83 and 2.81 (triplets, J = 6.5 Hz, 2 adjacent CH_2's); 6.17 and 7.54 (doublets, J = 9.5 Hz, pyrone ring protons); 6.71 and 7.14 (singlets, central ring protons).

Derivatives of **1***c*

(a) 2-Hydroxy-3-(3-methyl-2-butenyl)-4-benzyloxybenzaldehyde (Method 1)

Compound **1***c* (200 mg) was benzylated with phenyldiazomethane (8) in boiling ether. Gas chromatography of the reaction mixture showed a main component which matched (retention time, n.m.r. spectrum) the 4-benzyl ether (**1***f*).

(b) 2-Hydroxy-3-(3-methyl-2-butenyl)-4-benzyloxybenzaldehyde (Method 2)

The sodium salt of 4-benzyloxy-2-hydroxybenzaldehyde was prepared by treatment of the phenol **1***e* (15.5 g) in 100 ml methanol with 1.62 g sodium dissolved in 200 ml methanol, followed by rapid removal of the methanol and oven-drying of the product (15.6 g, 95%). The powdered salt was suspended in 300 ml dry benzene and refluxed 4 h with 7.5 g 3-methyl-1-chloro-2-butene. The filtered solution was evaporated to a syrup and dissolved in ether. This solution was adsorbed on 20 g silicic acid and chromatographed on a further 180 g silicic acid. Fractions of 20 ml were collected. Development with 1:9 ether–hexane gave 0.2 g **1***g*, m.p. 91–94.5° (fractions 40–43), 1.6 g **1***f*, m.p. 71.5–72.5° (fractions 46–53), and 2.6 g unchanged starting aldehyde (fractions 55 and onwards).

Anal. Calcd. for $C_{19}H_{20}O_3$ (**1***f*): C, 77.0; H, 6.8. Found: C, 76.8; H, 6.8.

The n.m.r. spectrum ($DCCl_3$) showed signals at δ 1.7 (singlets, 2 vinyl methyls); 3.41 (doublet, J = 7 Hz, CH_2 of butenyl chain); 5.16 (singlet, benzyl CH_2); 5.24 (triplet, J = 7 Hz, =CH); 6.58 and 7.30 (doublets, J = 8.5 Hz, H-5 and -6 of phenolic ring); 7.40 (singlet, phenyl); 9.70 (singlet, CHO); 11.46 (singlet, 2-OH).

The n.m.r. spectrum of **1***g* was similar to that of **1***f* except that the methyl signals were separated (δ 1.64, 1.74) and aromatic singlets at δ 6.48 and 7.25 replaced the doublets at 6.58 and 7.30.

(c) 3-Carboxyosthenol (2a)

Compound **1***c* (70 mg) and 120 mg malonic acid were warmed together 2 h at 50–60° in 1 ml 10% aniline in pyridine. After standing overnight the mixture was poured into 20 ml ice-cold 10% HCl; the yellow precipitate (50 mg, m.p. 180–204°) was filtered, washed with water, then chromatographed on a small column of Polyclar AT powder (General Aniline and Film Corporation), developing with increasing strengths of aqueous methanol. 3-Carboxyosthenol emerged as a brilliant blue-fluorescing band, melting at 209–212° after recrystallization from aqueous alcohol.

Anal. Calcd. for $C_{15}H_{14}O_5$: C, 65.7; H, 5.2. Found: C, 65.5; H, 5.2.

λ_{max}(EtOH) 262, 299 (sh), and 354 nm. The n.m.r. signals (d_6-DMSO) at δ 1.67 and 1.82 (singlets, 2 methyls); 3.40 (doublet, J = 7 Hz, CH_2); 5.18 (triplet, J = 7 Hz, =CH); 6.94 and 7.62 (doublets, J = 9 Hz, H-6 and -5 of coumarin system); 8.66 (singlet, H-4); 10.6–11.0 (broad singlet, 7-OH); the carboxyl proton was very broad, near δ 12–13.

(d) Dihydroseselin (3c)

Compound **2***a* (6 mg) was heated 5 min at 230–235° in 0.5 ml fresh quinoline containing a little copper powder. The cooled solution was diluted with 10 ml ether, decanted from the copper metal, and washed first with dilute HCl then twice with water. The blue-fluorescing solution was chromatographed on silicic acid, developing with ether. The major fluorescent band was dihydroseselin, co-chromatographing with authentic material and having the same spectral properties: λ_{max}(EtOH) 248, 258, 327 nm, unchanged by either $AlCl_3$ or NaOH.

The n.m.r. signals ($DCCl_3$) at δ 1.25 (singlet, 2 methyls); 1.83 and 2.88 (triplets, J = 7 Hz, 2 adjacent methylenes); 6.15 and 7.55 (doublets, J = 9.5 Hz, H-3 and -4 of coumarin ring system); 6.67 and 7.15 (doublets, J = 9 Hz, H-6 and -5 of coumarin ring system). No osthenol could be detected in the reaction mixture. Repeated attempts at decarboxylation of **2***a* in Cu–quinoline, using lower and higher temperatures, or in ethylene glycol, gave similar results. By heating *in vacuo* below 270°, 3-carboxyosthenol could be sublimed; above 270° a mixture containing some dihydroseselin (but no osthenol) was produced.

(±)-2,3-Dihydro-2-(1-hydroxy-1-methylethyl)-4-hydroxybenzofuran-5-aldehyde (5)

Compound **1***c* (0.5 g) in 20 ml chloroform was treated with 0.5 g technical (85%) *m*-chloroperoxybenzoic acid in 20 ml chloroform. After 24 h the solution was washed with dilute bicarbonate, then with water, and evaporated to a syrup. Gas chromatography showed a single component with n.m.r. signals ($DCCl_3$) at δ 1.24 and 1.36

Can. J. Chem. Downloaded from www.nrcresearchpress.com by 210.87.254.40 on 09/05/12
For personal use only.

(singlets, methyls); 1.82 (singlet, alcoholic OH); 3.12 (doublet, J = 8.5 Hz, CH_2); 4.76 (triplet, J = 8.5 Hz, —CH); 6.45 and 7.35 (doublets, J = 8.5 Hz, H-5 and -6); 9.70 (singlet, CHO); 11.74 (singlet, 2-OH). Removal of the hydroxyl signals by shaking the sample with D_2O did not alter the shape or position of the —CH triplet.

(±)-3-Carboxycolumbianetin (4a)

The aldehyde **5** (1.4 g) was kept 24 h with 1.2 g malonic acid in 5 ml pyridine and 0.5 ml aniline, then the solution was poured slowly into ice-cold 10% HCl (50 ml) and the resulting solution or suspension was continuously extracted with ether. This extract was passed through a column of silicic acid developing with ethyl acetate–hexane. The product, 0.3 g white crystals of m.p. 220–221°, was dried at 120° overnight.

Anal. Calcd. for $C_{15}H_{14}O_6$: C, 62.1; H, 4.9. Found: C, 62.2; H, 4.9.

λ_{max}(EtOH) 263 and 353 nm. The n.m.r. signals (d_6-DMSO) at δ 1.33 and 1.36 (singlets, methyls); 2.79 (doublet, CH_2); 3.81 (triplet, —CH); 5.2 (broad singlet, alcoholic OH); 6.83 and 7.67 (doublets, J = 9 Hz, H-6 and -5); 8.70 (singlet, H-4). The carboxyl proton was very broad at δ 12–13.

(±)-Columbianetin (4b)

Compound **4***a* (30 mg) was refluxed 10 min with 30 mg copper powder in 1 ml fresh dry quinoline. The cooled solution was then diluted with 15 ml ethyl acetate and 15 ml ether, decanted from the copper, shaken with two portions of 3 *N* HCl, washed with two portions of water, and dried over Na_2SO_4. Evaporation of the clear yellow solution gave 18 mg crude (±)-columbianetin, m.p. 164–167°, raised to 168–169° by recrystallization from chloroform–hexane [lit. 170–171° (5)]. Direct comparison of the product with authentic (+)-columbianetin showed no differences in chromatographic behavior (paper chromatography, three systems; g.l.c.) or in u.v. and n.m.r. spectra.

λ_{max}(EtOH) 251, 262, and 327 nm. The n.m.r. signals ($DCCl_3$) at δ 1.25 and 1.37 (singlets, methyls); 1.75 (singlet, OH); 3.30 (doublet, J = 8 Hz, CH_2); 4.77 (triplet, J = 8 Hz, CH); 6.17 and 7.58 (doublets, J = 9.5 Hz, H-3 and -4 respectively of coumarin ring system); 6.72 and 7.22 (doublets, J = 9.0 Hz, H-6 and -5).

(±)-2,2-Dimethyl-3,5-dihydroxychroman-6-aldehyde (6b)

Compound **1***c* (0.6 g) and *p*-toluenesulfonic acid (0.01 g) in 20 ml $HCCl_3$ were treated with 85% *m*-chloroperoxybenzoic acid (0.6 g) in 15 ml $HCCl_3$ and kept 18 h at room temperature. Work-up as for **5** above gave a light brown syrup. After chromatography on silicic acid a colorless viscous syrup (0.45 g) was obtained which, although chromatographically homogeneous, still could not be crystallized. It showed n.m.r. signals ($DCCl_3$) at δ 1.46 (singlet, two methyls); 1.73 (broad singlet?, OH); 2.70 and 2.94 (doublets of doublets, J_{AB} = 16 Hz, —CH_2); 3.84 (after removal of coupled HO, doublet of doublets, J_{AX} = 5, J_{BX} = 6 Hz, —CH); 6.46 and 7.27 (doublets, J = 9 Hz, aromatic H-5 and -6); 9.66 (singlet, CHO) and 11.75 (singlet, 2-HO).

(±)-3-Carboxylomatin (3b)

The above aldehyde (0.35 g) was kept 24 h with malonic acid (0.5 g) in 1.5 ml pyridine containing a little aniline. The mixture was poured in 25 ml cold 3 *N* HCl and extracted with chloroform. The chloroform solution was washed once with water then dried and evaporated, leaving 0.28 g pale yellow crystals, m.p. 223–223.5° from methanol.

Anal. Calcd. for $C_{15}H_{14}O_6$: C, 62.1; H, 4.9. Found: C, 62.1; H, 4.9.

The n.m.r. signals (d_6-DMSO) at δ 1.29 and 1.32 (singlets, methyls); 2.70 and 2.99 (doublets of doublets, J_{AB} = 16 Hz, CH_2); 3.77 (doublet of doublets, J_{AX} = 5, J_{BX} = 6 Hz, —CH); 5.31 (broad singlet?, OH); 6.83 and 7.66 (doublets, J = 8.5 Hz, aromatic H-6 and -5); 8.70 (singlet, H-4); 12–13 (very broad, carboxyl).

(±)-Lomatin (3a)

Decarboxylation of **3***b* as for 3-carboxycolumbianetin gave (±)-lomatin in 30–50% yield, m.p. 163–165.5° from benzene [lit. m.p. 165.5–167.0° (9)].

λ_{max}(EtOH) 246, 256, and 325 nm. The n.m.r. signals ($DCCl_3$) at δ 1.35 and 1.41 (singlets, methyls); 2.0 (broad singlet, alcoholic OH); 2.92 and 3.14 (doublets of doublets, J_{AB} = 17 Hz, —CH_2); 3.89 (doublet of doublets, J_{AX} = 5.5, J_{BX} = 6 Hz, —CH); 6.21 and 7.60 (doublets, J = 9.5 Hz, H-3 and -4 respectively); 6.76 and 7.23 (doublets, H-6 and -5 respectively); all in agreement with literature values (4).

Thanks are extended to Mr. W. Haid for the elemental analyses, to Mr. M. Mazurek for the n.m.r. spectra, and especially to Mr. B. K. Bailey for skillful technical assistance throughout. I am also indebted to Professor A. Kjaer (Technical University of Denmark, Lyngby, Denmark) for helpful advice.

1. R. E. Willette and T. O. Soine. J. Pharm. Sci. **53**, 275 (1964).
2. W. Steck and S. A. Brown. Tetrahedron Lett. 4805 (1969).
3. M. E. Perel'son, G. K. Nikonov, G. Yu. Pek, and Yu. N. Sheinker. Dokl. Akad. Nauk SSSR (Khim. izd.) **159**, 154 (1964).
4. T. O. Soine and F. H. Jawad. J. Pharm. Sci. **53**, 990 (1964).
5. M. Shipchandler, T. O. Soine, and P. K. Gupta. J. Pharm. Sci. **59**, 67 (1970).
6. P. W. Austin and T. R. Seshadri. Indian J. Chem. **6**, 412 (1968).
7. J. C. Bell, W. Bridge and A. Robertson. J. Chem. Soc. 1542 (1937).
8. C. G. Overberger and J-P. Anselme. J. Org. Chem. **28**, 592 (1963).
9. A. Mustafa, N. A. Starkovsky, and T. I. Salama. J. Org. Chem. **26**, 890 (1961).
10. J. Hlubucek, E. Ritchie, and W. C. Taylor. Chem. Ind. 1780 (1969).
11. R. D. H. Murray, M. M. Ballantyne, and K. P. Mathai. Tetrahedron Lett. 243 (1970).
12. F. E. King, J. R. Housley, and T. J. King. J. Chem. Soc. 1392 (1954).
13. L. Claisen. J. Prakt. Chem. **105**, 65 (1922).

Can. J. Chem. Downloaded from www.nrcresearchpress.com by 210.87.254.105 on 09/05/12
For personal use only.

Conformational Analysis of Trimethylene Sulfites. The Importance of Vicinal Unshared Electron Pairs[1]

GORDON WOOD, JOHN M. MCINTOSH, AND MAURICE H. MISKOW[2]
Department of Chemistry, University of Windsor, Windsor, Ontario

Received June 16, 1970

Dipole moments are reported for trimethylene sulfite and 11 alkyl derivatives in a variety of solvents (C_6H_{12}, CCl_4, C_6H_6, dioxan). The variation of dipole moment with solvent for one of the 5-*t*-butyltrimethylene sulfite isomers is confirmed, but this behavior is not shown by the other compounds. This latter fact is used to rule out rapid chair–chair interconversion for these compounds. Recent ultrasonic absorption experiments are reinterpreted in the context of vicinal electron pair interactions and their effect on conformational analysis of sulfites and similar six-membered compounds. The result is a general scheme which is consistent with available information and which we believe is preferable to analysis of these compounds by analogy with cyclohexane.

On a mesuré, dans quelques solvants (C_6H_{12}, CCl_4, C_6H_6, dioxane), les moments polaires du sulfite de triméthylène et de 11 dérivés alkylés. Nous avons confirmé que le moment polaire de l'un des *tert*-butyl-5 sulfite de triméthylène varie avec le solvant; cette variation n'est pas observée avec les autres composés. Ce dernier fait est utilisé pour exclure la possibilité d'une interconversion chaise–chaise rapide entre ces composés. Des résultats récents d'absorption ultrasonique sont réinterprétés dans le contexte d'interactions entre des paires d'électrons vicinaux et de leurs effets sur l'analyse conformationnelle des sulfites et des composés cycliques à six chaînons de nature similaire. Le résultat est un schéma général qui est consistant avec les informations disponibles et qui, nous le croyons, est préférable à une analyse de ces composés par analogie avec le cyclohexane.

Canadian Journal of Chemistry, 49, 1202 (1971)

Introduction

Much data has been reported on the conformations of substituted trimethylene sulfites since the initial attempt by Arbouzov (1) to assign a conformation to the parent ring system, but no clear picture of the shapes of these compounds has emerged. Although trimethylene sulfites are usually assumed to undergo rapid chair–chair interconversion at room temperature, all our attempts to find a coalescence of signals in n.m.r. spectra have been unsuccessful. While this result by itself could indicate the presence of only one chair form in measurable amounts (anancomeric system), dipole moment data will be presented here which rules out that possibility for at least some of the sulfites. The lack of coalescence temperature between -100 and $+30$ °C for the molecules[3] is sufficient to show that the barrier to ring inversion must lie either substantially above or substantially below the usual cyclohexane barrier of 10.3 kcal/mol.[4] We shall attempt to show that only the former is consistent with all the facts. Recently ultrasonic relaxation studies have been interpreted in terms of chair–chair equilibria for several trimethylene sulfites (2). We suggest that the analysis of the data obtained in these experiments errs by neglecting the effect of vicinal electron pairs.

Our aim is to present, point by point, the evidence which leads us to conclude that the presently held concepts about the conformation of trimethylene sulfites and some related molecules need revision and to develop a new model consistent with all the facts known at this time.

Results and Discussion

Dipole Moments and Solvent Dependence

The dipole moments were calculated by the method of Guggenheim (3) and are presented in Table 1. The values in parentheses were obtained by van Woerden and Havinga (4) and the agreement is satisfactory, considering the different methods of calculation. In keeping with a previous observation (4*b*), these dipole moments permit important conclusions on conformation to be made. In particular, the influence of a polar solvent on an equilibrium between two forms of different dipole moment is such that the form of higher moment is favored. This shift in equilibrium results in a higher (average) dipole moment.

[1]Presented in part at the Organic Symposium of the Chemical Institute of Canada, London, Ontario, September, 1970.

[2]Recipient of NRCC Scholarships, 1966–1970.

[3]Results of our n.m.r. experiments will be reported later.

[4]For a signal separation of 0.5 p.p.m., a coalescence temperature below -100 °C corresponds to a barrier < 8.5 kcal/mol; a temperature above $+30$ °C to a barrier > 15 kcal/mol. Differences in signal separation have only a small effect on these values.

TABLE 1. Dipole moments for the compounds of the general structure:

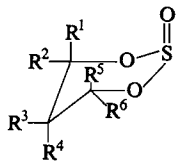

Compounds	Substituents*	Dipole Moment (D) C_6H_{12}	CCl_4	C_6H_6	Dioxane	$\Delta_{C_6H_6-CCl_4}$†	$\Delta_{C_6H_6-C_6H_{12}}$‡
1§		Insoluble	3.34				
2§	$R^2 = CH_3$		3.35	3.41		.06	
3	$R^1 = CH_3$		4.66	4.75		.09	
4§	$R^2 = R^6 = CH_3$	3.44	3.51	3.60		.09	.16
5	$R^2 = R^5 = CH_3$	3.97	3.93	3.93		.00	−.04
6	$R^1 = R^5 = CH_3$	Insoluble	5.31	5.37		.06	
7‖	$R^1 = R^2 = R^6 = CH_3$	3.91		3.86			−.05
8	$R^1 = R^2 = R^5 = CH_3$	4.53		4.71			.18
9‖	$R^1 = R^2 = R^5 = R^6 = CH_3$	4.22		4.30			.08
10§	$R^3 = R^4 = CH_3$	3.38					
11	$R^3 = (CH_3)_3C$	3.50	3.54(3.61)¶	3.60(3.66)¶	3.66	.06	.10
12	$R^4 = (CH_3)_3C$	3.54	3.63(3.76)¶	3.90(4.00)¶	4.15	.27	.36

*All R's not specified = H.
†$\mu_{C_6H_6} - \mu_{CCl_4}$.
‡$\mu_{C_6H_6} - \mu_{C_6H_{12}}$.
§Ultrasonic relaxation found.
‖No ultrasonic relaxation found.
¶From ref. 4*a*.

Several of these compounds have dipole moments corresponding at least approximately to a chair form with axial S=O[5] (compounds **1, 2, 4, 10, 11**). The only molecule with a moment which clearly corresponds to a chair with equatorial S=O is compound **6**.[6] This molecule has been assigned this conformation (5, 6) and recent n.m.r. evidence supports this assignment.[7] Compounds **3** and **8** must also have large amounts of this form or a non-chair form with similar geometry at the sulfite end of the molecule. Our analysis requires that the latter be the case.

The variation of dipole moment with solvent for compound **12** (4*a*) has been confirmed by measurement in two additional solvents. The difference in dipole moment between dioxane and cyclohexane solutions is 0.61 D which is well outside the experimental error and much larger than the corresponding change (0.16 D) for the other (rigid ?) isomer, compound **11**. The behavior exhibited by compound **12** is expected for a molecule existing as interconverting conformations with substantially different dipole moments (4*a* and references therein). In this situation the conformation of higher moment is favored in the more polar solvent. *None of the other compounds studied show enough variation of dipole moment with solvent to implicate a conformational equilibrium with certainty*, although some of them are borderline, *e.g.*, compound **8**.

Compound **9** has a dipole moment of intermediate value which is constant and it therefore seems likely that this compound exists in a non-chair form almost exclusively. Compounds **5** and **7** have moments near 3.9 D which implies either a distortion of the S=O axial chair or a non-chair form. Since both of these molecules have the same axial methyl – axial S=O interaction in the chair form, it is not surprising that they have similar moments, but it is not possible on this basis to decide between the chair and non-chair alternatives.[8]

The general constancy of the dipole moments in various solvents (except for compound **12**) even for compounds whose moments deviate considerably from the values expected for chair forms makes it highly unlikely that any of these

[5]Calculations give 3.4 D for trimethylene sulfite, see ref. 4*b*.
[6]The dipole moment for this form has been estimated as 5.0–5.2 D by H. F. van Woerden, private communication.
[7]Private communication from Professor R. E. Lack, University of Sydney, Sydney, Australia.
[8]Compound **5** has been assigned as existing as 70% chair and 30% non-chair (7). This result fits very well the general scheme to be developed later in this paper.

Can. J. Chem. Downloaded from www.nrcresearchpress.com by 210.87.254.105 on 09/05/12
For personal use only.

Can. J. Chem. Downloaded from www.nrcresearchpress.com by 210.87.254.105 on 09/05/12
For personal use only.

compounds exist as equilibrium mixtures of conformations with large differences in dipole moment. *In particular, with the possible exception of compound* ***12****,*[9] *none of these compounds exist as equilibrium mixtures of two chair conformations.* Where equilibria do exist, they probably involve chair and non-chair forms with similar moments.

In the remainder of this discussion an attempt will be made to reconcile the conclusions from the dipole moment study with other information available from conformation studies of cyclic sulfites and related molecules.

Ultrasonic Absorption and Conformational Equilibria

Sulfite barriers of 5–7 kcal/mol ($\Delta H^{\ddagger}$, more stable to less stable) are typical of the ultrasonic data. The assignment of these barriers to the chair–chair interconversion process depends on an interpretation of other data (8), chiefly spectral (2), which is less than compelling. In fact, all such interpretations to date implicitly use cyclohexane as the model for six-membered ring behavior.

The most relevant experimental evidence on the nature of the barrier being measured in the ultrasonic work arises from a comparison of the latter with low temperature n.m.r. results on related systems. For example, we have recently determined the ring inversion barrier for 5,5-dimethyltrimethylene sulfate (9). The n.m.r. result is 8.1–8.4 kcal/mol in contrast to the ultrasonic value of 4.6–6.2 kcal/mol for the related 4-methyltrimethylene sulfate. We prefer to handle this anomaly in the way that a similar one was handled for a 1,3-dioxane, namely by assigning the lower barrier observed in the ultrasonic work to a chair – non-chair interconversion (10).

A different kind of difficulty has arisen with compounds having two identical chair forms. Chair–chair interconversion cannot cause ultrasonic absorption for such a system (10), and yet relaxation has been observed. Once again, the assumption of a chair – non-chair equilibrium has been made.

Finally, ultrasonic absorption measurements on 4-phenyl-1,3-dioxan gave results unexpected for a chair–chair equilibrium (11). The most serious discrepancy was the large negative entropy associated with conversion of the less stable to the more stable form. That fact, coupled with the large $-\Delta G^{\circ}$ value expected for 4-axial substituents on this ring (12) can readily be accommodated by assignment of the less stable form to a non-chair conformation.

In conclusion, we suggest that the trimethylene sulfites which have been shown by ultrasonic measurements to exist as a conformational equilibrium (as little as 1% of minor conformer can be detected (8)) have a non-chair conformation of energy comparable to the preferred chair form. According to this notion, compounds which fail to give a relaxation result are limited to a single chair or non-chair conformation. Compound **9** and possibly **7** are examples of the latter and 5-nitro-5-methyltrimethylene sulfite (2) is presumably an example of the former. Compounds in our dipole moment study that have been studied by ultrasonics are noted in Table 1 along with the result.

The nature of the data from the ultrasonic experiment is such that one cannot use it to prove *any* structural assignments. Our claim is simply that considerable evidence can be brought forward from a re-evaluation of this data to support our interpretation of conformational behavior in these systems. The next section will show that there exists a large body of information on the influence of vicinal electron pairs on rotational barriers and conformation which is also consistent with our interpretation.

Vicinal Unshared Electron Pairs and Barriers to Rotation

The transition state for ring inversion in cyclohexane is considered to be the half-chair (13). In other six-membered ring compounds the minimum energy path for ring inversion may involve a twist or other form, but regardless of the form of the transition state, rotation about single bonds of the ring must accompany the process. Indeed, the barrier to ring inversion represents, in large part, the torsional energy required for rotation about these bonds (13, 14). Thus, the barrier of 10.3 kcal/mol in cyclohexane (15) should be related in part to the 3.4 kcal/mol about the C—C bond in propane (16),[10] and a ring containing single bonds with higher barriers to rotation would be expected to have a higher barrier to inversion.[11]

[9]Since compound **12** shows a constant n.m.r. spectrum from −100 to +180 °C, it is probable that it also fits the scheme proposed later, in spite of its dipole moment behavior.

[10]The choice of propane over ethane or butane for a model is an arbitrary one.

[11]There seems to be no dispute with this principle, see ref. 2, p. 314 and ref. 17. Our disagreement with ref. 2 involves only the choice of suitable acyclic models.

Can. J. Chem. Downloaded from www.nrcresearchpress.com by 210.87.254.105 on 09/05/12
For personal use only.

Rotational barriers about single bonds between atoms carrying unshared electron pairs have been measured (16, 18–21) and calculated (22–26) for a large variety of compounds. These barriers are generally of the order of 10 kcal/mol, a value seldom reached by the most hindered ethane derivatives lacking vicinal electron pairs. Although these high barriers may not be wholly resultant from vicinal electron pair interactions (18*b*, 19, 21, 25), all results thus far indicate these interactions make a most important contribution. A comprehensive paper by Wolfe and co-workers reduces the wealth of data and calculations now available on this point to two simple rules (26).

There is also abundant evidence that one or more bonds of this sort in a six-membered ring increase the barrier to ring inversion, in spite of the reduction in rotation barrier for neighboring bonds where only one atom has unshared electron pairs (27).

Thus, it seems to us that for trimethylene sulfites (with unshared electron pairs on three adjacent atoms) the choice between a high (>15 kcal/mol) and a low (<8.5 kcal/mol) barrier to ring inversion can be made with some confidence. The only conclusion compatible with these arguments is that the barrier to ring inversion is high and, further, that interactions of vicinal electron pairs are a major cause of this barrier as well as other conformational properties. The strong preference of the exocyclic S=O bond for the axial position is probably best understood in these terms.[12] Equatorial disposition of S=O would give rise to an arrangement which corresponds to an energy maximum for molecules of this sort ($\theta = 120°$, see Fig. 1 and ref. 28).

Two-fold Rotational Barriers and Minimum Energy Conformations

Attention is drawn by Wolfe *et al.* (26) to an important feature of their calculation of barriers for bonds with vicinal unshared electron pairs; *viz*, the total energy curves for 360° rotation about these bonds show only two maxima and two minima. Perhaps the clearest example of this can be seen by comparison of the calculated barriers for hydrogen methyl sulfoxide and its carbanion (28*c*).[13] Figure 1 shows a sketch combining these results with the corresponding curve for ethane. Note that CH_3SHO has an ethane-like barrier with the three maxima and three minima shifted about 20° to the right. The carbanion has had two of these maxima and the minimum between them ($\theta = 80$–$200°$) replaced by a single maximum ($\theta = 130°$), as well as other smaller shifts. When one considers that the conformational preference for the chair over non-chair forms in cyclohexane is equated with the preference of the staggered over the eclipsed conformation in ethane, it becomes clear that arbitrary assignment of the chair as preferred conformation in six-membered rings containing one or more bonds with vicinal unshared electron pairs is unjustified. The curve for $^-CH_2SHO$ shows energies of 4.4, 12.8, and 0 kcal/mol for the conformations corresponding to staggered ethane. Thus, in six-membered rings with vicinal electron pairs the staggered conformation characteristic of a perfect chair *may* correspond to an energy minimum, *but it also may correspond to the highest energy on the rotation curve or any intermediate value.*

Because of the increased height and, therefore, importance of these two-fold barriers we conclude that the preference for chair forms should decrease with the introduction of one or more bonds of this type. In fact, there is already experimental evidence for twist form preference in some of these molecules. One well-documented case involves 3,3,6,6-tetramethyl-1,2,4,5-tetrathian (29) where the twist form is preferred by 0.5–1 kcal/mol in the various activation parameters. The small entropy difference between the chair and twist forms of this molecule probably reflects the reduced flexibility of non-chair form in these systems. Several recent communications on phosphorus analogues of sulfites also implicate twist forms and high ring inversion barriers for these compounds (30–33).

The current view that trimethylene sulfite prefers the chair form, based mainly on X-ray data (34) may well be correct. However, the possibility of relatively low energy non-chair forms in solution seems to us to be strong. The n.m.r. work of Maroni and Cazaux referred to earlier (7), dipole moment data presented here, and our interpretation of the ultrasonic absorption data of Wyn-Jones may be cited in support

[12]No direct measure of this preference exists. Acid equilibration of compounds **4** and **6** gives values of 2.6 kcal/mol in CCl_4 and 1.7 kcal/mol in CH_3CN. However, persistent association of these sulfites (5) in dilute solution may influence these results.

[13]For comment on recent experimental work on related molecules, see ref. 26.

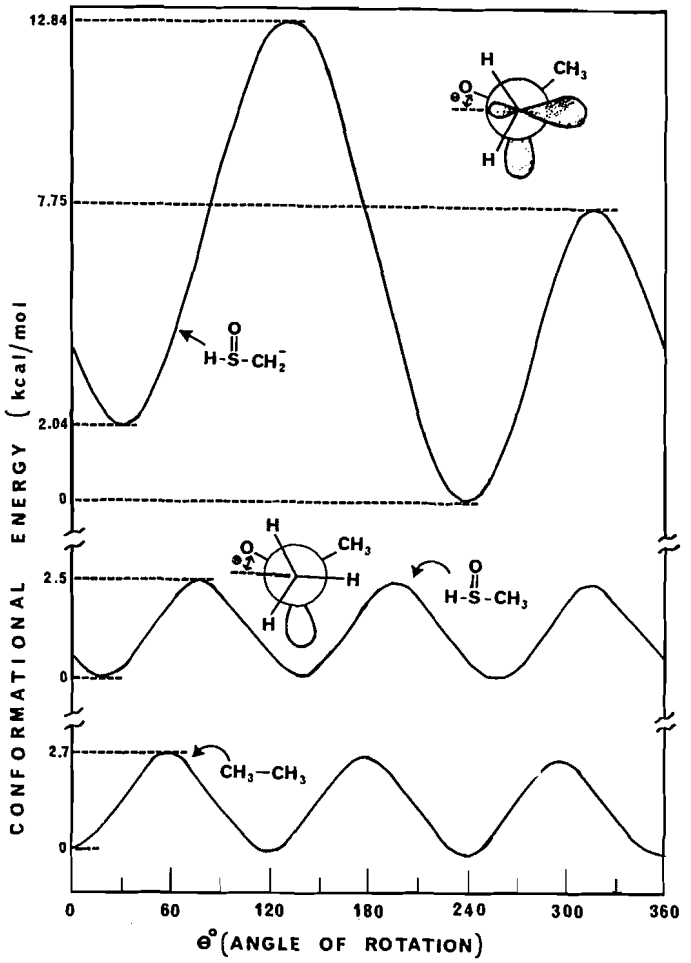

FIG. 1. Variation of the total energy of ethane, hydrogen methyl sulfoxide, and its carbanion as a function of rotation about the C—C or C—S bond (θ).

of this position. Further, it seems likely that steric interactions are capable of changing relative energy levels of sulfite conformations drastically. For example, it seems likely that compound **9** is predominantly non-chair.

Summary and Conclusions

The application of existing notions on trimethylene sulfite conformations to ultrasonic absorption data has led to an interpretation that contradicts a number of conformational studies documenting the importance of unshared electron pairs on adjacent atoms.

In this paper an attempt has been made, using the above results and new data on the sulfites, to define normal behavior for trimethylene sulfites with emphasis on the influence of electron pairs on sulfur and oxygen. This analysis leads to a coherent picture in which trimethylene sulfites have high barriers to chair–chair interconversion, low energy non-chair forms, and a strong preference for axial S=O. No conflict with previously reported facts has been uncovered, and the ultrasonic absorption experiments emerge as an important probe for chair to non-chair equilibria in these systems.

While we feel our conclusions are consistent with the data available at this time, we do not wish to imply that we have proven our contentions beyond any doubt. We offer our model as a possible solution to the difficulties encountered in viewing certain six-membered rings as close

Can. J. Chem. Downloaded from www.nrcresearchpress.com by 210.87.254.105 on 09/05/12
For personal use only.

Can. J. Chem. Downloaded from www.nrcresearchpress.com by 210.87.254.105 on 09/05/12
For personal use only.

relatives of cyclohexane in the hope that it will inspire more definitive experiments. Current work in this laboratory is directed toward that end.

Experimental

The n.m.r. spectra were obtained on a JEOL JNM-C60S or C60HL using TMS as internal standard.

Synthesis of Sulfites

The best synthetic method for the preparation of these sulfites was found to be the thionyl chloride – pyridine method. This gave not only a good yield of sulfites, but also the highest yield of the less stable isomers. The following procedure for 4-methyl-trimethylene sulfite is typical.

To 45 g (0.50 mol) 1,3-butanediol, dissolved in 300 ml dry benzene and 150 ml dry pyridine, was added dropwise with stirring and external cooling 44 ml thionyl chloride (0.60 mol) in 100 ml benzene over a period of 3 h. After filtering off the salt formed and neutralizing with bicarbonate, the organic layer was separated and washed with 0.1 *N* HCl, water, and dried over $MgSO_4$. After filtration and concentration on a rotary evaporator, the sulfites were collected by g.l.c. using either an 8 ft × 0.50 in. 10% DEGS (LAC 728) on 60–80 Diatoport W with an F and M 720, or a 14–19 ft × 3/8 in. 20% DEGS on 40–60 Chromosorb W with a Varian 712 Autoprep. All new compounds gave satisfactory elemental analyses and isomeric purity was in all cases greater than 99% by g.l.c.

Dipole Moments

Dipole moments were calculated by the method of Guggenheim (3) from dielectric constants determined on a Wissenschaftlich-Technische Werkstatten (Germany) Dipolemeter DMO1 at 20 °C. Solvents were spectrograde and dried over Linde molecular sieve type 4A. The determination equation is:

$$\mu^2 = 27kT/4\pi N_L \cdot 1/d_1(\varepsilon_1 + 2)^2 \cdot (a_\varepsilon + a_n) \cdot M_2$$

where

k = Boltzmann constant
N_L = Lohschmidt's number
d_1 = solvent density
ε_1 = solvent dielectric constant
M_2 = solute molecular weight
a_ε = slope of line $(\varepsilon_{12} - \varepsilon_1)$ *vs.* w_2
a_n = slope of line $(n^2_{12} - n_1^2)$ *vs.* w_2
ε_{12} = solution dielectric constant
n_{12} = solution refractive index
n_1 = solvent refractive index
w_2 = solute weight fraction $(m_2/m_1 + m_2)$

At 20 °C the first term is 1.433×10^{-37}

Slopes were determined from a least squares plot on an IBM 1620 Mk II and μ reproducibility was generally better than 0.1 D.

Sulfite Equilibrations

Solutions (1 *M* in sulfite with 100 l BF_3–etherate per 3 ml solution) initially on each side of equilibrium were stirred at room temperature in sealed vials for 2–10 weeks, neutralized with K_2CO_3 and gas chromatographed on a 6 ft × 0.25 in. Carbowax 20M on 60–80 Porapak S. Area ratios were measured by planimeter and corrected for response ratios determined with a standard mixture under identical conditions. Calculations were done according to Eliel and Reese (35) taking T as 298 °K.

NOTE ADDED IN PROOF: Similar conclusions to some of those drawn here are contained in a recent paper by Wucherpfennig (36).

The financial assistance of the National Research Council of Canada is gratefully acknowledged. We thank Professor Saul Wolfe for his helpful discussions and Professor E. Wyn-Jones for providing preprints.

1. B. A. ARBOUZOV. Bull. Soc. Chim. Fr. 1311 (1960).
2. G. ECCLESTON, R. A. PETHRICK, E. WYN-JONES, P. C. HAMBLIN, and R. F. M. WHITE. Trans. Faraday Soc. **66**, 310 (1970).
3. For pertinent references and a critical discussion of dipole moment methods see: (*a*) J. W. SMITH. Electric Dipole Moments. Butterworth's Scientific Publications, London, 1955. Chapt. 2; (*b*) C. J. BOTTCHER. Theory of Electric Polarization. Elsevier Publishing Company, New York, N.Y. 1952. pp. 303 *ff*.
4. (*a*) H. F. VAN WOERDEN and E. HAVINGA. Rec. Trav. Chim. Pays-Bas, **86**, 341 (1967); (*b*) Rec. Trav. Chim. Pays-Bas, **86**, 353 (1967).
5. G. WOOD and M. H. MISKOW. Tetrahedron Lett. 1775 (1970).
6. G. WOOD and M. H. MISKOW. Tetrahedron Lett. 1109 (1969).
7. P. MARONI and L. CAZAUX. Presented at the Fifty-first Conference of the Chemical Institute of Canada, University of British Columbia, Vancouver, British Columbia, June, 1968.
8. R. A. PETHRICK and E. WYN-JONES. Quart. Revs. **23**, 304 (1969).
9. G. WOOD, J. M. MCINTOSH, and M. MISKOW. Tetrahedron Lett. 4895 (1970).
10. G. ECCLESTON and E. WYN-JONES. Chem. Commun. 1511 (1969).
11. P. C. HAMBLIN, R. F. M. WHITE, and E. WYN-JONES. J. Mol. Structure, **4**, 275 (1969).
12. E. L. ELIEL. Accts. Chem. Res. **3**, 3 (1970).
13. J. B. HENDRICKSON. J. Amer. Chem. Soc. **83**, 4537 (1961).
14. R. K. HARRIS and R. A. SPRAGG. J. Chem. Soc. 684 (1968).
15. F. A. L. ANET and A. J. R. BOURN. J. Amer. Chem. Soc. **89**, 760 (1967).
16. J. P. LOWE. *In* Progress in physical organic chemistry. Vol. 6. *Edited by* A. Streitwieser, Jr., and R. W. Taft. Interscience Division, John Wiley and Sons, Inc., New York, N.Y., 1968. p. 1 and Table 2, pp. 36 *ff*.
17. J. E. ANDERSON. Chem. Commun. 417 (1970).
18. (*a*) M. RABAN, G. W. J. KENNEY, JR., and F. B. JONES, JR. J. Amer. Chem. Soc. **91**, 6677 (1969); (*b*) M. RABAN and F. B. JONES, JR. J. Amer. Chem. Soc. **91**, 2180 (1969).
19. A. H. COWLEY, M. J. S. DEWAR, and W. R. JACKSON. J. Amer. Chem. Soc. **92**, 5206 (1970).
20. J. R. FLETCHER and I. O. SUTHERLAND. Chem. Commun. 706 (1969).
21. H. GOLDWHITE and D. G. ROWSELL. Chem. Commun. 713 (1969).
22. B. M. GIMARC. J. Amer. Chem. Soc. **92**, 266 (1970).

23. M. J. S. DEWAR and M. SHANSHAL. J. Amer. Chem. Soc. **91**, 3654 (1969).
24. M. J. S. DEWAR, M. SHANSHAL, and B. JENNINGS. J. Amer. Chem. Soc. **91**, 3655 (1969).
25. M. S. GORDON. J. Amer. Chem. Soc. **91**, 3122 (1969).
26. S. WOLFE, A. RAUK, L. M. TEL, and I. G. CSIZMADIA. J. Chem. Soc. B, 136 (1971).
27. C. H. BUSHWELLER, J. GOLINI, G. U. RAO, and J. W. O'NEIL. J. Amer. Chem. Soc., **92**, 3055 (1970).
28. (*a*) S. WOLFE, A. RAUK, L. M. TEL, and I. G. CSIZMADIA. Chem. Commun. 96 (1970); (*b*) S. WOLFE, A. RAUK, and I. G. CSIZMADIA. J. Amer. Chem. Soc. **91**, 1567 (1969); (*c*) J. Amer. Chem. Soc. **89**, 5710 (1967).
29. C. H. BUSHWELLER, J. GOLINI, G. U. RAO, and J. W. O'NEIL. Chem. Commun. 51 (1970).
30. W. G. BENTRUDE, J. H. HARGIS, and P. E. RUSEK, JR. Chem. Commun. 296 (1969).
31. C. BODKIN and P. SIMPSON. Chem. Commun. 829 (1969).
32. W. WADSWORTH, JR. and H. HORTON. J. Amer. Chem. Soc. **92**, 3785 (1970).
33. W. G. BENTRUDE, K. C. YEE, and J. H. HARGIS. Presented at the 160th National Meeting of the American Chemical Society, Chicago, Illinois, September, 1970.
34. C. ROMERS, C. ALTONA, H. R. BUYS, and E. HAVINGA. *In* Topics in stereochemistry. Vol. 4. *Edited by* E. L. Eliel and N. L. Allinger. Interscience Division, John Wiley and Sons, Inc., New York, N.Y., 1969 and references contained therein.
35. E. L. ELIEL and M. C. REESE. J. Amer. Chem. Soc. **90**, 1560 (1968).
36. W. WUCHERPFENNIG. Ann. Chemie, **737**, 144 (1970).

Can. J. Chem. Downloaded from www.nrcresearchpress.com by 210.87.254.105 on 09/05/12
For personal use only.

Can. J. Chem. Downloaded from www.nrcresearchpress.com by 210.87.254.40 on 09/05/12
For personal use only.

Effect of Solvent Upon the Vicinal Proton Coupling Constants of Complex Substituted Ethanes. II. Anomalous Results for 1-Phenyl-1,2,2-trihaloethanes[1]

W. F. Reynolds and D. J. Wood
Lash Miller Chemical Laboratories, University of Toronto, Toronto 181, Ontario

Received September 9, 1970

The n.m.r. spectra of 11 tetra-substituted ethanes have been obtained in a number of solvents. Changes in the vicinal coupling constants of 1-phenyl-1,2,2-trihaloethanes with solvent do not fit the electrostatic model for solvent effects. It is concluded that the theory breaks down because solute–solvent hydrogen bonding specifically favors the *trans* rotamers of these compounds. The conditions under which the theory would be expected to break down are also discussed in more general terms.

Les spectres r.m.n. de 11 éthanes tetra-substitués ont été obtenus dans un certain nombre de solvants. Des changements, avec le solvant, des constantes de couplage vicinales des phényl-1 trihalo-1,2,2 éthanes ne peuvent être accomodés avec le modèle électrostatique des effets de solvant. Il en est conclu que la théorie ne tient pas parce que des ponts hydrogènes entre le solvant et le soluté favorisent le rotamère *trans* de ces composés. Les conditions où la théorie ne serait pas appropriée sont aussi discutées en termes plus généraux.

Canadian Journal of Chemistry, **49**, 1209 (1971)

Introduction

For substituted ethanes containing two or more polar groups, the fractional population of the most polar rotational isomer (rotamer) normally increases on going from the gas phase to a polar or polarizable medium (1). Observed differences for the rotationally averaged vicinal n.m.r. coupling constant(s) of the same compound in different solvents have been interpreted as due to changes in rotamer population (2–4). More recently, Abraham *et al.* have developed an electrostatic theory for the solvent reaction field (5), which enables one to calculate the energy difference between rotamers of a disubstituted ethane as a function of solvent dielectric constant, ε, and the energy difference in the gas phase. It can also be used to calculate vicinal coupling constants for the individual rotamers from changes in rotationally averaged vicinal coupling constants with solvent. The theory has been modified to allow for the presence of three or more dipolar substituents (6) and solvent–solute dipole–dipole interactions (7). It has been successfully used to predict differences between rotamer energy levels in a number of simple substituted ethanes in which two of the three rotamers have degenerate energy levels (8).

We have been interested in the problem of estimating relative rotamer energy levels of more complex substituted ethanes where all three rotamers have different energy levels and where gas phase energy differences are generally not known. We have shown that relative rotamer energy levels for 1-phenyl-1,2-dibromoethane can be correctly deduced from changes of vicinal coupling constants with ε and that reasonable values of relative rotamer energy levels for 1-phenyl-1,2-dibromopropanes can be deduced from the variation of vicinal coupling constants with ε and temperature (9). However, this approach will only be valid if the compounds investigated obey the electrostatic theory (5). In order to test the limits of applicability of the theory to more complex substituted ethanes, we have extended our investigation to include a large number of tetra-substituted ethanes, including 1-phenyl-1,2,2-trihaloethanes, 1-phenyl-1,2-dichloropropanes and 1,1,2-trihalopropanes. The results of these investigations are reported here.

Experimental

1-Phenyl-1,2,2-trichloropropane was produced as a by-product (20% yield) during the chlorination of styrene in CH_2Cl_2. It was separated and purified by v.p.c. Similarly, 1-(*p*-tolyl)-1,2,2-trichloroethane was produced from 4-methylstyrene. 1-Phenyl-1,2,2-tribromoethane was prepared by the addition of Br_2 to *trans*-β-bromostyrene in CH_2Cl_2. The solid product (m.p. 34°) was purified by low temperature recrystallization from methanol.

Bromination of *trans*-β-chlorostyrene in CH_2Cl_2 gave a 52–48 mixture of the two isomeric 1-phenyl-1,2-dibromo-2-chloroethanes. The products could not be separated by v.p.c. or fractional distillation because of their very similar physical properties. Therefore the mixture was purified by v.p.c. and n.m.r. data were obtained using the mixture. Chlorination of *trans*-β-bromostyrene

[1]For Part I, see ref. 9.

TABLE 1. Chemical shifts (δ scale) and vicinal coupling constants (Hz) for 1-phenyl-1,2,2-trihaloethanes

Compound	Solvent	Concentration (M)	ε	J_{AB}	δ_A	δ_B
1-Phenyl-1,2,2-tribromoethane	CCl_4	0.30	2.36	7.35	5.93	5.30
	$CDCl_3$	0.15	4.58	7.39	6.00	5.38
		0.30	4.70	7.39	6.00	5.38
		0.60	4.65	7.37	5.99	5.37
	$(CH_2)_4O$	0.30	6.79	7.77	6.45	5.61
	$(CH_3)_3CCl$	0.30	9.17	7.32	6.05	5.39
	$(CH_3)_2C{=}O$	0.15	19.1	7.83	6.55	5.71
		0.30	18.9	7.81	6.55	5.71
		0.60	17.6	7.72	6.53	5.68
	C_2H_5OH	0.30	23.8	7.41	6.30	5.49
	$CH_3C{\equiv}N$	0.30	33.6	7.69	6.31	5.60
	$(CH_3)_2S{=}O$	0.30	43.1	8.14	6.86	5.88
1-Phenyl-1,2,2-trichloroethane	CCl_4	0.30	2.33	5.98	5.89	5.09
	$CDCl_3$	0.30	4.59	5.86	5.98	5.18
	$(CH_3)_3CCl$	0.30	9.15	5.77	6.03	5.20
	$(CH_3)_2C{=}O$	0.30	18.5	5.93	6.53	5.55
	$CH_3C{\equiv}N$	0.30	33.4	5.80	6.31	5.44
	$(CH_3)_2S{=}O$	0.30	43.6	6.04	6.87	5.75
erythro-1-Phenyl-1,2-dibromo-2-chloroethane	CCl_4	0.21*	2.41	7.86	5.98	5.22
	$CDCl_3$	0.21	4.52	7.84	6.05	5.29
	$(CH_3)_3CCl$	0.21	8.97	7.75	6.11	5.31
	$(CH_3)_2C{=}O$	0.21	18.5	8.15	6.63	5.65
	$(CH_3)_2S{=}O$	0.21	42.2	8.46	6.98	5.85
threo-1-Phenyl-1,2-dibromo-2-chloroethane	CCl_4	0.19*	2.41	6.02	6.03	5.28
	$CDCl_3$	0.19	4.52	6.08	6.09	5.34
	$(CH_3)_3CCl$	0.19	8.97	6.01	6.13	5.37
	$(CH_3)_2C{=}O$	0.19	18.5	6.43	6.61	5.69
	$(CH_3)_2S{=}O$	0.19	42.2	6.71	6.93	5.87
erythro-1-Phenyl-1,2-dichloro-2-bromoethane	CCl_4	0.25*	2.42	5.66	5.93	5.17
	$CDCl_3$	0.25	4.70	5.60	6.00	5.24
	$(CH_3)_3CCl$	0.25	8.87	5.50	6.04	5.25
	$(CH_3)_2C{=}O$	0.25	18.4	5.73	6.53	5.58
	$(CH_3)_2S{=}O$	0.25	42.3	5.88	6.85	5.77
threo-1-Phenyl-1,2-dichloro-2-bromoethane	CCl_4	0.32*	2.43	6.58	5.90	5.14
	$CDCl_3$	0.32	4.67	6.52	5.98	5.23
	$(CH_3)_3CCl$	0.32	8.87	6.47	6.02	5.24
	$(CH_3)_2C{=}O$	0.32	18.4	6.66	6.54	5.57
	$(CH_3)_2S{=}O$	0.32	42.2	6.81	6.87	5.77

*Total solute concentration 0.40 M.

in CH_2Cl_2 gave an 80–20 mixture of the two isomeric 1-phenyl-1,2-dichloro-2-bromoethanes with the major product having the larger coupling constant. The corresponding reaction of *cis*-β-bromostyrene gave a 33–67 mixture of the same products. The isomers could not be separated and the two mixtures were purified by v.p.c. The n.m.r. spectra of both mixtures were recorded for each solvent. In every case, coupling constants for a given compound agreed within experimental error, suggesting that solute–solute interactions were unimportant. Assignment of each pair of isomers as *erythro* and *threo* is considered in the Discussion.

Erythro- and *threo*-1-phenyl-1,2-dichloropropane were prepared by addition of Cl_2 to *trans*-1-phenylpropene in CCl_4. The two liquid products were obtained in nearly equimolar quantities. They were separated and purified by v.p.c. 1,1,2-Tribromo- and 1,1,2-trichloropropane were obtained commercially and purified by v.p.c.

All halogenation reactions were carried out in the dark, using 0.3 M solutions of styrenes. The styrenes used in this investigation were obtained commercially and were used without further purification. All products were characterized by n.m.r. and mass spectra. Solvents were dried with appropriate drying agents and distilled in an N_2 atmosphere before use.

The n.m.r. spectra were recorded on a Varian HA-100 spectrometer operating in frequency sweep mode (ambient temperature 30°). Procedures followed were identical to those reported previously (9).

Solution dielectric constants were measured with a W.T.W. DKO3 dielectric constant apparatus with the cell thermostatted at 30°. The v.p.c. purifications were carried out using a Varian Aerograph Autoprep 700 gas chromatograph. Mass spectra were obtained with a C.D.C. 21490 mass spectrometer.

Results

The n.m.r. spectra of the substituted ethyl groups of the various 1-phenyl-1,2,2-trihalo-

Can. J. Chem. Downloaded from www.nrcresearchpress.com by 210.87.254.40 on 09/05/12
For personal use only.

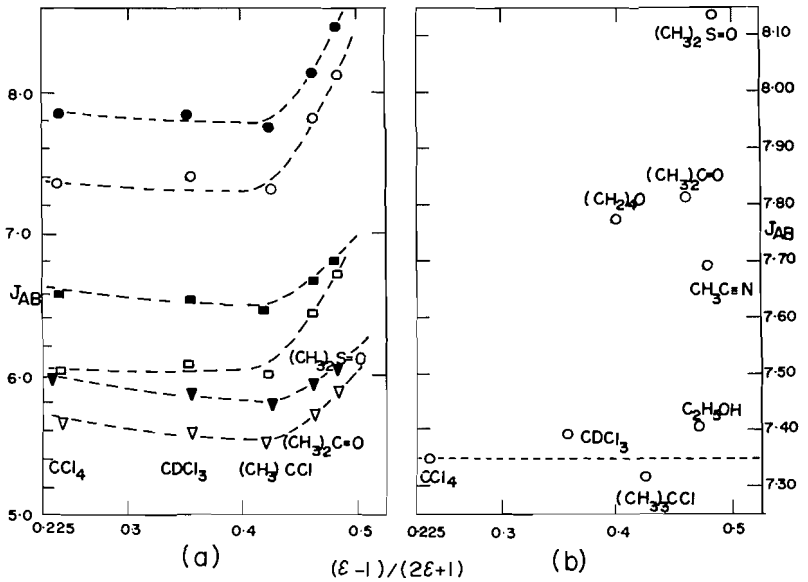

FIG. 1. (*a*) Plot of the vicinal coupling constant, J_{AB}, for 1-phenyl-1,2,2-trihaloethanes in five solvents *vs.* the dielectric function $(\varepsilon - 1)/(2\varepsilon + 1)$. ● *erythro*-1-phenyl-1,2-dibromo-2-chloroethane, ○ 1-phenyl-1,2,2-tribromoethane, ■ *threo*-1-phenyl-1,2-dichloro-2-bromoethane, □ *threo*-1-phenyl-1,2-dibromo-2-chloroethane, ▼ 1-phenyl-1,2,2-trichloroethane, ▽ *erythro*-1-phenyl-1,2-dichloro-2-bromoethane. (*b*) Expanded plot of J_{AB} *vs.* $(\varepsilon - 1)/(2\varepsilon + 1)$ for 1-phenyl-1,2,2-tribromoethane.

ethanes were analyzed as AB spectra. Results for room temperature measurements are given in Table 1 and Fig. 1. Results for variable temperature experiments for 1-phenyl-1,2,2-tribromoethane are given in Fig. 2.

The substituted propyl groups for the 1-phenyl-1,2-dichloropropanes and 1,1,2-trihalopropanes gave ABC_3 spectra. As previously reported (9), the splittings of the A and C protons corresponded, within 0.01 Hz, with $|J_{AC}|$ and $|J_{BC}|$. Therefore, the coupling constants were measured directly from these splittings. Values of the vicinal coupling constants are given in Table 2.

Results for 1-(*p*-tolyl)-1,2,2-trichloroethane are given in Table 3. The AA'BB' ring proton spectra were analyzed by an AB approximation. Assignment of ortho and meta protons was based upon the observation of greater long range coupling to the protons ortho to the methyl group (10) and was confirmed by a double resonance experiment in which the methyl group was decoupled.

The r.m.s. error for measurements of coupling constants was always less than 0.05 Hz. It is assumed that coupling constants are accurate within this value.

Rotamers for the various compounds included in this investigation are illustrated in Fig. 3.

Discussion

It is difficult to unambiguously assign pairs of *erythro* and *threo* compounds in the 1-phenyl-1,2,2-trihaloethane series. The actual assignments given are based upon the results of empirical energy calculations (11) similar to those of Scott and Scheraga (12). Pairs of compounds were assigned by assuming that the compound with the larger vicinal coupling constant (J_{AB}) corresponded to the compound with the larger fractional population of the *trans* rotamer. The assignments are believed to be correct since they correspond to predominant *cis* addition of chlorine and *trans* addition of bromine to ethylenic bonds, in agreement with previously reported results for the halogenation of 1-phenylpropene (13). It should be emphasized, however, that the following discussion would not be changed even if one or more of the assignments were incorrect since it is concerned with the anomalous solvent dependence of the vicinal coupling constants of these compounds and not primarily with the relative stabilities of rotamers.

(a) Evidence for Breakdown of the Electrostatic Theory

The effect of solvent upon the rotationally

Can. J. Chem. Downloaded from www.nrcresearchpress.com by 210.87.254.40 on 09/05/12
For personal use only.

TABLE 2. Chemical shifts (δ scale) and coupling constants (Hz) for 1,1,2-trisubstituted propanes (all solute concentrations 0.30 *M*)

Compound	Solvent	ε	J_{AB}	J_{BC}	δ_A	δ_B	δ_C
1,1,2-Tribromopropane	CCl_4	2.29	3.20	6.53	5.88	4.46	1.90
	$CDCl_3$	4.52	3.20	6.54	5.91	4.50	1.89
	$(CH_3)_3CCl$	8.58	3.19	†	5.94	4.49	†
	$(CH_3)_2C{=}O$	*	3.11	6.51	6.31	4.72	1.85
	$(CH_3)_2S{=}O$	44.3	2.94	6.50	6.54	4.82	1.75
1,1,2-Trichloropropane	CCl_4	2.32	3.60	6.54	5.81	4.29	1.70
	$CDCl_3$	4.65	3.56	6.56	5.85	4.35	1.69
	$(CH_3)_3CCl$	9.14	3.50	†	5.89	4.34	†
	$(CH_3)_2C{=}O$	*	3.24	6.52	6.30	4.58	1.65
	$(CH_3)_2S{=}O$	43.6	3.01	6.52	6.58	4.68	1.57
erythro-1-Phenyl-1,2-dichloropropane	CCl_4	2.30	8.03	6.43	4.80	4.28	1.70
	$CDCl_3$	4.48	7.82	6.44	4.88	4.36	1.70
	$(CH_3)_3CCl$	9.05	7.67	†	4.88	4.34	†
	$(CH_3)_2C{=}O$	18.6	7.63	6.43	5.16	4.59	1.66
	$(CH_3)_2S{=}O$	43.4	7.50	6.47	5.32	4.71	1.60
threo-1-Phenyl-1,2-dichloropropane	CCl_4	2.39	5.58	6.69	4.93	4.32	1.43
	$CDCl_3$	4.51	6.00	6.65	4.97	4.38	1.44
	$(CH_3)_3CCl$	9.28	5.94	†	4.97	4.35	†
	$(CH_3)_2C{=}O$	20.0	6.11	6.59	5.22	4.55	1.46
	$(CH_3)_2S{=}O$	44.4	5.98	6.59	5.39	4.65	1.43

*Cell malfunction prevented measurement.
†Solvent peak interference prevented measurement.

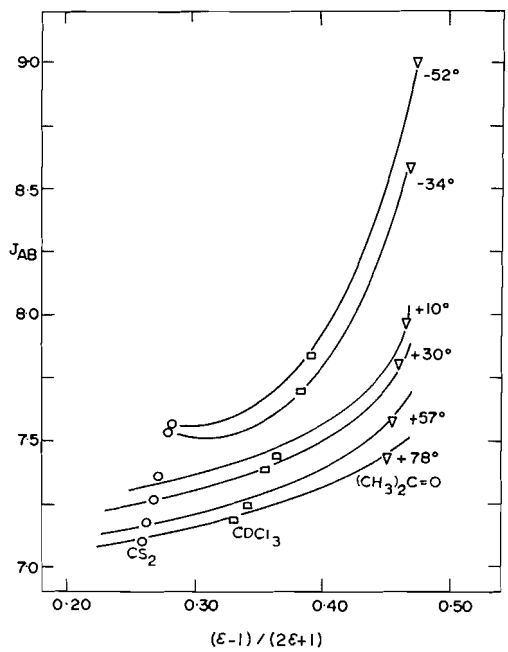

FIG. 2. Plot of J_{AB} for 1-phenyl-1,2,2-tribromoethane in three solvents at different temperatures *vs.* the dielectric function (ε − 1)/(2ε + 1).

averaged coupling constants of 1-phenyl-1,2,2-trihaloethanes is unusual (see Fig. 1*a*). The J_{AB} value decreases slightly or remains essentially constant on changing from solvents of low to intermediate ε but increases significantly in solvents of higher ε (particularly acetone and dimethylsulfoxide). Previous investigations of simpler substituted ethanes have revealed either a regular increase or a regular decrease in vicinal coupling constants with increasing ε for the solvents used in this investigation (8), although anomalous results have been noted for aromatic and hydroxylic solvents. Results of previous investigations have also been in general agreement with predictions of the electrostatic theory. However, as shown below, this theory does not predict the increase of J_{AB} for 1-phenyl-1,2,2-trihaloethanes in polar media.

Assuming staggered conformations for the three rotamers of 1-phenyl-1,2,2-tribromoethane and C—Br, H—C and C—phenyl bond dipole moments of respectively 1.48, 0.4 (14), and 0.35 D,[2] the predicted dipole moments of rotamers **1**, **2**, and **3** (see Fig. 3) are respectively 1.13, 2.08, and 3.11 D. According to the electrostatic theory, rotamer **3** would be stabilized relative to rotamers **1** and **2** by 0.33 and 0.23 kcal/mol respectively on going from the gas phase to carbon tetrachloride solution and by 0.52 and 0.35 kcal/mol on going from carbon tetrachloride to acetone solution (for details of calculations see Appendix). These predictions are not significantly altered if

[2]Based upon dipole moments for alkylbenzenes (15).

Can. J. Chem. Downloaded from www.nrcresearchpress.com by 210.87.254.40 on 09/05/12
For personal use only.

TABLE 3. Chemical shifts (δ scale) and coupling constants (Hz) for 1-(*p*-tolyl)-1,2,2-trichloroethane (all solutions 0.30 *M*)

Solvent	δ_{ortho}*	δ_{meta}	$\delta_{ortho} - \delta_{meta}$	J_{AB}	δ_A	δ_B
CCl_4	7.278	7.121	0.156	5.97	5.88	5.04
$(CH_2)_4O$	7.376	7.164	0.212	6.03	6.36	5.37
$(CH_3)_3CCl$	7.307	7.138	0.169	5.81	5.97	5.15
$(CH_3)_2C{=}O$	7.470	7.227	0.243	5.95	6.47	5.48
$(CH_3)_2S{=}O$	7.451	7.209	0.243	6.09	6.83	5.69

*Ortho to trichloroethyl group.

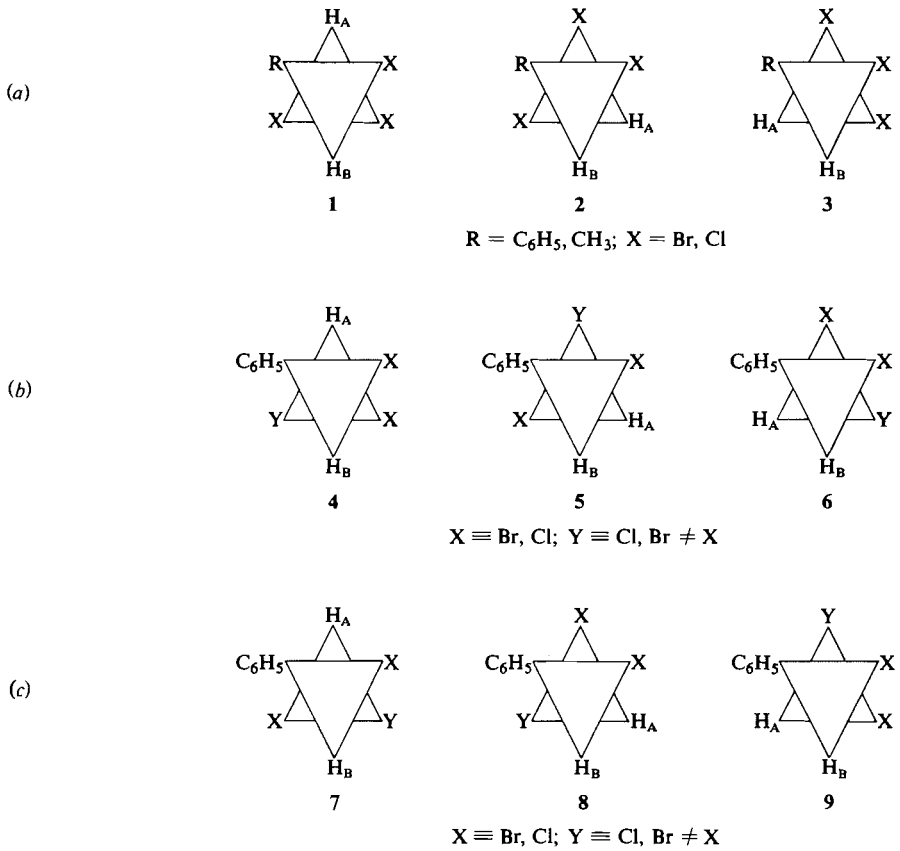

FIG. 3. Possible rotamers for the various tetrasubstituted ethanes which were investigated: (*a*) tribromo- and trichloro-compounds, (*b*) *threo*-1-phenyl-1,2,2-trihaloethanes, (*c*) *erythro*-1-phenyl-1,2,2-trihaloethanes (for *erythro*- and *threo*-1-phenyl-1,2-dihalopropanes see ref. 9).

one considers deviations from staggered conformations of as much as 15° or if one uses only C—Br group dipole moments in place of C—Br, H—C and C—phenyl bond dipole moments. Therefore, according to the electrostatic theory, the fractional population of rotamer **1** should decrease with increasing ε, leading to a decrease in J_{AB}. The same prediction would be made for all of the other 1-phenyl-1,2,2-trihaloethanes included in this investigation since C—Cl and C—Br bond dipole moments are only slightly different.

The electrostatic theory has recently been modified to include solvent–solute dipole–dipole interactions (7). However, inclusion of a term of this type would lead to the prediction of even greater stability of rotamer **3** (and a correspondingly smaller value of J_{AB}) in polar media

Can. J. Chem. Downloaded from www.nrcresearchpress.com by 210.87.254.40 on 09/05/12
For personal use only.

Can. J. Chem. Downloaded from www.nrcresearchpress.com by 210.87.254.40 on 09/05/12
For personal use only.

(an effect of this type has been demonstrated experimentally for 1,1,2-trichloroethane (7)). Therefore, it must be concluded that neither the simple nor the modified electrostatic theory can explain the observed increase of J_{AB} for 1-phenyl-1,2,2-trihaloethanes in acetone and dimethylsulfoxide.

(b) Evidence for Existence of Specific Hydrogen Bonding Interactions

As shown in Table 1, J_{AB} for 1-phenyl-1,2,2-trichloroethane is nearly independent of concentration in chloroform and acetone over a concentration range from 0.15 to 0.60 *M*. Consequently, it is improbable that anomalous results can be explained in terms of specific solute–solute interactions.

An alternate explanation, which we favor, is that specific hydrogen bonding occurs between the protons of 1-phenyl-1,2,2-trihaloethanes (either involving the ethyl protons or phenyl protons, *vide infra*) and strong hydrogen bonding solvents such as acetone and dimethylsulfoxide and that this hydrogen bonding favors the *trans* rotamer relative to the other rotamers. A similar explanation has been offered to account for the failure of the electrostatic theory to predict accurate rotamer energy differences for 1-chloro-1,2-dibromo-1-iodoethane in polar solvents (16).

In order to test the possibility of specific hydrogen bonding, 1-phenyl-1,2,2-tribromoethane was investigated in a number of additional solvents which were chosen because their hydrogen bonding properties did not parallel their dielectric constants. Assuming that CCl_4, $CDCl_3$, and $(CH_3)_3CCl$ are "normal" solvents, the order of magnitude of deviation of J_{AB} is acetonitrile < tetrahydrofuran < acetone < dimethylsulfoxide (see Fig. 1*b*). This parallels the hydrogen bonding abilities of these solvents as measured by association constants with phenol (17, 18), but is totally unrelated to ε. The large value of J_{AB} in tetrahydrofuran is particularly suggestive of hydrogen bonding in view of the relatively low ε for the tetrahydrofuran solution. Ethanol shows no tendency to stabilize the *trans* rotamer. This may indicate that ethanol preferentially hydrogen bonds to the halogen atoms.

Variable temperature measurements for 1-phenyl-1,2,2-tribromoethane in carbon disulfide, chloroform, and acetone provide support for the suggestion of specific hydrogen bonding in acetone. The J_{AB} value has a much larger negative temperature coefficient in acetone than in the other two solvents. When J_{AB} is plotted as a function of ε at different temperatures (Fig. 2), it is seen that J_{AB} increases rapidly with ε at low temperatures but that the plot becomes flatter as the temperature is increased, *i.e.* the solvent dependence of J_{AB} becomes closer to the predictions of the electrostatic theory at higher temperatures.

This is precisely the behavior which one would expect if the *trans* rotamer were being favored by specific hydrogen bonding in acetone. The extent of hydrogen bonding should decrease with increasing temperature. The negative temperature coefficient for J_{AB} in the other solvents is not surprising. Since rotamer **1** has a smaller total of steric and dipolar interactions than the other two rotamers, it should be the most stable rotamer. This is supported by the relatively large value of J_{AB} in all solvents and by empirical energy calculations (11). Consequently, the fractional population of rotamer **1** would be expected to increase with decreasing temperature, leading to an increase in J_{AB}. There will be a compensating change in each solvent due to the increase in ε with decreasing temperature, but the plots of J_{AB} *vs.* $(\varepsilon - 1)/(2\varepsilon + 1)$ at different temperatures indicate that the former effect predominates.

The chemical shift data for 1-phenyl-1,2,2-tribromoethane suggest specific hydrogen bonding to the protons of the substituted ethyl group. In acetone, H_A (see Fig. 3) shifts to high field by approximately 0.34 p.p.m. (relative to internal tetramethylsilane) when the temperature is increased from $-52°$ to $+78°$. Corresponding shifts in chloroform and carbon disulfide are 0.06 and -0.04 p.p.m. The large shifts in acetone are consistent with hydrogen bond breaking. At room temperature, H_A for 1-phenyl-1,2,2-tribromoethane shifts 0.12 p.p.m. to low field on going from carbon tetrachloride to *t*-butyl chloride but by 0.38, 0.52, 0.62, and 0.93 p.p.m. on going from carbon tetrachloride to acetonitrile, tetrahydrofuran, acetone, and dimethylsulfoxide, respectively. Similar, although smaller, shifts are noted for H_B and for the other compounds investigated (see Table 1).

It can be seen from the above discussion that the chemical shift and coupling constant data for 1-phenyl-1,2,2-tribromoethane are all consistent with the suggestion that basic hydrogen-bonding

Can. J. Chem. Downloaded from www.nrcresearchpress.com by 210.87.254.40 on 09/05/12
For personal use only.

solvents form hydrogen bonds with 1-phenyl-1,2,2-trihaloethanes, preferentially stabilizing the *trans* rotamers **1**, **4**, or **7**.

(c) General Discussion of Conditions for Breakdown of Electrostatic Theory

As stated in the Introduction, the primary purpose of this investigation was to establish the limitations of the application of the electrostatic theory to complex substituted ethanes. On the basis of available evidence, it would appear that di- and tri-substituted ethanes (with at least two halogen substituents) obey the simple (5) or modified (7) theory. Our results suggest that the theory may break down in the case of tetra-substituted ethanes in hydrogen-bonding media and should be used with caution in these systems.

One possible explanation for these observations is that in di- and tri-substituted ethanes all rotamers are hydrogen-bonded to a roughly equal extent while in tetra-substituted ethanes the *trans* rotamer is specifically favored by hydrogen bonding to ethyl C—H protons, possibly for steric reasons. The coupling constant data for 1-phenyl-1,2,2-trihaloethanes (Table 1 and Fig. 1) indicate that steric factors may be important in determining preferential stabilization of the *trans* rotamer. For example, the change in J_{AB} on going from *t*-butyl chloride to dimethylsulfoxide is only 0.27 Hz for 1-phenyl-1,2,2-trichloroethane while it is 0.82 Hz for 1-phenyl-1,2,2-tribromoethane. Average values for the bromodichloro and chlorodibromo compounds are respectively 0.36 and 0.71 Hz.

On the basis of the above explanation, one would expect the probability of breakdown of the theory to increase as the number of electron-withdrawing groups increases, due to increased hydrogen bonding. The evidence concerning this point is ambiguous. The electrostatic theory gives at least qualitatively correct predictions for meso-2,3-dibromobutane (7), *erythro-* and *threo-*1-phenyl-1,2-dibromo- (9) and dichloropropanes (Table 2) and 1,1,2-trihalopropanes (Table 2) while it breaks down for 1-phenyl-1,2,2-trihaloethanes. Three 1,1,2,2-tetrahaloethanes have been investigated. In both 1-chloro-1,2-dibromo-1-iodoethane (16) and 1,1,2,2-tetrafluoroethane (19), the electrostatic theory underestimates the stability of the *trans* rotamer in polar solvents. However, in both cases the deviations probably are less than the possible errors in the calculation. The theory gives good results for 1,1,2,2-tetrachloroethane (20). Consequently, it must be concluded that there is conclusive evidence for the breakdown of the electrostatic theory only in the case of 1-phenyl-1,2,2-trihaloethanes.

An alternative explanation involves specific hydrogen bonding of the solvent with phenyl protons. We have obtained some evidence that the phenyl group may be involved in specific hydrogen bonding. In non-polar solvents, the phenyl proton spectrum of each 1-phenyl-1,2,2-trihaloethane was essentially a single peak but in basic hydrogen bonding solvents a two proton multiplet appeared at slightly lower field. In order to investigate this phenomenon, we synthesized 1-(*p*-tolyl)-1,2,2-trichloroethane. The pattern of chemical shifts for this compound (see Table 3) is consistent with hydrogen-bonding to the phenyl protons. The protons ortho to the trihaloethyl group are shifted to a greater extent than the meta protons.

It is possible that hydrogen bonding may favor the *trans* rotamer simply by increasing the effective size of the phenyl group. On the basis of total steric and dipolar interactions, the *trans* rotamer (**1**, **4**, or **7**) and one of the *gauche* rotamers (**2**, **5**, or **8**) should be favored over the other *gauche* rotamer. The phenyl group is in a less sterically hindered environment than the favored *gauche* rotamer (see Fig. 3). Consequently an increase in size of the phenyl group should favor the *trans* rotamer.

However, in view of the bulk of the trihaloethyl group, it is surprising that the solvent should hydrogen bond to a greater extent to the ortho protons than to the meta protons. It has previously been reported that in 1-methyl-4-X-benzenes (where X was a polar group), acetone preferentially hydrogen bonded to the protons ortho to the methyl group (10*a*). Examination of molecular models suggests an alternate, although highly speculative, explanation for the low field shift of the ortho phenyl protons and, in part, for the increased stability of the *trans* rotamer (**1**, **4**, or **7**). In this rotamer, the β proton (H_A) and one of the ortho protons tend to align in a manner which allows them to simultaneously hydrogen bond to the same solvent molecule. No similar arrangement is possible with the *gauche* rotamer (**2**, **5**, or **8**) since the β proton is *trans* to the phenyl group in this rotamer.

It would obviously be useful to determine more

Can. J. Chem. Downloaded from www.nrcresearchpress.com by 210.87.254.40 on 09/05/12
For personal use only.

conclusively the reasons for the break-down of the electrostatic theory. Low temperature investigations, in which individual rotamers are observed, would be particularly useful in this respect. Our spectrometer cannot, at present, reach sufficiently low temperatures to "freeze out" individual rotamers but it is hoped to modify it to carry out experiments of this type.

In the absence of more definite information, our tentative conclusion is that the electrostatic theory probably breaks down in the case of 1-phenyl-1,2,2-trihaloethanes in polar media because of specific hydrogen bonding to the phenyl groups. However, the possibility that the breakdown is at least in part due to hydrogen bonding to the ethyl C—H protons also cannot be ruled out.

Conclusions

(*1*) Changes in the vicinal coupling constants of 1-phenyl-1,2,2-trihaloethanes with solvent cannot be explained by the electrostatic theory of solvent effects.

(*2*) Chemical shift and coupling data support the postulate that the *trans* rotamers of 1-phenyl-1,2,2-trihaloethanes are preferentially stabilized by hydrogen bonding in basic hydrogen bonding solvents.

(*3*) The preferential stabilization may be due to hydrogen bonding to either ethyl or phenyl protons or to some combination of both effects.

Appendix

The radius of the molecular cavity for 1-phenyl-1,2,2-tribromoethane was estimated by assuming that the difference in molar volume between 1-phenyl-1,2,2-tribromoethane and 1,1,2-tribromoethane was equal to that between 1-phenyl-1-bromoethane and bromoethane. The estimated molar volume and radius of the molecular cavity were respectively 168.4 cm^3 and 4.055 Å. The refractive index, n, was estimated as 1.617, using additive molar refraction parameters (21).

Bond dipole moments used in the calculation of rotamer dipole moments are listed in the discussion. The X—C—C and X—C—X (X ≡ Br or C_6H_5) angles were fixed at 111.5° and H—C—C angles at 109.5°. The following bond lengths (Å) were used: C—C = 1.54, C—C_6H_5 = 1.52, C—Br = 1.94, C—H = 1.11. Due to the completely non-spherical shape of the molecule, the quadrupole moment for each rotamer was calculated choosing the mid-point of the ethyl C—C bond as the origin. Since the calculation should be carried out with the geometrical center of the molecule as the origin, this may have introduced some error, particularly for the *gauche* rotamers (6). However, any significant change in the origin for rotamer **3** would result in an increase in the relatively small value (see below) for the quadrupolar reaction field parameter q_3 and a predicted greater stability for this rotamer.

The calculated values for the dipolar and quadrupolar reaction field parameters (5) are: $k_1 = 0.27_6$, $k_2 = 0.93_5$, $k_3 = 2.08_2$, $h_1 = 1.47_2$, $h_2 = 0.91_2$, $h_3 = 0.24_3$ kcal/mol. These values are generally smaller than previously calculated values for haloethanes (8). This is due to the significantly larger molar volume of this compound and to the use of bond dipole moments in place of group dipole moments.

The above values for k, h, and n lead to eqs. 1 and 2 for the rotamer energy differences (5);

$$[1]\quad \Delta E_{3-1}{}^{s} = \Delta E_{3-1}{}^{g} - [1.806X/(1 - 0.700X)] + [3.687X/(5 - X)]$$

$$[2]\quad \Delta E_{3-2}{}^{s} = \Delta E_{3-2}{}^{g} - [1.147X/(1 - 0.700X)] + [2.007X/(5 - X)]$$

where $\Delta E^g \equiv$ energy difference in the gas phase $\Delta E^s \equiv$ energy difference in a solution of dielectric constant ε, and $X \equiv (\varepsilon - 1)/(2\varepsilon + 1)$ (5). Insertion of solution dielectric constants into eqs. 1 and 2 yields the energy changes quoted in the discussion.

Financial support from the National Research Council of Canada is gratefully acknowledged.

1. S. Mizushima. Structure of molecules and internal rotation. Academic Press, Inc. New York, N.Y. 1954.
2. N. Sheppard and J. J. Turner. Proc. Roy. Soc. A**252**, 506 (1959).
3. H. Finegold. J. Chem. Phys. **41**, 1808 (1964).
4. E. I. Snyder. J. Amer. Chem. Soc. **88**, 1165 (1965).
5. R. J. Abraham, L. Cavalli, and K. G. R. Pachler. Mol. Phys. **11**, 471 (1966).
6. R. J. Abraham and M. A. Cooper. J. Chem. Soc. B, 202 (1967).
7. R. J. Abraham. J. Phys. Chem. **73**, 1192 (1969).
8. R. J. Abraham and G. Gatti. J. Chem. Soc. B, 961 (1969) and references therein.
9. W. F. Reynolds and D. J. Wood. Can. J. Chem. **47**, 1295 (1967).

10. (*a*) T. SCHAEFER and W. G. SCHNEIDER. J. Chem. Phys. **32**, 1218 (1960); (*b*) G. KOTOWYCZ and T. SCHAEFER. Can. J. Chem. **44**, 2743 (1966).
11. W. F. REYNOLDS and D. J. WOOD. To be published.
12. R. A. SCOTT and H. A. SCHERAGA. J. Chem. Phys. **45**, 2091 (1966).
13. (*a*) R. C. FAHEY and C. SHUBERT. J. Amer. Chem. Soc. **87**, 5172 (1965); (*b*) R. C. FAHEY and H. J. SCHNEIDER. J. Amer. Chem. Soc. **90**, 4429 (1968).
14. L. E. SUTTON. *In* Determination of organic structures by physical methods. Vol. 1. Academic Press, Inc., New York, N.Y., 1965. Chapt. 9.
15. A. L. MCCLELLAN. Tables of experimental dipole moments. W. H. Freeman and Co., San Francisco, California, 1963.
16. G. GOVIL and H. J. BERNSTEIN. J. Chem. Phys. **49**, 911 (1968).
17. (*a*) T. GRAMSTAD. Spectrochim. Acta, **19**, 497 (1962); (*b*) T. GRAMSTAD. Spectrochim. Acta, **19**, 829 (1962).
18. M. D. JOESTEN and R. S. DRAGO. J. Amer. Chem. Soc. **84**, 3817 (1962).
19. L. CAVALLI and R. J. ABRAHAM. Mol. Phys. **19**, 265 (1970).
20. R. J. ABRAHAM and M. A. COOPER. Chem. Commun. 588 (1966).
21. Handbook of chemistry and physics. 44th Ed. Chemical Rubber Publishing Co., Cleveland, Ohio, 1963.

Can. J. Chem. Downloaded from www.nrcresearchpress.com by 210.87.254.40 on 09/05/12
For personal use only.

Can. J. Chem. Downloaded from www.nrcresearchpress.com by 210.87.254.6 on 09/05/12
For personal use only.

Structure of the Second Coordination Sphere of Transition Metal Complexes. II. Substituted Anilines as Ligands

D. R. EATON, H. O. OHORODNYK, AND LINDA SEVILLE
Department of Chemistry, McMaster University, Hamilton, Ontario

Received[1] January 26, 1970

The role of substituted anilines as second coordination sphere ligands of cobalt(II) complexes has been investigated. Chemical shifts of the ligand nuclear magnetic resonance (n.m.r.) spectra arising from pseudo-contact interaction with the paramagnetic cobalt complex have been utilized for this purpose. It has been found that in each case the aniline preferentially occupies a position perpendicular to the three fold symmetry axis of the complex and tends to be aligned with the amino group directed towards the cobalt atom. Electron withdrawing substituents para to the amino group enhance the second coordination sphere binding and electron donating substituents diminish it. These results are consistent with the idea that the structure of the second coordination sphere is determined by electrostatic interaction with the negatively charged ligands comprising the first coordination sphere. There is competition between aniline molecules and solvent molecules for a position in the second sphere with the solvent competing with increasing effectiveness in the series carbon tetrachloride, benzene, and methylene chloride.

Le rôle des anilines substituées comme ligands de la seconde sphère de coordination des complexes du cobalt(II) est étudié. Les déplacements chimiques des spectres r.n.m. du ligand produits par les interactions de pseudo-contact avec le complexe paramagnétique du cobalt ont été utilisés à cette fin. On a trouvé que dans chaque cas l'aniline occupe préférentiellement une position perpendiculaire à l'axe de symétrie ternaire du complexe, et tend à s'aligner sur le groupe aminé en direction de l'atome de Cobalt. Des substituants-accepteur d'électrons en position para du groupe aminé augmentent la force de liaison de la seconde sphère de coordination, et des substituants-donneur d'électrons diminuent la force en question. Ces résultats sont en accord avec l'idée que la structure de la seconde sphère de coordination est déterminée par des interactions électrostatiques avec les ligands chargés négativement qui composent la première sphère de coordination. Il y a compétition entre les molécules d'aniline et les molécules du solvant pour une position en seconde sphère, l'efficacité de cette compétition du solvant croissant dans l'ordre de tétrachlorine de carbon, benzène et chlorure de méthylène.

Canadian Journal of Chemistry, 49, 1218 (1971)

Introduction

In the first paper in this series (1, and references therein) a method for studying the structure of the second coordination sphere of transition metal complexes based on pseudo contact interactions between a paramagnetic metal complex and protons on the complexing ligand was described. In the system studied it was demonstrated that aniline and pyridine interacted with the metal complex in preference to the solvent, that the enthalpy change involved in the formation of such a second sphere complex was of the order of 2 or 3 kcal/mol, and that there was a definite preferred geometry for the resulting complex. The present experiments were designed to investigate the effect of changes in the electronic nature of the ligand on the structure of the second sphere complexes. For this purpose the complexing of a number of substituted anilines has been investigated. The tentative conclusion reached in the first paper was that electrostatic attraction between the negatively charged nitrogen atoms surrounding the cobalt ion and the second coordination sphere ligand provided the binding energy for the complex. If this is correct, para substitution of the aniline with an electron withdrawing ligand should enhance the binding and para substitution with an electron donating ligand should diminish it. Data pertinent to this point are reported in the present paper.

Results

Co(II) trispyrazoylborate ($Co[HBpz_3]_2$) (2) was again used as the complexing agent. The structure of this compound and the preferred orientation of an aniline molecule in the second coordination sphere is shown in Fig. 1. Previously we have used carbon tetrachloride as an "inert" solvent. Limited solubility of some of the substituted anilines restricts the use of this solvent but data has been obtained for *p*-anisidine, *N*,*N*-dimethyl *p*-phenylenediamine, and *p*-aminobenzotrifluoride. The design of the experiments was similar to that developed in the earlier paper (1). Initially the chemical shifts of the aniline protons were measured in the presence of both Co(II) trispyrazoylborate and Zn(II) trispyrazoylborate. These latter two compounds are structurally

[1]Revision received December 3, 1970.

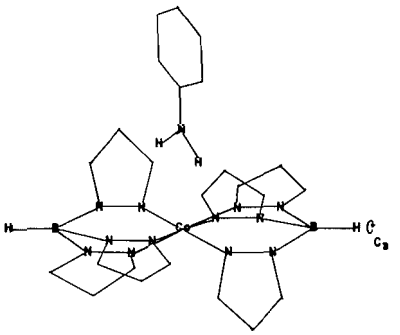

FIG. 1. Geometry of Co(II) trispyrazoylborate and preferred orientation of complexing aniline molecule.

TABLE 1. Aniline shifts in the presence of zinc and cobalt complexes*

Substituent	Position	Co shift	Zn shift
p-CF_3	Ortho	54	2
	Meta	26	1
	NH_2	47	14
p-OCH_3	Ortho	34	5
	Meta	15	3
	NH_2	32	1
p-$N(CH_3)_2$	Ortho	28	4
	Meta	17	7
	NH_2	27	12

*Data refer to shifts observed in 0.08 M solutions of $Co[HBpz_3]_2$ and $Zn[HBpz_3]_2$, respectively, in carbon tetrachloride. All shifts are in Hz and are to high field. Ortho and meta refer to the position with respect to the NH_2 group.

similar and differ only in the paramagnetism of the cobalt compound. The data of Table 1 show that the shifts of the aromatic protons of p-aminobenzotrifluoride in the presence of zinc complex are indeed small compared with those in the presence of cobalt complex and hence that the pseudo contact interaction is dominant. These shifts will be determined by the relationship

$$\Delta\nu = \frac{-D(3\cos^2\theta - 1)}{r^3}(g_{\parallel} - g_{\perp})$$

where r is the distance between the metal atom and the nuclear dipole under consideration, θ is the angle between the principal axis of the molecule and the vector joining the metal to the ligand nucleus, D is a constant, and $g_{\parallel}$ and $g_{\perp}$ are the principal values of the **g** tensor. It is the presence of the factor $(3\cos^2\theta - 1)/r^3$ which provides information on the geometry of the second coordination sphere complex. The D value for $Co[HBpz_3]_2$ is known (3) and it is therefore possible to use the pseudo contact shifts to obtain information on the geometry of the complex. However, for the purposes of the present paper it suffices to note that positive values of $\Delta\nu$ (*i.e.* high field shifts) correspond to negative values of $3\cos^2\theta - 1$ and hence that θ has values around $\pi/2$ and that the $1/r^3$ dependence of the shifts determines that the ligand protons closest to the cobalt will be shifted most. The situation for p-anisidine and N,N-dimethyl-p-phenylenediamine is somewhat less clear cut since the shifts with the cobalt compound are smaller and those with the zinc compound larger, but it is still apparent that pseudo contact effects make the main contribution to the shifts.

The aromatic protons of the anilines were assigned by reference to the mono substituted compounds which have been analyzed previously (4). Thus the ortho protons of p-anisole are found at lower field than those of aniline, hence it is deduced that the lower field resonance in p-anisidine arises from the protons ortho to the OCH_3 (meta to the NH_2) and the higher field resonance from those ortho to the NH_2. Similarly the protons ortho to the NH_2 of dimethylphenylenediamine are also assigned to higher field. At 100 Mc/s the aromatic protons of trifluorobenzoaniline are well separated and the chemical shifts can be measured directly. For p-anisidine and N,N-dimethylphenylenediamine the chemical shifts are of the same order as the larger spin–spin coupling constant and these were treated as AB spectra using the analytical expressions of Pople, Schneider, and Bernstein (5).

It has been shown previously (1) that for a model involving association between the aniline (L) and cobalt complex (X) of the simple type $X + L \rightleftharpoons XL$ with equilibrium constant K, providing the exchange between free and associated L is fast on the n.m.r. time scale, the observed shifts will be given by

$$[1] \qquad \Delta\nu_{obs} = \frac{K[X]\Delta\nu_0}{1 + K[X]}$$

where $\Delta\nu_0$ is the shift of the complexed ligand. It is apparent from this equation that providing $K[X] \ll 1$, a plot of $\Delta\nu_{obs}$ *vs.* [X] will be linear. This was found to be the case for aniline and also appears to hold for substituted anilines. Typical plots of $\Delta\nu_{obs}$ *vs.* [X] are shown in Fig. 2 and the derived slopes x are collected together in Table 2.[2]

It has also been shown that the temperature dependence is determined by the equation

[2]See footnote of Table 2.

Can. J. Chem. Downloaded from www.nrcresearchpress.com by 210.87.254.6 on 09/05/12
For personal use only.

TABLE 2. Experimental results in carbon tetrachloride*

Substituent	x (Hz) Ortho	Meta	NH_2	x_{ortho}/x_{meta}	y (kcal) Ortho	Meta	Hammett σ	Dipole moment (D)
p-H(ref. 1)	500	240	532	0.48	−2.5	−2.3	0.0	1.55
p-CF_3	740	343	889	0.46	−3.5	−3.7	0.55	4.28
p-$N(CH_3)_2$	360	214	—	0.59	−2.7	−2.5	−0.60	1.43
p-OCH_3	410	189	—	0.46	—	−2.1	−0.27	1.82

*From eq. 1 it is apparent that the slope x can be formally identified with the product $K\Delta\nu_0$ and from eq. 2 that the slope y similarly corresponds to ΔH. However, as has been discussed previously (1) these parameters do not have any rigorous thermodynamic significance since they represent only average values for a range of possible geometries rather than definitive data for a complex of well defined structure. We have therefore avoided the use of the symbols K and ΔH which have specific thermodynamic connotations. It remains true though, that x is a measure of the extent of second coordination sphere interaction even though we cannot distinguish between the effect of more molecules being complexed or the same number being more tightly bound and that y, although a complex average, is a measure of the difference in energy between a metal complex/aniline and a solvent/aniline environment.

$$[2] \quad \ln \Delta\nu_{obs} = \frac{-\Delta H}{RT} + \frac{\Delta S}{R} + \ln [X] + \ln \Delta\nu_0$$

Before applying this equation it is necessary to make an appropriate correction for the Curie law temperature dependence of $\Delta\nu_0$. This was effected by measuring the temperature dependence of the pyrazoyl protons of $Co[HBpz_3]_2$ and multiplying the observed aniline shifts at temperature T by the ratio of pyrazoyl shift at temperature T to that at a standard temperature (25 °C) in the manner described previously. A typical plot of $\ln \Delta\nu_{corr}$ *vs.* $1/T$ is shown in Fig. 3 and the measured slopes of these plots, y, are given in Table 2.[2] The agreement between the values obtained from the ortho and meta protons is seen to be quite good and with some allowance for possible systematic errors we obtain the values -3.6 ± 0.5 kcal for the *p*-CF_3 compound, -2.6 ± 0.2 kcal for the *p*-$N(CH_3)_2$ compound and -2.1 ± 0.6 kcal for the *p*-OCH_3 compound.

It would obviously be desirable to extend these measurements to a wider range of substituted anilines but this requires a change of solvent. Preliminary experiments indicated that the results obtained are very solvent dependent. Thus methylene chloride is a very suitable solvent for a wide range of anilines but in all cases the addition of $Co[HBpz_3]_2$ leads to no significant pseudo-contact shifts. It must be concluded either that the anilines cannot compete favorably with the methylene chloride in the solvation of the cobalt

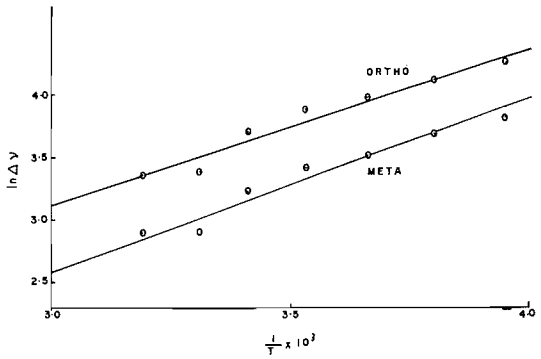

FIG. 3. Plot of $\ln \Delta\nu_{corr}$ *vs.* $1/T$ for *N*,*N*-dimethylphenylenediamine in carbon tetrachloride.

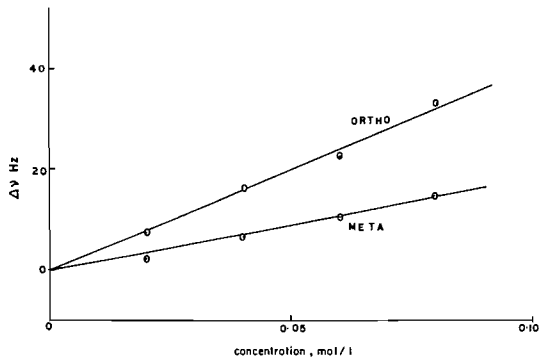

FIG. 2. Plot of $\Delta\nu_{obs}$ *vs.* concentration of cobalt complex for *p*-anisidine in carbon tetrachloride.

TABLE 3. Observed shifts in benzene and carbon tetrachloride

Substituent	Proton	Shift (Hz) in C_6D_6	CCl_4
p-$N(CH_3)_2$	Ortho	10	24
	Meta	5	15
p-OCH_3	Ortho	15	33
	Meta	6	16
p-CN	Ortho	35	—
	Meta	14	—
p-CF_3	Ortho	39	54
	Meta	16	26
p-NO_2	Ortho	37	—
	Meta	7	—

*All shifts relative to ligand. Solutions 0.08 *M* in $Co[HBpz_3]_2$. Temperature 30 °C.

Can. J. Chem. Downloaded from www.nrcresearchpress.com by 210.87.254.6 on 09/05/12
For personal use only.

TABLE 4. Results in benzene

Substituent	x (Hz) Ortho	Meta	Ratio	y* (kcal)	Hammett σ	Dipole moment (D)
p-NO_2	455	90	0.20	—	+0.78	6.29
p-CN	737	175	0.24	3	+0.63	5.96
p-CF_3	500	230	0.46	3	+0.55	4.28
H	250	108	0.43	—	0	1.55
p-CH_3	225	113	0.50	3	−0.17	1.66
p-OCH_3	218	106	0.49	5	−0.27	1.82
p-$N(CH_3)_2$	130	80	0.62	5	−0.60	1.43

*See footnote Table 2.

complex or that solvation of the aniline by the methylene chloride is too strong to allow preferential complexing with the $Co[HBpz_3]_2$. It is these factors of course which enhance the solubility of the cobalt complex or the anilines and it is apparent that meaningful results can only be obtained with a restricted range of solvents. Methylene chloride has a dipole moment comparable to that of aniline so it is perhaps not surprising that it is an equally efficient solvating agent.

It has been found that benzene has some advantages as a compromise solvent. A rather wide range of anilines are soluble but this advantage is to some extent off-set by the small shifts observed which is reflected in the lower accuracy of the derived parameters. In Table 3 the shifts of the ortho and meta protons of a number of anilines in carbon tetrachloride and benzene (C_6D_6) are shown to illustrate the magnitudes of the shifts observed. That the reduced shifts are caused at least in part by competition between the solvent and the aniline for positions in the second coordination sphere of the cobalt complex is illustrated by the shift in the position of the resonance of the residual hydrogen in the deuterated benzene with increasing concentration of cobalt complex which is clearly apparent in the spectra of Fig. 4. With increasing complex concentration the benzene resonance moves to high field showing that the solvent molecule competes with the aniline for a position perpendicular to the symmetry axis of the molecule as illustrated in Fig. 1. Analysis of the data follows the method previously outlined and values of x and y are contained in Table 4.

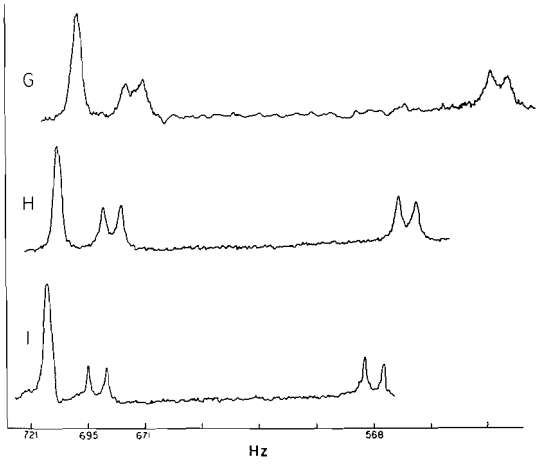

FIG. 4. 100 Mc/s proton magnetic resonance spectra of the aromatic protons of p-aminobenzonitrile in the presence of Co(II) trispyrazoylborate. Solvent benzene-d_6. Spectrum *G* 0.10 *M* $Co[HBpz_3]_2$; *H* 0.06 *M* $Co[HBpz_3]_2$; *I*, 0.02 *M* $Co[HBpz_3]_2$. The resonance on the left arises from C_6D_5H.

Discussion

Consider first the results in carbon tetrachloride. We might first note that the basic geometry of the second coordination sphere complex is unchanged by substitution on the aniline. All pseudo-contact shifts are to high field showing that the approach of the aniline is perpendicular to the three-fold symmetry axis of the $Co[HBpz_3]_2$. In each case the shift of the ortho proton is greater than that of the meta proton indicating that the amino end of the molecule is directed towards the cobalt. The ratio of the meta to ortho shifts is within experimental error identical for the p-H, the p-CF_3, and the p-OCH_3 derivatives (0.47, 0.46, and 0.46, respectively). The only other ratio which is available for comparison is that involving the amino protons. These protons are broadened to a greater extent than the aromatic protons by the addition of the paramagnetic complex and only in the case of the p-CF_3 derivative did it prove possible to measure their position with any degree of certainty. The observed x ratio of 1.20 agrees reasonably well with that of 1.07

Can. J. Chem. Downloaded from www.nrcresearchpress.com by 210.87.254.6 on 09/05/12
For personal use only.

Can. J. Chem. Downloaded from www.nrcresearchpress.com by 210.87.254.6 on 09/05/12
For personal use only.

previously reported for the unsubstituted anilines. It is concluded therefore that the geometries of the second sphere complexes formed by the above three compounds are closely similar.

The case of the p-$N(CH_3)_2$ derivative is less clear cut. The only ratio available for comparison is that of meta:ortho and the value of 0.59 is significantly different from those obtained for the compounds previously discussed. This compound has the smallest dipole moment of any of the molecules in this series and it might be argued that the second coordination sphere complex will have the least rigid structure. It has previously been pointed out that restricted tumbling or libration of the aniline will tend to make the shifts of different protons more nearly equal and the above observation could be rationalized on this basis.

It is apparent that qualitatively the expectation that electron withdrawing substituents on the aniline will enhance the binding of the second sphere ligands and electron donating substituents will diminish it is upheld. This is perhaps most clearly seen by noting the correlation between the x values for the protons ortho to the amino group and the Hammett σ values (6) for the substituent. Thus for the p-CF_3, p-H, p-OCH_3, and p-$N(CH_3)_2$ derivatives the ortho x values are 740, 462, 410, and 360 Hz, respectively, and the Hammett σ values are $+0.55$, 0.00, -0.27, and -0.60. It might also be noted that the dipole moments of these four compounds (7) are 4.28, 1.55, 1.82, and 1.43 D, respectively. The most plausible interpretation is that increasing positive charge on the amino group leads to stronger electrostatic interaction with the neighboring negatively charged nitrogens. Thus the idea of an electric "double layer" surrounding the metal ion with the first sphere ligands oriented with their negative ends towards the positive metal ion and the second sphere ligands oriented with their positive ends towards the metal ion receives additional support. It might next be asked whether the increasing x with electron withdrawing substituents is due to a change in K, the equilibrium constant, or a change in $\Delta\nu_0$, reflecting a contraction of the second coordination sphere due to tighter binding. However, as has been discussed previously, due to the relatively long time scale of the n.m.r. experiment it is not meaningful to try to separate these factors on the basis of the present type of experiment. We can only conclude that the average environment of the aniline involves increased interaction with the cobalt complex when an electron withdrawing substituent is present and can say nothing about the detailed kinetic processes which give rise to this average. It is possible to obtain a measure of the enthalpy changes for the formation of the second sphere complexes by studying the temperature dependences of the n.m.r. shifts. The values obtained of -3.6, -2.4, -2.1, and -2.6 kcal for the p-CF_3, p-H, p-OCH_3, and p-$N(CH_3)_2$ derivatives do not show a pronounced systematic variation with the donor ability of the substituent. These numbers represent the differences between the interaction energy of an aniline molecule with surrounding solvent molecules and with the $Co[HBpz_3]_2$ molecule. Since both of these quantities will vary with the substituent and the measured quantity is probably a small difference between two relatively large numbers it is perhaps not surprising that the data do not show a well defined trend.

The data obtained in deuterobenzene serve to compliment the carbon tetrachloride data discussed above. A rather wider range of anilines can be examined but the data are less accurate due to the smaller shifts and the more restricted temperature range available. In some cases there is also a problem of overlap from the resonance of the residual hydrogen in the solvent. The parameters given in Table 5, particularly the y values, are therefore somewhat less precise than those obtained in carbon tetrachloride. They do, however, serve to illustrate a number of points.

First of all it may be noted that all values of x are less than those obtained in carbon tetrachloride by a factor of about two. However, for the compounds for which there are data in both solvents the ratios of the ortho to meta shifts agree quite well. This includes the reproduction of an anomalously high value for N,N'-dimethylphenylenediamine. Taken together with the fact that there is a significant high field shift of the solvent resonance these observations suggest that the structure of the second sphere complexes is much the same in both solvents but that the competition between solvent and aniline molecules for a second sphere position is less favorable to the aniline when benzene is the solvent. This effect is of course reinforced by the known interaction between benzene and aniline. Data have also been obtained for two additional electron withdrawing substituents, p-NO_2 and p-CN, and

these show the expected behavior of stronger complex formation. In both cases the meta:ortho ratios are lower than for aniline and by an argument analogous to that developed for the *p*-$N(CH_3)_2$ this could be interpreted as implying that the second sphere complex structures are more rigid due to stronger binding. Arguments developed previously showed that either a smaller metal-to-amino nitrogen distance or a diminution in the tendency of the aniline molecule to tumble would lessen this meta-to-ortho ratio. Complexing with *m*-nitro aniline was also examined. In this case the shifts were all relatively small and it seems reasonable that steric factors are becoming important. The *y* values obtained are all of the expected order of magnitude and it would probably be unwise to attach too much significance to variations within the series.

The results of the present paper can be summarized as follows. The second sphere coordination complexes formed between substituted anilines and $Co[HBpz_3]_2$ have the same basic geometry as that previously found for aniline itself. Stronger complexes are formed if the substituent is electron withdrawing than if it is electron donating. This is consistent with the idea that the structure of the second sphere is determined by electrostatic interaction with the negatively charged first sphere ligands. The observation that the non-polar benzene molecule can also participate in the second sphere suggests that induced dipolar forces must also be considered. It is also apparent that steric factors will probably be important. An interesting implication of the present results is that if second sphere complexing does indeed play an important part in the mechanism of ligand substitution processes the electronic factors which tend to favor second sphere complexing and hence more facile substitution will tend to make the molecule less satisfactory as first sphere ligand. Such a result has interesting implications for the coupled ligand exchange reactions which constitute the cyclic mechanisms found in homogeneous catalysis. Experimental investigations in this area are underway and will be reported in subsequent papers in this series.

Experimental

The n.m.r. spectra were obtained on a Varian HA 100 spectrometer. The proton shifts were measured relative to tetramethylsilane used as an internal calibrant to obviate the need for susceptibility corrections. Cobalt and zinc trispyrazoyl borates were prepared by Dr. S. Trofimenko in a manner described previously and other chemicals were obtained commercially.

A number of experiments were carried out to investigate the possible effects of impurities in the anilines. Several were purified by vacuum distillation. This procedure had no appreciable effect on the observed shifts. It was also demonstrated that the maximum change in line position obtained by saturating the solutions with water was of the order of 1 Hz.

The authors are indebted to Dr. S. Trofimenko of the Central Research Department, E. I. Du Pont de Nemours and Co., Wilmington, Delaware for gifts of cobalt and zinc trispyrazoyl borates and to the National Research Council of Canada for financial support of this research.

1. D. R. EATON. Can. J. Chem. **47**, 2645 (1969).
2. S. TROFIMENKO. J. Amer. Chem. Soc. **88**, 1842 (1966).
3. J. P. JESSON. J. Chem. Phys. **47**, 582 (1967).
4. F. L. BOVEY. NMR Data Tables for Organic Compounds. Interscience Publ., New York.
5. J. A. POPLE, W. G. SCHNEIDER, and H. B. BERNSTEIN. High Resolution Nuclear Magnetic Resonance. McGraw Hill, 1959.
6. H. H. JAFFÉ. Chem. Rev. **53**, 222 (1953).
7. A. L. MCCLELLAN. Tables of Experimental Dipole Moments. Freeman.

Can. J. Chem. Downloaded from www.nrcresearchpress.com by 210.87.254.6 on 09/05/12
For personal use only.

Can. J. Chem. Downloaded from www.nrcresearchpress.com by 210.87.254.5 on 09/05/12
For personal use only.

The Motion of Guest Molecules in Clathrate Hydrates[1]

D. W. DAVIDSON
Division of Chemistry, National Research Council of Canada, Ottawa, Canada

Received September 25, 1970

The reorientation of molecules encaged in hydrates of structures I and II is controlled mainly by the cage geometry and the electrostatic fields of the water molecules. Departure from spherical symmetry of the short-range interactions between the guest molecule and the water molecules which form the cages leads to preferred orientations which become increasingly occupied at low temperatures. A modified Lennard–Jones potential energy calculation shows the preferred positions of Cl_2 to lie off-center and close to the equatorial plane of the tetrakaidecahedral cage with the Cl atoms near the axial planes of symmetry. In an attempt to account for the remarkable reorientational freedom of polar guest molecules, the electrostatic fields of the water molecules are treated in detail. It is shown that the geometry of the cages causes the sum of the fields of the cage water dipoles to almost vanish at points near the cage center, but that this is not true of the resultant quadrupolar fields. It is suggested that the quadrupolar fields are also relatively small because the hydrogen bonding to four neighbors considerably reduces the quadrupole moment of the water molecule. The orientational disorder of the water molecules results in a wide distribution of resultant electrostatic fields in different cages. This appears to be the origin of the great width of the dielectric absorption observed at low temperatures in tetrahydrofuran hydrate and of the wide temperature range of variation of the proton magnetic resonance (p.m.r.) line width in tetrahydrofuran deuterate.

La réorientation des molécules encagées dans des hydrates de structures I et II est principalement contrôlée par la géométrie de la cage et les champs électrostatiques des molécules d'eau. L'écart à la symétrie sphérique des intéractions à courte distance entre les molécules d'eau qui forment les cages et la molécule qui y est emprisonnée conduit à des orientations préférentielles qui deviennent plus fréquentes à basse température. Un calcul d'énergie potentiel de Lennard–Jones modifié montre que les positions préférentielles de Cl_2 sont décentrées et proches du plan équatorial de la cage tetrakaidecahedrale avec les atomes de Cl proches des *plans axiaux* de symétrie. Dans une tentative de rendre compte de la liberté remarquable de réorientation des molécules polaires emprisonnées, les champs électrostatiques des molécules d'eau sont traités en détail. On montre que la géométrie des cages entraînent la somme des champs dus aux dipôles aqueux de la cage à presque s'annuler en des points proches du centre de la cage, mais ceci n'est pas vrai des champs quadrupolaires résultants. On suggère que les champs quadrupolaires sont aussi relativement petits parce que la liaison hydrogène avec quatre voisins réduit considérablement le moment quadrupolaire de la molécule d'eau. Le désordre d'orientation des molécules d'eau entraîne une distribution étendue des champs électrostatiques résultant dans les différentes cages. Ceci apparaît être à l'origine de la grande largeur d'absorption diélectrique observée aux basses températures dans l'hydrate de tétrahydrofurane et du grand intervalle de température de variation de la largeur de raie r.m.p. dans le deuterate de tétrahydrofurane.

Canadian Journal of Chemistry, 49, 1224 (1971)

I. Introduction

This report is intended to serve as an introduction to a number of others in which the results of dielectric and wide-line nuclear magnetic resonance (n.m.r.) studies of the motions of a variety of molecules encaged in clathrate hydrates of von Stackelberg's structures I and II (1) will be presented. The first of these describes the dielectric properties of cyclobutanone hydrate and follows (2).

Among clathrate substances the clathrate hydrates are unique in the variety of cage geometries present and in the variety of guest molecules which may be incorporated in them (3). The lattices are ices in the sense that they consist of 4-coordinated hydrogen-bonded water molecules. In hydrates of structures I and II the hydrogen-bonded O---O---O angles are distorted from the tetrahedral angle by only, on average, 3.7 (4) and 3.0° (5), respectively (Table 1). The orientations of the water molecules, at least at relatively high temperatures, are disordered, as is shown by their dielectric relaxation. The disorder is not necessarily complete, as it is in cubic and hexagonal ices: that is, each of the six hydrogen-bonded orientations at each site may not be of equal average stability. But unlike the case of ice III (6), complete ordering is not possible within the unit cells which have been defined for the oxygen atoms. Indeed, any extensive degree of ordering is prevented by the correlations between neighboring water molecules which are required for full hydrogen bonding within the five- and six-membered rings of water molecules. Some of the consequences of this disorder are considered below (Section III).

The four cages which occur in hydrates of structures I and II are shown in Fig. 1. They con-

[1]NRCC No. 11 763.

TABLE 1. Geometry of clathrate hydrate cages

	Small cages			Large cages		
Structure I: *Pm3n*, $a = 12.03$ Å						
Number of cages in unit cell		2			6	
O site designation	*i*		*k*	*i*	*k*	*c*
Number of sites in cage	8		12	8	8 4	4
Distance to center (Å)	3.83		3.96	4.47	4.06 4.645	4.25
Average distance to center (Å)		3.91			4.33	
Average cage radius (Å)			4.22			
Structure II: *Fd3m*, $a = 17.31$ Å						
Number of cages in unit cell		16			8	
O site designation	*a*	*e*	*g*	*e*	*g*	
Number of sites in cage	2	6	12	4	12 12	
Distance to center (Å)	3.748	3.845	3.956	4.729	4.715 4.635	
Average distance to center (Å)		3.902			4.683	
Average cage radius (Å)			4.162			

	Structure I			Structure II		
O site designation	*i*	*k*	*c*	*a*	*e*	*g*
Sites in unit cell	16	24	6	8	32	96
Average departure at site from tetrahedral angle (degree)	1.2	5.1	1.2	0	2.1	3.6
Average departure (degree)		3.7			3.0	
Average distance of site to neighbors (Å)	2.769	2.802	2.811	2.767	2.774	2.795
Average O---O distance (Å)		2.793			2.790	

sist of 20 to 28 water molecules, each hydrogen-bonded to three neighbors within the cage wall and to a fourth neighbor outside the cage. The latter lies approximately on the extension of the line joining the center of the cage to the cage water molecule to which it is hydrogen-bonded. Distances from the cage centers of the water molecules which form the cages are given in Table 1, as given by the X-ray studies of the structure I hydrate of ethylene oxide (4) and the structure II double hydrate of tetrahydrofuran and hydrogen sulfide (5). In terms of these distances the most spherical cage is the large cage of structure II which shows a variation of no more than 2% in cage radius. In the large cage of structure I the variation is 14%.

It is significant that the formation of almost spherical cages in these and other related (3) hydrate structures is accompanied by no great distortion of the O---O---O angles from tetrahedral (Table 1) and by no great difference between the lattice energies and that of hexagonal ice (7, 8). A simple model suggests the geometrical reasons for this.

We suppose the O---O bonds between a water molecule and three of its neighbors a distance l away to make tetrahedral angles with one another. These four oxygen atoms then lie on an element

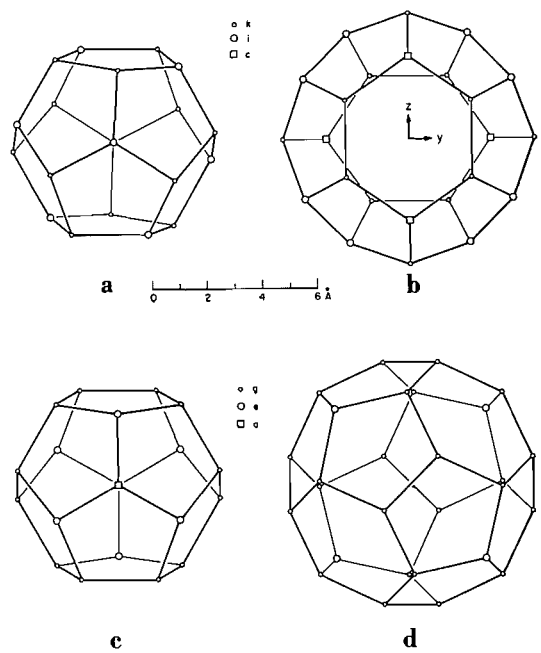

FIG. 1. The small and large cages of structure I (*a* and *b*) and of structure II (*c* and *d*) hydrates, viewed along an axis of greatest symmetry. The point group symmetries are respectively, $m3$, $\bar{4}2m$, $3m$, and $\bar{4}3m$. Literal identification of the non-equivalent oxygen sites follows the notation of *The International Tables for X-ray Crystallography* for space groups *Pm3n* and *Fd3m*.

Can. J. Chem. Downloaded from www.nrcresearchpress.com by 210.87.254.5 on 09/05/12
For personal use only.

Can. J. Chem. Downloaded from www.nrcresearchpress.com by 210.87.254.5 on 09/05/12
For personal use only.

of surface of a sphere whose center lies on the axis of 3-fold symmetry. A real cage consisting of an integral number of water molecules cannot of course be constructed in this way. However, if it be imagined that elements of the cage surface are so constructed, and to each molecule is assigned an appropriate element of surface area in the form of an equilateral spherical triangle bounded by the great circles which are the normal bisectors of the three bonds of each water molecule, it is found that each water molecule of this idealized cage occupies a fraction 1/24.09 of the area of the sphere. In structures I and II the cages are formed of 20, 24, and 28 water molecules. The model further leads to a cage radius of 3/2 l, or 4.14 Å for $l = 2.76$ Å as in hexagonal ice. This is only a few hundredths Å less than the mean cage radii found (Table 1) in structures I and II, in each of which the mean l is 2.79 Å. Thus it appears that the existence of cages is made possible and their general size determined by the tendency of water molecules to bond tetrahedrally, along with the circumstance that the angles in pentagonal and hexagonal faces need not depart greatly from the tetrahedral angle. A further requirement is, of course, that faces and edges be shared by cages in a way that permits formation of a unit cell. This is not possible if only one kind of cage is present (3).

The actual clathrate structure formed is determined by the nature of the guest molecule, particularly by its size (1, 3). With the exception of bromine (9) and various amines (3), which form clathrate hydrates of distinct and possibly unique structures, and of molecules which interact strongly and specifically with water to form, like ammonia and hydrogen chloride, stoichiometric hydrates, non-electrolyte molecules lying between about 3.8 (argon) and 6.5 Å (cyclobutanone) in maximum diameter form clathrate hydrates of structures I or II. Cyclopropane (10, 11) and trimethylene oxide (12) under suitable conditions can form either. The diameters of these molecules (5.3 to 5.5 Å) are intermediate between those of the small molecules which form hydrates of type I exclusively and of the larger molecules which form type II. The upper limit to the size of molecules which form each structure roughly agrees with the "free diameter" of the larger cage obtained by subtracting the van der Waals radius of the water molecule (1.45 Å) from the appropriate "average distance to center" given in Table 1. Complete occupancy of the smaller cages is approached for molecules less than about 5.0 Å in diameter, although partial occupancy is possible for somewhat larger molecules like chlorine and ethylene oxide (13). The larger cages of each structure seem generally to be almost completely occupied.

The absence of any strong interaction of a specific nature between individual water molecules and the guest molecule is clear not only from the prevalence of iso-structural hydrates for a wide variety of type of guest molecule but also by the exceptional degree of rotational mobility of the guest molecules. Reorientation rates of the order of 10^{10} s^{-1} and above at temperatures as low as 90 °K have been shown by microwave dielectric studies of ethylene oxide, tetrahydrofuran, and acetone hydrates (14, 15). The extent to which free rotation is approached at high temperatures is as yet uncertain. In their thermodynamic treatment (7) Platteeuw and van der Waals assumed that at 0 °C the rotational partition function of small guest molecules like methane was the same as that of the gas. Parsonage and Staveley (16) found a roughly gas-like contribution to the specific heat above 150 °K from the rotation of methane in the β-quinol clathrate in which the cages are approximately the same size, as, if less symmetric than, the pentagonal dodecahedral hydrate cages. Interaction with the cage walls, however, may well be expected to eliminate any possibility of a line structure in the microwave region associated with free molecular rotation.

The energy of a guest molecule depends on its position and orientation within the cage as determined by three major contributions: (*i*) short-range interactions between the guest and water molecules due to London dispersion and orbital overlap forces, and longer range interactions of guest molecules (*ii*) with the electrostatic fields of the water molecules and (*iii*) with the (mainly) dipolar fields of guest molecules in neighboring cages. Proper evaluation of each of these contributions is generally difficult but some conclusions may be drawn from the approximate analysis which follows.

II. Short Range Interactions with the Lattice Molecules

Monatomic Guests

The position-dependence of the energy of rare gas molecules in structure I cages and in the small cages of structure II has recently been considered by Barrer and Edge (8). The interaction

Can. J. Chem. Downloaded from www.nrcresearchpress.com by 210.87.254.5 on 09/05/12
For personal use only.

energy was taken as the sum of the pair-wise Lennard–Jones interactions between the rare gas atom k and individual water molecules i

$$[1] \qquad V_k = C_k \sum_i \left[\frac{1}{2}\left(\frac{r_{0k}}{r_{ik}}\right)^{12} - \left(\frac{r_{0k}}{r_{ik}}\right)^{6} \right]$$

where i included 1244 water molecules for structure I and 146 for structure II. The separation r_{0k} of minimum pair energy $-C_k/2$ was taken (8) as the sum of the van der Waals radii of the water molecule (1.40 Å for the oxygen atom) and of the rare gas atom. The enthalpies of encagement calculated with values of C_k obtained from the expressions of London, Slater and Muller, and Slater and Kirkwood were compared with those determined experimentally from the variation with temperature of the Langmuir equilibrium constant $K = \theta/(p(1 - \theta))$, which describes the degree of cage occupancy θ in terms of rare gas pressure p, for the small cages of chloroform structure II hydrate. There was best approximate agreement with the C_k values of Slater and Kirkwood. The "experimental" C_k values derived for chloroform double hydrates were used for calculation of the potential energies of the rare gases in the two cages of structure I.

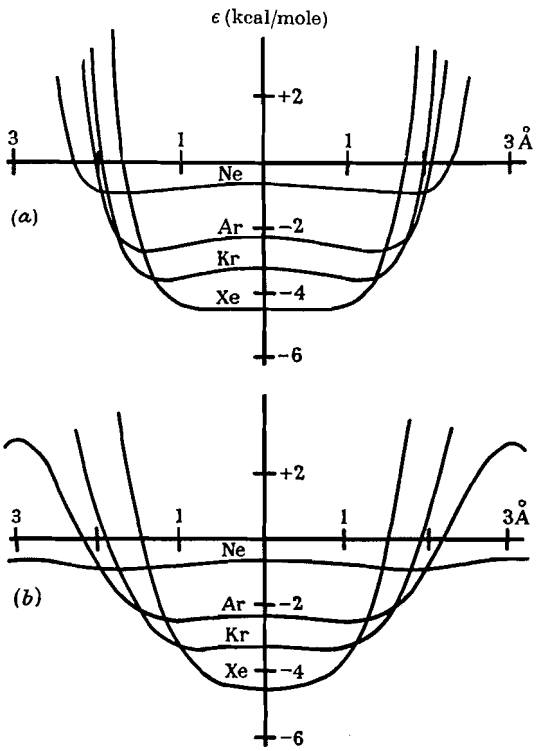

FIG. 2. Lennard–Jones potential energy of rare gas molecules (with London C_k) in the tetrakaidecahedron as a function of displacement from the center along a line (*a*) in the equatorial plane, (*b*) along the polar $\bar{4}$ axis. From ref. 8.

Figure 2 shows the variation of potential energy within the large cages of structure I along two directions through the cage center. For argon and krypton the energy hump at the center amounts to several hundred calories per mole. The directional dependence of the energy apparent for this cage is much less in the smaller cages of either structure and a small central energy maximum occurs only for argon (8).

Diatomic Guests

For homonuclear diatomic molecules the electrostatic fields of the water molecules may again be neglected to good approximation. (The orientation-dependent energies involve these electrostatic fields principally through the anisotropy of the polarizability and the quadrupole moment of the guest molecule. For magnitudes of field and field gradient of the order of those obtained later (Section III) both energies are less than 0.1 kcal/mol.)

Attempts to take the asymmetries of diatomic and polyatomic guest molecules into account for purposes of estimating clathrate hydrate dissociation pressures have been made by McKoy and Sinanoglu (17), who used a Kihara potential function (18) to represent the interaction between a guest molecule and an oxygen atom of water. As in earlier applications of the Lennard–Jones 12–6 potential by van der Waals and Platteeuw (19), the Lennard–Jones–Devonshire method of integrating the interactions with the oxygen atoms over the surface of a sphere of mean cage radius was adopted. The resulting form of the potential function (Fig. 3 for example) has a higher and broader central maximum than in the Lennard–Jones case, the effect being more pronounced for the pseudo-diatomic ethane molecule than for nitrogen and oxygen. The smearing-out of the cage oxygen atoms removes the orientation dependence of the energy and the potential function, having been effectively averaged over all orientations, becomes a function only of the position of the center of mass. Nevertheless, the results suggest that molecules of ethane, which according to Fig. 3 have an energy about 0.5 kcal/mol higher at the cage center than at positions 0.9 Å away, should tend at low temperatures to lie considerably off-center with the

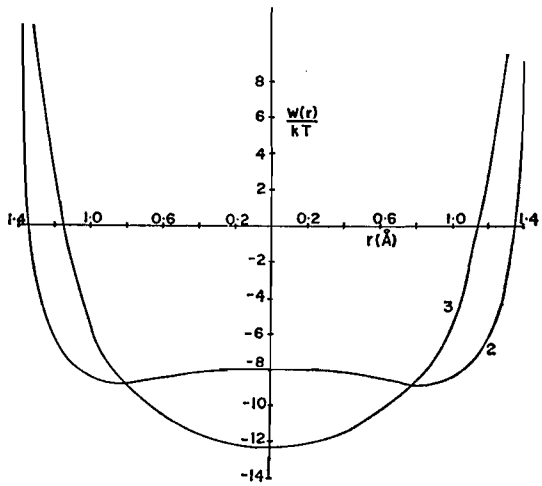

FIG. 3. Spherically symmetric (3) Lennard–Jones and (2) Kihara potential of ethane at 0 °C. From ref. 17.

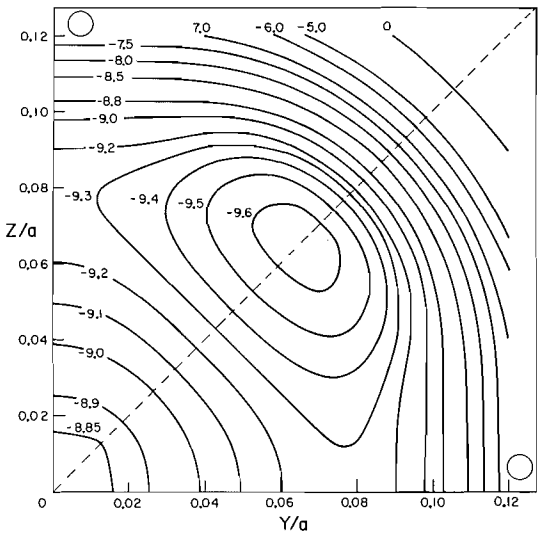

FIG. 4. Equipotential lines for center of mass of Cl_2 in the equatorial plane of the tetrakaidecahedron. The circles mark the positions of least energy of the Cl atoms.

methyl groups in van der Waals contact with cage water molecules. A similar tendency for other diatomic molecules to "stick" at low temperatures to the walls in off-center positions and therefore to experience finite barriers to reorientation is to be expected.

The case of chlorine hydrate is considered in more detail since some information about the X-ray structure factor of encaged chlorine is available (20). We represent the guest–host interaction in the large structure I cage by the superposition of two Lennard–Jones potential functions (eq. 1), one for each chlorine atom, and thereby neglect the presence of the bond. The value of r_{0k} was taken as 3.2 Å and the coordinates of the oxygen atoms from (4). The r_{ik}'s were expressed in terms of the coordinates of the center of mass of the chlorine molecule and the two angular coordinates specifying the direction of the chlorine bond (length = 1.988 Å). The right-handed coordinate system was that of Fig. 1(*b*).

The Lennard–Jones sum over the two chlorine atoms and the 24 water molecules of the cage wa found to have an absolute minimum at $x = 0$, $y = z = 0.065\,a$ (where the cubic lattice parameter $a = 12.1$ Å (20)), $\theta = 91.5°$ (measured from the $+x$ direction), and $\phi = 135°$ (measured from the $+y$ direction) and at three other equivalent positions generated by reflexion in the xy and xz symmetry planes. This energy is scarcely changed by a slight rotation to bring the molecule into the yz plane ($\theta = 90°$). The energy contours in one quadrant of this equatorial plane are shown in Fig. 4, where the numbers are the van der Waals sums as yet unmultiplied by the energy C_k. The potential defined at each point of the figure is for the value of ϕ at which the energy is a minimum. This value is 90° for points along the y axis, 0° along the z axis, and is usually but not always roughly defined by the direction of the equipotential line.

The value of C_k may be estimated from the heat of formation of chlorine hydrate from ice and gaseous chlorine, $\Delta H_h = -6.5 \pm 0.5$ kcal/mol at 0 °C (21). If the lattice energy is not appreciably affected by the presence of guest molecules, the heat of formation of $Cl_2 \cdot nH_2O$ is

$$[2] \qquad \Delta H_h = n\Delta H_0 + \Delta H_i$$

where ΔH_0 is the heat of formation of the empty lattice from ice and ΔH_i is the heat of intercalation of chlorine from the gas. We adopt Barrer and Edge's (8) average value of ΔH_0 for the rare gas hydrates, *viz.* 0.35 kcal/mol, and somewhat arbitrarily, in view of the range of composition of chlorine hydrate which has been reported (13), take $n = 6.6$. This is tantamount to complete occupancy of the larger cages and about half occupancy of the smaller cages. Since there are three times as many large as small cages in the lattice, only about 14% of the chlorine molecules occupy small cages and little error is introduced by ignoring the difference between the heats of

Can. J. Chem. Downloaded from www.nrcresearchpress.com by 210.87.254.5 on 09/05/12
For personal use only.

intercalation in the two cages, which is not likely to be great. We thus estimate $\Delta H_i = -8.8$ kcal/mol at 0 °C. This is related to the potential minimum $V_{min} = -9.64\ C_k$ of Fig. 4 approximately by

$$[3] \qquad \Delta H_i = V_{min} + 3RT/2$$

where the small zero-point energy of encaged chlorine has been neglected and $3RT/2$ refers to the excess of the enthalpy of translation and rotation of the encaged molecule over that of the gas, it being assumed that the encaged molecule makes the classical contribution from 5 translational and rotational vibrations. C_k then becomes 1.0 kcal/mol, with an uncertainty of perhaps 0.2 kcal/mol. This appears to be a reasonable value for the chlorine atom in Cl_2: the "experimental" value for argon was found (8) to be 0.93 kcal/mol.

The numbers on the equipotential lines of Fig. 4 may then be read, approximately, as kcal per mol.

The three-dimensional equipotential surfaces in the vicinity of the potential minimum are roughly ellipsoids with two principal axes in the equatorial plane in the direction of, and perpendicular to, the diagonal, and the third axis in the x direction. The approximately quadratic dependence on displacement in these three directions (particularly poor in the first case) gives 40, 23, and 27 cm^{-1} for the ground state translational oscillation frequencies. In a similar way the frequencies of rotational oscillation about the equilibrium orientation at (0, 0.065a, 0.065a) are found to be 18 cm^{-1} for rotation about the diagonal (variation of θ from 91.5°) and 28 cm^{-1} for rotation about the x axis (variation of ϕ from 135°).

Only at very low temperatures are the chlorine molecules in their ground oscillation states. With increase of temperature the motions become increasingly anharmonic and the molecules increasingly able to cross the ~300 cal/mol barriers separating the four regions of the potential minimum. The chlorine electron density, which at very low temperatures is concentrated in the vicinity of positions about 1.5 Å from the cage center along the y and z axes (*cf.* circles in Fig. 4), should as the temperature rises tend to become smeared out in a diffuse roughly circular ring.

The model gives a *relative* minimum of energy

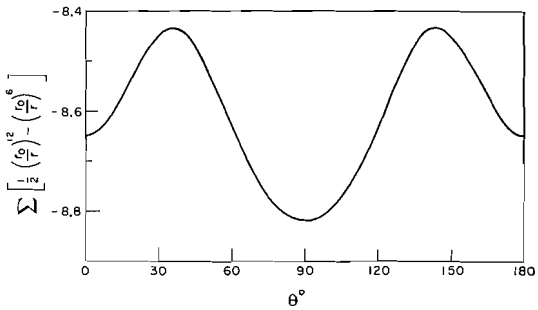

FIG. 5. Dependence of energy of Cl_2 centered in the cage on polar angle (θ); $\phi = 0$.

(−8.65 kcal/mol) when the axis of the chlorine molecule is aligned with the x axis and the center of mass is at the cage center. In Fig. 5 the energy is plotted *vs.* the polar angle, the center of mass being at the cage center, and ϕ is 0. (For each value of θ, the energy has equivalent minima at $\phi = 0, \pi/2, \pi, \ldots$; the energies at odd multiples of $\pi/4$ are as much as 100 cal/mol higher.) The axial configuration is about 1 kcal/mol less favorable than the configurations of least energy, in agreement with Pauling and Marsh's conclusion (20) that it could not account for the observed X-ray line intensities at 4 °C.

Pauling and Marsh made structure factor calculations for three other cases in which the center of mass coincided with the cage center. In these, the orientations were (*i*) distributed isotropically over a sphere, (*ii*) weighted by $\cos^2(\pi/2 - \theta)$ toward the equatorial plane, and (*iii*) confined to the equatorial plane. The best fit to the rather inaccurate observed intensities was found for (*ii*), with (*iii*) almost as good. This high-temperature result agrees with the present model with regard to electron density. We note, however, that the van der Waals model shows that the center of mass is not in general near the cage center and that reorientation of the chlorine molecule is accompanied by translation.

Rather similar results are expected for other nonpolar molecules like ethane and ethylene which resemble chlorine in size and shape. A more spherical but still off-center distribution is expected for smaller molecules like nitrogen and oxygen in the small as well as the large cages. Bromine, which is about 0.6 Å longer than chlorine, was first considered (1, 19) to partly occupy the larger structure I cages and its composition ($Br_2 . 8.47H_2O$) was the basis of a method of determining the difference in μ-potential be-

Can. J. Chem. Downloaded from www.nrcresearchpress.com by 210.87.254.5 on 09/05/12
For personal use only.

Can. J. Chem. Downloaded from www.nrcresearchpress.com by 210.87.254.5 on 09/05/12
For personal use only.

tween the empty structure I lattice and ice (19). Allen and Jeffrey (22) found, however, that bromine forms a structurally distinct tetragonal hydrate which contains 15-hedral as well as 12- and 14-hedral cages and has a composition of $Br_2 \cdot 8.6H_2O$ if the two largest cages are completely and exclusively occupied. A detailed structure has not been given but it may be suggested that the bromine molecule tends to be aligned along the long axis of 3-fold symmetry of the 15-hedron and to occupy nearly central positions in the equatorial plane of the 14-hedron.

Polyatomic Guests

The presence of hexagonal rings in the larger cages of both structures (Fig. 1) must contribute a degree of orientation dependence to the energy of many guest molecules, if only because atoms or atomic groups of the guest molecule which approach these rings may experience van der Waals contact with six water molecules rather than five. The "hole" in the center of a hexagonal ring is some 0.8 Å larger than in a pentagonal ring and may be partly penetrated by atoms of suitable size. Thus it is possible that in its most stable configuration in the large structure I cage the molecule of carbon dioxide is aligned with the polar axis of the cage. It is almost certain that the stable configurations of the large carbon tetrachloride molecule (known to form only a double structure II hydrate with hydrogen sulfide (23, 24) or other "help gas" (25) to occupy the small cages) are those in which the chlorine atoms are orientated toward the centers of the tetrahedrally disposed hexagonal rings. A relatively large barrier to rotation is probably present. Similar conclusions apply to neopentane, for which a clathrate hydrate appears not to have been reported, and, to a lesser degree, to isobutane, chloroform, and other molecules of similar geometry.

Oxygen atoms in guest molecules appear to be small enough to approach particularly close to the hexagonal faces if permitted to do so by adjacent groups. McMullan and Jeffrey (4) found that at −25 °C about one-half of the ethylene oxide molecules in large type I cages appeared to occupy the two "equilibrium" configurations shown in Fig. 6. Other ethylene oxide molecules appeared to occupy disordered positions somewhat displaced and rotated from the "equilibrium" ones. The possibility of additional disorder, including interchange of positions of the oxygen atom and a methylene group, was also suggested (4).

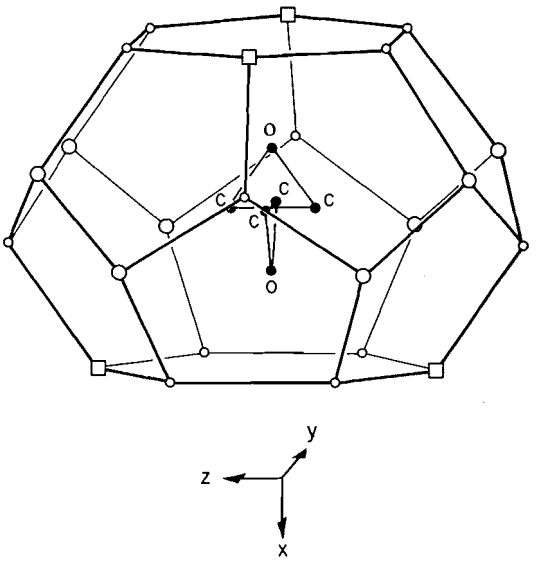

FIG. 6. Ethylene oxide in the two preferred positions in the tetrakaidecahedron suggested by ref. 4.

Tentative attempts were made to determine the configurations of greatest stability of ethylene oxide by using an expanded form of eq. 1 with individual values of r_{0k} and C_k chosen to represent the interaction of the cage oxygen atoms with the carbon, oxygen, and hydrogen atoms of ethylene oxide. Although the obvious inadequacies of this procedure give little quantitative meaning to the energies obtained, some conclusions are not sensitive to the particular parameters chosen.

The results failed to establish any preference for the axial configurations of Fig. 6. Many configurations of comparable and greater stability were found in which the molecule lay somewhat inclined to the equatorial plane. Even among axial configurations, increased stability resulted from translation of the ethylene oxide molecule along the $\bar{4}$ axis of the cage so as to bring the oxygen atom appreciably nearer to the adjacent hexagon. The results also showed no reason for the particular orientations about the axis shown in Fig. 6: these orientations were slightly less stable than those rotated by 90°.

The need for some reinterpretation of the X-ray results is also suggested by the rapid reorientation of the ethylene oxide dipole at temperatures down to 90 °K for which an "activation energy" of

Can. J. Chem. Downloaded from www.nrcresearchpress.com by 210.87.254.5 on 09/05/12
For personal use only.

only 0.5 kcal/mol has been found (14, 15). Moreover, at temperatures comparable to that of the X-ray study, the narrow proton resonance line of ethylene oxide deuterate (26) is indistinguishable from that expected for rapid isotropic rotation; that is, all intramolecular interproton vectors effectively average to zero in about 10^{-5} s.

In their X-ray study of the double hydrate of tetrahydrofuran and hydrogen sulfide at −20 °C, Mak and McMullan (5) found a spherically-symmetric distribution of electron density around the center of the 16-hedron, a result consistent (3) with either "free rotation" or the 12-fold orientational disorder required by the $\bar{4}3m$ symmetry of the cage. In the single hydrate of tetrahydrofuran the dipole reorientation rate is 15 GHz at 90 °K and increases at higher temperatures with an activation energy of *ca.* 0.3 kcal/mol (14, 15). Although the rotation is not free, the barriers to rotation are certainly comparable with kT at relatively high temperatures. At very low temperatures the dominant tetrahydrofuran configurations may well be those in which the oxygen atoms "point" toward the centers of the hexagonal rings.

III. Electrostatic Fields of the Water Molecules

The electrostatic field of the dipole moment of a *single* isolated water molecule an average cage radius away amounts to 44, 32, and 25 kesV/cm for the 12-, 14-, and 16-hedral cage, respectively. The corresponding energies of alignment of the ethylene oxide (μ = 1.90 D) and tetrahydrofuran (1.63 D) dipoles in their large cages are −980 and −590 cal/mol, respectively. Since the orientations of the water molecules are disordered, the resultant fields near the cage centers of the 20 to 28 water dipoles, each with six possible orientations consistent with full hydrogen bonding, should be expected to show wide variation according to the details of the cage configuration. The initial expectation is for fields which range from nearly zero to fields many times as great as the field of a single water molecule.

That large fields are not generally present, however, is shown by the dielectric results. The mean activation energies for orientation of ethylene oxide and tetrahydrofuran are less than 1 kcal/mol. For these and such other polar guest molecules (27) as trimethylene oxide (12), propylene oxide (12), dihydrofuran (12), acetone (28), and dioxolane (29) in structure II hydrates and methyl chloride (30) in structure I, the contribution of the guest molecule to the permittivity shows no significant departure at temperatures down to 77 to 100 °K from that expected for isotropic rotation, or the equivalent contribution to the permittivity from reorientation between two or more symmetrically disposed sites of the same energy. The electrostatic fields of the water molecules therefore appear to introduce no great anisotropy at high temperatures. One reason for this, as is shown below, is the almost complete cancellation of the dipolar fields of the water molecules at sites near the cage centers.

Dipolar Fields in an Idealized Cage Model

We suppose, as before, that the oxygen atoms of each water molecule and three of its neighbors are arranged tetrahedrally on the surface of a sphere of radius r. The fourth neighbor lies outside the sphere in the fourth tetrahedral direction which is also the direction of the position vector of the original molecule with respect to the cage center. The hydrogen bonding conforms to the Bernal–Fowler rules. The dipole moment of each water molecule is located on the oxygen atom and is resolved into two components m_{OH} along the O---O bonds to which hydrogen atoms are contributed.

For a cage of n water molecules, the $2n$ OH moments consist of $3n/2$ "internal" moments lying between the water molecules of the cage and $n/2$ moments lying external to the cage. The resulting field at the center of the cage is

$$[4]\quad \boldsymbol{E}(D) = \sum_{j=1}^{3n/2} [3(\boldsymbol{p}_j \cdot \boldsymbol{r}_j)\boldsymbol{r}_j - \boldsymbol{p}_j] + \sum_{k=1}^{n/2} [3(\boldsymbol{p}_k \cdot \boldsymbol{r}_k)\boldsymbol{r}_k - \boldsymbol{p}_k]$$

in units of m_{OH}/r^3. Here $\boldsymbol{p}_j$ is the unit vector in the direction of the jth internal moment located at $\boldsymbol{r}_j$ and k subscripts refer to external moments and positions (see Fig. 7).

Since $\boldsymbol{p}_k = \boldsymbol{r}_k$, the second sum becomes

$$[5]\quad \boldsymbol{E}_{ext} = 2 \sum_{k=1}^{n/2} \boldsymbol{r}_k$$

and, since $\boldsymbol{p}_j \cdot \boldsymbol{r}_j = -\frac{1}{3}$, the first

$$[6]\quad \boldsymbol{E}_{int} = -\sum_{j=1}^{3n/2} (\boldsymbol{r}_j + \boldsymbol{p}_j)$$

For tetrahedral angles the moment pointing from

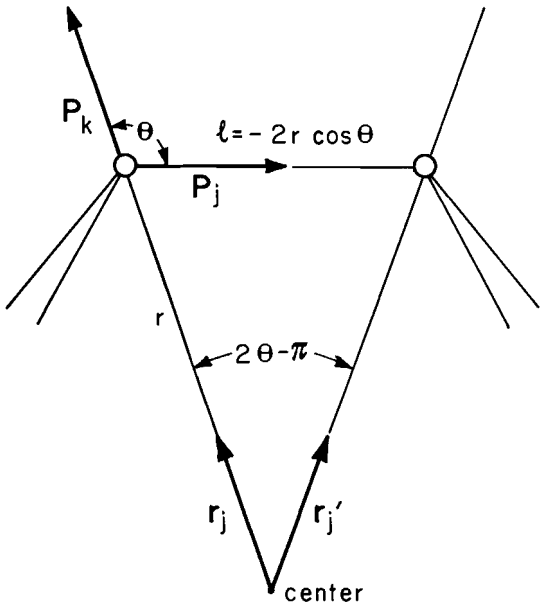

FIG. 7. Geometric model. θ is the tetrahedral angle, or, for the regular dodecahedron, 110° 54.3′.

site j to j' (Fig. 7) is $\boldsymbol{p}_j = 3(\boldsymbol{r}_{j'} - \boldsymbol{r}_j)/2$ and

$$[7] \qquad \boldsymbol{E}_{\text{int}} = \frac{1}{2}\sum_{j=1}^{3n/2} \boldsymbol{r}_j - \frac{3}{2}\sum_{j'=1}^{3n/2} \boldsymbol{r}_{j'}$$

The summation over j is taken once for each oxygen atom which has an external moment ($j = k$) and twice for each atom which does not ($j \neq k$). Thus

$$\sum_{j=1}^{3n/2} \boldsymbol{r}_j = \sum_{k=1}^{n/2} \boldsymbol{r}_k + 2\sum_{\substack{j=1 \\ j\neq k}}^{n/2} \boldsymbol{r}_j = -\sum_{k=1}^{n/2} \boldsymbol{r}_k$$

since the sum over all distinct sites

$$\sum_{k=1}^{n/2} \boldsymbol{r}_k + \sum_{\substack{j=1 \\ j\neq k}}^{n/2} \boldsymbol{r}_j = 0$$

(This condition does not follow from the model alone, but is fulfilled for all the actual cages.) Similarly, the summation over j' in eq. 7 occurs twice for $j' = k$, otherwise only once, and

$$\sum_{j'=1}^{3n/2} \boldsymbol{r}_{j'} = \sum_{k=1}^{n/2} \boldsymbol{r}_k$$

Substitution in eq. 7 gives

$$[8] \qquad \boldsymbol{E}_{\text{int}} = -2\sum_{k=1}^{n/2} \boldsymbol{r}_k$$

and addition of eq. 5

$$[9] \qquad \boldsymbol{E}(D) = 0$$

It is worth noting that this result is a consequence of the Bernal–Fowler rules and the tetrahedral bonding and is independent of the particular configuration of the water molecules. On the other hand, the vector sum of the dipole moments of the cage water molecules is

$$P = 4m_{\text{OH}}\sum_{k=1}^{n/2} \boldsymbol{r}_k$$

and does depend on this configuration.

In a discussion of the enthalpies of formation of clathrate hydrates, Glew suggested (31) that the attractive energy between guest and cage water molecules derives predominantly from short-range dispersion forces, since the cage symmetry and hydrogen bonding of the water molecules effectively reduce the dipole moments of the water molecules to zero. While providing support for Glew's main conclusion, the present treatment shows that it is based on the mutual cancellation of the *fields* of the dipoles.

Dipolar Fields in the Regular Dodecahedral Cage

Small resultant dipolar fields are to be expected for real cages in which the angles depart somewhat from tetrahedral. The idealized model may be slightly generalized to the case in which the three O---O directions on the cage surface make a common angle θ with the positive position vector (Fig. 7). With the other conditions as before, it is easily shown that

$$[10] \quad \boldsymbol{E}(D) = \frac{(1-\cos\theta)(1+3\cos\theta)}{\cos\theta}\sum_{k=1}^{n/2} \boldsymbol{r}_k$$

in units of m_{OH}/r^3. The value of the field now depends on the distribution of external OH groups over the cage. Since P is now

$$-(1-\cos\theta)(\cos\theta)^{-1} m_{\text{OH}}\sum_{k=1}^{n/2} \boldsymbol{r}_k$$

$$[11] \qquad \boldsymbol{E}(D) = -(1+3\cos\theta)\boldsymbol{P}/r^3$$

the proportionality factor being small for θ close to tetrahedral.

The pentagonal dodecahedral cages ($n = 20$) of structures I and II are slightly distorted from regular dodecahedra (32) for which θ is 110° 54.3′. For this value of θ

Can. J. Chem. Downloaded from www.nrcresearchpress.com by 210.87.254.5 on 09/05/12
For personal use only.

Can. J. Chem. Downloaded from www.nrcresearchpress.com by 210.87.254.5 on 09/05/12
For personal use only.

$$[12] \quad E(D) = 0.268 \frac{m_{OH}}{r^3} \sum_{k=1}^{10} r_k = -0.0705 \frac{P}{r^3}$$

The sum of the r_k's may take on all values from 0 to 4.91, the maximum value corresponding to the unlikely case that all ten external OH groups lie in the same half of the dodecahedron. Even the maximum dipolar field, 1.116 m_{OH}/r^3, is only 0.68 as large as the field of a single water dipole.

In order to find the distribution of dipolar fields in the regular dodecahedron, cage configurations were generated by assigning at random a hydrogen atom to either end of the thirty internal O---O bonds, excluding configurations which violated the Bernal–Fowler rules. The resulting distribution of fields for 4000 configurations is shown in Fig. 8, where $|E|$ is in units of m_{OH}/r^3. Without regard to direction, the number of distinct fields found was 71. Zero field occurred 25 times, the maximum field only twice. The median field was 0.44 m_{OH}/r^3 or 11.8 kesV/cm if m_{OH} is obtained from the dipole moment of the gas-phase water molecule, 1.84 D. (If a reaction-field enhanced dipole moment is assumed, the fields are increased in proportion.) The energy of alignment in this median field of a central dipole moment of 1 D (*e.g.*, hydrogen sulfide) is only −0.17 kcal/mol. The asymmetry introduced into the potential energy of the guest molecules by the dipolar fields therefore becomes important only at low temperatures, provided the molecular dipole is located close to the cage center.

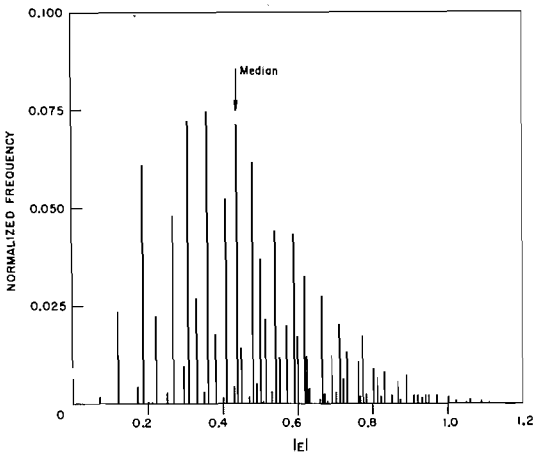

FIG. 8. Distribution of electrostatic fields for 4000 cage configurations of the regular dodecahedron. The fields are in units of m_{OH}/r^2 ($\cong$19 kesV/cm).

Quadrupolar Fields

Since, for geometric reasons, there is a high degree of mutual cancellation of dipolar fields, it is necessary to consider the fields of the higher moments of the charge distribution of the water molecules. Of these the quadrupolar fields are expected to be the most important.

In the coordinate system shown in Fig. 9 the only non-zero elements of the quadrupole moment tensor of the isolated water molecule are $Q_{xx}(=\int \rho(x,y,z)x^2 dv)$, Q_{yy}, and Q_{zz}. Here $\rho(x,y,z)$ is the charge density in the element of volume dv with coordinates x,y,z with respect to the oxygen nucleus as origin. For water molecules located and properly oriented in a lattice at sites where the symmetry is C_{2v} (or, as for tetrahedral symmetry, have C_{2v} as a factor group) the off-diagonal elements likewise vanish. In the clathrate hydrates, as in the ices (with the exception of Ic), most of the disordered orientations (except statistically) do not conform to the site symmetry with respect to O atoms and the quadrupole moment contains off-diagonal elements. These are expected to be small, however, since the local symmetry is approximately tetrahedral, and will be ignored.

The quadrupole potential at a point $r(x,y,z)$ with respect to the oxygen atom is

$$[13] \quad V(Q) = -\frac{1}{2r^3} \sum_{\alpha} Q_{\alpha\alpha}(1 - 3\alpha^2/r^2)$$

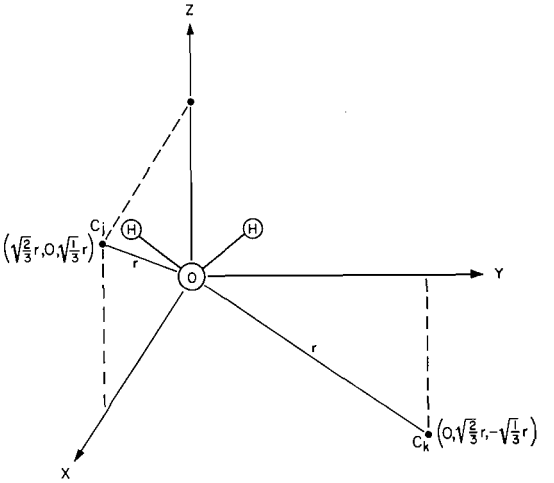

FIG. 9. Oxygen-centered coordinate system. C_j and C_k are the cage centers for tetrahedral O---O---O angles when both OH groups lie in the cage and when one OH group lies outside, respectively.

Can. J. Chem. Downloaded from www.nrcresearchpress.com by 210.87.254.5 on 09/05/12
For personal use only.

with $\alpha = x$, y, and z. The field in the α direction may be written

$$[14]\quad E_\alpha(Q) = -(\partial V/\partial\alpha) = \frac{3\alpha}{2r^5} \times \left[Q_{\alpha\alpha}(-3 + 5\alpha^2/r^2) + \sum_{\alpha'} Q_{\alpha'\alpha'}(-1 + 5\alpha'^2/r^2) \right]$$

where $\alpha' \neq \alpha$. Again, we express the quadrupolar fields in terms of the components in the directions of the donor O---O bonds and position vectors of the oxygen atoms with respect to the cage center.

For a water molecule with two internal OH groups, the cage center, in the coordinate system of Fig. 9, is at $(\sqrt{\frac{2}{3}}r, 0, \sqrt{\frac{1}{3}}r)$, where the field is

$$[15]\quad \boldsymbol{E}_j(Q) = E_x\boldsymbol{i} + E_z\boldsymbol{k} = E_{pj'}\boldsymbol{p}_{j'} + E_{pj''}\boldsymbol{p}_{j''} + E_{rj}\boldsymbol{r}_j$$

The unit vectors are

$$\boldsymbol{p}_{j'} = \sqrt{\tfrac{2}{3}}\boldsymbol{j} + \sqrt{\tfrac{1}{3}}\boldsymbol{k}$$
$$\boldsymbol{p}_{j''} = -\sqrt{\tfrac{2}{3}}\boldsymbol{j} + \sqrt{\tfrac{1}{3}}\boldsymbol{k}$$
$$\boldsymbol{r}_j = -\sqrt{\tfrac{2}{3}}\boldsymbol{i} - \sqrt{\tfrac{1}{3}}\boldsymbol{k}$$

whence

$$[16]\quad E_{pj'} = E_{pj''} = -\tfrac{1}{2}(\sqrt{\tfrac{3}{2}}E_x - \sqrt{3}E_z)$$
$$E_{rj} = -\sqrt{\tfrac{3}{2}}E_x$$

From eqs. 16 and 14

$$E_{pj'} = E_{pj''} = \frac{3}{2r^4}(Q_{xx} - Q_{zz})$$
$$E_{rj} = -\frac{1}{2r^4}(Q_{xx} - 3Q_{yy} + 2Q_{zz})$$

and by summation of eq. 15 over the $n/2$ "internal" sites

$$[17]\quad \boldsymbol{E}_{\text{int}}(Q) = \frac{9}{4r^4}(Q_{xx} - Q_{zz})(\sum \boldsymbol{r}_{j'} + \sum \boldsymbol{r}_{j''}) + \frac{1}{2r^4}(-10Q_{xx} + 3Q_{yy} + 7Q_{zz})\sum \boldsymbol{r}_j$$

Here, as before, we have used $\boldsymbol{p}_{j'} = (3/2)(\boldsymbol{r}_{j'} - \boldsymbol{r}_j)$, $\boldsymbol{p}_{j''} = (3/2)(\boldsymbol{r}_{j''} - \boldsymbol{r}_j)$, where $\boldsymbol{r}_{j'}$ and $\boldsymbol{r}_{j''}$ are the unit position vectors of the oxygen atoms which "receive" OH groups.

In the coordinate system of a water molecule with an external OH group the cage center is at $(0, \sqrt{\frac{2}{3}}r, -\sqrt{\frac{1}{3}}r)$ (Fig. 9). Since $E_x = 0$, there is no component of field perpendicular to the plane of $\boldsymbol{r}_k$ and $\boldsymbol{p}_{k'}$

$$[18]\quad \boldsymbol{E}_k(Q) = E_y\boldsymbol{j} + E_z\boldsymbol{k} = E_{pk'}\boldsymbol{p}_{k'} + E_{rk}\boldsymbol{r}_k$$

where

$$E_{pk'} = \tfrac{1}{2}(\sqrt{\tfrac{3}{2}}E_y + \sqrt{3}E_z)$$

and

$$E_{rk} = -\tfrac{1}{2}(\sqrt{\tfrac{3}{2}}E_y - \sqrt{3}E_z)$$

From [14]

$$E_{pk'} = \frac{3}{2r^4}(-Q_{yy} + Q_{zz})$$
$$E_{rk} = \frac{1}{2r^4}(3Q_{xx} - 4Q_{yy} + Q_{zz})$$

which, with $\boldsymbol{p}_{k'} = \frac{3}{2}(\boldsymbol{r}_{k'} - \boldsymbol{r}_k)$ and eq. 18 gives, for the sum over the $n/2$ external sites,

$$[19]\quad \boldsymbol{E}_{\text{ext}}(Q) = \frac{9}{4r^4}(-Q_{yy} + Q_{zz})\sum \boldsymbol{r}_{k'} + \frac{1}{4r^4}(6Q_{xx} + Q_{yy} - 7Q_{zz})\sum \boldsymbol{r}_k$$

The total quadrupolar field at the cage center $\boldsymbol{E}(Q)$ is the sum of eqs. 17 and 19. In addition to $\sum \boldsymbol{r}_j = -\sum \boldsymbol{r}_k$, as before, we have $\sum \boldsymbol{r}_{j'} + \sum \boldsymbol{r}_{j''} + \sum \boldsymbol{r}_{k'} = \sum \boldsymbol{r}_k$, since these three sums together include all $n/2$ internal sites once and all $n/2$ external sites twice. With these substitutions

$$[20]\quad \boldsymbol{E}(Q) = \frac{5}{4r^4}[-7(Q_{zz} - Q_{xx}) + (Q_{zz} - Q_{yy})]\sum \boldsymbol{r}_k + \frac{9}{4r^4}[(Q_{zz} - Q_{xx}) + (Q_{zz} - Q_{yy})]\sum \boldsymbol{r}_{k'}$$

There is thus no general geometric tendency for mutual cancellation of quadrupolar fields. However, since each k' is a nearest neighbor of some k, there is a statistical correlation between $\sum \boldsymbol{r}_{k'}$ and $\sum \boldsymbol{r}_k$. Not only may some $\boldsymbol{r}_{k'}$'s be identical with $\boldsymbol{r}_k$'s but they may occur twice.

Octupolar Fields

The field at the cage center due to the octupole moments of the water molecules may be similarly derived for the tetrahedral model. Again in the coordinate system of Fig. 9, the non-vanishing elements of the octupole moment tensor are R_{zzz}, R_{zxx}, and R_{zyy}, in terms of which the potential energy is

$$[21]\quad V(\text{O}) = \frac{z}{2r^5}\sum_\alpha (R_{zzz} - 3R_{z\alpha\alpha})\left(1 - \frac{5\alpha^2}{r^2}\right)$$

with $\alpha = x, y$.

Can. J. Chem. Downloaded from www.nrcresearchpress.com by 210.87.254.5 on 09/05/12
For personal use only.

The procedure of the last section leads to the simple result

$$[22] \quad \boldsymbol{E}(\mathrm{O}) = -\frac{14\sqrt{3}}{9r^5}\left[\sum_{\alpha}(R_{zzz} - 3R_{z\alpha\alpha})\right]\sum \boldsymbol{r}_k$$

Statistical Evaluation of Fields in the Tetrakaidecahedra

It is of interest to compare the predictions of the tetrahedral model with the fields calculated for actual cages. For this purpose, random 14-hedral cage configurations were generated for oxygen atom sites given by McMullan and Jeffrey (4) for ethylene oxide hydrate. Two protons were assigned randomly to those of the four O---O bonds of each water molecule which did not already bear a proton at the other end. If three bonds bore such a proton, or if the resulting assignment led to more than $12(=n/2)$ external protons, the entire process of assignment was restarted. The order of assignment of protons to water molecules was also random.

After generation of a cage configuration which conformed to the Bernal–Fowler rules, the axes of a coordinate system for each water molecule were determined to accord with Fig. 9. The coordinates of the 24 molecules outside the cage and directly hydrogen-bonded to it were included in the program to define the directions of the external bonds. The fields of the individual dipole, quadrupole, and octupole moments were found (from eqs. 4, 14, and differentiation of eq. 21) in the molecular coordinate system, transformed to a cage-fixed coordinate system, and summed over the 24 molecules. The resultant dipole moment of the cage was also found.

We illustrate the results for the following choice of moments: $\mu = 1.84 \times 10^{-18}$ e.s.u. cm; $Q_{xx} = -6.56$, $Q_{yy} = -5.18$, $Q_{zz} = -5.51 \times 10^{-26}$ e.s.u. cm^2; $R_{zzz} = -2.75$, $R_{zxx} = -1.08$, $R_{zyy} = -0.50 \times 10^{-34}$ e.s.u. cm^3. These quadrupole and octupole moment elements were calculated from relatively primitive wavefunctions by Glaeser and Coulson (33) and were used by Coulson and Eisenberg (34) to calculate the electrostatic field at the site of a water molecule in ice.

The distribution of magnitude of the dipolar field at the cage center given by 85 cage configurations is shown in the lower histogram of Fig. 10. As for the regular dodecahedron, the resultant dipolar fields are relatively small, the mean field (13.6 kesV/cm) being only 43% of the

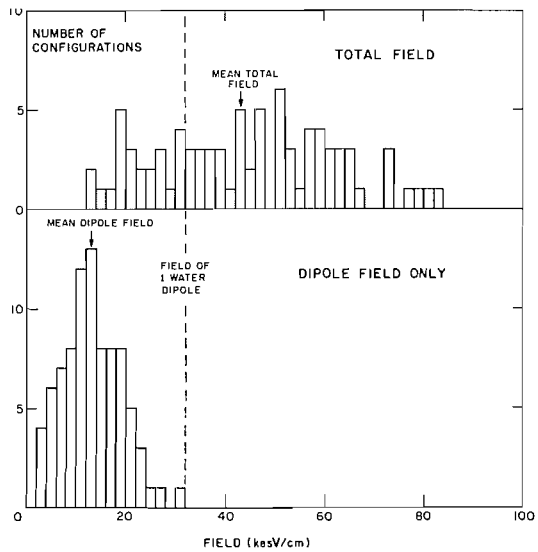

FIG. 10. Distribution of central fields for 85 configurations of the tetrakaidecahedron. The mean resultant dipole moment of the 24 water molecules was 6.93 μ.

dipolar field of a single water molecule. The energy of alignment of ethylene oxide in this mean field is −0.37 kcal/mol.

The field distribution when the fields of the quadrupoles and octupoles are added to those of the dipoles for the same configurations is also shown in Fig. 10. The distribution is considerably broadened and shifted to higher fields, the mean field being now more than three times as large as before. The increase is entirely the effect of the quadrupoles, since the contribution of the octupoles was found, in almost all cases, to slightly reduce the contribution of the quadrupoles. This is consistent with eqs. 20 and 22 (for the tetrahedral model). The latter now becomes $\boldsymbol{E}(\mathrm{O}) = 0.31 \sum \boldsymbol{r}_k$ kesV/cm. Since the resultant dipole moment of the cage molecules is $2\sqrt{3}\mu\sum \boldsymbol{r}_k$ for the tetrahedral model, and the mean value of this resultant was found to be 6.93 μ for the configurations of Fig. 10, the mean value of $\sum \boldsymbol{r}_k$ may be estimated to be about 2.0 and the mean octupolar field to be only about 0.62 kesV/cm. The actual mean field due to octupoles was found to be 3.0 kesV/cm and, like the resultant dipolar field, reflects departure from the tetrahedral model.

Since eq. 20, unlike eqs. 9 and 22, does not rely heavily on mutual cancellation effects implicit in the tetrahedral model, it is expected to give a reasonable estimate of the quadrupolar field of

TABLE 2. Calculated and experimental quadrupole moment elements ($\times 10^{26}$ e.s.u. cm^2) of water with respect to the O atom as origin

Workers	Reference number	Q_{xx}	Q_{yy}	Q_{zz}
Glaeser and Coulson	33	−6.56	−5.18	−5.51
Harrison	36	−7.80	−4.44	−6.17
Kern and Matcha	37	$Q_{zz} - Q_{xx} = 0.99$,		$Q_{zz} - Q_{yy} = -0.44$
Aung, Pitzer, and Chan	38	−7.71	−4.22	−5.77
Neumann and Moskowitz	39	−7.48	−4.18	−5.94
Arrighini, Guidotti, and Salvetti	40	−7.88	−4.20	−5.84
Verhoeven and Dymanus*	35	−7.15	−3.73	−5.32

*Experimental values.

the real cage. With $\overline{\sum r_k} = 2.0$ again, the mean contribution of the first term of eq. 20 is 55 kesV/cm, considerably greater than the 37 kesV/cm found for the actual mean quadrupolar field for the 85 configurations. Thus the term in $\sum r_{k'}$ reduces the contribution of the first term, as expected from a positive correlation between the directions of $\sum r_k$ and $\sum r_{k'}$ and the opposite signs of the factors in square brackets. We note too that for the moments assumed the signs of the coefficients of $\sum r_k$ in eqs. 20 and 22 are opposite.

A statistical tendency for the dipolar fields to favor the x direction (the $\bar{4}$ symmetry axis of the cage) was shown. The x component of this field averaged 36% higher than the y and z components which, for the 85 configurations considered, were the same to within 0.5%. After the quadrupolar and octupolar fields were added the mean preference for the x direction was reduced to 19%.

The mean dipolar field was found to be 68% higher at a point displaced 0.5 Å along the x axis than at the center, the major difference being in its x component. The total field however averaged only 2% higher.

Effect of Electrostatic Fields on Dielectric Properties

It is evident that the presence of a broad distribution of electrostatic fields and field directions within the cages will lead to a highly variable perturbation of the potential energy function which describes the short-range interactions. The symmetry imposed by cage geometry is removed and, at least at low temperatures, the reorientation should become distinguishable from isotropic reorientation. The contribution of the guest molecules to the permittivity should fall as, with fall of temperature, orientations favored by the electrostatic fields become increasingly populated at the expense of those which are not. The decline would be expected to cover a wide range of temperature because of the distribution of fields in different cages.

The barriers to reorientation ("activation energies") are also field-dependent and the distribution of fields should be reflected by a wide distribution of reorientation rates. Dielectric relaxation of the guest molecules should depart appreciably from Debye behavior.

It is difficult to make these qualitative conclusions more quantitative in the absence of an adequate knowledge of the charge distribution of the water molecule in the hydrate lattice, *i.e.* in an ice-like environment. The enhancement over the value of the gas-phase dipole moment may be reasonably estimated as the moment induced by the reaction field (Coulson and Eisenberg found $\mu = 2.60$ D in ice (34)), but the effect of the hydrogen bonding on the quadrupole moment, potentially the largest contributor to the field, is difficult to estimate.

Some recently calculated quadrupole moment elements are given in Table 2, together with an "experimental" value derived (35) from the magnetic moment tensor and the anisotropy of the magnetic susceptibility tensor obtained from analysis of the hyperfine microwave Zeeman spectrum. All the values listed are for the isolated water molecule, the calculated values having been obtained from a variety of electronic wave functions, of which those of refs. 38, 39, and 40 are presumably the most accurate. Where necessary the quadrupole moment elements have been converted from the Buckingham (41) form to the form which describes the second moment of the charge distribution, the origin has been shifted from the center of mass to the oxygen nucleus to conform with the present treatment, and axes have been transformed to conform to Fig. 9.

Can. J. Chem. Downloaded from www.nrcresearchpress.com by 210.87.254.5 on 09/05/12
For personal use only.

Can. J. Chem. Downloaded from www.nrcresearchpress.com by 210.87.254.5 on 09/05/12
For personal use only.

It is apparent that substitution of more recent gas-phase values for the quadrupole moment elements of Glaeser and Coulson will generally raise the resultant fields shown in Fig. 10 by a factor of between 2 and 3. The mean field is then about 100 kesV/cm and the energy of alignment of the ethylene oxide dipole at the cage center is about −3 kcal/mol. Dielectric and n.m.r. results for ethylene oxide hydrate at low temperatures have yet to be reported, but it seems quite clear that the high-temperature properties (14, 15, 26) are inconsistent with the presence of orientation-dependent energies of this magnitude. The second moment of the charge distribution of the water molecule in the hydrate lattice therefore appears to be much less anisotropic than in the gas.

Fields in the Hexakaidecahedra

The distribution of electrostatic fields in the more symmetrical large cages of structure II is shown in Fig. 11 for 241 randomly-generated configurations. The procedure was the same as for the 14-hedra, with modifications appropriate to a cage of 28 water molecules located at sites given by Mak and McMullan's X-ray analysis (5) of the structure II double hydrate of tetrahydrofuran and hydrogen sulfide.

The mean dipolar field (14.9 kesV/cm) was slightly larger than within the 14-hedra, the mean total field and resultant dipole moment slightly smaller.

Again, as expected, the resultant field is statistically a minimum at the cage center. For any given cage configuration, however, the position of minimum total field is diplaced from the cage center by, on average, some 1.45 Å. Only about 25% of the positions of least dipolar field were displaced from the center by more than 0.7 Å.

Figure 12 shows the variation of the *mean* field with displacement from the center along the directions of the mid points of the hexagons. The same 69 configurations were used for evaluation of the mean fields due to dipole moments (1.84 and 2.60 D) alone and with the multipole moments of Glaeser and Coulson (33) or Arrighini *et al.* (40) also included. It is apparent that the dipolar fields in general depend more on position within the cage than do the "total" fields and that for the quadrupole moment elements assumed, there is a strong tendency for the quadrupolar fields to reduce the increasing dipolar contributions with increase of off-center displacement.

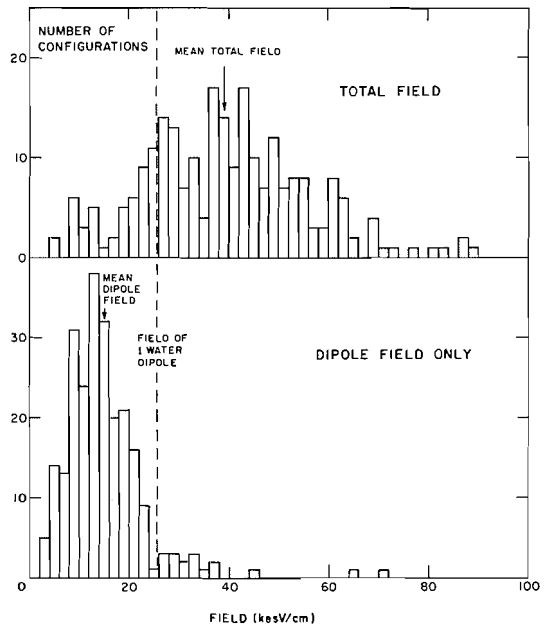

FIG. 11. Distribution of central fields for 241 configurations of the hexakaidecahedron. The mean resultant dipole moment was 6.89 μ.

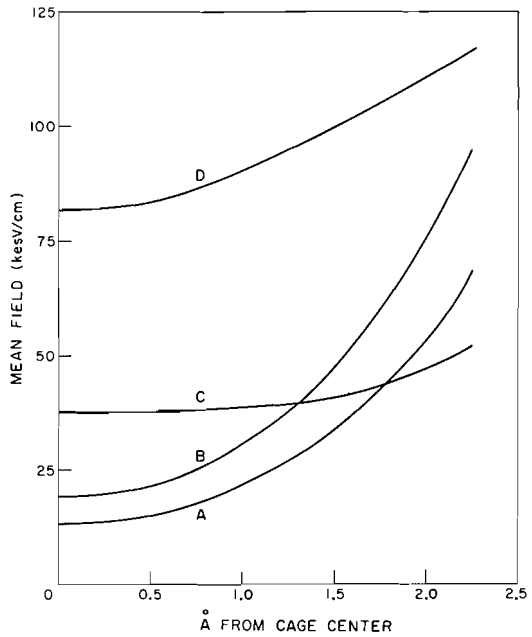

FIG. 12. Variation of mean fields with displacement along the 3-fold axes of the 16-hedra for *A*, μ = 1.84 D; *B*, μ = 2.60 D; *C*, μ = 1.84 D and higher moments of Glaeser and Coulson; *D* = 1.84 D and higher moments of Arrighini *et al.*

Can. J. Chem. Downloaded from www.nrcresearchpress.com by 210.87.254.5 on 09/05/12
For personal use only.

As long as the dipolar guest molecule has the ability to rotate it will be most stable where the field is largest. As it moves out from the center, however, the short-range repulsive forces eventually determine which orientations with respect to the field are possible. A model in which a molecular dipole is constrained by geometry to four mutually tetrahedral directions is considered in Section V.

IV. Interactions between Guest Molecules

The only interactions between adjacent guest molecules likely to contribute appreciably to the orientation-dependent energy are dipole–dipole interactions.

The centers of nearest-neighbor large cages in structure I lie on lines extending in 3 orthogonal directions, adjacent centers being 6.0 Å apart. There is a preference for parallel alignment of guest dipoles along the lines of centers, especially if the dipoles are constrained by geometry to point along these lines, as Fig. 6 suggests for ethylene oxide and may possibly be the case for trimethylene oxide at low temperatures. The energy of interaction between guest dipoles is affected by the presence of polarizable water molecules. If an isotropic polarizability α of 1.44 Å^3 is assigned to a water molecule, the reaction field of the dipoles induced in the water molecules of the cage enhances the dipole moment of a central ethylene oxide molecule ($\alpha = 4.8$ Å^3) by 0.11 D. Moreover, the field at the site of one guest molecule due to an adjacent parallel guest dipole is reduced by more than one-third by the fields of the dipoles induced in the 24 water molecules of the adjacent cage. (This shielding effect is equivalent to an effective permittivity of 1.6 for the medium between adjacent guest dipoles.) The energy of parallel alignment of an ethylene oxide molecule with a neighbor is then -350 cal/mol. If only parallel or anti-parallel alignment is permitted, the one-dimensional Ising model gives $\frac{1}{2}[1 + \tanh(350/RT)]$ for the probability of parallel alignment of a pair of adjacent molecules, or 0.91 at 150 °K. This leads to a chain of about 8 parallel dipoles in average length at this temperature and predicts a considerable enhancement of the permittivity.

No such enhancement has been found for ethylene oxide (14, 15) or trimethylene oxide (12) hydrates. This result does not conclusively show the absence of geometric preference for orientations along the polar axis of the cage since the electrostatic fields of the water molecules are in general larger than that of a neighboring guest, at most 12 kesV/cm for ethylene oxide. Even so, for such preferred orientations the statistical short range order should be great enough to give an appreciable dielectric increment.

Within the structure II hydrates interaction between the guest molecule dipoles is of minor importance. The lattice formed by centers of the large cages possesses simple tetrahedral symmetry. It is not certain whether any net statistical correlation of dipole directions is to be expected for this lattice. In any event the interaction energy between neighboring tetrahydrofuran molecules, with shielding, is no more than 110 cal/mol, which corresponds to a field of 5.1 kesV/cm at one molecule due to the other.

V. A Model of Guest Molecule Relaxation in Structure II Hydrates

An attempt is now made to make the previous discussion more quantitative by introducing a definite model to which to relate the dielectric results. The model is applied to structure II hydrates where the dipole–dipole interactions between guest molecules are assumed small enough to be neglected.

The simplest model that takes advantage of the tetrahedral symmetry of the large type II cages is the one which assumes that, in the absence of electrostatic fields of water molecules, there are four tetrahedrally disposed preferred orientations of equal energy. In the case of tetrahydrofuran these could be the orientations in which the oxygen atoms approach the hexagonal rings, that is, the dipole moment points toward the cage center along the line joining it to the center of a hexagon. We wish to find the temperature variation of the contribution of reorienting guest molecules to the permittivity when the symmetry is disturbed by the fields of the water molecules.

Consider first a collection of N cages per cm^3, all with identical configurations. The populations of the four orientations are given by $N_i(\mathrm{O})$, where

$$\sum_{i=1}^{4} N_i(\mathrm{O}) = N$$

In the presence of an applied field $\boldsymbol{E}_e$ there is a small adjustment of populations which now become $N_i(e)$ at equilibrium. For E_e small in com-

Can. J. Chem. Downloaded from www.nrcresearchpress.com by 210.87.254.5 on 09/05/12
For personal use only.

parison with kT/μ the four quotients of the form

$$\frac{N_i(\mathrm{e})}{N_i(\mathrm{O})(1 + \mu l_i E_\mathrm{e}/kT)}$$

may be equated to one another, which, along with

$$\sum_{i=1}^{4} N_i(\mathrm{e}) = N$$

leads to

[23] $$N_i(\mathrm{e}) = N_i(\mathrm{O}) \times \left[1 + \frac{\mu E_\mathrm{e}}{NkT} \sum_{j \neq i} N_j(\mathrm{O})(l_i - l_j)\right]$$

where l_i is the direction cosine between dipole orientation i and $\boldsymbol{E}_\mathrm{e}$. The polarization is

[24] $$P = \mu \sum_i l_i[N_i(\mathrm{e}) - N_i(\mathrm{O})] = \frac{\mu^2 E_\mathrm{e}}{kT} \sum_i \left[l_i N_i(\mathrm{O}) \sum_{j \neq i} \frac{N_j(\mathrm{O})}{N} (l_i - l_j)\right]$$

which for a polycrystalline sample yields an average polarization

[25] $$\bar{P} = \frac{\mu^2 E_\mathrm{e}}{kT} \sum_i \left[N_i(\mathrm{O}) \sum \frac{4N_j(\mathrm{O})}{9N}\right] = \frac{4}{9} \frac{\mu^2 E_\mathrm{e}}{kT} \sum_i N_i(\mathrm{O}) \left\{\frac{N - N_i(\mathrm{O})}{N}\right\}$$

since $\overline{l_i^2} = 1/3$ and $\overline{l_i l_j} = -1/9$, the latter for tetrahedral angles. This is the analogue of the Debye equation for an applied field E_e at the sites of the dipoles and reduces to the Debye case for all $N_i(\mathrm{O}) = N/4$.

After averaging over the distribution of electrostatic fields of the water molecules in different cages eq. 25 becomes

[26] $$\bar{\bar{P}} = \frac{4N\mu^2 E_\mathrm{e}}{9mkT} \sum_{n=1}^{m} \sum_i p_{in}(1 - p_{in})$$

where n specifies one of the m randomly generated cage configurations and p_{in}, the probability of orientation i within a cage of configuration n, is given by

[27] $$p_{in} = \frac{\exp(\boldsymbol{\mu}_i \cdot \boldsymbol{E}_{in}/kT)}{\sum_j \exp(\boldsymbol{\mu}_j \cdot \boldsymbol{E}_{jn}/kT)}$$

$\boldsymbol{E}_{in}$ being the cage electrostatic field at the site of orientation i.

The field $\boldsymbol{E}_\mathrm{e}$ is a consequence of the applied external field but is not equal to it. If all four orientations in each cage are equally probable the contribution to the dielectric constant from reorientation of guest molecules is not

[28] $$\Delta\varepsilon = \frac{4\pi N\mu^2}{3kT}$$

as given by eq. 26 with $\boldsymbol{E}_\mathrm{e}$ set equal to the external field, since the cavity and reaction fields are neglected and the contribution to the permittivity therefore considerably underestimated. A better representation is in terms of the Onsager equation (eq. 3 of ref. 2), especially, as discussed in the accompanying paper (2), if allowance is made for the enhanced polarizability of the guest molecule. For brevity we do not repeat the development here but simply note that modification of eq. 5 of ref. 2 by replacing the factor $\mu^2/3$ appropriate to high temperatures by the factor

$$(4\mu^2/9m) \sum_n \sum_i p_{in}(1 - p_{in})$$

appropriate to the present model at all temperatures leads to

[29] $$\frac{(\varepsilon_{02} - 1)(2\varepsilon_{02} + 1)}{3\varepsilon_{02}} = \frac{(\varepsilon_{\infty 2} - 1)(2\varepsilon_{\infty 2} + 1)}{3\varepsilon_{\infty 2}} + \frac{16\pi N\mu^2}{9mkT} \cdot \frac{1 + f(\alpha^* - \alpha)}{(1 - f\alpha^*)(1 - f\alpha)} \times \sum_{n=1}^{m} \sum_{i=1}^{4} p_{in}(1 - p_{in})$$

where ε_{02} is the permittivity of the hydrate which includes the contribution from reorientation of guest molecules but not of water molecules, $\varepsilon_{\infty 2}$ is the permittivity at frequencies too high for any reorientational contribution, α is the "normal" polarizability of the guest molecule, and α^* is the enhanced polarizability introduced in (2). The latter is related to the relatively large value of $\varepsilon_{\infty 2}$, which is found to be 3.47 for tetrahydrofuran hydrate at 4 °K, where reorientation makes no appreciable contribution to the permittivity at frequencies in the kHz region.

We have taken $\alpha = 7.9$ Å^3 and $\alpha^* = 16$ Å^3 (2) for tetrahydrofuran and applied eq. 29 with an effective cage radius $a = 3.4$ Å in $f = 2(\varepsilon_{02} - 1)/[(2\varepsilon_{02} + 1)a^3]$. The probabilities defined by eq. 27 were varied in two ways: by varying the assumptions made about the dipole and multipole moments of the water molecules, and by allowing the position of the dipole moment of the tetra-

Can. J. Chem. Downloaded from www.nrcresearchpress.com by 210.87.254.5 on 09/05/12
For personal use only.

hydrofuran molecule (that is, the point at which $\boldsymbol{E}_{in}$ was evaluated) to move from the cage center along the directions towards the mid-points of the hexagons. It is apparent that the dipole moment of tetrahydrofuran should be displaced from the center of mass toward the oxygen atom. Without a detailed knowledge of the charge distribution its proper position cannot be defined but it may be assumed to be close to a point lying on the axis bisecting the C—O—C bond and removed from the oxygen atom by about half the projection of an OC bond on this axis. If the center of mass lies at the cage center the dipole moment is then located about $0.04a$ away. Fields have been evaluated at positions $0.04a$, $0.08a$, and $0.12a$ from the cage center along the lines to the centers of the hexagons. The latter two positions correspond to increasing approach of the oxygen ends of the molecules to the hexagonal rings in conformity with the likely geometric preference for such positions.

In Fig. 13 the results of preliminary measurements of ε_{02} of tetrahydrofuran hydrate at low temperatures and of the earlier measurements (12) at higher temperatures are shown as a heavy solid line. The value of ε_{02} passes through a very broad maximum of 6.3 near 50 °K and falls off at an accelerating rate at lower temperatures. It proved impossible to estimate adequately this static permittivity below about 20 °K because the orientational relaxation became too slow. The dashed line joining the ε_{02} curve at low temperatures represents 1 kHz results through this dispersion region.

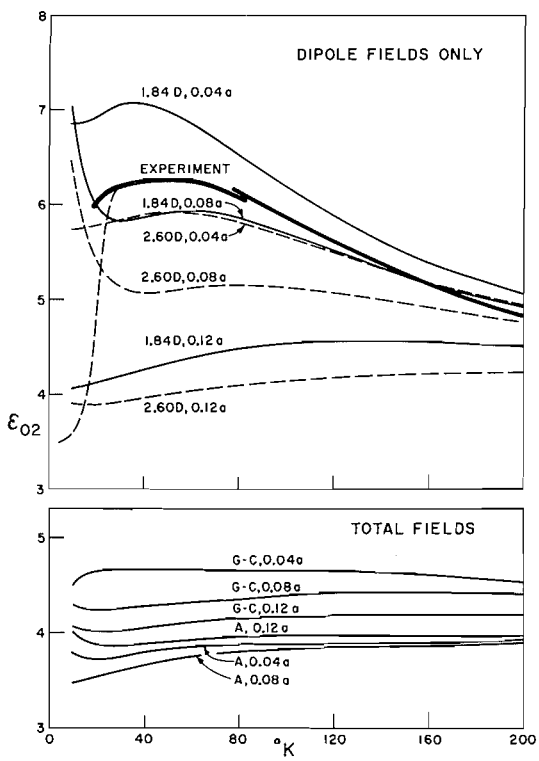

FIG. 13. Experimental and calculated ε_{02} *vs.* temperature curves of tetrahydrofuran hydrate.

The other curves of Fig. 13 represent various calculated values of ε_{02}, all for the same 70 randomly generated cage configurations. The curves in the upper part of the figure were calculated for dipole moments alone, two extreme values of the dipole moment, 1.84 and 2.60 D (34), being assumed. The lower curves include, besides the contribution of dipole moments of 1.84 D, quadrupole and octupole moment contributions using the smallest (Glaeser and Coulson) and largest (Arrighini *et al.*) quadrupole moments of Table 2. These curves are slightly depressed if the dipole moment is taken as 2.60 D.

It is apparent that the inclusion of any reasonable gas-phase quadrupole moment elements leads to dielectric constants which are much lower than the experimental ones. The agreement is much better when the fields are assumed to arise from dipole moments alone.

The model is obviously a very crude one. The rise in ε_{02} at the lower end of some curves as temperature goes down is contributed by only a few of the 70 configurations and would probably disappear for a more statistically significant number of configurations. We have neglected the possibility that guest molecules may occupy other than the orientational sites specified, that they may move to positions where the energy is more favorable, that the cavity and reaction fields are sensitive to displacement of the dipole moment from the center of the cage, and that the cage configurations may not be random. Most of these assumptions will lead to some under-estimation of ε_{02}. On the other hand the factor $f\alpha^*$ may be too large, especially at high temperatures. No great significance can therefore be attached to the particular choice of moments and sites which agrees best with experiment. However it is difficult to escape the qualitative conclusion that the second moment of the charge distribution of the water molecule in the hydrate lattice (and by

Can. J. Chem. Downloaded from www.nrcresearchpress.com by 210.87.254.5 on 09/05/12
For personal use only.

inference in ices and liquid water) is much more symmetrical than it is in the isolated water molecule.

VI. Distribution of Reorientation Rates

We conclude by offering some evidence of the variability of the electrostatic fields in different cages. Figure 14 shows the frequency-dependence of the dielectric absorption in tetrahydrofuran hydrate at liquid hydrogen temperature. The points at which $\varepsilon'' = \varepsilon''_{max}/2$ differ by a factor of 10^4 in frequency compared with the factor of ~ 14 characteristics of a Debye curve for a single relaxation time. Such a width corresponds to a very broad distribution of relaxation times at this low temperature, in qualitative agreement with the expectation of a wide variability of barrier heights resulting from the effects of the electrostatic fields. The same explanation seems appropriate to the proton magnetic resonance line width of tetrahydrofuran deuterate, shown in Fig. 15 as the square root of the second moment. This undergoes a very gradual change from its rigid lattice value at the lowest temperatures to the value characteristic of isotropic rotation at much higher temperatures.

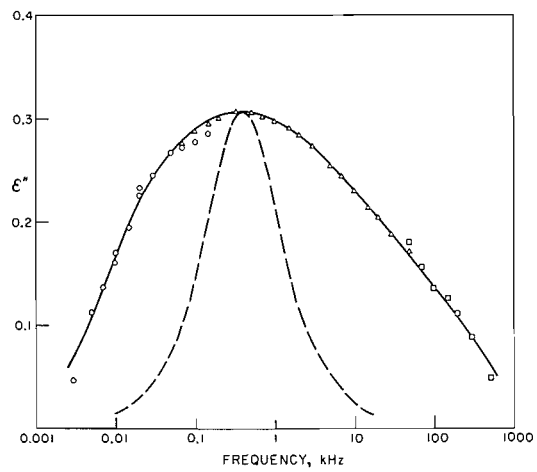

FIG. 14. Dielectric absorption in tetrahydrofuran hydrate at 20.4 °K.

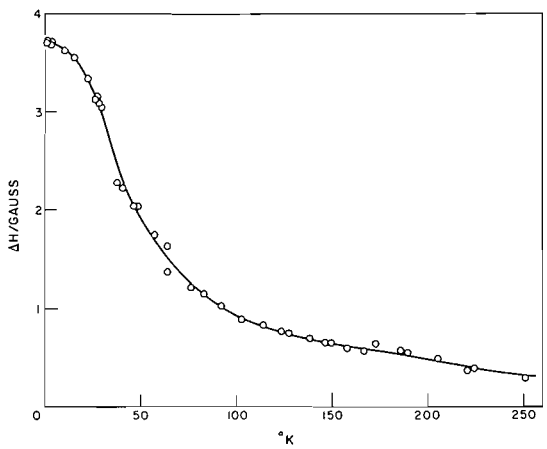

FIG. 15. Line width of the proton resonance line (as square root of the second moment) of $C_4H_8O \cdot 17.4D_2O$.

I am indebted to B. Morris for the low temperature dielectric measurements of tetrahydrofuran hydrate, to S. K. Garg for the n.m.r. measurements of tetrahydrofuran deuterate, and to M. Bedard for some of the calculations.

1. M. VON STACKELBERG and H. R. MÜLLER. Z. Elektrochem. **58**, 25 (1954).
2. B. MORRIS and D. W. DAVIDSON. Can. J. Chem. This issue.
3. G. A. JEFFREY and R. K. MCMULLAN. Progr. Inorg. Chem. **8**, 43 (1967).
4. R. K. MCMULLAN and G. A. JEFFREY. J. Chem. Phys. **42**, 2725 (1965).
5. T. C. W. MAK and R. K. MCMULLAN. J. Chem. Phys. **42**, 2732 (1965).
6. E. WHALLEY, J. B. R. HEATH, and D. W. DAVIDSON. J. Chem. Phys. **48**, 2362 (1968).
7. J. C. PLATTEEUW and J. H. VAN DER WAALS. Mol. Phys. **1**, 91 (1958).
8. R. M. BARRER and A. V. J. EDGE. Proc. Roy. Soc. London. Ser. A, **300**, 1 (1967).
9. K. W. ALLEN and G. A. JEFFREY. J. Chem. Phys. **38**, 2304 (1963).
10. D. R. HAFEMANN and S. L. MILLER. J. Phys. Chem. **73**, 1392 (1969).
11. Y. A. MAJID, S. K. GARG, and D. W. DAVIDSON. Can. J. Chem. **47**, 4697 (1969).
12. R. E. HAWKINS and D. W. DAVIDSON. J. Phys. Chem. **70**, 1889 (1966).
13. D. N. GLEW and N. S. RATH. J. Chem. Phys. **44**, 1710 (1966).
14. D. W. DAVIDSON, M. DAVIES, and K. WILLIAMS. J. Chem. Phys. **40**, 3449 (1964).
15. M. DAVIES and K. WILLIAMS. Trans. Faraday Soc. **64**, 529 (1968).
16. N. G. PARSONAGE and L. A. K. STAVELEY. Mol. Phys. **3**, 59 (1960).
17. V. MCKOY and O. SINANOGLU. J. Chem. Phys. **38**, 2946 (1964).
18. T. KIHARA. J. Phys. Soc. Japan, **6**, 289 (1951).
19. J. H. VAN DER WAALS and J. C. PLATTEEUW. Advan. Chem. Phys. **2**, 1 (1959).
20. L. PAULING and R. E. MARSH. Proc. Nat. Acad. Sci. (U.S.) **38**, 2304 (1963).
21. D. N. GLEW. J. Phys. Chem. **66**, 605 (1962).
22. K. W. ALLEN and G. A. JEFFREY. J. Chem. Phys. **38**, 2304 (1963).
23. M. VON STACKELBERG and H. FRÜHBUSS. Z. Elektrochem. **58**, 99 (1954).
24. M. VON STACKELBERG and W. JAHNS. Z. Elektrochem. **58**, 162 (1954).

25. M. VON STACKELBERG and W. MEINHOLD. Z. Elektrochem. **58**, 40 (1954).
26. S. BROWNSTEIN, D. W. DAVIDSON, and D. FIAT. J. Chem. Phys. **46**, 1454 (1967).
27. D. F. SARGENT and L. D. CALVERT. J. Phys. Chem. **70**, 2689 (1966).
28. G. J. WILSON and D. W. DAVIDSON. Can. J. Chem. **41**, 264 (1963).
29. A. VENKATESWARAN, J. R. EASTERFIELD, and D. W. DAVIDSON. Can. J. Chem. **45**, 884 (1967).
30. D. W. DAVIDSON. Unpublished results.
31. D. N. GLEW. Can. J. Chem. **38**, 208 (1960).
32. International Tables for X-Ray Crystallography. Vol. 2. 1967. p. 48.
33. R. M. GLAESER and C. A. COULSON. Trans. Faraday Soc. **61**, 389 (1965).
34. C. A. COULSON and D. EISENBERG. Proc. Roy. Soc. London. Ser. A. **291**, 445 (1966).
35. J. VERHOEVEN and A. DYMANUS. J. Chem. Phys. **52**, 3222 (1970).
36. J. F. HARRISON. J. Chem. Phys. **47**, 2990 (1967).
37. C. W. KERN and R. L. MATCHA. J. Chem. Phys. **49**, 2081 (1968).
38. S. AUNG, R. M. PITZER, and S. I. CHAN. J. Chem. Phys. **49**, 2071 (1968).
39. D. NEUMANN and J. W. MOSKOWITZ. J. Chem. Phys. **49**, 2056 (1968).
40. G. P. ARRIGHINI, C. GUIDOTTI, and O. SALVETTI. J. Chem. Phys. **52**, 1037 (1970).
41. A. D. BUCKINGHAM. J. Chem. Phys. **30**, 1580 (1958).

Can. J. Chem. Downloaded from www.nrcresearchpress.com by 210.87.254.5 on 09/05/12
For personal use only.

Can. J. Chem. Downloaded from www.nrcresearchpress.com by 210.87.254.105 on 09/05/12
For personal use only.

A Clathrate Hydrate of Cyclobutanone: Dielectric Relaxation of the Host and Guest Molecules[1]

B. MORRIS AND D. W. DAVIDSON
Division of Chemistry, National Research Council of Canada, Ottawa, Canada

Received September 25, 1970

A low-frequency dielectric study of $(CH_2)_3CO \cdot 17H_2O$ shows a water absorption region characteristic of a structure II clathrate hydrate which melts congruently at 0.0 °C. The relatively low Arrhenius energy of 6.5 kcal mol^{-1} is similar to that of acetone hydrate, for which new results are given. At low temperatures reorientation of encaged cyclobutanone molecules gives a very broad absorption region and a contribution to the static permittivity which falls with decrease of temperature. These properties are attributed to the effects of the electrostatic fields of the orientationally-disordered water molecules which form the cages. Such fields distort the tetrahedral symmetry of the cages to an extent which varies greatly from cage to cage. The high permittivity (~ 3.6) at 4.2 °K probably arises from rotational oscillations at frequencies near 20 cm^{-1} of the guest molecules in shallow potential minima. This enhancement of polarizability removes the difficulty previously noted in the applicability of the Onsager cavity model to structure II hydrates. The dipole moment of cyclobutanone in cyclohexane solution was found to be 2.78 ± 0.02 D.

Une étude diélectrique à basse fréquence de $(CH_2)_3CO \cdot 17H_2O$ montre un domaine d'absorption par l'eau caractéristique de la structure II de l'hydrate de clathrate ayant une fusion congruente à 0.0 °C. L'énergie d'Arrenius relativement basse de 6.5 kcal mol^{-1} est semblable à celle de l'hydrate d'acétone pour lequel on donne de nouveaux résultats. Aux basses températures la réorientation des molécules de cyclobutanone encagées donne une très large région d'absorption et contribue à la permitivité statique qui tombe quand la température décroit. Ces propriétés sont attribuées aux effets des champs électrostatiques des molécules d'eau en état de désordre d'orientation qui forment les cages. De tels champs introduisent une distorsion dans la symétrie tétrahédrique des cages qui varie beaucoup d'une cage à l'autre. La haute permitivité (~ 3.6) à 4.2 °K vient probablement des oscillations rotationnelles à des fréquences proches de 20 cm^{-1} des molécules prisonnières à des minima de potentiel peu profonds. Cette accuentation de polarisabilité fait disparaître la difficulté notée précédemment dans la possibilité d'appliquer le modèle de cavité d'Onsager aux hydrates de structure II. On a trouvé que le moment dipolaire de la cyclobutanone dans une solution de cyclohexanone est 2.78 ± 0.02 D.

Canadian Journal of Chemistry, 49, 1243 (1971)

Reference has already been made (1) to the dielectric evidence that cyclobutanone (CB) forms a clathrate hydrate of von Stackelberg's structure II (2), evidence since confirmed by powder X-ray examination (3).

Here we present the results of a dielectric study of the reorientation of both the lattice water molecules and the encaged cyclobutanone molecules. The dielectric properties of the lattice are compared with those of other structure II hydrates, including acetone hydrate (4), for which some new experimental data are presented. In previous studies (5, 6), the absorption by guest molecules in several clathrate hydrates was found to occur at microwave frequencies at 90 °K and above. In the present study the measurements have been made at temperatures sufficiently low that the absorption by cyclobutanone molecules occurs at low-radio and audio frequencies where it may be accurately defined.

[1]NRCC No. 11764.

Experimental Methods

Hydrate samples were prepared in dielectric cells by cooling solutions of cyclobutanone (< 0.2% impurity, mainly 2-butanone, by flame-detection vapor phase chromatography) in conductivity water. Compositions of the six samples studied varied between 16.7 and 17.5 mol of water per mol of cyclobutanone, *i.e.*, bracketed the 17:1 mole ratio of the ideal structure II hydrate with all large cages filled. Simple thermal analysis having shown that the hydrate formed and decomposed congruently at 0.0°, samples were conditioned for several hours at temperatures between −10 and −20° before measurements were started.

Two samples of acetone hydrate were conditioned for several days near −30°. This hydrate has an incongruent melting point at −20°. Its slow formation from ice and acetone-rich liquid was followed by the changes in the dielectric behavior of the system.

Most measurements above 77 °K were made with the 5 pF, stainless steel, three-terminal, coaxial cell and temperature control and measurement previously described (7). Capacitance and conductance were measured at frequencies between 0.01 and 700 kHz.

At lower temperatures the brass cell used was of the "split cylinder" type designed by Swenson and Cole (8) to minimize the development of gaps from thermal con-

TABLE 1. Measured dielectric parameters of cyclobutanone hydrate

Sample	Temperature (°C)	ε_0	$\varepsilon_{\infty 1}$	τ_0 (s)	α
CB·16.76H_2O	−6.4	64.4			
	−35.9	70.5		4.0×10^{-7}	0.03
	−58.8	74.0		8.8×10^{-7}	0.03
	−72.4	79.5	8.7	4.9×10^{-6}	0.03
	−109.6	96	10.04	1.92×10^{-4}	0.05
	−148.4		11.06		
CB·17.45H_2O	−2.5	62			
	−45.8	69	7.6	7.2×10^{-7}	0.04
	−89.1	71	9.1	1.89×10^{-5}	0.03
	−128.6	73	10.1	1.50×10^{-3}	0.07
	−178.0		10.29		
	−195.6		9.96		

traction of the sample. The guarded electrode assembly was held parallel to the high potential electrode by screws through the Teflon discs which formed the top and bottom of the cell. The cell was mounted in a copper can lined with a thin sheet of Teflon and threaded to a stainless steel supporting tube through which passed the coaxial Microdot leads from the electrode and the thermocouple leads. The assembly was supported within an Andonian Associates Cryogenic Dewar from a top plug, with leads brought out through vacuum seals. The sample thickness was 2.5 mm, sample volume 2.5 cm^3, and cell constant about 1 pF. Normally, after initial measurements at liquid helium temperature, the helium was vaporized and the vaporization heater and throttle control of the helium flow adjusted to maintain a heating rate of $\sim 0.1°$ per min. Measurements were made during heating at a number of fixed frequencies. Temperatures were measured by a copper–constantan thermocouple mounted in the cell and referred to liquid helium temperature.

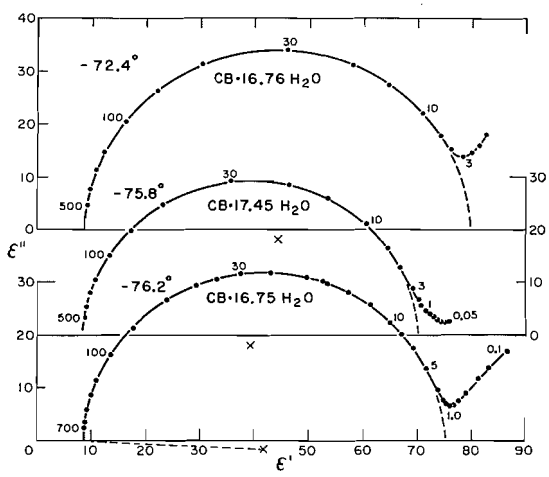

FIG. 1. Complex permittivity loci of various samples of cyclobutanone hydrate near −75°. Numbers on loci are frequencies in kHz.

Results

Absorption and Dispersion Associated with Water Molecules

Cyclobutanone Hydrate

Examples of a complex permittivity plots associated with relaxation of the hydrate lattice are given in Fig. 1 for three samples of somewhat different composition at temperatures near −75°. The CB·17.45H_2O sample clearly shows a region of extra absorption and dispersion at low frequencies which we attribute to the presence of a small quantity of ice. This feature is present in the loci of this sample at other temperatures but never evident in the loci of the other samples. It serves to fix the composition of the hydrate close to the ideal composition CB·17H_2O. The bottom locus is for a sample in the low-temperature cell.

The shapes of the loci are similar to those previously found (9) for the structure II hydrates of tetrahydrofuran, dihydrofuran, propylene oxide, trimethylene oxide, and 1,3-dioxolane (10) and appear to be characteristic of the type II lattice. They conform approximately to Cole–Cole arcs (with $\alpha = 0.03$ for the loci of Fig. 1) except at relatively high frequencies.

Representative dispersion parameters for a few of the 38 loci measured are given in Table 1. As before (9, 10), the mean relaxation time τ_0, static permittivity ε_0, and width parameter α refer to the Cole–Cole arc that "best" fits the locus, while $\varepsilon_{\infty 1}$ is the high-frequency intercept with the ε' axis, which is approached at right angles (*cf.* Fig. 8 below).

Values of the static permittivity for CB·16.76-H_2O measured in the high temperature cell were within a few permittivity units of those previously reported for dioxolane hydrate (11) and other isostructural hydrates (10) and are believed to represent the proper hydrate permittivities to about ±5%. The reasons for preferring a slight excess of hydrate-former in the sample have been dis-

Can. J. Chem. Downloaded from www.nrcresearchpress.com by 210.87.254.105 on 09/05/12
For personal use only.

Can. J. Chem. Downloaded from www.nrcresearchpress.com by 210.87.254.105 on 09/05/12
For personal use only.

cussed (9). Measured permittivities of samples containing excess water were lower at low temperatures, probably because of the presence of gaps and cracks. The results for CB·17.45H_2O are consistent with parallel air gaps constituting a few parts per thousand of the interelectrode separation (11).

Relaxation times are plotted in Fig. 2. The lower values for CB·17.45H_2O at low temperatures again reflect the presence of air gaps. Application of a correction of the form (11)

$$[1] \qquad \tau_0 = \left[\frac{\varepsilon_0(\text{true})}{\varepsilon_0(\text{exp})}\right]^{\frac{1}{1-\alpha}} \tau_0(\text{exp})$$

brings these points close to the line drawn in Fig. 2, which is described by

$$[2] \qquad \log_{10} \tau_0 = A + 1418/T$$

with $A = -12.395$.

Acetone Hydrate

New dielectric measurements of acetone hydrate were made primarily to check the static permittivity values found in the early study (4) which subsequent work with other structure II hydrates suggests are too low. Figure 3 is typical of the new loci obtained. Although better defined than before, the somewhat larger values of ε_0 are still considerably lower than expected for completely homogeneous samples.

The freezing point data of Benjamin (12) clearly

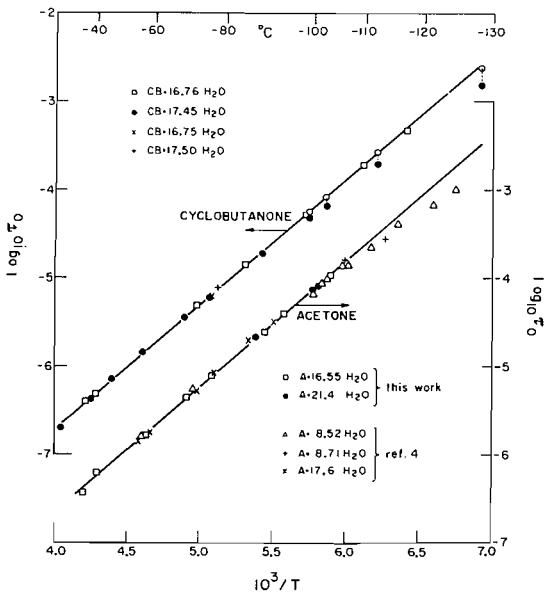

FIG. 2. Relaxation times of cyclobutanone and acetone hydrates.

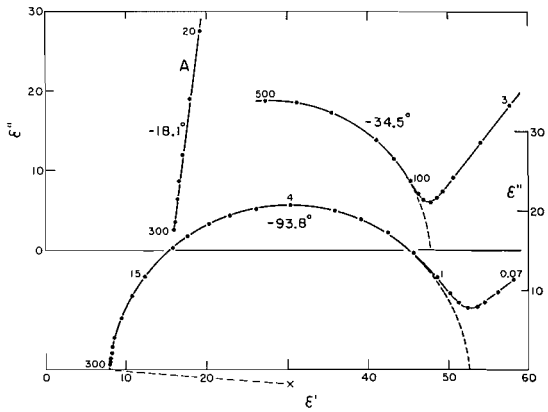

FIG. 3. Complex permittivity loci of $(CH_3)_2CO$·16.55H_2O. *A* is above the decomposition temperature of acetone hydrate.

show a change of slope at about −19° and 16.5 mol% acetone of the type characteristic of incongruent hydrate formation. At the composition of the ideal hydrate (5.6 mol% acetone) ice freezes at −5°. Hydrate therefore normally forms from ice and acetone-rich liquid by a process which is limited by the ability of the acetone to penetrate the hydrate crust as it forms on the ice. (The slowness of formation of argon and nitrogen hydrates has a similar cause (11).) Thus a sample containing 25% excess water after three days of conditioning at −30° still showed, by a small inflection in the high-frequency permittivity at the eutectic temperature, the presence of a trace of unreacted acetone.

The changes in ε' at a fixed frequency found when samples were slowly heated through the regions of the eutectic and decomposition temperatures identified these temperatures as −96.8 ± 0.4 and −19.8 ± 0.2°, respectively.

It appears that the main reason for the relatively low values of ε_0 (and of $\varepsilon_{\infty 1}$, see below) of acetone hydrate is the presence of irregular voids in the sample which result from the 4 to 5% contraction associated with the formation of hydrate from ice and acetone-rich liquid.

Relaxation times from the new measurements of acetone hydrate are plotted in Fig. 2, along with the earlier data (4). No attempt has been made to correct the results for the presence of gaps. Such a correction would raise the relaxation times somewhat, but the assumption that the effect of all the void space may be represented by a parallel air gap of uniform thickness seems unjustified in this instance.

The temperature-dependence of the water re-

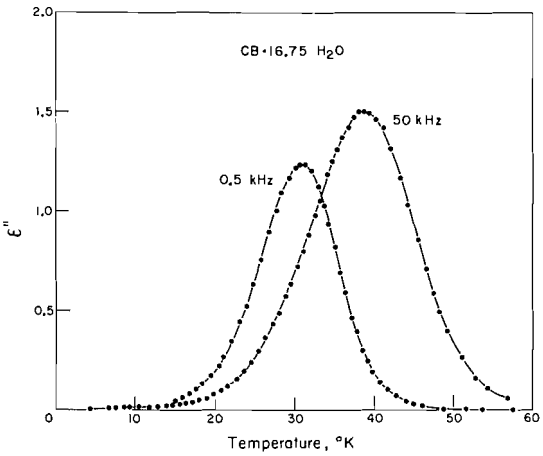

FIG. 4. Dielectric absorption of encaged cyclobutanone.

TABLE 2. Temperatures T_m of maximum loss ε_m'' at fixed frequencies f

f	ε_m''	T_m(°K)	ε' at T_m
10 Hz	~0.72	25.8	8.16
0.5 kHz	1.24	31.0	8.75
1.0 kHz	1.29	31.8	8.75
5 kHz	1.36	34.5	8.74
10 kHz	1.40	35.4	8.43
50 kHz	1.50	38.5	8.50

laxation times of acetone and cyclobutanone hydrates are very similar. At temperatures down to −106° these times for acetone hydrate average 18% higher and the best data may be described by eq. 2 with $A = -12.323$.

Dielectric Absorption by Cyclobutanone

The dielectric loss associated with reorientation of cyclobutanone in its cages is illustrated in Fig. 4. The absorption curves are very much broader than single relaxation-time Debye curves, as is evident from the extent of the overlap between the two curves for frequencies which differ by a factor of 100. In Table 2 the temperature at which ε'' reaches its maximum value is listed for a number of frequencies. The corresponding rate plot is linear between 30 and 40 °K, with the activation energy 1.44 kcal/mol. The slope appears to become smaller below 30°.

The variation with temperature of the contribution to the permittivity of reorienting cyclobutanone molecules is shown in Fig. 5. At the high-temperature end the values plotted are $\varepsilon_{\infty 1}$, the limiting permittivities on the high-frequency side of the water dispersion region. At low temperatures, down to 29 °K, the static permittivities of the cyclobutanone dispersion region, ε_{02}, are plotted. Also shown are dispersion curves at a number of fixed frequencies.

At high temperatures the variation of $\varepsilon_{\infty 1}$ is consistent with that expected (dashed curve) for an orientational contribution $\varepsilon_{02} - \varepsilon_{\infty 2}$ which is proportional to $1/T$. This behavior is characteristic of isotropic rotation or of reorientation between sites of about the same energy. Below about 150 °K departures become evident and $\varepsilon_{\infty 1} = \varepsilon_{02}$ passes through a flat maximum at about 45 °K and at lower temperatures begins to fall sharply. There is clearly a gradual depopulation of less stable orientational states over a large temperature range as energy differences between different orientations become more pronounced in comparison with kT.

The absorption and dispersion curves are so broad that they cannot be adequately defined at a fixed temperature by the frequency range available. However, it is possible to construct a Cole–Cole diagram (Fig. 6) using the reduced parameters $\varepsilon_r'' = \varepsilon''/(\varepsilon_{02} - \varepsilon_{\infty 2})$ and $\varepsilon_r' = (\varepsilon' - \varepsilon_{\infty 2})/(\varepsilon_{02} - \varepsilon_{\infty 2})$ measured at a number of temperatures. The resulting locus illustrates the extreme broadness of the absorption and its very slow fall at relatively high frequencies. Some absorption is still detectable at audio frequencies at 4.2 °K.

Discussion

Relaxation of Water Molecules in Structure II Hydrates

Although the shapes of the absorption–dispersion curves associated with reorientation of the water molecules in structure II hydrates appear to be insensitive to the nature of the guest molecule, the actual relaxation times and activation energies are dependent on the guest species. As Table 3 shows, there is no apparent correlation between the relaxation times τ_0 or the Arrhenius energies E_A and the estimated (3) maximum van der Waals diameter d of the guest or the lattice parameter a. There is a trend toward decrease of τ_0 and E_A with increase of dipole moment μ of the guest molecule, but no simple dependence on μ is suggested by these data nor by the results of study of the type II hydrates of CCl_3F ($\mu = 0.5$ D) and $CHCl_2F$ (1.3 D), for which E_A values as great as or greater than the value for ice (13.25 kcal/mol (13)) have been reported (14). (The relaxation times for these hydrates, however, may

Can. J. Chem. Downloaded from www.nrcresearchpress.com by 210.87.254.105 on 09/05/12
For personal use only.

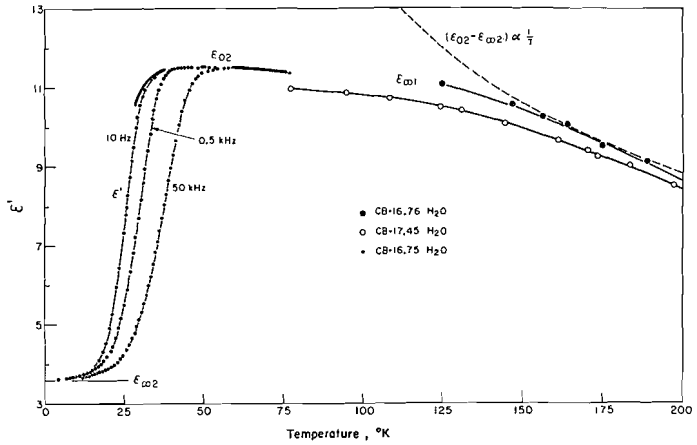

FIG. 5. Temperature dependence of $\epsilon_{\infty 1} = \epsilon_{02}$ and dispersion in cyclobutanone hydrate at low temperatures. Points O have been corrected for estimated series gaps.

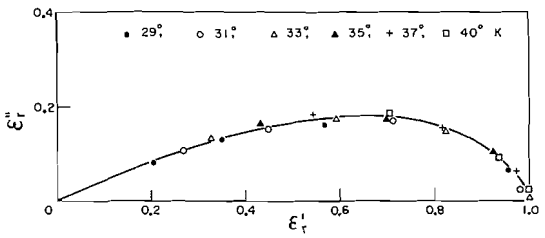

FIG. 6. Reduced complex permittivity plot for cyclobutanone hydrate for various temperatures between 29 and 40 °K.

have been affected by the presence of ice and incomplete filling factors: the loci (14) are much broader than found for other type II hydrates.)

As has been suggested elsewhere (11), it is possible that the relatively fast relaxation of the hydrates of ethers and ketones may be due to the occasional formation of hydrogen bonds between oxygen atoms of guest molecules and water molecules of the cage, with consequent injection of Bjerrum defects of the L type into the lattice. The listed values of τ_0 and E_A are not well correlated with the "strength" of hydrogen bonding between an OH group and an ethereal or ketonic oxygen atom as determined by infrared OH group frequency shifts and p.m.r. chemical shifts of, for example, phenol in solution (15). For the encaged molecules, however, the molecular geometry may well modify the extent of the proposed hydrogen bonding by affecting the distance and angle of approach of the oxygen atoms to the water molecules. This geometric factor should favor the formation of hydrogen bonds to the ketones over those to the ethers and to trimethylene oxide more than to propylene oxide, as required for consistency with the experimental data. It is also possible that molecular geometry may play a more general role by determining the nearness of approach and extent of electrostatic perturbation of the lattice by polar groups of the guest molecule.

When the relaxation time measurements of clathrate hydrates are extended to sufficiently low temperatures a fall in the slope of the log τ_0 *vs.* $1/T$ line is commonly found. Approximate temperatures and corresponding relaxation times at which these departures from linearity become significant are given in columns 7 and 8 of Table 3. Three reasons for this low-temperature behavior may be suggested.

The effect of the development and opening of cracks and gaps in the sample with decreasing temperature leads for the Cole–Cole arc approximation to a reduction in measured relaxation time given (11), at most, by eq. 1 above. This effect is tied to a negative departure from the expected linearity of ϵ_0 in $(1/T)$. It seems capable of accounting for the behavior of τ_0 of cyclobutanone and acetone hydrates at low temperatures (Fig. 2).

Another spurious effect may arise from the presence of "impurity" centers which give rise to extrinsic Bjerrum defects in numbers which dominate at low temperatures those intrinsic to the lattice. This is almost certainly the origin of the greatly reduced slope found for most samples of ice at low temperatures (16). It may determine the relaxation times of the structure I lattices of argon and nitrogen hydrates (11) prepared under

Can. J. Chem. Downloaded from www.nrcresearchpress.com by 210.87.254.105 on 09/05/12
For personal use only.

TABLE 3. Comparison of relaxation and other properties of structure II hydrates

Hydrate	d (Å)*	a(Å)* (−135 °C)	μ (D) (gas)	τ_0 at −40 °C (s)	E_A	Departure from linearity at τ_0 (s)	Departure from linearity at T (°C)	Reference
Sulfur hexafluoride	6.1	17.21 (0°)†	0	7.8×10^{-4}	12.3	1.8×10^{-3}	−49	21
1,3-Dioxolane	5.6	17.12	1.47 (Cyclohexane)	5.4×10^{-6}	8.7	10^{-4}	−73	10
2,5-Dihydrofuran	6.1	17.17	1.54 (Benzene)	1.5×10^{-6}	7.5	2.5×10^{-5}	−76	9
Tetrahydrofuran	5.9	17.17	1.63	1.0×10^{-6}	7.4	4×10^{-5}	−93	9
Trimethylene oxide	5.5	17.10	1.93	4.8×10^{-7}	7.0	1.2×10^{-5}	−81	9
Propylene oxide	6.5	17.12	2.00	2.0×10^{-6}	8.0	2.5×10^{-5}	−84	9
Cyclobutanone	6.5	17.16	2.78§ (Cyclohexane)	4.9×10^{-7}	6.5	3×10^{-4}	−113	This work
Acetone	6.3	17.16 (−40°)‡	2.88	5.7×10^{-7}	6.5	2×10^{-4}	−109	This work

*Generally from ref. 3.
†M. von Stackelberg and W. Jahns. Z. Elektrochem. 58, 163 (1954).
‡A. S. Quist and H. S. Frank. J. Phys. Chem. 65, 560 (1961).
§See Appendix.

high pressures of gas and relaxation times of the structure II hydrates of ethers (9, 10) which, at the lowest temperatures of measurement, are of the order of ten times as small as those given by extrapolation of the high-temperature behavior. This difference is much too great to be given by eq. 1.

A fall in effective activation energy at low temperatures may be characteristic of the lattice itself when some orientations become stabler than others by energies which are appreciable in comparison with kT. Such a process will be accompanied by a pronounced fall in ε_0 such as that observed during the gradual ordering transformation of ice III to ice IX (17). No appreciable change of slope of the log τ_0 *vs.* $1/T$ curve occurs during this transformation, however (17). It is unlikely that the curvature observed in the relaxation rate plots of water in the clathrate hydrates is due to this mechanism.

Contribution of Guest Molecules to the Permittivity

At relatively high temperatures this contribution is expected to be nearly proportional to the square of the dipole moment of the guest molecule. This is confirmed by Fig. 7, where $\varepsilon_{\infty 1} = \varepsilon_{02}$ at −105° is plotted *vs.* μ^2 for a series of eight structure II hydrates. The temperature is chosen for experimental convenience (9). It is also sufficiently high that any departure from isotropy of the rotation appears not to be great enough to appreciably affect the contribution to ε_{02}. In general

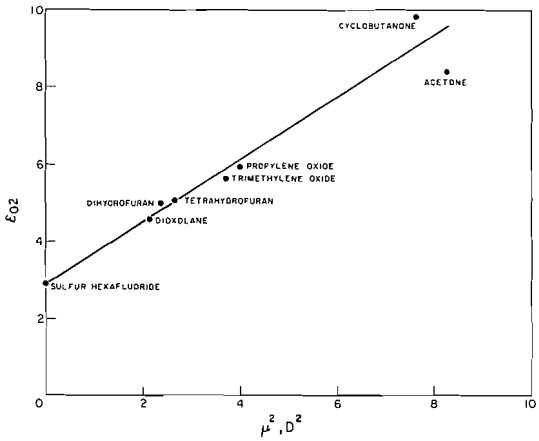

FIG. 7. ε_{02} at −105 °C *vs.* (dipole moment)² of guest molecules in structure II hydrates.

the values of ε_{02} are uncertain to at least 0.10. This uncertainty arises not from inability to fix the high-frequency limit of the permittivity of the water dispersion region for a given sample: Figure 8 illustrates how well this value may be defined. The main uncertainty arises from small air pockets and gaps and from possible traces of solid hydrate-former and ice in the sample. Such inclusions act to reduce the measured permittivity, as already discussed for acetone hydrate, in which the reduction is especially large.

It was previously pointed out (9, 10) for the hydrates of the cyclic ethers that the experimental values of ε_{02} were higher than those calculated from the Onsager theory if the radius of

Can. J. Chem. Downloaded from www.nrcresearchpress.com by 210.87.254.105 on 09/05/12
For personal use only.

TABLE 4. Calculated values of ε_{02} from the Onsager equation at −105 °C with "normal" polarizabilities

Molecule	α/Å³	ε_{02} (calcd) $a = 3.2$ Å	ε_{02} (calcd) $a = 2.8$ Å	$\varepsilon_{\infty 1}$ (exp)
Sulfur hexafluoride	6.46	3.04	3.05	2.9
1,3-Dioxolane	6.72	4.27	4.53	4.57
2,5-Dihydrofuran	7.74	4.51	4.91	5.03
Tetrahydrofuran	7.93	4.72	5.20	5.06
Trimethylene oxide	6.23	5.14	5.57	5.63
Propylene oxide	6.18	5.29	5.77	5.94
Cyclobutanone	7.57	8.07	9.66	9.85
Acetone	6.41	8.02	9.21	≥ 8.4

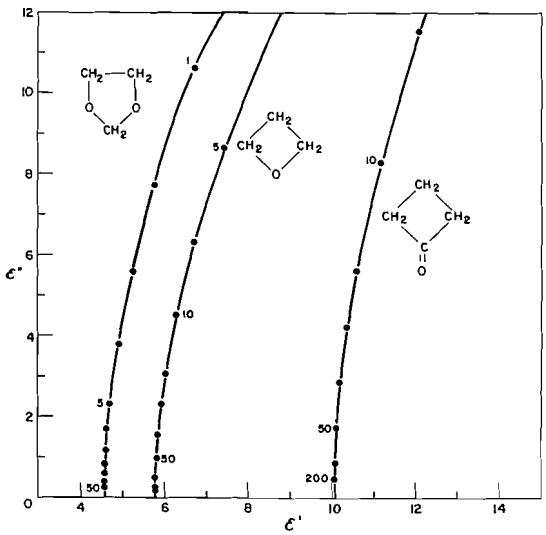

FIG. 8. Plots illustrating the perpendicular approach to $\varepsilon_{\infty 1}$ for some structure II hydrates. Temperatures from left to right are −102.5, −115.0, and −109.6 °C.

the Onsager cavity were taken to coincide with the free radius of the hydrate cage. With experimental estimates now available of $\varepsilon_{\infty 2}$ values for cyclobutanone and tetrahydrofuran hydrates, a reassessment of the Onsager model is possible.

Modification of the Onsager Model to Include Rotational Oscillations

With oxygen atoms of the water molecules at positions given by Mak and McMullan's study (19) of the tetrahydrofuran – hydrogen sulfide double hydrate and with an average lattice parameter of 17.18 Å at −105° (Table 3), one finds, for the large cage, 12 oxygen atoms at 4.68 Å, 12 at 4.60 Å, and 4 at 4.69 Å from the cage center. If the van der Waals radius of oxygen is 1.45 Å, the nearly spherical cage has a mean free radius of 3.20 Å.

We write the Onsager equation in the form (ref. 20, p. 191)

$$[3]\quad \frac{(\varepsilon_{02}-1)(2\varepsilon_{02}+1)}{3\varepsilon_{02}} = \frac{(\varepsilon_\infty{}^0-1)(2\varepsilon_\infty{}^0+1)}{3\varepsilon_\infty{}^0} + \frac{4\pi N_M \alpha_M}{1-f_M\alpha_M} + \frac{4\pi N_M \mu_M{}^2}{3kT(1-f_M\alpha_M)^2}$$

where $\varepsilon_\infty{}^0$ is the dielectric constant of the hypothetical empty lattice at frequencies too high for reorientation of the water molecules and N_M, α_M, μ_M, and f_M are, respectively, the number density, polarizability, dipole moment, and reaction field factor of the guest molecule. We take $\varepsilon_\infty{}^0 = 2.83$ as derived by equating the first term on the r.h.s. of eq. 3 to the product of the corresponding term for hexagonal ice (with $\varepsilon_\infty = 3.10$) by the ratio of the number densities of water molecules in hydrate and ice. This value is more consistent with the results (21) for the hydrate of nonpolar SF_6 than the somewhat higher value previously (9) assumed.

In the Onsager model the reaction field factor $f_M = 2(\varepsilon_{02}-1)/[a^3(2\varepsilon_{02}+1)]$ refers to a polarizable dipole located at the center of a spherical cavity of radius a, surrounded by a continuum of dielectric constant ε_{02}. For $a = 3.2$ Å, the free radius of the cage, values of ε_{02} from eq. 3 are listed in the third column of Table 4. The values of polarizabilities (mostly from sodium D molar refractions) used are also given in Table 4. All large cages are assumed occupied and $N_M = 1.59 \times 10^{21}$. It is seen that for polar guest molecules the derived values of ε_{02} are consistently and appreciably smaller than the measured values (column 5). Formally, the agreement may be greatly improved by allowing a to assume smaller values: column 4 gives ε_{02} for $a = 2.8$ Å.

Such a value for the cavity radius is however, unrealistically small. In applications of the Onsager equation to liquids a is invariably defined

Can. J. Chem. Downloaded from www.nrcresearchpress.com by 210.87.254.105 on 09/05/12
For personal use only.

Can. J. Chem. Downloaded from www.nrcresearchpress.com by 210.87.254.105 on 09/05/12
For personal use only.

by $4\pi a^3/3 = V/N$, where V is the molar volume of the liquid. The cavity radius is then larger than the radius of close-packed spheres which occupy the same volume. In liquid acetone, for which the Onsager equation fits the data well (ref. 20, p. 324), the value of a so defined is 3.04 Å at 0 °C. Similar values are obtained for other hydrate-forming liquids: for example $a = 3.18$ Å for liquid tetrahydrofuran at 22 °C. It is clear that for the molecules enclathrated in type II hydrates, with their exceptional degree of rotational mobility, values of a should be considerably larger than for the liquids. The free radius of the cage should be a *lower* limit to the proper value of a.

At the same time it may be noted that at very low temperatures, where guest-molecule reorientation makes no contribution to the permittivity, $\varepsilon_{02} = \varepsilon_{\infty 2}$ and

$$[4] \quad \frac{(\varepsilon_{\infty 2} - 1)(2\varepsilon_{\infty 2} + 1)}{3\varepsilon_{\infty 2}} = \frac{(\varepsilon_{\infty}{}^{0} - 1)(2\varepsilon_{\infty}{}^{0} + 1)}{3\varepsilon_{\infty}{}^{0}} + \frac{4\pi N_M \alpha_M}{1 - f_M \alpha_M}$$

Equation 4 predicts for cyclobutanone hydrate, with $a = 3.2$ Å and the polarizability in Table 4, a value of $\varepsilon_{\infty 2}$ of 3.08. The experimental value of the permittivity at 4.2 °K is about 3.6. This large value can be reconciled with the Onsager model (or any other reasonable model) only if the polarizability of the encaged molecule is greatly enhanced, to something like 18 Å^3. In a similar way it is found that the normal polarizability of tetrahydrofuran accounts for an $\varepsilon_{\infty 2}$ value of only 3.09 for its hydrate. The experimental value of 3.47 requires a polarizability of about 16 Å^3.

This enhanced polarizability probably arises mainly from the rotational oscillations of the encaged molecules around their equilibrium positions, oscillations of large amplitude expected to occur at far infrared frequencies. The increase in refractive index corresponding to the enhanced permittivity may be related (22) to the integrated infrared absorption. If the gross simplification is made that there is only one doubly-degenerate oscillation giving rise to a band of intensity proportional to $(\partial\mu/\partial Q)^2 \approx \mu^2 \sin^2\theta/(I\theta^2) \approx \mu^2/I$, where I is the moment of inertia corresponding to an angular displacement θ, it is found that the oscillation frequency is of the order of 20 cm^{-1} for both cyclobutanone and tetrahydrofuran. Actually, a great variety of depths and shapes of potential minima is expected from the wide distribution of fields and field directions in different cages (18) and broad structureless absorption is to be expected in the far infrared region.

It is to be noted that the contribution to the polarizability from rotational oscillation of the guest molecule is at right angles to the direction of the dipole moment of a molecule which possesses an axis of symmetry. The reaction field therefore increases the dipole moment by $1/(1 - f_M\alpha_M)$ where α_M may not differ much from the "normal" polarizability in Table 4. On the other hand the cavity field is increased on the average by $1/(1 - f_M\alpha_M{}^*)$, where $\alpha_M{}^*$ includes the contribution from rotational oscillations. For this case the Onsager equation takes the form

$$[5] \quad \frac{(\varepsilon_{02} - 1)(2\varepsilon_{02} + 1)}{3\varepsilon_{02}} = \frac{(\varepsilon_{\infty 2} - 1)(2\varepsilon_{\infty 2} + 1)}{3\varepsilon_{\infty 2}} + \frac{4\pi N_M \mu_M{}^2}{3kT} \cdot \frac{1 + f_M(\alpha_M{}^* - \alpha_M)}{(1 - f_M\alpha_M{}^*)(1 - f_M\alpha_M)}$$

If a is again taken to be 3.2 Å, eq. 5 is found to over-estimate ε_{02} of cyclobutanone and tetrahydrofuran hydrates. Such a result is to be expected since the assumption that the medium may be represented as a continuum of permittivity ε_{02} beyond the free radius ignores the structural details. The innermost shell of neighbors consists only of water molecules whose effective permittivity is less than ε_{02}. It is necessary to compensate for this by allowing a to assume somewhat larger values. That the value of a necessary to fit the observed value of ε_{02} of cyclobutanone hydrate is about 3.6 Å and that for tetrahydrofuran hydrate 3.4 Å agrees with this interpretation.

It thus appears that the inclusion of the relatively large contributions to the polarizability from low-frequency rotational oscillations in the Onsager equation leads to a satisfactory representation of the high-temperature values of ε_{02}.

Reorientation of Cyclobutanone Molecules

The very broad audio-frequency absorption associated with reorientation of guest molecules occurs at higher temperatures for cyclobutanone than for tetrahydrofuran. The temperatures of maximum absorption at 1 kHz, for example, are 31.8 and 21.6 °K, respectively, "corresponding" temperatures which are roughly proportional to the Arrhenius energies of 1.44 (between 30 and

Can. J. Chem. Downloaded from www.nrcresearchpress.com by 210.87.254.105 on 09/05/12
For personal use only.

40 °K) and 1.06 kcal/mol (between 18 and 25 °K). At these low temperatures the guest molecules appear to be undergoing restricted rotation between preferred orientations of unlike energy since the values of ε_{02} are small fractions of those given for an orientational contribution proportional to $1/T$ (Fig. 5). There is an increasing loss of population of unfavorable orientations with decrease of temperature. At the same time the absorption becomes broader, as shown by, for example, the data plotted in Fig. 6.

In these circumstances the interpretation of the experimental Arrhenius energy is far from straight-forward. One may perhaps infer that its larger value for cyclobutanone results from greater length of the molecule along its polar axis and the nearer approach of the oxygen atom to the center of a hexagonal ring of water molecules than is the case for tetrahydrofuran (18).

There appears to be a close similarity between the shapes of the absorption–dispersion curves (in frequency terms) of the two hydrates when compared at corresponding temperatures. Compared at temperatures where the 1 kHz absorption is greatest, for example, the ratio $\varepsilon_m''/(\varepsilon_{02} - \varepsilon_{\infty 2})$ is between 0.16 and 0.17 for both guests. It is suggested (18) that the shapes are mainly the result of variation from cage to cage of the electrostatic fields $\boldsymbol{E}$ of the orientationally-disordered water molecules. These fields modify the tetrahedral symmetry of the cages by introducing orientation-dependent energies of the form $-\boldsymbol{\mu}\cdot\boldsymbol{E}$ which lead, *inter alia*, to a distribution of barriers to reorientation, the spread of barrier heights being proportional to the dipole moment of the guest and therefore larger by a factor of about 1.7 for cyclobutanone ($\mu = 2.78$ D, see Appendix) than for tetrahydrofuran (1.63 D). For relaxation times of the simple form

$$\tau = \tau_0 \exp(\Delta E_A/RT)$$

the distributions of times will be similar when the distributions of $\Delta E_A/T$ are similar, that is, at temperatures which are about 1.7 times as high for cyclobutanone as for tetrahydrofuran. That these distributions are roughly the same at temperatures which differ by a factor of 1.5 provides a crude confirmation of the model.

Appendix

Dipole Moment of Cyclobutanone

This moment has been reported (23) from measurements of benzene solutions to be 2.76 D. Because of the relatively large values of ε_{02} found for cyclobutanone hydrate (Fig. 7), it appeared that new measurements in a more inert solvent would be worthwhile. From dielectric constant and refractive index measurements at 25 °C of five solutions in the weight fraction range between 0.0016 and 0.011 of cyclobutanone in cyclohexane Guggenheim's method (24) gave 2.78 ± 0.02 D. Because of possible solvent effects even in cyclohexane, however, it is not certain that the proper (*i.e.*, dilute gas phase) dipole moment of cyclobutanone is less than that of acetone. Figure 7 also suggests that the value for dihydrofuran (1.54 D) measured in benzene solution may be too low by as much as 0.1 D.

1. D. W. Davidson. *In* Molecular Relaxation Processes. Academic Press, London. 1966. p. 33.
2. M. von Stackelberg and H. R. Müller. Z. Elektrochem. **58**, 25 (1954).
3. D. F. Sargent and L. D. Calvert. J. Phys. Chem. **70**, 2689 (1966).
4. G. J. Wilson and D. W. Davidson. Can. J. Chem. **41**, 264 (1963).
5. D. W. Davidson, M. M. Davies, and K. Williams. J. Chem. Phys. **40**, 3449 (1964).
6. M. Davies and K. Williams. Trans. Faraday Soc. **64**, 529 (1968).
7. A. D. Potts and D. W. Davidson. J. Phys. Chem. **69**, 996 (1965).
8. R. W. Swenson and R. H. Cole. J. Chem. Phys. **22**, 284 (1954).
9. R. E. Hawkins and D. W. Davidson. J. Phys. Chem. **70**, 1889 (1966).
10. A. Venkateswaran, J. R. Easterfield, and D. W. Davidson. Can. J. Chem. **45**, 884 (1967).
11. S. R. Gough, E. Whalley, and D. W. Davidson. Can. J. Chem. **46**, 1673 (1968).
12. The Physico-chemical Constants of Binary Systems. Vol. 4. *Edited by* J. Timmermans. Interscience Publishers, New York. 1960.
13. R. P. Auty and R. H. Cole. J. Chem. Phys. **20**, 1309 (1952).
14. W. S. Brey, Jr. and H. P. Williams. J. Phys. Chem. **72**, 49 (1968).
15. See for example: L. J. Bellamy and R. C. Williams. Proc. Roy. Soc. (London) Ser. A. **254**, 119 (1960); D. P. Eyman and R. S. Drago. J. Amer. Chem. Soc. **88**, 1617 (1966).
16. S. R. Gough and D. W. Davidson. J. Chem. Phys. **52**, 5442 (1970), and references cited therein.
17. E. Whalley, J. B. R. Heath, and D. W. Davidson. J. Chem. Phys. **48**, 2362 (1968).
18. D. W. Davidson. Can. J. Chem. This issue.
19. T. C. W. Mak and R. K. McMullan. J. Chem. Phys. **42**, 2730 (1965).
20. C. J. F. Böttcher. Theory of Electric Polarisation. Elsevier Publishing Co., Amsterdam. 1952.
21. Y. A. Majid, S. K. Garg, and D. W. Davidson. Can. J. Chem. **46**, 1683 (1968).
22. J. E. Bertie, H. J. Labbé, and E. Whalley. J. Chem. Phys. **50**, 4501 (1969).
23. R. Arndt, H. H. Günthard, and T. Gaumann. Helv. Chim. Acta, **41**, 2213 (1958).
24. E. A. Guggenheim. Trans. Faraday Soc. **47**, 573 (1951).

Can. J. Chem. Downloaded from www.nrcresearchpress.com by 210.87.254.6 on 09/05/12
For personal use only.

Photochlorination of Perfluorocyclobutene

Z. R. Alberto, J. J. Cosa, C. A. Vallana, and E. H. Staricco

Departamento de Fisico-Química, Instituto de Ciencias Químicas, Universidad Nacional de Córdoba, Ciudad Universitaria, Córdoba, Argentina

Received October 19, 1970

The kinetics in the gas phase of the photochemical reaction between perfluorocyclobutene and chlorine was studied between 10 and 70 °C. The system was irradiated with light of 4360 Å. The rate of photochlorination was measured under full and intermittent light. The Arrhenius parameters for the reaction:

$$C_4F_6Cl + Cl_2 \rightarrow C_4F_6Cl_2 + Cl$$

are: $A_3 = (2.9 \pm 1.1) \times 10^8$ l mol^{-1} s^{-1} and $E_3 = 4.64 \pm 0.03$ kcal/mol and for

$$2\ C_4F_6Cl \rightarrow \text{Inactive products}$$

the constant rate value is: $k_4 = (7.23 \pm 4.3) \times 10^8$ l mol^{-1} s^{-1}.

On a étudié, entre 10 et 70° la cinétique en phase gazeuse de la réaction photochimique du perfluorocyclobutène avec le chlore; le système était irradié à 4360 Å. On a mesuré la vitesse de chloruration photochimique avec irradiation contenue et intermittente. Les paramètres d'Arrhénius pour la réaction

$$C_4F_6Cl + Cl_2 \rightarrow C_4F_6Cl_2 + Cl$$

sont: $A_3 = (2.9 \pm 1.1) \times 10^8$ l mol^{-1} s^{-1} et $E_3 = 4.64 \pm 0.03$ kcal/mol et pour la réaction

$$2\ C_4F_6Cl \rightarrow \text{Produits inactifs}$$

la constante de vitesse est: $k_4 = (7.23 \pm 4.3) \times 10^8$ l mol^{-1} s^{-1}.

Canadian Journal of Chemistry, 49, 1252 (1971)

Introduction

The addition of atoms or radicals to olefins has been subject to a rather extensive study (1–3). Less interest, however, has been devoted to processes involving cyclic olefins. Recently, the addition of CF_2Cl radicals to cyclic fluoroolefins has been studied (4). Also chlorine atoms produced photochemically have been added to perfluorocyclohexene (5). It was found that this reaction follows the well known chain chlorination mechanism (eqs. 1–4) (6) where A stands for the olefin and ACl for the chloroalkyl radical.

[1] $$Cl_2 + h\nu \rightarrow 2Cl$$

[2] $$A + Cl \rightarrow ACl$$

[3] $$ACl + Cl_2 \rightarrow ACl_2 + Cl$$

[4] $$2ACl \rightarrow \text{Inactive products}$$

Hence, it would be interesting to examine the behavior of other cyclic olefins such as perfluorocyclobutene (PFCB) and perfluorocyclopentene (PFCP).

Taking into account the above mechanism the rate law for these olefin reactions could be represented by eq. 5 where $k_0 = k_3/k_4^{1/2}$ and I_a is the

[5] $$\text{Rate} = k_0 \cdot Cl_2 \cdot I_a^{1/2}$$

absorbed light intensity.

In order to elucidate the influence of the ring structure on the kinetic parameters it is important to get the individual values of k_3 and k_4 at different temperatures. To accomplish this the intermittent light technique was used.

The present work deals with the kinetics of photochlorination of perfluorocyclobutene under steady and intermittent light.

Experimental

The reactor was a cylindrical quartz reaction vessel of 94.8 ml in volume. The other experimental arrangements have already been described (5). Light measurements and temperature control were also made as previously.

The experiments with intermittent light were performed at 30 and 60 °C following the suggestions given by Burnett and Melville (7). A 90° metal sector was used to cut the light beam off at its narrowest cross section. A set of synchronous a.c. motors at constant velocity was used for slow sector speeds. A low voltage d.c. motor connected to a power supply was used for high sector speeds and the rotation speed controlled electronically (8).

The PFCB from Pierce Chemical Company was sublimated several times in vacuum. Its purity was tested chromatographically with two different columns (Silica Gel and Halocarbon oil columns 10 and 30 ft long respectively) at room temperature, and no impurities were detected. After purification it was stored in a trap cooled with liquid air.

Cylinder chlorine was distilled trap-to-trap in vacuum five times between −78 and −135 °C, only the middle fraction being collected.

The CO_2 from a cylinder was dried by passage through sulfuric acid and then sublimated under vacuum at low temperature.

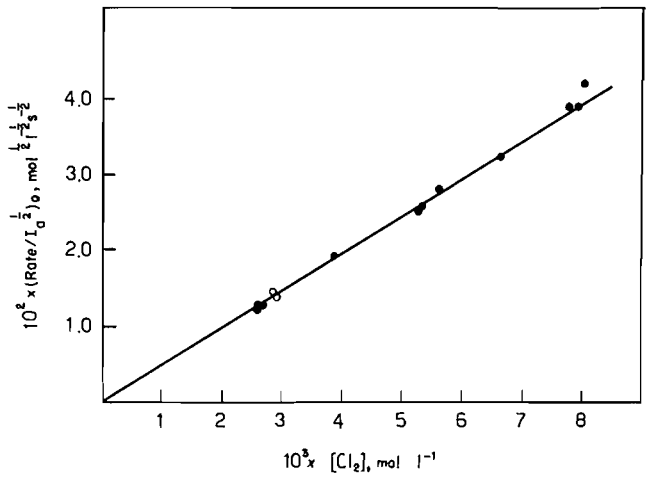

FIG. 1. Initial rate/$I_{abs}^{1/2}$ *vs.* initial pressure of Cl_2. ○, Runs with addition of 400 Torr CO_2. Temperature, 30 °C and pressure of C_4F_6, 50 Torr.

All samples were exhaustively degassed before using. Runs were always made up to 25% conversion under continuous light and up to 5% with intermittent light.

Results

(A) Experiments with Full Light

Preliminary observations at 30 °C showed the existence of a dark reaction less than 3% of the photochlorination rate. Therefore, all runs were performed in a darkened room. Under this condition experiments were reproducible and no dark reaction was observed at any temperature.

The analysis of products by gas chromatography and i.r. showed the existence of only one compound identified as 1,2-dichlorohexafluorocyclobutane. In addition, the i.r. spectrum showed that it was over 80% the *trans* isomer (9).

To test the eq. 5, the dependence upon rate of chlorine, olefin, total pressure, and light intensity was determined. An average value of the rate constant for each run was calculated assuming that the rate eq. 5 was valid at any moment through the course of the reaction within the studied range. The standard deviation of k for each run was less than 5% including some runs made up to 50% conversion. Initial rates given in all plots were calculated using that rate constant and the initial chlorine pressure.

The incident light intensity was changed in a series of runs using neutral glasses of known transmission and the rate was measured at different intensities. Chain termination by mutual interaction of radicals was also verified in experiments with the rotating sector (see below). The rate was found to be proportional to the square root of I_a as previously suggested.

In order to check the chlorine pressure effect the rate was measured at constant PFCB pressure and temperature. The rate was proportional to the first power of chlorine pressure within the whole range of pressure studied (25–150 Torr). Data are given in Fig. 1.

A plot of rate/$I_a^{1/2}$ *vs.* PFCB concentration at constant Cl_2 pressure and olefin between 25 and 150 Torr, given in Fig. 2, shows that the rate does not depend on olefin pressure.

Experiments with CO_2 as inert gas indicated that the total pressure does not have any effect on the rate at olefin pressure above 25 Torr (Fig. 1).

Hence, the results obtained with continuous light confirm the suggestion that the rate is proportional to the square root of I_a and to the first power of chlorine.

From experimental data, k_0 was found to be $4.989\ l^{1/2}\ mol^{-1/2}\ s^{-1/2}$ at 30 °C. With k_0 values at 10, 20, 30, 40, 50, 60, and 70 °C, obtained from similar plots to Fig. 1, an Arrhenius plot was made (Fig. 3). From this plot the kinetic parameters were obtained by the least squares method, being $E_0 = 4.64 \pm 0.03$ kcal/mol and $A_0 = (1.08 \pm 0.08) \times 10^4\ l^{1/2}\ mol^{-1/2}\ s^{-1/2}$. The incident light intensity was 1.4908×10^{-8} einstein $l^{-1}\ s^{-1}$.

(B) Experiments with Intermittent Light

The condition $\rho = 1 \pm 0.02$ at high sector speed was checked before and after a series of runs. Here ρ is the ratio between twice the rate with

Can. J. Chem. Downloaded from www.nrcresearchpress.com by 210.87.254.6 on 09/05/12
For personal use only.

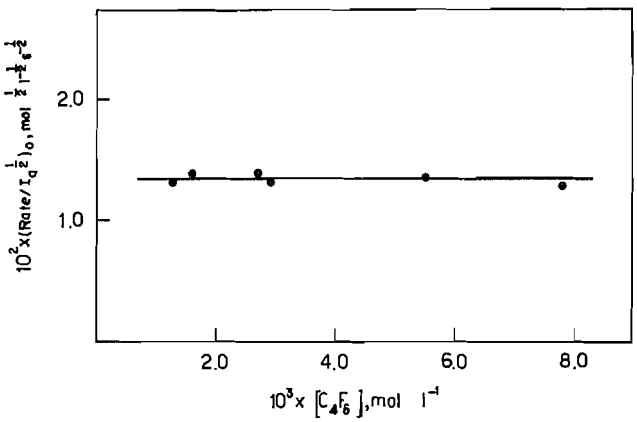

FIG. 2. Initial rate/$I_{abs}^{1/2}$ *vs.* initial pressure of C_4F_6. Temperature, 30 °C; pressure of Cl_2, 50 Torr.

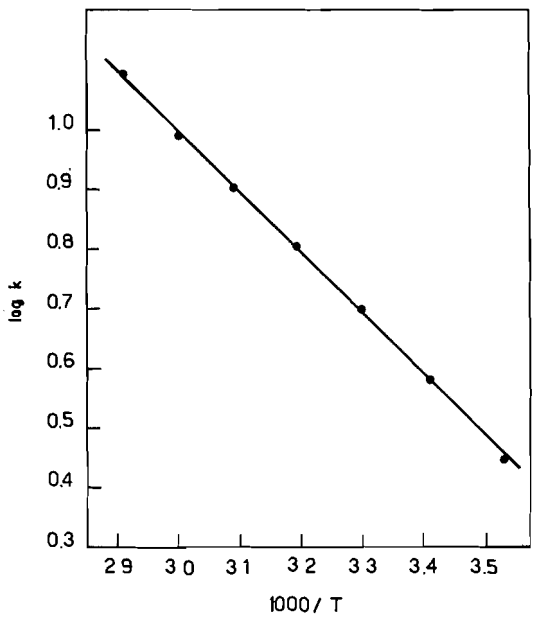

FIG. 3. Arrhenius plot; k in $mol^{-1/2}\ l^{1/2}\ s^{-1/2}$ of the overall reaction.

intermittent light to that with continuous light and it must be one when a 90° sector is used if rate is proportional to $I_a^{1/2}$. This ratio was also taken as a criterion of purity for reactants. When this condition was not fulfilled, the runs were rejected and the reactants purified again.

The plots of ρ *vs.* $\log_{10} \lambda I_0^{1/2}$ at 30 and 60 °C are shown in Fig. 4, where λ is the flash period. When the experimental plots are compared with the theoretical one, the value of $\log_{10} \lambda I_0^{1/2}$ was read off corresponding to the point at which $\log_{10} m = 0$, therefore $\lambda = \tau$. Since $\tau = \frac{1}{2}(k_4 I_a)^{-1/2}$, k_4 was obtained.

The value of k_4 appears independent of the temperature, within the experimental error. Hence, E_4 was taken as zero and the apparent activation energy E_0 assigned to E_3.

From the experimental plots follows that k_4 and therefore $A_4 = (7.23 \pm 4.3) \times 10^8$ l mol^{-1} s^{-1}. With this value and the overall reaction parameter A_0, A_3 results $(2.9 \pm 1.1) \times 10^8$ l mol^{-1} s^{-1}.

Discussion

The addition of inert gases showed that the vibrationally excited ACl radical formed in eq. 2 (2), because of the complexity of that radical, is deactivated in the pressure range used in the present work.

On the assumption that the apparent activation energy of 5.1 kcal/mol for perfluorocyclohexene (PFCH) arises as a result of a repulsive effect between the ring and the chlorine molecule (5), the 4.6 kcal/mol obtained with perfluorocyclobutene could account for the same effect. The difference may be justified by the smaller ring size or by a less electronic density on the carbon atom bearing the unpaired electron in PFCH.

With k_4 value (11) and k_0 (5), for PFCH, A_3 was evaluated as 3.1×10^8 l mol^{-1} s^{-1}. It appears that A_3 for PFCH and PFCB (3.1×10^8 and $2.9 \pm 1.1 \times 10^8$ respectively) are lower than A_3 for chloroethylenes as could be expected in a first approach, from the fact that cyclic radicals should have a more restricted zone of attack by Cl_2 molecule than alkyl radicals.

Regarding the k_4 value in the chloroethylene series (10) one could point out that k_4 decreases as the degree of substitution by chlorine atoms

Can. J. Chem. Downloaded from www.nrcresearchpress.com by 210.87.254.6 on 09/05/12
For personal use only.

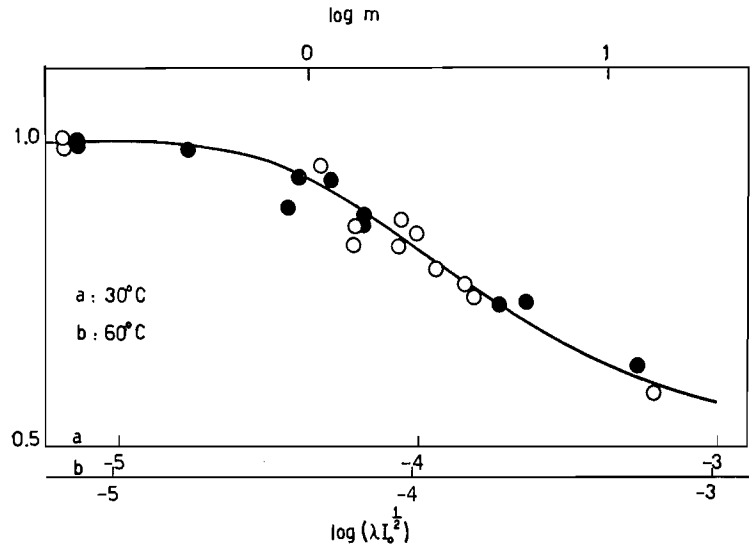

FIG. 4. Rotating sector curve: ρ *vs.* $\log_{10}$ ($\lambda I_0^{1/2}$); pressure of Cl_2, 100 Torr; pressure of C_4F_6, 50 Torr; ○ 30 °C; ●, 60 °C.

increases. In the present case it was found that k_4 is comparable with the smaller value of that series ($k_4 = 5 \times 10^8$ l mol^{-1} s^{-1} for C_2Cl_5) but slightly greater than the recently reported for $C_6F_{10}Cl$ (2.5×10^8 l mol^{-1} s^{-1}) (11).

It should be interesting to seek the value of k_4 in the chlorination of perfluorocyclopropene and perfluorocyclopentene because it likely would lead to an insight into the eventual trend of these values for a comparative set of cyclic olefins.

We thank the Consejo Nacional de Investigaciones Científicas y Técnicas (República Argentina) for financial support.

1. R. J. CVETANOVIC. *In* Advances in photochemistry. Vol. 1. Interscience Publishers. Inc. New York, N.Y., 1961. G. CHILTZ, P. GOLDFINGER, G. HUYBRECHTS, G. MARTENS, and G. VERBEKE. Chem. Revs. **63**, 355 (1963).
2. P. B. AYSCOUGH, F. S. DAINTON, and B. E. FLEISCHFRESSER. Trans. Faraday Soc. **62**, 1846 (1966).
3. J. H. KNOX and J. RIDDICK. Trans. Faraday Soc. **62**, 1190 (1966).
4. L. M. LEYLAND, J. R. MAJER, and J. C. ROBB. Trans. Faraday Soc. **66**, 904 (1970).
5. J. J. COSA, C. A. VALLANA, and E. H. STARICCO. Can. J. Chem. **47**, 1067 (1969).
6. P. A. GOSSELAIN, J. ADAM, and P. GOLDFINGER. Bull. Soc. Chim. Belg. **65**, 533 (1956).
7. H. W. MELVILLE and G. M. BURNETT. *In* Technique of organic chemistry. Vol. 8. Interscience Publishers Inc., New York, N.Y., 1953.
8. A. J. ARVIA, S. L. MARCHIANO, and J. J. PODESTÁ. Electrochim. Acta, **12**, 259 (1967).
9. J. R. LACHER, A. BÜCHLER, and J. D. PARK. J. Chem. Phys. **20**, 1014 (1952).
10. P. B. AYSCOUGH, F. S. DAINTON, and B. E. FLEISCHFRESSER. Trans. Faraday Soc. **62**, 1838 (1966). P. GOLDFINGER, G. HUYBRECHTS, and G. MARTENS. Trans. Faraday Soc. **57**, 2210 (1961).
11. L. BERTRAND, G. R. DE MARÉ, G. HUYBRECHTS, J. OLBREGTS, and M. TOTH. Chem. Phys. Lett. **5**, 183 (1970).

Can. J. Chem. Downloaded from www.nrcresearchpress.com by 210.87.254.6 on 09/05/12
For personal use only.

Can. J. Chem. Downloaded from www.nrcresearchpress.com by 210.87.254.5 on 09/05/12
For personal use only.

Nuclear Magnetic Resonance Study of Ring Inversion in Cycloheptene

MAURICE ST-JACQUES AND CAMBYSE VAZIRI
Department of Chemistry, University of Montreal, Montreal, Quebec

Received November 26, 1970

The p.m.r. spectrum of 4,4,5,6,6-pentadeuteriocycloheptene (**3**) has been studied down to −171 °C. Analysis of the spectral change below −160 °C yielded a $\Delta F^{\ddagger}$ value of 5.0 kcal/mol at −165 °C. Possible energy profiles for the ring inversion of cycloheptene are discussed.

On a étudié le spectre r.m.p. du pentadeuterio-4,4,5,6,6 cycloheptène (**3**) jusqu'à −171 °C. L'analyse des changements spectraux en bas de −160 °C permet d'évaluer à 5.0 kcal/mol la valeur du $\Delta F^{\ddagger}$ à −165 °C. Différents profils énergétiques pour l'interconversion du cycloheptène sont discutés.

Canadian Journal of Chemistry, 49, 1256 (1971)

Ring inversion has been studied in several seven-membered cyclic compounds (1). Out of the compounds investigated, 5,5-difluorocycloheptene (**1**) and 4,4,6,6-tetradeuteriobenzocycloheptene (**2**) have a carbon ring skeleton closely related to cycloheptene and yet the free energy barriers ($\Delta F^{\ddagger}$) to ring inversion are significantly different, being 7.4 (2)[1] and 10.9 kcal/mol (3) respectively.

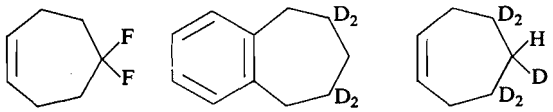

1 **2** **3**

We wish to report the results of a p.m.r. study of 4,4,5,6,6-pentadeuteriocycloheptene (**3**) which shows that $\Delta F^{\ddagger}$ for ring inversion is appreciably lower for this parent compound than for **1** and **2**.

Results and Discussion

Compound **3** was prepared from 4-cycloheptenone (4)[2] by the following sequence of reactions: (*1*) base-catalyzed exchange of α-protons by deuterium atoms, (*2*) reduction with lithium aluminum deuteride, and (*3*) reaction of the alcohol with *p*-toluenesulfonyl chloride and reduction with lithium aluminum hydride.

The deuterium decoupled 100 MHz p.m.r. spectrum at 25 °C of **3** in a mixture of vinyl chloride and chlorodifluoromethane (85:15 by volume) consists of a singlet at δ 1.680 (proton on C-5), a multiplet centered at δ 2.10 (methylene protons on C-3, and -7), and a lowfield multiplet due to the olefinic protons. Figure 1 shows the behavior of the two upfield bands as the temperature is decreased. The upfield singlet broadens and splits into a doublet whose upfield component is clearly visible at δ 1.40, the lowfield component

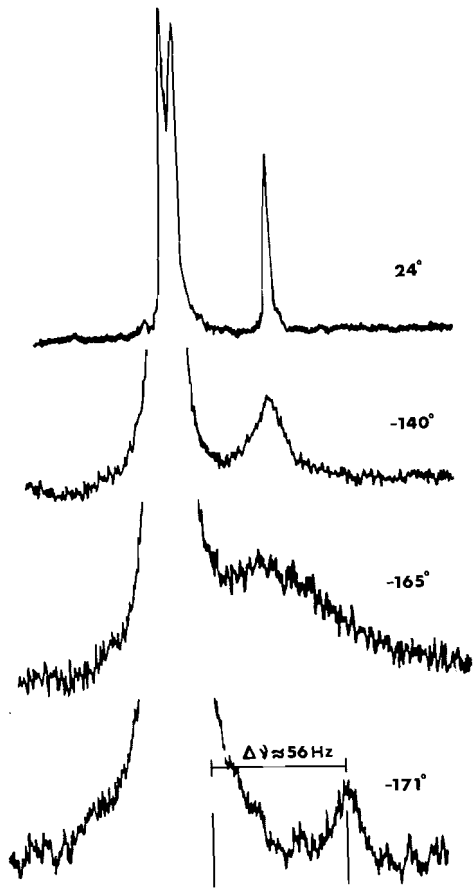

FIG. 1. The 100 MHz p.m.r. deuterium decoupled spectra of the high field peaks of **3** at several temperatures.

[1]The $\Delta F^{\ddagger}$ value was calculated from the data at −165 °C (2).

[2]We are very thankful to Professor G. Descotes for sending us a sample of this compound.

Can. J. Chem. Downloaded from www.nrcresearchpress.com by 210.87.254.5 on 09/05/12
For personal use only.

being under the intense band centered at about δ 2.10 which has broadened but not changed appreciably. The coalescence temperature (T_c) for this spectral change is estimated to be −165 °C. Since the chemical shift of the C-5 singlet changes by only 0.1 Hz from +25 to −140 °C, it is possible to assume that at −171 °C this peak has split into a doublet symmetrically disposed about δ 1.68 thus fixing the position of the downfield component at δ 1.96 as indicated with a line in Fig. 1. The chemical shift difference (Δν) at −171 °C is then about 56 ± 5 Hz, the uncertainty being due to the broadness of the lines because of increased viscosity and the closeness to T_c. This value is comparable to the 0.43 p.p.m. observed for the C-5 protons of **2** (3).

The rate constant (k, in s^{-1}) at T_c for the process of conformational interconversion responsible for the spectral change may be obtained from the relationship, $k = \pi\Delta\nu/\sqrt{2}$ (5). From $k = 124$ s^{-1}, a value of $\Delta F^{\ddagger}$ equal to 5.0 ± 0.3 kcal/mol was calculated using the Eyring equation (1) with a transmission coefficient of one-half (this value will be justified later in the discussion of the interconversion mechanism). The error in $\Delta F^{\ddagger}$ was estimated from the maximum uncertainties in T_c (±3 °C) and in Δν(±5 Hz). Since the spectra of **3** are not suitable for obtaining k with any accuracy over a reasonable range of temperature, it has not been possible to obtain values for $\Delta H^{\ddagger}$ and $\Delta S^{\ddagger}$ (1). However once the interconversion mechanism and the geometry of the transition state are known, it is possible to obtain a fair estimate for $\Delta S^{\ddagger}$ from symmetry contributions (1). We will now consider this aspect of the problem.

Although it has generally been assumed (1) that the most stable conformation of cycloheptene is a chair (**4**), the literature is somewhat ambiguous on this question. Semiempirical strain energy calculations by Allinger and coworkers (6) favor a boat form **5** whereas the results of similar calculations by Favini and co-workers (7) argue for a chair form. Experimentally, p.m.r. results[3] (8) for the benzocycloheptene system strongly favor the chair. It is therefore highly probable that the stable conformation of **3** is also a chair.

[3]The p.m.r. spectra of 2,3-benzocyclohepten-1,4-diol (*8a*) at room temperature and 5,5-dimethylbenzocycloheptene at −52 °C (*8b*) were interpreted in terms of a chair. The p.m.r. results in preparation from our laboratory on deuterated derivatives of benzocycloheptene indicate clearly that the seven-membered ring is a chair.

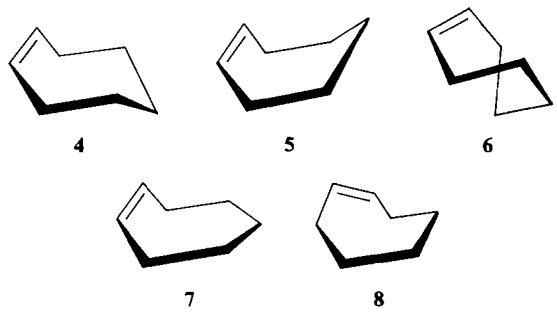

Our p.m.r. study therefore indicates that there are two equivalent (chair) forms in equilibrium which are separated by an energy barrier of 5.0 kcal/mol. A proposed itinerary for chair interconversion was described as involving the conformation changes described in Scheme 1 (9) (the asterisks indicated inverted conformations).

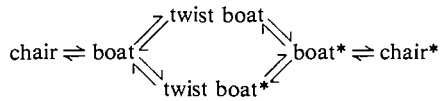

SCHEME 1

The free energy profile corresponding to this mechanism can take two limiting forms as shown in Fig. 2. Since Favini's results predict the correct stable conformation for cycloheptene, we have assumed that their calculated stabilities for the boat and twist boat forms are such that the latter is the least stable. The rate determining transition

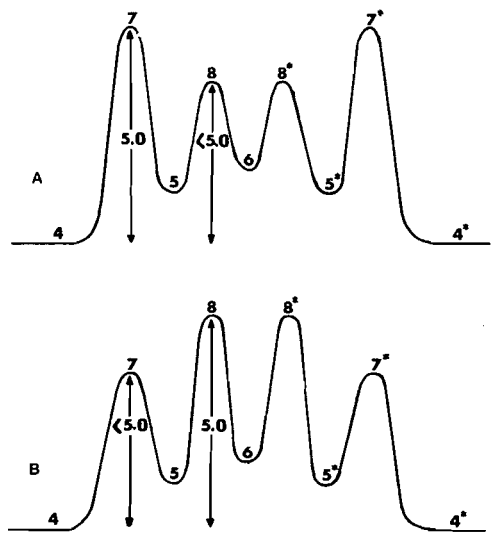

FIG. 2. Possible free energy profiles for the interconversion of cycloheptene chair forms. The asterisks indicate inverted conformations.

Can. J. Chem. Downloaded from www.nrcresearchpress.com by 210.87.254.5 on 09/05/12
For personal use only.

state could be the one for the chair to boat change (**4** → **5**, curve A); in this case the transition state is approximated by conformation **7** which contains five carbon atoms in an essentially planar arrangement. The other possibility (curve B) involves the transition state for the boat to twist boat pseudorotation for which conformation **8** has been proposed by Favini *et al.* (7). In that paper, the energy difference between **4** and **8** has been calculated as 5.6 kcal/mol, a value not incompatible with our p.m.r. result of 5.0 kcal/mol. It is very unfortunate that the energy of conformation **7** was not calculated by these workers. Other calculations for cycloheptane (10), however, have suggested that the barrier to pseudorotation is ordinarily lower than that of a symmetrical process as the change **4** → **5** through **7**. Furthermore, p.m.r. results (9) on cycloheptene derivatives containing two or three sulfur atoms instead of the C-4, -5, and -6 methylene groups have shown that the barrier to pseudorotation is appreciably smaller than chair-to-boat process (for 1,2-benzo-4,5,6-trithio-1-cycloheptene the values were found to be about 10 and 17.4 kcal/mol respectively) although for these compounds both barriers are much higher than the 5.0 kcal/mol observed for cycloheptene. It therefore appears that the energy profile B (Fig. 2) would represent a behavior different from other related systems. In addition, it is difficult to rationalize the barrier differences for **1**, **2**, and **3** by means of this profile. On the other hand, profile A (Fig. 2) offers a more comprehensive rationale for all cycloheptene derivatives through a consideration of substituent and structural effects on the energy of the transition state **7** in the rate determining step as will be discussed next.

Although fluorine substitution has been widely used (2, 11–16) to obtain information on the barrier to conformational interconversion, no comprehensive explanation has been advanced to account for the differences between fluorinated and non-fluorinated compounds. For example, perfluorocyclohexane has a lower $\Delta F^{\ddagger}$ barrier (~0.4 kcal/mol) than cyclohexane (12, 17) while for perfluorocyclohexene it is larger (~1.3 kcal/mol) than cyclohexene (16, 18). Similar differences have also been observed when only one or two fluorine atoms are present in the molecule. For example, 1,1-difluorocyclohexane and 4,4-dimethyl-1,1-difluorocyclohexane (12) have lower $\Delta F^{\ddagger}$ values than cyclohexane (17) and 1,1-dimethylcyclohexane (19) (9.7, 10.2, 10.3, and 11.1 kcal/mol respectively). For 4-fluorocyclohexene (20) the barrier has been found to be essentially equal to that for cyclohexene. In the cyclohexane series, steric interactions in the ground state chair conformation were used to rationalize the results whereas increased torsional energy in the transition state was invoked for halogenated cyclohexene derivatives (20). Solvent variations where possible have shown that these differences were not due to solvent effects (12, 14).

Any attempt to explain the higher barrier for **1** over **3** must consider steric, torsional, and electrostatic interactions. If steric (nonbonded) interactions were mainly responsible for the difference, we would expect the barrier to be lower since the larger size of fluorine would tend to destabilize the ground state chair conformation through axial-like H—F repulsion. Since the opposite is observed, this factor cannot be the sole or main contribution to the difference unless it leads to a larger destabilization of the transition state.

The replacement of the C-5 methylene protons by fluorine atoms is expected to increase the torsional energy to rotation about the C_4—C_5 and C_5—C_6 bonds only slightly if at all as suggested from a comparison of the barriers to methyl rotation in propane (3.4 kcal/mol)(21) and 2,2-difluoropropane (3.4–3.8 kcal/mol)(22). Electrostatic interactions would be manifested through increased dipole–dipole repulsion resulting from a decrease in the F—C—F angle accompanying a widening of the C_4—C_5—C_6 angle in reaching the rate determining transition state. An analogous repulsion has been considered as a possible reason for the much greater stability of 7,7-dicyanonorcaradiene over its cycloheptatriene form (~17 kcal/mol) (23).

The calculations by Favini *et al.* (7) indicate that the C-5 angle is about the same in **4** and **8** while torsional energy is lower and nonbonded energy is larger for **8**. If **8** were the transition state for ring inversion the larger $\Delta F^{\ddagger}$ for **1** would necessarily be due to a steric destabilization of this conformation. However an examination of Fieser models show that the only serious nonbonded interaction is between the interior C-4 and -7 protons, the H—F distances not being significantly shortened. It therefore appears that the fluorine atoms at C-5 would not raise the energy of conformation **8** appreciably over that expected for the parent compound. But since the nonbonded potential function for H—F

Can. J. Chem. Downloaded from www.nrcresearchpress.com by 210.87.254.5 on 09/05/12
For personal use only.

interaction is not available, we cannot be absolutely sure.

Profile A, with **7** as the rate determining transition state is better able to rationalize the 2.4 kcal/mol increase in energy for the inversion of **1** over **3**. The "flipping" of C-5 to reach **7** causes a slight (if any) increase in torsional energy and an increase in F—F repulsion because of the increase in the C_4—C_5—C_6 angle during this transition.

Incorporating the double bond of the cycloheptene ring into a benzene ring as in **2** raises the barrier by about 5.9 kcal/mol (3). The reason for this increase is not quite clear but appears to be related in part to the greater energy required to bend the C_1—C_2—C_3 and C_2—C_1—C_7 angles inward as Fieser models indicate they must to reach the transition state **7**. The origin of this effect is not obvious but is thought to depend in part on the magnitude of these angles in the chair conformation of both types of molecule. These angles are not known for these seven-membered rings but the values of 127° determined for naphthalene tetrachloride by X-ray analysis (24) and of 123.5° obtained for cyclohexene (25) from electron diffraction and microwave spectroscopy suggest that they should be larger in **2** than in **3**. (It is to be noted here that the 120° angles used by Favini *et al.* (7) are probably too small.) The larger deformation associated with the bending of bonds in **2** might account for part of the difference. Another contributing factor might be associated with differing facility for in-plane bending of the C_2—C_3 and C_1—C_7 bonds without introducing appreciable non-planarity into the C_3—C_2—C_1—C_7 part of the molecule (out-of-plane bending). Thus the constraint imposed by the aromatic ring is believed to increase the energy requirement of the in-plane distortions required to reach conformation **7**.

It is therefore reasonable that profile A is correct. The value to be chosen as the transmission coefficient in the Eyring equation for the calculation of $\Delta F^{\ddagger}$ depends on the inversion pathway (16–18, 26). The presence of the metastable intermediates (**5** and **6**) suggests that its value should be one-half to allow for the possibility that a molecule having once overcome the barrier **7** may return back to the initial chair and not go to an inverted chair. The p.m.r. experiment records only the complete inversion of the chair conformation.

Contributions to the entropy of activation ($\Delta S^{\ddagger}$) from differences in vibrational and rotational partition function are expected to be small and positive for ring inversion in similar classes of compounds in inert solvents (1, 16–18, 26) and for cyclohexane, a very accurate $\Delta S^{\ddagger}$ was found to be close to that calculated from symmetry considerations (17). For cycloheptene, the symmetry number (1) and the statistical weight of conformations **4** and **7** are equal since they both belong to the same symmetry group (C_s). The contribution of symmetry to $\Delta S^{\ddagger}$ is therefore $R\ln 1 = 0$ so that $\Delta F^{\ddagger}$ and $\Delta H^{\ddagger}$ are expected to be essentially equal, probably within experimental errors. Such a contention is supported by the determination of $\Delta S^{\ddagger} = -0.2 \pm 2$ e.u. for **1** (2) whose inversion mechanism is undoubtedly the same as that of cycloheptene. The energy difference between **4** and **8** must consequently be less that 5.0 kcal/mol and may turn out to be significantly smaller that the 5.6 kcal/mol calculated by Favini *et al.* (7). Our conclusion is not necessarily contradictory with the qualitative aspect of Favini's calculations. Our results indicate that the energy calculated for **8** is too high and it is highly probable that had the energy of **7** been calculated, its value would have been higher than **8** and qualitatively in accord with curve A. More comprehensive and accurate calculations for the conformations of the maxima and minima (**4** to **8**) of the energy profiles of Fig. 2 seem desirable in order to supply the missing thermodynamic parameters necessary to define completely the energetics of the mechanism of cycloheptene inversion. The results and discussion of this paper provide the necessary check value to lend credibility to such a calculation.

Finally, the results obtained for cycloheptene permit a comparision of the flexibility of the fundamentally important six-, seven-, and eight-membered cycloalkenes. Cyclohexene (18) and cycloheptene have comparable $\Delta F^{\ddagger}$ barriers (5.3 and 5.0 kcal/mol respectively) whereas *cis*-cyclooctene shows two p.m.r. spectral changes at low temperature characterized by $\Delta F^{\ddagger}$ values of 8.2 and 5.8 kcal/mol (27). *trans*-Cyclooctene is rigid on the p.m.r. time scale (28) and its conformation has recently been determined by Manor and co-workers (29).

Experimental

The v.p.c. analyses and separations were carried out on a Varian-Aerograph A90-P3 instrument using ¼ in. columns.

Routine analytical p.m.r. spectra were recorded on a JEOL C-60H spectrometer operating at 60 MHz in

Can. J. Chem. Downloaded from www.nrcresearchpress.com by 210.87.254.5 on 09/05/12
For personal use only.

external lock mode. The variable temperature p.m.r. spectra were recorded on a JEOL JNM-4H-100 spectrometer operating at 100 MHz using a 5% of **3** in a mixture of vinyl chloride and chlorodifluoromethane (85:15, v:v), m.p. −160 °C for both. A small quantity of tetramethylsilane was added and the sample was degassed and sealed. Temperatures were monitored by means of a JEOL temperature control unit model JES-VT-3 and read off a calibration chart obtained with a thermocouple inside a solvent-containing dummy n.m.r. tube. Checks on the accuracy of the calibration curve were made repeatedly and are believed accurate to within ±2 °C. Deuterium decoupling was effected by means of the JEOL Hetero Spin Decoupler model JNM-SD-HC.

2,2,7,7-Tetradeuterio-4-cycloheptenone

4-Cycloheptenone (4) was purified by v.p.c. on carbowax at 170 °C and 0.75 g (0.0068 mol) was added to a solution of 3.0 g of potassium carbonate in 30 ml of deuterium oxide. After 5 h of reflux, the organic material was extracted with ether, dried over magnesium sulfate, and stripped of its ether. The p.m.r. spectrum of the product in deuteriochloroform showed two multiplets at δ 2.43 and 5.95 which integrated for four and two protons respectively, thus indicating essentially complete deuteration next to the carbonyl group.

1,2,2,7,7-Pentadeuterio-4-cycloheptenol

The above deuterated ketone (0.72 g, 0.0062 mol) in 10 ml of anhydrous ether was added to 0.30 g of lithium aluminum deuteride (Fluka ⩾ 99% deuterium) in 10 ml of ether. The mixture was stirred for 1 h at room temperature and then the excess deuteride was decomposed with dilute sulfuric acid. The ether phase was separated, washed with a saturated solution of sodium bicarbonate, water, and dried over magnesium sulfate. The v.p.c. analysis on a silicone fluid, Dow 550 (15%) column at 170 °C indicated that the product, stripped of its ether, was entirely reduced to the alcohol. The p.m.r. spectrum of this compound showed peaks centered at δ 2.12 (multiplet, 4 protons), 2.62 (singlet, one proton), and 5.87 (multiplet, two protons).

4,4,5,6,6-Pentadeuteriocycloheptene (3)

p-Toluenesulfonyl chloride (1.25 g, 0.0065 mol) freshly crystallized from petroleum ether was slowly added to a solution 0.72 g (0.0061 mol) of the above alcohol in 12 ml of dry pyridine. After standing for 48 h at 0 °C, water was added and the solution was extracted three times with 20 ml of ether; the organic phase was then washed successively with 2 *N* hydrochloric acid, a solution of sodium bicarbonate and water. After drying over magnesium sulfate, the ether was evaporated.

The above tosylate (0.200 g, 0.0007 mol) was dissolved in 10 ml of dry tetrahydrofuran (freshly distilled) and this solution was added to a suspension of 0.150 g of lithium aluminum hydride in 10 ml of tetrahydrofuran. After 20 h of reflux, the excess hydride was decomposed with dilute sulfuric acid. Petroleum ether was added; the organic phase was separated and extracted three times with water and then dried over magnesium sulfate and the ether was stripped.

The v.p.c. analysis of the product on carbowax at 80 °C allowed the identification of the peak corresponding to **3** from a comparison with authentic cycloheptene. The deuterated cycloheptene **3** was then collected by v.p.c. on this same column.

The p.m.r. spectrum of this compound in carbon disulfide showed peaks at δ 1.65 (broad singlet, one proton), 2.10 (multiplet, four protons), and 5.70 (multiplet, two protons).

Identically prepared deuterated cycloheptene was used to prepare a sample for the low temperature study.

We are grateful to the National Research Council of Canada for financial assistance and to the Quebec Ministry of Education for a scholarship (France-Québec) to C. V.

1. A review with references for the original sources is given by G. BINSCH. *In* Topics in stereochemistry. Vol. 3. *Edited by* E. L. Eliel and N. L. Allinger. Interscience Publishers, New York, N.Y., 1968. p. 164.
2. R. KNORR, C. GANTER, and J. D. ROBERTS. Angew. Chem. Intern. Ed. Eng. **6**, 556, (1967).
3. S. KABUSS, H. FRIEBOLIN, and H. SCHMID. Tetrahedron Lett. 469 (1965).
4. G. DESCOTES, A. MENET, and P. ROBBE. Tetrahedron Lett. 2331 (1968).
5. J. A. POPLE, W. G. SCHNEIDER, and H. J. BERNSTEIN. High resolution nuclear magnetic resonance. McGraw-Hill Book Inc., New York, N.Y., 1959. p. 223.
6. N. L. ALLINGER, J. A. HIRSCH, M. A. MILLER, and I. J. TYMINSKI. J. Amer. Chem. Soc. **90**, 5773 (1968).
7. G. FAVINI, G. BUEMI, and M. RAIMONDI. J. Mol. Structure. **2**, 137 (1968).
8. (*a*) G. L. BUCHANAN and J. M. MCCRAE. Tetrahedron, **23**, 279 (1967). (*b*) S. KABUSS, H. G. SCHMID, H. FRIEBOLIN, and W. FAISST. Org. Magn. Resonance, **1**, 451 (1969).
9. S. KABUSS, A. LÜTTRINGHAUS, H. FRIEBOLIN, H. G. SCHMID, and R. MECKE. Tetrahedron Lett. 719 (1966).
10. J. B. HENDRICKSON. J. Amer. Chem. Soc. **89**, 7047 (1967).
11. J. B. LAMBERT and J. D. ROBERTS. J. Amer. Chem. Soc. **87**, 3884 (1965).
12. (*a*) F. A. BOVEY, E. W. ANDERSON, F. P. HOOD, and R. L. KORNEGAY. J. Chem. Phys. **40**, 3099 (1964); (*b*) S. SPASSOV, E. S. GLAZER, D. L. GRIFFITH, K. NAGARAJAN, and J. D. ROBERTS. J. Amer. Chem. Soc. **89**, 88 (1967); (*c*) G. V. D. TIERS. Proc. Chem. Soc. 389 (1960).
13. J. D. ROBERTS. Chem. Brit. **2**, 529 (1966).
14. J. T. GERIG and J. D. ROBERTS. J. Amer. Chem. Soc. **88**, 2791 (1966).
15. R. E. LACK, C. GANTER, and J. D. ROBERTS. J. Amer. Chem. Soc. **90**, 7001 (1968).
16. J. E. ANDERSON and J. D. ROBERTS. J. Amer. Chem. Soc. **92**, 97 (1970).
17. F. A. L. ANET and A. J. R. BOURN. J. Amer. Chem. Soc. **89**, 760 (1967).
18. F. A. L. ANET and M. Z. HAQ. J. Amer. Chem. Soc. **87**, 3147 (1965).
19. R. W. MURRAY and M. L. KAPLAN. Tetrahedron, **23**, 1575 (1967).
20. F. R. JENSEN and C. H. BUSHWELLER. J. Amer. Chem. Soc. **91**, 5774 (1969).
21. A review with references to original sources is given by J. P. LOWE. Progr. Phys. Org. Chem. **6**, 1 (1968).

22. K. D. MÖLLER, A. R. DE MEO, D. R. SMITH, and C. H. LONDON. J. Chem. Phys. **47**, 2609 (1967).
23. H. J. REICH, E. CIGANEK, and J. D. ROBERTS. J. Amer. Chem. Soc. **92**, 5166 (1970).
24. M. A. LASHEEN. Acta Cryst. **5**, 593 (1952).
25. (*a*) L. H. SCHARPEN, J. E. WALLRAB, and D. P. AMES. J. Chem. Phys. **49**, 2368 (1968); (*b*) J. F. CHIANG and S. H. BAUER. J. Amer. Chem. Soc. **91**, 1898 (1969).
26. R. K. HARRIS and N. SHEPPARD. J. Mol. Spectrosc., **23**, 231 (1967).
27. (*a*) M. ST-JACQUES. Ph.D. Thesis, University of California at Los Angeles, Los Angeles, California, December, 1967. (*b*) M. St-JACQUES, M. A. BROWN, and F. A. L. ANET. Tetrahedron Lett. 5947 (1966).
28. A. C. COPE and B. A. PAWSON. J. Amer. Chem. Soc. **87**, 3649 (1965).
29. P. C. MANOR, D. P. SCHOEMAKER, and A. S. PARKES. J. Amer. Chem. Soc. **92**, 5260 (1970).

Can. J. Chem. Downloaded from www.nrcresearchpress.com by 210.87.254.5 on 09/05/12
For personal use only.

Can. J. Chem. Downloaded from www.nrcresearchpress.com by 210.87.254.105 on 09/05/12
For personal use only.

The Effect of Sulfurhexafluoride on the Photochemistry of Aqueous Solutions[1]

R. C. RUMFELDT
Department of Chemistry, University of Windsor, Windsor, Ontario

Received July 6, 1970

The effect of SF_6 as a specific scavenger for e_{aq}^- in the photolysis of aqueous solutions has been studied. The photolysis of aqueous solutions of I^- with 2537 Å light and Br^-, Cl^-, and SCN^- with 1849 Å light containing $[SF_6] = 1.4 \times 10^{-3}$ *M* results in the formation of F^-, the yields of which are $\phi(F^-) = 1.38 \pm 0.05$, 1.98 ± 0.05, 2.40 ± 0.08, and 2.07 ± 0.05, respectively. By comparison with $\phi(N_2)$ from N_2O saturated solutions the relationship $\phi(e_{aq}^-) = \phi(F^-/6)$ was confirmed. Assuming the same ratio, $\phi(e_{aq}^-)$ for pure H_2O and aqueous HPO_4^{2-} with 1849 Å radiation and $[SF_6] = 2.4 \times 10^{-4}$ is 0.013 ± 0.002 and 0.30 ± 0.07, but these are considered minimum values due to the low concentration of SF_6. Despite these yields HPO_4^{2-} could be used as buffer in 1849 Å photolysis due to its low extinction at this wavelength.

On a étudié l'effet de SF_6 comme intercepteur spécifique des e_{aq}^- lors de la photolyse de solutions aqueuses. La photolyse de solutions aqueuses (contenant $[SF_6] = 1.4 \times 10^{-3}$ *M*) de I^- à 2537 Å et de Br^-, Cl^-, SCN^- à 1849 Å conduit à la formation de F^- avec des rendements respectifs de $\phi(F^-) = 1.38 \pm 0.05$, 1.98 ± 0.05, 2.40 ± 0.08 et 2.07 ± 0.05. Par comparaison avec les $\phi(N_2)$ mesurés à l'aide de solutions saturées de N_2O, on a pu confirmer que $\phi(e_{aq}^-) = \phi(F^-/6)$. En faisant l'hypothèse que ce rapport reste le même, les valeurs respectives de (e_{aq}^-) pour l'eau pure et HPO_4^{2-} aqueux à 1849 Å et $[SF_6] = 2.4 \times 10^{-4}$ sont de 0.013 ± 0.002 et 0.30 ± 0.07. En dépit de ces rendements, HPO_4^{2-} pourrait être utilisé comme tampon pour des photolyses à 1849 Å à cause de son faible coefficient d'extension à cette longueur d'onde.

Canadian Journal of Chemistry, 49, 1262 (1971)

Introduction

The irradiation of aqueous solutions of a variety of anions with light of short wavelength has been shown to produce solvated electrons (e_{aq}^-) as a primary product (1–3). Although flash photolysis (4, 5) has been used to identify e_{aq}^-, the principal technique in its quantitative measure has been the use of N_2O as a scavenger in the reaction

$$[1] \quad e_{aq}^- + N_2O \rightarrow N_2 + O^-(+H_2O \rightleftharpoons OH + OH^-)$$

From reaction 1 it is easily seen that $\phi(N_2)$ should give a quantitative measure of $\phi(e_{aq}^-)$, provided that there are no competing solutes or N_2 producing reactions.

When the photolyzing light is of wavelength 1849 Å, a direct photodissociation of N_2O can occur

$$[2] \quad N_2O + h\nu\,(1849\ Å) \rightarrow N_2 + O$$

with the result that a distinction must be made between N_2 formed via reactions 1 and 2.

The molecule SF_6 is also known to react rapidly with e_{aq}^- (6) with the proposed stoichiometry being

$$[3] \quad e_{aq}^- + SF_6 \rightarrow SO_4^{2-} + 6F^- + 8H^+$$

Since otherwise SF_6 is assumed to be extremely inert, reaction 3 represents a useful alternate to the use of N_2O as a specific scavenger of e_{aq}^-. Furthermore, it was found that SF_6 does not have any strong absorption bands in the region of 1849 Å. Thus, SF_6 should not undergo direct photodissociation at 1849 Å and any F^- formed would be the result of scavenging such as in reaction 3.

The potential of SF_6 as a specific scavenger in the quantitative measure of e_{aq}^- depends on the assumptions that e_{aq}^- is the only precursor to F^- and that the ratio 1:6 between e_{aq}^- and F^- given in reaction 3 is valid. It is the purpose of this investigation to examine these assumptions as well as to test the utility of SF_6 as an electron scavenger in photochemical systems.

The quantum yields of e_{aq}^- from the photolysis of I^-, Br^-, and Cl^- have previously been measured (1, 2) and provide a useful series with which to test SF_6. The pseudohalides, CN^- and SCN^-, have also been included to provide a broader range of conjugate radicals. While SF_6 does not react even with hydrogen atoms (6) (suggesting that its reactions are kinetically controlled), the possibility existed that the pseudohalogens through their antibonding π-orbitals might react with SF_6. Although there was no evidence of such reactions, some interesting effects were observed with the SCN^- system.

[1]This work was supported by the Defence Research Board of Canada, Grant Number 1675-08.

Can. J. Chem. Downloaded from www.nrcresearchpress.com by 210.87.254.105 on 09/05/12
For personal use only.

Experimental

Materials

The solutions were prepared with water which had been distilled from acid dichromate in a stream of oxygen over a hot platinum filament, condensed and redistilled from alkaline permanganate, and maintained under constant reflux over alkaline permanganate.

The salts KCl, KBr, KI, KCN, KSCN, and $Na_2HPO_4 \cdot 12H_2O$ were reagent grade and were used without further purification. The gases N_2O and SF_6 (The Matheson Company) were purified by repeated trap-to-trap distillations, stored in the vacuum system, and redistilled several times just prior to use.

Apparatus and Procedures

The standard photolysis vessel consisted of a cylindrical quartz cell 20 mm in depth to which was attached a 100 ml degassing bulb and a 10 mm pathlength spectrophotometer cell. The solutions were pipetted into the vessel through a side arm to which a stopcock could be joined for connecting to the vacuum system. After thorough deaeration, the solutions were equilibrated with the desired partial pressure of SF_6 or N_2O. Since the pressure of the additive gases was measured with a mercury manometer, the solutions were protected from contamination by mercury vapor by placing a trap (CO_2–acetone with N_2O and ice-salt slurry with SF_6) between the manometer and the reaction vessel.

Since SF_6 is only slightly soluble in H_2O (7), relatively high partial pressures were required to obtain millimolar concentrations and a high pressure cell was used for these experiments. This cell consisted of a heavy walled Pyrex cup and sidearm which were enclosed in a brass jacket. A quartz window was sealed on to the top of the cup by an O-ring and held tightly in place by a threaded metal cap which screwed over the window on to the brass jacket. A stopcock with a threaded Teflon tap was attached to the sidearm to close the system. This cell could withstand at least 15 atm internal pressure without leaking. The gas to be added to the cell was first measured in a calibrated bulb then distilled into the reaction vessel and the concentration of the gas in solution calculated from the solubility of SF_6 and the PV data with due corrections made for the volume of solution.

The photochemical lamp was a model PCQ011S low pressure mercury grid lamp (Ultra-Violet Products, Inc., San Gabriel, California). For irradiations with the 2537 Å line, the cells were immersed in a constant temperature water bath (25 ± 0.5 °C) with the radiation passing through a quartz window. When the desired line was 1849 Å, the cell was first brought to 25 °C in the bath, dried, and irradiated. Due to the brevity of the irradiation times and the proximity of the ambient temperature to 25 °C, the temperature of the solution under these conditions was assumed to be 25 ± 2 °C. Both cells contained magnetic stirring bars and all solutions were vigorously stirred during irradiation.

The intensity of the 2537 Å line was determined using the ferrioxalate actinometer (8), first with a water filter then replacing it with a degassed aqueous KI filter and measuring the difference. The approximate intensity was 4×10^{-4} einstein l^{-1} min^{-1}, the exact value depending on the particular cell and conditions employed. A deaerated solution of N_2O was used as the actinometer for the 1849 Å line. Following the work of Dainton and Fowles (9), the primary quantum yield of N_2 ($\phi_{N_2}{}^0$) was assumed to be unity and was related to the measured yield ($\phi(N_2)$) by the relationship

$$\phi(N_2) = \phi_{N_2}{}^0 \frac{\varepsilon_{N_2O}[N_2O]}{\varepsilon_{N_2O}[N_2O] + \Sigma_{H_2O}}$$

where $\varepsilon_{N_2O} = 60\ M^{-1}\ cm^{-1}$ and $\Sigma_{H_2O} = 1.8\ cm^{-1}$. The approximate intensity of the 1849 Å was 1.3×10^{-5} einstein l^{-1} min^{-1}.

Gaseous products were analyzed by removal from the reaction cell by successive freeze–pump–thaw cycles and injection into a Varian model 1521-B gas chromatograph employing a molecular sieve 13X column.

Fluoride and cyanide were measured by means of Orion specific ion electrodes with an Orion model 801 meter. The calibration curves were obtained using standardized solutions in reagent blanks. In the case of CN^- the solutions were made 0.1 N in NaOH to prevent hydrolysis. Due to the low yields sulfate was only measured qualitatively using the $BaSO_4$ turbidity technique.

Spectra were obtained using a Beckman DK-1A Far U.V. recording spectrophotometer. At wavelengths below 2000 Å the monochromator and cell compartment were vigorously purged with high purity N_2 to eliminate light absorption by atmospheric gases. Cells with a pathlength of 0.028 or 0.0074 cm were used in the region 2000 to 1700 Å to reduce absorption by the solvents H_2O and D_2O, thereby minimizing the slitwidth and the effects of scattered light. Using the 0.028 cm pathlength cell the slitwidth could be maintained at less than 0.1 mm to 1800 Å after which it increased to 0.5 mm at 1750 Å with a maximum value of 1.0 mm at the 1700 Å cutoff. Essentially the same values were obtained using the 0.0074 cm cell; however, the 0.028 cm cell was used preferentially as it provided greater ease in handling.

Results

(a) KI–SF_6 with 2537 Å Radiation

The only products on irradiation with 2537 Å light of solutions containing $[KI] = 5 \times 10^{-3}\ M$ and $[SF_6]$ in the range 1×10^{-4} to $1.4 \times 10^{-3}\ M$ were F^-, H^+, and $SO_4{}^{2-}$ with no $I_2(I_3{}^-)$ being formed. Beyond a yield of $[F^-] = 1 \times 10^{-4}\ M$, the F^- yields showed a nearly continuous curvature with irradiation time. While buffering the solution after irradiation caused an increase in the F^- yield, buffering with $10^{-3}\ M$ Na_2HPO_4 prior to irradiation resulted in even higher F^- yields which were now linear with irradiation time (Fig. 1). The variation of $\phi(F^-/6)$ from the buffered solutions with $[SF_6]$ is shown in Fig. 2 with the maximum value being $\phi(F^-) = 1.38 \pm 0.05$. Whereas $SO_4{}^{2-}$ was detected it could not be determined quantitatively due to the low concentration.

(b) Irradiation with 1849 Å Light

The spectra of $2.4 \times 10^{-4}\ M$ aqueous SF_6 showed no absorption bands in the region 3000 to

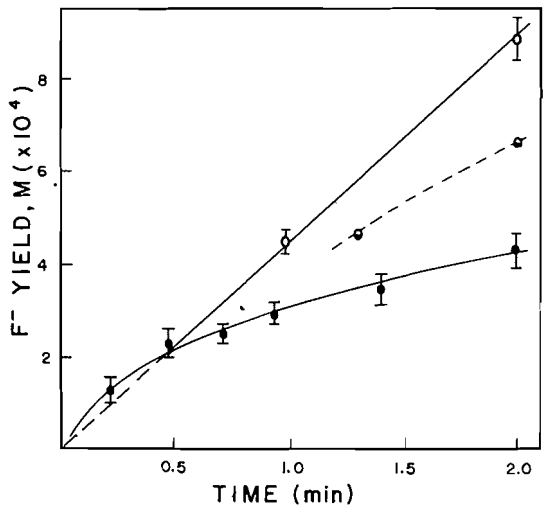

FIG. 1. The dependence of F^- yield on the time of irradiation with 2537 Å light of intensity 4.25×10^{-4} einstein l^{-1} min^{-1} for solutions containing [KI] = 5×10^{-3} M and [SF_6] = 2.4×10^{-4} M; ● unbuffered solutions, ◒ post-irradiation buffering, and ○ pre-irradiation buffering.

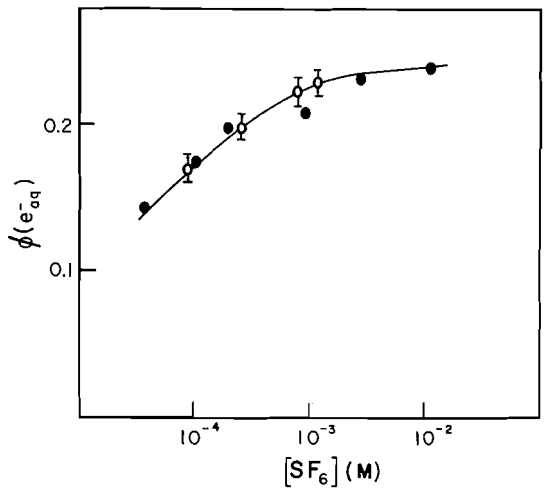

FIG. 2. The variation of $\phi(e_{aq}^-)$ with SF_6 concentration: ○, $\phi(e_{aq}^-) = \phi(F^-/6)$ using buffered solutions; ●, $\phi(e_{aq}^-) = \phi(N_2)$ where $[SF_6] = k_2/k_3[N_2O]$ to account for the difference in scavenging efficiencies and using $k_2/k_3 = 0.57$ (6).

1700 Å. Although irradiation with 2537 Å light of aqueous SF_6 produced no F^-, using the 1849 Å line caused the formation of a low yield of F^- corresponding to $\phi(F^-) = 0.08 \pm 0.01$. No other products could be detected. Since SF_6 is transparent to 1849 Å light, the F^- must arise by the reactions of SF_6 with a product of the photolysis of the solvent H_2O, presumably e_{aq}^- for which $0.2 < \phi(e_{aq}^-) < 0.4$ for pure H_2O has been reported (10).

When salt solutions are illuminated with 1849 Å light only a fraction of the incident light is absorbed by the anion with the remainder being absorbed by the solvent water. Therefore, eq. 1 has been used to calculate the quantum yields due to the photolysis of the solute anions.

$$[4] \qquad \phi'(A) = \phi(A)\frac{\varepsilon_S[S]}{\varepsilon_S[S] + \Sigma_{H_2O}}$$

$\phi'(A)$ is the yield based on the total light intensity, $\phi(A)$ is the yield if all the light had been absorbed by the solute (S), ε_S is the extinction coefficient of the solute, and $\varepsilon_S[S]/(\varepsilon_S[S] + \Sigma_{H_2O})$ gives the fraction of the total light intensity absorbed by the solute. Unless otherwise indicated, all the quantum yields have been calculated this way. The values of ε_S employed are given in Table 1. It can be seen that with the salt concentrations employed, the F^- yield resulting from photolysis of H_2O would be reduced to the magnitude of the experimental error and thus can be neglected.

(i) Buffered and Unbuffered KCl and KBr Solutions

In order to employ HPO_4^{2-} as a buffer in the photolysis of Cl^- and Br^-, it was necessary to establish the absence of a significant inner filter effect by the HPO_4^{2-}. Furthermore photolysis of HPO_4^{2-} by wavelengths shorter than 2000 Å has been shown to produce e_{aq}^- (13), however, $\phi(e_{aq}^-)$ is uncertain since the value appears to differ depending on the choice of scavenger (14).

The spectrum of aqueous Na_2HPO_4 was recorded over the region 3000 to 1700 Å and when plotted as a function of frequency showed a single weak asymmetric band with $\lambda_{max} = 1830$ Å for which $\varepsilon = 575 \pm 50$ M^{-1} cm^{-1}. At the

TABLE 1. Extinction coefficients of compounds absorbing light of wavelength 1849 Å

Compound	Extinction coefficient	Reference
H_2O	1.8 cm^{-1}	11
N_2O	60 M^{-1} cm^{-1}	9
HPO_4^{2-}	500 ± 50 M^{-1} cm^{-1}	This work
Cl^-	$3\,800 \pm 300$ M^{-1} cm^{-1}	9
	$3\,560 \pm 175$ M^{-1} cm^{-1}	This work
Br^-	$13\,000 \pm 1\,000$ M^{-1} cm^{-1}	9
	$11\,600 \pm 500$ M^{-1} cm^{-1}	This work
CN^-	610 ± 50 M^{-1} cm^{-1}	12
SCN^-	$14\,600 \pm 400$ M^{-1} cm^{-1}	12

Can. J. Chem. Downloaded from www.nrcresearchpress.com by 210.87.254.105 on 09/05/12
For personal use only.

TABLE 2. Yield data* for the photolysis of KSCN solutions

Solute	$\phi(CN^-)$	$\phi(F^-)$	$\phi(N_2)$
Deaerated	1.1 ± 0.1	—	—
O_2	1.29 ± 0.1	—	—
$[N_2O] = 2.0 \times 10^{-2}\ M$	1.44 ± 0.1	—	0.33 ± 0.02
$[SF_6] = 2.4 \times 10^{-4}\ M$	2.0 ± 0.2	1.26 ± 0.05	—
$[SF_6] = 1.4 \times 10^{-3}\ M$	—	2.07 ± 0.05	—

*Quantum yields have been calculated from linear yield *vs.* time plots.

photolyzing wavelength $\lambda = 1849$ Å, $\varepsilon = 500 \pm 50\ M^{-1}\ cm^{-1}$ and at $\lambda = 2537$ Å there was no appreciable absorption; these values being in good agreement with previously published data (15). Thus, at $10^{-3}\ M$ the HPO_4^{2-} would contribute only 0.5 OD units per cm of solution suggesting its feasibility as a buffer in 1849 Å photolyses.

Irradiation of solutions containing only $[HPO_4^{2-}] = 10^{-3}\ M$ and $[SF_6] = 2.4 \times 10^{-4}\ M$ results in a total yield of F^- corresponding to $\phi(F^-) = 0.45 \pm 0.09$, of which 0.06 units would be due to H_2O photolysis. Applying the light fraction correction to the residue, $\phi(F^-) = 1.8 \pm 0.4$ would be the value associated with the photolysis of HPO_4^{2-}. As is discussed later, further corrections should be made before this value can be related to any primary process. In any event, in the presence of $5 \times 10^{-3}\ M$ Cl^- or Br^-, the HPO_4^{2-} would absorb only 2.3 and 0.74% respectively of the incidental light, thus reducing the F^- yield from HPO_4^{2-} below the level of the experimental error. For these solutions when $[SF_6] = 2.4 \times 10^{-4}\ M$, $\phi(F^-) = 1.30 \pm 0.2$ for Cl^- and $\phi(F^-) = 1.0 \pm 0.1$ for Br^-. The relatively large error arises from the poor electrode response under these conditions. As an alternate, the same systems were repeated without the buffer and the irradiation times maintained sufficiently short so that $[F^-]$ did not exceed $5 \times 10^{-5}\ M$. Good linear yield–time plots were obtained from which $\phi(F^-) = 1.34 \pm 0.05$ and 2.40 ± 0.08 for Cl^- at $[SF_6] = 2.4 \times 10^{-4}$ and $1.4 \times 10^{-3}\ M$, respectively. For Br^- solutions where $[SF_6] = 2.4 \times 10^{-4}$ and $1.4 \times 10^{-3}\ M$, $\phi(F^-) = 1.1 \pm 0.05$ and 1.98 ± 0.05, respectively.

(ii) KCN

Due to hydrolysis, aqueous solutions of KCN are quite alkaline and it is essential to use a reagent blank in the F^- calibration curve since OH^- interferes with the F^- measurement. The F^- yields for $[CN^-] = 2 \times 10^{-2}\ M$ and $[SF_6] = 2.4 \times 10^{-4}\ M$ are linear with time. After correcting the yields for the anticipated contribution by photolysis of OH^-, the yield associated with photolysis of CN^- corresponds to $\phi(F^-) = 0.50 \pm 0.05$ where the error limit here refers only to the reproducibility.

(iii) KSCN

Irradiation of $[SCN^-] = 5 \times 10^{-3}\ M$ either deaerated, air saturated or with the solutes N_2O or SF_6 results in the formation of sulfur and CN^- with $\phi(CN^-)$ being independent of the total integrated absorbed intensity up to 2.5×10^{-4} einstein/l. The yield data are summarized in Table 2. Since some oxides of sulfur are known to interfere with CN^- determinations, some of the SF_6–SCN^- photolyte was mixed with a standardized CN^- solution with no deviation from the calibration curve being observed.

Discussion

The published values (1, 2) of $\phi(e_{aq}^-)$ for Cl^- and Br^- at 1849 Å and I^- at 2537 Å systems are 0.43, 0.34, and 0.23, respectively. Comparing these values with the F^- yield for the same systems using $[SF_6] = 1.4 \times 10^{-3}\ M$ it can be seen that $\phi(F^-/6) = \phi(e_{aq}^-)$.

While the rate constant for the reaction of e_{aq}^- with SF_6 has been measured (6), neither the exact reaction nor reaction sequence leading to the formation of $6F^-$ and SO_4^{2-} have been established. However, a parallel mechanism to that proposed for the γ-radiolysis of SF_6 solutions is given below

$$[5] \qquad X_{aq}^- + h\nu \rightarrow X + e_{aq}^-$$

$$[6] \qquad e_{aq}^- + SF_6 \rightarrow SF_6^- \rightarrow SF_5\cdot + F^-$$

$$[7] \qquad SF_5\cdot + X^- \rightarrow SF_4 + F^- + X$$

$$[8] \qquad SF_4 + H_2O \rightarrow SOF_2 + 2F^- + 2H^+$$

$$[9] \qquad SOF_2 + X_3^- + 3H_2O \rightarrow SO_4^{2-} + 2F^- + 3X^- + 6H^+$$

or alternately to reaction 8

Can. J. Chem. Downloaded from www.nrcresearchpress.com by 210.87.254.105 on 09/05/12
For personal use only.

Can. J. Chem. Downloaded from www.nrcresearchpress.com by 210.87.254.105 on 09/05/12
For personal use only.

[10] $SOF_2 + 2H_2O \rightarrow SO_3^{2-} + 2F^- + 4H^+$

[11] $SO_3^{2-} + X_3^- + H_2O \rightarrow SO_4^{2-} + 3X^- + 2H^+$

An important product of these reactions is H^+ since it will compete with SF_6 for e_{aq}^- to form H-atoms which do not react with SF_6. Likewise, H^+ reacts with F^- to form the weak acid HF to which the specific ion electrode is insensitive, thus further reducing the yield of F^-. The combination of these effects accounts for the pronounced curvature of the F^- yields and, while the latter effect is offset by post-irradiation buffering, both effects are suppressed by photolyzing buffered solutions.

Reaction 8 is stoichiometrically equivalent to reactions 9 and 10 and for the halide systems no distinction can be made. For other systems which may lack a sufficiently strong oxidizing agent reaction 9 may replace reaction 8 for which $\phi(e_{aq}^-) = \phi(F^-/6) = \phi(X_3^-)$. It is also possible since reaction 9 is reported to be slow (16) that the reaction sequence may terminate at reaction 7 for which $\phi(e_{aq}^-) = \phi(F^-/4) = \phi(X_3^-)$; however, there is no evidence for such a case either in the systems reported here or those studied by radiation chemistry (6).

In the HPO_4^{2-}, CN^-, or pure H_2O systems where a SO_4^{2-} yield could not be established, the relationship $\phi(e_{aq}^-) = \phi(F^-/6)$ is speculative. Furthermore, because of the relatively low concentrations of SF_6 used, these yields would not be expected to represent more than 60 to 70% of the scavengable yield of e_{aq}^- (17). Although the HPO_4^{2-} system was examined primarily to determine its suitability as a buffer in the 1849 Å photolysis of Cl^- and Br^-, applying the rough correction suggested above leads to a value of $\phi(e_{aq}^-)$ for HPO_4^{2-} of between 0.4 and 0.5. This value clearly supports the yield $\phi(e_{aq}^-) = 0.506$ reported by Halmann and Platzner (14) using N_2O rather than the lower yield of 0.14 determined by the same authors using CH_3OH.

For the SCN^- systems, although SO_4^{2-} could not be determined, since $\phi(F^-/6) = 0.35 \pm 0.02$ for $[SF_6] = 1.4 \times 10^{-3}$ and $\phi(N_2) = 0.33 \pm 0.02$ for $[N_2O] = 2.0 \times 10^{-2}$, the relationship $\phi(F^-/6) = \phi(e_{aq}^-)$ appears valid.

A corollary to the establishment of $\phi(e_{aq}^-) = \phi(F^-/6)$ is the exclusion of any reactions between SF_6 and the various radicals produced in these systems. This supports the conclusion that SF_6 is a specific scavenger of e_{aq}^-.

The formation of e_{aq}^- has been observed in the flash photolysis of SCN^- (4, 5) and the coincidence in $\phi(e_{aq}^-)$ for Br^- and SCN^- might seem consistent with the similarities in their absorption spectra. On the other hand, from a detailed study of the spectral region from 2750 to 2000 Å, Gusarsky and Treinin (18) assigned the absorption band at 2200 Å as CTTS and were supported in their assignment by the reported formation of e_{aq}^- on irradiation with 2288 Å light (19); however, the yield was very small ($\phi(e_{aq}^-) = 0.05$). While this seems to present a disagreement with the results observed here, it can be seen from Fig. 3 that the 2200 Å band does not appear to extend to 1849 Å nor does the broad asymmetric high frequency band extend to 2288 Å. Thus, the apparent discrepancy may only be the result of producing two different excited states by the two different exciting wavelengths. If in fact this is the case, then the apparent wavelength dependence of the yield of e_{aq}^- would not seem unreasonable.

In any event, if intersystem crossing is neglected, only the high frequency part of the SCN^- spectrum will contribute significantly to the absorption of the 1849 Å radiation. The asymmetry of the band suggests that more than one electronic transition is contained within this absorption band and the resultant excited states could then correlate with the photochemical processes

[12a] $SCN^- + h\nu\,(1849)\,Å \rightarrow S + CN^-$

[12b] $SCN^- + h\nu\,(1849)\,Å \rightarrow SCN\cdot + e_{aq}^-$

These reactions which have also been proposed (5) in the flash photolysis of SCN^- suggest a modification to eq. 1 since in effect reaction 12*a* is competing with 12*b* for the incident radiation via an intramolecular inner filter effect. Thus, the true quantum efficiency ($\phi^0(e_{aq}^-)$) would be given by

$$[13]\quad \phi(e_{aq}^-) = \phi^0(e_{aq}^-)\frac{\varepsilon'[SCN^-]}{\varepsilon_{SCN^-}[SCN^-] + \Sigma_{H_2O}}$$

where ε' is the extinction coefficient at 1849 Å of the absorption band leading to the excited state involved in reaction 12*b*. Consequently, $\phi^0(e_{aq}^-)$ may be substantially larger than the mean observed value of $\phi(e_{aq}^-) = 0.34$. Similar conclusions would also apply to the CN^- system and, in general, should be considered before interpreting $\phi(e_{aq}^-)$ for complex ions.

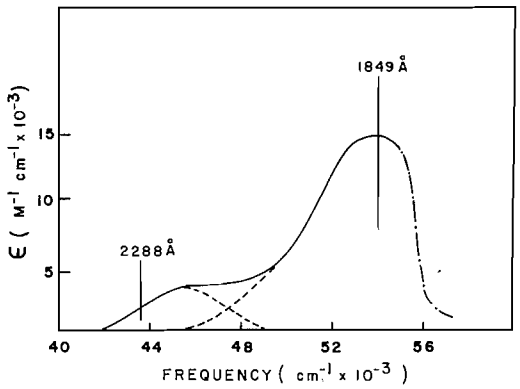

FIG. 3. The spectrum of KSCN in H_2O. The solid line represents the observed spectrum (mean of eight), the broken line (–·–) indicates the region of poor resolution due to increasing slit width and the dashed lines were calculated assuming a Gaussian shape for the band at 45 500 cm^{-1}.

The same considerations when applied to $\phi(CN^-)$ requires that reaction 12*a* cannot be the only source of CN^- and that the SCN produced must also lead to CN^-. This is supported by the difference in $\phi(CN^-)$ between the deaerated and N_2O system where the increase in $\phi(CN^-)$ is equal to $\phi(N_2)$. The use of N_2O in both the pulse radiolysis (20) and flash photolysis (5) of SCN^- solutions causes an increase in the species $(SCN)_2^-$.

[1] $e_{aq}^- + N_2O \rightarrow N_2 + O^- (+H_2O \rightleftharpoons OH + OH^-)$

[14] $OH + SCN^- \rightarrow OH^- + SCN$

[15] $SCN\cdot + SCN^- \rightarrow (SCN)_2^-$

The decay of the species $(SCN)_2^-$ in N_2O saturated systems is reported to be first order in the flash photolysis system whereas it is second order by pulse radiolysis. While the discrepancy between the two systems cannot presently be explained, CN^- could be the decay product in the first case by

[16] $2H_2O + (SCN)_2^- \rightarrow SCN^- + SO_2 + CN^- + 4H^+$

and in the second case by

[17] $(SCN)_2^- + (SCN)_2^- \rightarrow (SCN)_2 + 2SCN^-$

[18] $(SCN)_2 + 4H_2O \rightarrow 2SO_2 + 2CN^- + 8H^+$

In addition, Dogliotti and Hayon (5) have also proposed the reaction

[19] $S + SCN^- \rightarrow S_2 + CN^-$

The speculative nature of these reactions does not encourage a detailed interpretation of $\phi(CN^-)$. In particular, the anomalously high value for $\phi(CN^-)$ in the SF_6 system suggests the possibility that a more complex mechanism may be operative and further experimental data is required to resolve these problems.

The author wishes to acknowledge the assistance of Mr. R. K. Singal in performing the high pressure experiments and to Mr. J. L. Batiste for his assistance in resolving the SCN^- spectra.

1. F. S. DAINTON and S. LOGAN. Proc. Roy. Soc. A, **287**, 281 (1965).
2. F. S. DAINTON and P. FOWLES. Proc. Roy. Soc. A, **287**, 312 (1965).
3. J. JORTNER, M. OTTOLENGHI, and G. STEIN. J. Phys. Chem. **68**, 247 (1964).
4. M. S. MATHESON, W. A. MULAC, and J. RABANI. J. Phys. Chem. **67**, 2613 (1963).
5. L. DOGLIOTTI and E. HAYON. J. Phys. Chem. **72**, 1800 (1968).
6. K.-D. ASMUS and J. H. FENDLER. J. Phys. Chem. **72**, 4285 (1968).
7. H. L. FRIEDMAN. J. Amer. Chem. Soc. **76**, 3294 (1954).
8. C. G. HATCHARD and C. A. PARKER. Proc. Roy. Soc. A, **235**, 518 (1956).
9. F. S. DAINTON and P. FOWLES. Proc. Roy. Soc. A, **287**, 295 (1965).
10. N. GETOFF and G. O. SCHENCK. Photochem. Photobiol. **8**, 167 (1968).
11. J. L. WEEKS, G. M. A. C. MEABURN, and S. GORDON. Radiation Res. **19**, 559 (1963).
12. J. L. BATISTE. Ph.D. Thesis. University of Windsor, Windsor, Ontario. 1970.
13. J. R. HUBER and E. HAYON. J. Phys. Chem. **72**, 3820 (1968).
14. M. HALMANN and I. PLATZNER. J. Phys. Chem. **70**, 2281 (1966).
15. M. HALMANN and I. PLATZNER. J. Chem. Soc. 1440 (1965).
16. H. L. ROBERTS. Quart. Rev. **15**, 30 (1961).
17. J. JORTNER, M. OTTOLENGHI, and G. STEIN. J. Phys. Chem. **66**, 2029 (1962).
18. E. GUSARSKY and A. TREININ. J. Phys. Chem. **69**, 3176 (1965).
19. M. LURIA and A. TREININ. J. Phys. Chem. **72**, 305 (1968).
20. J. H. BAXENDALE, P. L. T. BEVAN, and D. A. STOTT. Trans. Faraday Soc. **64**, 2389 (1968).

Can. J. Chem. Downloaded from www.nrcresearchpress.com by 210.87.254.105 on 09/05/12
For personal use only.

Can. J. Chem. Downloaded from www.nrcresearchpress.com by 210.87.254.105 on 09/05/12
For personal use only.

Collisional Deactivation Rates of $N_2^+(B^2\Sigma_u^+)$

G. I. MACKAY AND R. E. MARCH
Department of Chemistry, Trent University, Peterborough, Ontario

Received September 24, 1970

Electron beam excitation of nitrogen was utilized to produce ions in the zeroth and first vibrational levels of the $B^2\Sigma_u^+$ state. The rate constants for the collisional deactivation of electronically excited N_2^+, for each of N_2 and NO, were determined individually for the $v' = 0$ and $v' = 1$ vibrational levels of the $N_2^+(B^2\Sigma_u^+)$ state. Charge transfer is the most probable mode of deactivation.

L'excitation de l'azote par un faisceau d'électrons a été utilisé pour produire des ions de niveau vibrationnels zéro et un de l'état $B^2\Sigma_u^+$. Pour N_2 ainsi que NO, les constantes de vitesse de désactivation par collision de N_2^+ excité électroniquement, ont été déterminées individuellement pour les niveaux vibrationnels $v' = 0$ et $v' = 1$ de l'état $N_2^+(B^2\Sigma_u^+)$. Le transfert de charge est le mode le plus probable de désactivation.

Canadian Journal of Chemistry, 49, 1268 (1971)

Measurements of a large number of ion–molecule reactions have been reported by Ferguson *et al.* (1) in recent years. While their experiments involved ground state ions exclusively some work has been reported (2) in which the reacting molecule may be excited. In this work we report the rate constants at room temperature for the collisional deactivation process (in which charge-transfer is energetically favored)

$$[1] \qquad NO + N_2^+(B^2\Sigma_u^+) \rightarrow NO^+ + N_2 \qquad k_1$$

where the nitrogen ion is electronically excited and is in either the ground vibrational level or in the first excited vibrational level. No attempt was made to ascertain the identities of the products.

Experimental[1]

A differentially-pumped beam of electrons, accelerated to 20 keV through an orifice 0.022 in. in diameter, was directed into a known mixture of nitrogen and nitric oxide in a flow system, perpendicular to the direction of flow. The beam current was maintained at a constant value of approximately 1 mA; fluctuations greater than $\pm 1\%$ could not be detected with the Keithley 601 electrometer once a reliable filament had been installed. The flow rate of each component was determined from the decrease in pressure of a known volume of gas; a calibrated McLeod gauge was used for the total pressure. An image of the slit of the spectrometer at a magnification of unity was formed at the axis of the beam using a combination of lens and front surfaced mirror. Direct observation of the first negative system (1N) of nitrogen in the beam was made with a SPEX 1700-II Czerny-Turner spectrometer. The spectrometer was equipped with a 100 mm × 100 mm grating (1200 lines/mm) blazed at 3000 Å. The spectrum was scanned in the first order with a Servo-Tek wavelength scanning control. The spectrometer, associated external optics, chopper, and detector were mounted on a movable platform which was operated by a 1 mm pitch screw to facilitate alignment with the central core of the beam. The beam diameter was 0.15 cm. The signal was detected with an EMI 6256S photomultiplier tube and amplified by an Ortec 486 Amplifier-Pulse Height Analyzer coupled with an Ortec 441 Linear Ratemeter. The output was recorded on a Leeds and Northrup Speedomax W Azar Recorder. The signal intensity was taken as the integrated area of an entire vibrational band.

[1]A complete description of the apparatus is given in the M.Sc. thesis of G. I. Mackay (11).

Results and Discussion

Electronically excited N_2^+, in the $B^2\Sigma_u^+$ state which lies some 3.1 eV above that of the ground state molecular ion, is produced by electron impact;

$$[2] \qquad N_2 + e^- \rightarrow N_2^+(B) + 2e^- \qquad k_2$$

where k_2 is an effective rate constant for the formation of $N_2^+(B)$ ions in a particular vibrational level, v'. The effects of secondary electron excitation are small at the pressures used here and are minimized by the optical arrangement in which the fluorescent beam is brought to a focus parallel to the spectrometer entrance slit rather than perpendicular to it. Removal of excited molecular ions may be effected by

(*i*) spontaneous emission of radiation (1N) which results in the production of nitrogen ions in the $X^2\Sigma_g^+$ state.

$$[3] \qquad N_2^+(B) \rightarrow N_2^+(X) + h\nu\,(1N) \qquad k_3$$

Bennett and Dalby (3) have measured the mean lifetime corresponding to the (0,0) band at 3914 Å as $6.53 \pm 0.22 \times 10^{-8}$ s. The rotational temperature of the 3914 Å band was 298 °K.

Can. J. Chem. Downloaded from www.nrcresearchpress.com by 210.87.254.105 on 09/05/12
For personal use only.

(*ii*) de-excitation by ground state nitrogen molecules, presumably through a charge transfer process

[4] $N_2^+(B) + N_2 \rightarrow N_2^+(X) + N_2 \quad k_4$

and

(*iii*) de-excitation by nitric oxide molecules, again presumably through a charge transfer process

[1] $N_2^+(B) + NO \rightarrow NO^+ + N_2 \quad k_1$

It was anticipated that k_1 would not differ considerably from the rate constant involving ground state ions (4).

[5] $N_2^+(X) + NO \rightarrow NO^+ + N_2 \quad k_5$

where $k_5 = 30(+6, -18) \times 10^{10}\ l\ s^{-1}$

In pure nitrogen, the steady state equation for the intensity of any given vibrational band of the 1N system, $I_{v',v''}$ is of the form

$$[6] \qquad \frac{1}{I_{v',v''}} = \frac{1}{k_2 i[N_2]} + \frac{k_4}{k_2 k_3 i}$$

where i is the electron beam current. Thus a plot of $1/I_{v',v''}$ *vs.* $1/[N_2]$, such as is shown in Fig. 1 (curve *a*), should yield a straight line of slope, $S_{N_2} = 1/k_2 i$ and intercept, $i_{N_2} = k_4/k_2 k_3 i$.

In the presence of nitric oxide, reaction 1 must be taken into account and thus

$$[7] \qquad I_{v',v''} = \frac{k_2 k_3 i[N_2]}{k_3 + k_4[N_2] + k_1[NO]}$$

When the total concentration of nitrogen and nitric oxide is kept constant, *i.e.*

$$[8] \qquad [N_2] + [NO] = C$$

eq. 7 may be re-arranged to yield

$$[9] \qquad \frac{1}{I_{v'v''}} = \frac{k_4 - k_1}{k_2 k_3 i} + \frac{k_3 + k_1 C}{k_2 k_3 i[N_2]}$$

A plot of $1/I_{v',v''}$ *vs.* $1/[N_2]$ at constant total pressure of mixtures of nitrogen and nitric oxide yields a straight line of slope, $S_{NO} = (k_3 + k_1 C)/k_2 k_3 i$ and intercept, $i_{NO} = (k_4 - k_1)/k_2 k_3 i$. It is readily seen that

$$[10] \qquad k_1 = \frac{k_3}{C}\left(\frac{S_{NO}}{S_{N_2}} - 1\right)$$

and k_1 was determined for a number of values of C. The rate constant for any given vibrational state of $N_2^+(B)$ in reaction 1 can be determined from observation of the emission from that given state. Thus reaction 1 can be expanded to include individual vibrational levels

$[1,v'=0]$ $N_2^+(B)_{v'=0} + NO \rightarrow NO^+ + N_2$

$[1,v'=1]$ $N_2^+(B)_{v'=1} + NO \rightarrow NO^+ + N_2$

etc.

In practice, it was possible to observe only the (0,0), (1,0), and (1,2) vibrational bands due to interference from the second positive (2P) system of nitrogen, and other minor background features excited by the electron beam.

In Figs. 1 and 2 are shown the linear relationship between $1/I_{v'v''}$ and reciprocal nitrogen

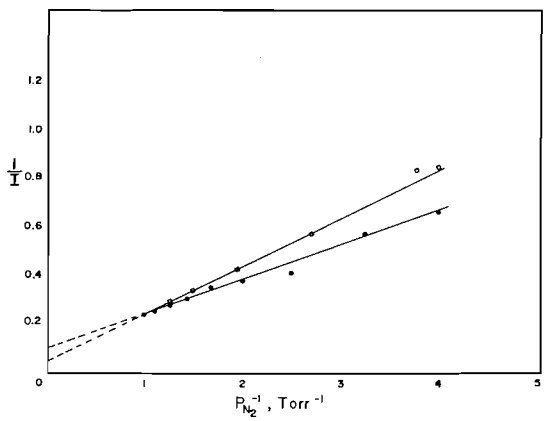

FIG. 1. Plot of the reciprocal intensity (arbitrary units) of the (0,0) band of the N_2 1N system *vs.* reciprocal nitrogen pressure, (*a*)●, pure nitrogen; (*b*) NO added, ○, $C = 1$ Torr; (*c*) NO added, ◇, $C = 0.9$ Torr; (*d*) NO added, △, $C = 0.8$ Torr.

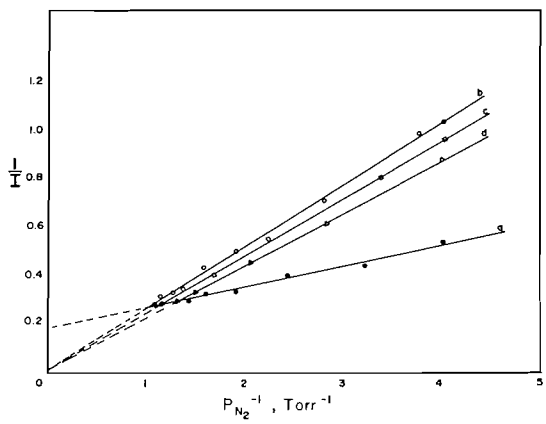

FIG. 2. Plot of the reciprocal intensity (arbitrary units) of the (1,0) band of the N_2 1N system *vs.* reciprocal nitrogen pressure. Pure nitrogen, ●; NO added, ◇, $C = 1$ Torr.

Can. J. Chem. Downloaded from www.nrcresearchpress.com by 210.87.254.105 on 09/05/12
For personal use only.

pressure up to a pressure of 1 Torr, for the $v' = 0$ and $v' = 1$ levels, respectively. The straight lines represent the least-squares curve fit of the points which are the experimental data. At a given pressure, nitrogen was partially replaced by successive amounts of nitric oxide. A series of curves, each originating from the pure nitrogen line, was then obtained. Values for k_1, calculated from each curve, are shown in Table 1. The mean value for $k_{1,v'=0}$ was $46 \pm 9 \times 10^{10}$ l s^{-1}, based on Bennett and Dalby's value for k_3. The rate constant for deactivation of $N_2^+(B)$ by nitric oxide agrees quite well with the value for charge transfer from $N_2^+(X)$ obtained by Ferguson *et al.*, though it lies at the upper limit of their range.

In the determination of $k_{1,v'=1}$, two vibrational bands (1,0) and (1,2) were monitored, and the results are shown also in Table 1; a mean value of $k_{1,v'=1} = 14(+6, -3) \times 10^{10}$ l s^{-1} was obtained. The radiative lifetime for the (1,0) and (1,2) bands was taken to be 7.58×10^{-8} s based on the value of Jeunehomme (5). The values of $k_{1,v'=1}$ are less accurate than those for $k_{1,v'=0}$ due to the diminished intensity of the $v' = 1$ bands. The rate constant is lower for the excited nitrogen ion with a single vibrational quantum than that for the vibrationally unexcited one. Schmeltekopf *et al.* (2) have reported enhancement of the rate constant for a vibrationally excited neutral in the ion–atom interchange reaction

$$[11] \qquad O^+ + N_2(v) \rightarrow NO^+ + N$$

No enhancement was observed in our case with a vibrationally excited ion; on the contrary, as shown above a decrease was noted.

A value for the rate constant $k_{4,v'=0}$ (for the de-excitation reaction of nitrogen ions with nitrogen molecules) may be estimated crudely in three ways:

TABLE 1. Mean values of the rate constant k_1 for N_2^+ in the $v' = 0$ and $v' = 1$ vibrational levels

Total pressure (Torr)	$k_{1,v'=0}$ (l s^{-1} × 10^{-10})	$k_{1,v'=1}$ (l s^{-1} × 10^{-10})	
1.00	47	14*	13†
0.90	41		
0.80	46		
0.70	44		
0.60	48		

*Mean value derived from the (1,0) band of the N_2^+ 1N system.
†Mean value derived from the (1,2) band of the same system.

(*i*) In the excitation of pure nitrogen, the ratio of the intercept to slope $i_{N_2}/S_{N_2} = k_4/k_3$. It was calculated, thus, from the data in Fig. 1 that $k_{4,v'=0} \approx 42 \times 10^{10}$ l s^{-1}.

(*ii*) On extrapolation of the nitric oxide curves to zero (such a procedure invokes negative concentrations of nitric oxide!), comparison may be made of the resulting common intercept with that for pure nitrogen, *i.e.* $i_{NO}/i_{N_2} = 1 - k_1/k_4$. The uncertainty in the value for i_{NO}, in this work, is too large to justify even a crude estimate.

(*iii*) Equation 7 may be rearranged to predict a linear plot of $1/I_{v'v''}$ *vs.* [NO] at constant [N_2]; the data are obtained from any vertical line on Fig. 1. The slope of this plot $S'_{NO} = k_1/(k_2k_3i[N_2])$. Now $i_{N_2} = k_4/k_2k_3i$, therefore

$$\frac{k_1}{k_4} = \frac{S'_{NO}}{i_{N_2}}[N_2]$$

The data present a range for $(k_1/k_4)_{v'=0}$ of from 1.1 to 1.4, corresponding to the minimum and maximum values for S'_{NO}. For the vibrationally excited ion $(k_1/k_4)_{v'=1}$ was found to be approximately 0.6. These ratios for k_1/k_4 were evaluated independently of k_3. One may then substitute the above values for $k_{1,v'=0}$ and $k_{1,v'=1}$ (based on the lifetimes of the $v' = 0$ and $v' = 1$ states, respectively) and show that, whereas the rate constant for deactivation by nitric oxide is decreased by a factor of 3 on the acquisition of a single vibrational quantum, the corresponding rate constant for deactivation by nitrogen molecules is decreased by a factor of 1.5 only.

As shown in Table 2, Brocklehurst and Downing (6), in two experiments using X-ray excitation and 50 keV electron excitation of nitrogen at 770 Torr, obtained values for $k_{4,v'=0} = 24 \pm 9 \times 10^{10}$ l s^{-1}, while Mitchell (7) reports a value for $27 \pm 3 \times 10^{10}$ l s^{-1} obtained by soft X-ray excitation in the pressure range 0.3–600 Torr. This is in fair agreement with the values obtained in this work which was carried out at low pressures and with 20 keV electron excitation.

The observation that $k_{1,v'=0}$ is slightly greater than k_5 may be accounted for by favored Franck–Condon transitions to vibrationally excited states of the $A^3\Sigma$ molecule. It has been shown (8, 9) that reaction 5 may yield molecules in the $A^3\Sigma_u^+$ state. Transitions from the N_2^+ $X^2\Sigma_g^+$ and $B^2\Sigma_u^+$ states to the $A^3\Sigma$ state

TABLE 2. Comparison of the quenching constants for $N_2^+(B^2\Sigma_u^+)$

	Quencher	k ($l\,s^{-1} \times 10^{-10}$) This work	Other workers
$k_{1,v'=0}$	NO	46 ± 9	$30(+6, -18)$‡
$k_{1,v'=1}$	NO	$14\ (+6, -3)$	—
$k_{4,v'=0}$	N_2	≈ 42* 33–42 (± 8)†	24 (± 9)§; 27(± 3)‖
$k_{4,v'=1}$	N_2	23 ($+9, -5$)†	—

*Method (*i*).
†Method (*iii*).
‡Reference 4. Note: reactant ion was $N_2^+(X)$ rather than $N_2^+(B)$.
§Reference 6.
‖Reference 7.

of nitrogen are compatible with the application of the Franck–Condon principle, and the spin-conservation rule is not violated. Reaction 5 is near-resonant while reaction 1 is exothermic by $\geqslant 3.1$ eV.

Little can be said of the mechanism of deactivation to explain the diminution of the rate constants for the vibrationally excited ions. No other results are available for the variation of quenching of ions with v'. Some data are available (10) for the molecular state $C^3\Pi_u$ where a 3-fold enhancement of the quenching constant is observed between $v' = 0$ and 1. There is, however, little reason to expect similar behavior for quenching of charged species. An attempt is being made to obtain more precise data for this species as it is an important constituent of the upper atmosphere.

The authors gratefully acknowledge the financial support of the National Research Council of Canada, Imperial Oil Limited (Canada) and one of us (G.I.M.), the Province of Ontario for a Graduate Fellowship.

1. F. C. FEHSENFELD, A. L. SCHMELTEKOPF, D. B. DUNKIN, and E. E. FERGUSON. ESSA Tech. Report EDL 135-AL 3.
2. A. L. SCHMELTEKOPF, F. C. FEHSENFELD, G. I. GILMAN, and E. E. FERGUSON. Planet. Space Sci. **15**, 401 (1967).
3. R. G. BENNETT and F. W. DALBY. J. Chem. Phys. **31**, 434 (1959).
4. P. D. GOLDAN, A. L. SCHMELTEKOPF, F. C. FEHSENFELD, H. I. SCHIFF, and E. E. FERGUSON. J. Chem. Phys. **44**, 4095 (1966).
5. M. JEUNEHOMME. J. Chem. Phys. **44**, 2672 (1966).
6. B. BROCKLEHURST and F. A. DOWNING. J. Chem. Phys. **46**, 2976 (1967).
7. K. B. MITCHELL. J. Chem. Phys. **53**, 1795 (1970).
8. N. G. UTTERBACK and B. VAN ZYL. Phys. Rev. Lett. **20**, 1021 (1968).
9. J. R. SHERIDAN and J. R. PETERSON. J. Chem. Phys. **51**, 3574 (1969).
10. B. BROCKLEHURST. Trans. Faraday Soc. **60**, 2151 (1964).
11. G. I. MACKAY. M.Sc. Thesis, Trent University, Peterborough, Ontario. 1971.

Can. J. Chem. Downloaded from www.nrcresearchpress.com by 210.87.254.105 on 09/05/12
For personal use only.

Can. J. Chem. Downloaded from www.nrcresearchpress.com by 210.87.254.5 on 09/05/12
For personal use only.

Removal of Wood Components During Chlorite Delignification of Black Spruce

P. A. AHLGREN[1] AND D. A. I. GORING

Physical Chemistry Section, Pulp and Paper Research Institute of Canada and Chemistry Department, McGill University, Montreal, Quebec

Received October 14, 1970

The pattern of component removal has been studied for black spruce during delignification by acidified sodium chlorite at 70 °C. Special emphasis was placed on the determination of the acid soluble portion of lignin remaining in the sample.

It was found that the chlorite procedure is selective in removing lignin only during the first 60% of delignification. At later stages of delignification some glucomannan is dissolved. A so-called holocellulose of 70% yield is thus composed of about 40% cellulose, 13% glucomannan and galactan, 12% xylan and other carbohydrates, and 5% lignin (all based on the original wood).

On a étudié la séquence de dissolution des différents composés de l'épinette noire durant la délignification par chlorite de sodium acidifié, à 70 °C. On s'est occupé surtout de suivre la mise en solution de la lignine par détermination de la teneur résiduelle en lignine de la fibre après la cuisson.

Durant une première étape de délignification le traitement au chlorite est sélectif pour la lignine seulement. Lorsque 60% de la lignine est éliminé, le glucomannan commence à se dissoudre et on trouve qu'un holocellulose de rendement 70% est composé d'environ: 40% cellulose, 13% glucomannan et galactan, 12% xylan et autres carbohydrates ainsi que 5% de lignine (les pourcentages étant basés sur la masse originale du bois).

Canadian Journal of Chemistry, 49, 1272 (1971)

Introduction

Although the chlorite method is widely used for the preparation of holocellulose few attempts have been made to study quantitatively the pattern of component removal. Previous investigations (1–3) were inadequate as few intermediate stages of delignification were reported and the degree of delignification was not determined accurately. That acidic chlorite does not leave the carbohydrate portion of the wood intact is suggested by the observed decrease in DP of the cellulose (4), as well as the observed decrease in carbohydrate yield toward the end of the delignification (3–5).

The main purpose of the present work was to establish quantitatively the degree to which acidic chlorite treatment at 70 °C is selective in removing lignin from spruce wood. A secondary purpose was to determine which polysaccharides and how much of them dissolved during the delignification.

The delignification was followed by Klason analysis of the remaining lignin. It has long been recognized that this procedure does not account for all the lignin in the sample. The analysis must be complemented by a determination of that part of the lignin soluble in the sulfuric acid used to hydrolyze the carbohydrates. High values have been reported for the amount of acid-soluble lignin in samples produced by the chlorite process (3, 6). In order to ensure accuracy in the measurement of the degree of lignin removal, special care was taken in determining acid-soluble lignin at various stages of chlorite treatment.

Previous investigators have isolated glucose and mannose from chlorite liquors (7–9). In the present work, the sugar composition of samples treated to different extents was determined in order to characterize quantitatively the loss of various types of carbohydrates during the chlorite process.

Materials and Methods

Wood

Black spruce (*Picea mariana*) whole wood was used in three forms: (*1*) 2 × 2 × 5 mm matchstick chips; (*2*) 0.3 mm thick longitudinal shavings cut to about 3 mm in the fiber direction; (*3*) 40–60 mesh meal from dry Wiley milling. The Klason lignin content of the samples was 27.8 ± 0.2% (n = 7, 95% confidence limits). The samples were extracted with hot water before chlorite treatment.

Chloriting Procedure

Chlorite treatment was done according to the procedure of Wise *et al.* (5) as adapted by Timell (10). The initial chemical charge was 0.3 g sodium chlorite and 0.1 ml glacial acetic acid per g of dry wood. The liquor to wood ratio was 15:1 and the temperature was 70 °C. Batches of 2 g of wood were treated for different lengths of time. At hourly intervals a fresh charge of chemicals was added without withdrawal of any liquor. The time required with

[1]On leave from Swedish Forest Products Research Laboratory (STFI), Stockholm, Sweden.

Can. J. Chem. Downloaded from www.nrcresearchpress.com by 210.87.254.5 on 09/05/12
For personal use only.

this procedure was 2 h 10 min and 7 h to reach 50 and 90% lignin removal respectively.

Lignin Determination

The Klason lignin analyses were done according to Tappi T 13m-54 for wood and Tappi T 222m-54 for the chlorite-treated samples.

The acid soluble portion was estimated spectrophotometrically by measuring the absorbance of the Klason hydrolysates in the u.v. Similar results were obtained when the measurements were made at 240 and 280 nm but the measurements at 240 nm gave greater precision because of the higher absorbance of the lignin at this wavelength.

There are several indications that the amount of acid-soluble lignin from untreated softwoods is sufficiently small to be neglected (3, 11, 12). The observed absorbance of a Klason hydrolysate from spruce wood is most probably due to carbohydrate degradation products of the furan type, such as furfural and hydroxymethylfurfural (3). Therefore it has been assumed in the present work that the portion of the absorbance in the acid soluble fraction of the treated samples due to non-lignin is equal to the absorbance of the Klason hydrolysate from untreated wood and the appropriate correction made. This correction for carbohydrate degradation products corresponded to less than 1% acid soluble lignin on wood. Lignin concentrations were then calculated from the corrected absorbances using an absorptivity of 30 l/g cm at 240 nm determined by Campbell and McDonald (6) for the acid soluble lignin from chlorited spruce wood.

Carbohydrate Determination

In the hydrolysates from Klason lignin analysis, the glucose contents were determined by the glucose–oxidase method (13, 14). The relative sugar compositions of the hydrolysates were determined by g.l.c. of the alditol acetates, essentially according to the method reported by Sjöström *et al.* (13, 15).

Results and Discussion

Figure 1 shows the results obtained for the acid soluble lignin at various Klason lignin contents. Each point is an average of the data from two separate hydrolyses (mean deviation ±0.1% lignin on wood). Noteworthy is the high level of the acid soluble lignin, in agreement with earlier findings (3, 6). A maximum is reached at about 50% delignification in agreement with the behavior found for other processes (11, 16).

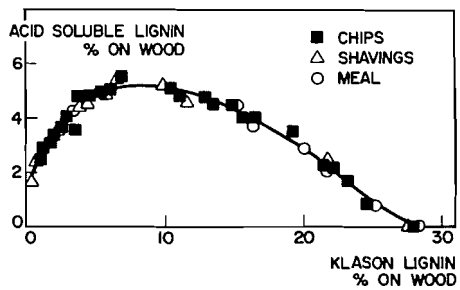

FIG. 1. The amount of acid-soluble lignin from chlorite treated spruce wood measured spectrophotometrically at different stages of delignification.

The removal of components during the course of chlorite delignification is shown in Fig. 2. The hot water extraction dissolved about 2% of the wood, giving a starting point at 98% yield. The total yield is determined from eq. 1.

$$[1]\quad \text{Yield} = \frac{\text{Oven-dried wt. of washed sample after treatment}}{\text{Oven-dried weight of original wood}} \times 100$$

The non-lignin yield is calculated by subtracting from the total yield the amount of lignin remaining in the sample (determined as insoluble Klason lignin plus the u.v.-estimated acid soluble lignin, Fig. 1). The total carbohydrate content of the samples is assumed to be the non-lignin yield. In order to facilitate use of the data by others, smoothed values from the curves in Figs. 1 and 2 are compiled in Table 1.

From Fig. 2, it is evident that acidic chlorite treatment dissolves only lignin during the first 60% of delignification. On further treatment, the non-lignin yield decreases, indicating that lignin-removal is accompanied by a loss of carbohydrates. In passing it is worth noting that, as the wood contains about 28% lignin and 2% water-soluble extractives in totally selective delignification, a residue obtained in 70% yield should be constituted entirely of carbohydrate. However, it was found that at 70% yield the carbohydrate content of the residue was only 93%, the loss being compensated for by the retained lignin.

The question then arises as to which of the

TABLE 1. The lignin contents of holocelluloses at different degrees of delignification

Delignification (%)	Klason lignin (% on wood)	Acid soluble lignin (% on wood)	Total yield (%)
0	27.8	0	100
10	23.2	1.7	95.4
20	19.2	3.1	92.5
30	15.4	4.2	89.7
40	12.0	4.8	86.9
50	8.7	5.2	84.0
60	6.2	5.0	81.2
70	4.0	4.4	77.4
80	2.1	3.4	72.3
85	1.3	2.8	69.0
90	0.6	2.1	64.6
92.5	0.3	1.8	61.3

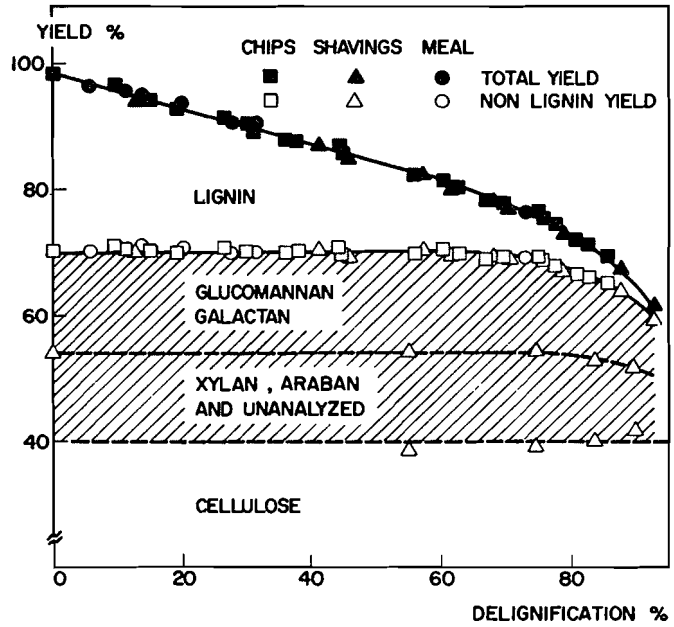

FIG. 2. Yield of the major wood components during chlorite treatment of spruce at different stages of delignification.

TABLE 2. Sugar composition of holocelluloses at different yields

Holocellulose yield (%)	Anhydrosugars from holocellulose (% on wood)				
	Glucose	Arabinose	Xylose	Mannose	Galactose
97.9	—	1.1	5.9	10.2	2.2
82.7	42.4	0.8	5.9	10.7	1.5
75.4	43.0	0.8	5.7	9.8	1.3
70.2	43.7	0.8	6.3	8.6	1.3
65.1	44.7	0.7	5.7	7.4	0.7

wood carbohydrates are lost in the later stages of the delignification. Bublitz (7), Meier (8), and Thompson *et al.* (9) have all found that the polysaccharide fraction isolated from chlorite liquors contains galactose, glucose, and mannose. Only small amounts of arabinose and xylose were found in the chlorite liquor. As seen in Table 2 this is in reasonable agreement with the analysis of the carbohydrates remaining in the chlorite treated samples; there is a well-defined decrease in mannose and galactose with decrease in yield, while xylose and arabinose remain constant. The glucomannan content of the samples in Table 2 was estimated by assuming the value of 2.6 for the ratio mannose/glucose (17). Glucose not in glucomannan was taken to be cellulose; the remainder was assumed to be xylan and other sugars. In Fig. 2 the non-lignin portion has been subdivided into carbohydrate fractions by means of the data in Table 2. The fractions are cellulose, xylan plus other sugars (partly unanalyzed), and glucomannan plus galactan. This graphical representation illustrates clearly that the predominant loss in carbohydrates towards the end of the chlorite process is in glucomannan and galactan.

It has been suggested that hemicelluloses are difficult to extract from softwoods because of the protective action of lignin (18, 19). If this is so, the present results imply that removal of about 60% of the lignin is necessary before the carbohydrate fraction is exposed. A possible reason for preferential retention of xylan could be that in acidic processes the glucomannan is easily dissolved whereas the xylan is resistant to hydrolysis unless the p*H* is very low (20). A similar prefer-

Can. J. Chem. Downloaded from www.nrcresearchpress.com by 210.87.254.5 on 09/05/12
For personal use only.

ential removal of glucomannan has been noted by Erikson and Samuelson (21) in the bisulfite cooking of spruce wood.

At this stage we may comment on the excellent agreement between the analyses shown in Figs. 1 and 2 for the different forms of wood used. The agreement extends over the entire range of delignification studied. An average minimum dimension of the wood meal was about 0.04 mm compared with 0.3 mm for the shavings and 2 mm for the chips. Evidently in this range of dimensions there is a negligible effect of particle size on the chemistry of chlorite delignification and carbohydrate solubilization.

Concluding Remarks

Many physicochemical studies have been made of the important commercial pulping processes (22–27), but interpretation is often difficult because of the simultaneous removal of lignin and hemicellulose from the wood (20). The present investigation has shown that the chlorite process is selective in removing lignin from spruce wood during the first 60% of delignification. Beyond this point small quantities of glucomannan are dissolved together with the lignin. There is no doubt, however, that the selectivity of the chlorite procedure is much greater than conventional pulping processes and offers advantages for studies of physicochemical effects of "pure" delignification.

Subsequent research will deal with the dimensional changes of the cell wall, the macromolecular properties of the lignin, and the porous structure of the cell wall developed during chlorite delignification.

It is anticipated that a comparison of the results of such work with the corresponding behavior in kraft and sulfite pulping will further elucidate the physicochemical phenomena which are important in chemical pulping.

1. W. J. POLGLASE. *In* Advances in carbohydrate chemistry. **10**, 283 (1955).
2. W. G. CAMPBELL and I. R. C. MCDONALD. J. Chem. Soc. 2644 (1952).
3. B. L. BROWNING and L. O. BUBLITZ. Tappi, **36**, 452 (1953).
4. T. E. TIMELL. Pulp Pap. Mag. Can. **60**, T26 (1959).
5. L. E. WISE, M. MURPHY, and A. A. D'ADDIECO. Paper Trade J. **122** No. 2, 35 (1946).
6. W. G. CAMPBELL and I. R. C. MCDONALD. J. Chem. Soc. 3180 (1952).
7. W. J. BUBLITZ. Tappi, **34**, 427 (1951).
8. H. MEIER. Acta Chem. Scand. **14**, 749 (1960).
9. N. S. THOMPSON, R. E. KREMERS, and O. A. KAUSTINEN. Tappi, **51**, 123, 127 (1968).
10. T. E. TIMELL. Tappi, **44**, 88 (1961).
11. A. G. SCHÖNING and G. JOHANSSON. Sv. Papperstidn. **68**, 607 (1965).
12. V. LORÅS, and F. LØSCHBRANDT. Norsk Skogind. **10**, 402 (1956).
13. Swedish Forest Products Research Laboratory, Internal Standard, 1969.
14. N. SOMOGYI. J. Biol. Chem. **195**, 19 (1952).
15. E. SJÖSTRÖM, P. HAGLUND, and J. JANSON. Sv. Papperstidn. **69**, 381 (1966).
16. D. MARTH. Tappi, **42**, 301 (1959).
17. N. S. THOMPSON and O. A. KAUSTINEN. Pap. Puu, **47**, 637 (1964).
18. R. NELSON. J. Pol. Sci. **51**, 27 (1961).
19. T. E. TIMELL. *In* Advances in carbohydrate chemistry. **19**, 247 (1964).
20. S. A. RYDHOLM. Pulping processes. Interscience, New York, N.Y., 1965. p. 359–360.
21. E. ERIKSON and O. SAMUELSON. Sven. Papperstidn. **66**, 407 (1963).
22. W. Q. YEAN and D. A. I. GORING. Pulp Pap. Mag. Can. **65**, T127 (1964).
23. J. G. MCNAUGHTON, W. Q. YEAN, and D. A. I. GORING. Tappi, **50**, 548 (1967).
24. W. Q. YEAN and D. A. I. GORING. Sv. Papperstidn. **71**, 739 (1968).
25. A. SZABO and D. A. I. GORING. Tappi, **51**, 440 (1968).
26. J. E. STONE and A. M. SCALLAN. J. Pol. Sci. C11, 13 (1965).
27. J. E. STONE and A. M. SCALLAN. Pulp Pap. Mag. Can. **69**, T288 (1968).

Can. J. Chem. Downloaded from www.nrcresearchpress.com by 210.87.254.5 on 09/05/12
For personal use only.

Can. J. Chem. Downloaded from www.nrcresearchpress.com by 210.87.254.42 on 09/05/12
For personal use only.

A ^{19}F Nuclear Magnetic Resonance Study of Halogen Exchange between Antimony Pentafluoride and Inorganic Chlorides. Complexes of Antimony and Arsenic Pentafluorides with Carbonyl Fluoride

J. BACON, P. A. W. DEAN, AND R. J. GILLESPIE
Department of Chemistry, McMaster University, Hamilton, Ontario

Received July 31, 1970

^{19}F nuclear magnetic resonance (n.m.r.) has been used to study the reactions occurring in the systems $SbCl_5$–SbF_5–SO_2ClF, SO_2Cl_2–SbF_5–SO_2ClF, COF_2–SbF_5–SO_2ClF, COF_2–AsF_5–SO_2ClF, and COClF –SbF_5–SO_2ClF. Ionization occurs in $SbCl_5$–SbF_5–SO_2ClF, yielding antimony chloro- and chlorofluorocations and antimony polyfluoroanions. Donor–acceptor complexes are formed between SbF_5 and SO_2Cl_2, COF_2 or COClF at low temperatures and also between AsF_5 and COF_2. In all the complexes the ligand is oxygen-bonded. At higher temperatures halogen exchange and ionization occurs in SO_2Cl_2–SbF_5–SO_2ClF and COClF–SbF_5–SO_2ClF giving SO_2ClF and COF_2 complexes, respectively, together with antimony cations and polyfluoroanions. The alkyl chloride – SbF_5 reaction is also shown to give chlorine-containing cations of antimony.

La r.m.n. du ^{19}F a été utilisée pour l'étude des réactions se produisant dans les systèmes $SbCl_5$–SbF_5–SO_2ClF, SO_2Cl_2–SbF_5–SO_2ClF, COF_2–SbF_5–SO_2ClF, COF_2–AsF_5–SO_2ClF et COClF–SbF_5–SO_2ClF. Une ionisation se produit dans $SbCl_5$–SbF_5–SO_2ClF conduisant à la formation de cations chloro- et chloro-fluoroantimoine et d'anions polyfluoro antimoine. Des complexes donneur–accepteur sont formés entre SbF_5 et SO_2Cl_2, COF_2 et COClF à basses températures et aussi entre AsF_5 et COF_2. Dans tous les complexes le ligand est lié à l'oxygène. A plus haute température des échanges d'halogènes et des ionisations se produisent dans SO_2Cl_2–SbF_5–SO_2ClF et COClF–SbF_5–SO_2ClF donnant respectivement des complexes de SO_2ClF et COF_2 avec des cations d'antimoine et des anions polyfluorés. Il est démontré que la réaction entre un chlorure d'alkyle et SbF_5 donne cations de l'antimoine contenant du chlore.

Canadian Journal of Chemistry, 49, 1276 (1971)

As part of a continuing study of the chemistry of antimony pentafluoride, we have used ^{19}F n.m.r. to investigate its interaction with $SbCl_5$, SO_2Cl_2, COClF, and COF_2, generally in sulfuryl chlorofluoride as solvent, and we have used our results for these systems as a basis for reinterpretation of the alkyl chloride – SbF_5 reaction.

^{19}F n.m.r., electrical conductivity, and viscosity measurements have previously been made on homogeneous liquid phase mixtures of SbF_5 and $SbCl_5$, and the complexity of the system demonstrated (1). On addition of $SbCl_5$ to SbF_5, both the viscosity and specific electrical resistance dropped precipitously, reaching a minimum at a F/Sb ratio of *ca.* 3.5. The results for the fluorine-rich part of the system were interpreted in terms of the equilibrium [1] which involves ionization and formation of a polyfluoroanion or mixture of polyfluoroanions.

$$[1]\quad 4SbCl_5 + (5n+1)SbF_5 \rightarrow 5SbCl_4^+ + 5Sb_nF_{5n+1}^-$$

Definitive ^{19}F n.m.r. spectra of the polyfluoroanions were not observed, however, presumably due to the relatively high temperatures ($> -10°$) necessary to prevent crystallization in the system. More recent work (2–4) has shown that temperatures of $-60°$ or below are necessary to slow down the fluorine exchange of the polyfluoroanions to the point where fine structure is observed in the ^{19}F n.m.r. spectrum.

Results and Discussion

SbF_5–$SbCl_5$ Solutions in SO_2ClF

At room temperature the fluorine-on-antimony region of the ^{19}F n.m.r. spectrum of a solution with $SbCl_5/SbF_5/SO_2ClF = 1/4.45/21.8$ was a single broad line due to fluorine exchange. At low temperatures, however, fine structure was observed. Figure 1 shows the 94.1 MHz ^{19}F n.m.r. spectrum of the F-on-Sb region at $-106°$. The doublet *C* at ϕ104.0 can be attributed to the four equivalent fluorines in the 1:1 complex $SbF_5.SO_2ClF$; this resonance has previously been observed (5) at ϕ105.1. The quintet resonance expected for the single axial fluorine of this species is not observed but is expected to lie under the intense quintet *H*. Comparison with a previous study (4) of *t*-BuF–SbF_5–SO_2ClF and $(n\text{-Bu})_4NSbF_6$–SbF_4–SO_2ClF shows that resonances *B*, *D*, *E*, *F*, and *H*, arise mainly from fluorines F_3, F_5, F_2, F_4, and F_1, respectively, of the *cis*-$Sb_3F_{16}^-$ anion **1**. However, the

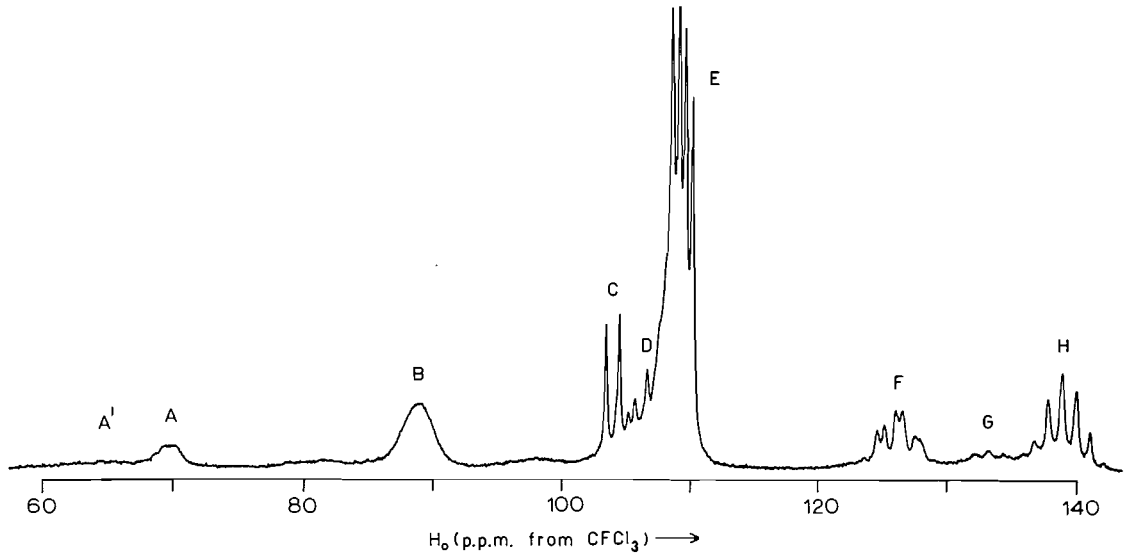

FIG. 1. The 94.1 MHz ^{19}F n.m.r. spectrum (F-on-Sb region only) of a solution with $SbCl_5/SbF_5/SO_2ClF$ = 1/4.45/21.8, at −106°.

broad quintet *G*, from F_1 of the $Sb_2F_{11}^-$ anion (**2**) can also be seen at ϕ133.4, and the asymmetry of the double-doublet *E* must be caused

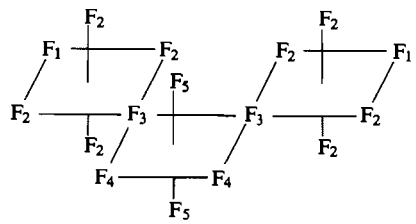

1

by partial overlap with the double-doublet resonance expected for F_2 of this anion. Likewise a minor part of the intensity of the resonance *B* is from F_3 of $Sb_2F_{11}^-$.

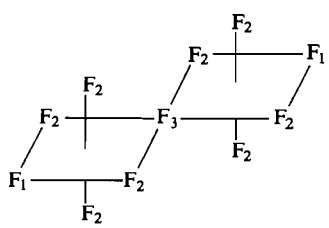

2

In the previous study (4) of the formation of the polyfluoroanions $Sb_nF_{5n+1}^-$ in SO_2ClF, it was shown that with increasing SbF_5 concentration $Sb_2F_{11}^-$ and then $Sb_3F_{16}^-$ are formed and are followed by the formation of both $Sb_4F_{21}^-$ and $SbF_5.SO_2ClF$, *i.e.*, $Sb_4F_{21}^-$ is solvolyzed to some extent according to the equation

$$Sb_4F_{21}^- + SO_2ClF \rightleftarrows Sb_3F_{16}^- + SbF_5.SO_2ClF$$

whereas solvolysis of $Sb_2F_{11}^-$ and $Sb_3F_{16}^-$ is negligible. Thus the observation of a small amount of $SbF_5.SO_2ClF$ in the spectrum in Fig. 1 indicates that a small amount of $Sb_4F_{21}^-$ is also formed.

The resonance *A*, at ϕ69.8, is not due to a polyfluoroanion or an SbF_5–SO_2ClF complex, and it seems most likely, therefore, that it arises from a fluorine-containing cation. There is a suggestion of a broad resonance *A'* to low field of *A* which is difficult to see in Fig. 1, but which is somewhat clearer in other spectra (*e.g.* it occurs at *ca.* ϕ65 in Fig. 2(*b*)).

In the fluorine-on-sulfur region of the ^{19}F n.m.r. spectrum, an intense sharp line due to the solvent is seen, together with another less intense sharp signal +396 Hz from the solvent line. The latter arises from SO_2ClF in $SbF_5.SO_2ClF$ (5), consistent with the observation of the remainder of the spectrum of this species in the F-on-Sb region.

Our results clearly support earlier evidence (1) for ionization in $SbCl_5$–SbF_5. It is unlikely, however, that the cation is solely $SbCl_4^+$ as indicated by reaction 1, since we observe ^{19}F

Can. J. Chem. Downloaded from www.nrcresearchpress.com by 210.87.254.42 on 09/05/12
For personal use only.

Can. J. Chem. Downloaded from www.nrcresearchpress.com by 210.87.254.42 on 09/05/12
For personal use only.

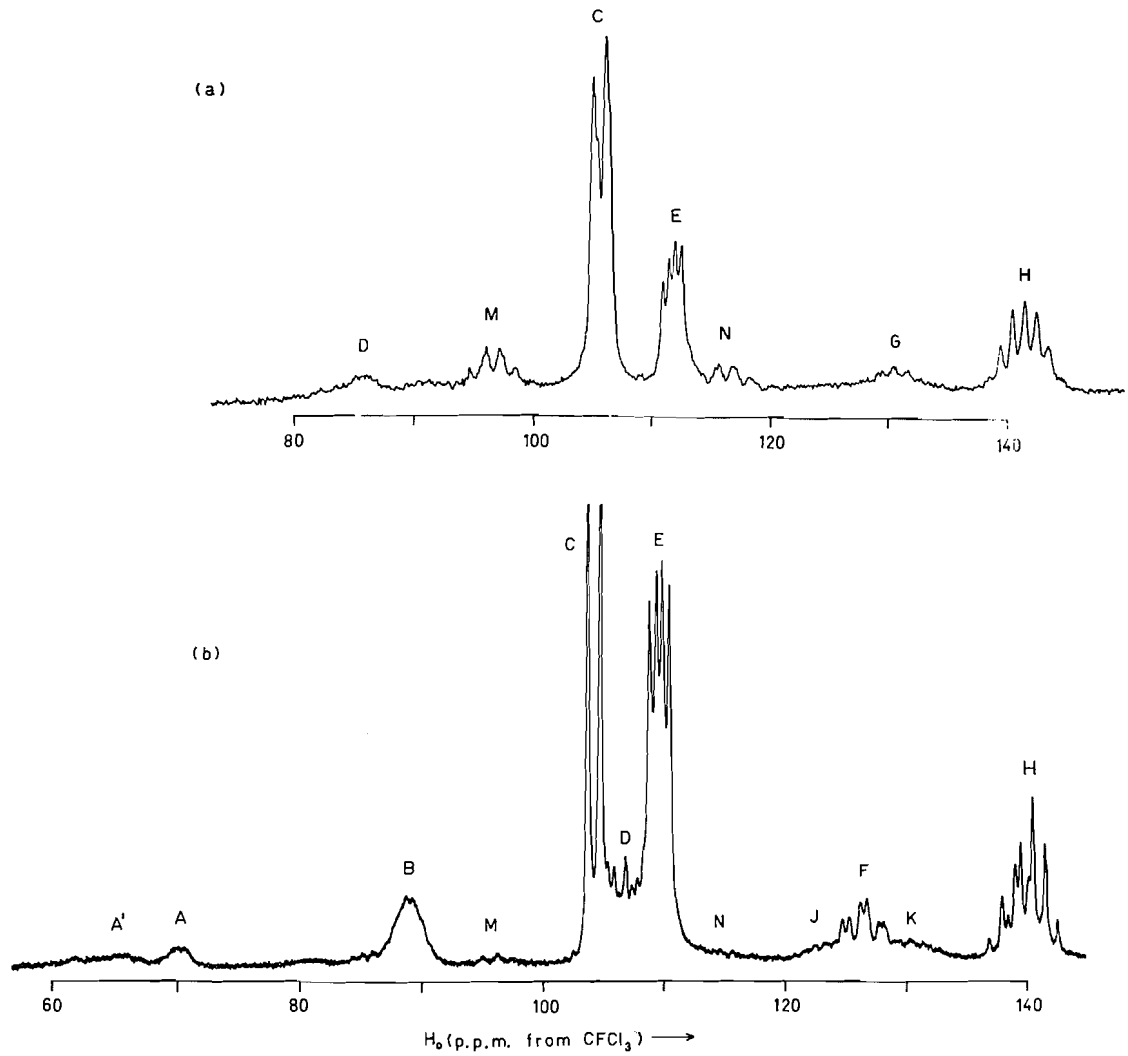

FIG. 2. The 94.1 MHz ^{19}F n.m.r. spectra (F-on-Sb region only) of a solution with $SO_2Cl_2/SbF_5/SO_2ClF$ = 1/1.61/5.09: (*a*) −75° spectrum after being kept at −23° or below; (*b*) −100° spectrum after standing at room temperature for 10 min.

n.m.r. signals which are very probably due to cationic species. We note that, assuming complete reaction according to [1], the stoichiometry of the solution leads to a value of 3.36 for n, the average number of antimony units in the polyfluoroanions. The n.m.r. spectrum in Fig. 1 shows that the amount of $SbF_5.SO_2ClF$, and presumably therefore also $Sb_4F_{21}^-$, is very small, suggesting a somewhat lower value for n. Reactions such as 2 and 3 produce chlorofluoro

[2] $3SbCl_5 + (5n + 2)SbF_5 \rightarrow 5SbCl_3F^+ + 5Sb_nF_{5n+1}^-$

[3] $2SbCl_5 + (5n + 3)SbF_5 \rightarrow 5SbCl_2F_2^+ + 5Sb_nF_{5n+1}^-$

cations and the occurrence of these would be consistent with the observation of ^{19}F n.m.r. signals from cations. The positions of *A* and *A'*, to relatively low applied fields, also support the suggestion that they arise from chlorofluoro species: the resonances of such species commonly lie to lower fields than those of their fully fluorinated analogs (6). If only reaction 2 occurred and this reaction was complete, the value of n would be 2.27 and similarly reaction 3

Can. J. Chem. Downloaded from www.nrcresearchpress.com by 210.87.254.42 on 09/05/12
For personal use only.

would lead to a value of 1.18 for n in the present solution; as noted above the observed spectrum shows $n \sim 3$. Thus reactions 2 and 3 appear to occur only to a minor extent. Our observations suggest the formation of a mixture of cationic species including $SbCl_4^+$ (which is probably the predominant cation) and chlorofluorocations of the type $SbCl_{4-n}F_n^+$. We tentatively assign resonance A' to $SbCl_3F^+$ and A to $SbCl_2F_2^+$. (The more chlorinated of the two species is expected to have a resonance at lower field (6).) The fluorine resonances of these cations are broad presumably due to relatively slow quadruple relaxation of the antimony nucleus in the quite symmetrical tetrahedral environment of the cations. A reasonable first step in the reaction of $SbCl_5$ and SbF_5 would be

$$SbCl_5 + nSbF_5 \rightarrow SbCl_4^+ + Sb_nF_{5n}Cl^-$$

but the reaction route from this initial cation-producing step to the final formation of the observed polyfluoroanions, $Sb_nF_{5n+1}^-$, must be complex.

SbF_5–SO_2Cl_2 Solutions in SO_2ClF

A solution of SbF_5 in SO_2Cl_2, allowed to stand for several hours at room temperature, provided good evidence for halogen exchange. Whilst it was not possible to attain low enough temperatures for observation of fine structure in the fluorine-on-antimony region of the ^{19}F n.m.r. spectrum, the room temperature spectrum showed a single line at $\phi - 99.9$ which is due to SO_2ClF.

A solution of composition $SO_2Cl_2/SbF_5/SO_2ClF = 1/1.61/5.09$ was prepared at low temperatures and homogenized at $-23°$. On cooling, a white solid quickly came out of the solution. It was possible, however, by rapid recording, to obtain the ^{19}F n.m.r. spectrum of the solution whilst crystallization was occurring. When the solution was cooled to $-75°$, the fluorine-on-sulfur region of the 94.1 MHz spectrum showed a sharp line from the bulk solvent and a second line due to $SbF_5.SO_2ClF$ 384 Hz upfield of the solvent line. The fluorine-on-antimony region of the spectrum is shown in Fig. 2(*a*). Though the resolution is not good owing to the conditions under which the spectrum was obtained, there are some features of interest. The signal C is comprised of two overlapping doublets at $\phi \sim 105.1$ and $\phi \sim 105.5$. One of these arises from the four equatorial fluorines in $SbF_5.SO_2ClF$, and the other must be due to the analogous fluorines in a 1:1 complex with oxygen-bonded SO_2Cl_2. The two quintets expected for these species make up part of the complex resonance H which is centered at $\phi \sim 142$. Because of the closeness of the chemical shifts we cannot make a definite assignment of either of the two AX_4 spectra to one or the other of the two possible species. In addition to the signals from the 1:1 complexes, the spectrum also shows the complex spectrum E, D, M, N, G previously shown (5) to be characteristic of neutral 2:1 SbF_5:base complexes of the type **3**. Signals E, D, M, N, and G at ϕ111.4, 85.1, 96.0, 115.9, and 130.4 are due to the fluorines F_2, F_3, F_5, F_6, and F_4, respectively. The signal

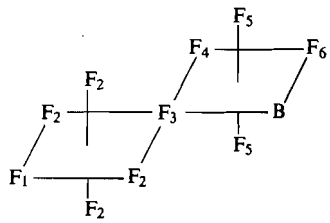

3

arising from F_1 is expected to occur in the region of H. The chemical shifts in the spectrum of the 2:1 complex are close to those reported (5) for $(SbF_5)_2.SO_2ClF$. Nevertheless, it seems unlikely that the latter species is formed, for the following reasons: (*i*) no signal attributable to SO_2ClF in $(SbF_5)_2.SO_2ClF$ is seen in the F-on-S region, whereas in SbF_5/SO_2ClF solutions of comparable dilution this signal is easily observed under the same conditions; (*ii*) in the F-on-Sb region E is a multiplet whereas in all comparable SbF_5/SO_2ClF solutions E was found to be a single line at the same temperature; (*iii*) SO_2Cl_2 is more basic than SO_2ClF: a complex $SbCl_5.SO_2Cl_2$ has been isolated at room temperature (7), whereas we have found no evidence from ^{19}F n.m.r. spectra for $SbCl_5$–SO_2ClF complexes even at very low temperatures. It is, therefore, more probable that E, D, M, N, G is the spectrum of a 2:1 SbF_5:SO_2Cl_2 complex; this spectrum is expected to resemble closely that of the analogous SO_2ClF complex. In this context it is noteworthy that the chemical shifts of the four equivalent fluorines in the 1:1 complexes $SbF_5.SO_2ClF$ and $SbF_5.SO_2Cl_2$ are very

Can. J. Chem. Downloaded from www.nrcresearchpress.com by 210.87.254.42 on 09/05/12
For personal use only.

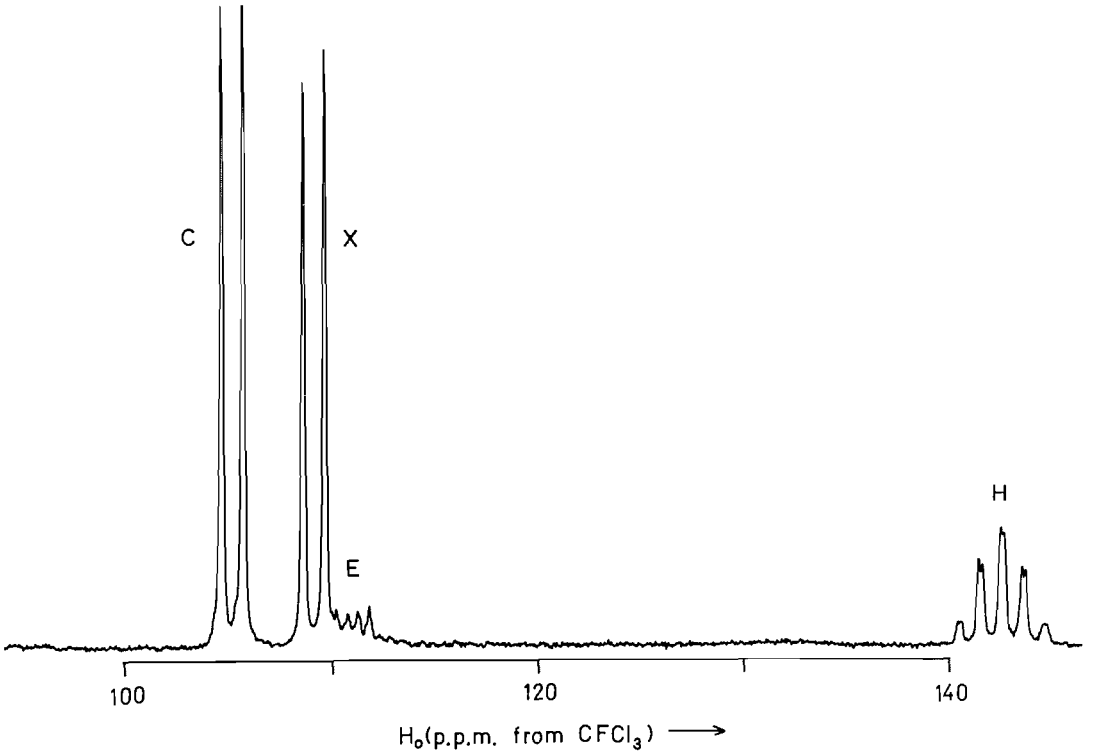

FIG. 3. The 94.1 MHz ^{19}F n.m.r. spectrum (F-on-Sb region only) of a solution with $COF_2/SbF_5/SO_2ClF$ = 1/2.17/10.0, at −100°.

similar: this chemical shift is as sensitive as any in either the 1:1 or 2:1 complexes to change in the donor (4).

The solution can be warmed to room temperature briefly and recooled with no change in the ^{19}F n.m.r. spectrum, but when it is allowed to stand at room temperature for 10 min, crystallization no longer occurs on cooling. The −100° 94.1 MHz ^{19}F n.m.r. spectrum at this time is as shown in Fig. 2(*b*). It differs considerably from the spectrum in Fig. 2(*a*) and there is a very obvious similarity to the spectrum in Fig. 1, the only apparent differences being the increased intensity of the doublet *C* due to $SbF_5.SO_2ClF$ in Fig. 2(*b*), and the apparent absence of any peaks due to $Sb_2F_{11}^-$ in this spectrum. In addition the resonances *J* and *K* are now seen on the low and high field sides of the signal *F*; these two resonances have previously been tentatively assigned (4) to fluorines F_6 and F_4 of *cis-cis*-$Sb_4F_{21}^-$ (**4**).

The small multiplets *M* and *N* can be assigned to F_5 and F_6 of $(SbF_5)_2.SO_2ClF$ (**3**). (These signals persist for weeks and hence cannot be due to the complex $(SbF_5)_2.SO_2Cl_2$, which, as noted above, has a very similar spectrum to $(SbF_5)_2.SO_2ClF$.)

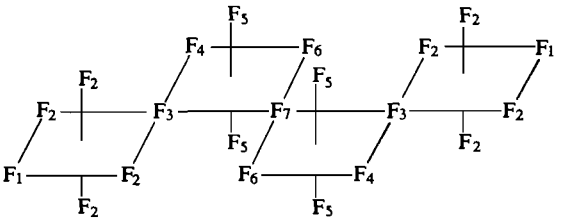

4

From the results above it is clear that in the cold solutions, donor–acceptor complexes of SbF_5 with O-bonded SO_2Cl_2 are formed. On warming, halogen exchange occurs, the SO_2Cl_2 being converted to SO_2ClF, and the chlorofluoro antimony species simultaneously formed ionize in a manner analogous to that which occurs in $SbCl_5$–SbF_5–SO_2ClF (reactions 1–3).

SbF_5–COF_2 Solutions in SO_2ClF

Fine structure is observed in the ^{19}F n.m.r. spectra of SbF_5–COF_2 solutions in SO_2ClF at

Can. J. Chem. Downloaded from www.nrcresearchpress.com by 210.87.254.42 on 09/05/12
For personal use only.

low temperatures. Figure 3 shows the fluorine-on-antimony region of a spectrum obtained from a solution with $COF_2/SbF_5/SO_2ClF$ = 1/2.17/10.0, when cooled to −100°. In addition to this spectrum and the solvent line, two lines are observed at +376 and +269 Hz from the solvent line (relative areas 10.5 and 1, respectively) which are attributable (5) to SO_2ClF bound in 1:1 and 2:1 complexes with SbF_5, and a relatively sharp singlet (half width ~18 Hz) is also seen at ϕ −2.1.

In the F-on-Sb region, the doublet *C* (chemical shift ϕ105.3; J_{F-F} = 98 Hz) is due to $SbF_5.SO_2ClF$, as is the more intense (lower field : ϕ142.5) of the two overlapping quintets *H*. The second doublet, X, (chemical shift ϕ109.2; J_{F-F} = 98 Hz) and the higher field (ϕ142.6) quintet constitute an AX_4 spectrum which must be due to a complex $SbF_5.OCF_2$, in which the carbonyl fluoride acts as a donor through oxygen. The multiplet *E* arises from the fluorines F_2 of the 2:1 complex $(SbF_5)_2.SO_2ClF$ (**3**), the observation of this spectrum being consistent with the presence of the line +269 Hz from the solvent line. In solutions with greater SbF_5/COF_2 ratios, larger amounts of SO_2ClF complexes occur, but we did not observe any spectrum attributable to a 2:1 SbF_5:COF_2 complex.

The singlet at ϕ −2.1 has an area half that of the doublet X and so results from the fluorine in the bound COF_2. At −65°, where fine structure is being lost in the F-on-Sb region, no signal is observed which could be due to F-on-C. (We presume it becomes too broad to see.) At higher temperatures the signal reappears, and at 25° is again quite sharp (~ 45 Hz half width) with a chemical shift ϕ14.3, much closer to the position of the signal from free COF_2 in SO_2ClF (ϕ19.6 in dilute SO_2ClF solution at −100°). The temperature dependent behavior of the F-on-C resonance shows increasing dissociation of $SbF_5.OCF_2$ with increasing temperature; the dissociation is incomplete even at 25°, however, since there is still a significant difference between the chemical shift of the COF_2 in the presence and absence of the pentafluoride at this temperature.

No change was observed in the n.m.r. spectra of the solutions even after standing for long periods at room temperature. Other than producing changes in resolution due to viscosity changes, changes in concentration were without significant effect on the spectra.

AsF_5–COF_2 Solutions in SO_2ClF

No fine structure was observed in the −100° ^{19}F n.m.r. spectrum of a solution with composition $COF_2/AsF_5/SO_2ClF$ = 1/2.0/4.0. In addition to the solvent line, a quite sharp (~ 16 Hz half width) signal from fluorine-on-arsenic was seen at ϕ49.4, together with a resonance due to COF_2 at ϕ5.2 (~ 12 Hz half width). The observation of a relatively sharp ^{19}F n.m.r. line from AsF_5 in the presence of a weak base has been shown (8) to indicate complex formation. By comparison with SbF_5–COF_2–SO_2ClF (above), the low field shift of the F-on-C signal relative to free COF_2, is also consistent with complexed COF_2 being present. This low field shift is not as great as in $SbF_5.OCF_2$, however, showing that complexing of the COF_2 by AsF_5 is most probably incomplete even at −100°.

As the temperature of the solution is increased there is a steady increase in the chemical shift of the F-on-C resonance (*e.g.* ϕ12.1 at −51°, 20.4 at 24°).

At room temperature the chemical shift is the same within experimental error as that of free COF_2 showing complete dissociation of the AsF_5–COF_2 complex (or complexes). Similar behavior is observed with AsF_5 and the weak base SOF_2 (8).

SbF_5–COClF in SO_2ClF Solution

A sample having $COClF/SbF_5/SO_2ClF$ = 1/2.9/3.1 was prepared by allowing COClF to distil into a cold (−63°) solution of SbF_5/SO_2ClF. A considerable amount of white solid formed immediately which could not be redissolved even at −23°. Outside the fluorine-on-antimony region, the 94.1 MHz fluorine spectrum of the supernatant liquid at −80° gave no resonance for COClF (ϕ −57.7 at 25° in SO_2ClF solution), but signals were observed at ϕ −2.1 and ϕ +17.7 (relative areas ~ 2 and 1) which, by comparison with $SbF_5/COF_2/SO_2ClF$ (above), can be attributed to co-ordinated and free COF_2. In addition, lines were observed from the solvent, and from SO_2ClF co-ordinated in $SbF_5.SO_2ClF$.

The fluorine-on-antimony region of the spectrum was complicated, but similar to Figs. 1 and 2(*b*). It showed resonances attributable to $SbF_5.SO_2$ (impurity), $SbF_5.SO_2ClF$, $(SbF_5)_2.SO_2ClF$, $Sb_2F_{11}^-$, and *cis*-$Sb_3F_{16}^-$. Also observed was a doublet (J_{F-F} ~ 95 Hz) centered on ϕ108.8 in the position expected for the signal

Can. J. Chem. Downloaded from www.nrcresearchpress.com by 210.87.254.42 on 09/05/12
For personal use only.

from the four equivalent fluorines in $SbF_5.OCF_2$ (see above). This resonance partly overlapped the signal from F_5 of *cis*-$Sb_3F_{16}^-$.

When a much more dilute solution was prepared ($COClF/SbF_5/SO_2ClF$ = 1/2.0/27) dissolution was complete at −63°. The −95° ^{19}F n.m.r. spectrum of this solution showed two equally intense doublet–quintet (AX_4) spectra. The first of these (chemical shifts: X, ϕ105.1; A, ϕ141.0, J_{F-F} = 96 Hz) arises from $SbF_5.SO_2ClF$ for which shifts of ϕ105.1 and ϕ141.8 are known (5). The second (chemical shifts: X, ϕ110.0; A, ϕ142.5, J_{F-F} = 96 Hz) cannot be due to $SbF_5.OCF_2$, since no signal from co-ordinated COF_2 was observed, and it must, therefore, show the presence of the complex $SbF_5.OCClF$. In agreement with this assignment, a resonance with intensity one quarter that of the ϕ110.0 doublet was observed at ϕ −59.9: this must result from co-ordinated COClF. This resonance is not seen in the spectrum of the sample having $COClF/SbF_5/SO_2ClF$ = 1/2.9/3.1 because all the COClF was converted to COF_2 in that solution. As for $SbF_5.SO_2Cl_2$ and $SbF_5.SO_2ClF$ (see earlier), the ^{19}F n.m.r. spectra of $SbF_5.OCClF$ and $SbF_5.OCF_2$ are very similar.

It is clear that, as in the case of SO_2Cl_2 and SbF_5, simple donor–acceptor behavior between SbF_5 and oxygen-bonded COClF occurs at low temperatures. At higher temperatures, however, halogen exchange occurs, the chlorofluoro-antimony species so produced ionizing in the manner demonstrated earlier for $SbCl_5/SbF_5$ to give a mixture of polyfluoroanions and chlorine-containing cations.

The Reaction of Alkyl Chlorides with SbF_5

Alkyl chlorides react with SbF_5 in SO_2 to produce carbonium ions (9) but there has been some controversy over the fate of the chlorine in this reaction. Olah *et al.* (9) suggested that the anion produced was SbF_5Cl^-. In a previous paper (3) we showed by ^{19}F n.m.r. that the anion was, in fact, $Sb_2F_{11}^-$, excess SbF_5 combining with the solvent to give $SbF_5.SO_2$; we suggested that the chlorine was present in some neutral species such as $SbF_4Cl.SO_2$ which precipitated from solution. Commeyras and Olah (10) used ^{19}F n.mr. to study the effect of adding HCl or alkyl chlorides to SbF_5/FSO_3H. The n.m.r. spectra of the solutions were complicated but very similar to those produced by adding HF or alkyl fluorides to SbF_5/FSO_3H. The authors therefore concluded that in the chloride solutions halogen exchange certainly occurred leading to anions of the type SbF_6^- and $Sb_2F_{11}^-$ more or less chlorine substituted, although they did not observe any n.m.r. signals assignable to these species. In view of the complex nature of the halogen exchange reaction occurring between SbF_5 and $SbCl_5$, SO_2Cl_2, or COClF, we have re-examined the evidence relating to the reaction of alkyl chlorides with antimony pentafluoride.

At −80° the 56.4 MHz ^{19}F n.mr. spectra of SO_2 solutions in which *t*-BuCl/SbF_5 = 1/5.5 or *t*-BuF/SbF_5 = 1/3.8 are very similar in the region above ϕ90 (3). Careful examination showed, however, that whilst in the latter mixture no signal was observed below ϕ90, the former shows two small broad singlets (half width 120 Hz) at ϕ71.8 and 79.9. At −50° the 56.4 MHz ^{19}F n.m.r. spectrum of the solution with $SbF_5/FSO_3H/HCl$ = 0.799/1/0.72 given in the work of Commeyras and Olah (10) also shows a low field broad line (ϕ ~ 84), which the authors labelled *H'* but did not comment on. The results given earlier, of our investigations into other systems which involve halogen exchange, provide evidence that the relatively low field lines observed in these two cases should be attributed to chlorofluorocations of antimony. Assigning these resonances to particular chlorofluoro-cations is somewhat difficult, as there may be a solvent dependence of the chemical shifts of the cations in the three solvents SO_2ClF, SO_2, and FSO_3H. We have previously reported solvent effects on the chemical shifts of the anions SbF_6^- and $Sb_2F_{11}^-$ in several systems (4). If we assume similar solvent effects in these anions and the chloro-fluoro-cations, then we can expect the difference in chemical shift between a particular cation and one of the anions, say $Sb_2F_{11}^-$, to be constant. The resonance in the fluorine spectrum of the solution having $SbF_5/FSO_3H/HCl$ = 0.799/1/0.72 which Commeyras and Olah label *H'* lies 31 p.p.m. below the "double-doublet" resonance of the eight equivalent fluorines of $Sb_2F_{11}^-$ in the same spectrum. The resonance at ϕ79.9 in the fluorine spectrum of our *t*-BuCl/SbF_5/SO_2 sample is 30 p.p.m. below the double-doublet resonance of $Sb_2F_{11}^-$ in the same spectrum, and can therefore be assigned to the same species. The resonance at ϕ71.8 in the spectrum of

Can. J. Chem. Downloaded from www.nrcresearchpress.com by 210.87.254.42 on 09/05/12
For personal use only.

t-BuCl/SbF_5/SO_2 is 38 p.p.m. below the double-doublet resonance, while resonance *A* in Fig. 1 of this work is about 39 p.p.m. below the same resonance in that spectrum, suggesting the same species in the two spectra. Since we expect that the resonances of the more highly chlorine-substituted cations will occur at lower field (6), the above analysis suggests that the SbF_5/FSO_3H/HCl solution of Commeyras and Olah contains $SbClF_3^+$ (ϕ84), that our *t*-BuCl/SbF_5/SO_2 solution contains $SbClF_3^+$(ϕ79.9) and $SbCl_2F_2^+$ (ϕ71.8), and that our $SbCl_5$/SbF_5/SO_2ClF solution contains $SbCl_2F_2^+$ (ϕ69.8) and $SbCl_3F^+$ (ϕ65).

We conclude that the reaction of alkyl chlorides with SbF_5 is more complicated than previously suspected. The reaction may be regarded as occurring in two steps: firstly, halogen exchange between the chloride and SbF_5 to give the alkyl fluoride together with antimony chloro- or chlorofluorocations and polyfluoroanions, and secondly, reaction of the alkyl fluoride with the polyfluoroanions to yield a carbonium ion and smaller polyfluoroanions.

Conclusions

Ionization occurs in $SbCl_5$/SbF_5 mixtures in SO_2ClF, polyfluoroanions, $Sb_nF_{5n+1}^-$, and chlorine-containing cations ($SbCl_4^+$ and probably $SbCl_3F^+$ and $SbCl_2F_2^+$) being formed. Evidence for ionization in mixtures of the pentachloride and pentafluoride has been given previously (1), but the nature of the ionization was not established with certainty.

At low temperatures both SO_2Cl_2 and COClF form donor–acceptor adducts (through oxygen) with SbF_5 in SO_2ClF, but at higher temperatures, halogen exchange and ionization occur, producing SO_2ClF and COF_2 adducts, together with a mixture of antimony cations and polyfluoroanions. It is not clear whether the low temperature complexes are intermediates in the halogen exchange process.

Both arsenic and antimony pentafluorides form donor–acceptor complexes with carbonyl fluoride in SO_2ClF. In contrast to the reactions of many acyl fluorides with SbF_5 (11), no ionization occurs in these solutions even at room temperature.

A re-examination of the evidence relating to the reaction of alkyl chlorides with SbF_5 shows that reaction to be more complex than hitherto supposed. In addition to carbonium ions and polyfluoroanions of antimony, chloro- and chlorofluorocations are among the reaction products.

Experimental

Nuclear Magnetic Resonance Spectra

These were obtained as described in earlier work (4).

Materials

Sulfuryl chlorofluoride was prepared by the method of Seel and Riehl (12). This and SbF_5 were purified as described previously (4). Sulfuryl chloride (Eastman Organic Chemicals) and antimony pentachloride (J. T. Baker Chemical Co.) were purified by vacuum fractionation. Carbonyl chlorofluoride (Ozark-Mahoning Co.) was vacuum distilled twice before use; the purified material showed only one ^{19}F n.m.r. resonance. The carbonyl fluoride (Matheson of Canada Ltd.) showed only one ^{19}F n.m.r. signal and was used without purification.

Sample Preparation

The basic methods of sample preparation have been described in earlier papers (3–5). For SbF_5/$SbCl_5$/SO_2ClF, SbF_5/SO_2Cl_2/SO_2ClF, and SbF_5/COF_2/SO_2ClF, the antimony compounds were added from all glass syringes to suitably adapted n.m.r. tubes under an inert atmosphere. Sulfuryl chloride was transferred in preweighed amount using a standard vacuum line; known amounts of SO_2ClF and/or COF_2 were added to the samples by gaseous volume. SbF_5/COClF/SO_2ClF samples were prepared by a method directly analogous to that used previously (4) for SbF_5/*t*-BuF/SO_2ClF mixtures. Low temperature homogenization of samples was achieved by stirring or shaking, the temperature being maintained by use of a suitable slush bath.

We thank the National Research Council of Canada for generous financial assistance. One of us (J.B.) thanks the National Research Council of Canada for the award of a studentship.

1. N. E. Aubrey and J. R. Van Wazer. J. Inorg. Nucl. Chem. **27**, 1761 (1965).
2. R. J. Gillespie and K. C. Moss. J. Chem. Soc. A, 1170 (1966).
3. J. Bacon, P. A. W. Dean, and R. J. Gillespie. Can. J. Chem. **47**, 1655 (1969).
4. J. Bacon, P. A. W. Dean, and R. J. Gillespie. Can. J. Chem. **48**, 3413 (1970).
5. P. A. W. Dean and R. J. Gillespie. J. Amer. Chem. Soc. **91**, 7260 (1969).
6. P. A. W. Dean and D. F. Evans. J. Chem. Soc. A, 1154 (1968).
7. I. Lindqvist and P. Einarsson. Acta Chem. Scand. **13**, 420 (1959).
8. M. Brownstein and R. J. Gillespie. J. Amer. Chem. Soc. **92**, 2718 (1970).
9. G. A. Olah, E. B. Baker, J. C. Evans, W. S. Tolgyesi, J. S. McIntyre, and I. J. Bastien. J. Amer. Chem. Soc. **86**, 1360 (1964).
10. A. Commeyras and G. A. Olah. J. Amer. Chem. Soc. **91**, 2929 (1969).
11. G. A. Olah and M. B. Comisarow. J. Amer. Chem. Soc. **88**, 4442 (1966).
12. F. Seel and L. Riehl. Z. Anorg. Allgem. Chem. **282**, 293 (1955).

Can. J. Chem. Downloaded from www.nrcresearchpress.com by 210.87.254.6 on 09/05/12
For personal use only.

Formation of Lower Nitro Alkanes by Vapor Phase Nitration of Cyclic Hydrocarbons

C. MATASA
IMNR Research Institute, Bucharest, Romania

AND

H. B. HASS
95 Fernwood Road, Summit, New Jersey

Received[1] July 17, 1969

Vapor-phase nitration of cyclohexane and cyclohexyl nitrite produces primary nitro alkanes, the yield of which decreases with decreasing number of carbon atoms. Both their structure and relative ratios of formation lead to the conclusion that they are formed from 1-pentyl radical, which in turn is formed from cyclohexoxyl radical. The intermediate phases are radical reactions already known from the vapor-phase oxidation of hydrocarbons.

La nitration en phase gazeuse du cyclohexane et du nitrite de cyclohexyle conduit à des nitroalcanes primaires avec des rendements qui diminuent lorsque le nombre d'atomes de carbone diminue. La structure et les quantités relatives de produits obtenus tendent à supposer que ces composés sont formés à partir du radical pentyle-1 qui proviendrait lui-même du radical hydroxycyclohexyle-1. Les phases intermédiaires seraient des réactions radicaliques déjà connues pour l'oxydation en phase gazeuse des hydrocarbures.

Canadian Journal of Chemistry, 49, 1284 (1971)

Introduction

The study of the formation of lower nitro alkanes produced by the nitration of a hydrocarbon (also called degradation nitro alkanes) is of interest from both theoretical and industrial point of view. It is well known that all the nitromethane and nitroethane now produced industrially are obtained by the nitration of propane. Different mechanisms have been proposed for the formation of these nitro derivatives by nitration of acyclic hydrocarbons under conditions where thermal cracking is avoided but none has been proved beyond doubt.

Omitting some mechanisms which have been previously rejected, *i.e.* the intermediate formation of alpha nitro acids (1), the oxidation or nitration of nitro derivatives initially formed, the addition of nitric acid to the hydrocarbon with the formation of a complex which is decomposed into nitro derivatives and alcohols (2), the following mechanisms are now considered as probable: (*A*) Breaking of the C—C bond of the hydrocarbon with simultaneous formation of two nitro derivatives (2)

$$R{-}CH_2{-}CH_3 + 2NO_2 \rightarrow R{-}CH_2{-}NO_2 + CH_3{-}NO_2$$

(*B*) Decomposition of alkyl nitrites with formation of nitric oxide and alkoxy radicals, the latter being decomposed to a lower alkyl radical and formaldehyde (3)

$$R{-}CH_2{-}CH_2\cdot + NO_2 \rightarrow R{-}CH_2{-}CH_2{-}ON{=}O$$
$$\xrightarrow{-NO} R{-}CH_2{-}CH_2O\cdot \rightarrow R{-}CH_2\cdot + CH_2O$$

(*C*) The intermediate formation of vicinal dinitro alkanes which react further to give aldehydes and lower nitro alkanes (4)

$$R{-}CH_2{-}CH_3 + 2NO_2 \rightarrow R{-}CHNO_2{-}CH_2NO_2 + 2HNO_2$$
$$R{-}CHNO_2{-}CH_2NO_2 \rightarrow R{-}CH{=}CHNO_2 + HNO_2$$
$$R{-}CH{=}CHNO_2 + H_2O \rightarrow RCHO + CH_3NO_2$$

The application of these mechanisms to the nitration of the branched or cyclic hydrocarbons can eliminate some possibilities. In fact, if for the linear hydrocarbons the formation of lower nitro alkanes can be explained by any of the foregoing mechanisms, for branched hydrocarbons, *e.g.* for neopentane, the two compounds which are identified, nitromethane and 2-nitro-2-methylpropane (5), lead to the *A* mechanism.[2]

The application of this mechanism to the nitration of cyclic hydrocarbons suggests the formation of α-ω-dinitro alkanes but these

[1]Revision received December 16, 1970.

[2]These products can also be explained, however, by mechanism *B* on the assumption that acetone rather than formaldehyde is the co-product (note added by Hass).

Can. J. Chem. Downloaded from www.nrcresearchpress.com by 210.87.254.6 on 09/05/12
For personal use only.

products have not been previously identified. For a long time it was considered that during the nitration of cyclic hydrocarbons in vapor phase, no opening of the ring took place, the lower nitro alkanes were not formed. (2, 6). Hass has repeated this assertion in his nitration rules. However, the presence of lower nitro alkanes in the reaction products obtained by the nitration of cyclic hydrocarbons was subsequently reported by some researchers. Quilico and Fusco (8) first reported that a mixture of nitro alkanes was obtained by the nitration of cyclohexane. Later the formation of nitropentane and nitrobutane was reported from the same nitration by Yasui and Yamada (9). The explanation for this has not been stated precisely.

In the following we propose to present the mechanism by which these lower nitro derivatives are obtained. We have considered cyclohexane to be the most appropriate hydrocarbon for this purpose because of the equivalence of its carbon atoms and the absence of strain in the ring.

Experimental

Raw Materials

Cyclohexane

A 99.8% cyclohexane, obtained by vapor-phase hydrogenation of benzene, was subjected to refining by sulfuric acid, washing with aqueous alkali, and then rectified.

Nitric Acid

Fifty percent analytical grade HNO_3 was used.

Cyclohexyl Nitrite

A 98% pure product was obtained from 99.5% cyclohexanol following Hunter and Marriott (11). The characteristics of the product were D_4^{20}, 0.990; n_D^{20} = 1.4430.

The Apparatus

The apparatus used is shown in Fig. 1. During a first series of experiments, nitric acid and liquid cyclohexane were introduced into the reactor using pumps made of stainless steel (Cr 18%, Ni 9%, Mn 2%, Si 1%), provided with polytetrafluoroethylene diaphragms. To prevent thermal decomposition of nitric acid before entering the reactor, the feed pipe was provided with an air-cooled jacket. The air flowing through the jacket was used to homogenize the bath surrounding the reactor, composed of a eutectic mixture of KNO_3 and $NaNO_3$. After evaporation and preheating at 400 °C by means of a stainless steel coil, cyclohexane was introduced at the base of the reactor where it met the nitric acid. The reactor (12), in the form of a truncated cone of stainless steel, was provided at its base with several U-tubes forming a thermosiphon system necessary to heat the inner salt bath composed also of an equimolar mixture of KNO_3 and $NaNO_3$. These melted salts were injected into the free

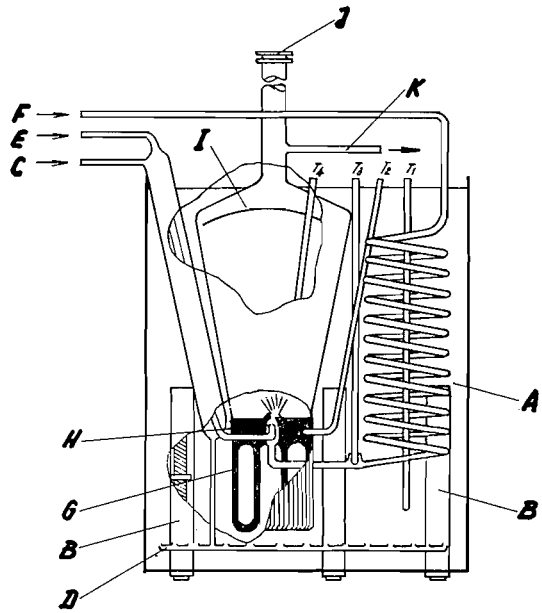

FIG. 1. The apparatus: *A*, molten salt thermostat; *B*, heating elements; *C*, air inlet for tube E cooling and molten salt agitation; *D*, perforated coil for air bubbling in the thermostat; *E*, nitric acid inlet; *F*, cyclohexane inlet; *G*, thermosiphon for heating molten salts; *H*, coaxial nozzles; *I*, baffles for separation of molten salt droplets; *J*, relief valve; *K*, outlet for reaction products.

space of the reactor through a concentric system of three nozzles. The first two were required for the cyclohexane and the nitric acid and the third for the salt.

The molten salt dispersion thus obtained acted as a heat transfer agent and, due to its wall effect, the oxidative chain reactions were greatly limited, at the same time having no effect on the nitration. The salts were then separated from the gases and returned on the wall to the thermosyphon system. The effluent gases were condensed and cooled to 5 °C by a brine condenser.

In a second series of experiments cyclohexyl nitrite was introduced together with nitric acid through the jacketed pipe. No cyclohexane was supplied.

(A) Cyclohexane Nitration

The nitration was carried out at 400 °C and atmospheric pressure; the reaction time was 1–1.1 s and the molar ratio cyclohexane/nitric acid was 2/1.

The condensate separated into two layers, the lower layer composed of water, some oxidation and nitration products, and a small quantity of nitric acid; the upper one composed of unreacted cyclohexane and the major part of the nitration and oxidation products. It was neutralized with a solution of 5% Na_2CO_3, washed and dried with anhydrous Na_2SO_4; the resulting solution of Na_2CO_3 and the aqueous layer were mixed together, adjusted to neutrality and extracted with ethyl ether. The residue obtained after distillation of the ether from the extract was added to the neutralized organic layer; the resulting mixture was extracted with a solution of

TABLE 1. Comparison of amounts of product of recovery

Product submitted to extraction with 10% NaOH solution	Acid used for recovery of nitro compounds	Refractive index of nitro compounds		Recovery, % by volume
		Before extraction	After extraction	
Pure nitrocyclohexane	10% H_2SO_4	1.4605	Impure	40–50
" "	95% CH_3COOH	1.4605	1.4603	96–97
" "	CO_2(gas)	1.4605	Nitrocyclohexane cannot be recovered	
90% Cyclohexane + 10% nitrocyclohexane	95% CH_3COOH		1.4600	95
Organic layer from cyclohexane nitration	95% CH_3COOH		1.4575–1.4535	96

10% $NaHCO_3$ to remove the fatty acids without solubilizing the nitro derivatives. The aqueous alkaline solution obtained as extract was subsequently extracted with ethyl ether; the ether layer was distilled and the residue added to the raffinate.

The organic mixture, freed from aliphatic acids, was then treated with a 10% aqueous solution of NaOH to convert the nitro derivatives to their salts, which were extracted in the aqueous layer. This was treated further with acetic acid to release the nitro derivatives; for a better separation NaCl was added. The tests performed showed a better recovery of nitrocyclohexane than those previously reported (over 95% *vs.* 74%) (14). An attempt to decompose the sodium salt of nitrocyclohexane with CO_2 did not succeed at atmospheric pressure. To the nitro derivatives thus obtained 1% boric acid was added, the mixture being subjected to a rectification at atmospheric pressure. The water and separate organic layer were continuously removed, the organic layer returned to the still and the aqueous layer extracted with ether to recover traces of organics which were added to the main part. The nitro compounds were distilled in an adiabatic column of the Podbielniak type having 10 theoretical plates. Nitromethane and nitroethane were distilled at atmospheric pressure, the higher homologs at 25 mm over nitrogen.

(B) Nitration of Cyclohexyl Nitrite

The nitration was carried out under the same conditions as for cyclohexane, the molar ratio of cyclohexyl nitrite to nitric acid being 2:1. The product was worked up in the manner already described.

Results

Table 1 presents a comparison of recovery obtained by extraction with NaOH and the subsequent treatment with acids of pure nitrocyclohexane, its synthetic mixtures and of the organic layers obtained by nitration. The following lower nitro alkanes were obtained by rectification of the nitration products of either cyclohexane or cyclohexyl nitrite: 1-nitropentane, 1-nitrobutane, 1-nitropropane, and nitroethane. Small quantities of nitromethane were found in the nitration product of cyclohexane.

Table 2 presents the relative weight range between the nitro alkanes obtained in both nitrations as well as their properties. In addition, a color identification was done with Meyer's reagent.

Discussion

The fact that primary nitro alkanes comprise almost the entire fraction of lower nitro alkanes obtained in the nitration of cyclohexane, and that the ratios of formation from two homologs are near halves for each decrease of one carbon atom (see Table 2) indicate that all these products are derived from 1-pentyl radical, initially formed by mechanism *B*.

The radical 1-pentyl can arise from the radical cyclohexoxyl, whose formation from cyclohexyl nitrite can readily be deduced.

This hypothesis is confirmed by the nitration of cyclohexyl nitrite in which both the identity and the ratios of lower nitro alkanes are the same as in the nitration of cyclohexane. Except for the mononitro alkanes already discussed,

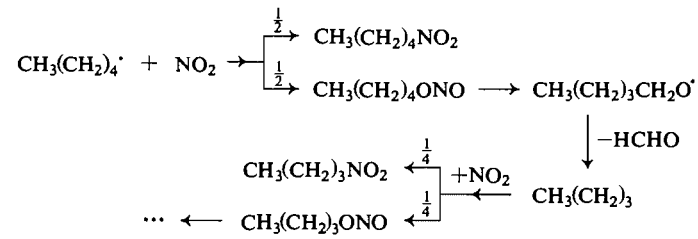

Can. J. Chem. Downloaded from www.nrcresearchpress.com by 210.87.254.6 on 09/05/12
For personal use only.

Can. J. Chem. Downloaded from www.nrcresearchpress.com by 210.87.254.6 on 09/05/12
For personal use only.

TABLE 2. Properties of nitration products

	Cyclohexane nitration					Cyclohexyl nitrate nitration					
Nitro compound (col. 1)	Distilled volume (ml) (col. 2)	Relative weight ratio (col. 3)	b.p./ (mm Hg) (col. 4)	D_4^{20} (col. 5)	n_D^{20} (col. 6)	Distilled volume (ml) (col. 7)	Relative weight ratio (col. 8)	b.p./ (mm Hg) (col. 9)	D_4^{20} (col. 10)	n_D^{20} (col. 11)	Ratio (col. 3) (col. 8)
Nitrocyclohexane	1200	150	98–99/25	1.0681	1.4620	—	—	—	—	—	—
1-Nitropentane	190	23.8	75–76/25	0.9480	1.4195	70	5	74/25	0.949	1.4200	4.77
1-Nitrobutane	100	12.6	56–57/25	0.9675	1.4102	35	2.5	55/25	0.9670	1.4100	5.0
1-Nitropropane	40	5	43–44/25	1.003	1.4015	14	1	42/25	—	1.4010	5
Nitroethane	18	2.25	114–5/760	1.052	1.3916	Traces	—	112–114/760	—	1.3920	—
Nitromethane	8	1	101–2/760	—	1.3818	—	—	—	—	—	—

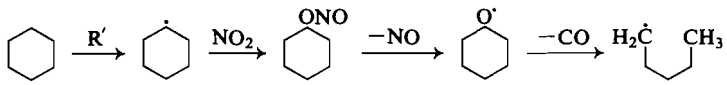

no other nitrogen-containing compounds were found in the distillate.

It is now possible to eliminate mechanisms *A* and *B* for the nitration of cyclohexane. The breakdown mechanism of the cycle can now be explained on the basis of literature on the vapor-phase oxidation of cyclohexane. The rupture of the ring of the cyclohexane radical with formation of 1-pentyl radical requires only 1.7 kcal/mol (15). The formation of 1-pentyl radical from cyclohexoxyl radical has already been described (16), the decomposition occurring through the intermediate formation of the radical shown.

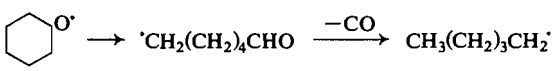

Such intermediates are commonly formed in the decomposition of hydroperoxides. This decarbonylation can probably take place after an internal hydrogen abstraction, as in other cases described even for cyclohexane derivatives (15), studies which were carried out using labeled oxygen in the cyclohexane oxidation have shown that nearly all the carbon oxide formed results from carbonyl compounds (17).

Another route can be the oxidation of the cyclohexoxyl radical or of carboxylic intermediates, followed by a decarboxylation (as described by Tipper for lower alkyl radical formation in cyclopentane oxidation) (18). In the case of cyclohexane nitration this route seems less probable due to the relatively small quantities of carbon dioxide which can be formed. It is interesting to show that the preceding arguments are supported also by the nitration of other substances having weak bonds. In these cases the nitro alkanes which can be formed are principally the primary ones.

This fact is confirmed by the results obtained by Hass and Hudgin (19) in the nitration of *n*-butyl ether. Both the structure of the nitro alkanes formed and their relative ratios show that the 1-butyl radical was initially formed.

The traces of secondary nitropentane which were found in the reaction mixture can arise from a vapor-phase isomerization of the 1-pentyl radical.

Examination of the foregoing data shows that for vapor-phase nitration of cyclo alkanes the formation of lower nitro alkanes can be explained by mechanism *B*, with the aid of certain radical reactions already known from oxidation studies.

1. H. B. Hass, E. B. Hodge, and B. M. Vanderbilt. I.E.C. **28**, 339 (1936).
2. H. B. Hass and E. F. Riley. Chem. Rev. 373 (1936).
3. G. B. Bachman, L. M. Addison, J. V. Hewett, L. Kohn, and A. Millikan. J. Org. Chem. 906 (1952).
4. T. Slebodzinski, J. Bimer, and D. Salbut. Przemysl Chemiczny, No. 1, Jan. 1962. pp. 18–20.
5. A. P. Howe and H. B. Hass. I.E.C. **38**, 251 (1946).
6. T. Urbanski and M. Slon. Roczniki Chem. **17**, 161 (1937).
7. H. B. Hass and H. Shechter. I.E.C. **39**, 817 (1947).
8. A. Quilico and R. Fusco. La Chimica e l'Industria, 5–6, 135 (1948).
9. E. Yasui and T. Yamada. Kogyo Kagaku Zasshi, **60**, 56–58 (1957).
10. I. Velea, I. Drimus, C. Matasa, and C. Cristescu. Rev. de l'Institut Francais du Petrole, XIX No. 2, Feb. 1964. p. 281.
11. L. Hunter and J. A. Marriot. J. Chem. Soc. 285 (1936).
12. I. Drimus, C. Matasa, and M. Klang. U.S.P. **3**, 115, 527 (1963).
13. I. Drimus, I. Velea, C. Matasa, and C. Cristescu. U.S.P. **3**, 173, 961 (1965).
14. N. Kornblum. J. Amer. Chem. Soc. **73**, 4041 (1951).
15. P. Gray and A. Williams. Chem. Rev. 239 (1959).
16. R. Guedj and J. Jullien. Bull. Soc. Chim. France, 1501 (1964).
17. A. B. Nalbandian *et al.* Radioisotopes Sci. Res. Proc. International Conf. Paris 1957. **27**, 72 (1958).
18. C. F. H. Tipper. Quart. Rev. Chem. Soc. London, **11**, 313 (1957).
19. H. B. Hass and D. E. Hudgin. J. Amer. Chem. Soc. **76**, 2692 (1954).

Can. J. Chem. Downloaded from www.nrcresearchpress.com by 210.87.254.6 on 09/05/12
For personal use only.

Can. J. Chem. Downloaded from www.nrcresearchpress.com by 210.87.254.6 on 09/05/12
For personal use only.

Infrared and Raman Spectroscopic Studies of Solid Alkali Metal Nitrites

M. H. BROOKER[1] AND D. E. IRISH
Department of Chemistry, University of Waterloo, Waterloo, Ontario

Received July 2, 1970

Infrared and Raman spectra of solid $LiNO_2.H_2O$, $LiNO_2$, $NaNO_2$, KNO_2, and $CsNO_2$ are presented and discussed. Pronounced changes in the spectra of $LiNO_2.H_2O$ during dehydration to anhydrous $LiNO_2$ are interpreted as evidence for an ordered distribution of NO_2^- ions over two non-equivalent sites (akin to linkage isomerism) in anhydrous $LiNO_2$. The frequencies of the internal modes of the nitrite ion shift to lower values with increasing cation size. Vibrational bands due to nitrate ion present as an impurity are assigned.

Les spectres infrarouge et Raman des $LiNO_2.H_2O$, $LiNO_2$, $NaNO_2$, KNO_2 et $CsNO_2$ sont présentés et discutés. Les changements prononcés qui se produisent dans les spectres pendant la déshydratation du sel $LiNO_2.H_2O$ à $LiNO_2$ sont interprétés comme preuve d'une distribution ordonnée des ions NO_2^- sur deux sites non équivalents (véritable isomérisme de liaison) dans le sel anhydre $LiNO_2$. Les fréquences des modes internes de l'ion nitrite sont abaissées lorsque la dimension du cation augmente. Les bandes vibrationnelles dues à l'ion nitrate présent comme impureté sont assignées.

Canadian Journal of Chemistry, 49, 1289 (1971)

Introduction

An interest in the vibrational spectra of concentrated electrolyte solutions and in N—O vibrations of ions similar to nitrate (1) has recently caused us to focus attention on metal nitrites, many of which are extremely water soluble. When interpreting data for concentrated solutions and melts, knowledge about the probe ion in static, cationic environments is an asset. Although $NaNO_2$ has been extensively studied and KNO_2 to a lesser extent (2–17), no systematic comparison including other alkali metal nitrites has been reported. In this study Raman spectra and multiple internal reflectance (m.i.r.) infrared spectra of powders have been obtained. The m.i.r. technique is particularly useful for disclosing features of intense absorption bands, the positions of which are not distorted by contributions from longitudinal optical (l.o.) modes or Christiansen filter effects (18). An interesting consequence of this study has been the observation of spectral changes on dehydration of the lithium nitrite monohydrate which can be attributed to a reorientation of nitrite ions into an ordered distribution over two non-equivalent orientations in the coordination sphere of the lithium (linkage isomerism).

The nitrites of lithium, potassium, and caesium are extremely hygroscopic. Lithium nitrite crystallizes from aqueous solution as a monohydrate which may be dehydrated at 110 °C but is reported to decompose at 200 °C before melting at 225 °C (19). The solid potassium and caesium nitrites take the form of unmanageable plastics with variable amounts of water; however, definite hydrates of these salts are not known (19, 20). Sodium nitrite, on the other hand, forms well defined single crystals. The discovery by Strijk and MacGillavry (21) of the ferroelectric phase transition in $NaNO_2$ prompted considerable infrared (12–15) and Raman (16, 17) spectral studies, most of which have been performed on single crystals and concerned with various phenomena associated with order–disorder ferroelectrics.

An important consideration prior to the measurement of the physical properties of nitrites must be sample purity. The assay of commercial reagent grade KNO_2 varies from 89 to 97% nitrite; even $NaNO_2$ seldom exceeds 98% minimum nitrite assay. Usual impurities are H_2O, OH^-, Cl^-, CO_3^{2-}, and NO_3^-; of these the NO_3^- is most serious. Potassium nitrite is known to form a solid solution with NO_3^- and consequently is extremely difficult to purify (19, 22, 23). In infrared studies of nitrite-doped alkali halides, vibrational bands due to NO_3^- were also observed (9–11). Kato and Rolfe (9) reported inability to obtain an infrared spectrum of NO_2^- in an alkali halide pellet without also observing vibrational bands due to NO_3^-. Sato *et al.* (12) observed the ν_2 vibration of NO_3^- *ca.* 840 cm^{-1} in the infrared spectrum of single crystal $NaNO_2$.

In a recent publication (23), bands present in the spectrum of KNO_2 which previously had

[1]Present address: Oak Ridge National Laboratory, Oak Ridge, Tennessee 37830.

TABLE 1. Vibrational frequencies (cm^{-1}) for $NaNO_2$, KNO_2, and $CsNO_2$

$NaNO_2$		KNO_2		$CsNO_2$		
Infrared	Raman	Infrared	Raman	Infrared	Raman	Assignments
829 (m, sp)	829 (m, sp)	806 (m, sp)	806 (m, sp)	803 (m, sp)	803 (m, sp)	ν_2 (A_1) NO_2^-
810 (w)	810 (w)*					ν_2 $^{14}N^{16}O^{18}O^-$
840 (w)		837 (vw)		835 (w)		ν_2 (A_2'') NO_3^- impurity
	1068 (w)		1058 (w)		1054 (w)	ν_1 (A_1') NO_3^- impurity
1230 (vs)	1232 (w, br)	1225 (vs)	1240 (br)	1210 (vs)	1230 (br)	ν_3 (B_2) NO_2^-
1322 (w)	1329 (vs, sp)		1322 (vs, sp)		1317 (vs, sp)	ν_1 (A_1) NO_2^-
		1390 (w)		1375 (w)		ν_3 (E') NO_3^- impurity

*The Raman intensity ratio of bands at 810 and 829 cm^{-1} is within experimental error of the predicted ratio 0.00413 on the basis of natural isotopic abundance of ^{18}O. Abbreviations: s, strong; m, medium; w, weak; sp, sharp; br, broad; sh, shoulder; v, very.

been incorrectly attributed to the NO_2^- ion perturbed by ionic interactions were reassigned to NO_3^- present as an impurity. Infrared and Raman methods of analyses for small amounts of NO_3^- in NO_2^- were advanced. Evidence for NO_3^- impurity in nitrite complexes has also been reported (24). Vibrational bands due to NO_2^- are thus assigned with full knowledge of NO_3^- impurity.

Experimental

Chemicals used were all high purity reagent grade. KNO_2 and $NaNO_2$ were Baker and Adamson 95 and 98% minimum nitrite assay, respectively. $Ba(NO_2)_2$ was supplied by Alfa Chemicals and listed at 97–99% nitrite assay. British Drug House reagent grade K_2SO_4, Cs_2SO_4, and AnalaR Li_2SO_4 were used as received. $NaNO_2$ and $Ba(NO_2)_2$ were recrystallized from aqueous solution. KNO_2 was purified by the ion exchange method of Ray (20), using Dowex 3-X8, 50–100 mesh anion exchange resin. Pure KNO_2 was also prepared by stoichiometric addition of K_2SO_4 to $Ba(NO_2)_2$ followed by filtration to remove insoluble $BaSO_4$. $LiNO_2$ and $CsNO_2$ were prepared in a similar manner from Li_2SO_4 and Cs_2SO_4. The potassium, lithium, and caesium salts were subsequently recrystallized from aqueous solution. The lithium salt crystallizes as the stable monohydrate, $LiNO_2.H_2O$. Anhydrous $LiNO_2$ was obtained by carefully drying the hydrate in the oven at 110 °C. Reconversion to the hydrate occurred slowly if the sample was left open to the atmosphere. The removal of 1 mol of water was confirmed by weight loss. $LiNO_2$, $NaNO_2$, KNO_2, and $CsNO_2$ were dried and stored in an oven at 110 °C. $LiNO_2.H_2O$ was used as recrystallized from aqueous solution. Analyses for nitrate by methods described previously (23) gave NO_3^- to NO_2^- ion ratios of 0.0054, 0.0031, 0.001, and 0.0002 for $CsNO_2$, $LiNO_2$, KNO_2, and $NaNO_2$, respectively. The solid powders except for $LiNO_2.H_2O$ were loaded into the sampling devices while still in the oven, sealed and allowed to cool in a desiccator over P_2O_5.

Raman spectra, excited by the 4358 Å mercury line of a "Toronto" lamp were obtained from powdered samples in a thermostated (25 °C) conical cell sealed from the atmosphere and were recorded on a Cary 81 spectrophotometer as described previously (25). Raman spectra from powders in a sealed capillary tube, excited by the 4880 Å line of the Spectra Physics 141 Argon ion laser, were recorded on the Jarrell-Ash model 25-300 Raman spectrometer. Frequency agreement between the two methods was excellent. Spectra recorded on the Jarrell-Ash instrument were obtained at the ambient temperature of the sample compartment (25 °C). Similarities between spectra recorded by both methods indicate no evidence of heating or decomposition of the samples by the laser beam. Further, the invariance of the relative intensities of nitrate and nitrite bands indicates that the samples were stable even in the laser beam. Spectra recorded on the Jarrell-Ash instrument were superior in quality. Vibrational bands of low intensity were only detected by the laser Raman method.

Infrared spectra were obtained from powdered solids pressed against the surface of a KRS-5 prism cut with a face angle of 60° and placed in the Wilks-model 9 m.i.r. attachment. Multiple internal reflectance spectra were recorded with a Beckman IR-9 operated at 3 times the "standard" program slits. The double beam mode was employed with some reference beam attenuation. Infrared spectra were recorded at the temperature of the infrared beam *ca.* 30 °C. The sample compartment of the IR-9 was purged with dry air and desiccated with P_2O_5. The extreme weakness of the water vapor bands *ca.* 1600 cm^{-1} attested to the dryness of the sample compartment. Infrared spectra were also recorded of Nujol mulls of $LiNO_2.H_2O$, anhydrous $LiNO_2$, and solids at intermediate stages of dehydration as well as for the other nitrites. Frequencies obtained by the two different infrared methods were identical in the 800–900 cm^{-1} region. In the 1200–1500 cm^{-1} region, bands due to the mulling agents complicated the infrared spectra and caused considerable uncertainty in the nitrite frequencies. The frequencies measured by m.i.r. methods are reported for this region since they are more reliable. The uncertainties for the reported infrared and Raman frequencies are expected to be ± 1 cm^{-1} for sharp peaks (ν_1 and ν_2) and ± 5 cm^{-1} for broad bands (ν_3).

Results

Infrared m.i.r. spectra of the solid alkali metal nitrites are shown in Fig. 1. A portion of the Raman spectrum of $NaNO_2$ is shown in Fig. 2. Portions of the infrared and Raman spectra of $LiNO_2.H_2O$, $LiNO_2$, and a partially dehydrated

Can. J. Chem. Downloaded from www.nrcresearchpress.com by 210.87.254.6 on 09/05/12
For personal use only.

Can. J. Chem. Downloaded from www.nrcresearchpress.com by 210.87.254.6 on 09/05/12
For personal use only.

sample of the salt are also shown (Fig. 3). Vibrational frequencies are collected in Tables 1 and 2. Except for anhydrous $LiNO_2$, the internal vibrations of the nitrite ion give rise to only three nearly coincident infrared and Raman bands.

Vibrational frequencies shift to lower values with increasing cation mass (Tables 1, 2). The symmetric stretching vibration $\nu_1(A_1)$, *ca.* 1330 cm^{-1}, is intense and polarized (*e.g.* see refs. 5, 16, 17, 23) in the Raman spectrum; it is weak in the infrared spectrum. The antisymmetric stretching vibration $\nu_3(B_2)$, *ca.* 1230 cm^{-1}, exhibits strong infrared absorbance but in the Raman spectrum the intensity is low. In the infrared spectra ν_3 absorbs strongly and masks ν_1 in the spectra of KNO_2 and $CsNO_2$ (Fig. 1). Dehydration of $LiNO_2.H_2O$ is accompanied by intensity decrease for bands at 1710, 1310, 857, 134, and 92 cm^{-1}, and intensity increase for bands at 1360, 1273, 872, 842, 335, 310, 170, and 86 cm^{-1} while bands at 1352, 126, and 70 cm^{-1} appear relatively constant (Fig. 3, Table 1). The dehydration process and the spectroscopic manifestations were observed to be reversible even after several dehydrations and no decomposition of nitrite was apparent.

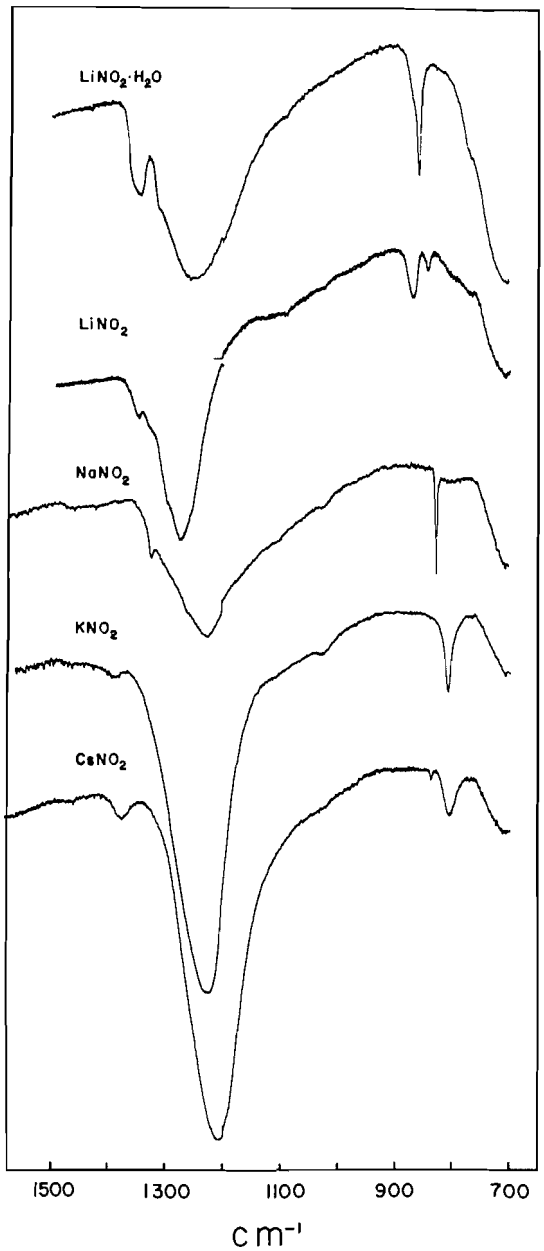

FIG. 1. Photographs of m.i.r. infrared spectra obtained from powdered-solid phase $LiNO_2.H_2O$, $LiNO_2$, $NaNO_2$, KNO_2, and $CsNO_2$.

Discussion

Weak bands *ca.* 835 and 1380 cm^{-1} in the infrared spectra and *ca.* 1050 cm^{-1} in the Raman spectra are due to the $\nu_2(A_2'')$, $\nu_3(E')$, and $\nu_1(A_1')$ modes, respectively, of NO_3^- present as an impurity (23). The frequencies are similar to but not exactly those found for the solid alkali metal nitrates (25, 26). Band intensities are in agreement with the known NO_3^- concentration in the alkali metal nitrite salt. It is possible that NO_3^- contributes to the band *ca.* 1350 cm^{-1} in the infrared spectrum of the lithium salts but it is extremely unlikely to be sole cause of this band. Note that a comparison of spectra of the lithium salts to the caesium salt (Fig. 1) provides a way to estimate the intensity of the NO_3^- band in $LiNO_2$.

The data for Na, K, and Cs nitrites are collected in Table 1 for comparison purposes. Assignments for $NaNO_2$ have previously been made (15, 17). Since the crystal is orthorhombic, space group C_{2v}^{20}–Im_2m_1 with two molecules per unit cell but one molecule per primitive cell (27–30) and since the nitrite ion is on a C_{2v} site, factor group analysis predicts three internal modes $2A_1(I,R) + B_2(I,R)$ and six external modes $A_1(I,R)$, $A_2(R)$, $2B_1(I,R)$, $2B_2(I,R)$. In the absence of crystal data to support any major departure from this analysis for K and Cs nitrites, the internal mode assignments (which are also the "free" ion assignments) are adopted for all

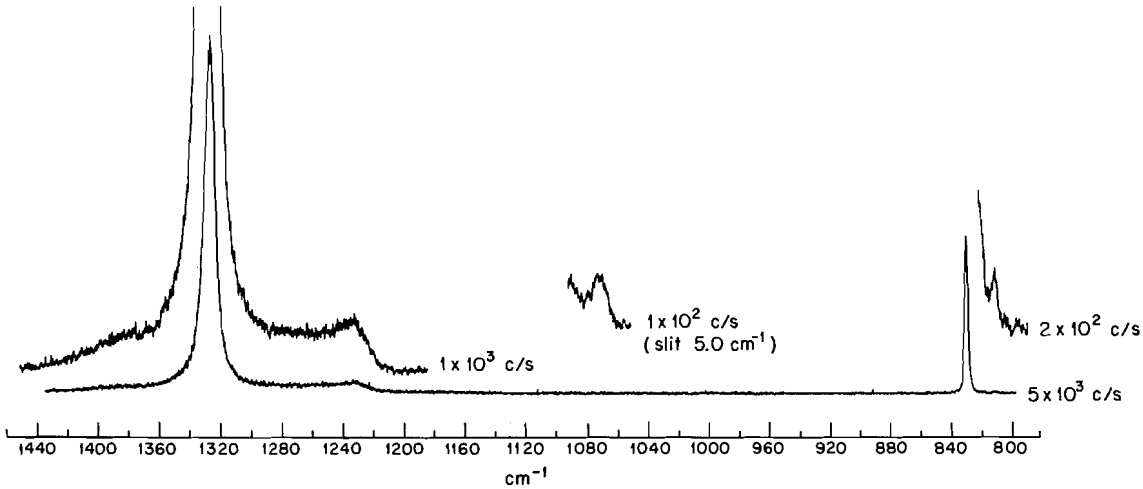

FIG. 2. A portion of the Raman spectrum of $NaNO_2$ obtained on the Jarrel-Ash model 25-300 Raman spectrometer after excitation with the 4880 Å Argon ion line. Slit width 2.0 cm^{-1} except where noted. Weak bands at *ca.* 810 and 1050 cm^{-1} are due to $^{14}N^{16}O^{18}O^-$ and NO_3^-, respectively.

TABLE 2. Vibrational frequencies (cm^{-1}) for $LiNO_2.H_2O$ and $LiNO_2$

$LiNO_2.H_2O$		$LiNO_2$		
Infrared	Raman	Infrared	Raman	Assignments
	72 (s, sp)		70 (m, sp)	
	84 (w, sh)		86 (s, sp)	
			92 (sh)	
	100 (m, sp)			
	118 (s, sp)			
			126 (m, sp)	
	134 (m, sp)			
	175 (m, br)		170 (s, sp)	
			310 (sh)	
			335 (w, br)	
		842 (m, sp)	842 (m, sp)	Nitro Linkage } ν_2
857 (m, sp)	857 (m, sp)			
		872 (m, sp)	872 (m, sp)	Nitrito Linkage }
	1070 (w)		1070 (w)	ν_1 (A_1') NO_3^- impurity
1260 (vs, br)		1275 (vs)	1273 (m, sp)	ν_3 NO_2^-
1310 (sh)	1310 (m, sp)			?
1348 (m)	1350 (s, sp)	1350 (w)	1352 (vs, sp)	} ν_1 NO_2^-
			1360 (sh)	
1710 (m, br)				ν_2 H_2O

the crystals except $LiNO_2$. The external modes of $NaNO_2$ observed in this work reproduce those in the literature; they are 122 (vs, sp), 155 (m), 164 (sh), 186 (w), and 222 (w). One point arising from the $NaNO_2$ study bears emphasis. The $\nu_3(B_2)$ mode is very broad in the Raman, peaking at 1232 cm^{-1} and extending to *ca.* 1360 cm^{-1} (Fig. 2). Tramer (5) and Tsuboi *et al.* (17) have observed that Raman frequency shifts for this band depend on the orientation of the single crystal. These authors proposed that the effect was due to the presence of a transverse optical mode (t.o.) at 1230 cm^{-1} and a longitudinal optical mode (l.o.) at 1360 cm^{-1}, in agreement with infrared reflectance studies (15). The true infrared absorption frequency corresponding to a normal mode of vibration is considered to be the frequency of the t.o. maximum, which is usually measured by thin film transmission techniques for which the l.o. mode is theoretically inactive (31). It has been recently shown (18) that the m.i.r. technique also provides a spectrum in which the activity of the l.o. mode is either absent or so low that it has no effect on the frequency of the band

Can. J. Chem. Downloaded from www.nrcresearchpress.com by 210.87.254.6 on 09/05/12
For personal use only.

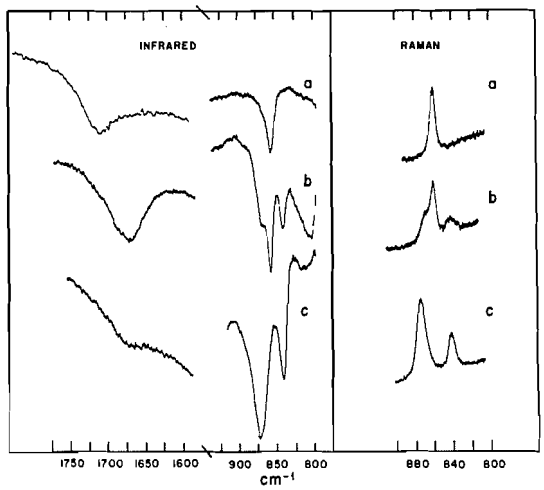

FIG. 3. Photographs of portions of infrared and Raman spectra of $LiNO_2.H_2O$ at various stages of dehydration: (*a*) $LiNO_2.H_2O$; (*b*) $LiNO_2.H_2O$ partially dehydrated; (*c*) $LiNO_2$ anhydrous. Infrared spectra were recorded as Nujol mulls between AgBr plates. Raman spectra were recorded on the Jarrel-Ash model 25-300 Raman spectrometer after excitation with the 4880 Å Argon ion line.

maximum, which corresponds identically to the t.o. frequency, provided $\theta \gg \theta_c$. The same cannot be said for single internal reflectance studies, specular reflection, or regular transmission studies when the incident radiation has non-normal incidence on a sample surface (31). This point is illustrated by the data for $NaNO_2$. Our m.i.r. frequency for ν_3 is $1230 \pm 5\ cm^{-1}$, identical to the t.o. frequencies independently determined by specular reflection (15) and Raman techniques (5, 17).

Zeigler (32) reported a face-centered monoclinic crystal for KNO_2 similar to $NaNO_2$ with space group C_s^3 and NO_2^- on a C_s site. However, Tanisaki and Ishimatsu (33) recently reported a trigonal structure for KNO_2. The latter authors concluded from the absence of superlattice reflections that there was a disordered arrangement of NO_2 groups. The absence of any lattice vibrations in the Raman spectrum of KNO_2 (Table 1) would be in accord with large-scale disorder in solid KNO_2. We have found that KNO_2 does not produce well formed crystals but acts rather as an unmanageable plastic. $CsNO_2$ resembles KNO_2 in physical appearance and properties. Crystallographic data for $CsNO_2$ are inconclusive. Ferrari *et al.* (20) reported that $CsNO_2$ forms a body-centered cube but lack of a sufficient number of reflections prevented determination of atomic positions. Raman and infrared spectra for KNO_2 and $CsNO_2$ are very similar (Fig. 1) (Table 1). Since no lattice bands can be found in the Raman spectrum of $CsNO_2$, it would appear that $CsNO_2$ also has a disordered crystal structure. It would be interesting to know if the apparent disorder in KNO_2 and $CsNO_2$ crystals is impurity induced or a real property of the room temperature crystal phase. However, the preparation of ultra-pure KNO_2 and $CsNO_2$ appears to be a formidable task.

Significant frequency discrepancies between the infrared and Raman frequencies for the ν_3 peaks (Table 1) are difficult to rationalize. It is possible that contributions from the l.o. component of ν_3 have shifted the Raman peak to higher frequencies. Weston and Brodasky (4) reported striking changes in the appearance of the ν_3 infrared peak which depended on the mulling procedure employed. Spectral variations of this type can be caused by contributions from the l.o. mode which becomes active when the incident beam propagates in an orientation other than parallel to the optic axis (31). Failure to observe similar effects in our m.i.r. spectra further support our claim that l.o. contributions are minimal.

Zeigler (32) reported that $LiNO_2.H_2O$ crystallized in a pseudo-orthorhombic monoclinic cell with 4 molecules per unit cell. The complete crystal structure was never determined. No crystallographic structural evidence exists for $LiNO_2$.

Appearance of the band at *ca.* $842\ cm^{-1}$ in the infrared spectrum of anhydrous $LiNO_2$ (Figs. 1, 3) was first suspected to be due to the $\nu_2(A_2'')$ nitrate vibration, but this explanation was ruled out for several reasons. The bands at 842 and $872\ cm^{-1}$ are both infrared and Raman active; if the band at $842\ cm^{-1}$ was $\nu_2(A_2'')$ of nitrate, it would not be Raman active (25, 26). The intensity ratio of bands at 842 and $872\ cm^{-1}$ is similar in both Raman and infrared and is much too large (on the basis of NO_3^- analysis above) for the band at $842\ cm^{-1}$ to be due to nitrate impurity. Finally, in the infrared spectrum of $LiNO_2.H_2O$ no band is visible at *ca.* $840\ cm^{-1}$ (Figs. 1, 3).

Dehydration of $LiNO_2.H_2O$ produces significant changes in the nitrite bending region at *ca.* $850\ cm^{-1}$ (Fig. 3). On conversion of $LiNO_2.H_2O$ to the anhydrous form, the bands at *ca.* 842 and $872\ cm^{-1}$ increase together at the same rate and at the expense of the band at $857\ cm^{-1}$.

Can. J. Chem. Downloaded from www.nrcresearchpress.com by 210.87.254.6 on 09/05/12
For personal use only.

Can. J. Chem. Downloaded from www.nrcresearchpress.com by 210.87.254.6 on 09/05/12
For personal use only.

A band at *ca.* 1700 cm^{-1} assigned to the bending mode of the water of hydration decreases in both frequency and relative absorbance as the sample is dehydrated. The loss of weight on dehydration of $LiNO_2.H_2O$ corresponds to the loss of 1 mol of water.

A nondegenerate vibration may be split in two ways, each of which requires more than one molecule per primitive cell. (*a*) Coupling between identical normal modes of vibration of molecules in the unit cell gives rise to correlation field splitting (34, 35). (*b*) The ordered distribution of molecules over sets of non-equivalent sites will give rise to a number of bands equal to the number of distinct sites occupied. Correlation field splittings are typically of the order of 5 cm^{-1} except for normal modes with very large dipole derivatives (34, 35). The 30 cm^{-1} separation between the two bands in the ν_2 region of $LiNO_2$ is considered too large to be due to correlation field splitting. On the other hand, the presence of two distinct sites will result in a pair of bands with separation that depends on the dissimilarity of the static fields at the occupied sites. In certain nitrate crystals where the nitrate ion is known to occupy two distinct sites, pairs of bands separated by 15 to 30 cm^{-1} have been observed in regions of the nondegenerate vibrations and interpreted in terms of a two site effect (36–38).

In studies of inorganic nitrite complexes, Goodgame and Hitchman (39) and Hathaway and Slade (40) have assigned bands above 860 cm^{-1} to ONO type vibrations of either a nitrito linkage or a bridged ligand. The presence of both low and high frequency vibrations in the deformation region has been used by these authors as a criterion for two types of nitrite bonding. The low frequency bands are attributed to nitro (bonding through nitrogen); whereas, the high frequency bands arise from nitrito (bonding through oxygen) linkages. In anhydrous lithium nitrite, it appears that two different environments are available to the nitrite ion. Different sites can be created by an asymmetric arrangement of nitrite ions about the lithium ions. From infrared and Raman intensity considerations, it appears that the site responsible for the band at 872 cm^{-1} is twice as plentiful as the one responsible for the 842 cm^{-1} band. One could argue that nitrito linkages are twice as plentiful as nitro. The nitrite is probably not specifically linked or bonded to the lithium. The nitrito, nitro terminology is used merely to suggest that the band at 872 cm^{-1} is associated with a nitrite site with short Li—O distances; whereas the band at 842 cm^{-1} is associated with a nitrite site with short Li—N distances. If a strongly covalent nitrito linkage was actually present (as in nitrito complexes of cobalt), one would anticipate a decrease in the symmetric stretching frequency (41–43); in fact, the symmetric stretching frequency does not shift. In the hydrate, only one band is present in the deformation region which would indicate that the nitrite ions lie on a single site.

The infrared and Raman spectra of $LiNO_2.H_2O$ and $LiNO_2$ differ in many respects other than those discussed above (Table 2). Changes in the lattice region are difficult to explain without a more detailed study of a single crystal. A shoulder *ca.* 1360 cm^{-1} on the ν_1 vibration in the Raman spectrum of $LiNO_2$ may reflect a doubling of the symmetric stretching vibration for reasons analogous to those discussed for the deformation region but this region is very complicated (*cf.* ref. 24).

Occasionally it was possible to detect a weak band in the 800 cm^{-1} region approximately 20 cm^{-1} removed from the ν_2 nitrite ion fundamental (Fig. 2, Table 1). This band may be due to either isotopic species $^{15}N^{16}O_2^-$ or $^{14}N^{16}O^{18}O^-$; expected intensity ratios based on natural isotopic abundances are 0.00366 and 0.00413, respectively. Sato *et al.* (12) assigned a band at $\sim(\nu_2 - 20)$ cm^{-1} in the $NaNO_2$ spectrum to the $^{15}N^{16}O_2^-$ species; however, ^{15}N isotopic substitution studies (2, 4, 9) have firmly established that the ν_2 mode of NO_2^- shifts only 5 cm^{-1} on ^{15}N substitution. Kato and Rolfe (9) have assigned a band at $(\nu_2 - 21)$ cm^{-1} to the $^{14}N^{16}O^{18}O^-$ species. There can be little doubt that this latter assignment is correct.

This work was supported by grants from the National Research Council of Canada. One of us (M.H.B.) acknowledges receipt of a NRCC Postdoctoral Fellowship. The authors are indebted to Dr. G. E. Boyd of the Oak Ridge National Laboratories for the use of the Jarrell-Ash model 25-300 Raman spectrometer.

1. D. E. IRISH. *In* Ionic Interactions, Dilute Solutions to Molten Salts. Vol. 2. (*Editor*). S. Petrucci. Academic Press, New York. 1971. Chap. 9. p. 187.
2. J. S. SIDMAN. J. Amer. Chem. Soc. **79**, 2669 (1957); **79**, 2675 (1957).
3. R. NEWMAN. J. Chem. Phys. **20**, 444 (1952).
4. R. E. WESTON, JR. and T. F. BRODASKY. J. Chem. Phys. **27**, 683 (1957).

5. A. TRAMER. Compt. Rend. **248**, 3546 (1959).
6. R. M. HOCHSTRASSER and A. P. MARCHETTE. J. Chem. Phys. **50**, 1727 (1969).
7. J. KETELAAR and J. VAN DER ELSKEN. J. Chem. Phys. **30**, 336 (1959).
8. W. A. MORGAN, E. SILBERMAN, and H. W. MORGAN. Spectrochim. Acta, **23A**, 2855 (1967).
9. R. KATO and J. ROLFE. J. Chem. Phys. **47**, 1901 (1967).
10. V. NARAYANAMURTI, W. D. SEWARD, and R. O. POHL. Phys. Rev. **148**, 481 (1966).
11. R. BONN, R. METSELAAR, and J. VAN DER ELSKEN. J. Chem. Phys. **46**, 1988 (1967).
12. Y. SATO, K. GESI, and Y. TAKAGI. J. Phys. Soc. Jap. **16**, 2172 (1961).
13. Y. ISHIBASHI, K. SIRATORI, and T. NAKAMURA. J. Phys. Soc. Jap. **21**, 809 (1966).
14. H. VOGT and H. HAPP. Phys. Status Solidi, **16**, 711 (1966).
15. J. D. AXE. Phys. Rev. **167**, 573 (1968).
16. E. V. CHISLER and M. S. SHUR. Phys. Status Solidi, **17**, 163 (1966).
17. M. TSUBOI, M. TERADA, and T. KAJIURA. Bull. Chem. Soc. Jap. **41**, 2545 (1968); **42**, 1871 (1969).
18. M. H. BROOKER. J. Chem. Phys. **53**, 4100 (1970).
19. J. BUREAU. Ann. Chim. Paris, **8**, 5 (1937).
20. A. FERRARI, L. CAVALCA, and M. E. TANI. Gazz. Chim. Ital. **87**, 310 (1957).
21. B. STRIJK and C. H. MACGILLAVRY. Rec. Trav. Chim. **62**, 705 (1943); **65**, 127 (1946).
22. J. D. RAY. J. Inorg. Nucl. Chem. **15**, 290 (1960).
23. M. H. BROOKER and D. E. IRISH. Can. J. Chem. **46**, 229 (1968).
24. M. H. BROOKER and D. E. IRISH. Inorg. Chem. **8**, 219 (1969).
25. M. H. BROOKER and D. E. IRISH. Can. J. Chem. **48**, 1183 (1970).
26. D. W. JAMES and W. H. LEONG. J. Chem. Phys. **49**, 5089 (1968)
27. G. B. CARPENTER. Acta Cryst. **5**, 132 (1952); **8**, 852 (1955).
28. M. R. TRUTER. Acta Cryst. **7**, 73 (1954).
29. M. I. KAY and B. C. FRAZER. Acta Cryst. **14**, 56 (1961).
30. R. W. G. WYCKOFF. Crystal Structures. Vol. 2. Interscience Publishers, Inc., New York. 1963.
31. D. W. BERREMAN. Phys. Rev. **130**, 2193 (1963).
32. G. E. ZIEGLER. Z. Krist. **90**, 95 (1935); **94A**, 491 (1936).
33. S. TANISAKI and T. ISHIMATSU. J. Phys. Soc. Jap. **20**, 1277 (1965).
34. M. H. BROOKER. J. Chem. Phys. **53**, 2670 (1970).
35. T. S. HERMAN, S. R. HARVEY, and C. N. HONTS. Appl. Spectry. **23**, 451 (1969).
36. J. P. MATHIEU and M. LOUNSBURY. Discuss. Faraday Soc. **9**, 196 (1950).
37. R. P. J. COONEY and J. R. HALL. Aust. J. Chem. **22**, 337 (1969).
38. D. E. IRISH, D. L. NELSON, and M. H. BROOKER. J. Chem. Phys. **54**, 654 (1971).
39. D. M. L. GOODGAME and M. A. HITCHMAN. Inorg. Chem. **3**, 1389 (1964); **6**, 813 (1967).
40. B. J. HATHAWAY and R. G. SLADE. J. Chem. Soc. A, 1485 (1966).
41. R. B. PENLAND, T. J. LANE, and J. V. QUAGLIANO. J. Amer. Chem. Soc. **78**, 887 (1956).
42. K. NAKAMOTO, J. FUJITA, and M. MURATA. J. Amer. Chem. Soc. **80**, 4817 (1958).
43. F. BASOLO and G. S. HAMMAKER. Inorg. Chem. **1**, 1 (1962).

Can. J. Chem. Downloaded from www.nrcresearchpress.com by 210.87.254.6 on 09/05/12
For personal use only.

Can. J. Chem. Downloaded from www.nrcresearchpress.com by 210.87.254.105 on 09/05/12
For personal use only.

NOTES

Mass Spectra of the Hydroxyindole-3-carboxylic Acids and the Hydroxyskatoles[1,2]

ROSANGELA MARCHELLI,[3] W. D. JAMIESON, S. H. SAFE, O. HUTZINGER, AND R. A. HEACOCK
Atlantic Regional Laboratory, National Research Council of Canada, Halifax, Nova Scotia

Received November 4, 1970

The electron impact fragmentations of the 4-, 5-, 6-, and 7-hydroxyskatoles and the 4-, 5-, 6-, and 7-hydroxyindole-3-carboxylic acids have been studied. The spectra of the four isomeric hydroxyskatoles are virtually indistinguishable, due to substituent randomization of the [M] and [M-1] ions. In the case of the hydroxyindole-3-carboxylic acids, loss of H_2O from the molecular ion is characteristic of the 4-isomer but initial loss of $\cdot OH$ from the molecular ion is the most important reaction of the other three isomers.

On a étudié la fragmentation sous l'impact d'électrons, des hydroxy-4, -5, -6, ou -7 skatoles et des acides hydroxy-4, -5, -6, ou -7 indolecarboxyliques-3. Les spectres des quatre hydroxyskatoles isomériques sont virtuellement indiscernables du à la randonisation des substituants dans les ions [M] et [M-1]. Dans le cas des acides hydroxyindolecarboxyliques-3, la perte d'eau est caractéristique de l'isomère 4 mais une perte initiale de $\cdot OH$ de la part de l'ion moléculaire est la réaction principale pour ces trois autres isomères.

Canadian Journal of Chemistry, 49, 1296 (1971)

The electron impact-induced fragmentations of indoles, substituted indoles (1–11), and oxindoles (12–14) have been extensively investigated. Marx and Djerassi (15) have shown that with [1-^{13}C]-*N*-methylindole considerable skeletal rearrangement involving the exocyclic methyl group occurs prior to formation of the [M-(H + HCN)] ion. Similar observations using deuterated oxindoles (12–14) also indicate considerable H/D randomization.

In the present study the mass spectra of several biologically important isomeric hydroxyskatoles and hydroxyindole-3-carboxylic acids have been investigated to determine if differences in their mass spectra would be useful for identification purposes and to study their respective fragmentation pathways.

4-, 5-, 6-, and 7-Hydroxyskatoles

The mass spectrum (Fig. 1) and fragmentation pattern (Scheme 1) for 4-hydroxyskatole are shown and are remarkably similar to the data obtained from the 5-, 6-, and 7-isomers. The constancy of the relative abundance of the [M], [M-H], [M-H-28], and [M-H-29] species (Table 1) shows that the differences in the primary ion spectra are small. One exception being that for the 7-isomer a slightly more intense [M-H-18] ion is observed. Inspection of the high resolution spectra confirmed that for all four isomers the reaction *m/e* 146 → 118 is primarily due to expulsion of CO (80–95%) rather than $H_2CN\cdot$ (5–20%), a fragment commonly lost in the breakdown of indoles (*cf.* ref. 6).

Using the kinetic approach (*cf.* refs. 16–18) it was of interest to compare ["metastable" ion]/[daughter ion] ratios for the *m/e* 147 $\xrightarrow{-H\cdot}$ 146 and 146 $\xrightarrow{-CO}$ 118 reactions of the isomeric hydroxyskatoles (Table 1). Strong "metastable" ions at *m/e* 145.0 (m_1*) and 95.4 (m_2*) respectively are observed for the above reactions in all four isomeric hydroxyskatoles; moreover the [m_1*]/[*m/e* 146] and [m_2*]/[*m/e* 118] ratios are all similar. The results indicate that under electron impact the molecular ions and [M-1] ions for the 4-, 5-, 6-, and 7-hydroxyskatoles have similar energy distributions which suggests substituent randomization in these ions. These results indicate why the spectra of the isomers are virtually indistinguishable.

The extent and mechanism of substituent randomization has not been ascertained since the mechanism of carbon and hydrogen scram-

[1]Issued as NRCC No. 11 696.
[2]This investigation was presented in part at the C.I.C./A.C.S. meeting in Toronto, May, 1970.
[3]NRCC Postdoctorate Fellow 1967–1969.

TABLE 1. Relative ion intensity data and [metastable ion]/[daughter ion] ratios for the hydroxyskatoles

Compound	[M]	[M-H]	[M-H-28]	[M-H-29]	[*m/e* 145]*/[*m/e* 146] $\times 10^{-3}$	[*m/e* 95.4]*/[*m/e* 118]
4-Hydroxyskatole	82	100	10	8	0.67	0.45
5-Hydroxyskatole	90	100	8	9	0.66	0.46
6-Hydroxyskatole	85	100	8	8	0.70	0.46
7-Hydroxyskatole	88	100	18	8	0.70	0.44

*Metastable ion.

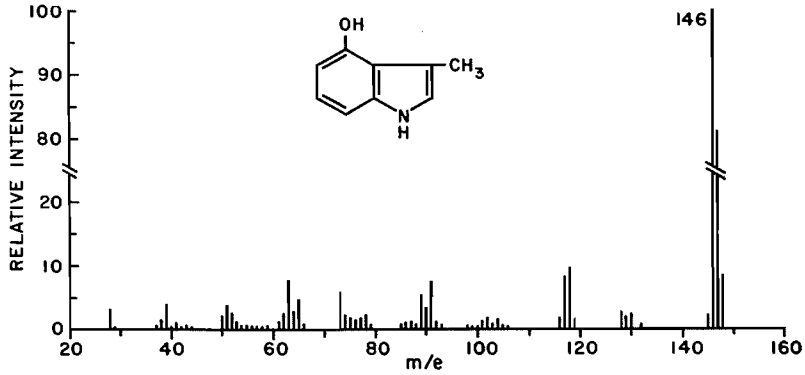

FIG. 1. Mass spectrum of 4-hydroxyskatole.

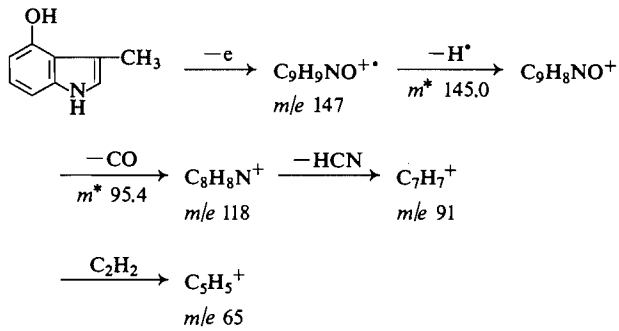

SCHEME 1

bling in aromatic systems is not yet fully established (*cf.* ref. 19).

4-, 5-, 6-, and 7-Hydroxyindole-3-carboxylic Acids

The mass spectral fragmentation patterns of the isomeric hydroxyindole-3-carboxylic acids are more complex than those of the corresponding hydroxyskatoles. The spectra of the 5-, 6-, and 7-isomers are similar to each other (*e.g.* 5-isomer, Fig. 2), except that for the 5-isomer the *m/e* 133 ion (100%) is much more intense than the same ion in the 6- (20%) and 7- (8%) isomers. Thermal decarboxylation of the hydroxyindole-3-carboxylic acids, prior to ionization, is probably an important factor here. The fragmentation patterns (Scheme 2) for the 5-, 6-, and 7-isomers show two main pathways featuring initial loss of ·OH and decarboxylation. The reaction *m/e* 177 $\xrightarrow{-OH\cdot}$ 160 yields an intense "metastable" ion at *m/e* 144.7 (m_3*) and the [m_3*]/[*m/e* 160] ratios for the 5-, 6-, and 7-isomers are identical (1.4×10^{-3}). As with the skatole derivatives the kinetic approach for the above reaction suggests substituent randomiza-

Can. J. Chem. Downloaded from www.nrcresearchpress.com by 210.87.254.105 on 09/05/12
For personal use only.

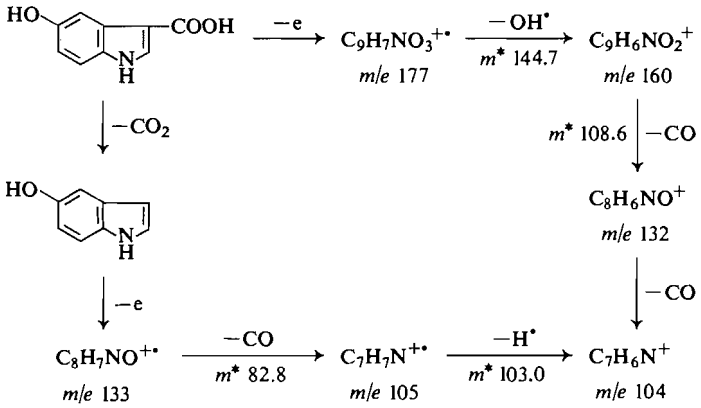

SCHEME 2

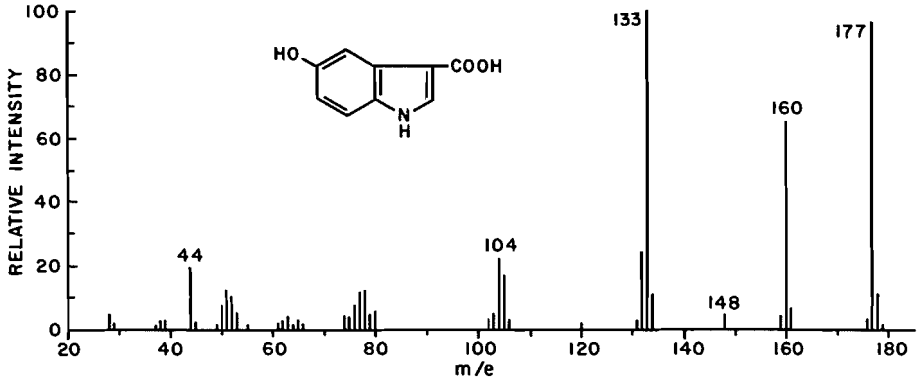

FIG. 2. Mass spectrum of 5-hydroxyindole-3-carboxylic acid.

tion has occurred because the molecular ions of the 5-, 6-, and 7-isomers have similar internal energies and energy distributions.

The mass spectrum (Fig. 3) and breakdown pattern (Scheme 3) of 4-hydroxyindole-3-carboxylic acid are in contrast to those of the other isomers. As a result of the 3,4-peri-interaction between the carboxyl and hydroxy substituents the initial loss of ·OH is entirely suppressed by the formation of an $[M\text{-}H_2O]$ ion. Thus with the mass spectra of the isomeric hydroxyindole-3-carboxylic acids only that of the 4-isomer is significantly different to the others due to the above-mentioned peri-interaction. In the case of the hydroxyskatoles, the methyl group, in place of the carboxyl group in the 3-position, prevents this interaction with the result that the mass spectra of the isomeric hydroxyskatoles are virtually indistinguishable. In the case of the hydroxyindole-3-carboxylic acids however, high resolution measurement of the ions at *m/e* 104, 105, and 106 indicated that the components of these doublets varied in relative abundance and that this depended on the isomer (see Table 2). Also an unusually abundant doubly charged ion at $[M\text{-}H_2O]$ was present in the spectrum of the 7-isomer. This information allows differentiation

TABLE 2. Nature and relative abundance of some doublet ions

Ion		Isomer*			
m/e	Formula	4-	5-	6-	7-
106	C_7H_6O	—	4	S	1
	C_7H_8N	—	1	—	20
105	C_7H_5O	1	10	7	1
	C_7H_7N	2	7	1	9
104	C_7H_4O	1	—	1	1
	C_7H_6N	1	S	8	73

*S, Single species only.

Can. J. Chem. Downloaded from www.nrcresearchpress.com by 210.87.254.105 on 09/05/12
For personal use only.

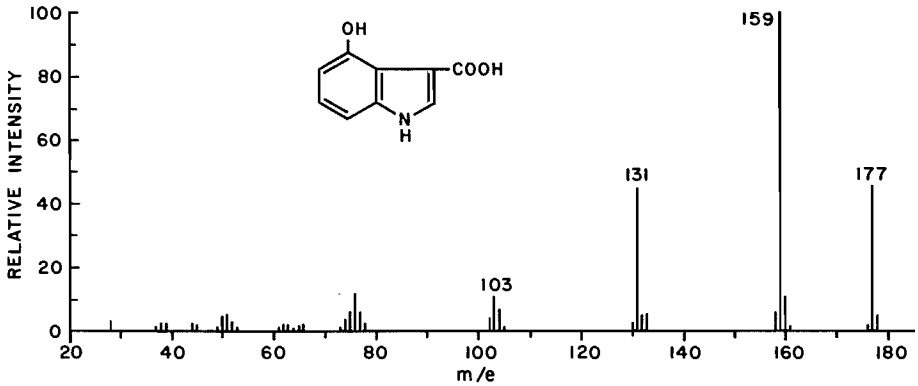

FIG. 3. Mass spectrum of 4-hydroxyindole-3-carboxylic acid.

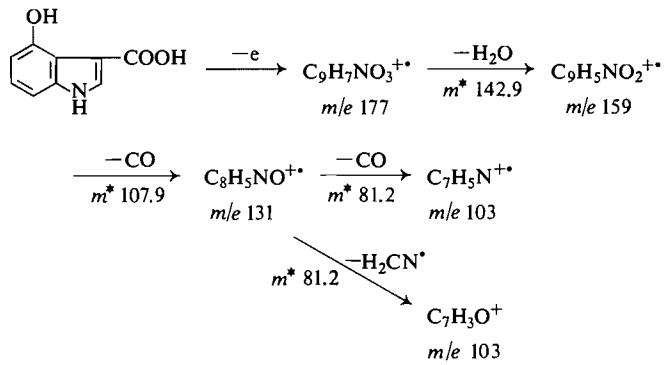

SCHEME 3

of these isomers. The above results indicate some of the difficulties in the way of structural identification of isomeric hydroxyindoles by mass spectrometry.

Experimental

Materials

The hydroxyindole-3-carboxylic acids (20) and hydroxyskatoles (21) were prepared by methods described in the literature.

Methods

Mass spectral data were obtained with a Dupont/CEC 21-110B double-focussing instrument equipped with an electron-impact ion source and fitted to record data either by photoplate (Ilford Q2 emulsion) or electrical detection.

The 70 eV spectra of the 4-, 5-, 6-, and 7-hydroxyindole-3-carboxylic acids were recorded at ionization chamber temperatures of: 4-, 203°; 5-, 196; 6-, 236; 7-, 223. The 70 eV mass spectra of the 4-, 5-, 6-, and 7-hydroxyskatoles were recorded with sample temperatures in the range 50–66° and block temperatures in the range 153–157°.

The authors wish to thank D. J. Embree, who recorded the mass spectra.

1. D. E. HALL and A. H. JACKSON. J. Chem. Soc. C, 1681 (1967).
2. B. HOLMSTEDT and J. E. LINDGREN. *In* Ethnopharmacologic search for psychoactive drugs. *Edited by* D. H. Efron, B. Holmstedt, and N. S. Kline. Public Health Service Publication No. 1645, U.S. Government Printing Office, Washington, D.C., 1967. p. 339.
3. S. W. BELLMAN. J. Ass. Offic. Anal. Chem. **51**, 164 (1968).
4. A. Y. LEUNG and A. G. PAUL. J. Pharm. Sci. **57**, 1667 (1968).
5. E. MUTSCHLER, H. ROCHELMEYER, and D. WÖLFFLING. Arch. Pharm. **301**, 287 (1968).
6. J. C. POWERS. J. Org. Chem. **33**, 2044 (1968).
7. W. D. JAMIESON and O. HUTZINGER. Phytochem. **9**, 2029 (1970).
8. O. BUCHARDT, A. M. DUFFIELD, and C. DJERASSI. Acta Chem. Scand. **22**, 2329 (1968).
9. Y. OMOTE, H. YASUDA, Y. FUJINUMA, and N. SUGIYAMA. Nippon Kagaku Zasshi, **89**, 594 (1968); Chem. Abstr. **69**, 86110*v* (1968).
10. M. WILCHEK, T. SPANDE, G. MILNE, and B. WITKOP. Biochem. **7**, 1777 (1968).
11. R. M. ACHESON, R. G. BOLTON, and I. HUNTER. J. Chem. Soc. C, 1067 (1970).
12. J. A. BALLATINE, F. G. FENWICK, and M. ALAM. Org. Mass Spec. **1**, 467 (1968).
13. R. HODGES, J. S. SHANNON, W. D. JAMIESON, and A. TAYLOR. Can. J. Chem. **46**, 2189 (1968).

Can. J. Chem. Downloaded from www.nrcresearchpress.com by 210.87.254.105 on 09/05/12
For personal use only.

14. T. HINO, M. NAKAGAWA, K. TSUNEOKA, S. MISAWA, and S. AKABOSHI. Chem. Pharm. Bull. **17**, 1651 (1969).
15. M. MARX and C. DJERASSI. J. Amer. Chem. Soc. **90**, 678 (1968).
16. M. M. BURSEY and F. W. MCLAFFERTY. J. Amer. Chem. Soc. **88**, 529 (1966).
17. M. M. BURSEY and F. W. MCLAFFERTY. J. Amer. Chem. Soc. **88**, 5023 (1966).
18. D. H. WILLIAMS, S. W. TAM, and R. G. COOKS. J. Amer. Chem. Soc. **90**, 2150 (1968).
19. R. G. COOKS and S. L. BERNASEK. J. Amer. Chem. Soc. **92**, 2131 (1970).
20. R. MARCHELLI, O. HUTZINGER, and R. A. HEACOCK. Can. J. Chem. **47**, 4375 (1969).
21. R. A. HEACOCK and O. HUTZINGER. Can. J. Chem. **42**, 514 (1964).

An Aspect of the Scope of the Phosphonic Acid Bis Amide – Carbonyl Method in the Synthesis of Exocyclic Olefins

J. BRYAN JONES AND PETER W. MARR
Lash Miller Chemical Laboratories, Department of Chemistry, University of Toronto, Toronto 181, Ontario

Received November 16, 1970

The synthesis of cyclohexylidene derivatives by condensation of α-lithiocyclohexylphosphonic acid bis(dimethylamide) with some carbonyl compounds has been studied. The desired olefin was obtained when the carbonyl moiety was an aldehyde but, probably for steric reasons, not when ketones were used.

On a étudié la synthèse de cyclohexylidènes substitués obtenus par condensation de composés carbonylés avec la bis(diméthylamide) de l'acide α-lithiocyclohexylphosphonique. Les oléfines désirées peuvent être obtenues lorsque le composé carbonylé est de nature aldéhydique; toutefois les composés attendus ne sont pas obtenus, probablement pour des raisons stériques, lors des essais de condensation de cétones.

Canadian Journal of Chemistry, 49, 1300 (1971)

During the course of some studies on non-steroidal potential androgens the need arose for olefin intermediates of the general structure **1**. Tetrasubstituted olefins of this type are not easily prepared and routes involving elimination reactions (1) were not considered suitable for steroid-like polycyclic compounds owing to the probability of double bond migration (2) under the vigorous reaction conditions required. Attention was therefore concentrated on the possibility of preparing the series of compounds **1** by condensation of the appropriate Wittig or related reagent with cyclohexanones.

Although the Wittig reaction has been used successfully to effect the preparation of alkylidene alkanes (3) attempts to condense cyclohexylidenetriphenylphosphorane with cyclohexanone did not produce any of the required olefin **1**, R = H.[1] The related phosphonamide route to tetrasubstituted and other recently described olefins (4, 5) was also evaluated. The required cyclohexylphosphonic acid bis(dimethylamide) starting material was prepared but disappointingly its α-lithioderivative **2** and cyclohexanone could not be induced to react to give any cyclohexylidenecyclohexane (**1**, R = H).[1]

The use of carbocyclic phosphonamide derivatives, such as **2**, in olefin synthesis has not previously been reported and it was recognized that steric factors might be interfering with the formation of the intermediate β-hydroxyphosphonamide adducts.[2] Accordingly a limited study on the scope and limitations of the cyclohexylphosphonamide reagent **2** in olefin synthesis was carried out.

The results obtained, which are generalized in Scheme 1, show that reactions of **2** with alde-

[1]The g.l.c. analysis of the reaction mixture prior to working-up showed only the presence of unchanged starting materials.

[2]That α-lithioisopropylphosphonic acid bis(dimethylamide), for which qualitatively similar steric factors obtain, reacted readily with benzophenone (4) was confirmed by repeating the literature experiment. However, condensation of the lithioisopropylphosphonamide with cyclohexanone did not go well and a 17% (by g.l.c., 15% isolated) yield only of isopropylidenecyclohexane was obtained.

Can. J. Chem. Downloaded from www.nrcresearchpress.com by 210.87.254.105 on 09/05/12
For personal use only.

14. T. HINO, M. NAKAGAWA, K. TSUNEOKA, S. MISAWA, and S. AKABOSHI. Chem. Pharm. Bull. **17**, 1651 (1969).
15. M. MARX and C. DJERASSI. J. Amer. Chem. Soc. **90**, 678 (1968).
16. M. M. BURSEY and F. W. MCLAFFERTY. J. Amer. Chem. Soc. **88**, 529 (1966).
17. M. M. BURSEY and F. W. MCLAFFERTY. J. Amer. Chem. Soc. **88**, 5023 (1966).
18. D. H. WILLIAMS, S. W. TAM, and R. G. COOKS. J. Amer. Chem. Soc. **90**, 2150 (1968).
19. R. G. COOKS and S. L. BERNASEK. J. Amer. Chem. Soc. **92**, 2131 (1970).
20. R. MARCHELLI, O. HUTZINGER, and R. A. HEACOCK. Can. J. Chem. **47**, 4375 (1969).
21. R. A. HEACOCK and O. HUTZINGER. Can. J. Chem. **42**, 514 (1964).

Can. J. Chem. Downloaded from www.nrcresearchpress.com by 210.87.254.6 on 09/05/12
For personal use only.

An Aspect of the Scope of the Phosphonic Acid Bis Amide – Carbonyl Method in the Synthesis of Exocyclic Olefins

J. BRYAN JONES AND PETER W. MARR
Lash Miller Chemical Laboratories, Department of Chemistry, University of Toronto, Toronto 181, Ontario

Received November 16, 1970

The synthesis of cyclohexylidene derivatives by condensation of α-lithiocyclohexylphosphonic acid bis(dimethylamide) with some carbonyl compounds has been studied. The desired olefin was obtained when the carbonyl moiety was an aldehyde but, probably for steric reasons, not when ketones were used.

On a étudié la synthèse de cyclohexylidènes substitués obtenus par condensation de composés carbonylés avec la bis(diméthylamide) de l'acide α-lithiocyclohexylphosphonique. Les oléfines désirées peuvent être obtenues lorsque le composé carbonylé est de nature aldéhydique; toutefois les composés attendus ne sont pas obtenus, probablement pour des raisons stériques, lors des essais de condensation de cétones.

Canadian Journal of Chemistry, 49, 1300 (1971)

During the course of some studies on non-steroidal potential androgens the need arose for olefin intermediates of the general structure **1**. Tetrasubstituted olefins of this type are not easily prepared and routes involving elimination reactions (1) were not considered suitable for steroid-like polycyclic compounds owing to the probability of double bond migration (2) under the vigorous reaction conditions required. Attention was therefore concentrated on the possibility of preparing the series of compounds **1** by condensation of the appropriate Wittig or related reagent with cyclohexanones.

Although the Wittig reaction has been used successfully to effect the preparation of alkylidene alkanes (3) attempts to condense cyclohexylidenetriphenylphosphorane with cyclohexanone did not produce any of the required olefin **1**, R = H.[1] The related phosphonamide route to tetrasubstituted and other recently described olefins (4, 5) was also evaluated. The required cyclohexylphosphonic acid bis(dimethylamide) starting material was prepared but disappointingly its α-lithioderivative **2** and cyclohexanone could not be induced to react to give any cyclohexylidenecyclohexane (**1**, R = H).[1]

The use of carbocyclic phosphonamide derivatives, such as **2**, in olefin synthesis has not previously been reported and it was recognized that steric factors might be interfering with the formation of the intermediate β-hydroxyphosphonamide adducts.[2] Accordingly a limited study on the scope and limitations of the cyclohexylphosphonamide reagent **2** in olefin synthesis was carried out.

The results obtained, which are generalized in Scheme 1, show that reactions of **2** with alde-

[1]The g.l.c. analysis of the reaction mixture prior to working-up showed only the presence of unchanged starting materials.

[2]That α-lithioisopropylphosphonic acid bis(dimethylamide), for which qualitatively similar steric factors obtain, reacted readily with benzophenone (4) was confirmed by repeating the literature experiment. However, condensation of the lithioisopropylphosphonamide with cyclohexanone did not go well and a 17% (by g.l.c., 15% isolated) yield only of isopropylidenecyclohexane was obtained.

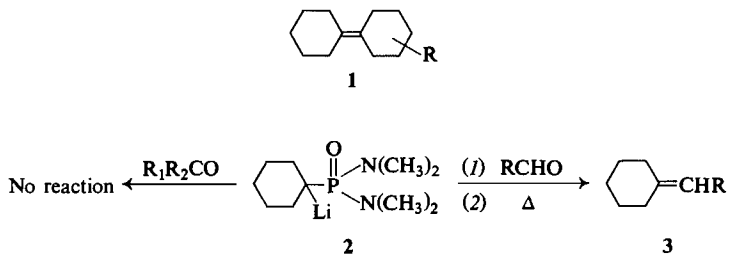

SCHEME 1

hydes[3] can occur to give ~40–60% yields of alkenes such as **3** but that no olefinic products could be detected[1] when a representative structural range of ketones[4] was used as the carbonyl moiety.

Experimental

Cyclohexylphosphonic Acid Bis(dimethylamide)

Chlorocyclohexane (30 g, 0.25 mol), phosphorous trichloride (68.7 g, 0.5 mol), and aluminum trichloride (68 g, 0.5 mol) were mixed (in that order) with stirring at 0° (6). After stirring for 20 min, methylene chloride (900 ml) was added and the solution cooled to −20°. Water (92 ml) was then added slowly with stirring and when the precipitate formed had coagulated (1 h), the mixture was filtered and the filtrate was rotary evaporated. The cyclohexylphosphonic dichloride (42 g) so obtained was added slowly with stirring to a cooled (0°) solution of dimethylamine (68 g, 1.5 mol) in diethyl ether (400 ml) (7). The mixture was stirred at 20° for a further 2 h and was then filtered and the filtrate dried ($MgSO_4$) and evaporated. Chromatography of the crude product on Florisil with methanol–acetone (1:1) elution followed by distillation yielded *cyclohexylphosphonic acid bis(dimethylamide)*, b.p. 118°/0.45 Torr, as a hygroscopic white solid (13.2 g): i.r. ($CHCl_3$) 1295 cm^{-1} (P=O); p.m.r. ($CDCl_3$) δ 1.2–1.8 (broad, 11H, C_6H_{11}) and 2.60 and 2.75 p.p.m. (two s, 12H, $[N(CH_3)_2]_2$).

Anal. Calcd. for $C_{10}H_{23}N_2OP$ (mol. wt. 218.1548): C, 55.03; H, 10.62; N, 12.83; P, 14.19. Found (218.1547 (mass spectrum)): C, 54.47; H, 10.69; N, 12.50; P, 14.20.

General Procedure for Reaction of α-Lithiocyclohexyl Phosphonic Acid Bis(dimethylamide) (2) with Aldehydes (1)

A solution of *n*-butyl lithium in hexane (9.9 ml, 1.6 *M*, 16.2 mmol) was added with stirring under dry nitrogen to cyclohexylphosphonic acid bis(dimethylamide) (3.51 g, 16.2 mmol) in dry tetrahydrofuran (80 ml) at −40°. After further stirring of the yellow solution at −40° for 1 h, the aldehyde (16.2 mmol) was added dropwise and the mixture kept at −40° for 30 min and then at 20° for a further 20 min. Water (2 ml) was added and the mixture concentrated by rotary evaporation. The residue was extracted with diethyl ether (60 ml) and the ether solution washed with water (4 × 10 ml), dried ($MgSO_4$), and evaporated. The resulting β-hydroxyphosphonamide was then heated under reflux in benzene (60 ml) in the presence of silica gel G (12 g) for 12 h. The mixture was filtered, the silica gel washed with diethyl ether (30 ml), and the combined organic solution washed with water (15 ml). Evaporation of the dried ($MgSO_4$) solution afforded an oil which was chromatographed on Florisil with petroleum ether (b.p. 30–60°) elution. Distillation (spinning band) of the product was used as the final purification step. All compounds obtained showed single peaks when analyzed by g.l.c. on a 3% SE-30 column. Following the above procedure *n*-butylidenecyclohexane[5] (**3**, R = C_3H_7), b.p. 35°/1.4 Torr, was obtained from 1-butanol in 38% yield; 1-cyclohexylidene-2-butene[5] (**3**, R = $CH{=}CHCH_3$), b.p. 47°/1.3 Torr (lit. (8) b.p. 66.5°/6 Torr) from 2-butenal in 48% yield, and benzylidenecyclohexane[5] (**3**, R = C_6H_5), b.p. 59°/0.08 Torr (lit. (9) b.p. 76°/0.05 Torr) from benzaldehyde in 57% yield.

Isopropylidenecyclohexane

Isopropylidenecyclohexane was obtained in 15% yield by the above general procedure from α-lithioisopropylphosphonic acid bis(dimethylamide) prepared *in situ* as described by Corey and Kwiatkowski (4), and cyclohexanone. The i.r. spectrum was identical with that reported previously (11); p.m.r.[6] ($CDCl_3$) δ 1.55 (broad s, 6H, C-3,4,5 CH_2), 1.66 (s, 6H, $=C(CH_3)_2$) and 2.20 p.p.m. (broad s, 4H, C-2,6 CH_2).

Mol. Wt. Calcd.: 124.1252. Found (mass spectrum): 124.1251.

The generous support of the National Research Council of Canada and the award (to P.W.M.) of an Ontario Government Fellowship are gratefully acknowledged.

1. J. JAQUES and C. WEIDMANN-HATTIER. Bull. Soc. Chim. Fr. 1478 (1958).
2. *Cf.* D. N. KIRK and P. M. SHAN. J. Chem. Soc. C, 182 (1970) and references therein.

[3]1-Butanal, 2-butenal, and benzaldehyde were surveyed.

[4]Acetone, cyclohexanone, 2-cyclohexenone, acetophenone, and benzophenone.

[5]Satisfactory elemental analyses were obtained for each of these previously reported compounds and the p.m.r., i.r., u.v., and high resolution mass spectra were in agreement with previously obtained data (8–10) and were consistent with the structures assigned.

[6]The p.m.r. data quoted for this compound in ref. 12 are not totally consistent with the structure of isopropylidenecyclohexane.

Can. J. Chem. Downloaded from www.nrcresearchpress.com by 210.87.254.6 on 09/05/12
For personal use only.

3. A. MAERCKER. *In* Organic reactions. *Edited by* A. C. Cope. J. Wiley and Sons, New York, N.Y. **14**, 420 (1965).
4. E. J. COREY and G. T. KWIATKOWSKI. J. Amer. Chem. Soc. **90**, 6816 (1968).
5. E. J. COREY and D. E. CANE. J. Org. Chem. **34**, 3053 (1969).
6. A. M. KINNEAR and E. A. PERREN. J. Chem. Soc. 3437 (1952).
7. G. M. KOSOLAPOFF and L. B. PAYNE. J. Org. Chem. **21**, 413 (1956).
8. K. J. CROWLEY. Tetrahedron, **21**, 1001 (1965).
9. v. H. OEDIGER and K. EITER. Ann. **682**, 58 (1965).
10. D. SEYFERTH, W. B. HUGHES, and J. K. HEEREN. J. Amer. Chem. Soc. **87**, 2847 (1965).
11. R. H. SIEGMANN, M. J. BEERS, and H. O. HUISMAN. Rec. Trav. Chim. **83**, 67 (1964).
12. V. J. TRAYNELIS, W. L. HERGENROTHER, H. T. HANSON, and J. A. VALICENTI. J. Org. Chem. **29**, 123 (1964).

Can. J. Chem. Downloaded from www.nrcresearchpress.com by 210.87.254.6 on 09/05/12
For personal use only.

Polysaccharides of the Red Alga *Rhodymenia pertusa* Part II. Cell-Wall Glucan; Proton Magnetic Resonance Studies on Permethylated Polysaccharides[1]

J. N. C. WHYTE AND J. R. ENGLAR
Fisheries Research Board of Canada, Vancouver Laboratory, 6640 N.W. Marine Drive, Vancouver 8, British Columbia

Received November 5, 1970

The cell-wall polysaccharide from *R. pertusa* has been shown, by g.l.c., mass spectrum, and p.m.r. studies on the methylated derivative, to consist of β-(1 → 4)-linked-D-glucopyranose residues. The assessment of anomeric configuration in polysaccharides by p.m.r. spectroscopy is illustrated by the spectra of methylated amylose and cellulose. The preparation of anilides for mass spectral analysis of sugars is suggested.

On a démontré par c.p.g., spectre masse, et par des études de r.m.n. du proton de dérivés méthylés que les polysaccharide des parois cellulaires de *R. pertusa* sont constitués de résidus de D-glucopyranose liés suivant la relation β-(1 → 4). La détermination par r.m.n. de la configuration anomérique des polysaccharides est démontrée grâce aux spectres de l'amylose et de la cellulose méthylée. Il est recommandé pour l'analyse des sucres par spectrométrie de masse, de préparer leur anilide.

Canadian Journal of Chemistry, **49**, 1302 (1971)

Few structural studies on the cell-wall glucans of Rhodophyceae have been presented (1). The residue from aqueous extraction of the red alga *Rhodymenia pertusa* (2) gave mainly glucose on hydrolysis and when successively treated with acid, alkali, and chlorine water furnished an insoluble glucan which was purified by dissolution and reprecipitation from cuprammonium hydroxide solution.

The constituent sugar was characterized as 2,3,4,6-tetra-*O*-acetyl-*N*-(*p*-nitrophenyl)-β-D-glucopyranosylamine which provided a mass spectrum with a parent peak at *m/e* 468 (11% of the base peak *m/e* 43), the A series of ions (3) and an ion at mass 180 which was derived from the rearrangement involving the transfer of the acetyl group on O-2 to the nitrogen of the glycosidic linkage in a manner analogous to the electron impact fragmentation of nucleosides (4). The abundance of the molecular ion in the spectrum of this *N*-glycoside, which is absent in corresponding *O*-glycoside spectra, indicates a possible use of anilides in the mass spectral analysis of oligosaccharides (5).

Treatment of the glucan with the Hakomori reagents (6) afforded a methylated derivative ($[\alpha]_D$ −15°, OCH_3 45.6%) a portion of which was hydrolyzed, reduced, and acetylated to yield partially methylated alditol acetates subsequently analyzed by g.l.c. and mass spectrometry (7). The methylated polymer contained 2,3,4,6-tetra- and 2,3,6-tri-*O*-methyl-D-glucose in the molar proportions of 1:110, providing evidence for a structure of linear (1 → 4)-linked-D-glucopyranose residues with a degree of polymerization (d.p.) of 110–120; a d.p. value of 120 was obtained from viscosity measurements of the derived nitrated polymer (8).

The p.m.r. spectra of the methylated derivatives of the glucan from *R. pertusa* and potato amylose in benzene-d_6: chloroform-*d* (6:1) are

[1]Part of a lecture presented at the C.I.C. "Marine Sciences" Conference held in Charlottetown, Prince Edward Island, August 16–18, 1970.

3. A. MAERCKER. *In* Organic reactions. *Edited by* A. C. Cope. J. Wiley and Sons, New York, N.Y. **14**, 420 (1965).
4. E. J. COREY and G. T. KWIATKOWSKI. J. Amer. Chem. Soc. **90**, 6816 (1968).
5. E. J. COREY and D. E. CANE. J. Org. Chem. **34**, 3053 (1969).
6. A. M. KINNEAR and E. A. PERREN. J. Chem. Soc. 3437 (1952).
7. G. M. KOSOLAPOFF and L. B. PAYNE. J. Org. Chem. **21**, 413 (1956).
8. K. J. CROWLEY. Tetrahedron, **21**, 1001 (1965).
9. v. H. OEDIGER and K. EITER. Ann. **682**, 58 (1965).
10. D. SEYFERTH, W. B. HUGHES, and J. K. HEEREN. J. Amer. Chem. Soc. **87**, 2847 (1965).
11. R. H. SIEGMANN, M. J. BEERS, and H. O. HUISMAN. Rec. Trav. Chim. **83**, 67 (1964).
12. V. J. TRAYNELIS, W. L. HERGENROTHER, H. T. HANSON, and J. A. VALICENTI. J. Org. Chem. **29**, 123 (1964).

Can. J. Chem. Downloaded from www.nrcresearchpress.com by 210.87.254.5 on 09/05/12
For personal use only.

Polysaccharides of the Red Alga *Rhodymenia pertusa* Part II. Cell-Wall Glucan; Proton Magnetic Resonance Studies on Permethylated Polysaccharides[1]

J. N. C. WHYTE AND J. R. ENGLAR
Fisheries Research Board of Canada, Vancouver Laboratory, 6640 N.W. Marine Drive, Vancouver 8, British Columbia

Received November 5, 1970

The cell-wall polysaccharide from *R. pertusa* has been shown, by g.l.c., mass spectrum, and p.m.r. studies on the methylated derivative, to consist of β-(1 → 4)-linked-D-glucopyranose residues. The assessment of anomeric configuration in polysaccharides by p.m.r. spectroscopy is illustrated by the spectra of methylated amylose and cellulose. The preparation of anilides for mass spectral analysis of sugars is suggested.

On a démontré par c.p.g., spectre masse, et par des études de r.m.n. du proton de dérivés méthylés que les polysaccharide des parois cellulaires de *R. pertusa* sont constitués de résidus de D-glucopyranose liés suivant la relation β-(1 → 4). La détermination par r.m.n. de la configuration anomérique des polysaccharides est démontrée grâce aux spectres de l'amylose et de la cellulose méthylée. Il est recommandé pour l'analyse des sucres par spectrométrie de masse, de préparer leur anilide.

Canadian Journal of Chemistry, **49**, 1302 (1971)

Few structural studies on the cell-wall glucans of Rhodophyceae have been presented (1). The residue from aqueous extraction of the red alga *Rhodymenia pertusa* (2) gave mainly glucose on hydrolysis and when successively treated with acid, alkali, and chlorine water furnished an insoluble glucan which was purified by dissolution and reprecipitation from cuprammonium hydroxide solution.

The constituent sugar was characterized as 2,3,4,6-tetra-*O*-acetyl-*N*-(*p*-nitrophenyl)-β-D-glucopyranosylamine which provided a mass spectrum with a parent peak at *m/e* 468 (11% of the base peak *m/e* 43), the A series of ions (3) and an ion at mass 180 which was derived from the rearrangement involving the transfer of the acetyl group on O-2 to the nitrogen of the glycosidic linkage in a manner analogous to the electron impact fragmentation of nucleosides (4). The abundance of the molecular ion in the spectrum of this *N*-glycoside, which is absent in corresponding *O*-glycoside spectra, indicates a possible use of anilides in the mass spectral analysis of oligosaccharides (5).

Treatment of the glucan with the Hakomori reagents (6) afforded a methylated derivative ($[\alpha]_D$ −15°, OCH_3 45.6%) a portion of which was hydrolyzed, reduced, and acetylated to yield partially methylated alditol acetates subsequently analyzed by g.l.c. and mass spectrometry (7). The methylated polymer contained 2,3,4,6-tetra- and 2,3,6-tri-*O*-methyl-D-glucose in the molar proportions of 1:110, providing evidence for a structure of linear (1 → 4)-linked-D-glucopyranose residues with a degree of polymerization (d.p.) of 110–120; a d.p. value of 120 was obtained from viscosity measurements of the derived nitrated polymer (8).

The p.m.r. spectra of the methylated derivatives of the glucan from *R. pertusa* and potato amylose in benzene-d_6: chloroform-*d* (6:1) are

[1]Part of a lecture presented at the C.I.C. "Marine Sciences" Conference held in Charlottetown, Prince Edward Island, August 16–18, 1970.

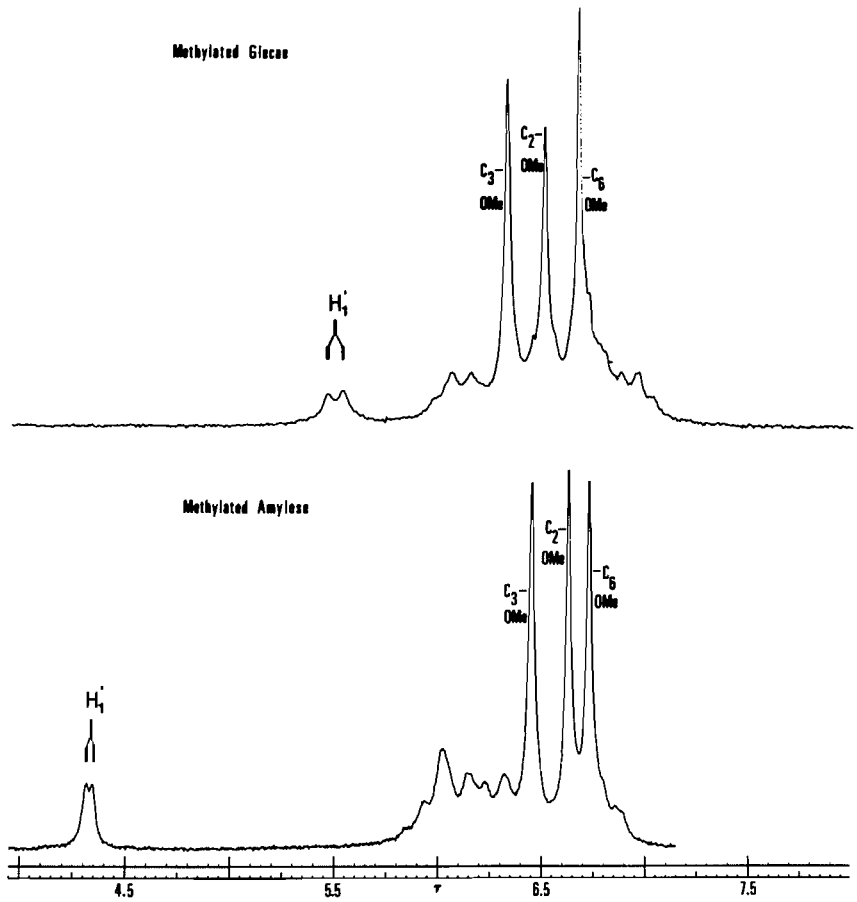

FIG. 1. The p.m.r. spectra (100 MHz) in benzene-d_6:chloroform-d (v/v 6:1) of the methylated derivatives of: Glucan from *R. pertusa* (top) and amylose from potato.

illustrated in Fig. 1. Devoid of the shielding effects of the methoxyl groups, the anomeric protons at the glycosidic linkages resonated to lower field than the remaining annular protons. The signals at τ 4.32 and 5.53 were assigned to the anomeric protons of the α- and β-linked linear polyglucans respectively and this was substantiated by the resonance of the proton at C-1 of the non-reducing moiety of methyl hepta-*O*-methyl-α- and β- maltoside and methyl hepta-*O*-methyl-α- and β-cellobioside at τ 4.29, 4.34 and 5.59 and 5.60 respectively. The spacings of 3.6 Hz for the doublet at τ 4.32 and 7.0 Hz for that at 5.53 are consistent with a *gauche* and *trans*-diaxial interaction between H-1 and -2 of the α- and β-linked glucose residues respectively. The signals at τ 6.44, 6.62, and 6.72 in the spectrum of methylated amylose (mol. wt. *ca.* 106 000) and τ 6.32, 6.51, and 6.68 in the spectrum of the methylated glucan (mol. wt. *ca.* 33 000) were ascribed (9) to the methoxyl groups at C-3, -2, and -6, respectively.

The anomeric configuration in this cell-wall β-(1 → 4)-linked glucan (cellulose) was verified chemically by the isolation of cellobiose and cellotriose as products of acetolysis. Callose, an insoluble β-(1 → 3)-linked glucan, reported to exist in the red seaweeds *Bangia* and *Porphyra* (10) was not evident as a polymer in *R. pertusa*.

The spectrum, Fig. 2, derived from a mixture (1:9, w/w) of methylated α-(1 → 4): β-(1 → 4)-linked glucan exhibited signals at τ 4.4 and 5.54 for the α- and β-anomeric protons and provided an integrated value of 9.5% content of α-linked residues. Together with the assessment of the overall anomeric configuration of the glycosidic linkages in polysaccharides (which is normally determined by isolation and characterization of

Can. J. Chem. Downloaded from www.nrcresearchpress.com by 210.87.254.5 on 09/05/12
For personal use only.

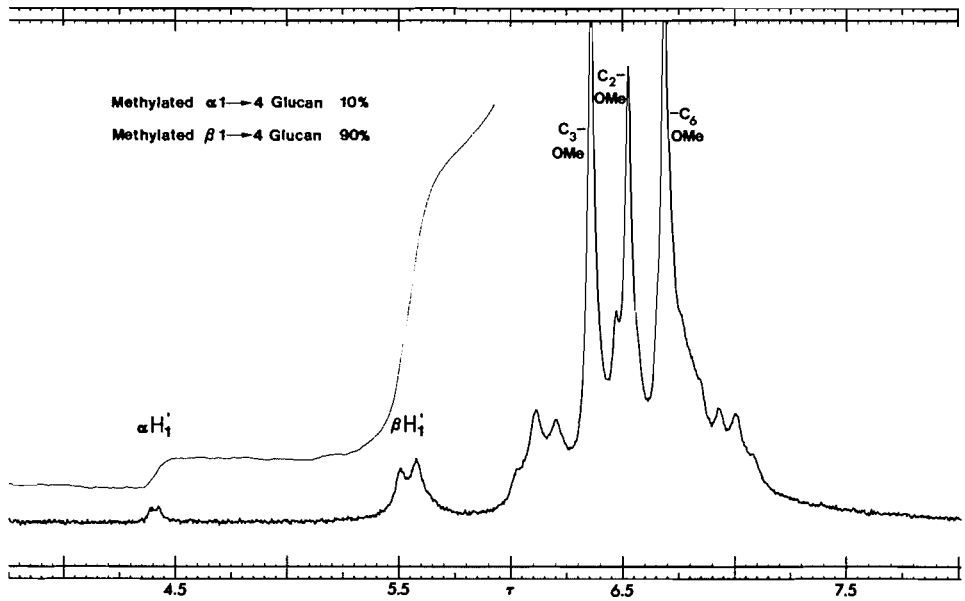

FIG. 2. The p.m.r. spectrum (100 MHz) in benzene-d_6: chloroform-d (v/v 6:1) of methylated α-(1 → 4): β-(1 → 4)-linked glucans (w/w 1:9).

partial depolymerization products), the p.m.r. spectra of methylated polysaccharides have provided for a distinction between α-linked branched and linear polyglucans (2). The insolubility or highly viscous nature of many polysaccharides in water preclude p.m.r. studies in deuterium oxide to assess anomeric configuration and the peracetylated derivatives have the disadvantage that the acetoxyl groups deshield the protons on C-2 and -3 into the region of the p.m.r. spectrum associated with the anomeric protons (11).

Experimental

The p.m.r. spectra were obtained with a Varian HA 100 spectrometer, τ values are relative to tetramethylsilane. The mass spectra were obtained with a Nuclide spectrometer. The g.l.c. was carried out on a column (170 × .45 cm) containing (w/w) 0.2% poly (ethylene glycol adipate), 0.2% poly (ethylene glycol succinate), and 0.4% silicone XF1150.

The residue (70 g) from aqueous extraction of the alga was treated with aqueous sulfuric acid (1%, 90°, 0.5 h), aqueous sodium hydroxide (1% under N_2, 6h), washed with water, resuspended in chlorine water (12 h) and the procedure repeated. After dialysis for 4 days, the slurry was freeze-dried to yield an insoluble polysaccharide (8 g; ash, 4.9%) which gave only glucose on hydrolysis.

The polysaccharide was dissolved in cuprammonium hydroxide solution (500 ml) then centrifuged to yield a siliceous residue and a centrifugate which on acidification with hydrochloric acid precipitated the polysaccharide (6.06 g; ash, 0.5%). The purified product (20 mg) was dissolved in sulfuric acid (72%, 0.2 ml, 1 h) then water (2.3 ml) was added and the solution heated at 100° for 6 h. The phenol – sulfuric acid estimation (12) of the hydrolysate gave 86.9% carbohydrate as glucose; cotton cellulose under the same conditions provided 88% carbohydrate as glucose. The hydrolysate of a sample of the polymer (50 mg) on treatment with *p*-nitroaniline followed by acetylation yielded 2,3,4,6-tetra-*O*-acetyl-*N*-(*p*-nitrophenyl)-β-D-glucopyranosylamine, m.p. and mixed m.p. 182–183°, $[\alpha]_D$ −101° (*c*, 1.0 in $CHCl_3$), which provided a mass spectrum with major peaks at *m/e* 468 (11%), 331 (10%), 169 (23%), 180 (11%), and 43 (100%). Nitration of the crude polysaccharide afforded a derivative which in ethyl acetate gave $[\eta] = 0.9$ corresponding to a d.p. of 120. The glucan (400 mg) was methylated with successive treatments of methyl sulfinyl carbanion and methyl iodide to give a product which was fractionated by dissolution in boiling mixtures of chloroform – light petroleum. The main fraction (420 mg, OCH_3 = 45.6%, $[\alpha]_D$ − 15° (*c*, 1.0 in benzene) was soluble in chloroform – light petroleum (1:4). A portion of the methylated polysaccharide (10 mg) was hydrolyzed with 90% formic acid for 1 h at 100° followed by 0.25 *M* sulfuric acid for 12 h at 100°, subsequently neutralized, the sugars converted into alditol acetates and analyzed by g.l.c. and mass spectrometry. Two fractions T_G 1.0 and 2.6 were shown to be chromatographically and mass spectrometrically identical to 1,5-di-*O*-acetyl-2,3,4,6-tetra-*O*-methyl-D-glucitol and 1,4,5-tri-*O*-acetyl-2,3,6-tri-*O*-methyl-D-glucitol in the molar proportions of 1:110. Methylated amylose, $[\alpha]_D$ + 212° (*c*, 1.0 in $CHCl_3$), OCH_3 45.5%, prepared and analyzed in a similar manner, contained 2,3,4,6-tetra- and 2,3,6-tri-*O*-methyl-D-glucose in the molar proportion 1:421.

A portion of the crude glucan (3 g) was stirred in a mixture of acetic anhydride (20 ml), acetic acid (20 ml), and concentrated sulfuric acid (2 ml) for 72 h. Separation

Can. J. Chem. Downloaded from www.nrcresearchpress.com by 210.87.254.5 on 09/05/12
For personal use only.

of the acetolysis products and deacetylation with barium methoxide yielded a mixture of mono- and oligomers (2.5 g) which were separated by chromatography on charcoal. The sugar (400 mg) eluted with water containing 5% ethanol, recrystallized from aqueous ethanol m.p. mixed m.p. 225°, $[\alpha]_D$ + 35° (*c*, 1.0 in H_2O) was identical to 4-*O*-β-D glucopyranosyl -D-glucose. Elution of the column with water containing 10% ethanol yielded a sugar (50 mg) recrystallized from aqueous ethanol m.p. and mixed m.p. 206° $[\alpha]_D$ + 21° (*c*, 1.0 in H_2O) which was identical to *O*-β-D-glucopyranosyl-(1 → 4)-*O*-β-D-glucopyranosyl-(1 → 4)-D-glucose.

Methyl hepta-*O*-methyl α-D-maltoside provided a p.m.r. spectrum in benzene-d_6: chloroform-*d* (6:1 v/v) with signals at τ 5.33, H-1 ($J_{1,2}$ = 3.6 Hz), 4.29, H-1′ ($J_{1',2'}$ = 3.6 Hz) and the corresponding β-glycoside exhibited signals at τ 5.92, H-1 ($J_{1,2}$ = 7.6 Hz) and 4.34, H-1′ ($J_{1',2'}$ = 3.6 Hz). Methyl hepta-*O*-methyl α- and β-cellobioside exhibited nomeric signals for the α-glycoside at τ 5.31, H-1 ($J_{1,2}$ = 3.6 Hz), 5.59, H-1′ ($J_{1',2'}$ = 7.3 Hz) with the corresponding β-glycoside signals at τ 5.88, H-1 ($J_{1,2}$ = 7.5 Hz) and 5.60, H-1′ ($J_{1',2'}$ = 7.3 Hz). The spectrum of 2,3,4,6-tetra-*O*-methyl-α-D-glucose in the solvent mixture exhibited 4-OMe signals at τ 6.76 (C-6), 6.67 (C-2), 6.54 (C-4), and 6.40 (C-3); the spectrum of the corresponding methyl glycoside was in accord with Gagnaire (9).

The authors are indebted to Mr. J. Love for p.m.r. and mass spectral analysis.

1. E. Percival and R. H. McDowell. Chemistry and enzymology of marine algal polysaccharides. Academic Press, London, 1967. p. 86.
2. J. N. C. Whyte. Carbohyd. Res. **16**, 220 (1971).
3. N. K. Kochetkov and O. S. Chizhov. Advan. Carbohyd. Chem. **21**, 39 (1966).
4. K. Biemann and J. A. McCloskey. J. Amer. Chem. Soc., **84**, 2005 (1962).
5. G. S. Johnson, W. S. Ruliffson, and R. Graham Cooks. J. Chem. Soc. D 587 (1970).
6. S. Hakomori. J. Biochem. Tokyo, **55**, 205 (1964).
7. H. Bjorndal, K. E. Ericksson, Per J. Garegg, B. Lindberg, and B. Swan. Acta Chem. Scand. **19**, 2309 (1965).
8. J. W. Green. Methods in carbohydrate chemistry VIII. Acad. Press, New York, N.Y. 1963. p. 213.
9. D. Gagnaire and L. Odier. Carbohyd. Res., **11**, 33 (1969).
10. M. L. Priou. Thèse presentée à la Faculté des Sciences de L'Université de Rennes, Série C, No. 14, Masson et Cie, Paris, France 1962, pp. 321–406.
11. B. Casu, M. Reggiani, G. G. Gallo, and A. Vigevani. Carbohyd. Res. **12**, 157 (1970).
12. M. Dubois, K. A. Gilles, J. K. Hamilton, P. A. Rebers, and F. Smith. Anal. Chem. **28**, 350, 1956.

Kinetic Isotope Effects in the Radiation-induced Oxidation of Alcohols by Hydrogen Peroxide in Aqueous Solution

C. E. Burchill and G. F. Thompson[1]

Department of Chemistry, University of Manitoba, Winnipeg 19, Manitoba

Received October 15, 1970

By using selectively deuterated alcohols it is demonstrated that abstractions from both α and β positions of 2-propanol and ethanol contribute to the overall mechanism for the radiation-induced chain oxidation of these alcohols by hydrogen peroxide. Kinetic isotope effects are measured for abstraction of H by OH from 2-propanol and ethanol at both α and β positions and for the H atom transfer reaction from the alcohol to the β radical. The chain oxidation of methanol shows no primary kinetic isotope effect on substitution of CD_3OH.

On a démontré, en utilisant des alcools deutérés sélectivement, que des abstractions faites en position α et en position β du propanol-2 et de l'éthanol contribuent au mécanisme global de l'oxydation, en chaîne et induite par des radiations, de ces alcools par le peroxyde d'hydrogène. On a mesuré les effets isotopiques cinétiques pour l'enlèvement de H· par des ·OH du propanol-2 et de l'éthanol aux positions α et β et pour la réaction de transfert de H· de l'alcool au radical β. L'oxydation en chaîne du méthanol ne présente aucun effet isotopique lorsqu'on lui substitue du CD_3OH.

Canadian Journal of Chemistry, 49, 1305 (1971)

The radiation-induced oxidation of several aliphatic alcohols by hydrogen peroxide has recently been investigated in these laboratories (1*a*, *b*). On the basis of the observed dependence of *G*(acetone) and $G(-H_2O_2)$ on alcohol concentration, Burchill and Ginns proposed eqs. 1–8 as a mechanism for the chain oxidation of 2-propanol by hydrogen peroxide (1*a*).

$$H_2O \rightsquigarrow e_{aq}^-, H, OH, H_2O_2, H_2, H_3O^+$$

[1] $$e_{aq}^- + H_2O_2 \rightarrow OH^- + OH$$

[1]Present address: Department of Pure and Applied Physics, The Queen's University of Belfast, Belfast, BT7 INN, N. Ireland.

Can. J. Chem. Downloaded from www.nrcresearchpress.com by 210.87.254.5 on 09/05/12
For personal use only.

of the acetolysis products and deacetylation with barium methoxide yielded a mixture of mono- and oligomers (2.5 g) which were separated by chromatography on charcoal. The sugar (400 mg) eluted with water containing 5% ethanol, recrystallized from aqueous ethanol m.p. mixed m.p. 225°, $[\alpha]_D$ + 35° (*c*, 1.0 in H_2O) was identical to 4-*O*-β-D glucopyranosyl -D-glucose. Elution of the column with water containing 10% ethanol yielded a sugar (50 mg) recrystallized from aqueous ethanol m.p. and mixed m.p. 206° $[\alpha]_D$ + 21° (*c*, 1.0 in H_2O) which was identical to *O*-β-D-glucopyranosyl-(1 → 4)-*O*-β-D-glucopyranosyl-(1 → 4)-D-glucose.

Methyl hepta-*O*-methyl α-D-maltoside provided a p.m.r. spectrum in benzene-d_6: chloroform-*d* (6:1 v/v) with signals at τ 5.33, H-1 ($J_{1,2}$ = 3.6 Hz), 4.29, H-1′ ($J_{1',2'}$ = 3.6 Hz) and the corresponding β-glycoside exhibited signals at τ 5.92, H-1 ($J_{1,2}$ = 7.6 Hz) and 4.34, H-1′ ($J_{1',2'}$ = 3.6 Hz). Methyl hepta-*O*-methyl α- and β-cellobioside exhibited nomeric signals for the α-glycoside at τ 5.31, H-1 ($J_{1,2}$ = 3.6 Hz), 5.59, H-1′ ($J_{1',2'}$ = 7.3 Hz) with the corresponding β-glycoside signals at τ 5.88, H-1 ($J_{1,2}$ = 7.5 Hz) and 5.60, H-1′ ($J_{1',2'}$ = 7.3 Hz). The spectrum of 2,3,4,6-tetra-*O*-methyl-α-D-glucose in the solvent mixture exhibited 4-OMe signals at τ 6.76 (C-6), 6.67 (C-2), 6.54 (C-4), and 6.40 (C-3); the spectrum of the corresponding methyl glycoside was in accord with Gagnaire (9).

The authors are indebted to Mr. J. Love for p.m.r. and mass spectral analysis.

1. E. Percival and R. H. McDowell. Chemistry and enzymology of marine algal polysaccharides. Academic Press, London, 1967. p. 86.
2. J. N. C. Whyte. Carbohyd. Res. **16**, 220 (1971).
3. N. K. Kochetkov and O. S. Chizhov. Advan. Carbohyd. Chem. **21**, 39 (1966).
4. K. Biemann and J. A. McCloskey. J. Amer. Chem. Soc., **84**, 2005 (1962).
5. G. S. Johnson, W. S. Ruliffson, and R. Graham Cooks. J. Chem. Soc. D 587 (1970).
6. S. Hakomori. J. Biochem. Tokyo, **55**, 205 (1964).
7. H. Bjorndal, K. E. Ericksson, Per J. Garegg, B. Lindberg, and B. Swan. Acta Chem. Scand. **19**, 2309 (1965).
8. J. W. Green. Methods in carbohydrate chemistry VIII. Acad. Press, New York, N.Y. 1963. p. 213.
9. D. Gagnaire and L. Odier. Carbohyd. Res., **11**, 33 (1969).
10. M. L. Priou. Thèse presentée à la Faculté des Sciences de L'Université de Rennes, Série C, No. 14, Masson et Cie, Paris, France 1962, pp. 321–406.
11. B. Casu, M. Reggiani, G. G. Gallo, and A. Vigevani. Carbohyd. Res. **12**, 157 (1970).
12. M. Dubois, K. A. Gilles, J. K. Hamilton, P. A. Rebers, and F. Smith. Anal. Chem. **28**, 350, 1956.

Kinetic Isotope Effects in the Radiation-induced Oxidation of Alcohols by Hydrogen Peroxide in Aqueous Solution

C. E. Burchill and G. F. Thompson[1]

Department of Chemistry, University of Manitoba, Winnipeg 19, Manitoba

Received October 15, 1970

By using selectively deuterated alcohols it is demonstrated that abstractions from both α and β positions of 2-propanol and ethanol contribute to the overall mechanism for the radiation-induced chain oxidation of these alcohols by hydrogen peroxide. Kinetic isotope effects are measured for abstraction of H by OH from 2-propanol and ethanol at both α and β positions and for the H atom transfer reaction from the alcohol to the β radical. The chain oxidation of methanol shows no primary kinetic isotope effect on substitution of CD_3OH.

On a démontré, en utilisant des alcools deutérés sélectivement, que des abstractions faites en position α et en position β du propanol-2 et de l'éthanol contribuent au mécanisme global de l'oxydation, en chaîne et induite par des radiations, de ces alcools par le peroxyde d'hydrogène. On a mesuré les effets isotopiques cinétiques pour l'enlèvement de H· par des ·OH du propanol-2 et de l'éthanol aux positions α et β et pour la réaction de transfert de H· de l'alcool au radical β. L'oxydation en chaîne du méthanol ne présente aucun effet isotopique lorsqu'on lui substitue du CD_3OH.

Canadian Journal of Chemistry, 49, 1305 (1971)

The radiation-induced oxidation of several aliphatic alcohols by hydrogen peroxide has recently been investigated in these laboratories (1*a*, *b*). On the basis of the observed dependence of *G*(acetone) and $G(-H_2O_2)$ on alcohol concentration, Burchill and Ginns proposed eqs. 1–8 as a mechanism for the chain oxidation of 2-propanol by hydrogen peroxide (1*a*).

$$H_2O \rightsquigarrow e_{aq}^-, H, OH, H_2O_2, H_2, H_3O^+$$

[1] $$e_{aq}^- + H_2O_2 \rightarrow OH^- + OH$$

[1]Present address: Department of Pure and Applied Physics, The Queen's University of Belfast, Belfast, BT7 INN, N. Ireland.

Can. J. Chem. Downloaded from www.nrcresearchpress.com by 210.87.254.42 on 09/05/12
For personal use only.

Can. J. Chem. Downloaded from www.nrcresearchpress.com by 210.87.254.42 on 09/05/12
For personal use only.

[2] $H + (CH_3)_2CHOH \rightarrow H_2 + (CH_3)_2\dot{C}OH$
$(CH_3)_2\dot{C}OH = \alpha$

[3] $H + (CH_3)_2CHOH \rightarrow H_2 + CH_3CHOH\dot{C}H_2$
$CH_3CHOH\dot{C}H_2 = \beta$

[4] $OH + (CH_3)_2CHOH \rightarrow H_2O + \alpha$

[5] $OH + (CH_3)_2CHOH \rightarrow H_2O + \beta$

[6] $\alpha + H_2O_2 \rightarrow (CH_3)_2CO + H_2O + OH$

[7] $\beta + (CH_3)_2CHOH \rightarrow (CH_3)_2CHOH + \alpha$

[8] $2\alpha \rightarrow$ 2,5-Hexanediol or other products

An expression for G(acetone) may be derived using the usual steady-state assumptions, eqs. 9, 10.

$$[9]\quad G(\text{acetone}) = \left[G_H \left\{ \frac{k_2}{k_5} \left(\frac{k_4 + k_5}{k_2 + k_3} \right) \right\} + \frac{k_4}{k_5} (G_{e_{aq}^-} + G_{OH}) \right] + \left(1 + \frac{k_4}{k_5} \right) k_7 \times \left(\frac{G_{e_{aq}^-} + G_H + G_{OH}}{2k_8 \cdot D} \right)^{1/2} [\text{2-propanol}]$$

where D is the dose rate in units of 6.023×10^{25} eV l^{-1} s^{-1}.

$$[10]\quad G(-H_2O_2) = G(\text{acetone}) + G_{e_{aq}^-} - G_{H_2O_2}$$

If $(CH_3)_2CDOH$ is substituted for $(CH_3)_2CHOH$, reactions 2, 4, and 7 would be expected to show a normal primary kinetic isotope effect if they are, in fact, hydrogen atom transfer reactions. Equation 9 predicts that this would lead to a decrease in both the slope and the intercept of a plot of G(acetone) as a function of alcohol concentration. Similarly, if $(CH_3)_2CHOH$ is replaced by $(CD_3)_2CHOH$, reactions 3 and 5 should show a primary kinetic isotope effect leading to an increase in both the slope and the intercept of the concentration dependence of G(acetone).

Burchill and Ginns have shown that the radiation-induced peroxidation of ethanol (1*b*) is very similar to that of 2-propanol and may be described by a reaction scheme analogous to eqs. 1–8. Hence selective deuteration of ethanol should have effects comparable to those outlined above for 2-propanol.

In the case of methanol, which has no β carbon, it was found (1*b*) that the results were adequately rationalized by a mechanism employing only one alcohol-derived radical. This simpler reaction scheme is outlined in eqs. 11–14. Equation 15 predicts that the first order consumption of peroxide under irradiation will be essentially identical for CH_3OH and CD_3OH, assuming that neither reaction 13 or 14 involves H atom transfer from a C—H bond.

[11] $H + CH_3OH \rightarrow H_2 + \dot{C}H_2OH$

[12] $OH + CH_3OH \rightarrow H_2O + \dot{C}H_2OH$

[13] $\dot{C}H_2OH + H_2O_2 \rightarrow H_2CO + H_2O + OH$

[14] $2\,\dot{C}H_2OH \rightarrow$ ethylene glycol or $H_2CO + CH_3OH$

$$[15]\quad \frac{-d[H_2O_2]}{dt} = (G_{e_{aq}^-} - G_{H_2O_2})D + k_{13} \left[\frac{(G_{e_{aq}^-} + G_H + G_{OH})D}{2k_{14}} \right]^{1/2} [H_2O_2]$$

In order to verify the mechanisms proposed above we have carried out a study of the radiation-induced peroxidation of three 2-propanols ($(CH_3)_2CHOH$, $(CH_3)_2CDOH$, and $(CD_3)_2CHOH$), three ethanols (CH_3CH_2OH, CH_3CD_2OH, and CD_3CH_2OH), and two methanols (CH_3OH and CD_3OH).

Experimental

2-Propanol (Fisher Certified Reagent), ethanol (Canadian Industrial Alcohols, absolute), methanol (Fisher Certified Reagent), and hydrogen peroxide (Fisher Reagent, 30%, unstabilized) were used without further purification. The following partially deuterated alcohols, all of guaranteed 99% isotopic purity, supplied by Merck, Sharp and Dohme were used as received: 2-d_1 2-propanol ($(CH_3)_2CDOH$); 1,1,1,3,3,3,-d_6 2-propanol ($(CD_3)_2CHOH$); 1,1-d_2 ethanol (CH_3CD_2OH); 2,2,2-d_3 ethanol (CD_3CH_2OH); and d_3 methanol (CD_3OH). Water was redistilled from alkaline $KMnO_4$ and then from acidic $K_2Cr_2O_7$ solution. Analytical reagents were of reagent grade and were used without further treatment.

Two milliliters aliquots of the solutions in 5 ml Pyrex bulbs were degassed by four freeze–pump–thaw cycles and irradiated at an average dose rate of 1.32×10^{19} eV l^{-1} s^{-1} using a ^{60}Co Gammacell 220 source (Atomic Energy of Canada, Ltd.). Dose rates were estimated using the Fricke dosimeter (2) and assuming $G(Fe^{3+}) = 15.6$. Absorbed dose rates in experimental solutions were assumed to be proportional to their electron densities.

Acetone was determined spectrophotometrically using salicylaldehyde (3), and hydrogen peroxide by the triiodide method (4).

Results

Acetone formation yields for a constant initial hydrogen peroxide concentration of 0.01 *M* and

Can. J. Chem. Downloaded from www.nrcresearchpress.com by 210.87.254.42 on 09/05/12
For personal use only.

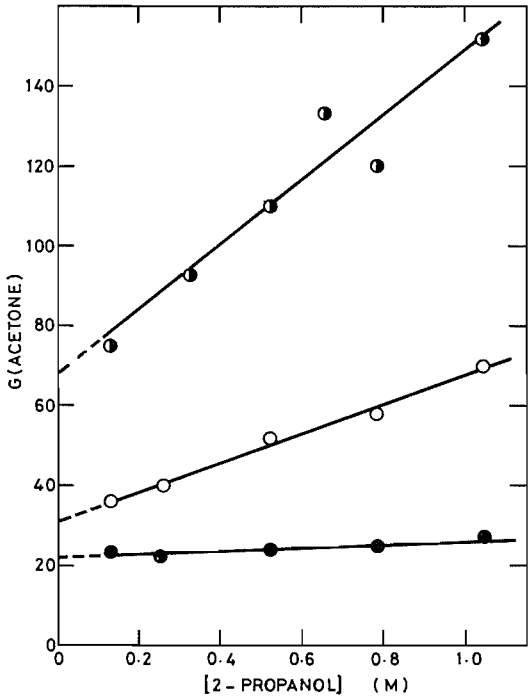

FIG. 1. Radiation-induced oxidation of 2-propanols by hydrogen peroxide in aqueous solution. Initial $[H_2O_2] = 0.01\ M$. Dose rate = 1.32×10^{19} eV l^{-1} s^{-1}. ◑ $(CD_3)_2CHOH$; ○ $(CH_3)_2CHOH$; ● $(CH_3)_2CDOH$.

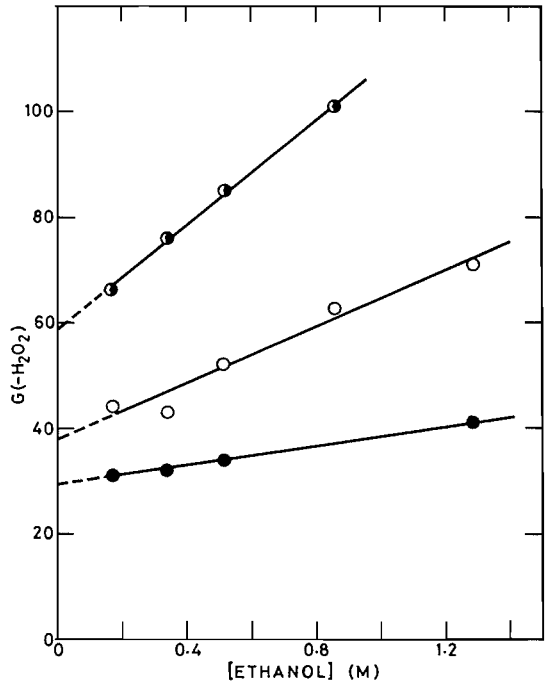

FIG. 2. Radiation-induced reduction of hydrogen peroxide by ethanols in aqueous solution. Initial $[H_2O_2] = 0.02\ M$. Dose rate = 1.32×10^{19} eV l^{-1} s^{-1}. ◑ CD_3CH_2OH; ○ CH_3CH_2OH; ● CH_3CD_2OH.

various concentrations of the three 2-propanols are shown in Fig. 1. The essential equivalence of acetone formation and peroxide consumption reported previously for $(CH_3)_2CHOH$ (1*a*) was found to hold also for the partially deuterated alcohols. Thus for solutions 0.131 *M* in alcohol and 0.01 *M* in H_2O_2, *G*(acetone) = 23.6 and $G(-H_2O_2) = 20.8$ for $(CH_3)_2CDOH$, and *G*(acetone) = 74.5 and $G(-H_2O_2) = 76.9$ for $(CD_3)_2CHOH$. For all three 2-propanols, *G*(acetone) is a linear function of alcohol concentration over the range 0.13–1.05 *M*. The slopes and extrapolated intercepts of the best-fit straight lines are given in Table 1.

The variation of the peroxide destruction yields with ethanol concentration for solutions of the three ethanols is shown in Fig. 2. The initial concentration of hydrogen peroxide was 0.02 *M* in each case. In the case of CH_3CH_2OH and CH_3CD_2OH, $G(-H_2O_2)$ increased linearly with increasing alcohol concentration over the range 0.17–1.28 *M* but for CD_3CH_2OH the yield leveled off above 0.9 *M* and was significantly less at 1.28 *M*. The slopes and extrapolated intercepts obtained from the linear portions of the curves are given in Table 2.

When methanol is the oxidizable substrate the reduction of hydrogen peroxide under irradiation shows a first-order dependence on peroxide concentration. Apparent first-order rate constants for peroxide removal have been determined for four different alcohol concentrations for both CH_3OH and CD_3OH. The results obtained are given in Table 3.

TABLE 1. Slopes and intercepts calculated for the lines of Fig. 1

Alcohol	G_0(acetone)	Slope (M^{-1})
$(CH_3)_2CHOH$	31.2±0.7	36.7±1.2
$(CH_3)_2CDOH$	22.1±0.5	4.2±0.8
$(CD_3)_2CHOH$	66.7±3.3	78.8±5.7

TABLE 2. Slopes and intercepts calculated for the lines of Fig. 2

Alcohol	$G_0(-H_2O_2)$	Slope (M^{-1})
CH_3CH_2OH	37.5±1.3	26.8±2.3
CH_3CD_2OH	29.2±0.2	8.9±0.4
CD_3CH_2OH	58.5±0.4	50.1±0.9

Can. J. Chem. Downloaded from www.nrcresearchpress.com by 210.87.254.42 on 09/05/12
For personal use only.

TABLE 3. Apparent first-order rate constants for the radiation-induced reduction of H_2O_2 by methanols in aqueous solution. Dose rate = 1.32×10^{19} eV l^{-1} s^{-1}

[Alcohol] (M)	$10^3 k'$ (s^{-1})	
	CH_3OH	CD_3OH
0.249	1.07 ± 0.06	1.01 ± 0.06
0.494	1.03	1.01
0.741	1.01	1.11
1.24	1.00	1.12

Discussion

It is apparent from Figs. 1 and 2 that selective deuteration of the alcohol has essentially the same effects on the radiation-induced chain oxidation of 2-propanol and ethanol by hydrogen peroxide. In both cases deuteration at the α position causes a marked decrease in both the slope and intercept of the yield *vs.* alcohol concentration plot whereas the opposite effect is observed on deuteration of the β position.

The effects are in excellent qualitative agreement with those predicted in the introduction on the basis of eq. 9 and thus provide further strong evidence in favor of the mechanism proposed by Burchill and Ginns (1*a*, *b*). Furthermore, the large increase in the chain yield observed on β deuteration of either 2-propanol or ethanol is, *per se*, a direct indication of the involvement of the β position in the reaction scheme.

The lack of significant effect observed on deuteration of the methyl group of methanol is evidence that reaction 13 (and its analogue, [6], for 2-propanol and ethanol) does not involve rupture of a C—H bond as a rate-determining process and is in accord with the prediction previously made on the basis of eq. 15.

In the case of 2-propanol and ethanol it is possible to estimate the magnitudes of the primary hydrogen kinetic isotope effects for reactions 4, 5, and 7 from the data of Tables 2 and 3. Assuming that secondary isotope effects are unimportant, it may be seen from eq. 9 that the ratio of the intercepts or the ratio of the slopes for $(CD_3)_2CHOH$ and $(CH_3)_2CHOH$ will give essentially $k_{5(H)}/k_{5(D)}$ while the ratio of the intercepts for $(CH_3)_2CHOH$ and $(CH_3)_2CDOH$ will be approximately $k_{4(H)}/k_{4(D)}$ and the ratio of their slopes will be

$$\left(\frac{k_{5(H)} + k_{4(H)}}{k_{5(H)} + k_{4(D)}}\right)\frac{k_{7(H)}}{k_{7(D)}}$$

For more precise values of the kinetic isotope effects it is necessary to assume specific values for the primary free radical yields, $G_{e_{aq}^-}$, G_{OH}, and G_H, the kinetic isotope effects on reactions 2 and 3, and the rate constant ratio k_2/k_3. This calculation is, however, very insensitive to the particular values chosen. The following values were assumed for the primary yields in irradiated aqueous solution as being more applicable to solutions containing appreciable scavenger concentrations than those previously assumed by Burchill and Ginns (1*b*):

$$G_H + G_{e_{aq}^-} = 3.18$$

$$G_{OH} = 2.72$$

$$G_{H_2O_2} = 0.68 \quad (5)$$

$$G_H = 0.55 \quad (6)$$

k_2/k_3 was taken as 20 for 2-propanol and as 10.5 for ethanol (7). Anbar and Meyerstein (8) have obtained a value of 7.5 ± 1 for $k_{2(H)}/k_{2(D)}$ and this figure has also been assumed for $k_{3(H)}/k_{3(D)}$. This value is somewhat less than that obtained by Vacek and von Sonntag (9) for hydrogen abstraction from $(CH_3)_2CHOH$ and $(CD_3)_2CDOH$ by hydrogen atoms. However, reactions 2 and 3 are not involved in chain propagation, with the result that the magnitudes of the isotope effects calculated for [4] and [5] are almost independent of the particular value assumed. The same values were assumed also for the isotope effects on reactions 2 and 3 for ethanols.

The results of these calculations are given in Table 4. The uncertainties quoted are probable deviations based on the scatter of the points from the best-fit lines in Figs. 1 and 2. Several comments should be made regarding the results. The values of k_4/k_5 given in Table 4 are somewhat different from those previously calculated (1*a*, *b*). For 2-propanol this simply reflects the different choice of primary yields used in calculation but with ethanol there was a significant difference in the observed reaction yields for the undeuterated alcohol from those reported earlier (1*b*) although the concentration dependence was similar. It was observed that the reduction of H_2O_2 in the presence of ethanol tended to become somewhat non-linear with dose at larger conversions. An average G value calculated from a non-linear yield-dose curve varies with the extent of the reaction and this may, in part, account for the

TABLE 4. Rate constants and rate constant ratios for H atom abstraction reactions from 2-propanol and ethanol. Values of k_4/k_5 and k_7 from previous work (1*a*, *b*) are included

	Rate constant ratio	Rate constant (M^{-1} s^{-1})
2-Propanol	$k_4/k_5 = 5.2 \pm 0.1 (6.2)$ (1*a*)	$k_4+k_5 = 1.4\times10^9$ (7)
	$k_{5(H)}/k_{5(D)} = 2.08\pm0.12$ (intercept)	$k_5 = 2.3\times10^8$
	$= 2.15\pm0.16$ (slope)	
	$k_{4(H)}/k_{4(D)} = 1.38\pm0.05$	$k_4 = 1.2\times10^9$
	$k_{7(H)}/k_{7(D)} = 7.3 \pm 1.5$	$k_7 = 51\pm2(53\pm10)$ (1*a*)
		(assuming $2k_8 = 2\times10^9$)
Ethanol		
	$k_4/k_5 = 6.0 \pm 0.2 (8.2)$ (1*b*)	$k_4+k_5 = 1.1\times10^9$ (7)
	$k_{5(H)}/k_{5(D)} = 1.55\pm0.06$ (intercept)	$k_5 = 1.6\times10^8$
	$= 2.28\pm0.20$ (slope)	
	$k_{4(H)}/k_{4(D)} = 1.24\pm0.04$	$k_4 = 9\times10^8$
	$k_{7(H)}/k_{7(D)} = 2.9 \pm 0.3$	$k_7 = 33\pm3(16\pm3)$ (1*b*)
		(assuming $2k_8 = 2\times10^9$)

differences. The difference in initial yields observed with ethanol is also reflected in a significantly higher value of k_7 reported for ethanol in this work. For ethanol the kinetic isotope effect calculated for reaction 5 differs by more than the estimated precision depending upon whether it is calculated from the slope or intercept ratio in Fig. 2. This is a further indication that the reliability of the calculated parameters for ethanol may be significantly poorer than the precision estimates given.

It is a feature of both the 2-propanol and ethanol systems that

$$\frac{k_{4(H)}}{k_{4(D)}} < \frac{k_{5(H)}}{k_{5(D)}} < \frac{k_{7(H)}}{k_{7(D)}}$$

which is the reverse order of the magnitudes of the specific rate constants. This is in agreement with the qualitative picture that if an atom is transferred from one site to another in a rate-determining step there will be a normal primary kinetic isotope effect observed if the bond strength to the atom (and hence the zero-point energy) is decreased in the transition state relative to that in the initial state. If the bond is not significantly weakened in forming the transition state (a situation corresponding to a small activation energy) the isotope effect will be small whereas if the bond is very weak in the transition state (corresponding to a large activation energy) the kinetic isotope effect will be large. Hence for a series of analogous reactions, such as abstraction of hydrogen atoms from C—H bonds by free radicals, the kinetic hydrogen isotope effects are expected to be in the reverse order of their activation energies (and their rate constants.)

The authors gratefully acknowledge financial support for this research from Atomic Energy of Canada Limited, Commercial Products Division and from the Graduate Research Fund of the University of Manitoba for contributions to a fellowship to G. F. T.

1. C. E. BURCHILL and I. S. GINNS. Can. J. Chem. **48**, (*a*) 1232, (*b*) 2628 (1970).
2. H. A. J. B. BATTAERD and G. W. TREGEAR. Rev. Pure and Appl. Chem. **16**, 83 (1966).
3. S. BERNTSSON. Anal. Chem. **28**, 1337 (1956).
4. A. O. ALLEN, C. J. HOCHANADEL, J. A. GHORMLEY, and T. W. DAVIS. J. Phys. Chem. **56**, 697 (1952).
5. I. G. DRAGANIĆ, M. T. NENADOVIĆ, and Z. D. DRAGANIĆ. J. Phys. Chem. **73**, 2564 (1969).
6. M. HAISSINSKY. J. Chim. Phys. **62**, 1141 (1965).
7. M. ANBAR and P. NETA. Int. J. Appl. Radiat. Isotop. **18**, 493 (1967).
8. M. ANBAR and J. MEYERSTEIN. J. Phys. Chem. **68**, 3184 (1964).
9. K. VACEK and C. VON SONNTAG. Chem. Commun. 1256 (1969).

Can. J. Chem. Downloaded from www.nrcresearchpress.com by 210.87.254.42 on 09/05/12
For personal use only.

Photolysis of 4-Methyl 3-Hexanone and 2-Methoxy 3-Pentanone in Hydrocarbon Solution

L. P-Y. LEE, B. MCANENEY, AND J. E. GUILLET
Department of Chemistry, University of Toronto, Toronto, Ontario

Received January 7, 1970[1]

Studies of the photolysis of 4-methyl 3-hexanone and the iso-electronic 2-methoxy 3-pentanone have been made in hydrocarbon solution using light of wavelength 313 nm. The latter compound gives only Norrish type II products with a quantum yield of 0.19 ± .01. The former gives a predominance of type I products with a total quantum yield of 0.23 ± .01 and the quantum yield for type II is reduced to 0.10 ± .01. The predominant type I reaction appears to involve α-scission to give an ethyl and a 2-methyl butyryl radical, which suggests a "cage effect". It is suggested that the reason for the suppression of the type I reaction in 2-methoxy 3-pentanone is the greater ease of γ-hydrogen abstraction due to the presence of the oxygen atom in a six-membered transition state.

On a étudié la photolyse en solution dans des hydrocarbures à 313 mm, de la méthyl-4 hexanone-3 et de la méthoxy-2 pentanone-3 qui lui est iso-électronique. Ce dernier composé ne donne, avec un rendement quantique de 0.19 ± 0.01, que des produits provenant d'une réaction de Norrish de type II. Par ailleurs le premier conduit de préférence à des produits de type I avec un rendement quantique de 0.23 ± 0.01 alors que le rendement quantique des produits de type II n'est que de 0.10 ± 0.01. La formation d'une quantité prépondérante de composés de type I semble impliquer une session α conduisant à des radicaux éthyle et méthyl-2 butyryle qui suggérerait un "effet de cage". On croit que le fait de la réaction de type I ne se produit pas provient de ce que dans la méthoxy-2 pentanone-3 l'hydrogène γ est enlevé plus facilement dû à la présence d'oxygène dans l'état de transition à six chaînons.

Canadian Journal of Chemistry, 49, 1310 (1971)

A considerable body of evidence (1–3) now supports the role of a cyclic six-membered transition state in the Norrish type II photoelimination reaction of aliphatic ketones containing hydrogen in the γ-position. It appeared to us of interest to determine if the substitution of a hetero atom such as oxygen for a methylene in the cyclic ring would alter the quantum yields for the various photochemical processes. Accordingly, we have studied the photolysis of two ketones, 4-methyl 3-hexanone and 2-methoxy 3-pentanone. The structure of the two ketones is identical except that in the latter compound an oxygen atom replaces a methylene group.

Srinivasan (4) has shown that the photolysis of methoxyacetone at 313 nm in the vapor phase leads to the formation of acetone and formaldehyde as the major products. Since these are the products expected from the type II reaction, it seemed likely that a similar reaction would occur for 2-methoxy 3-pentanone. The quantum yield of acetone obtained by Srinivasan was 0.32 as compared with 0.22 for 2-pentanone obtained by Ausloos and Rebbert (5). This was considered to be an indication that the presence of the hetero atom in the cyclic transition state increased the probability of the type II reaction. Similar results will be shown in the present work.

In other analogous studies, a series of alkoxy acetophenones was investigated by Turro and Lewis (6) and it was shown that only the type II products and the cyclic oxetanol were formed, the total quantum yield being unity for the sum of the two processes. However, Yates and Szabo (7) who studied a number of alkyl and aryl alkoxy ketones in the liquid phase, report that only a very low yield of cyclic product was formed in the photolysis of methoxy acetone and 1-methoxy-3,3-dimethyl-2-butanone. On this basis they concluded that formation of the cyclic compound was considerably less probable in aliphatic ketones than in the analogous aromatic ketones containing an α-alkoxy group.

Experimental

2-Methoxy 3-pentanone and 4-methyl 3-hexanone were synthesized from the appropriate acid chlorides by reaction with diethyl cadmium by the method of Cason and Prout (8). The crude reaction products were purified on a preparative gas chromatograph and are estimated to be better than 99.8% pure by v.p.c. analysis. 2-Methyl butyraldehyde was prepared by reaction of 2-butyl magnesium chloride with methyl formate. The compounds were identified by their u.v. and n.m.r. spectra.

Product analysis was made by gas chromatography using a Perkin–Elmer 800 Gas Chromatograph. The irradiation products were identified by the identity of their retention times on two different columns using authentic samples of the suspected compound as reference. The solvent used for the photolysis was *n*-undecane which had

[1]Revision received November 3, 1970.

Can. J. Chem. Downloaded from www.nrcresearchpress.com by 210.87.254.40 on 09/05/12
For personal use only.

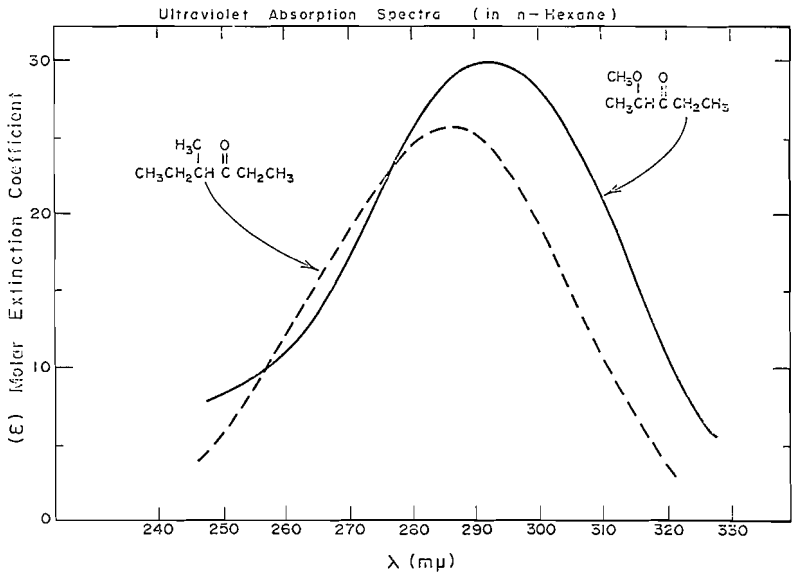

FIG. 1. The u.v. absorption spectra of 4-methyl 3-hexanone and 2-methoxy 3-pentanone in *n*-hexane.

been chromatographically purified and an internal standard (tetradecane) was used for quantitative work. Photolysis experiments were carried out both under nitrogen and in a cell sealed under vacuum.

The photolysis apparatus consisted of a medium pressure Mercury arc (B.T.H. type ME/D), a quartz lens, a solution filter, an interference filter, a heating block, and a quartz photolysis cell and photomultiplier all mounted rigidly on an optical bench. The system is similar to that described by Hartley and Guillet (3). The 3130 Å wavelength line was isolated by the use of a Carl Zeiss U.V.–P.I.L. line filter with a λ_{max} equal to 315 with a 70 Å half-width. The photolysis cell was a 1 mm path length quartz cell sealed to a side arm containing a quartz to pyrex graded seal. The cell was heated in an aluminum block the temperature of which was maintained constant by a circulating oil bath from a Lauda K-2 ultra thermostat. The light beam intensity was monitored by an RCA IP-28 photomultiplier tube whose response was calibrated against a uranyl oxalate actinometer.

Results and Discussion

The absorption spectra of the two ketones are shown in Fig. 1. Both ketones show the characteristic low intensity absorption of the $n \rightarrow \pi^*$ transition in the 250–330 mμ region. However, the band for the methoxy ketone has a somewhat higher molar extinction coefficient and shows a red shift. This red shift is due to the substitution of the methoxy group for an ethyl group. It can be attributed to a lowering of the energy level of the π^* antibonding orbital of the carbonyl group by the contribution of the lone pair electrons on the ether oxygen, which permits further delocalization of the electron over a four atom system (as for example in a conjugated diene). The n level of the non-bonding electrons localized on the carbonyl oxygen will not be affected to the same degree by the presence of the ether oxygen. Hence the energy corresponding to the $n \rightarrow \pi^*$ transition is reduced, and λ_{max} is shifted to longer wavelengths.

The analytical results for the photolysis of the two ketones in undecane solution are summarized in Table 1 and the quantum yields in Table 2. Each analysis was run in triplicate and the results are estimated to be precise to $\pm 1\%$ and accurate to $\pm 5\%$. It is clear from this table that the presence of the oxygen atom has changed markedly the photochemistry of the two ketones. The only products identified in the photolysis of 2-methoxy 3-pentanone are 3-pentanone and formaldehyde which constitute the type II products formed by the reaction shown in Scheme 1. Careful inspection of the gas chromatographic data indicated no other products exceeding 5% of the 3-pentanone. The total quantum yield for the type II process at 23 °C was 0.19. The almost total elimination of type I products is quite remarkable.

On the other hand the products isolated from the photolysis of 4-methyl 3-hexanone indicate a predominance of type I products even at the low

Can. J. Chem. Downloaded from www.nrcresearchpress.com by 210.87.254.40 on 09/05/12
For personal use only.

Can. J. Chem. Downloaded from www.nrcresearchpress.com by 210.87.254.40 on 09/05/12
For personal use only.

TABLE 1. Summary of analytical results for photolysis at 23 °C

Ketone	Light absorbed (einstein × 10^6)	Irradiation time (h)	3-Pentanone (mol × 10^6)	2-Methyl 1-butyraldehyde (mol × 10^7)	Propanal (mol × 10^7)	Ethane + ethylene (mol × 10^7)	*n*-Butane (mol × 10^7)
2-Methoxy 3-pentanone	50.6	7.0	9.60±0.03				
	83.5	7.0	15.4±0.1				
4-Methyl 3-hexanone	31.6	3.0	3.12±0.03	—	—	—	—
	18.0	3.0	1.80±0.03	37.6±0.3	3.6±0.1	27.7±0.3	3.7±0.1

TABLE 2. Summary of quantum yields at 23 °C

Ketone	Product	Process type	ϕ	Total ϕ
2-Methoxy 3-pentanone	3-Pentanone	II	0.19	0.19
	Formaldehyde*	II	—	—
4-Methyl 3-hexanone	2-Methyl, 1-butyraldehyde	I	0.21	0.23
	Ethane	I	0.16	
	Butane	I	0.021	
	Propanal	I	0.020	
	3-Pentanone	II	0.10	0.10
	Ethylene†	II	—	—

*Identified as DNPH derivative by t.l.c.
†Identified by gas chromatography.

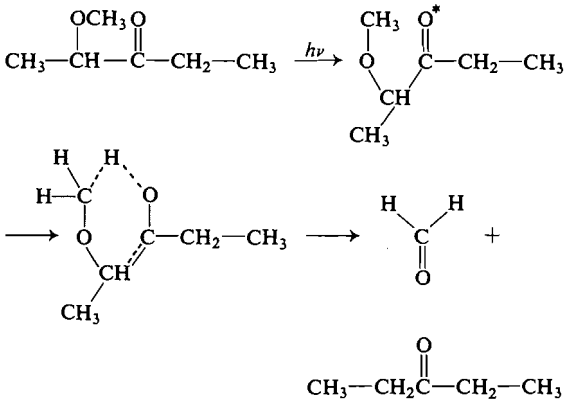

SCHEME 1

temperature of the experiment. The observed products can be explained by reaction Scheme 2. Smaller peaks which were tentatively identified as various combination products of radicals formed by the type I process were shown by the gas chromatograph, but the amounts observed were considerably smaller than for any of the compounds listed above.

Several conclusions can be drawn from these data. In the first place, it is interesting to note that the type I cleavage of the ethyl group is favored by a factor of 10 to 1 over cleavage of the isobutyl group. Since the bond strength of the carbon bond on the ethyl group would be expected to be greater than that of the isobutyl group, one might conclude that the reason for the higher efficiency for the cleavage of the smaller radical is due to a smaller "cage effect". In essence the smaller radical has a greater probability of escaping from the adjacent fragment and the quantum yield for scission of this bond is therefore higher.

The other factor of interest is that the quantum yield for the type I process is nearly double that for the type II process in this ketone whereas in the case of the methoxy ketone, practically no type I products were identified at all and the quantum yield for the type II process was double that for 4-methyl 3-hexanone. It is possible that the reason for the increased quantum yield for the type II reaction in 2-methoxy 3-pentanone is a greater ease in the formation of the six-membered transition state, and that this formation must compete with whatever state gives rise to the free radical type I split. Alternatively, one may argue that the six-membered ring is formed readily in both cases and the proportion of reaction into the type II photoelimination (as opposed to the type I) will depend on the relative ease of proton abstraction. This is suggested by the results of Wagner and Kamppainen (9) who estimate that the rate constant for γ-hydrogen abstraction in methoxy acetophenone is 230 times that in propiophenone.

In the case of both ketones a careful inspection of the chromatograms showed no product in the region where the cyclic oxetanol or cyclobutanol derivatives would be expected. It is estimated that unless these products are very unstable during the analysis, they could not amount to more than 5% of the yields of the major type I and type II products. This low yield of the cyclic derivative for aliphatic ketones corroborates the results of Yates and Szabo (7) with similar ketones.

The unusual distribution of the type I split in 4-methyl 3-hexanone suggests that perhaps a major mechanism for the dissipation of excited state energy involves the dissociation of the molecule into free radicals which lose some of their excess excitation energy by collision with the solvent and then recombine in the "cage". It would appear that this might represent a fairly efficient method for the conversion of the energy

Can. J. Chem. Downloaded from www.nrcresearchpress.com by 210.87.254.40 on 09/05/12
For personal use only.

Can. J. Chem. Downloaded from www.nrcresearchpress.com by 210.87.254.40 on 09/05/12
For personal use only.

Type I

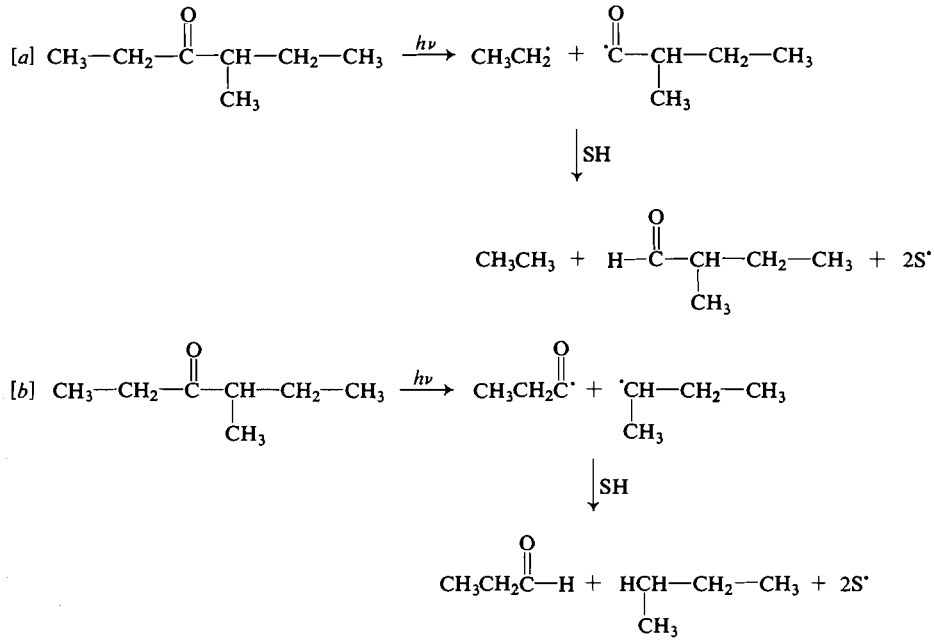

Type II

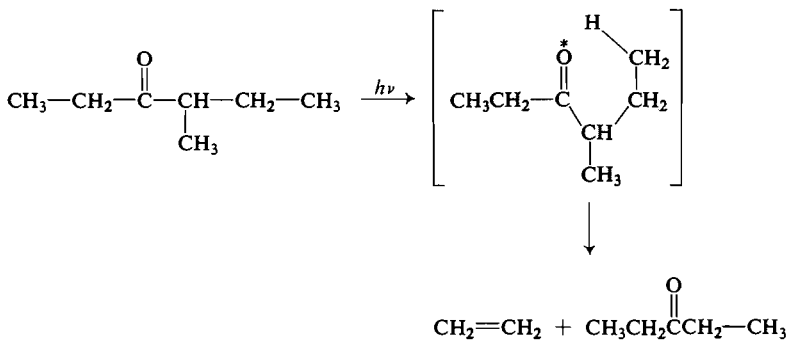

SCHEME 2

of the electronically excited states into thermal energy.

The authors wish to acknowledge the generous financial assistance of the National Research Council of Canada and one of us (L.P–Y.L.), financial support from the Paint Research Institute. Thanks are also due to Dr. G. Hartley, Mr. F. Golemba, Dr. P. Yates, and Dr. I. G. Csizmadia for helpful discussions.

1. G. R. MCMILLAN, J. G. CALVERT, and J. N. PITTS, JR. J. Amer. Chem. Soc. **86**, 3620 (1964).
2. R. SRINIVASAN. J. Amer. Chem. Soc. **81**, 5061 (1959).
3. G. H. HARTLEY and J. E. GUILLET. Macromolecules **1**, 165 (1968).
4. R. SRINIVASAN. J. Amer. Chem. Soc. **84**, 2475 (1961).
5. P. AUSLOOS and R. E. REBBERT. J. Amer. Chem. Soc. **83**, 4897 (1961).
6. N. J. TURRO and F. D. LEWIS. Tetrahedron Lett. **56**, 5845 (1968).
7. P. YATES and A. G. SZABO. Tetrahedron Lett. **9**, 485 (1965).
8. J. CASON and F. S. PROUT. J. Amer. Chem. Soc. **66**, 46 (1944).
9. P. S. WAGNER and A. E. KAMPPAINEN. J. Amer. Chem. Soc. **90**, 5896 (1968).

The Silver–Calcium System

A. N. CAMPBELL AND W. H. W. WOOD
Department of Chemistry, University of Manitoba, Winnipeg, Manitoba

Received November 4, 1970

The Ag–Ca system has been reinvestigated over the composition range 50–100 atomic% Ca, by differential thermal analysis and high temperature X-ray powder diffraction. Our results are in good agreement with those of Alexander *et al.* (1) and those of Pascal *et al.* (2) in the region 50–59 atomic% Ca, but the peritectic claimed by Alexander *et al.*, lying at 50% Ca and 598 °C, appears not to exist, according to our DTA and X-ray results. Here and elsewhere our results substantiate those of Pascal *et al.* We also find that the compound $AgCa_3$ is formed peritectically, and not congruently as suggested by Alexander *et al.*

Le système Ag–Ca a été réexaminé dans le domaine des compositions 50–100% at. Ca, par les techniques d'analyse thermique différentielle et de diffraction X de poudres à températures élevées. Nos résultats sont en accord avec ceux de Alexander et coll. (1) et ceux de Pascal et coll. (2) dans la région 50–59% at. Ca; cependant nos résultats d'ATD et de rayons-x ne confirment pas l'existence d'une réaction péritectique à 50% Ca et 598 °C, telle que rapportée par Alexander et coll. De façon générale, nos résultats s'accordent avec ceux de Pascal et coll. Nous trouvons de plus que le composé $AgCa_3$ est formé par une réaction péritectique et non pas, tel que suggéré par Alexander et coll., de façon congruente.

Canadian Journal of Chemistry 49, 1315 (1971)

Introduction

The equilibrium diagram of the system Ag–Ca is well established for the most part. The original work is that of Baar (3), whose results have been confirmed by Alexander *et al.* (1) and by Pascal *et al.* (2) as far as the region from 0 to 50 atomic% Ca is concerned. On the basis of DTA results only, Alexander *et al.* suggested the occurrence of a peritectic lying at 59 atomic% Ca and 598 °C, and that the compound $AgCa_3$, whose existence is not disputed, is produced from the melt with congruent freezing. Pascal *et al.* (2) working in the range 50–100% Ca failed to confirm the conclusions of Alexander *et al.* The aim of the present work was to settle these disputed points, using both DTA and X-ray powder photography.

Experimental

Materials

Silver, obtained from the Matheson, Coleman and Bell Company, was 99.999% pure. Calcium from Dominion Magnesium Ltd., was supplied with the following spectrographic analysis: N_2 = 0.0057%, Fe = 0.0008%, Mg = 0.10%, Al = 0.007%, and Mn = 0.013%.

The alloys were homogenized in a Leco induction furnace (Model 521) but some modifications were necessary to prevent oxidation. Stirring of the molten sample was assumed to have been sufficiently accomplished by the eddy currents established by the induction furnace. Microscopic examination and chemical analysis by the Volhard method for silver showed a variation in composition of up to 1% Ca between top and bottom sections. This variation in composition was undoubtedly due to the burning off of calcium at the top of the alloy, during the homogenization process. Accordingly, the tube in which the alloys were homogenized was purged several times with purified argon, before heating, and a final positive pressure of about 5 cm Hg maintained over the alloy during homogenization.

Zircon crucibles were found to be satisfactory for alloys with low calcium content but they were attacked by alloys containing more than 30% Ca. We, therefore, changed to boron nitride crucibles for all our definitive work. There appears to be no interaction between these alloys and boron nitride.

Experimental details of our DTA and X-ray work are to be found in a previous publication (4).

Results and Discussion

As noted by Alexander *et al.* (1), the liquidus points were fairly consistent but the solid state arrests were not very reproducible, both from alloy to alloy and also for successive thermal analyses of the same alloy. This is probably due to slight contamination of the alloy by the crucible.

We found no evidence for the existence of the peritectic claimed by Alexander *et al.* (1) at 59% Ca and 598 °C. In this region, our results confirm those of Pascal *et al.* (2). Between the compound Ag_3Ca_5 and pure Ca, Alexander *et al.* has suggested the existence of two eutectics, with $AgCa_3$ forming congruently at 75% Ca. This, however, is inconsistent with their own suggestion of a maximum at 77.5% Ca. Admittedly, the curve is very flat between 75 and 80% Ca and, were it not for the extreme sensitivity of our DTA method, we

Can. J. Chem. Downloaded from www.nrcresearchpress.com by 210.87.254.105 on 09/05/12
For personal use only.

should be inclined to leave it as an open question whether $AgCa_3$ forms peritectically or congruently. The matter is of no great moment but, obviously, if a maximum were to exist, it must lie at 75% Ca, since this is the composition of the compound itself. In our opinion, the compound $AgCa_3$ forms incongruently at 475 °C, at the composition of the compound. Our results are to be found in Table 1.

TABLE 1

Composition (at % Ca)	Temperature (°C) Liquidus	Solidus
49.9	666	554
53.9	657	553
55.6	649	557
57.3	621	555
59.0	594	556
60.1	567	555
62.3	—	555
65.2	550	475
68.5	539	474
71.0	525	476
75.1	—	475
76.9	474	—
77.8	472	468
78.6	471	469
80.1	—	469
85.0	635	468
91.1	749	470
100.0	840	

X-Ray photographs were taken with the high temperature camera, above and below 598 °C, the temperature suggested by Alexander *et al.* as that of a peritectic, but we found no evidence of the existence of any phase other than AgCa, above 555 °C, the temperature at which Ag_3Ca_5 is formed peritectically. On the basis both of DTA and X-ray work, we conclude that the peritectic proposed by Alexander at 59% Ca and 598 °C, does not exist.

1. W. A. ALEXANDER, L. D. CALVERT, A. DESAULNIERS, H. S. DUNSMORE, and D. G. SARGENT. Can. J. Chem. **47**, 611 (1969).
2. B. PASCAL, M. CAILLEY, and M. ALLIBERT. C. R. Acad. Sc. Paris, **270**, 520 (1970).
3. N. BAAR. Z. Inorg. Chem. **70**, 383 (1911).
4. A. N. CAMPBELL, R. WAGEMANN, and R. B. FERGUSON. Can. J. Chem. **48**, 1703 (1970).

Photolysis of Thiolane Vapor[1]

SILVIA BRASLAVSKY AND JULIAN HEICKLEN
Department of Chemistry and Center for Air Environment Studies, The Pennsylvania State University, University Park, Pa. 16802

Received October 26, 1970

The photolysis of thiolane vapor ($\overline{CH_2CH_2CH_2CH_2S}$) was studied at room temperature with 2139 Å radiation. The major product was C_2H_4, whose quantum yield decreased as the pressure was increased. Next in importance were 1-C_4H_8, C_3H_6, and C_2H_6. Also produced were CH_4, *c*-C_3H_6, 1,3-C_4H_6, CH_2CHSH, $\overline{CH_2CH_2S}$, 1-C_4H_9SH, H_2, C_3H_8, *n*-C_4H_{10}, *c*-C_4H_8, polymer, and an unstable product tentatively identified as 1-butene-1-thiol. All products were initial products of the reaction. Experiments with added C_3H_6 showed the absence of sulfur atoms. The results are interpreted in terms of two excited states and an intermediate which might be the diradical $\cdot CH_2CH_2CH_2CH_2S\cdot$.

La photolyse de vapeur de thiolane, ($\overline{CH_2CH_2CH_2CH_2S}$) a été étudiée à la température de la pièce à 2139Å. Le produit principal de la réaction est C_2H_4 dont le rendement quantique diminue inversement avec la pression. Les produits formés avec une importance moindre étaient le butène-1, C_3H_6 et C_2H_6. Les composés suivants: CH_4, C_3H_6, butadiène-1,3, CH_2CHSH, $\overline{CH_2CH_2S}$, butanethiol-1, H_2, C_3H_8, *n*-C_4H_{10}, *c*-C_4H_8, polymère et un produit instable qui pourrait être le butène-1-thiol-1 sont aussi formés. Tous ces produits étaient des produits initiaux de la réaction. Des expériences supplémentaires au cours desquelles du C_3H_6 avait été ajouté ont permis de démontrer l'absence d'atome de soufre. Les résultats sont expliqués en termes de deux états excités et d'un intermédiaire qui pourrait être le diradical $\cdot CH_2CH_2CH_2CH_2S\cdot$.

Canadian Journal of Chemistry, 49, 1316 (1971)

Previous reports from this laboratory have discussed the photolysis of thiophene vapor (1) ($\overline{CHCHCHCHS}$) and thietane vapor (2) ($\overline{CH_2CH_2CH_2S}$). In both cases photodecomposition proceeds in two ways: (*a*) direct fragmentation to molecular products and (*b*) the

[1]CAES Publication No. 155-70.

Can. J. Chem. Downloaded from www.nrcresearchpress.com by 210.87.254.105 on 09/05/12
For personal use only.

should be inclined to leave it as an open question whether $AgCa_3$ forms peritectically or congruently. The matter is of no great moment but, obviously, if a maximum were to exist, it must lie at 75% Ca, since this is the composition of the compound itself. In our opinion, the compound $AgCa_3$ forms incongruently at 475 °C, at the composition of the compound. Our results are to be found in Table 1.

TABLE 1

Composition (at % Ca)	Temperature (°C) Liquidus	Solidus
49.9	666	554
53.9	657	553
55.6	649	557
57.3	621	555
59.0	594	556
60.1	567	555
62.3	—	555
65.2	550	475
68.5	539	474
71.0	525	476
75.1	—	475
76.9	474	—
77.8	472	468
78.6	471	469
80.1	—	469
85.0	635	468
91.1	749	470
100.0	840	

X-Ray photographs were taken with the high temperature camera, above and below 598 °C, the temperature suggested by Alexander *et al.* as that of a peritectic, but we found no evidence of the existence of any phase other than AgCa, above 555 °C, the temperature at which Ag_3Ca_5 is formed peritectically. On the basis both of DTA and X-ray work, we conclude that the peritectic proposed by Alexander at 59% Ca and 598 °C, does not exist.

1. W. A. ALEXANDER, L. D. CALVERT, A. DESAULNIERS, H. S. DUNSMORE, and D. G. SARGENT. Can. J. Chem. **47**, 611 (1969).
2. B. PASCAL, M. CAILLEY, and M. ALLIBERT. C. R. Acad. Sc. Paris, **270**, 520 (1970).
3. N. BAAR. Z. Inorg. Chem. **70**, 383 (1911).
4. A. N. CAMPBELL, R. WAGEMANN, and R. B. FERGUSON. Can. J. Chem. **48**, 1703 (1970).

Photolysis of Thiolane Vapor[1]

SILVIA BRASLAVSKY AND JULIAN HEICKLEN
Department of Chemistry and Center for Air Environment Studies, The Pennsylvania State University, University Park, Pa. 16802

Received October 26, 1970

The photolysis of thiolane vapor ($\overline{CH_2CH_2CH_2CH_2S}$) was studied at room temperature with 2139 Å radiation. The major product was C_2H_4, whose quantum yield decreased as the pressure was increased. Next in importance were 1-C_4H_8, C_3H_6, and C_2H_6. Also produced were CH_4, *c*-C_3H_6, 1,3-C_4H_6, CH_2CHSH, $\overline{CH_2CH_2S}$, 1-C_4H_9SH, H_2, C_3H_8, *n*-C_4H_{10}, *c*-C_4H_8, polymer, and an unstable product tentatively identified as 1-butene-1-thiol. All products were initial products of the reaction. Experiments with added C_3H_6 showed the absence of sulfur atoms. The results are interpreted in terms of two excited states and an intermediate which might be the diradical $\cdot CH_2CH_2CH_2CH_2S\cdot$.

La photolyse de vapeur de thiolane, ($\overline{CH_2CH_2CH_2CH_2S}$) a été étudiée à la température de la pièce à 2139Å. Le produit principal de la réaction est C_2H_4 dont le rendement quantique diminue inversement avec la pression. Les produits formés avec une importance moindre étaient le butène-1, C_3H_6 et C_2H_6. Les composés suivants: CH_4, C_3H_6, butadiène-1,3, CH_2CHSH, $\overline{CH_2CH_2S}$, butanethiol-1, H_2, C_3H_8, *n*-C_4H_{10}, *c*-C_4H_8, polymère et un produit instable qui pourrait être le butène-1-thiol-1 sont aussi formés. Tous ces produits étaient des produits initiaux de la réaction. Des expériences supplémentaires au cours desquelles du C_3H_6 avait été ajouté ont permis de démontrer l'absence d'atome de soufre. Les résultats sont expliqués en termes de deux états excités et d'un intermédiaire qui pourrait être le diradical $\cdot CH_2CH_2CH_2CH_2S\cdot$.

Canadian Journal of Chemistry, 49, 1316 (1971)

Previous reports from this laboratory have discussed the photolysis of thiophene vapor (1) ($\overline{CHCHCHCHS}$) and thietane vapor (2) ($\overline{CH_2CH_2CH_2S}$). In both cases photodecomposition proceeds in two ways: (*a*) direct fragmentation to molecular products and (*b*) the

[1]CAES Publication No. 155-70.

Can. J. Chem. Downloaded from www.nrcresearchpress.com by 210.87.254.105 on 09/05/12
For personal use only.

Can. J. Chem. Downloaded from www.nrcresearchpress.com by 210.87.254.105 on 09/05/12
For personal use only.

formation of an intermediate which reacts with a second molecule to produce S_2 and hydrocarbon products. In both studies sulfur atoms were found to be absent. In this paper we report some results on the room-temperature photolysis of thiolane vapor ($\overline{CH_2CH_2CH_2CH_2S}$) with 2139 Å radiation.

There are two previous reports of the photolysis of thiolane. In a brief study Haines *et al.* (3) reported the products when liquid samples of $\overline{CH_2(CH_2)_nCH_2S}$ (n = 1 to 3) were irradiated with a mercury arc. For thiolane, the major products reported were C_2H_4 and H_2. A more detailed study of the photodecomposition of thiirane vapor ($\overline{CH_2CH_2S}$) and thiolane vapor irradiated with 2537 Å radiation was reported by Sidhu (4). In both cases $S(^3P)$ atoms were detected by episulfide formation in the presence of olefins. A primary process involving ring opening and leading to diradicals was proposed in both systems. Heavy molecular weight molecules were also produced in the presence of olefins which were explained as coming from the adduct of sulfur-bearing radicals with the olefins. When 10 Torr of pure thiolane was irradiated at 2537 Å, the products were 1-C_4H_9SH, 1-C_4H_8, C_3H_6, and c-C_3H_6 in the ratio of 3.6 to 1, equal amounts of C_2H_4 and $\overline{CH_2CH_2S}$, hydrogen, and polymer. The C_2 and C_3 hydrocarbons were about of equal importance. Furthermore c-C_4H_8 was absent. In the liquid phase the products were the same but their quantum yields were small.

Thiolane absorption is very weak at 2537 Å, but a strong transition occurs below 2350 Å, possibly involving two electronically excited states (5). With 2139 Å irradiation the major product is C_2H_4. Next in importance are 1-C_4H_8, C_3H_6, and C_2H_6. Minor products included CH_4, c-C_3H_6, 1,3-C_4H_6, CH_2CHSH, $\overline{CH_2CH_2S}$, and 1-C_4H_9SH. Traces of H_2, C_3H_8, n-C_4H_{10}, and c-C_4H_8 (cyclobutane) were produced. A very unstable product was also found which, according to its retention time and its high instability, was tentatively identified as 1-butene-1-thiol, an isomer of thiolane. A white polymer also formed. A careful search was made for H_2S, CS_2, C_2H_2, 2-C_4H_8, and i-C_4H_8, but these compounds were not found as products. (H_2S and CS_2 were also absent in the photolysis of thietane (2).) The effect of extent of conversion was studied and it was found that all the product quantum yields were invariant to exposure times between 10 and 60 min. Thus all the products are primary products of the photolysis.

With 2139 Å radiation, the products included those reported at 2537 Å, as well as several others. Furthermore the ratio C_3H_6 to c-C_3H_6 is about the same at both wavelengths. Three significant differences at the two wavelengths are: (*1*) the C_2 and C_3 hydrocarbons were of about equal importance at 2537 Å, whereas at 2139 Å, the amount of C_2H_4 was in great excess, (*2*) the ratio of $[C_2H_4]$ to $[\overline{CH_2CH_2S}]$ greatly exceeded unity with 2139 Å, whereas it was about one at 2537 Å, and (*3*) an experiment in which 9 Torr of thiolane was photolyzed at 2139 Å in the presence of 3 Torr of propylene produced neither propylene episulfide nor propanethiol, thus indicating the absence of sulfur atoms (6), contrary to the results at 2537 Å where $S(^3P)$ was found. Furthermore with 2139 Å radiation the quantum yields of 1,3-C_4H_6 and the sulfur bearing products remained unchanged in the presence of C_3H_6. Thus intermediates which react readily with C_3H_6 are not important in this system.

It is of interest to note that the photodecomposition of the electronically similar oxolane molecule ($\overline{CH_2CH_2CH_2CH_2O}$) with radiation principally at 1942 and 1973 Å gives similar products (7). The major products in that system were CO, H_2, CH_4, C_2H_6, C_2H_4, C_3H_6, c-C_3H_6, C_3H_8, and CH_2O. Minor products included C_4H_{10}, 2-C_4H_8, and 1,3-C_4H_6.

Table 1 lists the quantum yields for the more important gas-phase products at pressures between 0.78 and 11.6 Torr and absorbed intensities, I_a, between 10.8 and 48 $\times$ 10^{11} quanta/cc s. The yields for 1-C_4H_9SH and the product tentatively identified as 1-butene-1-thiol varied erratically between 0 and $\simeq$ 0.1. When one was present and important, so was the other. $\Phi\{C_2H_4\}$ drops measureably as the pressure (and I_a) is enhanced. Presumably this drop results from pressure quenching of the precursor, since intensity effects were absent in the thiophene and thietane systems (1, 2). The CH_4 yield rises with pressure and I_a, but the quantum yields of the other products show no marked trend with the experimental parameters, though the results are quite scattered due to the low quantum yields and the attendant analytical difficulties.

Since $\Phi\{C_2H_4\}$ is pressure quenched and the other gas-phase products are not, two electronically excited states of thiolane (designated Th* and Th**) are indicated, as was proposed in the

Can. J. Chem. Downloaded from www.nrcresearchpress.com by 210.87.254.105 on 09/05/12
For personal use only.

TABLE 1. Photolysis of thiolane vapor with 2139 Å radiation at 25 ± 3 °C

[Th] (Torr)	$I_a \times 10^{11}$ (quanta/cc s)	Irradiation time (min)	$\Phi\{CH_4\}$	$\Phi\{C_2H_4\}$	$\Phi\{C_2H_6\}$	$\Phi\{C_3H_6\}$	$\Phi\{c\text{-}C_3H_6\}$	$\Phi\{1\text{-}C_4H_8\}$	$\Phi\{1,3\text{-}C_4H_6\}$	$\Phi\{CH_2CHSH\}$*	$\Phi\{\overline{CH_2CH_2S}\}$*
0.78	10.8	60	0.003	0.74	—	0.059	0.028	0.083	0.036	0.020	0.00
2.60	28	30	—	0.60	0.064	—	—	—	—	—	—
4.1	33	20	—	—	—	0.046	0.014	0.063	0.018	0.022	0.010
6.0	26	30	0.011	0.50	0.040	0.082	0.026	0.103	0.032	0.051	0.020
9.2	48	20	—	—	—	0.071	0.015	0.083	0.042	—	—
11.6	48	20	0.023	0.27	0.046	—	—	—	—	0.035	0.007

*Not calibrated. Assumed chromatographic sensitivity same as for CS_2.

Can. J. Chem. Downloaded from www.nrcresearchpress.com by 210.87.254.105 on 09/05/12
For personal use only.

photolysis of thietane vapor (2). One electronically excited state produces C_2H_4, and the primary steps can be represented by

[1] $\quad Th^* \rightarrow C_2H_4 + \cdot C_2H_4S\cdot$

[2] $\quad Th^* + Th \rightarrow 2Th$

Th* might be formed by direct absorption of the 2139 Å radiation or might result from internal conversion of Th**. On the other hand Th* cannot be a precursor for Th** since the products arising from Th** show no pressure dependence; reaction 2 cannot produce Th**, but it might produce polymer. The fate of the $\cdot C_2H_4S\cdot$ fragment is uncertain. In this system $\Phi\{C_2H_4\}$ greatly exceeds $\Phi\{\overline{CH_2CH_2S}\} + \Phi\{CH_2CHSH\}$, contrary to the results at 2537 Å where the two quantities are about the same. In this system the $\cdot C_2H_4S\cdot$ fragment probably either polymerizes or produces more C_2H_4 via

[3] $\quad 2\cdot C_2H_4S\cdot \rightarrow 2C_2H_4 + S_2$

Reactions 1–3 lead to the result

$$[4] \quad (\Phi\{C_2H_4\})^{-1} = (1 + k_2[Th]/k_1)/2\alpha$$

where α is the fraction of the light absorbed which leads to Th* formation. However, if reaction 3 is negligible then

$$[5] \quad (\Phi\{C_2H_4\})^{-1} = (1 + k_2[Th]/k_1)/\alpha$$

Figure 1 is a plot of $(\Phi\{C_2H_4\})^{-1}$ *vs.* [Th]. The data points are fitted by a straight line of slope 0.20 $Torr^{-1}$ and intercept 1.2. The ratio of slope to intercept gives $k_2/k_1 = 0.17$ $Torr^{-1}$. The intercept yields a value for α of either 0.42 if reaction 3 is important or 0.83 if reaction 3 is negligible.

The CH_4 yield increases with pressure suggesting that reaction 2 might lead to CH_4 part of the time. The C_3 hydrocarbon products could be produced directly by decomposition of Th**. However, the C_4 hydrocarbon products cannot be produced in this way, since sulfur atoms were shown to be absent. In order to explain the absence of both sulfur atoms and a pressure effect, it is necessary that Th** revert to some intermediate, possibly $\cdot CH_2CH_2CH_2CH_2S\cdot$, which can react with unexcited thiolane to produce S_2 and the C_4 hydrocarbon products.

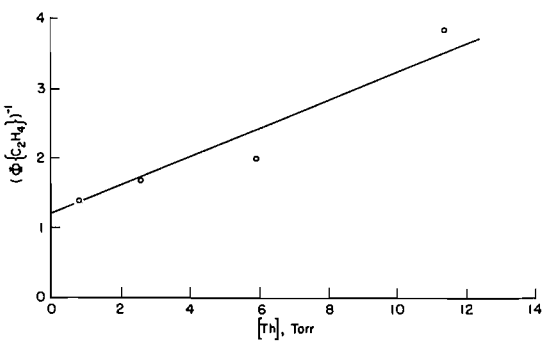

FIG. 1. Plot of the reciprocal ethylene quantum yield *vs.* thiolane pressure in the photolysis of thiolane vapor at 2139 Å and room temperature.

Experimental

Thiolane was obtained from Eastman Organic Chemicals. It contained two impurities (< 200 p.p.m.) which were removed by preparative gas chromatography using a 20 ft long column packed with 10% tricresyl phosphate on Chromosorb G, operating at 60 °C with a He flow rate of 60 cc/min. Furthermore the thiolane was distilled at −90 °C before each run. Matheson Co. Instrumental Grade C_3H_6 and C.P. grade O_2 were used without purification. The C_3H_6 showed no impurities, and the O_2 contained only traces of N_2.

The reaction vessel, radiation source, vacuum system, and HBr actinometry have been described previously (1). The extinction coefficient of thiolane at 2139 Å was found on a Cary 14 spectrophotometer to be 1.9×10^{-2} $Torr^{-1}$ cm^{-1} (to base 10). The absorbed radiation was obtained by comparison to the H_2 yield from HBr irradiations at matched absorbances. Since polymer formation was observed after long irradiations, air was admitted to the reaction vessel and heated with an oxygen torch to about 500 °C after each run to remove the polymer.

The products were analyzed with a Gow-Mac Model No. 40-05D gas chromatograph utilizing a thermistor detector and 1/4-in. diameter columns. The identification of the hydrocarbon products and 1-C_4H_9SH was made by adding an authentic commercial sample to the reaction products and checking the chromatographic retention time on two different columns. These products were also calibrated directly. H_2 was identified by collecting the gas noncondensable at −196 °C and passing it through a chromatograph using a Porapak Q column with Ar as a carrier gas. To identify CH_2CHSH and $\overline{CH_2CH_2S}$, these compounds were prepared from the photolysis of OCS in the presence of C_2H_4 (6). Both compounds gave retention times corresponding to products of the reaction. Furthermore the product with the same retention time as CH_2CHSH was collected and the identification confirmed by mass spectroscopy.

For complete analysis of the products three runs were performed under similar experimental conditions. From one run the gases noncondensable at −130 °C were collected with a Toepler pump, and analyzed on a 20 ft Porapak Q column at 0 °C using a He flow rate of 60 cc/min for 20 min after which the flow rate was increased to 110 cc/min. In this way CH_4, C_2H_4, and C_2H_6 were measured.

In a second run the C_3 and C_4 hydrocarbons were analyzed on a 40 ft column packed with 15% dimethyl-

sulfone on Chromasorb G at 0 °C with a He flow rate of 43 cc/min. The sulfur compounds were analyzed in the third run using a 2 ft column packed with 10% tricresyl phosphate on Chromasorb G at room temperature with a He flow rate of 43 cc/min.

The authors wish to thank Dr. H. A. Wiebe for his help. This work was supported by the U.S. Public Health Service, National Air Pollution Control Administration under Grant No. IR01 AP00718-02 for which we are grateful.

1. H. A. WIEBE and J. HEICKLEN. Can. J. Chem. **47**, 2965 (1969).
2. H. A. WIEBE and J. HEICKLEN. J. Amer. Chem. Soc. **92**, 7031 (1970).
3. W. E. HAINES, G. L. COOK, and J. S. BALL. J. Amer. Chem. Soc. **78**, 5213 (1956).
4. K. S. SIDHU. Ph.D. Thesis. University of Alberta, Edmonton, Alberta. 1965.
5. L. B. CLARK and W. T. SIMPSON. J. Chem. Phys. **43**, 3666 (1965).
6. H. A. WIEBE. Ph.D. Thesis. University of Alberta, Edmonton, Alberta. 1967.
7. B. C. ROQUITTE. J. Amer. Chem. Soc. **91**, 7664 (1969).

Can. J. Chem. Downloaded from www.nrcresearchpress.com by 210.87.254.105 on 09/05/12
For personal use only.

Can. J. Chem. Downloaded from www.nrcresearchpress.com by 210.87.254.105 on 09/05/12
For personal use only.

Pyrolysis of Oxime Carbonates: Novel Conversion of Aldehydes into Nitriles under Mild Conditions

J. M. PROKIPCAK AND P. A. FORTE
Department of Chemistry, University of Guelph, Guelph, Ontario

Received January 8, 1971

A new synthesis of nitriles is reported based on the pyrolysis of oxime carbonates.

On rapporte une nouvelle synthèse des nitriles qui fait appel à la pyrolyse de carbonates d'oximes.

Canadian Journal of Chemistry, 49, 1321 (1971)

Recently there have been reports for preparing nitriles using dialkyl hydrogen phosphonates (1), 3-chloro-1,2-benzisothiazole-*S*,*S*-dioxide (2), and chlorothionoformate (3) derivatives of oximes. Other methods generally used involve more vigorous fragmentation of oxime esters under a variety of conditions (4). We wish to report a new relatively mild method of effecting this conversion of aldehydes to nitriles without use of any acidic or basic reagents.

Various aldoximes **1** which were readily available from the aldehydes were treated with phenyl chloroformate to yield the desired oxime carbonate **2**. Thermal decomposition of these oxime carbonates produced high yields of the corresponding nitriles. A typical transformation is depicted in Scheme 1.

The method seems applicable to both aliphatic and aromatic systems. A summary of our results to date is given in Table 1.

Although the mechanistic details of the reaction are not yet understood, a possible six-centered transition state **3** could be involved.

TABLE 1. Preparation and pyrolysis* of oxime carbonates†

Starting oxime	Melting point of oxime carbonate (°C)	Yield of nitrile (%)
anti-p-Nitrobenzaldoxime	151 (dec)	90
syn-p-Chlorobenzaldoxime	115	90
syn-Benzaldoxime	83	85
syn-p-Methylbenzaldoxime	91	90
syn-p-Methoxybenzaldoxime	115 (dec)	85

*All decompositions were carried out at approximately 100–110°.

†Structure of carbonate is 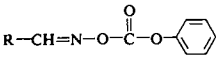

Further work on the synthetic scope as well as the mechanistic aspects of this reaction is now underway and will be reported in due course. The reaction itself has possible synthetic use because of the relatively mild temperatures required to effect the conversion, excellent yields of the nitriles, and no use of any acidic or basic reagents.

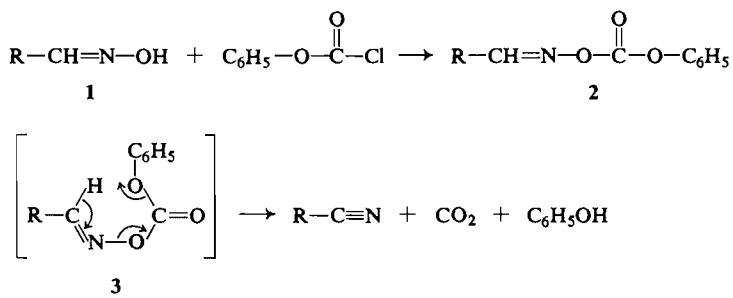

SCHEME 1.

All the oximes used were prepared by standard routes. The general experimental procedure is illustrated for the preparation of the carbonate of *syn*-anisaldoxime and its subsequent thermal breakdown. To a cooled (0°), stirred solution of *syn*-anisaldoxime (25.3 g, 0.17 mol) in 250 ml anhydrous ether containing 14 ml (0.18 mol) pyridine was added slowly 28.4 g (0.18 mol) of phenyl chloroformate. The resultant mixture was stirred for 10 h at room temperature and then poured on ice water (1000 ml). The ether layer was removed and the aqueous layer extracted with 800 ml methylene chloride. The combined organic extracts were washed with water, dried over sodium sulfate, and the solvent evaporated to yield the crude oxime carbonate. Recrystallization from hexane–chloroform gave 36.0 g (79%) of pure carbonate, m.p. 118° which had the following spectral data: ($CHCl_3$) 1759 (C=O stretch), 1259–1190 (ester C—O stretch), and 1024 cm^{-1} (C—O—C stretch); n.m.r. ($CDCl_3$) δ (p.p.m.) 8.44 (1H singlet, imino hydrogen H—C(=N)—) 7.84–6.92 (9H multiplet centered at 7.38, aromatic), 3.84 (3H singlet, phenyl CH_3—O—).

Anal. Calcd. for $C_{15}H_{13}NO_4$: C, 66.41; H, 4.83; N, 5.11. Found: C, 66.63; H, 4.76; N, 5.28.

The oxime carbonate (7.46 g, 0.028 mol) was then placed in a flask and heated until a steady stream of CO_2 evolved (110°). Then the reaction became very exothermic and external heating was discontinued. After CO_2 evolution had ceased, the resultant material was dissolved in 150 ml benzene. The benzene layer was extracted with 5% NaOH (3 × 50 ml), water (2 × 100 ml), and dried over sodium sulfate. The benzene was removed *in vacuo* yielding an oil which crystallized from hexane–chloroform. The pure nitrile (3.1 g, 85%) had a m.p. 59.0–61.0° (reported (5), 61–62°) and its spectral data (i.r. and n.m.r.) was consistent with the assigned structure.

The authors wish to thank the National Research Council of Canada for financial support of this research and for a NRCC Scholarship awarded to P. A. Forte.

1. P. J. Foley Jr. J. Org. Chem. **34**, 2805 (1969).
2. H. Hettler and H. Neygenfind. Chem. Ber. **103** 1397 (1970).
3. D. L. J. Clive. Chem. Commun. 1014 (1970).
4. See, for example (*a*) J. S. Buck and W. S. Ide. Org. Synth. Collect. Vol. **2**, 622 (1943). (*b*) J. H. Hant. Chem. Ind. 1873 (1961).
5. Tables for identification of organic compounds. 2nd Edition, Chemical Rubber Company, Cleveland, Ohio, 1964.

Can. J. Chem. Downloaded from www.nrcresearchpress.com by 210.87.254.105 on 09/05/12
For personal use only.

Can. J. Chem. Downloaded from www.nrcresearchpress.com by 210.87.254.42 on 09/05/12
For personal use only.

Canadian Journal of Chemistry

Published by THE NATIONAL RESEARCH COUNCIL OF CANADA

VOLUME 49 MAY 1, 1971 NUMBER 9

Coordination Compounds of Olefins with Anhydrous Silver Tetrafluoroborate. VI. Complexes with Vinyl Chloride and Vinyl Fluoride[1]

H. W. QUINN AND R. L. VANGILDER

Exploratory Research Laboratory, Dow Chemical of Canada, Limited, Sarnia, Ontario

Received February 27, 1970[2]

The stability of the complexes $AgBF_4 \cdot 2$ vinyl chloride and $AgBF_4 \cdot 2$ vinyl fluoride has been determined and compared with that of $AgBF_4 \cdot 2$ propylene. The much lower stability of the halo-olefin complexes has been attributed partly to weaker interaction of these less basic olefins with the silver ion and partly to configurational restrictions imposed upon the complexed halo-olefin molecules as a result of their higher permanent dipole moment.

On a déterminé les stabilités des complexes de $AgBF_4 \cdot 2$ chlorure de vinyle et $AgBF_4 \cdot 2$ fluorure de vinyle et on les a comparées avec celle de $AgBF_4 \cdot 2$ propylène. La stabilité beaucoup plus faible des complexes des olefines halogénées est attribuée en partie à une intéraction plus faible de ces oléfines moins basiques avec les ions d'argent et aussi en partie aux restrictions configurationnelles imposées aux molécules d'oléfines halogénées du au fait qu'elles ont des moments polaires plus élevés.

Canadian Journal of Chemistry, 49, 1323 (1971)

Introduction

Earlier studies of the interaction of solid silver tetrafluoroborate with propylene and some other gaseous mono-olefins (1, 2) have indicated that the stability of the π complexes (1) produced is dependent upon olefin basicity. In order to compare propylene with some less basic olefins a study has been made of the stability of the 1:2 silver tetrafluoroborate complexes of propylene, vinyl chloride, and vinyl fluoride. Equilibrium dissociation pressure–temperature data for the complexes have been determined experimentally over the temperature range -40 to 20 °C. From these the change in the values of the thermodynamic functions for complex dissociation has been calculated. A determination has been made also of the change which occurs in the frequency of the double bond stretching vibration in the olefin when the $AgBF_4$ complex is formed.

[1]Dow Chemical of Canada, Limited, contribution no. 181.

[2]Revision received August 31, 1970.

Experimental

Materials

Vinyl chloride and vinyl fluoride were Matheson C. P. grade with 99.9% purity.

Propylene and 1-pentene were Phillips Pure Grade (99%) and Phillips Research Grade (99.99%), respectively.

Anhydrous $AgBF_4$ was purchased from Peninsular Chemical Research Incorporated.

1,2-Dichloroethane was Dow Chemical of Canada material of 99.99% purity.

Preparation of Complexes

(a) $AgBF_4 \cdot 2$ (1-Pentene)

The $AgBF_4$ (2.0109 g, 10.328 mmol) under petroleum ether was transferred to a Pyrex vapor pressure cell. The petroleum ether was pumped off and the system thoroughly evacuated. The anhydrous $AgBF_4$ was exposed to 1.4515 g (20.697 mmol) liquid 1-pentene at 50 °C to yield the liquid 1:2 complex (3). The complex was distributed as a thin uniform layer on the wall of the vapor pressure cell, crystallized by cooling to room temperature, and the 1-pentene subsequently removed by pumping for 48 h. This procedure yields a thin layer of $AgBF_4$ on the cell wall which equilibrates more rapidly with olefin than does a thick deposit of $AgBF_4$ at the bottom of the cell.

TABLE 1. Dissociation equilibrium data

Complex	Dissociation pressure equation*		Temperature range (°C)	Dissociation pressure at 0 °C (Torr)
	A	*B*		
$AgBF_4 \cdot 2C_3H_6$	8.8258 ± 0.00001	2274.2 ± 14.0	+2.27 to +16.68	3.18
$AgBF_4 \cdot 2C_2H_3Cl$	10.3234 ± 0.00000	2081.7 ± 4.8	−39.28 to −12.48	506.30
$AgBF_4 \cdot 2C_2H_3F$	9.6827 ± 0.00004	1856.4 ± 22.4	−39.69 to −18.61	773.22

*$\log P$ (Torr) $= A - B/(273.15 + t\ °C)$.

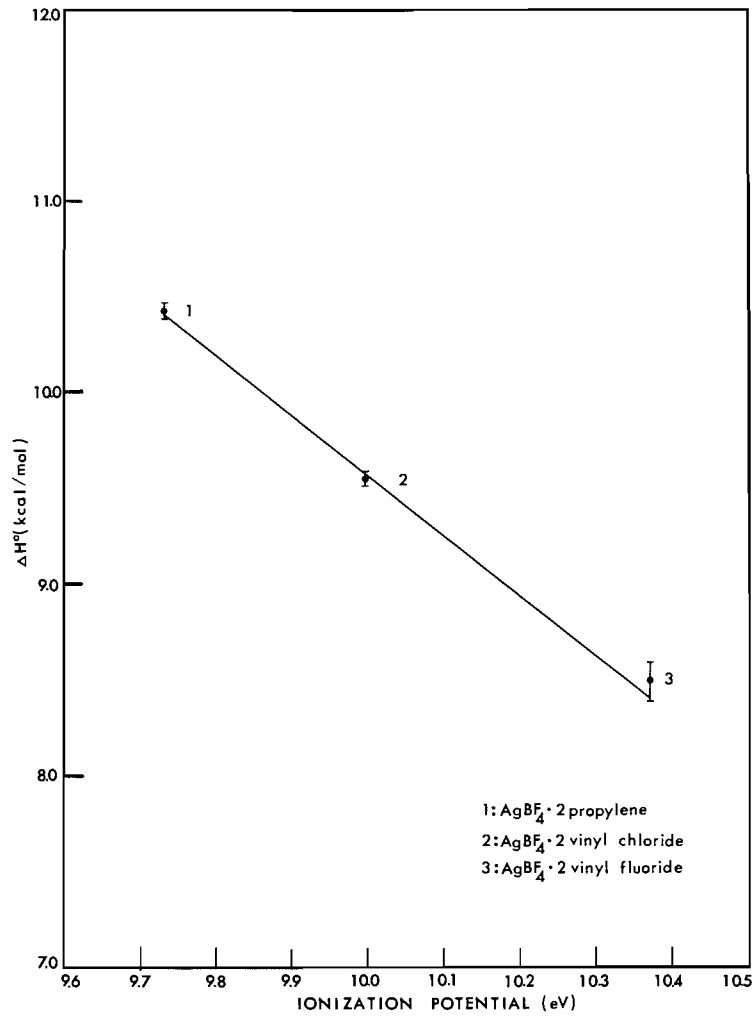

FIG. 1. Enthalpy change – olefin ionization potential correlation.

(b) $AgBF_4 \cdot 2$ Vinyl Chloride

The above described sample of anhydrous $AgBF_4$ was exposed at −22 °C to vinyl chloride (initial pressure 580 Torr). After 2 days the quantity of olefin in the cell was 1.3239 g (21.182 mmol), yielding the system $AgBF_4 \cdot 2$ 2.05 vinyl chloride.

(c) $AgBF_4 \cdot 2$ Vinyl Fluoride

After removal of the vinyl chloride, the same sample of anhydrous $AgBF_4$ was exposed at −45 °C to vinyl fluoride (initial pressure 690 Torr). After 4 days the quantity of olefin in the cell was 1.0339 g (22.456 mmol), yielding the system $AgBF_4 \cdot 2.17$ vinyl fluoride.

(d) $AgBF_4 \cdot 2$ Propylene

After removal of the vinyl fluoride, the same sample of $AgBF_4$ was exposed at ambient temperature to propylene (initial pressure 760 Torr). After 4 days the propylene

Can. J. Chem. Downloaded from www.nrcresearchpress.com by 210.87.254.42 on 09/05/12
For personal use only.

TABLE 2. Thermodynamic functions for the complex equilibria at 0 °C

Complex	$\Delta H°$ (kcal/mol)	$\Delta S°$ (cal/mol deg)	$\Delta G°$ (kcal/mol)
$AgBF_4 \cdot 2C_3H_6$	10.406±0.064	27.204±0.0000	2.975
$AgBF_4 \cdot 2C_2H_3Cl$	9.525±0.022	34.056±0.0000	0.223
$AgBF_4 \cdot 2C_2H_3F$	8.494±0.102	31.124±0.0002	−0.007

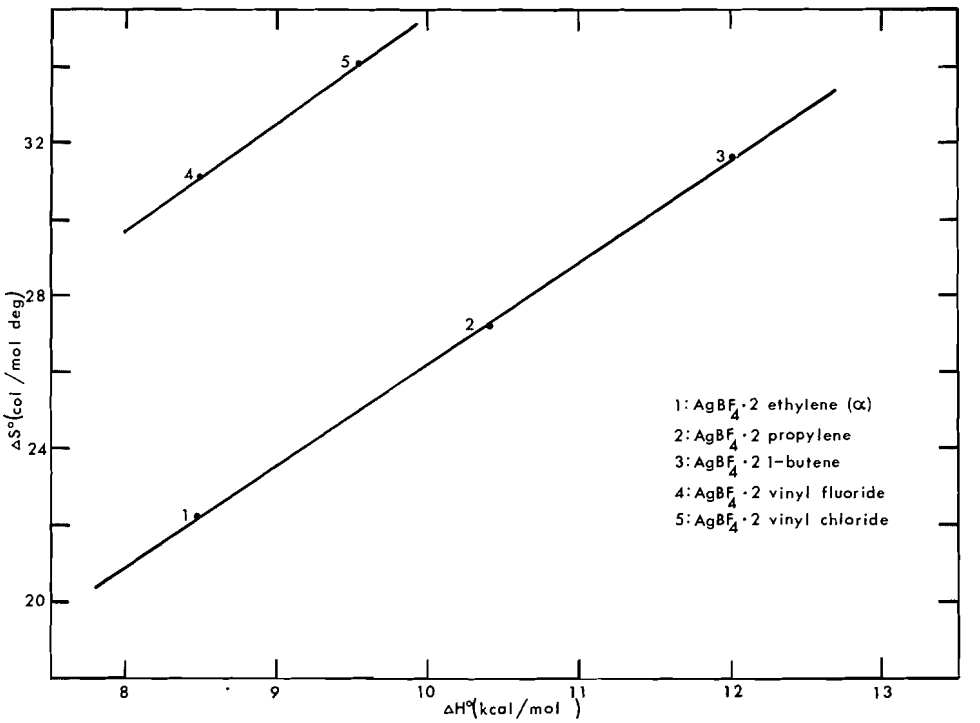

FIG. 2. Plot of entropy change *vs.* enthalpy change. Data for ethylene and 1-butene complexes taken from ref. 1.

uptake was 0.8580 g (20.428 mmol) yielding $AgBF_4 \cdot 1.98C_3H_6$.

The olefin uptake was determined gravimetrically. The discrepancy between the quantity of olefin in the cell and that expected for the 1:2 complex is attributable to the olefin still in the gas phase when the cell was removed for weighing. This excess was removed prior to determination of the dissociation pressure.

Pressure was measured with a Texas Instruments Fused Quartz Precision Pressure Gauge, Model 140A, operating within the range 0–1000 Torr with a sensitivity of 0.01 Torr. The temperature of the gauge capsule was controlled at 35 °C while the envelope of the capsule was continuously evacuated with a mercury diffusion pump backed by an oil pump.

The temperature dependence of the complex dissociation pressure was determined for vinyl chloride and vinyl fluoride complexes in the range −10 to −40 °C and for the propylene complex between 0 and +20 °C. The sample cell was evacuated for about 1 min between measurements after lowering the temperature to a point where the vapor pressure of the complex was very low.

After determination of the stability data for the 1:2 complex, the olefin content of the system was lowered to produce a 1:1 ratio of $AgBF_4$: olefin and another stability point was determined. The similarity of the dissociation pressure to that previously observed for the 1:2 complex ruled out the possibility of lower complexes.

Infrared Studies

A 10% solution of anhydrous $AgBF_4$ in 1,2-dichloroethane was exposed at −20 °C to vinyl chloride or vinyl fluoride (700 Torr) for 24 h. A Research and Industrial Instruments Company variable temperature i.r. unit, V-LTJ, equipped with an absorption cell, FH-01 Ag, was then used with a Beckman IR-9 Spectrophotometer to obtain the i.r. spectra of the solutions at −15 °C.

Results and Discussion

The dissociation pressure and resulting thermodynamic data for the three complexes are presented in Tables 1 and 2. The constants, *A* and *B*, for the dissociation pressure equation were determined by a least squares fit of five to nine

Can. J. Chem. Downloaded from www.nrcresearchpress.com by 210.87.254.42 on 09/05/12
For personal use only.

Can. J. Chem. Downloaded from www.nrcresearchpress.com by 210.87.254.42 on 09/05/12
For personal use only.

experimental points. The thermodynamic values for the propylene complex are slightly different from those reported earlier (1). The present data are considered to be the more accurate.

Upon complexation of the olefins, the shifts to lower frequency for the double bond stretching vibrations are 55 (2), 53, and 47 cm^{-1} for propylene, vinyl chloride, and vinyl fluoride respectively.

From the data of Table 2 it is obvious that the order of complex stability for the three olefins studied is $AgBF_4 \cdot 2C_3H_6 \gg AgBF_4 \cdot 2C_2H_3Cl > AgBF_4 \cdot 2C_2H_3F$. The stability of the corresponding ethylene complex, $AgBF_4 \cdot 2C_2H_4$ (α) (1), lies between those for propylene and vinyl chloride. The much lower stability of the vinyl chloride and vinyl fluoride complexes results both from smaller enthalpy and larger entropy changes upon interaction of these olefins with the silver salt.

As has been found earlier with a series of hydrocarbon olefins (1), there is a linear dependence, Fig. 1, of $\Delta H°$ on the ionization potential (4) of the olefin indicating a linear increase of $\Delta H°$ with increasing olefin basicity. The slope of this plot may be indeed a measure of the dependence of the coordinate bond energy upon the olefin basicity.

The shift to lower frequency, $\Delta\nu_{C=C}$, for the double bond stretching vibration in the olefin reflects the extent of perturbation of the double bond by the silver ion (2). The approximately linear variation of $\Delta H°$ with $\Delta\nu_{C=C}$ is then a further indication that the difference between the $\Delta H°$ values for the different olefins in this series is a measure of the difference between the coordinate bond energies.

The complexes of the hydrocarbon olefins (1) show a linear variation of $\Delta S°$ with $\Delta H°$ indicative of a progressive limitation of the freedom of the olefin with increasing silver ion – olefin interaction. On this plot, Fig. 2, the points for the vinyl fluoride and vinyl chloride complexes lie, however, far from the line for the hydrocarbon olefins because of their large $\Delta S°$ values and may lie, in fact, on another line essentially parallel to that for the hydrocarbon olefins.

Physical properties of the olefin such as molar volume and polarizability (5) are very similar for vinyl fluoride and ethylene and for vinyl chloride and propylene. Consequently, the larger $\Delta S°$ values for the halo-olefin complexes must be attributable to configurational limitations imposed upon the complexed molecule in addition to those determined by the strength of the coordinate bond and the size or shape of the molecule.

One physical characteristic of the halo-olefins which differs markedly from that of the hydrocarbon olefins is the permanent dipole moment (C_3H_6, 0.366; C_2H_3Cl, 1.445; C_2H_3F, 1.43 D (6)). As a result of their large dipole moment relative to those of ethylene and propylene, the complexed vinyl fluoride and vinyl chloride molecules will experience a greater ion–dipole interaction with the silver ion as well as a greater dipole–dipole interaction with other complexed molecules than do those of the hydrocarbon olefins. These additional interactions will further restrict the freedom of the complexed halo-olefin and will be reflected in higher $\Delta S°$ values for complex formation. Figure 3 provides an indication of the dependence of $\Delta S°$ on the dipole

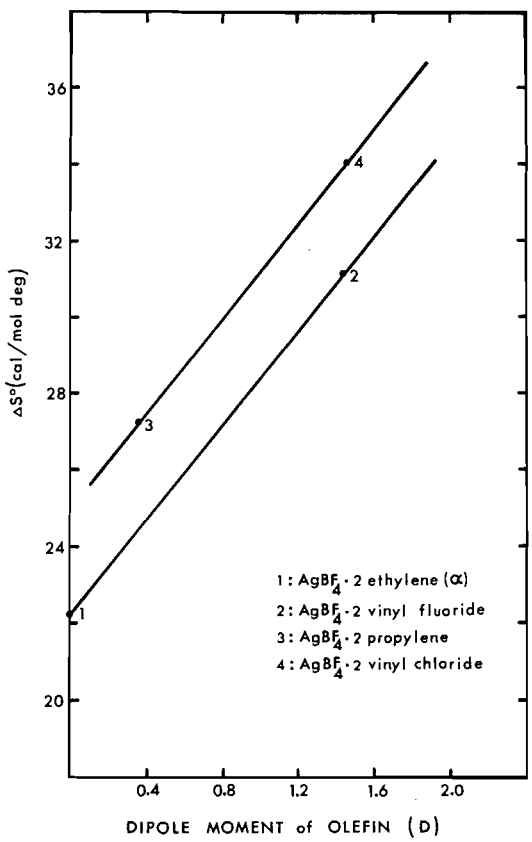

FIG. 3. Entropy change – dipole moment correlation.

moment of the olefin molecule for each pair of olefins with similar molar volume.

For olefins with relatively large dipole moments such as vinyl fluoride or vinyl chloride, the $\Delta S°$ for complex formation can be represented then by the two-term expression, $\Delta S° = C(\Delta H°) + D$ (dipole moment). The constant C is the slope of the line, ($\Delta S° = 2.627\ \Delta H° - 0.044$, by least squares), representing the hydrocarbon olefins in Fig. 2, while the constant D is the slope of either line in Fig. 3. Using the slope of the line for the ethylene and vinyl fluoride complexes, $D = 6.207$, one can calculate for the vinyl chloride complex a $\Delta S°$ value of 34.02 cal deg^{-1} mol^{-1} which compares very favorably with that, 34.06 cal deg^{-1} mol^{-1}, obtained directly from the equilibrium dissociation data.

The much lower stability of the vinyl chloride than of the propylene complex is due then both to the lower basicity of the halo-olefin which results in a weaker metal–olefin bond and to the presence of a much larger dipole moment in the halo-olefin which results in a larger entropy change; the latter effect is the larger. With vinyl fluoride, the reduced complex stability with respect to propylene is about equally attributable to reduced olefin basicity and to the effect of the dipole moment while the reduced stability with respect to ethylene results almost completely from the dipole moment effect.

The authors wish to acknowledge the contribution of A. R. McDowell, Analytical Laboratory, Dow Chemical of Canada, who has determined the i.r. spectra of the complexes.

1. H. W. QUINN and D. N. GLEW. Can. J. Chem. **40**, 1103 (1962).
2. H. W. QUINN, J. S. MCINTYRE, and D. J. PETERSON. Can. J. Chem. **43**, 2896 (1965).
3. H. W. QUINN and R. L. VANGILDER. Can. J. Chem. **46**, 2707 (1968).
4. R. BRALSFORD, P. V. HARRIS, and C. W. PRICE. Proc. Roy. Soc. A**258**, 459 (1960).
5. E. R. LIPPINCOTT, G. NAGARAJAN, and J. M. STUTMAN. J. Phys. Chem. **70**, 78 (1966).
6. Handbook of chemistry and physics. 50th Ed. Chemical Rubber Company, 1969–1970. p. E-70.

Can. J. Chem. Downloaded from www.nrcresearchpress.com by 210.87.254.42 on 09/05/12
For personal use only.

Can. J. Chem. Downloaded from www.nrcresearchpress.com by 210.87.254.40 on 09/05/12
For personal use only.

Chemical Shift. V. Further Studies on the Long-range Shielding Effects of the C—H and C=O Bonds

J. W. ApSimon and H. Beierbeck[1]

Department of Chemistry, Carleton University, Ottawa, Canada

Received November 9, 1970

The long-range shielding effects of the C=O and C—H bonds were reexamined by the method described in part IV of this series, with the objective of resolving the discrepancies between some of the conclusions presented and earlier findings by Zürcher. The C—H bond magnetic anisotropy was treated as a variable and found to be small enough to be negligible. Upon omission of this term, both electrostatic and magnetic anisotropy effects had to be invoked to account for the shielding effects of the carbonyl group.

The necessary geometric quantities were calculated from atomic coordinates for androsterone, as determined by X-ray crystallography, and freely rotating methyl groups were approximated by superpositions of 24 conformations of the group. The results were in essential agreement with those obtained with the use of geometric factors computed as described in part IV.

La méthode décrite dans notre travail précédent (4ème partie) est utilisée pour réexaminer l'effet de blindage à longue distance des liaisons C=O et C—H; le but de ce travail était de trouver une explication qui permettrait de concilier quelques-unes des conclusions présentées et des données rapportées précédemment par Zürcher. On a traité l'anisotropie magnétique du lieu C—H comme une variable et on a trouvé qu'elle est suffisamment faible pour être négligée. Si l'on omet ce terme des calculs ayant comme but d'évaluer les effets de déblindage du groupe carbonyle on doit ensuite faire intervenir les effets d'anisotropie magnétique et électrostatique.

Les quantités géométriques nécessaires ont été calculées à partir des coordonnées atomiques de l'androstanone telles que déterminées par cristallographie de rayons-X; on a simulé les groupes méthyles en rotation libre par superposition de 24 conformations de ce groupe. Les résultats obtenus sont généralement en accord avec ceux obtenus en utilisant les facteurs géométriques calculés par la méthode décrite dans la section IV de cette série.

Canadian Journal of Chemistry, 49, 1328 (1971)

Introduction

In part IV of this series (1–4) the derivation of values for the shielding parameters of the ketonic C=O bond was described. Chemical shifts were predicted in good agreement with experiment and with earlier calculations by Zürcher (5) for the same group of model compounds. However, our conclusions differed in two aspects from Zürcher's results. We did not find any preferred position for the (coincident) magnetic and electric dipole representing the carbonyl group. More importantly it appeared that, in contrast to Zürcher's findings, the electrostatic shielding effect of the carbonyl group was only of minor importance if not negligible. Apart from our simplified version of methyl groups the only difference in assumptions concerned the magnetic anisotropy $\Delta\chi_{xz}$(CH) of the C—H bond. We used a value of 7.54 for $\Delta\chi_{xz}$(CH),[2] derived previously (see note added in proof, ref. 2), whereas the latter author assumed the C—H bond to be practically magnetically isotropic and omitted this term in his calculations. Since this difference in the assumed values for $\Delta\chi_{xz}$(CH) must be responsible for the conflicting results and in the light of recent evidence (8) supporting Zürcher's view that the C—H bond is magnetically isotropic it was decided to repeat the calculations of Part IV (4), firstly treating $\Delta\chi_{xz}$(CH) as a variable, in the hope of confirming one or the other value, and secondly omitting in turn the terms for the C—H bond anisotropy effect and that for the electrostatic effect of the C=O group, in order to compare their relative importance.

[1]Taken from the M.Sc. thesis of H. Beierbeck, Carleton University, Ottawa, Canada, April, 1970.

[2]All shielding parameters are quoted in units: $\times 10^{-30}$ cm^3/molecule.

Can. J. Chem. Downloaded from www.nrcresearchpress.com by 210.87.254.40 on 09/05/12
For personal use only.

It also appeared useful to study the reproducibility of the C—H and C=O shielding parameters using geometric quantities obtained from atomic coordinates derived from X-ray crystallographic data and by the use of a more realistic methyl group model (5). Comparison of values obtained by these routes with those of part IV (4) (use of Dreiding models and methyl hydrogen approximation) would then give indication of the expected variations in shielding parameters on the use of approximate conformational data.

Results and Discussion

As in part IV (4) the change in chemical shift of a methyl group upon substitution of CH_2 by C=O is assumed to be due to two shielding mechanisms. The magnetic anisotropy effects of the C=O and C—H bonds are given by eqs. 1*a* and 1*b*[3] (4, 6).

$$[1a]\quad \delta^{M}(CO) = \Delta\chi_{yx}(CO)\,\langle(1 - 3\cos^2\theta_y)/3R^3\rangle + \Delta\chi_{zx}(CO)\,\langle(1 - 3\cos^2\theta_z)/3R^3\rangle$$
$$= \Delta\chi_{yx}(CO)\,\langle g_1{}^{M}(CO)\rangle + \Delta\chi_{zx}(CO)\,\langle g_2{}^{M}(CO)\rangle$$

$$[1b]\quad \delta^{M}(CH) = \Delta\chi_{xz}(CH)\,\langle(1 - 3\cos^2\theta_x)/3R^3\rangle$$
$$= \Delta\chi_{xz}(CH)\,\langle g^{M}(CH)\rangle$$

Equations 2*a* or 2*b*, depending on the methyl group model used (*vide infra*), are the expressions for the electrostatic shielding effect of the C=O bond (4, 7).

$$[2a]\quad \delta^{E}(CO) = K(CO)\,\langle\cos\omega(3\cos\phi\cos\theta_x - \cos\alpha)/R^3\rangle$$
$$= K(CO)\,\langle g^{E}(CO)\rangle$$

$$[2b]\quad \delta^{E}(CO) = K(CO)\,\langle(2\cos\theta_x\cos\phi + \sin\theta_x\cos\psi)/R^3\rangle$$
$$= K(CO)\,\langle g^{E}(CO)\rangle$$

The geometric quantities are defined in Fig. 1, $\Delta\chi_{yx}(CO)$, $\Delta\chi_{zx}(CO)$, and $\Delta\chi_{xz}(CH)$ are the magnetic anisotropies and $K(CO)$ is a proportionality constant descriptive of the electric screening effect. The angle brackets denote averages over the possible conformations of the rotating methyl groups. Thus, the change in chemical shift for a methyl group substitution of CH_2 by C=O is given by eq. 3 (4)

$$[3]\quad \Delta\delta = \Delta\chi_{yx}(CO)\,\langle g_1{}^{M}(CO)\rangle + \Delta\chi_{zx}(CO)\,\langle g_2{}^{M}(CO)\rangle + K(CO)\,\langle g^{E}(CO)\rangle$$
$$- \Delta\chi_{xz}(CH)[\langle g^{M}(CH_\alpha)\rangle + \langle g^{M}(CH_\beta)\rangle]$$

Two changes were introduced in the computation of the necessary geometric quantities. Firstly, in addition to measurements on Dreiding models, X-ray structural data were used.[4,5] The carbon coordinates for androsterone (9) seemed a suitable representation of the androstane backbone. The coordinates for the ring protons and carbonyl oxygens were derived using standard bond lengths and angles.

In the calculations of the oxygen coordinates it had to be assumed that the C—(C=O)—C and C—(CH_2)—C ring fragments are the same. In fact the valency angles increase from *ca.* 110°

[3]The corresponding terms in ref. 4 are:
$\langle g_1{}^{M}(CO)\rangle \equiv f(\theta_1 R_1)$
$\langle g_2{}^{M}(CO)\rangle \equiv f(\theta_1 R_1 \gamma_1)$
$\langle g^{E}(CO)\rangle \equiv f(R_1\omega\beta\psi\phi)$
$\langle g^{M}(CH_\alpha)\rangle \equiv f(\theta_2 R_2)$
$\langle g^{M}(CH_\beta)\rangle \equiv f(\theta_3 R_3)$

[4]Dr. Samek has informed us that his group at the Czechoslovak Academy of Sciences, Prague, is using a similar approach.

[5]Although conformational data from the solid state are used, the close agreement between geometric factors (Table 1) and shielding parameters (Table 4), obtained with X-ray data for six different steroids (Table 1, footnote *), supports the view that different packing in crystals does not seriously affect the molecular geometry.

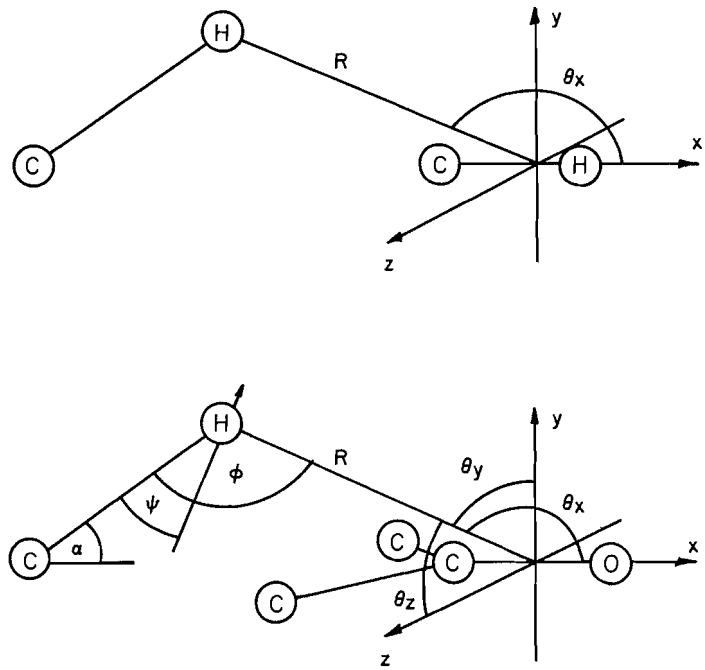

FIG. 1. Definition of geometric quantities.

in the saturated compound to about 116° in the ketones. However, this assumption does not seem to affect the results seriously. In Table 1, geometric factors and differences between calculated and experimental shifts are given for case 11/19, *i.e.*, the effect of substitution of CH_2 by CO in position 11 on the chemical shift of the C-19 methyl group. Carbonyl oxygen positions were calculated with the carbon coordinates for six different steroids, but in the last three cases the C—(CO)—C fragments were part of 11-keto steroids. The variations in geometric factors and calculated shifts between the two groups are of the same magnitude as the variations within both groups.

Secondly two methyl group models were compared. In one, the methyl shifts were represented by the effects at the center of the circle of rotation of the methyl hydrogens. In this case, eq. 2*a* was used and the angle brackets indicate that an average methyl proton position was assumed.

In a second series the shielding was approximated by the average of the shift increments at each of 72 points around the circle, 5° apart. In this case the electric field effect was expressed by eq. 2*b*, derived previously (4), and the angle brackets signify that the enclosed geometric quantities are averages of 72 values.

In order to separate changes in shielding parameters due to changes of the methyl group model from changes with the source of the skeletal coordinates, four series of geometric factors were derived, XR, XA, MR, and MA. The X and M stand for X-ray data and molecular models respectively, R and A denote the type of methyl group model that was employed (R = rotating methyl; A = average proton position (1–4)). Within each of these four series of geometric factors the C—H and C═O dipole positions were varied in steps of 0.2 Å. The geometric quantities from set XR are collated in Table 2; Table 3 shows a comparison of geometric factors from the four series XR, XA, MR, and MA.

Least squares calculations were carried out initially with the 22 equations derived from the methyl shifts in 5α,14α androstane and its monoketo derivatives, varying C═O and C—H point dipole positions independently. Again, it was found that the shielding effect of the C-11 keto

Can. J. Chem. Downloaded from www.nrcresearchpress.com by 210.87.254.40 on 09/05/12
For personal use only.

TABLE 1. Conformational comparison of 11-desoxy and 11-keto steroids*

	1	2	3	4	5	6*
			Torsional angles (deg)			
3-2-1-10†	55.7	58.0	56.3	55.1	57.6	57.1
2-1-10-9	188.9	195.5	190.6	193.5	192.1	189.9
1-10-9-11	60.2	64.1	53.9	56.2	58.7	60.2
10-9-11-12	182.5	181.5	181.3	183.8	186.9	184.0
9-11-12-13	54.8	58.3	56.0	54.3	56.2	55.1
			Geometric factors (10^{19} cm^{-3})‡			
$\langle g_1^M(CO)\rangle$	175	188	70	185	348	238
$\langle g_2^M(CO)\rangle$	−1059	−1096	−902	−981	−1181	−1065
$\langle g^E(CO)\rangle$	1069	1148	855	768	1037	977
			Difference between calculated and experimental shifts (Hz, at 100 MHz)			
Δδ	27.7	27.2	29.6	28.5	25.0	29.1
			Distances of closest approach of carbonyl oxygen and C-19 methyl protons (Å)§			
	2.20	2.12	2.36	2.41	2.36	2.28

*Atomic coordinates, as determined by X-ray crystallography, were available for the following steroids: 1, androsterone (9); 2, testosterone (10); 3, 2α,3β-dibromo-5α-cholestane (11); 4, 3β-acetoxy-17α-hydroxy-16β-bromo-5α-pregnane-11,20-dione (12); 5, 3β,17α-dihydroxy-21-bromo-5α-pregnane-11,20-dione (13); 6, 3β,17α-dihydroxy-16β-bromo-5α-pregnane-11,20-dione (14).

†The numbering system used follows the standard steroidal nomenclature as illustrated in the figure:

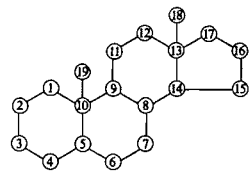

Thus, the angle 3-2-1-10 is the torsional angle about the C_1—C_2 bond axis.

‡See eq. 3 in the text.

§In all six cases the oxygen coordinates were calculated, as described in the text, from the coordinates for the C—C—C ring fragments.

TABLE 2. Geometric factors for C=O (0.6 Å) and C—H (0.8 Å) bonds. Set XR. All values in units: × 10^{19} cm^{-3}

	$\langle g_1^M(CO)\rangle$	$\langle g_2^M(CO)\rangle$	$\langle g^E(CO)\rangle$	$\langle g(CH_\alpha)\rangle$	$\langle g(CH_\beta)\rangle$
1/18*	91	−236	−100	141	76
2/18	28	−39	82	85	−35
3/18	39	51	27	−55	33
4/18	31	−48	86	87	−30
6/18	−41	47	211	196	−180
7/18	177	−266	108	305	−30
11/18	−828	359	1665	663	−684
12/18	−5	367	2463	1242	−932
15/18	−822	703	1764	1140	−978
16/18	−126	565	1439	1000	−892
17/18	−318	408	2791	1600	−1045
1/19	4	452	2476	1256	−990
2/19	−849	365	1637	722	−703
3/19	331	342	690	25	−309
4/19	−829	388	1581	690	−701
6/19	−879	399	1632	657	−705
7/19	336	345	710	19	−307
11/19	175	−1059	1069	617	394
12/19	230	49	232	63	−82
15/19	91	−238	127	184	41
16/19	76	68	71	20	−52
17/19	104	−39	56	23	32

*1/18, effect of substitution in position 1 on the chemical shift of the C-18 methyl group, etc.

Can. J. Chem. Downloaded from www.nrcresearchpress.com by 210.87.254.40 on 09/05/12
For personal use only.

Can. J. Chem. Downloaded from www.nrcresearchpress.com by 210.87.254.40 on 09/05/12
For personal use only.

TABLE 3. Variation of geometric factors for the C=O bond with the manner by which the atomic coordinates were obtained. All values in units: 10^{19} cm^{-3}

	XR*	XA	MR	MA	Reference 4
			$\langle g_1^M(CO)\rangle$		
7/18†	177	195	188	207	163
11/18	−828	−684	−1515	−1224	−1030
12/18	−5	206	118	308	385
15/18	−822	−644	−579	−442	−357
16/18	−126	−9	−185	−76	36
17/18	−318	−50	−273	−36	15
1/19	4	218	10	198	247
2/19	−849	−690	−1303	−1058	−859
3/19	331	346	371	380	406
11/19	175	381	−258	20	−276
12/19	230	231	248	250	244
			$\langle g_2^M(CO)\rangle$		
7/18	−266	−294	−224	−262	−174
11/18	359	361	745	713	656
12/18	367	332	508	495	513
15/18	703	713	567	592	601
16/18	565	584	498	522	544
17/18	408	350	332	298	188
1/19	452	420	501	460	329
2/19	365	360	540	527	502
3/19	342	359	356	372	431
11/19	−1059	−1357	−801	−1160	−876
12/19	49	45	148	140	111
			$\langle g^E(CO)\rangle$		
7/18	108	113	−8	78	117
11/18	1665	876	2106	1118	1030
12/18	2463	1329	2466	1339	1475
15/18	1764	990	1603	914	962
16/18	1439	874	1407	829	820
17/18	2791	1459	2666	1398	1564
1/19	2476	1342	2455	1323	1437
2/19	1637	878	1993	1016	937
3/19	690	496	749	526	543
11/19	1069	333	1045	338	329
12/19	232	216	236	232	201

*See explanation in the text.
†See footnote * in Table 2.

group on the C-19 methyl protons was anomalous. The corresponding equation was therefore excluded from further calculations.

The original suggestion to account for this discrepancy (4) was conformational disparity between the 11-ketone and androstane, caused by nonbonded interactions between the C-1 protons and the C-11 carbonyl oxygen. However, the six steroids in Table 1 do not show a distortion of either the A or the C ring large enough to produce additional downfield shifts of 0.3 p.p.m. More likely causes are van der Waals' deshielding and hindered rotation of the C-19 methyl group (also suggested by Zürcher (5)) and failure of the point dipole approximation. The distance of closest approach of the carbonyl oxygen and the C-19 methyl hydrogens is 2.2 to 2.4 Å as compared to the next shortest distance of *ca.* 3 Å in the case of the 1-ketone.

Conformational disparity, however, seems to be the reason for the large error in the prediction of the effect of the C-17 carbonyl group on the C-18 methyl hydrogens. Introduction of the C-17 C=O bond shifts the energy minimum along the pseudorotation path of the D ring relative to its position in the saturated ring (15). This change from one conformation to the other most likely contributes to the chemical shift of the C-18 methyl group. This case was also excluded from further calculations.

The least squares analyses were repeated with the remaining 20 equations, varying C—H and C=O dipole positions independently. The standard deviation between calculated and experimental shifts showed a minimum for a C=O dipole location at the bond center, but there was no preferred C—H dipole location. The

TABLE 4. Variation of C=O bond shielding parameters. Unless indicated otherwise, $\Delta\chi_{xz}$ (CH)=O, the geometric factors from set XR were used in the derivation, and cases 17/18 and 11/19 were excluded, solvent was CCl_4, the C=O dipole position was the point 0.6 Å from carbon. All values in units: 10^{-30} cm^3/molecule

	$\Delta\chi_{yx}$ (CO)	$\Delta\chi_{zx}$ (CO)	K(CO)
	Choice of geometric factors		
XR	−31.6	−20.9	−9.3
XA	−31.7	−19.2	−12.6
MR	−26.2	−18.5	−7.7
MA	−26.7	−16.0	−11.3
	Change of C=O dipole position		
0.4 Å	−27.8	−17.0	−9.5
0.6 Å	−31.6	−20.9	−9.3
0.8 Å	−36.1	−24.5	−9.0
	Change of Solvent		
C_6D_{12}	−31.2	−19.5	−7.5
CCl_4	−31.6	−20.9	−9.3
$CDCl_3$	−32.6	−18.2	−10.6
	Miscellaneous		
$\Delta\chi_{xz}$ (CH) included*	−31.7	−23.1	−8.6
5β and 14β†	−29.3	−20.0	−9.1
Steroids included ($CDCl_3$)			
X-Ray data for other steroids‡	−30.7	−21.3	−9.1

*A value of 3.1 was used for $\Delta\chi_{xz}$(CH). The C—H dipole location was 0.8 Å.
†Five additional cases were included. 5β-Androstane: 1/19, 3/19, 4/19; 14β-androstane: 15/18, 17/18; the experimental values were taken from ref. 4; the necessary geometric factors were calculated from the atomic coordinates for digitoxigenin, as determined by X-ray crystallography (16).
‡Derived with geometric factors that were calculated from the atomic coordinates for steroids 1 and 3–6 in footnote *, Table 1. The average deviations were, in the same order, ±0.8, ±1.1, ±0.3.

TABLE 5. Differences between calculated and experimental shifts (in Hz at 100 MHz); $\Delta\chi_{xz}$ (CH)=O. Solvent CCl_4, C=O point dipole 0.6 Å from carbon. Geometric factors as indicated. Corresponding shielding parameters from Table 4

	XR	XA	MR	MA	Reference 4†
1/18	3.0	2.3	4.4	3.4	1.2
2/18	−0.2	−0.4	0.9	0.4	0.2
3/18	1.0	0.9	0.9	0.8	0.4
4/18	0.7	0.4	1.7	1.2	1.1
6/18	1.9	1.4	2.8	2.1	0.5
7/18	−1.3	−2.2	−1.7	−3.0	3.1
11/18	0.5	0.9	2.5	2.1	3.1
12/18	−1.6	−1.0	−5.3	−5.2	2.6
15/18	4.3	3.5	−1.4	−1.5	2.6
16/18	−2.7	−3.5	0.6	0.5	0.2
17/18*	−12.2	−11.4	−7.9	−7.9	5.4
1/19	1.4	1.9	4.0	4.3	5.2
2/19	−0.7	−0.9	1.2	1.1	0.2
3/19	−0.5	−0.6	1.5	1.3	0.5
4/19	−1.3	−1.3	−1.0	−1.0	0.8
6/19	−1.5	−1.4	−2.7	−2.6	0.1
7/19	2.8	2.7	4.1	4.0	3.0
11/19*	27.6	30.7	33.1	32.8	—
12/19	−1.7	−2.2	−2.7	−3.1	1.7
15/19	3.2	2.7	3.7	3.0	0.7
16/19	−0.7	−0.9	−0.1	−0.3	0.4
17/19	−0.2	−0.5	−0.2	−0.7	0.6

*Not included in least squares calculations.
†Table 9, ref. 4, unsigned.

values for $\Delta\chi$(CH) were small for all points along the C—H bond, *e.g.*, 3.1 for the point 0.8 Å from carbon. The standard deviation remained practically unchanged when the term in $\Delta\chi_{xz}$(CH) was omitted and there were only small changes in the C=O bond shielding parameters. Thus, it is fairly certain that the C—H bond anisotropy is indeed small and normally it seems justified to set it equal to zero.

The electrostatic shielding effect of the C=O bond was found to be equally important as its anisotropy effect. The chemical shifts could not be accounted for by the use of only the anisotropy effects or only the electric field effect terms, in accord with Zürcher's findings (5). Thus, it appears that the conflicting conclusions regarding the C=O dipole location and the significance of the electrostatic screening mechanism were indeed due to the use of different C—H bond anisotropy values.

In contrast the use of geometric quantities obtained from measurements on molecular models and the simplifying assumptions concerning the actual methyl hydrogen positions, led to conclusions in general agreement with results obtained using more accurate conformational data. Although the results obtained with set XR of geometric factors have to be considered to be the best, the other parameters do not differ very much (Table 4) and they predict the chemical shifts equally well (Table 5).

Experimental

The steroids used were obtained as described in ref. 4. Calculations were performed on the SIGMA 7 computer at Carleton University. Programs are available upon request.

We thank Mrs. J. Lemke and Mr. S. Scharf for expert technical assistance, the National Research Council of Canada for generous financial support, and the Ontario Government for a Graduate Fellowship (H.B.).

1. J. W. APSIMON, W. G. CRAIG, P. V. DEMARCO, D. W. MATHIESON, L. SAUNDERS, and W. B. WHALLEY. Tetrahedron, **23**, 2339 (1967).
2. J. W. APSIMON, W. G. CRAIG, P. V. DEMARCO, D. W. MATHIESON, L. SAUNDERS, and W. B. WHALLEY. Tetrahedron, **23**, 2357 (1967).
3. J. W. APSIMON, W. G. CRAIG, P. V. DEMARCO, D. W. MATHIESON, and W. B. WHALLEY. Tetrahedron, **23**, 2375 (1967).
4. J. W. APSIMON, P. V. DEMARCO, D. W. MATHIESON, W. G. CRAIG, A. KARIM, L. SAUNDERS, and W. B. WHALLEY. Tetrahedron, **26**, 119 (1970).
5. R. F. ZÜRCHER. Progress in n.m.r. spectroscopy. Vol. II. *Edited by* J. W. Emsley, J. Feeney, and L. H. Sutcliffe. Pergamon Press, Oxford, 1967. p. 205.

Can. J. Chem. Downloaded from www.nrcresearchpress.com by 210.87.254.40 on 09/05/12
For personal use only.

6. H. M. McConnell. J. Chem. Phys. **27**, 226 (1957).
7. A. D. Buckingham. Can. J. Chem. **38**, 300 (1960).
8. J. Homer and D. Callaghan. J. Chem. Soc. A, 439 (1968).
9. D. F. High and J. Kraut. Acta Cryst. **21**, 88 (1966).
10. A. Cooper, E. M. Gopalakrishna, and D. A. Norton. Acta Cryst. **B24**, 935 (1968).
11. H. J. Geise and C. Romers. Acta Cryst. **20**, 257 (1966).
12. J. M. Ohrt, B. A. Haner, A. Cooper, and D. A. Norton. Acta Cryst. **B24**, 312 (1968).
13. J. M. Ohrt, A. Cooper, G. Kartha, and D. A. Norton. Acta Cryst. **B24**, 824 (1968).
14. J. M. Ohrt, A. Cooper, and D. A. Norton. Acta Cryst. **B25**, 41 (1969).
15. C. Altona, H. J. Geise, and C. Romers. Tetrahedron, **24**, 13 (1968).
16. I. L. Karle and J. Karle. Acta Cryst. **B25**, 434 (1969).

Can. J. Chem. Downloaded from www.nrcresearchpress.com by 210.87.254.40 on 09/05/12
For personal use only.

Can. J. Chem. Downloaded from www.nrcresearchpress.com by 210.87.254.105 on 09/05/12
For personal use only.

Chemical Shift. VI. The Long-range Shielding Effects of Ethylene–Ketal and –Thioketal Groups

J. W. ApSimon, H. Beierbeck,[1] and D. K. Todd[1]
Department of Chemistry, Carleton University, Ottawa, Canada

AND

P. V. DeMarco
Department of Molecular Structure Research, The Lilly Research Laboratories, Indianapolis, Indiana 46206, U.S.A.

AND

W. G. Craig
Department of Chemistry, University of Prince Edward Island, Charlottetown, Prince Edward Island, Canada

Received November 9, 1970

The calculation of chemical shift values by the method used in parts I–V (1–5) has been extended to a derivation of the shielding effects of the ethylene–ketal and –thioketal groups. For these studies ketal and thioketal derivatives of monoketoandrostanes were prepared. The chemical shifts of the C-18 and -19 methyl protons in these compounds are reported for the solvents $CDCl_3$, CCl_4 and benzene.

Representing both groups by point dipoles, values for the anisotropies and for *K*, a parameter descriptive of the electric field effect, were derived for various, coincidental, locations of the magnetic and electric dipoles along the symmetry axes of the two groups.

La méthode de calculs des déplacements chimiques développée dans nos communications I–V (1–5) a été étendue à la dérivation des effets de blindage provoqués par les groupes éthylène–cétals et –thiocétals. Afin de mener ces études à bien on a préparé des dérivés cétals et thiocétals de monocétoandrostanes. On rapporte les déplacements chimiques des protons des méthyles en C-18 et -19 de ces composés lorsqu'ils sont en solution dans le $CDCl_3$, CCl_4 et le benzène.

On a représenté les deux groupes par des dipoles ponctuels et il a été alors possible d'évaluer pour divers sites des dipoles électriques et magnétiques qui coincident le long des axes de symétrie des deux groupes, des valeurs pour leur anisotropie et pour *K*, un paramètre descriptif de l'effet de champ électrique.

Canadian Journal of Chemistry, 49, 1335 (1971)

Preceding papers in this series (1–5) have described the derivations of values for the long range shielding parameters of C—C, C—H, C=C, and C=O bonds. In this paper we report the results of the extension of the method to the ethylene–ketal **1** and –thioketal **2** groups.

1 **2**

We became interested in these groups in connection with our studies of the C=O bond shielding effect. Since only changes in chemical shifts upon exchange of one group by another can be predicted, it is necessary to have a reference group for every functional group of interest. In the studies of the C=O bond shielding effects (4–6) the substitution CO/CH_2 was used, *i.e.*, the parent hydrocarbon served as reference. In the general case, however, ketal or thioketal derivatives are more readily available. Therefore an understanding of the shielding effects of these groups could be of considerable value for structural assignments concerning the keto group.

One paper on the long-range shielding effects of the ketal groups has appeared recently in the literature (7). These workers estimated the shift increments due to the substitution of CH_2 by the ethylene–ketal group from the sum of the anisotropy effects (8) of the component bonds plus the electric field effect (9) of the total group. Values for the anisotropies for the C—C and C—O bonds were taken from the literature (10, 11), the C—H bonds were assumed to be magnetically

[1]Taken from the M.Sc. theses of H. Beierbeck and D. K. Todd, Carleton University, Ottawa, Canada, 1970.

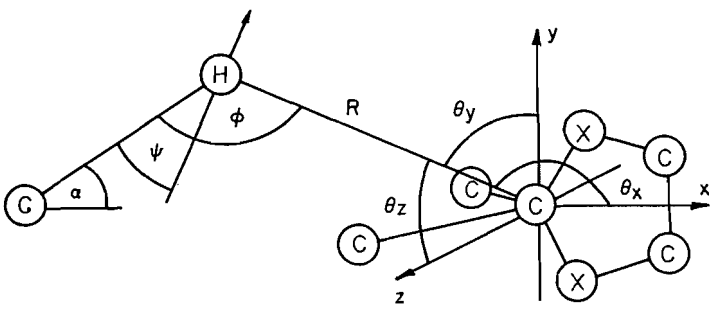

FIG. 1. Definition of geometric quantities.

isotropic. The electric field effect was assumed to arise from a point dipole, with the dipole moment of the group located at its center of gravity. Experimental shifts for C-18 and -19 methyl groups in 12 steroidal ketals, representing seven different situations, were quoted. Calculated shifts were given for three cases, in two cases agreement with experiment was satisfactory.

In the present study we attempted to treat the ketal and thioketal groups as point magnetic and electric dipoles as in the case of the carbonyl group. If average planarity is assumed, the two groups have the same symmetry as the C=O bond. Therefore, the same geometric quantities could be used that had previously been derived in the course of our studies of the C=O bond shielding effect (5). The requisite experimental data were derived from the chemical shifts of the C-18 and -19 methyl groups in ketal and thioketal derivatives of monoketoandrostanes, made in this laboratory (Table 1).

As in the case of the carbonyl group (4, 5) changes in chemical shift were assumed to be due to anisotropy effects δ^M (8) and to electric field effects δ^E (9), as defined by eqs. 1 and 2.[2]

The geometric quantities are defined in Fig. 1, $\Delta\chi_{yx}$ and $\Delta\chi_{zx}$ are the magnetic anisotropies in the yx and zx planes respectively, and K is a proportionality constant, descriptive of the

TABLE 1. Experimental shifts of C-18 and -19 methyl groups in androstane ketals and thioketals, in Hz [at 100 MHz] from TMS

	Ethylene-ketals			Ethylene-thioketals		
	$CDCl_3$	CCl_4	Bz	$CDCl_3$	CCl_4	Bz
	5α,14α-Androstane derivatives					
1/18*	66.0	68.4	75.7	70.4	69.8	75.2
2/18	66.8	69.0	68.0	68.6	69.3	64.1
3/18	68.0	69.2	67.5	69.7	68.9	66.0
4/18	68.0	69.5	69.6	68.3	68.5	66.2
6/18	70.2	72.3	69.5	73.0	74.3	70.5
7/18	69.2	69.8	75.0	74.0	74.2	71.0
12/18	83.8	78.8	98.2	96.3	93.1	104.3
16/18		82.2†		89.5	87.7	90.8
17/18	82.6	77.6	94.8	91.6	87.4	97.2
1/19	97.3	95.2	110.8	118.5	115.3	120.7
2/19	88.4	86.0	106.0	99.5	97.0	110.3
3/19	80.1	81.0	73.6	82.3	81.8	66.0
4/19	94.4	91.3	114.8	93.5	90.8	104.0
6/19	91.7	88.5	109.6	95.2	92.0	105.3
7/19	80.4	81.0	75.0	82.6	83.2	76.4
12/19	77.0	77.2	74.0	78.7	79.8	70.1
16/19		78.0†		78.2	77.8	71.2
17/19	77.4	77.6	76.2	79.1	78.6	73.7
	5β,14α-Androstane derivatives					
1/18					69.2	68.2
2/18	68.8	68.3	72.0	69.4	69.2	69.5
3/18	66.4	68.7	66.3	68.4	68.3	64.2
1/19					131.1	150.4
2/19	94.8	93.0	92.4	94.5	94.0	86.5
3/19	92.7	94.0	93.6	96.1	96.7	88.1

*1/18: substituent in position 1, shift of C-18 methyl group, etc.
†Determined in a mixture of ketone and ketal.

$$[1] \quad \delta^M = \Delta\chi_{yx}\langle(1 - 3\cos^2\theta_y)/3R^3\rangle + \Delta\chi_{zx}\langle(1 - 3\cos^2\theta_2)/3R^3\rangle = \Delta\chi_{yx}\langle g_1{}^M\rangle + \Delta\chi_{zx}\langle g_2{}^M\rangle$$

$$[2] \quad \delta^E = K\langle(2\cos\theta_x\cos\phi + \sin\theta_x\cos\psi)/R^3\rangle = K\langle g^E\rangle$$

[2]See part V, footnote 2 re nomenclature.

Can. J. Chem. Downloaded from www.nrcresearchpress.com by 210.87.254.105 on 09/05/12
For personal use only.

TABLE 2. Differences between calculated and observed shifts (in CCl_4), in Hz [at 100 MHz]

	Ke/CH_2	Ke/CO*	Ke/CO†	S/CH_2	S/CO*	S/CO†
1/18	0.6	−2.4	−0.3	−0.3	−3.3	−1.2
2/18	−0.1	0.1	0.3	−1.2	−1.0	−0.8
3/18	0.1	−0.9	−2.0	0.3	−0.7	−1.8
4/18	0.4	−0.3	0.1	−2.1	−2.8	−2.5
6/18	2.1	0.2	−0.2	2.9	1.0	0.6
7/18	2.1	3.4	4.5	1.3	2.6	3.6
12/18	−1.5	0.1	−3.0	−1.9	−0.3	−3.5
16/18	2.4	5.1	2.6	2.4	5.1	2.6
17/18	−4.4	7.8	0.1	−9.0	3.2	−4.1
1/19	4.8	3.4	0	10.8	9.4	6.0
2/19	−2.6	−1.9	−1.8	3.2	3.9	3.2
3/19	−1.0	−0.5	2.1	−3.1	−2.6	0
4/19	2.9	4.2	2.6	−2.0	−0.7	−2.1
6/19	−0.2	1.3	−0.1	−1.1	0.4	−0.8
7/19	−1.1	−3.9	−1.0	−1.9	−4.7	−1.9
12/19	−1.4	0.3	0.2	−1.3	0.4	0.2
16/19	−0.7	0	−1.0	−0.8	−0.1	−1.1
17/19	−0.6	−0.4	−0.4	−1.1	−0.9	−1.0

*Estimated from $\Delta\delta(\text{Ke/CO}) = \Delta\delta(\text{Ke/CH}_2) - \Delta\delta(\text{CO/CH}_2)$. Dipole positions: Ke at carbon, CO 0.6 Å from carbon.
†From direct least squares fit to $\delta(\text{Ke/CO})^{obs}$. Both dipoles at carbon.

electric field effect. Electric and magnetic dipoles were assumed to coincide. Their positions were varied along the symmetry axes in steps of 0.2 Å.

Shielding parameters for the ketal (thioketal) group were derived in two ways, namely by predicting the effect of the substitutions of either CH_2 or of C=O by the ketal (thioketal) group. With the abbreviations Ke = ketal, S = thioketal, Ke/CO = substitution of C=O by the ketal group, etc., eqs. 3 and 4 can be written,

$$[3]\quad \delta(\text{Ke/CH}_2) = \delta^M(\text{Ke}) + \delta^E(\text{Ke}) - \delta^M(\text{CH}_2)$$
$$= \Delta\chi_{yx}(\text{Ke})\langle g_1{}^M(\text{Ke})\rangle + \Delta\chi_{zx}(\text{Ke})\langle g_2{}^M(\text{Ke})\rangle + K(\text{Ke})\langle g^E(\text{Ke})\rangle$$
$$- \Delta\chi(\text{CH})[\langle g(\text{CH}_\alpha)\rangle + \langle g(\text{CH}_\beta)\rangle]$$

$$[4]\quad \delta(\text{Ke/CO}) = \delta^M(\text{Ke}) + \delta^E(\text{Ke}) - \delta^M(\text{CO}) - \delta^E(\text{CO})$$
$$= \Delta\chi_{yx}(\text{Ke/CO})\langle g_1{}^M(\text{CO})\rangle + \Delta\chi_{zx}(\text{Ke/CO})\langle g_2{}^M(\text{CO})\rangle$$
$$+ K(\text{Ke/CO})\langle g^E(\text{CO})\rangle$$

plus two analogous equations for the thioketal group.

Equation 4 was written in an attempt to use coincidental C=O and Ke(S) dipole positions. The actual center of gravity of the ketal group is *ca.* 1 Å from carbon, compared to 0.6 Å for the keto group. The shielding parameters obtained by employing eq. 4 are differences between the parameters for the Ke(S) and the C=O group. The use of two different dipole locations involves too many variables to promise reasonably accurate predictions of chemical shifts. Least squares calculations of δ(Ke/H) and δ(S/H), using eq. 3, again (5) showed little dependence of the standard deviation between calculated and experimental shifts on the C—H dipole position. Values obtained for the C—H bond anisotropy were small in agreement with previous results (5). In view of the nature of the other assumptions it seemed justified to ignore this term.

A plot of the standard deviation between calculated and experimental shifts $\delta(\text{Ke/CH}_2)$ and $\delta(\text{S/CH}_2)$ *vs.* the dipole positions had a minimum at the steroidal carbon, but there was only a slight increase of σ as the dipoles were moved out along the symmetry axes. Table 2 shows the differences between calculated and experimental shifts; the

Can. J. Chem. Downloaded from www.nrcresearchpress.com by 210.87.254.105 on 09/05/12
For personal use only.

[5] $$\Delta\delta(\mathrm{Ke/CO}) = \Delta\delta(\mathrm{Ke/CH_2}) - \delta(\mathrm{CO/CH_2})$$

since

[6] $$\delta(\mathrm{Ke/CO})^{\mathrm{obs}} = \delta(\mathrm{Ke/CH_2})^{\mathrm{obs}} - \delta(\mathrm{CO/CH_2})^{\mathrm{obs}}$$

corresponding shielding parameters are given in Table 3.

An estimate of the errors Δ(Ke/CO) of predictions of δ(Ke/CO) may be obtained from eq. 5.

Analogous expressions hold for $\Delta\delta$(S/CO). Alternatively the shifts δ(Ke/CO) and δ(S/CO) may be calculated by a direct least square fit to experimental shifts, using eq. 4. In this case, too, the steroidal carbon was found to be the best dipole location. Calculated shifts and shielding parameters are collated in Tables 2 and 3.

It is doubtful whether these shielding parameters have any physical significance. The point dipole approximation is certainly inadequate in this case and the electric center of gravity is not at the steroidal carbon atom. Only five of the experimental shifts δ(Ke/CO) in the 5 α series were larger than 10 Hz and these represent only two truly different situations, since substituents in the 2, 4, and 6 positions and those in the 3 and 7 positions are practically equivalently oriented with respect to the C-19 methyl group. In addition, it is likely that the 1,3-diaxial interactions between the methyl groups and the C—O (C—S) bonds are severe enough to cause substantial deformations in the steroid skeleton and to give rise to van der Waals shielding effects.

TABLE 3. Shielding parameters, in units: $\times 10^{-30}$ cm^3/molecule. All dipoles at the steroidal carbon. Solvent CCl_4

	$\Delta\chi_{yz}$	$\Delta\chi_{zx}$	K
Ke	2.6	−2.3	−3.1
Ke/CO	26.2	3.6	7.6
S	−0.1	9.8	−9.7
S/CO	23.3	15.8	0.9

Experimental

Ethylene-ketals and -thioketals were made in the standard manner by Mr. S. Scharf at Carleton University. The derivatives of 11 ketoandrostane could not be obtained. All calculations were performed on the Sigma 7 computer at Carleton University.

We thank the National Research Council of Canada for generous financial assistance and the Ontario Government for a Graduate Fellowship (H.B.).

1. J. W. APSIMON, W. G. CRAIG, P. V. DEMARCO, D. W. MATHIESON, L. SAUNDERS, and W. B. WHALLEY. Tetrahedron, **23**, 2339 (1967).
2. J. W. APSIMON, W. G. CRAIG, P. V. DEMARCO, D. W. MATHIESON, L. SAUNDERS, and W. B. WHALLEY. Tetrahedron, **23**, 2357 (1967).
3. J. W. APSIMON, W. G. CRAIG, P. V. DEMARCO, D. W. MATHIESON, and W. B. WHALLEY. Tetrahedron, **23**, 2375 (1967).
4. J. W. APSIMON, P. V. DEMARCO, D. W. MATHIESON, W. G. CRAIG, A. KARIM, L. SAUNDERS, and W. B. WHALLEY. Tetrahedron, **26**, 119 (1970).
5. J. W. APSIMON and H. BEIERBECK. Can. J. Chem. This issue.
6. R. F. ZÜRCHER. Progress in n.m.r. spectroscopy Vol. II. *Edited by* J. W. Emsley, J. Feeney, and L. H. Sutcliffe. Pergamon Press, Oxford, 1967. p. 205.
7. B. P. KOCH, H. ROSENBERGER, and R. ZEPTER. J. für prakt. chem. **311**, 983 (1969).
8. H. M. MCCONNELL. J. Chem. Phys. **27**, 226 (1957).
9. A. D. BUCKINGHAM. Can. J. Chem. **38**, 300 (1960).
10. J. I. MUSHER. J. Chem. Phys. **35**, 1159 (1961).
11. L. D. HALL. Tetrahedron Lett. 1457 (1964).

Can. J. Chem. Downloaded from www.nrcresearchpress.com by 210.87.254.105 on 09/05/12
For personal use only.

Can. J. Chem. Downloaded from www.nrcresearchpress.com by 210.87.254.40 on 09/05/12
For personal use only.

Total Synthesis of 4-*O*-Methyl-DL-lyxose and 4-Deoxy-DL-ribose. Further Evidence of the Stereoselective Hydroxylation of Double Bonds by Osmic Acid

R. M. SRIVASTAVA[1] AND R. K. BROWN

Department of Chemistry, University of Alberta, Edmonton, Alberta

Received December 7, 1970

Methyl 4-*O*-methyl-α-DL-lyxopyranoside (**6**) and methyl 4-deoxy-β-DL-*erythro*-pentopyranoside (**3**) were obtained in excellent yield as the sole isolable products of the reaction of osmic acid in pyridine on *cis*-2,5-dimethoxy-5,6-dihydro-2*H*-pyran (**2**) and 2-methoxy-5,6-dihydro-2*H*-pyran (**1**), respectively. Hydrolysis of **6** and **3** gave respectively 4-*O*-methyl-DL-lyxose (**9**) and 4-deoxy-DL-ribose (**8**).

The attack on the double bond of **1** and **2** occurs nearly completely if not exclusively from the unhindered side, remote from the substituent. These results indicate that **1** must be predominantly in the conformation in which the C-2 alkoxy group is *quasi* axial.

Le 4-*O*-méthyl-α-DL-lyxopyranoside de méthyle (**6**) et le déoxy-4 β-DL-*érythro*-pentopyranoside de méthyle (**3**) ont été obtenus avec un excellent rendement et comme seuls produits de la réaction entre l'acide osmique dans la pyridine et respectivement le diméthoxy-2,5-dihydro-5,6 2*H*-pyranne-*cis* (**2**) et le méthoxy-2 dihydro-5,6 2*H*-pyranne (**1**). L'hydrolyse de **6** et de **3** conduit respectivement au 4-*O*-méthyl DL-lyxose (**9**) et au déoxy-4 DL-ribose (**8**).

L'attaque de la double liaison de **1** et de **2** se produit presque complètement sinon complètement par le côté le moins empêché, à savoir celui le plus éloigné du substituant. Ces résultats impliquent que **1** doit être sous une conformation dans laquelle le groupe alcoxy en position 2 est *quasi* axial.

Canadian Journal of Chemistry, 49, 1339 (1971)

A recent report from this laboratory has described the stereoselective attack of osmic acid on the double bond of the bicyclo compound 1,6-anhydro-3,4-dideoxy-β-DL-*erythro*-hex-3-enopyranose to produce, after hydrolysis, both α,β-DL-allose and α,β-DL-galactose (1). As part of a program aimed at the total syntheses of monosaccharides, and also to determine whether the stereoselective attack by osmic acid could be extended to 2-alkoxydihydropyrans, the reaction of osmic acid on both 2-methoxy-5,6-dihydro-2*H*-pyran (**1** in Scheme 1) and *cis*-2,5-dimethoxy-5,6-dihydro-2*H*-pyran (**2** in Scheme 1) was investigated. This report describes the results obtained.

The reactions performed and the products obtained are summarized in Scheme 1.

By the improved procedure (2), the reaction of osmic acid with **1** gave a nearly quantitative yield of crude material whose 100 MHz p.m.r. spectrum showed the presence of only one anomeric proton signal. Distillation of this crude material provided methyl 4-deoxy-β-DL-*erythro*-pentopyranoside (**3**) in 93% yield. The 100 MHz p.m.r. spectrum of **3** agreed with the structure designated. The 100 MHz p.m.r. spectrum of its diacetate **4** when analyzed with the aid of double irradiation, fully confirmed that the configuration and conformation was that indicated by **4**. Hydrolysis of **3** with aqueous dioxane containing sulfuric acid gave 4-deoxy-DL-ribose (**8**) in 77% yield. The 100 MHz p.m.r. spectrum of **8** in D_2O showed at first only one anomeric proton signal as a doublet at τ 5.09 ($J \approx 5$ Hz). When the solution had stood for a period of 24 h a second doublet appeared in the anomeric proton region at τ 5.36 ($J \approx 1.7$ Hz) thus indicating that the α anomer was now present in the ratio β:α = 1.0:0.42 as shown by the integrated areas of the signals.

The reaction of osmic acid with **2** gave a nearly quantitative yield of crude material which showed only two spots on a t.l.c., one barely discernible. Distillation of this crude substance gave methyl 4-*O*-methyl-α-DL-lyxopyranoside (**6**) in 84% yield as the sole insoluble product. The i.r. spectrum of **6** in carbon tetrachloride showed a narrow band at 3600 cm^{-1} and a broad absorption band, 3260–3540 cm^{-1}. An extensively diluted solution gave an i.r. spectrum with only one narrow band at 3590 cm^{-1}, indicative of the absence of intramolecular hydrogen bonding. The 100 MHz p.m.r. spectrum of **6** in pyridine-d_5 showed the anomeric proton signal as a doublet ($J \approx 2.8$ Hz) centered at τ 5.05 in agreement with the configura-

[1]Postdoctoral Fellow, 1968–1970. Presently at the Department of Chemistry, University of Windsor, Windsor 11, Ontario.

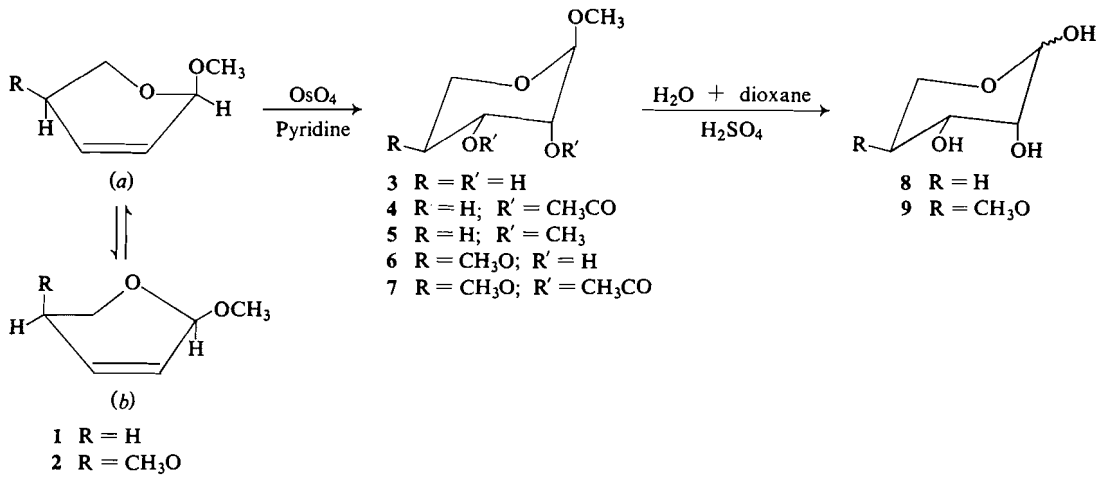

SCHEME 1

tion and conformation shown by **6**. Spin decoupling experiments provided no further corroboration of the structure proposed. However, the 100 MHz p.m.r. spectrum of the crystalline di-*O*-acetyl derivative **7** agreed with the proposed structure and spin decoupling experiments corroborated that **7** was in fact methyl 2,3-di-*O*-acetyl-4-*O*-methyl-α-DL-lyxopyranoside.

Hydrolysis of **6** with aqueous dioxane containing sulfuric acid afforded 4-*O*-methyl-DL-lyxose **9** as a viscous sirup in 75% yield. The 100 MHz p.m.r. spectrum of **9** in D_2O, after it had stood at room temperature for 16 h, showed two anomeric proton signals as doublets at τ 4.72 ($J \approx 5$ Hz) and 4.83 ($J \approx 1.5$ Hz) in the area ratio of 1.0:0.37, indicative of a mixture of the β and α anomers respectively. Final corroboration that **9** was indeed the structure indicated was obtained by the observation that the 100 MHz p.m.r. spectrum of **9** in D_2O was identical to that of authentic 4-*O*-methyl-D-lyxose.

It is clear that for both **1** and **2**, the attack by osmic acid on the double bond occurs nearly if not completely exclusively from the side remote from the substituent at C-2 and -4 and thus provides further evidence that the preferred direction of attack by osmic acid on a double bond of this six-membered ring structure is determined by steric factors. In this respect it is similar to the effect of substituents in directing the attack of peroxy acids on the double bond of 3-substituted cyclohexenes (3). This steric effect is readily discerned in either of the conformations *a* and *b* of compound **2** (Scheme 1). However, only in conformation *a* does compound **1** show such steric opposition by the C-2 methoxy group to the approach of osmic acid to the double bond on the same side of the ring occupied by the substituent. In conformation **1***b*, the double bond of compound **1** is readily accessible from either side of the ring. The fact that such a high proportion (84% at least) is obtained of the product resulting from attack of the double bond *trans* to the C-2 methoxy group indicates that compound **1** must prefer to a very large degree the conformation *a* in which the C-2 methoxy group is in the *quasi* axial orientation. It is well known that 2-alkoxytetrahydropyrans prefer that chair conformation in which the alkoxy group is axial. This phenomenon is known as the "anomeric effect" (4–6). This phenomenon is thought to be due to the polar character of the C_2—OCH_3 bond and the C_6—O_1 or C_2—O_1 bond of the 2-alkoxytetrahydropyran ring system (6–9). The similarity in these structural features of compound **1** leads to the reasonable assumption that the anomeric effect should be operative here also and thus conformer *a* would be preferred to conformer *b*. The great preponderance of attack by osmic acid on the side of the double bond remote from the C-2 methoxy group lends further support for this view.

Experimental

Boiling points and melting points are uncorrected. The b.p. of the viscous sirup was obtained in a sublimation apparatus. The lower end of this apparatus was

Can. J. Chem. Downloaded from www.nrcresearchpress.com by 210.87.254.40 on 09/05/12
For personal use only.

Can. J. Chem. Downloaded from www.nrcresearchpress.com by 210.87.254.40 on 09/05/12
For personal use only.

dipped into an oil bath and slowly heated. When the sirup started to deposit on the cold finger, the bath temperature was recorded as the b.p.

Elemental analyses were made by Mrs. Darlene Mahlow and Mrs. Andrea Dunn of this Department.

The 60 MHz p.m.r. spectra were made by Mr. R. Swindlehurst on a Varian A-60 spectrometer at 35 ± 1°. The 100 MHz p.m.r. spectra and spin decoupling experiments were done by Mr. Glen Bigam and associates of this Department, using a Varian HR-100 MHz instrument at 33 ± 1°. Unless otherwise specified, deuteriochloroform was the solvent used, with tetramethylsilane as internal or external reference. The couplings reported have been estimated from the spacings on the spectrum and are therefore approximate values.

The t.l.c. was done with Silica Gel G (E. Merck and Co.) as adsorbent. Iodine vapor was used to detect the spots.

Solvents were removed by rotary evaporator under vacuum unless otherwise stated.

*Methyl 4-O-Methyl-*α*-*DL*-lyxopyranoside (6)*

Osmium tetroxide (1.0 g, 3.39 mmol) in 4 ml of dry pyridine (2) was added to a solution of 0.563 g (3.90 mmol) of *cis*-2,5-dimethoxy-5,6-dihydro-2*H*-pyran (**2**) (10) in 9 ml of pyridine at room temperature. The solution was stirred for 20 h at room temperature and then treated with a solution of 1.8 g of sodium bisulfite in a mixture of 20 ml of pyridine and 30 ml of water and then stirred for an additional 4 h. The orange solution was extracted with methylene chloride (6 × 25 ml) and the extract dried (K_2CO_3) and filtered. The drying agent was washed with methylene chloride. The combined methylene chloride solutions were freed from solvent at room temperature under vacuum and gave 0.65 g of a sirup which showed two spots on a t.l.c. (solvent, 10% methanol in chloroform). Distillation at 70° at 0.05 mm gave 0.51 g (73%) of **6** as a colorless sirup.

Anal. Calcd. for $C_7H_{14}O_5$: C, 47.19; H, 7.92. Found: C, 46.99; H, 7.72.

The aqueous portion left after methylene chloride extraction was further extracted continuously for 48 h with methylene chloride and provided, after purification, 80 mg (11.4%) more of **6**. The t.l.c. of this pure material showed only one spot.

The i.r. spectrum in carbon tetrachloride showed a narrow band at 3600 (OH) and a broad band at 3260–3540 cm^{-1} (bonded OH). In highly dilute solution only one narrow band at 3590 cm^{-1} occurred (unbonded OH).

The 100 MHz p.m.r. spectrum in pyridine-d_5 showed a doublet ($J \sim 2.8$ Hz) at τ 5.05.

*Methyl 2,3-Di-O-acetyl-4-O-methyl-*α*-*DL*-lyxopyranoside (7)*

A solution of **6** (0.51 g, 2.86 mmol) in 2.5 ml of dry pyridine and 2.5 ml of acetic anhydride was warmed for 0.5 h at 60° and then stirred overnight at room temperature. The bulk of the pyridine and excess acetic anhydride was removed by fractional distillation under vacuum (5–6 mm) at room temperature. The residual liquid in 10 ml of chloroform was treated with 10 ml of cold 3 *N* aqueous ammonium hydroxide and the resulting solution then extracted with chloroform (5 × 25 ml). The chloroform extract was dried (Na_2SO_4), filtered, and freed from solvent. The residual sirup crystallized from chloroform–hexane; yield, 515 mg (69%), m.p. 79–82°, raised to 81–82.5° by two recrystallizations.

Anal. Calcd. for $C_{11}H_{18}O_7$: C, 50.38; H, 6.92. Found: C, 50.50; H, 6.87.

The i.r. spectrum in chloroform showed a strong band at 1750 cm^{-1} (—CO_2—).

The 100 MHz p.m.r. spectrum showed the anomeric proton signal at τ 5.41 (doublet, $J \sim 2.0$ Hz) and a multiplet (2H) at 4.79 due to H-2 and -3. Irradiation of the nucleus of H-1 at τ 5.41 resulted in loss of a small coupling in the multiplet at τ 4.79. Double irradiation of H-1 (τ 5.41) and H-4 (∼τ 6.36) produced an AB pattern for the signal of H-2 and -3 at τ 4.79 which appeared as a rather broad singlet. The loss of a large coupling in the signal at τ 4.79 due to this double irradiation shows that H-3 and -4 are *trans* diaxially disposed.

*4-O-Methyl-*DL*-lyxose (9)*

A solution of **6** (0.1 g, 0.56 mmol) in 1.2 ml of *p*-dioxane and 3 ml of 1.5% aqueous sulfuric acid was refluxed for 4 h, then cooled, neutralized with barium carbonate, and filtered. The solid was washed with a 1:1 mixture of *p*-dioxane and water (4 × 3 ml). The combined filtrate and washings were freed from solvent and gave 80 mg of crude viscous sirup. Distillation provided 69 mg (75%) of colorless sirup boiling at 80° at 0.07 mm.

Anal. Calcd. for $C_6H_{12}O_5$: C, 43.90; H, 7.37. Found: C, 43.94; H, 7.45.

The 100 MHz p.m.r. spectrum (tetramethylsilane as external reference) of a solution of **9** in D_2O after standing for 16 h, showed two anomeric proton signals at τ 4.72 (doublet, $J \sim 5$ Hz) and 4.83 (doublet, $J \sim 1.5$ Hz) in the area ratio of 1.0:0.37. Both the 60 and 100 MHz p.m.r. spectra of **9** were identical to those of authentic 4-*O*-methyl-D-lyxose.

*Methyl 4-Deoxy-*β*-*DL*-erythro-pentopyranoside (3)*

The reaction of osmic acid with **1** (11) was carried out essentially as described above for the formation of **6** except that after decomposition of the osmate ester the solution was extracted continuously with methylene chloride. The extract was then worked-up as described for the isolation of **6**. The crude product, obtained in almost quantitative yield, gave a 100 MHz p.m.r. spectrum whose amplified anomeric proton signal region gave only one anomeric proton signal, a doublet at τ 5.40 ($J \sim 4.0$ Hz). Distillation of the crude product in a sublimation apparatus afforded a colorless, viscous liquid in 93% yield, b.p. 72° at 1.5 mm. This showed a single spot on t.l.c. (5% methanol in chloroform).

Anal. Calcd. for $C_6H_{12}O_4$: C, 48.64; H, 8.16. Found: C, 47.92, 48.27; H, 7.85, 8.16.

An ether solution, cooled in ice, gave an hygroscopic solid, m.p. 49–51.5°.

The 100 MHz p.m.r. spectrum of the viscous oil showed the anomeric proton (H-1) signal as a doublet at τ 5.39 ($J \sim 4.0$ Hz). Irradiation of H-1 caused a collapse of the triplet (total $J \sim 7.5$ Hz) for H-2 at τ 6.38 to a doublet ($J \sim 3.5$ Hz). A one-proton multiplet at τ 5.97 with total width ∼16 Hz remained unaffected. This, as well as its

splitting pattern indicated that this multiplet at τ 5.97 was due to H-3.

*Methyl 4-Deoxy-2,3-di-O-acetyl-β-*DL*-erythro-pentopyranoside (4)*

Compound **3** (0.4 g) was converted to its diacetate **4** by the same procedure used to prepare the diacetate 7 above. Crystals (505 mg, 81%) from methylene chloride – hexane, m.p. 80–82.5°, raised to 82–83.5° by two recrystallizations.

Anal. Calcd. for $C_{10}H_{16}O_6$: C, 51.72; H, 6.94. Found: C, 51.53; H, 6.71.

The i.r. spectrum (Nujol mull) showed a strong band at 1750 cm^{-1} (—CO_2—).

The 100 MHz p.m.r. spectrum gave a triplet at τ 4.97 ($J \sim 2.5$–3.0 Hz) for H-2 and an eight-line multiplet for H-3 at 4.75 with total width $\simeq$ 19 Hz. Irradiation of H-1 at τ 5.36 (doublet, $J \sim 2.5$ Hz) caused the triplet for H-2 at 4.97 to change to a doublet ($J \sim 3.0$ Hz) thus corroborating the location of the H-2 signal. A slight sharpening of the eight-line multiplet at τ 4.75 occurred. This multiplet can be accommodated only if H-3 is axial. This information clearly confirms the structure and conformation of this diacetate as shown by **4**.

*Methyl 4-Deoxy-2,3-di-O-methyl-β-*DL*-erythro-pentopyranoside (5)*

Compound **3** was methylated by the following modification of the published general procedure (12). A solution of **3** (0.37 g, 2.5 mmol) in 5 ml of dry 1,2-dimethoxyethane (DME) was added dropwise over a period of 15 min to a stirred slurry of sodium hydride (0.15 g, 6.2 mmol) in 5 ml of dry DME containing 1 ml of methyl iodide (an excess). The mixture was stirred overnight at room temperature, then diluted with 50 ml of ether and filtered. The solvent was removed by fractional distillation. The residue was distilled in a two-bulb apparatus and gave 0.21 g (48%) of a colorless oil, b.p. 95° (oil bath temperature) at 11 mm, $n_D^{27.5}$, 1.4394.

Anal. Calcd. for $C_8H_{16}O_4$: C, 54.53; H, 9.15. Found: C, 54.68; H, 9.06.

The i.r. and 60 MHz p.m.r. spectra were consistent with the structure as shown by **5**.

*4-Deoxy-*DL*-ribose (8)*

Hydrolysis of **3** was carried out by the same procedure used above to hydrolyze **6**. From 200 mg of **3** there was obtained 175 mg of crude product. Distillation in a sublimation apparatus gave 139 mg (76.8%) of a semisolid, b.p. 74–76° (oil bath temperature) at 0.09 mm.

Anal. Calcd. for $C_5H_{10}O_4$: C, 44.77; H, 7.51. Found: C, 44.68; H, 7.57.

The i.r. spectrum (neat) showed a strong broad band at 3360 (OH) and two weak bands at 1720 (C=O) and 1650 cm^{-1} (unknown).

The 60 MHz p.m.r. spectrum in D_2O, with tetramethylsilane as external reference, was taken after the solution had stood at room temperature for a short time and showed one anomeric proton signal at τ 5.09 (doublet for H-1, $J \simeq 5$ Hz). The spectrum, obtained this time at 42° after the solution had stood for 24 h, showed two anomeric proton signals as doublets, one at τ 5.1 and the other at 5.36. Expansion of these signals to a sweep width of 100 Hz gave $J \simeq 5.2$ and $J \sim 1.7$ Hz respectively with the signals in the area ratio of 1.0:0.42.

The authors thank the National Research Council of Canada for financial support throughout the course of this work.

Particular thanks are given to Professor N. A. Hughes, Department of Organic Chemistry, The University of Newcastle upon Tyne, England, for kindly supplying us with a sample of 4-*O*-methyl-D-lyxose.

1. U. P. Singh and R. K. Brown. Can. J. Chem. **49**, 1179 (1971).
2. J. S. Baran. J. Org. Chem. **25**, 257 (1960).
3. H. B. Henbest. Proc. Chem. Soc. 159 (1963).
4. E. L. Eliel, N. L. Allinger, S. J. Angyal, and G. A. Morrison. Conformational analysis. John Wiley and Sons, Inc., New York, N.Y., 1965. Pp. 375–377.
5. C. B. Anderson and D. T. Sepp. Chem. and Ind. London, 2054 (1964).
6. E. L. Eliel and C. A. Giza. J. Org. Chem. **33**, 3754 (1968).
7. J. T. Edward. Chem. and Ind. London, 1102 (1955).
8. R. U. Lemieux. *In* Molecular rearrangements. *Edited by* P. de Mayo. John Wiley and Sons, Inc., New York, N.Y., 1964. Pp. 738–741.
9. F. Sweet and R. K. Brown. Can. J. Chem. **46**, 1543 (1968).
10. R. M. Srivastava and R. K. Brown. Can. J. Chem. **48**, 2341 (1970).
11. M. J. Baldwin and R. K. Brown. Can. J. Chem. **47**, 3099 (1969).
12. U. E. Diner, F. Sweet, and R. K. Brown. Can. J. Chem. **44**, 1591 (1966).

Can. J. Chem. Downloaded from www.nrcresearchpress.com by 210.87.254.40 on 09/05/12
For personal use only.

Can. J. Chem. Downloaded from www.nrcresearchpress.com by 210.87.254.5 on 09/05/12
For personal use only.

Synthesis of 2,3,6,7,8,9-Hexahydro-1*H*-cyclohepta[*gh*]phenalene

A. FISCHER AND D. R. A. LEONARD
Department of Chemistry, University of Victoria, Victoria, British Columbia

AND

D. A. R. HAPPER
Department of Chemistry, University of Canterbury, Christchurch, New Zealand

Received September 2, 1970

2,3,6,7,8,9-Hexahydro-1*H*-cyclohepta[*gh*]phenalene (**7**) has been prepared via the tricyclic ketone 3-oxo-1,2,3,7,8,9,10,10*a*-octahydrocyclohepta[*de*]naphthalene (**1**) and the tetracyclic ketone 1-oxo-2,3,6,7,8,9-hexahydro-1*H*-cyclohepta[*gh*]phenalene (**6**). Conversion of the tricyclic ketone **1** into 1-oxo-1,2,3,3*a*,5,5*a*,6,7,8,9-decahydro-4*H*-cyclohepta[*cd*]phenalene (**8**) and reduction of this tetracyclic ketone to 1,2,3,3*a*,5,5*a*,6,7,8,9-decahydro-4*H*-cyclohepta[*cd*]phenalene (**9**), followed by aromatization, gave 5,5*a*,6,7,8,9-hexahydro-4*H*-cyclohepta[*cd*]phenalene (**10**) (73%) together with the desired isomeric 2,3,6,7,8,9-hexahydro-1*H*-cyclohepta[*gh*]phenalene (**7**) (23%).

On a préparé l'hexahydro-2,3,6,7,8,9 1*H*-cyclohepta[*gh*] phénalène (**7**) en utilisant la cétone tricyclique, oxo-3 octahydro-1,2,3,7,8,9,10,10*a*-cyclohepta[*de*]naphtalène (**1**), et la cétone tétracyclique, oxo-1 hexahydro-2,3,6,7,8,9 1*H*-cyclohepta[*gh*]phénalène (**6**) comme intermédiaires. La transformation de la cétone tricyclique **1** en oxo-1 décahydro-1,2,3,3*a*,5,5*a*,6,7,8,9, 4*H*-cyclohepta[*cd*]phénalène (**8**) suivie d'une réduction de cette cétone tétracyclique en décahydro-1,2,3,3*a*,5,5*a*,6,7,8,9, 4*H*-cyclohepta[*cd*]-phénalène (**9**) et d'une aromatisation de ce dernier conduit à 73% de l'hexahydro-5,5*a*,6,7,8,9, 4*H*-cyclohepta[*cd*]phénalène (**10**) aux côtés de 23% de l'hydrocarbure (**7**) désiré.

Canadian Journal of Chemistry, 49, 1343 (1971)

2,3,6,7,8,9-Hexahydro-1*H*-cyclohepta[*gh*]phenalene (**7**) (Scheme 1) was synthesized for comparative studies with its homolog 1,2,3,4,7,8,9,10-octahydrodicyclohepta[*de*,*ij*]naphthalene (**1**). The Stobbe condensation of the tricyclic ketone 3-oxo-1,2,3,7,8,9,10,10*a*-octahydrocyclohepta[*de*]-naphthalene (**1**) with diethyl succinate gave the *exo* olefinic half-ester 3-carbethoxy-3-(1′,2′,3′,7′,8′,9′,10′,10′*a*-octahydrocyclohepta[*de*]naphthalen-3′-ylidene)propionic acid (**2***b*). Acid-catalyzed hydrolysis and concurrent decarboxylation of the half-ester (**2***b*) produced the lactone of 3-(3′-hydroxy-1′,2′,3′,7′,8′,9′,10′,10′*a*-octahydrocyclohepta[*de*]naphthalen-3′-yl)propionic acid (**3**) together with 3-(1′,2′,3′,7′,8′,9′,10′,10′*a*-octahydrocyclohepta[*de*]naphthalen-3′-yl)propionic acid (**4***a*) and 3-(7′,8′,9′,10′-tetrahydrocyclohepta[*de*]naphthalen-3′-yl)propionic acid (**5***a*). On refluxing in acetic acid with red phosphorous and iodine, the lactone **3** was converted into a mixture of the octahydro acid **4***a* and tetrahydro acid **5***a*. The mixture of acids **4***a* and **5***a* was converted into a mixture of the methyl esters **4***b* and **5***b* by treatment with diazomethane. The octahydro ester **4***b* component of the mixture was dehydrogenated and essentially pure tetrahydro ester **5***b* was obtained by heating the mixture with palladium-on-charcoal. Treatment of the ester **5***b* with anhydrous hydrogen fluoride brought about ring closure and gave an excellent yield of 1-oxo-2,3,6,7,8,9-hexahydro-1*H*-cyclohepta[*gh*]phenalene (**6**). Clemmensen reduction of the ketone **6** gave the desired hexahydrocyclohepta[*gh*]phenalene **7**, obtained in 49% overall yield from the ketone **1**.

Structure **2***b* was assigned to the Stobbe product on the basis of the n.m.r. spectrum which showed a singlet for an acid proton at τ 0.04 and insignificant absorption in the vinyl proton region. Attempts to crystallize the half-ester were not successful. On methylation with diazomethane, the methyl ethyl ester **2***c* was obtained. Hydrolysis of the half-ester **2***b* gave the diacid **2***a*. Sublimation of the diacid gave the anhydride **11** which, like the half-ester and di-ester, showed no vinyl proton absorption in the n.m.r. spectrum. The anhydride **11** had an u.v. absorption maximum at 308 mμ, indicative of the C_6H_3—C=C—CO_2 conjugated system and supporting the *exo* assignment of the double bond. Formation of only the *exo* olefinic half-ester in the Stobbe reaction of the tricyclic ketone **1** may be

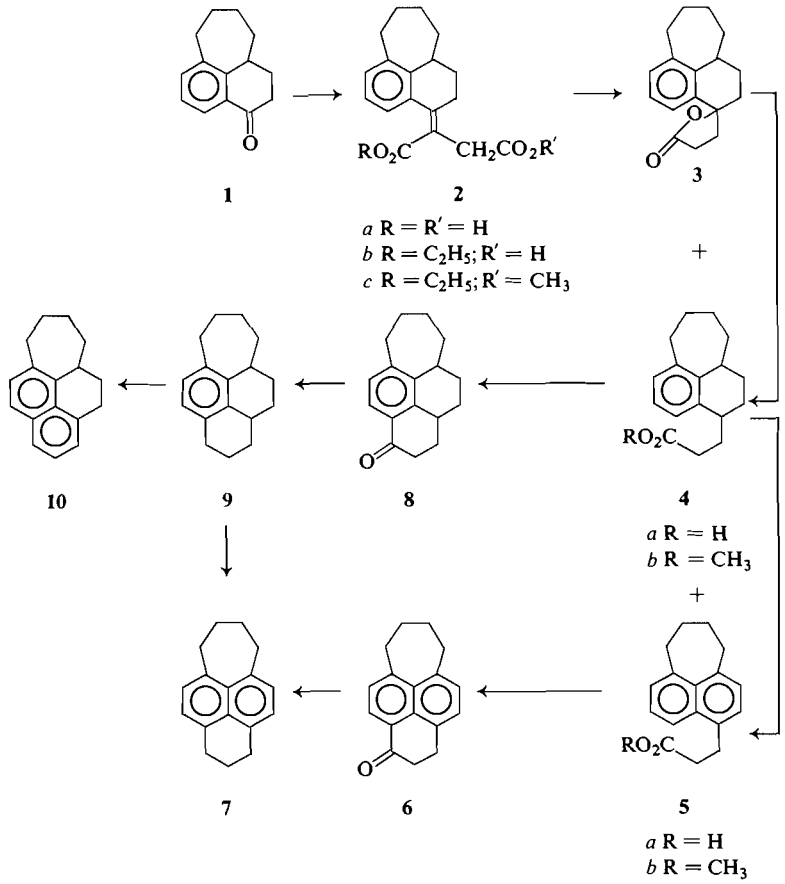

SCHEME 1

contrasted with the predominant formation of the *endo* olefinic half-ester when benzosuberone was the substrate (1). The implication is that in a seven-membered ring with a fused benzo substituent there is a steric preference for an *endo* rather than an *exo* double bond.

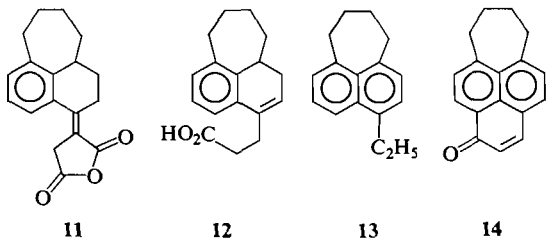

Hydrolysis–decarboxylation of the half-ester was expected to lead to a mixture of the lactone **3** and its isomeric olefinic acid **12**. The olefinic acid **12** could be detected as its methyl ester, after methylation with diazomethane of a sample of the reaction mixture isolated after a reaction of short duration. However, only the lactone **3** and the disproportionation products, **4***a* and **5***a*, of the olefinic acid were obtained from the reactions of extended period. The tetrahydro acid **5***a* was much less soluble than the octahydro acid **4***a* and almost pure acid **5***a* crystallized out from the hydrolysis mixture, as was shown by methylation with diazomethane and v.p.c. of the ester mixture. There is a considerable gain in resonance energy as a result of the disproportionation reaction. In the hydrolysis–decarboxylation of the Stobbe product from benzosuberone no disproportionation was observed (1) because the seven-membered ring cannot be aromatized. From the hydrolysis–decarboxylation followed by hydrogen fluoride-catalyzed ring closure of the Stobbe product from 1-

Can. J. Chem. Downloaded from www.nrcresearchpress.com by 210.87.254.5 on 09/05/12
For personal use only.

Can. J. Chem. Downloaded from www.nrcresearchpress.com by 210.87.254.5 on 09/05/12
For personal use only.

tetralone Johnson *et al.* (2) obtained 2,3,3*a*,4,5,6-hexahydro-1*H*-phenalen-1-one in addition to the expected tetrahydrophenalenone. They recognized the hexahydrophenalenone as being a disproportionation product, although they were not able to isolate the dehydrogenated counterpart. They were also unable to determine whether the acid disproportionated before ring closure, or whether the tetrahydrophenalenone itself disproportionated. However, the acid was known to disproportionate on distillation.

Small amounts of the ketone **8** and the hydrocarbon **13** were isolated as the neutral fraction from the products of reduction of the lactone **3**. These compounds are likely to have been formed by acid-catalyzed ring closure of acid **4***a* and by decarboxylation of acid **5***a* respectively. In the hydrolysis–decarboxylation of the half-ester **2***b* the products, which include **4***a* and **5***a*, are refluxed in acid solution for a lengthy period and under these conditions ring closure and decarboxylation are likely. The ketone **8** and the hydrocarbon **13** were present (v.p.c.) in the neutral (lactone) fraction from hydrolysis–decarboxylation reaction and it is possible that the samples isolated from after reduction of the lactone were actually formed in the previous (hydrolysis–decarboxylation) reaction.

An attempt to form acid **5***a* by aromatization of acid **4***a* led to considerable decarboxylation resulting in the formation of hydrocarbon **13**. The ester **4***b* was much less prone to decarbomethoxylation during aromatization. Similar observations were made by Newman and O'Leary (3) for the aromatization of 5,6,7,8-tetrahydro-2-naphthylacetic acid and its methyl ester. The ester **5***b* was much more soluble in hydrogen fluoride than the acid **5***a* and was therefore much more suitable as a substrate for the ring closure reaction to give the ketone **6**. When the condensation of the ester **5***b* with hydrogen fluoride was carried out for reaction times longer than 3 h or when polyphosphoric acid was used as the condensing agent, the ketone **6** was contaminated with the enone **14**. With polyphosphoric acid the enone **14** was the major product and a considerable amount of tar was also formed. The ketone **6** was also readily dehydrogenated to enone **14** with dichlorodicyanoquinone. In the closure of 3-(1′naphthyl)propionic acid with hydrogen fluoride Fieser and Gates (4) obtained 6% of the product of closure in the 2′ position as well as the dihydrophenalenone, the product of closure in the 8′ (*peri*) position. We did not observe any of the product of closure in the 2′ position from the tetrahydrocycloheptanaphthalen-3′-ylpropionate, **5***b*. The alicyclic ring activates the 4′ (*peri*) position more than the 2′ and thus enhances the 4′ closure.

The Clemmensen reduction of the ketone **6** to give the desired hydrocarbon **7** was conducted for a short time since prolonged treatment of either **6** or **7** with acid led to formation of enone **14** and its subsequent dimerization.

In the preparation of 1,2,3,4,7,8,9,10-octahydrodicyclohepta[*de*,*ij*]naphthalene the fourth (seven-membered) ring was constructed before the second six-membered ring was aromatized. This was necessary since ring closure would have otherwise preferentially occurred in this second aromatic ring and a cycloheptaphenanthrene system formed. Initially, we attempted to follow the same sequence for the preparation of the cycloheptaphenalene **7**. Ring closure of the ester **4***b* with polyphosphoric acid gave the ketone **8** in excellent yield. Clemmensen reduction of the ketone **8** gave the hydrocarbon **9**. Dehydrogenation of hydrocarbon **9**, by heating with palladium-on-carbon gave as major product (73%) the hydrocarbon **10** together with a lesser amount (23%) of the desired hydrocarbon **7**. The ketone **8** was dehydrated and dehydrogenated, by heating palladium-on-carbon, to the same mixture of hydrocarbons. The hydrocarbons **7** and **10** were separated by chromatography on alumina.

Experimental

The u.v. spectra were determined on a Unicam S.P. 800 spectrometer. The i.r. spectra were determined on a Perkin–Elmer model 337 spectrometer calibrated with polystyrene. The n.m.r. spectra were determined on a Varian HA-60-IL spectrometer using tetramethylsilane as internal standard. Mass spectra were determined on an AEI MS-902 instrument. Microanalyses were by Dr. A. D. Campbell, University of Otago, Dunedin, New Zealand. Melting points are uncorrected.

3-Carbethoxy-3-[1′,2′,3′,7′,8′,9′,10′,10′a-octahydrocyclohepta[de]naphthalen-3′-ylidene]propionic Acid (2b)

3-Oxo-1,2,3,7,8,9,10,10*a*-octahydrocyclohepta[*de*]-naphthalene (**1**) (10.0 g, 0.05 mol) and diethyl succinate (13.05 g, 0.075 mol) were added under 1 atm of nitrogen to a slurry of potassium *t*-butoxide (0.055 mol) which had been prepared by stirring potassium shavings (2.15 g) with dry *t*-butyl alcohol until all the potassium had dis-

Can. J. Chem. Downloaded from www.nrcresearchpress.com by 210.87.254.5 on 09/05/12
For personal use only.

solved. After heating under reflux for 40 min the solution was stood at room temperature for 24 h before being acidified with hydrochloric acid. The solvent was removed and the residue taken up in ether. The ether solution was washed with water, the product half-ester extracted into bicarbonate, and the bicarbonate solution washed. The product was extracted back into ether from the acidified bicarbonate solution and the ethereal solution dried. After removal of the ether the half-ester **2***b* (13.42 g, 82%) was obtained: i.r. 1710 cm^{-1} (conjugated ester C=O and acid C=O); n.m.r. (CCl_4) τ 0.04 (s, 1, CO_2H), 3.05 (m, 3, C_6H_3), 5.9 (q, 2, J = 7 Hz, $CO_2CH_2CH_3$), 6.45 (m, 2, C=C—CH_2CO_2H), 6.7–7.7 (5, $CH_2C_6H_3CH$ and CH_2C=C—CO_2), 7.7–8.7 (8, alicyclic CH_2), 9.0 p.p.m. (t, J = 7 Hz, CH_2—CH_3).

Methyl 3-Carbethoxy-3-(1′,2′,3′,7′,8′,9′,10′,10′a-octahydrocyclohepta[de]naphthalen-3′-ylidene)-propionate (2c)

The half-ester **2***b* (3.4 g) was treated with excess diazomethane, allowed to stand overnight at 5°, and the solvent then evaporated. The residue was taken-up in petroleum ether and chromatographed on neutral alumina (100 g, Brockmann activity II), using petroleum ether as solvent. The v.p.c. analyses on a 5 ft SE30 column of the crude di-ester showed that two compounds were present in an 80:20 ratio. These two compounds were not separated by the column chromatography nor by subsequent distillation. It is suggested that the two compounds are geometrical isomers with the carbethoxy group being *cis* to the aromatic ring in one case and *trans* in the other. The diester **2***c* had b.p. 176–178°/0.05 mm, i.r. 1740 and 1705 cm^{-1} (ester C=O); n.m.r. (CCl_4) τ 3.0 (m, 3, C_6H_3), 6.0 (q, 2, J = 7 Hz, $CO_2CH_2CH_3$), 6.35 (s, 3, CH_3O), 6.5 (m, 2, C=C—CH_2CO_2), 6.7–8.8 (13), 9.0 p.p.m. (t, J = 7 Hz, CH_2CH_3); mass spectrum (70 eV) *m/e* (relative intensity) 342.1832 (20, $M_r(^{12}C_{21}{}^{1}H_{26}{}^{16}O_4)$ = 342.1831), 311 (14, $C_{20}H_{23}O_3$), 310 (8), 298 (9), 297 (60), 296 (100), 282 (13), 268 (99), 264 (40).

Anal. Calcd. for $C_{21}H_{26}O_4$: C, 73.66; H, 7.65. Found: C, 74.20; H, 7.63.

1′,2′,3′,7′,8′,9′,10′,10′a-Octahydrocyclohepta[de]-naphthalen-3′-ylidenesuccinic Acid (2a)

The half-ester **2***b* (1.02 g) was dissolved in methanol (50 cm^3) and a solution of potassium hydroxide (50 g) in water (50 cm^3) was added and the mixture stirred for 1 week. The methanol was evaporated and the residue was taken up in water and acidified. The diacid **2***a* was extracted with benzene–ether, dried over magnesium sulfate, and concentrated to yield a light yellow crystalline solid (0.64 g). The acid was converted to the sodium salt which was recrystallized from water. The salt was converted back into the acid which was recrystallized from benzene; m.p. 173.7–174.0°; i.r. (KBr) 2700–2500 and 940 (acid OH), 1705 (acid C=O), 1680 (conjugated acid C=O), 1655 cm^{-1} (C=C); mass spectrum (70 eV) *m/e* (relative intensity) 300.1369 (9, $M_r(^{12}C_{18}{}^{1}H_{20}{}^{16}O_4)$ = 300.1362), 283 (17), 282 (84, $C_{18}H_{18}O_3$), 255 (19), 254 (100, $C_{17}H_{18}O_2$), 239 (5), 238 (12), 237 (10), 236 (9).

1′,2′,3′,7′,8′,9′,10′,10′a-Octahydrocyclohepta[de]-naphthalen-3′-ylidenesuccinic Anhydride (11)

Vacuum sublimation of the diacid **2***a* at 120–155°/0.005 mm gave as a white crystalline sublimate the octahydronaphthalenylidenesuccinic anhydride **11**: m.p. 165.2–165.4°; u.v. max (95% C_2H_5OH) 204 (ε 1560), 215 (shoulder, ε 1100), 235 (ε 660), 307 mμ (ε 1000 m^2 mol^{-1}); i.r. (Nujol) 1845, 1775, 1232 cm^{-1} (anhydride C=O); n.m.r. ($CDCl_3$) τ 2.43 (q, 1, 4′-*H*), 2.83 (m, 2, 5′-*H* and 6′-H), 6.33 (s, 2, C=C—CH_2CO_2), 7.2 (b, 3, CHC_6H_3-CH_2), 7.6 (b, 2, CH_2C=C—CO_2), 8.3 p.p.m. (b, alicyclic CH_2); mass spectrum (70 eV) *m/e* (relative intensity) 282.1249 (85, $M_r(^{12}C_{18}{}^{1}H_{18}{}^{16}O_3)$ = 282.1257), 255 (19), 254 (100), $C_{17}H_{18}O_2$), 238 (9, $C_{17}H_{18}O$), 237 (10), 236 (8), 226 (5), 225 (7), 211 (16), 210 (26), 209 (39), 208 (20), 207 (9).

Anal. Calcd. for $C_{18}H_{18}O_3$: C, 76.57; H, 6.42. Found: C, 76.69; H, 6.42.

The Hydrolysis–Decarboxylation of the Half-ester 2b; Methyl 3-(1′,2′,3′,7′,8′,9′,10′,10′a-Octahydrocyclohepta[de]naphthalen-3′-yl)propionate (4b); the Lactone of 3-(3′-Hydroxy-1′,2′,3′,7′,8′,9′,10′,-10′a-octahydrocyclohepta[de]naphthalen-3′-yl)-propionic Acid (3)

The half-ester **2***b* (13.3 g) was refluxed with a solution of concentrated hydrochloric acid (100 cm^3), acetic acid (200 cm^3), and water (150 cm^3). Isolation of the product after 48 h indicated that the hydrolysis–decarboxylation was incomplete[1] and the heating under reflux was continued with a fresh solution of the hydrochloric acid – acetic acid – water for an additional 72 h. More hydrochloric acid (50 cm^3) was added after 24 h and again after 48 h of the second reflux period. The acidic solution was concentrated, benzene was added, and the mixture filtered to remove the highly insoluble cycloheptanaphthalenylpropionic acid **5***a* (3.4 g, 33%). The benzene layer was separated, extracted with sodium carbonate solution, dried, and evaporated to give the lactone **3** (1.8 g, 17%) as a gum. The sodium carbonate solution was acidified and extracted with benzene. From this benzene solution (3.8 g, 36%) of an acidic gum was isolated.

The combined acid fractions (7.9 g) which contained mainly the tetrahydro **4***a* and octahydro **5***a* cycloheptanaphthalenylpropionic acids were taken up in a solution of ether (100 cm^3) and benzene (100 cm^3). Diazomethane (0.07 mol) in ether (200 cm^3) was added, with stirring to the solution at 0°. The mixture was stirred for 2 h, stood at 5° for 12 h, and the ether evaporated. The residue was taken-up in benzene (5 cm^3) and placed on a column of alumina (300 g deactivated with 50% acetic acid (18 cm^3)). Elution with petroleum ether (900 cm^3) gave, after discarding the initial fraction (300 cm^3) methyl octahydrocycloheptanaphthalenylpropionate **4***b* (2.2 g); i.r. (film) 1740 cm^{-1} (ester C=O); mass spectrum (70 eV) *m/e* (relative intensity) 272 (41, $M_r(C_{18}H_{24}O_2)$ = 272), 241 (17, $C_{17}H_{21}O$), 240 (22), 199

[1]A sample of the acid fraction of the incompletely reacted material was esterified with diazomethane and subjected to chromatography on alumina. The second fraction (5% of the total esters) obtained from the column contained, as the major component, an ester (i.r. 1735 cm^{-1}) which on v.p.c. on an SE30 column had retention time between that of the esters **4***b* and **5***b* and which had M_r = 270. This was presumably the methyl ester of the olefinic acid **12**.

Can. J. Chem. Downloaded from www.nrcresearchpress.com by 210.87.254.5 on 09/05/12
For personal use only.

(23), 198 (83), 186 (22), 185 (100), 158 (26). Further elution with petroleum ether (1800 cm^3) and then benzene (1200 cm^3) gave mixtures of the octahydro **4***b* and tetrahydro esters **5***b* (4.8 g). The ester mixtures were analysed by v.p.c. on an SE30 column and by mass spectrometry.

The neutral lactone fraction was recrystallized (×2) from ether–petroleum ether and sublimed (×2). The lactone **3** had m.p. 119.5–119.8°; i.r. (Nujol) 1775 cm^{-1} (lactone C=O), mass spectrum (70 eV) *m/e* (relative intensity) 256.1411 (59, $M_r(^{12}C_{17}{}^1H_{20}{}^{16}O_2)$ = 256.1463), 238 (1), $C_{17}H_{18}O$), 212 (24, $C_{16}H_{20}$), 202 (16), 201 (100), 183 (21), 169 (18), 158 (41).

Anal. Calcd. for $C_{17}H_{20}O_2$: C, 79.65; H, 7.87. Found: C, 79.91, H, 7.89.

3-(1′,2′,3′,7′,8′,9′,10′,10′a-Octahydrocyclohepta[de]-naphthalen-3′-yl)propionic Acid (4a)

The ester **4***b* (1 g) in methanol (50 cm^3) was stirred with sodium hydroxide (50 g) in water (50 cm^3) for 5 days. The methanol was evaporated, the solution acidified, and extracted with benzene. The benzene solution was dried and the solvent evaporated. The residual gum was recrystallized (×2) from methanol–water and sublimed at 120–125°/0.005 mm; m.p. 135–136.5°; i.r. (Nujol) 1705 cm^{-1} (acid C=O); n.m.r. (CCl_4) τ 1.6 (b, 1, CO_2H), 3.23 (s, 3, C_6H_3), 7.3 (b, $CH_2C_6H_3(CH)CHCH_2CH_2CO_2H$), 8.3 p.p.m. (b, alicyclic and aliphatic CH_2); mass spectrum (70 eV) *m/e* (relative intensity) 258.1615 (79, $M_r(^{12}C_{17}{}^1H_{22}{}^{16}O_2)$ = 258.1620), 240 (5), 230 (8), 217 (9), 216 (9), 212 (20), 199 (16), 186 (29), 185 (100).

Anal. Calcd. for $C_{17}H_{22}O_2$: C, 79.03; H, 8.59. Found: C, 78.94; H, 8.59.

The Reduction of Lactone 3

The lactone **3** (5.6 g) was heated under reflux for 24 h with a mixture of glacial acetic acid (125 cm^3), red phosphorous (7.5 g), iodine (2.5 g), and water (5 cm^3). The hot reaction mixture was filtered and added to water (400 cm^3) containing sufficient sodium bisulfite to reduce the iodine. The aqueous solution was extracted with benzene–ether and the benzene–ether solution then extracted with 10% sodium carbonate solution. The carbonate solution was acidified and extracted with benzene–ether. This benzene–ether solution was washed with water and concentrated to 200 cm^3. Diazomethane (0.04 mol) in ether (100 cm^3) was added and the mixture left to stand at 5° for 24 h. The solvent was evaporated and the ester taken up in benzene and filtered through a column of alumina (100 g). Removal of the benzene gave the ester **4***b* (4.1 g, 79%).

The benzene–ether solution containing the non-acidic portion of the reaction product was dried and the solvent removed to yield 0.6 g of a gum shown by comparison of retention times with authentic samples (*vide infra*) to be composed of approximately equal parts of ketone **8** and 3-ethyl-7,8,9,10-tetrahydrocyclohepta[*de*]naphthalene (**13**).

Methyl 3-(7′,8′,9′,10′,-Tetrahydrocyclohepta[de]-naphthalen-3′-yl)propionate (5b) and 3-Ethyl-7,8,9,10-tetrahydrocyclohepta[de]naphthalene (13)

A sample (12.7 g) of the mixed esters **4***b* (80%) and **5***b* (20%) was heated under 1 atm of nitrogen with 30% palladium-on-carbon (0.8 g) in a Claisen flask fitted with a cold finger and placed in a silicone-oil bath. Hydrogen evolution started at 240°, reached a maximum at 270° and continued for 8 h as the temperature was raised to 300°. The v.p.c. analysis after heating for 3.5 h, at which time the temperature had reached 275°, showed only the octahydro **4***b* (22%) and tetrahydro **5***b* (78%) esters. The product was isolated by taking it up in benzene, filtering off the catalyst, and evaporation of the solvent. The v.p.c. analysis of the crude product showed the presence of the tetrahydro ester **5***b* (95%) and its de-ethoxycarbonylation product, 3-ethyl-7,8,9,10-tetrahydrocyclohepta[*de*]naphthalene (**13**) (5%). Chromatography on alumina (300 g deactivated with 50% acetic acid (18 cm^3)) using petroleum ether then benzene as eluants gave a mixture (2.1 g) of **13** (25%) and **5***b* (75%) and then pure ester **5***b* (9.9 g).

The ester **5***b* was distilled: b.p. 160–170°/0.2 mm; i.r. (film) 1735 cm^{-1} (ester C=O); n.m.r. (CCl_4) τ 2.29 (q, 1, 4′-*H*), 2.93 (m, 2, 5′-*H* and 6′-*H*), 3.03 (s, 2, 1′-*H* and 2′-*H*), 6.50 (s, 3, CH_3O), 6.9 (b, 6, $C_{10}H_5CH_2$), 7.4 (m, 2, CH_2CO_2), 8.1 p.p.m. (b, 4, alicyclic CH_2); mass spectrum (70 eV) *m/e* (relative intensity) 268.1468 (100, $M_r(^{12}C_{18}{}^1H_{20}{}^{16}O_2)$ = 268.1463), 240 (15), 237 (14), 208 (17), 196 (31), 195 (99), 181 (19), 179 (21), 165 (40).

Anal. Calcd. for $C_{18}H_{20}O_2$: C, 80.56; H, 7.51. Found: C, 80.34; H, 7.70.

Further chromatography of the hydrocarbon-ester fraction on alumina, using petroleum ether as eluant, gave the hydrocarbon **13** (0.5 g) which was finally distilled: b.p. 120–122°/0.2 mm; n.m.r. (CCl_4) τ 2.23 (q, 1, 4-*H*), 2.87 (m, 2, 5-*H* and 6-*H*), 2.98 (s, 2, 1-*H* and 2-*H*), 6.8 (b, 4, $C_{10}H_5(CH_2)_2C_2H_4$) 7.0 (q, 2, J = 7 Hz, $CH_3CH_2C_{10}H_5$), 8.0 (b, 4, alicyclic CH_2), 8.69 p.p.m. (t, 3, J = 7 Hz, CH_3CH_2); mass spectrum (70 eV) *m/e* (relative intensity) 210.1405 (100, $M_r(^{12}C_{16}{}^1H_{18})$ = 210.1408), 196 (33), 195 (98), 182 (27), 181 (92), 179 (29), 178 (25), 167 (40), 166 (38), 165 (97), 153 (30), 152 (46).

Anal. Calcd. for $C_{16}H_{18}$: C, 91.37; H, 8.63. Found: C, 91.29; H, 8.78.

3-(7′,8′,9′,10′-Tetrahydrocyclohepta[de]naphthalen-3′-yl)propionic Acid (5a)

The ester **5***b* (1 g) in methanol (50 cm^3) was stirred with a solution of sodium hydroxide (50 g) in water (50 cm^3) for 5 days. The methanol was evaporated and the solution acidified with hydrochloric acid. The acid **5***a* was filtered off, recrystallized (×2) from acetic acid, and sublimed: m.p. 193–193.5° (with sublimation), i.r. (Nujol) 1705 cm^{-1} (acid C=O); mass spectrum (70 eV) *m/e* (relative intensity) 254.1308 (100, $M_r(^{12}C_{17}{}^1H_{18}{}^{16}O_2)$ = 254.1307), 196 (22), 195 (98), 165 (35).

Anal. Calcd. for $C_{17}H_{18}O_2$: C, 80.28; H, 7.13. Found: C, 80.80; H, 7.26.

1-Oxo-2,3,6,7,8,9-hexahydro-1H-cyclohepta[gh]-phenalene (6)

The ester **5***b* (0.43 g) was stirred in anhydrous hydrogen fluoride (20 cm^3) at 20°. The polyvinyl chloride reaction vessel was enclosed and had a tube in the top. The other end of the tube was immersed in hydrogen fluoride in a second polyvinyl chloride container which was cooled in ice. This arrangement allowed the reaction to be carried out at room temperature without excessive loss of hydrogen fluoride. After 3 h the hydrogen fluoride was evaporated in a stream of air. The product was taken-up

Can. J. Chem. Downloaded from www.nrcresearchpress.com by 210.87.254.5 on 09/05/12
For personal use only.

in benzene–ether and washed with water and with 5% sodium hydroxide solution. After drying over magnesium sulfate the solvent was evaporated. The residue was taken up in heptane and chromatographed on a column of acidic alumina (6 g, Brockmann activity II). Elution with petroleum ether and benzene – petroleum ether mixtures gave the ketone **6** (0.35 g, 92%). Further elution with benzene removed a bright yellow band of the enone **14** (4 mg). The ketone **6** was recrystallized from pentane and then had m.p. 81–82°. A sample was sublimed at 79–80°/0.005 mm: m.p. 83.5–83.9°; u.v. max (95% C_2H_5OH), 223 (ε 1600), 256 (ε 2000), 349 mμ (ε 700 m^2 mol^{-1}); i.r. (Nujol) 1690 cm^{-1} (aromatic C=O); n.m.r. (CCl_4) τ 2.08 (nq, 1, J = 7.5 Hz, 11-*H*), 2.79 (nq, 1, J = 7.5 Hz, 10-*H*), 2.92 (s, 2, 4-*H* and 5-*H*), 6.8 (b, 6, $C_{10}H_4CH_2$), 7.27 (m, 2, $COCH_2$), 8.0 p.p.m. (b, 4, alicyclic CH_2); mass spectrum (70 eV) *m/e* (relative intensity) 236.1206 (100, $M_r(^{12}C_{17}{}^1H_{16}{}^{16}O)$ = 236.1201), 221 (3), 208 (4), 207 (6), 195 (6), 194 (6), 193 (11), 179 (14), 178 (9), 165 (13), 152 (6).

Anal. Calcd. for $C_{17}H_{16}O$: C, 86.40; H, 6.83. Found: C, 86.52; H, 6.92.

*1-Oxo-6,7,8,9-tetrahydro-1H-cyclohepta[gh]phenalene (**14**)*

2,3-Dichloro-5,6-dicyanoquinone (DDQ) (125 mg, 0.55 mmol), which had been recrystallized from benzene–chloroform, was dissolved in dry benzene (10 cm^3) and the solution was added with stirring to a solution of the ketone **6** (118 mg, 0.51 mmol) in benzene (10 cm^3). After stirring for 1 h the solvent was evaporated and the residue extracted (×6) by heating with benzene (20 cm^3). The combined extracts were passed through a column of neutral alumina (6 g; Brockmann activity II). Elution with benzene (120 cm^3) gave a colorless fraction which was the ketone **6** (13 mg, 11%) and a lime-green fraction which was the enone **14** (98 mg, 84%). A sample of the enone **14** was recrystallized from methanol and sublimed at 125–128°/0.005 mm to give bright yellow crystals: m.p. 134.7–135.3°; u.v. max (95% C_2H_5OH) 207 (ε 2300), 231 (ε 880), 259 (shoulder, ε 1800), 264 (ε 2100), 324 (ε 370), 326 (s, ε 630), 415 mμ (ε 1050 m^2 mol^{-1}); i.r. (Nujol) 1635 cm^{-1} (aromatic and conjugated C=O); n.m.r. ($CDCl_3$) τ 1.58 (nq, 1, J = 7 Hz, 11-*H*), 2.42 (nq, 1, J = 10 Hz, 3-*H*), 2.52 (nq, 1, J = 7 Hz, 4-*H*), 2.55 (nq, 1, J = 7 Hz, 10-*H*), 2.74 (nq, 1, J = 7 Hz, 5-*H*), 3.41 (nq, 1, J = 10 Hz, 2-*H*), 6.76 (b, 4, $C_{10}H_4CH_2$), 8.0 p.p.m. (b, 4, alicyclic CH_2); mass spectrum (70 eV) *m/e* (relative intensity) 234.1046 (100, $M_r(^{12}C_{17}{}^1H_{14}{}^{16}O)$ = 234.1045), 219 (81), 218 (53), 206 (29), 205 (43), 202 (29), 193 (59), 191 (43), 189 (70), 178 (28), 177 (33), 176 (45), 165 (29), 152 (14).

Anal. Calcd. for $C_{17}H_{14}O$: C, 87.15; H, 6.02. Found: C, 87.17; H, 6.02.

*2,3,6,7,8,9-Hexahydro-1H-cyclohepta[gh]phenalene (**7**)*

The ketone **6** (0.50 g) in toluene (5 cm^3) was heated under reflux for 2 h with amalgamated zinc (5 g), concentrated hydrochloric acid (10 cm^3), and acetic acid (20 cm^3). The mixture was cooled, diluted with water (120 cm^3), and extracted with ether (4 × 25 cm^3). The combined ethereal extract was washed with saturated bicarbonate solution, dried over magnesium sulfate, and the solvent evaporated. The residue was chromatographed on alumina (Brockmann I) with heptane as eluant to give the hexahydrocycloheptaphenalene 7 (0.43 g, 92%). The hydrocarbon 7 was recrystallized (×2) from methanol and sublimed at 100°/0.005 mm: m.p. 111.8–112.2°; u.v. max (95%, C_2H_5OH) 236 (ε 2200), 275 (shoulder, ε 370), 288 (s, ε 700), 298 (ε 880), 309 (s, ε 660), 316 (ε 480), 325 (ε 190), 331 mμ (ε 300 m^2 mol^{-1}); i.r. (Nujol) 3070, 3035, 1610, 1595, 830 cm^{-1} (aromatic with two adjacent H); n.m.r. (CCl_4) τ 3.09 (s, 4, $C_{10}H_4$), 7.0 (b, 8, $C_{10}H_4CH_2$), 8.1 p.p.m. (b, 6, alicyclic CH_2); mass spectrum (70 eV) *m/e* (relative intensity) 222.1405 (100, $M_r(^{12}C_{17}{}^1H_{18})$ = 222.1408), 208 (6), 207 (32), 194 (29), 193 (15), 181 (12), 179 (25), 178 (19), 165 (25).

Anal. Calcd. for $C_{17}H_{18}$: C, 91.84; H, 8.16. Found: C, 91.91; H, 8.18.

*1-Oxo-1,2,3,3a,5,5a,6,7,8,9-decahydro-4H-cyclohepta-[cd]phenalene (**8**)*

The ester **4***b* (0.73 g) was heated on a steam bath with a solution of phosphorus pentoxide (25 g) in 85% orthophosphoric acid (24 g) for 2 h. The mixture was poured into ice-water (100 g) and extracted with benzene–ether (4 × 50 ml). The extract was washed with 5% sodium hydroxide solution (3 × 50 ml), dried, and the solvent evaporated yielding the ketone **8** (0.60 g, 93%). A sample was recrystallized from hexane, sublimed at 80–85°/0.01 mm and recrystallized (×3) from methanol; m.p. 85.0–86.5°; u.v. max (95% C_2H_5OH) 219 (ε 1400), 269 mμ (ε 1000 m^2 mol^{-1}); i.r. (melt) 1680 cm^{-1} (aromatic ketone C=O); n.m.r. (CCl_4) τ 2.35 (nq, 1, J = 7.5 Hz, 11-*H*), 3.07 (nq, 1, J = 7.5 Hz, 10-*H*), 7.3 (b, 6, C_6H_2CH, $C_6H_2CH_2$, $COCH_2$), 8.2 p.p.m. (b, 12, alicyclic CH_2); mass spectrum (70 eV) *m/e* (relative intensity) 240.1521 (100, $M_r(^{12}C_{17}{}^1H_{20}{}^{16}O)$ = 240.1514), 223 (8), 210 (21), 197 (16), 196 (45), 195 (13), 194 (19), 183 (21), 182 (57), 181 (56), 167 (22), 165 (12), 163 (14), 154 (22), 153 (33), 152 (13), 151 (21), 140 (21), 139 (60).

Anal. Calcd. for $C_{17}H_{20}O$: C, 84.95; H, 8.39. Found: C, 84.90; H, 8.57.

*1,2,3,3a,5,5a,6,7,8,9-Decahydro-4H-cyclohepta[cd]-phenalene (**9**)*

The ketone **8** (1 g) was reduced following the procedure described for the reduction of the ketone **6**. The hydrocarbon **9** (0.81 g, 88%) was obtained on chromatography of the crude product and then was distilled; m.p. 60.2–61.5°; b.p. 90°/0.008 mm; u.v. max (95% C_2H_5OH) 211 (ε 1430), 224 mμ (shoulder, ε 870 m^2 mol^{-1}); n.m.r. (CCl_4) τ 3.32 (s, 2, C_6H_2), 7.3 (b, 6, C_6H_2CH, $C_6H_2CH_2$), 8.3 p.p.m. (b, 14, alicyclic CH_2); mass spectrum (70 eV) *m/e* (relative intensity) 226.1716 (100, $M_r(^{12}C_{17}{}^1H_{22})$ = 226.1721), 199 (6), 198 (36), 197 (16), 185 (17), 184 (20) 183 (34), 170 (19), 169 (42), 155 (12).

Anal. Calcd. for $C_{17}H_{22}$: C, 90.20; H, 9.80. Found C, 90.16; H, 9.88.

*5,5a,6,7,8,9-Hexahydro-4H-cyclohepta[cd]phenalene (**10**)*

The decahydrocycloheptaphenalene **9** (0.2 g) was heated under an atmosphere of nitrogen with 30% palladium-on-carbon (0.02 g) at 300° for 4 h. The product was taken up in benzene, the catalyst filtered off, and the benzene evaporated. The v.p.c. and mass spectral analysis of the residue showed that it was a mixture of unchanged

decahydro compound **9** (4%) and the isomeric hexahydrocycloheptaphenalenes 7 (23%) and **10** (73%). When the decahydrophenalenone **8** (0.2 g) was heated with palladium-on-carbon under the conditions described the product consisted of unreacted ketone **8** (7%) and the hexahydrocycloheptaphenalenes **7** (24%) and **10** (69%).

The combined products from the two dehydrogenations (0.31 g) were taken up in benzene (0.5 cm^3) and chromatographed on alumina (10 g of activity I). The more symmetrical hexahydrocyclohepta[*gh*]phenalene was eluted first with petroleum ether. Further elution with petroleum ether and with 5% benzene – petroleum ether gave the hexahydrocyclohepta[*cd*]phenalene contaminated with the *gh*-isomer. The impure *cd*-isomer was rechromatographed. The final fractions from the second column were recrystallized (×2) from methanol and then sublimed at 65–70°/0.005 mm to give the pure hexahydrocyclohepta[*cd*]phenalene **10** as a white powder: m.p. 73.3–74.3°; u.v. max (95% C_2H_5OH) 236 (ε 2000), 271 (shoulder, ε 360), 281 (s, ε 600), 292 (ε 720), 297 (s, ε 640), 303 (s, ε 550), 311 (s, ε 310), 315 (s, ε 200), 325 (ε 140), 330 mμ (s, ε 80 m^2 mol^{-1}); n.m.r. (CCl_4) τ 2.83 (m, 5, $C_{10}H_5$), 7.03 (b, 5, $C_{10}H_5CH$, $C_{10}H_5CH_2$), 8.15 p.p.m. (b, 8, alicyclic CH_2); mass spectrum (70 eV) *m/e* (relative intensity) 222.1397 (100, $M_r(^{12}C_{17}{}^1H_{18})$ = 222.1408), 207 (4), 193 (17), 181 (13), 179 (12), 178 (11), 165 (41).

Anal. Calcd. for $C_{17}H_{18}$: C, 91.84; H, 8.16. Found: C, 91.65, H, 8.33.

We thank the University Grants Committee (New Zealand) for a postgraduate scholarship (D.R.A.L.), the National Research Council of Canada, and the University of Victoria for grants, and Dr. G. J. Wright for mass spectrometric measurements.

1. A. Fischer, D. R. A. Leonard, and D. A. R. Happer. Can. J. Chem. **48**, 1446 (1970).
2. W. S. Johnson, H. C. E. Johnson, and J. W. Petersen. J. Amer. Chem. Soc. **67**, 1360 (1945).
3. M. S. Newman and T. J. O'Leary. J. Amer. Chem. Soc. **68**, 258 (1946).
4. L. F. Fieser and M. D. Gates, Jr. J. Amer. Chem. Soc. **62**, 2335 (1940).

Can. J. Chem. Downloaded from www.nrcresearchpress.com by 210.87.254.5 on 09/05/12
For personal use only.

Can. J. Chem. Downloaded from www.nrcresearchpress.com by 210.87.254.40 on 09/05/12
For personal use only.

Hindered Rotation and Intramolecular Hydrogen Exchange in *N*-Phenyl-*o*-hydroxybenzylamines[1]

S. Brownstein, E. C. Horswill, and K. U. Ingold
Division of Chemistry, National Research Council of Canada, Ottawa, Canada

Received November 2, 1970

Non-equivalence of the benzylic hydrogens was found in several *N*-phenyl-ortho-hydroxybenzylamines and, where possible, activation parameters were calculated for the processes causing non-equivalence. Hindered rotation about the aromatic carbon–nitrogen bond was the rate determining process with an ortho-*t*-butyl group on the aniline ring. Exchange of phenolic and amino hydrogens was studied over a range of temperature and concentration. Both intermolecular and intramolecular exchange were observed. The latter may be the first example of such a process to be studied by n.m.r.

On a trouvé que les hydrogènes benzyliques de plusieurs *N*-phényl ortho-hydroxybenzylamines sont non-équivalents; dans certains cas, on a pu calculer les paramètres d'activation des processus causant cette non équivalence. On a établi que dans les cas où l'aniline possède un groupe *t*-butyle en position ortho, l'empêchement à la rotation libre autour du lien reliant le carbone aromatique et l'azote est le facteur déterminant la vitesse de réaction. On a de plus étudié à diverses températures et à diverses concentrations, l'échange des hydrogènes des groupes amino et phénols; on a observé que l'échange peut se faire soit par une réaction intermoléculaire soit par une réaction intramoléculaire. Ce dernier procédé pourrait être le premier exemple d'une telle réaction à être observé par r.m.n.

Canadian Journal of Chemistry, **49**, 1350 (1971)

Introduction

Proton resonance spectroscopy has frequently been used to study hindered rotation about nominally single bonds in organic compounds (1–4). The barrier to rotation about formally single carbon–nitrogen bonds has in most cases been attributed to some partial double bond character. We have previously shown (5) that for ortho-alkylphenyl substituted 1,3-benzoxazines, **1**, the barrier to rotation about the aromatic carbon–nitrogen bond, $\Delta H^{\neq}$, increases with increasing bulk of the ortho-substituent, R_1. Inhibition to free rotation in these cases must therefore arise from steric effects.

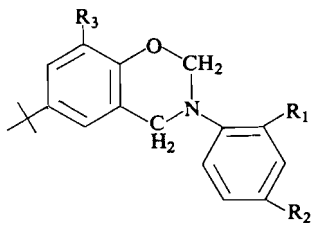

1

	$\Delta H^{\neq}$ kcal/mol
a R_1 = Me; R_2 = R_3 = H	<8.9
b R_1 = Pr^i; R_2 = H; R_3 = Me	10.8
c R_1 = R_2 = R_3 = Bu^t	16.9

ortho-Hydroxybenzylanilines, **2**, are structurally related to the benzoxazines, the six-membered heterocyclic ring being produced by an intramolecular hydrogen bond. In these compounds there are four processes which could

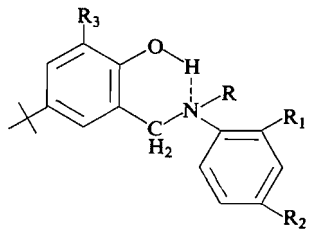

2

produce magnetic non-equivalence of the benzylic protons. When the phenyl ring is symmetrically substituted (*i.e.*, R_1 = H) non-equivalence could arise from hindered inversion about nitrogen (6, 7), or from hindered rotation about the benzyl–nitrogen bond (8), or by a slow inversion of the heterocyclic ring so as to produce quasi-axial and quasi-equatorial benzylic hydrogens. However, in this last case, the values of $\Delta H^{\neq}$ could not be greater than the strength of the OH---N hydrogen bond (probably ~4 kcal/mol). Finally, non-equivalence could arise from hindered rotation about the aromatic carbon–nitrogen bond if the aromatic group is asymmetrically substituted (*i.e.*, **2** with $R_1 \neq$ H).

[1]Issued as NRCC No. 11797.

Can. J. Chem. Downloaded from www.nrcresearchpress.com by 210.87.254.40 on 09/05/12
For personal use only.

Provided the ortho-hydroxybenzylanilines do not have an additional substituent on the nitrogen atom (*i.e.*, provided R = H in structure **2**) there is an additional process that can be studied by n.m.r., namely proton exchange between the amino hydrogen and the phenolic hydrogen. There are two possible mechanisms for such an exchange, an intermolecular reaction involving two molecules of **2** or an intramolecular reaction involving only a single molecule of **2**. In the present work we have observed both processes. The intramolecular exchange is of particular interest because it appears to be the first example of such a reaction. That is, although there have been several n.m.r. studies of intermolecular proton exchange between hydroxyl and amino groups (9) we have only been able to find one example of even an apparent intramolecular exchange. Sheinblatt (10) has reported that in water at 21° $k_f = 75\ s^{-1}$ for the reaction,

$$CH_3\overset{+}{N}H_2CH_2COO^- \underset{}{\overset{k_r}{\rightleftharpoons}} CH_3NHCH_2COOH$$

However, proton exchange is believed to occur via a water molecule solvent bridge (10) and therefore this reaction is only pseudo-intramolecular.

Experimental

Proton resonance spectra were obtained at 100 MHz on a Varian Associates HA100D spectrometer. Sample temperatures were controlled with a Varian Associates V-4343 temperature controller. The temperatures were measured by monitoring the voltage drop across the platinum sensing element of the temperature controller, which had been calibrated with variable temperature spectra of a standard methanol sample. Chemical shifts are reported as p.p.m. to low field of tetramethylsilane as internal reference. Rate constants were obtained by comparison of theoretical and experimental spectra as reported previously (5). All activation parameters were obtained from a least squares fit of the data and quoted errors are standard deviations. The solvent is carbon disulfide unless otherwise specified. All samples were prepared on a vacuum line using vigorously dried materials and should not contain any water or molecular oxygen.

Compounds **2***a*, *b*, and *e* were prepared as described previously (11).

*N-(3,5-Di-tert-butyl-2-hydroxybenzyl)-N-methylaniline (**2***c*)

A mixture of 2,4-di-*tert*-butylphenol (4.12 g, 20 mmol), *N*-methylaniline (2.14 g, 20 mmol), barium hydroxide octahydrate (0.18 g), and formalin solution (1.65 ml, 22 mmol) was stirred and heated in a bath at 94° for 1 h. The solid product was dissolved in 50 ml benzene, washed with 2 *N* HCl and with water and then dried over sodium sulfate. Vacuum removal of the solvent left a syrup which rapidly crystallized as beige prisms (5.61 g) m.p. 55–75°. Recrystallization from 95% ethanol yielded 3.98 g of product m.p. 87–92°. Further recrystallization gave an analytical sample, m.p. 89.5–91.1°.

Anal. Calcd. for $C_{22}H_{31}NO$: C, 81.18; H, 9.60; N, 4.30. Found: C, 81.10; H, 9.69; N, 4.22.

*N-(3,5-Di-tert-butyl-2-hydroxybenzyl)-ortho-toluidine (**2***d*)

Similar treatment of 3.1 g (15 mmol) 2,4-di-*tert*-butylphenol, 1.6 g (15 mmol) *o*-toluidine, 0.18 g barium hydroxide octahydrate, and 1.22 ml (16 mmol) formalin solution gave, after work-up, 4.39 g of crude solid. Recrystallization from hexane–benzene gave colorless, fluffy, needles, m.p. 149.5–151°.

Anal. Calcd. for $C_{22}H_{31}NO$: C, 81.18; H, 9.60; N, 4.30. Found: C, 81.32; H, 9.75; N, 4.27.

Results and Discussion

Hindered Rotation

The structural formulae of the compounds studied and the chemical shifts for the various types of protons are given in Fig. 1. The assignments of the *o*- and *p*-*tert*-butyl group chemical shifts were made by analogy with other similar compounds and cannot be considered to be definitely proven. Non-equivalent methylene protons could be observed in compounds **2***a* at room temperature and in the other four compounds at low temperatures.

The process causing equivalence of the methylene protons of **2***a* has $\Delta H^{\ddagger}_{298} = 14.1 \pm 0.9$ kcal/mol and $\Delta S^{\ddagger}_{298} = -11 \pm 14$ e.u. in tetrachloroethylene as the solvent. A plot of the experimental results is shown in Fig. 2. The activation parameters are sufficiently close to those of the correspondingly substituted benzoxazine, **1***c*, ($\Delta H^{\ddagger}_{298} = 16.9 \pm 0.3$ kcal/mol, $\Delta S^{\ddagger}_{298} = 0.4 \pm 0.2$ e.u. (5)) that we can be reasonably sure that the same process is being examined in both cases, *viz.*, hindered rotation about the aromatic carbon–nitrogen bond. Since $\Delta H^{\ddagger}_{298}$ for **2***a* is so much greater than the strength of the hydrogen bond which holds the heterocylic ring rogether, it is clear the non-equivalence of the methylene protons does not in fact require a six-membered ring incorporating the methylene protons and the nitrogen atom. That is, it can be confidently predicted that *N*-benzyl-*N*-methyl-*o*-*t*-butylaniline will also exhibit non-equivalent methylene protons and that $\Delta H^{\ddagger}$ for the process causing their equivalence will be somewhere around 16 kcal/mol.

Non-equivalent methylene protons were also observed in compound **2***b* which is similar to **2***a* except for the replacement of the amino methyl group by a hydrogen atom. However, in **2***b* the

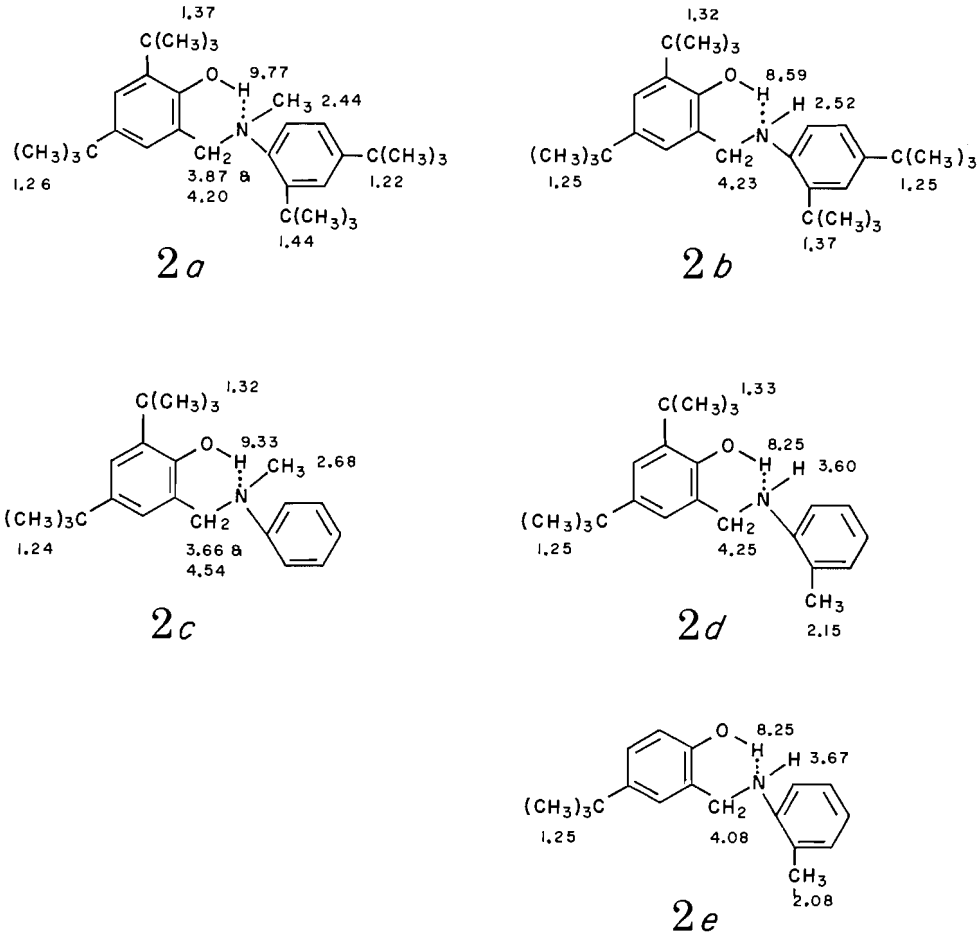

FIG. 1. Structural formulae and chemical shifts of some *N*-phenyl-*o*-hydroxybenzylamines.

chemical shift difference between the methylene protons is so small that accurate rates could not be measured.

Compound **2***c*, which does not have any ortho-substituent on the aniline ring, exhibited non-equivalent methylene protons at low temperatures. The process causing equivalence for this compound in CF_2Cl_2 solvent had $\Delta H^{\ddagger}_{298} = 6.1 \pm 0.5$ kcal/mol and $\Delta S^{\ddagger}_{298} = -12 \pm 12$ e.u. (see Fig. 2). Three possible causes of non-equivalence for compounds of this type were described in the Introduction, inversion at nitrogen, inversion of the ring, and rotation around the benzyl carbon–nitrogen bond. Of these we are inclined to disfavor inversion at nitrogen since we could find no evidence for non-equivalent methylene protons in *N*-benzyl-*N*-methylaniline even at temperatures below those required for non-equivalence with **2***c* (8). The barrier to rotation should be larger for **2***c* than for *N*-benzyl-*N*-methylaniline because of the ortho-hydroxy group, but the barrier to inversion is probably similar.

Non-equivalent methylene protons were observed in compounds **2***d* and **2***e* at low temperatures but, as with **2***b*, the chemical shift difference was too small for rate constants to be calculated. It would appear that an *N*-methyl substituent is necessary to give appreciable chemical shifts.

Hydrogen Exchange

The phenolic and amino hydrogen atoms in compounds **2***b*, *d*, and *e* undergo exchange since for each compound the signals due to these two protons undergo comparable changes in shape as the temperature is altered. The hydroxyl proton line was used for rate measurements since the

Can. J. Chem. Downloaded from www.nrcresearchpress.com by 210.87.254.40 on 09/05/12
For personal use only.

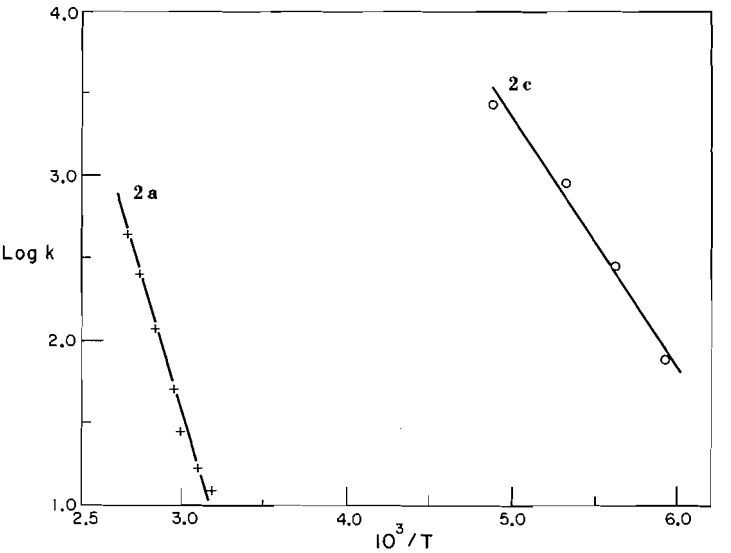

FIG. 2. The temperature variation for the rate of magnetic averaging of the methylene protons.

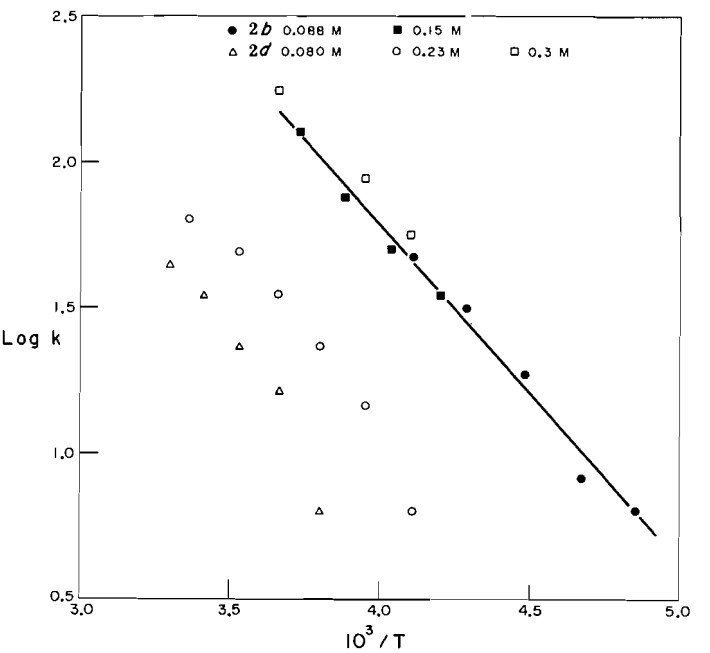

FIG. 3. The concentration and temperature dependence of the exchange of hydroxyl and amino protons.

amino hydrogen gave a broadened line in the slow exchange limit because of proton–nitrogen spin coupling. The solubility of compound **2***e* in CS_2 at low temperatures was unfortunately too low for accurate rate measurements but exchange rates were measured for **2***b* and *d* over a range of temperature and concentration. First order rate constants were calculated from the reciprocal of the measured lifetimes and have been plotted as their logarithms against the reciprocal of the temperature in Fig. 3. For compound **2***b* the rate constants are independent of concentration which indicates a unimolecular process, *i.e.*, an intramolecular hydrogen exchange. An excellent

Can. J. Chem. Downloaded from www.nrcresearchpress.com by 210.87.254.40 on 09/05/12
For personal use only.

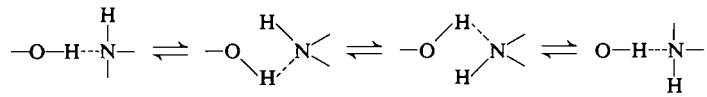

linear Arrhenius plot is obtained from which is calculated $\Delta H^{\ddagger}_{298} = 4.7 \pm 0.2$ kcal/mol and $\Delta S^{\ddagger}_{298} = -29 \pm 7$ e.u. for the exchange. In contrast, with **2***d* the rate constants at a particular temperature increase with increasing concentration of **2***d* which indicates the occurrence of a bimolecular or higher order process.[2] The Arrhenius plots with this compound show some evidence of curvature.

Space-filling molecular models indicate that the amino hydrogen in **2***b* (and in **2***d* and *e*) can approach fairly close to the phenolic oxygen if the angle formed by the O—H---N hydrogen bond is decreased to ~120° from its optimum 180°. In this configuration it is not unreasonable to suppose that the phenolic and amino hydrogens of **2***b* should change places.

The large negative entropy of activation for this exchange is indicative of a reaction requiring a highly constrained transition state.

From the data in Fig. 3 it is clear that with **2***d* the intermolecular exchange swamps out any intramolecular exchange at concentrations of **2***d* $\geqslant$ 0.08 *M*. This can be accounted for by the lesser steric hindrance of the reaction center in **2***d* compared with **2***b*. However, the question remains as to why **2***d* does not have a residual intramolecular exchange occurring at a rate comparable to the intramolecular rate with **2***b*. That is, why are the apparent rate constants at 0.08 *M* [**2***d*] not greater than the rate constants found with **2***b* (7). The only explanation that has occurred to us which might account for the ten-fold or more faster intramolecular exchange of **2***b* relative to **2***d* is based on the polar effect of the aniline ring's para-*t*-butyl group in compound **2***b*. The transition state for intramolecular exchange probably involves a significant degree of charge separation and, in fact, proton transfer from oxygen to nitrogen prior to that from nitrogen to oxygen is a distinct possibility. A reaction that involved

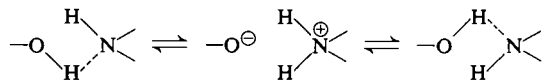

such an intermediate or transition state would be very sensitive to the acidity of the phenolic proton and to the basicity of the nitrogen atom. The *t*-butyl group at the para-position of the aniline ring (R_2) in compound **2***b* is electron donating and hence should accelerate the intramolecular exchange relative to the rate of intramolecular exchange in **2***d*. Our attempt to check this explanation by studying a compound with increased acidity of the phenolic hydrogen, as in compound **2***e*, was frustrated by the material's insolubility at low temperatures.

To judge by our present limited results, intramolecular proton transfers are very sensitive both to polar and to steric effects. It is therefore perhaps not so surprising that one has not, apparently, been previously observed.

[2]The rate constants at 0.23 *M* [**2***d*] are about twice those found at 0.08 *M* indicating a reaction order somewhat less than 2. However, the rate constants at 0.3 *M* are about ten times as great as those at 0.08 *M* indicating an order greater than 2.

1. D. S. THOMPSON, R. A. NEWMARK, and C. H. SEDERHOLM. J. Chem. Phys. **37**, 411 (1962).
2. T. D. ALGER, H. S. GUTOWSKY, and R. L. VOLD. J. Chem. Phys. **47**, 3130 (1967).
3. A. MANNSCHRECK and H. MUENSCH. Tetrahedron Lett. 3227 (1968).
4. H. KESSLER. Angew. Chem. Int. Ed. **9**, 219 (1970).
5. S. BROWNSTEIN, E. C. HORSWILL, and K. U. INGOLD. Can. J. Chem. **47**, 3243 (1969).
6. C. H. BUSHWELLER and J. W. O'NEIL. J. Amer. Chem. Soc. **92**, 2159 (1970).
7. M. J. S. DEWAR and W. B. JENNINGS. Tetrahedron Lett. 339 (1970).
8. S. BROWNSTEIN, E. C. HORSWILL, and K. U. INGOLD. J. Amer. Chem. Soc. **92**, 7217 (1970).
9. See for example; A. LOEWENSTEIN and T. M. CONNOR. Ber. Bunsen. Phys. Chem. **67**, 280 (1963). E. F. CALDIN. Fast reactions in solution. Blackwell Sci. Publ., Oxford, 1964. J. J. DELPUECH. Bull. Chim. Soc. Fr. 2697 (1964). E. GRUNWALD and M. COCIVERA. Disc. Faraday Soc. **39**, 105 (1965).
10. M. SHEINBLATT. J. Chem. Phys. **39**, 2005 (1963).
11. E. C. HORSWILL, D. A. LINDSAY, and K. U. INGOLD. Can. J. Chem. **48**, 579 (1970).

Can. J. Chem. Downloaded from www.nrcresearchpress.com by 210.87.254.40 on 09/05/12
For personal use only.

Can. J. Chem. Downloaded from www.nrcresearchpress.com by 210.87.254.40 on 09/05/12
For personal use only.

Methyl Glycosidation and Methyl Thioglycosidation of Some Fully Chlorosulfated Pentopyranosyl Chlorides Using Sodium Iodide as a Catalyst[1]

H. J. JENNINGS

Biochemistry Laboratory, National Research Council of Canada, Ottawa, Canada

Received November 2, 1970

The treatment of α- and β-D-xylopyranosyl chloride 2,3,4-tri(chlorosulfate) and the corresponding α-D-*lyxo* derivative with a catalytic quantity of sodium iodide in methanol solution resulted in the removal of the chlorosulfate groups and rapid methanolysis of the anomeric chlorine atoms. The methanolysis proceeded with predominant inversion in each case (80–90%), independent of the orientation of the C-2 substituent. In the presence of sodium methyl mercaptide, however, thioglycosides having an inverted configuration were produced from 1,2-*cis* chlorides, and thioglycosides having an unchanged anomeric configuration were formed from 1,2-*trans* chlorides. It is proposed that all these glycosidations occur via a free pentopyranosyl chloride intermediate, and that under the basic conditions of thioglycosidation a 1,2-anhydro intermediate is formed from 1,2-*trans* chlorides.

Le traitement des chloro-1 trichlorosulfate-2,3,4 α- et β-D-xylopyranose et α-D-lyxopyranose par des quantités catalytiques d'iodure de sodium en solution dans le méthanol conduit à une solvolyse rapide des groupes chlorosulfates et des atomes de chlore attachés aux carbones anomériques. Dans chaque cas, la méthanolyse se produit principalement (80–90%) avec inversion et ceci quelle que soit l'orientation du substituant en position 2. Toutefois, lorsque ces réactions sont effectuées en présence du sel de sodium du méthanethiol, la stéréochimie de la réaction dépend de l'orientation présente dans les composés de départ; la réaction des chlorures ayant la configuration *cis*-1,2 procède avec inversion alors que celle des dérivés *trans*-1,2 se produit avec rétention. On croit que toutes ces réactions conduisant à des glucosides se produisent par l'intermédiaire d'un chloro-1 pentopyranose; pour ce qui est des thioglucosides formés en milieu alcalin à partir de chlorures trans-1,2; ils proviendraient d'un dérivé anhydro-1,2 intermédiaire.

Canadian Journal of Chemistry, 49, 1355 (1971)

In earlier experiments it has been demonstrated that chlorosulfate groups can be removed from chlorosulfated glycoside derivatives by treatment with sodium iodide in aqueous methanol (1). This reaction is very rapid and regenerates the hydroxyl groups with retention of configuration. When glycosyl chlorides containing chlorosulfate groups were treated with sodium iodide in aqueous acetone the reaction involved in addition, hydrolysis of the anomeric chlorine atom, to give the free glycose (2, 3). It was of interest to study this reaction on chlorosulfated glycosyl chlorides using methanol as the solvent, to ascertain whether methyl glycosidation would occur under these conditions. As in some previously described dechlorosulfations (1, 4), barium carbonate was added in these reactions in order to neutralize hydrochloric acid and so to prevent, as much as possible, the formation of chloro–deoxy derivatives by displacement of chlorosulfate groups, and to minimize anomerization of the glycosides produced.

The reaction of β-D-xylopyranosyl chloride 2,3,4-tri(chlorosulfate) (1) gave good yields of a mixture of methyl α- and β-D-xylopyranosides. The methyl α-D-anomer (3) was shown to constitute approximately 90% of the mixture (g.l.c. analysis), and was isolated and characterized as its triacetate. Thus the methyl glycosidation of **1** occurs predominantly with inversion of configuration and similar results were obtained with α-D-anomeric chlorides. Both the α-D-anomer of **1** and its α-D-*lyxo* epimer yielded mixtures of methyl pyranosides in which the products of inversion (β-D-anomers) preponderated to the extent of approximately 80%, as indicated by p.m.r. spectroscopy. The fact that the methanolysis in both of these cases proceeded largely with inversion of the anomeric configuration indicates that the configuration at C-2 has little influence on the stereochemical course. It is interesting to note that when the reaction of **1** was carried out in the absence of sodium iodide, the methanolysis was not so rapid and only a very small amount of a methyl glycoside could be detected (p.m.r. spectroscopy). This seems to indicate that iodide ions assist in the displacement of the anomeric chlorine atom, either

[1]NRCC No. 11801.

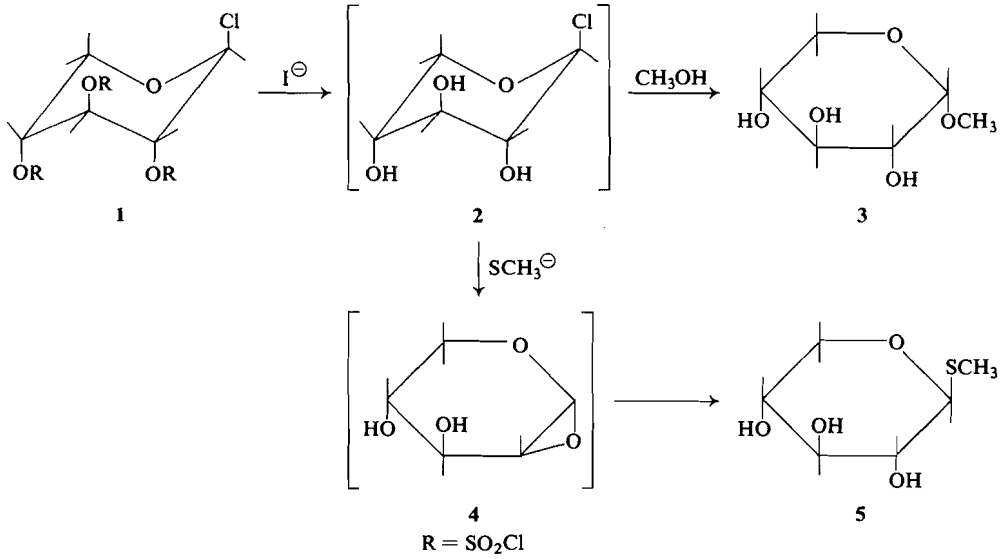

1 2 3

4
R = SO_2Cl

5

SCHEME 1

directly, or by the prior removal of the chlorosulfate groups, or possibly by a combination of these two modes. Our results provide no evidence for a direct action of iodide ions upon the anomeric center, but we do have evidence to suggest that the chlorosulfate groups of these glycosyl chloride derivatives are removed prior to methanolysis, and it is probable that a free glycopyranosyl chloride (2) is generated as a highly reactive intermediate in the solvolytic process (see Scheme 1). This evidence will be discussed below. Certainly the removal of the C-2 chlorosulfate group would contribute to a more rapid solvolysis as it has been demonstrated that the removal of a non-participating trichloroacetate group from the C-2 position of a glucopyranosyl chloride derivative does considerably enhance the rate of solvolysis (5). This has been attributed to a decrease in steric hindrance at the anomeric center (5), although the importance of the contribution of electronic factors has also been clearly demonstrated (6). It is also probable that the removal of the C-3 and -4 chlorosulfate groups from **1** would further assist in the solvolytic process, as it has been demonstrated that other groups besides the one situated at C-2 of glycopyranosyl halides do have some effect on the relative rates of anomeric exchange reactions (7, 8).

Some evidence for the formation of **2** was obtained when **1** was treated under reaction conditions similar to those described above except for the introduction of sodium methyl mercaptide. The addition of barium carbonate was omitted in this case as sufficient base was used to neutralize all the acid produced in this reaction. Sodium iodide was still employed for the rapid removal of the chlorosulfate groups because although sodium methoxide, too, will remove these groups, it will produce cyclic sulfate or epoxy derivatives from vicinal chlorosulfates (1). The β-D chloride (1) gave good yields of crystalline methyl 1-thio-β-D-xylopyranoside (5), which was also synthesized by the treatment of 2,3,4-tri-*O*-acetyl-α-D-xylopyranosyl bromide with potassium methyl mercaptide (9) for comparative reasons. Thus, in contrast to the previous results on the methyl glycosidation of **1**, the thioglycosidation proceeded with complete retention of configuration. This was confirmed since the only other detectable reaction product was in fact a small quantity of methyl β-D-xylopyranoside, estimated as approximately 10% of the crude reaction mixture. Obviously methoxide must compete with methyl mercaptide to a limited extent in this glycosidation process. Retention of configuration in the thioglycosidation of **1** can be explained on the basis that the reaction proceeds via a 1,2-anhydro intermediate **4** which is probably formed by the action of base on **2**. This would require that the C-1 and -2 groups of the original pentopyranosyl chloride derivative should be *trans* disposed as in **1**. Support for

Can. J. Chem. Downloaded from www.nrcresearchpress.com by 210.87.254.40 on 09/05/12
For personal use only.

Can. J. Chem. Downloaded from www.nrcresearchpress.com by 210.87.254.40 on 09/05/12
For personal use only.

this explanation was obtained when the thioglycosidation of α-D-lyxopyranosyl chloride 2,3,4-tri(chlorosulfate) also yielded products of complete retention of configuration. Methyl 1-thio-α-D-lyxopyranoside and methyl α-D-lyxopyranoside were the only two detectable products of the reaction (p.m.r. and g.l.c. analysis), the former constituting approximately 90% of the crude reaction product. Methyl 1-thio-α-D-lyxopyranoside was isolated crystalline from the crude reaction mixture and was assigned the α-D-configuration by virtue of its high positive specific rotation.

A similar methyl thioglycosidation procedure has been performed which proceeds through a 1,2-anhydro intermediate when 3,5-di-*O*-benzoyl-D-arabinofuranosyl chloride was treated with sodium methyl mercaptide (10). Also, a structural analogue of **2** having an anomeric fluorine atom has been isolated which on treatment with sodium methoxide yielded methyl β-D-xylopyranoside, presumably also via intermediate **4** (11). Although this evidence does not prove conclusively that all the chlorosulfate groups are removed prior to epoxide formation, nevertheless it does prove that the C-2 chlorosulfate group is, as this would be a requirement for such a retention (12). Also it would seem reasonable to assume that both the C-3 and -4 chlorosulfate groups would be removed at a rate comparable to that of the C-2 chlorosulfate group.

Further evidence in support of the formation of the 1,2-anhydro intermediate **4** was obtained when α-D-xylopyranosyl chloride 2,3,4-tri(chlorosulfate) was treated with sodium methyl mercaptide by an identical procedure to that used with its β-D-anomer **1**. The reaction produced two glycosidic products which were shown to be identical to those produced with **1** (g.l.c. analysis), and the major component was isolated crystalline and was characterized as methyl 1-thio-β-D-xylopyranoside. Thus the thioglycosidation occurs with predominant inversion of configuration with the α-D-anomer of **1** because the 1,2-*cis* arrangement of the anomeric chlorine and C-2 chlorosulfate group is sterically unfavorable for the formation of a 1,2-anhydro intermediate (12).

It is of interest to note that although no substantial quantity of free glycose was detected in any of the crude reaction products (g.l.c. analysis), it is nevertheless probable that water does play some role in the dechlorosulfation procedure. Although the precise mechanism is not known, mechanisms have been proposed which all involve the attack of iodide ion on the chlorosulfate group to liberate iodine and sulfur dioxide (13). In our reactions, only a catalytic quantity of iodide ion was used (approximately 0.1 mol equiv.), which would require that the iodide ion must be regenerated for complete dechlorosulfation. This is probably accomplished by the iodine oxidation of the liberated sulfur dioxide (or sulfite) to sulfur trioxide (or sulfate). This reaction requires the presence of water and is similar to the one utilized in the method of Karl Fischer for the estimation of water in methanol (14). It is probable that sufficient water is available in the reagent grade methanol to satisfy these requirements but not enough to compete extensively as a nucleophile at the anomeric center.

Experimental

Melting points were determined on a Kofler hot stage and are uncorrected, and optical rotations were measured at 21 ± 3°. Solutions were concentrated below 50° under diminished pressure. An F and M (model 420) chromatograph was used for g.l.c. and the column packings used were (*a*) 10% Carbowax 6000 on Chromosorb W, 100–120 mesh at 165°, and (*b*) 10% neopentylglycol sebacate on Gas Chrom A, 100–120 mesh at 180°. Relative amounts of the separated components were estimated by triangulation of the peaks on the g.l.c. The p.m.r. spectra were obtained from a Varian A60A spectrometer using the following solvents (*i*) deuteriochloroform with tetramethylsilane (τ 10.0) as the identical standard and (*ii*) deuterium oxide with 3-(trimethylsilyl)-propanesulfonic acid sodium salt (τ 10.0) as the internal standard. Barium carbonate was dried over phosphorus pentoxide under vacuum and "Anachemia" reagent grade methanol was used in all these experiments.

Methyl 2,3,4-Tri-O-acetyl-α-D-xylopyranoside

Crystalline β-D-xylopyranosyl chloride 2,3,4-tri(chlorosulfate) (**1**) (2 g, 0.0043 mol) (15) was dissolved in methanol (100 ml) and anhydrous barium carbonate (20 g) was added to the solution with continuous stirring. A solution of sodium iodide (0.07 g) (0.00046 mol) in methanol (5 ml) was then added to the mixture which caused an immediate evolution of iodine. The iodine (yellow coloration) rapidly disappeared and the reaction mixture was stirred for a further 15 min before being filtered. The clear filtrate was then concentrated to dryness and the residue was acetylated using pyridine and acetic anhydride. The inorganic salts were then removed by partitioning the acetylation mixture between chloroform and water and the chloroform layer was then washed with dilute sulfuric acid, water, and sodium bicarbonate solution. The chloroform solution was then dried over anhydrous sodium sulfate, filtered, and concentrated to a syrup (1.2 g) which rapidly crystallized.

Can. J. Chem. Downloaded from www.nrcresearchpress.com by 210.87.254.40 on 09/05/12
For personal use only.

Recrystallization of the crude acetate from ethanol gave crystals (0.95 g, 69%) of $[\alpha]_D$ +118° (*c*, 3.7 in chloroform) and m.p. 84° undepressed on admixture with authentic methyl 2,3,4-tri-*O*-acetyl-α-D-xylopyranoside (16). The p.m.r. spectrum of the crude acetylated product in solvent *i* was almost identical to that of authentic methyl tri-*O*-acetyl-α-D-xylopyranoside (methoxy singlet at τ 6.60) indicating a high yield of the methyl α-D-anomer. This was confirmed when a small quantity of the crude acetate was deacetylated (sodium methoxide) and the deacetylated product was trimethylsilylated and injected onto column *a*. Two components were detected with identical retention volumes to those of the trimethylsilyl derivatives of authentic samples of methyl α- and β-D-xylopyranosides. The amount of methyl α-D-anomer was estimated as 90%.

The above reaction was repeated and the reaction mixture was stirred for an identical period of time except that the addition of sodium iodide was omitted in this case. The mixture was filtered and the filtrate was poured into chloroform solution. The chloroform solution was washed with water, dried, and concentrated to a syrup. A p.m.r. spectrum of the syrupy product in solvent *i* was almost identical to the original β-D-chloride **1** except for a very small methoxy singlet at τ 6.50 indicating that only a negligible amount of methyl glycosidation had occurred.

Methyl 2,3,4-Tri-O-acetyl-β-D-xylopyranoside

Crystalline α-D-xylopyranosyl chloride 2,3,4-tri(chlorosulfate) (0.6 g) (15) was treated in methanol solution with sodium iodide and barium carbonate, and the product was acetylated by identical procedures used for **1**. The syrupy acetate (0.4 g) slowly crystallized and recrystallization from ethanol gave crystals (0.1 g, 24%) of $[\alpha]_D$ −59.6° (*c*, 1.0 in chloroform) and m.p. 116–118° undepressed on admixture with authentic methyl 2,3,4-tri-*O*-acetyl-β-D-xylopyranoside. A p.m.r. spectrum of the crude acetate in solvent *i* indicated two methoxy singlets at τ 6.52 (methyl β-D-anomer) and 6.60 (methyl α-D-anomer). Integration of these signals indicated that the amount of methyl β-D-anomer present in the mixture was approximately 80%.

Methyl β-D-Lyxopyranoside

α-D-Lyxopyranosyl chloride 2,3,4-tri(chlorosulfate) (1.5 g) (15) was treated in methanol solution with sodium iodide and barium carbonate, and the product was acetylated by identical procedures used for **1**. A p.m.r. spectrum of the syrupy acetate (0.9 g) in solvent *i* indicated two methoxy singlets at τ 6.54 (methyl β-D-anomer) and 6.58 (methyl α-D-anomer). These signals were assigned by comparison with the p.m.r. spectrum of an authentic mixture of methyl 2,3,4-*O*-acetyl-α- and β-D-lyxopyranosides in solvent *i*. Integration of these signals indicated that the amount of methyl β-D-anomer present in the mixture was approximately 80%. The syrupy acetate was deacetylated (sodium methoxide) and following deionization with Amberlite I.R. 120 (H^+ form) ion-exchange resin was concentrated to a syrup which crystallized. Recrystallization from propan-2-ol gave needles (0.25 g, 47%) of $[\alpha]_D$ −127° (*c*, 0.25 in water) and m.p. 115–116° undepressed on admixture with an authentic sample of methyl β-D-lyxopyranoside.

Methyl 1-Thio-β-D-xylopyranoside

Crystalline **1** (2 g, 0.0043 mol) was dissolved in methanol (25 ml) and the solution was quickly added to a previously prepared solution of sodium iodide (0.07 g, 0.00046 mol) and methyl mercaptan (5 ml) in 0.35 *M* sodium methoxide in methanol (100 ml). During the addition the solution was continuously stirred and was cooled in an ice-bath. A yellow coloration (iodine) was formed instantaneously on the addition of **1** which rapidly disappeared leaving a colorless solution. The solution then began to deposit inorganic salts. The reaction mixture was stirred for 45 min and was then neutralized with a few drops of dilute sulfuric acid (aqueous). The inorganic salts were removed by filtration and the filtrate was passed through Amberlite I.R. 120 (H^+ form) and Duolite A4 (OH^- form) ion-exchange resins. The eluate was concentrated to a syrup (1.1 g) which rapidly crystallized and recrystallization from ethanol gave colorless plates (0.38 g, 50%) of m.p. 162–164° and $[\alpha]_D$ −69° (*c*, 1.0 in water).

Anal. Calcd. for $C_6H_{12}O_4S$: C, 40.00; H, 6.67; S, 17.80. Found: C, 40.29; H, 6.82; S, 17.70.

These physical constants are in fairly good agreement with those quoted for authentic methyl 1-thio-β-D-xylopyranoside (9) and the m.p. of the above crystalline compound was undepressed on admixture with an authentic sample prepared essentially as described by Zinner *et al.* (9). The p.m.r. spectrum of the crystals in solvent *ii* indicated a methylthio singlet at τ 7.79 (3 protons) and an anomeric doublet at 5.60 (1 proton) with a spacing of 7.9 Hz. The g.l.c. analysis using column *b* of the trimethylsilylated crude product from the deionized eluate indicated two components with relative retention volume of 1.0:2.5. The faster minor component had an identical retention volume to that of the trimethylsilyl derivative of methyl β-D-xylopyranoside and the slower major component (estimated as 90% of the mixture) had an identical retention volume to that of the trimethylsilyl derivative of authentic methyl 1-thio-β-D-xylopyranoside above.

α-D-Xylopyranosyl chloride 2,3,4-tri(chlorosulfate) (2 g) (15) was treated with sodium iodide in sodium methyl mercaptide solution and the product was isolated by an identical procedure used for **1**. The product was a syrup (0.5 g) which crystallized and the crude product was shown to be a mixture of two components identical to those produced under the same reaction conditions by **1** (g.l.c. analysis) except that the methyl 1-thio-β-D-xylopyranoside constituted only 70% of the mixture in this case. Recrystallization (two times) of the crude product from ethanol gave crystals (0.1 g, 13%) of m.p. 162–164°, undepressed on admixture with authentic methyl 1-thio-β-D-xylopyranoside obtained above.

Methyl 1-Thio-α-D-lyxopyranoside

Crystalline α-D-lyxopyranosyl chloride 2,3,4-tri(chlorosulfate) (2 g) (15) was treated with sodium iodide in sodium methyl mercaptide solution and the product was isolated by identical procedures used for **1**. The product was a syrup which crystallized and a p.m.r. spectrum of the crude product in solvent *ii* indicated a methylthio singlet at τ 7.86 and a methoxy singlet at 6.62. The g.l.c. analysis using column *b* of the trimethylsilylated crude product indicated two components with relative retention times of 1.0:2.8. The faster minor component had

an identical retention volume to the trimethylsilyl derivative of methyl α-D-lyxopyranoside and the major slower component constituted 90% of the mixture. Recrystallization from chloroform – propan-1-ol gave crystals (0.3 g, 40%) of m.p. 120–122° and $[\alpha]_D$ +123° (*c*, 0.9 in water).

Anal. Calcd. for $C_6H_{12}O_4S$: C, 40.00; H, 6.67; S, 17.80. Found: C, 40.18, H, 6.72; S, 17.67.

The crystals did not reduce Fehlings' solution and a p.m.r. spectrum of the crystals in solvent *ii* indicated a methylthio singlet at τ 7.86 (3 protons) and an anomeric doublet at 5.09 (1 proton) with a spacing of 4.6 Hz.

The author wishes to thank Mrs. A. Martin for technical assistance and Mr. A. E. Castagne for determination of the microanalyses and the p.m.r. spectra.

1. H. J. JENNINGS and J. K. N. JONES. Can. J. Chem. **41**, 1151 (1963).
2. B. COXON, H. J. JENNINGS, and K. A. MCLAUCHLAN. Tetrahedron, **23**, 2395 (1967).
3. H. J. JENNINGS. Can. J. Chem. **48**, 1834 (1970).
4. H. J. JENNINGS and J. K. N. JONES. Can. J. Chem. **43**, 2372 (1965).
5. F. H. NEWTH and G. O. PHILLIPS. J. Chem. Soc. 2904 (1953).
6. R. U. LEMIEUX, C. BRICE and G. HUBER. Can. J. Chem. **33**, 134 (1955).
7. R. U. LEMIEUX and C. BRICE. Can. J. Chem. **34**, 1006 (1956).
8. G. L. MATTOCK and G. O. PHILLIPS. J. Chem. Soc. 130 (1958).
9. H. ZINNER, A. KOINE, and H. NIMZ. Chem. Ber. **93**, 2705 (1960).
10. E. J. REIST, P. A. HART, L. GOODMAN, and B. R. BAKER. J. Amer. Chem. Soc. **81**, 5176 (1959).
11. F. MICHEEL, A. KLEMER, and R. FLITSCH. Chem. Ber. **91**, 663 (1958).
12. S. PEAT. Advan. Carbohyd. Chem. **2**, 37 (1946).
13. E. BUNCEL. Chem. Revs. **70**, 323 (1970).
14. A. I. VOGEL, *editor*. Quantitative inorganic analysis. Longmans, Green and Co., London, 1951.
15. H. J. JENNINGS. Can. J. Chem. **47**, 1157 (1969).
16. R. L. WHISTLER, K. A. KIMMELL, and D. DURSO. J. Amer. Chem. Soc. **73**, 3530 (1951).

Can. J. Chem. Downloaded from www.nrcresearchpress.com by 210.87.254.40 on 09/05/12
For personal use only.

Can. J. Chem. Downloaded from www.nrcresearchpress.com by 210.87.254.105 on 09/05/12
For personal use only.

Tricyclic Unsaturated Hydrocarbons

R. H. WIGHTMAN, (Miss) R. J. WAIN, AND D. H. LAKE[1]
Department of Chemistry, Carleton University, Ottawa, Canada

Received December 7, 1970

Some new unsaturated tricyclic hydrocarbons have been synthesized using a sequence of some general usefulness.

De nouveaux hydrocarbures tricycliques insaturés ont été synthétisés utilisant une série de réactions qui pourraient s'avérer d'utilisation générale.

Canadian Journal of Chemistry, 49, 1360 (1971)

Introduction

Polycyclic unsaturated systems containing chiefly non-six-membered rings represent an area of organic chemistry currently full of theoretical interest (1) and synthetic challenges (2). From the synthetic point of view we wish to report a generally useful sequence which has provided us with several new tricyclic compounds containing a bicycloalkeno–benzenoid system. The compounds should serve as excellent precursors to test chemically the theoretical predictions (1) concerning stability and/or aromaticity of similar carbon skeletons containing more unsaturations. The general scheme is outlined in Scheme 1. Additionally, slight variations in the synthetic sequence (3*a*) or modification (3*b*) of the final products (*i.e.* **4***a–d*, **5***b–d*) would give other ring systems of potential interest in this expanding field.

Results and Discussion

The Synthetic Sequence

The pinacol reaction leading to the diols **1***a–d* is well-documented (4), even in the mixed series, *i.e.* preparation of **1***c* (5). Since we were primarily interested in the product from this "mixed-pinacol" reaction much of our effort was devoted to separation and characterization of the products **1***c*–**4***c* in this series.[2]

The mixed pinacol reaction gave a somewhat variable yield of products **1***a* (~10%), **1***b* (~40%), **1***c* (~50%); however, it was possible to obtain analytical samples of the mixed diol (1*c*), either by preparative t.l.c. or careful sublimation of the diol mixture. No useful methods were found for separation of preparative quantities of the diols, hence the mixture was carried through the next step.

Dehydration of the diols was accomplished with phosphorus oxychloride in pyridine (4, 6) to minimize possible rearrangements. Due to the varying instability of the dienes,[3] no rigorous attempt was made to purify them. However, separation of the diene mixture **2***a–c* could readily be accomplished by g.l.c. and preparative-scale g.l.c. techniques were employed at this stage. The individual dienes were then immediately allowed to react with maleic anhydride (4) to yield Diels–Alder adducts, **3***a–c*. Product distribution at the diene stage did not correspond exactly to that of the diol mixture, presumably due to the differences in stabilities of the various dienes.

Transformation of the anhydrides **3***a–d* into the corresponding aromatic products was accomplished by heating with a slight excess of phosphorus pentoxide, P_2O_5, or excess 10% palladium-on-charcoal. The synthesis of **4***a*, originally prepared via an alternate route (8), has already been reported using the P_2O_5 method (7*a*), while a similar "aromatization" was accomplished using Pd/C (7*b*). Treatment of **4***a* with 2,3-dichloro-5,6-dicyanobenzoquinone (DDQ) produced the dihydro-*as*-indacene (**6**) as indicated by comparison with the reported n.m.r. data (9). This final reaction was not further investigated,

[1]Taken in part from the thesis submitted by D.H.L. in partial fulfillment of the requirements of the M.Sc. degree at Carleton University, Ottawa, Canada, 1969. Present address: Cambrian College of Applied Arts and Technology, Sudbury, Ontario.

[2]No attempt had been made to characterize **1***c* and **2***c* by the original author (5).

[3]Stability of the dienes increases with ring size. We have an indication that the decomposition involves cycloaddition of oxygen and subsequent cleavage to keto-alcohols.

Can. J. Chem. Downloaded from www.nrcresearchpress.com by 210.87.254.105 on 09/05/12
For personal use only.

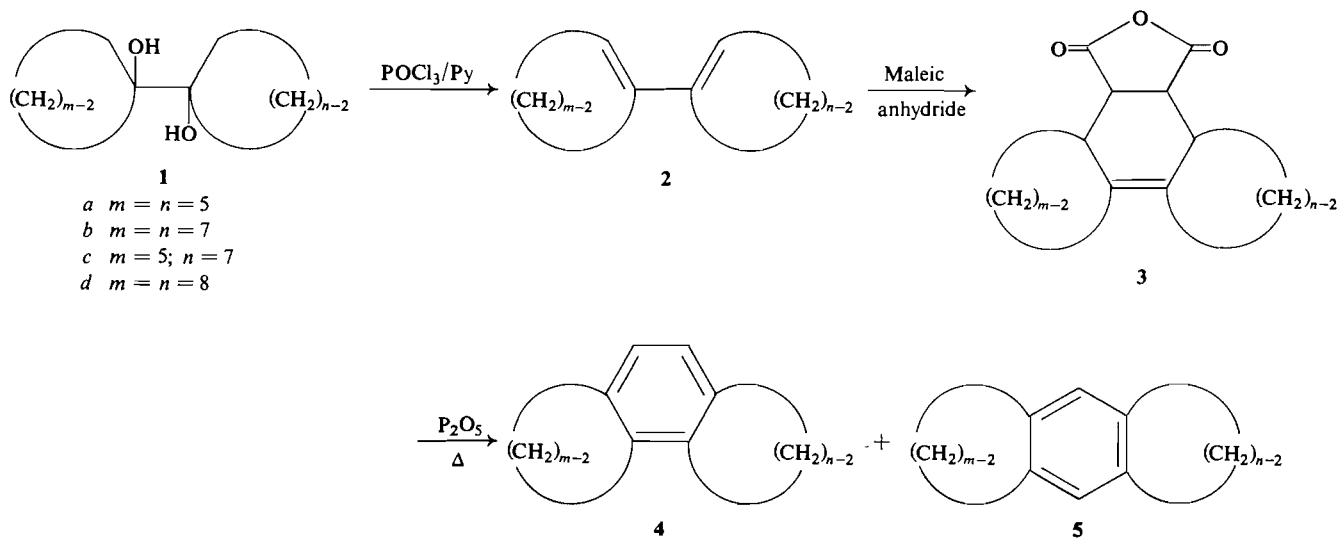

1

a $m = n = 5$
b $m = n = 7$
c $m = 5;\ n = 7$
d $m = n = 8$

2 **3** **4** **5**

SCHEME 1

since the chemistry of the system has already been elegantly investigated by Katz and coworkers (9). However, this method is a significantly simpler approach to **4***a* (21% overall yield in four steps from cyclopentanone after our modification of the P_2O_5 treatment). Also, it serves to illustrate how benzenoid products can be used in quest of the more interesting compounds containing additional unsaturations.

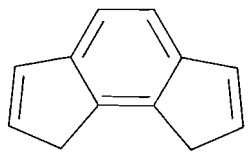

6

The reaction of **3***d* with phosphorus pentoxide usually yieded two hydrocarbons, easily separable by g.l.c. and partially separable by column chromatography. The minor constituent (*ca.* 10–20%), m.p. 133–135°, was identified as bicyclo-octeno-[*a*,*d*]-benzene (**5***d*) by comparison with an authentic sample[4] obtained via an unambiguous synthesis (10). The major product, m.p. 83–85°, has been characterized as the hitherto unknown bicyclo-octeno-[*a*,*c*]-benzene (**4***d*). Combustion analysis and mass spectral data established the empirical formula; n.m.r. data (two aromatic, eight benzylic, and 16 methylenic protons) indicated the functionality and i.r. and u.v. comparisons (*vide infra*) corroborated the correct isomeric designation.

The identification of **4***c* and **5***c* has been noted (11), albeit in milligram quantities and via a rather lengthy synthesis (12) which favors the linear[5] isomer **5***c*. Our sequence now makes available synthetically useful amounts of the potentially more interesting[6] angular isomer **4***c*. In our sequence the hydrocarbon mixture obtained by "aromatization" of **3***c* with P_2O_5 appears to contain approximately 90% of **4***c* and 10% of **5***c* as judged by i.r. and u.v. comparisons of reported values.

Treatment of the anhydride **3***b* with P_2O_5 at elevated temperatures produced a mixture of two hydrocarbons from which a crystalline solid, m.p. 140°, could easily be isolated. This product was identified as bicyclohepteno-[*a*,*d*]-benzene (**5***c*), primarily on the basis of strong i.r. bands in the region 860–900 cm^{-1} and comparative u.v. data. Once again the empirical formula was ascertained by mass spectrum and combustion analysis, while the three gross structural features (two aromatic, eight benzylic, and 12 methylenic protons) were clearly distinguishable in the n.m.r. The ratio of the two components varied greatly, depending on the duration and temperature of the P_2O_5 treatment. Removal of **5***c* was almost complete after several crystallizations and g.l.c. investigation showed that the mother liquors contained essentially the second compound which could be obtained as a solid, m.p. 54°. This product was identified as bicyclohepteno-[*a*,*c*]-benzene (**4***c*).[7] Structure proof was again dependent on combustion analysis plus mass spectral and n.m.r. data for the gross structure, while i.r. and u.v. data (*vide infra*) were necessary to identify the substitution pattern.

The Isomers: Formation and Characterization

The formation of the linear isomer, often in appreciable quantities from **3***b* with P_2O_5, was somewhat puzzling and frustrating at first. However, this isomerization, which had not previously been noted (7*a*), appears to be yet another example of the acid-catalyzed rearrangement of polyalkylated benzenes (16). Much work has been reported over the years on the *s*-octahydroanthracene : *s*-octahydrophenanthrene equilibrium under a variety of acidic conditions (*e.g.*, H_2SO_4, $AlCl_3$, HF/BF_3). A recent paper (17) suggests that the most plausible mechanism involves protonation of the ring system followed by rearrangement via a spiro-carbonium ion intermediate (similar to the dienone–phenol rearrangement). It seems quite probable, there-

[4]We thank Professor F. Sondheimer for kindly providing a sample and other relevant data.

[5]Angular and linear designate 1,2:3,4- and 1,2:4,5-substitution patterns respectively.

[6]Several unsuccessful attempts to prepare the fully unsaturated hydrocarbon derived from the linear isomer **5***c* have been reported (13*a*, *b*). Recently, however, it has been calculated that the non-benzenoid hydrocarbon containing the angular system **4***c* is more favorable (14*a*, *b*).

[7]Although very incomplete data were reported and only the melting points agree, it seems possible that our sample is the same as that reported by Rosenfelder and Ginsburg (15) via a completely different route. Unfortunately, Professor Ginsburg has no sample of his product (personal communication).

Can. J. Chem. Downloaded from www.nrcresearchpress.com by 210.87.254.105 on 09/05/12
For personal use only.

Can. J. Chem. Downloaded from www.nrcresearchpress.com by 210.87.254.105 on 09/05/12
For personal use only.

fore, that some rearrangement would be occurring under the conditions of the P_2O_5 experiments. Although not useful as a large-scale preparative method, it is interesting to note that isomerically pure angular hydrocarbons could be obtained if the corresponding anhydrides were treated under non-acidic conditions, *e.g.*, heating with excess Pd/C. Thermal reaction of **3***c* with catalytic amounts of Pd/C merely produced the aromatic anhydride **7**.[8]

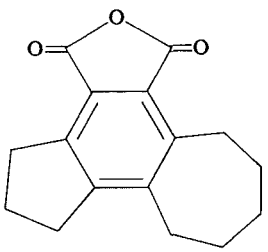

7

Proof of structure of the new aromatic hydrocarbons required a complete spectral investigation. The mass spectra of each pair of isomers exhibited fairly intense molecular ions and all other significant *m/e*'s were the same. The n.m.r. spectra could not be used to distinguish isomers; the only potentially useful value (the chemical shift of the singlet representing two aromatic protons) varied slightly but no significant trends were observed. The most useful values were the strong i.r. bands ascribed to out-of-plane C—H deformation vibrations of the hydrogens on the benzene ring (18). Good agreement with the values quoted was found: for the angular isomers a range of 830–800 cm^{-1} (two adjacent hydrogens), and for the linear isomers a range of 890–850 cm^{-1} (one isolated hydrogen). Another useful trend was noticed when comparing the u.v. spectra of various pairs of isomers. Although the λ_{max} were not always identical, the linear isomer invariably exhibited a larger extinction coefficient (ε) than the angular isomer. Finally, it was noted that the linear isomer always had the higher melting point.

In addition to making available several precursors for potential non-benzenoid aromatic hydrocarbons, this study has provided the missing compounds in an interesting series of tetraalkylated benzenes. Much spectroscopic information was unavailable in this series and we have repeated the syntheses of the 5–5 linear (**5***a*) (16) and 5–6 linear (21) compounds for a more complete comparison. Table 1 summarizes the pertinent information.

[8]The aromatization of anhydrides such as **3***c* can be readily accomplished (4, 7*b*) while similar decarboxylations involving prolonged heating with metals (Zn, Cu, Pd/C) have been previously noted (7*b* and refs. therein). Excess Pd/C appears to accelerate the latter process but no kinetic studies were attempted at this time.

Experimental

Melting points were determined on a Kofler hot stage and are uncorrected. The n.m.r. spectra were obtained on a Jeolco C-60 spectrometer and are expressed in p.p.m. (τ) from internal tetramethylsilane in deuterochloroform. The i.r. spectra (ν_{max} in cm^{-1}) were measured on a Perkin–Elmer 237B or 257 spectrophotometer either as solutions or liquid film, and u.v. spectra [λ_{max} in nm (ε)] were recorded with a Cary 14 or Perkin–Elmer 202 instrument. Mass spectra were obtained from an MS12 spectrometer (AEI). The g.l.c. was performed on Hewlett–Packard (F and M) instruments. Analytical investigations were performed on a Model 402 equipped with flame-ionization detector, helium carrier gas (50 ml/min), and a glass column (6′ × ¼″) packed with six-ring polyphenyl ether (PPE – 5% on Chromosorb W 80/100 mesh). For preparative separations a Model 776 was used with a stainless steel column (80″ × 3/4″) packed with UCW98 (2% on Chromosorb W 60/80 mesh) and nitrogen carrier gas (400 ml/min). Temperatures and retention times are noted as required. The t.l.c. was accomplished using Silica gel G (0.25 mm layers) on glass plates. Microanalyses were performed by Organic Microanalyses (Dr. C. Daesslé), Montreal, Quebec.

The preparation of some of the starting materials (**1***a, b, d* and **3***a, b, d*) has been adequately described elsewhere (4). Therefore the "mixed" series (**1***c*–**3***c*) will be used as the experimental example (5).

Preparation of "Mixed" Diols (1a–c)

To a well-stirred mixture of coarse aluminum powder (100 g, 3.7 mol) in dry benzene (600 ml), was added a solution of cycloheptanone (276 g, 2.46 mol), cyclopentanone (206 g, 2.46 mol), and mercuric chloride (46 g, 0.17 mol) in dry benzene (600 ml). The mixture was stirred and heated at reflux for 6 h, then cooled. Extra benzene (600 ml) then water (250 ml) was added dropwise and the stirred mixture was again heated for 3 h before being cooled and filtered. The solid was thoroughly washed with hot benzene and the combined organic filtrates were dried (anhydrous sodium sulfate). After removal of the solvent, the thick, residual oil was dissolved in a minimal amount of petroleum ether (b.p. 30–60°) and upon cooling, white crystals (m.p. 64–68°) slowly formed. Further concentration of the mother liquors eventually produced a total yield of 189 g (35%). The t.l.c. (30% ethyl acetate : 70% benzene) showed three spots with R_f values of 0.19, 0.31, and 0.42. Preparative t.l.c. or slow sublimation (90°/0.1 mm Hg) produced three crystalline solids (approximate ratio 1:5:4). The

Can. J. Chem. Downloaded from www.nrcresearchpress.com by 210.87.254.105 on 09/05/12
For personal use only.

TABLE 1. Physical and spectral data of various tetra-alkyl benzenes

	1,2:3,4-Substitution (angular)					1,2:4,5-Substitution (linear)				
Substituents	The u.v *	The i r.†	The n.m.r.‡	The m.p. (b.p./mm Hg)	Reference	The u.v.	The i.r.	The n.m.r.	The m.p. (b.p./mm Hg)	Reference
Tetramethyl-§	268 (265) 273 (220) 277 (208)	804	3.09	205°/760		269 (700) 278 (750)	869	3.09	79–81°	
Bicyclopenteno- 4*a* and 5*a*	269 (774)‖ 273 (643) 279 (904)	765 810	3.05	39–40‖	8,9	277 (3860) 281 (4040) 287 (4180)	870	2.97	52–54‖	16, 19
Cyclohexeno-, cyclopenteno-	269 (556)‖ 273 (468) 278 (556)	800‖ 830	3.12‖ 3.30	65/0.6‖	20	276 (2290) 280 (2350) 286 (2590)	851 908	3.08	125/6‖	21
Bicyclohexeno-§	270 (310)‖ 273 (360) 278 (215)	800	3.19	295/760	22	275 (1550)‖ 280 (1300) 285 (1950)	850	3.29	72–74	22
Cyclohepteno-, cyclopenteno- 4*c* and 5*c*	268 (575)¶ 274 (490)	812 (820)¶	3.05 (3.20)¶	275/760	11	272 (1650)¶ 276 (1580)	830¶ 880	3.14¶	170–172/16‖	11, 13*b*
Bicyclohepteno- 4*b* and 5*b*	269 (341) 278 (299)	806	3.22	53–54	7*b*	269 (919) 278 (1191)	830 895 965	3.15	139–140	
Bicycloocteno- 4*d* and 5*d*	270 (368) 276 (316) 280 (347)	825	3.10	83–85		271 (981) 275 (790) 280 (1235)	872	3.27‖	132–133‖	10

*λ_{max}(ε): measured in saturated hydrocarbon solvents.
†In cm^{-1} (carbon disulfide solution or neat liquid film) of benzene substitution pattern.
‡τ-Values (p.p.m.) in deuterochloroform of aromatic protons only.
§Obtained from commercial sources: tetramethyls- (J. T. Baker Chemical Co., U.S.A.); 1,2:3,4-bicyclohexeno- (Fluka AG, Switzerland); 1,2:4,5-bicyclohexeno- (Aldrich Chemical Co., U.S.A.).
‖Values obtained from literature sources (see indicated refs.).
¶Personal communication from Professor Sondheimer (data from thesis of J. Mayer).

Can. J. Chem. Downloaded from www.nrcresearchpress.com by 210.87.254.105 on 09/05/12
For personal use only.

slowest moving product, m.p. 108–109°, was identified as **1***a* (4) while the fastest moving component, m.p. 77–78°, was **1***b* (4). The product with intermediate mobility was **1***c*,[9] m.p. 63–64° (5). Spectra: i.r. 3400 (strong —OH); n.m.r. 7.90 (2H singlet, exchangeable in D_2O, —OH), 8.15–8.70 (20H multiplet, —CH_2's).

Anal. Calcd. for $C_{12}H_{22}O_2$: C, 72.73; H, 11.11. Found: C, 72.82; H, 11.17.

Preparation of Bicyclic Dienes (2a–c)

Essentially the method of Greidinger and Ginsburg (4) was followed. Thus the mixture of diols (189 g), excess phosphorus oxychloride (150 g), and dry pyridine (1500 ml) was stirred at room temperature for 0.5 h, then heated under reflux for 6 h. The pyridine was removed under reduced pressure, the residue dissolved in ice–water (4 l) and stirred for 2 h. This mixture was extracted with hexane (3 × 300 ml) and the combined organic extracts were washed successively with 5% aqueous hydrochloric acid (2 × 300 ml), 5% aqueous sodium bicarbonate (2 × 300 ml), water (1 × 300 ml), and saturated aqueous sodium chloride (1 × 200 ml) before drying (anhydrous sodium sulfate) and removing solvent. The yield of crude oily dienes was 153 g. Separation was achieved by repeated 8 ml injections on a preparative scale g.l.c. instrument at 165°. Yields of components were as follows: **2***a* (8.5 g), **2***b* (62.7 g), **2***c* (34.2 g), mixture of **2***b* and **2***c* (6.9 g).

Preparation of Anhydrides (3a–c)

The dienes were immediately dissolved in hexane, treated with excess maleic anhydride, and heated under reflux for several hours, as outlined by Greidinger and Ginsburg (4). The reaction mixture was dissolved in benzene and excess maleic anhydride removed by water extraction. After drying (anhydrous sodium sulfate) and removing the solvent, the residue was recrystallized from hexane. Thus, (*i*) **2***a* (8.5 g, 0.063 mol) and maleic anhydride (17.6 g, 0.180 mol) gave **3***a* (13.5 g, 92%), m.p. 103°; reported m.p. 104° (4). (*ii*) Compound **2***b* (62.7 g, 0.33 mol) and maleic anhydride (128 g, 1.3 mol) gave **3***b* (75 g, 80%), m.p. 157°; reported m.p. 158° (4); (*iii*) Compound **2***c* (34.2 g, 0.21 mol) and maleic anhydride (72 g, 0.74 mol) gave **3***c* (43.3 g, 62%), m.p. 135–137°. Spectra: i.r. 1850 and 1775 (anhydride); n.m.r. 6.65 (2H, d), 7.0–9.2 (18H, m).

Anal. Calcd. for $C_{16}H_{20}O_3$: C, 73.85; H, 7.70. Found: C, 73.91; H, 7.62.

Preparation of Aromatic Hydrocarbons.

The aromatic hydrocarbons were prepared by heating the corresponding anhydrides with a slight excess of phosphorus pentoxide at elevated temperatures (7*a*) for short periods of time (*ca.* 2–5 min). Our method involved mixing the two components in an elongated flask connected to a Hickman-type still and air condenser. The flask was briefly inserted into a preheated furnace (350°) and following a somewhat vigorous reaction, the distillate was collected. Filtration through a short column of silica gel (using petroleum ether as eluant) was usually sufficient to rid the product of any colored impurities.

The following reactions were carried out:

(*i*) **3***a* (3.5 g, 0.017 mol) and phosphorus pentoxide (3.0 g, 0.021 mol) gave a colorless oil (1.67 g, 65%) which formed white needles, m.p. 40°; reported for **4***a*, m.p. 40° (8, 9).

(*ii*) Compound **3***b* (5.0 g, 0.0192 mol) and phosphorus pentoxide (3.5 g, 0.021 mol) gave a colorless oil (2.50 g, 70%). Crystallization from methanol/ether produced **5***b*, white crystals, m.p. 139–140°. Spectra: n.m.r. 3.15 (2H, s, aromatic H), 7.0–7.5 (8H, m, benzylic H's) and 8.0–8.6 (12H, m —CH_2's); i.r. and u.v. (see Table 1) indicated a 1,2:4,5 tetra-substitution pattern; mass spectrum, molecular ion *m/e* 214.

Anal. Calcd. for $C_{16}H_{22}$: C, 89.72; H, 10.28. Found: C, 89.72; H, 10.28.

From the mother liquors could be isolated a second compound **4***b*, m.p. 53–54°. Spectra: n.m.r. 3.22 (2H, s, aromatic H's), 7.0–7.5 (8H, m, benzylic H's), and 8.0–8.6 (12H, m —CH_2's); i.r. and u.v. (see Table 1) consistent with a 1,2:3,4-substitution pattern; mass spectrum, molecular ion *m/e* 214.

Anal. Calcd. for $C_{16}H_{22}$: C, 89.72; H, 10.28. Found: C, 89.75; H, 10.21.

Analytical g.l.c. at 175° showed the two components to have retention times of 10.0 (**4***b*) and 11.5 min (**5***b*). The linear:angular ratio of approximately 1:3 in the reaction mixture could be changed dramatically in favor of the linear isomer by prolonging the contact time with phosphorus pentoxide.

(*iii*) The usual reaction between **3***c* (5.0 g, 0.019 mol) and phosphorus pentoxide (3.5 g, 0.025 mol) produced after column chromatography a colorless oil (2.98 g, 86%). The n.m.r., i.r., and u.v. comparisons with reported values (see Table 1) indicated that this material was composed of **4***c* and **5***c* (approximately 9:1 in favor of the angular isomer). The g.l.c. analysis at 175° showed only one (slightly unsymmetrical) peak with a retention time of 4.5 min.

(*iv*) The preparation of **3***d* was precisely as outlined by Greidinger and Ginsburg (4). The reaction of **3***d* (5.0 g, 0.016 mol) and phosphorus pentoxide (2.5 g, 0.018 mol) produced, after the usual work-up, a white crystalline residue (3.2 g, 80%). The g.l.c. analysis indicated two components with retention times at 175° of 21.3 and 25.7 min. The two compounds could be separated by column chromatography (silica gel) and crystallization (methanol/ether) and were identified as **5***d* and **4***d* respectively (ratio of approximately 1:5). Our linear isomer **5***d* had m.p. 135° and mixture m.p. 135° with an authentic sample[6] while all spectral data were in complete agreement with literature values. Compound **4***d* (white needles) had m.p. 83–85° and the following spectra: n.m.r. 3.10 (2H, s, aromatic H's), 7.0–7.5 (8H, m, benzylic H's) and 8.0–8.6 (16H, m, —CH_2's); i.r. and u.v. (see Table 1) indicated a 1,2:3,4-substituted benzene ring; mass spectrum, molecular ion *m/e* 242.

Anal. Calcd. for $C_{18}H_{26}$: C, 89.27; H, 10.73. Found: C, 89.20; H, 10.59.

Alternate Preparation of 4c

A mixture of **3***c* (500 mg, 0.0019 mol) and 10% palladium-on-charcoal (700 mg) was heated at 350° for a few

[9]Oxidation with lead tetraacetate and treatment with 2,4-dinitrophenylhydrazine showed two spots on t.l.c. corresponding to the 2,4-dinitrophenylhydrazones of cyclopentanone and cycloheptanone.

minutes. After evolution of gas (*ca.* 5 min) the mixture was cooled, filtered, and rinsed with ether. The filtrate was evaporated to dryness to yield an oily residue (300 mg, 85%) which was rendered colorless by filtration through a short column of silica gel. Spectroscopic examination (especially i.r. and u.v.) indicated isomerically pure **4***c* and g.l.c. comparison was identical with a sample prepared via the phosphorus pentoxide method.

Preparation of **7**

When a mixture of **3***c* (500 mg, 0.0019 mol) and 10% palladium-on-charcoal (100 mg) was treated in a manner similar to that outlined above, there was obtained a solid residue (400 mg, 80%). Crystallization from ethanol yielded white crystals of **7**, m.p. 199–201°. Spectra: i.r. (Nujol mull) 1835 and 1775 (aromatic anhydride).

Anal. Calcd. for $C_{16}H_{16}O_3$: C, 74.98; H, 6.24. Found: C, 74.67; H, 6.45.

Preparation of **6**

A solution of **4***a* (300 mg, 0.002 mol) and DDQ (1.0 g, 0.004 mol) in benzene (50 ml) was heated under reflux for 24 h. Hexane (100 ml) was added to precipitate phenolic by-products and the residue, after filtration and evaporation, was subjected to column chromatography on alumina (Woelm, neutral, activity I). Elution with hexane yielded a slightly colored viscous oil. The n.m.r. comparisons with a published spectra (9) indicated the presence of **6** (extra bands in the 3.0–4.0 τ region). The g.l.c. studies showed the sample to contain some starting material.

We wish to thank the National Research Council of Canada for generous financial support and the Ontario Department of University Affairs for a studentship (D.H.L.).

We wish to thank Professor J. W. ApSimon for assistance in obtaining the mass spectra and Mr. G. K. Diedrich and Mr. R. J. Sampson for technical assistance.

1. (*a*) R. ZAHRADNIK. Angew. Chem. Int. Ed. **4**, 1039 (1965); (*b*) G. BINSEH and E. HEILBRONNER. Tetrahedron, **24**, 1215 (1968); (*c*) C. F. WILCOX, JR. Tetrahedron Lett. 795 (1968).
2. (*a*) D. M. G. LLOYD. Carbocyclic non-benzenoid aromatic compounds. Elsevier, Amsterdam, 1966. Chapt. 8. (*b*) P. J. GARRATT and M. V. SARGENT. Advances in organic chemistry. Vol. 6. *Edited by* E. C. Taylor and H. Whyberg. Interscience Publishers, New York, N.Y., 1969. Chapt. 1.
3. (*a*) H. CHRISTOL, H. COMBE and Y. PIETRASANTA. Bull. Soc. Chim. Fr. 4493 (1969). (*b*) V. BOEKELHEIDE and C. D. SMITH. J. Amer. Chem. Soc. **88**, 3950 (1966).
4. D. S. GREIDINGER and D. GINSBURG. J. Org. Chem. **22**, 1406 (1957).
5. R. D. SANDS. Tetrahedron, **21**, 887 (1965).
6. H. CHRISTOL, A. P. KRAPCHO, and F. PIETRASANTA. Bull. Soc. Chim. Fr. 4059 (1969).
7. (*a*) V. R. SKVARCHENKO, R. YA. LEVINA, and O. YU. OKHLOBYSTIN. Doklady Akad. Nauk. S.S.S.R., **99**, 789 (1954) or Chem. Abstr. **49**, 5414*e* (1955); (*b*) Y. ALTMAN and D. GINSBURG. J. Chem. Soc. 1498 (1960).
8. H. RAPOPORT and G. SMOLINSKY. J. Amer. Chem. Soc. **82**, 1171 (1960).
9. T. J. KATZ, V. BALOGH, and J. SHULMAN. J. Amer. Chem. Soc. **90**, 734 (1968).
10. J. A. ELIX, M. V. SARGENT, and F. SONDHEIMER. J. Amer. Chem. Soc. **92**, 962 (1970).
11. J. MAYER and F. SONDHEIMER. J. Amer. Chem. Soc. **88**, 602, (1966).
12. R. GRANGER, H. ORZALESI, and A. MURATELLE. Compt. Rend. **255**, 720 (1965).
13. (*a*) D. J. BERTELLI. J. Org. Chem. **30**, 891 (1965); (*b*) A. D. CAMPBELL and S. N. SLATER. J. Chem. Soc. 4353 (1952).
14. (*a*) C. F. WILCOX, JR. J. Amer. Chem. Soc. **91**, 2731 (1969); (*b*) R. ZAHRADNIK, J. MICHL, and J. KOPECKY. Coll. Czech. Chem. Commun. **31**, 640 (1966).
15. W. J. ROSENFELDER and D. GINSBURG. J. Chem. Soc. 1301 (1957).
16. R. T. ARNOLD and R. A. BARNES. J. Amer. Chem. Soc. **66**, 960 (1944).
17. R. D. BUSHICK. J. Org. Chem. **33**, 4085 (1968).
18. L. J. BELLAMY. The infra-red spectra of complex molecules. 1st edition. John Wiley and Sons, Inc., New York, N.Y., 1958, Chapt. 5.
19. K. HAFNER. Angew. Chem. Int. Ed. **3**, 165 (1964).
20. W. F. ERMAN and H. C. KRETSCHMAR. Tetrahedron Lett. 1717 (1965).
21. S. C. SEN GUPTA. J. Ind. Chem. Soc. **16**, 89 (1939).
22. E. R. NES and E. MOSSETIG. J. Amer. Chem. Soc. **76**, 3182 (1954).

Can. J. Chem. Downloaded from www.nrcresearchpress.com by 210.87.254.105 on 09/05/12
For personal use only.

Can. J. Chem. Downloaded from www.nrcresearchpress.com by 210.87.254.105 on 09/05/12
For personal use only.

Some Aspects of the Mass Spectra of *N*-Nitrosamines

J. W. ApSimon and J. D. Cooney[1]
Department of Chemistry, Carleton University, Ottawa, Canada

Received November 26, 1970

The mass spectra of seven cyclic *N*-nitrosamines were examined for characteristic fragmentation patterns. Accurate mass measurements on three of the compounds indicated that the M-17 and M-30 peaks resulted from molecular ion losses of •OH and •NO respectively. The loss of •OH was rationalized in terms of a McLafferty-type rearrangement.

On a examiné les spectres de masse de sept *N*-nitrosoamines cycliques afin de déterminer s'il existe des modes de fragmentations caractéristiques. Des mesures précises des masses de trois de ces composés ont permis de mettre en évidence que les fragments de masses M-17 et M-30 résultent respectivement de la perte de •OH et •NO par l'ion moléculaire. La perte de •OH peut être rationalisée en faisant intervenir un réarrangement du type préconisé par McLafferty.

Canadian Journal of Chemistry, 49, 1367 (1971)

Several researchers have reported the mass spectra of dialkyl-*N*-nitrosamines (1–3) and dibenzyl-*N*-nitrosamines (3, 4) but little mass spectral data have been presented on cyclic *N*-nitrosamines (3). Schroll *et al.* (3) obtained the mass spectra of *N*-nitrosazacyclohexane and *N*-nitrosomorpholine and accurate mass measurements on the latter compound indicating molecular ion loss of •NO. In the course of another problem we had cause to determine the mass spectra of seven cyclic *N*-nitrosamines and some interesting facets of their fragmentation pathways are reported here.[2]

The compounds studied were the cyclic series **1** (n = 1–5), *N*-nitrosocamphidine (**2**), and *N*-nitroso-3-azabicyclo[3.2.2]nonane (**3**).

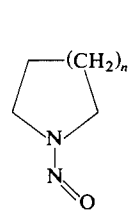

1
$n = 1$–5

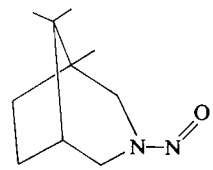

2

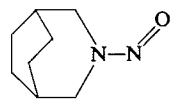

3

Two processes interested us in this study, the molecular ion loss of fragments of mass 17 and mass 30. Intuitively, these would be expected to be loss of •OH (5, 6) and •NO, respectively and this was confirmed by the accurate mass measurements summarized in Table 1.

Loss of •OH

Schroll *et al.* (3) had also noticed the loss of •OH from *N*-nitrosodi-*n*-propylamine but not from the di-*n*-butyl, diethyl or dimethyl derivatives. Examination of Collin's data (1) revealed an M-17 fragment for each of these compounds. These data are summarized in Table 2. A reasonable mechanism for •OH loss can be written as in Scheme 1 (7) assuming a preference for a six-membered McLafferty-type rearrangement (8) with transfer of a hydrogen atom β to the amine nitrogen.[3]

Fragments representing the expected loss of olefin from a McLafferty-type rearrangement

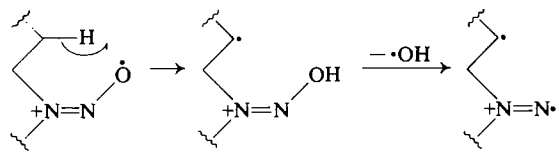

Scheme 1

[1]Taken from the M.Sc. thesis of J. D. Cooney, Carleton University, Ottawa, Canada, April, 1970. Present Address: Textile Chemistry Section, Division of Chemistry, National Research Council of Canada, Ottawa, Canada.

[2]We purposely refrain from extrapolation to more complete fragmentation patterns in the absence of deuterium labels and further accurate mass measurements. Those fragmentations mentioned are supported by metastable peaks.

[3]Attempts are in progress to confirm this by synthesis of specifically deuterated *N*-nitrosamines.

TABLE 1. Accurate mass measurements

Compound	Species	Calculated mass	Measured mass
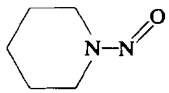	M^+	114.0793	114.0793
	M-OH	97.0766	97.0763
	M-NO	84.0813	84.0798
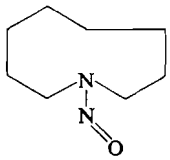	M^+	156.1263	156.1251
	M-OH	139.1235	139.1233
	M-NO	126.1283	126.1283
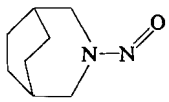	M^+	154.1106	154.1095*
	M-OH	137.1079	137.0964*
	M-NO	124.1126	124.1125
	$M-CH_3N_2O$	95.0861	95.0857
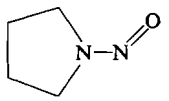	M^+	100.0637	100.0638
	$M-H_2NO$	68.0500	68.0501

*Errors of 12 and 15 p.p.m. due to unusual curve shapes.

TABLE 2. Molecular ion loss of •OH

N-Nitroso compound	Relative abundance	Percentage of total ionization	Type of hydrogen transferred	Reference
Dimethylamine	0.07	0.01 Σ_{35}	Primary	1
Diethylamine	1.46	0.19 Σ_{60}	Primary	1
Di-*n*-propylamine	5.28	0.93 Σ_{89}	Secondary	1
Di-*i*-propylamine	0.46	0.12 Σ_{76}	Primary	1
Di-*n*-butylamine	6.87	0.76 Σ_{91}	Secondary	1
Azacyclopentane	0.2	0.04 Σ_{76}	Secondary	This work
Azacyclohexane	1.2	0.13 Σ_{75}		
Azacycloheptane	6.2	1.1 Σ_{70}		
Azacyclooctane	3.8	0.41 Σ_{73}		
Azacyclononane	2.4	0.31 Σ_{52}		
3-Azabicyclo[3.2.2]nonane	8.6	0.60 Σ_{99}		
Camphidine	8.3	0.64 Σ_{94}		

were also observed for each of the dialkyl-*N*-nitrosamines examined by Collin (1) and a possible mechanism is illustrated in Scheme 2.

Generally speaking a large loss of •OH was accompanied by a small loss of olefin and *vice versa* (9) suggesting two pathways for molecular ion fragmentation involving hydrogen atom transfer.

In some respects the data in Table 2 support the contention of a six-membered process for transfer of a β-hydrogen, thus *N*-nitrosodi-*n*-propylamine and *N*-nitrosodi-*n*-butylamine have larger M-17 peaks than the other aliphatic cases since a weaker C—H bond (10) was broken during transfer of a secondary hydrogen. A preference of approximately 7:1 for secondary hydrogen abstraction over primary hydrogen abstraction is apparent from comparison of % total ionization (T.I.) values for *N*-nitrosodi-*n*-propylamine and *N*-nitrosodiethylamine. Preference for secondary

Can. J. Chem. Downloaded from www.nrcresearchpress.com by 210.87.254.105 on 09/05/12
For personal use only.

TABLE 3. The molecular ion and its loss of •NO

N-Nitroso compound	M^+ Relative abundance	M^+ Total ionization (%)	M-30 Relative abundance	M-30 Total ionization (%)
Azacyclopentane	15.8	3.4	22.4	4.8
Azacyclohexane	68.5	7.4	51.5	5.6
Azacycloheptane	57.3	10.1	8.0	1.4
Azacyclooctane	12.3	1.3	74.3	8.1
Azacyclononane	2.2	0.28	100	12.7
3-Azabicyclo[3.2.2]nonane	58.3	4.1	23.4	1.6
Camphidine	69.4	5.4	19.7	1.5

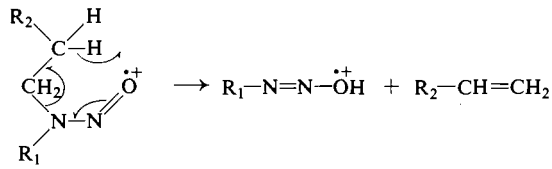

SCHEME 2

hydrogen abstraction has also been observed in the McLafferty rearrangement of ketones (11). The loss of •OH from *N*-nitrosodimethylamine is very small since this requires breakage of a stronger C—H bond as well as a strained five-membered ring process with transfer of a primary hydrogen. Since submission of this paper, a communication (12) has appeared on the dialkyl-*N*-nitrosamine molecular ion loss of •OH employing ion cyclotron resonance.

In the cyclic cases (see Table 2), *N*-nitrosoazacyclopentane (**1**, $n = 1$) shows very little •OH loss, perhaps a reflection of the geometrical restraints on hydrogen transfer by a five-membered process. We can also support a similar mechanism for loss of •OH for *N*-nitrosoazacyclohexane (**1**, $n = 2$), but in this more flexible system the oxygen can approach the hydrogen to be transferred much more readily (13). The loss of •OH from *N*-nitrosoazacycloheptane (**1**, $n = 3$) is fairly efficient (1.1% T.I.) since the medium ring system is more flexible and a six-membered arrangement is possible. The loss of •OH from *N*-nitrosoazacyclooctane (**1**, $n = 4$) and *N*-nitrosoazacyclononane (**1**, $n = 5$) (0.41 and 0.31% T.I. respectively) is not as large as anticipated for these more flexible systems, a possible reason being the higher efficiency of competing reactions.

From examination of the molecular models of *N*-nitrosocamphidine and *N*-nitroso-3-azabicyclo[3.2.2]nonane, it appears that tertiary hydrogen abstraction via a six-membered process is unlikely, thus the large M-OH peaks (0.64 and 0.60% T.I. respectively) probably result from secondary hydrogen abstraction (α to the amine nitrogen). If we extrapolate from the ground state molecular models to the excited state, the ease of hydrogen abstraction becomes apparent since in the case of *N*-nitrosoazacyclopentane and *N*-nitrosoazacyclohexane a five-membered ring process cannot attain coplanarity whereas in *N*-nitrosocamphidine and *N*-nitroso-3-azabicyclo-[3.2.2]nonane such a process is readily obtained. The planar process **4** is more efficient because it has a shorter oxygen to α-hydrogen distance which appears to be the critical factor in hydrogen atom transfer (13).

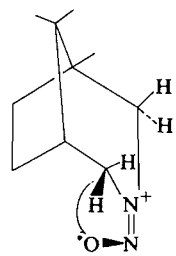

4

Loss of •NO

The accurate mass measurements (Table 1) indicate that the M-30 peak of three of the cyclic *N*-nitrosamines was due to the expected molecular ion loss of •NO. The ability to lose •NO (Table 3, % T.I. column) would be expected to indicate the relative strengths of the N—N bond. A large M-NO peak would indicate a weaker N—N bond and predominance of resonance form **5** while a small M-NO peak would indicate a stronger N—N bond and a larger contribution from resonance form **6**. In a similar manner the

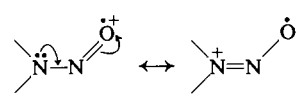

5 **6**

Can. J. Chem. Downloaded from www.nrcresearchpress.com by 210.87.254.105 on 09/05/12
For personal use only.

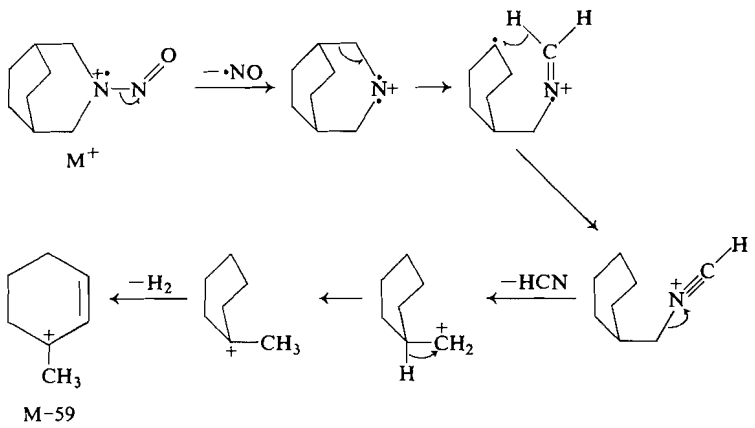

SCHEME 3

METASTABLE PEAKS

TRANSITION	m^*_{calcd}	m^*_{obs}
128 → 111	96.26	96.2
128 → 98	75.03	75.05

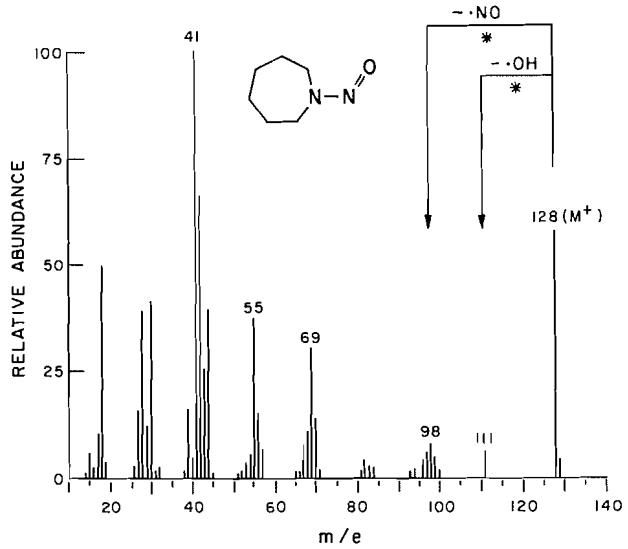

FIG. 1. The mass spectrum of *N*-nitrosoazacycloheptane.

size of the molecular ion and M-17 peaks should also be indicative of the N—NO bond strength. Consideration of the size of the M^+, M-17, and M-30 peaks in Tables 2 and 3 suggests that stronger N—NO bonds are present in *N*-nitrosoazacycloheptane, *N*-nitroso-3-azabicyclo[3.2.2]-nonane, and *N*-nitrosocamphidine. The possibility of differing contributions from **5** and **6** influencing the fragmentation pattern is supported by the observation that a small M-30 peak is accompanied by a large M-17 peak and *vice versa*.

Accurate mass measurement on the M-32 peak of *N*-nitrosoazacyclopentane indicated loss of H_2NO. Metastable peaks confirmed molecular ion loss of ·NO and then H_2.

M-59 Peak of N-Nitroso-3-azabicyclo[3.2.2]-nonane (3)

The accurate mass measurement (Table 1) on the M-59 peak of *N*-nitroso-3-azabicyclo[3.2.2]-nonane indicated molecular ion loss of CH_3N_2O. Metastable peaks suggested fragmentation by loss

Can. J. Chem. Downloaded from www.nrcresearchpress.com by 210.87.254.105 on 09/05/12
For personal use only.

of •NO, HCN, then H_2 in sequence. A possible process resulting in a stable allylic cation as the final M-59 fragment is illustrated in Scheme 3 (*cf.*, however, footnote 2). Metastable peak analysis also indicated a similar fragmentation process for *N*-nitrosoazacyclopentane, *N*-nitrosoazacyclohexane, and *N*-nitrosoazacycloheptane.

Other Fragments

It would not be opportune to discuss other fragments deeply but in this series there are some general similarities which would bear further study.

The base peak varies from compound to compound but in all spectra intense peaks were present at *m/e* 41, 42 (possibly $CH_2{=}N^+{=}CH_2$ (5)), and 55. Very few similarities to the parent amine spectra were noted (9).

Experimental

The *N*-nitrosamines were prepared by nitrosation of the parent amine with HNO_2 made *in situ* (14, 15) and showed all requisite spectral and analytical properties for the structures quoted. The mass spectra were determined with an Atlas CH 4 mass spectrometer operating at 70 eV and a source temperature of 180–250 °C. Most of the spectra were repeated on both an AEI MS-12 and a Thomson–Houston mass spectrometer. The mass spectra are available from the Depository of Unpublished Data, National Science Library, National Research Council of Canada, Ottawa, Canada. A typical mass spectrum of a cyclic *N*-nitrosamine is shown in Fig. 1. Accurate mass measurements were determined on an AEI MS-902 mass spectrometer by interpolation using an internal fluorinated mass marker with an error of less than 10 p.p.m. unless otherwise indicated.

We thank the National Research Council of Canada for generous financial assistance (grant in aid J.W.A. and study leave J.D.C.). J.W.A. thanks the administrators of the C. D. Howe Foundation for a fellowship, Professors Ourisson, Institut de Chimie, Strasbourg, France, and G. W. Kenner, University of Liverpool, Liverpool, England, for their hospitality and use of facilities. Mr. J. Barclay and his associates, University of Liverpool, kindly obtained the accurate mass measurements. Dr. R. F. Pottie, Division of Chemistry, National Research Council of Canada, Ottawa, Canada, is thanked for the Atlas CH 4 mass spectra and many helpful discussions.

1. J. COLLIN. Bull. Soc. Roy. Sci. Liège **23**, 201 (1954).
2. S. S. DUBOV and A. M. KHOKHLOVA. Zhur. obshchei Khim. **34**, 1961 (1964).
3. G. SCHROLL, R. G. COOKS, P. KLEMMENSEN, and S. O. LAWESSON. Ark. Kemi, **28**, 413 (1967).
4. T. AXENROD and G. W. A. MILNE. Chem. Commun. 67 (1968).
5. H. BUDZIKIEWICZ, C. DJERASSI and D. H. WILLIAMS. Mass spectrometry of organic compounds. Holden-Day, Inc., San Francisco, California, 1967. p. 329.
6. J. H. BEYNON, R. A. SAUNDERS and A. E. WILLIAMS. The mass spectra of organic molecules. Elsevier Publishing Co., New York, N.Y., 1968. p. 346.
7. N. M. M. NIBBERING, TH. J. DE BOER, and H. J. HOFMAN. Rec. Trav. Chim. **84**, 481 (1965).
8. F. W. MCLAFFERTY. Interpretation of mass spectra. W. A. Benjamin Inc., New York, N.Y., 1966. p. 123.
9. J. D. COONEY. M.Sc. Thesis. Carleton University, Ottawa, Canada, 1970.
10. S. W. BENSON. J. Chem. Ed. **42**, 502 (1965).
11. H. BUDZIKIEWICZ, C. FENSELAU, and C. DJERASSI. Tetrahedron **22**, 1391 (1966).
12. S. BILLETS, H. H. JAFFÉ, and F. KAPLAN. J. Amer. Chem. Soc. **92**, 6964 (1970).
13. C. DJERASSI, G. VON MUTZENBECHER, J. FAJKOS, D. H. WILLIAMS, and H. BUDZIKIEWICZ. J. Amer. Chem. Soc. **87**, 817 (1965).
14. H. H. HART. Organic syntheses. Coll. Vol. II. John Wiley and Sons Inc. New York, N.Y., 1943. p. 211.
15. S. MARBURG. J. Org. Chem. **30**, 2834 (1965).

Can. J. Chem. Downloaded from www.nrcresearchpress.com by 210.87.254.105 on 09/05/12
For personal use only.

Can. J. Chem. Downloaded from www.nrcresearchpress.com by 210.87.254.5 on 09/05/12
For personal use only.

Quelques imino-4 thiophènes particulièrement stables[1]

RÉAL LALIBERTÉ ET GEORGES MÉDAWAR
Département de Chimie, Laboratoires de Recherche Ayerst, Montréal, Québec

Reçu le 1 décembre, 1970

La réaction des dérivés sodés d'hydrazides des acides amino-3 cyano-2 mercapto-3 acryliques avec certains dérivés halogénés a donné des dérivés imino-4 thiophènes stables que nous avons caractérisés à l'i.r., à l'u.v., et au r.m.n.

Reaction between sodium salts of 3-amino-2-cyano-3-mercapto acrylhydrazides and two halocompounds resulted in the formation of some 4-iminothiophenes that were found to be quite stable. Their i.r., u.v., and n.m.r. spectra are described here together with one of their tautomeric forms obtained after acetylation.

Canadian Journal of Chemistry, **49**, 1372 (1971)

Introduction

Dans une publication récente (1) nous avons suggéré la formation d'imino-4 thiophènes se réarrangeant rapidement en amino-4 thiophènes lors de la réaction de dérivés sodés d'hydrazides des acides amino-3 cyano-2 mercapto-3 acryliques (**3**) avec des α-halocétones pour donner des hydrazides d'acides diamino-2,4 acyl-5 thiophène carboxyliques-3. Ces aminothiophènes sont d'une grande stabilité et leur examen à l'i.r. et au r.m.n. n'a pas permis de déceler de forme imine tautomérique soit en position 4 soit en position 2. La possibilité qu'ont ces amines de former des ponts hydrogènes avec les carbonyles adjacents ainsi que la contribution des azotes à l'aromaticité du thiophène nous ont semblé suffisant pour expliquer la grande stabilité du système. Comme la synthèse décrite est très souple et permet de modifier ces thiophènes nous avons essayé de dissocier ces deux facteurs pour évaluer leur importance relative. C'est ainsi que nous avons réussi à éliminer l'un des carbonyles et à obtenir quelques molécules aussi stables que les premières mais sous une forme différente.

Synthèse

La réaction de l'isothiocyanate de phényle (**1**) avec les hydrazides de l'acide cyano-2 acétique (**2**) en présence d'un équivalent d'éthylate de sodium dans l'éthanol donne les dérivés sodés d'hydrazides des acides amino-3 cyano-2 mercapto-3 acryliques (**3**) utilisés *in situ* comme produit de départ (schéma 1). Ils réagissent avec un dérivé halogéné convenable pour donner des thiophènes portant en 5 soit un groupe méthyle **12** soit un groupe phényle **8**. Dans le premier cas on fait réagir le dérivé sodé **3** avec un peu moins d'un équivalent de bromo-3 butanone dans l'éthanol sous reflux pendant quelques heures. La condensation s'accompagne de l'élimination du groupe acétyle de telle sorte qu'on obtient directement l'hydrazide de l'acide anilino-2 dihydro-4,5 imino-4 méthyl-5 thiophène carboxylique-3 (**12**) après addition sur le nitrile du carbanion **11** formé dans les conditions utilisées.

Pour introduire un groupe phényle on fait réagir le produit de départ **3** avec l'α-bromophénylacétate d'éthyle (**4**). Dans ce cas il n'y a pas d'élimination spontanée de la fonction ester de sorte qu'on obtient après addition sur le nitrile du carbanion **6** un imino-4 thiophène disubstitué en position 5 ne pouvant pas se tautomériser. L'acide chlorhydrique à 20% à chaud provoque l'élimination de la fonction ester pour donner l'hydrazide de l'acide anilino-2 dihydro-4,5 imino-4 phényl-5 thiophène carboxylique-3 (**8**) après addition de carbonate de sodium et extraction avec l'acétate d'éthyle.

Il est à noter que dans ce cas il n'y a pas hydrolyse du groupe hydrazide ou de la fonction imine. Celle-ci est donc très stable. Elle a aussi résisté à plusieurs essais d'acétylation avec l'anhydrique acétique. Cependant l'anhydride de l'acide trifluoracétique forme un trifluoracétamide en position 4 avec déplacement de la double liaison vers le cycle, pour donner un thiophène aromatique. Dans ce cas il y a simultanément formation de l'amide trifluoré du groupe aniline en 5 et le produit que l'on obtient est en fait le méthyl-5(*N*-phényltrifluoracéta-

[1]Ce travail a été exécuté grâce au Programme d'Aide à la Recherche Industrielle du Conseil National de Recherches du Canada.

Can. J. Chem. Downloaded from www.nrcresearchpress.com by 210.87.254.5 on 09/05/12
For personal use only.

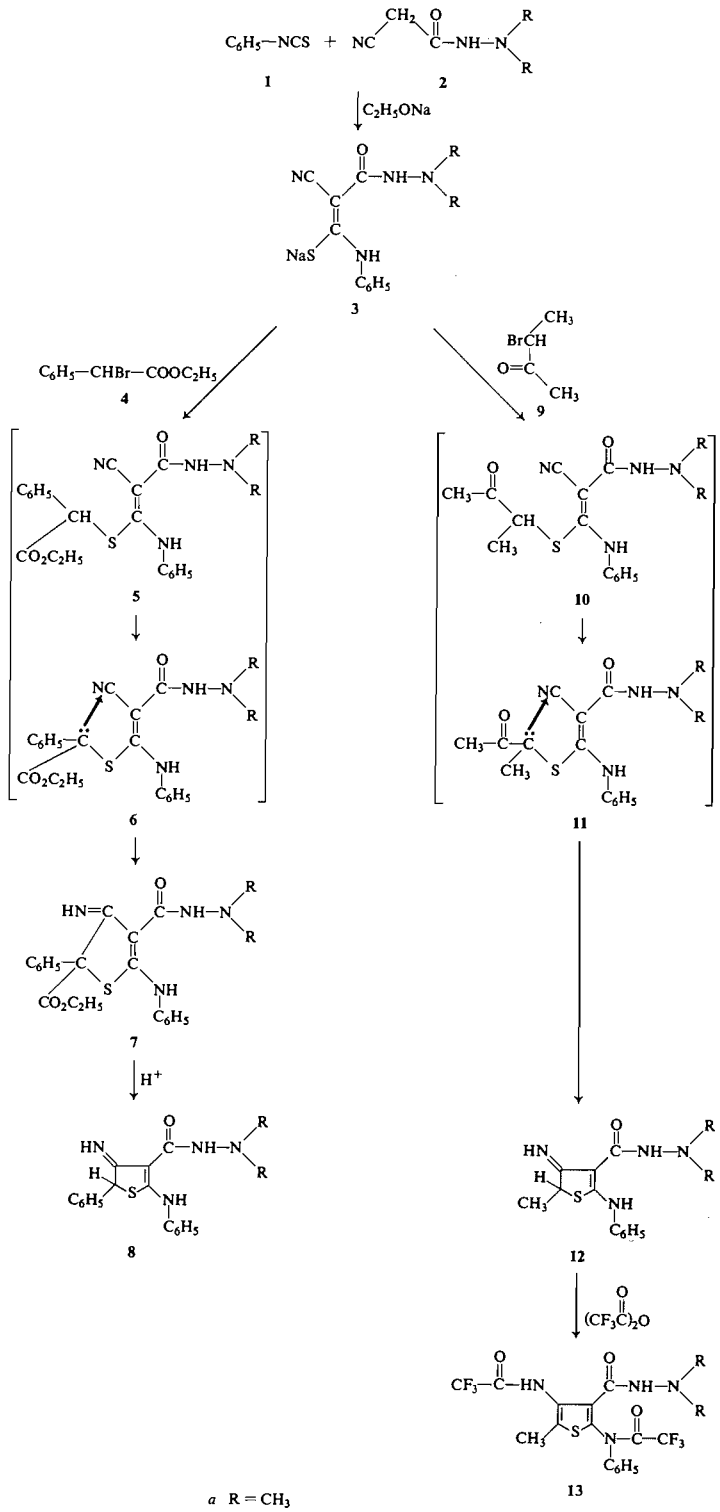

a R = CH_3

b R + R = $-CH_2-CH_2-CH_2-CH_2-CH_2-$

SCHÉMA 1. Synthèse d'imino-4 thiophènes

Can. J. Chem. Downloaded from www.nrcresearchpress.com by 210.87.254.5 on 09/05/12
For personal use only.

TABLEAU 1. Données i.r.* et r.m.n.† des imino-4 thiophènes

	NH Imine		NH Amide		NH Amine		O=C Ester	O=C Amide	H-5	R_1
	i.r. (cm^{-1})	r.m.n. (H_3 fine, éch.)	i.r. (cm^{-1})	r.m.n. (éch.)	i.r. (cm^{-1})	r.m.n. (éch.)	i.r. (cm^{-1})	i.r. (cm^{-1})	r.m.n.	r.m.n.
7a	3470	640	3250	420–450	3180	340–380	1725	1635		$2CH_3$ 164 (1)
7b	3470	640	3250	560–590	3170	330–370	1725	1635		$3CH_2$ 70–120
8a	3470	640(1)	3265	561	3220	320		1635	310 singulet	$2CH_3$ 159 (1)
12a	3485	643(1)	3340	568	3270	385		1630	252 quadruplet $J = 7$	CH 95 doublet $J = 7$ $N(CH_3)_2$ 158 singulet
12b	3310	620	3160	540	3120	480		1630	250 quadruplet $J = 7$	CH_3 80 doublet $3CH_2$ 70–100 $2CH_2$ 150–160

*L'i.r. dans $CHCl_3$ sauf ***12b*** dans le Nujol.
†Le r.m.n. dans $CDCl_3$ sauf ***12b*** dans le DMSO. Echanges avec D_2O.

Can. J. Chem. Downloaded from www.nrcresearchpress.com by 210.87.254.5 on 09/05/12
For personal use only.

mido)-2 trifluoracétamido-4 *N*-pipéridinothiophène carboxamide-3 (**13**).

Spectroscopie

L'aromatisation du système que l'on vient de décrire confirme la structure des iminothiophènes. On obtient des indications additionnelles en examinant les spectres i.r. et de r.m.n. des produits décrits dans le tableau 1.

On y voit immédiatement que l'i.r. dans le $CHCl_3$ montre une bande imine caractéristique à $3480 \pm 10\ cm^{-1}$. Cette bande est fine et peut être repérée facilement. On notera qu'elle est la même pour les produits **7***a* et **7***b* dont la structure est évidente et les imines **8***a* et **12***a*. On trouve aussi dans l'i.r. les deux bandes NH amides à 3340–3250 et 3270–3170 cm^{-1} ainsi que les bandes carbonyles à $1632 \pm 3\ cm^{-1}$. Le spectre du produit **12***b* a été fait dans le Nujol et présente des caractéristiques normales pour ce milieu. Les spectres de r.m.n. montrent une bande à 640–620 Hz attribuée à l'imine et deux bandes amines entre 560–420 et entre 385 et 320 Hz. Toutes les trois sont faciles à reconnaître parce qu'elles sont échangeables ce qui permet d'établir avec certitude le nombre de NH réel. La formation du trifluoracétamide modifie ce tracé et ce produit **13** montre deux bandes amides à 650 et 535 Hz. De plus l'imide **8***a* montre un singulet à 310 Hz pour H-5 et les imines **12***a* et **12***b* montrent chacune un quartet à 250–252 Hz ($J = 7$). Ce couplage ne peut s'expliquer que par la structure proposée.

Conclusion

Il est donc évident que l'équilibre imine–amine en -4 auquel nous avons fait allusion plus haut est possible comme le démontre les formes extrêmes **12** et **13** que nous décrivons ici. Il est tout aussi évident que l'aromaticité du thiophène est un facteur secondaire contribuant à la stabilité de ces molécules vu que des produits comme **8***a* et **12***a* n'existent que sous la forme imine non-aromatique. Ceci est d'autant plus surprenant que l'on pourrait s'attendre à ce que la présence d'un phényle en -5 favorise la forme amine en ajoutant à la conjugaison comme semblent le faire certains carbonyles déjà décrits (1).

Partie expérimentale

Remarques générales

Les spectres i.r. sont faits dans le $CHCl_3$ sur spectrophotomètre Perkin–Elmer 225. Les spectres u.v. sont pris dans l'éthanol sur spectrophotomètre Perkin–Elmer 350. Les spectres de r.m.n. ont été enregistrés sur un appareil Varian A-60-A en utilisant le tétraméthylsilane comme référence interne. Les positions sont exprimées en Hz. Les points de fusion sont pris au microscope chauffant Reichert.

N,N-Diméthylhydrazide de l'acide cyano-2 acétique (2a)

Nous avons utilisé les conditions décrites par Howard *et al.* (2).

Cyano-2 N-pipéridino acétamide (2b)

On laisse à température ambiante un mélange équimoléculaire de cyano-2 acétate d'éthyle et d'amino-1 pipéridine. Après 4 jours on filtre le solide obtenu et on le cristallise de l'isopropanol. On obtient ainsi un solide jaunâtre (65%) fondant à 131–132°. A l'i.r. il montre des bandes à 3210, 3080, 2260, et 1670 cm^{-1}.

Anal. Calc. pour $C_8H_{13}N_3O$: C, 57.46; H, 7.84; N, 25.13. Trouvé: C, 57.48; H, 7.88; N, 25.25.

Sel de sodium du N,N-diméthylhydrazide de l'acide anilino-3 cyano-2 mercapto-3 acrylique (3a)

On ajoute un équivalent du *N,N*-diméthylhydrazide de l'acide cyano-2 acétique **2** à une solution refroidie de sodium (0.1 mol) dans 300 ml d'éthanol sec. On ajoute ensuite un équivalent d'isothiocyanate de phényle et on chauffe la solution sous reflux pendant 1 h.

Sel de sodium de l'anilino-3 cyano-2 mercapto-3 N-pipéridinoacrylamide (3b)

On le prépare comme ci-haut en utilisant le cyano-2 *N*-pipéridino acétamide **2***b*.

N,N-Diméthylhydrazide de l'acide anilino-2 carbéthoxy-5 imino-4 phényl-5 dihydro-4,5 thiophène carboxylique-3 (7a)

On ajoute à la solution dans l'éthanol du sel de sodium **3***a* un peu moins d'un équivalent de α-bromophénylacétate d'éthyle **4** et on chauffe pendant 1 h. On acidifie avec quelques ml d'acide acétique puis on filtre. On évapore l'éthanol, on reprend à l'acétate d'éthyle puis on lave. On évapore à nouveau et on reprend dans l'isopropanol pour obtenir un solide que l'on précipite du benzène par addition d'hexane et que l'on cristallise du benzène seul. Il est blanc (45%) et fond à 83–85°. A l'i.r. il montre l'ester à 1725 cm^{-1} et une bande intense à 1578 cm^{-1}. L'u.v. montre un maximum à 305 (ε 19 700). Le groupe $N(CH_3)_2$ parait à 164 Hz dans le r.m.n.

Anal. Calc. pour $C_{22}H_{24}N_4O_3S$: C, 62.25; H, 5.70; N, 13.20; S, 7.50. Trouvé: C, 61.91; H, 5.79; N, 12.83; S, 7.55.

Anilino-2 carbéthoxy-5 dihydro-4,5 phényl-5 thiophène N-pipéridinocarboxamide-3 (7b)

On le prépare comme 7*a* en utilisant le dérivé sodé **3***b*. On le précipite du benzène par addition d'hexane et on le cristallise du méthylcyclohexane. Le solide blanc (35%) fond à 101–103°. L'i.r. montre l'ester à 1725 et une bande intense à 1575 cm^{-1}. L'u.v. montre un maximum à 300 (ε 19 200).

Anal. Calc. pour $C_{25}H_{28}N_4O_3S$: C, 64.64; H, 6.08; N, 12.06; S, 6.88. Trouvé: C, 64.94; H, 5.83; N, 12.28; S, 6.67.

N,N-Diméthylhydrazide de l'acide anilino-2 dihydro-4,5 imino-4 phényl-5 thiophène carboxylique (8a)

On obtient en traitant 3 g de 7*a* par 60 ml d'acide

chlorhydrique à 20% sous reflux pendant 2 h. On neutralise avec Na_2CO_3 et on reprend à l'acétate d'éthyle. Après lavage on évapore le solvant et on cristallise le résidu du benzène et de l'isopropanol. C'est un solide blanc (75%) qui fond à 191–193°. L'i.r. montre une bande intense à 1575 cm^{-1}. L'u.v. donne un maximum à 291 (ε 20 000). Le r.m.n. donne un singulet à 159 Hz pour le $N(CH_3)_2$.

Anal. Calc. pour $C_{19}H_{20}N_4OS$: C, 64.76; H, 5.72; N, 15.90; S, 9.08. Trouvé: C, 64.98; H, 6.24; N, 15.94; S, 8.96.

*N,N-Diméthylhydrazide de l'acide anilino-2 dihydro-4,5 imino-4 méthyl-5 thiophène carboxylique-3 (**12a**)*

On l'obtient en gardant sous reflux pendant 2 h le dérivé sodé **3***a* avec un peu moins d'un équivalent de bromo-3 butanone. On refroidit, on ajoute un peu d'acide acétique et on évapore. On dissout le résidu dans l'acétate d'éthyle, on lave, on sèche, et on évapore. On cristallise le produit du benzène et de l'isopropanol. Le solide est blanc (45%) et fond à 197–200°. L'u.v. montre un maximum à 289 (ε 21 350).

Anal. Calc. pour $C_{14}H_{18}N_4OS$: C, 57.92; H, 6.25; N, 19.30; S, 11.01. Trouvé: C, 57.97; H, 6.40; N, 19.07; S, 10.81.

*Anilino-2 dihydro-4,5 imino-4 méthyl-5 thiophène N-pipéridinocarboxamide (**12b**)*

On l'obtient en gardant sous reflux pendant 2 h le dérivé sodé **3***b* avec un peu moins d'un équivalent de bromo-3 butanone. On refroidit, on ajoute un peu d'acide acétique et on évapore. On dissout le résidu dans l'acétate d'éthyle, on lave puis on évapore à nouveau pour obtenir un solide jaune qu'on lave avec de l'isopropanol, et que l'on cristallise du méthanol. Il est blanc (55%) et fond à 275°. L'u.v. donne un maximum à 280 (ε 22 800).

Anal. Calc. pour $C_{17}H_{21}N_4OS$: C, 61.80; H, 6.39; N, 16.96; S, 9.84. Trouvé: C, 61.95; H, 6.37; N, 17.10; S, 9.72.

*Méthyl-5 (N-phényl trifluoracétamido)-2 trifluoracétamido-4 thiophène N-pipéridinocarboxamide (**13b**)*

On laisse à température ambiante pendant 5 h l'imino-4 thiophène **12***b* (0.03 mol) et 50 ml d'anhydride trifluoracétique. On filtre le solide qui se forme, on le lave à l'éther puis on le cristallise de l'isopropanol. Il a été nécessaire de sublimer l'échantillon analytique. Le solide est blanc (70%) et fond à 221–224°. L'u.v. montre un maximum à 330 (ε 1100).

Anal. Calc. pour $C_{21}H_{20}F_6N_4O_3S$: C, 48.27; H, 3.86; S, 6.14. Trouvé: C, 47.25; H, 3.99; S, 6.37.

1. R. Laliberté et G. Médawar. Can. J. Chem. **48**, 2709 (1970).
2. E. G. Howard, R. V. Lindsay, et C. N. Theobald. J. Amer. Chem. Soc. **81**, 4355 (1959).

Can. J. Chem. Downloaded from www.nrcresearchpress.com by 210.87.254.5 on 09/05/12
For personal use only.

Can. J. Chem. Downloaded from www.nrcresearchpress.com by 210.87.254.5 on 09/05/12
For personal use only.

Ion Association Effects on Nuclear Magnetic Resonance Parameters of Aromatic Ions. II. The Anions of Carbazole and 4,5-Methylenephenanthrene[1]

RICHARD H. COX
Department of Chemistry, University of Georgia, Athens, Georgia 30601

Received November 2, 1970

The ^1H n.m.r. spectra of carbazole nitranion, 4,5-methylene- and 9,10-dihydro-4,5-methylenephenanthrene carbanions with various alkali metal cations have been analyzed in terms of chemical shifts and coupling constants. Chemical shifts of the anions depend upon cation and solvent and are related to the type of ion pairs present. The ^7Li n.m.r. data indicate that Li is associated with the nitrogen of carbazole nitranion whereas with the 4,5-methylenephenanthrene carbanions, Li appears to be located in the π-cloud of the anions and associated equally with all carbons in the anion. The results are discussed in terms of the types of ion pairs present and the association of cation with anion.

On a analysé les spectres r.m.n. de proton du nitranion du carbazole et des carbanions des méthylène-4,5 et dihydro-9,10 méthylène-4,5 phénanthrènes en présence de divers cations de métaux alcalins et l'on a pu évaluer les déplacements chimiques et les constantes de couplage. Il a été démontré que les déplacements chimiques des anions varient avec le cation et le solvant et sont reliés avec le type de paires d'ions présents. Les données concernant les spectres r.m.n. du ^7Li indiquent que le Li est associé avec l'azote du nitranion du carbazole tandis que dans le cas des carbanions des méthylène-4,5 phénanthrènes, il semble que le Li se trouve dans le nuage d'électrons π des anions et qu'il est associé également avec tous les carbones de l'anion. On discute les résultats en termes des types de paires d'ions qui sont présents et de l'association entre le cation et l'anion.

Canadian Journal of Chemistry, **49**, 1377 (1971)

Introduction

Of all the factors given by Schaefer and Schneider (2) which affect aromatic proton chemical shifts ion association effects have been the least investigated. The effect of counterion on the proton spectrum of the pyridinium cation was interpreted in terms of ion pair formation which reduces the π-electron polarization in the pyridinium ion (3). Although the effect of cation on the n.m.r. spectra of aromatic anions has been reported in a few cases, the results have not been discussed to any extent. Cation was reported to have no effect on the n.m.r. spectrum of triphenylmethyl carbanion (4). The protons of cyclopentadienyl (2) and cyclononatetraenyl (5) anions are more shielded with lithium than with other alkali metal cations. However, the protons of 1-phenylallyl anion are less shielded with lithium than with either sodium or potassium (6). In order to more clearly define the effect of counterion and ion association on chemical shifts of aromatic ions, we have undertaken an extensive investigation of the n.m.r. spectra of aromatic ions.

Recently, we reported the effect of cation and temperature on the proton n.m.r. spectrum of fluorenyl carbanion (1). In THF, the protons were found to be shielded in the order Li > Rb > K > Na. Furthermore, at -70 °C the spectrum of fluorenyl sodium became identical with that of fluorenyl lithium at room temperature. The effect of cation was interpreted in terms of polarization of charge in the aromatic anion by the cation. The anomalous shielding with lithium and the temperature dependence with sodium is consistent with a change in the type of ion pair formed with these cations. From the effect of cation, solvent, and temperature on the absorption spectrum of fluorenyl carbanion, Smid and co-workers (7, 8) have clearly shown that fluorenyl carbanion exists in solution in equilibrium with two types of ion pairs (contact and solvent-separated). Since the n.m.r. results are consistent with the absorption data, we suggested that n.m.r. spectroscopy may be used to study ion pairing of aromatic anions. Recently, we have learned of another investigation where n.m.r. has been used to study equilibrium between ion pairs of similar carbanions. It appears, on the basis of n.m.r. shifts and their behavior with cation and temperature, that carbanions may be divided into three classes: (*1*) those which exist as solvent-separated ion pairs, (*2*) those which exist as contact ion pairs, and

[1]For Part I, see ref. 1.

(*3*) those which exist as rapidly equilibrating mixtures of contact and solvent-separated ion pairs (9).

We have extended our previous investigations and wish to report the effect of cation and solvent on the n.m.r. parameters of the anions of carbazole (**1**) and 4,5-methylenephenanthrene (**2** and **3**). The carbazole nitranion is of interest since it permits examination of possible differences in bonding between nitranions and carbanions with a given cation. Since the 4,5-methylenephenanthrene system forms both a $4n$ (**2**) and $4n + 2$ (**3**) π-electron anion upon alkali metal reduction (10), the relationship between the number of π-electrons in the anion and the effect of cation on the chemical shifts may be examined. The results are discussed in terms of bonding between cation and anion.

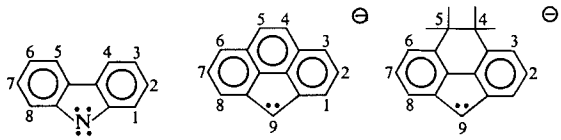

1 **2** **3**

Experimental

Carbazole and 4,5-methylenephenanthrene of commercial origin were used without further purification. Samples were prepared using vacuum-line techniques in the "onion-dome" cells as described previously (10). Solvents were stored over sodium benzophenone ketyl and were transferred to the n.m.r. tube under vacuum. A final concentration of 0.4 *M* for the starting hydrocarbon was used. Tetramethylsilane was added (3%) as internal reference and lock signal source. No impurity peaks were detected in any of the spectra of the starting hydrocarbons.

Proton n.m.r. spectra were obtained on a Varian Associates HA-100 spectrometer operating in the field-sweep mode. A probe temperature of 29 °C was used. Calibration of the spectra was by the usual frequency difference technique. Final line positions used in the calculation of the chemical shifts and coupling constants were obtained as the average of two upfield and two downfield scans. A scan width of 50 Hz was employed with a sweep time of 1000 s.

The ^{7}Li n.m.r. spectra were obtained on the HA-100 spectrometer operating in the HR mode at 38.8 MHz. Calibration of the spectra was by the usual side-band technique using an external reference of aqueous LiCl. The reported chemical shifts are the average of two upfield and two downfield scans. No attempt was made to correct the ^{7}Li chemical shifts for bulk susceptibility differences. Such effects are usually smaller than 0.1 p.p.m.

The *in situ* alkali metal reductions of carbazole and 4,5-methylenephenanthrene were carried out by allowing the respective hydrocarbon solution to remain in contact with the metal mirror until n.m.r. signals from either the methylene or N—H protons in the starting hydrocarbon were no longer detectable. At this point there was essentially complete conversion of the starting hydrocarbons to their respective anions. Both the phenanthrenide (**2**), and 9,10-dihydrophenanthrenide (**3**) anions are formed in each case with 4,5-methylenephenanthrene (11)[2] (Fig. 1). Carbazole nitranion is the only detectable anion in the reduction of carbazole (Fig. 2). Identical conditions (concentration and temperature) were used for the reductions of a given hydrocarbon so that with a given solvent, any differences in the spectra of the anions are due to the effect of cation.[3]

The proton n.m.r. spectra were analyzed in terms of chemical shifts and coupling constants with the aid of the computer program LAOCN3 (12). Chemical shifts were assigned on the basis of comparisons with the shifts of fluorenyl carbanion (1, 2) and substituted fluorenyl and carbazole anions (13). The chemical shifts are considered to be accurate to within ±0.1 Hz. Coupling constants for these anions have been previously reported (10). Neither cation nor solvent have any effect on the coupling constants within experimental error (±0.1 Hz).

Results and Discussion

Carbazole

The chemical shifts of carbazole nitranion are dependent upon the cation (Table 1). In THF, the protons are shielded in the order Rb > K > Na. With lithium as the counterion, carbazole nitranion was not soluble in THF at these concentrations. The order of shielding observed in THF is similar to that observed for fluorenyl (1) and 1-phenylallyl (6) carbanions. However, in the better cation-solvating solvent (14) DME, the protons are shielded in the reverse order (Li > Na > K). With potassium the chemical shifts are identical to within 1 Hz in both solvents.

Several features of the data in Table 1 are in contrast to those reported for fluorenyl carbanion (1). Firstly, the effect of cation on the shifts of fluorenyl carbanion was approximately identical

[2]Polarographic reduction of 4,5-methylenephenanthrene also produces both **2** and **3** (11).

[3]While it is true that solvent affects the ratio of ion pairs present in solution (7), there is no evidence to indicate that solvent affects the type of anions formed upon alkali metal reduction. In fact the n.m.r. spectra show that identical anions are formed in each case. The relative amounts of the two anions in the case of 4,5-methylenephenanthrene are dependent upon the solvent. With potassium, the ratio of **2** to **3** is 1.95:1 and 2.50:1 in THF and diethyl ether, respectively. This difference reflects the effect of solvent on the rate of proton transfer from 4,5-methylenephenanthrene to the 4,5-methylenephenanthrene radical anion (10).

Can. J. Chem. Downloaded from www.nrcresearchpress.com by 210.87.254.5 on 09/05/12
For personal use only.

Can. J. Chem. Downloaded from www.nrcresearchpress.com by 210.87.254.5 on 09/05/12
For personal use only.

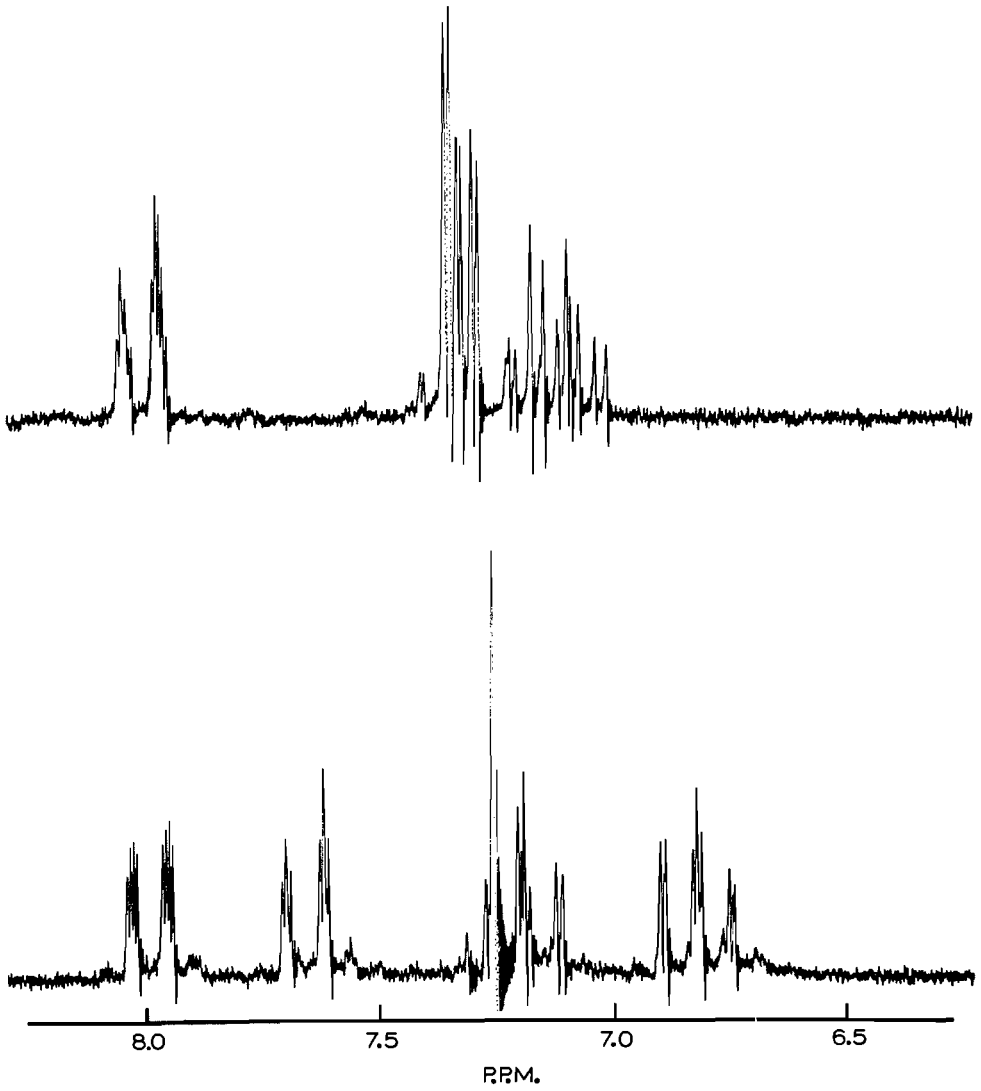

FIG. 1. Upper trace, the 100 MHz n.m.r. spectrum of 4,5-methylenephenanthrene in THF-d_8; lower trace, the 100 MHz n.m.r. spectrum of **2** and **3** with sodium in THF-d_8. The peaks at 1.7 and 3.5 p.p.m. are due to residual THF.

for all protons (~20 Hz). In THF, the total change in chemical shift with cation for the protons of carbazole nitranion is: H_1, 21; H_2, H_3, and H_4, 8 Hz. In DME the change is H_1, 23; H_2, 10; H_3 and H_4, 3 Hz. Secondly, the ^{7}Li chemical shift for fluorenyl lithium in diethyl ether was reported to be 6.2 p.p.m. upfield from an aqueous lithium chloride reference (15). The ^{7}Li chemical shift for lithium carbazole nitranion in DME is 0.13 p.p.m. downfield from lithium chloride. The differences in the observed ^{7}Li and ^{1}H shifts reflect the differences in the overall electronic structure of the carbanion and nitranion and hence, the bonding of cation to these two anions.

In the carbanion, the pair of electrons are in a p orbital and are delocalized throughout the carbon system. However, two pairs of electrons are donated to the system by nitrogen in the nitranion. The electronic structure about nitrogen in carbazole nitranion should be similar to that of pyrrole. Thus, a crude model for the electronic structure about nitrogen in carbazole nitranion

Can. J. Chem. Downloaded from www.nrcresearchpress.com by 210.87.254.5 on 09/05/12
For personal use only.

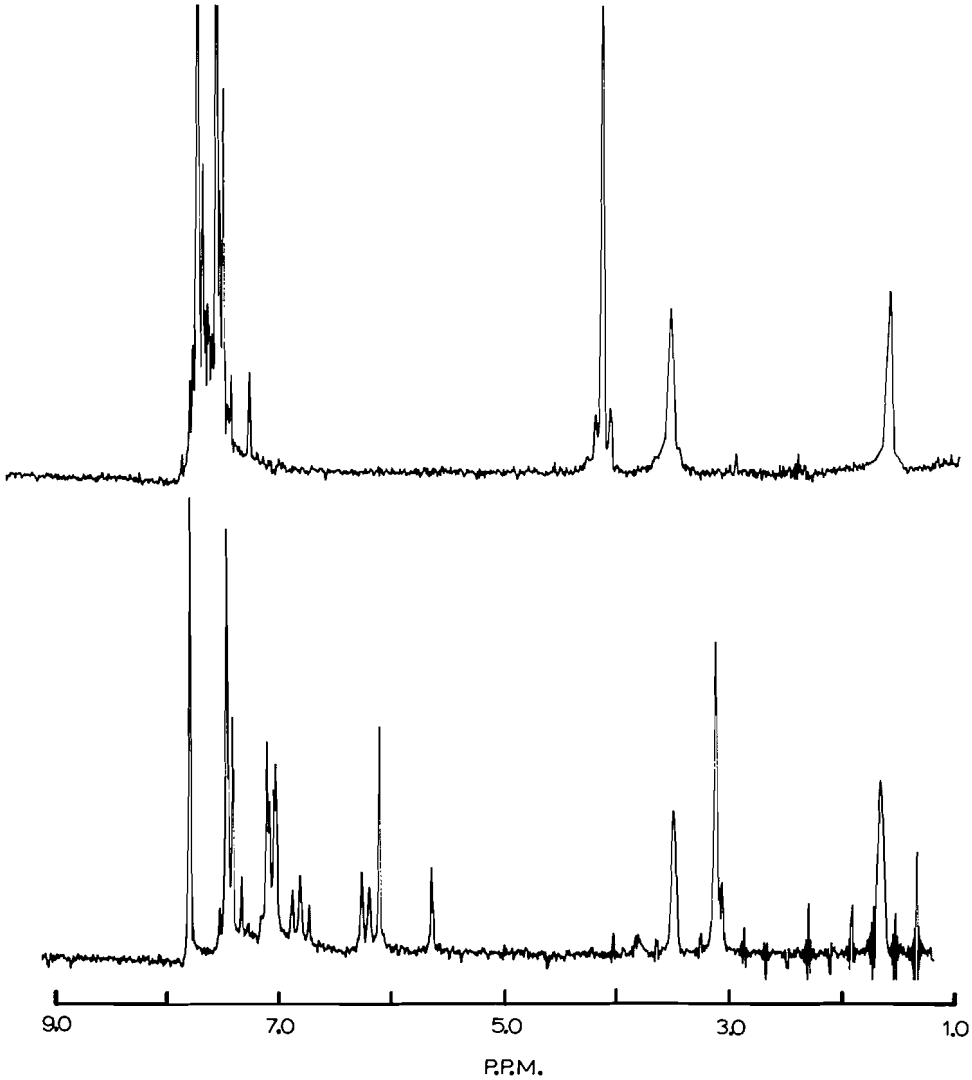

FIG. 2. Upper trace, the 100 MHz n.m.r. spectrum of carbazole in THF; lower trace, the 100 MHz n.m.r. spectrum of carbazole nitranion with sodium in THF. The sharp singlet at 7.24 p.p.m. is due to benzene impurity.

has one pair of electrons in a p orbital on nitrogen which are delocalized throughout the system and the second pair of electrons in an orbital (probably sp^2) orthogonal to the π-system. Using this model for the nitranion, one would expect the electrostatic interactions between carbazole nitranion and cation to be stronger than those between fluorenyl carbanion and cation. Furthermore, since the excess charge is located partially in a sigma orbital on nitrogen, the cation influences the chemical shifts of the six-membered ring protons largely through inductive effects which are thought to be attenuated rapidly and to be smaller than resonance or π-effects (16). The larger variation exhibited by H_1 with cation in the nitranion compared to the other protons is consistent with this model. The ^7Li chemical shift is also consistent with the above model. It was suggested with fluorenyl lithium that lithium was located in the π-cloud of the anion and hence, the upfield ^7Li shift was due to the shielding of the aromatic anion. The ^7Li shift observed for carbazole ni-

TABLE 1. The n.m.r. parameters of carbazole nitranion

Cation/ Solvent	$\nu_{1,8}$*	$\nu_{2,7}$	$\nu_{3,6}$	$\nu_{4,5}$	$J_{12,78}$†	$J_{13,68}$	$J_{14,58}$	$J_{23,67}$	$J_{24,57}$	$J_{34,56}$
H/THF‡	7.353	7.306	7.106	8.009	8.06	0.49	0.69	7.62	1.26	7.84
Na/THF	7.646	7.182	6.819	7.981	8.14	0.99	0.74	6.87	1.31	7.71
K/THF	7.596	7.152	6.755	7.947	8.09	1.08	0.74	6.86	1.37	7.63
Rb/THF	7.437	7.109	6.727	7.902	8.17	0.99	0.74	6.88	1.33	7.71
Li/DME§	7.362	7.043	6.715	7.889	8.19	0.94	0.73	6.86	1.33	7.69
Na/DME	7.416	7.057	6.713	7.896	8.16	1.01	0.76	6.85	1.33	7.67
K/DME	7.597	7.146	6.746	7.933	8.17	0.98	0.75	6.89	1.31	7.71

*In p.p.m. downfield from internal TMS.
†In Hz.
‡THF, tetrahydrofuran; this entry refers to neutral carbazole.
§DME, dimethoxyethane.

TABLE 2. The n.m.r. parameters for the carbanions of 4,5-methylenephenanthrene

Compound	Cation/Solvent	$\nu_{1,8}$*	$\nu_{2,7}$	$\nu_{3,6}$	$\nu_{4,5}$	ν_9
2	Li/THF-d_8†	7.347	7.281	6.932	7.657	6.023
	Na/THF	7.486	7.401	7.071	7.749	6.083
	K/THF-d_8	7.405	7.351	7.003	7.719	6.051
	Rb/THF-d_8	7.395	7.352	7.001	7.709	6.036
	K/Ether‡	7.478	7.464	7.093	7.776	5.971
3	Li/THF-d_8	6.952	6.690	6.111	3.026	5.516
	Na/THF	7.015	6.823	6.257	§	5.653
	K/THF-d_8	6.996	6.752	6.181	3.116	5.593
	Rb/THF-d_8	6.962	6.750	6.180	3.066	5.555
	K/Ether	7.037	6.902	6.328	§	5.482

*In p.p.m. downfield from internal TMS.
†Tetrahydrofuran.
‡Diethyl ether.
§Overlapping with solvent.

tranion suggests that lithium is strongly associated with nitrogen and is not located in the π-cloud of carbazole nitranion.

Even though the cation is associated with nitrogen, the degree of association is dependent upon both cation and solvent. In THF, the protons are shielded with cation in the order expected on the basis of polarizability of the cation (17). Since the chemical shifts of carbazole nitranion with potassium are identical in both THF and DME, the degree of association of potassium with nitrogen must be the same in both solvents (9). However, with sodium and lithium in DME, the protons of carbazole nitranion are more shielded, especially H_1, than with potassium indicating a difference in association of sodium and lithium with nitrogen than with potassium and nitrogen. On the basis of the shielding observed with cation and solvent (1, 9), it appears that contact ion pairs are formed in THF whereas with sodium and lithium in DME, an appreciable fraction of solvent-separated ion pairs are formed (18).

4,5-Methylenephenanthrene

The chemical shifts of both **2** and **3** are dependent upon the cation (Table 2) in a manner similar to that reported for fluorenyl carbanion (1). In THF, the protons of **2** and **3** are shielded in the order Li > Rb > K > Na. However, the effect of cation is smaller for **2** and **3** (~12 Hz) than for fluorenyl carbanion. From studies of the effect of temperature, cation, and solvent on the absorption spectrum of **2**, it was concluded that **2** forms both contact and solvent-separated ion pairs (19). The fraction of solvent-separated ion pairs in THF at 0° was reported to be: Li, 0.80; Na, 0.15; K, 0.0; and Cs, 0.0. Although the presence of **3** (10, 11) in solution was not considered by these investigators (18), their overall conclusions are probably correct.

The increased shielding observed for **2** and **3** with lithium, compared to the other cations, (Table 2) clearly indicates a larger separation between cation and anion (less distortion of charge in the anion) and is consistent with an appreciable

Can. J. Chem. Downloaded from www.nrcresearchpress.com by 210.87.254.5 on 09/05/12
For personal use only.

Can. J. Chem. Downloaded from www.nrcresearchpress.com by 210.87.254.5 on 09/05/12
For personal use only.

amount of solvent-separated ion pairs present in solution. With sodium the n.m.r. data are not consistent with the absorption data (19). At least three factors could be responsible for this difference: (*a*) the two investigations were conducted at different concentrations, (*b*) the two investigations were conducted at different temperatures, and (*c*) the n.m.r. data are characteristic of the average population in solution. It has been shown from u.v. data that the fraction of solvent-separated ion pairs is not dependent upon the concentration (10^{-2} to 10^{-3} *M*) (20). Similar studies of the n.m.r. spectrum of sodium triphenylmethanide over the concentration range of 1.5–7.6 $\times$ 10^{-1} *M* also show that concentration does not affect the ratio of ion pairs formed (9). Lowering the temperature causes a shift in the equilibrium which favors the solvent-separated ion pair (7, 8, 19). Therefore, it is reasonable that less than 15% of solvent-separated ion pairs are present in the present investigation since it was conducted at a higher temperature. The time scale for the interconversion between solvent-separated and contact ion pairs has been shown by e.s.r. studies on related radical anions (21, 22) to be of the order of 10^{-8} s. Therefore, the n.m.r. data represent the population average and hence, are probably characteristic of the contact ion pair present in greater concentration.

The effect of solvent on the chemical shifts of **2** and **3** with potassium was investigated. In the less basic solvent (14) diethyl ether, the protons of **2** and **3** are less shielded than in THF. Similar shifts to lower field upon changing to a less basic solvent have been observed for fluorenyl lithium (15) and 1-phenylallyl sodium and potassium (6). Since both **2** and **3** with potassium exists as contact ion pairs (19), the downfield shift reflects a decrease in ionic character of the anion–cation interaction upon changing to a less basic solvent.

The ^{7}Li n.m.r. spectra of **2** and **3** are quite revealing concerning the location of lithium with respect to the anions. In THF, the ^{7}Li chemical shift is 2.20 p.p.m. upfield from external aqueous lithium chloride. Furthermore, only a single peak is observed indicating that either there is fast exchange of lithium between the two carbanions relative to the n.m.r. time scale or the ^{7}Li shift is accidentally the same for **2** and **3**. The upfield ^{7}Li shift indicates that lithium is located in the π-cloud of the carbanions similar to fluorenyl lithium (15). Although the ^{1}H chemical shifts of **2** and **3** indicate that there is a greater attraction between cation and anion with sodium, potassium, and rubidium than with lithium, the observation that all protons of **2** and **3** are affected to approximately the same extent by cation indicates that sodium, potassium, and rubidium are also located in the π-clouds of the carbanions.

Concluding Remarks

The major difference in the bonding of cation to carbazole nitranion, compared to fluorenyl carbanion is the association of cation with nitrogen in **1**, whereas with fluorenyl carbanion the cation appears to be associated with all carbons in the molecule. Even though the cation is associated with nitrogen in **1**, the degree of association is both cation and solvent dependent. In DME, the results suggest that with lithium and sodium, carbazole nitranions form an appreciable fraction of solvent-separated ion pairs.

The results for the carbanions of 4,5-methylenephenanthrene (**2** and **3**) clearly show that the number of π-electrons has no effect on the type of ion pairs formed since the effect of cation is identical for both **2** and **3**. Furthermore, the results with sodium suggest that the fraction of solvent-separated ion pairs must be greater than 0.15 before deviations to the order of shielding with cation (1) will be observed.

Finally, the use of ^{7}Li n.m.r. to determine the locations of the cation with respect to the anion complements the proton data and allows a more complete picture to be drawn concerning the bonding between cation and anion and hence, the effect of ion association on n.m.r. chemical shifts.

The author wishes to thank Drs. J. F. Garst and E. G. Janzen, for many helpful discussions. This work was partially supported by a grant from the Petroleum Research Foundation administered by the American Chemical Society.

1. R. H. Cox. J. Phys. Chem. **73**, 2649 (1969).
2. T. Schaefer and W. G. Schneider. Can. J. Chem. **41**, 966 (1963).
3. G. Kotowycz, T. Schaefer, and E. Bock. Can. J. Chem. **42**, 2541 (1964).
4. V. R. Sandel and H. H. Freedman. J. Amer. Chem. Soc. **85**, 2328 (1963).
5. T. J. Katz and P. J. Garratt. J. Amer. Chem. Soc. **85**, 2852 (1963).
6. V. R. Sandel, S. V. McKinley, and H. H. Freedman. J. Amer. Chem. Soc. **90**, 495 (1968).

7. T. E. HOGEN-ESCH and J. SMID. J. Amer. Chem. Soc. **88**, 307, 318 (1966).
8. L. I. CHAN and J. SMID. J. Amer. Chem. Soc. **90**, 4654 (1968).
9. J. B. GRUTZNER, J. M. LAWLOR, and L. M. JACKMAN. Private communication.
10. R. H. COX, E. G. JANZEN, and J. L. GERLOCK. J. Amer. Chem. Soc. **90**, 5906 (1968).
11. J. JANATA, J. GENDELL, R. G. LAWTON, and H. B. MARK, JR. J. Amer. Chem. Soc. **90**, 5226 (1968).
12. A. A. BOTHNER-BY and S. M. CASTELLANO. Mellon Institute, Pittsburgh, Pa., 1966.
13. R. H. COX. J. Mag. Res. **3**, 223, (1970).
14. (*a*) J. F. GARST, C. HEWITT, D. WALMSLEY, and W. RICHARDS. J. Amer. Chem. Soc., **83**, 5034 (1961). (*b*) J. F. GARST, R. A. KLEIN, D. WALMSLEY, and E. R. ZABOLOTNY. J. Amer. Chem. Soc. **87**, 4080 (1965).
15. J. A. DIXON, P. A. GWINNER, and D. C. LINI. J. Amer. Chem. Soc. **87**, 1379 (1965).
16. For example, see H. SPIESECKE and W. G. SCHNEIDER. J. Chem. Phys. **35**, 731 (1961).
17. F. A. COTTON and G. WILKINSON. Advanced inorganic chemistry. Interscience Publishers, New York, N.Y., 1962. p. 157.
18. For a review of ion pairs see M. SZWARC. Accounts of Chem. Res. **2**, **87**, (1969) and references therein.
19. D. CASSON and B. J. TABNER. J. Chem. Soc. (B), 572 (1969).
20. T. E. HOGEN-ESCH and J. SMID. J. Amer. Chem. Soc. **87**, 669 (1965).
21. R. CHANG and C. S. JOHNSON. J. Amer. Chem. Soc. **88**, 2338 (1966).
22. N. HIROTA. J. Amer. Chem. Soc. **90**, 3603 (1968).

Can. J. Chem. Downloaded from www.nrcresearchpress.com by 210.87.254.5 on 09/05/12
For personal use only.

Can. J. Chem. Downloaded from www.nrcresearchpress.com by 210.87.254.42 on 09/05/12
For personal use only.

On the Reaction of *N*-Bromoacetamide with Olefins. Preparation and Chemistry of 2-Bromo-*N*-Bromoacetimidates, a New Class of Compounds[1]

SAUL WOLFE AND D. V. C. AWANG
Department of Chemistry, Queen's University, Kingston, Ontario

Received November 6, 1970

A historical and mechanistic review of the Wohl–Ziegler reaction (allylic bromination by *N*-bromoamides and imides) is presented as an introduction to the present work, a re-examination of the reaction of *N*-bromoacetamide (NBA) with some olefins. The reaction has been found to lead not to allylic bromination but, rather, to 2-bromo-*N*-bromoacetimidates, a new class of compounds. The stoichiometry of the reaction is: olefin + 2 NBA → adduct + acetamide. The process appears to occur in two stages, *viz.*, a free radical reaction of NBA with itself to form *N,N*-dibromoacetamide (NDBA), followed by ionic addition of NDBA to the double bond. Hofmann's synthesis of NDBA has been repeated; the compound reacts rapidly with cyclohexene to give the same adduct **10** as does NBA. A variety of stereochemical and selectivity data suggest that this is an ionic addition.

The chemical transformations of 2-bromo-*N*-bromoacetimidates under thermal, acidic, and basic conditions are discussed.

Comme introduction au présent travail qui est un réexamen de la réaction de la *N*-bromoacétamide avec quelques oléfines, nous présentons une revue historique et mécanistique de la réaction de Wohl–Ziegler (bromuration allylique par des *N*-bromoamides et imides). On a trouvé que la réaction ne conduit pas à la bromination allylique mais plutôt aux bromo-2 *N*-bromoacétimidates, une nouvelle classe de composés. La stoichiométrie de la réaction est: oléfine + 2 NBA → composé d'addition + acétamide. Le processus semble se produire en deux temps à savoir une réaction radicalique de la NBA sur elle-même pour conduire à la *N,N*-dibromoacétamide (NDBA) suivie d'une addition ionique de la NDBA à l'alcène. La synthèse de Hofmann de la NDBA a été repétée; ce composé réagit rapidement avec le cyclohéxène et conduit au produit **10** qui est aussi obtenu sous l'action de la NBA. La stéréochimie et la sélectivité de cette réaction suggèrent que l'addition est ionique.

On discute aussi des transformations chimiques que subissent les bromo-2 *N*-bromoacétamidates sous l'influence de la chaleur, des acides, et des bases.

Canadian Journal of Chemistry, 49, 1384 (1971)

Historical Introduction

In 1919, A. Wohl reported (1) that a mixture of 10 g of tetramethylethylene and 16 g of *N*-bromoacetamide (NBA), allowed to stand overnight in 36 ml of ether and then distilled, afforded in 16% yield a bromine-containing fraction, b.p. 60–90° at 15 mm. This liquid decolorized permanganate and contained 46.3% of bromine ($C_6H_{11}Br$ requires 49.0% bromine). A mixture of 50 g of trimethylethylene and 100 g of NBA, allowed to stand for one day and then vacuum distilled, afforded 10 g of an oil, b.p. 49–52.5° at 13.5 mm, which decolorized permanganate and contained 67.6% of bromine (C_5H_9Br requires 53.6%, and $C_5H_8Br_2$ requires 70.1% bromine). On the basis of these results, Wohl formulated the latter substance as an unsaturated dibromide, $C_5H_8Br_2$, and the product from tetramethylethylene as an unsaturated monobromide, $C_6H_{11}Br$, the reaction in this instance being described by eq. 1. A mechanism was proposed which involved exchange of bromine for an allylic hydrogen within a 1:1 olefin-NBA complex. The possibility that this complex

[1] $Me_2C{=}CMe_2 + CH_3CONHBr \rightarrow Me_2C{=}CMeCH_2Br + CH_3CONH_2$

might be an intermediate in an addition–elimination sequence was considered, and rejected on the grounds that HBr, rather than acetamide, ought to have been eliminated from such an adduct.

When equal amounts of NBA and trimethylethylene were mixed in ether at low temperature, the sparingly soluble NBA slowly dissolved and a viscous oil precipitated. The supernatant solution was then found to contain only traces of olefin and NBA. Wohl recognized that the viscous oil was an addition compound, but

[1]This work was presented, in part, at the 50th Canadian Chemical Conference, Toronto, Ontario, June 1967.

Can. J. Chem. Downloaded from www.nrcresearchpress.com by 210.87.254.42 on 09/05/12
For personal use only.

apparently believed that its formation was not related to the reactions which produced the unsaturated dibromide.

In a second paper in 1921 (2), Wohl and Jaschinowski extended this work to the substrates crotonic acid, ethyl β-ethoxycrotonate, ethyl β-ethoxycinnamate, propylene, allyl alcohol, allyl bromide, and methyl phenylacetylene. In each case the reactants were stirred in ether or acetone at room temperature or below until a negative starch–iodide test was obtained; products were then isolated by vacuum distillation and characterized by bromine analysis. Carbon and hydrogen analyses were recorded for the products from the enol ethers and from allyl alcohol. In all cases, the distilled sample subjected to analysis represented only a small fraction of an obviously complex mixture; in several cases the analytical data were not compatible with a simple molecular formula.

Wohl and Jaschinowski observed that 2 mol equiv of NBA reacted with 1 mol equiv of crotonic acid to produce a *mono*bromocrotonic acid. They also observed some yellow crystals in the reaction with propylene. Neither of these observations was followed up. Ethylene, acetylene, ethyl cinnamate, cinnamic acid, cinnamaldehyde, maleic acid, and fumaric acid did not react with NBA. Styrene gave styrene dibromide.

It is evident from this summary of Wohl's experimental work that, although some reaction does take place between certain olefins and NBA, unequivocal evidence for allylic bromination was not obtained. It is not surprising, therefore, that the next reference to this work appeared only in 1941 (3). An attempt to convert β-cyclogeranic acid to 3-bromo-β-cyclogeranic acid was not successful.

In 1942 (4), Ziegler and his co-workers presented the results of a systematic study, prompted by Wohl's work, of the reactions of alkenes with *N*-halo compounds. *N*-Bromoacetamide was not included in the study because "*die von Wohl mitgeteilten Ergebnisse auf einem nicht eben glatten Reaktionsverlauf schliessen lassen*". In Ziegler's work the unique ability of *N*-bromosuccinimide (NBS), in refluxing carbon tetrachloride, to effect allylic bromination was discovered and exploited. The synthetic implications of this discovery were very clear and, by 1948 (5), at least 100 examples had been reported. Djerassi's review, subtitled "The Wohl–Ziegler Reaction", left the impression that Wohl's work had been overlooked because of a failure to emphasize its practical implications, and the description "Wohl–Ziegler reaction" is taken to mean allylic bromination by *N*-bromoamides and imides, including NBA and NBS. Although allylic bromination by NBA has often been assumed since the appearance of the first review, in no case do the experimental descriptions indicate that an allylic bromide was ever isolated and characterized. Indeed, the work reported here was also founded on the assumption that allylic bromination by NBA does exist; and a close examination of Wohl's papers was not made until it had become clear (6) that this assumption is incorrect.

Introduction to the Present Work

That allylic bromination by NBS is a radical chain reaction is evident from the catalytic effect of peroxides, other radical sources, and u.v. light, the retarding properties of oxygen and other typical radical inhibitors (7), and kinetic studies (8). In allylic bromination of cyclohexene, initiated by decomposition of azobisisobutyronitrile (AIBN), the rate of disappearance of NBS is zero order in NBS, half order in AIBN and first order in olefin. This result is consistent with a succinimidyl radical chain and termination via two succinimidyl radicals. It is also consistent with a bromine atom chain and termination via two bromine atoms. The former pathway, proposed by Bloomfield in 1944 (9), was widely accepted for some time (7), but more recent work (10–13) has proved the latter process, first suggested by Goldfinger and his co-workers (14), to be the operative one.

The Goldfinger mechanism considers the elementary steps 2–5, where RH is an alkene. For low concentrations of X_2, the ratio of addi-

[2] $Br_2 \rightarrow 2Br\cdot$

[3s] $Br\cdot + HR \rightarrow HBr + R\cdot$ [3a] $Br\cdot + RH \rightarrow Br\dot{R}H$

[4s] $R\cdot + Br_2 \rightarrow RBr + Br\cdot$ [4a] $Br\dot{R}H + Br_2 \rightarrow BrRHBr + Br\cdot$

[5s] $R\cdot + HBr \rightarrow RH + Br\cdot$ [5a] $Br\dot{R}H \rightarrow RH + Br\cdot$

Can. J. Chem. Downloaded from www.nrcresearchpress.com by 210.87.254.42 on 09/05/12
For personal use only.

tion (a) to substitution (s) is given by eq. 6 so

[6] $$r_{a/s} = k_{3a} \cdot k_{4a}[Br_2] / k_{3s} \cdot k_{5a}$$

that addition would be favored by higher, and substitution by lower concentrations of Br_2. The function of NBS is two-fold: to maintain the required low concentration of Br_2 by reaction 7 (10); and, by serving as a scavenger for HBr, to maintain a non-polar medium.

[7] $$HBr + NBS \rightarrow Succinimide + Br_2$$

Two significant features of allylic bromination by NBS are that both NBS (15) and succinimide are virtually insoluble in CCl_4, the solvent of choice for the reaction, and that the rate of the reaction depends greatly upon the purity of the reagent and its surface area. High purity and/or the employment of large crystals lead to a reduction in the rate (8, 16). These facts have led Horner and Winkelmann to suggest (16) that the reaction takes place at the surface of the NBS, but an alternate explanation (8*a*) for the rate-diminishing effect of purification of the reagent is that this removes trace impurities which catalyze the adventitious formation of molecular bromine, and the surface mechanism is usually discounted (see *e.g.*, ref. 12*a*, footnote 28).

If the surface mechanism were unimportant, it could be expected that slow addition of a *solution* of NBS to an alkene might be equivalent to the usual heterogeneous reaction conditions. However, although addition to the double bond of cyclohexene is not detected under the heterogeneous conditions, when the reaction is performed in refluxing CH_2Cl_2 with slow addition of the NBS and catalysis by light and peroxides the conversion to dibromocyclohexane cannot be reduced to less than 25% (17).

Further, if there were no constraint upon the intermediates in the reaction, the mesomeric structure of an allyl radical should cause the product of kinetic control to be a mixture of two allyl bromides. In the case of a symmetrical substrate like cyclohexene-3,3,6,6-d_4 (**1**), the allyl radical will have structure **2**, and the products of kinetic control would be **3** and **4**, formed in equal amounts. It has been suggested, however, that an equimolar mixture of **3** and **4** is seen in the product of *thermodynamic* control, the product of kinetic control being mainly **3** (18). This result is not compatible with a "free" radical mechanism but might be compatible with a "trapped" radical if the surface mechanism were operative.

On the basis of the above results and considerations it appeared that Horner and Winkelmann's surface mechanism needed further examination. The approach selected involved repetition of the cyclohexene-3,3,6,6-d_4 experiment with NBA. It was assumed that NBA does effect allylic bromination and that the ratio of **3** to **4** in the product of kinetic control would differ from that given by NBS, either because NBA bromination affords a free radical, or because the surfaces of NBA and NBS are not the same. The choice of NBA for this study was also dictated by the fact that it, like NBS, is only slightly soluble in refluxing CCl_4 and was reported to effect allylic bromination in this medium (19–21).

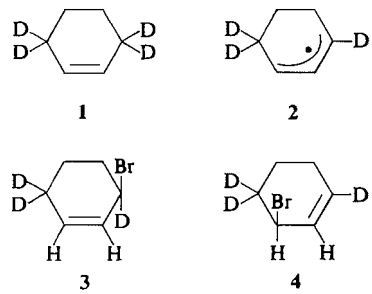

Results and Discussion

Reaction of NBA with Cyclohexene

In refluxing carbon tetrachloride, NBA is a solid and is only slightly soluble. Acetamide, the expected product of allylic bromination, is soluble in refluxing CCl_4; therefore, dissolution of the insoluble solid provides a convenient visual assay of the progress of an NBA reaction under these conditions. When cyclohexene was allowed to react with NBA in refluxing CCl_4, with catalysis by light and peroxide, the NBA disappeared within 5 min. The g.l.c. analysis of the reaction mixture at this point revealed only *trans*-1,2-dibromocyclohexane (**5**) and, surprisingly, no 3-bromocyclohexene. Continued refluxing caused darkening of the solution, and in the g.l.c. two new peaks appeared. The relative amounts of the new compounds gradually increased and, after 1 h, on the basis of the areas under the three peaks, one of the new compounds represented about 55% of the

Can. J. Chem. Downloaded from www.nrcresearchpress.com by 210.87.254.42 on 09/05/12
For personal use only.

mixture and the other about 5%. The new compounds were isolated by preparative g.l.c. and identified as *trans*-cyclohexene bromohydrin (**6**; major product) and 2-bromocyclohexanone (**7**; minor product). Repetition of the experiment, with addition of benzonitrile as an internal standard for the g.l.c. analyses, revealed that **6** and 7 were not formed at the expense of **5** and confirmed that 3-bromocyclohexene was not present at any time. (It was established that 3-bromocyclohexene is stable to the reaction conditions and to the g.l.c. procedure employed.)

5

6

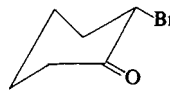

7

It seemed likely that **6**, especially, had been formed by thermal decomposition of a primary product of higher molecular weight or polarity whose retention time was too great to permit its detection under the g.l.c. conditions utilized. If **5** and **7** also were formed from this primary product, the course of the reaction could then be described tentatively as shown in eq. 8. For

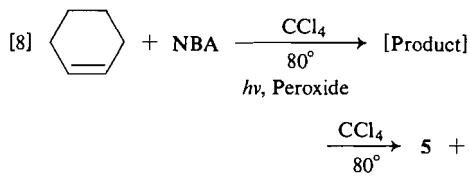

the isolation of this primary product, the reaction of cyclohexene with one molar equivalent of NBA was terminated by rapid cooling as soon as the NBA had disappeared. Acetamide precipitated and was removed by filtration; evaporation of the filtrate under reduced pressure at 30° yielded a colorless oil. Treatment of this oil afforded, besides a small amount (*ca.* 1%) of *trans*-2-acetamidocyclohexyl bromide (**8**), massive crystals melting at 28.0–28.5°. Microanalysis indicated a formula $C_8H_{13}Br_2NO$, *i.e.*, an *adduct* of cyclohexene plus NBA plus Br minus H. In view of the nature of the products **5**–**7** a part structure **9** could be assigned, and the gross structure **10**, 2-bromocyclohexyl-*N*-bromoacetimidate, became clear upon examination of the i.r. and n.m.r. spectra (6). The i.r. spectrum showed strong absorption at 6.2 and 7.85 μ assigned, respectively, to the C=N and C—O—C groupings (22); the n.m.r. spectrum showed 1-proton multiplets at τ 4.96 and 5.87, a methyl peak at 7.62, and a cyclohexane envelope (8 protons) centered at 8.34. The stereochemistry of the addition to the double bond was determined to be *trans* by preparation and n.m.r. analysis of the adduct **11** of cyclohexene-3,3,6,6-d_4. This adduct showed an AB quartet (τ_A 4.96; τ_B 5.87) for the tertiary protons with a coupling constant of 9 Hz; the chemical shift assignments shown in **11** are based on comparison with those of cyclohexene-3,3,6,6-d_4 bromohydrin (18) (τ_{CHBr} 6.13; τ_{CHOH} 6.4) and its derived acetate (τ_{CHBr} 5.95; τ_{CHOAc} 5.2). The geometry of the C=NBr grouping of **10** was not investigated.

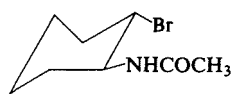

8

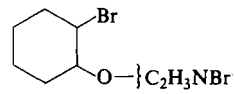

9

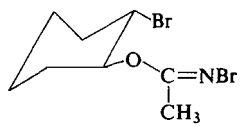

10

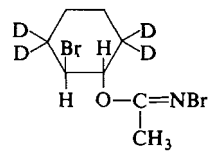

11

Because of its low m.p. no attempt was made to optimize the recovery of crystalline **10**. However, since the i.r. spectrum of the mother liquor obtained following removal of the first crop of **10** was superimposable upon that of **10**, it was concluded that **10** represented at least 90% of the non-volatile product of the primary reaction of equimolar amounts of cyclohexene and NBA. Since **10** contains two bromine atoms it seemed that at least 2 mol equiv of NBA per mol of alkene were necessary for the reaction. To check the stoichiometry, 0.5:1, 1:1, 2:1, 3:1, and 4:1 molar ratios of cyclohexene to NBA were allowed to react in refluxing CCl_4 with catalysis by light and peroxide. Each reaction mixture was rapidly cooled when the initial reaction was complete and the precipitated acetamide was collected and weighed; in each case this amounted to 90–95% of the theoretical based on eq. 9. Each filtrate was concentrated under reduced pressure and the distillate titrated with a standardized solution of Br_2 in CCl_4; except for the product from a

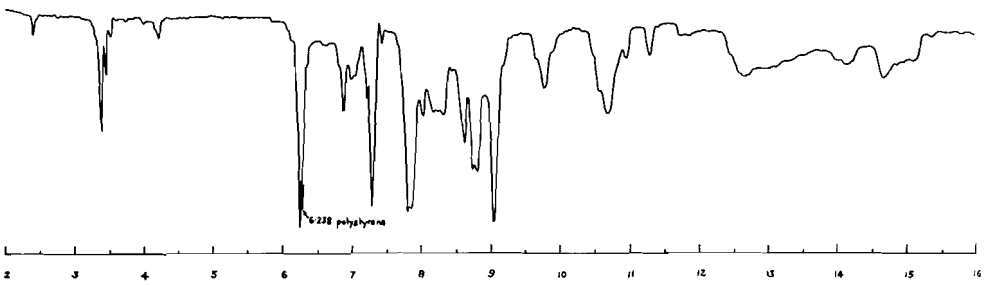

FIG. 1. The i.r. spectrum (KBr) of **12**.

0.5:1 molar ratio of reactants, which contained no cyclohexene, all distillates contained cyclohexene in amounts corresponding to 80–100% of that expected on the basis of eq. 9. The nonvolatile residue was then weighed and its i.r. spectrum recorded; in each case these i.r. spectra were virtually identical with the spectrum of pure **10**. It can be concluded that the reaction of cyclohexene with NBA is not an allylic bromination but an addition, closely obedient to the stoichiometry shown in eq. 9, in which **10**, a new class of compound, is produced.

[9] Cyclohexene + 2 NBA → **10** + Acetamide

Reaction of NBA with Tetramethylethylene

Since Wohl's initial experiment was performed with tetramethylethylene it was of interest to examine the reaction of this substrate with NBS employing the conditions and stoichiometry established for cyclohexene. A crystalline compound, m.p. 40–41°, was obtained. This compound analyzed as $C_8H_{15}Br_2NO$; its n.m.r. spectrum showed three methyl singlets, at τ 7.72, 7.99, and 8.17, in the ratio 1:2:2 and its i.r. spectrum, reproduced in Fig. 1, showed prominent peaks at 6.2 and 7.85 μ. All of these data are compatible with structure **12**, the 2-bromo-*N*-bromoacetimidate adduct of tetramethylethylene.

It was conceivable that the experimental conditions employed here, *viz.*, refluxing in CCl_4 in the presence of light and peroxide, had led to a reaction different from that envisaged by Wohl (1). To check this point, NBA was allowed to react with tetramethylethylene *in ether*. There was no reaction at 0° in the dark but, in 4.5 h at room temperature and in the diffuse light of the laboratory, a 75% conversion to **12** was achieved (*cf.* paragraph 2 of the Historical Introduction).

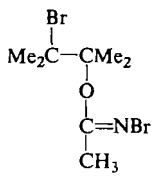

12

TABLE 1. Proton chemical shifts of some styrene derivatives (τ values)

Compound	τ_A	τ_B
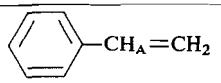	3.5	
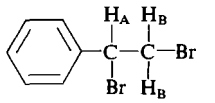	4.95	6.18
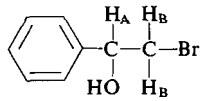	5.33	6.7
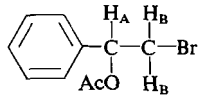	4.32	6.5
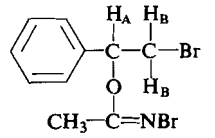	4.15	6.57

Reaction of NBA with Styrene and with 1-Methylcyclohexene

The adducts **10** and **12** are produced formally by the addition of bromine and *N*-bromoacetimidyl moieties to the double bond. To establish

Can. J. Chem. Downloaded from www.nrcresearchpress.com by 210.87.254.42 on 09/05/12
For personal use only.

Can. J. Chem. Downloaded from www.nrcresearchpress.com by 210.87.254.42 on 09/05/12
For personal use only.

the sequence of these two additions it was necessary to determine the regioselectivity (23) of addition to unsymmetrical olefins. The styrene adduct is assigned structure **13** rather than **14** on the basis of the chemical shifts of its tertiary (triplet) and secondary (doublet) protons, comparison of these chemical shifts with those of the authentic styrene derivatives shown in Table 1, and the assumption that *N*-bromoacetimidate resembles acetate in its effect upon the chemical shift of a geminal proton. The 1-methylcyclohexene adduct was assigned structure **15** rather than **16** on the basis of the chemical shift data shown in Table 2. This structure and the formulation of the adduct as a product of *trans*-addition are supported by the chemical properties of the compound, described below.

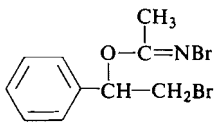

13

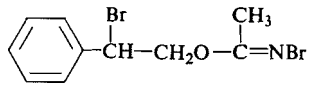

14

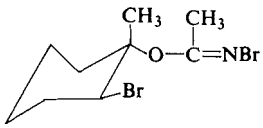

15

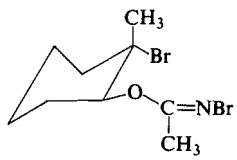

16

Mechanism of Formation of the Adducts

Adducts **13** and **15** contain bromine on the less-substituted carbon atom. Whether the addition of the two fragments is ionic (electrophilic) or radical, it follows that the C—Br bond is formed first. An ionic process for the addition seems more reasonable for the following reasons:

(*1*) Only the *trans*-adduct is obtained with cyclohexene. A radical addition reaction would have proceeded in a non-stereospecific manner. Thus, ionic chlorination of cyclohexene affords 1,2-dichlorocyclohexane which is at least 99% *trans* (24, 25) but, under radical conditions (25), the *cis* adduct is also observed, together with the products of vinylic, allylic, and homoallylic substitution. Similarly, ionic addition of bromine azide to cyclohexene and to 2-cholestene leads to the *trans*-adducts only; under radical conditions, the product from 2-cholestene is a 58:42 mixture of *trans* and *cis* adducts (26).

TABLE 2. Proton chemical shifts of some 1-methylcyclohexene derivatives

Compound	τ_A
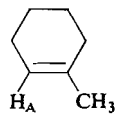	4.65
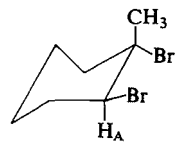	5.4
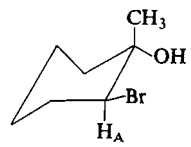	5.9
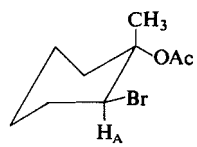	5.3
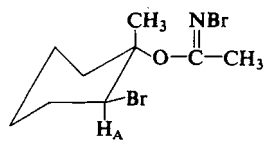	5.1

N,N-Dichlorourethane (DCU) adds to olefins by a free radical chain mechanism (27–29) to give 1:1 adducts **17**. With cyclohexene (27, 29) and cyclopentene (29) both *cis*- and *trans*-adducts are obtained together with the products of vinylic, allylic and homoallylic chlorination. Acyclic olefins react to give erythro–threo mixtures (27).

(*2*) Under ionic conditions, addition of IN_3 (26), ClN_3, and BrN_3 (30) to unsymmetrical olefins proceeds with attachment of halogen to the less substituted carbon atom, as in the present reaction. Under radical conditions the opposite regioselectivity is observed, *i.e.*, the *azido* group is attached to the less-substituted carbon atom. Similarly, in the radical addition of DCU, it is the nitrogen atom which becomes attached to the less-substituted carbon atom; *e.g.*, the styrene product is **18** (27).

(*3*) In the radical addition of DCU, as indi-

Can. J. Chem. Downloaded from www.nrcresearchpress.com by 210.87.254.42 on 09/05/12
For personal use only.

cated in **17** and **18**, a *nitrogen*–carbon bond is formed; in contrast, the addition reaction of NBA proceeds with formation of an *oxygen*–carbon bond.

(*4*) In a competition experiment involving reaction of NBA with a mixture of styrene and cyclohexene, only the cyclohexene adduct was formed. There is a variety of competition data which indicate that these two substrates display opposite selectivities in ionic and radical addition reactions (31). In a radical addition, styrene is several hundred times more reactive; and in an ionic addition, cyclohexene is five to ten times more reactive.

Although the final, adduct-forming stage of the NBA reaction with olefins thus appears to be ionic, the initial stage of the reaction is probably a free-radical chain process involving only the NBA. The over-all reaction is catalyzed by light and by peroxide. It is known (32) that u.v. irradiation of a refluxing solution of NBA in chloroform leads to rapid formation of a low equilibrium concentration of bromine. In the present work slow distillation of a refluxing suspension of NBA in carbon tetrachloride, illuminated by a 200 W bulb, led to the formation of bromine and acetamide in amounts compatible with the stoichiometry shown in eq. 10. Methyl isocyanate is indicated as a possible product of the decomposition, but attempts to detect this compound were not successful.

[10] $2NBA \rightarrow CH_3CONH_2 + Br_2 + [CH_3NCO]$

The elementary steps shown in eqs. 11–16 can be considered for the homolytic decomposition of NBA. The initiation step, eq. 11, must be followed by a rapid exchange, eq. 12 or eq. 13, which generates the *N*-bromoacetamidyl radical **19**. In each of these reactions there is a hydrogen abstraction *from NBA*; we believe that the availability of this hydrogen in NBA, and the absence of a reactive hydrogen in NBS,

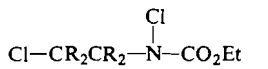

17

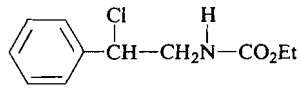

18

is a major source of the difference in behavior of the two brominating agents. Reaction **13** would be followed rapidly by 14 (10) and then 15, the latter being necessary to account for the failure to observe allylic bromide or dibromoolefin as primary products. The sequences 13–15 and 11, 12, 16 each lead to a compound $C_2H_3NOBr_2$ (**20**). Consideration of bond strengths (33) indicates that 16 would be strongly endothermic and 13–15 would be slightly exothermic.

It will be noted that addition of **20** to an olefin would afford a compound having the molecular formula of a 2-bromo-*N*-bromoacetimidate. Two structures can be considered for **20**, *viz.*, *N*,*N*-dibromoacetamide (**21**) and *N*,*O*-dibromoacetimide (**22**). A compound, assigned structure **21**, was prepared by Hofmann in 1882 (34) but no other reference to this substance could be found in the literature. Repetition of Hofmann's synthesis gave a yellow crystalline compound having the reported m.p. (100°) which analyzed correctly for $C_2H_3NOBr_2$. This compound is stable at room temperature in the solid state and as a solution in CH_2Cl_2 or $CHCl_3$. The n.m.r. spectrum in the latter solvent shows *one* singlet, at τ 7.50; in the same solvent the methyl protons of NBA appear as two singlets of unequal intensity at τ 7.8 and 8.0 (because of hindered rotation about the amide bond (35)). Acetamide shows a methyl singlet at τ 8.0. Thus the dibromo compound appears to exist in solution as a single species. Its constitution is clearly seen to be **21** (NDBA) rather than **22**

[11] $CH_3CONHBr \rightarrow CH_3CONH\cdot + Br\cdot$

[12] $CH_3CONH\cdot + CH_3CONHBr \rightarrow CH_3CONH_2 + CH_3\dot{C}ONBr$

19

[13] $Br\cdot + CH_3CONHBr \rightarrow HBr + CH_3\dot{C}ONBr$

[14] $HBr + CH_3CONHBr \rightarrow Br_2 + CH_3CONH_2$

[15] $Br_2 + CH_3\dot{C}ONBr \rightarrow Br\cdot + [CH_3CONBr]\cdot Br$

20

[16] $CH_3\dot{C}ONBr + CH_3CONHBr \rightarrow CH_3CONH\cdot + [CH_3CONBr]\cdot Br$

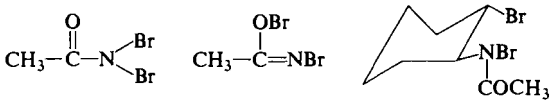

21 22 23

when the solution i.r. spectrum is compared to those of NBA and acetamide. Carbonyl stretching bands are observed for acetamide, NBA and NDBA at 5.95, 5.94, and 5.92 μ, respectively; and NDBA shows a strong band at 8.2 μ (N—Br?) approximately twice the intensity of a band at the same position in NBA.

In methylene chloride or carbon tetrachloride solutions, at 0 or 25°, **21** reacted rapidly with cyclohexene to give a greater than 9/1 mixture of **10** and the isomeric compound **23**, the latter being isolated as the hydrolysis product **8**. The addition proceeded smoothly, and the ratio of the two adducts was not significantly different, both in the dark and in the light of the laboratory. It is evident, therefore, that the reaction of this olefin with NBA can be discussed in terms of a radical reaction of NBA with itself to produce NDBA, followed by an ionic addition of the latter to the double bond. An as yet unexplained feature of the addition reaction is the formation of a C—O bond (to form **10**) in preference to a C—N bond (to form **23**). This point is under investigation and will be reported later along with the detailed discussion of the spectral and chemical properties of NDBA (36).

Reactions of 2-Bromo-*N*-bromoacetimidates

Rearrangement to Dibromides

One of the differences that had been noted previously in the reactions of NBA and NBS with olefins (2, 17*b*, 20, 37, 38) was the much greater tendency of NBA to give dibromo addition compounds. The observations recorded in eq. 8 indicate that these may form during the thermal decomposition of 2-bromo-*N*-bromoacetimidates. Thus, when heated at 100° in the absence of a solvent, **10** underwent violent decomposition to give *trans*-dibromocyclohexane (30%) and other (tarry) products. Following injection of a solution of pure **10** into a gas chromatograph at 130°, only *trans*-dibromocyclohexane was detected. Refluxing of a 10% solution of **10** in carbon tetrachloride caused complete decomposition in 1 h. Even at room temperature, in the absence of a solvent, crystalline **10** decomposed completely in 18 h; g.l.c. analysis of the product of this decomposition revealed the ratio of cyclohexene bromohydrin to cyclohexene dibromide to be 3:1. If the crude product of the NBA–cyclohexene reaction was similarly left to decompose at room temperature an identical ratio of **6** to **5** was observed. These observations demonstrate that the dibromide is indeed a product of the decomposition of **10**; and the latter result indicates further that *all* of the dibromide is produced during this decomposition.

In dimethylformamide, at 100°, **10** decomposed to give (by g.l.c.) a 35:25:40 mixture of **5**:**6**:**7**. The proportions of these three compounds were unchanged, and no bromochlorocyclohexane was formed, when this experiment was repeated in the presence of a molar equivalent of lithium chloride. This result is consistent with the description of the conversion of **10** to **5** as an intramolecular rearrangement. The presence of **5** and the absence of *dibromocyclopentane* in the products of decomposition of **10** in refluxing cyclopentene (b.p. 44°) support the conclusion that **5** is the result of an intramolecular rearrangement. There appears to be a formal analogy between the nature of this rearrangement and base-catalyzed rearrangements of *N*-bromoamides, in which retention of configuration is also observed (39–43), see eq. 17. Following this

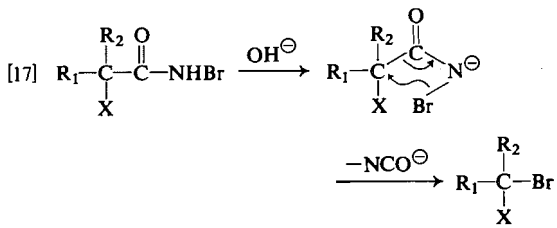

[17]

analogy, the conversion of **10** to **5** may be postulated to proceed by eq. 18. Methyl isocyanate

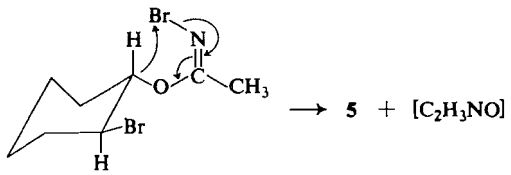

[18]

was considered to be a possibility for the species C_2H_3NO, by rearrangement of an acyl nitrene, but all attempts to isolate or trap the isocyanate were unsuccessful. It is relevant to note that recent investigations of the Curtius and Lossen rearrangements (44, 45) demonstrate that an isocyanate is formed from an acyl *azide*

Can. J. Chem. Downloaded from www.nrcresearchpress.com by 210.87.254.42 on 09/05/12
For personal use only.

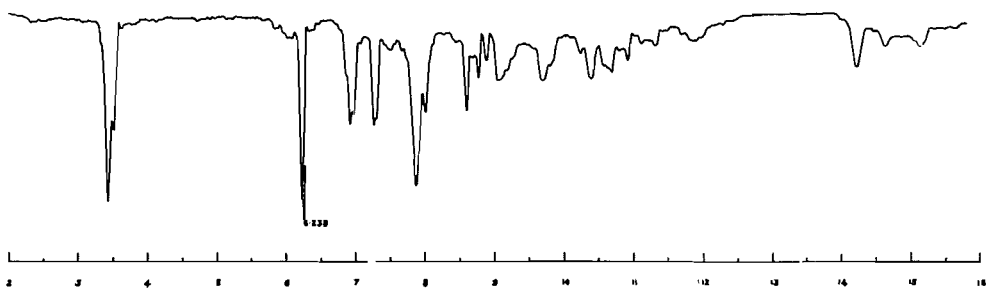

FIG. 2. The i.r. spectrum (KBr) of **15**.

in a concerted manner, intramolecular rearrangement of an acyl nitrene being much slower than intermolecular insertion, addition and abstraction reactions.

The rearrangement of a 2-bromo-*N*-bromoacetimidate to a dibromide just described is a general reaction of the adducts. After 60 h in ether at −20°, the styrene adduct had undergone 34% conversion to styrene dibromide. In chloroform at 30° this adduct decomposed completely within 1 h to give a mixture containing 30–40% of styrene dibromide. The 1-methylcyclohexene adduct was even less stable. The i.r. spectrum of **15** immediately after isolation is shown in Fig. 2; after 15 min in CCl_4 the peaks at 6.2 and 7.85 μ had disappeared completely. When this decomposition was followed by n.m.r., the disappearance of the tertiary proton absorption of **15** (τ 5.1) coincided with the appearance of peaks of equal intensity at τ 5.4 and 5.9, corresponding to 1-methylcyclohexene dibromide and 1-methylcyclohexene bromohydrin, respectively. In the reaction of NBA with stilbene, the adduct could not be detected; only stilbene dibromide (38%) was identified among the products of this reaction.

Reaction with HCl

In the investigations of Buckles *et al.* of the reaction of olefins with NBA (20, 37, 38), it was assumed that dibromides were primary products. This assumption caused some difficulty in the establishment of a stoichiometry. The reaction was clearly seen to be radical in nature, and acetamide was a product, but there was no obvious source of hydrogen to account for the formation of this compound or for the fate of the acetamidyl radical. In an attempt to optimize the recovery of the acetamidyl fragment, the product of the styrene reaction (0.1 mol of NBA to 0.05 mol of styrene) was treated with anhydrous hydrogen chloride (20); a precipitate was obtained and identified as bisacetamide hydrochloride on the basis of a "m.p. around 131°" (pure acetamide hydrochloride was also found to have "m.p. around 131°"). On the assumption that the precipitate had this structure, a 95–97% recovery of acetamide was claimed.

If this observation were correct, it would follow from the stoichiometry of the initial reaction (eq. 9) that half of the bisacetamide hydrochloride was derived from the adduct **13**. It is not immediately obvious how hydrogen chloride could react with **13** to give acetamide or bisacetamide hydrochloride, and it seemed desirable to examine the reaction of hydrogen chloride with a pure 2-bromo-*N*-bromoacetimidate. Because of its relative stability, the cyclohexene adduct was selected for this work. Titration of an ether solution of **10** at 0° with ethereal hydrogen chloride afforded in 91% yield a crystalline compound, m.p. 157.5–158.5°. This compound has the molecular formula $C_8H_{15}NOBrCl$. Its i.r. spectrum shows strong absorption at 6.0 μ (C=N), a broad peak at 3.5 μ (CH, NH_2^+), and no peak at 3.0 μ (NH). Structure **24** is assigned to this compound. The observation of an orange color during the reaction of **10** with hydrogen chloride is attributed to the formation of BrCl according to eq. 19.

Reaction with Triethylamine

It is known that *N*-bromo compounds react with triethylamine as shown in eq. 20 (8*a*, 16, 17*b*, 46). In agreement with eq. 20, the cyclohexene adduct **10** reacts with triethylamine to give triethylamine hydrobromide, 2-bromocyclohexanone (20%), and, in 75–80% yield, a compound assigned structure **25** on the basis of its i.r. spectrum which was identical with that of the acetimidic acid obtained upon neutralization

Can. J. Chem. Downloaded from www.nrcresearchpress.com by 210.87.254.42 on 09/05/12
For personal use only.

[19] 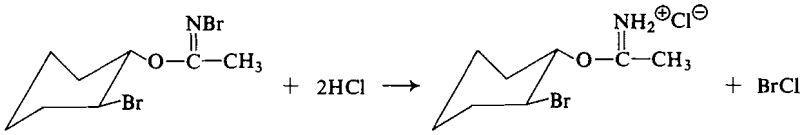

24

[20]

of **24** ($\lambda_{max}(CHCl_3)$ 3.0, 6.04 μ):

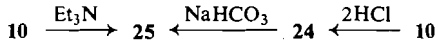

Further evidence that the reaction of the cyclohexene adduct with triethylamine occurs mainly at the nitrogen atom is found in the n.m.r. spectrum of the 3,3,6,6-tetradeuterio analog of **25**. Although the methyl peak of this compound shifts from τ 7.62 in the adduct **11** to τ 7.97, the position of the AB quartet for the *trans* tertiary protons is unchanged.

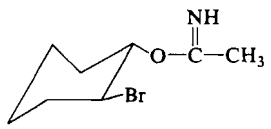

25

Formation of 2-bromocyclohexanone in this reaction is considered to be the result of the elimination shown in eq. 21.

[21] 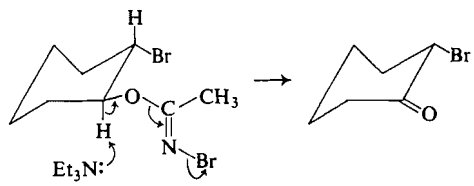

+ CH_3CN + $Et_3N{\cdot}HBr$

Formation from 10 of Cyclohexene Bromohydrin and 2-Bromocyclohexanone

If the acetimidic acid **25** is allowed to stand at room temperature, a slow conversion to cyclohexene bromohydrin is observed (*cf.* ref. 47). This observation provides an important clue to the mode of formation of the bromohydrin from the 2-bromo-*N*-bromoacetimidate. It was already noted in the initial experiments that continued refluxing of the mixture obtained from the reaction of cyclohexene with NBA leads to a steady increase in the ratio of cyclohexene bromohydrin to cyclohexene dibromide and that the bromohydrin is not formed at the expense of the dibromide. It has also been noted that refluxing of a 10% solution of pure **10** in carbon tetrachloride causes complete decomposition in one hour. The g.l.c. analysis of the latter mixture revealed a 44:36:20 mixture of **5**, **6**, and **7**. When the solvent was removed and the residue allowed to stand overnight at room temperature, this ratio changed to 22:65:13. Since **25** was not detected by the g.l.c. procedure employed to determine the proportions of the volatile products **5**, **6**, and **7** these results can be interpreted in terms of the sequence shown in eq. 22. The i.r. spectra shown in Fig. 3

[22] 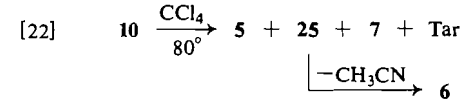

support this interpretation. The initial product of decomposition of **10** (lower spectrum) shows a strong absorption at 6.0 μ, assigned to the C=N group of **25**, and a weaker absorption at 5.8 μ, assigned to the carbonyl group of **7**. The upper spectrum is that of the product obtained after the solvent was removed and the residue allowed to stand at room temperature overnight.

If the formation of the bromohydrin from the 2-bromo *N*-bromoacetimidate is to be explained in terms of the sequence,

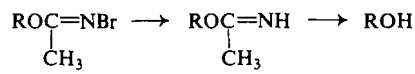

it is necessary to provide a hydrogen source for the reaction **10** → **25**. Two possible hydrogen sources can be suggested. The first is HBr (*cf.* eq. 19[2]) formed, together with 2-bromocyclohexanone, by the route suggested below.

[2]During the decomposition of **10** in dimethylformamide, already described, a bromine color developed and then faded, possibly because of reaction or distillation from the medium, or both.

Can. J. Chem. Downloaded from www.nrcresearchpress.com by 210.87.254.42 on 09/05/12
For personal use only.

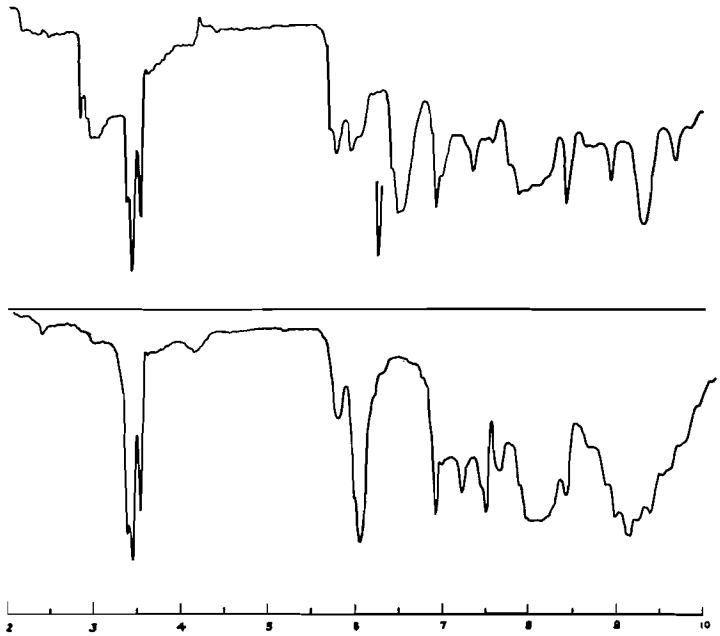

FIG. 3. The i.r. spectrum of the product resulting from thermal decomposition of **10**. The lower spectrum is that obtained when **10** was refluxed in CCl_4 for 1 h. The upper spectrum is that of the product obtained after the solvent was removed and the residue allowed to stand overnight at room temperature.

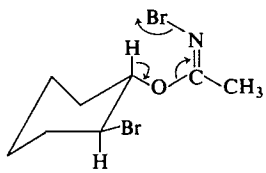

$\longrightarrow$ 7 + HBr + CH_3CN

This cannot be the sole hydrogen source for this transformation because, in the materials balance, equal amounts of bromohydrin and 2-bromocyclohexanone or derived products would be expected. In fact, the amount of bromohydrin always exceeds that of bromoketone. A second hydrogen source for the reaction **10** $\rightarrow$ **25** is the adduct **10** itself. It has been demonstrated recently (48) that heating of a solution of benzophenone *N*-bromoimine in cyclohexane affords cyclohexyl bromide. Although the mechanism of this bromination was not studied, the reaction does not provide precedent for a process, eq. 23. In the present case,

[23] $R_2C{=}NBr + R'H \rightarrow R_2C{=}NH + R'Br$

reaction of **10** with itself according to eq. 23 would be expected to afford, in addition to **25**, polybrominated adducts and/or the high boiling residues encountered in the decomposition of **10**.

Rearrangement to Aminoacetates

The i.r. spectrum displayed in the upper curve of Fig. 3 shows carbonyl absorption at 5.7 *and* at 5.8 μ. The 5.8 μ peak is attributed to 2-bromocyclohexanone; the 5.7 μ peak is consistent with an ester carbonyl absorption. Since the precursor of this material, with the spectrum shown in the lower curve of Fig. 3, appears to have no peak at 5.7 μ, it can be speculated that the decomposition of **25** leads not only to the bromohydrin but also to acetate-containing material. Attempts to obtain this compound in pure form were not successful, but the apparently analogous product of decomposition of the 1-methylcyclohexene adduct could be isolated in crystalline form, m.p. 208–210°. This compound has the formula $C_9H_8BrN_2O$; its n.m.r. and i.r. spectra, reproduced in Fig. 4, are compatible with structure **26**, 2-acetoxy-2-methylcyclohexylammonium bromide. Cyclization of the imidic acid **27** would afford the oxazoline hydrobromide **28**; hydrolysis of **28** could proceed to give the salt **26** or the acetamido alcohol **29**. A search for **29** was not made.

The scheme shown in eq. 24, if correct, provides chemical support for the structure and

Can. J. Chem. Downloaded from www.nrcresearchpress.com by 210.87.254.42 on 09/05/12
For personal use only.

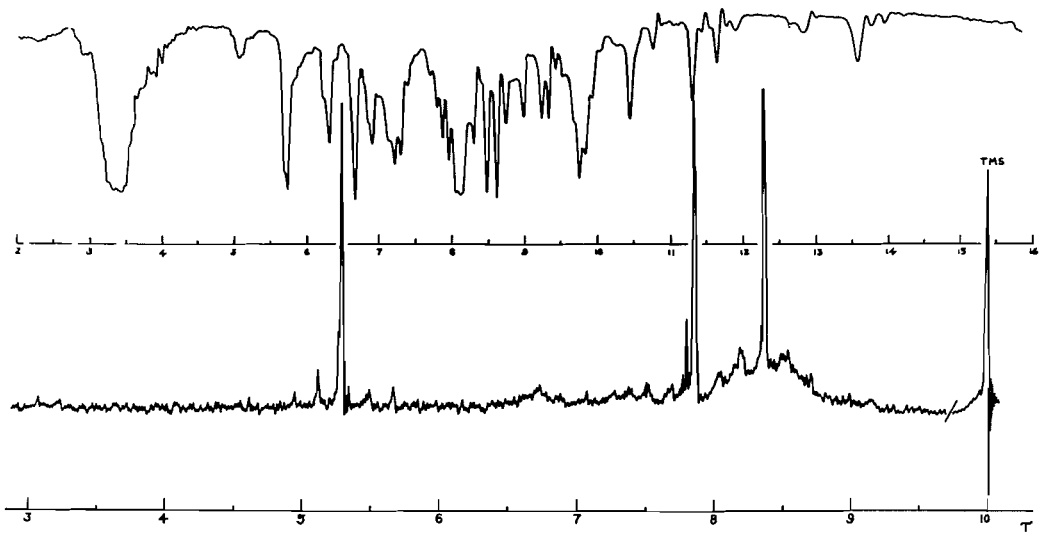

FIG. 4. The i.r. (KBr) and n.m.r. (D_2O) spectra of **26**.

[24]

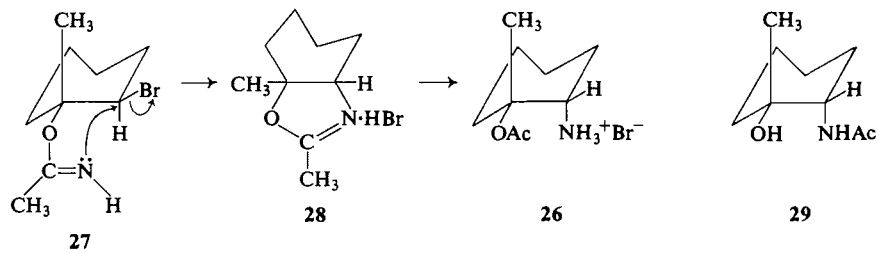

stereochemistry of the 1-methylcyclohexene adduct **15**. Formation of the oxazoline would require a *trans* relationship of the electronegative substituents; and attack on the C—Br bond with inversion of configuration would not be expected in the case of the tertiary bromide **16**.

Experimental

Melting points were determined on a Fisher–Johns m.p. apparatus, and are uncorrected. Boiling points are also uncorrected. The i.r. spectra were recorded on a Beckman IR 5A instrument unless otherwise indicated. The n.m.r. spectra were obtained on a Varian A60 spectrometer, tetramethylsilane (TMS) being employed as the internal standard, unless otherwise specified. The g.l.c. determinations were performed on a Beckman GC-2 chromatograph; a Fisher Prep. Partitioner was employed for preparative work. The column packing was 15% butanediol succinate on Embacel and separations were conducted at 130°. Microanalyses are by Dr. C. Daesslé, Montreal, Spang Microanalytical Laboratory, Ann Arbor, and J. Booker, Queen's University.

All solvents were Fisher Certified Reagent Grade and were used without further purification except for drying, where indicated, by conventional means.

N-Bromosuccinimide

BDH Reagent Grade material was employed.

N-Bromoacetamide

Commercial NBA was dissolved in boiling benzene, no attempt being made to remove the color of bromine in the solution. Perfectly formed colorless needles, m.p. 108°, were obtained when the solution was allowed to cool undisturbed at room temperature. The precipitated solid was collected, washed to whiteness with 30–60° petroleum ether and allowed to dry in the air. This material could be stored for long periods in the cold without apparent deterioration.

Olefins and Ketones

All substrate olefins and ketones except tetramethylethylene and 1-methylcyclohexene, were commercial products of "Reagent" or equivalent grade and were used unpurified if g.l.c. analysis indicated no significant (<1%) contamination. If color could be detected or g.l.c. analysis indicated significant impurity the material was distilled before use.

Tetramethylethylene

This material, b.p. 70–71° was synthesized by reduction of pinacolone, followed by acid-catalyzed dehydration of the resultant alcohol (49). Integration of the methyl peak at τ 8.36 against all extraneous peaks indicated greater than 90% purity.

Can. J. Chem. Downloaded from www.nrcresearchpress.com by 210.87.254.42 on 09/05/12
For personal use only.

Can. J. Chem. Downloaded from www.nrcresearchpress.com by 210.87.254.42 on 09/05/12
For personal use only.

1-Methylcyclohexene

This olefin, b.p. 108–110°, n_D^{25}, 1.4475, lit. (50) n_D^{25}, 1.4478, was prepared by acid-catalyzed dehydration of 1-methylcyclohexanol. Integration of the n.m.r. spectrum showed that the downfield multiplet centered at τ 4.66 was in the ratio 1:11 with the remaining upfield signals.

2-Bromocyclohexanone

Cyclohexanone was brominated with NBS (51) to yield 2-bromocyclohexanone, b.p. 82–84°/6 mm, lit. (52) 74°/3 mm.

3-Bromocyclohexene

This compound was prepared by treatment of cyclohexene with NBS (16) and had b.p. 60–62°/14 mm, lit. (8*a*) 55–57°/11 mm.

1,2-Dibromocyclohexane

A solution of molecular bromine in chloroform was added dropwise to a magnetically stirred solution of an equimolar amount of cyclohexene in chloroform maintained at 0–5°. Evaporation of the solvent and distillation gave a product b.p. 92–94°/10 mm, lit. (20) 93–96°/10 mm.

1,2-Dibromocyclopentane

The compound had b.p. 67–68°/11 mm, lit. (53) 75°/17 mm.

α,β-Dibromostyrene

This compound, m.p. 72–73°, lit. (38) 73–74°, and *trans-α,α′-dibromostilbene*, m.p. 225–228°, lit. (38) 235–237° were synthesized in the same manner as was 1,2-dibromocyclohexane.

Cyclohexene Bromohydrin

This compound, b.p. 85–87°/10 mm, lit. (54) 86.6–88.4°/10 mm, was prepared by ring opening of cyclohexene oxide with gaseous hydrogen bromide (55).

1-Methylcyclohexene Bromohydrin

This compound, b.p. 98–101°/10 mm, lit. (50*b*) 96.8°/8.5 mm, and *styrene bromohydrin* b.p. 134–136°/10 mm, lit. (56) 120–123°/5 mm, were synthesized by the method of Guss and Rosenthal (56) by reaction of the respective olefins with NBS and water.

The purity of all reference compounds, except α,α′-dibromostilbene and the styrene derivatives, was established by g.l.c. examination. The identity of the styrene derivatives was confirmed by determination of their n.m.r. spectra described later.

*2-Bromocyclohexyl-N-bromoacetimidate (**10**)*

A solution of cyclohexene (41.0 g, 0.5 mol) in carbon tetrachloride (100 ml) was added rapidly to a refluxing suspension of NBA (69.0 g, 0.5 mol) in carbon tetrachloride (400 ml) in a 1 l three-necked flask.[3] Refluxing was maintained by the heat from a 100 W Photoflood No. 2 lamp with reflector mounted close to the reaction flask. The reaction soon became vigorous and, after approximately 5 min, the solid NBA had disappeared and yellow droplets of acetamide could be discerned adhering to the sides of the vessel. The otherwise colorless reaction mixture was immediately cooled in an ice-bath until crystallization of the acetamide[4] was complete and this solid was then collected (15.4 g, 104% based on eq. 9). The mother liquor was distilled under reduced pressure below 40 °C to a residue of 81.1 g; the distillate was then found to contain 16.1 g (80%, based on eq. 9) of cyclohexene by titration of an aliquot with a standardized solution of bromine in carbon tetrachloride.

The residue, diluted with 30–60° *petroleum* ether (10 ml) and stored overnight at −20°, afforded 0.7 g (1%) of *trans*-2-acetamidocyclohexyl bromide, m.p. 110–111°, lit. (57) 109–110°. The i.r. spectrum of this product shows amide absorption at 6.05 and 6.38 μ, and the n.m.r. spectrum shows a peak at τ 7.93 consistent with the presence of an acetamidyl methyl group.

The filtrate was concentrated, *ethyl* ether (10 ml) was added and this solution was kept overnight at −20°. The massive camphor-like crystals then obtained weighed 26.4 g (36%) and melted at 28.0–28.5°.

Anal. Calcd. for $C_8H_{13}NOBr_2$: C, 32.12; H, 4.38; N, 4.72; Br, 53.46. Found: C, 32.34; H, 4.25; N, 4.69; Br. 53.57.

No attempt was made to optimize the recovery of crystalline **10**; however, it was noted that the i.r. spectrum of the residue following removal of **10** was superimposable upon that of the crystalline material.

*Reaction of NBA with Tetramethylethylene. Preparation of **12***

(i) In Carbon Tetrachloride

Tetramethylethylene (4.6 g, 0.055 mol) was added rapidly to a refluxing suspension of NBA (7.8 g, 0.059 mol) in carbon tetrachloride (25 ml), heat being supplied by a 100 W Photoflood No. 2 lamp mounted beneath the flask. When the crystalline NBA had disappeared and yellow droplets of acetamide could be seen, the reaction flask was immediately cooled in an ice–bath and the precipitated acetamide (1.3 g, 78%) was collected. The filtrate was evaporated to yield 5.7 g (66%) of a faintly yellow oil which was diluted with a small amount of ether and stored at −20°. The product crystallized overnight to a solid mass from which well-formed needles (4.7 g, m.p. 40–41°) were obtained; these crystals were washed with a small quantitiy of ice-cold anhydrous ether and analyzed.

Anal. Calcd. for $C_8H_{15}NOBr_2$: C, 31.90; H, 4.98. Found: C, 31.70; H, 4.97.

(ii) In Ether[5]

To a suspension of NBA (1.68 g, 0.013 mol) in anhydrous ether (10 ml), magnetically stirred and cooled in an ice-bath, was added dropwise a solution of tetramethylethylene (1.0 g, 0.012 mol) in anhydrous ether (5 ml). No apparent reaction had taken place by the end of the addition. A crystal of the solid residing at the bottom of the reaction flask was, therefore, extracted and its m.p. determined (107–108°); a mixture m.p. of this material with an authentic sample of NBA was 107–108°.

[3]Care should be taken to use a reaction flask of capacity at least twice the volume of solvent in order to obviate the possibility of overflow of its contents when the highly exothermic reaction begins.

[4]In all cases acetamide was identified by determination of its m.p. and a mixture m.p. with an authentic sample.

[5]Wohl (1) mixed 10 g of tetramethylethylene in 36 ml of ether with 16 g of NBA "under good cooling" and allowed the reaction to go to completion overnight. No other details, including the method of work-up, were mentioned.

Can. J. Chem. Downloaded from www.nrcresearchpress.com by 210.87.254.42 on 09/05/12
For personal use only.

No further change was apparent after the reaction mixture had been stored overnight at 0° in the dark.

After approximately 4½ h stirring at room temperature in the diffuse light of the laboratory, the needles of NBA could not be detected and a voluminous precipitate was dispersed throughout the reaction medium. Filtration yielded acetamide (0.43 g, 78%, m.p. 76–78°; mixture m.p. with acetamide 76–78°). Evaporation of the filtrate yielded 1.5 g (75%) of a colorless oil, whose i.r. spectrum was almost identical with that of the crystalline adduct **12** prepared in (*i*), and which could be crystallized to give material melting at 39–40° by seeding with the former product.

Reaction of NBA with Styrene. Preparation of ***13***

A solution of styrene (1.0 g, 0.01 mol) in carbon tetrachloride (10 ml) was added rapidly to a refluxing suspension of NBS (2.76 g, 0.02 mol) in carbon tetrachloride (50 ml), with irradiation by a 100 W Photoflood No. 2 lamp. As soon as the NBA had disappeared, the mixture was rapidly cooled in an ice-bath, the precipitated acetamide was collected (0.4 g, 68%) and the filtrate was concentrated under reduced pressure at room temperature. The i.r. spectrum of the residue (2.7 g, 80%) showed the characteristic adduct absorptions at 6.2 and 7.8 μ and, as well, some slight absorption at 5.8 and 5.95 μ. The product was dissolved in ether (20 ml) and stored at −20° for 60 h. Fine needles (0.8 g, m.p. 72–73°) separated out and were identified as α,β-dibromostyrene by a mixture m.p. with an authentic sample (72–74°) and by superimposition of the i.r. spectra of the two samples.

The adduct has not yet been crystallized; that this may be due to its instability is evident upon examination of the n.m.r. spectrum of the newly formed product of the NBA–styrene reaction as a function of time. Immediately after isolation this spectrum showed, in addition to unreacted styrene, a triplet (1H) centered at τ 4.15, a doublet (2H) centered at 6.57, and a sharp peak (3H) at 7.85. Within 1 h at room temperature, the peaks at τ 4.15, 6.57, and 7.85 disappeared completely; (in the i.r. spectrum the characteristic peaks at 6.2 and 7.8 μ also disappeared). A doublet, centered at τ 6.18, was now present and was attributed to the β-protons of α,β-dibromostyrene. In the n.m.r. spectrum of the latter compound the α- and β-protons are found, respectively, at τ 4.95 and 6.18; however, in the n.m.r. spectrum of the concentrated NBA–styrene product the signal at 4.95 is obscured by signals due to residual styrene. This proton was readily seen when the product of decomposition was exhaustively evaporated to remove the residual styrene.

Reaction of NBA with 1-Methylcyclohexene. Preparation of ***15***

1-Methylcyclohexene (0.96 g, 0.01 mol) was added rapidly to a refluxing suspension of NBA (1.38 g, 0.01 mol) in carbon tetrachloride (25 ml) with irradiation from a 100 W Photoflood No. 2 lamp. Work-up in the usual manner yielded 1.4 g (81%) of a colorless oil whose i.r. spectrum, shown in Fig. 2, has the characteristic peaks at 6.22 and 7.86 μ. Dilution with ether and storage at −20° failed to crystallize the adduct.

The n.m.r. spectrum of the colorless oil, immediately after isolation, showed, in addition to the two methyl peaks and the ring protons, a 1-proton quartet centered at τ 5.1. After 15 min this quartet had disappeared and a triplet centered at τ 5.4, and a multiplet centered at 5.9 were present. The proton geminal to bromine in 1,2-dibromo-1-methylcyclohexane appears as a triplet centered at τ 5.4. 1-Methylcyclohexene bromohydrin shows complex absorption centered at τ 5.9.

Variable quantities of a chloroform and carbon tetrachloride - insoluble white solid, m.p. 208–210°, were isolated following decomposition of the adduct **15** in these solvents. This solid, a crystalline compound soluble in water, was isolated by filtration, washing with ether, and air-drying. Its i.r. and n.m.r. spectra, shown in Fig. 4, are compatible with structure **26**.

Anal. Calcd. for $C_9H_8BrN_2O$: C, 42.8; H, 7.14. Found: C, 42.89, 43.15; H, 7.53, 7.62.

Reaction of NBA with trans-Stilbene

trans-Stilbene (4.5 g, 0.025 mol) was dissolved in carbon tetrachloride (300 ml) and to the magnetically-stirred solution was added NBA (6.9 g, 0.050 mol). The reaction flask was immersed in a cold water bath which was also magnetically stirred. The temperature of the water bath was slowly raised by irradiation with a 100 W Photoflood No. 2 lamp mounted close to it. No apparent reaction took place until the bath temperature reached 60°, at which point the rate of solution of NBA seemed to increase dramatically; before all of the NBA had dissolved, the reaction mixture became noticeably yellow. The irradiation was immediately halted and the reaction mixture was quickly cooled in an ice-bath. The carbon tetrachloride - insoluble material was collected and triturated with cold water. After drying, the water-insoluble residue weighed 3.2 g and had an i.r. spectrum, m.p., and mixture m.p. identical with those of an authentic sample of α,α′-dibromostilbene.

The i.r. spectrum of the carbon tetrachloride filtrate showed no trace of a bromoacetimidate. Removal of the solvent yielded 4.2 g of an intractable brownish semi-solid residue.

Thermal Decomposition of 2-Bromocyclohexyl-N-bromoacetimidate

(i) In Carbon Tetrachloride and Cyclopentene

The crystalline adduct **10** (1 g) was dissolved in carbon tetrachloride (10 ml) and the solution quickly brought to reflux on a steam bath. One milliliter aliquots of the refluxing solution were withdrawn at 15–20 min intervals and subjected to i.r. and g.l.c. analysis. The g.l.c. analysis indicated formation of three compounds. These compounds were isolated by preparative g.l.c. and shown to be (in order of increasing retention time) cyclohexene dibromide, cyclohexene bromohydrin, and 2-bromocyclohexanone. The identifications were made in each case by i.r. and g.l.c. analysis.

When cyclopentene was employed as the solvent, g.l.c. analysis readily revealed cyclohexene dibromide, but no trace of cyclopentene dibromide could be detected.

(ii) In Dimethylformamide

The crystalline adduct **10** (1 g) was dissolved in DMF (5 ml), and the solution was heated on the steam bath for 1 h. The product was then diluted with water, extracted with ether, and the ether extract dried over anhydrous sodium sulfate and evaporated. The composition

Can. J. Chem. Downloaded from www.nrcresearchpress.com by 210.87.254.42 on 09/05/12
For personal use only.

of the residue was established, as in (*i*) by i.r. and g.l.c. analyses.

This experiment was repeated in the presence of added lithium chloride (0.1 g, a molar equivalent) in order to test the effect of added chloride ions on the nature of the decomposition in DMF. There was no effect.

(iii) In a Closed System

The crystalline adduct **10** (0.6 g, 0.002 mol) was sealed in a pyrex tube and rapidly heated on the steam bath. The melt soon darkened and an eruption of vapor followed closely. When the reaction tube was cooled, a clear light brown oil was noted over a dark brown semi-solid residue. The tube was opened and the oil washed out with carbon tetrachloride. Evaporation of the solvent and distillation of the residue afforded 1,2-dibromocyclohexane (0.14 g, 30%) identified by comparison of its g.l.c. retention time and its i.r. spectrum with those of an authentic sample. The intractable semi-solid residue weighed 0.43 g.

*Preparation of 2-Bromocyclohexylacetimidium Chloride (**24**)*

Crystalline **10** (0.60 g, 0.002 mol) was dissolved in 10 ml of anhydrous ether. The solution was cooled to 0°, stirred, and treated dropwise with 45 ml of 0.07 *N* ethereal hydrogen chloride. In the course of the addition the reaction mixture acquired a decidedly orange tint and a white crystalline solid separated out. The mixture was stirred for 2 h in the ice-bath after the addition was complete and the solid was then collected. It weighed 0.34 g and melted at 154–155°. Concentration of the orange-colored filtrate caused loss of the orange color and precipitation of a further 0.15 g of the white solid, m.p. 152–155°. The total yield of the crystalline solid corresponded to 91% conversion of the bromoimidate to its derived salt on the basis of the hydrogen chloride utilized. Recrystallization from methanol–ether gave fine needles, m.p. 157.5–158.5° (sealed tube).

Anal. Calcd. for $C_8H_{15}NOBrCl$: C, 37.42; H, 5.85. Found: C, 37.26; H, 5.63.

*Neutralization of **24**. Preparation of 2-Bromocyclohexylacetimidic Acid (**25**)*

An ether suspension of the salt **24** was shaken with 1% aqueous bicarbonate. The ether layer was then separated, dried, freed of solvent, and the i.r. spectrum of the residue determined. Strong absorption at 6.0 μ was still present but the C–H region of the spectrum was now cleanly resolved and a sharp peak was observed at 3.0 μ. When an ether solution of this product (**25**) was shaken with D_2O, dried over anhydrous sodium sulfate, and the solvent removed, the i.r. spectrum of the residue showed no absorption at 3.0 μ. Instead a sharp peak was present at 4.1 μ indicating an N–H to N–D transformation. There was no change in the remainder of the spectrum.[6]

*Reaction of **10** with Triethylamine*

To an ice-cooled stirred solution of **10** (6.0 g, 0.02 mol) in anhydrous ether (20 ml), was added dropwise a solution of triethylamine (2.0 g, 0.02 mol) in anhydrous ether (20 ml). After the addition was complete, the product was stored in the refrigerator for 2 h and the precipitated solid was then collected (3.2 g) and identified as triethylamine hydrobromide on the basis of its i.r. spectrum and a mixture m.p. The filtrate was washed with cold water, dried over anhydrous sodium sulfate, and evaporated to yield 4.2 g of a light brown oil. The i.r. spectrum of this oil was found to contain all of the peaks of **25**, as well as absorption at 5.8 μ attributed to the carbonyl stretching band of 2-bromocyclohexanone. The presence of the latter compound was confirmed by g.l.c. comparison with an authentic sample of the bromoketone using a column of 1% SE 30 on Embacel in addition to the butanediol succinate column.

The n.m.r. spectrum of the product of triethylamine treatment of the adduct **11** from cyclohexene-3,3,6,6-d_4 is almost identical with that of the precursor adduct except for an upfield shift of the methyl peak to τ 7.97. The hydrogen atoms corresponding to H_A and H_B of the original adduct remain as a typical AB quartet with $J = 9$ Hz.

Decomposition of NBA

The NBA (6 g, 0.043 mol) was dissolved in refluxing carbon tetrachloride (500 ml) and the solution irradiated with an ordinary 200 W bulb.[7] Bromine was slowly codistilled with carbon tetrachloride as it formed, and collected in an ice-cooled receiver. After approximately 5 h, the residual solution was only faintly yellow. At this point crystals of a colorless solid were present in the water-cooled condenser; these were washed out with anhydrous ether and collected (0.2 g, m.p. 76–77°). The residual solution was then concentrated under reduced pressure below 40° and the residue triturated with ether to give a further 0.5 g of crystals, m.p. 76–78°. The volume of the bromine-containing distillate was then accurately measured, a sample retained for titration, and the remainder evaporated to dryness and the residue triturated with ether to yield a third crop of colorless crystals (0.2 g, m.p. 76–78°). The crystals were identified as acetamide by a mixture m.p. determination with an authentic sample (total yield, 0.9 g, 35% based on NBA; 70% based on eq. 10).

Titration of the bromine-containing aliquot with a standardized solution of cyclohexene in carbon tetrachloride indicated that the distillate contained 0.018 mol of Br_2, corresponding to 84% of that expected from the stoichiometry shown in eq. 10.

Methyl isocyanate and diacetylhydrazine (anticipated from coupling of two acetamidyl radicals) were, however, not detected.

Preparation of N,N-Dibromoacetamide (NDBA)

An ice-cooled solution of potassium hydroxide (112 g, 2.0 mol) in 1 l of water was added dropwise to a well-stirred mixture of acetamide (59 g, 1 mol) and bromine

[6]We thank Dr. H F. Shurvell for suggesting this procedure.

[7]The use of stronger illumination, such as the 100 W Photoflood No. 2 lamp used in bromoacetimidate preparations, led to more complex products; *bis*-acetamide hydrobromide m.p. 131°, lit. (32) 131° was isolated from such a decomposition. Buckles *et al.* (32) have reported deposition of impure *bis*-acetamide hydrobromide from a u.v. irradiated solution of NBA in chloroform.

Can. J. Chem. Downloaded from www.nrcresearchpress.com by 210.87.254.42 on 09/05/12
For personal use only.

(320 g, 2.0 mol), the temperature of the reaction mixture being maintained between 0 and 5° by cooling in an ice-salt bath. After the addition was complete the orange colored solid (obviously impregnated with bromine) was rapidly filtered and washed with ice-cold water. The wet bright orange solid was vacuum dried to yield 60.8 g (30%) of a bright yellow solid. This material could be recrystallized with care from hot water to give a 52% recovery of lustrous golden yellow plates, m.p. 100°, lit. (34) 100°.

Anal. Calcd. for $C_2H_3NOBr_2$: C, 11.06; H, 1.38. Found: C, 11.03; H, 1.55.

Reaction of NDBA with Cyclohexene

Cyclohexene (0.82 g, 0.01 mol) in methylene chloride (10 ml) was added dropwise to a magnetically-stirred solution of NDBA (2.17 g, 0.01 mol) in methylene chloride (20 ml), the reaction mixture being cooled in an ice-bath. At the end of the addition the solution was decidedly yellow. Evaporation of the solvent yielded 2.82 g of a yellow oil whose i.r. spectrum showed the absorptions at 6.2 and 7.85 μ characteristic of the bromoacetimidate adduct **10**, as well as a peak of much lower intensity at 5.9 μ. The oil was diluted with ether, and petroleum ether (30–60°) was added to the cloud point. Storage at 0° produced colorless needles, 50 mg, of **8**, m.p. 111–112° (yield 2.5%). The mother liquor was evaporated to dryness and the residue treated with ether (1 ml). After 1 day at −20° crystallization had occurred. The crystals were collected and identified as **10** by m.p. and i.r. determinations.

Competition Experiment of NDBA with Cyclohexene and Styrene

The above experiment was repeated except that a mixture of cyclohexene (0.01 mol) and styrene (1.04 g, 0.01 mol) was added to the NDBA solution. The n.m.r. spectrum of the resulting product showed the peaks of **10** and of styrene. Peaks corresponding to the adduct **13** and styrene dibromide were not observed.

We thank the National Research Council of Canada for financial support of this work.

1. A. Wohl. Chem. Ber. **52**, 51 (1919).
2. A. Wohl and K. Jaschinowski. Chem. Ber. **54**, 476 (1921).
3. G. Wendt. Chem. Ber. **74**, 1242 (1941).
4. K. Ziegler, A. Späth, E. Schaaf, W. Schumann, and E. Winkelmann. Ann. **551**, 80 (1942).
5. C. Djerassi. Chem. Rev. **43**, 271 (1948).
6. S. Wolfe and D. V. C. Awang. J. Amer. Chem. Soc. **89**, 5287 (1967).
7. C. Walling. Free radicals in solution. John Wiley, New York, N.Y., 1957. p. 381.
8. (*a*) H. J. Dauben and L. L. McCoy. J. Amer. Chem. Soc. **81**, 4863 (1959); (*b*) J. Org. Chem. **24**, 1577 (1959); (*c*) J. Amer. Chem. Soc. **81**, 5404 (1959).
9. G. F. Bloomfield. J. Chem. Soc. 14 (1944).
10. R. E. Pearson and J. C. Martin. J. Amer. Chem. Soc. **85**, 354, 3142 (1963).
11. (*a*) G. A. Russell, C. DeBoer, and K. M. Desmond. J. Amer. Chem. Soc. **85**, 366 (1963); (*b*) G. A. Russell and K. M. Desmond. J. Amer. Chem. Soc. **85**, 3139 (1963); (*c*) G. A. Russell and C. DeBoer. J. Amer. Chem. Soc. **85**, 3136 (1963).
12. (*a*) C. Walling, A. L. Rieger, and D. D. Tanner. J. Amer. Chem. Soc. **85**, 3129 (1963); (*b*) C. Walling and A. L. Rieger. J. Amer. Chem. Soc. **85**, 3134 (1963).
13. J. H. Incremona and J. C. Martin. J. Amer. Chem. Soc. **92**, 627 (1970).
14. J. Adam, P. A. Gosselain, and P. Goldfinger. Nature. **171**, 704 (1953); Bull. Soc. Chim. Belges. **65**, 523, 533 (1956).
15. P. S. Skell, D. L. Tuleen, and P. D. Readio. J. Amer. Chem. Soc. **85**, 2850 (1963).
16. L. Horner and E. H. Winkelmann. *In* Newer methods of preparative organic chemistry. Vol. III. *Edited by* W. Foerst. Academic Press Inc., New York, N.Y., 1964. p. 151.
17. (*a*) S. Wolfe and P. G. C. Campbell. Unpublished results; (*b*) E. A. Braude and E. S. Waight. J. Chem. Soc. 1116 (1952).
18. S. Wolfe and P. G. C. Campbell. Can. J. Chem. **43**, 1184 (1965).
19. J. D. Park, H. J. Gerjovich, W. R. Lycan, and J. R. Lacher. J. Amer. Chem. Soc. **74**, 2189 (1952).
20. R. E. Buckles, R. C. Johnson, and W. J. Probst. J. Org. Chem. **22**, 55 (1957).
21. E. Ucciani and M. Naudet. Bull. Soc. Chim. Fr. 1151 (1960).
22. L. J. Bellamy. The infrared spectra of complex molecules. John Wiley and Sons, Inc., New York, N.Y., 1962. pp. 267–270.
23. A. Hassner. J. Org. Chem. **33**, 2684 (1968).
24. J. R. Campbell, J. K. N. Jones, and S. Wolfe. Can. J. Chem. **44**, 2339 (1966).
25. M. L. Poutsma. J. Amer. Chem. Soc. **87**, 2161 (1965).
26. A. Hassner and F. Boerwinkle. J. Amer. Chem. Soc. **90**, 218 (1968).
27. T. A. Foglia and D. Swern. J. Org. Chem. **31**, 3625 (1966).
28. T. A. Foglia and D. Swern. J. Org. Chem. **33**, 766 (1968).
29. K. Schrage. Tetrahedron Lett. 5795 (1966).
30. A. Hassner and F. Boerwinkle. Tetrahedron Lett. 3309 (1969).
31. F. D. Greene and W. W. Rees. J. Amer. Chem. Soc. **80**, 3432 (1958).
32. R. E. Buckles, B. T. Simpson, and W. F. Edgell. J. Org. Chem. **23**, 483 (1958).
33. T. L. Cottrell. The strengths of chemical bonds. Butterworths, London, 1958.
34. A. W. Hofmann. Chem. Ber. **15**, 407 (1882).
35. W. A. Szarek, S. Wolfe, and J. K. N. Jones. Tetrahedron Lett. 2743 (1964).
36. S. Wolfe and A. Garbesi. To be published.
37. R. E. Buckles. J. Amer. Chem. Soc. **71**, 1157 (1949).
38. R. E. Buckles and J. E. Maurer. J. Org. Chem. **18**, 1585 (1953).
39. C. L. Stevens, T. K. Mukerjee, and V. J. Traynelis. J. Amer. Chem. Soc. **78**, 2264 (1956).
40. D. A. Barr and R. N. Haszeldine. J. Chem. Soc. 30 (1957).

41. S. BROWNSTEIN. J. Org. Chem. **23**, 113 (1958).
42. C. L. STEVENS, H. DITTMAN, and J. KOVACS. J. Amer. Chem. Soc. **85**, 3394 (1963).
43. C. L. STEVENS, M. E. MUNK, A. B. ASH, and R. D. ELLIOTT. J. Amer. Chem. Soc. **85**, 3390 (1963).
44. G. T. TISUE, S. LINKE, and W. LWOWSKI. J. Amer. Chem. Soc. **89**, 6303 (1967).
45. S. LINKE, G. T. TISUE, and W. LWOWSKI. J. Amer. Chem. Soc. **89**, 6308 (1967).
46. S. DUNSTAN and H. B. HENBEST. J. Chem. Soc. 4905 (1957).
47. R. ROGER and D. G. NEILSON. Chem. Rev. **61** 179 (1961).
48. D. Y. CURTIN and C. G. MCCARTY. J. Org. Chem. **32**, 223 (1967).
49. J. R. CAMPBELL. Ph. D. Thesis. Queen's University, Kingston, Ontario, 1969.
50. (*a*) W. A. MOSHER. J. Amer. Chem. Soc. **62**, 552 (1940); (*b*) R. FILLER, B. R. CAMARA, and S. M. NAQVI. J. Amer. Chem. Soc. **81**, 658 (1959).
51. H. SCHMID and P. KARRER. Helv. Chim. Acta, **29**, 573 (1946).
52. E. J. COREY. J. Amer. Chem. Soc. **75**, 2301 (1953).
53. J. D. ROBERTS and C. W. SAVER. J. Amer. Chem. Soc. **71**, 3925 (1949).
54. S. WINSTEIN. J. Amer. Chem. Soc. **64**, 2780 (1942).
55. E. J. LANGSTAFF. Ph.D. Thesis. Queen's University, Kingston, Ontario, 1967.
56. C. O. GUSS and R. ROSENTHAL. J. Amer. Chem. Soc. **77**, 2549 (1955).
57. T. L. CAIRNS, P. J. GRAHAM, P. L. BARRICK, and R. S. SCHREIBER. J. Org. Chem. **17**, 751 (1952).

Can. J. Chem. Downloaded from www.nrcresearchpress.com by 210.87.254.42 on 09/05/12
For personal use only.

Can. J. Chem. Downloaded from www.nrcresearchpress.com by 84.22.46.98 on 09/08/12
For personal use only.

On the Distinction between Reaction Fluxes and Phenomenological Rate Constants

R. K. BOYD
Chemistry Department, University of Guelph, Guelph, Ontario

Received October 19, 1970

The physical interpretation of the phenomenological rate constants of chemical kinetics is examined. For perfect gas systems, the traditional view of the rate constants for elementary reactions as one-way reaction fluxes is compared with a more recent interpretation (3) in terms of more complicated functions; it is concluded that, for real systems, the former view is a special case of the latter, while for systems in which the phenomenological rate equation is exact, the rate constants are shown to be one-way fluxes.

In any given system, the applicability of the special interpretation is a function of the detailed nature of the transport matrix, which is generally unknown; practical implications of these ideas are presented. For systems other than perfect gases, the problem is complicated by the absence of well-defined molecular states; however, it is suggested that the flux interpretation is the most reasonable.

L'interprétation physique des constantes de vitesse phénoménologiques en cinétique chimique est examinée. Pour des systèmes de gaz parfaits, le point de vue traditionnel, qui consiste à assimiler les constantes de vitesse des réactions élémentaires à des flux de réaction uni-directionnels, est comparé à une interprétation plus récente (3) en termes de fonctions plus complexes; il est conclu que, pour les systèmes réels, le premier point de vue est un cas particulier du dernier; cependant, dans le cas des systèmes, pour lesquels l'équation de vitesse phénoménologique est exacte, il est montré que les constantes de vitesse sont des flux uni-directionnels.

Pour un système donné, l'applicabilité de l'interprétation spéciale est fonction de la nature de la matrice de transport, laquelle est en général inconnue; l'implication pratique de ces idées est présentée. Pour des systèmes autres que de gaz parfaits, le problème est compliqué par l'absence d'états bien définis des molécules; toutefois, il est suggéré que l'interprétation en termes de flux est la plus raisonnable.

Canadian Journal of Chemistry, 49, 1401 (1971)

Introduction

For elementary chemical reactions in homogeneous systems, it is found experimentally that the observed reaction rate may be expressed as the difference of two terms, one of which contains only the concentrations of reactants, and the other only the concentrations of products. For example, consider an isomerization reaction in a perfect gas system

$$[1] \qquad X_1 + Y \rightleftharpoons X_2 + Y$$

X_1 and X_2 denote chemical isomers, which are undergoing interconversion through the agency of collisions with an inert collision partner Y, assumed present in large excess. The observed rate law is assumed to take the form,

$$[2] \qquad -d[X_1]/dt = k_f[X_1] - k_b[X_2]$$

where k_f and k_b are constants for a given value of [Y]. For present purposes, isomerizations involving low and high pressure limits are excluded, *i.e.* there are no "spontaneous" reactive transitions, which do not require a collision with Y.

The traditional interpretation of the rate constants is well expressed in the following quotation from Denbigh (1) "··· there is no specifically thermodynamic reason why the measured reaction rate must be expressible as a difference of two terms ··· the existence of the two terms must therefore be given an interpretation which is *kinetic*, and it has become customary to regard the observed reaction rate as being equal to the difference of the rates in the forward and backward directions ··· there is clearly an element of convention in identifying the two terms with the forward and backward rates."

More recently, this convention has been challenged by Widom (3), on the basis of an analysis due to Zwolinski and Eyring (2), later developed by Snider (4). As emphasized by Widom (3) as a result of this analysis, "the constants k_f and k_b are *not* the probabilities per unit time of an X_1 molecule making an $X_1 \rightarrow X_2$ transition, and an X_2 molecule making an $X_2 \rightarrow X_1$ transition; $k_f[X_1]$ and $k_b[X_2]$ are *not* the separate $X_1 \rightarrow X_2$ and $X_2 \rightarrow X_1$ fluxes." (The symbols used here are slightly different from those used by Widom (3).)

In the present work, the nature of this fundamental disagreement concerning the physical

Can. J. Chem. Downloaded from www.nrcresearchpress.com by 84.22.46.98 on 09/08/12
For personal use only.

meaning of rate constants will be further explored; some basic notation is first defined. The microscopic description of the chemical rate is given by

$$[3] \qquad (\mathrm{d}/\mathrm{d}t)|\boldsymbol{a}\rangle = -\mathbf{K}|\boldsymbol{a}\rangle$$

where a_i is the fraction of the total reactant molecules in internal state i, *i.e.* $a_i = x_i/\sum_{i=1}^{n} x_i$, where x_i is the concentration of molecules in internal state i. The transport matrix $\mathbf{K}$ is defined by

$$[4] \quad \mathbf{K}_{ii} = \sum_{j=1}^{n} k_{ji};\ \mathbf{K}_{ij} = -k_{ij} \quad \text{for } i \neq j$$

where the concentration [Y] is again conveniently included in the k_{ij}.

By assigning states 1 to m to species X_1, and states $m + 1$ to n, to X_2, Snider proposed (4) that eqs. 2 and 3 are mutually consistent after an incubation time, and that the rate constants are given by

$$[5] \quad k_f = \lambda_2 K_{eq}/(1 + K_{eq});\ k_b = \lambda_2/(1 + K_{eq})$$

where λ_2 is the smallest non-zero eigenvalue of $\mathbf{K}$, and K_{eq} is the thermodynamic equilibrium constant $([X_2]/[X_1])_{eq}$. Since λ_2 is a function of *all* microscopic rate constants k_{ij}, it is not possible (3), in general, to identify k_f and k_b, and the corresponding terms in eq. 2, with one-way fluxes.

Exact Solutions

The present approach is based on the elegant lumping analysis technique introduced by Wei and Kuo (5). Reduction of eq. 3 to eq. 2 corresponds to linear transformation of the n-tuple composition vector $|\boldsymbol{a}\rangle$ into a two-fold vector $|\hat{\boldsymbol{a}}\rangle$, by means of a $(2 \times n)$ proper (5) lumping matrix $\mathbf{M}$, of rank 2

$$[6] \qquad \mathbf{M} \equiv \left(\begin{array}{ccc|ccc} 1 & 1 & 1 \cdots & 0 & 0 & \cdots 0 \\ 0 & 0 & 0 \cdots & 1 & 1 & \cdots 1 \end{array}\right)$$

where the vertical division in $\mathbf{M}$ occurs between the mth and $(m + 1)$th columns.

In common with other work on this problem (3), the theoretical constructs $(\hat{a}_1 R)$ and $(\hat{a}_2 R)$ are now assumed to correspond *exactly* to the experimentally determined quantities $[X_1]$ and $[X_2]$, respectively; $R = [X_1] + [X_2]$ is the total concentration.

The system described by eq. 3 is said to be exactly lumpable (5) by $\mathbf{M}$ if, and only if, there exists a matrix $\hat{\mathbf{K}}$ such that

$$[7] \qquad (\mathrm{d}/\mathrm{d}t)|\hat{a}\rangle = -\hat{\mathbf{K}}|\hat{a}\rangle$$

Equation 7 corresponds to eq. 2, with

$$[8] \qquad \hat{\mathbf{K}} \equiv \begin{pmatrix} k_f & -k_b \\ -k_f & k_b \end{pmatrix}$$

Thus, in view of the above assumption, exact lumpability by $\mathbf{M}$ (eq. 6) implies that the phenomenological rate eq. 2 is *exactly* consistent with the microscopic description, eq. 3. The necessary and sufficient condition for exact lumpability (5) is

$$[9] \qquad \mathbf{MK} = \hat{\mathbf{K}}\mathbf{M}$$

For the present case, where $\mathbf{M}$ is given by eq. 6, this condition is readily shown to require that

$$[10] \quad \sum_{i=m+1}^{n} k_{i1} = \sum_{i=m+1}^{n} k_{i2} = \cdots = \sum_{i=m+1}^{n} k_{im} = k_f$$

and $$\sum_{i=1}^{m} k_{i,m+1} = \cdots = \sum_{i=1}^{m} k_{i,n} = k_b$$

It is clear that the conditions for exact lumpability are not met, in general; however, elucidation of the physical meaning of these conditions is a simple extension of earlier work of Widom (6), and will be only briefly sketched in here. The term $k_f[X_1]$, from eq. 2, may be transformed as follows

$$\begin{aligned}[11] \quad k_f[X_1] &= k_f \cdot [R] \cdot \sum_{i=1}^{m} a_i \\ &= [R] \cdot \sum_{i=1}^{m} \left[a_i \left(\sum_{j=m+1}^{n} k_{ji} \right) \right] \\ &= [X_1] \cdot \sum_{i=1}^{m} \left[b_i \left(\sum_{j=m+1}^{n} k_{ji} \right) \right] \\ &= r_f[X_1] \end{aligned}$$

with a similar relationship for $k_b[X_2]$. The first step uses the above assumption relating $[X_1]$ and $[X_2]$ to $\hat{a}_1$ and $\hat{a}_2$, and the second requires conditions [10]; the one-way reaction fluxes r_f and r_b (1, 2), are defined by eq. 1, with

$$\begin{aligned}[12] \quad b_i &= x_i \Big/ \sum_{i=1}^{m} x_i = a_i([R]/[X_1]) \\ &\qquad \text{for } 1 \leqq i \leqq m \\ b_j &= x_j \Big/ \sum_{j=m+1}^{n} x_j = a_j([R]/[X_2]) \\ &\qquad \text{for } (m + 1) \leqq j \leqq n \end{aligned}$$

Can. J. Chem. Downloaded from www.nrcresearchpress.com by 84.22.46.98 on 09/08/12
For personal use only.

Since the rate constants k_f and k_b are functions of temperature only, the equalities $k_f = r_f$ and $k_b = r_b$ can hold only if the b_i and b_j have their Boltzmann values (6); the corresponding fluxes will be denoted by R_f and R_b. Thus, the necessary and sufficient conditions [10], for eq. 2 to be an *exact* consequence of eq. 3, also ensure that the rate constants are given by the corresponding one-way fluxes, with the internal distribution functions Boltzmannized.

The sense in which the $\hat{\mathbf{K}}$ matrix, given by eqs. 5 and 8, may be said to be an exact solution, is now investigated. An entirely equivalent condition to eq. 9, for exact lumpability (5), is

$$[13] \qquad \mathbf{MX} = \hat{\mathbf{X}}(\mathbf{I}(2)|\mathbf{0})$$

where $\mathbf{X}$ is the eigenvector matrix of $\mathbf{K}$, defined as $(|\mathbf{x}_1\rangle, |\mathbf{x}_2\rangle, \cdots, |\mathbf{x}_n\rangle)$, and $\hat{\mathbf{X}}$ is the corresponding eigenvector matrix of $\hat{\mathbf{K}}$; $\mathbf{I}(2)$ is the 2×2 identity matrix, and $\mathbf{0}$ is a $2 \times (n-2)$ null matrix. Each of the non-vanishing vectors $\mathbf{M}|\mathbf{x}_i\rangle$ is an eigenvector of $\hat{\mathbf{K}}$, with the same eigenvalue $\lambda_i = \hat{\lambda}_i$ (5). If now $\hat{\mathbf{K}}$ is chosen to correspond to Snider's rate constants (4) given by eq. 5, and the nature of the corresponding exact lumping matrix $\mathbf{M}'$ is derived from eq. 13, it is easily shown that $\mathbf{M}'$ is an improper (5) lumping matrix. That is to say, although a vector $|\hat{a}'\rangle$ does exist, whose time-evolution is *exactly* described by eqs. 5 and 7, the quantities $\hat{a}_1'$ and $\hat{a}_2'$ bear no relation to the experimentally measured quantities $[X_1]$ and $[X_2]$.

The conclusions of the present section, while exact, are probably not applicable to any real system, since conditions [10] and [13] are unlikely to be fulfilled. Master equations like eq. 3 are unlikely to prove invalid for the present example, so that the range of validity of the rate eq. 2 must be questioned. Since this is a phenomenological equation found to be adequate to within experimental uncertainty, approximate solutions and their associated errors must be sought.

Approximate Solutions

The techniques of error estimation for approximately lumped systems, devised by Wei and Kuo (5), are here applied to the present problem; the conditions under which reaction system [3] is approximately lumpable by $\mathbf{M}$ (eq. 6) are required. By retaining this proper lumping matrix, the elements of the lumped distribution vector $|\hat{\boldsymbol{a}}\rangle$ correspond to $[X_1]$ and $[X_2]$; this section is concerned with the error associated with estimates of these observables.

For any given choice of the matrix $\hat{\mathbf{K}}$, the corresponding error matrix $\mathbf{E}$ is defined (5) as

$$[14] \qquad \mathbf{E} \equiv \mathbf{MK} - \hat{\mathbf{K}}\mathbf{M}$$

In addition, there are thermodynamic constraints upon the choice of the $\hat{\mathbf{K}}$ matrix (1, 7–9), since the rate and the reaction affinity must vanish together. For the case of reaction 1, this constraint is simply the rate-quotient law

$$[15] \qquad k_f/k_b = K_{eq}$$

There is an infinite set of possible $\hat{\mathbf{K}}$ matrices (eq. 8) fulfilling this condition, including that proposed by Snider (4), (eq. 5). The choice recommended by Wei and Kuo (5) involves specifying an error matrix such that

$$[16] \qquad \mathbf{EAM}^{\mathrm{T}} = \mathbf{0}(2)$$

where $\mathbf{A}$ is the diagonal matrix whose non-zero elements are the equilibrium fractions a_i^*, $\mathbf{M}^{\mathrm{T}}$ is the transpose of $\mathbf{M}$, and $\mathbf{0}(2)$ is the 2×2 null matrix. For the present example, combination of eqs. 8, 14, and 16 readily shows that the resulting rate constants are identifiable with R_f and R_b.

The concepts of one-way fluxes and Snider's rate coefficients have now both been introduced as acceptable approximate solutions for a system not exactly lumpable by the proper lumping matrix $\mathbf{M}$ (eq. 6). In order to investigate which of the two solutions is likely to be the more accurate, the error of lumping is defined (5) as

$$[17] \quad |\hat{\boldsymbol{a}}(t)\rangle - |\hat{\boldsymbol{a}}'(t)\rangle = (\mathbf{M}\, e^{-\mathbf{K}t}|\boldsymbol{a}(0)\rangle) - (e^{-\hat{\mathbf{K}}t}\mathbf{M}|\boldsymbol{a}(0)\rangle)$$

i.e. the difference between the true (observable) composition vector $|\hat{\boldsymbol{a}}(t)\rangle$, obtained by lumping the integrated form of the correct eq. 3, and the estimate $|\hat{\boldsymbol{a}}'(t)\rangle$, obtained from the lumped initial distribution $\mathbf{M}|\boldsymbol{a}(0)\rangle$, and eq. 7. Two exactly analogous expressions may be obtained for the errors in the approximate solutions in terms of Boltzmannized fluxes (eqs. 11 and 12), and Snider's rate coefficients (eq. 5); the former will be denoted by a superscript or subscript R, and the latter by S. Further, define a matrix $\mathbf{N}$ for each case by

$$\mathbf{N} \equiv \hat{\mathbf{X}}^{-1}\mathbf{MX}$$

Then, eq. 17 may be written (5) in the form

Can. J. Chem. Downloaded from www.nrcresearchpress.com by 84.22.46.98 on 09/08/12
For personal use only.

[18] $$|\hat{a}(t)\rangle - |\hat{a}'(t)\rangle = \hat{\mathbf{X}}\mathbf{P}\mathbf{X}^{-1}|a(0)\rangle$$

where $\mathbf{P}_{ij} = 0$, for $i = 1$ or $j = 1$; $\mathbf{P}_{ij} = n_{ij}(e^{-\lambda_j t} - e^{-\hat{\lambda}_i t})$, for $i,j \neq 1$. The error vector is thus a vector function of time, which asymptotically approaches zero as $t \to \infty$, provided the chosen $\hat{\mathbf{K}}$ satisfies condition [15]. In order to discover which of $\hat{\mathbf{K}}_R$ and $\hat{\mathbf{K}}_S$ gives the error vector with the more rapid approach to zero, examine the elements P_{ij}. Since $\hat{\lambda}_2{}^S = \lambda_2$, by choice, $P_{22}{}^S = 0 \neq P_{22}{}^R$, *i.e.* $\mathbf{P}^S$ has one additional zero element. If $\mathbf{X}^{-1}|a(0)\rangle \equiv |d\rangle$, the error vectors for the two cases may be written

[19] $$|\hat{a}(t)\rangle - |\hat{a}_R(t)\rangle = \hat{X}_2{}^R(1) \sum_{j=2}^{n} d_j n_{2j}{}^R(e^{-\lambda_j t} - e^{-\hat{\lambda}_2{}^R t}) \hat{X}_2{}^R(2) \sum_{j=2}^{n} d_j n_{2j}{}^R(e^{-\lambda_j t} - e^{-\hat{\lambda}_2{}^R t})$$

[20] $$|\hat{a}(t)\rangle - |\hat{a}_S(t)\rangle = \hat{X}_2{}^S(1) \sum_{j=3}^{n} d_j n_{2j}{}^S(e^{-\lambda_j t} - e^{-\lambda_2 t}) \hat{X}_2{}^S(2) \sum_{j=3}^{n} d_j n_{2j}{}^S(e^{-\lambda_j t} - e^{-\lambda_2 t})$$

For all $\hat{\mathbf{K}}$ matrices corresponding to eq. 8, which conserve mass, it is readily shown that $\hat{X}_2(1) = -\hat{X}_2(2)$, so that the sum of the elements of the error vector is zero, as required.

Equations 19 and 20 permit evaluation of the errors in the case that the detailed nature of $\mathbf{K}$ is known; however, it is the present purpose to determine whether any general conclusions, concerning the physical interpretation of observed rate constants, may be drawn in the case that $n_{ij}{}^R$, $n_{ij}{}^S$, λ_i, and $\hat{\lambda}_2{}^R = (R_f + R_b)$, are unknown. The summation over j, in eq. 20 has one term less than that in eq. 19, since $P_{22}{}^S = 0$; this suggests that the $\hat{\mathbf{K}}$ matrix proposed by Snider (4) should, in general, yield a satisfactory approximation to the true $|\hat{a}(t)\rangle$, after a shorter time than the Boltzmannized fluxes. (Such prediction of the experimental observables would seem to be the only possible criterion.) However, the incubation times, after which the error vectors corresponding to the two approximate solutions, become less than some appropriate measure of experimental uncertainty, are seen to be complex functions of $\mathbf{K}$. Thus, the above conclusion may not be regarded as a completely general result, but rather as a strong indication.

Through additional general considerations, the relationship between the two interpretations of phenomenological rate constants, in terms of one-way fluxes (1) and composite functions (3), would appear to be a reflection of the relationship between "equilibrium" and "steady state" theories of chemical kinetics; that is, the former is a special case of the latter. (The steady-state implied by Snider's analysis (4) is not the usual steady-state of conventional chemical kinetics, in that the quantity which is essentially time-independent (4) is $(a_i - a_i^*/a_j - a_j^*)$, for all i,j.) For, if the two incubation times are *both* much shorter than the characteristic time for reaction, it seems reasonable to suppose that the two interpretations should be equivalent. This suggestion may be formalized as follows: for times after which both error vectors [19] and [20] are acceptably small

[21] $$R_f[X_1] - R_b[X_2] \equiv k_f[X_1] - k_b[X_2] = -d[X_1]/dt$$

where eq. 21 has been written as an identity, to express the fact that at a given temperature rate constants measured in a reaction mixture of some arbitrary composition may be used directly to compute rates in *all* reaction mixtures. Identity [21] is valid if, and only if

[22] $$k_f \equiv R_f \quad \text{and} \quad k_b \equiv R_b$$

where k_f and k_b are here taken to represent the quantities defined in eq. 5. This analysis is applicable only to systems in which the microscopic rate constants governing internal relaxation are much larger than those describing "chemical" transitions, so that the appropriate incubation time is a small fraction of the reaction time. For cases where this condition is not met, the relevant fluxes are r_f and r_b, corresponding to time-dependent internal distribution functions for X_1 and X_2. An equation analogous to [21] is still valid, but since r_f and r_b are now functions of $[X_1]$ and $[X_2]$, the one-to-one correspondence of eq. 22 does not apply. Since, in general, the less stringent steady-state condition will be reached before the internal modes are approximately Boltzmannized, Snider's approximate solution (2, 4) is expected to have a wider range of validity than that in terms of one-way fluxes; this conclusion supports that drawn from eqs. 19 and 20.

Can. J. Chem. Downloaded from www.nrcresearchpress.com by 84.22.46.98 on 09/08/12
For personal use only.

Practical Application

As a practical illustration of these problems, the reaction system

[23] $$Br_2 + Y \rightleftharpoons 2Br + Y$$

will be considered. This system has non-linear recombination terms in the rate equation, and the above analysis cannot be applied directly; however, for present purposes, the broad conclusions concerning the physical interpretation of empirical rate constants will be assumed valid for this case also. Significant discrepancies have been found, both in absolute magnitude and temperature dependence, in rate coefficients measured by different experimental techniques (10) for this system. These discrepancies are readily explicable qualitatively on the assumption that the rate coefficients for dissociation, derived for initial rates immediately behind shock-waves, were measured before the necessary incubation times (2–4) were over. A simplified model (10) of the coupling of vibrational relaxation to dissociation, was able to account quantitatively for the observed discrepancies; this model involves several approximations, such as the assumption of a unique, time-dependent vibrational temperature T_v, for Br_2. Apart from such approximations, necessitated by the lack of more detailed information, a fundamental assumption of this model, relevant to the present work, is the identification of the experimental recombination rate constants, obtained from flash photolysis experiments at high temperatures (10), with the normalized recombinative flux R_r. As shown above, this requires that the internal modes were essentially fully relaxed in these recombination experiments. Using this assumption, the corresponding dissociative flux R_d could be evaluated, and the non-equilibrium flux r_d was approximated by

[24] $$r_d/R_d = [Q_v(T)/Q_v(T_v)] \exp [(-D/R)(1/T_v - 1/T)]$$

where Q_v and D are the vibrational partition function and dissociation energy, respectively, for Br_2. The right side of eq. 24 is simply the ratio of the fractional populations of states very close to the dissociation limit (assumed to be the only states involved in "chemical" transitions) for $T_v \neq T$ and $T_v = T$.

This evaluation of the observed behavior, during the incubation times, was possible only through the *assumption* that the observed recombination rate constants (10) correspond to R_r values; this implies that the incubation times for this system are true relaxation times, during which internal modes of Br_2 become essentially Boltzmannized. Direct experimental information on the latter assumption is not available, since the volume concentrations of states involved in the "chemical" transitions are not measurable by current techniques; the only justification for this procedure, in the present example, lies in its empirical success (10).

However, the present considerations have shown that there is no fundamental conflict between this model and the established theories of kinetics, as has been suggested (11). The rate quotient law [15] arises, as a special case, from general conditions for the mutual consistency of the thermodynamic and kinetic descriptions of reversible reactions at equilibrium (1, 7–9). As such, it is, indeed, an essential feature (11); however, the rate coefficients, observed immediately behind shock waves in Br_2, involved measurements of concentration, and its rate of change, at a single time (10). There is *no* experimental evidence that these coefficients are rate *constants*, which may be used at all times, including the equilibrium limit, to derive [15]; indeed, for the Br_2 example, the noted discrepancies (10) suggest that this may not be the case, and that the measurements were made during the incubation times. Equation 15 is known to be inapplicable to such quantities (2–4, 6, 12).

Discussion

The physical interpretation of phenomenological rate constants, as contained implicitly in microscopic theories of reaction rates (3, 4, 6, 12) has been shown above to depend on whether or not *exact* correspondence, with the microscopic master equation, is demanded. For real systems, with only approximate correspondence to within experimental uncertainty, no completely general and clearcut conclusions have been reached; however, the quantities defined by Snider (4) (eq. 5) do appear, indeed, to offer the most likely interpretation, but to be equivalent to one-way fluxes in special cases. For the exact case, it has been shown unambiguously that the rate constants are one-way fluxes.

The entire foregoing discussion, in terms of single-particle quantum states, is restricted to ideal gases. For reaction 1, proceeding in solution, the form of the rate equation, found to be generally satisfactory, is (ref. 1, pp. 447–450),

$$[25] \quad -\mathrm{d}[\mathrm{X}_1]\mathrm{d}t = k_\mathrm{f}' \cdot \beta \cdot a(\mathrm{X}_1) - k_\mathrm{b}' \cdot \beta \cdot a(\mathrm{X}_2)$$

where k_f' and k_b' are functions of temperature only, $a(\mathrm{X}_1)$ and $a(\mathrm{X}_2)$ are the activities of the reacting chemical species, and β depends on the concentrations of all species in the solution. The same problem arises here, *i.e.* can the two terms on the right side of eq. 25 be identified with one-way fluxes, assuming the latter can be defined. Strictly, any rigorous physical model would deal only with system states; however, the fact that distinct chemical species may be meaningfully inferred to exist in solution, indicates that "chemical" classifications must be somehow imposable upon the "physical" model of the reaction mixture. An account of this difficult problem has been given by Golden (13); unfortunately, "··· the formal theory which has been derived, is, without further embellishments, completely incapable of rendering unique theoretical expressions identifiable as the rate constants of chemical change" (ref. 13, p. 153). As emphasized by Golden (13), this particular conclusion has no bearing on the description of the observables, *i.e.* chemical composition and its rate of change, but is concerned only with the conventional identification of measured rate constants with theoretical constructs (1, 2).

On a less rigorous level, the only existing theory which has been usefully applied to reactions in solution is transition state theory; now, β (eq. 25) is identified as the reciprocal of the activity coefficient of the activated state. As applied to ideal gas reactions, this theory is explicitly an "equilibrium" theory, and the calculated rate constants are, indeed, normalized one-way fluxes; this latter feature is most clearly seen in the exposition given by Denbigh (ref. 1, pp. 450–459). The situation is not so clear for the "thermodynamic" formulation of the theory, applicable to solution reactions, but it seems that the same identification is the most reasonable that can be made; this is entirely consistent with the fact that relaxation of internal modes of molecules appears to be extremely fast in the liquid phase (14), even though a rigorous definition of such modes (13) involves conceptual difficulties.

The author's interest in these problems was originally stimulated by a period spent in the research group of Professor George Burns; the continued encouragement of Professor Burns is gratefully acknowledged. Professor B. Widom very kindly took time to offer valuable criticisms of an early version of the paper. The work was supported by financial assistance from the National Research Council of Canada.

1. K. G. Denbigh. Principles of Chemical Equilibrium. Cambridge University Press, Cambridge. 1955. p. 443.
2. B. J. Zwolinski and H. Eyring. J. Amer. Chem. Soc. **69**, 2702 (1947).
3. B. Widom. Sci. **148**, 1555 (1965).
4. N. S. Snider. J. Chem. Phys. **42**, 588 (1965).
5. J. Wei and J. C. W. Kuo. Ind. Eng. Chem. Fundam. **8**, 114 (1969); Ind. Eng. Chem. Fundam. **8**, 124 (1969).
6. B. Widom. J. Chem. Phys. **34**, 2050 (1961).
7. M. Manes, L. J. E. Hofer, and S. Weller. J. Chem. Phys. **18**, 1355 (1950).
8. C. A. Hollingsworth. J. Chem. Phys. **20**, 1649 (1952).
9. E. H. Blum and R. Luus. Chem. Eng. Sci. **19**, 322 (1964).
10. J. K. K. Ip and George Burns. Discuss. Faraday Soc. **44**, 241 (1967); J. Chem. Phys. **51**, 3425 (1969).
11. F. Kaufmann. Ann. Rev. Phys. Chem. **20**, 45 (1969).
12. C. A. Brau. J. Chem. Phys. **47**, 1153 (1967).
13. S. Golden. Quantum-Statistical Foundations of Chemical Kinetics. Oxford University Press, London. 1969.
14. B. J. Berne, J. Jortner, and R. Gordon. J. Chem. Phys. **47**, 1600 (1967).

Can. J. Chem. Downloaded from www.nrcresearchpress.com by 84.22.46.98 on 09/08/12
For personal use only.

Can. J. Chem. Downloaded from www.nrcresearchpress.com by 210.87.254.40 on 09/05/12
For personal use only.

Molecular Theory of Energy Conversion and of Initiation of Chemical Reactions in Solids[1]

CHARLES E. MELTON
Department of Chemistry, University of Georgia, Athens, Georgia 30601

Received October 8, 1970

A theory has been developed to describe the initiation of chemical reactions in solids. Two basic assumptions are made to formulate the model. First, the initiation of chemical reactions in solids ultimately results from the vibrational excitation of the individual molecules in the solid, and second, the lattice vibrations in a solid can be treated as pseudocollisions between the individual molecules in the lattice. In effect, the solid is treated as an ordered dense gas. These assumptions permit us to describe chemical reactions in a solid within the framework of collision theory. The resultant rate constant, k, depends on molecular and lattice parameters and on the temperature. It is of the form $k = P_{t\rightarrow f}v/\sqrt{2}Nb$, where N is the number of nearest neighbor molecules, b is the lattice spacing, v is the mean velocity of the individual molecules, and $P_{t\rightarrow f}$ is the probability of translational–vibrational energy conversion.

Conclusions based on the present model are in accord with qualitative results from a hard sphere model. For example, energy conversion (translational to vibrational) is many orders of magnitude greater in the region of a defect. Consequently, the probability for initiation of chemical reactions is orders of magnitude greater in the region of a defect.

Une théorie a été développée pour décrire l'initiation des réactions chimiques dans les solides. Le modèle utilisé est basé sur deux hypothèses. Premièrement, l'initiation des réactions chimiques dans les solides résulte tout compte fait de l'excitation vibrationnelle des molécules individuelles dans le solide et, deuxièmement, les vibrations de réseau dans un solide peuvent être traitées comme des pseudocollisions entre molécules individuelles dans le réseau. En effet, le solide est traité comme un gaz dense ordonné. Ces hypothèses nous permettent de décrire les réactions chimiques dans un solide en termes de la théorie des collisions. La constante de vitesse résultante, k, dépend des paramètres moléculaires, de ceux du réseau et de la température. Elle est de la forme $k = P_{t\rightarrow f}v/\sqrt{2}Nb$, où N est le nombre de molécules voisines les plus proches, b est l'espacement du réseau, v est la vitesse moyenne de la molécule individuelle et $P_{t\rightarrow f}$ est la probabilité de conversion de l'énergie translationnelle en énergie vibrationnelle.

Les conclusions, basées sur le modèle présenté, sont en accord avec des résultats qualitatives d'un modèle de sphères rigides. Par exemple, la conversion de l'énergie (translationnelle en vibrationnelle) est plus grande de plusieurs ordres de grandeur dans la région d'un défaut. Par conséquence, la probabilité de l'initiation de réactions chimiques est plus grande de quelques ordres de grandeur dans la région d'un défaut.

Canadian Journal of Chemistry, **49**, 1407 (1971)

Introduction

The primary purpose of this work was to develop a theory of initiation of chemical reactions in solids. Theories of reactions (1–5) in solids have generally been based on the macroscopic properties of the material. Thus, properties such as pressure, temperature, and energies suggested by a sense of preception were related within the framework of fluid flow to give the so called hydrodynamic theories. Within this framework, matter is a continuous substance and energy behaves like an incompressible weightless fluid. Consequently, the analysis of chemical processes provided by macroscopic theories can give only limited insight into the actual physical process. The chemist is not satisfied to look at the process from a macroscopic point of view. For him the properties and reactions of substances are determined by the configuration of the atoms which make up the individual molecules. Thus, the macroscopic theories are not aesthetically good despite their success in describing many aspects of the problem.

To attack the problem from a microscopic or molecular point of view, one simply tries to conceive of the elementary steps of the overall process. Each step is then described by an appropriate mathematical model. Formulation of the elementary steps is somewhat arbitrary. In the present approach, we define six elementary steps which occur in temporal sequence to give the overall reaction. The six steps are: (*1*) excitation

[1]Supported by the U.S. Atomic Energy Commission under contract No. At-(40-1) 3729 with the University of Georgia.

Can. J. Chem. Downloaded from www.nrcresearchpress.com by 210.87.254.40 on 09/05/12
For personal use only.

of molecules in the solid; (*2*) propagation of energy from the region of primary excitation to the region of initiation of chemical reactions (conduction through the lattice); (*3*) energy transition from the lattice to the internal degrees of freedom of the individual molecules (electronic, vibrational, and rotational); (*4*) decomposition of the individual molecules into primary products (ions, free radicals, excited species, etc.); (*5*) reaction of primary products with neighbors to form intermediate products (nonequilibrium conditions); (*6*) reactions of intermediate products to form final reaction products (equilibrium conditions).

Steps 1–6 are actually a step by step description of the reaction path of each species from initiation to its ultimate fate. Actually, this sequence is a description of the rate of attaining chemical equilibrium which is normally called chemical kinetics. The model is fully described qualitatively by steps 1–6. Our task is to develop a rigorous mathematical model which will qualitatively describe each step.

Much previous work has been carried out on steps 1 and 2. In general, however, these studies were within the framework of a hard sphere model. Nevertheless, it is instructive to briefly review the previous work because the hard sphere model gives considerable insight into the problem of energy transfer through the lattice.

In a previous report (6), we studied the problem of initiation of chemical reactions from the point of view of the hard sphere lattice of one molecule per unit cell and considered the effect of an impurity added to the molecular crystal. Relationships governing the transmission T' and reflection R' of energy for this type of lattice are known (7). They are

$$[1] \quad T' = \left[1 + \left(1 - \frac{M_1}{M_2}\right)^2 \frac{\omega^2}{\omega_L{}^2 - \omega^3}\right]^{-1}$$

$$[2] \quad R' = \left(1 - \frac{M_1}{M_2}\right)^2 \omega^2 \times \left[\omega_L{}^2 - \omega^2 \left(1 - \left(1 - \frac{M_1}{M_2}\right)^2\right)\right]^{-1}$$

where $\omega = 2\pi$ and ω_L is the maximum lattice frequency, M_1 and M_2 are the masses of the hard spheres. We note that the transmission coefficient is unity for the interior of a pure crystal because $M_1 = M_2$ in eq. 1. On the other hand, energy tends to concentrate near an impurity in an impure crystal. Thus, chemical reactions according to the hard sphere model occur in the region of an impurity. Similar conclusions are apparent from the work of Montroll and Potts (8) on the effect of defects in solids.

Propagation of energy through a two dimensional lattice has been investigated by Payton, Rich, and Visscher (9). These investigators approached the problem by numerical integration of the Newton's equations of motion. The lattice consisted of a ten by fifty array at fixed boundaries. An initial impulse of energy of about 7 kT was given to all atoms at the boundary. Results in Fig. 1 show the propagation of energy through the lattice. The energy in the lattice is proportional to the height of the grid. In Fig. 1, we see the effects of an impurity on the transmission of energy through the lattice. In Fig. 1*a*, the energy shows a dip in the region of the light impurity. The replacement of an atom in the lattice by a light impurity causes a local variation in mass, force constant, and consequently vibrational modes. In a simple cubic lattice, the introduction of an impurity changes six force constants considering only nearest neighbor interactions. Thus, in the region of the light impurity, localized modes are generated. The frequency of these local modes is higher than that of the host atoms which means the light impurity does not couple with the normal modes to increase its energy. This fact explains the dip in energy in the region of the light impurity in Fig. 1*a*. A heavy impurity, on the other hand, has a lower local mode. This means that the particle remains in phase with the energy pulse for a longer period and consequently more energy is transferred to the particle. This phenomenon is illustrated by the results of Fig. 1*b*. Note the spike in the energy pulse at the heavy

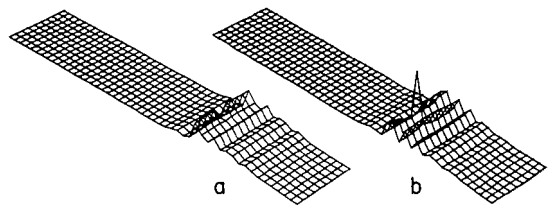

FIG. 1. Illustrations of the dip occurring in the energy wave as it passes over a light impurity (*a*) and the spike resulting from encounter with a heavy impurity (*b*).

Can. J. Chem. Downloaded from www.nrcresearchpress.com by 210.87.254.40 on 09/05/12
For personal use only.

impurity. Both light and heavy impurities in a 2D lattice cause energy to concentrate in the region of the impurity in accord with the conclusions drawn from the simple 1D model.

Theoretical Model

Thus far we have discussed an ideal system, namely, the hard sphere model. This model can never be used to describe the actual physical phenomena of chemical reactions in a solid although the model does provide considerable insight into the process of energy transfer. Let us restrict the molecules in the solid to two dimensions as shown in Fig. 2. We assume that line 5 is composed of impurities and further assume that collisions in the solid can be treated by the same techniques as those used for the gas phase. To make any real progress in the development of a theory of reactions in solids, the hard sphere restriction suggested in Fig. 2 must be removed. Specifically, the process must be described in terms of the properties of the individual molecules. This means we must formulate a mechanism for the transfer of energy from translation into internal energy (most likely vibrational). We now make the assumption that the initiation of chemical reactions in solids results from the excitation of vibrational modes of an individual molecule by some mechanism. This mechanism includes absorption of photons, conversion of kinetic energy to vibrational energy by collision, etc. In this treatment we consider vibrational excitation by collision with other molecules in the lattice. A collision, it should be emphasized, is simply an interaction between collisional partners. The basic assumption of vibrational excitation permits us to attack the problem of chemical reactions with the machinery of collision theory. In this approach the colliding partners suffer an inelastic collision which results in the vibrational excitation of one or more modes of the individual molecules. We now define a quantity which we call the molecular activation energy E_m. This quantity is the minimum vibrational excitation required to produce a chemical reaction. Thus, we have the requirement for chemical reaction

$$[3] \qquad E_m = \sum_{j=1}^{3N-6} n_j h\nu_j = \text{constant}$$

$$\{n_j\} = 0, 1, 2, \cdots$$

where N is the number of atoms in the molecule and $h\nu_j$ is the energy of the jth oscillator in the molecule, and $\{n_j\}$ is any set which will give the constant E_m. A bimolecular reaction in the gas phase can be described by the relationship

$$[4] \qquad A + B \xrightarrow{k'} C + D$$

where A, B, C, and D are any species: atoms, molecules, ions, electrons, etc, and k' is the rate constant. The rate constant can be expressed in terms of reaction cross section as

$$[5] \qquad k_\sigma = 2\left(\frac{2kT}{\pi\mu}\right)^{\frac{1}{2}}\sigma_R = \bar{v}\sigma_R$$

where v is the mean velocity. The reaction cross section is given by

$$[6] \qquad \sigma_R = \sigma_t P_{i\to f}$$

where σ_t is the total cross section and $P_{i\to f}$ is the probability that one of the collisional partners will undergo a transition from the initial state i to a final state f which corresponds to E_m of eq. 3. We have now reduced the problem of chemistry in solids to that of calculating $P_{i\to f}$. The other variables can be easily obtained from other considerations. If one deals with the gas phase, one must use a three dimensional theory. However, one can apply the approach to the solid state by simply assuming that lattice vibrations actually represent collisions of particles restricted to move along a straight line connecting their centers of mass. Thus, one can treat the problem as that of a one dimensional collision process.

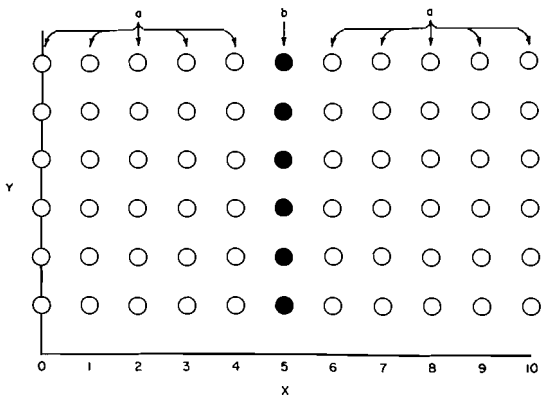

FIG. 2. Two dimensional gas with a line of impurities (*b*).

Can. J. Chem. Downloaded from www.nrcresearchpress.com by 210.87.254.40 on 09/05/12
For personal use only.

There have been a number of treatments of inelastic collisions in which an exchange of translational and rotational energy occurs. Most of these calculations are based on the original work of Zener (10) and of Landau and Teller (11). We now look briefly at the general method.

In an ideal treatment one would obtain a total wave function for the molecules. This would be done by expanding the complete set of eigenfunctions for the stationary states of the system to give

$$[7] \qquad \Psi = \sum_n c_n \psi_n$$

We then substitute the expansion into the Schrödinger equation. A set of coupled differential equations in the coefficients c_n is obtained from the property of orthogonality of the states. A solution to this set of equations with appropriate boundary conditions gives the transition probability. Unfortunately, a solution to the complete set of coupled differential equations is an arduous task. Thus, various simplifying approximations must be introduced to obtain a solution to the equations.

The simplest treatment is the first order perturbation approximation. In this approximation the wave function is taken as a linear combination of terms corresponding to the initial and final states

$$[8] \qquad \psi = c_i \Psi_i + c_f \Psi_f$$

The coefficient of the initial state c_i is set equal to unity throughout the collision. This is equivalent to assuming a small transition probability.

First order perturbation theory can be extended by removing the restrictions on c_i and c_f. Such a treatment is called the two state approximation. In this treatment, the wave function is given by [8], without setting $c_i = 1$.

If one cares to increase the complexity and presumably the accuracy, the Nth order perturbation approximation is used. In this approximation all energetically possible states between the initial and final state are retained as well as the initial and final states. Transition probabilities are assumed to be small thus restricting c_i to unity.

The most accurate and most complex method is the N state approximation in which all N states of [8] are used. In addition, virtual transitions among the N states are included. A solution is obtained by a variational type approach. The value of $P_{i\to f}$ is considered "best" when the addition of more states produce no significant change in $P_{i\to f}$.

A serious problem in calculating $P_{i\to f}$ is that of obtaining a suitable interaction potential. The assumption is sometimes made that the interaction can be approximated by a product which is a function of the intermolecular distance r and the normal vibrational coordinates, $s_i (i = 1, 2, 3, \cdots, n)$. Thus,

$$[9] \qquad V = V_0 V_{(r)} V_i(i) \cdots V_m(s_m)$$

Sometimes an exponential of the form

$$[10] \qquad V = V_0 \, e^{-r/a}$$

is used, where r is the intermolecular distance measured in atomic units and a is a length measured in atomic units and is of the order of the gas kinetic radius of the molecules.

The problem of evaluating $P_{i\to f}$ has been treated fairly successfully with a simple one dimensional model for the collision (10–13). Schwartz, Slawsky, and Herzfeld (12) obtained the relationship for an initial velocity of v_0 and a final velocity of v_f

$$[11] \quad P_{i\to f}(v_0) = \frac{16\pi^2 V_0^2}{v_0 v_f h^2} \times [V(i_1 \to f_1) \cdots V(i_n \to f_n) R]^2$$

where R is defined as

$$[12] \qquad R = \int_{-\infty}^{\infty} F_0 F_f V_r \, dr$$

and F_0, F_f are solutions of the Schrödinger equation for the motion of a free particle in the potential field V_r. The term $V(i_i \to f_i) \cdots$ is defined as

$$V(i_n \to f_n) \equiv \int_{-\infty}^{\infty} \psi_i V_n \psi_f \, ds_n$$

where s_n is the nth vibrational coordinate.

Results calculated by this approach (12) are given in Table 1. These data have implications for solids. Consider a hypothetical solid consisting of O_2 with a line of CO impurities. Let us give the solid translational energy. We see $P_{i\to f}$ for O_2 is 8.5×10^{-8} and $P_{i\to f}$ for pure CO is 7×10^{-10}. In sharp contrast $P_{i\to f}$ for O_2 colliding with CO is about two orders of magnitude greater 2×10^{-6}. Thus energy is converted more readily where unlike partners collided.

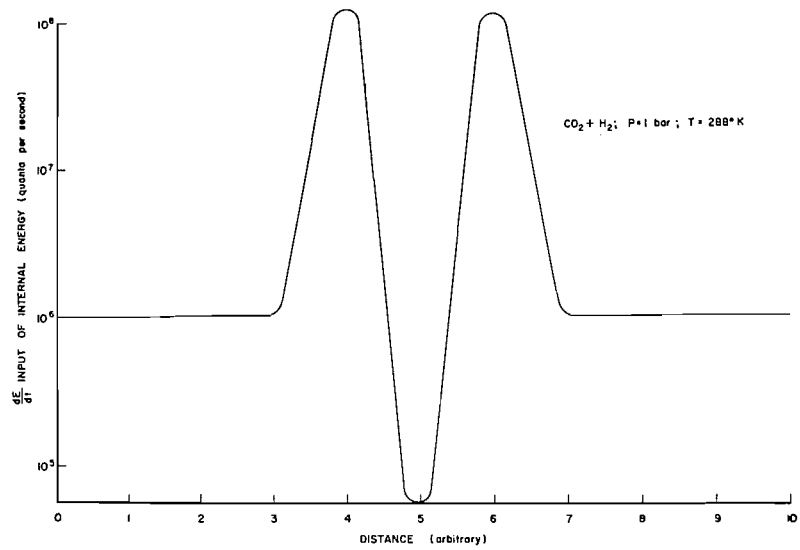

FIG. 3. Energy conversion as a function of distance in a solid of the type shown in Fig. 2 where $a = CO_2$ and $b = H_2$.

TABLE 1. Probability of collision induced vibrational excitation in pure gases and in mixtures*

Gases (a, b)	T (K°)	$P_{0\to1}$ Pure gas (a)	Pure gas (b)	Mixture (a, b)
O_2, N_2	288	8.5×10^{-8}	0	3×10^{-7}
O_2, CO	288	8.5×10^{-8}	7×10^{-10}	2×10^{-6}
CO_2, N_2	288	4×10^{-4}	0	7.5×10^{-4}
CO_2, H_2	288	4×10^{-4}	0	4.5×10^{-2}
N_2, Ar	600	7×10^{-9}	0	3×10^{-8}

*Reference 12.

Results for a system of CO_2 and H_2 $a = CO_2$ and $b = H_2$ (Fig. 2) are shown in Fig. 3 for a pressure of 1 bar and a temperature of 288°. This figure shows that the energy input to lines *4* and *6* (Fig. 2) is over two orders of magnitude greater than that to other areas of the system. Consequently, any chemical reaction would be expected to occur in this area, because of the higher effective temperature.

In summary, an impurity or unlike molecules in a system increases the transfer of translational to internal energy in the region near the impurity. If the treatment were extended to a three dimensional system the results would be qualitatively the same. In the three dimensional treatment, the relative motion of the molecules has an angular dependence. Several investigations (13–16) have developed relationships for the three dimensional gaseous system. The results of Tanczos (15) will be given here because they can be applied to complicated molecules. The probability that a pair of molecules in vibrational states i_a and i_b will, after collision, be in higher energy states f_a and f_b is given for nonresonant conditions by

$$[13]\quad P(a,b) = P_0(a)P_0(b)P_c V^2(a)V^2(b)8\left(\frac{\pi}{3}\right)^{1/2}\left[\frac{8\pi^3\mu\Delta E}{(a^*)^2h^2}\right]^2 X^{1/2}\exp\left[-\left(3X - \frac{\Delta E}{2kT} + \frac{\phi_0}{kT}\right)\right]$$

where

$$X = \frac{\mu(v^*_0)^2}{2kT} = \left[\frac{2\pi^4\mu(\Delta E)^2}{(a^*)^2h^2kT}\right]^{1/2}$$

and

$$\Delta E = h\nu_a(i_a - f_a) + h\nu_b(i_b - f_b)$$

The factors $P_0(a)$ and $P_0(b)$ are geometrical steric factors for the molecules a and b. The preexponential factor P_c relates probabilities as calculated for an elastic collision cross section and is given approximately by

$$[14]\quad P_c = 1.364(1 + C/T)^{-1}(r_c/r_0)^2$$

where C is the Sutherland constant, r_c the distance

Can. J. Chem. Downloaded from www.nrcresearchpress.com by 210.87.254.40 on 09/05/12
For personal use only.

between molecular centers at the point of closest approach, and r_0 is the distance for zero potential value. Combining all of these relationships one obtains for the transition probability under resonance conditions ($\Delta E = 0$) the relationship

$$[15] \quad P(a, b) = P_0(a)P_0(b)V^2(a)V^2(b)\frac{64\pi^2\mu kT}{\alpha^2 h^2} \times \exp[-(\phi_0/kT)]$$

Let us now apply the results to chemical reactions in solids. Consider the region of an impurity where $P_{i\to f}$ has a relatively large value. To form an activated complex, one molecule must receive an energy of E_m.

If the reaction occurs by bimolecular decomposition, the rate constant is given by eq. 5. We have already evaluated $P_{i\to f}$, *e.g.*, eq. 11, now all that remains is an evaluation of σ_t and v. We evaluate σ_t in the solid by means of the concept of the mean free path λ. We know that

$$[16] \quad \lambda = \int_0^\infty P(x)\,dq = \frac{1}{\sqrt{2}\sigma_t N}$$

where (P_x) is the probability that the particle goes a distance x without collision. In a solid the mean free path is the lattice spacing, b; thus σ_t is given by

$$[17] \quad \sigma_t = \frac{1}{\sqrt{2}bN}$$

where N is the number of nearest neighbor molecules substituting for and in eq. 5 one obtains the chemical rate constant, k

$$[18] \quad k = \frac{P_{i\to f}\bar{v}}{\sqrt{2}bN}$$

In summary, we have shown that the rate constant for chemical reactions in solids can be expressed in rather simple terms (eq. 18). Other techniques can be used to calculate the mean velocity of molecules in a solid and thereby increase the precision of the calculation. It should be mentioned that the same type of relationship could be used to describe reactions in the liquid state. Because of mathematical difficulties in calculating $P_{i\to f}$, results from the present model are considered of qualitative rather than quantitative significance.

The basic problem under study is that of energy transfer in a crystal from lattice vibrations, vibration of the molecule as a whole about its lattice position, to internal vibrations, vibrations of the atoms comprising the molecule within the molecule. Sometimes the higher lattice vibrational frequencies overlap the lowest internal mode, but usually there is little overlap. One can develop a model based on coupling between these vibrational modes. However, such a model requires, in general, high order perturbation theory (to tenth order) to explain the energy transfer. We investigated and rejected the "perturbation model" in favor of the present "collision model" mainly on the basis of the less complex mathematical treatment of the present model.

1. D. L. CHAPMAN. Phil. Mag. 213, Series A, **47**, 90 (1899).
2. J. M. JOUQUET. J. Math. Pure Appl. Vol. 70. Ser. 6. **1**, 347 (1905).
3. Y. B. ZEL'DOVICH. J. Exptl. Theo. Phys. (USSR) **10**, 542 (1940).
4. J. VON NEUMANN. OSRD Report No. 549. 1942.
5. R. A. STREHLOW and F. D. FERNANDES. Comb. Flame. **9**, 109 (1965).
6. C. E. MELTON, D. F. STRENZWILK, and P. D. YEDINAK. BRL Technical Note No. 1715. 1969.
7. A. A. MARADUDIN, E. W. MONTROLL, C. H. WEISS. Theory of lattice dynamics in the harmonic approximation, solid state physics. Supp. 3. 1963. p. 166.
8. E. W. MONTROLL and R. B. POTTS. Phys. Rev. **100**, 525 (1955).
9. D. N. PAYTON, III, M. RICH, and W. M. VISSCHER. Localized excitations in solids. *Edited by* R. F. Wallis. Plenum Press, New York. 1968. p. 657.
10. C. ZENER. Phys. Rev. **37**, 556 (1931).
11. L. D. LANDAU and E. TELLER. Phys. Z. Sowjetunion, **10**, 34 (1936).
12. R. N. SCHWARTZ, Z. I. SLAWSKY, and K. F. HERZFELD. J. Chem. Phys. **20**, 1591 (1952).
13. K. TAKAYANAGI. Progr. Theoret. Phys. Japan, **8**, 111 (1952).
14. R. N. SCHWARTZ and K. F. HERZFELD. J. Chem. Phys. **22**, 767 (1954).
15. F. I. TANCZOS. J. Chem. Phys. **25**, 439 (1955).
16. E. E. NIKITIN. Discuss. Faraday Soc. **57**, 14 (1961).

Can. J. Chem. Downloaded from www.nrcresearchpress.com by 210.87.254.40 on 09/05/12
For personal use only.

Can. J. Chem. Downloaded from www.nrcresearchpress.com by 210.87.254.40 on 09/05/12
For personal use only.

Infrared Studies of Water in Crystalline Hydrates: Sodium Nitroprusside Dihydrate, $Na_2[Fe(CN)_5NO].2H_2O$ [1]

MICHAELA HOLZBECHER AND OSVALD KNOP
Department of Chemistry, Dalhousie University, Halifax, Nova Scotia

AND

MICHAEL FALK
Atlantic Regional Laboratory, National Research Council of Canada, Halifax, Nova Scotia

Received October 14, 1970

Infrared spectra of polycrystalline $Na_2[Fe(CN)_5NO].2H_2O$ at different degrees of deuteration were studied as a function of temperature. The single peaks observed for the bending fundamentals of isotopically dilute H_2O and D_2O show that all the water molecules are equivalent, as required by Manoharan and Hamilton's structure determination; the doublets observed for the three fundamentals of isotopically dilute HDO show that the water molecules are asymmetric. Doublet separation decreases gradually with increasing temperature, indicating decreasing asymmetry. The water molecule appears to orient itself so as to maximize the strength of one OH···NC bond, while the other OH group interacts only very weakly with another CN group. The hitherto unknown extent to which the nitroprusside ion deviates from the ideal C_{4v} symmetry has been estimated from the $^{13}C^{14}N$ stretching spectrum. The $^{15}N^{16}O$ and $^{14}N^{18}O$ stretching spectrum was used to confirm that only one type of NO group is present in the crystal, and hence that all nitroprusside ions are equivalents.

Les spectres infrarouge du $Na_2[Fe(CN)_5NO].2H_2O$ polycristallin à des degrés différents de deutération ont été étudiés en fonction de la température. Les pics uniques observés pour les fondamentales de déformation angulaire de H_2O et D_2O isotopiquement dilués montrent que toutes les molécules d'eau sont équivalentes, comme il était requis par les déterminations de structure de Manoharan et Hamilton. Les doublets observés pour les trois fondamentales du HDO isotopiquement dilué montrent que les molécules d'eau sont asymétriques. La séparation du doublet décroît graduellement avec l'accroissement de température, montrant la diminution de l'asymétrie. La molécule d'eau semble s'orienter afin de maximiser la force d'un lien OH···NC, tandis que les autres groupements OH intéragissent seulement très faiblement avec un autre groupe CN. Jusqu'ici, la déviation de l'ion nitroprussique de la symétrie idéale C_{4v} a été estimée du spectre de valence du $^{13}C^{14}N$. Le spectre de valence de $^{15}N^{16}O$ et $^{14}N^{18}O$ a été utilisé pour confirmer qu'il y a seulement un type de groupement NO dans le cristal, et ainsi que tous les ions nitroprussique sont équivalents.

Canadian Journal of Chemistry, **49**, 1413 (1971)

The water molecule in the crystal structure of sodium nitroprusside dihydrate, $Na_2[Fe(CN)_5NO].2H_2O$,[2] has been quoted as an example of structural water not forming a definite pair of hydrogen bonds (1, 2). The evidence from a crystal-structure determination by photographic X-ray diffraction methods (1) is incomplete, as only the oxygen atoms, O_w, of the water molecule have been located. The shortest O_w–O_w distance is 3.63 ± 0.04 Å (O_wD–O_wC in Table 1 and Figs. 1 and 2) and thus outside the accepted range for O—H···O bonding. As for the possibility of the water molecule participating in two O_w—H···N bonds, the two distances singled out in ref. 1 as the shortest O_w–N distances in the SND structure, 3.27 ± 0.05 and 3.36 ± 0.05 Å,[3] involve oxygen and nitrogen atoms all of which are part of the same coordination octahedron about sodium. This has been considered to disqualify these two interatomic vectors as coincident with hydrogen bonds (2). However, there are other O_w–N distances between 3 and 4 Å in the structure, some of them just as short as the two used in Manoharan and Hamilton's argument (1) (Table 1); all of these must be examined in turn for the possibility of hydrogen-bond engagement with the water molecule.

The O_w atoms have been placed in the general equipoint 8(*h*) of the tetramolecular unit cell of

[1]NRCC No. 11 794.

[2]Abbreviated in the following to SND.

[3]The account, on p. 1046 of ref. 1, of the environment of the water molecule in SND contains misprints and ambiguities.

Can. J. Chem. Downloaded from www.nrcresearchpress.com by 210.87.254.40 on 09/05/12
For personal use only.

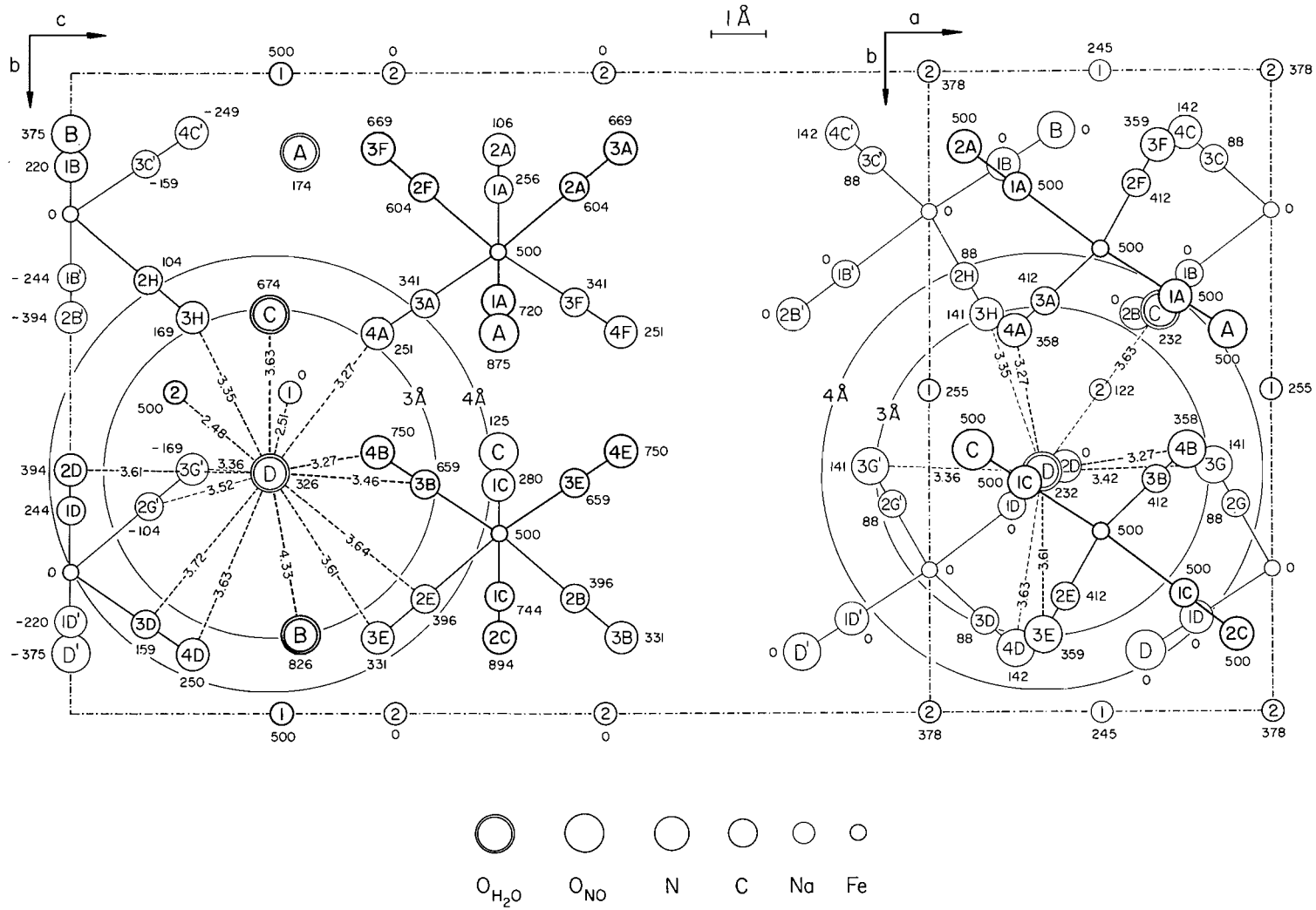

FIG. 1. Partial projections of the SND structure on the (100) and (001) planes (after ref. 1). The fractional coordinates shown in the projections have been multiplied by 1000; the interatomic distances are in Å. The complete environment of the water molecule *D* up to 4 Å is shown in both projections (*cf.* Tables 1 and 2).

TABLE 1. Interatomic distances O_wD–X up to 4 Å and bond angles calculated from the atomic coordinates of ref. 1

X	d(Å)*	Angle (deg) X—O_wD—Na1A	Angle (deg) X—O_wD—Na2D
Na2D	2.48±0.05		0
Na1A	2.51±0.03	0	
N4B	3.27±0.05	120.1±2.7	90.0±1.6
N4A	3.27±0.04	49.0±1.1	90.3±1.5
N3H	3.35±0.04	47.6±1.0	48.2±1.0
N3G'	3.36±0.05	47.2±1.0	45.6±2.4
N3G	3.42±0.05	141.8±3.9	46.9±1.1
C3B	3.46±0.05		
C2G'	3.52±0.06		
N2D	3.61±0.04	103.2±1.5	42.9±0.9
N3E	3.61±0.04	114.5±2.0	149.3±4.4
O_wC	3.63±0.04		
N4D	3.63±0.05	118.3±2.2	109.1±1.9
C2E	3.64±0.04		
C1D	3.68±0.03		
C3D	3.72±0.04		
N4B'	4.07±0.07		
N1C	4.15±0.03		
C2G	4.21±0.05		

*The uncertainty in d was calculated from the standard deviations of the positional coordinates of ref. 1 and multiplied by three. It would be increased by about 1% of d if one were to allow for the uncertainty in the unit-cell dimensions.

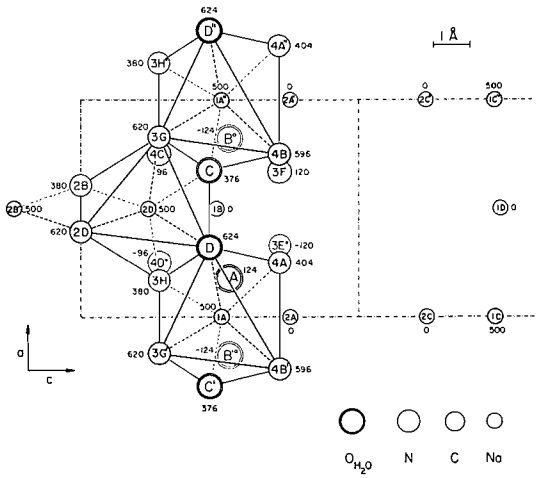

FIG. 2. Partial projection of the SND structure on the (010) plane. The environments of the Na atoms are shown.

symmetry D_{2h}^{12}-*Pnnm* (Table 2). This makes the eight water molecules in the unit cell equivalent, but their hydrogen atoms must belong to two nonequivalent sets, $8H_1 + 8H_2$. Like in gypsum (4, 5), the distances O_w–H_1 and O_w–H_2 are in principle different, but as the positions of the hydrogen atoms have not been determined, the extent of asymmetry of the water molecule is not known. The water molecules in SND differ from those in gypsum in that they do not participate

TABLE 2. Distribution of atoms in the unit cell of SND (*Pnnm*), their site symmetries and equivalence relations

Atom (This work and ref. 3)	Reference 1*	Equipoint	Site symmetry
N1	Nitroso N	4 (*g*)	C_s-*m*
O	Nitroso O	4 (*g*)	C_s-*m*
O_w	Water O	8 (*h*)	C_1-1
C1	C_1	4 (*g*)	C_s-*m*
N2	N_1	4 (*g*)	C_s-*m*
C2	C_2	8 (*h*)	C_1-1
N3	N_2	8 (*h*)	C_1-1
C3	C_3	8 (*h*)	C_1-1
N4	N_3	8 (*h*)	C_1-1
Fe	Fe	4 (*g*)	C_s-*m*
Na1	Na_1	4 (*f*)	C_2-2
Na2	Na_2	4 (*e*)	C_2-2

Symmetry relations of equivalent atoms (Figs. 1 and 2)

4 (*e*): $A(0, 0, z)$, $B(1/2, 1/2, 1/2 + z)$, $C = -A$, $D = -B$

4 (*f*): $A(0, 1/2, z)$, $B(1/2, 0, 1/2 - z)$, $C = -A$, $D = -B$

4 (*g'*): $A(x, y, 1/2)$, $B(1/2 + x, 1/2 - y, 0)$, $C = -A$, $D = -B$

8 (*h*): $A(x, y, z)$, $B(\bar{x}, \bar{y}, z)$, $C(1/2 + x, 1/2 - y, 1/2 - z)$, $D(1/2 - x, 1/2 + y, 1/2 - z)$, $E = -A$, $F = -B$, $G = -C$, $H = -D$

*Conversion of Table IV of ref. 1 to present notation: Coordination of Na_1 (= Na1B): W = O_wA, W' = O_wB', N_2 = N3F, N_2' = N3E', N_3 = N4C, N_3' = N4D'. Coordination of Na_2 (= Na2A): N_2 = N3E, N_2' = N3F', N_1 = N2A, N_1' = N2C'.

Can. J. Chem. Downloaded from www.nrcresearchpress.com by 210.87.254.40 on 09/05/12
For personal use only.

Can. J. Chem. Downloaded from www.nrcresearchpress.com by 210.87.254.40 on 09/05/12
For personal use only.

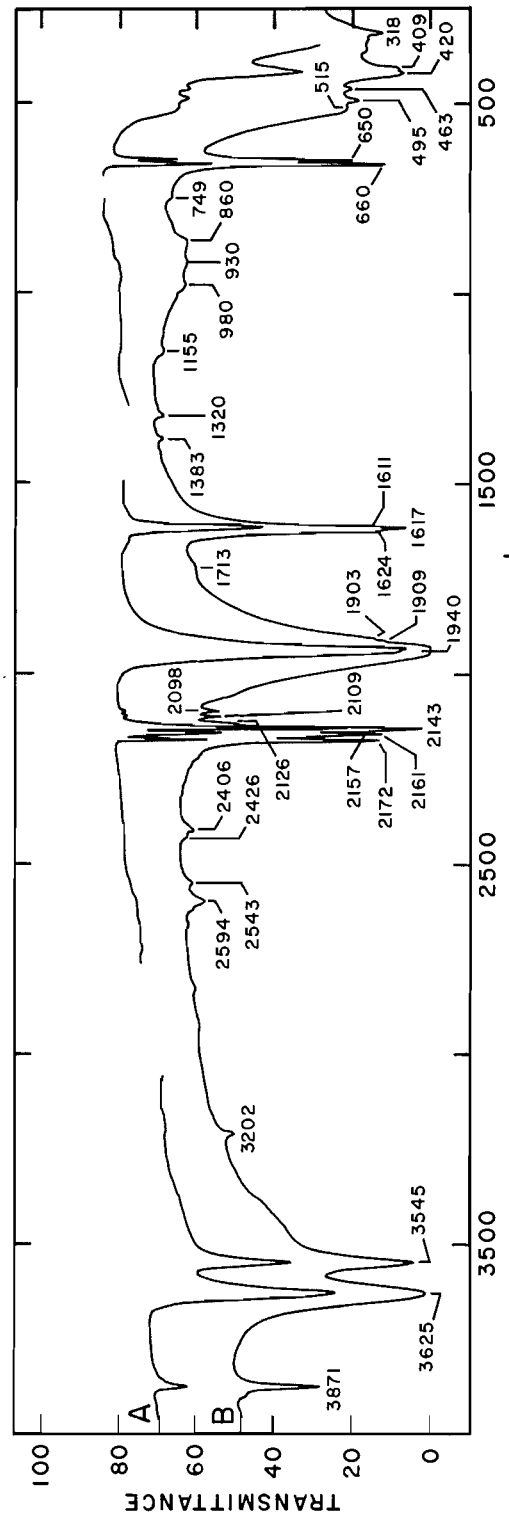

FIG. 3. Survey spectra of undeuterated SND at room temperature. *A*, mull in Nujol; *B*, KBr pellet (thicker sample).

Can. J. Chem. Downloaded from www.nrcresearchpress.com by 210.87.254.40 on 09/05/12
For personal use only.

in strong hydrogen bonding, as is apparent from the observed O_w–N distances. It was therefore of interest to see whether the two weakly bonded OH groups of the water molecule have fundamental frequencies that are sufficiently different to be distinguishable in the infrared (i.r.) spectrum of isotopically dilute HDO.

The subject of main interest to us has been the fundamentals of the water molecule. None of the many i.r. and Raman spectroscopic studies of SND that have been reported (6–17)[4] was primarily concerned with this aspect of the SND structure. The vibrational frequencies of the nitroprusside *ion*, $[Fe(CN)_5NO]^{2-}$, have been recently reviewed in detail in refs. 13 and 16 which appeared while the present work was in progress. We have restricted our attention to structural deductions from those vibrational bands of the anion that arise from minor isotopic species (^{13}C, ^{15}N, ^{18}O).

Experimental

The identity of the brownish-red crystals of SND (May and Baker, Ltd.; reagent-grade, recrystallized from distilled water) was verified by the i.r. spectrum.

The material was partially deuterated by crystallization from hot solutions in H_2O–D_2O mixtures. The higher deuterations were carried out by dissolving the sample in D_2O of 99.7% isotopic purity and evaporating the excess D_2O under reduced pressure into a cold trap. Three successive deuteration steps yielded samples of H:D ratio of about 1:20. The approximate H:D ratio was calculated from the areas of the HOH, DOD, and HOD bands (4).

Samples were studied as mulls in Nujol and as pressed pellets in KBr and NaCl matrices, as in earlier work (4). The spectra were recorded on a Perkin–Elmer Model 521 spectrophotometer [*cf.* ref. 4]. Survey spectra (*e.g.* those in Figs. 3 and 4) were recorded at a scanning speed of about 100 cm^{-1}/min. The more important spectral features (*e.g.* those in Figs. 5–10) were recorded with expanded abscissa scale at a scanning speed of about 10 cm^{-1}/min. Frequencies of the sharp peaks were read to the nearest 0.1 cm^{-1} and are believed to be accurate to ± 1.0 cm^{-1}. All frequencies quoted in the following are the averages of several runs.

Results

Spectrum of Undeuterated SND

Spectra of Nujol mulls and of KBr and NaCl pellets were essentially the same. Figure 3 shows typical survey spectra in a form useful for identification and catalogue purposes. In[5] Table 3 our frequencies for the major bands in the spectrum at room temperature are compared with values reported by other workers (6–8, 10, 13, 15, 16). Our values agree particularly well (within 1 cm^{-1} for most bands) with those of refs. 13, 15, and 16.

Partially Deuterated SND

Figure 4 shows the spectra in the regions of H_2O, HDO, and D_2O fundamental vibrations at increasing deuterium content. Details of interest are shown in Figs. 5–8 as a function of temperature,[5] and more detailed comments may be found in Appendix 1.[5]

Of major importance structurally are the fundamentals of the *isotopically dilute* water molecules; such molecules are vibrationally "isolated" (4). The bending fundamentals of isolated H_2O and D_2O in SND were sharp *singlets* at 1616.5 and 1191.2 cm^{-1}, respectively, essentially independent of temperature (Fig.[5] 8 and Table 4). All three of the fundamentals of isolated HDO were *doublets*, the separation of which decreases gradually with increasing temperature (Fig.[5] 5 and Table 4).

At higher isotopic concentrations the bending fundamentals of HDO, H_2O, and D_2O showed additional components (best resolved at low temperature), indicating vibrational coupling. As has been reported by Khanna, Brown, and Jones (13), the HOH and DOD bending fundamentals of undeuterated and highly deuterated SND were found to be triplets, the separations of which decreased with temperature (Figs.[5] 6 and 7).

The stretching fundamentals of HDO, H_2O, and D_2O did not appreciably change their frequencies and half-widths at higher isotopic concentrations, indicating absence of vibrational coupling.

CN and NO Stretching Fundamentals

The small bands on the low-frequency side of the CN stretching fundamentals in the spectra of undeuterated SND (Fig.[5] 9) are due to the minor isotopic species $^{13}C^{14}N$ and $^{12}C^{15}N$ (13, 16). All the CN stretching bands shifted to higher

[4]Reference 17 seems to convey the impression that *anhydrous* sodium nitroprusside was studied. However, the "deep dark red color" of the samples and the partial i.r. and Raman spectra reported there leave little doubt that the substance studied was in fact the dihydrate.

[5]Table 3, Figs. 5–11, and Appendices 1 and 2 have been placed in Depository of Unpublished Data. Photocopies may be obtained free of charge upon request, from: Depository of Unpublished Data, National Science Library, National Research Council of Canada, Ottawa, Canada.

Can. J. Chem. Downloaded from www.nrcresearchpress.com by 210.87.254.40 on 09/05/12
For personal use only.

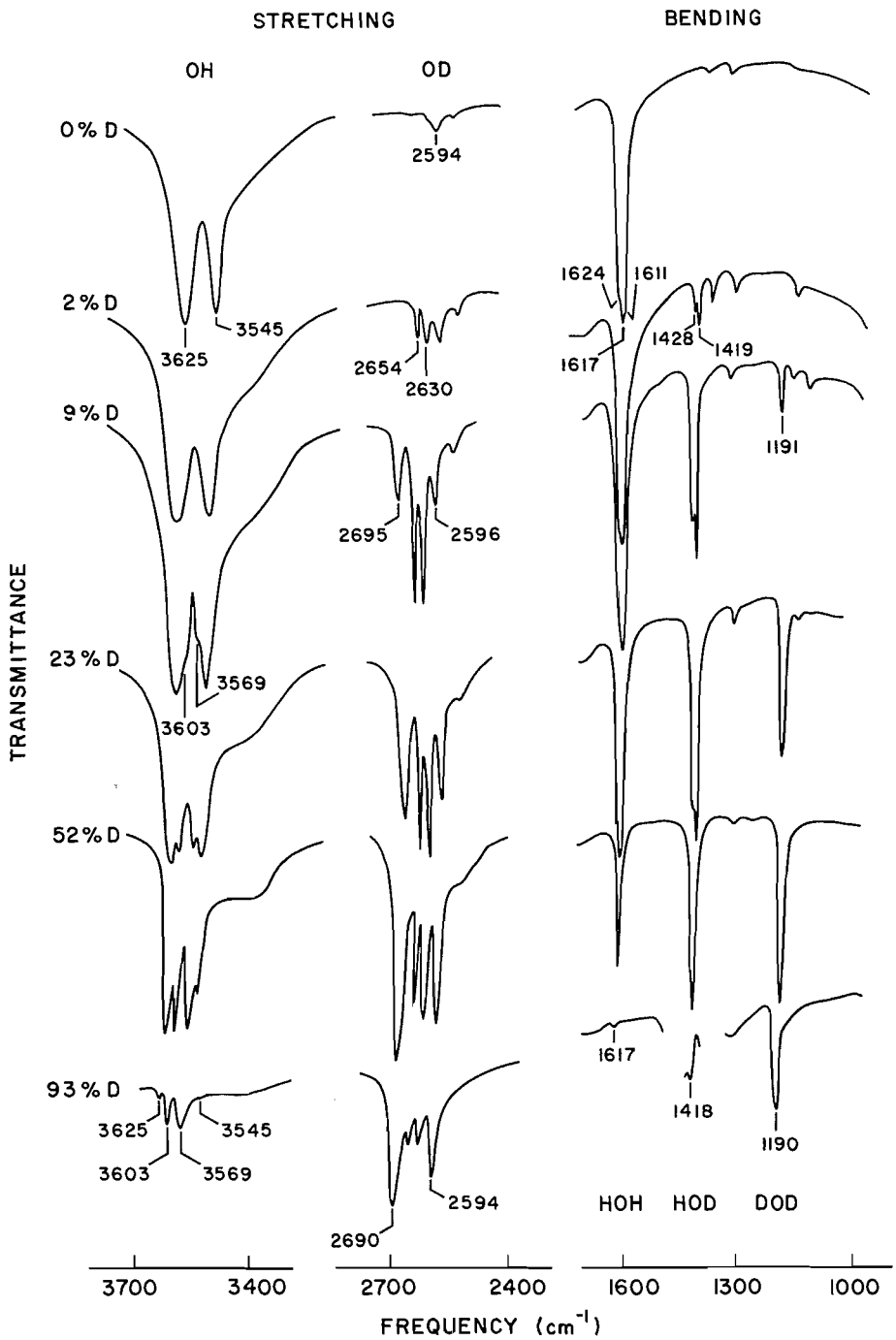

FIG. 4. Survey spectra of SND at different degrees of deuteration, in the regions of H_2O, D_2O, and HDO fundamentals (room temperature). 0–52% D, KBr pellets; 93% D, Nujol mull. Bands near 2594 cm^{-1}, visible at low deuteration, are due to a combination mode (1940 + 650 cm^{-1}).

TABLE 4. Fundamentals of isotopically dilute HDO, H_2O, and D_2O in SND (cm^{-1})

Assignment		Frequency (cm^{-1})			
		−165°	−80°	+30°	+80°
HDO	OH stretch	3607.0, 3562.5 (44.5)	3605.6, 3565.4 (40.2)	3603.0, 3568.0 (35.0)	3601.8, 3569.0 (32.8)
	OD stretch	2654.4, 2624.5 (30.1)	2654.0, 2627.4 (26.6)	2653.5, 2629.5 (24.0)	2653.0, 2631.0 (22.0)
	bend	1429.3, 1417.6 (11.7)	1428.4, 1418.0 (10.4)	1427.4, 1419.0 (8.4)	1427.3, 1419.2 (8.1)
HOH bend		1616.8		1616.5	
DOD bend		1191.4		1191.2	

frequencies at decreasing temperatures, by 2–4 cm^{-1} per 100°.

The small bands on the low-frequency side of the NO stretching fundamental (Fig.[5] 10) arise from the minor isotopic species $^{15}N^{16}O$ and $^{14}N^{18}O$ (13). The center of the major NO stretching band, as well as the two minor isotopic bands, shifted to higher frequencies with decreasing temperature, by 3.5 cm^{-1} per 100°.

Discussion

Site Symmetry of the Water Molecules

The single peaks observed for the bending fundamentals of isotopically dilute H_2O and D_2O show that all water molecules in SND are crystallographically equivalent. The doublets observed for the three fundamentals of isotopically dilute HDO indicate that the water molecules are asymmetric (4, 5). These conclusions agree with the expectations from the orthorhombic space-group symmetry of SND and the concomitant site symmetry for the water molecule, C_1-*1* (1). The OH:OD frequency ratios are the same for the two components of the doublet, 3603.0/2653.5 = 1.3578 and 3568.0/2629.5 = 1.3569, which confirms that the doublet is due to the presence of two nonequivalent OH groups rather than to other possible effects such as proton tunnelling (4, 5).[6] The gradual decrease in the doublet separation with increasing temperature, which occurred for all three fundamentals of HDO in proportion, indicates that the water molecule becomes effectively more symmetric, probably as a result of increased motion with respect to the neighboring atoms. A similar interpretation accounts satisfactorily for the observed temperature dependence of the split HDO fundamentals in other hydrates (18).

Correlation Field Splitting

It is seen from the correlation diagram of the site symmetry C_1 with the factor-group symmetry D_{2h} (Fig.[5] 11) that correlation field splitting (*i.e.* coupling of like vibrations within the unit cell) should cause each internal vibration of a water molecule to give rise to eight coupled vibrations of the unit cell, of which three (B_{1u}, B_{2u}, B_{3u}) are i.r. active. In agreement with Khanna *et al.* (13) and Tosi (16) we have found three components of the bending fundamentals of H_2O in undeuterated SND (and of D_2O in highly deuterated SND). Correlation splitting was also observed for the HOD bending fundamental. As may be expected, the correlation components increase their separation at lower temperature.

On the other hand, correlation splitting was not observed for the stretching fundamentals of HDO, H_2O, or D_2O. Hence it must be smaller than the half-widths of the stretching bands, 8 and 21 cm^{-1} for the two D_2O stretching peaks at −170 °C, and 14 and 21 cm^{-1} for the two H_2O stretching peaks at −160 °C. The magnitude of correlation field splitting commonly observed for stretching vibrations of water in crystals is 50–

[6]Khanna, Brown, and Jones previously reported the doubling of HDO fundamentals but could not explain it (13). Bates and Khanna have since ascribed the doubling to "orientational splitting" (15). This view appears to coincide with our analysis.

Can. J. Chem. Downloaded from www.nrcresearchpress.com by 210.87.254.40 on 09/05/12
For personal use only.

Can. J. Chem. Downloaded from www.nrcresearchpress.com by 210.87.254.40 on 09/05/12
For personal use only.

100 cm^{-1} (19, 20). The unusually small splitting in SND is probably due to the water molecules not being interconnected by hydrogen bonds (*vide infra*).

Hydrogen Bonding

The environment of the water molecule according to ref. 1 is shown in Figs. 1 and 2 (*cf.* Table 2 for symmetry relationships and site symmetries of the atoms). The two sodium atoms Na*1* (*A*) and Na*2* (*D*) are the only two neighbors of O_wD within 3 Å (for interatomic distances, see Table 1). The nitrogen atoms of the eight CN groups surrounding the water molecule are at distances between 3.27 ± 0.05 and 3.63 ± 0.05 Å. The carbon atoms are somewhat farther away than the corresponding nitrogen atoms, although the differences may be slight and well within the limits of uncertainty of the interatomic distances (compare, for example, N*3E* and C*2E*, or N*4D* and C*3D*).

Hydrogen bonds corresponding to O–N distances greater than 3.2 Å will necessarily be very weak;[7] still, it is reasonable to assume that the OH groups of the water molecule will seek to maximize the H···NC interactions and tend to orient themselves toward the closest-lying N atoms. Which of the latter will be available for such interaction is determined by the cation–proton repulsion between the sodium ions and the water molecule; the repulsion may be expected to cause the O—H bonds to point away from the Na^+ ions. Five of the eight N atoms (*4A*, *3H*, *3G'*, *3G*, and *2D* of Figs. 1 and 2) are ruled out because of the smallness of their N—O_w—Na*1* or N—O_w—Na*2* angles, which are all under 50°. Of the remaining three N atoms, N*4B* is 3.27 ± 0.05 Å away from O_wD compared with 3.61 ± 0.04 Å for N*3E* and 3.63 ± 0.05 Å for N*4D*. Aligning one of the OH groups, O_w—H_1, of the water molecule approximately along O_wD–N*4B* not only leads to the shortest O_w–N distance in this situation, but is also consistent with each of the two lone pairs on O_w pointing in the direction of one of the sodium ions, Na*1A* or Na*2D*. The most reasonable orientation for the second OH group, O_w—H_2, is then in the general direction of N*4D*: the angle N*4B*—O_wD—N*3E* is only 75.9 ± 1.3°, while the angle N*4B*—O_wD—N*4D* is 115.0 ± 2.3°, which is much closer to the H—O—H angle of about 109° usually found in crystalline hydrates (21). The orientation N*4B*···H_1—O_wD—H_2···N*4D*, which thus appears the most probable, may be viewed as the result of the tendency of the water molecule to maximize the strength of the one hydrogen bond it can make (exemplified by O_wD—H_1···N*4B*—C*3B*) at the price of the other OH group remaining essentially non-hydrogen-bonded.

The i.r. spectrum supports this deduction. The high-frequency component of the stretching doublets of isotopically dilute HDO is at 3603.0 cm^{-1} for OH and at 2653.5 cm^{-1} for OD. These are the highest stretching frequencies so far reported for HDO in crystalline hydrates. They clearly correspond to the stretching of O_w—H_2. The frequency of the other component of the stretching doublet, 3569.0 cm^{-1} for OH and 2629.5 cm^{-1} for OD, is sufficiently lower, and the intensity sufficiently higher, for this component to be considered as arising from the more strongly interacting OH group, O_w—H_1, which is oriented toward N*4B* and corresponds to an O_w–N distance of 3.27 ± 0.05 Å.

Comparison with Related Compounds

High OH (or OD) stretching frequencies appear to be characteristic of hydrates of cyano complexes. They indicate that the hydrogen bonding between water and CN groups is generally weak. The OD stretching frequencies of isotopically dilute HDO extend, at −165°, up to about 2624 cm^{-1} in $K_4[Fe(CN)_6].2H_2O$, and up to about 2630 cm^{-1} in $K_4[Ru(CN)_6].3H_2O$ (22). Another example is the unassigned sharp doublet in the spectra of partially deuterated $K_4[Mo(CN)_8].2H_2O$ and $K_4[W(CN)_8].2H_2O$ at room temperature (23): The doublet, at 2614 and 2640 cm^{-1} in the Mo compound and at 2614 and 2641 cm^{-1} in the W compound, undoubtedly corresponds to HDO, in analogy to the doublets in the spectrum of partially deuterated SND. The H_2O···N separations in the Mo compound range upward from 3.16 Å (24).

The CN Stretching Fundamentals

If the nitroprusside ion had the point-group symmetry C_{4v}-*4mm*, the four CN groups num-

[7]This is true regardless of whether the hydrogen-bonding interaction is considered to be between O_w and N or, more vaguely, between O_w and the π system of the CN group.

Can. J. Chem. Downloaded from www.nrcresearchpress.com by 210.87.254.40 on 09/05/12
For personal use only.

bered *2–5* in Fig.[8] 12 would be equivalent. In the crystal of SND the symmetry of the ion is lowered to C_s-*m*; the mirror plane passes through the atoms N_1C_1–Fe–N_6O and bisects the angles C_3—Fe—C_4 and C_2—Fe—C_5. Consequently the groups C_2N_2 and C_3N_3 are no longer equivalent by symmetry, and likewise C_4N_4 and C_5N_5. How closely the C_{4v} symmetry is simulated by *metric* similarity is difficult to determine because of the insufficient accuracy of the crystal-structure determination: Fe—C_2, 1.91 ± 0.06 Å; Fe—C_3, 1.93 ± 0.06 Å; Δ = 0.02 ± 0.09 Å; C_2—N_2, 1.15 ± 0.06 Å, C_3—N_3, 1.14 ± 0.06 Å; Δ = 0.01 ± 0.09 Å; similar uncertainties obtain in the bond angles.

The effective symmetry of the nitroprusside ion in SND can in principle, *i.e.* without reference to crystal structure determination, be deduced from the vibrational spectrum in the region of the CN

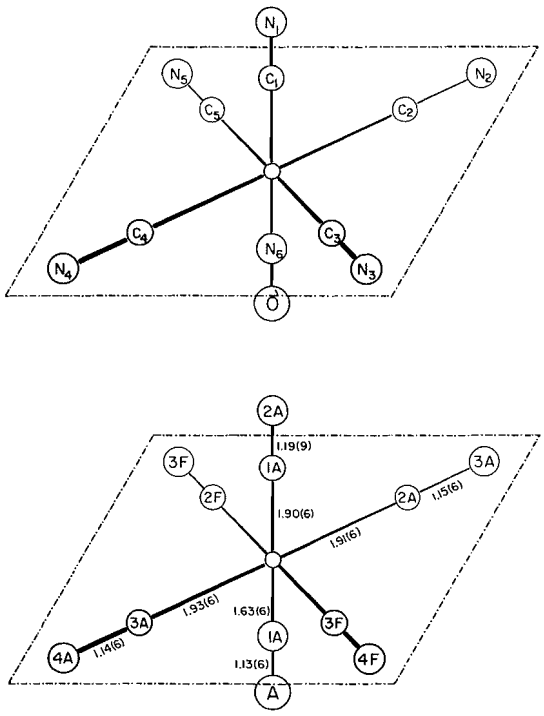

FIG. 12. Geometry of the $[Fe(CN)_5NO]^{2-}$ ion. The schematic coordination figure (*top*), which is drawn as if the symmetry of the ion were C_{4v}, can be correlated with Fig. 1 as indicated in the bottom drawing.

[8]This numbering refers only to Fig. 12; it is not to be confused with the notation for C and N atoms used in ref. 1 (*cf.* Table 2).

stretching fundamentals. However, that information is difficult to obtain from the $^{12}C^{14}N$ stretching spectrum, as discussed in Appendix[5] 2. On the other hand, a simple and unequivocal confirmation of the local symmetry of the nitroprusside ion, as well as an estimate of the extent to which the ion deviates from the ideal C_{4v} symmetry, can be derived from the minor isotopic bands due to ^{13}C and ^{15}N.

The natural abundance of these isotopes is sufficiently low for the $^{13}C^{14}N$ and $^{12}C^{15}N$ groups to have mostly $^{12}C^{14}N$ groups as neighbors. As a consequence the two factors that complicate the $^{12}C^{14}N$ stretching spectrum, the internal coupling of vibrations within the complex ion and the coupling of vibrations of neighboring ions in the unit cell cease to be important.[9] Every crystallographically distinct CN group will then yield one $^{13}C^{14}N$ and one $^{12}C^{15}N$ fundamental vibration, so that the number of observed $^{13}C^{14}N$ (or $^{12}C^{15}N$) fundamentals will be two under C_{4v}, C_4, or $C_{2v}[\sigma_d]$; three under $C_s[\sigma_d]$ or $C_{2v}[\sigma_v]$; four under $C_s[\sigma_v]$; and five under C_1 symmetry (*cf.* Table 5 and Fig. 12).[10]

The calculated frequencies and abundancies of the isotopic CN groups (Table 6) show that the species $^{13}C^{14}N$ will dominate the spectral region below the $^{12}C^{14}N$ stretching frequencies. Bands of $^{12}C^{15}N$ will be only one-third as intense, and those of $^{13}C^{15}N$ will be vanishingly small. Because the $^{13}C^{14}N$ and $^{12}C^{15}N$ stretching fundamentals occur in approximately the same spectral region, care must be taken to assign the observed bands correctly.

The observed spectrum in the CN stretching region (Fig.[5] 9) shows four features in the $^{13}C^{14}N$–$^{12}C^{15}N$ region, 2098–2130 cm^{-1}. The lowest-frequency peak, at 2098.2 cm^{-1} (2101.2 cm^{-1})[11] must be due to $^{13}C^{15}N$: if it were due to $^{12}C^{15}N$, a $^{13}C^{14}N$ peak three times more intense would be expected at a frequency 11–17 cm^{-1}

[9]Thus the assumption of correlation field splitting, *i.e.* vibrational coupling for $^{13}C^{14}N$ fundamentals, by Tosi (16) is incorrect.

[10]There are two ways in which the nitroprusside ion can assume C_s or C_{2v} symmetry. A mirror plane σ_d bisects a C—Fe—C angle involving *neighboring* equatorial C atoms (C_2—Fe—C_3 or C_3—Fe—C_4); a mirror plane σ_v bisects a C—Fe—C angle involving *alternating* equatorial C atoms (C_2—Fe—C_4 or C_3—Fe—C_5) and contains the remaining carbon atoms.

[11]Frequencies in parentheses refer to −160°.

Can. J. Chem. Downloaded from www.nrcresearchpress.com by 210.87.254.40 on 09/05/12
For personal use only.

TABLE 5. Possible point-group symmetries for the $[Fe(CN)_5NO]^{2-}$ ion (Fig. 12)

Symmetry	Equivalence of CN groups	Number of distinct CN groups
C_{4v}-*4mm*	$1\neq2=3=4=5$	2
C_4-*4*	$1\neq2=3=4=5$	2
$C_{2v}(\sigma_d)$-*mm*	$1\neq2=3=4=5$	2
$C_{2v}(\sigma_v)$-*mm*	$1\neq2=4\neq3=5$	3
$C_s(\sigma_a)$-*m*	$1\neq2=5\neq3=4$	3
$C_s(\sigma_v)$-*m*	$1\neq2\neq3=5\neq4$	4
C_1-*1*	$1\neq2\neq3\neq4\neq5$	5

TABLE 6. Relative natural abundances and vibrational frequencies of isotopic CN and NO groups

Species	Abundance (%)	Frequency shift (cm^{-1})* Calculated†		Observed
$^{12}C^{14}N$	98.6	0	0	0
$^{13}C^{14}N$	1.10	−45.6	−48.1	−46.3
$^{12}C^{15}N$	0.38	−33.8	−31.1	—
$^{13}C^{15}N$	0.004	−79.8	−79.4	—
$^{14}N^{16}O$	99.4	0	0	0
$^{15}N^{16}O$	0.38	−35.1	−41.1	−31.7
$^{14}N^{18}O$	0.20	−51.3	−39.3	−37.0
$^{14}N^{17}O$	0.04	−26.9	−20.8	—
$^{15}N^{18}O$	0.0008	−87.1	−81.6	—
$^{15}N^{17}O$	0.0002	−62.3	−62.5	—

*The shifts are relative to $^{12}C^{14}N$ stretching frequency of 2172.3 cm^{-1} and $^{14}N^{16}O$ stretching frequency of 1947.0 cm^{-1} (−150°).
†The first column refers to calculation by a harmonic diatomic-molecule approximation (CN or NO); the second column, to calculation by a harmonic linear triatomic-molecule approximation (FeCN or FeNO) neglecting the stretch–stretch interaction force constant.

lower. The corresponding $^{12}C^{15}N$ peak must occur at 2109–2115 (2112–2118) cm^{-1} with about one-third of its intensity. The band observed at 2109.4 (2114.4) cm^{-1} has an intensity comparable with that of the band at 2098.2 cm^{-1}, so it too must be largely due to $^{13}C^{14}N$. The weak shoulder at 2113.5 cm^{-1} (apparently too close to the 2114.4 cm^{-1} band to be resolved at −160 °C) must then arise from $^{12}C^{15}N$ stretching and corresponds to the $^{13}C^{15}N$ band at 2098.2 cm^{-1}. This leads to a $^{12}C^{15}N$–$^{13}C^{14}N$ frequency shift of 16.2 cm^{-1}, a reasonable value compared with a shift of 11.7 cm^{-1} calculated by a diatomic approximation and 17.0 cm^{-1} calculated by a simple triatomic approximation (Table 6).

The band at 2125.2 (2130.0) cm^{-1} lies 15.8 (15.6) cm^{-1} below the $^{13}C^{14}N$ band at 2109.4 (2114.4) cm^{-1}. This is the right value for a $^{12}C^{15}N$–$^{13}C^{14}N$ shift, but the 2125.2 cm^{-1} band is too intense to be due only to $^{12}C^{15}N$. A part of its intensity must therefore come from a $^{13}C^{14}N$ band. There are thus *three* $^{13}C^{14}N$ bands, at 2098.2, 2109.4, and 2125.2 cm^{-1} (2101.1, 2114.4, and 2130.0 cm^{-1} at −160°), with intensities in the approximate ratio 2:2:1. This is the expected intensity ratio if the two bands at lower frequency arise from the equatorial pairs C_3N_3, C_4N_4 and C_2N_2, C_5N_5; the high-frequency band is due to the axial C_1N_1 group. This agrees with the results of the analysis of the $^{12}C^{14}N$ vibrations, which also show that the axial C_1N_1 group has the highest stretching frequency (13, 14, 16).

The presence of three isotopically isolated $^{13}C^{14}N$ stretching bands proves unequivocally that there are three types of CN groups in the nitroprusside ion in SND. The symmetry of the ion must therefore be either $C_{2v}[\sigma_v]$ or $C_s[\sigma_d]$; it is the latter that is compatible with the reported space-group symmetry of SND. From the frequencies of the three bands, $\nu(CN)_{1,3} = 2098.2$ cm^{-1}, $\nu(CN)_{2,4} = 2109.4$ cm^{-1}, and $\nu(CN)_5 = 2125.2$ cm^{-1}, the distortion of the ion from the C_{4v} configuration can be approximately calculated. Badger's rule (25) provides an empirical relationship between the force constant for bond stretching, k_{CN}, and the C—N interatomic distance, r_{CN}

$$r_{CN} = 0.68 + (1.86 \times 10^5/k_{CN})^{1/3}$$

Using the harmonic diatomic approximation for the force constant,

$$k_{CN} = 4\pi^2\mu_{CN}c^2\nu_{CN}^2$$

where $c = 2.998 \times 10^{10}$ cm/s and $\mu_{CN} = 1.1189 \times 10^{-23}$ g, the reduced mass of the $^{13}C^{14}N$ group, the following bond lengths are obtained: $r_1 = 1.149$ Å, $r_{3,4} = 1.152$ Å, $r_{2,5} = 1.154$ Å. The absolute values of these distances have no claim to accuracy, but the relative values indicate that the three crystallographically nonequivalent CN groups have very similar bond lengths. The two pairs of equatorial CN groups differ by only about 0.002 Å, which makes the distortion of the ion, relative to interatomic distances though not necessarily to bond angles, from C_{4v} symmetry very small.

The NO Stretching Fundamental

Cotton *et al.* (7) reported the band at 1944 cm^{-1} as a doublet, 1943 and 1955 cm^{-1}. They attributed the splitting of this fundamental to the existence of "environmentally distinguishable ions in the crystal". This interpretation, which has not been

Can. J. Chem. Downloaded from www.nrcresearchpress.com by 210.87.254.40 on 09/05/12
For personal use only.

discussed by later workers (8–17), cannot be reconciled with the crystal-structure determination, according to which the four nitroprusside ions in the unit cell are equivalent (*cf.* Table 2). In refs. 8–10 the stretching band in the i.r. spectrum has been reported as a singlet. In ref. 13 it has been reported as a peak with a shoulder. In ref. 16 considerable fine structure has been observed in the polarized spectra of single crystals. Our spectra show the band to be a doublet at low temperature (Fig.[5] 10), although it is rather hard to resolve as the separation is only about 3 cm^{-1}, and the band is extremely intense. Thus Cotton's original claim that the band is a doublet is confirmed, although the splitting is much smaller than that reported in ref. 7.

The splitting of the NO stretching band is almost certainly due to correlation field splitting and not to crystallographically nonequivalent NO groups. The NO stretching fundamental is A' under the C_s site-group symmetry and should yield two i.r. active components, B_{2u} and B_{3u}, under the D_{2h} factor-group symmetry of the crystal (13, 16).

An unequivocal proof that all NO groups, and hence all nitroprusside ions, in SND are equivalent is obtained from the number of $^{15}N^{16}O$ and $^{14}N^{18}O$ stretching fundamentals. Table 6 shows that these fundamentals can be expected to occur at 30 to 55 cm^{-1} below the corresponding $^{14}N^{16}O$ fundamental.[12] In our spectrum two bands occur at 1909.1 and 1903.7 cm^{-1} at 25° and at 1915.3 and 1910.0 cm^{-1} at −150°. The temperature shift is the same as that for the main band (1941.0 cm^{-1} at 25° and 1947.0 cm^{-1} at −150°) as expected for satellite bands. There is little doubt that the two small bands should be assigned to $^{15}N^{16}O$ and $^{14}N^{18}O$ stretching, as their intensities are consistent with the natural abundances of ^{15}N and ^{18}O.[13] The occurrence of only one $^{15}N^{16}O$ and only one $^{14}N^{18}O$ stretching fundamental confirms that all the NO groups in the crystal belong to one crystallographic type.

[12]The calculated shifts for the isotopic NO species differ by as much as 12 cm^{-1}, depending on the model assumed, and so are uncertain by a similar amount.

[13]These bands are clearly visible in the spectrum of ref. 8, but were not assigned. They were correctly assigned in refs. 13 and 15, but no structural deductions were drawn from them. In ref. 16 both bands were incorrectly assigned to $^{15}N^{16}O$.

Conclusions

The results of the present i.r. study of SND are consistent with the conclusions from Manoharan and Hamilton's crystal-structure determination. In particular:

(*1*) The equivalence of the water molecules and their site symmetry C_1 are confirmed.

(*2*) The symmetry of the water molecule deviates considerably from C_{2v}: the uncoupled stretching frequencies of isotopically dilute HDO are 3603 and 3569 cm^{-1} for OH, and 2654 and 2630 cm^{-1} for OD.

(*3*) It is very likely that both O_w—H bonds of the water molecule point toward CN groups (or their N atoms), each CN group belonging to a different nitroprusside ion. One of the two O_w—H···N distances is significantly greater than the other, which explains the dissimilarity of the uncoupled OH (and OD) stretching frequencies.

(*4*) The two N atoms which we believe are involved in the O_w—H···N bonds do not correspond to those thought to be so involved in ref. 1. While the shorter of the two distances appears to be 3.27 Å in both descriptions, the longer distance is taken to be 3.36 Å in ref. 1 but 3.63 Å in the present work. Thus the difference between an O_w—H···N interaction at 3.27 Å and what must be a *very* weak interaction at 3.63 Å corresponds to 34 (24) cm^{-1} in the uncoupled OH (OD) stretching frequency. The frequency of the fundamental corresponding to the longer bond is the highest so far reported; high stretching frequencies appear to be typical of water in hydrates of cyano complexes

(*5*) The equivalence of the nitroprusside ions is confirmed. The symmetry of the ion, $[Fe(CN)_5NO]^{2-}$, must be either $C_s[\sigma_d]$ or $C_{2v}[\sigma_v]$, consistent with the site symmetry $C_s[\sigma_d]$ required by the crystal structure. The deviation from the C_{4v} symmetry of the idealized ion has been estimated to be very small, at least so far as the CN bond lengths are concerned. Minor isotopic bands have been found useful for structural deductions.

We thank Mr. P. F. Seto for assistance with some of the experimental work. Financial assistance from the Geological Survey of Canada is hereby acknowledged.

1. P. T. Manoharan and W. C. Hamilton. Inorg. Chem. 2, 1043 (1963).

2. W. C. HAMILTON and J. A. IBERS. Hydrogen bonding in solids. W. A. Benjamin, Inc., New York. 1968. p. 219.
3. R. W. G. WYCKOFF. Crystal structures. Vol. 3. 2nd ed. Interscience, New York. 1965. pp. 623–626.
4. V. SEIDL, O. KNOP, and M. FALK. Can. J. Chem. **47**, 1361 (1969).
5. J. SCHIFFER. Ph.D. Thesis. Princeton University. Princeton, N.J. 1963; Dissert. Abstr. **25**, 2786 (1964).
6. E. F. G. HERINGTON and W. KYNASTON. J. Chem. Soc. 3555 (1955).
7. F. A. COTTON, R. R. MONCHAMP, R. J. M. HENRY, and R. C. YOUNG. J. Inorg. Nucl. Chem. **10**, 28 (1959).
8. G. BOR. J. Inorg. Nucl. Chem. **17**, 174 (1961).
9. B. JEZOWSKA-TRZEBIATOWSKA and J. ZIÓŁKOWSKI. Bull. Acad. Polon. Sci., ser. sci. chim. **12**, 503 (1964).
10. P. GANS, A. SABATINI, and L. SACCONI. Inorg. Chem. **5**, 1877 (1966).
11. A. SABATINI. Inorg. Chem. **6**, 1756 (1967).
12. L. TOSI. C. R. **264B**, 1313 (1967).
13. R. K. KHANNA, C. W. BROWN, and L. H. JONES. Inorg. Chem. **8**, 2195 (1969).
14. L. TOSI. C.R. **270B**, 688 (1970).
15. J. B. BATES and R. K. KHANNA. Inorg. Chem. **9**, 1376 (1970).
16. L. TOSI. Spectrochim. Acta, **26A**, 1675 (1970).
17. W. KRASSER. Ber. Bunsenges. **74**, 476 (1970).
18. G. BRINK and M. FALK. Can. J. Chem. **49**, 347 (1971).
19. M. HASS and G. B. B. M. SUTHERLAND. Proc. Roy. Soc. London. Ser. A, **236**, 427 (1956).
20. E. WHALLEY. Dev. Appl. Spectrosc. **6**, 277 (1968).
21. W. C. HAMILTON. *In* Structural chemistry and molecular biology. *Edited by* A. Rich and N. Davidson. W. H. Freeman Co., San Francisco. 1968. p. 466.
22. M. HOLZBECHER. Unpublished spectra.
23. K. O. HARTMAN and F. A. MILLER. Spectrochim. Acta, **24A**, 669 (1968).
24. J. L. HOARD, T. A. HAMOR, and M. D. GLICK. J. Am. Chem. Soc. **90**, 3177 (1968).
25. R. M. BADGER. J. Chem. Phys. **2**, 128 (1934).

Can. J. Chem. Downloaded from www.nrcresearchpress.com by 210.87.254.40 on 09/05/12
For personal use only.

Can. J. Chem. Downloaded from www.nrcresearchpress.com by 210.87.254.5 on 09/05/12
For personal use only.

Oxidation of Pentoses in Alkaline Solution[1]

W. B. GLEASON AND R. BARKER
Department of Biochemistry, The University of Iowa, Iowa City, Iowa 52240

Received August 6, 1970

The reaction of pentoses with oxygen in dilute aqueous potassium hydroxide at 25.00 ± 0.05° has been studied by determining the initial rate of oxygen uptake and the rate of disappearance of reducing sugar. Pentose reactivity decreased through the series: D-xylose (2.0), D-ribose (1.4), L-arabinose (1.2), D-lyxose (1.0). The products formed were identified by paper chromatography, isolation, and n.m.r. spectroscopy. In all cases less than one molar equivalent of tetronic acid is produced. The results are discussed with reference to recent studies on the behavior of sugars in alkaline solution. The reaction of pentoses with oxygen in 0.5 *M* sodium carbonate at 25.00 ± 0.05° was also studied. The order of pentose reactivity in this system was changed to D-ribose (5.7), D-lyxose (2.2), D-xylose (1.9), L-arabinose (1.0).

On a étudié la vitesse de réaction des pentoses avec l'oxygène à 25.00 ± 0.05 °C en présence d'hydroxyde de potassium en solution aqueuse diluée; les mesures ont été effectuées en déterminant le taux initial d'absorption d'oxygène et le taux de disparition du sucre réducteur. La réactivité des pentoses diminue dans l'ordre suivant: D-xylose (2.0) D-ribose (1.4), L-arabinose (1.2), et D-lyxose (1.0). On a identifié les produits formés, et isolés, par chromatographie sur papier et spectroscopie r.m.n. Dans tous les cas la quantité d'acide tétronique produite correspond à moins d'un équivalent. On discute les résultats en fonction d'études récentes sur le comportement des sucres en milieu alcalin. On a aussi étudié la réaction des pentoses avec l'oxygène, à 25.00 ± 0.05 °C, en présence de solutions 0.5 *M* de carbonate de sodium. L'ordre de la réactivité des pentoses dans ce système est maintenant D-ribose (5.7), D-lyxose (2.2), D-xylose (1.9), L-arabinose (1.0).

Canadian Journal of Chemistry, 49, 1425 (1971)

Introduction

Our original goal was to develop a preparative synthesis of the D- and L-forms of erythronic and threonic acids because of the potential of their phosphorylated derivatives as substrate analogs for enolase (1, 2). Oxidation of pentoses in alkaline solution appeared to be a good route since pentoses with the desired configuration at C-3 and -4 are readily available.

Nef and his students (3) described a degradation of L-arabinose and D-xylose in which an alkaline solution of the pentose was aerated yielding formic, glycollic, glyceric, and tetronic acids as major products. In an analogous degradation of D-glucose, Spengler and Pfannenstiehl (4) showed that the yield of arabinonic acid was much increased when pure oxygen was used rather than air. Isbell (5), in an attempt to increase the yield of tetronic acids from pentoses, studied the alkaline degradation with pure oxygen, but succeeded in increasing Nef's yields only slightly. Hardegger *et al.* (6) have also described the synthesis of tetronic acids in yields of about 40% by oxygenation of an alkaline pentose solution.

In alkali, sugars undergo isomerization, internal oxidation–reduction reactions, and rearrangements of the carbon skeleton. Perhaps the best known of these transformations is the isomerization of glucose to fructose and mannose first described by Lobry de Bruyn and Alberda von Ekenstein (7), which is commonly considered to proceed with the initial formation of an enediol (8). Another well-known sugar rearrangement, that of saccharinic acid formation, is generally considered to proceed by the Nef-Isbell (9) mechanism which also invokes initial formation of an enediol.

A plausible reaction scheme involving enediol intermediates that might account for the main products of oxygenation of a basic pentose solution is given in Scheme 1. Similar schemes have been proposed by Dubourg and Naffa (10) and by Bamford and coworkers (11) for the oxidation of hexoses. This mechanism requires that the molar amount of formic acid produced should equal that of tetronic acid, that the molar amount of glyceric acid should equal glycollic acid, and that with a great excess of oxygen the only products should be formic and tetronic acids.

[1]Supported in part by a Public Health Service Grant (HD 02618) from the Institute of Child Health and Human Development and a National Science Foundation Predoctoral Fellowship to W.B.G.

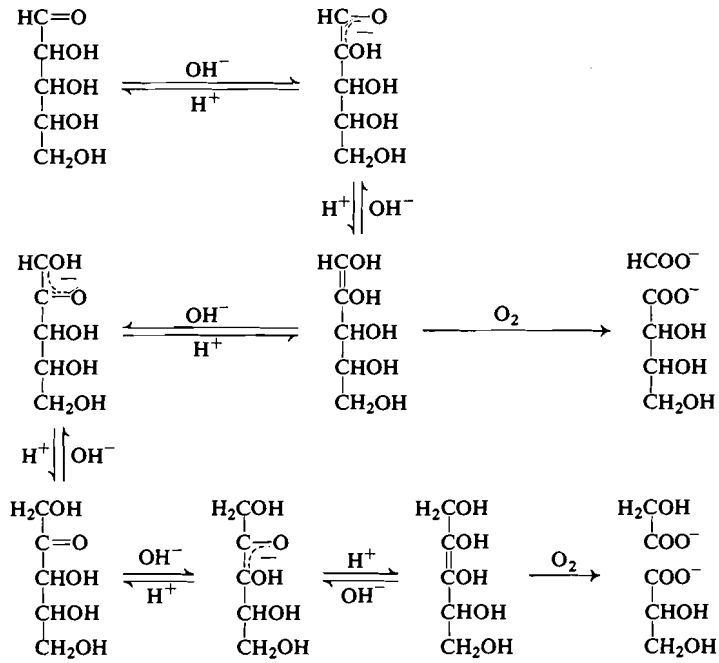

SCHEME 1

However, it was found that these compounds were never formed exclusively, even in very dilute sugar solutions with an oxygen pressure of 50 p.s.i. This finding casts doubt on a mechanism as simple as that of Scheme 1 and led us to study the initial rate of oxygen uptake and reducing sugar disappearance for the pentoses as well as the product distribution. Studies were also made of the behavior of D-ribose-2-*t* in alkali, the subject of the following paper.

Experimental

Pentoses were obtained from Pfansteihl Laboratories (Waukegan, Illinois) with the exception of D-lyxose which was prepared by Ruff degradation of calcium D-galactonate (12). The sugars were dried over phosphorus pentoxide under vacuum before use.

Rate of Initial Oxygen Uptake for the Pentoses

Oxygen uptake was measured by Warburg manometric technique (13) using the ferricyanide–hydrazine system for evaluation of flask constants. The Bunsen coefficient for oxygen in 0.833 *M* potassium hydroxide was obtained by interpolation of the data presented in the International Critical Tables. Temperature was maintained at 25.00 ± 0.05° and the shaking rate was 110 c.p.m. The sugar solution (0.5 ml) was placed in the Warburg flask side-arm and 2.5 ml of standard base in the main compartment. The concentrations of sugar solutions ranged from 6.6×10^{-5} to 5.68×10^{-1} *M*. For experiments in carbonate solution 0.6 *M* sodium carbonate was used in the main compartment of the Warburg flask and 1.2 *M* sugar solution in the side-arm.

Rate of Reducing Sugar Disappearance

Standard base (95.0 ml) was equilibrated with oxygen in a vessel which was connected to an oxygen reservoir. The system was alternately filled with oxygen and evacuated to remove air and then filled with oxygen to a final pressure of 1 atm. The vessel was shaken vigorously in a water bath at 25.00 ± 0.05°.

A calibrated syringe was used to inject 5.0 ml of a sugar solution through a side-arm fitted with a rubber septum. Concentrations of sugar solutions ranged from 1.32 to 2.24 *M* and were selected to give the same final concentrations as in the oxidation experiments. Samples of approximately 5 ml were removed with a syringe through the side-arm at various times.

An aliquot of the sample was placed in a 5 ml volumetric flask containing 0.1 ml of 0.05% bromocresol green and 2.0 ml of 1 *M* hydrochloric acid to stop the reaction and then back-titrated to green with 0.1 *M* potassium hydroxide and the final volume adjusted with water. The reducing sugar present in the sample was determined by the dinitrosalicylate method (14). First-order rate constants were calculated by a least squares fit of the data.

Determination of Formate by Nuclear Magnetic Resonance Spectroscopy

A 100 ml sample of reaction mixture was passed slowly over a small (1 × 10 cm) column of Rexyn 201 (OH^-) and then the column was washed with 200 ml of water. Acids were eluted with 90 ml of *M* potassium hydroxide. The eluate was passed through a column (3 × 60 cm) of Dowex 50 (H^+) to give a strongly acidic solution free of reducing sugars. To a sample of the acidic eluate containing approximately 2.0 mmol of acid was added 0.500 mmol of malonic acid. The mixture was brought to

Can. J. Chem. Downloaded from www.nrcresearchpress.com by 210.87.254.5 on 09/05/12
For personal use only.

TABLE 1. Initial rate of oxygen uptake, rate constants for reducing sugar disappearance of pentoses in 0.833 *M* KOH at 25.00 ± 0.05°

	Concentration (mmol)	Rate of oxygen uptake (mol O_2/mol/h × 10^2)	Reducing sugar disappearance pseudo-first order rate constant (h^{-1} × 10^2)	Rate of tritium uptake* 0.5 *M* Na_2CO_3 (h^{-1} × 10^3)
D-Xylose	56	8.20	8.6±0.2	3.2
	28	7.90		
D-Ribose	88	6.03	5.9±0.1	13.1
	44	6.15		
	22	5.90		
	11	6.35		
L-Arabinose	66	4.91	5.0±0.1	1.9
	33	4.95		
D-Lyxose	112	4.38	4.2±0.1	4.1
	56	4.44		
	28	4.20		

*H. S. Isbell *et al.*, ref. 24.

p*H* 6.5 with pyridine and concentrated to dryness at reduced pressure. The sample was dissolved in 0.5 ml pyridine to obtain the n.m.r. spectrum. The absorption peaks were separated sufficiently at a sweep width of 100 Hz to allow their complete resolution with a DuPont curve analyzer.

Preparation of Erythro- and Threonolactones

A 0.05 *M* solution of the appropriate pentose in 0.15 *M* aqueous potassium hydroxide was shaken in a 2 l bottle under an atmosphere of oxygen on a Parr pressure reaction apparatus at room temperature. After 40 h the reaction mixture was passed over a column containing 100 ml of Rexyn 101 (H^+) to remove cations and then over a column containing 200 ml of Rexyn 201 (OH^-) to remove the acidic products. The eluate from this column contains the unreacted and transformed neutral sugars. The Rexyn 201 column was eluted with *M* potassium hydroxide and the alkaline eluate containing the acid products was passed over a column of Rexyn 101 (H^+) to remove potassium. The acidic eluate from this column was concentrated several times from water to remove formic acid and then to a sirup and heated at 80° for 2 h to promote the formation of lactones. The acidic sirup was dissolved in water and passed over a column containing 50 ml of Rexyn 203 (HCO_3^-) to remove acids and the neutral eluate containing lactones was concentrated to dryness. Crystalline D-erythronolactone was obtained from D-ribose in 40% overall yield and crystalline D-threonolactone was obtained from D-xylose in 38% overall yield by this procedure.

Results and Discussion

The experimental rates of oxygen uptake for the pentoses in 0.833 *M* KOH at 25.00 ± 0.05° are given in Table 1. To demonstrate that these data reflect the rate of oxygen uptake for the pentoses, it must be shown that diffusion of oxygen into the solution is not rate-limiting. This was accomplished by varying the concentration of sugar. If the amount of oxygen taken up per h per mol of sugar is the same at various levels of sugar concentration, then oxygen diffusion into solution is not rate-limiting. The experimental results indicate that the measured rate of oxygen uptake (expressed as mol O_2/mol/h) is constant over the range of concentrations studied and oxygen diffusion is not rate limiting in the experiments reported here. Within experimental error, three of the pentoses showed strictly first-order oxygen uptake. D-Lyxose, the only sugar not obtained from a commercial source, did not. With this sugar an initial fast reaction was observed equivalent to the oxidation of 0.2% of the D-lyxose present. The fast reaction was followed by a slower, constant rate of oxygen uptake. The initial fast reaction is probably due to the presence of a small amount of impurity in the sample. The first preparation was quite brown and was decolorized with charcoal repeatedly and recrystallized from ethanol. The final preparation has an absorption (6.0 mg/ml) of 0.05 at 287 nm and showed a smaller rapid initial oxygen uptake. On this basis the rate of oxygen uptake for D-lyxose was computed from the period of slower oxygen uptake.

Pseudo-first order rate constants for the disappearance of reducing sugar at 25.00 ± 0.05° in 0.833 *M* potassium hydroxide are given in Table 1. It can be seen that the relative rate of disappearance of the pentoses agrees well with their relative rates of oxygen uptake; however, the relative reactivities of the pentoses was at first surprising because it differed significantly from the relative rates of enolization reported by Isbell and co-workers (15) who studied the uptake of

Can. J. Chem. Downloaded from www.nrcresearchpress.com by 210.87.254.5 on 09/05/12
For personal use only.

TABLE 2. Rate of oxygen uptake by 0.2 *M* sugars in 0.5 *M* sodium carbonate at 25.00 ± 0.05°

	Rate of oxygen uptake (mol O_2/mol/h)	Relative rate	Rate of ^3H uptake*	Relative rate
D-Ribose	0.0171	5.7	0.0131	6.8
D-Lyxose	0.0065	2.2	0.0041	2.2
D-Xylose	0.0056	1.9	0.0032	1.7
L-Arabinose	0.0029	1.0	0.0019	1.0
D-Glucose	0.00048	1	0.00046	1.0
D-Fructose	0.0056	11.7	0.0049	10.7

*H. S. Isbell *et al.*, ref. 15.

tritium by sugars in 0.5 *M* aqueous sodium carbonate. MacLaurin and Green (16) also found recently that the relative reactivities of glucose (1.0), fructose (3.0), and mannose (0.3) in interconversion reactions conducted in 1 *N* sodium hydroxide at 22° differed from rates of enolization reported by Isbell who found relative rates to be, glucose (1.0), fructose (10.7), and mannose (0.5) in 0.5 *M* sodium carbonate solution. Isbell *et al.* (15) found that ketoses, such as fructose, take up tritium faster than aldoses, and they suggested that this may be due to the reversible formation from the ketoses of glyceraldehyde and its enediol, to the presence of three replaceable hydrogens α to the carbonyl group, and to the possibility of a β-elimination reaction leading to an unsaturated sugar that can rearrange with hydrogen incorporation. Since a pentose could be converted to a ketose the figures given for tritium uptake of the pentoses may not reflect the primary rate of enolization alone. It is probable, however, that the tritium uptake in the early stages of the reaction is related to enolization rates. In this study 0.833 *M* potassium hydroxide and oxygen was used, whereas Isbell and co-workers used 0.5 *M* aqueous sodium carbonate under anaerobic conditions and it is possible that this difference alters the relative reactivities of the sugars.

That relative reactivities depend upon the conditions of the oxidation was shown by a study of the rates of oxygen uptake by the pentoses, glucose, and fructose in the carbonate system. The results are shown in Fig. 1 and Table 2. The rates given in Table 2 are maximum oxidation rates; those observed after the induction period apparent in Fig. 1. The agreement between the relative rates obtained by oxidation and by tritium uptake (Isbell *et al.* (15)) is quite good; however, the values for absolute rates are consistently higher for oxygen uptake than for tritium incorporation. It is possible that this difference is due to a dis-

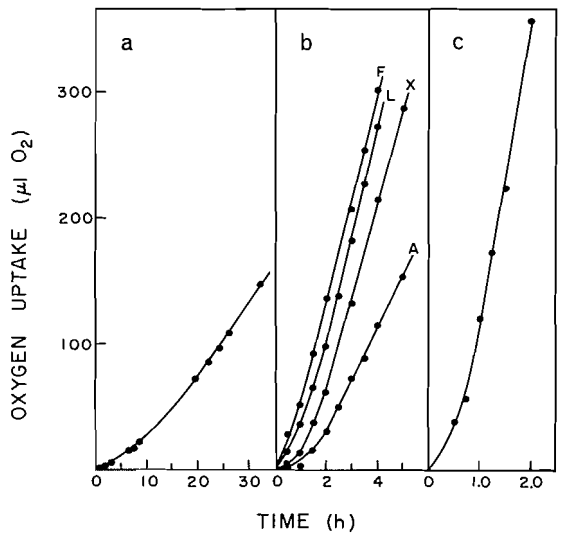

FIG. 1. The uptake of oxygen by 0.2 *M* sugars in 0.5 *M* sodium carbonate at 25°. a, D-glucose; b, F = D-fructose, L = D-lyxose, X = D-xylose, A = L-arabinose; c, D-ribose.

crimination against tritium incorporation from the solvent resulting in an under-estimation of the enolization rate by the method of Isbell *et al.* The agreement between the data presented here and that obtained by Isbell *et al.* (15) is good enough for us to conclude that both are measuring the same event and it seems reasonable to conclude, in agreement with others (10, 11), that an enolate anion is the species attacked by oxygen. A striking feature present in our data is the induction period which occurred for all of the sugars examined. Isbell *et al.* (15) did observe an increase with time in the rate of tritium uptake for D-glucose and certain other sugars and in most cases they obtained rates from observations made before the rate increase was significant, however, the induction period shown in Fig. 1 for the pentoses would have ended. We cannot explain this induction period, but it must be accounted for

Can. J. Chem. Downloaded from www.nrcresearchpress.com by 210.87.254.5 on 09/05/12
For personal use only.

Can. J. Chem. Downloaded from www.nrcresearchpress.com by 210.87.254.5 on 09/05/12
For personal use only.

in any mechanistic hypothesis. Bamford *et al.* (11) have reported that oxygen uptake by glucose in aqueous sodium hydroxide begins immediately and is first order. Our experiments on oxygen uptake by the pentoses in aqueous potassium hydroxide also lack an induction period; however, it is possible that a very short induction period is present in the reactions occurring in strong alkali. Tentative evidence that this may be the case is provided by our observation that in 0.2 *M* potassium hydroxide under anaerobic conditions D-ribose and D-xylose develop a strong absorbance at 305 nm that shows an induction period of approximately 5 min.

The occurrence of an induction period in the oxidation of sugars in 0.5 *M* sodium carbonate solution (p*H* 11) implies that the species derived from the sugar which is attacked by oxygen is formed in a multi-step process from the starting sugar. It is unlikely that mutarotation is a step of significance in limiting the rate of oxidation under these conditions although it may be that the species from which the oxidizable intermediate is derived is produced by mutarotation. It is more probable that an intermediate formed by ionization of a hydroxyl group (perhaps that at C-2) rearranges to an enolate anion which is susceptible to oxidation and that this rearrangement is responsible for the induction period. Differences in rate then would be due to differences in the ease with which the oxidizable species is formed. The differences in rate do not correspond to the differences in rate of mutarotation (17) or to the relative amounts of various tautomers present in solution (18).

Alternatively, the induction period could be due to the oxidation being a radical reaction that is initiated by the carbohydrate and becomes autocatalytic. Bamford *et al.* (11) were unsuccessful in accelerating the reaction by using free radical initiators; however, evidence for a free radical mechanism by initiation techniques may be difficult to obtain because of reaction of the initiator with oxygen.

The relative rates of oxidation of the pentoses in 0.833 *M* potassium hydroxide differ from those in 0.5 *M* sodium carbonate. If the hydroxide ion concentration is the only important difference between the two systems, then the two systems should yield the same relative reactivities with a series of sugars. The oxidation reaction is not first-order with respect to hydroxide ion. The carbonate system (p*H* 11.0) is equivalent to a hydroxide concentration of 0.001 *M*, but the rates of oxidation of the pentoses are only a factor of 3.5 to 17 lower than in 0.883 *M* potassium hydroxide. Similarly, when 0.02 *M* D-xylose is oxidized in 0.05 *M* potassium hydroxide at 25°, a rate of 0.06 mol of oxygen $mol^{-1}\ h^{-1}$ is observed compared to a rate of 0.08 mol of oxygen $mol^{-1}\ h^{-1}$ in 0.883 *M* potassium hydroxide. Although the carbonate ion may act as a base in catalyzing the reaction, the results with D-xylose in potassium hydroxide clearly demonstrate that the reaction is not first-order with respect to hydroxide ion. This finding does not explain the differences in relative rates since if the same rate-limiting step is involved in each case, the effect of configuration on that step should be a constant regardless of the order with respect to hydroxide ion. Nor can the differences be explained on the basis that different pK_a values of the pentoses determine the amount of ionic forms present that are capable of rearrangement, since the pK_a values of lyxose and ribose are identical and are not very different from that of xylose (19). Using the published pK_a values of the pentoses (19) and the assumptions that the rates measured in 0.833 *M* potassium hydroxide are maximum values, relative rates for the carbonate system can be calculated. They are L-arabinose, 1.0; D-lyxose, 2.2; D-ribose, 2.5; D-xylose, 2.9. Both D-ribose and D-xylose differ significantly from the observed values. Thus, the change in relative rates cannot be related to any obvious parameter and may reflect a specific effect of the carbonate ion or a change in mechanism with change in hydroxide ion concentration.

The carbonate system, although of great theoretical interest, does not lend itself to studies on degradations because of the slowness of reaction and an examination of reaction products was conducted only for the potassium hydroxide system.

In Fig. 2*a* is shown the n.m.r. spectrum of a complete xylose oxidation mixture after 8 h with added acetate as an internal standard. The acetate peak E is well separated from the complex part of the spectrum D which is due to the α- and β-pyranose forms of D-xylose, plus the acidic products. The peak C is due to HOD; the singlet A is due to formate. In Fig. 2*b* is shown the simplification that occurs when xylose is removed from such a mixture. In this spectrum C is due to the complex mixture of acidic products. Although apparently better resolution of the still complex

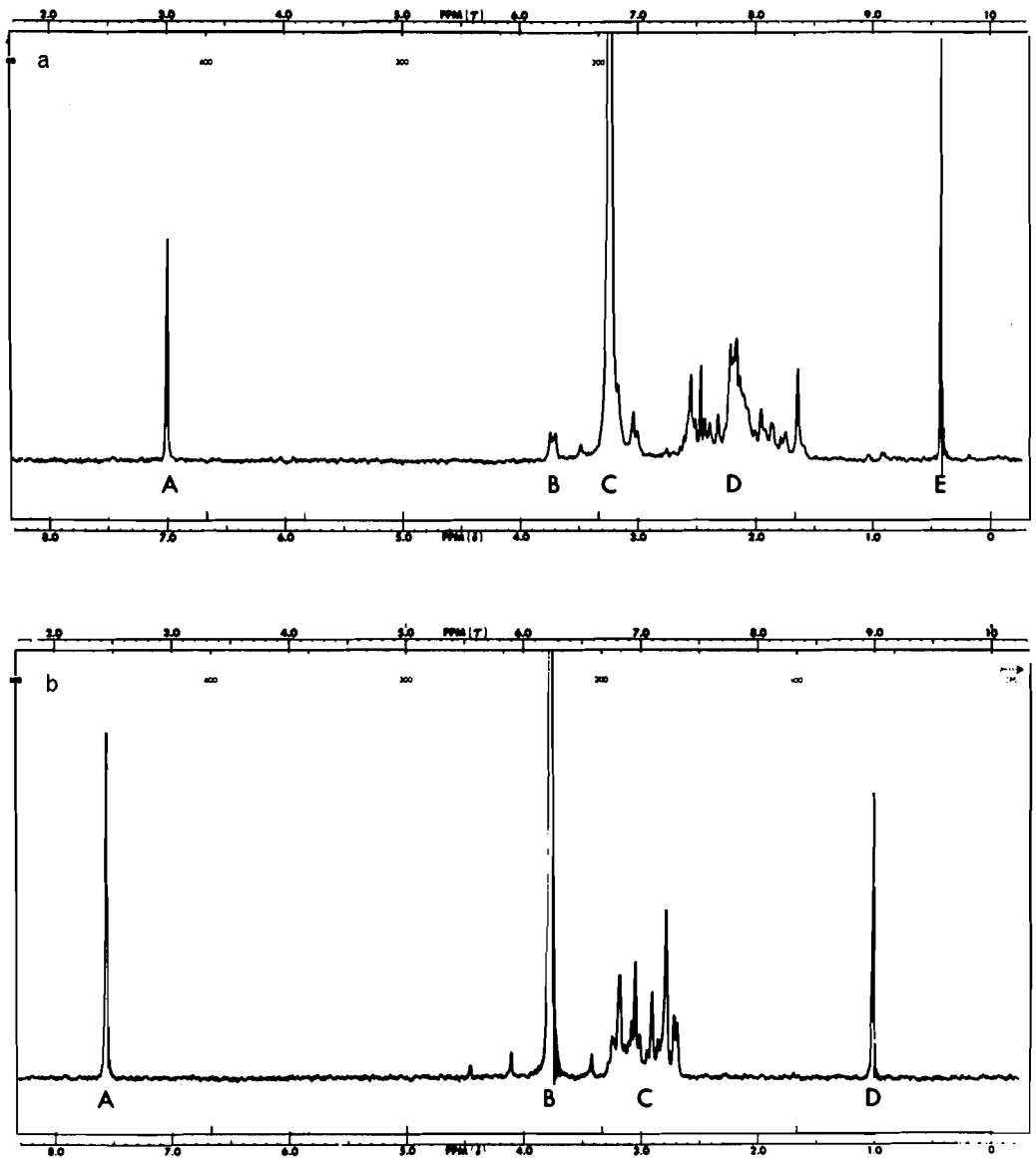

FIG. 2. The 60 MHz p.m.r. spectra of D-xylose oxidation reaction mixtures at 50% reaction. *a*, Total mixture with added acetate, A, formate; B, anomeric protons; C, HOD; D, non-exchangeable protons of xylose and acidic products. *b*, Acidic products only, A, formate; B, HOD; C, non-exchangeable protons of acidic products; D, acetate.

mixture of acidic products can be obtained by adding sulfuric acid, the tetronic acids lactonize making interpretation difficult. When pyridine is used as the solvent, the resolution at 100 Hz sweep width is good enough for product quantitation. In Fig. 3*a* is shown a standard mixture in pyridine of the acidic products from a xylose oxidation reaction with malonic acid added as an internal standard for quantification. The identification of peaks was made by running authentic samples individually. The doublet A is due to the C-2 proton of threonic acid split by the protons at C-3. Peak B is due to the methylene protons of glycollic acid. Peak C is a composite of the signals of the methylene protons of glyceric acid and threonic acid. In both acids the methylene proton peaks are doublets because there is a proton on the penultimate carbon. Quantitation can be achieved

Can. J. Chem. Downloaded from www.nrcresearchpress.com by 210.87.254.5 on 09/05/12
For personal use only.

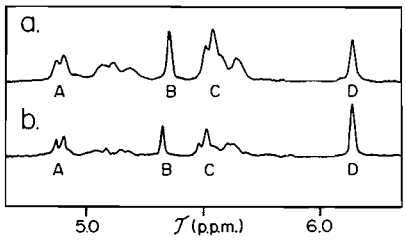

FIG. 3. The 60 MHz p.m.r. spectra of acids from D-xylose oxidation. *a*, A synthetic mixture of acids at 100 Hz; A, C-2 protons of threonic acid; B, methylene protons of glycollic acid; C, methylene protons of glyceric and threonic acid; D, methylene protons of malonic acid. *b*, The acids from D-xylose oxidation at 100 Hz.

by careful integration with a planimeter and by calculating the proportions of the various acids relative to the total acids from the peaks that characterize them. The proportion of glyceric acid was calculated from peak C by subtracting out 2 × the area of peak A. When erythronic acid is in the reaction mixture, the same procedure is used.

Mixtures of known amounts of acids were used to test the experimental procedure. Results from such experiments are given in Table 3. When the only products present are the acids of the synthetic reaction mixture, the results are highly reproducible; however, by paper chromatography in *n*-butanol : formic acid : water (*n*5:10:15) it was shown that there are other reaction products present, probably in small amounts. Thus, in the analysis of the reaction mixture, the amounts given are upper limits.

The n.m.r. analysis of pentose oxidation mixtures given in Table 4 indicates that with ribose, arabinose and lyxose there must be a source of formic acid other than the cleavage of a five carbon 1,2-enediol, since the molar proportions of formic acid and tetronic acid exceed the ratio of one predicted if the cleavage of that intermediate is the source of formic acid. Erythronic and threonic acids are stable under the conditions of the reaction. For example, when erythronic acid (5.05 mmol) was exposed to oxidizing conditions in 100 ml of 0.833 *M* KOH, no breakdown could be detected during 17 h. Thus, the formation of formic acid in a molar amount significantly greater than tetronic acid is not due to the breakdown of the latter.

TABLE 3. Quantitation of a synthetic reaction mixture by n.m.r.

	Actual (mmol)	Found (mmol)
Formate	1.15	1.15
Erythronate	0.69	0.68
Glycollate	0.36	0.38
Glycerate	0.31	0.31
Formate	1.41	1.42
Threonate	0.25	0.23
Glycollate	0.91	0.87
Glycerate	1.22	1.29

Excess formate might arise from oxidation of the products of a reverse aldol reaction as in Scheme 2.

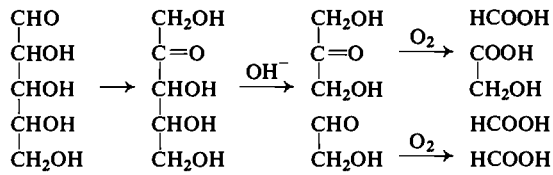

SCHEME 2

In this sequence glycollic acid is produced in excess of the molar amount of glyceric acid. This route cannot be ruled out in the case of arabinose, but for xylose, ribose, and lyxose apparently it is not a reaction of importance since for these sugars the ratio of glycollate to glycerate is close to unity.

If a 3-pentulose is formed, the reaction in Scheme 3 could result. If Schemes 2 and 3 both occurred to a similar extent, the molar amounts of glyceric and glycollic acid could be reasonably close.

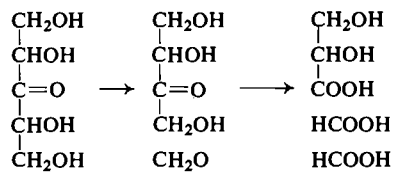

SCHEME 3

Similar conclusions concerning an alternative to the simple enolization mechanism were drawn by Dubourg and Naffa (10) from their studies on the oxidation of glucose in alkaline solution. There is, however, a dilemma regarding the nature and source of the compound which undergoes fragmentation. In the original reverse aldol mechanism of Schmidt (20) the initial formation of an enediol was postulated which should be oxygenated if enediols are the susceptible species. Isbell (21) has suggested that the reverse aldol may occur via a ketose; however, this requires that

Can. J. Chem. Downloaded from www.nrcresearchpress.com by 210.87.254.5 on 09/05/12
For personal use only.

TABLE 4. Products of pentose oxidation determined by n.m.r. spectroscopy*

	Acids (mmol)			
	D-Xylose	D-Ribose	L-Arabinose	D-Lyxose
Formate	2.05±0.05	2.78±0.08	2.82±0.13	3.33±0.10
Threonate	1.82±0.08	—	—	1.14±0.13
Erythronate	—	1.02±0.03	0.79±0.01	—
Glycerate	0.54±0.01	0.79±0.15	0.54±0.05	0.41±0.07
Glycollate	0.56±0.01	0.80±0.15	0.71±0.01	0.42±0.01
Ratio of formate to tetronate	1.1	2.7	3.6	2.9

*0.05 *M* Pentose, 0.833 *M* potassium hydroxide, 25.00 ± 0.05°.

the ketose be formed by other than an enolization mechanism.

Although the consensus seems to be that the Lobry de Bruyn – Alberda von Ekenstein reaction occurs by an enolization mechanism, there have been suggestions that a hydride transfer may operate under certain circumstances. Thus, Gutsche *et al.* (22) have drawn attention to the fact that glyceraldehyde in pyridine isomerizes to dihydroxyacetone but no aldolization occurs. Since an enolate anion is supposed to be involved in the aldol condensation, the failure of aldolization to occur in this reaction is puzzling. Thus, it was suggested that either pyridine interferes in some way with the aldolization step or that a route exists for interconversions which does not involve the formation of an enolate ion, namely a hydride transfer. Precedent was taken from the Cannizzaro reaction, the benzylic acid rearrangement and the base-catalyzed rearrangement of α-dicarbonyls.

Another observation that may be relevant is the report of Fodor and Saccheto (23) that in slightly alkaline D_2O, glucose-3-phosphate was converted to a 3-deoxyketose with no incorporation of deuterium. This behavior was interpreted in favor of a hydride shift mechanism.

It seems that a simple enolization scheme cannot account satisfactorily for the product distribution observed, nor for the inability to obtain exclusive cleavage of a 1,2-enediol even in very dilute alkali. These findings led us to investigate this reaction further by studying the oxidation of D-ribose labeled with tritium at C-2 (24).

1. R. BARKER and F. WOLD. J. Org. Chem. **28**, 1847 (1963).
2. F. WOLD and R. BARKER. Biochim. Biophys. Acta, **85**, 475 (1964).
3. J. U. NEF, O. F. HEDENBURG, and J. W. E. GLATTFELD. J. Amer. Chem. Soc. **39**, 1638 (1917).
4. O. SPENGLER and A. PFANNENSTIEHL. Z. Wirtschafts Zucher-Ind. **85**, 546 (1933).
5. H. S. ISBELL. J. Res. Nat. Bur. Stand. **29**, 227 (1942).
6. E. HARDEGGER, K. KREIS, and H. EL KHADEM. Helv. Chim. Acta, **34**, 2343 (1951).
7. C. A. LOBRY DE BRUYN and W. ALBERDA VON EKENSTEIN. Rec. Trav. Chim., **14**, 150 (1895).
8. R. U. LEMIEUX. *In* Molecular rearrangements. Part II. *Edited by* P. de Mayo. Interscience, 1964. p. 709.
9. H. S. ISBELL. J. Res. Nat. Bur. Stand. **32**, 45 (1944).
10. J. DUBOURG and P. NAFFA. Bull. Soc. Chim. Fr. 1353 (1959).
11. C. H. BAMFORD, D. BAMFORD, and J. R. COLLINS. Proc. Roy. Soc. London, **204**, 85 (1950).
12. H. G. FLETCHER. *In* Methods in carbohydrate chemistry. Vol. I. Academic Press, 1962. p. 77.
13. W. W. UMBREIT, R. BURRIS, and J. F. STAUFFER. Manometric techniques. 4th Edit. Burgess Publishing Co., Minneapolis, Minn., 1964.
14. J. M. CLARK (editor). Experimental biochemistry. W. H. Freeman and Co., San Francisco, California. p. 26.
15. H. S. ISBELL, H. L. FRUSH, C. W. R. WADE, and L. E. HUNTER. Carbohyd. Res. **9**, 163 (1969).
16. D. J. MACLAURIN and J. W. GREEN. Can. J. Chem. **47**, 3947 (1969).
17. W. PIGMAN and H. S. ISBELL. Adv. Carbohyd. Chem. **23**, 11 (1968).
18. S. J. ANGYAL. Angew. Chem. Internat. Edit. **8**, 157 (1969).
19. R. M. IZATT, J. H. RYTTING, L. D. HANSEN, and J. J. CHRISTENSEN. J. Amer. Chem. Soc. **88**, 2641 (1966).
20. O. SCHMIDT. Chem. Revs. **17**, 137 (1935).
21. H. S. ISBELL. Quoted in a review by J. C. SOWDEN. Adv. Carbohyd. Chem. **12**, 35 (1957).
22. C. D. GUTSCHE, D. REDMORE, R. BURICK, K. NOVOTNY, H. GRAESSNER, and C. W. ARMBRUSTER. J. Amer. Chem. Soc. **89**, 1235 (1967).
23. G. FODOR and J. P. SACCHETO. Tetrahedron. Lett. 401 (1968).
24. W. B. GLEASON and R. BARKER. Can. J. Chem. This issue.

Can. J. Chem. Downloaded from www.nrcresearchpress.com by 210.87.254.5 on 09/05/12
For personal use only.

Can. J. Chem. Downloaded from www.nrcresearchpress.com by 210.87.254.42 on 09/05/12
For personal use only.

Evidence for a Hydride Shift in the Alkaline Rearrangements of D-Ribose[1]

W. B. GLEASON AND R. BARKER
Department of Biochemistry, The University of Iowa, Iowa City, Iowa 52240

Received August 6, 1970

The synthesis of D-ribose-2-t from D-arabinose is described and its conversions in aqueous alkali in the presence and absence of oxygen reported. In both situations a significant amount of label is transferred from C-2 to -1 and a relatively small proportion is released to the solvent. It is concluded that hydride transfer is occurring and that enolization, which requires the loss of hydrogen from C-2, is not an obligatory first step in base-catalyzed rearrangements of D-ribose.

On décrit une synthèse du D-ribose-2-*t* à partir du D-arabinose et on rapporte ce qui lui survient en milieu alcalin en présence et en l'absence d'oxygène. Dans chaque cas une quantité significative de tritium est transférée du C-2 au -1 et une faible proportion se retrouve dans le solvant. On en conclut qu'un transfert d'hydrure se produit et qu'une enolisation, qui implique une pente d'hydrogène du C-2, n'est pas nécessairement la première étape lors du réarrangement du D-ribose au milieu alcalin.

Canadian Journal of Chemistry, **49**, 1433 (1971)

Introduction

In the preceding paper (1) circumstantial evidence was presented that the pentoses in aqueous potassium hydroxide, in the presence of oxygen, cannot react only by a simple enolization mechanism initiated by abstraction of the hydrogen at C-2. To further test this conclusion, we have studied the behavior of D-ribose-2-*t* in aqueous potassium hydroxide under both aerobic and anaerobic conditions.

Experimental

The n.m.r. spectra were obtained on a Varian A-60 spectrometer and i.r. spectra were obtained on a Perkin–Elmer Model 521. Elemental analyses were performed by Galbraith Laboratories, Inc., Knoxville, Tennessee. Evaporations were carried out at water-aspirator pressure. Melting points are corrected.

A Beckman LS-100 scintillation counter equipped with automatic external standardization was used for radioactivity determination. Aqueous samples were added in a volume of 0.100 to 10.0 ml of scintillation fluid containing 5 g PPO and 100 g napthalene with dioxane added to make 1 l. Water insoluble samples were added directly to the scintillation fluid and then 0.100 ml H_2O added to this mixture.

Gas chromatographic analyses were performed using a Varian Aerograph Hy-Fi, Model 600 D, with a flame ionization detector (hydrogen flow rate of 30 ml/min). The column was 1/8 in. × 6 ft copper tubing packed with 10% Hi-eff-3-CP (Applied Sciences Laboratories, Inc.) with helium carrier gas at 30 ml/min. Silyl derivatives were prepared by dissolving 10 mg of material in 0.5 ml pyridine and adding 0.2 ml hexamethyl disilazane and 0.1 ml trimethylchlorosilane (Applied Sciences Laboratories). The derivative mixture (2 μl) was injected after 10 min. Acetylated derivatives were prepared by warming a 10 mg sample in 0.5 ml pyridine and acetic anhydride (1:1) for 30 min. Peak areas were determined by planimetry.

The t.l.c. was carried out on plates prepared with Silica gel G (Merck) using isopropyl ether as solvent. Spots were visualized by spraying with 10% sulfuric acid and heating at 110° for 5 min.

Acidic products were separated by paper chromatography on Whatman 3MM paper to which a wick of Whatman 1 (10 × 57 cm) had been sewn. The freshly prepared solvent, *n*-butanol : formic acid : water (75:10:15), gave an adequate separation provided that samples of 100 mg or less were used. Standards of glyceric (R_f = 0.46), glycollic (R_f = 0.61), and erythronic or threonic (R_f = 0.31) acids were applied 3 cm from each edge and were used to locate the main reaction components. Acidic compounds could be located as yellow spots on a blue background with the indicator bromocresol green (0.05%) in slightly alkaline ethanol if the chromatograms were allowed to dry for several days to free them of formic acid. Alternate cycles of steaming and drying at 100° in an oven was used also to remove formic acid more rapidly.

For quantitation of the reaction products, strips were cut from the chromatogram and eluted with water. The eluted acids were titrated to p*H* 7.0 with 0.050 *M* potassium hydroxide. In cases where lactonization had occurred (indicated by a rapidly fading end-point) an excess of alkali was added and the sample was back titrated with 0.050 *M* hydrochloric acid to determine the total amount of acid and lactone.

Benzyl 3,4-O-Isopropylidene-β-D-ribopyranoside (4)

(A) By Dimethyl Sulfoxide – Acetic Anhydride Oxidation

The reaction sequence used to synthesize this compound is shown in Scheme 1. D-Arabinose was converted

[1]Supported in part by a Public Health Service Grant (HD 02618) from the Institute of Child Health and Human Development and an NSF Predoctoral Fellowship to W.B.G.

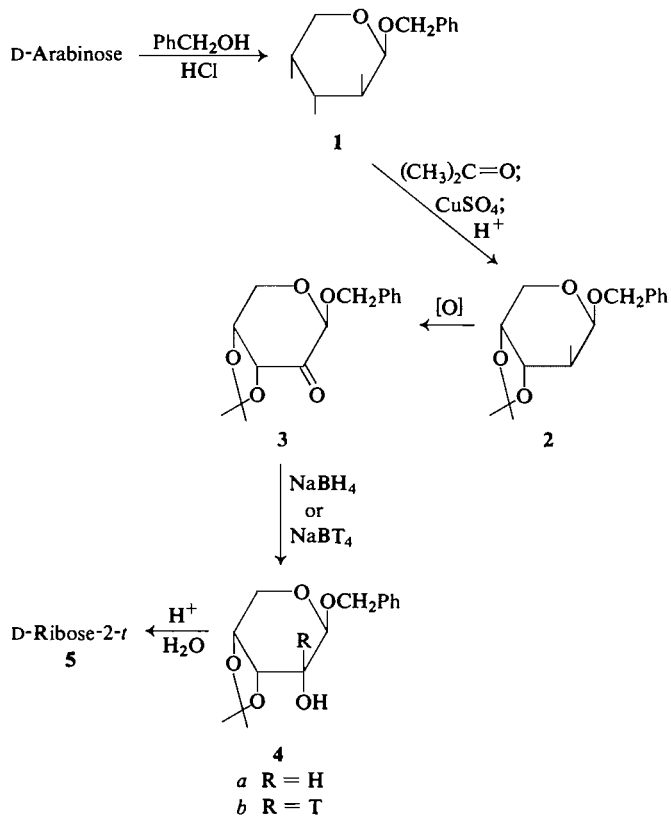

SCHEME 1

to benzyl β-D-arabinopyranoside (**1**) by the method of McCormick (2). Benzyl 3,4-*O*-isopropylidene-β-D-arabinopyranoside (**2**) was prepared from (**1**) by the method of Ballou (3).

Benzyl 3,4-*O*-isopropylidene-β-D-arabinopyranoside (**2**), 3.0 g, was oxidized in a mixture of 30 ml dimethylsulfoxide and 20 ml acetic anhydride (4). The progress of the reaction was monitored by t.l.c.; the starting material had $R_f = 0.15$. After 8 h reaction two new spots of about equal intensity appeared with $R_f = 0.37$ and 0.46. After 24 h only the two product spots were present. At this time the reaction mixture was quite yellow. Dimethylsulfoxide and acetic anhydride were removed by evaporation at 55°. The residue, a thin sirup, was reduced at 0° in 150 ml ethanol–water (3:1) using 3 g sodium borohydride. After 2 h acetic acid was added to destroy the excess borohydride and the reaction mixture was passed over 70 ml Rexyn 101 (H^+) and the eluate evaporated to dryness. Finally, boric acid was removed as its volatile methyl ester by three evaporations from 100 ml portions of methanol.

The t.l.c. of the mixture indicated that material of $R_f = 0.46$ was still present, but that the material of $R_f = 0.37$ had disappeared and a new spot with R_f approximately equal to that of the starting material had appeared. The mixture was dissolved in 15 ml ether and petroleum ether added to turbidity. After several hours at 4°, a cotton-like precipitate was removed by filtration and the filtrate was evaporated to dryness. The residue was dissolved in a minimum amount of absolute ethanol and petroleum ether was added to produce turbidity. The product, **4***a*, 1.25 g (41% from **2**), could be recrystallized from ether – petroleum ether and melted at 94–96°; $[\alpha]_D^{25} -105 \pm 5°$ (*c* 3.1, EtOH). Follmann and Hogenkamp report m.p. 92–94° (5). The n.m.r. data: τ 2.65 (singlet, 5 protons, phenyl ring hydrogens); 5.06 (doublet, 1 proton H-1, $J_{1,2}$ 3.5 Hz); 5.20, 5.36, and 5.55 (multiplet, 3 protons, H-2, -3, and -4); 6.20 (multiplet, 4 protons, H_2-5 and benzyl methylene hydrogens); 2.47 and 2.63 (singlets, 6 protons, acetal methyl hydrogens).

Anal. Calcd. for $C_{15}H_{20}O_5$: C, 64.27; H, 7.19. Found: C, 64.27; H, 7.29.

The cotton-like precipitate which was removed from the product by filtration as described above proved to be a methylthiomethyl ether, presumably benzyl 3,4-*O*-isopropylidene-2-*O*-methylthiomethyl-β-D-arabinopyranoside. It could be isolated in yields of approximately 40% and crystallized readily from ether – petroleum ether. It melted at 43.8–45°; $[\alpha]_D^{25} -175 \pm 8°$ (*c* 1.2, EtOH). The n.m.r. data: τ 2.67 (singlet, 5 protons, phenyl ring hydrogens); 5.06 (doublet, 1 proton, H-1, $J_{1,2}$ 3.3 Hz); 5.23, 5.31, and 5.39 (multiplet, 3 protons, H-2, -3, and -4); 5.76 (singlet, 2 protons, methylthiomethyl methylene hydrogens); 6.06 (multiplet, 4 protons, H_2-5 and benzyl

Can. J. Chem. Downloaded from www.nrcresearchpress.com by 210.87.254.42 on 09/05/12
For personal use only.

Can. J. Chem. Downloaded from www.nrcresearchpress.com by 210.87.254.42 on 09/05/12
For personal use only.

methylene hydrogens); 2.47 and 2.67 (singlets, 6 protons, acetal methyl hydrogens).

Anal. Calcd. for $C_{17}H_{24}O_5S$: C, 59.97; H, 7.11; S, 9.42. Found: C, 59.90; H, 6.98; S, 9.28.

This compound proved to be the material of $R_f = 0.46$ observed in thin layer chromatograms of the reaction mixture.

(B) Alternate Oxidation Procedures

Because the dimethyl sulfoxide – acetic anhydride oxidation gave such a large amount of side-product, other oxidation methods were investigated.

(1) Pfitzner–Moffat Oxidation (6)

Benzyl 3,4-*O*-isopropylidene-β-D-arabinopyranoside (837 mg) was added to a mixture of 1.85 g dicyclohexylcarbodiimide (DCC), 5 ml dimethylsulfoxide, 10 ml benzene, 0.24 ml pyridine, and 0.12 ml trifluoroacetic acid. After 24 h, benzene was removed by evaporation and 20 ml water added to the reaction mixture. After 2 h the DCC had been converted to insoluble dicyclohexylurea, which was removed by filtration. The filtrate was evaporated to a sirup and extracted three times with 10 ml portions of chloroform. The chloroform extract was dried to a sirup. This sirup was applied to a 60 × 1.5 cm column of silica gel (60–200 mesh, W. R. Grace and Co.) and eluted with isopropyl ether, 3 ml fractions were collected at a flow rate of 0.2 ml per min. The first peak, found in fractions 1–14, contained at least three components as judged by t.l.c. Fractions 14–30 contained only the product, **3**: overall yield 38–42%.

(2) Catalytic Ruthenium Dioxide – Sodium Metaperiodate Oxidation (7)

Benzyl 3,4-*O*-isopropylidene-β-D-arabinopyranoside (1.0 g) was dissolved in 20 ml carbon tetrachloride containing 20 mg of ruthenium dioxide (Englehard Industry). Sodium metaperiodate (5%) was added by a burette to a rapidly stirred solution. The p*H* was maintained between 6.0 and 7.0 by the addition of dilute sodium bicarbonate. After 3 h and the addition of 23 ml of periodate, the end of the reaction was signalled by a permanent yellow ruthenium tetroxide color which was not darkened by conversion to the dioxide. The excess oxidant was destroyed by adding *n*-propanol. The organic layer was removed, filtered, and evaporated to a colorless sirup (0.78 g) which gave one spot on t.l c ($R_f = 0.37$ in isopropyl ether) and a carbonyl absorption (5.8 μ) in the i.r.

Benzyl 3,4-O-isopropylidene-β-D-ribopyranoside-2-t (4)

Benzyl 3,4-*O*-isopropylidene-β-D-*erythro*-pentopyranos-2-uloside (150 mg) was dissolved in a mixture of 7.5 ml ethanol (distilled from 2,4-dinitrophenol) and 5 ml distilled water. Sodium borohydride-*t* (3 mg, New England Nuclear, 200 mc/mmol), dissolved in 5 ml H_2O, was added drop by drop. The solution was allowed to stand overnight at 4° and then 25 mg of unlabeled borohydride was added. The t.l.c. indicated complete reduction. The reaction mixture was partitioned between ether and water; the ether extracts were evaporated at reduced pressure, and the residue was taken-up in a small volume of ether and 1.5 g of unlabeled benzyl 3,4-*O*-isopropylidene-β-D-ribopyranoside was added. The addition of petroleum ether gave 1.40 g of chromatographically pure product which had a specific activity of 0.232 mc/mmol, a radiochemical yield of 77%.

D-*Ribose-2-t*

Benzyl 3,4-*O*-isopropylidene-β-D-ribopyranoside-2-*t* (250 mg) was hydrolyzed with 10 ml of 1 *N* HCl at 100° for 3 h. The reaction mixture was passed through Rexyn 203 (OH^-) and 6 g unlabeled D-ribose was added to the eluate as carrier. After removal of the solvent the product was recrystallized three times from ethanol to a constant specific activity of 4.14 μCi/mmol; 4.0 g of material equivalent to a radiochemical yield of 54% was obtained.

To show that label was present only at C-2 the following experiments were performed. D-Ribose-2-*t* was reduced with borohydride to ribitol which then was oxidized with periodic acid – bicarbonate as described by Reeves (8) and the dimedon derivative of formaldehyde isolated. The dimedon derivative from a ribose sample containing 215 000 c.p.m. had 78 c.p.m.; indicating that less than 0.04% of the radioactivity was at C-1. The phenylosazone of ribose was then prepared and found to be free of radioactivity, indicating that there was no tritium bound to C-1, -3, -4, or -5 and that the counts observed in the dimedon derivative could have been due to contamination with formic acid or to migration of label under the alkaline conditions of the borohydride reduction.

Treatment of Ribose-2-t with Alkali

Into a 10 ml vial equipped with a rubber septum 1 ml of sugar solution was injected. An outlet needle was inserted in the septum and the vial was flushed with nitrogen (or oxygen) for 10 min and then degassed potassium hydroxide (5 ml) was injected. Vials were incubated in a constant temperature water bath and aliquots of approximately 0.5 ml were removed at various times and assayed for tritium as described below.

For larger scale experiments the reaction vessel consisted of a flask having a side-arm equipped with a rubber septum and an outlet to a gas reservoir. The reaction vessel was immersed in a constant temperature bath and attached to a shaker mechanism. The reaction vessel was filled with an alkaline solution and flushed repeatedly with oxygen or nitrogen with shaking. The reaction was initiated by injecting the sugar solution with a calibrated syringe. Aliquots were removed at intervals by syringe through the septum.

Assay of Tritium Release to Solvent

Samples were placed in a standard taper test-tube and shell-frozen in liquid nitrogen. The sample tube was attached to one side of a standard taper U-tube equipped with a stop-cock and another standard taper test tube was attached to the other arm. The system was evacuated to 0.1 mm Hg while the sample side was immersed in liquid nitrogen. After the system had been evacuated, the stop-cock was closed and the receiver tube was placed in liquid-nitrogen. In 15 min enough water had sublimed so that 0.100 ml could be obtained and assayed for tritium by scintillation counting.

Isolation of Products from the Alkaline Treatment of D-Ribose-2-t

The oxidation mixture was passed through a column containing 100 ml Dowex 50 (H^+) to remove potassium

Can. J. Chem. Downloaded from www.nrcresearchpress.com by 210.87.254.42 on 09/05/12
For personal use only.

ions. The acidic solution was then passed over 25 ml Rexyn 203 (free base form) to remove acids; and the acids were recovered by elution with potassium hydroxide. The salts so obtained were converted back to the acids by treatment with Dowex 50 (H^+). The acidic fraction was resolved by preparative paper chromatography. The neutral sugar fraction was concentrated and applied to a column of Rexyn 101 (Ba^+) for fractionation (21).

Reduction of D-*Arabinose-t*

Unlabeled D-arabinose (53.5 mg) was added to a sample of 1.96 mg arabinose-*t* isolated from a reaction mixture; the mixture was dissolved in 7 ml of water and the solution was stirred at 0°. The p*H* was monitored and kept below 9 with dilute acetic acid while 50 mg of sodium borohydride dissolved in 5 ml water was added dropwise. The reaction was kept for 24 h at 4°. Excess borohydride was destroyed with acetic acid and the reaction mixture was passed over a small column of Dowex 50 (H^+). The eluate was evaporated to dryness, with five additional evaporations from 10 ml of methanol. The yield was 50.5 mg. The product gave a quantitative yield of pentabenzoate m.p. 151.0–151.7, undepressed on admixture with the authentic material.

Results and Discussion

This study was undertaken to determine the role of enolization in the oxidative degradation of sugars, specifically the pentoses. Two hypotheses have been advanced for the analogous degradation in the hexose series. Bamford and Collins (9), supported by subsequent experiments of Dubourg and Naffa (10), proposed that in the oxidation of glucose an enediolate anion intermediate is attacked by oxygen to produce a peroxide which cyclizes and decomposes to give formic and arabinonic acids. This mechanism requires that the starting material lose the proton at C-2.

Samuelson and Thede (11) have recently reported that after 26 h in 4.5 *N* sodium hydroxide, at 1 atm oxygen pressure, glucose was converted to a mixture of at least 13 monoprotic carboxylic acids, as well as small amounts of mannose, fructose, and arabinose. These workers suggested the intermediate formation of osones, because D-glucosone gives approximately the same mixture of products as D-glucose does. This mechanism also requires loss of the proton from C-2 of the starting material.

Because the reaction of the pentoses with oxygen at neutral p*H* values is negligible compared to the base-catalyzed reaction, it is apparent that some reaction of the sugar with base must occur prior to the actual oxidation. Thus, it is also of interest to study the reaction of the labeled sugar with alkali in the absence of oxygen. Many other base-catalyzed sugar reactions such as the Lobry de Bruyn – Alberda van Ekenstein rearrangement and the formation of saccharinic acids occur by mechanisms that have been much debated but which usually are thought to involve enolization as the first step (12). Although D-ribose-2-*t* might appear to be an ideal substrate to test the proposal that alkaline rearrangements of sugars involve an initial enolization resulting in the loss of the C-2 hydrogen, it is not. Reactions involving breaking the carbon–tritium bond in the rate-determining step can be expected to differ in rate from those involving the carbon–hydrogen bond by a factor of 10, or more. In addition, ribose is an unusual sugar, it reacts many times faster than other sugars in reactions involving ring opening. Nevertheless, one would expect that the loss of tritium to solvent would occur if enolization is a principal event and that other reactions involving the hydrogen at C-2 would be reflected by qualitatively, if not quantitatively, similar reactions of tritium.

The release of tritium to water in the absence of oxygen in 0.88 *M* potassium hydroxide solution is shown in Fig. 1. The conditions were chosen to be pseudo-first order in D-ribose-2-*t*, that is with a large relative excess of alkali so that the formation of acidic products would not decrease the effective hydroxide ion concentration. The first 50% of the reaction follows first-order kinetics, but it is clear that a portion of the tritium (40%) is incorporated into a position from which base-catalyzed exchange with solvent is very slow. The initial rate of tritium release to solvent is strongly temperature dependent and increases five-fold between 30 and 40°.

Although no extensive study was made, we find that tritium release is not first-order with respect to base concentration.

To investigate the effect of oxygen on tritium release from D-ribose-2-*t*, experiments were carried out at 25° in the presence and absence of oxygen. The results obtained are given in Table 1. The presence of oxygen depresses the rate of tritium release to the solvent by a factor of two. The release of tritium in volatile acids was estimated by distillation of an acidified sample of the reaction mixture; the acid was shown to be formic acid by DuClaux distillation (13) and by n.m.r. spectroscopic examination of the neutralized distillate.

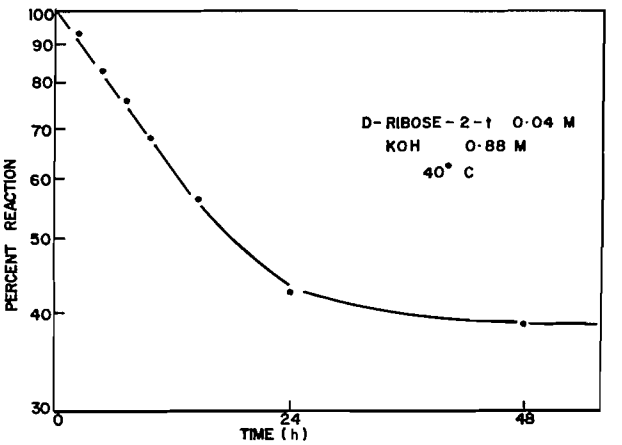

FIG. 1. The release of tritium to solvent from D-ribose-2-*t* in 0.88 *M* aqueous potassium hydroxide at 40°.

TABLE 1. Products from ribose-2-*t* (0.05 *M*) in 100 ml of 0.833 *M* KOH for 12 h at 25.00 ± 0.05 °C

Gas	Acid produced (mmol)	Percent of total counts released to		
		Solvent	Formic acid	Other acids
O_2	6.03	2.1	17.5	—
	5.92	2.0	17.2	—
N_2	1.73	4.15	0.0	1.87
	1.67	4.14	0.0	1.91

TABLE 2. Specific activity of acids from the aerobic degradation of D-ribose-2-*t* in c.p.m. per mmol

	Experiment 1	Experiment 2
Erythronic acid	5.1×10^4	1.2×10^5
Glyceric acid	3.1×10^4	3.8×10^4
Glycollic acid	2.0×10^5	2.6×10^5

The acids formed in the aerobic degradation of D-ribose-2-*t* were separated by paper chromatography, titrated and counted; their specific activities are listed in Table 2. The data for erythronic acid do not agree well and the counts in that fraction may be due partly to contamination with small amounts of starting material. There is no doubt, however, that tritium is present in significant amounts in glyceric and glycolic acids.

Acids produced under anaerobic conditions when 22% of the reducing sugar had been transformed were isolated, after removal of cations, by adsorption on a weakly basic anion exchange resin and elution with alkali. The whole fraction contained 1.5×10^4 c.p.m., 1.9% of the original activity; equivalent to 50% of the tritium released to solvent. The acids were regenerated by removal of solvent, converted to silyl derivatives, and examined by g.l.c. Two main peaks and at least eight minor peaks were present. The major peaks are probably the saccharinic acids, 3-deoxy-D-*erythro*-, and 3-deoxy-D-*threo*-pentonic acids. Attempts to isolate and separate these acids by fractional crystallization of their quinine salts (14) were unsuccessful.

The reaction of D-ribose-2-*t* was further examined by isolating the pentoses (neutral sugar fraction) after 12 h reaction and determining the proportion of label present at C-1 (or C-5) by reduction to the penitol with sodium borohydride, oxidation with periodate, and isolation of the dimedon derivative. The results of these experiments are shown in Table 3. Ribose was not purified after reisolation and the label present in the dimedon fraction, which is significantly greater than in the dimedon fraction from the starting material, could be due to the presence of small amounts of other pentoses or pentuloses. The increase in specific activity of the neutral sugars allows an approximate calculation to be made of the isotope effect. Under the conditions used in the aerobic degradation experiments 50% of the protium sugar had reacted in the 12 h reaction period. During the same time 19% of the tritium sugar had reacted; an apparent isotope effect (k_H/k_T) of 3.3. A similar calculation gives an isotope effect of 4.1 in the anaerobic reaction in which approximately 22% of the reducing sugar had been converted. By themselves, isotope effects cannot be used to demonstrate the operation of a specific mechanism, however, the isotope effects observed in

Can. J. Chem. Downloaded from www.nrcresearchpress.com by 210.87.254.42 on 09/05/12
For personal use only.

TABLE 3. The distribution of tritium in the neutral sugar fraction after incubating D-ribose-2-*t* in 0.833 *N* potassium hydroxide

	Percent reaction	Total neutral sugars (c.p.m./mmol)	Dimedon derivative (C-1 and -5) (c.p.m./mmol)
Original ribose	0	7.83×10^5	$<1.5\times10^2$
"Ribose" from aerobic treatment	50	1.23×10^6 1.26×10^6	2.09×10^3 2.12×10^3
"Ribose" from anaerobic treatment	22	1.11×10^6 1.15×10^6	1.3×10^3 1.2×10^3

this study are of the order expected for a hydride shift (15) but are smaller than expected for a simple enolization reaction (16, 17). The principal reaction occurring in the absence of oxygen is in a large part attributable to enolization since tritium is lost to the solvent. The small isotope effect is not incompatible with an enolization reaction even though a much larger effect is observed with acetone (16). The magnitude of the isotope effect depends on the symmetry of the transition state (15), changes in bending frequencies (18), the linearity of the transition state (19), and the occurrence of prerate-determining equilibria (20). All of these factors could be important in producing the small isotope effect observed here; however, the data do not permit a more detailed analysis of the mechanism.

The principal reaction in the presence of oxygen involves the transfer of hydrogen from C-2 to -1; it cannot be accomplished by an enolization reaction since tritium lost to solvent cannot return. In this case, the small isotope effect is probably attributable to the occurrence of a cyclic transition state, **6** (14, 18).

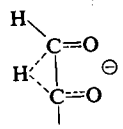

6

The possibility that tritium ribose and protium ribose react by different pathways must be considered. In Scheme 2 a hypothetical reaction sequence is shown in which two pathways are available to ribose; pathway *a* for enolization and pathway *b* for hydride shift. If we assume that protium ribose **7** reacts 100 times faster through pathway *a* than through pathway *b* and that the enolization isotope effect is 20 (pathway *a'*) while that for the hydride shift is 2 (pathway *b'*), then, of the tritium ribose **8** that

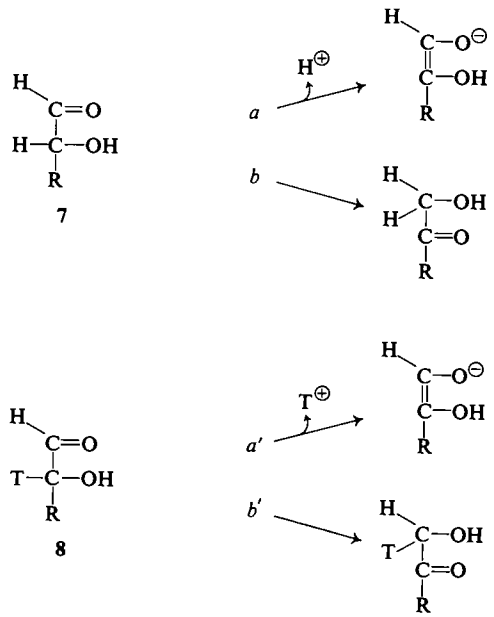

SCHEME 2

had reacted at any given time, 10 parts would have traversed pathway *a'* and one part pathway *b'*. Thus, the observation of an overall isotope effect less than 5 allows us to conclude that a substantial portion of the protium ribose is reacting by the same pathways as the tritium ribose, and that under both aerobic and anaerobic conditions a hydride shift to C-1 is important.

The evidence for a hydride shift in the aerobic degradation of D-ribose-2-*t* is very convincing, 17% of the label is present in formic acid and a small amount in the dimedon derivative from the recovered neutral sugars. In the anaerobic system, however, the evidence is weaker, although there is a significant increase in the tritium content of the dimedon derivative (*i.e.*, at C-1), and this is hard to explain by other than

Can. J. Chem. Downloaded from www.nrcresearchpress.com by 210.87.254.42 on 09/05/12
For personal use only.

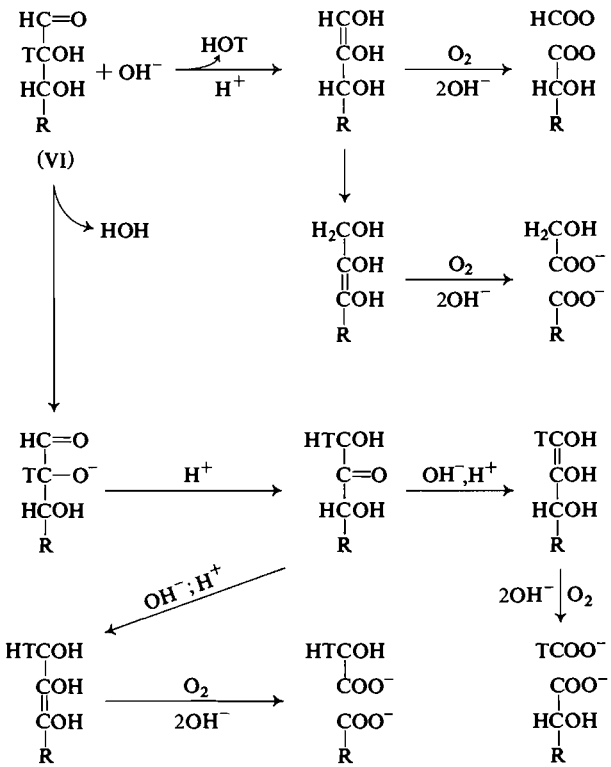

SCHEME 3

a hydride shift mechanism. To further demonstrate that a hydride shift does occur in this system, D-arabinose was isolated from the neutral sugar fraction of the anaerobic degradation when the reaction had proceeded to 22% completion (as judged by reducing sugar content). D-Arabinose was isolated by chromatography on the barium form of Rexyn 101 as described by Jones and Wall (21). Two fractions were obtained, the first fraction containing arabinose had 4% of the radioactivity of the neutral sugar fraction; the second fraction had 96% of the radioactivity. Unlabeled D-arabinose was added to the material of the first peak and the whole reduced to D-arabinitol with sodium borohydride. After recrystallization a sample was subjected to periodate oxidation and the dimedon derivative of the formaldehyde so released was prepared. A second sample of the D-arabinitol was converted to the pentabenzoate and recrystallized to constant specific activity. The results of this experiment are presented in Table 4. It is clear that D-arabinose is formed from D-ribose in the anaerobic reaction and that it contains a significant amount of radioactivity.

TABLE 4. Radioactivity present in D-arabinose derived from ribose-2-*t* treated with 0.833 *M* KOH, 12 h at 25.00 ± 0.05 °C; oxygen excluded

	Specific activity (c.p.m./mmol)
Starting material (ribose-2-*t*)	6.36×10^6
Arabinitol pentabenzoate	$2.13 \pm 0.02 \times 10^4$
Formaldehyde dimedon of periodate oxidized arabitol	$7.53 \pm 0.07 \times 10^3$
Arabinose-*t* from reaction mixture (= 28.3 × specific activity penta-benzoate)	6.03×10^5

At least 70% of the activity in the D-arabinose is present in hydrogen attached to C-1. The overall isotope effect for the conversion of D-arabinose can be estimated to be approximately 10 from the specific activities of the starting material and product. The conversion by hydride shift involves two equivalent steps, that is, conversion of D-ribose to an intermediate and conversion of the intermediate back to the epimer D-arabinose. Both steps should show approximately the same isotope effect and the overall isotope effect is the multiple of those for the

Can. J. Chem. Downloaded from www.nrcresearchpress.com by 210.87.254.42 on 09/05/12
For personal use only.

individual steps. Thus, in the conversion of D-ribose to D-arabinose each step has an isotope effect of approximately 3.0 consistent with the observed effect for the transfer of tritium from C-2 to -1.

The results of this investigation indicate that an intermediate enediol is not a necessary intermediate in the alkaline conversion of one aldose to another. This may explain the many contradictory findings in the literature concerning the incorporation of solvent deuterium during the treatment of carbohydrates with alkali. Thus, one reviewer (22) concluded that a pathway for the Lobry de Bruyn – Alberda von Ekenstein which does not permit the exchange of carbon bound hydrogen with the solvent was invalid, while another author (23) concluded that the reaction can proceed by two mechanisms (enolization and hydride transfer) the operation of which depends on the nature of the catalyst, temperature, and structure of reactant. Scheme 3 is based on these mechanisms; in it the reactions of a tritiated molecule are shown. The protium isomer would follow the same pathways in different proportion. This scheme accounts only for the major products of the aerobic conversion of D-ribose in alkali. The overproduction of formic acid (1, 9) and the formation of saccharinic acids are not shown since our data do not permit us to comment on the validity of proposals that have been made to explain their formation (9, 11).

Isbell *et al.* (17) have shown that sugars take up tritium from solvent in alkaline medium and have interpreted their data in terms of the rate of primary enolization of the sugars with incorporation at C-2 of the aldoses. Our data would suggest that this incorporation may be a secondary event, depending upon the prior formation of a ketose anion.

It is possible that our findings are peculiar to the D-ribose-2-*t*, potassium hydroxide system, but it appears that this is the first direct demonstration of the operation of a mechanism other than enolization for carbohydrate interconversions. Experiments are in progress in this laboratory to investigate the interconversion mechanism for glucose, fructose, and mannose in order to test the generality of the findings for ribose-2-*t*.

1. W. B. GLEASON and R. BARKER. This issue.
2. J. E. MCCORMICK. Carbohyd. Res. **4**, 262 (1967).
3. C. E. BALLOU. J. Amer. Chem. Soc. **79**, 165 (1957).
4. W. SOWA and G. H. S. THOMAS. Can. J. Chem. **44**, 836 (1966).
5. H. FOLLMANN and H. P. C. HOGENKAMP. J. Amer. Chem. Soc. **92**, 671 (1970).
6. K. E. PFITZNER and J. G. MOFFAT. J. Amer. Chem. Soc. **85**, 3027 (1963).
7. V. M. PARIKH and J. K. N. JONES. Can. J. Chem. **43**, 3452 (1965).
8. R. E. REEVES. J. Amer. Chem. Soc. **63**, 1476 (1941).
9. C. H. BAMFORD and J. R. COLLINS. Proc. Royal Soc. London, Series A, **228**, 100 (1954).
10. J. DOUBOURG and P. NAFFA. Bull. Soc. Chim. Fr. 1959, 1353.
11. O. SAMUELSON and L. THEDE. Acta Chim. Scand. **22**, 1913 (1968).
12. J. C. SOWDEN. Adv. Carbohyd. Chem. **12**, 35 (1957).
13. H. A. BARKER. *In* Methods in enzymology. Vol. III. Academic Press, New York, N.Y., 1957. p. 372.
14. I. U. NEF. Ann. **376**, 1 (1910).
15. F. H. WESTHEIMER. Chem. Rev. **61**, 265 (1961).
16. O. REITZ and J. KOPP. Z. Physik. Chim. **184A**, 429 (1939).
17. H. S. ISBELL, H. L. FRUSH, C. W. R. WADE, and L. E. HUNTER. Carbohyd. Res. **9**, 163 (1969).
18. R. F. W. BADER. Can. J. Chem. **42**, 1822 (1964).
19. E. S. LEWIS and M. C. R. SYMONS. Quart. Revs. London, **12**, 230 (1958).
20. W. T. FORD, E. W. GRAHAM, and D. J. CRAM. J. Amer Chem. Soc. **89**, 4661 (1967).
21. J. K. N. JONES and R. A. WALL. Can. J. Chem. **38**, 2290 (1960).
22. J. C. SPECK. Adv. Carbohyd. Chem. **13**, 63 (1958).
23. J. HINE. Physical organic chemistry. 2nd Edit. McGraw-Hill, New York, N.Y., 1962. p. 272.

Can. J. Chem. Downloaded from www.nrcresearchpress.com by 210.87.254.42 on 09/05/12
For personal use only.

Can. J. Chem. Downloaded from www.nrcresearchpress.com by 210.87.254.40 on 09/05/12
For personal use only.

Sulfonyl Chloride Kinetics. Part II. Solvolysis of a Series of Benzenesulfonyl Chlorides: An Unexpected Heat Capacity Variation[1]

R. E. ROBERTSON AND B. ROSSALL[2]

Department of Chemistry, The University of Calgary, Calgary, Alberta

Received July 8, 1970

First order rate constants for the solvolysis of a series of 4-X-benzenesulfonyl chlorides (where X = MeO, Me, Br, and NO_2) were measured by the conductance method in H_2O over the approximate temperature range of 0 to 25°. Pseudothermodynamic parameters, $\Delta G^{\ddagger}$, $\Delta H^{\ddagger}$, $\Delta S^{\ddagger}$, and $\Delta C_p^{\ddagger}$ were derived and the high accuracy of the rate constants enabled an estimation of $d\Delta C_p^{\ddagger}/dT$.

A trigonal bipyramidal transition state is favored for the nucleophilic attack which is probably by an S_N2 type mechanism. A novel explanation for the effect of 4-methoxy on $\Delta C_p^{\ddagger}$ involves a temperature dependent water–solute interaction, which has general applicability to the behavior of 4-methoxy substituents.

On a mesuré, par la méthode de la conductivité, dans l'eau et à des températures entre 0 et 25 °C, les constantes de vitesse du premier ordre pour la solvolyse d'une série de chlorures de benzenesulfonyles substitués en position 4. On en a dérivé les paramètres pseudothermodynamiques $\Delta G^{\ddagger}$, $\Delta H^{\ddagger}$, $\Delta S^{\ddagger}$, et $\Delta C_p^{\ddagger}$ et grâce à la grande précision des mesures, on a pu estimer la valeur de $d\Delta C_p^{\ddagger}/dT$.

On favorise un état de transition trigonal et bipyramidal pour l'attaque nucléophile qui est probablement un mécanisme S_N2. Une nouvelle explication pour l'effet du groupement méthoxy en position 4 sur $\Delta C_p^{\ddagger}$ implique une intéraction entre l'eau et le soluté qui serait dépendante de la température; cette explication serait d'application générale chaque fois que des substituants méthoxyle en position 4 seraient impliqués.

Canadian Journal of Chemistry, 49, 1441 (1971)

The practical importance of knowing relative reaction rates is readily apparent: corresponding energy relationships between structure and reactivity are more obscure, and generally so difficult to define that the search is frequently abandoned where it should begin. Indeed, practical arguments can be advanced to support the position that free energy differences are the proper end (1, 2).[3] This attitude may have gained credence from repeated failure of many to find sufficient analytical and predictive value in $\Delta H^{\ddagger}$ and $\Delta S^{\ddagger}$ differences to warrant a serious consideration. As a consequence, these pseudo-thermodynamic parameters frequently have been treated as a by-product of questionable value, or as an empirical tool for approximate interpolation and extrapolation of rate data. Because of the wide-spread belief that no useful information can be gained from such derived parameters, in planning a kinetic study, there is no imperative to meet the more stringent experimental requirements needed to ensure rate data of the required accuracy (3). Hence these less accurate rates (which may be adequate for free energy comparisons) lead inevitably to unreliable values of $\Delta H^{\ddagger}$ and $\Delta S^{\ddagger}$ and thus on each successive occasion apparently supply factual support to confirm the negative approach. Granted this attitude, our appreciation of structure–reactivity relationships must remain in its present primitive state.

We do not accept this philosophy of despair and would prefer to draw encouragement from those studies of the temperature dependence of the rate where progress has been recorded. In this paper we demonstrate that useful information can be gained from such studies of the hydrolysis of a series of para-substituted benzenesulfonyl chlorides in water.

Nucleophilic displacement from a tetrahedral sulfur has been treated generally as analogous to the corresponding displacement from carbon and the same terminology based on similar mechanistic distinctions has tended to be used (4–13). To the degree that the activation processes are similar, such a comparison is valid but in this and in the following paper we attempt to identify and evaluate the source of differences. Thus differences have been recognized in the

[1]The experimental work reported here was done at the National Research Council of Canada, Ottawa, Canada. For Part I, see ref. 18.

[2]NRCC Postdoctorate Fellow, 1968–1970.

[3]M. J. S. Dewar has described the study of temperature effect on the rate of reactions as a "fetish".

TABLE 1. Properties of 4-X-benzenesulfonyl chlorides

X	Solvent	Experimental m.p. (°C)	Literature m.p. (°C)	Reference
MeO	Petroleum ether (30–60°)	40–41	42	7
Me	Petroleum ether (60–80°)	68–69	69.5	9
Br		80–81	81–82	9
NO_2		78–79	79	9

higher selectivity ratio (12, 14) and the enhanced kinetic solvent isotope effect (15). Scott has reported evidence of different steric requirements for the solvolysis of a series of alkyl sulfonyl chlorides (16, 17). Some kinetic requirement other than that of solvent reorganization was needed to account for the large change in $\Delta S^{\ddagger}$ noted above in the hydrolysis of methanesulfonyl chloride and of benzenesulfonyl chloride (18). The latter study also led us to expect that there would be no change in $\Delta C_p^{\ddagger}$ through a series of para-substituted benzenesulfonyl chlorides. The degree to which these expectations are supported by experimental facts and the reasons for departure supply strong support for the value of derived parameters in detecting significant kinetic factors provided, as always, sufficiently accurate rate data are available.

Experimental

The hydrolysis of a sulfonyl chloride molecule produces four ions, two of which are protons, hence the system is particularly suited to rate determination by a conductimetric method. The details of the system, the methods of computation, of temperature control, and of rate measurement have been described elsewhere (19).

The 4-substituted benzenesulfonyl chlorides were commercial samples. 4-Nitrobenzenesulfonyl chloride contained a considerable amount of impurity and was subjected to a preliminary vacuum distillation (b.p. 144° at 2 mm Hg) (20). Further purification of all samples was achieved by recrystallization from petroleum ether to constant m.p. (see Table 1).

Recrystallized samples of 4-methyl and 4-bromobenzenesulfonyl chloride were further purified by zone refinement. Kinetic measurements on all samples gave excellent first order rate constants. This was considered to be the most reliable test of purity for the purpose of this study. Water was purified by preliminary distillation and then passed through an ion exchange column (Rexyn R 208-1-300 H–OH). Analar HCl ($<0.0001\ M$) was added as a backing electrolyte to adjust the solution conductance to the optimum range for accurate rate determination. Rate measurements were made using our Auto-Ram system (19). Since substituted benzenesulfonyl chlorides are only sparingly soluble in water, supersaturation had to be avoided to obtain consistent rate data. This was accomplished by the following dilution technique which has much wider application than in the present study. Kieselguhr (dried at 500° for 24 h) in large excess was intimately mixed with a small amount of the sulfonyl chloride and a suitable amount of this mixture added to a flask containing backing electrolyte at bath temperature and shaken. This solution was pressure filtered through a glass-sinter into Queen-type cells. Each cell had been 9/10 filled with backing electrolyte solution and brought to bath temperature. The resultant dilution of the reacting solution was sufficient to avoid any supersaturation. This process requires about 200 s to fill four cells. This time, together with that for the reestablishment of temperature equilibrium, sets an upper limit to the rates which can be determined by this method. Rates with $t_{1/2} \simeq 200$ s were the fastest which could be determined, corresponding to an upper temperature limit of about 25°. Rate studies[4] were carried out at 2 or 3° intervals from this upper temperature limit down to 0°.

Results

The temperature dependence of the rate constants was expressed by an equation of the general form

$$[1] \quad \log_{10} k = A_1 + A_2/T + A_3 \log_{10} T + A_4 T \ldots$$

TABLE 2. Empirical constants for the rate–temperature relation for the hydrolysis of 4-X-benzenesulfonyl chlorides in H_2O

X	A_1	$-A_2$	$-A_3$	$n_{T_1}{}^{T_2}$*
H†	89.12618	7284.232	27.1603	$38_4{}^{25}$
Me	112.36272	8240.901	35.2212	$34_4{}^{23}$
MeO	73.97095	6523.780	21.9353	$41_2{}^{20}$
NO_2	88.05989	7344.942	26.6700	$34_5{}^{30}$
Br	87.51848	7319.845	26.5254	$18_4{}^{22}$

*$n_{T_1}{}^{T_2}$ represents the number of individual rate determinations: T_1, T_2 define the lower and upper limits of the experimental temperature range.
†From ref. 18.

[4]Individual rate data have been filed with the Depository of Unpublished Data, National Science Library, Ottawa, 2, Canada.

Can. J. Chem. Downloaded from www.nrcresearchpress.com by 210.87.254.40 on 09/05/12
For personal use only.

TABLE 3. Pseudothermodynamic parameters of activation for the hydrolysis of 4-X-benzenesulfonyl chlorides in H_2O at 15°

X	$\Delta G^{\ddagger}$ (cal mol^{-1})	$\Delta H^{\ddagger}$ (cal mol^{-1})	$-\Delta S^{\ddagger}$ (cal deg^{-1} mol^{-1})	$-\Delta C_p^{\ddagger}$ (cal deg^{-1} mol^{-1})
MeO	20 305±1	16 718±18	12.45±0.06	46±4
Me	20 629±1	16 967±8	12.71±0.03	72±3
H*	20 747±1	17 206±6	12.29±0.01	56±1
Br	20 972±1	17 732±21	11.25±0.07	55±7
NO_2	20 841±1	17 764±5	10.68±0.02	55±1
Methanesulfonyl chloride*	22 433±1	20 300±11	7.41±0.03	53±1

*From ref. 18.

TABLE 4. Heat capacity of activation and its temperature coefficient* for the solvolysis of a series of 4-X-benzenesulfonyl chlorides in H_2O

X	Temperature (°C)	$-\Delta C_p^{\ddagger}$ (cal deg^{-1} mol^{-1})	$d\Delta C_p^{\ddagger}/dT$ (cal deg^{-2} mol^{-1})
H	10	48.9± 3.7	−1.4±0.8
	15	55.9± 1.6	
	20	62.8± 5.0	
Me	10	82.1± 7.4	2.6±1.8
	15	67.0± 3.5	
	20	55.9±11.3	
MeO	10	46.5± 3.7	1.8±2.2
	15	37.5±10.4	
	20	28.5±21.1	
NO_2	10	50.6± 5.2	−0.6±0.7
	15	53.8± 2.0	
	20	56.9± 2.6	

*Calculated from a four constant fit to eq. 1 assuming $d^2\Delta C_p^{\ddagger}/dT^2 = 0$.

using a modified form of the Clarke–Glew transformation (21). Corresponding constants for the benzenesulfonyl chloride series are given in Table 2. These permit calculation of rates, the values of which are in excellent agreement with experimental values. Pseudothermodynamic parameters $\Delta G^{\ddagger}$, $\Delta H^{\ddagger}$, $\Delta S^{\ddagger}$, and $\Delta C_p^{\ddagger}$ were derived from the constants A_1, A_2, A_3 making the *usual* assumptions with respect to the applicability of the transition state theory and also assuming that $d\Delta C_p^{\ddagger}/dT = 0$. The values so derived are given in Table 3.

The assumption that $d\Delta C_p^{\ddagger}/dT = 0$ has been made frequently in our work not from any strong experimental or theoretical reasons but rather because the rate data did not normally justify including such a term in the analysis. The kinetic rate data in this study are sufficiently accurate to warrant an examination of the coefficient $d\Delta C_p^{\ddagger}/dT$, assuming now that the derivative of the latter term with respect to temperature is zero. The kinetic rate–temperature data were therefore fitted to a four constant equation of the same form as eq. 1 with the added term in T. These constants are not given since the three-constant equation is adequate for interpolation. Nor are the values of $\Delta H^{\ddagger}$ and $\Delta S^{\ddagger}$ given since in the middle of the temperature range these values are identical with those in Table 3. The heat capacity of activation, $\Delta C_p^{\ddagger}$ and its temperature derivative are in Table 4.

It is recognized that the values of $d\Delta C_p^{\ddagger}/dT$ are small and not significantly different from the calculated uncertainty.

Discussion

While no detailed study of the structure of the RSO_2Cl molecule has been reported,[5] available evidence suggests that this class of molecules has a distorted tetrahedral shape (22). From X-ray analysis of the related structure 1-parabromobenzenesulfonyloxymethyl-bicyclo-2,2,2-octane, we learn that the O^2—S—O^3 bond angle is

[5]Such a study will be undertaken shortly by Professor K. Ann Kerr of The University of Calgary, Calgary, Alberta.

Can. J. Chem. Downloaded from www.nrcresearchpress.com by 210.87.254.40 on 09/05/12
For personal use only.

Can. J. Chem. Downloaded from www.nrcresearchpress.com by 210.87.254.40 on 09/05/12
For personal use only.

118.9 ± 5°, while O^1—S—O^3 is 103.9°, the remaining angles having intermediate values. The S—O bond lengths are shorter than those in SO_4^{2-} (1.49 Å) giving an estimated π-bond order of 0.7 (23). The corresponding O—S—O bond angle in SO_2Cl_2 is 119.8 ± 5° and Cl—S—O, 106.5 ± 5° with an S—O bond length of 1.43 ± 0.02 Å (24). Similar conclusions can be drawn from data for SO_2F_2 (25). From the above evidence we conclude that the stereochemistry of the RSO_2Cl molecules may be considered as a distorted tetrahedron but with shortened S—O bonds due to pπ–dπ interaction (26). The question of importance here is how this initial state structure will alter in the preliminary activation and how the resulting activated molecule will influence the approach of the displacing nucleophile.

It is assumed that only those molecules will react with a nucleophile which achieve some *critical* charge level. This activated state will be equivalent to the so-called intimate-ion-pair postulated by Winstein and co-workers (27)[6] and adopted by many writers. It might equally be considered equivalent to the activated molecule postulated by Arrhenius (29).

For the present purpose the equilibrium can be shown formally as

$$RX \underset{k_2}{\overset{k_1}{\rightleftharpoons}} [R^{\delta+} \cdots X^{\delta-}] \xrightarrow[+H_2O]{k_3} \text{Products}$$

$$k_{obs} = \frac{k_2}{k_1} \cdot k_3$$

in which $k_2/k_1 = K_e$.

Evaluation of K_e is difficult (28, 30, 31). Clearly, K_e will depend on the nature of the solute and on the solvent but such elementary questions as the following must be answered.

(*1*) Is the formation of the intimate-ion-pair accompanied by solvent reorganization?

(*2*) Is the same degree of charge separation required where the nucleophile is OH^-, F^-, or acetate$^-$ as when the agent is water?

(*3*) Is the activated intermediate, in fact, a series of states depending on the requirements of the particular reaction?

No clear answers have been provided either by those who proposed or by those who have adopted this working hypothesis (27, 28, 30–32). In the absence of such elementary information it remains a convenient working hypothesis.

Whatever the nature of the intimate-ion-pair, the lack of strong sensitivity to the ionizing power of the solvent points to a lower degree of charge separation at the intimate-ion-pair than, for example, the activated alkyl halides. The higher kinetic solvent isotope effect (k.s.i.e.) might be given a similar interpretation (15) as would the higher k_{OH^-}/k_{H_2O} ratio (12). However we do not know how to make a quantitative estimate of these differences since for both the halides and the sulfonyl chlorides the rate of activation can be regarded as the product of an initial activation equilibrium followed by the product forming step, or in the case of some reactants, a kinetically significant step preceding a kinetically insignificant product forming step(s).

It can be recognized that the distorted tetrahedral form of the sulfonyl chloride with π-bonding of oxygen pπ-electrons into empty dπ-orbitals on sulfur and leaves available an empty d_{z^2} orbital for the approaching nucleophile. Thus in the activation process corresponding to k_3 it is attractive to postulate a trigonal bipyramidal structure for the transition state with displacement of Cl^- from RSO_2Cl and the nucleophile approaching along the *z*-axis.

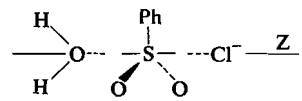

The steric requirements apparent in Scott's kinetic studies of alkyl sulfonyl chlorides (16) and the substituent effects on the rate and entropy of activation (see below) differ from the analogous S_N2 displacement from the sp^3 carbon. The enhanced k.s.i.e. values compared to corresponding values for displacement from carbon (15) are consistent with this hypothesis. A similar model was proposed by Bunton and Frei (33) for the hydrolysis of aryl sulfonates and by Christensen (34, 35) for the hydrolysis of aryl sulfonic anhydrides. This transition state configuration was favored by Kice and Kasperek (36) over several alternatives for the hydrolysis of diaryl sulfones and for aryl sulfinyl sulfones in the absence of compelling evidence in favor of a tetrahedral configuration. In the latter cases,

[6]For a review and assessment of this analysis see ref. 28.

TABLE 5. First order rate constants for the solvolysis of substituted benzenesulfonyl chlorides, $10^4\ k(s^{-1})$

Solvent	Temperature (°C)	Substituent 4-MeO	4-Me	4-H	4-Br	3-NO_2	4-NO_2	Reference
H_2O	15	23.89	13.57	11.04	7.447	—	9.373	This work, A
H_2O	15	—	13.43	11.04	—	4.783	9.417	5, A
H_2O	15	21.00	11.7	11.5	—	5.40	10.0	12, A
H_2O/0.199 mf Acetone	15	—	1.01	1.30	—	3.89	8.17	5, B
H_2O/0.198 mf Acetone	25	—	1.90	2.62	3.82	—	15.4	9, C
H_2O/0.083 mf Dioxan	30	0.50	0.59	0.867	1.38	4.13	12.33	7, D

in order to account for the much larger k.s.i.e. (2.3–2.7) compared to 1.2 for the hydrolysis of halides and 1.4–1.8 for hydrolysis of the sulfonyl chlorides (37) it was necessary to introduce an *ad hoc* Grottius chain extension (38) in order to accommodate the stereochemical implication of the bipyramidal transition state. On this evidence the above hypothesis is not unreasonable and the k.s.i.e. for the hydrolysis of the sulfonyl chlorides in water is at least consistent with such a proposal.

The fact that Jenkins and Hambly (9) found a linear correlation between log $k_3/(H_2O)^2$ and the first power of the dielectric constant might be taken as evidence supporting the requirement for two ligands in the transition state, implying an octahedral configuration. Such an hypothesis would require a much more extensive change in the O—S—O bond angle in contrast to the almost negligible change required in the above model and hence is not considered as a reasonable alternative. The evidence that the enhanced k.s.i.e. which characterizes the hydrolysis of the sulfonyl chlorides compared to the alkyl halides or to the diaryl sulfones derives from enhanced nucleophilic interaction rather than extended solvation requirements will be given in the accompanying paper (37).

para-Substitution and Relative Rates

The effect of para-substitution on the S—Cl bond in the initial state appears to be small judging by the negligible changes in the Raman spectra (375 cm^{-1} for *p*-Me, -H, -Cl, -Br) (39).

At the level of relative rates, no surprises were anticipated in view of previous work by Hedlund (5), Tommila and Hirsjärvi (6), Vizgert and Savchuk (7, 8), Jenkins and Hambly (9, 10), and most recently by Rogne (12), but such duplication was incidental to the purpose of this investigation. Corresponding data have been collected for convenience in Table 5. The changes in the relative effect of substituents on the rate with changes in solvent are illustrated in Fig. 1. This can be taken as evidence of the opposing electronic requirements of the two stages of the activation process ($k_{obs} = K_e k_3$), Under good ionizing conditions and with an uncharged nucleophile the effect of the substituents on the concentration of the activated intermediate (K_e) is dominant (ρ is negative). Under poorer ionizing conditions (mixed aqueous/organic solvents) or with a charged nucleophile in water (12) then those factors influencing the approach of the nucleophile take precedence and the corresponding Hammett constant changes sign (ρ is positive) (Fig. 1). To this point our work confirms but does not add any new insight. Only when the derived parameters are examined is new information provided.

Enthalpy and Entropy of Activation

While it is recognized that ionogenic reactions occurring in solution produce solvation changes which are reflected in the derived terms, $\Delta H^{\ddagger}$ and $\Delta S^{\ddagger}$ it is unlikely that such an explanation can account for the major differences in $\Delta S^{\ddagger}$ found in the hydrolysis of sulfonyl chlorides (18). This generalization is possible because of a lack of correlation between $\Delta S^{\ddagger}$ and $\Delta C_p^{\ddagger}$ (Fig. 2), the former quantity changing while the latter term, with two exceptions, remains relatively constant. Such constancy in $\Delta C_p^{\ddagger}$ was taken as an indication that solvent reorganization attending the activation process tended to be uniform through the series and prompted a search for some alternative source of change in $\Delta S^{\ddagger}$.

Can. J. Chem. Downloaded from www.nrcresearchpress.com by 210.87.254.40 on 09/05/12
For personal use only.

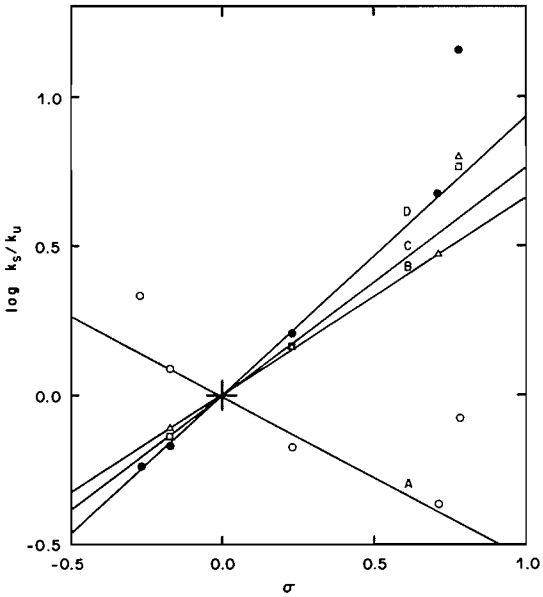

FIG. 1. Hammett plots for solvolysis of substituted benzenesulfonyl chlorides. See Table 5 for letter identification.

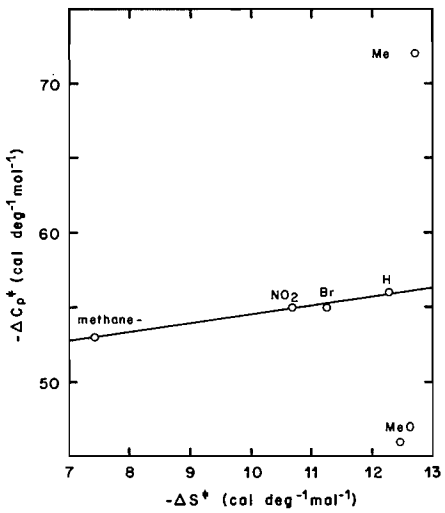

FIG. 2. $-\Delta C_p^{\ddagger}$ plotted against $-\Delta S^{\ddagger}$ for the solvolysis of sulfonyl chlorides in H_2O at 15°.

If an initial activated equilibrium precedes nucleophilic attack, then the expected effect of the para-substituent on that equilibrium will be just the opposite to that required for the approach of the nucleophile. The change in the sign of the Hammett plot with a change in solvent suggests

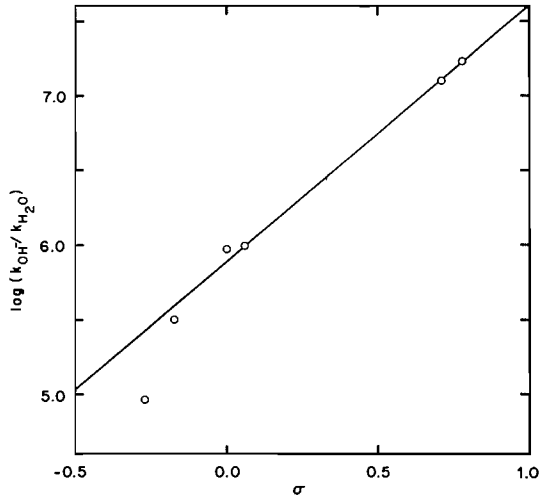

FIG. 3. Log (k_{OH^-}/k_{H_2O}) plotted against Hammett σ (rate data at 15°, this work and ref. 12).

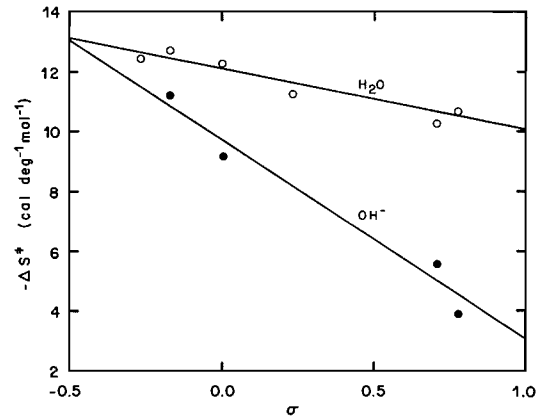

FIG. 4. $-\Delta S^{\ddagger}$ plotted against Hammett σ (H_2O reaction at 15°, this work and ref. 5, OH^- reaction ref. 12).

that in solvolysis these effects are just about balanced. Granted K_e for the reaction with OH^- and with H_2O are about the same throughout the series, then this constant will disappear in the ratio k_{OH^-}/k_{H_2O} (31). A plot of the latter *vs.* σ gives a linear correlation with a positive slope, Fig. 3, an indication that the nucleophilic displacement step (k_3) is dependent on the positive charge on the sulfur atom. Further $\Delta S^{\ddagger}$ values for solvolysis in water and for displacement with OH^- *vs.* σ give linear correlations reflecting a similar relationship between $\Delta H^{\ddagger}$ and $\Delta S^{\ddagger}$ (Fig. 4). It is apparent that the same or a related

Can. J. Chem. Downloaded from www.nrcresearchpress.com by 210.87.254.40 on 09/05/12
For personal use only.

Can. J. Chem. Downloaded from www.nrcresearchpress.com by 210.87.254.40 on 09/05/12
For personal use only.

factor which enhances the probability of reaction enhances enthalpy requirement. Such compensation has been noted frequently (40–43), but it is of particular interest here because solvation effects can be eliminated as a cause, in favor of short range interactions. It may be significant in this connection that the authors found that the degree of bond-making at the transition state (as reflected by the kinetic solvent isotope effect) is the same for the methanesulfonyl chloride and benzenesulfonyl chloride (18), is greater for the 4-nitro member of the series, and less for the 4-methoxy and 4-methyl members (37). We assume that these differences in k.s.i.e. are indications of corresponding differences in the electron sharing required to achieve a critical charge on the chloride ion but note that there is no obvious correlation between such indicated differences in bond-making and the trend in $\Delta H^{\ddagger}$ and $\Delta S^{\ddagger}$. Hence we suggest that the correlation of changes in these latter terms (Fig. 5) is a consequence of the difference in the electron supply to sulfur. The changes in $\Delta H^{\ddagger}$ reflect differences in the energy requirement for rehybridization; the changes in $\Delta S^{\ddagger}$ reflecting the probability of approach of the nucleophile. Other components in $\Delta S^{\ddagger}$ and $\Delta H^{\ddagger}$ are assumed to be about the same throughout the series.

Heat Capacity of Activation

For an S_N2 hydrolysis occurring in water, the temperature dependence of the enthalpy of activation ($\Delta C_p^{\ddagger}$) has been interpreted as reflecting the temperature dependence of the structural stability of the solvent shell about the reactant, or more particularly about the displaced group

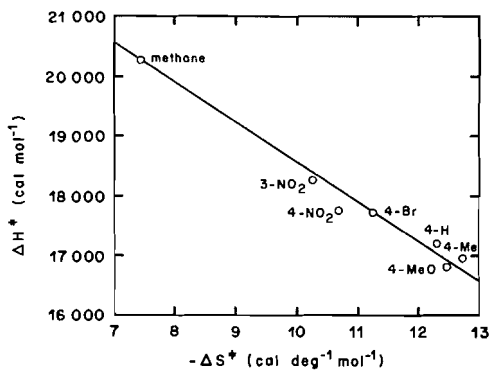

FIG. 5. $\Delta H^{\ddagger}$ plotted against $-\Delta S^{\ddagger}$ for sulfonyl chloride solvolysis in H_2O at 15° (3-NO_2 from ref. 5).

(44). Where displacement of a halide was from carbon, the charge development at the activated intimate-ion-pair was such that the degree of bond-making was minimal.[7]

Where displacement occurs from a tetrahedral sulfur, k.s.i.e. values are higher but as argued in our previous paper (18), it was anticipated that solvent reorganization would be about the same no matter what the substituent on the benzenesulfonyl chloride and that solvent reorganization would still be the major contributor to $\Delta C_p^{\ddagger}$. The results (Table 3) supported our expectations in part only. A plot of $\Delta C_p^{\ddagger}$ *vs.* $\Delta S^{\ddagger}$ (Fig. 2) showed little or no dependence of $\Delta C_p^{\ddagger}$ on $\Delta S^{\ddagger}$ for three para-substituents H, Br, NO_2, and methanesulfonyl chloride. The value of $\Delta C_p^{\ddagger}$ for two substituents, *p*-Me and *p*-MeO lie off this plot ($\Delta C_p^{\ddagger} = -72$ and -46 cal deg^{-1} mol^{-1} compared to the "normal" value of -55 cal deg^{-1} mol^{-1}). Both of these values are outside the expected error and were carefully checked to ensure that the deviation was not due to some experimental error.

In previous discussions of the significance of $\Delta C_p^{\ddagger}$ for ionogenic reactions occurring in water (44, 46) we have normally considered the contributions to $\Delta C_p^{\ddagger}$ arising from the effect of temperature on that solvent structure which was necessarily reorganized in the activation process. In exceptional cases the effect of competing reactions on $\Delta C_p^{\ddagger}$ was recognized (45–48). The latter explanation is unlikely in the two exceptions noted above. Less negative values of $\Delta C_p^{\ddagger}$ have been attributed to a modification of the initial state in the direction of less structure (49, 50). This might accommodate the value of $\Delta C_p^{\ddagger}$ for the *p*-methoxy substituent but not for the *p*-methyl group. A more likely explanation for the latter case is that in the formation of the transition state, sufficient electron demand occurs such that hyperconjugative interaction with the phenyl group raises the level of charge on the methyl group to the point where added solvent reorganization occurs about this group as well as at the seat of reaction. Preliminary results obtained in mixed solvents where water structure has been decreased tend to support this interpretation (51). If the above hypothesis is correct, then deuterium substitution on the *p*-methyl

[7]For MeBr and *t*-butyl Cl, $k_{H_2O}/k_{D_2O} = 1.2$–1.3 (45).

Can. J. Chem. Downloaded from www.nrcresearchpress.com by 210.87.254.40 on 09/05/12
For personal use only.

group should show a significant isotope effect, but this experiment was not done. The argument used previously to account for the reduction in $\Delta C_p^{\ddagger}$ ($= -63$ cal deg^{-1} mol^{-1}) for the solvolysis of $MeOCH_2(CH_3)_2CCl$ (50) was based on the reasonable assumption that the methoxy group would modify the initial state solvation shell thus reducing the extent of reorganization required in the activation process compared to that for *t*-butyl chloride ($\Delta C_p^{\ddagger} = -83$ cal deg^{-1} mol^{-1}). Clearly such an explanation is inadmissable here since there is no reason to assume that solvent reorganization occurs about the benzene group in the activation process (*cf.* $\Delta C_p^{\ddagger}$ for methanesulfonyl chloride and benzenesulfonyl chloride, Table 3). However, the unexpected value of $\Delta C_p^{\ddagger}$ obtained for the *p*-methoxybenzenesulfonyl chloride points to an important solvation effect, influencing substituent effects on rates and equilibria.

The more positive value of $\Delta C_p^{\ddagger}$ found in the case of the *p*-methoxy compound is related to: (*1*) the interaction of the *p*-methoxy group with the benzene ring is opposed by the interaction of this group with water; (*2*) the interaction of water with the methoxy group is opposed by water–water interaction, and the latter is associated with the tendency of water to form three-dimensional structures. This latter tendency is known to decrease as temperature increases (52–54).

Because of the presence of the methyl group, some degree of steric hindrance to hydrogen bonding toward structured water would be expected, but less so toward "freed"[8] water. Following the same reasoning, this steric hindrance to solvation will not exist in the case of an hydroxyl substituent (55).

It would seem reasonable that the more extensive hydrogen bonded co-ordination of structured water would be more sensitive to temperature than the hydrogen-bonding of "freed" water molecules to the methoxyl-oxygen. The number of "freed" water molecules will increase as the temperature increases (55). Hence as the temperature increases, interaction of the latter with water will increase and there will be a corresponding decrease in the electronic effect of the phenyl group on the sulfonyl-sulfur, with a consequent increase in the positive charge on sulfur. To predict the consequence of such a temperature dependent solvent effect it is necessary to examine the relationship between changes in the nominal charge on sulfur and the corresponding values of $\Delta H^{\ddagger}$ and $\Delta S^{\ddagger}$.

In Fig. 5, $\Delta H^{\ddagger}$ and $\Delta S^{\ddagger}$ are shown to be linearly dependent for the hydrolysis of sulfonyl chlorides. Here it is sufficient to note that in this series, electron withdrawal leads to higher values of $\Delta H^{\ddagger}$ and less negative values of $\Delta S^{\ddagger}$. We shall return to this fact presently. First let us examine how $\Delta H^{\ddagger}$ and $\Delta S^{\ddagger}$ will change as the effect of the *p*-methoxy group on $S^{\delta+}$ is modified through enhanced interaction with water as temperature increases. Clearly, as water interaction with the methoxy group increases, electron release to the phenyl group will *decrease* and the positive charge on $S^{\delta+}$ will *increase*. It follows, from Fig. 5, that there will be a corresponding *increase* in $\Delta H^{\ddagger}$, resulting in a positive ($d\Delta H^{\ddagger}/dT$) contribution to the apparent $\Delta C_p^{\ddagger}$. This positive contribution will be unrelated to the negative component arising from the need to reorganize water about the chloride quasi-ion in the activation process. Such an explanation must appear contrived unless supporting evidence can be found in other systems. In principle such a temperature dependent solvent effect would be expected to be quite general provided certain requirements are met. Firstly, the substituent group must be capable of relatively strong interaction with the solvent but not sufficiently strong to cause a breakdown of water–water interaction. Thus the effect is observed with MeO— but not with Br—, NO_2—, Me—, or H—. We would not expect the effect with OH— since the latter can fit into the water lattice in the initial state (52, 55). It is equally clear that changes in the effect of the substituent as a consequence of enhanced solvent interaction must be readily transmissible to the "seat of reaction", otherwise changes in electronic requirements will be unobserved between initial and transition states.

These simple corollaries to our interpretation of the exceptional $\Delta C_p^{\ddagger}$ value for the hydrolysis of *p*-methoxybenzenesulfonyl chloride find ready support from the changes in ΔC_p^{0} for the ionization of carboxylic acids and from our

[8]We have used the vague word "freed" intentionally since at this stage it would be speculative to suggest that only non-hydrogen bonded water molecules can interact, or some variant on this theme. The general principle seems implicit in the facts and that is all that is required here.

Can. J. Chem. Downloaded from www.nrcresearchpress.com by 210.87.254.40 on 09/05/12
For personal use only.

kinetic solvent isotope effects (discussed in the following paper). The ΔC_p^0 values for the ionization of substituted benzoic acids and acetic acids tend to lie in the range -31 to -40 cal deg^{-1} mol^{-1}, but the value for anisic acid is reported to be -50 cal deg^{-1} mol^{-1} while the value for vanillic acid is even more negative.[9]

The change in sign for the incremental contribution of $d\Delta H^0/dT$ to ΔC_p^0 follows directly from the electronic requirements of the ionization process and serves as a secondary check on the basic correctness of the postulate. Enhanced solvent interaction with the methoxy group will increase the relative strength of the acid, decreasing ΔG^0 and ΔH^0.

A consideration of these ΔC_p^0 values suggests that this temperature dependent solvation need not be specific to the methoxy-group in the latter system but rather varies according to the electronic nature of the substituent. Further, it will be obvious that the competition between the substituent and water–water interaction will also be present with respect to interaction with the π electrons of the benzene group, an interaction of possible importance in discussing solvation effects in the benzyl system (58).

The consequence of the temperature effect on the above temperature dependent competition is clearly illustrated by a consideration of the change in ΔC_p^0 for ΔH_1^0 and ΔH_2^0 as illustrated in the case of *o*-phthalic acid (59, 60). Thus the ΔC_p^0 value for the second ionization constant for a dibasic acid is normally much more negative than for the first ionization constant, *e.g.* *o*-phthalic (1) $\Delta C_p^0 = -22$ cal deg^{-1} mol^{-1}, while *o*-phthalic (2) $\Delta C_p^0 = -70$ cal deg^{-1} mol^{-1}. For this and similar cases the above hypothesis provides a reasonable explanation of observed ΔC_p^0 values.

We do not propose to discuss the application of the above concept to the ionization of weak acids at this time, preferring to cite the data as support for the basic idea. Inherent in this idea is the corrollary that as the temperature rises the carboxylic group can compete more successively with water in establishing a solvation sphere, hence from this effect the acid gets stronger with increasing temperature. It would appear that at still higher temperatures, this differential interaction of water with the carboxylic group which comes into play below 40° decreases as the temperature exceeds this value. This may account for the typical shape of the log K_a *vs.* T plots. This idea is related to, but somewhat different from, the explanation used to account for the large negative $\Delta C_p^{\neq}$ values which characterize ionogenic reactions in water (44).

One further observation is implicit in the above rationalization. In all of the examples cited the basis for the effect springs from the unique structure of water and the effect of temperature on that structure. It follows that if that structure is destroyed by a co-solvent then we should anticipate that the above effects would tend to disappear. This does not imply that the ΔC_p^0 for ionization in such systems or $\Delta C_p^{\neq}$ for the reaction kinetics in mixed solvents would disappear, but the available evidence suggests that this term will be much reduced (19, 44, 46) and the greatest reduction will be observed for those kinetic and equilibria situations where the most negative values were observed in water.

[9]Chaturvedi *et al.* report a value of -130 cal deg^{-1} mol^{-1} (56) but Larson and Hepler have questioned this value (57). Even were a truer value closer to one-half the quoted value, it would still support the argument.

1. M. G. Evans and M. Polanyi. Trans. Faraday Soc. **32**, 1333 (1936).
2. M. J. S. Dewar. Molecular orbital theory of organic chemistry. McGraw-Hill, New York N.Y., 1969. p. 283.
3. R. C. Petersen, J. H. Markgraf, and S. D. Ross. J. Amer. Chem. Soc. **83**, 3819 (1961).
4. G. Berger and S. C. J. Olivier. Rec. Trav. Chim. Pays-Bas, **46**, 516 (1929).
5. I. Hedlund. Ark. Kemi. **14A**, 1 (1940).
6. E. Tommila and P. Hirsjärvi. Acta Chem. Scand. **5**, 659 (1951).
7. R. V. Vizgert and E. K. Savchuk. Zh. Obshch. Khim. **26**, 2261 (1956).
8. R. V. Vizgert and E. K. Savchuk. Zh. Obshch. Khim. **26**, 2268 (1956).
9. F. E. Jenkins and A. N. Hambly. Aust. J. Chem. **14**, 190 (1961).
10. F. E. Jenkins and A. N. Hambly. Aust. J. Chem. **14**, 205 (1961).
11. H. K. Hall, Jr. J. Amer. Chem. Soc. **78**, 1450 (1955).
12. O. Rogne. J. Chem. Soc. B, 1294 (1968).
13. O. Rogne. J. Chem. Soc. B, 633 (1969).
14. C. G. Swain and S. B. Scott. J. Amer. Chem. Soc. **75**, 246 (1953).
15. R. E. Robertson and P. M. Laughton. Can. J. Chem. **35**, 1319 (1957).
16. R. B. Scott and H. L. McLeod. J. Org. Chem. **21**, 388 (1956).
17. R. B. Scott and R. E. Lutz. J. Org. Chem. **19**, 830 (1954).

18. R. E. ROBERTSON, B. ROSSALL, S. E. SUGAMORI, and L. TREINDL. Can. J. Chem. **47**, 4199 (1969).
19. R. E. ROBERTSON and S. E. SUGAMORI. J. Amer. Chem. Soc. **91**, 7254 (1969).
20. H. J. BARBER. J. Chem. Soc. 101 (1943).
21. E. C. W. CLARKE and D. N. GLEW. Trans. Faraday Soc. **62**, 539 (1966).
22. A. F. CAMERON, G. FERGUSON, and D. G. MORRIS. J. Chem. Soc. B, 1249 (1968).
23. D. W. J. CRUIKSHANK. J. Chem. Soc. 5486 (1961).
24. J. PALMER. J. Amer. Chem. Soc. **60**, 2360 (1938).
25. D. R. LIDE, D. E. MANN, and R. M. FRISTROM. J. Chem. Phys. **26**, 734 (1957).
26. D. P. CRAIG and C. ZAULI. J. Chem. Phys. **37**, 601 (1962).
27. S. WINSTEIN, P. E. KLINEDINST, JR., and G. C. ROBINSON. J. Amer. Chem. Soc. **83**, 885 (1961).
28. C. D. RITCHIE. Solute–solvent interactions. *Edited by* J. F. Coetzee and C. D. Ritchie. Dekker, New York, N.Y., 1969. p. 272.
29. S. ARRHENIUS. Z. Phys. Chem. **4**, 226 (1889).
30. R. A. SNEEN and J. W. LARSEN. J. Amer. Chem. Soc. **91**, 6031 (1969).
31. J. M. W. SCOTT. Can. J. Chem. **48**, 3807 (1970).
32. H. L. GOERING and E. C. LINSAY. J. Amer. Chem. Soc. **91** 7435 (1969).
33. C. A. BUNTON and Y. F. FREI. J. Chem. Soc. 1872 (1951).
34. N H. CHRISTENSEN. Acta Chem. Scand. **20**, 1955 (1966).
35. N. H. CHRISTENSEN. Acta Chem. Scand. **21**, 899 (1967).
36. J. L. KICE and G. J. KASPEREK. J. Amer. Chem. Soc. **91**, 5510 (1969).
37. B. ROSSALL and R. E. ROBERTSON. This issue.
38. C. A. BUNTON and V. J. SHINER. J. Amer. Chem. Soc. **83**, 3207 (1961).
39. N. S. HAM and A. N. HAMBLY. Aust. J. Chem. **6**, 135 (1953).
40. J. E. LEFFLER. Nature, **205**, 1101 (1965).
41. J. E. LEFFLER and E. GRUNWALD. Rates and equilibria of organic reactions. Wiley, New York, N.Y., 1963.
42. R. F. BROWN. J. Org. Chem. **27**, 3015 (1962).
43. P. RUETSCHI. Z. Phys. Chem. N. F. **14**, 213 (1967).
44. R. E. ROBERTSON. Progr. Phys. Org. Chem. **4**, 213 (1967).
45. L. J. BRUBACHER, L. TREINDL, and R. E. ROBERTSON. J. Amer. Chem. Soc. **90**, 4611 (1968).
46. G. KOHNSTAM. Advan. Phys. Org. Chem. **5**, 121 (1967).
47. J. R. HULETT. Quart. Rev. (London), **18**, 227 (1964).
48. W. J. ALBERY and B. H. ROBINSON. Trans. Faraday Soc. **65**, 980 (1969).
49. R. E. ROBERTSON. Can. J. Chem. **33**, 1536 (1955).
50. K. T. LEFFEK, R. E. ROBERTSON, and S. E. SUGAMORI. J. Amer. Chem. Soc. **87**, 2097 (1965).
51. C. LUMLEY, J. NEARING, R. E. ROBERTSON, and B. ROSSALL. Unpublished results.
52. H. S. FRANK and W-Y. WEN. Discuss. Faraday Soc. **24**, 133 (1957).
53. G. NEMETHY and H. A. SCHERAGA. J. Chem. Phys. **36**, 3382 (1962).
54. H. J. BERNSTEIN. Private communication.
55. E. M. ARNETT, W. B. KOVER, and J. V. CARTER. J. Amer. Chem. Soc. **91**, 4028 (1969).
56. R. K. CHATERVEDI, P. DINKAR, and B. BISWAS. Proc. Nat. Acad. Sci. India, **34**, 22 (1964).
57. J. W. LARSEN and L. G. HEPLER. Reference 28, p. 1.
58. W. M. J. STRACHAN and R. E. ROBERTSON. Unpublished results.
59. W. J. HAMER, G. D. PINCHING, and S. F. ACREE. J. Res. Nat. Bur. Stand. A. **35**, 539 (1945).
60. W. J. HAMER and S. F. ACREE. J. Res. Nat. Bur. Stand. A. **35**, 381 (1945). See Table 5 for letter identification.

Can. J. Chem. Downloaded from www.nrcresearchpress.com by 210.87.254.40 on 09/05/12
For personal use only.

Can. J. Chem. Downloaded from www.nrcresearchpress.com by 210.87.254.40 on 09/05/12
For personal use only.

Sulfonyl Chloride Kinetics. Part III. Nucleophilic Interaction on the Transition State for 4-X-Benzenesulfonyl Chloride Solvolyses[1]

B. ROSSALL[2] AND R. E. ROBERTSON

Department of Chemistry, The University of Calgary, Calgary, Alberta

Received July 8, 1970

The kinetic solvent isotope effect (k.s.i.e.) = k_{H_2O}/k_{D_2O}, was measured for 4-X-benzenesulfonyl chlorides (where X = MeO, Me, H, Br, and NO_2) and shown to vary systematically, giving linear correlations with Hammett σ values and with k_{OH^-}/k_{H_2O} ratios. These results contrast with the lack of sensitivity in k.s.i.e. to structural changes for displacement from a saturated carbon atom. This behavior is attributed to a greater degree of bond making required to achieve a critical charge on the chloride of the sulfonyl chloride at the transition state.

On a mesuré l'effet isotopique cinétique du solvant (e.i.c.s.) = k_{H_2O}/k_{D_2O}, pour des chlorures de benzenesulfonyles substitués en position 4 et on a démontré qu'il varie d'une façon systématique donnant une corrélation linéaire entre les valeurs σ de Hammet et les rapports k_{OH^-}/k_{H_2O}. Ces résultats sont en opposition avec ceux obtenus pour des réactions de substitutions sur des carbones saturés alors que e.i.c.s. est peu sensible aux changements structuraux. Ce comportement serait dû à ce que l'état de transition ressemble au produit final et nécessite un haut degré de formation de lieu pour atteindre une charge critique sur le chlorure du chlorure de sulfonyle.

Canadian Journal of Chemistry, 49, 1451 (1971)

Introduction

Robertson and Laughton (1) showed that the kinetic solvent isotope effect ((k.s.i.e.) = k_{H_2O}/k_{D_2O}) for benzenesulfonyl chloride and methane sulfonyl chloride were similar (1.58 at 10 and 20°, respectively) and larger than the values which characterize the hydrolysis of alkyl halides (1.2 to 1.3 over widely differing temperature ranges) (2, 3). These results are interesting since it seemed unlikely that a phenyl and a methyl group could have identical electronic effects. Especially so, since Rogne (4) measured k.s.i.e. for dimethylsulfamoyl chloride at 25° = 1.33. Hence our studies were extended to discover whether k.s.i.e. were dependent on changes in the para-substituent of the benzene ring. In our initial investigation (5) we noted the claim by Vizgert (6) that the solvolytic rate constant for mesitylenesulfonyl chloride was not increased by base addition. This is in contrast to a "normal" acceleration of 10^5–10^7 (7, 8). We expected this compound to have a k.s.i.e. distinct from that arising from nucleophilic interaction. Unfortunately, this substrate proved quite insoluble in water and the rate ratio was unavailable. However, since rate constants and pseudothermodynamic parameters of activation, $\Delta G^{\ddagger}$, $\Delta H^{\ddagger}$, $\Delta S^{\ddagger}$, and $\Delta C_p{}^{\ddagger}$ have been determined in H_2O (9), the rate studies were repeated in pure D_2O, over a similar temperature range. In view of the k.s.i.e. values previously reported (10–12), the results of this study must be regarded as surprising.

Experimental

Substituted benzenesulfonyl chlorides were commercial samples purified as previously described (9). The purification of D_2O and D analysis have been previously reported (5).

First order rate constants were measured using the Auto-RAM system (13). In all reactions excellent pseudo-first order kinetics were observed. Sulfonyl chlorides were only sparingly soluble in heavy water and supersaturation was carefully avoided by the use of Kieselguhr as a filter aid in a dilution technique (9).

Results

First order rate constants were computed from the conductance–time data. Rate constants, for 15°, are presented in Table 1, along with the corresponding data obtained in H_2O. These rate constants are recalculated smoothed curve values, obtained as described below.

The kinetic modification of the Clarke and

[1]Presented in part at the 52nd Conference of the Chemical Institute of Canada, Montreal, Quebec, May, 1969.

[2]NRCC Postdoctorate Fellow, 1968–1970.

Can. J. Chem. Downloaded from www.nrcresearchpress.com by 210.87.254.40 on 09/05/12
For personal use only.

TABLE 1. First order rate constants and kinetics solvent isotope effects* for 4-X-benzenesulfonyl chloride solvolysis at 15°

X	$10^4\ k_{D_2O}$ (s^{-1})	$10^4\ k_{H_2O}$[a] (s^{-1})	The k.s.i.e.
MeO	17.00	23.89	1.405
Me	9.025	13.57	1.504
H	6.986[b]	11.04	1.580
Br	4.576	7.447	1.627
NO_2	5.143	9.373	1.822

*The k.s.i.e. = k_{H_2O}/k_{D_2O}; *a* from ref. 9, *b* from ref. 5. For 2-nitrobenzenesulfonyl chloride, at 14.862°, $k_{D_2O} = 1.18 \times 10^{-4}\ s^{-1}$ and at 19.142°, $k_{H_2O} = 3.45 \times 10^{-4}$ and $k_{D_2O} = 1.93 \times 10^{-4}\ s^{-1}$.

Glew equation (14) was used to calculate pseudothermodynamic parameters from the rate constant – temperature data.[3]

The temperature dependence of the rate constants was expressed by an equation of the form

$$[1] \quad \log_{10}k = A_1 + A_2/T + A_3 \log_{10} T + A_4 T \ldots .$$

Empirical constants, A_1, A_2, A_3, for a three-parameter fit to eq. 1 are given in Table 2, and permit recalculation of rate constants, see Table 1, which are within the limits of experimental error.

Pseudothermodynamic parameters, $\Delta G^{\ddagger}$, $\Delta H^{\ddagger}$, $\Delta S^{\ddagger}$, and $\Delta C_p{}^{\ddagger}$ for solvolysis of 4-X-benzenesulfonyl chlorides in D_2O were calculated from the empirical constants, A_1, A_2, and A_3 assuming the transition state theory, well behaved differentiability of $\log_{10}k$ with respect to temperature and $d\Delta C_p{}^{\ddagger}/dT = 0$. These derived parameters are presented in Table 3.

The high degree of accuracy in the rate constants was sufficient for an evaluation of $d\Delta C_p{}^{\ddagger}/dT$, using a four parameter fit to eq. 1.

TABLE 2. Empirical constants for the three-parameter temperature–rate eq. 1 for hydrolysis of 4-X-benzenesulfonyl chlorides in D_2O

X	A_1	$-A_2$	$-A_3$	$n_{T_1}{}^{T_2}$*
MeO	63.58978	6120.961	18.3431	$37_4{}^{22}$
Me	117.56484	8535.781	36.9922	$31_4{}^{23}$
H†	90.85547	7430.415	27.7379	$39_4{}^{25}$
Br	92.34299	7598.220	28.1806	$20_4{}^{22}$
NO_2	93.41010	7673.163	28.4881	$30_5{}^{30}$

*$n_{T_1}{}^{T_2}$ represents the number of individual rate determinations; T_1, T_2 define the lower and upper limits of the experimental temperature range.
†Reference 5.

[3]Experimental rate constants have been filed with the Depository of Unpublished Data, National Science Library, Ottawa 2, Canada.

The values obtained for $d\Delta C_p{}^{\mp}/dT$ were not significant and the corresponding values for $\Delta G^{\ddagger}$, $\Delta H^{\ddagger}$, $\Delta S^{\ddagger}$, and $\Delta C_p{}^{\ddagger}$ were similar to those derived for the three parameter analysis and given in Table 3 (9).

Discussion

The effect of para-substitution on k.s.i.e. values for hydrolysis of aromatic substrates has attracted little interest (12, 15). In the sulfonate and halide series, the effects of structural changes on k.s.i.e. were small (16, 17), in contrast to the systematic changes evident in Table 1. These differences are illustrated in Fig. 1, where log(k.s.i.e.) was plotted against Hammett σ values (18) for 4-X-benzenesulfonyl chlorides and methyl 4-X-benzenesulfonates. In the former series significant bond-making was assumed from the larger values of k.s.i.e. (1.405 to 1.822 at 15°), in contrast with the methyl benzenesulfonates where it is probable that bond-making requirements are smaller. The k.s.i.e. of the latter appears to be independent of the para-substituent. From Fig. 1, we conclude that the bond-making requirement of the transition state for sulfonyl chloride solvolyses is a function of the electronic property of the para-substituent, slope $\rho = +0.11$, small but significant. In such a comparison it must be borne in mind that we are comparing displacement from a distorted tetravalent sulfur atom with displacement from a

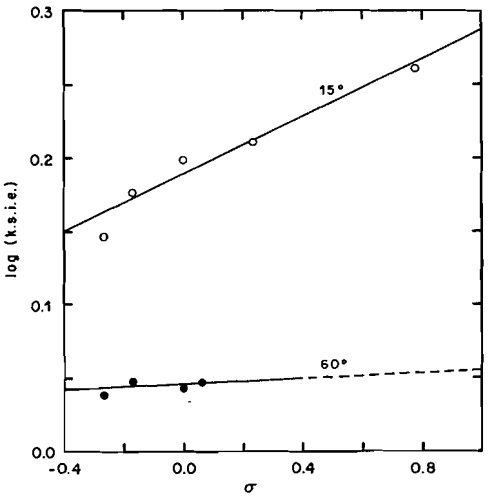

FIG. 1. Log(k.s.i.e.) plotted against Hammett σ values for 4-X-benzenesulfonyl chlorides, ⊙, and methyl 4-X-benzenesulfonates, ●.

TABLE 3. Pseudothermodynamic parameters of activation for the solvolysis of 4-X-benzenesulfonyl chlorides in D_2O at 15°

X	$\Delta G^{\ddagger}$ (cal mol^{-1})	$\Delta H^{\ddagger}$ (cal mol^{-1})	$-\Delta S^{\ddagger}$ (cal deg^{-1} mol^{-1})	$-\Delta C_p^{\ddagger}$ (cal deg^{-1} mol^{-1})
MeO	20 500 ± 1	16 932 ± 12	12.38 ± 0.04	38 ± 4
Me	20 862 ± 1	17 302 ± 11	12.35 ± 0.04	76 ± 4
H*	21 009 ± 1	17 544 ± 5	12.03 ± 0.02	57 ± 2
Br	21 251 ± 1	18 058 ± 16	11.08 ± 0.05	58 ± 6
NO_2	21 185 ± 1	18 225 ± 15	10.27 ± 0.05	59 ± 3

*From ref. 5.

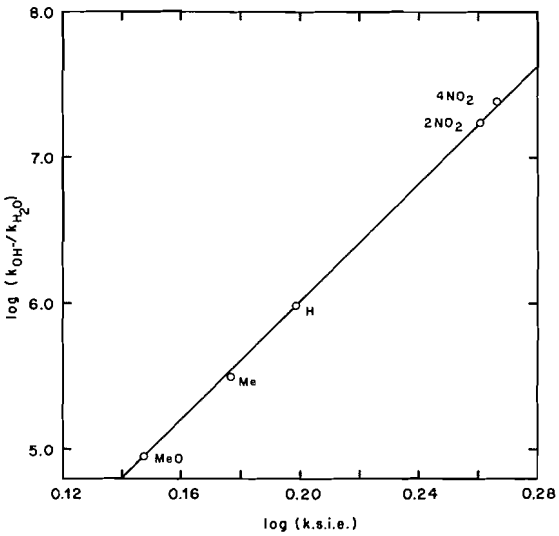

FIG. 2. Log (k_{OH^-}/k_{H_2O}) plotted against log (k_{H_2O}/k_{D_2O}), all rate constants at 15°.

tetravalent carbon atom. The electron supply to the SO_2Cl group required to raise the chloride to some critical charge level (δ^-) (16) would be expected to be greater than the sulfonate case where $ArSO_3^-$ is the leaving group.

If an intimate ion-pair mechanism is valid for the hydrolysis of the benzene sulfonyl chlorides it is reasonable to assume that K_e[4] (19) will be about the same in H_2O and D_2O. This is likely to be true for each substituent. The common assumption in such a correlation is that K_e is also about the same throughout the series or varies linearly with σ.[4] Then by consideration of log(k.s.i.e.), K_e will be eliminated, if indeed it exists. The correlation evident in Fig. 2, where $\log k_{OH^-}/k_{H_2O}$[5] was plotted against log(k.s.i.e.), reflects the charge characteristics of the product forming step. The large slope, +20.2, results from the acceleration of the base reaction relative to that of attack by a nucleophilic water molecule and is consistent with an S_N2 type of mechanism. We do not consider this plot as evidence of an ion-pair intermediate.

Since the pseudothermodynamic parameters of activation for the solvolysis in H_2O and D_2O are available we have inherently determined the temperature dependence of k.s.i.e. (17). By definition, $\delta_I\Delta G^{\ddagger}$, $\delta_I\Delta H^{\ddagger}$, $\delta_I\Delta S^{\ddagger}$, and $\delta_I\Delta C_p^{\ddagger}$ are considered as $\Delta X_{D_2O}^{\ddagger} - \Delta X_{H_2O}^{\ddagger}$, these data are presented in Table 4.

In the alkyl halide and sulfonate ester examples, the temperature dependence of k.s.i.e. was simply linear Arrhenius behavior, *i.e.* $\delta_I\Delta C_p^{\ddagger} = 0$ and $\delta_I\Delta H^{\ddagger}$ and $\delta_I\Delta S^{\ddagger}$ were constant over the experimental temperature range. A plot of log(k.s.i.e.) against reciprocal temperature for the sulfonyl chlorides was linear in each case and gave derived thermodynamic parameters identical to those in Table 4. The temperature dependence of the kinetic solvent isotope effects for all available examples was conveniently summarized by plotting $\delta_I\Delta H^{\ddagger}$ against $T \cdot \delta_I\Delta S^{\ddagger}$, see Fig. 3. Temperature was included in the entropy term to accommodate all the available data with common units. In the halide series, the larger values of $\delta_I\Delta H^{\ddagger}$ and $T \cdot \delta_I S^{\ddagger}$, which we relate to structural changes in the activation process, compensate each other to produce small values of $\delta_I\Delta G^{\ddagger}$, slope = +1.06 (20). Hence the small and relatively constant k.s.i.e. values observed for alkyl halides (1–3, 16, 17) are in fact the sum of two larger terms, $\delta_I\Delta H^{\ddagger}$ and $\delta_I\Delta S^{\ddagger}$, which have opposite sign and cancel each other

[4]Where $K_e = k_2/k_1$ and $k_{obs} = K_e \cdot k_3$ for the following mechanism

$$RX \underset{k_2}{\overset{k_1}{\rightleftharpoons}} [R^+X^-] \xrightarrow{k_3} \text{Products}$$

then, $\alpha = k_2/k_3$.

[5]The k_{OH^-} values are those determined by Rogne (8).

Can. J. Chem. Downloaded from www.nrcresearchpress.com by 210.87.254.40 on 09/05/12
For personal use only.

TABLE 4. Kinetic solvent isotope effects as pseudothermodynamic differences* for the solvolysis of 4-X-benzenesulfonyl chlorides at 15°

X	$\delta_I \Delta G^{\ddagger}$ (cal mol^{-1})	$\delta_I \Delta H^{\ddagger}$ (cal mol^{-1})	$\delta_I \Delta S^{\ddagger}$ (cal deg^{-1} mol^{-1})	$\delta_I \Delta C_p^{\ddagger}$ (cal deg^{-1} mol^{-1})
MeO	195 ± 1	218 ± 30	0.07 ± 0.10	7 ± 7
Me	233 ± 1	335 ± 19	0.36 ± 0.07	−4 ± 7
H†	262 ± 1	338 ± 11	0.26 ± 0.03	−1 ± 3
Br	279 ± 1	326 ± 37	0.17 ± 0.12	−3 ± 13
NO_2	344 ± 1	461 ± 20	0.41 ± 0.07	−4 ± 5
Methanesulfonyl chloride†	264 ± 1	363 ± 20	0.34 ± 0.07	−5 ± 4

*By definition $\delta_I \Delta X^{\ddagger} = \Delta X_{D_2O}^{\ddagger} - X_{H_2O}^{\ddagger}$.
†Reference 5.

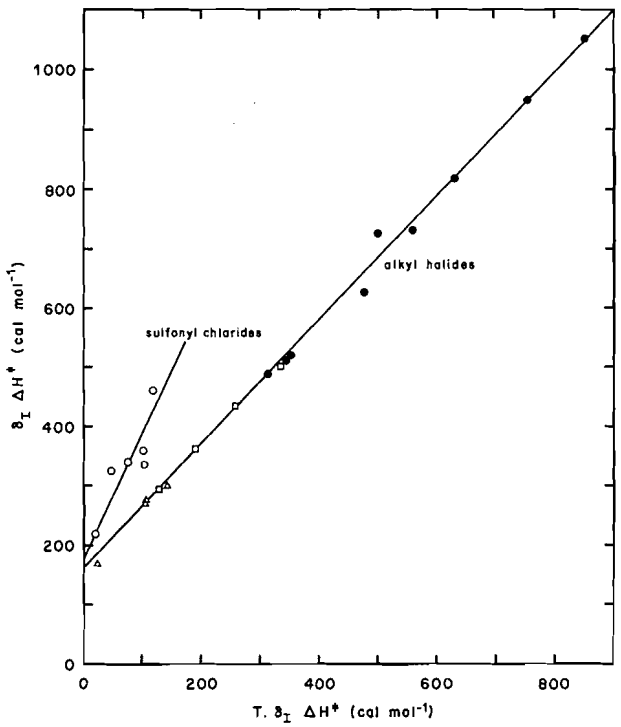

FIG. 3. $\delta_I \Delta H^{\ddagger}$ plotted against $T \cdot \delta_I \Delta S^{\ddagger}$ for solvolysis reactions; ⊙ sulfonyl chlorides, ● tertiary halides, ⊡ secondary halides, and △ primary halides.

to give small values for $\delta_I \Delta G^{\ddagger}$, which are equivalent to the k.s.i.e. term.

From Fig. 3, the sulfonyl chlorides behave quite differently from the halides, where the slope = +2.33 and the compensation effect is less important. The significance of the intercept at $T \cdot \delta_I \Delta S^{\ddagger} = 0$ is not obvious but corresponds to $\delta_I \Delta H^{\ddagger} = \delta_I \Delta G^{\ddagger} = 160$ cal mol^{-1}, that is k.s.i.e. = 1.2. We consider this common intercept to represent the minimum zero-point energy difference associated with the disruption of water structure about the displaced halide ion. Rogne has reported a k.s.i.e. (25°) = 1.33 for dimethylsulfamoyl chloride (4), and which according to Hall (21), hydrolyses by the S_N1 mechanism. We predict this compound would lie close to the intercept in Fig. 3.

In conclusion we consider that Fig. 3 is a useful summary of kinetic solvent isotope effects and illustrates a different nucleophilic process for attack of water molecules on sulfur from attack on carbon.

Can. J. Chem. Downloaded from www.nrcresearchpress.com by 210.87.254.40 on 09/05/12
For personal use only.

1. R. E. ROBERTSON and P. M. LAUGHTON. Can. J. Chem. **35**, 1319 (1957).
2. P. M. LAUGHTON and R. E. ROBERTSON. Can. J. Chem. **34**, 1714 (1956).
3. P. M. LAUGHTON and R. E. ROBERTSON. Can. J. Chem. **37**, 1491 (1959).
4. O. ROGNE. J. Chem. Soc. (B), 663 (1969).
5. R. E. ROBERTSON, B. ROSSALL, S. E. SUGAMORI, and L. TREINDL. Can. J. Chem. **47**, 4199 (1969).
6. R. V. VIZGERT. Zh. Obshch. Khim. **32**, 628 (1962).
7. C. G. SWAIN and S. B. SCOTT. J. Amer. Chem. Soc. **75**, 246 (1953).
8. O. ROGNE. J. Chem. Soc. (B), 1294 (1968).
9. R. E. ROBERTSON and B. ROSSALL. Can. J. Chem. This issue.
10. A. R. BUTLER and V. GOLD. J. Chem. Soc. 2212 (1962).
11. C. A. BUNTON, N. A. FULLER, S. G. PERRY, and V. J. SHINER. J. Chem. Soc. 2918 (1963).
12. S. L. JOHNSON. Adv. Phys. Org. Chem. **5**, 237 (1967).
13. R. E. ROBERTSON and S. E. SUGAMORI. J. Amer. Chem. Soc. **91**, 7254 (1969).
14. E. C. W. CLARKE and D. N. GLEW. Trans. Faraday Soc. **62**, 539 (1966).
15. R. E. ROBERTSON, A. STEIN, and S. E. SUGAMORI. Can. J. Chem. **44**, 685 (1966).
16. R. E. ROBERTSON. Prog. Phys. Org. Chem. **4**, 213 (1967).
17. L. TREINDL, R. E. ROBERTSON, and S. E. SUGAMORI. Can. J. Chem. **47**, 3397 (1969).
18. H. H. JAFFÉ. Chem. Revs. **53**, 191 (1953).
19. S. WINSTEIN, P. E. KLINEDINST, and G. C. ROBINSON. J. Amer. Chem. Soc. **83**, 885 (1961).
20. J. E. LEFFLER and E. GRUNWALD. Rates and equilibria of organic reactions. Wiley, New York, N.Y., 1963. p. 48.
21. H. K. HALL, JR. J. Amer. Chem. Soc. **78**, 1450 (1956).

Can. J. Chem. Downloaded from www.nrcresearchpress.com by 210.87.254.40 on 09/05/12
For personal use only.

Can. J. Chem. Downloaded from www.nrcresearchpress.com by 210.87.254.40 on 09/05/12
For personal use only.

Carbon Disulfide. II. Reaction with Active Methylene Compounds. The Structures of the Desaurins[1,2]

PETER YATES,[3] DONALD R. MOORE, AND THOMAS R. LYNCH
The Departments of Chemistry, Harvard University, Cambridge, Massachusetts 02138, and the University of Toronto, Toronto 5, Ontario

Received October 1, 1970

The desaurins, high-melting, neutral compounds formed by the reaction of active methylene compounds with base and carbon disulfide, have been shown to be derivatives of 2,4-bismethylene-1,3-dithietane.

On a montré que les désaurines, des composés neutres, à points de fusion élevés provenant de la réaction du sulfure de carbone avec de la base et des composés contenant des méthylènes actifs, sont des dérivés du bisméthylène-2,4-dithiétane-1,3.

Canadian Journal of Chemistry, 49, 1456 (1971)

Introduction

The reactions of active methylene compounds with carbon disulfide in the presence of bases have been observed to give both acidic and neutral products. The former have been shown to be dithio acids of type **1**; these acids have often been isolated as their more stable alkyl derivatives **2** and **3** (Scheme 1) (3–9). If an activating group is

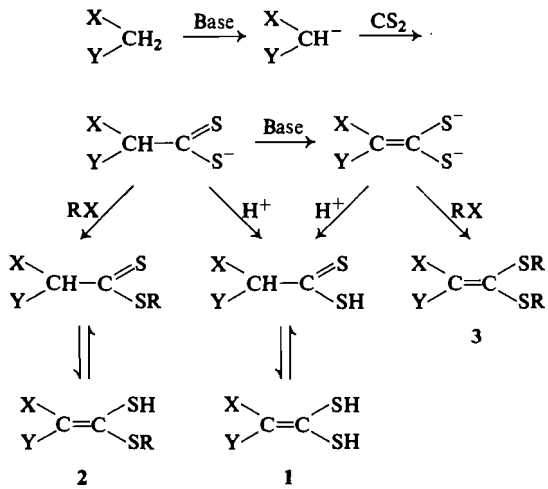

SCHEME 1

flanked on both sides by methylene groups, acidic products of type **4** (and/or tautomers) can also be formed (eq. 1) (6*b*, 10).

The first report of the formation of a neutral compound by the reaction of an active methylene

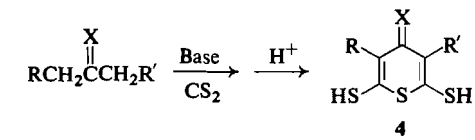

[1]

4

compound with carbon disulfide in the presence of a base is that of Norton and Oppenheim (11), who obtained a yellow product from the reaction of ethyl acetoacetate with carbon disulfide and zinc or lead oxide. Subsequently, Meyer and Wege (12) obtained a related compound by the reaction of deoxybenzoin with four equivalents of potassium hydroxide in carbon disulfide. The product was a high-melting, golden-yellow crystalline solid, that was identical with a compound formed on treatment of the sodio derivative of deoxybenzoin with thiophosgene (13). Meyer (14) showed that this compound has the molecular formula $C_{30}H_{20}O_2S_2$ and suggested that it has structure **5**.[4] He dubbed this class of compounds desaurins on account of their color [*des*oxybenzoin + *aur*um (L., gold)].

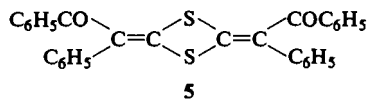

5

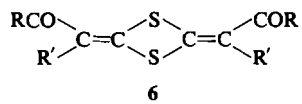

6

Analogs of **5** were subsequently prepared by treatment of compounds of type $ArCOCH_2Ar'$ and $ArCOCH_2CH_3$ with carbon disulfide and base (15, 16). Desaurins were also obtained by

[1]For Paper I see ref. 1.
[2]A preliminary report on part of this work has appeared (2).
[3]Lash Miller Chemical Laboratories, University of Toronto, Toronto 5, Ontario.
[4]In this and subsequent structures no assignment of configuration is implied, unless specifically discussed.

Can. J. Chem. Downloaded from www.nrcresearchpress.com by 210.87.254.40 on 09/05/12
For personal use only.

pyrolysis of the dibenzoyl derivatives or heavy metal salts of dithio acids of type **1** (16); pyrolysis of the acids themselves gave the desaurins, but in very poor yields. Recently, Gompper and Töpfl (*7a*) have obtained desaurins directly from compounds of type **1** by treatment with acylating agents or with oxidizing agents (bromine, iodine, or ammonium persulfate). However, the latter agents give rise to products containing three sulfur atoms in some cases (*7a*, 17). These reactions are related to the earlier observations by Wenzel (18) of the formation of desaurins and three-sulfur compounds on treatment of active methylene compounds with bromine in carbon disulfide.

The structural type **6** originally proposed by Meyer (14) for the desaurins has found general acceptance by most other workers [*cf.*, however, Wenzel (18*b*)]. However, the assignment of **6** rested almost solely on the elemental composition and molecular weights of the compounds. The only degradative studies, those of Wachter (19) on the desaurin from deoxybenzoin, were performed under vigorous conditions and provided little structural information. The present work was undertaken to establish the structures of the desaurins and to investigate further the chemistry of this interesting group of compounds.

Reactions and Structures of the Desaurins

The desaurin from deoxybenzoin was prepared by the procedure of Meyer and Wege (12), and the molecular formula, $C_{30}H_{20}O_2S_2$, previously assigned to it was confirmed by elemental analysis and mass spectrometry (1). Its i.r. and u.v. spectra [λ_{max}(KBr) 6.17μ; λ_{max}($CHCl_3$) 266 (ε 22 900) and 419 mμ (ε 38 100)] showed the presence of one or more highly conjugated carbonyl groups.[5] It was found to be highly resistant to acid hydrolysis; after treatment with a boiling solution of concentrated hydrochloric acid in dioxane for 50 h, 96% of the desaurin was recovered.

Oxidation with chromic acid in acetic acid gave >3 molar equivalents of benzoic acid, demonstrating that no ring closure on the phenyl rings occurs in the formation of the desaurin. Oxidation of the desaurin with potassium permanganate in boiling acetone or ozonolysis in dichloromethane at 0° gave benzil and benzoic acid. The formation of these products is in accord with the presence of the structural feature **7** in **5** (21).

Reaction of the desaurin with zinc in boiling acetic acid for 50 h gave 2-phenylpropiophenone (**8**), *erythro*-1,2-diphenyl-1-propyl acetate (**9**) (22), and *trans*-1,2-diphenylpropene (**10**) (23). The formation of these products is again in accord with the presence of one or more groupings of type **7** in the desaurin molecule. Moreover, the desaurin was found to be stable to the action of zinc and acetic acid at room temperature, which makes it most unlikely that thione groups or disulfide linkages are present.

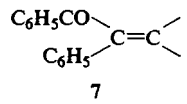

7

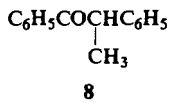

8

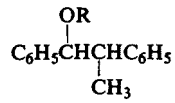

9 R = $COCH_3$
11 R = H

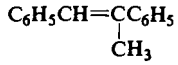

10

Treatment of the desaurin with Raney nickel in boiling dioxane also gave **8** together with *erythro*-1,2-diphenyl-1-propanol (**11**) (23). The same products were obtained when old sponge nickel catalyst was used; however, when fresh sponge nickel catalyst was used, a different product was obtained. This was a colorless crystalline compound, $C_{30}H_{22}O_2$, with a strong band at 5.91 μ in its i.r. spectrum and medium or weak bands at 6.25, 6.33, and 6.45 μ; its u.v. spectrum showed maxima at 249 (ε 31 600) and 291 mμ (ε 17 400), and its p.m.r. spectrum showed signals at δ 6.05 (s, 1H), 6.26 (s, 1H), 7.1–7.5 (m, 18H), 7.9–8.1 (m, 2H). It formed an orange 2,4-dinitrophenylhydrazone. These data suggested the presence of a benzoyl group attached to an sp^3 carbon atom, and a furan ring (24). The desulfurization product was cleaved by ethanolic potassium hydroxide to give benzoic acid and an oily product, $C_{23}H_{18}O$. This did not show a strong band in the carbonyl-stretching region of its i.r. spectrum, but retained a medium band at 6.45 μ, attributable to a furan ring. The cleavage product was oxidized by potassium permanganate to a ketone, $C_{23}H_{16}O_2$, that was characterized as its 2,4-dinitrophenylhydrazone. The spectra of the ketone [6.08 μ; 263 (ε 18 600) and 344 mμ (ε 19 100)] indicated that it was highly conjugated, a feature that was confirmed by the position of the long wavelength maximum in the u.v. spectrum of its 2,4-dinitrophenylhydrazone [418 mμ (ε 26 900)]. More vigorous oxidation with potassium permanganate

[5]The i.r. and u.v. spectra of the desaurins are discussed in detail in Paper III of this series (20).

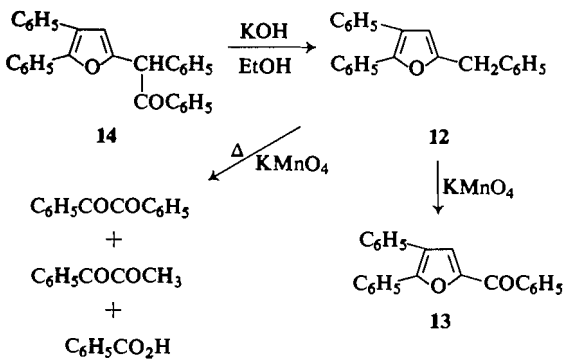

SCHEME 2

gave benzoic acid, benzil, and 1-phenyl-1,2-propanedione. These data establish the structure of the cleavage product as **12**; the ketone formed on mild oxidation is formulable as **13** (see Scheme 2). The desulfurization product itself can then be formulated as **14**, its cleavage to **12** finding close analogy in the cleavage of 2,2-diphenylacetophenone by ethanolic potassium hydroxide to diphenylmethane and benzoic acid (25). The products formed on vigorous oxidation of **12** can be interpreted as arising via hydroxylation of **13** (Scheme 3).

The formation of **14** from the desaurin can be rationalized in terms of structure **5** by a route of the type shown in Scheme 4. The formation of a new carbon–carbon bond during desulfurization reactions with nickel has been observed in other cases (26), and the proximity of the carbon atoms involved in **5** could undoubtedly represent a favorable factor for the occurrence of such a reaction in the present case.

The chemical reactions of the desaurin from deoxybenzoin discussed thus far can all be interpreted in terms of structure **5**; the only alternative structure that could possibly provide a basis for their interpretation and might be in accord with the spectroscopic data is **15**. This differs from **5** in possessing one rather than two carbonyl groups, and means were therefore sought to establish the number of carbonyl groups present in the desaurin. This could not be done by the preparation of simple derivatives, because of the very low solubility of the desaurin in organic solvents. Advantage was therefore taken of its solubility in concentrated sulfuric acid to subject it to a Schmidt reaction in this medium by the addition of sodium azide. Two isomeric yellow products, $C_{30}H_{21}O_2S_2N$, were obtained, whose i.r. spectra were very similar. These spectra showed weak bands at 2.96–2.97 μ, and bands in the carbonyl-stretching region at 6.02–6.03 and 6.14 μ, and are in good accord with the assignment to the products of structures of type **16** or **17**. The u.v. spectra of the products confirmed the retention of the desaurin nucleus in these products (20). The very close similarity of their spectra suggested that they are *cis*- and *trans*-stereoisomers of either **16** or **17**, rather than structural

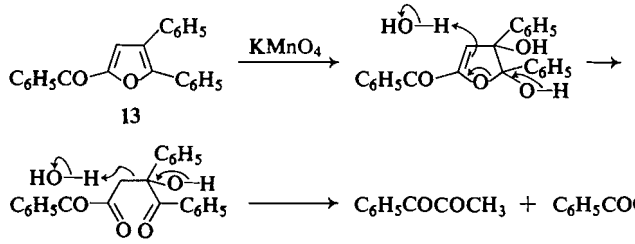

SCHEME 3

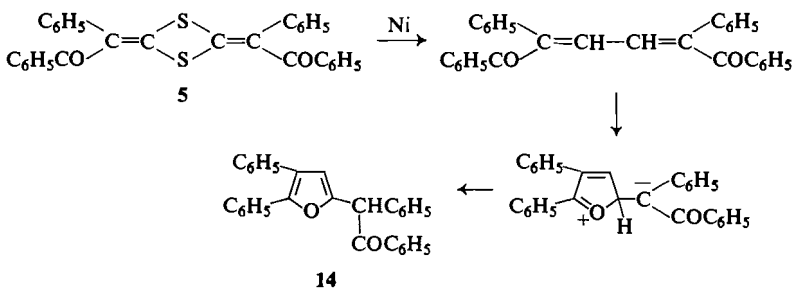

SCHEME 4

Can. J. Chem. Downloaded from www.nrcresearchpress.com by 210.87.254.40 on 09/05/12
For personal use only.

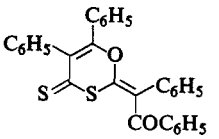

15

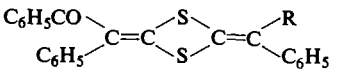

16 R = $CONHC_6H_5$
17 R = $NHCOC_6H_5$

isomers. Structure **16** can be assigned on the basis of the mass spectrum of one of the isomers, which shows, in addition to the molecular ion peak at *m/e* 491 (42%), a peak at *m/e* 399 (47%) corresponding to the ion $(M\text{-}C_6H_5NH)^+$. The formation of these amides that possess a second carbonyl group that gives rise to a carbonyl-stretching band in a similar position to that of the desaurin itself can readily be interpreted in terms of structure **5**, but not of structure **15**.

Because of the importance of establishing the presence of two ketonic carbonyl groups in the desaurins, and the possible ambiguity associated with the use of the Schmidt reaction for this purpose, *i.e.*, the possibility of cleavage or additional rearrangement reactions in the strongly acid medium, it was considered desirable to search for a more soluble desaurin, which would undergo derivative formation under mild reaction conditions. Apitzsch (10*a*) has previously reported the formation of an acidic product of type **4** from the reaction of phenylacetone with carbon disulfide and base; we have found that when the reaction is carried out under the conditions used for the preparation of the desaurin from deoxybenzoin, a lemon yellow neutral compound, $C_{20}H_{16}O_2S_2$, is formed whose spectra showed it to be a desaurin (20); it was considerably more soluble in organic solvents than the desaurin from deoxybenzoin.

Reduction with zinc and sodium hydroxide gave 1.44 molar equivalents of 3-phenyl-2-butanone (**18**), establishing the presence of *two* C_{10} moieties with structure **19**.

Treatment with 2,4-dinitrophenylhydrazine in ethanolic sulfuric acid gave a mono-2,4-dinitrophenylhydrazone that retained a carbonyl-stretching band in its i.r. spectrum, while treatment with this reagent in aqueous dioxane containing hydrochloric acid gave a bis-2,4-dinitrophenylhydrazone that showed no carbonyl-stretching band in its i.r. spectrum. Further, this desaurin could be converted to a dioxime, $C_{20}H_{18}N_2O_2S_2$, from which the desaurin could be regenerated by acid-catalyzed hydrolysis in the presence of formaldehyde, demonstrating that no skeletal change had occurred in its conversion to the derivative. These data show that the desaurin contains *two* carbonyl groups.

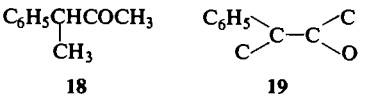

18 19

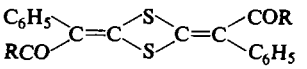

20 R = CH_3
21 R = OH

Treatment of the desaurin with sodium hypochlorite converted it to a yellow acidic product, $C_{18}H_{12}O_4S_2$, whose spectra demonstrated that it retained the desaurin nucleus (20). This transformation must involve the conversion of two *C*-acetyl groups to two carboxylic acid groups by haloform reactions; the occurrence of such reactions was confirmed by the isolation of iodoform when the desaurin was treated in basic solution with iodine and potassium iodide. Structure **20**, analogous to **5**, rather than a structure analogous to **15**, can thus be assigned unambiguously to the desaurin; this is in conformance with its p.m.r. spectrum, which shows signals at δ 2.10 (s, 6H) and 7.38 (m, 10H). The structure of the haloform reaction product is then **21**.

The chemical evidence discussed above (27) established that the structures of the desaurins investigated are of type **6**, as originally suggested by Meyer (14*a*). It did not, however, provide information concerning their configuration. This has been obtained in the case of the desaurin from acetophenone by a subsequent X-ray crystallographic study in collaboration with Nyburg and Mellor (28, 29). The desaurin was prepared by the method of Kelber and Schwarz (16) and obtained by slow crystallization from toluene or nitrobenzene as small plates, m.p. 270–272.5° (dec.). A complete three-dimensional X-ray analysis was performed and established the structure, configuration, and conformation of the desaurin as shown in **22**.[6]

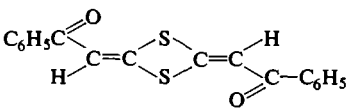

22

[6]The two α,β-unsaturated carbonyl systems and the two sulfur atoms are essentially coplanar, while the two phenyl rings make an angle of 11° with this plane (29).

Can. J. Chem. Downloaded from www.nrcresearchpress.com by 210.87.254.40 on 09/05/12
For personal use only.

[2] 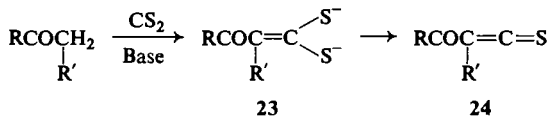

[3] 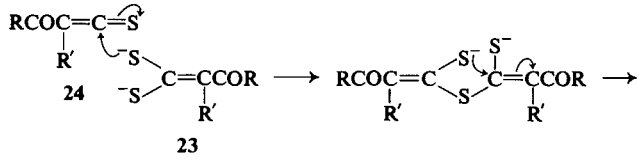

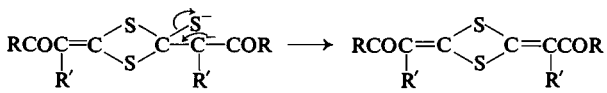

[4] 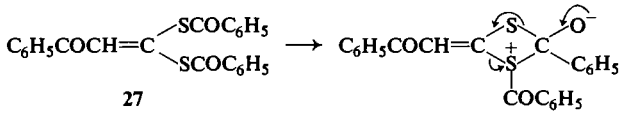

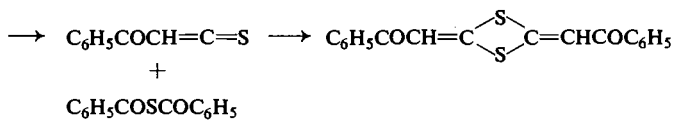

Mechanism of Desaurin Formation

The desaurins are formally dimers of thioketenes, **24**. In the preparation of desaurins by the action of carbon disulfide and bases on active methylene compounds, thioketenes (**24**) could be formed by the elimination of sulfide ion from the dianions **23** (eq. 2). However, formation of the desaurins by dimerization of the thioketenes **24** is unlikely, since the latter would be expected to undergo attack by the nucleophiles present more rapidly than dimerization. The probable pathway, then, would involve attack by **23** on **24** with elimination of sulfide ion (eq. 3). An alternative type of route, without thioketene formation, could involve direct dimerization of **23** followed by elimination of two sulfide ions; however, the dimerization of such dianions is counted improbable on electrostatic grounds (the intervention of the monoanions is also improbable under the highly basic conditions).

Very recently a novel method for the synthesis of the desaurins of type **25** has been reported by Chan, Crow, and Gosney (30), involving treatment of the corresponding *N*-alkyl-3-isothiazolones **26** with bases. These authors also rejected a mechanism for these reactions involving thioketene dimerization for a similar reason to that referred to above. They favored a pathway involving reaction of **26** with its C-5 anion, but did not consider explicitly the possibility of attack of this anion on the thioketene.

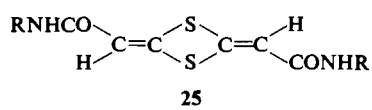

25

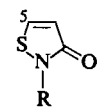

26

The formation of desaurins via thermal cleavage of diacyl derivatives of type **27** (16) [or the related alkyl derivatives (7*a*)] may well proceed via thioketene dimerization (*e.g.*, eq. 4); a related pathway could also account for the formation of desaurins by treatment of compounds of type **1** with phthalyl chloride (7*a*).

The dimerization of thioketenes has been implicated in related reactions (26*b*, 31) and Dickore and Wegler (31*b*) have trapped the thioketene intermediate with nitrile oxides (Scheme 5). However, Raasch (32) has observed that bis(trifluoromethyl)thioketene dimerizes only very slowly at room temperature in the absence of Lewis bases.

Can. J. Chem. Downloaded from www.nrcresearchpress.com by 210.87.254.40 on 09/05/12
For personal use only.

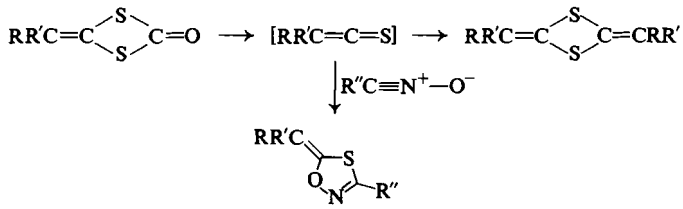

SCHEME 5

Experimental

Melting points were taken on a Fisher–Johns micro hot stage and are uncorrected, unless otherwise indicated. Solutions in organic solvents were dried over anhydrous sodium sulfate.

The Desaurin from Deoxybenzoin (5)

The desaurin was prepared essentially according to the procedure of Meyer and Wege (12). Deoxybenzoin (49.0 g, 0.250 mol) and powdered potassium hydroxide (56.0 g, 1.00 mol) were heated in boiling carbon disulfide (600 ml) under reflux for 8 h. The excess carbon disulfide was removed under reduced pressure, and the solid cake remaining was triturated with water. The suspension was filtered, and the solid was washed with successive small portions of water, alcohol, and ether and air dried to give **5** (23.7 g, 40%) as a bright yellow powder. An additional 2.0 g of the desaurin could be recovered by evaporation of the combined washings to one-half volume.

The desaurin could be purified most conveniently by extraction with chloroform in a Soxhlet apparatus. It crystallized from the hot chloroform as small golden needles, m.p. 300–302° (dec.). An analytical sample was prepared by recrystallization from nitrobenzene, and was dried under reduced pressure at 100° for 10 h; m.p. 300.5–302.5° (dec.).[5]

Anal. Calcd. for $C_{30}H_{20}O_2S_2$: C, 75.60; H, 4.23; S, 13.46. Found: C, 75.81; H, 4.38; S, 13.20.

The desaurin was insoluble in the usual organic solvents at room temperature; at elevated temperatures small amounts could be dissolved in chloroform, dioxane, xylene, and nitrobenzene. It was readily soluble in cold concentrated sulfuric acid to give a deep purple solution, from which it was precipitated unchanged (mixed m.p.) upon addition of water.

Attempted Acid-catalyzed Hydrolysis of 5

The desaurin **5** (1.14 g, 2.39 mmol) was added to concentrated hydrochloric acid (25 ml) and dioxane (50 ml), and the mixture was boiled under reflux for 100 h and filtered. The yellow crystalline solid (1.10 g) was identified as **5** by a mixed m.p.; recovery 96%. The acidic filtrate was extracted with dichloromethane, and the extract was dried, filtered, and evaporated. There was no residue.

Oxidation of 5 with Chromic Acid

The desaurin **5** (1.00 g, 2.10 mmol) was suspended in glacial acetic acid (75 ml), and chromic anhydride (5.00 g, 50 mmol) was added in portions. The mixture was stirred for 15 h at room temperature, then diluted with water (200 ml), and extracted with ether. The ethereal solution was extracted with aqueous 10% sodium hydroxide, washed with water, dried, and filtered. Removal of the solvent gave a gummy solid (0.05 g), whose i.r. spectrum showed it to be largely benzoic acid.

The basic extracts were combined, acidified to p*H* 1, and extracted with four portions of dichloromethane. The combined extracts were dried, filtered, and evaporated by gentle warming on the steam bath to give a white crystalline solid (0.76 g), m.p. 119–120.5°, undepressed on admixture with benzoic acid. The i.r. spectrum of the product was identical with that of benzoic acid. The total yield of benzoic acid was 0.81 g (79%, based on the formation of 4 mol from 1 mol of **5**).

Attempted oxidation of the desaurin with chromic anhydride in concentrated sulfuric acid, or with the chromic anhydride – pyridine complex led only to intractable red tars from which no pure organic compounds could be isolated.

Ozonolysis of 5

A suspension of **5** (1.00 g, 2.09 mmol) in dichloromethane (50 ml) was cooled to 0° in an ice bath. The mixture was maintained at this temperature throughout the ozonization. Ozonized oxygen from a Welsbach Ozonizer was passed through the mixture for 3 h. Additional dichloromethane was added as necessary to maintain the volume of the solution. The ozonide was decomposed by the addition of water (20 ml), removal of the dichloromethane under reduced pressure at room temperature, and heating of the mixture on the steam bath for 0.5 h.

Unconsumed desaurin (0.27 g, 0.564 mmol) was removed by filtration, and the filtrate was extracted with four portions of ether. The aqueous layer was acidified to p*H* 1 with 10% hydrochloric acid and warmed on the steam bath to 80°. Excess dilute aqueous barium chloride was added dropwise, the solution was allowed to cool, and the precipitate of barium sulfate (0.11 g) was collected.

The combined ethereal extracts were partitioned into acid and neutral fractions by extraction with four portions of aqueous 10% sodium hydroxide, combination and acidification of the basic extracts to p*H* 1, and extraction with four portions of dichloromethane. Both organic solutions were dried and stripped of solvent under reduced pressure.

A portion (0.20 g) of the acid fraction (0.25 g) was sublimed at a bath temperature of 55–60° and 2 mm pressure for 5 h. The white crystalline sublimate (0.16 g) was recrystallized from water to give colorless needles (0.12 g), m.p. and mixed m.p. with benzoic acid, 120.5–121.5°. The i.r. spectrum of the product was superimposable on that of benzoic acid.

A portion (0.23 g) of the neutral fraction (0.28 g) was dissolved in cyclohexane and chromatographed on silica gel (15 g). The major fraction, eluted with benzene, was a

Can. J. Chem. Downloaded from www.nrcresearchpress.com by 210.87.254.40 on 09/05/12
For personal use only.

Can. J. Chem. Downloaded from www.nrcresearchpress.com by 210.87.254.40 on 09/05/12
For personal use only.

yellow solid (0.19 g), m.p. 88–92°, whose i.r. spectrum indicated it to be nearly pure benzil. A portion of this material was crystallized from ethanol to give yellow needles, m.p. and mixed m.p. with benzil, 93.5–95°; another portion was converted to the 2,4-dinitrophenylhydrazone by the method of Shriner *et al.* (33), and this was crystallized from ethanol – ethyl acetate; m.p. and mixed m.p. 188–190°.

The yield of benzil was 35%, based on a theoretical yield of 2 mol equiv from unrecovered **5**; that of benzoic acid was 20%, based on a theoretical yield of 4 mol equiv from unrecovered **5**.

Oxidation of 5 with Potassium Permanganate

The desaurin **5** (0.772 g, 1.62 mmol) was mixed with potassium permanganate (5.00 g, 31.6 mmol) in acetone (150 ml), and the mixture was boiled under reflux for 4 h, cooled, and filtered. The brown precipitate was treated with acidified aqueous sodium bisulfite, and the mixture was warmed gently. The desaurin **5** (0.2989 g, 0.627 mmol) was recovered as a yellow, insoluble precipitate.

The filtrate was poured into water, and the solution was extracted five times with ether. The combined ethereal extracts were extracted five times with aqueous 10% potassium hydroxide and once with water. The ethereal solution was dried and filtered, and the solvent was removed under reduced pressure to give a yellow crystalline product, m.p. 92.5–94.5° (0.128 g). This was shown to be benzil by a mixed m.p. determination and comparison of its i.r. spectrum with that of an authentic sample. The yield, based on the formation of 2 mol equiv from the unrecovered desaurin, was 39%.

The combined basic extracts were acidified to p*H* 1 with 10% hydrochloric acid, and the solution was extracted five times with dichloromethane. The extracts were combined, dried, filtered, and evaporated by gentle warming on the steam bath to give a colorless, crystalline mass (0.221 g). This material was sublimed at 50–60° (4–5 mm) for 5 h. The sublimate (0.208 g) had m.p. 119–120.5°. Recrystallization from water gave colorless needles, m.p. and mixed m.p. with benzoic acid, 120.5–121.5°. The i.r. spectrum was identical with that of benzoic acid. The yield, based on the formation of 4 mol equiv from the unrecovered desaurin, was 35%.

Reduction of 5 with Zinc and Acetic Acid

The desaurin **5** (5.00 g, 10.5 mmol) was suspended in glacial acetic acid (150 ml) and a large excess of powdered zinc (*ca.* 30 g) was added. The mixture was boiled under reflux for 50 h, during which time an odor resembling that of carbon oxysulfide was noticed at the top of the condenser. The mixture was cooled and filtered, and the excess zinc was thoroughly washed with acetic acid. The combined filtrate and washings were diluted with water (600 ml), acidified to p*H* 1 with 10% hydrochloric acid, and extracted with three portions of dichloromethane. The extracts were combined, washed three times with aqueous 10% sodium carbonate and once with water, dried, filtered, and evaporated to give a pale yellow-orange, neutral oil (3.94 g). The combined basic washings were acidified to p*H* 1 with 10% hydrochloric acid and extracted with three portions of dichloromethane. The combined extracts were dried, filtered, and evaporated to give a trace of acidic, gummy solid, m.p. 109–116°.

The neutral fraction was dissolved in benzene and chromatographed on alumina (Merck; 100 g) packed in petroleum ether. Early fractions (70% petroleum ether – 30% benzene eluent) crystallized upon evaporation to give a colorless solid (0.14 g), m.p. 57–65°, which after two crystallizations from ethanol gave colorless crystals, m.p. 81–82°, which did not depress the m.p. of authentic *trans*-1,2-diphenyl-1-propene (**10**) (*vide infra*). The two samples had identical i.r. spectra, and each decolorized neutral potassium permanganate in acetone.

Middle fractions (50% petroleum ether – 50% benzene eluent; 0.77 g) gave a product with an i.r. spectrum showing all the bands of methyldeoxybenzoin (**8**). The product was converted to its 2,4-dinitrophenylhydrazone by the method of Vogel (34). After two crystallizations from ethanol – ethyl acetate this had m.p. 153–155°, undepressed on admixture with authentic methyldeoxybenzoin 2,4-dinitrophenylhydrazone (*vide infra*).

Later fractions (benzene eluent; 0.80 g) gave a product that was crystallized twice from ethanol to give transparent squares, m.p. 108–109.5°, identified as *erythro*-1,2-diphenyl-1-propyl acetate (**9**) by a mixed m.p. and i.r. spectral comparison with an authentic sample (*vide infra*).

Stripping of the column with ethanol gave a mixture (0.82 g) whose i.r. spectrum showed bands attributable to **8** and **9** and an unidentified alcohol.

Attempted reduction of the desaurin with the same amounts of reagents at room temperature was unsuccessful.

Methyldeoxybenzoin (8)

Methyldeoxybenzoin was prepared by the method of Meyer and Oelkers (35). A recrystallized sample had m.p. 48–49°; $\lambda_{max}(CHCl_3)$ 5.94(s) and 7.28 μ(m).

The 2,4-dinitrophenylhydrazone was prepared by the procedure of Shriner *et al.* (33). Two recrystallizations from ethanol afforded orange prisms, m.p. 153–155° [lit. (36) m.p. 151.5–152.5°].

erythro-1,2-Diphenyl-1-propanol (11) and erythro-1,2-Diphenyl-1-propyl Acetate (9)

A mixture of methyldeoxybenzoin (2.40 g, 11.4 mmol), ethanol (50 ml), and sodium borohydride (0.75 g, 19.8 mmol) was boiled under reflux for 2 h, poured into water (150 ml), and extracted with three portions of dichloromethane. The combined extracts were dried, filtered, and evaporated. An i.r. spectrum of the crude product (2.14 g) revealed complete reduction, as evidenced by the disappearance of all carbonyl absorption.

The crude alcohol was purified by chromatography on alumina (Merck) with ether as eluent. The purified product was crystallized from petroleum ether to give **11** as fine, colorless needles, m.p. 47.5–49° [lit. (37) m.p. 48°]; $\lambda_{max}(CHCl_3)$ 2.82(m), 7.24 μ(m).

The acetate **9** was prepared by acetylation of **11** with pyridine – acetic anhydride in the normal fashion, and was crystallized three times from ethanol; m.p. 107–109° [lit. (22) m.p. 109–110°]; $\lambda_{max}(CHCl_3)$ 5.78(s), 7.30 μ(m).

trans-1,2-Diphenyl-1-propene (10)

erythro-1,2-Diphenyl-1-propanol (0.65 g, 3.06 mmol) was heated with potassium hydrogen sulfate (2.40 g, 17.6 mmol) at 200° for 0.5 h. The mixture was cooled, water was added, and the solution was extracted with three

Can. J. Chem. Downloaded from www.nrcresearchpress.com by 210.87.254.40 on 09/05/12
For personal use only.

portions of dichloromethane. The combined extracts were dried, filtered, and evaporated to give the crude alkene (0.53 g). Two recrystallizations from ethanol gave colorless plates, m.p. 80–81.5° [lit. (23) m.p. 81–82°]; $\lambda_{max}(CHCl_3)$ 6.10(w), 7.28 μ(m).

Reduction of **5** *with Nickel. Formation of* **14**

(A) Sponge nickel catalyst (Davison; 50.0 g) from a freshly opened bottle was washed 11 times by decantation with dioxane. Dioxane (200 ml) and **5** (5.00 g, 10.5 mmol) were added and the mixture, protected from atmospheric moisture with a calcium chloride drying tube, was boiled under reflux for 50 h. The catalyst was removed by filtration through a sintered glass disc and washed with several portions of boiling absolute ethanol. The combined filtrate and washings were evaporated under reduced pressure at room temperature. The residue was taken up in a small volume of hot ethanol and the solution was allowed to stand for 12 h. Filtration yielded 1.5 g (35%) of **14** as pale yellow needles, m.p. 126–127.5°. Four recrystallizations from ethanol afforded an analytical sample as fine, colorless needles, m.p. 129–130°; $\lambda_{max}(CHCl_3)$ 5.91(s), 6.25(m), 6.33(w), 6.45 μ(w); $\lambda_{max}(C_2H_5OH)$ 249 (ε 31 600), 291 mμ (ε 17 400); $\delta(CDCl_3)$ 6.05(s, 1H), 6.26(s, 1H), 7.1–7.5(m, 18H), 7.9–8.1(m, 2H).

Anal. Calcd. for $C_{30}H_{22}O_2$: C, 86.93; H, 5.35. Found: C, 86.94; H, 5.53.

The 2,4-dinitrophenylhydrazone was prepared by the method of Shriner *et al.* (33). Four recrystallizations from ethanol – ethyl acetate gave orange cubes, m.p. 160–162° (dec.).

Anal. Calcd. for $C_{36}H_{26}O_5N_4$: C, 72.71; H, 4.41; N, 9.42. Found: C, 72.65; H, 4.48; N, 9.20.

(B) Reduction of **5** with old Davison sponge nickel catalyst or W-6 Raney nickel (38), by the same procedure as in section A led to a mixture of products, from which no **14** could be isolated.

In a typical reduction desaurin **5** (5.00 g, 10.5 mmol) gave a crude mixture (4.14 g) whose i.r. spectrum showed no absorption at 6.45 μ. A mixture (5.00 g) from two reductions was chromatographed on alumina (Woelm, activity grade 3). From the early fractions (70% petroleum ether – 30% benzene eluent) there was obtained a product (1.78 g) whose i.r. spectrum was very similar to that of methyldeoxybenzoin (**8**). A portion of this material was converted to its 2,4-dinitrophenylhydrazone by the procedure of Shriner *et al.* (33), and this was chromatographed on alumina (Merck). The major fraction gave, after three crystallizations from ethanol – ethyl acetate, orange plates, m.p. 149.5–151°, undepressed on admixture with authentic methyldeoxybenzoin 2,4-dinitrophenylhydrazone.

Later fractions (80% benzene – 20% ether eluent) (0.75 g) from the original chromatogram were combined and rechromatographed on alumina (Merck). Benzene eluted a material which solidified, and whose i.r. spectrum was identical with that of *erythro*-1,2-diphenyl-1-propanol (**11**). Recrystallization from petroleum ether gave fine, colorless needles, m.p. 47–49°.

Base-catalyzed Hydrolysis of **14**. *Formation of* **12**

A solution of **14** (0.554 g, 1.34 mmol) in 95% ethanol (25 ml) containing potassium hydroxide (1.50 g, 26.7 mmol) was heated under reflux on the steam bath for 3 h. Water (25 ml) was added, and the solution was cooled and extracted with four portions of dichloromethane. The combined extracts were dried and stripped of solvent under reduced pressure to give a pale yellow oil (0.306 g).

The basic aqueous solution was acidified to p*H* 1 with 10% hydrochloric acid and extracted as above. The acidic product (0.133 g) was obtained as a white crystalline solid, m.p. 119–120.5°, undepressed upon admixture with benzoic acid. The i.r. spectrum of this product was identical with that of benzoic acid.

The neutral oily fraction was purified by chromatography on non-basic alumina (Woelm, activity grade 1) with elution with petroleum ether (b.p. 30–60°). Evaporation of the solvent at 10° under reduced pressure and for 12 h at 0.5 mm gave **12** as a colorless oil; $\lambda_{max}(CHCl_3)$ 6.24(m), 6.34(w), 6.45 μ(m); $\lambda_{max}(C_2H_5OH)$ 225 (ε 23 400), 297 mμ (ε 13 800).

Anal. Calcd. for $C_{23}H_{18}O$: C, 89.00; H, 5.85. Found: C, 88.88; H, 6.28.

Oxidation of **12** *with Neutral Potassium Permanganate. Formation of* **13**

A solution of **12** (2.13 g, 6.86 mmol) in anhydrous acetone (50 ml) was stirred with anhydrous magnesium sulfate (2.0 g). A solution of potassium permanganate (0.80 g, 5.06 mmol) in anhydrous acetone (30 ml) was added, and the mixture was stirred at room temperature for 2.5 h. The precipitate of manganese dioxide was filtered off and washed with acetone. The combined filtrate and washings were diluted with water (70 ml), and saturated aqueous sodium bisulfite was added until the pink color was discharged. The resulting solution was acidified with concentrated hydrochloric acid to p*H* 1 and extracted with three portions of ether. The combined ethereal extracts were washed with water and with aqueous 10% sodium bicarbonate, dried, filtered, and evaporated under reduced pressure to give the neutral fraction (1.08 g) as a pale yellow oil. This fraction was dissolved in benzene and chromatographed on alumina (Merck; 50 g). Elution with petroleum ether (b.p. 30–60°) and benzene led to recovery of 0.85 g of colorless oil, which was identified as **12** by its i.r. spectrum. The column was then eluted with dichloromethane to give **13** as a yellow viscous oil (0.18 g); $\lambda_{max}(CHCl_3)$ 6.08(vs), 6.25(m), 6.34(m), 6.62 μ(m); $\lambda_{max}(C_2H_5OH)$ 263 (ε 18 600), 344 mμ (ε 19 100).

Compound **13** was characterized as its 2,4-dinitrophenylhydrazone (33), which was purified by twice eluting it from alumina (Merck) with benzene, followed by three recrystallizations from ethanol – ethyl acetate to give deep orange microcrystals, m.p. 185–186° (dec.); $\lambda_{max}(CHCl_3)$ 290(sh, ε 17 800), 331 (ε 17 400), 418 mμ (ε 26 900).

Anal. Calcd. for $C_{29}H_{20}O_5N_4$: C, 69.04; H, 4.11; N, 11.11. Found: C, 69.02; H, 4.31; N, 10.71.

Oxidation of **14** *with Basic Potassium Permanganate*

A solution of **14** (0.593 g, 1.91 mmol) in acetone (100 ml) was treated with potassium permanganate (1.00 g, 7.97 mmol) and water (10 ml), and the mixture was boiled under reflux for 2.5 h. It was then cooled, acidified with 10% hydrochloric acid to p*H* 1, and treated with aqueous 10% sodium bisulfite (10 ml). After dissolution of the manganese dioxide was complete, the solution was extracted with four portions of dichloromethane. The ex-

Can. J. Chem. Downloaded from www.nrcresearchpress.com by 210.87.254.40 on 09/05/12
For personal use only.

tracts were combined, washed with four portions of aqueous 10% potassium hydroxide and one of water, dried, filtered, and evaporated to give the neutral fraction (0.172 g).

The combined basic extracts and washings were acidified to p*H* 1 with 10% hydrochloric acid, and extracted with four portions of dichloromethane. The organic extracts were combined, filtered through anhydrous sodium sulfate, and evaporated under reduced pressure to give the acid fraction (0.333 g) as colorless crystals, m.p. 115–118°, undepressed upon admixture with benzoic acid. The i.r. spectrum of the acid fraction was identical with that of benzoic acid.

The neutral fraction was dissolved in benzene and chromatographed on Florisil. Two distinct yellow bands were developed and eluted with benzene. The first, when freed of solvent, furnished yellow needles (0.082 g), m.p. 91.5–93°, undepressed upon admixture with benzil; its i.r. spectrum was identical with that of benzil. The second gave a yellow oil (0.027 g), whose i.r. spectrum indicated it to be largely 1-phenyl-1,2-propanedione. It was converted *in toto* to its bis-2,4-dinitrophenylhydrazone (0.032 g) (33); this was recrystallized once to give orange micro-crystals, m.p. 153.5–155°, undepressed on admixture with 1-phenyl-1,2-propanedione bis-2,4-dinitrophenylhydrazone [lit. (39) m.p. 155–156°].

Reaction of **5** *with Hydrazoic Acid. Formation of* **16**

The desaurin **5** (0.48 g, 1.00 mmol) was dissolved in concentrated sulfuric acid (50 ml) and sodium azide (0.20 g, 2.3 mmol) was added in small portions. The mixture was allowed to stand for 12 h, and then an additional quantity of sodium azide (0.10 g, 1.2 mmol) was added. After standing for 24 h the color of the solution had changed from an initial intense red–violet to a deep red.

The solution was poured onto ice, the mixture was filtered, and the precipitate was air-dried. This yellow solid was thoroughly triturated with hot ethanol, and the mixture was allowed to cool and then filtered.

The resulting solid (0.22 g) was dissolved in chloroform and chromatographed on alumina (Merck; 50 g). A bright yellow band moved rapidly with chloroform as eluent and gave a fraction, which, after removal of solvent, was obtained as a yellow powder (0.80 g). This was purified by three recrystallizations from chloroform–cyclohexane to give fluffy yellow needles, m.p. 258–259°; *m/e* 491 (42), 399 (47), 161 (32), 105 (100).[5]

Anal. Calcd. for $C_{30}H_{21}O_2NS_2$: C, 73.29; H, 4.31; N, 2.85. Found: C, 73.56; H, 4.28; N, 2.70.

A second yellow band that was eluted more slowly with chloroform gave a fraction which, after removal of solvent, yielded small yellow crystals (0.06 g). This product was purified by three recrystallizations from ethanol–water to give yellow micro-crystals, m.p. 210–211°.[5]

Anal. Calcd. for $C_{30}H_{21}O_2NS_2$: C, 73.29; H, 4.31; N, 2.85. Found: C, 73.02; H, 4.33; N, 2.92.

*The Desaurin from Phenyl-2-propanone (***20***)*

A mixture of finely powdered potassium hydroxide (56.0 g, 1.00 mol) and phenyl-2-propanone (33.5 g, 0.250 mol) in carbon disulfide (300 ml) was boiled under reflux for 15 h. The excess carbon disulfide was removed under reduced pressure at room temperature, and the residue was treated with water (500 ml). The basic mixture was extracted with four portions of dichloromethane, and the extracts were combined, dried, filtered, and evaporated. The neutral fraction was thus obtained as a dark red tar (22.40 g).

The basic solution was acidified with 20% sulfuric acid at 10°, and extracted three times with dichloromethane. The combined organic extracts were dried over sodium sulfate, filtered, and freed of solvent under reduced pressure to give the acidic fraction as a red-brown tar (12.5 g). A portion (3.0 g) of this acidic material was dissolved in benzene and chromatographed on silica gel (100 g). A light orange band (70% petroleum ether – 30% benzene eluent) was collected and evaporated to give a deep red tar; $\lambda_{max}(CHCl_3)$ 2.84–4.2(w), 6.24(m), 6.44(s), and 6.90 μ(s). The remainder of the acid fraction was dissolved in benzene (200 ml), and the solution was poured into petroleum ether (500 ml) with vigorous stirring to give a curdy light orange precipitate, which on filtration turned to a viscous deep red oil. The i.r. spectrum of the freshly filtered material was compared with that of a sample dried *in vacuo*. The spectra were similar with no extraneous bands unattributable to solvent and the spectrum of the dried sample was indistinguishable from that of the sample obtained by chromatography.

The neutral fraction was dissolved in benzene (50 ml), and chromatographed on alumina (Merck; 500 g). Early fractions (30% benzene – 70% petroleum ether eluent) on evaporation gave dark red oils whose i.r. spectra indicated the presence of large amounts of phenyl-2-propanone. Elution with benzene yielded red oils which solidified either spontaneously or upon trituration with ligroin (b.p. 66–75°). Increasingly polar solvents eluted tars which were not further investigated. The benzene-eluted solid was purified by five recrystallizations from benzene–cyclohexane to give **20** as lemon yellow needles (2.5 g), m.p. 233–233.5°; δ($CDCl_3$) 2.10 (s, 6H), 7.38 (m, 10H).[5]

Anal. Calcd. for $C_{20}H_{16}O_2S_2$ (mol. wt. 352): C, 68.15; H, 4.58; S, 18.20; 2 C—CH_3, 8.53. Found (355 (isothermal distillation)): C, 68.30; H, 4.50; S, 18.23; C—CH_3, 7.34.

The desaurin **20** was readily soluble in hot benzene, ethanol, dioxane, and sparingly soluble in ligroin (b.p. 66–75°). It was soluble in concentrated sulfuric acid to give an orange solution from which it was precipitated by the addition of water.

Reduction of **20** *with Zinc and Base*

The desaurin **20** (0.50 g, 1.42 mmol) was mixed with zinc dust (3.00 g, 45.9 mg-atoms), sodium hydroxide (5.00 g, 125 mmol), water (150 ml), and ethanol (25 ml), and the mixture was boiled under reflux for 5 days. Fresh zinc dust (1.00 g, 15.3 mg-atoms) and sodium hydroxide (1.00 g, 25 mmol) were added daily.

The reaction mixture was cooled and filtered, and the unchanged zinc was washed with several portions of ethanol. The combined filtrate and washings were diluted with water (100 ml) and extracted with three portions of dichloromethane. The extracts were combined, dried, filtered, and evaporated to give a pale yellow oil (0.30 g), whose i.r. spectrum was very similar to that of 3-phenyl-2-butanone. It was converted *in toto* to its 2,4-dinitrophenylhydrazone (33) to give a product (0.53 g), m.p. 166–169°. Two recrystallizations from ethanol – ethyl acetate afforded orange needles, m.p. 170.5–171.5°, undepressed by admixture with 3-phenyl-2-butanone 2,4-

Can. J. Chem. Downloaded from www.nrcresearchpress.com by 210.87.254.40 on 09/05/12
For personal use only.

dinitrophenylhydrazone (*vide infra*), with an i.r. spectrum identical with that of the authentic material.

The yield of crude ketone based on 2 mol from 1 mol of **20** was 72%; the overall yield of crude 2,4-dinitrophenylhydrazone based on 2 mol from 1 mol of **20** was 57%.

3-Phenyl-2-butanone

3-Phenyl-2-butanone was prepared by the method of Suter and Weston (40).

Its 2,4-dinitrophenylhydrazone (33) was recrystallized from ethanol – ethyl acetate to give fine orange needles, m.p. 173–174° [lit. (41) m.p. 171–172°].

*The Mono-2,4-dinitrophenylhydrazone of **20***

The mono-2,4-dinitrophenylhydrazone of **20** was prepared by the method of Shriner *et al.* (33). The crude product was purified by elution with benzene from alumina (Merck), and crystallized three times from benzene–ligroin (b.p. 66–75°) to give fluffy, deep red needles, m.p. 250–251°; λ_{max}(CHCl$_3$) 3.01(w), 6.05(m), 6.18(s), 6.27(s), 6.65(s), 6.72(s), 7.36(m), 7.48 μ(s); λ_{max}(CHCl$_3$) 356 (ε 23 400), 450 mμ (ε 22 900).

Anal. Calcd. for $C_{26}H_{20}O_5N_4S_2$: C, 58.63; H, 3.79; N, 10.52. Found: C, 58.75; H, 3.99; N, 10.41.

*The Bis-2,4-dinitrophenylhydrazone of **20***

The desaurin **20** (0.43 g, 1.28 mmol) was dissolved in dioxane and treated with 2,4-dinitrophenylhydrazine (0.60 g, 3.03 mmol), concentrated hydrochloric acid (1 ml), and water (5 ml). The mixture was warmed briefly on the steam bath to effect complete solution, then allowed to cool and stand at room temperature for 2 weeks. A deep purple–brown solid slowly separated from the solution and was collected from time to time by filtration. The combined, dried solid weighed 0.85 g (93%).

This product was extremely insoluble in all common solvents, including ethyl acetate, chloroform, nitromethane, dimethylformamide, pyridine, and quinoline. Purification was effected by extraction of the powder with boiling pyridine for 0.5 h, filtration of the undissolved solid, and drying at 100° (0.5 mm) for 12 h to give a deep purple-brown powder, m.p. 285–286°; λ_{max}(KBr) 6.19(s), 6.32(s), 6.63(s), 6.75 μ(s); λ_{max}(CHCl$_3$) 260 (ε 18 200), 341 (ε 30 000), 505 mμ (ε 21 900).

Anal. Calcd. for $C_{32}H_{24}O_8N_8S_2$: C, 53.92; H, 3.39; N, 15.72. Found: C, 53.92; H, 3.57; N, 15.54.

*The Dioxime of **20***

The dioxime was prepared in pyridine by the method of Shriner *et al.* (42). Five recrystallizations from ethanol–water afforded yellow needles, m.p. 209.5–210° (dec.); λ_{max}(KBr) 3.00(m), 6.17(m), 6.25(w), 6.44 μ(s); λ_{max} (C_2H_5OH) 250 (sh, ε 11 000), 267 (sh, ε 7800), 347 (ε 20 400), 368 mμ (ε 19 500).

Anal. Calcd. for $C_{20}H_{18}O_2N_2S_2$: C, 62.80; H, 4.74; N, 7.33; S, 16.77. Found: C, 62.78; H, 4.78; N, 7.00; S, 16.53.

The dioxime was hydrolyzed in ethanol in the presence of hydrochloric acid and a large excess of 37% aqueous formaldehyde. After being stirred at room temperature for 24 h, the solution was diluted with water, and the product was isolated by filtration. After four recrystallizations from aqueous ethanol, the product was obtained as fine, pale yellow needles, m.p. 232–232.5°, undepressed upon admixture with **20**, and having an identical i.r. spectrum with that of **20**.

*Reaction of **20** with Sodium Hypochlorite. Formation of **21***

A solution of **20** (0.50 g, 1.42 mmol) in dioxane and a solution of sodium hydroxide (0.70 g) in water (10 ml) were stirred together at room temperature for 1 min. Commercial sodium hypochlorite [Chlorox(5.25% NaOCl): fresh bottle; 10 ml], was added, and stirring was continued for 5 min. Water (100 ml) was added, and the solution was filtered and acidified with 30% hydrochloric acid. The curdy precipitate was filtered, washed thoroughly with water, and air-dried. Purification of the crude product (0.35 g) was effected by one recrystallization from ethyl acetate – cyclohexane, followed by four recrystallizations from 2-butanone-cyclohexane, to give **21** as pale yellow microcrystals, m.p. 298–299° (dec.).

Anal. Calcd. for $C_{18}H_{12}O_4S_2$: C, 60.66; H, 3.39. Found: C, 60.75; H, 3.47.

The sample dissolved in concentrated sulfuric acid to give a yellow brown solution, unchanged on standing.

Reaction of **20** with sodium hypoiodite under a variety of conditions led to mixtures of products in both the acidic and neutral fractions. From the neutral fractions low yields of iodoform, m.p. 117–119°, could be isolated by chromatography on Florisil.

*Preparation of the Desaurin from Acetophenone (**22**)*

The desaurin **22** was prepared by the pyrolysis of the mercury salt of benzoyldithioacetic acid (20) according to the method of Kelber and Schwarz (16). The yield of the crude product was 24%. It could also be obtained by pyrolysis of the dibenzoate of benzoyldithioacetic acid in acetophenone. The desaurin was purified by slow recrystallization from toluene or nitrobenzene. Several crystallizations from toluene gave **22** as small plates, m.p. 270–272.5° (dec.) (corrected); λ_{max}(Nujol) 6.18(s), 6.26(m), 6.34(m), 7.26(m), 7.59(m), 8.17(s), 9.80(m), 12.11(m), 12.98(s), 14.4 μ(s); λ_{max}(CHCl$_3$) 274 (ε 17 000), 377 (sh ε 45 700), 392 mμ (ε 49 000).

Anal. Calcd. for $C_{18}H_{12}O_2S_2$: C, 66.64; H, 3.73; S; 19.78. Found: C, 66.66; H, 3.78; S, 19.83.

Rapid crystallization from toluene followed by several recrystallizations gave **22** as small needles, m.p. 237–238° (corrected), with resolidification, followed by remelting with decomposition at *ca.* 265°; λ_{max}(Nujol) 6.18(s), 6.26(m), 6.34(m), 7.26(s), 7.49(m), 8.16(s), 9.80(m), 12.00(w), 12.96(m), 14.39 μ(m); λ_{max}(CHCl$_3$) 273 (ε 18 200), 379 (ε 45 700), and 391 mμ (ε 49 000).

Anal. Calcd. for $C_{18}H_{12}O_2S_2$: C, 66.64; H, 3.73; S, 19.78. Found: C, 66.71; H, 3.77; S, 19.44.

We thank the National Research Council of Canada for generous support of part of this work. D.R.M. thanks the Standard Oil Co. of Indiana, the Procter and Gamble Co., and the U.S. National Institutes of Health for fellowship support. T.R.L. thanks the National Research Council of Canada for fellowship support.

1. P. Yates, T. R. Lynch, and L. S. Weiler. Can. J. Chem. **46**, 365 (1968).
2. P. Yates and D. R. Moore. J. Amer. Chem. Soc. **80**, 5577 (1958).
3. (*a*) C. Kelber. Ber. **43**, 1252 (1910). (*b*) C. Kelber and A. Schwarz. Ber. **44**, 1693 (1911).
4. P. Laakso. Suomen Kemistilehti, B, **17**, 1, 3, 13, 23, 27 (1944); **18**, 19 (1945); **19**, 31 (1946).

5. J. D. KENDALL and H. D. EDWARDS. U.S. Pat. 2 493 071 (1950); Chem. Abstr. **44**, 7346 (1950).
6. (*a*) A THUILLIER and J. VIALLE. Bull. Soc. Chim. Fr. 1398 (1959). (*b*) A. THUILLIER and J. VIALLE. Bull. Soc. Chim. Fr. 2182 (1962). (*c*) A. THUILLIER and J. VIALLE. Bull. Soc. Chim. Fr. 2187 (1962).
7. (*a*) R. GOMPPER and W. TÖPFL. Chem. Ber. **95**, 2861 (1962). (*b*) R. GOMPPER and H. SCHAEFER. Chem. Ber. **100**, 591 (1967).
8. E. SÖDERBÄCK. Acta Chem. Scand. **17**, 362 (1962).
9. K. A. JENSEN and L. HENRIKSEN. Acta Chem. Scand. **22**, 1107 (1968).
10. (*a*) H. APITZSCH. Ber. **38**, 2888 (1905). (*b*) H. APITZSCH. Ber. **37**, 1599 (1904); **41**, 4028, 4047 (1908); H. APITZSCH and G. A. BAUER. Ber. **41**, 4039 (1908); A. SCHÖNBERG and W. ASKER. J. Chem. Soc. 198 (1945); 604 (1946).
11. T. NORTON and A. OPPENHEIM. Ber. **10**, 701 (1877).
12. V. MEYER and H. WEGE. Ber. **24**, 3535 (1891).
13. H. BERGREEN. Ber. **21**, 337 (1888).
14. V. MEYER. Ber. **21**, 353 (1888); Ber. **23**, 1571 (1890).
15. P. PETRENKO-KRITSCHENKO. Ber. **25**, 2239 (1892).
16. C. KELBER and A. SCHWARZ. Ber. **45**, 137 (1912).
17. P. YATES and T. R. LYNCH. Can. J. Chem. This issue.
18. (*a*) G. WENZEL. Ber. **33**, 2041 (1900). (*b*) G. WENZEL. Ber. **34**, 1043 (1901).
19. W. WACHTER. Ber. **25**, 1727 (1892).
20. P. YATES, T. R. LYNCH, and D. R. MOORE. Can. J. Chem. This issue.
21. R. CRIEGEE. Ann. **583**, 1 (1953).
22. F. A. A. ELHAFEZ and D. J. CRAM. J. Amer. Chem. Soc. **75**, 339 (1953).
23. D. J. CRAM and F. A. A. ELHAFEZ. J. Amer. Chem. Soc. **74**, 5828 (1952).
24. M. FÉTIZON and P. BARANGER. Bull. Soc. Chim. Fr. [5] **24**, 1311 (1957); C.N.R. RAO. Chemical applications of infrared spectroscopy. Academic Press, New York, N.Y., 1963. p. 324; H. MINATO and T. NAGASAKI. J. Chem. Soc. C, 377 (1966).
25. H. BILTZ. Ber. **26**, 1952 (1893).
26. (*a*) H. HAUPTMAN and B. WLADISLAW. J. Amer. Chem. Soc. **72**, 707 (1950); A. SCHÖNBERG, K.-H. BROSOWSKI, and E. SINGER. Chem. Ber. **95**, 2984 (1962). (*b*) A. SCHÖNBERG, E. FRESE, and K.-H. BROSOWSKI. Chem. Ber. **95**, 3077 (1962).
27. D. R. MOORE. Ph.D. Thesis. Harvard University, Cambridge, Massachusetts, 1958.
28. (*a*) T. R. LYNCH, I. P. MELLOR, S. C. NYBURG, and P. YATES. Tetrahedron Lett. 373 (1967). (*b*) T. R. LYNCH. Ph.D. Thesis. University of Toronto, Toronto, Ontario, 1967.
29. S. C. NYBURG. Private communication; I. P. MELLOR. Ph.D. Thesis. University of Keele, Keele, England, 1968.
30. A. W. K. CHAN, W. D. CROW, and I. GOSNEY. Tetrahedron, **26**, 1493 (1970); W. D. CROW and I. GOSNEY. Aust. J. Chem. **22**, 765 (1969).
31. (*a*) A. SCHÖNBERG, L. V. VARGHA, and H. KALTSCHMITT. Ber. **64**, 2582 (1931); A. SCHÖNBERG, A. STEPHENSON, H. KALTSCHMITT, E. PETERSEN, and E. SCHULTEN. Ber. **66**, 237 (1933); E. V. ELAM and H. E. DAVIS. J. Org. Chem. **32**, 1562 (1967). (*b*) K. DICKORE and R. WEGLER. Angew. Chem. Intl. Ed. Engl. **5**, 970 (1967).
32. M. S. RAASCH. Chem. Commun. 577 (1966).
33. R. L. SHRINER, R. C. FUSON, and D. Y. CURTIN. The systematic identification of organic compounds. 5th ed. John Wiley and Sons, Inc., New York, N.Y., 1964. p. 253.
34. A. I. VOGEL. A textbook of practical organic chemistry. 3rd ed. Longmans, Green and Co., London, 1956. p. 344.
35. V. MEYER and L. OELKERS. Ber. **21**, 1295 (1888).
36. B. G. CHRISTENSEN. Ph.D. Thesis. Harvard University, Cambridge, Massachusetts, 1956.
37. F. KAYSER. Compt. Rend. **199**, 1424 (1934).
38. H. ADKINS and H. R. BILLICA. J. Amer. Chem. Soc. **70**, 695 (1948).
39. P. YATES. J. Amer. Chem. Soc. **74**, 5376 (1952).
40. C. M. SUTER and A. W. WESTON. J. Amer. Chem. Soc. **64**, 533 (1942).
41. T. TAKESHIMA. J. Sci. Res. Inst. (Tokyo), **48**, 113 (1954); Chem. Abstr. **49**, 13153 (1955).
42. R. L. SHRINER, R. C. FUSON, and D. Y. CURTIN. The systematic identification of organic compounds. 5th ed. John Wiley and Sons, Inc., New York, N.Y. 1964. p. 289.

Can. J. Chem. Downloaded from www.nrcresearchpress.com by 210.87.254.40 on 09/05/12
For personal use only.

Can. J. Chem. Downloaded from www.nrcresearchpress.com by 210.87.254.6 on 09/05/12
For personal use only.

Carbon Disulfide. III. Reaction with Active Methylene Compounds. The Infrared and Ultraviolet Spectra of the Desaurins[1,2]

PETER YATES,[3] THOMAS R. LYNCH, AND DONALD R. MOORE

The Departments of Chemistry, University of Toronto, Toronto, Ontario, and Harvard University, Cambridge, Massachusetts 02138

Received October 1, 1970

The position of the carbonyl-stretching bands in the i.r. spectra of the desaurins, 2,4-bis(acylmethylene)- and 2,4-bis(carboxymethylene)-1,3-dithetane derivatives, establishes that there is a strong interaction between the sulfur atoms and the carbonyl groups. This is considered to involve mainly conjugative interaction rather than interaction through space, although the latter may account for the abnormally weak intensity of the carbonyl-stretching bands. These bands are split in the case of several desaurins and related compounds, and evidence has been obtained in one case that the splitting is due to Fermi resonance. The u.v. spectra of the desaurins and related compounds also indicate a strong conjugative interaction between the sulfur atoms and the carbonyl groups.

La position des bandes de vibration des carbonyles dans les spectres i.r. des désaurines, des dérivés des bis(acylméthylène)-2,4 et bis(carboxyméthylène)-2,4 diéthane-1,3, démontre qu'il existe une interaction forte entre les atomes de soufre et les groupes carbonyles. Ces résultats proviendraient principalement d'une interaction conjugative plutôt que d'une interaction à travers l'espace, quoique cette dernière hypothèse pourrait expliquer l'intensité anormalement faible des bandes de vibration des carbonyles. Dans le cas de plusieurs désaurines et composés analogues, les bandes sont divisées et des indications ont été obtenues dans un cas, que cette division est due à de la résonance de Fermi. Les spectres ultraviolets des désaurines et des composés voisins indiquent aussi qu'une interaction conjugative forte existe entre les atomes de soufre et les groupes carbonyles.

Canadian Journal of Chemistry, 49, 1467 (1971)

Preparation of Desaurins and Related Compounds

The desaurins, neutral compounds formed by the reaction of active methylene compounds **1** with base and carbon disulfide (eq. 1) have been shown to have structures of type **2**[4] (1, 3). We have described the preparation of the desaurins **3–7** previously (1). In studying the spectra of

[1] 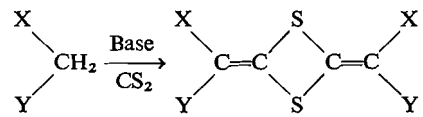

1 **2**

these desaurins, it was considered to be of importance to compare them with the spectra of a desaurin derived from a dialkyl ketone.

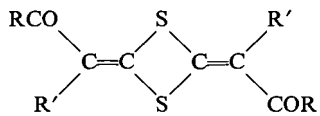

3 R = R′ = C_6H_5
4 R = CH_3; R′ = C_6H_5
5 R = OH; R′ = C_6H_5
6 R = C_6H_5; R′ = H
10 R = $(CH_3)_3C$; R′ = H

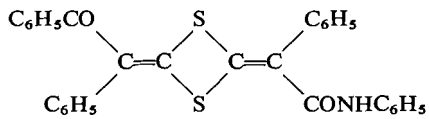

7

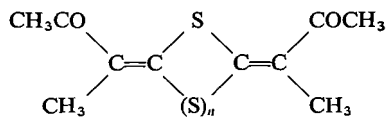

8 *n* = 1
9 *n* = 2

Previous to our investigation (3*b*), such a desaurin had not been prepared; however, during its course Kirby (4) reported the formation of the desaurin **8** by treatment of the trithiolane derivative **9** with triethyl phosphite. We pre-

[1]For Paper II see ref. 1.
[2]The mass spectra of several desaurins have been discussed previously (2).
[3]Lash Miller Chemical Laboratories, University of Toronto, Toronto 5, Ontario.
[4]In this and subsequent structures, no assignment of configuration is implied, except in the case of **6** (3).

Can. J. Chem. Downloaded from www.nrcresearchpress.com by 210.87.254.6 on 09/05/12
For personal use only.

pared the desaurin **10** by a modification of the general method of Gompper and Töpfl (5), whereby the dianion of the dithio acid formed by reaction of pinacolone with carbon disulfide and base was treated with oxalyl chloride.

Four model compounds were also prepared for spectroscopic comparison with the desaurins. Compound **12** was first obtained by Kelber (6) by treatment of acetophenone with carbon disulfide and base to give benzoyldithioacetic acid (**11**), followed by methylation with methyl iodide and sodium; in the present work it was also prepared by methylation of **11** with methyl iodide and sodamide or with diazomethane. Its structure was confirmed by our spectroscopic observations and those of Gompper and Schaefer (7), and by an X-ray crystallographic study by Nyburg and Mellor (8).

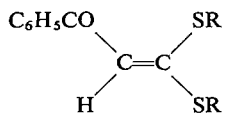

11 R = H
12 R = CH_3

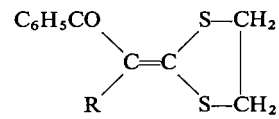

13 R = H
14 R = C_6H_5

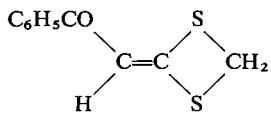

15

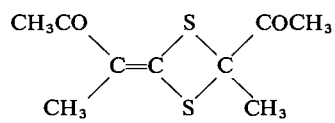

16

Compound **13** was prepared by the method of Kelber and Schwarz (9) by alkylation of **11** with 1,2-dibromoethane and base. These workers had established its structure by demonstrating that on reduction with zinc and sodium hydroxide it gave propiophenone and 1,2-ethanedithiol, thus establishing that both alkylations had occurred on sulfur.

Compound **14** was prepared by a similar alkylation with 1,2-dibromoethane of the salt of the β-keto dithio acid obtained from the action of carbon disulfide on the sodium derivative of deoxybenzoin. Its structure was established chemically by its reduction with zinc and sodium hydroxide to give *erythro*-1,2-diphenyl-1-propanol, isolated as its acetate (10), and 1,2-ethanedithiol, isolated as its dibenzoate (11). It has subsequently been confirmed by an X-ray crystallographic study by Schmidt and Tulinsky (12).

Compound **15** was prepared by alkylation of **11** with dibromomethane. Its structure is assigned on the basis of the close relationship of its i.r. and u.v. spectra (*vide infra*) to those of compounds **12** and **13**; its p.m.r. spectrum, with signals at δ 4.23 (s, 2H), 6.97 (s, 1H), 7.4–7.6 (m, 3H), and 7.8–8.0 (m, 2H), is in accord with this assignment. A related compound, **16**, has been obtained by Kirby (4) by the reaction of 3-diazo-2-butanone with carbon disulfide; its structure was established by an X-ray crystallographic study by Kapecki *et al.* (13).

Infrared Spectra of Desaurins and Related Compounds

Bands in the 2.8–3 and 5–6.5 μ regions of the i.r. spectra of the desaurins and of model compounds are listed in Tables 1 and 2, respectively. The spectra of the symmetrical desaurins **4**, **8**, and **10** with the group **17** show bands attributable to carbonyl-stretching vibrations at 6.05–6.07 μ. This position is at longer wavelength than that

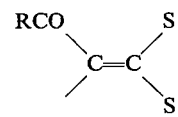

17 R = alkyl

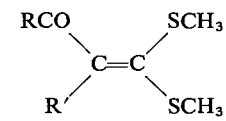

18 R = alkyl; R′ = H
19 R = R′ = alkyl

normally observed for simple α,β-unsaturated ketones, and indicates that the sulfur atoms interact with the carbonyl groups through the conjugated π-electron system and/or directly through space (*vide infra*).

Thuillier and Vialle (14) have examined the spectra of a number of compounds of type **18** and **19**. The former type of compound was found to have its carbonyl-stretching band at *ca.* 6.10 μ, while the latter type showed this band at *ca.* 5.90 μ. The striking effect of the introduction of an alkyl substituent in place of hydrogen at the vinylic carbon atom adjacent to the carbonyl group is most readily interpreted as being the result of a change in the nature of the preferred conformation (15). In these terms, a planar or near-planar *s-cis* conformation, **23**, is assigned to the compounds of type **18** (the *s-trans* conformation, **24**, would involve steric crowding of the R group and one of the sulfur

TABLE 1. The i.r. spectra of the desaurins

Compound	R = R′	R″	Medium*	λ_{max} (μ)
3	C_6H_5	C_6H_5	K	6.17, 6.26(m), 6.36(m)
4	CH_3	C_6H_5	C	6.05, 6.24(m), 6.35(w)
5	OH	C_6H_5	K	3.0–4.0, 6.02, 6.25(w), 6.32(m)
6	C_6H_5	H	N	6.18, 6.26(m), 6.34(m)
8†	CH_3	CH_3	C	6.06
10	$(CH_3)_3C$	H	C	6.07, 6.15(sh)
20‡	$NHCH_3$	H	N	3.12, 6.10
21‡	NHC_2H_5	H	N	3.02, 6.14
22‡	$NHCH_2C_6H_5$	H	N	3.05, 6.10
	R	R′ R″		
7	C_6H_5	NHC_6H_5 C_6H_5	K	(*i*)§ 2.96(w), 6.02, 6.14, 6.25(m), 6.35(m) (*ii*)‖ 2.97(w), 6.03, 6.14, 6.27(m), 6.35(m)

*K, potassium bromide or iodide disc; N, Nujol mull; C, chloroform solution.
†Reference 4.
‡Reference 16.
§Melting point 258–259°.
‖Melting point 210–211°.

TABLE 2. The i.r. spectra of compounds related to the desaurins*

	Compound	Medium†	λ_{max} (μ)
12	$C_6H_5COCH{=}C(SCH_3)_2$	C	6.13, 6.18, 6.25(m), 6.34(m)
13	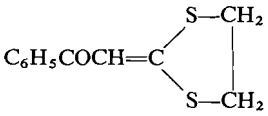	C	6.18, 6.25(m), 6.34(m)
14	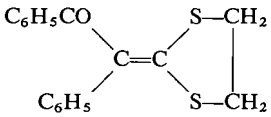	C	6.20, 6.25, 6.35(m)
15	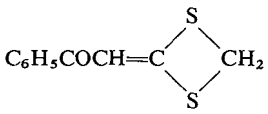	C	6.15, 6.21, 6.24(sh), 6.34(m)
18‡	$RCOCH{=}C(SCH_3)_2$ (R = alkyl)	K	6.09–6.10
19‡	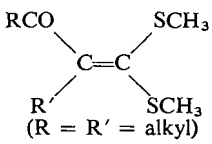	K or L	5.88–5.91

*For the spectra of additional related compounds, see refs. 5 and 17.
†C, chloroform solution; K, potassium bromide disc; L, liquid film.
‡Reference 14.

Can. J. Chem. Downloaded from www.nrcresearchpress.com by 210.87.254.6 on 09/05/12
For personal use only.

Can. J. Chem. Downloaded from www.nrcresearchpress.com by 210.87.254.6 on 09/05/12
For personal use only.

atoms). In compounds of type **19**, the analogous conformation, **25**, suffers from severe steric interaction between an S—CH_3 group and the R′ group, and probably also a further inter-

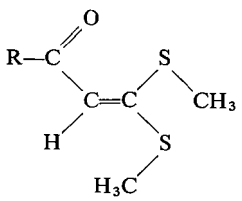

23

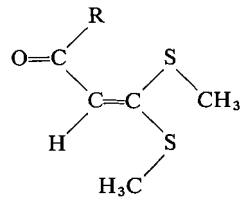

24

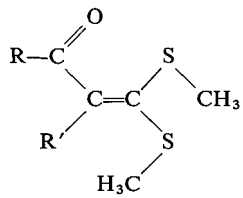

25

action between the R and R′ groups, due to a buttressing effect. As a result, compounds of type **19** are considered to take up a conformation in which there is a considerable departure from coplanarity, thus inhibiting the interaction of the carbonyl, ethylenic, and methylthio groups.

The desaurin **10** is expected to have the preferred conformation **26**, analogous to **23**, and this is reflected in the similarity of the position of its carbonyl-stretching band to that in the case of compounds of type **18**. The small shift to shorter wavelength may be due to the fact that in **23**, the two sulfur atoms interact through the conjugated system with a single carbonyl group, whereas in **26**, the two sulfur atoms inter-

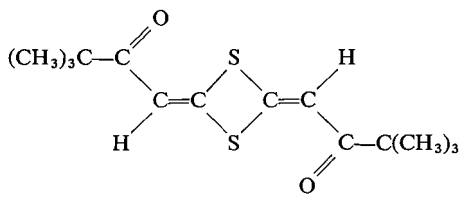

26

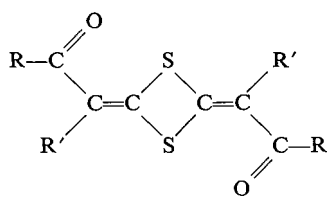

27

act with two carbonyl groups. The similarity of the carbonyl-stretching band positions for the desaurins **4**, **8**, and **10** suggests that **4** and **8** have preferred conformations of type **27**, analogous to **26**. In the case of **4**, this would require that the phenyl substituents (R′) be rotated considerably out of the plane of the conjugated carbonyl system.

The symmetrical desaurins **3** and **6** and the model compounds **12**–**15**, all having the grouping **28**, give rise to carbonyl-stretching bands at

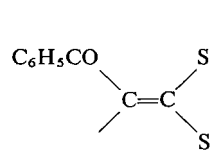

28

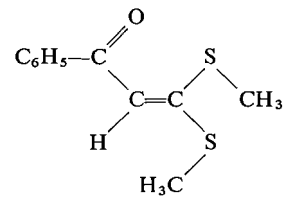

29

longer wavelengths than those of the compounds with the grouping **17**. A double *s-cis* conformation has been established for **6** in the solid state (3) and the shift of its carbonyl-stretching band relative to the desaurin **10**, which has been assigned this conformation also, is attributable to the additional conjugation of the carbonyl groups with the aromatic rings. The magnitude of the shift (*ca.* 0.10 μ) is similar to that found in cognate cases (18). The spectrum in the 6.1–6.4 μ region of the model compound **13** resembles that of **6**; however in the spectra of **12**[5] and **15** two bands of approximately equal intensity appear between 6.13 and 6.21 μ in addition to lower intensity bands at 6.25 and 6.34 μ, attributable to the phenyl rings. Thus it appears that in these compounds the carbonyl bands are split.[6] The origin of the splitting will be discussed subsequently; it may be noted here that if the unsplit band positions are approximated by the average of the positions of the split bands, the range of carbonyl-stretching absorption for the compounds with the grouping **28** is 6.15–6.20 μ.

The positions of the carbonyl-stretching bands of the non-ketonic desaurins listed in Table 1 are readily related to those of the ketonic

[5]This compound has been shown to have the *s-cis* conformation **29** in the solid state with a close approach of the α,β-unsaturated carbonyl system and the sulfur atoms to coplanarity (8).

[6]Ill-defined shoulders on the low wavelength sides of the bands at 6.18 and 6.20 μ of **13** and **14**, respectively, suggest that there may be some splitting in these cases also.

Can. J. Chem. Downloaded from www.nrcresearchpress.com by 210.87.254.6 on 09/05/12
For personal use only.

desaurins discussed already. The acid **5** has its carbonyl-stretching band at slightly shorter wavelength than the bands of **4**, **8**, and **10**, in conformity with the usual relationship between conjugated acids and conjugated ketones. Further, the amides **20–22** (16) have their carbonyl-stretching bands at slightly longer wavelength than the bands of **4**, **8**, and **10** in accord with the usual relationship between conjugated ketones and conjugated amides.

It has previously been reported (19) that the carbonyl-stretching bands of the desaurin **8** and the model compound **14** are abnormally weak; this conclusion was based on a qualitative examination of the spectra. Quantitative measurements have confirmed this in the case of **3**. The integrated intensity[7] of its 6.17 μ band measured in potassium bromide discs,[8] was 1.71, corresponding to 0.86 per carbonyl group, while the integrated intensity of the carbonyl-stretching band of benzophenone, measured in potassium bromide discs under the same conditions, was 1.20. However, similar measurements on the desaurin **6** gave a value of 2.86, or 1.43 per carbonyl group. The sum of the integrated intensities of the bands at 6.13 and 6.18 μ of **12** in solution in chloroform was determined to be 1.39. This value is low in comparison with values reported in chloroform solution for dialkyl ketones and benzophenone, *i.e.*, 1.9 and 2.4[9] (22), respectively.[10] In the case of planar chromophores, conjugation with an ethylenic double bond or aromatic ring brings about an increase in the carbonyl-stretching band intensity (20, 22). While the positions of the carbonyl-stretching bands of **3**, **6**, and **12** show a considerably higher degree of conjugation than that in benzophenone, their intensities per carbonyl group are similar to, or less than, that of the carbonyl-stretching band of benzophenone. This suggests that there is a significant reduction in intensity relative to simple conjugated ketones associated with the grouping **28** present in these compounds. The intensity relationships among **3**, **6**, and **12** may well reflect differences in the extent of coplanarity between the phenyl rings of the benzoyl groups and the α,β-unsaturated carbonyl system.[11]

The abnormally long wavelength of the carbonyl-stretching bands of the desaurins and related compounds and the reduced intensity of these bands raises the question whether these effects are due to an interaction through space between the sulfur and oxygen atoms in the *s-cis* conformations of these compounds. Recent X-ray crystallographic data have made it clear that for several of these compounds in the solid state the S—O distance is considerably shorter than the sum of the van der Waals' radii of sulfur and oxygen (3.05 Å),[12] *i.e.*, **6** (2.64 Å) (3, 8), **12** (2.72 Å) (8), **14** (2.70 Å) (12), and **16** (2.63 Å) (13).[13] However, 3-methylthio-2-cyclohexenone (**30**), which perforce has an *s-trans* relationship between the sulfur atom and the carbonyl group, gives rise to a carbonyl-stretching band in its neat or solution i.r. spectrum at 5.98–6.01 μ (26). This suggests that the effect of direct sulfur–oxygen interaction on the wavelength of the carbonyl-stretching vibrations in the desaurins and related compounds is relatively small, since compounds of type **18** absorb at 6.09–6.10 μ and the bathochromic shift of 0.10 μ is attributable in major part to increased conjugation resulting from the presence of the second sulfur atom.[14] Such an interaction may contribute significantly, however, to the reduction of band intensities, since the integrated intensity reported for **30** in solution is 2.70 (26), which is comparable or larger in magnitude than the values measured or estimated for the much

[7]Integrated absorption intensities are given in absorbance units (20): 1 absorbance unit = 1×10^4 mol^{-1} l cm^{-2}.

[8]Although integrated intensities are not normally measured in potassium bromide discs, this medium has been used with success for the analysis of mixtures (21*a*), and Lambert's and Beer's laws have been shown to hold (21).

[9]This was measured in the present work also and found to be 2.35.

[10]It has previously been found that absorptivities are greater in solution than in the solid state (23).

[11]The planes of these phenyl rings in **6** and **12** in the solid state have been shown to be inclined at 10 and 19°, respectively, to the planes of the α,β-unsaturated carbonyl systems (8). The angle is expected to be significantly larger in the case of **3** (*cf.* 12). It may be noted that benzophenone is itself nonplanar (24).

[12]This figure is based on a van der Waal's radius for sulfur of 1.65 Å (3*b*, 8), derived from the S—S contact distances in rhombic sulfur (25).

[13]For interpretations of these short S—O distances in terms of partial bonding between sulfur and oxygen, see refs. 3*b* and 8.

[14]Mollier *et al.* (27) have concluded that partial sulfur–oxygen bonding in the related case of 1,2-dithiol-3-ylidene ketones brings about a large shift of the carbonyl-stretching band to longer wavelength. However, Kapecki and Baldwin (28) have concluded from extended Hückel molecular orbital calculations that covalent bonding between sulfur and oxygen is negligibly weak in related cases.

TABLE 3. The u.v. spectra of the desaurins and related compounds

Compound*	Solvent†	λ_{max} (mμ) (ε)
3	C	266(22 900), 419(38 100)
4	C	246(9120), 374(27 500)
5	E	342(31 600)
6	C	274(17 000), 377(sh, 45 700), 392(49 000)
8	E	241(sh, 1440), 359(28 700), 370(28 700)
10	E	242(2510), 350(29 500)
20	E′	293(sh), 305(35 500), 322(30 420)
21	E′	293(sh), 306(36 600), 325(30 950)
22	E′	295(sh), 309, 325
7	C	(*i*) 263(18 200), 401(37 200)
	C	(*ii*) 265(18 600), 387(39 800)
12	E	263(8710), 280(8710), 344(20 400)
13	E	258(7940), 287(6030), 344(20 900)
14	E	257(10 700), 350(15 800)
15	E	257(14 500), 344(22 900)
16	E	243(5360), 317(8950)

*See Tables 1 and 2 for structures of compounds and references.
†C, chloroform; E, 95% ethanol; E′, 90% ethanol.

more highly conjugated ketones **3**, **6**, and **12** in solution. Further investigation is necessary to establish this, since the carbonyl-stretching band intensities are often weaker for *s-cis* than for *s-trans* α,β-unsaturated ketones in the absence of any special interactions of the oxygen atom (15*a*).

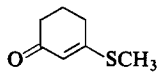

30

As has been noted earlier, several compounds with the grouping **28** have split carbonyl bands. A preliminary examination of the origin of the splitting was made in the case of compound **12**. In carbon tetrachloride solution the bands of equal intensity at 6.13 and 6.18 μ in chloroform solution were replaced by a sharp, intense band at 6.11 μ and a weak band at 6.18 μ. Such behavior could be due either to vibrational coupling or rotational isomerism (29). However, the latter origin is contra-indicated by the spectrum of **12** in a potassium bromide disc, which showed a sharp band at 6.20 μ with a medium intensity shoulder at 6.15 μ, and in a Nujol mull, which showed a broad band at 6.22 μ with a shoulder of medium intensity at 6.17 μ. Furthermore, the n.m.r. spectrum of **12** showed no temperature dependence in the range 27 to −60°. Thus the most probable sources of the bifurcation is vibrational coupling. Corroboration was sought by the preparation of **31**, *i.e.*, **12** with the vinylic hydrogen replaced by deuterium; n.m.r. spectroscopy indicated that there was *ca.* 70% incorporation of deuterium in the vinylic position.[15] In chloroform solution the i.r. spectrum of the labelled compound exhibited strong bands at 6.15 and 6.18 μ with a shoulder at 6.13 μ; in carbon tetrachloride the spectrum showed a strong, sharp band at 6.13 μ; in both spectra a band at 6.25 μ was also present. These observations are in accord with the attribution of the splitting of the carbonyl band of **12** to vibrational coupling, which is absent in the deuterated derivative **31**; the unperturbed carbonyl-stretching band positions are then 6.15 ($CHCl_3$) and 6.13 μ (CCl_4). This coupling could be with the fundamental stretching vibration of the ethylenic double bond or with an overtone or combination vibration (*i.e.*, Fermi resonance). If coupling to a fundamental vibration is involved, the estimates of the carbonyl-stretching band intensities made earlier may be too high, since they will also include the intensity of the other fundamental band; however, if Fermi resonance is involved, this error is unlikely to be significant because of the low intensity of overtone and combination bands. The data available do not permit a definitive choice between the two types of coupling, but the latter appears more probable. Jensen and Henriksen (17) have assigned a very intense band in the 6.5–7.0 μ region of the spectra of a series of compounds containing the function **32** to the ν_1 vibration of this grouping; they favored this assignment over one to a simple ethylenic stretching vibration because of the unusual intensity and long wavelength of the

[15]We thank Mr. A. Hepworth for the preparation of the labelled compound and obtaining the related spectra.

Can. J. Chem. Downloaded from www.nrcresearchpress.com by 210.87.254.6 on 09/05/12
For personal use only.

Can. J. Chem. Downloaded from www.nrcresearchpress.com by 210.87.254.6 on 09/05/12
For personal use only.

bands. In the spectra of all of the desaurins and related compounds that we have examined, a strong or very strong band appears in the 6.5–6.9 μ region, which is probably analogous to the bands in this region observed by Jensen and Henriksen. If this is the case, the splitting of the carbonyl-stretching bands cannot involve coupling with an ethylenic stretching vibration and must have their origin in Fermi resonance.[16] Again, further work is needed to establish this unequivocally, since strong bands due to aromatic C—C stretching and aliphatic C—H bending vibrations can also occur in the 6.5–6.9 μ region.

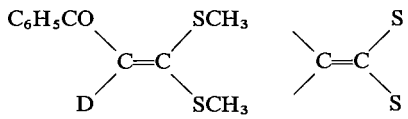

31 **32**

Ultraviolet Spectra of Desaurins and Related Compounds

The u.v. maxima of the desaurins and related compounds are listed in Table 3. The spectra of compounds **12**, **13**, and **15** with the grouping **33** have a high intensity, long wavelength maximum[17] at 344 mμ (ε 20 400 – 22 900) and another maximum at 257–263 mμ (ε 7940 –14 500).

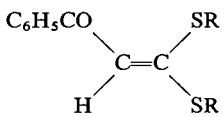

33

R = CH_3 or $(CH_2)_n$

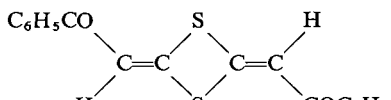

6

[16]Jensen and Henriksen (17) have also observed splitting of the carbonyl bands of certain of the compounds they have examined that have the ethylenic double bond of the grouping **32** conjugated with carbonyl groups. However, each of these has two such carbonyl groups, and the splitting may be due here to vibrational coupling between the carbonyl groups.

[17]These maxima are broad and unsymmetrical and may well represent the near superimposition of two peaks, as is suggested by the fact that some other compounds in Table 3 show either a high intensity shoulder on the long wavelength maximum or two close-lying long wavelength maxima of similar intensity; in the latter cases comparison is made with the average position of the maxima.

Introduction of a phenyl group in place of the vinylic hydrogen atom, as in **14**, causes a bathochromic and hypochromic shift of the long wavelength maximum to 350 mμ (ε 15 800), most probably due to extension of the chromophoric system with reduction in coplanarity (*vide supra*). The desaurin that is most closely related to compounds **12**, **13**, and **15** is **6**; its long wavelength maximum shows a bathochromic and hyperchromic shift with respect to the corresponding maxima of these compounds. The bathochromic shift is *ca.* 50 mμ and the hyperchromic shift >1500 per carbonyl group. The spectrum of the desaurin **3** in which the vinylic hydrogen atoms of **6** are replaced by phenyl groups bears a similar relationship to that of **14**, showing a bathochromic shift of the long wavelength maximum of 69 mμ and a hyperchromic shift of *ca.* 3000 per carbonyl group. These shifts are consistent with transmission of delocalization through the sulfur atoms in the desaurins (4, 16). The suggestion (16) that such effects may be due in part to the unusual short S–S distance in the desaurins and the resulting enhanced transannular S–S overlap must be viewed with some reserve on the basis of the present data. In compound **15** it may be anticipated that the S–S distance will be very short and similar to that in **6** rather than that in **12** or **13**.[18] Yet, although the long wavelength maximum of **15** shows a hyperchromic shift with respect to the maxima of **12** and **13**, it shows no bathochromic shift whatsoever and differs markedly from **6** in this regard.

As would be anticipated, the long wavelength maximum of **16** occurs at appreciably lower

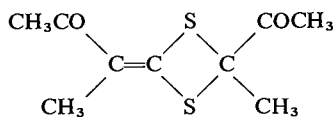

16

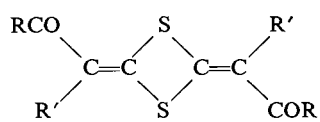

8 R = R′ = CH_3
10 R = $C(CH_3)_3$; R′ = H
4 R = CH_3; R′ = Ph

wavelength than those of the phenyl ketones **12**, **13**, and **15** ($\Delta\lambda \sim -25$ mμ); its intensity is

[18]*Cf.* the S–S distance in **16** (2.71 Å) (13) with that in **6** (2.67 Å) (3, 8), **12** (2.94 Å) (8), and **14** (2.95 Å) (12).

Can. J. Chem. Downloaded from www.nrcresearchpress.com by 210.87.254.6 on 09/05/12
For personal use only.

considerably lower also. The related desaurin **8** shows bathochromic and hyperchromic shifts analogous to those encountered in the phenyl ketone series ($\Delta\lambda \sim 50$ mμ; $\Delta\varepsilon \sim 5000$ per carbonyl group). The desaurin **10** that has no alkyl substituents on the ethylenic double bonds shows a shift of its longer wavelength maximum relative to that of **8** to lower wavelength ($\Delta\lambda \sim -15$ mμ), as expected. Conversely, substitution of phenyl for alkyl substituents on the ethylenic double bonds of **8** as in **4** leads to a bathochromic shift ($\Delta\lambda \sim 10$ mμ); the relatively small effect may be attributed to the deviation from coplanarity.

The non-ketonic desaurin spectra listed in Table 3 are readily related to those of the ketonic desaurins discussed above. The high intensity, long wavelength maximum of **5** occurs at shorter wavelength than that of the analogous ketone **4** ($\Delta\lambda \sim -30$ mμ; *cf.* benzoic acid *vs.* acetophenone: $\Delta\lambda \sim -15$ mμ). The amides **20–22** also give maxima at shorter wavelength than the maximum of the analogous ketone **10** ($\Delta\lambda \sim -35$ mμ; *cf.* benzamide *vs.* acetophenone: $\Delta\lambda \sim -20$ mμ). The spectra of the keto amides **7** are clearly also closely related to the spectrum of the diketone **3**.

Experimental

Melting points were taken on a Fisher–Johns micro hot stage and are uncorrected. Solutions in organic solvents were dried over anhydrous sodium sulfate.

The Desaurin from Pinacolone (10)

Pinacolone (20.0 g, 0.200 mol) was added dropwise to a cooled, stirred suspension of sodamide (8.00 g, 0.2005 mol) in anhydrous ether. When anion formation was complete, carbon disulfide (6.0 ml, 0.100 mol) was added slowly, and the yellow suspension formed was stirred for a further 5 min. Methanol (*ca.* 50 ml) was added to dissolve the suspension, and oxalyl chloride (10.0 ml, 0.120 mol) was added with great caution. The solution was stirred for a further 0.5 h, then transferred to a separatory funnel, and water and benzene were added. The organic layer was separated and washed several times with aqueous 10% sodium hydroxide, once with water, and dried. After removal of the solvent, hexane was added to the residue, and the precipitate (1.0 g) was filtered off. Crystallization of the solid from chloroform–hexane gave **10** (0.50 g, 4%), m.p. *ca.* 258°. Four further recrystallizations from chloroform–hexane gave an analytical sample, m.p. 259.5–260° (corrected).

Anal. Calcd. for $C_{14}H_{20}O_2S_2$: C, 59.11; H, 7.09; S, 22.55. Found: C, 59.00; H, 7.09; S, 22.62.

Benzoyldithioacetic Acid (11)

Acetophenone (120.6 g, 1.00 mol) was added dropwise to a stirred suspension of commercial sodamide (39.0 g, 1.00 mol) in benzene (250 ml) at room temperature under nitrogen. When the brisk evolution of ammonia was nearly complete, the sodium derivative of acetophenone separated suddenly to form a thick off-white paste. Additional benzene (100 ml) was added to facilitate stirring, which was continued while the system was swept with nitrogen until the evolution of ammonia appeared to be complete (negative test with moist litmus paper).

Carbon disulfide (100 g, 1.31 mol) was added under a current of nitrogen, and the deep orange suspension was stirred for 1 h. The slurry was poured onto ice (300 g), and the mixture was stirred thoroughly; the benzene layer was separated and washed with three portions of aqueous 10% sodium hydroxide. The combined basic extracts and original aqueous layer were cooled to 5° and neutralized with ice-cold 10% sulfuric acid while the temperature was maintained below 10°. At the neutral point a red-brown mass separated, accompanied by a vigorous evolution of hydrogen sulfide. Excess acid was added, and the mixture was filtered. The crude solid acid was washed with ice-cold water and air-dried at room temperature. The yield of crude benzoyldithioacetic acid was 90 g (46%).

Two recrystallizations of the crude acid from petroleum ether (b.p. 30–60°) gave golden leaflets, m.p. 62–64°, satisfactory for further reactions. Two further recrystallizations afforded a sample, m.p. 62.5–64° [lit. (30) m.p. 63–64°]; $\lambda_{max}(CHCl_3)$ 3.9–4.2 (w), 6.25 (m), 6.29 (ms), 6.45 μ (s); $\lambda_{max}(C_2H_5OH)$ 231 (ε 9300), 266 (ε 7800), 355 mμ (ε 14 800).

Methylation of 11. Preparation of 12

(A) Benzoyldithioacetic acid (**11**; 2.00 g, 10.2 mmol) was methylated by treatment with sodium and methyl iodide by the method of Kelber (6). Two recrystallizations of the product from ethyl acetate – ligroin (b.p. 66–75°) gave **12** as bright yellow needles (0.80 g, 35%), m.p. 93.5–94.0°, [lit. (6) m.p. 93–94°]; $\delta(CDCl_3)$ 2.52 (s, 3H), 2.54 (s, 3H), 6.73 (s, 1H), 7.42 (m, 3H), 7.86 (m, 2H); the n.m.r. spectrum was unchanged when recorded at −60°.

(B) A solution of **11** (1.00 g, 5.1 mmol) in ether (25 ml) was treated with 0.6 *N* ethereal diazomethane (20 ml). The mixture was allowed to stand at room temperature for 3 days. The ether was then removed on the steam bath, and the residue was chromatographed on alumina (Merck; 75 g). A small amount of yellow oil (0.035 g) was eluted with 50% petroleum ether in benzene. The major yellow band was eluted with dichloromethane to give **12** (0.85 g, 74%). After crystallization from ethyl acetate – ligroin this had m.p. 93.0–93.5°, undepressed on admixture with the product obtained by the procedure of Kelber (6).

Alkylation of 11 with 1,2-Dibromoethane. Preparation of 13

Benzoyldithioacetic acid (**11**; 10.00 g, 51.0 mmol) was alkylated with 1,2-dibromoethane by the method of Kelber and Schwarz (9) to give **13** (6.0 g, 53%). Two recrystallizations from ligroin (b.p. 66–75°) afforded bright yellow needles, m.p. 83–83.5° [lit. (9) m.p. *ca.* 80°].

Alkylation of 11 with Dibromomethane. Preparation of 15

Benzoyldithioacetic acid (**11**; 5.00 g, 25.5 mmol) was

Can. J. Chem. Downloaded from www.nrcresearchpress.com by 210.87.254.6 on 09/05/12
For personal use only.

dissolved in water (100 ml) containing potassium hydroxide (6.00 g, 107 mmol). Dibromomethane (8.00 g, 59.7 mmol) was added, and the mixture was stirred at room temperature for 12 h and then extracted with four portions of dichloromethane. The combined extracts were dried, filtered, and stripped of the bulk of the dichloromethane on the steam bath. The crude product was dissolved in benzene (25 ml), and the solution was boiled briefly to expel dichloromethane, cooled, and chromatographed on alumina (Merck; 150 g). The major fraction was eluted immediately with benzene to give **15** as stout yellow needles (2.0 g, 38%). Three recrystallizations from cyclohexane afforded fine, pale cream needles, m.p. 128–129°.

Anal. Calcd. for $C_{10}H_8OS_2$ (mol. wt 208): C, 57.66; H, 3.97; S, 30.79. Found (241 (Rast)): C, 57.50; H, 3.73; S, 30.54.

Preparation of ***14***

Deoxybenzoin (10.00 g, 50.9 mmol) was dissolved in benzene (300 ml), sodamide (2.0 g, 51.2 mmol) was added, and the mixture was boiled under reflux under nitrogen with stirring for 12 h. The sodium derivative of deoxybenzoin separated as a pale yellow suspension, and ammonia could no longer be detected in the effluent (moist litmus paper test). The stirred suspension was cooled and carbon disulfide (4.00 g, 51.3 mmol) was added. Stirring was continued for 5 days at room temperature; the suspension gradually assumed an orange–red color.

One-half of this reaction mixture was treated with 1,2-dibromoethane (4.80 g, 25.6 mmol), and the resulting mixture was boiled under reflux under nitrogen with stirring for 2 days. The mixture was filtered, and the solvent was removed from the filtrate under reduced pressure to give an orange solid (3.53 g). This was dissolved in benzene and chromatographed on alumina (Merck; 100 g). The column was thoroughly eluted with benzene, to give a yellow semi-solid product (1.70 g), whose i.r. spectrum indicated it to be largely deoxybenzoin. Elution of the column with chloroform gave **14** as a yellow–orange solid (1.40 g, 18%). This was recrystallized four times from aqueous ethanol to give small yellow needles, m.p. 157.5–158°.

Anal. Calcd. for $C_{17}H_{14}OS_2$: C, 68.42; H, 4.73; S, 21.49. Found: C, 68.42; H, 4.79; S, 21.69.

Reduction of ***14*** *with Zinc and Base*

A mixture of **14** (0.100 g, 0.335 mmol), sodium hydroxide (1.00 g, 25 mmol), zinc dust (1.00 g, 15.3 mg-atoms), ethanol (10 ml), and water (20 ml) was boiled under reflux. After 2 days additional sodium hydroxide (1.00 g, 25 mmol) and zinc dust (0.50 g, 7.6 mmol) were added. After 5 days the solution was cooled, filtered, and extracted with dichloromethane. The extract was dried, filtered, and stripped of solvent on the steam bath to give a pale yellow oil (0.058 g), whose i.r. spectrum showed it to be largely *erythro*-1,2-diphenyl-1-propanol. This was treated with pyridine (2.0 ml) and acetic anhydride (1.0 ml), and the mixture was heated for 4 h on the steam bath. The solution was poured into water, acidified to p*H* 1 with 10% hydrochloric acid, and extracted with dichloromethane. The extract was dried, filtered, and evaporated to give a crystalline mass (0.038 g), which was recrystallized from ethanol to give fine, colorless cubes, m.p. 107–108.5°, undepressed on admixture with *erythro*-1,2-diphenyl-1-propyl acetate (1, 10). The i.r. spectra of the two samples were identical.

The aqueous basic layer from the original extraction was diluted to 75 ml with water and evaporated nearly to dryness under reduced pressure. Water (50 ml) and benzoyl chloride (2.0 ml) were added. The mixture was shaken until no further warming was apparent and then filtered. The white precipitate (0.032 g) was recrystallized from ethanol–water to give colorless prisms, m.p. 92–92.5°, undepressed upon admixture with 1,2-ethanedithiol dibenzoate [lit. (11) m.p. 94.5–95°]. The i.r. spectra of the two samples were identical.

The yields of *erythro*-1,2-diphenyl-1-propyl acetate and 1,2-ethanedithiol dibenzoate were 45 and 31%, respectively.

Preparation of ***31***

A solution of acetophenone (2.50 g, 20.8 mmol) in dioxane (40 ml) containing deuterium oxide (18 ml, 1.00 mol) and a catalytic quantity of anhydrous potassium carbonate was boiled under reflux for 1 h. When cool, the solution was extracted with ether, and the dioxane was removed from the ethereal solution by washing with water. The acetophenone obtained after removal of the solvent showed 75% exchange of the α-hydrogen atoms by n.m.r. spectroscopy. The treatment was repeated using sodium-dried dioxane, and the product was distilled to give acetophenone-2-d_3 with 92% of the α-hydrogen atoms replaced by deuterium.

Acetophenone-2-d_3 (0.120 g, 1.00 mmol) was added to a suspension of sodamide (0.030 g, 1.00 mol) in anhydrous benzene. When anion formation was complete, carbon disulfide was added in excess, and after 15 min the excess carbon disulfide was boiled off. Sodamide (0.039 g, 1.00 mmol) was added, followed by methyl iodide (0.280 g, 2.00 mmol), and the reaction mixture was stirred overnight. Water was added, and the organic layer was separated, dried, and stripped of solvent. Addition of hexane to the residue caused it to crystallize, and filtration gave crude **31** (0.040 g, 18%). Recrystallization of the crude material from ethyl acetate – pentane gave **31**, m.p. 92.5–93.5° (corrected), undepressed on admixture with **12**. The ratio of the intensity of the vinylic proton signal at δ 6.73 to the intensities of the methyl proton signals at δ 2.52 and 2.54 in the n.m.r. spectrum of **31** showed *ca.* 70% incorporation of deuterium at the vinylic position.

Infrared Spectral Intensity Measurements

The spectra were recorded with a Perkin–Elmer 521 Grating Infrared Spectrophotometer [linear in frequency (ν)], whose horizontal scale was expanded by a factor of 4. Absorption bands, measured by the machine as percent transmittance, were replotted on the absorbance (A) scale, and integrations were performed by the method of cutting out and weighing. The solution spectra were obtained in chloroform solution with the use of two 0.5 mm cells, with Teflon spacers; the path length of the sample cell was determined to be 0.501 mm by the method of Sutherland and Willis (31). Potassium bromide pellets were made by adding a weighed sample of the compound to *ca.* 250 mg of anhydrous potassium bro-

mide (Harshaw) in a "Wig-L-Bug"; the mixture was then ground for 3 min, and all pellets were pressed for identical times and at identical pressures; a blank pellet was placed in the reference beam.

The integrated intensities, B (mol l^{-1} cm^{-2}), for the solution spectra were obtained by the use of the formula:

$$B = \frac{1}{cl}\int A \, dv,$$

where c is the concentration in mol l^{-1} and l is the path length in cm. For the pellet spectra, since c = mol/(area of pellet $\times$ l), the formula becomes:

$$B = \frac{\text{area of pellet}}{\text{mol}}\int A \, dv$$

We thank the National Research Council of Canada for generous support of part of this work. D.R.M. thanks the Standard Oil Co. of Indiana, the Procter and Gamble Co., and the U.S. National Institutes of Health for fellowship support. T.R.L. thanks the National Research Council of Canada for fellowship support.

1. P. YATES, D. R. MOORE, and T. R. LYNCH. Can. J. Chem. This issue.
2. P. YATES, T. R. LYNCH, and L. S. WEILER. Can. J. Chem. **46**, 365 (1968).
3. (*a*) T. R. LYNCH, I. P. MELLOR, S. C. NYBURG, and P. YATES. Tetrahedron Lett. 373 (1967). (*b*) T. R. LYNCH. Ph.D. Thesis. University of Toronto, Toronto, Ontario, 1967.
4. A. J. KIRBY. Tetrahedron, **22**, 3001 (1966).
5. R. GOMPPER and W. TÖPFL. Chem. Ber. **95**, 2861 (1962).
6. C. KELBER. Ber. **43**, 1252 (1910).
7. R. GOMPPER and H. SCHAEFER. Chem. Ber. **100**, 591 (1967).
8. S. C. NYBURG. Private communication. I. P. MELLOR. Ph.D. Thesis. University of Keele, Keele, England, 1968.
9. C. KELBER and A. SCHWARZ. Ber. **44**, 1693 (1911).
10. F. A. A. ELHAFEZ and D. J. CRAM. J. Amer. Chem. Soc. **75**, 339 (1953).
11. S. MATHIAS. Bols. faculdade filosofia cienc. letras. Univ. São Paulo **14**, Quimica No. 1, 75 (1942); Chem. Abstr. **40**, 2792 (1946).
12. A. TULINSKY. Private communication. W. H. SCHMIDT and A. TULINSKY. Tetrahedron Lett. 5311 (1967).
13. J. A. KAPECKI, J. E. BALDWIN, and I. C. PAUL. Tetrahedron Lett. 5307 (1967); J. Amer. Chem. Soc. **90**, 5800 (1968).
14. A. THUILLIER and J. VIALLE. Bull. Soc. Chim. Fr. 2187 (1962).
15. (*a*) R. MECKE and K. NOACK. Spectrochim. Acta, **12**, 391 (1958); R. L. ERSKINE and E. S. WAIGHT. J. Chem. Soc. 3425 (1960). (*b*) K. NOACK and R. N. JONES. Can. J. Chem. **39**, 2225 (1961).
16. A. W. K. CHAN, W. D. CROW, and I. GOSNEY. Tetrahedron, **26**, 1493 (1970); W. D. CROW and I. GOSNEY. Aust. J. Chem. **22**, 765 (1969).
17. K. A. JENSEN and L. HENRIKSEN. Acta. Chem. Scand. **22**, 1107 (1968).
18. J. KOSSANYI. Compt. Rend. **256**, 5308 (1963).
19. P. YATES and D. R. MOORE. J. Amer. Chem. Soc. **80**, 5577 (1958).
20. R. N. JONES, D. A. RAMSAY, D. S. KEIR, and K. DOBRINER. J. Amer. Chem. Soc. **74**, 80 (1952).
21. (*a*) J. J. KIRKLAND. Anal. Chem. **27**, 1537 (1955). (*b*) R. J. BROWNING, S. E. WIBERLEY, and F. C. NACHOD. Anal. Chem. **27**, 7 (1955).
22. G. M. BARROW. J. Chem. Phys. **21**, 2008 (1953).
23. N. E. SHARPLESS and D. A. GREGORY. Appl. Spectrosc. **17**, 47 (1963).
24. K. BANERJEE and A. HAGUE. Ind. J. Phys. **12**, 87 (1938); Chem. Abstr. **32**, 8399 (1938).
25. B. E. WARREN and J. T. BURWELL. J. Chem. Phys. **3**, 6 (1935).
26. (*a*) L. BATEMAN and F. W. SHIPLEY. J. Chem. Soc. 1896 (1955). (*b*) H. N. A. AL-JALLO and E. S. WAIGHT. J. Chem. Soc., B, 73 (1966).
27. Y. MOLLIER, F. TERRIER, and N. LOZAC'H. Bull Soc. Chim. Fr. 1778 (1964); R. PINEL, Y. MOLLIER, and N. LOZAC'H. Bull. Soc. Chim. Fr. 1049 (1966).
28. J. A. KAPECKI and J. E. BALDWIN. J. Amer. Chem. Soc. **91**, 1120 (1969).
29. P. YATES and L. L. WILLIAMS. J. Amer. Chem. Soc. **80**, 5896 (1958).
30. C. KELBER and A. SCHWARZ. Ber. **45**, 137 (1912).
31. G. B. B. M. SUTHERLAND and H. A. WILLIS. Trans. Faraday Soc. **41**, 181 (1945).

Can. J. Chem. Downloaded from www.nrcresearchpress.com by 210.87.254.6 on 09/05/12
For personal use only.

Can. J. Chem. Downloaded from www.nrcresearchpress.com by 210.87.254.105 on 09/05/12
For personal use only.

Carbon Disulfide. IV. Reaction with Active Methylene Compounds. The Formation of 3,5-Bismethylene-1,2,4-trithiolanes[1]

PETER YATES AND THOMAS R. LYNCH
Department of Chemistry, Lash Miller Chemical Laboratories, University of Toronto, Toronto 5, Ontario

Received October 1, 1970

The three-sulfur compounds formed on oxidation of the β-keto dithio acids prepared by the reaction of active methylene compounds with base and carbon disulfide have been shown to be 3,5-bis(acylmethylene)-1,2,4-trithiolane derivatives. In several cases, two of the three possible geometrical isomers have been isolated and provisional stereochemical assignments have been made. The i.r. and u.v. spectra of the trithiolanes have been compared with those of corresponding 2,4-bis(acylmethylene)-1,3-dithietane derivatives (desaurins) and interpreted in terms of a strong conjugative interaction between the sulfur atoms and carbonyl groups.

Il a été démontré que les composés contenant des trois atomes du soufre et formés par oxydation des acides dithio β-cétoniques obtenus lors de la réaction du sulfure de carbone avec de la base et des composés contenant des méthylènes actifs sont des dérivés du bis(acylméthylène)-3,5 trithiolane-1,2,4. Dans plusieurs cas, deux des trois isomères géométriques possibles ont été isolés et des configurations stéréochimiques provisoires ont pu être attribuées. Les spectres infrarouge et ultraviolet des trithiolanes ont été comparés à ceux des dérivés bis(acylméthylène)-2,4 dithiétane-1,3(désaurines) correspondants et ont été interprétés en termes d'une interaction conjugative forte entre les atomes de soufre et les groupes carbonyles.

Canadian Journal of Chemistry, 49, 1477 (1971)

Introduction

In the course of our investigation of the desaurins (1), it was observed that during recrystallization of benzoyldithioacetic acid (**1**), the product obtained by treatment of acetophenone with base and carbon disulfide, an insoluble yellow material was obtained. This gave on further recrystallization yellow needles, m.p. 236–238° (dec.), with the formula $C_{18}H_{12}O_2S_3$.

Many years ago Wenzel (2, 3) had observed the formation of compounds containing three sulfur atoms when the sodium derivatives of active methylene compounds, such as diethyl malonate, were treated in carbon disulfide with bromine or iodine. These compounds were assigned structures of type **2** and were considered to arise via oxidation by the bromine of the salts of dithioacetic acids analogous to **1**.

Subsequently, Kelber (4) found that oxidation of the disodium salt of **1** with ammonium persulfate gave a three-sulfur compound, $C_{18}H_{12}O_2S_3$, m.p. 206–207°; he also obtained this compound by oxidation of **1** with iodine followed by recrystallization of the crude product from high boiling solvents, when hydrogen sulfide was eliminated. More recently, Gompper and Töpfl (5) have reinvestigated the oxidation by bromine, iodine, and ammonium persulfate of the disodium salts of dithio acids derived by reaction of active methylene compounds with carbon disulfide. In some cases they again obtained three-sulfur compounds, but in others two-sulfur compounds were isolated. The latter were shown to be desaurins (**3**)[2] (1); the former were assigned structures of type **4** on the basis of their chemical properties and the similarity of their spectra with those of the desaurins.

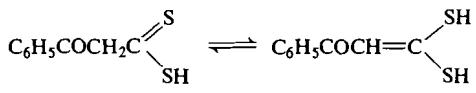

1

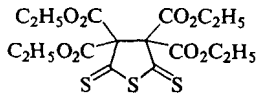

2

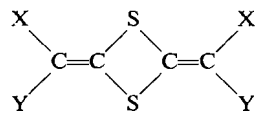

3

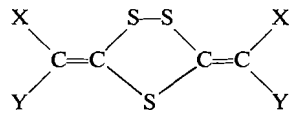

4

[1]For Paper III see ref. 1*a*.

[2]In this and subsequent structures, no assignment of configuration is implied, unless specifically discussed.

TABLE 1. The n.m.r. spectra of 3,5-bismethylene-1,2,4-trithiolanes

Compound*	R	R′	Solvent†	δ (p.p.m.)
19	$(CH_3)_3C$	Cl	C	1.33(s)
23	$(CH_3)_3C$	H	C	1.20(s, 18H), 6.95(s, 2H)
27*a*	*p*-$CH_3C_6H_4$	H	C	2.42(s, 6H), 7.29(d, J = 8.5 Hz, 4H) 7.48(s, 1H), 7.68(s, 1H) 7.89(d, J = 8.5 Hz, 4H)
27*b*	*p*-$CH_3C_6H_4$	H	S	2.47(s), 7.54(d, J = 8.5 Hz) 7.75(s), 7.98(d, J = 8.5 Hz)
28*a*	C_6H_5	H	C	7.5(m, 8H), 8.0(m, 4H)
28*b*	C_6H_5	H	S	7.9(m)
29*a*	C_6H_5	C_6H_5	C	7.3(m)
29*b*	C_6H_5	C_6H_5	S	7.40(br s)
30	Mesityl	H	C	2.17(s, 12H), 2.30(s, 6H), 6.83(s, 6H)

*See text for stereochemical assignments.
†C, Deuteriochloroform; S, 96% sulfuric acid.

Among the cases investigated by Gompper and Töpfl was that of the disodium salt of **1**; this on treatment with bromine gave in high yield a yellow crystalline compound, $C_{18}H_{12}O_2S_3$, m.p. 216–220° (dec.). We found that on repeated recrystallization from toluene the m.p. of the product formed in this reaction is raised to 236–238° (dec.) and that this m.p. is undepressed on admixture of the product with that obtained during our recrystallization of **1**; the spectra of the two products were also identical. It is thus clear that these products are the same and probable that our product was formed by air-oxidation during the recrystallization.

We embarked on a fuller study of these three-sulfur compounds for several reasons. First, to provide further evidence for the assignment of structure; although the spectral data excluded structures of type **2** for these compounds, they did not definitively establish structures of type **4**. Second, to examine the possibility of stereoisomerism among these compounds. Third, to examine in detail the relationship between their spectra and those of the desaurins.

Reactions and Structures of the Three-sulfur Compounds

The compound whose chemistry has been examined most extensively is that derived from pinacolone. This was prepared in 34% yield by the general method of Gompper and Töpfl (5) with the use of ammonium peroxydisulfate as oxidant. It was shown to have the molecular formula $C_{14}H_{20}O_2S_3$ by elemental analyses and mass spectrometry. Its n.m.r., i.r., and u.v. spectra are given in Tables 1–3; they are in accord with the assignment of a structure of type **8** and will be discussed subsequently.

Reduction of this substance with zinc and acetic acid gave three products. One was shown to be ethyl *t*-butyl ketone (**5**) by its i.r. and n.m.r. spectra and by the m.p. of its 2,4-dinitrophenylhydrazone.

One of the other products was a colorless, crystalline solid, $C_{14}H_{20}S_2$. Its i.r. spectrum showed a weak band at 6.15 μ, characteristic of ethylenic or aromatic bonds, and a doublet at 7.18 and 7.32 μ, assignable to *t*-butyl groups. Its n.m.r. spectrum exhibited two singlets at δ 1.40 (18H) and

TABLE 2. The i.r. spectra of the 3,5-bismethylene-1,2,4-trithiolanes

Compound*	Medium†	λ_{max} (μ)
19	C	6.25
23	C	6.18, 6.26(sh)
27*a*	N	6.23, 6.25, 6.43
27*b*	N	6.26, 6.42
28*a*	N	6.21, 6.26, 6.40
28*b*	N	6.26, 6.39
29*a*	N	6.25, 6.35, 6.44
29*b*	N	6.25, 6.35, 6.44
30	N	6.21, 6.29
36‡	U	6.19

*See Table 1 for structures of compounds.
†N, Nujol mull; C, chloroform; U, unspecified.
‡Reference 16.

Can. J. Chem. Downloaded from www.nrcresearchpress.com by 210.87.254.105 on 09/05/12
For personal use only.

TABLE 3. The u.v. spectra of 3,5-bismethylene-1,2,4-trithiolanes

Compound*	Solvent†	λ_{max} (mμ) (ε)
19	D	241(15 100), 352(19 500)
23	E	241(17 800), 339(19 500)
27*a*	C	282(21 400), 361(sh, 34 700) 378(39 800), 392(sh, 35 500)
27*b*	C	282(22 900), 372(sh, 32 400), 389(35 500)
28*a*	E	220(22 900), 268(21 400) 364(sh, 30 200), 378(33 900)
28*b*	E	228(20 900), 268(27 500) 370(sh, 28 800), 382(29 500)
29*a*	C	265(21 900), 392(32 400)
29*b*	C	265(25 100), 395(33 900)
30	E	247(10 000), 355(12 000)
36	E	232(15 200), 347(19 800)

*See Table 1 for structures of compounds.
†C, Chloroform; D, dioxane; E, 95% ethanol.

6.82 (2H). The high field signal could tentatively be assigned to two *t*-butyl groups in equivalent chemical environments; the position of the signal suggested that these groups might be attached to an aromatic ring system. The low field signal could then be due to two protons attached directly to this system in equivalent chemical environments. These spectral data, the origin of the compound, and the fact that its molecular formula requires the presence of a total of five double bonds and/or rings, suggested that it might be 2,5-di-*t*-butylthieno[3,2-*b*]thiophene (**6**).

$(CH_3)_3CCOCH_2CH_3$

5

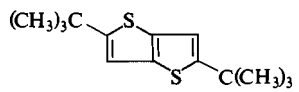

6

$(CH_3)_3CCOCH_2CH_2SCH_2CH_2COC(CH_3)_3$

7

Strong confirmatory evidence for the presence of the ring system was provided by the u.v. spectrum which exhibited maxima at 269 (ε 17 400) and 280 mμ (ε 12 600), while the parent compound, thieno[3,2-*b*]thiophene, has u.v. maxima at 259 (ε 12 600), 268 (ε 10 000), and 278 mμ (ε 10 000) (7). The related thieno[2,3-*b*]thiophene and thieno[2,3-*c*]thiophene systems, however, give u.v. spectra (8, 9) that differ markedly from the spectrum of the product.

Conclusive evidence for the presence of the thieno[3,2-*b*]thiophene system was afforded by the observation (10) that *t*-butylation of the parent compound gave, *inter al.*, a compound whose i.r. and n.m.r. spectra and m.p. were identical with those of our product; a mixture m.p. point showed no depression.[3] Given this proof of the nature of the aromatic nucleus of the compound $C_{14}H_{20}S_2$, the only structures other than **6** that can be entertained are the corresponding 2,3- and 3,5-di-*t*-butyl derivatives. The former is most unlikely to give the simple n.m.r. spectrum observed for this compound, and both, unlike **6** (*vide infra*), could arise only by a complex series of rearrangements. Structure **6** is thus preferred for this product.

The third reduction product was an oil, which gave a yellow bis-2,4-dinitrophenylhydrazone, $C_{26}H_{34}N_8O_8S$. The formula of the oil was thus indicated to be $C_{14}H_{26}O_2S$, indicating that it is acyclic and has no double bonds other than those of the two carbonyl groups. Its i.r. spectrum showed a single carbonyl-stretching band at 5.84 μ. Its n.m.r. spectrum in carbon tetrachloride solution showed two singlets at δ 1.14 (18H) and 2.67 (8H); this simplicity was deceptive, however, since in benzene solution the lower-field signal appeared as a symmetrical multiplet at δ 2.62. On the basis of these data, structure **7** is assigned to this product; this was confirmed by the fact that on desulfurization with Raney nickel it gave **5**.

The formation of the three reduction products **5**, **6**, and **7** from the three-sulfur compound can readily be interpreted in terms of the assignment

[3]We thank Professor S. Gronowitz, University of Lund, for undertaking this synthesis and carrying out the mixture m.p. determination.

Can. J. Chem. Downloaded from www.nrcresearchpress.com by 210.87.254.105 on 09/05/12
For personal use only.

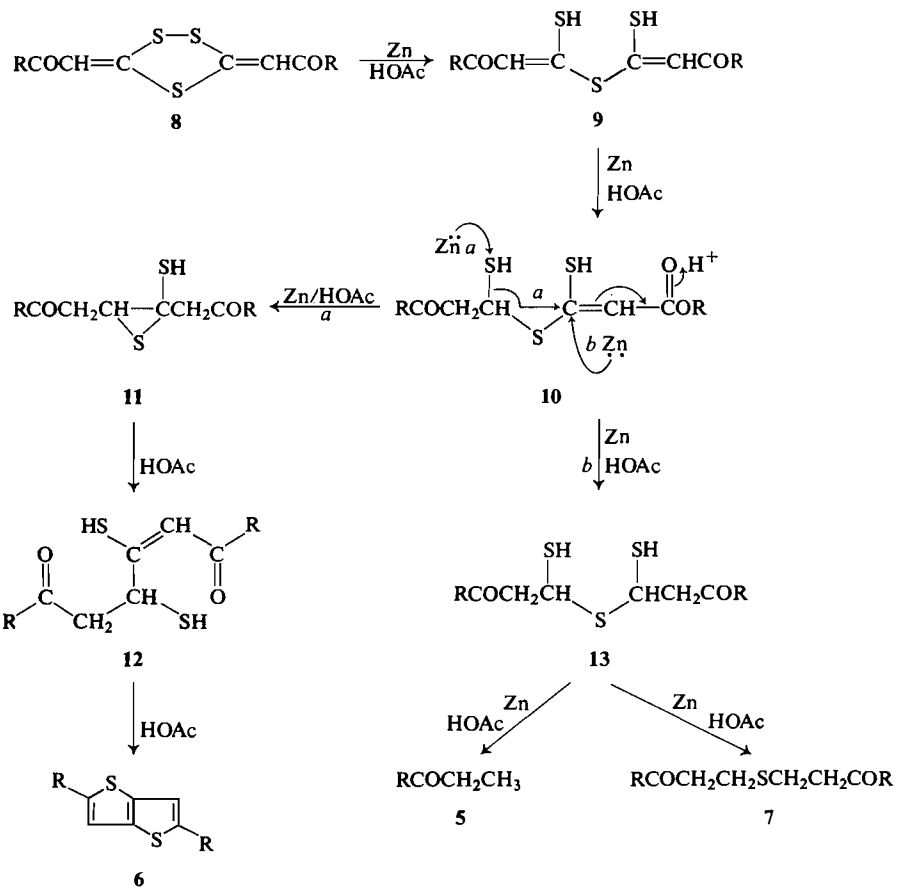

SCHEME 1

to it of a structure, **8**, of the type proposed by Gompper and Töpfl (Scheme 1). Reduction of the disulfide link would lead to **9**, which would give **10** on reduction of one of the α,β-unsaturated carbonyl systems (or of its thione tautomer). Reductive carbon–carbon bond formation as in path *a* could then lead to **11**,[4] which after ring cleavage to **12** followed by dehydration would give **6**. Alternatively, **10** could undergo reduction of its remaining α,β-unsaturated ketone system (or of its thione tautomer) to give **13**, which on further reduction would give **5** and **7**.

Reaction of the three-sulfur compound with phosphorus pentasulfide in boiling xylene gave a compound $C_7H_{10}S_3$, m.p. 69.0–69.5°. This product showed no bands in the 5–6.5 μ region of its i.r. spectrum. Its n.m.r. spectrum showed two singlets at δ 1.43 (9H) and 7.18 (1H). These data showed the product to be 5-*t*-butyl-1,2-dithiole-3-thione (**14**) (11). This structural assignment was corroborated by the similarity of the product's u.v. spectrum with that of **15** (12). The yield of **14**

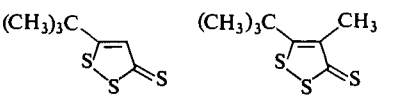

14 **15**

was 56%, based on the formation of 2 mol from 1 mol of the original three-sulfur compound. This reaction can again be readily interpreted in terms of the assignment of structure **8** to the latter compound (Scheme 2). Conversion of the diketone in the usual fashion to the corresponding dithione **16** could be followed by processes (**17** and **18**, arrows) that lead to two molecules of **14**.

[4] *Cf.* the occurrence of C—C bond formation in the nickel reduction of the desaurin derived from deoxybenzoin (1).

Can. J. Chem. Downloaded from www.nrcresearchpress.com by 210.87.254.105 on 09/05/12
For personal use only.

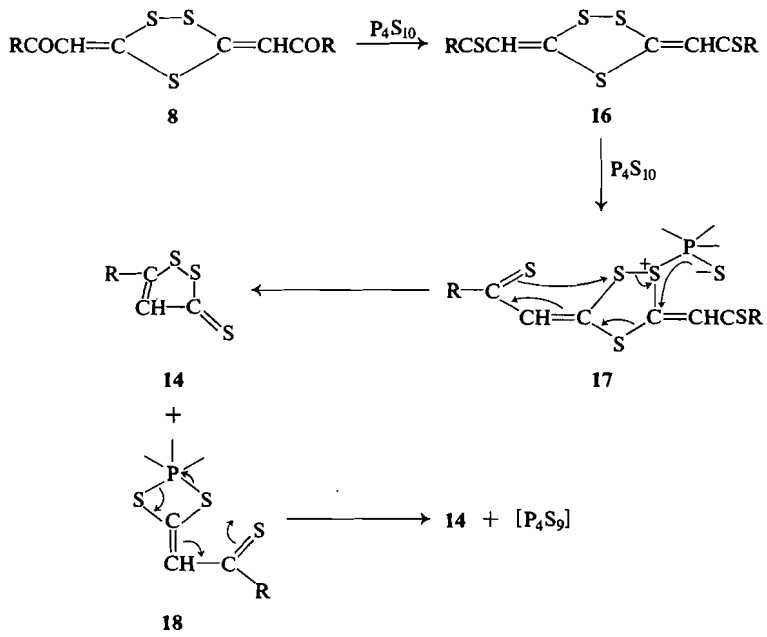

SCHEME 2

Reaction of **8** with phosphorus pentachloride gave a product, $C_{14}H_{18}Cl_2O_2S_3$. The u.v. spectrum of this product indicated that the original chromophore was intact (*vide infra*). Its n.m.r. spectrum showed only a singlet at δ 1.33. These data are clearly in accord with the assignment to this product of structure **19**, in which the vinyl hydrogen atoms are replaced by chlorine atoms. A related substitution reaction has been reported recently (13) in which treatment of the desaurin **20** with bromine gives **21**.

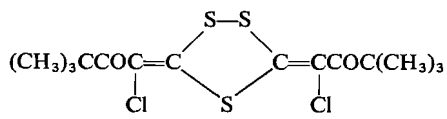

19

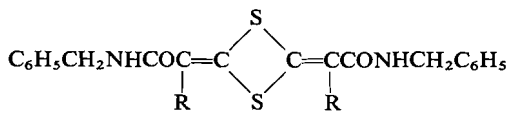

20 R = H
21 R = Br

Thus, these reactions of the three-sulfur compound from pinacolone can all be interpreted in terms of structure **8**. The only possible alternative appears to be the 2,4-bismethylene-1-thiono-1,3-dithietane, **22**. However, branched bonding at sulfur is unlikely in the present case. Such bonding appears to occur only in cases where the sulfur atom to which the branch is attached is also bonded to highly electronegative atoms (14). The assignment of structure **8** has subsequently been confirmed by an X-ray crystallographic study by Nyburg and Mellor (15), which has shown the compound to have the structure, configuration, and conformation shown in **23**.

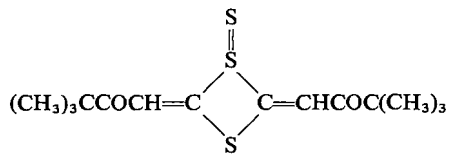

22

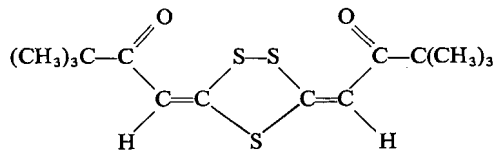

23

Compounds with the gross structure **4** can exist as three geometrical isomers: *trans* (**24***a*), *cis*$_2$

Can. J. Chem. Downloaded from www.nrcresearchpress.com by 210.87.254.105 on 09/05/12
For personal use only.

(**24***b*), and *cis*$_1$ (**24***c*).[5] As expected on the basis of the assignment of the *cis*$_2$ configuration **23** to the trithiolane from pinacolone, this compound shows a single vinyl proton signal in its n.m.r. spectrum (Table 1). The n.m.r. spectrum of the crude product and that of a sample recovered after solution of the pure product in 96% sulfuric acid and quenching on ice showed an additional, weak signal at δ 7.10, indicating the presence of a second geometrical isomer. Attempts to isolate this were unsuccessful, however.

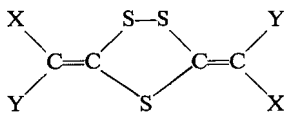

24*a*

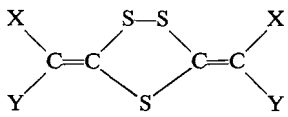

24*b*

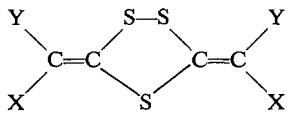

24*c*

More success was met in the case of the product from *p*-methylacetophenone. Two isomeric trithiolanes, $C_{20}H_{16}O_2S_3$, were obtained. The major product was insoluble in chloroform and had m.p. 251–252°, while the minor product was chloroform-soluble and had m.p. 213.5–214.5°. The i.r. and u.v. spectra of these products (Tables 2 and 3) were in accord with the assignment of structures analogous to that of the trithiolane from pinacolone. Furthermore, reduction of the higher-melting isomer with zinc and acetic acid followed by lithium aluminum hydride gave 1-*p*-tolyl-1-propanol (**25**), confirming the assigned carbon skeleton, and treatment with phosphorus pentasulfide gave a product, $C_{10}H_8S_3$, whose spectra (see Experimental) showed it to be **26**, the analog of **14**.

The n.m.r. spectrum ($CDCl_3$) of the lower-melting isomer (Table 1), showed in addition to

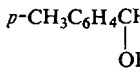

25

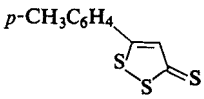

26

signals attributable to the *p*-tolyl protons, two singlets at δ 7.48 and 7.68 that can be assigned to the vinyl protons. This isomer must therefore be the *trans* compound **27***a*, since this is the only one of the three isomers of type **24***a–c* that has chemically non-equivalent vinyl protons. The two *p*-tolyl rings in **27***a* also are non-equivalent; however the difference between their environments must be too small to lead to differentiation of their proton signals. The n.m.r. spectrum of the higher-melting isomer could not be taken in conventional solvents because of its insolubility. Its spectrum in 96% sulfuric acid showed in addition to *p*-tolyl proton signals a singlet at δ 7.75 attributable to the vinylic protons. This is in accord with the assignment to it of either a *cis*$_2$ or *cis*$_1$ structure, each of which has chemically equivalent vinyl protons.[6] No firm basis for choice between their two structures is available, but the *cis*$_2$ structure **27***b* is provisionally assigned by analogy with **23**.

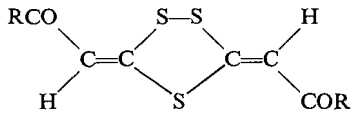

27*a* R = *p*-$CH_3C_6H_4$
28*a* R = C_6H_5

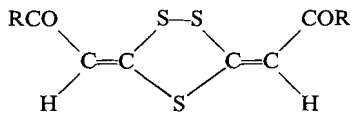

27*b* R = *p*-$CH_3C_6H_4$
28*b* R = C_6H_5

When the lower melting isomer was heated under nitrogen at 225° it was converted to the higher-melting isomer. The observation that thermal interconversion of one isomer to another can occur and that the higher-melting isomer is favored provides some evidence that this isomer has the *cis*$_2$ rather than the *cis*$_1$ structure. For it has been found that in this type of compound there is an attractive interaction between the oxy-

[5]In the general case the designations *cis*$_1$ and *cis*$_2$ are arbitrary. However for all the cases examined by us, X = RCO ≠ Y, and we define **24***b* as *cis*$_2$ (RCO groups *cis* to two-sulfur bridge) and **24***c* as *cis*$_1$ (RCO groups *cis* to one-sulfur bridge).

[6]The use of sulfuric acid as solvent leads to the possibility of isomerization in solution (*vide supra*); however, in this case there was no spectral evidence of such isomerization, and the higher-melting isomer was recovered unchanged on quenching the solution on ice.

Can. J. Chem. Downloaded from www.nrcresearchpress.com by 210.87.254.105 on 09/05/12
For personal use only.

Can. J. Chem. Downloaded from www.nrcresearchpress.com by 210.87.254.105 on 09/05/12
For personal use only.

gen and sulfur atoms (1, 15),[7] and it may be anticipated that the cis_2 isomer will be more stable than the cis_1 isomer because the two oxygen atoms interact with a common sulfur atom in the latter case while in the former they interact with two different sulfur atoms.

The observation that two isomeric trithiolanes are formed from *p*-methylacetophenone led us to reexamine the case of acetophenone. As has been discussed previously, the major product, $C_{18}H_{12}O_2S_3$, has m.p. 236–238° (dec.). Work-up of the mother liquors from the crystallization of this compound led to the isolation of a more soluble, isomeric compound, m.p. 167.5–168.5°. The vinylic proton signals in the n.m.r. spectra of both isomers are embedded in the aromatic proton multiplets and do not serve to distinguish between the isomers in this case. A tentative assignment of stereostructures **28***a* and *b* to the lower- and higher-melting isomers is made on the basis of the m.p. and solubility relationships and analogy with **23**. The fact that the lower-melting isomer resolidified above its m.p. and melted again with decomposition at *ca.* 225° strongly indicates that thermal conversion of the lower- to the higher-melting isomers occurs in this case also.

A third instance of the formation of two stereoisomeric trithiolanes was observed in the case of deoxybenzoin. The major product, $C_{30}H_{20}O_2S_3$, m.p. 277–278° (dec.), was accompanied by a minor, isomeric, more soluble product, m.p. 219–220°. Since these products lack vinyl hydrogen atoms, the *trans* isomer cannot be recognized by n.m.r. spectroscopy. A tentative assignment of stereostructures **29***a* and *b* to the lower- and higher-melting isomers, respectively, is again made on the basis of the m.p. and solubility relationships and analogy with **23**.

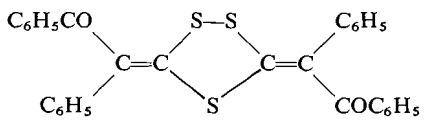

29*a*

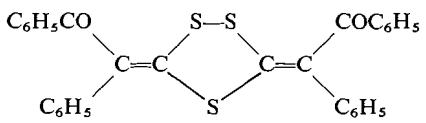

29*b*

From mesityl methyl ketone only a single trithiolane, $C_{24}H_{24}O_2S_3$, was obtained. Its n.m.r. spectrum (Table 1) showed a single low-field singlet attributable to superimposition of the signals due to both the vinylic and phenyl protons. Thus this is most probably a *cis* stereoisomer and it is provisionally assigned the stereostructure **30** by analogy.

We conclude this discussion of the reactions and structures of the 3,5-bismethylene-1,2,4-trithiolanes by noting that two reactions have been reported in which these compounds are converted to desaurins, *i.e.*, 2,4-bismethylene-1,3-dithietanes (**3**) (1). Wenzel (3) observed that saponification of the trithiolane **31** with sodium hydroxide in ethanol followed by acidification gave the desaurin **33**.[8] This transformation most probably involves the reductive cleavage of the disulfide linkage by the alcoholic base (*cf.* Scheme 1, **8** → **9**) to give **32** followed by closure to the desaurin with elimination of sulfide ion (Scheme 3).

More recently, Kirby (16) has converted the trithiolane **36** to the desaurin **37** by treatment with boiling triethyl phosphite. The trithiolane **36** was obtained by an analogous, novel method, *viz.*, reaction of triethyl phosphite with the tetrathiane **35** at room temperature (or by heating **35** in boiling toluene). The tetrathiane **35** (16, 17) was obtained by reaction of **34**, the adduct of biacetyl and trimethyl phosphite with carbon disulfide (Scheme 4).

Spectra of the 3,5-Bismethylene-1,2,4-trithiolanes[9]

Aspects of the n.m.r. spectra of the trithiolanes have already been discussed in the discussion of stereochemistry. It remains here to comment that the expected relationship between the vinylic proton signals in the spectra of the alkyl ketone **23** and the aryl ketones **27***b* and **28***b* holds in that the former appears at δ 6.95, while the latter are shifted to lower field (δ 7.4–7.7). Further, the mesityl ketone **30** more closely resembles the alkyl ketone than the other aryl ketones in this respect, as anticipated to result from a considerable departure from coplanarity of the mesityl and α,β-unsaturated carbonyl systems (18). It is of interest to note that the vinylic proton signals of

[7]Nyburg and Mellor (15) have found the shortest S—O distances (2.51 Å) in **23** to be markedly smaller than the sum of the van der Waals' radii of sulfur and oxygen (*cf.* ref. 1).

[8]The desaurin was originally considered to be a cyclobutane-1,2-dithione on the basis of the erroneous assignment of structure **2** to the trithiolane (3).

[9]For a discussion of the mass spectra of several 3,5-bismethylene-1,2,4-trithiolanes see ref. 6.

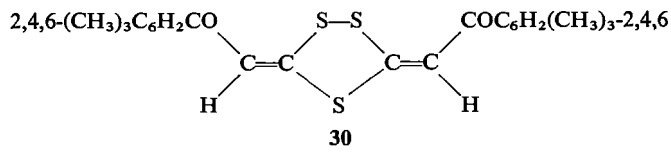

30

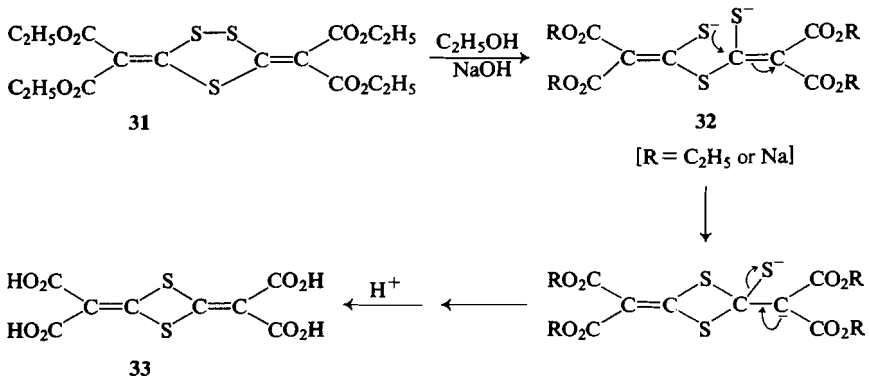

SCHEME 3

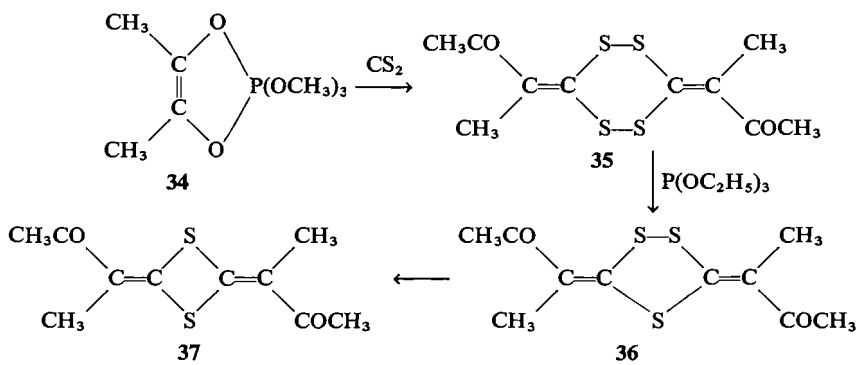

SCHEME 4

27*b* and **28***b* in sulfuric acid are only at slightly lower field than those of **27***a* and **28***a* in deuteriochloroform. Presumably, the species present in the sulfuric acid solutions are cations of type **38** (or the corresponding dications). Protonation of simple α,β-unsaturated ketones normally causes a shift of 0.6–1.0 p.p.m. to lower field of the α-vinylic proton signal (19, 20), *e.g.* protonated mesityl oxide (**39**) shows this signal at δ 6.96 (19) ($\Delta\delta$ = 1.0). The n.m.r. data in the present case indicate that the positive charge is more extensively delocalized, thus reducing the effect on the vinylic proton.

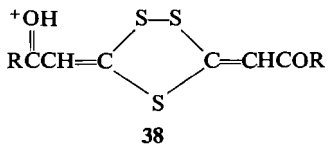

38

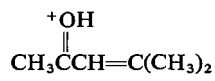

39

Bands in the 5–6 μ region of the i.r. spectra of the trithiolanes are listed in Table 2. These bands resemble those in this region in the spectra of the

Can. J. Chem. Downloaded from www.nrcresearchpress.com by 210.87.254.105 on 09/05/12
For personal use only.

Can. J. Chem. Downloaded from www.nrcresearchpress.com by 210.87.254.105 on 09/05/12
For personal use only.

desaurins (1) in that the carbonyl-stretching bands are at unusually long wavelength and often appear to be unusually weak. The trithiolanes **23** and **36** of type **40** (R′ = H or alkyl) have their carbonyl-stretching band at 6.18–6.19 μ.[10] This represents a significant shift to longer wavelength relative to the corresponding desaurins. It is possible that this shift is related to the fact that the S—O distance in the trithiolane **23** has been found to be shorter than that in one of the desaurins (15). In more general terms, the geometry of the trithiolanes may be more favorable for delocalization of the unshared electrons on sulfur than that of the dithietanes. It is noteworthy that the carbonyl-stretching band of **19**, in which the vinylic hydrogen atoms of **23** are replaced by chlorine atoms, is shifted to 6.25 μ. In the case of cyclic enones substitution of chlorine for α-vinyl hydrogen usually causes a shift of the carbonyl-stretching band to lower wavelength (21). The present result can be interpreted as due to the existence of **19** in an *s-cis* conformation; the dipoles of the carbon–halogen bonds would then facilitate the stretching of the carbonyl bonds, in contrast to their effect in the *s-trans* cyclic enones.

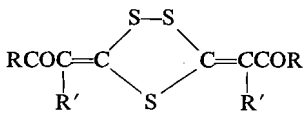

40 R = alkyl
41 R = aryl

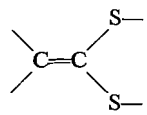

42

As in the case of the desaurins, the carbonyl-stretching bands of compounds of type **27** and **28** with an aryl group in conjugation with the carbonyl group (**41**) are moved to longer wavelength. Again they occur at longer wavelength than in the case of the corresponding desaurins. Their range cannot readily be defined because of overlap with aromatic stretching vibrations; the lower wavelength limit, however, is 6.21 μ. Compound **30**, the mesityl derivative falls at this lower limit as expected, due to departure from coplanarity of the aryl rings and the carbonyl groups (18). Another feature of the trithiolane spectra that resembles those of the desaurins is the occurrence of strong or very strong bands in the region 6.8–7.2 μ.[11] These are probably similar in origin to strong bands observed in the 6.5–7.0 μ region of the spectra of the desaurins and related two-sulfur compounds (1, 22). These have been assigned by Jensen and Henriksen (22) to the ν_1 vibration of the grouping **42**. As previously noted (1), this assignment must be considered as provisional because strong bands due to aromatic C—C stretching and aliphatic C—H bending vibrations can also occur in this region.

Examination of the i.r. spectra of the trithiolanes suggests that the carbonyl-stretching bands have unusually weak intensities relative to other bands in the spectra, as in the case of the desaurins (1). Measurement of the integrated absorption intensity for **27***a* in chloroform solution gave a value of 4.17, *i.e.*, 2.09 per carbonyl group, and for **27***b* in a potassium bromide disc a value of 2.24, *i.e.*, 1.12 per carbonyl group.[12] These values are comparable with those for benzophenone in chloroform and in a potassium bromide disc, *i.e.*, 2.35 and 1.20, respectively. The apparent abnormal weakness of the carbonyl-stretching bands observed on qualitative examination of the spectra is presumably due to the presence of unusually strong bands in other regions of the spectra and the fact that most of the spectra were recorded in the solid state.[13] In the case of planar chromophores, conjugation with an ethylenic double bond or aromatic ring brings about an increase in the carbonyl-stretching band intensity (23, 25). While the positions of the carbonyl-stretching bands of **27***a* and *b* show a considerably higher degree of conjugation than that in benzophenone, their integrated intensities per carbonyl group are slightly lower than the intensity of the carbonyl-stretching band of benzophenone. Thus, there does in fact appear to be a significant reduction in intensity relative to simple conjugated ketones when carbonyl groups are conjugated with the grouping **42**. As for the desaurins (1), this may be due to an interaction through space between the sulfur and oxygen atoms (15) in these compounds.

The u.v. maxima of the trithiolanes are listed in Table 3. The spectra of compounds **19**, **23**, and **36**

[10]The actual range may extend to slightly longer wavelength, since the shoulder at 6.26 μ in the spectrum of **23** suggests that the carbonyl-stretching band in this case may be split (*cf.* ref. 1).

[11]Although most of the spectra were recorded in Nujol mulls, it is clear that strong absorption due to the sample is superimposed on the Nujol absorption in this region.

[12]See ref. 1 for details of these integrated intensity measurements; the values are given in absorbance units (23), *i.e.*, 1×10^4 mol^{-1} l cm^{-2}.

[13]It has previously been found that absorptivities are less in the solid state than in solution (24).

Can. J. Chem. Downloaded from www.nrcresearchpress.com by 210.87.254.105 on 09/05/12
For personal use only.

of type **40** (R′ = H, CH_3, or Cl) have a high intensity long wavelength maximum at 339–352 mμ (ε 19 500 – 19 800) and another maximum at 232–241 mμ (ε 15 100 – 17 800). These may be compared with the spectra of analogous desaurins which have maxima at 350–370 mμ (ε 28 700 – 29 500) and *ca.* 242 mμ (ε 1440–2510) (1, 16), and of the related compound **43**, which has maxima at 317 (ε 8950) and 243 mμ (ε 5360) (16, 26). The relationship among these spectra is consistent with transmission of delocalization through one or more of the sulfur atoms in the trithiolanes, but to a lesser extent than in the desaurins (13, 16). This reduction most probably reflects reduced transmission through the disulfide linkage relative to that through the single sulfide linkage. The relationship among the spectra of **19**, **23**, and **36** is in accord with expectation in that substitution of alkyl groups or chlorine atoms for vinylic hydrogen atoms leads to a bathochromic shift of the long wavelength maximum.

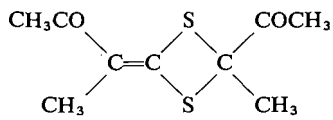

43

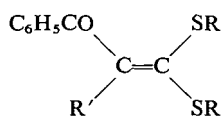

44 R = CH_3 or $(CH_2)_n$

The stereoisomers of the trithiolanes **27**, **28**, and **29** of type **41** show maxima in their u.v. spectra at 378–395 mμ (ε 29 500 – 35 500) and 265–282 mμ (ε 21 400 – 27 500). The bathochromic and hyperchromic shifts of the long wavelength maxima relative to those of the trithiolanes of type **40** clearly reflect the additional conjugation of the carbonyl groups with the phenyl groups. Again, the spectra give evidence of transmission of delocalization through one or more of the sulfur atoms [*cf.* the spectra of the related compounds of type **44**: λ_{max} 344–350 mμ (ε 15 800 – 22 900) and 257–263 mμ (ε 7940 – 14 500) (1)], but indicate that this is less than in the case of the related desaurins [λ_{max} 392–419 mμ (ε 38 100 – 49 000) and 266–274 mμ (ε 17 000 – 22 900) (1)]. The relationship among the spectra of the stereoisomers of **27**, **28**, and **29** is analogous to that in the case of the related desaurins in that substitution of phenyl groups for vinylic hydrogen atoms leads to a bathochromic shift of the long wavelength maximum. The relationship between the spectra of each pair of stereoisomers indicates that the *cis* isomers have long wavelength maxima at somewhat longer wavelengths than the corresponding *trans* isomers; the relationship is clouded, however, by the fact that the long wavelength maxima can show shoulders at either shorter or longer wavelength.

The trithiolane **37** of type **41**, but with R = mesityl, has a u.v. spectrum that more closely resembles the spectra of the trithiolanes of type **40** than the spectra of the other trithiolanes of type **41**. This difference is readily attributable to the usual marked departure from coplanarity of the aryl ring and the carbonyl group in mesitoyl derivatives (18).

Experimental

Melting points were taken on a Fisher-Johns micro hot stage and are corrected. Solutions in organic solvents were dried over anhydrous sodium sulfate. The n.m.r., i.r., and u.v. spectroscopic data for the trithiolanes are listed in Tables 1–3 in the text.

Preparation of the Trithiolane ***23*** *(≡* ***8****) from Pinacolone*

Pinacolone (5.00 g, 50.0 mmol) was added dropwise to a stirred suspension of sodamide (1.95 g, 50.0 mmol) in anhydrous ether (40 ml) cooled in ice. When anion formation was complete, carbon disulfide (1.50 ml, 25.0 mmol) was added slowly. The bright yellow precipitate that formed was dissolved by the addition of methanol (5 ml). Ammonium peroxydisulfate (5.70 g, 25 mmol) in water was then added slowly, and, when the addition was complete, the solution was stirred for a further 0.5 h and filtered. The solid was dissolved in chloroform, the solution was filtered and dried, and the solvent was removed to give **8** (**23**) as a pale yellow solid (1.34 g, 34%), m.p. 202–204°. Five crystallizations from chloroform–hexane gave fine, very pale yellow needles, m.p. 211.5–212.5°.

Anal. Calcd. for $C_{14}H_{20}O_2S_3$: C, 53.12; H, 6.37; S, 30.39. Found: C, 53.23; H, 6.22; S, 30.24.

Reduction of ***8*** *with Zinc and Acetic Acid*

A mixture of **8** (6.80 g, 21.5 mmol), zinc dust (21.3 g, 325 mg-atoms), and glacial acetic acid was boiled under reflux with stirring for 5 h. After cooling, the reaction mixture was diluted with ether and filtered, and the filtrate was washed with water until free of acetic acid. The ethereal solution was dried, and the solvent was removed by careful distillation until only a few milliliters remained. The residual solvent and the volatile product were removed by distillation at 80° (10 mm) into a series of Dry Ice traps. Distillation of the material in the traps gave ethyl *t*-butyl ketone (**5**; 1.78 g, 36%), b.p. 120–125°, identified by its i.r. and n.m.r. spectra, and the formation of a 2,4-dinitrophenylhydrazone, m.p. 144.5–146° [lit. (27) m.p. 143.5–144.5°].

Can. J. Chem. Downloaded from www.nrcresearchpress.com by 210.87.254.105 on 09/05/12
For personal use only.

The non-volatile material (2.2 g) was chromatographed on silica gel. Elution with 2% benzene-pentane gave **6** as a white crystalline solid (0.10 g), m.p. 161.5–162°, after two sublimations at 100° (15 mm); $\lambda_{max}(CCl_4)$ 6.15 (w), 6.7 (w), 6.85 (m), 7.18 (w), 7.32 μ(w); $\lambda_{max}(C_2H_5OH)$ 269 (ε 17 400), 280 mμ (ε 12 600); δ (CCl_4) 1.40(s, 9H), 6.82(s, 1H); *m/e* = 252 (mol. ion; 33.5%), 237 (100%), 222 (16.3%), 207 (9%).

Anal. Calcd. for $C_{14}H_{20}S_2$: C, 66.61; H, 7.99; S, 25.41. Found: C, 66.47; H, 7.94; S, 25.24.

The third reduction product, **7**, was obtained as an oil (2.0 g) by elution of the column with 2–5% ether–benzene. Purification was effected by further chromatography followed by molecular distillation at 70° (0.2 mm); $\lambda_{max}(CCl_4)$ 5.84 (s), 6.76 (m), 7.18 (w), 7.31 μ(m); δ (CCl_4) 1.14 (s, 18H), 2.67 (s, 8H); δ (C_6H_6) 0.93 (s), 2.62 (m).

A bis-2,4-dinitrophenylhydrazone was prepared by the method of Shriner *et al.* (28) and purified by five crystallizations from ethanol – ethyl acetate; m.p. 196–197.5°.

Anal. Calcd. for $C_{26}H_{34}N_8O_8S$: C, 50.47; H, 5.54; N, 18.11; S, 5.18. Found: C, 50.62; H, 5.52; N, 17.86; S, 5.35.

*Desulfurization of **7** with Raney Nickel*

A mixture of **7** (0.19 g, 0.720 mmol) and W-2 Raney nickel (*ca.* 2 g) in ethanol (15 ml) was boiled under reflux for 3.25 h under a slow stream of nitrogen. Nitrogen was bubbled through the solution for a short time after it had cooled to remove any acetaldehyde present. The solution was filtered, and the filtrate was treated with an excess of 2,4-dinitrophenylhydrazine reagent (28). After standing overnight, the mixture was filtered to give the 2,4-dinitrophenylhydrazone of ethyl *t*-butyl ketone (0.082 g, 20%), m.p. 136–138°. One crystallization from 95% ethanol gave crystals, m.p. 142–143°, undepressed upon admixture with an authentic sample, m.p. 144.5–146°.

*Reaction of **8** with Phosphorus Pentasulfide. Formation of **14***

A mixture of **8** (0.54 g, 1.70 mmol) and phosphorus pentasulfide (1.00 g, 2.30 mmol) in *p*-xylene (40 ml) was boiled under reflux for 2 h. When cool, the dark solution was washed successively with aqueous 10% potassium hydroxide, aqueous 10% hydrochloric acid, and water and dried. The solvent was removed and the crude product was crystallized from hexane to give **14** as yellow needles (0.37 g, 56%), m.p. 69.0–69.5, after three crystallizations from methanol; $\lambda_{max}(CHCl_3)$ 6.84 (m), 7.31 μ(s); $\lambda_{max}(C_2H_5OH)$ 230 (ε 9600), 246 (ε 5900), 268 (ε 6900), 317 mμ (ε 4400), 408 mμ (11 000); δ ($CDCl_3$) 1.43 (s, 9H), 7.18 (s, 1H).

Anal. Calcd. for $C_7H_{10}S_3$: C, 44.17; H, 5.30; S, 50.54. Found: C, 44.21; H, 5.30; S, 50.46.

*Reaction of **8** with Phosphorus Pentachloride. Formation of **19***

Compound **8** (0.100 g, 0.316 mmol) was mixed with phosphorus pentachloride (0.150 g, 0.680 mmol) and the mixture was heated at 140–145° under nitrogen for 50 min. Water and chloroform were added to the dark yellow product after it had cooled, and the organic layer was washed several times with water and dried. Removal of the solvent and crystallization of the residue from acetone gave **19** as pale yellow needles (0.040 g, 35%), m.p. 222.5–223.5° after three further crystallizations from acetone.

Anal. Calcd. for $C_{14}H_{18}Cl_2O_2S_3$: C, 43.63; H, 4.71; Cl, 18.40; S, 24.96. Found: C, 43.78; H, 4.75; Cl, 18.50; S, 24.56.

*Preparation of the Trithiolanes **27a** and **b** from p-Methylacetophenone*

p-Methylacetophenone (6.70 g, 50.0 mmol) in anhydrous ether (10 ml) was converted to a mixture of **27*a*** and ***b*** by the method used for the preparation of **23**. The resulting yellow solid (3.87 g, 80%) was washed with water and methanol, air-dried, and heated briefly in chloroform. The insoluble material was filtered off, and the filtrate was retained. The chloroform-insoluble material was recrystallized five times from toluene to give **27*b***, m.p. 251–252°.

Anal. Calcd. for $C_{20}H_{16}O_2S_3$: C, 62.47; H, 4.19; S, 25.02. Found: C, 62.55; H, 4.49; S, 24.81.

Evaporation of the chloroform filtrates to dryness gave a yellow solid, which was crystallized from benzene to give yellow crystalline clumps, m.p. 210–212° (0.60 g, 13%). Four recrystallizations from benzene gave **27*a***, m.p. 213.5–214.5°.

Anal. Calcd. for $C_{20}H_{16}O_2S_3$: C, 62.47; H, 4.19; S, 25.02. Found: C, 62.73; H, 4.20; S, 24.90.

Compound **27*a*** (0.027 g) was heated at 225° for 3 min. After cooling, the reddish solid was crystallized twice from toluene to give yellow needles (0.018 g, 66%), m.p. 249–251°, undepressed on admixture with **27*b***.

*Reduction of **27b**. Formation of **25***

Compound **27*b*** (3.14 g, 8.10 mmol) and zinc dust (18.5 g) were suspended in glacial acetic acid (50 ml), and the mixture was boiled under reflux with stirring for 6 h. When the mixture had cooled, ether was added, and the acetic acid was removed by washing with water. Removal of the solvent gave a yellow oil (1.94 g) which was chromatographed on silica gel. Fractions eluted with ether–benzene mixtures were combined and evaporated. The product was treated with excess lithium aluminum hydride in anhydrous ether, and the oil obtained was chromatographed on silica gel. Elution with ether–benzene gave 1-*p*-tolyl-1-propanol (**25**) as an oil (0.52 g, 21%): $\lambda_{max}(CCl_4)$ 2.74 μ(m); δ (CCl_4) 0.82 (t, J = 7 Hz, 3H), 1.55 (m, 2H), 2.26 (s, 3H), 4.35 (t, 1H), 7.01 (s, 4H). The identity of this compound was confirmed by comparison of its spectra with those of an authentic sample prepared by reduction of *p*-methylpropiophenone with lithium aluminum hydride.

*Reaction of **27b** with Phosphorus Pentasulfide. Formation of **26***

A mixture of **27*b*** (1.00 g, 2.60 mmol) and phosphorus pentasulfide (2.00 g, 4.60 mmol) in xylene was boiled under reflux for 2 h. When cool, the xylene solution was washed successively with aqueous 10% potassium hydroxide, 10% hydrochloric acid, and water and dried. The solvent was removed to give a reddish residue which was chromatographed on neutral alumina (Woelm). Elution with benzene gave yellow–red oils, which crystallized spontaneously. These were combined and the product was recrystallized from benzene to give yellow crystals (0.757 g, 65%). Five further crystallizations gave **26**,

m.p. 119–120°; $\lambda_{max}(CHCl_3)$ 6.22 (m), 6.73 (s), 7.10 μ(w); $\lambda_{max}(C_2H_5OH)$ 230 (ε 12 600), 271 (ε 8300), 327 (ε 21 400), 433 mμ (ε 10 700); δ ($CDCl_3$) 2.40 (s, 3H), 7.42 (s, 1H), 7.23 and 7.55 (dd, J = 8.5 Hz, 4H).

Anal. Calcd. for $C_{10}H_8S_3$: C, 53.53; H, 3.59; S, 42.88. Found: C, 53.49; H, 3.56; S, 42.84.

Preparation of the Trithiolanes ***28a*** *and b from Acetophenone*

The method of Gompper and Töpfl (5) was followed, giving the crude product in 65% yield. The material was purified by recrystallization from toluene to give **28*b*** as fine yellow needles, m.p. 236–238° (dec.). The same material was also obtained by recrystallization of a yellow, insoluble, material obtained during the purification of benzoyldithioacetic acid. A mixed m.p. with the material obtained by Gompper and Töpfl's method showed no depression.

Anal. Calcd. for $C_{18}H_{12}O_2S_3$: C, 60.64; H, 3.39; S, 26.99. Found: C, 60.53; H, 3.44; S, 26.77.

The mother liquors from the first method of preparation were stripped of solvent, and the residue was crystallized several times from benzene–hexane to give **28*a***, m.p. 167.5–168.5°.

Anal. Calcd. for $C_{18}H_{12}O_2S_3$: C, 60.64; H, 3.39; S, 26.99. Found: C, 60.71; H, 3.52; S, 26.58.

Preparation of the Trithiolanes ***29a*** *and b from Deoxybenzoin*

Deoxybenzoin (2.00 g, 10.0 mmol) in anhydrous ether (10 ml) was converted to a mixture of **29*a*** and *b* by the method used for the preparation of **23**. The resulting yellow precipitate (0.49 g, 38%) was washed with water, air dried, and heated briefly in chloroform. The solution was filtered, and the filtrate was retained. The chloroform-insoluble material (0.40 g, 31%) was crystallized three times from toluene to give **29*b***, m.p. 277–278° (dec.).

Anal. Calcd. for $C_{30}H_{20}O_2S_3$: C, 70.83; H, 3.96; S, 18.91. Found: C, 70.85; H, 3.98; S, 18.60.

Evaporation of the chloroform filtrates gave **29*a***, m.p. *ca.* 213° (0.085 g, 7%). After several recrystallizations from benzene–hexane, this had m.p. 219–220°, with subsequent solidification and remelting at *ca.* 245° (dec.).

Anal. Calcd. for $C_{30}H_{20}O_2S_3$: C, 70.83; H, 3.96; S, 18.91. Found: C, 70.90; H, 4.29; S, 18.85.

Preparation of the Trithiolane ***30*** *from Mesityl Methyl Ketone*

Mesityl methyl ketone (2.0 g, 12.5 mmol) in anhydrous ether (15 ml) was converted to **30** by the method used for the preparation of **23**. Benzene was added to the reaction mixture, and the organic layer was washed several times with water and dried. The solvent was removed, and the crude product was crystallized from chloroform–hexane to give **30** as small plates (0.38 g, 29%), which after five further crystallizations from chloroform–hexane had m.p. 208.5–210°.

Anal. Calcd. for $C_{24}H_{24}O_2S_3$: C, 65.42; H, 5.49; S, 21.83. Found: C, 65.35; H, 5.52; S, 21.45.

We thank the National Research Council of Canada for generous support of this work and for fellowship support (T.R.L.).

1. (*a*) P. YATES, T. R. LYNCH, and D. R. MOORE. Can. J. Chem. This issue. (*b*) P. YATES, D. R. MOORE, and T. R. LYNCH. Can. J. Chem. This issue.
2. G. WENZEL. Ber. **33**, 2041 (1900).
3. G. WENZEL. Ber. **34**, 1043 (1901).
4. C. KELBER. Ber. **43**, 1252 (1910).
5. R. GOMPPER and W. TÖPFL. Chem. Ber. **95**, 2861 (1962).
6. P. YATES, T. R. LYNCH, and L. S. WEILER. Can. J. Chem. **46**, 365 (1968).
7. Ultraviolet spectral data. American Petroleum Research Institute No. 44. Serial No. 731.
8. O. DANN and W. DIMMLING. Chem. Ber. **87**, 373 (1954).
9. J. GODART. J. Chim. Phys. **34**, 70 (1937).
10. S. GRONOWITZ. Private communication.
11. A. THUILLIER and J. VIALLE. Bull. Soc. Chim. Fr. 2187 (1962).
12. R. S. SPINDT, D. R. STEVENS, and W. E. BALDWIN. J. Amer. Chem. Soc. **73**, 3693 (1951).
13. A. W. K. CHAN, W. D. CROW, and I. GOSNEY. Tetrahedron, **26**, 1493 (1970).
14. *Cf.* R. L. KUCZKOWSKI and E. B. WILSON, JR. J. Amer. Chem. Soc. **85**, 2028 (1963). Q. E. THOMPSON, M. M. CRUTCHFIELD, and M. W. DIETRICH. J. Amer. Chem. Soc. **86**, 3891 (1964).
15. S. C. NYBURG. Private communication. I. P. MELLOR. Ph.D. Thesis. University of Keele, Keele, England. 1968.
16. A. J. KIRBY. Tetrahedron, **22**, 3001 (1966).
17. N. W. ALCOCK and A. J. KIRBY. Tetrahedron, **22**, 3007 (1966).
18. L. L. INGRAHAM. *In* Steric effects in organic chemistry. *Edited by* M. S. Newman. John Wiley and Sons, Inc., New York, N.Y., 1956. Chapt. 11.
19. N. C. DENO, H. G. RICHEY, JR., N. FRIEDMAN, J. D. HODGE, J. J. HOUSER, and C. U. PITTMAN, JR. J. Amer. Chem. Soc. **85**, 2991 (1963).
20. P. YATES and P. M. BURKE. Unpublished results. P. M. BURKE. Ph.D. Thesis. University of Toronto, Toronto, Ontario, 1966.
21. H. N. A. AL-JALLO and E. S. WAIGHT. J. Chem. Soc. B, 73 (1966).
22. K. A. JENSEN and L. HENRIKSEN. Acta Chem. Scand. **22**, 1107 (1968).
23. R. N. JONES, D. A. RAMSAY, D. S. KEIR, and K. DOBRINER. J. Amer. Chem. Soc. **74**, 80 (1952).
24. N. E. SHARPLESS and D. A. GREGORY. Appl. Spectrosc. **17**, 47 (1963).
25. G. M. BARROW. J. Chem. Phys. **21**, 2008 (1953).
26. J. A. KAPECKI, J. E. BALDWIN, and I. C. PAUL. Tetrahedron Lett. 5307 (1967); J. Amer. Chem. Soc. **90**, 5800 (1968).
27. F. A. WHITMORE, C. I. NOLL, and V. C. MEUNIER. J. Amer. Chem. Soc. **61**, 683 (1939).
28. R. L. SHRINER, R. C. FUSON, and D. Y. CURTIN. The systematic identification of organic compounds. 5th ed. John Wiley and Sons, Inc., New York, N.Y., 1964. p. 253.

Can. J. Chem. Downloaded from www.nrcresearchpress.com by 210.87.254.105 on 09/05/12
For personal use only.

Can. J. Chem. Downloaded from www.nrcresearchpress.com by 210.87.254.105 on 09/05/12
For personal use only.

Application of Proton Magnetic Resonance to Rotational Isomerism in Halotoluenes. VII. Barriers to Rotation and Conformational Preferences in α,α,α′,α′,2,4,5,6-Octachloro-*m*-xylene

J. PEELING,[1] B. W. GOODWIN,[2] T. SCHAEFER, AND C. WONG
Chemistry Department, University of Manitoba, Winnipeg, Manitoba

Received December 14, 1970

At low temperatures α,α,α′,α′,2,4,5,6-octachloro-*m*-xylene exists as three conformers in solution and the proton resonance spectrum can be assigned by comparison to the spectrum of α,α,α′,α′,2,4,6-heptachloro-*m*-xylene. The temperature dependent spectra of the former in toluene-d_8 solution are fitted to computed spectra based on a set of coupled Bloch equations. The activation parameters for the rotation about the sp^2–sp^3 carbon–carbon bonds are $E_a = 14.93 \pm 0.13$ kcal/mol, $\log A = 12.45 \pm 0.09$, $\Delta H^* = 14.30 \pm 0.14$ kcal/mol, $\Delta S^* = -2.0 \pm 0.5$ e.u., $\Delta G^* = 14.9 \pm 0.05$ kcal/mol at 293 °K. The quoted errors are standard deviations.

Le bis(dichlorométhyl)-1,3 tétrachloro-2,4,5,6 benzène en solution existe, à basse température, sous trois conformations et son spectre r.m.n. qui varie avec la température peut être analysé par comparaison avec celui du bis(dichlorométhyl)-1,3 trichloro-2,4,6 benzène. Son spectre déterminé dans le toluène-d_8 peut être superposé à un spectre théorique calculé à l'aide d'une série d'équations de Bloch. Les paramètres d'activation pour la rotation autour de la liaison carbone–carbone sp^2–sp^3 sont $E_a = 14.93 \pm 0.13$ kcal/mol, $\log A = 12.45 \pm 0.09$, $\Delta H^* = 14.30 \pm 0.14$ kcal/mol, $\Delta S^* = -2.0 \pm 0.5$ u.e., $\Delta G^* = 14.9 \pm 0.05$ kcal/mol à 293 °K. Les erreurs mentionnées sont les déviations standards.

Canadian Journal of Chemistry, 49, 1489 (1971)

Introduction

In a series of experiments designed to determine the stable conformations of the side-chain and the barrier to rotation about the sp^2–sp^3 carbon–carbon bond in halotoluene derivatives, the temperature dependence of the ring p.m.r. spectra of α,α,2,4,6-pentachlorotoluene (PCT), α,α-dichloro-2,4,6-tribromotoluene (DCTBT), and of α,α,2,3,6-pentachlorotoluene (3PCT) was studied (1–4). The undetected presence of systematic errors in DNMR techniques (5) is always a danger and therefore the study of the rotation of the dichloromethyl group in α,α,α′,α′,2,4,5,6-octachloro-*m*-xylene (MOCX) was undertaken. In contrast to the above molecules, it is the protons of the side-chains which are temperature dependent, the exchange takes place between four sites instead of two; and because there exists no observable long-range coupling between the protons, a set of coupled Bloch equations can be used to describe the exchange process. In other words, any systematic errors in the analysis of PCT at 60 MHz are expected to be of rather different origin in the study of MOCX at 100 MHz, while the barrier to rotation should not be greatly different in the two cases.

This paper describes the results of a careful study of the barrier to rotation in MOCX.

Experimental

(1) Preparation of MOCX

Free radical chlorination of 2,4,5,6-tetrachloro-*m*-xylene, as described for PCT (1), was monitored by observing the proton chemical shifts of the side-chain protons and was terminated when the peaks arising from chloromethyl protons were no longer present. These peaks occur some p.p.m. to high field of those from the protons in the dichloromethyl groups.

(2) Preparation of α,α,α′,α′,2,4,6-Heptachloro-m-xylene (MHCX)

Ring chlorination of 3,5-dimethylaniline, in a manner similar to that used in the preparation of PCT from *m*-toluidine (1), followed by deamination and chlorination of the side-chains as for MOCX, yielded MHCX.[3]

(3) Spectral Measurements

A 6.1 mol % solution of MOCX in toluene-d_8 (C_7D_8) containing tetramethylsilane (TMS) as internal reference was carefully degassed. A similar solution containing about 5 mol % of MHCX was also prepared. Toluene-d_8 is a good solvent of these molecules between −50 and 110 °C and the temperature dependence of the proton chemical shifts can be accurately measured. Solvents like CCl_4, CH_2Cl_2, and acetone do not fulfill all of these conditions.

The p.m.r. spectra were recorded at a sweep rate of 0.02 Hz/s on a HA-100D spectrometer, taking care not

[1]Manitoba Research Fellowship, 1969–1970.
[2]NRCC Scholarship, 1968–1969.

[3]We are grateful to Mr. K. Chum, summer student 1970, for this preparation.

to use excessive filtering of the d.c. signal.[4] Calibration of peak positions and of the sample temperature was done as previously described (3). Absolute temperatures are accurate to at least 1 °K and relative temperatures to 0.5 °K. Peak positions of MOCX were measured over a range of temperatures in the region of slow exchange. The magnetic field homogeneity was monitored by the width of a single sharp impurity peak (see Fig. 3).

Results and Discussion

(1) Assignment of Peaks to Conformations in the Region of Slow Exchange

In view of the results for PCT (1, 2), it is clear that there exist three stable conformations of MOCX, **1** to **3**. The protons are isochronous in **1**

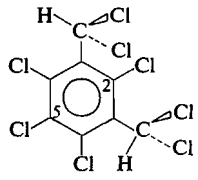

1

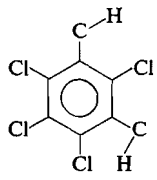

2

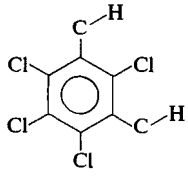

3

and in **3** but are anisochronous in **2**. In Fig. 1 the proton spectrum displays the expected four peaks but their assignment to the various conformers is not obvious because the peaks occur as pairs of apparently equal intensity within the pair.

On the basis of the zig–zag rule, coupling between the protons in **1** is possible but is unobservable because of the shift degeneracy. The zig–zag rule predicts zero coupling of the protons in **2** while shift degeneracy gives no observable coupling in **3**. Accordingly, the four peaks do not display any splitting.

Detailed electric field calculations, based on a dipole model as outlined by Buckingham (6), were carried out using scale diagrams and standard dipole moments for C—Cl bonds. The

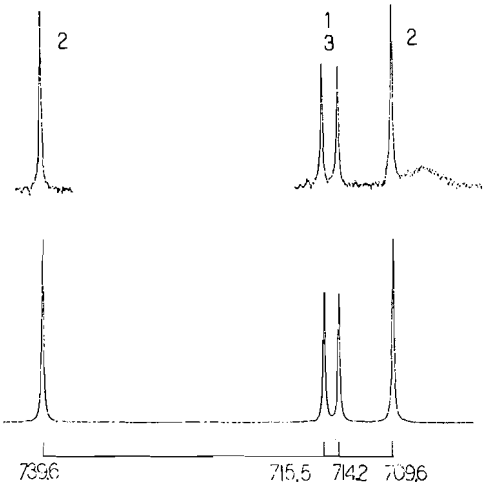

FIG. 1. The p.m.r. spectrum at 100 MHz of α,α,α′,α′-2,4,5,6-octachloro-*m*-xylene as a 6.1 mol % solution in toluene-d_8 at −41 °C. The chemical shift is given in Hz to low field of internal TMS. Note the broad resonance peak at high field due to incompletely deuterated toluene. The spectrum shown at the bottom of the figure was calculated using the computer program described in the text. The taller pair of peaks is assigned to the unsymmetrical conformation **2** with the methine proton at position 1 to lowest field. The smaller pair of peaks belongs to the symmetrical conformations **1** and **3**.

predicted shifts for the various conformers would assign **1** at highest field (739.7 Hz) and one proton of **2** at lowest field, clearly incompatible with the observed intensities in Fig. 1. It is unlikely that aromatic solvent shifts are responsible for the disagreement because the specific shifts induced by C_7D_8 on the methine protons are very small relative to those induced on the ring protons in PCT (1, 2). (At any rate, the calculated shifts do not qualitatively agree with a spectrum taken in CCl_4.) It is much more likely that the relative shifts of the protons in MOCX are dominated by intramolecular van der Waals (steric) interactions (see Appendix).

The assignment was therefore made on the basis of the spectrum of MHCX shown in Fig. 2. The ring proton peaks are broader than the methine peaks. The three conformations of MHCX can be represented by **4**, **5**, and **6**, where the presence of the chlorine atoms is understood. On the basis of the stereospecific five-bond coupling between ring and side-chain protons in PCT (1), the methine protons in **6** are coupled to the ring proton by 0.5 Hz (equal to the doublet splitting in PCT and in Fig. 2). Similarly, no

[4]A referee suggests that a sweep rate of 0.02 Hz/s is unusually slow and may well lead to signal distortion via saturation. In our opinion this sweep rate is more of an *upper* limit if other kinds of distortion are to be avoided. We emphasize that the signals showed no saturation effects.

Can. J. Chem. Downloaded from www.nrcresearchpress.com by 210.87.254.105 on 09/05/12
For personal use only.

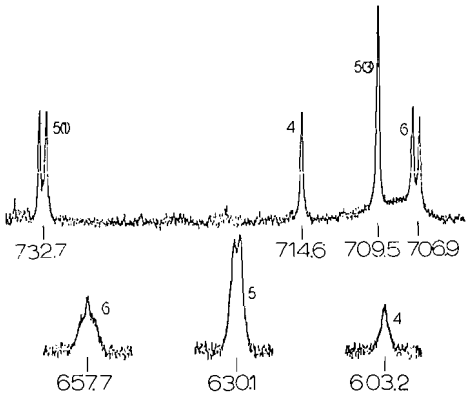

FIG. 2. The p.m.r. spectrum at 100 MHz and −41 °C of α,α,α′,α′,2,4,6-heptachloro-*m*-xylene as 7 mol % solution in toluene-d_8. The broad hump between 707 and 710 Hz to low field of internal TMS arises from incompletely deuterated toluene. The assignment is discussed in the text. The lower part of the figure gives the ring proton resonance peaks of the conformations **4** to **6** of the text. The splitting of the doublets at high and low field of the methine protons in the upper part of the figure is 0.5 Hz.

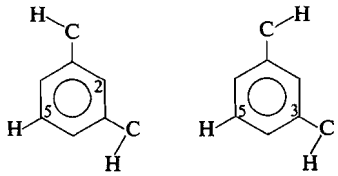

4 **5**

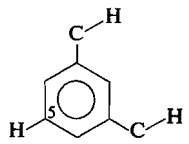

6

coupling will occur in **4** while in **5** the ring proton couples only to the methine proton in the dichloromethyl group at position 1 of the ring. Simple decoupling experiments and the relative peak intensities confirmed the assignments given in Fig. 2.

Assuming that the replacement of chlorine by hydrogen meta to the methine carbons has little effect on the methine proton shifts, it follows that in MOCX the most abundant conformer is **2** and the assignment of the peaks is given in Fig. 1. The unsymmetric **2** has been distinguished from the symmetric **1** and **3**. Which of the two smaller peaks belongs to **1** is irrelevant to the rate study because the populations of **1** and **3** are equal in C_7D_8 to within experimental error.

(2) Relative Populations of the Conformers in MOCX and MHCX

In MHCX the relative populations at −41 °C in C_7D_8 are **4**:**5**:**6** = 1:3.6:1.7 as determined by weighing of peaks. In MOCX the populations at −41 °C in C_7D_8 are **1**:**2**:**3** = 1:2.9:1, based on repeated measurements of peak areas by weighing. The larger population of the unsymmetrical conformer **2** in MOCX is likely an entropy effect (see below). The decrease in the stability of **4** relative to the other conformers of MHCX compared to the corresponding stability of **1** in MOCX is very likely a direct result of the absence of chlorine at position 5 in MHCX. Thus **5** and **6** become more stable in MHCX because steric crowding of the ortho C—Cl bonds by the dichloromethyl groups can be relieved by bending of the C—Cl bonds at positions 4 or 6 towards the C—H bond at position 5, whereas **4** and **1** have a very similar steric interaction of the two dichloromethyl groups with the C—Cl bond at position 2.

In the calculation of line-shapes for MOCX the relative populations of **1**, **2**, and **3** as a function of temperature are needed. But the peak area measurements in the limited temperature region of slow exchange are not accurate enough to determine enthalpy differences reliably. Therefore the following approach was adopted. At −41 °C, where no broadening from exchange was present, repeated peak area measurements yielded $\Delta G = G_2 - G_1 = G_2 - G_3 = -RT\ln K = RT\ln P_2/P_3 = 490 \pm 20$ cal/mol. Following Govil and Bernstein (7) it was assumed that the vibrational entropy differences between the conformers were negligible, particularly in view of the large barriers in the wells of which the torsional modes of the dichloromethyl groups are active (translational entropy differences are, of course, zero). The rotational entropy differences were then calculated from the product of the principal moments of inertia for each conformer, assuming tetrahedral angles in the side-chains and 120° bond angles in the benzene ring. This approximation is unimportant because the rotational entropy differences between the conformers turned out to be only about 0.02 e.u. and were therefore neglected.

From symmetry considerations it follows that $S_2 - S_1 = S_2 - S_3 = R\ln 2 = 1.38$ e.u. Hence

Can. J. Chem. Downloaded from www.nrcresearchpress.com by 210.87.254.105 on 09/05/12
For personal use only.

[1] Shift of **2** = $-11.340 \times 10^3/T + 788.54$ $r = 0.9997$

[2] Shift of **1** or **3** = $-15.603 \times 10^3/T + 782.78$ $r = 0.9999$

[3] Shift of **3** or **1** = $-13.823 \times 10^3/T + 773.82$ $r = 0.9998$

[4] Shift of **2** = $-17.804 \times 10^3/T + 786.34$ $r = -0.9999$

$H_2 - H_3 = -164$ cal/mol at -41 °C, so that the entropy effect on the relative stabilities is dominant. Then at 373 °K, near the highest temperature at which rate studies were carried out, one has $G_2 - G_1 = -680$ cal/mol. Therefore the population ratios change from $P_2/P_1 = 2.9$ at -40 °C to 2.5 at 373 °K. Calculated and experimental rate dependent spectra were fitted with these populations as well as under the assumption of temperature independent populations. As shown below, the activation parameters are insensitive to population changes of this extent.

(3) The Line-shape Theory and Computer Program

In terms of conformers **1** to **3** and with reference to Fig. 1, where the four resonance peaks display no spin–spin coupling, the McConnell formulation (8) of the Bloch equations under conditions of exchange was applied to this four-site problem. It can be seen that, in fact, only two independent preexchange lifetimes, τ, exist here by nature of the conformations and of the rate process, which is always a rotation by π radians from one in-plane C—H conformation to another (1). The other τ values are related to these via population ratios.

The final expression for the complex magnetization was written in terms of τ_1 and τ_2 which are, respectively, the mean preexchange lifetimes of conformers **1** and **3**, these conformers converting to **2** on rotation of either of the dichloromethyl groups. The expression carries four effective T_2 terms, one for each of the peaks, but only three population terms because the separate resonance peaks of **2** must have equal intensities.

A computer program in Fortran IV was written which took as input data the three populations, the four effective T_2 values, the two preexchange lifetimes, a scaling factor, and the frequencies of the exchange sites. The use of the program in line-shape fitting then follows the procedure described for the program ABXFIT(1) and a plotting procedure can be called for the line printer or the Calcomp plotter on an IBM 360/65 computer.

(4) Fitted Spectra and Activation Parameters

(a) Temperature Dependence of Peak Positions (Due to Solvent Effects) in the Absence of Exchange

As discussed previously (1), it is essential that this correction be made if severe errors in rate constants are to be avoided. In the region of slow exchange between -41 and -20 °C, the peak positions are best reproduced when plotted *vs.* T^{-1}. They are represented by eqs. 1–4, where the shift is measured in Hz at 100 MHz to low field of internal TMS and T is in °K.

As an example of the reliability of these equations in the region of fast exchange, the weighted mean of the four calculated nonexchanging peak positions at 94 °C is 743.04 Hz and can be compared with the exchange-averaged peak of width 0.76 Hz found at 743.11 Hz. Although the agreement is excellent it was found necessary to change the calculated shift of a few peaks by a few tenths of a Hz at some temperatures in order to obtain a sensible fit between calculated and observed spectra.

(b) Calculated Spectra

At low temperatures the linewidths of the four peaks were equal within experimental error. An impurity peak (to be seen in Fig. 3) was used to monitor the resolution of the spectrometer at each temperature. The T_2 values ranged from 1.59 to 1.72 s, depending on the temperature, and were used in the fitting procedure. Only those spectra showing substantial exchange broadening were fitted, those between -10 and 99 °C. It was further assumed that the barriers to rotation of the dichloromethyl group in **1** and **3** were equal. Their ground state free energies are the same (at least at -41 °C) and there appeared to be no reliable way in which a difference in barrier could be measured by the fitting method. The error introduced in this way is probably small (see below).

At 318 and 323 °K the spectra were so broad due to the low concentration of 6 mol %, that the line-shape could not be reliably measured in our opinion. Preexchange lifetimes were found

Can. J. Chem. Downloaded from www.nrcresearchpress.com by 210.87.254.105 on 09/05/12
For personal use only.

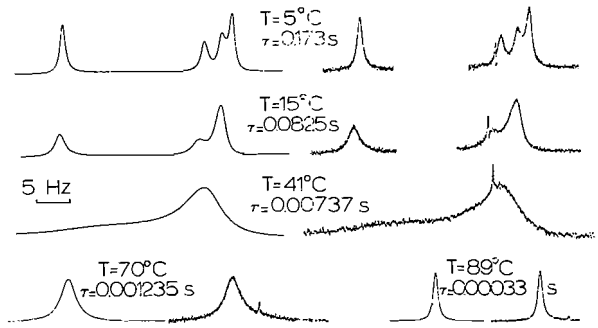

FIG. 3. A few representative observed and calculated proton resonance spectra of the methine protons of MOCX at various temperatures and preexchange lifetimes, τ. The small sharp peak observable in some spectra arises from an impurity.

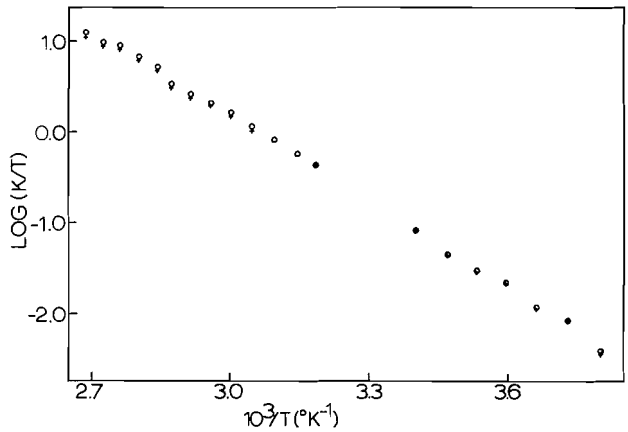

FIG. 4. A plot of log k/T *vs.* $1/T$ for the activated rotation of the dichloromethyl groups in MOCX dissolved in toluene-d_8. The open circles refer to the rate constants, k, obtained on the assumption of constant populations of the conformations. The crosses refer to the k values extracted when the populations of the conformations change with temperature in the manner described in the text. Both plots give a least squares fit with a correlation coefficient, $r = 0.999$.

at 20 temperatures and the rate constant, k, ranged from about 0.3 to 1400 s^{-1} between -10 and 99 °C.

Best fits were found on the assumption of no population change as well as with the populations calculated as described above. In Fig. 3 calculated and observed spectra are displayed at a few representative temperatures. In Fig. 4 a plot of log k/T *vs.* $1/T$ ($r = 0.9993$) indicates the differences obtained by using the two population assumptions above.

(c) The Activation Parameters

Plots of log k *vs.* $1/T$, log k/T *vs.* $1/T$, and $\Delta G^{\ddagger}$ *vs.* T were prepared based on the Arrhenius and transition state formulations of an activated process (5). Least squares analyses gave the parameter values shown in Table 1. It is customary to add the caveat that the least squares errors in Table 1 should be multiplied by a factor of from 2 to 4 to allow for systematic errors. In the present instance it is felt that the statistical errors may well lie near the true error. The temperature range is 110 °K and there are four peaks, presenting a number of coalescence temperatures. The temperature range falls into the region where it is most easily controlled in the probe and where temperature gradients near the receiver coil are relatively small.

Another way of estimating the uncertainty in the entropy of activation caused by errors in the rate constant k uses eq. 5 (9) where T_1 and T_2 are

$$[5]\quad \Delta(\Delta S^{\ddagger}) = (\pm R/T_2 - T_1)[(T_2\Delta k_2/k_2)^2 + (T_1\Delta k_1/k_1)^2]^{1/2}$$

Can. J. Chem. Downloaded from www.nrcresearchpress.com by 210.87.254.105 on 09/05/12
For personal use only.

TABLE 1. Activation parameters for the hindered rotation in α,α,α′,α′,2,4,5,6-octachloro-*m*-xylene

Parameter	Constant populations	Variable populations
E_A (kcal/mol)	15.08±0.12	14.93±0.13
log A	12.59±0.08	12.45±0.09 (r = 0.9994)
ΔH (kcal/mol)	14.46±0.12	14.32±0.13
$\Delta S^{\ddagger}$ (e.u.)	−1.6±0.4	−2.2±0.4
From log k/T vs. 1/T (r = 0.9993)		
$\Delta H^{\ddagger}$ (kcal/mol)	14.40±0.13	14.27±0.14
$\Delta S^{\ddagger}$ (e.u.)	−1.8±0.4	−2.4±0.4
From $\Delta G^{\ddagger}$ vs. T (r = 0.79)		
$\Delta G^{\ddagger}$ (kcal/mol at 293 °K)	14.9±0.05 at 293 °K	

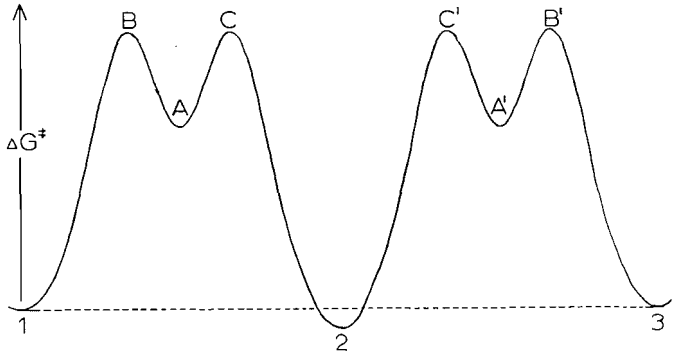

FIG. 5. A representation of the free energy profile for the interconversion of the conformers **1**, **2**, and **3** of α,α,α′,α′,-2,4,5,6-octachloro-*m*-xylene dissolved in toluene-d_8. Note that the unsymmetrical **2** has a lower free energy of about 0.5 kcal/mol than **1** and **3** at the temperatures under consideration. States B, B′, C, and C′ lie near 15 kcal/mol and A and A′ are about 10 kcal/mol above the ground state.

the end temperatures with corresponding rate constants k_1 and k_2 and errors Δk_1 and Δk_2. In this study we found $k_1 = 0.28_5 \pm 0.01$ s^{-1} at 263 °K and $k_2 = 1380 \pm 100$ s^{-1} at 372 °K. Then $\Delta(\Delta S^{\ddagger}) = 0.5$ e.u., in close agreement with the least squares errors given above.

(5) Discussion of Activation Parameters

Structures **1** and **3** are of equal stability and are less stable than **2** by about 0.5 kcal/mol in the temperature region under consideration. The free energy profile for the rotations can be depicted as in Fig. 5, where B, C, C′, and B′ represent transition states in which C—Cl bonds on the ring eclipse C—Cl bonds on the side-chain. The A and A′ represent intermediate conformers in which the C—H bonds of the side-chain are rotated by 90° out of the plane of the ring. As borne out by potential energy calculations (10), A and A′ are much too high in energy (A ≈ 0.7 B) to be appreciably populated at these temperatures.[5]

If B and C (and B′ and C′) are isoenergetic then the measured $\Delta G^{\ddagger}$ refers to the rate of rotation in **2** because the free energy barrier to rotation in **2** is then the higher by about 0.5 kcal/mol and is therefore rate controlling. The same conclusion holds if C (and C′) is lower or higher in free energy than B (and B′). It is not known which of the four transition states is of highest energy nor is it known that C and C′ (and B and B′) are isoenergetic. If, for example, B′ and C′ are both of lower energy than B and C, the measured $\Delta G^{\ddagger}$ refers to the rate of rotation from **2** to **1**. No difficulty in line-shape fitting was encountered, however, by assuming B and B′ (or C and C′) to be isoenergetic.

[5]The shape of the barrier justifies the use of a transmission coefficient near 1/2 (11).

Can. J. Chem. Downloaded from www.nrcresearchpress.com by 210.87.254.105 on 09/05/12
For personal use only.

Can. J. Chem. Downloaded from www.nrcresearchpress.com by 210.87.254.105 on 09/05/12
For personal use only.

In a similarly crowded molecule, α,α,α′,α′,2,3,5,6-octachloro-*p*-xylene (POCX), the entropy of activation lies near −7 e.u. (10), substantially more negative than in MOCX. The obvious difference between POCX and MOCX is that in POCX the ground states are symmetrical (each has a two-fold axis or a plane of symmetry). In MOCX the measured $\Delta S^{\ddagger}$ of near −2 e.u. evidently refers to the conversion of the unsymmetrical **2** to the symmetrical **1** and **3**. But **2** has greater entropy in the ground state than **1** or **3**, assuming the estimates in a previous section are correct. Then, if C (or C′) represents the transition state and if it partakes more of the ground state **2** than of **1** or **3** (C and C′ are obtained from **2** by a rotation of 60° about the sp^2–sp^3 carbon–carbon bond) the less negative $\Delta S^{\ddagger}$ of MOCX compared to POCX is perhaps understandable. If this line of argument is correct then $\Delta S^{\ddagger}$ for the conversion of **1** or **3** to **2** should be more negative than −2 e.u. There is no obvious method by which this prediction can be tested.

Appendix

Rationalization of Relative Proton Shifts in MOCX and MHCX

(a) Ring Proton Shifts in MHCX

The relative shifts cannot be explained on the basis of electric dipolar fields (6) because it is clear that the C—Cl dipoles in **4** would deshield the ring proton more than in **6**. Yet **4** lies to highest field in Fig. 2. However, a combination of solvent and steric effects can rationalize the relative shifts. It is well-known (12) that the aromatic solvent molecules avoid electron-rich regions of an aromatic solute molecule. Thus in **4** the C_7D_8 molecule can approach H-5 much more easily than in **5** or **6**, causing a preferred high-field shift in **4**. The aromatic solvent induced shifts are additive (12) and hence it is not surprising to note an increase of 27 Hz both from **6** to **5** and from **5** to **4**. In **6** the dichloromethyl groups have the C—Cl bonds near H-5 thus repelling the solvent molecules (12) while in **5** only one dichloromethyl group is so situated.

Again, the nonzero mean square electric fields originating in the C—Cl bonds of the dichloromethyl groups will deshield H-5 most in **6** and least in **4**, consistent with the observed order of the ring proton shifts.[6] Measurements of the ring proton shifts of MHCX in CCl_4 solution at low enough temperatures compatible with slow exchange are hampered by broadening effects due to precipitation of solute as well as freezing of the solution. Nevertheless, such measurements indicated that aromatic solvent shifts are the predominant cause of the observed relative shifts of the ring protons (in CCl_4 the ring proton shifts do not lie upfield from the methine proton shifts).

(b) Methine Proton Shifts in MHCX and MOCX

These shifts are relatively insensitive (2) to the aromatic solvent anisotropy probably because the proton is protected from a close approach of solvent molecules by the proximity of ring C—Cl bonds. The proton at position 3 of the unsymmetrical conformer occurs at 709.5(6) Hz to low field of internal TMS in both compounds. The proton at position 1 in this conformer occurs 7 Hz to lower field in MOCX than in MHCX. Both protons are strongly deshielded relative to those in the other sites. Steric crowding of the C—Cl bond at position 2 by the C—Cl bonds of the dichloromethyl group at position 3 forces a closer proximity of the coplanar C—H and C—Cl bonds (Cl and H overlap by 0.5 Å even in an uncrowded, coplanar situation), consistent with greater interference of the diamagnetic circulation of electrons in the C—H bond.[6] None of the other methine proton sites are characterized by such an interaction, indicated by Cl_2C—H···Cl···Cl_2-CH. In MHCX this interaction can be relieved somewhat by back-tilting of the dichloromethyl bearing the proton (chlorine at position 6 in MHCX can move away against the C—H bond at position 3), leading to less deshielding by 7 Hz.

If the single peaks at 714.3(6) Hz for MOCX and MHCX are assigned to **1** (**4**) then the upfield shift of 8.5 Hz of the proton in **6** of MHCX rela-

[6]A referee prefers to call these hydrogen-bonding shifts. Although the large shifts observed on the formation of hydrogen bonds arise to a large extent from fluctuating electric fields on the proton acceptor, we prefer to reserve the term for situations in which the hydrogen bond is mainly responsible for the stable conformation of a molecule. In our molecule, the coplanarity of the ring and the C—H bonds arises mainly from the steric interactions of the C—Cl bonds with each other (10).

tive to that of **3** at MOCX can be understood as a result of greater steric crowding of the dichloromethyl groups in **3** relative to **6**. In **6** crowding of the dichloromethyl groups by the C—Cl bonds at positions 4 and 6 can be relieved relative to **3** because these C—Cl bonds can bend towards the C—H bond at position 5 in MHCX, whereas there is a bulkier C—Cl bond at position 5 in MOCX. Consequently the C—H bonds of the dichloromethyl groups in **3** are forced closer to the C—Cl bond at position 2 leading to a deshielding of these protons relative to the ones in **6**.

We are grateful to the University of Manitoba and to the National Research Council of Canada for financial assistance.

1. B. J. FUHR, B. W. GOODWIN, H. M. HUTTON, and T. SCHAEFER. Can. J. Chem. **48**, 1558 (1970).
2. H. GYULAI, B. J. FUHR, H. M. HUTTON, and T. SCHAEFER. Can. J. Chem. **48**, 3877 (1970).
3. J. PEELING, T. SCHAEFER, and C. M. WONG. Can. J. Chem. **48**, 2839 (1970).
4. M. A. H. STEWART, T. SCHAEFER, H. M. HUTTON, and C. M. WONG. Can. J. Chem. **49**, 1085 (1971).
5. G. BINSCH. *In* Topics of stereochemistry. Vol. 3. *Edited by* E. L. Eliel and N. L. Allinger. Interscience Publishers, New York, N.Y., 1968.
6. A. D. BUCKINGHAM. Can. J. Chem. **38**, 300 (1960).
7. G. GOVIL and H. J. BERNSTEIN. J. Chem. Phys. **47**, 2818 (1967); **49**, 911 (1968).
8. H. M. MCCONNELL. J. Chem. Phys. **28**, 430 (1958).
9. L. L. SCHALEGER and F. A. LONG. Advances. Phys. Org. Chem. **1**, 8 (1963).
10. B. H. BARBER and T. SCHAEFER. Can. J. Chem. **49**, 789 (1971).
11. D. HOUALLA, R. WOLF, D. GAGNAIRE, and J. B. ROBERT. Chem. Commun. 443 (1969).
12. R. WASYLISHEN, T. SCHAEFER, and R. SCHWENK. Can. J. Chem. **48**, 2885 (1970).

Can. J. Chem. Downloaded from www.nrcresearchpress.com by 210.87.254.105 on 09/05/12
For personal use only.

Can. J. Chem. Downloaded from www.nrcresearchpress.com by 210.87.254.42 on 09/05/12
For personal use only.

Empirical σ Molecular Orbital Parameters and their Correlation with Rates of Substitution Reactions in Quadrate Cr(III) and Co(III) Complexes[1]

C. H. LANGFORD[2]

Department of Chemistry, Carleton University, Ottawa 1, Canada

Received December 1, 1970

Empirical measures of σ bonding involving metal 3d orbitals are derived from Perumareddi's (4) complete analysis of the quartet spectral bands of quadrate complexes in the families $Cr(NH_3)_5X^{n+}$ and $Cr(OH_2)_5X^{n+}$. These are shown to correlate with lability of X in the Cr(III) complexes and in $Co(NH_3)_5X^{n+}$ complexes in a sense indicating that relative reactivity is controlled by variation of ligand metal 3d σ interaction. The relationship between the two Cr(III) series implies that the non-labile ligands can labilize the leaving group in proportion to their σ donor capacities. This observation bears on some well-known difficulties in crystal field theories of reactivity. In evaluating the correlation of spectral parameters with reactivity, the role of solvation in reactivity of Cr(III) and Co(III) complexes is discussed with emphasis on the surprisingly small solvent effects that have been observed.

Les mesures empiriques des liaisons σ, impliquant les orbitales 3d d'un métal sont dérivées de l'analyse complète de Perumareddi des bandes spectrales quadruplet des complexes carrés de la famille $Cr(NH_3)_5X^{n+}$ et $Cr(OH_2)_5X^{n+}$. Ceux-ci montrent une corrélation avec la labilité de X dans les complexes Cr(III) et dans les complexes $Co(NH_3)_5X^{n+}$ dans un sens indiquant que la réactivité relative est contrôlée par les variations des intéractions σ du métal 3d ligande. La relation entre les deux séries Cr(III) implique que les ligandes non labiles peuvent rendre plus labile le groupe sortant, proportionnellement à leurs capacités de donneur σ. Cette observation porte sur des difficultés bien connues dans les théories de réactivité du champ cristallin. En évaluant la corrélation des paramètres spectraux avec la réactivité, le rôle de la solvatation sur la réactivité des complexes Cr(III) et Co(III) est discuté avec un accent sur le fait très surprenant, que les effets de solvant observés sont très petits.

Canadian Journal of Chemistry, 49, 1497 (1971)

Introduction

A calculation performed by Gray and Basch was reported (1) showing that the main features of the *trans* effect series, nucleophilicity series, and lability series, for ligands involved in substitution reactions at square planar Pt(II) may be correlated with the variation in values of ligand σ to metal 6p orbital overlap integrals. This result is strongly suggestive that the main feature governing the relationship between the ground state and transition state in a substitution reaction at the third transition series metal Pt is *sigma* bonding between the ligand and a metal p orbital. For halide ligands, lability in Pt(II) increases along the series $I^- < Br^- < Cl^-$. It has been remarked that the same lability order is observed in the substitution reactions of octahedral Rh(III) complexes. These complexes, like the octahedral complexes of the metals of the first transition series such as those of Cr(III) and Co(III), show little sensitivity to choice of entering ligand and must, therefore, react by a predominantly dissociative mechanism. It seems that metal p-ligand σ interaction also governs the bond that must be broken in a Rh(III) dissociative process.

In complexes of metals in the first transition series, the lability order is reversed, iodide is most labile and chloride is least labile. This reversal has been explained on the grounds that σ bonding in complexes of the first transition series is dominated by the interaction of ligand σ with metal d orbitals and that it is a bond of mainly σ-3d character which must be broken in reaching the substitution transition state (2, 3). This hypothesis helps to account for the absence of *large trans* effects in Cr(III) and Co(III) complexes since the four-fold symmetry of 3d orbitals does not uniquely relate a *trans* pair of ligands as metal p orbitals do (3). *Trans* effects are a feature of Rh(III) chemistry (3).

Intuitively, an m.o. (molecular orbital) theory for metal complex lability which can explicitly treat σ bonding is the most appealing. However, crystal field treatments have so far enjoyed greater, if limited, success as quantitative theories

[1]Supported financially by the National Research Council of Canada.

[2]Research fellow of the Alfred P. Sloan Foundation 1968–1970.

Can. J. Chem. Downloaded from www.nrcresearchpress.com by 210.87.254.42 on 09/05/12
For personal use only.

because empirical spectroscopic parameters are easily derived for correlation with reactivity. The purpose of this report is to illustrate the use of an empirical spectroscopic parameter measuring ligand interaction with 3d metal orbitals of symmetry correct for σ bonding ($3d_{x^2-y^2}$, $3d_{z^2}$) derived from recent careful analysis of the spectra of numerous quadrate Cr(III) complexes of the type CrA_5X^{n+} where A is either NH_3 or H_2O and X is usually an anionic ligand.

Energy Levels of Quadrate d^3 Complexes

An octahedral d^3 complex such as $Cr(NH_3)_6^{3+}$ displays two easily assigned spin allowed absorption bands in the d–d region. The states accounting for these are shown on the left in Fig. 1. As the microsymmetry is reduced to C_{4v} in a complex like $Cr(NH_3)_5Cl^{2+}$, the ^4T octahedral states split as shown on the right of Fig. 1. The C_{4v} complexes should exhibit four d–d bands. The spectra have been extensively studied and analyzed, see ref. 4 and earlier work cited therein. Resolution of the $^4A_2$ and ^4E has been accomplished in only a few cases but the $^4B_2$ band is observed in most cases and remains essentially constant. Orbitally, this band corresponds to the transition $xy \rightarrow x^2 - y^2$ in strong field. (The unique ligand is placed on the z axis.) It is not only constant but also found at the position of the $^4T_{2g}$ band of the octahedral parent complex (*e.g.* $Cr(NH_3)_6^{3+}$). This means that the equatorial orbitals xy and $x^2 - y^2$ are not demonstrably affected by variation in the axial ligand. The strong field one electron orbitals

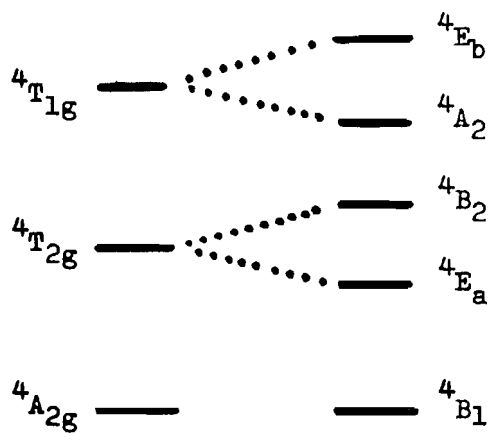

FIG. 1. Spectroscopic states of d^3 complexes in O_h and C_{4v} symmetry. O_h states are on the left and correlated with C_{4v} states (not to scale).

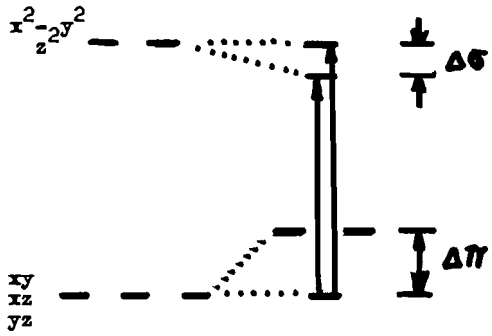

FIG. 2. Strong field d orbital energies in O_h and C_{4v} complexes of Cr(III). The specific ordering would be correct for $Cr(NH_3)_6^{3+}$ and $Cr(NH_3)_5Cl^{2+}$ (not to scale).

are shown in Fig. 2 with two transitions designated. The $^4B_2$ has been considered, the $^4A_2$ is the band of main interest here. The splitting of the orbitals $x^2 - y^2$ and z^2 is designated by Δσ since these are the σ *antibonding* orbitals in m.o. theory. Δσ is positive for z^2 lying above $x^2 - y^2$ and this implies stronger σ bonding by the unique ligand on the z axis. The energy of the $^4A_2$ band is $\Delta_0 + \Delta\sigma + f(B,C)$ where Δ_0 is the orbital splitting in the parent octahedral complex (or the difference between xy and $x^2 - y^2$ in the C_{4v} complex) and $f(B,C)$ is the appropriate combination of Racah's interelectronic repulsion parameters. As the unique ligand is varied (*e.g.* from Cl to Br to I), the quantities determining the shifts of the $^4A_2$ band should be only Δσ and $f(B,C)$.

If the evolution of the $^4A_2$ position in a series of complexes can be determined with suitable choice of B and C, relative σ bonding may be estimated. Recently Perumareddi and his colleagues have completed a comprehensive study of C_{4v} and D_{4h} Cr(III) complexes, which is reviewed in ref. 4. Although it was possible to achieve explicit resolution of the $^4A_2$ band in only a minority of examples, the constancy of the $^4B_2$ band and the small variation of B and C parameters permitted complete fitting and assignment of all bands within a crystal field framework of parameters that was highly "precise" (± 50 cm^{-1} (4)). Using Perumareddi's $^4A_2$ values for $Cr(NH_3)_5X$ and $Cr(OH_2)_5X$, the variation of Δσ with changing X is recorded in Table 1. There the parameter $\delta\Delta\sigma$ is defined, which is the difference between $^4T_{2g}$ of CrA_6 and $^4A_2$ of CrA_5X. This is the same as the

Can. J. Chem. Downloaded from www.nrcresearchpress.com by 210.87.254.42 on 09/05/12
For personal use only.

TABLE 1. $\delta\Delta\sigma$ ($^4A_2 - {}^4T_{2g}$) for CrA_5X complexes

X	$\delta\Delta\sigma$* $Cr(NH_3)_5X$	$Cr(OH_2)_5X$
CN^-	1.31	2.47
NH_3 (or H_2O)	0.00	0.00
CNS^-	−1.00	0.11
N_3^-	−1.36	−0.25
F^-	−1.41	−0.31
Cl^-	−2.12	−1.09
Br^-	−2.51	−1.43
I^-	−2.97	−1.90

*Values in kK after spectra of Perumareddi (4).

splitting of $x^2 - y^2$ and z^2 in CrA_5X according to Perumareddi (4).

Model of a Dissociative Substitution Transition State

To relate empirical sigma bonding parameters of complexes of the type CrA_5X to reactivity, we require a model for the transition state of the reaction. The reaction to be considered is

[1] $$CrA_5X + H_2O \rightarrow CrA_5OH_2 + X$$

and this reaction has been assigned a dissociative mechanism on the basis of several lines of evidence reviewed in ref. 3. The transition state must be supposed to have at most weak bonds to the leaving X and the entering H_2O. In compensation, it is expected to have stronger bonds to the remaining five A ligands. This transition state is crudely represented as

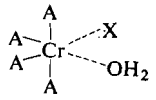

If σ bonding of ligand orbitals to metal 3d orbitals is crucial, this transition state model implies two consequences: (*i*) lability will increase nearly *proportionately* to *decreasing* $\Delta\sigma$, which measures reduction of the 3d-ligand σ interaction, and (*ii*) lability of a given leaving X will increase as the energy of the $x^2 - y^2$ orbital (determined by the A ligand and measured from the position of $^4T_{2g}$ of CrA_6 or $^4B_2$ of CrA_5X) increases. This is because strong σ donor properties of the A ligands can stabilize the transition state of reduced coordination by "capturing" the released metal 3d-σ orbital.

Results of Spectra–Rate Correlation

In Fig. 3, the values of $\delta\Delta\sigma$ are plotted against

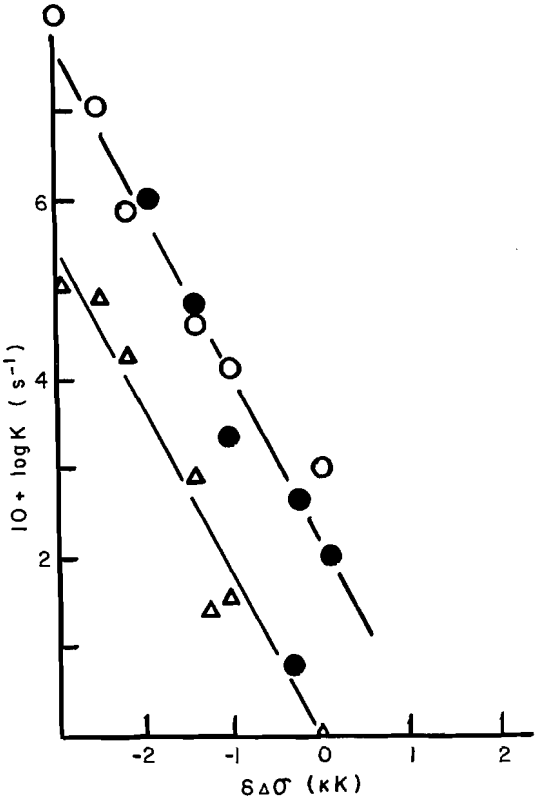

FIG. 3. Correlation of solvolysis rates with spectroscopic sigma bonding parameter defined in the text. (Rate data are from the compilations in refs. 5 and 6.) ○ = $Cr(NH_3)_5X$ with X = I^-, Br^-, Cl^-, F^-, NCS^-, NH_3 in decreasing order of rate. ● = $Cr(OH_2)_5X$ with X = I^-, Br^-, Cl^-, N_3^-, NCS^-, F^- in decreasing order of rate. △ = $Co(NH_3)_5X$ with X = I^-, Br^-, Cl^-, F^-, NCS^-, N_3^-, NH_3 in decreasing order of rate.

the log of the rates of acid hydrolysis for $Cr(NH_3)_5X$ and $Cr(OH_2)_5X$. Rate data are derived from compilations by Swadde and Guastalla (5) and Basolo and Pearson (ref. 6, chap. 3). The hydrolysis rates fit a linear correlation. The slope of the correlation is close to *unity* in consistent energy units (−0.88). The figure also shows points correlating the hydrolysis of complexes $Co(NH_3)_5X$ with $\delta\Delta\sigma$ values for $Cr(NH_3)_5X$. This correlation is successful and the slope (−0.92) is very nearly the same as the slope of the Cr(III) correlations. Such successful correlation of Co(III) rates with Cr(III) spectral parameters follows from the great similarity of Co(III) and Cr(III) spectra (7) and the substantial

Can. J. Chem. Downloaded from www.nrcresearchpress.com by 210.87.254.42 on 09/05/12
For personal use only.

evidence of similar substitution reaction mechanisms in Co(III) and Cr(III) chemistry (3, ref. 6, chap. 3).

Discussion

The near unit slope of the correlation supports the transition state model in which a bond to the leaving ligand is nearly entirely broken. Moreover, it implies that metal 3d to ligand σ interaction dominated variations of that bond. The contrast between Pt(II), Rh(III), and Co(III), Cr(III) (including stereochemistry) appears to be satisfactorily explained by the shift of emphasis from σ bonding through metal *p* orbitals to σ bonding through metal *d* orbitals. It is worth noting that the correlation of near unit slope extends over six decades in rates and more than 3000 cm^{-1} in spectral shifts.

An important feature of Fig. 3 is that the $Cr(OH_2)_5X^{n+}$ and $Cr(NH_3)_5X^{n+}$ complexes correlate satisfactorily on the *same* line. The values of $\delta\Delta\sigma$ are differently defined for the two series. For the amines $\delta\Delta\sigma$ is a shift from the $x^2 - y^2$ level determined by four ammonia ligands (or from the $^4T_{1g}$ level of $Cr(NH_3)_6^{3+}$). The reference level for the aquo systems is determined by H_2O ligands. The single correlation for both systems implies that the increased lability of the ammine systems (relative to aquo systems) is *proportional* to the difference in the $x^2 - y^2$ energy in the two series of complexes. This is not entirely unexpected. The model octahedral substitution transition state has a vacancy in the bonding to the σ type d orbitals. Remaining ligands with stronger σ donor properties can *stabilize* the transition state more effectively. (This is an exact parallel to the concept used to explain the *trans* effect in Rh(III) and Pt(II).)

This last idea, that non-labile ligands can labilize the leaving group in proportion to their σ donor ability, has two consequences that suggest resolution of two major puzzles in octahedral substitution studies. First, we can understand the weakness of the simple crystal field treatments of lability of the complexes $M(OH_2)_n^{2+}$ ($M = V^{2+}$ to Cu^{2+}). Calculations of losses of crystal field stabilization energy have given a correct ordering of labilities in these systems but have quantitatively *over-estimated* the differences (8). This overestimate results from the assumption that 10 *Dq* for the transition states is the same as that for the ground state. Thus, the loss of crystal field stabilization energy has been over-estimated! Second, the surprising similarity of rates of solvent exchange for $Ni(solvent)_6^{2+}$ in solvents from NH_3 to CH_3SOCH_3 (3) can be understood. When the Ni(II) ion is transferred from one solvent to another, there is a change in the leaving group *and* a corresponding change in the other ligands. As weaker σ donors become leaving groups, the bond becomes easier to break, *but* the remaining groups are less effective in their role in stabilization of the transition state of reduced coordination number. Consequently, solvent exchange reactions are subject to a "levelling" effect. Relatively non-labile solvent molecules are labilized by the rest of the coordination sphere. Relatively labile solvent molecules are not labilized by the rest of the coordination sphere.

The Co(III) complexes do not correlate on the same line as the Cr(III) complexes. This, of course, is expected. Among other things, $\delta\Delta\sigma$ parameters derived from Cr(III) spectra were used. In fact, the main justification for treating Co(III) complexes in this way at all is that there are detailed parallels between quadrate Cr(III) and quadrate Co(III) spectra but there is no available analysis of the Co(III) case which compares in extent and precision to Perumareddi's analysis of Cr(III) spectra. (In fact, some reliable kinetic results are not included in the correlation because the relevant spectral data are not available from Perumareddi's precise studies.)

Finally, a difficult aspect of the correlation must be approached. Correlation of $\Delta G^{\ddagger}$ with $\Delta\sigma$ implicitly minimizes the importance of differences in *solvation* energy between the reaction ground state and transition state. It should, first, be observed that there is a significant tradition behind the argument that solvation effects are expected to loom large in $\Delta H^{\ddagger}$ and $\Delta S^{\ddagger}$ but to cancel in $\Delta G^{\ddagger}$ (ref. 5, and earlier citations therein). But that is too easy an excuse for avoiding an issue that has not received the attention that it's due when significant experimental results are available. For example, a large body of evidence assigns the dissociative mechanism to solvolysis of *trans* $Coen_2Cl_2^{+}$. This should imply that a bound chloride becomes solvated on going from the ground state to the transition state. Now, the rate of solvolysis increases by only about a factor of *three* (ref. 6, p. 214) when the complex is transferred from *N,N*-dimethylformamide (DMF) to methanol. According to Parker's (11)

reliable extra-thermodynamic assessments of chloride ion activities, a free chloride ion should change activity by about 10^6 on transfer from DMF to CH_3OH. Parker's (9) methods of analysis would lead to the conclusion that the transition state for the solvolysis is "tight" (that is that chloride is still strongly bound to the metal in the transition state). This conclusion is contrary to a very large body of other evidence (1, 3, ref. 6, chap. 3) and the evidence of the present correlations. Reconciliation can be achieved if it is assumed that solvation of a bound ground state halide ligand is not profoundly dissimilar to solvation of the free halide ion. This is reasonable to the extent that metal halide bonding to "hard" metal centers may be considered "ionic".

Finally, solvation factors would tend to explain the largest deviations from the correlations in Fig. 3. For example, F^- ion, which fits very poorly in the case of $Cr(OH_2)_5F^{2+}$, is known to have a quite atypical $\Delta S^{\neq}$ (10).

I am indebted to Dr. V. S. Sastri for stimulating discussions and a key suggestion with respect to the role of non-labile ligands.

1. C. H. LANGFORD and H. B. GRAY. Ligand substitution processes. W. A. Benjamin, New York. 1965. Chap. 2.
2. H B. GRAY and C. H. LANGFORD. Chem. Eng. News 146, April 1, 1968. p. 68.
3. C. H. LANGFORD and T. R. STENGLE. Ann. Revs. Phys. Chem. **19**, 193 (1968).
4. J. R. PERUMAREDDI. Coord. Chem. Revs. **4**, 73 (1969).
5. T. W. SWADDLE and G. GUASTALLA. Inorg. Chem. 7, 1915 (1968).
6. F. BASOLO and R. G PEARSON. Mechanisms of inorganic reactions. 2nd ed. John Wiley & Sons, New York. 1967. Chap. 3.
7. R. A. D. WENTWORTH and T. S. PIPER. Inorg. Chem. **4**, 1524 (1965).
8. T. J. SWIFT and R. E. CONNICK. J. Chem. Phys. **37**, 307 (1962).
9. A. J. PARKER. Advan. Phys. Org. Chem. **5**, 173 (1967).
10. T. W. SWADDLE. J. Am. Chem. Soc. **89**, 4338 (1967).

Can. J. Chem. Downloaded from www.nrcresearchpress.com by 210.87.254.42 on 09/05/12
For personal use only.

Can. J. Chem. Downloaded from www.nrcresearchpress.com by 210.87.254.42 on 09/05/12
For personal use only.

The Nickel(II)–γ-Picoline–Perchlorate Complex System

M. S. SUN AND D. G. BREWER

Department of Chemistry, University of New Brunswick, Fredericton, New Brunswick

Received November 9, 1970

Three compounds have been isolated; *viz.*, $NiL_4(ClO_4)_2$, $NiL_4(H_2O)_2(ClO_4)_2$, and $NiL_6(H_2O)_2(ClO_4)_2$ (L = γ-picoline), and their spectral, magnetic, and other properties compared. Some tentative suggestions as to the possible structure of the last complex are offered; the first two compounds were reported previously (1).

On a isolé trois composés: $NiL_4(ClO_4)_2$, $NiL_4(H_2O)_2(ClO_4)_2$ et $NiL_6(H_2O)_2(ClO_4)_2$ (L = γ-picoline); on compare leurs propriétés spectrales, magnétiques et autres. Alors que des deux premiers complexes ont fait l'objet d'une communication antérieure (1), on fait maintenant des suggestions plausibles concernant la structure du dernier complexe.

Canadian Journal of Chemistry, 49, 1502 (1971)

Introduction

In the course of an investigation into the nuclear magnetic resonance (n.m.r.) isotropic shifts of some nickel(II) complexes with substituted pyridines, it was found necessary to become involved with the Ni(II)–γ-picoline–perchlorate system. Procedures in the literature (1) were used to obtain two compounds, *viz.*, $NiL_4(ClO_4)_2$ and $NiL_4(H_2O)_2(ClO_4)_2$, but under other conditions, a third compound was obtained, *viz.*, $NiL_6(H_2O)_2(ClO_4)_2$. The reversible conversion of the yellow $NiL_4(ClO_4)_2$ to the blue $NiL_4(H_2O)_2(ClO_4)_2$ when exposed to moisture, and the conversion of the blue $NiL_6(H_2O)_2(ClO_4)_2$ to the yellow $NiL_4(ClO_4)_2$ upon drying have led to a more detailed investigation of the spectral and physical properties of these compounds.

Experimental

$NiL_4(ClO_4)_2$ and $NiL_4(H_2O)_2(ClO_4)_2$ were prepared according to previously published procedures (1). Better crystals of the former compound were obtained from a solution of γ-picoline and nickel(II) perchlorate hexahydrate (molar ratio 4:1) in hot butanol.

$NiL_6(H_2O)_2(ClO_4)_2$ was precipitated as blue crystals upon the addition of an aqueous solution of $Ni(ClO_4)_2 \cdot 6H_2O$ to an aqueous solution of excess ligand. These crystals were filtered off and air dried for several hours.

TABLE 1. Properties

Parameter	Description		
	$NiL_4(ClO_4)_2$	$NiL_4(H_2O)_2(ClO_4)_2$	$NiL_6(H_2O)_2(ClO_4)_2$
Color	Yellow	Blue	Blue
μ_{eff} (B.M.)‖	Diamagnetic	3.12	3.11
Thermal stability	Melts and decomp. 222–252 °C	Loses water at 76 °C	Loses water and 2L at 73 °C
Molar conductance¶ (mho cm^2 mol^{-1}) 0.01 *M* in CH_2Cl_2 at 23 °C	1.29 (21.30)* (28.40)†	1.55 (2.54)‡	2.68 (3.36)‡
Reaction with H_2O	Blue ppte.§ green soln.	Blue ppte.§ green soln.	No reaction (very slightly soluble)
Reaction with CH_2Cl_2 or $CHCl_3$	Green soln.	Blue-green soln.	Blue soln.
Reaction with anhydrous ether	No reaction	Turns yellow (loss of water)	Turns yellow (loss of water and ligand)

*Solution in γ-picoline.
†After heating and cooling in γ-picoline.
‡Solution in CH_2Cl_2 sat. with H_2O.
§The blue ppte. was found to be $NiL_6(H_2O)_2(ClO_4)_2$.
‖Magnetic measurements were made on a Guoy type balance supplied by Newport Instruments (U.K.) and through the courtesy of Dr. F. Bottomley of this department.
¶Conductance measurements were made on an Industrial Instruments Model RC 16B2 Conductivity bridge. The cell was calibrated with a standard aqueous solution of KCl. The conductivity of the solvent methylene chloride or γ-picoline was found to be negligible.

TABLE 2. Infrared spectra*

Compound	Frequency (cm^{-1}) in medium: KBr	Nujol	$CHCl_3$ or CH_2Cl_2	Assignment
$Ni(ClO_4)_2.6H_2O$	3380(s)			HOH asym str. ν_3
	3210(sh)			HOH asym. str. ν_1
	1625(m)			HOH bend ν_2
	1143(s),1112(s)			ClO_4 ν_3
	1089(s)			
	939(w)			ClO_4 ν_1
	627(s)			ClO_4 ν_4
γ-Picoline			1600(vs)	ν_{8a}
			516(m)	ν_{6a}
			485(s)	ν_{16b}
$NiL_4(ClO_4)_2$	1624(s)			ν_{8a}
	576(m), 545(w)		544(m)	ν_{6a}
	514(s), 500(s)		496(s)	ν_{16b}
	1145(vs), 1121(vs)		1140(vs), 1032(vs)	ClO_4 ν_3
	1115(sh), 1090(vs)			
	940(w), 930(w)		930(s)	ClO_4 ν_1
	628(s)		630(sh), 619(s)	ClO_4 ν_4
		275(w), 262(w)		Ni—N str.
$NiL_4(H_2O)_2(ClO_4)_2$	3420(s)			H_2O ν_3
	3280(sh)			H_2O ν_1
	1640(sh)			H_2O ν_2
	1615(s)			ν_{8a}
	540(w)			ν_{6a}
	493(s)			ν_{16b}
	1140(vs), 1110(vs)		1130(vs), 1030(vs)	ClO_4 ν_3
	1085(vs)			
	926(w), 937(w)		929(m)	ClO_4 ν_1
	632(sh), 626(s)		623(s)	ClO_4 ν_4
		272(w)		Ni—N str.
		237(m), 225(sh)		?
$NiL_6(H_2O)_2(ClO_4)_2$	3450(m)	3420(m)	3420(w)	H_2O ν_3
	3280(sh)			H_2O ν_1
	1660(sh)	1682(m)	1670(sh)	H_2O ν_2
	1616(s)	1619(s), 1607(sh)	1622(s), 1607(sh)	ν_{8a}
	1141(vs), 1108(sh)	1110–1055(br.vs)	1130(vs)	
	1091(vs)		1030(vs)	ClO_4 ν_3
	937(w)	925(w)	928(m)	ClO_4 ν_1
	627(s)	621(s)	620(s)	ClO_4 ν_4
	540(w)	540(w), 520(w)	544(w), 515(sh)	ν_{6a}
	495(s)	495(s), 486(sh)	492(s), 482(sh)	ν_{16b}
		270(w), 277(sh)		Ni—N str.
		228(m), 237(sh)		?

*s = strong, m = medium, w = weak, v = very, sh = shoulder, br = broad. Infrared spectra were taken on a Beckman IR-12 spectrophotometer. Both KBr and Nujol mulls were used for the solid compounds in the 4000–200 cm^{-1} region. Solutions of the compounds in both chloroform and methylene chloride were also run using caesium bromide cells and polyethylene bags.

Anal. Calcd.: C, 50.70; H, 5.44; O, 18.76; N, 9.86; Cl, 8.32; Ni, 6.89. Found: C, 49.88; H, 5.44; O, 19.58; N, 9.92; Cl, 8.47; Ni, 6.67.

Analyses were performed by Dr. F. Pascher, Mikroanalytische Laboratorium, Bonn, West Germany.

Results and Discussion

It is apparent that γ-picoline, water, and perchlorate compete in solution for the nickel(II). It would also appear that some of these are not very strongly bound to the central metal, and ready conversion from one compound to another is observed.

In view of the previously assigned structures for Ni(II) complexes (1, 4) a square planar arrangement of four γ-picoline molecules is assumed for all three compounds. The two blue compounds could then have water and γ-picoline, respectively, occupying the octahedral positions. It is possible that the latter compound could be formulated as $NiL_4(H_2O)_2(ClO_4)_2.2L$, analogous to the compounds such as $Ni(pyr)_4(NCO)_2.2pyr$ reported by Norbury *et al.* (2). The perchlorate in all three solid compounds would be presumably ionic.

The infrared (i.r.) spectra of the three compounds (Table 2) tend to confirm these structural

Can. J. Chem. Downloaded from www.nrcresearchpress.com by 210.87.254.42 on 09/05/12
For personal use only.

TABLE 3. Electronic spectra*

Complex	Frequency (nm)			
	Ligand band		Metal d and d band	
	Chloroform	Nujol	Chloroform	Nujol
$NiL_4(ClO_4)_2$†	256.9	259	370 (18) 602 (6.4) 792‡	435
$NiL_4(H_2O)_2(ClO_4)_2$	256.5	263.5	370 (16) 605 (6.3) 860‡	365
$NiL_6(H_2O)_2(ClO_4)_2$	256.5	261.5	368 (15) 599 (6.1) 860‡	364 590 860‡

*Electronic spectra were taken by Miss M. Tong on a Hitachi SP3-T spectrophotometer, both in solution and as Nujol mulls. Numbers in parentheses are molar extinction coefficients.
†In chloroform solution, this compound gives rise to a green solution.
‡Very weak absorption.

assignments. Free ligand peaks were observed in Nujol and $CHCl_3$ (or CH_2Cl_2) for $NiL_6(H_2O)_2(ClO_4)_2$, although they are not well-defined in KBr. Assignment of these peaks is based on that for the corresponding pyridine complexes (2, 5). The water peaks in both this compound and $NiL_4(H_2O)_2(ClO_4)_2$ are within the range of those for lattice water (ν_3:3465–3407 cm^{-1}) (6), indicating that the water is at most weakly bound to the metal. The thermal data in Table 1 also confirms this observation. Comparing the spectra in the perchlorate region with that of $Ni(ClO_4)_2.6H_2O$ (7, 8) in KBr and Nujol one can conclude that the perchlorate in all cases is ionic in solid state although there is some activation of the ν_1 mode and splitting of the ν_3 mode, presumably due to the effects of low site symmetry of the crystal lattice. However, in CH_2Cl_2 or $CHCl_3$ solutions, the spectra show that coordination of the perchlorate to the metal ion has taken place in all three compounds as the result of removal of this lattice effect in solution. The far infrared of the blue compounds show some unassigned peaks in the region 225–240 cm^{-1}, and could be an indication of a weaker Ni—N bond resulting from a constrained ligand conformation imposed by the waters at the octahedral positions. Similar peaks were observed in the compounds $Ni(\gamma\text{-pic})_4Cl_2$ and $Ni(\gamma\text{-pic})_4Br_2$ (3).

The electronic spectral data (Table 3) are consistent with a change from a square planar configuration in the yellow $NiL_4(ClO_4)_2$ to an octahedral geometry in the other two cases.

The conductance data (Table 1), taken in methylene chloride, indicate that 0.01 *M* solutions of all the complexes are very little ionized indicating coordination of the perchlorate in solution, consistent with the i.r. solution data. The solutions of these compounds, when saturated with water, increase these values only slightly; apparently the small amount of water thus added competes equally well with γ-picoline for the metal. The yellow compound dissolved in γ-picoline as solvent, shows a large increase in conductance consistent with increased concentrations of NiL_4^{2+}, $ClCO_4^-$, and NiL_6^{2+}. Upon heating and cooling, the solution turned yellow-green and the conductance increased even further, consistent with the greater stability of NiL_4^{2+} over NiL_6^{2+}.

The complex $NiL_6(H_2O)_2(ClO_4)_2$ has been turned over to Dr. H. Lynton of this department for an X-ray crystallographic determination of its structure.

The continued financial support of the National Research Council of Canada and the award of a U.N.B. demonstratorship to M. S. Sun are gratefully acknowledged. Thanks are also extended to Mr. M. Sears and Miss M. Tong for recording some of the spectra.

1. L. M. VALLARINO, W. E. HILL, and J. V. QUEGLIANO. Inorg. Chem. **4**, 1598 (1965).
2. A. H. NORBURY, E. A. RYDER, and R. F. WILLIAMS. J. Chem. Soc. A, 1439 (1967).
3. M. S. SUN. Unpublished data, this laboratory.
4. S. BUFFAGNI, L. M. VALLARINO, and J. V. QUEGLIANO. Inorg. Chem. **3**, 671 (1964).
5. N. S. GILL, R. H. NUTTALL, D. E. SCAIFED, and D. W. A. SHARP. J. Inorg. Nucl. Chem. **18**, 79 (1961).
6. P. J. LUCCHESI and W. A. GLASSON. J. Am. Chem. Soc. **78**, 1347 (1956).
7. R. W. G. WYCKOFF. Crystal structures. Vol. 3. 2nd ed. Interscience Publishers. p. 814.
8. C. D. WEST. Z. Krist. **91A**, 480 (1935).

Can. J. Chem. Downloaded from www.nrcresearchpress.com by 210.87.254.42 on 09/05/12
For personal use only.

Can. J. Chem. Downloaded from www.nrcresearchpress.com by 210.87.254.42 on 09/05/12
For personal use only.

Studies of Substitution Reactions in Chromium(VI)–Fluorine Species

A. M. AKENA, D. S. BROWN, AND D. G. TUCK[1]

Department of Chemistry, Simon Fraser University, Burnaby 2, British Columbia

Received September 22, 1970

Nuclear magnetic resonance (n.m.r.) studies show that the exchange between fluorochromate(VI) and fluoride in dimethylsulfoxide is slow, in agreement with previous work on oxygen exchange between water and chromates(VI). No substitution was detected in the system CrO_3F^-/Cl^- in acetonitrile. Mixtures of chromyl fluoride and chromyl chloride show rapid fluorine exchange, both as the pure compounds, and in solution in trichlorofluoromethane. Possible mechanistic implications of these results are discussed.

Des études par r.m.n. permettent de démontrer que l'échange entre le fluorochromate(VI) et les ions fluorures dans le DMSO est une réaction lente; cette conclusion est en accord avec des travaux antérieurs sur l'échange d'oxygène entre l'eau et des chromates(VI). Dans l'acétonitrile, il n'est pas possible de détecter de substitutions dans le système CrO_3F^-/Cl^-. Toutefois des mélanges de fluorure de chromyle et de chlorure de chromyle s'échangent rapidement soit à l'état pur soit en solution dans le trichlorofluoromethane. On discute des implications mécanistiques possibles de ces résultats.

Canadian Journal of Chemistry 49, 1505 (1971)

Introduction

Much of the work on the inter-relationship of the various chromium(VI) species which may exist in aqueous solution has been based on the study of equilibria, but kinetic measurements can also provide significant information. The most recent studies in this field are those of Holyer and Baldwin (1), who investigated the rate of exchange of ^{18}O between chromium(VI) oxyanions and bulk water, as a function of p*H* and total chromium(VI) concentration. These authors, who also review the earlier literature, discuss their results in terms of the possible transition states for oxygen exchange.

During studies of the coordination chemistry of chromium(VI), we attempted to measure the equilibrium constant for substitution processes of the type

$$[1] \qquad CrO_3F^- + Cl^- \rightleftarrows CrO_3Cl^- + F^-$$

in non-aqueous solution, conditions chosen to eliminate competing hydrolytic processes such as

$$[2] \qquad CrO_3F^- + H_2O \rightleftarrows HCrO_4^- + HF$$

which must occur in aqueous solution. The rate of equilibration in [1] was found to be slow relative to the time limits imposed by the oxidative stability of the solvent. We subsequently investigated the exchange of ^{19}F between fluorochromate(VI) and fluoride in non-aqueous solution by n.m.r. methods. These latter results in particular bear upon the work of Holyer and Baldwin, and earlier workers, in that CrO_3F^- is isoelectronic with the $HCrO_4^-$ anion. Fluorine exchange in related systems, including chromyl fluoride plus chromyl chloride, was also studied, again in non-aqueous media.

The number of possible solvents for this work was rather restricted. For the n.m.r. studies of the CrO_3F^-/F^- and CrO_3F^-/Cl^- systems, the requirements for high solute concentration and reasonable resistance to chromium(VI) oxidation were met by dimethylsulfoxide, and the solubility was enhanced by using the tetraphenylarsonium or tetraalkylammonium salts throughout, and where necessary by working at temperatures above ambient. Ultraviolet spectroscopic studies of the CrO_3F^-/Cl^- system required a solvent which does not obscure the absorption bands of the halochromate anions, or (preferably) the fine structure of these bands (see below); acetonitrile proved satisfactory for this purpose. Nuclear magnetic resonance studies of chromyl fluoride either alone or mixed with chromyl chloride were carried out in trichlorofluoromethane, which has the necessary resistance to oxidation by these substances.

Experimental

Materials

(*1*) Solvents. Acetonitrile (Eastman, Spectroscopic grade) was distilled several times from phosphorus pentoxide before use. Dimethylsulfoxide (Fisher Scientific) was distilled three times from calcium hydride

[1]To whom correspondence should be addressed.

Can. J. Chem. Downloaded from www.nrcresearchpress.com by 210.87.254.42 on 09/05/12
For personal use only.

(40 °C, 15 mm pressure), and stored over calcium hydride. Trichlorofluoromethane (Matheson Co., Inc., "Freon 11", 99.9% purity) was dried over Linde molecular sieve for several days before use.

(*2*) Halide salts. Tetraethylammonium chloride and fluoride (Eastman Kodak) were recrystallized in vacuo from absolute ethanol, and stored over phosphorus pentoxide. Analysis of the material showed a low fluorine figure (found (ionic) F 11.6; $(C_2H_5)_4NF$ requires F 12.7%); since the compound picks up solvent or moisture very rapidly, this result suggests the presence of solvent in the solid. Tetraphenylarsonium chloride was used as supplied.

(*3*) Tetraphenylarsonium fluorochromate(VI). An aqueous solution of tetraphenylarsonium nitrate, prepared by titration of the corresponding chloride with silver nitrate, was added to an aqueous solution of potassium dichromate in 2 *M* hydrofluoric acid. The yellow precipitate so formed was redissolved in 1:1 acetone:chloroform, and reprecipitated with petroleum ether. Analysis confirmed that this method, which is known to give the corresponding chlorochromate salt (2), yields tetraphenylarsonium fluorochromate.

Anal. Calcd. for $C_{24}H_{20}AsCrO_3F$: C, 57.4; H, 4.0; As, 14.9; Cr, 10.4; F, 3.5. Found: C, 57.2; H, 4.1; As, 14.9; Cr, 10.3; F, 3.5.

The infrared (i.r.) spectrum was in agreement in all relevant features with that of potassium fluorochromate(VI) (3).

Solutions of halochromate salts were found to undergo decomposition on exposure to light, and were therefore handled in the dark as far as possible.

(*4*) Chromyl chloride. The pure liquid (Alfa Inorganics Inc.) was distilled in a dry apparatus with phosphorus pentoxide traps immediately before use.

(*5*) Chromyl fluoride. Chromium trioxide was treated with sulfur tetrafluoride (4) in a glass apparatus, and the red product collected at −35° (5). The solid was then sublimed onto either $CFCl_3$ or chromyl chloride frozen at −78°; the resulting solutions were used for n.m.r. spectroscopy. All handling of such mixtures was carried out in a dry-box over phosphorus pentoxide.

Spectral Studies

^{19}F n.m.r. spectra were run on a Varian A56/60 Spectrometer, operating at an oscillator frequency of 56.4 MHz. Unless otherwise stated, the sample temperature was 35°. Chemical shifts for ^{19}F, defined as $\delta = -(\nu_{sample} - \nu_{ref})/\nu_{ref}$, were measured relative to $CFCl_3$ as either internal or external standard.

Visible/ultraviolet spectra were measured with Unicam SP 800 or Cary 14 spectrophotometers.

Results and Discussion

Fluorochromate(VI)–Chloride System

The electronic spectrum of tetraphenylarsonium fluorochromate(VI) in acetonitrile consists of a high intensity cation absorption, plus an anion band centered at 28 400 cm^{-1} ($\varepsilon = 794$). This latter showed symmetrical vibrational fine structure, with a frequency spacing of approximately 700 cm^{-1}. The spectrum of tetraphenylarsonium chlorochromate(VI) has the corresponding maximum at 27 500 cm^{-1} ($\varepsilon = 1.43 \times 10^3$), with a similar fine structure. The absorption spectrum of a millimolar solution of the fluorochromate salt in acetonitrile was unaffected by the addition to the solution of an equimolar quantity of tetraphenylarsonium chloride; no change could be detected over a time span of three days. The addition of a tenfold molar excess of the chloride salt ultimately produced a small change in the fluorochromate spectrum, but the rate of change was too slow to allow any significant rate measurements to be made, in view of the limitations imposed by the oxidation of the solvent.

The ^{19}F resonance of a 0.25 *M* solution of tetraphenylarsonium fluorochromate in dimethylsulfoxide (DMSO) is at $\delta = 161.4$ p.p.m. from (external) $CFCl_3$. The line width at half-height is 2.5 ± 0.5 Hz. The addition of equimolar quantities of either tetraphenylarsonium or tetraethylammonium chloride in DMSO had no effect; the ^{19}F resonance signal was unchanged in both frequency and intensity over 1 h. The only change in the ^{19}F resonance of mixed solutions stored in the dark for 12 h was a broadening of the peak.

Upper limits for the rate constant (k_f) for the forward reaction in [1] can be obtained from these results. We estimate that the minimum change which would have escaped detection in the u.v./visible spectroscopic measurements is 5%; this is almost certainly a generous overestimate. For a time interval of 3 days, this implies an upper limit for k_f in acetonitrile of 2×10^{-4} l mol^{-1} s^{-1}. Similarly, analysis of the n.m.r. results shows that the decrease in CrO_3F^- concentration over 1 h could not have exceeded 5%; the rate constant in DMSO is then less than 5×10^{-5} l mol^{-1} s^{-1}. We return to these conclusions below.

Fluorochromate(VI)–Fluoride System

A solution of tetraethylammonium fluoride in DMSO at 50° had the ^{19}F resonance at $\delta = 142.7$ p.p.m. Mixing equal volumes of 0.25 *M* solutions of this salt and tetraphenylarsonium fluorochromate(VI) produced no alteration in the resonance frequency of either fluoro species. Some difficulty was experienced in making measurements on the ^{19}F resonance of tetraethylammonium fluoride

Can. J. Chem. Downloaded from www.nrcresearchpress.com by 210.87.254.42 on 09/05/12
For personal use only.

in the mixed solutions, and for this reason all results refer to the more readily detectable ^{19}F resonance of the fluorochromate anion. No change in this resonance could be detected after 2 h, indicating the absence of significant ^{19}F exchange in the CrO_3F^-/F^- system in DMSO at this temperature. The average lifetime of each species can be calculated from standard formulae (6) as $> 10^{-3}$ s, corresponding to a gross upper limit for the rate constant for the fluorine exchange in

[3] $$CrO_3F^- + F^- \rightleftarrows CrO_3F^- + F^-$$

of 10^3 l mol^{-1} s^{-1}.

Holyer and Baldwin (1) have reported a value of 7×10^{-7} s^{-1} for the pseudo-first order rate constant k_1' ($= k_1/[H_2O]$) for the aqueous phase exchange

[4] $$CrO_4^{2-} + H_2O^* \rightleftarrows CrO_3O^{*2-} + H_2O$$

which is one of two possible paths for oxygen exchange between water and chromium(VI) species at high pH in aqueous solution. These authors note however that the process

[5] $$HCrO_4^- + \overset{*}{O}H^- \rightleftarrows HCrO_3\overset{*}{O}^- + OH^-$$

provides an alternative path for oxygen exchange; the rate constant deduced for the forward reaction in [5] is 70 l mol^{-1} s^{-1}.

There are of course significant differences in the nature of the species present in aqueous solution and in DMSO or acetonitrile. In particular, the lower dielectric constants of the organic solvents ($\varepsilon = 46.6$ for DMSO (7), $\varepsilon = 36.2$ for acetonitrile (8)) must bring about more extensive ion-pairing than in aqueous solution, so that coulombic repulsion between two anions forming the transition state must be lower than in water. Despite the problems raised by these differences, we believe that the slow exchange observed in CrO_3F^-/F^- and CrO_3F^-/Cl^- argues against the identification of [5] as a rate-controlling process in the aqueous system. A more important question, to which we return below, is the mode of formation of the transition state for ligand exchange in chromium(VI) species.

The water content of the DMSO used in the exchange experiments described above was shown by gas–liquid chromatography to be 0.03% by weight. When the water content was deliberately increased above this value, the ^{19}F resonance peak of the fluorochromate anion collapsed at a readily measureable rate. With a solution of tetraphenylarsonium fluorochromate in DMSO containing 10% H_2O, the peak height decreased by approximately 50% within the time necessary for mixing the solutions and running the spectrum (approximately 3 min). Some broadening of the resonance signal was also observed. In similar solutions left for longer periods (up to 24 h), the formation of chromium(III) species was observed spectroscopically for both fluorochromate(VI) and chlorochromate(VI) systems; with CrO_3Cl^- in DMSO/H_2O, broad absorptions at 24 700 and 16 250 cm^{-1} appeared, and with CrO_3F^-, a new absorption at 25 300 cm^{-1} was detected. These results are consistent with the presence of $[Cr(H_2O)_5Cl]^{2+}$ and $[Cr(H_2O)_5F]^{2+}$, respectively, following the work of Swaddle and King (9). The broadening observed in the ^{19}F n.m.r. spectrum is presumably due to the growth of paramagnetic species in the solution, and for this reason no attempt was made to follow the hydrolysis process [2] by n.m.r. methods.

Chromyl Fluoride/Chromyl Chloride System

The ^{19}F resonance of chromyl fluoride in trichlorofluoromethane solution is a sharp singlet at 30.4 ± 0.4 p.p.m. downfield from the $CFCl_3$ resonance, independent of temperature and concentration over the ranges studied, within experimental error (see Table 1). The addition of chromyl chloride causes this resonance to move downfield, but in all cases we observed a singlet, whose frequency was dependent on the CrO_2F_2:CrO_2Cl_2 molar ratio, and to a slight extent upon the temperature. In dilute solution in trichlorofluoromethane, the half-width of the signal was < 1 Hz; in solvent-free mixtures, some broadening was observed. Our results do not allow any deductions as to the origin of the small temperature dependence.

The ready exchange of ^{19}F, shown by the presence of a single resonance, can be ascribed to the rapid establishment of the equilibrium

[6] $$CrO_2F_2 + CrO_2Cl_2 \rightleftarrows 2CrO_2FCl$$

The existence of a chromyl fluorochloride has previously been reported by Flesch and Svec (10) on the basis of infrared and mass-spectrometric observations; a value of 2.0 was found for the equilibrium constant for [6] in a solvent-free mixture of the parent chromyl halides. We assume the ^{19}F spectrum observed in the presence of a

TABLE 1. ^{19}F resonance frequencies in chromyl fluoride/chromyl chloride systems*

Exp. No.	Temperature (°C)	$[CrO_2F_2]$ (*M*)	$[CrO_2Cl_2]$ (*M*)	$\frac{[CrO_2Cl_2]}{[CrO_2F_2]}$	^{19}F resonance, downfield from $CFCl_3$ (p.p.m.; ±0.4)
1	0	< 0.02	0	—	30.3
2	−30	< 0.02	0	—	30.8
3	0	0.6	0	—	30.1
4	20	2	2	1	31.9
5	−30	0.3	6	20	29.0
6	0	< 0.02	6	> 300	38.8
7	−30	< 0.02	6	> 300	39.0
8	−30	6	6	1	39.0
9	0	6†	6	1	38.3
10	20	6†	6	1	38.3

*All results refer to solutions in $CFCl_3$, except for exp. 8, 9, and 10, which involved solvent-free mixtures of CrO_2F_2 and CrO_2Cl_2.
†Approximate value.

large excess of chromyl chloride (exp. 6 and 7 in Table 1) is essentially that of CrO_2FCl in $CFCl_3$ ($\delta = 38.9$ p.p.m.). If the resonance from an equimolar mixture in this (exp. 4) represents the time-averaged environment of the fluorine exchanging between CrO_2F_2 and CrO_2FCl, then one can calculate the relative concentration of all the species involved (11), from which we find the equilibrium constant for [6] is ~ 0.15. This value is of course for conditions which are different from those used by Flesch and Svec (10), but allowing for this, and for the differences inherent in the methods of measuring *K*, the agreement appears reasonable.

General Conclusions

The results reported show that chromium(VI) oxyfluoro-species undergo ligand exchange at rates which depend sharply on the nature of the compound. In seeking to explain such variations in terms of possible exchange mechanisms, we should first note that with few exceptions the normal coordination number of chromium(VI) is four. One group of higher coordination species is the peroxy complexes, which have been discussed elsewhere (12), and another exception is CrF_6, which decomposes above about −100°, but which probably has O_h symmetry (13). Chromium(VI) may have a coordination number greater than four in the 1:1 adduct of CrO_2F_2 and $K[HF_2]$ (14). No compound with a coordination number below four has been reported; even solid CrO_3 involves four-coordinate chromium(VI) (15). It is interesting that chromium(VI) does not show the easy 4 → 6-coordination expansion found in the corresponding oxidation states of molybdenum and tungsten.

On this evidence, substitution processes in chromium(VI) species must involve an S_N2 mechanism, but for CrO_4^{2-}/H_2O (or $HCrO_4^-/OH^-$), CrO_3F^-/Cl^- and CrO_3F^-/F^-, the formation of a five-coordinate transition state appears to be energetically unfavorable. A common factor in all these systems is the high molecular symmetry of the initial chromium(VI) species, and it seems probable that the highly symmetrical σ- and π-bonding system resists any rearrangement to a five-coordinate state. A useful analogy here is the energy barrier to rearrangement in $BF_3 \rightarrow BF_4^-$ (16).

For the CrO_2F_2/CrO_2Cl_2 system, exchange will be favored by two factors not applicable in the above discussion. These are; (*a*), the exchange involves neutral species, so that there will be no coulombic repulsion to be overcome in forming the transition state, and (*b*), the lower molecular symmetry could result in a weakening of those bonds which stabilize the initial structure. A number of possible transition states can be pictured; a model such as

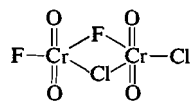

clearly permits dissociation either to the starting materials, or to CrO_2FCl. The existence of $(CrO_2X_2)_2$ dimers in the gas phase has been deduced from mass-spectrometric experiments (10). It must be emphasized, however, in any

Can. J. Chem. Downloaded from www.nrcresearchpress.com by 210.87.254.42 on 09/05/12
For personal use only.

discussion of rapid halogen exchange between CrO_2F_2 and CrO_2Cl_2, that catalysis by residual traces of water cannot be excluded with absolute certainty.

This work was supported in part by Operating Grants from the National Research Council of Canada. Dr. E. J. Wells is thanked for a number of stimulating discussions.

1. R. H. Holyer and H. W. Baldwin. Can. J. Chem. **45**, 413 (1967).
2. D. G. Tuck and B. D. Faithful. J. Chem. Soc. 5753 (1965).
3. H. Stammreich, O. Sala, and D. Bassi. Spectrochim. Acta, **19**, 593 (1963).
4. C. W. Tullock, F. S. Fawcett, W. C. Smith, and D. D. Coffman. J. Am. Chem. Soc. **82**, 539 (1960).
5. H. L. Kraus and F. Schwarzbach. Chem. Ber. **94**, 1205 (1961).
6. H. S. Gutowsky and C. H. Holm. J. Chem. Phys. **25**, 1228 (1957).
7. P. G. Sears, E. D. Wilhoit, and L. R. Dawson. J. Phys. Chem. **60**, 169 (1956).
8. A. Weissberger, E. S. Proskauer, J. A. Riddick, and E. E. Toops. Techniques of organic chemistry. Vol. VII. Interscience, New York, 2nd ed. 1959. p. 219.
9. T. W. Swaddle and E. J. King. Inorg. Chem. **4**, 532 (1965).
10. G. D. Flesch and H. J. Svec. J. Am. Chem. Soc. **80**, 3189 (1958); **81**, 1787 (1959).
11. H. S. Gutowsky and A. Saika. J. Chem. Phys. **21**, 1688 (1953).
12. D. G. Tuck and R. M. Walters. Inorg. Chem. **2**, 428 (1963).
13. O. Glemser, H. Roesky, and K. H. Helberg. Angew. Chem. (Int.) **2**, 266 (1963).
14. A. Englebrecht and A. V. Grosse. J. Am. Chem. Soc. **74**, 5262 (1954).
15. A. F. Wells. Structural inorganic chemistry. Oxford University Press, 3rd ed. 1962. p. 442.
16. F. A. Cotton and J. R. Leto. J. Chem. Phys. **30**, 993 (1959).

Can. J. Chem. Downloaded from www.nrcresearchpress.com by 210.87.254.42 on 09/05/12
For personal use only.

Can. J. Chem. Downloaded from www.nrcresearchpress.com by 210.87.254.6 on 09/05/12
For personal use only.

Vibrational Spectral Studies of Hexaquozinc Nitrate and Hexaquozinc Nitrate-d_2

M. H. BROOKER[1] AND D. E. IRISH

Department of Chemistry, University of Waterloo, Waterloo, Ontario

Received July 9, 1970

Infrared and Raman spectra are reported for the hexaquozinc nitrate crystal. Replacement of water by deuterium oxide causes a remarkable intensity reversal of components in the ν_3 nitrate region and provides Raman spectra free from interference in the $2\nu_2$ and ν_4 regions. The nitrate spectrum is interpreted in terms of a site group approximation. The spectra are compared with those of concentrated aqueous solutions and partially dehydrated crystals to point up changes which result from a lowered site symmetry and those which result from ionic association.

Des spectres infrarouge et Raman sont présentés pour le cristal de nitrate de zinc hexahydraté. La substitution de l'oxyde du deutéreum à l'eau produit un renversement remarquable de l'intensité des composantes du ν_3 du nitrate et il crée des spectres Raman libres d'interférence dans les régions de la $2\nu_2$ et de ν_4. Le spectre du nitrate est interprété en termes d'une approximation des groupes de site. La comparaison des spectres avec ceux de solutions aqueuses concentrées et ceux des cristaux partiellement déshydratés a pour but de montrer les changements qui résultent d'une symétrie de site réduite et ceux qui résultent d'une association ionique.

Canadian Journal of Chemistry, 49, 1510 (1971)

Introduction

Vibrational studies of hydrated crystalline nitrate salts have received very little attention. Ferraro (1) and Addison and Gatehouse (2) have reported infrared spectra of some hydrated transition metal nitrates. Frequencies reported by these authors exhibit variations which are apparently dependent on the sampling technique used. Mathieu and Lounsbury (3) have reported Raman spectra for several hydrated metal nitrate crystals and have noted that the vibration spectra of the hydrated crystals resemble those of the aqueous solutions from which the crystal was precipitated. Infrared and Raman spectra have been recorded for room-temperature hexaquozinc nitrate crystals and interpreted in the light of the recently proposed crystal structure (4). Additional information has been obtained from substitution of water by heavy water. When D_2O is substituted for H_2O in the crystals, interesting intensity changes in the components of the ν_3 and ν_4 vibrations are observed. Partially dehydrated samples were also studied. Comparison of spectra for a system in which nitrate ion is influenced by an aquated cation with those for a system in which zinc and nitrate ion are in contact broadens the base for the interpretation of spectra of ionic solutions.

[1]Present address: Oak Ridge National Laboratory, Oak Ridge, Tennessee 37830.

Experimental

"Baker Analyzed" reagent $Zn(NO_3)_2.6H_2O$ was recrystallized from an aqueous solution saturated at 36 °C. $Zn(NO_3)_2.6D_2O$ was prepared as follows: $Zn(NO_3)_2.6H_2O$ was partially dehydrated at 45 °C, dissolved in excess D_2O and slowly concentrated to half volume. D_2O was added and the process repeated twice; crystals obtained after this process were recrystallized from a D_2O solution saturated at 36 °C. Bands attributable to H_2O were absent in the spectra of these crystals. The infrared spectrum of polycrystalline $Zn(NO_3)_2.6H_2O$ (thermostated at 15 °C) (Fig. 1) was recorded against a KRS-5 prism with face angle of 60° placed in a Wilks model-9 M.I.R. attachment. The usefulness of this technique for solid samples has been discussed elsewhere (5). Raman spectra (Fig. 2) were obtained employing the Jarrell-Ash model 25–300 Raman spectrometer. Excitation of samples was achieved with the 4880 Å line of a Spectra Physics model 141 Argon ion laser. Plasma lines were removed with an appropriate narrow band interference filter. Polycrystalline samples were contained in thin-walled Pyrex tubes and thermostated at 25 °C. Raman spectra remained unchanged after prolonged exposure to the laser light. Local heating of the sample and subsequent dehydration did not occur. Excessive grinding of the crystals caused partial dehydration whereas the crystals picked up moisture and melted if exposed to the atmosphere for prolonged periods. Both effects could be detected by spectral changes. Some samples were partially dehydrated in an oven at 40 and 100 °C. No orientational or polarization effects were observed, as expected for polycrystalline samples.

Results and Discussion

$Zn(NO_3)_2.6H_2O$ crystals are orthorhombic, space group D_{2h}^{16}-*Pnma* with 4 molecules per

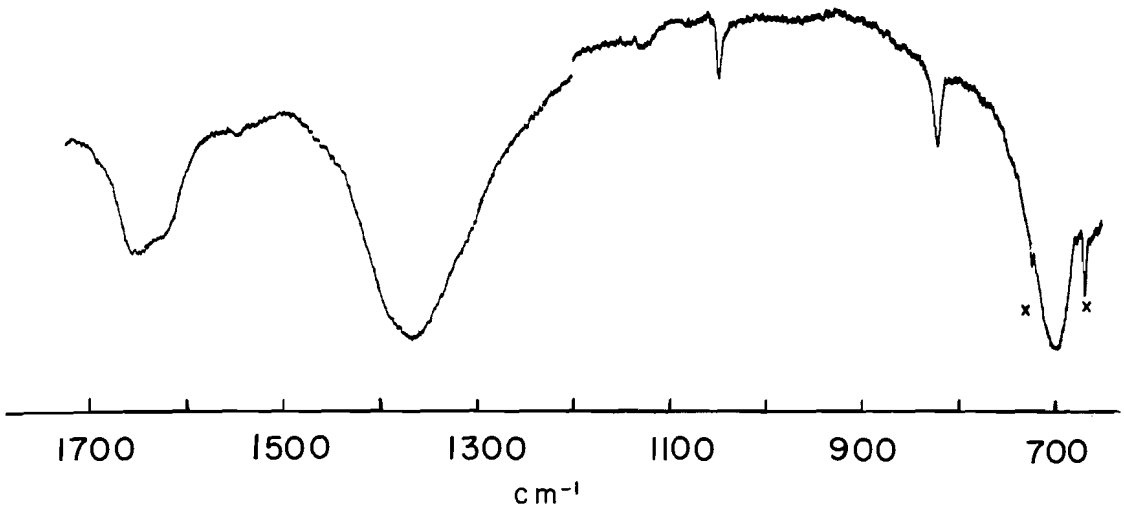

FIG. 1. Photograph of the multiple internal reflection spectrum of $Zn(NO_3)_2.6H_2O$ from 660 to 1750 cm^{-1}.

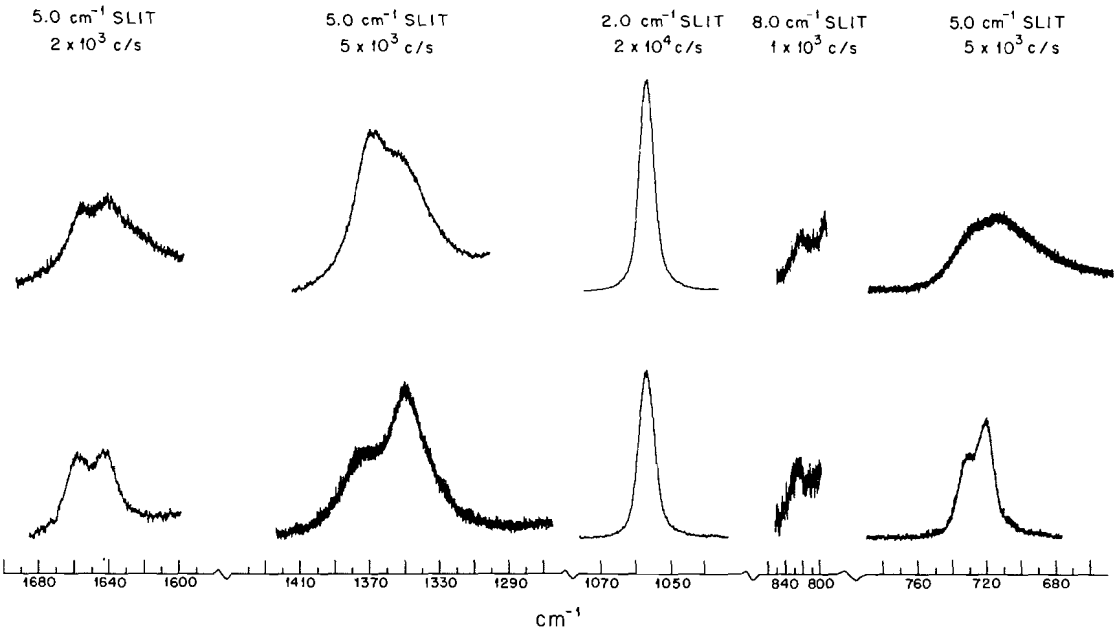

FIG. 2. Photograph of portions of the Raman spectra of $Zn(NO_3)_2.6H_2O$ (top) and $Zn(NO_3)_2.6D_2O$ (bottom).

primitive unit cell. The structure is composed of $[Zn(OH_2)_6]^{2+}$ cations and NO_3^- anions (4). All NO_3^- ions occupy general sites. The hexaquozinc has nearly octahedral symmetry. The two axial water molecules are somewhat closer to zinc, however, and occupy general sites; the four equatorial water molecules occupy C_s sites.

Infrared and Raman spectra are presented in Figs. 1 and 2. Frequencies and tentative assignments for hexaquozinc nitrate crystals are collected in Table 1. Broad Raman bands centered at 376 and 241 cm^{-1} for $Zn(NO_3)_2.6H_2O$ and at 358 and 226 cm^{-1} for $Zn(NO_3)_2.6D_2O$ are assigned to δ(Zn—O) stretching and deformation

Can. J. Chem. Downloaded from www.nrcresearchpress.com by 210.87.254.6 on 09/05/12
For personal use only.

TABLE 1. Vibrational frequencies for hexaquozinc nitrate

Frequency* (cm^{-1})			
$Zn(NO_3)_2.6H_2O$		$Zn(NO_3)_2.6D_2O$	
Infrared	Raman	Raman	Assignments
	50	49	
	60		
	73	70	
	85	85	
	111	110	
		226	$Zn—OD_2$
		358	
	241		$Zn—OH_2$
	376		
690	~ 700(br)		H_2O Librational mode
~ 725(br)†	~ 718	723	ν_4 NO_3^-
	~ 730	732	
821			ν_2 NO_3^-
	828	828	
1052			ν_1 NO_3^-
	1057	1057	
		1230 (w)	ν_2 D_2O
1330	1350	1350	ν_3 NO_3^-
1362	1368	1370	
1625			ν_2 H_2O (C_1 site)
1650	1640 (w)		ν_2 H_2O (C_s site)
	1642	1642	$2\nu_2$ NO_3^-
	1657	1656	

*br = broad, w = weak.
†Obtained from transmission spectrum. A layer of powdered sample was placed between AgBr plates and recorded at 15 °C.

vibrations of the hexaquozinc cations (6, 7). A broad Raman band *ca.* 700 cm^{-1} which appears to obscure the ν_4 NO_3^- vibration (Fig. 2) corresponds to a strong infrared absorption *ca.* 690 cm^{-1}, both of which are thought to be due to a water librational mode (8). This band appears weakly in aqueous nitrate solutions (9). In the ν_2 H_2O bending region of the infrared spectrum (Fig. 1) two components can be detected at 1650 and 1625 cm^{-1} which are assigned to water molecules on C_s and C_1 sites, respectively, on the basis of relative intensities.

The occupation of a C_1 site by nitrate ion of D_{3h} point group results in the removal of the degeneracy of the $\nu_3(E')$ and $\nu_4(E')$ modes and the activity of all modes in both infrared and Raman. The lifting of the degeneracy of ν_3 and ν_4, the low intensity of ν_2 in the Raman spectrum (forbidden under D_{3h} selection rules), and ν_1 in the infrared spectrum are clearly visible in Figs. 1 and 2. The spectra do not show sufficient detail to warrant factor group analysis although small differences between infrared and Raman frequencies can be attributed to correlation field coupling. In the infrared spectrum ν_4 was only barely detected even by thick-sample, transmission studies but the ν_3 band at 1362 cm^{-1} is intense and appears to have a shoulder *ca.* 1330 cm^{-1}. The magnitude of the site splitting is less than that observed in other crystalline ionic nitrates in which the NO_3^- ion occupies a general site (5) because the polarizing power of the cation is reduced by the hydration sphere.

The Raman spectrum of the crystal containing D_2O was obtained in order to observe features which could be masked by spectral lines arising from H_2O. In addition to clarification of the spectra in the regions of ν_4 and $2\nu_2$, an intensity reversal of the two components of the ν_3 nitrate vibration was observed (Fig. 2). It is assumed, in the absence of X-ray data and because of similarities in spectra, that the crystal containing D_2O is isomorphous with that containing H_2O, although some expansion of the lattice is probable (Ubbelohde Effect) (10). Strong hydrogen bonds exist in $Zn(NO_3)_2.6H_2O$ (4) and changes in these bond distances probably account for the spectral changes. The possibility that the intensi-

Can. J. Chem. Downloaded from www.nrcresearchpress.com by 210.87.254.6 on 09/05/12
For personal use only.

Can. J. Chem. Downloaded from www.nrcresearchpress.com by 210.87.254.6 on 09/05/12
For personal use only.

ties of the components of ν_4 (E') are similarly sensitive to deuteration could not be checked because of interference from the H_2O librational mode in this region. No corresponding librational mode was apparent in $Zn(NO_3)_2.6D_2O$.

Infrared and Raman components of ν_1 and ν_2 NO_3^- vibrations are non-coincident (Table 1). Lack of coincidence for the two ν_2 components is emphasized by the presence of two Raman bands at 1642 and 1656 cm^{-1} which correspond to twice the 821 cm^{-1} (infrared) and 828 cm^{-1} (Raman) bands. It is a general rule that overtones of non-degenerate fundamentals are Raman active. Thus the weak 828 cm^{-1} band (forbidden under D_{3h} but activated by the environment) possesses a more intense overtone. Since $Zn(NO_3)_2.6H_2O$ has a centrosymmetric space group the overtones, $2\nu_2$, remain infrared forbidden. Non-coincidence of infrared and Raman bands is required as a consequence of the centrosymmetric crystal structure; this implies that ν_1 and ν_2 vibrations are coupled with similar vibrations of other ions of the unit cell. Dipole–dipole coupling interactions have an inverse cube distance dependence (11). Considering that the minimum nitrogen–nitrogen distance is 6.2 Å in $Zn(NO_3)_2.6H_2O$ (4), it is hard to explain why correlation field coupling is so large compared to that observed for the same vibrations of other nitrates with shorter nitrogen–nitrogen distances (11, 12). Lack of coincidence has also been reported for the saturated aqueous solution (13) with a concentration less than that required to force the NO_3^- ion into the first coordination sphere of the zinc.

Interesting comparisons can be made between the vibrational spectra of solid $Zn(NO_3)_2.6H_2O$ and saturated aqueous $Zn(NO_3)_2$ solutions which are also considered to contain an octahedral hexaquozinc cation (14). Splitting of the ν_3 vibration of NO_3^- in saturated $Zn(NO_3)_2$ at 25 °C (8.2 mol water per mol salt) is 89 cm^{-1} (14) compared to only 20 cm^{-1} in solid $Zn(NO_3)_2.6H_2O$. This difference can partially be accounted for by the increase in the strength of the fluctuating field at the anion site in the more dense fluid state. Only one band has been observed in the ν_4 *ca.* 720 cm^{-1} region of saturated $Zn(NO_3)_2$ at 25 °C, whereas two bands can be resolved in solid $Zn(NO_3)_2.6H_2O$. These latter two bands do not arise from two forms of nitrate ion, however, but from site splitting. The magnitude of the split in the ν_4 region is usually considerably less than in the ν_3 region (5).

Gross changes in the vibrational spectra of solid $Zn(NO_3)_2.6H_2O$ and concentrated aqueous $Zn(NO_3)_2$ solutions only occur when the ratio of the moles of water to moles salt is less than 6 and the NO_3^- ion is allowed to enter the coordination sphere of the cation forming an actual complex *i.e.* an asymmetric field about the NO_3^- ion with a longer lifetime than the time of the measurement. At concentrations less than that required to force cation–anion contact the NO_3^- retains the basic vibrational spectrum of solvated ion modified by the field of the aquated cation environment (14) as noted above.

On dehydration a sharp line at 1047 cm^{-1} was observed in the Raman spectrum in addition to the 1057 cm^{-1} line. As dehydration was continued the new line increased in intensity and shifted to 1015 cm^{-1} at the expense of the 1057 cm^{-1} line. Clearly the new line is characteristic of nitrate ion in the first coordination sphere of zinc (*cf.* ref. 15). Additional Raman bands at 145, 408, 470, 771, 803, 1325, and 1558 cm^{-1} were observed. The 771 cm^{-1} line is higher in frequency than in the concentrated aqueous solution studied earlier (755 cm^{-1} with 2.5 mol water per mol of salt) (14). Hester and Scaife (16) report 775 cm^{-1} for 1.94 mol water per mol of salt at 85 °C. This high value suggests covalence in the zinc–nitrate interaction. The pair of lines, 771 cm^{-1} for inner-sphere nitrate and 718–730 cm^{-1} (site splitting) for outer-sphere, further support the criterion recently advanced for contact ion-pairing in aqueous nitrate solutions (17).

This work was supported by a grant from the National Research Council of Canada. One of us (M.H.B.) gratefully acknowledges support in the form of a NRCC postdoctoral fellowship and maintenance assistance from the Oak Ridge National Laboratory.

1. J. R. Ferraro. J. Mol. Spectrosc. **4**, 99 (1960).
2. C. C. Addison and B. M. Gatehouse. J. Chem. Soc. 613 (1960).
3. J. P. Mathieu and M. Lounsbury. Discuss. Faraday Soc. **9**, 196 (1950).
4. A. Ferrari, A. Braibanti, A. M. M. Lanfredi, and A. Tiripicchio. Acta. Cryst. **22**, 240 (1967).
5. M. H. Brooker and D. E. Irish. Can. J. Chem. **48**, 1183 (1970).
6. A. da Silveira, M. A. Marques, and N. M.

MARQUES. Compt. Rend. **252**, 3983 (1961); Mol. Phys. **9**, 271 (1965).
7. D. E. IRISH, B. MCCARROLL, and T. F. YOUNG. J. Chem. Phys. **39**, 3436 (1963).
8. J. R. FERRARO and A. WALKER. J. Chem. Phys. **42**, 1278 (1965).
9. D. E. IRISH and A. R. DAVIS. Can. J. Chem. **46**, 943 (1968).
10. J. PIRENNE. Physica, **21**, 971 (1955) and references therein.
11. J. C. DECIUS. J. Chem. Phys. **22**, 1941 (1954); **23**, 1290 (1955).
12. M. H. BROOKER. J. Chem. Phys. **53**, 2670 (1970).
13. R. E. HESTER and R. A. PLANE. J. Chem. Phys. **45**, 4588 (1966).
14. D. E. IRISH, A. R. DAVIS, and R. A. PLANE. J. Chem. Phys. **50**, 2262 (1969).
15. G. J. JANZ, K. BALASUBRAHMANYAM, and B. G. OLIVER. J. Chem. Phys. **51**, 5723 (1969).
16. R. E. HESTER and C. W. J. SCAIFE. J. Chem. Phys. **47**, 5253 (1967).
17. D. E. IRISH, G. CHANG, and D. L. NELSON. Inorg. Chem. **9**, 425 (1970).

Can. J. Chem. Downloaded from www.nrcresearchpress.com by 210.87.254.6 on 09/05/12
For personal use only.

Can. J. Chem. Downloaded from www.nrcresearchpress.com by 210.87.254.5 on 09/05/12
For personal use only.

The Adsorption of Tetrachloroethylene and Trichlorofluoromethane on Anhydrous Nickel Sulfate[1]

G. A. KINLOCH[2] AND W. D. MACHIN

Department of Chemistry, Memorial University of Newfoundland, St. John's, Newfoundland

Received[3] March 24, 1970

Several anomalous features of the adsorption isotherms obtained with tetrachloroethylene and trichlorofluoromethane on anhydrous nickel sulfate at 20.0, 5.8, and −7.5 °C, have been explained using a parallel plate pore model. Application of the Kelvin equation to the system indicates that adsorption hysteresis is due primarily to contact angle hysteresis, and that the thickness of the adsorbed layer that does not participate in meniscus formation is independent of relative pressure. Heats of immersion calculated from the estimated contact angles, and from heats of adsorption, have provided some support for the model.

Les diverses anomalies des isothermes d'adsorption de tétrachloroéthylène et de trichlorofluorométhane sur sulfate de nickel anhydre à 20.0, 5.8, et −7.5 °C, ont été expliquées à l'aide du modèle à pores en feuillets. L'application de l'équation de Kelvin au système indique que l'hystérésis d'adsorption est principalement dû à l'hystérésis d'angle de contact, et l'épaisseur du film adsorbé, qui ne participe pas à la formation du ménisque, est indépendant de la pression relative. Les chaleurs d'immersion, calculées à partir des angles de contact estimés et des chaleurs d'adsorption tendent à supporter le modèle.

Canadian Journal of Chemistry, 49, 1515 (1971)

Introduction

Hysteresis, when it occurs in adsorbent–adsorbate systems, is generally ascribed to capillary condensation of adsorbate in the pores of the adsorbent (1). The Kelvin equation has been applied to obtain information concerning the size (2), and in some cases, the shape (3) of the pores. The utility of this approach is limited by the necessary assumptions that the molar volume and surface tension of the adsorbate are the same as the bulk liquid, and that the contact angle of the capillary held liquid is zero.

The adsorption of tetrachloroethylene and trichlorofluoromethane on anhydrous nickel sulfate yields isotherms having anomalous features. In particular, the lower closure point of the hysteresis loop is temperature dependent, and may occur within the monolayer region of the isotherm.

Using a relatively simple model for the adsorbent structure, it has been possible to account for these anomalies and to obtain some insight into the applicability of the Kelvin equation.

Experimental

The adsorption system consisted of a vacuum microbalance, similar to that described by Hales and Turner (4), having a sensitivity of ±4 μg and a total capacity of *ca.* 0.5 g; a spoon gauge having a sensitivity of ±0.004 Torr (5), and which, at higher pressures, overlapped with a mercury manometer. Adsorbate purification and storage facilities were also included in the system. Metal valves and O-ring seals were used throughout the equilibrium part of the system.

The sample and counterweight legs of the balance were partially immersed in a large constant temperature bath controlled to ±0.05 °C. At the lowest experimental temperature (−7.5 °C), the water in the bath was replaced with a water–alcohol solution and cooling was provided using a commercial refrigeration unit.

The adsorbent was prepared *in situ* from Reagent Grade $NiSO_4.6H_2O$ by careful dehydration *in vacuo* at temperatures up to 200 °C with most of the water (ca. 90%) being removed below 100 °C. Subsequent degassing of the sample was carried out at 120 °C.

Spectral grade tetrachloroethylene (Eastman Kodak) and trichlorofluoromethane of minimum purity 99.5 mol% (Matheson) were vacuum distilled at least twice, with generous discard of head and tail fractions.

Results

Adsorption isotherms at 20.0, 5.8, and −7.5 °C were determined for both adsorbates. Typical isotherms are shown in Fig. 1. Only those parts of the desorption branches which were reproducible, *i.e.* independent of the point at which desorption was commenced, are shown.

[1]Presented, in part, at the Annual Conference of the Chemical Institute of Canada, May, 1969.

[2]Based on a thesis prepared by G. A. Kinloch in partial fulfillment of the requirements for the degree of Master of Science.

[3]Revision received December 14, 1970.

TABLE 1. Summary of isotherm data*

Adsorbate	Temperature (°C)	Monolayer capacity (μmol)	Surface area (m^2)	Hysteresis closure point (P/P_0)	Saturation pressure (Torr)
$CFCl_3$	20.0	36.9	6.60	0.45	666.23
	5.8	34.4	6.15	0.36	385.02
	−7.5	36.4	6.50	0.28	215.98
	Average	35.9	6.42		
C_2Cl_4	20.0	45.5	—	0.15	13.82
	5.8	44.4	—	0.10	6.00
	−7.5	42.5	—	0.05	2.45
	Average	44.1			

*All data refer to a sample weight of 0.4515 g.

Table 1 summarizes the important features of the isotherms. Monolayer capacities for both adsorbates were determined from B.E.T. plots. Surface areas have been calculated from the $CFCl_3$ isotherms using a molecular area of 29.7 $Å^2$ (6). On this basis, the apparent molecular area of C_2Cl_4 (24.2 $Å^2$) is appreciably lower than the area calculated from liquid density (33.4 $Å^2$). A similar effect has been reported with carbon tetrachloride (7).

Saturation vapor pressures were determined at the various temperatures and are also reported in Table 1. The calculated heats of vaporization are: $CFCl_3$ 6.35 kcal mol^{-1}; C_2Cl_4 9.74 kcal mol^{-1}.

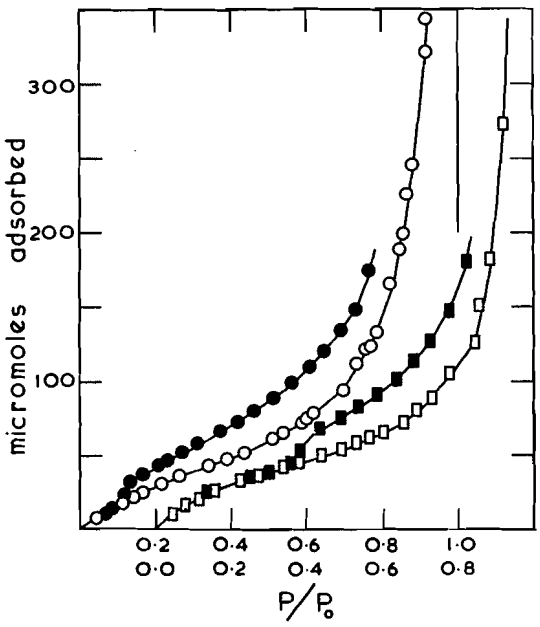

FIG. 1. Adsorption isotherms at 5.8 °C; ○, C_2Cl_4; □, $CFCl_3$. Desorption points are solid. Lower scale P/P_0 refers to $CFCl_3$ data.

Isosteric heats of adsorption, and differential entropies of adsorption are presented in Figs. 2 and 3. The entropies have been calculated according to the procedure given by Young and Crowell (8). Bulk liquid entropies are also shown in Fig. 3.

Discussion

The general form of the Kelvin equation as given by Gregg and Sing (1) is

$$[1] \qquad \frac{dv}{dS} = -\frac{\bar{V}\gamma \cos\theta}{RT \ln (P/P_0)}$$

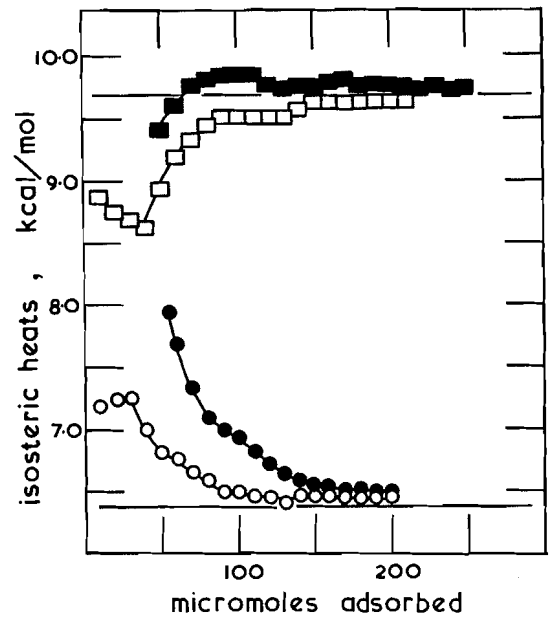

FIG. 2. Isosteric heats of adsorption; □, C_2Cl_4; ○, $CFCl_3$. Desorption points are solid. Latent heats of vaporization as calculated from adsorbate saturation vapor pressures are indicated by solid horizontal lines.

Can. J. Chem. Downloaded from www.nrcresearchpress.com by 210.87.254.5 on 09/05/12
For personal use only.

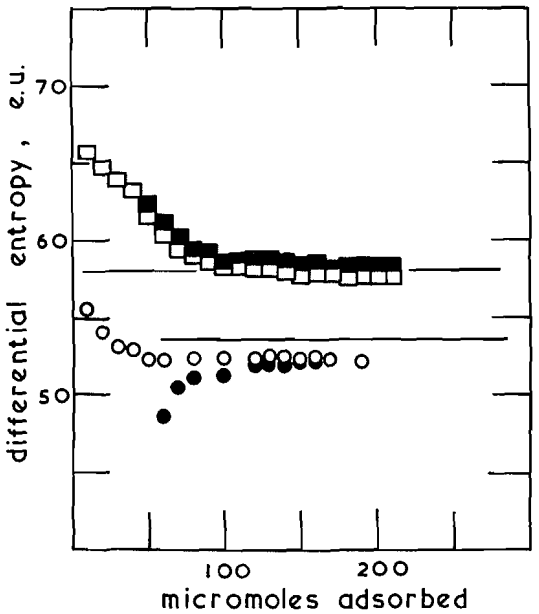

FIG. 3. Differential entropies of adsorption, calculated at 20 °C; □, C_2Cl_4; ○, $CFCl_3$. Desorption points are solid. Solid horizontal lines correspond to entropy of bulk liquid.

where v is the volume and S the surface area of those capillaries capable of inducing capillary condensation at a relative pressure of P/P_0. $\bar{V}$ and γ are the molar volume and surface tension of the adsorbate and θ is the contact angle. These authors also show that, irrespective of the pore geometry, dv/dS is constant, and may be considered a pore size parameter.

The simplest solution to the equation

$$[2] \qquad \left(\frac{\partial v}{\partial S}\right)_d = \text{constant} \quad (\text{at given } P/P_0)$$

is

$$[3] \qquad \left(\frac{\partial v}{\partial S}\right)_d = \frac{v}{S} \quad (\text{at given } P/P_0)$$

and where S is now assumed to be the total surface area, and v is the total volume of adsorbate at P/P_0. This solution defines a particular type of pore structure, the parallel plate model, with the additional condition that the plates are free to move apart in order to accommodate additional quantities of adsorbate, the spaces between all the plates being filled with adsorbate at all relative pressures in the region of hysteresis, and the distance between the plates being variable and dependent on the relative pressure. Some support for this model has been provided by various workers using adsorbents such as montmorillonite clays (9) and boehmite (10) which are known to have parallel plate structures. Isotherms reported by these workers have shapes similar to those reported here.

Accepting this model, we obtain

$$[4] \qquad \frac{v}{S} = -\frac{\bar{V}\gamma \cos\theta}{RT \ln (P/P_0)}$$

and since $v/\bar{V} = M$, the number of moles of adsorbate, and

$$[5] \qquad S = M_m BN$$

where S is the total surface area, M_m is the number of moles of adsorbate required to form a monolayer, and B is the molecular area, we obtain

$$[6] \qquad \frac{-1}{\ln (P/P_0)} = \frac{RT}{BN\gamma \cos\theta} \cdot \frac{M}{M_m}$$

which indicates that a plot of $-1/\ln (P/P_0)$ against M/M_m should be linear. That this is the case is demonstrated in Fig. 4, but the linear portions, when extrapolated, do not pass through the origin.

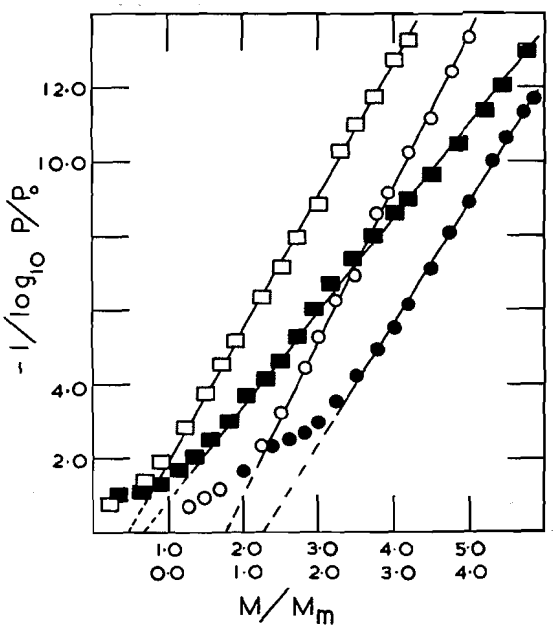

FIG. 4. Inverse Kelvin plots at 5.8 °C; □, C_2Cl_4; ○, $CFCl_3$. Desorption points are solid. Lower M/M_m scale refers to $CFCl_3$ data.

Can. J. Chem. Downloaded from www.nrcresearchpress.com by 210.87.254.5 on 09/05/12
For personal use only.

TABLE 2. Contact angles and "t" values

Temperature (°C)	Surface tension (erg cm^{-2})	Adsorption			Desorption		
		cos θ	θ	t	cos θ	θ	t
			$CFCl_3$				
20.0	19.5	0.376	67.9	0.67	0.510	59.3	1.01
5.8	21.4	0.352	69.3	0.63	0.432	64.3	1.22
−7.5	23.1	0.318	71.5	0.69	0.408	65.8	1.36
			C_2Cl_4				
20.0	31.7	0.364	68.7	0.40	0.469	62.0	0.76
5.8	33.3	0.312	71.8	0.43	0.441	63.8	0.62
−7.5	34.9	0.262	74.8	0.38	0.362	68.8	0.91

In our derivation of eq. 6 we have implicitly assumed that all of the adsorbate is present as capillary-held liquid, but both heats and entropies of adsorption indicate that this may not be the case. If we assume that a portion of the adsorbate is not liquid-like, then

$$[7] \qquad v/\bar{V} = M - x$$

where x is the quantity of adsorbate not having liquid properties, and $v/\bar{V}$ is now the quantity of adsorbate having liquid properties.

We now obtain the equation

$$[8] \qquad \frac{-1}{\ln (P/P_0)} = \frac{RT}{BN\gamma \cos\theta}\left[\frac{M}{M_m} - t\right]$$

where $t = x/M_m$, and which provides a satisfactory description of the linear plots in Fig. 4.

Contact angles and values for t calculated from these plots are reported in Table 2. The experimental molecular areas were used in the calculation of cos θ. It is not possible to verify these contact angles by direct measurement, but some measure of support is provided by the following approach.

The heat of immersion, q_{imm}, is related to the contact angle through the equation (11)

$$[9] \qquad q_{imm} = E_L \cos\theta - T\gamma \mathrm{d}\cos\theta/\mathrm{d}T$$

where E_L is the total surface energy and can be evaluated from

$$[10] \qquad E_L = \gamma - T\mathrm{d}\gamma/\mathrm{d}T$$

The heat of immersion may also be calculated (1) from the heat of adsorption, as

$$[11] \qquad \Delta H_i = \Delta H_{SV} - n\Delta H^0 = q_{imm}S$$

where ΔH_i is the net integral heat of adsorption, ΔH_{SV} is the integral heat of adsorption, and ΔH^0 is the latent heat of evaporation of the liquid, and S is the surface area. Unfortunately, both methods of calculation involve small differences between relatively large quantities.

The calculated heats of immersion at 20 °C are: $CFCl_3$ +9.7 erg cm^{-2} (contact angle); +27.8 erg cm^{-2} (heat of adsorption); C_2Cl_4 −10.0 erg cm^{-2} (contact angle); −44.0 erg cm^{-2} (heat of adsorption). While agreement is only qualitative, it should be remembered that the effect of experimental error on these values is large, being *ca.* ±20 erg cm^{-2} for those values calculated from heats of adsorption.

The assumption of contact angle hysteresis provided one of the earliest explanations for the occurrence of hysteresis loops in adsorption isotherms (12), but later work has shown that this cannot be the only reason for their occurrence. We feel that the present work provides some support for the idea that, in the present systems at least, contact angle hysteresis may influence the shape of the adsorption hysteresis loop. In this context, it should be noted that Jones and Wade (13), investigating the adsorption of various *n*-aliphatic alcohols on porous Vycor, found it necessary to assume various contact angles in order to obtain self-consistent pore size distributions.

It is also generally assumed, in pore size calculations, that the thickness of the adsorbed layer that does not participate in meniscus formation (t) is not constant, but increases with increasing relative pressure (2). In the present case, the linearity of the inverse Kelvin plots suggests that t is constant over a large range of relative pressures.

The authors thank the National Research Council of Canada for financial support of this work.

Can. J. Chem. Downloaded from www.nrcresearchpress.com by 210.87.254.5 on 09/05/12
For personal use only.

1. S. J. GREGG and K. S. W. SING. Adsorption, surface area, and porosity. Academic Press, New York. 1967. pp. 123–137, 298.
2. E. P. BARRETT, L. G. JOYNER, and P. H. HALENDA. J. Am. Chem. Soc. **73**, 373 (1951).
3. J. H. DE BOER and B. C. LIPPENS. J. Catal. **3**, 38 (1964).
4. J. L. HALES and A. R. TURNER. Lab. Pract. **5**, 245 (1956).
5. W. D. MACHIN. Can. J. Chem. **45**, 1904 (1967).
6. W. D. MACHIN. Trans. Faraday Soc. **65**, 529 (1969).
7. W. D. MACHIN. J. Phys. Chem. **73**, 1170 (1969).
8. D. M. YOUNG and A. D. CROWELL. Physical adsorption of gases. Butterworths, London. 1962. p. 84.
9. R. M. BARRER and D. M. MACLEOD. Trans. Faraday Soc. **50**, 980 (1954); Trans. Faraday Soc. **51**, 1290 (1955).
10. J. H. DE BOER. *In* The structure and properties of porous materials. *Edited by* D. H. Everett and F. S. Stone. Academic Press, New York. 1958.
11. A. W. ADAMSON. Physical chemistry of surfaces. 2nd ed. Interscience, New York. 1967. pp. 353, 354.
12. A. ZSIGMONDY. Z. Anorg. Chem. **71**, 356 (1911).
13. B. R. JONES and W. H. WADE. J. Colloid Interfac. Sci. **28**, 415 (1968).

Can. J. Chem. Downloaded from www.nrcresearchpress.com by 210.87.254.5 on 09/05/12
For personal use only.

Can. J. Chem. Downloaded from www.nrcresearchpress.com by 210.87.254.42 on 09/05/12
For personal use only.

Oxygen Interchange on Vanadium Oxide Catalysts

R. F. MANN

Department of Chemistry and Chemical Engineering, Royal Military College of Canada, Kingston, Ontario

Received September 23, 1970

It is often difficult to compare results for heterogeneous reactions as the data reported in the literature are presented in various ways. A common example of this difficulty is the reporting of oxygen adsorption rate constants in units such as l (g-catalyst)$^{-1}$ s^{-1}, l m^{-2} h^{-1}, g m^{-2} h^{-1}, g-mol m^{-2} h^{-1}, etc. In this paper a number of studies involving oxygen interchange with vanadium pentoxide or vanadium pentoxide – potassium sulfate promoted catalysts are re-examined. Where possible, a first-order oxygen adsorption rate constant is evaluated from published data on rates of oxidation and rates of isotopic exchange, and expressed in units of l h^{-1} m^{-2} of catalyst surface. The rate constants so evaluated and compared as to catalyst composition, temperature, and activation energy show reasonable agreement, even though a variety of catalysts, processes, and techniques are involved.

Dû au fait qu'ils sont souvent présentés sous diverses formes, il est souvent difficile de comparer les résultats rapportés dans la littérature pour des réactions hétérogènes. Un exemple commun de ces difficultés a trait à la façon de rapporter les constantes de vitesses d'adsorbtion de l'oxygène pour lesquelles les unités ont été: l (g-catalyseur)$^{-1}$ s^{-1}, l m^{-2} h^{-1}, g m^{-2} h^{-1}, mol-g m^{-2} h^{-1}, etc. Dans la présente communication, on réexamine un certain nombre d'études au sujet des échanges d'oxygène impliquant des catalyseurs activés par l'oxyde de vanadium ou un mélange d'oxyde de vanadium et de sulfate de potassium. Dans les cas où ce fut possible, nous avons évalué une constante de vitesse du premier ordre pour l'adsorption de l'oxygène; à cette fin, nous avons utilisé les données publiées pour les vitesses d'oxydation et les vitesses d'échanges isotopiques et nous exprimons ces vitesses en litres par heure par m^2 de surface de catalyseur. Quoique les catalyseurs, les procédés de préparation et les techniques employées varient grandement, les constantes de vitesse que nous avons évaluées présentent une corrélation raisonable suivant la composition du catalyseur, la température et l'énergie d'activation.

Canadian Journal of Chemistry, 49, 1520 (1971)

Introduction

Much work has been reported in recent years concerning systems where gas-phase oxygen interacts with vanadium oxide, as well as other metal oxide catalysts. These works involve processes such as catalytic oxidation of a hydrocarbon, oxidation of a reduced catalyst, adsorption of oxygen on a catalyst, and oxygen isotope exchange.

A number of such works, where the catalyst was vanadium pentoxide or vanadium pentoxide promoted with potassium sulfate, were reviewed and, where possible, a first-order oxygen adsorption rate constant was evaluated. It was assumed that the oxygen adsorption stage could be described by

$$[1] \qquad r_{ads} = k_a C_0(1 - \theta)$$

where r_{ads} = rate of oxygen adsorption or uptake by the catalyst surface, in g-mol m^{-2} h^{-1}; k_a = oxygen adsorption first-order rate constant, in l m^{-2} h^{-1}; C_0 = concentration of oxygen in the gas phase, in g-mol l^{-1}; and θ = fraction of the available surface covered by the oxygen being adsorbed.

The k_a values evaluated suffer, of course, from uncertainties. In some cases the values obtained can only be called estimates. The parameters subsequently evaluated, *e.g.* E_a, ln k_0 (E_a = activation energy of k_a, in kcal g-mol^{-1}, k_0 = Arrhenius pre-exponential, in l m^{-2} h^{-1}), will also be in error by varying amounts depending on the source of the original data, the method of k_a estimation, etc. In general the magnitude of these errors is unknown.

The object of this paper, however, is to examine the general characteristics of the various oxygen interchange processes and to discover general similarities in the data.

Data from Catalytic Oxidation of Hydrocarbons

A reaction model was proposed and described by Hinshelwood (1) and Mars and van Krevelen (2) and has been employed by a number of workers as the "steady-state adsorption model". The derivation of this model includes the assumption that eq. 1 describes the interaction between the gas-phase oxygen and the catalyst, and leads to

$$[2] \qquad r_R = \frac{k_a k_r C_0 C_R}{k_a C_0 + n k_r C_R}$$

where r_R = rate of reaction of hydrocarbon reactant, in g-mol m^{-2} h^{-1}; k_r = reaction rate

TABLE 1. k_a evaluated from catalytic oxidation studies (P = 1 atm)

Set	Reference	Reactant	Temperature (°C)	k_a	E_a	ln k_0
A	3, 4	*o*-Methyl-benzyl alcohol	280 to 360	7.13×10^{-3} to 1.24×10^{-1}*	24.6	17.45
B	5, 6	Toluene	300 to 350	7.68×10^{-4} to 1.09×10^{-2}†	37.3	25.7
C	6	Benzene	350 to 400	3.78×10^{-3} to 1.72×10^{-2}†	26.4	15.8
D	6, 7	Naphthalene	312 to 335	1.25×10^{-3} to 4.26×10^{-3}†	38.1	26.1
E	8	*o*-Xylene	290 to 310	6.0×10^{-4} to 1.32×10^{-3}†	26.0	15.9
F	9	Naphthalene	330 to 360	3.07×10^{-4} to 9.0×10^{-4}‡	27.0	14.7

*Fuzed V_2O_5, 99.9% pure, about 2 m²/g.
†An industrial V_2O_5/K_2SO_4 catalyst, about 0.35 mol of K_2SO_4 per mol V_2O_5, 52 m²/g.
‡A V_2O_5/K_2SO_4 catalyst, relative amounts not known, about 75 m²/g.

TABLE 2. k_a evaluated from rates of oxidation of reduced V_2O_5 catalyst (P = 0.023 atm)*

Set	Degree of reduction of catalyst (ΔO_2) (m l g^{-1})	Temperature (°C)	k_a	E_a	ln k_0
G	1	436 to 509	1.81 to 11.5	25.8	19.0
H	2	436 to 509	3.01 to 16.6	24.6	18.6
J	3	436 to 509	3.61 to 21.1	25.5	19.45
K	5	436 to 509	3.94 to 30.2	28.5	21.7
L	8	436 to 509	5.13 to 39.1	28.2	21.8

*Reference 10.

constant, in l m^{-2} h^{-1}; C_R = concentration of hydrocarbon reactant in the gas phase, in g-mol l^{-1}; and n = stoichiometric number = mol of oxygen required/mol of reacted hydrocarbon. Various units for these variables have been used by various workers. The k_a values have been re-evaluated as described earlier and the results are summarized in Table 1.

Data from Oxidation of Reduced Catalyst

Roiter and Yuza (10) reported rates of oxidation of a V_2O_5 catalyst which had been reduced various amounts with hydrogen. Rates of oxidation were given at various oxygen concentrations so that it was possible to estimate a slope in the low pressure region (*i.e.* as $\theta \rightarrow 0$ in eq. 1) and obtain an estimated k_a. These data are given in Table 2. The degree of reduction, ΔO_2, is expressed in terms of the volume of oxygen that was removed per gram of catalyst by the previous hydrogen oxidation reaction.

Data from Oxygen Isotope Exchange Studies

A number of Russian workers have carried out catalytic activity studies in conjunction with heteromolecular and homomolecular oxygen

Can. J. Chem. Downloaded from www.nrcresearchpress.com by 210.87.254.42 on 09/05/12
For personal use only.

TABLE 3. k_a evaluated from oxygen isotope exchange studies

Set	Reference	Exchange process	System pressure (atm)	Temperature (°C)	k_a	E_a	ln k_0
M	12	Simultaneous hetero- and homomolecular	0.014	450 to 500	1.44×10^{-2} to 1.53×10^{-1}*	52.0	32.0
N	13	Homomolecular	0.0065	500 to 550	5.55 to 2.37×10†	37.0	25.8
P	14		0.053	440 to 480	2.23×10^{-2} to 1.18×10^{-1}‡	45.3	28.1
Q	14		0.053	400 to 480	1.39×10^{-1} to 3.97§	42.6	29.9
R	14		0.053	400 to 480	8.35×10^{-1} to 9.75‖	~30	~22.6
S	14		0.053	440 to 480	1.66 to 6.0¶	35	25.2

*V_2O_5, 6 m^2/g.
†V_2O_5, 2.7 m^2/g.
‡V_2O_5, 1–2 m^2/g.
§V_2O_5, 0.1 K_2SO_4 1–2 m^2/g.
‖V_2O_5, 0.3 K_2SO_4 1–2 m^2/g.
¶V_2O_5, 0.5 K_2SO_4 1–2 m^2/g.

isotope exchange measurements. The exchange techniques have been extensively discussed by Boreskov (11) who also presented rate data for exchange on various oxide catalysts. Several of the original papers have been examined and the k_a values in Table 3 were obtained.

Other Work Examined

Other published works on the catalytic oxidation of naphthalene (2, 15), toluene (2), anthracene (2), benzene (2, 16), sulfur dioxide (17), *o*-xylene (18), and methyl alcohol (19) were also examined as were other oxygen adsorption and isotope exchange studies (20, 21). First order adsorption constants k_a could not be evaluated from these works because of insufficient data on oxygen concentrations, catalyst specific areas, units, etc.

Results and Treatment of Data

(1) Arrhenius Correlation

The temperature coefficient of k_a, the apparent Arrhenius activation energy of adsorption E_a, was calculated for each set of k_a values. The accompanying pre-exponential, as ln k_0, was also obtained for each set. The data so obtained are shown in Tables 1, 2, and 3.

(2) Compensation Behavior of ln k_0 with E_a

The great range of k_a values for the first-order adsorption process and the variety of E_a and ln k_0 values are partly explained in Fig. 1, where ln k_0 is plotted against adsorption activation energy, E_a. There appears to be a relationship between the activation energy and the pre-exponential factor for each catalyst, roughly of the form

$$[3] \qquad \ln k_0 = aE_a + b$$

where, in Fig. 1, $a \simeq 0.53$ and $b \simeq 6.0$. As discussed by Ashmore (22) this has been called the "theta rule" by Schwab (23) and the "com-

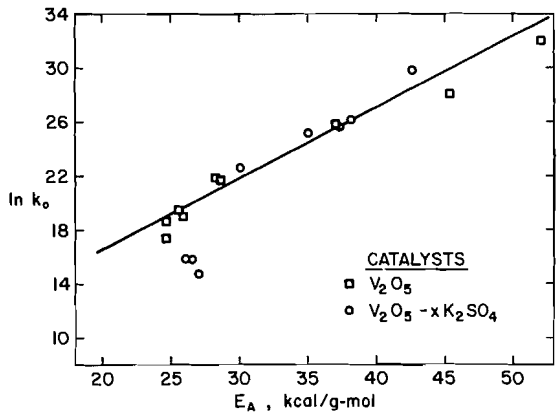

FIG. 1. Data from Arrhenius correlation of $k_a(T)$.

Can. J. Chem. Downloaded from www.nrcresearchpress.com by 210.87.254.42 on 09/05/12
For personal use only.

Can. J. Chem. Downloaded from www.nrcresearchpress.com by 210.87.254.42 on 09/05/12
For personal use only.

pensation effect'' by Cremer (24). Cremer called the temperature of intersection of the Arrhenius correlation lines T_s without saying much about the significance of such a temperature. Various possible explanations of the compensation effect were discussed by Cremer (24) but no single explanation was endorsed. Surface heterogeneity of the catalyst is likely a major factor with more than one type of ''active center'' existing. The compensation effect must still be regarded as an empirical relationship, however.

The major objective of the present work is to indicate that oxygen adsorption rate constants obtained by different methods for different processes show some relationship to each other. The present data for V_2O_5 catalysts do illustrate a certain compensation effect as the data for Sets *A*, *G*, *H*, *J*, *K*, *L*, *M*, *N*, and *P* show the general convergence characteristic with the T_s temperature in the range 900 to 1000 °K. (Note that V_2O_5 melts at 963 °K.) As is obvious in Fig. 1, the V_2O_5–xK_2SO_4 data (x = mol K_2SO_4 in catalyst per mol V_2O_5) are not as well correlated as are the V_2O_5 data and, therefore, no clear compensation effect is evident when the k_a values for Sets *B*, *C*, *D*, *E*, *F*, *Q*, *R*, and *S* are plotted on an Arrhenius basis.

Conclusions

While some of the data are admittedly approximate and, therefore, some aspects of the subsequent data analysis must also be approximate, it is concluded that a relationship does exist between k_a data from a variety of sources, for a variety of processes and for a variety of catalysts.

The relationship appears to be of the form described by Cremer as the ''compensation effect'' where an increase in the activation energy of the adsorption rate constant is accompanied (or compensated for) by an increase in the pre-exponential factor. This effect is illustrated most clearly where a number of different processes have been studied on the same catalyst, V_2O_5.

This preliminary examination of data from seventeen different studies of a variety of processes is sufficiently encouraging to warrant continued work. The determination and comparison of k_a data should initially be confined to single catalyst compositions and further information on the relationship between surface and E_a should be a major objective. Re-evaluation of other published work should be continued to give a broader picture of the oxygen interchange process on vanadium oxide catalysts.

On the applied aspects of heterogeneous catalysis, a long-range objective must be the prediction of reactor performance by the proper use of predicted rate equations. This present paper is a further contribution to the problem of predicting the rate of oxygen interaction with a particular family of metal oxide catalysts for catalytic oxidation processes.

The research for this paper was supported in part by the Defence Research Board of Canada, Grant number 9530-64.

1. C. N. HINSHELWOOD. The Kinetics of Chemical Change. Oxford University Press, 1942.
2. P. MARS and D. W. VAN KREVELEN. Chem. Eng. Sci. Special Supplement, **3**, 41 (1954).
3. T. VRBASKI and W. K. MATTHEWS. J. Phys. Chem. **69**, 457 (1965).
4. R. F. MANN and J. DOWNIE. (Re-evaluation of the data in ref. 3.) Unpublished.
5. J. DOWNIE, K. A. SHELSTAD, and W. F. GRAYDON. Can. J. Chem. Eng. **39**, 201 (1961).
6. I. S. JASWAL, R. F. MANN, J. A. JUUSOLA, and J. DOWNIE. Can. J. Chem. Eng. **47**, 284 (1969).
7. K. A. SHELSTAD, J. DOWNIE, and W. F. GRAYDON. Can. J. Chem. Eng. **38**, 102 (1960).
8. J. A. JUUSOLA, R. F. MANN, and J. DOWNIE. J. Catal. **17**, 106 (1970).
9. V. A. ROITER, V. P. USHAKOVA, G. P. KORNEICHUK, and T. G. SKORBILINA. Kinet. Catal. **2**, 83 (1961).
10. V. A. ROITER and V. A. YUZA. Kinet. Catal. **3**, 302 (1962).
11. G. K. BORESKOV. The Catalysis of Isotope Exchange in Molecular Oxygen. Advan. Catal. **15**, 285 (1964).
12. V. S. MUZYKANTOV, V. V. POPOVSKII, G. K. BORESKOV, and N. I. MIKICHUR. Kinet. Catal. **5**, 665 (1964).
13. A. P. DZISYAK, G. K. BORESKOV, L. A. KASATKINA, and V. E. KOCHURIKHIN. Kinet. Catal. **2**, 355 (1961).
14. G. K. BORESKOV, L. A. KASATKINA, V. V. POPOVSKII, and YU. A. BALOVNEV. Kinet. Catal. **1**, 207 (1960).
15. P. H. CALDERBANK. The Industrial Chemist, 291 (July, 1952).
16. J. D. BUTLER and B. G. WESTON. J. Catal. **2**, 8 (1963).
17. P. H. CALDERBANK. J. Appl. Chem. **2**, 482 (1952).
18. J. HERTEN and G. F. FROMENT. I. and E.C. Proc. Des. and Dev. **7**, 516 (1968).
19. S. K. BHATTACHARYYA, K. JANAKIRAM, and N. D. GANGULY. J. Catal. **8**, 128 (1967).
20. L. YA. MARGOLIS and E. G. PLYSHEVSKAYA. Akad. Nauk. SSSR, Izvestia (Leningrad), Otdelenie Khimicheskikh Nauk, 415 (1952).
21. V. N. BIBIN and L. A. KASATKINA. Kinet. Catal. **5**, 653 (1964).
22. P. G. ASHMORE. Catalysis and Inhibition of Chemical Reactions. Butterworths, London. 1963.
23. G. M. SCHWAB. Advan. Catal. **2**, 251 (1950).
24. E. CREMER. Advan. Catal. **7**, 75 (1955).

Can. J. Chem. Downloaded from www.nrcresearchpress.com by 210.87.254.105 on 09/05/12
For personal use only.

Photochemistry of the *cis*- and *trans*-Dichlorobisethylenediamine Chromium(III) Cations in Acidic Aqueous Solutions. Observation of a Stereochemical Change in Photoaquation

A. D. KIRK[1], K. C. MOSS, AND J. G. VALENTIN[2]

Department of Chemistry, University of Victoria, Victoria, British Columbia

Received October 23, 1970

The photoreactions of *cis*- and *trans*-$[CrCl_2(en)_2]^+$ have been investigated in acidic aqueous solution at p*H* 3 and 0 °C. On photolysis in the ligand field bands the *cis* isomer was found to undergo mainly ethylenediamine aquation, apparently to a thermally unstable monodentate protonated ethylenediamine complex, with a quantum yield of 0.13. In addition chloride aquation occurred with $\phi(Cl^-) = 0.02$. In contrast, the *trans* isomer underwent exclusive chloride aquation with quantum yield 0.32. The results are qualitatively, but not quantitatively, in agreement with predictions of Adamson's empirical rules. It was found that for *trans*-$[CrCl_2(en)_2]^+$ photolysis, the reaction product $[CrCl(H_2O)(en)_2]^{2+}$ was produced at least 70% in the *cis* configuration.

Les réactions photochimiques du *cis*- et *trans*-$[CrCl_2(en)_2]^+$ ont été étudiées en solution aqueuse acide à p*H* 3 et à 0 °C. Lors de la photolyse dans les bandes du champ liant, on a trouvé que l'isomère *cis* subit principalement l'hydrolyse de l'éthylènediamine, apparemment pour donner un complexe monodentate protoné de l'éthylènediamine, avec un rendement quantique de 0.13. De plus, l'hydrolyse du chlore a eu lieu avec $\phi(Cl^-) = 0.02$. Par opposition, l'isomère *trans* a subit exclusivement l'hydrolyse du chlore avec un rendement quantique de 0.32. Les résultats sont qualitativement, mais non quantitativement, en accord avec les prévisions des règles empiriques d'Adamson. Il a été trouvé que pour la photolyse du *trans* $[CrCl_2(en)_2]^+$ le produit de réaction $[CrCl(H_2O)(en)_2]^{2+}$ a été produit au moins à 70% dans la configuration *cis*.

Canadian Journal of Chemistry, 49, 1524 (1971)

Introduction

Adamson (1) has proposed a set of empirical rules governing the modes and approximate quantum yields for photolysis of Cr(III) complexes. An interesting prediction of these rules is that for certain *cis*/*trans* complex pairs the photolysis modes and yields for the two isomers would be quite different. To the best of our knowledge the only system of this type previously investigated has been the *cis*/*trans* pair $[Cr(OH)_2(en)_2]^+$ (1, 2). The results of this investigation were rendered somewhat ambiguous by the complexity of the possible reaction modes and ignorance as to the extent of photochemical solvent exchange. Thus although the results are not inconsistent with the rules, they do not allow firm conclusions regarding them.

We wish to report a study of the photochemical reactions of the pair of complexes *cis*- and *trans*-$[CrCl_2(en)_2]^+$. Experimentally this system has the advantage that detailed studies of the thermal reactions have been made (3) and the loss of either ligand from the compounds can easily be followed experimentally. For this pair of compounds, Adamson's rules predict that the *cis* isomer would undergo predominantly ethylenediamine aquation, with a quantum yield of about 0.1 to 0.3, whereas the *trans* compound would undergo predominantly chloride aquation with a low quantum yield of about 0.1 or less. It seemed to us, therefore, that this system offered an excellent opportunity to test critically the extent to which Adamson's rules are valid.

Results and Conclusions

Photolysis of cis-$[CrCl_2(en)_2]^+$

The absorption spectrum of *cis*-$[CrCl_2(en)_2]^+$ is shown in Fig. 1*a*. Photolysis of this compound at p*H* 3.0, 0 °C and at wavelengths (400 and 540 nm) corresponding to absorption into the two ligand field bands Q_1 and Q_2 ($^4T_{2g} \leftarrow {}^4A_{2g}$ and $^4T_{1g} \leftarrow {}^4A_{2g}$ in O_h symmetry, respectively) resulted in hydrogen ion uptake corresponding to the aquation and protonation of the basic ethylenediamine ligand

[1] *cis*-$[CrCl_2(en)_2]^+ + H_2O + H^+ \rightarrow [CrCl_2(H_2O)en(enH)]^{2+}$

[1]To whom correspondence should be addressed.

[2]Present address: Analytical Chemistry Department, Dow Chemical Company, Sarnia, Ontario.

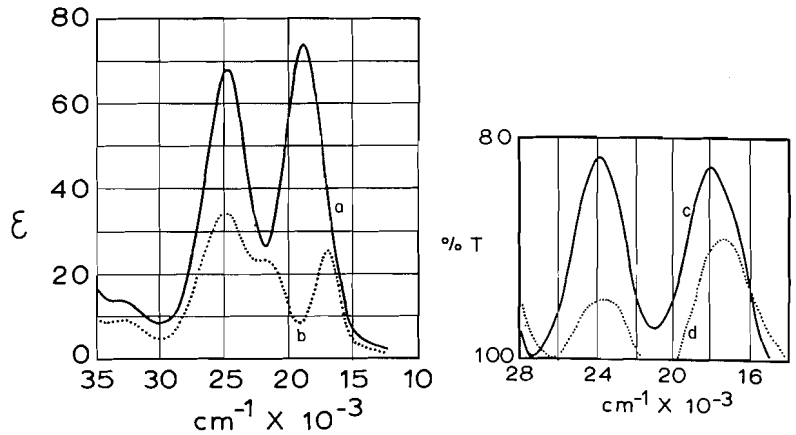

FIG. 1. *a*, solution spectrum of *cis*-$[CrCl_2(en)_2]$; *b*, solution spectrum of *trans*-$[CrCl_2(en)_2]$; *c*, spectrum obtained for the unstable product from photolysis of *cis*-$[CrCl_2(en)_2]^+$; *d*, spectrum obtained after the thermal ageing of the product from photolysis of *cis*-$[CrCl_2(en)_2]^+$.

or

[2] *cis*-$[CrCl_2(en)_2]^+ + H_2O + 2H^+ \rightarrow$
$[CrCl_2(H_2O)_2en]^+ + enH_2^{2+}$

Simultaneously with this reaction, the major thermal reaction

[3] *cis*-$[CrCl_2(en)_2]^+ + H_2O \rightarrow$
cis-$[CrCl(H_2O)(en)_2]^{2+} + Cl^-$

also occurred and was followed by the thermal chloride release. By working at low temperature and maximum possible light intensity it was possible to ameliorate the complicating effects of this process.

Ion exchange chromatography (Rexyn 101) on solutions photolyzed to about 50% decomposition resulted in the elution of a band of compound having the absorption spectrum seen in Fig. 1*c*. This band eluted after the unchanged starting material which was the first observable band off the column. The substance was thermally unstable and, if left on the column at p*H* 0 and 0 °C, decomposed fairly rapidly yielding a compound having the spectrum shown in Fig. 1*d*. It is seen that the long wavelength band maxima in spectra 1*c* and 1*d* are progressively shifted about 500 cm^{-1} towards the red relative to the starting material. Thus, these spectra are close to those expected for the thermally unstable protonated ethylenediamine complex $[CrCl_2(H_2O)en(enH)]^{2+}$ and its ethylenediamine aquation product $[CrCl_2(H_2O)_2en]^+$. Such an identification is also consistent with the chromatographic behavior of the compounds. It was unfortunately not possible to identify the isomers of $[CrCl_2(H_2O)en(enH)]^{2+}$ or $[CrCl_2(H_2O)_2en]^+$ produced. No other significant products were present and the minor amounts of other species found appear to be associated with chloride aquation and secondary photolysis and thermal reactions. In particular *trans*-$[CrCl_2(en)_2]^+$, which would have eluted first in the chromatographic separation, was absent.

The above identification of the major reaction product is rendered somewhat tentative because of the difficulty due to its thermal instability. However, the spectral and chromatographic evidence obtained, the fact of the thermal instability of the product, the absence of other major products, and previous experience with the photolysis of other ethylenediamine complexes (8, 11) all suggest that the major photolysis process occurring in this system is reaction 1. Parallel to this reaction a small yield of photochemical chloride aquation occurred (reaction 3, although the product chloroaquo species may not be *cis*). A small contribution from reaction 2 can not be completely excluded.

On the assumption that reaction 1 is the sole photochemical reaction resulting in proton uptake, one obtains the quantum yields for ethylenediamine aquation shown in Table 1. It is unlikely that any serious error is incurred by neglect of possible thermal aquation of the enH product during the run as this would have caused a curvature in the hydrogen ion time plots and

Can. J. Chem. Downloaded from www.nrcresearchpress.com by 210.87.254.105 on 09/05/12
For personal use only.

TABLE 1. Photolysis quantum yields for *cis*- and *trans*-$[CrCl_2(en)_2]^+$ at 0 °C and p*H* 3.0

Complex	Wavelength (nm)	Reaction mode	Quantum yield
cis-$[CrCl_2(en)_2]^+$	400	en	0.13 ± 0.02
		Cl^-	0.011 ± 0.005
	540	en	0.12 ± 0.02
		Cl^-	0.02 ± 0.01
	All	Isomerism	< 0.01
trans-$[CrCl_2(en)_2]^+$	400	Cl^-	0.35 ± 0.02
	424	Cl^-	0.32 ± 0.02
	540	Cl^-	0.32 ± 0.02
	565	Cl^-	0.31 ± 0.02
	All	Isomerism	< 0.05
		en	< 0.001

none was observed. Occurrence of reaction 2 would lead to an error in equating the quantum yield of hydrogen ion uptake to the yield of the species $[CrCl_2(H_2O)en(enH)]^{2+}$, but since no $[CrCl_2(H_2O)_2en]^+$ was observed in the chromatography such error cannot be large.

Direct measurements of the overall chloride yields, corrected for the thermal chloride release, led to the values of Table 1 for the chloride aquation quantum yields. On the assumption of one chloride ion released per photolyzed complex ion, these yields may be taken to be for the primary aquation process, reaction 3. Table 1 also shows a maximum isomerization quantum yield based on our failure to observe any *trans*-$[CrCl_2(en)_2]^+$ amongst the products and our estimate of the maximum amount of the compound that could have gone undetected.

Photolysis of trans-$[CrCl_2(en)_2]^+$

The absorption spectrum of *trans*-$[CrCl_2(en)_2]^+$ is shown in Fig. 1*b*. Because *trans*-$[CrCl_2(en)_2]^+$ is thermally much more stable to aquation than the *cis* isomer, the photochemical work on this complex was uncomplicated by thermal reaction of the starting material. Photolysis of the compound at p*H* 3.0, 0 °C and 400, 424, 540, or 565 nm resulted in chloride ion release, with no detectable hydrogen ion uptake.

Ion exchange chromatography on solutions photolyzed to more than 50% decomposition yielded four substances. Using the Rexyn 101 column and eluting with 0.6 *M* nitric acid one obtained Band 1: *trans*-$[CrCl_2(en)_2]^+$, 39% of the total Cr; Band 2: unidentified, 9% of the total Cr; Band 3, *cis*-$[CrCl(H_2O)(en)_2]^{2+}$, 33% of total Cr; and Band 4, unidentified, 19% of total Cr. Band 2, 9% of the total Cr, was present in too small an amount to allow certain identification by our present techniques. However, since the *trans* isomers of these complexes generally elute before the *cis* it may consist of either or both of *cis*-$[CrCl_2(en)_2]^+$ or *trans*-$[CrCl(H_2O)(en)_2]^{2+}$. The observed color of the band is more consistent with the latter identification. Band 4 was not studied in detail at this juncture. It is almost certainly a secondary product resulting from the high conversion necessary to obtain identifiable amounts of the primary products. Its elution characteristics and color suggest it is $[Cr(H_2O)_2(en)_2]^{3+}$ or $[CrCl(H_2O)_2en(enH)]^{3+}$ arising from secondary photochemical reactions of *cis*-$[CrCl(H_2O)(en)_2]^{2+}$.

These results show that the main process occurring on photolysis of *trans*-$[CrCl_2(en)_2]^+$ in acid aqueous solution is

[4] *trans*-$[CrCl_2(en)_2]^+ \rightarrow [CrCl(H_2O)(en)_2]^{2+} + Cl^-$

where the product $[CrCl(H_2O)(en)_2]^{2+}$ is produced at least 70% in the *cis* configuration.

Because of the latitude allowed by the unidentified Band 4, it remains possible that direct photolysis to $[Cr(H_2O)_2(en)_2]^{3+}$ with loss of both chloride ions also occurs to some extent. This would prevent us from equating the yields of chloride and $[CrCl(H_2O)(en)_2]^{2+}$. However, chromatographic data show that in the worst case, *i.e.*, that Band 4 consists entirely of $[Cr(H_2O)_2(en)_2]^{3+}$ arising from such a direct process, the maximum error incurred by neglect of this process would be 35%. Having recognized this uncertainty, we proceed on the likely assumption that reaction 4 is the only photochemical process releasing chloride and that the ϕ_{Cl} values are equal to $\phi_{[CrCl(H_2O)(en)_2]^{2+}}$.

In all the quantitative work the reactions were

Can. J. Chem. Downloaded from www.nrcresearchpress.com by 210.87.254.105 on 09/05/12
For personal use only.

Can. J. Chem. Downloaded from www.nrcresearchpress.com by 210.87.254.105 on 09/05/12
For personal use only.

followed continuously by potentiometric chloride determination and by p*H* measurements and the conversions were always $\leqslant 5\%$. Table 1 shows quantum yield data for chloride aquation together with upper limit estimates for other reaction modes based on the chromatographic data and our estimate of observable p*H* changes. The chloride aquation quantum yields for the *trans* complex showed a small increase with decreasing photolysis wavelength while the ethylenediamine yields for the *cis* complex appeared wavelength independent.

Discussion

From the above results it is seen that the photochemistry of the *cis*- and *trans*-$[CrCl_2(en)_2]^+$ complexes illustrates that geometrical configuration can indeed determine the course of chemical reactions undergone by the excited state of a complex ion. The major photoaquation modes are exactly as predicted by Adamson's rules.

The study provides some support for the contention that the photochemical activation of quadrate complexes occurs along the weak-field axis, a suggestion which was not, in our opinion, confirmed by previous reported evidence. Invariably the complexes studied were of such a nature that the results did not allow unequivocal mechanistic conclusions.

For example, for the $[CrX(NH_3)_5]^{2+}$ complexes, the observation that ammonia aquation was the main photochemical reaction did not prove that the ammonia molecule released was that on the weak field axis, but could equally well have arisen from activation of the plane orthogonal to the weak field axis.[3] In fact, the studies of Schläfer and co-workers on the complexes $[CrCl(NH_3)_5]^{2+}$ (4) and $[CrBr(NH_3)_5]^{2+}$ (5) in which the product aquo complex was apparently in the *cis* configuration, could on one interpretation be considered to support such a mechanism. Similar ambiguities of interpretation arise with previous studies of $[Cr(OH)_2(en)_2]^{3+}$ (2) and $[Cr(NCS)_4(NH_3)_2]^-$ (6). In the present work an ambiguity remains for the *cis* isomer but the observation of exclusive chloride aquation in *trans*-$[CrCl_2(en)_2]^+$ unequivocally confines the activation to the weak field axis.

Adamson has suggested that the quantum yields for these photoaquation reactions of non-octahedral complexes should be about the same as for a complex having the same overall average ligand field strength as on the weak field axis. This would suggest a lower quantum yield for the *trans* isomer (about 0.1 to 0.01 by analogy to $[Cr(H_2O)_6]^{3+}$ and $[Cr(urea)_6]^{3+}$ (8) than for the *cis* (about 0.3). Our findings, 0.32 for the *trans* isomer and 0.13 for the *cis*, are very much contrary to this prediction. We conclude that there exists at present little experimental support for any correlation relating the relative magnitudes of quantum yields to the average ligand field on the weak field axis. The pursuit of such quantitative correlations should await the accumulation of much more evidence than is presently available.

As a final aspect of Adamson's rules there is the question as to whether they predict the stereochemistry of the photosubstitution reactions. Earlier work has again been contradictory and equivocal on this point. As stated, Schläfer and co-workers found $[CrCl(NH_3)_5]^{2+}$ and $[CrBr(NH_3)_5]^{2+}$ aquated ammonia to give predominantly the *cis* isomer of the product. It was not, however, completely certain that a post irradiation isomerization was not responsible.[4] In contrast, *trans*-$[Cr(NCS)(H_2O)(NH_3)_4]^{2+}$ (7) appeared to be the product from photoaquation of $[Cr(NCS)(NH_3)_5]^{2+}$.

In the present study it was not possible to identify the isomeric form of the product of the *cis* photoaquation. However, the chloro aquo product complex from photolysis of *trans*-$[CrCl_2(en)_2]$ was found to be at least 70% in the *cis* configuration. Under the temperature and conditions of the experiments the measured rate constants for isomerization (3) exclude any possibility of this amount of thermal isomerization and photochemical *cis*/*trans* isomerization of the reaction product could not occur to this extent. Thus, the photochemical aquation in this complex occurs mainly with stereochemical change, suggesting that the entering water molecule attacks the excited state of the complex *trans* to the leaving chloride ion.

This is in complete contrast to the thermal reaction and, together with our recent findings

[3]We are indebted to Dr. Vincenzo Balzani for useful discussions on this point.

[4]Recent work (12) has confirmed the *cis* configuration of the chloroaquotetraammine product from the photolysis of chloropentaammine Cr(III) ion.

for $[Cren(ox)_2]^-$ (8), represents the first unambiguous demonstration of stereomobility in Cr(III) complex aquation reactions, photochemical or thermal. The result suggests strongly that reaction occurs from some precursor having quite different properties from the ground state, and renders it unlikely that this reaction occurs from vibrationally excited ground state molecules produced by internal conversion.

Experimental

(a) Preparation of Complexes

trans-$[CrCl_2(en)_2]Cl$ was prepared as described in the literature (9), except that it was found necessary to bubble chlorine through the $[Cr(NCS)_2(en)_2]SCN$ slurry overnight in order to obtain good yields.

trans-$[CrCl_2(en)_2]NO_3$ was prepared by adding concentrated nitric acid to a solution of *trans*-$[CrCl_2(en)_2]Cl$ and cooling on ice, filtering and drying.

Anal. Calcd. for *trans*-$[CrCl_2(en)_2]NO_3$: Cr, 17.0. Found: Cr, 16.9.

cis-$[CrCl_2(en)_2]Cl$ was prepared as described in the literature (10).

cis-$[CrCl_2(en)_2]NO_3$ was prepared from the chloride by dissolving in the minimum amount of water at room temperature, adding a large excess of ammonium nitrate, and cooling on ice. The separated salt was filtered and dried.

Anal. Calcd. for *cis*-$[CrCl_2(en)_2]NO_3$: Cr, 17.0. Found: Cr, 16.8.

(b) Photolysis Apparatus and Actinometry

These have been previously described (8). The interference filters for 424 and 565 nm were obtained from Rolyn Corp (Filtraflex B-20) and had half-widths of 9 and 6 nm, respectively. For the ion exchange chromatographic separations, solutions were extensively decomposed using a wide band color filter (CS-496, Corning Glass Co.) to allow greater light intensity. The photolysis cell was a modified 1.0 cm quartz spectrophotometer cell, solutions being stirred by means of a stream of presaturated nitrogen gas along the rear face of the cell.

(c) pH and Chloride Determinations

For the quantitative work, photolysis solutions were prepared at the run temperature 0 °C in semidarkness. Solutions, 5.0×10^{-3} *M*, made up with 1.0×10^{-3} *M* perchloric acid were used for both p*H* and chloride determinations and in addition the solutions were 0.01 *M* in potassium perchlorate.

The p*H* measurements were made using a Fisher microprobe combination electrode in conjunction with a Metrohm Compensator E 388 p*H* meter.

Determinations of the free chloride present in the solutions were made using a concentration cell without transference. The internal reference cell contained 1.00×10^{-2} *M* potassium chloride and the apparatus was calibrated over the range of chloride concentration 1.00×10^{-4} to 2.00×10^{-3}. Silver/silver chloride electrodes were used and that in the photolysis cell was masked to avoid difficulties experienced with photopotentials.

In the quantitative work both p*H* and chloride measurements were made continuously throughout separate series of runs, and percentage conversions were always held to a few percent ($2 \rightarrow 5\%$).

(d) Ion Exchange Chromatography

For both complexes adequate separations of the reaction products were obtained by chromatography on Rexyn 101 with 0.6 *M* nitric acid as eluent. A 1.0 cm diameter, 4.0 cm long column, jacketed at 0 °C was used.

The authors are grateful for the financial support of the National Research Council of Canada and the University of Victoria Faculty Research Fund by grants-in-aid of research (A.D.K. and K.C.M.) and for an NRCC Bursary (J.G.V.).

1. A. W. ADAMSON. J. Phys. Chem. **71**, 799 (1967).
2. A. W. ADAMSON. Adv. Chem. Ser. Amer. Chem. Soc. Washington, D.C. **49**, 237 (1965).
3. D. J. MACDONALD and C. S. GARNER. J. Amer. Chem. Soc. **83**, 4152 (1961).
4. H. F. WASGESTIAN and H. L. SCHLÄFER. Z. Phys. Chem. Frankfurt, **57**, 282 (1968); **62**, 127 (1968).
5. P. RICCIERI and H. L. SCHLÄFER. Inorg. Chem. **9**, 727 (1970).
6. E. WEGNER and A. W. ADAMSON. J. Amer. Chem. Soc. **88**, 394 (1966).
7. E. ZINATO, R. D. LINDHOLM, and A. W. ADAMSON. J. Amer. Chem. Soc. **91**, 1076 (1969).
8. A. D. KIRK, K. C. MOSS, and J. G. VALENTIN. Can. J. Chem. **49**, 375 (1971).
9. G. BRAUER. Handbook of Preparative Inorganic Chemistry, 2nd ed. Academic Press, New York, **2**, 1357 (1965).
10. W. C. FERNELIUS. Inorganic Synthesis. McGraw-Hill Inc., New York, **2**, 201 (1946).
11. H. L. SCHLÄFER and W. GEISS. Z. Phys. Chem. Frankfurt, **65**, 107 (1969).

Can. J. Chem. Downloaded from www.nrcresearchpress.com by 210.87.254.105 on 09/05/12
For personal use only.

A Study of Cation-exchange Reactions in the System Potassium Durosemiquinone – Potassium Tetraphenylboride – Tetrahydrofuran

T. E. GOUGH[1] AND P. R. HINDLE

Department of Chemistry, University of Waterloo, Waterloo, Ontario

Received November 9, 1970

The electron spin resonance (e.s.r.) spectrum of potassium durosemiquinone in tetrahydrofuran has been studied as a function of temperature and found to exhibit line-width alternation indicating the presence of an intramolecular migration of the potassium ion between the oxygens of the semiquinone. The addition of potassium tetraphenylboride to the system produces intermolecular scrambling of potassium, the spectral effects of which are superimposed upon those of the intramolecular exchange. From the spectral line-shapes approximate values of the activation energies and frequency factors were derived. The tetraphenylboride anion did not play a detectable role in the various exchange mechanisms.

On a étudié le spectre r.p.e. du sel de potassium de la durosemiquinone en fonction de la température et on a trouvé qu'ils présentent une alternation des largeurs de raie qui indiquerait que l'ion de potassium effectue des migrations intramoléculaires entre les divers atomes d'oxygène de la semiquinone. L'addition de tétraphénylborure de potassium au système a comme effet de permettre une permutation des ions potassium entre les molécules; ces migrations provoquent des changements spectraux qui se superposent à ceux provoquées par les échanges intramoléculaires. A partir des formes des bandes dans les spectres, on a pu donner les énergies d'activation et les facteurs de fréquence de ces réactions. Il ne semble pas que l'anion tétraphénylborure joue un rôle détectable dans les divers mécanismes d'échange.

Canadian Journal of Chemistry, **49**, 1529 (1971)

Can. J. Chem. Downloaded from www.nrcresearchpress.com by 210.87.254.42 on 09/05/12
For personal use only.

Introduction

Electron spin resonance spectroscopy has been used to probe the kinetics of both intra- and intermolecular cation-exchange reactions of systems in which the paramagnetic anion has two sites at which ionic association may occur. The intramolecular case has, to date, received more attention and a number of rate-constants and activation energies have been determined for these processes (1–5); however, the mechanistic details of the exchanges are still somewhat uncertain (6). Intermolecular exchange of cations, occurring in the presence of a second electrolyte, has also been studied, and shown to occur *via* a mechanism in which the incoming cation associates with the uncomplexed site of the anion (7, 8). For semiquinone ion-pairs, these exchanges have been found to proceed *via* the triple ion M_2Q^+ (9, 10), and the role of the anion of the second electrolyte elucidated (10). When this second anion has an affinity for the cation comparable with that of the semiquinone, then the dissociation of the triple ion may be written as

$$[1] \qquad MQM^+ + X^- \rightarrow MQ + MX$$

The principle of microscopic reversibility then demands that MX (rather than M^+) is the attacking species in the intermolecular cation exchange. A quantitative estimation of the kinetic parameters for such an exchange, in the "slow" limit, has been made for the system sodium 2,5-di-*t*-butyl-*p*-benzosemiquinone – sodium iodide – tetrahydrofuran, in which the rate of intramolecular exchange is negligible (9). Here we present the results of a similar kinetic analysis carried through from the "slow" to the "fast" exchange limits for a system showing simultaneous intra- and intermolecular cation exchange.

Experimental

Experimental techniques for the production of samples and the recording of electron spin resonance spectra were as previously described (11). Potassium tetraphenylboride was precipitated *via* the standard literature method (12), from dilute aqueous solutions of sodium tetraphenylboride and potassium chloride.

Results

Electron spin resonance spectra of the system potassium durosemiquinone – potassium tetraphenylboride – tetrahydrofuran were recorded for several concentrations ratios of semiquinone to tetraphenylboride for sample temperatures between −80 and +40 °C. In the absence of potassium tetraphenylboride, spectra of the ion-

[1]To whom all correspondence should be addressed.

TABLE 1. Electron spin resonance spectral parameters of the system potassium durosemiquinone – potassium tetraphenylboride – tetrahydrofuran (values in G ± 0.02 G)

Temperature (°C)	Triple ion a_{Me}	Ion-pair a_{Me},I	Ion-pair a_{Me},II	ΔH^*
−70	1.92	2.49	1.38	0.210
−40	1.92	2.50	1.34	0.230
−20	1.91	2.52†	1.32†	0.250
+20	1.90	2.57†	1.26†	0.300

*ΔH, in G, between center of triple ion and ion-pair spectra.
†Extrapolated values, see text.

pair were obtained: at low temperatures this species was locked into a static asymmetric configuration but, as the temperature was increased, line-width alternation, attributed to the intramolecular exchange of potassium, was observed.

Addition of potassium tetraphenylboride to the ion-pair produced spectra which, at low temperatures, contained resonances due to the ion-pair and the triple ion $[K_2\text{-durosemiquinone}]^+$. Since no potassium hyperfine interaction was resolvable, the spectrum of the triple ion was very similar to that of unassociated durosemiquinone, consisting of 13 lines, with binomial intensity distribution and $a_{Me} = 1.92 \pm 0.05$ G; however, the center of this spectrum occurred to high field of the ion-pair spectrum, not to low field as does that of the free ion. Increasing the sample temperature led to intermolecular exchange of potassium ions between the triple ion and the ion-pair. The spectra selected for detailed evaluation of the kinetic parameters characterizing both intra- and intermolecular exchange reactions are given in Fig. 1.

When the intermolecular exchange of potassium nears its "fast" limit, the spectra of mixtures of the triple ion and ion-pair show three interesting features, which we have found to be generally indicative of the participation of triple ions in the intermolecular cation exchange reactions of ion-pairs. These are: (*i*) lines to low field of the center of the spectrum are broader than their high field counterparts (because g and a_{Me} for the triple ion are slightly less than g and $\bar{a}_{Me}$ for the ion-pair); (*ii*) the line shapes are asymmetric; (*iii*) the apparent hyperfine splitting constant varies by as much as 10% across the spectrum in a systematic large–small–large–small pattern. All three features were reproduced in our simulation of such spectra.

In order to extract the required kinetic parameters from the spectra in Fig. 1, it is necessary to know as a function of temperature the difference in magnetic field between the centers of the triple ion and ion-pair spectra, and the values of both methyl hyperfine splitting constants of the ion-pair. Unfortunately, at the higher sample temperatures the ion pair hyperfine splitting constants are not directly obtainable from the spectra. However, for the corresponding system in which potassium is replaced by sodium these parameters are measurable over the range of interest; wherever similar measurements were possible for both systems, trends in these parameters with temperature were independent of cation. Hence, we have used the results for the sodium system to guide the extrapolation of the potassium data to the higher sample temperatures. Table 1 contains the data on hyperfine splitting constants and g-shifts used in the kinetic analysis of the spectra in Fig. 1.

Discussion

We now propose the equilibria depicted in [2] to be occurring in the system potassium durosemiquinone – potassium tetraphenylboride – tetrahydrofuran, and show how this reaction scheme can account quantitatively for the line shapes in Fig. 1.

[2] $$K^+ + DK \rightleftharpoons KDK^+ \rightleftharpoons K^+ + KD$$

[D = duroquinone]

For convenience we represent [2] by [3] and define τ_{IP} as the mean

[3] $$A \rightleftharpoons B \rightleftharpoons C$$

residence time of durosemiquinone as the ion-pair A before intramolecular exchange converts

Can. J. Chem. Downloaded from www.nrcresearchpress.com by 210.87.254.42 on 09/05/12
For personal use only.

Can. J. Chem. Downloaded from www.nrcresearchpress.com by 210.87.254.42 on 09/05/12
For personal use only.

FIG. 1*a*. Sample temperatures for each figure: −70, −40, −20, +20 °C from top to bottom of diagram. Observed electron spin resonance spectra of KD (in the absence of KPh_4B, the structure is complicated by that of D^-) in tetrahydrofuran.

Can. J. Chem. Downloaded from www.nrcresearchpress.com by 210.87.254.42 on 09/05/12
For personal use only.

b

FIG. 1*b*. Computed electron spin resonance spectra of KD in tetrahydrofuran.

Can. J. Chem. Downloaded from www.nrcresearchpress.com by 210.87.254.42 on 09/05/12
For personal use only.

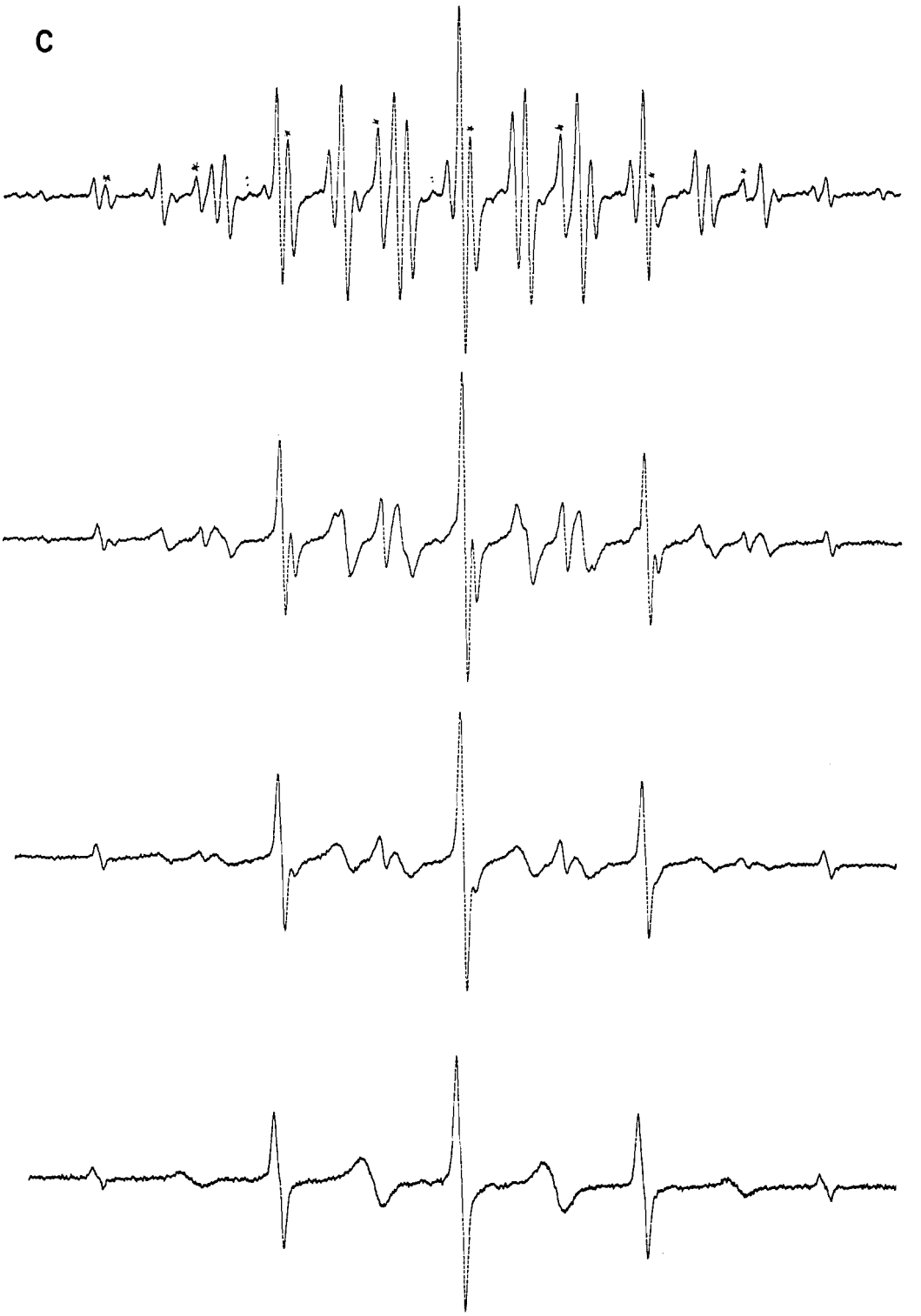

FIG. 1*c*. Observed electron spin resonance spectra of KD–K_2D^+ in tetrahydrofuran. $[KPh_4B] = 2 \times 10^{-4}$ *m*; $[K_2D^+]/[KD] = 0.2$.

Can. J. Chem. Downloaded from www.nrcresearchpress.com by 210.87.254.42 on 09/05/12
For personal use only.

FIG. 1*d*. Computed electron spin resonance spectra of $KD-K_2D^+$ in tetrahydrofuran. $[KPh_4B] = 2 \times 10^{-4}$ *m*; $[K_2D^+]/[KD] = 0.2$.

FIG. 1*e*. Observed electron spin resonance spectra of KD–K_2D^+ in tetrahydrofuran [KPh_4B] = 10^{-3} *m*; [K_2D^+]/[KD] = 1.0.

Can. J. Chem. Downloaded from www.nrcresearchpress.com by 210.87.254.42 on 09/05/12
For personal use only.

Can. J. Chem. Downloaded from www.nrcresearchpress.com by 210.87.254.42 on 09/05/12
For personal use only.

f

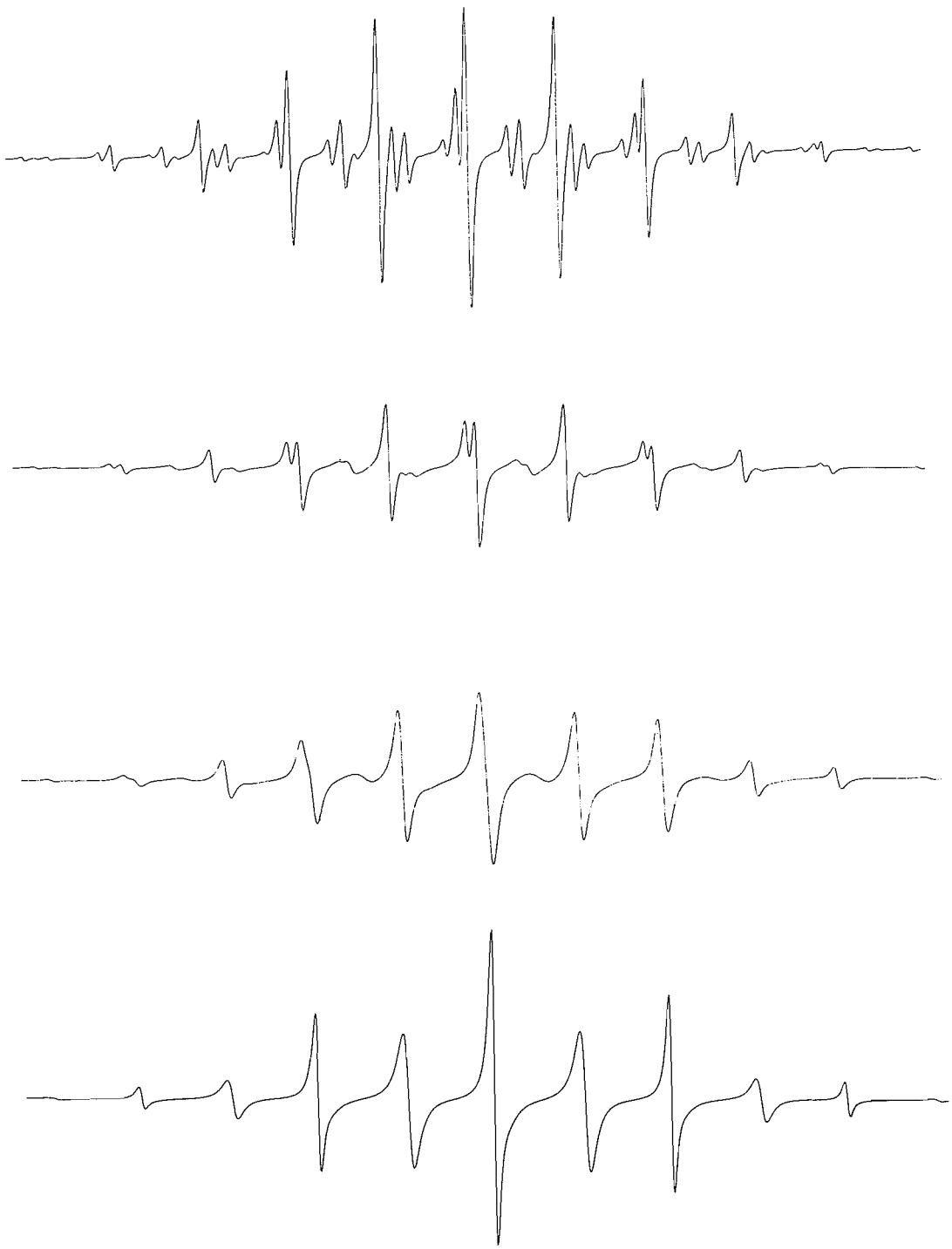

FIG. 1*f*. Computed electron spin resonance spectra of KD–K_2D^+ in tetrahydrofuran. [KPh_4B] = 10^{-3} *m*; [K_2D]/[KD] = 1.0.

Can. J. Chem. Downloaded from www.nrcresearchpress.com by 210.87.254.42 on 09/05/12
For personal use only.

it to the ion-pair C (or *vice versa*), define τ_A as the residence time as the ion-pairs A or C before reaction with a potassium ion forms the triple ion, and define τ_B as the residence time as the triple ion B before dissociation to an ion-pair. Note then that $2\tau_B$ is the residence time before dissociation to a particular ion pair. Defining G_A, G_B, and G_C as the complex magnetizations of the sites A, B, and C we may then write the Bloch Equations, under slow passage conditions, and modified after the fashion suggested by McConnell (13) as [4].

$$[4]\quad \begin{aligned} \alpha_A G_A &= p_A - G_A(\tau_A^{-1} + \tau_{IP}^{-1}) + G_B/2\tau_B + G_C/\tau_{IP} \\ \alpha_B G_B &= p_B - G_B/\tau_B + (G_A + G_C)/\tau_A \\ \alpha_C G_C &= p_C - G_C(\tau_A^{-1} + \tau_{IP}^{-1}) + G_B/2\tau_B + G_A/\tau_{IP} \end{aligned}$$

where α_j has the usual significance of $1/T_2 - i(\omega_j - \omega)$, p_j represents the fractional population of site j, and the scaling factor $-i\gamma H_1 M_0$ has for simplicity been omitted from the fractional populations. Solution of [4] for G_A, G_B, and G_C gives the result shown in [5].

$$[5]\quad G_A = \frac{(\alpha_C + \tau_A^{-1} + 2\tau_{IP}^{-1})(p_A(\alpha_B + \tau_B^{-1}) + 0.5p_B\tau_B^{-1})}{(\alpha_A + \tau_A^{-1} + 2\tau_{IP}^{-1})[(\alpha_B + \tau_B^{-1})(\alpha_C + \tau_A^{-1} + \tau_{IP}^{-1}) - 0.5\tau_A^{-1}\tau_B^{-1}] - (\alpha_C + \tau_A^{-1} + 2\tau_{IP}^{-1})(0.5\tau_A^{-1}\tau_B^{-1} + (\alpha_B + \tau_B^{-1})\tau_{IP}^{-1})}$$

$$G_C = \frac{(\alpha_A + \tau_A^{-1} + 2\tau_{IP}^{-1})G_A}{(\alpha_C + \tau_A^{-1} + 2\tau_{IP}^{-1})}$$

$$G_B = \frac{(\beta_B + (G_A + G_C)\tau_A^{-1})}{\alpha_B + \tau_B^{-1}}$$

$$G = G_A + G_B + G_C$$

The values of G_A, G_B, G_C may then be added to form the total complex magnetization, G, the imaginary part of which represents the intensity of resonant absorption at the frequency defined by ω. To compute the simulations in Fig. 1 values of ω_A, ω_B, and ω_C, expressed relative to the center of the ion-pair spectrum, were calculated for the 49 nuclear spin wave functions each of which defines a line in the ion-pair spectrum. At each of the 1000 values of ω used to define the spectrum it is then necessary to sum the 49 contributions to the overall signal intensity. The number of parameters to be determined is rather large and so the following assumptions and approximations were made.

The transverse relaxation time of all three species was assumed the same; the fractional populations were taken as independent of temperature, though experimentally we have noticed small variations ($\sim$ 5%) in fractional populations for some ion-pair triple ion equilibria; τ_{IP} and τ_B were assumed independent of the concentration of potassium tetraphenylboride, consistent with the reaction scheme being as shown in [2].

In Fig. 2 Arrhenius plots are used to express the temperature dependences of τ_{IP}, τ_A, and τ_B. The plots are reasonable straight lines which, coupled with the excellent agreement between experimental and computed spectra, indicate that the simple reaction scheme [2] adequately describes the present system. Thus, as previously argued for the triple ion Na_2D^+ (10), the dissociation of the triple ion K_2D^+ in the system potassium durosemiquinone – potassium tetraphenylboride – tetrahydrofuran is not brought about by attack of the tetraphenylboride anion; likewise, the association reaction forming the triple ion does not proceed *via* attack of KPh_4B ion pairs upon KD, but rather K^+ must be the attacking species.

Since the intramolecular cation migration and the dissociation of the triple ion are both first order processes, the intercepts of the appropriate Arrhenius plots may be used to determine frequency factors. For the migration process $\log_{10} A = 12.1$ while for the dissociation $\log_{10} A = 11.7$; for both reactions the activation energy was identical (6.6 kcal/mol) within experimental accuracy. The two reactions are, therefore, kinetically very similar and it is tempting to speculate, on this basis, on the mechanism of the intramolecular migration; however, we feel that it is preferable to examine further systems to see whether the observed kinetic similarity is merely a coincidence.

The association reaction forming the triple-ion

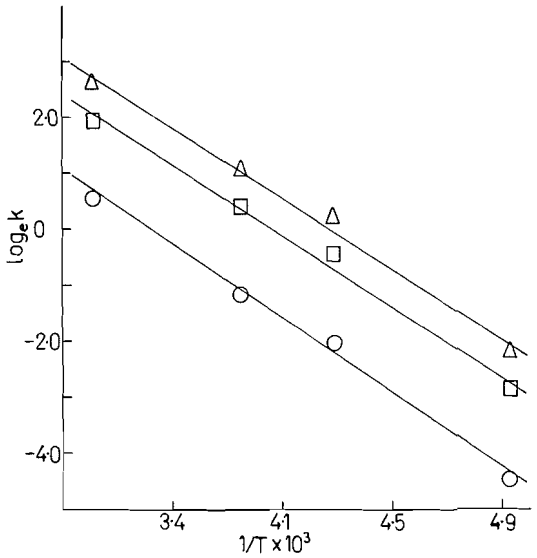

FIG. 2. Arrhenius plots for the system potassium durosemiquinone – potassium tetraphenylboride – tetrahydrofuran; △, intramolecular migration; □, dissociation of triple ion and formation of triple ion at [KPh_4B] *c.* 10^{-3} *m*; ○, formation of triple ion at [KPh_4B] *c.* 2×10^{-4} *m*.

is a second order reaction and so the intercept of the Arrhenius plot is equal to $\log_{10}(A[K^+])$. The concentration of unassociated potassium ions was not determined in the present work, because the dissociation constant of potassium tetraphenylboride in tetrahydrofuran has been measured only at 25 °C (14), and furthermore, there is no guarantee that the species defined by these conductivity measurements as the unassociated potassium ion is in fact the same species as the kinetically significant unassociated potassium ion. However, from a knowledge of the approximate concentration of potassium tetraphenylboride we estimate that $\log_{10} A$ for the association reaction is approximately 14, which is a reasonable value for a positively charged species attacking the negative end of a dipole. The identity of the activation energies for the dissociation and association reaction is, of course, a consequence of our approximation that the fractional populations are independent of temperature.

Thus, using the reaction scheme [2] we are able to account satisfactorily for the observed spectra of the system under discussion and to derive kinetically reasonable parameters characterizing the constituent reactions of the scheme.

This work received financial support in the form of an operating grant from the National Research Council of Canada.

1. N. M. ATHERTON and A. E. GOGGINS. Trans. Faraday Soc. **61**, 1399 (1965).
2. P. S. GILL and T. E. GOUGH. Trans. Faraday Soc. **64**, 1997 (1968).
3. J. C. CHIPPENDALE and E. WARHURST. Trans. Faraday Soc. **64**, 2332 (1968).
4. B. S. PRABHANANDA, M. P. KHAKKAR, and M. R. DAS. J. Indian Chem. Soc. **56**, 659 (1969).
5. J. OAKES and M. C. R. SYMONS. Trans. Faraday Soc. **66**, 10 (1970).
6. J. A. CLAXTON. Trans. Faraday Soc. **65**, 2289 (1969).
7. R. F. ADAMS and N. M. ATHERTON. Trans. Faraday Soc. **64**, 7 (1968).
8. A. W. RUTTER and E. WARHURST. Trans. Faraday Soc. **64**, 2338 (1968).
9. A. W. RUTTER and E. WARHURST. Trans. Faraday Soc. **66**, 1866 (1970).
10. T. E. GOUGH and P. R. HINDLE. Can. J. Chem. **48**, 3959 (1970).
11. T. E. GOUGH and P. R. HINDLE. Can. J. Chem. **47**, 3393 (1969).
12. R. P. PFLAUM and L. C. HOWICK. Anal. Chem. **28**, 1542 (1956).
13. H. M. MCCONNELL. J. Chem. Phys. **28**, 430 (1958).
14. D. N. BHATTACHARYYA, C. L. LEE, J. SMID, and M. SYWARC. J. Phys. Chem. **69**, 608 (1965).

Can. J. Chem. Downloaded from www.nrcresearchpress.com by 210.87.254.42 on 09/05/12
For personal use only.

Can. J. Chem. Downloaded from www.nrcresearchpress.com by 210.87.254.6 on 09/05/12
For personal use only.

Anharmonicity and Hydrogen Bonding. The in-plane OH Bending and its Combination with the OH Stretching Vibration

M. Asselin and C. Sandorfy

Département de Chimie, Université de Montréal, Montréal, Québec

Received December 17, 1970

The infrared spectra of isopropanol, tert-butanol, and their deuterated homologues were measured between 1600 and 1160 cm^{-1} in a mixture of CCl_3F and methylcyclohexane-d_{14} at temperatures ranging from 20 to −182 °C. The assignments of the in-plane OH deformation (δ_{OH}) bands of alcohols are confirmed by these low temperature measurements. An explanation is proposed for the great apparent differences between the δ_{OH} frequencies of primary and secondary alcohols on the one hand, and tertiary alcohols on the other. The effect of temperature on the δ_{OH} frequency of hydrogen bonded alcohols is found to be slight. Hydrogen bonding increases significantly the anharmonic coupling constant between ν_{OH} and δ_{OH}. It remains, however, much smaller than the anharmonicity constant of ν_{OH} itself.

Les spectres infrarouge des l'isopropanol, du tert-butanol et de leurs homologues deutérés ont été mesurés entre 1600 et 1160 cm^{-1} dans un mélange de CCl_3F et méthyl-cyclohexane-d_{14} pour un intervalle de température de 20 à −182 °C. Les attributions des bandes de déformation OH dans le plan (δ_{OH}) des alcools sont confirmées par ces mesures à basses températures. Une explication est proposée pour les grandes différences apparentes entre les fréquences δ_{OH} des alcools primaires et secondaires d'une part et les alcools tertiaires de l'autre. On a trouvé que l'effet de la température sur la fréquence δ_{OH} des alcools liés par liaison hydrogène est faible. La liaison hydrogène augmente de façon significative la constante de couplage anharmonique entre ν_{OH} et δ_{OH}. Elle reste, cependant, beaucoup plus petite que la constante d'anharmonicité de ν_{OH}.

Canadian Journal of Chemistry, **49**, 1539 (1971)

Introduction

The effect of hydrogen bonding on the anharmonicity of the OH stretching vibration (ν_{OH}) of alcohols has been examined previously (1–4) but the anharmonic coupling between ν_{OH} and the in-plane bending vibration (δ_{OH}) of these molecules has not been studied. δ_{OH} is located in a crowded part of the infrared spectrum and is expected to be much less "purely OH" than the stretching vibration. Stuart and Sutherland (5) assigned the free and associated δ_{OH} vibrations to bands observed at about 1250 and 1370 cm^{-1} for primary and secondary alcohols. This was based on isotopic substitution experiments and the great breadth of the 1370 band. Later works by Tarte and Deponthière (6) and Maclou and Henry (7) were basically in agreement with these assignments. It is known that hydrogen bond formation increases the frequency of δ_{OH} (although Ratajczak and Orville-Thomas (8) drew the attention to some exceptions in the case of short hydrogen bonds) but $\Delta\delta$ is much less than $\Delta\nu$.

In the present paper we report results on δ_{OH} and the $\nu_{OH} + \delta_{OH}$ combination band of isopropanol and tertiary butanol. The assignment and anharmonic coupling of these vibrations will be discussed on the basis of low temperature measurements and isotopic substitution.

Outline of the Work

The δ_{OH} bands were measured at 20, −60, −120, and −182 °C in a 1:1 mixture of CCl_3F (freon-11) and methylcyclohexane-d_{14} which is sufficiently translucent between 1600 and 1160 cm^{-1} at thicknesses below 0.1 mm. The location of the free band was ascertained by dilution using a 2.0 mm cell in CS_2 solution at −60 °C. At this temperature most of the OH groups are associated and the free δ_{OH} band disappears. Unfortunately under 2 mm CS_2 is translucent at frequencies lower than 1360 cm^{-1} only.

The $\nu_{OH} + \delta_{OH}$ combination band was measured in a 3 cm cell in a 1:1 mixture of CCl_3F (freon-11) and $C_2Br_2F_4$ (fréon-114-B-2) at 20 and at −193 °C.

Experimental details were given in previous publications (3, 4).

Results

Tertiary Butanol

Figures 1 and 2 show the spectra of C_4H_9OH, C_4D_9OH, C_4D_9OD, and C_4H_9OD at 20 and at

Can. J. Chem. Downloaded from www.nrcresearchpress.com by 210.87.254.6 on 09/05/12
For personal use only.

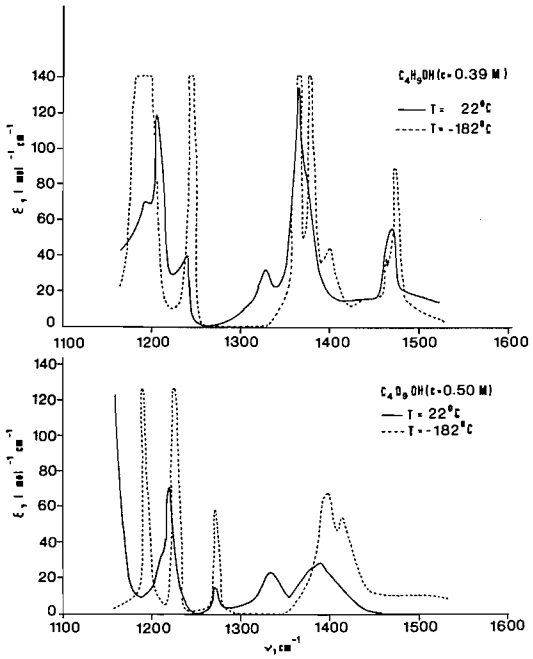

FIG. 1. The infrared spectra (1100–1600 cm^{-1}) of tert-butanol (C_4H_9OH and C_4D_9OH) in a 1:1 mixture of CCl_3F and methylcyclohexane-d_{14} at 22 and −182 °C.

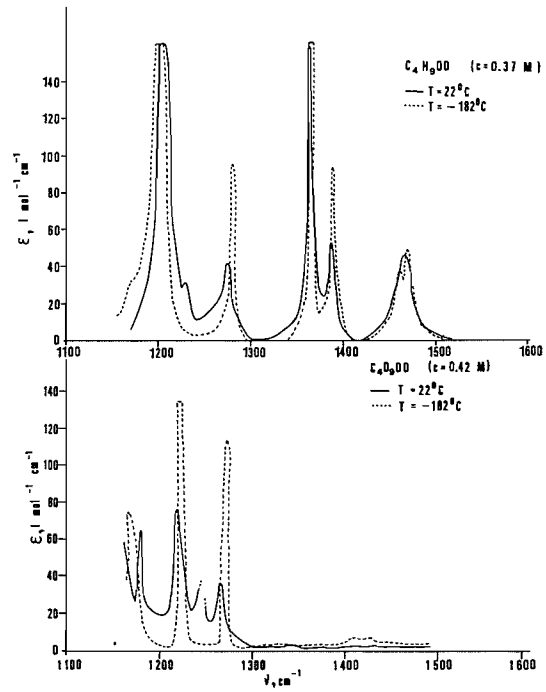

FIG. 2. The infrared spectra (1100–1600 cm^{-1}) of tert-butanol (C_4H_9OD and C_4D_9OD) in a 1:1 mixture of CCl_3F and methylcyclohexane-d_{14} at 22 and −182 °C.

−182 °C. It is seen clearly that the 1328 cm^{-1} band of C_4H_9OH and the 1334 cm^{-1} band of C_4D_9OH disappear in going to low temperature confirming the assignment of this band to the free δ_{OH} vibration. At low temperatures the associated band appears at 1400 cm^{-1} for C_4H_9OH. C_4D_9OH has a doublet at 1415 and 1397 cm^{-1}. The splitting is probably due to Fermi-resonance and since the bands are of nearly equal intensity we used the average, 1406 cm^{-1}, in our calculations.

Unfortunately, solvent problems and near-coincidences with CH bands make it impossible to locate the first overtone of δ_{OH} with any degree of accuracy. We could, however, locate the $\nu_{OH} + \delta_{OH}$ combination tone. Figure 3 shows it for 20 and −193 °C. C_4H_9OH has a sharp band at 4944 cm^{-1} which belongs to the free OH band. It disappears completely at low temperatures. It is replaced by the broad and strong band at 4669 cm^{-1} due to the polymer. C_4D_9OH has these bands at 4949 and 4688 cm^{-1}. They all disappear for C_4D_9OD and C_4H_9OD (Fig. 4). Table 1 contains the frequencies of the fundamentals of ν_{OH} (3, 4), δ_{OH}, and $\nu_{OH} + \delta_{OH}$ for tert-butanol.

Isopropanol

Figures 5 and 6 give the spectra of C_3H_7OH, C_3D_7OH, and $(CH_3)_2CDOH$ at 20 and −182 °C in a 1:1 mixture of CCl_3F and methylcyclohexane-d_{14}. The concentration we had to use to obtain these spectra (0.5 *M*) makes it impossible to identify the bands due to the monomer. We obtained these at 0.1 *M* concentration in CS_2. The associated δ_{OH} band is found at 1397 cm^{-1} for C_3D_7OH and 1400 cm^{-1} for $(CH_3)_2CDOH$

TABLE 1. Wavenumbers of the stretching vibration (ν_{OH}), the in-plane OH bending vibration (δ_{OH}), and of the combination band ($\delta_{OH} + \nu_{OH}$) of free tertiary butanol in solution at 20 °C and of the associated alcohol in solution at −193 °C

	Value			
	C_4H_9OH		C_4D_9OH	
Parameter	Free	Associated	Free	Associated
ν_{OH}	3621	3250	3621	3250
δ_{OH}	1328	1400	1334	1406
$\delta_{OH} + \nu_{OH}$	4943	4669	4949	4688

Can. J. Chem. Downloaded from www.nrcresearchpress.com by 210.87.254.6 on 09/05/12
For personal use only.

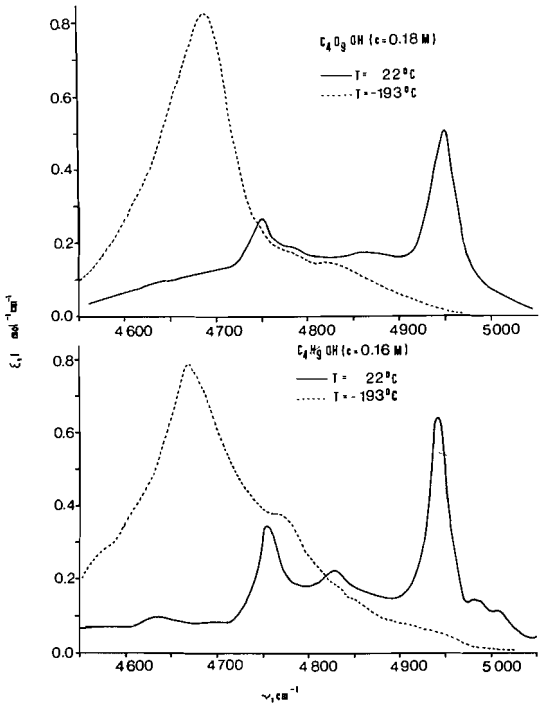

FIG. 3. The infrared spectra (4600–5100 cm^{-1}) of tert-butanol (C_4H_9OH and C_4D_9OH) in a 1:1 mixture of CCl_3F and $C_2Br_2F_4$ at 22 and −193 °C.

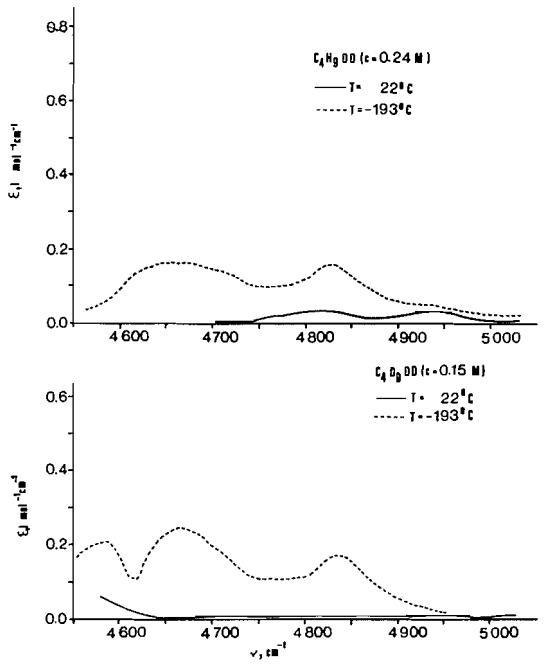

FIG. 4. The infrared spectra (4600–5100 cm^{-1}) of tert-butanol (C_4H_9OD and C_4D_9OD) in a 1:1 mixture of CCl_3F and $C_2Br_2F_4$ at 22 and −193 °C.

while C_3H_7OH has two bands at 1310 and 1415 cm^{-1}. The free bands are at 1328 (C_3D_7OH), 1318 ($(CH_3)_2CDOH$), and 1248 cm^{-1} (C_3H_7OH). According to Krimm, Liang and Sutherland (9), the presence of two bands in the case of associated C_3H_7OH is due to a mixing between δ_{OH} and the CH or CH_2 deformation modes at the same carbon. No explanation was given, however, for the great difference in frequency between the free δ_{OH} of tertiary alcohols (1330 either deuterated or undeuterated), and of primary and secondary alcohols (1256) if the CH hydrogens which are on the same carbon as the OH group are not deuterated.

We observe similar features for the $\nu_{OH} + \delta_{OH}$ combination band of C_3H_7OH. The polymer shows two bands, at 4700 and 4600 cm^{-1}. Both are broad and partly overlap each other (Fig. 7). They are obviously the combinations of ν_{OH} with the bands at 1415 and 1310 cm^{-1}. For the monomer we find a sharp band at 4879 cm^{-1} which is easily assigned to $\nu_{OH} + \delta_{OH} = 3630 + 1248 = 4878\ cm^{-1}$. We find a weaker band at 4995 cm^{-1} which disappears upon association and is absent in the spectra of C_3D_7OH and $(CH_3)_2CDOH$ (Figs. 7, 8). This could be interpreted as a combination between 3630 and a band located at about 1365 which is not observed. It seems logical then to suppose that the strong mixing between OH and CH bending (*cf.* the normal coordinate analysis of Fukushima and Zwolinski (10)) yields two bands for the free species, the one observed at 1248 and one at 1365 assumed coincident with the CH_3 bending bands. This would explain the great difference between the 1250 of the primary and secondary alcohols and the 1330 of tertiary alcohols.

Table 2 summarizes the ν_{OH}, δ_{OH}, and $\nu_{OH} + \delta_{OH}$ frequencies for isopropanol.

Tables 3 and 4 contain the anharmonicity constants for ν_{OH} ($X \equiv \omega_e x_e$ and $Y = \omega_e y_e$; index 1 stands for ν_{OH} and 2 for δ_{OH}) computed from the usual second order formulas. X_{12}* is the anharmonic coupling constant for ν_{OH} and δ_{OH} and the ω are the harmonic frequencies

$$[1] \quad \omega_1 = \nu_1 + 2X_1 + W_1 + (13/4)Y_1 + (1/2)X_{12}^*$$

Can. J. Chem. Downloaded from www.nrcresearchpress.com by 210.87.254.6 on 09/05/12
For personal use only.

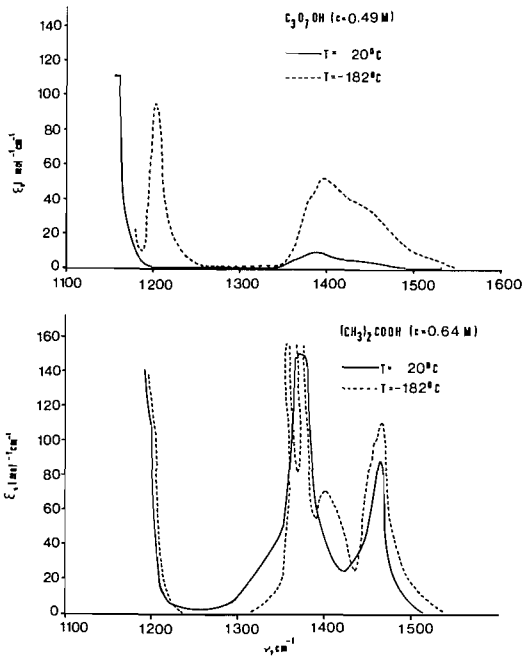

FIG. 5. The infrared spectra (1100–1600 cm^{-1}) of isopropanol (C_3D_7OH and $(CH_3)_2CDOH$) in a 1:1 mixture of CCl_3F and methylcyclohexane-d_{14} at 22 and −182 °C.

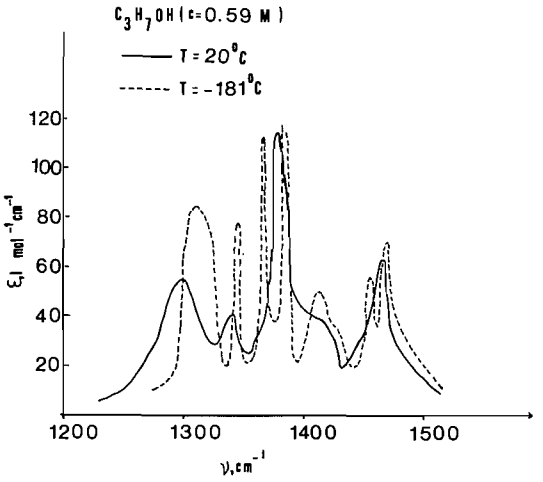

FIG. 6. The infrared spectra (1100–1600 cm^{-1}) of isopropanol (C_3H_7OH) in a 1:1 mixture of CCl_3F and methylcyclohexane-d_{14} at 22 and −182 °C.

where

$$[2] \quad -X_{12} = (\nu_{OH} + \delta_{OH}) - \nu_{OH} - \delta_{OH}$$

W_1, X_1, and Y_1 are the successive anharmonicity constants of ν_{OH} (taken from ref. 4) and $\omega_1{}^*$ is

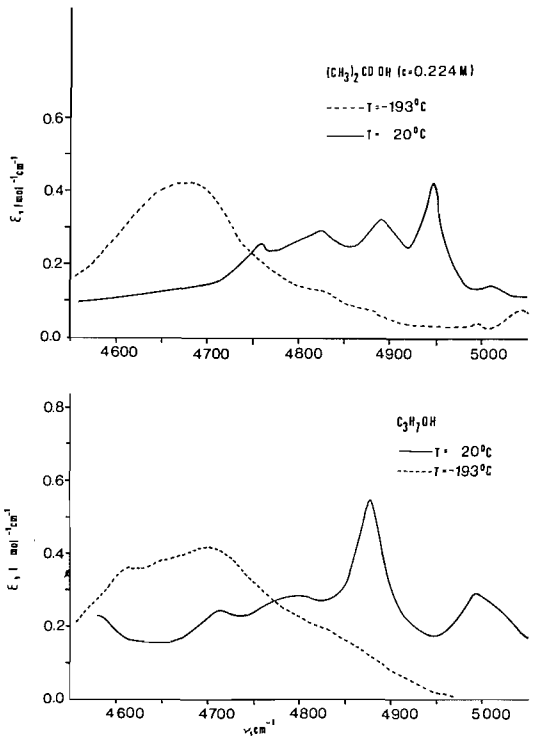

FIG. 7. The infrared spectra (4600–5100 cm^{-1}) of isopropanol (C_3H_7OH and $(CH_3)_2CDOH$) in a 1:1 mixture of CCl_3F and $C_2Br_2F_4$ at 22 and −193 °C.

computed in taking $X_{12}{}^*$ into account (as in eq. 1) and ω_1 without it.

The temperature effect on the associated δ_{OH} band was found to be very slight, between −60 and −182 °C it remains within experimental error. This contrasts with the pronounced temperature shift of ν_{OH} (4). Since vibrations are more sensitive to environmental and temperature effects the more anharmonic they are (11) this indicates a very slight anharmonicity for δ_{OH}. So the shift of δ_{OH} between −182 and −193 °C was neglected in the computation of X_{12} and $\omega_1{}^*$ as well as the very slight differences which might exist between solutions in CS_2, (CCl_3F + methylcyclohexane-d_{14}) and ($CCl_3F + C_2Br_2F_4$). The shift to higher frequencies due to hydrogen bond formation amounts to 72 cm^{-1} for tertiary butanol, 69 cm^{-1} for isopropanol, and 82 cm^{-1} for $(CH_3)_2CDOH$. $\Delta\delta/\Delta\nu$ is of the order of 0.200. As expected $\nu_{OH} + \delta_{OH}$ has a much larger temperature shift, slightly less than ν_{OH} itself.

The coupling constant $X_{12}{}^*$ is only about

TABLE 2. Wavenumbers of the stretching vibration (ν_{OH}), the in-plane OH bending vibration (δ_{OH}), and of the combination band ($\delta_{OH} + \nu_{OH}$) of free isopropanol in solution at 20 °C and of the associated alcohol in solution at −193 °C

	Value					
	C_3D_7OH		$(CH_3)_2CDOH$		C_3H_7OH	
Parameter	Free	Associated	Free	Associated	Free	Associated
ν_{OH}	3634	3225	3634	3225	3630	3225
δ_{OH}	1328	1397	1318	1400	1248 (1365)* 1415	1310
$\delta_{OH} + \nu_{OH}$	4957	4680	4947	4672	4879 (4995)*	4600 4700

*See text.

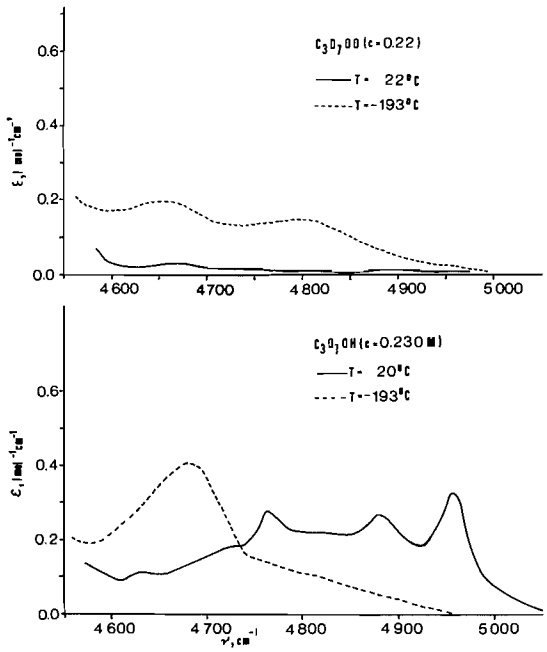

FIG. 8. The infrared spectra (4600–5100 cm^{-1}) of isopropanol (C_3D_7OH and C_3D_7OD) in a 1:1 mixture of CCl_3F and $C_2Br_2F_4$ at 22 and −193 °C.

$-5\ cm^{-1}$ for the monomers. Upon association it increases to 25 ± 5 for tertiary butanol and 52 ± 5 for isopropanol. This means that hydrogen bond formation increases greatly the coupling between OH stretching and in-plane bending vibrations. The value of this coupling constant is relatively low, however, and its effect on the harmonic frequency of ν_{OH} (polymer) is only about 10–20 cm^{-1} compared to about 400 cm^{-1} (Tables 1–4) due to the anharmonicity of the ν_{OH} vibration itself. It can be understood, then, that it can be neglected in computing the isotopic ratios of the frequencies and that the ratios expected in the diatomic approximation can still be obtained (4) as we have shown previously.

TABLE 3. The anharmonicity constants (X_1, Y_1) of the stretching vibration (ν_{OH}), the anharmonic coupling constant (X_{12}*) as given by [2], the harmonic frequency (ω_1*) of the OH vibration as computed by [1], and the harmonic frequency ω_1 computed without X_{12}* for free and self-associated tertiary butanol

	Value			
	C_4H_9OH		C_4D_9OH	
Parameter	Free	Associated	Free	Associated
X_1	85	253	85	253
Y_1	~1	−27.1	~1	−27.1
X_{12}*	−6	19	−6	32
ω_1	3795	3635	3795	3635
ω_1*	3792	3645	3792	3651

TABLE 4. The anharmonicity constants (X_1, Y_1) of the stretching vibration (ν_{OH}), the anharmonic coupling constant (X_{12}*) as given by [2], the harmonic frequency (ω_1*) of the ν_{OH} vibration as computed with [1], and the harmonic frequency ω_1 computed without X_{12}* for free and self-associated isopropanol

	Value			
	C_3D_7OH		$(CH_3)_2CDOH$	
Parameter	Free	Associated	Free	Associated
X_1	83	179	83	170
Y_1	0	−14.8	0	−14.8
X_{12}*	−5	58	−5	47
ω_1	3800	3526	3800	3526
ω_1*	3798	3555	3798	3549

We express our thanks to the National Research Council of Canada for financial help and for a scholarship granted to one of us (M.A.).

Can. J. Chem. Downloaded from www.nrcresearchpress.com by 210.87.254.6 on 09/05/12
For personal use only.

1. G. DUROCHER and C. SANDORFY. J. Mol. Spectry, **15**, 22 (1965).
2. A. FOLDES and C. SANDORFY. J. Mol. Spectry, **20**, 262 (1966).
3. M. ASSELIN, G. BÉLANGER, and C. SANDORFY. J. Mol. Spectry, **30**, 96 (1969).
4. M. ASSELIN and C. SANDORFY. J. Mol. Struct. In press.
5. A. V. STUART and G. B. B. M. SUTHERLAND. J. Chem. Phys. **24**, 559 (1956).
6. P. TARTE and R. DEPONTHIÈRE. J. Chem. Phys. **26**, 962 (1957).
7. M. MACLOU and L. HENRY. Compt. Rend. Acad. Sci. **244**, 1494 (1957).
8. H. RATAJCZAK and W. J. ORVILLE-THOMAS. J. Mol. Struct. **1**, 449 (1968).
9. S. KRIMM, C. Y. LIANG, and G. B. B. M. SUTHERLAND. J. Chem. Phys. **25**, 778 (1956).
10. K. FUKUSHIMA and B. J. ZWOLINSKI. J. Mol. Spectry, **26**, 368 (1968).
11. A. D. BUCKINGHAM. Trans. Faraday Soc. **56**, 753 (1960).

Can. J. Chem. Downloaded from www.nrcresearchpress.com by 210.87.254.6 on 09/05/12
For personal use only.

Can. J. Chem. Downloaded from www.nrcresearchpress.com by 210.87.254.42 on 09/05/12
For personal use only.

Thermodynamic Investigation of the Reaction: $CoSO_{4\,(s)} \rightleftharpoons CoO_{(s)} + SO_{3\,(g,i)}$ by Electromotive Force Measurements

A. W. ESPELUND[1] AND S. N. FLENGAS

Department of Metallurgy and Materials Science, University of Toronto, Toronto 5, Ontario

Received November 12, 1970

The thermodynamic properties of the system CoO–$CoSO_4$ have been investigated over the temperature range 560 to 916 °C, by an electrochemical method using a ZrO_2–CaO solid electrolyte and an oxygen reference electrode. The standard free energy change for the reaction

$$CoSO_{4(s)} \rightleftharpoons CoO_{(s)} + SO_{3(1\ atm)}$$

can be expressed by

$$\Delta G^0_R = 69\,213 + 27.631\,T \log T - 137.07\,T$$

and is given with an accuracy of ± 400 cal.

On a étudié les propriétés thermodynamiques du système CoO–$CoSO_4$ entre 560 et 916 °C en utilisant une méthode électrochimique qui fait appel à un électrolyte solide (ZrO_2–CaO) et de l'oxygène comme électrode de référence. Le changement d'énergie libre pour la réaction

$$CoSO_{4(s)} \rightleftharpoons CoO_{(s)} + SO_{3(1\ atm)}$$

peut être exprimé par l'équation

$$\Delta G^0_R = 69\,213 + 27.631\,T \log T - 137.07\,T$$

et est donné avec une précision de ± 400 cal.

Canadian Journal of Chemistry, 49, 1545 (1971)

Introduction

Most previous investigations on simple oxide–sulfate equilibria have been conducted by static methods involving the measurement of the total equilibrium pressure of the gases SO_2, SO_3, and O_2, resulting from thermal decomposition. The partial pressure of SO_3, defining the thermodynamic properties of the reaction

$$[1] \qquad MSO_{4(s)} \rightleftharpoons MO_{(s)} + SO_{3(gas)}$$

(M is a divalent metal cation) was then calculated from the known values of the equilibrium constant of the decomposition reaction

$$SO_{3(g)} \rightleftharpoons SO_{2(g)} + \tfrac{1}{2}\,O_{2(g)}$$

For the calculation the basic assumption was made that at the reaction zone temperature, $P_{SO_2} = 2P_{O_2}$.

The accuracy of the method is usually restricted by the rather low sensitivity of the all glass Bourdon type gauges, which have been employed because of the corrosive nature of the SO_3 gas, and in addition, the validity of the assumption regarding the ratio for the partial pressures given above has not been fully established; the equilibrium between O_2, SO_2, and SO_3 is highly temperature dependent and the actual partial pressures at the sample site could be influenced by the existence of a temperature gradient along the pressure cell. Ingraham and Kellogg (1) demonstrated in one case by circulating the gas with an all glass pump, that such mixing had no influence on the measured total pressure. Warner (2) improved the method by introducing an "oxygen couple" in a position adjacent to the reacting mixture, or as a part of the sample, thus fixing the oxygen pressure. In this way data for the CoO–O–SO_2 system were obtained, using the mixtures of Cu_2O–CuO and CoO–Co_3O_4 as oxygen couples.

In the present investigation, the application of a ZrO_2–CaO type solid electrolyte and an oxygen electrode allows direct determination of the oxygen partial pressures of the reacting mixture at various temperatures. Unambiguous values for the composition of the gas phase at the sample site are obtained by simultaneous measurements of the total gas pressure. The cell design is schematically represented by

$$CoO_{(s)}\text{–}CoSO_{4(s)},\ SO_{2(g)}\ Pt/ZrO_2\text{–}CaO/Pt,\ O_{2(1\ atm)}$$

In this cell the *total* pressure is fixed by using a

[1]Present address: Metallurgisk Institutt, Norges Tekniske Høgskole, Trondheim.

Can. J. Chem. Downloaded from www.nrcresearchpress.com by 210.87.254.42 on 09/05/12
For personal use only.

flow of SO_2 gas. The method is similar to that employed recently by Larson and Elliott for the investigation of oxide–sulfide equilibria (3).

In this paper, the results of e.m.f. measurements on the system CoO–$CoSO_4$ are presented and a comparison is made with other available thermodynamic data.

Experimental

The essential features of the cell are shown in Fig. 1. The sample was held in a crucible of silica glass, supported by the SO_2 admission tube. Electrical contact on the sample side of the ZrO_2–CaO electrolyte was provided through a platinum grid, upon which the ZrO_2 + CaO ($\frac{1}{2}$ in. o.d.) tube was resting. Additional material was filled around the tube.

Pure oxygen at atmospheric pressure was utilized in the reference electrode. The gas was admitted through a spring loaded silica tube, that provided good contact between the platinum foil inner electrode and the inner surface of the electrolyte tube.

The platinum leads from each electrode were introduced through the two gas admission tubes. In addition, Pt + 13% Rh leads were welded to the electrodes for temperature measurement. The cell was placed in a vertical position in a conventional tube furnace provided with a grounded Inconel tube for electrical shielding. The temperature of the furnace was controlled with a proportional type controlling unit.

CoO was prepared from the hydrated salt, $CoSO_4 \cdot 7H_2O$ Fisher certified reagent, with a total of 0.12% impurities, by the method used by Ingraham (4): *i.e.* drying to $CoSO_4$ at 400 °C, formation of Co_3O_4 at 850 °C, and conversion of Co_3O_4 to CoO in vacuum at 850 °C. The compositions were verified by X-ray analysis including comparison with the standard ASTM-file.

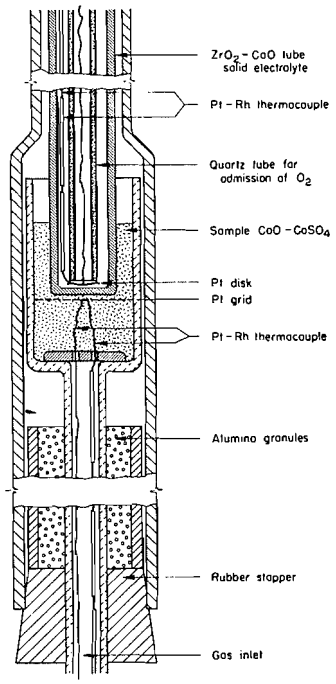

FIG. 1. Apparatus for e.m.f. measurements.

The sulfur dioxide gas was Matheson Anhydrous Grade, with a minimum of 99.98% SO_2. The flow rate was normally varied between 0 and 10 cc/min, and was measured with a calibrated rotameter.

The e.m.f. across the cell was measured with a high impedance p*H*-meter having a scale expander attachment, which could be read to the nearest millivolt.

Results

Electromotive force measurements were taken in the temperature range from 560 to 916 °C. Extension to lower temperatures was not possible because of the erratic behavior of the p*H*-meter, due to the increasing total resistance of the cell.

In the flow rate range of 3 to 10 cc/min of SO_2, the e.m.f. remained independent of flow rate to within ± 1.5 mV. The measurements at the lower flow rate were used for the calculations. The overall calculations involved the following sequence:

(*1*) From the barometric pressure and the measured e.m.f., the partial pressure of oxygen at the reaction site was determined using the equation

$$E_{cell} = \frac{-RT}{4F} \ln \frac{P_{O_2'}}{P_{O_2''}}$$

where $P_{O_2'}$ and $P_{O_2''}$ are the oxygen partial pressures in the reference electrode and at the reaction site, respectively.

(*2*) A preliminary value for p_{SO_2} was obtained, by subtracting the measured oxygen pressure from the total pressure.

(*3*) A preliminary value for p_{SO_2} was determined from the equation for the SO_2/SO_3 equilibrium recommended by Kellogg (5), based upon Evans and Wagman's study of the SO_2–SO_3 system (6).

(*4*) The value obtained was incorporated in the sum of partial pressures, giving a new final value for p_{SO_2}.

(*5*) A second final value for p_{SO_3} was calculated.

At the lowest oxygen pressures, *i.e.* below about 800 °C the first value for p_{SO_3} was sufficiently accurate (less than 20 cal difference between ΔG^0_R resulting from steps (*3*) and (*5*)) and could be calculated from step (*3*) only. Electromotive force measurements and calculated partial pressures in this system are given in Table 1.

The data were fitted into a Σ-plot, using a C_p

TABLE 1. Electromotive force measurements and partial pressure calculations in the system CoO–$CoSO_4$

Temperature (°K)	E_{cell} (mV)	log p_{O_2}	log K	log p_{SO_3}	ΔG^0_R (cal/mol)
982	380	−7.8075	−0.3491	−3.5583	15 980
1027	311	−6.1099	−0.1266	−2.9335	13 780
1069	254	−4.7950	+0.6128	−2.4645	12 050
1111	196	−3.5614	+0.2341	−2.0241	10 280
1154	143	−2.5029	+0.3955	−1.6633	8 780
1078	242	−4.5318	+0.0974	−2.3702	11 680
1047	281	−5.4154	−0.0351	−2.6778	12 820
914	469	−10.3505	−0.7228	−4.4577	18 640
881	516	−11.8136	−0.9273	−4.9847	20 090
849	562	−13.3505	−1.1415	−5.5383	21 510
827	595	−14.5152	−1.3025	−5.9597	22 540
926	455	−9.9145	−0.6522	−4.3132	18 270
850	563	−13.3632	−1.1380	−5.5529	21 590
883	513	−11.7161	−0.9144	−4.9465	19 980
901	491	−10.9898	−0.8015	−4.6963	19 350
936	445	−9.5881	−0.6176	−4.1794	17 890
986	370	−7.6849	−0.3289	−3.5165	15 860
1010	336	−6.7105	−0.2073	−3.1517	14 560
1058	271	−5.1675	0.0136	−2.6018	12 590
1104	207	−3.7843	0.2063	−2.1061	10 630
1130	171	−3.0550	0.3079	−1.8444	9 530
1157	138	−2.4088	0.4083	−1.6304	8 630
1166	125	−2.1654	0.4406	−1.5426	8 220
1177	111	−1.9054	0.4795	−1.4558	7 830
1095	221	−4.0731	0.1699	−2.2138	11 090
866	534	−12.4349	−1.0256	−5.1947	20 580
838	579	−13.9329	−1.2191	−5.7502	22 040
866	534	−12.4349	−1.0256	−5.1947	20 580

value of −12 cal/deg mol, as recommended by Warner (2). The corresponding sigma function is

$$\Sigma = -R \ln p_{SO_3} - 12 \ln T$$

and the plot of Σ vs. $1/T$ is shown in Fig. 2. There is no marked deviation from the straight line given by the equation

$$\Sigma = -137.07 + \frac{69\,213}{T}$$

Accordingly, for the reaction

$$CoSO_{4(s)} = CoO_{(s)} + SO_{3(g,\ 1\ atm)}$$

$$\Delta H^0_R = 69\,213 - 12\,T$$

$$\Delta G^0_R = 69\,213 + 27.631\,T \log T - 137.07\,T$$

$$\Delta S^0_R = 125.07 - 27.63 \log T$$

in the temperature range 833 to 1189 °K. Figure 3 represents the plot of ΔG^0_R *vs.* temperature.

The accuracy in the reported free energy data is subject to the following possible uncertainties. The maximum error due to a fluctuation of ±1 °C in the temperature measurements contributes an error of ±50 cal. The uncertainty of ±1.5 mV in the e.m.f. readings represents an added uncertainty of ±100 cal, and for the SO_2–SO_3 equi-

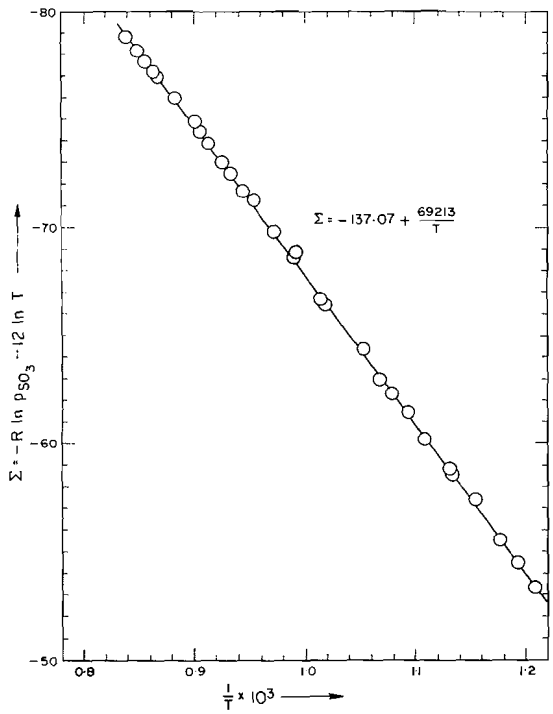

FIG. 2. Σ-plot of experimental results.

Can. J. Chem. Downloaded from www.nrcresearchpress.com by 210.87.254.42 on 09/05/12
For personal use only.

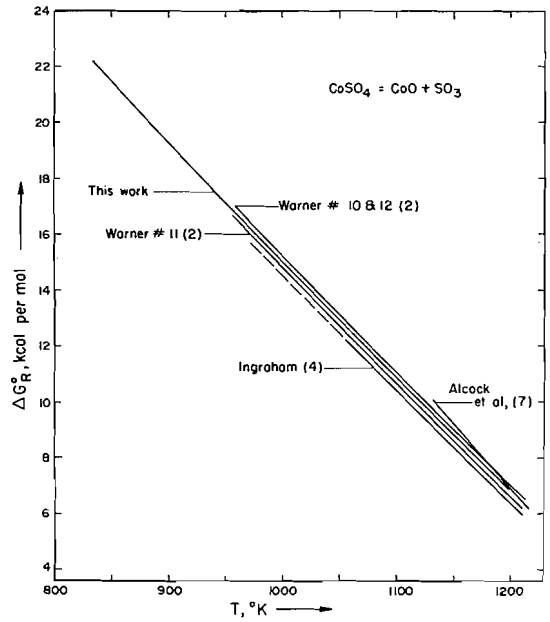

FIG. 3. Plot of ΔG^0_R against T, and comparison of data.

librium Kellogg's equation is given with an accuracy of ± 200 cal. Therefore, the overall accuracy for the free energies calculated from the present results should be better than ± 400 cal/mol.

Discussion

The results shown in Fig. 2 refer to experiments with a sample consisting of the two phases CoO and $CoSO_4$, the latter formed in the apparatus. The source of SO_2 gas was the same for all runs. In order to determine the oxygen potential of the gas in the cylinder, a non-reacting sample of only CoO was used deliberately in the e.m.f. cell at a temperature of 900 °C. The measurements gave an oxygen pressure of $10^{-5.5}$ atm, in good agreement with the gas analysis quoted earlier. This value corresponds to a temperature of about 775 °C at which the CoO–$CoSO_4$ mixture has the same equilibrium oxygen pressure as above. The lack of any abnormal behavior during measurements at temperature below this point of balance indicates that both the sulfation and the decomposition reactions do not have a noticeable kinetic restriction within the range of flow rates and temperatures applied.

In Fig. 3, a comparison is made with the results by Ingraham (4), Warner (2), and Alcock, Sudo, and Zador (7). Ingraham, using direct pressure measurements, obtained as products of decomposition, CoO above 782 °C and Co_3O_4 below this temperature. The values for the $CoSO_4$–CoO equilibrium in the temperature range 700–782 °C (dotted line) were obtained by additional measurements on the Co_3O_4–CoO system.

Warner (2) in his final treatment has averaged his own measurements taken together with those by Ingraham (4), using the Σ-function calculation. However, the application by the former of the oxygen couple with a known oxygen pressure, in addition to a measurement of the total pressure, seems to justify a separate treatment of the data.

The Σ-function equations for experiments #11, and a composite for #10, and #12, reported by Warner (2), are available and have been converted to the ΔG^0_R–T curves shown in Fig. 3. The present results are in excellent agreement with the average of Warner's results, and in addition they extend to a much wider temperature range.

Warner (2) and Ingraham (4) mention the presence of an α–β transition for $CoSO_4$ at 615 ± 5 °C. However, the Σ-plot in Fig. 2 does not show a change in slope below this temperature. This can be explained by the rather low value of ΔH^0_t (600 cal) associated with the phase change according to Ingraham (4), and by the uncertainty of about 400 cal in the present results.

The temperature dependence of the results by Alcock *et al.* (7), obtained over a short temperature range, differs from all others, as shown in Fig. 3. The difference is in the entropy of the reaction and cannot be explained by the use of another equation for the treatment of the SO_2–SO_3 equilibria. The method used by the former was a combination of thermal and gravimetric thermal analysis carried out in a flowing mixture of SO_2, O_2, and N_2 gases and could be limited by nonequilibrium conditions in the gas phase or, during the gas solid reaction. Lack of sensitivity of the equipment registering the onset of reaction in the solid sample could also account for the discrepancy. It is, therefore, proper to question if the present results suffer from the same handicaps. As indicated, in the present method the e.m.f. measurements were practically independent of flow rate of the SO_2 gas, and therefore should represent equilibrium conditions. Furthermore the results were totally reproducible on increasing and decreasing the temperature.

Can. J. Chem. Downloaded from www.nrcresearchpress.com by 210.87.254.42 on 09/05/12
For personal use only.

The formation of Co_3O_4 can also be excluded during these measurements, as the oxygen pressures which are required for the oxidation of CoO, in the temperature range 800 to 1100 °K, are of the order of 10^{-8} and 10^{-2} atm, respectively. From the results in Table 1, it may be seen that the partial pressures of oxygen which were present in the reaction site were much lower and oxidation of CoO should not be expected to have taken place.

The authors acknowledge the valuable assistance of Mr. R. Chappell for the construction of the quartz cells used for these experiments.

The financial assistance (A.W.E.) by the Norwegian Science Council is also gratefully acknowledged.

1. T. R. INGRAHAM and H. H. KELLOGG. Trans. Met. Soc. A.I.M.E. **227**, 1419 (1963).
2. J. S. WARNER. D. Eng. Sc. Dissertation, Columbia University, New York. May, 1964.
3. H. R. LARSON and J. F. ELLIOTT. Trans. Met. Soc. A.I.M.E. **239**, 1713 (1967).
4. T. R. INGRAHAM. Can. Met. Quart. **3**, 221 (1964).
5. H. H. KELLOGG. Trans. Met. Soc. A.I.M.E. **230**, 1622 (1964).
6. W. EVANS and D. WAGMAN. J. Res. Nat. Bur. Std. **49**, 141 (1952).
7. C. B. ALCOCK, K. SUDO, and S. ZADOR. Trans. Met. Soc. A.I.M.E. **233**, 655 (1965).

Can. J. Chem. Downloaded from www.nrcresearchpress.com by 210.87.254.42 on 09/05/12
For personal use only.

Can. J. Chem. Downloaded from www.nrcresearchpress.com by 210.87.254.6 on 09/05/12
For personal use only.

Drop Calorimetric Measurements on some Chlorides, Sulfides, and Binary Melts

W. T. THOMPSON[1] AND S. N. FLENGAS
Department of Metallurgy and Materials Science, University of Toronto, Toronto 181, Ontario

Received September 9, 1970

Enthalpy content measurements on pure KCl, AgCl, CuCl, $PbCl_2$, Ag_2S, and PbS were made at temperatures up to 1000 °C using a sapphire calibrated drop calorimeter. Similar measurements were performed on AgCl–Ag_2S and AgCl–KCl melts. These results determined values for the integral enthalpy of liquid–liquid mixing.

Des mesures d'enthalpie furent faites sur des échantillons purs de KCl, AgCl, CuCl, $PbCl_2$, Ag_2S et PbS à des températures allant jusqu'à 1000 °C utilisant un calorimètre à chute. Des mesures similaires ont été effectuées sur des mélanges fondus de AgCl–Ag_2S et AgCl–KCl. Ces résultats ont permis de déterminer des valeurs pour l'enthalpie intégrale de mélange liquide–liquide.

Canadian Journal of Chemistry, 49, 1550 (1971)

Introduction

The physical chemistry of base metal sulfide – molten chloride solutions, and their use as potential electrolytes in the recovery of metal and elemental sulfur from sulfide minerals, has been under continuous investigation in this laboratory for the past few years. Included in this program are conductivity (1–3), density (3–5), phase diagram (3–6), and electromotive force (e.m.f.) studies (7, 8). Correlation of the complementary e.m.f. and phase diagram investigations requires accurate thermal data for the pure chlorides and sulfides, but it appears that some of the information is lacking or in possible error. The present investigation therefore was undertaken in order to determine or to re-evaluate the enthalpy contents and associated thermodynamic properties of the sulfides and chlorides involved in the previous work of this laboratory. For this purpose, an aluminum block drop calorimeter was designed and constructed commensurate with the accuracy required. After calibration with N.B.S. synthetic sapphire, measurements were made on pure KCl, AgCl, CuCl, $PbCl_2$, Ag_2S, and PbS for temperatures up to about 1000 °C. Approximate measurements of the enthalpy of mixing were also made for the AgCl–Ag_2S melts by determining the enthalpy contents as a function of temperature and composition. This procedure was checked by performing similar measurements and calculations on the AgCl–KCl system for which independent measurements are available.

[1]Present address: Department of Metallurgical Engineering, McGill University, Montreal 110, Quebec, Canada.

Experimental

Calorimeter Design

The essential features of the drop calorimeter constructed for this investigation are shown in Fig. 1. This instrument consists of three main assemblies: a furnace to heat samples to the desired temperature, the calorimeter proper consisting of an aluminum billet, and a mechanism to prevent the transfer of heat by radiation from the furnace to the calorimeter proper.

The heating furnace was made from a Kanthal element wound on a 1 in. diameter Inconel tube. This was insulated with Fiberfrax placed within a copper jacket. The jacket was water cooled to maintain the furnace exterior near room temperature. The furnace assembly was mounted on wheels and located on a track so that it could be rolled away from the calorimeter proper after performing an experiment or during the temperature equilibration of a sample. The drop samples consisted of weighed quantities of the desired compounds sealed within weighed evacuated quartz capsules equipped with quartz hooks. The samples were about 14 mm in diameter and about 6 cm in length. These were suspended within the furnace on 0.005 in. diameter platinum filament strung across thick platinum electrodes. This suspension method made it possible to release the sample by electrically fusing the filament. The small amount of platinum that fell with the sample as a bead attached to the glass hook contributed negligibly to the total heat content. The sample and the suspension assembly are shown in detail A of Fig. 1. The temperature gradient along the length of the sample was reduced to about 1 °C at the average operating temperature of 500 °C by adjusting the furnace insulation. The temperature of the sample was precisely regulated with a proportional electronic controller. The temperature of the sample was measured using a Pt/Pt–13%Rh thermocouple located adjacent to it. The couple was calibrated against the melting points of gold, sodium chloride, tin, and the boiling point of water. Considering the temperature gradient along the sample, the precision of the temperature controller, and the reliability of the calibrated thermocouple, the reported temperatures are within 1 to 1½ °C of the true sample temperatures at the average furnace operating temperature of 500 °C.

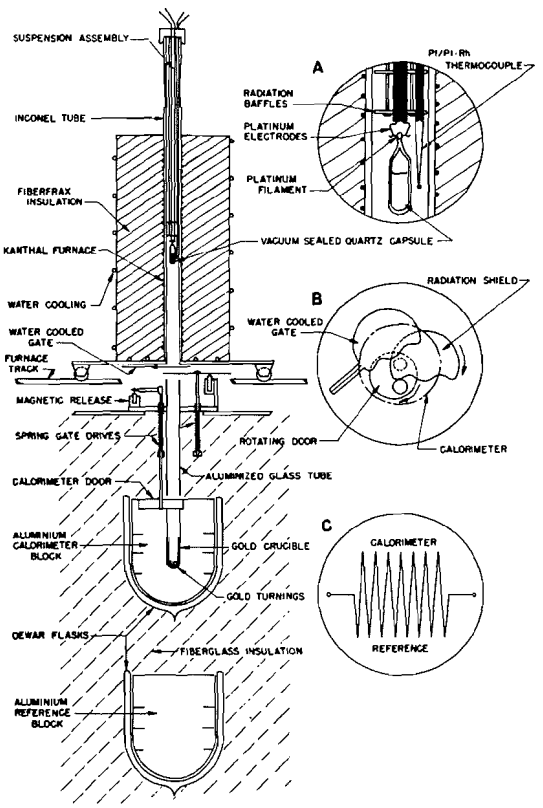

FIG. 1. The drop calorimeter.

The calorimeter proper consisted of a 45 lb aluminum billet suspended within a large Dewar flask. A gold crucible having a $\frac{1}{8}$ in. wall thickness was located at the bottom of a 1 in. diameter hole bored into the billet. This was forced into place so that it made complete thermal contact with the billet. The function of the gold crucible was to prevent the aluminum from oxidizing when the heat from the hot sample was transferred to the calorimeter. Gold turnings placed in the bottom of the crucible absorbed the shock of a falling sample. The calorimeter was equipped with a 1 in. thick disc-shaped aluminum door. This appears in a top view in detail B of Fig. 1. The function of the door was to reduce the loss of heat to the surroundings when a sample was resting within the calorimeter. The door was opened and closed by rotation; it rolled on three small ball bearing wheels located on the bottom face of the disc-shaped door. In the fully closed position, these wheels dropped into small depressions machined into the calorimeter block so that the door made thermal contact with the billet. Before an experiment, the door was rotated manually into the fully open position; however, after releasing a sample from the furnace, it was automatically closed by a relay actuated spring drive mechanism.

The temperature rise of the calorimeter proper, after the admission of a sample, was measured relative to a second block of similar size using a thermopile containing 36 copper–constantan junctions constructed from 0.003 in. diameter insulated thermocouple wire. The thermopile is represented in detail C of Fig. 1. The couples were arranged in three banks of twelve; each couple in each bank was 30° removed from its neighbors, and the banks were displaced 10° from each other. In this way, no matter which way the sample rested in the calorimeter, the signal from the thermopile was the same. The junctions of the thermopile were inserted into snug fitting holes drilled 1 in. into the billet. This depth of penetration assured that at no time during the delivery of heat to the aluminum billet would the thermoelectric signal from the pile rise above the final value when the heat was uniformly distributed in the billet. The shorting of couples through contact with the aluminum was prevented by coating the exposed metal at each junction with lacquer. The output from the thermopile was fed to a Sargent SRG recorder. The chart scale could be adjusted from 0.4 to 2.0 mV for full scale deflection.

Both the calorimeter block and the reference block were insulated from the room with 18 in. of fiberglass wool; a similar quantity of insulation thermally separated the two blocks. Therefore, small changes in the temperature of the room in which the instrument was located resulted in long term monotonic changes in the temperatures of the calorimeter and reference blocks. Heat transfer from the calorimeter to the reference block was negligible during the period following an experiment. This was chiefly a result of the large thermal mass of the calorimeter which resulted in temperature increases of only 0.3 °C during an experiment. Small quantities of heat eventually reached the aluminum reference block. This, however, did not constitute a source of systematic error since heat transfer in this manner is the same for both samples of unknown heat content and known heat content (sapphire) with which the instrument was calibrated.

In order to reduce the transfer of heat from the furnace to the calorimeter and/or make this reproducible from run to run, a radiation shield, shown in detail B of Fig. 1, was incorporated into the design. During temperature equilibration, a water cooled gate closed the bottom of the furnace. This was opened manually just before an experiment when the furnace was over the calorimeter. At this time, the radiation shield prevented short term transfer of heat from the furnace to the calorimeter. When the sample was dropped, an automatic magnetic release allowed this shield to rotate at such a rate that the section removed from the periphery opened the furnace to the calorimeter for a sufficient time interval to allow the sample to pass freely through. As the rotation continued, the shield again passed into a closed position. In coming to rest against a mechanical stop, a microswitch was actuated which released the calorimeter door, thereby enclosing the hot sample within the instrument. The water cooled gate on the furnace was then closed manually and the entire furnace assembly was rolled away from its position over the calorimeter.

Operation

The measurements of the enthalpy contents required compensating for the thermoelectric voltage due to billet temperature differences resulting from previous experiments. In this way, the sensitivity of the recorder could

Can. J. Chem. Downloaded from www.nrcresearchpress.com by 210.87.254.6 on 09/05/12
For personal use only.

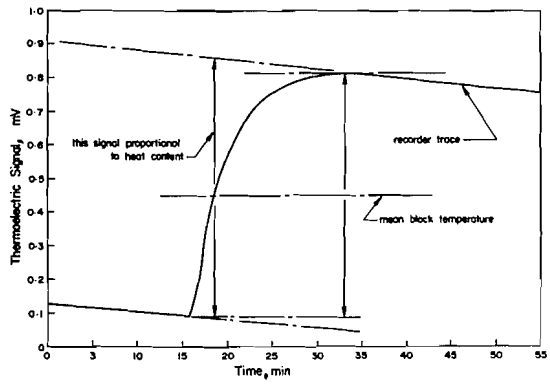

FIG. 2. Typical thermoelectric signal from drop calorimeter.

be used to full advantage. After recording the thermopile output for about 20 min to establish a baseline, the temperature of the calorimeter was measured by withdrawing a mercury thermometer that had been lowered into it 2 or 3 h prior to the experiment. The furnace temperature was then measured and the sample was dropped into the calorimeter. The recorder continued to run for about three quarters of an hour by which time a complete trace of the type shown in Fig. 2 was established. For such behavior, the heat increase of the calorimeter is proportional to the increase in the thermopile output at a point corresponding to half the determined total increase (9). In order to eliminate small errors due to chart paper shrinkage and changes in the electrical characteristics of the recorder, the paper was calibrated at regular intervals using a Leeds and Northrup K-3 potentiometer. The measured thermoelectric signals were all referred to a standard temperature of 25 °C using a simple linear correction (10). This correction gives the signal that would have been measured if the temperature of the sample and calorimeter after an experiment were exactly 25 °C. This correction is quite small since actual final temperatures were generally within 1 or 2 °C of 25 °C.

Calibration

The relationship between the thermopile output and the heat increase of the calorimeter block was determined using U.S. Bureau of Standards synthetic sapphire (11). Since silica glass was used as a container material for the sapphire and compounds studied, a large number of initial experiments were performed to determine the recorded output per gram of silica for temperatures up to 1200 °C. The slugs of silica used in those experiments were similar in surface area to capsules used subsequently to contain compounds. Heat loss by radiation should therefore be similar for slugs and capsules, and hence not lead to a source of systematic error. These results with silica slugs are given in Fig. 3. A smooth curve through these data was determined by the method of least squares. The equation is

$$[1]\quad V_1 = 4.5038\,T^{-1} - 4.3816 \times 10^{-2} + 9.6981 \times 10^{-5}\,T + 1.8370 \times 10^{-9}\,T^2$$

where V_1 is the signal in mV/g SiO_2, and T is the temperature in °K. The standard deviation for this fit is 3.0×10^{-4} mV/g.

A second series of experiments was performed with platinum cuttings sealed in silica capsules. The results are also given in Fig. 3. The equation of the curve is

$$[2]\quad V_2 = -3.037 \times 10^{-3} + 9.629 \times 10^{-6}\,T + 1.751 \times 10^{-9}\,T^2$$

where V_2 is the signal in mV/g Pt. The standard deviation is 5.8×10^{-5} mV/g.

A third series of experiments was performed with the standard sapphire sample sealed in the silica capsule. To prevent possible reaction between the sapphire and silica at high temperature, a platinum foil liner separated the sapphire from the walls of the capsule. The signal corresponding to the enthalpy content of the platinum lined container, obtained by calculating values from eq. 1 and 2, was subtracted from the results of these experiments. The resultant signal corresponded to the enthalpy content of the sapphire.

The enthalpy content of sapphire is known to be the following function of temperature relative to 0 °K (11)

$$[3]\quad H_T - H_0 = 148.5704\,T - 1.7106 \times 10^{-3}\,T^{-2} - 46\,994.87 \log T + 82\,146.1$$

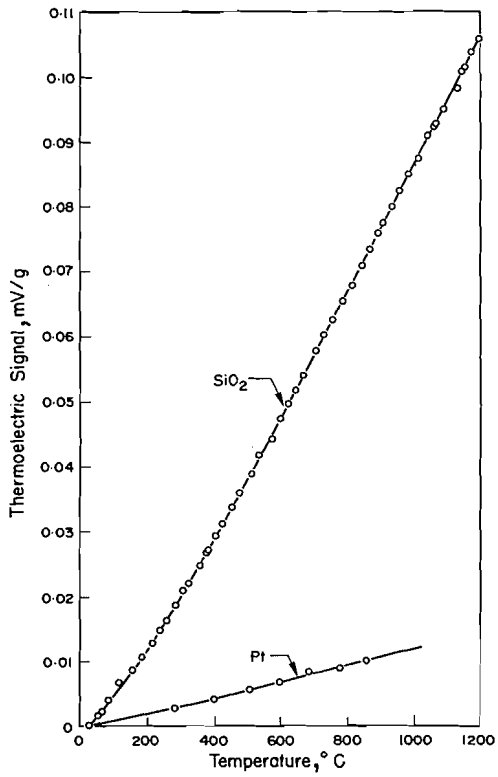

FIG. 3. Thermoelectric signal from silica and platinum.

Can. J. Chem. Downloaded from www.nrcresearchpress.com by 210.87.254.6 on 09/05/12
For personal use only.

Can. J. Chem. Downloaded from www.nrcresearchpress.com by 210.87.254.6 on 09/05/12
For personal use only.

where the enthalpy difference is in absolute J/g-mol. Using this equation, the calorimetric constant was determined. The mean of twelve such determinations from 201 to 1074 °C is 2885 cal/mV with a standard deviation of 34.6 cal/mV. There was no detectable temperature dependence of this factor.

Using this constant, the enthalpy content of silica at 1000 °K relative to 298 °K was calculated from eq. 1 to be 10 320 cal/mol. This compares with 10 280 cal/mol at 1000 °K given by Kelley (12) which is considered accurate to 3% (9). Based on this comparison and the reproducibility of results, it is estimated that the present instrument is capable of measuring enthalpy contents with an absolute accuracy of at least 2%.

Enthalpy Measurements on Pure Compounds

The calorimetric measurements reported on the following materials apply to the condensed state in equilibrium with its vapor. Consequently, the enthalpy change involves an enthalpy effect due to condensing vapor within the silica capsule as the sample cools in the calorimeter, and an enthalpy effect due to changing pressure on the condensed phase as well as that due to the heat capacity of the condensed material. As a result of the small vapor pressure of the compounds studied, and the small volume occupied by the vapor in the capsule, the former effects may be neglected as they contribute collectively no more than about 10 cal/mol of sample to the total enthalpy change. Therefore, to a good approximation and well within the error limits of the present measurements, the enthalpy change may be ascribed entirely to the heat capacity so that

$$[4] \qquad H_T - H_{298} = n \int_{298}^{T} C_p \, dT$$

where H is enthalpy, n is the number of moles of compound, T is temperature, and C_P is the heat capacity at constant pressure.

Of the materials used AgCl, $PbCl_2$, and KCl were vacuum-oven dried Fisher reagent grade materials. CuCl was prepared by SO_2 reduction of $CuCl_2$ as previously described (3). Ag_2S was prepared by precipitation from aqueous $AgNO_3$ solution using $(NH_4)_2S$ solution. The material was washed with distilled water and vacuum dried. To assure crystallinity, Ag_2S was prefused in an evacuated cell before sealing it into a drop capsule. PbS was prepared by reacting stoichiometric quantities of pure lead (five nines) with doubly distilled sulfur in sealed evacuated silica capsules. Heating to 1000 °C resulted in complete reaction; however, to assure crystallinity, the material was prefused in an evacuated double walled silica container. Such a container was necessary because the freezing of the PbS tended to crack the primary container wall.

The experimental measurements for the pure compounds are given in Table 1; for each state of each compound the enthalpy content was expressed as a function of temperature using the least squares method. These data are given in Table 2. Errors quoted represent one standard deviation. The enthalpies of transformation are given in Table 3. The standard deviations were calculated by taking the square root of the sum of the squares of the standard deviations for the enthalpy contents of the high and low temperature phases. The heat capacities of the compounds are given by

$$[5] \qquad C_p = a_1 + 2a_2T$$

where the constants a_i are as in Table 2.

Potassium Chloride

The enthalpy of fusion of potassium chloride has been relatively well established by several investigators using modern instruments calibrated with the sapphire standard. The purpose in studying KCl in this investigation was to provide a further check on the accuracy of the present instrument.

Dworkin and Bredig (13) have determined the enthalpy of fusion of all the alkali halides; for KCl, they give a value of 6340 cal/mol with an estimated accuracy of 1–2%. Douglas of the National Bureau of Standards (14) gives the value of 6270 cal/mol. Earlier literature reports values as high as 6410 and as low as 6100 cal/mol (15, 16). It is evident, therefore, that the enthalpy of fusion is about 6300 ± 100 cal/mol. The results of the present work are shown in Fig. 4. A value of 6250 cal/mol is indicated. This rather good agreement with previous measurements was taken to indicate that the present instrument was free of any gross systematic errors.

The procedure used by Dworkin and Bredig (13) did not give a complete enthalpy content curve, so a detailed comparison of results could not be made. Kelley (12), in his critical review of the older literature, has expressed the enthalpy content of solid KCl as a function of temperature. His evaluation of the thermal data appears in recent tabulations by Blander (17) and Kubaschewski *et al.* (9). At the melting point, the enthalpy content relative to 298 °K and the heat

TABLE 1. Enthalpy content measurements on pure compounds

KCl		AgCl		CuCl		$PbCl_2$		Ag_2S		PbS	
t (°C)	$H_T - H_{298}$ (cal/mol)	t (°C)	$H_T - H_{298}$ (cal/mol)	t (°C)	$H_T - H_{298}$ (cal/mol)	t (°C)	$H_T - H_{298}$ (cal/mol)	t (°C)	$H_T - H_{298}$ (cal/mol)	t (°C)	$H_T - H_{298}$ (cal/mol)
102	1 030	104	1 070	218	2 460	304	5 460	54	460	80	680
158	1 670	158	1 740	219	2 480	369	6 510	83	1 130	140	1 430
217	2 480	217	2 540	265	3 130	407	7 570	112	1 620	195	2 040
282	3 260	251	3 060	306	3 670	429	7 910	131	1 970	244	2 630
462	5 780	306	3 720	329	4 160	449	8 130	162	2 620	245	2 710
601	7 650	356	4 480	342	4 350	472	8 430	181	3 950	308	3 430
677	9 050	404	5 210	379	4 920	506	14 910	192	4 170	369	4 210
741	9 820	444	5 930	399	5 240	540	15 680	204	4 390	437	5 080
789	17 030	470	9 270	413	6 950	581	17 100	259	5 450	496	5 760
809	17 280	529	10 270	417	6 920	613	17 660	303	6 280	556	6 600
813	17 240	584	10 990	438	9 160	652	18 800	364	7 580	609	7 300
837	17 780	648	11 940	468	9 340	672	19 730	410	8 480	670	8 000
865	18 340	696	12 590	502	9 840			460	9 490	720	8 750
891	18 840	744	13 070	526	10 190			512	10 540	776	9 490
919	19 450	790	13 710	562	10 780			577	11 780	828	10 270
943	19 810	842	14 490	607	11 300			593	12 240	892	11 090
977	20 410	865	14 720	644	11 950			602	12 440	949	11 950
1 033	21 350	896	15 220					622	12 940	1 008	12 740
		942	15 990					649	13 210		
		989	16 450					695	14 360		
								741	15 000		
								789	16 250		
								820	16 720		
								838	18 980		
								865	19 680		
								880	19 830		
								940	21 300		
								967	21 850		
								995	22 450		
								1 037	23 430		

TABLE 2. Enthalpy content functions $H_T - H_{298} = a_0 + a_1T + a_2T^2$ (cal/mol)

Compound	a_0	a_1	$a_2 \times 10^3$	Accuracy	Range (°K)
KCl (solid)	−3369	10.738	2.290	75	298–1043
KCl (liquid)	−2618	18.412	—	84	1043–1306
AgCl (solid)	−3261	9.870	3.971	49	298–727
AgCl (liquid)	−783	13.695	—	88	727–1262
CuCl (solid, α)	−4289	13.755	—	15	491–570
CuCl (solid, α)	−5159	15.460	—	50	600–680
CuCl (solid, β)	−3706	15.460	—	47	680–696
CuCl (liquid)	−867	13.894	—	87	696–917
$PbCl_2$ (solid)	−5208	18.494	—	144	577–772
$PbCl_2$ (liquid)	−7210	28.284	—	172	772–945
Ag_2S (solid, α)	−4966	14.798	6.027	40	298–449
Ag_2S (solid, β)	−4969	19.440	0.351	29	449–859
Ag_2S (solid, γ)	−4876	19.769	—	126	859–1103
Ag_2S (liquid)	−5742	22.255	—	65	1103–1310
PbS (solid)	−3288	10.775	1.359	34	298–1281

capacity are given as 10 150 cal/mol and 15.4 cal/°K mol, respectively. The values in the present study are 10 320 cal/mol and 15.5 cal/°K mol. The value for the heat capacity of liquid KCl was estimated by Kelley to be 16.0 cal/°K mol. This value has appeared in recent tabulations in spite of a more up-to-date measurement of 17.6 cal/°K mol (18). The average heat capacity of liquid over the 250 °C range of the present study was 18.4 cal/°K mol. Considering the temperature range and the small random errors in enthalpy contents evident in Fig. 4, this value is probably more reliable than the former values.

Silver Chloride

The enthalpy content of silver chloride was determined by Goodwin and Kalmus (19) and Kobayashi (20). Both investigations were charac-

Can. J. Chem. Downloaded from www.nrcresearchpress.com by 210.87.254.6 on 09/05/12
For personal use only.

TABLE 3. Enthalpies of transformation

Compound	Transformation	Temperature (°C)	ΔH_{trans} (cal/mol)	Accuracy
KCl	Fusion	770	6250	112
AgCl	Fusion	454	3160	101
CuCl	α–β	407	1450	69
CuCl	Fusion	423	1750	99
$PbCl_2$	Fusion	499	5560	224
Ag_2S	α–β	176	940	49
Ag_2S	β–γ	586	120	129
Ag_2S	Fusion	830	1880	142

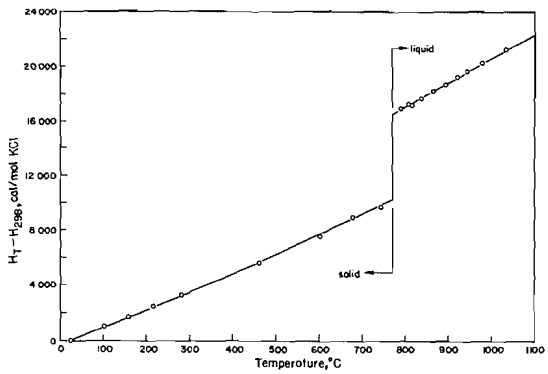

FIG. 4. Enthalpy content of potassium chloride.

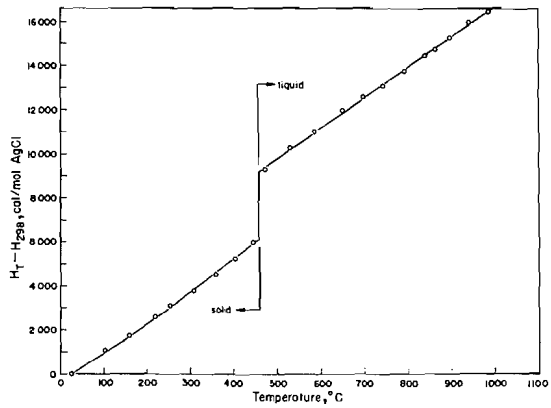

FIG. 5. Enthalpy content of silver chloride.

terized by a limited study of the liquid and were performed before the sapphire standard was available. A value of 3080 cal/mol for the enthalpy of fusion is indicated (12, 21). By way of comparison, a recent estimate of the enthalpy of fusion by Blanc and Petit (22), based on cryoscopic studies with KCl and RbCl, is 2900 cal/mol. Figure 5 shows the results of the present investigation. A value for the enthalpy of fusion of 3160 cal/mol is indicated. There is also good agreement of the present work with previous enthalpy content and heat capacity data on solid AgCl. From Kelley's equation (12), the enthalpy content and heat capacity at the melting point are 6080 cal/mol and 15.1 cal/°K mol, respectively, as compared with 6010 cal/mol and 15.6 cal/°K mol in the present study.

Kelley's reported heat capacity of liquid AgCl of 16.0 cal/°K mol has been generally accepted (9, 17). More recently, a critical appraisal by Lumsden (21) has suggested the value 14.7 cal/°K mol. This, however, is based exclusively on the calorimetric work of Goodwin and Kalmus (19) which shows considerable scatter. The value determined in this investigation of 13.7 cal/°K mol is significantly lower than any value previously reported. In spite of this, the present value is probably more reliable because of the large temperature range studied and the use of sapphire to calibrate the calorimeter. In addition, very recent work independently conducted in this laboratory (23) supports this low heat capacity. From precise e.m.f. measurements of the cell

$$-\text{Ag/AgCl (liquid)/Cl}_2, \text{C}+$$

the free energy of formation of liquid AgCl was determined. The curvature of the ΔG^0 *vs.* T plot requires that the heat capacity of liquid AgCl be about 13.8 cal/°K mol, if the heat capacity of the elements are to be considered correct (12).

Lead Chloride

There is considerable disagreement in the literature concerning the enthalpy of fusion and associated thermal properties of lead chloride. Suggested values for the enthalpy of fusion vary from 3000 to 5800 cal/mol. Using the freezing point depression of $PbCl_2$ with AgCl additions (24) and the e.m.f. data of Salstrom (25) for this system to demonstrate Temkin ideality, Lumsden (21) calculates the enthalpy of fusion of $PbCl_2$ to be 4400 cal/mol. Recent cryoscopic studies of Blanc and Petit (22) using LiCl and NaCl as solutes give an enthalpy of fusion of 5800 cal/mol. Similar work by Bell and Flengas (4), using NaCl

Can. J. Chem. Downloaded from www.nrcresearchpress.com by 210.87.254.6 on 09/05/12
For personal use only.

Can. J. Chem. Downloaded from www.nrcresearchpress.com by 210.87.254.6 on 09/05/12
For personal use only.

as a solute, gives a value of 5400 cal/mol. Since Lumsden's calculation involved an old phase diagram, the more recent cryoscopic estimates of the enthalpy of fusion are probably more reliable, although these may be somewhat high as a result of solubility of the solutes in solid $PbCl_2$. Based upon the calorimetric work of Goodwin and Kalmus (19) mainly, and neglecting the study of Krestovnikov and Karetnikov (26) which gives a very low value, Kelley (12) suggested 5800 cal/mol for the enthalpy of fusion. Lumsden (21) in considering the same data reports 5000 cal/mol. With all of the foregoing in mind, the most probable value for the enthalpy of fusion lies between 5000 and 5800 cal/mol. The enthalpy content measurements in the present investigation appear in Fig. 6. These lead to a value of 5560 cal/mol.

Modestova (27) has reported a transformation of lead chloride at 422 °C. This has not been observed by other workers, but may exist and might account for the arrangement of enthalpy content points shown in Fig. 6 just below the melting point. These points show a small systematic deviation with respect to the straight line drawn through them. Since phase diagrams do not show an abrupt change in curvature of the $PbCl_2$ liquidus at 422 °C, the enthalpy of transformation, if the transformation exists, must be quite small. Thus, to evaluate the enthalpy content of solid $PbCl_2$ at the melting point for purposes of determining the enthalpy of fusion, no large error results by drawing a straight line through all the points. The value of the enthalpy content of solid $PbCl_2$, so determined, is 9070 cal/mol at 499 °C. This compares rather poorly with older measurements assessed by Kelley to be 9570 cal/mol.

It is very difficult to make a worthwhile comparison of heat capacities because of the large scatter in the older data. The study of Goodwin and Kalmus (19), however, does substantiate the conclusion of the present study to the extent that the heat capacity of the liquid is considerably greater than that of the solid near the melting point. This feature is most evident in Fig. 6.

Copper(I) Chloride

As with lead chloride there is considerable disagreement in the literature concerning the enthalpy of fusion of CuCl. The appraisals of Kelley (12) and Lumsden (21) refer to Krestovnikov and Karetnikov (26) and give a value of 2620 cal/mol at 430 °C. Considering that the melting point was in error, a more recent value being 423 °C (3), and that the enthalpy of transformation (28) at 407 °C was not detected, this value for the enthalpy of fusion is probably incorrect. The results of the present study are shown in Fig. 7 and indicate two first order transformations at 407 and 423 °C having enthalpy changes 1450 and 1750 cal/mol, respectively. Independent cryoscopic studies (3) using NaCl, KCl, and $BaCl_2$ as solutes, suggest a value of 1800 cal/mol for the enthalpy of fusion, and from the change in slope of the CuCl liquidus at 407 °C, a value of 1500 cal/mol for the enthalpy of the solid state transformation. The higher reported values (3) for the enthalpy of fusion are apparently due to lack of awareness of the 407 °C transformation, causing the apparent enthalpy of fusion to be approximately the sum of the first order enthalpy changes shown in Fig. 7.

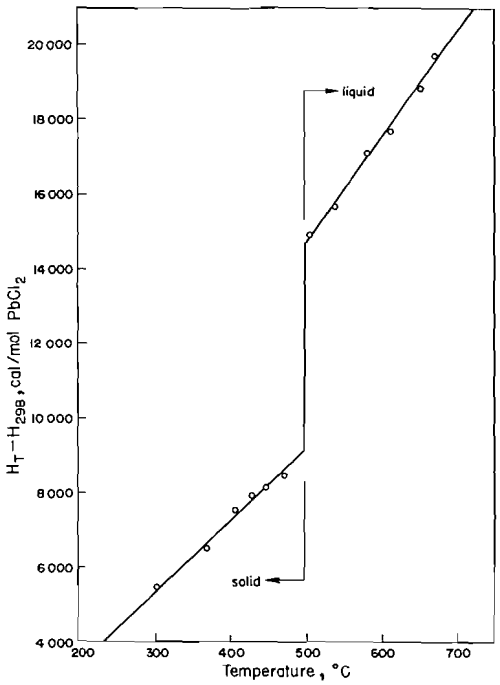

FIG. 6. Enthalpy content of lead chloride.

The determination of the enthalpy content of solid CuCl at the melting point is complicated by the presence of an apparent second order transformation in the low temperature modification of CuCl just prior to the 407 °C transformation. The interesting feature of this phenomenon is its

Can. J. Chem. Downloaded from www.nrcresearchpress.com by 210.87.254.6 on 09/05/12
For personal use only.

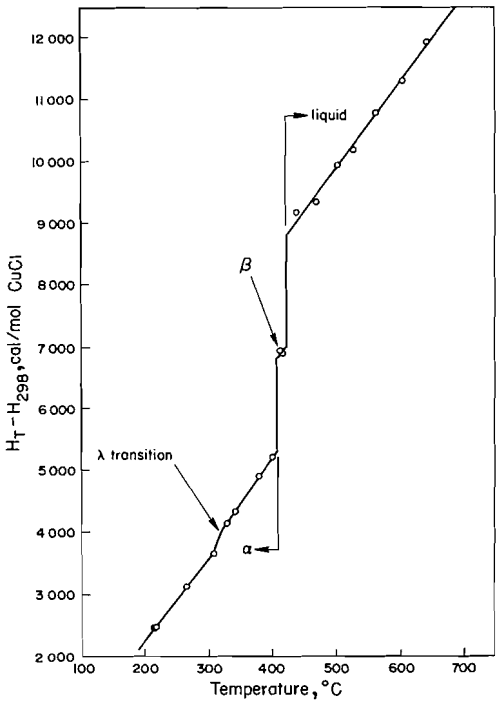

FIG. 7. Enthalpy content of copper(I) chloride.

relation to electrical conductivity measurements on solid CuCl (29). These measurements indicate that cuprous chloride changes from an electronic conductor to an ionic conductor in this temperature range with the transport number of cuprous ion approaching unity at 365 °C. This suggests that at temperatures below the second order transformation, cuprous ions are constrained to a limited number of lattice sites. However, as the temperature rises the lattice expands and cuprous ions are free to occupy all of the tetrahedral positions in the alpha phase (zinc blende). This ability is consistent with an increase in the capacity to store heat over a limited temperature range, a second order transformation.

Because of the numerous transformations taking place near the melting point, the exact heat capacity of the solid phases were difficult to determine with accuracy from the enthalpy content data collected in the present study. For purposes of evaluating the enthalpy of transformation and enthalpy of fusion, a least squares straight line was drawn through the four high temperature points in the alpha phase shown in Fig. 7. A line of the same slope was formed through the points in the beta phase since an adequate temperature range was not available to determine the heat capacity of this phase directly. It is unlikely that the heat capacity of this phase differs significantly enough from 15.5 cal/°K mol to seriously alter the enthalpy of transformation and fusion.

The present heat capacity measurement of liquid CuCl is much lower than that reported by Krestovnikov and Karetnikov (26); their enthalpy content points, spreading over nearly 300 °C, fall on a nearly straight line and would therefore appear to give a reliable mean heat capacity. However, in view of the oversights mentioned previously and the lack of a good calorimetric standard when the work was performed, the determination in the present study of 13.9 cal/°K mol for the heat capacity of liquid CuCl is probably more reliable, particularly since it compares well with that determined for AgCl.

Silver Sulfide

Enthalpy content measurements on silver sulfide are shown in Fig. 8. The solid state transformations are known to be prompt (30); the measurements may therefore be expected to be

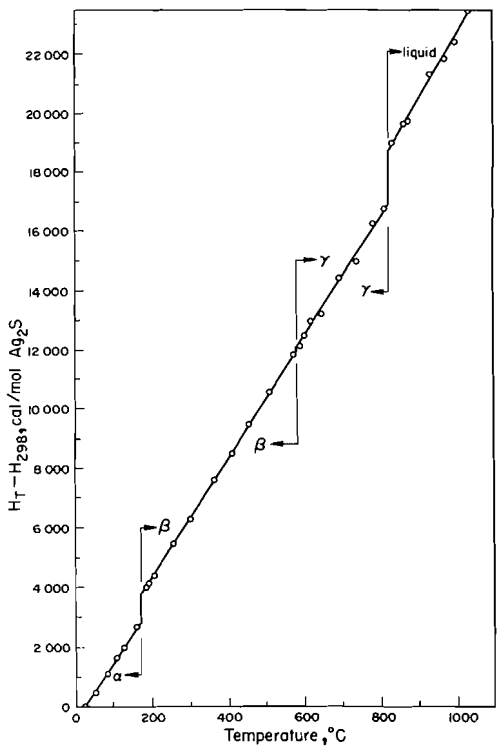

FIG. 8. Enthalpy content of silver sulfide.

Can. J. Chem. Downloaded from www.nrcresearchpress.com by 210.87.254.6 on 09/05/12
For personal use only.

reliable. Several values for the enthalpy of the alpha–beta transformation are available in the literature. Kelley (12) suggests 1010 cal/mol based on rather old calorimetric data. Roy *et al.* (31) investigated the pressure effect on this transformation, and from estimates of the volume change on transformation, calculated the enthalpy of transformation to be 1524 cal/mol, using the Clapeyron–Clausius equation. However, this has the rather broad error limit of ±420 cal/mol. Recently, Perrott and Fletcher (32) in an adiabatic calorimeter measured a value of 950 cal/mol ± 100 for this transformation. At 350 °C they observed a second order phase change during which the enthalpy content rose quickly by about 600 cal/mol. The measurements, however, only extended up to 375 °C. This second order transformation was not observed in the present case nor has it been mentioned in previous literature. In particular, the thermal analysis of Kracek (30) reports no such change. It seems that Perrott reports the heat capacity of a metastable compound produced at the time of aqueous precipitation. Therefore, although there is very good agreement of Perrott's enthalpy of alpha–beta transformation with the value of 940 cal/mol in the present study, this may be fortuitous. It is significant to mention here that in early experiments on powdered Ag_2S, which formed part of the present investigation, great difficulty was experienced in obtaining reproducible results, presumably because of structural metastability which could only be alleviated by freezing the sulfide from its liquid state.

It is possible to calculate the enthalpy of alpha–beta transformation from other thermochemical data. From the study of Kiukkola and Wagner (33), the enthalpy of the reaction

[6] $$2Ag_{(s)} + S_{(l)} \rightarrow Ag_2S_{(s,\beta)}$$

is, at 176 °C, −7040 cal/mol. Kubaschewski *et al.* (9) gives the enthalpy of formation of alpha Ag_2S at 298 °K from rhombic sulfur and solid silver to be −7500 cal/mol. Applying the Kirchhoff equation, using the existing enthalpy content data (12) for silver and sulfur, and the present data for alpha Ag_2S, the enthalpy change for the reaction

[7] $$2\,Ag_{(s)} + S_{(l)} \rightarrow Ag_2S_{(s,\alpha)}$$

is, at 176 °C, −7930 cal/mol. The calculated enthalpy of transformation, the difference between the enthalpy of reactions 6 and 7, is thus 890 cal/mol. This value, however, could be in error by as much as ±300 cal/mol. Nevertheless, it is in fair agreement with the present calorimetric determination of the enthalpy of transformation.

The beta–gamma transformation was discovered by Urazov (34) and has been recognized to have a low enthalpy of transformation; however, no direct experimental value appears to have been recorded. The differential thermal analysis of Kracek (30) suggests that this enthalpy change has about one tenth of the magnitude of the alpha–beta transformation. This is in agreement with the present work which gives a value of 120 cal/mol. It is apparent from Table 3 that the error in the measurement of this quantity is as large as the quantity itself, a consequence of subtracting large experimental measurements. Therefore, the present measurement has limited quantitative significance. Qualitatively, the measurement serves to verify that the enthalpy change accompanying this transformation is negligible for most purposes.

The enthalpy of fusion of Ag_2S has been in question for many years with values ranging from 900 to 3600 cal/mol (30, 35). The present work indicates a value of 1880 cal/mol at 830 °C. This is small for such a temperature, but it is consistent with the low entropy change associated with the small alteration in atomic order occurring during fusion of Ag_2S (35).

Lead Sulfide

The experimental measurements are shown in Fig. 9. It appears that no transformations exist in the solid state over the temperature range shown. The enthalpy content was initially expressed as a function of T involving a $1/T$ term. This, however, resulted in a point of inflection which was thought to be statistically meaningless. Accordingly, the simple parabolic form was used. The present measurements are slightly lower than those previously reported. At 900 °K Bornemann and Hengstenberg (36) give 7880 cal/mol. The present measurement at this temperature is 7510 cal/mol. The former value was reported before the sapphire standard was available.

Lead sulfide melts at 1113 °C (6). It is therefore possible, in principle, to make measurements of the enthalpy content of liquid PbS in the present calorimeter, thereby determining the enthalpy of fusion. These experiments were not performed

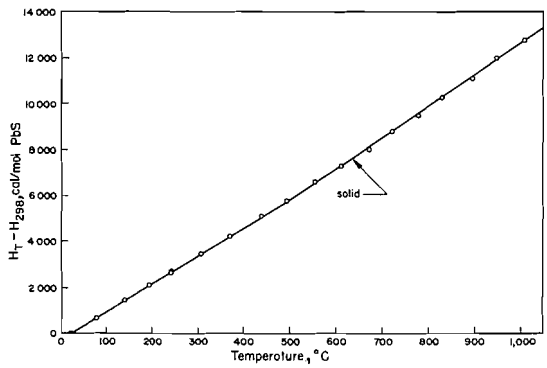

FIG. 9. Enthalpy content of lead sulfide.

because the freezing PbS invariably cracked the silica capsule.

Measurements of Enthalpy Content of Molten Solutions

The enthalpy contents of certain solutions, such as AgCl–KCl and AgCl–Ag_2S melts, include heat effects due to the integral enthalpy of mixing. For such systems, therefore, it is possible to assess the enthalpy of mixing by drop calorimetric methods.

From basic definitions, the integral enthalpy of liquid–liquid mixing ΔH_{mix} of components *1* and *2* at any temperature T is given by

$$[8] \quad \Delta H_{mix} = H_{soln} - X_1 H_1^0 - X_2 H_2^0$$

where H_{soln}, H_1^0, and H_2^0 are the enthalpy of one mole of solution, and pure components *1* and *2*, respectively, and X_1 and X_2 are mole fractions. If the components are not mutually soluble in the solid state at 298 °K

$$[9] \quad (H_{298})_{soln} = X_1(H_{298}^0)_1 + X_2(H_{298}^0)_2$$

where $(H_{298})_{soln}$ is the enthalpy content of a mechanical mixture of the two components at 298 °K having the same composition as the solution in eq. 8. Adding eqs. 8 and 9

$$[10] \quad \Delta H_{mix} = (H_T - H_{298})_{soln} - [X_1(H_T^0 - H_{298}^0)_1 + X_2(H_T^0 - H_{298}^0)_2]$$

The final two terms in eq. 10 are measurable in a drop calorimeter; collectively they represent the additive enthalpy contents of the pure components at temperature T. The first term in this equation may be similarly measured for melts of various compositions. This term represents the enthalpy content per mole of solution at temperature T, and any composition X_1, relative to a mechanical mixture of the two components at 298 °K. Thus the deviation of the enthalpy content of the solution from additivity at temperature T represents the integral enthalpy of mixing.

At constant temperature, the additive enthalpy content of the pure components is given by

$$[11] \quad (H_T - H_{298})_{add} = b_1 + b_2 X_1$$

where b_i are constants. The integral enthalpy of mixing for systems which do not form compounds can generally be adequately expressed as a function of composition using the equation

$$[12] \quad \Delta H_{mix} = b_3 X_1 X_2 + b_4 X_1^2 X_2$$

This form allows for some asymmetry or a change in the sign of the enthalpy effect with respect to composition. Substituting eqs. 11 and 12 into 10, the variation of the enthalpy content of the solution with respect to composition may be represented by the equation

$$[13] \quad (H_T - H_{298})_{soln} = b_1 + b_2 X_1 + b_3 X_1 - b_3 X_1^2 + b_4 X_1^2 - b_4 X_1^3$$

The coefficients in eq. 13 are temperature dependent. The coefficient b_1 is the enthalpy content of pure component *2* at temperature T (X_1 is zero). Similarly $(b_1 + b_2)$ is the enthalpy content of pure component *1* at temperature T (X_1 is one). Previous experiments have shown that the enthalpy contents of pure melts do not detectably vary from linearity with respect to temperature. This is apparent in Figs. 4–8. Therefore

$$[14] \quad b_1 = c_1 + c_2 T$$

and

$$[15] \quad (b_1 + b_2) = c_3 + c_4 T$$

where c_i are constants. The magnitude of the enthalpy of mixing may, in general, vary slightly with temperature. As a first approximation, this dependence will be considered to be linear.

$$[16] \quad b_3 = c_5 + c_6 T$$

The asymmetry term, b_4, may also vary with temperature. The precision of drop calorimetric data, however, does not warrant expressing b_4 as a function of temperature; b_4 may therefore be considered a constant for a particular system. Let

$$[17] \quad b_4 = c_7$$

Substituting eqs. 14, 15, 16, and 17 into eq. 13,

Can. J. Chem. Downloaded from www.nrcresearchpress.com by 210.87.254.6 on 09/05/12
For personal use only.

TABLE 4. Enthalpy content measurements on KCl–AgCl melts

0.23 X_{KCl}		0.42 X_{KCl}		0.57 X_{KCl}		0.72 X_{KCl}		0.88 X_{KCl}	
t (°C)	$H_T - H_{298}$ (cal/mol)	t (°C)	$H_T - H_{298}$ (cal/mol)	t (°C)	$H_T - H_{298}$ (cal/mol)	t (°C)	$H_T - H_{298}$ (cal/mol)	t (°C)	$H_T - H_{298}$ (cal/mol)
587	11 120	651	12 440	601	12 070	649	13 130	744	15 580
651	12 140	694	12 940	648	12 800	655	13 420	793	16 370
747	13 560	750	13 960	697	13 510	695	14 110	840	17 240
785	13 980	786	14 640	744	14 160	705	14 200	895	18 330
891	15 580	848	15 490	794	15 200	744	15 080	985	19 890
942	16 360	893	16 280	845	15 980	786	15 550	1 036	20 700
993	16 980	950	17 100	908	17 000	842	16 700		
		1 004	17 850	944	17 570	893	17 330		
				991	18 160	936	18 240		
						949	18 360		
				104	1 030	987	19 000		
				158	1 730	990	19 020		
				219	2 500				
				282	3 350				
				310	3 690				

the enthalpy content of the solution becomes, as a function of temperature and composition

$$[18]\quad (H_T - H_{298}{}^0)_{soln} = c_1 + c_2T + (c_3 - c_1 + c_5)X_1 + (c_4 - c_2 + c_6)TX_1 + (c_7 - c_5)X_1{}^2 - c_6TX_1{}^2 - c_7X_1{}^3$$

renaming the coefficients,

$$[19]\quad (H_T - H_{298}{}^0)_{soln} = d_1 + d_2T + d_3X_1 + d_4TX_1 + d_5X_1{}^2 + d_6TX_1{}^2 + d_7X_1{}^3$$

From eqs. 16, 17, 18, and 19

$$[20]\quad b_3 = -d_5 - d_7 - d_6T$$

and

$$[21]\quad b_4 = -d_7$$

Substituting eqs. 20 and 21 into eq. 12

$$[22]\quad \Delta H_{mix} = X_1(1 - X_1)(-d_5 - d_7 - d_6T - d_7X_1)$$

This equation gives the enthalpy of mixing when the enthalpy content of the binary melt can be expressed by eq. 19.

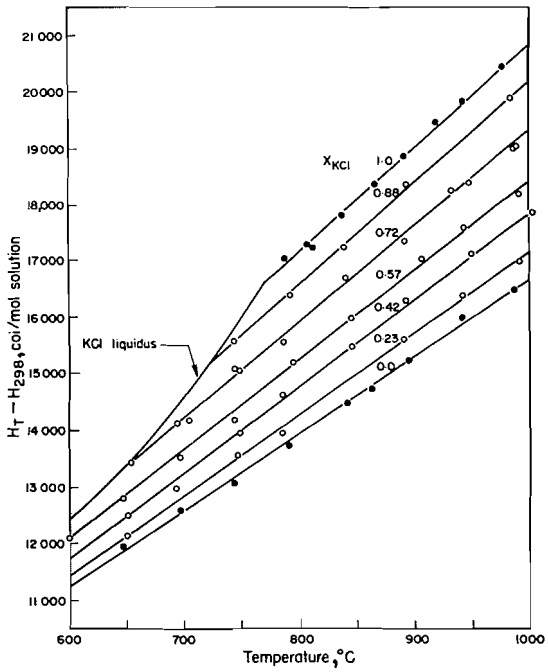

FIG. 10. Enthalpy content of KCl–AgCl melts *vs.* temperature.

The AgCl–KCl System

Enthalpy content measurements of AgCl–KCl melts are given in Table 4. Figure 10 shows these measurements as a function of temperature for solutions of various compositions. The KCl liquidus curve comes from the study of Baboian and Flengas (37). Originally, each of the lines in Fig. 10 was individually constructed by the method of least squares. Isothermal enthalpy contents, interpolated using these equations, yielded the plots in Fig. 11. The deviation from the additivity lines is the integral enthalpy of liquid–liquid mixing. A few measurements on solidified mixtures were made. These are reported in Table 4. There was no detectable deviation from additivity indicating that the salts freeze at the eutectic to form a simple mechanical mixture of nearly pure phases. This is consistent with the phase diagram (37).

Can. J. Chem. Downloaded from www.nrcresearchpress.com by 210.87.254.6 on 09/05/12
For personal use only.

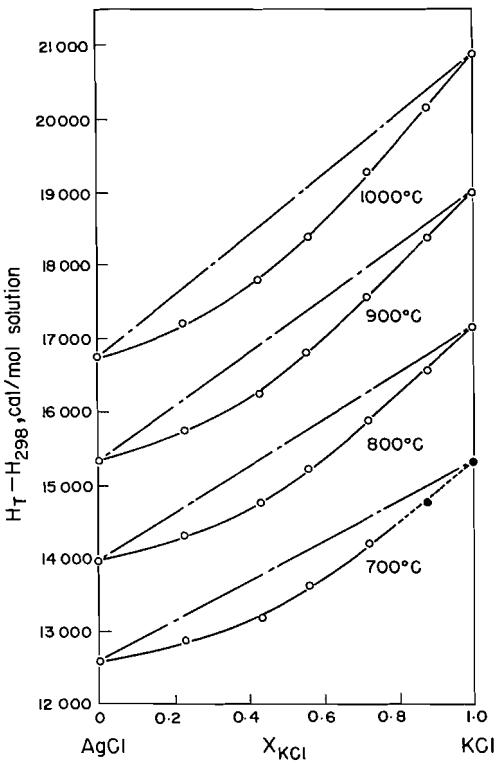

FIG. 11. Enthalpy content of KCl–AgCl melts *vs.* composition.

The actual determination of the position of the lines, shown in Fig. 10, involved fitting the experimental measurements at the various temperatures and compositions to eq. 19 where X_1 is X_{KCl}. The determination of the coefficients d_1 to d_7 was accomplished by multiple linear regression. The coefficients so determined are

$$\begin{aligned} d_1 &= -764.1 \\ d_2 &= 13.68 \\ d_3 &= -3319.0 \\ d_4 &= 3.835 \\ d_5 &= 2031.0 \\ d_6 &= 0.9277 \\ d_7 &= -596.0 \end{aligned} \qquad [23]$$

The standard deviation of the experimental points from the mathematical surface defined by these coefficients was 82 cal/mol. This represents 0.6% of the average total enthalpy content of the salt solution.

From eqs. 22 and 23, the integral enthalpy of mixing for liquid AgCl and liquid KCl is given by

$$\Delta H_{mix} = X_{KCl}(1 - X_{KCl})(-1435 - 0.9277\,T + 596\,X_{KCl}) \qquad [24]$$

Baboian and Flengas (37) measured the integral enthalpy of mixing of this system in an isothermal calorimeter (38) by directly recording the heat liberated when the two liquid salts were mixed. For 0.5 X_{KCl} they report −470 cal/mol at 788 °C and −544 cal/mol at 860 °C. From eq. 24, the values resulting from the present experiments are −531 and −548 cal/mol at the same composition and temperatures, respectively. In addition, the data compare well with respect to the asymmetry of the enthalpy of mixing; both are skewed slightly to the AgCl side of this system. Hersh and Kleppa (39) report integral enthalpies of mixing based on solid–liquid mixing experiments. For 0.5 X_{KCl}, they report −552 cal/mol at 660 °C. In view of the agreement of the present measurements with those previously reported, the present drop calorimetric technique may be considered as a reliable way of quickly determining enthalpies of mixing when great precision is not required.

The AgCl–Ag_2S System

Enthalpy content measurements of AgCl–Ag_2S melts are given in Table 5. These data are plotted in Fig. 12 as a function of temperature for various Ag_2S concentrations; the Ag_2S liquidus was constructed from the phase diagram of Bell and Flengas (4). The straight lines through the data points were determined for each concentration of Ag_2S using eq. 19 in which X_1 was X_{Ag_2S}. The coefficients in this equation were determined by multiple linear regression. Since it was desirable for comparison with other measurements to have average enthalpies of mixing over the temperature range studied, the coefficient d_6 was set equal to zero prior to processing the data. The coefficients are as follows

$$\begin{aligned} d_1 &= -983.7 \\ d_2 &= 13.88 \\ d_3 &= -2223.0 \\ d_4 &= 8.417 \\ d_5 &= -8206.0 \\ d_6 &= 0.0 \\ d_7 &= 5613.0 \end{aligned} \qquad [25]$$

The standard deviation of the enthalpy content measurements from the surface defined by these coefficients was 94 cal/mol. This represents 0.6%

Can. J. Chem. Downloaded from www.nrcresearchpress.com by 210.87.254.6 on 09/05/12
For personal use only.

TABLE 5. Enthalpy content measurements on Ag_2S–AgCl melts

0.16 X_{Ag_2S}		0.35 X_{Ag_2S}		0.46 X_{Ag_2S}		0.70 X_{Ag_2S}		0.85 X_{Ag_2S}	
t (°C)	$H_T - H_{298}$ (cal/mol)	t (°C)	$H_T - H_{298}$ (cal/mol)	t (°C)	$H_T - H_{298}$ (cal/mol)	t (°C)	$H_T - H_{298}$ (cal/mol)	t (°C)	$H_T - H_{298}$ (cal/mol)
475	9 790	545	11 090	656	13 240	646	13 710	718	15 490
612	12 020	599	12 130	707	14 300	758	15 780	786	16 870
684	13 070	665	13 240	755	15 110	811	16 820	854	18 230
760	14 090	729	14 270	801	15 740	852	17 680	917	19 640
824	15 400	802	15 480	854	16 820	917	18 920		
894	16 370	866	16 510	901	17 700				
961	17 330	933	17 740	954	18 760				
		989	18 610	1 009	19 590				

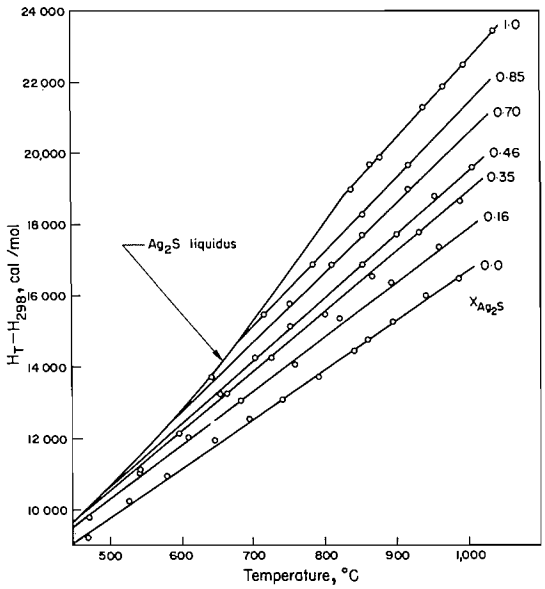

FIG. 12. Enthalpy content of Ag_2S–AgCl melts *vs.* temperature.

of the average total enthalpy content of the solution.

From eqs. 22 and 25, the integral enthalpy of mixing for liquid AgCl and liquid Ag_2S is given by

$$[26] \quad \Delta H_{mix} = X_{Ag_2S}(1 - X_{Ag_2S}) \times (2593 - 5613\, X_{Ag_2S})$$

This equation requires that the integral enthalpy of mixing be endothermic at Ag_2S concentrations less than 0.46 X_{Ag_2S}, and exothermic at higher concentrations. This is uncommon behavior. It is, however, qualitatively consistent with previous e.m.f. measurements on this system (7, 8). These indicate that the partial molar enthalpy of mixing of Ag_2S relative to liquid Ag_2S decreases rapidly from about 2400 cal/mol at 0.0 X_{Ag_2S} to zero near 0.14 X_{Ag_2S}. By differentiating eq. 26, the partial molar enthalpy of mixing of Ag_2S is

$$[27] \quad (\Delta \bar{H}_m)_{Ag_2S} = 2593 - 16\,412\, X_{Ag_2S} + 25\,045\, X_{Ag_2S}^2 - 11\,226\, X_{Ag_2S}^3$$

This equation indicates that the partial molar enthalpy of mixing decreases from about 2600 cal/mol at 0.0 X_{Ag_2S} to zero at 0.23 X_{Ag_2S}. This agreement suggests that the enthalpy of mixing does change sign in this system. Furthermore, it appears that there may be some connection between this effect and the change in mode of electrical conduction (1) although a quantitative model cannot be advanced at this time.

The authors wish to thank the National Research Council of Canada for financial assistance in the form of equipment grants and a fellowship for W.T.T.

1. M. C. BELL and S. N. FLENGAS. J. Electrochem. Soc. **111**, 575 (1964).
2. M. C. BELL and S. N. FLENGAS. J. Electrochem. Soc. **113**, 31 (1966).
3. A. K. CARBEE. Ph.D. Thesis, University of Toronto. 1969.
4. M. C. BELL and S. N. FLENGAS. J. Electrochem. Soc. **111**, 569 (1964).
5. M. C. BELL and S. N. FLENGAS. J. Electrochem. Soc. **113**, 27 (1966).
6. A. D. PELTON and S. N. FLENGAS. Can. J. Chem. **48**, 2016 (1970).
7. W. T. THOMPSON and S. N. FLENGAS. Can. J. Chem. **46**, 1611 (1968).
8. W. T. THOMPSON and S. N. FLENGAS. J. Electrochem. Soc. In press.
9. O. KUBASCHEWSKI, E. W. EVANS, and C. B. ALCOCK. Metallurgical Thermodynamics. Pergamon Press, New York. 1967.
10. J. GOODKIN, C. SOLOMONS, and G. JANZ. Rev. Sci. Instr. **29**, 105 (1958).
11. G. FURUKAWA, T. DOUGLAS, R. MCCOSKEY, and D. GINNINGS. J. Research Nat. Bur. Standards, **57**, 67 (1956).
12. K. K. KELLEY. Bull. U.S. Bur. Mines, No. 584 (1960).

Can. J. Chem. Downloaded from www.nrcresearchpress.com by 210.87.254.6 on 09/05/12
For personal use only.

13. A. S. DWORKIN and M. A. BREDIG. J. Phys. Chem. **64**, 269 (1960).
14. T. B. DOUGLAS. Natl. Bur. of Standards, Private communication in ref. 13.
15. K. K. KELLEY. Bull. U.S. Bur. Mines, No. 476 (1949).
16. Selected Values of Chemical Thermodynamic Properties. Circular 500, Natl. Bur. Standards (1952).
17. M. BLANDER. Molten Salt Chemistry. Interscience, New York. 1964.
18. T. B. DOUGLAS. Declass. Rep. U.S. Atom. Energy Comm. BNL 2446, 13 (1955).
19. H. M. GOODWIN and T. H. KALMUS. Phys. Rev. **28**, 1 (1909).
20. K. KOBAYASHI. Sci. Repts. Tohoku Univ. **34**, 112 (1950).
21. J. LUMSDEN. Thermodynamics of Molten Salt Mixtures. Academic Press, London. 1966.
22. M. BLANC and G. PETIT. C.R. Acad. Sci. Paris, **248**, 1305 (1959).
23. A. D. PELTON and S. N. FLENGAS. J. Electrochem. Soc. **117**, 1130 (1970).
24. K. TREIS. Neues Jb. Miner, Geol. Palaont. Beil Bd. **37**, 766 (1914).
25. E. J. SALSTROM. J. Amer. Chem. Soc. **56**, 1272 (1934).
26. A. N. KRESTOVNIKOV and G. A. KARETNIKOV. Zh. Obshch. Khim. **6**, 955 (1936).
27. T. P. MODESTOVA. Zh. Neorg. Khim. **5**, 1955 (1960).
28. M. R. LORENZ and A. PRENER. Acta Cryst. **9**, 538 (1956).
29. W. GARNER. Chemistry of the Solid State. Butterworths, London. 1955. p. 31.
30. F. G. KRACEK. Trans. Amer. Geo. Union, **27**, 364 (1946).
31. R. ROY, A. J. MAJUNDAR, and C. W. HULBE. Econ. Geol. **54**, 1278 (1959).
32. C. M. PERROTT and N. H. FLETCHER. J. Chem. Phys. **50**, 2344 (1969).
33. K. KIUKKOLA and C. WAGNER. J. Electrochem. Soc. **104**, 308 (1957).
34. G. URAZOV. Annales de l'Inst. Polytechnique Pierre le Grand à Petrograd, **23**, 593 (1915).
35. T. ROSENQVIST. J. Metal. **185**, 451 (1949).
36. K. BORNEMANN and O. HENGSTENBERG. Metall. u. Erz. **17**, 313 (1920).
37. R. BABOIAN and S. N. FLENGAS. Can. J. Chem. **45**, 813 (1967).
38. R. BABOIAN and S. N. FLENGAS. Can. J. Chem. **45**, 383 (1967).
39. L. S. HERSH and O. J. KLEPPA. J. Chem. Phys. **42**, 1309 (1965).

Can. J. Chem. Downloaded from www.nrcresearchpress.com by 210.87.254.6 on 09/05/12
For personal use only.

Can. J. Chem. Downloaded from www.nrcresearchpress.com by 210.87.254.6 on 09/05/12
For personal use only.

NOTES

Semicarbazide Complexes with Metal Chlorides

P. BOLDRINI

Département des Sciences, Université du Québec à Trois-Rivières, Trois-Rivières, Québec

Received[1] March 25, 1970

Complexes of semicarbazide with bivalent metal chlorides were characterized. Crystal data are reported, together with some optical properties and general relations among their crystal structures.

On a caractérisé des complexes formés par réaction de la semicarbazide avec les chlorures de métaux bivalents.

On rapporte les données cristallographiques concernant ces complexes de même que quelques unes de leurs propriétés optiques et les relations générales entre leurs structures cristallines.

Canadian Journal of Chemistry, 49, 1564 (1971)

Semicarbazide (sem), $H_2NNHCONH_2$, is a reagent for identification of aldehydes and ketones, and has applications in medicine as a lathyrogenic (1) and a teratogenic (2). It forms complexes with polynucleotides (3) and enhances growth of Polio (4) and Rubella (5) viruses. The possibility for sem to act as a bidentate ligand has been suggested (6) and verified (7). Sem metal complexes were then prepared as part of an investigation of the reactions of bivalent metal compounds with mono and bidentate ligands (8–10). The synthesis, X-ray crystal data, and some optical properties of 14 salts are reported. Seven of these were previously known (6, 7, 11–13), but their analytical and preparative data were incomplete.

Experimental

Synthesis and Analysis

Sem was isolated from the hydrochloride (11) of Fisher Scientific Co. At room temperature, a cooling of about 30 cal/mol was observed during the solution of the freshly prepared base. The optimum molar ratio for preparing each complex is reported in Table 1, column 2.

Chemical analyses were performed as follows: N by Dumas method; Cl as AgCl after oxidation of sem with H_2O_2; Ni, Cu, Zn by electrolysis; Cd and Pb as sulfates; Mn as pyrophosphates; and Fe as Fe_2O_3.

Densities were obtained, in most cases, by flotation in $CHBr_3$–benzene mixtures at room temperature and then calculated in terms of water at 4 °C.

Density measurements for the two Pb complexes, in contrast, were done pycnometrically. Standard Weissemberg and precession methods, employing CuKα radiation, were used to obtain the X-ray densities; a Co target was used for Co and Mn complexes.

Cell constants were calculated as an average of all axial reflections and, although measured with a calibrated camera, were still affected by absorption. When good crystal forms were available the axial ratio was measured at the optical goniometer and compared with the roentgenographical value. Space groups were deduced from systematic absences of reflections. Results of these analyses are summarized in Table 1, where the density and formula weight for each compound are reported as well. Values in parentheses after each parameter represent calculated root mean square deviations.

Mn(sem)Cl₂ was obtained as dendritic rose microcrystals, orthorhombic and highly soluble in water. The compound showed optical extinction and examination of the cell constants indicated that it was isostructural with $Cd(sem)Cl_2$. $Mn(sem)_2Cl_2$ was always formed when $Mn(sem)Cl_2$ was recrystallized.

Mn(sem)₂Cl₂ was prepared as white needle crystals, orthorhombic and biaxial. They presented orthogonal extinction and appeared isostructural with $Cd(sem)_2Cl_2$. $Mn(sem)_2Cl_2$ showed two equideveloped forms: ((001)) and ((110)) in Buerger's modern symbolism (14). $(a/b)_{goniom.} = 1.527(4)$; $(a/b)_{roentg.} = 1.534(4)$.

Fe(sem)₂Cl₂ was always separated with this stoichiometry, even if prepared from equimolar ratios or solutions richer in sem. Crystals were pale-green, prismatic, monoclinic, optically biaxial, with orthorhombic extinction. They were superficially oxidized when left in the open air and turned brown. Acidic solutions favored the synthesis.

Co(sem)₂Cl₂.2H₂O was crystallized as red-amaranth, pseudohexagonal, tabular crystals; they were monoclinic and highly soluble in water. Preparation of the anhydrous compound (11) was tried without success.

Ni(sem)₂Cl₂ was reprepared (6) as green microcrystals, orthorhombic and easily recrystallizable from water.

Ni(sem)₃Cl₂.3H₂O was obtained as tiny blue-violet needles, aggregated in a sheaf-like manner. These crystals were monoclinic and showed parallel extinction. The

[1]Revision received October 16, 1970.

TABLE 1. Preparation and chemical analysis

Compounds	Preparative molar ratio*	M%		Cl%		N %		Density $\frac{20}{4^\circ}$(g/cm³)		Formula weight
		Obsd.	Calcd.	Obsd.	Calcd.	Obsd.	Calcd.	Obsd.	Calcd.	
$Mn(sem)Cl_2$	0.7*a*	27.7	27.3	33.1	35.3	21.1	20.9	2.03	2.14	200.915†
$Mn(sem)_2Cl_2$	3*a*	20.2	19.9	25.6	25.7	31.0	30.5	1.92	1.84	275.987†
$Fe(sem)_2Cl_2$	2*a*	20.2	20.2	25.1	25.6	31.5	30.4	1.97	1.95	276.895†
$Co(sem)_2Cl_2.2H_2O$	2*a*	18.1	18.6	22.3	22.4	26.9	26.6	1.83	1.82	316.012†
$Ni(sem)_2Cl_2$	2*b*	21.0	21.0	25.5	25.4	30.2	30.0	1.94	1.97	279.76
$Ni(sem)_3Cl_2.3H_2O$	5*b*	13.5	14.4	16.6	17.3	30.0	30.8	1.76	1.68	408.87
$Cu(sem)Cl_2$	2.5*a*	30.3	30.3	33.9	33.8	20.4	20.1	2.39	2.39	209.52
$Cu(sem)_2Cl_2$	4*a*	22.3	22.3	24.6	24.9	30.1	29.5	2.16	2.01	284.59
$Zn(sem)Cl_2$	0.5*a*	30.5	30.9	33.7	33.6	20.2	19.9	2.10	2.11	211.35
$Zn(sem)_2Cl_2$	2*a*	21.3	22.8	24.2	24.8	29.1	29.3	2.10	2.08	286.42
$Cd(sem)Cl_2$	1.5*a*	43.1	43.5	26.8	27.4	16.3	16.3	2.59	2.64	258.38
$Cd(sem)_2Cl_2$	9*a*	33.5	33.7	21.2	21.3	25.4	25.2	2.19	2.20	333.45
$Pb(sem)Cl_2$	5*c*	58.1	58.7	19.3	20.1	11.7	11.9	3.66	3.65	353.17
$Pb(sem)_2Cl_2$	9*c*	47.8	48.4	16.5	16.6	20.0	19.6	2.66	2.75	428.24

*The ratio is intended as sem:MCl_2. Letters *a*, *b*, *c* after the molar ratio indicate: *a*, preparation from aqueous solutions; *b*, preparation from ethanol 95% solutions; *c*, preparation carried out by slow cooling of aqueous solutions.
†Atomic weights for Mn, Fe, Co are known with higher accuracy and, therefore, the formula weights of these compounds have three decimals.

cell given in Table 2 results from an improvement of single crystal data by a powder diagram. The anhydrous complex (6) was not obtained, but preparation of the trihydrated complex (11) was confirmed.

Cu(sem)Cl₂ crystals were easily obtained (13), frequently as twins. The crystals were decomposed by mild heating and left a white residue of CuCl, thus confirming the known reductive character of sem. Spectra of this compound have recently been studied (12, 15), $(a:b:c)_{\text{gonlom.}} = 0.672(2):1:0.803(3)$; $(a:b:c)_{\text{roentg.}} = 0.675(3):1:0.808(3)$. Other crystal data for this and the three following compounds have been reported (7).

Cu(sem)₂Cl₂ has been studied spectroscopically (12, 15). At room temperature these crystals showed a tendency to be spontaneously reduced, but can be maintained in an unaltered state at 4 °C and are properly prepared under such conditions.

Zn(sem)Cl₂ was monoclinic and presented extinction parallel to the elongation axis. Preparation of this and the following compound was facilitated by adjusting the solutions to p*H* 5 with HCl.

Zn(sem)₂Cl₂ was also found to be monoclinic. A thin lamina, in a tilted direction under the microscope, showed an optical hyperbola which was almost resolved.

Cd(sem)Cl₂ separated as white prismatic crystals, optically biaxial in a direction normal to the elongation axis, and was isostructural with $Mn(sem)Cl_2$. A procedure differing from that devised by Smith (11) was found to be more suitable for the synthesis of this complex and, in addition, led to the formation of $Cd(sem)_2Cl_2$, which could not be prepared by the previous method (11).

Cd(sem)₂Cl₂ was procured as white irregular prisms, orthorhombic and with parallel extinction. The complex was isostructural with $Mn(sem)_2Cl_2$. A p*K* intermediate between the analogous thiosemicarbazide and urea compounds has been measured in solution (16).

Pb(sem)Cl₂ was prepared as thick, short, shining, white crystals which showed inclined extinction and triclinic symmetry. $Pb(sem)_2Cl_2$ was also obtained from the mother liquid.

Pb(sem)₂Cl₂ crystals were prismatic, brittle, shining needles, monoclinic and sometimes 1 in. long. Observed forms were: ((100)), ((111)), ((1̄11)), (14). $(a:b:c)_{\text{gonlom.}}$, 1.860(8):1:1.123(2); $(a:b:c)_{\text{roentg.}}$, 1.856(3):1:1.123(2).

Discussion

A study of the crystal structuresof $Cu(sem)_2Cl_2$ and $Zn(sem)_2Cl_2$ (7) has shown that each metal is surrounded by a trans-planar arrangement of two oxygens and two hydrazinic nitrogens which are found at the corners of a distorted square. Coordination is completed by two chlorines on opposite sites of the square. Such an octahedral coordination, more or less distorted, is also likely to be found in the Cd complexes and in the other disemicarbazide compounds as well.

$M(sem)Cl_2$ complexes have been reported to be polymeric (15). The monosemicarbazide compounds of Fe, Co, and Ni have not as yet been obtained and it has to be expected that such a stoichiometry does not satisfy the stereochemical requirements of these metals (17). Furthermore, success has not been achieved in the preparation of sem complexes with Hg(II) and Ag(I) chlorides. The behavior of Hg(II), however, is somewhat surprising in view of the fact that $Hg(sem)SO_4$ and $Hg(sem)_2SO_4$ have been obtained (18). On the other hand, polymeric complexes of AgCl with thiosemicarbazide are known (19).

There is no doubt that the Co compound of Table 1 differs from the anhydrous compound synthesized by Smith (11). However, existence of both compounds is quite probable as in the case of $Co(thiourea)_4(NO_3)_2$ (9) and that of

Can. J. Chem. Downloaded from www.nrcresearchpress.com by 210.87.254.6 on 09/05/12
For personal use only.

Can. J. Chem. Downloaded from www.nrcresearchpress.com by 210.87.254.6 on 09/05/12
For personal use only.

TABLE 2. Crystallographic data*

Compounds	Space groups	a (Å)	b (Å)	c (Å)	α (deg)	β (deg)	γ (deg)	Z	V (Å^3)	Rotation axis
$Mn(sem)Cl_2$	*Pna*2$_1$-33 *Pnam*-62	6.77(1)	8.56(1)	10.77(2)				4	624.13	[001]
$Mn(sem)_2Cl_2$	*Pbcn*-6	12.46(2)	8.12(2)	9.87(3)				4	998.60	[001]
$Fe(sem)_2Cl_2$	*C*2/*c*-15 *Cc*-9	14.74(4)	6.78(2)	10.88(3)		119.8(2)		4	943.54	[001]
$Co(sem)_2Cl_2.2H_2O$	P2$_1$/*c*-14	9.10(1)	9.62(1)	6.77(1)		103.6(2)		2	576.04	[001]
$Ni(sem)_2Cl_2$	*P*222$_1$-17	6.88(4)	9.18(7)	7.48(5)				2	472.43	[100]
$Ni(sem)_3Cl_2.3H_2O$	*P*2$_1$/*c*-14	4.90(1)	18.03(4)	18.32(5)		94.1(2)		4	1614.38	[100]
$Cd(sem)Cl_2$	*Pna*2$_1$-33 *Pnam*-62	6.96(1)	8.69(1)	10.76(1)				4	650.79	[001]
$Cd(sem)_2Cl_2$	*Pbcn*-60	12.63(3)	8.33(1)	9.57(3)				4	1006.84	[001]
$Pb(sem)Cl_2$	*P*1-1 *P*$\bar{1}$-2	6.54(1)	8.67(1)	12.22(1)	108.6(2)	100.9(3)	94.7(3)	4	642.69	[001]
$Pb(sem)_2Cl_2$	*C*2/*c*-15 *Cc*-9	15.00(1)	8.08(1)	9.07(1)		110.1(3)		4	1032.33	[001]

*Crystallographic data for $Cu(sem)Cl_2$; $Cu(sem)_2Cl_2$; $Zn(sem)Cl_2$; $Zn(sem)_2Cl_2$ have already been reported (7). Z of column 9 is the number of formula weights in the asymmetric unit.

$Ni(sem)_2Cl_2$ mentioned above. It is in fact the author's experience that such analogous possibilities are more numerous than those reported in the literature.

Finally, the ribbon-like structure of sem (10) is probably responsible for the cooling when sem is dissolved in water.

Financial help for the final stage of the research was provided by Ministère de l'Education, Québec. Thanks are also due to L. Cavalca, M. Nardelli, and A. Perley.

1. C. I. LEVENE. Lab. Invest. **19**, 25 (1968). M. ADAM, Z. DEYL, and J. ROSMUS. Med. Farmacol. Exp. **14**, 129 (1966). H. B. BENSUSAN, S. D. MCKNIGHT, and M. S. R. NAIDU. Biochem. Biophys. Res. Commun. **23**, 128 (1966). J. J. LALICH. Proc. Soc. Exp. Biol. Med. **123**, 214 (1966). R. DELLAVOLPE, A. GANDINI, and G. M. MERLI. Biochim. Biol. Sper. **3**, 388 (1964).
2. F. BODIT. C. R. Soc. Biol. **160**, 960 (1966).
3. H. SEIDEL. Biochem. Biophys. Acta, **129**, 412 (1966).
4. J. PAGES. Ann. Inst. Pasteur, **112**, 581 (1967). S. E. GROSSBERG, M. LWOFF, and A. LWOFF. J. Bacteriol. **92**, 1473 (1996).
5. A. VAHERI, M. D. SEDWICK, and S. A. PLOTKIN. Proc. Soc. Exp. Biol. Med. **125**, 1092 (1967).
6. K. A. JENSEN and E. RANCKE-MADSEN. Z. Anorg. Allgm. Chem. **227**, 25 (1936).
7. M. NARDELLI, G. F. GASPARRI, P. BOLDRINI, and G. G. BATTISTINI. Acta Cryst. **19**, 491 (1965).
8. D. A. BERTA, W. A. SPOFFORD, P. BOLDRINI, and E. L. AMMA. Inorg. Chem. **9**, 136 (1970).
9. W. A. SPOFFORD, P. BOLDRINI. E. L. AMMA, P. CARFAGNO, and P. S. GENTILE. Chem. Commun. 40 (1970).
10. P. BOLDRINI. Acta Cryst. In Press.
11. G. S. SMITH. J. Chem. Soc. 1354 (1937).
12. H. ELKHADEM, M. F. ISKANDER, and S. E. ZAYAN. Z. Anorg. Allgm. Chem. **320**, 261 (1963).
13. J. THIELE and O. STANGE. Lieb. Ann. **24**, 283 (1894).
14. M. J. BUERGER. Elementary Crystallography. 2nd ed. Wiley, New York. 1963. p. 114.
15. M. J. CAMPBELL and R. GRZESKOWIAK. Spectrochim. Acta, **24A**, 1149 (1968). and references herewith included.
16. V. F. TOPOROVA and K. V. NAIMUSHIMA. Zh. Neorg. Khim. **5**, 874 (1960).
17. M. NARDELLI and I. CHIERICI. Ric. Sci. **30**, 276 (1960). M. K. AKHMEDLI, and L. I. ZHIROVA. Russ. J. Inorg. Chem. **5**, 1326 (1960). R. A. HAINES and K. K. W. SUN. Can. J. Chem. **46**, 3241 (1968).
18. P. BOLDRINI. To be published.
19. G. F. GASPARRI, A. MANGIA, A. MUSATTI, and M. NARDELLI. Acta Cryst. **B24**, 367 (1968).

Spectrofluorometric Studies. X. The Photochemistry of Pentafluorobenzene

S. L. LEM, G. P. SEMELUK, AND I. UNGER

Department of Chemistry, University of New Brunswick, Fredericton, New Brunswick, Canada

Received September 18, 1970

The vapor phase photochemistry of pentafluorobenzene has been examined at a variety of exciting wavelengths starting at 2540 Å and extending to 2780 Å. Most of the studies were carried out at 2620, 2660, and 2700 Å. Below 2600 Å pentafluorobenzene does not exhibit any detectable fluoroscence, above 2600 Å a very weak fluorescent emission was observed. Addition of biacetyl does not markedly reduce the fluorescent yield, while addition of cyclohexane, CO_2, and *cis*-butene-2 causes an increase in the fluorescent yield. The triplet yield of pentafluorobenzene excited at 2620, 2660, and 2700 Å, measured by the sensitized emission of biacteyl technique, is also very low and is increased by the addition of cyclohexane, CO_2, and *cis*-butene-2. *cis*-Butene-2 is the most effective gas, of the three examined, in increasing the fluorescent and triplet yields of pentafluorobenzene. The fate of the majority of pentafluorobenzene molecules excited in the 2600 Å region is unknown.

La photolyse en phase gazeuse du pentafluorobenzène a été étudiée en fonction de la longueur d'onde de la raie excitatrice entre 2540 et 2780 Å. Pour des longueurs d'onde inférieures à 2600 Å, on n'a pu déceler aucune fluorescence, tandis qu'au-dessus de 2600 Å, on a observé une faible émission. L'addition de biacétyle ne réduit pas le rendement en fluorescence mais l'addition de cyclohexane, de CO_2 et de *cis*-butène-2 l'augmente. Le rendement en triplet, lorsque le pentafluorobenzène est irradié à 2620, 2660, et 2700, tel que mesuré par la technique du biacétyle par émission sensibilisée, est aussi très faible et augmente avec l'addition de cyclohexane, CO_2 et *cis*-butène-2. Des trois gaz examinés, le *cis*-butène-2 est le plus efficace pour accroître le rendement en triplet. On ne sait pas ce qui arrive à la majorité des molécules lorsqu'on photolyse le pentafluorobenzène dans la région de 2600 Å.

Canadian Journal of Chemistry, 49, 1567 (1971)

Introduction

In recent years a number of publications have appeared dealing with various aspects of the photochemical behavior of the fluorinated benzenes (1–6). To date there have been no published reports dealing with the photochemistry of pentafluorobenzene (PFB). Although it is not possible to discern many systematic changes

Can. J. Chem. Downloaded from www.nrcresearchpress.com by 210.87.254.6 on 09/05/12
For personal use only.

$Ni(sem)_2Cl_2$ mentioned above. It is in fact the author's experience that such analogous possibilities are more numerous than those reported in the literature.

Finally, the ribbon-like structure of sem (10) is probably responsible for the cooling when sem is dissolved in water.

Financial help for the final stage of the research was provided by Ministère de l'Education, Québec. Thanks are also due to L. Cavalca, M. Nardelli, and A. Perley.

1. C. I. LEVENE. Lab. Invest. **19**, 25 (1968). M. ADAM, Z. DEYL, and J. ROSMUS. Med. Farmacol. Exp. **14**, 129 (1966). H. B. BENSUSAN, S. D. MCKNIGHT, and M. S. R. NAIDU. Biochem. Biophys. Res. Commun. **23**, 128 (1966). J. J. LALICH. Proc. Soc. Exp. Biol. Med. **123**, 214 (1966). R. DELLAVOLPE, A. GANDINI, and G. M. MERLI. Biochim. Biol. Sper. **3**, 388 (1964).
2. F. BODIT. C. R. Soc. Biol. **160**, 960 (1966).
3. H. SEIDEL. Biochem. Biophys. Acta, **129**, 412 (1966).
4. J. PAGES. Ann. Inst. Pasteur, **112**, 581 (1967). S. E. GROSSBERG, M. LWOFF, and A. LWOFF. J. Bacteriol. **92**, 1473 (1996).
5. A. VAHERI, M. D. SEDWICK, and S. A. PLOTKIN. Proc. Soc. Exp. Biol. Med. **125**, 1092 (1967).
6. K. A. JENSEN and E. RANCKE-MADSEN. Z. Anorg. Allgm. Chem. **227**, 25 (1936).
7. M. NARDELLI, G. F. GASPARRI, P. BOLDRINI, and G. G. BATTISTINI. Acta Cryst. **19**, 491 (1965).
8. D. A. BERTA, W. A. SPOFFORD, P. BOLDRINI, and E. L. AMMA. Inorg. Chem. **9**, 136 (1970).
9. W. A. SPOFFORD, P. BOLDRINI. E. L. AMMA, P. CARFAGNO, and P. S. GENTILE. Chem. Commun. 40 (1970).
10. P. BOLDRINI. Acta Cryst. In Press.
11. G. S. SMITH. J. Chem. Soc. 1354 (1937).
12. H. ELKHADEM, M. F. ISKANDER, and S. E. ZAYAN. Z. Anorg. Allgm. Chem. **320**, 261 (1963).
13. J. THIELE and O. STANGE. Lieb. Ann. **24**, 283 (1894).
14. M. J. BUERGER. Elementary Crystallography. 2nd ed. Wiley, New York. 1963. p. 114.
15. M. J. CAMPBELL and R. GRZESKOWIAK. Spectrochim. Acta, **24A**, 1149 (1968). and references herewith included.
16. V. F. TOPOROVA and K. V. NAIMUSHIMA. Zh. Neorg. Khim. **5**, 874 (1960).
17. M. NARDELLI and I. CHIERICI. Ric. Sci. **30**, 276 (1960). M. K. AKHMEDLI, and L. I. ZHIROVA. Russ. J. Inorg. Chem. **5**, 1326 (1960). R. A. HAINES and K. K. W. SUN. Can. J. Chem. **46**, 3241 (1968).
18. P. BOLDRINI. To be published.
19. G. F. GASPARRI, A. MANGIA, A. MUSATTI, and M. NARDELLI. Acta Cryst. **B24**, 367 (1968).

Spectrofluorometric Studies. X. The Photochemistry of Pentafluorobenzene

S. L. LEM, G. P. SEMELUK, AND I. UNGER

Department of Chemistry, University of New Brunswick, Fredericton, New Brunswick, Canada

Received September 18, 1970

The vapor phase photochemistry of pentafluorobenzene has been examined at a variety of exciting wavelengths starting at 2540 Å and extending to 2780 Å. Most of the studies were carried out at 2620, 2660, and 2700 Å. Below 2600 Å pentafluorobenzene does not exhibit any detectable fluoroscence, above 2600 Å a very weak fluorescent emission was observed. Addition of biacetyl does not markedly reduce the fluorescent yield, while addition of cyclohexane, CO_2, and *cis*-butene-2 causes an increase in the fluorescent yield. The triplet yield of pentafluorobenzene excited at 2620, 2660, and 2700 Å, measured by the sensitized emission of biacteyl technique, is also very low and is increased by the addition of cyclohexane, CO_2, and *cis*-butene-2. *cis*-Butene-2 is the most effective gas, of the three examined, in increasing the fluorescent and triplet yields of pentafluorobenzene. The fate of the majority of pentafluorobenzene molecules excited in the 2600 Å region is unknown.

La photolyse en phase gazeuse du pentafluorobenzène a été étudiée en fonction de la longueur d'onde de la raie excitatrice entre 2540 et 2780 Å. Pour des longueurs d'onde inférieures à 2600 Å, on n'a pu déceler aucune fluorescence, tandis qu'au-dessus de 2600 Å, on a observé une faible émission. L'addition de biacétyle ne réduit pas le rendement en fluorescence mais l'addition de cyclohexane, de CO_2 et de *cis*-butène-2 l'augmente. Le rendement en triplet, lorsque le pentafluorobenzène est irradié à 2620, 2660, et 2700, tel que mesuré par la technique du biacétyle par émission sensibilisée, est aussi très faible et augmente avec l'addition de cyclohexane, CO_2 et *cis*-butène-2. Des trois gaz examinés, le *cis*-butène-2 est le plus efficace pour accroître le rendement en triplet. On ne sait pas ce qui arrive à la majorité des molécules lorsqu'on photolyse le pentafluorobenzène dans la région de 2600 Å.

Canadian Journal of Chemistry, 49, 1567 (1971)

Introduction

In recent years a number of publications have appeared dealing with various aspects of the photochemical behavior of the fluorinated benzenes (1–6). To date there have been no published reports dealing with the photochemistry of pentafluorobenzene (PFB). Although it is not possible to discern many systematic changes

Can. J. Chem. Downloaded from www.nrcresearchpress.com by 210.87.254.42 on 09/05/12
For personal use only.

Can. J. Chem. Downloaded from www.nrcresearchpress.com by 210.87.254.42 on 09/05/12
For personal use only.

as one progresses from monofluorobenzene to hexafluorobenzene, two trends are worth noting: (*1*) simple HMO calculations (2) predict singlet and triplet energies to decrease as fluorination increases; (*2*) with some exceptions the singlet and triplet yields appear to decrease with increasing fluorination (4, 5) and account for less than 10% of all the excited molecules by the time one reaches hexafluorobenzene (7, 8). An account of the photochemistry of PFB serves to provide a link in this chain and to check on theoretical predictions.

Experimental

The pentafluorobenzene was obtained from Peninsular Chemresearch Incorporated. The v.p.c. showed its purity to be in excess of 99.9%. A comparison of its excitation spectrum with its absorption spectrum indicated no interfering impurities. It was, therefore, used without further purification. Biacetyl (BiA) was obtained from the Aldrich Chemical Company and was purified by bulb-to-bulb distillation "in vacuo" and stored in a blackened reservoir. Fluorometric grade benzene and cyclohexane (CH) obtained from the Hartman Leddon Company and Philips research grade *cis*-butene-2 (*c*-B-2) having less than 0.1% impurity were used without further purification. Dry-Ice was used as the source of CO_2. All chemicals were thoroughly degassed prior to being introduced into the cell.

All experiments were carried out in a conventional grease- and mercury-free high vacuum line equipped exclusively with Hoke packless diaphram metal valves. Pressure measurements were performed by means of a spiral gauge constructed at the National Research Council of Canada in Ottawa. Mixing was effected by flash vaporization followed by circulating the vapors through a flow through cell with an all-glass pump also constructed at the National Research Council of Canada in Ottawa. The flow-through cell was a cuvette-type with dimensions 1 cm × 1 cm × 4.5 cm, polished on all four sides.

All emission measurements were performed on a modified Aminco–Bowman spectrophotofluorometer. Details concerning the light source, phototube, photomultiplier tube, microammeter, recorder and the experimental procedure have been given previously (2). The entrance slit of the excitation monochromator was set at 0.5 mm and the exit slits were set at 1.0, 0.5, and 1.0 mm. The half band pass and spectral distribution at several excitation wave lengths for this combination have been given (9).

Quantum yields of fluorescence and of sensitized emission reported in this paper were based on the singlet and triplet yields of benzene, excited at 2580 Å, being 0.183 (10) and 0.63 (11), respectively.

Results and Discussion

(A) Fluorescence Measurements

The absorption and fluorescent spectrum of PFB is given in Fig. 1. With excitation wavelengths below 2600 Å no fluorescent emission was detected. Above 2600 Å the fluorescent emission is very weak, does not appear to be self-quenched and increases with increasing exciting wavelength; the data are summarized in Table 1. The fluorescent yield with excitation at 2620, 2660, and 2700 Å increases on the addition of CH, CO_2, and *c*-B-2. Cyclohexane and CO_2 exhibit approximately the same efficiency in increasing the fluorescent yield, while *c*-B-2 is the most efficient (see Fig. 2).

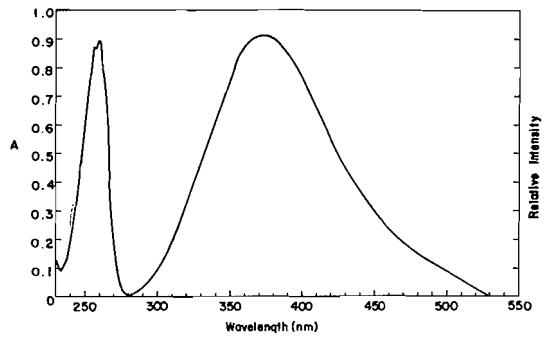

FIG. 1. The absorption and emission spectrum of PFB. The absorption spectrum was recorded on a Hitachi–Coleman Spectrophotometer, Model EPS-3T.

(B) Triplet Yields

The sensitized emission of BiA technique (12) was used to determine triplet yields.[1] The triplet

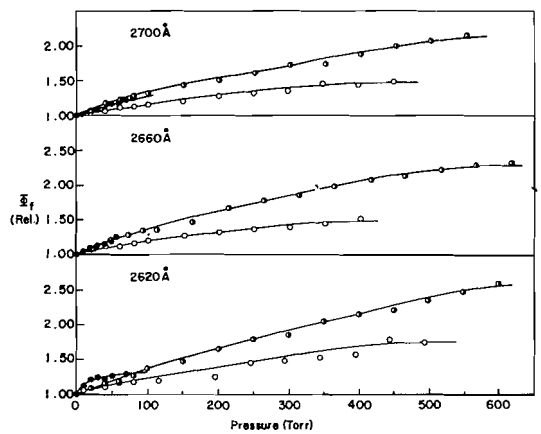

FIG. 2. The effect of CH, ●; CO_2, ○; and *c*-B-2, ◑ on relative fluorescent emission yield of PFB excited at various wavelengths.

[1]Triplet yields reported in this paper are upper limits only, since it is quite probable that excited singlet PFB sensitizes biacetyl emission as well. This phenomenon will be discussed in a forthcoming paper on difluorobenzene photochemistry.

TABLE 1. Fluorescent yield of PFB excited at various wavelengths

Pressure (Torr)	Φ_f	Pressure (Torr)	Φ_f	Pressure (Torr)	Φ_f
λ_{ex} = 2540, 2580 Å		λ_{ex} = 2620 Å		λ_{ex} = 2660 Å	
10–45	0	3.5	0.007	2.8	0.019
		6.4	0.011	5.2	0.018
		6.8	0.009	6.2	0.019
		10.8	0.009	9.9	0.019
λ_{ex} = 2600 Å		15.2	0.009	14.1	0.019
4.6	0.008	17.3	0.012	15.1	0.019
9.3	0.006	19.8	0.012	19.9	0.019
12.6	0.007	20.3	0.009	20.0	0.019
15.7	0.007	25.2	0.009	24.9	0.020
20.4	0.006	25.9	0.012	25.2	0.019
25.6	0.007	30.5	0.010	29.8	0.020
29.8	0.007	34.3	0.009	34.1	0.021
35.2	0.007	34.7	0.012	35.0	0.020
40.5	0.006	39.8	0.010	39.9	0.021
44.0	0.007	44.1	0.010	43.3	0.021
		44.9	0.013	43.9	0.021
λ_{ex} = 2680 Å		λ_{ex} = 2700 Å		λ_{ex} = 2720 Å	
3.6	0.020	3.8	0.024	4.2	0.026
5.8	0.019	5.1	0.025	7.1	0.027
10.4	0.019	6.3	0.026	11.7	0.025
15.4	0.019	10.4	0.024	16.6	0.025
20.4	0.019	14.1	0.024	21.0	0.025
24.2	0.019	15.6	0.025	27.3	0.025
28.9	0.019	19.4	0.024	32.1	0.026
35.0	0.019	20.2	0.025	38.0	0.027
40.2	0.019	24.3	0.024	42.7	0.026
44.6	0.019	25.2	0.024	46.7	0.027
		30.0	0.024		
		34.4	0.025		
		35.2	0.024		
		39.3	0.025		
		43.8	0.026		
		44.8	0.025		
λ_{ex} = 2750 Å		λ_{ex} = 2780 Å			
6.8	0.029	16.2	0.037		
12.7	0.031	21.8	0.041		
20.2	0.032	27.7	0.036		
24.3	0.035	33.8	0.037		
32.3	0.035	40.3	0.039		
38.1	0.035	48.1	0.038		
45.1	0.035				

yield of PFB excited at 2620, 2660, and 2700 Å increases with increasing BiA pressure. However, BiA does not markedly quench the fluorescent yield (see Fig. 3). The triplet yields are very low and increase with increasing excitation wavelength. Addition of CH, CO_2, and *c*-B-2 to PFB causes an increase in the triplet yield. These data are summarized in graphical form in Fig. 4.

The two most striking features of the photochemistry of PFB excited in the 2600 Å region are: (*1*) the very low total fluorescent and triplet yield even in the presence of large quantities of inert gas and (*2*) the increase in the sensitized emission, (*i.e.*, triplet yield) on the addition of *c*-B-2.

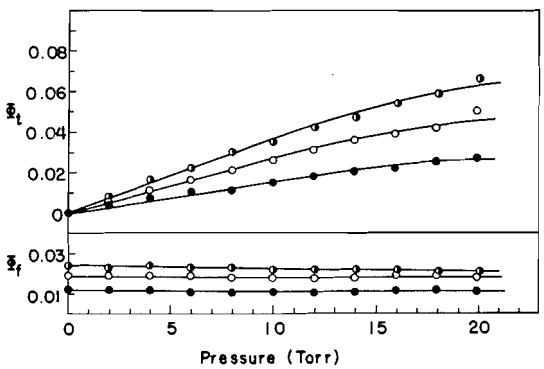

FIG. 3. Triplet and fluorescent yields of PFB excited at various wavelengths as a function of BiA pressure. λ_{ex} = 2620 Å, ●; λ_{ex} = 2660 Å, ○; and λ_{ex} = 2700 Å, ◑. PFB pressure = 20 Torr.

Can. J. Chem. Downloaded from www.nrcresearchpress.com by 210.87.254.42 on 09/05/12
For personal use only.

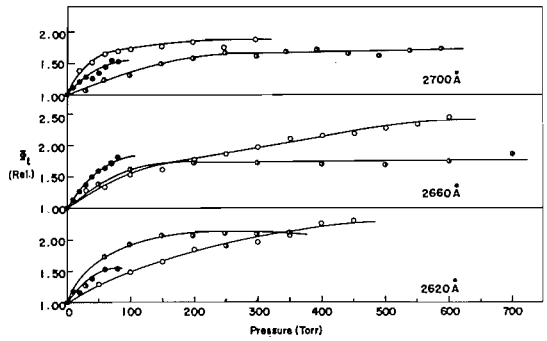

FIG. 4. The effect of CH, ●; CO_2, ○; and *c*-B-2, ◑ on the relative triplet yield of PFB excited at 2620, 2660, and 2700 Å. PFB pressure = 20 Torr, BiA pressure = 10 Torr.

The first phenomenon may be due to any of the following: (*a*) rapid internal conversion from the first singlet to the ground state, a process which has been postulated to account for the very low total singlet and triplet yield in perfluorotoluene (13); (*b*) intramolecular rearrangement occurring from either the singlet or triplet states (14); (*c*) very short PFB triplet lifetime which would require using greater BiA pressures than can be used in order to intercept all the triplet PFB molecules before their radiationless return to the ground state.

Most likely a combination of all of these factors contribute to the low total singlet and triplet yield. Pentafluorobenzene thus follows the pattern observed in the trifluorobenzenes, the tetrafluorobenzenes, and hexafluorobenzene.

With respect to the second phenomenon mentioned above, the "Schenck mechanism" (15) is not operative when aromatics transfer energy to *c*-B-2 (16). Thus when fluorinated aromatics, having triplet energies above the triplet of *c*-B-2, are excited in the presence of BiA and *c*-B-2 is added to the system, it would be expected that the sensitized emission of BiA would decrease. This is indeed the observation for all the fluorinated benzenes up to and including 1,3,5-trifluorobenzene (4). Starting with 1,2,4-trifluorobenzene and continuing to hexafluorobenzene, the triplet energies are predicted theoretically (2) to be lower than that of *c*-B-2 (17, 5). Hence these molecules may not be able to transfer triplet energy to *c*-B-2, and addition of *c*-B-2 to these molecules should then produce the same effect as the addition of any other inert gas. Within the *c*-B-2 pressure range used, this is confirmed for 1,2,4-trifluorobenzene, for all the tetrafluorobenzenes, and in the present case for pentafluorobenzene. However, an alternative explanation involving triplet energy transfer efficiency which seems to apply to 1,2,4-trifluorobenzene (18) cannot be excluded at this time.

Since this work was submitted, a description of some similar experiments has appeared (19). In the case of fluorescent yields where the results are directly comparable there is substantial agreement between the two sets of results.

The authors wish to thank the National Research Council of Canada for financial assistance.

1. D. PHILLIPS. J. Phys. Chem. **71**, 1839 (1967).
2. F. W. AYER, F. GREIN, G. P. SEMELUK, and I. UNGER. Ber. Bunsenges. Phys. Chem. **72**, 282 (1968).
3. J. L. DURHAM, G. P. SEMELUK, and I. UNGER. Can. J. Chem. **46**, 3177 (1968).
4. G. P. SEMELUK, R. D. S. STEVENS, and I. UNGER. Can. J. Chem. **47**, 597 (1969).
5. B. H. SCHOLZ and I. UNGER. Can. J. Chem. **48**, 2324 (1970).
6. I. HALLER. J. Amer. Chem. Soc. **88**, 2070 (1966).
7. R. B. CUNDALL, A. S. DAVIES, and K. DUNNICLIFF. The Triplet State, Proc. Int. Symp, Beirut, Lebanon. 1967. pp. 183–194.
8. D. PHILLIPS. J. Chem. Phys. **46**, 4679 (1967).
9. S. H. NG, G. P. SEMELUK, and I. UNGER. Ber. Bunsenges. Phys. Chem. **74**, 29 (1970).
10. W. A. NOYES, JR., W. A. MULAC, and D. A. HARTER. J. Chem. Phys. **44**, 2100 (1966).
11. W. A. NOYES, JR. and D. A. HARTER. J. Chem. Phys. **46**, 674 (1967).
12. H. ISHIKAWA and W. A. NOYES, JR. J. Chem. Phys. **37**, 583 (1962).
13. H. M. ROSENBERG and S. D. CARSON. J. Phys. Chem. **72**, 3531 (1968).
14. K. E. WILZBACH and L. KAPLAN. J. Amer. Chem. Soc. **86**, 2307 (1964).
15. G. O. SCHENCK and R. STINEMETZ. Bull. Soc. Chim. Belges, **71**, 781 (1962).
16. M. W. SCHMIDT and E. K. C. LEE. J. Amer. Chem. Soc. **92**, 3579 (1970).
17. R. B. CUNDALL and A. S. DAVIES. Progr. React. Kinet. **4**, 149 (1967).
18. G. P. SEMELUK and R. D. S. STEVENS. Can. J. Chem. To be published.
19. KH. AL-ANI and DAVID PHILLIPS. J. Phys. Chem. **70**, 4046 (1970).

Can. J. Chem. Downloaded from www.nrcresearchpress.com by 210.87.254.42 on 09/05/12
For personal use only.

Dissociative Electron Attachment Processes in SO_2 and NO_2

D. A. RALLIS AND J. M. GOODINGS
Centre for Research in Experimental Space Science, York University, Toronto, Ontario

Received October 28, 1970

A trapped electron apparatus has been used to identify the processes involved in negative ion formation for the triatomic oxides SO_2 and NO_2. Two O^- peaks are observed in SO_2 with onset values at $4.2 \pm 0.1_5$ and 6.3 ± 0.2 eV, and peak values at $5.0 \pm 0.1_5$ and $7.4 \pm 0.1_5$ eV, respectively. From kinetic energy analysis of the O^- ions, both peaks are found to have the same dissociation limit involving SO in its ground state. For NO_2, two dissociative electron attachment peaks are observed with onset values at 1.6 ± 0.2 and 7.3 ± 0.3 eV, and peak values at 3.0 ± 0.2 and 8.1 ± 0.2 eV, respectively. The first broad peak is explained by overlapping contributions from two processes having the same dissociation limit involving ground state NO; they differ only in the amount of kinetic energy possessed by the fragments. The second peak appears to involve electronic excitation of the neutral fragment NO* with zero kinetic energy at onset.

Un appareil à électron piégé a été utilisé pour identifier les procédés impliqués dans la formation d'ion négatif pour les oxydes triatomiques SO_2 et NO_2. Deux pics de O^- sont observés dans SO_2 avec des valeurs au commencement de $4.2 \pm 0.1_5$ et 6.3 ± 0.2 eV, et des valeurs pour les pics à $5.0 \pm 0.1_5$ et $7.4 \pm 0.1_5$ eV, respectivement. D'après des analyses d'énergie cinétique des ions O^-, on a trouvé que les deux pics ont la même limite de dissociation impliquant SO dans son état fondamental. Pour NO_2, deux pics d'attachement d'électron dissociatif sont observés avec des valeurs au commencement à 1.6 ± 0.2 et 7.3 ± 0.3 eV, et des valeurs pour les pics à 3.0 ± 0.2 et 8.1 ± 0.2 eV, respectivement. Le premier pic large est expliqué par les contributions qui se recouvrent de deux processus ayant la même limite de dissociation impliquant l'état fondamental NO. Ils diffèrent seulement dans la quantité d'énergie cinétique que possédaient les segments. Apparemment, le second pic implique l'excitation électronique du fragment NO* avec une énergie cinétique nulle au commencement.

Canadian Journal of Chemistry, 49, 1571 (1971)

Introduction

Negative ion formation in both SO_2 (1) and NO_2 (2) has been examined using mass spectrometry in the 0–10 eV range. In both cases, the only appreciable negative ion detected was O^- produced in a number of dissociative electron attachment processes. These unambiguous determinations of the fragments complement the present trapped electron studies in which kinetic energy analysis of the O^- ions is possible: together they serve to identify the processes involved. Possible kinetic energy discrimination in the mass spectrometric results is not a factor in the present work.

For these triatomic oxides, dissociative electron attachment can be represented by

$$[1] \qquad XO_2 + e(E_e) \rightarrow O^- + XO(E') + \text{k.e.}$$

where E_e is the kinetic energy of the electron projectile, E' is the excitation energy of the neutral fragment, and k.e. is the total kinetic energy of the separating fragments. It has been assumed that the thermal energy of the target gas is negligible and that there is no excited state of O^-.

The energetics of the process are given by

$$[2] \qquad E_e = D - A + E' + \text{k.e.}$$

where $D \equiv D(\text{OX—O})$ is the dissociation energy of the OX—O bond and A is the electron affinity of O. In terms of the O^- ion

$$[3] \qquad E_0 = (1 - \beta)[E_e - (D - A + E')]$$

where E_0 is the kinetic energy of the negative ion and β = mass (O^-)/mass (XO_2). A plot of E_0 *vs.* E_e is a straight line of slope $(1 - \beta)$ providing a mass identification of the negative ion. The intercept with the E_e-axis is the quantity $(D - A + E')$ which yields information concerning electron affinities, dissociation energies, and the energy states of the neutral fragment. The present study presents such negative ion data with kinetic energy determinations for SO_2 and NO_2.

Experimental

The trapped electron apparatus combines a retarding potential difference (r.p.d.) electron gun (3) with a Lozier-type collision chamber (4), and is similar to that developed by Schulz (5, 6). The apparatus has been described in detail elsewhere (7); hence, only essential details are given here. A pseudo-monoenergetic electron

Can. J. Chem. Downloaded from www.nrcresearchpress.com by 210.87.254.42 on 09/05/12
For personal use only.

Can. J. Chem. Downloaded from www.nrcresearchpress.com by 210.87.254.42 on 09/05/12
For personal use only.

beam aligned by a magnetic field (~250 G) traverses the axis of a collision region having the form of a cylindrical potential well. The potential well at the axis is formed by field penetration of an outer cylindrical collector electrode through an inner concentric grid. A pressure ratio of about 100 between the filament and collision chamber was achieved by good differential pumping.

Inelastically scattered electrons are "trapped" and measured at the collector if their residual kinetic energy k.e.$_e \leq W$, where W is the depth of the potential well expressed in eV. The collection mechanism for negative ions is different since their trajectories are not greatly influenced by the weak axial magnetic field; the collection efficiency depends primarily on the solid angle subtended at the outer collector by the collision volume near the axis. By sufficiently reducing W, only the ion current is collected out of a total negative signal comprised of both ions and electrons. By further reducing W to negative values, ion kinetic energy measurements can be made.

Results and Discussion for SO_2

A negative ion spectrum of O^- from SO_2 with a constant well depth $W = 0$ eV is shown in Fig. 1. Two peaks are observed with onset values at $4.2 \pm 0.1_5$ and 6.3 ± 0.2 eV, and with maxima at $5.0 \pm 0.1_5$ and $7.4 \pm 0.1_5$ eV, respectively. These results are in excellent agreement with recent mass spectrometric work by MacNeil and Thynne (1). The narrowness of the first peak supports their suggestion that the cross-section responsible for its production is resonant.

Figure 2 shows a plot of E_0 *vs.* E_e in SO_2. The E_e scale was calibrated against the onset of He^+ formation; the k.e. scale was calibrated from an ion retarding curve for SO_2^+. The line marked "theory" is drawn with a theoretical slope

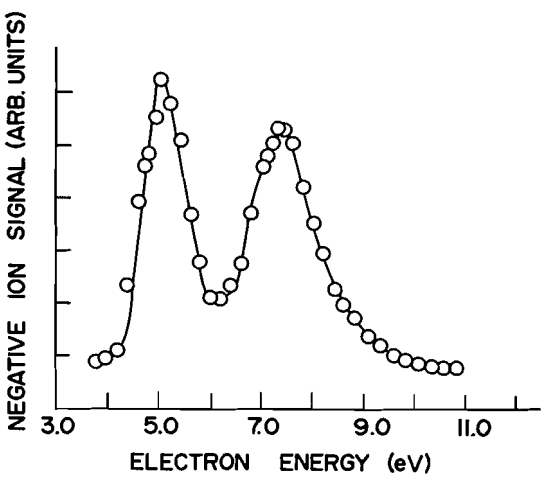

FIG. 1. Negative ion signal as a function of electron energy for SO_2 with $W = 0$.

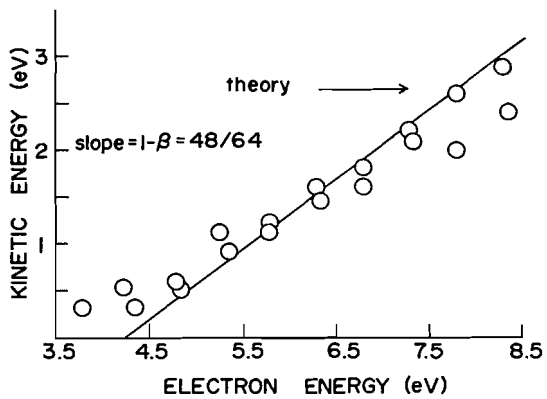

FIG. 2. Kinetic energy as a function of electron energy for the O^- ions produced by dissociative electron attachment processes in SO_2.

$(1 - \beta) = 48/64$ and an intercept $(D - A) = 4.14$ eV, using D(OS—O) = 5.61 eV (8) and A(O) = 1.465 eV (9). These values are consistent with the reaction

[4] $\quad SO_2 + e \rightarrow [SO_2^-]^* \rightarrow SO + O^- + \text{k.e.}$

where SO is in its ground state, and the thermal motion of the target gas has been neglected (10).

The experimental points in the energy range covering both peaks lie approximately along the theoretical line. Thus the products giving rise to the two peaks must be the same at infinite separation. The deviations are greatest at the wings of the peaks where the ion signal is small.

Results and Discussion for NO_2

Figure 3 shows a negative ion spectrum for NO_2 obtained with $W = 0$ eV. Two peaks have been clearly identified with onset values at 1.6 ± 0.2 and 7.3 ± 0.3 eV, and maxima at 3.0 ± 0.2 and 8.1 ± 0.2 eV, respectively. Figure 4 is a plot of E_0 *vs.* E_e for NO_2. The E_e scale was calibrated using the onset for He^+ formation while a retarding curve for NO_2^+ was used to calibrate the k.e. scale. In the range of the broad low-energy peak, the experimental points are in fair agreement with the theoretical line of slope $(1 - \beta) = 30/46$ and E_e-intercept $(D - A) = 1.65$ eV; at higher energy they assume a roughly constant value. A value for $D \equiv D$(ON—O) = 3.114 eV (8) has been assumed, with A(O) = 1.465 eV as before.

In a mass spectrometric study by Fox (2), three O^- peaks were observed in the range 0–10 eV. This work was concerned more with the informa-

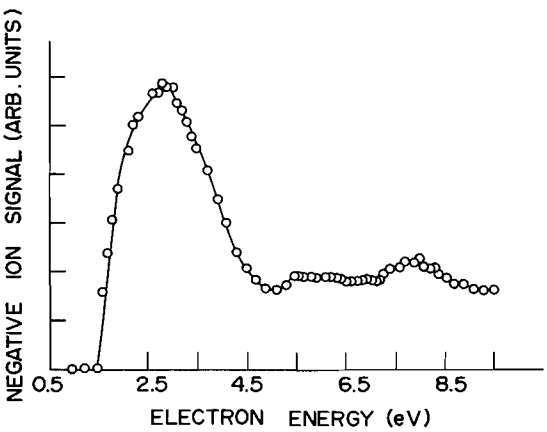

FIG. 3. Negative ion signal as a function of electron energy for NO_2 with $W = 0$.

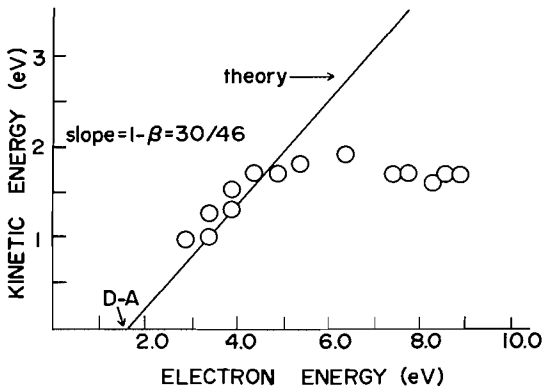

FIG. 4. Kinetic energy as a function of electron energy for the O^- ions produced by dissociative electron attachment processes in NO_2.

tion obtainable from the peak shapes than with the processes involved. The three peaks, designated here by *I*, *II*, and *III* are reported with maxima at 1.90, 3.0, and 8.75 eV, respectively. *I* has an onset at 1.35 eV and is about eleven times as intense as *II* and *III*, which are of comparable magnitude. Using Fig. 4, we believe the relevant processes for *I* and *II* to be

[5] $NO_2 + e \rightarrow [NO_2^-]^* \rightarrow NO + O^- + \text{k.e.}$ (*zero* at onset)

[6] $NO_2 + e \rightarrow [NO_2^-]^{**} \rightarrow NO + O^- + \text{k.e.}$ (*non-zero* at onset)

respectively, involving different excited states of the negative ion intermediate $[NO_2^-]$. Thus the broad low-energy peak in Fig. 3 arises from approximately equal overlapping contributions from [5] and [6]; its onset agrees reasonably well with that of *I* while its maximum is in good agreement with that of *II*. Due to kinetic energy discrimination, Fox's magnetic sector mass spectrometer may have considerably underestimated the relative intensity of *II*. The present results, for which such discrimination is not a problem, indicate that the cross sections for [5] and [6] are comparable, with [6] somewhat in predominance.

Above about 5 eV and in the region of the second peak near 8 eV in Fig. 3, E_0 in Fig. 4 assumes an approximately constant value. A similar behavior was observed by Schulz (11) for N_2O, and attributed to the process

[7] $N_2O + e \rightarrow [N_2O^-]^* \rightarrow N_2\dagger + O^- + \text{k.e.}$

based on his previous observation (12) of the process

[8] $N_2 + e \rightarrow [N_2^-]^* \rightarrow N_2\dagger + e$

where $N_2\dagger$ indicates vibrational excitation. However, a comparable explanation for NO_2 is not reasonable since it would involve the presence of $NO\dagger$ in analogy with eq. 7 for N_2O involving $N_2\dagger$. In a careful investigation by Chantry (13), no mention is made of any peak attributable to $NO\dagger$ in analogy with eq. 8, nor was any evidence obtained during a similar study of NO in these laboratories. Instead, the behavior of Fig. 4 above 5 eV is thought to be instrumental in origin, and indicates that the sensitivity limit of the apparatus has been reached. As noted in Fig. 2 for SO_2, the deviations of the k.e. data are greatest when the O^- signal is small.

Without reliable k.e. data, a conclusive mechanism for the peak near 8 eV in Fig. 3 is not possible. However, of the two probable processes

[9] $NO_2 + e \rightarrow [NO_2^-]^{***} \rightarrow NO(X^2\Pi) + O^- + \text{k.e.}$ (*non-zero* at onset)

[10] $NO_2 + e \rightarrow [NO_2^-]^{***} \rightarrow NO^*(A^2\Sigma^+) + O^- + \text{k.e.}$ (*zero* at onset)

[10] involving electronic excitation of NO is favored for a number of reasons.

(*a*) The separation of the onset values for the two peaks in Fig. 3 is about 5.7 eV. The energy required to excite the NO fragment into its $A(^2\Sigma^+)$ first excited electronic state is 5.45 eV (8) in approximate agreement with the onset separation.

Can. J. Chem. Downloaded from www.nrcresearchpress.com by 210.87.254.42 on 09/05/12
For personal use only.

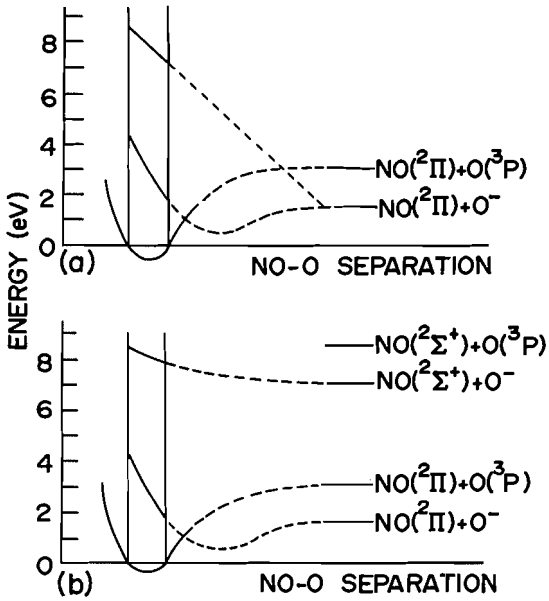

FIG. 5. Hypothetical potential energy curves for NO_2. (*a*) and (*b*) illustrate the behavior for processes [9] and [10], respectively.

(*b*) Fox (2) notes that peak *III* in his work with a maximum at 8.75 eV may be due to an impurity which produces O^- either from NO or from H_2O in this energy range. The peak at 8.1 eV in the present work, believed to arise from NO_2, is not in very good agreement with *III* as to its maximum value. For the present argument, however, suppose the 8.1 eV peak and *III* refer to the same process involving NO_2. *II* and *III* were observed by Fox with comparable low intensity. If [9] is the correct process, the same k.e. discrimination inferred previously for *II* should also be operative for *III* in the mass spectrometric results. In the present work which does not suffer from k.e. discrimination, the 8.1 eV peak should be observed with relatively increased intensity. Since this is not the case, [10] is again the more probable process.

(*c*) Hypothetical potential energy curves are drawn in Figs. 5(*a*) and (*b*) corresponding to [9] and [10], respectively. The points of intersection of the repulsive curves with the vertical Franck–Condon boundaries were taken to be the E_e values at which the peak height decreased to $1/e$ of its maximum value. In Fig. 5(*a*) the Franck–Condon energy range of the $[NO_2^-]^{***}$ state has been stretched somewhat to admit the extreme values possible considering the estimated experimental error; a reasonably shaped repulsive curve terminating at the $NO(^2\Pi) + O^-$ limit is only marginally possible. The smaller Franck–Condon energy range drawn for the $[NO_2^-]^{***}$ state in Fig. 5(*b*) is a more realistic fit to the experimental data. Alternatively, at the experimental onset of 7.3 eV, the total k.e. from eq. 2 of the separating fragments is 5.7 eV if [9] is the correct process. This value corresponds to the Coulomb repulsion of O^- and NO^- considered as point charges 2.5 Å apart. On this comparative basis, it is very unlikely that the repulsion between O^- and *neutral* NO could approach 5.7 eV stemming from a situation where the NO—O^- separation would be expected to exceed 2.5 Å. From either point of view, the process represented in [10] is favored.

The authors acknowledge the National Research Council of Canada for support of this work under Grant No. A-1604, and wish to thank Dr. H. K. Moe and Professor H. O. Pritchard for a number of helpful discussions.

1. K. A. G. MACNEIL and J. C. J. THYNNE. J. Phys. Chem. **74**, 52 (1970).
2. R. E. FOX. J. Chem. Phys. **32**, 285 (1960).
3. R. E. FOX, W. M. HICKAM, D. J. GROVE, and F. KJELDAAS. Rev. Sci. Instrum. **26**, 1101 (1955).
4. W. W. LOZIER. Phys. Rev. **36**, 1285 (1930).
5. G. J. SCHULZ. Phys. Rev. **112**, 150 (1958).
6. G. J. SCHULZ. J. Chem. Phys. **33**, 1661 (1960).
7. H. K. MOE. Ph.D. Thesis. McGill University. 1968.
8. G. HERZBERG. Electronic spectra of polyatomic molecules. D. Van Nostrand Co., Inc., Princeton, New Jersey. 1966.
9. L. M. BRANSCOMB, D. S. BURCH, S. J. SMITH, and S. GELTMAN. Phys. Rev. **111**, 504 (1958).
10. P. J. CHANTRY and G. J. SCHULZ. Phys. Rev. Lett. **12**, 449 (1964).
11. G. J. SCHULZ. J. Chem. Phys. **34**, 1778 (1961).
12. G. J. SCHULZ. Phys. Rev. **116**, 1141 (1959).
13. P. J. CHANTRY. Phys. Rev. **172**, 125 (1968).

Can. J. Chem. Downloaded from www.nrcresearchpress.com by 210.87.254.42 on 09/05/12
For personal use only.

A Simple Diffusion Cell for the Determination of Absolute Diffusion Constants using Radioactive Tracers

WILLY DYCK
Geological Survey of Canada, Ottawa, Canada

Received August 10, 1970

Using microscope slides for the diffusion grating, a glass diffusion cell was constructed which permitted the determination of absolute diffusion constants of γ-ray emitting elements in aqueous solutions.

The cell was tested at 25 °C with ^{110}Ag as tracer and gave a bulk-diffusion coefficient of 1.64×10^{-5} cm²/s and a self-diffusion coefficient of 1.48×10^{-5} cm²/s using 0.01 *M* $AgNO_3$.

The hydrogen ion concentration had no detectable effect on the diffusion coefficient of $AgNO_3$ in the p*H* range −0.48 to 7.5. The presence of Na or Fe(III) ions, or sucrose molecules at moderate concentrations (> 0.1 *M*) resulted in a marked decrease in the diffusion coefficient.

En utilisant des plaques de microscope comme grille de diffusion, on a construit une cellule de diffusion en verre qui a permis la détermination des constantes absolues de diffusion en solution aqueuse d'éléments émettant des rayonnements gamma.

La cellule a été testée en utilisant l'argent-110 comme traceur; on a obtenu un coefficient de diffusion globale de 1.64×10^{-5} cm²/s et un coefficient d'autodiffusion de 1.48×10^{-5} cm²/s en utilisant $AgNO_3$ 0.1 *M*.

La concentration d'ions hydrogène n'a pas eu d'effet mesurable sur le coefficient de diffusion de $AgNO_3$ dans la gamme de p*H* −0.48 à 7.5. La présence d'ions Na ou de Fe(III) ou de molécules de sucrose à concentration modérée (> 0.1 *M*) a produit une diminution marquée du coefficient de diffusion.

Canadian Journal of Chemistry, 49, 1575 (1971)

Introduction

The simplest way to determine diffusion coefficients in aqueous solutions is by the McBain–Northrop method (1–4). However, the sintered glass cell used in this method has to be calibrated using an electrolyte such as KCl with known diffusion coefficients. Also adsorption of ions such as silver on the porous diaphragm of sintered glass precludes the use of very dilute solutions. Harned and French (5) and Harned and Blander (6) have developed conductance cells for the measurement of absolute diffusion coefficients of electrolytes. Starik and Yurtov (7) have devised a cell for the measurement of self-diffusion coefficients of radioactive isotopes in dilute solutions. Various modifications of the sintered disc method have been used for diffusion studies (8–10). A capillary method is described by Mills and Godbole (11).

Whiteway *et al.* (12) used the sintered disc and a number of workers (13–17) have used the rotating disc method to measure the diffusion coefficient of Ag^+ in aqueous solutions.

This report describes a diffusion cell suitable for the determination of absolute diffusion coefficients of γ-ray emitting elements in solution and gives the results obtained with silver using ^{110}Ag as a tracer.

Experimental[1]

A sketch of the cell constructed for this work is shown in Fig. 1. The cell grating, or diffusion layer, was constructed as follows:

Approximately 50 to 75 ordinary microscope slides measuring 75 × 25 × 1 mm were encapsuled tightly in a hand-made box and cut approximately to the desired height using a diamond blade. While still in the bakelite box, the exposed edges were ground and polished on a rotating wheel using carborundum powders. The slides were then removed from the bakelite enclosure, their height and thickness measured accurately with calipers, cleaned thoroughly, dried, and cemented together with Canada Balsam using 0.2 mm microscope slide covers as spacers between them. The Canada Balsam cement was diluted with toluene so it would flow freely and give a thin glue line. The spacers were placed near the end of the slides in such a way as to give a series of 0.2 mm parallel slits. The length of these slits was varied to give a grating which approximated a circular opening. The slides and spacers were assembled and glued on an inclined stand and dried at 80 °C. When the cement had hardened the grating was ground into a circular shaped disc. The height of the grating (length of diffusion path), the total thick-

[1]The experiments were carried out by Mr. J. C. Pelchat, Geochemistry Section, Geological Survey of Canada.

Can. J. Chem. Downloaded from www.nrcresearchpress.com by 210.87.254.6 on 09/05/12
For personal use only.

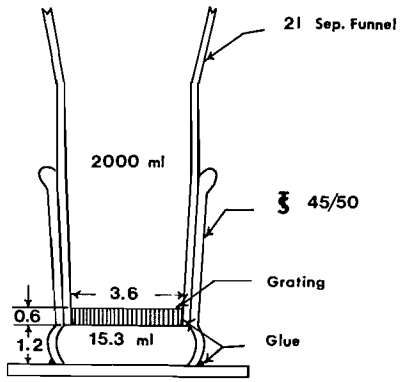

FIG. 1. Cross-section of diffusion cell (all dimensions are in cm).

ness (thickness of all slides plus the thickness of all spaces between them), and the length of each slit were measured accurately. From these measurements a value of a/d = 2.354 cm (eq. 1) was obtained. By weighing the empty and the water filled disc several times and making use of the previously measured d an independent measure of a was obtained. The value for a/d by this method was equal to 2.317 cm. After calibration of the grating it was cemented with epoxy glue into the bottom of a 45/50 male joint and the joint attached to a 2 l separatory funnel. This funnel filled with 2.00 l makes up the volume of the upper compartment. The female part of the joint was cut off about 1.5 cm below the ground surface, ground to a smooth flat edge, and cemented with epoxy glue to a 3 mm thick, 7.5 cm diameter glass disc. When the upper compartment is inserted into this joint the volume below the grating comprises the volume of the lower compartment. This volume was determined by weighing the cell empty and filled with water to the top of the grating and subtracting the volume of the grating as determined earlier.

If the composition in each compartment is kept constant so that diffusion through the grating governs the overall rate, it can be shown that

$$[1] \qquad \ln(\Delta c/\Delta c_0) = -(a/d)(1/v + 1/V)Dt$$

Δc and Δc_0 are the differences in the specific activities in the two compartments at time t and 0, respectively, v and V are the volumes of liquid, a is the total area, and d the length of the diffusion path. Rearranging, the diffusion coefficient is given by

$$[2] \qquad D = \log(\Delta c_0/\Delta c)/(bt)$$

For the cell described here $b = 0.0667\ \text{cm}^{-2}$.

Preliminary tests showed that the assumption that the composition throughout each compartment is constant is not valid (D for 0.01 M $AgNO_3$ fluctuated between 1.4 and 1.7 $\times$ 10^{-5}). Stirring the solutions gently in both compartments gave more reproducible results.

The experiments were carried out as follows: excess silver solution containing ^{110}Ag tracer was poured into the lower compartment making certain that no air remained trapped below or in the grating. After removing the excess tracer solution the upper compartment was filled slowly with 2.00 l of the desired test solution so as not to cause mixing between the compartments. At least once a day the cell was placed on top of a NaI (Tl activated) crystal and the change in γ-ray activity of the 0.656 MeV peak measured using a single channel pulse height analyzer. Between measurements the cell was placed on a stand which permitted gentle stirring of both compartments. A small magnet in glass turning at about 0.3 r.p.s. in the lower compartment and a rod turning at about 2 r.p.s. in the upper compartment were used for stirring. At the end of an experiment (usually one week) the lower compartment was cleaned and the activity of the solution in the upper compartment, still in the diffusion cell, determined giving the background plus upper compartment activity at the end of the experiment. Background plus initial activity of the upper compartment was determined by measuring the activity of the clean cell filled with inactive solution used for that test. A linear interpolation between the above values was used for inbetween values of the activity in the upper compartment. To ascertain that diffusion rather than mechanical mixing was responsible for the transfer of silver between compartments, a plot of $\log(\Delta c)$ *vs.* t was drawn for each experiment. If the points deviated appreciably from the straight line relationship predicted by the above equation, the experiment was rejected. On the few occasions where it was necessary to reject the experiment, it is believed that the solution in the upper compartment had become more dense than in the lower one because of a thermal gradient set up by heat generated by the magnetic stirrer below the cell. Several typical plots of $\log(\Delta c)$ *vs.* t are shown in Fig. 2. D is calculated from the slope of the straight line drawn through the experimental points.

All experiments were carried out at room temperature which was kept fairly constant near 25 °C. It is estimated that over the course of a week (the length of the average experiment) the error in the diffusion coefficient due to

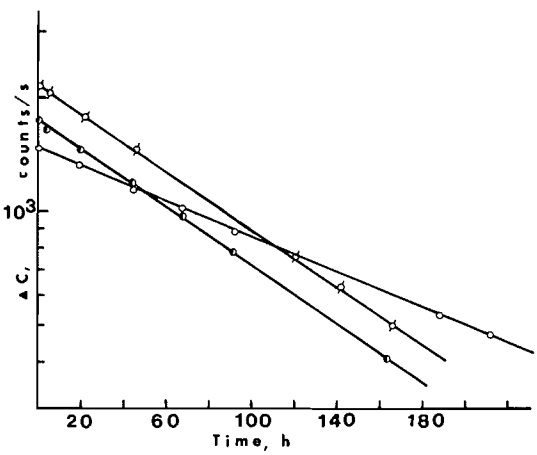

FIG. 2. Relationship between the change in the silver concentration between the cell compartments and time. ○, 0.01 M $AgNO_3$ into H_2O, pH = 0.0; ◐, 0.01 M $AgNO_3$ into H_2O, pH = 3.5; ○, 0.01 M $AgNO_3$ in 0.33 M $Fe(NO_3)_3$ into 0.33 M $Fe(NO_3)_3$, pH = 0.8.

Can. J. Chem. Downloaded from www.nrcresearchpress.com by 210.87.254.6 on 09/05/12
For personal use only.

TABLE 1. Effect of pH and salt content of solutions on the diffusion coefficient of 0.01 M $AgNO_3$

Concentration (mol/l)	pH	$D \times 10^5$ (cm²/s)	Concentration (mol/l)	pH	$D \times 10^5$ (cm²/s)	$\bar{D} \times 10^5$ (cm²/s)
	HNO_3			$NaNO_3$		
3.3×10^{-8}	7.5	1.51	0.10	2.0	1.57	
1.0×10^{-7}	7.0	1.72	0.10	2.0	1.52	1.55
1.0×10^{-6}	6.0	1.69				
1.0×10^{-5}	5.0	1.68	1.0	2.0	1.23	
1.0×10^{-4}	4.0	1.58	1.0	2.0	1.43	
3.2×10^{-4}	3.5	1.61	1.0	2.0	1.37	1.35
1.0×10^{-3}	3.0	1.62				
1.0×10^{-2}	2.0	1.70		$Fe(NO_3)_3$		
1.0×10^{-2}	2.0	1.70	0.033	1.9	1.23	
1.0×10^{-2}	2.0	1.64	0.033	1.6	1.50	
1.0×10^{-1}	1.0	1.62	0.033	1.6	1.51	1.41
1.0×10^{-1}	1.0	1.67				
1.0×10^{-1}	1.0	1.53	0.17	1.6	1.27	
1.0×10^{0}	0.0	1.62	0.17	1.6	1.18	1.22
3.0×10^{0}	−0.48	1.66				
3.0×10^{0}	−0.48	1.75	0.33	0.8	0.94	
			0.33	0.8	0.98	0.96
	$\bar{D}$	1.64				
	S_D	0.07		$C_{12}H_{22}O_{11}$		
	$S_{\bar{D}}$	0.02				
			1.0	2.0	1.08	
			1.0	2.0	0.88	0.98

temperature fluctuations was not more than ±3%. Other smaller errors were due to mixing during transport of the cell between counter and stirrers, statistical error in activity measurements (this was easily kept below ±1%), errors in the calibration of the grating, and background interpolations.

Results and Discussion

The results of this work are summarized in Table 1 and Fig. 3. From Fig. 3 we can deduce a bulk-diffusion coefficient of 1.68×10^{-5} cm²/s and a self-diffusion coefficient of 1.48×10^{-5} cm²/s for a 0.01 M $AgNO_3$ solution. These values are in fairly good agreement with those obtained by Whiteway *et al.* (12) using a sintered disc, *i.e.* 1.63×10^{-5} and 1.58×10^{-5}, respectively, except that the difference between the bulk and self-diffusion coefficients as determined in this work is somewhat larger. Other reported values of the diffusion coefficient of Ag^+ range from 1.42×10^{-5} to 1.69×10^{-5} cm²/s (13–17) as determined by the rotating disc and/or the Cottrell method.

The cell described in this report is simple to make, gives absolute diffusion constants, and is simple to use with γ emitting elements. By changing the relative sizes of the two compartments, β emitting elements or nonradioactive elements can be used. In fact, the first working prototype, based on this principle, consisted of two 250 ml beakers facing each other through a grating made from standard 75 × 25 × 1 mm microscope slides which had not been cut or ground at all.

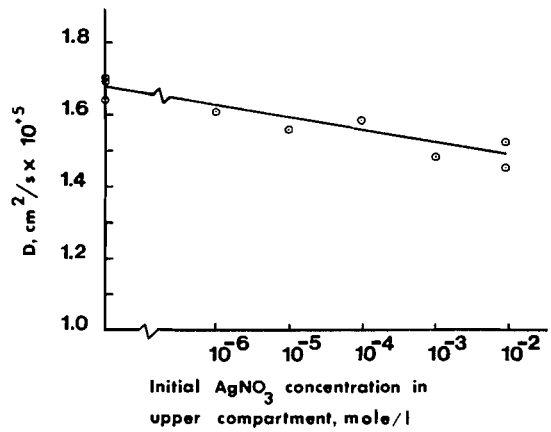

FIG. 3. Relationship between self-diffusion and bulk-diffusion coefficient of silver in aqueous solutions at 25 °C and a pH = 2.0 (initial $AgNO_3$ concentration in lower compartment = 0.01 M).

The use of cements limits its useful life and the type of solutions that can be studied with it. Perhaps a professional glass blower could make such a grating without the use of cements. The cement also offsets somewhat the advantage gained over the sintered disc cell with regard to the adsorption of ions from very dilute solutions.

From the pH series listed in Table 1 a mean

Can. J. Chem. Downloaded from www.nrcresearchpress.com by 210.87.254.6 on 09/05/12
For personal use only.

bulk-diffusion coefficient of $1.64 \pm 0.02 \times 10^{-5}$ cm^2/s for a 0.01 *M* $AgNO_3$ solution is calculated. The hydrogen ion concentration has no noticeable effect on *D* over the p*H* range −0.48 to 7.5 but silver, sodium, iron, and sucrose quite an appreciable one; quite in accord with laws known to govern ionic diffusion processes.

1. J. W. McBain and T. H. Liu. J. Am. Chem. Soc. **53**, 59 (1931).
2. J. H. Northrop and M. L. Anson. J. Gen. Physiol. **12**, 543 (1928–1929).
3. A. R. Gordon. Ann. N.Y. Acad. Sci. **46**, 285 (1945).
4. R. H. Stokes. J. Am. Chem. Soc. **72**, 763 (1950).
5. H. S. Harned and D. M. French. Ann. N.Y. Acad. Sci. **46**, 267 (1945).
6. H. S. Harned and M. Blander. J. Phys. Chem. **63**, 2078 (1959).
7. I. E. Starik and A. I. Yurtov. Transl. Radiokhimiya, **6**, 448 (1964).
8. F. T. Wall, P. F. Grieger, and C. W. Childers. J. Am. Chem. Soc. **74**, 3562 (1952).
9. F. T. Wall and C. W. Childers. J. Am. Chem. Soc. **75**, 3550 (1953).
10. F. Gruenn and Chr. Blattner. J. Am. Chem. Soc. **80**, 3838 (1958).
11. R. Mills and E. W. Godbole. Aust. J. Chem. **11**, 1 (1958).
12. S. G. Whiteway, D. F. MacLennan, and C. C. Coffin. J. Chem. Phys. **18**, 229 (1950).
13. R. R. M. Johnston and M. Spiro. J. Phys. Chem. **12**, 3784 (1967).
14. D. J. Macero and C. L. Rulfs. J. Am. Chem. Soc. **81**, 2942 (1959).
15. M. B. Kraichman and E. A. Hogge. J. Phys. Chem. **59**, 986 (1955).
16. M. v. Stackelberg, M. Pilgram, and V. Toome. Z. Elektrochem. **57**, 342 (1953).
17. H. A. Laitinen and I. M. Kolfhoff. J. Am. Chem. Soc. **61**, 3344 (1939).

Use of N^{im}-*t*-Butyloxycarbonyl in the Synthesis of Poly-L-histidine

M. Fridkin[1]

The Department of Biophysics, The Weizmann Institute of Science, Rehovot, Israel

AND

H. J. Goren[2]

Division of Medical Biochemistry, Faculty of Medicine, The University of Calgary, Calgary 44, Alberta

Received December 2, 1970

N^{α},N^{im}-Di-*t*-butyloxycarbonyl-L-histidine, N^{α}-benzyloxycarbonyl-N^{im}-*t*-butyloxycarbonyl-L-histidine and poly-L-histidine have been synthesized. The role in peptide synthesis of *t*-butyloxycarbonyl as an imidazole-blocking group is discussed and compared to other currently available imidazole-blocking groups.

On a synthétisé les N^{α},N^{im}-di-*t*-butyloxycarbonyl L-histidine, N^{α}-benzyloxycarbonyl N^{im}-*t*-butyloxycarbonyl L-histidine et poly-L-histidine. On discute du rôle dans les synthèses peptidiques du groupe *t*-butyloxycarbonyl pour bloquer l'imidazole et on le compare avec celui que peuvent jouer d'autres groupes qui sont disponibles présentement pour remplir cette fonction.

Canadian Journal of Chemistry, 49, 1578 (1971)

One of the main requirements associated with the synthesis of histidine-containing peptides has been the selection of a suitable protecting group for the imidazole nitrogen of the amino acid. A useful protecting group should satisfy a number of requirements such as ready availability, stability to the manipulations needed to purify the blocked peptides, stability to the removal conditions of some N and C protecting groups to assure conventional stepwise peptide synthesis, and the selective removal of the protective group under conditions that will not lead to racemization or to the destruction of labile peptide bonds. In addition, it is of great importance that the basicity of the imidazole nitrogen will be minimized while protected.

The benzyl group (1) has been used most often

[1]Present address: Department of Biology, Massachusetts Institute of Technology, Cambridge, Massachusetts 02139; on leave of absence from the Weizmann Institute of Science.

[2]NRCC Postdoctoral Fellow 1968–1970, The Department of Biophysics, The Weizmann Institute of Science, Rehovot, Israel. To whom reprint requests should be sent.

Can. J. Chem. Downloaded from www.nrcresearchpress.com by 210.87.254.6 on 09/05/12
For personal use only.

bulk-diffusion coefficient of $1.64 \pm 0.02 \times 10^{-5}$ cm^2/s for a 0.01 *M* $AgNO_3$ solution is calculated. The hydrogen ion concentration has no noticeable effect on *D* over the p*H* range −0.48 to 7.5 but silver, sodium, iron, and sucrose quite an appreciable one; quite in accord with laws known to govern ionic diffusion processes.

1. J. W. McBain and T. H. Liu. J. Am. Chem. Soc. **53**, 59 (1931).
2. J. H. Northrop and M. L. Anson. J. Gen. Physiol. **12**, 543 (1928–1929).
3. A. R. Gordon. Ann. N.Y. Acad. Sci. **46**, 285 (1945).
4. R. H. Stokes. J. Am. Chem. Soc. **72**, 763 (1950).
5. H. S. Harned and D. M. French. Ann. N.Y. Acad. Sci. **46**, 267 (1945).
6. H. S. Harned and M. Blander. J. Phys. Chem. **63**, 2078 (1959).
7. I. E. Starik and A. I. Yurtov. Transl. Radiokhimiya, **6**, 448 (1964).
8. F. T. Wall, P. F. Grieger, and C. W. Childers. J. Am. Chem. Soc. **74**, 3562 (1952).
9. F. T. Wall and C. W. Childers. J. Am. Chem. Soc. **75**, 3550 (1953).
10. F. Gruenn and Chr. Blattner. J. Am. Chem. Soc. **80**, 3838 (1958).
11. R. Mills and E. W. Godbole. Aust. J. Chem. **11**, 1 (1958).
12. S. G. Whiteway, D. F. MacLennan, and C. C. Coffin. J. Chem. Phys. **18**, 229 (1950).
13. R. R. M. Johnston and M. Spiro. J. Phys. Chem. **12**, 3784 (1967).
14. D. J. Macero and C. L. Rulfs. J. Am. Chem. Soc. **81**, 2942 (1959).
15. M. B. Kraichman and E. A. Hogge. J. Phys. Chem. **59**, 986 (1955).
16. M. v. Stackelberg, M. Pilgram, and V. Toome. Z. Elektrochem. **57**, 342 (1953).
17. H. A. Laitinen and I. M. Kolfhoff. J. Am. Chem. Soc. **61**, 3344 (1939).

Use of N^{im}-*t*-Butyloxycarbonyl in the Synthesis of Poly-L-histidine

M. Fridkin[1]

The Department of Biophysics, The Weizmann Institute of Science, Rehovot, Israel

AND

H. J. Goren[2]

Division of Medical Biochemistry, Faculty of Medicine, The University of Calgary, Calgary 44, Alberta

Received December 2, 1970

N^{α},N^{im}-Di-*t*-butyloxycarbonyl-L-histidine, N^{α}-benzyloxycarbonyl-N^{im}-*t*-butyloxycarbonyl-L-histidine and poly-L-histidine have been synthesized. The role in peptide synthesis of *t*-butyloxycarbonyl as an imidazole-blocking group is discussed and compared to other currently available imidazole-blocking groups.

On a synthétisé les N^{α},N^{im}-di-*t*-butyloxycarbonyl L-histidine, N^{α}-benzyloxycarbonyl N^{im}-*t*-butyloxycarbonyl L-histidine et poly-L-histidine. On discute du rôle dans les synthèses peptidiques du groupe *t*-butyloxycarbonyl pour bloquer l'imidazole et on le compare avec celui que peuvent jouer d'autres groupes qui sont disponibles présentement pour remplir cette fonction.

Canadian Journal of Chemistry, 49, 1578 (1971)

One of the main requirements associated with the synthesis of histidine-containing peptides has been the selection of a suitable protecting group for the imidazole nitrogen of the amino acid. A useful protecting group should satisfy a number of requirements such as ready availability, stability to the manipulations needed to purify the blocked peptides, stability to the removal conditions of some N and C protecting groups to assure conventional stepwise peptide synthesis, and the selective removal of the protective group under conditions that will not lead to racemization or to the destruction of labile peptide bonds. In addition, it is of great importance that the basicity of the imidazole nitrogen will be minimized while protected.

The benzyl group (1) has been used most often

[1]Present address: Department of Biology, Massachusetts Institute of Technology, Cambridge, Massachusetts 02139; on leave of absence from the Weizmann Institute of Science.

[2]NRCC Postdoctoral Fellow 1968–1970, The Department of Biophysics, The Weizmann Institute of Science, Rehovot, Israel. To whom reprint requests should be sent.

Can. J. Chem. Downloaded from www.nrcresearchpress.com by 210.87.254.105 on 09/05/12
For personal use only.

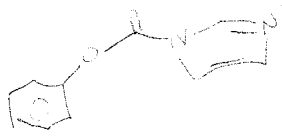

Can. J. Chem. Downloaded from www.nrcresearchpress.com by 210.87.254.105 on 09/05/12
For personal use only.

for the protection of the imidazole (im)[3] of histidine but it does not mask the basicity of the ring. In addition, the use of sodium in liquid ammonia for the removal of the benzyl group is drastic, leading in some cases to the cleavage of peptide bonds (2). Removal of the benzyl group from the imidazole group effected by catalytic hydrogenation is very slow, and impossible when sulfur-containing amino acids are present in the peptide. The im-benzyloxycarbonyl (Cbz) group (3) is very labile to basic conditions and to various nucleophilic reagents. Thus the reaction of N^{α},N^{im}-di-Cbz-L-histidine *N*-hydroxysuccinimide ester with L-alanine in a mixture of water and dioxane in the presence of two equivalents of $NaHCO_3$ led to the formation of dipeptide with a free imidazole group.[4] The new imidazole-protecting groups 2,2,2-trifluoro-1-benzyloxycarbonylaminoethyl (4) and 2,2,2-trifluoro-1-butyloxycarbonylaminoethyl (4) which are removed from imidazole by strong acids, the dinitrophenyl which is removed readily from imidazole by thiolysis (5), and the piperidinocarbonyl (6) which is labile to basic conditions and stable to acids, are most promising. However, little information on their use in peptide synthesis is available. The use of *t*-butyloxycarbonyl (*t*-Boc) as an imidazole-blocking group has been briefly described (7, 8). Some further properties of this blocking group have been investigated and its role as a blocking group is discussed.

N^{α},N^{im}-Di-*t*-Boc-L-histidine was obtained in 50% yield on reacting histidine with *t*-Boc azide in the presence of MgO (9). The im-*t*-butyloxycarbonyl (*im*-Boc) group could be removed by strong acids such as HBr in trifluoroacetic acid, HBr in acetic acid, or anhydrous HF, however it is stable to the action of HCl in dioxane. It would thus appear to be compatible with the *t*-Boc or nitrophenylsulfenyl α-amino protecting groups. In addition the *im*-Boc group was found to be much more stable towards alkali than *im*-Cbz group (3, 8). Thus when N^{α},N^{im}-di-*t*-Boc-L-histidine *N*-hydroxysuccinimide ester was coupled with L-alanyl-γ-benzyl-L-glutamic acid the corresponding di-Boc-tripeptide was obtained[4] in 80% yield. Moreover, the basicity of the imidazole ring was reduced markedly by its protection with the *t*-Boc group, since various derivatives such as N^{α},N^{im}-di-*t*-Boc-L-histidine or N^{α}-Cbz-N^{im}-*t*-Boc-L-histidine were not soluble in dilute aqueous acid solutions.

Poly-L-histidine has, in the past, been synthesized by polymerizing N^{im}-benzyl-L-histidine *N*-carboxylanhydride (10). The benzyl group was subsequently removed by treatment with sodium in liquid NH_3. We wish to report here the use of the new imidazole-protecting group, *im*-Boc, in the synthesis of this polymer.

The synthesis of poly-L-histidine is summarized in Scheme 1: N^{im}-*t*-Boc-L-histidine *N*-carboxylanhydride hydrochloride (**2**), prepared from N^{im}-*t*-Boc-N^{α}-Cbz-L-histidine (**1**), was converted to the free base **3** and polymerized in dioxane, using triethylamine as initiator. The blocked polymer, poly-N^{im}-*t*-Boc-L-histidine (**4**), with an average molecular weight of 21 000 as determined by its sedimentation and diffusion constants in dimethylformamide, assuming a partial specific volume ($\bar{v}$) of 0.75, was converted to poly-L-histidine hydrobromide (**5**) with HBr in trifluoroacetic acid.

From these preliminary studies one can conclude that the *t*-Boc blocking group on the imidazole ring has several advantages: (*i*) availability, (*ii*) ease of synthesis, (*iii*) ease of removal with no chance of racemization since carried out under anhydrous HBr treatment, (*iv*) the insolubility of *im*-Boc histidine peptides in aqueous acid solution indicates decreased basicity which results in higher yields in peptide synthesis illustrated by the large poly-L-histidine molecule synthesized (average degree of polymerization is approximately 100 compared to 50 obtained when the imidazole-blocking group was benzyl (10), and (*v*) stable to methods of purification.

Experimental

All melting points are uncorrected. Prior to analysis the compounds were dried at room temperature *in vacuo* over phosphorus pentoxide and NaOH.

N^{α},N^{im}-Di-t-butyloxycarbonyl-L-histidine

Histidine hydrochloride (31.5 g, 0.164 mol) was dissolved in 480 ml of water and added to a solution of *t*-butyloxycarbonyl azide (70 g, 0.49 mol) in 480 ml of dioxane. Magnesium oxide (24 g, 0.62 mol) was then added and the mixture was stirred for 4 days at room temperature. The excess MgO was filtered and the solution was evaporated in high *vacuo* (~25 °C). The oily residue obtained was dissolved in 100 ml of water, cooled

[3]Abbreviations: imidazole, im; benzyloxycarbonyl, Cbz; *t*-butyloxycarbonyl, *t*-Boc; im-*t*-butyloxycarbonyl, *im*-Boc.

[4]H. J. Goren, M. Fridkin, and E. Katchalski. Unpublished data.

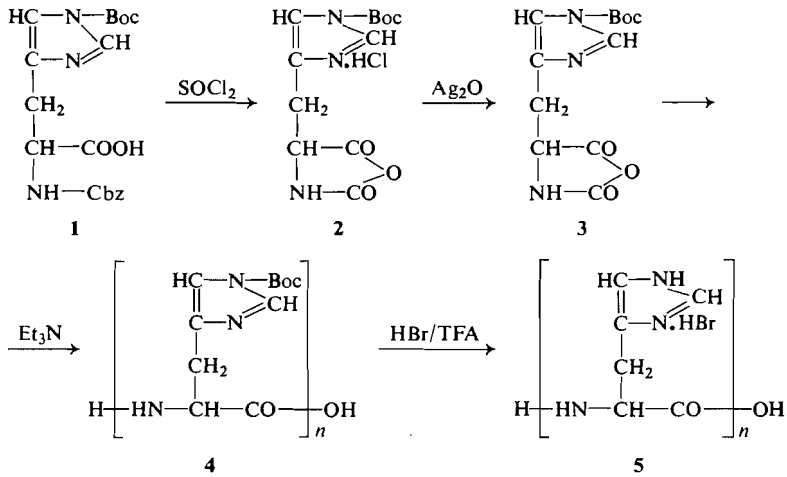

Boc = $(CH_3)_3COCO-$; Cbz = $C_6H_5CH_2OCO-$

SCHEME 1

to 0 °C, and acidified with 50% aqueous citric acid. The oily product was extracted into ethyl acetate, the organic solution dried over Na_2SO_4, filtered, and evaporated *in vacuo* to give a colorless amorphous solid; 29 g (50% yield). All attempts to crystallize the product were unsuccessful; m.p. 70° (starts to soften slowly at 53°); $[\alpha]_D^{23}$ +13.9 (*c* 1.1, methanol).

Anal. Calcd. for $C_{16}H_{25}N_3O_6$: C, 54.07; H, 7.09; N, 11.83. Found: C, 54.77; H, 7.37; N, 11.85.

Neutralization equivalent Calcd.: 355. Found: 349, determined by anhydrous titration with sodium methoxide (11); 365, determined by anhydrous titration with perchloric in acetic acid (12).

N^{im}-t-Butyloxycarbonyl-N^{α}-benzyloxycarbonyl-L-histidine

Compound **1** was prepared similarly to the above compound on reaction of N^{α}-benzyloxycarbonyl-L-histidine (3) with *t*-butyloxycarbonyl azide in presence of MgO. Yield of amorphous solid 50%; m.p. 80° (starts to soften slowly at 55°); $[\alpha]_D^{23}$ +16.5 (*c* 1, methanol).

Anal. Calcd. for $C_{19}H_{23}N_3O_6$: C, 58.60; H, 5.95; N, 10.79. Found: C, 59.29; H, 5.75; N, 11.13.

Neutralization equivalent Calcd.: 389. Found: 380 (12) and 383 (11).

N^{im}-t-Butyloxycarbonyl-L-histidine N-Carboxylanhydride Hydrochloride (2)

To a solution of N^{im}-*t*-butyloxycarbonyl-N^{α}-benzyloxycarbonyl-L-histidine (**1**) (1.1 g, 2.8 mmol) in 10 ml of dioxane, thionyl chloride (0.64 ml, 8.5 mmol) was added. The mixture was then stirred at room temperature when the anhydride hydrochloride started to precipitate from the reaction mixture after 30 min. Stirring was effected for an additional 4 h. The product was filtered, and washed with dioxane and ether. It was then suspended in dry acetone, stirred for 15 min, and absolute ether was added. Compound **2** was filtered, washed with ether, and dried *in vacuo* over P_2O_5 and NaOH. Yield 0.80 g (90%); m.p. 260–265° dec. (evolution of CO_2 starts slowly at 200 °C); $[\alpha]_D^{25}$ −34.0 (*c* 1.1, dimethylformamide).

Anal. Calcd. for $C_{12}H_{16}O_5N_3Cl$: C, 45.36; H, 5.08; N, 13.23; Cl, 11.5. Found: C, 44.71; H, 4.81; N, 13.41; Cl, 10.97.

Mol. Wt. Calcd.: 317.6. Found: 330 (11), assuming the presence of two titrable groups per molecule.

Poly-N^{im}-t-butyloxycarbonyl-L-histidine (4)

The anhydride **2** (1 g, 2.5 mmol) was dissolved in dry acetone (75 ml) and dry silver oxide (1 g) was added. The mixture was stirred until it showed negative in a chloride test (~15 min) and then the AgCl and excess of Ag_2O was filtered, washed with acetone, and the combined filtrate and washings were evaporated in high *vacuo* (~30 °C) to yield the neutral anhydride **3**. The oily anhydride **3** was dissolved in absolute dioxane (10 ml) and triethylamine (0.004 ml, 28.8 μmol) was added as an initiator. The polymerization proceeded at room temperature with evolution of CO_2 and a slight precipitate of polymer **4** appeared. After 4 days absolute ether (50 ml) was added, and the polymer which was thus precipitated was filtered, washed with ether, and dried *in vacuo* over P_2O_5 and NaOH. Yield 0.47 g (80%); $[\alpha]_D^{25}$ −8.2 (*c* 0.88, dimethylformamide).

Anal. Calcd. for $(C_{11}H_{15}N_2O_3)_n$: C, 55.68; H, 6.37; N, 17.71. Found: C, 55.63; H, 6.46; N, 17.65.

Neutralization equivalent Calcd.: 237. Found: 242 (12).

The polymer **4** obtained as above is soluble in chloroform, dimethylformamide, acetic acid, 50% aqueous acetic acid, and methanol.

Poly-L-histidine Hydrobromide (5)

Poly-N^{im}-*t*-butyloxycarbonyl-L-histidine (0.24 g, 1 mmol) was dissolved in anhydrous trifluoroacetic acid (10 ml) and HBr gas was passed through the solution for 90 min. The trifluoroacetic acid was removed in high *vacuo* (30° C) and the residue was triturated with dry ether, ethyl acetate and petroleum–ether (b.p. 30–60 °C) and dried *in vacuo* over NaOH and P_2O_5. Yield 0.2 g (90%); $[\alpha]_D^{25}$ −19.3 (*c* 0.6, water).

Can. J. Chem. Downloaded from www.nrcresearchpress.com by 210.87.254.105 on 09/05/12
For personal use only.

Anal. Calcd. for $(C_6H_8N_3OBr)_n \cdot n/2\ H_2O$: C, 31.73; H, 4.00; N, 18.50. Found: C, 31.45; H, 4.10; N, 18.00.

Neutralization equivalent Calcd.: 227. Found: 218, determined by titration of the bromide ions (13).

N^{im}-t-Butyloxycarbonyl-L-histidine Dihydrochloride

N^{α},N^{im}-Di-*t*-butyloxycarbonyl-L-histidine was dissolved in 2 *N* HCl in dioxane and after 5–10 min a white precipitate was formed. After another 45 min the mixture was triturated with absolute ether, the precipitate filtered, washed with ether, and dried over NaOH and P_2O_5 *in vacuo*: yield 87%.

Anal. Calcd. for $C_{11}H_{19}N_3O_4Cl_2$: N, 12.80; Cl, 21.65. Found: N, 12.83; Cl, 21.21.

Mol. Wt. Calcd.: 328. Found: 330 (11) assuming the presence of three titrable groups per molecule, and 336 (13) assuming the presence of two titrable groups per molecule.

On reactions of N^{α},N^{im}-di-*t*-butyloxycarbonyl-L-histidine with HBr in TFA or in acetic acid the dihydrobromides of histidine were obtained as shown by paper electrophoresis and nonaqueous titrations.

1. V. DU VIGNEAUD and O. K. BEHRENS. J. Biol. Chem. **117**, 27 (1937).
2. (*a*) K. HOFMANN and H. YAJIMA. J. Amer. Chem. Soc. **83**, 2289 (1961); (*b*) M. WILCHEK, S. SARID, and A. PATCHORNIK. Biochim. Biophys. Acta, **104**, 616 (1965).
3. A. PATCHORNIK, A. BERGER, and E. KATCHALSKI. J. Amer. Chem. Soc. **79**, 6416 (1957).
4. (*a*) F. WEYGAND, W. STEGLICH, and P. PIETTA. Tetrahedron Lett. 3751 (1966); (*b*) F. WEYGAND, W. STEGLICH, and P. PIETTA. Chem. Ber. **100**, 3841 (1967).
5. (*a*) S. SHALTIEL. Biochem. Biophys. Res. Commun. **29**, 178 (1967); (*b*) F. CHILLEMI and R. B. MERRIFIELD. Biochem. **8**, 4344 (1969).
6. G. JAGER, R. GEIGER, and W. SIEDEL. Chem. Ber. **101**, 3537 (1968).
7. E. SCHNABEL, H. HERZOG, P. HOFFMAN, E. KLAUKE, and I. UGI. *In* Peptides. North-Holland, Publishing Company, Amsterdam, 1968. p. 91.
8. B. O. HANDFORD, T. A. HYLTON, K. T. WANG, and B. WEINSTEIN. J. Org. Chem. **33**, 4251 (1968).
9. (*a*) R. SCHWYZER, P. SIEBER, and H. KAPPELER. Helv. Chim. Acta, **42**, 2622 (1959); (*b*) L. A. CARPINO. J. Amer. Chem. Soc. **79**, 4427 (1957).
10. A. PATCHORNIK, A. BERGER, and E. KATCHALSKI. J. Amer. Chem. Soc. **79**, 5227 (1957).
11. S. J. FRITZ and N. M. LISKICKI. Anal. Chem. **23**, 589 (1951).
12. S. SHALTIEL and A. PATCHORNIK. J. Amer. Chem. Soc. **85**, 2799 (1963).
13. L. N. LAPIN and R. K. ZAMANOV. Zhur. Anal. Khim. **10**, 364 (1955).

Erratum: Synthesis of *p-O*-(Tetra-*O*-acetyl-α-D-glucopyranosyl)-penicillin G

T. L. NAGABHUSHAN AND C. G. CHIN

R & L Molecular Research Ltd., 8045 Argyll Road, Edmonton 82, Alberta

Received February 4, 1971

(Ref.: Can. J. Chem. **48**, 3097 (1970))

Canadian Journal of Chemistry, 49, 1581 (1971)

On page 3099 in the right hand column, the title and compound **7** should be "*p-O*-(tetra-*O*-acetyl-α-D-glucopyranosyl)-hydroxy-penicillin G". The word "hydroxy" is absent in the article.

Can. J. Chem. Downloaded from www.nrcresearchpress.com by 210.87.254.105 on 09/05/12
For personal use only.

Can. J. Chem. Downloaded from www.nrcresearchpress.com by 210.87.254.5 on 09/05/12
For personal use only.

Canadian Journal of Chemistry

Published by THE NATIONAL RESEARCH COUNCIL OF CANADA

VOLUME 49 MAY 15, 1971 NUMBER 10

Spectroscopie de masse des dérivés dans la série des dicéto-2,5 pipérazines. III[1]

KRZYSZTOF JANKOWSKI[2]

Département de Chimie, Université de Moncton, Moncton, Nouveau Brunswick

ET

LOUIS VARFALVY

Département de Chimie, Université de Montréal, Montréal, Québec

Reçu le 9 novembre, 1970

On rapporte le spectre de masse de la dibenzyl-3,6 dicéto-2,5 pipérazine. On propose et discute un mécanisme général pour expliquer les principaux modes de fragmentation.

The fragmentation of 3,6-dibenzyl, 2,5-diketo piperazine in the mass spectrometry is presented. The general mechanism is proposed and discussed.

Canadian Journal of Chemistry, 49, 1583 (1971)

Nos deux dernières publications (1, 2) dans cette série nous a amené aux quelques conclusions générales concernant la fragmentation des dicéto-2,5 pipérazines dans la spectroscopie de masse. La fragmentation de la dibenzyl-3,5 dicéto-2,5 pipérazine (**1**) (anhydride de la phénylalanine) a démontré quelques particularités. D'abord ce produit possède trois centres facilement ionisables: deux hétéroatomes et les noyaux benzéniques. Les trois ions moléculaires formés sont donc par ordre d'importance: **A**, **B**, **C**. On peut noter

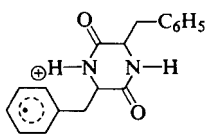

A

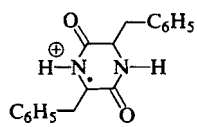

B

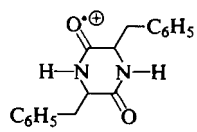

C

[1]Pour les parties I et II voir réfs. 1, 2.

[2]A qui il faut adresser toute la correspondence concernée.

TABLEAU 1. Intensité des fragments

m/e	I (%)	*m/e*	I (%)
296	0.75 P + 2 (2.93%)	66	0.7
295	5.49 P + 1 (21.06%)	65	10.1
294	25.54* P (100%)	63	1.9
204	2.2	57	5.4
203	15.4	56	0.2
176	3.6	55	1.0
175	28.7	52	1.0
148	0.5	51	3.4
147	3.0	50	0.7
146	0.9	44	0.3
132	1.7	43	0.4
131	2.7	42	1.9
130	2.6	41	1.7
128	2.0	39	4.0
121	1.4	30	1.1
120	14.1	29	2.3
119	1.7	28	9.1
118	2.6	27	1.2
117	1.5		
113	0.9		
112	2.5	Ions métastables	
105	0.8	46.6 intensité 0.3%	
104	3.3	47.4 intensité 0.2%	
103	0.8	140.3 intensité 0.2%	
93	1.8		
92	6.7		
91	*100.00*		
90	1.9		
89	2.2		
84	0.7		
79	0.6		
78	2.6		
77	7.1		

*Calculé (3) P + 1, 20.6; P + 2, 2.36%.

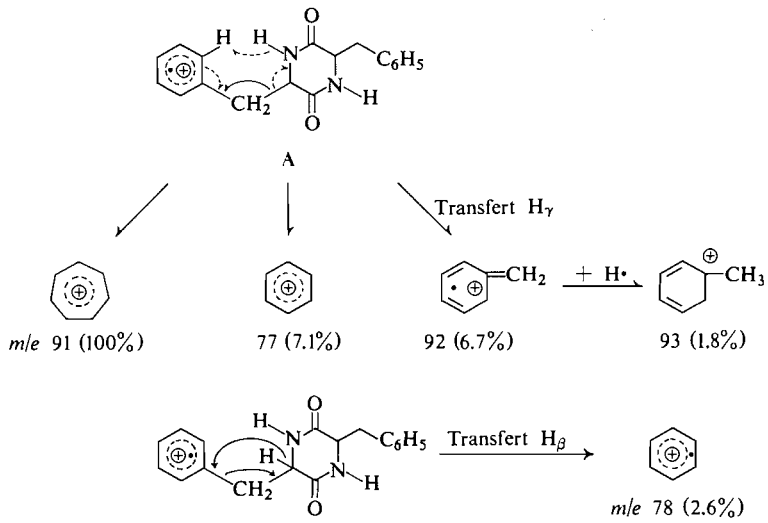

SCHÉMA 1

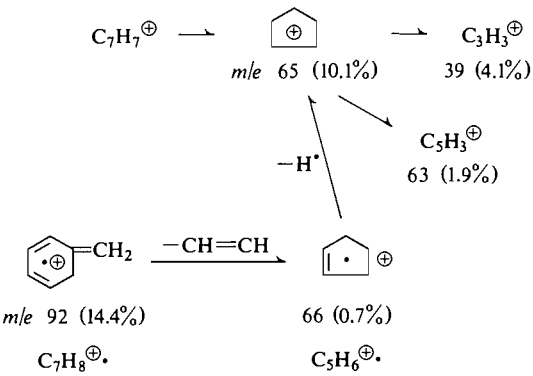

$M^* = 66^2/92 = 47.34$ (observé 47.4); $M^* = 65^2/91 = 46.4$ (observé 46.6)

SCHÉMA 2. *La tolérance + 0.1 ÷ 0.4 unité de masse pour le spectromètre semicirculaire a été suggérée (6).

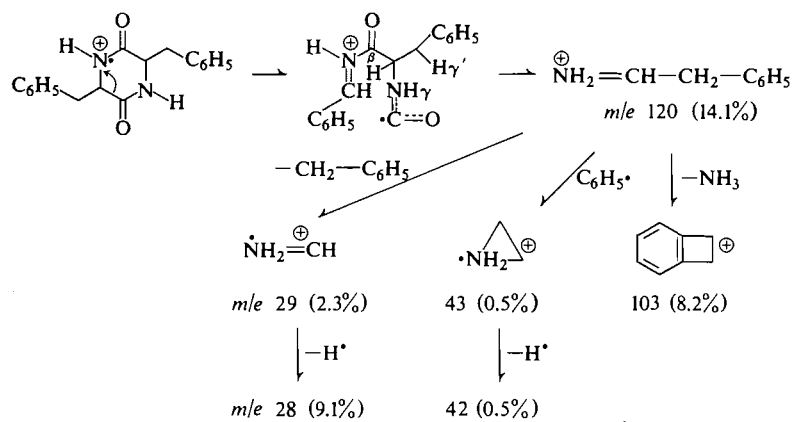

SCHÉMA 3

Can. J. Chem. Downloaded from www.nrcresearchpress.com by 210.87.254.5 on 09/05/12
For personal use only.

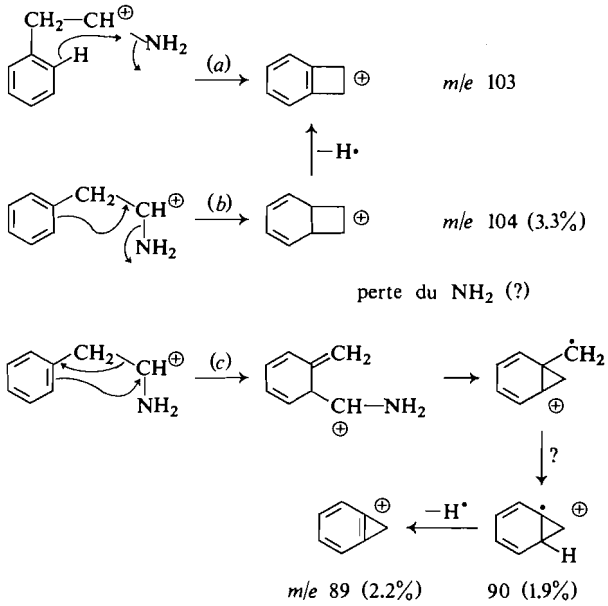

SCHÉMA 4

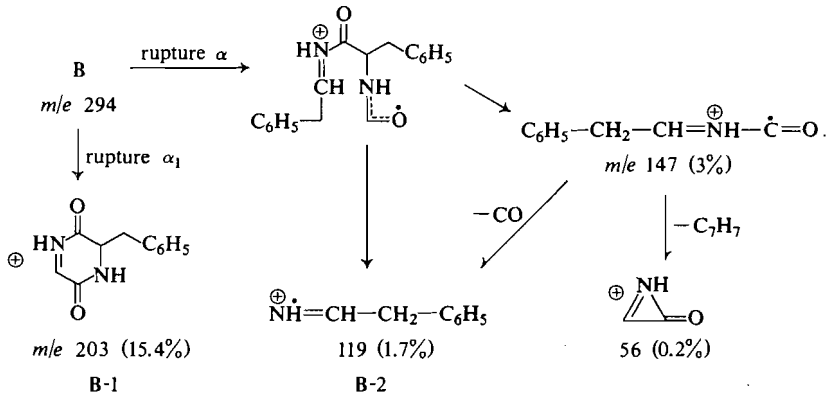

SCHÉMA 5

de nouveau, tout comme pour les anhydrides de la glycine et de l'alanine (1, 2) l'absence totale de fragment correspondant à $P^{\oplus}$-1, et la présence d'ion moléculaire assez abondant (25.5%) (tableau 1).

Ionisation du noyau benzénique conduit aux fragments les plus abondants. Cette ionisation conduit aux fragments connus (4) (schéma 1).

Le transfert de l'hydrogène γ a été supporté par l'obtention des ions 93 et 94 pour le produit **1** *N*-deutérié. On retrouve également le fragment $C_6H_7^{\oplus}$ (*m/e* 79, 0.6%) caractéristique pour le noyau substitué (5).

La fragmentation de schéma 2, élimination d'une molécule d'acéthylène à partir d'ion tropylium, a été supporté par les ions métastables.

Les fragmentations intenses à partir d'ion moléculaire **A** ont dérangé l'interpretation.

A partir de l'ion moléculaire **B** (ionisation de l'azote) on observe uniquement quatre fragments plus intense que 4%. D'abord, avec clivage de la liaison α on observe le transfert d'hydrogène β ou γ (ou γ'), schéma 3.

On peut envisager de différentes façons la formation du fragment à *m/e* 103; surtout qu'on donne les fragments à 104 ($C_8H_8^{\oplus}\cdot$), schéma 4.

Can. J. Chem. Downloaded from www.nrcresearchpress.com by 210.87.254.5 on 09/05/12
For personal use only.

Can. J. Chem. Downloaded from www.nrcresearchpress.com by 210.87.254.5 on 09/05/12
For personal use only.

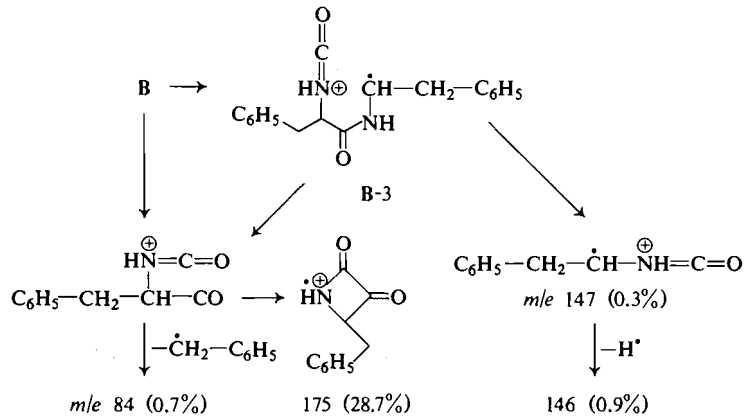

SCHÉMA 6

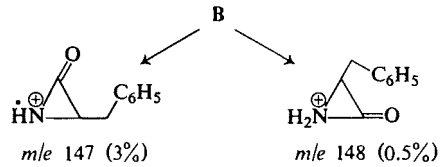

SCHÉMA 7

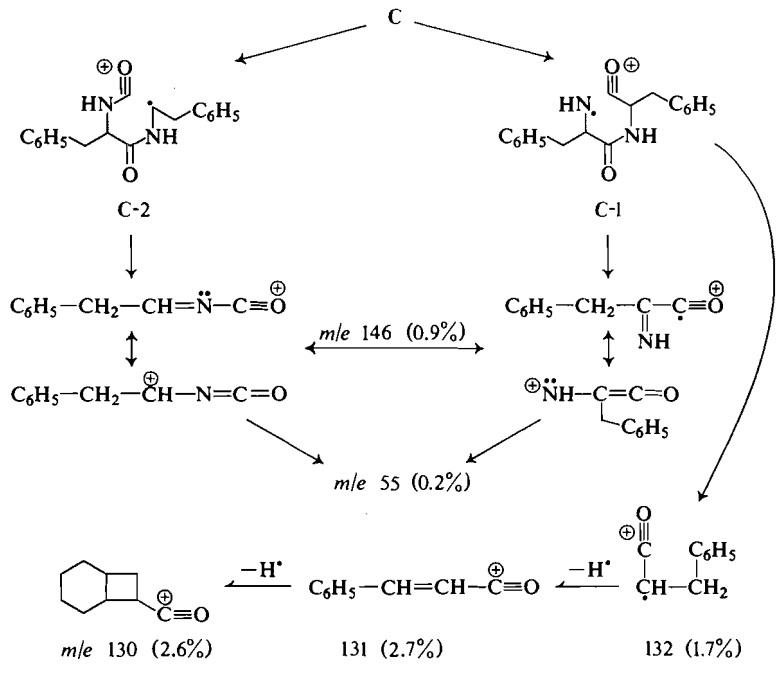

SCHÉMA 8

La fragmentation de schéma 5 par clivage de la liaison en α d'azote suivi de rupture simple de liaison.

Le fragment **B**-2 donne par la suite 118, 42, et 28 correspondant aux pertes du H·, C_6H_5·, ou radical benzyl. Les fragments 203, 119, et 118 sont spécifiques pour cette sorte du clivage. Le passage du fragment **B** au **B**-1 est supporté par le pic métastable donné à 140.3 (calculé 140.14).

Ouverture du cycle par clivage de la liaison β

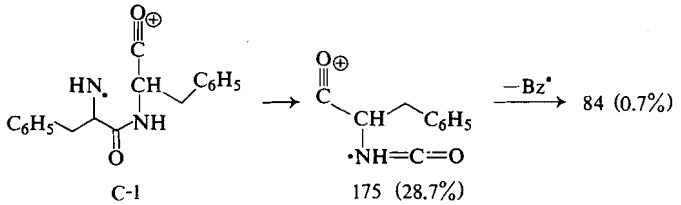

SCHÉMA 9

suivie de la rupture simple des liaisons ne donne aucun pic unique sauf le pic à *m/e* 175, schéma 6.

Les fragments $\overset{\oplus}{N}H{=}\dot{C}O$ ou $\overset{\oplus}{N}\dot{H}_2{=}CO$ (43 et 44) peuvent être également obtenu à partir de la structure **B**-3. Les clivages de la liaison en β de l'azote chargé donne naissance aux fragments déjà observés 147 et 148 (1, 2) suivi par les fragments avec une perte du H·, $\cdot CH_2C_6H_5$, schéma 7.

L'ionisation de l'oxygène du groupement carboxylique donne deux intermédiaires lesquels sont mis en évidence par les fragments de schéma 8.

La fragmentation 132, 131, 130 est analogue à celle pour les *N*-trifluoro acétyl phénylalanate de méthyle (7).

On peut former le fragment 175 à partir de la structure précédente, schéma 9.

Toutefois la fragmentation avec une perte du radical benzyl (203) et le fragment 147 peuvent être également obtenu à partir de cette structure. Une perte du CO, accompagnée par un transfert de charge, conduit à l'obtention du fragment à *m/e* 147, schéma 10.

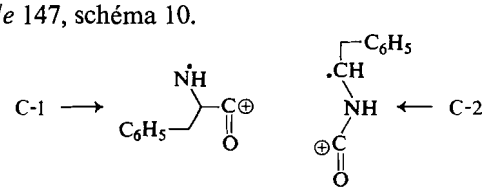

SCHÉMA 10

$\frac{M^{\oplus}}{2} + 1 = 148$

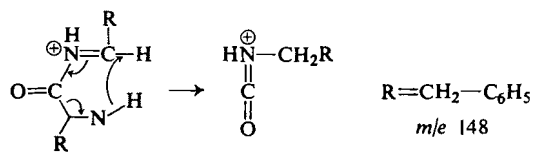

SCHÉMA 11

On a observé aussi le réarrangement qui donne un pic à *m/e* 57 + R. Ce réarrangement est également caractéristique pour les anhydrides de la glycine (à 58) et alanine (à 72) (1). La formule générale du réarrangement est donnée par schéma 11.

Le réarrangement analogue est observé pour les peptides et certains amides (8). Autres fragments non expliqués sont d'intensité plus petite que 3%.

Partie expérimentale

Les spectres de masse ont été enregistrés avec l'aide d'un appareil Hitachi RMU-6D et Picker–AEI MS-30 (200°, 70 eV). La dibenzyl-3,6 dicéto-2,5 pipérazine (**1**) p.f. 279–285° (9) a été obtenu par la cyclisation du NH_2-PhePheOC_2H_5 ou par la dimérisation du phénylalanate d'éthyle dans l'éthylène glycol (1). Le produit **1** a été libéré des fractions polymères par la recristalisation. La phénylalanine racémique a été utilisée. La présence des ions metastables a été prouvée par les méthodes habituellement utilisées.

Les auteurs remercient le Conseil National de Recherches du Canada pour l'aide apporté à ce travail sous forme de l'octroi de recherche (K.J.) A 5976. Nos remerciements vont également à Dr Yves Rousseau, Université de Montréal, Montréal, Québec, pour l'enregistrement de ces spectres.

1. K. JANKOWSKI et L. VARFALVY. Bull. Soc. Chim. Fr. Sous presse.
2. K. JANKOWSKI et L. VARFALVY. Tetrahedron, Sous presse.
3. K. BIEMANN. Mass spectrometry, application to organic chemistry. McGraw-Hill, New York, N.Y., 1962. p. 59.
4. R. SILVERSTEIN et G. BASSLER. Spectrometric identification of organic compounds. J. Wiley & Sons, New York, N.Y., 1967. p. 16.
5. Référence 3, p. 84.
6. Référence 3, 155.
7. Référence 3, 292.
8. Référence 3, 286 et 296.
9. E. FISCHER. Ber. **34**, 436 (1901).

Can. J. Chem. Downloaded from www.nrcresearchpress.com by 210.87.254.5 on 09/05/12
For personal use only.

Can. J. Chem. Downloaded from www.nrcresearchpress.com by 210.87.254.42 on 09/05/12
For personal use only.

Orientation in the Crossed Aldol Condensation of Chloral with Unsymmetrical Aliphatic Ketones

EBERHARD KIEHLMANN AND PUI-WAH LOO
Department of Chemistry, Simon Fraser University, Burnaby 2, British Columbia

Received November 9, 1970

The reactivity of a series of 14 aliphatic ketones in the crossed aldol condensation with chloral has been studied in glacial acetic acid and in dimethoxyethane. The reaction is irreversible and not accompanied by dehydration of the resulting 1,1,1-trichloro-3-hydroxy-4-alkanones. Except for butanone, condensation occurs preferentially at the least-hindered position of an unsymmetrical ketone. The α-methyl/α-methylene condensation product ratio obtained from ketones of the general formula RCH_2COCH_3 is higher in acetic acid than in dimethoxyethane as solvent when sodium acetate is used as catalyst. The steric size and chain length of the alkyl groups of methyl alkyl ketones have a marked effect on the reactivity of the α-methyl group toward chloral. Condensation at the α-methylene group results in the formation of diastereomeric ketols which epimerize under the preparative reaction conditions.

On a étudié la réactivité, dans l'acide acétique et dans le diméthoxyéthane, d'une série de quatorze cétones aliphatiques vis à vis le chloral et conduisant à des produits d'aldolisation mixtes. La réaction est irréversible et les trichloro-1,1,1 hydroxy-3 alcanones-4 formées ne se déshydratent pas. Dans le cas des cétones non symétriques la condensation se fait généralement au niveau de la position la moins empêchée; la butanone est toutefois une exception. Lorsque l'acétate de sodium est utilisé comme catalyseur les quantités de produits provenant d'une condensation sur le méthyle en α par rapport au méthylène α dans des cétones de formule générale RCH_2COCH_3 sont plus grandes dans l'acide acétique que dans le diméthoxyéthane. L'effet stérique et la longueur de la chaîne alkylée des méthylalkylcétones ont un effet marqué sur la réactivité du groupe méthyle sur le chloral. La condensation du chloral sur la position méthylénique conduit à la formation de cétols diastéréoisomères qui s'épimèrisent lorsque des conditions de réaction préparative sont utilisées.

Canadian Journal of Chemistry, 49, 1588 (1971)

Of the numerous reactions leading to the formation of new carbon-to-carbon bonds, the aldol condensation has been studied most extensively. The mechanism of this reaction, scope and limitations, experimental conditions and procedures, and a tabular survey (by reactants) of the literature data through August 1966 have been the subject of a recent comprehensive review by Nielsen and Houlihan (1). Although kinetic and deuterium exchange experiments in protic solvents have firmly established a two-step enolization–addition mechanism, frequently followed by dehydration, for both the acid-catalyzed and the base-catalyzed reaction (2), relatively little is known on the factors determining the orientation of the crossed aldol condensation of aldehydes with unsymmetrical aliphatic ketones, *i.e.*, the relative reactivities of the α-methyl group (C-1) and the α-methylene or α-methine group (C-3) of ketones of the general formula $CH_3COCHRR'$ (R = alkyl, R′ = H or alkyl) toward an aldehydic carbonyl group under kinetically controlled conditions (3, 4).

The reason for the paucity of systematic studies of the effects of ketone structure, aldehyde structure, catalyst, and solvent on the ratio of the isomeric crossed condensation products (ketol *c*/sum of ketols *a* and *b*, Scheme 1) appears to be threefold:

(*a*) The complexity of the reaction sequence makes it extremely difficult to obtain rate constants for all individual steps involved, especially since it has been shown by Noyce and Snyder (5) and Stiles *et al.* (6) that the condensation of certain aromatic aldehydes with butanone is reversible, and that ketol dehydration may be the product-determining step. Thus, neither the ratio of isomeric ketols nor the ratio of isomeric enones were found to be valid measures of the relative reactivities of the two α-carbons of an unsymmetrical ketone toward an aldehydic carbonyl group in these specific cases.

(*b*) The quantitative determination of the ratio of isomeric crossed aldol condensation products is further complicated by the formation of by-products due to self-condensation of aldehydes and ketones containing α-hydrogens. Since isomeric β-ketols differ very little in their spectro-

Can. J. Chem. Downloaded from www.nrcresearchpress.com by 210.87.254.42 on 09/05/12
For personal use only.

scopic properties, spectroscopic methods are not suitable for analytical measurements.

(*c*) Although the aldol addition step is believed to be preceded by enolization, few systematic studies have been reported on the equilibrium composition of enol and/or enolate mixtures formed from ketones of the general structure $CH_3COCHRR'$, and on the relative rates of enolization toward C-1 and -3. The extensive data published by House (7) on relative enolate stabilities in 1,2-dimethoxyethane permit qualitative conclusions on the orientation of base-catalyzed enolization in aprotic solvents. However, attempts to formulate similar rules for the orientation of enolization in protic solvents have met with limited success since the relative rates of deuteration or halogenation[1] at C-1 *vs.* C-3 of $CH_3COCHRR'$ have been found to depend not only on the structure of R and R′ but also on the catalyst and the solvent (10–13).

In the course of our studies on the synthesis and properties of 1,1,1-trichloro-2-hydroxy-4-alkanones we have found that the crossed aldol condensation of chloral with aliphatic ketones is effectively irreversible and not accompanied by dehydration or other side reactions (14, 15). The resulting β-ketols were found to be thermally stable thus permitting determination of the isomer distribution by gas chromatography. On account of these desirable characteristics, we undertook a systematic investigation of the effect of ketone structure and reaction conditions on the composition of the product mixture of isomeric 1,1,1-trichloro-2-hydroxy-4-alkanones in order to gain further insight into the factors determining the orientation in crossed aldol condensations of aldehydes with unsymmetrical aliphatic ketones under kinetically controlled conditions.

Results and Discussion

The condensation of chloral with aliphatic ketones has been reported to give 1,1,1-trichloro-2-hydroxy-4-alkanones in satisfactory yields in glacial acetic acid or propionic acid as solvent and in the presence (14) or absence (16) of the corresponding sodium or potassium carboxylate as catalyst; chloral hydrate is known to undergo the same reaction when acetic anhydride and sodium acetate are used as solvent and catalyst, respectively (15, 17).

In order to optimize the yield of the desired ketol and to minimize the formation of by-products, the condensation of chloral with 4-methyl-2-pentanone as model compound (14) was reinvestigated in a variety of solvent/catalyst systems as well as at various temperatures and reagent concentrations. Dipolar aprotic solvents (DMSO, DMF, and pyridine) and sodium acetate gave large quantities of unidentified black products together with small amounts (yield $< 5\%$) of the desired ketol **6***c*. Dimethyoxyethane (DME)/sodium acetate, acetic acid/sodium acetate and acetic acid (no added base catalyst) were found to be satisfactory to warrant their use for quantitative studies of ketol product ratios as a function of ketone structure.

Gas-chromatographic measurements of the product yield as a function of time (in the acetic acid/sodium acetate system) and graphic determination of the limiting slope at 20% completion of the reaction (for details, see Experimental, kinetic procedures) have shown that the limiting rate of product formation increases approximately linearly with increasing catalyst concentration (Fig. 1). The large positive intercept of this line and the observed ketol formation (although at a slower rate) in the absence of sodium acetate suggest that the reaction is also catalyzed by acetic acid. Although it was shown by further kinetic experiments that the initial rate of ketol formation increases as the temperature is raised (Fig. 2) and as the molar ratio ketone/chloral is increased from 1.00 to 1.50, the following reaction conditions were chosen for subsequent studies with other ketones in order to minimize discoloration due to by-product formation: molar ratio of ketone/chloral/solvent (HOAc or DME)/NaOAc 1.25:1.00:2.00:0.25, temperature 100°, and reaction time 52 h. No significant amounts ($\leq 0.5\%$ if any) of ketol dehydration products and only traces of other by-products were detected by v.p.c. analysis of the crude product mixtures under these conditions.

Kinetic control of the condensation reaction, as suggested by Reeve and Kiehlmann (14), was demonstrated by several types of experiments.

[1]Recent experiments by Rappe (8, 9) on the competitive acid-catalyzed halogenation and deuteration of butanone indicate that, contrary to the generally accepted mechanism, halogenation is not always preceded by rate-determining enolization, *i.e.*, literature reports on enolization kinetics as determined by halogenation experiments must be considered with caution!

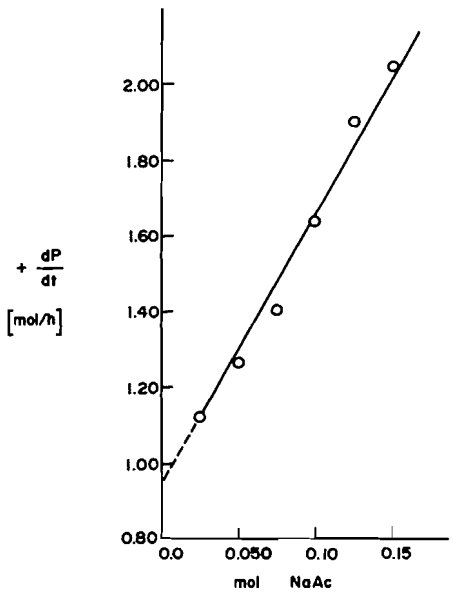

FIG. 1. Effect of catalyst concentration on limiting rate of product (**6***c*) formation. Initial reagent quantities: 0.80 mol chloral, 1.05 mol 4-methyl-2-pentanone, 0.20 mol **6***c*, 2.00 mol HOAc, temperature 100 ± 0.02 °C.

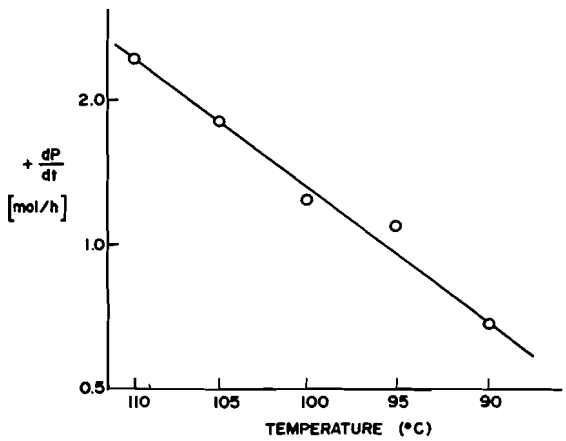

FIG. 2. Effect of temperature on limiting rate of product (**6***c*) formation. Initial reagent quantities: 0.80 mol chloral, 1.05 mol 4-methyl-2-pentanone, 0.20 mol **6***c*, 2.00 mol HOAc, 0.050 mol NaOAc.

involving three different unsymmetrical ketones and their respective chloral condensation products. When pure 1,1,1-trichloro-2-hydroxy-6-methyl-4-heptanone (**6***c*) was dissolved in glacial acetic acid and heated at 100° for 15 h in the presence of anhydrous sodium acetate, no 4-methyl-2-pentanone was formed as shown by v.p.c. of the reaction mixture on a Reoplex-400 column at 70°. Ninety percent of the starting material was recovered. No 1,1,1-trichloro-2-hydroxy-3-isopropyl-4-pentanone (isomeric condensation product) was detected in this experiment or in any crude product mixture resulting from the condensation of chloral with 4-methyl-2-pentanone.

Essentially the same result was obtained when mixtures of 1,1,1-trichloro-2-hydroxy-4-hexanone (**2***c*) and the two diastereomeric 1,1,1-trichloro-2-hydroxy-3-methyl-4-pentanones (**2***a* and *b*) containing the three isomeric ketols in various molar ratios were subjected to the preparative reaction conditions: no butanone was formed, 85% of the starting material was recovered after 15 h at 100°, and the ratio of the structural isomers, **2***c*/(**2***a* + **2***b*), remained constant within experimental error. However, the two diastereomeric ketols **2***a* and *b* were found to epimerize slowly via a common enol intermediate (Scheme 1). The v.p.c. analysis of the reaction mixture obtained from chloral and butanone under standard conditions, determination of the total yield of isomeric ketols (**2***a*, *b*, and *c*) formed and empirical comparison of the butanone peak areas before and after the reaction revealed a 94% yield of the desired condensation products based on the amount of ketone consumed. This product balance is considerably higher than the 80% yield reported by Reeve and Kiehlmann for the reaction of chloral with 4-methyl-2-pentanone (14) and provides further evidence that chloral-ketone condensations and the interpretation of the isomeric product ratios are not complicated by retrogression, dehydration, or other undesirable side reactions.

Finally, kinetic studies of the reaction of chloral with 2-heptanone have shown that the ratio of isomeric ketols (78:22) formed by condensation of chloral at C-1 and -3, respectively, does not change as the reaction proceeds (based on 16 kinetic assays taken over a period of 27 h which correspond to 42% completion of the reaction). Since 1,1,1-trichloro-2-hydroxy-4-nonanone (**5***c*) does not isomerize to 1,1,1-trichloro-2-hydroxy-3-(*n*-butyl)-4-pentanone (**5***a* and *b*) under the preparative reaction conditions, this result clearly demonstrates that the condensation reaction is irreversible and that the observed ratio of struc-

Can. J. Chem. Downloaded from www.nrcresearchpress.com by 210.87.254.42 on 09/05/12
For personal use only.

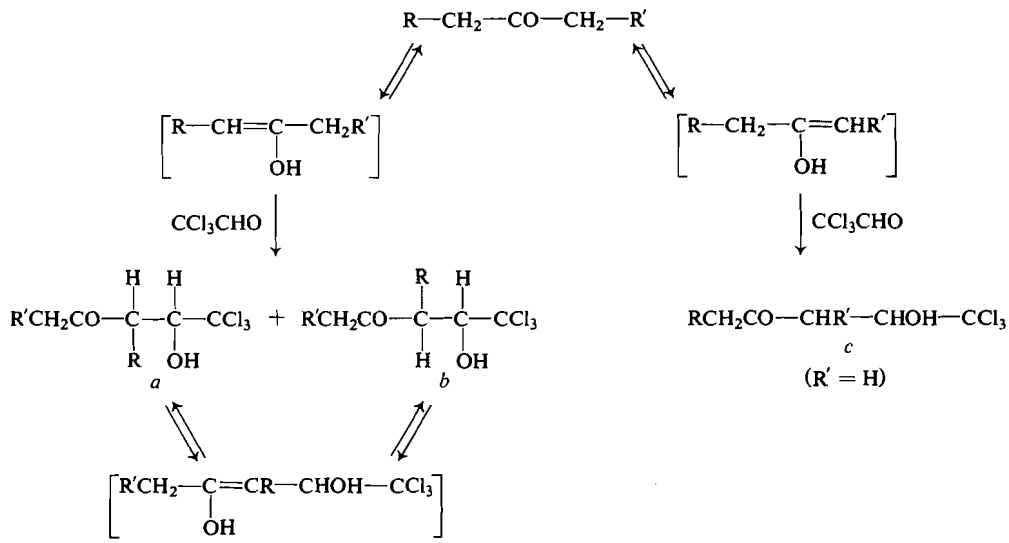

1 R = R′ = H
2 R = Me; R′ = H
3 R = Et; R′ = H
4 R = *n*-Pr; R′ = H
5 R = *n*-Bu; R′ = H
6 R = *i*-Pr; R′ = H
7 R = *t*-Bu; R′ = H
8 R = *i*-Bu; R = H
9 R = R′ = Me
10 R = R′ = Et
11 R = *n*-Pr; R′ = Me
12 R = Me; R′ = *n*-Pr
13 R − R′ = —$(CH_2)_3$—

SCHEME 1

TABLE 1. Percentage yields of condensation products formed from chloral and aliphatic ketones under standard conditions*

Ketone	Methylene condensation				Methyl condensation	
	Product structure†	Yield‡ (%)	Product structure†	Yield‡ (%)	Product structure	Yield‡ (%)
CH_3—CO—CH_3	—	—	—	—	**1***c*	31.0§
C_2H_5—CO—CH_3	**2***a*	18.0	**2***b*‖	22.3	**2***c*	31.7
CH_3—$(CH_2)_2$—CO—CH_3	**3***a*	8.0	**3***b*	4.2	**3***c*	40.8
CH_3—$(CH_2)_3$—CO—CH_3	**4***a*	9.3	**4***b*	7.0	**4***c*	41.8
CH_3—$(CH_2)_4$—CO—CH_3	**5***a*	13.0	**5***b*	5.8	**5***c*	53.3
$(CH_3)_2CH$—CH_2—CO—CH_3	—	—	—	—	**6***c*	61
$(CH_3)_3C$—CH_2—CO—CH_3	—	—	—	—	**7***c*	74
$(CH_3)_2CH$—$(CH_2)_2$—CO—CH_3	**8***a*	18.8	**8***b*	5.4	**8***c*	42.9
$(CH_3)_2CH$—CO—CH_3	—	—	—	—	—	38
$(CH_3)_3C$—CO—CH_3	—	—	—	—	—	48
C_2H_5—CO—C_2H_5	**9***a*‡	12.7§	**9***b*‖	14.3§	—	—
CH_3—$(CH_2)_2$—CO—$(CH_2)_2$—CH_3	**10***a*	8.9§	**10***b*	6.7§	—	—
CH_3—$(CH_2)_3$—CO—C_2H_5¶	**11***a*	5.0	**11***b*	3.6	—	—
	12*a*	14.4	**12***b*	13.0	—	—
Cyclohexanone	**13***a*‖	9.3‡	**13***b*‖	26.3‡	—	—

*Standard conditions: 1.25 mol ketone, 1 mol CCl_3CHO, 2 mol HOAc, 0.25 mol NaOAc, 100°, 52 h.
†*a*, Low-boiling diastereomer: *b*, high-boiling diastereomer.
‡Average figure of at least three runs (± 2% relative deviation) determined by v.p.c. of crude product mixture on a 5 ft × 1/8 in. SE-30 column at 120–140°.
§Corrected for statistical factor of 2 (true yields are twice the values given).
‖Configuration and conformation of these compounds have been discussed in ref. 15.
¶11, Product of condensation at C-4; 12, product of condensation at C-2.

Can. J. Chem. Downloaded from www.nrcresearchpress.com by 210.87.254.42 on 09/05/12
For personal use only.

TABLE 2. Condensation of chloral with aliphatic ketones.* Isomer distribution and product yields obtained in three solvent–catalyst systems

Ketone	Solvent	Catalyst	Weight (g)†	Structure*	Composition (%)†			Total yield§ (%)
					*a**‡	*b**‡	*c**	
CH_3COCH_3	HOAc	NaOAc	31.9	**1**	—	—	100	46
	DME	NaOAc	25.7	**1**	—	—	100	35
	HOAc	—	30.0	**1**	—	—	100	43
$C_2H_5COCH_3$	HOAc	NaOAc	39.6	**2**	25	31	44	52
	DME	NaOAc	23.0	**2**	24	38	38	28
	HOAc‖	—	20.0	**2**	7	8	75	24
$CH_3(CH_2)_2COCH_3$	HOAc	NaOAc	31.0	**3**	15	8	77	41
	DME	NaOAc	21.0	**3**	22	15	63	25
	HOAc‖	—	22.3	**3**	8	3	81	27
$CH_3(CH_2)_3COCH_3$	HOAc	NaOAc	36.0	**4**	16	12	72	40
	HOAc‖	—	24.2	**4**	10	5	76	26
$CH_3(CH_2)_4COCH_3$	HOAc	NaOAc	47.1	**5**	15	7	78	51
	DME	NaOAc	30.1	**5**	24	16	60	22
	HOAc‖	—	36.0	**5**	9	2	80	32
$(CH_3)_2CHCH_2COCH_3$	HOAc	NaOAc	37.8	**6**	—	—	100	50
	DME	NaOAc	22.5	**6**	—	—	100	30
	HOAc‖	—	24.0	**6**	—	—	96	31
$(CH_3)_3CCH_2COCH_3$	HOAc	NaOAc	48.4	**7**	—	—	100	62
	HOAc	—	39.0	**7**	—	—	100	49
$(CH_3)_2CH(CH_2)_2COCH_3$	HOAc	NaOAc	44.0	**8**	28	8	64	50
	HOAc	—	26.8	**8**	20	3	77	30
$(CH_3)_2CHCOCH_3$	HOAc	NaOAc	22.2	—	—	—	100	34
	HOAc	—	16.2	—	—	—	100	24
$(CH_3)_3CCOCH_3$	HOAc	NaOAc	29.7	—	—	—	100	44
	HOAc	—	24.0	—	—	—	100	34
$C_2H_5COC_2H_5$	HOAc	NaOAc	31.5	**9**	47	53	—	43
	DME	NaOAc	25.8	**9**	43	57	—	29
	HOAc	—	9.3	**9**	51	49	—	13
$CH_3(CH_2)_2CO(CH_2)_2CH_3$	HOAc	NaOAc	20.3	**10**	57	43	—	21
	HOAc	—	6.5	**10**	64	36	—	7
$CH_3(CH_2)_3COC_2H_5$¶	HOAc	NaOAc	23.6	**11**	14	10	—	26
	HOAc	NaOAc		**12**	40	36	—	
	HOAc	—	10.5	**11**	20	12	—	12
	HOAc	—		**12**	37	31	—	
Cyclohexanone	HOAc	NaOAc	43.6	**13**	26	74	—	43
	DME	NaOAc	30.7	**13**	23	77	—	29
	HOAc	—	0	**13**	—	—	—	0

*Scheme 1.
†Crude product obtained from 0.25 mol CCl_3CHO, 0.313 mol of ketone, 0.50 mol of solvent, and 0.0625 mol NaOAc (if any) after 52 h at 100°; analyzed by v.p.c. on a 5 ft × 1/8 in. SE-30 column (120-140°).
‡*a*, Low-boiling diastereomer: *b*, high-boiling diastereomer.
§Total yield of all isomeric condensation products ($a + b + c$) after purification by high-vacuum distillation (or one recrystallization in those cases where *c* is the only product) based on chloral.
‖Sum of composition data < 100% because of partial product decomposition.
¶**11**, Product of condensation at C-4; **12**, product of condensation at C-2.

turally isomeric ketols reflects the relative reactivities of the α-methylene and the α-methyl group of 2-heptanone toward chloral.

On the basis of these preliminary results, the orientation in the crossed aldol condensation of chloral with 14 aliphatic ketones was studied by quantitative determination of the ratios of isomeric ketols formed under standard conditions of time, temperature, and reagent concentration before completion of the reaction. The results are summarized in Tables 1 and 2.

Although the methyl condensation products of all ketones listed (except **7***c*) have been described in the literature (14–19), the formation and separation of diastereomeric products resulting from the condensation of chloral at the α-methylene group of butanone, 3-pentanone, and cyclohexanone was not reported until 1969 (15). In agreement with the results of configurational and hydrogen-bonding studies reported for these three ketones (15), the low-boiling isomer of each diastereomeric pair (designated "*a*") listed in Tables 1 and 2 has been found to exhibit strong intramolecular hydrogen bonding. The melting points reported by Caujolle *et al.* (17) for the methylene condensation products of butanone, 3-pentanone, and cyclohexanone with chloral indicate that these authors had obtained only the

Can. J. Chem. Downloaded from www.nrcresearchpress.com by 210.87.254.42 on 09/05/12
For personal use only.

Can. J. Chem. Downloaded from www.nrcresearchpress.com by 210.87.254.42 on 09/05/12
For personal use only.

high-melting (and less volatile) diastereomer in pure form. Although Mastagli and de Champs (19) have recently described a "chelated" and a "non-chelated" isomer of 1,1,1-trichloro-2-hydroxy-3-methyl-4-pentanone (**2***a* and *b*), they have characterized the methylene condensation products of chloral with 2-pentanone and 2-hexanone, respectively, as homogeneous liquids and thus failed to detect the presence of two diastereomers in each case. The same applies to the single chloral-butanone condensation product described by Baluja *et al.* (18). We conclude from this analysis of the literature that **3***a*, **4***a*, **5***a*, **5***b*, **7***c*, **8***a*, **8***b*, **10***a*, **10***b*, **11***a*, **11***b*, **12***a*, and **12***b* are new compounds which have not been characterized before.

Analysis of the percentage yields of the various condensation products listed in Tables 1 and 2 reveals certain trends which permit qualitative conclusions to be drawn with respect to the reaction mechanism.

A comparison of the product yields obtained from the first four ketones in the homologous series $CH_3(CH_2)_nCOCH_3$ shows that methyl condensation becomes more facile as *n* increases from one (31.7% yield) to four (53.3%). Excepting butanone (*vide infra*), the same general trend of increasing reactivity with increasing alkyl chain length is observed for the α-methylene groups. Wamhoff and coworkers (20) have reported similar results for the enol content of acetoacetic esters substituted in the α- or γ-position by alkyl groups of varying chain lengths. They have explained this phenomenon by postulating a high density of σ-electrons at the end of a paraffin chain and delocalization of these electrons into the π-orbital of the enolic C=C double bond which leads to increasing resonance stabilization with increasing alkyl chain length. This analogy suggests that relative enol stabilities (and/or enolization rates) are a determining factor in the crossed aldol condensation of chloral with straight-chain aliphatic methyl ketones.

The effect of alkyl branching on the reactivity of the α-methyl group of aliphatic methyl ketones toward chloral confirms the above conclusion. The data of Table 1 show that the rate of condensation of chloral at the α-methyl group increases from R = *n*-propyl (41.8% yield) via isopropyl (61%) to *t*-butyl (74%) for CH_3COCH_2R, and from R′ = ethyl (31.7%) via isopropyl (38%) to *t*-butyl (48%) for CH_3COR'. Delocalization of the σ-electrons of the alkyl group leads to favorable resonance interaction with the enolic system, and the stability of the 1-enol increases in the indicated order. If one assumes that the energy of activation for the addition of chloral at the unhindered methylene carbon of the 1-enol changes insignificantly from one methyl ketone to another, increasing enol stability would be expected to lead to an increased overall condensation rate.

The observed reactivity sequence is in qualitative agreement with the order of acid-catalyzed deuteration rates reported by Rappe and Sachs (21) for alkyl-substituted methyl ketones but opposite to the order of base-catalyzed deuteration rates of the corresponding ketones (10, 12). We conclude that the mechanism of the acetate-catalyzed condensation of chloral with aliphatic ketones in glacial acetic acid has the characteristics of an acid-catalyzed reaction, and that the transition state of the initial enolization step closely resembles the intermediate enol (22) rather than a negatively charged enolate ion.[2]

It should be pointed out that these trends, as noted by Rappe and Sachs (21), are opposite to what would be predicted on the basis of hyperconjugative enol stabilization. We are presently studying deuteration rates of aliphatic methyl ketones under experimental conditions similar to those employed for the crossed aldol condensation in order to determine whether the formation of 1-enol is the rate-determining step in the enolization–addition sequence.

A qualitative comparison of the relative reactivities of the α-methylene group in ketones of the type CH_3COCH_2R indicates that in most cases the rate of chloral addition is comparable to or slower than the rate of enolization. The reactivity of the methylene group of monoalkyl-substituted acetones drops off rapidly with increasing bulk of the alkyl substituent, *e.g.*, from butanone (R = CH_3, 40.3% yield of ketol) via 2-pentanone (R = Et, 12.2%) to 4-methyl-2-pentanone (R = *i*-Pr, 0%) and 4,4-dimethyl-2-pentanone (R = *t*-Bu, 0%). 3-Methyl-2-butanone, the only 1,1-disubstituted acetone tested, reacts exclusively at the α-methyl group. Apparently the

[2]A study of the relative rates of base-catalyzed enolization of butanone led Warkentin and Tee (11) to suggest that even with bases as strong as $OD^{\ominus}$ in D_2O, the α-carbon does not bear negative charge at the transition state.

Can. J. Chem. Downloaded from www.nrcresearchpress.com by 210.87.254.42 on 09/05/12
For personal use only.

aforementioned electron-releasing effect of alkyl groups which leads to increased stabilization of the enol relative to the keto form with an increasing number of carbon atoms in the alkyl residue is superimposed on and swamped by a rate-retarding steric effect in the case of methylene condensation. The same rapid reactivity decrease, in the order shown above, has been reported by Rappe, Warkentin, and coworkers for the acid-catalyzed (21) and base-catalyzed (10,12) deuteration of the α-methylene carbon of methyl alkyl ketones in aqueous solution, and by Wesslén (23) for the acid-catalyzed condensation of formaldehyde at the α-methylene group of methyl alkyl ketones in glacial acetic acid as solvent. These authors have interpreted this behavior in terms of steric hindrance to enolization and of decreasing hyperconjugative stabilization of the "3-enol", $RCH{=}C(OH)CH_3$, with increasing substitution at the β-carbon of butanone.

The failure of the methylene group of 4-methyl-2-pentanone and 4,4-dimethyl-2-pentanone to react with chloral indicates that there is also severe steric hindrance to the addition of chloral at the methylene carbon. When the condensation of chloral with 4,4-dimethyl-2-pentanone was performed in deuterated acetic acid (CH_3COOD) and the condensation product was analyzed by mass spectrometry at 80 meV, a five-fold increase in the $(m + 1)/m$ intensity ratio (1.37) was observed for both the $C_5H_{11}^{\oplus}$ cation and the $(CH_3)_3CCH_2CO^{\oplus}$ acylium ion, relative to the corresponding ratio (0.072) measured for a product sample prepared in non-deuterated acetic acid. Thus deuterium exchange at the methylene group occurs at a measurable rate under the experimental conditions of the crossed aldol condensation. We conclude that both the enolization, as measured by deuteration rates, and the chloral addition step are slow, and that the addition step is rate-determining in the case of ketones with bulky alkyl substituents. The observation by Wesslén (23, 24) that acid-catalyzed deuteration of the methylene carbon of butanone in glacial acetic acid occurs faster than addition of formaldehyde at the same position provides further support for this interpretation. The finding that a significant amount of formaldehyde condenses at the methylene carbon of 4-methyl-2-pentanone (23) and the detection of a trace amount of the methylene condensation product of fluoral with the same ketone under comparable reaction conditions indicate that the overall condensation rate is also retarded by bulky substituents (CF_3, CCl_3) on the aldehydic carbon.

It can be seen from Table 1 that the condensation of chloral at the methylene carbon of the ethyl groups of butanone, 3-pentanone, and 3-heptanone, respectively, is especially facile. Warkentin and Barnett (12), who observed the same phenomenon for deuteration rates, have attributed this exceptionally high reactivity of the methylene group of butanone to a rate-accelerating polar effect of the alkyl group which "opposes the steric effect and is swamped by it in all the ketones except butanone". Our data extend this interpretation to other ethyl alkyl ketones and suggest that in these cases of minor steric hindrance to addition, the enolization step is product-determining. In all other cases, kinetic control favors formation of the least-substituted enol (7) and chloral addition at the least-substituted α-carbon.

The data listed in Table 2 show that similar reactivity trends are observed when the reactions are performed in glacial acetic acid without added base catalyst or in the aprotic solvent dimethoxyethane (DME).[3] In the latter case, the reaction proceeds at a slower rate and generally gives higher ratios of 3-condensation/1-condensation product which may be due to a change in mechanism. In the absence of a proton donor (acetic acid), chloral will not be activated toward nucleophilic addition by protonation of its carbonyl oxygen, and the condensation is likely to proceed via an enolate (rather than enol) intermediate. The lower overall yields and higher 1-condensation/3-condensation product ratios observed in glacial acetic acid without added sodium acetate cannot be meaningfully interpreted in mechanistic terms since the ketols, especially the methylene condensation products, were found to decompose slowly under these conditions.

In summary, our studies of the acetate-catalyzed crossed aldol condensation of chloral with aliphatic ketones in glacial acetic acid as solvent indicate that the following factors govern the rate and orientation of this reaction:

(*1*) The reaction is acid- and base-catalyzed, proceeds via an enol-like transition state, and

[3]Solvent effects on the orientation of the acid-catalyzed deuteration and bromination of unsymmetrical ketones have recently been discussed by Sachs and Rappe (25), and by Gaudry and Marquet (26).

Can. J. Chem. Downloaded from www.nrcresearchpress.com by 210.87.254.42 on 09/05/12
For personal use only.

chloral adds preferentially at the least-highly substituted α-carbon of unsymmetrical dialkyl ketones other than butanone.

(*2*) The rate of condensation at the α-methyl carbon of $CH_3CO(CH_2)_nCH_3$ increases with increasing chain length *n* and thus parallels the stability order of the corresponding 1-enols relative to the keto forms.

(*3*) The rate of condensation at the α-methylene carbon of CH_3COCH_2R decreases with increasing bulk of the alkyl substituent R as a result of steric hindrance to both enolization and rate-determining chloral addition.

(*4*) The rate of condensation at the α-methylene carbon of butanone and other ethyl alkyl ketones is unusually high due to special stabilization of the 2-enol $CH_3CH{=}C(OH)R$ by the polar effect of the methyl group which predominates in these cases over the rate-retarding steric effect.

Experimental

Melting points are uncorrected. The u.v. spectra were run in 95% ethanol using a Unicam SP-200 spectrometer. The n.m.r. spectra were recorded on a Varian A 56/60 spectrometer using TMS as internal standard and $CDCl_3$ as solvent. Chemical shifts are reported in τ units. All spectral measurements were performed at room temperature.

The v.p.c. analyses were carried out on a Varian Aerograph Model 1200-1 HY-FI III gas chromatograph using a 5 ft × 1/8 in. column packed with 5% SE-30 on Aeropak 30 (column temperature 120–140°) and nitrogen as carrier gas (35 ml/min). All quantitative estimates of the composition of product mixtures by g.l.c. analysis (Tables 1 and 2) are based on comparison of integrated peak areas obtained for the various components of a crude product mixture with those obtained for standard mixtures prepared from the pure components. The v.p.c. peak areas were measured by a disc chart integrator. For the purpose of analysis and identification, pure samples of all compounds (except **11***b*) were isolated by fractional distillation, crystallization, and/or liquid partition chromatography on silica (Mallinckrodt, Silicic Acid A.R. 100 Mesh, Chromatographic Grade).

Anhydrous chloral was prepared from the commercially available material (Matheson, Coleman and Bell; Chloral, Practical, Stabilized) by distillation from phosphorus pentoxide under dry nitrogen. All ketones were obtained from commercial sources and purified by fractional distillation. Glacial acetic acid (Baker and Adamson, U.S.P.) and anhydrous sodium acetate (Baker and Adamson, Reagent Grade) were used without further purification in all preparative experiments. For the kinetic studies, reagent grade acetic acid (Baker) was used, and the anhydrous sodium acetate was purified by heating at 160° for 2 h and storage in a desiccator.

Kinetic Procedures

A specific quantity of anhydrous sodium acetate, 4-methyl-2-pentanone (or 2-heptanone), glacial acetic acid, and anhydrous chloral was weighed into each of a series of 10–20 10-ml ampules under the exclusion of atmospheric moisture. The ampules were immediately sealed and immersed in a constant-temperature oil bath (±0.02°). Timing was started after 1 min of temperature equilibration. At room temperature, no discernible reaction was found to occur inside the ampule over a period of 10 days.

Ampules were withdrawn from the oil bath at appropriate time intervals and immediately chilled in ice water. Each sample was then quantitatively transferred and rinsed with chloroform into a 50-ml calibrated volumetric flask which was allowed 2 h to reach temperature equilibrium (23.0 ± 0.01°) before filling up to the mark. Using a 10-μl syringe, at least three aliquots of 5.0 ± 0.02 μl each were withdrawn from each volumetric flask for v.p.c. analysis. In each case, the average reading of all integrated peak areas was used to determine graphically the product yield by comparison with a calibration curve prepared under the same experimental conditions using known quantities of product. The limiting rate of product formation at 20% completion was determined graphically from a plot of the product yield *vs.* reaction time. (The peak area *vs.* concentration plot was found to deviate from linearity at product concentrations corresponding to less than 13% yield.)

Condensation of Chloral with Ketones

Reaction Procedure

A mixture of 36.9 g (0.25 mol) of anhydrous chloral, 0.31 mol of ketone, 5.1 g (0.063 mol) of anhydrous sodium acetate (where required), and 0.50 mol of glacial acetic acid or dimethoxyethane was heated at 100° for 52 h in a 500-ml flask equipped with reflux condenser and calcium chloride tube. Solvent, unreacted starting materials, and acetic acid were removed by vacuum distillation. The residue was dissolved in 200 ml of ether and 100 ml of water, and the layers were separated. The aqueous layer was extracted with 50 ml of ether, and the combined organic extracts were washed with 5% aqueous sodium bicarbonate solution and water and dried with anhydrous magnesium sulfate. Evaporation of the ether gave the crude product quantities listed in Table 2 which were analyzed by v.p.c. as described before. The experiments performed in acetic acid in the absence of sodium acetate resulted in black crude product mixtures which were found by v.p.c. analysis to contain up to 10% of unidentified products.

Product Isolation and Purification

The single condensation product (Scheme 1, structure *c*) formed from chloral and acetone, 4-methyl-2-pentanone, 4,4-dimethyl-2-pentanone, 3-methyl-2-butanone, and 3,3-dimethyl-2-butanone, respectively, was isolated from the crude product mixture and purified by recrystallization from carbon tetrachloride and cyclohexane. In all other cases, *i.e.*, where mixtures of two, three, or four isomeric ketols were formed, small samples of the individual components were isolated by liquid partition chromatography on silica using 20% (by volume) petroleum ether (30–60°) in benzene as eluent. Larger quantities of the pure isomers melting above 30° were obtained by fractional distillation of the product mixture through a Vigreux

Can. J. Chem. Downloaded from www.nrcresearchpress.com by 210.87.254.42 on 09/05/12
For personal use only.

TABLE 3. Physical constants of 1,1,1-trichloro-2-hydroxy-4-alkanones

Structure (Q = —CHOH—CCl_3)	Melting point (°C)	Boiling point (°/mm)	Nuclear magnetic resonance chemical shift (τ value)				
			—*CH*OH—	—*OH*	—CO—*CH*QR	—CHQ—CH_2R	—*CH*R′—CO—
CH_3COCH_2Q (1*c*)	74–75	84–86/0.02	5.35	5.90	7.00	—	7.75
C_2H_5—CO—CH_2Q (2*c*)	56–56.5	88/0.02	5.35	5.85	7.01	—	7.47
CH_3—CHQ—CO—CH_3 (2*a*)	33.5–34.5	70/0.02	5.90	4.27	6.55	8.61	7.71
CH_3—CHQ—CO—CH_3 (2*b*)	59.5–60.5	81/0.02	5.31	6.25	6.79	8.65	7.71
CH_3—$(CH_2)_2$—CO—CH_2Q (3*c*)	51.5–53	85–90/0.04	5.33	5.93	7.01	—	7.50
C_2H_5—CHQ—CO—CH_3 (3*a*)	—	75–80/0.04	5.81	4.15	6.69	8.20	7.69
C_2H_5—CHQ—CO—CH_3 (3*b*)	—	80–85/0.04	5.45	6.09	6.93	8.17	7.75
CH_3—$(CH_2)_3$—CO—CH_2Q (4*c*)	41–42.5	99–101/.005	5.30	5.86	7.00		7.45
CH_3—$(CH_2)_2$—CHQ—CO—CH_3 (4*a*)	—	90–92/.005	5.90	4.20	6.50	8.21	7.79
CH_3—$(CH_2)_2$—CHQ—CO—CH_3 (4*b*)	—	95–97/.005	5.45	6.02	6.95	8.23	7.79
CH_3—$(CH_2)_4$—CO—CH_2Q (5*c*)	51.5–53.5	110/0.01	5.37	5.90	7.03	—	7.50
CH_3—$(CH_2)_3$—CHQ—CO—CH_3 (5*a*)	—	95/0.01	5.83	4.13	6.65	8.23	7.70
CH_3—$(CH_2)_3$—CHQ—CO—CH_3 (5*b*)	—	103/0.01	5.43	6.00	6.83	8.23	7.77
$(CH_3)_2$CH—CH_2—CO—CH_2Q (6*c*)	86–87	—	5.37	5.97	7.05	—	7.60
$(CH_3)_3$C—CH_2—CO—CH_2Q (7*c*)	109–109.5	—	5.38	6.01	7.05	—	7.62
$(CH_3)_2$CH—$(CH_2)_2$—CO—CH_2Q (8*c*)	78–79	111–114/0.02	5.35	5.89	7.01	—	7.50
$(CH_3)_2$CH—CH_2—CHQ—CO—CH_3 (8*a*)	—	92–94/0.02	5.86	4.05	6.55	8.30	7.70
$(CH_3)_2$CH—CH_2—CHQ—CO—CH_3 (8*b*)	52–54	105–108/0.02	5.50	5.95	6.90	8.31	7.73
$(CH_3)_2$CH—CO—CH_2Q	79.5–80.5	—	5.33	5.90	7.00	—	7.33
$(CH_3)_3$C—CO—CH_2Q	108.5–109	—	5.33	6.11	6.90	—	—
CH_3—CHQ—CO—C_2H_5 (9*a*)	37–38	65–66/0.01	5.89	4.17	6.53	8.61	7.33
CH_3—CHQ—CO—C_2H_5 (9*b*)	57.5–58.5	72–74/0.01	5.33	6.15	6.78	8.71	7.37
CH_3—CH_2—CHQ—CO—CH_2—C_2H_5 (10*a*)	—	81–83/0.05	5.83	4.05	6.73	8.31	7.40
CH_3—CH_2—CHQ—CO—CH_2—C_2H_5 (10*b*)	—	90–94/0.05	5.41	6.13	6.97	8.23	7.45
CH_3—$(CH_2)_3$—CO—CHQ—CH_3 (12*a*)	—	79–81/0.01	5.93	4.25	6.56	8.50	7.41
CH_3—$(CH_2)_3$—CO—CHQ—CH_3 (12*b*)	—	83–85/0.01	5.40	6.23	6.83	8.50	7.45
CH_3—$(CH_2)_2$—CHQ—CO—C_2H_5 (11*a*)	—	77–79/0.01	5.97	4.08	6.63	8.63	7.37
CH_3—$(CH_2)_2$—CHQ—CO—C_2H_5 (11*b*)	—	81–83/0.01	5.43	6.20	6.83	8.53	7.47
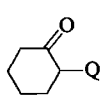 (13*a*)	43–44.5	110/0.04	6.03	3.62	6.95	—	—
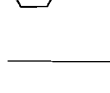 (13*b*)	101-102	120/0.04	4.99	6.37	6.93	—	—

column at high vacuum, v.p.c. analysis of each of the fractions collected, seeding of selected fractions with the appropriate pure compound and recrystallization from cyclohexane. Crystallization of **2***a*, **8***b*, 9*a*, and **13***a* was extremely slow and inhibited by small amounts of impurities. The mixture of four isomeric ketols (**11***a*, **11***b*, **12***a*, **12***b*) formed from chloral and 3-heptanone was resolved by partition chromatography on silicic acid using 10% petroleum ether (65–110°) in benzene as eluent. Although this procedure gave only **11***a*, **12***a*, and **12***b* in pure form, the n.m.r. of a fraction containing 65% **11***b* and 35% **12***b* allowed a satisfactory structure assignment for this isomer.

Physical Constants

The melting points, boiling points, and chemical shifts of the reaction products are summarized in Table 3. The 1,1,1-trichloro-2-hydroxy-4-alkanones were found to exhibit two weak u.v. absorption maxima at 210–219 (ε 40–60) and 275–285 mμ (ε 25–30). 1,1,1-Trichloro-2-hydroxy-6-methyl-4-heptanone showed an additional peak at 239 mμ (ε 32).

Reaction of Chloral with 2,4-Dimethyl-3-pentanone

Following the standard condensation procedure, 3.6 g of crude product was obtained from 0.31 mol (35.6 g) of 2,4-dimethyl-3-pentanone and the appropriate quantities of chloral, acetic acid and sodium acetate. The product mixture which exhibited five major peaks in the gas chromatogram was not further investigated since none of the desired condensation product was detected by spectroscopic analysis.

Epimerization of Diastereomeric 1,1,1-Trichloro-2-hydroxy-4-alkanones

A mixture of 5.50 g (0.025 mol) of 1,1,1-trichloro-2-hydroxy-3-methyl-4-pentanone (**2***a*), 0.43 g (0.0060 mol) of butanone, 0.51 g (0.0063 mol) of anhydrous sodium acetate and 3.00 g (0.050 mol) of glacial acetic acid was heated at 100° for 15 h. The standard work-up procedure gave a product mixture containing the two diastereomeric ketols **2***a* and *b* in the approximate ratio 4:5 but no detectable amount of the structural isomer **2***c* (analysis by v.p.c.). Application of the above procedure to **2***b* (instead of **2***a*) gave the same result. When 1,1,1-trichloro-2-hydroxy-4-hexanone (**2***c*) was subjected to these reaction conditions, v.p.c. analysis of the product did not disclose any **2***a* or *b*. The same type of experiment was performed with **9***a*, **9***b*, **13***a*, **13***b*, **5***c*, and mixtures of **5***a* and *b*, respectively, replacing **2***a* in the above procedure. In all cases, epimerization of diastereomers but no structural isomerization was observed.

The following specific heats of combustion (kcal/g) were determined calorimetrically to estimate relative thermodynamic product stabilities (product structure in parentheses): 3.66 (**2***a*), 3.63 ± 0.01 (**2***b*), 3.73 ± 0.03 (**2***c*), 4.20 ± 0.03 (**9***a*), and 4.15 ± 0.02 (**9***b*).

The authors wish to express their gratitude to the National Research Council of Canada for providing the financial support for these investigations, and to Miss N. McGillivray for her assistance in the performance of laboratory experiments.

1. A. T. Nielsen and W. J. Houlihan. The aldol condensation. *In* Organic reactions, **16** (1968).
2. Reference 1, pp. 4–11.
3. A. T. Nielsen and E. B. W. Ovist. J. Am. Chem. Soc. **76**, 5165 (1954).
4. J. E. Dubois. Ann. Chim. (Paris), **6**, 406 (1951).
5. D. S. Noyce and L. R. Snyder. J. Am. Chem. Soc. **80**, 4033 (1958).
6. M. Stiles, D. Wolf, and G. V. Hudson. J. Am. Chem. Soc. **81**, 628 (1959).
7. H. O. House. Record of Chem. Prog. **28**, 99 (1967).
8. C. Rappe. Acta Chem. Scand. **22**, 1359 (1968).
9. C. Rappe. Acta Chem. Scand. **21**, 1823 (1967).
10. C. Rappe and W. H. Sachs. J. Org. Chem. **32**, 4127 (1967).
11. J. Warkentin and D. S. Tee. J. Am. Chem. Soc. **88**, 5540 (1966).
12. J. Warkentin and C. Barnett. J. Am. Chem. Soc. **90**, 4629 (1968).
13. M. Gaudry and A. Marquet. Bull. Soc. Chim. Fr. 1849 (1967).
14. W. Reeve and E. Kiehlmann. J. Org. Chem. **31**, 2164 (1966).
15. E. Kiehlmann and P. W. Loo. Can. J. Chem. **47**, 2029 (1969).
16. F. L. Breusch and H. Keskin. Arch. Biochem. Biophys. **18**, 305 (1948).
17. F. Caujolle, P. Couturier, and C. Dulaurans. Bull. Soc. Chim. Fr. **17**, 19 (1950).
18. G. Baluja, A. M. Municio, and S. Vega. Anales Real Soc. Esp. Fis. Quim. (Madr.), Ser. B, **60**, 639 (1964).
19. P. Mastagli and F. de Champs. C.R. Acad. Sci. Ser. C, **270**, 1247 (1970).
20. H. Wamhoff, G. Höffer, H. Lander, and F. Korte. Justus Liebigs Ann. Chem. **722**, 12 (1969).
21. C. Rappe and W. H. Sachs. J. Org. Chem. **32**, 3700 (1967).
22. C. Rappe. Acta Chem. Scand **20**, 376 (1966).
23. B. Wesslén. Doktorsavh. Chalmers Tek. Hoegsk. **82** (1968).
24. B. Wesslén. Acta Chem. Scand. **23**, 1017 (1969).
25. W. H. Sachs and C. Rappe. Acta Chem. Scand. **22**, 2031 (1968).
26. M. Gaudry and A. Marquet. C.R. Acad. Sci. Ser. C, **268**, 1174 (1969); Bull. Soc. Chim. Fr. 4169 (1969).

Can. J. Chem. Downloaded from www.nrcresearchpress.com by 210.87.254.42 on 09/05/12
For personal use only.

Can. J. Chem. Downloaded from www.nrcresearchpress.com by 210.87.254.105 on 09/05/12
For personal use only.

Studies on Acyl Alkyl Diimides

THOMAS R. LYNCH,[1] FREDERICK N. MACLACHLAN, AND YUM KUEN SIU[2]
Chemistry Department, Scarborough College, University of Toronto, West Hill, Ontario

Received November 26, 1970

A number of acyclic acyl alkyl diimides have been obtained by oxidation of the corresponding alkyl hydrazides. A new method for the synthesis of α-cyanoalkyl hydrazides, the reaction of acid hydrazides with ketones in the presence of sodium cyanide, has been explored. All the acyl alkyl diimides so obtained exhibit a medium to weak i.r. band at *ca.* 1550 cm^{-1}; evidence supporting the assignment of this band to the —N=N— stretch is given. The results of oxidation of 5-methyl and 5-phenyl-pyrazolidin-3-one are reported, together with the synthesis and oxidation of tetrahydro-6-methyl-3(2*H*)-pyridazinone.

Par l'intermédiaire de l'oxydation des hydrazides alkylées correspondantes, on a obtenu un certain nombre de diimides acycliques substituées par des groupes acylés et alkylés. On a de plus exploré une nouvelle méthode de synthèse d'hydrazides substituées par des groupes α cyanoalkyles qui fait appel à la réaction d'hydrazides d'acides avec des cétones en présence de cyanure de sodium. Toutes les diimides ainsi préparées montrent, dans leur spectre i.r., une bande légèrement faible à environ 1550 cm^{-1}; on présente des données permettant d'attribuer cette bande à la vibration de fréquence du groupe —N=N—. On rapporte aussi les résultats obtenus lors de l'oxydation des méthyl-5 et phényl-5 pyrazolidinone-3 ainsi que la synthèse et l'oxydation de la tétrahydro méthyl-6 pyridazinone 3(2*H*).

Canadian Journal of Chemistry, 49, 1598 (1971)

Introduction

Whereas the chemistry of diacyl and dicarbalkoxy diimides and related compounds have been widely investigated (1), that of acyl alkyl diimides has received less attention since the early studies of Wieland *et al.* (2). Chaco and Rabjohn have synthesized the carbethoxy alkyl diimides **1** and **1***a* by oxidation of the corresponding hydrazides with bromine water, and silver oxide in benzene, respectively (3). The diimide **1** tautomerized readily to the corresponding hydrazone at room

R—N=N—CO_2Et

1 R = *n*-Bu

1*a* R = *t*-Bu

temperature, whereas **1***a*, lacking an α-H, decomposed only on heating to 170°; both diimides exhibited n–π* bands in their u.v. spectra at *ca.* 375 mμ. Hoffmann and Eicken (4) have found lead tetraacetate (LTA) to be a convenient reagent for oxidation of benzohydrazides to the corresponding diimides, a number of which were obtained as unstable red oils, with n–π* bands of unspecified extinction coefficient in the 395–420 mμ region, but no further spectral information was given. The alkoxide-induced decomposition of these (4) and of benzoyl *t*-butyl diimide (5) have been investigated, carbanionic intermediates being suggested, with the possible additional intervention of radicals in the latter case. In the present work we reported on the synthesis of a variety of acyl alkyl diimides, including some acetyl cases which have not previously been reported, together with some discussion on their i.r. and u.v. spectra.

Results and Discussion

The hydrazides **2***a*, **2***b*, **4***a*, and **4***b* were synthesized by catalytic hydrogenation of the corresponding hydrazones over 5% Pt/C in alcohol (6). Reaction of a 4.1 *M* excess of phenyl-

PhCONHNHR → PhCON=N—R

2 **3**

AcNHNHR → AcN=N—R

4 **5**

R	R
a Et	*e* C(CN)*cyclo*-C_5H_{10}
b *i*-Pr	*f* $C(CN)Me_2$
c CMe_2Ph	*g* C(CN)MeEt
d *t*-Bu	

magnesium bromide with benzoyl acetonehydrazone in refluxing ether/benzene for 2.5 days, according to the method of Yale *et al.* (7), gave the hydrazide **2***c* in 25% yield. Attempts to

[1]To whom correspondence should be addressed.
[2]Taken in part from the M.Sc. Thesis of Y.-K. Siu, University of Toronto, Toronto, Ontario, 1970.

Can. J. Chem. Downloaded from www.nrcresearchpress.com by 210.87.254.105 on 09/05/12
For personal use only.

extend this reaction to obtain the hydrazides **2***d*, **4***c*, and **4***d*, using phenylmagnesium bromide, methyl lithium, or methylmagnesium bromide were unsuccessful.

The benzoyl diimides **3***a–c* and the acetyl diimides **5***a* and *b* were obtained by LTA oxidation of the corresponding hydrazides essentially according to the method of Hoffmann and Eicken. The diimides thus obtained were, with the exception of **3***c*, unstable red oils, which tautomerized to the hydrazones on standing at room temperature, the acetyl cases being more unstable in this regard than the benzoyl examples. However, satisfactory n.m.r., i.r., and u.v. spectra could be obtained (*vide infra*). As expected, **3***c* was more stable, an analytically pure sample being obtained by two molecular distillations at 70°/0.5 mm.

Azobisnitriles have been widely investigated as sources of free radicals, due to their inability to tautomerize, and their clean decomposition on mild heating. We therefore attempted the synthesis of some acyl α-cyanoalkyl hydrazides by modification of the method of Overberger *et al.* (8) for the preparation of symmetrical α-cyanoalkyl hydrazines. Reaction of benzohydrazide and acetohydrazide with cyclohexanone, acetone, and butanone, in the presence of aqueous sodium cyanide and 1 equiv of mineral acid, gave the hydrazides **2***e–g* and **4***e–g* respectively, in yields of 50–88%. Compound **2***f* has previously been prepared by addition of liquid hydrogen cyanide to the corresponding hydrazone (9). Oxidation of **2***e* and *f* was conveniently accomplished with yellow mercuric oxide; the acetylhydrazides **4***e* and *f* were resistant to this reagent, but could be oxidized with activated manganese dioxide (10) in methylene chloride. Of these four diimides so formed, only **3***e* was obtained analytically pure, being isolated as yellow–orange crystals, m.p. 66.5–67.5°. Diimide **3***f* was obtained spectroscopically pure as an oil, but could not be obtained crystalline; attempted molecular distillation appeared to cause decomposition. Samples of **4***e* and *f* obtained by oxidation either with manganese dioxide at 25°, or with *N*-chlorobenzotriazole at −20°, in methylene chloride, exhibited in their i.r. spectra an additional carbonyl band at *ca.* 1710 cm^{-1} of varying intensity. Also, during manganese dioxide oxidations of **4***e* and *f*, mild effervescence of a gas was observed, suggesting that some decomposition was occurring on the surface of the metal oxide.[3]

We have also examined the oxidation of some cyclic hydrazides. Kent and Anselme (12) observed that mercuric oxide oxidation of **8** afforded styrene, and assumed, without identification, the intermediacy of the substituted 1-pyrazolin-3-one **9**. In our hands, LTA oxidation of **8** at −70° afforded a yellow solution with $\lambda_{max}(CH_2Cl_2)$ 430 mμ, consistent with the presence of **9**. When allowed to warm up, this absorption disappeared, and styrene, as the dibromide, was isolated. Similar oxidation of **10** (13), gave a solution with $\lambda_{max}(CH_2Cl_2)$ 443 mμ, consistent with the presence of **11**; however, attempts to isolate **11**, or trap it with 2,3-dimethylbutadiene or diphenylketene (14) were unsuccessful. After completion of our work in this area, Nagata and Kamata (15) reported the successful isolation of **13** and **15**, as unstable solids, having $\lambda_{max}(CH_2Cl_2)$ 448 (ε 190), 436 (ε 251), 445 (sh), and 460 mμ (sh), respectively, in agreement with our values.

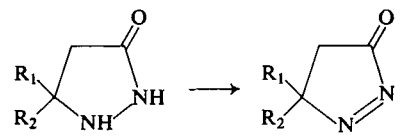

8 R_1 = Ph; R_2 = H
10 R_1 = Me; R_2 = H
12 R_1, R_2 = Me
14 R_1, R_2 = H

9 R_1 = Ph; R_2 = H
11 R_1 = Me; R_2 = H
13 R_1, R_2 = Me
15 R_1, R_2 = H

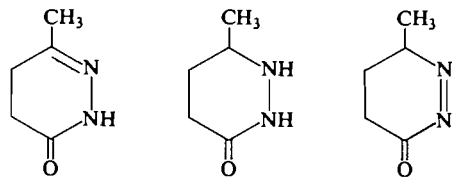

16 **17** **18**

Reduction of the previously known 4,5-dihydro-6-methyl-3(2*H*)-pyridazinone (**16**) (16), in methanol containing a slight excess of acetic acid occurred smoothly to give the previously unknown tetrahydro-6-methyl-3(2*H*)-pyridazinone (**17**), m.p. 71–72°. Oxidation of **17** with mercuric oxide at room temperature gave only **16**. Oxidation with LTA or with activated manganese

[3]While this manuscript was in preparation, the chlorine oxidation of hydrazides **2***e–g* and **4***e–g* to **3***e–g* and **5***e–g* respectively, was reported (11).

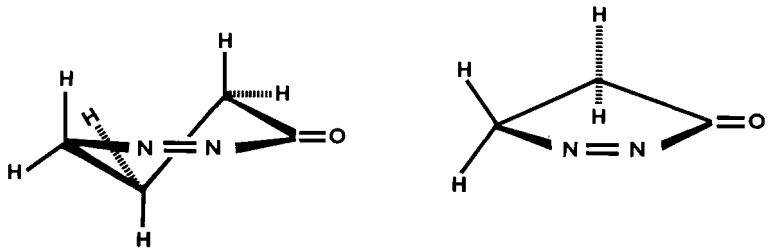

FIG. 1. Dihydro-1-pyridazin-3-one and 1-pyrazolin-3-one conformations.

dioxide at −70° gave purple solutions with $\lambda_{max}(CH_2Cl_2)$ 512 mμ, not considered consistent with the presence of **18**. It is possible that the product with λ_{max} 512 mμ arises by rapid tautomerism of **18** to **16**, followed by subsequent oxidation of **16**, since LTA oxidation of **16** alone yields the same purple solution. The rapid tautomerism of **18** to **16** compared to the stability of the 1-pyrazolin-3-ones is perhaps interpretable in terms of the conformations of the molecules. In the dihydro-1-pyridazin-3-ones effective overlap of a developing p orbital on C-6 is aided by the near axial orientation of one of the C_6—H bonds, a situation which is not so favorable in the 1-pyrazolin-3-one cases[4] (Fig. 1).

The i.r. spectra of the acetyl and benzoyl diimides obtained above exhibit carbonyl absorptions at 1755–1762 and 1710–1725 cm^{-1}, in good agreement with the carbonyl band positions of diacetyl diimide (1762 cm^{-1}) and dibenzoyl diimide (1726 cm^{-1}). In addition, the spectra of the acetyl and benzoyl diimides, with the exception of **3***c*, obtained by LTA oxidation contain bands of variable intensity at 1825–1827 and *ca.* 1810 cm^{-1}, respectively, which may be due to the presence of traces of acetic anhydride and acetyl benzoyl anhydride, formed by nucleophilic attack of acetate ion or acetic acid on the diimides. The n.m.r. spectra of the diimides indicate the percentage of these anhydrides to be very small.

In dialkyl diimides, the stretching frequency of the N=N group is fairly well established to lie in the region 1540–1576 cm^{-1} from Raman (17) and i.r. (18, 19) studies. However, with substituents other than alkyl, a variety of i.r. frequencies have been proposed, *e.g.*, in *trans*-diaryl diimides, 1410–1440 (20), *cis*-diphenyldiimide, 1511 (20), a variety of aromatic azo compounds, *ca.* 1406 or 1577 (21), formazans, 1450 (22), and aryl azo naphthols, *ca.* 1450 cm^{-1} (23). In a recent review (1) it has been stated that "the position of the N=N stretching band of α-carbonyl azo compounds has not yet been determined." Raman spectra of esters and the potassium salt of azodicarboxylic acid (24, 25) attribute this vibration to a band at 1553–1562 cm^{-1}, whereas Chaco and Rabjohn (3) appear to assign bands at 1610 and 1635 cm^{-1} to this vibration in the i.r. spectra of diethyl azodicarboxylate, and ethyl *t*-butylazocarboxylate, (**1***a*), respectively, while Le Fèvre *et al.* (26), in the i.r. spectra of esters of azodicarboxylic acid, has suggested that it lies at *ca.* 1780 cm^{-1}.

It was therefore with some interest that we observed that the i.r. spectra of all the acyclic diimides obtained above exhibited a sharp band of weak to medium intensity between 1545 and 1551 cm^{-1}. It is difficult to attribute this band to any common structural feature in these diimides other than the —N=N— group. Further support for this assignment comes from examination of the i.r. spectra of dibenzoyl diimide and diacetyl diimide; the spectra of these symmetrically substituted diimides exhibit no absorption between 1500 and 1580 cm^{-1}. To provide further information, we have also examined the laser Raman spectrum of a crystalline sample of dibenzoyl diimide.[5] This spectrum exhibits two intense sharp bands at 1712 and 1600 cm^{-1}, attributable, respectively, to carbonyl and aromatic absorptions. In addition, there occurs a much weaker sharp band at 1545 cm^{-1}, which can be assigned, in the light of the evidence above, to the —N=N—stretching vibration.

[4]This explanation follows that of R. Moore in a somewhat similar system (R. Moore, Ph.D. Thesis. University of Alberta, Edmonton, Alberta, 1967).

[5]The authors are indebted to Prof. G. A. Ozin for obtaining the Raman spectrum and for helpful discussions. The instrument used was a Spex 1401 Raman spectrometer.

Can. J. Chem. Downloaded from www.nrcresearchpress.com by 210.87.254.105 on 09/05/12
For personal use only.

TABLE 1. The u.v. spectra of acyl alkyl diimides

Diimide	Solvent	λ_{max} mμ (ε)
5*a**	C_6H_{12}	227(2200), 275(155), 405(27)
5*b**	C_6H_{12}	225(sh, 440), 276(210), 407(37)
5*f*	C_6H_{12}	229, 271(sh), 396
5*e*	CH_2Cl_2	232, 270(sh), 404
3*a**	C_6H_{12}	239(7960), 286(sh, 916), 312(231), 329(sh, 192), 409(37)
3*b**	C_6H_{12}	236(6920), 286(sh, 718), 316(192), 329(sh, 170), 410(37)
3*c*	C_6H_{12}	241(11500), 287(sh, 1272), 317(314), 330(sh, 299), 413(89)
3*f*	C_6H_{12}	241(9000), 288(sh, 1700), 325(sh, 300), 404(49)
3*e*	C_6H_{12}	244(9000), 288(sh, 1700), 322(sh, 230), 406(40)

*For comments on the purities of these compounds, see Discussion.

It was of interest to determine whether direct attachment of an aromatic ring to the diimide functional group might affect the position of the —N=N— stretching band. Indeed, in the spectrum of phenyl benzoyl diimide one observes no absorption in the region between 1510 and 1580 cm^{-1}. Sharp bands are observed at 1450, 1501, and 1600 cm^{-1}, the last absorption having a weak shoulder at 1585 cm^{-1}. It would thus appear, as has already been shown in the case of diaryl diimides (20), that direct attachment of an aromatic ring to the diimide group does have a profound effect on the position of the —N=N— stretching vibration.

The u.v. spectra for the diimides prepared here are collected in Table 1. Intensity data for **5***e* and *f* are not given due to the presence of impurities. All exhibit broad weak n–π* bands in the 396–410 mμ region; these bands undergo hypsochromic shifts of 1–3 mμ on increasing the polarity of the solvent. The acetyl cases exhibit additional, relatively weak, maxima at *ca.* 226 and 275 mμ. The benzoyl diimides have more intense bands below 400 mμ, characteristic maxima occurring at *ca.* 240 and 312–325 mμ. All benzoyl cases exhibit shoulders at *ca.* 286 mμ, some cases having shoulders at 330 mμ.

Experimental

Melting points were determined on a Fisher–Johns apparatus, and are uncorrected. The i.r. spectra were obtained in chloroform solution unless otherwise stated, on a Beckman IR-10, n.m.r. spectra in deuterochloroform using a Varian T-60 instrument, u.v. spectra on a Bausch and Lomb 505 recording spectrophotometer, and mass spectra on a CEC 490 instrument. A Series 3910 Shaker Type Hydrogenation Apparatus (Parr Instrument Co.) was used for the hydrogenations. Microanalyses were performed either by A. B. Gygli, Toronto, Ontario, or by Bernhardt Mikroanalytisches Laboratorium, 5251 Elbach uber Engelskirchen, Fritz-Pregl-Strasse 14–16, West Germany.

2-Isopropyl acetohydrazide (**4***b*), m.p. 55–56° (lit. (27) m.p. 54°) and 2-ethyl benzohydrazide (**2***a*), m.p. 85–87° (lit. (28) m.p. 86–87°) were obtained by catalytic reduction of the corresponding hydrazones.

2-Acetyl Acetaldehyde Hydrazone

A mixture of 29 g (0.39 mol) acetohydrazide and 60 g (1.36 mol) acetaldehyde was stirred at room temperature for 2.5 h. The excess acetaldehyde was removed and the crude product (31.7 g, 81%), m.p. 94–96°, was recrystallized from benzene–hexane to give pure material, m.p. 107.5–109°; ν_{max} 3328 (w) and 1666 cm^{-1} (s); n.m.r.: δ 7.25 (q, 1, J = 5.4 Hz), 2.20 (s, 3) and 1.90 (d, 3, J = 5.4 Hz).

Anal. Calcd. for $C_4H_8N_2O$: C, 47.98; H, 8.05; N, 27.98. Found: C, 48.14; H, 8.24; N, 28.05.

*2-Ethyl Acetohydrazide (**4***a*)*

A solution of 17 g (0.17 mol) 2-acetyl acetaldehydehydrazone in 200 ml absolute alcohol with 3 g 5% platinum-on-carbon was hydrogenated under 50 p.s.i. for 2 days. The catalyst was removed by filtration and washed with additional absolute alcohol. Removal of the solvent and recrystallization of the residue from benzene–pentane yielded white needles (13.29 g, 77%) m.p. 42–46°; b.p. 67–68° (0.5 mm); ν_{max} 3447 (w) and 1675 cm^{-1} (s); n.m.r.: δ 4.51 (br s, 1), 2.90 (q, 2, J = 7.2 Hz), 1.99 (s, 3) and 1.10 (t, 3, J = 7.2 Hz).

Anal. Calcd. for $C_4H_{10}N_2O$: C, 47.03; H, 9.87; N, 27.43. Found: C, 47.18; H, 9.63; N, 27.22.

*2-Isopropyl Benzohydrazide (**2***b*)*

A solution of 18.32 g (0.104 mol) 2-benzoyl acetonehydrazone in 400 ml absolute alcohol with 4 g 5% platinum-on-carbon was hydrogenated under 50 p.s.i. overnight. The catalyst was removed by filtration and washed with additional absolute alcohol. The filtrates were combined, the solvent was removed, and the residue was recrystallized from benzene – petroleum ether (b.p. 60–80°) to give pure material (17.5 g, 98%) m.p. 116–117°; ν_{max} 3443 (w) and 1656 cm^{-1} (s); n.m.r.: δ 7.88–7.27 (m, 5), 3.31 (sept, 1, J = 6.2 Hz) and 1.11 (d, 6, J = 6.2 Hz).

Anal. Calcd. for $C_{10}H_{14}N_2O$: C, 67.38; H, 7.92; N, 15.72. Found: C, 67.57; H, 7.95; N, 15.70.

*2-(1,1-Dimethylbenzyl)-benzohydrazide (**2***c*)*

A solution of phenylmagnesium bromide in anhydrous ether (130 ml) prepared from bromobenzene (0.143 mol) and magnesium metal (0.143 g at), was added dropwise with stirring to 2-benzoyl acetone hydrazone (4.89 g, 27.8 mmol) in 60 ml benzene. The reaction mixture was

Can. J. Chem. Downloaded from www.nrcresearchpress.com by 210.87.254.105 on 09/05/12
For personal use only.

Can. J. Chem. Downloaded from www.nrcresearchpress.com by 210.87.254.105 on 09/05/12
For personal use only.

refluxed with stirring for 2.5 days, cooled, and hydrolyzed with water. The mixture was extracted with three 600 ml portions of chloroform, and the combined chloroform extracts were dried and concentrated. The residue solidified on cooling and was recrystallized from benzene – petroleum ether (b.p. 60–80°) to give pure material (1.63 g, 25%) m.p. 115.5–116.5°; ν_{max} 3430 (w) and 1650 cm^{-1} (s); n.m.r.: δ 7.65–7.15 (m, 10), 5.2 (broad, 1), and 1.41 (s, 6).

Anal. Calcd. for $C_{16}H_{18}N_2O$: C, 75.56; H, 7.13; N, 11.02. Found: C, 75.26; H, 7.26; N, 10.79.

Benzoyl 1,1-Dimethylbenzyl Diimide (3c)

A solution of 1.2 g (2.7 mmol) LTA in 30 ml methylene chloride was added dropwise to a stirred solution of 0.52 g (2.05 mmol) 2-(1,1-dimethylbenzyl)-benzohydrazide in 20 ml methylene chloride cooled to −20°. When addition of the oxidant was complete, stirring was continued at −20° for 30 min. The red-orange solution was poured into 20 ml ice water. The organic phase was separated and washed four times with 20 ml ice water, once with 20 ml saturated aqueous sodium bicarbonate solution, and finally with 20 ml ice water. After drying, the solvent was removed at ice-bath temperature to give the crude product as a red-brown oil (0.47 g, 90%); the product was purified by two molecular distillations at 70°/0.5 mm; ν_{max} (CCl_4) 1723 (s), 1600 (m), 1540 cm^{-1} (w). n.m.r.: δ 7.97–7.21 (m, 10) and 1.69 (s, 6).

Anal. Calcd. for $C_{16}H_{16}N_2O$: C, 76.16; H, 6.39; N, 11.10. Found: C, 76.01; H, 6.29; N, 11.00.

The diimides **3***a*, **3***b*, **5***a*, and **5***b* were similarly obtained in 18–90% yield and were not further purified (for comments on their purity, see Discussion); i.r. and n.m.r. data for these are as follows: **3***a*, ν_{max} 1810 (m), 1715 (s), and 1550 cm^{-1} (w); n.m.r.: δ 8.08–7.08 (m, 5), 4.10 (q, 2, J = 7.2 Hz), and 1.34 (t, 3, J = 7.2 Hz); **3***b*, ν_{max} 1810 (m), 1712 (s), and 1550 cm^{-1} (w); n.m.r.: 7.98–7.28 (m, 5), 4.07 (sept, 1, J = 6.0 Hz), and 1.40 (d, 6, J = 6.0 Hz); **5***a*, ν_{max} 1825 (s), 1756 (s) and 1550 cm^{-1} (vw); n.m.r.: δ 4.07 (q, 2, J = 7.6 Hz), 2.24 (s, 3), and 1.35 (t, 3, J = 7.6 Hz); **5***b*, ν_{max} 1825 (w), 1758 (s), and 1549 cm^{-1} (m); n.m.r.: δ 3.83 (sept, 1, J = 6.6 Hz), 2.18 (s, 3), and 1.26 (d, 6, J = 6.6 Hz).

The pyrazolidin-3-ones, **8** (29) and **10** (13) were obtained by previously reported procedures.

Tetrahydro-6-methyl-3(2H)-pyridazinone (17)

4,5-Dihydro-6-methyl-3(2*H*)-pyridazinone (**16**) (7 g, 0.06 mol) was dissolved in 100 ml methanol containing glacial acetic acid (7 g, 0.12 mol) and hydrogenated in the presence of 7 g 5% platinum-on-carbon under 50 p.s.i. for 2 days. After filtration to remove the catalyst, the methanol was evaporated. The residue was dissolved in 10 ml chloroform and neutralized with saturated sodium bicarbonate solution. After drying, the solvent was removed to give the crude product (3.49 g, 49%). Recrystallization from benzene – petroleum ether (b.p. 60–80°) gave white crystals (1.8 g, 25%), m.p. 71.5–72.5°; ν_{max} 3410 (w) and 1655 cm^{-1} (s); n.m.r.: δ 3.09 (m, 1), 1.36–2.60 (m, 4) and 1.10 (d, 3, J = 6 Hz).

Anal. Calcd. for $C_5H_{10}N_2O$: C, 52.61; H, 8.83; N, 24.54. Found: C, 52.38; H, 8.81; N, 24.31.

Synthesis of the α-Cyanoalkyl Hydrazides, 2e–g and 4e–g

The general method of synthesis was as follows; a solution of sodium cyanide (1 mol) in water (10 ml/g sodium cyanide) containing the ketone (1 mol) (with butanone and cyclohexanone, 4 and 10 ml, respectively, of dioxane/g ketone were added), was poured into a mixture of the acylhydrazide (1 mol) in water (10 ml/g benzohydrazide, 7 ml/g acetohydrazide; in the case of benzohydrazide, 8 ml alcohol/g benzohydride were also added). The combined solutions were stirred in tightly stoppered flasks for several days, and the products were isolated by filtration or extraction with chloroform. Yield, m.p., i.r., n.m.r., and analytical data for these hydrazides are as follows: **2***e*, 88%, 131–132.5°, ν_{max} 3410 (m), 2220 (vw), and 1666 cm^{-1} (s); n.m.r.: δ 7.25–7.8 (m, 6), 3.6 (br s, 1), 1.2–2.2 (br m, 10).

Anal. Calcd. for $C_{14}H_{17}N_3O$: C, 69.69; H, 6.27; N, 17.41. Found: C, 69.45; H, 6.07; N, 17.33.

Compound **2***f*, 59%, 122.5–125° (lit. (9) m.p. 120–123°), ν_{max} 3410 (m), 3290 (m), 2220 (vw), and 1669 cm^{-1} (s); n.m.r.: δ 7.3–8.1 (m, 6), 5.0 (br, 1), 1.53 (s, 6).

Anal. Calcd. for $C_{11}H_{13}N_3O$: C, 65.01; H, 6.45; N, 20.68. Found: C, 64.81; H, 6.34; N, 20.63.

Compound **2***g*, 61%, 103–104°, ν_{max} 3410 (m), 2220 (vw), and 1666 cm^{-1} (s); n.m.r.: δ 8.2 (br s, 1), 7.25–7.9 (m, 5), 5.3 (br s, 1), 1.0–2.0 (m, 8).

Anal. Calcd. for $C_{12}H_{15}N_3O$: C, 66.34; H, 6.96; N, 19.34. Found: C, 66.33; H, 6.74; N, 19.19.

Compound **4***e*, 59%, 101.5–103°, ν_{max} 3410 (m), 2220 (vw), and 1690 cm^{-1} (s); n.m.r.: (pyridine): δ 2.05 (s), 1.1–1.9 (br).

Anal. Calcd. for $C_9H_{15}N_3O$: C, 59.64; H, 8.34; N, 23.19. Found: C, 59.53; H, 8.39; N, 23.40.

Compound **4***f*, 50%, 79.5–82°, ν_{max} 3410 (m), 3290 (m), 2220 (vw), and 1685 cm^{-1} (s); n.m.r.: δ 8.1 (br s, 1), 5.0 (br s, 1), 2.0 (s, 3), 1.5 (s, 6).

Anal. Calcd. for $C_6H_{11}N_3O$: C, 51.05; H, 7.85; N, 29.77. Found: C, 51.03; H, 8.07; N, 29.84.

Compound **4***g*, 55%, 69–72°, ν_{max} 3410 (m), 3290 (m), 2220 (vw), and 1685 cm^{-1} (s); n.m.r.: δ 7.95 (br s, 1), 4.4 (br s, 1), 2.0 (s, 3), 0.9–1.9 (m, 8).

Anal. Calcd. for $C_6H_{13}N_3O$: C, 66.34; H, 6.96; N, 19.34. Found: C, 66.33; H, 6.74; N, 19.19.

Oxidation of 2e to 3e

2-α-Cyanocyclohexyl benzohydrazide (**2***e*, 0.50 g) was stirred in benzene (25 ml) with anhydrous sodium sulfate (0.50 g) and yellow mercuric oxide (0.886 g) for 0.5 h. After filtration, the solvent was removed to give crude **3***e* (0.122 g, 25%), which was crystallized from pentane, m.p. 66.5–67.5°, ν_{max} 2220 (w), 1721 (s), and 1550 cm^{-1} (m); n.m.r.: δ 7.4–8.0 (m, 5), 1.3–2.3 (m, 10).

Anal. Calcd. for $C_{14}H_{15}N_3O$: C, 69.69; H, 6.27; N, 17.41. Found: C, 69.45; H, 6.07; N, 17.33.

Compound **2***f* was similarly oxidized to give **3***f* as a yellow oil, ν_{max} 2220 (w), 1721 (s), and 1552 cm^{-1} (m); n.m.r.: 7.28–8 (m, 5), 1.8 (s, 6). Attempted purification of the oil by molecular distillation was unsuccessful.

Compounds **4***e* and *f* were oxidized to **5***e* and *f*, respectively, by stirring with excess manganese dioxide (10) in methylene chloride at room temperature. Mild effervescence of a gas was observed to occur. Oxidation of **4***e* was also accomplished using *N*-chlorobenzotriazole at −20° in methylene chloride. Spectral measurements were made on the samples of **5***e* and *f* so obtained; **5***e*, ν_{max} 2220 (vw), 1760 (s), 1710 (sh, w), 1550 cm^{-1} (m); **5***f*,

Can. J. Chem. Downloaded from www.nrcresearchpress.com by 210.87.254.105 on 09/05/12
For personal use only.

ν_{max} 1760 (s), 1710 (sh, m), 1555 cm^{-1} (w); n.m.r.: δ 2.15 (s), 1.70 (s).

*5-Phenylpyrazolin-3-one (**9**)*

A solution of 0.29 g (0.65 mmol) LTA in 15 ml methylene chloride was added dropwise to a stirred solution of **8** (0.073 g, 0.45 mmol) in 5 ml methylene chloride cooled to −70°. When addition of the oxidant was complete, stirring was continued at −70° for 10 min; the u.v. spectrum of this solution exhibited a maximum at 430 mμ.

In a subsequent preparation, 0.98 g **8** was oxidized at −20°, and when oxidation was complete, the solution was poured into water, and the organic phase was separated, washed successively with 40 ml portions of water, saturated aqueous sodium bicarbonate, and water, dried, and evaporated to give styrene (0.5 g, 67%), identified as the dibromide, m.p. 72–73° (lit. (32) m.p. 73–74°).

*5-Methylpyrazolin-3-one (**11**)*

A solution of 0.94 g (2.1 mmol) LTA in 30 ml methylene chloride was added to a stirred solution of **10** (0.178 g, 1.7 mmol) in 10 ml methylene chloride cooled to −70°. Stirring was continued at −70° for 10 min after addition of the oxidant was complete. The u.v. spectrum of the solution exhibited a maximum at 443 mμ.

Diacetyl diimide was prepared by iodine oxidation of the mercuric salt of 1,2-diacetylhydrazine according to the literature method (30). The product was once distilled.

Dibenzoyl diimide, m.p. 119–121° (lit. (31) m.p. 119.5–121.5°) was conveniently obtained by oxidation of 1,2-dibenzoylhydrazine with an equimolar quantity of *N*-chlorobenzotriazole in methylene chloride at room temperature.

We thank the National Research Council of Canada and the Ontario Department of University Affairs for support of this research.

1. E. Fahr and H. Lind. Angew. Chem. Int. Ed. Engl. **5**, 372 (1966).
2. H. Wieland *et al.* Ann. **514**, 145 (1935); Ann. **518**, 166 (1938).
3. M. C. Chaco and N. Rabjohn. J. Org. Chem. **27**, 2765 (1962).
4. R. W. Hoffmann and K. R. Eicken. Chem. Ber. **100**, 1465 (1967).
5. G. Fraenkel and E. Pecchold. Tetrahedron Lett. 4821 (1969).
6. M. Freifelder, W. B. Martin, G. R. Stone, and E. L. Coffin. J. Org. Chem. **26**, 383 (1961).
7. H. L. Yale, K. Losee, J. Martins, M. Holsing, F. M. Perry, and J. Bernstein. J. Am. Chem. Soc. **75**, 1933 (1953).
8. C. G. Overberger, M. T. O'Shaughnessy, and H. Shalit. J. Am. Chem. Soc. **71**, 2661 (1949).
9. E. G. Howard, Jr. U.S. Patent, 2 580 919 (1952); Chem. Abstr. **46**, 7119 (1952).
10. J. Attenburrow, A. F. B. Cameron, J. H. Chapman, R. M. Evans, B. A. Hems, A. B. A. Jansen, and T. Walker. J. Chem. Soc. 1094 (1952).
11. Fr. Pat. 1 582 440 (1969); Chem. Abstr. **73**, 45098*m* (1970).
12. R. H. Kent and J.-P. Anselme. Can. J. Chem. **46**, 2322 (1968).
13. C. F. H. Allen and E. W. Magder. J. Heterocycl. Chem. **6**, 349 (1969).
14. W. Ried and E. Kahr. Chem. Ber. **103**, 331 (1970).
15. W. Nagata and S. Kamata. J. Chem. Soc. C, 540 (1970).
16. D. Libermann and A. Rouaix. Bull. Soc. Chim. Fr. 1793 (1959).
17. G. Herzberg. Molecular spectra and molecular structure. Vol. 2. D. Van Nostrand, Princeton, New Jersey, 1945. p. 359.
18. L. Spialter, D. H. O'Brien, G. L. Untereiner, and W. A. Rush. J. Org. Chem. **30**, 3278 (1965).
19. R. J. Crawford, A. Mishra, and R. J. Dummel. J. Am. Chem. Soc. **88**, 3959 (1966).
20. R. Kubler, W. Lüttke, and S. Weckherlin. Zeit. Elektrochem. **64**, 650 (1960).
21. R. J. W. Le Fèvre, M. F. O'Dwyer, and R. L. Werner. Aust. J. Chem. **6**, 341 (1953).
22. R. J. W. Le Fèvre, J. B. Sousa, and R. L. Werner. Aust. J. Chem. **9**, 151 (1956).
23. K. J. Morgan. J. Chem. Soc. 2151 (1961).
24. S. S. Dubov and V. A. Ginsburg. Zh. Vses. Khim. Obshchestva im. D. I. Mendeleeva, **7**, 583 (1962); Chem. Abstr. **58**, 4041 (1963).
25. A. Simon and H. Wagner. Naturwissenschaften, **47**, 540 (1960).
26. R. J. W. Le Fèvre, W. T. Oh, I. H. Reece, R. Roper, and R. L. Werner. Aust. J. Chem. **11**, 92 (1958).
27. H. Rohnert. Z. Chem. **5**, 302 (1965).
28. R. L. Hinman. J. Am. Chem. Soc. **79**, 414 (1957).
29. L. A. Carpino. J. Am. Chem. Soc. **80**, 599 (1958).
30. H. H. Inhoffen, H. Pommer, and F. Bohlmann. Chem. Ber. **81**, 507 (1948).
31. L. Horner and W. Naumann. Ann. **587**, 81 (1954).
32. W. L. Evans and L. H. Morgan. J. Am. Chem. Soc. **35**, 56 (1913).

Can. J. Chem. Downloaded from www.nrcresearchpress.com by 210.87.254.40 on 09/05/12
For personal use only.

Preparations of Some Tetrahydronaphthalenone and Dihydroindanone Derivatives of Potential Value as Intermediates for the Synthesis of Steroids and Related Compounds

J. Bryan Jones, Jeffrey D. Leman,[1] and Peter W. Marr

Lash Miller Chemical Laboratories, Department of Chemistry, University of Toronto, Toronto 181, Ontario

Received December 17, 1970

The difficulties which in the past have precluded the preparation of some synthetically potentially useful ethylenedioxy-tetrahydronaphthalenone and -dihydroindanone derivatives have been overcome. The proclivity of the tetrahydronaphthalenone compounds to undergo acid- and base-catalyzed rearrangements has been shown to be paralleled to some extent by the analogous dihydroindanone compounds.

On a pu surmonter les difficultés qui dans le passé ont empêché la préparation de certains dérivés éthylenedioxitétrahydronaphtalènone ou -dihydroindanone qui sont potentiellement utiles au point de vue synthétique. On a démontré que les dihydroindanones en milieux acide ou basique, se réarrangent pratiquement avec autant de facilité que les tétrahydronaphtalénones.

Canadian Journal of Chemistry, 49, 1604 (1971)

During synthetic studies on androgen analogues the need arose to prepare the tetrahydronaphthalenone and dihydroindanone derivatives **1**, **2**, **3**, and **4**. Such compounds have

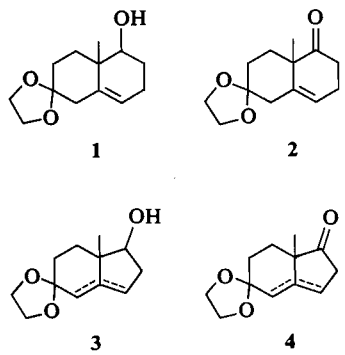

obvious potential as intermediates in steroid and related syntheses and in view of their desirability in this regard it was somewhat surprising to discover that their preparations had not been reported. However, examination of the pertinent literature revealed that the parent ketones of **1** and **2**, the hydroxynaphthalenone **5**, and the dione **6** respectively, and related compounds were extremely susceptible to rearrangement under acidic, basic, and photochemical conditions (1–4) and that a previous attempt to effect the ketalization of **5** with ethylene glycol and toluene-*p*-sulfonic acid (PTSA) had yielded only the tetrahydronaphthyloxyethanol **7** and related rearrangement products (3) (Scheme 1). We have subsequently reinvestigated the latter reaction and our results confirm the rearrangement product **7** to be the major isolable product.

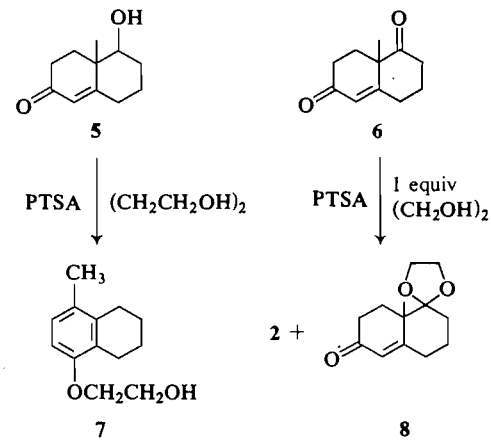

Scheme 1

Attention was then turned towards the possibility of selective ketalization of the unsaturated ketone function of **6** by using one equivalent only of ethylene glycol in the presence of an appropriate acid. This method had proven valuable for a variety of steroid ketals (5) and it was found that using toluene-*p*-sulfonic acid

[1]Abstracted in part from the Ph.D. thesis of J.D.L., University of Toronto, Toronto, Ontario, 1969.

Can. J. Chem. Downloaded from www.nrcresearchpress.com by 210.87.254.40 on 09/05/12
For personal use only.

catalysis, the dione **6** could be converted into a mixture containing up to 40% of the desired ketal **2**.[2] However, although separation of **2** from the other ketal product **8** was readily effected by chromatography, the reaction proved to be a very temperamental one and considerable variations in the ratios of the ketals formed were observed from one run to another. Reproducible results were not attainable even under very carefully controlled conditions and no satisfactory procedure could be developed. Substitution of oxalic acid as the catalyst (5) gave some 6,6-ethylenedioxy-8*a*β-methyl-3,4,8,8*a*-tetrahydro-1(2*H*,7*H*)-naphthalenone[2] but application of the method as an acceptable route to this desirable synthetic intermediate was precluded by the low (<12%) yields obtained. Attempted ketalizations of **6** using adipic acid catalysis (5) were not successful and the starting tetrahydronaphthalenedione was recovered unchanged.

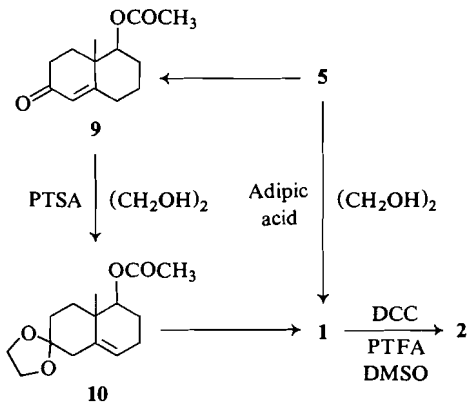

SCHEME 2

The preparations of **1** and **2** in sufficient quantities for our future synthetic studies were finally achieved by the two methods outlined in Scheme 2. Acetylation of the hydroxyl group of **5** prior to ketalization precluded the possibility of the previously observed (3) rearrangement reactions and the acetate **9** was readily converted into the ethylene ketal **10** under normal ethylene glycol toluene-*p*-sulfonic acid conditions (5, 7). Hydrolysis of **10** with methanolic sodium hydroxide yielded the desired hydroxyethylene ketal **1** in 69% overall yield from **5**. Subsequently, it was discovered that rearrangement of **5** under ketalization conditions could be prevented by using a weaker acid catalyst. In the presence of adipic acid, the reaction of **5** with ethylene glycol proceeded smoothly to give **1** in 30% yield. However, owing to the presence of the hydroxyl group, the ketal **1** retained its potential for rearrangement and proved to be a relatively unstable compound.

In refreshing contrast to the difficulties encountered with the other reactions in this series oxidation (8) of the hydroxy ketal **1** into the ethylenedioxynaphthalenone **2** was effected very readily in 58% yield. The oxoketal **2** obtained by this method was identical with the samples obtained by the less satisfactory selective ketalization route. Unlike its hydroxy analogue **1**, it was a stable solid which could be fully characterized and its structure was further verified by conversion into its oxime and by hydrolysis back to its parent dione **6**.

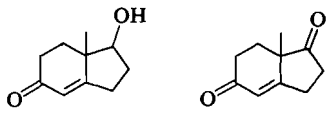

11 **12**

With the problems regarding ketalization in the tetrahydronaphthalenone series having been overcome, the study was then extended to the corresponding indanone ketals **3** and **4**. In view of the well documented sensitivity of the above naphthalenones to acids and bases (1–4), the stability of the analogous dihydroindanones **11** and **12** under similar conditions was investigated prior to any attempted ketalization experiments. Treatment of the hydroxyindanone **11** and the dione **12** with a variety of bases, including triethylamine, sodium hydroxide, and potassium-*t*-butoxide afforded complex reaction mixtures which contained no residual starting material. Disappointingly, no rearrangement products analogous to those reported previously in the naphthalenone series (1–4) could be isolated. However, the effect of toluene-*p*-sulfonic acid in refluxing benzene on the hydroxyindanone **11** paralleled the octalone results very closely and a 36% yield of the rearranged "dimer" **13** was obtained. One of the possible pathways which accounts for the formation of **13** is outlined in Scheme 3 (*cf.* ref. 3).

[2]The designations of the double bonds of **1** and **2** as Δ^4 and of the oxalic acid derived product as Δ^{4a} were made on the basis of comparisons of the p.m.r. spectra with those of analogous steroid ketals (6).

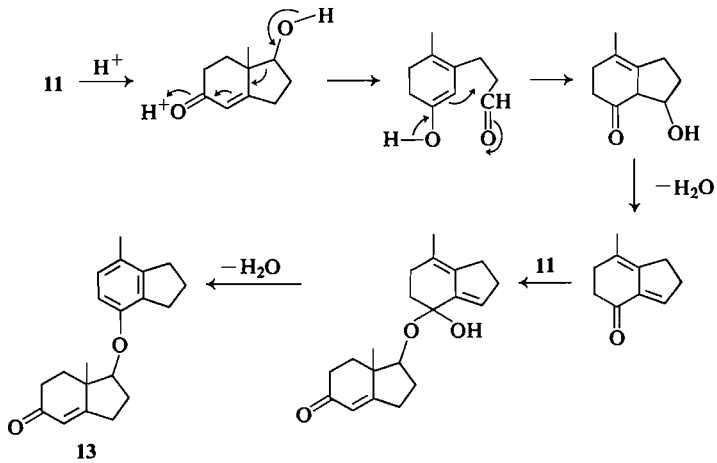

SCHEME 3

Very unexpectedly, when ethylene glycol was added to the above reaction mixture, the anticipated rearrangement (*cf.* **7**) did not occur and we were able to isolate the desired ketal **3**[3] in 30% yield (Scheme 4). Use of oxalic acid to promote ketalization gave a similar yield of **3** but adipic acid proved to be ineffective as a catalyst.

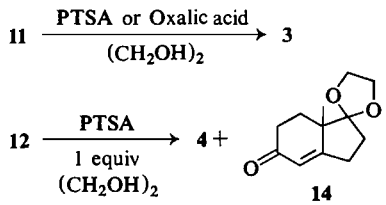

SCHEME 4

The ethylenedioxy indanone **4** was prepared from the dione **12** by the selective ketalization procedure. Following chromatographic purification a 22% yield of **4** was obtained and in addition, 41% of the isomeric ketal **14** was isolated. Since our particular interest in **4** as a synthetic intermediate was minimal at this time, no further studies of this reaction nor on the preparation of **4** by oxidation of **3** were considered warranted. However, if in the future the indanone **4** is required in quantity, our experiences in the tetrahydronaphthalenone series suggest that oxidation of the hydroxyindanone ketal **3** should be the preferred method.

[3]Comparisons of the vinylic proton peak widths and multiplicities in the p.m.r. spectra of **1**, **2**, and **8** with those of **3** and **4** indicated that the position of the double bonds of the latter two compounds is Δ^{3a}. However, the possibility that **3** and **4** possess the isomeric Δ^{3}-olefin structures cannot be eliminated (*cf.* ref. 6) and at present an unequivocal decision in this regard cannot be made. In the Experimental section, **3** and **4** have been named as Δ^{3a}-olefins in order to avoid the complexities inherent in either/or type nomenclature.

Experimental

Melting points were determined on a Fisher–Johns apparatus and are uncorrected. The i.r. spectra were obtained on a Perkin–Elmer 237B spectrophotometer using chloroform solutions. The p.m.r. spectra were measured on deuterochloroform solutions with Varian T-60 or HA-100 instruments and with tetramethylsilane as internal standard. A Varian Aerograph 1740 gas chromatograph equipped with a 6′ × 2 mm, 3% SE-30 glass column, and with temperature programming in the range 130–230°, was used to monitor most of the ketalization reactions. The t.l.c. and preparative layer chromatographic separations were effected on phosphor-containing silica gel G. Chromatograms were visualized both with u.v. light and with 5% ceric sulfate in 2 *N* sulfuric acid. Mass spectra were obtained on Bell and Howell 21-490 (low resolution) and AEI MS 902 (high resolution) mass spectrometers. All compounds reported were purified until no impurities could be detected by either t.l.c. or g.l.c. analysis.

8*a*β-Methyl-3.4,8 8*a*-tetrahydro-1,6(2*H*,7*H*)-naphthalenedione (**6**, catalogue name 9-methyl-$\Delta^{5(10)}$-octalin-1,6-dione) was purchased from Aldrich.

Acid-catalyzed Rearrangement of 1β-Hydroxy-8aβ-methyl-3,4,8,8a-tetrahydro-6(2H,7H)-naphthalenone (5) in the Presence of Ethylene Glycol

A solution of 1β-hydroxy-8*a*β-methyl-3,4,8,8*a*-tetrahydro-6(2*H*,7*H*)-naphthalenone (**5**, 1.17 g, 6.5 mmol, prepared by reduction of 8*a*β-methyl-3,4,8,8*a*-tetrahydro-1,6(2*H*,7*H*)-naphthalenedione (**6**) with recrystallized

Can. J. Chem. Downloaded from www.nrcresearchpress.com by 210.87.254.40 on 09/05/12
For personal use only.

Can. J. Chem. Downloaded from www.nrcresearchpress.com by 210.87.254.40 on 09/05/12
For personal use only.

sodium borohydride as described by Boyce and Whitehurst (9*a*)) and ethylene glycol (10 ml) in toluene (60 ml) containing toluene-*p*-sulfonic acid (10 mg) was slowly distilled with the addition of fresh toluene at intervals to maintain the starting volume. Distillation for 5 h afforded approximately 200 ml of distillate. The mixture was cooled, washed thoroughly with saturated sodium hydrogen carbonate solution, and dried ($MgSO_4$). The solvent was evaporated and the resulting yellow oil (1.40 g) was shaken with warm petroleum ether (40–60°). The solvent was decanted off and was kept overnight at −10°. 2-(1,2,3,4-Tetrahydro-8-methyl-5-naphthyloxy)ethanol (**7**) was obtained as a crystalline powder (240 mg, 18%), m.p. 72–73° (lit. (3) m.p. 73–74°).

1β-Acetoxy-8aβ-methyl-3,4,8,8a-tetrahydro-6(2H,7H)-naphthalenone (9)

1β-Hydroxy-8aβ-methyl-3,4,8,8*a*-tetrahydro-6(2*H*,7*H*)-naphthalenone (**5**, 320 mg, 1.8 mmol) was treated with acetic anhydride (1 ml) and pyridine (1.4 ml) and allowed to stand overnight at 20°. The solvent was removed under reduced pressure and the residue was recrystallized from petroleum ether (30–60°) to give the acetate (**9**, 360 mg, 91%), m.p. 82–85° (lit.(9*a*) 89°); i.r. 1730 and 1664 cm^{-1}; p.m.r. δ 1.28 (3H, s, CCH_3), 2.08 (3H, s, $COCH_3$), 4.67 (1H, m, *H*COCOCH_3), and 5.80 p.p.m. (1H, structured s, vinyl H).

1β-Acetoxy-6,6-ethylenedioxy-8aβ-methyl-2,3,8,8a-tetrahydro-(5H,7H)-naphthalene (10)

A mixture of 1β-acetoxy-8aβ-methyl-3,4,8,8*a*-tetrahydro-6(2*H*,7*H*)-naphthalenone (**9**, 1.45 g, 65 mmol), ethylene glycol (25 ml), benzene (300 ml), and a few crystals of toluene-*p*-sulfonic acid was heated under reflux with stirring for 12 h, and water which formed during the reaction was removed by a Dean–Stark moisture trap containing molecular sieves. The mixture was then washed with saturated aqueous sodium hydrogen carbonate solution (3 × 50 ml) and dried ($MgSO_4$). The solvent was evaporated and the residue (1.72 g) was recrystallized from petroleum ether (40–60°). The acetate **10** was obtained as plates (1.40 g, 80%), m.p. 95–97°; i.r. 1730, 1104 and 1093 cm^{-1}; p.m.r. δ 1.15 (3H, s, C-8*a* CH_3), 2.16 (3H, s, $OCOCH_3$), 3.93 (4H, s, OCH_2CH_2O), 4.83 (1H, "t", J = 7.0 Hz, *C*HOCOCH_3), and 5.35 p.p.m. (1H, m, vinyl H).

Anal. Calcd. for $C_{15}H_{22}O_4$: C, 67.65; H, 8.33. Found: C, 67.47; H, 8.16.

6,6-Ethylenedioxy-1β-hydroxy-8aβ-methyl-2,3,8,8a-tetrahydro-(5H,7H)-naphthalene (1)

(a) From the Ketal (5)

A mixture of 8aβ-methyl-3,4,8,8*a*-tetrahydro-1,6-(2*H*,7*H*)-naphthalenedione (**6**, 0.80 g, 4.4 mmol), ethylene glycol (2.4 ml), adipic acid (80 mg, 4.4 mmol), and benzene (160 ml) was stirred and heated under reflux for 12 h, the water formed during the reaction being removed by molecular sieves contained in a Dean–Stark moisture trap. The cooled reaction mixture was diluted with benzene (200 ml) and was then washed with saturated aqueous sodium hydrogen carbonate solution (2 × 50 ml). The aqueous phase was extracted with benzene (2 × 20 ml) and the combined benzene solutions were washed with water (2 × 100 ml) and filtered through Celite. The dried ($MgSO_4$) benzene solution was evaporated to yield a yellow oil which was then shaken with petroleum ether (40–60°). The supernatant was decanted and evaporated to give the ethylene ketal **1** as a clear colorless oil (300 mg, 30%); i.r. 3623, 3497, and 1089 cm^{-1}; p.m.r. δ 1.09 (3H, s, CH_3), 3.48–3.81 (1H, m, HOC*H*); 3.96 (4H, s, OCH_2CH_2O), and 5.34 p.p.m. (1H, m, vinyl H).

(b) From the Acetate (10)

A solution of 1β-acetoxy-6,6-ethylenedioxy-8aβ-methyl-2,3,8,8*a*-tetrahydro(5*H*,7*H*)-naphthalene (**10**, 200 mg, 0.75 mmol) in methanol (6 ml) containing sodium hydroxide (140 mg, 3.5 mmol) was kept at 20° for 16 h and was then poured into water (50 ml). The mixture was reduced to half volume under reduced pressure and was then extracted with ether (3 × 10 ml). The combined ether extracts were dried ($MgSO_4$) and evaporated to produce the hydroxyketal **1** as a yellow oil (160 mg, 95%) identical in all respects to the material obtained above.

6,6-Ethylenedioxy-8aβ-methyl-2,3,8,8a-tetrahydro-1(5H,7H)-naphthalenone (2)

(a) By Oxidation of the Hydroxyketal 1

6,6-Ethylenedioxy-1β-hydroxy-8aβ-methyl-2,3,8,8*a*-tetrahydro-(5*H*,7*H*)-naphthalene (**1**, 0.43 g, 1.9 mmol), dicyclohexyl carbodiimide (1.18 g, 1.9 mmol), and pyridinium trifluoroacetate (0.19 g, 0.95 mmol) were dissolved in dimethyl sulfoxide (5 ml) and benzene (5 ml) and the solution heated at 50° for 2 h. Ethyl acetate (25 ml) was then added and the precipitated dicyclohexylurea (m.p. 235–236°) was removed by filtration. The solution was extracted with phosphate buffer (0.01 *M*, p*H* 7.0, 2 × 25 ml) and was then washed with water (2 × 25 ml). The dried solution ($MgSO_4$) was evaporated to give a yellow oil (1.10 g) which was chromatographed on neutral alumina. Elution with benzene – petroleum ether (40–60°) (3:1) gave the ethylenedioxy ketone (**2**, 0.15 g, 58%), m.p. 63–64.5°; i.r. 1706, 1110 and 1092 cm^{-1}; p.m.r. δ 1.30 (3H, s, CH_3), 1.77 (2H, d, superimposed on other proton signals, J_{AX} = 0.5 Hz, $O_2CCH_2^AC{=}CH^X$), 3.99 (4H, s, OCH_2CH_2O), and 5.61 p.p.m. (1H, m, vinyl H).

Anal. Calcd. for $C_{13}H_{18}O_3$ (mol. wt. 222.1256): C, 70.14; H, 8.16. Found (222.1254 (mass spectrum)): C, 69.92; H, 8.09.

The oxime (prepared in 58% yield by treatment of **2** with hydroxylamine hydrochloride in aqueous ethanolic pyridine) recrystallized from ethanol as feathery plates, m.p. 175–175.5°; i.r. (KBr) 3257, 1675, 1099, and 1089 cm^{-1}; p.m.r. δ 1.32 (3H, s, CH_3), 1.81 (2H, s, superimposed on other proton signals, O_2CCH_2), 3.93 (4H, s, OCH_2CH_2O), 5.52 (1H, m, vinyl H), and 9.02 p.p.m. (1H, s, C=C—OH). Mass spectrum *m/e* 237 (molecular ion).

Anal. Calcd. for $C_{13}H_{19}NO_3$ (mol. wt. 237): C, 65.80; H, 8.07; N, 5.90. Found: C, 66.03; H, 8.03; N, 5.99.

Toluene-*p*-sulfonic acid catalyzed hydrolysis of **2** in aqueous acetone-chloroform solution regenerated the parent dione **6** in 75% yield.

(b) By Selective Ketalization of the Dione 6

8aβ-Methyl-3,4,8,8*a*-tetrahydro-1,6(2*H*,7*H*)-naphthalenedione (**6**, 100 mg, 0.6 mmol), ethylene glycol (37

Can. J. Chem. Downloaded from www.nrcresearchpress.com by 210.87.254.40 on 09/05/12
For personal use only.

mg, 0.6 mmol), and toluene-*p*-sulfonic acid (12 mg) in dry benzene (5 ml) were refluxed under a molecular sieve containing Dean–Stark trap for 1 h. The reaction mixture was cooled, diluted with benzene (5 ml), and washed with saturated aqueous sodium bicarbonate solution (2 ml) followed by water (2 ml). The dried ($MgSO_4$) benzene solution was evaporated and the yellow oil (130 mg) obtained was preparative layer chromatographed using 60% diethyl ether – 40% petroleum ether (b.p. 40–60°) as developing solvent. The higher R_f band was extracted to give the ethylenedioxy ketone **2** (50 mg) which was identical with the sample obtained above.

The lower R_f band yielded 1,1-ethylenedioxy-8*a*β-methyl-3,4,8,8*a*-tetrahydro-6(2*H*,7*H*)-naphthalenone (**8**) as a colorless oil (26 mg) which decomposed on attempted distillation[4]; i.r. 1665 and 1070 cm^{-1}; p.m.r. δ 1.35 (3H, s, CH_3), 3.96 (4H, s, OCH_2CH_2O), and 5.78 (1H, s, vinylic H).

Mol. wt. Calcd. for $C_{13}H_{18}O_3$: 222.1256. Found (mass spectrum): 222.1254.

*7,7a-Dihydro-7a*β*-methyl-1,5(6H)-indanone (12)*

The indandione **12** was prepared in 45% yield from 2-methylcyclopentane-1,3-dione (synthesized[5] by the method of Schick and co-workers (11)) and methyl vinyl ketone according to the procedure of Boyce and Whitehurst (9*b*); it formed prisms from diethyl ether – *n*-hexane, m.p. 68.5–70° (lit. (9*b*) m.p. 72–73°)

*Acid-catalyzed Rearrangement of 7,7a-Dihydro-1*β*-hydroxy-7a*β*-methyl-5(6H)-indanone (11)*

7,7*a*-Dihydro-1β-hydroxy-7*a*β-methyl-5(6*H*)-indanone (**11**, 500 mg, prepared in 76% yield by reduction of the indandione **12** with recrystallized sodium borohydride as described by Boyce and Whitehurst (9*c*)) and toluene-*p*-sulfonic acid (30 mg) in dry benzene (15 ml) were refluxed under a Soxhlet extractor containing molecular sieves for 20 h. The cooled solution was then washed with saturated aqueous sodium bicarbonate (5 ml) followed by water (5 ml). The dried ($MgSO_4$) benzene solution was evaporated and the residue (307 mg) column chromatographed on Florisil. Elution with diethyl ether – benzene (1:2) yielded 7,7*a*-dihydro-7*a*β-methyl-1β-(7-methyl-4-indanoxy)-5(6*H*)-indanone(**13**,180 mg, 36%). Preparative layer chromatography (diethyl ether development) followed by recrystallization from ethanol afforded an analytical sample m.p. 101.5–102.5°; i.r. 1680 and 1082 cm^{-1}; p.m.r. δ 1.30 (3H, s, CH_3), 2.18 (3H, s, $C_6H_5CH_3$), 4.30 (1H, t, J = 4 Hz, *H*CO), 5.84 (1H, s, vinylic H), 6.66 (1H, d, J = 4 Hz, aromatic H) and 6.93 p.p.m. (1H, d, J = 4 Hz, aromatic H). Mass spectrum *m/e* 296 (molecular ion).

Anal. Calcd for $C_{20}H_{24}O_2$ (mol. wt. 296): C, 81.08; H, 8.11. Found: C, 81.19; H, 8.14.

*5,5-Ethylenedioxy-1*β*-hydroxy-7a*β*-methyl-7,7a-dihydro-(6H)-indane (3)*[3]

7,7*a*-Dihydro-1β-hydroxy-7*a*β-methyl-5(6*H*)-indanone (**11**, 100 mg, 0.6 mmol), ethylene glycol (37 mg, 0.6 mmol), and toluene-*p*-sulfonic acid (or oxalic acid) (12 mg) were heated under reflux for 4 h with a Dean–Stark trap containing molecular sieves. The cooled, discolored solution was then washed with saturated aqueous sodium bicarbonate (2 ml), then with water (2 ml), and the dried ($MgSO_4$) benzene layer evaporated. Preparative layer chromatography of the residual oil (96 mg) with diethylether as the developing solvent yielded the hydroxy indane ketal **3** (38 mg, 30%) m.p. 82–83.5° which decomposed on attempted recrystallizations from a variety of solvents; i.r. 3640, 3480, 1090, and 1110 cm^{-1}; p.m.r. δ 1.00 (3H, s, CH_3), 2.4 (2H, "s", C-3 or -4 CH_2), 3.96 (4H, s, OCH_2CH_2O), 4.12 (1H, t, J = 4 Hz, C*H*-OH) and 5.26 (1H, "s", vinylic H).

Anal. Calcd. for $C_{12}H_{18}O_3$ (mol. wt. 210.1256): C, 68.54; H, 8.62. Found (210.1253): C, 68.64; H, 8.77.

*5,5-Ethylenedioxy-7a*β*-methyl-7,7a-dihydro-1(6H)-indanone (4)*[3]

7,7*a*-Dihydro-7*a*β-methyl-1,5(6*H*)-indandione (**12**, 100 mg, 0.6 mmol) and ethylene glycol (37 mg, 0.6 mmol) were reacted and worked-up as described above for the preparation of **3** by selective ketalization of the dione **6**. The higher R_f preparative layer chromatography band contained the ketal **4** (26 mg) which recrystallized from *n*-hexane as small prisms m.p. 54–56°;[6] i.r. 1740 and 1090 cm^{-1}; p.m.r. δ 1.10 (3H, s, CH_3), 2.36 (2H, broad s), and 2.83 (2H, m, C-2 and -3, or -4 CH_2), 3.83 (4H, s, OCH_2CH_2O) and 5.60 p.p.m. (1H, "s", vinylic H).

Anal. Calcd. for $C_{12}H_{16}O_3$ (mol. wt. 208.1099): C, 69.20; H, 7.74. Found (208.1105); C, 68.73; H, 7.72.

The preparative layer chromatography band of lower R_f yielded the isomeric 1,1-ketal **14** as an oil (48 mg) which decomposed on attempted purification by distillation; i.r. 1660, 1160, and 1135 cm^{-1}; p.m.r. δ 1.28 (3H, s, CH_3), 2.45 (2H, "s") and 2.95 (2H, m, C-2 and -3, or -4 CH_2).

Mol. Wt. Calcd. for $C_{12}H_{16}O_3$: 208.1099. Found (mass spectrum): 208.1105.

Financial support from the National Research Council of Canada and the National Cancer Institute of Canada, and the awards of an NRCC Scholarship (to J.D.L.) and an Ontario Graduate Fellowship (to P.W.M.) are gratefully acknowledged.

1. M. S. Newman and A. B. Mekler. J. Am. Chem. Soc. **82**, 4039 (1960).
2. S. Swaminathan, J. P. Hohn, and S. Ramachandran. Tetrahedron Lett. 729 (1962); S. Swaminathan, R. K. Natarajan, S. Ramachandran, and S. K. Sankarappa. J. Org. Chem **31**, 656 (1966).
3. M. Los and A. D. Mighell. Tetrahedron, **21**, 2297 (1965).

[4]No further studies were carried out on this compound since its preparation by a superior alternative method has already been reported (10).

[5]Alternatively this compound may be purchased from Aldrich.

[6]The preparation of a compound, m.p. 68–69°, described as the Δ^3-isomer, has been reported (12). However, the data upon which the latter structural assignment were made (12) are not unequivocal and the position of the double bond in either compound cannot be regarded as proven at the present time (*cf.* footnote 3).

4. D. GRAVEL and J. GAUTHIER. Tetrahedron Lett. 5489 (1968).
5. J. J. BROWN, R. H. LENHARD, and S. BERNSTEIN. J. Am. Chem. Soc. **86**, 2183 (1964).
6. J. F. W. KEANA. *In* Steroid reactions. *Edited by* C. Djerassi. Holden-Day, San Francisco, California, 1963. pp. 1–88.
7. *Cf.* E. J. SALMI. Ber. **71**, 1803 (1938).
8. K. E. PFITZNER and J. G. MOFFAT. J. Am. Chem. Soc. **87**, 5670 (1965).
9. (*a*) C. B. C. BOYCE and J. S. WHITEHURST. J. Chem. Soc. 2680 (1960); (*b*) J. Chem. Soc. 2022 (1959); (*c*) J. Chem. Soc. 4547 (1960).
10. J. E. MCMURRY. J. Am. Chem. Soc. **90**, 6821 (1968).
11. H. SCHICK, G. LEHMANN, and G. HILETAG. Chem. Ber. **102**, 3238 (1969).
12. V. F. KUCHEROV, I. A. GURVICH, and B. A. RUDENKO. Izv. Akad. Nauk. SSSR Ser. Khim. 1456 (1964).

Can. J. Chem. Downloaded from www.nrcresearchpress.com by 210.87.254.40 on 09/05/12
For personal use only.

Can. J. Chem. Downloaded from www.nrcresearchpress.com by 210.87.254.40 on 09/05/12
For personal use only.

Reaction of 1-Nitroso-2-naphthylamine with 3-Aroylaziridines

J. W. LOWN AND M. H. AKHTAR[1]

Department of Chemistry, University of Alberta, Edmonton 7, Alberta

Received December 21, 1970

Reaction of 1-nitroso-2-naphthylamine with a series of 3-aroylaziridines affords (*a*) 3-arylbenzo[*f*]-quinoxalines, (*b*) cyclohexylimino derivatives of 2-aroylnaphtho[1,2-*d*]imidazoles, and (*c*) a 2-aryl-naphtho[1,2-*d*]imidazole. Electron-withdrawing substituents in either the 2 or 3 aryl moieties of the aziridine lead to preferential formation of products of type *a* whereas electron-donating substituents in either of these positions result in the formation of products of type *b*. The results of deuterium labelling and unambiguous synthetic studies in support of the proposed 1,3-dipolar cycloaddition mechanism are discussed.

La réaction de la nitroso-1 naphtylamine-2 avec une série de benzoyl-3 arizidines conduit à (*a*) des phényl-3 benzo[*f*]quinoxalines, (*b*) des dérivés cyclohéxylimino des benzoyl-2 naphto[1,2-*d*]imidazoles, et (*c*) une phényl-2 naphta[1,2-*d*]imidazole. Si le noyau aromatique de l'aziridine porte des substituants électro-affinitaires en positions 2 ou 3, les produits formés d'une façon préférentielle sont ceux du type *a*; par ailleurs si des substituants sont électro-répulsifs les produits formés d'une façon préférentielle sont ceux du type *b*. On discute de nos résultats-molécules marquées par du détérium et synthèses non-ambigues-en fonction d'un mécanisme de cycloaddition dipolaire-1,3.

Canadian Journal of Chemistry, 49, 1610 (1971)

We recently described the reaction of 3-aroylaziridines with 1-nitroso-2-naphthol to produce both 2-aryl and 2-aroylnaphtho[1,2-*d*]oxazoles in good yield (1, 2). The reaction was interpreted as proceeding via initial 1,3-dipolar addition of an azomethine ylide, derived by thermal cleavage of the aziridine, to the nitrogen–oxygen bond in both orientations. Spontaneous 1,3-cleavage of the intermediate oxadiazolidines produced nitrones which cyclodehydrate to produce the observed products. In these reactions the aziridines behave as ylides and the reactions parallel the classic work of Krohnke and Gerlach on the chemistry of pyridinium ylides with nitrosonaphthols (3, 4). The latter type of reaction was used to prove the structure of the 2-aroylnaphtho-[1,2-*d*]oxazoles obtained in the aziridine reactions. 2-Nitroso-1-naphthol behaves differently with 3-aroylaziridines than with pyridinium ylides however and affords in the former case 2-arylnaphtho[2,1-*d*]oxazoles, 2,2′-azodi-1-naphthol, and examples of the hitherto undescribed naphtho[2,1-*f*]-1,3,5-oxadiazepine system (5), whereas in the latter case only naphtho[2,1-*d*]oxazoles are produced.

The simplicity and versatility of the reactions of aziridines with nitroso compounds suggested an extension to include other participating groups to be worthwhile. We describe the reaction of 1-nitroso-2-naphthylamine with 3-aroylaziridines to produce 3-arylbenzo[*f*]quinoxalines, cyclohexylimino derivatives of 2-aroylnaphtho[1,2-*d*]-imidazoles, and a 2-arylnaphtho[1,2-*d*]imidazole.

Treatment of 3-benzoyl-1-cyclohexyl-2-*p*-nitrophenylaziridine with an equimolar quantity of 1-nitroso-2-naphthylamine in refluxing benzene for 24 h and chromatographic separation of the product on alumina gave 3-phenylbenzo[*f*]quinoxaline (**1**), $C_{18}H_{12}N_2$, in 49% yield and 2-*p*-nitrophenylnaphtho[1,2-*d*]imidazole(**3**),$C_{17}H_{11}N_3O_2$, in 16% yield.

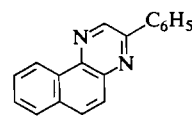

1

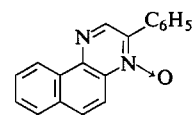

2

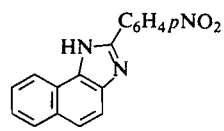

3

The structure of **1** was proven by oxidation to the known 3-phenylbenzo[*f*]quinoxaline-4-oxide (**2**) (6) in 53% yield with *m*-chloroperbenzoic acid. Owing to the existence of tautomerism in the

[1]NRCC Postdoctorate Fellow, 1970 to present.

Can. J. Chem. Downloaded from www.nrcresearchpress.com by 210.87.254.40 on 09/05/12
For personal use only.

2-*p*-nitrophenylnaphtho[1,2-*d*]imidazole (**3**) the position of the NH proton (clearly indicated by a band at 3330 cm^{-1} in the i.r. spectrum) cannot be assigned (7). Such structures had been considered for the sole products obtained in the parallel reaction of nitrosonaphthylamines with pyridinium ylides by Krohnke which were formulated as the benzo[*f*]quinoxaline-*N*-oxides *e.g.* **4** and **5** obtained by reaction of pyridinium

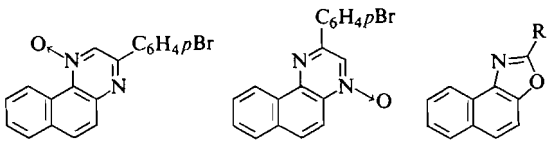

4 **5** **6**

p-bromophenacylide on 1-nitroso-2-naphthylamine and 2-nitroso-1-naphthylamine respectively (3, 4). In our reactions therefore the azomethine ylides derived from thermal cleavage of the 3-aroylaziridines behave quite differently from their pyridinium ylide analogs in contrast to their parallel behavior in their reactions with 1-nitroso-2-naphthol to produce 2-arylnaphtho-[1,2-*d*]oxazoles **6** (1, 2).

The obvious pathway to benzoquinoxalines such as **1** in the reaction with 3-aroylaziridines, namely, initial formation of a benzoquinoxaline-*N*-oxide analogous to **4** followed by deoxygenation, does not apply. While aromatic nitroso compounds can effect oxygen transfer reactions in many instances especially at elevated temperatures (8) nevertheless representative benzo[*f*]-quinoxaline-1-oxides prepared separately with pyridinium ylides proved to be completely unreactive towards 1-nitroso-2-naphthylamine under conditions in which **1** and similar compounds are formed readily.

The 3-*p*-bromophenylbenzo[*f*]quinoxaline-1-oxide (**4**) (4) could however be deoxygenated with lithium aluminum hydride to 3-*p*-bromophenylbenzo[*f*]quinoxaline which was shown to be identical with the product obtained from the reaction of 3-*p*-bromobenzoyl-1-cyclohexyl-2-phenylaziridine with 1-nitroso-2-naphthylamine.

Reaction of 1-cyclohexyl-2-phenyl-3-*p*-toluoylaziridine with 1-nitroso-2-naphthylamine in refluxing benzene for 24 h followed by chromatographic separation afforded a third type of product, 2-(cyclohexylimino-2-*p*-toluoyl)naphtho[1,2-*d*]imidazole (**7**), $C_{25}H_{25}N_3$, in 35.3% yield.

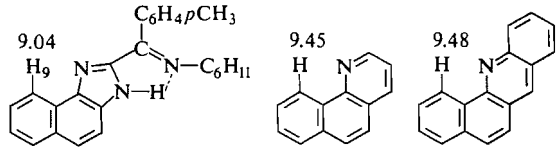

7 **8** **9**

The i.r. spectrum of **7** showed an NH absorption at 3440 cm^{-1} [compared with reported values of 3470–3400 cm^{-1} for hydrogen bonded NH in solution for benzimidazoles (9)]. The n.m.r. spectrum showed two bands at 5.08 and 5.21 δ, together equal to one proton, and both exchangeable in deuterium oxide and assigned to the NH proton in tautomeric hydrogen-bonded forms such as **7**; and a band at 3.83–4.50 characteristic of cyclohexyl methine adjacent to a C=N bond (10). The strongly shifted aromatic proton at 9.04 δ is ascribed to proton-9 *peri* to the aza-nitrogen of the imidazole ring by comparison with model compounds **8** and **9** (11).

The benzo[*f*]quinoxalines and cyclohexylimino 2-aroylnaphtho[1,2-*d*] imidazoles produced by reaction of 1-nitroso-2-naphthylamine with a variety of 3-aroylaziridines are listed in Tables 1 and 2 together with analytical data. In several instances the same naphthoimidazole or benzoquinoxaline was obtained from reactions with different aziridines when the appropriate groups were common.

The formation of the three types of products benzo[*f*]quinoxalines, cyclohexylimino-2-aroylnaphtho[1,2-*d*]imidazoles, and 2-arylnaphtho-[1,2-*d*]imidazoles is rationalized in Scheme 1.

The reactions are interpreted in terms of initial 1,3-dipolar cycloadditions in both orientations of the azomethine ylide (derived by cleavage of the aziridine) to the N—O bond of the nitrosonaphthylamine although most of the products correspond to one particular orientation of addition **10**. Formation of products of types **16** and **17** are envisaged as involving cleavage (*y*) of the intermediate oxadiazolidines **10** and **11** to the nitrones **13** and **14** respectively (a reaction for which precedents and strong analogies exist (1, 2)) and cyclodehydration of the latter to **16** and **17** respectively. Although Schiff bases have occasionally been isolated from 1,3-dipolar cycloaddition reactions of 4-oxazolines, they are more often hydrolyzed to aldehyde and cyclohexylamine during the reaction (12) and so cyclohexylamine would be available for condensation to form **16**.

TABLE 1. 3-Arylbenzo[*f*]quinoxalines

No.	3-Substituent	Melting point (°C)	Found (%) C	H	N	Molecular ion (mass spectrum)	Calculated (%) C	H	N	Molecular ion (mass spectrum)
a	*p*-$NO_2C_6H_4$	216–218	72.43	3.57	13.60	301.0845	71.75	3.67	13.94	301.0851
b	*m*-$NO_2C_6H_4$	247–249	71.90	3.49	13.73	301.0845	71.75	3.67	13.94	301.0851
c	C_6H_5	163–164.5	84.48	4.57	10.93	256.0997	84.50	4.70	10.83	256.1001
d	*p*-BrC_6H_4	200–201.5	64.55	3.34	8.11	334.0101	64.48	3.30	8.35	334.0105

TABLE 2. 2-Cyclohexyliminoaroylnaphtho[1,2-*d*]imidazoles

No.	2-Aroyl substituent	Melting point (°C)	Found (%) C	H	N	Molecular ion (mass spectrum)	Calculated (%) C	H	N	Molecular ion (mass spectrum)
d	*p*-$CH_3O{\cdot}C_6H_4$	130–131	77.77	6.40	10.53	383.1994	78.27	6.57	10.80	383.1998
e	*p*-$CH_3{\cdot}C_6H_4$	134–135	81.52	6.83	11.49	367.2045	81.70	6.85	11.45	367.2049
f	C_6H_5	110–112	81.40	6.50	11.83	353.1888	81.55	6.57	11.88	353.1892
g	*p*-BrC_6H_4	149–150.5	66.83	4.84	9.60	431.0997	66.66	5.13	9.71	431.1000

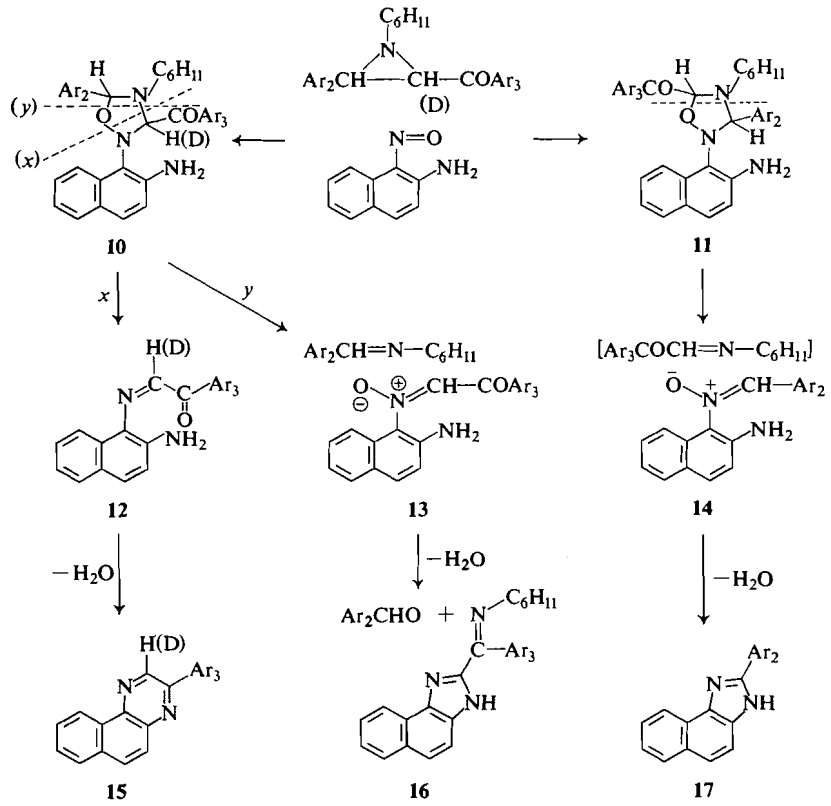

SCHEME 1

Can. J. Chem. Downloaded from www.nrcresearchpress.com by 210.87.254.40 on 09/05/12
For personal use only.

Can. J. Chem. Downloaded from www.nrcresearchpress.com by 210.87.254.40 on 09/05/12
For personal use only.

Formation of **16** and **17** from the nitrones **13** and **14** is the intramolecular counterpart of the reaction of aromatic 1,2-diamines with nitrones to form naphtho[1,2-*d*]imidazoles and benzimidazoles described by Krohnke and Leister (13) (see eq. 1). In the case of **13** the initially formed 2-aroylnaphtho[1,2-*d*]imidazole condenses with cyclohexylamine to form **16**.

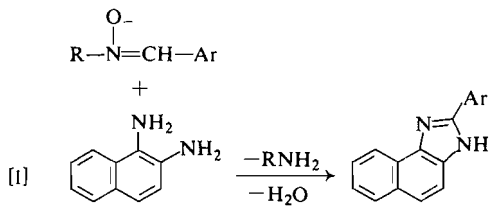

[1]

An alternative rationale for the formation of benzo[*f*]quinoxalines rather than benzo[*f*]-quinoxaline-1-oxides in these reactions suggested by a referee involves the reversible cycloaddition of Schiff bases to the *N*-oxide 1,3-dipoles (see Scheme 2).

However two benzo[*f*]quinoxaline-1-oxides were found to be completely unreactive towards benzal cyclohexylamine eliminating route *a*. Similarly route *b* is unlikely in view of the observed rapid cyclization of **13** (generated with pyridinium ylides at 15°) to the benzo[*f*]quinoxaline-1-oxide in contrast to the known sluggish dipolarophilic activity of Schiff bases (19) even at high temperatures.

1 - Nitroso - 2 - methylaminonaphthalene (**18**), when allowed to react with 3-benzoyl-1-cyclohexyl-2-*p*-nitrophenyl aziridine, gave the 1-*N*-methyl-2-*p*-nitrophenylnaphtho[1,2-*d*]imidazole (**19**), $C_{18}H_{13}N_3O_2$, m.p. 246–248° as the only isolable product. Compound **19** showed a singlet at 3.99 δ in the n.m.r. spectrum for the *N*-methyl group but showed no NH absorption in the i.r. spectrum. The benzo[*f*]quinoxaline is not formed in this reaction since condensation to the carbonyl group as in **12** is precluded.

Formation of products of type **15** without the intermediacy of the benzo[*f*]quinoxaline-1-oxide

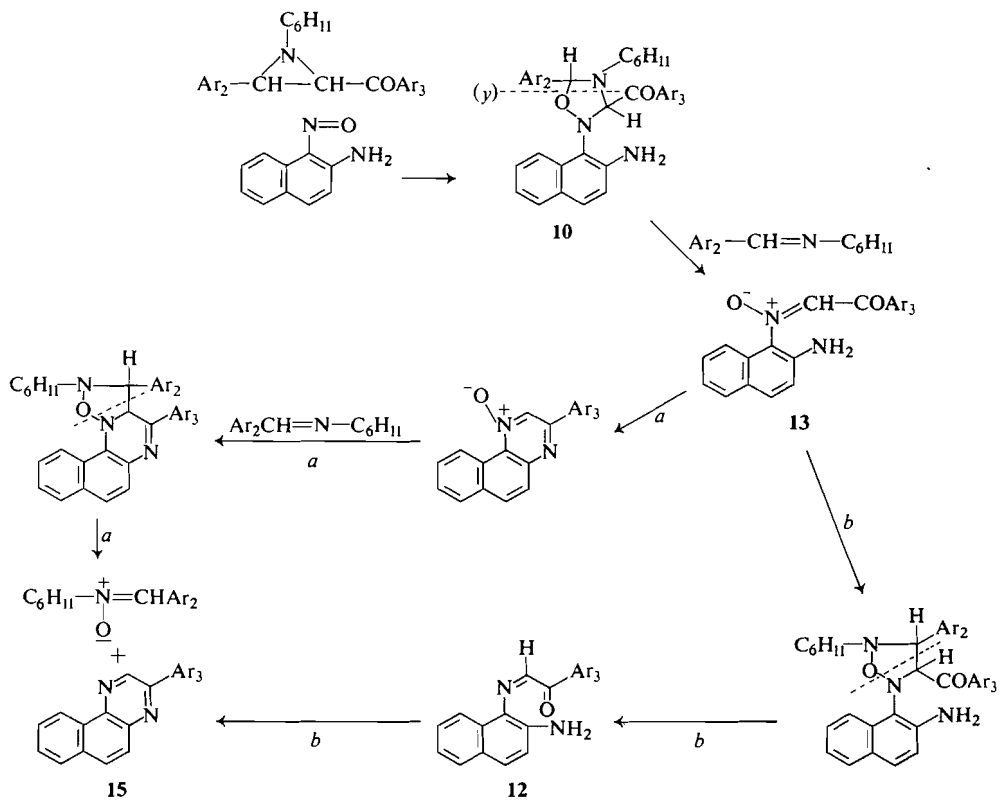

SCHEME 2

TABLE 3. Reaction of 3-aroylaziridines with *p*-nitrosodiphenylamine

Aziridine substituents*				Schiff base formed†		Yield (%)	Melting point (°C)	Reference
R_1	R_2	R_3	R_4	R_1	R_2			
(*cis*)H	NO_2	C_6H_{11}	H	H	NO_2	30.0	120	15
(*trans*)H	NO_2	C_6H_{11}	H	H	NO_2	26.3	121	15
NO_2	H	C_6H_{11}	H	NO_2	H	34.0	172	15
H	H	CH_3	CH_3	H	H	26.0	105	15
OCH_3	H	C_6H_{11}	H	OCH_3	H	33.9	103	16

*Refers to structure:

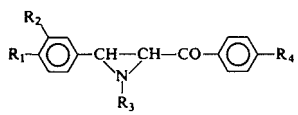

†Refers to structure: $C_6H_5NHC_6H_4-N=CH-C_6H_3(R_2)-R_1$

implies a second mode of cleavage (*x*) of intermediate **10** in which the substituted Schiff bases **12** are formed and subsequently cyclodehydrate to the benzo[*f*]quinoxalines **15**. At this latter stage the reaction becomes the counterpart of the

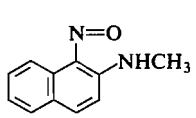

18

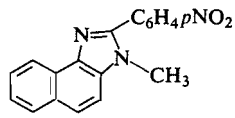

19

reaction of 1,2-diamines with α-diketones to form quinoxalines. The latter reaction would be favored over formation of an imidazole ring since the C=N bond in **12** is less susceptible to nucleophilic attack than the strongly polarized $C=\overset{+}{N}-O^{\ominus}$ bond in **13** or **14**. This reaction pathway to **15** receives confirmation by the reaction of 1-nitroso-2-naphthylamine with specifically deuterium labelled 3-benzoyl-1-cyclohexyl-3-deutero - 2 - *p* - nitrophenylaziridine (containing 54% deuterium incorporation) which gave 2-deutero-3-phenylbenzo[*f*]quinoxaline in which 56% of the original label was incorporated into the 2 position (see Scheme 1).

To support the above proposal involving cleavage of the intermediate oxadiazolidine by mode (*x*), examples were sought in which Schiff bases were isolable directly. Such should be the case if cyclization were prevented by a suitable positioning of substituents.

p-Nitrosodiphenylamine reacted readily with either *cis* or *trans* 3-benzoyl-1-cyclohexyl-2-*m*-nitrophenylaziridine to give the known *N*-[*m*-nitrobenzal]-4-phenylaminoaniline (**20**), m.p. 121°, in 30 and 26% yields respectively. Similarly *p*-nitrosodiphenylamine reacted with 2-*p*-anisyl-3-benzoyl-1-cyclohexylaziridine to give *N*-[4-methoxybenzal]-4-phenylaminoaniline in 34% yield (see Table 3).

$$pC_6H_5NHC_6H_4N{=}CHC_6H_4mNO_2$$

20

It is very improbable that a nitrone comparable with **14** is an intermediate in the formation of **20** and similar Schiff bases. Nitrones like the *N*-oxides **2**, **4**, and **5** may be deoxygenated to imines but require reagents such as triphenylphosphine (14).

It may be noted from Table 4 that electron-withdrawing substituents in either the 2 or 3 aryl moieties of the aziridine lead to a clear preference for formation of the benzo[*f*]quinoxalines. In contrast electron-donating substituents in either the 2 or 3 positions of the aziridine result in formation of the naphtho[1,2-*d*]imidazole derivative and groups which have zero (H) or small inductive effects (Br) lead to mixtures of the two principal products. The 2-arylnaphtho[1,2-*d*]-imidazole was isolated in only one instance. The marked effects of the substituents on the mode of cleavage of the intermediate oxadiazolidine **10** indicate a highly polar transition state for the reaction and suggest heterolytic cleavage.

Reactions of 3-aroylaziridines with 1-nitroso-naphthalenes bearing other neighboring groups in the 2 position are currently under investigation.

Experimental

Melting points were determined on a Fisher–Johns apparatus and are uncorrected. The i.r. spectra were

Can. J. Chem. Downloaded from www.nrcresearchpress.com by 210.87.254.40 on 09/05/12
For personal use only.

TABLE 4. Reaction of 3-aroylaziridines with 1-nitroso-2-naphthylamine

Aziridine		3-Arylbenzo[*f*]quinoxaline		Cyclohexylimino-2-aroylnaphthol	
Ar_2	$COAr_3$	Product no.	Yield (%)	Product no.	Yield (%)
C_6H_5	*p*-$NO_2C_6H_4$	*a*	80.5		—
C_6H_5	*m*-$NO_2C_6H_4$	*b*	78.5		—
p-$NO_2C_6H_4$	C_6H_5	*c*	49.4		15.5*
m-$NO_2C_6H_4$	C_6H_5	*c*	47.8		—
C_6H_5	*p*-$CH_3OC_6H_4$		—	*d*	36.3
C_6H_5	*p*-$CH_3C_6H_4$		—	*e*	35.3
p-$CH_3OC_6H_4$	C_6H_5		—	*f*	39.0
p-$CH_3C_6H_4$	C_6H_5	*c*	12.5	*f*	27.6
C_6H_5	C_6H_5	*c*	42.5	*f*	4.5
C_6H_5	*p*-BrC_6H_4	*d*	32.7	*g*	10.0

*2-*p*-Nitrophenylnaphtho[1,2-*d*]imidazole.

recorded on a Perkin–Elmer model 421 spectrophotometer, and only the principal, sharply defined peaks are reported. The n.m.r. spectra were recorded on Varian A-60 and A-100 analytical spectrometers. The spectra were measured on approximately 10–15% (W/V) solutions in $CDCl_3$, with tetramethylsilane as a standard. Line positions are reported in p.p.m. from the reference. Absorption spectra were recorded in 'spectro'-grade solvents on a Beckman DB recording spectrophotometer. Mass spectra were determined on an Associated Electrical Industries MS-9 double focusing high resolution mass spectrometer. The ionization energy, in general, was 70 eV. Peak measurements were made by comparison with perfluorotributylamine at a resolving power of 15 000. Kieselgel DF-5 (Camag, Switzerland) and Eastman Kodak precoated sheets were used for t.l.c. Microanalyses were carried out by Mrs. D. Mahlow of this department.

General Preparation of 3-Aroylaziridines

The aziridines used in this study were prepared by the Gabriel synthesis involving Claisen–Schmidt condensations to form chalcones, addition of bromine to form the dibromochalcones, and treatment of the dibromochalcones with an excess of a primary aliphatic amine to provide 3-aroylaziridines (17).

Preparation of 1-Nitroso-2-naphthylamine

1-Nitroso-2-naphthylamine was prepared by dissolving 1-nitroso-2-naphthol (technical grade, Eastman Organic Chemicals) in water, adding an equimolar quantity of 0.88 aqueous ammonia, and heating the mixture on the steam bath for 2 h. 1-Nitroso-2-naphthylamine formed as a moss-green precipitate which was collected and purified by recrystallization from aqueous ethanol m.p. 150–152° in 69% yield (lit. m.p. 150–152° (18)).

Preparation of 1-Nitroso-2-(N-methyl)-naphthylamine

To a suspension of 8.6 g (0.05 mol) of 1-nitroso-2-naphthol in 40 ml of water were added 10 ml of methylamine (40% in water, Eastman Organic Co). The reaction mixture was heated in a pressure bottle in a steam bath for 30 min. On cooling a greenish-brown precipitate deposited, which was filtered, boiled in water twice (20 ml), filtered, dried *in vacuo* to give 5.4 g (69% yield) of 1-nitroso-2-(*N*-methyl)-naphthylamine, m.p. 135–137 °C.

Anal. Calcd. for $C_{11}H_{10}N_2O$ (mol. wt. 186.0793): C, 70.96; H, 5.38; N, 15.05. Found (186.0790 (mass spectrum)): C, 70.82; H, 5.08; N, 14.73.

The i.r. spectrum, $\nu_{max}(CHCl_3)$: 3410 cm^{-1} (N—H); n.m.r. spectrum: $\delta_{TMS}(CDCl_3)$: 2.85 (3H, doublet, —N—CH_3, J = 5.0 Hz); 4.18–5.18 (1H, broad, —NH, D_2O-exchangeable); 6.55–7.62 (5H, multiplet, aromatic protons); 8.81–8.95 (1H, multiplet, *peri*-proton at C-8 position).

General Procedure for the Reaction of 3-Aroylaziridines with 1-Nitroso-2-naphthylamine

Representative examples of the preparation of 3-arylbenzo[*f*]quinoxalines, 2-cyclohexyliminoaroylnaphtho[1,2-*d*]imidazoles, and 2-arylnaphtho[1,2-*d*]imidazoles are described in detail. The analytical and spectral data on further examples prepared in a similar fashion are summarized in Tables 1–3.

Reaction of 3-Benzoyl-1-cyclohexyl-2-p-nitrophenylaziridine with 1-Nitroso-2-naphthylamine

A solution of 1.75 g (5 mmol) of 2-*p*-nitrophenyl-1-cyclohexyl-3-benzoylaziridine and 0.86 g (5 mmol) of 1-nitroso-2-naphthylamine in 40 ml of dry benzene was stirred and heated under reflux for 24 h. The reaction mixture was concentrated *in vacuo*, and the dark oil was subjected to chromatography on 60 g of alumina (BDH) with hexane–benzene (8:2) as eluant. Removal of the solvent afforded white flakes of 3-phenylbenzo[*f*]quinoxaline, 0.632 g (49.4% yield), m.p. 163–164 °C [from 95% ethanol (lit. m.p. 163–164° (6)].

Anal. Calcd. for $C_{18}H_{12}N_2$ (mol. wt. 256.1001): C, 84.50; H, 4.70; N, 10.83. Found (256.0997 (mass spectrum)): C, 84.48; H, 4.57; N, 10.93.

The n.m.r. spectrum $\delta_{TMS}(CDCl_3)$: 7.16–8.22 (10H, multiplet, aromatic protons); 9.03–9.18 (1H, multiplet, *peri*-proton at C-10), and 9.25 (1H, singlet, proton at C-2).

Further elution with benzene gave after removal of the solvent *in vacuo* a brownish solid of 2-*p*-nitrophenylnaphtho[1,2-*d*]imidazole 0.224 g (15.5% yield), m.p. 290–293 °C.

Anal. Calcd. for $C_{17}H_{11}N_3O_2$ (mol. wt. 289.0851): C, 70.58; H, 3.83; N, 14.52. Found (289.0858 (mass spectrum)): C, 70.57; H, 4.19; N, 13.69.

The i.r. spectrum ν_{max}(KBr) 3330 (—N—H); 1510 and 1335 cm^{-1} (aromatic nitro group).

Can. J. Chem. Downloaded from www.nrcresearchpress.com by 210.87.254.40 on 09/05/12
For personal use only.

Can. J. Chem. Downloaded from www.nrcresearchpress.com by 210.87.254.40 on 09/05/12
For personal use only.

Reaction of 3-Benzoyl-1-cyclohexyl-3-deutero-2-p-nitrophenylaziridine with 1-Nitroso-2-naphthylamine

A solution of 0.88 g (2.5 mmol) of 3-benzoyl-1-cyclohexyl-3-deutero-2-*p*-nitrophenylaziridine (54% D incorporation) (11) and 0.43 g (2.5 mmol) of 1-nitroso-2-naphthylamine in 30 ml of dry benzene was heated under reflux for 24 h. The reaction mixture worked-up exactly as described above affording 2-deutero-3-phenylbenzo-[*f*]quinoxaline, m.p. 162–163°, 0.240 g (36% yield) m.p. of protium analog 163–164°.

The n.m.r. spectrum δ_{TMS} ($CDCl_3$): 7.16–8.22 (10H, multiplet, aromatic protons), 9.03–9.18 (1H, multiplet, *peri*-protons at C-10), and 9.25 (0.67H, singlet, proton at C-2, 33% deuterium incorporation at C-2 position *i.e.* overall incorporation 55.5%).

Reaction of 1-Cyclohexyl-2-phenyl-3-p-toluoylaziridine with 1-Nitroso-2-naphthylamine

A solution of 1.59 g (5 mmol) of 1-cyclohexyl-2-phenyl-3-*p*-toluoylaziridine and 0.87 g (5 mmol) of 1-nitroso-2-naphthylamine in 40 ml of dry benzene was stirred and heated under reflux for 24 h. The reaction mixture was concentrated *in vacuo*, and the oil was subjected to chromatography on 60 g of alumina (BDH) with hexane–benzene (9:1) as eluant. Removal of the solvent and trituration of the resulting yellow oil with petroleum ether (30–60) gave the cyclohexylamino adduct of 2-toluoylnaphtho[1,2-*d*]imidazole as a yellow solid, 0.645 g (35.3% yield), m.p. 134–135.5° (95% ethanol).

Anal. Calcd. for $C_{25}H_{25}N_3$ (mol. wt. 370.2049): C, 81.70; H, 6.85; N, 11.45. Found (367.2045 (mass spectrum)): C, 81.52; H, 6.83; N, 11.49.

The i.r. spectrum ν_{max}($CHCl_3$): 3440 cm^{-1} (—NH). The n.m.r. spectrum δ_{TMS}($CDCl_3$): 0.83–2.33 (10H, multiplet, cyclohexyl protons); 2.42 (3H, singlet, methyl protons); 3.83–4.50 (1H, multiplet, methine proton), 5.08 and 5.21 (1H, 2 singlet, D_2O exchangeable, —NH). 7.18–7.96 (9H, multiplet, aromatic protons), and 8.96–9.12 (1H, multiplet *peri*-proton at C-9).

Oxidation of 3-Phenylbenzo[f]quinoxaline with m-Chloroperbenzoic Acid

To a solution of 0.256 g (1 mmol) of 3-phenylbenzo-[*f*]quinoxaline in 10 ml chloroform was added 0.207 g (1.2 mmol) of *m*-chloroperbenzoic acid (80%). The reaction mixture was stored at 0 °C for 4 days, concentrated, made alkaline with 2 *N* aqueous sodium carbonate, and extracted with chloroform to give the yellow 3-phenylbenzo[*f*]quinoxaline-4-oxide, 0.144 g (53% yield), m.p. 231–233 °C (lit. m.p. 234–235° (6)).

Deoxygenation of 3-p-Bromophenylbenzo[f]quinoxaline-1-oxide with Lithium Aluminum Hydride

To a suspension of 0.38 g (10 mmol) of lithium aluminum hydride in 125 ml of dry benzene was added 0.9 g (2.5 mmol) of 3-*p*-bromophenylbenzo[*f*]quinoxaline-1-oxide prepared from published procedures (4) and the suspension was heated under reflux for 24 h. The usual work-up procedure afforded a cream-colored solid of 3-*p*-bromophenyl-benzo[*f*]quinoxaline, 0.078 g (8%), m.p. 199–201 °C. The n.m.r. and i.r. spectra of this compound were identical to those prepared by reaction of 3-*p*-bromobenzoyl-1-cyclohexyl-2-phenylaziridine with 1-nitroso-2-naphthylamine. The mixed melting points of 3-*p*-bromophenylbenzo[*f*]quinoxaline from these two sources were undepressed. In comparable reactions between 3-*p*-bromophenylbenzo[*f*]quinoxaline-1-oxide and an equimolar quantity of 1-nitroso-2-naphthylamine, the benzo-[*f*]quinoxaline-1-oxide was recovered unchanged, even after prolonged refluxing in benzene.

Reaction of 3-Benzoyl-1-cyclohexyl-2-p-nitrophenylaziridine with 1-Nitroso-2-(N-methyl)-naphthylamine

A solution of 1.75 g (5 mmol) of 3-benzoyl-1-cyclohexyl-2-*p*-nitrophenylaziridine and 0.93 g (5 mmol) of 1-nitroso-2-(*N*-methyl)naphthylamine in 40 ml of dry benzene was stirred and heated under reflux for 24 h during which time the solution turned dark brown. Upon cooling of the reaction mixture, a green–brown solid which had precipitated, 0.982 g (65% yield) was collected and purified by extraction of the impurities with benzene–acetone (8:2) to give yellow solid, m.p. 246–248 °C.

Anal. Calcd. for $C_{18}H_{13}N_3O_2$ (mol. wt. 303.1008): C, 71.28; H, 4.31; N, 13.85. Found (303.1004 (mass spectrum)): C, 70.80; H, 3.70; N, 13.91.

The i.r. spectrum, ν_{max}($CHCl_3$): ν_{max} 1515 and 1340 cm^{-1} (aromatic nitro group); n.m.r. spectrum δ_{TMS} ($CDCl_3$): 3.99 (3H, singlet, CH_3), and 7.20–8.94 (10H, multiplet, aromatic protons).

Reaction of p-Nitrosodiphenylamine with 2-Anisyl-3-benzoyl-2-cyclohexylaziridine

A solution of 1.675 g (5 mmol) of 2-anisyl-3-benzoyl-1-cyclohexylaziridine and 0.99 g (5 mmol) of *p*-nitrosodiphenylamine in 40 ml of dry benzene was heated under reflux for 24 h when a red–brown color developed. After removal of the solvent *in vacuo*, the residual brown oil was subjected to chromatography on 80 g of B.D.H. alumina. Elution with benzene afforded a yellow oil after evaporation of the solvent. The oil crystallized upon trituration with hexanes yielding *N*-[4-methoxybenzal]-4-phenylaminoaniline 0.51 g (34% yield), m.p. 103° (lit. m.p. 105° (16)).

Reaction of cis-3-Benzoyl-1-cyclohexyl-2-p-nitrophenylaziridine with p-Nitrosodiphenylamine

A solution of 1.75 g (5 mmol) of *cis*-3-benzoyl-1-cyclohexyl-2-*p*-nitrophenylaziridine and 0.99 g (5 mmol) of *p*-nitrosodiphenylamine in 50 ml of dry benzene was heated under reflux for 24 h. After removal of the solvent *in vacuo*, the residual oil was subjected to chromatography on 85 g of B.D.H. alumina. Elution with benzene afforded a red oil which crystallized upon trituration with hexanes yielding *N*-[3-nitrobenzal]-4-phenylaminoaniline as deep yellow plates, 0.464 g (30% yield), m.p. 120° (lit. m.p. 123° (14)).

Reaction of trans-3-Benzoyl-1-cyclohexyl-2-p-nitrophenylaziridine with p-Nitrosodiphenylamine

A similar reaction between 1.75 g (5 mmol) of *trans*-3-benzoyl-1-cyclohexyl-2-*p*-nitrophenylaziridine and 0.99 g (5 mmol) of *p*-nitrosodiphenylamine afforded *N*-[3-nitrobenzal]-4-phenylaminoaniline, 0.402 g (26% yield), m.p. 121° identical with that obtained above.

Reaction of other 3-aroylaziridines with *p*-nitrosodiphenylamine to give Schiff bases were carried out in a similar fashion and the results are summarized in Table 4.

Reaction of 3-Phenylbenzo[f]quinoxaline-1-oxide with Benzal Cyclohexylamine

A solution of 1.36 g (0.05 mmol) of 3-phenylbenzo-[*f*]quinoxaline-1-oxide [prepared from 1-nitroso-2-

naphthylamine and pyridinium phenacylide (4) [Mol. Wt. Calcd. for $C_{18}H_{12}N_2O$: 272.0950. Found (mass spectrum): 272.0944)] and 0.91 g (0.05 mol) of benzal cyclohexylamine (20) in 40 ml of benzene was heated under reflux for 24 h. Upon cooling the solution the *N*-oxide precipitated unchanged as an orange–red solid which was collected, 1.31 g (98% recovery), m.p. 222–224° (mixed m.p. with authentic sample 222–224°).

Reaction of 3-p-Bromophenylbenzo[f]quinoxaline-1-oxide with Benzal Cyclohexylamine

Similarly a suspension of 1.75 g (0.05 mol) of 3-*p*-bromophenylbenzo[*f*]quinoxaline and 0.91 g (0.05 mol) of benzal cyclohexylamine in 40 ml of benzene was heated under reflux for 24 h. Upon cooling the solution, the unchanged *N*-oxide was recovered 1.72 g (99% recovery), m.p. 301° (mixed m.p. with authentic sample 301°).

This research was supported by a National Research Council of Canada grant to J. W. Lown. We thank Mr. R. Swindlehurst and Dr. A. Hogg for the n.m.r. spectra and Mr. J. P. Moser and Miss B. Cole for able technical assistance.

1. J. W. LOWN and J. P. MOSER. Can. J. Chem. **48**, 2227 (1970).
2. J. W. LOWN and J. P. MOSER. Chem. Commun., 247 (1970).
3. F. KROHNKE. Angew. Chem. Int. Ed. **2**, 380 (1963).
4. K. GERLACH and F. KROHNKE. Chem. Ber., **95**, 1124 (1962).
5. J. W. LOWN and J. P. MOSER. Tetrahedron Lett. 3019 (1970).
6. E. HAYASHI and H. SAITO. Yakugaku Zasshi, **86**, 687 (1966). Chem. Abstr. **65**, 16970c (1966).
7. (*a*) A. R. KATRITZKY and J. M. LAGOWSKI. Adv. Heterocycl. Chem. **2**, 27 (1963); K. HOFMANN. Imidazole and its derivatives. Part 1. *In* The chemistry of heterocyclic compounds. A. Weissberger, *editor*. Interscience, New York, N.Y., 1953. pp. 26–30.
8. P. A. S. SMITH. Open-chain nitrogen compounds. Vol. 2. Benjamin Press, New York, N.Y., 1966, p. 363.
9. A. R. KATRITZKY and A. P. AMBLER. Physical methods in heterocyclic chemistry. Vol. II. Academic Press, New York, N.Y., 1963, p. 239
10. J. W. LOWN and K. MATSUMOTO. J. Org. Chem. In press.
11. E. V. DONCKT, R. H. MARTIN, and F. GEERTS-EVRARD. Tetrahedron, **20**, 1495 (1964).
12. J. W. LOWN, R. K. SMALLEY, G. DALLAS, and T. W. MALONEY. Can. J. Chem. **48**, 103 (1970).
13. F. KROHNKE and H. LEISTER. Ber. **91**, 1479 (1958).
14. L. HORNER and H. HOFFMANN. Angew. Chem. **68**, 480 (1956).
15. C. HEUCKE. Ann. **255**, 190 (1889).
16. F. J. MOORE and R. G. WOODBRIDGE. J. Am. Chem. Soc. **30**, 1001 (1908).
17. N. H. CROMWELL, N. G. BARKER, R. A. WANKEL, P. J. VANDERHORST, F. W. OLSON, and J. H. ANGLIN. J. Am. Chem. Soc. **73**, 1044 (1951).
18. M. ILINSKI. Chem. Ber. **17**, 391 (1884).
19. J. W. LOWN, J. P. MOSER, and R. WESTWOOD. Can. J. Chem. **47**, 4335 (1969).
20. E. D. BERGMANN, E. ZIMKIN, and S. PINEHAS. Rec. Trav. Chim. **71**, 168 (1952).

Can. J. Chem. Downloaded from www.nrcresearchpress.com by 210.87.254.40 on 09/05/12
For personal use only.

Photolysis of 1,1-Diphenylsilacyclohexanone in Diethyl Fumarate. The Trapping of a Siloxycarbene by an Electron-Deficient Olefin

A. G. Brook, H. W. Kucera, and Ronald Pearce
Department of Chemistry, University of Toronto, Toronto 181, Ontario

Received December 4, 1970

Photolysis of diphenylsilacyclohexanone in diethyl fumarate yields a product shown to be the cyclopropane resulting from trapping of a siloxycarbene by the alkene.

On montre que le produit formé lors de la photolyse de la diphénylsilacyclohexanone dans le fumarate d'éthyle est un cyclopropane provenant de la condensation d'un syloxycarbène sur l'alcène.

Canadian Journal of Chemistry, 49, 1618 (1971)

Can. J. Chem. Downloaded from www.nrcresearchpress.com by 210.87.254.6 on 09/05/12
For personal use only.

Introduction

In our investigations of the photochemistry of acylsilanes, we have obtained evidence for a ready photoisomerization of acylsilanes to siloxycarbenes, these latter species being trapped in the presence of alcohols (1) (eq. 1). Confirmation of the formation of the siloxycarbenes in these photolyses was required, and since the formation of cyclopropanes by the addition of carbenes to the double bond of olefins is characteristic of such species (2) the photolysis of acylsilanes in alkenes was investigated. This report describes the isolation and characterization of the spirocyclopropane obtained from the photolysis of 1,1-diphenyl-1-silacyclohexan-2-one (**1**) in the presence of diethyl fumarate.

$$[1]\quad R_3SiC(=O)R' \xrightarrow{h\nu} R_3SiO\ddot{C}R' \xrightarrow{R''OH} R_3SiOCHR'(OR'')$$

Results and Discussion

Photolysis of **1** in diethyl fumarate solution proceeded readily to give the adduct, *trans*-1,2-dicarbethoxy-4,4-diphenyl-3-oxa-4-silaspiro-[2.6]nonane (**2**) in 78% yield (Scheme 1). Its n.m.r. spectrum showed two doublets at δ 2.29 and 2.72 (J = 7 Hz) assigned to the cyclopropyl protons, in addition to other expected features. No evidence of the presence of other isomers was noted.

Mild acid hydrolysis of **2** afforded the acyclic ester, **3**, while a more vigorous, basic hydrolysis gave the acyclic acid, **4**, which was characterized as its methyl ester, **5**, after reaction with diazomethane. The formation of **3** presumably takes place via attack of water (or hydroxide ion) at silicon. Saponification of **3**, and decarboxylation of the resulting β-keto acid, accounts for the formation of **4**.

The structure of the methyl ester, **5**, was confirmed by the alternate synthesis outlined in Scheme 2. 5-(Diphenylhydroxysilyl)pentanal (3) prepared by photolysis of **1** in wet ether, was treated with 3-butenylmagnesium bromide to give 9-diphenylhydroxysilyl-5-hydroxynon-1-ene (**6**). Ozonolysis of this alkene gave a product believed to be the 2-hydroperoxytetrahydrofuran, **7** (4). Without being isolated this was reduced with zinc in acetic acid and oxidized with chromic acid to give the γ-lactone, **8**, along with a small quantity of the γ-keto acid, **4**. The predominance of the γ-lactone in the oxidation product is not unexpected since it is known that 4-hydroxybutanals exist mainly as their tautomeric cyclic hemi-acetals (5). Hydrolysis of **8**, followed by oxidation with chromic acid, afforded the γ-keto acid, **4**, which was converted to its methyl ester, **5**, on treatment with diazomethane. The spectra of **5** obtained from this synthesis and from the material obtained by the degradation of the spiro compound, **2**, were identical.

The isolation of the adduct **2** is, therefore, good evidence for the intermediacy of a siloxycarbene, **1***a*, in the photolysis of **1**.

Photolysis of **1** in the presence of a number of other olefins failed to give significant quantities of the expected spiro adducts. The olefins used were cyclohexene, 2,3-dimethylbut-2-ene, 1,1-dimethoxyethene, *cis*- and *trans*-1,2-dichloroethene, and tetracyanoethene (this olefin appeared

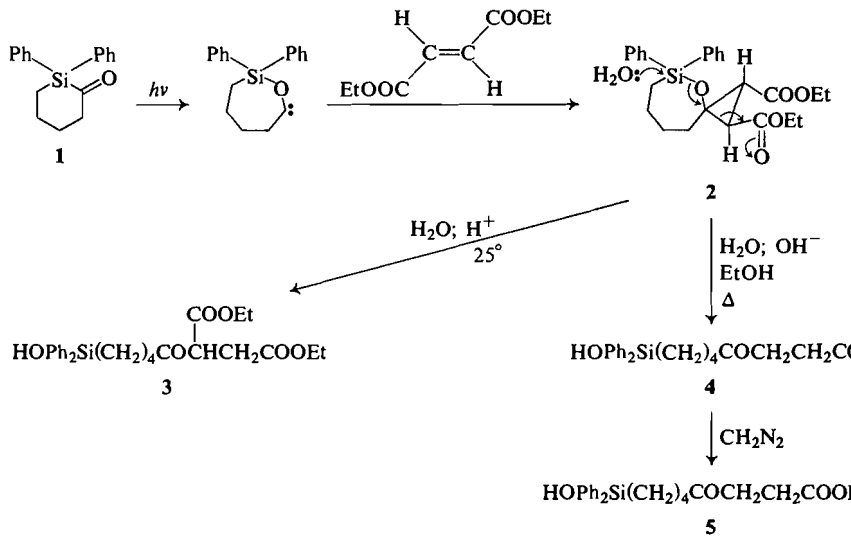

SCHEME 1

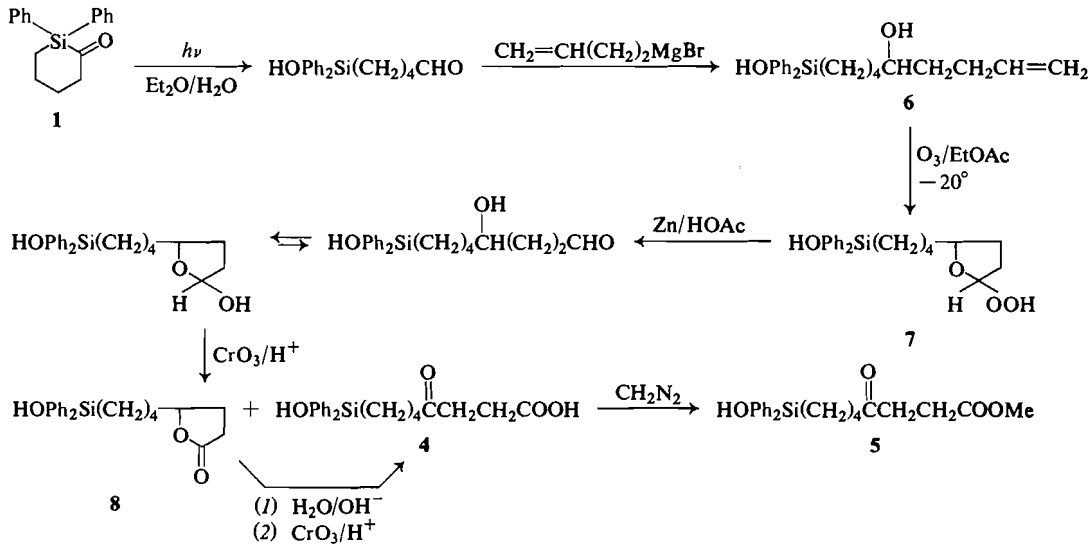

SCHEME 2

to form a charge-transfer complex with **1**). The presence of very small quantities of what may be the expected adducts with *cis*- and *trans*-1,2-dichloroethene was indicated by weak signals in the n.m.r. spectra of the crude products: absorptions at δ 3.28 and 2.77 p.p.m. were observed with the *cis*-olefin and a pair of doublets (AB system, $J = 4$ Hz) at δ 2.89 and 3.27 p.p.m. were observed with the *trans*-olefin.

The facile reaction with diethyl fumarate and the lack of reactivity with electron-rich olefins such as cyclohexene or tetramethylethylene suggest that the cyclic siloxycarbene behaves as a nucleophile, a behavior observed previously with a variety of other oxacarbenes (2, 6). The nucleophilic properties of oxacarbenes can be ascribed to the importance of contributions from the canonical form **9*a*** of the hybrid. If this interpre-

Can. J. Chem. Downloaded from www.nrcresearchpress.com by 210.87.254.6 on 09/05/12
For personal use only.

$$R—O—\ddot{C}—R' \leftrightarrow R—\overset{+}{O}=\bar{C}—R'$$
9 **9a**

tation is correct then the siloxycarbenes may be expected to be more nucleophilic than their carbon analogues since electron release by the relatively electropositive silyl group R should stabilize this contribution. The results presented here are in accord with this order of relative nucleophilicity.

Experimental

Photolysis of 1,1-Diphenylsilacyclohexan-2-one (1) in Diethyl Fumarate

A solution of **1** (5.0 g, 0.019 mol) in freshly distilled diethyl fumarate (31 g, 0.18 mol) was irradiated under nitrogen for 6 h using a low pressure mercury lamp.[1] Fractionation afforded *trans*-1,2-dicarbethoxy-4,4-diphenyl-3-oxa-4-silaspiro[2.6]nonane (**2**), 6.5 g (78%); b.p. 190–200°/0.01 mm (Kugelröhr); n_D^{22} 1.5462; i.r. (film) λ_{max} 5.78 (C=O) μ; n.m.r. (CCl_4) δ 7.7–7.1 (Ar, m, 10), 4.0 (OCH_2—, two overlapping q (J = 7 Hz), 4), 2.72, 2.29 (cyclopropyl, AB system (J = 7 Hz), 2), 2.2–0.9 (aliphatic and O—C—CH_3, m with two overlapping t at 1.1 (J = 7 Hz), 14), p.p.m.

Anal. Calcd. for $C_{25}H_{30}O_5Si$: C, 68.45; H, 6.90. Found: C, 68.24; H, 6.91.

Acid Hydrolysis of 2

A solution of **2** (1.11 g, 0.0025 mol), acetone (15 ml), and 2 *M* hydrochloric acid (1 ml) was stirred at room temperature for 24 h. The solvent was removed on a rotary evaporator and the residue was extracted with ether. The ethereal extract was washed with sodium carbonate solution and dried ($MgSO_4$). Evaporation of the ether gave 0.90 g (80%) of viscous oil. Elution with 5% acetone in chloroform from silica gel gave pure ethyl-8-diphenylhydroxysilyl-3-carbethoxy-4-oxooctanoate (**3**); i.r. (film) λ_{max} 2.7–3.1 (OH), 5.77, 5.85 (C=O) μ; n.m.r. (CCl_4) δ 7.7–7.2 (Ar, m, 10), 3.98 and 4.02 (OCH_2, two overlapping q, (J = 7 Hz), 4), 3.8 (—COCH(COOEt)-CH_2—, t (J = 8 Hz), 1), 2.70 (CH_2COOEt, two d (J = 8 Hz), 2), 2.5 (CH_2CO—, m, 2), 1.7–0.9 (aliphatic OH and O—C—CH_3, m with two overlapping t at 1.1 (J = 7 Hz), 13) p.p.m.

Anal. Calcd. for $C_{25}H_{32}O_6Si$: C, 65.75; H, 7.06. Found: C, 66.16; H, 7.09.

An n.m.r. spectrum in DMSO showed a singlet at δ 6.48 p.p.m. (—SiOH) which disappeared on addition of D_2O.

Base Hydrolysis of 2

A solution containing **2** (1.64 g, 0.0036 mol), potassium hydroxide (1.3 g, 0.023 mol), ethanol (20 ml), and water (4 ml) was heated at reflux for 2 h. The solution was acidified and the crude γ-keto acid, **4**, was isolated by extraction with sodium bicarbonate solution. To a solution of **4** in ether was added dropwise a solution of diazomethane in ether until the yellow color of the diazomethane was no longer rapidly discharged. Work-up gave a viscous oil (0.95 g, 50%) which was eluted with chloroform from silica gel to give methyl-8-(diphenylhydroxysilyl)-4-oxooctanoate (**5**); i.r. (film) λ_{max} 2.7–3.1 (OH), 5.74, 5.81 (C=O) μ; n.m.r. (CCl_4) δ 7.6–7.1 (Ar, m, 10), 4.9 (OH, broad, s, 1), 3.45 (OMe, s, 3), 2.4 ($COCH_2CH_2CO$, broad, s, 4), 2.4–2.1 (CH_2CO, m, 2), 1.6–0.8 (aliphatic, m, 6) p.p.m.

Anal. Calcd. for $C_{21}H_{26}O_4Si$: C, 68.08; H, 7.07. Found: C, 67.91; H, 7.03.

An n.m.r. spectrum in DMSO showed a singlet at δ 6.36 p.p.m. attributed to the silanol proton.

Synthesis of Methyl 8-(Diphenylhydroxysilyl)-4-oxooctanoate

To a solution of 5-(diphenylhydroxysilyl)pentanal (**3**) (prepared from **1** (4.4 g, 0.0165 mol in ether (50 ml)) was added at −70° a solution of 3-butenylmagnesium bromide (excess) in ether. After the addition the solution was allowed to warm to room temperature. Work-up gave an oil which was purified by elution with 7% acetone in chloroform from silica gel to give 8-(diphenylhydroxysilyl)-5-hydroxynon-1-ene (**6**), 4.6 g, 82%; i.r. (CCl_4) λ_{max} 2.70 (SiOH), 2.75 (C—OH), 6.10 (C=C) μ; n.m.r. (CCl_4) δ 7.7–7.1 (Ar, m, 10), 6.0–4.6 (CH_2=CH, m, 3), 4.2 (OH, broad, s, 2), 3.5–3.1 (C*H*—OH, m, 1), 2.1–0.8 (aliphatic, m, 12) p.p.m.

Anal. Calcd. for $C_{21}H_{28}O_2Si$: C, 74.08; H, 8.29. Found: C, 74.01; H, 8.41.

Ozone in dry oxygen was bubbled through a solution of **6** (3.78 g, 0.0112 mol) in dry ethyl acetate (100 ml) at −20° until the effluent gases liberated iodine on passage through a solution of potassium iodide in aqueous acetic acid. The solvent was removed on a rotary evaporator and the residual oil was dissolved in glacial acetic acid (50 ml). To this solution was added zinc dust (8.0 g, 0.12 g atom) and water (25 ml) and the resulting mixture was stirred for 3.5 h. Work-up gave 3.11 g of a viscous oil, believed to be 8-(diphenylhydroxysilyl)-4-hydroxyoctanal and its tautomeric cyclic hemi-acetal. To this product (2.45 g, 0.0072 mol) in acetone (25 ml) at 0° was added dropwise 1.67 *M* chromic acid solution (12.5 ml, 0.021 mol). The mixture was warmed to ambient temperature over 15 min. The solvent of the organic layer was removed on a rotary evaporator, and the residue was taken up in ether and extracted with sodium bicarbonate solution. Reacidification of the bicarbonate extracts gave an oil (0.22 g, 10%) which contained some of the γ-keto acid, **4**. The ethereal extracts afforded the γ-lactone, **8**, as a crude oil. An analytical sample was separated by elution with chloroform from silica gel; i.r. (CCl_4) λ_{max} 2.70 (OH), 5.60 (C=O) μ; n.m.r. (CCl_4) δ 7.7–7.2 (Ar, m, 10), 4.3 (CH—O, m, 1), 3.7 (OH, broad, s, 1), 2.5–2.0 (CH_2C=O, m, 2), 2.0–0.9 (aliphatic, m, 10).

Anal. Calcd. for $C_{20}H_{24}O_3Si$: C, 70.55; H, 7.10. Found: C, 70.77; H, 7.30.

A solution of the crude γ-lactone in ethanol (10 ml) and 3 *M* sodium hydroxide (10 ml) was heated at reflux for 15 min. The mixture was acidified, and the crude

[1]Blak-Ray Model B-100A, lamp and transformer with filter removed, available from Fisher Scientific. This unit contains a 100 W Westinghouse H44-4GS Lifeguard Mercury Spot.

Can. J. Chem. Downloaded from www.nrcresearchpress.com by 210.87.254.6 on 09/05/12
For personal use only.

product, isolated by ether extraction, was reoxidized with 1.67 *M* chromic acid solution (8.5 ml, 0.014 mol). The product was separated into its acidic and neutral components by extraction with sodium bicarbonate as before. The organic extract contained the γ-lactone, 0.58 g (25%), while the bicarbonate extract gave the γ-keto acid, **4**, 0.45 g (19%). This was treated with diazomethane in ether to give the methyl ester, **5**. The n.m.r. and i.r. spectra of **5** prepared by the two routes were identical.

This research was supported by the National Research Council of Canada.

1. A. G. Brook and J. M. Duff. J. Am. Chem. Soc. **89**, 454 (1967).
2. W. Kirmse. Carbene chemistry. Academic Press, New York, N.Y., 1964.
3. A. G. Brook and J. B. Pierce. J. Org. Chem. **30**, 2566 (1965), and unpublished studies.
4. A. Rieche, M. Schulz, and D. Becker. Chem. Rev. **58**, 925 (1958).
5. R. Breslow. Organic reaction mechanisms. Benjamin, New York, N.Y. 1965.
6. P. Yates. Pure Appl. Chem. **16**, 93 (1968).

Can. J. Chem. Downloaded from www.nrcresearchpress.com by 210.87.254.6 on 09/05/12
For personal use only.

Can. J. Chem. Downloaded from www.nrcresearchpress.com by 210.87.254.40 on 09/05/12
For personal use only.

Nucleophilic Attack of Siloxycarbenes on Carbonyl Groups. The Formation of Oxiranes

A. G. Brook, Ronald Pearce, and J. B. Pierce
Department of Chemistry, University of Toronto, Toronto 181, Ontario

Received December 24, 1970

Siloxycarbenes, formed by the photolysis of dimethyl- or diphenylsilacyclohexanone have been trapped as oxiranes or as the ring-opened hydrolysis products of oxiranes, with simple aldehydes and ketones such as acetaldehyde, or cyclohexanone. The reactions are interpreted as arising from the nucleophilic attack of the siloxycarbene on the carbonyl group. The structures of the oxiranes and their hydrolysis products have been established.

La photolyse de diméthyl- ou diphénylsilacyclohexanones fournit des siloxycarbènes qui réagissent avec les aldéhydes et les cétones simples comme l'acétaldéhyde et la cyclohexanone pour fournir des oxirannes ou les produits provenant d'une hydrolyse de ces hétérocycles. Ces produits proviendraient d'une attaque nucléophile du siloxycarbène sur les groupes carbonylés. On a bien établi la structure des oxirannes et de leurs produits d'hydrolyse.

Canadian Journal of Chemistry, 49, 1622 (1971)

It has recently been shown that acylsilanes yield siloxycarbenes on photolysis which can be trapped with alcohols as mixed acetals (eq. 1)

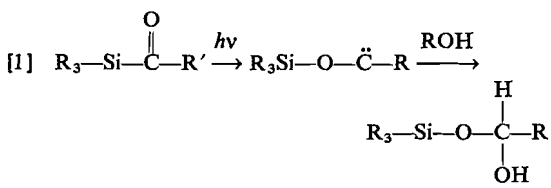

[1] $R_3Si-\overset{\overset{O}{\|}}{C}-R' \xrightarrow{h\nu} R_3Si-O-\ddot{C}-R \xrightarrow{ROH} R_3Si-O-\underset{OH}{\overset{H}{\underset{|}{\overset{|}{C}}}}-R$

(1). A cyclic siloxycarbene has also been trapped as a spirocyclopropane by reaction with diethyl fumarate (2). These and other studies suggest that siloxycarbenes display nucleophilic character.

Additional support for this concept is now provided by the finding that siloxycarbenes, generated by photolysis of acylsilanes, will react with acetaldehyde or a simple ketone to give the oxirane, or compounds formally derivable therefrom, as reaction products.

Photolysis of 1,1-dimethyl-1-silacyclohexanone (**1**), in cyclohexane at 0° in the presence of excess acetaldehyde using a low pressure mercury floodlamp with λ_{max} about 360 nm gave the oxirane **2**, as a mixture of two isomers (Scheme 1). The mixture was unstable and hence the isomers could not be separated nor the mixture analyzed but the structures of the major components were confirmed by spectral data and derivatization reactions. The methyl group and hydrogen atom on the oxirane ring appeared as two sets of doublets and quartets in the ratio of 1 to 1.6, in the δ 1.2 and 2.8 p.p.m. regions of the n.m.r. spectra, compared with 1.3 and 3.0 p.p.m. for propylene oxide (3). The i.r. spectrum showed a doublet at 7.95–8.0 μ, corresponding to overlapping absorptions by the epoxide and Si—Me groups in the molecule.

Oxirane **2** slowly decomposed spontaneously, or rapidly in the presence of added water, being hydrolyzed to the acyloin **3**, which was characterized by analysis, the presence of a methyl doublet, hydrogen quartet and broad singlet in the n.m.r. spectrum, and OH, C=O, and SiOSi absorption in the i.r.

When treated with methylmagnesium bromide the carbinol **4** was formed almost quantitatively. This reaction appears surprising at first, but the isomerization of trisubstituted oxiranes in ring opening reactions is known to be facile (4). Further, treatment of the oxirane **2** with anhydrous magnesium bromide, a mild Lewis acid, gave the rearranged product, the methyl ketone **5**, in almost quantitative yield. This showed the expected carbonyl absorption at 5.82 μ. On treatment with methyl Grignard reagent, **5** also gave **4** as expected. On exposure to moisture **4** gave the acyloin **6**, isomeric to that given by **2**, as shown by the methyl ketone singlet at δ 2.13 p.p.m. together with the other expected spectral features.

The above data fully support the structure of **2** as that of the oxirane. While the reaction of carbenes with carbonyl groups is relatively

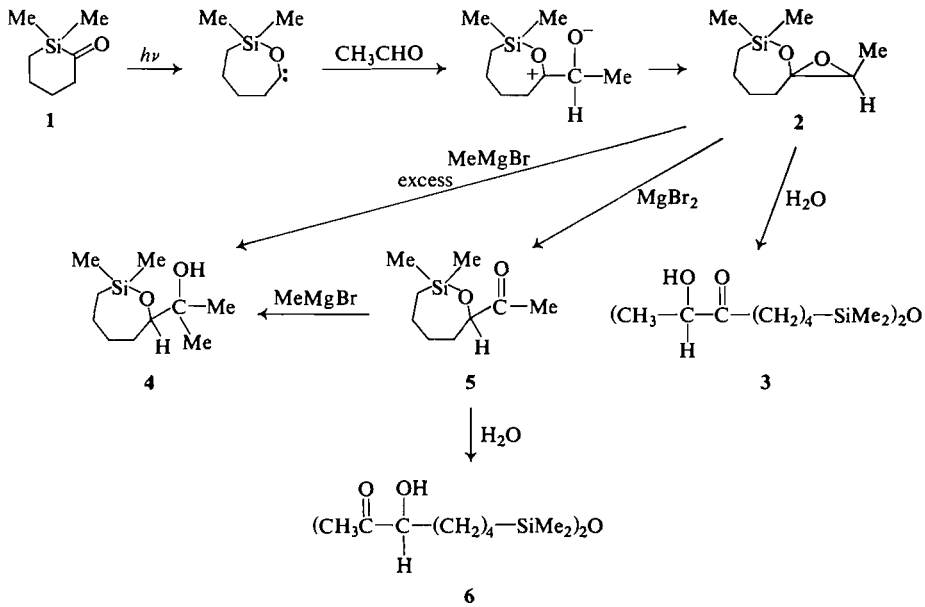

1 2 3 4 5 6

SCHEME 1

unknown, recent studies by Seyferth and Tronich (5) have shown that dihalocarbenes will form oxiranes only with highly fluorinated ketones such as hexafluoroacetone: the mechanism of this reaction has not been thoroughly established.

Attempts to trap the siloxycarbene using benzaldehyde were unsuccessful, and the fact that almost no decomposition of the acylsilane had occurred after 6 h irradiation, double that required for complete reaction with acetaldehyde, suggests that the benzaldehyde is acting as a quenching agent. Preliminary studies using pivaldehyde indicated that a mixture of products was formed. The n.m.r. data of the mixture could be interpreted as containing a mixture of the two diastereomeric oxiranes corresponding to **2**, with Me replaced by *t*-Bu.

When diphenylsilacyclohexanone **7** was photolyzed in acetone, related behavior was observed (Scheme 2). The sole product isolated was the acyloin **10**, which is derivable at least formally from the oxirane **9**, which was not detected in this case. It seems probable that sufficient water to hydrolyze the oxirane (or other intermediate) was present in the excess acetone used as solvent.

The structure of **10** was confirmed by analysis, by the presence of Si—OH, C—OH, and C=O absorption in the i.r., by a six-proton singlet signal for the two methyl groups and by two sharp singlets (in DMSO) at δ 6.48 and 5.10 p.p.m. in the n.m.r. spectrum corresponding to the Si—OH and C—OH signals. Diphenylmethylsilanol also has OH absorption at 6.48 p.p.m. (6). The structure of **10** was further confirmed by its reduction to the diol–silanol **11**, which on cleavage with lead tetraacetate gave the known 5-diphenylhydroxysilylpentanal, **12** (7) which can be produced also by photolysis of **7** in damp ether, or by photolysis in methanol to give the acetal **8** which readily hydrolyzes to **12** on treatment with dilute acid.

A similar photochemical reaction appeared to take place when 2-butanone was used as the solvent for the diphenylsilacyclohexanone photolysis, as judged by the similar spectroscopic properties of the product isolated to those of **10**. However, somewhat different behavior was observed when cyclohexanone was employed as the solvent (Scheme 3). In addition to the acyloin **16** obtained in about 50% yield, a second compound, **15**, was obtained in 25% yield. This compound is isomeric with the oxirane, **14**, which would have been formed had ring closure of **13**, the dipolar product of nucleophilic addition to the carbonyl group, occurred. It is not clear why **15** is formed in this case instead of the

Can. J. Chem. Downloaded from www.nrcresearchpress.com by 210.87.254.40 on 09/05/12
For personal use only.

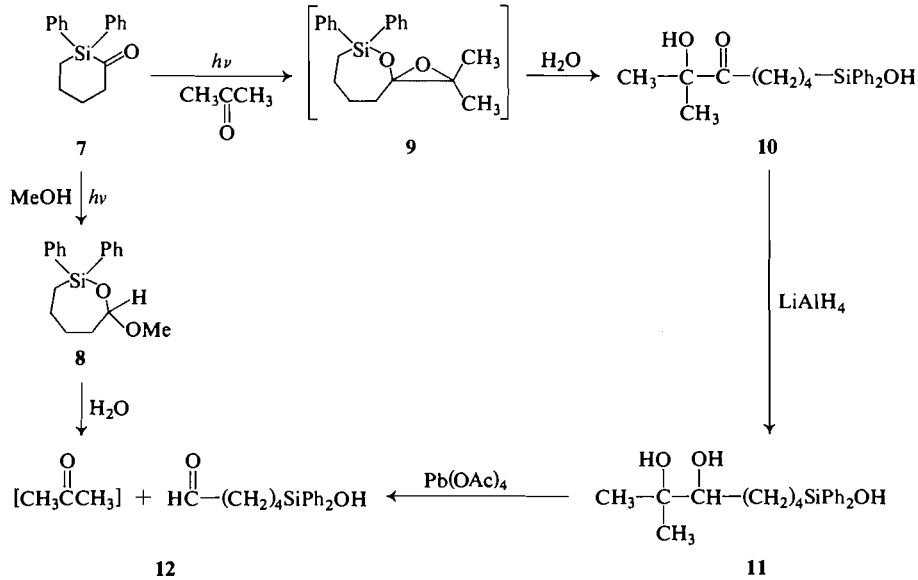

SCHEME 2

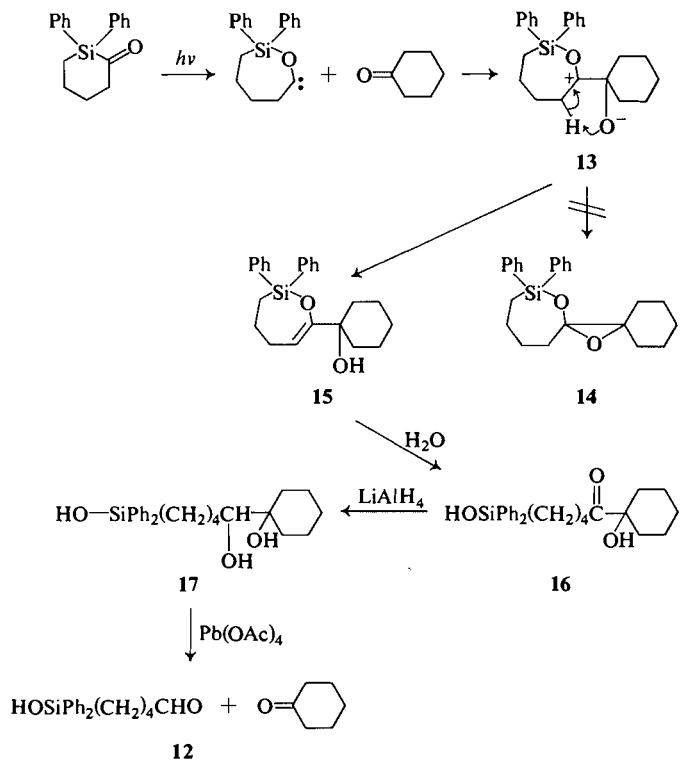

SCHEME 3

Can. J. Chem. Downloaded from www.nrcresearchpress.com by 210.87.254.40 on 09/05/12
For personal use only.

Can. J. Chem. Downloaded from www.nrcresearchpress.com by 210.87.254.40 on 09/05/12
For personal use only.

oxirane **14**, since molecular models do not suggest that **14** is unduly sterically hindered. Indeed, it is possible that **14** is formed and transformed into **15** during the course of the reaction or its work-up.

The structure of **16** was confirmed by its reduction to the silanol–diol **17**, which on cleavage with lead tetraacetate gave the known compound **12**, and cyclohexanone, isolated as the 2,4-dinitrophenylhydrazone. The structure of **15** was inferred from the presence of OH, Si—O—C, and C=C stretching absorption in the i.r., and the n.m.r. spectrum showed a single vinyl proton, as a triplet centered at 4.98 p.p.m. On treatment with acetone containing a drop of aqueous 5% hydrochloric acid, **15** was rapidly converted to **16**. This facile hydrolysis, observed before for siloxyalkenes (8), is consistent with **15** being the precursor of **16**, hydrolysis being accomplished by traces of water introduced with the cyclohexanone.

The reactions described above are all consistent with the photochemical generation, from an acylsilane, of a siloxycarbene which possesses nucleophilic character. While all acylsilanes readily undergo photolysis in polar reagents such as alcohols (1), within our limited experience cyclic acylsilanes appear to yield siloxycarbenes which react as nucleophilic carbenes more rapidly and cleanly with other kinds of electrophiles than do their acyclic analogs. The scope of this nucleophilic reactivity is being explored further.

Experimental

General

The n.m.r. spectra were run on either an A-60 or T-60 Varian spectrometer, using TMS as internal standard in most cases. The i.r. spectra were recorded on a Perkin–Elmer Model 237B instrument. Melting points and boiling points are uncorrected.

It was important to carry out the photolyses in the absence of oxygen, since in at least some cases its presence diverted the reaction and other products were formed.

The Oxirane 2 from Dimethylsilacyclohexanone 1 and Acetaldehyde

A solution of 1,1-dimethyl-1-silacyclohexan-2-one (9) (2.0 g, 0.014 mol), freshly distilled acetaldehyde (2 ml), and cyclohexane (80 ml) was placed in a vessel, flushed with nitrogen, sealed, and irradiated with a 100 W low pressure mercury floodlamp for about 3 h while being cooled in ice-water. The solution became colorless. After removal of the solvent by rotary evaporation, the residual liquid was distilled to give 1.1 g (43%) of colorless material, **2**, b.p. 35–36° (0.8 mm), 62–64° (2.5 mm). Freshly distilled material had the following spectral characteristics: i.r.; 7.0 (Si—Me), 9.3 (Si—O—C) μ; n.m.r.; δ (CCl_4), (isomer **1***a*, relative amount 1) 2.94 (Me—C*H*, q, J = 5.5 Hz, 1H), 1.13 (*Me*—CH, d, J = 5.5 Hz, 3H) and (isomer **1***b*, relative amount 1.6) 2.64 (Me—C*H*, q, J = 5.0 Hz, 1H), 1.22 (*Me*—CH, d, J = 5.0 Hz, 3H) together with 1.65 (CH_2, m), 0.73 (CH_2Si, poorly resolved t), 0.05 (Me_2Si, m) p.p.m. in relative ratio 6:2:6; δ (C_6H_6) (isomer **1***a*) 3.17 (J = 5.5 Hz, q), 1.00 (J = 5.5 Hz, d), and (isomer **1***b*) 2.65 (J = 5 Hz, q), 1.33 (J = 5 Hz, d) together with 1.73 (CH_2, m), 0.80 (s, CH_2, poorly resolved triplet), and 0.17 (three peak multiplet with separations of about 5 Hz due to nonequivalent Me groups on Si) p.p.m.

Formation of $(CH_3CHOHCO(CH_2)_4SiMe_2)_2O$ (3) by Hydrolysis of 1

When 0.5 g of **2** in ether was shaken with water for 30 min, or when exposed to air for 12 h, a pale-yellow liquid **3** was obtained on removal of the solvent, n_D^{21} 1.4597; i.r. (film) 2.7–3.2 (OH), 5.84 (C=O), 9.5 (SiOSi) μ; n.m.r. (CCl_4 with benzene as internal standard) δ 4.15 (C*H*OH, q, J = 7 Hz, 1H), 3.6 (OH, s (broad), 1H), 2.5 (CH_2CO, t (partially resolved) 2H), 2.0–0.9 (CH_2CH_2, m with d centered at δ 1.33, J = 7 Hz due to CH_3—CHOH, 7H), 0.7–0.3 (CH_2Si, m, 2H), 0.10 ($SiMe_2$, s, 6H) p.p.m.

Anal. Calcd. for $C_{18}H_{38}Si_2O_5$: C, 55.34; H, 9.80. Found: C, 55.34; H, 9.77.

Reaction of Oxirane 2 with Methylmagnesium Bromide

The oxirane produced from photolysis of 2.5 g (0.018 mol) of the acylsilane with acetaldehyde was added to excess methylmagnesium bromide in ether. After stirring for 15 min the reaction was worked-up rapidly with aqueous ammonium chloride solution to give 3.0 g (85%) of crude carbinol **4**. Distillation gave a colorless liquid in 50% yield, $n_D^{22.5}$ 1.4538; b.p. 54–55° (0.8 mm); i.r. (film) 2.7–3.1 (OH), 9.25 (Si—O—C) μ; n.m.r. (CCl_4 with benzene as internal standard) δ 3.3 (CH, m, 1H), 2.0–0.5 (CH_2 and OH, m, 9H), 1.1 (CMe_2, s (broad), 6H), 0.13 ($SiMe_2$, s, 6H) p.p.m.

Anal. Calcd. for $C_{10}H_{22}O_2Si$: C, 59.35; H, 10.96. Found: C, 59.48; H, 11.06.

Isomerization of Oxirane 2 to Siloxyketone 5

The photolysate from 3.0 g (0.021 mol) of **1** in acetaldehyde was poured into a solution of anhydrous magnesium bromide in ether (prepared from excess magnesium and 0.5 ml of 1,2-dibromoethane). The solution was stirred for 1 h and worked-up rapidly using aqueous ammonium chloride to give 3.45 g (91%) of pale-yellow liquid. Distillation gave 2.8 g (64%) of pure **5**, b.p. 85–88°/10 mm, n_D^{22} 1.4488; i.r. (film) 5.82 (C=O), 7.41 (COMe) μ; n.m.r. (CCl_4 with benzene as internal standard) δ 4.0 (C*H*COMe, m, 1H), 2.08 (MeCO, s, 3H), 2.1–0.5 (CH_2, m, 8H), 0.15 and 0.10 (Me_2Si, two s, 6H) p.p.m.

Anal. Calcd. for $C_9H_{18}O_2Si$: C, 58.02; H, 9.74. Found: C, 57.99; H, 9.96.

Formation of the Dimethylcarbinol 4 from Methyl Ketone 5 with Methyl Grignard Reagent

A solution of 0.5 g (0.0027 mol) of the ketone **5** was added to excess methylmagnesium bromide in ether. The

Can. J. Chem. Downloaded from www.nrcresearchpress.com by 210.87.254.40 on 09/05/12
For personal use only.

solution was stirred for 15 min and then was rapidly worked-up with aqueous acid to give 0.52 g (85%) of material identical in all respects to the dimethylcarbinol **4** described above.

Hydrolysis of the Methyl Ketone 5 to Give Acyloin 6

Hydrolysis of **5** could be rapidly accomplished by shaking with water or with aqueous sodium hydroxide but exposure to air over a period of 4 weeks gave the purest product. The mixture, a pale-yellow liquid, n_D^{21} 1.4647 had i.r. (CCl_4) 2.85 (OH), 5.84 (C=O) μ; n.m.r. (CCl_4 with benzene as internal standard) δ 4.0 (C*H*OH, m (broad) 1H), 3.2 (OH, broad, 1H), 2.13 (MeCO, s, 3H), 1.4 (CH_2, m, 6H), 0.6 (CH_2Si, m, 2H), 0.06 (Me_2Si, s, 6H) p.p.m.

Anal. Calcd. for $C_{18}H_{38}Si_2O_5$: C, 55.34; H, 9.80. Found: C, 55.18; H, 10.04.

Photolysis of Dimethylsilacyclohexanone 1 in Benzaldehyde

Photolysis of 1.0 g of **1** in excess freshly redistilled benzaldehyde in cyclohexane was examined after 6 h. Spectra of the crude material indicated much **1** was still present and only traces of unidentified material (n.m.r. (CCl_4): δ 4.2, 3.8 p.p.m., both singlets of unequal intensity) were observed.

Photolysis of Dimethylsilacyclohexanone in Pivaldehyde

When the material obtained from a photolysis similar to the above but using pivaldehyde in place of benzaldehyde was examined, little **1** remained. The n.m.r. spectrum in CCl_4 showed absorptions at δ 3.4 (broad singlet), 1.10 and 0.90 (singlets), and 0.10 (m) assignable to the C—H, *t*-Bu, and Si—Me signals of a mixture of oxiranes like **2**, where *t*-Bu replaces Me on the three-membered ring. Other signals were also present indicating the presence of at least one other compound. The mixture could not be separated.

Photolysis of 1,1-Diphenylsilacyclohexane-2 in Methanol

Twenty-five milliliters of dry methanol (freshly distilled from MeOMgI) were placed in a flask and dry nitrogen was bubbled through for about 1/2 h to displace all the dissolved oxygen. Then 1.0 g (0.00377 mol) of 1,1-diphenylsilacyclohexanone-2 (**7**) was added in one lot and the 100 W mercury floodlamp was turned on. The solution was irradiated for 1/2 h while maintaining a constant flow of nitrogen. After this time the solution was blown over into a receiving flask with nitrogen and the photolysis flask was rinsed once with dry methanol. The methanol was removed under reduced pressure to give the cyclic acetal (**8**). The product was not absolutely pure as judged by the presence of a small carbonyl peak at 5.78 μ. It was distilled under high vacuum to give 0.404 g or 36% of **8**, b.p. 130–132° (0.04 mm) but little purification was obtained: i.r. (CCl_4) 3.51 (OMe), 7.0, 9.0 (Si—Ph) μ; n.m.r. (CCl_4) δ 7.10–7.75 (Ar, m, 10H), 4.80–5.00 (C*H*OMe, m, 1H), 3.23 (OMe, s, 3H), 0.91–2.15 (CH_2, m, 8H) p.p.m.

Anal. Calcd. for $C_{18}H_{22}SiO_2$: C, 72.46; H, 7.43. Found: C, 72.93; H, 7.47.

Hydrolysis of the Cyclic Acetal 8

To 0.40 g (0.00134 mol) of the cyclic acetal **8** (prepared in the above photolysis) in 20 ml of THF was added a solution consisting of 2 ml of a 1% solution of KOH in water and 10 ml of THF. After stirring for 15 min 5% HCl was added and the mixture was extracted with diethyl ether. The ether phase was washed with water, dried, and the solvent was then removed. The residue was chromatographed on silica gel using benzene, 50:50 benzene–chloroform, and then chloroform as eluents. Isolated in the benzene fractions was 0.12 g or 30% of the starting acetal. The aldehyde, 5-(diphenylhydroxysilyl)-pentanal, 2.5 g (68%), was eluted with benzene–chloroform and gave an i.r. spectrum identical to that of authentic material (**7**): n.m.r. (CCl_4) δ 9.44 (CHO, t, 1H), 6.80–7.70 (Ar, m, 10H), 1.90–2.34 ($COCH_2$ + OH, m, 3H), 0.81–1.80 (CH_2, m, 6H).

Photolysis of 1,1-Diphenylsilacyclohexanone-2 in Acetone Saturated with Nitrogen; Isolation of 10

Nitrogen was bubbled through a solution of 0.200 g (0.000753 mol) of 1,1-diphenylsilacyclohexanone-2 in 40 ml of dry acetone (freshly distilled from anhydrous $MgSO_4$) while maintaining the solution in the dark. After 15 min the lamp was started and the photolysis was continued for 2 h with a constant stream of nitrogen passing through the solution. An i.r. spectrum of a small aliquot taken 2 h after the start of the photolysis indicated that none of the starting acylsilane remained. The solution was collected under nitrogen in the conventional way and after removal of the solvent gave a residue which was purified by chromatography on silica gel. The majority of the material was eluted with chloroform to give 0.130 g (54%) of **10**: i.r. (CCl_4) 2.70 (Si—OH), 2.85 (C—OH), 5.85 (C=O), 7.0, 8.95 (Si—Ph) μ; n.m.r. (CCl_4), δ 7.18–7.67 (Ar, m, 10H), 3.60–3.82 (Si—OH + COH, broad, 2H), 2.13–2.50 (CH_2CO, m (broad), 2H), 1.0–2.02 (CH_2, m), with 1.19 (CMe_2, s, 6H) superimposed p.p.m.; (DMSO) δ 7.22–7.33 (Ar, m, 10H), 6.48 (Si—OH, s, 1H), 5.10 (C—OH, s, 1H) p.p.m.

Anal. Calcd. for $C_{20}H_{26}SiO_3$: C, 70.18; H, 7.66. Found: C, 70.15; H, 7.57.

Reduction of 10 with Lithium Aluminum Hydride

A mixture consisting of 0.089 g (0.000260 mol) of 7-(diphenylhydroxysilyl)-2-hydroxy-2-methylheptanone-3 (**10**) and 50 mg (0.00132 mol) of lithium aluminum hydride in 20 ml of dry ether was stirred for 20 min at room temperature. An aqueous solution of 5% HCl was added to destroy the excess lithium aluminum hydride and the mixture was then extracted with ether. The ether phases were dried and the solvent was removed under reduced pressure. An i.r. spectrum of the isolated material indicated that reduction had been complete (no carbonyl band). A total of 72 mg or 81% of the diol **11** was obtained; i.r. (CCl_4) 2.70 (Si—OH), 2.91, very broad (C—OH), 7.00, 8.96 (Si—Ph) μ.

Cleavage of 7-(Diphenylhydroxysilyl)-2-methylheptane-2,3-diol (11) with Lead Tetraacetate

A sample of lead tetraacetate was recrystallized from glacial acetic acid and dried under high vacuum. A mixture of 100 mg (0.000226 mol) of this purified material and 72 mg (0.000209 mol) of the above-produced 7-(diphenyl-

Can. J. Chem. Downloaded from www.nrcresearchpress.com by 210.87.254.40 on 09/05/12
For personal use only.

hydroxysilyl)-2-methylheptane-2,3-diol in 75 ml of dry benzene was allowed to stand for 1½ h. After this time the mixture was poured onto a saturated solution of sodium bicarbonate and was extracted with ether. The organic phases were washed with water and were then dried with $MgSO_4$. Evaporation of the solvents left an oily residue which gave spectra identical in every way to those of authentic 5-(diphenylhydroxysilyl)-pentanal (**12**) (7).

Photolysis of 1,1-Diphenylsilacyclohexanone-2 in Butanone-2 Saturated with Nitrogen

Purified butanone-2 was distilled from phosphorus pentoxide and a central cut was stored over Drierite for 2 days. After this time it was again distilled and a central cut was taken. The oxygen was displaced from a solution consisting of 0.200 g (0.000753 mol) of 1,1-diphenylsilacyclohexanone-2 in 30 ml of this purified solvent by bubbling nitrogen through the solution while maintaining it in the dark. An i.r. spectrum, taken 1 h after the beginning of the irradiation, indicated that no starting material remained. The solution was collected under nitrogen and the solvent was removed. Attempts to crystallize the residue from dry hexane failed. An i.r. spectrum of the material indicated that it was probably 8-(diphenylhydroxysilyl)-3-methyl-3-hydroxyoctanone-4. The n.m.r. spectra in CCl_4 and dimethyl sulfoxide confirmed this structure: i.r. (CCl_4) 2.70 (Si—OH), 2.85 (C—OH), 5.85 (C=O), 7.00, 9.00 (Si—Ph) μ; n.m.r. (CCl_4) δ 6.95–7.72 (Ar, m, 10H), 0.78–2.52 (complex), 1.12 (broad, possibly a singlet superimposed on band above) p.p.m.; n.m.r. (DMSO) δ 7.16–7.75 (Ar, m, 10H), 6.48 (Si—OH, s, 1H), 5.11 (C—OH, s, 1H) p.p.m.

*Photolysis of 1,1-Diphenylsilacyclohexanone-2 in Oxygen-Free Cyclohexanone; Isolation of **15** and **16***

Purified cyclohexanone was distilled at atmospheric pressure and a central cut retained. This cut was redistilled under nitrogen in "flamed out" apparatus and another central cut collected. A solution of 1.0 g (0.00377 mol) of 1,1-diphenylsilacyclohexanone-2 in 35 ml of this purified solvent was freed from oxygen and then was photolyzed for 8 h while a stream of nitrogen was constantly bubbled through the solution. The solution was collected after 8 h of irradiation and the solvent was removed by distillation under high vacuum. Two methods of purification of the residue were attempted. About half of the residue was distilled under high vacuum through a short column and three fractions boiling in the range 180–190 °C (0.05 mm) were collected. However, i.r. spectra of these fractions were all identical with the i.r. spectrum of the crude material indicating that no separation had occurred. Chromatography on silica gel collecting 75 ml fractions and using a series of solvents was more successful. With benzene as eluent, fractions 7 to 15 yielded compound **15** and after using 375 ml of chloroform, which eluted nothing, fractions 22 and 23 using ether as eluent gave compound **16**. The yields of **15** and **16** were approximately 25 and 51% respectively, as observed from a second experiment. Samples of **15** and **16** were pumped down under high vacuum at 100 °C for 18 h to prepare them for analysis. Both compounds were viscous oils. The cyclic siloxyalkene **15** had: i.r. (CCl_4) 2.76 (Si—OH), 6.01 (C=C) 7.00, 9.00 (Si—Ph) μ; n.m.r. (CCl_4) δ 7.20–7.65 (Ar, m, 10H), 4.97 (=CH, t, J = 7 Hz, 1H), 0.90–2.40 (m, 17H) p.p.m.

Anal. Calcd. for $C_{23}H_{28}SiO_2$: C, 75.77; H, 7.74. Found: C, 75.80; H, 7.82.

The hydrolysis product of **15**, the acyloin **16** had: i.r. (CCl_4); 2.70 (Si—OH), 2.85 (C—OH), 5.87 (C=O), 7.00, 8.97 (Si—Ph) μ; n.m.r. (CCl_4) δ 7.10–7.68 (Ar, m, 10H), 3.68–4.10 (C—OH + Si—OH, broad, 2H), 2.10–2.55 (CH_2CO—, m (broad), 2H), 0.82–1.95 (m, 16H) p.p.m.

Anal. Calcd. for $C_{23}H_{30}SiO_3$: C, 72.18; H, 7.90. Found: C, 72.62; H, 8.12.

*Reduction of Acyloin **16** with Lithium Aluminum Hydride*

A solution consisting of 120 mg (0.000314 mol) of compound **16** and 100 mg (0.00264 mol) of lithium aluminum hydride in 10 ml of dry ether was stirred for 1/2 h. A solution of 5% HCl was then added and the mixture was extracted with ether. The ether phases were dried and then evaporated to leave a residue whose i.r. spectrum indicated that reduction of the carbonyl group was complete. The yield of crude reduction product **17** was 112 mg or 93%: i.r. (CCl_4) 2.70 (Si—OH), 2.99 (C—OH, very broad), 7.00, 9.00 (Si—Ph) μ.

*Treatment of **17** with Lead Tetraacetate*

A solution consisting of 112 mg (0.000293 mol) of **17** as isolated from the experiment above and 129 mg (0.000293 mol) of freshly crystallized lead tetraacetate in 10 ml of dry benzene was stirred for 1/2 h at room temperature. It was then poured onto a saturated solution of sodium bicarbonate and was extracted with ether. After drying, the solvents were distilled from the products at atmospheric pressure. The flask containing the residue was then connected to a vacuum apparatus and all volatile material was collected in a cold trap. The volatile material (cyclohexanone + benzene) gave an i.r. spectrum (using benzene in the reference cell) which compared very favorably with an i.r. spectrum of authentic cyclohexanone. The 2,4-dinitrophenylhydrazone of this isolated ketone was prepared by the method of Parrick and Rasburn (10) by adding 2 ml of dimethyl sulfoxide and 100 mg of 2,4-dinitrophenylhydrazine followed by 1 drop of concentrated HCl to the residue. After 15 min the benzene was removed from the sample under reduced pressure and 0.049 g or 65% of the crystalline 2,4-dinitrophenylhydrazone of cyclohexanone was deposited. This material was filtered off, washed with dilute HCl, water, and then 95% ethanol, m.p. 161–163 °C, mixed m.p. with an authentic sample 162–163 °C. The non-volatile material consisted of 0.076 g or 91% of 5-(diphenylhydroxysilyl)-pentanal **12**, whose i.r. and n.m.r. spectra were identical to those of authentic material.

*Hydrolysis of Siloxyalkene **15***

A small sample of chromatographically pure **15** as isolated from the photolysis above was dissolved in acetone and about 5 drops of a 5% v/v HCl solution was added. After standing at room temperature for 1/2 h the sample was added to water and extracted with ether. The ether phases were dried and the solvents were then

removed to leave a residue which gave an i.r. spectrum identical to that of authentic **16**. An n.m.r. spectrum taken in dimethyl sulfoxide confirmed the structure of the product.

The authors are grateful for the support of this research by the National Research Council of Canada.

1. A. G. BROOK and J. M. DUFF. J. Am. Chem. Soc. **89**, 454 (1967).
2. A. G. BROOK, H. KUCERA, and R. PEARCE. Can. J. Chem. This issue.
3. Varian NMR Spectra Catalogue. Varian Associates, 1962. Spectrum 32.
4. A. ROSOWSKY. Heterocyclic compounds. Vol. 19. Interscience, New York, N.Y. 1964. Part 1, p. 1.
5. D. SEYFERTH and W. TRONICH. J. Organomet. Chem. **18**, 8 (1969).
6. J. F. HAMPTON, C. W. LACEFIELD, and J. F. HYDE. J. Inorg. Chem. **4**, 1659 (1965).
7. A. G. BROOK and J. B. PIERCE. J. Org. Chem. **30** 2566 (1965),
8. A. G. BROOK, W. W. LIMBURG, D. M. MACRAE, and S. A. FIELDHOUSE. J. Am. Chem. Soc. **89**, 704 (1967).
9. A. G. BROOK and H. KUCERA. Unpublished results.
10. J. PARRICK and J. W. RASBURN. Can. J. Chem. 43, 3453 (1965).

Can. J. Chem. Downloaded from www.nrcresearchpress.com by 210.87.254.40 on 09/05/12
For personal use only.

Can. J. Chem. Downloaded from www.nrcresearchpress.com by 210.87.254.105 on 09/05/12
For personal use only.

Refinement of the Structure of $Mg_3(VO_4)_2$

N. KRISHNAMACHARI AND C. CALVO

Department of Chemistry and Institute for Materials Research, McMaster University, Hamilton, Ontario

Received June 29, 1970

Magnesium orthovanadate crystallizes in the orthorhombic space group *Cmca* with $a = 6.053(3)$, $b = 11.442(6)$, $c = 8.330(3)$ Å, and $Z = 4$. The structure was refined by full matrix least square methods to a final R value of 0.047 using 1697 reflections measured by a quarter circle General Electric automatic diffractometer. The structure was assumed to be isomorphous with that of $Ni_3(VO_4)_2$, reported by Durif and Bertaut (2), and the refinement started using the same fractional atomic coordinates. The structure consists of nearly cubic closest packing of oxygen atom layers roughly normal to the [01$\bar{1}$] direction with the Mg ions in two types of octahedral sites and the V ion in a tetrahedral site. The VO_4 group has a crystallographic mirror plane. The cations lying on sites of C_m symmetry show an average Mg—O bond length of 2.092 Å, compared to 2.098 Å for cations lying at sites of C_{2h} symmetry. The anion deviates significantly and substantially from regularity with the three oxygen atoms shared with only two cations showing V—O bond lengths within 0.015 Å of their mean, 1.70 Å, whereas the remaining oxygen atom, which is shared with three Mg ions, lies 1.809 Å from the V ion. The structure has characteristics similar to those of spinel.

L'orthovanadate de magnésium cristallise dans le système orthorhombique avec une maille de dimensions: $a = 6.053(1)$, $b = 11.422(2)$ et $c = 8.330(1)$ Å. Le groupe d'espace est *Cmca* et $Z = 4$.

L'affinement de la structure, par moindres-carrés (matrice complète), conduit à un facteur d'accord final $R = 0.047$ pour les 1697 réflexions mesurées sur un diffractomètre automatique General Electric. On a admis que la structure était isomorphe de celle de $Ni_3(VO_4)_2$, telle que rapportée par Durif et Bertaut, et on a utilisé les mêmes coordonnées fractionnaires pour commencer l'affinement.

La structure consiste en un arrangement compact presque cubique de couches d'atomes d'oxygène approximativement paralléles à la direction [01$\bar{1}$]. Les ions magnésium sont répartis sur deux sites octaèdriques tandis que le vanadium occupe un site tétraèdrique. Le groupe VO_4 possède un plan de symétrie cristallographique. La longueur de liaison moyenne Mg—O est de 2.092 Å pour les cations dans la position de symétrie C_m, et de 2.098 Å pour ceux qui sont sur les sites de symétrie C_{2h}. L'anion est fortement déformé: les distances du vanadium aux trois oxygènes communs à deux cations chacun diffèrent de 0.015 Å de la moyenne de 1.70 Å, tandis que la distance du vanadium à l'oxygène commun à trois ions Mg est de 1.809 Å. La structure a des caractéristiques semblables à celles des spinelles.

Canadian Journal of Chemistry, 49, 1629 (1971)

Introduction

Pope and Dale recently indicated "a detailed structure of a crystalline orthovanadate has yet to appear in the literature" (1). However, approximate atomic positions have been reported for $Ni_3(VO_4)_2$ by Durif and Bertaut (2). The powder pattern of $Mg_3(VO_4)_2$ has been indexed on the basis of a cell similar to that of $Ni_3(VO_4)_2$ (3) as has $Zn_3(VO_4)_2$ and the high temperature form of $Co_3(VO_4)_2$ (4). Joubert and Durif have shown that the low temperature form of $Co_3(VO_4)_2$ is cubic probably transforming to a spinel structure with disordered vacancies and finally becomes orthorhombic at high temperature (5).

The average V—O bond lengths in $Cd_2V_2O_7$ (6) and $Mn_2V_2O_7$ (7) suggest that for orthovanadates showing tetrahedrally coordinated V ions, the V—O bond length should be near 1.70 Å. For closest packing of oxygen atoms as spheres of radii 1.40 Å, the tetrahedral holes would give rise to V—O bond lengths of 1.71 Å. In $Co_3(AsO_4)_2$ (8), where the mean As—O bond length is 1.69 Å the oxygen atom pack as layers with an *ABCB* arrangement while the $Ni_3(VO_4)_2$ structure is based upon an *ABC* stacking sequence. Thus the structure of $Mg_3(VO_4)_2$ has been refined in order to examine the source of the detailed difference between the packing in $Co_3(AsO_4)_2$ and $Co_3(VO_4)_2$. As a prototype of the latter structure, $Mg_3(VO_4)_2$, containing the lightest cation of the series, has been examined.

Experiments

Crystals of $Mg_3(VO_4)_2$ were grown in a Pt crucible by slowly cooling a melt of hydrated $Mg_3(VO_4)_2$ obtained from Alpha Inorganic, Inc. Several crystals with dimensions of the order of $0.1 \times 0.1 \times 0.2$ mm^3 were chosen for study. Unit cell parameters were obtained from a least squares refinement using 2θ values of 17 lines measured with the quarter circle General Electric XRD6

Can. J. Chem. Downloaded from www.nrcresearchpress.com by 210.87.254.105 on 09/05/12
For personal use only.

TABLE 1. Atomic coordinates for $Mg_3(VO_4)_2$*

Atom	Site symmetry	Positional coordinates			Thermal coordinates†					
		x	y	z	U_{11}	U_{22}	U_{33}	U_{12}	U_{13}	U_{23}
Mg(1)	$2/m$	0	0	0	0.0056(3)	0.0082(3)	0.0042(3)	—	—	−0.0014(2)
Mg(2)	2	1/4	0.13533(5)	1/4	0.0042(2)	0.0055(2)	0.0060(2)	—	−0.0006(2)	−0.0020(3)
V	m	0	0.37978(2)	0.12098(3)	0.0040(1)	0.0033(1)	0.0042(1)	—	—	0.0000(1)
O(1)	m	0	0.25136(9)	0.2274(2)	0.0054(1)	0.0042(3)	0.0083(3)	—	—	0.0023(2)
O(2)	m	0	0.00375(9)	0.2442(1)	0.0050(1)	0.0047(3)	0.0050(3)	—	—	0.0004(3)
O(3)	1	0.2723(1)	0.11791(7)	0.9974(1)	0.0063(2)	0.0069(2)	0.0058(2)	−0.0010(2)	0.0014(2)	0.0002(2)

*Estimated standard deviations obtained from the least square refinement are in parentheses.
†Calculated from $\beta_{ij} = 2\pi^2 b_i b_j U_{ij}$ where $T = \exp[-(\beta_{11}h^2 + 2\beta_{12}hk + \cdots)]$ is the thermal factor appearing in the structure factor expression and b_i's are the reciprocal lattice vectors.

Can. J. Chem. Downloaded from www.nrcresearchpress.com by 210.87.254.105 on 09/05/12
For personal use only.

Diffractometer with MoKα radiation ($\lambda_\alpha = 0.71069$ Å). The cell parameters obtained are $a = 6.053(3)$, $b = 11.442(6)$, $c = 8.330(3)$ Å where the estimated standard deviations in the parentheses represent 3 × the values obtained from the refinement. The crystals are orthorhombic with reflections *hkl* extinct when $h + k$ is odd, *h0l* absent for *l* odd and *hk*0 absent for *h* and/or *k* odd. Hence the space group is D_{2h}^{18}-*Cmca* or C_{2v}^{15}-*C2ca*. The former space group, that of $Ni_3(VO_4)_2$ (3), was chosen for the initial trial. *Z* was taken as four in agreement with the value assigned to $Ni_3(VO_4)_2$. The calculated density is 3.486 g/cm³. It cannot be compared to an experimental one since the product did not appear uniform. A total of 1697 symmetry independent reflections were collected with the diffractometer from a crystal, with dimensions 0.08 × 0.08 × 0.23 mm³, mounted parallel to the long axis. Filtered Mo radiation was used and the peaks were scanned at a rate of 1°/min through 2 to 3° in 2θ depending upon this angle. The total counts for each peak were corrected for the average background, counted at fixed angles on either side of the peak for a time period of 40 s. The 113 reflections with background intensity greater than that of the reflection were ignored. If the net counts were less than that three standard deviation above background but greater than zero, the intensities were considered as unobserved. The intensities were corrected for Lorentz and polarization but not for absorption. The linear absorption coefficient, μ, equal to 37 cm^{-1} leads to transmission factors that vary by less than 10% for the range of angles used. The structure was refined initially using the atomic positional parameters of $Ni_3(VO_4)_2$ together with measured photographic intensity data and the results of this refinement used as the trial model for the diffractometer data. Weights, $w = (10.5 - 0.476|F_o| + 0.006|F_o|^2)^{-1}$, were chosen so that the value of $w(|F_o| - |F_c|)^2$ would be independent of the local average $|F_o|$. Zero weights were assigned to those reflections whose calculated structure was less than the local minimum observed value. Scattering factor curves for Mg^{2+}, V^{5+} corrected for dispersion, and for O^-, were obtained from the International Tables for X-Ray Crystallography (10). The structure was refined to a minimum in

$$R_W = \left\{\frac{\sum w||F_o| - |F_c||^2}{\sum w|F_o|^2}\right\}^{1/2}$$

using a full matrix least squares program and the refinement terminated when the calculated shifts were less than 1/3 of the estimated standard deviations. The final *R* and R_W values are 0.047 and 0.031, respectively. The final atomic positional coordinates are listed in Table 1, $|F_o|$ and $|F_c|$ in Table 2. Structure factors were calculated for those 113 reflections whose derived intensities were negative. Only one appeared to be larger than the estimated minimum observable value obtained from the examination of the unobserved limit in the same region of reciprocal space.

Description of the Structure

The structure of $Mg_3(VO_4)_2$ is based upon a pseudocubic, that is *ABC*, arrangement of close packed layers of oxygen atoms, as seen in Fig. 1. The normal to these layers nearly parallel the $-2b^* + c^*$ direction which lies within 2° of the [011] in the direct lattice. The oxygen atom layers alternate between pairs containing tetrahedrally coordinated V ions and pairs devoid of such ions. Some of the Mg(1) ions occur between the same layers as do the V ions. All the Mg ions have nearly regular octahedral coordination.

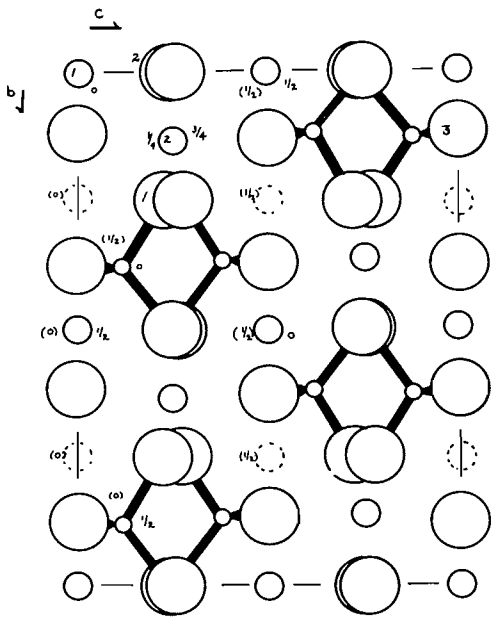

FIG. 1. The projection of the structure of $Mg_3(VO_4)_2$ onto the *bc* plane. Large circles represent oxygen atoms, smaller circles the Mg ions while the smallest circles are vanadium ions. The dotted circles, are the cations to be added. These together with the changes in *x* coordinates indicated by parentheses and small shift in oxygen atom positions will generate the spinel structure.

The Mg(1) site has 2/*m* symmetry with four equal, symmetry related Mg—O(3) bond lengths of 2.130(1) Å and two equal, symmetry related Mg—O(2) bond lengths of 2.034(1) Å. Mg(2) lies at a site with two fold symmetry with independent Mg—O bond lengths of 2.022(1), 2.118(1), and 2.135(1) Å. The independent bond lengths and angles can be found in Table 3. The two V—O bonds lying in the mirror planes, V—O(1) and V—O(2), are 1.716(1) and 1.809(1) Å long, respectively, while the two mirror planes related V—O(3) bonds are 1.695 Å in length. Since the estimated standard deviations in these bond lengths are of the order of 0.001 Å all these differences appear to be significant. The cause of the large difference of the V—O(2) bond and the other V—O bonds lies in the fact that O(2) is shared with three cations while the remaining oxygen atoms are shared with only two Mg ions. The bond angles also show substantial deviations from tetrahedral symmetry. The major distortion from a regular tetrahedron arises from the displacement of O(2) from the ideal position and not the displacement of V from the center.

The Mg(2)—O_6 groups form chains of O(1)—O(2) edge sharing octahedra running parallel to the *a* axis.

Table 2. OBSERVED AND CALCULATED STRUCTURE FACTOR AMPLITUDES FOR $Mg_3(VO_4)_2$

UNOBSERVED REFLECTIONS ARE MARKED BY (L) AND UNRELIABLE REFLECTIONS BY (U)

K	L	|FOBS|	|FCALC|
		H = 0	
-2	0	56	48
4	0	136	150
6	0	12	4
8	0	205	198
12	0	70	69
14	0	L 16	8
16	0	102	96
18	0	30	29
20	0	28	28
22	0	21	21
24	0	48	48
2	1	U 31	21
4	1	25	23
6	1	28	25
8	1	49	48
12	1	35	35
14	1	27	26
16	1	42	41
18	1	21	21
20	1	23	25
22	1	22	23
24	1	31	31
2	2	54	54
4	2	79	75
6	2	15	12
8	2	16	17
10	2	60	59
12	2	19	20
14	2	24	24
16	2	L 6	4
18	2	37	37
20	2	19	19
22	2	17	18
24	2	L 7	2
2	3	U 127	155
4	3	L 4	0
6	3	117	120
8	3	12	12
10	3	89	88
12	3	L 6	4
14	3	54	54
18	3	40	40
20	3	13	13
22	3	23	23
2	4	29	29
4	4	77	75
6	4	54	52
8	4	51	49
12	4	11	11
14	4	56	56
16	4	L 7	5
18	4	20	19
20	4	43	42
22	4	28	28
24	4	8	6
4	5	L 5	4
6	5	88	88
10	5	67	66
12	5	L 6	2
14	5	42	42
16	5	L 7	7
18	5	31	31
20	5	9	7
22	5	18	18
24	5	7	0
2	6	28	26
4	6	L 5	2
8	6	20	21
10	6	38	37
14	6	19	18
16	6	10	9
18	6	24	25
22	6	12	14
24	6	L 7	5
2	7	23	22
6	7	25	26
8	7	33	32
10	7	23	23
12	7	26	26
16	7	35	35
18	7	22	22
20	7	22	22
22	7	24	24
2	8	32	31
4	8	88	90
8	8	124	121
10	8	31	31
12	8	56	56
14	8	L 7	4
16	8	74	72
18	8	29	30
20	8	27	28
22	8	14	15
4	9	11	11
6	9	12	12
8	9	23	24
10	9	12	13
12	9	21	21
14	9	17	16
16	9	26	28
18	9	15	14
20	9	18	18
22	9	15	12
4	10	15	15
6	10	14	15
8	10	15	14
12	10	18	17
14	10	25	25
16	10	13	12
18	10	22	23
20	10	14	15
2	11	72	73
4	11	65	64
6	11	57	56
8	11	8	9
10	11	41	41
11	11	35	34
12	11	13	15
2	12	17	18
4	12	29	29
6	12	29	30
8	12	L 7	3
10	12	L 7	2
12	12	23	28
14	12	28	30
16	12	L 8	7
18	12	L 8	6
2	13	34	33
4	13	L 7	1
6	13	30	30
8	13	26	25
10	13	17	18
12	13	9	6
14	13	12	15
16	13	15	15
18	13	8	10
20	13	9	8
22	13	8	6
24	13	8	10
11	14	13	13
12	14	23	21
14	14	8	6
16	14	10	10
18	14	56	56
20	14	10	10
22	14	23	23
24	14	7	9
12	15	14	15
14	15	23	22
16	15	17	18
18	15	48	48
20	15	10	10
22	15	36	37
24	15	9	6
12	16	17	L 8
14	16	17	C 8
16	16	8	6
18	16	L 8	1
20	16	13	13
22	16	13	13
		H = 1	
K	L		
1	1	51	46
3	1	98	105
5	1	104	107
7	1	18	17
9	1	41	39
11	1	43	43
13	1	61	61
17	1	31	31
19	1	15	14
21	1	37	37
25	1	23	23
1	2	95	104
3	2	83	83
5	2	60	58
7	2	90	89
9	2	49	49
11	2	62	62
13	2	21	21
15	2	57	56
17	2	17	17
19	2	42	42
21	2	L 7	4
23	2	39	39
1	3	76	79
3	3	18	16
5	3	26	24
7	3	53	53
9	3	7	6
11	3	24	23
13	3	21	21
17	3	36	36
19	3	7	2
21	3	20	21
23	3	L 7	6
1	4	12	11
3	4	28	26
5	4	23	22
7	4	12	14
9	4	11	10
11	4	6	0
13	4	L 7	9
15	4	7	6
17	4	L 7	0
19	4	82	85
21	4	15	15
23	4	27	26
25	4	65	65
1	5	6	5
3	5	26	27
5	5	43	42
7	5	24	24
9	5	8	9
11	5	45	46
13	5	82	82
15	6	64	64
17	6	51	51
19	6	22	23
21	6	64	63
23	6	30	30
25	6	40	41
1	7	47	46
3	7	11	12
5	7	31	29
7	7	23	23
9	7	11	12
11	7	25	25
13	7	24	24
15	7	39	39
17	7	23	22
19	7	10	8
21	7	27	26
23	7	26	25
1	8	L 6	3
3	8	L 6	6
5	8	22	22
7	8	17	18
9	8	L 6	1
11	8	16	16
13	8	12	11
15	8	L 7	6
17	8	11	11
19	9	25	25
21	9	56	58
23	9	63	63
25	9	11	12
1	9	30	30
3	9	50	50
5	9	7	2
7	9	28	28
9	9	15	15
11	9	35	35
13	10	51	52
15	10	33	34
17	10	22	23
19	10	55	54
21	10	34	35
23	10	9	8
25	10	45	46
1	11	17	18
3	11	29	28
5	11	24	25
7	11	10	9
9	11	12	12
11	11	18	18
13	11	25	24
15	11	8	6
17	11	13	13
19	11	9	8
21	11	20	19
23	12	L 7	2
25	12	19	21
1	12	20	19
3	12	L 7	2
5	12	19	18
7	12	15	13
9	12	L 8	6
11	12	L 7	5
13	12	12	14
15	12	42	42
17	13	33	33
19	13	18	19
21	13	42	41
23	13	22	22
25	13	19	20
1	13	33	33
3	14	21	21
5	14	37	37
7	14	31	30
9	14	25	26
11	14	13	12
13	14	38	37
15	14	19	19
17	14	25	25
19	15	9	11
21	15	13	14
23	15	17	17
25	15	8	8
1	15	15	12
3	15	8	7
5	15	18	16
7	16	16	15
9	16	8	7
11	16	13	12
13	16	9	9
15	16	7	0
17	17	15	16
19	17	31	31
21	17	37	35
23	17	8	8
25	17	21	20
1	18	21	23
3	18	19	20
5	18	14	14
7	18	14	14
9	18	57	58
11	18	6	5
13	18	37	36
15	18	29	29
17	18	26	27
19	18	35	35
21	18	19	19
23	18	21	21
25	18	8	6
1	19	29	29
3	19	32	31
5	19	26	28
7	19	22	23
9	19	28	29
11	19	26	27
13	19	33	33
15	19	16	15
17	19	32	31
19	19	25	25
21	19	21	21
23	19	18	18
25	19	7	5
1	20	22	22
3	20	6	5
5	20	39	38
7	20	36	36
9	20	19	19
11	20	17	17
13	20	52	52
15	20	11	11
17	20	34	33
19	20	9	4
21	20	26	27
23	20	46	46
25	20	32	32
1	20	29	28
3	20	6	7
5	20	42	43
7	20	9	5
9	20	39	38
11	20	12	10
13	20	37	37
15	20	33	31
17	20	8	6
19	20	14	14
21	20	57	58
23	20	6	7
25	20	14	13
1	21	24	23
3	21	21	21
5	21	32	31
7	21	16	15
9	21	21	21
11	21	8	8
13	21	16	15
15	21	8	7
17	21	11	11
19	21	11	11
21	21	34	33
23	21	9	4
25	21	27	27
1	21	46	46
3	21	32	32
5	21	28	28
7	21	29	28
9	21	6	7
11	21	58	58
13	21	14	14
15	21	28	27
17	21	7	4
19	21	38	36
21	21	8	6
23	21	7	5
25	21	8	6
1	22	8	7
3	22	8	8
5	22	8	8
7	22	8	8
9	22	8	8
11	22	8	8
13	22	8	8
15	22	8	8
17	22	8	8
19	22	8	8
21	22	8	8
23	22	8	8
25	22	8	8
1	23	8	8
3	23	8	8
5	23	8	8
7	23	8	8
9	23	8	8
11	23	8	8
13	23	8	8
15	23	8	8
17	23	8	8
19	23	8	8
21	23	8	8
23	23	8	8
25	23	8	8
1	24	8	8
3	24	8	8
5	24	8	8
7	24	8	8
9	24	8	8
11	24	8	8
13	24	8	8
15	24	8	8
17	24	8	8
19	24	8	8
21	24	8	8
23	24	8	8
25	24	8	8
1	25	8	8
3	25	8	8
5	25	8	8
7	25	8	8
9	25	8	8
11	25	8	8
13	25	8	8
15	25	8	8
17	25	8	8
19	25	8	8
21	25	8	8
23	25	8	8
25	25	8	8

Can. J. Chem. Downloaded from www.nrcresearchpress.com by 210.87.254.105 on 09/05/12
For personal use only.

Table 2 (Continued)

	FOBS	FCALC		FOBS	FCALC		FOBS	FCALC		FOBS	FCALC		FOBS	FCALC
1 4	9	8	9 16	15	12	20 16	11	13	11 7	21	22	22 2	17	18
3 4	19	19	1 17	9	10	2 11	63	64	13 7	46	41	2 3	18	19
5 4	17	17	3 17	27	26	4 11 L	6	3	17 7	27	27	4 3	16	16
11 4	10	12	5 17	28	29	6 11	57	57	19 7 L	7	6	6 3	18	19
13 4	11	9	9 17	14	14	8 11 L	7	6	21 7	29	29	8 3	24	26
17 4 L	7	5	1 18	19	21	10 11	50	51	1 8	18	18	10 3	23	23
19 4	9	8	3 18	17	18	12 11	8	9	3 8 L	6	2	14 3	21	20
21 4 L	7	6				16 11 L	7	4	5 8 L	6	5	16 3	22	22
1 5	90	96	K L		H = 4	18 11	32	32	7 8	17	17	18 3	24	23
3 5	28	29				0 12	7	3	9 8	13	14	20 3	30	30
7 5	58	58	0 0	190	208	2 12	16	15	11 8 L	6	0	22 3	15	17
9 5	72	73	2 0	29	29	4 12	30	29	13 8 L	6	6	0 4	73	74
11 5	9	9	4 0	99	103	8 12 L	7	1	15 8	15	13	2 4	16	16
13 5	36	37	6 0	15	14	10 12 L	7	1	17 8	9	10	4 4	132	128
15 5	23	24	10 0	25	26	12 12	29	28	19 8 L	7	1	6 4	26	29
17 5	47	49	12 0	56	56	16 12	10	8	21 8 L	7	6	8 4	56	57
19 5 L	7	1	18 0	25	25	18 12	9	7	1 9	30	30	10 4 L	6	3
21 5	28	30	20 0	25	25	2 13	30	30	3 9	52	52	12 4	93	89
23 5	8	6	22 0	18	19	6 13	26	27	7 9	16	16	14 4	22	21
5 6	56	56	24 0	44	44	8 13 L	7	5	9 9	35	36	16 4	31	32
9 6	21	21	2 1	18	16	10 13	23	23	11 9	30	31	18 4	11	10
11 6	59	60	4 1	18	18	16 13 L	7	5	15 9 L	7	4	20 4	52	52
13 6	28	28	6 1	35	36	0 14	13	11	17 9	33	32	22 4	22	21
15 6	38	39	10 1	18	19	4 14	15	15	19 9	14	12	2 5	13	13
17 6 L	7	5	12 1	28	29	6 14 L	8	8	1 10	43	44	4 5	14	14
19 6	45	45	18 1	19	19	8 14 L	8	10	3 10	30	30	6 5	14	13
21 6	12	11	20 1	23	23	10 14 L	7	4	5 10	19	20	8 5	16	18
23 6	28	29	22 1	22	21	12 14	11	11	7 10	47	47	12 5	28	27
1 7	9	7	24 1	28	29	2 15	21	20	9 10	30	30	16 5	20	20
3 7	33	33	2 2	35	34	4 15 L	8	5	11 10	31	31	18 5	20	18
5 7	34	35	4 2	18	17	6 15	22	21	13 10 L	7	7	20 5	27	27
7 7 L	6	5	8 2	16	17	8 15	14	13	15 10	42	41	0 6	7	6
9 7	11	11	10 2	44	44	10 15	20	18	17 10	16	16	2 6 L	6	3
11 7	20	19	12 2	12	14	0 16	60	58	19 10	26	26	4 6 L	3	5
17 7	14	13	18 2	30	30	2 16	13	17	1 11	11	14	6 6	23	22
19 7	9	8	22 2	14	15	4 16	42	43	3 11 L	7	3	8 6	9	10
21 7	18	19	24 2 L	7	3	6 16	11	10	5 11 L	7	4	10 6	11	13
23 7 L	6	2	2 3	108	111	8 16	51	51	7 11	13	11	14 6	23	24
1 8	23	23	4 3 L	5	0	10 16	20	20	9 11	11	13	16 6	13	14
3 8 L	5	1	8 3	7	8	4 17 L	8	4	11 11	8	4	18 6	15	16
5 8 L	6	4	10 3	72	72	6 17 L	8	7	13 11	8	5	20 6 L	7	1
7 8	20	21	12 3 L	6	4				17 11	12	11	2 7	71	70
9 8	16	17	18 3	37	37	K L		H = 5	1 12	7	2	6 7	65	64
13 8 L	7	6	20 3	11	12				3 12	18	19	8 7 L	6	4
15 8	15	16	22 3	22	22	1 1	43	43	5 12	16	17	10 7	52	51
17 8	10	11	24 3 L	7	4	3 1	80	81	7 12 L	7	5	12 7 L	7	1
19 8 L	7	2	0 4	55	54	7 1	19	20	11 12	19	17	14 7	42	43
21 8 L	7	6	2 4	19	18	9 1	42	43	13 12	11	12	16 7	16	11
1 9	11	12	6 4	42	41	11 1	36	35	17 12 L	7	4	18 7	28	29
3 9	44	45	8 4	28	27	13 1	58	58	1 13	31	30	0 8	43	43
5 9	47	48	10 4	13	11	15 1 L	7	5	3 13 L	0	6	2 8	21	22
9 9	18	18	12 4	51	52	17 1	35	35	5 13	12	11	4 8	8	7
11 9	28	29	16 4 U	7	2	19 1	12	11	7 13	25	25	6 8 L	6	2
13 9	38	39	18 4	20	19	21 1	39	39	9 13	30	30	8 8	41	41
17 9	20	20	20 4	40	40	23 1 L	7	4	11 13 L	8	3	10 8	31	31
19 9	14	15	22 4	27	27	1 2	62	63	13 13	14	14	14 8	11	11
21 9	28	29	6 5	69	70	5 2	40	41	15 13	14	17	16 8	34	35
1 10	47	48	8 5	9	10	9 2	35	36	1 14	19	19	20 8	9	8
3 10	30	31	10 5	55	55	11 2	48	49	3 14	33	33	2 9	42	43
5 10	20	21	12 5 L	6	0	13 2	16	18	5 14	26	27	4 9 L	6	3
9 10	35	33	18 5	28	28	15 2	48	49	11 14	32	32	6 9	39	39
11 10	32	32	20 5	11	7	17 2	12	15	13 14	16	17	8 9 L	7	1
13 10	8	8	22 5	17	16	19 2	37	38	1 15	9	15	10 9	32	31
15 10	45	43	0 6	30	29	23 2	34	35	3 15	16	16	12 9 L	7	5
17 10	17	18	2 6	19	19	3 3	6	2	5 15	18	21	14 9	25	25
19 10	27	27	4 6	11	10	5 3 L	5	6	7 15	11	10	18 9	17	17
1 11	32	31	6 6	6	6	7 3	29	31	9 15	16	17	0 10	15	16
5 11	19	21	8 6	20	21	9 3	32	32	11 15	8	7	4 10	18	18
7 11	22	21	10 6	28	28	15 3	16	16	1 16	13	12	6 10 L	7	7
9 11	32	31	12 6 L	6	6	17 3	22	23	7 16	13	13	8 10	11	11
11 11	7	8	16 6	10	10	19 3	8	3	9 16 L	8	10	10 10	8	9
13 11	19	21	18 6	19	20	21 3	11	13	1 17	17	19	12 10	11	12
15 11 L	8	8	20 6 L	8	6	23 3 L	7	7	3 17	30	32	18 10	10	9
17 11	24	25	22 6	10	11	3 4	15	15				2 11	22	21
19 11 L	7	2	2 7	20	21	5 4	14	14	K L		H = 6	4 11	11	9
3 12	19	19	4 7	12	12	9 4 L	6	4				6 11	20	21
5 12	18	17	6 7	23	24	11 4	14	11	0 0	64	66	8 11	12	12
7 12 L	7	3	8 7	26	27	13 4	9	9	2 0	29	25	10 11	24	23
11 12	15	17	10 7	21	22	15 4 L	7	0	4 0	30	30	12 11	21	21
13 12	13	13	18 7	21	21	17 4	7	4	6 0 L	7	5	14 11	19	19
15 12 L	8	5	20 7	21	21	21 4 L	7	5	8 0	57	59	16 11	16	16
17 12 L	7	5	22 7	20	22	23 4 L	7	1	10 0	35	36	0 12	50	49
1 13	45	47	0 8	131	126	1 5	46	46	14 0	17	20	2 12	13	14
3 13	17	18	2 8	23	24	5 5	9	10	16 0	46	47	4 12	72	70
5 13	25	27	4 8	72	73	7 5	36	36	18 0	30	31	6 12	26	19
7 13	36	35	6 8	13	13	9 5	39	40	20 0 L	7	4	8 12	44	43
9 13	47	46	8 8	107	103	11 5	6	3	22 0	22	22	12 12	55	54
11 13 L	8	7	10 8	26	26	13 5	15	15	2 1	80	81	14 12	21	21
13 13	28	28	12 8	47	48	15 5	20	20	4 1 L	6	5	16 12	28	28
15 13	19	20	16 8	67	65	17 5	28	30	6 1	71	72	2 13 L	8	9
17 13	37	37	18 8	25	26	19 5 L	7	1	8 1 L	6	0	6 13	9	9
1 14	22	21	20 8	25	25	21 5	17	16	10 1	53	54	8 13	11	9
3 14	36	37	2 9	8	10	1 6	34	35	14 1	42	42	10 13	9	10
5 14	28	29	4 9	8	9	3 6	58	59	16 1	8	6	12 13	16	15
7 14	27	26	6 9	13	12	5 6	46	47	18 1	26	27	14 13	10	9
9 14 L	8	12	10 9	13	13	7 6	39	40	20 1 L	7	0	0 14 L	8	9
11 14	37	36	12 9	17	18	9 6	18	19	22 1	21	22	2 14 L	8	6
13 14	19	18	16 9	26	25	11 6	53	53	0 2 L	5	4	4 14	14	13
15 14	25	25	18 9	12	13	13 6	26	26	2 2	9	10	8 14	10	10
1 15	8	5	20 9	15	16	15 6	34	35	4 2	29	30	10 14	15	15
3 15	10	8	0 10	9	7	17 6 L	7	5	6 2	29	29	12 14	13	12
7 15	8	5	2 10	9	7	19 6	41	41	8 2 U	6	1	2 15	43	43
9 15 L	8	5	4 10	11	12	21 6	12	11	10 2 L	7	8	6 15	40	41
13 15 L	8	9	8 10	9	10	1 7	28	28	12 2	17	16	8 15 L	7	6
1 16	15	15	10 10	20	20	3 7	42	42	14 2	26	26	0 16	20	21
3 16 L	8	8	12 10	12	14	5 7	49	50	16 2	11	10	4 16	15	16
5 16 L	8	4	16 10	9	9	7 7	16	16	18 2	11	11	6 16 L	8	7
7 16	13	16	18 10	19	20	9 7	32	32	20 2	10	8	8 16	7	6

Can. J. Chem. Downloaded from www.nrcresearchpress.com by 210.87.254.105 on 09/05/12
For personal use only.

Table 2 (Concluded)

K	L	|FOBS|	|FCALC|
		H = 7	
3	1	30	31
5	1	31	31
7	1	L 8	2
9	1	7	7
11	1	21	21
13	1	24	25
15	1	L 7	3
17	1	13	11
19	1	12	12
21	1	18	19
1	2	43	43
3	2	31	32
5	2	50	50
7	2	28	30
9	2	41	42
11	2	15	16
13	2	42	42
15	2	15	13
17	2	33	34
19	2	55	56
21	2	26	26
1	3	35	36
3	3	37	37
5	3	10	11
7	3	35	35
9	3	14	15
11	3	41	40
13	3	L 1	1
15	3	27	27
17	4	L 6	3
19	4	11	10
21	4	9	9
1	5	L 6	2
3	5	8	8
5	5	8	7
7	5	L 8	4
9	5	7	5
11	5	59	61
13	5	27	27
15	5	37	38
17	5	59	58
19	5	11	11
21	5	37	37
1	6	20	19
3	6	45	45
5	6	29	30
7	6	49	49
9	6	36	36
11	6	17	16
13	6	47	47
15	6	23	23
17	6	33	32
19	6	37	38
21	6	17	17
1	7	L 7	4
3	7	12	12
5	7	15	14
7	7	L 8	6
9	7	8	7
11	7	17	17
13	8	L 6	1
15	8	18	17
17	8	13	14
19	8	13	14
21	8	9	9
1	9	L 7	2
3	9	27	27
5	9	29	29
7	9	L 7	3
9	9	18	18
11	9	28	28
13	9	36	36
15	9	L 14	15
17	9	13	13
19	9	37	37
1	10	23	24
3	10	16	17
5	10	39	40
7	10	28	27
9	10	24	26
11	10	10	7
13	10	36	36
15	10	14	15
17	10	29	29
1	11	23	23
3	11	18	17
5	11	23	23
7	11	19	18
9	11	31	30
11	11	8	9
13	11	25	23
15	11	L 7	7
17	12	13	14
19	12	12	13
21	12	9	10
1	13	43	42
3	13	19	19
5	13	28	28
7	13	32	31
9	13	42	43
11	13	L 9	8

K	L	|FOBS|	|FCALC|
1	14	19	18
3	14	31	31
5	14	25	25
7	14	21	23
9	14	11	10
11	14	L 7	4
13	14	L 7	4
15	14	L 7	2
1	15	13	13
		H = 8	
0	0	114	111
2	0	12	13
4	0	51	52
6	0	8	7
8	0	97	94
10	0	14	14
12	0	35	35
14	0	L 7	5
16	0	64	62
18	0	14	16
20	0	17	18
2	1	14	15
4	1	10	9
6	1	20	21
8	1	15	17
10	1	19	19
12	1	19	20
14	1	27	27
16	1	16	18
18	1	17	16
20	1	16	18
0	2	22	23
2	2	15	14
4	2	L 6	2
6	2	15	17
8	2	21	21
10	2	9	8
12	2	L 8	9
14	2	16	18
16	2	9	11
18	2	63	63
20	2	L 6	1
0	3	56	56
2	3	U 8	3
4	3	49	48
6	3	L 7	5
8	3	35	35
10	3	29	29
12	3	11	10
14	3	11	8
16	3	L 7	7
18	3	25	26
20	3	10	12
0	4	45	45
2	4	30	30
4	4	10	9
6	4	20	19
8	4	34	34
10	4	L 7	4
12	4	37	38
14	4	L 7	2
16	4	27	27
18	4	L 7	3
20	4	23	23
0	5	26	26
2	5	L 7	8
4	5	12	10
6	5	L 7	2
8	5	21	21
10	5	L 7	2
12	5	L 7	7
14	5	13	12
16	5	10	11
18	5	21	20
20	5	L 7	7
0	6	21	21
2	6	12	13
4	6	L 7	2
6	6	7	7
8	6	12	10
10	6	L 7	2
12	6	21	21
14	6	12	13
16	6	L 7	2
18	6	7	7
20	6	10	11
0	7	21	20
2	7	7	7
4	7	21	21
6	7	16	16
8	7	23	22
10	7	24	25
12	7	16	17
14	7	85	81
16	7	14	14
18	7	45	45
20	7	8	9
0	8	73	71
2	8	17	17
4	8	49	49
6	8	33	33
8	8	11	11
10	8	19	20
12	8	L 7	7
14	8	13	13
16	8	L 7	1
18	8	L 7	6
20	8	L 9	6

K	L	|FOBS|	|FCALC|
8	10	L 7	3
10	10	10	11
12	10	9	9
14	10	13	14
2	11	49	48
4	11	L 8	3
6	11	L 44	43
8	11	L 8	1
10	11	39	40
12	11	7	8
14	11	29	30
0	12	10	7
2	12	12	10
4	12	31	30
6	12	21	21
8	12	9	8
12	12	27	27
2	13	23	23
4	13	L 7	0
6	13	21	21
10	13	19	19
0	14	15	15
4	14	16	16
6	14	L 7	5
2	15	18	17
K	L	H = 9	
1	1	30	31
3	1	43	43
5	1	52	51
7	1	18	18
9	1	34	36
11	1	23	24
13	1	44	45
15	1	L 7	5
17	1	31	31
19	1	10	8
1	2	36	37
3	2	35	36
5	2	26	26
7	2	40	41
9	2	25	24
11	2	36	36
13	2	38	37
15	2	12	11
17	2	29	30
1	3	18	18
3	3	L 7	2
5	3	L 7	3
7	3	14	16
9	3	17	17
11	3	L 7	3
13	3	L 7	6
15	3	9	11
17	3	12	14
1	4	10	10
3	4	L 7	0
5	4	10	8
7	4	L 7	3
9	4	23	24
11	4	L 7	3
13	4	L 7	6
15	4	24	20
17	4	L 7	3
1	5	23	24
3	5	L 7	3
5	5	L 7	6
7	5	20	20
9	5	22	23
11	5	7	3
13	5	9	9
15	5	14	14
17	5	18	20
1	6	24	24
3	6	32	32
5	6	29	28
7	6	16	14
9	6	19	19
11	6	27	27
13	6	16	15
15	6	28	28
17	6	L 7	4
1	7	23	25
3	7	29	30
5	7	37	37
7	7	16	15
9	7	28	28
11	7	17	16
13	7	32	34
15	7	10	12
17	7	11	10
1	8	10	12
3	8	12	11
5	8	11	10
7	8	L 7	4
9	8	16	18
11	8	10	12
13	8	32	31
15	8	39	39
17	8	16	16
1	9	32	32
3	9	24	24
5	9	41	42
7	9	33	33
9	9	23	23
11	9	16	15
13	9	17	16
15	9	32	32
17	9	25	24
1	10	37	37
3	10	24	23
5	10	25	25
7	10	L 7	6

K	L	|FOBS|	|FCALC|
1	11	8	6
3	11	L 7	2
5	11	U 7	2
7	11	8	6
9	11	7	6
11	11	L 7	3
1	12	L 7	3
3	12	14	15
5	12	14	14
7	12	L 7	5
1	13	20	20
5	13	9	7
7	13	17	17
K	L	H =10	
0	0	51	51
2	0	12	13
6	0	7	6
8	0	47	48
10	0	21	25
12	0	7	5
14	0	18	18
16	0	38	39
2	1	46	46
4	1	43	43
8	1	L 7	2
10	1	35	35
12	1	L 7	2
14	1	30	30
16	1	L 7	6
0	2	L 7	5
2	2	L 7	5
4	2	24	24
6	2	13	12
8	2	L 7	1
12	2	17	17
14	2	13	12
16	2	L 7	4
2	3	17	18
4	3	8	9
6	3	18	17
8	3	11	12
10	3	21	19
12	3	20	21
14	3	17	16
16	3	16	16
0	4	38	38
2	4	8	8
4	4	78	75
6	4	11	10
8	4	33	32
10	4	L 7	2
12	4	60	58
14	4	12	12
16	4	21	20
2	5	14	13
4	5	7	8
6	5	15	13
8	5	8	10
10	5	15	15
12	5	19	18
14	5	13	13
2	6	L 7	1
4	6	11	11
6	6	11	9
8	6	L 7	4
12	6	8	7
14	6	11	12
2	7	47	45
6	7	43	43
8	7	L 7	4
10	7	36	36
12	8	41	39
2	8	15	14
4	8	8	8
6	8	L 7	1
8	8	36	37
10	8	23	24
12	8	L 7	9
2	9	29	29
6	9	28	27
8	9	L 7	1
10	9	23	22
12	9	L 7	3
0	10	16	15
2	10	L 7	1
4	10	20	19
6	10	L 7	2
10	10	L 8	4
2	11	18	18
4	11	L 7	7
6	11	18	17
8	11	9	9
12	11	31	31
2	12	10	10
4	12	47	47
K	L	H =11	
1	1	16	16
3	1	L 7	1
5	1	L 7	3
11	1	13	13

K	L	|FOBS|	|FCALC|
13	1	15	16
1	2	30	30
3	2	27	28
5	2	21	21
7	2	34	33
9	2	20	20
11	2	36	29
13	2	12	11
1	3	21	20
3	3	28	27
5	3	22	24
7	3	36	36
9	3	11	10
11	3	27	28
K	L	H =10	
0	4	L 7	6
2	4	L 7	7
4	4	L 7	5
6	4	40	39
8	4	22	21
10	4	27	29
12	4	29	28
14	4	42	41
16	4	10	10
1	5	27	29
3	5	25	25
5	5	34	34
7	5	27	27
9	5	25	25
11	5	12	14
13	5	34	34
1	6	7	6
3	6	35	34
5	6	27	27
7	6	25	25
9	6	12	12
11	6	34	33
13	6	27	28
1	7	L 7	7
3	7	L 8	9
5	7	L 7	7
7	7	L 7	7
9	7	8	7
11	7	13	12
13	7	8	8
1	8	L 7	8
3	8	8	10
5	8	L 7	7
7	8	10	12
9	8	8	10
11	8	L 7	5
13	8	17	17
1	9	L 7	5
3	9	17	17
5	9	20	19
7	9	L 7	3
9	9	20	19
11	9	25	26
13	9	17	17
1	10	12	12
K	L	H =12	
0	0	64	63
2	0	28	26
4	0	L 7	4
6	0	57	56
8	0	8	7
10	0	20	19
12	0	14	14
14	0	8	5
16	0	14	15
18	0	13	13
20	0	13	13
0	1	13	13
2	1	19	20
4	1	8	6
6	1	L 7	1
8	1	17	17
10	1	38	36
12	1	30	30
14	1	7	7
16	1	36	34
18	1	25	25
20	1	11	12
0	2	35	34
2	2	27	27
4	2	25	25
6	2	12	12
8	2	7	7
10	2	19	20
12	2	8	6
14	2	L 7	1
16	2	17	17
18	2	24	23
20	2	23	23
0	3	18	17
2	3	24	23
4	3	10	10
6	3	22	24
8	3	17	17
10	3	17	17
12	3	11	11
14	3	7	3
16	3	9	4
18	3	8	6
20	3	15	15
0	4	13	13
2	4	11	11
4	4	11	11
6	4	8	8
8	4	12	12
10	4	9	9
12	4	7	7
14	4	11	11
16	4	8	8
18	4	8	8
20	4	8	8
0	5	13	13
2	5	13	13
4	5	13	13
6	5	13	13
8	5	13	13
10	5	13	13
12	5	13	13
14	5	13	13
16	5	13	13
18	5	13	13
20	5	13	13

Can. J. Chem. Downloaded from www.nrcresearchpress.com by 210.87.254.105 on 09/05/12
For personal use only.

TABLE 3. Bond lengths and angles for $Mg_3(VO_4)_2$*

Bond	Distance (Å)	Bonds	Angles (deg)	Bonds	Angles (deg)
VO_4 group					
V—O(1)	1.716(1)	O(1)—V—O(2*a*)	110.51(6)	O(2*a*)—V—O(3*b*)	110.43(5)
—O(2*a*)	1.809(1)	—O(3*b*)	108.30(4)	O(3*b*) —O(3*b*)	108.81(5)
—O(3*b*)	2×1.695(1)				
Mg(1)—O_6 group					
Mg(1)—O(2)	2×2.034(1)	O(2)—Mg(1)—O(3)	89.82(3)		
—O(3)	4×2.130(1)	O(3) —O(3*c*)	78.60(3)		
Mg(2)—O_6 group					
Mg(2)—O(1)	2×2.022(1)	O(1)—Mg(2)—O(1*d*)	97.91(6)	O(2)—Mg(2)—O(2*d*)	90.32(5)
—O(2)	2×2.135(1)	—O(2)	86.01(1)	—O(3)	87.49(4)
—O(3)	2×2.118(1)	—O(2*d*)	174.60(5)	—O(3*e*)	84.90(4)
		—O(3*e*)	96.11(4)	O(3) —O(3*e*)	169.20(6)
		—O(3)	90.98		

*Estimated standard deviations in parentheses. Transformations: $a = x, 1/2 + y, 1/2 - z$; $b = 1/2 + x, 1/2 - y, -z$; $c = x, -y, -z$; $d = 1/2 + x, y, 1/2 - z$; $e = 1/2 - x, y, 1/2 - z$.

The O(1)—Mg(2)—O(2) angle, subtending this edge, is contracted to 86.0°, presumably as a result of cation repulsion. Between these chains lie rows of octahedral sites which are either alternately filled or empty as shown in Fig. 2. The Mg(1)—O_6 and Mg(2)—O_6 share O(2)—O(3) edges which are also contracted (89.8 and 87.5°, respectively). The unshared edges of Mg(2)—O_6, involving O(1) and O(1′), and O(2) and O(2′) are both larger than 90° and substantially so in the former case. The O(3)—O(3′) edge subtended at Mg(1) shows the greatest contraction (77.8°) and involves oxygen atoms which are separately shared with two Mg(2) ions lying in an x = constant plane. The reason for this contraction is a greater net Mg(1)–Mg(2) and Mg(1)–V repulsion compared to the Mg(2)–Mg(2) repulsion.

The three dimensional packing can be appreciated by a comparison of the $Mg_3(VO_4)_2$ structure with that of spinel whose stoichiometry is M_2TO_4. The spinel structure is shown in a projection analogous to that of $Mg_3(VO_4)_2$ in Fig. 1. Here we note that octahedral sites at (0,1/4,0) are filled, leading to octahedral layers as seen in Fig. 2. The chains of filled octahedral sites alternate with chains where half the octahedral sites are filled. These layers alternate with layers of oxygen atoms where both octahedral and tetrahedral sites are occupied. In $Mg_3(VO_4)_2$, the Mg(1) and V both alternate between lying at $x = 0$ and 1/2 along b while in spinel these ions are colinear with the b axis.

Figures 3*a* and *b* compare the relative disposition of the filled octahedral and tetrahedral sites in a double layer of close packed oxygen atoms in $Mg_3(VO_4)_2$ and spinel. Both structures contain double rows of filled tetrahedral sites with the apexes of adjacent tetrahedra directed oppositely with respect to the normal to the oxygen atom layers. These rows run parallel to the a axis of the diagram with adjacent double rows equivalent and related either by a translation perpendicular to the original row or a diagonal to this row. In spinel every double row is related to its neighbors by this latter translational operation while in $Mg_3(VO_4)_2$ the two translational operations alternate. The maximum stoichiometry for these layers obtainable in spinel is one filled octahedral site for every two filled tetrahedral sites while for the magnesium orthovanadate the maximum stoichiometry is a filled octahedral site for every four filled tetrahedral sites. We will assume that the tetrahedral groups do not share oxygen atoms, and that face sharing between octahedra or

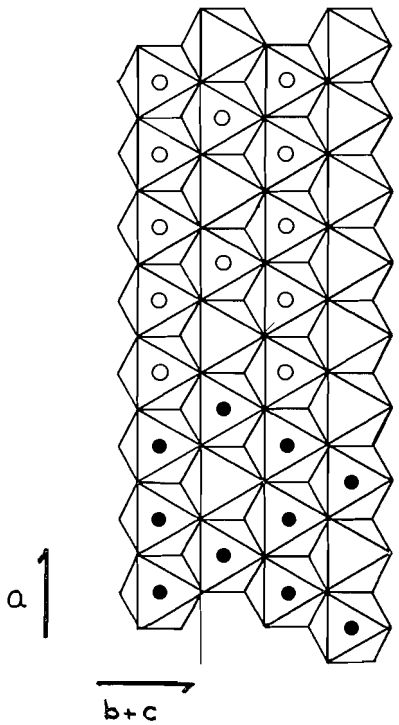

FIG. 2. The octahedrally coordinated cation layers in $Mg_3(VO_4)_2$ and spinel. The open circles are the filled cation sites in $Mg_3(VO_4)_2$. The rows parallel to a, where the cation sites are filled half the time, correspond to those containing Mg(1) and the filled rows to Mg(2). The black circles represent the filled cation sites in spinel for these types of layers.

Can. J. Chem. Downloaded from www.nrcresearchpress.com by 210.87.254.105 on 09/05/12
For personal use only.

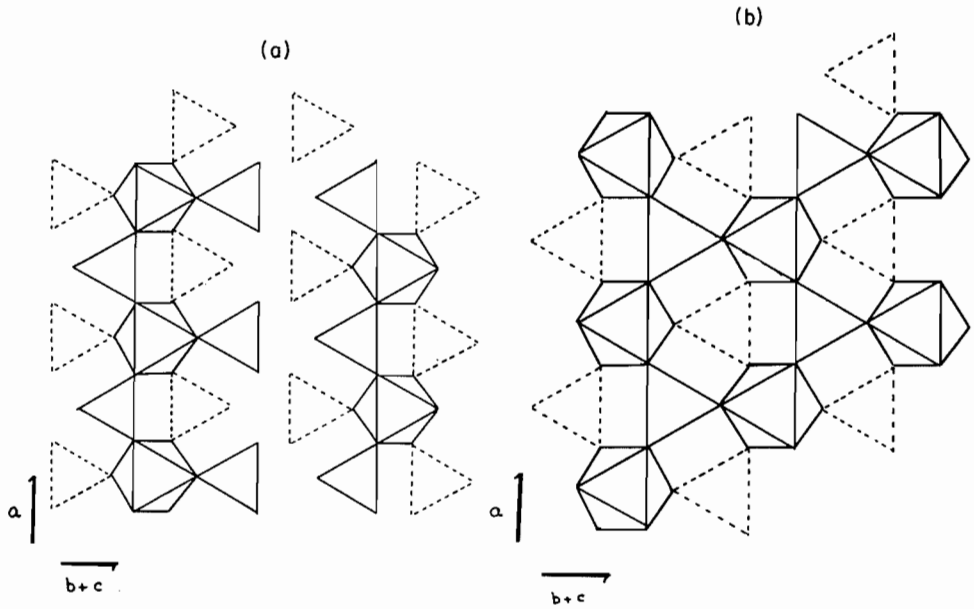

FIG. 3. (*a*) The oxygen atom layer containing tetrahedrally coordinated cations in $Mg_3(VO_4)_2$. The broken triangles represent three oxygen atoms bonded tetrahedrally to the fourth oxygen atom in the layer of the oxygen atoms represented with solid lines. The tetrahedra shown in projection with solid lines have their fourth oxygen atom in the plane of the broken triangles. Only occupied tetrahedral and octahedral sites are shown. (*b*), The oxygen atom layers containing tetrahedrally coordinated cations in spinel.

between tetrahedra and octahedra are not acceptable. The oxygen layer adjacent to the two layers depicted in Fig. 3 can either form a hexagonally close packed oxygen arrangement (*ABA*) or a cubically close packed arrangement (*ABC*). By applying the above restrictions and by disallowing edge sharing between filled octahedra and tetrahedra, a stoichiometry greater than one filled octahedral per filled tetrahedral site can be achieved only when the third layer is added cubically. For this packing the maximum stoichiometry obtainable corresponds to that of spinel, M_2TX_4, when the motif of Fig. 3*b* is used and $M_{7/4}TX_4$ when that of Fig. 3*a* is employed.

Discussion

The average V—O bond length in VO_4^{3-} is 1.729 Å and is slightly larger than that recently determined for other structures containing VO_4^{3-} tetrahedra with non-bridging oxygen atoms. In $Zn_3(VO_4)_2$, an isostructure of $Mg_3(VO_4)_2$, and YVO_4 the average V—O bond lengths are 1.71 Å (11, 12). In $Ca_3(VO_4)_2$ the average bond lengths for the three independent VO_4 groups are 1.69, 1.69, and 1.70 Å (13), with individual V—O bond lengths ranging from 1.67 to 1.72 Å. In YVO_4 the V ion lies on a $\bar{4}$ axis and thus all the V—O distances are equivalent. In $Zn_3(VO_4)_2$ the situation is quite parallel to that in $Mg_3(VO_4)_2$ with the V—O(2) bond length at 1.78(1) Å while V—O(1) and V—O(3) are 1.74(1) and 1.67(1) Å long, respectively. The bridging bond lengths in the meta-vanadates are of the same order as those found for V—O(2) in the ortho-vanadates. Thus in NH_4VO_3 (14) and $CsVO_3$ (15) the bridging V—O bond length is 1.81 Å and in KVO_3 it is 1.80 Å long (16). The V—O(2) bond with O(2) shared with three cations (Zn or Mg) have bond orders of 1.00, based upon a scale proposed by Evans (17) while the remaining bonds, involving oxygens shared with only two cations, have bond orders near 1.5. The high sensitivity of X—O bond lengths to their environment have been noted for X = P (18) and silicate systems are described in some detail by Brown and Gibbs (19).

The relationship between the spinel and $Mg_3(VO_4)_2$ structures has been considered above. Kamb (20) has recently discussed the conditions favoring the appearance of a spinel or olivine form for a M_2TX_4 compound where X ions are close-packed spheres. These compounds show an almost universal deviation from the ideal close-packed arrangement of X ions, resulting in an enlarged occupied tetrahedral site in the spinel form and a contracted occupied

Can. J. Chem. Downloaded from www.nrcresearchpress.com by 210.87.254.105 on 09/05/12
For personal use only.

TABLE 4. B—O/A—O ratios for $B_3(AO_4)_2$ and related structures

Compound	B—O/A—O	Packing	
		Tetrahedra	Oxygen atoms
$Co_3(AsO_4)_2$*	1.25	*N*/2,*N*/2,*N*/2	*ABAC*
$Mg_3(VO_4)_2$	1.21	*N*/2,0,*N*/2,0	*ABC*
$Zn_3(VO_4)_2$†	1.23	*N*/2,0,*N*/2,0	*ABC*
$Co_{7.0}As_{3.6}O_{16}$‡	1.28	*N*/2,*N*/2,*N*/2	*AB*

*Reference 8.
†Reference 11.
‡Reference 22.

tetrahedral site in the olivine form. In the latter case a contraction of the tetrahedral T—X bond length leads to a shortening of the shared edges between the tetrahedron and octahedron. A similar phenomenon occurs in spinel with the pertinent edges being shared between MX_6 groups. It is the shortening of shared edges separating the positively charged cations which Kamb claims explains the relative stability of these phases. The boundary defining the stability limit of the two phases should lie near an ideal ratio of the M—X to T—X bond lengths. However, Kamb finds that the spinel structure is stable to progressively larger values of this ratio as the charge on the T ion increases. For pentavalent T ions the value of this ratio seems to be near 1.22.

Kamb's concepts should find application to other stoichiometries in addition to M_2TX_4. The appearance of the $Mg_3(VO_4)_2$ structure for the ortho-vanadates of Co, Ni, and Zn while a structure based upon an olivine-like packing for the ortho-arsenates of Ni(21) and Co(8) provide some test data. Table 4 summarizes the value of this ratio for the known vanadates and arsenates in this series. The mode of oxygen atom packing is indicated together with the number of filled tetrahedral sites out of *N* possible filled sites. Filled tetrahedral sites sharing bridging X ions are excluded. The layer sequence in spinel and $Mg_3(VO_4)_2$ both have the tetrahedral sites showing *N*, 0, *N*, 0, · · · sequence while in olivine the sequence is *N*/2, *N*/2, · · ·. This datum provides support for the extension of Kamb's criterion to these stoichiometries with the ratio at the boundary near 1.24.

This research was supported by a grant by the National Research Council of Canada.

1. M. T. POPE and B. W. DALE. Q. Rev. **22**, 527 (1968).
2. A. DURIF and E. F. BERTAUT. J. Phys. Radium, **20**, 45S (1959).
3. A. DURIF. Anal. Chem. **31**, 1741 (1959).
4. C. BRISI. Ricerca Sci. **30**, 1339 (1960).
5. J. C. JOUBERT and A. DURIF. Bull. Soc. Fr. Min. Crist. **87**, 47 (1964).
6. P. K. L. AU and C. CALVO. Can. J. Chem. **45**, 2297 (1967).
7. E. DORM and B. MARINDER. Acta Chem. Scand. **21**, 590 (1967).
8. N. KRISHNAMACHARI and C. CALVO. Can. J. Chem. **48**, 881 (1970).
9. D. J. CROMER and K. HERRINGTON. J. Am. Chem. Soc. **77**, 4708 (1955).
10. International Tables for X-Ray Crystallography. Vol. II. Kynoch Press. 1952.
11. R. GOPAL and C. CALVO. To be published.
12. J. A. BAGLIO and G. GASHUROV. Acta Cryst. B**24**, 292 (1968).
13. C. CALVO and R. GOPAL. American Crystallographic Association, Summer meeting, 1970. Carlton, Ontario.
14. H. T. EVANS, JR. and S. BLOCK. Am. Min. **39**, 326 (1954).
15. J. OZOG and C. CALVO. Unpublished results.
16. V. SYNEVEK and F. HANIC. Phy. J. Czech. **4**, 120 (1954).
17. H. J. EVANS, JR. Zeits. für Kristallog. **114**, S257 (1960).
18. C. CALVO and P. K. L. AU. Can. J. Chem. **47**, 3409 (1969).
19. G. E. BROWN and G. V. GIBBS. Am. Min. **54**, 1528 (1969).
20. B. KAMB. Am. Min. **53**, 1439 (1969).
21. R. J. DAVIS, M. H. HEY, and A. W. G. KINGSBURY. Min. Mag. **35**, 72 (1965).
22. N. KRISHNAMACHARI. Ph.D. Thesis. McMaster University, Hamilton, Ontario. 1970.

Can. J. Chem. Downloaded from www.nrcresearchpress.com by 210.87.254.105 on 09/05/12
For personal use only.

Can. J. Chem. Downloaded from www.nrcresearchpress.com by 210.87.254.6 on 09/05/12
For personal use only.

Stereochemistry of Hexahydrocarbazoles; the Temperature-dependent Nuclear Magnetic Resonance Spectra of *N*-Acetyl Derivatives

STEWART MCLEAN, U. O. TROTZ, C. J. MACDONALD, W. F. REYNOLDS, AND D. J. WOOD
Department of Chemistry, University of Toronto, Toronto 181, Ontario

Received November 25, 1970

The configuration of certain substituted hexahydrocarbazoles **2**, of significance in connection with earlier work, has been established. A study of the temperature dependence of the n.m.r. spectra of *N*-acetyl derivatives, initiated with the intention of distinguishing between *cis*- and *trans*-fused isomers, has led to the conclusion that the distinction could not be made on this basis since all of the temperature-dependent phenomena, even in cases where the *cis*-fusion had been established by other means, could be associated with rotational isomerism of the *N*-acetyl group and no observable effects in the temperature range studied could be related to conformational mobility of the ring system. Nevertheless, the results obtained provide information of value and interest regarding the stereochemistry of hexahydrocarbazoles.

On a établi la configuration de certaines hexahydrocarbazoles substituées **2** qui présentaient de l'intérêt en fonction de nos travaux antérieurs dans ce domaine. Nous avons examiné les spectres r.m.n. des dérivés *N*-acétylés en fonction de la température afin d'évaluer s'il est possible de déterminer la configuration-*cis* ou -*trans* de la jonction entre les cycles; nous avons été amenés à conclure que cette méthode ne peut être utilisée parce que, dans les limites des températures examinées, toutes les variations spectrales dépendantes de la température qui sont observées peuvent être reliées à l'isomérie rotationnelle du groupe *N*-acétyle et que de plus aucune variation détectable ne peut être attribuée à la mobilité conformationnelle et ce même dans les cas où on a pu établir par d'autres méthodes que la jonction entre les cycles est *cis*. Malgré ces limitations nos résultats fournissent des informations importantes et intéressantes concernant la stéréochimie des hexahydrocarbazoles.

Canadian Journal of Chemistry, 49, 1638 (1971)

Recently we reported on the results of our studies which led to the synthesis of certain derivatives of 2,3-benzo-1-azabicyclo[2.2.1]hept-2-ene and the discovery that compounds of this structure underwent an unusual ring opening on treatment with acetic anhydride; for example, compound **1**, formally derived from hexahydrocarbazole by the introduction of a two-carbon bridge, afforded **2***a* (1). In contrast to the case of the analog formally derived from 2,3-dimethylindoline, where two stereoisomers were obtained and confident stereochemical assignments could be made both to the ring-closed isomers, analogs of **1**, and to the ring-opened isomers, analogs of **2***a*, only one isomer was obtained in the hexahydrocarbazole case and it was not possible to present conclusive evidence for the stereochemistry of either the ring-closed or ring-opened compounds. We did, however, point out that the burden of the evidence, mainly based on the n.m.r. spectroscopic characteristics of the ring-closed and the ring-opened compounds, favored a configuration, as depicted in **1** and **2***a*, based on a *cis*-hexahydrocarbazole parent structure.[1]

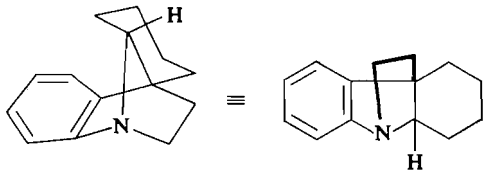

1

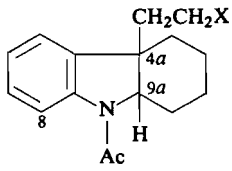

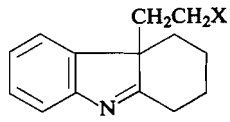

2

a X = OAc
b X = H
c X = OTs
d X = OH
e X = Br

3

a X = Br
b X = H

In order to establish conclusively the configuration in this series, we undertook two simultaneous lines of investigation. In the first we converted **2***a* to the 4*a*-ethyl derivative, **2***b*, by borohydride reduction of the tosylate **2***c* obtained from the alcohol **2***d*, the hydrolysis product of **2***a*. Compound **2***b* was then subjected to an X-

[1]Since the major part of this paper concerns hexahydrocarbazole derivatives, locants based on this system will be used throughout.

Can. J. Chem. Downloaded from www.nrcresearchpress.com by 210.87.254.6 on 09/05/12
For personal use only.

ray analysis which established unequivocally that its configuration was that shown (2), and since none of the reactions used to effect the interrelationship are expected to affect position 9*a*, the configuration of **1** and that of each of the compounds of formula **2** are also firmly established. It can be noted at this point that one chemically significant conclusion that follows from this result is that the reaction which formed **1**, the reduction of **3***a* by either borohydride or catalytic hydrogenation, delivered hydrogen to C-9*a* exclusively from the side of the molecule carrying the C-4*a* side chain; in contrast the reduction of the corresponding 2,3-dimethylindolenine led to both stereoisomers, but with delivery of hydrogen to the other side of the molecule as the predominant path (1). No good explanation for the stereochemical outcome of the reduction of **3***a*, particularly by catalytic hydrogenation, is apparent, but it can be shown that the presence of bromine in the molecule is not a significant factor since catalytic hydrogenation of the 4*a*-ethyl derivative **3***b* in the presence of acetic anhydride also leads to the *cis* product **2***b*. (Under these conditions **3***a* is transformed directly into **2***e*.)

Our second line of investigation involved a more careful examination of the n.m.r. spectra of the ring-opened compounds since our original tentative stereochemical assignment (1) was based on the appearance of the spectra of a number of derivatives, but in each case only one member of a pair of epimers was available. It was our intention, therefore, to prepare suitable model *cis*- and *trans*-hexahydrocarbazoles and compare their behavior with that of our compounds. However, it became apparent that the original assignments of configuration to the model compounds were made a number of years ago on an empirical basis (3) and some element of doubt existed about them; the assignments have not been challenged, but very recently others have also noted the need for placing them on firmer ground (4), and, once **2***a* proved amenable to X-ray analysis, one outcome of our present study has been to do that, the converse of what we had originally intended.

It is well known that a fused ring system such as *cis*-hexahydrocarbazole is flexible and can adopt two extreme conformations, one with the 4*a* substituent axial and the 9*a* substituent equatorial and the other with the relationship reversed, but, with suitable substitution, one conformation may be predominantly or exclusively populated; in contrast, the *trans*-fused isomer is rigid and both 4*a* and 9*a* substituents are axial. Our previous studies (1) had led us to conclude that the 9*a* proton in our compounds of structure **2** was axial, indicative of a *trans*-hexahydrocarbazole or a *cis* isomer in which one conformation was populated predominantly, and of these two possibilities we favored the latter. (It may be noted that the X-ray study (2) has now shown that the molecule does in fact adopt this conformation, with the hydrogen at 9*a* axial, in the crystal.) It was our intention to verify this conclusion by examining the temperature dependence of the n.m.r. spectra of compounds of formula **2**, since it was anticipated that the conformational mobility of the ring system, if *cis*-fused, would exhibit some temperature dependent feature in these spectra. However, we recognized that the compounds of interest to us all carried an *N*-acetyl group which could also lead to temperature dependent changes in the spectra (5), and the conclusion we now draw from our present study is that the temperature dependence of the n.m.r. spectra in the range in which we have studied it can be entirely attributed to the conformational mobility of the *N*-acetyl group.

When the spectra of compounds of formula **2** were examined, three features showing a significant temperature dependence could be associated with each compound: the signals concerned were those attributed to the protons at C-8 and -9*a* and those of the *N*-acetyl group. In the best cases where there was a minimum of overlap with other signals, each set of protons gave rise at the low temperature limit to two groups of signals of appropriate multiplicity, indicative of the presence of two species in the sample; the abundance ratio, as judged by the relative intensities of the signals, depended primarily on the specific compound examined, but was also affected by variables such as solvent and temperature. As the temperature was raised, the signals associated with each set of protons broadened and converged on an average position, coalesced, and, at the upper temperature limit, appeared as one signal, again showing the appropriate multiplicity. It is clear that rotation of the *N*-acetyl group, for which two rotamers, **A** and **B**, are favored by π-orbital stabilization, can affect the signals associated with all three sets of protons, while conformational inversion of the ring system is highly unlikely to have any effect on the signals of the C-8 proton. If both conformational variations were occurring together, it would be expected that the temperature dependence of each set of

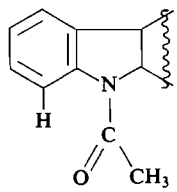
A

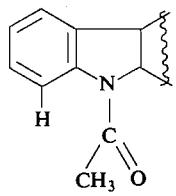
B

signals would be different, and ideally a precise analysis of each would be required. Unfortunately, the system in hand is a complex one; the chemical shift differences at the low temperature limit are different in each set of protons, signals are often obscured by overlap of other signals, and it is difficult to obtain data with the precision required for a quantitative analysis. Nevertheless, by making use of observable values and by interpolating or extrapolating where necessary, we have concluded that the presence of the two interconverting *N*-acetyl rotamers is sufficient to provide an explanation for all of the temperature dependent phenomena in the range we have studied, and that any conformational mobility of the ring system has a minimal effect. In terms of our original aim of using this technique to study the configuration of the ring fusion, this result is not helpful, but since the X-ray analysis has provided the answer to this question, we can simply state that the conformational mobility of a *cis*-fused hexahydrocarbazole does not lead to observable temperature-dependent phenomena in the n.m.r. spectrum, at least in the temperature range we have studied, while rotation of an *N*-acetyl substituent has a pronounced effect.

Results were obtained for the 4*a*-ethyl derivative **2***b* as a solution in toluene-d_8 over the temperature range -84 to $+96°$. The C-8 proton (6) was associated at the lowest temperatures with a doublet, $J = 8$ Hz, at τ 1.20, which moved upfield as the temperature was raised, began to collapse at about 0° (at intermediate temperatures better resolution was obtained and the doublet showed further fine structure), and at $+40°$ appeared as a broad featureless envelope; at the higher temperatures a doublet, $J = 8$ Hz, again appeared and at 96° it was centered at τ 1.94. The doublet at the highest temperature is clearly the time-averaged signal for the C-8 proton in both rotamers, while at the lowest temperatures interconversion of rotamers is sufficiently slow that two sets of signals are obtained, the τ 1.20 doublet being attributed to the C-8 proton of rotamer **A**, but the corresponding signal for rotamer **B** being lost among the other aromatic signals near τ 3. The signals we attributed to the C-9*a* proton at the lowest temperatures were a smaller multiplet centered near τ 5.5 and a larger multiplet centered near 6.9 (which in well resolved spectra appeared as a symmetrical three-peak pattern with 8 Hz spacing and further fine structure); as the temperature was raised these signals moved together and collapsed, appearing at about $+40°$ as a very broad envelope, and at the highest temperature the three-peak pattern reappeared, centered at τ 6.2. The signal for the *N*-acetyl protons appeared at the lowest temperatures as an unresolved peak at τ 8.15, but at $-60°$, where resolution was generally better, two components could be discerned, a smaller singlet at τ 8.09 and a larger singlet at 8.14; by the time 0° was reached only one singlet, at τ 8.10, was visible and at the highest temperature this appeared at 8.01. These observations are again compatible with the existence of two rotamers, **A** and **B**, which are seen separately at low temperatures but lead to a time-averaged signal at high temperatures. (The appearance of the *N*-acetyl signal at the lowest temperatures may result from poorer resolution at these temperatures, an accidental convergence arising from a different temperature dependence of the chemical shift of the protons in the two rotamers, or a combination of both effects.) In these cases the relative peak areas indicated the rotamer ratio **A**:**B** is roughly 3:1; the value based on the C-8 protons is not directly available because of overlap, but the signal strength of the observed doublet is compatible with this figure.

An approximate free energy of activation ($\Delta G^{\ddagger}$) for the interconversion between rotamers **A** and **B** was obtained by observation of the broadening of the individual components of the low field C-8 doublet in the slow exchange limit. At 10 °C, the individual lines were broadened beyond the limiting value in the absence of exchange by between 3 and 4 Hz. Since, in the slow exchange limit (8),

$$\pi(\Delta\nu - \Delta\nu_0)_A = 1/\tau_A$$

where $\Delta\nu$ and $\Delta\nu_0$ are line widths in Hz (at half height) in the presence and absence of exchange and τ_A is the lifetime at site A. Therefore, $\tau_A \simeq 10^{-1}$ s. This corresponds to $\Delta G^{\ddagger} = 15$ kcal/mol. In addition, values of $\Delta G^{\ddagger}$ of 14 to 15 kcal/mol were obtained from the coalescence temperatures for C-8, -9*a*, and the *N*-acetyl protons. While both sets of measurements are only approximate, the

Can. J. Chem. Downloaded from www.nrcresearchpress.com by 210.87.254.6 on 09/05/12
For personal use only.

Can. J. Chem. Downloaded from www.nrcresearchpress.com by 210.87.254.6 on 09/05/12
For personal use only.

former because the above equation should strictly only be applied to a system in which protons at sites A and B are not coupled to other protons and the latter because the temperature dependence of the chemical shift was ignored, it is believed that at least the former value is accurate to within 1 kcal/mol since this would allow for an error of greater than a factor of 5 in the measurement of line width and lifetime.[2] The value of 15 kcal/mol is of the same order of magnitude as has been obtained by others for related processes (5); this combined with the relative constancy of the value obtained from different processes provides support for the conclusion that the temperature dependence of all three sets of signals can be attributed to interconversion of *N*-acetyl rotamers and that it is not necessary to invoke further effects arising from the conformational mobility of the ring system.

Other derivatives of formula **2** have been examined less extensively as chloroform-*d* solutions and they show behavior corresponding to that of **2***b*. For the bromo compound **2***e*, the relevant data are that the C-8 proton produces a sharp doublet, $J = 8$ Hz, at τ 1.80 (a second component is presumably lost in the aromatic multiplet between τ 2.5 and 3.0) at $-60°$, the coalescence temperature is about $+30°$, but at 65°, the highest temperature used, the upper limiting condition is not reached and the signal appears as an unresolved multiplet centered at τ 2.05; the C-9*a* proton produces two signals at $-60°$, a smaller multiplet at τ 5.55 and a larger at 6.10 (both are three-peak patterns with fine structure and the ratio of areas is approximately 1:4), which have coalesced by $+40°$, but still appear as an unresolved multiplet centered at τ 5.90 at 65°; the two components of the *N*-acetyl signal at the lowest temperature, the smaller singlet at τ 7.54 and the larger at 7.67, appear as one singlet at 7.70 at the highest temperatures; in addition, the CH_2Br protons which form a simple three-peak pattern centered at 6.85 at the highest temperatures appear as a much more complex multiplet at the lowest temperatures, but with very little change in chemical shift. The C-8, -9*a*, and *N*-acetyl protons of the alcohol **2***d*, show the same behavior with only very small chemical shift differences; in addition the OH proton moves from about τ 5.45 to 8.0 as the temperature is raised over the range -60 to $+70°$.

The parent *N*-acetylhexahydrocarbazole to which the *cis* configuration was previously assigned on empirical grounds (3) shows a marked correspondence in behavior to that of our 4*a*-substituted derivatives. In toluene-d_8 at $-73°$ the C-8 proton appears at τ 1.30 as a doublet, $J = 8$ Hz, which moves upfield and broadens with increasing temperature, has its maximum width at about $+30°$, and then sharpens to a doublet at τ 2.00, $J = 8$ Hz, at 97°; the *N*-acetyl protons, which are unresolved at $-73°$, form two singlets at $-56°$, the smaller at τ 8.17 and the larger at 8.23 (in this case the ratio of areas is two or three times greater than in the case of **2***b*), coalesce by $+10°$, and appear as a singlet at τ 8.05 at the highest temperatures. The behavior of the C-9*a* proton signals is made somewhat more difficult to follow in this case by the presence of peaks associated with the C-4*a* proton, and a rational explanation of the observed spectra is as follows: the C-4*a* proton is responsible for a multiplet that appears at τ 7.20 at $-73°$ and moves slowly downfield without significant broadening as the temperature is raised, appearing at τ 6.88 at $+97°$, while the C-9*a* proton is associated with a multiplet at τ 6.90 at $-73°$ which moves downfield and broadens as the temperature is raised, having its greatest width at $+30°$, and then sharpens to a multiplet at τ 6.04 at $+97°$; at low temperatures a small, broad, and very poorly defined signal can be discerned against the background noise near τ 5.2, and is consistent with the description already given (which requires the C-9*a* proton signal from rotamer **B** to appear in this region and to move upfield to meet the signal associated with rotamer **A** as the temperature is raised). It follows that the stereochemistry of the *cis* isomer is analogous to that of **2***b* with the C-9*a* proton axial and with no conformational inversion involving the ring fusion giving rise to a temperature-dependent change in the spectra, despite the fact that it could be anticipated that this conformational equilibrium might be significantly affected by the

[2]In principle, a more accurate value for ΔG^* could be obtained from the temperature dependence of the *N*-acetyl signals, by use of total line shape analysis. In practice, this would be extremely difficult for this system. Firstly, exchange rate, chemical shift, and rotamer populations would all be adjustable parameters in the calculation (previous calculations have involved no more than two parameters). Secondly, the signal-to-noise ratio is poor due to limited solubility at low temperature and the peaks of interest partially overlap with other spectral peaks. Consequently, we believe that a detailed total lineshape analysis would not give a significantly more accurate value for ΔG^*.

Can. J. Chem. Downloaded from www.nrcresearchpress.com by 210.87.254.6 on 09/05/12
For personal use only.

presence or absence of a bulky substituent at C-4*a*. The account given for the *cis*-*N*-acetylhexahydrocarbazole case does require that the preponderance of rotamer **A** over rotamer **B** be significantly greater than in the case of **2***b* in the same solvent, and no good explanation for this difference is apparent at present. Although it does not appear to bear directly on this question, we can note that the **A**:**B** ratio does have a solvent dependence and the corresponding spectra in chloroform-*d* show signals, albeit at slightly different positions because of the effect of the solvent on the chemical shift, which are consistent with a smaller **A**:**B** ratio; moreover, in support of the case made above, the signal at lower field associated with the C-9*a* proton of rotamer **B** is now more clearly visible.

The spectrum of *trans*-*N*-acetylhexahydrocarbazole (3) shows a temperature dependence that is related to those already described but is sufficiently distinctive in detail that it serves to support the assignments made previously. In toluene-d_8 at $-73°$, the C-8 proton of rotamer **A** gives rise to a doublet, $J = 8$ Hz, at τ 1.18 and in this case the corresponding signal from rotamer **B**, the minor component, appears at τ 3.54, to high field of the other aromatic resonances; as the temperature is raised, these signals converge and broaden, coalesce at about $-30°$, reappear as a doublet at about $+30$, and, at $+77°$, appear as a sharp doublet, $J = 8$ Hz, at τ 2.35. The *N*-acetyl protons give rise to two singlets at $-73°$, the smaller at τ 8.11 and the larger at 8.32, which coalesce near $-45°$, and appear as a sharp singlet at τ 8.03 at $+77°$. These features are consistent with a rotamer ratio **A**:**B** of between 2:1 and 3:1 at the lowest temperatures and a rotational barrier significantly lower (by 3 to 4 kcal/mol) than in the *cis* case; no ready steric explanation for this difference can be discerned from molecular models. As with the *cis* isomer, an account of the behavior of the C-9*a* proton is made more difficult by the presence of the C-4*a* proton, and a further difficulty becomes apparent when the spectra of the *trans* isomer are examined. At $-73°$ two multiplets are clearly visible, centered at τ 6.47 and 6.93, in the region where the C-4*a* and -9*a* resonances may be expected and a further multiplet appears to be present near τ 7.8 at the edge of the envelope to higher field (which includes solvent peaks); at $+77°$ two three-peak patterns with further fine structure appear in this region, one at τ 6.92 and one at 7.63 and a two-peak pattern appears at 7.30, and each of these patterns appears to correspond to one proton; since the multiplets are both broadened and shifted at intermediate temperatures and a considerable amount of overlap of signals occurs, it is difficult to follow their progress in detail, but it is possible that the multiplet near τ 6.9 is associated with the C-4*a* proton and does not move significantly as the temperature is varied, while the τ 7.63 multiplet at high temperatures is the time-averaged signal for the C-9*a* proton; the τ 7.30 multiplet at higher temperatures must then be associated with another proton in the cyclohexane ring, such as the equatorial proton at C-1, which experiences an unusually strong deshielding effect from the acetyl group (time-averaged at this temperature); at the lowest temperature the low field pattern at about τ 6.47 would, if this explanation were correct, correspond to a superimposition of signals from the latter proton and the C-9*a* proton in one rotamer, the corresponding signals from the other rotamer being at τ 7.8 or higher. A 220 MHz spectrum obtained at 60° supports these conclusions; each set of peaks is more clearly resolved than in the 100 MHz spectrum and the integrated areas of the peaks are in accord with the proposals made. As we have already stated, the assignments are not considered to be rigorously established, but it is clear that any analysis requires the assignment of some rather unusual chemical shift values, and it is a judgment of the probable pattern of behavior of the chemical shifts over the temperature range studied that has led us to the assignments we have made.

We have also examined the spectra of *cis*-*N*-ethylhexahydrocarbazole (obtained by reduction of the *N*-acetyl derivative), in which *N*-acetyl rotation is obviously no longer a factor but the possibility still exists of conformational inversion associated with the ring fusion, and the spectra of aspidocarpine, in which hydrogen bonding between the *N*-acetyl group and a hydroxyl group at the position corresponding to C-8 holds the molecule in a conformation corresponding to rotamer **A** (7). In neither case did the spectra show appreciable variation with temperature over a range of about 100°, particularly with respect to the signals arising from protons corresponding to those on which the present discussion has centered.

In summary, we have established that the 4*a*-

substituted hexahydrocarbazoles that we isolated previously are *cis*-fused and this information has been used to deduce the stereochemistry of the azabicycloheptene from which they were derived and the steric course of the reduction of the precursor tetrahydrocarbazolenine. No temperature-dependent phenomena in the n.m.r. spectra of the hexahydrocarbazoles could be traced to conformational mobility of the ring fusion, but *N*-acetyl substituents led to temperature-dependent effects which could be associated with the interconversion of two rotamers. Comparison of this behavior with that of *cis*- and *trans*-hexahydrocarbazole provided supporting evidence for the configurational assignments originally made for these isomers.

Experimental

The n.m.r. spectra were recorded on a Varian HA-100 spectrometer operating in frequency sweep mode at a sweep rate of 1 Hz/s. Spectra were calibrated by measuring the difference between sweep and manual (lock) oscillators. The variable temperature unit was calibrated with standard Varian samples before each run.

All solute concentrations were approximately 0.5 *M*; 5% tetramethylsilane was added as a lock and internal reference. Sample tubes were degassed and sealed under vacuum before use.

The 220 MHz spectrum of *trans*-*N*-acetylhexahydrocarbazole was recorded on a Varian HR-220 at the Canadian 220 MHz N.M.R. Center.

Model compounds were synthesized by standard procedures (3).

9-Acetyl-4a-ethyl-1,2,3,4,4a,9a-hexahydrocarbazole (2b)

Preparation A

A solution of the tosylate **2***c* (1) (65 mg; 0.16 mmol) in 6 ml dimethyl sulfoxide was stirred with excess sodium borohydride (800 mg) for 10 h at room temperature. The solution was diluted with water and extracted with methylene chloride; the extract afforded an oil (35 mg; 0.14 mmol) which, on recrystallization from hexane, was isolated as colorless crystals, m.p. 63.5–64.5°.

Preparation B

A solution of 4*a*-ethyl-1,2,3,4-tetrahydrocarbazolenine (**3***b*) (1) (2.40 g; 12 mmol) in 6 ml acetic anhydride was hydrogenated in the presence of prereduced platinum oxide at room temperature and atmospheric pressure for 10 h (11.3 mmol hydrogen was consumed). This afforded **2***b* (2.92 g; 12 mmol) identical with that described above. Repeated recrystallization afforded an analytical sample, m.p. 65.5–66.5°.

Anal. Calcd. for $C_{16}H_{21}NO$: C, 78.97; H, 8.70; N, 5.76. Found: C, 79.07; H, 8.68; N, 5.99.

The i.r., λ_{max} (CCl_4) 6.01 μ; u.v., λ_{max} (MeOH) 254 (ε 11 700) 276 (ε 3600), 287 mμ (ε 2900).

We are grateful to the National Research Council for financial support of this research, to the Canadian Commonwealth Scholarship and Fellowship Committee for a Fellowship (U.O.T.), and to the Province of Ontario for a Fellowship (D.J.W.).

1. S. McLEAN, A. L. FALLAS, U. O. TROTZ, and W. F. REYNOLDS. Can. J. Chem. **47**, 3647 (1969).
2. S. McLEAN, U. O. TROTZ, K. S. DICHMANN, J. K. FAWCETT, and S. C. NYBURG. Tetrahedron Lett. 4561 (1970).
3. J. GURNEY, W. H. PERKIN, JR., and S. G. P. PLANT. J. Chem. Soc. 2676 (1927).
4. O. L. CHAPMAN and G. L. EIAN. J. Am. Chem. Soc. **90**, 5329 (1968). A. BLOOM and J. CLARDY. Chem. Commun. 531 (1970).
5. F. A. L. ANET. Can. J. Chem. **41**, 883 (1963). K. NAGARAJAN, M. D. NAIR, and P. M. PILLAI. Tetrahedron, **23**, 1683 (1967). A. M. MONRO and M. J. SEWELL. Tetrahedron Lett. 595 (1969).
6. S. McLEAN. Can. J. Chem. **38**, 2278 (1960).
7. S. McLEAN, K. PALMER, and L. MARION. Can. J. Chem. **38**, 1547 (1960). S. McLEAN. Can. J. Chem. **42**, 191 (1964).
8. J. A. POPLE, W. G. SCHNEIDER, and H. J. BERNSTEIN. High-resolution nuclear magnetic resonance. McGraw-Hill, Toronto, Ontario, 1959. Chapt. 10.

Can. J. Chem. Downloaded from www.nrcresearchpress.com by 210.87.254.6 on 09/05/12
For personal use only.

Can. J. Chem. Downloaded from www.nrcresearchpress.com by 210.87.254.40 on 09/05/12
For personal use only.

The Effect of Pressure on the Aquation of Chromium(III) Complexes

DAVID L. GAY AND ROBERT NALEPA[1]

Received December 21, 1970

The effect of pressure on the rates of aquation of $Cr(NCS)_6^{3-}$ and $Cr(NH_3)_2(NCS)_4^-$ has been studied over the pressure range 1 to 2043 atm, at 50 °C. The activation volumes for these reactions are found to be 16 ± 2 and −2.4 ± 0.8 ml/mol, respectively. The pressure dependence of the activation volumes, $(\partial\Delta V^*/\partial P)_T$, are 15 ± 5 and 0 ± 1 ml/katm mol, respectively. These results are consistent with a dissociative interchange (I_d) process for the aquation of $Cr(NCS)_6^{3-}$ and an S_N2 front-side process for the aquation of $Cr(NH_3)_2(NCS)_4^-$.

On a étudié, à 50 °C et à différentes pressions entre 1 et 2043 atmosphères, l'effet de la pression sur les taux d'hydratation de $Cr(NCS)_6^{3-}$ et $Cr(NH_3)_2(NCS)_4^-$. On a trouvé que les volumes d'activation de ces réactions sont respectivement de 16 ± 2 et de −2.4 ± 0.8 ml/mol; on a aussi établi pour chacune de ces réactions que la dépendance de leur volume d'activation sur la pression, $(\partial\Delta V^*/\partial P)_T$, est de 15 ± 5 et de 0 ± 1 ml/katm mol. Ces résultats seraient consistants avec l'hypothèse que l'hydratation du $Cr(NCS)_6^{3-}$ se fait par un processus d'échange dissociatif alors que l'hydratation du $Cr(NH_3)_2(NCS)_4^-$ se produit par une substitution S_N2 impliquant le devant de la molécule.

Canadian Journal of Chemistry, 49, 1644 (1971)

Introduction

The aquation reactions 1 and 2,

[1] $Cr(NCS)_6^{3-} + H_2O \rightarrow Cr(NCS)_5(H_2O)^{2-} + NCS^-$

[2] $Cr(NH_3)_2(NCS)_4^- + H_2O \rightarrow Cr(NH_3)_2(NCS)_3(H_2O) + NCS^-$

are thought to proceed via transition states involving one and two molecules of water, respectively (1, 2). However, it is believed that the role of solvent water is not that of a nucleophile (1–3). In addition, it assumed that a fair degree of Cr...NCS bond stretching is involved in the activation processes of these reactions, but no direct evidence for this has been presented (1, 2).

This study was therefore performed to obtain evidence which would clarify the role of Cr... NCS bond stretching as well as the role of water in these reactions.

Experimental

Materials

Reagent grade $K_3Cr(NCS)_6$, Alpha Inorganics stock No. 24115, and Fisher Certified grade $NH_4Cr(NH_3)_2(NCS)_4$ were used without further purification. Deionized water was obtained from boiled out distilled water by passing it through a mixed bed, acid–base, ion-exchange resin column. The mixed bed resin was Fisher certified, Rexyn H–OH resin, analytical grade.

[1]Summer student, 1970.

Kinetics

The rates of the aquation reactions 1 and 2 were estimated from the rate of production of free thiocyanate. The free thiocyanate was measured spectrophotometrically as $FeSCN^{2+}$ complex ion, by Adamson's method (3).

All rate studies were carried out in the high pressure vessel using the sampling technique outlined previously (4). For studies at atmospheric pressure, the reaction vessel inside the pressure bomb was not pressurized. The reaction vessel was a 5 ml hypodermic syringe with the barrel sawed off. In order to minimize complications from photolysis, a photographic red light replaced the normal fluorescent room lights. All solutions were 10^{-3} *M* in complex and 6×10^{-3} *M* in perchloric acid. Reactions were followed for no more than 3 h and less than 25% completion. In all experiments no deviations from first order kinetics were observed.

First order rate constants, reproducible to ±1%, were obtained for the aquation of $Cr(NCS)_6^{3-}$ and $Cr(NH_3)_2(NCS)_4^-$ as a function of pressure at 50 °C (see Table 1). The activation volume, ΔV^*, is usually extracted from the pressure dependence of the rate constant by eq. 3.

$$[3] \qquad \Delta V^* = -2.303RT(\partial \log k/\partial P)_T$$

However, this can only be used in cases where the activation volume is independent of pressure,

Can. J. Chem. Downloaded from www.nrcresearchpress.com by 210.87.254.40 on 09/05/12
For personal use only.

TABLE 1. Rate constants for the aquation of $Cr(NH_3)_2(NCS)_4^-$ and $Cr(NCS)_6^{3-}$ in 6×10^3 *M* perchloric acid solution at 50 °C as a function of pressure

	Rate constant, 10^4k, min^{-1} at 50 °C	
P (atm)	$Cr(NH_3)_2(NCS)_4^-$	$Cr(NCS)_6^{3-}$
1	0.93_1	9.7_4
340	—	8.0_5
681	0.97_0	7.4_6
1362	1.00	6.8_2
2043	1.11	7.1_9

as exhibited by the linearity of log *k vs. P* plots. This is illustrated for the aquation of $Cr(NH_3)_2(NCS)_4^-$ in Fig. 1. When the activation volume is dependent of pressure, that is the plot of log *k vs. P* is non-linear, resort to other approaches in extracting ΔV^* from pressure-rate data becomes essential (5, 6). The approach taken here will be that of Baliga and Whalley (6). Thus the activation volume of reaction 1 was obtained by plotting the mean activation volumes given by eq. 4

$$[4] \quad \Delta V^* = -(2.303RT \log k_2/k_1)/(P_2 - P_1)$$

in the pressure interval P_1 and P_2, against the mean pressure $(P_1 + P_2)$, and extrapolating to zero pressure; k_1 and k_2 are the first order rate constants at pressures P_1 and P_2, respectively.

The activation volumes are found to be -2.4 ± 0.8 and 16 ± 2 ml/mol for the aquation of $Cr(NH_3)_2(NCS)_4^-$ and $Cr(NCS)_6^{3-}$, respectively. The activation volume for the $Cr(NH_3)_2(NCS)_4^-$ aquation is independent of pressure (*i.e.* $(\partial\Delta V^*/\partial P)_T = 0$), whereas the activation volume for the $Cr(NCS)_6^{3-}$ aquation is strongly pressure dependent $(\partial\Delta V^*/\partial P)_T = 15 \pm 5$ ml/katm mol.

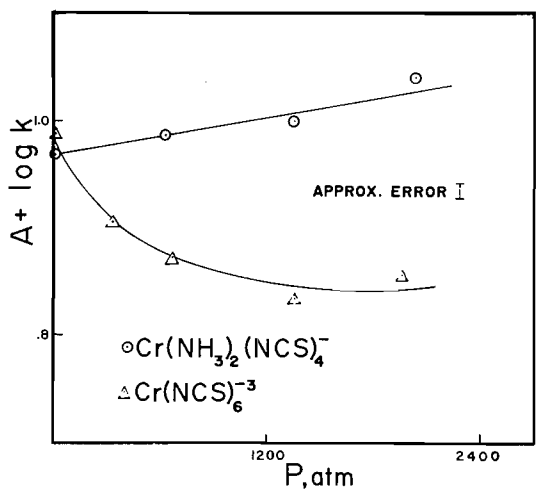

FIG. 1. Plot of log *k* against pressure for the aquation reactions 1 and 2.

Discussion

As far as the mechanistic interpretation of activation volumes is concerned, by far the simplest and most straightforward approach would be to compare the activation volumes of the reactions concerned with those for reactions of known mechanism. This approach becomes more acceptable since theory does not allow *a priori* calculation of activation volumes (4).

Suppose the aquation reactions 1 and 2 proceed via a dissociative interchange process (I_d) involving the non-nucleophilic participation of water molecule, as stated by Langford and co-workers (1, 2), then the only important activational process will be that involving Cr...NCS bond stretching, according to eqs. 5 and 6.

$$[5] \quad (NCS)_5CrNCS^{3-} \rightarrow (NCS)_5Cr^{2-}...NCS^-$$

$$[6] \quad (NH_3)_2(NCS)_3CrNCS^- \rightarrow (NH_3)_2(NCS)Cr...NCS^-$$

Since in neither of these cases is there a net creation nor destruction of charge, it is reasonable to assume that the formation of the transition states does not involve appreciable changes in the electrostriction of the solvent. Therefore, the ΔV^* of $+16 \pm 2$ ml/mol for the $Cr(NCS)_6^{3-}$ aquation can be attributed to Cr...NCS bond stretching. Furthermore, this value falls in the range (about +12 ml/mol) found for unimolecular dissociative reaction of both anions and cations (7–9). However, complications arising from charge dispersal in the transition state of reaction 5 may not be unimportant and could result in a positive contribution to the activation volume. If this is so, then a rough estimate of this given in ref. 15 of +5 ml/mol may be used. The net positive contribution to the activation volume due to Cr...NCS bond stretching is found to be +11 ml/mol. Using a value of 4.9 Å for the radius of the $Cr(NCS)_6^{3-}$ ion (10), the observed ΔV^* is the result of 5 to 8% stretching in the

Can. J. Chem. Downloaded from www.nrcresearchpress.com by 210.87.254.40 on 09/05/12
For personal use only.

Cr...NCS bond.[2] This value is in the range (10%) estimated for unimolecular processes (11, 12). On the other hand ΔV^* of -2.4 ml/mol is not in keeping with a unimolecular dissociative aquation for $Cr(NH_3)_2(NCS)_4^-$. In any case a process involving the estimated "normal" amount of bond stretching is not involved.

The only other mechanism worth exploring, for the aquation of $Cr(NH_3)_2(NCS)_4^-$, is the one proposed by Langford and White (1). In this mechanism, one of the two water molecules involved is hydrogen bonded to the leaving NCS^- anion in the activation process; the other water molecule has a non-nucleophilic role and is not important from an energy point of view. If this is so then the ΔV^* should be about -1 to -3.6 ml/mol; this being the volume difference between a water molecule in the bulk solvent and the first coordination (4, 13). The value of -2.4 ml/mol found for the aquation of $Cr(NH_3)_2(NCS)_4^-$ is in good agreement with this estimate. This mechanism is in effect the S_N2 front-side mechanism proposed by Adamson (3). However, a small amount of Cr...NCS bond stretching facilitated by the NCS...H_2O hydrogen bonding cannot be ruled out.

Lateef and Hyne (14) have correlated the value of $(\partial\Delta V^*/\partial P)_T$ found for many solvolytic reactions of organic substrates with reaction mechanism. Large values (of about 45 ml/katm mol) are associated with unimolecular solvolytic processes and small values (of about 10 ml/katm mol) with bimolecular processes. If this type of analysis is at all applicable here, then the implication is that a molecule of water may be involved in the activation processes of reactions 1 and 2, since the values of $(\partial\Delta V^*/\partial P)_T$ for these aquations are 15 ± 5 and 0 ± 1 ml/katm mol, respectively. These small values may then be a result of the small differences between the volume of a water molecule in the bulk solvent and the first coordination sphere (13).

From this study the authors conclude that the aquation of $Cr(NH_3)_2(NCS)_4^-$ proceeds via a mechanism involving at least one molecule of water. It is assumed on the basis of previous studies (13) that the role of this water molecule is non-nucleophilic but rather facilitates Cr...NCS bond cleavage through hydrogen bonding to the leaving NCS^- anion (3). However, the presence of another water molecule in the transition state, as indicated by the studies of Langford and White (1), cannot be ruled out completely. It may also be concluded that the aquation of $Cr(NCS)_6^{3-}$ goes by a mechanism involving at least one molecule of water. In this mechanism the Cr...NCS bond is thought to be excessively broken and the H_2O...Cr bond only very slightly formed. This mechanism is taken to be the dissociative interchange (I_d) mechanism proposed by Langford and co-workers (2), for this aquation process. This study, therefore, essentially confirms the conclusions of Langford and co-workers (1, 2) and Adamson (3). However, it provides direct evidence for a large degree of Cr...NCS bond stretching involved in the $Cr(NCS)_6^{3-}$ aquation which had been previously assumed without proof (2). Also, no significant amount of Cr...NCS bond stretching seems to be involved in the aquation of $Cr(NH_3)_2(NCS)_4^-$, as previously proposed (1), but this is not absolutely certain.

[2]A crude calculation of ΔV^* is given by the product of the effective cross-sectional area of the molecule and the amount of bond stretching (15). Therefore, the amount of bond stretching, x, is obtained as follows

$$x = \frac{\Delta V^*}{\text{cross-sectional area}}$$

$$= \frac{16 \times 10^{24}}{\pi \times (4.9)^2 \times 6 \times 10^{23}}$$

$$= 0.4 \text{ Å}$$

If the Cr...NCS bond length is assumed to be 4.9 Å (10), then the percentage bond stretching is about 8%. This value is based on the assumption that all 16 ml/mol found for ΔV^* is due to bond stretching. However, if the value corrected for electrostriction changes (11 ml/mol) is used, then the percentage bond stretching is found to be about 5%.

The authors wish to thank the National Research Council of Canada and St. Francis Xavier University Council for Research for support of this work.

1. Cooper H. Langford and John F. White. Can. J. Chem. **45**, 3049 (1967).
2. Stefan Behrendt, Cooper H. Langford, and Lawrence S. Frankel. J. Am. Chem. Soc. **91**, 2236 (1969).
3. A. Adamson. J. Am. Chem. Soc. **80**, 3183 (1958).
4. D. L. Gay and R. Nalepa. Can. J. Chem. **48**, 910 (1970).
5. H. S. Golinkin, W. G. Laidlaw, and J. B. Hyne. Can. J. Chem. **44**, 2193 (1966).
6. B. T. Baliga and E. Whalley. Can. J. Chem. **48**, 528 (1970).

7. W. J. LENOBLE and M. DUFFY. J. Am. Chem. Soc. **86**, 4512 (1964).
8. K. R. BROWER, B. GAY, and T. L. KONKOL. J. Am. Chem. Soc. **85**, 1401 (1963).
9. K. R. BROWER. J. Am. Chem. Soc. **82**, 4535 (1960).
10. LAWRENCE S. FRANKEL. J. Phys. Chem. **73**, 3897 (1969).
11. A. E. STEARN and H. EYRING. Chem. Rev. **29**, 509 (1941).
12. A. E. STEARN and H. EYRING quoted in S. Glasstone, K. J. Laidler, and H. Eyring. Theory of rate processes. McGraw-Hill, N.Y. 1941. p. 141.
13. H. R. HUNT and H. TAUBE. J. Am. Chem. Soc. **80**, 2642 (1958).
14. A. B. LATEEF and J. B. HYNE. Can. J. Chem. **47**, 1369 (1969).
15. W. J. LENOBLE. Prog. Phys. Org. Chem. **5**, 207 (1967).

Can. J. Chem. Downloaded from www.nrcresearchpress.com by 210.87.254.40 on 09/05/12
For personal use only.

Can. J. Chem. Downloaded from www.nrcresearchpress.com by 210.87.254.6 on 09/05/12
For personal use only.

Cyclization and Fragmentation of *N*-Chloro Lactams. The Transannular Synthesis of Bicyclic Lactams with Bridgehead Nitrogen[1]

O. E. EDWARDS AND J. M. PATON[2]

Biochemistry Laboratory, National Research Council of Canada, Ottawa 7, Canada

AND

M. H. BENN, R. E. MITCHELL, CHURAI WATANATADA, AND K. N. VOHRA

Chemistry Department, The University of Calgary, Calgary 44, Alberta

Received November 5, 1970

High yield peroxide initiated and photochemical conversion of *N*-chloroazacyclooctanone to 5-chloroazacyclooctanone and of *N*-chloroazacyclononanone to a mixture of azabicyclo[4.3.0]nonan-2-one and azabicyclo[4.3.0]nonan-9-one is described. *N*-Chloro-2-azabicyclo[2.2.2]octan-3-one gave 4-chlorocyclohexylamine derivatives under similar conditions, while *N*-chloro-*N*-methylpentanoamide gave γ-valerolactone. An apparent ionic, silver ion, and base-catalyzed cyclization of *N*-chloroazacyclononanone was observed.

On décrit une réaction photochimique et initiée par les péroxydes qui permet de transformer avec de bons rendements la *N*-chloroazacyclooctanone en chloro-5 azacyclooctanone et la *N*-chloroazacyclononanone en un mélange d'azabicyclo[4.3.0]nonanone-2 et d'azabicyclo[4.3.0]nonanone-9. Dans des conditions expérimentales semblables, la *N*-chloro aza-2 bicyclo[2.2.2]octanone-3 fournit des dérivés de la chloro-4 cyclohexylamine alors que la *N*-chloro *N*-méthylpentanoamide donne la γ-valéro lactone. On a aussi observé une cyclisation de la *N*-chloroazacyclononanone qui s'effectue en présence d'ion argent et de base et qui serait apparemment ionique.

Canadian Journal of Chemistry, 49, 1648 (1971)

Some time ago it was reported (1) that when the medium ring *N*-chloro lactams, *N*-chloroazacyclooctan-2-one (**1***a*) and *N*-chloroazacyclononan-2-one (**2***a*), were heated with silver perchlorate in aqueous dioxane. they cyclized, in low yield, to bicyclic lactams. We now report conditions under which these cyclizations can be effected in high yield. The reaction was initially considered to involve the generation of nitrenium ions ($R—\overset{+}{\underset{\cdot\cdot}{N}}COR'$). However, experimental evidence is now presented that these efficient cyclizations proceed by a radical-chain mechanism.

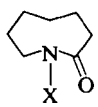

1

a X = Cl
b X = H

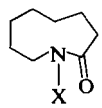

2

a X = Cl
b X = H

In our further investigations of the reactions of medium ring chloro lactams, we first endeavored to optimize conditions for the cyclization of the nine-membered *N*-chloro lactam **2***a*, a compound which had, in the original investigation, given a better yield (13%) of bicyclic products than the eight-membered **1***a* (5%). It was discovered that: (*a*) the *N*-chloro lactams were inert to silver ions in peroxide-free solvents; (*b*) traces of peroxide in the dioxane used as solvent, catalytic amounts of benzoyl peroxide, or metallic silver initiated the reaction; (*c*) in order to obtain reasonable yields of bicyclic products the presence of bases such as silver oxide, silver carbonate or calcium carbonate was needed to prevent accumulation of acid during reaction; (*d*) the presence of water in the solvent markedly reduced the amount of parent lactam produced, and led to high yields of bicyclic products.

In 1 h at 80° in 80% dioxane – 20% water in the presence of 1.5 mol % of benzoyl peroxide and calcium carbonate, *N*-chloroazacyclononane was converted into a mixture of **3** (34%), **4** (63%), and **2***b* (3%). A similar result was obtained in aqueous dimethylformamide. Neither of the bicyclo[5.2.0] compounds **5** or **6** was produced. The preparation of authentic reference lactams is outlined in Scheme 1.

Under comparable conditions *N*-chloroaza-

[1]Submitted as NRCC No. 11695.
[2]NRCC Postdoctorate Fellow.

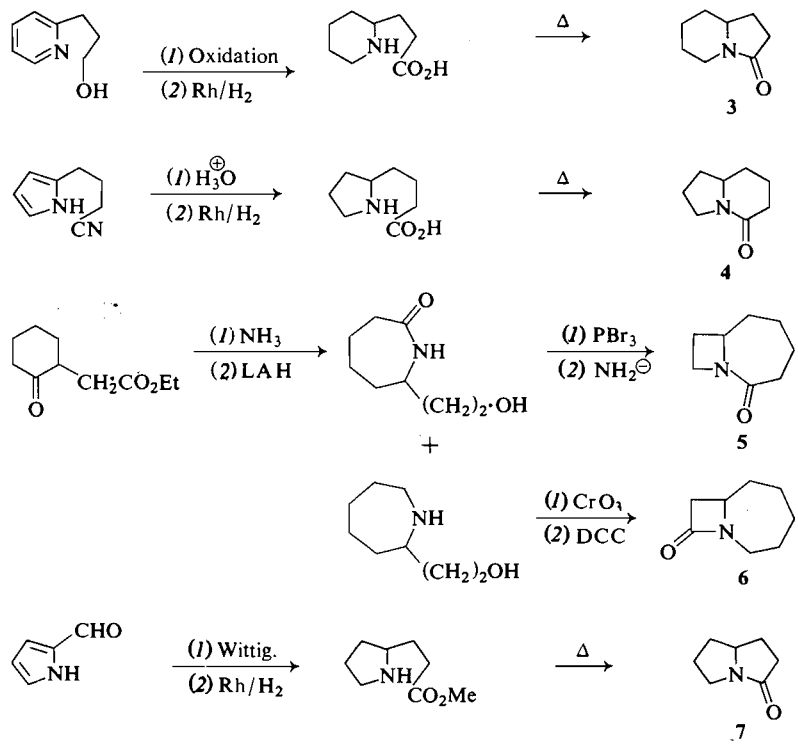

SCHEME 1

cyclooctan-2-one (**1***a*) was converted in over 70% yield into 5-chloroazacyclooctan-2-one (**8**). The structure of this product was proven by base or silver ion promoted conversion into 1-azabicyclo[3.3.0]octan-2-one (**7**).

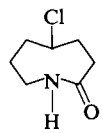

8

Under the above conditions, *N*-chloroazacycloheptan-2-one (**9***a*) gave only the parent lactam **9***b* (*ca.* 100%).

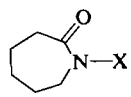

9

a X = Cl

b X = H

A further and remarkable variation in behavior was provided by the reaction of *N*-chloro-2-azabicyclo[2:2:2]octan-3-one (**10***a*) in aqueous dioxane, which yielded a urea, to which we ascribe structure **12**. The intermediacy of the isocyanate **11** could be demonstrated when the reaction was carried out in anhydrous dioxane.[3] Small amounts of the lactam **10***b* were also formed, in both cases.

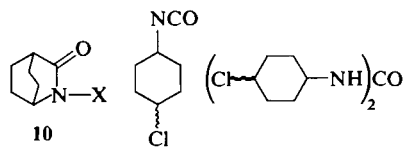

10 **11** **12**

a X = Cl

b X = H

Thus we have a set of observations in which, under the same reaction conditions, *N*-chloro lactams produce predominantly either the parent lactam (**9***a* → **9***b*), a *C*-chloro lactam

[3]This is in accord with the report that *N*-bromosuccinimide is converted to 3-bromopropionyl isocyanate when it is heated with benzoyl peroxide in the presence of allyl halides in chloroform, or bromoform, solution (2). Similarly several *N*-bromo-α-haloamides gave chlorobromoalkanes in a chain reaction that appeared to be homolytic in character. However *N*-chloromandelamide gave comparable fission in an apparent ionic process (3).

Can. J. Chem. Downloaded from www.nrcresearchpress.com by 210.87.254.6 on 09/05/12
For personal use only.

Can. J. Chem. Downloaded from www.nrcresearchpress.com by 210.87.254.6 on 09/05/12
For personal use only.

(**1***a* → **8**), bicyclic lactams (**2***a* → **3** + **4**), or fragment to an isocyanate (**10***a* → **11**). This diversity of products implies that the reaction must be very sensitive to substrate structure.

Under our optimum cyclization conditions an acyclic chloramide *N*-chloro-*N*-methylpentanoamide **13** gave the γ-lactone **14**. This parallels

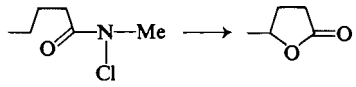

13 **14**

the observation of Neale *et al.* (4) on the photolysis of the *N*-bromo analogue of **13** followed by thermal cyclization *i.e.* the internal nucleophilic displacement in the intermediate *C*-haloamide was by oxygen rather than nitrogen.

The above reactions appeared to be homolytic chain reactions. In agreement with this, photolysis of **1***a* or **2***a* in aqueous dioxane resulted in rapid conversion into the same products as in the peroxide catalyzed process. The yield of bicyclic products was near 90% from **2***a*. However, photolysis in *dry* dioxane gave only 29% of bicyclic products.

Since metallic silver has been shown to produce nitrogen radicals from chloramines (5) at room temperature, we examined its action on **1***a* and **2***a*. The reaction proved to be very slow at room temperature, but fairly rapid at 80°. The yield of transannular product was much lower than in the photochemical or peroxide-initiated reaction (25% for **1***a*, 15% for **2***a*), the main product being the parent lactams.

In the light of our initial interest in the generation of nitrenium ions (1) we made attempts to find ionic conditions for cyclizing *N*-chloro lactams to bicyclic ones. Since silver ions alone were inert, it was argued that both a base and silver ions might provide a push–pull mechanism. The system chosen, silver oxide – $Ag(NH_3)_2^+$ – ammonia did indeed give a rapid room temperature reaction. Chloro lactam **2***a* was converted into **2***b* (37%), **3** (16%), and **4** (47%) when aqueous dioxane was used as solvent. In aqueous acetonitrile 50% of bicyclic products was obtained. Blank runs showed that **2***a* was inert to ammonia or silver oxide under these conditions.

In contrast to the case of the nine-membered ring, *N*-chloroazacyclooctanone gave less than 5% of bicyclic products when treated with silver oxide – ammonia at room temperature.

It seemed probable (see Discussion) that 5- and 6-chloroazacyclononan-2-one (**15** and **16**) were being formed as primary products from the corresponding *N*-chloro lactam in the reactions initiated by peroxide or metallic silver, and that these were spontaneously cyclizing to the bicyclic derivatives **3** and **4**. To test this we attempted to synthesize authentic **15**.

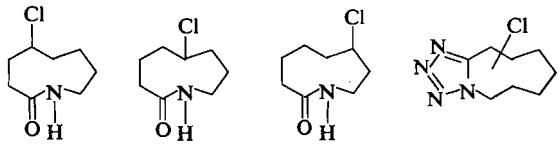

15 **16** **17** **18**

A Schmidt reaction on 4-chlorocyclooctanone gave one of the expected 5- or 7-chloro lactams as a crystalline product. However this proved to be the 7-isomer (**17**) since it could be cyclized cleanly with potassium amide in liquid ammonia to **5**. Investigation of the non-crystalline product from the Schmidt reaction showed it to be rich in **3**, hence cyclization of **15** had already occurred. Another product isolated was the tetrazole **18**.

Discussion

The present work, and our related study of the reaction of medium ring chloramines with silver ions (5), has provided no evidence for the formation of discrete nitrenium ions [see however the special cases studied by Gassman (6)].

Although no previous transannular replacement of unactivated hydrogen in *N*-halo lactams seems to have been observed, the intramolecular analogues for *N*-iodo (7), *N*-bromo, and *N*-chloro amides (4, 8) and *N*-halo imides (9) have been studied. Photolysis (4, 7–9) or initiation by one-electron reducing agents (8) converted these to 4-halo amides or imides.

The fact that dioxane peroxides or benzoyl peroxide at 80° were sufficient to catalyze the decomposition of the medium ring chloro lactams suggested that a homolytic chain reaction was involved. Scheme 2 outlines three pathways open to an initially formed amidyl radical. Pathway (*a*) leads to a *C*-chloro lactam. In the case of **1***a* this could be isolated, but **15** and **16** cyclized below room temperature to the bicyclic lactams. Pathway (*b*) gives solvent radicals and parent lactams. The former give rise to products such as **19** and **19***a* (via 2-

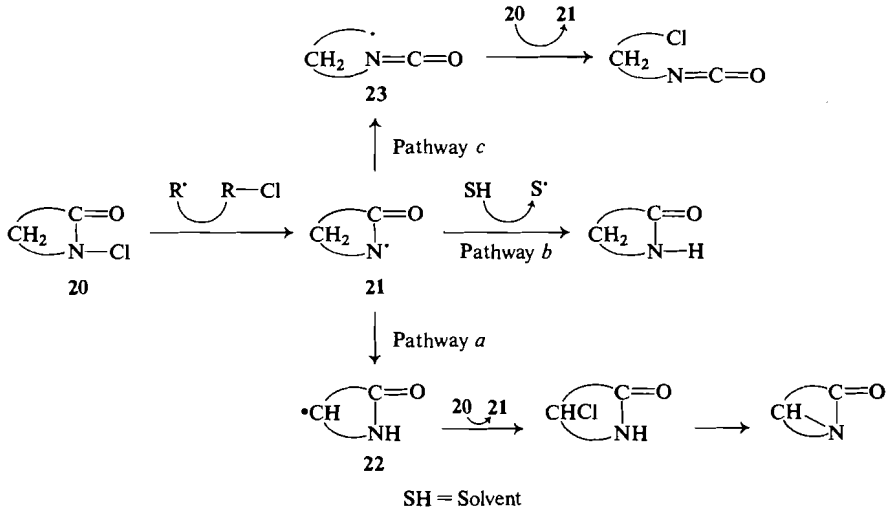

SCHEME 2

chlorodioxane). Pathway (*c*) is the course followed by amidyl radicals from **10***a* and from *N*-bromosuccinimide (2).

The high yield of parent lactam formed at the expense of transannular products in the silver initiated reactions contrasts sharply with the results of the peroxide initiated reactions. We assume that the silver produces the same amidyl radicals (see eq. 1) as are formed in the peroxide catalyzed reaction. Hence we are faced

[1] 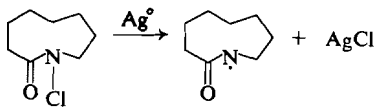

with the puzzle why a very small amount of chain reaction ensues (more than 90 mol % of silver chloride formed) and why hydrogen abstraction from solvent now is favored over transannular hydrogen abstraction followed by chlorine abstraction. A possible explanation of the difference is that the amidyl radical or corresponding carbon radical (see **22**) remains associated with the silver surface for some time, and that access to solvent as a source of hydrogen in this state is better than access to a chloro lactam molecule.

The ring fission undergone by **10***a* seems to be a consequence of the inaccessibility of internal hydrogen in the most probable configuration **24** of the derived radical (amide resonance), and the fact that its geometry is ideal for ring opening.

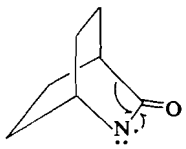

24

One striking factor affecting the course of the homolytic reactions is the solvent composition. In *dry* dioxane or dimethyl formamide, the radical **24** and the medium ring ones (see **21**) derived from **1***a* and **2***a* abstract the reactive hydrogens of the solvent in preference to the unactivated transannular ones. However in all cases, the presence of 20% water in the solvent reverses this nearly completely. A possible explanation is that the amidyl radicals are exclusively water-solvated, and that this shields the nitrogen radical from attack on the dioxane or dimethylformamide. It is reasonable to expect that the carbon radicals (**22**) formed by transannular hydrogen abstraction would then abstract chlorine from another molecule of *N*-chloro lactam, in preference to hydrogen abstraction from other species, and thus promote a chain reaction. As expected from the above results, in the photochemical decomposition of **2***a* in dioxane, the presence of 20% water

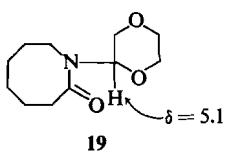

19

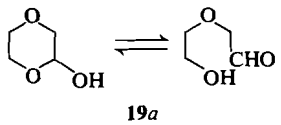

19*a*

Can. J. Chem. Downloaded from www.nrcresearchpress.com by 210.87.254.6 on 09/05/12
For personal use only.

Can. J. Chem. Downloaded from www.nrcresearchpress.com by 210.87.254.6 on 09/05/12
For personal use only.

dramatically suppressed hydrogen abstraction from solvent.[4] The peroxide initiated reaction in dry dimethylformamide was much slower than in dry dioxane, perhaps because of solvent shielding of the chloro lactam.

The striking difference between the ease of cyclization of the nine-membered and eight-membered *C*-chloro lactams must be of purely geometric origin. Indeed, if one assumes that the reactions involve overlap of the π electrons of the planar amide function with the rear lobe of the C—Cl bond, Courtauld molecular models do show a significant difference between the proximity in the two cases (see **25** and **26**).

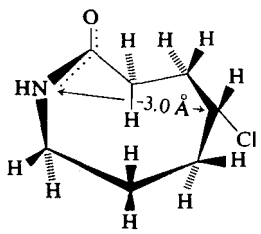

25

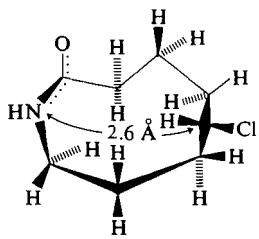

26

The apparent ionic reaction between *N*-chloroazacyclononanone and silver oxide–ammonia combination in aqueous dioxane or acetonitrile can be formulated as a push–pull process (eq. 2). However the other main product

[2]

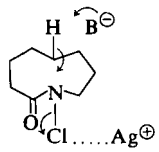

was parent lactam, and with the eight-membered ring this was the main product. These are certainly formed by a homolytic process. Since the chloro lactams were inert to dioxane peroxide at room temperature, and no peroxide was present in the acetonitrile, it appears possible that colloidal metallic silver produced in some oxidation–reduction reaction may be the initiator of radical chains leading to these lactams.

Experimental

The i.r. spectra were recorded on a Perkin–Elmer Model 257 grating spectrometer and n.m.r. spectra on a Varian A60A spectrometer using deuterochloroform as solvent and tetramethylsilane as internal standard unless otherwise specified. Mass spectra were obtained using a Hitachi–Perkin Elmer RMU-60 instrument. Intensities are given in parentheses.

Solvents

Acetonitrile used throughout was of spectroscopic quality. Dioxane was distilled after refluxing over sodium and was stored under nitrogen in the presence of sodium. Elimination of traces of peroxide was achieved by the passage of the solvent through a column of alumina (activity 1) prior to use.

Silver Oxide

This was prepared by the addition of 10% sodium hydroxide solution to an aqueous solution of silver nitrate until precipitation was complete. The oxide was repeatedly washed with water until the washings were free of base, filtered, and used immediately.

Silver

The silver oxide prepared as described above was dissolved in the minimum volume of ammonia solution (28%). Formaldehyde solution was added with rapid stirring until precipitation was complete. The silver was washed repeatedly with water until free of base, filtered, and used immediately.

Gas–Liquid Chromatography

The lactams were analyzed by g.l.c. on 4′ glass columns of 10% versamid 900 on HMDS treated Chromosorb W (60/80 mesh) at 200° using a flame ionization detector. The response of this detector towards azacyclononan-2-one, and the azabicyclononanones was determined using the authentic compounds, and the analyses reported for these compounds are estimated as having a maximum error of 5%.

Parent Lactams

With the exception of azacycloheptan-2-one which was a commercial product, and the mixed *C*-chloroazacyclononan-2-ones (see below), the monocyclic lactams used in this study were prepared by the sulfuric acid induced (10) Beckmann rearrangement of the oximes of the corresponding cyclic ketones. 2-Azabicyclo[2.2.2]-octan-3-one was prepared from *cis*-4-aminocyclohexanecarboxylic acid (11).

N-Chloro Lactams

These were conveniently prepared by the addition of excess 10% sodium hypochlorite solution to a stirred aqueous solution of the medium ring lactams at 10 °C. A reaction time of 1 h was sufficient for an almost quantitative conversion to the *N*-chloro derivative, which conveniently separated as an oil. The reaction mixture was extracted with hexane–dichloromethane (7:3), and the extracts washed (H_2O), dried (Na_2SO_4), and the solvents removed *in vacuo* at < 50°. The colorless chloro lactams, whose iodometric assay gave a purity > 95% (traces of solvent remain), were used without further purification.

Alternatively a 10% excess of freshly prepared *t*-butyl hypochlorite was added to a solution of lactam in benzene, or chloroform, and the reaction mixture kept in the dark, at room temperature for 6–12 h (t.l.c. analysis

[4]We are grateful to a referee for suggesting this experiment.

Can. J. Chem. Downloaded from www.nrcresearchpress.com by 210.87.254.6 on 09/05/12
For personal use only.

indicated that *N*-chlorination was essentially complete within 1 h). Evaporation under reduced pressure then yielded the *N*-chloro lactams as oils which usually crystallized spontaneously when stored overnight at 0°. As before, the purity of the products was determined by iodometry, and t.l.c. Certain of the *N*-chloro lactams were recrystallized and further characterized.

N-Chloroazacycloöctan-2-*one*, m.p. 43–44° (ether – petroleum ether).

Anal. Calcd. for $C_7H_{12}ClNO$: C, 52.02; H, 7.48; N, 8.67. Found: C, 51.97; H, 7.66; N, 8.64.

N-Chloroazaclononan-2-one, m.p. 32–36° (pentane).

Anal. Calcd. for $C_8H_{14}ClNO$: C, 54.70; H, 8.03; N, 7.98. Found: C, 55.05; H, 8.27; N, 7.80.

N-Chloro-2-azabicyclo[2.2.2]octan-3-one, m.p. 97–99° (benzene).

Anal. Calcd. for $C_7H_{10}ClNO$: C, 52.67; H, 6.32; N, 8.77. Found: C, 52.85; H, 6.52; N, 8.84.

N-Chloro-*N*-methylpentanoamide. This chloramide was prepared from the parent amide by the *t*-butyl hypochlorite procedure, and obtained as an oil, homogeneous by t.l.c. analysis; ν_{max}(film) 1675 cm^{-1}; n.m.r. (CCl_4) τ 6.72 (3H, s, NCH_3), 7.30 (2H, tr. J = 7 Hz, CH_2CO), 8.2–8.8 (4H, broad multiplet, H-3 and -4), and 9.05 (3H, tr. J = 6 Hz, CH_3CH_2).

Preparation of Reference 1-Azabicyclo[m.n.o]alkanones

(1) 1-Azabicyclo[4.3.0]nonan-2-one (3-Ketooctahydropyrrocoline) (3)

This compound was prepared, in 80% yield, by the thermal cyclization of 3-(2-piperidyl)propionic acid (12), and obtained as a colorless oil, homogeneous by g.l.c. analysis, b.p. 70°/0.02 mm (lit. (12) b.p. 126–127°/12 mm).

(2) 1-Azabicyclo[4.3.0]nonan-9-one (5-Ketooctahydropyrrocoline) (4)

Mixed methyl 4-(2′- and 3′-) pyrrolylbutyrates (13) (70% 2′-isomer by g.l.c.) were dissolved in hot aqueous ethanol (1:1 v/v) and saponified by titration with 2.5 *N* aqueous sodium hydroxide to a persistent (1 h) phenolphthalein end point. The solution was concentrated to small volume, diluted with water, and extracted with ether. The aqueous phase was then brought to p*H* 2 with 2 *N* hydrochloric acid and extracted with ether. Evaporation of the combined, dried ($MgSO_4$) ether extracts afforded a golden, crystalline residue of the mixed 4-(3′- and 2′-pyrrolyl) butyric acids which was used without further purification.

A solution of the acids (7.5 g, 49 mmol) in water (100 ml) containing concentrated aqueous ammonia (5 ml, *d* 0.88) was shaken with 5% rhodium-on-alumina (2.5 g) at room temperature in an atmosphere of hydrogen (50 p.s.i.). Hydrogen uptake appeared complete in 1 h. The suspension was filtered, the catalyst washed with water, and the filtrate and washings were evaporated (bath 50°) under reduced pressure. The syrupy residue was dried by azeotropic distillation with benzene under reduced pressure, and finally over P_2O_5, *in vacuo*, yielding the 4-(3′- and 2′-pyrrolidyl) butyric acids as a colorless solid m.p. 112–115°.

These mixed acids (7 g) were heated for 10 min (bath 125–130°) under a slow current of nitrogen. After cooling, the resulting oil was partitioned between 1 *N* aqueous sulfuric acid (5 ml) and ether (10 ml). The aqueous phase was then re-extracted with ether (4 × 10 ml), and then with chloroform (5 × 5 ml). Evaporation of the dried ($MgSO_4$) extracts yielded an oil which was distilled to give 5-ketooctahydropyrrocoline, as a colorless liquid b.p. 66–67°/0.15 mm (4.26 g, 98% based on 2′-pyrrolyl isomer content of the starting ester): ν_{max}(film) 1650 cm^{-1}; n.m.r. τ 8.9–7.5 (10H, complex) and 6.8–6.2 (3H, complex, $-CH_2-\underset{|}{N}-CH\langle$).

Anal. Calcd. for $C_8H_{13}NO$: C, 69.04; H, 9.42; N, 10.07. Found: C, 69.28; H, 9.71; N, 10.05.

(3) 1-Azabicyclo[5.2.0]nonan-9-one (5)

(*a*) Ethyl (2-oxocyclohexyl) acetate (44 g, 240 mmol) dissolved in chloroform was submitted to a Schmidt reaction with hydrazoic acid (190 ml of a 1.55 *M* solution in chloroform, 290 mmol) at 3–5° (14). After 3 h the reaction mixture was worked-up by the standard procedure (14) to give a crystalline product, which recrystallized from ethanol–hexane to give ethyl 2-oxohexahydro-7-azepinyl acetate as colorless prisms, m.p. 113–114°; n.m.r. τ 3.30 (1H, br. singlet, NH), 5.81 (2H, quartet, J = 7 Hz, $-CO_2CH_2CH_3$), 6.22 (1H, br. multiplet $NHCHCH_2CO_2$), 7.45 (2H, doublet, J = 7 Hz, $CHCH_2CO_2$), 7.52 (2H, broad multiplet, $-CH_2CO$), 8.0–8.6 (6H, broad complex multiplet, ring CH_2), and 8.73 (3H, triplet, J = 7 Hz, $CO_2CH_2CH_3$).

Anal. Calcd. for $C_{10}H_{17}NO_3$: N, 7.03. Found: N, 6.87.

This ester (5.0 g, 25 mmol) was reduced with lithium aluminum hydride (1.5 g) in refluxing dioxane (50 ml) for 4 h. Excess reagent was decomposed by the dropwise addition of water (2 ml), and then 15% aqueous sodium hydroxide (4.5 ml) to the cold, stirred, reaction mixture. The precipitated inorganic salts were removed by filtration, and the filter-cake was washed well with methylene dichloride. The combined, dried ($MgSO_4$) filtrate and washings were evaporated to yield a solid residue, which recrystallized from chloroform–benzene to give 7-(2-hydroxyethyl)hexahydroazepin-2-one as fine colorless needles, m.p. 138° (2.9 g, 74%); ν_{max}($CHCl_3$) 3400, 3325 (br.), and 1660 cm^{-1}; n.m.r. τ 3.15 (1H, br. singlet, NH) 6.22 (3H as a 2H triplet, J = 5 Hz, plus a 1H singlet which disappeared upon addition of D_2O, $-CH_2OH$), 6.47 (1H, broad complex, $-CHCH_2$), 7.53 (2H, multiplet, CH_2CO), and 7.9–8.7 (8H, broad complex signal, hydrogens at C-4, -5, -6, and -1′); m/e 157 (16) (M^+), 112 (100) $(M-CH_2CH_2OH)^+$.

Anal. Calcd. for $C_8H_{15}NO_2$: N, 8.91. Found: N, 9.16.

Phosphorus tribromide (0.8 g, 2.95 mmol) was added to the alcohol (1.2 g, 7.5 mmol). The mixture was stirred, and kept at 40–50° for 2 h, then poured into ice-water (10 ml), and extracted with chloroform (3 × 25 ml). The chloroform extracts were washed with saturated aqueous sodium bicarbonate (2 × 5 ml) and water (5 ml). The crystalline residue (1.5 g), which remained after removing the solvent from the dried chloroform extracts, was recrystallized from benzene – hexane to yield 7-(2-bromoethyl)hexahydroazepin-2-one, m.p. 121–122° (1.3 g, 5.9 mmol) (77%); ν_{max}(KBr) 3200 and 1670 cm^{-1}; n.m.r. τ 3.2 (1H, br. singlet, NH), 6.48 (3H, triplet, [2H, J = 7 Hz (CH_2Br) superimposed on 1H multiplet ($-CH-$N)], 7.52 (2H, br. multiplet, CH_2CO) and 7.6–8.6 (8H broad complex multiplet, H

Can. J. Chem. Downloaded from www.nrcresearchpress.com by 210.87.254.6 on 09/05/12
For personal use only.

at C-4, -5, -6 and -1′); *m/e* 121 (3) and 119 (3) (M^+), and 112 (100) ([$M—CH_2CH_2Br^+$]).

Anal. Calcd. for $C_8H_{14}BrNO$: C, 43.64; H, 6.37; N, 6.36. Found: C, 43.98; H, 6.19; N, 6.71.

The bromoethyl compound (1.2 g, 5.4 mmol) was added to a solution of potassium amide (from 0.21 g, 5.4 mmol potassium) in liquid ammonia (30 ml), and the reaction mixture was stirred overnight, while the ammonia was allowed to evaporate. The residue was extracted with benzene (3 × 25 ml), and the extracts were washed successively with 0.01 *N* aqueous hydrochloric acid (5 ml) and then with water (5 ml). Removal of solvent from the dried ($MgSO_4$) extract left a residual oil which was distilled to yield 1-azabicyclo[5.2.0]nonan-9-one as a colorless liquid, b.p. 132°/15 mm (0.47 g, 3.4 mmol) (63%); ν_{max}(film) 1630 cm^{-1}; n.m.r. τ 5.7 (1H, broad multiplet, H-7), 6.15 (2H, triplet J = 7 Hz, H-9), and 7.3–9.0 [10H, broad overlapping signals at *ca.* 7.6 (H at C-3) and 7.7–9.0 (H at C-4, -5, -6, and -8)]; *m/e* 137 (84) (M^+), and 56 (100).

Anal. Calcd. for $C_8H_{13}NO$: N, 10.07. Found: N, 9.93.

(*b*) To a solution of potassium amide (prepared from 0.14 g, 3.6 mmol of potassium) in liquid ammonia was added 7-chloroazacyclononan-2-one (0.53 g, 3.0 mmol). The reaction mixture, protected by a soda-lime tube, was stirred overnight while the solvent was allowed to evaporate. The residue was extracted with benzene (3 × 50 ml) and the extracts were washed with dilute hydrochloric acid, and water, then dried ($MgSO_4$), and evaporated under reduced pressure to yield a residual oil (0.31 g, 74%) (> 95% (**5**) by g.l.c.).

(4) 1-Azabicyclo[5.2.0]nonan-2-one (6)

The mother liquors from the lithium aluminum hydride reduction of ethyl (2-oxohexahydro-7-azepinyl) acetate (see preparation of reference 1-azabicycloalkanones) upon evaporation yielded a residual oil which was part-soluble in cold ether. Evaporation of the ether solution, followed by fractional distillation, gave 2-(2′-hydroxyethyl)-hexahydroazepine as an oil b.p. 71°/0.03 mm; $\nu_{max}(CHCl_3)$ 3200 cm^{-1} (very broad), no C=O absorption; n.m.r. τ 3.15 (1H, br., NH), 6.22 (3H, 2H triplet J = 6 Hz, H at C-2′, with a superimposed 1H singlet, OH), 6.45 (1H, br. multiplet, H at C-2), 7.53 (2H, multiplet, H at C-7), and 8.1–8.6 (8H, H at C-1′, -3, -4, -5, and -6). The 1H signals at τ 3.15, and 6.22 were removed upon addition of D_2O.

The imino alcohol (1.0 g) was dissolved in a solution of sulfuric acid (2.0 g) and chromium trioxide (1.2 g) in water (17 ml), and the reaction mixture was kept at 80° for 30 min. Excess chromic acid was reduced by passing SO_2 through the mixture, which was then boiled briefly with a slight excess of aqueous barium hydroxide solution. The mixture was filtered, and the filtrate evaporated to dryness to leave a syrupy residue which solidified upon storage under vacuum. This hygroscopic material was extracted with ethanol (3 ml), and the ethanol extract was then diluted with ether (200 ml). Hexahydro-2-azepinylacetic acid separated as a non-hygroscopic white solid (0.35 g) with m.p. 173–174°, ν_{max} 3115 and 1580, together with broad absorption in the region 2780–2325 cm^{-1}.

Anal. Calcd. for $C_8H_{15}NO_2$: C, 61.15; H, 9.55; N, 8.92. Found: C, 60.69; H, 10.16; N, 8.70.

The identity of this acid was further confirmed by its conversion with diazomethane to a methyl ester, b.p. 75°/0.3 mm; ν_{max} 3350 and 1725 cm^{-1}; n.m.r. τ 6.30 (3H, s, CO_2CH_3), 6.70–7.20 (3H, overlapping broad multiplets for H at C-2′, and -7′), 7.62 (2H, doublet J = 7 Hz, H at C-2), and 9.0 (8H, multiplet, H at C-3′, -4′, -5′, and -6′); *m/e* 171 (M^+) with base peak at 98 corresponding to α-cleavage and loss of $CH_2CO_2CH_3$.

A solution of the hexahydroazepinylacetic acid (150 mg) in dry nitromethane (8 ml) was treated with dicyclohexylcarbodiimide (120 mg), and the reaction mixture was stirred at room temperature for 4 days. The *N,N′*-dicyclohexylurea which separated was removed by filtration. Evaporation of the filtrate yielded an oil (125 mg) which was subjected to t.l.c. on alumina with chloroform–hexane (1:1) as the developing solvent. The major band yielded 1-azabicyclo[5.2.0]nonan-2-one as an oil (51 mg); $\nu_{max}(CHCl_3)$ 1745 cm^{-1}; mass spectrum, M^+ 139 (base peak); n.m.r. τ 6.39 (1H, br. singlet, H-7), 7.15 (1H, dd, J = 5 and 14 Hz, H-8), and 7.70 (1H, dd, J = 3 and 14 Hz, H-8).

(5) 1-Azabicyclo[3.3.0]octan-2-one (Pyrrolizidin-3-one) (7)

Methyl *trans*-2-(2-pyrrolyl) acrylate was prepared from pyrrole-2-aldehyde and carboethoxymethyltriphenylphosphorane as described for the ethyl ester (15) and obtained as pale yellow crystals, m.p. 88–89°, b.p. 110°/0.1 mm (64%).

This ester (5.4 g, 36 mmol), dissolved in ethanol (100 ml), was hydrogenated over 5% rhodium-on-alumina (5g) at atmospheric pressure for 20 h. The reaction mixture was then filtered and the filtrate evaporated to yield a dark oil, fractionation of which gave 3-ketopyrrolizidine b.p. 107–108°/12 mm, > 99% pure by g.l.c. (80%);[5] ν_{max}(film) 1680 cm^{-1}, (lit. (16) b.p. 90–100°/10 mm).

Schmidt Reaction on 4-Chlorocyclooctanone

A 1.0 *M* solution of hydrazoic acid in chloroform (30 ml, 30 mmol), containing 4-chlorocycloöctanone (17) (4.4 g, 27 mmol) was added dropwise to a mixture of chloroform (25 ml) and concentrated sulfuric acid (10 ml). The temperature of the reaction mixture was maintained at 3–5° by external cooling. After addition was complete the reaction mixture was stirred for 30 min, then poured into ice-water (200 ml) and neutralized with sodium carbonate. The chloroform phase was separated, and the aqueous phase extracted with chloroform (2 × 30 ml). The combined chloroform extracts were dried ($MgSO_4$) and evaporated under reduced pressure to yield an oil (*ca.* 6 g), which was shown by t.l.c. to consist of some unchanged ketone (R_f 0.70) together with two other major products, R_f 0.33 and 0.45 (chloroform:methanol:hexane, 85:5:10).

The material with R_f 0.33 crystallized out from the crude reaction product when this was stored at 0°. Recrystallization from benzene and ether gave 7-chloroazacyclononan-2-one (**17**) (0.80 g, 17%) as colorless

[5]We also obtained this product, in poorer yield, and less pure, by treating pyrrolyl magnesium chloride with propiolactone, at 0°. The mixed 2- and 3-pyrrolylbutyric acids so obtained were methylated with diazomethane, the methyl ester purified by distillation (b.p. 125–128°/15 mm), and hydrogenated as described above for the acrylate.

Can. J. Chem. Downloaded from www.nrcresearchpress.com by 210.87.254.6 on 09/05/12
For personal use only.

prisms, m.p. 109–111°; ν_{max} 3400 and 1600 cm^{-1}; *m/e* 175 and 177 (*ca.* 2.5:1) M^+, with M + 1 ions of comparable intensity at *m/e* 176 and 178; n.m.r. τ 5.7–6.0 (1H, multiplet, CHCl).

Anal. Calcd. for $C_8H_{14}ClNO$: C, 54.70; H, 8.03; N, 7.97. Found: C, 54.77; H, 8.11; N, 8.21.

The mother liquors from the original crystallization were evaporated to a residual oil which was subjected to t.l.c. (chloroform:methanol:hexane 85:5:10) by which means the component with R_f 0.45 was separated as an oil, free of the lower R_f product. If had ν_{max}(film) 1685 cm^{-1}. Its n.m.r. was complex, but had no significant absorption at τ 5.5–6.0 for CHCl. The identity of the product with 1-azabicyclo[4.3.0]nonan-2-one (**3**) was established by comparison of mass spectra and g.l.c. retention time.

In other cases, the crude Schmidt product was subjected, directly, to fractional distillation, yielding a material with b.p. 60–65°/0.01 mm rich in **3** (g.l.c. analysis), followed by the *C*-chloro lactam **18**, b.p. 85–125°/0.02 mm which crystallized in the receiver.

Also isolated in small amounts, from some reactions conducted in acetic acid containing sulfuric acid and sodium azide at 60–65°, was a substance R_f 0.57 (chloroform:methanol:hexane 85:5:10), m.p. 72–74°, identified as the tetrazole derivative, **18**; ν_{max}(KBr) no NH or CO absorptions; *m/e* 200 and 202 (*ca.* 3:1, M^+); n.m.r. τ 5.40 (2H, br. triplet, *J ca.* 6 Hz), 5.90 (1H, width *ca.* 14 Hz), 2.87 (2H, broad multiplet), 6.5 (2H, AB quartet, J = 6 Hz), 8.15 (4H, broad complex), and 8.5 (2H, broad multiplet).

Anal. Calcd. for $C_8H_{13}ClN_4$: N, 27.78. Found: N, 27.77.

(A) Reaction of the N-Chloro Lactams "under Ionic-reaction Conditions"

(1) N-Chloroazacyclononan-2-one

To a solution of the *N*-chloro lactam (0.72 g, 4.1 mmol) in dioxane–water (4:1, 15 ml) was added ammonia solution (0.56 ml of 30%; 10 mmol), followed by freshly prepared silver oxide (from 4.74 g silver nitrate), and the resultant mixture stirred at room temperature under nitrogen. The reaction rate was determined by iodometric assay of 0.5 ml samples, withdrawn from the flask at appropriate intervals. After the reaction was completed (2 h), sodium chloride solution was added to precipitate any silver remaining in solution, and the mixture was filtered and the cake washed with dioxane. The filtrates were evaporated to low bulk; taken up in chloroform, dried (Na_2SO_4), evaporated, and the residue distilled on the oil pump. The distillate (b.p. 70–95°/0.01 mm, 0.5 g) was analyzed by g.l.c. The products, the lactams **3**, **4**, and **2***b* were found in the ratio 1:2.8:1.85, which corresponded to a yield of 63% of bicyclic products.

When the above reaction was carried out in acetonitrile–water (9:1) the following result was obtained. After 3 h reaction, the product analysis showed the lactams **3**, **4**, and **2***b* to be in the ratio 1:2.8:3.6, corresponding to a 50% yield of bicyclic products.

When a solution of the *N*-chloro-2-azacyclononanone (1.23 mmol) in acetonitrile–water 9:1 (5 ml) containing ammonia (0.14 cc, 30%, 2.5 mmol) was left under nitrogen at room temperature for 3 days, the concentration of *N*-chloro amide remained unchanged (iodometric assay).

(2) N-Chloroazacyclooctan-2-one

The reaction of the *N*-chloro compound with silver oxide – ammonia, under the standard conditions described previously was complete in 3 h in aqueous dioxane, and 4.5 h in aqueous acetonitrile. Product analysis by g.l.c. and n.m.r. showed the parent lactam **1***b* (90% recovery) to be the sole product of reaction in the case where aqueous acetonitrile was used as solvent. A trace (< 5%) of 1-azabicyclo[3.3.0]octanone-2 was detected in the reaction mixture when aqueous dioxane was used as solvent (95% recovery).

(3) N-Chloroazacycloheptan-2-one

Under the reaction conditions described previously, the parent azacycloheptan-2-one was the sole product of reaction (90%).

(B) Reaction of the N-Chloro Lactams "under Free-radical Conditions"

(1) N-Chloroazacyclooctan-2-one

(*a*) This *N*-chloro lactam (1.01 g, 6.3 mmol) was dissolved in 4:1 (v/v) peroxide-free dioxane–water (75 ml) containing precipitated calcium carbonate (3.0 g) and benzoyl peroxide (20 mg, 0.01 mmol). The reaction mixture was stirred and heated at 80°, under nitrogen. The reaction was complete in 1.5 h, and the mixture was then filtered and the filter-cake washed with dioxane. The combined filtrate and washings were evaporated to small bulk and the residue taken up in chloroform. Removal of solvent from the dried solution yielded an oil which was taken up in acetone–hexane. The solution deposited white prisms of the *C*-chloro lactam **8**, m.p. 85–87° (750 mg, 75%), ν_{max}($CHCl_3$) 1660 and 3400 cm^{-1}; n.m.r. τ 2.8–3.5 (broad, 1H, NH), 5.5–5.9 (multiplet, 1H, CH—Cl), 6.4–6.85 (multiplet, 2H, —CONH—CH_2—), and 7.1–8.5 (complex multiplet, 8H, ring protons).

Anal. Calcd. for $C_7H_{12}ClNO$: C, 52.02; H, 7.48; N, 8.64. Found: C, 52.37; H, 7.51; N, 8.78.

The g.l.c. behavior of the *C*-chloro lactam **8** on two columns, versamid at 200°, and SE30 at 165°, provided evidence of the thermal cyclization of **8** to the bicyclic lactam **7** *i.e.* retention times of **8** and **7** were identical on versamid at 200°, but **8** on SE30 at 165° gave two peaks (R_t = 4 min: 12 min), the faster peak corresponding to bicyclic lactam **7**.

(*b*) The above reaction could be duplicated using dioxane containing traces of hydroperoxides instead of benzoyl peroxide (*i.e.* by using dioxane distilled from sodium, but not percolated through alumina). Calcium carbonate could also be replaced by silver carbonate without altering the course of the reaction.

(*c*) *N*-Chloroazacycloöctan-2-one (0.465 g, 2.9 mmol) in 4:1 (v/v) peroxide-free dioxane – water (25 ml) containing calcium carbonate was heated at 80° under nitrogen. After 6 h no decrease in *N*-chloro lactam concentration could be detected, as judged by iodometry.

(*d*) The reaction at 80° in pure dioxane containing added peroxide, but no water or calcium carbonate, was very fast (complete in under 30 min), and gave a mixture of products; the major being the parent lactam **1***b*, with less than 5% of the *C*-chloro lactam, as estimated by the intensity of the *H*—C—Cl signal in the n.m.r. spectrum of the crude product. Further analysis of the n.m.r. spectrum revealed a singlet at τ 6.3 (dioxane hydrogens) together with a doublet at τ 5.1 (J = 3 Hz),

Can. J. Chem. Downloaded from www.nrcresearchpress.com by 210.87.254.6 on 09/05/12
For personal use only.

consistent with the presence of a coupled product **19** formed by combination of amidyl and dioxanyl radicals.

(*e*) When the reaction was run as in (*a*) or (*b*), but without calcium carbonate, the reaction mixture became slightly acidic, and the rate of reaction decreased considerably. Addition of calcium carbonate accelerated the reaction. In cases where the reaction was allowed to go to completion in the absence of carbonate, lower yields (30–40%) of *C*-chloro lactam **8** were obtained.

(*f*) When the reaction was conducted as in (*a*), but in pure dry dioxane, the reaction was fast (complete within 1 h) but gave lower yields of the desired *C*-chloro lactam. Examination of the n.m.r. spectrum of the crude product revealed absorptions similar to those described in (*d*) *i.e.* products such as **19** were again forming.

(*g*) When the reaction was conducted as in (*a*), but in dimethylformamide–water (4:1) an 80% yield of the *C*-chloro lactam **8** was obtained. In contrast, a comparable run in anhydrous dimethylformamide, showed that only 20% of the *N*-chloro lactam had decomposed in 1 h (*c.f.* 100% in the aqueous DMF case). Further additions of benzoyl peroxide (up to 25 mol %) were required over a period of 25 h to complete the decomposition in the dry solvent.

Cyclization of the C-Chloro Lactam 8

(*a*) The crystalline lactam (1.0 g, 6.2 mmol) was dissolved in dioxane–water (7:3, 200 ml), containing silver perchlorate (2.5 g, 12 mmol), and the mixture refluxed with stirring for 4 h, during which time silver chloride precipitated. Saturated sodium bicarbonate was added to precipitate the silver remaining in solution and the mixture was filtered; the filtrate was reduced to low bulk, taken up in chloroform, dried (Na_2SO_4), and the residue on evaporation distilled in vacuum. The fraction b.p. 60–70°/3 × 10^{-2} mm (500 mg, 58%) had ν_{max} ($CHCl_3$) 1680 cm^{-1} (5 ring lactam).

Anal. Calcd. for $C_7H_{11}NO$: C, 67.16; H, 8.85. Found: C, 67.06; H, 8.81.

The mass spectrum, M^+ = 125 (78); 97 (100) ($M^+ - 28$); 69 (61) (97–28), was consistent with the formulation of the product as 1-azabicyclo[3.3.0]octan-2-one (**7**).

Lithium aluminum hydride reduction of the bicyclic lactam **7** in dioxane, afforded a base whose picrate, m.p. 254–256° was identical (m.p. and mixed m.p. 253–255°) with an authentic sample of pyrrolizidine picrate (lit. (16) m.p. 255–258°).

(*b*) A solution of potassium amide in liquid ammonia was prepared from potassium metal (22 mg, 0.57 mmol) and liquid ammonia (25 ml). To this solution was added **8** (81 mg, 0.5 mmol) and the reaction mixture was stirred overnight while the ammonia was allowed to evaporate. The residue was extracted with a little benzene, and the benzene solution was washed with dilute hydrochloric acid, and dried ($MgSO_4$). Removal of solvent under reduced pressure left a residual oil which was >95% 3-ketopyrrolizidine by g.l.c. analysis, and comparison with the above sample.

(2) N-Chloroazacycloheptanone

(*a*) The *N*-chloro compound (0.42 g, 2.86 mmol) was dissolved in 4:1 (v/v) pure dioxane–water (40 ml), containing calcium carbonate (2 g) and benzoyl peroxide (20 mg, 0.01 mmol). Reaction was complete within 1 h at 80° under nitrogen, and work-up as before gave a product (%Cl = 0.07) whose i.r. spectrum was almost identical with that of azacycloheptan-2-one. The n.m.r. spectrum of the crude product revealed significant absorptions at τ 6.3 (singlet) and 5.1 (doublet, J = 3 Hz) consistent with products such as **19** derived from radical attack on dioxane.

(*b*) *N*-Chloro lactam (from 0.51 g, (4.41 mmol) of lactam) dissolved in 4:1 v/v dioxane–water (25 ml) in which was suspended silver carbonate (4 g), was stirred and heated at 100° (bath) for 3 h (reaction was complete after 1 h as judged by iodometry). The reaction mixture was filtered (Celite) and the filter-cake was washed with hot dioxane. Upon cooling, the combined filtrate and washings deposited colorless micro-needles (200 mg), soluble in water, insoluble in chloroform, containing silver but no nitrogen ν_{max}(KBr) 3400–3200, 1610, 1125, and 1075 cm^{-1}; n.m.r. (D_2O) τ 6.30 and 6.27 (4H, apparently the superposition of two triplets, J = 3 Hz, $HOCH_2CH_2O$—) and 5.97 (2H, singlet, —OCH_2CO_2) consistent with this material being silver 2′-hydroxyethoxyacetate, presumably derived by the further oxidation of **19***a*.

Evaporation of the aqueous dioxane filtrates, followed by partitioning of the residue between chloroform and water, gave a chloroform extract which was dried ($MgSO_4$) and evaporated to yield an oil (500 mg). The g.l.c. analysis revealed that this product was more than 90% azacycloheptan-2-one, and crystallization of the material from solution in petroleum ether afforded **9***b* as colorless plates. Its i.r. spectrum was superimposable upon that of authentic material.

(3) N-Chloroazacyclononan-2-one

(*a*) The *N*-chloro lactam (1.02 g, 5.75 mmol) was dissolved in 4:1 (v/v) "sodium-dry" dioxane–water (30 ml) containing calcium carbonate (2 g), and the reaction mixture was stirred and heated at 85° under nitrogen. The reaction appeared complete (iodometric assay) after 3 h. The reaction mixture was worked-up in the usual manner to yield an oil (0.96 g) which was shown by g.l.c. analysis to consist of the three lactams (**3**) (32%), (**4**) (63%), and (**2***b*) (5%).

(*b*) In a similar experiment, in which silver carbonate was used instead of the calcium salt, the products were fractionated by distillation under reduced pressure on a micro spinning-band column, yielding pure 5-ketooctahydropyrrocoline (**3**) (b.p. 96°/0.003 mm, n_D^{24} 1.4879) and 3-ketooctahydropyrrocoline (**4**) of greater than 90% purity (b.p. 110°/0.001 mm, n_D^{24} 1.5003). The i.r. spectra of these preparations were superimposable upon those of authentic specimens of the bicyclic lactams.

(*c*) The decomposition of *N*-chloroazacyclononan-2-one in wet, and dry dimethylformamide containing calcium carbonate and benzoyl peroxide, was also investigated.

As usual, the *N*-chloro lactam was completely destroyed within 20 min at 88°, in the wet solvent. The major products, as determined by g.l.c. analysis consisted of **3**, **4**, and **2***b* (*ca.* 1:3.3:1).

In anhydrous DMF the reaction was complete within 4 h at 88°, and the major products were the same as in the aqueous solvent, but with increased amounts of **2***b* (**3**:**4**:**2***b* *ca.* 1:1.9:2.0).

Can. J. Chem. Downloaded from www.nrcresearchpress.com by 210.87.254.6 on 09/05/12
For personal use only.

(4) N-Chloro-2-azabicyclo[2.2.2]octan-3-one ("Isoquinuclidone")

(*a*) The *N*-chloroazabicyclolactam (3.0 g, 18.8 mmol) was dissolved in 4:1 "sodium-dry" dioxane–water (150 ml), containing 12 g of suspended calcium carbonate, and heated at 80° under nitrogen. After all the *N*-chloro lactam had disappeared, the reaction mixture was worked-up in the usual fashion. However in this instance, a white precipitate separated from the filtrate, and considerable amounts of organic material were present in the filter-cake, which was therefore washed thoroughly with hot chloroform. The chloroform washings were used to extract the original filtrates, and the combined, dried chloroform extracts were then evaporated to yield a white solid which was recrystallized from acetone–hexane, m.p. 225–226° (1.9 g, 69%); ν_{max}(KBr) 3340 and 1635 cm^{-1}, *m/e* 292:294:296 *ca.* 9:6:1 corresponding to "M^+" species for $C_{13}H_{22}Cl_2N_2O$.

Anal. Calcd. for $C_{13}H_{22}Cl_2N_2O$: C, 53.06; H, 7.58; N, 9.58. Found: C, 53.29; H, 7.84; N, 9.49.

The mother liquors contained, in addition to this *N,N'*-di-(4'-chlorocyclohexyl) urea, a little parent 2-azabicyclo[2.2.2]octan-3-one, as judged by t.l.c. and g.l.c. (*ca.* 10%).

(*b*) When the *N*-chlorobicyclolactam was heated in "sodium-dry" dioxane, reaction was again rapid. The solution became acid. Evaporation, with exclusion of moisture, gave an oil containing some suspended solids. The i.r. spectrum of this crude product had ν_{max}(film) 2265 (—N=C=O), as well as 3200 and 1700 cm^{-1}.

Freshly distilled aniline was added to a solution of the crude product in dry ether. A mildly exothermic reaction ensued. The reaction mixture was kept for several hours at room temperature, then washed with dilute aqueous sulfuric acid, and then with bicarbonate solution. Evaporation of the dried ether extracts gave a solid which consisted of two major components (t.l.c.). Separation was achieved by fractional recrystallization from benzene–hexane to give the less-soluble substance as colorless crystals m.p. 179–183°; *m/e* 284:286 (*ca.* 3:1) as required for $C_{14}H_{21}ClN_2O_2$.[6]

The other substance was obtained by t.l.c. of the residues obtained upon evaporation of the mother liquors as colorless crystals m.p. 243°; *m/e* 252 and 254 (*ca.* 3:1) as required for *N*-(4-chlorocyclohexyl)-*N'*-phenylurea.

(*c*) The reaction was repeated in dry dioxane, with the addition of silver carbonate. After 1 h the reaction was complete, and work-up under anhydrous conditions gave an oily product which was distilled under reduced pressure to give a colorless liquid, b.p. 67–70°/14 mm (65%); ν_{max}(film) 2265 cm^{-1}.

Addition of aniline to a solution of this oil in ether gave a quantitative yield of the *N*-(4-chlorocyclohexyl)-*N'*-phenylurea; flat-sided needles from ethanol–hexane, m.p. 237–238° raised to 241–242° on further recrystallization; *m/e* 252 and 254 (*ca.* 3:1); n.m.r. (DMSO-d_6) τ 1.72 (1H, singlet, NH Ar), 2.5–3.2 (5H, multiplet, ArH), 3.95 (1H, doublet, J = 8 Hz, N*H*—CH), 5.92 (1H, very broad "singlet" (width *ca.* 24 Hz), C*H*Cl)), 6.47 (1H, very broad singlet (width *ca.* 20 Hz) C*H*—NH)), and 7.65–9.0 (8H, overlapping multiplets, ring CH_2). Irradiation at τ 6.47 collapsed the signal at τ 3.95 to a singlet, but the reverse operation, although it sharpened the τ 6.47 signal, did not resolve its structure. From the width of the τ 6.47 and 5.92 signals it seems most likely that the urea has a *trans*, diequatorial arrangement of the chloro and ureido groups.

Anal. Calcd. for $C_{13}H_{17}ClN_2O$: C, 61.78; H, 6.78; N, 11.09. Found: C, 61.66; H, 6.71; N, 10.98.

(5) N-Chloro-N-methylpentanoamide

A solution of the *N*-chloramide (1.49 g, 0.01 mol) in aqueous dioxane (100 ml, 1:4 v/v) containing benzoyl peroxide (*ca.* 20 mg) and suspended calcium carbonate (1.1 g, 0.011 mol) was stirred and heated at 85° (bath) for 18 h, after which time the *N*-chloro amide had been completely decomposed.

The reaction mixture was cooled, filtered, and evaporated to small volume (*ca.* 20 ml). Aqueous sodium bicarbonate solution was added, after which the mixture was extracted with chloroform (4 × 50 ml). The combined dried ($MgSO_4$) extracts were then evaporated to yield a residual yellow oil (1.21 g), shown by t.l.c. analysis (silica gel G, ethyl formate – benzene 4:1 v/v) to consist of two major, and one minor products. The crude reaction product had ν_{max} 3300, 1770, and 1650 cm^{-1}.

Fractional distillation gave two fractions: b.p. 75–80°/14 mm (290 mg), and b.p. 110–120°/*ca.* 14 mm (529 mg). The first fraction had ν_{max} 1790 cm^{-1} (v. strong), n.m.r. τ 5.35 (m) (1H), 7.65 (m) (2H), 7.9–8.5 (br. m.) (2H), and 8.65 (d, J = 7 Hz) (3H); this was identified as γ-valerolactone.

The second fraction had ν_{max} 3310 (strong) and 1655 cm^{-1} (strong); n.m.r., τ 2.15 (1H, broad), 5.8 (1H, multiplet), 7.3 (3H, d, J = 5 Hz), 7.8 (2H multiplet), 8.55 (2H multiplet) and 9.10 (3H, d, J = 6 Hz) consistent with it being γ-chloro-*N*-methylpentanoamide. The fraction also contained a small amount of *N*-methylpentanoamide.

Photolyses

The *N*-chloro amides were photolyzed at 5 °C in aqueous dioxane solutions (peroxide-free) under an atmosphere of nitrogen in a Vycor apparatus with a central well using a Hanovia (8A36) lamp (254 mμ).

N-Chloro-2-azacyclooctanone

The *N*-chloro amide (0.467 g, 2.9 mmol) in peroxide-free dioxane–H_2O (4:1, 50 ml) was completely photolyzed in 15 min (iodometric assay). The solution was evaporated to dryness at low temperature and the residue taken up in methylene chloride, dried (Na_2SO_4), and evaporated. The gum so obtained (0.51 g) was shown by n.m.r. and halogen analysis (%Cl = 16.24) to contain the *C*-chloro lactam **8**, in a yield of 75%.

[6]We ascribe structure **i** to this material.

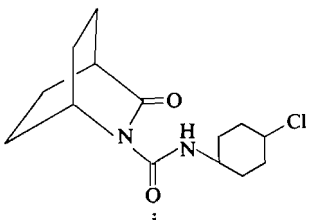

i

N-Chloro-2-azacyclononanone

The *N*-chloro amide (0.41 g, 2.34 mmol) in dioxane–water (4:1, 50 ml) was completely photolyzed in 10 min. The resulting acidic solution was stirred at 0 °C with a little calcium carbonate, filtered, and worked-up at ice temperature in the manner described previously. All attempts to isolate the suspected intermediate *C*-chloro lactams failed, the bicyclic lactams **3** and **4** being the major products isolated in all cases in yields of 70–80%.

Comparison of Photolysis in Wet and Dry Dioxane

Solutions of *N*-chloroazacyclononan-2-one in aqueous dioxane (1:4 v/v) and dry dioxane (both peroxide-free) were photolyzed under nitrogen at 0–5° using a 450 W Hanovia high pressure mercury lamp in a quartz well. The reaction in aqueous dioxane was complete in 20 min and gave a ratio of **3** to **4** to **2***b* of 1:2:0.3. The reaction dry dioxane was complete in 30 min and gave a ratio of **3** to **4** to **2***b* of 1.5:1:6.

Reaction of the N-Chloroamides with Silver

N-Chloro-2-azacyclooctanone (0.505 g, 3.13 mmol) was dissolved in dioxane–water (4:1, 40 ml), containing calcium carbonate (2 g). Silver (prepared from 7.5 g silver nitrate) was then added and the stirred reaction mixture heated at 80° under nitrogen. After the reaction was completed (5 h) the solids were removed by filtration and washed well with dioxane. The filtrates, on working-up in the manner described previously, gave an oil whose chlorine analysis (8.62%) and n.m.r. spectrum indicated a yield of *C*-chloro lactam **8** of around 25%. Extraction of the dried filter-cake (3x) with aqueous ammonia, and acidification of the extracts gave a precipitate of silver chloride (0.271 g, 1.91 mmol). *N*-Chloro-2-azacyclononanone under the above conditions gave a low yield (*ca.* 10–15%) of the bicyclic lactams **4** and **5**, the major product being the parent lactam **2***b* (over 90 mol % of silver chloride was found in this case).

Reaction of the N-Chloro amides with Silver Oxide

The following experiment was conducted using dioxane which had been stored over sodium wire, but which contained traces of peroxide. *N*-Chloro-2-azacyclononanone (0.405 g, 2.3 mmol) in dioxane–water (4:1, 20 ml) containing silver oxide (prepared from 3 g silver nitrate), was heated at 90° under nitrogen. Complete reaction occurred in 4 h, and the reaction mixture was worked-up in the manner described previously. The distilled residue (0.26 g) contained the lactams **3**, **4**, and **2***b* in the ratio 1:2.8:0.4, the total yield of bicyclic lactams being in the region of 85%.

1. O. E. Edwards, D. Vocelle, J. W. ApSimon, and F. Haque. J. Am. Chem. Soc. **87**, 678 (1965).
2. H. W. Johnson, Jr. and D. E. Bublitz. J. Am. Chem. Soc. **80**, 3150 (1958).
3. W. P. Judd and B. E. Swedlund. Chem. Commun. 43 (1966).
4. R. S. Neale, N. L. Marcus, and R. G. Schepers. J. Am. Chem. Soc. **88**, 3051 (1966); Y. L. Chow and T. C. Joseph. Chem. Commun. 490 (1969).
5. O. E. Edwards, D. Vocelle, and J. W. ApSimon. Can. J. Chem. In preparation.
6. P. G. Gassman. Acc. of Chem. Res. **3**, 26 (1970).
7. D. H. R. Barton, A. L. J. Beckwith, and A. Goosen. J. Chem. Soc. 181 (1965).
8. A. L. J. Beckwith and J. E. Goodrich. Aust. J. Chem. **18**, 747 (1965).
9. R. C. Petterson and A. Wambsgans. J. Am. Chem. Soc. **86**, 1648 (1964).
10. W. Z. Heldt and L. G. Donaruma. Org. React. **11**, 57 (1960).
11. F. J. Villani and C. A. Ellis. J. Med. Chem. **9**, 185 (1966).
12. K. Loffler and H. Kaim. Chem. Ber. **42**, 94 (1909).
13. A. J. Castro, J. F. Deck, N. C. Ling, J. P. Marsh, Jr., and G. E. Means. J. Org. Chem. **30**, 344 (1965).
14. L. Birkofer and C. D. Barnikel. Chem. Ber. **91**, 1996 (1958).
15. R. A. Jones and J. A. Lindner. Aust. J. Chem. **18**, 875 (1965).
16. F. Galinovsky and A. Reichard. Chem. Ber. **77B**, 138 (1944).
17. P. W. Henniger, L. J. Dukker, and E. Havinga. Rec. Trav. Chim. **85**, 1177 (1966); J. G. Traynham and T. M. Couvillon. J. Am. Chem. Soc. **89**, 3205 (1967).

Can. J. Chem. Downloaded from www.nrcresearchpress.com by 210.87.254.6 on 09/05/12
For personal use only.

Can. J. Chem. Downloaded from www.nrcresearchpress.com by 210.87.254.42 on 09/05/12
For personal use only.

The Reaction of S(^{3}P) Atoms with Molecular Oxygen

R. W. Fair,[1] A. Van Roodselaar, and O. P. Strausz
Department of Chemistry, University of Alberta, Edmonton, Alberta

Received November 27, 1970

The rate constant of the reaction of ground state S(^{3}P) atoms with molecular oxygen, S(^{3}P) + $O_2(X^3\Sigma_g^-) \rightarrow SO(X^3\Sigma^-) + O(^3P)$, has been determined as $(1.7 \pm 0.2) \times 10^{12}$ cm^3 mol^{-1} s^{-1} at 298 °K by means of kinetic spectroscopy in the vacuum ultraviolet region. The source of S(^{3}P) atoms was the isothermal flash photolysis of COS in the presence of Ar or CO_2.

On a déterminé par spectroscopie cinétique dans l'ultraviolet lointain que la constante de vitesse à 298 °K de la réaction des atomes S(^{3}P) dans leur état fondamental avec de l'oxygène moléculaire, S(^{3}P) + $O_2(X^3\Sigma_g^-) \rightarrow SO(X^3\Sigma^-) + O(^3P)$, est de $(1.7 \pm 0.2) \times 10^{12}$ cm^3 mol^{-1} s^{-1}. On a utilisé la photolyse éclair de COS en présence de Ar ou de CO_2 comme source d'atomes S(^{3}P).

Canadian Journal of Chemistry, **49**, 1659 (1971)

The spin and symmetry allowed reaction of ground state $^3P_{2,1,0}$ atomic sulfur with molecular oxygen

[1] $S(^3P) + O_2(X^3\Sigma_g^-) \rightarrow SO(X^3\Sigma^-) + O(^3P)$

has often been postulated as an elementary process occurring in the oxidation of simple sulfur compounds (1–6). Two conflicting rate constants have been reported for this reaction. Homan *et al.* (7) obtained the relation

$$k_1 = 1 \times 10^{13} \exp(-5600 \text{ cal/mol})/RT \quad \text{cm}^3 \text{ mol}^{-1} \text{ s}^{-1}$$

in the temperature range 675–1090 °K, but extrapolation of this expression to 298 °K yields a value which is three orders of magnitude lower than the value $(1.2 \pm 0.3) \times 10^{12}$ cm^3 mol^{-1} s^{-1} obtained by Fair and Thrush (8). In view of this discrepancy it was considered desirable to reinvestigate reaction 1.

Experimental

The technique of flash photolysis with kinetic spectroscopy in the vacuum ultraviolet region was used in this work. The reaction cell, made of quartz with LiF end windows, was 17.6 cm long and 1.9 cm in diameter. It was positioned parallel to the limbs of a U-shaped flash lamp and the cell-lamp assembly surrounded by an aluminum reflector. The lamp was filled with 2–6 Torr N_2 to prevent firing during the charging period, and the total pressure was made up to 50 Torr with Kr. It was discharged at 3–9 kV from a 30 μF capacitor. Maximum flash intensity was reached at 14 μs and half peak intensity at 20 μs after initiation. Over 90% of the flash energy was dissipated by 40 μs after initiation, which was the shortest time delay used in the kinetic runs. The spectroscopic source was a conventional quartz capillary discharge lamp which was filled with 10 Torr Kr and discharged at 12–16 kV from a 2.5 μF capacitor; its intensity rose to a maximum in 4 μs and had a duration of 10 μs at half peak intensity. Light from the spectroscopic lamp was focused onto the entrance slit of the spectrograph by a LiF lens placed between the reaction cell and the slit. The LiF end windows of the cell also served as the windows for the spectroscopic lamp and the spectrograph, thus minimizing the number of optical components in the light path.

The spectrograph was a 1 m McPherson 225 normal incidence vacuum scanning instrument fitted with a 30 000 grooves/in. grating, which provided a dispersion of 8.3 Å/mm. A slit width of 20 μ was used. Spectra were recorded on Kodak SWR film which was developed in half strength Kodak D-19 developer for 5 min. The plates were photometered with a Joyce Loebl double beam recording microdensitometer. The three multiplets of S(3^{3}P) were detected by the absorption lines at 1807 ($^3P_2$), 1820 ($^3P_1$), and 1826 Å ($^3P_0$). The dependence of the microdensitometer peak heights, h, of these transitions on the concentrations, c, of the species and the path length, l, was assumed to be of the form

$$h = kc^n l^n$$

The value of n was determined by comparing the peak heights obtained by flashing half the cell length and the full cell length. For the $^3P_2$ line at 1807 Å, n was found to be 0.5 ± 0.1 (Fig. 1). The same value was obtained for the $^3P_1$ line, but the $^3P_0$ line was too weak for quantitative measurements.

Carbonyl sulfide (Matheson) was purified by the procedure of Wiebe *et al.* (9) and carbon dioxide by passing it over P_2O_5 and outgassing at 77 °K. Airco assayed reagent grade argon and oxygen were used without further purification.

[1]Present address: Department of Chemistry, University of Essex, Colchester, Essex, England.

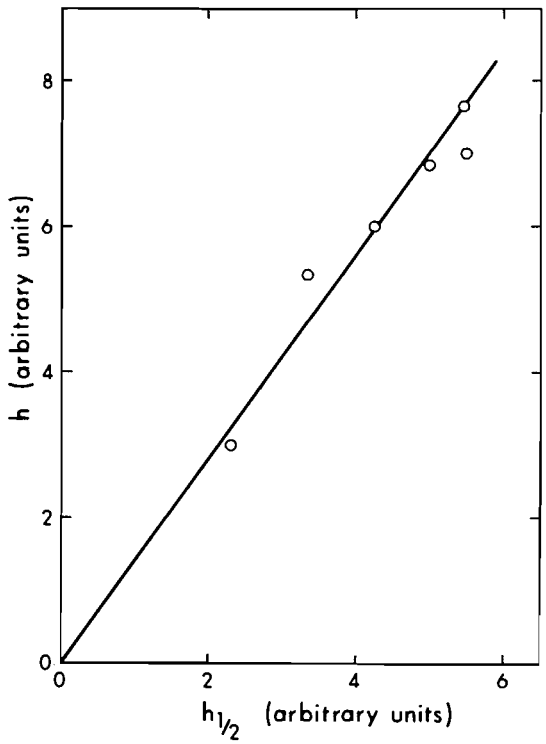

FIG. 1. Determination of Beer–Lambert exponent for the $S(4s^3S_1 \leftarrow 3p^3P_2)$ transition at 1807 Å. h and $h_{\frac{1}{2}}$ are microdensitometer peak heights for path lengths of 17.6 and 8.8 cm, respectively.

Results

The flash photolysis of mixtures containing 0.1 Torr COS with 200 Torr of CO_2 or of Ar was investigated briefly. $S(3^3P_{2,1,0})$ atoms were observed and they decayed over a period of a few milliseconds. The fraction of COS decomposed by flashing COS + Ar mixtures was estimated to be $(2 \pm 1)\%$ by monitoring the intensity of the COS absorption in the wavelength region 1730–1785 Å. Similar measurements were not carried out with COS + CO_2 mixtures since CO_2 also absorbs at these wavelengths. The $S(^3P_2)$ decay fitted first order plots, Fig. 2, with first order rate constants of $(1.1 \pm 0.3) \times 10^3$ and $(0.7 \pm 0.3) \times 10^3$ s^{-1} in the presence of CO_2 and of Ar, respectively. First order $S(^3P_1)$ decay plots showed rather more scatter since the microdensitometer peak heights of the $S(^3P_1)$ absorption were a factor of about 4.5 lower than the corresponding $S(^3P_2)$ line, but the first order rate constants obtained were the same as those for the $S(^3P_2)$ decays.

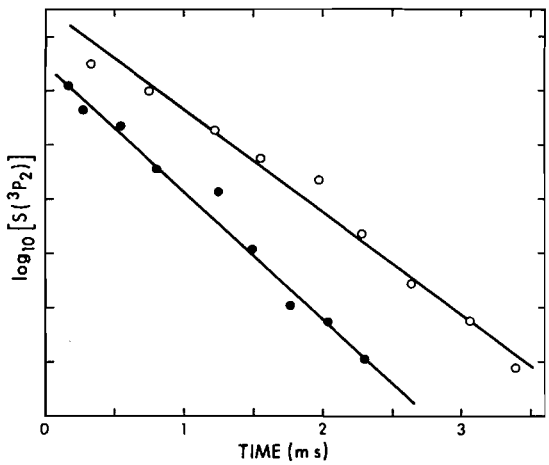

FIG. 2. First order plots of $S(^3P_2)$ decay from flash photolysis of 0.1 Torr COS with: ○, 200 Torr Ar; ●, 200 Torr CO_2. The ordinate axis is marked in intervals of 0.2.

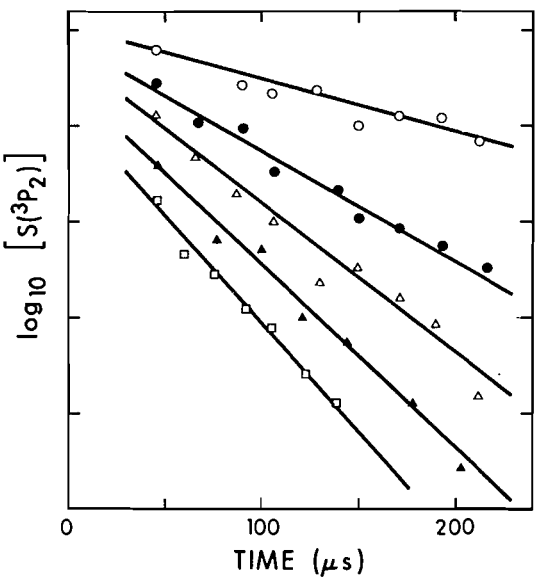

FIG. 3. First order plots of $S(^3P_2)$ decay. $10^9[O_2]$-(mol cm^{-3}): ○, 3.3; ●, 6.7; △, 9.9; ▲, 13.8; □, 15.5. Total pressure = 200 Torr. The ordinate axis is marked in intervals of 0.5.

The addition of 0.06–0.29 Torr of O_2 to COS (0.1 Torr) + CO_2 (200 Torr) mixtures considerably enhanced the rate of removal of atomic sulfur. Typical first order plots obtained for the $S(^3P_2)$ decays are shown in Fig. 3 and the pseudo first order rate constants, k_{uni}, are given in Table 1. Figure 4 shows that k_{uni} is linearly related to the oxygen concentration. A three-fold variation

Can. J. Chem. Downloaded from www.nrcresearchpress.com by 210.87.254.42 on 09/05/12
For personal use only.

Can. J. Chem. Downloaded from www.nrcresearchpress.com by 210.87.254.42 on 09/05/12
For personal use only.

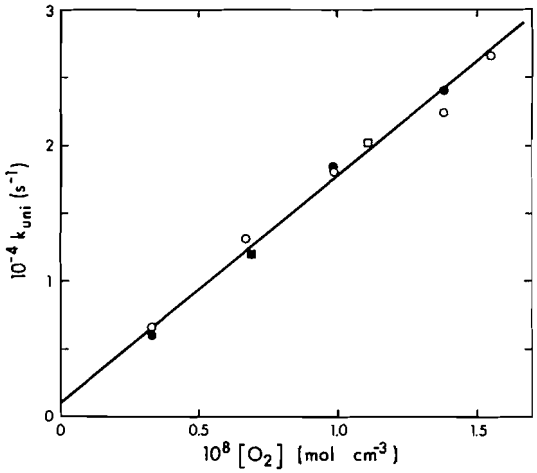

FIG. 4. Plot of k_{uni} *vs.* $[O_2]$. ○, $S(^3P_2)$ decay at 200 Torr total pressure; ●, $S(^3P_1)$ at 200 Torr; ■, $S(^3P_2)$ at 100 Torr; □, $S(^3P_2)$ at 60 Torr.

TABLE 1. Kinetic data for the reaction of $S(^3P)$ with O_2

$10^8[O_2]$ (mol cm^{-3})	$S(^3P)$ species monitored	No. of runs	$10^{-4}k_{uni}$* (s^{-1})
0.33	$^3P_2$	4	0.66
0.33	$^3P_1$	2	0.60
0.67	$^3P_2$	2	1.31
0.69	$^3P_2$	1	1.20[a]
0.99	$^3P_2$	4	1.80
0.99	$^3P_1$	1	1.84
1.11	$^3P_2$	4	2.02[b]
1.38	$^3P_2$	4	2.24[c]
1.38	$^3P_1$	4	2.40[c]
1.55	$^3P_2$	3	2.66

*Listed values of k_{uni} are averages from the number of runs given in column 3. All experiments were carried out with 0.1 Torr COS and 200 Torr CO_2 except: (*a*) 0.05 Torr COS, 70 Torr Ar, 30 Torr CO_2; (*b*) 0.1 Torr COS, 60 Torr CO_2; (*c*) 0.1 Torr COS, 140 Torr Ar, 60 Torr CO_2.

in the flash energy did not affect the value of k_{uni}. The latter was also unaltered when the total pressure was reduced to 60 Torr and when a mixture of CO_2 and Ar in the ratio 1:2.4 was used instead of CO_2 as the thermalizing gas.

The ratio of the microdensitometer peak heights of $S(^3P_2)$ and $S(^3P_1)$ in flashed COS + O_2 + CO_2 mixtures was (4.5 ± 1):1 and was independent of the reaction time. The $S(^3P_1)$ decay was measured in some of the runs and its kinetics were identical with those of the $S(^3P_2)$ decay (*cf.* Table 1 and Fig. 4). The line in Fig. 4 is drawn as the best fit to all the data. Its slope is $(1.7 \pm 0.2) \times 10^{12}$ cm^3 mol^{-1} s^{-1}. Since the oxygen consumed was always less than 5% of the initial $[O_2]$, no correction was made for the concentration change during the reaction.

SO could not be detected under the conditions used for the kinetic runs (0.1 Torr COS). However, when the COS pressure was increased to 0.3 Torr the (14,0), (15,0), (16,0), (17,0), (18,0), (19,0), and (21,0) bands of the $B^3\Sigma^- \leftarrow X^3\Sigma^-$ system of SO were observed weakly in the region 1950–2040 Å. Quantitative measurements of the kinetics of the SO formation were not possible due to the low intensity of the bands, but the rise in the SO concentration appeared to correspond to the decay of atomic sulfur.

A very weak diffuse band centered at 1831.5 Å was observed in flashed COS (0.1 Torr) + O_2 + CO_2 mixtures. Its intensity increased during the period of the atomic sulfur decay. With 0.3 Torr COS additional bands centered at 1838 and 1844 Å were observed. These are the most intense members of a set of six bands which McGarvey and McGrath (3) attributed to an isomeric form of sulfur dioxide. More recently, however, this assignment has been questioned by two independent groups of workers (10, 11) who concordantly suggest that the band system in fact is due to the $D^3\Pi \leftarrow X^3\Sigma^-$ transition of the SO molecule.

Discussion

The absorption spectrum and photodissociation of carbonyl sulfide have been discussed in detail in the literature (12–15). The quartz cell and photo lamp used in the present work limited photolysis to the first absorption band, which lies in the region 1900–2600 Å. The predominant primary process occurring at these wavelengths is

[2*a*] $COS(\tilde{X}^1\Sigma^+) + h\nu \rightarrow CO(X^1\Sigma^+) + S(^1D_2)$

with possibly a small contribution from the spin forbidden process

[2*b*] $COS(\tilde{X}^1\Sigma^+) + h\nu \rightarrow CO(X^1\Sigma^+) + S(^3P_{2,1,0})$

The $^1D_2$ sulfur atoms are removed by reaction with COS and collision-induced relaxation to the ground state (14, 16)

[3*a*] $S(^1D_2) + COS(\tilde{X}^1\Sigma^+) \rightarrow S_2(a^1\Delta_g) + CO(X^1\Sigma^+)$

[3*b*] $S(^1D_2) + COS(\tilde{X}^1\Sigma^+) \rightarrow S(^3P_{2,1,0}) + COS$

[4] $S(^1D_2) + M \rightarrow S(^3P_{2,1,0}) + M$

The half-lives of the decay of $S(^1D_2)$ under our conditions would be ~ 4 μs for reactions 3 with 0.1 Torr COS (16) and ~ 0.1 μs for reaction 4

Can. J. Chem. Downloaded from www.nrcresearchpress.com by 210.87.254.42 on 09/05/12
For personal use only.

with 200 Torr Ar (17). Removal of $S(^1D_2)$ by [4] in the presence of 60 Torr CO_2 would have a half-life of approximately 0.01 μs since the data of Wiebe *et al.* (9) indicate that k_3 and k_4 have comparable magnitudes for $M = CO_2$. Hence with the pressures used in the present work, the $S(^1D_2)$ atoms generated by [2*a*] were almost exclusively quenched to the ground state, and the rate of this quenching was extremely rapid on our time scale. This was also the case in the flash photolysis of the $COS + CO_2 + O_2$ mixtures since the oxygen would remove negligible amounts of $S(^1D_2)$ even if the reaction occurred with unit collision efficiency. The photolysis of COS under our conditions therefore provides a clean source of $S(3^3P_{2,1,0})$ atoms.

The low intensity of the $S(^3P_0)$ line and the constant ratio of the intensities of the $S(^3P_1)$ and $S(^3P_2)$ lines strongly suggest that a Boltzmann distribution was maintained among the three triplet components. An alternative explanation is that the chemical reactivities of the triplet components are equal; provided the $S(^3P)$ decay is first order in [S], the intensities of the multiplets would then represent the relative amounts initially formed by reaction 4. However, in view of Donovan's observation (17) on the rapidity of the thermalization process for sulfur atoms and of the reported high efficiency of spin–orbit relaxation of $Se(4^3P_0)$ (18), a species for which the triplet splitting is much larger than for sulfur, the latter explanation is improbable. Hence, it was not possible in the present work to determine the relative reactivities of the different *J* states of $S(^3P)$, but monitoring the $S(^3P_2)$ line or the $S(^3P_1)$ line yields the total reaction rate of all the *J* states.

Previous studies (19, 20) have shown that $S(^3P)$ atoms generated by the isothermal flash photolysis of COS decay by a recombination process rather than by the abstraction reaction

[5] $S(^3P) + COS(\tilde{X}^1\Sigma^+) \rightarrow S_2(X^3\Sigma_g^-) + CO(X^1\Sigma^+)$

The apparent first order decay of $S(^3P)$ observed in the present work in flashed $COS + CO_2$ and $COS + Ar$ mixtures demonstrates that simple atomic recombination

[6] $S(^3P) + S(^3P) + M \rightarrow S_2 + M$

is not the dominant process removing $S(^3P)$. In order to contribute significantly to the observed rate, this reaction would require an improbably high rate constant of $k_6 \sim 2 \times 10^{17}$ cm^6 mol^{-2} s^{-1}. A mechanism involving strong, irreversible complexing

[7] $S + COS + M \rightarrow COS_2 + M$

with $k_7 = 1.4 \times 10^{16}$ cm^6 mol^{-2} s^{-1} (M = Ar), followed by

[8] $COS_2 + COS_2 \rightarrow 2COS + S_2$

would be consistent with the observed first order decay of S-atoms. However, more work is clearly required on this problem and with the limited data available, further speculation about the mechanism is not justified.

In the presence of molecular oxygen, the pseudo first order rate constant, k_{uni}, for the $S(^3P)$ decay increased linearly with the concentration of O_2 added (Fig. 4). The intercept of the line in Fig. 4 at $[O_2] = 0$ is 1.0×10^3 s^{-1} and is identical within experimental error with the value of $k_{uni} = (1.1 \pm 0.3) \times 10^3$ s^{-1} ($M = CO_2$) determined directly in the absence of oxygen. Therefore, the $S(^3P)$ decay rate due to the oxygen and the decay which occurs in the absence of oxygen are strictly additive with no interaction between the two processes.

According to correlation rules the following reactions are possible within the confines imposed by energy limitations

[1] $S(^3P) + O_2(X^3\Sigma_g^-) \rightarrow SO(X^3\Sigma^-) + O(^3P)$

[9*a*] $\rightarrow SO_2(X^1A_1)$

[9*b*] $\rightarrow SO_2(a^3B_1)$

[9*c*] $\rightarrow SO_2(A^1B_1)$

To date no evidence has been found for the formation of SO_2 and it is doubtful if reactions 9 occur at all. Therefore the most likely structure for the reaction complex is SOO. Correlation rules predict nine states for this molecule: three singlets, three triplets, and three quintets. The latter would probably lie too high to be attainable energetically. This leaves three singlets and three triplets possible, none of which appears to possess a finite lifetime. Decomposition of the complex should preferentially follow the lower energy path SOO → SO + O, according to the sequence

[1] $S(^3P) + O_2(X^3\Sigma_g^-) \rightarrow SOO\dagger(2^1A' + 2^3A'' + {}^1A'' + {}^3A'') \rightarrow SO(X^3\Sigma^-) + O(^3P)$

where the dagger signifies vibrational excitation.

Can. J. Chem. Downloaded from www.nrcresearchpress.com by 210.87.254.42 on 09/05/12
For personal use only.

Thus we assign the rate constant, $(1.7 \pm 0.2) \times 10^{12}$ cm^3 mol^{-1} s^{-1}, measured at 298 °K to reaction 1. The possibility of the intervention of other reactions removing S atoms were considered. The combination reactions

[10] $S + SO + M \rightarrow S_2O + M$

[11] $S + O + M \rightarrow SO + M$

[12] $S + SO_2 + M \rightarrow S_2O_2 + M$

were insignificant under our conditions since rate constants of $\sim 10^{19}$ cm^6 mol^{-2} s^{-1} would be required. The bimolecular reactions

[13] $S(^3P) + SO(X^3\Sigma^-) \rightarrow S_2(X^3\Sigma_g^-) + O(^3P)$

[14] $S(^3P) + SO_2 \rightarrow 2SO$

would also require unreasonably large rate coefficients. Additional evidence against the occurrence of these steps is the lack of light intensity dependence of the S atom decay (and the 22 kcal/mol endothermicity of step 13). Although oxygen does absorb light weakly at wavelengths above the quartz cut-off (21), any decomposition products or excited intermediates formed by this photolysis did not remove S(³P) since k_{uni} was independent of the flash energy. Reactions such as

[15] $O + O_2 + M \rightarrow O_3 + M$

[16] $S + O_3 \rightarrow SO + O_2$

or

[17] $O + SO + M \rightarrow SO_2 + M$

[18] $S + SO_2 + M \rightarrow S_2O_2 + M$

could not proceed at a rate sufficient to remove significant amounts of S(³P) atoms.

The rate constant obtained in the present study for the removal of S(³P) atoms by O_2 shows satisfactory agreement with the value of $(1.2 \pm 0.3) \times 10^{12}$ cm^3 mol^{-1} s^{-1} which Fair and Thrush (8) measured by monitoring the formation of the products of reaction 1. The maximum value of the activation energy consistent with these values of the rate constant is 2.8 kcal if the A factor is equal to the gas kinetic collision frequency. Therefore, the high activation energy reported by Homann *et al.* (7) is in error. The overall reaction, step 1, is exothermic by 6 kcal and its activation energy would not be expected to be higher than that of the thermoneutral isotopic exchange reaction (22–24)

[19] $^{18}O(^3P) + {}^{16}O_2 \rightarrow {}^{18}O{}^{16}O + {}^{16}O(^3P)$

which is reported to have $E_a = 1.1$ kcal (22).

Considering the analogous sequence for the reaction of O(³P) atoms with O_2 (25)

$$O + O_2 \underset{}{\overset{a}{\rightleftarrows}} O_3^* \begin{cases} \nearrow O_2 + O \\ \xrightarrow{M} O_3 \end{cases}$$

the calculated value of $k_a = 0.9 \times 10^{12}$ cm^3 mol^{-1} s^{-1} corresponds closely with our results on the S + O_2 reaction. In this case, however, the reaction complex, the excited ozone molecule has a finite lifetime and can be deactivated by collision to the stable ground state.

From the measured rate coefficient, the upper limit for the activation energy of the reverse reaction of [1],

$$SO(X^3\Sigma^-) + O(^3P) \rightarrow O_2(X^3\Sigma_g^-) + S(^3P)$$

may be estimated to be < 9 kcal.

We wish to thank the National Research Council of Canada for continuing financial support and Mr. R. Kadlecz for help in electronics.

1. A. L. Myerson, F. R. Taylor, and P. L. Hanst. J. Chem. Phys. **26**, 1309 (1957).
2. F. J. Wright. J. Phys. Chem. **64**, 1648 (1960).
3. J. J. McGarvey and W. D. McGrath. Proc. Roy. Soc. Ser. A. **278**, 490 (1963).
4. M. A. Pollack. Appl. Phys. Lett. **8**, 237 (1966).
5. D. W. Gregg and S. J. Thomas. J. Appl. Phys. **39**, 4399 (1968).
6. G. Hancock and I. W. M. Smith. Chem. Phys. Lett. **3**, 573 (1969).
7. K. H. Homann, G. Krome, and H. Gg. Wagner. Ber. Bunsenges. Phys. Chem. **72**, 998 (1968).
8. R. W. Fair and B. A. Thrush. Trans. Faraday Soc. **65**, 1557 (1969).
9. H. A. Wiebe, A. R. Knight, O. P. Strausz, and H. E. Gunning. J. Am. Chem. Soc. **87**, 1443 (1965).
10. R. J. Donovan, D. Husain, and P. T. Jackson. Trans. Faraday Soc. 2930 (1969).
11. N. Basco and R. D. Morse. Proc. Roy. Soc. Ser. A. **313**, 111 (1969).
12. R. J. Donovan. Trans. Faraday Soc. **65**, 1419 (1969).
13. W. H. Breckenridge and H. Taube. J. Chem. Phys. **52**, 1713 (1970).
14. H. E. Gunning and O. P. Strausz. Advan. Photochem. **4**, 143 (1966).
15. K. S. Sidhu, I. G. Csizmadia, O. P. Strausz, and H. E. Gunning. J. Am. Chem. Soc. **88**, 2412 (1966).

16. R. J. DONOVAN, L. J. KIRSCH, and D. HUSAIN. Nature, **222**, 1164 (1969).
17. R. J. DONOVAN, L. J. KIRSCH, and D. HUSAIN. Trans. Faraday Soc. **66**, 774 (1970).
18. W. J. R. TYERMAN and A. B. CALLEAR. Trans. Faraday Soc. **62**, 2313 (1966).
19. P. FOWLES, M. DE SORGO, A. J. YARWOOD, O. P. STRAUSZ, and H. E. GUNNING. J. Am. Chem. Soc. **89**, 1352 (1967).
20. N. BASCO and A. E. PEARSON. Trans. Faraday Soc. **63**, 2684 (1967).
21. J. R. MCNESBY and H. OKABE. Advan. Photochem. **3**, 157 (1964).
22. S. JAFFE and F. S. KLEIN. Trans. Faraday Soc. **62**, 3135 (1966).
23. J. T. HERRON and F. S. KLEIN. J. Chem. Phys. **40**, 2731 (1964).
24. N. BRENNEN and H. NIKI. J. Chem. Phys. **42**, 3725 (1965).
25. J. T. HERRON and F. S. KLEIN. J. Chem. Phys. **41**, 1285 (1964).

Can. J. Chem. Downloaded from www.nrcresearchpress.com by 210.87.254.42 on 09/05/12
For personal use only.

Can. J. Chem. Downloaded from www.nrcresearchpress.com by 210.87.254.6 on 09/05/12
For personal use only.

Anionic Dimerization in Reductive Cleavage of an Allyl Ether with Sodium–Potassium Alloy

D. H. HUNTER AND D. W. MOORE
Department of Chemistry, University of Western Ontario, London, Ontario

Received September 30, 1970

The reaction of 9-methoxy-9-vinylfluorene (**2a**) with sodium–potassium alloy does not yield the expected 9-vinylfluorenylanion (**1**). The anions derived from the reaction were characterized by carbonation and subsequent methylation. Four esters (**5**, **6**, **7**, and **8**) accounting for about two-thirds of the starting material were isolated and characterized. Structures were assigned on the basis of mass spectra and n.m.r. spectra in particular using decoupling experiments. A brief mechanistic scheme is presented.

La réaction du méthoxy-9 vinyl-9 fluoréne (**2a**) avec un alliage sodium–potassium ne conduit pas à l'anion vinyl-9 fluorényle (**1**). On a caractérisé les anions dérivés de cette réaction en effectuant successivement une carbonatation et une méthylation. On a pu isoler et caractériser quatre esters (**5**, **6**, **7** et **8**) qui permettent de tenir compte d'environ les deux tiers du produit de départ. On a attribué des structures à ces composés en se basant principalement sur les spectres de masse et de r.m.n. en faisant appel aux techniques de découplage. On présente un bref mécanisme réactionnel.

Canadian Journal of Chemistry, 49, 1665 (1971)

Introduction

Reductive cleavage of ethers by alkali metals has proved to be one of the more successful routes to organic derivatives of the alkali metals. The presence of a site of unsaturation in the ether, often a phenyl ring, facilitates the reaction and allyl- and benzyl-type carbanides have been prepared most commonly (1–6). In an attempt to prepare and study restricted rotation in the alkali metal derivatives of anion **1**, a sample of 9-methoxy-9-vinylfluorene **2a** was prepared and reacted. Unlike analogous 9-substituted-9-methoxy-fluorenes (**2b** (7), **2c** (8), and **2d** (8)), the expected anion was not observed (**1** in this case). Other analogous ethers which have been reacted successfully to produce their potassium salts are **3** and **4** (9).

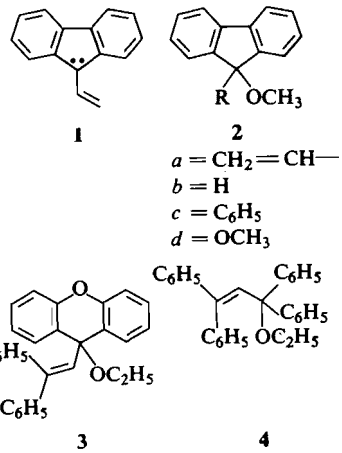

1 **2** **3** **4**

Results

A sample of 9-methoxy-9-vinylfluorene (**2a**) was prepared as described in the Experimental section. A dilute solution (*ca.* 0.1 *M*) of **2a** in freshly distilled tetrahydrofuran was stirred under an argon atmosphere for two days with a slight excess over the stoichiometric amount of sodium–potassium alloy. During the course of the reaction a dissolving deep-red coloration developed on the surface of the alloy and the final solution was deep red. In an attempt to characterize the organometallics present, this solution was passed into a room temperature solution of carbon dioxide in tetrahydrofuran. The acids accounted for 85 wt% of the total isolated materials and no **2a** could be detected in the neutral fraction.

Instead of a mixture of the two acids expected upon carbonation of the desired anion, thin layer chromatography indicated a mixture of at least nine components and n.m.r. suggested that neither of the predicted products was present. This result proved to be reproducible. The acids were converted to their methyl esters on treatment with diazomethane and again both thin layer chromatography and n.m.r. showed about nine components. By a combination of thick layer chromatography and vapor phase

Can. J. Chem. Downloaded from www.nrcresearchpress.com by 210.87.254.6 on 09/05/12
For personal use only.

chromatography (v.p.c.), four components of the mixture were isolated and characterized as described in the Experimental section.

Structures **5**, **6**, **7**, and **8** have been assigned

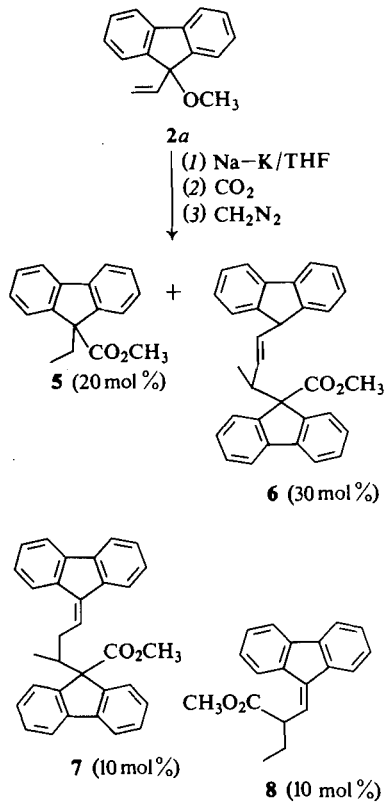

on the basis of their n.m.r. and mass spectra. The structure assigned to **5** has been verified by mixed melting point with an authentic sample.[1] All the esters proved to be crystalline solids except **8** which remained a viscous oil. Both the n.m.r. and analytical results for **8** suggest the presence of a small amount of impurities which, however, do not interfere with the structural assignment.

Integration of the 100 MHz n.m.r. spectrum of **6** (Fig. 1) indicated the presence of two fluorenyl groupings and this was substantiated by the mass spectrum parent peak at $m/e = 442$. A first order analysis of this and the decoupled n.m.r. spectra yielded $\delta a = 0.81$, $\delta b = 3.47$, $\delta c = 5.53$, $\delta d = 5.14$, $\delta e = 4.14$, and $J_{ab} = 6.8$ Hz, $J_{bc} = 8.0$ Hz, $J_{cd} = 15.0$ Hz, $J_{de} = 8.8$ Hz. The structure of the carbon chain was clarified by proton–proton decoupling experiments. The high field methyl doublet (protons *a*) collapsed to a singlet when proton *b* was irradiated. At the same time the low field quartet due to a vinyl proton (*c*) collapsed to a doublet. Irradiation of the doublet at $\delta = 4.14$ (proton *e*) collapsed the upfield vinyl proton (*d*) to a doublet. These results require a carbon chain of the following type. The large coupling ($J_{cd} = 15.0$ Hz) between the vinyl protons is consistent with a *trans* geometry. Introduction of two fluorenyl ring systems and a carbomethoxy group lead to structure **6**.

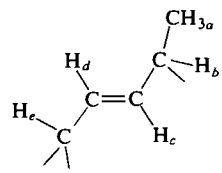

The n.m.r. spectrum of **7** is shown in Fig. 2 along with the results of integration. The mass spectrum (parent peak at $m/e = 442$) show that **6** and **7** are isomers. The n.m.r. again suggests the presence of two fluorenyl rings and a carbomethoxy grouping. Again homonuclear decoupling experiments proved very useful in the assignment of the structure of the carbon chain. The methyl doublet (protons *a*) collapsed to a singlet when the signal at $\delta = 3.14$ due to a single proton (*b*) was irradiated. Furthermore the multiplet due to two protons (*c* and *d*) at $\delta = 2.4$ simplified to an unsymmetrical triplet. Irradiation at $\delta = 2.4$ caused the triplet due to a single vinyl proton (*e*) to collapse to a singlet. These results are consistent with the following skeleton.

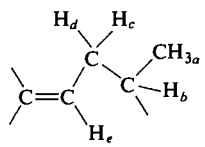

Further decoupling experiments showed that irradiation of the signal due to the vinyl proton *e* changed the character of the multiplet due to protons *c* and *d* so that it appeared as the AB part of an ABX. The multiplet at $\delta = 3.14$ (proton *b*) could be changed to a quartet by irradiation of either protons *a* or protons *c*

[1]The authors wish to thank F. A. L. Anet for providing a sample of 9-ethyl-9-carbomethoxyfluorene for comparison.

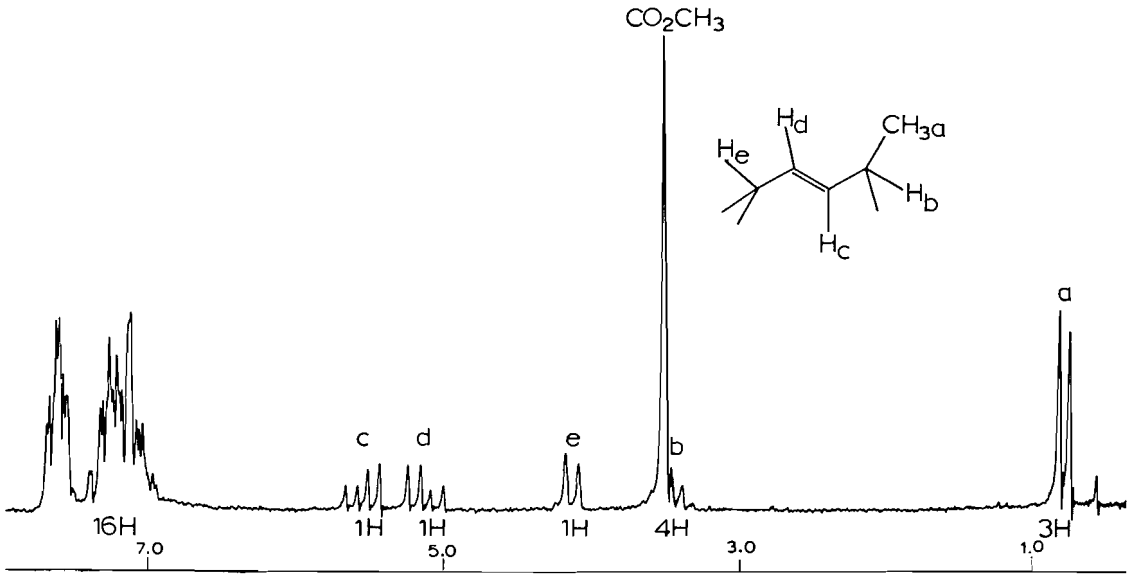

FIG. 1. The 100 MHz n.m.r. spectrum of ester **6**.

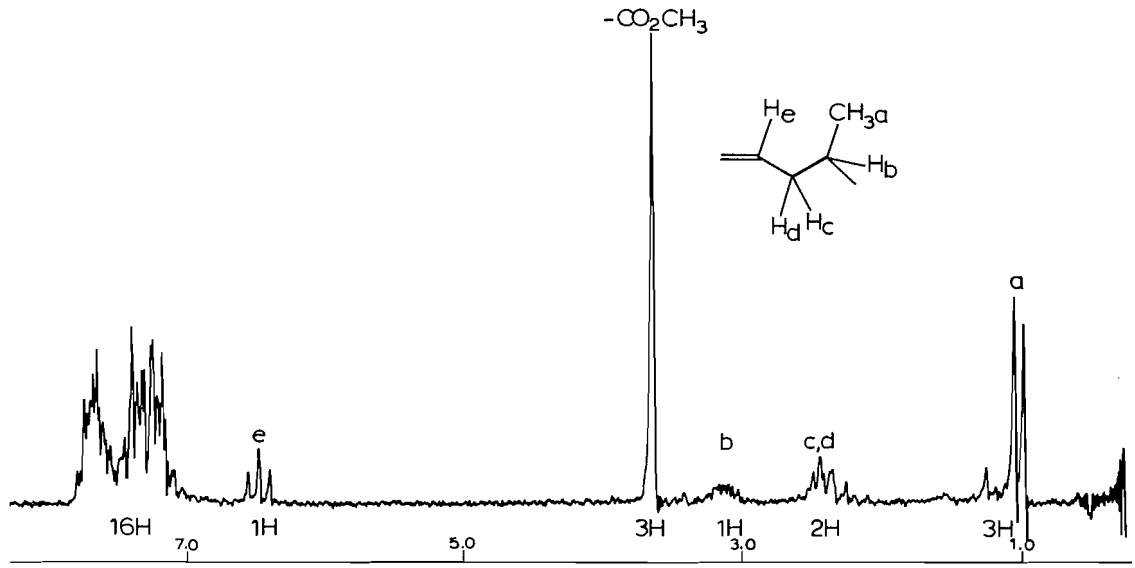

FIG. 2. The 100 MHz n.m.r. spectrum of ester **7**.

and *d*. This latter piece of evidence and the complex pattern due to protons *c* and *d* show that protons *c* and *d* are magnetically nonequivalent due to the asymmetric center. Inclusion of the fluorenyl rings and the carbomethoxy group leads to structure **7**. The signals formed by protons *b*, *c*, and *d* on successive irradiation of protons *a* and *e* were analyzed as an ABC pattern. The following parameters were obtained for the entire system: $\delta_a = 1.02$, $\delta_b = 3.16$, $\delta_c = 2.32$, $\delta_d = 2.50$, $\delta_e = 6.49$ and $J_{ab} = 6.9$, $J_{bc} = 10.3$, $J_{bd} = 4.1$, $J_{cd} = -14.8$, and J_{ce}, $J_{de} = 7.9$.

It can be seen that **6** and **7** are just double bond isomers. An attempt was made to determine which is the thermodynamically more stable

Can. J. Chem. Downloaded from www.nrcresearchpress.com by 210.87.254.6 on 09/05/12
For personal use only.

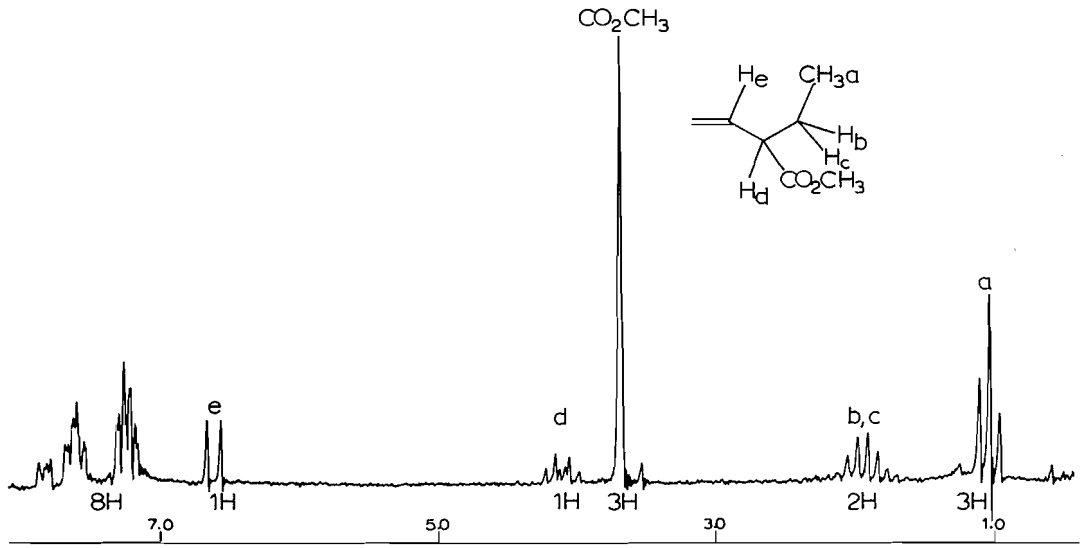

FIG. 3. The 100 MHz n.m.r. spectrum of ester **8**.

isomer and to provide further evidence on the interrelationship of the structures. Treatment of **6** in methanol with 0.4 *M* potassium methoxide at 60° led to nearly complete conversion of **6** to **7**. Further reaction led to the complete disappearance of **7** and the formation of new and unidentified products. This result requires that the isomer with the conjugated double bond (**7**) is the more stable of the two.

Unlike esters **6** and **7**, the mass spectrum (parent peak at $m/e = 278$) and the integrated n.m.r. spectrum (Fig. 3) of ester **8** are consistent with the presence of just one fluorenyl nucleus and one carbomethoxy group. The structure of the attached carbon chain for this compound also was elucidated with decoupling experiments.

Irradiation in the region of the signals due to the two protons labelled *b*, *c* resulted in the collapse of the perturbed methyl triplet (proton *a*) at high field to a singlet and the collapse of the one proton doublet of triplets (proton *d*) at $\delta = 4.13$ into a doublet. This same multiplet (*d*) at $\delta = 4.13$ changes to a triplet when irradiation is applied to the signal at $\delta = 6.62$ (proton *e*). Conversely irradiation of the signal at 4.13 p.p.m. collapses the doublet at 6.62 (proton *e*) to a singlet and the character of the two proton multiplet (proton *b*, *c*) at 1.96 p.p.m. alters but to more than four lines. The following carbon skeleton is suggested.

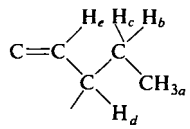

From the complexity of both the decoupled and undecoupled signal due to protons *b*, *c* it is apparent that the methylene protons are magnetically nonequivalent. On the basis of a first order analysis, the spectral parameters have been partially assigned: $\delta_a = 1.24$, $\delta_{b,c} \approx 1.96$, $\delta_d = 4.13$, $\delta_e = 6.62$, and $J_{ab} = 7.4$, $J_{bd} = 7.0$, and $J_{ed} = 9.8$ Hz. The structure of ester **8** is completed by attaching the fluorenyl ring and the carbomethoxy grouping.

The separation of these four esters (**5**, **6**, **7**, and **8**) was sufficiently involved that only low yields of purified materials were obtained. The yields of the various esters, indicated under their formulas, were estimated from the n.m.r. spectrum of the original ester mixture and account for about two-thirds of the original material.

Discussion

The unique feature of the reaction of **2a** is the apparent absence of the monomeric anion **1**, as judged by n.m.r. of the anions and of the CO_2 quenched material. Instead, significant amounts of dimeric products were produced. As was mentioned in the Introduction section, reductive cleavage of unsaturated ethers by alkali metals usually succeeds and has been applied fairly widely (1). Reagents commonly

Can. J. Chem. Downloaded from www.nrcresearchpress.com by 210.87.254.6 on 09/05/12
For personal use only.

Can. J. Chem. Downloaded from www.nrcresearchpress.com by 210.87.254.6 on 09/05/12
For personal use only.

used are potassium, sodium, sodium–potassium alloy, lithium or magnesium in ether, tetrahydrofuran, or hexamethylphosphoramide (2). Thus allylmagnesium phenoxide (3), allyllithium (4), allylsodium (5), and allylpotassium (6) have all been prepared in reasonable yield from allylphenylether or diallylether.

Unlike ethers **2b–d**, **3**, and **4**, ether **2a** produces an anion which reacts further to eventually dimerize. Aside from ester **5**, the other isolated products, **6**, **7**, and **8**, seem to have arisen from an end to middle coupling of the original carbon skeleton. This structural feature can be accommodated if 9-ethylidenefluorene **9** is generated as an intermediate in the reaction (see Scheme 1).

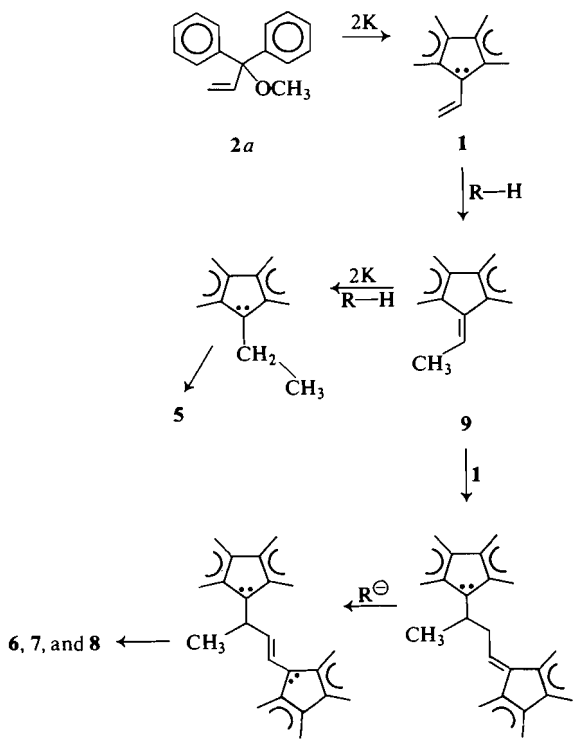

This olefin **9** could arise by protonation of **1** (10) as the monoanion or in a more highly charged form (11–13). Reduction of **9** to the 9-ethylfluorenylanion with eventual production[2] of ester **5** and addition of **1** across the double bond (14) of **9** could follow. The polymerization reaction could terminate at the dimeric stage with formation of the dianion. Ester **8** apparently arises following carbon–carbon bond cleavage (1) of one of the dimeric species. Esters **6** and **7** arise upon carbonation and methylation of the dimeric anions. While a variety of ions and radicals can be involved as intermediates, the present results do not bear on this feature and only a simplified mechanism is included.

Polymerization has been reported for cinnamylethers and 2-phenylallylphenylether during reductive cleavage by alkali metals (2, 3). Unlike **2a**, these ethers could be viewed as substituted styrenes and thus are prone to polymerize in the presence of carbanions (15). Ether **2a** first required a double bond shift and then reaction in a manner similar to the styrenes.

Experimental

Infrared spectra were obtained of carbon tetrachloride solutions with a Beckman IR-10. The n.m.r. spectra (CCl_4 or $CDCl_3$) were run on a Varian HA-100 spectrometer using internal TMS. Mass spectra were obtained using a Varian M-66 mass spectrometer. Melting points and boiling points are uncorrected. Microanalyses were run by A. B. Gygli, Toronto.

The tetrahydrofuran used as solvent was freshly distilled from lithium hydride onto sodium–potassium alloy. The tetrahydrofuran-d_8 (Stohler Isotope Chemicals) was dried with sodium–potassium alloy before use.

9-Methoxy-9-vinylfluorene

Reaction of 90 g (0.5 mol) of 9-fluorenone with a 300 ml tetrahydrofuran solution of vinylmagnesium bromide prepared from 14.6 g (0.6 g-atoms) of magnesium turnings and 70 g (0.65 mol) of vinylbromide yielded 9-vinyl-9-fluorenol. Recrystallization from ether-ligroin gave 121 g (0.45 mol, 90%) of material (m.p. 89–90°, lit. (16) m.p. 91°).

The methyl ether was prepared (17) by stirring a mixture of 50 g (0.25 mol) of 9-vinyl-9-fluorenol, 60 ml (0.96 mol) of methyl iodide, 129 g of barium oxide and 0.8 g of water in 20 ml of dimethylformamide for 40 h at 20 °C. Water–methylene chloride extraction was followed by elution chromatography on alumina using 5% ether in pentane. Recrystallization from 2:1 methanol–water yielded 49 g (88%) of colorless crystals, m.p. 50–51°.

The infrared (i.r.) showed band at 1186 cm^{-1} attributable to the ether C—O stretch. The n.m.r. spectrum in CCl_4 appeared consistent with the expected structure. The aromatic protons appeared as a multiplet δ 7.04 to 7.52 (8H), the methoxy protons appeared as a singlet δ 2.75 (3H) and the vinyl protons (3H) appeared as a multiplet which was analyzed as an ABC pattern with $\delta_A = 5.83$, $\delta_B = 5.42$, $\delta_C = 5.04$, and $J_{AB} = 17.2$ Hz, $J_{BC} = 1.7$ Hz, and $J_{AC} = 10.6$ Hz.

Anal. Calcd. for $C_{16}H_{14}O$: C, 86.45; H, 6.34. Found: C, 86.34; H, 6.41.

Reaction of 9-Methoxy-9-vinylfluorene

Sodium–potassium alloy (5.7 wt% sodium; 6 ml, 108 mmol) was added to a solution of 9-methoxy-9-

[2]Treatment of a sample of **9** with sodium–potassium alloy under the reaction conditions followed by carbonation and methylation produced **5** in about 15% yield.

Can. J. Chem. Downloaded from www.nrcresearchpress.com by 210.87.254.6 on 09/05/12
For personal use only.

vinylfluorene (12 g, 54 mmol) in 450 ml of tetrahydrofuran. The tetrahydrofuran solution was degassed and the atmosphere exchanged for argon before addition of the alloy. The solution was stirred at room temperature for 48 h and acquired a deep red color.

The anions were carbonated by slow addition of the deep red solution to 100 ml of tetrahydrofuran saturated with dried carbon dioxide. The reaction mixture was stirred at room temperature and carbon dioxide was constantly bubbled into the solvent. The resulting pale green solution was stirred for another hour and the majority of the tetrahydrofuran removed with a rotary evaporator.

The reaction products were extracted with dilute sodium hydroxide – ether. The aqueous layer was acidified and extracted with ether to yield 10.2 g (85 wt%) of acids, and neutrals amounting to 1.2 g were obtained.

Thin layer chromatography of the neutral fraction indicated the absence of 9-methoxy-9-vinylfluorene while t.l.c. of the acid fraction using 3% acetic acid in chloroform on silica gel suggested at least 9 components.

The mixture of acids was methylated using both diazomethane and boron trifluoride etherate-methanol. The ester mixture prepared by either route appeared to be of the same composition as judged by t.l.c. on silica gel using 30% ether-pentane and contained about nine components. The conversion of acids to esters appeared to be complete on the basis of weight (103 wt.% yield) and n.m.r.

Separation of the Esters

A gross separation of the ester mixtures from the diazomethane reactions was obtained with elution column chromatography. The esters were chromatographed on silica gel eluting with 30% ether in pentane. Two major components, labelled esters **6** and 7, were collected in a purified state. Further purification with thick layer chromatography, eluting three times with 10% ether–pentane yielded nearly pure samples of both esters. Each ester was then recrystallized from methanol to yield sharp melting colorless crystals.

Ester **6**: m.p. 118–119°. The i.r. peak due to the ester carbonyl appeared at 1730 cm^{-1}.

Anal. Calcd. for $C_{32}H_{26}O_2$: C, 86.86; H, 5.93. Found: C, 86.76; H. 5.92.

Ester 7: m.p. 162–163°. The i.r. carbonyl peak appeared at 1730 cm^{-1}.

Anal. Calcd. for $C_{32}H_{26}O_2$: C, 86.86; H, 5.93. Found: C, 86.61; H, 5.90.

The less pure fractions containing ester **6** from the column chromatography showed three carbomethoxy signals in the n.m.r. spectrum. The remaining ester **6** was removed from this material by thick layer chromatography eluting three times with 10% ether–pentane. The remaining band was extracted and n.m.r. indicated a mixture of two esters. These were separated and collected using g.l.p.c. ($\frac{1}{4}$ in. × 6 ft column of 10% SE-30 on 45-60 Chromosorb W) with a column temperature of 220 °C.

The two components were labelled esters **5** and **8**. Ester **8** was a liquid which was distilled using a molecular still (b.p. 60–63° @ 0.05 mm of Hg). The i.r. showed an ester carbonyl at 1727 cm^{-1}.

Anal. Calcd. for $C_{19}H_{18}O_2$: C, 81.98; H, 6.52. Found: C, 80.42; H, 6.73.

Ester **5** was a solid which was sublimed under vacuum to yield material of m.p. 77–78°. Admixture with an authentic sample **1** of the methyl ester of fluorene-9-ethyl-9-carboxylic acid gave m.p. 77–78°.

A comparison of the n.m.r. spectra of the separated esters **5** and **8** with the mixture before g.l.p.c. indicated that no chemical changes had occurred during the separation.

The authors wish to thank the National Research Council of Canada for financial support of this research.

1. M. SCHLOSSER. Angew. Chem. Int. Ed. **3**, 362 (1964).
2. H. NORMANT and T. CUVIGNY. Bull. Soc. Chim. France, 3344 (1966).
3. A. MAERCKER. J. Organometal. Chem. **18**, 249 (1969).
4. J. J. EISCH and A. M. JACOBS. J. Org. Chem. **28**, 2145 (1963).
5. R. L. LETSINGER and J. G. TRAYNHAM. J. Amer. Chem. Soc. **70**, 3342 (1948).
6. A. A. MORTON, E. E. MAGAT, and R. L. LETSINGER. J. Amer. Chem. Soc. **69**, 950 (1947).
7. A. KLIEGEL. Ber. Dtsch. Chem. Ges. **62**, 1327 (1929).
8. W. SCHLENK and E. BERGMANN. Liebigs Ann. Chem. **463**, 188 (1928).
9. K. ZIEGLER and F. THIELMANN. Ber. Dtsch. Chem. Ges. **56**, 1740 (1923).
10. A. MAERCKER. Liebigs Ann. Chem. **730**, 91 (1969).
11. E. G. JANZEN and J. L. GERLOCK. J. Organometal. Chem. **8**, 354 (1967).
12. E. G. JANZEN and J. G. PACIFICI. J. Amer. Chem. Soc. **87**, 5504 (1965).
13. G. LEVIN, J. JAGUR-GRODZINSKI, and M. SZWARC. J. Amer. Chem. Soc. **92**, 2268 (1970).
14. (*a*) L. L. CHAN and J. SMID. J. Amer. Chem. Soc. **90**, 4654 (1968). (*b*) K. ZIEGLER. Liebigs Ann. Chem. **473**, 7 (1929).
15. M. SZWARC. Carbanions, Living Polymers, and Electron-Transfer Processes. Interscience Publ. 1968. Chap. III for example.
16. R. KUHN, H. FISCHER, F. A. NEUGEBAUER, and H. FISCHER. Ann. **654**, 64 (1962).
17. R. KUHN and H. TAISCHMANN. Chem. Ber. **94**, 2258 (1961).

Can. J. Chem. Downloaded from www.nrcresearchpress.com by 210.87.254.5 on 09/05/12
For personal use only.

The Effect of Trace Impurities on Condensed Electrode and Microwave Discharges through Nitrogen

R. R. BAKER, A. JACOB,[1] AND C. A. WINKLER
Department of Chemistry, McGill University, Montreal, Quebec

Received November 26, 1970

Traces of various gases have been added to a stream of purified nitrogen gas prior to entering either a microwave or a condensed electrode discharge, and the effect of the presence of these gases on the steady flow rate of nitrogen atoms obtained from the discharge has been measured. Suggestions for the effect of the impurity gases on the possible reactions occurring in the discharge have been put forward. It seems probable that an important feature of the presence of the impurities may be their effect on the electron temperature in the discharge.

A un jet d'azote purifié qui est ensuite soumis à une décharge soit de micro-ondes ou soit d'électrode condensé, on ajoute des traces de divers gaz et l'on mesure leur effet sur le débit constant des atomes d'azote qui sont obtenus. On propose des suggestions concernant les effets possibles de ces impuretés sur les réactions se produisant au cours de la décharge électrique. Il semble probable qu'une caractéristique importante de la présence de ces impuretés soit leur effet sur la température des électrons dans la décharge.

Canadian Journal of Chemistry, 49, 1671 (1971)

Introduction

It has been known for many years that very small amounts of certain impurities increase the extent of dissociation of diatomic molecules (H_2, O_2, N_2) in electrical discharges. Although one report indicated that the yellow afterglow in pure nitrogen which has been activated by an electrical discharge was not produced in the presence of a trace of hydrogen (1), there seems little doubt that the afterglow is more intense when traces of gaseous "dissociation catalysts" such as H_2, O_2, or H_2O have been added to the nitrogen before or after the discharge tube (2–4). As a result of previous investigations on the subject, it has been suggested (ref. 5, pp. 25–27, ref. 6) that the effect of the impurities is to increase the afterglow mainly by inhibiting the wall destruction of a precursor to the afterglow, probably by their adsorption onto the wall of the discharge tube and reaction vessel, with reduction in the heterogeneous recombination of N atoms (7).

The present report records some related observations on the effect of catalysts on the behavior of continuous and discontinuous discharges through nitrogen. The corresponding results were reproducibly observed over a period of months on more than one apparatus, and it is believed that such studies should help to define operating conditions most conducive to meaningful data.

[1]Present address: Trapelo Division of L.F.E. Corporation, 1601, Trapelo Road, Waltham, Mass., 02154.

Experimental

The systems were of the fast flow type, similar to those described in earlier studies (*e.g.* refs. 8, 9). Linde "Bone Dry" nitrogen was purified by passing it over copper turnings at 500 °C and copper oxide at 750 °C to remove oxygen, and hydrogen and hydrocarbon impurities respectively, and finally through two traps surrounded by liquid nitrogen, to remove condensible impurities. The purified nitrogen stream either entered the discharge tube directly, or was premixed with measured traces of catalyst gases before entering the discharge tube. The condensed electrode discharge occurred between aluminum electrodes in a tube of new design, shown in Fig. 1. When glass wool was introduced into the "U" bends, and these were immersed in cooling water, no aluminum dust accumulated in any part of the reactor or product traps, even after prolonged operation of the discharge unit. The pulse rate in the systems used could be varied from a distinctly discontinuous discharge to a virtually continuous one by changing the time constant of the electric circuit for a constant input voltage at a given pressure. The microwave discharges occurred in vycor tubing using a Raytheon diathermy unit of 125 W power output at 2450 Mcs^{-1} continuous wave radiation.

The reaction vessels used were straight Pyrex tubes, about 70 cm long and having internal diameters in the range 2.0 to 2.6 cm. The average nitrogen atom flow rates at points 12 to 16 cm downstream from the discharge tube were determined with the NO gas-phase titration (10).

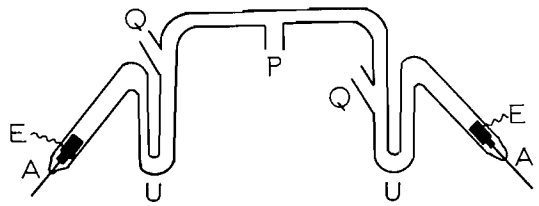

FIG. 1. Diagram of modified discharge tube. A, tungsten-to-glass seal; E, aluminum electrode; P, inlet to reaction vessel; Q, feed lines; U, bends packed with glass wool and cooled in water.

Results

With a flow of pure nitrogen and a distinctly discontinuous condensed discharge, at total pressures of 2.0 to 3.5 Torr, the NO titration (*i.e.* the N atom flow rate) continued to decrease for as long as 2.5 h before it became constant at about one half its initial value. On the other hand, with a microwave discharge and a flow of pure nitrogen, a constant value for the N atom flow rate was reached in only about 10 min.

In the presence of trace amounts of catalysts, constant levels of atomic nitrogen were usually attained much more quickly than in the absence of a catalyst. For instance, with H_2O vapor as catalyst at flow rates of 0.1×10^{-6} and 5×10^{-6} mol s^{-1} in a discontinuous condensed discharge, the N atom flow rate reached a steady value within 30 min of operation at about 10 and 18 times, respectively, the level without catalyst present. However, when the H_2O flow rate was changed from the higher to the lower value without interrupting the discharge, the decrease in N atom flow rate from one level to the other required up to 3 h of operation.

Similar results were obtained using other catalysts. When the pulse rate was increased until the condensed discharge operated almost continuously ("pseudo-continuous"), steady N atom flows were usually obtained in 5–15 min. When the catalyst flow was stopped in either the discontinuous or pseudo-continuous discharges, it required several hours for the N atom flow to decrease to the steady value in the absence of catalyst. However, when I_2 was used as catalyst, it required only 15 min for the N atom flow to decrease to the steady uncatalyzed value, after the I_2 flow was stopped (11). With a microwave discharge, on the other hand, a steady N atom flow was reached after only 10 to 15 min operation of the discharge in the presence of the various catalysts. When the flow of the catalyst was stopped, the steady condition corresponding to its absence was restored in about the same short time of operation, except with catalysts containing F atoms, when about 1 h of operation was required. This could be due to the strong adsorption onto the walls of the discharge tube and reaction vessel of species derived from the F-containing compounds, probably F atoms.

Some typical plots of N atom flow against the flow of the added catalyst are shown in Figs. 2 and 3 for the microwave and continuous condensed electrode discharge units, respectively. In all cases, the points on the plots are the steady values of the N atom flow rate for the corresponding flow of the catalyst. The temperature and total pressure in the reaction vessel, and the flow of molecular nitrogen through the reaction vessel, were kept constant at the values given in Table 1 for all the catalysts used. These data show an initial linear dependence of N atom flow rate on the flow rate of the catalyst, and in all cases, either a plateau value of N atom flow is reached with a sufficiently high catalyst flow rate, or the gradient falls towards a plateau value (zero gradient) at high catalyst flow rates. The plateau values appear to be reached either sharply, as with H_2S and CH_3Cl, for example (Fig. 2), or gradually, as with C_2H_2 (Fig. 2). The effects of the various catalysts are summarized in Table 1. In the table, $(\Delta[N]/\Delta[M])_i$ is the initial gradient of the plot of N atom flow rate against catalyst flow rate, for a given catalyst M, $N_{plateau}$ is the value of the N atom flow rate at the plateau in the curve, and $M_{plateau}$ is the minimum flow rate of the catalyst that gives the plateau value of the N atom flow. The latter quantity is obtained for a given catalyst from a plot of the gradient of the catalyst curve (Figs. 2 and 3), $\Delta[N]/\Delta[M]$, against the flow rate of the catalyst. $M_{plateau}$ is then the value of the intercept where the plot cuts the catalyst flow rate axis. The approximation signs ($\sim$) in Table 1 indicate that $N_{plateau}$ or $M_{plateau}$ for that particular catalyst has been obtained by extrapolation. Table 1 shows that, with the exceptions of Ar, He, and SF_6, the value of $(\Delta[N]/\Delta[M])_i$ for a given catalyst is much smaller in the microwave discharge than in the condensed discharge, the value in the microwave discharge being about 30% that in the condensed discharge, on average. To a first approximation, the value of $(\Delta[N]/$

Can. J. Chem. Downloaded from www.nrcresearchpress.com by 210.87.254.5 on 09/05/12
For personal use only.

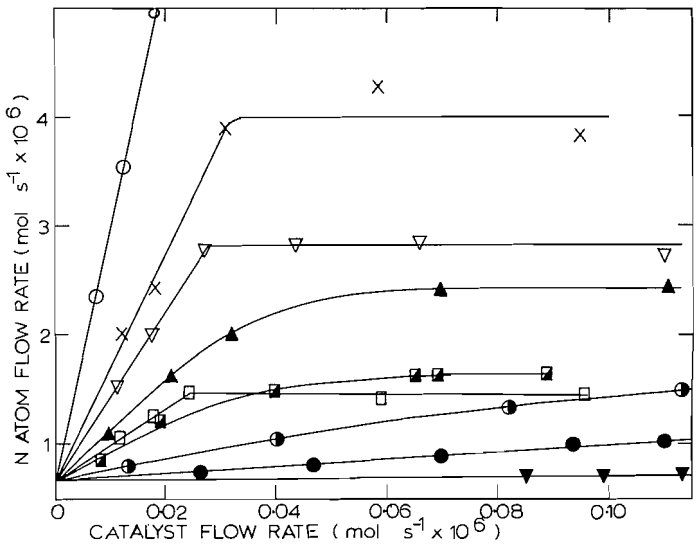

FIG. 2. Effect of different catalysts in the microwave discharge. ○ = CF_4, × = CH_3F, ▽ = H_2S, ▲ = C_2H_2, □ = CH_3Cl, ◪ = HBr, ◑ = NH_3, ● = N_2O, ▼ = He.

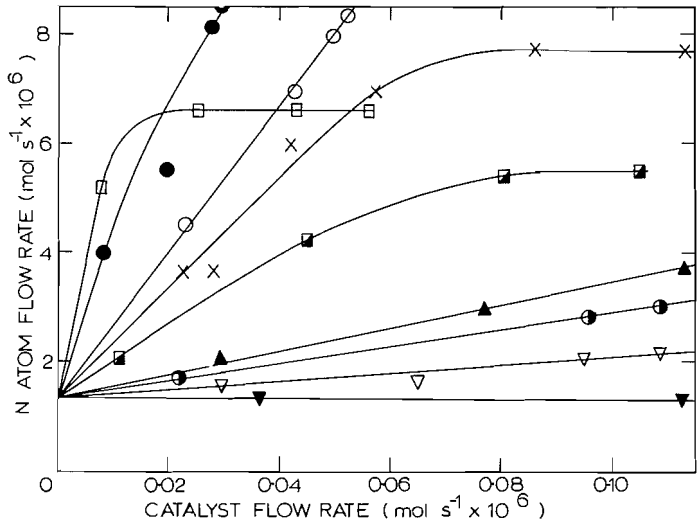

FIG. 3. Effect of different catalysts in the condensed electrode discharge. □ = CF_4, ● = CH_3Cl, ○ = SF_6, × = CH_4, ◪ = HCl, ▲ = CO_2, ◑ = H_2, ▽ = O_2, ▼ = Ar.

$\Delta[M])_i$ in either discharge depends on the electronegativity of the molecule, and the number of degrees of freedom in the molecule. Thus large, electronegative molecules such as SF_6, CF_4, and CCl_3F give large values of $(\Delta[N]/\Delta[M])_i$, while smaller and more electroneutral molecules such as O_2, CO, and NO have small values. For molecules with the same number of degrees of freedom, such as CH_4, CH_3Cl, CCl_4, CH_3F, CCl_3F, and CF_4, the value of $(\Delta[N]/\Delta[M])_i$ increases with the overall electronegativity of the molecule. The inert gases Ar and He are virtually without any catalytic effect.

The effect of using O_2, NO, and SF_6 as catalysts has also been investigated by Young, Sharpless, and Springham (12), who used a microwave discharge and measured the concentration of N atoms produced in an electron spin resonance

Can. J. Chem. Downloaded from www.nrcresearchpress.com by 210.87.254.5 on 09/05/12
For personal use only.

TABLE 1. The effect of catalysts on the concentration of N atoms produced*

Catalyst	Microwave discharge†			Condensed electrode discharge‡		
	$(\Delta[N]/\Delta[M])_i$	$N_{plateau}$	$M_{plateau}$	$(\Delta[N]/\Delta[M])_i$	$N_{plateau}$	$M_{plateau}$
Ar	0.20	—	>5.0	0.06	—	—
He	0.29	—	~5.5	0.20	—	—
H_2	9.8	2.2	0.90	15	6.9	1.6
NH_3	12	2.0	0.30	41	8.0	0.22
H_2O	71	—	—	210	—	—
H_2S	77	2.8	0.028	190	8.4	0.044
HCl	8.6	1.5	0.22	75	5.5	0.090
HBr	33	1.6	0.075	200	4.8	0.096
O_2	3.4	1.5	0.60	8.3	3.9	0.65
CO	4.7	~1.4	~0.26	15	9.2	0.41
CO_2	6.0	~1.3	~0.20	20	5.5	0.19
NO	5.5	1.3	0.16	7.5	3.0	0.26
NO_2	6.4	1.3	0.18	11	8.0	0.44
N_2O	4.3	1.2	0.31	8.8	2.8	0.19
CH_4	18	1.9	0.073	100	7.7	0.084
C_2H_2	48	2.4	0.068	130	8.9	0.10
C_2H_4	36	2.3	0.051	110	11.2	0.088
C_2H_6	39	2.1	0.036	120	8.3	0.080
CH_3Cl	37	1.5	0.024	340	13	0.090
CCl_4	63	2.3	0.040	270	~9.4	~0.15
CCl_3F	130	~3.9	~0.030	400	11	0.063
CH_3F	110	4.0	0.033	330	14	0.071
CF_4	240	5.3	0.022	520	6.6	0.022
SF_6	240	4.6	0.016	140	—	>0.10
I_2	21	~2.2	~0.20	120	~8	~0.20

*Unheated reaction vessel at a total pressure of 2.3 Torr; N_2 flow = 190×10^{-6} mol s^{-1}.
†Steady N flow in absence of catalyst = 0.66×10^{-6} mol s^{-1}.
‡Steady N flow in absence of catalyst = 1.3×10^{-6} mol s^{-1}. $N_{plateau}$ and $M_{plateau}$ have the units of 10^{-6} mol s^{-1}.

TABLE 2. Results of the present investigation using a microwave discharge compared to those of Young *et al.* (12)*

Catalyst	$(\Delta[N]/\Delta[M])_i$	
	This work	Young *et al.* (12)
O_2	3.4	17
NO	5.5	6.2
SF_6	240	230

*Young *et al.* (12) used a N_2 flow of 872×10^{-6} mol s^{-1}, and the N flow in the absence of catalyst was about 0.1×10^{-6} mol s^{-1}.

(e.s.r.) cavity well removed from the discharge. Their results are compared to those of the present investigation with a microwave discharge in Table 2. The results with NO and SF_6 are very similar, indicating that the effect of these catalysts is very reproducible, but the results with O_2 differ for some yet inexplicable reason.

It was also observed in the present study that the short-lived, energetic pink afterglow observed downstream from the microwave discharge was increased from a distance corresponding to a flow time of 5 ms in the absence of a catalyst to distances corresponding to about 30, 40, and 70 ms in the presence of H_2S, SF_6, and CF_4, respectively. With the other catalysts, the pink afterglow was reduced, usually to zero seconds.

Discussion

When the flow of catalyst is stopped in the microwave discharge, the steady N atom flow rate reverts back to the uncatalyzed condition in a few minutes (1 h for compounds containing F atoms), whereas several hours are usually required to produce the same effect in a condensed discharge. This suggests that the effect of the catalyst is unlikely to be due solely to heterogeneous reactions (*cf.* ref. 7). It appears that traces of catalyst are involved in some way in the dissociation process to increase the yield of N atoms. This is indicated also by the observation that a condensed discharge could be initiated and sustained at a lower voltage in the presence of traces of catalyst than in a system containing pure N_2.

The main problem in interpreting the effect of catalysts on the steady concentration of N atoms is that the fundamental processes occurring in the discharge are not known. Young and

Can. J. Chem. Downloaded from www.nrcresearchpress.com by 210.87.254.5 on 09/05/12
For personal use only.

Can. J. Chem. Downloaded from www.nrcresearchpress.com by 210.87.254.5 on 09/05/12
For personal use only.

St. John have shown that under appropriate conditions electrical discharges both produce and destroy N atoms (13). Their results (14) indicate that, in the discharge, the dissociation of pure N_2 results from stepwise excitation involving intermediate excited states susceptible to deactivation. The suggested mechanism below gives various possible reactions that may contribute to the final concentration of N atoms.

[1] $e_{fast} + N_2 \rightarrow N_2^* + e_{slow}$

[2] $e_{slow} + N_2^* \rightarrow N_2 + e_{fast}$

[3] $N_2^* \rightarrow$ (N atoms)

[4] $N + N_2^* \rightarrow N_2 + N$

[5] $e + N_2^* \rightarrow N_2^+ + 2e$

[6] $e + N_2 \rightarrow N_2^+ + 2e$

[7] $N_2 + N_2 + N_2^+ \rightleftarrows N_4^+ + N_2$

[8] $N + N_4^+ \rightarrow N_3^+ + N_2$

[9] $N + N_3^+ \rightarrow N_2^+ + N_2$

Reaction 3 represents some unspecified reaction of N_2^* that gives N atoms, possibly reaction with an electron, $e + N_2^* \rightarrow 2N + e$. The radiative lifetime of N_2^* must be sufficient, of course, so that reaction 3 is reasonably probable before radiation to a lower level occurs, and metastable species such as $N_2(A^3\Sigma_u^+)$ might be particularly effective. In reaction 1, e_{fast} represents an electron with sufficient energy to produce metastable N_2^* molecules from molecules in the $X^1\Sigma_g^+$ state. The deactivation of N_2^* by N atoms in reaction 4 has been postulated previously (15, 16), in this case with N_2^* identified as $N_2(A^3\Sigma_u^+)$.

Since N_2^* is probably a metastable species, the cross section for reaction 1 will be a maximum for some specific electron energy, and the production of N_2^* will be most efficient over a relatively narrow range of electron energy (ref. 17, pp. 196–228). By the principle of detailed balancing (ref. 17, pp. 57–58, ref. 18) the deactivation of N_2^* by electron attachment (reaction 2) peaks near 0 eV (18). Thus reactions 1 and 2, which both govern the concentration of N_2^* and hence N atoms, will be very sensitive to the electron temperature in the discharge.

The presence of small amounts of impurities is known to affect the electron temperature in electrical discharges (19, 20), with polyatomic molecules causing large decreases in the electron temperature, and the inert gases having a small effect. The degree of effect on the electron temperature is very approximately similar to the degree of effect which impurities have on the steady state concentration of N atoms (Table 1). While this correlation should not be unduly emphasized, perhaps, it does suggest the possibility that added impurities in the present systems might exert their effects primarily through an influence on the electron energy in the discharge. Four possible effects that traces of impurities can have on reactions 1–9 are given below.

(*1*) Polyatomic molecules, with many degrees of freedom, can undergo a wide variety of low energy (< 1 eV), inelastic collisions with very energetic electrons. These collisions may lead to electrons with energy in the range where reaction 1, and hence the production of N atoms by reaction 3, is most efficient.

(*2*) Low energy electrons may be removed from the system by forming negative ions with electronegative catalysts, thus lowering the possibility of reaction 2. This should promote an increase in the steady concentration of N_2^* in the system, and hence in the production of N atoms by reaction 3. SF_6, in particular, can readily form SF_6^- by a highly resonant process in which an electron of energy 0 ± 0.05 eV can be attached without radiation, the process having the very high attachment cross section of at least 10^{-15} cm^2 (ref. 17, pp. 285–286; ref. 20, pp. 417–419). Dissociative attachment to form SF_5^- is also possible (21) with the process peaking around 0.1 eV.

(*3*) N atom consumption by reactions 8 and 9 will be minimized if the nitrogen ionic species are removed by the following types of charge transfer reactions with the impurity, M (13),

[10] $N_2^+ + M \rightarrow N_2 + M^+$ (or $m_1 + m_2^+$)

[11] $N_4^+ + M \rightarrow 2N_2 + M^+$ (or $m_1 + m_2^+$)

where m_1 and m_2 are decomposition products of M. These types of reactions explain the supression of the first negative bands of N_2^+ ($B^2\Sigma_u^+ \rightarrow X^2\Sigma_g^+$) in the pink afterglow in the presence of traces of H_2, O_2, and C-containing compounds (ref. 5, pp. 48–50, ref. 22). However, they cannot explain the catalytic effects of H_2, CF_4, and SF_6 since the ionization and appearance potentials for these gases are larger than for N_2 (23). Furthermore, they cannot be important catalytic reactions for the other gases, since there is no apparent correlation between the observed value

of $(\Delta[N]/\Delta[M])_i$ for a catalyst, and its ionization or appearance potential.

(*4*) A reduction in the breakdown potential in the presence of a catalyst might be due to a sequence of reactions, such as

[12] $$N_2^* + M \rightarrow m_1 + m_2 + N_2$$

[13] $$e + m_1 \text{ (or } m_2) \rightarrow m_1^+ \text{ (or } m_2^+) + 2e$$

where m_1 and m_2 possess ionization potentials lower than that of N_2. By such a process, the same extent of positive ion formation (m_1^+ or m_2^+) might be maintained by electrons that have enough energy to create metastable N_2 (by reaction 1) but not N_2^+. In this way, one molecule of M introduces more than one extra electron into the system, which, if they have the correct energy, could then produce more than one N_2^* by reaction 1.

The much smaller effect which catalysts usually have on the N atom yield in a microwave discharge than in a condensed electrode discharge (Table 1) might then simply reflect a lower concentration of excited molecular nitrogen species in the microwave discharge. This would be in accord with the observations that active nitrogen from a condensed discharge is capable of promoting chemical changes that do not seem to occur significantly with active nitrogen from a microwave system, *e.g.* the decomposition of NH_3 and SO_2 (ref. 5, pp. 505–511, refs. 6, 24). Presumably, the condensed discharge produces a higher concentration of excited molecular species capable of initiating such reactions.

Thus, the possible ways in which a particular catalyst may influence the steady concentration of N atoms are varied and complex, and probably more complex than is indicated above. However, they provide a ready interpretation, for example, of the observation that He and Ar have virtually no catalytic effect on the production of N atoms. Since these gases have no vibrational and rotational degrees of freedom, the first possible effect enumerated above cannot operate; formation of negative ions as required by *2* is unlikely; their high ionization potentials make *3* energetically improbable; and *4* cannot occur for monatomic species. On the other hand, electronegative polyatomic molecules, such as SF_6, have large catalytic effects since the first two possibilities above are readily available. However, it is not possible as yet to resolve the varied and complex ways in which a given impurity may exert its catalytic effect from its possible inhibition of N-atom recombination (homogeneously or heterogeneously), and the final yield of N atoms may be strongly affected by both.

The authors would like to thank Dr. J. S. Bulger for helpful discussion.

1. J. KAPLAN. Nature, **136**, 549 (1935).
2. R. J. STRUTT. Proc. Roy. Soc. Ser. A. **85**, 219 (1911).
3. B. LEWIS. J. Am. Chem. Soc. **51**, 654 (1924).
4. E. J. B. WILLEY. J. Chem. Soc. 336 (1930).
5. A. N. WRIGHT and C. A. WINKLER. Active nitrogen. Academic Press, New York. 1968.
6. B. BROCKLEHURST and K. R. JENNINGS. Progress in reaction kinetics. Vol. 4. *Edited by* G. Porter. Pergamon, London. 1967.
7. R. W. WOOD. Phil. Mag. **44**, 538 (1922).
8. P. A. GARTAGANIS and C. A. WINKLER. Can. J. Chem. **34**, 1457 (1956).
9. E. M. LEVY and C. A. WINKLER. Can. J. Chem. **40**, 686 (1962).
10. F. KAUFMAN and J. R. KELSO. J. Chem. Phys. **27**, 1209 (1957).
11. G. R. BROWN. Ph.D. Thesis. McGill University, Montreal, Quebec. 1970.
12. R. A. YOUNG, R. L. SHARPLESS, and R. SPRINGHAM. J. Chem. Phys. **40**, 117 (1964).
13. R. A. YOUNG and G. A. ST. JOHN. J. Phys. Chem. **69**, 1763 (1965).
14. R. A. YOUNG and G. A. ST. JOHN. J. Chem. Phys. **48**, 3505 (1968).
15. R. A. YOUNG and G. A. ST. JOHN. J. Chem. Phys. **48**, 895 (1968).
16. R. A. YOUNG and G. A. ST. JOHN. Adv. Chem. (Editor) R. F. Gould. Am. Chem. Soc. Washington, **80**, 105 (1969).
17. J. B. HASTED. Physics of atomic collisions. Butterworths, London. 1964.
18. A. VON ENGEL. Br. J. Appl. Phys. **18**, 1661 (1967).
19. J. D. COBINE. Gaseous conductors. Dover Publication, New York. 1958. pp. 181–184.
20. E. W. MCDANIEL. Collision phenomena in ionized gases. John Wiley and Sons, New York. 1964. pp. 553–548.
21. F. C. FEHSENFELD. J. Chem. Phys. **53**, 2000 (1970).
22. B. BROCKLEHURST and R. M. DUCKWORTH. J. Phys. B (Proc. Phys. Soc.) **1** (2), 990 (1968).
23. J. L. FRANKLIN, J. G. DILLARD, H. M. ROSENSTOCK, J. T. HERRON, K. DRAXL, and F. H. FIELD. National Bureau of Standards, NSRDS-NBS 26 (1969).
24. G. R. BROWN and C. A. WINKLER. Angew. Chem. **9**, 181 (1970).

Can. J. Chem. Downloaded from www.nrcresearchpress.com by 210.87.254.5 on 09/05/12
For personal use only.

Can. J. Chem. Downloaded from www.nrcresearchpress.com by 210.87.254.42 on 09/05/12
For personal use only.

Radiolysis of Hydrogen Sulfide at Very High Dose Rates. The Effect of SF_6[1]

C. WILLIS, A. W. BOYD, AND O. A. MILLER

Physical Chemistry Branch, Chalk River Nuclear Laboratories, Atomic Energy of Canada Limited, Chalk River, Ontario

Received November 26, 1970

Gaseous H_2S has been irradiated with electron pulses from a Febetron 705 at a dose rate of $\sim 2 \times 10^{27}$ eV g^{-1} s^{-1}. For single pulse experiments, the yield of hydrogen is $G(H_2) = 12.0 \pm 0.5$, independent of pressure from at least 350 to 1600 Torr. Addition of SF_6 reduces the yield to $G(H_2) = 7.9 \pm 0.3$ which is fairly close to that observed for pure H_2S at low dose rates. The reduction, $\Delta G(H_2) = 4.1 \pm 0.3$, agrees very well with the ion pair yield based on a W value of 25.3 eV.

In multi-pulse irradiations, for pure H_2S, the yield falls off with dose giving a limiting yield close to $G(H_2) = 8.0$. No similar fall-off is observed for H_2S–SF_6 mixtures. It is proposed that at high absorbed doses and at low dose rates, there is no contribution to the hydrogen yield from neutralization processes; and that this is due to neutralization of H_3S^+ by an ion of the type S_n^- rather than a free electron.

L'hydrogène sulfuré a été irradié en phase gazeuse par pulsations électroniques au moyen d'un Febetron 705 à une dose de 2×10^{27} eV g^{-1} s^{-1}. A pulsation unique, le rendement en hydrogène est $G(H_2) = 12.0 \pm 0.5$, et ne dépend pas de la pression entre 350 et 1600 Torr. L'addition de SF_6 réduit le rendement à $G(H_2) = 7.9 \pm 0.3$, ce qui est très proche du rendement observé pour H_2S pur, irradié à faibles intensités. Cette diminution de $\Delta G(H_2) = 4.1 \pm 0.3$ est en excellent accord avec le rendement en paires d'ions basé sur une valeur de $W = 25.3$ eV.

Pour des irradiations à pulsations multiples de H_2S pur le rendement décroît avec la dose jusqu'à une valeur limite proche de $G(H_2) = 8.0$. Pour des mélanges H_2S–SF_6, une telle décroissance n'est pas observée. Il est suggéré que des processus de neutralisation ne contribuent pas au rendement en hydrogène pour l'absorption de fortes doses, ou à faibles intensités à un taux de doses faibles; ceci pouvant être attribué à la neutralisation de H_3S^+ par un ion du type S_n^- plutôt que par un électron libre.

Canadian Journal of Chemistry, **49**, 1677 (1971)

Introduction

The γ-radiolysis of H_2S has been the subject of several recent papers. Meissner and Henglein (1) γ-irradiated solid, liquid, and gaseous H_2S and report $G(H_2) = 9.3$ at 1 atm and that N_2O had little or no effect on this H_2 yield. Perner and Franken (2) in a pulse radiolysis study of gaseous H_2S, devoted mainly to the formation and reactions of SH radicals, reported $G(H_2) = 11.5 \pm 0.7$[2] at high dose rates. They also reported that this yield is reduced by the addition of SF_6, although they did not state by how much. Huyton and Woodward (7, 8) γ-irradiated gaseous H_2S and measured the dose by ion chamber measurements. They report $G(H_2) = 7.0 \pm 0.2$ at 800 Torr and that neither N_2O nor SF_6 has any effect on this yield (7).

The α-radiolysis of gaseous H_2S also has been studied recently by Forys and Jezierska (9) and by Torrey (10). The former (9) obtained $G(H_2) = 7.9$ based on a series of dosimeter systems and the latter (10) obtained a hydrogen yield of $M/N = 1.82$ molecules per ion pair relative to $W_{H_2S} = 23.4$ eV per ion pair giving $G(H_2) = 7.8$. As with the γ-radiolysis, both refs. 9 and 10 report no effect of electron scavengers on the hydrogen yield.

The difference between the hydrogen yields of Meissner and Henglein and of Huyton and Woodward may be due to dosimetry as the former give no details of their dose measurements. The difference between the yields and the effect of electron scavengers at high and low dose rates is more fundamental.

Perner and Franken propose the following mechanism for the primary processes and subsequent neutral reactions in irradiated H_2S.

[1] Primary processes: $H_2S \rightsquigarrow H + SH$

[2] Primary processes: $H_2S \rightsquigarrow H_2 + S$

[3] Primary processes: $H_2S \rightsquigarrow H + H + S$

[4] $H_2S \xrightarrow{\text{ionic processes}}$ (H and/or H_2) + (SH and/or S)

---

[1] AECL No. 3848.

[2] These authors used a Febetron 706 pulsed electron accelerator and we can assume a dose rate of $\sim 10^{25}$–10^{27} eV g^{-1} s^{-1}. Perner and Franken reported $G(H_2) = 8.8$ based on N_2O dosimetry assuming $G(N_2) = 10$. As we have pointed out (3–6), at these dose rates $G(N_2) = 12.4$ and the yields of Perner and Franken have been corrected using this value. These authors also used a stopping power for H_2S relative to air which is 6% too high.

Can. J. Chem. Downloaded from www.nrcresearchpress.com by 210.87.254.42 on 09/05/12
For personal use only.

[5] $H + H_2S \rightarrow H_2 + SH$

[6] $SH + SH \rightarrow H_2S_2^*$

[7] $S' + H_2S \rightarrow H_2S_2^*$

[8] $H_2S_2^* + M \rightarrow H_2S_2$

[9] $H_2S_2^* \rightarrow H_2 + S_2$

As Perner and Franken point out there is some uncertainty as to the importance of reactions 7 to 9. However, because of the large rate constant for reaction 5, $k_5 = 7 \pm 2 \times 10^8\ M^{-1}\ s^{-1}$,[3] and the inherent high concentration of H_2S it can be assumed that all H atoms formed in the system, even at dose rates as high as 10^{28} eV $g^{-1}\ s^{-1}$, will react to form hydrogen. The reaction of H atoms with SH radicals, [10],

[10] $H + SH + M \rightarrow H_2S + M$

would have to have the improbably high rate constant of k_{10} [M] $= 5 \times 10^{10}\ M^{-1}\ s^{-1}$ at 1000 Torr to compete measurably with [5] at 10^{28} eV $g^{-1}\ s^{-1}$.

It appears then that the effect of dose rate on the H_2 yield is due to a change in the ionic reactions and this is supported by the change in behavior with electron scavengers. Huyton and Woodward (7) suggested from their low dose rate work that the neutralization process in H_2S–SF_6 mixtures is [11]

[11] $H_3S^+ + SF_6^- \rightarrow H + H_2S + SF_6$

giving the same H atom yield as in pure H_2S where they suggested the neutralization process is [12]

[12] $H_3S^+ + X^- \rightarrow H + H_2S + X$

where X^- may be H_2S^- or some other negative species. Clearly, reaction 11 contradicts the earlier observation of Perner and Franken that at high dose rates SF_6 does reduce the hydrogen yield.

Because of this contradiction, we have irradiated H_2S at dose rates similar to those of Perner and Franken and have measured quantitatively the effect of SF_6 and of dose. We have also examined the ionic processes grouped in reaction 4.

[3]Perner and Franken (2) report $k_5 = 7.7 \pm 1.5 \times 10^8\ M^{-1}\ s^{-1}$ giving D. Mihelcic and R. N. Schindler's (private communication) value of $k_5 = 8.3 \pm 0.4 \times 10^8\ M^{-1}\ s^{-1}$ as supporting evidence. Dzantiev and Shiskov (11) report $k_5 = k_{H+C_2H_4}$ and a recent reliable value for this reaction at high pressures is $k_H + C_2H_4 = 5.5 \pm 0.5 \times 10^8\ M^{-1}\ s^{-1}$ (12).

Experimental

Radiation Source and Dosimetry

The accelerator used in the present experiments was a Febetron 705. This is a high intensity, pulsed electron accelerator and we have described previously its use in high dose rate studies (13–15). The gas samples were irradiated in quartz cells (13) fitted with Teflon O ring type stopcocks (Ace Glass Company Inc.).

The mean absorbed dose in the cell, measured using nitrous oxide dosimetry with $G(N_2) = 12.4$ (3–6), was 1×10^{20} eV g^{-1} per pulse. The mean dose rate was $\sim 2 \times 10^{27}$ eV $g^{-1}\ s^{-1}$. The stopping power correction in going from N_2O to H_2S is 1.006 g^{-1} (16).

Materials and Analyses

The H_2S and SF_6, Matheson C. P. grade, were used without further purification other than the elimination of impurities non-condensible at 77 °K by several freeze–pump–thaw cycles. The volume of gas non-condensible at 77 °K produced by the radiolysis was measured with a McLeod gauge and its composition determined by mass spectrometry.

Results

The hydrogen yield from single pulse irradiations of H_2S at different pressures is shown in Fig. 1. The yield of hydrogen is independent of pressure over the range shown at $G(H_2) = 12.0 \pm 0.5$.

Figure 2 shows the effect of SF_6 at 350 and 1000 Torr H_2S. The yields are not corrected for the slight increase in dose due to the SF_6 addition. Although there is a more rapid initial decrease in $G(H_2)$ at the higher pressure both give the same limiting yield of $G(H_2) = 7.9 \pm 0.3$, giving a reduction in yield of $\Delta G(H_2) = 4.1 \pm 0.3$.

The amounts of hydrogen formed in multipulse irradiations for pure H_2S are shown in Fig. 3*A* for 350 and 1000 Torr. There is marked

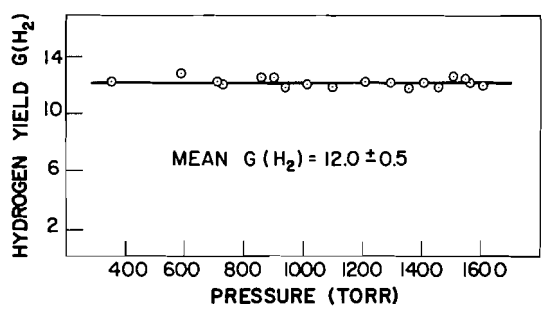

FIG. 1. Hydrogen yields from radiolysis of H_2S at a dose rate of $\sim 2 \times 10^{27}$ eV $g^{-1}\ s^{-1}$ as a function of pressure of H_2S.

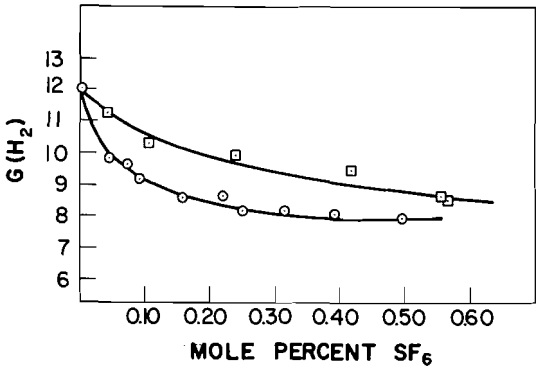

FIG. 2. Effect of added SF_6 on the hydrogen yield from the radiolysis of H_2S at a dose rate of $\sim 2 \times 10^{27}$ eV g^{-1} s^{-1}. ○, 1000 Torr pressure; □, 350 Torr pressure.

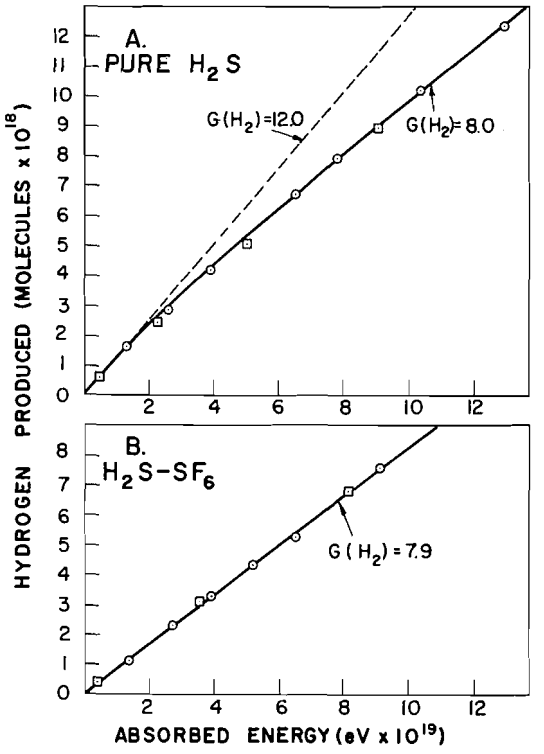

FIG. 3. Amount of hydrogen produced as a function of absorbed energy. Increase in absorbed dose was achieved by use of several pulses. Volume of quartz irradiation cell approximately 78 ml. *A*: □, 350 Torr H_2S, ○, 1000 Torr H_2S; *B*: □, 350 Torr H_2S + ~1.0 mol% SF_6, ○, 1000 Torr H_2S + ~0.5 mol% SF_6.

decrease in yield at higher doses for both pressures. The results for H_2S–SF_6 mixtures are given in Fig. 3*B*. In direct contrast to pure H_2S there is no fall-off in yield at the higher doses.

Discussion

The hydrogen yield, $G(H_2) = 12.0 \pm 0.5$, we observe in the radiolysis of H_2S at a dose rate of $\sim 2 \times 10^{27}$ eV g^{-1} s^{-1} is in good agreement with that of Perner and Franken (2) of $G(H_2) = 11.5 \pm 0.7$ for similar conditions.

We also agree with the qualitative observations of these authors in that SF_6 reduces the hydrogen yield. The decrease we observe is in good agreement with the ion pair yield for H_2S based on the value of $W = 25.3$ eV per ion pair (8). This value of W measured by Huyton and Woodward is probably more reliable than the lower value used in ref. 9.

Primary Ionic Processes

From mass spectrometric studies (17), the predominant positive ions formed in the radiolysis of H_2S will be H_2S^+ (52%), SH^+ (22%), S^+ (23%), and H^+ (3%). Accepting the energy required to form an ion pair as $W_{H_2S} = 25.3$ eV (8), the yields of these should then be $G(H_2S^+) = 2.08$, $G(SH^+) = 0.88$, $G(S^+) = 0.92$, and $G(H^+) = 0.12$. These ions are presumably formed in reactions such as [13]–[16].

[13] $H_2S \rightsquigarrow H_2S^+ + e$

[14] $H_2S \rightsquigarrow SH^+ + H + e$

[15] $H_2S \rightsquigarrow S^+ + H + H + e$

[16] $H_2S \rightsquigarrow H^+ + SH + e$

Both H_2S^+ and SH^+ will react very rapidly with H_2S to form H_3S^+ (18–20)

[17] $H_2S^+ + H_2S \rightarrow H_3S^+ + SH$
$k_{17} \simeq 8 \times 10^9\ M^{-1}\ s^{-1}$

[18] $SH^+ + H_2S \rightarrow H_3S^+ + S$
$k_{18} \simeq 1 \times 10^{10}\ M^{-1}\ s^{-1}$

as we shall assume does the trace of H^+,

[19] $H^+ + H_2S + M \rightarrow H_3S^+ + M$

The fate of S^+ is not as clear. Since SF_6 reduces the hydrogen yield by ~4 G units, each neutralization reaction must give an H atom. Thus some reaction sequence involving S^+ which can be suppressed by SF_6 must be capable of producing H atoms. A possibility is charge exchange with H_2S, reaction 20. This is slightly endothermic (i.p.$_{H_2S}$ = 10.47 eV, i.p.$_S$ = 10.36 eV (21))

[20] $S^+ + H_2S \rightarrow H_2S^+ + S$

Can. J. Chem. Downloaded from www.nrcresearchpress.com by 210.87.254.42 on 09/05/12
For personal use only.

Can. J. Chem. Downloaded from www.nrcresearchpress.com by 210.87.254.42 on 09/05/12
For personal use only.

but is possible if the S^+ ion is formed with a slight excess of energy. The H_2S^+ ion would then form H_3S^+ by reaction 17. Reaction with H_2S to yield S_2^+, reaction 21, would be favored on grounds of ionization potentials (i.p.$_S$ = 10.36 eV, i.p.$_{S_2}$ = 8.3 eV (21))

[21] $$S^+ + H_2S \rightarrow S_2^+ + H_2$$

but this reaction would not be suppressed by SF_6.

Assuming S^+ reacts as in [20] then [17], or by some other reaction sequence, to yield H_3S^+, the net yields from primary ionic processes before neutralization are predicted to be: $G(H_3S^+)$ = 4.0 = G(e), $G(SH)_i$ = 3.12, $G(H)_i$ = 2.72, and $G(S)_i$ = 1.80.

Neutralization Processes

At high dose rates, for single pulse experiments in pure H_2S, the fate of H_3S^+ and e must be to neutralize each other. The predominant neutralization reactions most probably are

[12] $$H_3S^+ + e \rightarrow H + H_2S$$

[22] $$H_3S^+ + e \rightarrow H_2 + SH$$

Since H atoms react so rapidly with H_2S, [5], we are unable to distinguish between these two reactions.

Sulfur hexafluoride will rapidly attach thermal electrons (22), [23]

[23] $$e + SF_6 \rightarrow SF_6^-$$
$$k_{23} = 1.8 \times 10^{14}\, M^{-1}\, s^{-1}$$

and this can suppress contributions from dissociative neutralization reactions. Since addition of SF_6 reduces the hydrogen yield and since SF_6 does not react rapidly with hydrogen atoms, we must assume the reduction is due to reaction 24 competing with reaction 12

[24] $$H_3S^+ + SF_6^- \rightarrow H_2S + HF + SF_5$$

[12] $$H_3S^+ + e \rightarrow H\cdot + H_2S$$

or reaction 25 competing with reaction 26.

[25] $$H_3S^+ + SF_6^- \rightarrow H\cdot + HF + SH + SF_5$$

[26] $$H_3S^+ + e \rightarrow 2H + SH$$

Both these competitions lead to a reduction in hydrogen yield of $\Delta G(H_2) = G(e) = 4.0$. Reactions 25 and 26, however, are an improbable sequence. It is unlikely that four product fragments arise from a single neutralization. Even less likely is the small yield of H atoms from neutral excitation processes that these reactions would require. The maximum possible yield of H atoms is $G(H)_{total}$ = 12.0. If reaction 26 occurred it would yield $G(H)_{26} = 2G(e) = 8.0$. The yield from ion–molecule reactions is $G(H)_i$ = 2.72 leaving 12.0 − 8.0 − 2.72 = 1.28 from direct neutral excitation processes. This gives an unreasonably low value for the ratio of $G_{excitation}$ to $G_{ionization}$. Thus it appears that one H atom is formed per neutralization as in [12] and that this can be suppressed by SF_6, as in [24].

The effect of pressure on the decrease in the yields with SF_6 shown in Fig. 2 cannot be precisely explained. A reduction in the effectiveness of SF_6 at lower pressures has been observed in Febetron irradiations of N_2O and HCl (5, 6). It was proposed that this was due to an increase in electron energy at low pressures. The rate constant of reaction 23 decreases rapidly for electrons above thermal energies (22–24). This should be reflected by an inverse dependence of k_{23} on pressure. A measure of the reduction in k_{23} can be obtained from a reciprocal plot of the yields given in Fig. 2. These plots are shown in Fig. 4 and are based on the expression

$$\frac{1}{G(H_2)_0 - G(H_2)_s} = \frac{1}{G(H_2)_0 - G(H_2)_\infty}\left[1 + \frac{\text{constant} \times [H_2S]}{k_{23}[SF_6]}\right]$$

From the slopes in the figure, SF_6 is seen to be more than three times as effective at 1000 Torr

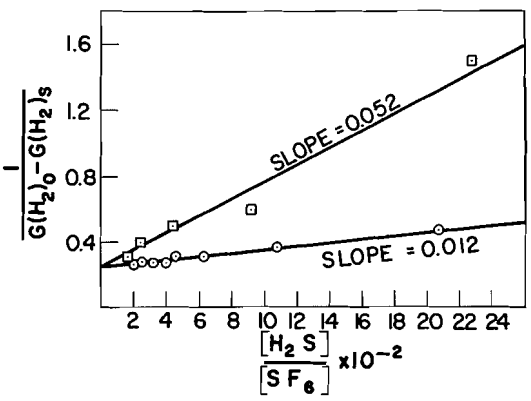

FIG. 4. Reciprocal plot of reduction in hydrogen yield *vs.* amount of SF_6 added. ○, 1000 Torr H_2S; □, 350 Torr H_2S.

Can. J. Chem. Downloaded from www.nrcresearchpress.com by 210.87.254.42 on 09/05/12
For personal use only.

as it is at 350 Torr. Using a computer program[4] to test the system and assuming $k_{12} = 1 \times 10^{15}$ M^{-1} s^{-1}, even at 1000 Torr, k_{23} (effective) is more than 10 times smaller than that given in the literature for thermal electrons (22).

Low Dose Rate Yields

As discussed in the previous section, the fair agreement between the low dose rate yield of $G(H_2) = 7.0$–7.9 (7, 9, 10) and the limiting yield of $G(H_2) = 7.9 \pm 0.3$ with SF_6 at high dose rates suggests that there is no contribution from neutralization at low dose rates. This is confirmed by the absence of an effect of SF_6 and N_2O on $G(H_2)$ at low dose rates (1, 7, 9, 10) and it is further confirmed by the limiting yield in multipulse irradiations at high dose rates where $G(H_2) \approx 8$, and is unaffected by SF_6, Figs. 3*A* and 3*B*.

For conditions where no neutralization contribution to $G(H_2)$ is observed, there must be some neutralization process other than reaction 12. At low dose rates this could be due to clustering or charge transfer reactions of the H_3S^+ ion. Because of the high proton affinity of H_2S (p.a. $\geqslant$ 7.6 eV (25)), however, charge transfer is unlikely. Because reaction 26 is unlikely, neutralization of H_3S^+ should only give one H atom and this should not be affected by clustering. The fall-off in yield at high doses at high dose rates, Fig. 3, also eliminates clustering as an explanation for the difference in yields. The amount of clustering will be the same for any number of pulses as the life-time of ions with respect to neutralization is essentially independent of absorbed dose.

The reduction in yield at low dose rates or at high doses in high dose rate experiments is probably due to electron attachment to products. Perner and Franken (2) have reported that H_2S_2 has no effect on the H_2 yield and therefore the most likely product involved is sulfur. Assuming that a negative ion of the type S_2^-, S_4^- etc. is formed, the neutralization reaction could be

$$[27] \qquad H_3S^+ + S_n^- \rightarrow H_2S + HS_n$$

Whatever the species responsible, it must attach electrons very efficiently. From Fig. 3, at a dose of $\sim 6 \times 10^{20}$ eV g^{-1}, $G(H_2) \simeq 10$ and therefore electrons are disappearing equally by neutralization [12] and by attachment to this species. Assuming the species to be S_2, its maximum concentration at this dose is 8×10^{-5} M. Since the mean lifetime of the electron with respect to neutralization is ~ 10 ns at a dose rate of 2×10^{27} eV g^{-1} s^{-1} (6), the attachment rate constant must be $k_{28} \geqslant 3 \times 10^{12}$ M^{-1} s^{-1}.

$$[28] \qquad e + S_2 \rightarrow S_2^-$$

Conclusions

The initial hydrogen yield of $G(H_2) = 12.0$ obtained at high dose rates is reduced to $G(H_2) \simeq 7.9 \pm 0.3$ either by the addition of SF_6 or increasing the absorbed dose. This reduction, which is equal to the ion pair yield, is due to the replacement of the neutralization of H_3S^+ with an electron by the SF_6^- ion or a negative ion of the type S_n^-. The fair agreement between this and the yield observed at low dose rates of $G(H_2) = 7.0$–7.9 and the lack of effect of SF_6 at low dose rates is probably due to similar neutralization processes.

[4]The program was WR16 and we have previously described its use in similar calculations, *e.g.* ref. 6.

1. G. Meissner and A. Henglein. Z. Natuforsch. **20b**, 1005 (1965).
2. D. Perner and T. Franken. Ber. Bunseges. phys. chem. **73**, 897 (1969).
3. C. Willis, O. A. Miller, A. E. Rothwell, and A. W. Boyd. Adv. Chem. Ser. **81**, 539 (1968).
4. A. W. Boyd, C. Willis, and O. A. Miller. Can. J. Chem. **47**, 3783 (1969).
5. A. W. Boyd, D. A. Armstrong, C. Willis, and O. A. Miller. Rad. Res. **40**, 255 (1969).
6. C. Willis, A. W. Boyd, and D. A. Armstrong. Can. J. Chem. **47**, 3783 (1969).
7. D. W. Huyton and T. W. Woodward. Can. J. Chem. **48**, 2300 (1970).
8. D. W. Huyton and T. W. Woodward. Trans. Faraday Soc. **66**, 1648 (1970).
9. M. Forys and K. Jezierska. Radiochem. Radioanal. Lett. **1**, 237 (1969).
10. R. M. P. Torrey. Ph.D. Thesis. Syracuse University. 1969.
11. B. G. Dzantiev and A. V. Shiskov. Khimija Vysokikh Energij, **1**, 192 (1967).
12. J. A. Eyre, T. Hikida, and L. M. Dorfman. J. Chem. Phys. **53**, 1281 (1970).
13. C. Willis, A. W. Boyd, and O. A. Miller. Can. J. Chem. **47**, 3007 (1969).
14. C. Willis, O. A. Miller, A. E. Rothwell, and A. W. Boyd. Rad. Res. **35**, 428 (1968).
15. C. Willis, A. W. Boyd, and P. E. Bindner. Can. J. Chem. **48**, 1951 (1970).
16. A. T. Nelms. N.B.S. Circular, 577 (1956).
17. A. Cornu and R. Massot. Compilation of mass spectral data. Heyden and Sons, London. 1966.
18. F. H. Field and F. W. Lampe. J. Am. Chem. Soc. **80**, 5583 (1958).

19. A. G. HARRISON and J. C. THYNNE. Trans. Faraday Soc. **62**, 3345 (1966).
20. S. K. GUPTA, E. G. JONES, A. G. HARRISON, and J. J. MYHER. Can. J. Chem. **45**, 3107 (1967).
21. J. L. FRANKLIN *et al.* Ionization potentials, appearance potentials, and heats of formation of gaseous positive ions. NSRDS-NBS-26 (1969).
22. B. H. MAHAN and C. E. YOUNG. J. Chem. Phys. **44**, 2192 (1966).
23. R. N. COMPTON, L. G. CHRISTOPHOROU, G. S. HURST, and P. W. REINHARDT. J. Chem. Phys. **45**, 4634 (1966).
24. R. N. COMPTON, R. H. HUEBNER, P. W. REINHARDT, and L. G. CHRISTOPHOROU. J. Chem. Phys. **48**, 901 (1968).
25. V. I. VEDENEYEV *et al.* Bond energies, ionization potentials, and electron affinities. Edward Arnold Publishers, London. 1962.

Can. J. Chem. Downloaded from www.nrcresearchpress.com by 210.87.254.42 on 09/05/12
For personal use only.

Can. J. Chem. Downloaded from www.nrcresearchpress.com by 210.87.254.5 on 09/05/12
For personal use only.

Kinetics of Reactions of 8-Quinolinol and Acetate with Hydroxyaluminum Species in Aqueous Solutions. 1. Polynuclear Hydroxyaluminum Cations[1]

R. C. TURNER AND WAN SULAIMAN[2]

Soil Research Institute, Research Branch, Canada Department of Agriculture, Ottawa, Canada

Received[3] April 27, 1970

The effect of varying 8-quinolinol and acetate concentration on the rate of decomposition of polynuclear hydroxyaluminum cations was studied. It was found that the concentration of the undissociated 8-quinolinol and acetic acid molecules determined the magnitude of the first order rate constant for the decomposition of the polynuclear hydroxyaluminum cations, except when the acetate concentrations were relatively high. With high acetate concentrations, it appeared that polynuclear acetate species were involved in the reactions. An empirical equation was developed showing the effect of 8-quinolinol and acetic acid molecule concentrations on the pseudo first order rate constant for the decomposition reaction.

L'effet de la variation de la concentration de l'hydroxy-8 quinoléïne et de l'acétate sur la vitesse de décomposition des cations hydroxy-aluminium polynucléaires a été étudié. Il a été trouvé que la grandeur de la constante de vitesse d'ordre un est déterminée par la concentration de l'hydroxy-8 quinoléïne et de l'acide acétique non dissociés, excepté à relativement haute concentration en acétate. A haute concentration en acétate, il est apparu que la réaction impliquait des complexes polynucléaires contenant de l'acétate. On a développé une équation empirique qui donne l'effet de la concentration de l'hydroxy-8 quinoléïne et de l'acide acétique sur la constante de vitesse d'ordre un de la réaction de décomposition.

Canadian Journal of Chemistry, **49**, 1683 (1971)

Introduction

It was shown in an earlier publication (1) that three forms of Al could be determined in partially neutralized $AlCl_3$ solutions by 8-quinolinolate extraction procedures. The three forms of Al were mononuclear and polynuclear hydroxyaluminum cations (mono- and polynuclear with respect to Al) and an initial solid phase. The rate of the reaction with the mononuclear cations was essentially instantaneous, while with the polynuclear cations it could be represented by a first order process and with the initial solid phase it could be represented reasonably well by a 2/3 order process, which went to completion because the reaction mixtures were swamped with 8-quinolinol.

Goto and Yotsuyanagi (2) studied the effect of 8-quinolinol and acetate concentrations on the initial rate of the reaction with hydroxyaluminum material. They concluded that the reaction was first order but that the rate constant was affected to a great extent by the 8-quinolinol concentration and to a lesser extent by the acetate concentration. They found that the rate of the reaction with varying acetate concentrations (but with the 8-quinolinol and pH kept constant) could be represented by the equation

$$[1] \quad \frac{d[Al]}{dt} = k_2[Ac_T]^n[Al_p] + k_2^0[Al_p]$$

where [Al] is the concentration of mononuclear Al, $[Ac_T]$ the total concentration of acetate, $[Al_p]$ the concentration of polynuclear material expressed as Al, k_2 and k_2^0 are constants and the experimental value of n was 2. Similarly, when the 8-quinolinol was varied but the acetate concentration and pH kept constant the rate of the reaction was

$$[2] \quad \frac{d[Al]}{dt} = k_3[OX_T]^m[Al_p] + k_3^0[Al_p]$$

where $[OX_T]$ is the total concentration of 8-quinolinol, k_3 and k_3^0 are constants, and the experimental value of m was 2. Goto and Yotsuyanagi (2) did not differentiate between polynuclear hydroxyaluminum cations and the initial solid phase, thus it is uncertain whether their results referred to the two forms together or to only one of them.

The objective of the work reported here was to determine the effect of the concentrations of 8-quinolinol and acetate on the rate of the

[1]Contribution No. 332.

[2]Present address: Soil Science Department, University of Guelph, Guelph, Ontario.

[3]Revision received January 4, 1971.

Can. J. Chem. Downloaded from www.nrcresearchpress.com by 210.87.254.5 on 09/05/12
For personal use only.

reaction with the polynuclear hydroxyaluminum cations and to determine whether it was the undissociated 8-quinolinol and acetic acid molecules or their ions that determined the magnitude of the first order rate constant for the reaction.

Experimental

The polynuclear hydroxyaluminum cations were prepared by titrating a solution of $AlCl_3$ slowly with NaOH to an NaOH/Al mole ratio of 2.4, the time required for titration being about 24 h. The final total concentration of Al in a system was usually 10^{-3} *M* although in some experiments higher concentrations were used. After ageing for at least 24 h, aliquots were filtered through VS Millipore filters under suction and the filtrates were used in the rate studies.

The method for determining the concentration of mononuclear Al ions was based on the fact that the complex formed between this form of Al and 8-quinolinol was essentially instantaneous. The complex was extracted into chloroform and its concentration determined colorimetrically.

Before presenting the procedures followed, it is important to point out that rather small concentrations of phosphate in the reaction mixtures increased the rate of the reactions. It was found, however, that this source of error was eliminated by ensuring that the phosphate concentration was less than 3×10^{-7} *M*.

The standard procedure was as follows: 25 ml of 8-quinolinol stock solution (which was prepared by dissolving 10 g 8-quinolinolate in 25 ml acetic acid and diluting to 1000 ml with H_2O) was added to 150 ml of H_2O, followed by 25 ml of 1 *N* NaOAc. This solution was then added to 50 ml of an aqueous test solution in which the Al concentration was between 5×10^{-5} and 2×10^{-4} *M*. The reaction flask was suspended in a constant-temperature water bath at 26 °C and $NaOH–H_2SO_4–H_2O$ washed air was bubbled through the solution. Twenty-five ml aliquots were pipetted from the flask at predetermined time intervals and extracted with exactly 10 ml of chloroform. Extraction with chloroform consisted of shaking the mixture in a separatory funnel for 10 s allowing the chloroform to separate from the aqueous layer and drawing the chloroform off through the drainage tube which contained a cotton plug to remove H_2O. This procedure gave a reaction mixture with 8-quinolinol and acetate concentrations of 6.9×10^{-3} and 1.44×10^{-1} *M*, respectively, with a p*H* of 5.05 ± 0.02.

Variations in the concentrations of 8-quinolinol and acetate were made by varying the amounts of the stock solutions used, adjusting the p*H* by adding acetic acid or NaOH but keeping the volume of the reaction mixture constant by varying the amount of H_2O added. When the desired acetate concentration in the reaction mixture was less than that in the stock solution of the 8-quinolinol, it was necessary to use a special stock solution of 8-quinolinol dissolved in perchloric acid rather than acetic acid.

With both 8-quinolinol and acetate present the reactions went to completion via a first order process. When the concentration of either 8-quinolinol or acetate was zero, the reactions did not go to completion via a first order process. In fact, the reactions appeared to reach equilibria when there was an appreciable concentration of the polynuclear hydroxyaluminum cations remaining in solution. Consequently, when the acetate concentration was zero, the rates were determined during the first minute of reaction, and when the 8-quinolinol concentration was zero the rates were determined over the first 35% of reaction. In both cases the rates were proportional to the concentration of polynuclear cations present. It was assumed therefore that the processes were first order and the rate constants were calculated on the basis of the concentration of polynuclear cations present.

Results and Discussion

The concentrations of both OX_T and Ac_T, except when either was zero, were much greater than the total concentrations of Al in the reaction mixtures so that their concentrations remained essentially constant during the reactions. Thus the reactions appeared to be first order processes with respect to $[Al_p]$.

The effect of acetate concentration on the reaction with constant p*H* and 8-quinolinol concentrations is shown in the upper section of Fig. 1 as the plot of first order rate constant *k vs.* $[Ac_T]^2$. These plots are essentially the same as those used by Goto and Yotsuyanagi (2) and show, in agreement with their results, that the plots could be represented by straight lines over the entire range of $[Ac_T]$ used including zero. Thus *n* in eq. 1 is equal to 2. When the 8-quinolinol concentration was 6.9×10^{-3} *M*, however, *k* was equal to 3.0 min^{-1} M^{-2} whereas when $[OX_T]$ was zero *k* was 3.3 min^{-1} M^{-2} which indicates that the two reactants did not react independently with the polynuclear hydroxyaluminum cations.

The results in Fig. 1*b* show that when the first order rate constant *k* was plotted against $[OX_T]^2$ with constant p*H* and $[Ac_T]$, the plots could not be represented by a straight line. This is contrary to the conclusion reached by Goto and Yotsuyanagi (2) but they did not use the low concentrations of 8-quinolinol which were necessary to show the definite curves in the plots. The upper curve is included to show the increased rates over those in the middle curve due to phosphate in the reaction mixture. It is ignored in the following treatment. Before proceeding with the effect of $[OX_T]$ on the first order rate constant, eqs. 1 and 2 will be combined into one equation.

Equations 1 and 2 imply that 8-quinolinol and acetate react independently with the polynuclear

Can. J. Chem. Downloaded from www.nrcresearchpress.com by 210.87.254.5 on 09/05/12
For personal use only.

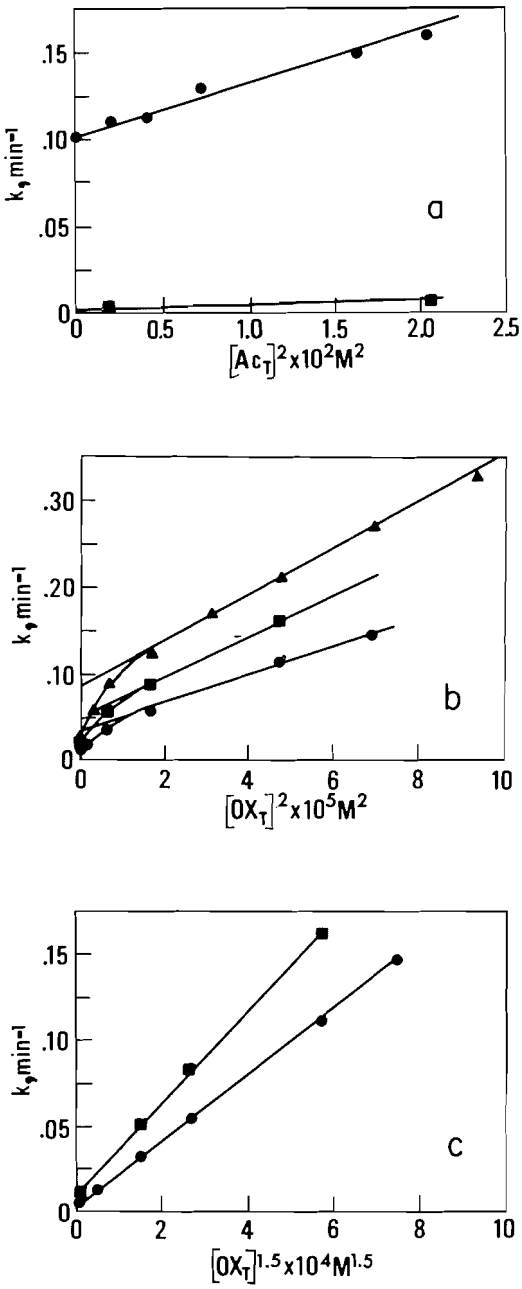

FIG. 1. Effect of 8-quinolinol and acetate concentrations on the rate constant for the decomposition of polynuclear hydroxyaluminum cations. (*a*) Varying $[Ac_T]$: ●, $[OX_T] = 6.9 \times 10^{-3}$ *M*; ■, $[OX_T] = 0$. (*b*) Varying $[OX_T]$: ▲, $[Ac_T] = 1.44 \times 10^{-1}$ and $[P] = 1.6 \times 10^{-5}$; ■, $[Ac_T] = 1.44 \times 10^{-1}$; ●, $[Ac_T] = 4.4 \times 10^{-2}$ *M*. (*c*) Varying $[OX_T]$: ■, $[Ac_T] = 1.44 \times 10^{-1}$; ●, $[Ac_T] = 4.4 \times 10^{-2}$ *M*.

cations and they therefore can be combined to give

$$[3] \quad \frac{d[Al]}{dt} = (k_2[Ac_T]^n + k_3[OX_T]^m)[Al_p]$$

which shows that $k_2[Ac_T]^n$ is equal to k_2^0 when $[OX_T]$ is zero and $k_3[OX_T]^m$ is equal to k_3^0 when $[Ac_T]$ is zero. According to eq. 3 the pseudo first order rate constant k at constant pH is expressed by the equation

$$[4] \quad k = k_2[Ac_T]^n + k_3[OX_T]^m$$

where n is equal to 2.

The value of m was determined from the experimental results represented in Fig. 1*b* by plotting the log k minus $k_2[Ac_T]^2$ *vs.* log $[OX_T]$. The slopes of the straight lines of best fit drawn through the experimental points showed m equal to 1.5. Figure 1*c* shows the same plots as Fig. 1*b* but with m equal to 1.5. The experimental values follow a straight line over the entire range of $[OX_T]$ used including zero. The slopes of the lines were different, however, for the two concentrations of $[Ac_T]$ so that the value for k_3 with $[Ac_T]$ equal to 14.4×10^{-2} was 2.7×10^{-2} $M^{-1.5}\,min^{-1}$, while with $[Ac_T]$ equal to 4.4×10^{-2} it was 2.0×10^{-2}. It appeared, therefore, as was the case when $[Ac_T]$ was varied with $[OX_T]$ and pH constant, the 8-quinolinol and acetate did not react independently with the polynuclear cations.

Since the acetate and 8-quinolinol did not react independently with the polynuclear cations, it was necessary to modify eq. 4 by adding at least one term which involved both reactants. Furthermore, this new term or terms must be consistent with the experimental fact that the plot of k *vs.* $[Ac_T]^2$ at constant $[OX_T]$ and k *vs.* $[OX_T]^{1.5}$ at constant $[Ac_T]$ both gave straight lines (Fig. 1). The simplest equation that was consistent with the experimental facts was

$$[5] \quad k = k_2[Ac_T]^2 + k_4[Ac_T]^2[OX_T]^{1.5} + k_3[OX_T]^{1.5}$$

The constants k_2, k_3, and k_4 in eq. 5 can be readily evaluated graphically. Specifically, the slope of k *vs.* $[Ac_T]^2$ plot in which $[OX_T]$ and the pH are held constant (Fig. 1*a*) is equal to $k_2 + k_4[OX_T]^{1.5}$. Likewise, the slope of the plot of k *vs.* $[OX_T]^{1.5}$ with $[Ac_T]$ and pH held constant, (Fig. 1*c*) is equal to $k_3 + k_4[Ac_T]^2$. The value of k_2 obtained from the intercept of the plot in Fig. 1*c*

Can. J. Chem. Downloaded from www.nrcresearchpress.com by 210.87.254.5 on 09/05/12
For personal use only.

where $[OX_T] = 0$ and $[Ac_T] = 1.44 \times 10^{-1}$ was 3.4×10^{-1} min^{-1} M^{-2}. Also, the value of k_3 from the intercept at $[Ac_T] = 0$ and $[OX_T] = 6.9 \times 10^{-3}$ in Fig. 1*a* was 1.8×10^{-2} min^{-1} $M^{1.5}$. With these values for k_2 and k_3 and the slopes from the same plots the calculated value of k_4 was 4.5×10^3 min^{-1} $M^{-3.5}$.

The equations developed above as well as the values for k_2, k_3, and k_4, are based on the total concentrations of acetate and 8-quinolinol in the reaction mixtures. This is legitimate regardless of the specific species derived from the acetate or 8-quinolinol which may be rate determining because at constant p*H* a specific species is proportional to the total concentrations, except in special cases, which will be discussed later.

To determine whether it was the concentration of protonated 8-quinolinol $[OX^+]$, 8-quinolinol [OX], dissociated quinolinolate $[OX^-]$ or the sum of the three, *i.e.*, $[OX_T]$, that controlled the rate of the reaction, experiments were made with $[OX_T]$ and $[Ac_T]$ kept constant at 6.9×10^{-3} and 4.4×10^{-2} *M*, respectively, and the p*H* of the reaction mixture was varied from 4.8 to 5.6. At this concentration of acetate the solution was strongly buffered so that the p*H* was not affected by the reactions and the concentration was too low relative to that of 8-quinolinolate to have an appreciable effect on the rate of the reaction. When the p*H* was raised from 4.8 to 5.6 the rate constant increased from 0.06 to 0.21 min^{-1}, a 3.5-fold increase. Thus, according to eq. 5, the concentration of the species controlling the magnitude of the rate constant must have increased 2.3 fold. The value of $[OX_T]$ is independent of p*H* and can therefore be ruled out. Using $10^{-9.89}$ (3) and $10^{-5.13}$ (3) as the equilibrium constants for $OX \rightleftharpoons OX^- + H^+$ and $OX^+ \rightleftharpoons OX + H^+$, respectively, it can be shown that increasing the p*H* from 4.8 to 5.6 decreases $[OX^+]$ by a factor of 2.7 but increases $[OX^-]$ and [OX] 15 and 2.3-fold, respectively. Since a 2.3-fold increase in concentration corresponds to a 3.5-fold increase in the rate constant, it is obvious that the concentration of OX controls the rate of the reaction. Consequently, eq. 5 was modified to

$$[6] \quad k = 3.4 \times 10^{-1}[Ac_T]^2 + 1.47 \times 10^4[Ac_T]^2[OX]^{1.5} + 5.88 \times 10^2[OX]^{1.5}$$

In the case of acetate there were a number of possibilities including polynuclear forms of acetic acid. Providing relatively low concentrations of acetate were involved, however, only three possibilities needed to be considered, *i.e.*, that it was the concentration of total acetate $[Ac_T]$, acetate ion $[Ac^-]$, or undissociated acid [Ac] that governed the rate of the reaction. In all experiments in which 8-quinolinol was absent and $[Ac_T]$ was constant, decreasing the p*H* increased the rate constant. When the p*H* was decreased from 5.05 to 4.70 the rate constant increased 3.3-fold which corresponds to an increase of 1.8-fold in the concentration of the reacting species (eq. 6). Using $10^{-4.75}$ (4) for the dissociation constant of acetic acid, it can be shown that this decrease in p*H* would decrease $[Ac^-]$ by a factor of 1.4 but increase [Ac] 1.6-fold. It was concluded therefore that it was the concentration of undissociated acid, *i.e.*, [Ac] that controlled the rate of the reaction. Consequently, eq. 6 was modified to

$$[7] \quad k = 3.09[Ac]^2 + 1.32 \times 10^5[Ac]^2[OX]^{1.5} + 5.88 \times 10^2[OX]^{1.5}$$

Equation 7 was tested by either varying $[OX_T]$ and $[Ac_T]$ simultaneously while keeping $[OX_T]/[Ac_T]$ and p*H* constant or by keeping $[OX_T]$ and $[Ac_T]$ constant and varying p*H*. The upper part of Table 1 shows that there was excellent agreement between the calculated and experimental results when the p*H* was kept constant, and, although much of the total calculated rates came from the third term of the equation which involves only [OX], as much as 40% was contributed by the second term which involves [Ac] as well as [OX]. The second section of the table shows that there was also excellent agreement between calculated and experimental results when the p*H* was varied but in these experiments the acetate concentration was low with the result that practically all of the calculated values were derived from the last term of the equation which involves only [OX]. In both of these experiments, the first term of the equation which involves [Ac] alone contributed essentially nothing to the total calculated values. To have conditions in which the first term of the equation contributed materially to the total values, it was necessary to either increase the concentration of acetate to relatively high values or to decrease the 8-quinolinol concentration to zero. The first two rows of the third section of the table show that when only acetate was present, changing the p*H* from 5.05 to 4.70 increased the

TABLE 1. Comparison of first order rate constants calculated from eq. 7 with those determined experimentally

pH	$[OX_T]$ $M \times 10^3$	$[Ac_T]$ $M \times 10^2$	k (min^{-1}) Calculated 1*	2*	3*	Total	Experimental
5.05	8.28	17.3	0.0102	0.101	0.135	0.25	0.25
5.05	6.90	14.4	0.00704	0.0534	0.103	0.16	0.16
5.05	5.25	11.5	0.00449	0.0244	0.0738	0.10	0.10
5.05	2.76	5.76	0.00113	0.00217	0.0261	0.029	0.028
5.05	1.38	2.88	0.00028	0.00017	0.00844	0.0089	0.0092
5.60	6.90	4.40	0.00009	0.00145	0.217	0.22	0.21
5.39	6.90	4.40	0.00021	0.00263	0.174	0.18	0.18
5.28	6.90	4.40	0.00038	0.00410	0.151	0.16	0.16
5.05	6.90	4.40	0.00067	0.00497	0.103	0.11	0.11
4.80	6.90	4.40	0.00134	0.00585	0.0606	0.067	0.063
4.77	6.90	4.40	0.00143	0.00585	0.0565	0.064	0.065
4.40	6.90	4.40	0.00286	0.00431	0.0208	0.028	0.028
5.05		15.1	0.00709			0.0071	0.0070
4.70		15.1	0.0191			0.019	0.023
5.05	6.90	28.8	0.0284	0.213	0.102	0.34	0.34
4.87	6.90	28.8	0.0479	0.247	0.0412	0.34	0.34
5.05	2.76	43.2	0.0641	0.122	0.0261	0.21	0.26
4.77	2.76	43.2	0.138	0.143	0.0143	0.30	0.45
4.80	2.76	64.0	0.283	0.315	0.0153	0.61	1.20

*First, second, and third term on the right-hand side of eq. 7.

experimental rate constant. The next two rows show that the experimental values agreed with those calculated by the equation when the pH was either 5.05 or 4.87 and $[OX_T]$ and $[Ac_T]$ were respectively 6.9×10^{-3} and 2.88×10^{-1} M. At these concentrations decreasing the pH increased the contribution from the $[Ac]^2$ term and decreased the contribution from the $[OX]^{1.5}$ term with the result that rate constant was the same at the two pH values. The final three rows of the table show that increasing the acetate concentration beyond 2.88×10^{-1} M caused the experimental values to be significantly greater than the calculated ones.

The very real discrepancy observed between the calculated and experimental values of the first order rate constant with relatively high acetate concentration is probably due to a simplifying assumption made in the derivation of eq. 7. This assumption was that only the two mononuclear forms, undissociated acid and acetate ion, would be involved. At acetate concentrations greater than 5×10^{-2} M, however, the polynuclear forms $H_2(OAc)_2$ and $H(OAc)_2^-$ cannot be ignored (5). Since at constant ionic strength and pH the concentrations of these two species are proportional to $[Ac]^2$, their concentrations increase with increasing $[Ac_T]$ much more rapidly than [Ac].

Regardless of the discrepancies between calculated and experimental rate constants at the higher total acetate concentrations, the evidence is convincing that it is the 8-quinolinol and acetic acid molecules, rather than the charged ions derived from them, that react directly with the polynuclear hydroxyaluminum cation. The polynuclear acetate species have very little effect at the concentration of acetate used in the proposed method (1).

The phosphorus analyses were done by Ian Duncan.

1. R. C. TURNER. Can. J. Chem. **47**, 2521 (1969).
2. K. GOTO and T. YOTSUYANAGI. Nippon Kagaku ZASSHI, **89**, 49 (1968).
3. A. ALBERT and A. HAMPTON. J. Chem. Soc. 505 (1954).
4. Stability constants of metal-ion complexes. Section 1. Compiled by S. G. Sillen. Special publication No. 17. The Chem. Soc., Burlington House, W.1. London.
5. D. L. MARTIN and F. J. C. ROSSOTTI. Proc. Chem. Soc. 60 (1959).

Can. J. Chem. Downloaded from www.nrcresearchpress.com by 210.87.254.5 on 09/05/12
For personal use only.

Can. J. Chem. Downloaded from www.nrcresearchpress.com by 210.87.254.5 on 09/05/12
For personal use only.

Kinetics of Reactions of 8-Quinolinol and Acetate with Hydroxyaluminum Species in Aqueous Solutions. 2. Initial Solid Phases[1]

R. C. TURNER

Soil Research Institute, Research Branch, Canada Department of Agriculture, Ottawa, Canada

Received[2] April 27, 1970

The effects of p*H* and concentrations of 8-quinolinol and acetate on the rate of release of mononuclear Al from an initial solid phase formed by the rapid precipitation of mononuclear Al cations and from another formed by the precipitation of polynuclear hydroxyaluminum cations with NaOH were determined. With the solid formed by precipitation of the mononuclear Al cations, the rate was governed by the rate of dissolution of the solid. Dissolution occurred because the solution was undersaturated with respect to the solid. With the solid formed by the precipitation of the polynuclear cations the reaction behaved as if the rate determining step in the release of the mononuclear Al was the decomposition of the polynuclear cations after dissolution of the solid, indicating that the polynuclear cations persisted as such in the precipitate.

Independent evidence that the two initial solid phases were entirely different was indicated by the fact that the one formed by precipitation of mononuclear cations developed into gibbsite in a few days whereas the other did not.

L'influence du p*H* et de la concentration de l'hydroxy-8 quinoléïne et de l'acétate sur la formation de Al mononucléaire à partir d'une phase solide initiale, obtenue par précipitation rapide de cations Al mononucléaires, et d'une autre, formée par la précipitation de cations hydroxy-aluminium polynucléaires par NaOH, a été déterminée. Avec le solide, formé par précipitation des cations Al mononucléaires, la vitesse a été contrôlée par la dissolution du solide. La dissolution a eu lieu parce que la solution était insaturée par rapport au solide. Avec le solide formé par précipitation de cations polynucléaires, la réaction s'est comportée comme si l'étape déterminante de la vitesse de formation de Al mononucléaire était la décomposition des cations polynucléaires après dissolution du solide, indiquant que les cations polynucléaires sont restés comme tels dans le précipité.

Une preuve supplémentaire que les deux phases solides initiales sont différentes peut être apporteé par le fait suivant : celle obtenue par précipitation des cations mononucléaires se développe sous une forme gibbsite en quelques jours tandis que l'autre phase ne se développe pas sous cette forme.

Canadian Journal of Chemistry, **49**, 1688 (1971)

Introduction

It was shown in a previous publication (1) that the reaction between 8-quinolinol plus acetate at p*H* 5.05 and the initial solid phase formed by the rapid precipitation of $Al(OH)_3$ from an $AlCl_3$ solution with NaOH could be represented reasonably well by a 2/3 order process. It was assumed that the reaction was irreversible and went to completion via a 2/3 order process because the reaction mixture contained a high concentration of 8-quinolinol which remained essentially constant during the reaction. This implied that there was a direct reaction between the 8-quinolinol and the surface of the solids. Later (2) it was shown that both the 8-quinolinol and the acetic acid in the reaction mixture reacted with polynuclear hydroxyaluminum cations. Thus, the acetate played a double role; it not only acted as buffer to keep the reaction mixture at a constant p*H* but also was a source of acetic acid molecules which entered into the reaction. Studies similar to those made with the polynuclear hydroxyaluminum cations were therefore made with the initial solid phase.

It has been shown that, whereas the initial solid phase formed by the rapid precipitation from an $AlCl_3$ solution occurs near p*H* 4.5 (3, 4), the precipitation resulting from the neutralization of the polynuclear hydroxyaluminum cations occurs near p*H* 6.0 (4). The reaction between the initial solid formed in the latter way and 8-quinolinol plus acetate was also studied.

The object of the study, besides determining the kinetics of the reactions, was to see whether there was any real difference between the two initial solid phases, one formed by precipitation of mononuclear Al cations and the other by the precipitation of polynuclear hydroxyaluminum cations.

[1]Contribution No. 334.

[2]Revision received January 4, 1971.

Can. J. Chem. Downloaded from www.nrcresearchpress.com by 210.87.254.5 on 09/05/12
For personal use only.

Experimental

Initial solid phases were prepared by titrating Al salt solutions to pH 7.0 with NaOH solutions. In some cases the Al in the salt solution was in the form of mononuclear cations while in others it was in the form of polynuclear hydroxyaluminum cations. The solid formed from mononuclear cations will be referred to as ISP(M) and the other, formed from the polynuclear cations, will be referred to as ISP(P). The NaOH, in both cases, was added rapidly while the solutions were stirred vigorously. The final total Al concentrations in the suspensions were either 10^{-3} or 5×10^{-3} M. These suspensions were used in the rate studies without filtering. The procedure for the determination of the rate of release of mononuclear Al was the same as that used with the polynuclear cations (2).

Results and Discussion

It was shown previously (1) that the reaction of 8-quinolinol plus acetate at pH 5.05 with the initial solid phase ISP(M) could be represented by the equation

$$[1] \qquad C_0^{1/3} - C^{1/3} = k_c t$$

where C_0 is the concentration of ISP(M) expressed as Al^{3+} at t equals zero, C is the concentration at time t, and k_c is a constant for any given value of C_0 and temperature.

The experiments made to determine the effect of 8-quinolinol concentration on the rate constant k_c were done with the acetate concentration 1.44×10^{-1} M in the reaction mixture at pH 5.0 or 6.0 at 35 °C. As shown in the lower section of Fig. 1, the reaction at pH 5.0 or 6.0 could be represented reasonably well by eq. 1 with k_c equal to 3.3×10^{-4} $M^{-1/3}$ min^{-1} when the 8-quinolinol concentration was varied from 1.38×10^{-3} to 6.9×10^{-3} M. When the 8-quinolinol concentration was zero the reaction was somewhat faster than in the presence of 8-quinolinol when the pH was 5.0, but when the pH was raised to 6.0 the reaction rate was reduced to almost zero.

Calculations showed that at pH 5.0 when all of the solid was dissolved even if no complexing occurred between mononuclear Al and 8-quinolinol and/or acetate, the ion activity product $(Al)(OH)^3$ would be less than $10^{-31.7}$, the solubility product of the initial solid phase (3, 4). When the pH was 6.0, however, the solution would be saturated with respect to the initial solid phase after very little dissolution unless considerable complexing of the mononuclear Al occurred. Apparently with only acetate present there was not sufficient complexing of mononuclear Al at pH 6.0 to maintain the solution undersaturated with respect to the solid and therefore dissolution did not occur. On the other hand, when 8-quinolinol was present as well as the acetate there was apparently sufficient complexing of the mononuclear Al ions to maintain the solution undersaturated with respect to the solid at pH 6.0 and dissolution occurred as fast at pH 6.0 as at 5.0. The conclusion, on the basis of this interpretation, is that there is no direct reaction

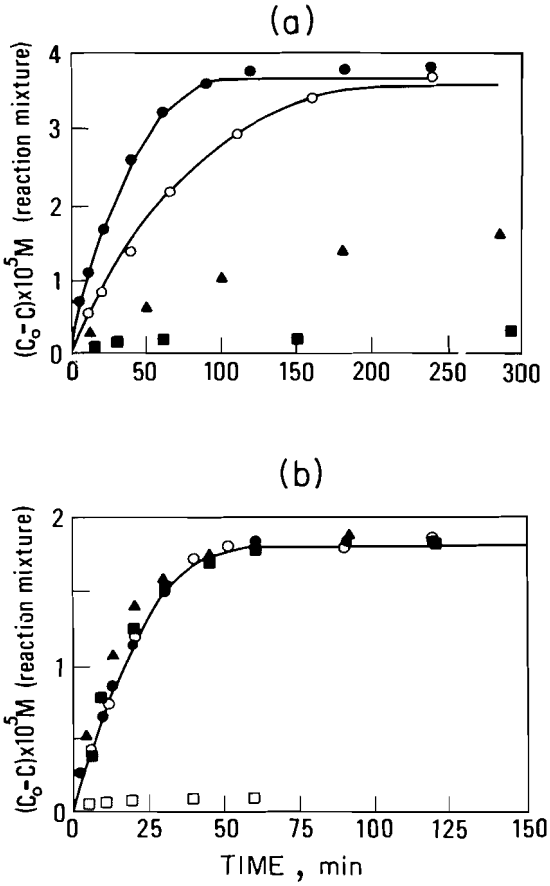

FIG. 1. Rate of decomposition of initial solid phase formed by precipitation of mononuclear Al cations. (*a*) Effect of ageing the precipitate on the rate of decomposition at 26 °C. ●, less than 1 min and the smooth curve is eq. 1 with $k_c/C_0^{1/3} = 7.8 \times 10^{-3}$ min^{-1}. ○, 40 min and the smooth curve is eq. 1 with $k_c/C_0^{1/3} = 3.9 \times 10^{-3}$ min^{-1}. ▲, 24 h; ■, 9 days. (*b*) Effect of varying concentrations of 8-quinolinol and pH at 35 °C. pH either 5.0 or 6.0 and 8-quinolinol ●, 6.9×10^{-3} M; ○, 3.7×10^{-3} M; ■, 1.38×10^{-3} M. 8-Quinolinol zero and ▲, pH 5.0; □, pH 6.0. The smooth curve is eq. 1, with $k_c = 3.3 \times 10^{-4}$ min^{-1} $M^{-1/3}$.

Can. J. Chem. Downloaded from www.nrcresearchpress.com by 210.87.254.5 on 09/05/12
For personal use only.

between 8-quinolinol or acetate and the solid phase; dissolution occurs because the solution is undersaturated with respect to the solid. The 8-quinolinol and acetate play an indirect role, *i.e.*, they contribute to maintaining the solution undersaturated by complexing the mononuclear aluminum cations. Thus the assumption made in the earlier publication (1) that the dissolutions of the ISP(M) goes to completion via a 2/3 order process because there is a direct reaction between 8-quinolinol and the surface of the solid must be modified.

Figure 1*a* shows the effect of ageing the ISP(M) on the rate of the reaction. When the length of time of ageing was as short as it was physically possible to make it, less than 1 min from the beginning of addition of NaOH to the $AlCl_3$ solution to the beginning of the rate experiment, $k_c/C_0^{1/3}$ was 7.8×10^{-3} min^{-1} at 26 °C whereas when the length of time ageing was 40 min it was 3.9×10^{-3} min^{-1}. With 24 h ageing the rate was very slow and could not be represented by eq. 1, and after nine days ageing only a very small fraction of the solid was dissolved in 5 h.

When the initial solid phase was ISP(P), *i.e.*, when it was formed by precipitation of polynuclear hydroxyaluminum cations rather than mononuclear Al cations, its reaction with 8-quinolinol plus acetate was entirely different. As shown in Fig. 2 the rate of release of mononuclear Al from the solid was not affected by ageing and was similar to that which occurred with polynuclear hydroxyaluminum cations, *i.e.*, it approximated a first order process with rate constant equal to 0.16 min^{-1} (2). It appeared therefore that the rate determining step was the decomposition of the polynuclear cation resulting from dissolution of the solid. To check this possibility the following experiments were made.

An aliquot of the suspension containing the ISP(P) was filtered through a VS Millipore filter and the filtrate was found to contain only a trace of Al showing that the precipitation was essentially complete. Another aliquot was suspended in 0.1 *N* NaOAc which had been adjusted to p*H* 5.0 and filtered immediately through a VS Millipore filter. All of the solid was dissolved and the Al passed through the filter but only a very small fraction of it was measured as mononuclear cations. The remainder reacted with the 8-quinolinol plus acetate reaction mixture at p*H* 5.0 via a first order process with rate constant 0.16 min^{-1} (Fig. 2). Thus, although the dissolution

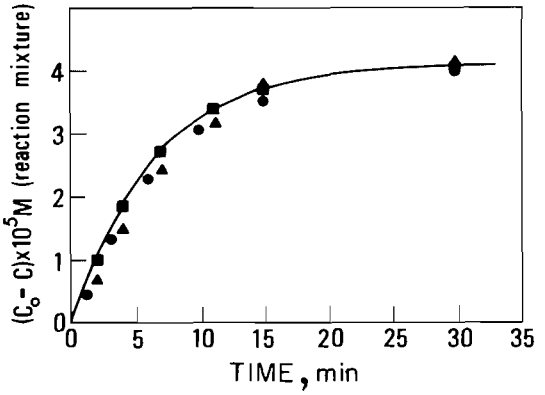

FIG. 2. Rate of decomposition of initial solid phase formed by precipitation of polynuclear hydroxyaluminum cations. ●, Immediately after precipitation; ▲, 8 days after precipitation; ■, filtrate from acetate treatment of precipitate. Smooth curve is the first order rate curve with $k = 0.16$ min^{-1}.

of the solid in the acetate solution at p*H* 5.0 was very rapid, the result of dissolution was polynuclear hydroxyaluminum cations. The polynuclear cations could not have been formed from mononuclear Al cations in the 0.1 *N* NaOAc at p*H* 5.0 because it has been shown that they are destroyed under these conditions (2). Furthermore, when the initial solid phase formed by the precipitation of mononuclear Al cations ISP(M), was suspended, immediately after precipitation, in 0.1 *N* NaOAc adjusted to p*H* 5.0, only about 20% of the solid dissolved and passed through a VS Millipore filter; and this 20% was in the mononuclear Al form. It must be concluded, therefore, that the polynuclear hydroxyaluminum cations are sufficiently stable to go through precipitation by NaOH and redissolution as well as exchange reactions with clays (5) and resins (6).

Further evidence that the two initial solid phases were entirely different was the fact that at the end of the 8 days ageing, the one formed from precipitation of the polynuclear cations was amorphous to X-rays whereas the other showed a good gibbsite pattern.

The X-ray analysis was done by N. M. Miles.

1. R. C. TURNER. Can. J. Chem. **47**, 2521 (1969).
2. R. C. TURNER and WAN SULAIMAN. Can. J. Chem. This issue.
3. C. R. FRINK and B. L. SAWHNEY. Soil Sci. **103**, 144 (1967).
4. R. C. TURNER. Soil Sci. **106**, 338 (1968).
5. R. C. TURNER. Can. J. Soil Sci. **47**, 217 (1967).
6. M. HONDA. J. Chem. Soc. Japan (Pure Chem. Sect.) **72**, 555 (1951).

Can. J. Chem. Downloaded from www.nrcresearchpress.com by 188.143.235.115 on 09/06/12
For personal use only.

Carbon Disulfide. V. Reaction with Azibenzil[1,2]

PETER YATES,[3] B. G. CHRISTENSEN, AND L. L. WILLIAMS
The Departments of Chemistry, Harvard University, Cambridge, Massachusetts 02138, and the University of Toronto, Toronto 5, Ontario

Received December 8, 1970

The product formed by the reaction of azibenzil (2-diazo-2-phenylacetophenone) with carbon disulfide has been shown to be 2-(α-phenylphenacylidene)-5,5-diphenyl-1,3-dithiolan-4-one (**9**).

On démontre que le produit de la réaction entre l'azibenzil (diazo-2 phényl-2 acétophénone) et le sulfure de carbone est la (α-phénylphénylacylidène)-2 diphényl-5,5 dithiolanone-1,3,4 (**9**).

Canadian Journal of Chemistry, 49, 1691 (1971)

The reaction of carbon disulfide with azibenzil (2-diazo-2-phenylacetophenone, **1**) was first described by Meyer (4). He found that when a solution of **1** in carbon disulfide was boiled under reflux, a yellow crystalline product, $C_{29}H_{20}O_2S_2$, was formed readily in high yield. Basic hydrolysis of this material was found to give benzoic, phenylacetic, and diphenylacetic acids, together with another acid that was considered to be thiobenzilic acid (**2**). On this basis Meyer proposed **3** as the structure of the reaction product.

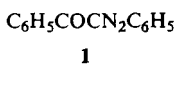

1

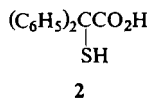

2

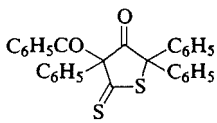

3

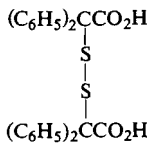

4

In our hands Meyer's experimental results were reproduced, except that in the basic hydrolysis 2,2,5,5-tetraphenyl-3,4-dithiaadipic acid (**4**) was isolated rather than **2**. This product is doubtless produced by air oxidation of **2**, and the structural implications of its formation are the same as for **2**. However, the i.r. and u.v. spectra of the compound $C_{29}H_{20}O_2S_2$ were not in accord with structure **3**. Its i.r. spectrum showed bands at 5.86(s), 5.98(w), and 6.17 μ (mw), in addition to bands associated with the phenyl ring vibrations. Its u.v. spectrum showed maxima at 254 (ε 17 000) and 347 mμ (ε 13 800) and very strong end absorption. These spectra strongly suggested the presence of the part structure **5**; they may be compared with the spectra of **6** (5*a*): λ_{max} 6.20 μ; 257 (ε 10 700) and 350 mμ (ε 15 800).[4] A further spectroscopic analogy supports this conclusion: a set of strong bands in the 7.4–7.9 μ region of the i.r. spectra of the product $C_{29}H_{20}O_2S_2$, compound **6**, the desaurin **7**[5] (5), and both the trithiolane **8** and one of its *cis* isomers (1).

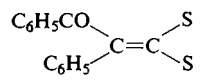

5

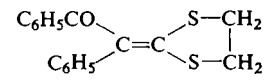

6

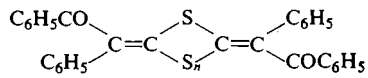

7 $n = 1$
8 $n = 2$

Given the part structure **5**, two structures must be considered for the compound $C_{29}H_{20}O_2S_2$, *viz.* **9**[6] and **10**. Of these, **9** may be preferred on the

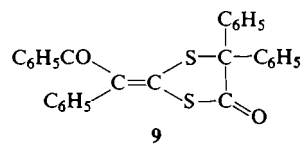

9

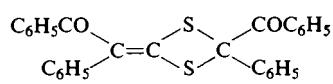

10

[1]For Paper IV see ref. 1.

[2]Preliminary reports of this work have appeared (2, 3).

[3]Lash Miller Chemical Laboratories, Department of Chemistry, University of Toronto, Toronto 5, Ontario.

[4]The differences in these spectra may be attributed to the presence of an additional chromophore in the compound $C_{29}H_{20}O_2S_2$.

[5]The stereochemical assignment for the desaurin is provisional (5).

[6]No stereochemical assignment is implied by this and subsequent structures, unless specifically discussed.

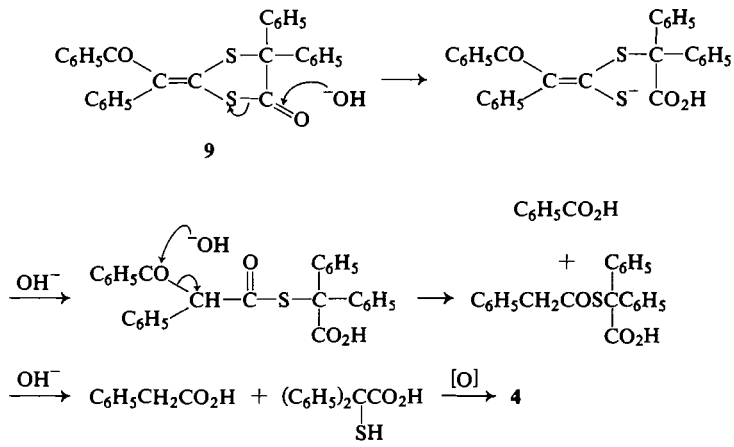

SCHEME 1

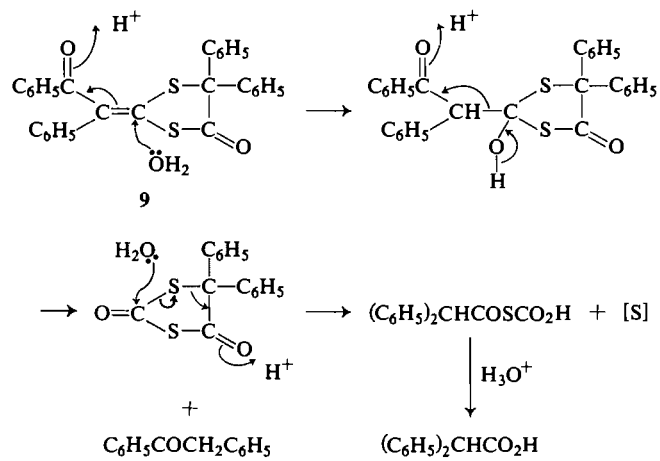

SCHEME 2

basis of the formation of products with geminal phenyl groups in several of the degradation reactions of the compound $C_{29}H_{20}O_2S_2$ now to be discussed.

It may first be noted that the products obtained on basic hydrolysis can readily be interpreted in terms of structure **9** (Scheme 1).[7]

Acidic hydrolysis of the compound $C_{29}H_{20}O_2S_2$ gave diphenylacetic acid, deoxybenzoin, and sulfur, products whose formation can again be readily interpreted in terms of structure **9** (Scheme 2).

Desulfurization of the compound $C_{29}H_{20}O_2S_2$ with deactivated Raney nickel in ethanol gave principally ethyl diphenylacetate and α-methyldeoxybenzoin (**11**), together with a small amount of diphenylmethane. These products could arise from **9** as shown in Scheme 3; alternatively, ethyl diphenylacetate could be formed via diphenylketene.

Reduction of the compound $C_{29}H_{20}O_2S_2$ with zinc in boiling acetic acid gave a colorless dihydro product, whose i.r. spectrum showed a broad band at 5.94 μ. Its u.v. spectrum had a maximum at 252 mμ (ε 15 900), and its p.m.r. spectrum showed an AB signal system (δ 4.62 and 5.28, J = 11 Hz, 2H). Basic hydrolysis gave deoxybenzoin and diphenylacetic acid, and desulfurization with

[7]This and the following schemes are illustrative only; it is clear that many variations in detail are possible.

Can. J. Chem. Downloaded from www.nrcresearchpress.com by 188.143.235.115 on 09/06/12
For personal use only.

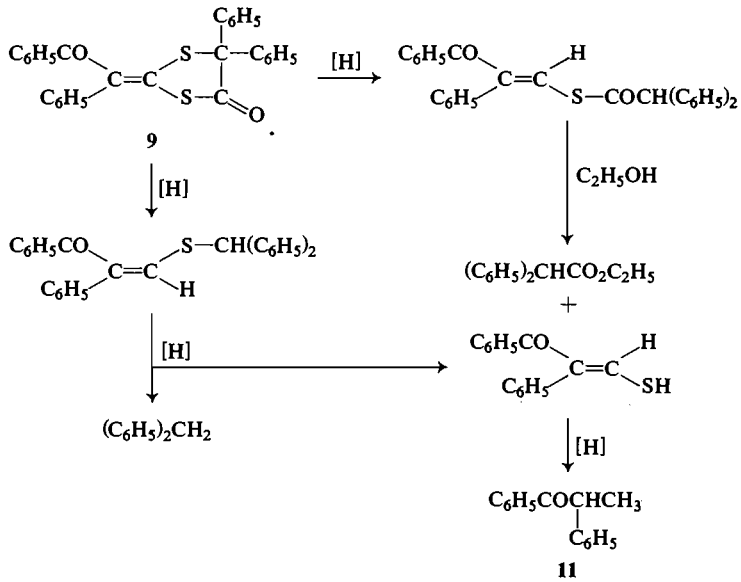

SCHEME 3

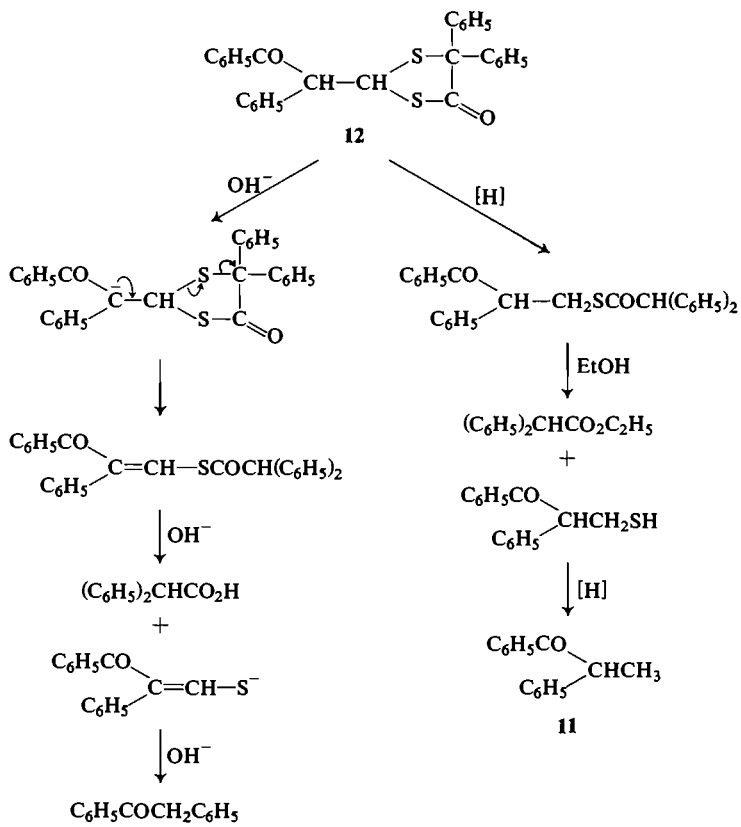

SCHEME 4

Can. J. Chem. Downloaded from www.nrcresearchpress.com by 188.143.235.115 on 09/06/12
For personal use only.

Can. J. Chem. Downloaded from www.nrcresearchpress.com by 188.143.235.115 on 09/06/12
For personal use only.

Raney nickel in ethanol gave ethyl diphenylacetate, methyldeoxybenzoin (**11**), and a trace of 1,1,2,2-tetraphenylethane. These data can be interpreted in terms of structure **12** for the dihydro product, derived by reduction of the ethylenic double bond of the α,β-unsaturated carbonyl system of **9**. The broad carbonyl-stretching band can be assigned to overlapping absorption of the benzoyl and thio lactone groups, and the u.v. maximum to the former group.[8] The degradation products can arise by the routes shown in Scheme 4 (the formation of the tetraphenylethane as a minor product on treatment with Raney nickel is probably related to the formation of diphenylmethane from **9**, proceeding via the diphenylmethyl radical).

Ozonolysis of the compound $C_{29}H_{20}O_2S_2$ followed by hydrolytic work-up gave benzil and benzoic acid, together with a small amount of diphenylacetic acid. When reductive work-up with zinc and hot aqueous acetic acid was used, the neutral product was benzoin rather than benzil. The formation of benzoic acid from a compound with the structural feature **13** can proceed via benzoic anhydride, whose formation finds analogy, for example, in the ozonolysis of **14** (7). The failure to isolate more than small amounts of geminal diphenyl derivatives may be due to the incorporation of water-soluble sulfonic acid residues. Evidence was obtained that indicated the formation of sulfuric acid in the reaction, but this accounted for only a small fraction of the sulfur in the starting material.

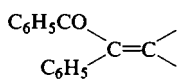

13

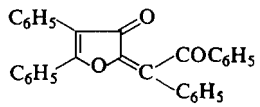

14

Oxidation of the compound $C_{29}H_{20}O_2S_2$ with perphthalic acid led to the formation of a compound $C_{29}H_{20}O_3S_2$. Since this product regenerates the compound $C_{29}H_{20}O_2S_2$ on treatment with zinc and acetic acid at room temperature, it is highly probable that it has been formed without skeletal change. Three structures then come into consideration on the basis of structure **9** for the compound $C_{29}H_{20}O_3S_2$, *viz.*, **15**, **16**, and **17**. Of these **17** may be rejected, since it is most unlikely that the electron poorer of the two sulfur atoms of **9** would undergo preferential attack by peracid. Treatment of the compound $C_{29}H_{20}O_3S_2$ with aqueous ethanolic sodium hydroxide gave benzophenone and the desaurin **7**. The formation of these products can be interpreted in terms of structure **16** as shown in Scheme 5. The cleavage of the sulfenic acid **18** to give thiobenzophenone finds analogy in the observation that the disulfide **4** undergoes partial conversion to thiobenzophenone (**20**) in aqueous base (8); the further conversion of **20** to benzophenone with aqueous ethanolic sodium hydroxide has also been observed previously. The conversion of the thioketene **19** to the desaurin **7** may well not involve simple dimerization, but may proceed via attack of hydroxide or methoxide ion to give a β-keto thio acid or ester as an intermediate (*cf.* ref. 5*b*).

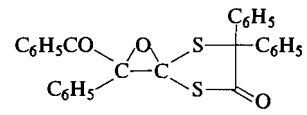

15

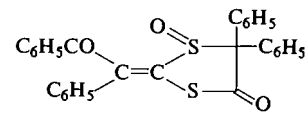

16

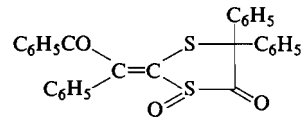

17

The formation of these products is more difficult to interpret in terms of structure **15** in that the segment of the molecule that would have to serve as the source of the desaurin is in too high an oxidation state, while that which must serve as the source of the benzophenone is in too low an oxidation state. Furthermore, the i.r. and u.v. spectra of the compound $C_{29}H_{20}O_3S_2$ are in better accord with structure **16**. Thus, its i.r. spectrum ($CHCl_3$) showed carbonyl-stretching bands at 5.83 and 5.97 μ that may be assigned to the thio lactone and benzoyl carbonyl groups in **16**, respectively. The conversion of the thio ether function to a sulfoxide function should inhibit the

[8]Thiol esters have absorption maxima at *ca.* 235 mμ (ε 4000) (6) and thus the thio lactone absorption would be expected to be masked by the maximum due to the benzoyl group and the intense end absorption.

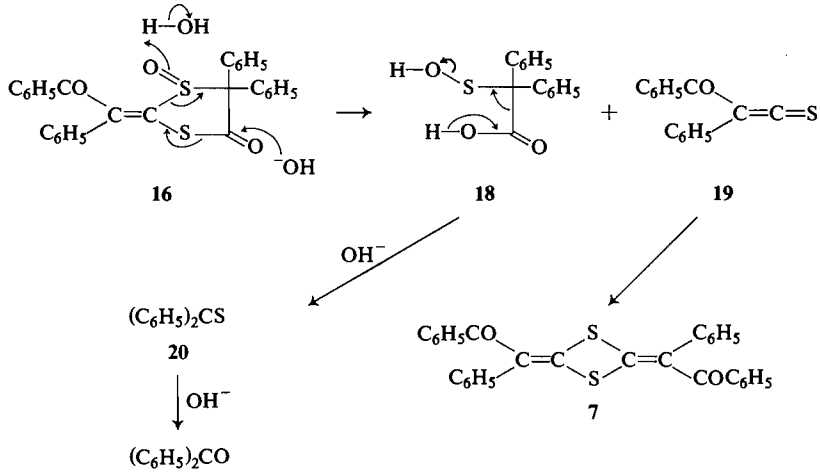

SCHEME 5

interaction of this sulfur atom with the benzoyl carbonyl group and also partially inhibit the interaction of this carbonyl group with the ethylenic double bond, thus accounting for the fact that the carbonyl-stretching band due to the benzoyl group occurs at a wavelength only slightly longer than that observed for simple benzoyl groups [*cf.* methylenedeoxybenzoin (**21**): $\lambda_{max}(CCl_4)$ 5.95 μ (10)].[9] The sulfoxide function could also be responsible for the observed small hypsochromic shift of the thio lactone band relative to that of **9**. Finally, it may be noted that a strong band occurs at 9.27 μ, close to the range assigned to the sulfoxide group (9). On the other hand, it is unlikely that the benzoyl group in structure **15** would have its carbonyl-stretching band at longer wavelength than that for simple benzoyl compounds, and it would be expected that the thio lactone carbonyl-stretching band would occur at longer rather than shorter wavelength than that for **9**.

The u.v. spectrum of the perphthalic acid oxidation product showed a maximum at 263 mμ (ε 23 400) with a shoulder at 287 mμ (ε 16 500). This spectrum is in good accord with structure **16**; the considerable hypsochromic shift relative to the long wavelength maximum in the spectrum of **9** being again attributable to inhibition of the interaction between the thio ether sulfur atom and the α,β-unsaturated carbonyl system upon oxidation of this sulfur to a sulfoxide function. The spectrum may be compared with that of **21**, which shows a maximum at 247 mμ (ε 20 900) (10). Although models are lacking for the epoxy ketone structure **15**, it seems unlikely that this would show such strong absorption at 287 mμ.

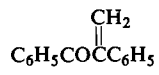

21

Thus, although no single observation rigorously excludes structure **15**, the weight of the evidence favors the assignment of structure **16**. It may be noted that in simpler cases it has been found that oxidation of vinyl sulfides with peracids gives sulfoxides rather than epoxides (11).

As pointed out earlier, the formation of geminal diphenyl derivatives in several of the degradation reactions of the compound $C_{29}H_{20}O_2S_2$ favors the assignment of **9** rather than **10** as its structure. However, most of these reactions were carried out under vigorous conditions, and the possibility existed that the residue **22** arose by rearrangement of the residue **23**. Furthermore, in none of the degradation reactions had products been isolated that provided direct evidence of the environment of both sulfur atoms. A very mild method of degradation was therefore sought.

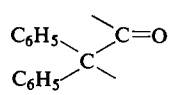

22

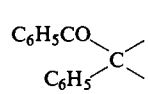

23

[9]As has been noted earlier, it is anticipated that the other sulfur atom would not interact strongly with the α,β-unsaturated carbonyl system because of its incorporation into a thio lactone function.

Can. J. Chem. Downloaded from www.nrcresearchpress.com by 188.143.235.115 on 09/06/12
For personal use only.

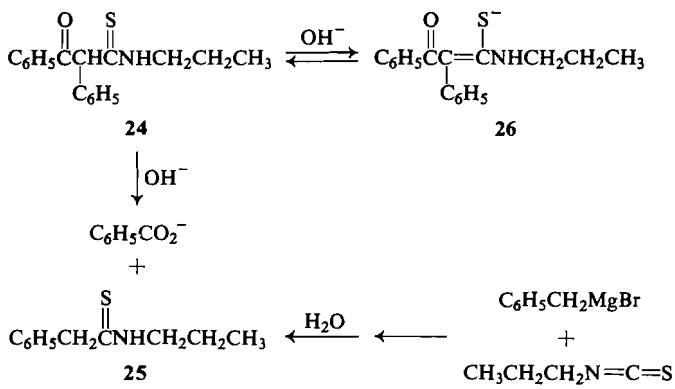

SCHEME 6

Treatment with propylamine in chloroform solution at room temperature provided such a method. The reaction mixture rapidly assumed a bright red color, which slowly faded; further addition of amine resulted in regeneration of the red color until 2 molar equivalents had been added. The characteristic odor of hydrogen sulfide indicated its formation during the reaction. Two compounds were isolated by fractional crystallization of the product mixture.

The lower melting, more soluble compound, $C_{18}H_{19}NOS$, is assigned structure **24** on the following basis. On treatment with dilute aqueous sodium hydroxide at room temperature, it slowly dissolves, after which an oily product separates from solution. The latter product was shown to be the thio amide **25** by direct comparison with a sample prepared from the reaction of benzylmagnesium chloride with propyl isothiocyanate. Acidification of the basic solution from the hydrolysis reaction gave benzoic acid. Thus the compound $C_{18}H_{19}NOS$ must be a benzoyl derivative of **25**; the only such derivative that would be expected to be base-soluble is **24**, which could form the anion **26** (Scheme 6). In accord with this assignment, a solution of the compound rapidly gave a black precipitate when treated with mercuric oxide, indicating the presence of a thiocarbonyl group (12).

The spectroscopic data for compound **24** are in good accord with the assigned structure and show that this compound has the preferred conformation ***24a*** in solution. Its i.r. spectrum showed a single carbonyl-stretching band at 5.98 μ, assigned to the hydrogen-bonded benzoyl carbonyl group in ***24a***; it also showed a band at 3.01 μ (with shoulder at 2.95 μ) attributable to a hydrogen-bonded N—H stretching vibration (the shoulder may result from the presence of conformations other than ***24a***). Its u.v. spectrum in methanol showed maxima at 249 (ε 15 900) and 265 mμ (infl., ε 12 300), attributable to the benzoyl and thio amide groups, respectively [*cf.* thioacetamide λ_{max}(EtOH) 265 mμ (ε 13 800) (13)].

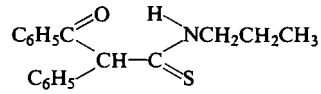

24a

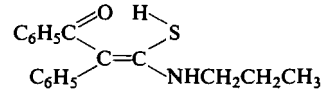

24b

When the u.v. spectrum was recorded in methanolic sodium methoxide these maxima were shifted to 273 (ε 7800) and 340 mμ (ε 15 100), a change that can be attributed to formation of the anion **26**. Its p.m.r. spectrum showed signals at δ 0.9(t), 1.55(m), and 3.42(m), assigned to the *N*-propyl protons, a singlet at 6.30, assigned to the benzylic proton, multiplets at 7.33 and 8.05, assigned to the phenyl protons, and a broad signal at 9.30, in good accord with the presence of a strongly hydrogen-bonded thio amide proton.

The spectral data exclude the possibility that **24** exists in solution as the enethiol tautomer ***24b***. This would be expected to show i.r. and u.v. bands at much longer wavelengths than those observed (1, 5, 10). Further, the p.m.r. spectrum of such a species would be expected to show a signal at $\delta \gg 10$, due to chelate-type hydrogen bonding. Although β-keto dithio acids and their derivatives

Can. J. Chem. Downloaded from www.nrcresearchpress.com by 188.143.235.115 on 09/06/12
For personal use only.

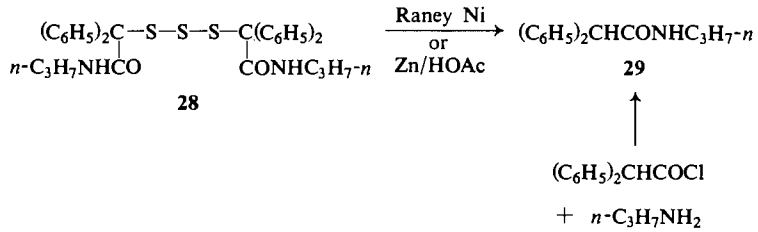

SCHEME 7

often exist to a significant extent as the corresponding enethiol tautomers (5, 10), it is not surprising in the present case that **24***a* should be favored over **24***b*. Gompper and Schaefer (14) have found that the β-keto thioamide **27** exists in the solid state in the unenolized form **27***a*, and that in solution in chloroform the tautomer ratio **27***a*:**27***b* is 6:4. It would be expected in the case of

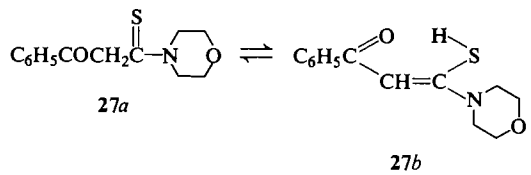

27*a* **27***b*

24 that the unenolized form **24***a* would be considerably more favored than in the case of **27***a*, both because **24***a* derives additional stabilization from hydrogen bonding and because **24***b* is destabilized more than **24***a* by steric interactions between the phenyl groups.

The second compound isolated from the aminolysis of the compound $C_{29}H_{20}O_2S_2$ was found to have the formula $C_{34}H_{36}N_2O_2S_3$. It is assigned structure **28** on the basis of the following data. Reduction with either Raney nickel or zinc and acetic acid gave 2 molar equivalents of the amide **29**, whose structure was established by direct comparison with a sample prepared from diphenylacetyl chloride and propylamine (Scheme 7). The compound $C_{34}H_{36}N_2O_2S_3$ was insoluble in dilute aqueous sodium hydroxide and failed to give a sodium nitroprusside test, indicating the absence of sulfhydryl groups (15); it also failed to react with mercuric oxide, indicating the absence of thione groups (12). The sulfur atoms must then be present as sulfide or polysulfide linkages joining two residues related to **29**. The removal of all three sulfur atoms by treatment with zinc and acetic acid can then only be interpreted in terms of the structural assignment **28** or the closely related branched trisulfide **30**. Although the latter structure cannot be excluded rigorously, structure **28** is preferred since branched bonding at sulfur appears to occur only in those cases in which the sulfur atom to which the branch is attached is also bonded to a highly electronegative atom (16).

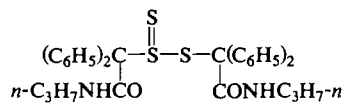

30

The i.r. and u.v. spectra of the compound $C_{34}H_{36}N_2O_2S_3$ are in good accord with the assignment of structure **28**. The former showed all the bands of **29** and no others of appreciable intensity. This is in agreement with expectation since neither C—S nor S—S single bonds give rise to bands of high intensity (17). The u.v. spectrum showed no clear cut maxima but medium intensity absorption at 300 mμ rising steadily to high intensity end absorption with an inflection at *ca.* 270 mμ (ε 6500). In appearance it is strikingly similar to the u.v. spectrum of dibenzyl disulfide (18), although greater in intensity. It can be interpreted in terms of overlap of absorption due to geminal phenyl groups (19) and the trisulfide group (*cf.* ref. 20).

The three-sulfur compound **28** must have arisen in a secondary reaction after the primary aminolysis (Scheme 8). Its precursor is clearly the thiol **31**. It could be formed from this via air oxidation to the disulfide **32** (*cf.* the formation of the disulfide **4** during the hydrolysis of **9**) followed by attack of hydrosulfide ion (the formation of hydrogen sulfide during the reaction has already been noted) to give **33** and oxidative coupling of this with **31**; alternatively, **33** might arise via oxidative coupling of **31** with hydrogen sulfide. The yield of **28** was only 39%, and it is possible that the reaction mixture also contained **32** and the tetrasulfide corresponding to **33**.

The formation of **24** and **31** on treatment of the

Can. J. Chem. Downloaded from www.nrcresearchpress.com by 188.143.235.115 on 09/06/12
For personal use only.

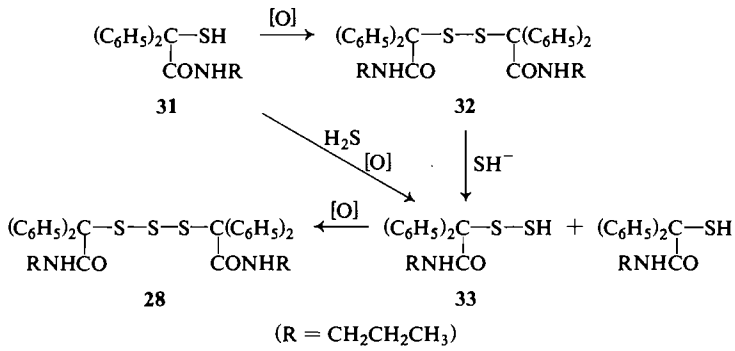

(R = $CH_2CH_2CH_3$)

SCHEME 8

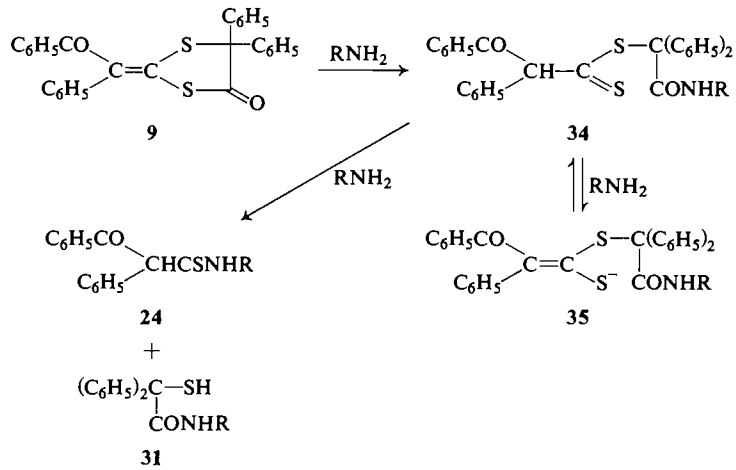

(R = $CH_2CH_2CH_3$)

SCHEME 9

compound $C_{29}H_{20}O_2S_2$ is readily interpretable in terms of structure **9** for that compound as shown in Scheme 9. This scheme accounts for the formation of a red-colored species during the course of the reaction, the anion **35** of the β-keto dithio ester **34**. The hydrogen sulfide observed to be formed could arise by reaction of **24** or **35** with propylamine (*cf.* ref. 21).

The isolation of the product **28** from a reaction carried out under such mild conditions supports the earlier conclusion that a geminal phenyl grouping is present in the compound $C_{29}H_{20}O_2S_2$ and that its structure is better represented by **9** than by **10**.

The choice of structure **9** was finally vindicated by an alternative synthesis of the compound $C_{29}H_{20}O_2S_2$, albeit in very low yield, by the route shown in Scheme 10. This route was adopted in analogy to that used for the synthesis of **6** (5). The product obtained in this way was identical in all respects with that formed in the reaction of azibenzil with carbon disulfide.

The degradative and synthetic evidence presented in favor of the assignment of structure **9** do not exclude the closely related structure **36**, a valence bond isomer of **9** containing a tetracovalent sulfur atom. This might account for the apparent [10] relatively low intensity of the band assigned to the carbonyl-stretching vibration of the benzoyl group in **9**. However, X-ray crystallographic studies in related cases of compounds with the *s-cis* grouping **37** have shown that although the S—O distances are considerably

[10]No quantitative intensity measurements have been made; *cf.* refs. 1 and 5.

Can. J. Chem. Downloaded from www.nrcresearchpress.com by 188.143.235.115 on 09/06/12
For personal use only.

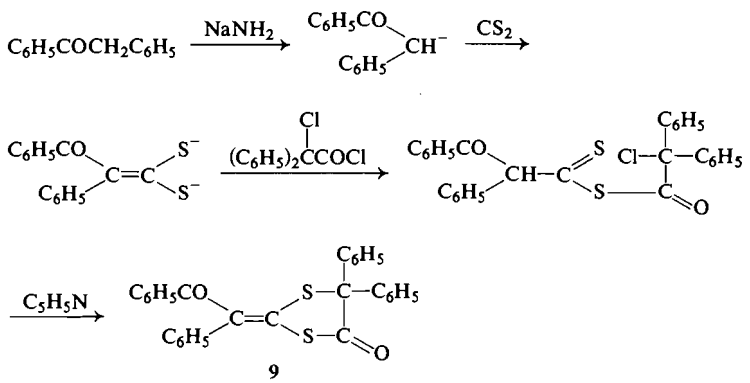

9

SCHEME 10

shorter than the sum of the van der Waals' radii of sulfur and oxygen, they are appreciably longer than the normal S—O covalent bond length (22). Furthermore, Kapecki and Baldwin (23) have concluded from extended Hückel molecular orbital calculations that covalent bonding between sulfur and oxygen is negligibly weak in related cases. Thus structure **9** is considered to be the best representation of the compound $C_{29}H_{20}O_2S_2$, although there may be weak bonding between the oxygen atom of the benzoyl group and one of the sulfur atoms.[11]

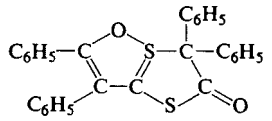

36

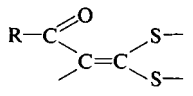

37

A variety of pathways can be envisaged for the formation of **9** from azibenzil and carbon disulfide. All must involve at some stage the rearrangement of one of the two azibenzil residues that are incorporated into the product. In one type of mechanism this is accomplished by a Wolff rearrangement of azibenzil to diphenylketene. However, it has been found that addition of diphenylketene to the reaction mixture of azibenzil and carbon disulfide does not increase the yield of the product, and it thus appears unlikely that diphenylketene is an intermediate. An alternative type of mechanism is illustrated in Scheme 11. Electrophilic attack by carbon disulfide on azibenzil could give **38**; loss of nitrogen would then give **39**. Alternatively, this could be formed via **40**, whose formation would find analogy in the reaction of aliphatic diazo compounds with thiones (24). Reaction of **39** with a second molecule of azibenzil would give **42**, either directly or via **41**. Elimination of nitrogen from **42** accompanied by phenyl group migration would give **9**.[12]

The reaction of two other α-diazo ketones with carbon disulfide have been reported recently. 3-Diazo-2-butanone (**43**) was found to react with carbon disulfide to give a product, $C_9H_{12}O_2S_2$, that was originally assigned structure **44** by analogy with the case of azibenzil (25). However, its structure was subsequently shown to be **45** by

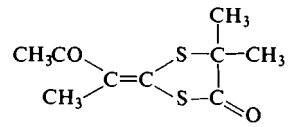

44

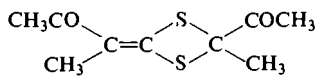

45

X-ray crystallography (22*b*). It is possible to interpret this behavior in terms of Scheme 11. In the case of 3-diazo-2-butanone the rearrangement corresponding to the step **42** → **9** requires the migration of a methyl group rather than a phenyl group as in the case of azibenzil. It may be anticipated that such a migration will be less ready,

[11]It should be reemphasized here that the geometry depicted about the ethylenic double bond in **9** is arbitrary and no evidence is available regarding the configuration or conformation of the product.

[12]It is not excluded that the processes depicted in Scheme 11 occur in a more concerted fashion.

Can. J. Chem. Downloaded from www.nrcresearchpress.com by 188.143.235.115 on 09/06/12
For personal use only.

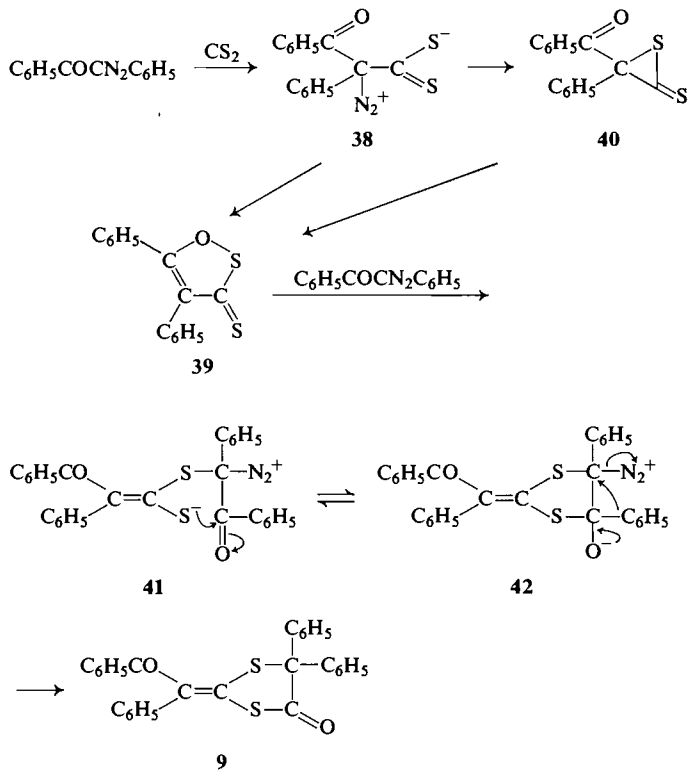

SCHEME 11

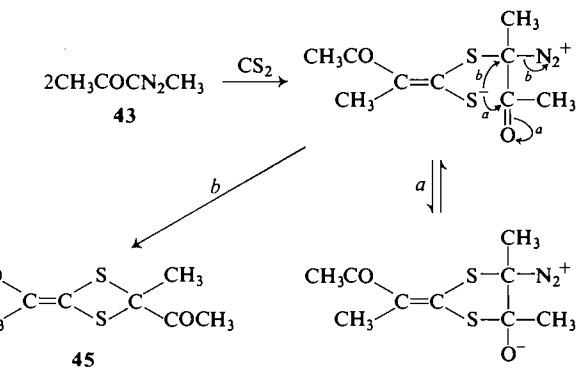

SCHEME 12

and, if the intermediate corresponding to **42** is formed reversibly from that corresponding to **41**, an alternative pathway could be traversed from the latter, leading to the formation of **45** (Scheme 12).

Baldwin and Kapecki (26) have investigated the reaction of *p*-fluorobenzoyl-*p*-fluorophenyldiazomethane (**46**) with carbon disulfide. They obtained as the major product a compound $C_{29}H_{16}F_4O_2S_2$, analogous in composition to **9** and **45**. They concluded that this product was better represented by structure **47**, analogous to **9**, than by a structure analogous to **45**, on the basis of its ^{19}F n.m.r. spectrum, which showed three signals with an intensity ratio of 1:1:2 in both tetrahydrofuran and bromoform solution [*cf.* **45**, which shows in its p.m.r. spectrum four methyl proton signals (25)]. The preferential for-

Can. J. Chem. Downloaded from www.nrcresearchpress.com by 188.143.235.115 on 09/06/12
For personal use only.

Can. J. Chem. Downloaded from www.nrcresearchpress.com by 188.143.235.115 on 09/06/12
For personal use only.

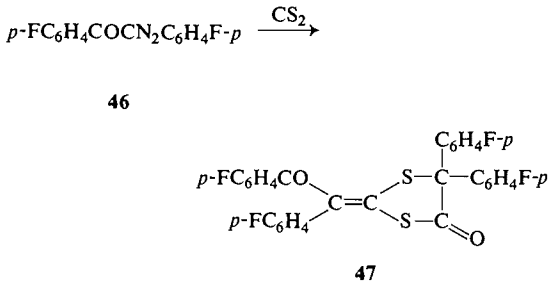

46 47

mation of **47** can again be interpreted in terms of the above rationale.

Experimental

Solutions in organic solvents were dried over anhydrous sodium sulfate, unless otherwise indicated. The i.r. spectra were taken in chloroform solution unless otherwise indicated.

Reaction of Azibenzil with Carbon Disulfide (4). Formation of 9

Azibenzil (22.0 g, 106 mmol), prepared by the method of Nenitzescu and Salomonica (27), was dissolved in carbon disulfide (120 ml, 1.99 mol). The solution was boiled under reflux for 36 h. Carbon disulfide was removed by heating the solution on the steam bath at water aspirator pressure until the product began to crystallize. The mixture was then cooled in an ice bath, and the product was filtered. It was washed with ether and recrystallized from carbon disulfide to give **9** as a pale yellow crystalline solid (22.5 g, 92%), m.p. 154–155° [lit. (4) m.p. 153–154°]; λ_{max} 5.86, 5.98 (w), 6.17 μ (mw); $\lambda_{max}(CHCl_3)$ 254 (ε 17 000), 347 mμ (ε 13 800).

Anal. Calcd. for $C_{29}H_{20}O_2S_2$: C, 74.97; H, 4.34; S, 13.80. Found: C, 74.83; H, 4.46; S, 13.71.

Compound **9** was recovered unchanged after treatment with yellow mercuric oxide in boiling benzene for 30 min and with boiling 2% alcoholic silver nitrate for 15 min.

Basic Hydrolysis of 9

A mixture of **9** (12.0 g, 25.8 mmol) and a solution of potassium hydroxide (16.0 g, 285 mmol) in 95% ethanol (50 ml) was boiled under reflux for 7 h. It was cooled to room temperature, diluted with a four-fold excess of water, and acidified to p*H* 1 with concentrated hydrochloric acid, when hydrogen sulfide was evolved. The mixture was heated on the steam bath for a few minutes, cooled, neutralized with aqueous 10% sodium bicarbonate, and filtered. The filtrate was acidified (p*H ca.* 1) and extracted three times with ether. The combined ethereal extracts were dried and evaporated on the steam bath to give a solid (10.4 g). This was extracted three times with petroleum ether (b.p. 30–60°). The red oil (4.8 g) that remained undissolved was extracted with benzene. Evaporation of the benzene from this extract afforded a white solid (100 mg), m.p. 194–196° (dec.). This product was soluble in aqueous 5% sodium bicarbonate with evolution of carbon dioxide and after several recrystallizations from carbon disulfide had m.p. 199.5–200.5° dec.; λ_{max}(KI) 5.99 μ.

Anal. Calcd. for $C_{28}H_{22}O_4S_2.H_2O$ (mol. wt. 504): C, 66.64; H, 4.80; S, 12.71. Found (neut. equiv. 247): C, 66.32; H, 4.76; S, 13.13.

The m.p. of authentic 2,2,5,5-tetraphenyl-3,4-dithiaadipic acid (**4**) (*vide infra*) was undepressed on admixture with this product; the i.r. spectra of the two samples were identical.

An ethereal solution of diazomethane (5.9 mmol) was added to a solution of the degradation product (100 mg, 2.0 mmol) in dioxane. The dioxane was evaporated at oil pump pressure on the steam bath, and the resulting methyl ester was crystallized from benzene: m.p. 130.5–131.5°; λ_{max} 5.79 μ.

Anal. Calcd. for $C_{30}H_{26}O_4S_2$: C, 70.01; H, 5.09; S, 12.46. Found: C, 69.65; H, 5.08; S, 12.12.

The m.p. of the methyl ester was undepressed on admixture with authentic dimethyl 2,2,5,5-tetraphenyl-3,4-dithiaadipate (*vide infra*); the i.r. spectra of the two samples were identical.

The petroleum ether - soluble fraction from the basic hydrolysis of **9** weighed 5.0 g. Examination of the i.r. spectra of this fraction in both carbon disulfide and chloroform corroborated Meyer's earlier observation (4) that this was a mixture of benzoic and phenylacetic acid. Quantitative analysis by means of i.r. spectroscopy demonstrated that it was composed of 2.2 g (70%) of benzoic acid and 2.8 g (80%) of phenylacetic acid.

It was subsequently found that such drastic conditions are not necessary to effect the basic hydrolysis of **9**, which was completely hydrolyzed in a 2.5% sodium hydroxide solution in dioxane–water at room temperature overnight.

2,2,5,5-Tetraphenyl-3,4-dithiaadipic Acid (4)

2,2,5,5-Tetraphenyl-3,4-dithiaadipic acid was prepared by the method of Becker and Bistrzycki (28) from thiobenzilic acid (28) in 70% yield; m.p. 192.0–193.5° (dec.).

Dimethyl 2,2,5,5-Tetraphenyl-3,4-dithiaadipate

Dimethyl 2,2,5,5-tetraphenyl-2,4-dithiaadipate was prepared by reaction of **4** with ethereal diazomethane as above; m.p. 130.5–131.5°.

Acidic Hydrolysis of 9

Compound **9** (10.0 g, 21.5 mmol) was added to a mixture of glacial acetic acid (300 ml), concentrated sulfuric acid (50 ml), and water (50 ml). The mixture was boiled under reflux for 2 days, poured into water (2 l), and extracted six times with ether. The combined ethereal extracts were extracted with aqueous 5% sodium bicarbonate until carbon dioxide was no longer evolved. The sodium bicarbonate extract was acidified to p*H ca.* 1 with concentrated hydrochloric acid and extracted six times with ether. Both the acidic and neutral fractions were dried and evaporated to dryness on the steam bath.

The acidic fraction, which contained much acetic acid, was kept in a vacuum desiccator over potassium hydroxide pellets until the odor of acetic acid was absent. It was crystallized from aqueous ethanol to give colorless crystals of diphenylacetic acid (3.10 g, 68%), m.p. 145–147°, undepressed on admixture with an authentic sample. The neutral fraction yielded sulfur (1.30 g, 94%) as yellow needles, m.p. 116–118.5° [lit. (29) m.p. of monoclinic sulfur, 119°]. Its identity was confirmed by the fact that it burned with a blue flame, liberating sulfur dioxide and leaving no residue.

Can. J. Chem. Downloaded from www.nrcresearchpress.com by 188.143.235.115 on 09/06/12
For personal use only.

The remainder of the neutral fraction (5.30 g) showed all the bands of deoxybenzoin in its i.r. spectrum. It was converted to its 2,4-dinitrophenylhydrazone by the method of Shriner *et al.* (30). This was recrystallized from ethyl acetate to give orange crystals (3.60 g, 50%), m.p. 200–201°, undepressed on admixture with an authentic sample of the 2,4-dinitrophenylhydrazone of deoxybenzoin.

Desulfurization of **9** *with Raney Nickel*

The W-2 Raney nickel catalyst was prepared by the method of Mozingo (31). This was deactivated by a modification of the procedure of Spero *et al.* (32). The W-2 Raney nickel catalyst (50.0 g) was washed twice by decantation with acetone and heated in boiling acetone (150 ml) under reflux for 2 h. The catalyst was then washed twice by decantation with ethyl acetate, heated in boiling ethyl acetate (150 ml) under reflux for 2 h, and washed twice by decantation with ethanol.

The deactivated W-2 Raney nickel catalyst (50.0 g, 1.78 g-atoms) was suspended in ethanol (250 ml), **9** (5.00 g, 10.8 mmol) was added, and the mixture was boiled under reflux in a nitrogen atmosphere for 24 h. Examination of the i.r. spectrum of an aliquot of the reaction mixture showed that all of the starting material had been consumed. The mixture was filtered free of the catalyst and evaporated to dryness on the steam bath at water aspirator pressure to give an oil (4.70 g).

A solution of this oil (4.35 g) in petroleum ether (b.p. 30–60°; 75 ml) was chromatographed on Merck alumina (150 g). The column was developed with petroleum ether, and 50 ml fractions were collected. Fractions 1 and 2 gave diphenylmethane (190 mg), which was purified by vacuum distillation; b.p. 70–75° (1 mm); n_D^{24} 1.5761. This was identified by its characteristic odor and the identity of its i.r. spectrum with that of an authentic sample; n_D^{24} 1.5763.

Further elution of the column gave an oil (fractions 13–15). One gram of this oil was subjected to a series of seven successive chromatographic separations. In each case Merck alumina (40 g) was used, and 10 ml fractions were collected. The oil was thus separated into two components. The i.r. spectra of these two compounds were identical in every respect to those of methyldeoxybenzoin and ethyl diphenylacetate.

To corroborate the identification of these products, the oil (1.00 g) was heated for 3 h with boiling aqueous 5% sodium hydroxide (25 ml) and ethanol (10 ml) under reflux. The reaction mixture was diluted three-fold with water and extracted three times with ether to give the neutral fraction. The aqueous layer was acidified to p*H ca.* 1 with concentrated hydrochloric acid and extracted three times with ether to give the acidic fraction. Both fractions were dried and evaporated to dryness on the steam bath. The acidic fraction was crystallized from aqueous ethanol to give diphenylacetic acid (300 mg, 66%), m.p. 144–145.5°, undepressed on admixture with an authentic sample; the i.r. spectra of the two samples were identical.

The neutral fraction (410 mg, 73%) was a colorless oil. This was converted to its 2,4-dinitrophenylhydrazone by the method of Shriner *et al.* (30). The orange crystalline product was recrystallized from ethyl acetate: m.p. 151.5–152.5°, undepressed on admixture with an authentic sample of the 2,4-dinitrophenylhydrazone of methyldeoxybenzoin (*vide infra*).

When W-6 Raney nickel catalyst (33) was used for the desulfurization in place of the less reactive deactivated W-2 Raney nickel catalyst, a product mixture of different composition was obtained. Reaction with **9** (5.00 g) yielded 640 mg of diphenylmethane, and the amount of methyldeoxybenzoin was greatly reduced. The product mixture was separated by chromatography and vacuum distillation. Ethyl diphenylacetate was isolated and crystallized from aqueous ethanol: m.p. 57–58°, undepressed on admixture with an authentic sample; the i.r. spectra of the two samples were identical.

Methyldeoxybenzoin 2,4-Dinitrophenylhydrazone

Methyldeoxybenzoin was prepared by the method of Meyer and Oelkers (34) in 65% yield; b.p. 140–145° (5 mm); λ_{max} 5.95, 7.28 μ (m). It was converted to its 2,4-dinitrophenylhydrazone by the method of Shriner *et al.* (30); m.p. 151.5–152.5°.

Anal. Calcd. for $C_{21}H_{18}O_4N_4$: C, 64.60; H, 4.65; N, 14.35. Found: C, 64.78; H, 4.86; N, 14.81.

Reduction of **9** *by Zinc and Acetic Acid. Formation of* **12**

To a boiling solution of **9** (1.00 g, 2.15 mmol) in glacial acetic acid (15 ml), zinc dust (1.00 g, 15.3 mg-atoms) was added with swirling over a period of 20 min. The solution was filtered, and three drops of concentrated hydrochloric acid were added to the filtrate (p*H ca.* 1). The solution was added to a large excess of water, and the mixture was extracted with dichloromethane. The extract was washed three times with saturated aqueous sodium bicarbonate and three times with water, dried, and evaporated on the steam bath. The residual oil (700 mg) was crystallized from benzene – petroleum ether (b.p. 30–60°) to yield **12** (140 mg, 14%) as a colorless, crystalline solid, m.p. 209.5–210.5°; λ_{max} 5.94 μ (br), λ_{max}(EtOH) 252 mμ (ε 15 900); δ ($CDCl_3$) 4.62 (d, J = 11 Hz, 1H), 5.28 (d, J = 11 Hz, 1H), 7.2–7.5 (m, 18H), 7.67 (m, 2H).

Anal. Calcd. for $C_{29}H_{22}O_2S_2$: C, 74.67; H, 4.75; S, 13.72. Found: C, 74.69; H, 5.03; S, 13.90.

Although the i.r. spectrum of the oil showed only the bands of the reduction product **12**, attempts to obtain further crystalline product from it failed.

Basic Hydrolysis of **12**

A mixture of **12** (1.00 g, 2.15 mmol) and a solution of potassium hydroxide (1.50 g, 26.7 mmol) in 95% ethanol (10 ml) was boiled under reflux for 7 h. The reaction mixture was diluted with water, acidified to p*H ca.* 1 with concentrated hydrochloric acid, heated on the steam bath for 10 min, and allowed to cool to room temperature. It was then extracted three times with ether, and the combined ethereal extracts were extracted three times with aqueous 5% sodium bicarbonate. The bicarbonate extract was acidified with concentrated hydrochloric acid to p*H ca.*1 and extracted three times with ether to obtain the acidic fraction. Both acidic and neutral fractions were dried and evaporated on the steam bath.

The neutral fraction (330 mg, 79%) showed all of the bands of deoxybenzoin in its i.r. spectrum. A 2,4-dinitrophenylhydrazone of this fraction was made (30) and crystallized from ethanol: m.p. 200–201°, undepressed

Can. J. Chem. Downloaded from www.nrcresearchpress.com by 188.143.235.115 on 09/06/12
For personal use only.

upon admixture with authentic deoxybenzoin 2,4-dinitrophenylhydrazone.

The acidic fraction (420 mg, 91%), whose i.r. spectrum was identical with that of diphenylacetic acid, was crystallized from aqueous ethanol to yield colorless crystals of diphenylacetic acid, m.p. 145–146°, undepressed on admixture with an authentic sample.

Desulfurization of ***12*** *with Raney Nickel*

A mixture of **12** (1.00 g, 2.14 mmol), W-2 Raney nickel catalyst (31) (2.00 g), and ethanol (50 ml) was stirred under a nitrogen atmosphere for 2 days. The mixture was filtered, and the filtrate was stripped of ethanol on a steam bath under vacuum. The resulting oil had an i.r. spectrum identical with that of the oil from the Raney nickel desulfurization of **9**. It was heated with a boiling mixture of aqueous 5% sodium hydroxide (15 ml) and ethanol (3 ml) for 3 h. After cooling to room temperature, the mixture was poured into a three-fold excess of water and extracted with ether to give the neutral fraction. The aqueous layer was acidified with concentrated hydrochloric acid to p*H ca.* 1 and extracted with ether three times to give the acidic fraction. Both fractions were dried and evaporated on the steam bath.

The acid fraction on crystallization from aqueous ethanol gave diphenylacetic acid (160 mg, 36%) m.p. 144–146°, undepressed on admixture with an authentic sample.

Lixiviation of the partially crystalline neutral fraction with ethanol yielded *sym*-tetraphenylethane (30 mg) as colorless crystals, m.p. 210–211° after recrystallization from benzene. The m.p. was undepressed upon admixture with authentic *sym*-tetraphenylethane.

Excess ethanol was evaporated from the filtrate to give an oil (400 mg, 89%) whose i.r. spectrum showed all of the bands of methyldeoxybenzoin. Its 2,4-dinitrophenylhydrazone was prepared (30) and crystallized from ethanol; m.p. 151–152.5°. A mixture melting point with an authentic sample of the 2,4-dinitrophenylhydrazone of methyldeoxybenzoin showed no depression.

Ozonolysis of ***9***

A solution of **9** (1.00 g, 2.15 mmol) in dichloromethane (50 ml) was cooled to 0°, and maintained at this temperature throughout the ozonolysis. Ozone from a Welsbach ozonizer was bubbled through the solution for 3 h.The ozonide was decomposed by the addition of water (20 ml). The dichloromethane was removed under water aspirator pressure, first at room temperature and finally on the steam bath. The aqueous solution was extracted four times with ether, and the combined ethereal extracts were extracted six times with aqueous 5% sodium hydroxide. The ethereal layer was dried and evaporated on the steam bath to give the neutral fraction. The aqueous layer was neutralized with concentrated hydrochloric acid to p*H ca.* 1 and extracted four times with ether. The combined ethereal extracts were dried and evaporated on the steam bath to give the acidic fraction.

The original aqueous solution was allowed to stand at room temperature until it had evaporated. The residue (150 mg) was dissolved in water to give an acidic solution (p*H ca.* 1). Neutralization of this solution to the methyl red end-point with aqueous 5% barium hydroxide gave a precipitate of barium sulfate (20 mg).

The neutral fraction (630 mg) was distilled at 100° (1 mm) to give an oil (410 mg) that showed all of the bands of benzil in its i.r. spectrum. This was treated with 2,4-dinitrophenylhydrazine reagent (30), and the product was crystallized from ethanol to give benzil 2,4-dinitrophenylhydrazone, m.p. 194–195°, undepressed on admixture with an authentic sample.

The acidic fraction (170 mg) was sublimed at 50° (1 mm) for 6 h. The sublimate (110 mg) was crystallized from water to give benzoic acid, m.p. 120–121.5°, undepressed on admixture with an authentic sample. Distillation of the sublimation residue from the acidic fraction at 150° (1 mm) gave an oil (30 mg). This oil showed all of the bands of diphenylacetic acid in its i.r. spectrum; however, it contained benzoic acid since all of the bands of the latter were also present in the spectrum.

In another ozonolysis, the ozonide was decomposed with zinc and acetic acid by the method of Noller and Adams (35). Glacial acetic acid (10 ml) was added to the ozonide, and the dichloromethane was removed at water aspirator pressure and room temperature. Ether (40 ml) was added, and the mixture was stirred and treated with zinc dust (1.00 g) and three drops of water. Further zinc dust (9.00 g) was added in small portions, followed by water (1 ml). The mixture was boiled under reflux until it gave a negative test with starch–iodide paper (*ca.* 15 min). It was then filtered, and the zinc salts were washed several times with ether. The combined filtrate and washings were washed several times with aqueous 10% sodium carbonate and once with water. The sodium carbonate extract was acidified to obtain the acidic fraction. The ethereal layer was dried and evaporated on the steam bath to give the neutral fraction (250 mg), which was crystallized from benzene to give benzoin, m.p. 132–134°, undepressed on admixture with an authentic sample; the i.r. spectra of the two samples were identical.

Oxidation of ***9*** *with Perphthalic Acid. Formation of* ***16***

Compound **9** (5.00 g, 10.8 mmol) was added to a solution of perphthalic acid (33.5 mmol) in ether (500 ml). The mixture was stirred at room temperature for 2 days. The solution was evaporated at water aspirator pressure without the application of external heat. The residue was digested with chloroform (250 ml) that had stood over anhydrous sodium sulfate for 3 h. The mixture was filtered, and the filtrate was evaporated to dryness. The product was crystallized from ethanol to give **16** (4.10 g, 79%), m.p. 148–150° (dec.); λ_{max} 5.83, 5.97 μ; λ_{max} 263 (ε 23 400), 287 mμ (sh, ε 16 000).

Anal. Calcd. for $C_{29}H_{20}O_3S_2$: C, 72.47; H, 4.20; S, 13.35. Found: C, 72.28; H, 4.19; S, 13.14.

Reduction of ***16*** *with Zinc and Acetic Acid*

A mixture of **16** (82 mg, 0.17 mmol), acetic acid (10 ml), and zinc dust (39 mg, 0.70 mmol) was stirred at room temperature for 30 min. The solution was decanted into ether (30 ml), and the ethereal solution was washed twice with water, three times with aqueous 5% sodium bicarbonate, and again with water. It was dried over anhydrous magnesium sulfate and evaporated to give a yellow glass (80 mg). This was crystallized from ether to give **9** as pale yellow crystals (10 mg, 13%), m.p. 153–155°. One recrystallization from carbon disulfide gave material, m.p. 153.5–155°, undepressed on admixture with an authentic sample of **9**, the i.r. spectra of the two samples were identical.

Can. J. Chem. Downloaded from www.nrcresearchpress.com by 188.143.235.115 on 09/06/12
For personal use only.

Basic Hydrolysis of ***16***

A mixture of compound **16** (1.00 g, 2.09 mmol), ethanol (25 ml), and aqueous 5% sodium hydroxide (25 ml) was boiled under reflux for 3 days. The mixture was poured into an excess of water, acidified to p*H ca.* 1 with concentrated hydrochloric acid, and extracted three times with ether, with filtration to remove the insoluble yellow precipitate that appeared. This precipitate was crystallized from chloroform to give **7** (220 mg, 45%), m.p. 300.5–302.5° (dec.), undepressed on admixture with an authentic sample (*5b*).

The ethereal extract was dried and evaporated to give a liquid (330 mg, 87%) that showed all of the bands of benzophenone in its i.r. spectrum. Its 2,4-dinitrophenylhydrazone was prepared (30) and crystallized from ethyl acetate – ethanol; m.p. 238–240°, undepressed on admixture with an authentic sample of the 2,4-dinitrophenylhydrazone of benzophenone.

Acidic Hydrolysis of ***16***

A mixture of **16** (1.00 g, 2.09 mmol), ethanol (25 ml), and concentrated hydrochloric acid (25 ml) was boiled under reflux for 2 days. The mixture was poured into a four-fold excess of water and extracted four times with ether, and the combined ethereal extracts were extracted four times with aqueous 10% sodium bicarbonate. The sodium bicarbonate extract was acidified to p*H ca.* 1 with concentrated hydrochloric acid and extracted four times with ether. These ethereal extracts were combined, dried, and evaporated on the steam bath to give the acidic fraction (160 mg). This was crystallized from aqueous ethanol to give benzilic acid, m.p. 148–149°, undepressed on admixture with an authentic sample; the i.r. spectra of the two samples were identical.

The neutral fraction showed all of the bands of the starting material **16** in its i.r. spectrum.

Reaction of ***9*** *with n-Propylamine. Formation of* ***24*** *and* ***28***

To a solution of **9** (5.00 g, 11.0 mmol) in chloroform (50 ml) was added *n*-propylamine (2.0 ml, 1.4 g, 24 mmol). The pale yellow solution rapidly acquired a bright red color, which faded to pale orange after the solution had stood for 2 h at room temperature, when the characteristic odor of hydrogen sulfide could be detected. Addition of further *n*-propylamine (0.50 ml, 350 mg, 6.0 mmol) produced only a slight intensification of the orange color. After a further 4 h at room temperature the chloroform and excess amine were removed by evaporation at room temperature and water aspirator pressure. The residual orange oil was dissolved in a small amount of ether, and the solution was stored at −10°. After 2 days the solid (750 mg) that had separated was filtered and washed well with ether; the mother liquor was concentrated and again cooled to −10°. After a further 3 days a second crop of solid (600 mg) was separated as before. The first crop had m.p. 164–166°, and the second had m.p. 166–168°; their i.r. spectra were virtually identical. Combination and recrystallization from benzene–ligroin gave fine colorless needles of **28** (1.30 g, 39%), m.p. 167–168°. Two more recrystallizations from benzene–ligroin gave an analytical sample, m.p. 167–168°; λ_{max} 2.91 (w), 2.94 (sh), 2.98 (sh), 6.01 μ; λ_{max}(MeOH) *ca.* 270 mμ (inflexion, ε 6500); ε_{235} 25 000.

Anal. Calcd. for $C_{34}H_{36}N_2O_2S_3$: C, 68.02; H, 6.03; N, 4.65; S, 15.98. Found: C, 67.87; H, 5.98; N, 4.67; S, 16.20.

A benzene solution of **28** on treatment with yellow mercuric oxide underwent no reaction in 30 min.

Crystallization of the remainder of the original reaction product from ether yielded a yellowish solid (1.05 g) whose i.r. spectrum suggested that it was a mixture. The remaining product was crystallized from ether – petroleum ether by cooling at −10° to give **24** as a faintly yellow solid (1.20 g, 37%), m.p. 62–64°. Four more recrystallizations from ether – petroleum ether gave fluffy white needles, m.p. 66–67°; $\lambda_{max}(CCl_4)$ 2.95 (sh), 3.01 (m), 5.98 μ; λ_{max}(MeOH) 249 (ε 15 900), 265 (inflexion, ε 12 300) mμ; λ_{max}(MeOH–MeONa) 273 (ε 7800), 340 mμ (ε 15 100); δ 0.90 (t, J = 7 Hz, 3H), 1.55 (m, 2H), 3.42 (m, 2H), 6.30 (s, 1H), 7.33 (m, 8H), 8.05 (m, 2H), 9.30 (br, s, 1H).

Anal. Calcd. for $C_{18}H_{19}NOS$: C, 72.70; H, 6.44; N, 4.71; S, 10.76. Found: C, 72.76; H, 6.63; N, 4.52; S, 10.65.

A benzene solution of **24** on treatment with yellow mercuric oxide developed a black precipitate within 10 min.

Reaction of ***24*** *with Aqueous Base*

A mixture of **24** (271 mg, 0.91 mmol) and aqueous 5% sodium hydroxide (20 ml) was stirred vigorously at room temperature. After 20 min all but a few crystals had dissolved to give a yellow solution, from which an oil soon began to separate. After 3 h the mixture was extracted with two 20 ml portions of ether. The extracts were combined, dried over anhydrous magnesium sulfate, and evaporated to give a pale yellow oil (105 mg) that crystallized on standing; the i.r. spectrum of this material showed only very weak absorption in the 5.8–6.1 μ region. Two recrystallizations from ether – petroleum ether gave α-phenyl-*N*-*n*-propylthioacetamide (**25**) as colorless needles (49 mg, 28%), m.p. 55.5–57°, undepressed on admixture with an authentic sample (*vide infra*); the i.r. spectra of the two samples were identical.

In another run **24** (192 mg, 0.65 mmol) was stirred for 3 h with aqueous 5% sodium hydroxide (10 ml). After separation of the neutral product, the solution was acidified with hydrochloric acid and extracted with two 20 ml portions of ether. These were dried over magnesium sulfate and evaporated to give an off-white solid (86 mg), whose i.r. spectrum was very similar to that of benzoic acid. Sublimation of the solid at 50° (1 mm) gave colorless crystals (55 mg), m.p. 106–113°. Recrystallization first from aqueous ethanol and then cyclohexane gave benzoic acid as colorless crystals (14 mg, 18%), m.p. 120–122°, undepressed on admixture with an authentic sample.

*α-Phenyl-N-n-propylthioacetamide(****25****)*

n-Propyl isothiocyanate was prepared by the method used previously for the preparation of methyl isothiocyanate (36). It was obtained in 73% yield as a colorless liquid, b.p. 150–152° [lit. (37) b.p. 153°]; $\lambda_{max}(CCl_4)$ 4.60 (sh), 4.71 (sh), 4.82 μ.

n-Propyl isothiocyanate was converted to **25** by treatment with benzylmagnesium bromide following the method described by Blicke and Zinnes (38) for the preparation of α-phenyl-*N*-ethylthioacetamide. Com-

Can. J. Chem. Downloaded from www.nrcresearchpress.com by 188.143.235.115 on 09/06/12
For personal use only.

pound **25** was obtained in 43% yield as off-white needles, m.p. 51.5–53.5°. Four recrystallizations from ether – petroleum ether gave colorless needles, m.p. 55.5–56.5°; $\lambda_{max}(CCl_4)$ 2.89 (m), 6.25 (w), 6.63, 7.16, 9.36 μ; λ_{max}(MeOH) 267.5 (ε 12 700), 271 (sh, ε 12 400) mμ; λ_{max}(MeOH–MeONa) 268 (ε 11 500), 271 mμ (sh, ε 11 300).

Anal. Calcd. for $C_{11}H_{15}NS$: C, 68.37; H, 7.82; N, 7.25; S, 16.56. Found: C, 68.55; H, 8.01; N, 7.45; S, 16.59.

When a benzene solution of **25** was treated with yellow mercuric oxide a black precipitate developed within 10 min.

*Reduction of **28** with Nickel*

A solution of **28** (52 mg, 0.087 mmol) in ethanol (20 ml) was boiled under reflux for 20 h with a large excess of sponge nickel catalyst (Davison). The solution was cooled to room temperature, the catalyst was separated by gravity filtration, and the solvent was evaporated at the water aspirator. The residual solid (45 mg) had m.p. 86–88°; crystallization from benzene-ligroin gave α,α-diphenyl-*N*-*n*-propylacetamide (**29**; 28 mg, 64%) as colorless needles, m.p. 94–94.5°. One further recrystallization gave **29** (21 mg), m.p. 94.5–95°, undepressed on admixture with an authentic sample (*vide infra*).

*Reduction of **28** with Zinc and Acetic Acid*

A solution of **28** (69 mg, 0.120 mmol) in acetic acid (5 ml) was boiled under reflux for 3 h with zinc dust (100 mg). The supernatant solution was poured into ice-water, and the mixture was extracted with three 10 ml portions of ether. The extracts were combined, washed well with aqueous 5% sodium bicarbonate, and dried over anhydrous magnesium sulfate. The ether was evaporated at reduced pressure, and the solid residue was sublimed at 120° (1 mm) to give a white solid (42 mg), m.p. 87–90°. Recrystallization from cyclohexane gave **29** as colorless needles (32 mg, 55%), m.p. 94–94.5°, undepressed on admixture with an authentic sample (*vide infra*).

*α,α-Diphenyl-N-n-propylacetamide (**29**)*

The preparation of **29** was accomplished by the general method of Shriner *et al.* (39). Diphenylacetic acid (500 mg, 2.40 mmol) was dissolved in a large excess of thionyl chloride (10 ml), and the solution was boiled gently under reflux for 30 min. The excess thionyl chloride was evaporated at the water aspirator, and a solution of *n*-propylamine (1.0 ml, 0.70 g, 12 mmol) in benzene (15 ml) was added to the residual oil. The resulting solution was boiled under reflux for a few minutes, cooled to room temperature, and washed once with 5% hydrochloric acid, once with water, and twice with aqueous 5% sodium hydroxide. Drying over anhydrous magnesium sulfate followed by evaporation of the benzene under reduced pressure gave a tan solid (500 mg). Recrystallization from benzene–ligroin gave **29** as off-white needles (400 mg, 67%) m.p. 94–95°. Six recrystallizations from benzene–ligroin gave colorless needles, m.p. 95–95.5°; λ_{max} 2.84 (m), 5.97, 6.66 μ.

Anal. Calcd. for $C_{17}H_{19}NO$: C, 80.57; H, 7.56; N, 5.53. Found: C, 80.58; H, 7.36; N, 5.58.

*Alternative Synthesis of **9***

To a stirred suspension of sodium amide (400 mg, 10.0 mmol) in dry benzene (75 ml) was added a solution of deoxybenzoin (2.00 g, 10.0 mmol) in benzene (40 ml), and the mixture was stirred and boiled under reflux under nitrogen for 10 h. The yellow suspension was cooled to room temperature, and to it was added carbon disulfide (0.65 ml, 820 mg, 11.0 mmol). The mixture rapidly acquired a bright red color, which intensified during an additional 24 h of stirring. Addition of a solution of α-chlorodiphenylacetyl chloride (40) (2.70 g, 10.0 mmol) in benzene (20 ml) rapidly discharged the red color, after which the mixture was stirred for 1 h. Dry pyridine (1 ml) was added, and the mixture was boiled under reflux for 5 h, during which time a heavy precipitate formed. The mixture was cooled to room temperature, and the precipitate was filtered and washed with benzene. The benzene was evaporated from the filtrate at reduced pressure leaving a viscous reddish oil. This was triturated with a small amount of ether, and the brownish solution was decanted, leaving a sticky solid (600 mg).

The ethereal solution was evaporated, and the residual oil (3.0 g) was dissolved in benzene – petroleum ether (3:2) and chromatographed on silica gel (Davison, 300–400 mesh; 50 g); 80 ml fractions were collected. Elution with benzene – petroleum ether (9:1) gave fractions that appeared from their i.r. spectra to be largely mixtures of deoxybenzoin and **9**. These were combined and rechromatographed on silica gel (50 g). The column was eluted with benzene – petroleum ether (7:3), and 80 ml fractions were collected. Fractions 3 and 4 were combined and recrystallized from carbon disulfide to give a first crop of yellow prisms (97 mg), m.p. 154–156°, and a second crop (57 mg), m.p. 153–155°, undepressed on admixture with **9**.

The residue from evaporation of the mother liquors from the recrystallizations was combined with fractions 2, 5, and 6 of the second chromatogram, and this material was again chromatographed on silica gel (18 g). The column was eluted with benzene – petroleum ether (3:2), and 50 ml fractions were collected. Recrystallization of fraction 4 from ether – carbon disulfide gave yellow crystals (14 mg), m.p. 153–155°, while a combination of fractions 3 and 5 gave yellow solid (20 mg), m.p. 142–147°. Trituration of the residues from evaporation of the mother liquors with ether and cooling gave more yellow solid (14 mg), m.p. 151–153°. The last two, low-melting crops were recrystallized from carbon disulfide to give yellow prisms (20 mg), m.p. 154–155°, undepressed on admixture with **9**. The i.r. spectra of all four crops were identical with the spectrum of **9**; the total combined product (188 mg) represents a yield of 8%.

Reaction of Azibenzil with Carbon Disulfide in the Presence of Diphenylketene

Diphenylketene (5.00 g, 25.7 mmol), prepared by the method of Smith and Hoehn (41), azibenzil (5.72 g, 25.7 mmol), and carbon disulfide (55 ml) were boiled under reflux in a nitrogen atmosphere overnight. The excess carbon disulfide was removed by evaporation on the steam bath at the water aspirator, and the residue was crystallized from acetic acid to give **9** (5.00 g, 84% based on azibenzil alone); m.p. 152–154°, undepressed on admixture with a sample of **9** prepared by the reaction of azibenzil with carbon disulfide in the absence of diphenylketene. The i.r. spectrum of the product showed all of the bands of **9**.

1. P. YATES and T. R. LYNCH. Can. J. Chem. In press.
2. P. YATES and B. G. CHRISTENSEN. Chem. Ind. (London), 1442 (1958).
3. P. YATES and L. L. WILLIAMS. Tetrahedron Lett. 1205 (1968).
4. J. MEYER. Helv. Chim. Acta, **8**, 38 (1925).
5. (*a*) P. YATES, T. R. LYNCH, and D. R. MOORE. Can. J. Chem. In press. (*b*) P. YATES, D. R. MOORE, and T. R. LYNCH. Can. J. Chem. In press.
6. L. H. NODA, S. A. KUBY, and H. A. LARDY. J. Am. Chem. Soc. **75**, 913 (1953).
7. P. YATES and J. A. WEISBACH. J. Am. Chem. Soc. **85**, 2943 (1963).
8. A. SCHOBERL. Ber. **70**, 1186 (1937).
9. A. D. CROSS. Introduction to practical infrared spectroscopy. 2nd ed. Butterworths, London, 1964. p. 78.
10. J. A. WEISBACH. Ph.D. Thesis, Harvard University, Cambridge, Massachusetts, 1959.
11. L. N. LEWIN. J. Prakt. Chem. **127**, 77 (1930). P. WARREN, N. J. ANTIA, and R. SCHWYZER. Helv. Chim. Acta, **34**, 1392 (1951).
12. E. SCHMIDT, W. STRIEWSKY, and F. HITZLER. Ann. **560**, 222 (1948). A. KJAER. Acta Chem. Scand. **6**, 1374 (1952).
13. C. N. R. RAO. Ultraviolet and visible spectroscopy. 2nd ed. Butterworths, London. 1967. p. 28.
14. R. GOMPPER and H. SCHAEFER. Chem. Ber. **100**, 591 (1967).
15. N. D. CHERONIS and J. B. ENTREKIN. Semimicro qualitative organic analysis. 2nd ed. Interscience Publishers, Inc., New York, N.Y., 1947. pp. 274–275.
16. P. L. KUCZKOWSKI and E. B. WILSON, JR. J. Am. Chem. Soc. **85**, 2028 (1963). Q. E. THOMPSON, M. M. CRUTCHFIELD, and M. W. DIETRICH. J. Am. Chem. Soc. **86**, 3892 (1964).
17. L. J. BELLAMY. The infrared spectra of complex molecules. 2nd edition. John Wiley and Sons, Inc., New York, N.Y. 1958. pp. 352–354.
18. W. A. BONNER. J. Am. Chem. Soc. **73**, 464 (1951).
19. A. E. GILLAM and E. S. STERN. Electronic absorption spectroscopy. 2nd edition. Edward Arnold, Ltd., London, 1958. p. 135.
20. H. P. KOCH. J. Chem. Soc. 394 (1949).
21. R. N. HURD and G. DELAMATER. Chem. Rev. **61**, 45 (1961).
22. (*a*) T. R. LYNCH, I. P. MELLOR, S. C. NYBURG, and P. YATES. Tetrahedron Lett. 373 (1967). W. H. SCHMIDT and A. TULINSKY. Tetrahedron Lett. 5311 (1967). I. P. MELLOR. Ph.D. Thesis. University of Keele, Keele, England, 1968. (*b*) J. A. KAPECKI, J. E. BALDWIN, and I. C. PAUL. Tetrahedron Lett. 5307 (1967); J. Am. Chem. Soc. **90**, 5800 (1968).
23. J. A. KAPECKI and J. E. BALDWIN. J. Am. Chem. Soc. **91**, 1120 (1969).
24. A. SCHÖNBERG and L. V. VARGHA. Ann. **483**, 176 (1930). R. SCHÖNBERG and S. NICKEL. Ber. **64**, 2323 (1931).
25. A. J. KIRBY. Tetrahedron, **22**, 3001 (1966).
26. J. E. BALDWIN and J. A. KAPECKI. J. Org. Chem. **34**, 724, (1969).
27. C. D. NENITZESCU and E. SALOMONICA. Organic syntheses. Coll. Vol. 2. John Wiley and Sons, Inc., New York, N.Y., 1943. p. 496.
28. H. BECKER and A. BISTRZYCKI. Ber. **47**, 3149 (1914).
29. R. C. Weast, *editor* Handbook of chemistry and physics. 45th ed. The Chemical Rubber Co., Cleveland, Ohio, 1964. p. B-137.
30. R. L. SHRINER, R. C. FUSON, and D. Y. CURTIN. The systematic identification of organic compounds. 5th ed. John Wiley and Sons, Inc., New York, N.Y., 1964. p. 253.
31. R. MOZINGO. Organic syntheses. Coll. Vol. 3. John Wiley and Sons, Inc., New York, N.Y., 1955. p. 181.
32. G. B. SPERO, A. V. MCINTOSH, JR., and R. H. LEVIN. J. Am. Chem. Soc. **70**, 1907 (1948).
33. H. BILLICA and H. ADKINS. Organic syntheses. Coll. Vol. 3. John Wiley and Sons, Inc., New York, N.Y. 1955. p. 176.
34. V. MEYER and L. OELKERS. Ber. **21**, 1297 (1888).
35. C. R. NOLLER and R. ADAMS. J. Am. Chem. Soc. **48**, 1074 (1926).
36. M. L. MOORE and F. S. CROSSLEY. Organic syntheses. Coll. Vol. 3. John Wiley and Sons, Inc., New York, N.Y., 1955. p. 599.
37. G. M. DYSON and R. F. HUNTER. Rec. Trav. Chim. **45**, 421 (1926).
38. F. F. BLICKE and H. ZINNES. J. Am. Chem. Soc. **77**, 4849 (1955).
39. R. L. SHRINER, R. C. FUSON, and D. Y. CURTIN. The systematic identification of organic compounds. 5th ed. John Wiley and Sons, Inc., New York, N.Y., 1964. p. 236.
40. J. H. BILLMAN and R. H. HIDY. J. Am. Chem. Soc. **65**, 760 (1943).
41. L. I. SMITH and H. H. HOEHN. Organic syntheses. Coll. Vol. 3. John Wiley and Sons, Inc., New York, N.Y., 1955. p. 356.

Can. J. Chem. Downloaded from www.nrcresearchpress.com by 188.143.235.115 on 09/06/12
For personal use only.

Can. J. Chem. Downloaded from www.nrcresearchpress.com by 210.87.254.40 on 09/05/12
For personal use only.

The Reaction of Hydroperoxides with Triphenylphosphine

R. HIATT, R. J. SMYTHE, AND CHRISTINE MCCOLEMAN
Chemistry Department, Brock University, St. Catharines, Ontario

Received September 9, 1970

The reductions of *n*-butyl, *sec*-butyl, and *tert*-butyl hydroperoxides by triphenylphosphine in ethanol have been shown to follow second-order kinetics with k_2's equal, respectively to $10^{7.2}e^{-8.4/RT}$, $10^{9.0}e^{-10.8/RT}$, $10^{8.8}e^{-11.2/RT}$. Similar results obtain in CH_2Cl_2, but in hexane the rate equation requires an additional term, $k_3[Ph_3P][RO_2H]^2$, though the overall reaction is somewhat faster than in the other solvents.

Retardation, apparently by adventitious impurities, has been observed in some cases, but attempts to inhibit the reaction by free radical traps were unsuccessful. Parallels with reduction of hydroperoxides by organic sulfides suggest a similar non-radical mechanism.

On a établi que la réduction des hydropéroxydes de *n*-butyle, *sec*-butyle et *tert*-butyle par la triphénylphosphine dans l'éthanol est d'ordre deux et que les constantes de vitesses sont de $10^{7.2}e^{-8.4/RT}$, $10^{9.0}e^{-10.8/RT}$ et $10^{8.8}e^{-11.2/RT}$ respectivement pour chacun de ces composés. On a obtenu des résultats semblables dans le CH_2Cl_2 mais dans l'hexane l'équation de vitesse nécessite un terme supplémentaire et devient $k_3[Ph_3P][RO_2H]^2$ quoique dans l'ensemble la réaction devient plus rapide que dans les autres solvants.

On a observé que la réaction est ralentie dans certains cas, apparemment par des impuretés, mais on n'a toutefois pas pu inhiber la réaction par addition de substances susceptibles d'éliminer les radicaux libres. Les parallèles qui peuvent être faits avec la réaction de réduction des hydropéroxydes par les sulfures organiques permettent de suggérer que le mécanisme de la réaction sous considération n'est pas de nature radicalique.

Canadian Journal of Chemistry, 49, 1707 (1971)

Introduction

The facile reduction of hydroperoxides to alcohols by phosphines (1, 2) or phosphites (3) has been used extensively in the analysis of autoxidation products (4). The 1:1 stoichiometry of the reaction provides a method for quantitative analysis (5, 6). Stereochemical studies have shown that

[1] $$RO_2H + R'_3P \rightarrow ROH + R'_3PO$$

the phosphine abstracts the hydroxyl oxygen (7); the cleanness of reduction and the absence of inhibition by trinitrobenzene (3) have suggested a polar rather than radical mechanism (3, 7).

Nonetheless the reaction occurs extremely rapidly in non-polar solvents, "instant" reduction in hexane solution at $-40°$ (7) being an oft quoted claim. There is evidence that the reduction *can* be inhibited, or at least retarded, by adventitious impurities (8), and misgivings about its cleanness when applied to non-tertiary hydroperoxides have been expressed (4). Such findings suggested a free radical chain mechanism propagated by steps [2] and [3].

[2] $$RO_2^{\cdot} + R'_3P \rightarrow RO^{\cdot} + R'_3PO$$

[3] $$RO^{\cdot} + RO_2H \rightarrow ROH + RO_2^{\cdot}$$

Differences between tertiary and non-tertiary hydroperoxides could thus be ascribed to the much faster self-termination of non-tertiary peroxy radicals acting in competition with reaction 2.

The following describes what we believe to be the first rate studies of the phosphine–hydroperoxide reaction, undertaken in the hope that a kinetic analysis would settle the mechanistic question conclusively.

Experimental

Triphenylphosphine obtained from Eastman Organic Products, Limited, (m.p. 74–80 °C) was purified by chromatography on alumina followed by recrystallization from ethanol; m.p. 79–80°. Simple sublimation of the crude material did not improve its melting range.

t-Butyl hydroperoxide (Lucidol 90%) was purified by vacuum distillation. *n*-Butyl and *s*-butyl hydroperoxides were synthesized by the method of Williams and Mosher (9) and used as the 80–81% pure materials (by iodometric titration) afforded by this procedure.

t-BuO_2D was obtained by hydrolysis of the potassium salt of *t*-BuO_2H with D_2O. The recovered hydroperoxide (by ether extraction and vacuum distillation) was 90.5% pure and contained 88% O—D (by i.r.). *The dry t-$BuO_2^-K^+$, prepared by reaction of KNH_2 with t-BuO_2H in liquid ammonia, was found to be considerably more hazardous than expected.* While small quantities did not explode even on scratching or hammering, a 70 g batch

Can. J. Chem. Downloaded from www.nrcresearchpress.com by 210.87.254.40 on 09/05/12
For personal use only.

left unattended for several minutes detonated violently and without warning.

Methylene chloride and *n*-hexane to be used in solvents for kinetic runs were fractionally distilled and dried over molecular sieves. Ethanol was dried with the magnesium ethoxide. EtOD (99.5%) was obtained from Merck, Sharp and Dohme, Ltd.

Rates of reaction were measured by scanning the disappearance of the triphenylphosphine maximum absorbance at 2600–2800 Å (10) using a Hitachi–Perkin–Elmer model 124 u.v. spectrophotometer. Since both hydroperoxides and triphenylphosphine oxide absorb weakly in this region, reactions using approximately equal concentrations of RO_2H and Ph_3P were difficult to analyze. Consequently all kinetic runs were carried out with at least a 10 fold excess of peroxide, using plots of log [Absorbance$_t$ − Absorbance$_\infty$] *vs.* *t* to obtain pseudo first-order rate constants. These latter were independent of the actual wave length followed over the range of 2500–2800 Å.

Results

Exclusion of a Free Radical Mechanism

The reaction of triphenylphosphine with *t*-BuO_2H in styrene solution at 0 °C resulted in a virtually quantitative yield of Ph_3PO and *t*-BuOH but *no* polystyrene. Attempts to inhibit the reaction in benzene or methylene chloride solution using either hydroquinone or the stable free radical galvinoxyl (11) were unsuccessful.[1] The products of reaction of *n*-BuO_2H or *s*-BuO_2H with Ph_3P were shown by g.l.c. to be the corresponding alcohols exclusively. No traces of the aldehydes or ketones resulting from self-termination of peroxy radicals could be detected.

While none of these tests in itself is conclusive, they together tend to substantiate the generally held view (3, 7) that the reaction is non-radical.

Rates and Kinetics of Reaction, t-Butyl and n-Butyl Hydroperoxides

Reductions were carried out in three solvents, ethanol, methylene chloride, and hexane, using initial concentrations of 0.5–2.0 × 10^{-4} *M* Ph_3P and 0.001–0.1 *M* hydroperoxide. Rates of reaction were sufficiently slow for convenient measurement by following the decrease in u.v. absorption due to triphenylphosphine. With the uniformly large excess of hydroperoxide, disappearance of the phosphine followed first order kinetics; plots of log [Ph_3P] *vs.* time were linear to at least 95% reaction (Fig. 1), with slopes that were independent of [Ph_3P]$_0$ (Table 1).

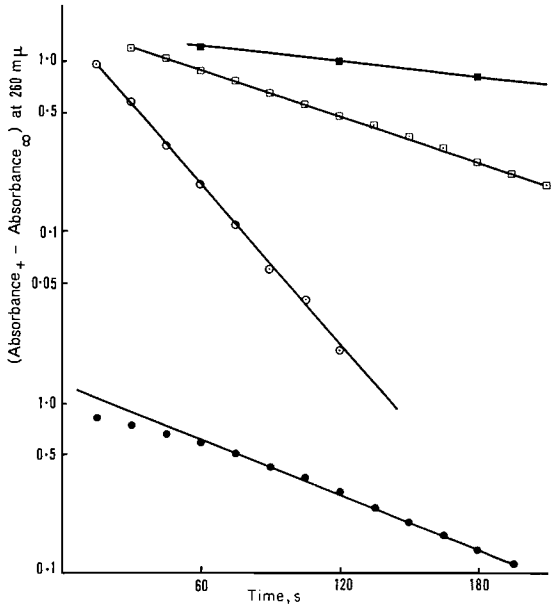

FIG. 1. Pseudo-first order plots for the reduction of hydroperoxides by 2 × 10^{-4} *M* Ph_3P. ■, 0.01 *M* *t*-BuO_2H at 23.5° in EtOH; □, 0.013 *M* *n*-BuO_2H at 20.0° in EtOH; ○, 0.013 *M* *n*-BuO_2H at 21.5° in *n*-hexane; ●, 0.010 *M* *s*-BuO_2H at 21.5° in *n*-hexane.

In ethanol[2] or methylene chloride the pseudo-first order rate constants ("k_1") were directly proportional to hydroperoxide concentration,[3] (Table 1), *i.e.*,

$$[4] \qquad -\partial[Ph_3P]/\partial t = k_2[Ph_3P][RO_2H]$$

Reactions in *n*-hexane were not second order, however. Plots of log "k_1" *vs.* log [RO_2H] showed a close fit to 3/2-order in hydroperoxide, but the data could be fitted equally well to an ex-

[1]These tests were necessarily qualitative since the u.v. absorption of the inhibitors was so intense as to preclude the following reaction by the decrease of the Ph_3P maximum. Instead a crude form of differential thermal analysis was used. Mixing 0.001 mol each of Ph_3P and *t*-BuO_2H in 30 ml of solvent at 20–22 °C caused a rapid temperature rise of 2.5 °C. The pattern was completely unaffected by the presence of the free radical traps.

[2]The reaction of *t*-BuO_2H in ethanol was scrutinized particularly for the effect of impurities. Hydroperoxide and Ph_3P in all stages of purification were used, but in no case did the rate of reaction differ significantly from that using the purest starting materials.

[3]For *t*-BuO_2H, k_2's increased slightly as RO_2H was decreased from 0.1 to 0.001 *M*. The increase was, however, barely outside the limits of reproducibility for individual runs at a given concentration. Since the hundredfold change in peroxide concentration produced a hundredfold change in rate, approaching the high and low limits for accurate measurement, the variation can probably be ascribed to experimental error.

TABLE 1. Reduction of hydroperoxides by triphenylphosphine

R	$10^2[RO_2H]_0$ (M)	$10^4[Ph_3P]_0$ (M)	T (°C)	k_2 (M^{-1} s^{-1})*	log A†	E_a†
			In ethanol			
t-Bu	1.00	1.79	17.5	0.220		
	6.5	2.00	24.0	0.323		
	6.5	1.00	24.0	0.356		
	6.5	0.50	24.0	0.356		
	10.0	1.00	24.0	0.330	8.8±0.2	11.2±0.2
	1.00	1.00	24.0	0.375		
	0.10	1.00	24.0	0.427		
	1.00	1.97	40.0	0.937		
	0.70‡	1.67‡	24.0	0.364‡		
n-Bu	1.30	2.10	20.0	0.773		
	1.00	1.0	25.0	1.43		
	2.00	1.0	25.0	1.30	7.2±0.3	8.4±0.5
	8.25	1.0	25.0	1.32		
	24.3	1.0	25.0	1.36		
	50.8	1.0	25.0	1.38		
	101.5	1.0	25.0	1.33		
	1.30	2.10	39.5	1.98		
s-Bu	1.06	1.60	25.5	1.04	9.0±0.3	10.8±0.4
	1.06	1.60	40.0	2.51		
			In methylene chloride			
t-Bu	1.00	2.08	17.5	0.296		
	10.0	1.06	24.0	0.533		
	1.00	1.06	24.0	0.574	7.8±0.3	9.8±0.5
	0.10	1.06	24.0	0.680		
	1.00	2.08	35.5	0.843		
n-Bu	1.04	2.00	24.0	1.53	7.4±0.3	8.4±0.4
	1.04	2.00	37.0	2.77		
	0.83	1.60	23.5	0.835	8.3±0.3	10.1±0.4
s-Bu	0.83	1.60	44.5	2.53		
			In hexane			
t-Bu	1.01	2.00	22.5	0.752		
	1.01	2.00	55.0	1.79	5.3±0.1§	6.0±0.2§
	1.08‖	2.00	22.5	0.446‖		
n-Bu	1.35	2.00	21.5	2.63		
	1.35	2.00	36.5	3.80	4.9±0.4§	4.7±0.6§
s-Bu	1.04	2.00	21.5	1.14		
	1.04	2.00	42.5	2.26	5.8±0.3§	6.5±0.4§

*Average of 3 runs in most cases.
†Least squares value for runs at 2–3 °C intervals from lowest to highest indicated temperature.
‡In EtOD.
§From k_2's calculated arbitrarily at the given hydroperoxide concentration over the temperature range shown.
‖Hydroperoxide titrating 90.5% pure and containing 88% O—D by infrared.

pression, "k_1" = $k_2[RO_2H] + k_3[RO_2H]^2$ (Table 2, Fig. 2), an analysis which we prefer.[4]

[4]A 3/2-order reaction might be explained on the assumptions (*a*) that the hydroperoxide is extensively dimerized in this solvent and (*b*), reaction in aprotic solvents requires both RO_2H monomer and a proton transfer agent, which could be hydroperoxide dimer. (The parallel with reductions by organic sulfides is discussed in a later section.) However, this interpretation falls short on several grounds; even in hexane, the hydroperoxide is probably not dimerized to the necessary extent at the concentrations used. Assuming the association constant for *t*-BuO_2H in CCl_4 (12) is a satisfactory approximation, dimer would account only 8% of the hydroperoxide at 0.02 M and 0.5% at 0.001 M; in methylene chloride, also aprotic, higher order kinetics are not observed; reduction by organic sulfides are second order, not 3/2-order, in hydroperoxide under similar circumstances (13, 14).

For *t*-BuO_2H, $k_2 = 0.185 \pm 0.008$ and $k_3 = 37.77 \pm 0.50$ at 22 °C. For *n*-BuO_2H, $k_2 = 1.25 \pm 0.15$ and k_3, 207 ± 17 at 27.6 °C. The constants in Table 1 were computed as if the reaction were simple second order, owing to insufficient data at other temperatures to compute the second- and third-order constants.

Deuterium Isotope Effects

Reduction of partially deuterated hydroperoxide (*t*-BuO_2D (H), 88% O—D) in hexane gave an overall rate about 0.6 times as fast as the undeuterated material. (Table 2, shown arbitrarily as an effect on "k_2", but readily translatable to the pseudo-first order rate since the comparable run with *t*-BuO_2H is at the same initial concen-

Can. J. Chem. Downloaded from www.nrcresearchpress.com by 210.87.254.40 on 09/05/12
For personal use only.

TABLE 2. Reduction of hydroperoxides by triphenylphosphine in hexane rate dependence on hydroperoxide concentration

$[RO_2H]_0$ ($M \times 10^3$)	"k_1" $\times 10^3$ Experimental	Calculated as $k_{3/2}[RO_2H]^{3/2}$	Calculated as $k_2[RO_2H] + k_3[RO_2H]^2$
	t-BuO₂H at 22.0 °C		
18.6	16.5	15.2	16.5
10.1	5.77	6.09	5.72
5.35	2.01	2.35	2.07
1.95	0.525	0.516	0.504
1.00	0.190	0.190	0.222
	n-BuO₂H at 27.6 °C		
10.1	33.6	33.3	33.7
5.00	11.5	11.6	11.4
4.50	10.6	9.91	9.81
2.50	3.85	4.10	4.41
1.97	2.58	2.87	3.26
1.01	1.14	1.05	1.47

*Pseudo first-order rate constant for disappearance of Ph_3P (initial concentration of 1×10^{-4} *M*).

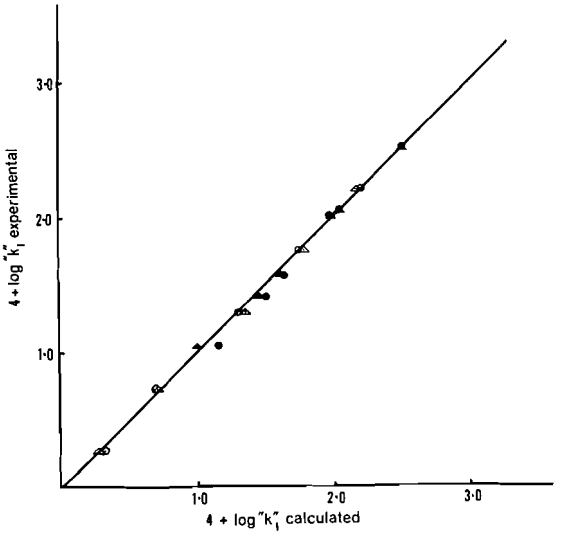

FIG. 2. "k_1" experimental *vs.* "k_1" calculated for reduction of hydroperoxides by Ph_3P in *n*-hexane. "k_1" = $k_2[RO_2H] + k_3[RO_2H]^2$; ●, *t*-$BuO_2H$, ○, *n*-$BuO_2H$; "$k_1$" = $k_{3/2}[RO_2H]^{3/2}$, ▲, *t*-BuO_2H, ○, *n*-BuO_2H.

tration.) While it would have been nice to have a more accurate estimate of the isotope effect and to have resolved the separate contributions to the bimolecular and termolecular parts of the reaction in hexane, work in this direction was abandoned when efforts to prepare 100% *t*-BuO_2D proved unexpectedly hazardous (Experimental section).

To see whether solvent deuteration had any effect, *t*-BuO_2H was reduced in EtOD (Table 1). The reacting species was, of course, *t*-BuO_2D, due to the rapid exchange with solvent. However, rates were the same within experimental error as for *t*-BuO_2H in EtOH.

s-Butyl hydroperoxide in ethanol or methylene chloride gave results consistent with those obtained using *n*- or *t*-BuO_2H (Table 1). In hexane, however, rates were not reproducible, and in some cases reactions exhibited induction periods (Fig. 1). (Rates given in Table 1 are typical and reliable, perhaps, to ±50%.) The variability appeared linked to impurities in the hydroperoxide.[5] Different batches having approximately the same peroxide titer (80–83%) gave different results which could not be traced to known or suspected contaminants such as 2-butanol, methyl-ethyl-ketone, acetaldehyde, or 2-butyl methanesulfonate.

Differing purities of triphenylphosphine had no effect on the results with a given batch of hydroperoxide, a surprising result since slow and incomplete reductions of hydrocarbon solutions of *s*-BuO_2H on a large scale (prior to g.l.c. analysis of reaction mixtures) have been traced to the use of unpurified Ph_3P more than once (8).

Discussion

Generally speaking, these results confirm earlier contentions (3, 7) that phosphine reduc-

[5]Impurities were much less important when ethanol was the solvent; hydroperoxide which had been allowed to deteriorate on standing over several months to a titer of 30% gave rates of reduction only 10% less than those obtained for the purest material.

Can. J. Chem. Downloaded from www.nrcresearchpress.com by 210.87.254.40 on 09/05/12
For personal use only.

TABLE 3. Comparisons of reduction of t-BuO_2H by triphenylphosphine and by organic sulfides

System	10^4k_2 M^{-1} s^{-1}	E_a	$\Delta S^{\ddagger}$	k_{SH}/k_{SD}*
Thioxane† in H_2O, 25 °C	1.35	14.1	−27	1.42
Ph_3P in EtOH, 24 °C	3600.0	10.8	−24	1.0

*H_2O/D_2O and EtOH/EtOD, respectively.
†From ref. 14.

tions belong to a sizable class of nucleophilic displacements on the peroxide bond. Examples include reactions with I^-, organic sulfides and sulfones, amines and olefins (15), all of which require for ease of accomplishment either a readily transferred proton (hydroperoxides), generation of a stable anion (acyl peroxides), or both (peroxy acids).

Of these examples cited the reaction of hydroperoxides with organic sulfides, though much less rapid (13, 14), bears the most resemblance to that with Ph_3P (Table 3). Similarities include relative insensitivity to solvent, cleanness of reduction without the need for added catalysts, and large negative entropies of activation. The sulfide reduction appears to require a greater degree of assistance in transferring the proton from one oxygen to the other (14), since in non-polar, aprotic solvents the reaction is strictly second order in hydroperoxide, whereas, as we have shown, for Ph_3P the $[RO_2H]^2$ contribution is

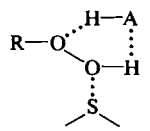

1

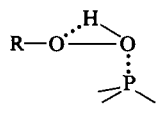

2

balanced by an almost equally rapid reaction which is unimolecular in hydroperoxide.[6] Likewise the effect is greater for reduction by sulfides, insofar as effects in D_2O *vs.* H_2O and EtOD *vs.* EtOH are comparable (Table 3). (The reduction of RO_2D by sulfides in aprotic solvents seems not to have been investigated.)

The lower sensitivity of the RO_2H–Ph_3P reaction to such factors need not be interpreted as a concerted proton shift, as in **2**; more likely it reflects a transition state closely related to the reactants in which there is little weakening of the O—H bond. The low activation energy and the insensitivity to solvent polarity would tend to support this conclusion.

The relative reactivities of the three hydroperoxides t-Bu < s-Bu < n-Bu are line with both expected steric effects and relative electrophilicities of the peroxidic oxygen. The differences are so small, however, as to discourage any detailed rationalization.

The inhibition or retardation of the reduction of s-BuO_2H by small amounts of as yet undefined species has some peculiar aspects, to say the least, and will be the subject of continuing research.

The authors gratefully acknowledge financial support received from the National Research Council of Canada.

1. F. CHALLENGER and V. K. WILSON. J. Chem. Soc. 213 (1927).
2. V. L. HORNER and W. JURGELEIT. Ann. **591**, 138 (1955).
3. C. WALLING and R. RABINOWITZ. J. Am. Chem. Soc. **81**, 1243 (1959).
4. D. E. VAN SICKLE, F. R. MAYO, R. M. ARLUCK, and M. SYZ. J. Am. Chem. Soc. **89**, 967 (1967) and references therein.
5. L. DULOG and K. H. BURG. Z. Anal. Chem. 203 (1964).
6. R. A. STEIN and V. SLAWSON. Anal. Chem. **35**, 1008 (1963).
7. D. B. DENNY, W. F. GOODYEAR, and B. GOLDSTEIN. J. Am. Chem. Soc. **82**, 1393 (1960).
8. Unpublished work in this laboratory.
9. H. R. WILLIAMS and H. S. MOSHER. J. Am. Chem. Soc. **76**, 2984, 2987 (1954).
10. G. SHAW and J. K. BECCONSTALL. J. Am. Chem. Soc. **79**, 979 (1957).
11. G. M. COPPINGER. J. Am. Chem. Soc. **79**, 501 (1957).
12. C. WALLING and L. HEATON. J. Am. Chem. Soc. **87**, 48 (1965).
13. L. BATEMAN and K. R. HARGRAVE. Proc. Roy. Soc. Ser. A. **224**, 389 (1954).
14. M. A. P. DANKLEFF, R. CURCI, J. O. EDWARDS, and H.-Y. PYUN. J. Am. Chem. Soc. **90**, 3209 (1968).
15. E. J. BEHRMAN and J. O. EDWARDS. *In* Progress in physical organic chemistry. *Edited by* A. Streitweiser and R. W. Taft. Interscience, New York. 1967. p. 93*ff*.

[6]The $[RO_2H]^2$ term may, in fact, indicate that the small amount of dimer present reacts independently. Such an assumption would fit our data equally well since $[RO_2H]_2 \cong K_{assoc.}[RO_2H]^2$ over the concentration range employed ($K_{assoc.}$ = 2–3 M^{-1} (12)).

Can. J. Chem. Downloaded from www.nrcresearchpress.com by 210.87.254.40 on 09/05/12
For personal use only.

Can. J. Chem. Downloaded from www.nrcresearchpress.com by 210.87.254.40 on 09/05/12
For personal use only.

Catalysis of the Reduction of Hydroperoxides by Triphenylphosphine

R. HIATT AND CHRISTINE MCCOLEMAN

Chemistry Department, Brock University, St. Catharines, Ontario

Received September 9, 1970

The reaction of hydroperoxides with triphenylphosphine is catalyzed by the addition of strong acid. Likewise in hydroxylic solvents, the log of the bimolecular rate constant increases linearly with the solvents' autoprotolysis constants. Soluble salts of molybdenum or vanadium are 10^4 to 10^5 times more effective catalysts than H^+. The reaction shows promise as a method for quantitative comparison of the effectiveness of these compounds in augmenting the electrophilic character of hydroperoxides.

On observe que la réaction entre les hydropéroxydes et la triphénylphosphine est catalysée par les acides forts. Il en est de même dans les solvants hydroxyliques où le log de la constante de vitesse bimoléculaire augmente d'une façon linéaire avec les constantes d'autoprotolyse des solvants. Les sels solubles de molybdène ou de vanadium sont des catalyseurs de 10^4 à 10^5 fois plus efficaces que H^+. Il semble que cette réaction pourrait éventuellement être utilisée pour déterminer d'une façon quantitative l'efficacité de ces composés pour augmenter le caractère électrophile des hydropéroxydes.

Canadian Journal of Chemistry, 49, 1712 (1971)

Introduction

The reduction of hydroperoxides by triphenylphosphine has been shown not to involve a free radical chain, and to have similar characteristics to reductions by organic sulfides (1). It seemed useful to determine whether this similarity extended to catalysis by strong acids and by more protic solvents (2), even though the reaction itself is fast enough to scarcely require added acceleration. In the same vein we have explored the effect of compounds of molybdenum, vanadium, and tungsten, metal ions known to catalyze the reaction of hydroperoxides with olefins (3), amines (4), and sulfoxides (5).

Experimental

Hydroperoxides and triphenylphosphine were obtained or prepared as previously reported. Solvents were Reagent Grade, used without further purification. Perchloric acid was used as the 70% solution in water. Compounds of Mo, V, or W were used as obtained from K & K Laboratories, molarities for naphthenate solutions being calculated on the basis of their containing 3%, by weight, of metal ion.

Rate studies were based on the u.v.-monitored, unimolecular disappearance of Ph_3P, hydroperoxide being in uniformly large excess, as previously described (1). Excellent first-order plots for Ph_3P disappearance were obtained in every case. Most constants reported are averages of duplicate runs.

Results and Discussion

Acid Catalysis

Table 1 shows second-order rate constants for the reaction of n-BuO_2H with Ph_3P in ethanol with added amounts of 70% $HClO_4$. The constants increase linearly with $HClO_4$ up to 0.1 M. At higher concentrations of acid there is a slight tailing off (Fig. 1), due possibly to the activity of $HClO_4$ (or H^+) in ethanol not being a linear function of concentration at these higher values. Alternatively sufficient protonation of the phosphine may be occurring to reduce the effective concentration of the active species.

TABLE 1. Reduction of n-BuO_2H by Ph_3P in ethanol,* effect of added $HClO_4$

10^3 [n-BuO_2H]$_0$ (mol/l)	$HClO_4$ (mol/l)	"k_2"† (M^{-1} s^{-1})
1.00	—	1.28 (ref. 1)
1.00	0.025	1.88
1.00	0.050	2.50
1.00	0.100	3.23
1.00	0.200	5.08
1.00	0.600	10.36

*At 25 °C, $[Ph_3P]_0 = 1 \times 10^{-4}$ mol/l.
†Defined by $-d[Ph_3P]/dt =$ "k_2"$[Ph_3P][n\text{-}BuO_2H]$.

[1] $$Ph_3P + H^+ \rightleftharpoons Ph_3PH^+$$

Over the linear portion,

$$-d[Ph_3P]/dt = k_2[Ph_3P][RO_2H] + k_3[HClO_4][Ph_3P][RO_2H]$$

where

$$k_2 = 1.28\ M^{-1}\,s^{-1} \text{ and } k_3 = 24.0\ M^{-2}\,s^{-1}.$$

Solvent Effects

While the comparative effects of non-polar, polar-aprotic, and polar-protic solvents admit no

Can. J. Chem. Downloaded from www.nrcresearchpress.com by 210.87.254.40 on 09/05/12
For personal use only.

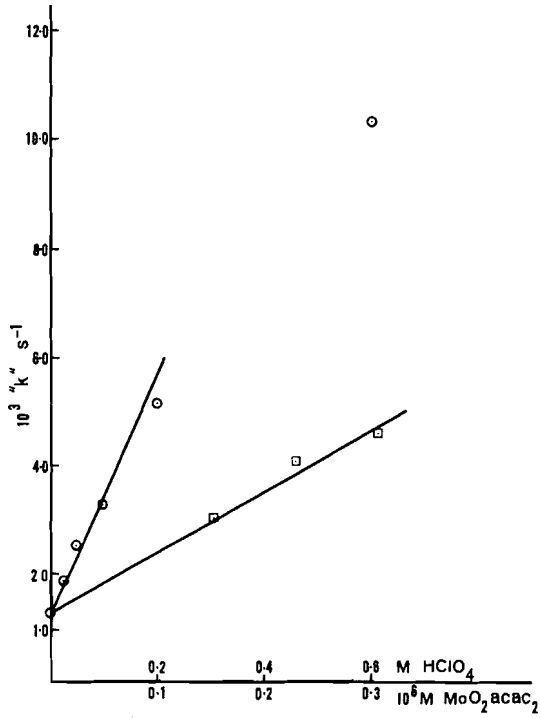

FIG. 1. Pseudo first-order rate constants for the reduction by 10^{-4} *M* Ph_3P of 10^{-3} *M* *n*-BuO_2H in ethanol at 25 °C, catalyzed by; ○, $HClO_4$; and □, MoO_2acac_2.

ready interpretation (1), those of a structurally similar series fall nicely into line (Table 2, Fig. 2); log k_2's for reaction in alcohols being correlated with their autoprotolysis constants (6). While no such correlation coefficient is available for 80% ethanol, the increase in rate over that in 100% ethanol is clearly in the right direction.

Determination of the effect of added acetate ion on the rate in acetic acid was limited to the extent that no attempt was made to maintain a constant ionic strength. However, it is clear from the slight increase in rate constant that there is no common ion effect, as should be the case if the accelerating effect of acetic acid were due to protonation of the hydroperoxide. It may be noted that acetic acid as solvent exerts a levelling effect on rate differences due to hydroperoxide

[2] $$HOAc + RO_2H \rightleftharpoons RO_2H_2^+ + {}^-OAc$$

structure. While the differences between *n*-BuO_2H and *t*-BuO_2H in ethanol, CH_2Cl_2 or hexane are small, a factor of 3–4 (1), in HOAc their rates are the same within experimental error (Table 2).

TABLE 2. Reduction of *t*-BuO_2H by Ph_3P in protic solvents*

10^3 [*t*-BuO_2H]$_0$ (mol/l)	Solvent	k_2 (M^{-1} s^{-1})
10.5	*i*-PrOH	0.220
	EtOH	0.350 (ref. 1)
1.5	MeOH	0.734
2.10	MeOH	0.764
5.20	MeOH	0.760
1.10	80% EtOH	0.748
2.20	80% EtOH	0.792
3.60	80% EtOH	0.758
0.50	HOAc	6.6
1.00	HOAc	5.70
1.2	HOAc†	6.51
1.6‡	HOAc	5.52

*At 25 °C, [Ph_3P]$_0$ = 1 × 10^{-4} mol/l.
†Containing 0.10 *M* KOAc.
‡*n*-BuO_2H.

The effects of different protic solvents and of strong acid on the reaction of Ph_3P with hydroperoxides are strikingly similar to those for the hydroperoxide – organic sulfide reaction (2), not only as to direction and lack of common ion effect, but even approximate magnitude of the correlation constants. Thus for catalysis by $HClO_4$ at 25 °C, k_3 for *t*-BuO_2H + thioxolane is 14.1 times as large as k_2 for the uncatalyzed component (2), whereas for *n*-BuO_2H + Ph_3P at 25°, $k_{3[HClO_4]}$ is 18 times as large as k_2. While the differences in solvent (H_2O *vs.* EtOH) and hydroperoxide might argue that this agreement is coincidental, the effects of different alcohols as solvents on the bimolecular rate constant for

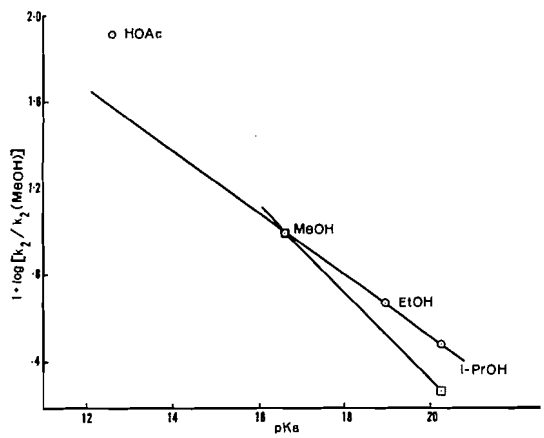

FIG. 2. Log of second-order rate constants for the reduction of *t*-BuO_2H at 25° *vs.* autoprotolysis constants of the solvent (taken from ref. 6.). ○, by Ph_3P; □, by thioxolane, (from ref. 2).

TABLE 3. Effects of metal ions on the reduction of hydroperoxides by Ph_3P*

10^3 $[RO_2H]_0$ (mol/l)	Additive	mol/l × 10^6	"k_2"† (M^{-1} s^{-1})	$10^{-5}k_3$‡ (M^{-2} s^{-1})
		t-BuO₂H		
1.2	Mo naphthenate	3.12	0.692	1.11
1.2	Mo naphthenate	6.2	1.13	1.25
1.2	V naphthenate	70.0	0.959	0.0870
1.2	V naphthenate	140.0	1.82	0.1050
6.0	MoO_2acac_2	3.0	0.67	1.0
		n-BuO₂H		
1.0	Mo naphthenate	3.7	5.5	11.4
1.0	MoO_2acac_2	1.53	3.04	11.5
1.0	MoO_2acac_2	2.29	4.06	12.1
1.0	MoO_2acac_2	3.06	4.61	10.9

*In ethanol at 25 °C, $[Ph_3P]_0 = 1 \times 10^{-4}$ mol/l.
†Defined as $-d[Ph_3P]/dt = "k"_2[Ph_3P][RO_2H]$.
‡Defined as $-d[Ph_3P]/dt = k_2[Ph_3P][RO_2H] + k_3[M][Ph_3P][RO_2H]$.

t-BuO_2H (Fig. 2) are directly comparable and are about half as large for Ph_3P as for the sulfide.

Catalysis by Metal Ions

A select group of metal ions, molybdenum, vanadium, and to a lesser extent, tungsten, have been shown to increase the electrophilicity of hydroperoxides, via complexation (3–5), to the extent that hitherto unknown reactions are possible (vide infra). Such compounds in exceedingly low concentrations have been found to exert a profoundly accelerating effect on the rate of reaction of hydroperoxides with Ph_3P (Table 3). Over the admittedly small range of concentrations experimentally available, catalysis was reasonably close to first order in metal ion (Table 3 and Fig. 1); *i.e.*, conforming to

$$-d[Ph_3P]/dt = [Ph_3P][RO_2H][k_2 + k_3[M^{n+}]]$$

The low concentrations were only in part dictated by the necessity of keeping the reaction rate within measurable bounds. The high coloration imparted to their solutions extended into the u.v. region and interfered with the method of Ph_3P analysis. In fact, solutions containing carbonyls of the mentioned metals, as well as the acetyl acetonate of vanadium could not be used due to absorbtion changes of the metal compound during the course of reaction. This was doubly unfortunate, since catalysis of the RO_2H–Ph_3P reaction appears to offer a clean method for quantitatively assessing the effect of these substances on hydroperoxide reactivity. That is, reactions appeared to suffer little of the autoretardation (Fig. 3) commonly noted for other reactions catalyzed by these species (3*b*, 4*b*). (This has led to as yet unresolved difficulties in making other than qualitative comparisons of catalyst efficiency in those cases.[1])

It is particularly interesting that the effectiveness of molybdenum is independent of whether it is added as naphthenate or oxyacetylacetonate, and is some ten times greater than that of vanadium (Table 3). It would be precipitous and doubtless an oversimplification to assert that ligands had no effect, and that previous ratings of Mo over V and *vice versa* were entirely due to extraneous effects. However, further experiments in the Ph_3P–RO_2H system would appear to offer a profitable avenue for ascertaining the true situation.

Catalysis

Generally speaking, catalysis of the electrophilic reactions of hydroperoxides can be ascribed to two factors, not always easily separable, facilitation of hydrogen transfer, and increase in the electrophilic character of the hydroperoxide. Both are easily visualized in terms of a hydroperoxide–catalyst complex.

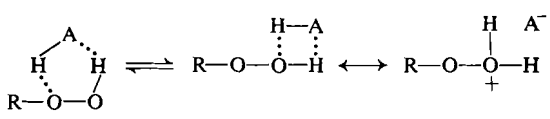

[1]This is not to say that catalyst solutions were not subject to degradation. They were, and were consequently made up fresh immediately prior to reactions. Most noticeably, solutions of MoO_2acac_2 in hexane deteriorated to the point of virtual inactivity over the course of a few hours. This was perhaps not surprising in view of the low concentration and the tendency of acetylacetonates to autoxidize rapidly (7).

Can. J. Chem. Downloaded from www.nrcresearchpress.com by 210.87.254.40 on 09/05/12
For personal use only.

The present data suggest that whatever its effect, complexation is in itself the most important factor. That is, acetic acid which probably has low steric requirements for complex formation tends to level out differences between n-BuO_2H and t-BuO_2H, while metal ion aggregates, undoubtedly more bulky, tend to exaggerate them (Table 3).

While the catalytic influence of complexing with molybdenum or vanadium certainly derives from an increased electron demand of the peroxidic oxygen (3*b*), this is not to say all, if indeed any, of the effect of acids or protic solvents

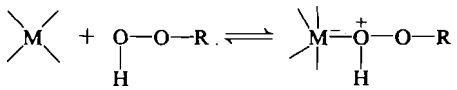

is similarly founded. Factors affecting electrophilic reactions of peroxides require better understanding, and will be the subject of continued research in these laboratories.

The authors gratefully acknowledge financial support received from the National Research Council of Canada.

1. R. HIATT, R. J. SMYTHE, and CHRISTINE McCOLEMAN. Can. J. Chem. This issue.
2. M. A. P. DANKLEFF, R. CURCI, J. O. EDWARDS, and Y.-Y. PYUN. J. Am. Chem. Soc. **90**, 3209 (1968).
3. (*a*) N. M. SHENG and J. G. ZAJACEK. Advances in Chemistry Series, No 75, American Chemical Society, Washington, D.C., 1968. (*b*) E. S. GOULD, R. HIATT, and K. C. IRWIN. J. Am. Chem. Soc. **90**, 4573 (1968).
4. (*a*) N. M. SHENG and J. G. ZAJACEK. J. Org. Chem. **33**, 588 (1968). (*b*) G. R. HOWE and R. HIATT. J. Org. Chem. To be published.
5. VON F. LIST and L. KUHNEN. Erdol und Kohle Erdgas Petrochemie, 192 (1967).
6. K. BOWDEN. Chem. Rev. **66**, 119 (1966).
7. M. MENDELSOHN, E. M. ARNETT, and H. FRASER. J. Phys. Chem. **64**, 664 (1960).

Can. J. Chem. Downloaded from www.nrcresearchpress.com by 210.87.254.40 on 09/05/12
For personal use only.

Can. J. Chem. Downloaded from www.nrcresearchpress.com by 210.87.254.105 on 09/05/12
For personal use only.

Hydrates of Tetra-*n*-butylammonium Picrate in Benzene and Chlorobenzenes

SAUL GOLDMAN AND G. C. B. CAVE
Department of Chemistry, McGill University, Montreal, Quebec
Received[1] December 23, 1969

The first two hydration constants of the ion pair tetra-*n*-butylammonium picrate in the solvents *o*-dichlorobenzene, chlorobenzene, and a binary mixture benzene–chlorobenzene (1:1 *v/v*) at 25.0, 35.1, and 45.1 °C were determined by an isopiestic method. In addition, algebraic treatment of the data permitted evaluation of the hydration constants of the dimer and higher aggregates known to co-exist with the monomer in the solutions. The effect of bulk dielectric constant of the solvent on the hydration constants of the monomer is discussed.

Les deux premières constantes d'hydratation de la paire d'ion, picrate de tétra-*n*-butylammonium, dans l'*o*-dichlorobenzene, le chlorobenzene et le mélange binaire benzène–chlorobenzène (1:1 *v/v*) à 25, 35.1 et 45.1 °C ont été déterminées par une méthode isopiestique. De plus le traitement algébrique des données a permis une évaluation des constantes d'hydratation des agrégats dimères et polymères qui existent en solutions avec le monomère. L'effet de la constante dielectrique globale du solvant sur les constantes d'hydratation du monomère est discutée.

Canadian Journal of Chemistry, **49**, 1716 (1971)

Introduction

Ion pairs (monomers) and co-existing ion-pair aggregates occur in many solvent extraction systems of analytical importance. At least partial hydration of these species in the organic phase of such systems is expected. Characterization of the species extracted in a solvent extraction system and evaluation of their thermodynamic properties in the organic phase require, therefore, similar knowledge of these hydrates.

The thermodynamic properties ΔG^0, ΔH^0, and ΔS^0 of the aggregation reactions of the monomer of tetra-*n*-butylammonium picrate in benzene and in substituted benzenes have been evaluated from solvent extraction data (1). These evaluations required prior evaluation of the hydration constants of the monomer and its aggregates, as well as the activity values of the unbound water in the organic phase.

The sought-for hydration constants were evaluated from isopiestic data. Thus, standard nonaqueous solutions of tetra-*n*-butylammonium picrate (hereafter usually abbreviated Bu_4NPi) were equilibrated in closed, thermostatted vessels with the water vapor from an adjoining standard aqueous solution of calcium chloride. The equilibrium stoichiometric concentrations of water in the nonaqueous solutions, together with the stoichiometric concentrations of Bu_4NPi, as well as the activities of the water in the aqueous solutions gave on algebraic treatment the required constants.

The use of an isopiestic technique, rather than direct equilibration of the two liquid phases, avoided the possibility of chemical reaction between the solutes Bu_4NPi and $CaCl_2$. In the case of solutes Bu_4NPi and $CaBr_2$, preliminary experiments showed that reaction was extensive.

Experimental

Apparatus

Karl Fischer Titration Assembly

The stoichiometric concentrations of water in the equilibrated nonaqueous solutions of Bu_4NPi were determined by a conventional Karl Fischer dead-stop back-titration (2). The titration was carried out in a standard, completely closed Radiometer Titration Assembly (type TTA1); and the two platinum electrodes in the electrode head of this Assembly were connected to a Radiometer Titrator (type TTT1a), for determination of the dead-stop end point.

Isopiestic Assembly

The apparatus was similar to that described by Christian *et al.* (2). The equilibration flasks were 250 ml, conical, ground-glass stoppered iodine flasks, dried before use. The nonaqueous solution of Bu_4NPi for equilibration was contained in the bottom of the iodine flask. The aqueous solution of $CaCl_2$ was in an open 10 cm × 1 cm test tube which rested obliquely inside the stoppered flask. The upper rim of the ground-glass stopper was lightly greased. The flask and its contents were then placed in a water thermostat maintained to within ±0.1 °C.

Materials

The tetra-*n*-butylammonium picrate (Bu_4NPi) was prepared by a method similar to that of Flaherty and Stern (3). The product was re-crystallized 3 times from hot ethanol solutions, by adding a large excess of cold, distilled water. The resulting product was dried in vacuo over P_2O_5, for 12 h at 65 °C: m.p. 89.3–89.8 °C; lit. 89.5 °C (4). This final product was also assayed for pic-

[1]Revision received December 1, 1970.

Can. J. Chem. Downloaded from www.nrcresearchpress.com by 210.87.254.105 on 09/05/12
For personal use only.

rate, by means of a potentiometric titration with a standard 0.1 *N* solution of $HClO_4$ in glacial acetic acid (5); the product was thereby found to be 100.0 ± 0.1% pure.

Reagent grade benzene, chlorobenzene, and *o*-dichlorobenzene were further purified by washing each of them successively with concentrated sulfuric acid, water, 1 *N* NaOH solution for benzene and 1 *N* $NaHCO_3$ solution for the chlorobenzenes, and finally with water. Each resulting product was then fractionally distilled over silica gel, the center two-thirds cut being kept for use. These final products were stored over silica gel. Their densities at 25.0 °C were found to be: benzene, 0.8734 (lit. 0.8734 (6)); chlorobenzene, 1.1010 (lit. 1.1008 (3)); *o*-dichlorobenzene, 1.3005 (lit. 1.3007 (6)).

Conventional, stabilized Karl Fischer reagent and diluent (Fisher So-K-3 and So-K-5) were used for the dead-stop determination of water in the nonaqueous solutions of Bu_4NPi. Spectrophotometric grade methanol (Fisher A-408) containing approximately 0.1% water was the titrant for the back-titration step.

Calcium chloride was anhydrous reagent grade (Fisher C-76). Distilled water was used to prepare the aqueous solutions of $CaCl_2$.

Silver nitrate was reagent grade (Engelhard 99.98%), dried at 120 °C before use.

Sodium chloride was best quality reagent grade (Fisher 271), dried at 120 °C before use.

Linde dry nitrogen was used to flush the Karl Fischer titration vessel before use.

Procedures

Preparation of Solutions

The nonaqueous solutions of Bu_4NPi were prepared by accurately weighing the salt, considered as a primary standard, into calibrated volumetric flasks, and diluting to volume with the solvent (*o*-dichlorobenzene, chlorobenzene, and the mixed solvent benzene–chlorobenzene (1:1 *v/v*)).

The aqueous solutions of $CaCl_2$ were prepared by suitable dilutions of a near-saturated aqueous stock solution of $CaCl_2$. Those resulting working solutions that were used at 25 °C were standardized after the isopiestic equilibration experiments.

Equilibration

Approximately 20–50 ml of the nonaqueous solution of Bu_4NPi were placed in the dried iodine flask. The 10 cm × 1 cm test tube containing 7 ± 0.5 ml of water or a standard aqueous solution of $CaCl_2$ was then placed in the iodine flask so that the rim of the test tube rested against the upper inside wall of the flask. The flask was then stoppered, the upper rim of the stopper having been lightly greased. The flask and its contents were then placed in a water thermostat maintained to within ±0.1 °C. Care was taken to ensure that the water level in the thermostat was kept above the bottom of the stopper in the iodine flask; condensation inside the flask was thereby prevented.

Trials showed that the stoichiometric concentration of water in the nonaqueous solution did not change after equilibration for 2 days. In the present work, 5 days were allowed. As further proof of equilibrium, pure benzene equilibrated at 25 °C with water by the isopiestic method had the same water content as benzene equilibrated with water by direct liquid–liquid extraction.

Water Content of the Nonaqueous Solutions of Bu_4NPi

The stoichiometric concentration of water in a nonaqueous solution of Bu_4NPi after the isopiestic equilibration was determined by a Karl Fischer titration. Thus, the Karl Fischer reagent was dispensed by using a dried pipet, into the dried titration cell of the Radiometer Titration Assembly. Then an aliquot of the nonaqueous solution for analysis was added via a pipet which had been prerinsed with the same solution. The volume of this aliquot was so chosen that only a small excess of Karl Fischer reagent remained unreacted. This small excess was then back-titrated with the methanol–water titrant, which consisted of approximately 0.1% water in pure methanol.

In practice, the following sequence of operations was followed, for every water determination: (*i*) The titre of the methanol–water titrant was determined with respect to the Karl Fischer reagent; (*ii*) the Karl Fischer reagent itself was standardized against a stock standard solution that for convenience consisted of water-saturated benzene kept at 25.0 °C; (*iii*) a measured aliquot of the nonaqueous solution for analysis was titrated by the procedure outlined in the preceding paragraph.

The water content of the water-saturated benzene at 25.0 °C was also found by Karl Fischer titration. In this case, the Karl Fischer reagent was first standardized against a standard solution of water in methanol, prepared by adding an accurately measured amount of water to methanol. The solubility of water in benzene at 25.0 °C was found in this way to be 0.0347 *M* (standard deviation 0.0015 for 5 replicates), in good agreement with the literature value (2) of 0.0349 *M* (standard deviation 0.0005 for 4 replicates).

Trials had shown that even virtually anhydrous solvents showed, on Karl Fischer titration, measurable traces of water. The source of water was attributed to a small amount of atmospheric moisture believed to have entered the titration cell during addition of the sample solution. Therefore this small blank correction (0.017 mmol of water) was determined in replicate by using very carefully dried benzene as the sample, and the correction found was applied to all subsequent titrations.

Trials also showed that dried Bu_4NPi had no effect on the titration results.

Equilibrium Water Activities

The molality of each aqueous solution of $CaCl_2$, after the isopiestic equilibration at 25 °C, was determined by titration of a diluted aliquot with a standard aqueous solution of silver nitrate. Dichlorofluorescein was the indicator. The silver nitrate solution was standardized against dried sodium chloride (the primary standard).

The molalities of the equilibrium calcium chloride solutions were found to be within 1% of the initial molalities, as a result of the small volumes of the nonaqueous solutions used in the isopiestic studies, and the low solubility of water in those solutions.

From the measured molalities of those calcium chloride solutions which were at 25.0 °C, the corresponding water activities at 25.0 °C were found from published tabulations (7).

Results

The equilibrium data for the isopiestic systems are summarized in Table 1. Literature values for

Can. J. Chem. Downloaded from www.nrcresearchpress.com by 210.87.254.105 on 09/05/12
For personal use only.

TABLE 1. Equilibrium isopiestic hydration data (organic phase: Bu_4NPi in solvent; aqueous phase: $CaCl_2$ solution)*

25.0 °C					35.1 °C				45.1 °C			
Aqueous		Organic			Aqueous	Organic			Aqueous	Organic		
			H_2O				H_2O				H_2O	
$CaCl_2$ (m)	H_2O (Activity)	Bu_4NPi (M)	($M \times 10^4$)	(s.d. $\times 10^4$)	$CaCl_2$ (m)	Bu_4NPi (M)	($M \times 10^4$)	(s.d. $\times 10^4$)	$CaCl_2$ (m)	Bu_4NPi (M)	($M \times 10^4$)	(s.d. $\times 10^4$)
					(Solvent: *o*-dichlorobenzene)							
6.96	0.314	Nil	91	5	7.0	Nil	123	3	7.0	Nil	166	1
6.96		0.100	149	1	7.0	0.099	184	1	7.0	0.098	260	19
6.96		0.200	226	0	7.0	0.198	287	7	7.0	0.196	358	2
5.02	0.496	Nil	125	5	5.0	Nil	175	1	5.0	Nil	232	0
5.02		0.100	232	17	5.0	0.099	295	4	5.0	0.098	376	1
5.02		0.200	334	6	5.0	0.198	441	5	5.0	0.196	545	0
3.62	0.675	Nil	170	3	3.5	Nil	232	3	3.5	Nil	315	5
3.62		0.100	320	7	3.5	0.099	411	2	3.5	0.098	529	12
3.62		0.200	493	2	3.5	0.198	603	6	3.5	0.196	775	17
1.97	0.863	Nil	218	5	2.0	Nil	274	1	2.0	Nil	393	1
1.97		0.100	412	23	2.0	0.099	505	8	2.0	0.098	655	7
1.97		0.200	635	8	2.0	0.198	760	23	2.0	0.196	940	23
Nil	1.000	Nil	241	10	Nil	Nil	321	5	Nil	Nil	439	8
Nil		0.100	479	2	Nil	0.099	574	16	Nil	0.098	745	9
Nil		0.200	753	23	Nil	0.198	866	27	Nil	0.196	1100	30
					(Solvent: chlorobenzene)							
6.82	0.323	Nil	96	5	6.81	Nil	137	3	7.0	Nil	200	3
6.82		0.100	180	5	6.81	0.099	238	6	7.0	0.098	310	12
6.82		0.200	251	5	6.81	0.198	319	4	7.0	0.196	417	0
4.97	0.500	Nil	145	1	4.96	Nil	205	2	5.0	Nil	266	7
4.97		0.100	272	6	4.96	0.099	344	7	5.0	0.098	414	10
4.97		0.200	398	6	4.96	0.198	485	2	5.0	0.196	559	28
3.57	0.680	Nil	215	3	3.58	Nil	276	3	3.5	Nil	356	2
3.57		0.100	391	4	3.58	0.099	477	4	3.5	0.098	562	4
3.57		0.200	570	6	3.58	0.198	677	10	3.5	0.196	783	2
1.95	0.865	Nil	254	4	1.94	Nil	363	4	2.0	Nil	459	9
1.95		0.100	489	6	1.94	0.099	618	6	2.0	0.098	735	14
1.95		0.200	703	6	1.94	0.198	906	1	2.0	0.196	1070	2
Nil	1.000	Nil	290	3	Nil	Nil	411	7	Nil	Nil	535	1
Nil		0.100	545	5	Nil	0.099	683	30	Nil	0.098	872	18
Nil		0.200	834	20	Nil	0.198	1010	20	Nil	0.196	1230	30

Can. J. Chem. Downloaded from www.nrcresearchpress.com by 210.87.254.105 on 09/05/12
For personal use only.

TABLE 1. (*Concluded*)

25.0 °C					35.1 °C				45.1 °C			
Aqueous		Organic			Aqueous	Organic			Aqueous	Organic		
			H_2O				H_2O				H_2O	
$CaCl_2$ (*m*)	H_2O (Activity)	Bu_4NPi (*M*)	($M \times 10^4$)	(s.d. $\times 10^4$)	$CaCl_2$ (*m*)	Bu_4NPi (*M*)	($M \times 10^4$)	(s.d. $\times 10^4$)	$CaCl_2$ (*m*)	Bu_4NPi (*M*)	($M \times 10^4$)	(s.d. $\times 10^4$)
(Solvent: benzene–chlorobenzene (1:1 *v/v*))												
6.43	0.354	Nil	105	2	6.5	Nil	161	2	7.0	Nil	202	8
6.43		0.107	187	5	6.5	0.098	275	5	7.0	0.098	295	20
6.43		0.197	264	2	6.5	0.195	368	6	7.0	0.196	422	35
5.00	0.498	Nil	157	4	5.0	Nil	232	8	5.0	Nil	316	8
5.00		0.107	297	3	5.0	0.103	417	17	5.0	0.098	487	6
5.00		0.197	399	1	5.0	0.195	582	30	5.0	0.196	640	12
3.59	0.677	Nil	216	1	3.5	Nil	348	10	3.5	Nil	437	13
3.59		0.107	398	2	3.5	0.098	538	16	3.5	0.098	660	10
3.59		0.197	531	5	3.5	0.195	810	40	3.5	0.196	910	17
1.95	0.865	Nil	275	7	2.0	Nil	417	3	2.0	Nil	553	16
1.95		0.107	540	6	2.0	0.098	692	0	2.0	0.098	839	30
1.95		0.197	768	2	2.0	0.195	950	15	2.0	0.196	1190	30
Nil	1.000	Nil	311	3	Nil	Nil	466	10	Nil	Nil	601	7
Nil		0.107	613	1	Nil	0.098	810	5	Nil	0.098	946	10
Nil		0.197	853	12	Nil	0.195	1100	40	Nil	0.196	1330	20

*s.d. means standard deviation for 1 degree of freedom.

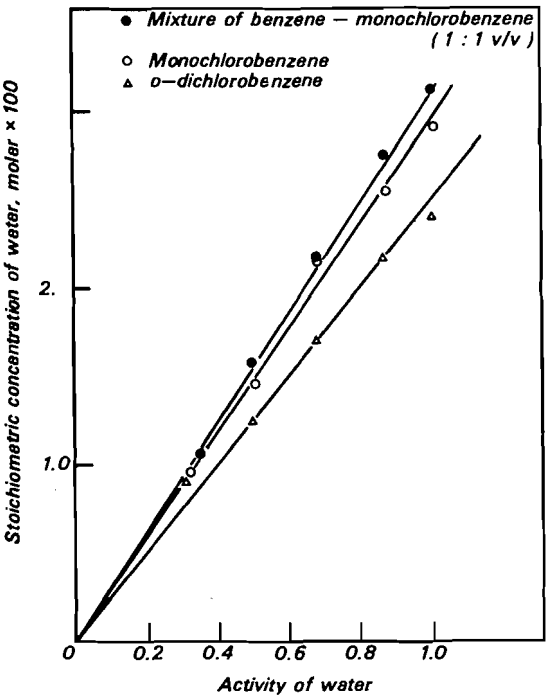

FIG. 1. Concentration of water *vs.* its activity, in three solvents at 25.0 °C, from isopiestic experiments.

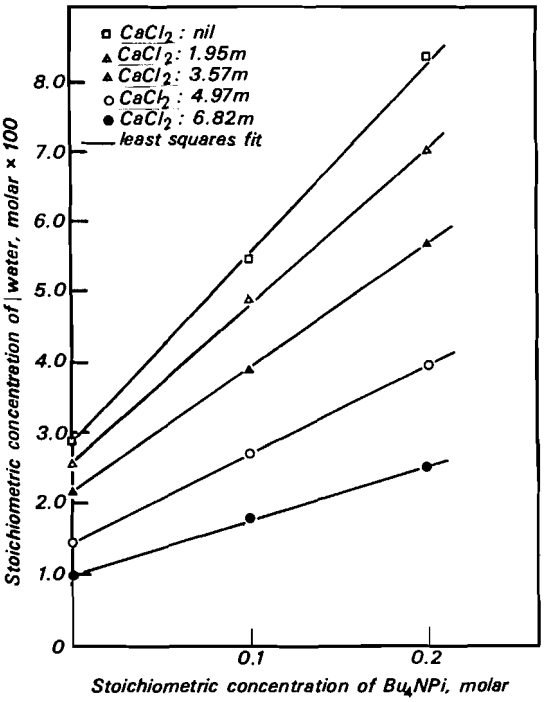

FIG. 2. Stoichiometric concentration of water *vs.* stoichiometric concentration of Bu_4NPi in chlorobenzene at 25.0 °C, in equilibrium with five aqueous solutions of $CaCl_2$ (isopiestic experiments).

the activity of water in aqueous solutions of calcium chloride were available only for 25 °C. Therefore only at this temperature were the equilibrium calcium chloride molalities measured; at 35.1 and 45.1 °C the molalities given in Table 1 are initial values calculated from the known dilution of a stock solution of calcium chloride.

In Fig. 1, the stoichiometric concentration of water in each of the pure nonaqueous solvents is plotted against the activity of water, for 25.0 °C. For each solvent, the graphs are linear. Consequently Henry's law was obeyed by water. This conclusion is in accord with similar results reported (8) for water in benzene, toluene, carbon tetrachloride, and cyclohexane. It was considered reasonable to assume that the unbound water (*i.e.* water not bound as hydrates to the Bu_4NPi monomer and its aggregates) was monomeric in the three solvents and in their Bu_4NPi solutions, at the three temperatures studied.

From the data in Table 1, it was found that for a fixed temperature, solvent, and water activity, a linear relationship exists between the equilibrium stoichiometric concentration of water in the nonaqueous solution, and the stoichiometric concentration of Bu_4NPi in that solution. All systems showed this linear relationship. In Fig. 2 it is illustrated for the chlorobenzene solutions at 25.0 °C. The intercept of each of these straight-line plots represents the concentration of unbound water, $[H_2O]_f$, that was present in all the solutions that belong to that particular straight line. The slope of each line represents the average number ($\bar{n}$) of bound moles of water per stoichiometric mole of Bu_4NPi (monomers and aggregates, anhydrous and hydrated).

Actually, $\bar{n}$ and $[H_2O]_f$ were evaluated for each system by a conventional least squares treatment of the relevant data from Table 1. The resulting values and their standard deviations are entered in Table 2, and are used in the following section. Plots of $\bar{n}$ *vs.* $[H_2O]_f$ are illustrated in Fig. 3 for the chlorobenzene systems; similar curves were obtained for the other two solvent systems.

Treatment of the Data

Solvent extraction studies of Bu_4NPi between water and each of the solvents benzene, chlorobenzene, and *o*-dichlorobenzene have been carried out (1). These data showed that Bu_4NPi in the organic phase of the solvent extraction system existed as an equilibrium mixture of several

Can. J. Chem. Downloaded from www.nrcresearchpress.com by 210.87.254.105 on 09/05/12
For personal use only.

TABLE 2. Concentration of free water and $\bar{n}$ for isopiestic systems*

Solvent	Temperature (°C)	$CaCl_2$ in aqueous phase (*m*)	Free water in organic phase		$\bar{n}$ for organic phase	
			$M \times 10^4$	s.d. $\times 10^4$	value $\times 10^3$	s.d. $\times 10^3$
Mixture, 1:1 *v/v* benzene–chlorobenzene	25.0	6.43	104	3	80.6	3
		5.00	160	6	123	5
		3.59	219	8	160	6
		1.95	274	2	250	2
		Nil	313	6	275	5
	35.1	6.5	164	7	106	6
		5.0	232	1	179	0
		3.5	334	31	237	24
		2.0	420	6	273	5
		Nil	475	20	325	16
	45.1	7.0	196	13	112	10
		5.0	319	7	165	5
		3.5	433	10	241	8
		2.0	542	24	325	19
		Nil	594	15	372	12
Chlorobenzene	25.0	6.82	98	5	77.5	4
		4.97	145	0	126	0
		3.57	214	1	177	1
		1.95	258	8	224	6
		Nil	284	13	272	10
	35.1	6.81	140	7	91.9	6
		4.96	205	1	141	0
		3.58	276	0	203	0
		1.94	357	12	274	10
		Nil	402	21	303	16
	45.1	7.0	200	1	111	1
		5.0	266	1	149	1
		3.5	354	6	218	4
		2.0	449	22	312	17
		Nil	531	8	355	6
o-Dichlorobenzene	25.0	6.96	88	7	67.5	6
		5.02	126	2	104	1
		3.62	166	9	161	7
		1.97	213	11	208	8
		Nil	235	13	256	10
	35.1	7.0	116	16	82.8	12
		5.0	169	18	134	14
		3.5	230	5	187	4
		2.0	270	9	245	7
		Nil	314	15	275	11
	45.1	7.0	165	2	98.0	1
		5.0	228	9	160	7
		3.5	310	12	235	9
		2.0	389	9	279	7
		Nil	431	18	337	14

*s.d. means standard deviation for 1 degree of freedom.

species, namely ions, ion pair (monomer), dimer (aggregate of two pairs), trimer (aggregate of three pairs), and others. A proportion of each of these species was considered to be hydrated. However, the charged species were found (1) to contribute only very slightly to the stoichiometric concentration of Bu_4NPi, in the range of concentrations studied in the present work. Therefore, their existence is ignored in the following treatment.

A treatment of the isopiestic data is now described which allows calculation of the step-wise hydration constants of the coexisting uncharged species in the organic phases.

Let $[X_i(H_2O)_j]$ denote the molar concentration of any neutral species in the solution of Bu_4NPi. For example, $[X_1(H_2O)_0]$ will denote the molarity of the anhydrous monomer; and $[X_2(H_2O)_2]$ will denote the molarity of the dihydrated dimer

Let $\bar{n}$ denote the total number of moles of bound

Can. J. Chem. Downloaded from www.nrcresearchpress.com by 210.87.254.105 on 09/05/12
For personal use only.

Can. J. Chem. Downloaded from www.nrcresearchpress.com by 210.87.254.105 on 09/05/12
For personal use only.

water per stoichiometric mole of Bu_4NPi (monomers and aggregates, anhydrous and hydrated). Then

$$[1] \qquad \bar{n} = \frac{\sum_{j=0}^{m} \sum_{i=1}^{n} j[X_i(H_2O)_j]}{\sum_{j=0}^{m} \sum_{i=1}^{n} i[X_i(H_2O)_j]}$$

Let ${}^{j}k_i$ denote the stepwise hydration constants where

$$[2] \qquad {}^{j}k_i = \frac{(X_i(H_2O)_j)}{(H_2O)_f(X_i(H_2O)_{j-1})} \qquad i, j \geq 1$$

and where round brackets denote activity, and $(H_2O)_f$ denotes the activity of the unbound water in the organic phase. Since this unbound water was shown to obey Henry's law, it is permissible to write $(H_2O)_f = [H_2O]_f$. If the assumption is made that $(X_i(H_2O)_j) = [X_i(H_2O)_j]$, then

$$[3] \qquad {}^{j}k_i = \frac{[X_i(H_2O)_j]}{[H_2O]_f[X_i(H_2O)_{j-1}]} \qquad i, j \geq 1$$

Substitution of eq. 3 into eq. 1 gives, on rearrangement,

$$[4] \qquad \sum_{i=1}^{n} C_i(\theta_i - \bar{n}i\psi_i) = 0$$

where

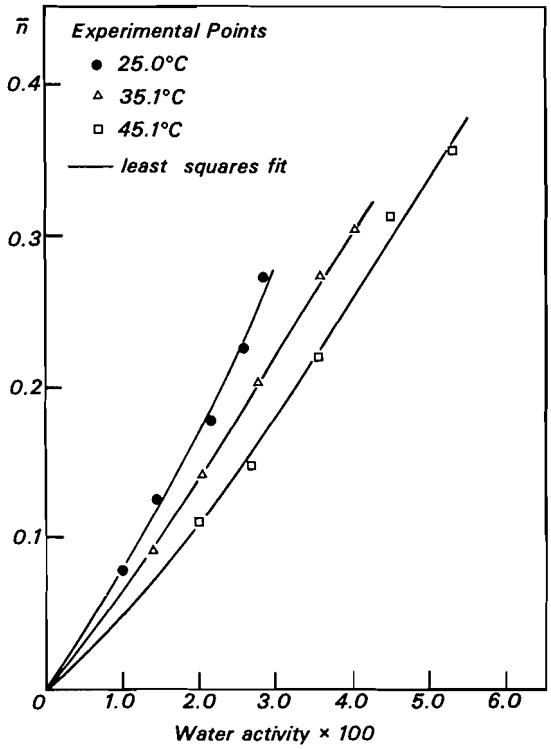

FIG. 3. Activity of water *vs.* $\bar{n}$ for solutions of Bu_4NPi in chlorobenzene at three temperatures.

$C_i = [X_i(H_2O)_0]$, the molarity of anhydrous species X_i

$$\theta_i = {}^{1}k_i[H_2O]_f + 2{}^{1}k_i{}^{2}k_i[H_2O]_f{}^{2} + \cdots + m\prod_{r=1}^{m} {}^{r}k_i[H_2O]_f{}^{m}$$

$$\psi_i = 1 + {}^{1}k_i[H_2O]_f + {}^{1}k_i{}^{2}k_i[H_2O]_f{}^{2} + \cdots + \prod_{r=1}^{m} {}^{r}k_i[H_2O]_f{}^{m}$$

For the present systems, it was shown experimentally, from the data in Table 1 (vide Fig. 2), that the value of $\bar{n}$ was independent of the stoichiometric concentration of Bu_4NPi. Moreover, for a fixed temperature, solvent, and water activity θ_i and ψ_i were also constants. Under those conditions

$$[5] \qquad (\theta_i - \bar{n}i\psi_i) = 0 \qquad \text{for all } i$$

That is,

$$[6] \qquad \bar{n} = \frac{\theta_1}{\psi_1} = \frac{\theta_2}{2\psi_2} = \cdots = \frac{\theta_n}{n\psi_n}$$

Equation 6 was used in order to evaluate the hydration constants for these species present in significant concentrations in the organic phase of the isopiestic experiments. These species are considered in turn.

Monomer (Ion Pair)

For the monomer, eq. 6 becomes

$$[7] \qquad \bar{n} = \frac{\theta_1}{\psi_1} = \frac{{}^{1}k_1[H_2O]_f + 2{}^{1}k_1{}^{2}k_1[H_2O]_f{}^{2} + \cdots + n\prod_{r=1}^{n} {}^{r}k_1[H_2O]_f{}^{n}}{1 + {}^{1}k_1[H_2O]_f + {}^{1}k_1{}^{2}k_1[H_2O]_f{}^{2} + \cdots + \prod_{r=1}^{n} {}^{r}k_1[H_2O]_f{}^{n}}$$

Can. J. Chem. Downloaded from www.nrcresearchpress.com by 210.87.254.105 on 09/05/12
For personal use only.

The sought-for constants ${}^1k_1$ to ${}^n k_1$ inclusive can be evaluated for each solvent system by applying eq. 7 to the values of $\bar{n}$ and $[H_2O]_f$ in Table 2.

If only one hydrate of the monomer were formed, eq. 7 would reduce to

$$[8] \qquad \bar{n} = \frac{{}^1k_1[H_2O]_f}{1 + {}^1k_1[H_2O]_f}$$

However, eq. 8 did not fit the data.

If only a mono- and a dihydrate of the monomer were formed, then

$$[9] \qquad \bar{n} = \frac{{}^1k_1[H_2O]_f + 2{}^1k_1{}^2k_1[H_2O]_f{}^2}{1 + {}^1k_1[H_2O]_f + {}^1k_1{}^2k_1[H_2O]_f{}^2}$$

The same results may be obtained by analogy with B.E.T. theory for the special case of a maximum of two adsorption layers (9).

Equation 9 can be written as

$$[10] \qquad Y = {}^1k_1 + {}^1k_1{}^2k_1X$$

where

$$Y = \bar{n}/[H_2O]_f(1 - \bar{n})$$

$$X = [H_2O]_f(2 - \bar{n})/(1 - \bar{n})$$

Plots of X *vs.* Y resulted in straight lines (within experimental error) for all the solvent systems. Therefore it was concluded that the monomer formed a monohydrate and a dihydrate. However, the data are not accurate enough to permit the unequivocal exclusion of small concentrations of higher hydrates.

The constants ${}^1k_1$ and ${}^2k_1$ were evaluated for each system by a conventional least-squares fit of eq. 10 to the data in Table 2. The resulting values and their standard deviations are entered in Table 3.

Dimer

Based on the monomer forming only the mono- and dihydrate, eq. 6 becomes

$$[11] \qquad \frac{{}^1k_1[H_2O]_f + 2{}^1k_1{}^2k_1(H_2O)_f{}^2}{1 + {}^1k_1[H_2O]_f + {}^1k_1{}^2k_1[H_2O]_f{}^2} = \frac{{}^1k_2[H_2O]_f + 2{}^1k_2{}^2k_2[H_2O]_f{}^2 + \cdots + m\prod_{r=1}^{m} {}^rk_2[H_2O]_f{}^m}{2\left[1 + {}^1k_2[H_2O]_f + {}^1k_2{}^2k_2[H_2O]_f{}^2 + \cdots + \prod_{r=1}^{m} {}^rk_2[H_2O]_f{}^m\right]}$$

Equation 11 led to chemically and mathematically consistent values of ${}^1k_2$ to ${}^m k_2$ inclusive only if $m = 4$. With $m = 4$, then on cross-multiplying eq. 11 and equating the coefficients of $[H_2O]_f{}^1$, $[H_2O]_f{}^2$, . . . , $[H_2O]_f{}^6$, 6 simultaneous equations resulted, which were solved to give the following 4 relationships

$${}^1k_2 = 2{}^1k_1$$

$${}^2k_2 = {}^2k_1 + \frac{{}^1k_1}{2}$$

$${}^3k_2 = \frac{2{}^1k_1{}^2k_1}{2{}^2k_1 + {}^1k_1}$$

$${}^4k_2 = \frac{{}^2k_1}{2}$$

From those 4 relationships and the values already found for ${}^1k_1$ and ${}^2k_1$, the 4 stepwise hydration constants for the dimer can be calculated.

Trimer

The same mathematical method was used in treating the trimer case, as that described for the dimer. Consistent values for ${}^jk_3$ for the trimer hydrates were obtained when the first 6 hydrates of the trimer were taken into account, and no others. The method then led to the following 6 relationships, from which the 6 stepwise hydration constants of the trimer can be calculated from the values already found for ${}^1k_1$ and ${}^2k_1$

$${}^1k_3 = 3{}^1k_1$$

$${}^2k_3 = {}^1k_1 + {}^2k_1$$

$${}^3k_3 = \frac{({}^1k_1)^2 + 6{}^1k_1{}^2k_1}{3({}^1k_1 + 2{}^2k_1)}$$

$${}^4k_3 = \frac{3{}^1k_1{}^2k_1({}^1k_1 + {}^2k_1)}{({}^1k_1)^2 + 6{}^1k_1{}^2k_1}$$

$${}^5k_3 = \frac{{}^1k_1{}^2k_1}{{}^1k_1 + {}^2k_1}$$

$${}^6k_3 = \frac{{}^2k_1}{3}$$

It is to be noted that the mathematical method

TABLE 3. Stepwise hydration constants for the monomer Bu_4NPi in organic solvents at three temperatures*

Solvent	Temperature (°C)	$^1k_1$ (l/mol) Mean	s.d.	$^2k_1$ (l/mol) Mean	s.d.
Benzene–chloro-benzene (1:1 *v/v*)	25.0	6.11	1.02	13.5	5.4
	35.1	7.11	0.96	3.5	2.1
	45.1	4.34	0.58	7.6	2.2
Chlorobenzene	25.0	7.18	0.73	10.5	3.1
	35.1	6.04	0.30	7.9	1.1
	45.1	4.08	0.42	11.6	2.3
o-Dichlorobenzene	25.0	5.14	0.68	30.1	7.2
	35.1	5.16	0.71	18.2	5.0
	45.1	4.84	0.72	12.4	3.7

*s.d. means standard deviation for 3 degrees of freedom.

described for the dimer and used for the trimer can in fact be applied to any neutral aggregate of the monomer, provided that (*i*) the stoichiometric concentrations of water and of salt (Bu_4NPi here) are related in a linear way, and (*ii*) the species of interest is present as a significant proportion of the total salt concentration.

Discussion

Equation 6 may be written as

$$[12] \qquad \bar{n} = \frac{\theta_i C_i}{i\psi_i C_i}; \qquad i = 1, 2, \ldots, n$$

where C_i is the stoichiometric concentration of the unhydrated species i, which is either the monomer Bu_4NPi, or one of its neutral aggregates. The numerator represents the stoichiometric concentration of water bound to species i, and the denominator the stoichiometric concentration of monomer present as species i (*e.g.* $2\psi_2 C_2$ is the stoichiometric concentration of monomers present as dimers). Therefore eq. 12 shows that the average number of mol of bound water per mol of monomer is constant, and therefore independent of whether the monomer is free or combined in an aggregate. That is, the tendency (as measured by ΔG^0) of water to hydrate the Bu_4NPi monomer is unaffected by self-association of the monomer.

By assigning two hydrates to the monomer Bu_4NPi, exactly the first $2n$ hydrates could then be found for a given aggregate of n monomers. The stepwise formation constants for these $2n$ hydrates are algebraically related through eq. 6 to the two stepwise hydration constants ($^1k_1$ and $^2k_1$) of the free monomer. Therefore only these latter two constants will be discussed; their values are in Table 3. The standard deviations of these values are too large to justify the evaluation of the standard enthalpies and entropies of the two hydration reactions, from the measured temperature dependence of the two constants.

The relationship between the standard free energy of hydration of the monomer, and the bulk dielectric constant (D) of the solvent was studied. Thus, the values of $\log {}^1k_1$ taken from Table 3 were plotted against $1/D$ for the three solvents, at each of the 3 temperatures; corresponding plots were also made for $\log {}^2k_1$. On taking into account the standard deviations found for $^1k_1$ and $^2k_1$, the plots were linear in every case. Least squares equations were calculated for the lines, together with the standard deviations of their slopes. Conventional statistical tests then showed that of the 6 slopes none was significantly different from the others, nor were they significantly different from zero, at the 95% confidence level.

Resonance forms of the models we postulate for the monohydrate and the dihydrate of the

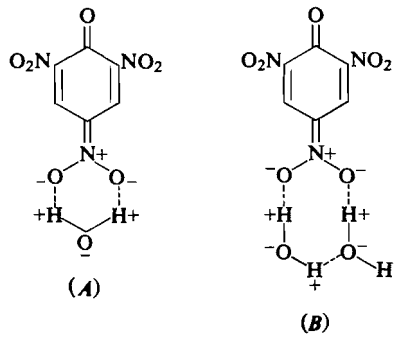

FIG. 4. One resonance form for the monohydrate (*A*) and the dihydrate (*B*) of the picrate anion.

Can. J. Chem. Downloaded from www.nrcresearchpress.com by 210.87.254.105 on 09/05/12
For personal use only.

Bu_4NPi monomer are illustrated in Fig. 4. Nitrobenzene has been reported (10) to form a monohydrate and a dihydrate through its nitro group, with the dihydrate forming a ring. Moreover, any other possible site for the addition of the water to the monomer would appear to be sterically less favorable due to the *n*-butyl groups on the cation.

The formation of rings, as shown in Fig. 4, makes possible the enhancement of those inductive effects that would normally exist. Thus, a cooperative inductive effect would then operate all around the rings. Such an enhanced effect due to ring formation has already been postulated (11) in order to explain the greater stability of trimers over dimers of alcohol in chloroform solutions.

The creation of these extra charges due to ring formation would require an amount of electrostatic energy proportional to $1/D$. Hence this electrostatic term in the standard free energy of formation of a hydrate would decrease linearly with $1/D$. If in addition the formation of a hydrate is considered to result from dipole–dipole (water–nitro group) interaction, then this electrostatic contribution to the standard free energy of formation of the hydrate would increase linearly with $1/D$. The overall contribution to ΔG^0 of hydrate formation would then be the difference between these two energies of interaction. If the other contributions to ΔG^0, including the standard entropy of formation of the hydrate are considered to depend only slightly or not at all on $1/D$, then plots of ΔG^0 *vs.* $1/D$ will provide information on the relative values of the two opposing electrostatic terms in ΔG^0. As noted above, the values of ΔG^0 for formation of the monohydrate and of the dihydrate were in fact found statistically not to depend on the solvent. These results therefore do not indicate any difference in the magnitude of the two opposing electrostatic terms in ΔG^0; but the large standard deviations of the values of ΔG^0 in Table 3 would enable only gross differences to be detected.

We are grateful to the National Research Council of Canada for financial support, and for a Scholarship to one of us (S.G.).

1. S. GOLDMAN. Ph.D. Thesis. McGill University, Montreal, Quebec, 1969.
2. S. D. CHRISTIAN, H. E. AFFSPRUNG, and J. R. JOHNSON. J. Chem. Soc. 1896 (1963).
3. P. H. FLAHERTY and K. H. STERN. J. Amer. Chem. Soc. **80**, 1034 (1958).
4. J. A. GEDDES and C. A. KRAUS. Trans. Faraday Soc. **32**, 585 (1936).
5. W. SEAMAN and E. ALLEN. Anal. Chem. **23**, 592 (1951).
6. W. R. GILKERSON and R. E. STAMM. J. Amer. Chem. Soc. **82**, 5295 (1960).
7. R. A. ROBINSON and R. H. STOKES. Electrolyte Solutions. 2nd Ed. Butterworths, London. 1959. p. 478.
8. J. R. JOHNSON, S. D. CHRISTIAN, and H. E. AFFSPRUNG. J. Chem. Soc. A, 77 (1966).
9. S. D. CHRISTIAN. Private communication.
10. J. R. JOHNSON, S. D. CHRISTIAN, and H. E. AFFSPRUNG. J. Chem. Soc. A, 1924 (1967).
11. A. D. COHEN and C. REID. J. Chem. Phys. **25**, 790 (1956).

Can. J. Chem. Downloaded from www.nrcresearchpress.com by 210.87.254.105 on 09/05/12
For personal use only.

Can. J. Chem. Downloaded from www.nrcresearchpress.com by 210.87.254.6 on 09/05/12
For personal use only.

Ions and Aggregates of Tetra-*n*-butylammonium Picrate in Nonaqueous Solvents at 25 °C: A Solvent Extraction Study

SAUL GOLDMAN AND G. C. B. CAVE
Department of Chemistry, McGill University, Montreal, Quebec

Received[1] December 23, 1969

The values of ΔG^0 at 25 °C were determined for the ionization, dimerization, and trimerization of tetra-*n*-butylammonium picrate (**1**) in benzene, chlorobenzene, and *o*-dichlorobenzene by a solvent extraction method. Corrections were applied for the presence of hydrates in the organic phase, in order to report ΔG^0 values for the anhydrous solvents. In chlorobenzene, hexamers of **1** were also indicated in measurable concentrations. The various values of ΔG^0 are related in a simple way to the bulk dielectric constant of the solvent.

La valeur de ΔG^0 à 25 °C pour l'ionisation, la dimérisation et la trimérisation du picrate du tétrabutylammonium (**1**) a été déterminée par une méthode d'extraction par solvants dans le benzène, le chlorobenzène et l'*o*-dichlorobenzène. De façon à pouvoir rapporter des valeurs de ΔG^0 pour des solvants anhydres des corrections ont été faites pour tenir compte de la présence d'hydrates dans la phase organique. Des concentrations mesurables de l'hexamère de **1** semblent présentes dans le chlorobenzène. Les diverses valeurs de ΔG^0 sont reliées d'une façon simple avec la constante diélectrique globale du solvant.

Canadian Journal of Chemistry, 49, 1726 (1971)

Introduction

Ion association in solvents of low dielectric constant to form ion pairs (monomers) and higher aggregates has been known for several decades. Cryoscopy (1), conductance measurements (2, 3), and dielectric studies (4) were the techniques most widely used in the earlier studies of ion association phenomena.

In cryoscopy neither the solvent nor the temperature can conveniently be altered. Therefore, it is difficult to measure the variation of equilibrium constants with changes in temperature, and with changes in the dielectric constant of the solvent.

Conductance measurements (2, 3) provided the first (and only) evidence for the existence of triple ions and higher charged aggregates in ion-pairing systems. However, the total concentration of these charged aggregates in low-dielectric solvents is small (5).

Dielectric studies have been interpreted (6) to indicate that monomers associate to form aggregates of two main types. One type results from lateral association of the monomer, to produce an aggregate with a dipole moment lower than that of the monomer. The second type results from end-to-end association of the monomer, to produce an enhanced dipole moment. Without prior knowledge of the shapes of the aggregates, dielectric studies alone cannot yield the equilibrium constants of aggregation reactions.

Solvent extraction was used in the present work, in order to evaluate ΔG^0 at 25 °C for the aggregation reactions of an ion pair in low dielectric solvents. This equilibration technique was well suited to the purpose; both the temperature, and the dielectric constant of the solvent could readily be varied. In addition, by appropriate choice of the concentration range several different aggregation reactions could be studied in turn.

Tetra-*n*-butylammonium picrate was the salt chosen for study. It has suitable solubilities in the solvents. Moreover, the cation is important in analytical solvent extraction procedures. The solvents chosen were benzene, chlorobenzene, and *o*-dichlorobenzene. They are geometrically similar, are relatively immiscible with water, and they covered a particularly convenient range of dielectric constants (2.27, 5.63, and 10.1, respectively at 25 °C).

The solvent extraction technique consisted in measuring at 25 °C the distribution ratio of tetra-*n*-butylammonium picrate between an aqueous phase and the nonaqueous phase, over a wide range of stoichiometric concentrations of the salt. The data, after applying corrections for the presence of hydrates in the organic phase, were fitted to a derived polynomial. Thereby, the species present were identified, and their standard free energies of formation from the monomer were evaluated.

[1]Revision received December 1, 1970.

Can. J. Chem. Downloaded from www.nrcresearchpress.com by 210.87.254.6 on 09/05/12
For personal use only.

Experimental

Apparatus

Equilibration Vessels

The two phases in the solvent extraction system were equilibrated in 165-ml "milk-dilution" bottles fitted with bakelite screw caps having Teflon inserts. The rim of the opening in each bottle had been ground flat with emery paper, so that a tight, leak-proof fit with the cap was attained. Plastic tape wound around the neck and tightly screwed cap of each bottle was an additional precaution against leakage while the bottles were in a water thermostat.

Thermostat

The water thermostat used for the solvent extraction equilibrations was 70 cm long, 40 cm wide, and 37 cm deep. The temperature was maintained to within ± 0.1 °C of the required value. Stirring was by a centrifugal pump and a rotor.

The 165-ml bottles for equilibration were clamped lengthwise on a Plexiglass rotor immersed in the water thermostat, with the axis of rotation horizontal. The rotor was driven at 15 r.p.m. from an external motor and gear-reduction box, and gave the bottles an end-over-end rotation.

Dielectric Constant

The dielectric constant of the three solvents presaturated by isopiestic equilibration with pure water were measured. A Sargent Model V Oscillometer with a Sargent cell compensator was used. The temperature of the sample in the Sargent cell was maintained to within ± 0.1 °C of the required temperature by a snug-fitting, hollow brass jacket through which constant-temperature water was circulated.

A calibration curve was prepared by using benzene, chlorobenzene, and *o*-dichlorobenzene purified and dried by a previously described procedure (7), then further dried by storage over Drierite for at least 2 weeks (8). Literature values (9, 10) were used for the dielectric constants.

Materials

The preparation, purification, and analysis of the tetra-*n*-butylammonium picrate (hereafter abbreviated to Bu_4NPi), and the purification and densities of the solvents benzene, chlorobenzene, and *o*-dichlorobenzene have been described elsewhere (7). The Bu_4NPi was found to be $100.0 \pm 0.1\%$ pure. Distilled water was used as the aqueous phase in the solvent extraction experiments.

Procedures

Preparation of Solutions

Stock standard solutions of Bu_4NPi were prepared both in water and in the water-saturated organic solvents by weighing the salt to ± 0.1 mg, into calibrated volumetric flasks, and diluting to the mark with the solvent. Aqueous stock solutions under 10^{-3} *M*, and nonaqueous stock solutions under 10^{-2} *M* were prepared by accurate dilution of more concentrated stock solutions.

The titre of nonaqueous stock solutions more dilute than 10^{-4} *M* was found to drop slowly with time, when anhydrous solvent had been used. A comparable phenomenon with phenolate-type indicators has been reported (11), and interpreted then as being due to an adsorption reaction. Specifically, the indicator was presumed to form with the sodium compounds in the glass of the container, an insoluble coating of the sodium salt. However, it was also found in the present work that aqueous solutions of Bu_4NPi even as dilute as 10^{-5} *M* retained their original titre for at least 2 years and possibly longer. This fact suggested that a strongly adsorbed water layer on the glass wall prevented the adsorption reaction observed for the anhydrous nonaqueous solvent. This in turn suggested in the present work that Bu_4NPi in a water-saturated organic solvent would also not lose salt to the glass wall; the activity of water in the solvent would be almost that of pure water. It was indeed found that when the nonaqueous solutions of Bu_4NPi had been prepared with water-saturated solvents, their titre remained constant to within 1% for at least 1 month. The publications on conductance and dielectric studies on Bu_4NPi in anhydrous solvents performed during the past 35 years appear not to mention this adsorption effect. The repetitive rinsing of the cells with solution, prior to the actual measurements of conductance or dielectric constant, evidently conditioned the cell walls.

Equilibration of Solutions

Equal volumes (10 ml–50 ml) of the two phases were transferred by pipet into the 165 ml equilibrating bottle. One phase contained a known concentration of Bu_4NPi, the other none. The capped bottle was fastened to the Plexiglass rotor in the water thermostat, and it received one end-over-end rotation every 4 s.

This gentle rotor motion was superior to mechanical shaking. When a shaker was tried, precision of the measured distribution ratios of Bu_4NPi was poor. This was attributed to the formation of a copious suspension of the organic phase in the aqueous phase. Precision by using the rotor method, on the other hand, was good.

An equilibration period of 1 h was allowed, although extensive tests had shown that 15 min were enough, regardless of which phase the Bu_4NPi was initially in.

Analysis of Equilibrated Phases

After the 1-h equilibration, the bottle was removed from the rotor, and was suspended vertically in the water thermostat, with only the cap and the neck above the water surface; the upper level of the lighter phase was well under the surface.

An aliquot of the required phase was transferred from the uncapped bottle still in the water thermostat, into a centrifuge tube. In sampling the heavier phase, air was always bubbled through the pipet during its descent through the lighter phase. The aliquot was centrifuged for 15 min to remove any droplets of the other phase present; but in practice the invariable absence of such droplets made centrifugation apparently only a precaution.

When an aliquot of the organic phase containing a low concentration of Bu_4NPi was being processed for analysis, the glassware used was pre-rinsed several times with the solution. Thereby, loss of Bu_4NPi due to adsorption on the glass walls was avoided.

The stoichiometric concentration of Bu_4NPi in the centrifuged aliquot was then determined with a Unicam SP 500 spectrophotometer, by measuring the absorbance at the wavelength of the absorption peak. The concen-

TABLE 1. Absorptivity of tetra-*n*-butylammonium picrate in four solvents at 25.0 °C

Solvent	λ_{max} (mμ)	Molar absorptivity × 10^{-4} Mean	Standard deviation	Degrees of freedom
Water	353	1.43	0.01	20
Benzene*	362	1.71	0.01	5
Chlorobenzene*	370	1.73	0.01	5
o-Dichlorobenzene*	377	1.83	0.01	5

*Water-saturated solvent.

tration was then found from the value of the molar absorptivity previously determined from standard solutions.

The wavelength of maximum absorption of Bu_4NPi depended on the solvent, as shown in Table 1. For the organic phases and the corresponding solutions for calibration, the spectrophotometric blank was the water-saturated solvent. For the aqueous phases, the blank was distilled water except when *o*-dichlorobenzene was the organic phase. In that case only did solvent-saturated water have a very slightly different absorptivity than that of pure water at the wavelength used. For the case of all 3 solvents, the molar absorptivity of Bu_4NPi in an aqueous solution, in which the water had been pre-saturated with the solvent, was the same as the molar absorptivity of Bu_4NPi in pure water, using the designated blanks.

Beer's law was obeyed by the Bu_4NPi both in water and in the water-saturated organic solvents over the tested concentration ranges of interest, namely 1×10^{-6} to 5×10^{-4} *M* for water, and 1×10^{-6} to 1×10^{-4} *M* for the organic solvents. The molar absorptivities are in Table 1.

Results and Treatment of the Data

All the distribution experiments were in triplicate. The standard deviation of most measured concentrations was within 1% of the mean, and never more than 2%.

In some experiments, both equilibrium phases were analyzed for Bu_4NPi content in order to check mass balance. Systems were chosen for which the distribution ratio was in the range 0.4–3. For all three solvents, it was found that mass balance was attained to within 1%.

For most systems, only the equilibrium phase containing the lesser concentration was analyzed for Bu_4NPi. The equilibrium concentration in the other phase was then found from the known total initial amount of Bu_4NPi, and the volumes.

The results of the distribution experiments at 25.0 °C are entered in Table 2.

A polynomial expression was derived which related the stoichiometric concentration of Bu_4NPi in the equilibrated organic phase, to its stoichiometric concentration in the equilibrated aqueous phase. A least squares fit of the data in Table 2 to that polynomial permitted the evaluation of sought-for equilibrium constants of the various species in the nonaqueous solutions.

In deriving the polynomial, three assumptions were made:

(*i*) In the concentration range studied, the aqueous phase contained only the simple ions Bu_4N^+ and Pi^-, and negligible concentrations of all other species. This assumption is supported by conductivity experiments (12, 13) in water, with salts similar to Bu_4NPi, namely Et_4NPi (12), Me_4NPi (13), $(n\text{-Am})_4NBr$ (13), $(n\text{-Bu})_4NBr$ (13), and $(n\text{-Pr})_4NI$ (13). The Onsager equation was found (12, 13) to be obeyed by these aqueous solutions at salt concentrations below 10^{-3} *M*, which indicated that dissociation was virtually complete in them. The maximum concentration of Bu_4NPi in the aqueous phases of the present extraction systems was 8×10^{-4} *M*.

(*ii*) The total contribution to the stoichiometric concentration of Bu_4NPi in the organic phase, made by charged species other than the simple ions Bu_4N^+ and Pi^- was negligibly small. This assumption is supported by the low conductivity of salts of the type used in the present work, in solvents of low dielectric constant (2, 3, 14). That charged aggregates contribute only slightly to the stoichiometric concentration of salts in such systems has been previously deduced (5) from conductivity data.

(*iii*) The monomer and neutral aggregates of Bu_4NPi in both phases had activity coefficients of unity (but the activity coefficients of the ions in both phases were not taken to be unity). The justification for this assumption is that the potential energy of interaction of two dipolar species falls off fairly rapidly with distance. The

Can. J. Chem. Downloaded from www.nrcresearchpress.com by 210.87.254.6 on 09/05/12
For personal use only.

TABLE 2. Distribution of tetra-*n*-butylammonium picrate between water and three organic solvents at 25.0 °C

Equilibrium stoichiometric molarity* of $Bu_4NPi \times 10^5$					
Water	*o*-Dichlorobenzene	Water	Chlorobenzene	Water	Benzene
0.294	0.706	0.596	0.404	0.944	0.0556
0.513	1.49	0.963	1.04	1.78	0.202
0.893	3.11	1.59	2.41	2.58	0.417
1.18	4.82	2.04	3.96	3.30	0.696
1.45	6.55	2.46	5.54	3.97	1.03
1.69	8.31	2.78	7.22	4.69	1.31
2.66	17.3	4.18	15.8	5.92	2.08
3.99	36.0	6.14	33.9	7.06	2.94
5.01	55.0	7.66	52.3	11.8	8.20
5.84	74.2	8.97	71.0	18.8	21.2
6.55	93.5	9.98	90.0	24.4	35.6
9.67	190	14.5	186	28.9	51.1
13.8	386	20.2	380	32.7	67.3
17.1	583	24.6	575	46.8	153
19.8	780	28.3	772	62.4	338
22.0	978	30.8	969	71.7	528
29.9	1970	40.0	1960	76.7	723
38.6	3960	48.5	3950	79.3	821
44.3	5960	52.8	5950		
48.2	7950	56.3	7940		
51.5	9950	57.9	9940		
57.2	14 900				
61.6	19 900				

*Mean of triplicates.

interaction at close distance is interpreted solely in terms of aggregation of monomers, and numerically is reflected in the calculated formation constants of the aggregates.

A previously reported (7) hydration study showed that Bu_4NPi and its aggregates were partially hydrated in the solvents used in the present work, when the solvent also contained dissolved water. Moreover, in that study it was considered reasonable to suppose that only the picrate ion was hydrated in the organic phase, and not the cation. This supposition is made in the present work.

Then for the organic phases of the present extraction systems,

$$[1] \qquad C_T = [X_{ion}]\psi_{ion} + \sum_{i=1}^{n} i[X_i]\psi_i$$

where C_T = stoichiometric concentration of Bu_4NPi in the equilibrium organic phase of the extraction system; $[X_{ion}]$ = molar concentration of unhydrated picrate ion in the equilibrium organic phase; $[X_i]$ = molar concentration of the unhydrated species X_i in the equilibrium organic phase, where X_i ($i = 1, 2, \cdots$) represents respectively the monomer and the neutral aggregates of Bu_4NPi; ψ_{ion}, ψ_i = water-correction factors for species X_{ion} (picrate ion) and X_i, respectively, in the organic phase.

$$[2] \qquad \psi_i = 1 + \sum_{m=1}^{n} [H_2O]_f^m \prod_{m=1}^{m} {}^mk_i$$

where $[H_2O]_f$ = molar concentration of unbound (to Bu_4NPi aggregates, and ions) water in the equilibrium organic phase; ${}^mk_i$ = mth stepwise hydration constant for species X_i in the organic phase.

Thus

$$[3] \qquad {}^mk_i = \frac{[X_i.mH_2O]}{[X_i.(m-1)H_2O][H_2O]_f}$$

In the previous study (7) on hydration, the values of ${}^mk_i$ for Bu_4NPi and its aggregates were determined for three solvents, *o*-dichlorobenzene, chlorobenzene, and a mixture of benzene and chlorobenzene (1:1 *v/v*). The plots of log ${}^mk_i$ *vs.* $1/D$ were linear for that sequence of solvents, D being the bulk dielectric constant. Therefore the values of ${}^mk_i$ for benzene as solvent were readily found from the least squares equation of the lines. Moreover, it was shown (7) that Henry's law was obeyed by the water in those solvents; and the activity of water in the nonaqueous solutions of Bu_4NPi was measured there by an

Can. J. Chem. Downloaded from www.nrcresearchpress.com by 210.87.254.6 on 09/05/12
For personal use only.

Can. J. Chem. Downloaded from www.nrcresearchpress.com by 210.87.254.6 on 09/05/12
For personal use only.

isopiestic method. Those activity values were applicable to the present extraction systems. Therefore these previous data (7) were used in eq. 2, and each ψ_i except ψ_{ion} was thereby evaluated. The evaluation of ψ_{ion} for the solvents is considered separately below.

Let the subscript T denote the stoichiometric concentration of Bu_4NPi in a particular phase. Let the subscript w denote the aqueous phase, and let the absence of a subscript denote the organic phase.

The notations used for eqs. 1 and 2 will be used, including square brackets to denote molarities. Then, with assumption (*iii*) above applied, the partition coefficient p of species X_1 (the monomer Bu_4NPi) is given by

$$[4] \qquad p = [X_1]/[X_1]_w$$

Let k denote the ion-pair formation constant of Bu_4NPi in the aqueous phase and $\gamma_{\pm w}$ the mean activity coefficient. Then

$$[5] \qquad k = \frac{[X_1]_w}{[X_{ion}]_w^2 \gamma_{\pm w}^2}$$

Let K denote the ion-pair dissociation constant of Bu_4NPi in the organic phase, and $\gamma_\pm$ the mean activity coefficient, for the case of unhydrated monomer and ions. Then

$$[6] \qquad K = [X_{ion}]^2 \psi_{ion} \gamma_\pm^2 / [X_1]$$

Let K_n be the aggregation constant for aggregation of unhydrated Bu_4NPi monomer to unhydrated aggregate $(Bu_4NPi)_n$.

$$[7] \qquad K_n = [X_n]/[X_1]^n$$

On combining eqs. 1 with 4 to 7 inclusive, and on recognizing that assumption (*i*) above indicates that $[X_{ion}]_w = C_{Tw}$ (the stoichiometric concentration of Bu_4NPi in the aqueous phase), then

$$[8] \quad C_T = \frac{\psi_{ion}^{\frac{1}{2}} (Kkp)^{\frac{1}{2}} C_{Tw} \gamma_{\pm w}}{\gamma_\pm} + \sum_{i=1}^{n} i \psi_i K_i (kp)^i (C_{Tw} \gamma_{\pm w})^{2i}$$

where $K_1 = 1$.

Equation 8 can be written

$$[9] \qquad C_T = \frac{A_{ion} x}{\gamma_\pm} + \sum_{i=1}^{n} A_i x^{2i}$$

where $x = C_{Tw}\gamma_{\pm w}$ and A_{ion}, A_i $(i = 1, 2, \cdots, n)$ are constants.

The C_T and C_{Tw} data required for least squares evaluation of the constants in eq. 9 are in Table 2. The values of $\gamma_{\pm w}$ and $\gamma_\pm$ were calculated by using the Debye–Hückel expression for activity coefficients. In the case of $\gamma_\pm$, the computation was necessarily an iterative one (15).

The standard deviation in C_T was a function of the value of C_T. Therefore, evaluation of the constants in eq. 9 from the data in Table 2 required the use of a weight function. For a given point, this weight function will be given by the reciprocal of the variance. However, in the present work only 3 independent replicates were available for each point, and the estimates of variance found therefrom proved inadequate to give the best fit of eq. 9 to the data. Therefore a weight function was derived, which was a function of x and of the constants in eq. 9. It was based on the vertical distance (C_T axis) of the experimental point (C_T, $C_{Tw}\gamma_{\pm w}$) from the curve of best fit, being taken as the standard deviation of that particular value of C_T. This weight function was of necessity obtained by using an iterative technique, because the constants in eq. 9 were initially unknown. Evaluation of these constants by a least squares treatment and the concomitant evaluation of the weight function and of $\gamma_\pm$ were carried out by several iterations. The detailed technique has been described elsewhere (15).

It proved to be the case that for the benzene system and the *o*-dichlorobenzene system, inclusion of the species simple ions, monomer (ion pair), dimer, and trimer resulted in a satisfactory fit of eq. 9 to the data in Table 2. Inclusion of additional, higher aggregates did not significantly improve the goodness of fit. Therefore, for these two solvents, eq. 9 was used with $n = 3$.

For the chlorobenzene system, eq. 9 with $n = 3$ did not provide a satisfactory fit to the data. In the high concentration region, the curve of best fit consistently lay below the upper experimental points (C_T, x). This fact indicated that for the chlorobenzene system, simple ions, monomers, dimers, trimers, and at least one still higher aggregate were present. The present data do not permit the unequivocal identification of this higher aggregate. Indeed, there may be more than one such aggregate higher than the trimer.

Can. J. Chem. Downloaded from www.nrcresearchpress.com by 210.87.254.6 on 09/05/12
For personal use only.

However, Rutgers and de Smet (16) reported the presence of hexamers of tetra-isoamylammonium picrate, in equilibrium with monomers and trimers in low-dielectric solvents. Therefore eq. 9 was written to include not only ions, monomers, dimers, and trimers, but also hexamers, as follows

$$[10] \quad C_T = \frac{A_{ion}x}{\gamma_\pm} + \sum_{i=1}^{3} A_i x^{2i} + A_6 x^{12}$$

When eq. 10 was fitted to the chlorobenzene data in Table 2, a good fit resulted, and in particular the above-described negative deviations in the high-concentration range disappeared.

The least squares values of the parameters A_{ion} and A_i in eqs. 9 and 10 together with their standard deviations are given in Table 3, for the three solvent systems at 25.0 °C. As an illustration of the goodness of the fit, the data in Table 2 are plotted as individual points in Figs. 1 and 2 for the *o*-dichlorobenzene system. The solid curve in each case is the least squares curve. The corresponding curves for the benzene system and the chlorobenzene system were similar in shape to those in Figs. 1 and 2, and they also fitted the experimental points equally well.

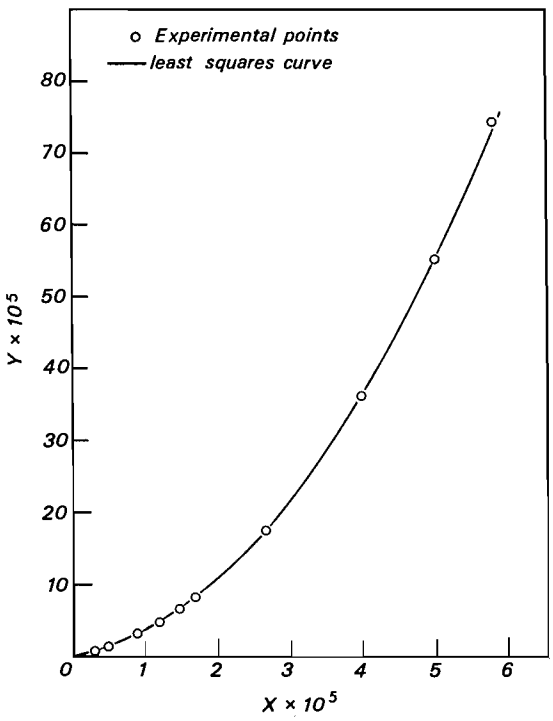

FIG. 1. Solvent extraction data for the system Bu_4NPi–H_2O–*o*-dichlorobenzene at 25.0 °C; low concentration range.

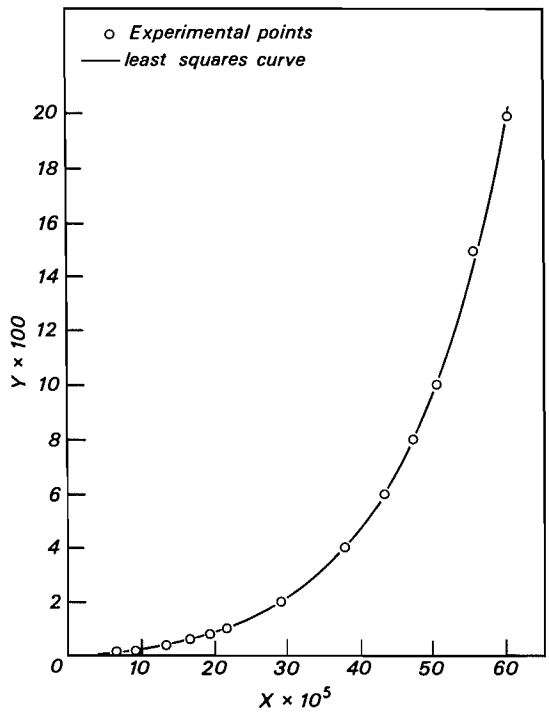

FIG. 2. Solvent extraction data for the system Bu_4NPi–H_2O–*o*-dichlorobenzene at 25.0 °C; entire concentration range.

From eqs. 8 and 9 it is seen that the sought-for equilibrium constants K, K_2, K_3, K_6, and pk could be evaluated at once from the values of A_{ion}, A_1, A_2, A_3, and A_6, provided the ψ values were available. A previous hydration study (7) had provided values for ψ_1, ψ_2, ψ_3, and ψ_6, but not for ψ_{ion}. Therefore for the present study it was assumed that $\psi_{ion} = \psi_1$. This assumption is equivalent to assuming that in the organic phase the simple ion Pi^- was hydrated to the same extent as was the monomer Bu_4NPi. This assumption is discussed below. The equilibrium constants were then evaluated, and the values are entered in Table 3. The term water-corrected equilibrium constant is used there, to emphasize that the equilibria involved are for the unhydrated species in the organic phases. The standard deviations tabulated for the benzene systems are larger percentage-wise than the corresponding values for the other two solvent systems. This

Can. J. Chem. Downloaded from www.nrcresearchpress.com by 210.87.254.6 on 09/05/12
For personal use only.

TABLE 3. Water-corrected equilibrium constants and parameters A_{ion}, A_l for Bu_4NPi in three solvents at 25 °C*

Solvent	A_{ion}		A_1 (l mol^{-1})		A_2 (l mol^{-1})^3		A_3 (l mol^{-1})^5		A_6 (l mol^{-1})^{11}	
	Value	s.d.	Value	s.d.	Value	s.d.	Value	s.d.	Value	s.d.
o-Dichlorobenzene	1.79	0.042	1.76×10^{5}	0.034×10^{5}	3.47×10^{11}	0.039×10^{11}	1.93×10^{18}	0.053×10^{18}		
Chlorobenzene	0.166	0.034	8.74×10^{4}	0.16×10^{4}	1.05×10^{11}	0.21×10^{11}	9.46×10^{17}	0.98×10^{17}	2.84×10^{37}	0.54×10^{37}
Benzene	2.03×10^{-3}	7.85×10^{-3}	6.18×10^{3}	0.23×10^{3}	7.53×10^{8}	5.40×10^{8}	2.04×10^{16}	0.20×10^{16}		

Solvent	K (mol l^{-1})		pk (l mol^{-1})		K_2 (l mol^{-1})		K_3 (l mol^{-1})^2		K_6 (l mol^{-1})^5	
	Value	s.d.	Value	s.d.	Value	s.d.	Value	s.d.	Value	s.d.
o-Dichlorobenzene	1.82×10^{-5}	0.08×10^{-5}	1.45×10^{5}	0.04×10^{5}	5.57	0.72	117	11		
Chlorobenzene	3.15×10^{-7}	1.00×10^{-7}	6.88×10^{4}	0.20×10^{4}	6.82	1.42	471	67	1.06×10^{7}	0.28×10^{7}
Benzene	6.67×10^{-10}	39.1×10^{-10}	4.68×10^{3}	0.59×10^{3}	9.86	7.69	2.86×10^{4}	1.32×10^{4}		

*Parameters are for eqs. 8 and 9 with $n = 3$; standard deviations for approximately four degrees of freedom; K is defined by eq. 6, pk by eqs. 4 and 5, and K_2, K_3, K_6 by eq. 7.

TABLE 4. Dissociation constants of Bu_4NPi monomer in 3 solvents at 25.0 °C

Solvent	Dissociation constant (mol/l)			
	Value (this work)	s.d.*	Literature	Reference
o-Dichlorobenzene	1.82×10^{-5}	0.08×10^{-5}	1.71×10^{-5}	14
			1.92×10^{-5}	17, 18
			2.14×10^{-5}	9
Chlorobenzene	3.15×10^{-7}	1.00×10^{-7}	2.02×10^{-8}	9
			1.88×10^{-8}	19
Benzene	6.67×10^{-10}	39.1×10^{-10}	1.84×10^{-17}	17

*Standard deviation for 5 degrees of freedom.

reduced precision is due partly to the fact that for the benzene systems the values of ψ_i were obtained from extrapolated values of the hydration constants (7), and partly to the relative scarcity of monomers and dimers in the benzene phase.

Discussion

The values found in the present work for the dissociation constants of the Bu_4NPi monomer are compared in Table 4 with literature values obtained from conductance data in anhydrous systems. Agreement for the *o*-dichlorobenzene system is reasonably good, but for the chlorobenzene it is poor. For the benzene system the large standard deviation (due to the relative scarcity of single ions in the benzene phase, even at the lowest concentrations studied) makes comparison of the two values of the dissociation constant of little value, even though statistically they agree.

The solvent systems in the present work were water-saturated, whereas the literature values in Table 4 were for anhydrous solvents. Therefore, the dielectric constants of the water-saturated solvents were measured, and the values are compared in Table 5 with values reported for the anhydrous solvents. Clearly, the presence of unbound water produced an increase in dielectric constant that was much too small to cause a measurable increase in the dissociation constants. Presumably the presence of hydrated species of Bu_4NPi and its aggregates and ions did not affect the dissociation constant of the anhydrous monomer. Therefore, another explanation was sought for the difference between the present and the literature values of that dissociation constant in chlorobenzene.

In treating the data for all the present systems, the somewhat arbitrary assumption had been made that $\psi_{ion} = \psi_i$ (see eq. 1). For the *o*-dichlorobenzene system, the agreement between present and literature values for the dissociation constant of Bu_4NPi suggests that the assumption was valid. To obtain similar agreement for the chlorobenzene system requires that $\psi_{ion} \sim 10\psi_1$. This indicates that the degree of hydration of the ions, compared to that of the monomer, was greater in chlorobenzene than in *o*-dichlorobenzene. A reasonable explanation for this difference in hydration is as follows. The dissociation constant of Bu_4NPi is approximately 1000 times greater in anhydrous *o*-dichlorobenzene than in anhydrous chlorobenzene. Hence *o*-dichlorobenzene is a stronger solvator of ions relative to monomers, than is chlorobenzene. Therefore *o*-dichlorobenzene would more successfully compete with dissolved water to solvate the ions, than would chlorobenzene. Moreover, hydration of ions would be expected to exceed hydration of the monomer, in both solvents; ion–dipole (ion–water) interactions are stronger than dipole–dipole (monomer–water) interactions. In addition, the phenolate oxygen on the picrate ion is exposed for hydration in the ion, but not in the monomer. These two factors would be less important in *o*-dichlorobenzene than in

TABLE 5. Dielectric constants of anhydrous and water-saturated solvents at 25.0 °C

Solvent		Dielectric constant	Reference
o-Dichlorobenzene	Dry	10.06	9
	Wet	10.07	*
Chlorobenzene	Dry	5.63	9
	Wet	5.64	*
Benzene	Dry	2.27	10
	Wet	2.28	*

*Present work.

Can. J. Chem. Downloaded from www.nrcresearchpress.com by 210.87.254.6 on 09/05/12
For personal use only.

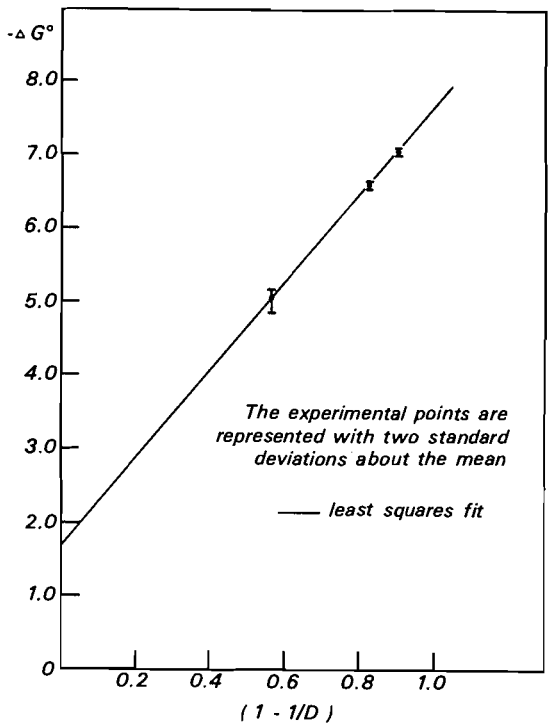

FIG. 3. The relationship between ΔG^0 for the transfer Bu_4NPi (water) → Bu_4NPi (org. solvent) of the ion pair, and the reciprocal of the dielectric constant (D) of the organic solvent, at 25.0 °C.

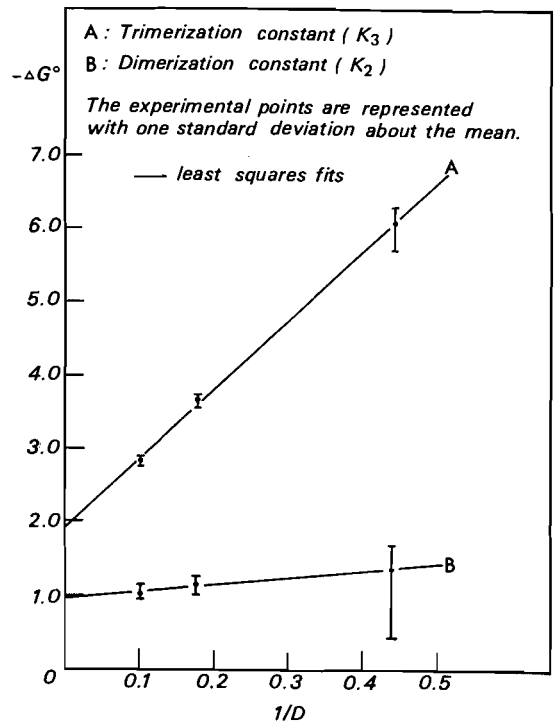

FIG. 4. The relationship between ΔG^0 for the formation of the dimer and the trimer of Bu_4NPi from the ion pairs, and the reciprocal of the dielectric constant of the solvent, for three solvents at 25.0 °C.

chlorobenzene if the former solvent solvates the ions more strongly than does the chlorobenzene.

The standard free energy of transfer of the pair of ions Bu_4N^+ and Pi^- from the aqueous phase to the organic phase, there to exist as the monomer, was calculated for the three solvents from the values of pk given in Table 3.

These values of ΔG^0 at 25 °C are plotted in Fig. 3 as a function of $(1 - 1/D)$, where D is the bulk dielectric constant of the water-saturated solvent. The values of ΔG^0 at 25 °C for the dimerization and the trimerization of the monomer in the three solvents were calculated from the values of K_2 and K_3 respectively, listed in Table 3. Plots of ΔG^0 of dimerization and of trimerization *vs.* $1/D$ are also shown in Fig. 4. Each plot in Figs. 3 and 4 is a straight line. The theoretical basis for this linearity is the subject of a separate communication.

Measurable concentrations of the hexamer did not appear in the benzene system, although benzene has a lower dielectric constant than chlorobenzene. No doubt the reason is that the highest stoichiometric concentrations $[C_T]$ of Bu_4NPi in the benzene phase were an order of magnitude lower (due to solubility limitations) than those in the upper concentration range of the chlorobenzene system.

Hexamers were also not detected in the *o*-dichlorobenzene systems. The highest stoichiometric concentrations of Bu_4NPi in that solvent were about twice those in the chlorobenzene phases. However, the dielectric constant of *o*-dichlorobenzene is also about twice that of chlorobenzene.

At higher concentrations of Bu_4NPi in benzene and in *o*-dichlorobenzene, hexamers would be expected, and no doubt, other higher aggregates as well.

We are grateful to the National Research Council of Canada for financial assistance.

1. D. T. COPENHAFER and C. A. KRAUS. J. Amer. Chem. Soc. **73**, 4557 (1951).
2. R. M. FUOSS and C. A. KRAUS. J. Amer. Chem. Soc. **55**, 2387 (1933).

Can. J. Chem. Downloaded from www.nrcresearchpress.com by 210.87.254.6 on 09/05/12
For personal use only.

3. R. M. FUOSS and C. A. KRAUS. J. Amer. Chem. Soc. **57**, 1 (1935).
4. A. A. MARYOTT. J. Res. Nat. Bur. Stand. **41**, 1 (1948).
5. L. D. PETTIT and S. BRUCKENSTEIN. J. Amer. Chem. Soc. **88**, 4783 (1966).
6. J. A. GEDDES and C. A. KRAUS. Trans. Faraday Soc. **32**, 585 (1936).
7. S. GOLDMAN and G. C. B. CAVE. Can. J. Chem. To be published.
8. R. G. BATES. N.B.S. Technical Note 271. 1965. p. 86.
9. P. H. FLAHERTY and K. H. STERN. J. Amer. Chem. Soc. **80**, 1034 (1958).
10. Handbook of Chemistry and Physics. 46th ed. The Chemical Rubber Company, Cleveland, Ohio. PE-49. 1965–1966.
11. J. STEIGMAN and P. M. LORENZ. J. Amer. Chem. Soc. **88**, 2093 (1966).
12. F. ACCASCINA, A. D'APRANO, and R. M. FUOSS. J. Amer. Chem. Soc. **81**, 1058 (1959).
13. H. M. DAGGETT, JR., E. J. BLAIR, and C. A. KRAUS. J. Amer. Chem. Soc. **73**, 799 (1951).
14. F. ACCASCINA, E. L. SWARTS, P. L. MERCIER, and C. A. KRAUS. Proc. Nat. Acad. Sci. **39**, 917 (1953).
15. S. GOLDMAN. Ph.D. Thesis. Department of Chemistry, McGill University, Montreal, Quebec. 1969.
16. A. J. RUTGERS and M. DE SMET. Trans. Faraday Soc. **48**, 635 (1952).
17. W. R. GILKERSON and R. E. STAMM. J. Amer. Chem. Soc. **82**, 5295 (1960).
18. H. L. CURRY and W. R. GILKERSON. J. Amer. Chem. Soc. **79**, 4021 (1957).
19. R. L. MCINTOSH, D. J. MEAD, and R. M. FUOSS. J. Amer. Chem. Soc. **62**, 506 (1940).

Can. J. Chem. Downloaded from www.nrcresearchpress.com by 210.87.254.6 on 09/05/12
For personal use only.

Can. J. Chem. Downloaded from www.nrcresearchpress.com by 210.87.254.105 on 09/05/12
For personal use only.

A ^{19}F Nuclear Magnetic Resonance and Raman Spectroscopic Study of Complex Formation between Antimony Pentafluoride and the Pentafluorides of Niobium and Tantalum

P. A. W. DEAN AND R. J. GILLESPIE

Department of Chemistry, McMaster University, Hamilton, Ontario

Received August 12, 1970

The low temperature ^{19}F nuclear magnetic resonance (n.m.r.) spectra of NbF_5–SbF_5–SO_2ClF and TaF_5–SbF_5–SO_2ClF systems appear to indicate ionization of the pentafluorides to form niobium (tantalum) fluorocations and antimony polyfluoroanions, but the solutions show an unusual distribution of species and have very low conductivities. It is concluded that neutral "fluxional" MF_4–Sb_nF_{5n+1} molecules are formed. The ^{19}F n.m.r. spectra and conductivities of the liquid systems NbF_5–SbF_5 and TaF_5–SbF_5 are consistent with the formation of neutral fluorine-bridged polymers with mixed transition metal and antimony units. These polymers may be "fluxional" on the n.m.r. time scale. The Raman spectra of the liquid systems and the crystalline pentafluoride mixtures show that both contain mixed *cis* fluorine-bridged units. The Raman spectrum of crystalline SbF_5 and the ^{19}F n.m.r. spectrum of the $NbSbF_{11}^-$ ion are reported.

Les spectres r.m.n. de fluor à basse température pour les systèmes NbF_5–SbF_5–SO_2ClF et TaF_5–SbF_5–SO_2ClF semblent indiquer que les pentafluorures s'ionisent pour former des fluorocations de niobium (tantale) et des polyfluoroanions d'antimoine; les solutions sont toutefois composés par une distribution surprenante des entités et ont de très basses conductivités. On en conclut que des molécules "fluxionnelles" neutres du type MF_4–Sb_nF_{5n+1} se forment. Les spectres r.m.n. du fluor et les conductivités des systèmes liquides NbF_5–SbF_5 et TaF_5–SbF_5 sont consistants avec la formation de polymères neutres comportant des ponts fluorés reliant des unités comportant des métaux de transition et de l'antimoine; par rapport à l'échelle de temps de la r.m.n., ces polymères peuvent être considérés comme fluxionnels.

Les spectres Raman des systèmes liquides et des mélanges cristallins de pentafluorures montrent que chacun des systèmes comporte des unités avec des ponts mixtes avec le fluor *cis*. On rapporte aussi le spectre Raman du SbF_5 cristallin et le spectre r.m.n. du fluor de l'ion $NbSbF_{11}^-$.

Canadian Journal of Chemistry, 49, 1736 (1971)

Liquid antimony pentafluoride and solid niobium and tantalum pentafluorides are all known to have fluorine-bridged structures which indicates that, in addition to their well-known Lewis acidity or acceptor properties, they also possess some basicity or donor strength. It was felt that it should be possible to obtain some information about the relative acceptor and donor strengths of these pentafluorides by studying mixtures of them. The formation of an unsymmetrical fluorine bridge would in the limit lead to ionization, for example

$$NbF_5 + SbF_5 \rightarrow NbF_4^+ + SbF_6^-$$

and the possible formation of such fluorocations was also of interest. We have, therefore, studied the mixtures NbF_5–SbF_5 and TaF_5–SbF_5 both in SO_2ClF and as liquids in the absence of a solvent using ^{19}F n.m.r. Raman spectra were obtained for the liquid and solid mixtures with no solvent; the Raman spectrum of crystalline SbF_5 is also reported. Some conductimetric measurements were made on solutions of $(n\text{-}Bu)_4NBF_4$, NbF_5–SbF_5, and TaF_5–SbF_5 in SO_2ClF and also on solutions of Et_4NSbF_6, NbF_5, and TaF_5 in SbF_5.

Recently Davies and Moss (1) reported the fluorine-on-antimony region of the ^{19}F n.m.r. spectrum of a dilute solution of NbF_5 in SbF_5. On the basis of this spectrum they concluded that simple dissolution of NbF_5 in SbF_5 occurred, but alluded to a change in the ^{19}F chemical shift of fluorine-on-niobium which led them to suggest that solute–solvent interactions were strong. Subsequently, since the completion of the present study, Edwards (2) has reported the preparation and crystal structure of a 1:1 NbF_5:SbF_5 adduct. The complex was obtained by sublimation from a mixture containing a slight excess of NbF_5. The structure consists of zig-zag chains of alternating antimony and niobium atoms linked asymmetrically by *cis*-bridging fluorine atoms in such a way that an important contribution to the structure from the ionic form $NbF_4^+SbF_6^-$ is indicated.

Can. J. Chem. Downloaded from www.nrcresearchpress.com by 210.87.254.105 on 09/05/12
For personal use only.

Results and Discussion

^{19}F n.m.r. Spectra and Conductivities of NbF_5–SbF_5–SO_2ClF and TaF_5–SbF_5–SO_2ClF

NbF_5–SbF_5 and TaF_5–SbF_5 mixtures are quite soluble in sulfuryl chlorofluoride at room temperature, but become much less so at the low temperatures required to obtain fine structure in the ^{19}F n.m.r. spectra of the solutions. Low temperature n.m.r. spectra can be obtained, however, by cooling the solutions quickly and recording the spectra rapidly.

We have investigated solutions with compositions $NbF_5/SbF_5/SO_2ClF$ = 1/1.94/4.03 and $TaF_5/SbF_5/SO_2ClF$ = 1/2.22/7.76. The ^{19}F n.m.r. spectra of both these solutions show broad lines at room temperature probably due to fast fluorine exchange, but at low temperatures fine structure can be observed in the spectra of the rapidly quenched solutions. Figure 1*a* shows the fluorine-on-antimony region of the −95° 56.4 MHz ^{19}F n.m.r. spectrum of the NbF_5 solution. Outside this region there is a single broad line (110 Hz half-width) from fluorine-on-niobium, at ϕ −278.4, and also a sharp single line from the solvent together with a smaller line +228 Hz from the solvent line which has been shown (3) to be due to SO_2ClF in the complex $SbF_5.SO_2ClF$. Figure 1*b* shows the fluorine-on-antimony region of the ^{19}F n.m.r. spectrum of the TaF_5 solution under the same conditions. The total spectrum of this solution includes a single line from the solvent, a line +215 Hz from the solvent arising from SO_2ClF in $SbF_5.SO_2ClF$, and a second line +150 Hz from the solvent line which is known (3) to result from SO_2ClF in the 2:1 complex $(SbF_5)_2.SO_2ClF$. The signal from fluorine-on-tantalum is a single broad line (240 Hz half-width) at ϕ −170.1.

The fluorine-on-antimony region of the n.m.r. spectra of both solutions are similar and the same assignments apply to both. By comparison with previous studies using SO_2ClF as solvent (3, 4) the doublet *H* and quintet *J* can be assigned to $SbF_5.SO_2ClF$ and *A*, *C*, and *F* to $Sb_2F_{11}^-$ (in Fig. 1*a* *C* is not observed due to the high intensity of *D*). *E* is part of the previously reported (4) spectrum of *cis*-$Sb_3F_{16}^-$ as is the quintet *G* which is overlapped by quintet *J* in Fig. 1*b* (other components of the spectrum of *cis*-Sb_3F_{16} are overlapped by more intense resonances and not observed); *K* may be part of the spectrum of $(SbF_5)_2.SO_2ClF$ (3). The broad signal *D* at ~ϕ 110 may reasonably be assigned to SbF_6^-.

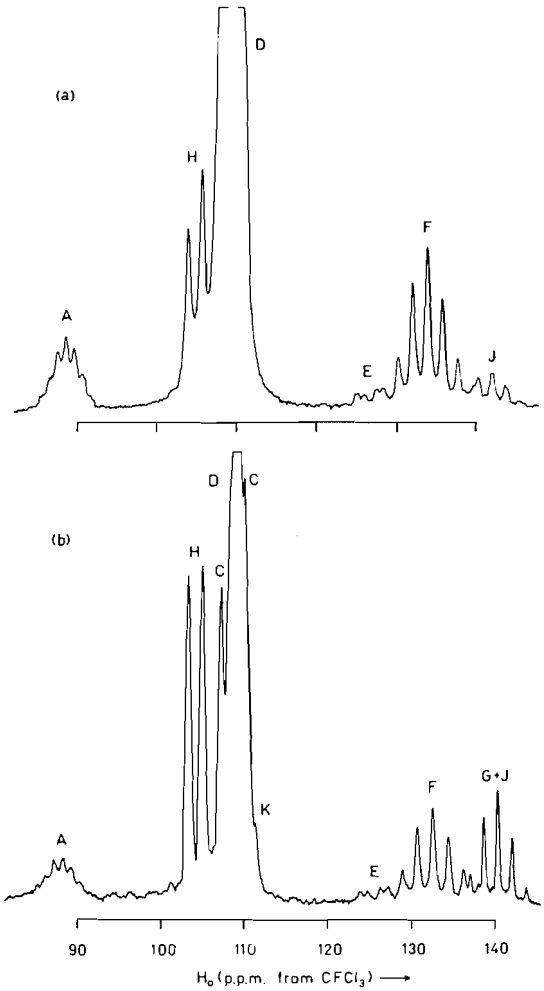

FIG. 1. The −95° 56.4 MHz ^{19}F n.m.r. spectra (F-on-Sb region only) of (*a*) a solution with $NbF_5/SbF_5/SO_2ClF$ = 1/1.94/4.03, and (*b*) a solution with $TaF_5/SbF_5/SO_2ClF$ = 1/2.22/7.76.

The n.m.r. spectra of the solutions appear to indicate ionization of the MF_5–SbF_5 mixtures to give the anions SbF_6^-, $Sb_2F_{11}^-$, and *cis*-$Sb_3F_{16}^-$, together with quite appreciable formation of $SbF_5.SO_2ClF$ which arises from solvolysis reactions such as $Sb_3F_{16}^- + SO_2ClF \rightleftarrows Sb_2F_{11}^- + SbF_5.SO_2ClF$. There must also be a cation, presumably MF_4^+, which gives rise to the broad line observed to low applied fields in these spectra. The distribution of the anions, and the amount of solvolysis product formed in the solu-

TABLE 1. Conductivities in SO_2ClF and SbF_5

Composition	Solvent	Temperature (°C)	Specific conductivity ($ohm^{-1}\ cm^{-1} \times 10^{-6}$)
$(n\text{-Bu})_4NBF_4$(0.104 *m*)	SO_2ClF[a]	0	719
NbF_5(0.111 *m*), SbF_5(0.214 *m*)	SO_2ClF	0	18.2
TaF_5(0.098 *m*), SbF_5(0.249 *m*)	SO_2ClF	0	10.8
Et_4NSbF_6(0.512 *m*)[b,c]	SbF_5[d]	25	822
NbF_5(0.456 *m*)	SbF_5	25	8.45
TaF_5(0.462 *m*)	SbF_5	25	1.63

[a]Specific conductivity of SO_2ClF used $< 10^{-8}$ ohm^{-1} cm^{-1} (0°).
[b]0.512 *m* $Et_4NSbF_6 \equiv$ 0.460 *m* Et_4NF.
[c]This solution becomes inhomogeneous at lower temperatures.
[d]Specific conductivity of SbF_5 used $= 0.23 \times 10^{-6}$ ohm^{-1} cm^{-1} (25°).

tions are, however, somewhat anomalous in the light of an investigation (4) of the systems *t*-BuF–SbF_5–SO_2ClF and $(n\text{-Bu})_4NSbF_6$–SbF_5–SO_2ClF. In this study it was shown that solvolysis of the anions $Sb_nF_{5n+1}^-$ is negligible up to $n = 3$, and that *cis-cis*-$Sb_4F_{21}^-$, which *is* partly solvolyzed, is not produced in solutions containing appreciable amounts of the SbF_6^- ion. For instance, in a solution where *t*-BuF/SbF_5/SO_2ClF = 1/2.5/2.2, there is an almost equimolar mixture of the anions $Sb_2F_{11}^-$ and *cis*-$Sb_3F_{16}^-$, a much smaller amount of SbF_6^- and an extremely small amount of $SbF_5.SO_2ClF$. Significant amounts of $SbF_5.SO_2ClF$ are formed only in solutions with higher SbF_5/F^- ratios, and in the spectra of these solutions there is no observable SbF_6^- signal.

Changing the cation from $C(CH_3)_3^+$ or $(n\text{-Bu})_4N^+$ to MF_4^+ clearly produces a change in the distribution of the fluorine-containing species in the SO_2ClF solutions. Whereas the *t*-BuF/SbF_5/SO_2ClF solutions contain predominately $Sb_2F_{11}^-$ and $Sb_3F_{16}^-$ and no $SbF_5.SO_2ClF$ or SbF_6^- all four species are present in the MF_5–SbF_5 solutions.

Changes of cation could produce changes in the distribution of a series of anions in equilibrium if there were a significant change in one or more cation–anion interactions with variation in cation. To assess the importance of cation–anion interactions in the SO_2ClF solutions of MF_5–SbF_5, conductivity measurements were made. The results are given in Table 1, together with a measurement on $(n\text{-Bu})_4NBF_4$ as a standard electrolyte. (Neither of the more desirable standards Et_4NSbF_6 or $(n\text{-Bu})_4NSbF_6$ showed sufficient solubility in SO_2ClF to be useful.) The MF_5–SbF_5 mixtures have conductivities very much lower than that of the tetrafluoroborate salt. Although the dielectric constant of SO_2ClF has not been reported, it is presumably low, and it is therefore expected that extensive ion-multiplet formation will occur in the BF_4^- solution. In the pentafluoride mixtures ion-multiplet formation must be even more extensive or alternatively a different type of interaction must be involved. Both NbF_4^+ and TaF_4^+ are expected to be extremely strong Lewis acids and it would not be surprising, therefore, if the cation–anion interaction in MF_5–SbF_5 took the form of strong fluorine bridging between MF_4^+ and $Sb_nF_{5n+1}^-$. We conclude that neutral fluorine bridged MF_4–Sb_nF_{5n+1} molecules are formed which are ionized to the extent of a few percent only.

The fluorine-on-antimony region of the ^{19}F n.m.r. spectrum of a neutral fluorine-bridged molecule MF_4–Sb_nF_{5n+1} would normally be expected to differ from that of an $Sb_nF_{5n+1}^-$ anion due to association of the MF_4 entity with some of the fluorines in the Sb_nF_{5n+1} section of the molecule but not with others. However, the n.m.r. spectra of the MF_5–SbF_5–SO_2ClF solutions (Fig. 1) show what appear to be the spectra of unperturbed $Sb_nF_{5n+1}^-$ ions and thus the n.m.r. measurements are apparently at variance with the above interpretation of the conductivity experiments.

It is possible to reconcile the conductivity and n.m.r. results if the molecules MF_4–Sb_nF_{5n+1} are "fluxional". In these "fluxional" molecules there occurs very rapid (on an n.m.r. time scale) intramolecular exchange of potential MF_4^+ cations between various fluorine positions on the potential $Sb_nF_{5n+1}^-$ anion, in such a way that the ^{19}F n.m.r. spectrum of the potential anion is indistinguishable from that of the free anion. Such an intramolecular exchange could be rapid and facile if the MF_4 moiety were fluorine-bridged to antimony as in **1**, the exchange then taking place by continued fission of one M···F bond at a time,

Can. J. Chem. Downloaded from www.nrcresearchpress.com by 210.87.254.105 on 09/05/12
For personal use only.

TABLE 2. 56.4 MHz ^{19}F n.m.r. spectra of the system NbF_5-SbF_5 at 33°

NbF_5/SbF_5	Chemical shift (p.p.m.),[a] fluorine-on-niobium	Approximate half-width, fluorine-on-niobium (Hz)	Intensity of fluorine-on-niobium[b] / Intensity of fluorine-on-antimony
0.063	−274.5	200	0.055
0.093	−274.3	340	0.078
0.200	−274.4	440	0.15
0.324	−272.3	480	0.22
0.504	−270.0	530	0.32
0.587	−266.4	570	0.42
0.921	−250.1	600	0.68
0.990	−249.0	500	0.68
1.27	−231.4	330	1.1
1.35	−234.2	390	1.0
1.95	−217.3	210	1.6
3.31	−201.9	170	[c]
3.61	−195.6	160	[c]
3.90	−197.0	160	[c]
5.56	−193.5	160	[c]
∞[d]	−180.3	65	
∞[e]	−180.7	900	

[a]Measured, relative to external $CFCl_3$, by sample interchange.
[b]Estimated error ±10%.
[c]No area measurement possible due to rapid crystallization.
[d]At 120°.
[e]Saturated solution in SO_2ClF.

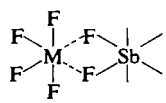

1

followed by formation of another such bond to a different fluorine on the antimony.

As the structures of crystalline NbF_5 and TaF_5 (5) and of $NbF_5.2SbF_5$ (2) involve two *cis* fluorine-bridges per niobium or tantalum it is most probable that in the present case the number of fluorine-bridges per M is also two. As the MF_4 unit is strongly electron withdrawing it is reasonable to expect that the molecule $MF_4.Sb_3F_{16}$ will be more easily solvolyzed than the free $Sb_3F_{16}^-$ ion. Therefore the unusually large amount of solvolysis observed in the MF_5–SbF_5 solutions is consistent with the proposed model.

Formation of "fluxional" molecules has recently been postulated to explain the ^{19}F and ^1H n.m.r. spectra of MeF–SbF_5 (6, 7) and EtF–SbF_5 (7) solutions in SO_2 and SO_2ClF. In these systems the fluorine n.m.r. showed what were apparently the spectra of the free anions $Sb_nF_{5n+1}^-$, but the proton n.m.r. showed the absence of ionization. It is noteworthy that the "fluxional" molecule Et-Sb_3F_{16} is apparently more easily solvolyzed in SO_2ClF than the free *cis*-$Sb_3F_{16}^-$ anion (7).

^{19}F n.m.r. Spectra and Conductivities of SbF_5–NbF_5 and SbF_5–TaF_5

Mixtures of NbF_5 and SbF_5 are stable as liquids or supercooled liquids at room temperature when $NbF_5/SbF_5 \gtrsim 0.7$, as are mixtures of TaF_5 and SbF_5 when $TaF_5/SbF_5 \gtrsim 0.5$. In systems containing more of the transition metal pentafluoride, crystallization occurred fairly rapidly but it was nevertheless possible to obtain some information from ^{19}F n.m.r. spectra recorded quickly on the melts supercooled to room temperature. Low temperature n.m.r. spectra could be obtained for both NbF_5–SbF_5 and TaF_5–SbF_5 mixtures in which $MF_5/SbF_5 \leq 0.3$.

The room temperature n.m.r. spectra of the MF_5–SbF_5 mixtures showed, to low applied fields, a broad resonance from the fluorine-on-transition element, and, in the fluorine-on-antimony region, either a single broad resonance or a more incompletely resolved set of several resonance. Table 2 gives details of the room temperature spectra of the NbF_5–SbF_5 mixtures; Table 3 presents similar information for TaF_5–SbF_5 mixtures. The intensity measurements for both systems indicate extensive transfer of fluorine from the transition element to antimony. In addition there is considerable variation in the chemical shift of the fluorine-on-Nb(Ta) signal

Can. J. Chem. Downloaded from www.nrcresearchpress.com by 210.87.254.105 on 09/05/12
For personal use only.

TABLE 3. 56.4 MHz n.m.r. spectra of the system TaF_5-SbF_5 at 33°

TaF_5/SbF_5	Chemical shift (p.p.m.),[a] fluorine-on-tantalum	Approximate half-width, fluorine-on-tantalum (Hz)	Intensity of fluorine-on-tantalum[b] / Intensity of fluorine-on-antimony
0.067	−165.0	940	0.050
0.096	−165.1	1085	0.067
0.187	−163.0	1095	0.12
0.316	−158.3	1170	0.21
0.571	−152.6	1680	[c]
0.937	−141.3	1420	[c]
1.95	−124.2	1049	[c]
3.00	−113.6	800	[c]
∞[d]	−100.7	36	
∞[e]	− 95.5	130	

[a]Measured, relative to external $CFCl_3$, by sample interchange.
[b]Estimated error ±10%.
[c]No area measurement possible due to rapid crystallization.
[d]At 140°.
[e]Saturated solution in SO_2ClF.

with composition, whereas the fluorine-on-Sb resonance, when a single line, is always in the range ϕ 107–112 (as noted above this part of the spectrum was more complex in some solutions). For compositions with small amounts of antimony the F-on-Nb(Ta) chemical shifts approach those of MF_5, and limiting values in the antimony-rich region are observed when the mole fraction of $SbF_5 \geqslant 0.8$. The total variation of the F-on-Nb(Ta) chemical shifts, about 100 p.p.m. for the NbF_5–SbF_5 system and 65 p.p.m. for the TaF_5–SbF_5 system,[1] provides good evidence for strong interaction between the components of the mixtures.

Figure 2 shows the fluorine-on-Sb region of the low temperature ^{19}F n.m.r. spectra of NbF_5–SbF_5 mixtures with $0.324 \geqslant NbF_5/SbF_5 \geqslant 0.093$. The fluorine-on-niobium chemical shifts of these mixtures did not change significantly from their room temperature values though there was some variation in half-width of the signal, probably resulting mostly from changes in viscosity. Essentially identical spectra were obtained for liquid TaF_5–SbF_5 mixtures with the same mole ratios. The spectrum of a dilute NbF_5–SbF_5 (or TaF_5–SbF_5) solution (Fig. 2*a*) is very similar to the ^{19}F n.m.r. spectrum of SbF_5 which shows three regions of resonance, *A*, *B*, and *C*, with intensities 1:2:2 (1, 4, 8). Davies and Moss (1) have previously remarked upon this similarity for a dilute solution of NbF_5 in SbF_5; however, they did not notice the distortion (compared to the spectrum of SbF_5) of the resonance *B* which arises from the growth of a new resonance *D* beneath the high field side of *B*. As the amount of solute is increased the intensity of the broad line *D* increases but the intensity ratio *C*/*A* remains equal to two as it is in SbF_5 itself, strongly suggesting that some free SbF_5 or another SbF_5-like species is present even at the highest M/Sb ratios studied (there is some loss in resolution of *C* which most probably results from increased viscosity at the higher M/Sb ratios). Over the range of composition studied at low temperatures, the ratio of the intensity of the signal *D* to that of the F-on-M resonance is approximately two.

Although the intensities given in Tables 2 and 3 suggest extensive ionization in these systems, with donation of fluoride ion from the transition element to antimony, the relatively good resolution obtained in the low temperature spectra is not consistent with an ionic model. In the system Et_4NSbF_6–SbF_5, which *must* be ionic, very broad lines are observed in the ^{19}F n.m.r. spectrum at all temperatures studied, almost certainly as a result of rapid fluorine exchange (9). In view of this apparent anomaly and the unusual results obtained for solutions of MF_5–SbF_5 in SO_2ClF (see above), conductivity measurements were made on the SbF_5 solutions of MF_5. The results are shown in Table 1, together with a measurement for Et_4NSbF_6 as a standard electrolyte. It is clear by comparison with the ionic Et_4NSbF_6–SbF_5 system that the MF_5–SbF_5 mixtures can be at most slightly ionized.

[1]As the solutions showed no electron spin resonance (e.s.r.) signals these cannot be contact shifts.

Can. J. Chem. Downloaded from www.nrcresearchpress.com by 210.87.254.105 on 09/05/12
For personal use only.

Can. J. Chem. Downloaded from www.nrcresearchpress.com by 210.87.254.105 on 09/05/12
For personal use only.

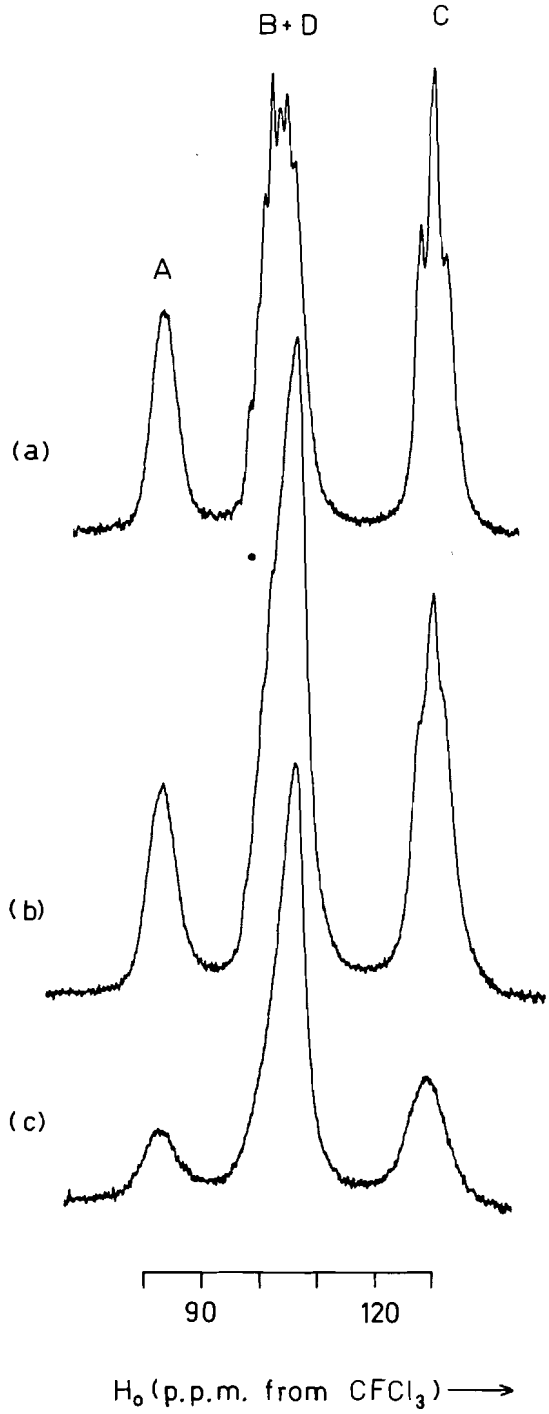

FIG. 2. The 56.4 MHz ^{19}F n.m.r. spectra (F-on-Sb region only) of liquid NbF_5/SbF_5 mixtures: (*a*) $NbF_5/SbF_5 = 0.093$, and $-36°$; (*b*) $NbF_5/SbF_5 = 0.200$, at $-36°$; (*c*) $NbF_5/SbF_5 = 0.324$, at $-28°$.

The NbF_5 solution was blue (as were those used for n.m.r.) apparently due to a very small amount of highly colored impurity;[2] thus part of the difference between the conductivities of the NbF_5 and TaF_5 solutions could be due to impurities.

The n.m.r. and conductivity measurements show that the MF_5–SbF_5 systems are essentially covalent, and the n.m.r. spectra also show that free SbF_5 is probably present at least up to MF_5/SbF_5 ratios of *ca.* 0.3. It seems very likely that $NbF_5.SbF_5$ has a polymeric structure in the liquid state similar to that found for the solid (2). However, our results cannot be satisfactorily accounted for in terms of the formation of a 1:1 mixed polymer only [*e.g.*, the ^{19}F chemical shift of F-on-Nb or F-on-Ta is, at the 1:1 point, considerably different from its value in dilute SbF_5 solution (Tables 2 and 3)] and we suggest that polymers of the general type **2** are formed.

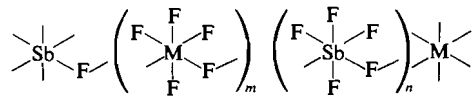

2

Like $NbF_5.SbF_5$ (2), these contain both antimony and transition metal units linked by *cis*-fluorine bridges. In principle **2** could also contain *trans*-fluorine bridges, but the Raman spectra discussed below provide no evidence for *trans* bridging. As SbF_5 is present at some compositions, completely random mixing of Sb and M cannot occur over the whole range of composition, but apparently the antimony-rich polymers tend to disproportionate to give the SbF_5 polymer and a less antimony-rich Nb(Ta)–Sb polymer, *i.e.*, there is a limiting value for *n*, the average antimony chain length in the mixed polymer. This situation resembles that in the system Et_4NSbF_6–SbF_5, where $Sb_nF_{5n+1}^-$ ions are not formed indefinitely but at higher values of *n* disproportionation occurs to give SbF_5 and a smaller polyfluoroanion (9). Since the intensities of *A* and *C* show quite a large amount of SbF_5 to be present in mixtures with $Nb(Ta)/Sb \simeq 0.3$, the average limiting value for *n* must be small, probably two or less.

In the polymers containing a maximum amount of antimony we can reasonably expect that few M—F—M bridges are present, *i.e.*, the value of

[2]We note that solutions of NbF_5 in ethanol are reported to be purple (10).

Can. J. Chem. Downloaded from www.nrcresearchpress.com by 210.87.254.105 on 09/05/12
For personal use only.

m, the average MF_5 chain length in the polymer, is close to unity. On increasing the M/Sb ratio the value of n, the average SbF_5 chain length approaches unity, and simultaneously the value of m increases. Both these factors probably affect the chemical shift of F-on-M. As the transition metal positions are averaged by fast exchange, we might expect a smooth variation in the average chemical shift of F-on-M, from a limiting value in solutions with a low M/Sb ratio towards the value for MF_5 itself as m increases with increasing M/Sb. Such variation is indeed observed (Tables 2 and 3). The rapid exchange which averages the F-on-M chemical shifts could occur by homo- or heterolytic cleavage and reformation of Sb—F—M or M—F—M bridges (or both).

There still remains the problem of the inconsistency between the apparently extensive ionization indicated by the intensities in the ^{19}F n.m.r. spectra and the very limited ionization indicated by the conductivity measurements. In view of the results for MF_5–SbF_5–SO_2ClF, one possible explanation is that polymers of the type **2** are "fluxional". Unfortunately we were unable to obtain spectra at a low enough temperature to observe the definitive n.m.r. spectra of the $Sb_nF_{5n+1}^-$ ions and so confirm that the polymers are "fluxional". We presume that, at the temperatures we could reach, the chemical shifts of the various fluorines-on-antimony in the M—Sb polymers are averaged to the single line D, just as the chemical shifts of F-on-M are averaged. If the value of n is between one and two then in the most antimony-rich polymers, where for reasons given above $m \simeq 1$, the intensity ratio of D to the F-on-M signal should be between 1.5 (for MF_4–SbF_6) and 2.75 (for MF_4–Sb_2F_{11}) and the ratio is found to be about two experimentally.

An alternative explanation for the apparent ionization is that not all the intensity attributed to fluorine-on-antimony is in fact due to fluorine bonded solely to antimony. To investigate this possibility further we studied the spectrum of another system containing a fluorine bridge between niobium and antimony. $(n\text{-Bu})_4NSbF_6$ has very low solubility in SO_2ClF but dissolves in the presence of an equimolar amount of NbF_5. At $-135°$, the 94.1 MHz ^{19}F n.m.r. spectrum of the mixture showed, in addition to the solvent line, a broad (approximately 225 Hz half-width) line at ϕ -157.1 which can be attributed to fluorine-on-niobium, and three broad structureless lines of intensity 1:4:1 at ϕ 101.7, 117.7, and 131.5 (half widths $\simeq$479, $\simeq$280, and $\simeq$470 Hz, respectively) in the region normally attributable to fluorine-on-antimony. The ratio of the intensities F-on-Nb/F-on-Sb was found to be 5/6. The spectrum may be assigned to the $NbSbF_{11}^-$ ion (**5**). By comparison with the spectra of the $Sb_2F_{11}^-$ ion (9, 11) and the $AsSbF_{11}^-$ ion (12),

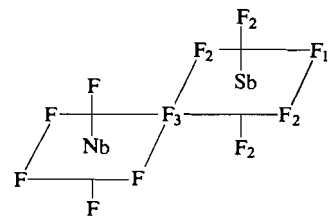

5

we can probably assign the line at ϕ 131.5 to the fluorine F_1. The intense signal at ϕ 117.7 must arise from the fluorines F_2, and hence we conclude that the resonance at ϕ 101.7 is due to the fluorine F_3, *bonded to both niobium and antimony*, even though it appears in the "fluorine-on-antimony" region. (Note that reversal of the assignments for F_1 and F_2 does not alter the conclusion.) This result probably signifies considerable asymmetry of the Nb—F—Sb bridge, the fluorine lying much closer to the antimony than to the niobium just as the bridging fluorines do in $NbF_5.SbF_5$ (2). The lack of fine structure in the lines in the F-on-Sb region may be due to residual coupling with the Nb nucleus ($I = 9/2$). The single signal from fluorine-on-niobium is probably a result of fast inter- or intramolecular exchange of the terminal fluorines attached to niobium.

Raman Spectra

In order to be able to interpret the Raman spectra of the pentafluoride mixtures, a knowledge of the individual Raman spectra of SbF_5, NbF_5, and TaF_5 as liquids and crystalline solids is desirable. Raman spectra have been reported for liquid SbF_5 (13–15), liquid (13, 16) and solid (13) NbF_5, and liquid (13, 16) and solid (13) TaF_5. We have now obtained the Raman spectrum of crystalline SbF_5 which can be obtained by cooling a solution of SbF_5 in C_4F_8, SO_2F_2 or SF_6 and removing the solvent at low temperature. We have also found that some samples of SbF_5 crystallize on cooling after having been stored in

TABLE 4. Raman spectra of a TaF_5–SbF_5 mixture and molten and crystalline SbF_5 and TaF_5 (cm^{-1})[a]

TaF_5/SbF_5 = 1.00/1.13		SbF_5		TaF_5	
Solid[b, c]	Liquid[b, d]	Solid[b, e]	Liquid[f, g]	Solid[f, h]	Liquid[f, i]
764 vs	762 vs (p)	745 m		755 vvs	755 vs (p)
743 mw		736 w		727 m	712 vw
713 m	705 s (p)	723 m		699 ms	690 w
695 s	680 m (p)	717 vs	718 s (p)	671 w	
668 s	668 vs (p)	712 m		273 ms	
532 w br	525 w br	693 w		254 w	251 m
305 w	~302 w	668 vs	670 s (p)	236 m	
279 s sh			(489)[j]	221 vw	222 w
272 s	272 m		349 w		184 w
236 m	238 s		(302)[j]	183 vw	
197 w	~197 w sh	268 m	268 mw	119 vw	
182 w		~264 m sh		106 w	
124 mw	135 mw (p)	258 m			
		241 m			
		234 m	231 mw		
		217 w			
		206 m	189 mw (p?)		
		171 m			
		141 m	140 vw		
		132 m			
			116 vw		

[a]s = strong, m = medium, w = weak, v = very, sh = shoulder, br = broad, p = polarized.
[b]This work.
[c]At 23°.
[d]At 65°.
[e]At −100°.
[f]Reference 13.
[g]At 25 and 125° (also supercooled liquid (present work)).
[h]Room temperature.
[i]At 110°.
[j]Reference 15.

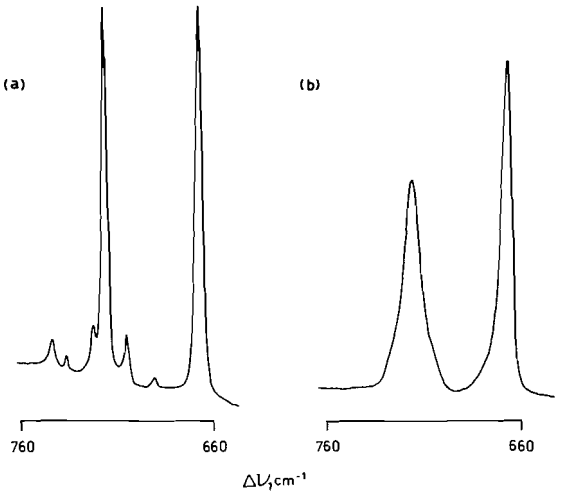

FIG. 3. The Raman spectra (high frequency region) of (*a*) crystalline SbF_5 (ex SO_2F_2) at −100°, and (*b*) liquid SbF_5 supercooled to −100°.

glass tubes for a period of months. Details of the Raman spectrum of crystalline SbF_5 are given in Table 4. The high frequency region of the −100° spectrum of the material is shown in Fig. 3*a*; Fig. 3*b* shows the same region for liquid SbF_5 supercooled to −100°. The spectra of crystalline and liquid pentafluoride show marked differences; in particular more and sharper bands are observed in the high frequency (antimony-terminal fluorine stretching) region of the spectrum of the solid than of the liquid. Nevertheless the two most intense bands observed in the spectrum of the liquid (717 and 668 cm^{-1}) are essentially unchanged in position in the solid (718 and 670 cm^{-1}) which must therefore have a structure based on *cis* fluorine-bridged SbF_5 units, as has been shown by ^{19}F n.m.r. to be the case for the liquid (1, 4, 8). The two most likely structures for the solid are the infinite *cis* fluorine-bridged chain structure of liquid SbF_5 and crystalline VF_5 (17) or the cyclic fluorine-bridged tetrameric structure of crystalline NbF_5 and TaF_5 (5), but we cannot definitely assign either structure on the basis of the Raman spectrum alone.

TaF_5–SbF_5 and NbF_5–SbF_5

Table 4 gives the details of the Raman spectrum of a system with TaF_5/SbF_5 = 1/1.13 both as a crystalline solid at room temperature, and as a

Can. J. Chem. Downloaded from www.nrcresearchpress.com by 210.87.254.105 on 09/05/12
For personal use only.

Can. J. Chem. Downloaded from www.nrcresearchpress.com by 210.87.254.105 on 09/05/12
For personal use only.

liquid at 65°. It also includes the spectra of solid and liquid SbF_5 and TaF_5 for comparative purposes. The spectrum of the system is complicated and it is difficult to make definite assignments. However, useful information can be obtained from the region above 600 cm^{-1}. In this region the spectrum of the solid closely resembles a superimposition of the spectra of solid SbF_5 and TaF_5 having strong bands at 764, 713, 695, and 668 cm^{-1} compared with 755 and 699 cm^{-1} for TaF_5 and 717 and 668 cm^{-1} for crystalline SbF_5. By variation of the composition of the mixtures studied, it was possible to associate increased intensity of the bands at 764 and 695 cm^{-1} with increased amount of TaF_5 in the system, and increased intensity of the bands at 743, 713, and 695 cm^{-1} with increased SbF_5.

The formation of crystalline products melting above room temperature (*e.g.*, 50–56° and 40–45° when TaF_5/SbF_5 = 1/1.13 and 1/2.01, respectively) and therefore well above the melting point of crystalline SbF_5 of 5–10 °C is good evidence that in the solid there is more than a simple mixture of the components with no interaction. In view of the similarity of bands in the Raman spectrum to those of either crystalline SbF_5 or crystalline TaF_5, both of which contain *cis* fluorine-bridging between MF_6 units (4, 5), it is reasonable to conclude that in the present case we also have *cis* fluorine-bridged MF_6 units but with some alternation of Sb and Ta as the central atom. The structure is presumably that of an infinite chain, similar to the structure of $NbF_5.SbF_5$ (2), though we cannot, on the basis of the Raman spectrum alone, rule out a cyclic fluorine-bridged structure.

The 65° Raman spectrum of the liquid of composition TaF_5/SbF_5 = 1/1.13 (Table 4) is similar to that of the solid with like composition, and also to a combination of the spectra of liquid SbF_5 and liquid TaF_5. Thus the liquid shows an intense strongly polarized band at 668 cm^{-1} where SbF_5 alone has a similar band, and a second intense strongly polarized band at 762 cm^{-1} close to the frequency (755 cm^{-1}) where such a band is observed in the spectrum of liquid TaF_5. The single rather broad polarized band at 705 cm^{-1} in this TaF_5–SbF_5 mixture must be a composite of two bands: in the spectrum of a liquid with TaF_5/SbF_5 = 1/2.01 a higher frequency band (712 cm^{-1}) with a lower frequency shoulder (~700 cm^{-1}) is observed, both bands being polarized. (These most probably correspond to the two distinct bands observed at 713 and 695 cm^{-1} in the solid.) Bands occur at 718 and 690 cm^{-1} in the spectra of liquid SbF_5 and TaF_5, respectively. Comparison of the spectra of mixtures of different composition shows that the band at 762 cm^{-1} increases in intensity with increasing mole ratio of TaF_5 and the band at 668 cm^{-1} with increasing amount of SbF_5.

As in the case of the solid product, the Raman spectrum of the liquid mixture is close to that expected for no interaction of the components. However, the ^{19}F n.m.r. spectra of the pentafluoride mixtures (see earlier) show that reaction does occur, a conclusion strengthened by the Raman evidence presented above for mixing of TaF_6 and SbF_6 units in the solid. It seems certain that if such mixing occurs in the solid it will also occur in the liquid. In view of the Raman spectra of the solids, the bands at 764 and 668 cm^{-1} in the spectrum of the liquid indicate the presence of *cis* fluorine-bridged TaF_6 and SbF_6 units, respectively, in the liquid also. We conclude that our results are consistent with formation of a mixed fluorine-bridged polymer of the type **2** with *cis* fluorine bridges on both Ta and Sb.

Since the bands observed at 755, 762, and 764 cm^{-1} in the Raman spectra of crystalline TaF_5, and the crystalline and liquid TaF_5/SbF_5 mixture, respectively, are diagnostic of the presence of *cis* fluorine-bridged TaF_6 octahedra, it seems highly probable that the observation of a band at 755 cm^{-1} in the spectrum of liquid TaF_5 also show the presence of such units, and is therefore consistent with the polymeric structure proposed by Beattie *et al.* (13) for this material. In view of our results for the mixed pentafluoride systems, we conclude that the monomeric structure proposed by other authors (16, 18) for liquid TaF_5 is highly unlikely.[3] Such a structure is in any case doubtful in view of the high Trouton's constants of 25.9 cal/°K for TaF_5 and of 25.4 cal/°K for NbF_5, (20).

We were able to obtain good Raman spectra of liquid NbF_5–SbF_5 mixtures and no spectra at all were obtained from the corresponding solids.

[3]In the only proven case of depolymerization of a fluorine-bridged material in the liquid phase, that of VF_5 (20), the Raman frequencies of the monomer differ significantly from those of the polymer, whereas the frequencies of the liquid and solid polymer are almost identical (13, 20).

Can. J. Chem. Downloaded from www.nrcresearchpress.com by 210.87.254.105 on 09/05/12
For personal use only.

TABLE 5. Raman spectra of a liquid NbF_5–SbF_5 mixture and molten and crystalline NbF_5 (cm^{-1})

NbF_5/SbF_5 = 1.00/2.13 Liquid[a]	NbF_5 Liquid[b, c]	NbF_5 Solid[b, d]
770 s (p)	763 s (p)	766 vvs
746 m (p)	689 m (p)	752 w
711 s (p)	256 mw	716 vs
699 s (p)	227 w	668 w
678 m (p)	180 w	656 m
667 s (p)		270 ms
~273 w		252 vw
~241 m		238 vw
~153 w		226 w
		182 w
		~163 w
		130 w

[a]At 23°.
[b]Reference 13.
[c]90°.
[d]Room temperature.

The spectra of the liquid mixtures were generally similar to those of the TaF_5–SbF_5 mixtures. Detailed frequencies for a typical spectrum (NbF_5/SbF_5 = 1/2.13) are given in Table 5, together with those of the spectra of liquid and solid NbF_5. All three spectra show an intense band in the region 763–770 cm^{-1} which, by the same arguments used for TaF_5–SbF_5, must be diagnostic of *cis* flourine-bridged NbF_6 units, known to occur in crystalline NbF_5; the spectrum of the mixture also shows an intense polarized band at 667 cm^{-1} shown above to be diagnostic of *cis*-bridged SbF_6 units. We conclude that, as in the TaF_5–SbF_5 system, the liquid has a polymeric structure involving mixed *cis* fluorine-bridged antimony and transition element MF_6 octahedra. It is reasonable to suppose that solids isolable from the system NbF_5–SbF_5 will have structures similar to $NbF_5.SbF_5$ (2) even when of different stoichiometry.

Experimental

Fluorine n.m.r. spectra were obtained using a Varian DA-60 operating at 56.4 MHz in the field sweep unlock mode described previously (3). The spectrometer was equipped with a Varian variable temperature probe and controller. Spectra were calibrated using sidebands from an audio oscillator, and referencing to external $CFCl_3$ was made either by sample interchange (in samples with no SO_2ClF solvent) or, in SO_2ClF solutions, by measuring relative to the internal SO_2ClF solvent line and applying the appropriate conversion ($\delta(CFCl_3) = \delta(SO_2ClF) - 99.1$ p.p.m.). Areas were measured by cutting out lines and weighing them; at least four spectra were averaged.

Raman spectra were taken with a Spex Industries Model 1400 spectrometer using argon ion (5145 Å) excitation from a Spectra Physics Model 140 laser. The 90° viewing technique of Gillespie and Pez (21) was used. Low temperature spectra were obtained using a Dewar insert cooled by boiling liquid nitrogen as already described (22). For high temperature work the same Dewar insert was used and heating was provided by directing the thrust of a hot air blower through the insert *via* a cone of aluminum foil. Temperatures were measured using a thermocouple which lay next to the sample in the Dewar insert. Samples were contained in either melting point capillary tubes or in 5 mm o.d. glass tubes.

Conductivity measurements were made using an Industrial Instruments Incorporated Bridge, model R.C. 18. The cell was like that previously used (11) with anhydrous hydrogen fluoride; it was calibrated in the normal manner.

Antimony pentafluoride (Ozark Mahoning Co.) was purified by double distillation under an atmosphere of dry nitrogen in a glass apparatus. Niobium and tantalum pentafluorides (Ozark Mahoning Co.) were purified by triple sublimation in vacuo in a Vycor apparatus. Sulfuryl chlorofluoride was synthesized from KSO_2F and chlorine by the method of Seel and Riehl (23). Sulfur dioxide impurity in the product was removed by condensing the SO_2ClF onto SbF_5 using a vacuum line, then distilling off the SO_2ClF *in vacuo*, leaving the SO_2 behind as the relatively involatile $SbF_5.SO_2$. The absence of SO_2 was confirmed by the absence of the characteristic ^{19}F n.m.r. spectrum of either $SbF_5.SO_2$ or $(SbF_5)_2.SO_2$ (3) in the n.m.r. spectra of the SO_2ClF solutions, and also by the absence of the band at 1361 cm^{-1} (24) in the infrared spectrum of the gas.[4]

Samples in 5 mm o.d. n.m.r. and Raman tubes were prepared by adding weighed amounts of the pentafluorides under a nitrogen atmosphere in a dry box. SbF_5 was transferred to the tubes using an all-glass syringe. The tubes were closed with detachable tops and attached to a standard glass vacuum line. If no solvent was to be added the tubes were evacuated and sealed, otherwise the SO_2ClF was condensed in prior to sealing and the sealed tube with top weighed afterwards. The samples with no solvent were homogenized by heating to *ca.* 100° in an oven with frequent shaking and turning. Thereafter these samples were kept molten until used since they exhibited a frustrating tendency to crack the container on crystallization. Raman samples in capillary tubes were prepared by carefully allowing the larger molten samples to crystallize, cracking open the 5 mm tube in the dry box, and transferring the solid to the capillary which was sealed immediately on leaving the box.

Antimony pentafluoride samples sometimes crystallized spontaneously on cooling in Dry Ice. Alternatively SbF_5 was added to a U-shaped apparatus, the arms of which were 5 mm o.d. glass tubes, *via* a 1/4 in. o.d. tube attached at the bend. SO_2F_2 was condensed into the apparatus on a vacuum line and the 1/4 in. opening sealed. On warming and shaking, a homogeneous solution was formed at room temperature and tipped into one arm. This arm was cooled in a chloroform slush bath and the other arm in an ethyl acetate slush bath. After some time all the solvent had condensed in the low temperature arm and

[4]This band has previously been incorrectly assigned (25) to a combination band of SO_2ClF.

crystalline SbF_5 remained in the higher. Last traces of SO_2F_2 were removed by cooling the low temperature arm to $-196°$. The tube containing the *crystalline* SbF_5 was sealed off and kept at low temperature until used.

For conductivity measurements in SO_2ClF, weighed amounts of antimony pentafluoride and the other pentafluoride, or of $(n\text{-Bu})_4NBF_4$, were added to the cell in the dry box. The cell was closed with a teflon "Swagelock" valve and attached to the vacuum line. On the vacuum line an appropriate amount of SO_2ClF was collected in a preweighed vessel closed by a teflon-in-glass stopcock. This vessel was removed from the line and weighed; it was then reconnected and the solvent was condensed into the conductivity cell.

Conductivity samples with no SO_2ClF were made up in glass tubes as for the similar n.m.r. and Raman samples, but on a larger scale. Following homogenization, the tubes were opened in the dry box and the fluid transferred to the conductivity cell.

Though both the niobium and antimony pentafluorides used were colorless, mixtures of these two, with or without solvent, were blue, presumably due to a small amount of highly colored impurity. TaF_5–SbF_5 mixtures were colorless.

We thank the United States Air Force Office of Scientific Research and the National Research Council of Canada for financial support of this work.

1. T. K. Davies and K. C. Moss. J. Chem. Soc. A, 1054 (1970).
2. A. J. Edwards. Chem. Commun. 820 (1970).
3. P. A. W. Dean and R. J. Gillespie. J. Amer. Chem. Soc. **91**, 7260 (1969).
4. J. Bacon, P. A. W. Dean, and R. J. Gillespie. Can. J. Chem. **48**, 3143 (1970).
5. A. J. Edwards. J. Chem. Soc. 3714 (1964).
6. G. A. Olah, J. R. DeMember, and R. H. Schlosberg. J. Amer. Chem. Soc. **91**, 2112 (1969).
7. J. Bacon and R. J. Gillespie. To be published.
8. C. J. Hoffman, B. E. Holder, and W. L. Jolly. J. Phys. Chem. **62**, 364 (1958).
9. J. Bacon, P. A. W. Dean, and R. J. Gillespie. Can. J. Chem. **47**, 1655 (1969).
10. J. V. Hatton, Y. Saito, and W. G. Schneider. Can. J. Chem. **43**, 47 (1965).
11. R. J. Gillespie and K. C. Moss. J. Chem. Soc. A, 1170 (1966).
12. S. Brownstein. Can. J. Chem. **47**, 605 (1969).
13. I. R. Beattie, K. M. S. Livingston, G. A. Ozin, and D. J. Reynolds. J. Chem. Soc. A, 958 (1969).
14. J. Gaunt and J. B. Ainscough. Spectrochim. Acta, **10**, 57 (1956).
15. A. Commeyras and G. A. Olah. J. Amer. Chem. Soc. **91**, 2929 (1969).
16. H. Selig, A. Reis, and E. L. Gasner. J. Inorg. Nucl. Chem. **30**, 2087 (1968).
17. A. J. Edwards and G. R. Jones. J. Chem. Soc. A, 1651 (1969).
18. T. J. Ouellette, C. T. Ratcliffe, and D. W. A. Sharp. J. Chem. Soc. A, 2351 (1969).
19. H. H. Claassen and H. Selig. J. Chem. Phys. **44**, 4032 (1966).
20. F. Fairbrother and W. C. Frith. J. Chem. Soc. 3051 (1951).
21. R. J. Gillespie and G. P. Pez. Inorg. Chem. **8**, 1229 (1969).
22. R. J. Gillespie and M. J. Morton. Inorg. Chem. **9**, 811 (1970).
23. F. Seel and L. Riehl. Z. anorg. allgem. Chem. **282**, 293 (1955).
24. E. A. Robinson. Can. J. Chem. **39**, 247 (1961).
25. T. Birchall and R. J. Gillespie. Spectrochim. Acta, **22**, 681 (1966).

Can. J. Chem. Downloaded from www.nrcresearchpress.com by 210.87.254.105 on 09/05/12
For personal use only.

Can. J. Chem. Downloaded from www.nrcresearchpress.com by 210.87.254.5 on 09/05/12
For personal use only.

Evidence for a Radical Chain Mechanism in the Autoxidation of Triethylbismuth

R. V. WINCHESTER[1]

School of Natural Resources, University of the South Pacific, P.O. Box 1168, Suva, Fiji

Received December 11, 1970

The autoxidation of triethylbismuth in cyclohexane at 25 °C produces as major products ethanol, acetaldehyde, and a solid suggested to be Bi_2O_3 with oxygen atoms randomly replaced by $=CHCH_3$ or $—CH_2CH_2—$ groups. Minor products include diethyl peroxide, diethyl ether, acetic acid, and probably ethylene. The reaction is strongly inhibited by diphenylamine and a radical chain reaction is proposed to account for the observed products.

L'autoxydation du triéthyle de bismuth, dans le cyclohexane à 25 °C, conduit principalement à l'éthanol, l'acétaldéhyde et un produit solide qui serait du Bi_2O_3 dans lequel des atomes d'oxygène ont été remplacés au hasard par des groupes $=CHCH_3$ et $—CH_2CH_2—$. Parmi les produits formés en quantités mineures on retrouve le peroxyde d'éthyle, l'éther éthylique, l'acide acétique et probablement l'éthylène. La réaction est fortement inhibée par la diphénylamine et on croit que la réaction se produit par un mécanisme en chaîne de nature radicalique.

Canadian Journal of Chemistry, 49, 1747 (1971)

Introduction

The autoxidation of organometallic alkyls was originally thought to proceed by a nucleophilic rearrangement mechanism to yield first a peroxide, then an alkoxide (for a summary, see ref. 1), but more recent evidence (2–5) suggests that a radical chain mechanism is favored.

The autoxidation of triethylbismuth has been investigated once previously (6) and though products suggestive of a radical chain reaction were found, no attempt was made to substantiate this point. This paper reports the results of a short investigation intended to determine whether or not the reaction is in fact a radical chain and if possible to suggest a mechanism for it.

Results and Discussion

In all cases, when the alkyl was introduced into the solvent and stirring commenced, a period of 1 to 3 min followed in which there was no apparent reaction. Immediately following this period a yellow precipitate suddenly appeared, accompanied by a rapid uptake of oxygen. The yellow compound then faded slowly until after 2 h it was entirely white. The maximum oxygen uptake of 1.5 ± 0.2 mol per mol of alkyl occurred about 5 min after injection of the alkyl; subsequently the contained gas volume increased slightly, due to evolution of gas in the reaction. Under identical conditions but with the addition of 0.1 mol% of diphenylamine, a known radical inhibitor, the oxygen uptake and solid deposition were extremely slow, with solid continuing to deposit on allowing the solution to stand for several weeks.

Results of analysis of the solid product from various reaction times are shown in Table 1. Traces of titratable peroxide were found in the product isolated after the reaction had proceeded for 5 min, but not in the product of any longer reaction period. Gas–liquid chromatography, though not absolutely reliable as an identification method, showed that ethanol, and to a lesser extent acetaldehyde, were probably the major products, together with smaller amounts of diethyl ether, diethyl peroxide, and acetic acid. All were tentatively identified by comparison with the retention times and volumes of authentic samples on two different columns.

TABLE 1. Analyses of solid autoxidation products of triethylbismuth

Reaction time (min)	Analysis				
	C,%	H,%	Bi (± 4%)	C:H	Bi:C (± 0.05)
5	2.90	0.55	81.41	1:2.29	1:0.62
30	3.28	0.57	85.94	1:2.09	1:0.67
60	3.67	0.60	88.18	1:1.96	1:0.73
120	3.60	0.59	84.37	1:1.97	1:0.74

[1]This work was performed in the Department of Chemistry, University of Auckland, Auckland, New Zealand.

Can. J. Chem. Downloaded from www.nrcresearchpress.com by 210.87.254.5 on 09/05/12
For personal use only.

The only gaseous product appeared to be a small amount of an unsaturated hydrocarbon.

In the earlier investigation of this reaction (6), the only ethyl containing solid product at 25 °C was EtOBiO, with Bi:C = 1:2 and C:H = 2.50, where the corresponding ratios obtained in this work are approximately 1:0.7 and 1:2.0, respectively (with the exception of the product of 5 min reaction), suggesting that intact ethyl groups are not generally present in the product. Mixture of sufficient Bi_2O_3 with EtOBiO would depress the Bi:C ratio to the observed figure but would not affect the C:H ratio.

Since inhibition of the reaction by diphenylamine indicates that a radical reaction does occur, and as traces of peroxide and a compound with a higher C:H ratio than 1:2 are found in a sample of the solid reaction product isolated after the reaction had proceeded for 5 min it is thought that a short-lived peroxide $Et_2BiOOEt$ is probably formed initially. Fission of the Et_3Bi into radicals, attachment of oxygen to form peroxy-radicals and abstraction by them of an ethyl group from another Et_3Bi molecule would achieve this. Homolytic fission of the peroxide to produce EtO· and Et_2BiO· radicals is likely, with the radicals then abstracting either hydrogen or ethyl groups from further Et_3Bi molecules to produce ethanol and further radicals to continue the chain. Chain termination reactions involving EtO· and Et· radicals can account for the formation of diethyl peroxide, diethyl ether, and possibly acetaldehyde, though the latter may arise directly from the peroxide.

$$Et_2BiOOEt \rightarrow Et_2BiOH + MeCHO$$

A similar scheme has been proposed in the gas-phase autoxidation of triethylindium (3); there seems little reason why this should not occur in solution provided that the solvent is not involved.

As the micro-analyses indicate few intact ethyl groups in the final product (C:H $\approx$ 1:2.0) it is suggested that this product is a compound similar to Bi_2O_3 but with some of its oxygen atoms replaced by $-CH_2CH_2-$ or $\rangle CH-CH_3$ groups and that this product eventually arises from $Et_2BiCH_2\dot{C}H_2$ or $Et_2Bi\dot{C}HCH_3$ radicals produced by hydrogen abstraction from an Et_3Bi molecule.[2] Since each Et_3Bi molecule reacts with 1.5 oxygen molecules the overall scheme might be represented by

$$2Et_3Bi + 3O_2 \rightarrow Bi_2O_{3/2}(C_2H_4)_{3/2} + 3EtOH + \tfrac{3}{2}CH_3CHO$$

also accounting for the fact that ethanol and acetaldehyde are the major liquid products.

Anal. Calcd. for $Bi_2O_{3/2}(C_2H_4)_{3/2}$: C, 7.44; H, 1.25; O, 4.96; Bi, 86.35; C:H = 1:2.0, and Bi:C = 1:1.5.

It is likely though that Bi_2O_3 is also a product (*cf.* ref. 6), and a mixture of Bi_2O_3 and the proposed product in, for example, a 1:1 ratio would give a solid of composition C, 3.79; H, 0.64; O, 7.58; Bi, 87.99; C:H = 1:2.0, and Bi:C = 1:0.75. These figures are reasonably close to those found in the microanalysis and suggest that such a scheme as proposed may occur.

To elucidate this mechanism further requires considerably more evidence of both kinetic and spectroscopic nature. This paper represents only an effort to suggest a reasonable mechanism based on a small amount of experimental evidence.

Experimental

Preparations

Triethylbismuth was prepared from ethylmagnesium bromide and bismuth trichloride as described by Gilman and Nelson (7). A yield of 22% was obtained. The method of transfer of the alkyl into sealed glass capsules, and other aspects of its handling in an oxygen-free atmosphere have been described by Abraham and Davies (10, and other papers in this series) for other inflammable alkyls.

Diethyl peroxide was prepared as described by Baeyer and Villiger (9). The fraction boiling at 55–75° was collected and purified as described. Gas–liquid chromatography showed two peaks, one of which corresponded to that obtained from pure diethyl ether; the other was assumed to be diethyl peroxide.

Analyses

The original preparation was found to contain 70 ± 4% triethylbismuth, the remainder being a solid believed to be Bi_2O_3. To remove the impurities before use, a capsule was broken under cyclohexane in a small nitrogen-filled vessel fitted with a self-sealing cap. The im-

[2]A referee has suggested that the acetic acid formed in the oxidation may be incorporated in the solid and that this possibility, together with the two outlined above, could probably be distinguished by n.m.r. Unfortunately in the author's present circumstances it is not possible to obtain further samples of the product in order to clarify this point.

purities were allowed to settle and an aliquot of the alkyl in cyclohexane withdrawn and introduced into the reaction vessel as described later. A similar aliquot was allowed to oxidize in air, the bismuth determined, and from this figure was found the amount of alkyl used and its purity (98 ± 4%). In all cases, including product analyses, the bismuth determination was made by the EDTA titration method of Cheng (8).

Peroxidic oxygen was measured by titration of the iodine liberated by the oxidation product from a solution of sodium iodide in isopropanol (11).

Liquid products were examined on a "Pye Panchromatograph" gas–liquid chromatography unit operating at ambient temperature. Columns of silicone oil (5 ft × 5 mm) and dinonyl phthalate (5 ft × 5 mm and 7 ft × 5 mm) were used with nitrogen as the carrier gas. Compounds were identified by comparison with retention times of standards, the result from the silicone oil and one of the DNP columns having to agree before an identification was confirmed.

Gases were examined with an Orsat's gas analysis apparatus, using acid mercuric sulfate and acid chromous chloride solutions as absorbents for unsaturated hydrocarbons and oxygen, respectively.

Autoxidations

The general method was as described by Abraham and Davies (10) except that the flask and swan-neck adaptor was replaced by a water-jacketed reaction vessel carrying a side arm with a self-sealing rubber cap. Aliquots of the alkyl in cyclohexane were injected through this after being withdrawn from the smaller vessel described earlier.

All oxidations were carried out at 25 °C using B.D.H. "Special for Spectroscopy" Grade cyclohexane as solvent. When diphenylamine was used as an inhibitor the required amount was dissolved in the solvent prior to introduction of the alkyl.

The interest and advice of Dr. J. E. Packer in this work is gratefully acknowledged. Microanalyses were performed by the Microanalytical Service of the University of Otago.

1. (*a*) G. E. Coates, M. L. H. Green, and K. Wade. Organometallic compounds. Methuen, London. 1967. (*b*) A. G. Davies. Organic peroxides. Butterworths, London. 1961.
2. S. A. Buckler. J. Am. Chem. Soc. **84**, 3093 (1962).
3. C. F. Cullis, A. Fish, and R. T. Pollard. Trans. Faraday Soc. **60**, 2224 (1964).
4. A. G. Davies and B. P. Roberts. J. Chem. Soc 17 (1967).
5. A. G. Davies and B. P. Roberts. J. Chem. Soc. 1074 (1968).
6. G. Calingaert, H. Soroos, and V. F. Hnizda. J. Am. Chem. Soc. **64**, 392 (1942).
7. H. Gilman and J. F. Nelson. J. Am. Chem. Soc. **59**, 935 (1937).
8. K. L. Cheng. Anal. Chem. 26, 1978 (1954).
9. A. Baeyer and V. Villiger. Chem. Ber. **33**, 3387 (1900).
10. M. H. Abraham and A. G. Davies. J. Chem. Soc. 429 (1959).
11. A. G. Davies and J. E. Packer. J. Chem. Soc. 3164 (1959).

Can. J. Chem. Downloaded from www.nrcresearchpress.com by 210.87.254.5 on 09/05/12
For personal use only.

Can. J. Chem. Downloaded from www.nrcresearchpress.com by 210.87.254.5 on 09/05/12
For personal use only.

Cobalt(II) Complexes of Isothiazole

R. RIVEST AND A. WEISZ
Département de Chimie, Université de Montréal, Montréal, Québec

Received August 25, 1970

The preparation and spectral properties are reported for complexes of CoX_2 (X = Cl, Br, I) and $Co(ClO_4)_2$ with isothiazole (L). The following complexes have been prepared: CoL_2X_2, CoL_4X_2, and $CoL_6(ClO_4)_2$. In the solid state, CoL_2X_2 (X = Br, Cl) are octahedral and polymeric, CoL_4X_2 (X = Br, Cl) are octahedral, CoL_2I_2 is tetrahedral, $[CoL_6](ClO_4)_2$ is octahedral. Except for $[CoL_6](ClO_4)_2$ which remains octahedral, all the other complexes give solutions in which Co(II) has a tetrahedral environment. In all the complexes, the ligand L is N-bonded to cobalt(II).

Ce mémoire décrit la préparation et les propriétés spectrales des complexes de CoX_2 (X = Cl, Br, I) et de $Co(ClO_4)_2$ avec le ligand isothiazole (L). Les complexes suivants ont été préparés: CoL_2X_2, CoL_4X_2 et $[CoL_6](ClO_4)_2$. A l'état solide, CoL_2X_2 (X = Br, Cl) sont octaédriques et polymériques, CoL_4X_2 (X = Br, Cl) sont octaédriques, CoL_2I_2 est tétraédrique et $[CoL_6](ClO_4)_2$ est octaédrique. A l'exception de $[CoL_6](ClO_4)_2$ qui reste octaédrique en solution, tous les autres complexes donnent des solutions dans lesquelles Co(II) a un environnement tétraédrique. Dans tous les complexes, le ligand L est lié au cobalt par l'azote.

Canadian Journal of Chemistry, 49, 1750 (1971)

Introduction

Thiazole in which the two donor atoms nitrogen and sulfur are separated by $—CH_2—$, has been reported to form N-bonded complexes with $CoCl_2$ (1). It was thought interesting to see if isothiazole (L) in which nitrogen and sulfur are neighboring atoms would have the same ligand properties. This was extended to other cobalt(II) salts to see if the anion has some influence on the type of complexes formed.

Experimental

Materials and Manipulations

Cobalt(II) halides and hexaquacobalt(II) perchlorate were obtained from Alfa Inorganics, isothiazole from Raylo Chemicals Ltd. and used as such.

For spectral work and conductivity measurements, Fisher spectro-analyzed nitromethane was used without further purification. All manipulations were performed in a dry box flushed with dry nitrogen. Unless otherwise stated all compounds were dried *in vacuo*, for 15 min at room temperature.

Preparation of the Complexes

CoL_2X_2 (X = Cl, Br, or I)

Anhydrous cobalt(II) halide (10 mmol) was dissolved in the minimum volume of hot absolute ethanol and added to an ethanolic solution of isothiazole (20 mmol). The chloride and bromide complexes precipitated on standing overnight, were filtered off and washed with ethanol and *n*-hexane. For the iodo-complex, 75% of the ethanol was evaporated and then *n*-hexane was added. After standing for a few days small green crystals were formed. These were filtered off and washed with *n*-hexane. These preparations can equally be performed in acetone.

CoL_4X_2 (X = Cl, Br)

Isothiazole (90 mmol) was added to a suspension of anhydrous cobalt(II) halide (3 mmol) in *n*-hexane. After standing overnight the products were filtered off, washed with *n*-hexane, and dried by suction under dry nitrogen for 10 min only. Drying under dry nitrogen and for a shorter length of time was necessary since preliminary experiments had shown that part of the ligand was lost if the drying was done under vacuum for 15 min.

CoL_4I_2

Isothiazole (90 mmol) was added to a suspension of anhydrous cobalt(II) iodide (3 mmol) in *n*-hexane. After standing for a week, the compound was filtered off and washed with *n*-hexane containing isothiazole to avoid exposure to dry nitrogen; only a very short drying time was therefore possible. If the yellow green iodo-complex is exposed to dry nitrogen, the color instantaneously turns to dark green indicating a partial decomposition. Then, it was not possible to prepare small samples for complete analysis on a micro-scale but by using a large sample, we could determine the iodine content. The storage of the iodo-complex is only possible in sealed containers.

$[CoL_6](ClO_4)_2$

To a solution of 15 mmol of $[Co(H_2O)_6](ClO_4)_2$ in 10 ml acetone and 25 ml dimethoxy propane (for dehydration) (2) an excess of isothiazole (263 mmol) was added; pink crystals immediately separated, which were washed once with acetone and twice with *n*-hexane.

Analysis

C, H, N, S, Co, and halogen analysis were made by Galbraith Lab. Inc., Knoxville, Tennessee. Only the iodide determination of CoL_4I_2 was carried out via titration with 0.1 *N* silver nitrate solution in the presence of K_2CrO_4 as indicator. The analytical results are included in Table 1.

Can. J. Chem. Downloaded from www.nrcresearchpress.com by 210.87.254.5 on 09/05/12
For personal use only.

TABLE 1. Analytical results and magnetic moment

		Analysis (%)												
		Cobalt		Halogen		Carbon		Hydrogen		Nitrogen		Sulfur		
Complex	Color	Calcd.	Found	Calcd.	Found	Calcd.	Found	Calcd.	Found	Calcd.	Found	Calcd.	Found	μ (B.M.)
CoL_2Cl_2	Violet	19.64	19.45	23.63	23.91	24.01	24.09	2.02	1.81	9.33	9.17	21.36	21.04	5.04
CoL_2Br_2	Violet	15.15	14.98	41.08	40.99	18.52	18.74	1.55	1.78	7.20	7.03	16.48	16.23	5.19
CoL_2I_2	Green	12.20	12.42	52.55	51.38	14.92	14.33	1.25	1.26	5.80	5.51	13.28	12.93	4.6
CoL_4Cl_2	Pink	12.53	12.50	15.07	15.33	30.64	30.64	2.57	2.58	11.91	12.08	27.27	26.71	5.12
CoL_4Br_2	Pink-violet	10.54	10.39	28.57	29.03	25.77	25.77	2.17	2.25	10.92	9.81	22.93	22.03	5.28
CoL_4I_2*	Yellow-green			38.85	39.9									4.90
$[CoL_6][ClO_4]_2$	Pink	7.66	7.48	9.23	9.50	28.13	28.25	2.36	2.50	10.93	10.73	25.03	24.69	4.99

*The high iodide content is due to the loss of ligand by exposure to air.

TABLE 2. Electronic spectral data in kK.† Diffuse reflectance and solution spectra in nitromethane

Complexes	Color	R or S*	Visible range	Near infrared range
CoL_2Cl_2	Violet	R	18.87; 17.76; 16.31	
	Blue	S	17.24(330); 16.31(445); 15.67(405); 14.99 sh	9.08(26); 7.10 br(44); 6.25(43)
CoL_2Br_2	Violet	R	19.23 sh; 18.32; 17.24 sh; 15.34	
		S	16.75(350); 15.67(550); 15.34(580)	8.80(34); 6.73(72); 5.85(53)
CoL_2I_2	Green	R	16.00; 15.27; 14.49	
	Green	S	15.92(350); 15.20(560); 14.49(600); 13.70 sh(380)	8.62(55); 6.63(82); 5.98 sh(50)
CoL_4Cl_2	Pink	R	19.61 sh, br; 18.87; 17.92	
	Blue	S	17.24(340); 16.31(450); 15.67(410); 14.99 sh(320)	9.08(26); 7.10 br(44); 6.25 sh(43)
CoL_4Br_2	Pink-Violet	R	19.23; 18.32; 17.09 sh; 15.34	
	Blue	S	16.75(340); 15.67(540); 15.34(570)	8.80(54); 6.82(72); 5.85(53)
CoL_4I_2	Yellow-green‡	R	16.05; 15.27; 14.49	
	Green	S	15.92 sh(350); 15.20(560); 14.49(600); 13.70 sh(380)	8.62(55); 6.63(82); 5.98 sh(50)
$[CoL_6](ClO_4)_2$	Pink	R	20.20; 18.76 sh	
	Pink	S	20.20(26); 18.75 sh	9.17(8)

*R = reflectance; S = solution.
†Molar extinction coefficients given in parentheses; sh = shoulder; br = broad.
‡The color turned to dark green during the recording of the spectrum.

Physical Measurements

Infrared spectra were recorded as Nujol mulls between polyethylene sheets or NaCl plates using Perkin–Elmer 621. Electronic spectra were obtained on a Cary 14 spectrophotometer between 25 and 5 kK for solutions. For solids, the same spectrometer was fitted with a reflectance attachment using $MgCO_3$ as reference and covered the range 25 to 12.5 kK. Magnetic measurements were made at room temperature on a Gouy balance. As a calibrant $Hg[Co(CNS)_4]$ (3) was used. The diamagnetic corrections were estimated by the method outlined by Figgis and Lewis (4). The electrolytic conductance measurements were made with a Radiometer direct-reading conductivity meter type CDM, 2d, No. 47477 and the Radiometer conductivity cell type CDC 104.

Result and Discussion

Electronic Spectra

The diffuse reflectance spectra of CoL_2X_2 complexes (Table 2) (X = Cl, Br) are similar to those of the previously prepared Co(II) complexes of pyridine (5, 6), thiazole (1), and 3-Br-pyridine (7) which are all showing a polymeric structure (8). We are therefore suggesting the same band assignment and the same structure for the CoL_2X_2 complexes.

The reflectance spectra of both CoL_4Cl_2 and CoL_4Br_2 are very similar to the respective CoL_2X_2 spectra, the only difference being for CoL_4Cl_2 a little shifting of the higher frequencies and the appearance of a shoulder at 16.5 kK, and for CoL_4Br_2 a broadening of the band at 15.34 kK. This is suggesting that in the solid state these complexes are octahedral.

The CoL_2X_2 and the CoL_4X_2 complexes dissolve in nitromethane to give blue solutions well known for tetrahedral cobalt(II) complexes (9, 10).

The behavior of CoL_2I_2 is quite different. Its reflectance spectrum with an intense band between 14.5 and 16.0 kK suggests a tetrahedral stereochemistry. The reflectance spectrum of CoL_4I_2 shows no difference with the spectrum CoL_2I_2. It is worth mentioning that, after recording, the sample of CoL_4I_2 shows the same green color as the complex CoL_2I_2 thus indicating that during the recording, a decomposition into CoL_2I_2 and the ligand occurs. Both iodo-complexes give green solutions in nitromethane having identical spectra which are also identical to their reflectance spectra and very similar to the spectrum of $Co(pyridine)_2I_2$ (9). This and the high molecular extinction coefficient indicates a tetrahedral stereochemistry.

For $CoL_6(ClO_4)_2$ there are no differences between the reflectance spectrum and the solution spectrum in nitromethane as solvent. The band at 20.2 kK can be assigned to $^4T_1(F) \rightarrow {}^4A_2$, at 18.75 kK to $^4T_1(F) \rightarrow {}^4T_1(P)$ and at 9.17 kK to $^4T_1(F) \rightarrow {}^4T_2$ for an octahedral environment. Nitromethane is the only suitable solvent since the more polar solvents react with the complex

Can. J. Chem. Downloaded from www.nrcresearchpress.com by 210.87.254.5 on 09/05/12
For personal use only.

TABLE 3. Infrared spectra (600–200 cm^{-1}) of cobalt(II) compounds with isothiazole*

Species	Infrared spectra (cm^{-1})				
L	590 s	478 s	—	—	—
CoL_2Cl_2	590 sh 585 s	478 s	250 sh	235 mbr	215 mbr
CoL_2Br_2	585 sh 580 s	472 s	250 sh	215–230 mbr	205 br
CoL_2I_2	580 s	472 s	250 sh	232 m	220 m
CoL_4Cl_2	585 s	475 s	255 sh	230 mbr	—
CoL_4Br_2	585 s	475 s	—	225 w	210 mbr
CoL_4I_2	585 s	480 s	255 sh	230 m	210 mbr
$CoL_6(ClO_4)_2$	585 s	478 s	250 sh	210–230 mbr	200 mbr

*s = strong; sh = shoulder; m = medium; br = broad.

and the non polar organic solvents give solutions too dilute to permit spectral measurements.

Magnetic and Conductance Studies

The magnetic susceptibility data (Table 1) of the complexes fall, with the exception of the iodide complexes within the normal range for octahedral complexes of cobalt(II) (4.8–5.2 B.M.) (11). The magnetic moment of CoL_2I_2 is in the range usually found for tetrahedral species (4.4–4.8 B.M.) (11). This definitely supports the tetrahedral stereochemistry of this complex as found by spectral studies. The moment of CoL_4I_2 (4.9 B.M.) is in the range of octahedral complexes. This may indicate that the size of the sample is such that the decomposition into $CoL_2I_2 + 2L$ is less important here than it is for the samples used to measure the reflectance spectrum.

The spectral studies have indicated that the dissolution of the halogeno-complexes changes their structure, all the solutions containing the tetrahedral blue Co(II) species. The conductance measurements on these complexes indicate that they are non-electrolytes. The perchlorate complex has a conductance value of 172 cm^2 mho/mol which indicates that it is a 1:2 electrolyte.

Infrared Spectra

The infrared spectra covering the range 600–200 cm^{-1} are given in Table 3. The spectrum of the complexes for the whole range 4000–200 cm^{-1} was recorded but for the region above 600 cm^{-1} they were essentially the same as the one of the pure ligand reported recently (12), except for an increase in ring vibrations and for the splitting of these vibrations on coordination. The far i.r. spectra of all complexes are all similar and consist of poorly resolved bands in the 200–260 cm^{-1} region. Since essentially the same bands are observed in this region for the perchlorate and all the halogeno-complexes, it is assumed that one of these bands is due to the Co—L stretching vibration. Exactly the same results were found by Clark and Williams (13) who investigated the violet $Co(pyridine)_2Cl_2$. In addition Goldstein and Unsworth (14) reported that in the case of the violet $Co(pyridine)_2Cl_2$ the ν(M—X) frequencies are below 200 cm^{-1} even for chlorine, and that the bands above 200 cm^{-1} are more clearly attributable to ν(M—N).

The similarity of the electronic and i.r. spectra to those of similar complexes with N-coordinated heterocyclic ligands *e.g.* pyridine (9), halogenopyridines (8), suggests that coordination is probably through nitrogen rather than through sulfur. Thiazole, benzothiazole, 2-methyl and 2-chlorobenzothiazole, 2-aminobenzothiazole (15–19) have all been reported to form N-coordinated complexes with cobalt(II).

We gratefully acknowledge the financial support of the National Research Council of Canada.

1. W. J. EILBECK, F. HOLMES, and A. E. UNDERHILL. J. Chem. Soc. A, 757 (1967).
2. K. STARKE. J. Inorg. Nucl. Chem. **11**, 77 (1959).
3. B. N. FIGGIS and R. S. NYHOLM. J. Chem. Soc. 4190 (1958).
4. B. N. FIGGIS and J. LEWIS. Modern coordination chemistry. *Edited by* J. Lewis and R. C. Wilkins. Interscience Publishers, Inc., New York. 1960. p. 403.
5. L. I. KATZIN and E. GEBERT. J. Am. Chem. Soc. **75**, 2830 (1953).
6. J. FERGUSON. J. Chem. Phys. **32**, 528 (1960).
7. D. E. BILLING and A. E. UNDERHILL. J. Chem. Soc. A, 29 (1968).
8. J. D. DUNITZ. Acta Cryst. **10**, 307 (1957).

Can. J. Chem. Downloaded from www.nrcresearchpress.com by 210.87.254.5 on 09/05/12
For personal use only.

9. N. S. GILL, R. S. NYHOLM, G. A. BARCLAY, T. I. CHRISTIE, and P. J. PAULING. J. Inorg. Nucl. Chem. **18**, 88 (1961).
10. A. B. P. LEVER and S. M. NELSON. J. Chem. Soc. A, 859 (1966).
11. B. N. FIGGIS and R. S. NYHOLM. J. Chem. Soc. 12 (1954); 338 (1959). B. N. FIGGIS and J. LEWIS. Prog. Inorg. Chem. **6**, 37 (1964).
12. S. CALIFANO, P. PIACENTI, and G. SBRANA. Spectrochim. Acta, **20**, 339 (1964).
13. R. J. H. CLARK and CH. S. WILLIAMS. Inorg. Chem. **3**, 350 (1965).
14. M. GOLDSTEIN and W. D. UNSWORTH. Inorg. Nucl. Chem. Lett. **6**, 25 (1970).
15. E. J. DUFF, M. N. HUGUES, and K. J. RUTT. J. Chem. Soc. A, 2354 (1968); 2101 (1969); 2126 (1969).
16. M. GOODGAME and M. J. WEEKS. J. Chem. Soc. A, 1156 (1966).
17. M. J. M. CAMPBELL, D. W. CARD, R. GRZESKOWIAK, and M. GOLDSTEIN. J. Chem. Soc. A, 672 (1970).
18. N. N. Y. CHAN, M. GOODGAME, and M. J. WEEKS. J. Chem. Soc. A, 2499 (1968).
19. J. A. WEAVER, P. HAMBRIGHT, P. T. TALBERT, E. KANG, and A. N. THORPE. Inorg. Chem. **9**, 268 (1970).

Can. J. Chem. Downloaded from www.nrcresearchpress.com by 210.87.254.5 on 09/05/12
For personal use only.

Nuclear Magnetic Resonance Evidence Concerning the Effect of Remote Polar Substituents upon Conformational Equilibrium in Substituted Ethanes

G. K. HAMER, W. F. REYNOLDS, AND D. J. WOOD
Department of Chemistry, University of Toronto, Toronto 5, Ontario

Received November 12, 1970

The vicinal coupling constants of 1-(4-X-phenyl)-1,2-dibromoethanes vary with substituent. The coupling constants correlate with parameters which measure the polarity of the C—X bond. It is concluded that the observed changes in coupling constants with substituent are due to electrostatic interactions between the C—X and C_2—Br bonds. Two different types of electrostatic calculations confirm that this interaction should stabilize the rotamers in which the phenyl and C_2—Br groups are in a *gauche* orientation when the C—X group has polarity $C^{\delta+}$—$X^{\delta-}$.

Les constantes de couplage vicinales des (X-4 phényl)-1 dibromo-1,2 éthanes varient avec le substituant X. Les constantes de couplage varient linéairement avec les paramètres qui mesurent la polarité des liens C—X. On en conclue que les changements observés dans les constantes de couplage en fonction du substituant sont dus à des intéractions électrostatiques entre les liens C—X et C_2—Br. Deux types de calculs électrostatiques ont permis de confirmer que cette intéraction devrait stabiliser les rotamères dans lesquels les groupes phényle et C_2—Br prennent une orientation *gauche* si la polarité du groupe C—X est $C^{\delta+}$—$X^{\delta-}$.

Canadian Journal of Chemistry, 49, 1755 (1971)

Introduction

It is well established that electrostatic interactions between polar groups can affect conformational equilibria in both substituted ethanes and cyclohexane derivatives (1–5). However, it is often difficult to separate electrostatic or dipolar interactions from steric interactions. We have determined the n.m.r. spectra of a series of eight compounds of the type 1-(4-X-phenyl)-1,2-dibromoethane where X is a substituent. These compounds are useful for determining the importance of electrostatic interactions since (*1*) a substituent in the 4 position should not alter the steric interaction of the phenyl group with other substituents and (*2*) the position of the remote dipole is well defined and is independent of rotation about the C–phenyl bond. In this note we present evidence that electrostatic interactions cause predictable changes in conformational equilibrium for the above-mentioned compounds.

Experimental

1-(4-X-phenyl)-1,2-dibromoethanes were prepared by the bromination of the corresponding 4-substituted styrenes in methylene chloride. Products were recrystallized from methanol–water and purities were checked by n.m.r. spectroscopy.

Spectra were recorded on a Varian HA-100 operating in frequency sweep mode at a probe temperature of 30°. Procedures used were identical to those previously described (6).

Results and Discussion

The ABC spectra of the substituted ethyl groups were analyzed by the exact method (7). Results are given in Table 1. Some of the data were taken from a previous publication (6). In the cases where the r.m.s. error between measured and calculated line positions exceeded 0.03 Hz these data have been redetermined. It is difficult to estimate the accuracy of the coupling constants since they do not correspond to first order splittings. We believe that a reasonable error limit is 0.05 Hz. The greatest uncertainties occur for compounds with relatively non-polar substituents since in these systems, one of the AB quartets in each ABC system is nearly collapsed to a singlet, reducing the number of measurable lines.

It is obvious from the data presented in Table 1 that there is a variation of the vicinal coupling constants J_{AC} and J_{BC} which is well in excess of

TABLE 1. Coupling constants (in Hz) and chemical shifts (in p.p.m. to low field of tetramethylsilane) for 1-(4-X-phenyl)-1,2-dibromoethane derivatives*

Substituent	F	J_{AB}	J_{AC}	J_{BC}	δ_A	δ_B	δ_C	Root mean square†
$C(CH_3)_3$‡	−0.104	−10.16	10.95	5.06	3.950	4.007	5.060	0.01
CH_3‡	−0.052	−10.13	11.13	5.00	3.933	3.998	5.034	0.01
H§	0	−10.12	11.07	5.00	3.950	4.015	5.055	0.02
OCH_3‡	0.413	−10.15	11.27	4.86	3.937	4.011	5.064	0.01
F‡	0.708	−10.23	11.35	4.83	3.909	4.022	5.052	0.01
Cl‡	0.690	−10.24	11.39	4.79	3.906	4.013	5.030	0.03
Br‡	0.727	−10.26	11.33	4.83	3.902	4.007	5.015	0.01
NO_2§	1.109	−10.38	11.52	4.74	3.962	4.069	5.134	0.02

*All solutions 0.30 M in CCl_4 with approximately 5% added tetramethylsilane.
†Root mean square error (in Hz) between calculated and experimental peak positions.
‡This work.
§Reference 6.

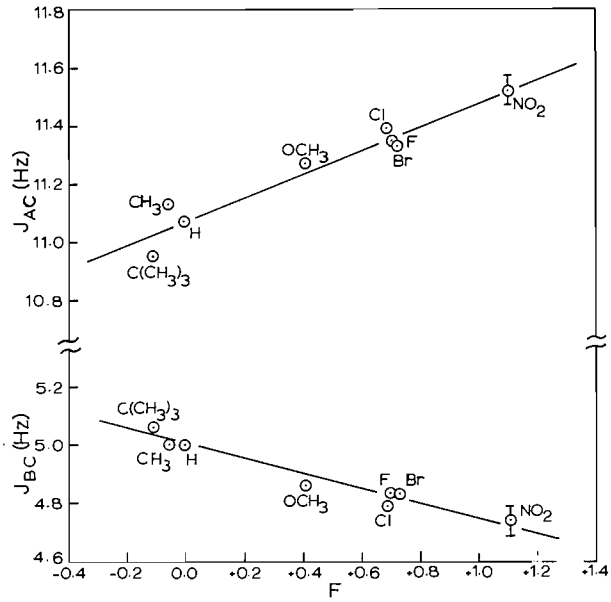

FIG. 1. Plot of vicinal coupling constants for 1-(4-X-phenyl)-1,2-dibromoethane derivatives *vs.* substituent parameter F. Estimated uncertainties in coupling constants are included for nitro derivative.

the experimental error in measuring the coupling constants. It is unlikely that this variation is due to changes in coupling constants of the individual rotational isomers (rotamers) with substituent. The *cis* and *trans* coupling constants of the corresponding 4-substituted styrenes are constant within experimental error (8). Similarly, the vicinal coupling constants of 4-X-phenylhexachloro[2.2.1]heptene derivatives (these compounds roughly correspond to our compounds frozen in an eclipsed conformation) do not vary with substituent (9). The vicinal coupling constants for the parent compound and the nitro derivative have been shown to be nearly concentration independent (6). Consequently, it is highly improbable that the observed variation in coupling constants is due to concentration effects. We believe that the observed changes in coupling constants are due to changes in rotamer populations.[1]

[1]The variation of J_{AB} with substituent may also reflect conformational changes. However, the observed variation may, in part, reflect substituent effects upon individual coupling constants since the corresponding geminal coupling constant in 4-substituted styrenes varies markedly with substituent. It is difficult to separate the two possible effects but they probably both contribute to the variation in J_{AB}.

Changes in rotamer populations with substituent cannot reflect steric interactions since H and *t*-butyl derivatives have similar coupling constants. We believe that they reflect electrostatic interactions between the remote dipolar substituent and the C_2—Br bond (interactions between the substituent and the C_1—Br bond should be essentially equal in all rotamers). In an attempt to confirm this, we have plotted J_{AC} and J_{BC} *vs.* the substituent parameter F (see Fig. 1). Parameter F is a pure field effect substituent parameter derived by Swain and Lupton (the companion parameter R is a measure of resonance interactions) (10). Since F measures the field effect of a substituent, it should be proportional to the polarity of the C—X bond. Therefore, the good correlation of F with J_{AC} (correlation coefficient, $r = 0.966$) and J_{BC} ($r = 0.976$) strongly suggests that the variation of J_{AC} and J_{BC} with substituent has an electrostatic origin. A good correlation also exists between coupling constants and the bond dipole moments (11) of the substituents ($r = 0.949$, 0.943).[2] There is no correlation between coupling constants and R ($r = 0.083$, 0.013).

The three possible rotamers for 1-phenyl-1,2-dibromoethane derivatives are shown in Fig. 2. It is known that the order of energy levels for the parent compound is $E_1 < E_2 \ll E_3$ (6, 12). J_{AC} is a *trans* coupling constant in rotamer **1** while J_{BC} is a *gauche* coupling constant, confirming the assignment $J_{AC} > J_{BC}$ given in Table 1. Since J_{AC} increases and J_{BC} decreases when H is replaced by an electron-withdrawing substituent, the population of rotamer **1** must increase when the latter group has polarity $C^{\delta+}$—$X^{\delta-}$, *i.e.* the interaction between C_2—Br and $C^{\delta+}$—$X^{\delta-}$ groups in rotamer **1** must be relatively stabilizing. We originally rejected the present explanation on the naive grounds that this interaction should destabilize rotamer **1** relative to rotamer **2** (6). While this would be true if X were bonded directly to C-1, it is not true when it is bonded to a more remote carbon. This can be shown in two ways. The C—X and C_2—Br dipoles can be represented as separated charges calculated from the group dipole moments. For example, consider the 4-bromo derivative. The distance between the remote polar group and C-2 is independent of rotation angle. Therefore, electrostatic interactions involving C-2 are equal in all rotamers and need not be considered in a calculation of relative energies. The distances of the two ends of the remote polar group from bromine for *gauche* (rotamer **1**) and *trans* (rotamer **2**) conformations are shown in Fig. 3 (assuming normal bond lengths (13) and tetrahedral bond angles). Assuming a dipole moment of 2.03 D for each group,[3] the calculated energy of interaction is -0.35×10^{-13} ergs/molecule or -0.50 kcal/mol for rotamer **2** and -0.55×10^{-13} ergs/molecule or -0.79 kcal/mol for rotamer **1**. Therefore, rotamer **1** is predicted to be stabilized relative to rotamer **2** by 0.29 kcal/mol due to a remote C—Br bond at the 4 position of the phenyl group. A similar approach has been used by Wood *et al.* (4) to account for the stability of 1,4 dipolar cyclohexane derivatives.

Alternately one could calculate the energy of interaction between the groups as an interaction between two point dipoles acting half way along the bonds, following the method of Allinger and Allinger (3). In this case the predicted relative stabilization is 0.27 kcal/mol, in very good agree-

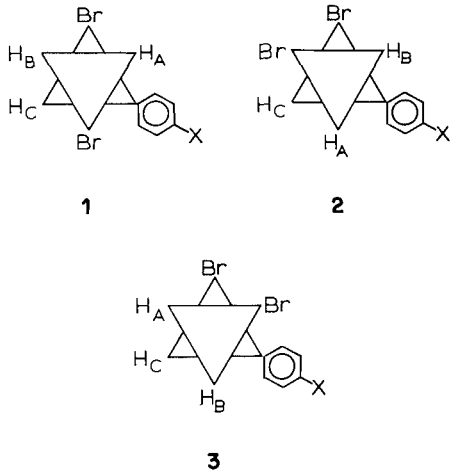

FIG. 2. Possible staggered rotamers for 1-(4-X-phenyl)-1,2-dibromoethane derivatives (looking along C_2—C_1 bond).

[2]The F value was chosen for the primary correlation due to the variety of bond dipole moments quoted in the literature.

[3]The actual numbers would be slightly altered if one used bond dipole moments in place of group dipole moments or assumed different Br–alkyl and Br–aryl moments. The predicted stabilization of rotamer **1** would be slightly less if one assumed an angle of 65–70° between phenyl and bromine instead of 60°. However, none of these changes would alter the basic conclusion. Similarly, calculated energies are positive if interactions involving C-2 are included but rotamer **2** is destabilized relative to rotamer **1** by 0.29 kcal/mol.

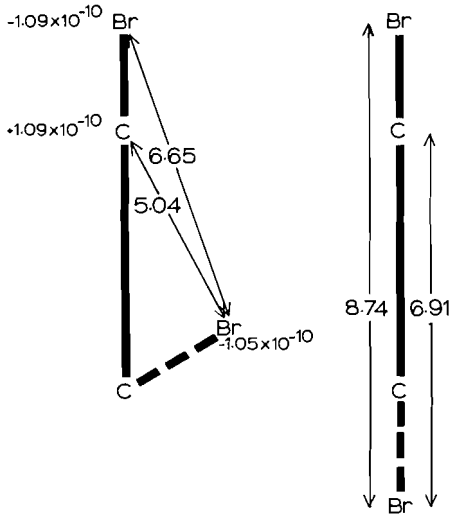

FIG. 3. Distances (Å) of remote polar group from bromine attached to C-2 in *gauche* and *trans* orientations and separated charges (e.s.u.) for polar groups based upon a C—Br dipole moment of 2.03 D and Br–alkyl and Br–aryl bond lengths of 1.94 and 1.86 Å respectively (looking along C_1—C_2 bond).

ment with the previous calculation. If one assigns an effective dielectric constant of 2.0 for the molecular cavity (3), all calculated interactions will be halved. Replacement of a $C^{\delta+}$—$X^{\delta-}$ group by one of polarity $C^{\delta-}$—$X^{\delta+}$ leads to a relative destabilization of rotamer **1**.

Rotamer **3** should also be stabilized relative to rotamer **2** by a $C^{\delta+}$—$X^{\delta-}$ group. However, since the former is by far the least stable rotamer (6, 12), its fractional population should remain negligibly small and the main effect of a remote dipolar group will be to change the relative populations of rotamers **1** and **2**. Precise solution rotamer energy differences and coupling constants for the individual rotamers of the parent compound are unknown. Consequently, it is impossible to precisely determine the expected variation of J_{AC} and J_{BC} with substituent. However, our calculations do show that the variation is in the correct direction, and a variation of 0.2 to 0.4 Hz for a change in energy difference of 0.1 to 0.3 kcal/mol does not seem unreasonable. Furthermore, the variation of J_{AC} and J_{BC} with substituent is generally less in dimethylsulfoxide than in carbon tetrachloride (6). This would be expected since the polar solvent should solvate the remote dipole, reducing its effect. These observations, along with the good correlation of J_{AC} and J_{BC} with parameters which measure the polarity of the C—X bond suggest to us that there is a small but predictable variation of conformational equilibrium in 1-(4-X-phenyl)-1,2-dibromoethanes due to electrostatic interactions involving the remote polar substituent.

Financial support from the National Research Council of Canada is gratefully acknowledged.

1. S. MIZUSHIMA. Structure of molecules and internal rotation. Academic Press, Inc., New York, N.Y. 1954.
2. E. L. ELIEL, N. L. ALLINGER, S. J. ANGYAL, and G. A. MORRISON. Conformational analysis. Interscience, New York, N.Y. 1965.
3. J. ALLINGER and N. L. ALLINGER. Tetrahedron, **2**, 67 (1958).
4. G. WOOD, E. P. WOO, and M. H. MISKOW. Can. J. Chem. **47**, 429 (1969).
5. R. J. ABRAHAM and K. PARRY. J. Chem. Soc. B, 539 (1970).
6. W. F. REYNOLDS and D. J. WOOD. Can. J. Chem. **47**, 1295 (1969).
7. (*a*) S. CASTELLANO and J. S. WAUGH. J. Chem. Phys. **35**, 1900 (1961). (*b*) J. R. CAVANAUGH. J. Chem. Phys. **39**, 2378 (1963).
8. (*a*) G. K. HAMER and W. F. REYNOLDS. Can. J. Chem. **46**, 3813 (1968). (*b*) G. K. HAMER and W. F. REYNOLDS. To be published.
9. K. L. WILLIAMSON, N. C. JACOBUS, and K. J. SOUCY. J. Am. Chem. Soc. **86**, 4021 (1964).
10. C. G. SWAIN and E. C. LUPTON. J. Am. Chem. Soc. **90**, 4328 (1968).
11. L. E. SUTTON. Determination of organic structures by physical methods. Vol. 1. Academic Press, Inc., New York, N.Y., 1965. Chapt. 9.
12. M. BUZA and E. I. SNYDER. J. Am. Chem. Soc. **88**, 1165 (1966).
13. Tables of interatomic distances and configuration in molecules and ions. Chem. Soc. Special Publication 11, 1958.

1,3-Substituted Benzocycloheptanes

TERRENCE W. DOYLE
Bristol Laboratories of Canada Limited, 100 Industrial Boulevard, Candiac, Québec

Received November 3, 1970

We describe some derivatives of benzocycloheptan-1-one-3-carboxylic acid (**2**) which was obtained by reduction of benzo[6,7]cyclohepta-3,6-dien-1-one-3-carboxylic acid (**1**).

On décrit quelques dérivés de l'acide benzocycloheptanone-1 carboxylique-3 (**2**) obtenus par réduction de l'acide benzo[6,7]cycloheptadiène-3,6 one-1 carboxylique-3 (**1**).

Canadian Journal of Chemistry, 49, 1759 (1971)

Can. J. Chem. Downloaded from www.nrcresearchpress.com by 210.87.254.42 on 09/05/12
For personal use only.

Recently we reported the synthesis of benzo-[6,7]cyclohepta-3,6-dien-1-one-3-carboxylic acid (**1**) (1). We would now like to report some transformations of **1** directed at the synthesis of potentially biologically active compounds.

Reduction of **1** gave benzocycloheptan-1-one-3-carboxylic acid **2** (> 95%) which was converted to the methyl ester **3** (87%). Esterification of **1** went with enol ether formation to give methyl 1-methoxybenzo[6,7]-5-*H*-cycloheptatriene-3-carboxylate **4** (70%).

Treatment of **2** with phosphorous pentachloride gave **5** (unstable to distillation) which was readily converted to the amide **6** (45%). An excess of phosphorous pentachloride converted **2** into the trichloride 7 which gave **8** on distillation (50%). Treatment of either **7** or **8** with an excess of benzylamine gave **9** (85%).

The acid chloride **5** was converted to its azide (2) and thence to the urethane **10** through the isocyanate. Urea **11** was also isolated. The overall conversion to **10** from **2** was 57%.

Reduction of **10** with sodium borohydride gave alcohol **12** (97%) which on treatment with sodium hydride gave 9-oxa-7-azabenzo[2,3]bicyclo[4.3.1]-decan-8-one (**13**) (77%). On this basis the *cis* configuration is assigned to **12** since formation of cyclic urethane **13** from the diaxial conformer (3) would be expected to be facile whereas the *trans* isomer would cyclize only with great difficulty, if at all.

Reduction of **13** with lithium aluminum hydride gave *cis*-aminoalcohol **14**. Treatment of **10** with phenyl magnesium bromide followed by acidic work-up gave the olefin **15** rather than the desired alcohol.

Treatment of **10** with benzyl magnesium chloride gave **16** (46%) which on treatment with sodium hydride gave the cyclic urethane **17**

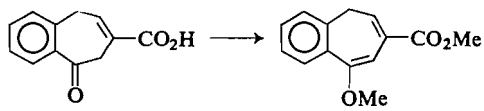

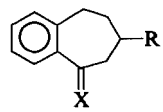

2 X = O; R = CO_2H
3 X = O; R = CO_2Me
5 X = O; R = COCl
6 X = O; R = CONHMe
7 X = Cl_2; R = COCl
10 X = O; R = $NHCO_2Et$

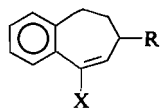

8 X = Cl; R = COCl
9 X = Cl; R = $CONHCH_2C_6H_5$
15 X = C_6H_5; R = $NHCO_2Et$

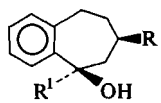

12 R = $NHCO_2Et$; R^1 = H
14 R = NHMe; R^1 = H
16 R = $NHCO_2Et$; R^1 = $CH_2C_6H_5$
19 R = NMe_2; R^1 = $CH_2C_6H_5$

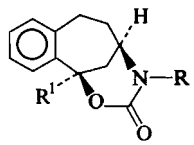

13 R = H; R^1 = H
17 R = H; R^1 = $CH_2C_6H_5$
18 R = Me; R^1 = $CH_2C_6H_5$

TABLE 1. Infrared spectra and analytical data

Compound	The i.r. spectra (cm^{-1})	Calculated (%)			Found (%)		
		C	H	N	C	H	N
2	1700, 1645, 1600*	70.58	5.88	—	70.80	5.90	—
3	1730, 1680, 1600†	71.54	6.46	—	71.33	6.47	—
4	1725, 1720, 1600†	73.03	6.13	—	72.77	6.16	—
5	1785, 1680, 1595†			‡			
6	3340, 1680§	71.86	6.96	6.45	71.81	6.90	6.46
8	1785, 1620, 1595†	59.77	4.18	—‖	60.14	4.40	—
9	3420, 1670, 1515§	73.19	5.82	4.49	73.36	5.82	4.59
10	3320, 1712, 1680, 1600	68.10	6.88	5.67	67.73	6.82	5.74
11	3390, 1680, 1670(sh), 1600§	73.38	6.42	7.45	72.93	6.38	7.49
12	3600, 3420, 3280, 1710§	67.44	7.68	5.62	67.48	7.70	5.55
13	3430(s), 3245(b) 1700§	70.91	6.44	6.89	70.47	6.47	6.68
14	2400–3100(b), 3320(b)*	63.18	7.96	6.15	62.85	8.07	6.09
15	3330, 1715	78.14	6.89	4.56	78.01	6.90	4.52
16	1695, 1685§	78.14	6.89	4.56	77.78	6.95	4.51
17	3425(s), 3240, 1700§	77.79	6.53	4.78	77.58	6.59	4.64
18	1695, 1685§	78.14	6.89	4.56	77.88	6.95	4.51
19	3400b†	72.37	7.89	4.22¶	71.98	7.83	4.19

*Nujol mull.
†Neat.
‡Not analyzed.
§In $CHCl_3$.
‖Anal. Calcd. for Cl: 29.41. Found: 28.96.
¶Anal. Calcd. for Cl: 10.68. Found: 10.65.

(37%). The addition of methyl iodide to the sodium hydride reaction mixture gave *N*-methyl urethane **18** (80%). Reduction of **18** with lithium aluminum hydride gave *cis*-aminoalcohol **19** (96%). All attempts to esterify this alcohol have failed.

Summary

We have prepared a number of compounds (see Table 1) for biological evaluation as medicinal agents. None of the reported compounds exhibited significant activity although compound **15** did show marginal activity in the test for reversal of reserpine induced ptosis[1] (75 mg/kg in mice) and compound **19** showed slight C.N.S. stimulation (150 mg/kg in mice).

Experimental

The i.r. spectra were recorded on a Unicam SP-200G grating i.r. spectrometer. The n.m.r. spectra were determined on a Varian A60-A spectrometer using tetramethylsilane as an internal standard. Melting points are uncorrected and were determined on a Gallenkamp m.p. apparatus. The analyses were performed by Micro-Tech Laboratories, Skokie, Illinois.

Benzocycloheptan-1-one-3-carboxylic Acid (2)

Benzocyclohept-3-en-1-one-3-carboxylic acid (**1**) (20.2 g, 0.10 mol) was hydrogenated over prehydrogenated platinum oxide in methanol to give 17.5 g (87%) of **2**; m.p. 132–134°. An additional 2.0 g (9.8%) of **2** was recovered from the mother liquors.

Methyl Benzocycloheptan-1-one-3-carboxylate (3)

Compound **2** (2.04 g, 0.01 mol) was esterified in methanol containing hydrogen chloride to give 1.75 g (82%) of **3** after distillation; b.p. 130–134°/0.1 mm.

Methyl 1-Methoxybenzo[6,7]-5-H-cycloheptatriene-3-carboxylate (4)

Esterification of compound **1** (2.02 g, 0.1 mol) gave 2.06 g of an oil. On distillation 1.60 g (70%) of the enol ester **4** was obtained; b.p. 138–140°/0.1 mm. The n.m.r. spectrum (CCl_4): 2.40 τ (m, 1H), 2.90 (m, 3H), 3.35 (t, J = 7.1 Hz, 1H), 3.87 (s, 1H), 6.18 (s, 3H), 6.34 (s, 3H), 6.98 (d, J = 7.1 Hz, 2H).[2]

N-Methylbenzocycloheptan-1-one-3-carboxamide (6)

A solution of 3.06 (0.015 mol) of **2** and 3.12 g (0.015 mol) phosphorous pentachloride in 50 ml of phosphorous oxychloride – ether (1:1) mixture was refluxed for 30 min. The solution was evaporated at reduced pressure to yield **5** as an oil.

Treatment of the crude acid chloride with an excess of methylamine in ether gave 1.5 g (45%) crystalline amide **6**, m.p. 141–142 °C after one recrystallization from benzene.

1-Chlorobenzocyclohept-1-en-3-carboxoyl Chloride (8)

A solution of 1.02 g (0.005 mol) **2** and 3.12 g (0.015 mol) phosphorous pentachloride in 50 ml phosphorous oxychloride was refluxed for 20 min and let stand for 18 h. The solvent was evaporated at reduced pressure and the residue distilled (gas evolution was observed on

[1]The general screening procedure used has been described by Bergmann and Goldschmidt (4).

[2]For the n.m.r. spectra of a number of similar benzocycloheptatrienes see ref. 1.

Can. J. Chem. Downloaded from www.nrcresearchpress.com by 210.87.254.42 on 09/05/12
For personal use only.

heating the oil); b.p. 160–170°/0.3 mm, to give 0.60 g (50%) of **8**. The n.m.r. spectrum (CCl_4) 2.2–3.0 τ (m, 4H), 3.57 (d, J = 6 Hz, 1H), 6.5–8.0 (m, 5H).

N-Benzyl-1-chlorobenzocyclohept-1-en-3-carboxamide (9)

Treatment of crude trichloride **7** (prepared from 2.04 g, 0.01 mol **2** as above) with an excess of benzylamine in ether gave an oil which on trituration with ether and filtration yielded 1.75 g (56.5%) of **9**, m.p. 168–169 °C after recrystallization from methanol–water. An additional 0.9 g (29%) of amide was recovered from the mother liquors of trituration.

N-Carboethoxy-3-aminobenzocycloheptan-1-one (10)

The acid chloride **5** prepared as previously described from 2.41 g (0.12 mol) of **2** was added over a period of 20 min to a solution of 1.6 g sodium azide in 8 ml of a 1:1 mixture of dioxane–water precooled to 0–5 °C in an ice bath. The slurry was maintained at this temperature for 2 h, poured into 40 ml of cold water, and extracted with three 20 ml portions of chloroform. The extracts were dried over anhydrous $MgSO_4$ and concentrated below 15 °C at reduced pressure. The i.r. spectrum of the residual oil showed bands at 2135, 1700, and 1670 cm^{-1}.

The azide was then taken up in 20 ml of toluene and warmed gently until gas evolution commenced (~40 °C) after which the solution was brought to reflux for 20 min and evaporated to give 2.5 g of an oil the i.r. spectrum of which had bands at 2255 and 1672 cm^{-1}.

The isocyanate was taken up in 50 ml of benzene. To this solution, 5 ml of absolute ethanol was added and the solution then refluxed 18 h. Evaporation of the solvent gave 2.40 g of a brown oil which was chromatographed on 80 g of Florisil (60–100 mesh, Fisher Scientific) with benzene. The oil which was eluted crystallized on standing. Trituration with 5 ml of ether and filtration gave 1.40 g of white needles, m.p. 86–87.5 °C. The compound could not be recrystallized as the compound partially decomposed and darkened on heating.

In addition to **10** another compound was obtained from a large scale (40 g) experiment in < 2% yield which was identified as the urea **11**, m.p. 189–190 °C after recrystallization from ethanol–water.

N-Carboethoxy-1-hydroxy-3-aminobenzocycloheptane (12)

Reduction of **10** (1.25 g, 0.005 mol) with $NaBH_4$ (0.5 g) in ethanol at 0 °C for 30 min gave 1.20 g of a white solid, m.p. 184–187 °C (raised to 191–192 °C on recrystallization from methanol). The compound was homogeneous by t.l.c. on both silica gel and alumina plates using a number of solvent systems.

9-Oxa-7-azabenzo[2,3]bicyclo[4.3.1]decan-8-one (13)

To 0.25 g of NaH (55% mineral oil dispersion washed free of oil using hexane) suspended in 50 ml of dry THF was added 1.21 g (0.00485 mol) of **12**. A vigorous gas evolution ensued. The solution was refluxed 10 min and let stand 18 h. To the solution was added 10 ml of 10% HCl followed by 200 ml water. The solution was extracted with ether, the extracts dried over anhydrous $MgSO_4$, and concentrated to give an oily solid 1.05 g (~ 100%). Trituration with 3 ml of ether and filtration gave 0.75 g (77%) of pure crystalline **13**, m.p. 184–185 °C.

N-Methyl-1-hydroxy-3-aminobenzocycloheptane (14)

To a solution of 0.8 g $LiAlH_4$ in 50 ml of THF was added 1.02 g (0.005 mol) of **13** in 10 ml THF. The solution was refluxed 3 h after which time 3 ml of water was added to the cooled solution. The solution was filtered and the filtrate evaporated. The resultant oil was taken up in 25 ml of ether and dry HCl gas bubbled in. The salt was then filtered and recrystallized from methanol–ethyl acetate to give 0.62 g of **14** as its hydrochloride, m.p. 196–197 °C.

N-Carboethoxy-1-phenyl-3-aminobenzocyclohept-1-ene (15)

To a solution of 1.235 g (0.005 mol) of **10** in 100 ml of ether was added (at 0 °C) 5 ml of a 2.14 M solution of phenyl lithium in benzene–ether (7:3). The solution was stirred for 10 min and then 25 ml of 10% HCl was added. The layers were separated, the ethereal extract dried over anhydrous $MgSO_4$, and concentrated to give an oil. The oil was chromatographed on alumina (Fluka, neutral activity grade 1) with benzene followed by ether–ethanol (95:5). An oil (1.15 g) was collected in the later fractions from the column. On standing, the oil crystallized, m.p. 114–115 °C.

N-Carboethoxy-1-benzyl-1-hydroxy-3-aminobenzocycloheptane (16)

To a solution of 0.052 mol benzylmagnesium chloride in 50 ml ether was added 4.22 g (0.017 mol) of **10**. After 1 h at reflux the reaction was worked-up by addition of 30 ml of 10% H_2SO_4 and extraction into ether. An oil was obtained which was chromatographed on florisil with benzene to remove toluene and bibenzyl. The column was flushed with ether to give 2.65 g of a pale yellow gum (46%), which could not be induced to crystallize nor could it be distilled.

1-Benzyl-9-oxa-7-azabenzo[2,3]bicyclo[4.3.1]decan-8-one (17)

Treatment of 0.90 g (0.00265 mol) of **16** with an excess of NaH in THF as before gave 0.51 g of an oily solid. Trituration with ether and filtration gave 0.29 g (37%) pure **17**, m.p. 227–228°.

1-Benzyl-7-methyl-9-oxa-7-azabenzo[2,3]bicyclo-[4.3.1]decan-8-one (18)

To a suspension of 2.0 g NaH (55% mineral oil dispersion) in 50 ml of THF was added 4.4 g (0.013 mol) of **16**. The solution was refluxed 10 min and 5 ml (large excess) of methyl iodide added. Reflux was continued for 1 h. The reaction was worked-up as described for compound **13** to give 4.8 g of an oil. Trituration with 10 ml of ether and filtration gave 2.2 g (55%) of pure **18**, m.p. 167–168° after recrystallization from methanol. An additional 1.0 g (25%) was obtained by column chromatography of the residue on Florisil (60–100 mesh) using benzene then ether as eluent.

1-Benzyl-1-hydroxy-3-dimethylaminobenzocycloheptane (19)

To 1.0 g of $LiAlH_4$ in 20 ml of dry THF was added 2.0 g (0.0065 mol) of **18**. The solution was refluxed for 3.5 h, cooled to 0 °C, and the excess hydride decomposed with 3.5 ml of 40% aqueous potassium hydroxide. The granular precipitate was filtered and the filter cake

Can. J. Chem. Downloaded from www.nrcresearchpress.com by 210.87.254.42 on 09/05/12
For personal use only.

washed thoroughly with ether. The filtrate was evaporated to yield 1.85 g (96%) of a pale yellow oil. This oil was taken up in 50 ml of ether and dry HCl bubbled in to give the hydrochloride salt, m.p. 229–230° recrystallized from methanol – ethyl acetate.

We gratefully acknowledge the assistance of Dr. R. Martel and Dr. R. Berman of our Pharmacology Department in obtaining the cited results.

1. T. W. DOYLE. Can. J. Chem. **48**, 1629 (1970); **48**, 1633 (1970).
2. M. A. GOLDBERG, E. P. ORDAS, and C. CARSCH. J. Am. Chem. Soc. **69**, 261 (1967).
3. E. L. ELIEL, N. L. ALLINGER, S. J. ANGYAL, and G. A. MORRISON. Conformational analysis. Interscience, New York, N.Y., 1965. p. 209–210.
4. E. D. BERGMANN and Z. GOLDSCHMIDT. J. Med. Chem. **11**, 1121 (1968).

On the Isolation of (+)3-Thujone

V. HACH, R. W. LOCKHART, ELIZABETH C. MCDONALD, AND D. M. CARTLIDGE
MacMillan Bloedel Research Limited, Vancouver, British Columbia

Received September 18, 1970

Conditions necessary for the formation of the (+)3-thujone bisulfite adduct **1***a* and its utilization for the isolation of pure (+)-thujone have been established.

On a déterminé les conditions nécessaires pour former le complexe bisulfitique de la (+)-thujone-3 (**1***a*) et pour son utilisation afin d'isoler cette cétone à l'état pur.

Canadian Journal of Chemistry, 49, 1762 (1971)

In our work on western red cedar [Thuja Plicata Donn] leaf oil we have been concerned with the isolation of (+)3-thujone (**1**)[1] and particularly with its separation from (−)3-isothujone (**2**). In regard to the larger amounts of **1** desired, fractional spinning band column distillation of the two ketones which differ in their b.p. by about 1°, proved tedious and time consuming. The same applied to large scale preparative g.l.c. Therefore we became interested in the use of $NaHSO_3$ for the separation of the two ketones.

Bruylants (1) observed that (+)3-thujone (**1**) formed an adduct **1***a* with $NaHSO_3$. Subsequent work has shown that (−)3-isothujone (**2**) does not form a $NaHSO_3$ adduct. Formation of the adduct **1***a* has been used repeatedly for the isolation of (+)3-thujone from various oils (tansy, cedar leaf, artemisia) and for its separation from (−)3-isothujone (3–7). Recently Eastman and Winn (8*a*, *b*) studied in detail the formation and decomposition of **1***a* and described the difficulties they met. However, none of the work recorded has dealt with the quantitative aspects of the (+)3-thujone bisulfite adduct formation. The implication has been that this method is generally applicable for the complete separation of (+)3-thujone from its isomer **2** and from a natural oil.

We now wish to report quantitative studies showing that this method has severe limitations with regard to the yield of adduct **1***a* and the necessary concentration of (+)3-thujone in the starting mixture.

In our work we used western red cedar leaf oil obtained by steam distillation of freshly harvested leaves. This oil contained 70–80% (−)3-isothujone and 5–10% (+)3-thujone. However, using either the conditions of Eastman and Winn (8*a*, *b*) or varying these conditions, we failed to obtain the bisulfite adduct **1***a* of (+)3-thujone from this oil. Subsequently, we utilized the known fact, (2, 7, 9, 10) that the base-catalyzed epimerization of either of the two ketones gives a mixture of (+)3-thujone and (−)3-isothujone in a ratio of 65:35 respectively, to enhance the (+)3-thujone content in our oil to about 55%. From this oil we then obtained the bisulfite adduct using the above mentioned conditions.

This result prompted us to investigate in detail the limits of the bisulfite adduct **1***a* formation using mixtures containing varying proportions of ketones **1** and **2** and cedar leaf oil samples containing varying amounts of **1**. Our results can be summarized as follows. Pure (+)3-thujone forms

[1]We have adopted the nomenclature proposal of H. C. Brown, see ref. 2.

Can. J. Chem. Downloaded from www.nrcresearchpress.com by 210.87.254.42 on 09/05/12
For personal use only.

washed thoroughly with ether. The filtrate was evaporated to yield 1.85 g (96%) of a pale yellow oil. This oil was taken up in 50 ml of ether and dry HCl bubbled in to give the hydrochloride salt, m.p. 229–230° recrystallized from methanol – ethyl acetate.

We gratefully acknowledge the assistance of Dr. R. Martel and Dr. R. Berman of our Pharmacology Department in obtaining the cited results.

1. T. W. DOYLE. Can. J. Chem. **48**, 1629 (1970); **48**, 1633 (1970).
2. M. A. GOLDBERG, E. P. ORDAS, and C. CARSCH. J. Am. Chem. Soc. **69**, 261 (1967).
3. E. L. ELIEL, N. L. ALLINGER, S. J. ANGYAL, and G. A. MORRISON. Conformational analysis. Interscience, New York, N.Y., 1965. p. 209–210.
4. E. D. BERGMANN and Z. GOLDSCHMIDT. J. Med. Chem. **11**, 1121 (1968).

On the Isolation of (+)3-Thujone

V. HACH, R. W. LOCKHART, ELIZABETH C. MCDONALD, AND D. M. CARTLIDGE
MacMillan Bloedel Research Limited, Vancouver, British Columbia

Received September 18, 1970

Conditions necessary for the formation of the (+)3-thujone bisulfite adduct **1***a* and its utilization for the isolation of pure (+)-thujone have been established.

On a déterminé les conditions nécessaires pour former le complexe bisulfitique de la (+)-thujone-3 (**1***a*) et pour son utilisation afin d'isoler cette cétone à l'état pur.

Canadian Journal of Chemistry, 49, 1762 (1971)

In our work on western red cedar [Thuja Plicata Donn] leaf oil we have been concerned with the isolation of (+)3-thujone (**1**)[1] and particularly with its separation from (−)3-isothujone (**2**). In regard to the larger amounts of **1** desired, fractional spinning band column distillation of the two ketones which differ in their b.p. by about 1°, proved tedious and time consuming. The same applied to large scale preparative g.l.c. Therefore we became interested in the use of $NaHSO_3$ for the separation of the two ketones.

Bruylants (1) observed that (+)3-thujone (**1**) formed an adduct **1***a* with $NaHSO_3$. Subsequent work has shown that (−)3-isothujone (**2**) does not form a $NaHSO_3$ adduct. Formation of the adduct **1***a* has been used repeatedly for the isolation of (+)3-thujone from various oils (tansy, cedar leaf, artemisia) and for its separation from (−)3-isothujone (3–7). Recently Eastman and Winn (8*a*, *b*) studied in detail the formation and decomposition of **1***a* and described the difficulties they met. However, none of the work recorded has dealt with the quantitative aspects of the (+)3-thujone bisulfite adduct formation. The implication has been that this method is generally applicable for the complete separation of (+)3-thujone from its isomer **2** and from a natural oil.

We now wish to report quantitative studies showing that this method has severe limitations with regard to the yield of adduct **1***a* and the necessary concentration of (+)3-thujone in the starting mixture.

In our work we used western red cedar leaf oil obtained by steam distillation of freshly harvested leaves. This oil contained 70–80% (−)3-isothujone and 5–10% (+)3-thujone. However, using either the conditions of Eastman and Winn (8*a*, *b*) or varying these conditions, we failed to obtain the bisulfite adduct **1***a* of (+)3-thujone from this oil. Subsequently, we utilized the known fact, (2, 7, 9, 10) that the base-catalyzed epimerization of either of the two ketones gives a mixture of (+)3-thujone and (−)3-isothujone in a ratio of 65:35 respectively, to enhance the (+)3-thujone content in our oil to about 55%. From this oil we then obtained the bisulfite adduct using the above mentioned conditions.

This result prompted us to investigate in detail the limits of the bisulfite adduct **1***a* formation using mixtures containing varying proportions of ketones **1** and **2** and cedar leaf oil samples containing varying amounts of **1**. Our results can be summarized as follows. Pure (+)3-thujone forms

[1]We have adopted the nomenclature proposal of H. C. Brown, see ref. 2.

Can. J. Chem. Downloaded from www.nrcresearchpress.com by 210.87.254.42 on 09/05/12
For personal use only.

Can. J. Chem. Downloaded from www.nrcresearchpress.com by 210.87.254.42 on 09/05/12
For personal use only.

the bisulfite adduct **1***a* quantitatively. The adduct does not form when the content of (+)3-thujone (**1**) is lower than 35% in a mixture from which it is to be separated. A mixture of 70% (−)3-isothujone and 30% (+)3-thujone does not give a bisulfite adduct. The same applies *e.g.* to a mixture containing 70% fenchone and 30% (+)3-thujone (**1**). Fenchone itself does not form a bisulfite adduct. Cedar leaf oil containing less than 35% of ketone **1** does not give any adduct. For practical preparative purposes a (+)3-thujone content of 55% or more in the starting material is necessary to achieve a reasonable yield of the adduct. However, the complete utilization of all (+)3-thujone present in a mixture is apparently not possible. From our extensive experimental series we conclude that a yield of about 25–40% of the (+)3-thujone available in the mixture is attainable with a starting concentration of 55–60% of this ketone.

The reasons why (+)3-thujone (**1**) forms the adduct and ketone **2** does not, still remain obscure. The hypothesis put forward by Eastman and Winn (8*a*, *b*) and based on the steric interference of the SO_3Na and CH_3 groups is not convincing because the authors assumed a wrong configuration of the CH_3 group and the conformation of the bicyclohexane skeleton in ketones **1** and **2** is yet to be proven (13). We inspected Fisher–Hirshfelder molecular models constructed with a flat five-membered ring and observed that the SO_3Na and CH_3 groups could possibly be accommodated even in the *cis*-position. That steric hindrance by an alkyl group is not an important factor in the bisulfite adduct formation of terpenic ketones is shown in the case of piperitone (**3**), pulegone (**4**), and isopulegone (**5**). Whereas ketones **3** and **4** form adducts, isopulegone does not (11). Apparently the CO group in **4** and **5** is rendered more active by conjugation. It is known (12) that conjugated ketones add two molecules of $NaHSO_3$. We prepared the bisulfite adducts of piperitone and pulegone. Due to their instability we were unable to reach completely satisfactory analysis. However, it appeared that two molecules of $NaHSO_3$ were indeed added. Therefore, we hypothesize, that the bisulfite adduct **1***a* formation from (+)3-thujone (**1**) as compared to the unreactivity of (−)3-isothujone (**2**) may be governed by electronic factors such as the hydrogen bonding between a suitably placed OH group and the cyclopropane ring (13) in addition to any steric factors that might be contemplated.

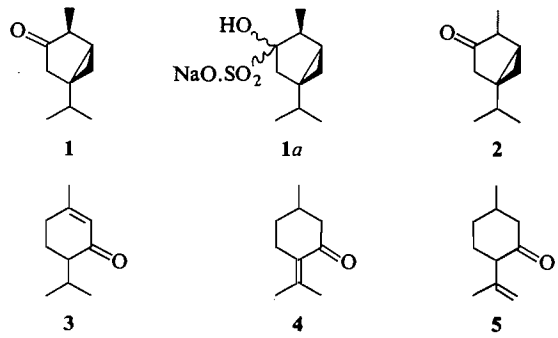

1 **1***a* **2**

3 **4** **5**

Experimental

All determinations of the isomeric thujones were carried out by isothermal g.l.c. at 120°, column 30 ft × 3/8 in., 25% Carbowax 20M on 40–60 mesh Chromosorb A, helium as carrier gas 150 ml/min. Elemental analyses by Galbraith Laboratories, Knoxville, Tennessee. Water in samples of adduct **1***a* was determined by xylene distillation.

Bisulfite Adduct of (+)3-Thujone (1a)

A mixture of 2 g of (+)3-thujone (99%+), 5 ml of a *fresh saturated $NaHSO_3$ solution*, 0.6 g $NaHCO_3$ and 0.8 ml of (95%) ethanol was shaken overnight at room temperature. The separated solid was filtered off and air dried giving 3.54 g (93%) of the bisulfite adduct. Extraction of the filtrate with ether yielded 0.03 g of an oily residue confirming the completion of the reaction.

Anal. Calcd. for $C_{10}H_{17}NaO_4S \cdot 2H_2O$: C, 41.09; H, 7.24; Na, 7.86; O, 32.84; S, 10.96. Found: C, 40.71; H, 7.67; Na, 7.85; O, 32.43; S, 11.04.

The bisulfite adduct was decomposed by heating in water under reflux for 1 h. After an exhaustive (6 times) ether extraction 1.65 g (83%) of pure (+)3-thujone was recovered.

The same amounts of reagents and identical reaction conditions were applied to: (*a*) 2 g of a mixture containing 30% (+)3-thujone and 70% (−)3-isothujone and (*b*) 2 g of a mixture containing 70% (−) fenchone and 30% (+)3-thujone. In both cases there was no bisulfite adduct formation.

Preparation of (+)3-Thujone from Cedar Leaf Oil

The cedar leaf oil used in this experiment contained 10.3% (+)3-thujone and 79.1% (−)3-isothujone. In order to enhance the (+)3-thujone content the (−)3-isothujone-(+)3-thujone equilibration was carried out by stirring the cedar leaf oil (700 g) with a 5% NaOH solution in 95% ethanol (475 ml) for 30 min. The content of (+)3-thujone and (−)3-thujone then was respectively 56.8 and 26.6%. The $NaHSO_3$ solution used to form the bisulfite adduct **1***a* was prepared by dissolving 570 g $NaHSO_3$ in 875 ml H_2O. The freshly prepared $NaHSO_3$–$NaHCO_3$ solution was added to the solution of the "isomerized" cedar leaf oil and the two phase system was stirred vigorously for 16 h by an efficient paddle

stirrer. The separated solid was collected on a glass fritt, pressed to remove excess H_2O and oil, and washed thoroughly with ether (2 × 100 ml). The air dried solid weighed 409 g. We found that in large scale preparations of this type, varying amounts of $NaHSO_3$ (10–40% of the collected solid) separated with the bisulfite adduct. Thus the weight of the collected solid cannot be used to calculate the yield of the adduct.

The adduct was decomposed by heating with 10% aqueous H_2SO_4 (1200 ml) to a gentle reflux for 3 h. The (+)3-thujone was isolated by separating the oil from the aqueous phase and exhaustively extracting the aqueous phase with ether (7 × 200 ml). The ether extracts and the separated oil were combined, washed with 5% Na_2CO_3 solution, H_2O, dried with Na_2SO_4, and evaporated. The weight of crude (+)3-thujone was 111.2 g. Distillation of the crude ketone gave 91.1 g (22.9% based on **1** available in the isomerized oil) of pure (99.9%+) (+)3-thujone, b.p. 40.9° (0.5 mm) uncorrected; $[\alpha]_D^{25}$ +78.8° (neat).

1. G. BRUYLANTS. Chem. Ber. **11**, 449 (1878).
2. S. P. ACHAKYA, H. C. BROWN, A. SUZUKI, S. NOZAWA, and M. ITOH. J. Org. Chem. **34**, 3015 (1969).
3. F. W. SEMMLER. Chem. Ber. **25**, 3343 (1892).
4. O. WALLACH. Justus Liebigs Ann. Chem. **286**, 92 (1895).
5. E. GUENTHER. The essential oils. Vol. II. D. Van Nostrand Co., New York, N.Y., 1949. pp. 423–429.
6. J. D. HUXTABLE, J. D. A. JOHNSON, and M. J. SAXBY. Perfum. Essent. Oil Rec. 492 (1966).
7. D. V. BANTHORPE and H.FF. DAVIES. J. Chem. Soc. B, 1356 (1968).
8. (*a*) R. H. EASTMAN and A. V. WINN. J. Am. Chem. Soc. **82**, 5908 (1960); (*b*) A. V. WINN. Ph.D. Thesis. Stanford University, Stanford, California, 1959.
9. A. G. SHORT and J. READ. J. Chem. Soc. 2016 (1938).
10. M. B. BADOCHE. Bull. Soc. Chim. Fr. 1029 (1952).
11. J. J. SIMMONSEN and L. N. OWEN. The terpenes. Vol. I. 2nd ed. Cambridge University Press, Cambridge, Great Britain, 1953. pp. 363, 372, 373.
12. E. MULLER, *editor*. Methoden der organischen chemie. Vol. IX. 4th ed. G. Thieme, Stuttgart, 1955. p. 384.
13. V. HACH, R. F. RAIMONDO, D. CARTLIDGE, and E. C. MCDONALD. Tetrahedron Lett., 3175, 1970.

Can. J. Chem. Downloaded from www.nrcresearchpress.com by 210.87.254.42 on 09/05/12
For personal use only.

Preparation of β-Cyclocitral

R. N. GEDYE, PARKASH C. ARORA, AND K. DECK
Department of Chemistry, Laurentian University, Sudbury, Ontario

Received December 10, 1970

An improved method for the preparation of pure β-cyclocitral by cyclization of citral anil with 95% sulfuric acid is reported. By avoidance of steam distillation of the reaction product, the formation of the by-products *p*-cymene and 1-acetyl-4,4-dimethyl-1-cyclohexene was prevented. The formation of this ketone by treatment of α- or β-cyclocitral anil with dilute sulfuric acid followed by steam distillation supports the mechanism proposed by Henbest *et al.*

On rapporte une méthode améliorée de préparation de β-cyclocitral pur basée sur la cyclisation de l'anil de citral en présence d'acide sulfurique à 95%. En évitant de faire un entraînement à la vapeur des produits de la réaction, on élimine la formation des produits secondaires *p*-cymène et acétyl-1 diméthyl-4,4 cyclohexène-1. La formation de cette cétone lors du traitement de l'anil de l'α ou du β-cyclocitral par de l'acide sulfurique dilué suivi par un entraînement à la vapeur d'eau corrobore le mécanisme proposé par Henbest *et al.*

Canadian Journal of Chemistry, 49, 1764 (1971)

Introduction

β-Cyclocitral has been used as starting material in the synthesis of vitamin A and related compounds (1–4). The synthesis involves essentially the addition of two isoprene units to β-cyclocitral using two successive Reformatsky reactions with methyl 4-bromo-3-methylbut-2-enoate. One important disadvantage of this method is the lack of availability of pure β-cyclocitral.

β-Cyclocitral is most conveniently prepared by the cyclization of citral anil (**1**) with sulfuric acid at low temperatures (5–7). The accepted method consists of the reaction of citral anil (**1**) in ether with a large excess of 95% sulfuric acid at −20° followed by steam distillation of the product. Henbest *et al.* (6) have shown that under these conditions a mixture of three isomers is formed: α-cyclocitral (**2**), β-cyclocitral (**3**), and a ketone **4**

stirrer. The separated solid was collected on a glass fritt, pressed to remove excess H_2O and oil, and washed thoroughly with ether (2 × 100 ml). The air dried solid weighed 409 g. We found that in large scale preparations of this type, varying amounts of $NaHSO_3$ (10–40% of the collected solid) separated with the bisulfite adduct. Thus the weight of the collected solid cannot be used to calculate the yield of the adduct.

The adduct was decomposed by heating with 10% aqueous H_2SO_4 (1200 ml) to a gentle reflux for 3 h. The (+)3-thujone was isolated by separating the oil from the aqueous phase and exhaustively extracting the aqueous phase with ether (7 × 200 ml). The ether extracts and the separated oil were combined, washed with 5% Na_2CO_3 solution, H_2O, dried with Na_2SO_4, and evaporated. The weight of crude (+)3-thujone was 111.2 g. Distillation of the crude ketone gave 91.1 g (22.9% based on **1** available in the isomerized oil) of pure (99.9%+) (+)3-thujone, b.p. 40.9° (0.5 mm) uncorrected; $[\alpha]_D^{25}$ +78.8° (neat).

1. G. BRUYLANTS. Chem. Ber. **11**, 449 (1878).
2. S. P. ACHAKYA, H. C. BROWN, A. SUZUKI, S. NOZAWA, and M. ITOH. J. Org. Chem. **34**, 3015 (1969).
3. F. W. SEMMLER. Chem. Ber. **25**, 3343 (1892).
4. O. WALLACH. Justus Liebigs Ann. Chem. **286**, 92 (1895).
5. E. GUENTHER. The essential oils. Vol. II. D. Van Nostrand Co., New York, N.Y., 1949. pp. 423–429.
6. J. D. HUXTABLE, J. D. A. JOHNSON, and M. J. SAXBY. Perfum. Essent. Oil Rec. 492 (1966).
7. D. V. BANTHORPE and H.FF. DAVIES. J. Chem. Soc. B, 1356 (1968).
8. (*a*) R. H. EASTMAN and A. V. WINN. J. Am. Chem. Soc. **82**, 5908 (1960); (*b*) A. V. WINN. Ph.D. Thesis. Stanford University, Stanford, California, 1959.
9. A. G. SHORT and J. READ. J. Chem. Soc. 2016 (1938).
10. M. B. BADOCHE. Bull. Soc. Chim. Fr. 1029 (1952).
11. J. J. SIMMONSEN and L. N. OWEN. The terpenes. Vol. I. 2nd ed. Cambridge University Press, Cambridge, Great Britain, 1953. pp. 363, 372, 373.
12. E. MULLER, *editor*. Methoden der organischen chemie. Vol. IX. 4th ed. G. Thieme, Stuttgart, 1955. p. 384.
13. V. HACH, R. F. RAIMONDO, D. CARTLIDGE, and E. C. MCDONALD. Tetrahedron Lett., 3175, 1970.

Preparation of β-Cyclocitral

R. N. GEDYE, PARKASH C. ARORA, AND K. DECK

Department of Chemistry, Laurentian University, Sudbury, Ontario

Received December 10, 1970

An improved method for the preparation of pure β-cyclocitral by cyclization of citral anil with 95% sulfuric acid is reported. By avoidance of steam distillation of the reaction product, the formation of the by-products *p*-cymene and 1-acetyl-4,4-dimethyl-1-cyclohexene was prevented. The formation of this ketone by treatment of α- or β-cyclocitral anil with dilute sulfuric acid followed by steam distillation supports the mechanism proposed by Henbest *et al.*

On rapporte une méthode améliorée de préparation de β-cyclocitral pur basée sur la cyclisation de l'anil de citral en présence d'acide sulfurique à 95%. En évitant de faire un entraînement à la vapeur des produits de la réaction, on élimine la formation des produits secondaires *p*-cymène et acétyl-1 diméthyl-4,4 cyclohexène-1. La formation de cette cétone lors du traitement de l'anil de l'α ou du β-cyclocitral par de l'acide sulfurique dilué suivi par un entraînement à la vapeur d'eau corrobore le mécanisme proposé par Henbest *et al.*

Canadian Journal of Chemistry, 49, 1764 (1971)

Introduction

β-Cyclocitral has been used as starting material in the synthesis of vitamin A and related compounds (1–4). The synthesis involves essentially the addition of two isoprene units to β-cyclocitral using two successive Reformatsky reactions with methyl 4-bromo-3-methylbut-2-enoate. One important disadvantage of this method is the lack of availability of pure β-cyclocitral.

β-Cyclocitral is most conveniently prepared by the cyclization of citral anil (**1**) with sulfuric acid at low temperatures (5–7). The accepted method consists of the reaction of citral anil (**1**) in ether with a large excess of 95% sulfuric acid at −20° followed by steam distillation of the product. Henbest *et al.* (6) have shown that under these conditions a mixture of three isomers is formed: α-cyclocitral (**2**), β-cyclocitral (**3**), and a ketone **4**

Can. J. Chem. Downloaded from www.nrcresearchpress.com by 210.87.254.6 on 09/05/12
For personal use only.

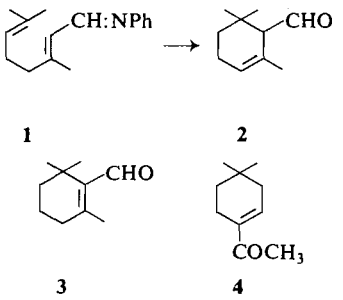

which was shown to be 1-acetyl-4,4-dimethyl-1-cyclohexene.

While α- and β-cyclocitral may be separated by fractional distillation, **3** and **4** have almost identical boiling points. The latter two compounds can be separated by conversion into semicarbazones followed by steam distillation in the presence of phthalic anhydride. Our investigations have indicated, however, that the recovery of pure β-cyclocitral by this method is only fair.

The present study has resulted in an improved method for the formation of pure β-cyclocitral from citral anil. According to Henbest *et al.* (6) the ketone **4** is probably formed during the steam distillation of the diluted product from the reaction of citral anil with sulfuric acid. By avoiding the use of steam distillation in the work-up procedure, we were able to obtain a mixture of α- and β-cyclocitral only from the cyclization in the ratio, 3 parts of α-cyclocitral to 1 part of the β-isomer. It was shown (using g.l.c.) that α-cyclocitral was rapidly converted to a mixture of approximately 8 parts of β-cyclocitral to 1 part of α-cyclocitral, when treated with methanolic KOH. It was also shown the formation of *p*-cymene, formed in about 10% yield, by the method of Henbest *et al.*, was avoided when steam distillation was not used.

It was observed that considerable quantities of black polymeric material were formed during the reaction of citral anil and sulfuric acid even at low temperature (−20°). The extent of polymer formation was reduced by conducting the reaction under nitrogen, with a resulting increase in the total yield of the α- and β-cyclocitrals from about 50% in air to 60% when nitrogen was used. It was also observed that, when conducted under nitrogen, the product was almost pure α-cyclocitral.

Henbest *et al.* (6) suggested the mechanism shown in Scheme 1 to explain the formation of

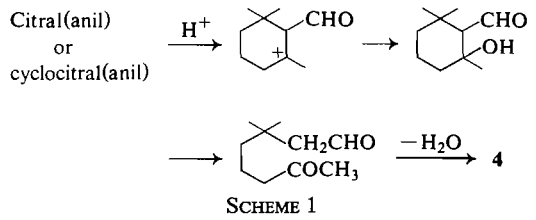

SCHEME 1

the ketone **4** from citral anil, with hydration occurring at the steam distillation stage.

Our observation that the ketone was not formed when steam distillation was not used, would add support to this mechanism. Further support was offered by the observation that considerable amounts of ketone were formed when pure β-cyclocitral anil was refluxed with dilute sulfuric acid and then steam distilled. Under similar conditions α-cyclocitral anil also gave some ketone. A partial isomerization of α-cyclocitral to β-cyclocitral occurred during the steam distillation of the former in the presence of H_2SO_4. This is to be expected, since loss of a proton from the carbonium ion would result in the formation of a mixture of α- and β-cyclocitral.

Experimental

All melting points are uncorrected. The v.p.c. analysis was carried out using commercial (Varian Aerograph) 10 ft × 1/4 in. stainless steel columns containing the appropriate packing. Fractional distillations were carried out on an annular spinning band column, boiling points being uncorrected.

β-*Cyclocitral*

(*a*) Citral anil (from 76 g citral) in 75 ml ether was added dropwise to 95% sulfuric acid (500 g) at −20° during 30 min in a nitrogen atmosphere, and stirred for a further 45 min at −15°. The product was added to ice (1.5 kg) and extracted several times with ether. Distillation of the extracts gave a colorless liquid (43 g, 57%), b.p. 83–90°/13 mm. Gas chromatography on FFAP and Carbowax 20M showed only two peaks (area ratio 15:1) with relative retention times of 1 to 2 on FFAP and 1.7 to 3.0 on Carbowax 20M. Treatment of a sample with semicarbazide hydrochloride and sodium acetate in 50% aqueous ethanol gave α-cyclocitral semicarbazone, m.p. 202–203°; the other isomer formed in the cyclization was shown to be β-cyclocitral (when nitrogen was not used the cyclization yielded a mixture of 3 parts α- to 1 part β-cyclocitral in 48% yield, a larger amount of dark brown polymer being evident).

The crude α-cyclocitral (30 g) was treated with potassium hydroxide (10 g) in methanol (200 ml) at 0 °C for a few min. The mixture was diluted with water (500 ml), saturated with sodium chloride, and extracted with ether. Distillation of the extracts yielded a colorless liquid (21.6 g, 72%), b.p. 88–94°/12 mm which was shown by

Can. J. Chem. Downloaded from www.nrcresearchpress.com by 210.87.254.6 on 09/05/12
For personal use only.

TABLE 1. Physical data of fractions obtained from the cyclization of citral anil

Fraction	Boiling point (8 mm °C)	Weight (g)	n_D^{18}	λ_{max} (mμ)	Semicarbazone m.p. (°C)	% α	% β
1	60–62	1.5	1.4700	235	199–201	95	0
2	62–69	1.0	1.4831	—	—	40	45
3	69–73	1.0	1.4948	—	163–165	8	90
4	73–74	14.0	1.4944	275	165–167	0	99

gas chromatography to contain approximately 8 parts β-cyclocitral to 1 part of the α-isomer.

Fractional distillation of the product using the annular spinning band column gave the fractions listed in Table 1.

Gas chromatography on the FFAP column indicated the product ratios given in Table 1. No ketone semicarbazone was isolated from any of these fractions. The overall yield of pure β-cyclocitral was 25%.

(*b*) Citral anil was cyclized by the method of Henbest *et al.* (6). In agreement with the results of Henbest *et al.*, the products were *p*-cymene, α-cyclocitral, β-cyclocitral, and the ketone, 1-acetyl-4,4-dimethyl-1-cyclohexene, in the approximate ratio 2:6:10:1. The product of the steam distillation was analyzed using gas chromatography on the FFAP column. The ketone and β-cyclocitral were partially separated at 130° using FFAP. The identity of the products was confirmed by the melting points of their semicarbazones and their u.v. spectra.

Isomerization of α- and β-Cyclocitral to 1-Acetyl-4,4-dimethyl-1-cyclohexene

β-Cyclocitral (20 g) was refluxed with 50% sulfuric acid (200 ml) for 3 h and the product steam distilled. The distillate was extracted with ether and the ether evaporated. The residue was shown by gas chromatography on the FFAP column to consist of 60% ketone, 35% β-cyclocitral together with a small amount of α-cyclocitral and other unidentified products.

A similar reaction with α-cyclocitral and with α-cyclocitral anil was shown to give mainly β-cyclocitral together with smaller amounts of the ketone and some unchanged α-cyclocitral.

1. S. H. HARPER and J. F. OUGHTON. Chem. Ind. 574 (1950).
2. S. AKIYOSHI and K. MENO. J. Chem. Soc. Jap. Pure Chem. Sect. 73, 126 (1952).
3. K. TANABE. Pharm. Bull. Jap. 3, 25 (1955).
4. H. O. HUISMAN, A. SMIT, S. VROMEN, and L. G. M. FISSCHER. Rec. Trav. Chem. 71, 899 (1952).
5. L. COLOMBI, A. BOSSHARD, H. SCHINZ, and C. F. SCIDEL. Helv. Chem. Acta, 34, 265 (1951).
6. H. B. HENBEST, B. L. SHAW, and G. WOODS. J. Chem. Soc. 1154 (1952).
7. I. M. MOUSSERON CANET, M. MOUSSERON, and J. BOCH. Bull. Soc. Chim. Fr., 597 (1959).

Occurrence and Origin of the Tropylium Ion in the Mass Spectra of Arylboronic Acid Esters

R. J. BOSE AND M. D. PETERS

Fisheries Research Board of Canada, Vancouver Laboratory, Vancouver 8, British Columbia

Received September 8, 1970

The mass spectra of a number of phenylboronic acid esters of 1,2- and 1,3-diols are examined and the presence and origin of the tropylium rearrangement ion is established.

On rapporte les spectres de masse d'un certain nombre d'esters dérivés de l'acide phénylboronique d'une part et de diols-1,2 et -1,3 d'autre part; on explique la présence et l'origine d'un ion tropylium.

Canadian Journal of Chemistry, 49, 1766 (1971)

Increasing attention is being given to electron impact induced rearrangements involving the migration of atoms other than hydrogen (1, 2). Failure to recognize such skeletal rearrangements could lead to erroneous conclusions regarding the structures of unknown compounds. Conversely, a full understanding of the factors governing such rearrangements could provide useful stereochemical information.

The occurrence of the tropylium ($C_7H_7^+$, *m/e* 91) rearrangement ion is one of the most characteristic features of the mass spectra of aromatic

Can. J. Chem. Downloaded from www.nrcresearchpress.com by 210.87.254.6 on 09/05/12
For personal use only.

TABLE 1. Physical data of fractions obtained from the cyclization of citral anil

Fraction	Boiling point (8 mm °C)	Weight (g)	n_D^{18}	λ_{max} (mμ)	Semicarbazone m.p. (°C)	% α	% β
1	60–62	1.5	1.4700	235	199–201	95	0
2	62–69	1.0	1.4831	—	—	40	45
3	69–73	1.0	1.4948	—	163–165	8	90
4	73–74	14.0	1.4944	275	165–167	0	99

gas chromatography to contain approximately 8 parts β-cyclocitral to 1 part of the α-isomer.

Fractional distillation of the product using the annular spinning band column gave the fractions listed in Table 1.

Gas chromatography on the FFAP column indicated the product ratios given in Table 1. No ketone semicarbazone was isolated from any of these fractions. The overall yield of pure β-cyclocitral was 25%.

(*b*) Citral anil was cyclized by the method of Henbest *et al.* (6). In agreement with the results of Henbest *et al.*, the products were *p*-cymene, α-cyclocitral, β-cyclocitral, and the ketone, 1-acetyl-4,4-dimethyl-1-cyclohexene, in the approximate ratio 2:6:10:1. The product of the steam distillation was analyzed using gas chromatography on the FFAP column. The ketone and β-cyclocitral were partially separated at 130° using FFAP. The identity of the products was confirmed by the melting points of their semicarbazones and their u.v. spectra.

Isomerization of α- and β-Cyclocitral to 1-Acetyl-4,4-dimethyl-1-cyclohexene

β-Cyclocitral (20 g) was refluxed with 50% sulfuric acid (200 ml) for 3 h and the product steam distilled. The distillate was extracted with ether and the ether evaporated. The residue was shown by gas chromatography on the FFAP column to consist of 60% ketone, 35% β-cyclocitral together with a small amount of α-cyclocitral and other unidentified products.

A similar reaction with α-cyclocitral and with α-cyclocitral anil was shown to give mainly β-cyclocitral together with smaller amounts of the ketone and some unchanged α-cyclocitral.

1. S. H. HARPER and J. F. OUGHTON. Chem. Ind. 574 (1950).
2. S. AKIYOSHI and K. MENO. J. Chem. Soc. Jap. Pure Chem. Sect. **73**, 126 (1952).
3. K. TANABE. Pharm. Bull. Jap. **3**, 25 (1955).
4. H. O. HUISMAN, A. SMIT, S. VROMEN, and L. G. M. FISSCHER. Rec. Trav. Chem. **71**, 899 (1952).
5. L. COLOMBI, A. BOSSHARD, H. SCHINZ, and C. F. SCIDEL. Helv. Chem. Acta, **34**, 265 (1951).
6. H. B. HENBEST, B. L. SHAW, and G. WOODS. J. Chem. Soc. 1154 (1952).
7. I. M. MOUSSERON CANET, M. MOUSSERON, and J. BOCH. Bull. Soc. Chim. Fr., 597 (1959).

Occurrence and Origin of the Tropylium Ion in the Mass Spectra of Arylboronic Acid Esters

R. J. BOSE AND M. D. PETERS

Fisheries Research Board of Canada, Vancouver Laboratory, Vancouver 8, British Columbia

Received September 8, 1970

The mass spectra of a number of phenylboronic acid esters of 1,2- and 1,3-diols are examined and the presence and origin of the tropylium rearrangement ion is established.

On rapporte les spectres de masse d'un certain nombre d'esters dérivés de l'acide phénylboronique d'une part et de diols-1,2 et -1,3 d'autre part; on explique la présence et l'origine d'un ion tropylium.

Canadian Journal of Chemistry, 49, 1766 (1971)

Increasing attention is being given to electron impact induced rearrangements involving the migration of atoms other than hydrogen (1, 2). Failure to recognize such skeletal rearrangements could lead to erroneous conclusions regarding the structures of unknown compounds. Conversely, a full understanding of the factors governing such rearrangements could provide useful stereochemical information.

The occurrence of the tropylium ($C_7H_7^+$, *m/e* 91) rearrangement ion is one of the most characteristic features of the mass spectra of aromatic

Can. J. Chem. Downloaded from www.nrcresearchpress.com by 210.87.254.5 on 09/05/12
For personal use only.

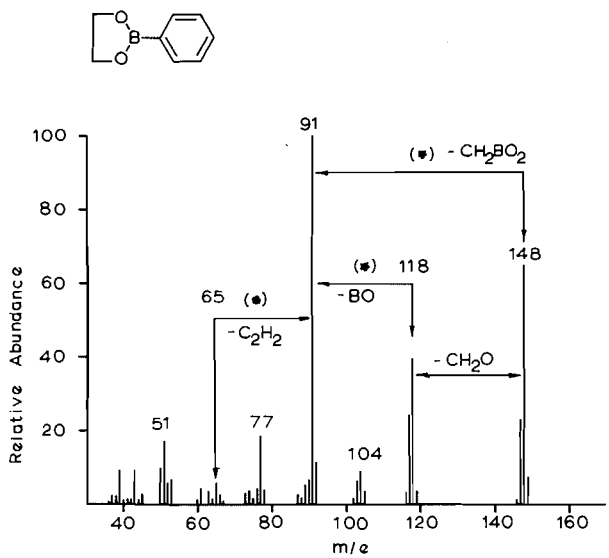

FIG. 1. The mass spectrum of ethylene glycol phenylboronate (**1**).

hydrocarbons (2, 3) and, although a few examples of skeletal rearrangement giving rise to the tropylium ion have been reported in which a contributing carbon was not directly bonded to a phenyl substituent in the parent molecule, the relative abundance of the *m/e* 91 ion in these cases is generally low. The presence of the tropylium ion in the mass spectra of alkylphenylthioethers (4), phenylvinylsulfide (5), and alkylphenylphosphonates and related compounds (6) has been observed. Recent reports (7, 8) on the presence of an intense *m/e* 91 ion in the mass spectra of ethylene glycol phenylboronate (**1**) have prompted us to present our findings in support of the identity and origin of the *m/e* 91 ion in the spectra of this (**1**) (Fig. 1) and other cyclic phenylboronates.

The constitution of the *m/e* 91 ion is inferred from the presence of an ion at *m/e* 65 (attributed to either the cyclopentadienyl cation or more probably an acyclic isomer (9, 10), a metastable peak centered at *m/e* 46.4 corresponding to the transformation $C_7H_7^+ \rightarrow C_5H_5^+$ and the occurrence of the base peak two mass units higher at *m/e* 93 in the mass spectra of ethylene glycol-d_4 phenylboronate (**2**), Fig. 2.

The tropylium ion arises from the parent ion of **1** (**2**) by either a one-step process, *m/e* 148 (152) → *m/e* 91 (93) for which a metastable ion (m*) appears at 55.9 (56.9) or by a two-step process in which CH_2O is lost from the parent ion, giving *m/e* 118 (120) followed by the elimination of a BO radial. An intense metastable peak appears at *m/e* 70.2 (72.1) in support of the latter transformation.

We propose to explain the transformation by the following scheme (Scheme 1) in which the parent ion (*a*) undergoes α-cleavage and the resulting stabilized oxycarbonium ion (*b*), by a cationic site mechanism (11, 12) gives the common intermediate (*c*). Further transformations of (*c*) by a process of one electron shifts give the tropylium ion directly or in two steps, $c \rightarrow d \rightarrow C_7H_7^+$.

Alternately, (*b*) could rearrange by two electron shifts through a four-membered spiran transition state (*f*), analogous to that arbitrarily proposed for the migration of dimethylsilyl groups in both the trimethylsilyl benzoates (*g*) (13) and benzyltrimethylsilyl ethers (*h*) (14).

To further delineate the origin of the tropylium rearrangement ion, the mass spectra of both phenyl-1,3,2-dioxaborinane (**3**) and phenyl-5,5-dideutero-1,3,2-dioxaborinane (**4**) were examined, Figs. 3 and 4, respectively.

By far the most intense ions in the spectra of **3** (**4**) correspond to the parent ion, *m/e* 162 (164) and *m/e* 104, C_6H_5BO, corresponding to the loss of trimethyleneoxide. Although a metastable peak appears at *m/e* 66.8 in **3**, the corresponding metastable ion at *m/e* 65.9 in the spectra of **4** could not be confirmed, and leaves in doubt the

Can. J. Chem. Downloaded from www.nrcresearchpress.com by 210.87.254.5 on 09/05/12
For personal use only.

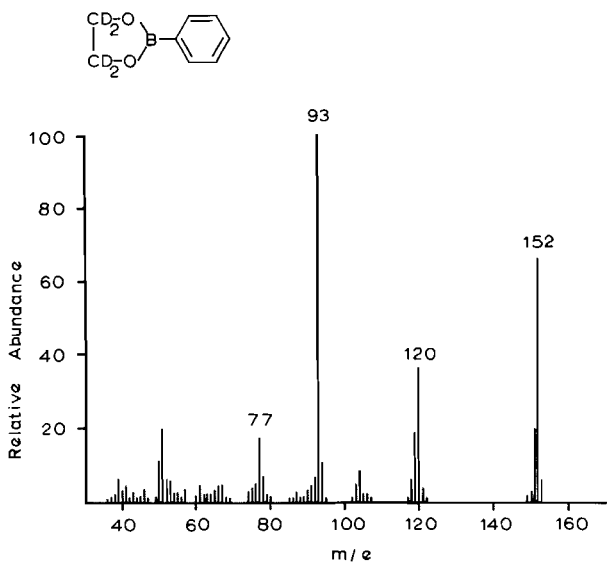

FIG. 2. The mass spectrum of d_4-ethylene glycol phenylboronate (2).

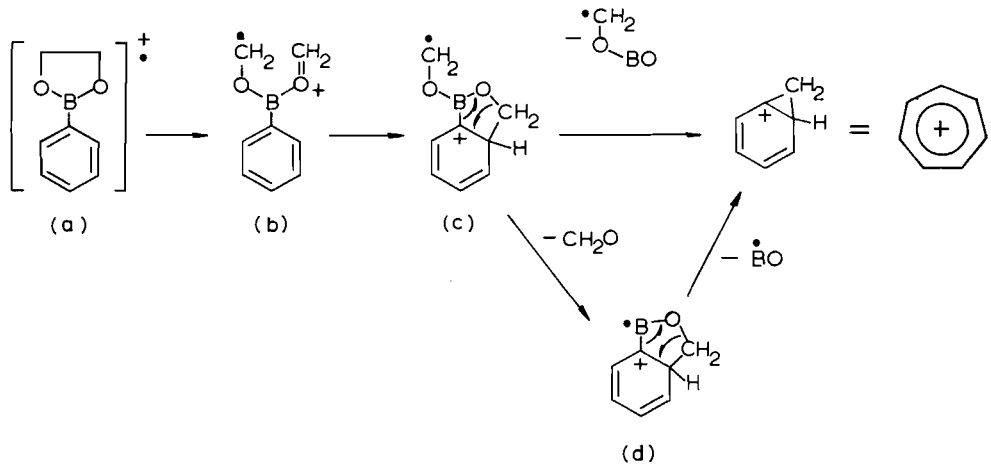

SCHEME 1

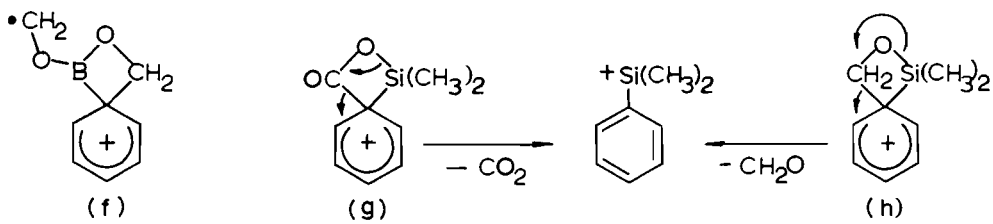

possible direct elimination of trimethylene oxide from the parent ion. Further, the expulsion of CH_2O from **3** and **4** generates a fragmentation sequence leading to the phenyl cation, and intense metastable ions are observed at *m/e* 107.4 (109.6), 82 (80.7), and 56.9 (56.9) in support of each reaction in this sequence (Scheme 2).

The tropylium ion occurs at *m/e* 91 in the mass

Can. J. Chem. Downloaded from www.nrcresearchpress.com by 210.87.254.5 on 09/05/12
For personal use only.

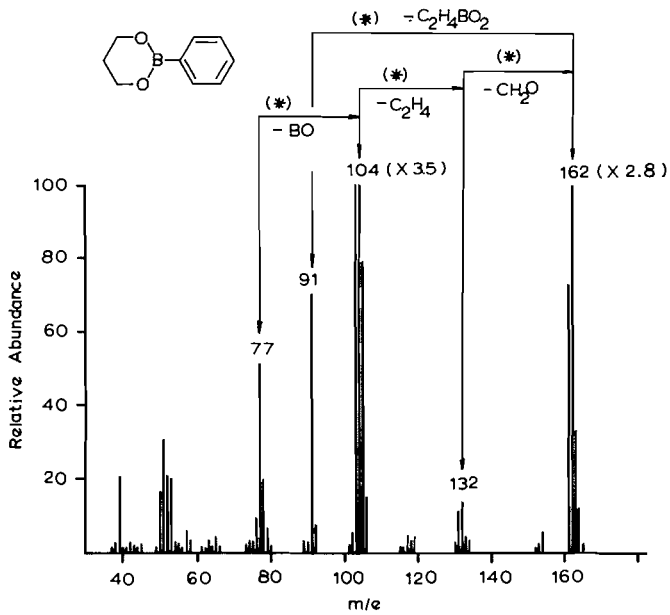

FIG. 3. The mass spectrum of propane-1,3-diol phenylboronate (**3**).

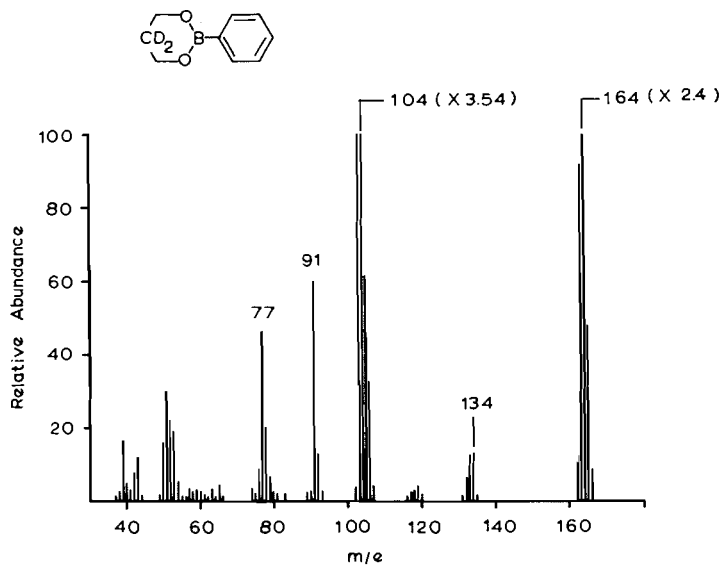

FIG. 4. The mass spectrum of 2,2-dideuteropropane-1,3-diol phenylboronate (**4**).

spectra of both **3** and **4** and is derived from the parent ion, *m/e* 162 (164) directly, m* 51.15 (50.5). By analogy to the transition state *c* proposed for **1** and **2**, **3**, and **4** would generate *cc* (Scheme 3) which on further rearrangement would be expected to give the tropylium ion directly or by the loss of C_2H_4O and BO in a two step process. The absence of a metastable ion corresponding to M-44 (118) $\rightarrow C_7H_7^+$ in the spectra of **3** and **4** is consistent with a one-step process. The low ion abundance of the *m/e* 118 fragment ion does not permit the confirmation of the expected two-step reaction *i.e.* the loss of C_2H_4O from (*cc*), leading to $C_7H_7^+$. The nearly complete absence of

Can. J. Chem. Downloaded from www.nrcresearchpress.com by 210.87.254.5 on 09/05/12
For personal use only.

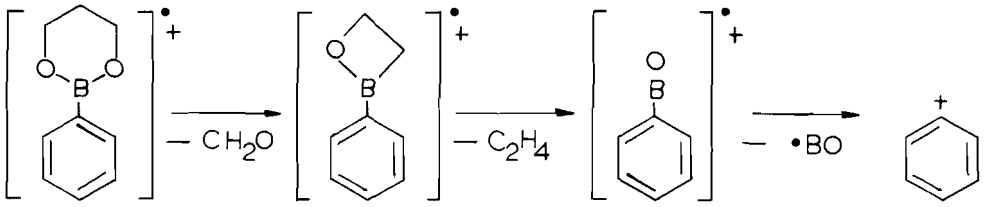

SCHEME 2

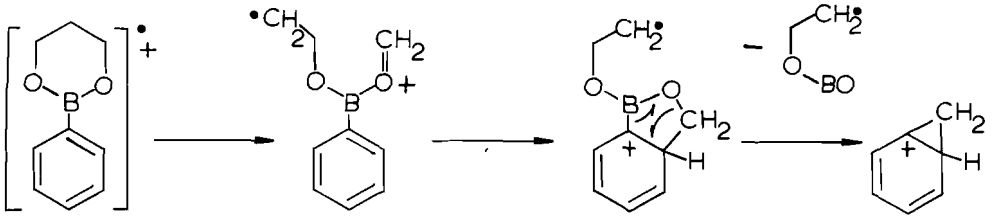

SCHEME 3

deuterium labelling of the tropylium ion in the mass spectra of **4** adds support to the proposed intermediate (*cc*), and rules out the possibility of the expulsion of a neutral BO_2 fragment and recombination of the hydrocarbon and aromatic portions.

Experimental

The mass spectra were obtained on a nuclide 12-90-G mass spectrometer at 70 eV potential and 100 μA trap current. The source was maintained at 150 °C and the compounds were introduced as neat liquids on an unheated direct insertion probe. Individual ion intensities were corrected by reference to the total ion current

The cyclic esters were prepared from the appropriate diols by standard procedures (15). Ethylene glycol-d_4 was a commercial sample, Merck, Sharp and Dohme Canada Ltd., while 2,2-dideuteropropane-1,3-diol was prepared by several times exchanging diethylmalonate with D_2O followed by $NaBH_4$ reduction in D_2O. The isotope purity of **4** was determined to be better than 95% from the integrated n.m.r. signal obtained at 100 MHz.

1. P. BROWN and C. DJERASSI. Angew. Chem. Int. Ed. **6**, 477 (1967).
2. H. BUDZIKIEWICZ, C. DJERASSI, and D. H. WILLIAMS. Interpretation of mass spectra of organic compounds. Holden Day Inc., San Francisco, California, 1964.
3. H. M. GRUBB and S. MEYERSON. *In* Mass spectrometry of organic ions *Edited by* F. W. McLafferty. Academic Press, New York, N.Y., 1963. p. 453ff.
4. J. H. BOWIE, S. O. LAWESSON, J. MADSON, G. SCHROLL, and D. H. WILLIAMS. J. Chem. Soc. B, 951 (1966).
5. W. D. WERINGA. Tetrahedron Lett. 273 (1969).
6. H. BUDZIKIEWICZ and Z. PELAH. Monatsh. Chem. **96**, 1739 (1965).
7. R. H. CRAGG and J. F. J. TODD. Chem. Commun. 386 (1970).
8. I. R. MCKINLEY and H. WEIGEL. Chem. Commun. 1022 (1970).
9. K. R. JENNINGS. Chem. Commun. 283 (1966).
10. A. G. HARRISON, P. HAYNES, S. MCLEAN, and F. MEYER. J. Am. Chem. Soc. **87**, 5099 (1965).
11. F. W. MCLAFFERTY. Chem. Commun. 78 (1966).
12. F. W. MCLAFFERTY, G. E. VAN LEAR, and R. KORNFELD. J. Am. Chem. Soc. **90**, 6240 (1968).
13. R. M. TEETER. Abstracts, Tenth Conference on Mass Spectrometry of the American Society for Testing Materials, New Orleans, Louisiana, 1962. p. 51.
14. J. DIEKMAN, J. B. THOMSON, and C. DJERASSI. J Org. Chem. **32**, 3904 (1967).
15. J. M. SUGIHARA and C. M. BOWMAN. J. Am. Chem. Soc. **80**, 2443 (1958).

Can. J. Chem. Downloaded from www.nrcresearchpress.com by 210.87.254.5 on 09/05/12
For personal use only.

Proton Magnetic Resonance Investigation of Some Weak Interactions Between Naphthalene and Alkyl Iodides in Carbon Tetrachloride[1]

R. SAHAI AND S. H. LIN
Department of Chemistry, Arizona State University, Tempe, Arizona 85281

Received November 27, 1970

A p.m.r. investigation of the interactions between naphthalene and alkyl iodides has been reported. The equilibria, the heats and the entropy changes for the complexation, and the chemical shifts of the acceptor protons in the pure complex have been determined. A crude dipole model for these interactions has been suggested.

On rapporte les résultats obtenus lors d'une étude par r.m.n. des intéractions entre le naphtalène et les iodures d'alkyle. On a pu déterminer la position d'équilibre, les changements d'enthalpie et d'entropie pour la complexation et les déplacements chimiques des protons accepteurs du complexe pur. On croit que ces intéractions peuvent être expliquées en utilisant un modèle dipolaire simple.

Canadian Journal of Chemistry, 49, 1771 (1971)

Theoretical and experimental results (1–5), carried out recently in this laboratory, on the mechanisms for the quenching of the phosphorescence of aromatic hydrocarbons in the presence of heavy atoms (3–5) or paramagnetic species (1, 2), led us to suggest that a complex (exciplex) (4, 5) is formed between lumiphor (the excited molecule) and quencher containing heavy atoms. It seemed then desirable to investigate the equilibria in the formation of charge-transfer complexes between alkyl iodides and naphthalene, quantitatively, since only limited or no information was available about these equilibria and related thermodynamic quantities. The present communication reports a p.m.r. investigation of these complexes. The equilibrium constants, the heats and the entropy changes for the formation of these weak complexes in carbon tetrachloride have been determined over the temperature range -10 to $+50$ °C.

All chemicals used in this study were AR grade. Naphthalene was obtained from Matheson, Coleman & Bell and was recrystallized from alcohol. Methyl iodide (Mallinckrodt Chemical Works), ethyl iodide, and carbon tetrachloride (Baker analyzed reagent) were checked before use and indicated no detectable impurities in these materials. Solutions were prepared by dissolving varying amounts of naphthalene (0.2 to 2.0 M) and a constant amount of methyl iodide (0.01 M) or ethyl iodide (0.08 M) in carbon tetrachloride. All solutions were freshly prepared on the day of measurement. The n.m.r. spectra were taken on a Varian Associates A-60 spectrometer operating at 60 MHz. Line positions of the proton resonance of the acceptor molecule were measured using an internal cyclohexane (0.008 M) resonance reference. Chemical shifts were reproducible to better than 0.3 Hz, the uncertainty being determined by the line width. Measurements were made at -10, $+10$, $+30$, and $+50$°, the temperatures of the probe. All shifts in the signal, caused by additions of electron donor to the system, were to higher field values.

Because n.m.r. spectroscopy is extremely sensitive to small changes in the electronic environment of a magnetic nucleus, a study of the appropriate n.m.r. parameters has recently become a useful method of determining equilibrium constants for charge-transfer complexes (6–8). The method of Foster and Fyfe (7) was used for the determination of K. For a series of solutions in which the concentration of donor is much higher than that of acceptor [D] $\gg$ [A], the difference in chemical shift δ of a particular proton absorption in the acceptor moiety was measured relative to an internal reference of cyclohexane. If δ_0 is the chemical shift of the same proton absorption in the absence of donor species, then for a series of solutions,

$$[1] \qquad \Delta/[D] + \Delta K = \Delta_0 K$$

where $\Delta = \delta - \delta_0$ and Δ_0 is the chemical shift of the particular proton of the acceptor moiety of the pure complex relative to the shift in the acceptor alone. From eq. 1, a plot of $\Delta/[D]$

[1]Supported by the National Science Foundation and ACS Petroleum Research Fund.

Can. J. Chem. Downloaded from www.nrcresearchpress.com by 210.87.254.5 on 09/05/12
For personal use only.

TABLE 1. Association constants K, maximum observed shifts Δ_{max}, and the calculated shifts for the pure complex Δ_0, for naphthalene complexes with some alkyl iodide acceptors

	Acceptor								
	Methyl iodide			Ethyl iodide					
Temperature (°C)	K (l mol^{-1})	Δ_{max} (Hz)	Δ_0 (Hz)	K† (l mol^{-1})	K‡ (l mol^{-1})	Δ_{max}† (Hz)	Δ_{max}‡ (Hz)	Δ_0† (Hz)	Δ_0‡ (Hz)
−10	0.160	15.1*	93.1	0.140	0.159	13.1*	13.2*	90.7	82.2
+10	0.113	20.0	108.5	0.088	0.104	17.5	18.2	117.0	105.7
+30	0.074	18.5	140.1	0.051	0.060	16.4	17.0	197.1	158.8
+50	0.068	16.1	134.5	0.038	0.046	14.0	14.5	199.3	171.7

*Maximum donor concentration was 1.2 M due to solubility restriction at low temperature; in other cases it was 2.0 M.
†Obtained with respect to methyl protons.
‡Obtained with respect to methylene protons.

against Δ gave a straight line with slope $-K$. The typical plots are shown in Figs. 1 and 2. The Δ_0 value was measured from the intercept. The values of K and Δ_0 at various temperatures were computed by using a standard least squares curve fit programme. The results are summarized in Table 1. Concentrations have been expressed in moles of donor or acceptor per litre of solution, so that values of K have obviously the dimensions of the reciprocal of this concentration.

The plot of $\ln K$ against $1/T$ gave a good straight line (Fig. 3). The heat of formation, ΔH, and the entropy change, ΔS, for the complexation were

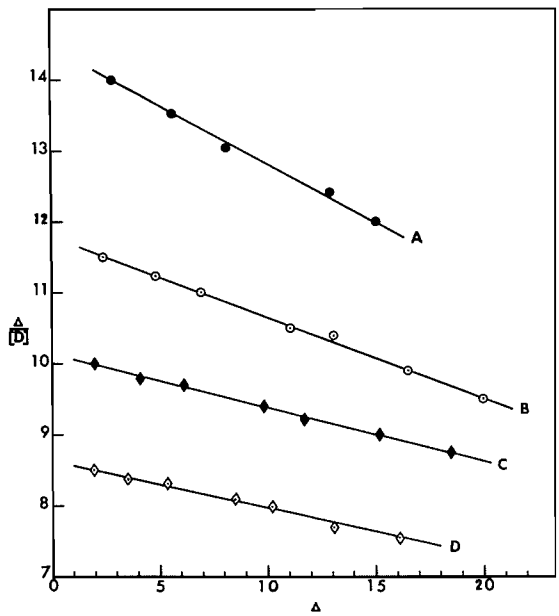

FIG. 1. Plots of Δ/[D] against Δ for complexes of methyl iodide with naphthalene at: (A) −10, (B) +10, (C) +30, and (D) +50°; all in carbon tetrachloride.

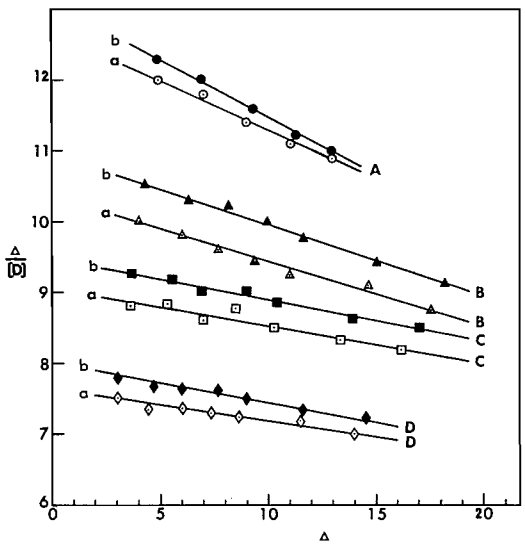

FIG. 2. Plots of Δ/[D] against Δ for complexes of naphthalene with ethyl iodide with respect to: (*a*) methyl protons, (*b*) methylene protons at: (A) −10, (B) +10, (C) +30, and (D) +50°; all in carbon tetrachloride.

obtained from the slope of the straight line and its intersection with ordinate, respectively. These values are given in Table 2.

The methyl and methylene proton resonance of alkyl iodides were observed in the absence of donor species, to vary only within 3 Hz in the temperature range investigated here, with respect to cyclohexane as internal reference. It is apparent from Table 1 that the K values for complexes of alkyl iodides with naphthalene are of the same order of magnitude having a slightly higher value for methyl iodide than for ethyl iodide, and are temperature dependent. The individual maximum proton shifts Δ_{max}, Δ_0, and equilibrium constants for CH_3 and CH_2 groups in ethyl iodide

Can. J. Chem. Downloaded from www.nrcresearchpress.com by 210.87.254.5 on 09/05/12
For personal use only.

TABLE 2. Thermodynamic constants* for charge-transfer complexes of naphthalene with alkyl iodide acceptors

Acceptor	$-\Delta H$† (kcal/mol)	$-\Delta H$‡ (kcal/mol)	$-\Delta S$† (e.u.)	$-\Delta S$‡ (e.u.)
CH_3I	2.54	—	13.34	—
CH_3CH_2I	3.28	4.12	16.47	19.21

*Based on equilibrium constants measured in l mol^{-1}.
†Obtained with respect to methyl protons.
‡Obtained with respect to methylene protons.

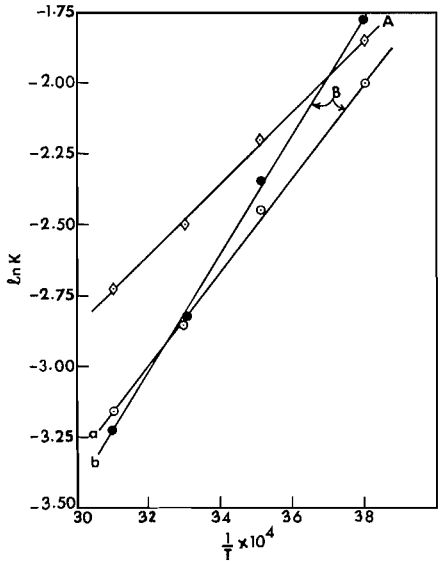

FIG. 3. Plots of ln$K$ *vs.* $1/T$ for complexes of naphthalene with: (A) methyl iodide and (B) ethyl iodide with respect to: (*a*) methyl protons; (*b*) methylene protons.

are listed in Table 1. From Table 1 we can see that the equilibrium constants and the observed shifts are small, and, hence, the errors must be relatively large (9). The standard deviation of K in this investigation is in the range of 5–10%. Thus the differences in K given in Table 1 are within the experimental errors, and we cannot draw any conclusion as to whether there is only 1:1 complex, or more 1:1 complexes or an even more complex situation taking place. The n.m.r. study of the formation of a set of isomeric dimers from a given donor molecule and a given acceptor molecule has been discussed by Kuntz and Johnston (10).

If the crude dipole model of the interaction with naphthalene is valid then we would expect that the measured shifts Δ should be directly proportional to the dipole moment μ of the alkyl iodides and inversely to its molecular volume (V). The molecular volume comes in because after rotational averaging this will determine the mean distance of approach of acceptor to the donor molecule. So we expect larger shift and hence larger equilibrium constant for methyl iodide than ethyl iodide because methyl iodide has comparatively larger μ/V value (0.026) than for ethyl iodide (0.024). These expectations are supported experimentally by the present investigation. This suggests that in these cases the interaction has probably a dipole type of origin in accordance with the observation of Schneider (11) for directed solute–solvent interactions in benzene solutions. Present investigation is further supported by the recent observed charge-transfer band (λ_{max} = 340 mμ) for the intermolecular interaction between naphthalene and ethyl bromide at 77 °K in cyclohexane by Bolotnikova and Sichkar (12).

Comparing the observed and estimated K values for the interaction of alkyl iodides with naphthalene in ground electronic state (0.04–0.16 l mol^{-1}) and excited electronic state (13) (0.50–0.80 l mol^{-1}), respectively, it is apparent that these values are found to be comparatively greater for excited state than for ground state and are within the expectation limit.

In conslusion, this investigation seems to provide further substantial support on the proposed charge-transfer mechanism of quenching by heavy atoms (4, 5).

The authors wish to thank Mr. G. L. Loper for some helpful discussions.

1. S. H. LIN and D. TWEED. Int. J. of Quantum Chem. **3s**, 315 (1969).
2. C. O. HILL and S. H. LIN. Int. J. of Quantum Chem. **3s**, 307 (1969).
3. C. O. HILL and S. H. LIN. J. Chem. Phys. **53**, 608 (1970).
4. R. H. HOFELDT, R. SAHAI, and S. H. LIN. J. Chem. Phys. **53**, 4512 (1970).
5. R. SAHAI, R. H. HOFELDT, and S. H. LIN. Trans. Faraday Soc. In press.

Can. J. Chem. Downloaded from www.nrcresearchpress.com by 210.87.254.5 on 09/05/12
For personal use only.

6. M. W. HANNA and A. L. ASHBAUGH. J. Phys. Chem. **68**, 811 (1964).
7. R. FOSTER and C. A. FYFE. Trans. Faraday Soc. **61**, 1626 (1965).
8. R. S. MULLIKEN and W. B. PERSON. Molecular complexes. A Lecture and Reprint Volume, John Wiley, New York, N.Y., 1969.
9. R. FOSTER. Organic charge-transfer complexes. Academic Press, New York, N.Y., 1969. Chaps. 5, 6.
10. I. D. KUNTZ, JR., and M. D. JOHNSTON, JR. J. Am. Chem. Soc. **89**, 6008 (1967).
11. W. G. SCHNEIDER. J. Phys. Chem. **66**, 2653 (1962).
12. T. N. BOLOTNIKOVA and O. N. SICHKAR. Opt. Spectrosc. **26**, 411 (1969).
13. R. H. HOFELDT, R. SAHAI, and S. H. LIN. To be published.

Can. J. Chem. Downloaded from www.nrcresearchpress.com by 210.87.254.5 on 09/05/12
For personal use only.

Nuphar Alkaloids: 3-Epinupharamine

T. P. FORREST AND S. RAY
Department of Chemistry, Dalhousie University, Halifax, Nova Scotia

Received December 17, 1970

The structure of a new alkaloid isolated from *Nuphar variegatum* is shown to be that of 3-epinupharamine (**4**).

On a établi que la structure d'un nouvel alcaloïde isolé du *Nuphar variegatum* est celle de la 3-epinupharamine (**4**).

Canadian Journal of Chemistry, 49, 1774 (1971)

The genus *Nuphar* has been the source of several quinolizidine alkaloids as well as some piperidine alkaloids of similar structure in which the second ring of the quinolizidine nucleus remains open. The major alkaloid of the North American yellow water lily, *Nuphar variegatum* Engelm., has been shown to be nuphenine (**1**) (1), a piperidine alkaloid differing in relative configuration from the alkaloids (*e.g.* anhydronupharamine (**2**) (2)) isolated from the yellow water lilies of Japanese origin, *Nuphar japonicium* (3). Another piperidine alkaloid, 3-epinuphamine (**3**) (4) having the same stereochemistry as nuphenine has recently been found in *Nuphar variegatum*. We now wish to report the isolation of a third such alkaloid 3-epinupharamine (**4**) from the same source.

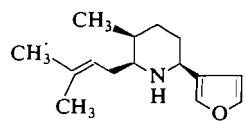

1

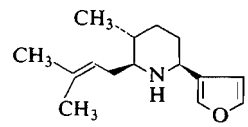

2

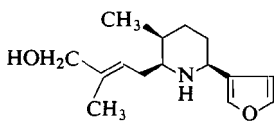

3

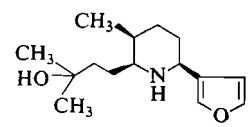

4

The structure of 3-epinupharamine (picrolonate m.p. 83–85 °C, *N*-acetate m.p. 107–109 °C) was proved by analysis of its various spectra and by its synthesis from the known alkaloid nuphenine (**1**). The molecular formula was determined to be $C_{15}H_{25}NO_2$ by mass spectrometry. Evidence for the presence of the hydroxyl group was obtained from the i.r. spectrum, 3575 (sharp) and 3150 cm^{-1} (broad) and the n.m.r. spectrum (in $CDCl_3$) (τ 7.35, 2H, OH and NH). The furan ring was indicated by the i.r. bands at 1500, 1170, and 875 cm^{-1} and by peaks in the n.m.r. spectrum at τ 2.63 (2α-H's) and 3.57 (1β-H). The ring methyl group was observed as a doublet at τ 9.03 (J = 6.6 Hz) and the gem-dimethyl groups as singlets τ 8.83 and 8.75. The magnetic nonequivalence of these gem-dimethyl groups, separated by two methylene groups from the nearest chiral center, is apparently accentuated by hydrogen bonding of the hydroxyl group with the nitrogen. The methyl groups appear as a single peak when the spectrum is determined in dimethyl sulfoxide. One proton α to the nitrogen (position 6) was seen as a doublet of doublets (J = 3 and 10 Hz) centered at τ 6.39 and the other proton α to the nitrogen (position 2) as a triplet (J = 7 Hz)

6. M. W. HANNA and A. L. ASHBAUGH. J. Phys. Chem. **68**, 811 (1964).
7. R. FOSTER and C. A. FYFE. Trans. Faraday Soc. **61**, 1626 (1965).
8. R. S. MULLIKEN and W. B. PERSON. Molecular complexes. A Lecture and Reprint Volume, John Wiley, New York, N.Y., 1969.
9. R. FOSTER. Organic charge-transfer complexes. Academic Press, New York, N.Y., 1969. Chaps. 5, 6.
10. I. D. KUNTZ, JR., and M. D. JOHNSTON, JR. J. Am. Chem. Soc. **89**, 6008 (1967).
11. W. G. SCHNEIDER. J. Phys. Chem. **66**, 2653 (1962).
12. T. N. BOLOTNIKOVA and O. N. SICHKAR. Opt. Spectrosc. **26**, 411 (1969).
13. R. H. HOFELDT, R. SAHAI, and S. H. LIN. To be published.

Can. J. Chem. Downloaded from www.nrcresearchpress.com by 210.87.254.40 on 09/05/12
For personal use only.

Nuphar Alkaloids: 3-Epinupharamine

T. P. FORREST AND S. RAY
Department of Chemistry, Dalhousie University, Halifax, Nova Scotia

Received December 17, 1970

The structure of a new alkaloid isolated from *Nuphar variegatum* is shown to be that of 3-epinupharamine (**4**).

On a établi que la structure d'un nouvel alcaloïde isolé du *Nuphar variegatum* est celle de la 3-epinupharamine (**4**).

Canadian Journal of Chemistry, 49, 1774 (1971)

The genus *Nuphar* has been the source of several quinolizidine alkaloids as well as some piperidine alkaloids of similar structure in which the second ring of the quinolizidine nucleus remains open. The major alkaloid of the North American yellow water lily, *Nuphar variegatum* Engelm., has been shown to be nuphenine (**1**) (1), a piperidine alkaloid differing in relative configuration from the alkaloids (*e.g.* anhydronupharamine (**2**) (2)) isolated from the yellow water lilies of Japanese origin, *Nuphar japonicium* (3). Another piperidine alkaloid, 3-epinuphamine (**3**) (4) having the same stereochemistry as nuphenine has recently been found in *Nuphar variegatum*. We now wish to report the isolation of a third such alkaloid 3-epinupharamine (**4**) from the same source.

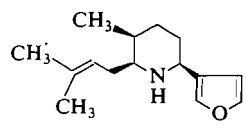

1

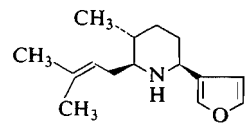

2

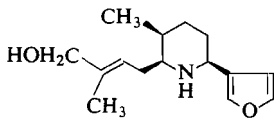

3

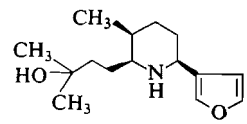

4

The structure of 3-epinupharamine (picrolonate m.p. 83–85 °C, *N*-acetate m.p. 107–109 °C) was proved by analysis of its various spectra and by its synthesis from the known alkaloid nuphenine (**1**). The molecular formula was determined to be $C_{15}H_{25}NO_2$ by mass spectrometry. Evidence for the presence of the hydroxyl group was obtained from the i.r. spectrum, 3575 (sharp) and 3150 cm^{-1} (broad) and the n.m.r. spectrum (in $CDCl_3$) (τ 7.35, 2H, OH and NH). The furan ring was indicated by the i.r. bands at 1500, 1170, and 875 cm^{-1} and by peaks in the n.m.r. spectrum at τ 2.63 (2α-H's) and 3.57 (1β-H). The ring methyl group was observed as a doublet at τ 9.03 (J = 6.6 Hz) and the gem-dimethyl groups as singlets τ 8.83 and 8.75. The magnetic nonequivalence of these gem-dimethyl groups, separated by two methylene groups from the nearest chiral center, is apparently accentuated by hydrogen bonding of the hydroxyl group with the nitrogen. The methyl groups appear as a single peak when the spectrum is determined in dimethyl sulfoxide. One proton α to the nitrogen (position 6) was seen as a doublet of doublets (J = 3 and 10 Hz) centered at τ 6.39 and the other proton α to the nitrogen (position 2) as a triplet (J = 7 Hz)

Can. J. Chem. Downloaded from www.nrcresearchpress.com by 210.87.254.40 on 09/05/12
For personal use only.

further split into doublets (J = 2.5 Hz) centered at τ 7.21. The presence of the 3-methyl-3-hydroxybutyl side chain on position 2 was substantiated by the appearance of the base peak in the mass spectrum at *m/e* 164 (M—$C_4H_{11}O$). The presence of only two α protons on the piperidine ring and the coupling of the 2-proton to only one 3-proton established the substitution pattern shown (**4**).

This assignment of the structure and stereochemistry was verified by the conversion of nuphenine (**1**) into a compound identical in all respects with the naturally occurring **4**. The isolation of **4** by extraction conditions which would not hydrate a double bond indicated that this compound is indeed a natural product and not formed by acid catalyzed hydration of nuphenine. It is of interest to note that no quinolizidine alkaloids having the relative configuration of nuphenine have been reported, whereas the quinolizidine alkaloids are the major alkaloids of the other stereochemical series.

Experimental

All n.m.r. data were recorded on a Varian A-60 spectrometer in deuterochloroform with tetramethylsilane as internal standard. Optical rotation was measured on a Perkin–Elmer model 141 polarimeter and u.v. spectra on a Coleman-Hitachi 124 double beam spectrometer. The i.r. spectra were determined on a Perkin–Elmer 237B grating spectrometer. The melting points are uncorrected.

Isolation of Alkaloids

Air dried powdered rhizomes (1.15 kg) of *Nuphar variegatum* were continuously extracted with petroleum ether (40–60 °C) for 3 days, then air dried, soaked overnight with 10% Na_2CO_3, and filtered under suction. The residue was then extracted with chloroform at room temperature (over an extended period). Evaporation of the chloroform *in vacuo* gave a viscous residue (47 g). This was dissolved again in chloroform, filtered, and the filtrate repeatedly washed with 5% HCl solution until the aqueous phase showed no cloudiness with Mayers reagent. The combined washings were made basic (*ca.* p*H* 8) with Na_2CO_3 and the bases (25.3 g) obtained by chloroform extraction.

Isolation of 3-Epinupharamine (4)

A quantity of crude bases (12.7 g) was chromatographed on Silicar CC7 (Malinckrodt) by gradient elution using benzene and methanol. Fractions were collected in 100ml portions and were monitored by t.l.c. 3-Epinupharamine (0.5 g) was obtained from the fraction eluted with benzene–methanol (9:1 v/v) and purified by repeated chromatography on preparative alumina plates.

3-Epinupharamine was also obtained by column chromatography of the crude chloroform extract of the rhizomes (without separation of the bases) on neutral alumina and then repeated preparative t.l.c. on alumina plates.

Pale yellow oil: $[\alpha]_D^{23°} = -24.8$ (1.45 MeOH); λ_{max}(MeOH) 274 nm (440) and λ_{max}(CCl_4) 263 nm (400); i.r. (CCl_4), 3575, 3150, 2794 (weak), 2710 (weak), 1500, 1450, 1381, 1170, 1155, 1065, 1025, 875 cm^{-1}; n.m.r. ($CDCl_3$) τ 2.63 (2H, α-furan), 3.57 (1H, β-furan), 8.78 and 8.83 (6H, gem-CH_3), 9.03 (3H, C_3—CH_3), 6.4 (1H, C_6—H), 7.22 (1H, C_2—H), 7.35 (2H, OH and NH), 8.1–8.7 (9H); mass spectrum: major peaks at *m/e* 251.1884 (M^+), 236, 164 (base peak), 107, and 94.

3-Epinupharamine Picrolonate

3-Epinupharamine (170 mg) was dissolved in a small quantity of methanol and picrolonic acid (180 mg) dissolved in a small amount of methanol was added to it. The mixture was kept at 50° for 1/2 h and then the solvent was evaporated producing a semi-solid mass which was crystallized from methanol–acetone, m.p. 83–85 °C.

N-Acetyl-3-epinupharamine

3-Epinupharamine (140 mg) was dissolved in a mixture of freshly distilled pyridine and acetic anhydride (2 ml, 1:1) and left overnight at room temperature. The solvents were removed *in vacuo*, the residue dissolved in chloroform and washed successively with cold 5% $NaHCO_3$, 5% HCl, and finally with distilled water. The chloroform was removed *in vacuo* and the residue crystallized from acetone, m.p. 107–109 °C; i.r. (KBr pellet) 3450, 1615, 1500, 1415, 1375, 1360, 1310, 1260, 1130, 1020, 870, 745 cm^{-1}; n.m.r. ($CDCl_3$, room temperature, showing the presence of both amide conformations) τ 9.03 (d, 3H, C_3—CH_3, J = 6.5 Hz), 8.73 (s, 3H, gem-CH_3), 8.68 (s, 3H, gem-CH_3), 7.8 (s, 3H, *N*-acetyl CH_3), 7.68 (s, 1H, OH), 6.27 (br, 1H, C_2—H), 4.05 (br, 0.7H, C_6—H), 3.56 (br, 0.3H, C_6H), 3.5 (m, 1H, furan βH), 2.6 (m, 2H, furan αH).

Conversion of Nuphenine to 3-Epinupharamine

Nuphenine (0.45 g) was dissolved in 25 ml of 5% HCl and maintained at room temperature for 2 weeks. The solution was made basic with solid Na_2CO_3, extracted with chloroform, the chloroform extract dried over $MgSO_4$, and the solvent removed *in vacuo* to give crude 3-epinupharamine. The crude product was purified on preparative scale alumina plates to yield 0.38 g of pure 3-epinupharamine. The i.r. and n.m.r. spectra were superimposable with those of natural 3-epinupharamine.

The authors wish to thank the National Research Council of Canada for financial support.

1. R. Barchet and T. P. Forrest. Tetrahedron Lett. **21**, 4229 (1965).
2. Y. Arata, T. Ohasi, M. Yonemitsu, and Y. Asuda. J. Pharm. Soc. Jap. **87**, 1094 (1967).
3. Y. Arata and T. Ohasi. Chem. Pharm. Bull. Jap. **13**, 392 (1965).
4. C. F. Wong and R. T. LaLonde. Phytochem. **9**, 1851 (1970).

L'isomérisation des acétates énoliques en série décalinique

H. FAVRE, F. HUET, ET L. VARFALVY
Département de chimie, Université de Montréal, Montréal, Québec

Reçu le 9 juin 1970[1]

Le réactif d'acétylation énolique préconisé par Edwards et Rao (anhydride acétique et acide perchlorique dans l'acétate d'éthyle) est tout à fait adapté à la préparation d'acétates d'énols et à leur mise en équilibre en série décalinique *cis* et *trans*.

The reagent (acetic anhydride and perchloric acid in ethylacetate) proposed by Edwards and Rao for the enolacetylation of ketones is particularly well suited to the preparation of the enolacetates of *cis* and *trans* 2-decalones, and to the study of their equilibrium.

Canadian Journal of Chemistry, 49, 1776 (1971)

Can. J. Chem. Downloaded from www.nrcresearchpress.com by 210.87.254.6 on 09/05/12
For personal use only.

L'acétylation énolique constitue un moyen d'étudier la direction de l'énolisation de cétones substituées dissymétriquement. Elle a été mise en œuvre dans les séries stéroïdiques A/B *trans* (1–4) et *cis* (5, 6), cyclohexanique (7), et décalinique (8, 9). D'une manière générale, on utilise l'acétate d'isopropényle et l'acide sulfurique (1), réactif I, pour obtenir une commande cinétique et l'anhydride acétique et l'acide perchlorique 70% dans le tétrachlorure de carbone (10) ou dans le mélange tétrachlorure de carbone–benzène (5–9), réactif II, pour la commande thermodynamique; une étude récente (11) confirme les premières observations (7) sur l'action de ces réactifs, mais une généralisation ne semble pas encore possible; en effet, en séries décalinique et stéroïdique (5, 8, 11), le réactif I ne provoque aucune isomérisation des acétates formés, alors qu'il le fait en série aliphatique (12). Le réactif II, selon (11), présente la caractéristique d'une commande cinétique initiale, suivie d'une mise à l'équilibre; nous avons remarqué que ce réactif présente toutefois le désavantage marqué de conduire en série décalinique *cis* à de forts pourcentages de produits secondaires, et en série décalinique *trans*, à l'hydrolyse des acétates d'énols plutôt qu'à leur mise en équilibre. On a rapporté que l'anhydride acétique en présence d'acide *p*-toluène sulfonique anhydre (13) ou d'acide bromhydrique dans le benzène (14) sont de bons agents d'isomérisation des acétates énoliques. De notre côté, nous avons trouvé que le réactif préconisé par Edwards et Rao (15), anhydride acétique, acide perchlorique 70% dans l'acétate d'éthyle, est particulièrement intéressant: (*a*) il ne donne aucune réaction secondaire; les résultats sont facilement reproductibles, (*b*) la réaction est juste assez lente pour permettre de faire les observations suivantes: en série *cis* (*a*) (cétones **1** et **2**), la réaction débute par une commande cinétique et aboutit à un équilibre des acétates d'énols; en série *cis* (*e*) (cétone **3**) il n'y a pas de différence entre les résultats des commandes cinétiques et thermodynamique. En série *trans* (cétone **4**), il y a d'abord acétylation, avec commande cinétique, puis isomérisation et lent retour à la décalone de départ; au bout de 162 h, la réaction s'arrête à toutes fins pratiques; la mise en équilibre de chaque acétate énolique pur indique qu'il y a d'abord hydrolyse en décalone, puis isomérisation des acétates d'énols. Les résultats apparaissent au tableau 1.

La structure Δ^1 correspond, en r.m.n. aux acétates qui donnent un singulet en série *cis* (*a*) (5, 15) et un doublet (J = 4.8 Hz) en série *cis* (*e*): ceci est conforme (16) au fait qu'en série *cis* (*a*) (**5***a* et **6***a*) les protons 1 et 9 forment un angle de 90° et qu'en série *cis* (*e*) (**7***a*) cet angle est de 35° environ (mesuré sur un modèle de Dreiding). Le signal du proton vinylique en position 3 est un multiplet (5, 15).

Les structures découlant des spectres de r.m.n. nous obligent à reviser les pourcentages obtenus par méthode chimique et décrits précédemment (8, 9) pour les décalones **1** et **2**. Nos nouveaux résultats confirment l'absence de différences appréciables dans la direction de l'énolisation de décalones *cis* (*a*) et *cis* (*e*). Ils indiquent aussi que le groupe *gem* diméthyles n'a que peu d'influence sur cette direction en série *cis* (*a*), par rapport au groupe *tert*-butyle.

Partie expérimentale

1. Cétones

Les décalones *cis* **1** et **3** (préparées selon (17)) sont absolument pures et exemptes d'isomère *trans*, après

[1]Revision reçu le 21 décembre 1970.

TABLEAU 1. Résultats de la formation et de la mise à l'équilibre des acétates énoliques

Cétone de départ	Méthode cinétique* % Acétates Δ^1	Δ^2	%C=O‡	Durée (min)	Equilibre† % Acétates Δ^1	Δ^2	%C=O‡	Durée (min)
1	43.5	56.5	0.7	60	*i* 45	55	7.5	5
					i 59	41	5.5	120
					ii 60	40	4.5	180
					iii 60	40	4.6	210
2	40	60	1.2	90	*i* 38	62	6.4	5
					i 59	41	5.1	360
					ii 59	41	6.1	300
					iii 59	41	6.2	300
3	59	41	1.2	60	*i* 65	35	6.5	5
					i 65	35	7.5	120
					ii 65	35	6.4	150
					iii 64	36	5.2	240
4	33	67	2.2	60	*i* 30	70	24.0	2.5
					25	75	10.9	18
					24	76	11.6	60
					23	77	13.0	120
					24	77	42.0	162 h
					ii 90	10	10.8	2.5
					59	41	12	5
					38	62	11.3	17
					24	76	13.9	90
					24	76	35.6	42 h
					iii 4	96	9.6	2.5
					8	92	10.7	5
					17	83	11.7	17
					23	77	13.8	90
					24	76	24.8	41 h

*Acétate d'isopropényle et acide sulfurique; pour la préparation, voir (8, 9).
†Action de l'acide perchlorique 70% et l'anhydride acétique dans l'acétate d'éthyle sur: (*i*) la décalone, (*ii*) l'acétate énolique Δ^1, (*iii*) l'acétate énolique Δ^2.
‡%C=O indique le pourcentage de cétone de départ, dans le mélange, au temps indiqué; les pourcentages des acétates énoliques ont été recalculés pour donner les proportions respectives des acétates.

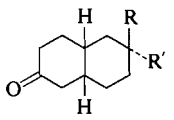

1 R = R′ = CH_3
2 R = H; R′ = *tert*-butyle

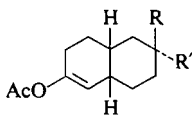

5*a* R = R′ = CH_3
6*a* R = H; R′ = *tert*-butyle

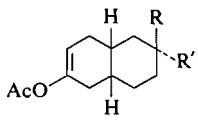

5*b* R = R′ = CH_3
6*b* R = H; R′ = *tert*-butyle

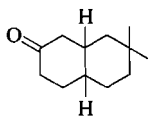

3

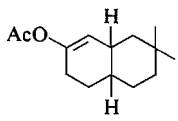

7a

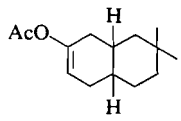

7b

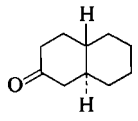

4

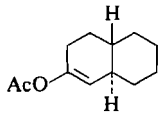

8*a*

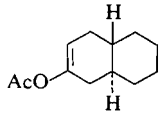

8*b*

Can. J. Chem. Downloaded from www.nrcresearchpress.com by 210.87.254.6 on 09/05/12
For personal use only.

TABLEAU 2. Caractérisation des acétates énoliques par c.p.g. et r.m.n.

Isomères	Temps de rétention (min)	Pureté (%)*	Spectre r.m.n. (60 MHz, TMS) δ	Largeur à mi-hauteur (Hz)	Signal
5*a*	63	99.4	5.03	3.3	s
5*b*	87	99.2	5.26	8.5	m
6*a*	35	99.3	4.98	3.5	s
6*b*	44	99.6	5.16	9.4	m
7*a*	26	99.1	5.16	6.3	d $J_{1,2}$ = 4.8 Hz $J_{1,3}$ = 0.9 Hz
7*b*	28	98.9	5.17	7.5	m
8*a*	116	99.6	5.12†	3.7	s
8*b*	132	99.3	5.26†	8.6	m

*La pureté est définie par rapport aux deux isomères Δ^1 et Δ^2.
†On indique 5.07 (s) et 5.22 (doublet de triplets) (13).

analyse en c.p.g. sur: (*a*) 5% QFI (FS 1265) sur Chromosorb G 80/100, A.W. DMCS, 3.6 m, 3 mm, 170–220°, 5–40 ml N_2/min; (*b*) 4% Carbowax 20M sur Chromosorb G 80/100, A.W. DMCS, 2.4 m, 3 mm, 130–200°, 5–40 ml N_2/min; (*c*) 20% Polyester Succinique de Craig sur Chromosorb P 80/100, 4.8 m, 6 mm, 180–200°, 30–60 ml N_2/min.

La cétone *cis* **2** qui résulte de la synthèse décrite précédemment (9) contient deux autres composés, décelés par c.p.g. (colonne *b* plus haut), représentant d'une part 3.2% d'isomère *trans* et d'autre part 8.7% d'un composé non identifié. La cétone pure **2**, homogène en c.p.g., cristallise lentement du mélange brut, abandonné pendant plusieurs semaines à 15–18°; elle fond à 32–33°.[2] Nous avons obtenu la cétone **4** pure par c.p.g. préparative à partir d'un mélange commercial des décalones-2 *trans* et *cis*, dans les conditions suivantes: 20% Carbowax 20M TPA sur Chromosorb P 80/100, A.W., 3.0 m, 6 mm de diamètre, 186°, 70 ml He/min.

2. Acétates énoliques

(2.1) Les mélanges d'acétates énoliques se séparent en c.p.g. analytique:

(*a*) Acétates **5***a* et *b*: sur 5% QFI (FS 1265) sur Chromosorb G 80/100, A.W. DMCS, 3.9 m, 3 mm, 176°, 20 ml N_2/min. Temps de rétention: Δ^1, 7.9 min; Δ^2, 9.2 min.

(*b*) Acétates **6***a* et *b*: sur 5% QFI (FS 1265) sur Chromosorb G 80/100, A.W. DMCS, 3.9 m, 3 mm, 176°, 18 ml N_2/min; temps de rétention: Δ^1, 10.0 min.; Δ^2, 12.2 min.

(*c*) Acétates **7***a* et *b*: sur 4% Carbowax 20M sur Chromosorb G 80/100, A.W. DMCS, 2.4 m, 3 mm, 180°, 42 ml N_2/min; temps de rétention: Δ^1, 8.5 min.; Δ^2, 9.3 min.

(*d*) Acétates **8***a* et *b*: sur 3% Carbowax 20M TPA, sur Chromosorb G 80/100, A.W., DMCS, 3.6 m, 4 mm de diamètre, 170°, 25 ml N_2/min; temps de rétention: Δ^1, 6.0 min.; Δ^2, 6.6 min.

(2.2) La séparation des acétates énoliques, préparés selon les méthodes décrites en (8, 9), se fait en c.p.g. préparative, dans les conditions suivantes, et les résultats figurent au tableau 2.

(*a*) Acétates **5***a* et *b*: sur 5% QFI (FS 1265) sur Chromosorb G 80/100, A.W. DMCS, 6 m, 9 mm, 185°, 60 ml N_2/min.

(*b*) Acétates **6***a* et *b*: sur 15% QFI (FS 1265) sur Chromosorb G 80/100, A.W. DMCS, 6 m, 6 mm, 198°, 60 ml He/min.

(*c*) Acétates **7***a* et *b*: sur 25% Carbowax 20M sur Chromosorb P 60/80, A.W. DMCS, 3 m, 6 mm, 175°, 47 ml He/min.

(*d*) Acétates **8***a* et *b*: sur 20% Carbowax 20M TPA sur Chromosorb P 80/100, A.W. 6 m, 6 mm de diamètre, 182°, 70 ml He/min.

Note: Les acétates énoliques correspondants aux trois décalones **1–4** peuvent très bien être séparés en c.p.g. analytique sur les phases stationnaires suivantes: QFI (FS 1265), Carbowax 20M, Carbowax 20M TPA ou sur Polyester Succinique de Craig en utilisant des taux d'imprégnation faibles (3–5%) et en c.p.g. préparative en utilisant des taux d'imprégnation plus élevés (20–25%).

La position des décalones est variable (il reste toujours quelques % de décalone lors de la formation des acétates énoliques dans les conditions thermodynamiques, voir tableau 1) suivant la phase stationnaire employée. Notamment dans le cas de la phase stationnaire Polyester succinique de Craig, la décalone se trouve masquée par l'un des deux acétates ce qui exclut l'emploi de cette phase stationnaire pour fins de c.p.g. analytique ou préparative dans les cas où il reste une certaine quantité de décalone. D'autre part sur Carbowax 20M nous avons constaté une certaine décomposition thermique des acétates énoliques, en c.p.g. préparative seulement. La phase stationnaire QFI (FS 1265) ne représente par contre aucun inconvénient en c.p.g. préparative.

3. Acétylation énolique et mise à l'équilibre

Le réactif utilisé a la composition suivante: 10^{-2} *M* $HClO_4$, 70% 1 *M* Ac_2O dans l'acétate d'éthyle (18). Un essai typique se déroule comme suit: 2.5 mmol de cétone (ou d'acétate énolique dans le cas d'une isomérisation) sont ajoutées à 24.8 ml de réactif; on laisse la solution,

[2]Pour une synthèse récente (voir 18).

Can. J. Chem. Downloaded from www.nrcresearchpress.com by 210.87.254.6 on 09/05/12
For personal use only.

sous agitation, à la température ambiante pour une durée pré-déterminée.

Le mélange réactionnel est par la suite lavé par une solution saturée de bicarbonate de sodium, par une solution saturée de sel, séché sur sulfate de sodium; puis l'acétate d'éthyle est évaporé sous vide. Les résultats sont rapportes au tableau 1, tels qu'obtenus par analyse par c.p.g. dans les conditions décrites à la section 2.1.

Les rendements sont en général de l'ordre de 90–95%, on ne note aucune formation de produits secondaires.

Un réactif vieux de plusieurs semaines perd de sa force d'acétylation (au bout de 360 min, le rapport **6***a*/**6***b* est 39–61 avec 6.8% de cétone **2**) et de sa force d'isomérisation (au bout de 600 min l'isomère **6***a*, pur à 99.9% s'isomèrise pour donner un mélange **6***a*/**6***b* de 93/7).

Nous remercions le Conseil National de Recherches du Canada de son aide financière (H.F.) et d'une bourse d'étude (L.V.).

1. W. G. Dauben, R A Micheli, et J. F. Easthan. J. Am. Chem. Soc. **74**, 3852 (1952).
2. Y. Mazur et F. Sondheimer. J. Am. Chem. Soc. **80**, 5220 (1958).
3. M. P. Hartshorn et E. R. H. Jones. J. Chem. Soc. 1312 (1962).
4. B. Berkoz, E. P. Chavez, et C. Djerassi. J. Chem. Soc. 1323 (1962).
5. A. J. Liston. J. Org. Chem. **31**, 2105 (1966).
6. A. J. Liston et M. Horwath. J. Org. Chem. **32**, 1034 (1967).
7. J. Champagne, H. Favre, D. Vocelle, et I. Zbikowski. Can. J. Chem. **42**, 212 (1964).
8. H. Favre et A. J. Liston. Can. J. Chem. **42**, 268 (1964).
9. H. Favre et A. J. Liston. Can. J. Chem. **47**, 3233 (1969).
10. D. H. R. Barton, R. M. Evans, J. C. Hamlet, P. G. Jones, et T. Walker. J. Chem. Soc. 747 (1954).
11. J. Libman et Y. Mazur. Tetrahedron, **25**, 1699 (1969).
12. W. B. Smith et T. K. Chen. J. Org. Chem. **30**, 3095 (1965).
13. H. O. House et B. M. Trost. J. Org. Chem. **30**, 1341 (1965).
14. P. Toft et A. J. Liston. Chem. Commun. 111 (1970).
15. B. E. Edwards et P. N. Rao. J. Org. Chem. **31**, 324 (1966).
16. A. A. Bothner-By. Adv. Magn. Resonance, **1**, 195 (1965).
17. H. Bruderlein, N. Dufort, H. Favre, et A. J. Liston. Can. J. Chem. **41**, 2908 (1963).
18. H. O. House, R. W. Giese, K. Kronberger, J. P. Kaplan, et J. F. Simeone. J. Am. Chem. Soc. **92**, 2800 (1970).

CNDO/2 Electron Densities and Proton Chemical Shifts

John F. Sebastian and John R. Grunwell
Department of Chemistry, Miami University, Oxford, Ohio 45056

Received October 30, 1970

An approximate linear dependence of the proton shifts on the CNDO/2[1] calculated electron densities on hydrogen for $C_5H_5^-$, C_6H_6, $C_7H_7^+$, $C_5H_5NH^+$, and $C_6H_5CH_2^-$ has been found. The significance and limitations of the correlation are discussed.

On a trouvé une relation linéaire approchée entre les déplacements chimiques des protons et les densités électroniques calculées d'après la méthode CNDO/2[1] pour les hydrogènes du $C_5H_5^-$, C_6H_6, $C_7H_7^+$, $C_5H_5NH^+$ et $C_6H_5CH_2^-$. On discute de la signification et des limitations de cette corrélation.

Canadian Journal of Chemistry, 49, 1779 (1971)

Linear correlations of ^1H and ^{13}C chemical shifts with carbon charge densities have been established previously (1–4). We wish to report an approximate linear correlation of the hydrogen electron densities with the ^1H chemical shifts for $C_5H_5^-$, C_6H_6, $C_7H_7^+$, $C_5H_5NH^+$ (*para*-hydrogen), and $C_6H_5CH_2^-$ (*para*-hydrogen). All densities were calculated using the CNDO/2 method (5) and, except for pyridine and pyridinium ion, standard geometries were used. The geometries of pyridine and pyridinium ion were taken from a microwave study and X-ray diffraction analysis, respectively (see Table 1 for shift values and densities taken from the literature). The shifts for $C_5H_5^-$ and $C_7H_7^+$ have been corrected for the effect of ring size on the ring current (3).

[1]Program 141, Quantum Chemistry Program Exchange, Indiana University.

Can. J. Chem. Downloaded from www.nrcresearchpress.com by 210.87.254.6 on 09/05/12
For personal use only.

sous agitation, à la température ambiante pour une durée pré-déterminée.

Le mélange réactionnel est par la suite lavé par une solution saturée de bicarbonate de sodium, par une solution saturée de sel, séché sur sulfate de sodium; puis l'acétate d'éthyle est évaporé sous vide. Les résultats sont rapportes au tableau 1, tels qu'obtenus par analyse par c.p.g. dans les conditions décrites à la section 2.1.

Les rendements sont en général de l'ordre de 90–95%, on ne note aucune formation de produits secondaires.

Un réactif vieux de plusieurs semaines perd de sa force d'acétylation (au bout de 360 min, le rapport **6***a*/**6***b* est 39–61 avec 6.8% de cétone **2**) et de sa force d'isomérisation (au bout de 600 min l'isomère **6***a*, pur à 99.9% s'isomèrise pour donner un mélange **6***a*/**6***b* de 93/7).

Nous remercions le Conseil National de Recherches du Canada de son aide financière (H.F.) et d'une bourse d'étude (L.V.).

1. W. G. Dauben, R A Micheli, et J. F. Easthan. J. Am. Chem. Soc. **74**, 3852 (1952).
2. Y. Mazur et F. Sondheimer. J. Am. Chem. Soc. **80**, 5220 (1958).
3. M. P. Hartshorn et E. R. H. Jones. J. Chem. Soc. 1312 (1962).
4. B. Berkoz, E. P. Chavez, et C. Djerassi. J. Chem. Soc. 1323 (1962).
5. A. J. Liston. J. Org. Chem. **31**, 2105 (1966).
6. A. J. Liston et M. Horwath. J. Org. Chem. **32**, 1034 (1967).
7. J. Champagne, H. Favre, D. Vocelle, et I. Zbikowski. Can. J. Chem. **42**, 212 (1964).
8. H. Favre et A. J. Liston. Can. J. Chem. **42**, 268 (1964).
9. H. Favre et A. J. Liston. Can. J. Chem. **47**, 3233 (1969).
10. D. H. R. Barton, R. M. Evans, J. C. Hamlet, P. G. Jones, et T. Walker. J. Chem. Soc. 747 (1954).
11. J. Libman et Y. Mazur. Tetrahedron, **25**, 1699 (1969).
12. W. B. Smith et T. K. Chen. J. Org. Chem. **30**, 3095 (1965).
13. H. O. House et B. M. Trost. J. Org. Chem. **30**, 1341 (1965).
14. P. Toft et A. J. Liston. Chem. Commun. 111 (1970).
15. B. E. Edwards et P. N. Rao. J. Org. Chem. **31**, 324 (1966).
16. A. A. Bothner-By. Adv. Magn. Resonance, **1**, 195 (1965).
17. H. Bruderlein, N. Dufort, H. Favre, et A. J. Liston. Can. J. Chem. **41**, 2908 (1963).
18. H. O. House, R. W. Giese, K. Kronberger, J. P. Kaplan, et J. F. Simeone. J. Am. Chem. Soc. **92**, 2800 (1970).

CNDO/2 Electron Densities and Proton Chemical Shifts

John F. Sebastian and John R. Grunwell
Department of Chemistry, Miami University, Oxford, Ohio 45056

Received October 30, 1970

An approximate linear dependence of the proton shifts on the CNDO/2[1] calculated electron densities on hydrogen for $C_5H_5^-$, C_6H_6, $C_7H_7^+$, $C_5H_5NH^+$, and $C_6H_5CH_2^-$ has been found. The significance and limitations of the correlation are discussed.

On a trouvé une relation linéaire approchée entre les déplacements chimiques des protons et les densités électroniques calculées d'après la méthode CNDO/2[1] pour les hydrogènes du $C_5H_5^-$, C_6H_6, $C_7H_7^+$, $C_5H_5NH^+$ et $C_6H_5CH_2^-$. On discute de la signification et des limitations de cette corrélation.

Canadian Journal of Chemistry, 49, 1779 (1971)

Linear correlations of ^1H and ^{13}C chemical shifts with carbon charge densities have been established previously (1–4). We wish to report an approximate linear correlation of the hydrogen electron densities with the ^1H chemical shifts for $C_5H_5^-$, C_6H_6, $C_7H_7^+$, $C_5H_5NH^+$ (*para*-hydrogen), and $C_6H_5CH_2^-$ (*para*-hydrogen). All densities were calculated using the CNDO/2 method (5) and, except for pyridine and pyridinium ion, standard geometries were used. The geometries of pyridine and pyridinium ion were taken from a microwave study and X-ray diffraction analysis, respectively (see Table 1 for shift values and densities taken from the literature). The shifts for $C_5H_5^-$ and $C_7H_7^+$ have been corrected for the effect of ring size on the ring current (3).

[1]Program 141, Quantum Chemistry Program Exchange, Indiana University.

Can. J. Chem. Downloaded from www.nrcresearchpress.com by 210.87.254.105 on 09/05/12
For personal use only.

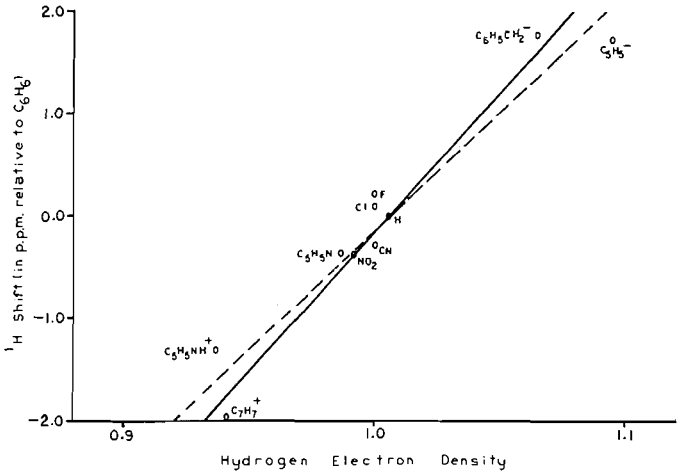

FIG. 1. Correlation of *para*-^{1}H shifts (relative to benzene) of monosubstituted benzenes pyridine, C_6H_6, and aromatic ions and the hydrogen electron densities as calculated by the CNDO/2 method. The solid line was chosen to have a slope of 26.6 p.p.m./*e* and to pass through the point for benzene. The slope of the best line (least squares; dashed line) is 23.4 p.p.m./*e*.

TABLE 1. Summary of chemical shifts and hydrogen electron densities

Compound	Chemical shift*	Hydrogen electron density
$C_7H_7^+$	−1.98	0.941
$C_5H_5NH^+$	−1.30†	0.937†
C_5H_5N	−0.37†	0.987†
$C_6H_5NO_2$	−0.38‡	0.992
C_6H_5CN	−0.28‡	1.001
C_6H_6	0.00	1.006
C_6H_5Cl	0.09‡	1.001
C_6H_5F	0.22§	1.001
$C_6H_5CH_2^-$	1.77§	1.065‖
$C_5H_5^-$	1.73	1.095

*In p.p.m. relative to benzene. A minus sign indicates a downfield shift. *Para*-hydrogen only.
†Reference 11.
‡Reference 15.
§Reference 13, p. 265; δ for $C_6H_5CH_2Li$ corrected to $\delta(C_6H_6) = 0.0$ p.p.m. scale.
‖Reference 16.

A plot of hydrogen electron densities *vs.* ^{1}H chemical shifts is shown in Fig. 1. The solid line drawn through the points was chosen to have a slope of 26.6 p.p.m./*e* and to pass through the point for benzene. This value of the slope is the best estimate for the shielding of a proton in the hydrogen molecule (6). The local diamagnetic shielding in a hydrogen atom has been calculated to be 17.8 p.p.m./*e* (7). The best straight line (least squares, dashed line in Fig. 1) for all points has a slope of 23.4 p.p.m./*e*. The similarity of the two slopes and the observed approximate linear correlation suggest that large differences in the chemical shift (*cf.* aromatic ions of opposite charge type, Table 1) are dominated by changes in the hydrogen electron densities. The deviation from the line of the points may be due to non-linear electric field effects (8, 9), overestimation of charge dipole sigma polarization (10) or other factors. The view presented here suggests that the shift difference between the *para*-hydrogen (γ-H) of pyridine and the corresponding proton of pyridinium ion is largely due to a change in hydrogen 1s electron density. This view differs from that reported earlier (11) and supports the conclusions of Yonezawa and co-workers (12).

Shift data (13) and the calculated hydrogen electron densities for the *para*-hydrogens of some neutral monosubstituted benzene derivatives and pyridine are included in Fig. 1. The *ortho*- and *meta*-hydrogens are not plotted since they may be subject to substituent field effects (14). The deviation of the points is a result of the small values for the charges and chemical shifts (relative to benzene) as compared to the corresponding values for the aromatic ions. The scatter may reflect the intervention of long range shielding effects, to which proton shifts are quite sensitive, and deviations from the standard geometries assumed in the calculations.

Normally, the order of proton shifts in a molecule having two or more chemically distinct protons cannot be predicted correctly by hydrogen charge density considerations alone.

The *para*-hydrogen charge density (−0.001)

Can. J. Chem. Downloaded from www.nrcresearchpress.com by 210.87.254.105 on 09/05/12
For personal use only.

calculated for chlorobenzene and plotted in Fig. 1 is obtained by excluding d-orbitals from the basis set. Including d-orbitals insignificantly changes the hydrogen charge density to +0.001. However, the total charge density on the *para*-carbon atom *is* dependent on inclusion of d-orbitals in the basis set (−0.002 without d-orbitals, +0.014 with). A plot of *para*-^{13}C shifts (14) *vs.* *para*-carbon charge densities (CNDO/2 method) for the neutral monosubstituted benzene derivatives, $C_5H_5^-$, and $C_7H_7^+$ yields a straight line (slope = 280 p.p.m./*e*). The charge density which gave the best fit to the line for the *para*-carbon atom in chlorobenzene was calculated by excluding d-orbitals from the basis set.

One of us (J.F.S.) thanks the Miami University Research Committee for a Summer Faculty Research Fellowship. We are indebted to Mr. Wally Danison and Mr. Art Fiser for getting the CNDO/2 program operational. Finally we wish to express our appreciation to the Miami University Computer Center for the generous amount of computer time.

1. G. Fraenkel, R. E. Carter, A. McLachlan, and J. H. Richards. J. Am. Chem. Soc. **82**, 5846 (1960).
2. H. Spiesecke and W. G. Schneider. Tetrahedron Lett. 368 (1961).
3. T. Schaefer and W. G. Schneider. Can. J. Chem. **41**, 966 (1963).
4. J. E. Bloor and D. L. Breen. J. Phys. Chem. **72**, 716 (1968).
5. J. A. Pople and D. L. Beveridge. Approximate molecular orbital theory. McGraw-Hill, New York. 1970.
6. J. I. Musher. *In* Advances in magnetic resonance. Vol. 2. *Edited by* J. S. Waugh. Academic Press, New York. 1966. p. 199.
7. J. A. Pople, W. G. Schneider, and H. J. Berstein. High-resolution nuclear magnetic resonance. McGraw-Hill, New York. 1958. p. 175.
8. T. W. Marshall and J. A. Pople. Mol. Phys. **1**, 199 (1958).
9. J. I. Musher. J. Chem. Phys **37**, 34 (1962).
10. R. G. Jesaitis and A. Streitwieser, Jr. Theor. Chim. Acta, **17**, 165 (1970).
11. J. W. Emsley. J. Chem. Soc. A, 1387 (1968).
12. H. Katô, H. Kato, and T. Yonezawa. Bull. Chem. Soc. Jap. **43**, 1921 (1970).
13. L. M. Jackman and S. Sternhell. Applications of nuclear magnetic resonance spectroscopy in organic chemistry. Pergamon Press, London. 1969. p. 202.
14. H. Speisecke and W. G. Schneider. J. Chem. Phys. **35**, 731 (1961).
15. K. Hayamizu and O. Yamaoto. J. Mol. Spectry. **28**, 89 (1968).
16. A. Streitwieser, Jr., P. C. Mowery, R. G. Jesaitis, J. R. Wright, P. H. Owens, and D. M. E. Reuben. The Jerusalem symposia on quantum chemistry and biochemistry. Vol. II. 1970. p. 160.

Can. J. Chem. Downloaded from www.nrcresearchpress.com by 210.87.254.105 on 09/05/12
For personal use only.

Can. J. Chem. Downloaded from www.nrcresearchpress.com by 210.87.254.40 on 09/05/12
For personal use only.

Electron Spin Resonance Detection of Electrochemical Intermediates Formed During Oxygen Evolution[1]

C. L. GARDNER AND E. J. CASEY

Defence Research Board, Defence Research Establishment Ottawa, Ottawa 4, Canada

Received January 7, 1971

Electron spin resonance detection has been made of ozonide ion (O_3^-) and another unidentified species (X) formed during anodic oxygen evolution in concentrated KOH solutions at low temperature. The relative amounts observed depend on the metal used for the anode. New insight into the mechanism of oxygen evolution results.

Nous avons détecté, par la r.p.e., des ions (O_3^-) ozonides et aussi une autre espèce inconnue qui est engendrée pendant l'émission de l'oxygène par une anode dans une solution concentrée de KOH à basse température. Les quantités relatives observées dépendent du métal utilisé pour l'anode. Une meilleure compréhension du mécanisme de l'émission de l'oxygène est ainsi obtenue.

Canadian Journal of Chemistry, 49, 1782 (1971)

In the course of a recent study of the anodic oxidation of metals in concentrated potassium hydroxide at low temperatures, we have been able to detect several paramagnetic intermediates including the ozonide ion (O_3^-) and an unidentified species, "X". Controlled potential measurements have demonstrated that the O_3^- is formed only during oxygen evolution. In addition, as shown in Table 1, the intermediates observed depend on the metal used.

Anodic oxidations of the various metals were carried out in 45% KOH and at high current densities ($\sim$ 90 mA/cm^2) at -40 °C. The experimental technique necessary to observe the species X involved plunging a cooled, open-ended 4 mm silica tube into the anolyte and transferring this tube as rapidly as possible into liquid nitrogen. The O_3^- is sufficiently long-lived at -40 °C that it could be observed by flowing the anolyte down into a low temperature aqueous cell where the species could then be observed either in solution and the decay kinetics studied or else frozen and the polycrystalline spectrum studied. The electron spin resonance (e.s.r.) spectrum formed during the anodic oxidation of a silver foil electrode is shown in Fig. 1. The spectrum is characterized by

TABLE 1. Species detected by e.s.r. during the anodic process

Anode material	Species detected*
Silver	O_3^-(s); X(w)
Cadmium	O_3^-(s); X(w)
Lead	O_3^-(w); X(w)
Nickel	X(w)
Platinum	X(w)
Copper	CuO_2^{2-}(s); X(w)

*w = weak; s = strong e.s.r. signal.

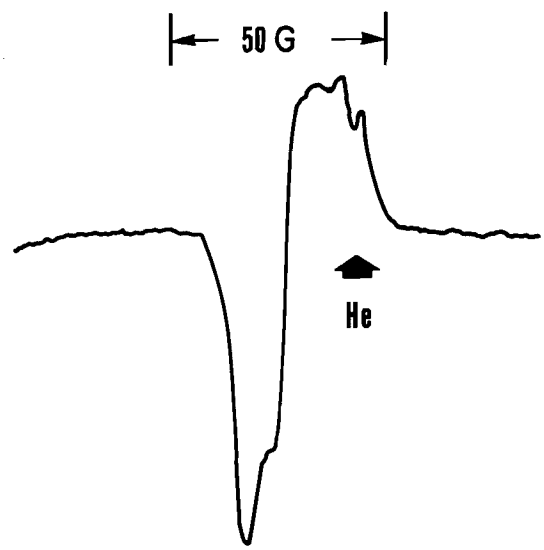

FIG. 1. Electron spin resonance spectrum of O_3^- formed in the anolyte during the anodic oxidation of silver at -40 °C in 45% KOH, then frozen at 77 °K.

[1]DREO Technical Note No. 71-9.

Can. J. Chem. Downloaded from www.nrcresearchpress.com by 210.87.254.40 on 09/05/12
For personal use only.

TABLE 2. Principal g-values for O_3^-

Matrix	g_{xx}	g_{yy}	g_{zz}
$KClO_4$ (ref. 3)	2.0174	2.0113	2.0025
$KClO_4$ (ref. 4)	2.018	2.011	2.0034
NaO_3 (ref. 1)	2.015	2.015	2.003
This work	2.0181	2.0112	2.0019

a non-axial g-tensor (Table 2). Identification of the species as O_3^- can be made by comparison with the results of other workers on alkali ozonides (1, 2), γ-irradiation of $KClO_4$ (3, 4) and the u.v.-irradiation of alkaline glasses containing H_2O_2 (2). Parameters from some of these systems are included in Table 2.

The e.s.r. spectrum due to the species X consists of a narrow line (linewidth $\simeq$ 2 G) with $g = 2.002$. This species causes the small inflection at He in Fig. 1. In other spectra, this line can be much more pronounced. The absence of hyperfine interactions or g-shifts indicates that this spectrum is due to a species with an essentially "free" electron. In our opinion the most likely identity is either a solvated electron (5) or else it is due to conduction electrons (6) in small metal or metal oxide particles ejected into solution during the oxidation. Additional work is in progress in order that a more positive identification can be made.

The mechanism of oxygen evolution in alkaline solution is generally considered (7) to involve discharge of adsorbed hydroxyl ions as the first step

[1] $$OH^- \rightarrow OH\cdot + e^-$$

Other steps involving adsorbed species, such as those given in reactions 2–4, could follow

[2] $$OH\cdot + OH^- \rightarrow H_2O + O^-$$

[3] $$O^- \rightarrow O\cdot + e^-$$

[4] $$O\cdot + O\cdot \rightarrow O_2$$

The O_3^- formed in our system could arise from reaction

[5] $$O^- + O_2 \rightarrow O_3^-$$

or alternatively by dissociation of HO_3 to O_3^- in strong base following reaction 6

[6] $$OH\cdot + O_2 \rightarrow HO_3$$

Addition of a small amount of methanol to the solution in the electrolysis cell almost completely eliminated the e.s.r. signal due to O_3^-. Since it is known (8) that the formation of O_3^- during the radiolysis of alkaline solutions can be suppressed by the addition of a hydroxyl radical scavenger such as methanol, this observation provides strong evidence that hydroxyl radicals are a precursor to the *anodic* formation of O_3^- as well.

It is interesting to speculate on the observation that the species detected depends on the metal used (Table 1). This result must indicate that the mechanism of oxygen evolution differs amongst the metals. In particular, there appears to be a fundamental difference in the oxygen evolution mechanism between active metals such as silver and cadmium, and the passive metals such as nickel and platinum. One could argue that if the $OH\cdot$ is weakly bound it can leave the surface and form O_3^- by reaction 5 or 6 (Ag or Cd), but if the $OH\cdot$ is strongly bound no O_3^- is produced (Ni or Pt). Lead appears to be intermediate.

Some preliminary results of the anodic oxidation of cadmium at higher temperatures (−10 °C) and lower KOH concentrations (30%) have indicated that O_2^-, rather than O_3^-, is the major product detected by e.s.r. under these conditions.

This work is part of a continuing study of battery electrode mechanisms at low temperature. More complete results including kinetic results and effects of pH on these species will be included in a future publication.

1. J. E. BENNETT, D. J. E. INGRAM, and D. SCHONLAND. Proc. Phys. Soc. London, **A69**, 556 (1956).
2. A. D. MCLACHLAN, M. C. R. SYMONS, and M. G. TOWNSEND. J. Chem. Soc. 952 (1959).
3. P. W. ATKINS, J. A. BRIVATI, N. KEEN, M. C. R. SYMONS, and P. A. TREVALION. J. Chem. Soc. 4785 (1962).
4. A. V. DUBOVITSKII and G. B. MANELIS. Kin. Katal. **6**, 828 (1965).
5. L. KEVAN. J. Am. Chem. Soc. **87**, 1481 (1965).
6. F. VESCIAL, N. S. VANDERVEN, and R. T. SCHUMAKER. Phys. Rev. **134**, 1286 (1964).
7. J. O'M. BOCKRIS. J. Chem. Phys. **24**, 817 (1956).
8. G. CZAPSKI and L. M. DORFMAN. J. Phys. Chem. **68**, 1169 (1964).

Can. J. Chem. Downloaded from www.nrcresearchpress.com by 210.87.254.42 on 09/05/12
For personal use only.

Canadian Journal of Chemistry

Published by THE NATIONAL RESEARCH COUNCIL OF CANADA

VOLUME 49 JUNE 1, 1971 NUMBER 11

Sur la formation de composés bicycliques lors de réactions de Friedel–Crafts

N. DUFORT, B. JODOIN, ET J. LAFONTAINE

Département de chimie, Université de Montréal, Montréal, Québec

Reçu le 29 décembre 1970

Le méthyl-1 cyclohexène est condensé avec le chlorure de propionyle, de butyryle, et de benzoyle en présence de différents acides de Lewis. Les isomères *exo* et *endo* acyl-1 méthyl-6 bicyclo[3.1.0]hexane se forment avec des pourcentages variables dépendant du catalyseur utilisé. La condensation avec le chlorure de benzoyle en plus de conduire à des composés bicycliques donne également le benzoyl-3 méthyl-2 cyclohexanol. La condensation du chlorure d'acétyle sur le pentaméthyl-1,3,3,5,5 cyclohexène en présence de chlorure stannique ne donne pas de composés bicycliques.

The acylation of 1-methylcyclohexene with propionyl, butyryl, and benzoyl chloride in the presence of different Lewis acids is reported. The *exo* and *endo* 1-acyl-6-methyl bicyclo[3.1.0]hexane isomers are formed with variable percentages depending upon the catalyst used. An unexpected compound, 3-benzoyl-2-methylcyclohexanol, was isolated from the reaction of 1-methylcyclohexene with benzoyl chloride. The acylation of 1,3,3,5,5-pentamethylcyclohexene with acetyl chloride – stannic chloride gave no bicyclic compounds.

Canadian Journal of Chemistry, 49, 1785 (1971)

Lors d'une publication antérieure (1), nous rapportions la formation de l'*endo* et de l'*exo* acétyl-1 méthyl-6 bicyclo[3.1.0]hexane lors d'une réaction de Friedel–Crafts. Nous avons poussé plus loin cette étude, en particulier l'effet de la grosseur de l'agent acylant et la nature du catalyseur sur la formation de composés bicycliques et nous en rapportons les résultats dans la présente publication.

Le méthyl-1 cyclohexène est condensé avec le chlorure de propionyle, le chlorure de butyryle, et le chlorure de benzoyle en présence de différents acides de Lewis: $AlCl_3$, $SnCl_4$, $ZnCl_2$, et BF_3. Le mélange réactionnel est ensuite traité par une solution méthanolique d'hydroxyde de sodium. Les résultats obtenus sont rapportés dans le tableau 1. Tous les composés indiqués au tableau 1 sont isolés à l'état pur par c.p.g. préparative sauf le composé **3***a* à cause du fait qu'il ne se forme qu'en très petite quantité et qu'il est alors impossible de le séparer de ses isomères.

Les cétones α,β et β,γ éthyléniques formées sont identifiées comme on l'indique dans la partie expérimentale par leurs spectres i.r., u.v., et de r.m.n. Le spectre de masse ou l'analyse élémentaire des nouveaux composés vient confirmer leur structure. Les spectres i.r. des composés **1***a* et *d* montrent une bande à 1685 cm^{-1}. Dans l'u.v., ces composés présentent respectivement un maximum à 213 et 211 mμ. Le spectre r.m.n. des composés **1***a* et *d* n'indique aucun proton éthylénique. De plus, ces composés résistent à l'ozone mais s'isomérisent en présence d'acide oxalique pour conduire à un mélange formé de 34% de

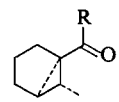

1*a* R = C_2H_5
2*a* R = C_3H_7
3*a* R = C_6H_5

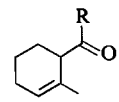

1*b* R = C_2H_5
2*b* R = C_3H_7
3*b* R = C_6H_5

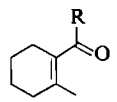

1*c* R = C_2H_5
2*c* R = C_3H_7
3*c* R = C_6H_5

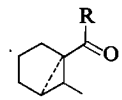

1*d* R = C_2H_5
2*d* R = C_3H_7
3*d* R = C_6H_5

TABLEAU 1. Composés obtenus lors des différentes condensations

Réactifs	Catalyseurs	Produits	Pourcentage des produits formés a:b:c:d
Chlorure de propionyle	$AlCl_3$	**1**	10:47:23:20*
	$SnCl_4$		5:12:33:50
	$ZnCl_2$		0:23:68:9
	BF_3		0:60:40:0
Chlorure de butyryle	$AlCl_3$	**2**	2:49:39:10*
	$SnCl_4$		3:13:36:48
	$ZnCl_2$		1:21:64:14
	BF_3		0:64:36:0
Chlorure de benzoyle	$AlCl_3$	**3**	0:30:55:15*
	$SnCl_4$		2:9:41:48
	$ZnCl_2$		0:46:24:30
	BF_3		0:90:10:0

*L'analyse par c.p.g. des produits de la condensation en utilisant $AlCl_3$ comme catalyseur indique la présence d'une petite quantité d'un produit dont le pic sort avant celui qui représente l'isomère *exo*. Ce produit n'a pas été identifié et est exclu du calcul du pourcentage des différents isomères.

composé **1***b* et de 66% de composé **1***c* ce qui permet de conclure que ces composés comportent un anneau cyclopropanique conjugué avec le groupe carbonyle. Il s'agirait donc de l'*exo* propionyl-1 méthyl-6 bicyclo[3.1.0]hexane (**1***a*) et de l'*endo* propionyl-1 méthyl-6 bicyclo[3.1.0]hexane (**1***d*).

Pour confirmer ces structures, on a fait la synthèse de l'isomère *exo* selon le cheminement indiqué sur le schéma 1. Le composé **1***b* est d'abord transformé sous forme d'acétal **4** et ensuite soumis à l'hydroboration selon la méthode de Brown et Subba Rao (2) pour conduire au composé **5** dans lequel les groupes méthyle et hydroxyle sont nécessairement *trans* l'un par rapport à l'autre. Après hydrolyse et tosylation du composé **5**, on obtient le composé **7** qui traité par NaOH alcoolique conduit à la formation d'un seul composé bicyclique; l'*exo* propionyl-1 méthyl-6 bicyclo[3. 1.0]hexane. Ce composé se superpose parfaitement en c.p.g. avec le composé **1***a* obtenu à 5% lors de la condensation ce qui confirme la structure proposée. Les composés **2***a* et *d* présentent respectivement une bande à 1685 et 1680 cm^{-1} dans l'i.r. et une absorption à 215 et 212 mμ dans l'u.v. Ces composés qui ne présentent pas de proton éthylénique dans leur spectre r.m.n., résistent à l'ozone; mais ils s'isomérisent pour donner 34% de composé **2***b* et 66% de composé **2***c*. En se basant sur les différentes données spectrales, les composés **2***a* et *d* ont été identifiés comme étant respectivement l'*exo* et l'*endo* butyryl-1 méthyl-6 bicyclo[3.1.0]hexane.

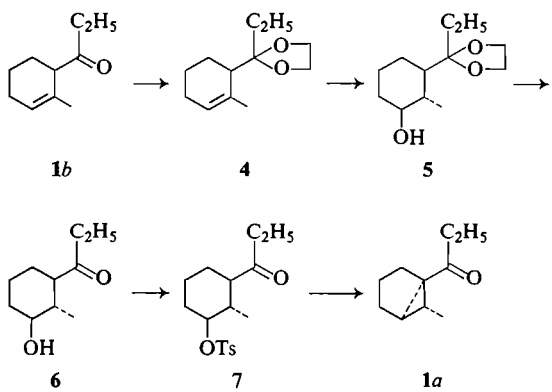

SCHÉMA 1

De plus, l'analyse par c.p.g. de ces composés et des composés analogues de la série propionyle sur trois colonnes différentes comme l'indique le tableau 2 vient confirmer les structures proposées puisque l'ordre d'élution des différents isomères est toujours le même quelle que soit la colonne utilisée; il n'y a que le temps de rétention qui varie.

Le composé **3***a* n'a pas pu être isolé à cause de sa formation en très petite quantité (2%). Le composé **3***d* absorbe à 1660 cm^{-1} dans i.r. et à 241 mμ dans u.v. Le spectre r.m.n. qui présente un doublet à 1.20 p.p.m. pour le méthyle sur le cyclohexane et aucun proton éthylénique est tout à fait conforme à la structure proposée en l'occurence l'*endo* benzoyl-1 méthyl-6 bicyclo[3.1.0]-hexane.

Si lors de la condensation du chlorure de benzoyle avec le méthyl-1 cyclohexène, le mélange

Can. J. Chem. Downloaded from www.nrcresearchpress.com by 210.87.254.42 on 09/05/12
For personal use only.

TABLEAU 2. Temps de rétention (en min) des composés analogues sur différentes colonnes

Colonnes utilisées	Température (°C)	R		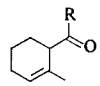	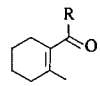	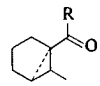
Polyester de Craig 3% sur Chromosorb G; longueur: 15 p	155	C_2H_5	3	3.5	4	5
	155	C_3H_7	4	4.6	5.5	6
	190	C_6H_5	10.6	11.8	13.2	15
QF1 3% sur Diatoport S; longueur: 20 p	145	C_2H_5	14	16	18	22
	170	C_3H_7	12	14	16	18
	190	C_6H_5	20	22	25	30
Carbowax 20M TPA 3% sur Chromosorb G; longueur: 20 p	130	C_2H_5	2.2	2.8	3.6	4
	130	C_3H_7	12	14	18	19
Carbowax 20M TPA 25% sur Chromosorb P; longueur: 10 p	200	C_6H_5	42	48	54	60

réactionnel obtenu après déshydrochloruration est laissé quelques heures à la température de la pièce, il cristallise un produit avec un rendement de 12.5%. Ce composé fond à 116–117 °C après recristallisation dans un mélange éther – éther de pétrole. Ce composé présente une bande carbonyle à 1665 cm^{-1} et une bande hydroxyle à 3450 cm^{-1} dans i.r. Le spectre r.m.n. indique également la présence d'un groupe hydroxyle puisqu'un massif à 3.26 p.p.m. (1H) disparaît par échange avec de l'eau deutérée. Il apparaît deux multiplets à 7.60 et 7.95 p.p.m. pour les protons du groupe phényle et un doublet à 0.85 p.p.m. pouvant correspondre à un méthyle sur le cyclohexane.

En se basant sur les données spectrales et l'analyse élémentaire, ce composé a été identifié comme étant le benzoyl-3 méthyl-2 cyclohexanol (**8**). Ce composé indique à l'analyse par c.p.g. la présence d'un seul produit dont le temps d'élution est le même que pour le composé **3***b*. Une injection mixte des deux composés conduit à la présence d'un seul pic. Il se produit donc une déshydratation. D'ailleurs par c.p.g. préparative, on a pu isoler le composé **3***b* à partir du composé **8**.

Afin de vérifier si ce produit se forme lors de la condensation ou lors de la déshydrochloruration, le chlorure de benzoyle a été condensé au méthyl-1 cyclohexène en présence de chlorure stannique et le mélange réactionnel après extraction fut laissé à la température de la pièce sans traitement par une base forte. Après quelques heures, le composé **8** commença à cristalliser. Le composé **8** pourrait s'expliquer par un mécanisme analogue à celui qui a été proposé par Ahmad *et al.* (3) pour la formation de l'acétyl-10β *trans* décalol-2β

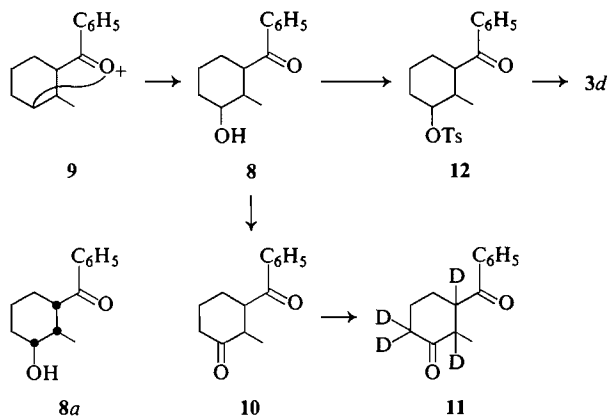

SCHÉMA 2

(schéma 2). L'ion carbonium serait stabilisé par le doublet de l'oxygène pour donner l'intermédiaire **9** qui traité par de l'eau donnerait le composé **8**. Afin de prouver avec certitude la position du groupe hydroxyle qui pouvait occuper la position 3 ou 4 comme dans le cas des cétones chlorées (4), l'alcool est oxydé par l'anhydride chromique dans la pyridine (5) en dicétone **10** qui traitée par de l'eau deutérée donne la dicétone **11**. Comme dans le spectre r.m.n., le méthyle sur le cyclohexane passe d'un doublet à un singulet en traitant la dicétone par de l'eau deutérée, la présence du groupe hydroxyle en position-3 est confirmée.

Comme l'alcool **8** est un composé analogue au composé **6**, il devenait intéressant de le tosyler et de le déshydrotosyler pour savoir s'il y aurait formation de l'*exo* benzoyl-1 méthyl-6 bicyclo[3.1.0]-hexane (**3***a*) comme lors de la synthèse décrite précédemment. Quand le tosylate **12** est traité par une solution méthanolique d'hydroxyde de so-

Can. J. Chem. Downloaded from www.nrcresearchpress.com by 210.87.254.42 on 09/05/12
For personal use only.

Can. J. Chem. Downloaded from www.nrcresearchpress.com by 210.87.254.42 on 09/05/12
For personal use only.

dium à 20%, l'analyse par c.p.g. indique la présence d'un seul pic qui se superpose parfaitement avec celui de l'isomère *endo* **3***d*.

A la lumière de ces résultats, on peut donc déduire que les groupes méthyle et hydroxyle doivent être dans une configuration *cis* puisqu'une configuration *trans* de ces deux substituants conduirait exclusivement à l'isomère *exo* tel que prouvé lors de la synthèse de l'*exo* méthyl-6 propionyl-1 bicyclo[3.1.0]hexane (**1***a*). De plus, si la formation du composé **8** se fait par l'intermédiaire **9**, le cétoalcool **8** devrait être représenté par la structure **8***a*. On a également fait la condensation du chlorure d'acétyle sur le pentaméthyl-1,3,3,5,5 cyclohexène en présence de chlorure stannique suivi d'un traitement par l'hydroxyde de sodium alcoolique afin d'étudier l'influence des *gem*-diméthyles en position-3,5 sur la formation de composés cyclopropaniques. Cette condensation donne à l'analyse par c.p.g. l'acétyl-1 pentaméthyl-1,3,3,5,5 cyclohexène (**14**) et l'acétyl-1 pentaméthyl-2,4,4,6,6 cyclohexène (**15**) dans une proportion de 1 à 10 et il n'apparaît pas de pic pouvant correspondre à des composés cyclopropaniques. De plus, le mélange réactionnel ozoné indique à l'analyse par c.p.g. la disparition des pics correspondants aux composés **14** et **15** et le chromatogramme ne présente aucun pic qui pourrait être attribué à des composés bicycliques.

Il est intéressant de noter que l'isomération de ce mélange même pendant quatorze jours en présence d'acide oxalique ne permet pas d'augmenter le pourcentage du composé **15**. Comme il était alors impossible d'obtenir le composé **15** à l'état pur par c.p.g. préparative à cause de son faible pourcentage et des temps de rétention trop voisins, il est synthétisé comme l'indique le schéma 3.

L'hydroboration du composé **13** conduit au *trans* pentaméthyl-2,2,4,4,6 cyclohexanol (**16**) qui

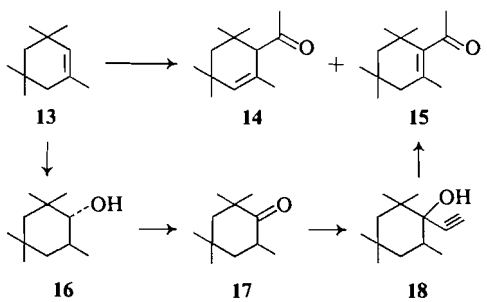

SCHÉMA 3

traité par l'anhydride chromique dans la pyridine (5) donne la pentaméthyl-2,2,4,4,6 cyclohexanone (**17**). Cette cétone traitée par l'acétylure de lithium selon la méthode de Beumel et Harris (6) donne l'éthynyl-1 pentaméthyl-2,2,4,4,6 cyclohexanol (**18**) qui chauffé à reflux en présence d'acide formique donne la cétone conjuguée (**15**).

Ce travail permet de déduire que les chlorures d'acide condensés avec le méthyl-1 cyclohexène conduisent généralement à la formation de composés bicycliques avec des pourcentages variables dépendant du catalyseur utilisé. Le chlorure stannique s'avère de beaucoup le meilleur catalyseur pour la formation de ces composés bicycliques tandis qu'avec le trifluorure de bore, on en retrouve aucune trace.

Enfin, la condensation du chlorure d'acétyle sur le pentaméthyl-1,3,3,5,5 cyclohexène a montré que les groupes *gem*-diméthyles créaient trop d'interactions pour conduire à la formation de composés bicycliques.

Partie expérimentale

Les points de fusion ont été déterminés à l'aide d'un appareil de marque "Büchi" et ne sont pas corrigés. Les spectres i.r. ont été déterminés en solution dans le tétrachlorure de carbone à l'aide d'un spectrophotomètre Beckmann modèle IR-8 à double faisceau.

Les spectres u.v. ont été déterminés en solution dans l'éthanol 95% à l'aide d'un appareil "Bausch & Lomb Spectronic 505". Les spectres de r.m.n. ont été déterminés avec un appareil "Jeol type C 60 H" pour des solutions dans le tétrachlorure de carbone et utilisant le tétraméthylsilane comme référence interne. Les spectres de masse ont été déterminés à l'aide d'un appareil "Hitachi–Perkin" modèle RMU-6D. Les analyses par c.p.g. ont été effectuées à l'aide d'un appareil F et M modèle 810. Les longueurs des colonnes et les adsorbants utilisés sont rapportés dans le tableau 2. Les séparations préparatives ont été effectuées à l'aide d'un appareil "Prep/Partitioner" de Fisher modèle 24 en utilisant des colonnes renfermant 15% de Polyester de Craig supporté par du chromosorb P ou à l'aide d'un appareil "Varian Aerograph" modèle 90 P en utilisant des colonnes renfermant 25% de carbowax 20M TPA supporté sur du chromosorb P. Les analyses élémentaires ont été effectuées par "Schwarzkopf Micro-analytical Laboratory" de New York et par Dr. C. Daesslé "Organic Microanalyses" de Montréal.

Condensation du méthyl-1 cyclohexène avec le chlorure de propionyle en présence de $SnCl_4$

Le méthyl-1 cyclohexène (18 g), en solution dans 54 ml de CS_2 est condensé avec 15 g de chlorure de propionyle en présence de 49 g de $SnCl_4$ selon le procédé décrit par Turner et Voitle (7). Les résultats de l'analyse par c.p.g. sont rapportés dans le tableau 1. Le mélange cétonique (5

Can. J. Chem. Downloaded from www.nrcresearchpress.com by 210.87.254.42 on 09/05/12
For personal use only.

g) est ozoné selon le procédé décrit par Dufort et Lafontaine (1). Les composés **1***a* et *d* sont ensuite séparés par c.p.g. préparative. Le composé **1***a* distille à 203° à 755 mm; spectre u.v.: λ_{max} 213 mμ (ε 2960); spectre i.r.: bande carbonyle à 1685 cm^{-1}; spectre r.m.n.: multiplet à 0.96 p.p.m. (6H) méthyle de la chaine et méthyle sur le cycle; pas de proton éthylénique.

Anal. Calc. pour $C_{10}H_{16}O$: C, 78.94; H, 10.53. Trouvé: C, 78.57; H, 10.73.

La semicarbazone cristallisée dans le méthanol fond à 207–208°.

Anal. Calc. pour $C_{11}H_{19}N_3O$: C, 63.15; H, 9.09; N, 20.09. Trouvé: C, 63.14; H, 9.33; N, 20.14.

Le composé **1***d* a un point d'ébullition de 221° à 755 mm; spectre u.v.; λ_{max} 211 mμ (ε 4530); spectre i.r.: bande carbonyle à 1685 cm^{-1}; spectre r.m.n.: multiplet à 0.94 p.p.m. (6H) méthyle de la chaine et méthyle sur le cycle; pas de proton éthylénique.

Anal. Calc. pour $C_{10}H_{16}O$: C, 78.94; H, 10.53. Trouvé: C, 78.79; H, 10.48.

La semicarbazone cristallisée dans le méthanol fond à 203–204°.

Anal. Calc. pour $C_{11}H_{19}N_3O$: C, 63.15; H, 9.09; N, 20.09. Trouvé: C, 63.05; H, 9.03; N, 20.11.

Le mélange cétonique (5 g) est traité par 13 g d'acide oxalique en solution dans 65 ml d'eau comme décrit par Dufort et Lafontaine (1). Le composé **1***b* distille à 213–214° à 750 mm; spectre i.r.: bande carbonyle à 1705 cm^{-1}; spectre r.m.n.: triplet à 0.96 (3H, J = 6 Hz) méthyle de la chaine; singulet émergeant d'un massif à 1.53 (3H) méthyle sur le cycle; multiplet à 5.50 p.p.m. (1H) hydrogène éthylénique.

Anal. Calc. pour $C_{10}H_{16}O$: C, 78.94; H, 10.53. Trouvé: C, 78.84; H, 10.37.

La semicarbazone cristallisée dans le méthanol fond à 174–175°.

Anal. Calc. pour $C_{11}H_{19}N_3O$: C, 63.15; H, 9.09; N, 20.09. Trouvé: C, 62.89; H, 9.20; N, 20.06.

Le composé **1***c* distille à 218–219° à 750 mm; spectre u.v.: λ_{max} 248 mμ (ε 4330); spectre i.r.: bande carbonyle à 1680 cm^{-1}; spectre r.m.n.: triplet à 0.96 (3H, J = 6 Hz) méthyle de la chaine; singulet à 1.75 p.p.m. (3H) méthyle sur la double liaison.

Anal. Calc. pour $C_{10}H_{16}O$: C, 78.94; H, 10.53. Trouvé: C, 78.95; H, 10.45.

La semicarbazone cristallisée dans le méthanol fond à 201–202°.

Anal. Calc. pour $C_{11}H_{19}N_3O$: C, 63.15; H, 9.09; N, 20.09. Trouvé: C, 63.12; H, 9.20; N, 20.36.

Préparation de l'acétal **4**

Le composé **1***b* (30 g) est transformé en acétal comme décrit par Dufort et Lafontaine (1) sauf que le mélange d'alcool et d'acétal obtenu est séparé sur une colonne de "Florisil" au lieu d'alumine. On recueille 21 g du composé **4** qui distille à 122–124° à 17 mm; spectre i.r.: bandes à 1145, 1070, et 1045 cm^{-1}; pas de bande à 1705 cm^{-1}; spectre r.m.n.: triplet à 0.80 (3H, J = 6 Hz) méthyle de la chaine propionyle; singulet émergeant d'un massif à 1.70 (3H) méthyle sur la double liaison, singulet à 3.84 (4H) hydrogènes du groupe acétal, et multiplet à 5.45 p.p.m. (1H) hydrogène sur la double liaison.

Anal. Calc. pour $C_{12}H_{20}O_2$: C, 73.43; H, 10.27. Trouvé: C, 73.56; H, 10.28.

Hydroboration de l'acétal **4**

L'acétal **4** (10 g) est soumis à l'hydroboration selon le procédé décrit par Brown et Subba Rao (2); on recueille 9.4 g de composé **5** qui est directement soumis à l'hydrolyse; spectre i.r.: bandes à 3450, 1145, 1070, et 1045 cm^{-1}.

Hydrolyse de l'acétal **5**

Le composé **5** (5 g), en solution dans 110 ml d'éthanol, est chauffé à reflux durant 2½ h et agité à la température de la pièce durant 16 h. Après extraction et évaporation des solvants, on recueille 2.9 g de cétoalcool **6** qui distille 158° à 0.8 mm; spectre i.r.: bande hydroxyle à 3450 et bande carbonyle à 1710 cm^{-1}.

Tosylation du cétoalcool **6**

Le cétoalcool **6** (2.9 g) est tosylé comme décrit par Dufort et Lafontaine (1). Après évaporation des solvants, on obtient un résidu huileux jaune de 2.7 g qui dissous dans l'éther de pétrole, cristallise lentement. Après quatre cristallisations dans un mélange éther – éther de pétrole, on obtient des cristaux qui fondent à 72–73°; spectre i.r.: bandes à 1710, 1600, 1175, 1100 cm^{-1}; spectre r.m.n.: doublet à 0.66 (3H, J = 6 Hz) méthyle du cycle, triplet à 0.96 (3H, J = 8 Hz) méthyle de la chaine propionyle, singulet à 2.45 (3H) méthyle du toluène, multiplet à 4.15 p.p.m. (1H) hydrogène attaché au carbone qui porte le tosylate.

Anal. Calc. pour $C_{17}H_{24}O_4S$: C, 62.95; H, 7.46; S, 9.86. Trouvé: C, 62.90; H, 7.59; S, 9.93.

Déshydrotosylation du cétotosylate **7**

A une solution formée de 60 mg de NaOH dans 0.3 ml de méthanol sont ajoutés 70 mg de cétotosylate **7**. Après une agitation de 20 h à la température de la pièce et extraction de la façon habituelle et évaporation du solvant, le résidu analysé par c.p.g. sur une colonne de Polyester de Craig 15% et une colonne de QF1 3% indique la présence d'un seul composé. Une injection mixte sur les deux colonnes de ce composé et du composé **1***a* formé à 5% lors de la condensation montre que ces deux composés sont identiques. D'ailleurs les donnés spectrales du produit déshydrotosylé correspondent à celles du composé **1***a* obtenu par la réaction de Friedel–Crafts.

Condensation du méthyl-1 cyclohexène avec le chlorure de butyryle en présence de $SnCl_4$

Le méthyl-1 cyclohexène (24 g), en solution dans 64 ml de CS_2 est condensé avec 36 g de chlorure de butyryle en présence de 67 g de $SnCl_4$ selon le procédé décrit par Turner et Voitle (7). Les résultats de l'analyse par c.p.g. sont rapportés dans le tableau 1. L'ozonolyse de 5 g du mélange cétonique suivie d'une séparation par c.p.g. préparative permet d'isoler les composés **2***a* et *d*. Le composé **2***a* distille à 67–68° à 0.1 mm; spectre i.r.: bande carbonyle à 1685 cm^{-1}; spectre u.v.: λ_{max} 215 mμ (ε 7500); spectre r.m.n.: multiplet à 0.96 p.p.m. (6H) méthyle de la chaine et celui du cycle; pas d'hydrogène éthylénique. Le composé **2***d* distille à 68–69° à 0.1 mm; spectre u.v.: λ_{max} 212 mμ (ε 3500); spectre i.r.: bande carbonyle à 1680 cm^{-1}; spectre r.m.n.: multiplet à 1.00

Can. J. Chem. Downloaded from www.nrcresearchpress.com by 210.87.254.42 on 09/05/12
For personal use only.

p.p.m. (6H) méthyle de la chaine et celui du cycle; pas d'hydrogène éthylénique.

Anal. Calc. pour $C_{11}H_{18}O$: C, 79.46; H, 10.91. Trouvé: C, 79.17; H, 10.94.

La semicarbazone cristallisée dans le méthanol fond à 178–179°.

Anal. Calc. pour $C_{12}H_{21}N_3O$: C, 64.54; H, 9.48; N, 18.82. Trouvé: C, 64.55; H, 9.72; N, 19.08.

L'isomérisation de 5 g du mélange cétonique par 13 g d'acide oxalique en solution dans 65 ml d'eau donne 34% de composé **2***b* et 66% de composé **2***c*. Ces deux composés sont séparés par c.p.g. préparative. Le composé **2***b* distille à 52–53° à 0.3 mm; spectre i.r.: bande carbonyle à 1710 cm^{-1}; spectre r.m.n.: triplet à 0.92 (3H, $J = 6$ Hz) méthyle de la chaine butyryle, singulet émergeant d'un massif à 1.58 (3H) méthyle sur la double liaison, multiplet à 5.58 p.p.m. (1H) hydrogène sur la double liaison.

Anal. Calc. pour $C_{11}H_{18}O$: C, 79.46; H, 10.91. Trouvé: C, 79.30; H, 10.91.

La semicarbazone cristallisée dans le méthanol fond à 160°.

Anal. Calc. pour $C_{12}H_{21}N_3O$: C, 64.54; H, 9.48; N, 18.82. Trouvé: C, 64.33; H, 9.21; N, 18.72.

Le composé **2***c* distille à 54–55° à 0.3 mm: spectre i.r.: bande carbonyle à 1685 cm^{-1}; spectre u.v.: λ_{max} 247 mμ (ε 4080); spectre r.m.n.: triplet à 0.93 (3H, $J = 6$ Hz) méthyle de la chaine butyryle, singulet émergeant d'un massif à 1.80 p.p.m. (3H) méthyle sur la double liaison.

Anal. Calc. pour $C_{11}H_{18}O$: C, 79.46; H, 10.91. Trouvé: C, 79.36; H, 10.71.

La semicarbazone cristallisée dans le méthanol fond à 187°.

Anal. Calc. pour $C_{12}H_{21}N_3O$: C, 64.54; H, 9.48; N, 18.82. Trouvé: C, 64.32; H, 9.61; N, 18.99.

Condensation du méthyl-1 cyclohexène avec le chlorure d'acide benzoïque en présence de $SnCl_4$

Le méthyl-1 cyclohexène (18 g) en solution dans 54 ml de CS_2 est condensé avec 26.5 g de chlorure d'acide benzoïque en présence de 49 g de $SnCl_4$ selon le procédé décrit par Turner et Voitle (7). Les résultats de l'analyse par c.p.g. sont rapportés dans le tableau 1. Les produits sont obtenus à l'état pur par c.p.g. préparative. Le composé **3***b* distille à 102–103° à 0.1 mm; spectre i.r.: bande carbonyle à 1680 cm^{-1}; spectre r.m.n.: singulet à 1.62 (3H) méthyle sur la double liaison, massif à 3.90 (1H) hydrogène en α du carbonyle, massif à 5.75 (1H) hydrogène sur la double liaison, multiplets à 7.50 et 8.00 p.p.m. (5H) hydrogènes du noyau aromatique.

Anal. Calc. pour $C_{14}H_{16}O$: C, 83.96; H, 8.05. Trouvé: C, 83.95; H, 8.09.

Le composé **3***c* distille à 102–103° à 0.1 mm; spectre i.r.: bande carbonyle à 1650 cm^{-1}; spectre r.m.n.: singulet à 1.50 (3H) méthyle sur la double liaison, multiplets à 7.50 et 7.86 p.p.m. (5H) hydrogènes du noyau aromatique.

Anal. Calc. pour $C_{14}H_{16}O$: C, 83.96; H, 8.05. Trouvé: C, 83.82; H, 8.01.

Le composé **3***d* distille à 102–104° à 0.2 mm; spectre i.r.: bande carbonyle à 1660 cm^{-1}; spectre u.v.: λ_{max} 241 mμ (ε 10 350); spectre r.m.n.: doublet à 1.20 (3H, $J = 6$ Hz) méthyle sur le cycle, multiplets à 7.46 et 7.65 p.p.m. (5H) hydrogènes du noyau aromatique.

Anal. Calc. pour $C_{14}H_{16}O$: C, 83.96; H, 8.05. Trouvé: C, 84.27; H, 8.22.

La semicarbazone cristallisée dans le méthanol fond à 186°.

Anal. Calc. pour $C_{15}H_{19}N_3O$: C, 70.01; H, 7.44; N, 16.33. Trouvé: C, 69.86; H, 7.23; N, 16.62.

De 28 g de produit brut non déshydrochloré, il cristallise 5 g de composé **8** qui recristallisé dans un mélange éther – éther de pétrole fond à 116–117°; spectre i.r.: bande carbonyle à 1665 et bande hydroxyle à 3450 cm^{-1}; spectre r.m.n.: doublet à 0.85 (3H, $J = 7$ Hz) méthyle du cycle, massif à 3.26 (1H) hydrogène de l'hydroxyle, disparition de ce massif par échange avec D_2O, multiplets à 3.64 et 3.90 (2H) hydrogène carbinolique et hydrogène qui est en α de la cétone, multiplets à 7.60 et 7.95 p.p.m. (5H) hydrogènes sur le noyau aromatique.

Anal. Calc. pour $C_{14}H_{18}O_2$: C, 77.06; H, 8.25. Trouvé: C, 77.16; H, 8.20.

*Oxydation chromique du cétoalcool **8***

Le cétoalcool **8** (0.77 g) est oxydé par le complexe anhydride chromique – pyridine selon la méthode de Poos *et al.* (5). On obtient 0.6 g de composé **10** qui fond à 90° après recristallisation dans un mélange éther – éther de pétrole. Spectre i.r.: bandes carbonyles à 1710 et 1670 cm^{-1}; spectre r.m.n.: doublet à 1.00 (3H, $J = 7$ Hz) méthyle sur le cycle, massif dans la région de 2 (7H) protons cyclohexaniques, multiplet à 4.12 (1H) hydrogène en α du groupe benzoyle, multiplets à 7.50 et 7.90 p.p.m. (5H) hydrogènes sur le noyau aromatique. Le spectre de masse indique un ion moléculaire à *m/e* 216.

*Echange de protons de la dicétone **10** en présence d'eau deutérée*

La dicétone **10** (100 mg) et 5 ml de D_2O sont portés à reflux avec 0.5 g de K_2CO_3 durant 72 h. Après extraction de la manière habituelle et évaporation des solvants, le spectre r.m.n. indique la disparition du multiplet à 4.12 p.p.m. et la diminution du massif dans la région de 2.00 p.p.m. Le doublet à 1.00 p.p.m. est maintenant transformé en singulet.

*Tosylation du cétoalcool **8***

Le cétoalcool **8** (5.1 g) est tosylé selon le procédé expérimental décrit précédemment. Après recristallisation dans un mélange éther – éther de pétrole, on recueille 3.6 g de tosylate **12** qui fond à 100°.

Anal. Calc. pour $C_{20}H_{24}O_4S$: C, 68.29; H, 5.69; S, 8.70. Trouvé: C, 68.11; H, 5.44; S, 8.97.

*Déshydrotosylation du composé **12***

Le cétotosylate **12** (3.5 g) est déshydrotosylé selon le procédé décrit précédemment. On obtient 2 g de produit qui indique à l'analyse par c.p.g. la présence d'un seul composé identifié comme étant l'*endo* benzoyl-1 méthyl-6 bicyclo[3.1.0]hexane (**3***d*). D'ailleurs une injection mixte de ce composé et du composé formé à 48% lors de la condensation, montre qu'ils sont parfaitement identiques.

Condensation du méthyl-1 cyclohexène avec le chlorure d'acide en présence de $AlCl_3$

A un mélange de 0.11 mol de $AlCl_3$ dissous dans 30 ml de CS_2 et de 0.1 mol de méthyl-1 cyclohexène refroidi à 0°, on ajoute lentement 0.1 mol de chlorure d'acide. Après une agitation de 1 h à la température de la pièce, le mélange est extrait de la manière habituelle. Après évaporation des solvants, le résidu est traité par une solution

méthanolique de NaOH à 20% pendant une nuit. Après extraction et évaporation des solvants, le résidu est analysé par c.p.g. et les résultats sont rapportés dans le tableau 1.

Condensation du méthyl-1 cyclohexène avec le chlorure d'acide en présence de $ZnCl_2$

A un mélange de 0.1 mol de $ZnCl_2$ en solution dans 30 ml de CS_2 et de 0.1 mol de méthyl-1 cyclohexène, on ajoute lentement 0.1 mol de chlorure d'acide en maintenant la température du milieu réactionnel à 0°. Après une agitation de 20 h à la température de la pièce, le mélange est extrait de la manière habituelle. Le résidu est traité par une solution méthanolique de NaOH à 20% pendant une nuit. Les résultats de l'analyse par c.p.g. sont rapportés dans le tableau 1.

Condensation du méthyl-1 cyclohexène avec le chlorure d'acide en présence de fluorure de bore

A un mélange de 0.1 mol de méthyl-1 cyclohexène et de 0.1 mol de chlorure d'acide refroidi à 0°, on ajoute lentement 0.12 mol de fluorure de bore éthéré. Après une agitation de 20 h à la température de la pièce, le mélange est extrait de la manière habituelle puis traité par une solution méthanolique de NaOH à 20%. Les résultats de l'analyse par c.p.g. sont rapportés dans le tableau 1.

Condensation du pentaméthyl-1,3,3,5,5 cyclohexène avec le chlorure d'acétyle en présence de chlorure stannique

A un mélange de 5 g du composé **13** et de 3.3 g de chlorure d'acétyle refroidi à 0°, on ajoute lentement 3.9 ml de $SnCl_4$. La solution est agitée pendant 5 min puis extraite de la manière habituelle. Le résidu obtenu est déshydrochloré par une solution méthanolique d'hydroxyde de sodium à 20% puis extrait de la manière habituelle. Le résidu analysé par c.p.g. indique la présence des composés **14** et **15** dans une proportion de 1 à 10. L'ozonolyse de 500 mg du résidu indique à l'analyse par c.p.g. la disparition de ces deux composés: on ne décèle pas la présence de composés cyclopropaniques. Le composé **14** est obtenu à l'état pur par c.p.g. préparative. Il distille à 100–101° à 12 mm (rapporté 92–93° à 11 mm (8)); spectre i.r.: bande carbonyle à 1710 cm^{-1}; spectre r.m.n.: singulet à 0.90 (3H), à 1.02 (3H) et à 1.05 (6H) *gem*-diméthyles sur le cycle; doublet à 1.62 (3H, $J = 2$ Hz) méthyle sur la double liaison; singulet à 2.10 (3H) méthyle en α du carbonyle; multiplet à 5.22 p.p.m. (1H) hydrogène sur la double liaison.

Hydroboration du pentaméthyl-1,3,3,5,5 cyclohexène

Le composé **13** (24 g) en solution dans 44 ml de tétrahydrofuranne est soumis à l'hydroboration selon le procédé décrit précédemment. Il se forme 16 g de *trans* pentaméthyl-2,2,4,4,6 cyclohexanol (**16**) qui distille à 65° à 1.5 mm. Cet alcool cristallise lentement à la température de la pièce et fond à 34°. Spectre i.r.: bande hydroxyle à 3450 cm^{-1}; spectre r.m.n.: multiplet à 0.95 (15H) méthyles sur le cycle, singulet à 2.52 (1H) hydrogène de l'hydroxyle, doublet à 2.74 p.p.m. (1H, $J = 9$ Hz) hydrogène carbinolique. Le spectre de masse indique un ion moléculaire à *m/e* 170.

Oxydation du trans pentaméthyl-2,2,4,4,6 cyclohexanol

L'alcool (5.2 g) est oxydé en suivant le même procédé expérimental que pour l'oxydation de l'alcool **8**. On recueille 5 g de cétone **17** qui distille à 43° à 1.5 mm; spectre i.r.: bande carbonyle à 1710 cm^{-1}; spectre r.m.n.: singulets à 0.90, 0.98, et 1.00 (12H) *gem*-diméthyles sur le cycle; doublet à 1.25 p.p.m. (3H, $J = 2.3$ Hz) méthyle en α du carbonyle; multiplet à 2.70 p.p.m. (1H) hydrogène en α de la cétone.

Anal. Calc. pour $C_{11}H_{20}O$: C, 78.51; H, 11.98. Trouvé: C, 78.54; H, 12.14.

La semicarbazone cristallisée dans le méthanol fond à 191–192°.

Anal. Calc. pour $C_{12}H_{23}N_3O$: C, 63.96; H, 10.29; N, 18.65. Trouvé: C, 64.20; H, 10.34; N, 18.64.

Préparation de l'acétyl-1 pentaméthyl-2,4,4,6,6 cyclohexène

La cétone **17** (2.6 g) est traité par 1.9 g d'acétylure de lithium selon le procédé de Beumel et Harris (6). On obtient un résidu de 2.7 g qui distille à 55–60° à 0.1 mm. Le spectre i.r. présente une bande hydroxyle à 3500 cm^{-1}; 1 g de cet alcool est ensuite chauffé à reflux pendant 2 h avec 16 ml d'acide formique 98%. Après neutralisation de l'acide et extraction de la manière habituelle, on recueille 0.9 g de produit qui distille à 45–47° à 0.07 mm. L'analyse par c.p.g. indique la présence d'un seul pic représentant le composé **15**. Spectre i.r.: bande carbonyle à 1685 cm^{-1}; spectre r.m.n.: singulets vers 1.00 (12H) *gem*-diméthyles sur le cycle, singulet à 1.35 (2H) hydrogènes entre les groupes *gem*-diméthyles, singulet à 1.60 (3H) méthyle sur la double liaison, singulet à 1.75 (2H) hydrogènes allyliques, singulet à 2.20 p.p.m. (3H) méthyle en α du carbonyle.

Anal. Calc. pour $C_{13}H_{22}O$: C, 80.35; H, 11.41. Trouvé: C, 80.47; H, 11.43.

Les auteurs remercient le Conseil National de Recherches du Canada pour l'aide financière accordée sous forme d'octroi de recherches (A2030).

1. N. DUFORT et J. LAFONTAINE. Can. J. Chem. **46**, 1065 (1968).
2. H. C. BROWN et B. C. SUBBA RAO. J. Am. Chem. Soc. **81**, 6428 (1959).
3. M. S. AHMAD, G. BADDELEY, B. G. HEATON, et J. W. RASBURN. Proc. Chem. Soc. 395 (1959).
4. C. L. STEVENS et E. FARKAS. J. Am. Chem. Soc. **75**, 3306 (1953).
5. G. I. POOS, G. E. ARTH, R. E. BEYLER, et L. H. SARRETT. J. Am. Chem. Soc. **75**, 422 (1953).
6. O. F. BEUMEL et R. F. HARRIS. J. Org. Chem. **29**, 1872 (1964).
7. R. B. TURNER et D. M. VOITLE. J. Am. Chem. Soc. **73**, 1403 (1951).
8. R. VONDERWAHL et H. SCHINZ. Helv. Chim. Acta, **35**, 2368 (1952).

Can. J. Chem. Downloaded from www.nrcresearchpress.com by 210.87.254.42 on 09/05/12
For personal use only.

Can. J. Chem. Downloaded from www.nrcresearchpress.com by 210.87.254.42 on 09/05/12
For personal use only.

Reactions of 1-Phenyl-1,2,3-triazolyllithium Compounds; Formation of Ketenimines, Alkynylamines, and Heterocycles from the Ambident (*N*-Phenyl)phenylketenimine Anion

R. RAAP

R & L Molecular Research Ltd., 8045 Argyll Road, Edmonton 82, Alberta

Received November 2, 1970

At room temperature 1,4-diphenyl-1,2,3-triazolyllithium rapidly undergoes fragmentation to nitrogen and lithium (*N*-phenyl)phenylketenimine anion **8***c*, $(C_6H_5{\equiv}C{-\!\!-}NC_6H_5)^{\ominus}Li^{\oplus}$. Some of the reactions of this ambident anion have been studied. Reaction of **8***c* with methyl iodide results in *C*-methylation to a mixture of (*N*-phenyl)methylphenylketenimine and 3-methyl-1,3-diphenyl-4-(2′-phenylethylene)-2-phenyliminoazetidine. A six-membered heterocyclic compound, 6-anilino-1,3,5-triphenyluracil, results from the reaction between **8***c* and phenyl isocyanate. With dimethyl sulfate and methyl chloroformate *N*-alkylation and *N*-acylation takes place predominantly, forming *N*-methyl-*N*-phenyl-2-phenylethynylamine and *N*-carbomethoxy-*N*-phenyl-2-phenylethynylamine respectively. Reaction of **8***c* with methanol and ethanethiol gives an iminoester and an iminothioester respectively.

1-Phenyl-1,2,3-triazolyllithium and 4-methyl-1-phenyl-1,2,3-triazolyllithium undergo fragmentation at somewhat higher temperatures.

Le sel de lithium du diphényl-1,4 triazolyl-1,2,3 se fragmente rapidement à la température de la pièce pour donner de l'azote et le sel de lithium de l'anion **8***c*, $(C_6H_5{-}C{\equiv}C{-\!\!-}N{-}C_6H_5)^{\ominus}Li^{\oplus}$. On a étudié quelques unes des réactions de cet anion ambivalent. La réaction de **8***c* avec l'iodure de méthyle conduit à une *C*-méthylation fournissant un mélange de (*N*-phényl) méthylphénylcitinimine et de méthyl-3 diphényl-1,3 (phényléthylène-2)-4 phénylimino-2 azètidine. Un composé hétérocyclique à six chaînons, l'amino-6 triphényl-1,3,5 uracile, se forme par réaction entre **8***c* et l'izocyanate de phényle. Avec le sulfate de méthyle et le chloroformate de méthyle des réactions de *N*-alkylation et de *N*-acylation se produisent de façon prépondérante et conduisent respectivement à la formation du *N*-méthyl *N*-phényl phényl-2 éthynylamine et de *N*-carbométhoxy *N*-phényl phényl-2 éthynylamine et de carbométhoxy *N*-phényl phényl-2 éthynylamine. Les réactions de **8***c* avec le méthanol et l'éthanethiol fournissent respectivement une iminoester et une iminothioester.

Par ailleurs la fragmentation des sels de lithium des phényl-1 triazolyl-1,2,3 et méthyl-4 phényl-1 triazolyl-1,2,3 s'effectuent à des températures un peu plus hautes.

Canadian Journal of Chemistry, 49, 1792 (1971)

Lithiation of five-membered heteroaromatics has in several instances provided a useful method for the introduction of ring substituents (1). Certain ring systems however undergo fragmentation with elimination of nitrogen under the influence of base, resulting in alkynylthiolates from 1,2,3-thiadiazoles (2, 3), diphenylacetylene from 4,5-diphenyl-1,2,3-thiadiazole (4), carbodiimides from 1,4-disubstituted tetrazolium salts (5), and phenylcyanamide from the reaction between 5-chloro-1-phenyltetrazole and magnesium or *n*-butyllithium (6). In the following we report our results on the lithiation of some 1-phenyl-1,2,3-triazoles. This investigation was of interest not only for the syntheses of substituted 1,2,3-triazoles, but also for the possible interesting products resulting from a fragmentation of the triazole ring.

In tetrahydrofuran (THF) the triazoles **1** and **4** were all readily lithiated with *n*-butyllithium at -20 to $-60°$ (Scheme 1). Ring lithiation takes place preferentially at the 5-position as was indicated by the products **2**, **3**, **6**, and **7** obtained by methylation or carboxylation. Whereas the reaction product of **1***a* with *n*-butyllithium upon reaction with methyl iodide provided **2** as the only isolable product, **4***a* and *b* under these conditions gave high yields of the 5-methyl-1,2,3-triazoles **5***a* and *b*. Solutions of **5***a* and *b* were stable at room temperature but decomposed with gas evolution when heated at 40–50°. A solution of **5***c* readily decomposed at 20° to a yellow to green solution of the ambident *N*-phenylketenimine anion **8***c*, displaying strong absorption at 2140 cm^{-1} in the i.r. The various reactions performed with **8***c* are outlined in Scheme 2.

Reaction of **8***c* with methyl iodide resulted exclusively in *C*-methylation and the formation

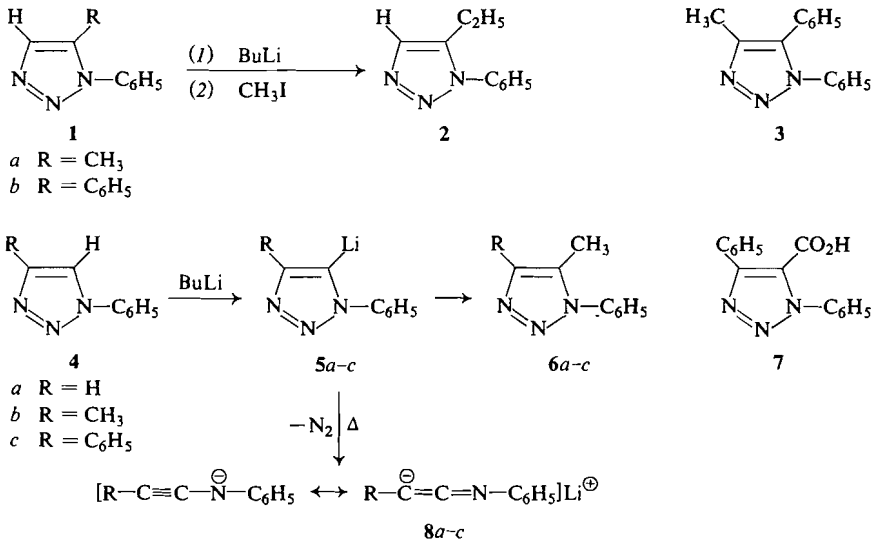

1
a R = CH_3
b R = C_6H_5

2 3 4 5*a–c* 6*a–c* 7

a R = H
b R = CH_3
c R = C_6H_5

$[R-C\equiv C-\overset{\ominus}{N}-C_6H_5 \leftrightarrow R-\overset{\ominus}{C}=C=N-C_6H_5]Li^{\oplus}$

8*a–c*

SCHEME 1

of two products, one being the expected (*N*-phenyl)methylphenylketenimine[1] (**9**). The structure of **9** was indicated by the n.m.r. and i.r. spectra, the latter showing strong absorption at 2000 cm^{-1} in agreement with reported ketenimine absorption (8), and was further proven by conversion to *N*,2-diphenylpropionamide (**10**) with dilute acid and to the imino ester **11** by reaction with methanol in the presence of a catalytic amount of sodium methoxide. The empirical formula $C_{30}H_{26}N_2$ of the second product, a pale yellow solid melting at 114–115°, indicated a dimer of **9**. The n.m.r. spectrum showed the presence of four phenyl groups and two different *C*-methyl groups; the i.r. spectrum contained bands at 1730 and 1655 cm^{-1}. The compound hydrolyzed slowly upon heating in a mixture of THF and 3 *N* hydrochloric acid to aniline and a highly viscous compound, $C_{24}H_{21}NO$. The n.m.r. spectrum of this latter compound showed the presence of three phenyl groups and two *C*-methyl groups; the i.r. spectrum contained strong bands at 1780 and 1680 cm^{-1}, the former band indicating the presence of a β-lactam carbonyl group (9). These observations point to 3-methyl-1,3-diphenyl-4-(2′-phenylethylene)-2-phenyliminoazetidine (**12**) as being the other alkylation product, hydrolysis of which should lead to 3-methyl-1,3-diphenyl-4-(2′-phenylethylene)-2-azetidinone (**13**). The formation of **12** can be explained by attack of **8***c* on the initially formed ketenimine **9** followed by methylation of the intermediate **14** with methyl iodide (Scheme 3). In agreement with this it was found that although the relative amounts of **9** and **12** were little affected by the reaction temperature and the mode of addition of the methyl iodide, it strongly depended on the amount of methyl iodide used. The yields of isolated **9** when a 10, 25, and 100% excess of methyl iodide was employed were 17, 28, and 45% respectively, the yields of isolated **12** being 46, 36, and 19% respectively.

In an attempt to extend the synthesis of azetidine derivatives to compounds derived from the anion **15** (Scheme 3), the reaction between equivalent amounts of **8***c* and phenyl isocyanate was investigated. However no indication for the formation of **15** was obtained and the only product isolated, after treatment of the reaction mixture with water, was 6-anilino-1,3,5-triphenyluracil (**16**; 37%). The structural assignment of **16** is based on the elemental analyses, the n.m.r. and i.r. spectra, and on its hydrolysis to 1,3,5-triphenylbarbituric acid (**17**) in a boiling mixture of 6 *N* hydrochloric acid and acetic acid. Apparently the first addition product of **8***c* to phenyl isocyanate, rather than cyclizing to **15**,

[1]The photochemical decomposition of 1-phenyl-1,2,3-triazoles has been reported and also results in the formation of ketenimines, *e.g.* from **4***c* an 80% yield of diphenylketenimine was obtained (7).

Can. J. Chem. Downloaded from www.nrcresearchpress.com by 210.87.254.42 on 09/05/12
For personal use only.

Can. J. Chem. Downloaded from www.nrcresearchpress.com by 210.87.254.42 on 09/05/12
For personal use only.

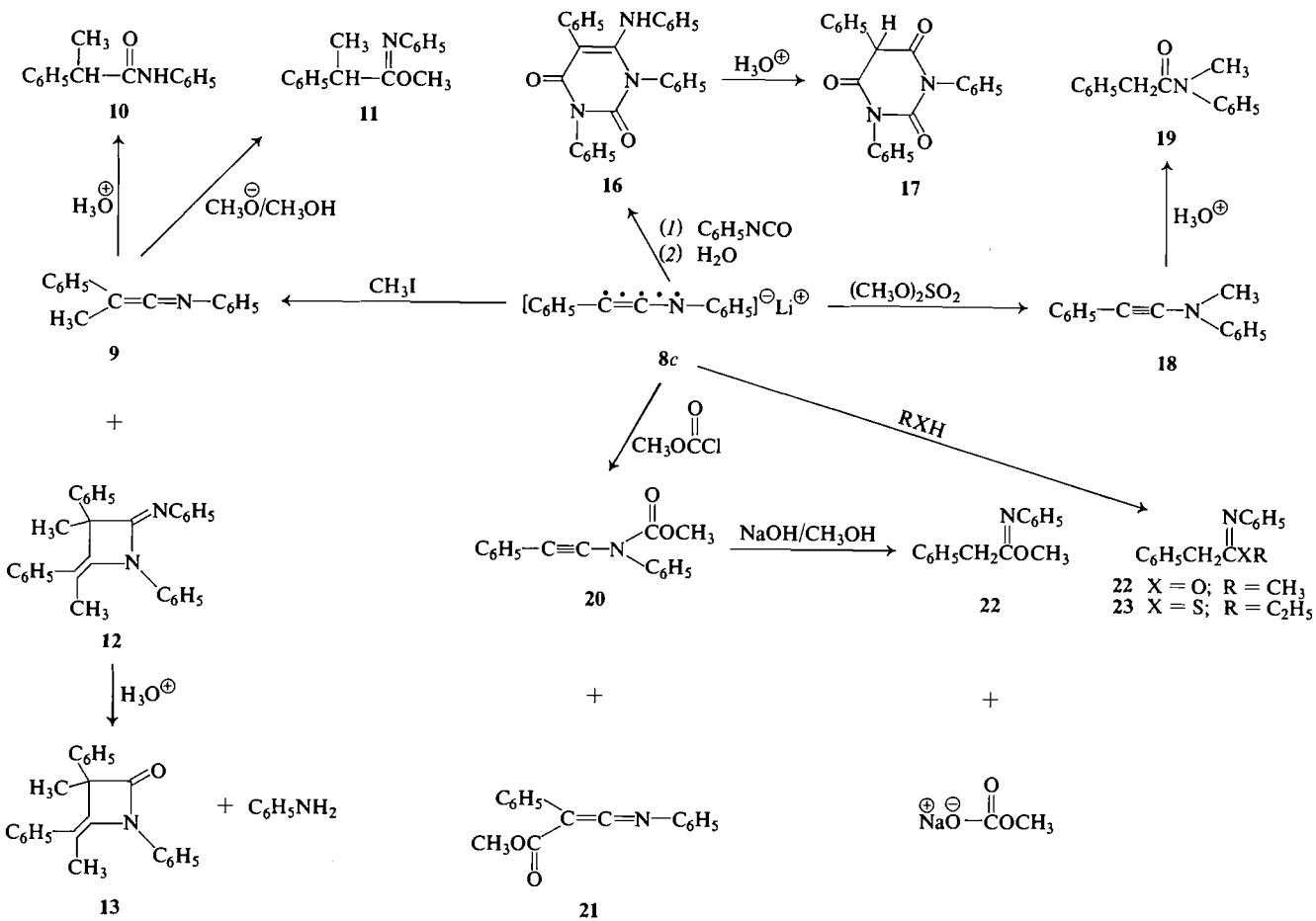

SCHEME 2

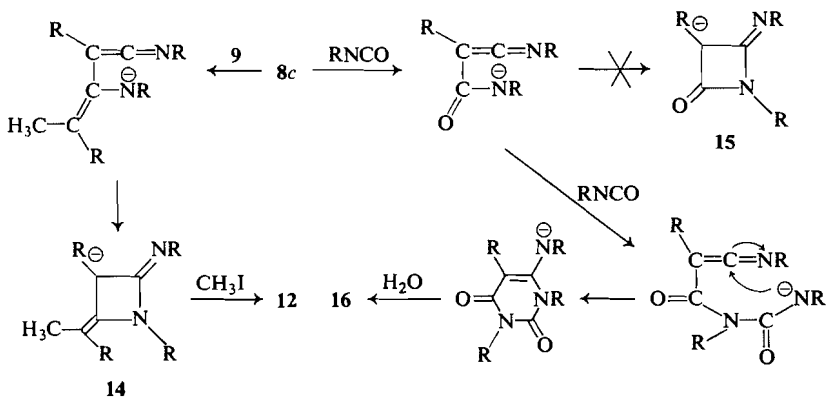

(R = C_6H_5)

SCHEME 3

reacts with a second molecule of phenyl isocyanate followed by cyclization to a uracil derivative.

The methylation of **8***c* took a different course with dimethyl sulfate, for *N*-methyl-*N*-phenyl-2-phenylethynylamine (**18**; 42%) was the only product isolated. Only trace amounts of **9** and **12** were detectable in the n.m.r. and i.r. spectra of the crude reaction product. The product showed strong i.r. absorption at 2230 cm^{-1} in agreement with reported absorptions of alkynylamines (10). Compound **18**, m.p. 47–48°, was further characterized by hydrolysis with dilute acid to (*N*-methyl-*N*-phenyl)phenylacetamide (**19**).

Acylation of **8***c* with methyl chloroformate gave *N*-carbomethoxy-*N*-phenyl-2-phenylethynylamine (**20**; 40%) as the main product. The formation of a small amount of the ketenimine **21** was evident from the n.m.r. and i.r. spectra of the crude product, but attempts to isolate this material by chromatography or distillation were unsuccessful. Compound **20** represents a new type of alkynylamine. Whereas **18** undergoes an exothermic reaction with dilute acid, **20** was recovered unchanged from a mixture of THF and 1 *N* sulfuric acid when left at room temperature for 1 h. With methanolic sodium hydroxide **20** underwent a rapid reaction resulting in the formation of sodium methylcarbonate and methyl (*N*-phenyl)phenylacetimidate (**22**), the latter material being identical with that obtained from the reaction between methyl phenylthionacetate and aniline (11).

The iminoester **22** was also obtained when methanol was added to the THF solution of **8***c* (45%). An 80% yield of the iminothioester **23** was obtained from the reaction between **8***c* and ethanethiol, indicating that ethanethiolate is a more efficient reactant for the intermediate ketenimine.

The fragmentation of **5***a* to **8***a* produced a dianion as the alkylation of both **8***a* and *b* with dimethyl sulfate gave the same product, *N*-methyl-*N*-phenyl-1-propynylamine (**24**), in yields of 21 and 31% respectively. The addition of methanol to a solution of **8***a* provided a 47% yield of the iminoester **25** and a 37% recovery of **4***a* (Scheme 4).

Experimental

All melting points and boiling points are uncorrected. The i.r. spectra were recorded on a Perkin–Elmer Model 137 "Infracord" spectrophotometer. The n.m.r. spectra were measured using a Varian Associates Model A-60 spectrometer with tetramethylsilane as a reference. Microanalyses were performed by Dr. F. B. Strauss, Microanalytical Laboratory, Oxford, England.

Substitution Reactions with 1-Phenyl-1,2,3-triazolyllithium Compounds

To a stirred solution (or suspension) of 0.040 mol of either 1-phenyl-1,2,3-triazole (12), 4-methyl-1-phenyl-1,2,3-triazole (13), 5-methyl-1-phenyl-1,2,3-triazole (12), 1,4-diphenyl-1,2,3-triazole (14), or 1,5-diphenyl-1,2,3-triazole (14) in 80 ml of anhydrous THF was added dropwise in 15 min, 26 ml of 1.6 *M* *n*-butyllithium in *n*-hexane at −20 to −60° (depending on the solubility of the triazole) in a nitrogen atmosphere. When the addition was completed the mixture was stirred and cooled for an additional 0.5–1 h whereafter a solution of methyl iodide (8.5 g, 0.060 mol) in 15 ml of THF was added in one portion. The reaction mixtures were worked up by standard procedures. The following compounds were thus prepared:

5-Ethyl-1-phenyl-1,2,3-triazole (2) (42%), m.p. 79–81°; reported m.p. 79–80° (15). The identity was confirmed by the n.m.r. spectrum and the elemental analyses. The n.m.r. spectrum of the crude product indicated that little (if any) 4,5-dimethyl-1-phenyl-1,2,3-triazole was present.

Can. J. Chem. Downloaded from www.nrcresearchpress.com by 210.87.254.42 on 09/05/12
For personal use only.

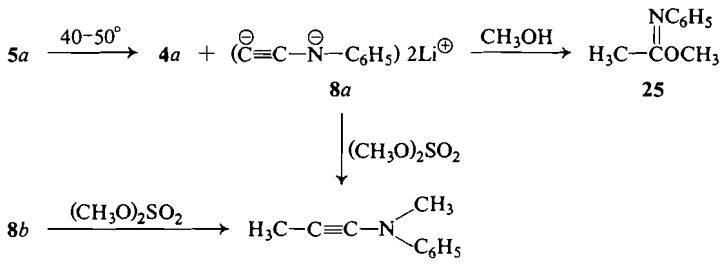

SCHEME 4

1,5-Diphenyl-4-methyl-1,2,3-triazole (3) (99%), m.p. 122–124°; n.m.r. ($CDCl_3$): τ 2.5–3.0 (m, 10H) and 7.58 (s, 3H).

Anal. Calcd. for $C_{15}H_{13}N_3$: C, 76.57; H, 5.57; N, 17.86. Found: C, 76.63; H, 5.70; N, 17.67.

5-Methyl-1-phenyl-1,2,3-triazole (6a) (94%), m.p. 63–65°; reported m.p. 64° (12). The material was identical with an authentic sample.

4,5-Dimethyl-1-phenyl-1,2,3-triazole (6b) (81%), m.p. 87–88°; reported m.p. 98° (16). The structure was confirmed by the n.m.r. spectrum and elemental analyses.

1,4-Diphenyl-5-methyl-1,2,3-triazole (6c) (78%), m.p. 156–159° (C_6H_6 – *n*-C_6H_{14}); n.m.r. ($CDCl_3$): τ 2.1–2.8 (m, 5H), 2.52 (s, 5H) and 7.59 (s, 3H).

Anal. Calcd. for $C_{15}H_{13}N_3$: C, 76.57; H, 5.57; N, 17.86. Found: C, 76.56; H, 5.46; N, 17.72.

1,4-Diphenyl-1,2,3-triazole-5-carboxylic Acid (7)

This compound was prepared in 62% yield by pouring the 1,4-diphenyl-1,2,3-triazolyllithium solution on solid carbon dioxide, followed by acidification of an aqueous solution of the salt; m.p. 169–170° (dec.); reported m.p. 177.5° (17). The structure was confirmed by an elemental analysis.

Lithium (N-Phenyl)phenylketenimine Anion (8c)

To a stirred suspension of 1,4-diphenyl-1,2,3-triazole (8.8 g, 0.040 mol) in 80 ml of anhydrous THF was added dropwise in 10–15 min 26 ml of 1.6 *M* *n*-butyllithium in *n*-hexane at −20 to −40° in a nitrogen atmosphere. The mixture was cooled for an additional 15 min (a white precipitate had formed) and was then allowed to warm up. At approximately 10° gas evolution became noticeable. At room temperature the gas evolution became rapid and was complete within one hour to give a yellow to green solution, the i.r. spectrum of which contained a very intense absorption at 2140 cm^{-1}.

Reaction of 8c with Methyl Iodide

The above prepared solution of **8c** was cooled to −60° and a solution of methyl iodide (11.4 g, 0.080 mol) in 20 ml of THF was added in one portion. After the mixture had reached room temperature the solvent was removed, the residue was dissolved in 75 ml of ether and this solution was washed with two 25 ml portions of water. The ether solution was dried and the solvent removed giving 8.1 g of liquid residue, the n.m.r. spectrum of which indicated that it consisted only of the ketenimine **9** (61%) and the dimer **12** (39%). A solution of the residue in 50 ml of *n*-hexane was cooled to give 1.6 g (19%) of crystalline **12**, m.p. 109–111°. The material could be recrystallized from methanol to pale yellow crystals, m.p. 114–115°; ν_{max} (Nujol) 1730, 1655, and 1590 cm^{-1}; n.m.r. ($CDCl_3$): τ 2.6–3.7 (multiplet, 20H), 8.16 (s, 3H), and 8.31 (s, 3H).

Anal. Calcd. for $C_{30}H_{26}N_2$ (mol. wt. 414.5): C, 86.92; H, 6.32; N, 6.76. Found (409 (Rast)): C, 86.92; H, 6.26; N, 7.18.

The hexane filtrate was concentrated and the residue distilled *in vacuo* to give 3.7 g (45%) of **9** as a yellow liquid, b.p. 128–129° (0.5 mm), which crystallized upon cooling and could be recrystallized from a small amount of methanol to long yellow needles, m.p. 35–37°; ν_{max} (Nujol) 2000 cm^{-1}; n.m.r. ($CDCl_3$): τ 2.6–2.9 (m, 10H) and 7.92 (s, 3H).

Anal. Calcd. for $C_{15}H_{13}N$: C, 86.92; H, 6.32; N, 6.76. Found: C, 86.96; H, 6.45; N, 7.00.

The crude reaction product could also be distilled directly, in which case the dimer **12** could be isolated by recrystallization of the distillation residue from methanol.

N,2-Diphenylpropionamide (10)

A mixture of (*N*-phenyl)methylphenylketenimine (0.35 g, 0.0017 mol), 1 *N* aqueous sulfuric acid (10 ml), and THF (10 ml) was briefly heated at 50°. The product isolated was recrystallized from benzene – *n*-hexane to give 0.31 g (82%) of white crystals, m.p. 135–136°; reported m.p. 133–134° (18). The n.m.r. and i.r. spectra and the elemental analyses were also in agreement with the assigned structure.

Methyl N,2-Diphenylpropionimidate (11)

A mixture of ketenimine **9** (1.24 g, 0.006 mol), sodium methoxide (0.10 g), and methanol (25 ml) was left at room temperature for 1 h, by which time the yellow color had disappeared. From the reaction mixture was isolated 1.3 g (77%) of pale yellow product, b.p. 110–112° (0.1 mm); ν_{max} (neat) 1655 cm^{-1}; n.m.r. (CCl_4): τ 2.87 (s, 5H), 2.5–3.5 (m, 5H), 6.20 (q, 1H), 6.25 (s, 3H), and 8.59 (d, 3H).

Anal. Calcd. for $C_{16}H_{17}NO$: C, 80.32; H, 7.16; N, 5.85. Found: C, 80.18; H, 7.09; N, 6.10.

Hydrolysis of 12

A mixture of **12** (1.0 g), THF (30 ml), and 3 *N* hydrochloric acid (30 ml) was heated under reflux for 5 h. The mixture was cooled and extracted with two 50 ml portions of ether. The aqueous solution was made alkaline and extracted with ether to give 0.25 g of a liquid residue,

Can. J. Chem. Downloaded from www.nrcresearchpress.com by 210.87.254.42 on 09/05/12
For personal use only.

Can. J. Chem. Downloaded from www.nrcresearchpress.com by 210.87.254.42 on 09/05/12
For personal use only.

the i.r. spectrum of which was superimposable with that of aniline. The ether solution was dried, the solvent removed, and the residue distilled *in vacuo* to give 0.52 g (63%) of a very viscous liquid, distilling at approximately 190° (0.1 mm) with slight decomposition. An analytical sample was obtained by chromatography on silica gel and elution with benzene; ν_{max} (neat) 1780 and 1680 cm^{-1}; n.m.r. ($CDCl_3$): τ 2.3–3.3 (m, 15H), 8.01 (s, 3H), and 8.06 (s, 3H).

Anal. Calcd. for $C_{24}H_{21}NO$ (**13**): C, 84.93; H, 6.24; N, 4.13. Found: C, 84.82; H, 6.43; N, 3.99.

*6-Anilino-1,3,5-triphenyluracil (**16**)*

A solution of phenyl isocyanate (2.4 g, 0.020 mol) in 10 ml of THF was added in one portion to a stirred solution of **8***c* in THF, prepared from 4.4 g (0.020 mol) of 1,4-diphenyl-1,2,3-triazole, at −60°. The cooling bath was removed and when the temperature of the reaction mixture had reached −20°, 20 ml of water was added followed by some ethyl acetate. The organic layer was washed with water, dried, and concentrated. The residue was treated with 40 ml of ether and cooled, resulting in the formation of a white solid precipitate (2.0 g). A small amount of starting material **4***c* could be removed by treating this solid with cold methylene chloride which dissolved **16** but not **4***c*. The product thus obtained amounted to 1.6 g (37%), m.p. 230–234°. The m.p. could be raised to 242–243° by recrystallization from a 1:4 mixture of chloroform and carbon tetrachloride; ν_{max} ($CHCl_3$) 3400, 1700, and 1640 cm^{-1}; n.m.r. ($CDCl_3$): complex phenyl absorption at τ 2.5–3.6 and a singlet at 4.37 with an integrated area ratio of approximately 20:1.

Anal. Calcd. for $C_{28}H_{21}N_3O_2$ (mol. wt. 431.5): C, 77.93; H, 4.91; N, 9.74. Found (432 (osmometric)): C, 77.47; H, 4.96; N, 9.61.

*1,3,5-Triphenylbarbituric Acid (**17**)*

A mixture of **16** (1.0 g, 2.3 mmol), acetic acid (30 ml), and 6 *N* hydrochloric acid (15 ml) was heated under reflux for 1.5 h, then diluted with 15 ml of water and cooled. The solid precipitate was collected by filtration, washed with water, dried, and recrystallized from ethyl acetate – *n*-hexane to give 0.5 g (63%) of fine white needles, m.p. 262–263°; reported m.p. 261–262° (19). The i.r. spectrum (in $CHCl_3$) contained no absorption at 3100–3600 cm^{-1}, but showed a strong carbonyl band at 1690 cm with a shoulder at 1710 cm^{-1}; the n.m.r. spectrum (in DMSO-d_6) contained singlets at τ 2.55 and 4.62 (broad) with an integrated area ratio of approximately 15:1.

Anal. Calcd. for $C_{22}H_{16}N_2O_3$ (mol. wt. 356): C, 74.14; H, 4.53; N, 7.86. Found (380 (Rast)): C, 73.95; H, 4.55; N, 7.96.

*N-Methyl-N-phenyl-2-phenylethynylamine (**18**)*

To the previously described solution of **8***c* (prepared from 0.040 mol of **4***c*) in THF, cooled at −60°, was added in one portion a solution of dimethyl sulfate (5.05 g, 0.040 mol) in 20 ml of THF. The mixture was worked-up as before to give 7.5 g of crude reaction product which upon distillation *in vacuo* provided 3.5 g (42%) of pale yellow liquid, b.p. 134–136° (0.1 mm), which crystallized from *n*-hexane to colorless crystals, m.p. 47–48°; ν_{max} (Nujol) 2230 and 1595 cm^{-1}; n.m.r. ($CDCl_3$): τ 2.5–3.2 (m, 10H) and 6.73 (s, 3H).

Anal. Calcd. for $C_{15}H_{13}N$: C, 86.92; H, 6.32; N, 6.76. Found: C, 86.67; H, 6.46; N, 6.86.

Treatment of a solution of the product in THF with 1 *N* aqueous sulfuric acid resulted in an exothermic reaction to give a quantitative amount of (*N*-methyl-*N*-phenyl)phenylacetamide, identical with an authentic sample prepared from phenylacetyl chloride and *N*-methylaniline.

*N-Carbomethoxy-N-phenyl-2-phenylethynylamine (**20**)*

To a solution of **8***c* in THF, prepared from 4.42 g (0.020 mol) of 1,4-diphenyl-1,2,3-triazole, was added, at −60°, a solution of methyl chloroformate (2.3 g, 0.024 mol) in 10 ml of THF in one portion. After the usual work-up, 5.4 g of crude product was obtained. The i.r. spectrum contained bands at 2250 and 2020 cm^{-1} of approximately equal intensity and a strong band at 1740 cm^{-1} with a shoulder at 1710 cm^{-1}, indicating the presence of both **20** and **21**. The amount of the ketenimine was small as was also indicated by the n.m.r. spectrum. The crude product was extracted with *n*-hexane (5 × 50 ml) to remove some hexane-insoluble resinous material. The residue (3.3 g) obtained by removal of the hexane was chromatographed on silica gel in an attempt to separate **20** and **21**. Although no separation was effected, the material eluted with a 1:4 mixture of ether and benzene contained only a trace of the ketenimine as most of this compound had decomposed on the column. The eluted product (2.8 g) was distilled *in vacuo* to give 2.0 g (40%) of pale yellow viscous liquid, b.p. 150–152° (0.1 mm); ν_{max} (neat) 2250 and 1740 cm^{-1}; n.m.r. (CCl_4): τ 2.3–3.0 (multiplet, 10H) and 6.16 (s, 3H).

Anal. Calcd. for $C_{16}H_{13}NO_2$: C, 76.49; H, 5.21; N, 5.58. Found: C, 76.22; H, 5.38; N, 5.75.

*Methyl (N-Phenyl)phenylacetimidate (**22**)*

*(a) From **8c***

Methanol (10 ml) was added in one portion to a solution of **8***c*, prepared from 2.21 g (0.010 mol) of 1,4-diphenyl-1,2,3-triazole, in THF at −60°. The reaction mixture was worked-up in the usual manner to give 1.0 g (45%) of yellow oil, b.p. 114–115° (0.5 mm), the i.r. spectrum of which was superimposable with that of the product obtained from aniline and methyl phenylthionacetate (11).

*(b) From **20***

Methanolic sodium hydroxide (1.3 ml of 3 *N*) was added to a solution of **20** (0.64 g, 0.0025 mol) in 3 ml of methanol. After 15 min at room temperature the mixture was diluted with ether and cooled. A white solid (0.09 g) precipitated, the i.r. spectrum of which was identical with that of sodium methylcarbonate. The ether solution was washed with water and dried. Removal of the solvent gave 0.53 g (95%) of liquid residue, identical with the material obtained under method *a*. Distillation *in vacuo* gave 0.38 g of colorless liquid, b.p. 110–112° (0.3 mm).

*Ethyl (N-Phenyl)phenylthioacetimidate (**23**)*

A solution of ethanethiol (3.1 g, 0.050 mol) in 10 ml of THF was added in one portion to a solution of **8***c*, prepared from 4.42 g (0.020 mol) of 1,4-diphenyl-1,2,3-triazole, in THF at −60°, followed by the usual work-up. After distillation there was obtained 4.1 g (80%) of yellow oil, b.p. 125–127° (0.05 mm); ν_{max} (neat) 1610 and

1595 cm^{-1}; n.m.r. (CCl_4): τ 2.5–3.5 (multiplet, 10H), 6.38 (s, 2H), 7.06 (q, 2H), and 8.75 (t, 3H).

Anal. Calcd. for $C_{16}H_{17}NS$: C, 75.25; H, 6.71; N, 5.49; S, 12.56. Found: C, 75.47; H, 6.83; N, 5.43; S, 12.28.

Methyl N-Phenylacetimidate (25)

To a stirred solution of 1-phenyl-1,2,3-triazole (4.35 g, 0.030 mol) in 45 ml of THF was added, in 15 min, 19 ml of a 1.6 *M* solution of *n*-butyllithium in *n*-hexane, at −60° in a nitrogen atmosphere. The reaction mixture was heated at 40–45° for 30 min when the gas evolution was complete. The darkly colored mixture was cooled to −60° and 10 ml of methanol was added. After work-up there was obtained 4.0 g of crude product, from which 1.6 g (37%) of starting material, m.p. 55–56°, was recovered by the addition of *n*-hexane. The remaining material was distilled *in vacuo* to give 1.3 g (47%, based on unrecovered starting material) of product, b.p. 64–65° (3 mm); reported b.p. 81–82° (12 mm) (20). The n.m.r. and i.r. spectra and the elemental analyses were in agreement with the assigned structure.

N-Methyl-N-phenyl-1-propynylamine (24)

A solution of **5***b*, prepared from 4-methyl-1-phenyl-1,2,3-triazole (3.20 g, 0.020 mol) in the usual manner, in THF was heated at 40–50° for 2 h in a nitrogen atmosphere. The darkly colored solution was cooled to −60° and a solution of dimethyl sulfate (2.52 g, 0.020 mol) in 10 ml of THF was added in one portion. From the reaction mixture was isolated 0.9 g (31%) of product, b.p. 60–62° (0.2 mm); ν_{max} (neat) 2250 and 1595 cm^{-1}; n.m.r. ($CDCl_3$): τ 2.5–3.3 (m, 5H), 6.83 (s, 3H), and 8.00 (s, 3H). Reported b.p. 96° (6 mm) (21). The material was readily hydrolyzed with dilute acid to *N*-methyl-*N*-phenylpropionamide, m.p. 57–58°; reported m.p. 58° (21).

Compound **24** was also obtained, in 21% yield, when the reaction was repeated with 1-phenyl-1,2,3-triazole.

The author thanks Professor R. U. Lemieux for his interest and encouragement, Dr. R. G. Micetich for many enlightening discussions, and Mr. P. K. Wolfert for his capable technical assistance.

1. R. G. Micetich and C. G. Chin. Can. J. Chem. **48**, 1371 (1970), and references cited therein.
2. R. Raap and R. G. Micetich. Can. J. Chem. **46**, 1057 (1968).
3. R. Raap. Can. J. Chem. **46**, 2251 (1968).
4. R. G. Micetich. Private communication.
5. (*a*) D. M. Zimmerman and R. A. Olofson. Abstracts of the 158th National Meeting of the American Chemical Society, New York, N.Y., September 7–12, 1969, paper ORGN 133; (*b*) Tetrahedron Lett. 3453 (1970).
6. J. C. Kauer and W. A. Sheppard. J. Org. Chem. **32**, 3580 (1967).
7. J. J. M. Rowe, K. B. Gibney, M. T. Yang, and G. G. S. Dutton. J. Am. Chem. Soc. **90**, 1923 (1968).
8. C. L. Stevens and J. C. French. J. Am. Chem. Soc. **76**, 4398 (1954).
9. L. J. Bellamy. The infrared spectra of complex molecules, 2nd edition, John Wiley & Sons, Inc., New York, 1964. p. 214.
10. H. G. Viehe. Angew. Chem. Internat. Edit. **6**, 767 (1967).
11. R. Raap. Can. J. Chem. **46**, 2255 (1968).
12. O. Dimroth. Ber. **35**, 1029 (1902).
13. A. Bertho. Ber. **58**, 859 (1925).
14. W. Kirmse and L. Horner. Ann. **614**, 1 (1958).
15. D. Pocar, G. Bianchetti, and P. D. Groce. Chem. Ber. **97**, 1225 (1964).
16. C. A. Rojahn and H. Trieloff. Ann. **445**, 296 (1925).
17. J. C. Sheehan and C. A. Robinson. J. Am. Chem. Soc. **73**, 1207 (1951).
18. H. Staudinger and L. Ruzicka. Ann. **380**, 278 (1911).
19. A. J. Vazakas and W. Walden Bennetts, Jr. J. Med. Chem. **7**, 342 (1964).
20. A. Buhner. Ann. **333**, 289 (1904).
21. J. Ficini and C. Barbara. Bull. Soc. Chim. Fr. 2787 (1965).

Can. J. Chem. Downloaded from www.nrcresearchpress.com by 210.87.254.42 on 09/05/12
For personal use only.

Can. J. Chem. Downloaded from www.nrcresearchpress.com by 210.87.254.105 on 09/05/12
For personal use only.

Proton Magnetic Resonance of the Methyl Derivatives of 2-Fluoropyridine. Sigma and Pi Electron Contributions to Spin–Spin Coupling Constants

J. B. ROWBOTHAM, R. WASYLISHEN AND T. SCHAEFER

Department of Chemistry, University of Manitoba, Winnipeg, Manitoba

Received January 26, 1971

The p.m.r. spectra of the methyl derivatives of 2-fluoropyridine are analyzed. The signs and magnitudes of the long-range spin–spin coupling constants between the methyl protons and the ring protons and between the methyl protons and fluorine are consistent with a model in which the nitrogen atom polarizes the sigma electron system but leaves the pi electron contribution to the coupling constants relatively unchanged. There are dramatic changes in the ring proton – fluorine couplings while the couplings involving the methyl protons vary little from those in the corresponding toluene derivatives. Thus the coupling over six bonds between fluorine and methyl protons is 1.25 ± 0.03 Hz in 2-fluoro-5-methyl pyridine compared to 1.15 ± 0.02 Hz in *p*-fluorotoluene.

On a analysé les spectres r.m.n. des fluoro-2 pyridines méthylées. Les signes et les valeurs des constantes de couplage à longue distance entre les protons des groupes méthyles et d'une part ceux du noyau et d'autre part les atomes de fluor sont en accord avec un modèle dans lequel on fait l'hypothèse que l'azote polarise le système électronique sigma tout en laissant la contribution des électrons pi aux constantes de couplage relativement intacte. On note des changements dramatiques dans les couplages entre les protons du cycle et le fluor; toutefois les couplages impliquant les protons des groupes méthyles ne varient pratiquement pas par rapport à ce qui est observé dans les toluènes correspondants. Par exemple le couplage reparti sur six liaisons entre le fluor et les protons du groupe méthyle est de 1.25 ± 0.03 Hz dans la fluoro-2 méthyl-5 pyridine alors qu'une valeur de 1.15 ± 0.02 Hz est observée dans le *p*-fluorotoluène.

Canadian Journal of Chemistry, 49, 1799 (1971)

Introduction

The full analysis of the p.m.r. spectrum of 2-fluoro-3-methylpyridine (**1**) has been described (1). The signs and magnitudes of the long-range spin–spin coupling constants, $J_{o,m,p}^{H,CH_3}$ and J_o^{F,CH_3}, between methyl protons and the ring protons or fluorine in **1** are consistent with the assumption (2, 3) that the nitrogen atom primarily polarizes the nearby σ bonds in the molecule, leaving the π electron contribution to the coupling constants relatively unaffected. Because it is a coupling over four bonds only, J_o^{F,CH_3} may contain a sizeable σ electron contribution (4), *i.e.*, $J_o^{F,CH_3} = 1.4_5$ Hz in **1** but is nearer 2 Hz in *o*-fluorotoluene (5) and its derivatives (6). In this paper the spectral parameters of the isomers of **1**, *viz.*, **2**, **3**, and **4**, are reported and discussed in spirit of the σ–π model. A knowledge of the contents of ref. 1 is assumed throughout.

Experimental

(1) Preparation of 2, 3, and 4

These compounds were prepared from the amines by the Schiemann reaction (7, 8) via the diazonium fluoroborates. Colorless **2**, 2.6 g, was collected under vacuum between 30–32 °C. Compound **3**, 22.6 g, was collected as a pale yellow liquid, b.p. 153 °C; lit. 155–156 °C at 752 mm (7). Compound **4**, 0.6 g, was obtained on distillation from the CCl_4 extract and probably contained some CCl_4. All compounds gave p.m.r. spectra consistent with their structure and with no detectable proton-containing impurities in the spectral region of interest.

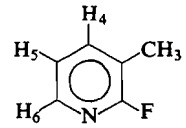

1

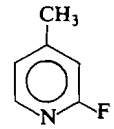

2

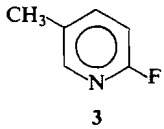

3

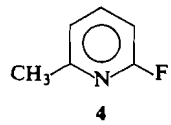

4

(2) Proton Resonance Measurements

Solutions of **2**, **3**, and **4** (20 mol %) in CS_2 containing trace amounts of trifluoroacetic acid (TFA) and internal tetramethylsilane (TMS) as locking material, were degassed. As described for **1** (1) the amount of TFA was sufficient to cause rapid relaxation of ^{14}N, leading to sharp peaks for proton 6, but insufficient to cause changes in the spectral parameters. However, addition of even

Can. J. Chem. Downloaded from www.nrcresearchpress.com by 210.87.254.105 on 09/05/12
For personal use only.

TABLE 1. Proton chemical shifts* and coupling constants† in methyl derivatives of 2-fluoropyridines

Parameter	1‡	2§	3¶	4¶	4‖,¶
ν_3	—	395.72	403.86	394.97	395.054
ν_4	458.58	—	452.78	453.45	453.502
ν_5	426.12	413.27	—	415.16	415.247
ν_6	479.82	475.9	475.72	—	—
ν_{CH_3}	132.72	139.55	136.72	143.70	143.763
$J_o^{H,H}$	[7.50(4, 5); 5.01(5, 6)]	5.07	8.34	[8.17(3, 4); 7.30]	[8.132; 7.352]
$J_m^{H,H}$	1.98	1.36	2.55	0.73	0.737
$J_p^{H,H}$	—	0.67	0.70	—	—
$J_m^{H,F}$	[9.93(2, 4); −1.02(2, 6)]	−0.7	[7.62; −0.7]	8.32	8.296
$J_p^{H,F}$	1.83	2.13	—	2.48	2.499
$J_o^{H,F}$	—	−2.18	−2.81	−3.12	−3.084
J_o^{H,CH_3}	−0.85	[−0.81(3, 4); −0.66]	[−0.68(4, 5); −0.80(5, 6)]	−0.58	−0.566
J_m^{H,CH_3}	0.40	0.29	0.38	0.27	0.269
J_p^{H,CH_3}	−0.7	—	—	−0.64	−0.643
J_o^{F,CH_3}	1.45	—	—	—	—
J_m^{F,CH_3}	—	−0.24	—	−0.61	−0.604
J_p^{F,CH_3}	—	—	1.25	—	—

*In Hz at 60 MHz to low field of internal TMS.
†In Hz, probable errors normally less than 0.01 Hz for 2, 3, and 4.
‡In TMS solution, from ref. 1.
§In CS_2 solution at 20 mol %.
‖Independent calibration and analysis using LAME. See text.
¶These solutions contained trace amounts of TFA, see Experimental.

Can. J. Chem. Downloaded from www.nrcresearchpress.com by 210.87.254.105 on 09/05/12
For personal use only.

very small amounts of TFA to the solution of **2** in CS_2 caused a separation into two layers. The final spectra of **2** were, therefore, taken on solutions containing no TFA, leading to relative large uncertainties in the peak positions of H-6. Addition of as much as 8 mol % of TFA to a more dilute solution of **3** caused significant changes in $J_o^{H,F}$ and $J_m^{H,F}$. An 18 mol % solution of **3** in benzene-d_6 yielded coupling parameters insignificantly different from those in CS_2 solution. In particular, the long-range coupling constants all lay within 0.02 Hz of their values in CS_2 solution.

The proton spectra were recorded at a sweep width of 50 Hz at sweep speeds of 2500 or 5000 s on a DA60I spectrometer. Calibrations were done by reading sweep and manual oscillator frequencies at 5 Hz intervals or less. Double and triple resonance experiments were carried out to find the relative signs of the coupling constants, as described for **1** (1).

Results and Discussion

(1) Spectral Analyses

The analytical techniques followed those for **1** (1), except that the computer program LAOCN 3 (9) was used to optimize the parameters. Therefore, the spectra obtained in the single ($ABCX_3R$) and in the multiple resonance experiments are not reproduced here. Their quality is not inferior to those displayed for **1** (1). Note, however, that the necessary absence of TFA in the sample of **2** led to broad peaks for H-6 resulting in larger errors in some of the parameters involving this proton.

The final parameters in CS_2 solution are given in Table 1. As many as 177 peaks per compound were assigned in iterating to these numbers. The r.m.s. errors in the fits varied between 0.009 and 0.033 (for **2**). The probable errors in the parameters ranged from 0.002 to 0.009 Hz and the worst assignment was 0.095 Hz (for some of the broad peaks in **2**). Calcomp plots of the spectra using the parameters in Table 1 agreed very well with the experimental spectra, in particular with the methyl proton resonances in a manner demonstrated for *p*-fluorotoluene (10*a*).

In a separate experiment on **4**, a recalibration of the spectrum at 0.01 Hz/s and its analysis using the program LAME (10*a*) gave the results listed in the last column of Table 1. In this analysis the r.m.s. error was 0.0088, the maximum standard deviation in the parameters was 0.005 Hz (otherwise between 0.001 and 0.003 Hz), and in the correlation matrix of dimension 14, there were two elements with a magnitude above 0.2 and none with a magnitude greater than 0.3. Over 250 transitions were assigned and the biggest deviation between observed and calculated transitions was 0.033 Hz (normally below 0.02 Hz).

(2) The Methyl Proton–Ring Proton Coupling Constants

To within experimental error, J_p^{H,CH_3} in **1** and **4** is the same as in toluene (11). By the methyl group replacement technique (12, 13), Macdonald and Reynolds (4) have shown that J_p^{H,CH_3} in toluene derivatives arises from a π electron mechanism. Consequently the nitrogen atom does not significantly alter the π electron contribution to this coupling constant or to J_p^{HF} in **1** and **4**.

In ref. 1 evidence is adduced that the J_o^{H,CH_3} value of -0.85 Hz in **1** is consistent with a contribution from the resonance structure **5**. This

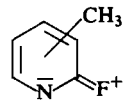

5

structure increases the mobile bond order between C-3 and -4 and between C-5 and -6 relative to that between C-4 and -5. Because the negative π electron contribution to J_o^{H,CH_3} is expected to increase as the bond order of the intervening C···C bond increases (14), structure **5** implies a larger magnitude of $J_o^{H_3,CH_3}$ in **2** and of $J_o^{H_5,CH_3}$ in **3** than of $J_o^{H_5,CH_3}$ in **2** and of $J_o^{H_4,CH_3}$ in **3**. Indeed, the former are larger in magnitude than the latter by up to 0.2 Hz (see Table 1).

However, $J_o^{H_5,CH_3} = -0.58$ Hz in **4**, rather smaller than predicted by structure **5**. There are two possible reasons. The first invokes structure **6**,

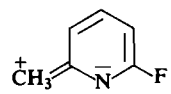

6

supported by ^{14}N quadrupole resonance studies (15), which decreases the mobile bond order[1] between C-5 and -6. The second possible reason lies in an indicated negative σ electron contribution (4) to J_o^{H,CH_3}, suggesting a decrease in the

[1]A referee points out that the larger and unequal values of J_o^{H,CH_3} in **2** can be taken as evidence against a resonance form for **2** analogous to **6**. He points out that in this connection the methyl derivatives of 3- and 4-fluoropyridine should be examined. We have synthesized a number of these compounds and are studying their proton resonance spectra.

Can. J. Chem. Downloaded from www.nrcresearchpress.com by 210.87.254.105 on 09/05/12
For personal use only.

magnitude of this contribution in **4** and caused by polarization of the σ core by the nitrogen atom. Qualitatively, it is simply that the electronegative nitrogen atom reduces the σ electron density near the bonded C-6 atom thereby reducing the σ contribution to J_o^{H,CH_3} in **4**.

Because there is very likely a positive σ contribution to J_m^{H,CH_3} (perhaps as large as 0.2 Hz (1, 4)), the second reason above implies a decrease in this contribution to J_m^{H,CH_3} in both **4** and **2** because C-6 is involved in the coupling path. In fact, J_m^{H,CH_3} is 0.1 Hz smaller in **4** and **2** than in **1** and **3**. In the latter two compounds J_m^{H,CH_3} has the same magnitude as in toluene (11). Other workers (2) have noted that polarization of the σ core in pyridine does not appreciably extend beyond the ortho carbon atoms.

(3) The Methyl Proton – Fluorine Coupling

In **3**, $J_p^{F,CH_3} = 1.25$ Hz, only 0.10 Hz larger than in *p*-fluorotoluene (10*a*). Since it is unlikely that other than a π mechanism is important for this coupling in the latter, the present result strongly suggests that the heteroatom does not appreciably affect the π contribution to J_p^{F,CH_3} in **3**. A similar, less strong, conclusion was reached for J_o^{F,CH_3} in **1** (1).

In 4-amino-5-bromo-3-fluorotoluene $J_m^{F,CH_3} = -0.4_3$ Hz (6), little different in magnitude from the value originally estimated for this coupling in *m*-fluorotoluene (5). The values of J_m^{F,CH_3} in **2** and **4** suggest that, again, the presence of the heteroatom has little effect on the π contribution to this coupling. By the methyl group replacement criterion, the effect of the nitrogen atom on J_m^{F,H_6} occurs predominantly through the σ electron system. For, $J_m^{H,F} = 5.6$ Hz in fluorobenzene (16) but is −1 Hz in **1**; yet J_m^{F,CH_3} remains constant to within 0.2 or 0.3 Hz even when a nitrogen atom replaces the carbon atom in the "coupling path".

(4) The Ring Proton and Ring Proton – Fluorine Couplings

The magnitudes of all these couplings are consistent with an alternating electronegativity effect of the substituents (2, 17) as discussed for **1** (1) and for *p*-fluorotoluene (10*a*); an effect acting primarily through the σ electron system, as suggested originally by Castellano and Kostelnik (2), and now also supported by the couplings with methyl protons reported here.

The additivity of substituent effects on coupling constants between protons in benzene derivatives (1, 18, 19) can be extended to the present pyridine derivatives. Using the coupling constants reported for pyridine dissolved in CCl_4 (20), for benzene (18, 21), fluorobenzene (16), and toluene (11), the predicted and observed values for **1**, **2**, and **3** agree to at least 0.2 Hz for $J_o^{H,H}$ and $J_m^{H,H}$ and to better than 0.1 Hz for $J_p^{H,H}$. In other words, the substituent effects of CH_3 and F on benzene are substantially the same as in pyridine in this regard. The deviations of the predicted from the calculated values are generally in the direction expected if the substituent effects of F (22) and CH_3 are somewhat less than in the monosubstituted benzenes themselves, *i.e.*, as if a saturation effect were occurring; as already noted for trisubstituted benzenes (23). These deviations become as large as 0.4 Hz for $J_o^{H,H}$ in **4** where both substituents are attempting to polarize the σ core at C-2 and -6 when it is already markedly polarized by the heteroatom, in agreement with the idea of a saturation effect.

In **3**, partial protonation of the nitrogen atom by addition of TFA (see Experimental) causes an algebraic increase of 1 Hz in $J_o^{H,F}$, an increase of 0.2 Hz in $J_m^{H_6,F}$, and a decrease of 0.2 Hz in $J_m^{H_4,F}$ of the values in Table 1. These changes are in order if the proton acts as an electronegative substituent polarizing the σ system (2). On this basis the long-range couplings involving methyl protons, particularly J_p^{F,CH_3}, should remain unchanged, as observed experimentally.

Conclusions

A model in which σ and π electron contributions to ring proton and ring proton – fluorine spin–spin coupling constants are distinguished can be extended to pyridine derivatives. In this model the nitrogen atom polarizes the σ electron system but does not strongly alter the π electron contribution to the coupling constants. The most dramatic effects are observed for $J_{o,m,p}^{H,F}$. Thus in fluorobenzene $J_o^{H,F} = 8.9$, $J_m^{H,F} = 5.6$, $J_p^{H,F} = 0.2$ Hz (16). In 2-fluoropyridine $J_o^{H,F} = -2.8$, $J_m^{H_6,F} = -1.0$, and $J_p^{H,F} = 2$ Hz (24). Yet $J_{o,m,p}^{F,CH_3}$ in **1**, **2**, **3**, and **4** are almost the same as in the fluorotoluenes and are a measure of the π electron contributions to the corresponding ring proton and ring proton – fluorine couplings.

This work was supported by the National Research Council of Canada. We are grateful to Mr. L. Olynyk for the synthesis of 2-fluoro-5-methylpyridine.

1. T. SCHAEFER, S. S. DANYLUK, and C. L. BELL. Can. J. Chem. **47** 1507 (1969).
2. S. CASTELLANO and R. KOSTELNIK. J. Am. Chem. Soc. **90**, 141 (1968).
3. J. B. MEMORY and J. H. GOLDSTEIN. J. Am. Chem. Soc. **88**, 5560 (1966).
4. C. J. MACDONALD and W. F. REYNOLDS. Can. J. Chem. **48**, 1002 (1970).
5. R. E. RICHARDS and T. SCHAEFER. Trans. Faraday Soc. **54**, 1447 (1958).
6. D. J. BLEARS, S. S. DANYLUK, and T. SCHAEFER. J. Chem. Phys. **47**, 5037 (1967).
7. J. T. MINOR, G. F. HAWKINS, C. A. VANDERWERF, and A. ROE. J. Am. Chem. Soc. **71**, 1125 (1949).
8. A. ROE, P. H. CHECK, and G. K. HAWKINS. J. Am. Chem. Soc. **71**, 4152 (1949).
9. S. CASTELLANO and A. A. BOTHNER-BY. J. Chem. Phys. **41**, 3863 (1964).
10. (*a*) R. WASYLISHEN and T. SCHAEFER. Can. J. Chem. **49**, 94 (1971). (*b*) C. W. HAIGH and J. M. WILLIAMS. J. Mol. Spectrosc. **32**, 398 (1969).
11. M. P. WILLIAMSON, R. J. KOSTELNIK and S. M. CASTELLANO. J. Chem. Phys. **49**, 2218 (1968).
12. R. HOFFMAN. Arkiv Kemi, **17**, 1 (1961).
13. R. HOFFMAN and S. GRONOWITZ. Arkiv Kemi, **16**, 471 (1960).
14. K. D. BARTLE. D. W. JONES, and R. S. MATTHEWS. Rev. Pure and Appl. Chem. **19**, 191 (1969).
15. L. GUIBÉ and E. A. C. LUCKEN. Mol. Phys. **14**, 79 (1968).
16. J. E. LOEMKER, J. M. READ, JR., and J. H. GOLDSTEIN. Mol. Phys. **13**, 433 (1967).
17. A. D. COHEN and T. SCHAEFER. Mol. Phys. **10**, 209 (1965).
18. S. CASTELLANO and R. KOSTELNIK. Tetrahedron Lett. **51**, 5211 (1967).
19. J. M. READ, JR., R. M. CRECELY, R. S. BUTLER, J. E. LOEMKER, and J. H. GOLDSTEIN. Tetrahedron Lett. **10**, 1215 (1968).
20. S. CASTELLANO, C. SUN, and R KOSTELNIK J. Chem. Phys. **46**, 327 (1967).
21. J. M. READ, JR., R. E. MAYO, and J. H. GOLDSTEIN. J. Mol. Spectrosc. **22**, 419 (1967).
22. J. E. LOEMKER, J. M. READ, JR., and J. H. GOLDSTEIN. J. Phys. Chem. **72**, 991 (1968).
23. T. SCHAEFER, G. KOTOWYCZ, H. M. HUTTON, and J. W. S. LEE. Can. J. Chem. **46**, 2531 (1968).
24. J. C. DECK. Ph.D. Thesis. University of Illinois, Urbana, Illinois, 1966.

Can. J. Chem. Downloaded from www.nrcresearchpress.com by 210.87.254.105 on 09/05/12
For personal use only.

Can. J. Chem. Downloaded from www.nrcresearchpress.com by 210.87.254.42 on 09/05/12
For personal use only.

A Glucan from *Tremella mesenterica* NRRL-Y6158[1]

C. G. FRASER[2] AND H. J. JENNINGS
Biochemistry Laboratory, National Research Council of Canada, Ottawa 7, Canada

Received July 30, 1970[3]

A dextrorotatory glucan has been isolated in good yields from the culture medium of *Tremella mesenterica* NRRL-Y6158. The glucan consumed 1.32 mol of periodate and released 0.33 mol of formic acid per mol anhydroglucose and reduction and hydrolysis of the periodate-oxidized glucan yielded glycerol and erythritol in the ratio 1.0:1.9. Partial hydrolysis of the glucan released maltose, isomaltose, panose, isomaltotriose and *O*-α-D-glucopyranosyl-(1 → 4)-*O*-α-D-glucopyranosyl-(1 → 6)-D-glucose. The fully methylated glucan was composed of 2,3,4,6-tetra-*O*-methyl glucose (0.5%), 2,3,4-tri-*O*-methyl glucose (31.4%), and 2,3,6-tri-*O*-methyl glucose (67.6%).

These results indicate that the glucan was a linear molecule composed of approximately 200 α-D-glucopyranose units linked 1 → 6 and 1 → 4 in the ratio 2:1. Structurally the glucan resembles to varying extents the neutral glucans obtained from the yeast-like fungi of the *Pullularia* species.

L'extraction d'un milieu de culture de *Tremella mesenterica* NRRL-Y6158 a permis d'isoler avec de bons rendements, un glucan dextrorotatoire. Le composé réagit avec 1.32 mol de périodate et fournit 0.33 mol d'acide formique par mole d'anhydroglucose; la réduction et l'hydrolyse du glucan oxydé au périodate conduit à la formation de glycérol et d'érythritol dans le rapport de 1.0 à 1.9. L'hydrolyse partielle du glucan fournit du maltose, de l'isomaltose, du panose, de l'isomaltotriose, et du *O*-α-D-glucopyranosyl-(1 → 4)-*O*-α-D-glucopyranosyl-(1 → 6)-D-glucose. Le glucan méthylé complètement est composé de tétra-*O*-méthyl-2,3,4,6 glucose (0.5%), de tri-*O*-méthyl-2,3,4 glucose (31.4%), et de tri-*O*-méthyl-2,3,6 glucose (67.6%).

Ces résultats indiquent que le glucan est une molécule linéaire composée d'environ 200 unités d'α-D-glucopyranose liées 1 → 6 et 1 → 4 dans un rapport de 2 à 1. Au point de vue structural, ce glucan ressemble aux glucans neutres obtenus à partir de champignons ressemblant à des levures de l'espèce *Pullularia*.

Canadian Journal of Chemistry, 49, 1804 (1971)

In our structural studies on the extracellular polysaccharides of *Tremella mesenterica* NRRL-Y6158 (1), it was found in one preliminary growth experiment that a glucan and not an acidic xylomannan was the predominant polysaccharide in the culture medium. This preponderance of the glucan was probably a direct result of the prolongation of the growth period (to 17 days) which we attempted in an effort to increase the very poor yields of the acidic xylomannan that were obtained with shorter growth periods (7–9 days). Prolongation of the growth period produced the glucan in very high yield, although traces of the acidic xylomannan were still detectable by the presence of xylose, mannose, and glucuronic acid in the hydrolysate of the crude glucan. The yeast *Cryptococcus laurentii* also produces a glucan in addition to an acidic xylomannan (2), and in view of the possible phylogenetic relationship between these two species (3, 4), a structural study of this glucan from *T. mesenterica* was undertaken.

T. mesenterica was grown for 17 days in a glucose medium and following removal of the suspended cells the polysaccharide was obtained by ethanol precipitation of the concentrated supernatant. This polysaccharide was separated into two fractions by precipitation of the acidic xylomannan with 5% cetyltrimethylammonium bromide (5). The material not precipitated by the detergent was isolated by filtration and ethanol precipitation and the product, after washing, contained no ash, and no acetyl or methoxyl groups. This polysaccharide gave glucose only on hydrolysis, gave a single symmetrical peak on moving boundary electrophoresis, and sedimented as a single component on ultracentrifugal analysis.

The presence of α-D-glucoside linkages was shown by the change in the specific rotation of the glucan (+185°) to +51° on hydrolysis, and by an absorption at 845 cm^{-1} in the i.r. (6). The glucan gave no coloration with iodine, and was unattacked by α-, and β-amylases, and consisted

[1]Issued as NRCC No. 11887.
[2]NRCC Postdoctorate Fellow, 1969–1970.
[3]Revision received March 11, 1971.

Can. J. Chem. Downloaded from www.nrcresearchpress.com by 210.87.254.42 on 09/05/12
For personal use only.

of about 200 glucopyranose units. This was determined by the estimation of the percentage of end-group (2,3,4,6-tetra-*O*-methyl glucose) released in the methanolysis of the methylated glucan and therefore must be regarded as a minimum value.

The glucan consumed 1.32 mol of periodate with production of 0.33 mol of formic acid per mol anhydroglucose and the periodate-oxidized glucan, after reduction and hydrolysis, yielded glycerol and erythritol; the ratio of glycerol to erythritol was estimated to be 1.0:1.9 by g.l.c. of the derived acetates.

These results attest to the presence of $1 \rightarrow 6$- and $1 \rightarrow 4$-α-D-glucopyranose linkages in the ratio of 1:1.9, and this result was in fairly good agreement with the results obtained from methylation studies. The permethylated glucan which was obtained in good yield was methanolyzed and the components, methyl 2,3,4,6-tetra-*O*-methyl glucoside (0.5%), 2,3,4-tri-*O*-methyl glucoside (31.4%), and 2,3,6-tri-*O*-methyl glucoside (67.6%) were identified by comparison with authentic samples and the quantitative data were obtained by estimation of the areas under the peaks. The ratio of $1 \rightarrow 6$- to $1 \rightarrow 4$-α-D-glucopyranose linkages in this case was calculated as 1:2.1. This value did not change when the duration of methanolysis was both shortened and lengthened indicating that complete methanolysis had been achieved and that no preferential degradation of one of the components had occurred. One unidentified component (0.5%), which may be 1,6-anhydro-2,3,4-tri-*O*-methyl glucose, a known artefact from this type of system (7), was present. The methylated glucan was hydrolyzed and examined by chromatography and the 2,3,4,6-tetra-, 2,3,4-tri-, and 2,3,6-tri-*O*-methyl derivatives of glucose were identified by comparison with authentic samples.

Partial hydrolysis of the glucan with oxalic acid gave a mixture of disaccharides and trisaccharides which were chromatographically indistinguishable from maltose, isomaltose, panose, isomaltotriose, and *O*-α-D-glucopyranosyl-$(1 \rightarrow 4)$-*O*-α-D-glucopyranosyl-$(1 \rightarrow 6)$-D-glucose.

The above evidence indicates that the extracellular glucan from *T. mesenterica* is essentially a linear glucan consisting of approximately 200 α-D-glucopyranose units linked $1 \rightarrow 4$ and $1 \rightarrow 6$ in the ratio of about 2:1. In these respects the glucan closely resembles the one obtained from *Pullularia fermentans* (8) and also exhibits structural similarities to the extracellular glucans (pullulans) obtained from different growths of the yeast-like fungus *Pullularia* pullulans (9–15). Although the $1 \rightarrow 4$- and $1 \rightarrow 6$-α-D-glucopyranose linkages are the main structural features of all these glucans (pullulans) nevertheless they do exhibit variations in overall structure. Wallenfels and coworkers isolated a linear glucan composed of 300 α-D-glucopyranose units linked $1 \rightarrow 4$ and $1 \rightarrow 6$ in the ratio 3:2 (9, 10). Bouveng *et al.* reported a linear glucan having 250 α-D-glucopyranose units linked $1 \rightarrow 4$ and $1 \rightarrow 6$ in the ratio 2:1; however, they did suggest the presence of a small amount of $1 \rightarrow 3$ linkages (1–2%) as a small amount of glucose remained after periodate oxidation of the glucan (11). Unequivocal evidence for the presence of $1 \rightarrow 3$ linkages (6%) in a pullulan was obtained by Sowa *et al.* and they obtained a ratio of $1 \rightarrow 4$ to $1 \rightarrow 6$ linkages of 2.2:1 (14). The ratio of $1 \rightarrow 4$ to $1 \rightarrow 6$ linkages in the latter two preparations of pullulan are very similar to that obtained in the glucan from *T. mesenterica* except that no evidence for $1 \rightarrow 3$ linkages in the glucan from *T. mesenterica* could be found. This appears to be the first reported isolation and study of a glucan with $1 \rightarrow 4$ and $1 \rightarrow 6$ glucosidic linkages from a yeast other than those from the *Pullularia* species, although there is some preliminary evidence to suggest that the glucan from *C. laurentii* may also contain these linkages (2). One major structural difference between the extracellular glucans of *T. mesenterica* and *C. laurentii* is that there is definite evidence for the presence of $1 \rightarrow 3$ linkages in the latter (2, 16), whereas none were detected in the former.

Experimental

Paper chromatography was performed on Whatman No. 1 paper, and t.l.c. on Silica Gel G (Merck, Darmstadt) layers. The irrigants used (v/v) were (*A*) ethyl acetate : pyridine : water, 72:20:23; (*B*) ethyl acetate : acetic acid : formic acid : water, 18:3:1:4; (*C*) benzene : ethanol : water : acetic acid, 200:47:15:1; (*D*) chloroform : methanol, 92:8; (*E*) ethyl acetate : pyridine : water, 8:2:1; (*F*) butan-2-one : water, 10:1; (*G*) butan-1-ol : ethanol : water, 4:1:5; (*H*) butan-1-ol : pyridine : 0.1 *N* hydrochloric acid, 5:3:2; (*I*) butan-1-ol : pyridine : benzene : water, 5:3:1:3. Sugars were detected on chromatograms by *p*-anisidine hydrochloride (17), alkaline silver nitrate (18), or by ethanolic sulfuric acid. A Tiselius-type Spinco model H apparatus was used for moving boundary electrophoresis in 0.05 *M* borate buffer. A Beckman

Can. J. Chem. Downloaded from www.nrcresearchpress.com by 210.87.254.42 on 09/05/12
For personal use only.

model E analytical ultracentrifuge was used for sedimentation analysis of 0.3% polysaccharide solutions. An F and M model 500 chromatograph was used for g.l.c. Evaporations were carried out under reduced pressure below 40°. Specific rotations are equilibrium values and were measured on a Perkin–Elmer 141 polarimeter.

Preparation of the Crude Glucan

T. mesenterica NRRL-Y6158, kindly provided by the United States Department of Agriculture, Peoria, Illinois, was grown with aeration in a 12 l baffled flask in an identical glucose medium (8 l) to that previously described for the growth of *C. laurentii* (2). The culture was continuously shaken on a rotary shaker, and was maintained at 25°. A starter culture was prepared by inoculation of the same medium (2 × 250 ml) from a slant of the organism; growth was allowed to occur for 4 days in continuously swirled Erlenmeyer flasks before transfer to the aerated medium was effected. Growth was allowed to continue for a further 17 days during which time the medium became viscous and then began to lose its viscous nature toward the end of the growth period. The culture was then centrifuged on a Sharples ultracentrifuge to remove suspended yeast cells. The supernatant was dialyzed against tap-water for 5 days, and was then concentrated to a viscous solution. The solution was poured into ethanol (5 vol) with stirring, and the fibrous white precipitate recovered, washed successively with ethanol, acetone, and ether, and air-dried to yield 80 g of the polysaccharide (a yield of 27% based on the initial glucose).

A sample of the polysaccharide was hydrolyzed with sulfuric acid in a sealed tube at 100° for 7 h. Chromatographic examination (irrigants *B* and *G*) of the neutralized (barium carbonate) hydrolyzate showed that glucose was the major component together with traces of mannose, xylose, and glucuronic acid.

Isolation of the Glucan

A sample (75 g) of the crude glucan was dispersed in water (1 l), the solution clarified by centrifugation, and 5% cetyltrimethylammonium bromide added until no further precipitation occurred. The mixture was filtered through celite, and the filtrate concentrated to 1 l and poured into ethanol (10 l). The precipitate was washed with ethanol (7 l), dissolved in water (1 l), filtered through celite, and the filtrate poured into ethanol (6 l). The precipitate was dissolved in water (1 l) and freeze-dried to yield 42.5 g of polysaccharide, hereafter referred to as the glucan.

Properties of the Glucan

The glucan gave a single symmetrical peak on moving boundary electrophoresis, and sedimented as a single component on ultracentrifugal analysis. The glucan had $[\alpha]_D^{26}$ +185° (*c*, 0.42 in water) which after hydrolysis (8 h, 100°) changed to $[\alpha]_D^{26}$ +51.4° (*c*, 0.67 in *N* sulfuric acid). Chromatographic examination (irrigants *A*, *B*, *E*, *F*, and *G*) of the neutralized (barium carbonate) hydrolyzate showed glucose alone. The glucan gave no coloration with iodine, and was unattacked by α- or β-amylases. The i.r. spectrum (KBr disc) showed an absorption at 845 cm^{-1}.

Periodate Oxidation

Preliminary experiments showed that the glucan consumed 1.32 mol of periodate and released 0.33 mol of formic acid per mol anhydroglucose.

A sample (1.6 g) of the glucan was dissolved in water (20 ml), 0.05 *M* sodium metaperiodate (500 ml) added, and the solution kept at 4° in the dark for 19 days. Excess periodate was destroyed by the addition of ethylene glycol (10 ml), the solution dialyzed, and sodium borohydride (5 g) added. After 24 h excess borohydride was destroyed by addition of glacial acetic acid, the solution dialyzed, and the resultant polyalcohol (1.2 g) isolated by freeze-drying. A sample (140 mg) of the polyalcohol was hydrolyzed by *N* sulfuric acid at 100° for 12 h. Paper chromatography (irrigant *A*) of the neutralized hydrolyzate showed the presence of two components that were identical to glycerol and erythritol. The hydrolyzate was acetylated with acetic anhydride and sodium acetate, and the product examined by g.l.c. on a column (4′ × 3 mm) of 3% ECNSS-M on Gas-Chrom Q (100–120 mesh) at 185° (19).

Two components were detected having retention times corresponding to those of authentic samples of glycerol triacetate and erythritol tetraacetate. The ratio of glycerol triacetate to erythritol tetraacetate was 1.0:1.9, as determined from the relative areas under the peaks.

Methylation Analysis

A sample of the glucan (300 mg) was dissolved in dry dimethyl sulfoxide (20 ml) and was treated with dimethylsulfinyl cation and methyl iodide by the Hakomori procedure (20). The reaction mixture was poured into water (100 ml) and the resultant solution was dialyzed against water for 24 h. A clear dialyzate was obtained which was then lyophylized to yield the methylated product (300 mg) having a small hydroxyl absorption in its spectrum and OCH_3, 38.0%. Further methylation of the glucan with silver oxide and methyl iodide by the Purdie procedure (21) yielded the permethylated glucan (285 mg, 80%) which showed no hydroxyl absorption in its i.r. spectrum and had $[\alpha]_D^{26}$ +212° (*c*, 0.1 in chloroform) and OCH_3, 43.0%.

A sample of the methylated glucan was heated at 100° with methanolic hydrogen chloride (3%) in a sealed tube for 7 h. After neutralization with silver carbonate the mixture was examined by g.l.c. on a column (8′ × 3 mm) of 15% diethylene glycol succinate on Gas-Chrom S (60–80 mesh) at 170°. The methyl glycosides of 2,3,4,6-tetra-*O*-methyl glucose (0.5%), 2,3,4-tri-*O*-methyl glucose (31.4%), and 2,3,6-tri-*O*-methyl glucose (67.6%) were detected and identified by comparison of their retention times with authentic samples of these methylated derivatives, and their quantitative estimation was carried out by mensuration of the peak areas. Thus the ratio of 2,3,4- to 2,3,6-tri-*O*-methyl glucopyranosides was 1:2.1. To ensure the accuracy of this ratio further methanolyses of the methylated glucan were carried out as above except for varying the time of methanolysis. At both shorter (4 h) and longer (12 h) periods of time the ratio of 2,3,4- to 2,3,6-tri-*O*-methyl glucopyranosides was found to be 1:2.1 in each case.

A small sample of the methylated glucan was hydrolyzed by the formic acid–sulfuric acid method (11) and the neutralized hydrolyzate was examined by paper

chromatography (irrigants *C*, *F*, and *G*) and t.l.c. (irrigants *C* and *D*). The 2,3,4,6-tetra- and 2,3,4-tri- and 2,3,6-tri-*O*-methyl derivatives of glucose were detected and identified by comparison with authentic samples.

Partial Hydrolysis

A sample (160 mg) of the glucan was heated at 100° with 0.1 *M* oxalic acid for 6 h (sealed tube). Chromatographic examination of the neutralized (barium carbonate) hydrolysate (irrigants *E* and *I*) revealed the presence of glucose, maltose, isomaltose, panose, isomaltotriose, and the trisaccharide *O*-α-D-glucopyranosyl-(1 → 4)-*O*-α-D-glucopyranosyl-(1 → 6)-D-glucose.

The authors wish to thank Mrs. A. Martin for technical assistance and Mr. A. E. Castagne for the microanalyses.

1. H. J. JENNINGS. Unpublished results.
2. M. J. ABERCROMBIE, J. K. N. JONES, M. V. LOCK, M. B. PERRY, and R. J. STOODLEY. Can. J. Chem. **38**, 1617 (1960).
3. M. E. SLODKI, L. J. WICKERHAM, and R. J. BANDONI. Can. J. Microbiol. **12**, 489 (1966).
4. M. E. SLODKI. Can. J. Microbiol. **12**, 495 (1966).
5. J. E. SCOTT. Chem. and Ind. 1568 (1955).
6. S. A. BARKER, E. J. BOURNE, and D. H. WHIFFEN. Methods in Biochem. Anal. **3**, 213 (1956).
7. H. W. KIRCHER. Anal. Chem. **32**, 1103 (1960).
8. E. NINOMIYA and T. KIZAKI. J. Agric. Chem. Soc. Jap. **43**, 115 (1969).
9. H. BENDER, J. LEHMANN, and K. WALLENFELS. Biochim. Biophys. Acta, **36**, 309 (1959).
10. K. WALLENFELS, H. BENDER, G. KEILICH, and G. BECHTLER. Angew. Chem. **72**, 522 (1960).
11. H. O. BOUVENG, H. KIESSLING, B. LINDBERG, and J. MCKAY. Acta Chem. Scand. **16**, 615 (1962).
12. H. O. BOUVENG, H. KIESSLING, B. LINDBERG, and J. MCKAY. Acta Chem. Scand. **17**, 797 (1963).
13. H. O. BOUVENG, H. KIESSLING, B. LINDBERG, and J. MCKAY. Acta Chem. Scand. **17**, 1351 (1963).
14. W. SOWA, A. C. BLACKWOOD, and G. A. ADAMS. Can. J. Chem. **41**, 2314 (1963).
15. K. WALLENFELS, G. KIELICH, G. BECHTLER, and D. FREUDENBERGER. Biochem. Zeit. **341**, 433 (1965).
16. R. J. STOODLEY. Ph.D. Thesis. Queen's University, Kingston, Ontario, 1959.
17. L. HOUGH, J. K. N. JONES, and W. H. WADMAN. J. Chem. Soc. 1702 (1950).
18. W. E. TREVELYAN, D. P. PROCTER, and J. S. HARRISON. Nature, **166**, 444 (1950).
19. J. W. SAWARDEKER, J. H. SLONEKER, and A. JEANES. Anal. Chem. **37**, 1602 (1965).
20. S. HAKOMORI. J. Biochem. Tokyo, **55**, 205 (1964).
21. T. PURDIE and J. C. IRVINE. J. Chem. Soc. 1021 (1903).

Can. J. Chem. Downloaded from www.nrcresearchpress.com by 210.87.254.42 on 09/05/12
For personal use only.

Can. J. Chem. Downloaded from www.nrcresearchpress.com by 210.87.254.5 on 09/05/12
For personal use only.

The Reaction of the Electronically Excited Oxygen Atom $O(^1D_2)$ with Nitrous Oxide[1]

P. M. SCOTT,[2] K. F. PRESTON, R. J. ANDERSEN,[3] AND L. M. QUICK[4]
Division of Chemistry, National Research Council of Canada, Ottawa, Canada

Received January 15, 1971

An investigation has been made of the relative importance of the possible pathways [2*a*]–[2*d*]

[2*a*] $O(^1D_2) + N_2O \rightarrow N_2 + O_2$

[2*b*] $O(^1D_2) + N_2O \rightarrow 2NO$

[2*c*] $O(^1D_2) + N_2O \rightarrow N + NO_2$

[2*d*] $O(^1D_2) + N_2O \rightarrow O(^3P) + N_2O$

for the reaction in the gas phase at room temperature between the excited oxygen atom $O(^1D_2)$ and N_2O, using the photolysis of NO_2, O_3, and N_2O as sources of the excited atom. Measurement of the yields of N_2 and NO from the photolysis at 2288 Å of mixtures of NO_2 and N_2O has led to a value of 1.01 ± 0.06 for k_{2a}/k_{2b}, the ratio of the rate constants for [2*a*] and [2*b*], in excellent agreement with the value of 0.99 ± 0.06 obtained from determination of the yields of N_2 and NO_2 arising from the flash photolysis of O_3–N_2O mixtures. The isotopic composition of the N_2 produced in the photolysis of $^{15}NO_2$–N_2O mixtures indicated that $k_{2c}/k_{2a} < 5 \times 10^{-3}$. Furthermore, the value of $k_{2a}/(k_{2b} + k_{2d}) = 1.08 \pm 0.19$, obtained from a study of the effect of CO_2 and Xe additions on the yield of N_2 from the photolysis of N_2O at 2288 Å, suggests that deactivation [2*d*] does not make an important contribution to the total rate constant for destruction of $O(^1D_2)$.

On rapporte les résultats obtenus lors d'une étude entreprise afin de déterminer l'importance relative des diverses réactions possibles [2*a*]–[2*d*]

[2*a*] $O(^1D_2) + N_2O \rightarrow N_2 + O_2$

[2*b*] $O(^1D_2) + N_2O \rightarrow 2NO$

[2*c*] $O(^1D_2) + N_2O \rightarrow N + NO_2$

[2*d*] $O(^1D_2) + N_2O \rightarrow O(^3P) + N_2O$

pour la réaction en phase gazeuse et à température de la pièce, entre l'atome d'oxygène excité $O(^1D_2)$ et le N_2O; on a utilisé la photolyse de N_2O, O_3 et NO_2 comme source d'atome excité. En mesurant les rendements de N_2 et NO obtenus lors de la photolyse, à 2288 Å de mélanges de NO_2 et N_2O, on a pu établir que le rapport des constantes de vitesse pour les réactions [2*a*] et [2*b*], k_{2a}/k_{2b}, est égal à 1.01 ± 0.06; cette valeur est en excellent accord avec celle, 0.99 ± 0.06, obtenue en déterminant les rendements de N_2 et NO_2 obtenus lors de la photolyse éclair de mélanges de O_3 et N_2O. En se basant sur la composition isotopique de N_2 produit lors de la photolyse de mélanges de $^{15}NO_2$–NO_2, on peut déduire que $k_{2c}/k_{2a} < 5 \times 10^{-3}$. Par ailleurs en étudiant l'effet que produit l'addition de CO_2 et de Xe sur le rendement de N_2 lors de la photolyse de N_2O à 2288 Å, on peut établir que $k_{2a}/(k_{2b} + k_{2d}) = 1.08 \pm 0.19$; ce résultat suggère que la contribution de la réaction de désactivation, [2*d*], à la constante de vitesse totale de la destruction de $O(^1D_2)$ est négligeable.

Canadian Journal of Chemistry, 49, 1808 (1971)

Introduction

In the course of our investigations of the chemistry of $O(^1D_2)$ atoms, we have become aware of serious disagreements in the literature concerning the nature and relative rates of the secondary reactions in the photolysis of N_2O. This paper describes work designed to clarify this situation.

The photolysis of N_2O in the wavelength region 1850–2300 Å is believed (1) to yield electronically excited oxygen atoms which are principally, if not entirely in the $^1D_2$ state

[1*a*] $N_2O + h\nu \rightarrow N_2 + O^*$

Recent observations (1, 2) suggest that [1*a*] is the only important primary process in that wavelength region so that the subsequent course of the photodecomposition is controlled entirely by the reaction of O^* with N_2O.

[1]NRCC No. 11 838.

[2]NRCC Postdoctorate Fellow 1968–1970. Present address: AERE, Materials Development Branch, Harwell, Berks., U.K.

[3]Summer student 1969.

[4]NRCC Postdoctorate Fellow 1968–1970.

Can. J. Chem. Downloaded from www.nrcresearchpress.com by 210.87.254.5 on 09/05/12
For personal use only.

The electronically excited atom $O(^1D_2)$ reacts rapidly with N_2O at room temperature (3–5), in contrast to the behavior of the ground-state $O(^3P)$ atom (6, 7). The rate of N_2 formation from the reaction

[2*a*] $$O(^1D_2) + N_2O \rightarrow N_2 + O_2$$

is a most convenient measure of the stationary concentration of the excited atoms which may be used to determine primary quantum yields of $O(^1D_2)$ production in the photolysis of gaseous oxides and the relative rates of reaction of $O(^1D_2)$ with other gases. Unfortunately there is evidence from quantum yield measurements (8–13) for the photolysis of N_2O that [2*a*] is not the exclusive pathway for reaction and that [2*b*]

[2*b*] $$O(^1D_2) + N_2O \rightarrow 2NO$$

is important. In addition, the spin-forbidden processes

[2*c*] $$O(^1D_2) + N_2O \rightarrow N + NO_2$$

[2*d*] $$O(^1D_2) + N_2O \rightarrow O(^3P) + N_2O$$

may conceivably contribute to the rate constant for the total reaction of $O(^1D_2)$ with N_2O. This investigation was undertaken to establish the relative rates of [2*a*]–[2*d*].

In principle, if [1*a*] is the sole primary process, one can derive information on the relative rates of the secondary processes from measurements of the quantum yields of the products of N_2O photolysis. Data so obtained are, however, subject to considerable experimental error, quite apart from any systematic error incurred through the assumption of unit efficiency for [1*a*]. In this investigation we have avoided uncertainties associated with the primary process in N_2O photolysis by using NO_2 and O_3 as sources of $O(^1D_2)$. From measurements of the yields of products specific to the individual steps [2*a*]–[2*c*], we have obtained their relative rate constants with greater precision than was possible from a study of N_2O photolysis alone. The results of a separate investigation of the effect of added inert gases on the yield of N_2 in N_2O photolysis have confirmed our value for k_{2a}/k_{2b} and have indicated that [2*d*] is unimportant.

Experimental

NO_2 Photolysis

Mixtures of NO_2 and N_2O were photolyzed in a 10 cm long cylindrical cell having plane quartz windows 5 cm in diameter. After an exposure, the contents of the cell were shared with the glass sample loop ($\simeq$ 20 cc volume) of a gas chromatographic analysis train. This aliquot was subjected to several freeze–thaw cycles (at least 3 were required) in which the sample loop was alternately cooled to −196 °C and warmed to room temperature. As experiments with an irradiated sample of pure NO_2 showed, this procedure removed O_2 and NO from the mixture according to $2NO + O_2 = 2NO_2$. Separation of the components of the sample was subsequently effected with three columns in series: NO_2 was removed by adsorption on a 1 ft column of 60/80 mesh silanized glass beads at −78 °C; the remaining components were eluted from an 18 ft column of 80/100 mesh Porapak Q held at room temperature, in the order (N_2, O_2), NO, N_2O and were passed through a thermistor detector; separation and detection of N_2 and O_2 were achieved with a 6 ft column of 60/80 mesh Molecular Sieve 5A at room temperature and a second thermistor element. Calibrations for NO and O_2 relative to N_2 were obtained by measuring peak heights for known mixtures of NO and N_2 or O_2 and N_2. The NO/N_2 calibration mixtures were diluted with sufficient pure NO_2 to simulate approximately an actual reaction mixture since it was found that NO_2 caused a slight broadening of the NO peaks.

Ozone Photolysis

Mixtures of pure, dry ozone and nitrous oxide contained in an all-vycor (7910 glass), cylindrical cell (20 cm long, 17 mm i.d.) having parallel, plane end-windows were subjected to a 3500 J light pulse of $\sim$ 20 μs duration to half peak height. A surrounding flash lamp of annular design (5, 14) was used Two methods of product analysis were used. Products noncondensible at −196 °C (N_2 and O_2) were collected by conventional vacuum techniques and were analyzed by gas chromatography (5). In addition, the nitrogen dioxide concentration in the cell was monitored continuously throughout an experiment with a home-made, double-beam photometer: A parallel beam of light from a 100 W P.E.K. lamp No. 110 was filtered by Corning filters 0–52 and 7–51, giving light in the wavelength region 3400–4200 Å (and a somewhat weaker emission at $\lambda > 6900$ Å), and was split by a partially silvered vycor plate placed at 45° to the beam. The deflected reference beam was focussed onto an RCA 935 phototube; the other (analyzing) beam traversed the length of the reaction cell before being focussed onto a second 935 phototube. The phototubes, two 18 kΩ resistors, and a dry cell formed a simple bridge circuit whose output voltage, which was proportional to the difference between the photocurrents, was recorded during an experiment by an oscilloscope with a polaroid camera attachment. Measurements of the output immediately before and several minutes after a flash and of the output of the reference phototube alone were superimposed on the photograph for each run (Fig. 1). From these readings it was possible to determine the optical density of the reaction cell contents and hence the NO_2 concentration as a function of time. A calibration plot of optical density *vs.* P_{NO_2} was linear for the range of pressures (0.05–0.35 Torr) investigated, and gave an extinction coefficient for NO_2 which agreed well with the established value (15) for the wavelength region used.

In a few experiments the ozone concentration was followed during a photolysis by monitoring light absorption in the region 2900–3000 Å. A monochromator was used to isolate the wavelength region required from the P.E.K. lamp.

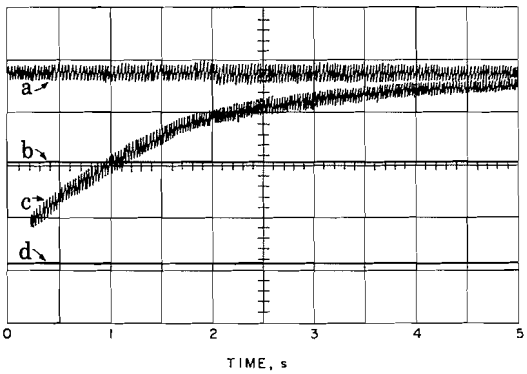

FIG. 1. Oscilloscope traces of the double-beam photometer output in run No. 231 (see Table 2). Curves (*a*) and (*c*) represent the differential output, *i.e.* the difference between the outputs of the reference and the analyzing phototubes, on an ordinate scale of 5 mV per large division. Curve (*a*) is the superimposed trace obtained before and several minutes after the flash; (*c*) is the trace obtained immediately after flash photolysis; (*d*) gives the output of the reference phototube alone on a scale of 0.2 V per large division; and (*b*) is the origin of the ordinate axis.

N_2O Photolysis

Light from a Philips 93107 Cadmium lamp was filtered by a 5 cm path length of NO at 100 Torr and was split into two beams of approximately equal intensity by a partially silvered quartz plate. The light beams were incident upon the plane end-windows of two identical, cylindrical quartz cells each of $\simeq$ 250 ml volume. Prior to an exposure both cells were filled with precisely the same pressure of N_2O ($\simeq$ 50 Torr). One of the vessels served as a reference cell; to the other (the reaction vessel) was added a measured pressure of CO_2 or Xe. After an irradiation period of from 24 to 96 h the noncondensible products at -196 °C of each cell were pumped through three liquid N_2 traps with diffusion and Toepler pumps and were collected in a gas burette. The contents of the first cold trap were distilled into the second and then into the third trap to ensure complete degassing. (When using Xe as an additive the final cold trap was held at -210 °C.) The products were analyzed by gas chromatography using a 20 ft column of Molecular Sieve 13X at room temperature for separation and a thermistor for detection.

The preparation and purification of the materials used in these experiments have been described elsewhere (4, 5). Reactant gases, and in the case of the NO_2 photolyses product gases also, were manipulated in mercury-free vacuum systems.

Results

NO_2 Photolysis

Table 1 summarizes the conditions employed in the photolysis of mixtures of NO_2 and N_2O and gives the values of k_{2a}/k_{2b} derived from the measurements of nitrogen and *excess* nitric oxide yields. The expression

$$[3] \quad [\text{excess NO}]/[N_2] = 3k_{2b}/k_{2a} - 1$$

used to calculate the rate constant ratio results from a consideration of the reaction mechanism consisting of [2*a*], [2*b*], and [2*d*] (for the moment we ignore reaction [2*c*]) and the reactions responsible (4) for the photodecomposition of NO_2

$$NO_2 + h\nu \rightarrow \begin{cases} NO + O^* \\ NO + O \end{cases}$$

$$O^* \text{ (or O)} + NO_2 \rightarrow NO + O_2$$

Contributions to excess NO formation, defined according to

$$[\text{excess NO}] = [NO] - 2[O_2]$$

arise solely from those $O(^1D_2)$ atoms (O*) which react with N_2O. Ground-state O atoms and those O* atoms which react with the NO_2 make no contribution to the excess yield of NO since they simply effect the overall change: $2NO_2 = 2NO + O_2$. Thus, the rate of formation of excess NO is given by

$$[4] \quad [2k_{2b} - 2k_{2a} + (k_{2b} + k_{2a})][O^*][N_2O]$$

where the first two terms represent the rate of formation of NO and twice the rate of O_2 formation, respectively, in reaction 2, and the third term represents a rate of formation of NO in the primary process equivalent to the rate of production of the O* which ultimately react chemically with N_2O. Equation 3 follows immediately from [4] and the expression for the rate of N_2 production, $k_{2a}[O^*][N_2O]$.

The simple mechanism which we have adopted predicts that the yield of excess NO relative to the yield of N_2 should be independent of the pressures of NO_2 and N_2O and of the yield of O*. Our values of k_{2a}/k_{2b} (Table 1) derived from [3] for the photolysis at 2288 Å were certainly constant (within 10%) within the range of reactant concentration ratios studied and did not differ significantly from the values obtained at 2420 Å. (At 2288 Å, the primary quantum yield of $O(^1D_2)$ in the photolysis of NO_2 is in the region 0.3–0.4 (4, 16), and at 2420 Å it is probably (16) close to 0.2.) Although this in itself was an indication that the assumed mechanism was essentially correct, we carried out additional experiments to make certain that [2*a*] was the sole source of N_2 in the system. Since approximately 10% decomposition of the NO_2 was permitted in most runs, the secondary photolysis of NO by light at 2265 and

Can. J. Chem. Downloaded from www.nrcresearchpress.com by 210.87.254.5 on 09/05/12
For personal use only.

TABLE 1. Values of k_{2a}/k_{2b} derived from measurements of the yields of products from the photolysis of mixtures of NO_2 and N_2O

Light source	Wavelength[a] (Å)	Temperature (°C)	P_{NO_2}[b] (Torr)	P_{N_2O}/P_{NO_2}	k_{2a}/k_{2b}
Cd[c] lamp + Cl_2 filter[e]	2288	23	5.57	1.17	1.12
	+	23	4.76	7.16	1.08
	2265	23	6.20	11.41	1.03[d]
	+	23	6.38	12.72	1.01[d]
	2144	23	5.60	15.31	1.00
Cd[c] lamp + Cl_2[e] + $CoSO_4/NiSO_4$[f]	2288 + 2265	23	5.31	12.72	0.92
Cd[c] lamp + Cl_2[e] + NO[g]	2288 only	150	5.99	16.23	0.99
		150	6.15	15.60	1.02
Hg lamp[h] + monochromator	2420	23	5.97	27.18	0.93
	± 80	23	5.42	24.43	0.97[d]
	Mean k_{2a}/k_{2b} = 1.01				
	Standard deviation = ± 0.06				

[a]Those wavelengths observed in the emission spectrum which were capable of dissociating NO_2.
[b]At 23 °C, 6 Torr NO_2 contains ~0.4 Torr N_2O_4; at 150 °C, 6 Torr NO_2 contains ~4×10^{-4} Torr N_2O_4.
[c]Philips 93107E cadmium lamp.
[d]O_2 added to reactants; result based on analysis for O_2, N_2.
[e]4 cm path of Cl_2 at 700 Torr.
[f]2 cm path of $CoSO_4.7H_2O$ (90 g/l) and $NiSO_4.6H_2O$ (25 g/l) in water.
[g]5 cm path of NO at 700 Torr.
[h]Osram HBO 200 W lamp.

2144 Å from the Cd lamp was considered a real possibility. The removal of the extraneous light by chemical filters did not, however, lead to a significant change in the measured rate constant ratio (Table 1). A few experiments were also conducted at 150 °C to eliminate light absorption by N_2O_4 and N_2O_3 which was significant (16) in the runs at room temperature. There was, however, no noticeable effect on the value of k_{2a}/k_{2b}. Calculations based on a primary quantum yield of 0.35 for O* from NO_2 and a value for the ratio of extinction coefficients of N_2O and NO_2 at 2288 Å of 4×10^{-4} (16) showed that at the highest ratio of P_{N_2O}/P_{NO_2} used in our experiments at that wavelength the direct photolysis of N_2O would have increased the observed rate constant ratio by only 4%. At 2420 Å, it was demonstrated experimentally that at most only 1% of the N_2 produced in the photolysis of the NO_2–N_2O mixtures employed arose from the direct photolysis of N_2O.

The scatter in the relative rate constant values obtained by this method is largely a reflection of the uncertainty associated with the gas chromatographic analysis for NO. Repeated analyses made with a mixture of NO and N_2 diluted with sufficient NO_2 to simulate an actual reaction mixture indicated that the product ratio [NO]/[N_2] could not be determined with greater accuracy than ±5%. Small, but varying extents of decomposition of NO_2 on the glass beads precolumn, resulting in NO formation, and varying degrees of adsorption of NO on the same column were believed responsible for the irreproducibility. All reaction mixtures were analyzed both before and (several times) after photolysis. Reactant chromatograms were examined closely for the presence of traces of NO, N_2, or O_2; product chromatograms were checked to ensure that the removal of O_2 by reaction with NO was complete. Duplicate analyses of product mixtures made up to 24 h after the initial analyses indicated no changes in composition and therefore no contributions to the formation or destruction of the products from thermal reactions. In a few experiments (indicated by a superscript *d* in Table 1) sufficient pure O_2 (< 3% of [NO_2]) was added initially to the reactants to ensure the complete oxidation of the excess NO produced in the photolysis. Calculations of k_{2a}/k_{2b} were then based on analysis for the O_2 and N_2 contents of the reactant and product mixtures, and the values so obtained were in good agreement with those based on the measurement of NO and N_2 yields.

An estimate of the importance of reaction [2*c*] was made from measurements of the isotopic composition of the N_2 arising from the photolysis of mixtures of $^{15}NO_2$ (95.3% $^{15}NO_2$) and natural N_2O at 2288 Å. Since N atoms reacted only with

Can. J. Chem. Downloaded from www.nrcresearchpress.com by 210.87.254.5 on 09/05/12
For personal use only.

Can. J. Chem. Downloaded from www.nrcresearchpress.com by 210.87.254.5 on 09/05/12
For personal use only.

the NO_2 under the conditions used, the yield of $^{29}N_2$ from

$$^{15}N + NO_2 \rightarrow {}^{29}N_2 + O_2 \text{ (or } 2O)$$

which accounts for approximately 23% of N atoms destroyed in reaction with NO_2 (17), was a measure of the N atom yield. $^{29}N_2$ contents of 0.88 and 0.84% were obtained for the photolysis of a 15:1 N_2O:$^{15}NO_2$ mixture at 23 and 150 °C, respectively, compared to a natural abundance of 0.76% determined with the same mass spectrometer. These results show that k_{2c}/k_{2a} is no larger than 5×10^{-3}.

Ozone Photolysis

The results (5) of a recent study of the flash photolysis of mixtures of ozone and nitrous oxide under conditions similar to those employed here are consistent with the assumption that the only reactions leading to significant decomposition of N_2O are [2*a*] and [2*b*]. In the presence of O_3 the NO produced in [2*b*] is oxidized to N_2O_5 through the intermediate formation of NO_2 and NO_3 (18, 19).

[5] $$NO + O_3 \rightarrow NO_2 + O_2$$

[6] $$NO_2 + O_3 \rightarrow NO_3 + O_2$$

[7] $$NO_3 + NO_2(+ M) \rightarrow N_2O_5(+ M)$$

In principle the rate constant ratio k_{2a}/k_{2b} can be obtained simply by measurement of the ratio of the yields of N_2 and N_2O_5, but trial experiments showed that the observed yields of N_2O_5 were irreproducible owing to erratic and irrecoverable losses probably at the reaction cell walls. We chose instead to use the yield of NO_2, determined by absorption photometry at short delays after the photolyzing flash, as a measure of k_{2b}. (Measurement of the NO yield at very short delays would, of course, have been preferable, but was unfortunately not possible with the equipment at our disposal.) The lifetimes of NO and NO_2 with respect to destruction in [5] and [6] at 1 Torr O_3, the pressure used throughout this study, were estimated from available rate constants (19, 20) to be $\sim 10^{-3}$ and ~ 1 s, respectively, so that extrapolation to zero time of our measurements for $[NO_2]$ in the time interval 0.2–5 s was expected to give a reliable value for the initial yield of NO. (An electronic disturbance prevented the direct measurement of $[NO_2]$ at times less than 0.2 s and necessitated the extrapolation procedure.) A typical oscilloscope trace of light absorption in the reaction cell is shown in Fig. 1 and the corresponding semilogarithmic plot used for extrapolation to zero time is given in Fig. 2.

In most experiments total pressures of 400 Torr or more were used in order to minimize the temperature rise in the reaction vessel due to the flash. N_2O pressures were always sufficiently large to ensure that practically all $O(^1D_2)$ atoms reacted with N_2O, rather than with O_3, and where necessary, the required total pressure was reached by adding SF_6, a very inefficient (1, 4, 5) deactivator of the excited atoms. The yields of N_2 and of NO_2 at zero time obtained in such high-pressure experiments are summarized in Table 2. The mean value of k_{2a}/k_{2b} deduced from those data is in excellent agreement with the value derived from the study of the photolysis of mixtures of NO_2 and N_2O (Table 1).

At high total pressures, the kinetics of decay of $[NO_2]$ were those expected for a reaction controlled by step [6] when $[O_3]$ is in appreciable excess of $[NO_2]$. Plots of $\log_{10}[NO_2]$ against time (Fig. 2) were linear during the first 70% of the reaction and estimates of k_6 (Table 2) were obtained from the slopes and from ozone con-

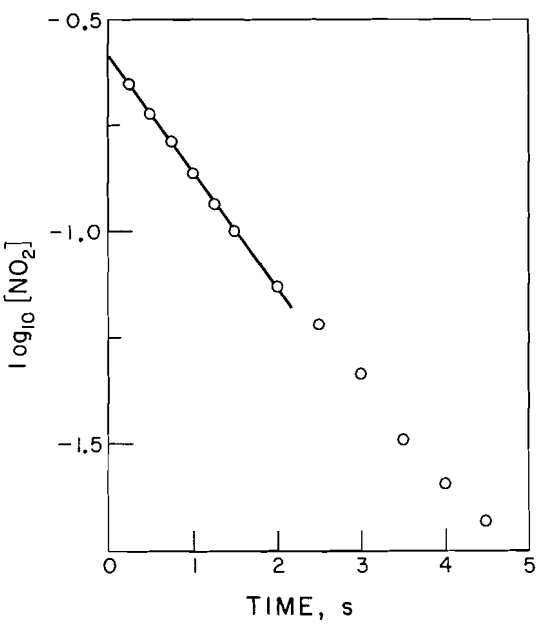

FIG. 2. Plot against time of the logarithm of the nitrogen dioxide yield (μmol) as calculated from the photometer traces (Fig. 1) of run No. 231. The straight line is a least-squares fit to the first seven points.

TABLE 2. Values of k_{2a}/k_{2b} and k_6 derived from a study of the yield of N_2 and the time dependence of NO_2 in the flash photolysis of O_3–N_2O mixtures[a]

Run No.	P_{O_3} (Torr)	P_{N_2O} (Torr)	P_{SF_6} (Torr)	NO_2 at zero time[b] (μmol)	N_2 (μmol)	$\frac{k_{2a}}{k_{2b}} = \frac{2[N_2]}{[NO_2]}$	$k_6 \times 10^{-4}$ (l mol^{-1} s^{-1})
223	1.10	103	445	0.332	0.161	0.97	1.05
228	1.07	533	—	0.298	0.153	1.03	0.73
229	1.06	103	429	0.302	0.139	0.92	1.09
230	1.13	104	418	0.331	0.155	0.935	1.25
231	1.11	103	410	0.258	0.125	0.97	0.84
232	1.11	482	—	0.269	0.141	1.09	0.59
233	1.16	104	377	0.249	0.126	1.01	0.83
234	1.16	103	367	0.355	0.167	0.94	0.24
235	1.10	104	362	0.249	0.131	1.05	0.57
236	1.10	104	631	0.267	0.130	0.975	0.82
						Average 0.99	0.8
						Standard deviation ±0.06	±0.3

[a]Reaction vessel volume = 45.9 cc.
[b]Obtained by extrapolation to zero time of plots such as Fig. 2.

TABLE 3. Stoichiometry of the flash-initiated reaction between O_3 and N_2O[a]

Run No.	P_{O_3} (initial) (Torr)	P_{N_2O} (Torr)	P_{SF_6} (Torr)	P_{O_3} (final)[b] (Torr)	$-\Delta O_3$ (μmol)	N_2 (μmol)	$\frac{-\Delta[O_3]}{[N_2]}$
242	0.98	103	574	0.54	1.10	0.133	8.3
243	1.03	104	289	0.46	1.42	0.173	8.2
245	1.08	103	539	0.49	1.47	0.163	9.0
247	1.12	104	276	0.56	1.39	0.128	10.8
249	1.10	103	309	0.61	1.14	0.140	8.1
							Average 9.0

[a]Reaction vessel volume = 45.9 cc.
[b]The final, steady value which was reached some 15 s after the flash and which remained constant for at least 2 min.

centrations calculated from an expression

$$[8] \qquad \Delta[O_3] = -8[N_2]$$

relating the decrease in O_3 concentration to the yield of N_2. This relationship, which assumed (5) that [6] was preceded by [2*a*], [2*b*] (with $k_{2a} = k_{2b}$, as found in this study), [5], and

$$O_3 + h\nu \rightarrow O_2(^1\Delta_g) + O(^1D_2)$$
$$O_2(^1\Delta_g) + O_3 \rightarrow 2O_2 + O(^3P)$$
$$O(^3P) + O_3 \rightarrow 2O_2$$

was shown to be approximately correct in independent experiments (Table 3) in which the ozone concentration was monitored. (The value of 9 obtained for $-\Delta[O_3]/[N_2]$ upon completion of all reaction in those experiments corresponds to a value of 8 at the commencement of [6].) Our mean k_6 value so derived is smaller by a factor of approximately 2 than the most recent value in the literature (20) and is six times smaller than an earlier value (21). While the agreement is only fair, we feel that it provides some justification for our assumptions regarding the fate of NO produced in the flash photolysis of O_3–N_2O mixtures, and certainly validates our extrapolation procedure for the determination of $[NO_2]$ at zero time. By contrast, the light absorption traces obtained in experiments at ~ 100 Torr pressure ($N_2O \simeq 100$ Torr, $O_3 \simeq 1$ Torr) clearly indicated that the simple mechanism formulated above was not applicable at low pressures. NO_2 apparently disappeared at a much slower rate in these experiments and semi-logarithmic plots, although linear, suggested a value for k_6 some 5–6 times smaller than that obtained in the high-pressure runs. Furthermore, the apparent yield of NO_2 and the loss of O_3 relative to the yield of N_2 were significantly larger: an average value $k_{2a}/k_{2b} = 0.87 \pm 0.04$ was obtained from five experiments at $O_3 = 1$ Torr, $N_2O = 100$ Torr, and a value $-\Delta[O_3]/[N_2] \simeq 12$ from experiments under the same conditions. We have chosen to dismiss the value of k_{2a}/k_{2b} obtained at low pressures because of our imperfect understanding of the kinetics and because of a strong suspicion that NO_3 may have contributed

Can. J. Chem. Downloaded from www.nrcresearchpress.com by 210.87.254.5 on 09/05/12
For personal use only.

TABLE 4. Effect of helium on k_{2a}/k_{2b}[a]

Run No.	P_{O_3} (Torr)	P_{N_2O} (Torr)	P_{SF_6} (Torr)	P_{He} (Torr)	NO_2 at zero time (μmol)	N_2 (μmol)	$\frac{k_{2a}}{k_{2b}} = \frac{2[N_2]}{[NO_2]}$
238	1.08	31	302	—	0.245	0.137	1.12
239	1.10	31	302	93	0.273	0.130	0.95
241	1.09	31	295	—	0.266	0.147	1.10

[a]See footnotes to Table 2.

significantly to light absorption in the low-pressure experiments. The rapidity of [7] would normally ensure a very low, stationary concentration of NO_3, but at the temperatures reached in a flash photolysis at 100 Torr (calculated adiabatic temperature rise ~ 50 °C) the reverse of [7] would probably have been important, resulting in a higher NO_3 concentration, a slower removal of NO_3 by

[9] $$2NO_3 \rightarrow 2NO_2 + O_2$$

[10] $$NO_3 + NO_2 \rightarrow NO + O_2 + NO_2$$

(18) and a slower decay of NO_2. If the effective extinction coefficient of NO_3 were higher than that for NO_2, a distinct possibility (22, 23) for the light source used here, the measured yield of NO_2 would then be too high. The greater extent of O_3 decomposition relative to N_2 formation which was noted in the low-pressure runs is consistent with a partial contribution to NO_3 removal from [9] and [10] at low pressures. Confirmation of this explanation of the observations at low pressures must await the results of more detailed studies; meanwhile we accept only the values of k_{2a}/k_{2b} obtained at high pressures where there are apparently no complications.

Following a recent suggestion of Heicklen (24) that the rate constant ratio k_{2a}/k_{2b} is markedly dependent on the translational energy of the $O(^1D_2)$ atom, we examined in one experiment (Table 4) the effect of added helium on the ratio. Compared to the values obtained in control experiments the ratio for the run with added He was somewhat smaller, although the change was barely significant and in any case in the opposite direction to that predicted by Heicklen (24). Our technique for the recovery of product N_2 unfortunately precluded the addition of larger pressures of He, so that we were unable to establish with certainty that the small effect observed was genuine. However, a comparison of the results (Tables 2 and 4) obtained with and without inert gas additions indicated that if excess translational energy is possessed by the $O(^1D_2)$ atom generated in O_3 photolysis, it has little or no effect on the rate constant ratio k_{2a}/k_{2b}. Thus, on the basis of the theory of collisions between hard-sphere molecules and the assumption of a reaction probability of 1 in 3 collisions between $O(^1D_2)$ and N_2O (4, 25), we calculate that the $O(^1D_2)$ atoms which reacted with N_2O in runs 228, 238, and 239 possessed, on average, the fractions 0.56, 0.13, and 0.09, respectively, of the original excess translational energy which the atom acquired in the photodissociation process. (For reaction at every collision between O* and N_2O the corresponding fractions would be 1.0, 0.34, and 0.25.) In spite of this considerable spread of possible excess energy content of O* the observed values of the rate constant ratio did not deviate significantly from the mean.

N_2O Photolysis

Figure 3 illustrates the observed effect of Xe and CO_2 additions on the yield of N_2 from the photolysis of N_2O at 2288 Å. Relative quantum yields $\Phi_{N_2}/\Phi_{N_2}{}^0$ (that is the ratio of the quantum yield of N_2 in the presence to that in the absence of inert gas) were derived from measurements of the N_2 produced in the reaction cell and in the

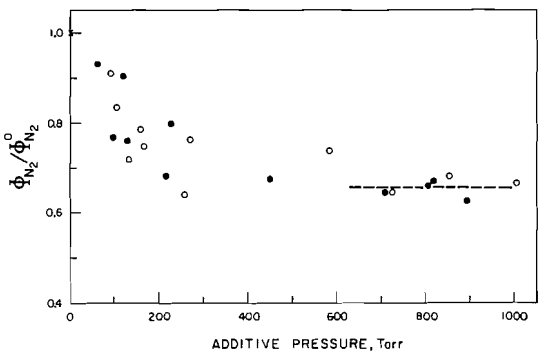

FIG. 3. The effect of Xe (○) and CO_2 (●) additions on the quantum yield of N_2 relative to the quantum yield in the absence of additives for the photolysis of 51 Torr of N_2O at 2288 Å and 23 °C. The dashed line is the average of the relative quantum yield values obtained at additive pressures > 600 Torr.

Can. J. Chem. Downloaded from www.nrcresearchpress.com by 210.87.254.5 on 09/05/12
For personal use only.

Can. J. Chem. Downloaded from www.nrcresearchpress.com by 210.87.254.5 on 09/05/12
For personal use only.

reference cell. The use of a nitric oxide filter ensured that only the Cd resonance line at 2288 Å was absorbed by N_2O and also prevented secondary photolysis of product nitric oxide. At 2288 Å [1*a*] is unquestionably (1, 2) the only primary photolytic process of importance and the excited oxygen atoms are exclusively in the $^1D_2$ state. Quenching of the $O(^1D_2)$ atoms limits the production of N_2 to the primary process at high Xe or CO_2 pressures (1, 4, 5), since ground-state O atoms do not react with N_2O at room temperature (6, 7). In the limit of complete quenching of the excited atoms we may write

$$\Phi_{N_2}{}^0/\Phi_{N_2}{}^\infty = 1 + k_{2a}/(k_{2a} + k_{2b} + k_{2d})$$

Using this expression and our value (Fig. 3) of the limiting relative quantum yield at high additive pressure, we obtain $k_{2a}/(k_{2b} + k_{2d}) = 1.08 \pm 0.19$ (standard deviation). In view of the appreciable scatter in our data we regard this value as only a crude estimate of the rate constant ratio. It does, however, confirm the values obtained using O_3 and NO_2 as sources of $O(^1D_2)$, and furthermore suggests that k_{2a} is small relative to k_{2b}.

In order to convince ourselves that the primary production of $O(^3P)$ atoms in the photolysis of N_2O at 2288 Å was unimportant, we analyzed the products of the photolysis of a mixture containing 92.6 mol% neopentane, 0.6% butene-1, and 6.8% nitrous oxide. The observed product ratios, [neopentanol]/[N_2] = 0.67 and [1,2-butylene oxide]/[N_2] = 0.013, were identical within experimental error to those obtained in similar experiments at 2139 Å (1), indicating that the total yield of $O(^3P)$, including a possible contribution from quenching of $O(^1D_2)$, was at most only 3% of the primary yield of excited oxygen atoms.

Discussion

Of the possible pathways [2*a*]–[2*d*] for the reaction between $O(^1D_2)$ and N_2O we have shown that at room temperature [2*c*] makes an insignificant contribution to the reaction and that [2*d*] is probably unimportant also. Evidence adduced by Young, Black, and Slanger (3) and by Greenberg and Heicklen (26) supports the assumption that physical deactivation of $O(^1D_2)$, [2*d*], is of negligible importance compared to chemical quenching, [2*a*] and [2*b*]. Our two values for the rate constant ratio k_{2a}/k_{2b} (Tables 1 and 2) obtained by completely independent methods are in excellent agreement and have a mean of 1.00 with a standard deviation of 0.04. This value differs markedly from that of the recent and only previous determination (26), but falls well within the range of the estimates (Table 5) of the ratio which one can derive from absolute product quantum yields reported for the photolysis of N_2O and the assumptions

$$[11] \quad \phi_{O(^1D_2)} = 1.0 \qquad k_{2c} = k_{2d} = 0$$

For the same assumptions, our value for k_{2a}/k_{2b} suggests a nitrogen quantum yield for the photolysis of N_2O of 1.50 ± 0.01, in good agreement with the results of recent determinations at 2139 Å (26) and at 1849 Å (11). Provided the assumptions [11] are exact, absolute quantum yields evidently can be predicted in this manner with greater precision than can be achieved in a direct measurement.

Greenberg and Heicklen (26) have reported a value for k_{2a}/k_{2b} at room temperature of 0.59 ± 0.01 based upon their value of 0.059 ± 0.007 for the quantum yield of O_2 from the photolysis of N_2O at 2139 Å, the postulates [11] and the assumption that the product oxygen which they measured was that remaining after the product NO had been completely consumed according to the stoichiometry $4NO + O_2 = 2N_2O_3$. For an assumed stoichiometry $2NO + O_2 = 2NO_2$, which is usually adopted and which applied in our experiments with mixtures of NO_2 and N_2O (see above), their measured quantum yield of O_2 corresponds to a ratio $k_{2a}/k_{2b} = 1.12 \pm 0.01$ in somewhat better accord with our result and with their value (Table 5) based on a measurement of the quantum yield of N_2. The good agreement between the values which we obtained by three independent methods supports our adoption of a 2:1 stoichiometry for the reaction between NO and O_2 in the determinations using NO_2 as a source of $O(^1D_2)$. Additional support for our value of unity for k_{2a}/k_{2b} comes from the coincidence of predicted and measured values of $-\Delta[O_3]/[N_2]$ for the flash photolysis of O_3–N_2O mixtures. The mechanism outlined above for the flash photolysis predicts values for $-\Delta[O_3]/[N_2]$ of 11.5 when $k_{2a}/k_{2b} = 0.59$ and of 8, the observed value, when $k_{2a}/k_{2b} = 1.0$.

We have found no evidence in this investigation for an effect of excess translational energy of the $O(^1D_2)$ atom on the ratio k_{2a}/k_{2b}. The

TABLE 5. Values of k_{2a}/k_{2b} derived from quantum yield data for the photolysis of N_2O and the assumptions [11]

Quantum yields	Wavelength (Å)	Calculated k_{2a}/k_{2b}	Reference number
$\Phi_{-N_2O} = 2.0$ $\Phi_{NO} = 1.0$, $\Phi_{O_2} = 0.5$	1849	1.0	11
$\Phi_{N_2} = 1.44 \pm 0.08$	1900	$0.79^{+0.29}_{-0.23}$	9
$\Phi_{NO} = 0.82$	1900	1.44	9
$\Phi_{-N_2O}/\Phi_{N_2} = 1.24 \pm 0.07$	1849	$1.56^{+0.77}_{-0.48}$	10
$\Phi_{-N_2O}/\Phi_{O_2} = 3.47 \pm 0.20$	1849	1.36 ± 0.20	10
$\Phi_{N_2} = 1.51 \pm 0.11$	2139	$1.04^{+0.59}_{-0.37}$	26
$\Phi_{O_2}{}^a = 0.059 \pm 0.007$	2139	0.59 ± 0.01^b 1.12 ± 0.01^c	26

[a]Measured after NO had been completely consumed.
[b]Assumed stoichiometry for NO removal: $4NO + O_2 = 2N_2O_3$.
[c]Assumed stoichiometry for NO removal: $2NO + O_2 = 2NO_2$.

same value within experimental error was found for all three sources of $O(^1D_2)$ in spite of the considerable variation in the excess energy available for translational excitation of the atom in the three cases

$$NO_2 \xrightarrow{2420\ Å} NO + O(^1D_2) \qquad \text{0.1 kcal/g-atom max. available}$$

$$NO_2 \xrightarrow{2288\ Å} NO + O(^1D_2) \qquad \text{4.5 kcal/g-atom max. available}$$

$$O_3 \xrightarrow{\sim 2500\ Å} O_2(^1\Delta_g) + O(^1D_2) \qquad \text{14.4 kcal/g-atom max. available}$$

$$N_2O \xrightarrow{2288\ Å} N_2 + O(^1D_2) \qquad \text{25.6 kcal/g-atom max. available}$$

Furthermore, the value obtained with O_3 as the source was not altered by additions of inert moderators.

We note that values close to unity have also been reported (27–30) for the ratio of the rate constants of the reactions [2*a*] and [2*b*] when the oxygen atom is in the ground state (although not all workers agreed on this value (31)). The energy barriers for the two pathways are identical, or nearly so (27, 28, 32), for the reactions with $O(^3P)$ and evidently (4, 25) are both very small in the case of reaction with $O(^1D_2)$. If the transition complexes involved differ little in the two cases, the proximity of the k_{2a}/k_{2b} values for ground- and excited-state oxygen atoms is understandable.

1. G. PARASKEVOPOULOS and R. J. CVETANOVIĆ. J. Am. Chem. Soc. **91**, 7572 (1969).
2. K. F. PRESTON and R. F. BARR. J. Chem. Phys. In press.
3. R. A. YOUNG, G. BLACK, and T. G. SLANGER. J. Chem. Phys. **49**, 4758 (1968).
4. K. F. PRESTON and R. J. CVETANOVIĆ. J. Chem. Phys. **45**, 2888 (1966).
5. P. M. SCOTT and R. J. CVETANOVIĆ. J. Chem. Phys. **54**, 1440 (1971).
6. R. J. CVETANOVIĆ. J. Chem. Phys. **23**, 1203 (1955).
7. F. KAUFMAN. Prog. React. Kinet. **1**, 1 (1961).
8. W. A. NOYES, JR. J. Chem. Phys. **5**, 807 (1937).
9. G. A. CASTELLION and W. A. NOYES, JR. J. Am. Chem. Soc. **79**, 290 (1957).
10. M. ZELIKOFF and L. M. ASCHENBRAND. J. Chem. Phys. **22**, 1680, 1685 (1954); **27**, 123 (1957).
11. N. R. GREINER. J. Chem. Phys. **47**, 4373 (1967).
12. W. E. GROTH and H. SCHIERHOLZ. Planet. Space Sci. **1**, 333 (1959).
13. J. Y. YANG and F. M. SERVEDIO. J. Chem. Phys. **47**, 4817 (1967).
14. P. L. GOODFRIEND and H. P. WOODS. Rev. Sci. Instr. **36**, 10 (1965).
15. J. G. CALVERT and J. N. PITTS, JR. Photochemistry. Wiley, New York. 1966.
16. R. J. NORSTROM, K. F. PRESTON, and R. J. CVETANOVIĆ. Unpublished results.
17. L. F. PHILLIPS and H. I. SCHIFF. J. Chem. Phys. **42**, 3171 (1965).

Can. J. Chem. Downloaded from www.nrcresearchpress.com by 210.87.254.5 on 09/05/12
For personal use only.

18. H. S. JOHNSTON. Gas phase reaction rate theory. Ronald Press Co., New York. 1966.
19. K. SCHOFIELD. Planet. Space Sci. **15**, 643 (1967).
20. H. W. FORD, G. J. DOYLE, and N. ENDOW. J. Chem. Phys. **26**, 1336 (1957).
21. H. S. JOHNSTON and D. M. YOST. J. Chem. Phys. **17**, 386 (1949).
22. E. J. JONES and O. R. WULF. J. Chem. Phys. **5** 873 (1937).
23. G. SCHOTT and N. DAVIDSON. J. Am. Chem. Soc. **80**, 1841 (1958).
24. J. HEICKLEN. Private communication, Sept. 1970.
25. D. BIEDENKAPP and E. J. BAIR. J. Chem. Phys. **52**, 6119 (1970).
26. R. I. GREENBERG and J. HEICKLEN. Int. J. Chem. Kinet. **2**, 185 (1970).
27. D. GUTMAN, R. L. BELFORD, A. J. HAY, and R. PANCIROV. J. Phys. Chem. **70**, 1793 (1966).
28. S. C. BARTON and J. E. DOVE. Can. J. Chem. **47**, 521 (1969).
29. H. HENRICI and S. H. BAUER. J. Chem. Phys. **50**, 1333 (1969).
30. A. A. BORISOV. Kinet. Katal. **9**, 482 (1968).
31. W. JOST, K. W. MICHEL, J. TROE, and H. Gg. WAGNER. Z. Naturforsch. **19a**, 59 (1964).
32. F. KAUFMAN, N. J. GERRI, and R. E. BOWMAN. J. Chem. Phys. **25**, 106 (1956).

Can. J. Chem. Downloaded from www.nrcresearchpress.com by 210.87.254.5 on 09/05/12
For personal use only.

Can. J. Chem. Downloaded from www.nrcresearchpress.com by 210.87.254.105 on 09/05/12
For personal use only.

The Effect of α-Substituents on Benzylic Spin–Spin Coupling Constants. Derivatives of 2,6-Dichlorotoluene

A. F. JANZEN[1] AND T. SCHAEFER

Chemistry Department, University of Manitoba, Winnipeg, Manitoba

Received November 9, 1970

Spin–spin coupling constants between methylene protons and ring protons over six and five bonds, $J_{m,p}^{H,CH_2}$, are reported for α-substituted derivatives of 2,6-dichlorotoluene. Potential energy calculations suggest that the C—X bond of the CH_2X group lies perpendicular to the plane of the ring. The six-bond coupling is dominated by a π electron mechanism and depends on the conformation of CH_2X with respect to the aromatic plane and on the electronegativity of the substituent, X. The five-bond coupling is independent of X and it is suggested that the decrease in the π electron contribution to this coupling caused by the increasing electronegativity of X, is compensated by a corresponding increase in the sigma electron contribution.

On rapporte les constantes de couplage, $J_{m,p}^{H,CH_2}$, qui se font par l'intermédiaire de cinq ou six liens entre les protons méthylèniques et les protons du noyau de dichloro-2,6 toluènes substitués en α. Des calculs d'énergie potentielle permettent de suggérer que le lien C—X du groupe CH_2X est perpendiculaire au plan du noyau aromatique. Le couplage qui se fait par l'intermédiaire de six liens est dû à un mécanisme dominé par les électrons π et dépend de la conformation du groupe CH_2X par rapport au plan du noyau aromatique et de l'électronégativité du substituant X. Le couplage qui se fait par l'intermédiaire de cinq liaisons est indépendant de X; on croit que la diminution de la contribution des électrons π à ce couplage due à une augmentation de l'électronégativité de X-est compensée par une augmentation correspondante de la contribution des électrons sigma.

Canadian Journal of Chemistry, 49, 1818 (1971)

Introduction

In toluene derivatives long-range proton–proton spin–spin coupling constants between methyl protons and ring protons over four, five, and six bonds, $J_{o,m,p}^{H,CH_3}$, are known for numerous ring substitution patterns (1, 2). J_p^{H,CH_3} and J_m^{H,CH_3} are insensitive to ring substitution (1) whereas J_o^{H,CH_3} may vary by about 10% of its value in toluene, apparently in a manner related to the mobile bond order of the intervening C—C bond in the aromatic ring (3, 4). J_p^{H,CH_3} has its origin in a π electron mechanism (1) but there exist appreciable σ electron contributions to $J_{o,m}^{H,CH_3}$.

Relatively little is known about the behavior of the analogous couplings when the methyl group is replaced by a CH_2X moiety. In this paper we report on the effect of a series of α-substituents on $^5J_m^{H,CH_2}$ and $^6J_p^{H,CH_2}$ in α-derivatives of 2,6-dichlorotoluene. The presence of the ring substituents, while denying information on $^4J_o^{H,CH_2}$, stabilizes one conformation of the CH_2X group with respect to the plane of the ring and thereby facilitates the isolation of other factors influencing the long-range couplings.

[1]Holder of an NRCC scholarship 1969–1970.

Experimental

The compounds were obtained from the usual commercial sources and were used without further purification. 2,6-Dichloroethylbenzene was prepared by hydrogenation of 2,6-dichlorostyrene. 2,6-Dichlorostyrene (3 ml) was dissolved in about 20 ml of distilled methanol containing one drop of concentrated hydrochloric acid. An amount of 50 mg of a palladium-on-charcoal catalyst was used. Air was swept out of the reaction vessel by repeatedly lowering the pressure in the vessel and then admitting hydrogen gas. The reaction vessel was left on a shaker overnight. The solvent was distilled off. Chloroform (10 ml) was added and distilled off and this procedure was repeated. Infrared and nuclear magnetic resonance (n.m.r.) spectra of the resulting compound were consistent with the structure of 2,6-dichloroethylbenzene and no impurity peaks were observed.

Samples were prepared as degassed 10 mol% solution in benzene-d_6 containing internal tetramethylsilane as a locking signal. Proton magnetic resonance spectra were recorded in the sweep frequency mode at a sweep rate of 0.02 Hz/s over a sweep width of 1 Hz/cm on a DA60IL spectrometer. Peak positions were repeatedly calibrated by reading sweep and manual oscillator frequencies at intervals of a few Hz, using period averaging techniques.

The temperature dependence of the long-range coupling constants in 2,6-dichlorobenzylbromide dissolved in toluene-d_8 was measured between −20 and 80 °C. Temperature calibrations depended on the standard methanol and glycol samples from Varian Associates. Temperatures are accurate to at least ±2 °C.

TABLE 1. Proton–proton coupling constants of some α-substituted 2,6-dichlorotoluenes

α-Substituent	$^6J_p^{H,CH_2}$ (Hz)	$^5J_m^{H,CH_2}$ (Hz)	$^3J_o^{H,H}$ (Hz)	E_x*
—H	−0.63±0.01	0.41±0.03	8.04±0.04	2.10
—CH_3	−0.29±0.02	0.36±0.03	8.08±0.06	2.32
—CN	−0.33±0.02	0.35±0.04	8.14±0.05	2.52
—SCN	−0.27±0.02	0.34±0.02	8.13±0.035	2.70
—Br	−0.21±0.02	0.36±0.02	8.04±0.03	2.94
—NH_2	−0.20±0.02	0.35±0.02	8.27±0.03	2.99
—Cl	−0.21±0.02	0.36±0.04	8.09±0.05	3.19
—OCH_3	−0.20±0.02	0.31±0.02	8.07±0.03	3.31
—OH	−0.19±0.03	0.33±0.02	8.07±0.03	3.51
—F†	−0.16±0.02	0.34±0.04	8.14±0.05	3.93

*Taken from ref. 22.
†Reference 6.

Results and Discussion

(1) Spectral Analysis

Rapid rotation of the CH_2X group in **1** ensures that the spin system can be designated as A_2BX_2. The properties of such a spectrum are well-known (5).

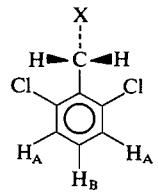

1

$J_{BX} = {}^6J_p^{H,CH_2}$ is easily obtained directly from the splittings of the transitions between antisymmetric states of the spin system. The extraction of $J_{AX} = {}^5J_m^{H,CH_2}$ is only a little more complex. When X = CH_3, no coupling between the methyl protons and ring protons is observable. When X = F the system corresponds to the case A_2BX_2R and has been previously analyzed (6).

The signs of $^5J_m^{H,CH_2}$ and of $^6J_p^{H,CH_2}$ were determined relative to $J_o^{H,H}$ for 2,6-dichlorotoluene and 2,6-dichlorobenzylfluoride by double resonance techniques, as described previously (6). The magnitudes of $^6J_p^{H,CH_2}$ in these two compounds bracket the magnitudes of this coupling in the other compounds (see Table 1) and therefore there is little doubt that the coupling is negative in all compounds. $^5J_m^{H,CH_2}$ does not vary appreciably as X changes in **1** and is no doubt positive for all X.

The coupling constants are given in Table 1. The spectra were taken in benzene-d_6 because the well-known aromatic solvent induced shifts (7) result in a relatively large internal shift for the ring protons, facilitating the extraction of precise values of the small long-range coupling constants from A_2BX_2 spectra.[2] Consequently the chemical shifts do not primarily reflect the electronic nature of the α-substituent and are not given here (the interested reader may write for a copy).

(2) The Six-bond Coupling, J_p^{H,CH_2}

(a) Conformational Dependence

The benzylic coupling over six bonds is transmitted by a π electron mechanism and for toluene one may write (4, 8)

$$[1] \qquad {}^6J_p^{H,CH_3} = B\cos^2\theta$$

where θ is the dihedral angle between the p_π orbital and the plane containing the methyl C—H bond and the carbon atom bearing the p_π orbital. The barrier to rotation of the methyl group in toluene is only 0.014 kcal/mol in the gas phase (9) and hence $\cos^2\theta = \frac{1}{2}$ while $J_p^{H,CH_3} = -0.62$ Hz (2). Consequently $B = -1.3_4$ Hz. In 2,6-dichlorotoluene, $J_p^{H,CH_3} = -0.63 \pm 0.02$ Hz, suggesting relatively rapid and almost free rotation of the methyl group. Furthermore, J_p^{H,CH_3} is constant to within experimental error in 3,5-dichlorotoluene (10), 2,3,5,6-tetrachlorotoluene (11), 2,6-dinitrotoluene (12), and 2,6-dichloro-3-ethyl-5-hydroxytoluene (13). Therefore it is assumed in the following that the ring chlorine atoms act on J_p^{H,CH_2} primarily via steric interactions in **1**.

[2]In many experiments on similar compounds dissolved in solvents ranging in polarity from cyclohexane to acetone we have never found a solvent dependence of the long-range couplings.

Can. J. Chem. Downloaded from www.nrcresearchpress.com by 210.87.254.105 on 09/05/12
For personal use only.

Can. J. Chem. Downloaded from www.nrcresearchpress.com by 210.87.254.105 on 09/05/12
For personal use only.

Introduction of one α-substituent into 2,6-dichlorotoluene changes the small 6-fold barrier into a 2-fold barrier, expected to be considerably larger. The preferred conformation is as in **2**, with each C—H bond lying at 30° to the plane of the ring. If the rotational barrier is high enough, say $5kT$, the motion of the methylene rotor may be treated as simple harmonic, provided the angular amplitude is small enough (14). The angular displacement from **2** (or **1**) is given classically (14) by

$$[2] \qquad \theta(t) = \theta_0 + \phi \sin x,\ x = 2\pi t/\tau$$

where $\theta_0 = 60°$ in **2**, ϕ is the maximum amplitude of the motion, and τ is the period of the oscillation.

The frequency of oscillation is clearly much larger than J_p^{H,CH_2}. In this approximation one has

$$[3] \qquad J_p^{H,CH_2} = -1.34 \langle \cos^2 \theta(t) \rangle$$

where

$$[4] \qquad \langle \cos^2 \theta(t) \rangle = \langle \cos^2 (60° + \phi \sin x) \rangle$$

For $\theta \leqslant 20°$ one finds, to within 10%, $J_p^{H,CH_2} = \frac{1}{4} \times 1.34 = -0.33$ Hz, *i.e.*, $J_p^{H,CH_2} = \frac{1}{2} J_p^{H,CH_3}$ in toluene. In other words, for small amplitudes of oscillation about the equilibrium conformation **2** of an α-X-2,6-dichlorotoluene, $J_p^{H,CH_2} \approx 0.3$ Hz if X does not affect the magnitude of B in eq. 1.

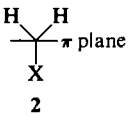

2

(b) Effect of the Electronegativity of X

It is clear from Table 1 that J_p^{H,CH_2} depends on the substituent, X. If this π electron coupling is dependent on hyperconjugation (15) then it is reasonable that an electron-withdrawing X will polarize the C—H bonds in CH_2X and thereby decrease their hyperconjugative overlap with the p_π orbital of the aromatic ring. In Fig. 1 a plot of J_p^{H,CH_2} *vs.* the electronegativity, E_x, of the substituent, X, is shown. In terms of the model an electronegative substituent decreases the magnitude of B in eq. 1. The plot extrapolates back to X = H giving $J_p^{H,CH_3} = -0.32$ Hz, half the observed value in 2,6-dichlorotoluene, as predicted by the model.

The point for X = CN probably deviates significantly from the least squares line in Fig. 1. A possible explanation calls on the hyperconjugation between CN and CH_3 in methylcyanide, as described by CNDO/2 calculations (16). In 2,6-dichlorobenzylcyanide there then exists an extended hyperconjugated system, encompassing the orbitals of the cyano and methylene groups and the aromatic ring, leading to the enhanced magnitude of J_p^{H,CH_2}.

(c) Amplitude of Oscillation, φ

The present model of a conformationally dependent π electron mechanism for J_p^{H,CH_2}, as modified by the polarization of the C—H bonds by the electronegative α-substituent, is in apparent agreement with the data in Table 1. The agreement depends on the assumed small amplitude of oscillation of the CH_2X group about the minimum energy depicted by **2**.

Rate studies on α,α-dichloro-2,4,6-tribromotoluene yield a barrier of about 16 kcal/mol to the rotation of the dichloromethyl group about the sp^2–sp^3 carbon–carbon bond (17). Calculations (18, 19) based on van der Waals and on modified Buckingham potentials verify that steric interaction of the C—Cl and C—Br bonds where in an eclipsed position gives rise to the barrier. In Fig. 2 is shown a potential energy curve for 2,6-dichlorobenzylbromide. It is based on calculations[3] using van der Waals function (19). The height of the barrier, A, is 22 kcal/mol when tetrahedral bond angles at the α-carbon and 120° bond angles for the ring moiety are assumed. It drops to 15 kcal/mol when all bonds are bent by less than 2°: the bonds at the α-carbon towards the extension of the sp^2–sp^3 bond axis and the ring C—Cl bonds in the plane of the ring away from this axis. Therefore the curve represents the barrier reasonably well in the region of high potential energy where the C—Br bond eclipses the C—Cl bond on the benzene ring.

In Fig. 2 the angle of rotation of 90° corresponds to the conformation **2** of minimum energy. If $A = 16$ kcal, then at an oscillation amplitude $\phi = 20°$ about this position, the potential energy has increased by about 0.4 kcal, somewhat more than the $\frac{1}{2} RT$ needed by the rotor to reach this amplitude of oscillation. Within the limitations of the assumption of simple harmonic oscillation, the potential energy curve supports the model used above for J_p^{H,CH_2}.

[3]We are grateful to Mr. Brian Barber for these computations.

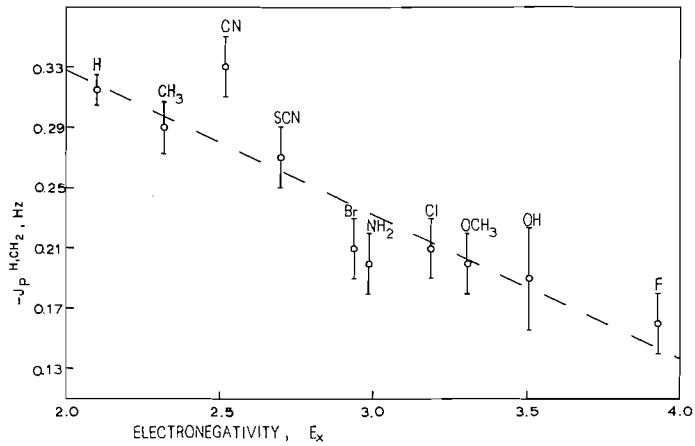

FIG. 1. The coupling constant over six bonds, J_p^{H,CH_2}, in some α-substituted 2,6-dichlorotoluene derivatives, is plotted *vs.* the electronegativity, E_x, of the α-substituent. Parameters are taken from Table 1. The correlation coefficient $r = 0.915$ for the least squares line. If the cyano group, CN, is omitted from the correlation, then $r = 0.954$. Note that $\frac{1}{2}J_p^{H,CH_3}$ is entered for 2,6-dichlorotoluene itself as discussed in the text.

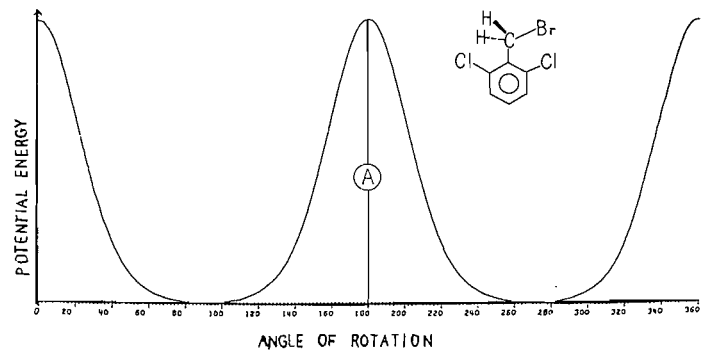

FIG. 2. The potential energy curve for rotation of the bromomethyl group about the sp^2–sp^3 carbon–carbon bond in 2,6-dichlorobenzylbromide as given by a van der Waals potential function. The angle of rotation is 0° when the C—Br bond eclipses a C—Cl bond, *i.e.*, when the former lies in the plane of the aromatic ring. The minimum energy occurs for conformation **1** in the text, where the C—Br bond lies 90° out of the plane of the ring. The barrier, *A*, is about 16 kcal/mol, as discussed in the text.

The fact that J_p^{H,CH_2} in 2,6-dichlorobenzylbromide does not vary between −20 and 80 °C is also in agreement with this picture because φ will remain within the limit of about 20°.

However, a similar calculation for 2,6-dichlorobenzylfluoride yields a barrier *A* of only 3 kcal/mol and, apart from the consideration that such a small barrier may invalidate the classical assumptions, the potential energy curve now apparently allows φ to attain values as large as 50° (although there occur subsidiary maxima at $\phi = \pm 20°$ which, if rather larger, would restrict φ to the smaller value). Since a classical oscillator spends most time near the limits of the motion, one might have expected J_p^{H,CH_2} in the fluoride to be much larger than observed. Yet it has the smallest magnitude in Table 1. Quantum effects on the oscillation will decrease $|J_p^{H,CH_2}|$ insofar as the ground state oscillator then exists most probably in the equilibrium position.

(3) The Five-bond Coupling, J_m^{H,CH_2}

The average value of J_m^{H,CH_2} is 0.35 ± 0.025 Hz, suggesting little, if any, effect of the α-substituent. Coupling between methyl protons in *m*-xylene derivatives (1) implies a π electron contribution of up to 0.25 Hz to J_m^{H,CH_3}. Because the π contribution to J_p^{H,CH_2} decreases as E_x of

Can. J. Chem. Downloaded from www.nrcresearchpress.com by 210.87.254.105 on 09/05/12
For personal use only.

the α-substituent increases, one may infer a proportional decrease in the π contribution to J_m^{H,CH_2} in the compounds of Table 1. On this assumption, a compensating increase in the σ electron contribution to J_m^{H,CH_2} occurs and therefore the observed values do not vary appreciably with the α-substituent.

There are known five-bond couplings which increase on α-substitution by a more electronegative substituent. Thus $^5J_p^{H,H} = 0.65$ Hz in benzene (20) and is 0.98 Hz in pyridine (21). Although $J_p^{H,H}$ in benzene is apparently dominated by a π electron mechanism (1), perturbation of the σ core by the substituent may, of course, give rise to a nonzero σ electron contribution to this five-bond coupling.

Just as for J_p^{H,CH_3}, ring substitution does not markedly alter J_m^{H,CH_3}. Thus $J_m^{H,CH_3} = 0.36$ Hz in toluene (2), 0.36 ± 0.02 Hz in 2,3,4,6-tetrachlorotoluene (11), 0.41 ± 0.02 Hz in 2,3,6-trichloro-4-nitrotoluene (12), 0.40 ± 0.02 Hz in 2,4,6-trimethoxytoluene (12), 0.36 ± 0.02 Hz in 2,4,6-tribromobenzylbromide (12), and 0.40 ± 0.02 Hz in 2,6-dinitro-4-*t*-butyltoluene (12).

We are grateful to the National Research Council of Canada for financial assistance.

1. C. J. MACDONALD and W. F. REYNOLDS. Can. J. Chem. **48**, 1002 (1970) and references therein.
2. M. P. WILLIAMSON, R. J. KOSTELNIK, and S. M. CASTELLANO J. Chem. Phys. **49**, 2218 (1968).
3. T. SCHAEFER, S. S. DANYLUK, and C. L. BELL. Can. J. Chem. **47**, 1506 (1969).
4. D. J. BLEARS, S. S. DANYLUK, and T. SCHAEFER. J. Chem. Phys. **47**, 5037 (1967).
5. P. DIEHL and J. A. POPLE. Mol. Phys. **3**, 557 (1960).
6. T. SCHAEFER, C. M. WONG, and K. C. TAM. Can. J. Chem. **47**, 3688 (1969).
7. P. LASZLO. *In* Progress in nuclear magnetic resonance spectroscopy. Vol. 3. *Edited by* L. H. Sutcliffe, J. Feeney, and J. W. Emsley. Pergamon Press, Oxford. 1967.
8. C. HELLER and H. M. MCCONNELL. J. Chem. Phys. **32**, 1535 (1960).
9. H. RUDOLPH, H. DREIZLER, A. JAESCHKE, and P. WENDLING. Z. Naturforsch. **22**a, 940 (1967).
10. R. SCHWENK. M.Sc. Thesis. University of Manitoba, Winnipeg, Manitoba. 1968.
11. S. STERNHELL and R. H. ROTTENDORF. Aust. J. Chem. **17**, 1315 (1964).
12. A. F. JANZEN. M.Sc. Thesis. University of Manitoba, Winnipeg, Manitoba. 1970.
13. R. WASYLISHEN. Private communication.
14. E. W. STONE and A. H. MAKI. J. Chem. Phys. **37**, 1326 (1962).
15. J. P. COLPA and E. DEBOER. Mol. Phys. **7**, 333 (1964).
16. J. A. POPLE and M. S. GORDON. J. Am. Chem. Soc. **89**, 4253 (1967).
17. J. PEELING, T. SCHAEFER, and C. M. WONG. Can. J. Chem. **48**, 2839 (1970).
18. B. H. BARBER and T. SCHAEFER. Can. J. Chem. **49**, 789 (1971).
19. B. H. BARBER. M.Sc. Thesis. University of Manitoba, Winnipeg, Manitoba. 1970.
20. S. CASTELLANO and R. KOSTELNIK. Tetrahedron Lett. 5211 (1967).
21. S. CASTELLANO, C. SUN, and R. KOSTELNIK. J. Chem. Phys. **46**, 327 (1967).
22. B. P. DAILEY and J. N. SHOOLERY. J. Am. Chem. Soc. **77**, 3977 (1955).

Can. J. Chem. Downloaded from www.nrcresearchpress.com by 210.87.254.105 on 09/05/12
For personal use only.

On the Theory of Linear Electro-Optical Rotation.[1] II. The Three-Photon Effect

HENDRIK F. HAMEKA
Department of Chemistry, University of Pennsylvania, Philadelphia, Pa., 19104

Received August 28, 1970

We present a theoretical description of an effect that we call three-photon electro-optical rotation. We consider a high-intensity beam of polarized monochromatic light, which interacts with an assembly of identical molecules. We calculate the probability of the absorption of two photons from this beam of light and the simultaneous reemission of a third photon, which has the same direction of propagation as the incident light and a direction of polarization that is perpendicular to the incident light. The energy of the emitted photon is the sum of the energies of the absorbed photons. We found that the effect is observable in the presence of a homogeneous electric field F, directed along the direction of polarization of the emitted beam of light. The effect is proportional to F and to the molecular dipole moment and it is inversely proportional to the absolute temperature T.

Nous présentons une description théorique d'un effet que nous appelons la rotation électro-optique impliquant trois photons. Nous considérons un faisceau de lumière monochromatique polarisée d'intensité élevée qui intéragit avec un ensemble de molécules identiques. Nous calculons la probabilité de l'absorption de deux photons de ce faisceau de lumière et la réémission simultanée d'un troisième photon, qui a la même direction de propagation que la lumière incidente et une direction de polarisation qui est perpendiculaire à la lumière incidente. L'énergie du photon émis est la somme des énergies des photons absorbés. Nous avons trouvé que l'effet est observable en la présence d'un champ électrique F homogène, dirigé selon la direction de polarisation du faisceau de lumière émise. L'effet est proportionnel à F et au moment dipolaire moléculaire et il est inversément proportionnel à la température absolue T.

Canadian Journal of Chemistry, 49, 1823 (1971)

Introduction

Conventional optical rotation is a two-photon process because it involves the absorption and simultaneous reemission of a photon by a molecule. The two photons have the same energies and directions of propagation, they differ in their directions of polarization, which are perpendicular to one another. If the molecule is placed in an electric or a magnetic field we speak of electro-optical rotation or magneto-optical rotation, respectively. Both these effects are also two-photon processes.

In the first paper of this series (1) we considered the two-photon electro-optical rotation and specifically the effect that is linear in the electric field. It follows easily from symmetry considerations that this effect is zero unless the electric field F is parallel to the beam of light. Hence we considered the case where F is parallel and our calculations showed that the effect is zero also in that case.

In the present paper we wish to consider higher-order effects in electro-optical rotation, in particular three-photon processes. These processes involve the absorption of two photons k_λ and k_μ by a molecule and the simultaneous reemission of a third photon $k_{\nu'}$. Since we treat the effect as photon scattering by a single molecule our approach is valid only for an assembly of noninteracting molecules, that is, a gas or a liquid.

In our theoretical approach we look upon the effect as some form of optical rotation because we are considering situations where all three protons have the same directions of propagation and where the direction of polarization of the emitted photons is different from the direction of polarization of the incident photons. It should be noted though that the same effect has already been studied from a different view point. Here it is considered as some form of second harmonic generation and since the polarizations of the photons are relatively of minor importance in this approach it is known as electric-field induced second harmonic generation.

If two beams of high-intensity light of frequency ω_1 and ω_2 pass through a medium, they can combine under certain conditions to produce a new beam of light with frequency $\omega_1 + \omega_2$. This is known as second-harmonic generation (2, 3). It was discovered a few years ago that in the presence of an electric field sum frequency

[1]Research supported by the National Science Foundation.

generation can occur if the two incident beams of light coincide. Here we have the situation where a high intensity beam of light of frequency ω produces light of frequency 2ω in the presence of an electric field. The effect is known as electric-field induced optical second harmonic generation; it was first measured in solids by Terhune *et al.* (4) and it was measured in gases and liquids by Mayer (5).

The theoretical description of electric-field induced second harmonic generation in gases was derived by Kielich (6). This derivation is essentially based on the classical Maxwell equations which are solved in higher order. In this way the theoretical results are expressed in terms of higher order electric susceptibilities, which must then be related to molecular quantities. This approach has been used also to derive the theory of conventional optical rotation.

In our theoretical derivation the effect is treated by considering the scattering of photons by individual molecules where we used the quantized radiation field. We have previously used this approach to derive the theory of ordinary optical rotation (7) and we found that this description is mathematically simpler than the theories that were derived from the classical Maxwell equations. Also, we feel that a second theoretical derivation of electric-field induced second harmonic generation or three-photon electro-optical rotation will add to our understanding of the effect.

It is easily seen from symmetry considerations what the most favorable direction of the electric field is. We will consider the experimental situation where the incident beam of light is propagating along the Z direction and polarized along the X direction. The effluent photons propagate also along the Z direction and they are polarized along the Y direction. Consequently, the photons k_λ and k_μ are X polarized and the photon $k_{\nu'}$ is Y polarized. We will show that the probability for this scattering process is non-zero only in first order if the exterior field is directed along the Y axis. We will first derive the general theory for the above described three-photon effect in the absence of exterior fields. In the subsequent section we then calculate the effect of an electric field. Finally, we should point out that we have already calculated this situation if the exterior field is a magnetic field (8) but in that case there was reason to believe that the effect is too small to be observable.

Three-Photon Effect

We wish to calculate the probability for the absorption of two photons k_λ and k_μ and the simultaneous reemission of a photon $k_{\nu'}$ by a molecule. We make use of the Heitler–Ma perturbation method (9) and we use the notation that we introduced previously (10). The molecular eigenvalues and eigenfunctions are denoted by E_n and ψ_n, respectively, and the initial state of the radiation field is denoted by 0. Furthermore, we denote photons that are polarized in the X direction by k_λ, k_μ, etc., photons that are polarized in the Y direction are denoted by primes, such as $k_{\nu'}$, $k_{\alpha'}$, etc. Consequently, the initial state is (0,0) and the final state is $(\bar{\lambda},\bar{\mu},\nu',0)$. Here we use a bar to indicate that a photon is removed from the reference state 0 of the radiation field. Additional states that occur in our calculation are $(\bar{\lambda},\nu',n)$, $(\bar{\lambda},\bar{\mu},n)$, $(\bar{\lambda},n)$ etc. Obviously the state 0 is the molecular ground state.

It has been shown (9, 10) that the probability of a radiative process from an initial state (0,0) to a final state α may be derived from a quantity $U(\alpha;E)$, which is determined from the equations

$$[1] \qquad U(\alpha;E) = H(\alpha;0,0) + \sum_{\beta \neq (0,0)} H(\alpha;\beta)U(\beta;E)\zeta(E - E_\beta)$$

where ζ is the Dirac ζ function. In our situation the above equation becomes

$$[2] \quad U(\bar{\lambda}\bar{\mu},\nu',0;E) = \sum_{n \neq 0} [H(\bar{\lambda}\bar{\mu},\nu',0;\bar{\lambda},\nu',n)U(\bar{\lambda},\nu',n;E)\zeta(E - E_{\lambda\nu' n}) + H(\bar{\lambda}\bar{\mu},\nu',0;\bar{\mu},\nu',n)U(\bar{\mu},\nu',n;E)\zeta(E - E_{\mu\nu' n}) + H(\bar{\lambda}\bar{\mu},\nu',\bar{\lambda}\bar{\mu},n)U(\bar{\lambda}\bar{\mu},n;E)\zeta(E - E_{\lambda\mu n})]$$

The functions U on the right hand side of eq. 2 may be further expressed by using eq. 1,

$$[3]\quad U(\bar{\lambda},\nu',n;E) = \sum_{m\neq 0}[H(\bar{\lambda},\nu',n;\bar{\lambda},m)U(\bar{\lambda},m;E)\zeta(E - E_{\lambda m}) + H(\bar{\lambda},\nu',n;\nu',m)U(\nu',m;E)\zeta(E_\nu - E_{\nu' m})], \text{ etc.}$$

Finally, we observe that

$$[4]\quad \begin{aligned} U(\bar{\lambda},m;E) &= H(\bar{\lambda},m;0,0)\\ U(\bar{\mu},m;E) &= H(\bar{\mu},m;0,0)\\ U(\nu',m;F) &= H(\nu',m;0,0)\end{aligned}$$

Substitution of eqs. 3 and 4 into eq. 2 gives

$$\begin{aligned}[5]\quad U(\bar{\lambda}\bar{\mu},\nu',0,E) = \sum_{n\neq 0}\sum_{m\neq 0\neq n}\Big(&H(\bar{\lambda}\bar{\mu},\nu',0;\bar{\lambda},\nu',n)H(\bar{\lambda},\nu',n;\bar{\lambda},m)H(\bar{\lambda},m;0,0)\zeta(E - E_{\lambda\nu' n})\zeta(E - E_{\lambda m})\\ &+ H(\bar{\lambda}\bar{\mu},\nu',0;\bar{\lambda},\nu',n)H(\bar{\lambda},\nu',n;\nu',m)H(\nu',m;0,0)\zeta(E - E_{\lambda\nu' n})\zeta(E - E_{\nu' m})\\ &+ H(\bar{\lambda}\bar{\mu},\nu',0;\bar{\mu},\nu',n)H(\bar{\mu},\nu',n;\bar{\mu},m)H(\bar{\mu},m;0,0)\zeta(E - E_{\mu\nu' m})\zeta(E - E_{\mu m})\\ &+ H(\bar{\lambda}\bar{\mu},\nu',0;\bar{\mu},\nu',n)H(\bar{\mu},\nu',n;\nu',m)H(\nu' m;0,0)\zeta(E - E_{\mu\nu' n})\zeta(E - E_{\nu' m})\\ &+ H(\bar{\lambda}\bar{\mu},\nu',0;\bar{\lambda}\bar{\mu},n)H(\bar{\lambda}\bar{\mu},n;\bar{\lambda},m)H(\bar{\lambda},m;0,0)\zeta(E - E_{\lambda\mu n})\zeta(E - E_{\lambda m})\\ &+ H(\bar{\lambda}\bar{\mu},\nu',0;\bar{\lambda}\bar{\mu},n)H(\bar{\lambda}\bar{\mu},n;\bar{\mu},m)H(\bar{\mu},m;0,0)\zeta(E - E_{\lambda\mu n})\zeta(E - E_{\mu m})\Big)\end{aligned}$$

The matrix elements in eq. 5 should be taken with respect to the interaction Hamiltonian

$$[6]\quad H_{\text{int}} = (e\hbar/mi)(4\pi)^{\frac{1}{2}}\textstyle\sum_j\sum_\lambda[q_\lambda \exp(ik_\lambda\cdot r_j/\hbar c) + q_\lambda^* \exp(-ik_\lambda\cdot r_j/\hbar c)](e_\lambda\cdot\nabla_j)$$

In order to transform eq. 5 further we may take the exponentials in eq. 6 equal to unity. Furthermore, we make use of the relation

$$[7]\quad \langle\psi_n|(\partial/\partial x_j)|\psi_m\rangle = -(m/e\hbar^2)(E_n - E_m)\langle\psi_n|ex_j|\psi_m\rangle$$

This enables us to transform eq. 5 to

$$\begin{aligned}[8]\quad U(\bar{\lambda}\bar{\mu},\nu',0;E_{\lambda\mu 0'0}) = -i(8\pi^3/k_\lambda k_\mu k_{\nu'})^{\frac{1}{2}}(n_\lambda n_\mu)^{\frac{1}{2}}(n_{\nu'}+1)^{\frac{1}{2}}\sum_{n\neq 0}\sum_{m\neq n\neq 0}(E_0 - E_n)(E_n - E_m)(E_m - E_0)\\ [P_{0,n;x}P_{n,m;y}P_{m,0;x}\zeta(-k_\mu + E_0 - E_n)\zeta(-k_\mu + k_{\nu'} + E_0 - E_m)\\ + P_{0,n;x}P_{n,m;x}P_{m,0;y}\zeta(-k_\mu + E_0 - E_n)\zeta(-k_\lambda - k_\mu + E_0 - E_m)\\ + P_{0,n;x}P_{n,m;y}P_{m,0;x}\zeta(-k_\lambda + E_0 - E_n)\zeta(-k_\lambda + k_{\nu'} + E_0 - E_m)\\ + P_{0,n;x}P_{n,m;x}P_{m,0;y}\zeta(-k_\lambda + E_0 - E_n)\zeta(-k_\lambda - k_\mu + E_0 - E_m)\\ + P_{0,n;y}P_{n,m;x}P_{m,0;x}\zeta(k_{\nu'} + E_0 - E_n)\zeta(-k_\mu + k_{\nu'} + E_0 - E_m)\\ + P_{0,n;y}P_{n,m;x}P_{m,0;x}\zeta(k_{\nu'} + E_0 - E_n)\zeta(-k_\lambda + k_{\nu'} + E_0 - E_m)]\end{aligned}$$

where

$$[9]\quad P_{k,l} = \langle\psi_k|\textstyle\sum_j er_j|\psi_l\rangle$$

We wish to consider the specific situation where the radiation field, that is its state 0, consists of an almost monochromatic beam of photons, which are polarized in the X direction and propagating in the Z direction. The energies of these photons are all very close to an energy k_0 so that we may substitute

$$[10]\quad k_\lambda \simeq k_\mu \simeq k_0$$

In addition, we need consider only those values of U for which the energy is preserved (10) so that

$$[11]\quad k_{\nu'} \simeq 2k_0$$

Since we are not concerned with resonance situations we may replace in eq. 9 the function $\zeta(x)$ by $(1/x)$. We find then that for an assembly of N non-interacting randomly oriented molecules eq. 9 becomes

$$[12]\quad U(\bar{\lambda}\bar{\mu},\nu',0;E_{\lambda\mu\nu'0}) = 2iN(4\pi^3/k_0{}^3)^{\frac{1}{2}}(n_\lambda n_\mu)^{\frac{1}{2}}\sum_{n\neq 0}\sum_{m\neq n\neq 0}(E_n - E_0)(E_m - E_0)(E_n - E_m)$$
$$\times G_{op}[(-k_0 + E_0 - E_n)^{-1}(k_0 + E_0 - E_m)^{-1}P_{0,n;x}P_{m,0;x}P_{n,m;y}$$
$$+ (-k_0 + E_0 - E_n)^{-1}(-2k_0 + E_0 - E_m)^{-1}P_{0,n;x}P_{m,0;y}P_{n,m;x}$$
$$+ (2k_0 + E_0 - E_n)^{-1}(k_0 + E_0 - E_m)^{-1}P_{0,n;y}P_{m,0;x}P_{n,m;x}]$$

Finally, this may be transformed to

$$[13]\quad U(\bar{\lambda}\bar{\mu},\nu',0;E_{\lambda\mu\nu'0}) = 2iN(4\pi^3 n_\lambda n_\mu/k_0)^{\frac{1}{2}}G_{op}\Big[\sum_{n\neq 0}\sum_{m\neq n}(A_{n,m}P_{0,n;x}P_{m,0;x}P_{n,m;y} + B_{n,m}P_{n,m;x}P_{m,0;x}P_{0,n;y})\Big]$$

with

$$[14]\quad A_{n,m} = (E_n - E_0)(E_m - E_0)(E_n - E_m)^2[(E_n - E_0)^2 - k_0{}^2]^{-1}[(E_m - E_0)^2 - k_0{}^2]^{-1}$$
$$B_{n,m} = (E_n - E_0)(E_m - E_0)(E_n - E_m)[2(E_n - E_0) + 4(E_m - E_0)][(E_n - E_0)^2 - 4k_0{}^2]^{-1}$$
$$\times [(E_m - E_0)^2 - k_\lambda{}^2]^{-1}$$

It is easily verified that eq. 13 yields zero in the absence of exterior fields because

$$[15]\quad G_{op}(a_x b_x c_y) = 0$$

However, we will show in the following section that eq. 13 yields in principle a non-zero result if we place our sample in a homogeneous electric field that has a suitable direction.

Electro-Optical Rotation

The probability $U(\bar{\lambda}\bar{\mu}\nu',0;E_{\lambda\mu\nu'0})$ of the three-photon process in the presence of a homogeneous electric field $\boldsymbol{F}$ may be derived from eq. 14 if we take E_n and ψ_n as the eigenvalues and eigenfunctions of the molecule in the presence of $\boldsymbol{F}$ and if we consider the Maxwell distribution of the molecular orientations with respect to $\boldsymbol{F}$.

The Hamiltonian H in the presence of $\boldsymbol{F}$ may be written as

$$[16]\quad H = H_0 - e\textstyle\sum_j r_j\cdot\boldsymbol{F} = H_0 - \boldsymbol{\mu}\cdot\boldsymbol{F}$$

We take E_n and ψ_n as the eigenvalues and eigenfunctions of the operator H and we denote the eigenvalues and eigenfunctions of H_0 by ε_n and ϕ_n. The relations between these two sets of eigenvalues and eigenfunctions are

$$[17]\quad E_n = \varepsilon_n - \boldsymbol{\mu}_{n,n}\cdot\boldsymbol{F}$$
$$\psi_n = \phi_n + \sum_{m\neq n}(\varepsilon_m - \varepsilon_n)^{-1}\phi_m(\boldsymbol{\mu}_{m,n}\cdot\boldsymbol{F})$$

with

$$[18]\quad \boldsymbol{\mu}_{m,n} = \langle\phi_m|\boldsymbol{\mu}|\phi_n\rangle$$

Equation 17 is accurate up to effects that are linear in $\boldsymbol{F}$, which is sufficient for our purpose. It is easily seen now that the three-photon electro-optical rotation is given by

$$[19]\quad U(\bar{\lambda}\bar{\mu},\nu',0;E_{\lambda\mu\nu'0}) = 2iN(4\pi^3 n_\lambda n_\mu/k_0)^{\frac{1}{2}}\Big[G_{op}\sum_{n\neq 0}\sum_{m\neq n}(A_{n,m}P_{0,n;x}P_{m,0;x}P_{n,m;y} + B_{n,m}P_{n,m;x}P_{m,0;x}P_{0,n;y})\exp(\boldsymbol{\mu}_{0,0}\cdot\boldsymbol{F}/kT)\Big][G_{op}\exp(\boldsymbol{\mu}_{0,0}\cdot\boldsymbol{F}/kT)]^{-1}$$

This expression should be transformed further by expressing the vectors $\boldsymbol{P}$ in terms of the vectors $\boldsymbol{\mu}$ and by expressing the energies E in terms of ε and μ. After these substitutions we should evaluate the effects of the operator G_{op}.

We derived previously (1) that for products of four vectors we have

[20] $$G_{op}(a_x b_x c_x d_x) = (1/15)[(\boldsymbol{a}\cdot\boldsymbol{b})(\boldsymbol{c}\cdot\boldsymbol{d}) + (\boldsymbol{a}\cdot\boldsymbol{c})(\boldsymbol{b}\cdot\boldsymbol{d}) + (\boldsymbol{a}\cdot\boldsymbol{d})(\boldsymbol{b}\cdot\boldsymbol{c})]$$

$$G_{op}(a_x b_x c_y d_y) = (1/30)[4(\boldsymbol{a}\cdot\boldsymbol{b})(\boldsymbol{c}\cdot\boldsymbol{d}) - (\boldsymbol{a}\cdot\boldsymbol{c})(\boldsymbol{b}\cdot\boldsymbol{d}) - (\boldsymbol{a}\cdot\boldsymbol{d})(\boldsymbol{b}\cdot\boldsymbol{c})] \text{ and cycl.}$$

All other products of four vector components are zero.

Equation 19 is now evaluated by expanding all its terms as power series in $\boldsymbol{F}$ and by limiting ourselves to the linear terms. It follows from eq. 20 that we obtain a non-zero result only if we take $\boldsymbol{F}$ along the Y direction. In that case $U(\bar{\lambda}\bar{\mu}\nu',0;E_{\lambda\mu\nu'0})$ may be written as a sum of three terms,

[21] $$U(\bar{\lambda}\bar{\mu},\nu',0;E_{\lambda\mu\nu},0) = U_1 + U_2 + U_3$$

Here U_1 results from expanding the Boltzmann exponentials, U_2 from expanding the energies in $A_{n,m}$ and $B_{n,m}$, and U_3 from expanding the eigenfunctions in the vectors $\boldsymbol{P}_{n,m}$.

Let us first consider U_1, which may be written as

[22] $$U_1 = (2iNF/kT)(4\pi^3 n_\lambda n_\mu/k_0)^{\frac{1}{2}}\Big[G_{op}\sum_{n\neq 0}\sum_{m\neq n}(A_{n,m}{}^0\mu_{0,n;x}\mu_{m,0;x}\mu_{n,m;y}\mu_{0,0;y} + B_{n,m}{}^0\mu_{n,m;x}\mu_{m,0;x}\mu_{0,n;y}\mu_{0,0;y})\Big]$$

Here $A_{n,m}{}^0$ and $B_{n,m}{}^0$ are derived from eq. 14 by replacing everywhere the energies E by ε. It follows from eq. 20 that eq. 22 is reduced to

[23] $$U_1 = (iNF/15kT)(4\pi^3 n_\lambda n_\mu/k_0)^{\frac{1}{2}}\Big[G_{op}\sum_{n\neq 0}\sum_{m\neq n}(A_{n,m}{}^0\{4(\boldsymbol{\mu}_{n,m}\cdot\boldsymbol{\mu}_{m,0})(\boldsymbol{\mu}_{0,n}\cdot\boldsymbol{\mu}_{0,0}) - (\boldsymbol{\mu}_{0,n}\cdot\boldsymbol{\mu}_{n,m})(\boldsymbol{\mu}_{m,0}\cdot\boldsymbol{\mu}_{0,0}) - (\boldsymbol{\mu}_{0,n}\cdot\boldsymbol{\mu}_{0,0})(\boldsymbol{\mu}_{m,0}\cdot\boldsymbol{\mu}_{n,m})$$
$$+ B_{n,m}{}^0\{4(\boldsymbol{\mu}_{n,m}\cdot\boldsymbol{\mu}_{m,0})(\boldsymbol{\mu}_{0,n}\cdot\boldsymbol{\mu}_{0,0}) - (\boldsymbol{\mu}_{n,m}\cdot\boldsymbol{\mu}_{0,n})(\boldsymbol{\mu}_{m,0}\cdot\boldsymbol{\mu}_{0,0}) - (\boldsymbol{\mu}_{n,m}\cdot\boldsymbol{\mu}_{0,0})(\boldsymbol{\mu}_{m,0}\cdot\boldsymbol{\mu}_{0,n})\}\Big]$$

or

[24] $$U_1 = (iNF/15kT)(4\pi^3 n_\lambda n_\mu/k_0)^{\frac{1}{2}}\sum_{n\neq 0}\sum_{m\neq 0\neq n}[(4A_{n,m}{}^0 - B_{n,m}{}^0)(\boldsymbol{\mu}_{0,n}\cdot\boldsymbol{\mu}_{m,0})(\boldsymbol{\mu}_{n,m}\cdot\boldsymbol{\mu}_{0,0}) + (4B_{n,m}{}^0 - A_{n,m}{}^0)(\boldsymbol{\mu}_{0,n}\cdot\boldsymbol{\mu}_{0,0})(\boldsymbol{\mu}_{n,m}\cdot\boldsymbol{\mu}_{m,0}) - (A_{n,m}{}^0 + B_{n,m}{}^0)(\boldsymbol{\mu}_{0,n}\cdot\boldsymbol{\mu}_{n,m})(\boldsymbol{\mu}_{m,0}\cdot\boldsymbol{\mu}_{0,0})]$$
$$= (iNF/15kT)(4\pi^3 n_\lambda n_\mu/k_0)^{\frac{1}{2}}\sum_{n\neq 0}\sum_{m\neq 0\neq \pm n}[(4A_{n,m}{}^0 - B_{n,m}{}^0)(\boldsymbol{\mu}_{0,n}\cdot\boldsymbol{\mu}_{m,0})(\boldsymbol{\mu}_{n,m}\cdot\boldsymbol{\mu}_{0,0}) + (4B_{n,m}{}^0 - A_{n,m}{}^0 - A_{m,n}{}^0 - B_{m,n}{}^0)(\boldsymbol{\mu}_{0,n}\cdot\boldsymbol{\mu}_{0,0})(\boldsymbol{\mu}_{n,m}\cdot\boldsymbol{\mu}_{m,0})]$$

Here it has been assumed that the eigenfunctions ϕ_n are all real.

Let us now proceed to the calculation of U_2. It follows easily from eqs. 17 and 19 that it is given by

[25] $$U_2 = -2iNF(4\pi^3 n_\lambda n_\mu/k_0)^{\frac{1}{2}}G_{op}\sum_{n\neq 0}[(\partial A_{n,m}{}^0/\partial\varepsilon_0)\mu_{0,n;x}\mu_{m,0;x}\mu_{n,m;y}\mu_{0,0;y} + (\partial A_{n,m}{}^0/\partial\varepsilon_n)\mu_{0,n;x}\mu_{m,0;x}\mu_{n,m;y}\mu_{n,n;y} + (\partial A_{n,m}{}^0/\partial\varepsilon_m)\mu_{0,n;x}\mu_{m,0;x}\mu_{n,m;y}\mu_{m,m;y}$$
$$+ (\partial B_{n,m}{}^0/\partial\varepsilon_0)\mu_{n,m;x}\mu_{m,0;x}\mu_{0,n;y}\mu_{0,0;y} + (\partial B_{n,m}{}^0/\partial\varepsilon_n)\mu_{n,m;x}\mu_{m,0;x}\mu_{0,n;y}\mu_{n,n;y} + (\partial B_{n,m}{}^0/\partial\varepsilon_m)\mu_{n,m;x}\mu_{m,0;x}\mu_{0,n;y}\mu_{m,m;y}]$$

This may be transformed further by calculating the various derivatives and by making use of eq. 20 and it should lead to a rather involved and unwieldy expression. However, even at this point it may be seen already that U_2 should be much smaller than U_1, the order of magnitude of their ratio is given by

[26] $$(U_2/U_1) \simeq (kT/\Delta\varepsilon)$$

Here $\Delta\varepsilon$ is the order of magnitude of the energy differences $(\varepsilon_n - \varepsilon_0)$, $(\varepsilon_m - \varepsilon_0)$ or $(\varepsilon_n - \varepsilon_m)$ which we roughly take as 1 eV. At room temperature the ratio of eq. 26 should be about 2% and it follows that U_2 is generally much smaller than U_1. We feel that it is somewhat pointless to transform eq. 25 any further because the result is too complicated to be of much help to us and in general we may expect it to be negligible compared to eq. 25.

Similar arguments apply to the calculation of U_3. It may be derived from eq. 13 by substituting

[27] $$\boldsymbol{P}_{k,l} = \boldsymbol{\mu}_{k,} + \sum_{j\neq k} (\varepsilon_j - \varepsilon_k)^{-1} F \mu_{j,k;y} \mu_{j,e} + \sum_{j\neq l} (\varepsilon_j - \varepsilon)^{-1} F \mu_{j,k;y} \boldsymbol{\mu}_{k,j}$$

and by collecting the terms that are linear in $\boldsymbol{F}$. Again, this leads to an unwieldy expression that is not going to be of much help towards understanding the effect. However, it is easily seen that the ratio (U_3/U_1) is again given by eq. 26. We feel that it is both convenient and justifiable to neglect U_2 and U_3 with respect to U_1, so that the probability of three-photon electro-optical rotation is given by eq. 24.

Discussion

Our considerations agree with Kielich's work (6) in the conclusion that in general the term U_1 is much larger than the others. It should be relatively easy to verify this conclusion because this term is temperature dependent and Kielich refers to it as the temperature effect. Unfortunately, Mayer (5) does not mention any temperature dependence and we presume that all of Mayer's measurements were performed at room temperature.

It seems that the theoretical expressions that we derived for U_1 are too complicated to make their numerical evaluation feasible. However, they are suitable for order of magnitude estimates and they can be used to derive some general features of the effect.

The order of magnitude of the effect may be estimated by making a comparison with the conventional Kerr effect. We consider U_1 and the corresponding expression $U_{1,k}$ for the conventional Kerr effect. It is easily seen then that

[28] $$\frac{U_1}{U_{1,k}} = \left(\frac{\boldsymbol{F}_{\text{rad}}}{\Delta\varepsilon}\right)\cdot\left(\frac{kT}{\boldsymbol{F}}\right) = \left(\frac{\boldsymbol{F}_{\text{rad}}}{\boldsymbol{F}}\right)\cdot\left(\frac{kT}{\Delta\varepsilon}\right)$$

Here $\boldsymbol{F}_{\text{rad}}$ is the electric field vector of the radiation field, $\boldsymbol{F}$ is the applied electric field and $\Delta\varepsilon$ is the energy difference that we introduced in eq. 26. The second term of eq. 28 is about 1% and the first term varies between 1 and 20 in Mayer's experiment, so that the ratio of eq. 28 is of the order of 0.1. We expect therefore that the effect is large enough to be measured if a laser is used. Since the effect has already been measured by Mayer this prediction is not of much practical use.

Kielich's result is expressed in terms of higher order electric susceptibilities whereas our result has a more detailed form and it is expressed in terms of matrix elements of the molecular eigenfunctions. Both expressions have their advantages and disadvantages but our result is more suitable for considering the intensity distribution of the incoming and outgoing radiation. Let the incoming radiation be described by

[29] $$I(k_\lambda) = \frac{I_0}{(k_\lambda - k_0)^2 + h^2\Gamma^2}$$

All its photons are polarized in the X direction. The outgoing radiation is the sum of $I(k_\lambda)$ of eq. 29 and of a much weaker line which is polarized in the Y direction and which has an intensity distribution

[30] $$I'(k_{\nu'}) = \frac{I_0^2 U_1^2}{(k_{\nu'} - 2k_0)^2 + h^2\gamma^2}$$

It follows that the term "optical rotation" is not entirely accurate for describing our effect because we do not predict a continuous rotation of the plane of polarization of the light. Instead we find that the effluent light is rotated by 90° and that its intensity is a continuous function of the optical activity of the sample. Of course, the frequency of the reemitted light is double the frequency of the incident light, which is quite different from any of the conventional optical activity effects.

Finally, let us determine the type of molecule for which the effect should be the largest. It follows from eq. 24 that U_1 is proportional to $\mu_{0,0}$ so that it is desirable that the molecule has a large electric dipole moment in its ground state. Obviously, the effect is zero if the molecule has a

center of symmetry, or even if the molecule has two symmetry planes or a symmetry axis. It is desirable that the molecule has a low lying state of appropriate symmetry. Also, U_1 is proportional to $(1/T)$ and the intensity of the emitted light is proportional to $(1/T)^2$ so that it is desirable to perform the experiment at low temperatures. We leave it to the reader to decide which molecules best satisfy the above conditions.

1. H. F. HAMEKA. Chem. Phys. Lett. **7**, 157 (1970).
2. J. A. GIORDMAINE. Phys. Rev. **138A**, 1599 (1965).
3. M. RENTZEPIS, J. A. GIORDMAINE, and K. W. HECHT. Phys. Rev. Lett. **16**, 792 (1966).
4. R. W. TERHUNE, P. D. MAKER, and C. M. SAVAGE. Phys. Rev. Lett. **8**, 404 (1962). R. W. MINCK, R. W. TERHUNE, and C. C. WANG. Appl. Opt. **5**, 1595 (1966).
5. G. MAYER. Compt. Rend. **267B**, 54 (1968).
6. S. KIELICH. Chem. Phys. Lett. **2**, 569 (1968).
7. H. F. HAMEKA. Ann. Phys. N.Y. **26**, 122 (1964).
8. N. V. COHAN and H. F. HAMEKA. Physica, **38**, 320 (1967).
9. W. HEITLER and S. T. MA. Proc. Roy. Irish Acad. **52**, 109 (1949).
10. H. F. HAMEKA. Advanced quantum chemistry. Addison Wesley Publishing Co., Inc., Reading, Mass. 1965.

Can. J. Chem. Downloaded from www.nrcresearchpress.com by 210.87.254.40 on 09/05/12
For personal use only.

Aqueous Nonelectrolyte Solutions. Part IX. Enthalpies of Mixing of Water and Deuterium Oxide with Ethylene Oxide[1]

D. N. GLEW AND HARRY WATTS

Exploratory Research Laboratory, Dow Chemical of Canada, Limited, Sarnia, Ontario

Received September 30, 1970

Calorimetric enthalpies of mixing have been measured over the whole composition range for the water – ethylene oxide system at 10.75 and 20.00 °C and for the deuterium oxide – ethylene oxide system at 13.45 and 20.00 °C. Less extensive measurements have been made for dilute ethylene oxide solutions in water at 0.6 °C and in deuterium oxide at 4.1 and 7.3 °C. The experimental S-shaped, enthalpy of mixing – composition curves are interpreted in terms of solution hydrogen bonding changes, with particular reference to the hydrogen bonding of water. At low ethylene oxide mole fractions the deuterium oxide systems are more exothermal and at high ethylene oxide mole fractions more endothermal than the corresponding water systems. A good correlation is found between the enthalpy of mixing and the water proton magnetic resonance chemical shift for solutions with greater than 0.55 mol fraction of ethylene oxide.

Des mesures calorimétriques d'enthalpies de mélange ont été effectuées sur tout le domaine de concentration pour les systèmes eau-oxyde d'éthylène à 10.75 et à 20.00 °C et oxyde de deutérium-oxyde d'éthylène à 13.45 et à 20.00 °C. Quelques mesures ont été faites pour des solutions diluées d'oxyde d'éthylène dans l'eau à 0.6 °C et dans l'oxyde de deutérium à 4.1 et à 7.3 °C. Les courbes expérimentales en forme de S de l'enthalpie de mélange en fonction de la concentration sont interprétées en termes de changements de ponts hydrogène dans la solution impliquant tout particulièrement les ponts hydrogène de l'eau. Les systèmes oxyde d'éthylène-oxyde de deutérium sont plus exothermiques que les systèmes oxyde d'éthylène-eau correspondants aux faibles fractions molaires d'oxyde d'éthylène et plus endothermiques aux fractions molaires élevées. Il existe une bonne corrélation entre l'enthalpie de mélange et le déplacement chimique en résonance magnétique nucléaire de l'eau pour les solutions dont la fraction molaire d'oxyde d'éthylène est supérieure à 0.55.

Canadian Journal of Chemistry, 49, 1830 (1971)

Introduction

As part of our study of the properties of solid and liquid aqueous nonelectrolyte solutions (1, 2), measurements in a new mixing calorimeter (3) are reported for the enthalpies of mixing of ethylene oxide (EO) with water and with deuterium oxide. The only earlier calorimetric study of the mixing of H_2O–EO is by Berthelot (4) in 1882, who reported two measurements at 13 °C giving a molar enthalpy of mixing $\Delta_m h = -39.0$ J at EO mole fraction $x_2 = 0.0062$.

The mixing of EO with both H_2O and D_2O has been measured to give a greater insight to the nature of the aqueous dissolution process. Benjamin and Benson (5) measured the enthalpy of mixing for CH_3OH with H_2O and for CH_3OD with D_2O, but the small differences between the enthalpies of mixing for these systems are related not only to the differences between H_2O and D_2O but also to the differences between CH_3OH and CH_3OD. The present investigation with EO is believed to be the first reported for the enthalpies of mixing of both H_2O and D_2O with the same substance.

The behavior observed for the enthalpy of mixing in simple, non-polar, hydrocarbon systems has been interpreted and quantitatively represented using the lattice theory of liquids and the principle of congruence (6, 7). For more polar systems, in which the liquids being mixed are subject to specific molecular interactions, the model of the ideal mixture of associated species has reasonably accounted for the enthalpy of mixing of hydrogen bonded (H-bonded) aniline with toluene, but does not adequately represent the mixing of aniline with cyclohexane (8, 9). The lattice theory of liquids has been partially successful in accounting for the enthalpy of mixing of some H-bonded systems containing alcohols (10). However, for the polar, strongly associated, H-bonded, aqueous systems with EO (1), propylene oxide, acetone, tetrahydrofuran, 1,4-dioxane, and *t*-butyl alcohol (2), and with alcohols (11), there is no solution theory yet developed which permits the *ab initio* calculation of the enthalpy of mixing behavior. This arises

[1]Contribution No. 188.

TABLE 1. Enthalpy of mixing of water and ethylene oxide at 10.75 °C

Weight H_2O (g)	Weight C_2H_4O (g)	Heat change (J)	Temperature (°C)	Mole fraction H_2O x_1	$\Delta_m h$ (J/mol)
4.4762	0.1876	+31.48	11.007	0.98315	−125.1
4.0123	0.2313	37.79	10.711	0.97697	−165.7
4.1822	0.5222	73.15	10.713	0.95142	−299.6
3.3029	0.4544	59.36	10.967	0.94673	−307.5
4.1207	0.6053	79.50	10.710	0.94333	−327.7
3.9253	0.6039	74.93	10.716	0.94081	−323.4
3.8723	0.8159	90.59	10.918	0.92067	−389.4
4.1563	1.7542	100.20	10.783	0.85281	−371.6
4.1625	2.7093	84.35	10.674	0.78978	−288.0
3.9829	3.7391	53.50	10.762	0.72259	−175.3
1.9878	3.6188	−16.30	10.702	0.57324	+84.9
1.3289	3.7051	−41.44	10.718	0.46726	+262.6
0.9864	3.6015	−46.01	10.720	0.40111	+337.2
0.7936	3.7032	−51.85	10.698	0.34385	+404.9
0.5874	3.6831	−53.04	10.706	0.28057	+456.7
0.3851	3.5507	−49.47	10.734	0.20962	+485.2
0.3019	3.6659	−48.04	10.720	0.16763	+480.7
0.2400	3.6727	−44.95	10.714	0.13780	+465.0
0.1377	3.6416	−34.01	10.719	0.08460	+376.7
0.0535	3.6906	−16.68	10.726	0.03420	+192.3

both from the lack of a quantitative theory of water (12) and from the lack of physically realistic models representing aqueous nonelectrolyte solutions (13, 14). In this paper we provide a semi-quantitative explanation for the S-shaped enthalpy of mixing curves for aqueous EO in terms of solution H-bonding changes (1, 2).

Experimental

Materials

Ethylene oxide was selected from the production of Dow Chemical of Canada, Limited; analysis for aldehydes, water, and nonvolatiles showed that the total of these impurities was less than 80 p.p.m.

Deuterium oxide was obtained from Atomic Energy of Canada, Limited; analysis 99.72 mol% D_2O, 0.28 mol% H_2O.

Water was triply distilled and had a specific conductivity 3.5×10^{-7} ohm^{-1} at room temperature of about 25 °C.

Apparatus and Procedure

The calorimeter has been described previously (3). A small modification in the filling procedure was required owing to the low boiling point of EO. The section of the filling system used for handling EO was packed with ice and the calorimeter was cooled to 10 °C. When the required amount of EO had been introduced into the calorimeter, the opening of the expansion chamber was closed with a plug (Fig. 1, ref. 3) and the calorimeter allowed to warm up to room temperature for weighing.

Previously only the conduct of endothermal mixing experiments was described. Exothermal mixings were encountered in the present systems. Standard calorimetric technique was used in which the temperature rise due to the mixing was compared with a subsequent nearly equal temperature rise due to known electrical energy dissipation in the heater. Allowance was made for the thermal effect of stirring and for heat losses as before.

Results

Measurements were made over the complete composition range for H_2O–EO at 10.75 and 20.00 °C, and for D_2O–EO at 13.45 and 20.00 °C. Tables 1, 2, 4, and 5 record the weight of H_2O or D_2O and of EO taken in each experiment, together with the temperature of the experiment and the heat change observed. The last two columns give the mole fraction of water, x_1, and the enthalpy change per mol of mixture formed, $\Delta_m h$, corrected to the reference temperature of the table.

At lower temperatures clathrate hydrate formation (15, 16) prevented study over the complete composition range so that measurements were made over restricted ranges for the H_2O–EO system at 0.6 °C and for D_2O–EO at 4.1 and 7.3 °C. These less extensive measurements are reported in Tables 3 and 6, which give $\Delta_m h$ values at the experimental temperatures. All measurements were made at a total pressure of 3 atm since many were above the normal boiling point of EO at 10.5 °C.

The experimental results for each system have been fitted by the method of least squares to the equation

Can. J. Chem. Downloaded from www.nrcresearchpress.com by 210.87.254.40 on 09/05/12
For personal use only.

TABLE 2. Enthalpy of mixing of water and ethylene oxide at 20.00 °C

Weight H_2O (g)	Weight C_2H_4O (g)	Heat change (J)	Temperature (°C)	Mole fraction H_2O x_1	$\Delta_m h$ (J/mol)
4.2886	0.0698	+11.47	20.000	0.99338	−47.88
4.0895	0.2683	35.97	20.004	0.97387	−154.3
4.2319	0.4493	57.56	19.999	0.95839	−234.8
4.1547	0.5798	65.16	20.000	0.94601	−267.3
4.1506	0.7001	74.48	19.997	0.93547	−302.4
5.1089	1.1379	104.86	19.996	0.91652	−338.9
4.0262	1.0360	87.59	19.999	0.90479	−354.6
4.2620	1.3683	91.72	19.988	0.88395	−342.7
4.2034	1.4048	93.60	19.997	0.87976	−352.9
4.1292	1.9447	80.32	19.983	0.83851	−293.7
4.1249	2.6569	74.82	19.979	0.79151	−258.6
4.1479	3.5349	58.39	19.985	0.74156	−188.0
2.5248	3.6047	−5.062	19.980	0.63137	+22.85
1.5108	3.5321	−36.98	19.974	0.51123	+225.5
0.9240	3.6515	−54.51	19.958	0.38225	+406.5
0.8072	3.6972	−57.13	19.964	0.34806	+444.0
0.6092	3.5788	−56.78	19.968	0.29391	+493.6
0.4908	3.6475	−56.83	19.975	0.24758	+516.6
0.3740	3.6069	−53.96	19.959	0.20227	+525.9
0.2509	3.8910	−49.74	19.953	0.13620	+486.6
0.1993	3.8403	−44.54	19.976	0.11261	+453.5
0.1246	3.8556	−33.92	20.006	0.07324	+359.1

TABLE 3. Enthalpy of mixing of water and ethylene oxide

Weight H_2O (g)	Weight C_2H_4O (g)	Heat change (J)	Temperature (°C)	Mole fraction H_2O x_1	$\Delta_m h$ (J/mol)
4.5210	0.0383	+6.807	0.577	0.99655	−27.03
5.7759	0.1043	19.96	0.601	0.99267	−61.80
5.7532	0.1383	25.53	0.601	0.99027	−79.15
4.4926	0.2037	33.76	0.679	0.98180	−132.9
4.6473	0.3401	15.90	0.554	0.97094	−244.9
0.1100	2.8996	−26.21	0.495	0.08489	+364.4

$$[1] \quad \Delta_m h\ (\text{J/mol}) = x_1(1-x_1)\sum_{k=0}^{k=m} B_k(1-2x_1)^k$$

with the water mole fraction x_1. To obtain an adequate fit of the measurements over the whole composition range, at least ten terms of the equation are required to minimize the residual variance. Values for the regression coefficients B_k are given in Table 7, together with the assessed standard errors for a single determination, $\sigma(\Delta_m h)$.[2] When the exothermal and endothermal results are fitted separately the number of terms is reduced to six, the value of $\sigma(\Delta_m h)$ remains about the same in the exothermal region but is significantly reduced to about 2 J/mol in the endothermal region. This properly reflects the greater calorimetric accuracy of the endothermal measurements, for which the calorimeter is maintained nearly isothermally by heater compensation. Smoothed values for $\Delta_m h$ calculated from [1] at regular mole fraction intervals are given in Table 8.[2] In Fig. 1 we show a typical S-shaped curve for the H_2O–EO system at 10.75 °C. The root mean squared deviation for this data from the smoothed curve is 4 J/mol.

At low EO concentrations $\Delta_m h$ values in D_2O lie below those for H_2O but at high EO concentrations they lie above. We have observed the same behavior in the $\Delta_m h$ values for tetrahydrofuran with D_2O and H_2O (36).

[2]Photocopies of Tables 7, 8, 10, 11, and 12 may be obtained free of charge, upon request, from the Depository of Unpublished Data, National Science Library, National Research Council of Canada, Ottawa, Canada.

Can. J. Chem. Downloaded from www.nrcresearchpress.com by 210.87.254.40 on 09/05/12
For personal use only.

TABLE 4. Enthalpy of mixing of deuterium oxide and ethylene oxide at 13.45 °C

Weight D_2O (g)	Weight C_2H_4O (g)	Heat change (J)	Temperature (°C)	Mole fraction D_2O x_1	$\Delta_m h$ (J/mol)
4.4875	0.0571	+10.56	13.427	0.99425	−46.85
4.5572	0.1507	26.68	13.443	0.98519	−115.5
4.6600	0.3202	48.43	13.451	0.96972	−201.8
4.5964	0.3791	55.78	13.442	0.96387	−234.2
4.6616	0.4738	65.91	13.431	0.95585	−270.4
4.6139	0.7409	83.31	13.444	0.93198	−336.9
4.5524	0.7503	82.77	13.439	0.93031	−338.6
4.6109	0.9740	91.11	13.442	0.91240	−360.9
4.6263	1.2909	95.25	13.445	0.88725	−365.8
4.6292	1.7486	92.16	13.446	0.85348	−340.2
4.6565	2.2068	84.37	13.448	0.82278	−298.5
4.6436	2.7638	70.77	13.433	0.78709	−240.1
4.6327	3.5271	49.99	13.444	0.74293	−160.5
3.2945	3.6027	5.049	13.451	0.66800	−20.47
2.2146	3.6467	−33.05	13.448	0.57195	+170.9
1.6873	3.2668	−34.52	13.446	0.53193	+217.9
1.3328	3.4720	−47.19	13.458	0.45788	+324.5
0.8738	3.0640	−46.71	13.451	0.38583	+413.0
1.0313	3.7058	−57.21	13.446	0.37978	+421.8
0.8739	3.5729	−56.87	13.469	0.34988	+455.8
0.7349	3.9335	−63.69	13.472	0.29133	+505.4
0.5185	3.5638	−56.77	13.476	0.24249	+531.5
0.4101	3.6887	−55.83	13.487	0.21573	+535.6
0.3330	3.7022	−52.65	13.490	0.16521	+522.9
0.2319	3.7630	−46.16	13.491	0.11940	+475.8
0.1356	3.7226	−34.04	13.485	0.07420	+373.0

TABLE 5. Enthalpy of mixing of deuterium oxide and ethylene oxide at 20.00 °C

Weight D_2O (g)	Weight C_2H_4O (g)	Heat change (J)	Temperature (°C)	Mole fraction D_2O x_1	$\Delta_m h$ (J/mol)
4.6615	0.1141	+18.66	19.987	0.98887	−79.25
4.6158	0.2228	33.94	19.951	0.97853	−144.0
4.5732	0.4264	56.49	19.989	0.95935	−237.2
4.6261	0.5277	64.88	20.010	0.95071	−267.0
4.4877	0.7935	78.90	19.948	0.92562	−326.6
4.5179	0.8679	81.25	19.974	0.91970	−331.1
4.5967	1.2165	88.81	19.886	0.89263	−344.9
4.6193	1.4116	90.03	19.883	0.87805	−342.3
4.6210	1.8544	84.22	19.889	0.84575	−308.3
4.6457	2.5856	69.78	19.931	0.79812	−239.8
4.6438	4.0030	30.71	19.909	0.71806	−94.86
3.3535	3.5442	3.757	19.923	0.67552	−14.94
2.2299	3.4781	−30.65	19.920	0.58517	+161.2
1.6727	3.8072	−51.51	19.947	0.49153	+303.4
1.1117	3.7160	−60.27	19.931	0.39695	+431.2
0.8967	3.3980	−58.20	19.936	0.36734	+477.7
0.6574	3.5174	−59.87	19.956	0.29140	+531.5
0.5503	3.5177	−59.28	19.947	0.25607	+552.5
0.4248	3.6771	−58.57	19.953	0.20267	+562.6
0.3036	3.8075	−54.34	19.962	0.14926	+535.0
0.2411	3.8046	−48.55	19.958	0.12237	+493.4
0.1456	3.5960	−34.58	19.967	0.08180	+389.0

Can. J. Chem. Downloaded from www.nrcresearchpress.com by 210.87.254.40 on 09/05/12
For personal use only.

TABLE 6. Enthalpy of mixing of deuterium oxide and ethylene oxide

Weight D_2O (g)	Weight C_2H_4O (g)	Heat effect (J)	Temperature (°C)	Mole fraction D_2O x_1	$\Delta_m h$ (J/mol)
5.9808	0.0215	+3.643	4.090	0.99837	−12.18
6.2270	0.0605	10.86	4.097	0.99560	−34.78
6.9953	0.0714	14.95	4.084	0.99538	−42.60
6.4841	0.1814	35.01	4.094	0.98744	−106.8
1.4038	0.0496	8.477	4.177	0.98420	−119.0
5.5662	0.2819	41.57	4.085	0.97750	−146.2
3.5632	0.0197	+7.806	7.298	0.99749	−43.75
3.9499	0.0408	4.878	7.306	0.99533	−24.61
3.2883	0.0491	10.59	7.302	0.99326	−64.04
4.3728	0.1954	35.06	7.292	0.98009	−157.4
2.2849	0.1108	20.54	7.284	0.97844	−176.1

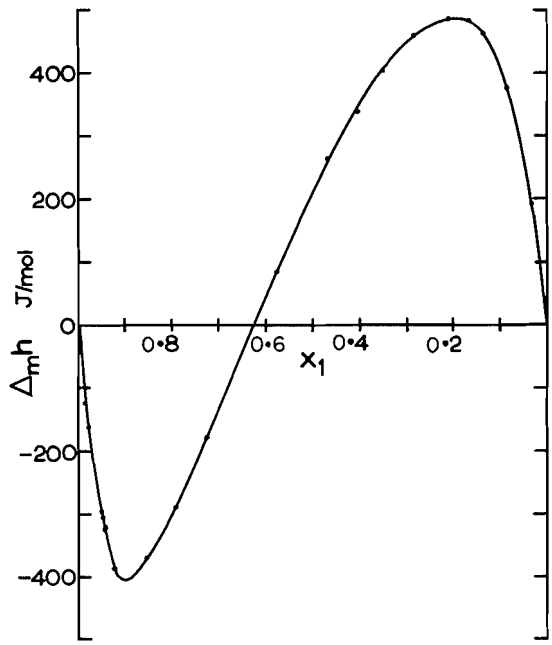

FIG. 1. S-shaped curve for the molar enthalpy of mixing $\Delta_m h$, dependence on water mole fraction x_1 for the H_2O–EO system at 10.75 °C.

Discussion

The Nature of Liquid Water

Before we can discuss the nature of aqueous nonelectrolyte solutions we must consider the nature of pure liquid water. Numerous models for water have been proposed, but no single one of them has been able to account satisfactorily for most of the properties of water. Since this has been adequately discussed elsewhere recently (12) we propose only to focus attention on a few relevant points. Liquid water is unique in its capability of forming a three-dimensional network of H-bonds. Each water molecule can form up to a maximum of four H-bonds, but whether or not liquid water is in fact fully H-bonded at temperatures not far above its freezing point has been the subject of much investigation and speculation. Falk and Ford (17) have pointed out that estimates of the number of broken H-bonds in water vary from 0 to over 70%. We believe that the answer to the question "What proportion of H-bonds are broken in pure water?" must depend on the type and time scale of the experiment that purports to answer this question. Let us consider the Pople model for water (18). In terms of this model no H-bonds are broken on melting ice but rather they are subject to considerable distortion. The bending of H-bonds causes weakening, so that in liquid water there is a range of energies associated with a H-bond. However, as Pople points out, each water molecule must be continually breaking its H-bonds and reforming them with different neighbors. If this were not so then water would not be a liquid. When one accepts the fact that H-bonds are being broken and remade, the crucial factor then becomes the time for which the H-bond is broken before reforming. Any experiment designed to detect broken bonds, that is to detect unbonded O—H groups, will only reveal broken bonds if the time scale of measurement is shorter than the time for which the bond is broken. For example, if one seeks evidence from the vibrational spectrum for the existence of unbonded O—H groups as distinct from those H-bonded O—H---O, the unbonded species must exist for at least one vibration to give rise to a quantized band of characteristic frequency.

Can. J. Chem. Downloaded from www.nrcresearchpress.com by 210.87.254.40 on 09/05/12
For personal use only.

Can. J. Chem. Downloaded from www.nrcresearchpress.com by 210.87.254.40 on 09/05/12
For personal use only.

Broken H-bonds appear to be fairly definitely indicated in the Raman spectrum of water (19–21) but detectable with difficulty in the infrared (22). This implies that the lifetime of an unbonded O—H group is at least greater than 10^{-14} s, and possibly 10 to 100 times longer than this depending on temperature. The importance of the time scale in considering H-bonding interactions seems to have been largely ignored until recently when Eisenberg and Kauzmann gave it detailed consideration (12).

In the present work considering the longer time periods for proton magnetic resonance and thermodynamic property measurements, we are interested in the ability of water molecules to form three-dimensional, H-bonded networks in which most water molecules form four, tetrahedrally oriented, H-bonds with four near neighbors. Here the formation and rupture of individual H-bonds is very rapid compared with the measurement time so that we observe the average over many formations and ruptures of all H-bonds. Since there is much evidence indicating the persistence of tetrahedral co-ordination in water at lower temperatures (12, 18, 23, 24) and since energy is absorbed in breaking H-bonds, it appears that most water molecules form four H-bonds with neighbors, and of those not forming four bonds the majority form three H-bonds with near neighbors, with progressively decreasing fractions forming two, one, and zero H-bonds to neighbors.

Let us now consider the effect on water of the addition of a nonelectrolyte. If the added solute is non-polar, such as argon, nitrogen, and methane, the solubility is very low. Eley (25) formulated a theory for the solubility of inert gases in water, in which the solute gas molecules were accommodated interstitially between the H-bonded water molecules. This theory permitted quantitative calculation of some of the aqueous solute properties. More recently, several authors have considered that the interstices between the water molecules in solution resemble the cages of clathrate hydrates (1, 2, 26–28). We believe that there has been much misinterpretation of this model, largely due to ignoring the importance of the time scale. It is not realistic to talk of clathrates in solution as though an ordered shell of water around the solute molecule had a permanent existence. It must be considered that any ordered shell is continually breaking and re-forming with different molecules, and the reality of such a shell as an entity relates to the time of its existence, compared with the time taken for a water molecule to move from a position of nearest neighbor to that of next nearest neighbor of a given solute molecule. One must also be wary of attributing to the H-bonds between water within this shell of nearest neighbors values of bond lengths and angles that conform rigidly to those found in a clathrate hydrate. We believe that an ordered shell of nearest-neighbor water molecules around a solute can be readily accounted for in terms of the Pople model for water. We visualize the solute as a template around which water molecules can be placed and so reduce the distortion of their H-bonds below that in pure liquid water (1, 2, 28, 29). Thus the bonds being less distorted have a greater stability, consequently the initial dissolution of a gaseous nonelectrolyte in water at low temperature is invariably exothermal.

If the solute added to water is polar, or is able to form H-bonds with water, then eventually, when sufficient solute has been added, a complete disruption of the H-bonded network of liquid water must occur. This will be discussed more fully later in this paper. We point out here, however, that any breaking of water H-bonds must be step-wise. It is common experience that breaking of bonds is step-wise in any process, such as the ionization of hydrogen sulfide or ortho-phosphoric acid, and there is no reason to expect that the breaking of the four-fold H-bonding of water should be supernatural.

Interpretation of the Enthalpy of Mixing of Water and Ethylene Oxide

The S-shaped composition dependence for $\Delta_m h$ observed in these systems and shown in Fig. 1 is typical of many aqueous nonelectrolyte systems (30–32, 38). A composition dependence curve of this shape is indicative of complex interactions between the species being mixed. When mixtures of two nonelectrolytes are considered the interpretation of such S-shaped curves may be straightforward, as, for example, in Barker and Smith's (10) application of the lattice theory of liquids to the ethanol–chloroform system, for which the calculated $\Delta_m h$ composition curve was in reasonable agreement with the experimental curve. In that system H-bonding occurs between ethanol molecules and between

Can. J. Chem. Downloaded from www.nrcresearchpress.com by 210.87.254.40 on 09/05/12
For personal use only.

ethanol and chloroform molecules. However, Barker and Smith had no success in the application of the theory to aqueous nonelectrolyte systems. We have attempted to apply their theory to the systems in this paper without success.

Water-rich Region (100–80% Water)

Consider the progressive addition of EO to water at lower temperatures. As pointed out earlier, there is probably a small concentration of unbonded O—H groups in pure water, so that H-bond formation may initially occur between these O—H groups and the oxygen atoms of the EO. However, bonding of these originally unbonded O—H groups disturbs the water–water H-bond equilibrium and causes more water to dissociate. In the absence of other effects the enthalpy change on adding EO to water would seem to be predictable by simple equilibrium constant theory, given values for the equilibrium constants and enthalpy changes for each of the relevant reactions. It is known that H-bonds between water molecules are stronger than those between water and ethers (2, 33, 34). At this point we must be clear about our meaning of the word strong. If we mean that the enthalpy of formation of a water–water H-bond is larger than that of a water–EO H-bond, then we cannot mean also that the equilibrium constant K_H for water–water H-bond formation is larger than K_E for water–EO H-bond formation, except in a limited temperature range (35). Accordingly, calculations have been made with K_H both larger and smaller than K_E, and for similar variations of ΔH_H and ΔH_E, the corresponding enthalpy changes for H-bond formation. We have found it impossible even to obtain the correct sign variation of $\Delta_m h$ with composition. The shortcoming of this calculation appears to lie in our use of concentrations rather than activities of the equilibrium species, but we are unaware of any method for determining the activities of the various H-bonded species.

The exothermal mixing of dilute nonelectrolytes with water can be described in qualitative terms as follows. On adding a small amount of EO to water some H-bonds are formed between unbonded O—H groups of water and EO. Other things being equal, some water–water H-bonds will dissociate. However, on adding EO to water we have changed the nature of the medium and we may in fact not dissociate any water–water H-bonds, or we may even form more or stronger water–water H-bonds (1, 2). This could arise if the activities of all species, both H-bonded and unbonded, were strongly composition dependent in this region. We know that the overall activity of EO and water does vary remarkably in this region (1, 2), but we can get no information on the individual H-bonded species.

As pointed out earlier, the reorientation of the H-bonded network around the solute species to give water H-bond angles nearer to the regular tetrahedral angles could occur and result in stronger and/or more H-bonds between water molecules (1, 2, 28, 29). The increase in strength or number of water–water H-bonds would readily account for the initial negative $\Delta_m h$ values found in this region. There is obviously a limit to the extent that reorientation effects are important although they are probably mainly responsible for the large negative excess entropies associated with this water-rich region. At higher EO levels the competition of the EO oxygen atoms forming H-bonds with the water protons will lead to the breakdown of the three-dimensionally H-bonded water network. Since the EO–water H-bond has a smaller enthalpy of formation than the water–water H-bond that it replaces, this breakdown of the water network will be accompanied by increases of enthalpy, which give rise to the enthalpy minima observed.

The concentration variation of $\Delta_m h$ for the D_2O–EO and H_2O–EO systems is closely similar so that our analysis above applies equally to the deuterium oxide system. The smoothed data given in Table 8[2] show that up to EO mole fraction 0.11 the $\Delta_m h$ values are negative and of greater magnitude with D_2O than with H_2O, implying greater strengthening of the three-dimensionally bonded network in the D_2O solutions, and/or stronger EO bonds with D_2O.

Intermediate Region (80–20% Water)

Once the minimum in enthalpy has been passed, $\Delta_m h$ changes almost linearly with composition while the EO mole fraction x_2 increases from 0.2 to 0.6. Since EO forms only one H-bond with water (1), we invisage this linear composition dependence as arising from the replacement of water–water H-bonds by EO–water H–bonds, so that at mole fraction 0.5, half of the EO is H-bonded to water, and the water molecules on the

Can. J. Chem. Downloaded from www.nrcresearchpress.com by 210.87.254.40 on 09/05/12
For personal use only.

average make three water–water H-bonds. This linear concentration dependence of the enthalpy of mixing of nonelectrolytes with water in this intermediate region is not confined to EO solutions, for example we have observed it with aqueous tetrahydrofuran (36), while others have shown it with aqueous dioxane (31) and acetone (37). Most recently Morcom and Smith (38) have furnished similar S-shaped enthalpy of mixing curves for other cyclic ethers with water.

A linear composition dependence of $\Delta_m h$ is also observed in the D_2O–EO system and the smoothed values given in Table 8 show that the $\Delta_m h$ values increase more rapidly for the D_2O solutions. This implies that the enthalpy difference between a D_2O bond with D_2O and a D_2O bond with EO is of greater magnitude than the corresponding difference for the H_2O–EO system. Thus the breakdown of the stronger bonds in the D_2O system leads to the larger endothermal enthalpies in this composition region.

Correlation of Enthalpy of Mixing with Water Proton Magnetic Resonance Chemical Shift

In aqueous EO solutions containing more than 0.5 mole fraction EO the large excess of unbonded basic oxygen atoms, that is unbonded oxide atoms or unbonded water lone pairs, reduces the fraction of unbonded water O—H groups to negligibly low levels. In this case we can say that all water protons are H-bonded either to EO oxygen atoms or to water lone pairs, so that the proton magnetic resonance (p.m.r.) chemical shift gives a direct measure of the water H-bonding to these two species. In this region we find that the enthalpy of mixing can be accurately related to the p.m.r. chemical shift.

In our earlier work (1) the water protons chemical shift ν at water mole fraction x_1 was interpreted as the resulting average for a fraction f_1 of water protons forming H-bonds with water lone pairs, and a fraction $(1 - f_1)$ forming H-bonds with EO. The extrapolated chemical shifts, $\nu_1 = 132.9$ Hz in pure water and $\nu_2 = -12.6$ Hz in pure EO, were taken as characteristic of water protons completely bonded to water lone pairs and to EO, respectively, so that the observed solution shift was given by the relation

$$[2] \qquad \nu = f_1\nu_1 + (1 - f_1)\nu_2$$

Thus, f_1, the fraction of water protons H-bonded to water lone pairs, was evaluated from each ν over the range of x_1. For ideal averaging f_1 would be identical with x_1, but for every solution measured f_1 was found to be greater than x_1, indicating that the water protons invariably formed more than the ideal fraction of H-bonds with water lone pairs and fewer than the ideal fraction with EO. This was to be expected since water H-bonds with water are on the average stronger, using p.m.r. chemical shift as criterion, than those to EO.

We define the standard molar enthalpy of pure liquid water as $H_{11}{}^0$ and the molar enthalpy for water in EO solution as, (*i*) H_{11} when H-bonded to two water lone pairs, (*ii*) H_{12} when H-bonded to two EO molecules, and (*iii*) $(H_{11} + H_{12})/2$ when H-bonded to one water and one EO molecule. For the molar enthalpy of mixing $\Delta_m h$ we obtain

$$[3] \quad \Delta_m h = x_1 f_1(H_{11} - H_{11}{}^0) + x_1(1 - f_1)(H_{12} - H_{11}{}^0)$$

where it is assumed that the enthalpy change arises predominantly from the change of H-bonding of the water, and that the enthalpy changes from other non-H-bonded interactions are included within the H-bonding terms. As the EO mole fraction $x_2 = (1 - x_1)$ tends to zero, so H_{11} should tend to $H_{11}{}^0$, so that the composition dependence of $H_{11} - H_{11}{}^0$ was taken as the simplest linear function

$$[4] \qquad H_{11} - H_{11}{}^0 = b_{11}(1 - x_1)$$

where the constant b_{11} is the molar enthalpy difference for water H-bonded to water between infinite dilution in EO and pure water. The composition dependence of $H_{12} - H_{11}{}^0$ was taken as the linear function

$$[5] \qquad H_{12} - H_{11}{}^0 = a_{12} + b_{12}(1 - x_1)$$

where a_{12} and b_{12} are constants and $(a_{12} + b_{12})$ is the molar enthalpy difference between water at infinite dilution H-bonded to EO and water H-bonded to water in the pure liquid. Substitution of [4] and [5] into [3] gives the three-parameter equation

$$[6] \quad \Delta_m h = x_1(1 - x_1)f_1 b_{11} + x_1(1 - f_1)a_{12} + x_1(1 - x_1)(1 - f_1)b_{12}$$

relating $\Delta_m h$ to x_1 and to the p.m.r. chemical shift through f_1.

TABLE 9. Comparison of $\Delta_m h$ for H_2O–EO at 10.75 °C with values from eq. 7

x_1	f_1	$\Delta_m h$(obs.) (J/mol)	$\Delta_m h$(calcd.) (J/mol)	$\delta(\Delta_m h)$
0.46726	0.7139	262.6	262.3	0.3
0.40111	0.6698	337.2	339.5	−2.3
0.34385	0.6256	404.9	400.3	4.6
0.28057	0.5659	456.7	456.4	0.2
0.20962	0.4787	485.2	492.6	−7.4
0.16763	0.4200	480.7	481.7	−1.1
0.13780	0.3688	465.0	459.8	5.2
0.08460	0.2526	376.7	373.2	3.5
0.03420	0.1147	192.3	196.3	−4.1
			$\sigma(\Delta_m h)$ =	4.4

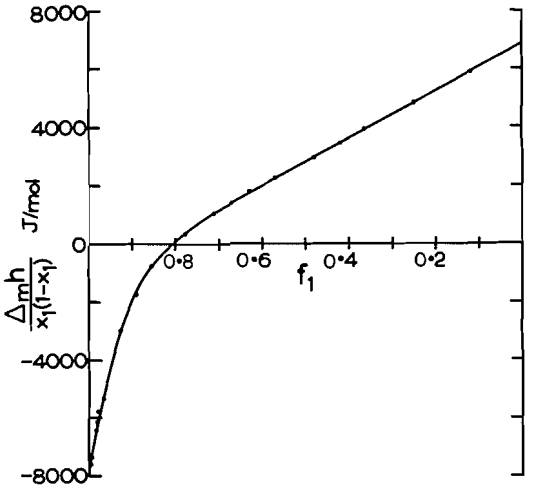

FIG. 2. Correlation of enthalpy of mixing with water proton magnetic resonance chemical shift for the H_2O–EO system at 10.75 °C. Enthalpy of mixing function $\Delta_m h/x_1(1 - x_1)$ variation with the fraction of water protons H-bonded to water, f_1, showing the linear region with $0.7 > f_1 > 0$.

For the systems H_2O–EO at 10.75 and 20.00 °C and D_2O–EO at 13.45 and 20.00 °C at EO mole fractions larger than 0.53, the endothermal $\Delta_m h$ values were fitted by [6] using the method of least squares, assuming constant enthalpy errors and error-free x_1 and f_1. The f_1 values were interpolated from the p.m.r. chemical shifts for the H_2O–EO system at 0 °C (1). The representation of the experimental $\Delta_m h$ by [6] showed that the value of a_{12} was not significantly different from zero. The least squares fits of the data were then redetermined using the two-parameter equation

$$[7]\quad \Delta_m h = x_1(1 - x_1)f_1 b_{11} + x_1(1 - x_1)(1 - f_1)b_{12}$$

Results for this curve-fitting are presented[2] in Tables 9–12, which include x_1, f_1, the experimental $\Delta_m h$(obs.) corrected to the tabulated temperature, the calculated $\Delta_m h$(calcd.) derived from [7], their difference $\delta(\Delta_m h)$, and $\sigma(\Delta_m h)$ the standard error on a single enthalpy determination assessed from the fit of [7].

A plot is shown in Fig. 2 of $\Delta_m h/x_1(1 - x_1)$ against f_1 for the H_2O–EO system at 10.75 °C, where the linear section obeying [7] is seen in the region $0 < f_1 < 0.7$, corresponding with $0 < x_1 < 0.46$. This corresponds with the region in which we previously suggested (1) that water formed one-dimensional H-bonded chains, which at higher water concentrations were further cross-linked to give two-dimensional H-bonded surfaces. At higher water mole fractions the experimental $\Delta_m h/x_1(1 - x_1)$ values become progressively more exothermal than predicted by [7]. In this region water forms three-dimensional H-bonded networks within which EO is included, causing orientation of the network around the solute as discussed earlier.

Tables 9–12[2] show the very good representations of $\Delta_m h$(obs.) by the two-parameter eq. 7, from which the $\sigma(\Delta_m h)$ values of between 2.8 and 4.4 J/mol are realistic estimates of the errors of measurement on $\Delta_m h$. In Table 12 the $\Delta_m h$ values shown in parentheses were not used to determine the least-squares fit of [7] because of their unreasonably large $\delta(\Delta_m h)$ values, which are also shown in parentheses: neglecting these two possibly erroneous measurements yields a reasonable $\sigma(\Delta_m h)$ value of 3.8 J/mol.

Rearrangement of eq. 7 gives

$$[8]\quad \Delta_m h/x_1(1 - x_1) = b_{12} + f_1(b_{11} - b_{12})$$

which defines b_{12} as the intercept when f_1 is zero and b_{11} as the intercept when f_1 is unity. The very

Can. J. Chem. Downloaded from www.nrcresearchpress.com by 210.87.254.40 on 09/05/12
For personal use only.

TABLE 13. Regression coefficients for eq. 7

System	Temperature (°C)	b_{11} (J/mol)	b_{12} (J/mol)
H_2O–C_2H_4O	10.75	−1282 ± 30	6881 ± 43
H_2O–C_2H_4O	20.00	−1107 ± 24	7140 ± 30
D_2O–C_2H_4O	13.45	−1148 ± 24	7323 ± 35
D_2O–C_2H_4O	20.00	−1054 ± 40	7518 ± 49

good fits of eq. 7 to the $\Delta_m h$ measurements, or the corresponding linearity of the plots of $\Delta_m h/x_1(1 - x_1)$ against f_1, suggests that the f_1 values for the systems H_2O–EO at 10.75 and 20.00 °C and D_2O–EO at 13.45 and 20.00 °C are directly proportional to those f_1 values derived from the proton chemical shifts of H_2O–EO at 0 °C. Since the b_{12} values are the intercepts at $f_1 = 0$, these values are unaffected by the fact that f_1 is determined from the chemical shifts measured at 0 °C. This is not the case for the b_{11} values, which may change in magnitude but probably not in sign if correct f_1 values replace those at 0 °C.

Table 13 presents the best b_{11} and b_{12} parameters and their standard errors, obtained from [7] for the measurements in Tables 9–12. The b_{12} values show that the molar transfer of pure water or deuterium oxide to infinite dilution in EO is attended by an enthalpy increase of about 7000 J/mol, which values become larger at higher temperature. This means that the two water H-bonds with EO are each some 3500 J/mol weaker, using enthalpy as a criterion, than the two water H-bonds to water in pure water. Further, the increase of the b_{12} values with temperature shows that the water H-bonds with EO weaken more rapidly at higher temperature than do those in liquid water.

The b_{12} values for the D_2O–EO system are significantly larger than those for H_2O–EO at the same temperature, the differences with standard errors are 366 ± 52 J/mol at 13.45 °C and 378 ± 58 at 20.00 °C: these differences at each temperature are the same within experimental error. On the assumption that EO bonds to D_2O at infinite dilution are not weaker than EO bonds to H_2O, we find that D-bonds in liquid D_2O are on a minimum estimate some 186 ± 55 J/mol stronger than H-bonds in liquid H_2O in the range 10–20 °C.

The negative b_{11} values of about −1100 J/mol for solutions with $0 < x_1 < 0.46$ indicate that water H-bonds to water in these EO solutions are on the average some 550 J/mol stronger, lower in enthalpy, than water H-bonds in pure water. The temperature coefficients of b_{11} show that this difference is reduced at higher temperatures. These negative values for b_{11} are consistent with the interpretation of the p.m.r. chemical shifts in terms of strongly bonded, unbranched water chains in solutions with $x_1 < 0.2$, as suggested earlier (1). This means that the water H-bonds to water along these one-dimensional chains are stronger, of lower enthalpy, than those in the three-dimensionally cross-linked water. We believe that the weaker water–water H-bonds in liquid water arise from the mutual repulsions between the pairs of like bonds at the four-coordinated water molecules, that is, from the mutual repulsions of the first bond with proton H_1 by the second bond with proton H_2, and

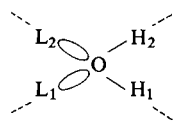

similarly from the mutual repulsions of the first bond with lone pair L_1 by the second bond with lone pair L_2. Whereas, for the one-dimensional water chains there is no second bond to L_2 and a weaker second bond to H_2 by EO, both of which lead to stronger bonds for lone pair L_1 and for proton H_1 with water along the chains. Similarly even stronger bonds are formed along the well-known alcohol polymer chains which have only the mutually enhancing bonding to H_1 and L_1 (34).

The b_{11} values for the D_2O–EO system are larger than for H_2O–EO by 83 ± 37 J/mol at 13.45 °C and by 53 ± 47 at 20.00 °C: both differences are just significant, arising by chance alone at the 4.5 and 30.8% probability levels, respectively. The differences at 13.45 and 20.00 °C are the same within experimental error.

We note a recent correlation between the water activity coefficient and p.m.r. chemical shift in the systems H_2O–1,4-dioxane and H_2O–acetone (39, 40).

Can. J. Chem. Downloaded from www.nrcresearchpress.com by 210.87.254.40 on 09/05/12
For personal use only.

This work was supported in part by a grant under the National Research Council of Canada Industrial Research Assistance Program, 1966.

1. D. N. GLEW, H. D. MAK, and N. S. RATH. Can. J. Chem. **45**, 3059 (1967).
2. D. N. GLEW, H. D. MAK, and N. S. RATH. *In* Hydrogen-bonded solvent systems. Taylor and Francis Ltd., London. 1968.
3. H. WATTS, E. C. W. CLARKE, and D. N. GLEW. Can. J. Chem. **46**, 815 (1968).
4. M. BERTHELOT. Ann. Chim. [5] **27**, 374 (1882).
5. L. BENJAMIN and G. C. BENSON. J. Phys. Chem. **67**, 858 (1963).
6. M. L. MCGLASHAN, K. W. MORCOM, and A. G. WILLIAMSON. Trans. Faraday Soc. **57**, 601 (1961).
7. TH. HOLLEMAN. Ph.D. Thesis. University of Amsterdam, Amsterdam, Holland. 1964.
8. H. KEHIAIAN. Bull. Acad. Polon. Sci. (Ser. Sci. Chim.) **12**, 567 (1964), and several references quoted therein.
9. K. SOSNKOWSKI-KEHIAIAN and H. KEHIAIAN. Bull. Acad. Sci. (Ser. Sci. Chim.) **13**, 659 (1965).
10. J. A. BARKER and F. SMITH. J. Chem. Phys. **22**, 375 (1954).
11. F. FRANKS and D. J. G. IVES. Quart. Rev. **20**, 1 (1966).
12. D. EISENBERG and W. KAUZMANN. The structure and properties of water. Clarendon Press, Oxford. 1969.
13. J. L. KAVANAU. Water and solute-water interactions. Holden-Day Inc., San Francisco. 1964.
14. J. S. ROWLINSON. Liquids and liquid mixtures. 2nd ed. Butterworths Scientific Publications, London. 1969.
15. O. MAASS and E. H. BOOMER. J. Am. Chem. Soc. **43**, 1709 (1922).
16. D. N. GLEW and N. S. RATH. J. Chem. Phys. **44**, 1710 (1966)
17. M. FALK and T. A. FORD. Can. J. Chem. **44**, 1699 (1966).
18. J. A. POPLE. Proc. Roy. Soc. London, Ser. A. **205**, 163 (1951).
19. G. BOLLA. Nuovo cimento, **9**, 290 (1932).
20. J. W. SCHULTZ and D. F. HORNIG. J. Phys. Chem. **65**, 2131 (1961).
21. G. E. WALRAFEN. J. Chem. Phys. **47**, 114 (1967).
22. W. K. THOMPSON, W. A. SENIOR, and B. A. PETHICA. Nature, **211**, 1086 (1966).
23. J. MORGAN and B. E. WARREN. J. Chem. Phys. **6**, 666 (1938).
24. A. H. NARTEN, M. D. DANFORD, and H. A. LEVY. Discuss. Faraday Soc. **43**, 97 (1967).
25. D. D. ELEY. Trans. Faraday Soc. **35**, 1281, 1421 (1939).
26. W. F. CLAUSSEN and M. F. POLGLASE. J. Am. Chem. Soc. **61**, 593 (1952).
27. D. N. GLEW and E. A. MOELWYN-HUGHES. Discuss. Faraday Soc. **15**, 150 (1953).
28. D. N. GLEW. J. Phys. Chem. **66**, 605 (1962).
29. D. N. GLEW, H. D. MAK, and N. S. RATH. Chem. Commun. 264 (1968).
30. A.-L. VIERK. Z. anorg. Chem. **261**, 283 (1950).
31. J. R. GOATES and R. J. SULLIVAN. J. Phys. Chem. **62**, 188 (1958).
32. J. ERVA. Suomen Kemistil. B**28**, 131 (1955).
33. E. M. ARNETT. *In* Progress in physical organic chemistry. Vol. 1. Interscience Publishers, New York. 1963.
34. D. N. GLEW and N. S. RATH. Can. J. Chem. **49**, 837 (1971).
35. M. L. MCGLASHAN, D. STUBLEY, and H. WATTS. J. Chem. Soc. A, 673 (1969).
36. D. N. GLEW and H. WATTS. Unpublished data.
37. A. T. KISTER and D. C. WALDMAN. J. Phys. Chem. **62**, 245 (1958).
38. K. W. MORCOM and R. W. SMITH. Trans. Faraday Soc. **66**, 1073 (1970).
39. W. KÖHLER, H.-J. BITTRICH, and R. RADEGLIA. J. Prakt. Chem. **311**, 643 (1969).
40. W. KÖHLER, H.-J. BITTRICH, and R. RADEGLIA. Z. Chem. **9**, 72 (1969).

Can. J. Chem. Downloaded from www.nrcresearchpress.com by 210.87.254.40 on 09/05/12
For personal use only.

Can. J. Chem. Downloaded from www.nrcresearchpress.com by 210.87.254.40 on 09/05/12
For personal use only.

Cycloaddition Reactions of Silyldiazoalkanes

A. G. Brook and Peter F. Jones
Lash Miller Chemical Laboratories, University of Toronto, Toronto 181, Ontario

Received November 23, 1970

The products of cycloaddition of silyldiazoalkanes with representative alkenes are described, together with their photolysis products. The photolysis of silyldiazoalkanes yields silylcarbenes which undergo typical reactions.

On décrit les produits obtenus lors de la cycloaddition de silyldiazoalcanes avec des alcènes représentatives; on a aussi déterminé la nature de leurs produits de photolyse. Par ailleurs la photolyse des silyldiazoalcanes fournit des silylcarbènes qui donnent des réactions typiques.

Canadian Journal of Chemistry, 49, 1841 (1971)

A variety of silyl- and germyldiazoalkanes is available from the decomposition of the lithium salts of acylmetalloid tosylhydrazones (1) and a preliminary account of the reactions of silylaryldiazoalkanes with acids has been presented (2). The results are reported here of 1,3-cycloaddition reactions of representative silyldiazoalkanes with suitable alkenes, and of their conversions to carbenes.

The reaction of 1-triphenylsilyl-1-diazoethane (**1**) with methyl vinyl ketone led to the initial formation of a 1-pyrazoline, **2** (eq. 1). However, on attempted purification of **2**, partial isomerization occurred to the corresponding 2-pyrazoline, **3**. Complete rearrangement to the conjugated isomer was effected by the use of pyridine as catalyst. Similar results have been reported by Seyferth *et al.* for the reactions of trimethylsilyldiazomethane with acrylonitrile (3). Reaction of **1** with methyl acrylate (R = CO_2Me) also gave a 1-pyrazoline, **4**, which did not isomerize spontaneously. The geometries described for these and other cases to follow have not been unequivocally established, but because of the great bulk of the triphenylsilyl group, it appears probable that the methyl and R groups will be in a *cisoid* relationship. No evidence was noted for mixtures of stereoisomers in any case.

The identity of the two 1-pyrazoline adducts was clearly established from their n.m.r. spectra. The signal from the single proton at C-3, the X component of an ABX system, was found as a doublet of doublets in both compounds, while the complex AB signal due to the non-equivalent methylene hydrogens at C-4 was extremely broad, extending in both cases over 1 p.p.m. Such large chemical shift differences for geminal protons are characteristic of 1-pyrazolines, whose C-4 methylene protons experience unequal anisotropic effects from the π electrons in the azo linkage due to the puckered pyrazoline ring but to speculate on possible conformations or geometries based on differential shielding effects is unwise in the presence of the very bulky anisotropic triphenylsilyl group (4). Both reactions showed the expected direction of addition, involving bond formation between the nucleophilic α-diazo carbon atom and the electrophilic β-carbon atom of the α,β-unsaturated compound (5).

Attention was next turned to more highly substituted alkenes. Although diethyl fumarate was more reactive than diethyl maleate toward **1**, both reacted very sluggishly giving complex mixtures of products and hence the reactions of **1** with the isomeric pair of esters were found to be of no synthetic utility. However **1** reacted readily with maleic anhydride (**5**, R = H) to give the 1-pyrazoline, **6**, in good yield, and with citraconic anhydride, (**5**, R = Me) to give the 1-pyrazoline adduct, **7** (eq. 2). In the latter case reaction occurred more slowly than with maleic anhydride (several days instead of a matter of hours), and the direc-

[1] Ph_3SiCN_2Me (**1**) + 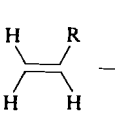 → 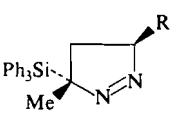 → 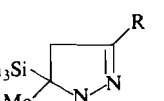

2 R = COMe
4 R = CO_2Me

3 R = COMe

[2] 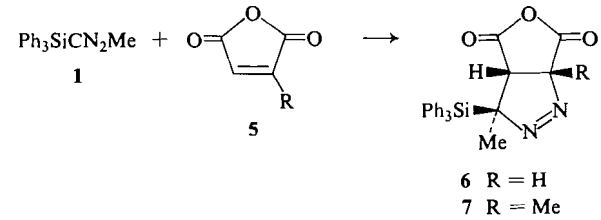

[3] 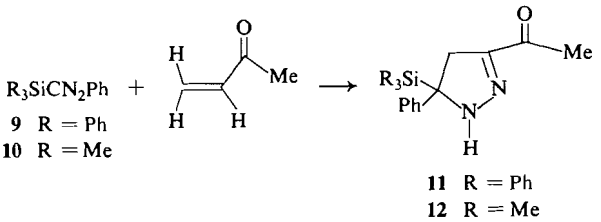

tion of addition occurred to give the less sterically hindered of the two possible products. The direction of addition of diazoalkanes to alkenes is known to be highly subject to steric factors and the mode of addition expected from electronic effects is frequently reversed under such circumstances (5). The structure of **7** was demonstrated by comparison of its n.m.r. spectrum, which contained a one proton singlet at δ 3.25 p.p.m. assigned to the hydrogen at C-4, with that of the corresponding maleic anhydride adduct, **5**, which showed two doublets, J = 10 Hz, at δ 4.88 and 3.62 p.p.m. The low field doublet is due to the hydrogen at C-3, which is deshielded by both the adjacent carbonyl and azo groups (4). The stereochemistry of **5** and **7** has not been rigorously established but a *cis* ring juncture with the bulky triphenylsilyl group *trans* to the anhydride ring appears from models to be the only reasonable geometry.

In all of the cases studied, it was possible to isolate the 1-pyrazoline adduct although all the compounds prepared, with the exception of the adduct **7** from citraconic anhydride, contain a hydrogen atom at C-3 activated by an adjacent electron-withdrawing substituent and are therefore capable of isomerizing to the corresponding conjugated 2-pyrazolines. It is not uncommon in diazo cycloadditions for the conjugated 2-isomers to be obtained (5) directly and reports of stable 1-pyrazolines of this type are rare (6).

The u.v. spectra of the silyl-1-pyrazolines were examined and the position of this long wavelength n-π* transition of the azo group was found to occur, like other 1-pyrazoline (4, 7, 8), in the region of 320–330 mm. These results indicate little interaction between the silyl group and the distant azo linkage, in contrast to the marked spectral changes that occur when silyl groups are attached directly to an azo group (9).

The reactions of two aryldiazomethanes, phenyltriphenylsilyldiazomethane (**9**) and its trimethylsilyl analogue, **10**, with methyl vinyl ketone have also been studied (eq. 3). The triphenylsilyl compound, **9**, exhibited low reactivity, complete reaction to give the 2-pyrazoline, **11**, requiring in excess of 1 month at room temperature. Since the corresponding reaction of **1** with methyl vinyl ketone was complete in a matter of hours it can be seen that replacement of a methyl by a phenyl group at the α-diazo carbon atom causes a large decrease in the reactivity of the silyldiazoalkane. This result is probably due both to stabilization of the diazo compound by mesomeric delocalization into the aromatic ring (10), and to steric effects. The sluggish reactivity of the triarylsilylaryldiazoalkanes towards methyl vinyl ketone, a fairly good dipolarophile, suggests that as a class they possess limited synthetic utility as dipolar cycloaddition reagents under mild conditions.

Phenyltrimethylsilyldiazomethane (**10**) was found to be much more reactive, since reaction with methyl vinyl ketone was complete over 16 h. The 2-pyrazoline, **12**, was the reaction product. Since the two silyldiazoalkanes appear to show similar ground state stabilities (1), the difference in their dipolar cycloaddition reactivity must be due largely to steric factors. The triphenylsilyl group should have a far larger spatial bulk than a trimethylsilyl group. Again, the direction of addition of both silylaryldiazoalkanes to methyl vinyl ketone was that expected on electronic grounds (5).

Since the photolysis of 1-pyrazolines is an ex-

Can. J. Chem. Downloaded from www.nrcresearchpress.com by 210.87.254.40 on 09/05/12
For personal use only.

Can. J. Chem. Downloaded from www.nrcresearchpress.com by 210.87.254.40 on 09/05/12
For personal use only.

[4] 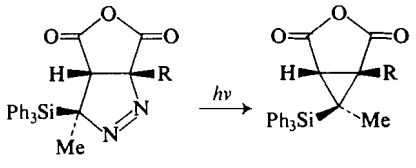

5 R = H
7 R = Me

13 R = H
14 R = Me

[5] 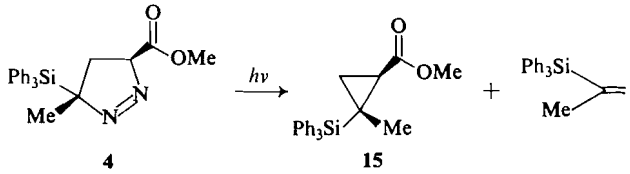

4 **15**

[6] 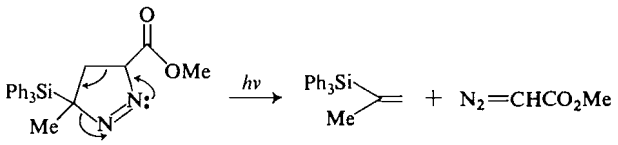

[7] $Ph_3SiCN_2Me \xrightarrow[Et_2O]{h\nu} Ph_3Si\ddot{C}Me \longrightarrow Ph_3SiCH{=}CH_2$

[8] $Ph_3SiCN_2CH_2Ph \xrightarrow[Et_2O]{h\nu} Ph_3Si\ddot{C}CH_2Ph \longrightarrow Ph_3SiCH{=}CHPh$

16 **17**

cellent method for the synthesis of cyclopropanes (7, 11–13), the photolyses of the stable silyl-1-pyrazolines obtained from **1** were examined as possible routes to silylcyclopropanes. Both **5** and **7**, the adducts from maleic and citraconic anhydrides, gave the corresponding cyclopropanes, **13** and **14**, in good yields as the sole isolated product in each case (eq. 4). No evidence was observed for isomeric products. However, the adduct **4** from methyl acrylate gave a mixture of 2-triphenylsilylpropene (13%) and the cyclopropane **15** (35%) (eq. 5) which, like **13** and **14**, is presumed to have *cis* carbonyl and methyl groups to minimize steric crowding. As has been found with other 1-pyrazolines (7), the silylalkene probably arose by elimination of diazoacetic ester, through reversal of the cycloaddition reactions by an alternative pathway (eq. 6).

Finally, a limited investigation of the conversion of silyldiazoalkanes to silylcarbenes was made, mainly using photochemical methods. 1-Triphenylsilyl-1-diazoethane was slowly converted to vinyltriphenylsilane in reflexing toluene in moderate yield. It smoothly underwent the same transformation when irradiated in ether at room temperature (eq. 7). Similarly, diazoalkane **16** gave a mixture of the isomeric triphenylsilylstyrenes **17**, with the *trans* product (54% yield) predominating over the *cis* compound (21%) as anticipated (eq. 8). Photolysis of phenyltriphenylsilyldiazomethane in methanol gave α-methoxylbenzyltriphenylsilane **18**, as expected from carbene insertion into an O—H bond, and thermolysis of the same compound in dimethylsulfoxide, a reagent known to be capable of oxidizing carbenes (14), gave benzoyltriphenylsilane **19** (see Scheme 1).

From the results described, it is evident that the silyldiazoalkanes undergo cycloaddition reac-

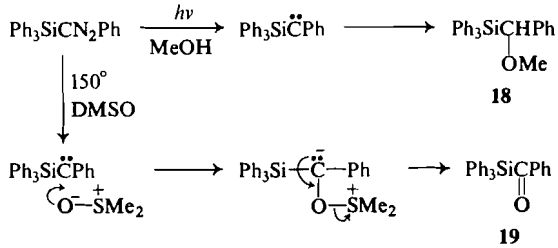

18 **19**

SCHEME 1

Can. J. Chem. Downloaded from www.nrcresearchpress.com by 210.87.254.40 on 09/05/12
For personal use only.

tions typical of diazoalkenes, although they are generally more stable and less reactive than their carbon analogs. The behavior of the silylcarbenes derived from their photolysis is unexceptional, although studies in progress on cyclopropane formation have been found to be very unclean reactions.

Experimental

Diethyl ether was dried over sodium metal and was distilled immediately prior to use. Photolyses of 1-pyrazolines were carried out in Pyrex glassware irradiated by a Hanovia high-pressure mercury arc. The n.m.r. spectra were measured on Varian A60, A56/60, or T60 spectrometers, using TMS as an internal standard. The i.r. spectra were taken on a Perkin–Elmer Model 237B with polystyrene calibration. The u.v. spectra were run on a Unicam SP800 spectrometer and were calibrated by means of a Holmium filter. Mass spectra were recorded using an AEI MS-902 instrument. Melting points were taken on a Fisher–Johns hot stage and are uncorrected. Microanalyses were performed by A. B. Gygli, Toronto, Ontario.

The Reaction of 1-Triphenylsilyl-1-diazoethane with Methyl Vinyl Ketone

To a solution of 1.0 g (0.00318 mol) of 1-triphenylsilyl-1-diazoethane in 50 ml of anhydrous ether was added an excess, 2 ml, of methyl vinyl ketone. The reaction flask was stoppered and allowed to stand in the dark at room temperature. After 2 h the mixture had decolorized and the solvent was evaporated to give a thick oil, whose spectra indicated the exclusive formation of a 1-pyrazoline. The i.r. spectrum (CCl_4 solution) showed a strong carbonyl band at 5.80 μ (non-conjugated ketone), with strong Si—Ph bands at 7.0 and 9.0 μ. There was no NH stretching band in the region of 3 μ. The n.m.r. spectrum confirmed the structure of the adduct as 3-acetyl-5-methyl-5-triphenylsilyl-1-pyrazoline by signals at δ ($CDCl_3$), 7.8–7.2 (multiplet, 15H, Si*Ph*), 4.47(1H, doublet of doublets, $J_{AX} = 9$, $J_{BX} = 11$ Hz, C*H*COMe), 2.43(3H, s, CO*Me*), 2.20–1.25(2H, multiplet, ring CH_2), 1.66(3H, singlet superimposed on above multiplet, SiC*Me*) p.p.m.

The oil was crystallized from benzene–hexane to give 1.1 g (90%) of adduct, m.p. 50–65°. However, an i.r. spectrum showed by the appearance of a conjugated carbonyl band at 5.98 μ the formation of some of the isomeric 2-pyrazoline. In a previous experiment, it had also been found that the 1-pyrazoline was slowly converted to the conjugated 2-isomer on repeated recrystallization from methanol. It was therefore decided to isolate the reaction product as the 2-isomer. Isomerization was carried out by adding 5 drops of pyridine to a methanol solution of the above product and allowing the reaction mixture to stand for 24 h. A white solid obtained on evaporation gave, on recrystallization from benzene–pentane, 0.47 g (39%) of 3-acetyl-5-methyl-5-triphenylsilyl-2-pyrazoline, m.p. 184–186°. The analytical sample had m.p. 185–186°.

Anal. Calcd. for $C_{24}H_{24}N_2OSi$: C, 74.98; H, 6.29; N, 7.29. Found: C, 74.44; H, 6.28; N, 7.26.

The n.m.r. spectrum: δ($CDCl_3$), 7.7–7.3(multiplet, 15H, Si*Ph*), 6.0(broad s, 1H, N*H*), 3.04(AB q, J_{AB} = 17 Hz, 2H, ring CH_2), 2.36(s, 3H, CO*Me*), 1.20(s, 3H, SiC*Me*) p.p.m. The i.r. spectrum: λ_{max}(CCl_4), 2.93(w), 3.23(w), 3.36(w), 5.98(s), 6.73(w), 7.00(m), 7.18(m), 7.48(w), 8.00(w), 8.42(w), 9.00(s), 9.25(w), 10.65(w), 11.50(w), 14.35(s) μ.

The Reaction of 1-Triphenylsilyl-1-diazoethane with Methyl Acrylate

To a solution of 1.50 g (0.00478 mol) of 1-triphenylsilyl-1-diazoethane in 50 ml of anhydrous ether was added an excess, ~2 ml, of methyl acrylate. The reaction flask was stoppered and allowed to sit in the dark. After 4 h the mixture had decolorized and the solvent was evaporated to give a clear glass. Crystallization from dichloromethane–hexane gave 1.53 g (80%) of 3-carbomethoxy-5-methyl-5-triphenylsilyl-1-pyrazoline, m.p. 130–133°. Several recrystallizations from dichloromethane–hexane gave the analytical sample, m.p. 135–137°.

Anal. Calcd. for $C_{24}H_{24}N_2O_2Si$: C, 71.97; H, 6.04; N, 7.00. Found: C, 71.90; H, 6.13; N, 6.90.

The n.m.r. spectrum: δ(CCl_4), 7.7–7.2(multiplet, 15H, Si*Ph*), 4.28(doublet of doublets, $J_{AX} = 9$, $J_{BX} = 11$ Hz, 1H, C*H*CO_2Me), 3.68(s, 3H, COO*Me*), 2.5–1.5(multiplet, 2H, ring CH_2), 1.71(singlet superimposed on above multiplet, 3H, SiC*Me*) p.p.m. The i.r. spectrum: λ_{max} (CCl_4), 3.26(m), 3.27(m), 3.3(w), 3.38(m), 3.41(w), 3.48(w), 5.73(s), 6.73(w), 6.90(m), 7.00(s), 7.28(w), 7.43(m), 7.90(m), 8.16(m), 8.38(m), 8.54(m), 9.00(s), 9.50(m), 11.32(m), 14.32(s) μ. The u.v. spectrum: λ_{max} (C_6H_{12}), 327(340), 273(1100), 266(1390), 261(1260), 255(s; 1180), 211(s; 26 800), 214(30 000) mμ.

The Reactions of 1-Triphenylsilyl-1-diazoethane with Dimethyl Fumarate and Dimethyl Maleate

(*a*) A solution of 0.63 g (0.022 mol) of the diazoalkane and 0.29 g (0.002 mol) of dimethyl fumarate in 50 ml of anhydrous ether was allowed to stand in the dark at room temperature. The mixture had decolorized after 16 days. Evaporation gave an oil which on crystallization from dichloromethane–hexane gave a partially solid oil. An n.m.r. spectrum indicated that an extremely complex mixture of products had been formed and no further purification was attempted.

(*b*) A similar complex mixture was obtained from a reaction with dimethyl maleate, using identical quantities to the above. In this case decolorization occurred only after 44 days.

The Reaction of 1-Triphenylsilyl-1-diazoethane with Maleic Anhydride

To a solution of 1.50 g (0.00478 mol) of 1-triphenylsilyl-1-diazoethane in 50 ml of anhydrous ether was added 0.45 g (0.00460 mol) of maleic anhydride. The mixture decolorized after standing in the dark for 15 min, with the formation of a white crystalline precipitate. Evaporation of the solvent gave a white solid, which was recrystallized from dichloromethane–hexane to give 1.64 g (86%) of 5-methyl-5-triphenylsilyl-1-pyrazoline-3,4-dicarboxylic acid anhydride, m.p. 152–154° (dec.).

Anal. Calcd. for $C_{24}H_{20}N_2O_3Si$: C, 69.90; H, 4.89; N, 6.79. Found: C, 70.18; H, 5.14; N, 6.76.

The n.m.r. spectrum: δ($CDCl_3$), 7.7–7.2(multiplet, 15H, aromatic), 4.88(d, J = 10 Hz, 1H, N=N—C*H*CO),

Can. J. Chem. Downloaded from www.nrcresearchpress.com by 210.87.254.40 on 09/05/12
For personal use only.

3.62(d, J = 10 Hz, 1H, CHC*H*CO), 1.85(s, 3H, SiC*Me*) p.p.m. The i.r. spectrum: λ_{max}(CCl_4), 3.24(w), 3.25(w), 3.32(w), 3.35(w), 5.33(m), 5.57(s), 7.00(m), 8.22(m), 9.00(s), 9.37(m), 9.60(w), 10.78(w), 10.91(s), 12.40(s), 13.90(s) μ. The u.v. spectrum: λ_{max}(C_6H_{12}), 326(289), 273(965), 266(1270), 260(1375), 251(s, 1575), 220(s, 21 000), 210(s, 27 000) mμ.

The Reaction of 1-Triphenylsilyl-1-diazoethane with Citraconic Anhydride

To a solution of 0.56 g (0.0050 mol) of citraconic anhydride in 50 ml of anhydrous ether was added 1.50 g (0.00478 mol) of 1-triphenylsilyl-1-diazoethane. The reaction flask was stoppered and allowed to stand in the dark. After 4 days the mixture had decolorized and white crystals had precipitated. These were filtered off and washed with anhydrous pentane to give 1.85 g (91%) of 3,5-dimethyl-5-triphenylsilyl-1-pyrazoline-3,4-dicarboxylic acid anhydride, m.p. 165–167° (dec.). Recrystallization from dichloromethane–hexane raised the m.p. to 167–168° (dec.).

Anal. Calcd. for $C_{25}H_{22}N_2O_3Si$: C, 70.39; H, 5.20; N, 6.57. Found: C, 70.32; H, 5.34; N, 6.57.

The n.m.r. spectrum: δ($CDCl_4$), 7.8–7.1(multiplet, 15H, aromatic), 3.25(s, 1H, CMeC*H*CO), 1.76(s, 3H, SiC*Me*), 0.87(s, 3H, N=N–C*Me*CO) p.p.m. The i.r. spectrum: λ_{max}(CCl_4), 3.25(w, 5.35(m), 5.58(s), 7.00(m), 8.28(m), 9.00(m), 9.88(m), 10.84(m), 14.34(m) μ. The u.v. spectrum: λ_{max}(C_6H_{12}), 330(257), 273(1110), 266(1325), 260(1470), 255(s, 1580), 249(s, 1920), 225(s, 11 700), 206(18 600) mμ.

The Reaction of Phenyltriphenylsilyldiazomethane with Methyl Vinyl Ketone

To a solution of 0.30 g (0.0008 mol) of phenyltriphenylsilyldiazomethane in 50 ml of anhydrous ether was added excess, ~2 ml, of methyl vinyl ketone. The reaction flask was stoppered and was allowed to sit in the dark at room temperature. After 35 days the mixture had decolorized. Following evaporation and crystallization from hexane–benzene there was obtained 0.24 g (66%) of impure 3-acetyl-5-triphenylsilyl-5-phenyl-2-pyrazoline, m.p. 153–163°. The impurity, present to the extent of ~10%, appeared from the n.m.r. spectrum to be 3(5)-acetyl-5(3)-phenylpyrazole, as found in a later experiment with the analogous trimethylsilyldiazo compound. Several recrystallizations from hexane–benzene and hexane–dichloromethane failed to remove this impurity. Finally, recrystallization from methanol gave 0.06 g (17%) of pure 2-pyrazoline, m.p. 170–175° (dec.).

Anal. Calcd. for $C_{29}H_{26}N_2OSi$: C, 78.00; H, 5.87; N, 6.28. Found: C, 78.02; H, 5.86; N, 6.04.

The n.m.r. spectrum: δ($CDCl_3$), 7.6–6.7(multiplet, 15H, aromatic), 3.56(AB q, J_{AB} = 17 Hz, 2H, ring CH_2), 2.34(s, 3H, CO*Me*) p.p.m. The i.r. spectrum: λ_{max}(CCl_4), 2.90(w), 3.25(m), 5.98(s), 6.90(w), 7.00(m), 7.17(m), 7.47(w), 8.03(w), 8.40(w), 9.02(s), 9.66(m), 10.02(w), 10.22(w), 10.58(w), 14.32(s), 14.82(m) μ.

The Reaction of Phenyltrimethylsilyldiazomethane with Methyl Vinyl Ketone

To a solution of 4.10 g of impure diazoalkane, estimated by n.m.r. spectroscopy to contain 3.0 g (0.0158 mol) of phenyltrimethylsilyldiazomethane, in 100 ml of anhydrous ether was added an excess, 4.0 ml, of methyl vinyl ketone. The reaction flask was stoppered and the mixture was allowed to stand overnight in the dark. After 16 h a colorless solution was obtained which on shaking deposited white crystals. These were filtered off to give 3.32 g (81%) of 3-acetyl-5-trimethylsilyl-5-phenyl-2-pyrazoline, m.p. 140–150°. The i.r. spectrum of a solution in chloroform showed the appropriate bands at 2.49 (NH) and 6.02 μ (conjugated ketone), while the n.m.r. spectrum ($CDCl_3$) had signals at δ 7.5–7.0(multiplet, 5H, aromatic), 3.33(s, 2H, ring CH_2), 2.40(s, 3H, CO*Me*), and 0.03(s, 9H, Si*Me*) p.p.m. (external TMS). The n.m.r. spectrum also showed the presence of ~5% of an impurity, later shown to be 3(5)-acetyl-5(3)-phenylpyrazole. The pyrazoline could not be obtained pure, therefore no elemental analyses were attempted. However, the mass spectrum of the initial crude pyrazoline showed a molecular ion at *m/e* 260 (calculated for $C_{14}H_{20}N_2OSi$, 260).

Attempted purification by recrystallization from benzene–pentane led to extensive decomposition, as shown in the n.m.r. spectrum of the products by the removal of the Si*Me* signal and the increase in the signals due to the pyrazole. A 0.3 g sample of the initial crude pyrazoline was dissolved in benzene and the solution was allowed to stand at room temperature for a nominal period of 10 days. The solvent was evaporated to give 0.20 g (93%) of 3(5)-acetyl-5(3)-phenylpyrazole, m.p. 152–154° (lit. (15) 154°). The pyrazole (chloroform solution) showed bands in the i.r. spectrum at 2.90 (NH) and 5.94 μ (conjugated ketone). The n.m.r. spectrum showed signals at δ($CDCl_3$), 7.9–7.2(multiplet, 5H, aromatic), 7.05(singlet, 1H, vinylic H), and 2.61(singlet, 3H, CO*Me*) p.p.m. The molecular formula was confirmed using high-resolution mass spectrometry by the appearance of a molecular ion at 186.0789 (calcd. for $C_{11}H_{10}N_2O$, 186.07931).

Photolyses of 5-Silyl-1-pyrazolines

The Photolysis of 3-Carbomethoxy-5-methyl-5-triphenylsilyl-1-pyrazoline

A solution of 1.23 g (0.00308 mol) of the pyrazoline in 75 ml of anhydrous ether was photolyzed. After 24 h, reaction, as shown by n.m.r. spectroscopy, appeared to be complete. The solvent was evaporated to give a clear glass which was chromatographed on silica gel. Elution with carbon tetrachloride gave a solid which, in recrystallization from methanol, yielded 0.12 g (13%) of 2-triphenylsilylpropene, m.p. 101–102°. A mixed m.p. with an authentic sample (16) was undepressed. Further elution with 1:1 carbon tetrachloride – benzene gave a series of clear oils. Spectral examination indicated a mixture of the desired cyclopropane together with unsaturated esters. Crystallization from methanol gave 0.4 g (35%) of 1-triphenylsilyl-1-methyl-2-carbomethoxycyclopropane, m.p. 90–93°. Several recrystallizations from methanol gave the analytical sample, m.p. 98–99°.

Anal. Calcd. for $C_{24}H_{24}O_2Si$: C, 77.39; H, 6.49. Found: C, 77.21; H, 6.42.

The n.m.r. spectrum: δ($CDCl_3$), 7.7–7.2(multiplet, 15H, Si*Ph*), 3.68(s, 3H, CO_2*Me*),1.59(doublet of doublets, 1H, J_{AX} + J_{AB} = 13 Hz, C*H*CO), 1.4–0.8(multiplet, 2H, cyclopropyl CH_2), 1.31(singlet superimposed on above multiplet, 3H, SiC*Me*) p.p.m. The i.r. spectrum: λ_{max} (CCl_4), 3.25(m), 3.30(m), 3.40(m), 3.50(w), 5.75(s), 6.73(w), 6.94(m), 7.00(m), 7.22(m), 7.50(w), 7.63(w), 8.05(w), 8.28(m), 8.38(m), 8.52(s), 9.00(s), 9.28(w),

Can. J. Chem. Downloaded from www.nrcresearchpress.com by 210.87.254.40 on 09/05/12
For personal use only.

9.42(w), 9.70(w), 10.02(w), 10.60(w), 11.51(m), 14.32(s), 14.64(w) μ.

The methanol filtrate was evaporated to give a trace of an oil, whose n.m.r. spectrum showed it was a complex mixture of unsaturated esters. The oil was not examined further.

The Photolysis of 3,5-Dimethyl-5-triphenylsilyl-1-pyrazoline-3,4-dicarboxylic Acid Anhydride

A solution of 1.37 g (0.00333 mol) of the pyrazoline in an anhydrous solvent mixture of 50 ml of ether and 60 ml of dichloromethane was photolyzed. The course of the reaction was monitored by examination of the n.m.r. spectra of aliquots removed at various intervals. After 6 h, ~66% of the starting material was present, being reduced to ~33% after 18 h. After 30 h, ~10% of the pyrazoline remained, while reaction appeared to be complete after 38 h. Evaporation of the reaction mixture gave an aerated solid which, on recrystallization from dichloromethane–hexane, gave 0.85 g (67%) of 1,2-dimethyl-1-triphenylsilylcyclopropane-2,3-dicarboxylic acid anhydride, m.p. 195–197°. The n.m.r. spectrum of the crude reaction mixture had indicated that this cyclopropane was the sole reaction product. The analytical sample, from dichloromethane–hexane, had m.p. 196–198°.

Anal. Calcd. for $C_{25}H_{22}O_3Si$: C, 75.34; H, 5.56. Found: C, 75.30; H, 5.76.

The n.m.r. spectrum: δ($CDCl_3$), 7.8–7.3(multiplet, 15H, aromatic), 2.94(s, 1H, C*H*CO), 1.40(s, 3H, SiC*Me*), 1.35(s, 3H, *Me*CCO) p.p.m. The i.r. spectrum: λ_{max} (CCl_4), 3.25(w), 5.40(m), 5.62(s), 7.00(m), 7.90(m), 8.32(m), 9.00(m), 10.00(m), 10.22(w), 10.45(w), 10.98(s), 14.23(s) μ.

The Photolysis of 5-Methyl-5-triphenylsilyl-1-pyrazoline-3,4-dicarboxylic Acid Anhydride

A solution of 1.05 g(0.00246 mol) of the pyrazoline in an anhydrous solvent mixture of 50 ml of ether and 50 ml of dichloromethane was photolyzed. The course of the reaction was monitored by examination of the n.m.r. spectra of aliquots removed at various intervals. After 5 h, ~70% of the starting pyrazoline was present, being reduced to ~50% after 11 h. After 23 h, ~15% of the pyrazoline remained, while reaction appeared to be complete after 35 h. Evaporation of the reaction mixture gave a cream colored solid which was recrystallized from dichloromethane–hexane to give 0.70 g (72%) of 1-methyl-1-triphenylsilylcyclopropane-2,3-dicarboxylic acid anhydride, m.p. 165–175°. The n.m.r. spectrum of the crude reaction mixture indicated that this cyclopropane was the sole reaction product. The analytical sample, from dichloromethane–hexane, had m.p. 175–180°. A sharply melting sample could not be obtained despite repeated recrystallization.

Anal. Calcd. for $C_{24}H_{20}O_3Si$: C, 74.99, H, 5.24. Found: C, 75.04, H, 5.29.

The n.m.r. spectrum: δ($CDCl_3$), 7.8–7.2(multiplet, 15H, aromatic), 2.66(s, 2H, C*H*CO), 1.48(s, 3H, SiC*Me*) p.p.m. The i.r. spectrum: λ_{max}(CCl_4), 3.25(m), 5.39(s), 5.61(s), 6.75(w), 7.00(m), 7.25(w), 7.50(w), 7.60(w), 8.10(m), 8.40(w), 8.60(w), 9.02(s), 10.20(w), 10.49(m), 11.00(s), 11.60(m), 14.40(s), 14.80(m), 15.25(m) μ.

Attempted Cycloaddition of 1-Triphenylsilyl-1-diazoethane with Diphenylacetylene

A mixture of 0.60 g (0.00191 mol) of 1-triphenylsilyl-1-diazoethane and 0.34 g (0.00192 mol) of diphenylacetylene was dissolved in 50 ml of anhydrous ether to give a yellow solution. No fading of the color was observed after the mixture had stood in the dark for 48 h at room temperature, or after 16 h refluxing in ether or 48 h reflux in benzene. The benzene solvent was evaporated and replaced with 50 ml of anhydrous toluene and after heating under reflux for 48 h, the mixture had decolorized. Evaporation gave a thick, colorless oil. An n.m.r. spectrum indicated vinyltriphenylsilane to be the sole product derived from the diazoalkane since no C—*Me* singlets were present. The oil was chromatographed on silica gel. Elution with 60–70° petrol gave a total of 0.20 g (59%) of recovered diphenylacetylene, m.p. 55–60°. Recrystallization from ethanol raised the m.p. to 61–65°. A mixed m.p. with diphenylacetylene was undepressed. Further elution with carbon tetrachloride gave a total of 0.20 g (37%) of vinyltriphenylsilane, m.p. 63–66°. A mixed m.p. with an authentic sample (17) was undepressed.

The Photolysis of 1-Triphenylsilyl-1-diazoethane in Ether

A yellow solution of 0.90 g (0.00286 mol) of 1-triphenylsilyl-1-diazoethane in 75 ml of anhydrous ether was photolyzed under nitrogen using a long wavelength "Blak-Ray" lamp. The solution had decolorized after a total of 6 h of illumination. Evaporation gave an oil, which was chromatographed on silica gel. Elution with carbon tetrachloride gave a total of 0.45 g (55%) of vinyltriphenylsilane, m.p. 65–68° on recrystallization from ethanol. A mixed m.p. with an authentic sample was undepressed.

The Photolysis of 1-Triphenylsilyl-2-phenyl-1-diazoethane in Ether

A yellow solution of 0.26 g (0.00067 mol) of 1-triphenylsilyl-2-phenyl-1-diazoethane in 50 ml of anhydrous ether was photolyzed under nitrogen using a long wavelength "Blak-Ray" lamp. The solution had decolorized after 4 h. Evaporation gave an oil, whose n.m.r. spectrum showed the presence of the alkene protons due to *cis*- and *trans*-β-triphenylsilylstyrene. No signals due to α-triphenylsilylstyrene could be observed. Crystallization from hexane gave 0.13 g (54%) of *trans*-β-triphenylsilylstyrene, m.p. 141–144°. Further recrystallization from methanol raised the m.p. to 148–150°. A mixed m.p. with an authentic (18) sample was undepressed.

Evaporation of the initial mother liquor gave an oil. Crystallization from methanol gave 0.05 g (21%) of *cis*-β-triphenylsilylstyrene, m.p. 90–94°. A mixed m.p. with an authentic sample (19) was undepressed.

The Pyrolysis of Phenyltriphenylsilyldiazomethane in Dimethyl Sulfoxide

A 0.10 g (0.000266 mol) sample of phenyltriphenylsilyldiazomethane was heated in 5 ml of dimethyl sulfoxide for 10 min at 150°. The mixture was poured into ether and was washed several times with water. The organic layer was dried over magnesium sulfate and the solvent was evaporated to give a yellow oil, whose i.r. spectrum showed the complete removal of the strong diazo band. Crystallization from ethanol gave 0.025 g (27%) of benzoyltriphenylsilane, m.p. 102–104°.

When a similar pyrolysis had been carried out on a 0.50 g (0.00133 mol) sample of the diazoalkane in 10 ml of dimethyl sulfoxide for 10 min at 130°, the diazoalkane

was recovered intact. No trace of benzoyltriphenylsilane could be detected in the i.r. spectrum.

The Photolysis of Phenyltriphenylsilyldiazomethane in Methanol

A solution of 0.50 g (0.00133 mol) of the diazoalkane in 50 ml of methanol and 15 ml of benzene (to effect solution) was photolyzed under nitrogen using a long wavelength "Blak-Ray" lamp. The solution decolorized after 1 h. Evaporation gave a solid, whose n.m.r. spectrum indicated the formation of α-methoxybenzyltriphenylsilane and triphenylmethoxysilane in the ratio of 75:25. The mixture was chromatographed on silica gel. Elution with carbon tetrachloride followed by benzene gave a series of solids which on combination and recrystallization from ethanol gave 0.19 g (37%) of α-methoxybenzyltriphenylsilane, m.p. 146–148°. A mixed m.p. with an authentic sample (20) was undepressed. Continued elution with chloroform gave 0.08 g (21%) of triphenylsilanol, the hydrolysis product of triphenylmethoxysilane, m.p. 150–153°.

The authors gratefully acknowledge support of this research by the National Research Council of Canada, and for a scholarship to PFJ by the Dow-Corning Corporation (1966–1968).

1. A. G. Brook and Peter F. Jones. Can. J. Chem. **47**, 4353 (1969).
2. A. G. Brook and Peter F. Jones. Chem. Commun. 1324 (1969).
3. D. Seyferth, A. W. Dow, H. Menzel, and T. C. Flood. J. Am. Chem. Soc. **90**, 1080 (1968).
4. R. J. Crawford, A. Mishra, and R. J. Dummel. J. Am. Chem. Soc. **88**, 3959 (1966); D. E. McGreer, N. W. Chin, and M. F. Vinge. Can. J. Chem. **43**, 1398 (1965).
5. R. Huisgen. Angew. Chem. Internat. Ed. **2**, 565, 633 (1963).
6. C. G. Overberger and J.-P. Anselme. J. Am. Chem. Soc. **84**, 869 (1962).
7. T. V. van Auken and K. L. Rinehart, Jr. J. Am. Chem. Soc. **84**, 3736 (1962).
8. R. F. Rekker, J. P. Brombacher, and W. Th. Nauta. Rec. Trav. Chim. **73**, 417 (1954).
9. H. Seidl, H. Bock, N. Wiberg, and M. Veith. Angew. Chem. Internat. Ed. **9**, 69 (1970).
10. P. Yates, B. Shapiro, N. Yoda, and J. Fugger. J. Am. Chem. Soc. **79**, 5756 (1957).
11. K. L. Rinehart, Jr. and T. V. van Auken. J. Am. Chem. Soc. **82**, 5251 (1960).
12. T. H. Kinstle, R. L. Welch, and R. W. Exley. J. Am. Chem. Soc. **89**, 3660 (1967).
13. K. Kocsis, P. G. Ferrini, D. Arigoni, and O. Jeger. Helv. Chem. Acta **43**, 2178 (1960).
14. R. Oda, M. Mieno, and Y. Hayaski. Tetrahedron Lett. 2363 (1967).
15. W. Ried and J. Omran. Ann. **666**, 144 (1963).
16. H. Gilman and G. D. Lichtenwalter. J. Am. Chem. Soc. **80**, 2680 (1958).
17. L. F. Cason and H. G. Brooks. J. Am. Chem. Soc. **74**, 4582 (1952).
18. R. A. Benkeser and R. A. Hickner. J. Am. Chem. Soc. **80**, 5298 (1958).
19. A. G. Brook and J. Duff. Unpublished studies.
20. A. G. Brook and P. J. Dillon. Can. J. Chem. **47**, 4347 (1969).

Can. J. Chem. Downloaded from www.nrcresearchpress.com by 210.87.254.40 on 09/05/12
For personal use only.

Can. J. Chem. Downloaded from www.nrcresearchpress.com by 210.87.254.42 on 09/05/12
For personal use only.

Dehydrogenation of 7,12-Dihydropleiadene Compounds with High Potential Quinones

J. W. LOWN AND A. S. K. AIDOO
Department of Chemistry, University of Alberta, Edmonton, Alberta

Received December 7, 1970

Dehydrogenation with high potential quinones has been extended to dihydro derivatives of non-aromatic hydrocarbons using 7,12-dihydropleiadenes as models. Reaction of 7-phenyl-7,12-dihydropleiadene with high potential quinones resulted in dehydrogenative cyclization whereas preparative scale and rate studies in 9-aryl-9,10-dihydroanthracenes gave no evidence of aryl participation during quinone dehydrogenation due to geometrical restrictions on this system.

Utilisant les dihydro-7,12 pléiadènes comme modèles, on a étendu aux dérivés dihydrogénés des hydrocarbures non aromatiques la méthode de déshydrogénation faisant appel aux quinones à haut potentiel. La réaction du phényl-7 dihydro-7,12 pléiadène avec de telles quinones provoque une cyclisation déshydrogénante; par ailleurs des études tant préparatives que cinétiques sur des aryl-9 dihydro-9,10 anthracènes n'ont fourni aucune preuve que les restrictions géométriques imposées à ce système provoquent une participation du groupe aromatique au cours de ces déshydrogénations.

Canadian Journal of Chemistry, 49, 1848 (1971)

Dehydrogenation of hydroaromatic compounds with high potential quinones is an important reaction widely used in synthetic schemes and in the oxidation of natural products (1). A substantial part of the driving force for the two-step ionic mechanism, proceeding by initial hydride transfer to the quinone is thought to be provided by the net resonance energy gain in both the quinone (acceptor) and the hydroaromatic compound (donor) which is thereby aromatized (2). In previous publications (3, 4) we demonstrated that aralkyl groups may react further with quinones often with surprising ease (*e.g.* 9,10-dimethylanthracene and 7,12-dimethylbenzanthracene) giving rise to cyclic and acyclic quinol ethers some of which are plausibly interpreted as arising via the intermediacy of para-quinodimethane intermediates. We report studies of the reaction of high potential quinones on derivatives of 7,12-dihydropleiadene (**1**), the parent compound of which, pleiadene (**2**) is expected not to exhibit substantial resonance stabilization (5, 6). Compounds **1** had the added interest of containing a potential ortho-quinodimethane moiety which could be expected to result from quinone dehydrogenation. The results on these systems extend the range of quinone dehydrogenation, limited to hydroaromatic donors hitherto, and also one compound proved ideal for testing predictions of cyclodehydrogenation.

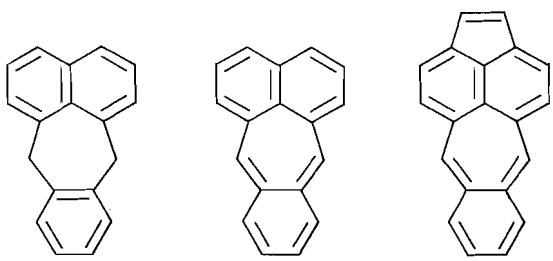

1 **2** **3**

7,12-Dihydropleiadene as Donors

Pleiadene has been generated in solution by Cava and Schlessinger by the elimination of sulfur dioxide from 7,12-dihydropleiadene-7,12-sulfone (**4**) both thermally and photochemically (see eq. 1) and by dehalogenation of 7,12-dibromo-7,12-dihydropleiadene with zinc or copper bronze at moderate temperatures (7). Pleiadene, in contrast to acepleiadylene (**3**) cannot be regarded as a peripherally conjugated system, and consequently exhibits a greater degree of ortho-quinodimethane character than **3** and dimerized readily to **5** in solution or could be trapped with *N*-phenylmaleimide in a Diels–Alder reaction to form **6**, however, only at higher temperatures.

Reaction of **1** (8) with 2 equiv of tetrachloro-

Can. J. Chem. Downloaded from www.nrcresearchpress.com by 210.87.254.42 on 09/05/12
For personal use only.

[1]

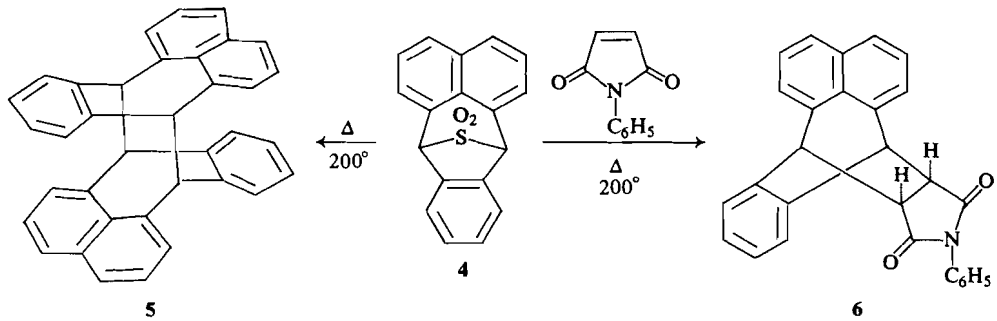

5 4 6

1,2-benzoquinone (TOQ) in refluxing chlorobenzene readily gave compound **7**. Examination

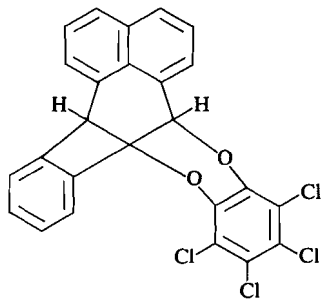

7

of the products of the reaction of quinones with alkenes by Horner and Merz (9) and in our own work with arenes (3, 4) have shown that products may be formed of types **8**, **9**, and **10** from ortho

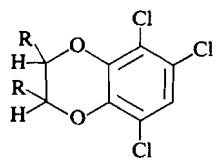

8

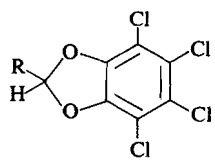

9

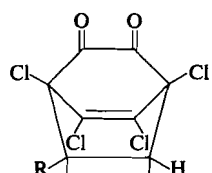

10

quinones (*e.g.* TOQ) and of types **11** and **12** from para quinones such as 2,3-dichloro-5,6-dicyano-1,4-benzoquinone (DDQ).

Compounds of types **8** and **9** are white or pale

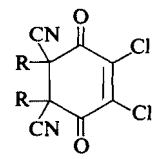

11

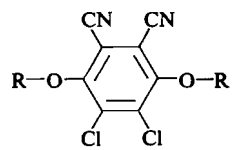

12

yellow solids the i.r. spectra of which exhibit strong and characteristic ether bands in the region 1420–1450 cm^{-1} due to tetrachlorobenzodioxan and tetrachlorobenzodioxole moieties (10). Adducts of type **10** are formed when TOQ acts as a diene and are characteristically bright yellow and exhibit strong α-diketone i.r. bands near 1680 cm^{-1}. In adducts of type **11** DDQ acts as a dienophile at the more reactive (nitrile substituted) double bond, an assumption which has recently been justified by X-ray analysis of a DDQ adduct of 1,3,5,5-tetramethylcyclohexa-1,3-diene (11).

Compound **7**, $C_{24}H_{12}Cl_4O_2$ showed a benzodioxan absorption at 1454 cm^{-1} but no hydroxyl or ketone absorption.

In contrast **1** reacted with DDQ to give compound **13**, $C_{26}H_{12}N_2Cl_2O_2$ in 47% yield, the formation of which can plausibly be interpreted by initial dehydrogenation of **1** to **2** followed by Diels–Alder addition to the nitrile substituted bond of DDQ. Compound **13** showed i.r. bands

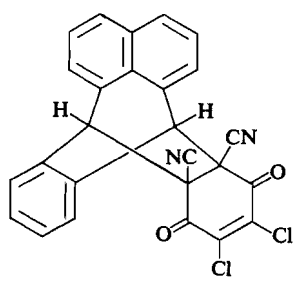

13

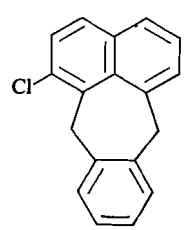

14

Can. J. Chem. Downloaded from www.nrcresearchpress.com by 210.87.254.42 on 09/05/12
For personal use only.

at 1705 (C=O) and 2250 cm^{-1} (C≡N) and the n.m.r. spectrum showed, besides aryl protons, a singlet at 5.05 δ (2H) demonstrating the equivalence of the 7- and 12-protons and therefore the symmetry of the molecule. (The signals of the corresponding protons in **7** are shifted by the adjacent oxygens into the aromatic region.)

Evidently 7,12-dihydropleiadene, lacking the driving force available to hydroaromatic donors, is still dehydrogenated readily by the two different quinones.

Cava and Schlessinger have convincingly demonstrated that Diels–Alder addition products of **2**, *e.g.* **6**, have the *exo* configuration illustrated (7). Accordingly we have assigned the *exo* configuration to **13** and tentatively assigned the conformation of **7** as *exo* as shown.

In contrast to the formation of **7** reaction of 1-chloro-7,12-dihydropleiadene (**14**) with TOQ gave rise to two isomeric products to which structures **15** and **16** were assigned the com-

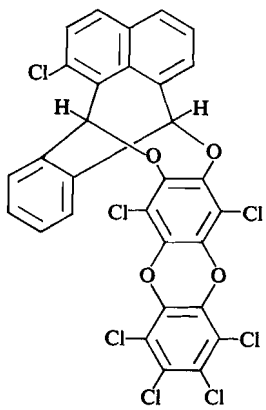

15

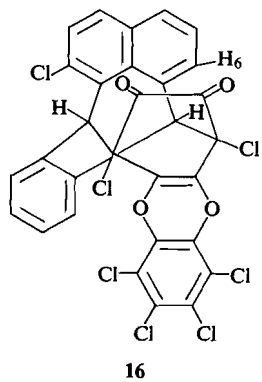

16

position which corresponded to $C_{30}H_{10}Cl_4O_4$, *i.e.* 1:2 pleiadene:quinone −2HCl. Compound **15** showed two strong ether bands in the i.r. at 1420 (=C—O—C) and 1445–1453 cm^{-1} (=C—O—C=) and no C=O bands, the 7- and 12-protons as in the case of **7** appeared in the aromatic region in the n.m.r. The isomer **16** was a bright yellow solid the i.r. spectrum of which showed bands due to both tetrachlorobenzodioxan (1445 cm^{-1}) and α-diketone (1680 cm^{-1}). The n.m.r. spectrum showed, in addition to aryl protons, two singlets at 5.26 and 6.31 δ (1H each) unambiguously assigned to the 7- and 12-pleiadene bridge protons since the corresponding adduct prepared from 1-chloro-7,7,12,12-tetradeuteropleiadene lacked these signals. In addition a doublet at 6.26 δ (J = 10.6 Hz), unaffected by the deuteration, was shown to be an aromatic proton by double irradiation experiments. It is tentatively assigned to the C-6 proton, adjacent to a carbonyl group in the proposed structure **16**.

Compound **14** is far less reactive than **1** because the electron-withdrawing 1-chloro substituent in **14** so deactivates the potential hydride ion at the benzylic positions, that higher reaction temperatures and longer reaction times are required for dehydrogenation. A similar sensitivity to electron-withdrawing substituents reflected in the Hammett ρ value of −2.5 has been observed in the dihydronaphthalene series (12). Under these forcing conditions TOQ undergoes a preceding reaction with the corresponding quinol to form **17** (see eq. 2).

[2]

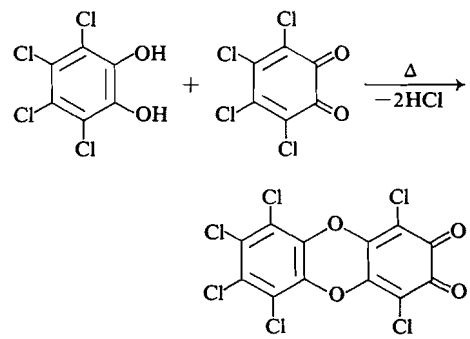

17

Compound **17** prepared independently (13) was allowed to react with **14** and gave rise to both compounds **15** and **16**.

In view of the reactions discussed above, the formation of **15** and **16** can be envisaged as involving similar reaction paths to those implied in the formation of **7** and **13** respectively, *i.e.* via an acyclic quinol ether to form **15** and by addition to 1-chloropleiadene to form **16**.

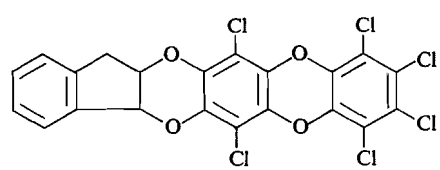

18

Indane, which like **14** requires forcing conditions to react with TOQ, similarly affords com-

Can. J. Chem. Downloaded from www.nrcresearchpress.com by 210.87.254.42 on 09/05/12
For personal use only.

pound **18** (14). Compound **14** reacted with DDQ to give adduct **19**, $C_{26}H_{11}Cl_3N_2O_2$ similar to **13**.

Substitution of an alkyl group at the 7-position of 1-chloro-7,12-dihydropleiadene has a pronounced effect on the course of reaction with

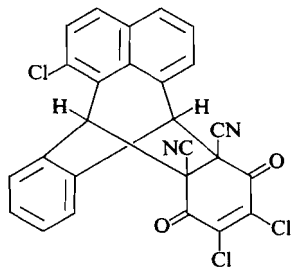

19

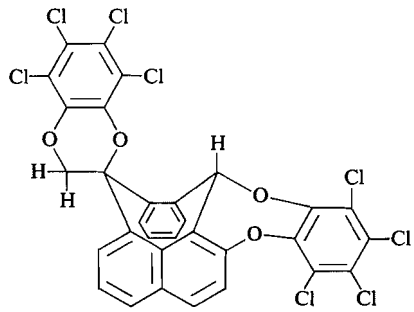

20

TOQ. The major product obtained from the 7-methyl derivative **21** was a pale yellow solid, $C_{31}H_{12}Cl_8O_4$, corresponding to the addition of 2 mol of TOQ and the elimination of H_2 and HCl. The product shows two distinct tetrachloroquinol ether bands at 1420 and 1445 cm^{-1} and is formulated as **20**. Supporting evidence for dehydrogenation into the methyl group of **21** to form the methylene compound followed by addition of TOQ to form the cyclic quinol ether is provided by reaction of **22** to form adduct **23**, $C_{25}H_{11}Cl_5O_3$, which shows a strong quinol ether absorption at 1423 cm^{-1}. In addition the methyl-

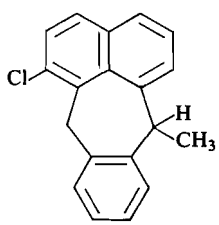

21

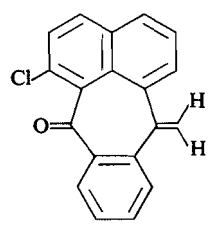

22

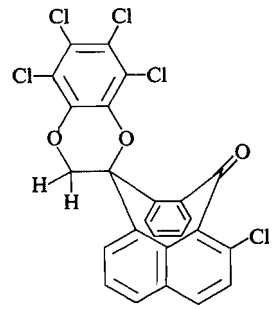

23

ene compound **24** forms **20** by reaction with 2 mol of TOQ. Reaction of the second quinone molecule results in substitution of the 1-chlorine by the quinone oxygen to form the cyclic ether.

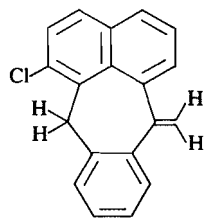

24

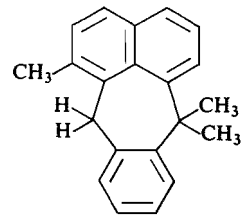

25

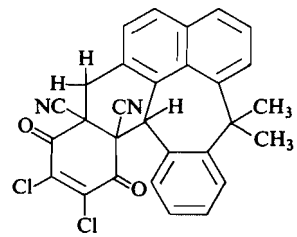

26

Reaction of 1,7,7-trimethyl-7,12-dihydropleiadene (**25**) with DDQ gave compound **26** $C_{29}H_{18}N_2Cl_2O_2$. The i.r. spectrum was typical of a Diels–Alder adduct of DDQ to the nitrile substituted double bond such as **13** and **19** and the n.m.r. spectrum showed the 7-methyl groups intact at 1.6 and 1.9, an AB quartet (J = 16 Hz) at 3.85 and 4.20 due to the methylene protons, and the methine singlet at 5.20 δ. Formation of **26** presumably involves Diels–Alder addition of DDQ to the reactive intermediate **27** which contains an ortho quinodimethane moiety and would resemble **2** in its reactivity towards dienophiles. Product **26** resembles those obtained from **22** and **24** with DDQ which gave **28** $C_{27}H_9Cl_3O_2N_2$, and **29**, $C_{27}H_{11}Cl_3N_2O_2$, respectively. In

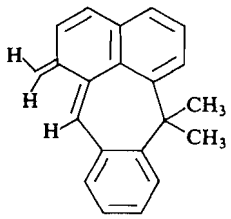

27

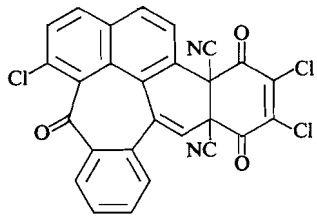

28

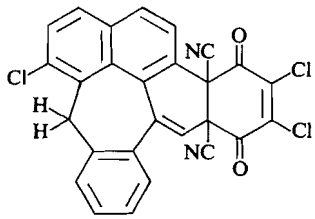

29

the case of **28** and **29** however the initial Diels–Alder addition products undergo further dehydrogenation to aromatize the naphthalene moiety. A corresponding subsequent dehydrogenation does not take place in the case of **26** since this would result in formation of a high energy ortho-quinodimethane structure. Compound **29** shows an AB quartet in the n.m.r. spectrum due to the C-12 methylene proton at 4.4 δ J = 16 Hz.

Compound **25** reacted with TOQ in refluxing benzene to give a white solid $C_{27}H_{18}Cl_4O_2$, the n.m.r. spectrum of which like **26** showed the 7-methyl groups unaffected at 1.8 and 2.05 δ and an AB quartet (2H) centered at 5.95 and 6.56 δ (J = 16 Hz) corresponding in chemical shift to a methylene bonded to oxygen. Since the i.r. spectrum showed a strong quinol ether absorption at 1405 cm^{-1} and no hydroxyl absorption this compound is formulated as **30**.

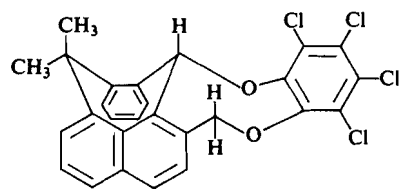

30

Thus the 1-methyl group in **25** shows a reactivity towards quinones comparable with that of methylnaphthalenes and 9-methylanthracene which also form quinol ethers under comparable conditions (3, 4).

Quinone Dehydrogenation of 9-Aryl-9,10-dihydroanthracenes and 7-Aryl-7,12-dihydropleiadenes

(i) Anthracene Models

The general quinone dehydrogenation reaction involves in the rate-determining initial step a hydride transfer from the donor (an arene or hydroaromatic compound) to the acceptor (quinone) with the concomitant generation of an electron deficient carbon (1, 2). It follows that in model compounds with a suitable geometry some degree of participation by a neighboring group could be anticipated (see eq. 3) and in the limit dehydrogenative cyclization could result.

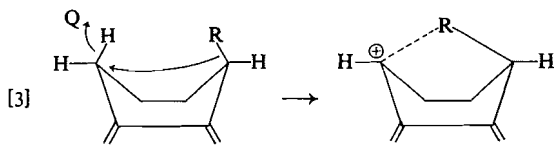

[3]

31

As a first approach we have examined the dehydrogenation with some high potential quinones of some 9-aryl-9,10-dihydroanthracenes since their geometry is reasonably well defined (15). 9,10-Dihydroanthracene, and its 9-phenyl, 9-*p*-tolyl, and 9-*p*-anisyl derivatives reacted with TOQ (in benzene at moderate temperatures) to give the corresponding anthracenes quantitatively. The rates of these reactions could be followed conveniently by a spectrokinetic procedure (16) by observing the rate of disappearance of the red quinone. Individual reactions obeyed the second order rate law strictly and the rate data obtained are summarized in Table 1.

9-Phenyl, 9-*p*-tolyl, and 9-*p*-anisyl-9,10-dihydroanthracenes have reaction rates with TOQ very close to that of 9,10-dihydroanthracene when allowance is made for the statistical factor of 2. 9,10-Dihydroanthracenes adopt a quasi-boat conformation of the central ring and a 9-aryl substituent adopts the quasi-axial position preferentially so as to minimize interactions with the flanking benzene rings. Inspection of models suggests that the quasi-axial hydrogen atom at the 10-position is correctly disposed with respect to the aromatic rings of the anthracene structure to provide maximum stabilization of the incipient carbonium ion, in contrast to the quasi-equational hydrogen atom which is unfavorably oriented. We therefore make the reasonable

Can. J. Chem. Downloaded from www.nrcresearchpress.com by 210.87.254.42 on 09/05/12
For personal use only.

TABLE 1. Kinetic data for reaction of 9-aryl-9,10-dihydroanthracenes with tetrachloro-1,2-benzoquinone in 1,2-dichlorobenzene

Donor	Second order rate constant (80°)	Arrhenius parameters	
		E (kcal mol^{-1})	$\text{Log}_{10} B$
9,10-Dihydroanthracene	$3.10 \pm 0.20 \times 10^{-1}$	12.06 ± 0.17	6.95
9,10-Dihydro-9-phenylanthracene	$1.37 \pm 0.04 \times 10^{-1}$	14.55 ± 0.58	8.15
9,10-Dihydro-9-*p*-tolylanthracene	$1.56 \pm 0.05 \times 10^{-1}$	13.48 ± 0.47	7.45
9,10-Dihydro-9-*p*-anisylanthracene	$1.75 \pm 0.12 \times 10^{-1}$	13.43 ± 0.23	7.65

assumption that the quasi-axial hydrogen atoms are potential hydride ions in the anthracene series.

In view of the known sensitivity of the quinone dehydrogenation reaction to substituent electronic effects in the dihydronaphthalene series (Hammett $\rho = -2.5$) (12) one would have anticipated a greater spread in the relative reactivities as reflected in the reaction rates, had hydride abstraction occurred at the 9-position.

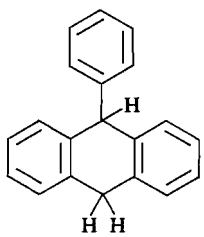

32

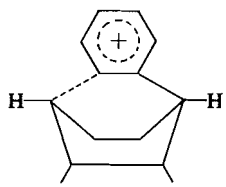

33

It is apparent therefore that hydride abstraction occurs at the 10-position in this series of hydroaromatic donors (a conclusion which is borne out by experiments in the dihydropleiadene series described below) and we may also conclude that the axial 9-substituent does not participate in the removal of the hydride ion by bridging to the cationic center as in **33**.

We infer from the rate data that the geometry of the quasi-boat in the anthracene series is such that the 9-aryl substituent is not in a suitable position for this kind of interaction.

(ii) Pleiadene Models

The experience of the quinone dehydrogenation of the pleiadene system outlined in preceding sections and an examination of molecular models suggested that the geometry of this system in contrast to the anthracene case might be suitable to allow attack of a 7-arylsubstituent at the cationic center generated at the 12-position by hydride abstraction leading to dehydrogenative cyclization as illustrated in eq. 4. 7-Phenyl-7,12-dihydropleiadene (**34**) reacted with TOQ in benzene to give the bridged hydrocarbon **36** as the sole product. Evidently aryl attack as represented by **35** is so effective with this molecular geometry as to prevent loss of the 7-proton from the carbonium ion with formation of a 7-phenylpleiadene.

Recently Lansbury and coworkers (17) have prepared a similar compound **38** in an attempted dehydration of the alcohol **37** and this reaction must proceed by a similar mechanism once the cationic center has been generated at position 12 (see eq. 5).

7-Phenyl-7,12-dihydropleiadene (**34**) also reacted with DDQ to give pure **36**. Compound **36** is completely unreactive towards further reaction with either TOQ or DDQ, a result which is in accordance with the observed lack of reactivity of the bridgehead hydrogens in trypticene **39**. This may be attributed to the inability of an incipient carbonium ion generated from **36** or **39** to attain coplanarity with the aryl rings despite the additional flexibility allowed in **36** by the

[4]

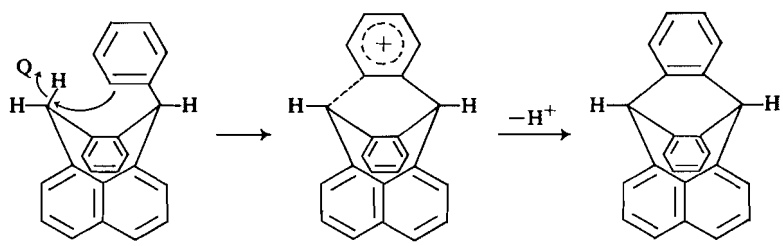

34 35 36

Can. J. Chem. Downloaded from www.nrcresearchpress.com by 210.87.254.42 on 09/05/12
For personal use only.

Can. J. Chem. Downloaded from www.nrcresearchpress.com by 210.87.254.42 on 09/05/12
For personal use only.

[5]

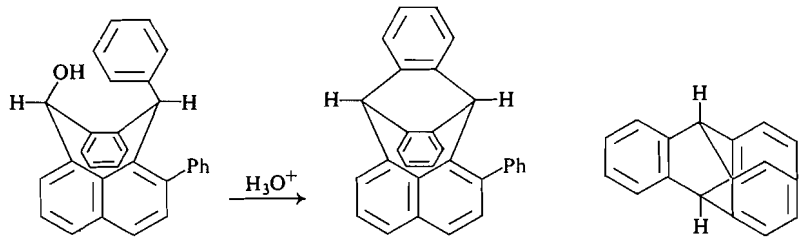

37 38 39

introduction of another fused aromatic ring compared with **39**.

Reaction of 7-isopropyl-7,12-dihydropleiadene (**40**) with TOQ gave compound **41**, similar in structure to **7** and **15**. The n.m.r. spectrum of **41**

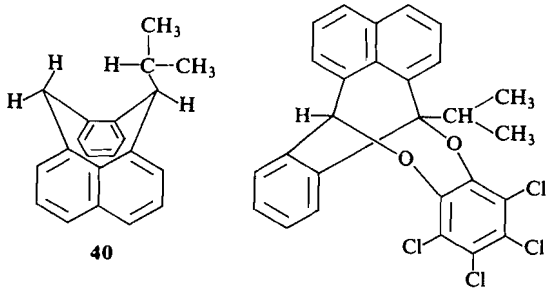

40 41

shows bands characteristic of an intact isopropyl group and also reveals an absence of absorption characteristic of the 7,12-protons in **40**. A strong quinol ether absorption at 1455 cm^{-1} and the absence of carbonyl absorption support structure **41**.

The results obtained with the 9,10-dihydro-9-arylanthracenes lead one to expect the 12-axial proton in **40** to be the potential hydride ion in the first step of the reaction since Lansbury has shown the isopropyl group in **40** adopts a pseudo-axial conformation. Had 1,5-hydride shift occurred from the isopropyl group in **40** such as occurs in the dehydration of **42** studied by Lansbury (see eq. 6 (17)), one would have expected a final product of addition of TOQ to the isopropenyl or isopropylidene group such as **23** to have resulted. We conclude that, unlike the rapid dehydrogenative cyclization in **34** to form **36**, **41** results from collapse of the quinol anion to the initially formed carbonium ion which prevents a 1,5-transannular hydride shift, and that a second dehydrogenation step involving participation by the quinol hydroxyl results in the formation of **41**.

Experimental

Melting points were determined on a Fisher–Johns apparatus and are uncorrected. The i.r. spectra were recorded on a Perkin–Elmer model 421 spectrophotometer, and only the principal, sharply defined peaks are reported. The n.m.r. spectra were recorded on Varian A-60 and A-100 analytical spectrometers. The spectra were measured on approximately 10–15% (w/v) solutions in $CDCl_3$, with tetramethylsilane as a standard. Line positions are reported in p.p.m. from the reference. Mass spectra were determined on an Associated Electrical Industries MS-9 double focusing high resolution mass spectrometer. The ionization energy, in general, was 70 eV. Peak measurements were made by comparison with perfluorotributylamine at a resolving power of 15 000. Kieselgel DF-5 (Camag, Switzerland) and Eastman Kodak precoated sheets were used for t.l.c. Microanalyses were carried out by Dr. C. Daesslé, Organic Microanalysis Ltd., Montreal, Quebec and by Mrs. D. Mahlow of this Department. Values for carbon microanalysis of some adducts were unacceptable owing to difficulties in combustion of high molecular weight compounds. In such cases an accurate peak measurement by mass spectrometry was performed.

1-Chloro-7,12-dihydropleiadene

1-Chloro-7,12-dihydropleiadene was prepared from 1-chloro-7,12-dihydropleiadene-7,12-dione by the method of Cava and Schlessinger (7). The crude product was

[6]

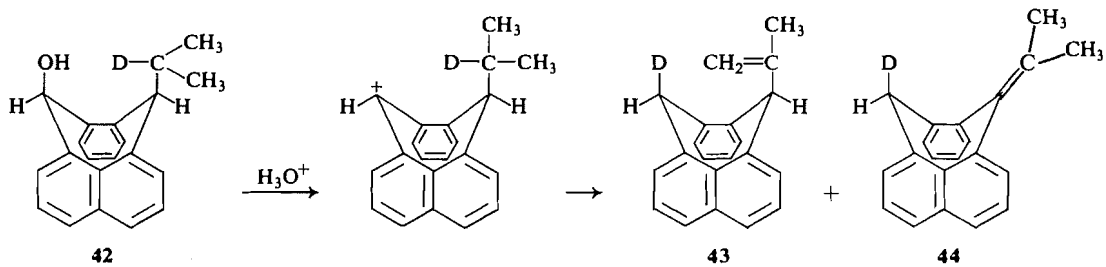

42 43 44

Can. J. Chem. Downloaded from www.nrcresearchpress.com by 210.87.254.42 on 09/05/12
For personal use only.

purified by chromatography on alumina using hexane as eluent. Crystallization from hexane gave white needles, m.p. 116–119° (lit. 117–119° (7)).

7,12-Dihydropleiadene

7,12-Dihydropleiadene was prepared from 1-chloro-7,12-dihydropleiadene by a modification of the method of Cava and Schlessinger (7). A mixture of 25 g (0.095 mol) of 1-chloro-7,12-dihydropleiadene, 5 g of 10% palladium-on-charcoal, 100 ml of 85% hydrazine hydrate, and 1000 ml of 95% ethanol was refluxed for 1 h. The filtered solution was concentrated to *ca.* 100 ml, acidified with 2 *N* hydrochloric acid, and the solid product collected, washed repeatedly with water, and dried. Recrystallization from hexane gave 20 g (91.8% yield) of 7,12-dihydropleiadene, m.p. 115–117° (lit. 113–114° (7), 116° (8)).

Reaction of 7,12-Dihydropleiadene with Tetrachloro-1,2-benzoquinone

A solution of 4 g (0.017 mol) of 7,12-dihydropleiadene in 50 ml of dry chlorobenzene was added to a solution of 10 g (0.041 mol) of tetrachloro-1,2-benzoquinone in 250 ml of chlorobenzene and the mixture heated under reflux for 72 h. The solvent was removed *in vacuo*, the residue taken up in benzene and subjected to chromatography on BDH alumina using (1:1) benzene:hexane as eluent. The main fraction consisted of a buff-white solid recrystallized from benzene, m.p. 266–268°, 4.3 g (52.4% yield) of 7.

Anal. Calcd. for $C_{24}H_{12}Cl_4O_2$ (mol. wt. 471.9593): C, 60.78; H, 2.56; Cl, 29.90. Found (471.9594 (mass spectrum)): C, 61.26; H, 2.51; Cl, 29.05.

The i.r. spectrum $\nu_{max}(CHCl_3)$: 1454 cm^{-1} (C—O—C); n.m.r. spectrum $\delta_{TMS}(CDCl_3)$: 7.1–8.2 (m, aryl, C-7 and -12 protons).

Reaction of 7,12-Dihydropleiadene with 2,3-Dichloro-5,6-dicyano-1,4-benzoquinone

A solution of 5 g (0.022 mol) of 7,12-dihydropleiadene in dry chlorobenzene was added to a solution of 10 g (0.044 mol) of 2,3-dichloro-5,6-dicyano-1,4-benzoquinone in 350 ml of chlorobenzene and the mixture refluxed for 30 min during which time a brown solid separated. Refluxing was continued for a further 1½ h, the mixture cooled, and the solid collected and washed with benzene. The filtrate was concentrated *in vacuo*, benzene added whereupon a yellow solid separated which was collected and washed with benzene yielding **13** 4.7 g (47.1% yield) m.p. > 300°.

Anal. Calcd. for $C_{26}H_{12}N_2Cl_2O_2$ (mol. wt. 454.0276): N, 6.16; Cl, 15.42. Found (454.0275 (mass spectrum)): N, 6.08; Cl, 15.31.

The i.r. spectrum ν_{max}(Nujol mull): 1705 (C=O), 2250 cm^{-1} (C≡N); n.m.r. spectrum $\delta_{TMS}((CD_3)_2SO)$: 5.05 (2H, s, C-7 and -12 protons), 7.1–8.2 (m, 10H, aromatic protons).

Reaction of 1-Chloro-7,12-dihydropleiadene with Tetrachloro-1,2-benzoquinone

A solution of 3.01 g (9 mmol) of 1-chloro-7,12-dihydropleiadene in 100 ml of dry *o*-dichlorobenzene was added to a solution of 8.36 g (0.0336 mol) of tetrachloro-1,2-benzoquinone in 300 ml of *o*-dichlorobenzene and the mixture refluxed for 48 h. The solvent was removed *in vacuo* (0.05 mm) and the residual solid taken up in benzene and subjected to chromatography on acid washed alumina. Elution with benzene gave **16**, 1 g, (13% yield) m.p. 280–281°.

Anal. Calcd. for $C_{30}H_{11}Cl_7O_4$: C, 52.94; H, 1.62; Cl, 36.03. Found: C, 53.05; H, 2.05; Cl, 36.48.

Mass Spectrum Calcd. for $C_{30}H_{10}{}^{35}Cl_6{}^{37}ClO_4$ (M^+-1): 680.8369. Found: 680.8372.

The i.r. spectrum $\nu_{max}(CHCl_3)$(Nujol): 1680 (C=O) 1454 cm^{-1} (—C—O—C); n.m.r. spectrum $\delta_{TMS}(CDCl_3)$: 5.26 and 6.31 (1H each, s, C-7 and -12 pleiadene bridge protons), these signals disappear in the analogous compound obtained from 1-chloro-7,7,12,12-tetradeuteropleiadene, 6.26 (1H, d, J = 10.6 Hz ortho coupling, C-6(?) aromatic proton. Irradiation at 7.45 causes collapse of the 6.26 signal to a singlet, 7.0–8.0 (8H, m, aromatic protons).

Further elution with chloroform gave **15** 1.2 g (20% yield), m.p. > 300°.

Anal. Calcd. for $C_{30}H_{11}Cl_7O_4$: Cl, 36.03. Found: Cl, 35.62.

The i.r. spectrum $\nu_{max}(CHCl_3)$: 1420 (—C—O—C—), 1445–1453 cm^{-1} (—C=C—O—C); n.m.r. spectrum $\delta_{TMS}(CDCl_3)$: 6.7–8.2 (m, aromatic, C-7 and -12 bridge protons).

Reaction of 1-Chloro-7,12-dihydropleiadene with Hexachloro-ortho-quinopyrocatechin Ether

A solution of 0.61 g (25 mmol) of 1-chloro-7,12-dihydropleiadene in 50 ml of dry chlorobenzene was added to a solution of 2.09 g (50 mmol) of hexachloro-ortho-quinopyrocatechin ether (13) in 300 ml of warm chlorobenzene and the mixture refluxed for 72 h. The solvent was removed *in vacuo* and the residue dissolved in benzene and subjected to chromatography on BDH alumina using benzene as eluant to give a bright yellow solid, m.p. > 300°, 0.5 g (29.4% yield).

Mol. Wt. Calcd. for $C_{30}H_{11}Cl_7O_4$: 679.8480. Found (mass spectrum): 679.8470.

The i.r. spectrum $\nu_{max}(CHCl_3)$: 1672 (—CO—CO—) 1452 cm^{-1} (C=C—O—C=C). This compound proved to be identical with adduct **16** obtained above.

Further elution with chloroform gave a violet compound 0.43 g (25.3% yield) the i.r. spectrum of which in $CHCl_3$ showed bands at 1453 and 1422 cm^{-1} (—C—O—C) and which proved to be identical with adduct **15** obtained above.

1-Chloro-7,7,12,12-tetradeutero-7,12-dihydropleiadene

Aluminum chloride (2.7 g, 0.02 mol) and 0.84 g (0.02 mol) of lithium aluminum hydride were added to ether at 0°. To this mixture was added with stirring 2.54 g (8 mmol) of 1-chloro-7,12-dihydropleiadene-7,12-dione and the mixture stirred for 45 min, decomposed with ice, the ether layer washed with water and dried (Na_2SO_4), and the ether removed *in vacuo* to give a slightly yellow solid. The latter was chromatographed on BDH alumina to give 2 g of 1-chloro-7,7,12,12-tetradeutero-7,12-dihydropleiadene, m.p. 119–121°.

Mol. Wt. Calcd. for $C_{18}H_9D_4Cl$: 268.0876. Found (mass spectrum): 268.0879.

Reaction of 1-Chloro-7,7,12,12-tetradeutero-7,12-dihydropleiadene with Tetrachloro-1,2-benzoquinone

A solution of 0.5 g (1.86 mmol) of 1-chloro-7,7,12,12-tetradeutero-7,12-dihydropleiadene in 25 ml of *o*-dichlorobenzene was added to a solution of 1.05 g (4.26 mmol) of tetrachloro-1,2-benzoquinone in 50 ml of

Can. J. Chem. Downloaded from www.nrcresearchpress.com by 210.87.254.42 on 09/05/12
For personal use only.

o-dichlorobenzene and the mixture refluxed for 48 h. The solvent was removed *in vacuo* and the residue subjected to chromatography using benzene as eluant to give 0.3 g (29.4% yield) of D-**16** m.p. 280–281°.

Mol. Wt. Calcd. for $C_{30}H_9D_2O_4{}^{35}Cl_6{}^{37}Cl$: 683.8581. Found (mass spectrum): 683.8576.

The i.r. spectrum ν_{max}(Nujol): 1660 (C=O), 1445 cm^{-1} (—C—O—C=C—O).

Reaction of 1-Chloro-7,12-dihydropleiadene with 2,3-Dichloro-5,6-dichloro-1,4-benzoquinone

A solution of 4 g (15 mmol) of 1-chloro-7,12-dihydropleiadene in 75 ml of dry chlorobenzene was added to a solution of 10 g (0.044 mol) of 2,3-dichloro-5,6-dicyano-1,4-benzoquinone in 350 ml of chlorobenzene and the mixture heated under reflux for 2 h. The insoluble quinol which separated from the reaction mixture was collected and the filtrate concentrated *in vacuo*. The residual solid was taken up in chloroform and subjected to chromatography on silica gel with benzene:chloroform (2:1) as eluent giving **19** as bright yellow crystals in m.p. 270°, 3.8 g (51.2% yield).

Anal. Calcd. for $C_{26}H_{11}Cl_3N_2O_2$ (mol. wt. 487.9886): C, 63.95; H, 2.25; Cl, 21.52; N, 5.73. Found: 487.9888 (mass spectrum): C, 63.35; H, 2.39; Cl, 21.39; N, 5.64.

The i.r. spectrum ν_{max}(Nujol mull): 2246 (C≡N), 1700, 1715(sh) cm^{-1} (C=O); n.m.r. spectrum δ_{TMS}-($(CD_3)_2SO$): 5.15 (1H, s, C-7 proton), 5.64 (1H, s, C-12 proton), 7.2–8.2 (9H, m, aromatic protons).

Reaction of 1-Chloro-7-methyl-7,12-dihydropleiadene with Tetrachloro-1,2-benzoquinone

A solution of 0.556 g (2 mmol) of 1-chloro-7-methyl-7,12-dihydropleiadene in dry chlorobenzene was added to a solution of 0.976 g (4 mmol) of the quinone in 150 ml of dichlorobenzene and the mixture refluxed for 10 h. The solvent was removed *in vacuo* and the residual solid purified by chromatography on BDH alumina using hexane:benzene (2:1) as eluent to give 0.13 g (8.9% yield) of **20**, m.p. 286–289.

Anal. Calcd. for $C_{31}H_{12}Cl_8O_4$ (mol. wt. 727.8248): C, 51.10; H, 1.65; Cl, 38.47. Found (727.8237 (mass spectrum)): C, 51.71; H, 1.65; Cl, 37.03.

The i.r. spectrum $\nu_{max}(CHCl_3)$: 1445, 1420 cm^{-1} (—C—O—C).

1-Chloro-7-methylene-7,12-dihydropleiadene and 1-Chloro-7-methyl-7,12-dihydropleiadene

A stirred suspension of 10 g (0.036 mol) of 1-chloro-7-pleiadenone in 200 ml anhydrous ether was treated dropwise with a solution of methyllithium in ether added through a serum cap until a pink coloration persisted. The mixture was stirred for 2 h, then poured on to ice, and acidified with dilute hydrochloric acid. The ether layer was separated, washed with water and dried ($NaSO_4$). The ether was removed *in vacuo*, the residual solid dissolved in hexane and purified by chromatography on BDH alumina giving 1-chloro-7-methylene-7,12-dihydropleiadene (**24**) 6 g (60.4% yield). The latter (5.52 g) was dissolved in 250 ml of 95% ethanol and hydrogenated over 1.5 g of 5% palladium-on-charcoal at atmospheric pressure giving 5.5 g (99% yield) of 1-chloro-7-methyl-7,12-dihydropleiadene (**21**), m.p. 95°.

Anal. Calcd. for $C_{19}H_{15}Cl$ (mol. wt. 292.0655): Cl, 12.59. Found (292.0653 (mass spectrum)): Cl, 12.40.

The n.m.r. spectrum $\delta_{TMS}(CDCl_3)$: 1.80 (3H, d, CH_3), 4.6–4.97 (3H, m, C-7 and -12 protons), 7.05–7.70 (9H, m, aromatic protons).

1-Chloro-7,12-epoxy-7,12-dihydro-7-methylpleiaden-12-ol

1-Chloro-7,12-dihydropleiadene-7,12-dione (10 g, 34 mmol) was added during 20 min to a stirred solution of methyl magnesium iodide (prepared from 15 g of methyl iodide, 3 g of magnesium, and 200 ml of anhydrous ether). After completed addition, stirring was continued for 8 h and worked-up in the usual way with saturated aqueous ammonium chloride giving 6.2 g (59% yield) of 1-chloro-7,12-epoxy-7,12-dihydro-12-methylpleiaden-7-ol as a white solid m.p. 205–207°.

Anal. Calcd. for $C_{19}H_{13}ClO_2$: C, 74.03; H, 4.22; Cl, 11.36. Found: C, 74.00; H, 4.28; Cl, 11.47.

The i.r. spectrum $\nu_{max}(CHCl_3)$ 3560, 3360 cm^{-1} (OH), 1450 cm^{-1} (—C—O—C); n.m.r. spectrum $\delta_{TMS}(CDCl_3)$: 2.2 (3H, s, CH_3), 4.95 (1H, s, OH), 7.0–8.0 (9H, m, aromatic protons).

1-Chloro-7-methylene-7,12-dihydropleiaden-12-one

1-Chloro-7,12-epoxy-12-methyl-7,12-dihydropleiaden-12-ol (6.2 g, 2 mmol) was dissolved in 100 ml of benzene, a catalytic quantity of *p*-toluenesulfonic acid added, and the mixture refluxed for 8 h, allowed to cool, and washed successively with 10% aqueous sodium hydrogen carbonate and water. The benzene layer was removed and dried ($MgSO_4$). Removal of the solvents *in vacuo* gave 1-chloro-7-methylene-7,12-dihydropleiaden-12-one (**22**), m.p. 169–171°, 5.3 g (91.4% yield).

Anal. Calcd. for $C_{19}H_{11}ClO$: C, 78.61; H, 3.79; Cl, 12.07. Found: C, 78.64; H, 3.79; Cl, 12.01.

The i.r. spectrum $\nu_{max}(CHCl_3)$ 1685 cm^{-1} (C=O); n.m.r. spectrum $\delta_{TMS}(CDCl_3)$: 5.65, 5.45 (2H, pair of doublets, J = 1.5 Hz, methylene protons), 7.25–7.85 (9H, m, aromatic protons).

Reaction of 1-Chloro-7-methylene-7,12-dihydropleiaden-12-one with Tetrachloro-1,2-benzoquinone

A solution of 1.45 g (5 mmol) of 1-chloro-7-methylene-7,12-dihydropleiaden-12-one in 75 ml of dry dichlorobenzene was added to a solution of 2.44 g (0.01 mol) of tetrachloro-1,2-benzoquinone in 125 ml of dichlorobenzene and the mixture refluxed for 24 h. The solvent was removed *in vacuo* and the residue triturated with benzene and recrystallized from benzene to give 1.3 g, m.p. 292–293° of **23**. The mother liquor was subjected to chromatography on BDH alumina to give an additional 0.5 g of **23** making a total yield of 67%.

Anal. Calcd. for $C_{25}H_{11}Cl_5O_3$ (mol. wt. 533.9153): C, 56.16; H, 2.07; Cl, 32.77. Found (533.9150 (mass spectrum)): C, 56.24; H, 2.07; Cl, 32.69.

The i.r. spectrum $\nu_{max}(CHCl_3)$, 1685 (C=O), 1423 cm^{-1} (—C—O—C—).

Reaction of 1-Chloro-7-methylene-7,12-dihydropleiadene with 2,3-Dichloro-5,6-dicyano-1,4-benzoquinone

A solution of 0.552 g (2 mmol) of 1-chloro-7-methylene-7,12-dihydropleiadene in 25 ml of benzene was added to a solution of 0.904 g (4 mmol) of 2,3-dichloro-5,6-dicyano-1,4-benzoquinone in 200 ml of benzene and the mixture refluxed for 10 h, cooled, and filtered. Concentration of the filtrate gave a brick-red solid purified by recrystallization from benzene to give **29**, 0.68 g (68% yield), m.p. 242–245° (dec.).

Can. J. Chem. Downloaded from www.nrcresearchpress.com by 210.87.254.42 on 09/05/12
For personal use only.

Anal. Calcd. for $C_{27}H_{11}Cl_3N_2O_2$ (mol. wt. 499.9888): C, 64.80; H, 2.20; Cl, 21.00. Found (499.9886 (mass spectrum)): C, 64.79; H, 2.37; Cl, 20.95.

The i.r. spectrum ν_{max}(Nujol mull): 1718 (C=O); 2250 cm^{-1} (CN), n.m.r. spectrum $\delta_{TMS}((CD_3)_3SO)$: quartet centered at 4.4 (2H, C-12 bridge protons J_{AB} = 15 Hz broad lines), 6.1, 6.47 (1H, singlets, vinyl proton), 6.95–8.5 (8H, aromatic protons).

1,7,7-Trimethyl-7,12-dihydropleiadene

To a stirred solution of 6.5 g of methyl-2-[2′-methyl-1′naphthylmethyl]benzoate in ether (prepared by treating the acid with methanol in the presence of a catalytic quantity of sulfuric acid), was added excess of a solution of methyllithium in ether. The mixture was poured on to ice, acidified with 2 *N* hydrochloric acid, and the ether layer separated and dried ($MgSO_4$). Evaporation of the solvent gave 1-[2′-(1′′-hydroxy-1′′-methylethyl)tolyl]-2-methylnaphthalene as a yellow oil. The oil was dissolved in 100 ml of formic acid containing a catalytic amount of *p*-toluenesulfonic acid and the mixture heated on the steam bath for 3 h. The solution was diluted with water extracted with ether, and the ether layer separated and washed with 10% sodium hydrogen carbonate solution then water and dried ($MgSO_4$). Evaporation of the solvent gave a yellow oil, chromatography of which on alumina gave 1-(2-isopropenyltolyl)-2-methylnaphthalene as a white crystalline solid identified by its n.m.r. spectrum $\delta_{TMS}(CDCl_3)$: 2.25 (3H, s, isopropenyl protons), 2.40 (3H, s, aryl methyl protons), 4.50 (2H, s, bridge methylene protons), 5.15, 5.40 (2H, m, isopropenyl vinylic protons), 6.40–8.0 (9H, m, aromatic protons). The latter was dissolved in 50 ml of anhydrous ether, treated with 25 ml of boron trifluoride-etherate in ether (48%) and the mixture stirred for 2 h. The reaction mixture was decomposed with ice, the ether layer removed, washed with water, and dried ($MgSO_4$). Evaporation of the solvent gave a brown solid purified by chromatography on BDH alumina to give 2.5 g (40% yield overall from the ester) of 1,7,7-trimethyl-7,12-dihydropleiadene (**25**), m.p. 165–166°.

Anal. Calcd. for $C_{21}H_{20}$: C, 92.64; H, 7.36. Found: C, 92.62; H, 6.7.

The n.m.r. spectrum $\delta_{TMS}(CDCl_3)$: 1.74 (6H, s, C-7 methyl groups), 2.73 (3H, s, C, methyl group), 4.18 (2H, s, C-12 methylene protons), 7.00–8.00 (9H, m, aromatic protons). This compound has previously been reported but no experimental details were given (18).

Reaction of 1,7,7-Trimethyl-7,12-dihydropleiadene with 2,3-Dichloro-5,6-dicyano-1,4-benzoquinone

A solution of 0.34 g (1.25 mmol) of 1,7,7-trimethyl-7,12-dihydropleiadene in 25 ml of benzene was added to 0.565 (2.5 mmol) of 2,3-dichloro-5,6-dicyano-1,4-benzoquinone in 150 ml of benzene and the mixture refluxed for 30 min during which time the hydroquinone separated as a brown solid. The solution was refluxed for a further 1½ h, cooled, and filtered. Concentration of the filtrate to *ca.* 50 ml deposited bright orange-red crystals of **26** purified by recrystallization from benzene 0.531 g (85.6% yield), m.p. 209–212°.

Anal. Calcd. for $C_{29}H_{18}N_2Cl_2O_2$ (mol. wt. 496.0746): C, 70.17; H, 3.63; Cl, 14.11. Found (496.0753 (mass spectrum)): C, 70.33; H, 3.41; Cl, 14.03.

The i.r. spectrum $\nu_{max}(CHCl_3)$: 1718 (C=O), 2225 cm^{-1} (C≡N); n.m.r. spectrum $\delta_{TMS}(CDCl_3)$: 1.6 (3H, s, C-7 equatorial CH_3), 1.9 (3H, s, C-7 axial CH_3), AB quartet centered at 3.85 and 4.20 (2H, q, J_{AB} = 16 Hz, C-12 CH_2), 5.20 (1H, s, C-12 methine proton), 7.20–8.30 (9H, m, aromatic protons).

Reaction of 1-Chloro-7-methylene-7,12-dihydropleiaden-12-one with 2,3-Dichloro-5,6-dicyano-1,4-benzoquinones

A solution of 1.37 g (5 mmol) of 1-chloro-7-methylene-7,12-dihydropleiadene in 100 ml of chlorobenzene was added to a solution of 2.230 g (10 mmol) of 2,3-dichloro-5,6-dicyano-1,4-benzoquinone in 150 ml of chlorobenzene and the mixture heated under reflux for 6 h. The filtered solution was concentrated to a small volume to give **28** as a yellow ocher solid, m.p. 225–228°, 1.77 g (67.3% yield).

Anal. Calcd. for $C_{27}H_9Cl_3O_3N_2$: Cl, 20.43; N, 5.45. Found: Cl, 21.65; N, 5.50.

The i.r. spectrum ν_{max}(Nujol mull): 1736, 1705 (C=O of quinone) 1680 cm^{-1} (C=O at C-12), n.m.r. spectrum $\delta_{TMS}((CD_3)_2SO)$: 6.45, 6.7 (1H, s, vinyl proton) 6.95–8.4 (8H, m, aromatic protons).

The appearance of two singlets for the vinyl protons is tentatively attributed to the presence of stereoisomeric adducts, resulting from the two possible modes of addition of DDQ to the diene system.

Reaction of 1,7,7-Trimethyl-7,12-dihydropleiadene with Tetrachloro-1,2-benzoquinone

A solution of 0.34 g (1.25 mmol) of 1,7,7-trimethyl-7,12-dihydropleiadene in 25 ml of dry benzene was added to a solution of 0.61 g (2.5 mmol) of tetrachloro-1,2-benzoquinone in 125 ml of benzene and the mixture heated under reflux for 48 h, cooled, and concentrated to *ca.* 25 ml yielding a gray solid which on crystallization from benzene gave **30**, m.p. 197–199°, 0.263 g (41% yield).

Anal. Calcd. for $C_{27}H_{18}Cl_4O_2$: C, 63.02; H, 3.50; Cl, 27.24. Found: C, 63.48; H, 3.45; Cl, 27.12.

The i.r. spectrum $\nu_{max}(CHCl_3)$: 1405 cm^{-1} (C—O—C); n.m.r. spectrum $\delta_{TMS}(CDCl_3)$: 1.8 (3H, s, C-7 equatorial CH_3), 2.05 (3H, s, C-7 axial CH_3), 5.95, 6.56 (AB quartet, J_{AB} = 16 Hz, C-19 CH_2 protons), 7.2–8.3 (9H, m, aromatic protons).

Synthesis of 9-Arylanthracenes and 9,10-Dihydro-9-arylanthracenes

The general method is described for 9-*p*-tolylanthracene and 9,10-dihydro-9-*p*-tolylanthracene.

(a) 9-p-Tolylanthracene

Anthrone (10 g, 0.0515 mol) was extracted with ether during 12 h into a refluxing solution of *p*-tolyl magnesium bromide (prepared from 26 g, 0.152 mol of *p*-bromotoluene, 3.7 g, 0.154 mol of magnesium turnings, and 100 ml of ether). The solution was cooled and hydrolyzed with aqueous ammonium chloride. The mixture was extracted with ether and the extract washed with (*a*) 2 *N* sodium hydroxide solution, (*b*) 2 *N* hydrochloric acid, (*c*) aqueous sodium hydrogen carbonate solution, and dried ($MgSO_4$). The filtered solution was concentrated to 75 ml and refluxed for 1 h, the solvent removed, and the residual oil heated at 100°/0.5 mm for 12 h. Recrystallization of the yellow solid residue from ethanol and chromatography on grade 1 alumina (BDH) in benzene afforded pure *p*-tolyl-

TABLE 2. 9-Arylanthracenes

9-Substituent	Melting point (°C)	Yield (%)	Formula	Observed C	Observed H	Calculated C	Calculated H	λ_{max}(mμ)	log ε
C_6H_5	155–157	80	$C_{20}H_{14}$	94.61	5.72	94.23	5.62	255 364.5 384	5.15 4.10 4.10
p-$CH_3C_6H_4$	145–147	29	$C_{21}H_{16}$	94.02	6.13	94.00	6.00	256 364 384	5.16 4.01 3.99
p-$CH_3OC_6H_4$	165–167	24	$C_{21}H_{16}O$	88.82	5.71	88.73	5.70	257 364 384	5.10 4.02 4.00

TABLE 3. 9,10-Dihydro-9-arylanthracenes

9-Substituent	Melting point (°C)	Yield (%)	Formula	Observed C	Observed H	Calculated C	Calculated H
C_6H_5	89	49	$C_{20}H_{16}$	93.73	6.31	93.80	6.30
p-$CH_3C_6H_4$	104–106	69	$C_{21}H_{18}$	93.33	6.91	93.30	6.70
p-$CH_3OC_6H_4$	130–132	24	$C_{21}H_{18}O$	88.33	6.31	88.10	6.30

anthracene in pale yellow needles, 4.0 g (29% yield), m.p. 145–147°.

(b) 9,10-Dihydro-9-p-tolylanthracene

Sodium (10 g) was added in small portions to a refluxing solution of 2 g (7.47 mmol) of 9-*p*-tolylanthracene in 150 ml of ethanol, until the solution no longer fluoresced in u.v. light. The solution was diluted with 600 ml of water and the resulting precipitate collected. Recrystallization from ethanol afforded 9,10-dihydro-9-*p*-tolylanthracene in colorless plates, m.p. 104–106°, 1.4 g (69% yield). The properties of other 9-arylanthracenes together with their 9,10-dihydro derivatives prepared by this method are summarized in Tables 2 and 3.

Preparative Scale Dehydrogenations

The general method is exemplified for 9,10-dihydro-9-*p*-tolylanthracene.

A mixture of 0.242 g (0.9 mmol) of 9,10-dihydro-9-*p*-tolylanthracene and 0.271 g (1.1 mmol) of tetrachloro-1,2-benzoquinone in 7 ml of benzene was heated under reflux for 8 h. The resulting mixture was passed down a column of grade 1 alumina and the column eluted with benzene. The evaporated eluent (0.23 g) had λ_{max} 255, 364, 384 mμ (log ε, 5.19; 4.01; 4.10). Pure 9-*p*-tolylanthracene has λ_{max} 256, 364, 384 mμ (log ε, 5.15, 4.01, 4.10). The product therefore contained 9-*p*-tolylanthracene (99.5%) and the overall yield of the latter was 94.5%.

Similarly 9,10-dihydro-9-phenylanthracene afforded 9-phenylanthracene (95% yield) and 9,10-dihydro-9-*p*-anisylanthracene afforded 9-*p*-anisylanthracene (92.5% yield).

Dehydrogenation Reaction Rate Studies

Materials

Pure 1,2-dichlorobenzene was dried over sodium and then distilled and had b.p. 177–178° at 750 mm. Commercial samples of tetrachloro-1,2-benzoquinone were purified by sublimation *in vacuo*.

Reaction Rates

The rates were determined by following spectrophotometrically the disappearance of the red quinone. The E_0 values were determined by graphical extrapolation. The experimental method used and detailed treatment of the rate data have been described previously (16). Values for the second order rate constants for reaction of the dihydroanthracenes with the quinone at 80° together with the Arrhenius parameters are summarized in Table 1.

A representative kinetic run at one temperature is recorded in Table 4. A summary of the rate constants for all the runs at different temperatures is given in Table 5. Unless otherwise stated the initial concentration of both the acceptor and the donor were 0.0100 *M* and 1,2-dichlorobenzene was the solvent.

Control Reaction Between Triptycene and Tetrachloro-1,2-benzoquinone

Reaction between 187 mg of triptycene and 429 mg of tetrachloro-1,2-benzoquinone in 5 ml of refluxing benzene for 8 days resulted in the recovery of unchanged triptycene, m.p. 250–252° in 81% yield, which set an approximate upper limit for any reaction as $k = 2 \times 10^{-6}$ l mol^{-1} s^{-1}.

TABLE 4. Dehydrogenation of 9-*p*-tolylanthracene by tetrachloro-1,2-benzoquinone at 73.10°

Time (min)	*E* (560 mμ)	10*k* (l mol^{-1} s^{-1})
0	1.007	—
8	0.640	1.19
10	0.589	1.19
12	0.545	1.18
15	0.443	1.16
24	0.367	1.21
28	0.334	1.20
47	0.232	1.19

Can. J. Chem. Downloaded from www.nrcresearchpress.com by 210.87.254.42 on 09/05/12
For personal use only.

TABLE 5. Summary of rate constants*

9,10-Dihydro-anthracene		9,10-Dihydro-9-phenylanthracene (0.00862 *M*)		9,10-Dihydro-9-*p*-tolylanthracene		9,10-Dihydro-9-*p*-anisylanthracene	
T^0	10^2k†	T^0	10^2k†	T^0	10^2k†	T^0	10^2k†
30.7	1.88	58.9	3.69	56.8	4.18	52.5	3.43
38.2	3.02	68.0	6.43	58.7	4.46	57.2	4.71
52.2	6.98	69.2	7.43	59.5	4.83	62.4	6.48
60.7	11.10	74.2	9.53	63.6	5.89	63.7	6.75
68.2	17.5	76.3	9.87	66.4	7.19	68.7	9.31
				73.1	11.90	71.5	10.7

*Initial concentrations of donors where different from 0.01 *M* are given in brackets.
†The units are l mol^{-1} s^{-1}.

7-Phenyl-7,12-dihydropleiadene

7-Phenyl-7,12-dihydropleiadene **34** was prepared from 1-(β-benzhydryl)naphthylcarbinol by the method of Lansbury in 80% yield, m.p. 180–181° (lit. m.p. 179–179.5) (19).

Reaction of 7-Phenyl-7,12-dihydropleiadene with 2,3-Dichloro-5,6-dicyano-1,4-benzoquinone

A solution of 1.53 g (5 mmol) of 7-phenyl-7,12-dihydropleiadene in 25 ml of benzene was added to a solution of 2.26 g (0.01 mol) of 2,3-dichloro-5,6-dicyano-1,4-benzoquinone in 150 ml of benzene and the mixture refluxed for 8 h, then concentrated to about 20 ml and chromatographed on BDH alumina using hexane:benzene (3:1) as eluent. Crystallization of the resulting solid in benzene gave 0.81 g (53.3% yield) of **36**, m.p. 271–273°.

Anal. Calcd. for $C_{24}H_{16}$: C, 94.73; H, 5.27. Found: C, 94.67; H, 5.45.

The n.m.r. spectrum $\delta_{TMS}(CDCl_3)$: 5.16 (2H, s, C-7 and -12 protons); 6.95–7.67 (14H, m, aromatic protons).

Reaction of 7-Phenyl-7,12-dihydropleiadene with Tetrachloro-1,2-benzoquinone

A solution of 1.53 g (5 mmol) of 7-phenyl-7,12-dihydropleiadene in 50 ml of dry benzene was added to a solution of 3.66 g (15 mmol) of tetrachloro-1,2-benzoquinone in 125 ml of benzene and the mixture refluxed for 72 h. The solution was concentrated *in vacuo* to a small volume and chromatographed on BDH alumina using hexane:benzene as eluant. Recrystallization of the main fraction from benzene gave 1.22 g of **36**, (80.3% yield) m.p. 272°.

Anal. Calcd. for $C_{24}H_{16}$: C, 94.73; H, 5.27. Found: C, 94.53; H, 5.66.

This material was identical in every respect with that obtained in the preceding experiment.

7-Isopropyl-7,12-dihydropleiadene

7,12-Dihydropleiadene (6.9 g, 0.03 mol) was dissolved in 150 ml of anhydrous ether in a pressure bottle under an atmosphere of nitrogen and 14 ml of 2.25 *M* *n*-butyllithium in hexane added to it gradually with stirring. The bottle was securely stoppered and the complex stirred magnetically for 2 h. After cooling the mixture to −20°, 2.6 g (0.033 mol) of isopropylchloride in 10 ml of anhydrous ether was added from a syringe with stirring and under nitrogen. The bottle was stoppered again and the contents stirred at room temperature for 8 h. The complex was decomposed with ice and the ether layer dried (Na_2SO_4) and the solvent removed to give a thick yellow oil. This oil was treated with a hot methanolic solution of 2,4,7-trinitro-9-fluorenone when only the unreacted starting material formed a complex, which was removed by filtration. The solvent was removed from the filtrate and the residual oil extracted subjected to chromatography on BDH alumina using hexane as eluent to give **40** as a yellow oil. The n.m.r. spectrum $\delta_{TMS}(CDCl_3)$: 0.8–1.05 (6H, m, $CH(CH_3)_2$), 2.55 (1H, m, $CH(CH_3)_2$), 3.6 (1H, d, J_{AB} = 10.5 Hz, C-7 bridge proton), 3.84, 5.14 (2H, q, $J_{A'B'}$ = 16 Hz, C-12 bridge protons), 7.0–7.83 (10H, m, aromatic protons) (20).

Reaction of 7-Isopropyl-7,12-dihydropleiadene with Tetrachloro-1,2-benzoquinone

A solution of 1.7 g (6.25 mmol) of 7-isopropyl-7,12-dihydropleiadene in 75 ml of dry chlorobenzene was added to a solution of 3.20 g (0.0120 mol) of tetrachloro-1,2-benzoquinone in 125 ml of chlorobenzene and the mixture refluxed for 72 h. The solvent was removed *in vacuo* and the residue dissolved in benzene and subjected to chromatography on BDH alumina using 1:1 hexane:benzene as eluent to give 1.56 g **41**, m.p. 160–165°.

Anal. Calcd. for $C_{27}H_{18}Cl_4O_2$ (mol. wt. 514.0063): Cl, 27.24. Found (514.0050 (mass spectrum)): Cl, 27.44.

The i.r. spectrum $\nu_{max}(CHCl_3)$: 1455, 1425 cm^{-1} (—C—O—C—); n.m.r. spectrum $\delta_{TMS}(CDCl_3)$: 0.5–1.5 (6H, m, $CH(CH_3)_2$), 1.87 (1H, m, J = 5 Hz, $CH(CH_3)_2$), 7.0–8.2 (8H, m, aromatic protons).

1. L. M. JACKMAN. Advances in organic chemistry. Vol. II. Interscience Publishers, London, 1960. p. 329.
2. E. A. BRAUDE, L. M. JACKMAN, and R. P. LINSTEAD. J. Chem. Soc. 3548 (1954).
3. J. W. LOWN and A. S. K. AIDOO. Can. J. Chem. **44**, 2507 (1966).
4. J. W. LOWN, R. WESTWOOD, and A. S. K. AIDOO. Can. J. Chem. **48**, 327 (1970).
5. G. BINSCH and I. TAMIR. J. Am. Chem. Soc. **91**, 2450 (1969).
6. D. P. CRAIG. Theoretical organic chemistry. The Kekulé Symposium. Butterworths Scientific Publications, London, 1959. p. 20.
7. M. P. CAVA and R. H. SCHLESSINGER. Tetrahedron, 3073 (1965).
8. L. F. FIESER. J. Am. Chem. Soc. **53**, 3546 (1931).
9. L. HORNER and H. MERZ. Ann. **570**, 89 (1950).
10. E. A. BRAUDE, L. M. JACKMAN, R. P. LINSTEAD, and G. LOWE. J. Chem. Soc. 3123 (1960).
11. D. J. POINTER, J. B. WILFORD, and O. J. R. HODDER. Chem. Commun. 1440 (1969).

Can. J. Chem. Downloaded from www.nrcresearchpress.com by 210.87.254.42 on 09/05/12
For personal use only.

12. L. M. JACKMAN and D. T. THOMPSON. J. Chem. Soc. 4794 (1961).
13. C. L. JACKSON and R. D. MACLAURIN. Am. Chem. J. **37**, 7 (1907).
14. L. M. JACKMAN and J. W. LOWN. Unpublished results.
15. A. H. BECKETT and A. L. MULLEY. J. Chem. Soc. 4159 (1955).
16. E. A. BRAUDE, L. M. JACKMAN, R. P. LINSTEAD, and J. S. SHANNON. J. Chem. Soc. 3116 (1960).
17. P. T. LANSBURY, J. B. BIEBER, F. D. SAEVA, and K. R. FOUNTAIN. J. Am. Chem. Soc. **91**, 399 (1969).
18. P. T. LANSBURY, J. F. BIERON, and M. KLEIN. J. Am. Chem. Soc. **88**, 1477 (1966).
19. P. T. LANSBURY. J. Am. Chem. Soc. **81**, 4325 (1959).
20. P. T. LANSBURY, A. J. LACHER, and F. D. SAEVA. J. Am. Chem. Soc. **89**, 4361 (1967).

Can. J. Chem. Downloaded from www.nrcresearchpress.com by 210.87.254.42 on 09/05/12
For personal use only.

Can. J. Chem. Downloaded from www.nrcresearchpress.com by 210.87.254.40 on 09/05/12
For personal use only.

Quinodimethane Analogs in the Pleiadene and Acepleiadene Systems

J. W. LOWN AND A. S. K. AIDOO
Department of Chemistry, University of Alberta, Edmonton 7, Alberta

Received January 6, 1971

5,10-Dimethylene-5,10-dihydroacepleiadene and 7,12-dimethylene-7,12-dihydropleiadene have been synthesized. Their facile hydration to bridged epoxide structures suggests a non-planar boat structure in which they react as dienes. Evidence is presented for the base-catalyzed tautomerization of the former to the 18π peripheral aromatic 5,10-dimethylacepleiadylene. The isoelectronic diketone and methylene ketones in the acepleiadene series similarly tautomerize with potassium *t*-butoxide in dimethyl sulfoxide giving rise to stable radical anions.

On a synthétisé le diméthylène-5,10 dihydro-5,10 acépléiadène et le diméthylène-7,12 dihydro-7,12 pléiadène. Le fait que ces composés s'hydratent facilement pour conduire à des composés ayant une structure époxyde permet de croire qu'ils réagissent comme diènes dans une conformation bateau non-planaire. Des données sont présentées qui permettent de conclure que le premier de ces composés se tautomérise en milieu basique pour donner le diméthyl-5,10 acépléiadylène qui est aromatique et qui possède 18 électrons π périphériques. De la même manière les composés isoélectroniques, dicétone et méthylène-cétone de la série acépléiadène, se tautomérisent, en présence de *t*-butylate de potassium dans le DMSO, pour fournir des radicaux anions stables.

Canadian Journal of Chemistry, 49, 1861 (1971)

The possible intermediacy of 9,10-anthraquinodimethane (**1**) in the quinone dehydrogenation of 9,10-dimethylanthracene (1) and the generation of pleiadenes containing an ortho-quinodimethane moiety from 7,10-dihydropleiadenes by the same method (2) suggested that analogs of **1** could be prepared in the pleiadene **2** and acepleiadene **3** series.

The synthesis of **2** and **3** could be used to test theoretical predictions of their properties of either (*i*) pseudoaromaticity in which case they would possess non-planar structures and react as dienes or (*ii*) aromaticity like **1** and exhibit high free valence reactivity of the exocyclic methylene groups requiring planar structures. Also the possible tautomerization of **3** to the 18π peripheral aromatic compound **4** could be studied.

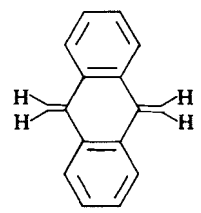

1

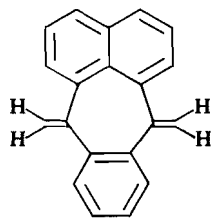

2

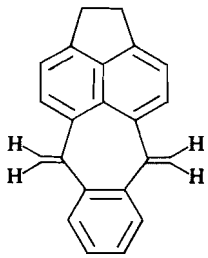

3

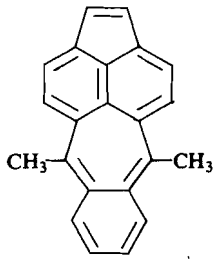

4

Synthesis of 7,12-Dimethylene-7,12-dihydropleiadene and 5,12-Dimethylene-5,10-dihydroacepleiadene

Reaction of 7-methylene-7,12-dihydropleiaden-12-one (**5**) with methylmagnesium iodide in ether at room temperature gave only 7-hydroxy-7-methyl-12-methylene-7,2-dihydro pleiadene (**6**). This reaction has been reported recently not to proceed under these conditions (3). In contrast when **5** was added to methylmagnesium iodide in ether/benzene and the mixture refluxed, a mixture of 7,12-dimethyl-7,12-epoxy-7,12-dihydropleiadene (**7**) and 7,12-dimethylene-7,12-dihydropleiadene (**2**) were obtained (see Scheme 1). Compound **6** was converted quantitatively into **7** upon brief heating with acid, whilst **7** in turn could be dehydrated to **2** in fair yield by heating with potassium hydrogen sulfate. The preparation of **2** has been reported recently employing a similar route (3). 5,12-Dihydroacepleiadene-5,12-dione (**8**) (4), was added to methyl magnesium iodide in ether to give 5-methyl-5,12-epoxy-5,12-dihydropleiaden-12-ol (**9**) (compare **6** above) which was readily dehydrated by treat-

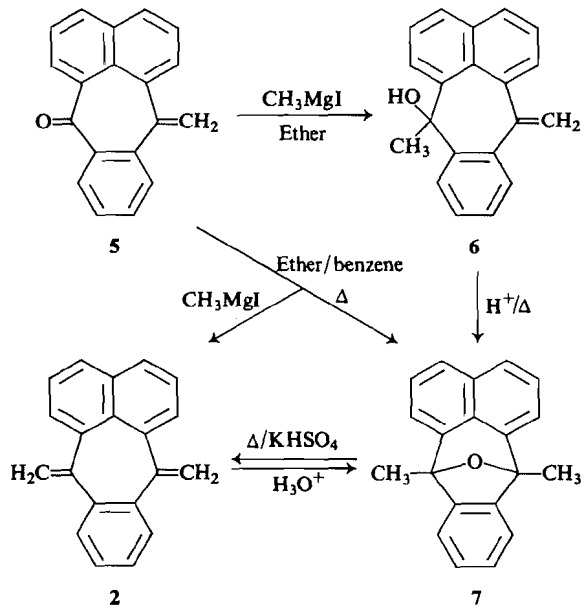

SCHEME 1

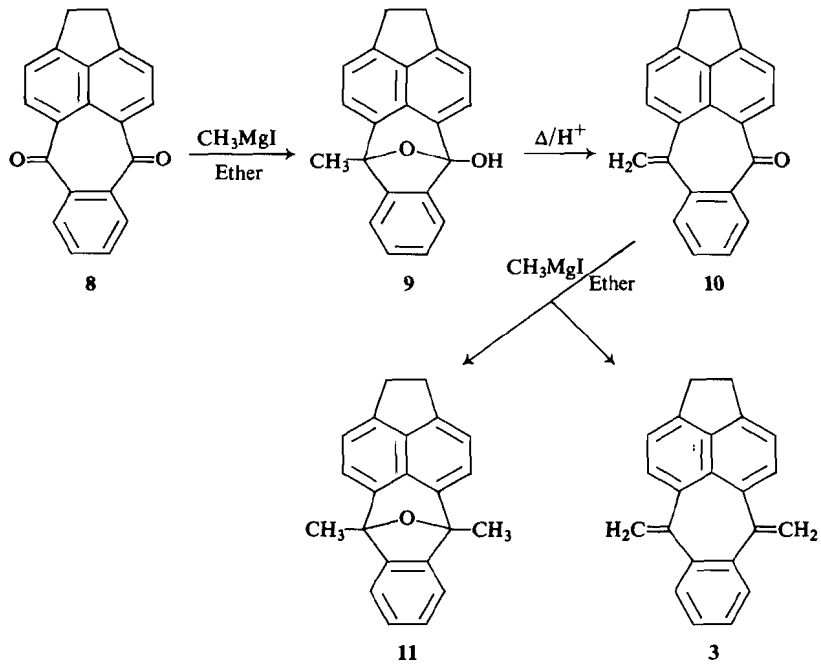

SCHEME 2

ment with *p*-toluenesulfonic acid in benzene to give 5-methylene-5,12-dihydropleiaden-12-one (**10**).

Treatment of **10** with methylmagnesium iodide in ether gave a mixture of **11** and the required compound **3** which were separated by chromatography on a silicic acid column (see Scheme 2).

Can. J. Chem. Downloaded from www.nrcresearchpress.com by 210.87.254.40 on 09/05/12
For personal use only.

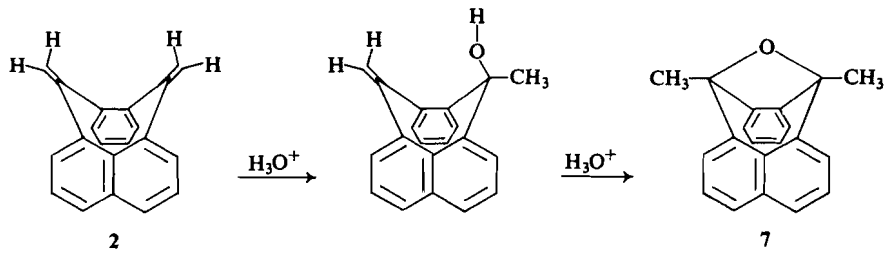

2 7

SCHEME 3

Properties of 7,12-Dimethylene-7,12-dihydropleiadene and 5,10-Dimethylene-5,10-dihydroacepleiadene

Compound **2** is quite hygroscopic and a solution of **2** in benzene gradually absorbed atmospheric moisture and was converted into **7**, a reaction which could be easily monitored by n.m.r. spectroscopy. The appearance of a sharp singlet (6H) at 2.13 δ indicated the formation of **7** while the diminution of the vinyl absorption at 5.22 and 5.49 δ signaled the disappearance of **2**. This conversion becomes very rapid when a solution of **2** is refluxed in the presence of acid catalysts. Compound **3** is similarly readily converted into the ether **11**. This ready formation of **7** from both **6** and **2** and the marked stability of **7** and of **11** made dehydration of the latter difficult.

The facile ring closure observed in the formation of **7** and **11** is attributed to the geometry of the seven-membered rings and to the known conformational preference of the hydroxyl group for an axial position and of the methyl group for the equatorial position in pleiadene systems (5) (see Scheme 3).

Another example of such transannular participation attributed to the ideal geometry of the pleiadene system and conformational preference of substituents at the bridge positions is in the quinone dehydrogenative cyclization of 7-phenyl-7,12-dihydropleiadene (2).

The stability of **2** and **3** compared with **1** leads to the conclusion that these hydrocarbons lack coplanarity in the seven-membered ring and react as dienes.

When a 2.5×10^{-2} *M* solution of potassium *t*-butoxide in dimethylsulfoxide was added to a 10^{-2} *M* solution of **3** in the same solvent a deep greenish-blue color was obtained which showed absorption maxima at 248, 326, 354, 498, and 625 mμ in the visible and u.v. regions, characteristic of the acepleiadylene moiety (4). This is attributed to base-catalyzed tautomerization of **3** to the aromatic 5,10-dimethylacepleiadylene (**12**). Cava and Schlessinger similarly obtained a blue solution of acepleiadylene by treatment of 5,10-dihydroxy-5,10-dihydroacepleiadene with hydrogen bromide. Compound **12**, like acepleiadylene, is stable only in solution, and upon attempted work-up yielded only polymers. Acepleiadylene upon attempted isolation gives a mixture of polymers and dimer (4).

Generation of Radical Anions from Acepleiadene Derivatives

The facile tautomerization in solution of **3** to **12** suggested examination of the properties of the diketone **8** which is isoelectronic with **3**. This led to the generation of stable radical anions.

Treatment of a 1×10^{-2} *M* solution of the diketone **8** in dimethylsulfoxide with a 2.5×10^{-2} *M* solution of potassium *t*-butoxide solu-

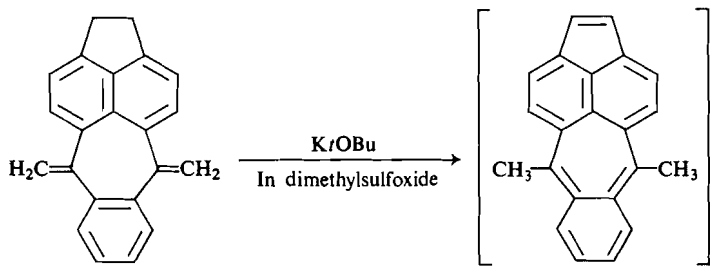

3 12

Can. J. Chem. Downloaded from www.nrcresearchpress.com by 210.87.254.40 on 09/05/12
For personal use only.

Can. J. Chem. Downloaded from www.nrcresearchpress.com by 210.87.254.40 on 09/05/12
For personal use only.

tion at ambient temperature gave a deep blue solution containing a paramagnetic species **14** as evidenced by a strong e.p.r. signal which persisted for 72 h.

Russell and coworkers (10) have generated many semidione anions by treatment of diones with potassium *t*-butoxide or the enolate anion of propiophenone in dimethylsulfoxide solution. The e.p.r. spectrum showed extensive hyperfine coupling with a spectrum width of 11.0 Oe (see Fig. 1). The blue solution in dimethylsulfoxide showed absorption in the u.v. and visible region at 342, 362(sh), 552 and 688 mμ, characteristic of an acepleiadylene structure (4) (compare absorption spectrum of 12).

The identical e.p.r. spectrum was obtained when a 1×10^{-2} *M* solution of 5,10-dihydroacepleiadylene-5,10-dione (**15**) in dimethylsulfoxide was treated with 2×10^{-2} *M* potassium *t*-butoxide in dimethylsulfoxide (see Scheme 4).

Compound **15** was prepared as illustrated in Scheme 5. 5,10-Dihydroacepleiadene-5,10-dione was treated with 2 mol equiv of *N*-bromosuccinimide to give the dibromide **16** which was then dehalogenated by refluxing an acetone solution of **16** with potassium iodide.

Dauben *et al.* have suggested that a similar mechanism to that outlined in Scheme 4 is operative in the conversion of certain cyclic 1,4-diketones by shaking an alkaline alcoholic solution in air, via the dianion thence to the radical anion to an enedione (6).

Further support for the structure of the radical anion **14** is provided by the reduction of the diketone **15** with potassium in dimethoxyethane. The e.p.r. spectrum obtained had the same gross features as that obtained in dimethyl sulfoxide but differed in details as expected for radicals generated under two quite different conditions. The distribution of spin density in an aromatic radical anion is affected by the polarity of the solvent (7). The spin density variation with solvents is assumed, to a first approximation, to be affected only by localized complexes between solvent and polar substituents in the radical anion (7*b*). The identity of the radical anion species obtained under both oxidizing and reducing conditions from **8** and **15** respectively precludes the possibility of oxidation at the 1 and

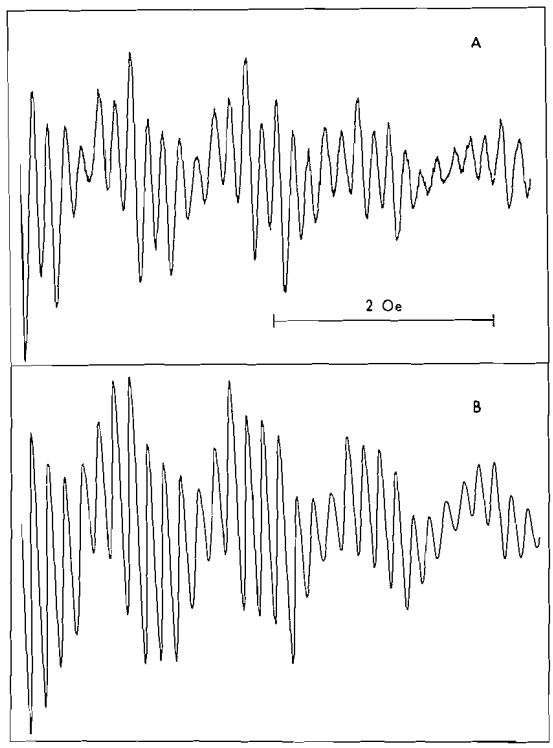

FIG. 1. (A) Experimental partial e.p.r. spectrum of 7,12-acepleiadylene semidione anion obtained from 1×10^{-2} *M* solution of 5,12-dihydroacepleiadene-5,12-dione with 2.5×10^{-2} *M* potassium *t*-butoxide in dimethylsulfoxide solution at room temperature. (B) Simulated partial e.p.r. spectrum using Lorentzian lines with a peak to peak width of 0.100 Oe (see Experimental for values of hyperfine coupling constants).

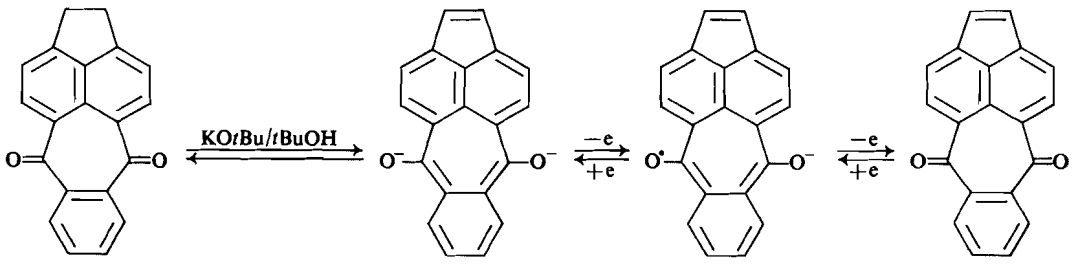

8 **13** **14** **15**

SCHEME 4

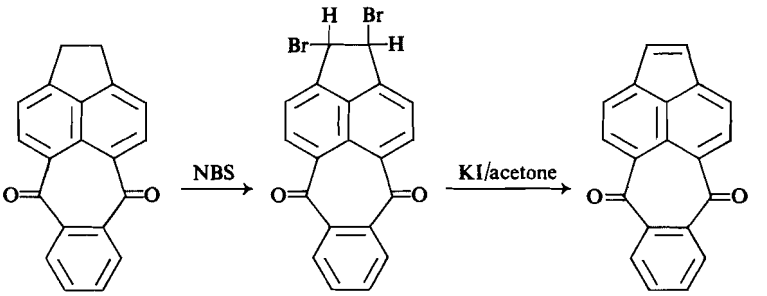

8 16 15

SCHEME 5

2 positions of **8** upon treatment with potassium *t*-butoxide.

Trost and coworkers found differences in the e.p.r. spectra of the related pyracyclosemiquinone anion **18** generated from 1,2-diketopyracene **17** by (*i*) potassium *t*-butoxide reduction in dimethylsulfoxide and (*ii*) irradiation of a 1,2-dimethoxyethane solution in the presence of sodium hydroxide or potassium hydroxide (8).

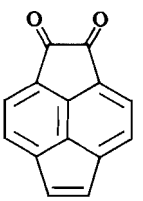

17

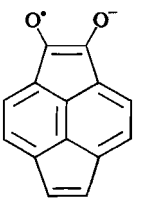

18

Values for the hyperfine coupling constants in the radical anion **14** were derived by obtaining the closest fit of a simulated spectrum, using Lorentzian lines with a peak to peak width of 0.100 Oe, with the experimental spectrum (see Fig. 1 and Experimental). Experiments are in hand to make the assignments of the coupling constants in **14** and analogous radical anions involving the syntheses of specifically deuterated compounds.

One of the most stable paramagnetic species is the super-oxide anion $O^{\cdot}—O^{-}$. The phenylogues of this species, the semi-quinones, are well known and have been explored exhaustively (9) while the vinylogues, the semidiones, have been examined by Russell and his coworkers (10). The 7,12-acepleiadylene semidione anion **14** represents an extension of this series, and evidently owes its stability to the aromaticity of the acepleiadylene moiety which possesses an 18 π-electron periphery since 7,12-pleiadenedione could not be induced to form a radical anion under similar conditions. The radical anion **14** appears to be much more stable than the parent hydrocarbon acepleiadylene which retains its blue color in solution for only 40 min (4).

The successful isomerization of the diene **3** to the acepleiadylene **12** and the generation of the radical anion **14** from the diketone **8** suggested examination of derivatives of **8** such as **10** under similar conditions. Accordingly a 1×10^{-3} *M* solution of 5-methylene-5,10-dihydroacepleiaden-10-one (**10**) in dimethyl sulfoxide was treated with potassium *t*-butoxide to give a stable paramagnetic species which gave a strong e.p.r. spectrum, which is attributed to the radical anion **19**. 5-Benzylidene-5,10-dihydroacepleiaden-12-one (**20**) was also observed to give a strong e.p.r. spectrum on treatment with potassium *t*-butoxide in dimethylsulfoxide which is ascribed to the radical anion **21**. Compound **20** was prepared by a similar sequence of reactions as was employed to synthesize **10**, *i.e.* by reaction of **8** with benzylmagnesium chloride in ether and acid-catalyzed dehydration of the resulting alcohol to give **20**.

Radical anions of the type **19** and **21** are a logical extension of species **14** and are analogs of benzophenone ketyl.

Experimental

Melting points were determined on a Fisher–Johns apparatus and are uncorrected. The i.r. spectra were recorded on a Perkin–Elmer model 421 spectrophotometer, and only the principal, sharply defined peaks are reported. The n.m.r. spectra were recorded on Varian A-60 and A-100 analytical spectrometers. The spectra were measured on approximately 10–15% (w/v) solutions in $CDCl_3$, with tetramethylsilane as a standard. Line positions are reported in p.p.m. from the reference.

Can. J. Chem. Downloaded from www.nrcresearchpress.com by 210.87.254.40 on 09/05/12
For personal use only.

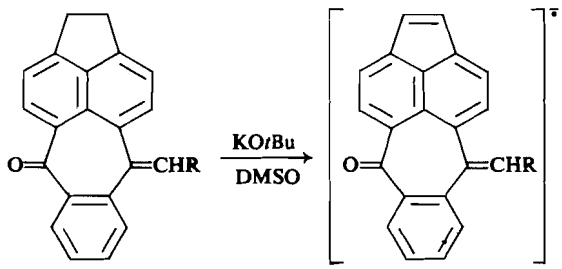

10 R = H **19** R = H; spectrum width, 15.53 Oe
20 R = Ph **21** R = Ph; spectrum width, 15.75 Oe

Absorption spectra were recorded in 'spectro'-grade solvents on a Beckman DB recording spectrophotometer. Mass spectra were determined on an Associated Electrical Industries MS-9 double focussing high resolution mass spectrometer. The ionization energy, in general, was 70 eV. Peak measurements were made by comparison with perfluorotributylamine at a resolving power of 15000. First derivative e.p.r. spectra were measured on a Varian V-2503 spectrometer fitted with a V-4532 dual cavity, operating at a nominal frequency of 9.5 GHz. The microwave power incident on the cavity was attenuated to 10 db below maximum. Hyperfine couplings were measured by comparison with a peroxylamine disulfonate solution in the audio cavity. The triplet spacing of the standard was taken to be 13.0 Oe. Kieselgel DF-5 (Camag, Switzerland) and Eastman Kodak precoated sheets were used for thin layer chromatography. Microanalyses were carried out by Mrs. D. Mahlow of this department.

7,12-Dihydropleiadene

7,12-Dihydropleiadene was prepared from 1-chloro-7,12-dihydropleiadene by a modification of the method of Cava and Schlessinger (11). A mixture of 25 g (0.095 mol) of 1-chloro-7,12-dihydropleiadene, 5 g of 10% palladium-on-charcoal, 100 ml of 85% hydrazine hydrate, and 1000 ml of 95% ethanol was refluxed for 1 h. The filtered solution was concentrated to *ca.* 100 ml, acidified with 2 *N* hydrochloric acid, and the solid product collected, washed repeatedly with water, and dried. Recrystallization from hexane gave 20 g (91.8% yield) of 7,12-dihydropleiadene, m.p. 115–117° (lit. (11), 116°).

7,12-Dihydropleiadene-7,12-dione

7,12-Dihydropleiadene-7,12-dione was prepared in 93% yield from 7,12-dihydropleiadene by the method of Cava and Schlessinger (11), m.p. 166–168° (lit. 168° (11)).

7,12-Epoxy-7-hydroxy-12-methyl-7,12-dihydropleiadene

7,12-Dihydropleiadene-7,12-dione (20 g, 77 mmol) was added during 30 min to a stirred solution of methyl magnesium iodide (prepared from 6 g of magnesium and 30 g of methyl iodide in 200 ml of anhydrous ether). After addition was completed, stirring was continued for 12 h. The complex was decomposed with cold saturated ammonium chloride solution, the ether layer washed with water, dried (Na_2SO_4), and concentrated to give 19.6 g (92.3% yield) of the ether, m.p. 186–188° (lit. (3) 184–186°).

Anal. Calcd. for $C_{19}H_{14}O_2$ (mol. wt. 274.0994): C, 83.21; H, 5.11. Found (274.0996 (mass spectrum)): C, 82.96; H, 5.08.

7-Methylene-7,12-dihydropleiaden-12-one

A catalytic amount of *p*-toluenesulfonic acid was added to a solution of 13.7 g (0.05 mol) of 7,12-epoxy-7-methyl-7,12-dihydropleiadene-7-ol in 400 ml benzene and the mixture refluxed for 8 h. After cooling, the solution was washed successively with water, 10% sodium bicarbonate, and water; dried and concentrated to give 10 g (85% yield) of **5**, m.p. 155–157° (lit. (3) 154–156°).

Anal. Calcd. for $C_{19}H_{12}O$ (mol. wt. 256.0888): C, 89.06; H, 4.69. Found (256.0888 (mass spectrum)): C, 89.09; H, 4.77.

7-Hydroxy-7-methyl-7,12-dihydropleiaden-12-ene

7-Methylene-7,12-dihydropleiaden-12-one (0.5 g, 19.5 mmol) was added to a Grignard reagent (0.5 and 3 g iodomethane in 30 ml of anhydrous ether) and stirred for 30 min. The mixture was then refluxed gently for another 30 min, stirring continued overnight, cooled, and the complex decomposed with ice and saturated solution of ammonium chloride. The ether layer was washed with water, dried ($MgSO_4$), and solvent removed to yield a gum which was triturated with hexane to give 0.41 g (77.3% yield) of **6** as a crystalline solid, m.p. 114–116°.

Anal. Calcd. for $C_{20}H_{16}O$ (mol. wt. 272.1201): C, 88.24; H, 5.88. Found (272.1200 (mass spectrum)): C, 88.08; H, 5.90.

The i.r. spectrum ν_{max} ($CHCl_3$): 3690, 3610, 3580 cm^{-1} (O—H); n.m.r. spectrum δ_{TMS} ($CDCl_3$): 1.97 (3H, singlet, C-7 methyl protons); 5.6, 5.2 (2H, pair of doublets J_{AB} = 1.5 Hz, C-12 methylene protons); 7.3–8 (11H, multiplet, aromatic ring protons and O—*H*).

7-12-Dimethylene-7,12-dihydropleiadene and 7,12-Dimethyl-7,12-epoxy-7,12-dihydropleiadene

7-Methylene-7,12-dihydropleiaden-12-one (1 g, 0.004 mol) was added with stirring over 30 min to a Grignard reagent, prepared from 1 g of magnesium and 6 g of iodomethane in 30 ml of anhydrous ether. Dry benzene (30 ml) was then added to the mixture and refluxed with stirring overnight, cooled, and decomposed with ice and ammonium chloride solution. The organic layer was washed with water, dried, and solvent removed *in vacuo* to yield a gum. This gum was dissolved in benzene and subjected to chromatography on B.D.H. silica gel using hexane as eluant to give 26 mg (25% yield) of **2**, m.p. 91–93° (lit. (3) 88–90°). The i.r. spectrum ν_{max} (CCl_4): 1625 cm^{-1} (C=C); n.m.r. spectrum δ_{TMS} (CCl_4): 5.22,

Can. J. Chem. Downloaded from www.nrcresearchpress.com by 210.87.254.40 on 09/05/12
For personal use only.

Can. J. Chem. Downloaded from www.nrcresearchpress.com by 210.87.254.40 on 09/05/12
For personal use only.

5.49 (4H, a pair of doublets, J = 2 Hz, CH_2); 7.0–7.8 (10H, multiplet, aromatic protons).

Further elution with benzene gave 0.65 g (60% yield) of **7**, m.p. 152–153°.

Anal. Calcd. for $C_{20}H_{16}O$ (mol. wt. 272.1201): C, 88.24; H, 5.88. Found (272.1200 (mass spectrum)): C, 88.13; H, 5.69.

The n.m.r. spectrum δ_{TMS} ($CDCl_3$): 2.13 (6H, singlet, methyl protons); 7.0–7.75 (8H, multiplet, aromatic protons).

Dehydration of 7,12-Dimethyl-7,12-epoxy-7,12-dihydropleiadene

A mixture of 1.4 g (5 mmol) of **7**, and 0.5 g of potassium hydrogen sulfate was heated in an oil bath at 140° for 15 min. The mixture was cooled and extracted with hexane, and the hexane solution subjected to chromatography on silicic acid (p*H* 7) to give 1.1 g (85% yield) of **2**.

5-Methylene-5,10-dihydroacepleiaden-12-one

A suspension of 2.84 g (0.01 mol) of 5,10-dihydropleiadene-5,10-dione (4) in 50 ml of dry benzene was added to a Grignard reagent prepared from 4.3 g of magnesium and 22.5 g of iodomethane in 150 ml of anhydrous ether. The mixture was stirred for 30 min; 70 ml of ether was distilled off and replaced by 50 ml of dry benzene. The reaction mixture was then refluxed overnight, cooled, decomposed with ice, and saturated ammonium chloride solution, the organic layer dried ($MgSO_4$), and solvent removed *in vacuo* to give a light yellow solid, **9**. The i.r. spectrum ν_{max} ($CHCl_3$): 3605, 3576 cm^{-1} (O—H); n.m.r. δ_{TMS} ($CDCl_3$): 2.1 (3H, singlet methyl protons); 3.26 (4H, C-1 and -2 protons).

Compound **9** without further purification was dissolved in benzene and a small amount of *p*-toluenesulfonic acid added to the solution. The mixture was refluxed for 4 h, cooled, washed with water, sodium bicarbonate solution, and water; the benzene solution dried, concentrated, and the residue subjected to chromatography on B.D.H. alumina using benzene as eluant to give 1.5 g (88.2%) of **10** as a brilliant yellow solid, m.p. 202–205°.

Anal. Calcd. for $C_{21}H_{14}O$ (mol. wt. 282.1045): C, 89.37; H, 4.96. Found (282.1040 (mass spectrum)): C, 88.94; H, 4.95.

The i.r. spectrum ν_{max} ($CHCl_3$): 1648 cm^{-1} (C=O); n.m.r. spectrum δ_{TMS} ($CDCl_3$): 3.41 (4H, singlet, C-1 and -2 protons); 5.42, 5.50 (2H, pair of doublets, J = 1.5 Hz, $=CH_2$); 7.2–8.4 (8H, aromatic protons).

Reaction of 5-Methylene-5,10-dihydroacepleiaden-12-one with Methylmagnesium Iodide

A methylmagnesium iodide solution was prepared from 2.4 g of magnesium and 14.5 g of iodomethane, in 100 ml of anhydrous ether; and 2.0 g (0.007 *M*) of 5-methylene-5,10-dihydroacepleiaden-12-one was added to it a little at a time, with stirring. Stirring was continued for 8 h, the complex decomposed with ice and ammonium chloride, the ether layer dried (Na_2SO_4) and solvent removed to give a light yellow oil. This oil was dissolved in benzene and subjected to chromatography on silicic acid (p*H* 7), using hexane as eluant to give 0.5 g (25.3% yield) of **3** as a light yellow oil, which solidified on standing, m.p. 85–87°.

Anal. Calcd. for $C_{22}H_{16}$ (mol. wt. 280.1252): C, 94.28; H, 5.72. Found (280.1253 (mass spectrum)): C, 94.30; H, 5.78.

The n.m.r. spectrum δ_{TMS} ($CDCl_3$): 3.27 (4H, singlet, C-1 and -2 protons); 5.3, 5.56 (4H, a pair of doublets, J = 1.5 Hz, $=CH_2$); 7.05–7.65 (8H, multiplet, aromatic ring protons).

Further elution with benzene gave 0.7 g (33.6% yield) of **11**, m.p. 222–224°.

Anal. Calcd. for $C_{22}H_{18}O$ (mol. wt. 298.1357): C, 88.59; H, 6.04. Found (298.1355): C, 88.46; H, 6.12.

The n.m.r. spectrum δ_{TMS} ($CDCl_3$): 2.15 (6H, singlet, methyl protons); 3.23 (4H, singlet, C-1 and -2 bridge protons); 7.05–7.43 (8H, multiplet, aromatic protons).

1,2-Dibromo-5,10-dihydroacepleiadene-5,10-dione

N-Bromosuccinimide (5.34 g, 0.030 mol) was added to a refluxing solution of 4.26 g (0.015 mol) 5,10-dihydroacepleiadene-5,10-dione and benzoyl peroxide in carbon tetrachloride, over a period of 10 min and refluxing was continued for an additional 1½ h. The succinimide was removed, and the mother liquor concentrated and cooled to give a dull yellow solid. This was further crystallized from carbon tetrachloride to give 6.5 g (98% yield) of **16**, m.p. 200°.

Anal. Calcd. for $C_{20}H_{10}Br_2O_2$ (mol. wt. 439.9047): C, 54.30; H, 2.26; Br, 36.20. Found (439.9046 (mass spectrum)): C, 54.40; H, 2.27; Br, 36.41.

The i.r. spectrum ν_{max} ($CHCl_3$) 1650 cm^{-1} (C=O); n.m.r. spectrum δ_{TMS} ($CDCl_3$): 5.95 (2H, singlet, C-1 and -2 protons); 7.5–8.1 (8H multiplet, aromatic protons).

5,10-Dihydroacepleiadylene-5,10-dione

1,2-Dibromo-5,10-dihydroacepleiadene-5,10-dione (3.08 g 0.07 mol) was dissolved in 300 ml of acetone, and 15 g of potassium iodide was added to the solution under nitrogen. The reaction mixture was refluxed for 3 h, cooled, poured into sodium thiosulfate solution, and extracted with chloroform. The chloroform layer was dried (Na_2SO_4) and solvent concentrated to give a red solid, which was recrystallized from methanol to give brick red flakes of **15**, 1.4 g (71% yield), m.p. 196–198°.

Anal. Calcd. for $C_{20}H_{10}O_2$ (mol. wt. 282.0681): C, 85.11; H, 3.55. Found (282.0678 (mass spectrum)): C, 84.87; H, 3.53.

The i.r. spectrum ν_{max} ($CHCl_3$): 1660 cm^{-1} (C=O); n.m.r. spectrum: δ_{TMS} ($CDCl_3$): 7.05 (2H, singlet, C-1 and -2 protons); 7.55–8.40 (8H, multiplet, aromatic protons).

5-Benzylidene-5,10-dihydroacepleiaden-12-one

5,10-Dihydroacepleiadene-5,10-dione, 2.84 g (0.001 mol), was added a little at a time to a Grignard reagent prepared from 2 g of magnesium and 13 g of benzyl-chloride in 200 ml of ether. Ether was distilled off (100 ml) and replaced by 100 ml of dry benzene and the mixture refluxed for 8 h. The complex was then decomposed with ice and saturated solution of ammonium chloride. The organic layer was dried (Na_2SO_4) and the solvent was removed *in vacuo* to give the hydroxyketone as a brilliant yellow solid. The i.r. spectrum ν_{max} ($CHCl_3$): 3530 (O—H) 1653 cm^{-1} (C=O); n.m.r. spectrum δ_{TMS} ($CDCl_3$): 3.5 (4H, singlet, C-1 and -2 protons); 5.13 (2H, singlet, $—CH_2—$Ph); 7.25–8.2 (13H, multiplet, aromatic protons).

This yellow solid, without further purification was dissolved in benzene, *p*-toluenesulfonic acid was added, and the solution was refluxed for 3 h. The reaction mixture was worked-up as for **10** to give 1.4 g (37.2%

yield) of 5-benzylidene-5,10-dihydroacepleiaden-12-one (**20**), m.p. 182–184°.

Anal. Calcd. for $C_{27}H_{18}O$: C, 90.48; H, 5.25. Found: C, 90.51; H, 5.24.

The i.r. spectrum ν_{max} ($CHCl_3$): 1645 cm^{-1} (C=O); n.m.r. spectrum δ_{TMS} ($CDCl_3$) 3.6 (4H, singlet, C-1 and -2 protons); 6.7 (1H, singlet, $=\!\!<^{Ph}_{H}$); 6.87–8.4 (13H, multiplet, aromatic protons).

Electron Spin Resonance Determinations

(a) Generation of Radical Anions in Dimethylsulfoxide

The dimethylsulfoxide used was dried with sodium sulfate, distilled, and kept standing on molecular sieve.

The radical anions were generated according to the method of Russell *et al.* (12). Solutions of the diketones in dimethylsulfoxide were placed in one leg of an inverted U-cell; the potassium *t*-butoxide in dimethylsulfoxide was placed in the other leg, and both solutions simultaneously deoxygenated by streams of prepurified nitrogen. After about 15–20 min of deoxygenation, the solutions were mixed by inverting the cell and the final solution was shaken into the sample cell, and the e.p.r. spectrum recorded. Fremy's salt in saturated sodium carbonate was used as a calibration standard.

(b) Generation of Radical Anion by Reduction of 5,10-Dihydroacepleiadylene-5,10-dione with Potassium in 1,2-Dimethoxyethane

The dimethoxyethane used was dried over sodium and distilled. It was kept standing on freshly-cut sodium.

The apparatus used is sketched in Fig. 2. About 6 mg of **15** was placed in the sample tube and the apparatus set up as shown in the diagram. Small pieces of freshly cut potassium were placed in bulb A, and the cell sealed off at D. The complete apparatus was evacuated and some potassium distilled into the bulb B. The cell was then sealed off at E. Dimethoxyethane was then distilled into the sample tube C, to dissolve the sample. The cell was then sealed off at F, allowed to cool, and inverted to allow the solution to come into contact with the potassium for about 2 min. After about 15 min, the solution went blue, indicating the formation of the radical anion, and the e.p.r. spectrum was recorded as for section *a*.

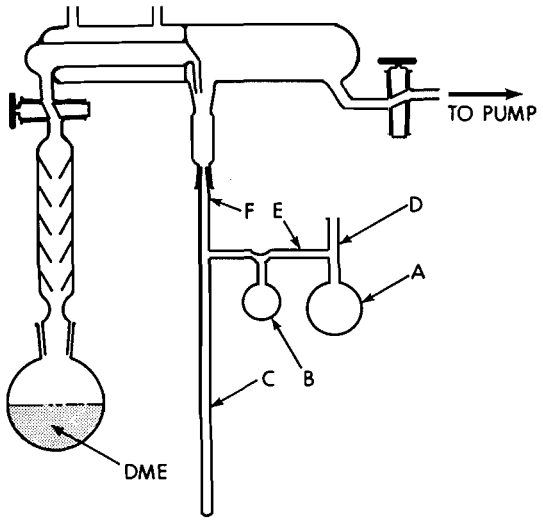

FIG. 2. Diagram of apparatus used in generation of acepleiadylene-5,10-semidione anion from 5,10-dihydroacepleiadylene-5,10-dione by reduction with potassium metal in 1,2-dimethoxyethane.

The hyperfine coupling constants for species **14** determined by the best fit of the simulated spectrum with that of the experimental spectrum were 2.50, 2.05, 1.11, 0.30, and 0.15 Oe.

This research was supported by a National Research Council of Canada grant to J. W. Lown. We thank Mr. R. Swindlehurst, Dr. A. Hogg, and Mr. G. Bigam for the n.m.r., mass, and e.p.r. spectra respectively. We also thank Dr. R. E. D. McClung for helpful discussions on the interpretation of the e.p.r. spectra.

1. J. W. LOWN and A. S. K. AIDOO. Can. J. Chem. **44**, 2507 (1966).
2. J. W. LOWN and A. S. K. AIDOO. Can. J. Chem. This issue.
3. D. C. C. SMITH and D. E. STEERE. J. Chem. Soc. C, 2305 (1967).
4. M. P. CAVA and R. H. SCHLESSINGER. Tetrahedron, **21**, 3051 (1965).
5. P. T. LANSBURY, A. J. LACHER, and F. D. SAEVA. J. Am. Chem. Soc. **89**, 4361 (1967).
6. W. G. DAUBEN, G. A. BOSWELL, and W. TEMPLETON. J. Org. Chem. **25**, 1853 (1960).
7. (*a*) E. W. STONE and A. H. MAKI. J. Chem. Phys. **36**, 1944 (1962). (*b*) J. GENDELL, J. H. FREED, and G. K. FRAENKEL. J. Chem. Phys. **37**, 2832 (1962). (*c*) P. LUDWIG, T. LAYLOFF, and R. N. ADAMS. J. Am. Chem. Soc. **86**, 4568 (1964). (*d*) P. B. AYSCOUGH and F. P. SARGENT. J. Chem. Soc. B, 907 (1966). (*e*) A. G. EVANS, J. C. EVANS, and E. H. GODDEN. J. Chem. Soc. 149 (1970).
8. S. F. NELSEN, B. M. TROST, and D. H. EVANS. J. Am. Chem. Soc. **89**, 3034 (1967).
9. (*a*) R. W. BRANDON and E. A. C. LUCKEN. J. Chem. Soc. 4273 (1961). (*b*) I. YAMAZAKI and L. H. PIETTE. J. Am. Chem. Soc. **87**, 986 (1965). (*c*) J. E. WERTZ and J. L. VIVO. J. Chem. Phys. **23**, 2441 (1955). (*d*) B. VENKATARAMAN and G. K. FRAENKEL. J. Am. Chem. Soc. **77**, 2707 (1955). (*e*) J. R. BOLTON and A. CARRINGTON. Proc. Chem. Soc. 385 (1961). (*f*) R. DEHL and G. K. FRAENKEL. J. Chem. Phys. **39**, 1793 (1963).
10. (*a*) G. A. RUSSELL, C. L. MYERS, P. BRUNI, F. A. NEUGEBAUER, and R. BLANKESPOOR. J. Am. Chem. Soc. **92**, 2762 (1970). (*b*) G. A. RUSSELL, E. T. STROM, E. R. TALATY, K. Y. CHANG, R. D. STEPHENS, and M. C. YOUNG. Rec. Chem. Prog. **27**, 3 (1966).
11. M. P. CAVA and R. H. SCHLESSINGER. Tetrahedron, **21**, 3073 (1965).
12. G. A. RUSSELL, E. G. JANZEN, and E. T. STROM. J. Am. Chem. Soc. **86**, 1807 (1964).

Can. J. Chem. Downloaded from www.nrcresearchpress.com by 210.87.254.40 on 09/05/12
For personal use only.

Can. J. Chem. Downloaded from www.nrcresearchpress.com by 210.87.254.40 on 09/05/12
For personal use only.

Electron Spin Resonance Studies of the Radiolysis of Aliphatic Amines at 77 °K[1]

P. WARDMAN[2] AND D. R. SMITH[3]

Physical Chemistry Branch, Atomic Energy of Canada Limited, Chalk River Nuclear Laboratories, Chalk River, Ontario

Received January 13, 1971

Several frozen aliphatic amines have been γ-irradiated at 77 °K and the electron spin resonance (e.s.r.) spectra of the trapped radicals obtained at 77 °K and on warming. Radiolysis of methyl, ethyl and isopropyl amines produces predominantly alkylamino (RĊNH) radicals. The proton hyperfine (h.f.) couplings of RĊNH radicals are 10–30% larger than those in the corresponding isoelectronic alkyl radicals and the parallel component of the ^{14}N coupling is about 35 G. Restricted rotation of alkyl groups occurs at 77 °K in some cases. On warming from 77 °K, the RĊNH radicals generally abstract from the solvent or isomerize to produce radicals of the aminoalkyl type (*e.g.* $R\dot{C}HNH_2$). The alkyl proton h.f. splittings of these latter radicals are 20–40% lower than in the corresponding alkyl radicals, and the observed ^{14}N coupling was $A_{14_{N,\parallel}} = 12 \pm 3$ G in $\dot{C}H_2NR_2$ and $A_{14_{N,iso}} \simeq 4$ G in $(CH_3)_2\dot{C}NH_2$ and $CH_3\dot{C}HNH_2$. The amino proton couplings in the aminoalkyl radicals were not resolved. Irradiated dimethylamine produces both $(CH_3)_2\dot{N}$ and $\dot{C}H_2N(CH_3)$ radicals, but $(CH_3)_2\dot{N}$ disappears on warming. Only $\dot{C}H_2N(CH_3)_2$ was observed after irradiation of $(CH_3)_3N$ at 77 °K. Solid methoxyamine (giving CH_3ONH) and *tert*-butylamine were also studied.

Plusieurs amines aliphatiques à l'état solide ont été irradiées à 77 °K par des rayons-γ et les spectres de résonance paramagnétique électronique (R.p.e.) ont été obtenus à 77 °K et à des températures plus élevées. La radiolyse des méthyl, éthyl et isopropyl amines produit en prépondérance les radicaux alkylamino (RNH). Lesécarts hyperfins (e.h.) du proton des radicaux RNH sont de 10–30% plus grand que ceux des radicaux alkyles isoélectriques correspondant et le composant parallèle du couplage de ^{14}N est d'environ 35 G. En réchauffant l'échantillon qui est à 77 °K les radicaux RNH généralement abstraient du solvant ou s'isomérisent pour produire des radicaux du type amino-alkyle (*e.g.* $R\dot{C}HNH_2$). Les écarts hyperfins des protons des groupements alkyles sont 20–40% plus bas que les radicaux alkyles correspondants et le couplage ^{14}N observé était $A_{14_{N,\parallel}} = 12 \pm 3$ G pour $\dot{C}H_2NR_2$ et $A_{14_{N,iso}} \simeq 4$ G pour $(CH_3)_2\dot{C}NH_2$ et $CH_3\dot{C}HNH_2$. Le couplage du proton sur l'azote dans les radicaux aminoalkyles n'était pas résolu. L'irradiation de la diméthylamine produit les deux radicaux $(CH_3)_2\dot{N}$ et $\dot{C}H_2N(CH_3)$, mais $(CH_3)_2\dot{N}$ disparait lorsqu'on élève la température. Seulement le radical $\dot{C}H_2N(CH_3)_2$ fut observé après irradiation de $(CH_3)_3N$ à 77 °K. La méthoxyamine (donnant CH_3ONH) et la *tert*-butylamine ont aussi été étudiées.

Canadian Journal of Chemistry, 49, 1869 (1971)

Introduction

Little is known about the radiolysis of solid aliphatic amines. Pukhal'skaya *et al.* (1, 2) γ-irradiated several methyl and ethyl amines at 77 °K and, for example, ascribed the e.s.r. spectrum of the radicals trapped in solid CH_3NH_2 to the aminomethyl radical, $\dot{C}H_2NH_2$. Their spectra were poorly resolved and no hyperfine (h.f.) splittings were derived. Hadley and Volman (3) found quite different e.s.r. spectra after ultraviolet photolysis of frozen CH_3NH_2 and suggested that in this case only $CH_3\dot{N}H$ was produced. The relative strengths of the C—H and N—H bonds in alkyl amines are not known, but in the gas phase, both $\dot{C}H_2NH_2$ and $CH_3\dot{N}H$ are produced (to about equal extents (4)) from methylamine in the ion–molecule reaction [1]

$$[1a] \quad CH_3NH_2^+ + CH_3NH_2 \rightarrow CH_3NH_3^+ + \dot{C}H_2NH_2$$

$$[1b] \quad \rightarrow CH_3NH_3^+ + CH_3\dot{N}H$$

In an attempt to provide further information about the radicals produced by radiolysis of amines, we have irradiated several of the lower aliphatic amines at 77 °K.

Experimental

Materials

Matheson CH_3NH_2, $(CH_3)_2NH$, $(CH_3)_3N$, and $C_2H_5NH_2$, Baker Analyzed Reagent grade $(C_2H_5)_2NH$, Eastman n-$C_3H_7NH_2$ and $(CH_3)_2CHNH_2$ and Fisher Certified grade n-$C_4H_9NH_2$ were distilled *in vacuo* and

[1]AECL No. 3872.

[2]NRCC Postdoctorate Fellow 1967–1969. Present address: Department of Chemistry, University of Manchester, Manchester M13 9PL, England.

[3]To whom correspondence should be addressed.

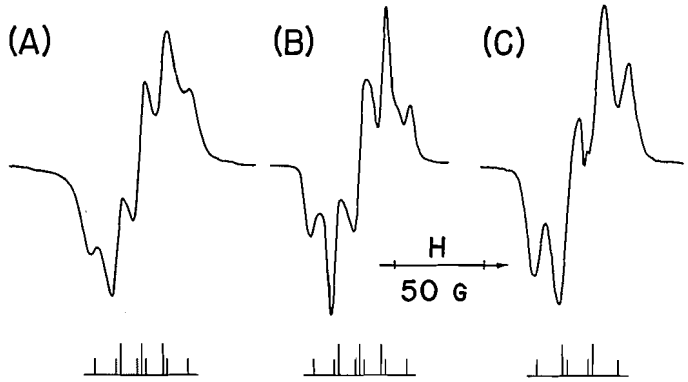

FIG. 1. First derivative e.s.r. spectra of γ-irradiated glassy methylamine at 77 °K: (*A*), CH_3NH_2; (*B*), CH_3ND_2; (*C*), $CH_3{}^{15}NH_2$.

stored over a Na mirror. Eastman $(CH_3)_3CNH_2$ was fractionated using a 1 m column of stainless steel gauze rings and stored over Na *in vacuo*. Eastman CH_3ONH_2. HCl was added to NaOH in aqueous solution, CH_3ONH_2 separated by fractionation as above (b.p. 48.5–49.5 °C) and stored over CaO *in vacuo*. Isotopes Inc. supplied $CH_3{}^{15}NH_2$.HCl and $(CH_3)_2{}^{15}NH$.HCl (96% ^{15}N), which were added to KOH in aqueous solution and separated by distillation *in vacuo* through two traps at 193 °K to a bulb at 77 °K. CH_3OND_2, $(CH_3)_2CHND_2$, and $(CH_3)_3CND_2$ were prepared by refluxing the protiated amine with at least five times its volume of D_2O (A.E.C.L. high grade material), separating the amine by fractionation and repeating the process a further three times before storage *in vacuo* over CaO. CD_3NH_2, CD_3ND_2, CH_3ND_2, $(CD_3)_2NH$, $(CD_3)_3N$, $C_2H_5ND_2$, and $CH_3CD_2NH_2$ were supplied sodium-dried by Merck, Sharp and Dohme.

Sample Preparation, Irradiation, and e.s.r. Spectroscopy

Amines deuterated in the amino group were handled on a mercury- and grease-free vacuum system that had been exposed to repeated lots of D_2O at 200 °C for several days, then flushed several times with ND_3 and finally with the amine in use. All samples were degassed on grease-free vacuum lines and distilled *in vacuo* into 3 mm i.d. Spectrosil tubes before ^{60}Co γ-irradiation at 77 °K. Doses between 0.1 and 0.5 Mrads were used. A Varian V-4502 X-band e.s.r. spectrometer was used with Fieldial, TE_{104} cavity and X–Y recorder. Samples were warmed from 77 °K by a stream of cold N_2 gas. Temperatures quoted are accurate to ±3 °K.

Results

Methylamine forms a glass rather than a polycrystalline solid if 10% H_2O is added before freezing to 77 °K: somewhat different spectra were obtained for these two types of solid. In some cases the effects of isotopic substitution were quite unexpected: we present fuller consideration of these effects, and of the hyperfine coupling parameters derived, in the Discussion section. Unless shown as ^{15}N, the nitrogen isotope is ^{14}N. Support for some of our assignments, including better resolved spectra in some cases, is to be found in our studies of the radiolysis of amines adsorbed on silica gel (see accompanying paper).

(i) Glassy Methylamine (+10% H_2O)

Glassy methylamine is deep blue after γ-irradiation at 77 °K but illumination with $\lambda > 640$ nm removes the color and the associated e.s.r. singlet spectrum of the trapped electron (1). We are concerned here only with the radical remaining after photobleaching. *In all cases, the spectra presented are those obtained after photobleaching.* In Fig. 1(*A*) we show the spectrum from CH_3NH_2 at 77 °K which is similar to that obtained by Pukhal'skaya *et al.* (1) but with superior resolution. Glassy CH_3ND_2 (10% D_2O) gave a similar spectrum (Fig. 1(*B*)), with slightly better resolution, showing that the amino proton h.f. coupling is too small to be resolved in our experiments. (A very weak 14.3 G quartet from CH_3ND_2 was just detectable on 2nd derivative presentation, which may be a very small amount of another radical.) The quintet spectra in Figs. 1(*A*) and (*B*) have $A_{av} = 13.0 \pm 0.5$ G. Glassy $CH_3{}^{15}NH_2$ gave a quartet spectrum, Fig. 1(*C*), with $A_{av} = 15.5 \pm 0.5$ G.

If the radical is the same in glassy CH_3NH_2, CH_3ND_2, and $CH_3{}^{15}NH_2$ and contains one interacting N atom, then the difference in the separation of the outermost lines in the spectra for the ^{15}N and ^{14}N isotopes will equal $(2A_{^{14}N} - A_{^{15}N}) = 0.58A_{^{14}N}$. Thus $A_{^{14}N} = 12 \pm 3$ G. The

Can. J. Chem. Downloaded from www.nrcresearchpress.com by 210.87.254.40 on 09/05/12
For personal use only.

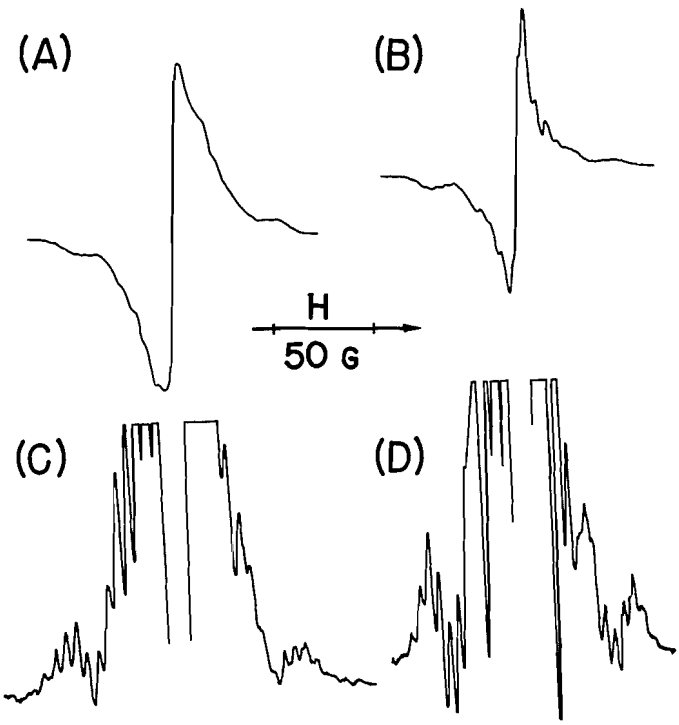

FIG. 2. Electron spin resonance spectra of γ-irradiated glassy methylamine at 77 °K: (*A*), CD_3NH_2 and (*B*), CD_3ND_2 (first derivative); (*C*), CD_3NH_2 and (*D*), CD_3ND_2 (2nd derivative).

spectra in Fig. 1 may then be assigned to $\dot{C}H_2NH_2$ with $A_H^{CH_2} = 14.5 \pm 3$, $A_{^{14}N} = 12 \pm 3$ ($A_{^{15}N} = 17 \pm 4$), and $A_H^{NH_2} \leq 5$ G, the "stick" spectra being for this assignment.

On this basis we expect to obtain spectra from CD_3NH_2 and CD_3ND_2 which are basically ~12 G ^{14}N triplets with the 2.2 G methylene *D* splitting unresolved. The spectra observed were quite different from those expected and are shown in Fig. 2. (Second derivative presentation gives the line positions as minima.) Both amines gave similar triplet spectra with the outer lines considerably broadened, and similar to the spectrum observed for $CD_3\dot{N}H$ by Hadley and Volman (3). Superimposed on the major triplet splitting are 5 ± 1 G deuterium splittings, very characteristic of the ~34 G methyl proton splitting of $CH_3\dot{N}H$. For this radical, these authors assigned $A_H^{CH_3} \simeq A_H^{NH} \simeq A_{^{14}N} = 32$ G. The observed ^{14}N coupling is the parallel component (see Discussion). For CD_3NH_2 we observed about 26 lines over 135 G, and for CD_3ND_2 about 25 lines over 117 G. This broadening (we expect ~ 136 and 110 G total separation, respectively, if the ^{14}N perpendicular component is neglected) was also observed by Hadley and Volman (3). Apparently the broadening of the $M_I(^{14}N) = \pm 1$ lines masks the amino proton splitting in $CD_3\dot{N}H$. By analogy with NH_2 (32) we might expect $A_{^{14}N,\parallel} \simeq 37$ G, $A_{^{14}N,\perp} \simeq 1$ G, $A_{H,\parallel}^{NH} \simeq 31$ G, and $A_{H,\perp}^{NH} \simeq 25$ G. The perpendicular features, especially if they are broad, would further inhibit resolution of the amino proton splitting in this case.

(ii) Polycrystalline (Anhydrous) Methylamine

Polycrystalline CH_3NH_2 and $CH_3{}^{15}NH_2$ gave the asymmetrical and poorly resolved spectra shown in Fig. 3(*A*) and (*B*). There are 7 major lines ($A_{av} \simeq 30$ G) for CH_3NH_2 and 6 major lines ($A_{av} \simeq 33$ G) for $CH_3{}^{15}NH_2$. We have not completely analyzed these spectra, but it is noteworthy that both spectra show 33 G h.f. splittings (therefore probably due to H) and that the difference in separation of outermost lines of the spectra of the two N isotopes gives $A_{^{14}N} \simeq 33$ G. On warming CH_3NH_2 to 100 °K for 15 min, the two outer pairs of lines disappeared leaving an ill-resolved singlet (and a small amount of $CH_2{=}\dot{N}$ (5) detectable). In Fig. 3(*C*) we show the spectrum of γ-irradiated CH_3NH_2 after

Can. J. Chem. Downloaded from www.nrcresearchpress.com by 210.87.254.40 on 09/05/12
For personal use only.

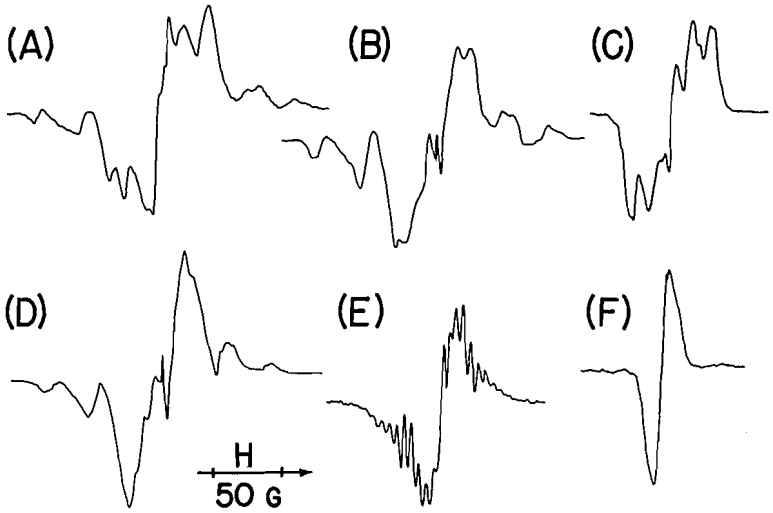

FIG. 3. First derivative e.s.r. spectra of γ-irradiated polycrystalline methylamine: (*A*), CH_3NH_2 at 77 °K; (*B*), $CH_3{}^{15}NH_2$ at 77 °K; (*C*), CH_3NH_2 after warming to 165 °K for 15 min and re-cooling to 77 °K; (*D*) CH_3ND_2 at 77 °K; (*E*), CD_3NH_2 after 10 min at 125 °K; (*F*), CD_3ND_2 after warming to 150 °K for 15 min and re-cooling to 77 °K.

warming to 165 °K for 15 min and then re-cooling to 77 °K. The resultant quintet structure has $A_{av} \simeq 13$ G, and the shape and width of the spectrum was similar at 165 and 77 °K. Thus although polycrystalline CH_3NH_2 and $CH_3{}^{15}NH_2$ gave ill-resolved spectra, the spectra at 77 °K were ascribable to $CH_3\dot{N}H$ and those after warming to 165 °K and re-cooling, to $\dot{C}H_2NH_2$ (the formation of $\dot{C}H_2NH_2$ from $CH_3\dot{N}H$ being non-reversible). The spectra of $CH_3\dot{N}H$ were not as well resolved as those of Hadley and Volman (3), and we note that in all cases, u.v. photolysis after γ-irradiation not only produced the $CH_2{=}\dot{N}$ radical (1) but also increased the resolution of the $CH_3\dot{N}H$ spectrum.

The major features of the e.s.r. spectrum of the radical(s) in irradiated polycrystalline CH_3ND_2 at 77 °K are seen in Fig. 3(*D*) to be six lines with $A_{av} \simeq 30$ G, *i.e.* near to that expected for $CH_3\dot{N}D$. CD_3NH_2 gave at 77 °K a spectrum similar to that found for the glass (Fig. 2(*A*)) but with a better defined ~35 G triplet. Optimum resolution for $CD_3\dot{N}H$ was after 10 min at 125 °K (Fig. 3(*E*)) but above 140 °K the outer lines almost disappeared (irreversibly), leaving a singlet spectrum with no resolved structure and peak-to-peak first derivative linewidth $\Delta H_{ms} \simeq 20$ G. This is compatible with $\dot{C}D_2NH_2$. Behavior identical to CD_3NH_2 was found for CD_3ND_2 and in Fig. 3(*F*) we show the spectrum observed for CD_3ND_2 after warming to 150 °K for 15 min and re-cooling to 77 °K. The singlet has $\Delta H_{ms} \simeq 11$ G, illustrating the linewidth contribution of the amino proton coupling in $\dot{C}D_2NH_2$. With both CD_3NH_2 and CD_3ND_2 the linewidth of this singlet did not change between ~150 and 77 °K.

(iii) Polycrystalline Ethylamine

The resolution of the spectrum obtained from $C_2H_5NH_2$ after irradiation at 77 °K was improved considerably (without change in line positions) by warming to 120 °K for 20 min. In Fig. 4(*A*) and (*B*) we show spectra for $C_2H_5NH_2$ which although still slightly asymmetric, may readily be analyzed into a 45 G doublet, a 36 G triplet, and a 25 G triplet. We assign this pattern to $CH_3CH_2\dot{N}H$ with $A_{^{14}N,\parallel} = 36$ G, $A_H{}^{NH} = 25$ G, and two inequivalent methylene protons $A_{H_1}{}^{CH_2} = 45$ G, $A_{H_2}{}^{CH_2} = 25$ G. The "stick" diagram shows that 16 of the 18 lines are resolved. The alternative assignment from these line positions of $A_{^{14}N} = 25$ G, $A_H{}^{NH} = 36$ G, $A_{H_1}{}^{CH_2} = 45$ G, and $A_{H_2}{}^{CH_2} = 36$ G is excluded by comparison with similar radicals (see Discussion).

With $CH_3CD_2\dot{N}H_2$, no overall change in the spectrum was observed on heating to 170 °K for 10 min and in Fig. 4(*C*) we see that ~5 G *D* hyperfine splittings are resolved. The width and overall shape of the spectrum are compatible with $CH_3CD_2\dot{N}H$ and the couplings derived above, but because of poor resolution we cannot confirm this assignment.

Can. J. Chem. Downloaded from www.nrcresearchpress.com by 210.87.254.40 on 09/05/12
For personal use only.

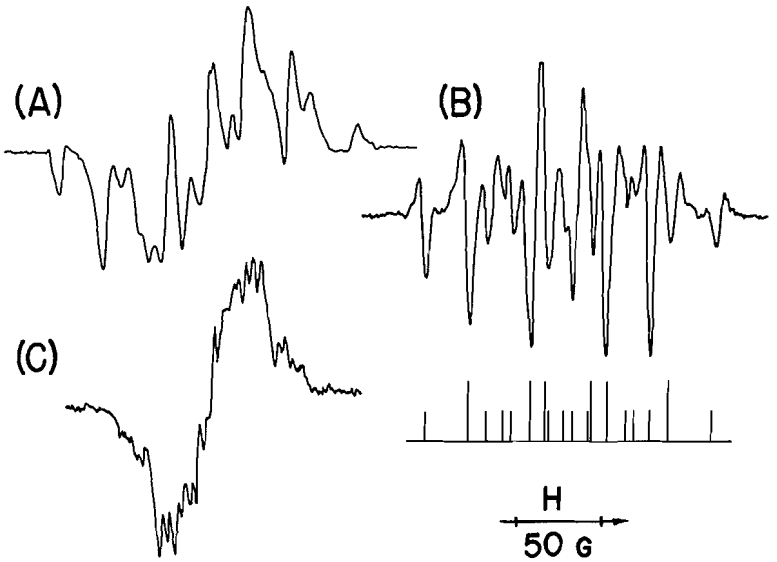

FIG. 4. Electron spin resonance spectra of γ-irradiated polycrystalline ethylamine: (*A*), $C_2H_5NH_2$ after 20 min at 120 °K (first derivative) and (*B*), (2nd derivative); (*C*), $CH_3CD_2NH_2$ after 10 min at 170 °K.

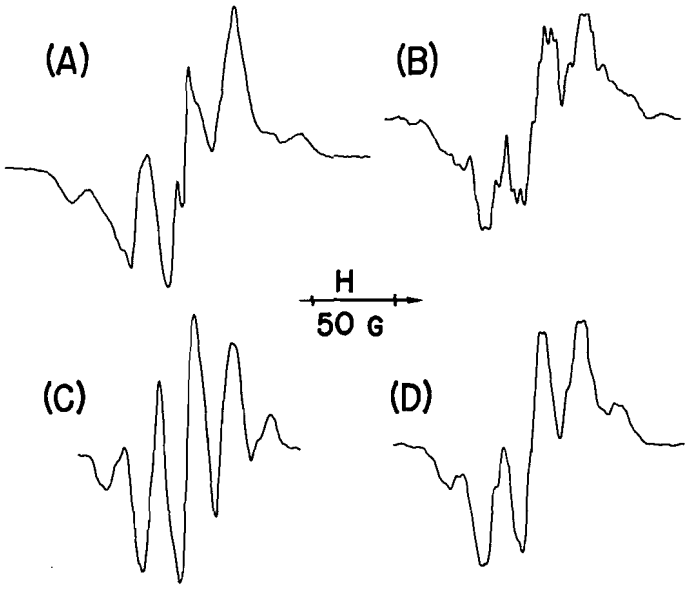

FIG. 5. First derivative e.s.r. spectra of γ-irradiated polycrystalline ethylamine: (*A*), $C_2H_5ND_2$ at 77 °K; (*B*), $C_2H_5NH_2$ after 30 min at 155 °K; (*C*), $C_2H_5ND_2$ after 10 min at 170 °K; (*D*), $C_2H_5ND_2$ after warming to 170 °K for 15 min and re-cooling to 77 °K.

Irradiated polycrystalline $C_2H_5ND_2$ gave at 77 °K a spectrum (Fig. 5(*A*)) quite unlike that of $C_2H_5NH_2$, suggesting that if a similar radical was formed in both cases, the radical was $C_2H_5\dot{N}D$ rather than $\dot{C}H_2CH_2ND_2$ or $CH_3\text{-}\dot{C}HND_2$. Both these latter alternatives would have small amino proton h.f. splitting (see Discussion). Although the spectrum computed for $C_2H_5\dot{N}D$ is somewhat different from that observed at 77 °K, the separation of the outermost lines of the spectrum was ~135 G, which is similar to that expected for this assignment and

Can. J. Chem. Downloaded from www.nrcresearchpress.com by 210.87.254.40 on 09/05/12
For personal use only.

Can. J. Chem. Downloaded from www.nrcresearchpress.com by 210.87.254.40 on 09/05/12
For personal use only.

much larger than that thought reasonable for the two alternatives mentioned above. It may be that $CH_3\dot{C}HND_2$ is already present at 77 °K as a minor radical in addition to $CH_3CH_2\dot{N}D$ (see below), and this prevents exact analysis of the spectrum.

Although the radical in irradiated CH_3CD_2-NH_2 did not appear to change on warming to 170 °K for 20 min, when irradiated $C_2H_5ND_2$ or $C_2H_5NH_2$ was warmed to 150–155 °K for 20 min, major changes in the spectra occurred. These changes were non-reversible on re-cooling to 77 °K and it was clear that a new radical had been formed on warming, which had the same e.s.r. spectra for both $C_2H_5ND_2$ and $C_2H_5NH_2$. Figures 5(*B*), (*C*), and (*D*) show the spectra for $C_2H_5NH_2$ and $C_2H_5ND_2$, respectively. The deuterated amine showed considerably better resolution as a 1:4:6:4:1 quintet ($A_{av} = 22 \pm 1$ G) with little further splitting observable after 10 min at 170 °K (Fig. 5(*C*)), but on re-cooling to 77 °K (Fig. 5(*D*)), the spectrum resembled that of $C_2H_5NH_2$ after 30 min at 155 °K (Fig. 5(*B*)). The second derivative spectra for both $C_2H_5ND_2$, re-cooled to 77 °K after warming to 150 °K (corresponding to Fig. 5(*D*)), and for $C_2H_5NH_2$ at 155 °K (Fig. 5(*B*)), showed the 22 ± 1 G quintet but with a 5 or 6 G quartet splitting superimposed. These features are not characteristic of $\dot{C}H_2CH_2NH_2$, the isotropic h.f. parameters of which are known (6). This radical would be expected to have two inequivalent β protons in solids at low temperatures similar to those observed in (isoelectronic) $\dot{C}H_2CH_2CH_3$ (7). We consider the radical to be $CH_3\dot{C}HNH_2$ ($CH_3\dot{C}HND_2$), although the 22 G average coupling seems rather larger than that thought likely for this radical even if the alkyl protons are nearly equivalent. The α and β proton couplings for the $CH_3\dot{C}HNH_2$ radical are 15.3 and 20.2 G, respectively (8). However, although the h.f. splittings for the α and β protons in the CH_3-$\dot{C}HOH$ radical are 15.4 and 22 G, respectively, in solution at 25 °C (9), this radical in the solid phase at 100 °K shows 5 lines ($A_{av} = 22$ G) of binomial intensity distribution (for a review, see ref. 10). The minor 5–6 G quartet splitting observed in $C_2H_5NH_2$ at 155 °K may result both from the isotropic ^{14}N splitting and the amino proton coupling, both about this magnitude in $CH_3\dot{C}HNH_2$ (see Discussion). Without superior resolution we cannot be sure it is definitely a quartet splitting.

(iv) Polycrystalline Isopropylamine

After irradiation at 77 °K, $(CH_3)_2CHNH_2$ gave the spectrum shown in Fig. 6(*A*). The major feature is a quintet, $A_{av} \simeq 33$ G with the central line showing clear evidence of a poorly resolved doublet splitting. A different spectrum (Fig. 6(*B*)) with a quartet structure predominating, was obtained with $(CH_3)_2CHND_2$, which was warmed to 104 °K for 20 min to increase the resolution without major overall change in the spectrum. The line envelopes are compatible with $(CH_3)_2$-$CH\dot{N}H$ ($(CH_3)_2CH\dot{N}D$), with $A_H^{CH} \simeq 40$ G, $A_H^{NH} \simeq 25$ G ($A_D^{ND} \simeq 4$ G), and $A_{^{14}N,\parallel} \simeq 35$ G.

Major (and similar) changes in the spectra of irradiated $(CH_3)_2CHNH_2$ and $(CH_3)_2CHND_2$ occurred on warming to ~140 °K or higher. Figure 6(*C*) and (*D*) are for $(CH_3)_2CHND_2$ after 30 min at 176 °K. The septet has approximate binomial intensity distribution with a major splitting of 18.0 ± 0.5 G and a minor triplet splitting of 4.5 ± 0.3 G. An almost identical spectrum was observed for $(CH_3)_2\dot{C}NH_2$ at 170 °K, an 18.5 ± 0.8 G binomial septet but with a minor 7 ± 1 G doublet splitting. Katayama and Gordy (11) showed that a poorly resolved triplet may appear as a doublet with second derivative presentation. This would explain the apparent 7 G doublet in the less well resolved, protiated amine instead of the expected 4.5 G triplet, although an amino proton coupling (~5 G (8)) may also contribute to the minor splitting. The amino proton coupling must also be small since deuteration has little effect on the spectrum. This observation plus the low nitrogen coupling indicates that these spectra are due to $(CH_3)_2\dot{C}NH_2(D_2)$ (8).

When either the protiated or deuterated amine was warmed to 170 °K for ~20 min to isolate the $(CH_3)_2\dot{C}NH_2(D_2)$ radical, and then re-cooled to 77 °K, the spectrum changed from the 18 G septet to a markedly different ~36 G triplet. Spectra from $(CH_3)_2CHND_2$ are shown in Fig. 6(*E*) and (*F*). The second derivative may be fitted to a 36 ± 2 G triplet with a 12 ± 1 G splitting superimposed. This change in the spectrum of the $(CH_3)_2\dot{C}NH_2$ radical with temperature is ascribed to restricted rotation of the methyl groups at 77 °K. A similar effect is known for $(CH_3)_2\dot{C}OH$ (12) and other radicals (13), and it may be that two of the 6 protons give the 36 G triplet, the other 4 giving much smaller (~12 G) splittings. The apparent quartet splitting may result from incomplete resolution, and from the

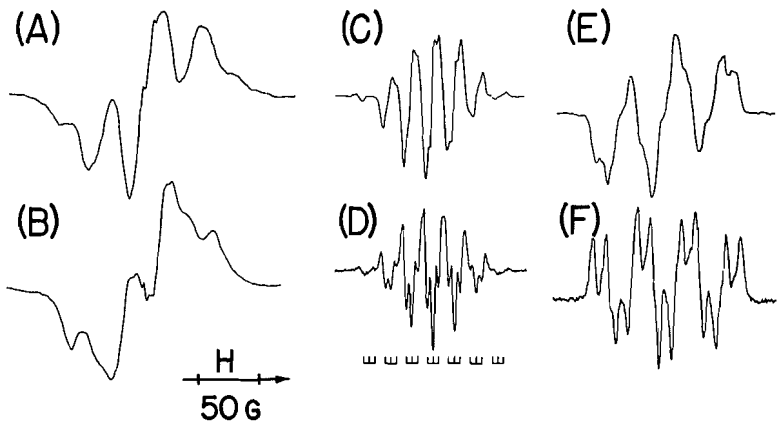

FIG. 6. Electron spin resonance spectra of γ-irradiated polycrystalline isopropylamine: (*A*), $(CH_3)_2CHNH_2$ at 77 °K; (*B*), $(CH_3)_2CHND_2$ after 20 min at 104 °K; (*C*) and (*D*), $(CH_3)_2CHND_2$ after 30 min at 175 °K (first and 2nd derivative); (*E*) and (*F*), $(CH_3)_2CHND_2$ after warming to 175 °K for 30 min and re-cooling to 77 °K (first and 2nd derivative).

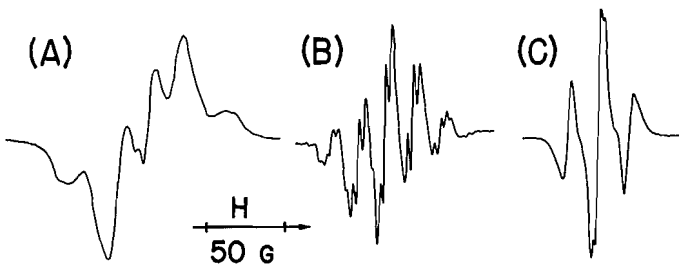

FIG. 7. First derivative e.s.r. spectra of γ-irradiated polycrystalline *tert*-butylamine: (*A*), $(CH_3)_3CNH_2$ at 77 °K; (*B*), $(CH_3)_3CNH_2$ after 30 min at 179 °K; (*C*), $(CH_3)_3CND_2$ after 20 min at 184 °K.

^{14}N splitting (which may be increased to $A_{^{14}N} \simeq$ 10–15 G at the lower temperature). At elevated temperatures the 18 G splitting represents the average value for the 6 methyl protons which are now equivalent due to rapid rotation. These data are consistent with $B_1 = 3.7$ G and $B_2 = 32.8$ G in the equation

$$A = B_1 + B_2 \cos^2 \theta$$

When rotation is restricted at 77 °K, θ (see standard texts for definition) approximately equals 0° for one proton in each methyl group and 60° for the other 4 protons. This value of B_2 is low compared to the normal value of about 50 G, presumably due to spin density delocalization onto the nitrogen, similar to the $\dot{C}H_2NH_2$ radical.

(v) Polycrystalline tert-Butylamine

The spectrum of γ-irradiated $(CH_3)_3CNH_2$ was five lines which were neither equally spaced nor of binomial intensities at 77 °K (Fig. 7(*A*)), but warming to 179 °K for 30 min resolved the spectrum into an approximately binomial quintet ($A = 18 \pm 1$ G) with a minor splitting (probably a quintet) $A = 4.0 \pm 0.5$ G, Fig. 7(*B*). This change was reversible on re-cooling to 77 °K. Irradiated $(CH_3)_3CND_2$ gave a 20 ± 1 G triplet spectrum with the outer lines considerably broadened. Figure 7(*C*) shows the spectrum after 20 min at 184 °K, when a minor 4 ± 1 G triplet splitting of the central line was evident. There was no change in the shape of this spectrum to 99% of the radical decay at 190 °K, nor on re-cooling to 77 °K.

These results are considered in the Discussion section.

(vi) Polycrystalline Di- and Tri-methylamines

Pukhal'skaya (1) suggested that $\dot{C}H_2NR_2$ radicals were formed by radiolysis of these amines, although their spectra were inadequate for analysis. If our assignment for $\dot{C}H_2NH_2$ in glassy CH_3NH_2 is correct, then we might expect

Can. J. Chem. Downloaded from www.nrcresearchpress.com by 210.87.254.40 on 09/05/12
For personal use only.

Can. J. Chem. Downloaded from www.nrcresearchpress.com by 210.87.254.40 on 09/05/12
For personal use only.

similar spectra from $\dot{C}H_2NHCH_3$ or $\dot{C}H_2N(CH_3)_2$.

Irradiated $(CH_3)_2NH$ showed at 77 °K a central broad singlet ($\Delta H_{ms} \simeq 40$ G) with lines from $(CH_3)_2\dot{N}$ radicals superimposed, as observed by Pukhal'skaya (1) and confirmed by our observation of a ~30 G ^{14}N triplet (parallel component) and 4.0 G *D* splitting (at least 30 lines over 124 G) with $(CD_3)_2NH$. On warming irradiated $(CH_3)_2NH$ to 125 °K for 10 min, the $(CH_3)_2\dot{N}$ radicals disappeared, leaving only a singlet which on further warming for 20 min at 155 °K was seen to be a quintet, $A_{av} = 15 \pm 1$ G, similar to that observed in glassy CH_3NH_2 and in the case of $(CH_3)_2NH$ thought to be the $\dot{C}H_2NHCH_3$ radical, with $A_H^{CH_2} \simeq A_{^{14}N} \simeq 15$ G.

The spectrum of irradiated $(CH_3)_3N$ at 77 °K was a broad singlet ($\Delta H_{ms} \sim 40$ G) but after 20 min at 143 °K a quintet ($A_{av} = 14 \pm 1$ G) was resolved (Fig. 8(*A*)). Radiolysis of $(CD_3)_3N$ at 77 °K gave a 13.5 G triplet with two small satellite lines (separation 80 G), the latter probably arising from a small amount of another radical. At 140 °K a further ~ 4 G splitting was observed, but after 10 min at 156 °K (Fig. 8(*B*)) a 2 G splitting was clearly resolved on the central line. These spectra are compatible with $\dot{C}H_2N(CH_3)_2$ or $\dot{C}D_2N(CD_3)_2$ with $A_{^{14}N} = 13.5 \pm 1.0$, $A_H^{CH_2} = 14.5 \pm 1.0$ ($A_D^{CD_2} \simeq 2$), and $A_H^{CH_3} \simeq 0$ G, an assignment supported by the isolation of $(CH_3)_2NCH_2CH_2N(CH_3)_2$ from irradiated liquid $(CH_3)_3N$ (14).

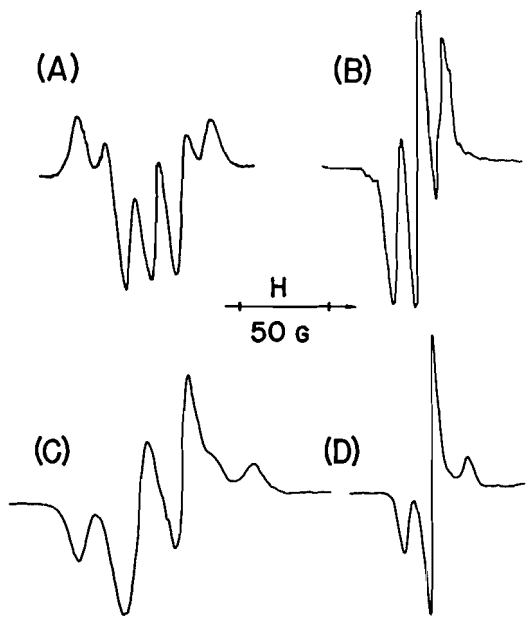

FIG. 8. Electron spin resonance spectra of γ-irradiated polycrystalline trimethylamine or methoxyamine: (*A*), $(CH_3)_3N$ after 20 min at 143 °K (2nd derivative); (*B*), $(CD_3)_3N$ after 10 min at 156 °K (first derivative); (*C*), CH_3ONH_2 and (*D*), CH_3OND_2 at 77 °K (first derivative).

(vii) Glassy (Anhydrous) Methoxyamine

We irradiated methoxyamine because the radicals produced by C—H and N—H bond breakage should have readily distinguishable e.s.r. spectra and because the N—H bond strength is ~ 4 kcal mol^{-1} lower than in methylamine (15) and is therefore probably lower than the H—CH_2ONH_2 bond strength.

Both CH_3ONH_2 and CH_3OND_2 were pale yellow after irradiation at 77 °K. The yellow color and minor lines in the e.s.r. spectra from both amines were removed by illumination with (visible) light from a quartz–iodine (tungsten) lamp at 77 °K. The minor signal removed by illumination was a 14 ± 2 G triplet for CH_3OND_2 but only a central line was removed in CH_3ONH_2. In the latter case the major spectrum would mask the outer lines of such a triplet. This minor species is probably $\dot{C}H_2ONH_2$ ($\dot{C}H_2OND_2$). The signal remaining after illumination was a quartet for CH_3ONH_2 (Fig. 8(*C*)) and a 30–35 G triplet for CH_3OND_2 (Fig. 8(*D*)). These spectra are assigned to $CH_3O\dot{N}H$ ($CH_3O\dot{N}D$) with $A_{^{14}N,\parallel} \simeq 30$ G, $A_H^{NH} \simeq 25$ G, and $A_H^{CH_3} \simeq 0$.

(viii) g-Values

All our spectra had $g = 2.003 \pm 0.001$, which is within the range found for $\dot{C}H_2NR_2$ or $R\dot{N}R'$ radicals in the literature.

Discussion

(i) Formation of the Radicals

The most likely routes for the formation of the majority of the radicals observed in glassy or polycrystalline solid amines are ion–molecule reactions such as [1]. In glassy CH_3NH_2 or CH_3ND_2, only $\dot{C}H_2NH_2$ ($\dot{C}H_2ND_2$) was observed, but in glassy CD_3NH_2 or CD_3ND_2, the predominant radical observed at 77 °K was $CD_3\dot{N}H$ ($CD_3\dot{N}D$). This sensitivity to selective deuteration may result from a close similarity in C—H and N—H bond strengths. Deuteration of the methyl group may change the crystal

TABLE 1. Hyperfine splittings (in G) for radicals trapped in solid amines

Radical	$A_H^{CH_3}$	$A_H^{CH_2}$	A_H^{CH}	A_H^{NH}	$A_H^{NH_2}$	$A_{14N,\parallel}$	$A_{14N,Iso}$
$CH_3\dot{N}H$	30–35	—	—	25–31	—	30–35	—
$(CH_3)_2\dot{N}$	27	—	—	—	—	30	—
$CH_3CH_2\dot{N}H$	—	45, 25	—	25	—	36	—
$(CH_3)_2CH\dot{N}H$	—	—	40	25	—	35	—
$\dot{C}H_2NH_2$	—	14.5 ± 3	—	—	≤5	12 ± 3*	—
$\dot{C}H_2NHCH_3$	≤5	15	—	≤5	—	15*	—
$\dot{C}H_2N(CH_3)_2$	≤5	14.5 ± 1	—	—	—	13.5 ± 1*	—
$CH_3\dot{C}HNH_2$	~22	—	~22	—	≤5	—	≤5
$(CH_3)_2\dot{C}NH_2$	18.0 ± 0.5	—	—	—	≤5	—	≤5
$\dot{C}H_2ONH_2$	—	14 ± 2	—	—	—	—	—

*Largest component of anisotropic hyperfine tensor (see Discussion).

structure (16) (see below). On the other hand some of the effect may not be genuine. There may be mixtures of aminoalkyl and alkylamine radicals in all cases. The predominance of the spectrum of one over the other in a particular case may arise partly from an isotopic effect on the relative yield and also from linewidth effects.

In all the polycrystalline methylamines, the $CH_3\dot{N}H$ radical was observed at 77 °K but was transformed into $\dot{C}H_2NH_2$ on warming, suggesting that $D(H—CH_2NH) < D(CH_3NH—H)$. This conclusion was also reached by Smithies and Whitworth (17) (who observed ethylenediamine as a major product of radical combination in irradiated liquid methylamine, but found no dimethyl hydrazine), and contrasts with the selectivity of methyl radical attack on amines (18). The transformation of $RCH_2\dot{N}H$ to $R\dot{C}HNH_2$ radicals was also observed on warming $C_2H_5NH_2$, $C_2H_5ND_2$, $(CH_3)_2CHNH_2$, and $(CH_3)_2CHND_2$. The effect of deuteration of the alkyl group on this transformation of $RCH_2\dot{N}H$ radicals was seen by the absence of such reaction of $CH_3CD_2\dot{N}H$ after 10 min at 170 °K, and by the fact that the reaction was occurring at 100 °K in polycrystalline CH_3NH_2, but required warming to about 140 °K in CD_3NH_2. A similar thermal reaction has been reported for dimethylamine (1).

The absence of spectra attributable to $\dot{C}H_2CH_2NH_2$ in irradiated $C_2H_5NH_2$ results from the almost negligible reactivity of the methyl protons both in ion–molecule reactions similar to [1] (19), and also in attack by methyl radicals (18). In contrast, reaction of the Ti^{3+}/H_2O_2 system with $C_2H_5NH_2$ *in acid solution* produces the $\dot{C}H_2CH_2NH_2$ radical (6).

The differences between glassy and polycrystalline CH_3NH_2 and CH_3ND_2 are not thought to originate directly from the 10% water added to the glass, since the ionization potential of water is much higher than that of CH_3NH_2. It seems likely to reflect an importance of the structure of the solid on the ion–molecule reaction. A hydrogen-bonded collision complex with the amino groups adjacent may be preferentially formed in the polycrystalline solid, resulting in preferential formation of $R\dot{N}H$ radicals. This may not be the case in the glassy mixture with 10% water since this water will disrupt the hydrogen bonding between amino groups to a significant extent.

Effects of phase modifications and deuteration have been observed in other systems (20). The radicals observed in irradiated glycine depend on the crystal structure and on deuteration (21).

(ii) The e.s.r. Parameters of the Radicals

By using extensive isotopic labelling, we have been able to make reasonable spectral assignments without reference to published hyperfine parameters for similar radicals prepared by other methods. However, since this work was completed, high resolution spectra of some amines have been reported. Wood and Lloyd (8) obtained isotropic spectra for some radicals of the type $R\dot{C}HNR'_2$ in an adamantane matrix and Neta and Fessenden (22) observed $\dot{C}H_2NR_2$ and other radicals in aqueous solutions of amines. Danen and Kensler (23) have reported parameters for $R_2\dot{N}$ radicals in cyclopropane solution. In Table 1 we summarize our data for amine radicals trapped in solid amines to facilitate comparison with these new high resolution data. The radicals for which h.f. parameters have recently been reported are $(CH_3)_2\dot{N}$ (23); $\dot{C}H_2NH_2$ (22),

Can. J. Chem. Downloaded from www.nrcresearchpress.com by 210.87.254.40 on 09/05/12
For personal use only.

TABLE 2. Hyperfine splittings (in G).

Radical	$A_{^{14}N,\parallel}$	$A_{^{14}N,\perp}$	$A_{^{14}N,Iso}$	Reference number
$\dot{C}H_2CH_2\dot{N}^+$	33	5	14.3	27
$\dot{N}H\overset{+}{N}H_3$ (α N)	~34	~8	16.9±1	28
$H_2C{=}\dot{N}$	34.4	3	9.5	5, 29
$\dot{N}H_2$ (in ice)	31			26, 30
$\dot{N}H_2$ (silica gel)	~38	~1	~13	31
$\dot{N}H_2$(in KNH_2SO_3)*	~37	~1	13.2	32
$(CH_3)_3\overset{+}{\dot{N}}$	49	2	18	29
$\overset{+}{\dot{N}}H_3$ at 77 °K*	~36	~11	19.1	33

*From ^{15}N data.

$\dot{C}H_2NHCH_3$, and $\dot{C}H_2N(CH_3)_2$ (8, 22); and $CH_3\dot{C}HNH_2$ and $(CH_3)_2\dot{C}NH_2$ (8). Our results are in substantial agreement with these recent reports and in addition permit clarification of earlier anomalies such as the assignment of the ~32 G ^{14}N splitting in $R\dot{N}H$ radicals to an isotropic coupling (3).

The 30–35 G ^{14}N coupling we observed for $R\dot{N}H$ (R = CH_3, C_2H_5, $(CH_3)_2CH$, CH_3O) and $R_2\dot{N}$ (R = CH_3) radicals is much larger than the 14.8 G isotropic ^{14}N splitting of $(CH_3)_2\dot{N}$ (23) or the 10.4 G ^{14}N isotropic coupling for $\dot{N}H_2$ in an argon matrix (24). The ^{14}N coupling for $\dot{N}H_2$ varies with the radical environment (25), possibly because of differing bond angles (26). However, a matrix effect is unlikely to raise the isotropic coupling for $R\dot{N}H$ or $R_2\dot{N}$ to 30–35 G and we assign our observed splitting to the parallel component of the ^{14}N interaction. This interpretation is supported by the published isotropic and anisotropic ^{14}N h.f. splittings of the related radicals shown in Table 2, and by calculation of the anisotropic couplings expected for these radicals.

We may estimate the anisotropic h.f. interaction for ^{14}N in $R_2\dot{N}$ and $R\dot{N}H$ type radicals if the isotropic splittings and the spin density in the ^{14}N 2p orbital ($\rho_{2p}{}^N$) are known. The axially symmetric h.f. tensor for the interaction with the electron in the ^{14}N 2p orbital will have magnitudes $A_{^{14}N,\parallel} = A + 2B$ and $A_{^{14}N,\perp} = A - B$, using Morton's nomenclature (34).[4] A is the isotropic ^{14}N splitting and B the anisotropic parameter associated with p character. The latter is estimated from the relation $B = \rho_{2p}{}^N.B_0{}^N$ where $B_0{}^N$ = 17.1 G (34). For $(CH_3)_2\dot{N}$ (23), electron density in proton 1s orbitals is $6 \times A_{CH_3}{}^H/A_0{}^H = 0.324$ and in the ^{14}N 2s orbital is $A_{^{14}N,iso}/A_0{}^N = 0.027$, leaving 0.649 in the ^{14}N 2p orbital. Hence B = 11.1 G and $A_{^{14}N,\parallel} = 37.0$, $A_{^{14}N,\perp} = 3.7$ G, very similar to observed values for $\dot{N}H_2$ (32). Thus this treatment, although simple, gives values for $A_{^{14}N,\parallel}$ which are similar to those listed in Table 1, *i.e.* 30–35 G for $R\dot{N}R'$ radicals. Since we observe a ^{14}N coupling in $\dot{C}H_2NH_2$ in the solid of 12 ± 3 G and the isotropic ^{14}N coupling is 5.0 G (22), the observed splitting in the solid must be the largest component of the ^{14}N anisotropic hyperfine tensor and the other two principal values must be close to zero. (That the ^{14}N coupling for $\dot{C}H_2NR_2$ in solid amines is considerably larger than the ~5 G isotropic value (22) is without doubt the cause of the marked differences between $CH_3{}^{14}NH_2$ and $CH_3{}^{15}NH_2$. We assign $A_H{}^{CH_2}$ = 14.5 ± 3 G, which is close to the isotropic value (22) and there are no satellite lines characteristic of methylene proton anisotropy. The total width of the spectrum therefore requires an ~11 G ^{14}N coupling. The larger ^{14}N coupling is also particularly apparent in $\dot{C}D_2N(CD_3)_2$, shown in Fig. 8(*B*)). Surprisingly, both $CH_3\dot{C}HNH_2$ and $(CH_3)_2\dot{C}NH_2$ show ^{14}N h.f. couplings in the solid which are close to the isotropic values (8) and the limit of our resolution, and are certainly not the 10–15 G anisotropic components found for $\dot{C}H_2NR_2$. This effect is probably not one of temperature, since $\dot{C}H_2NH_2$ shows a similar ^{14}N coupling at ~165 and 77 °K.

The low (4–5 G) amino proton h.f. couplings in $R\dot{C}HNH_2$ radicals (8, 22) confirm our observations that we are generally not resolving these splittings in the solid amines. The inequivalence

[4]The terms parallel and perpendicular refer to the direction of the applied external field with respect to the nitrogen 2p orbital containing the odd electron.

Can. J. Chem. Downloaded from www.nrcresearchpress.com by 210.87.254.40 on 09/05/12
For personal use only.

Can. J. Chem. Downloaded from www.nrcresearchpress.com by 210.87.254.40 on 09/05/12
For personal use only.

of methylene protons in $CH_3CH_2\dot{N}H$ in solid ethylamine is similar to the effects of restricted rotation in the isoelectronic alkyl radicals in solids (7). The increase in methyl proton coupling from 24.7 G in $(CH_3)_2\dot{C}$ (35) to 27.4 G in $(CH_3)_2\dot{N}$ (23) is in accord with the ~32 G methyl proton coupling in $CH_3\dot{N}H$.

We are unable to positively interpret our results from irradiated *tert*-butylamine. Smith and Swan (14) found products which may result from both $(CH_3)_3C\dot{N}H$ and $\dot{C}H_2C(CH_3)_2NH_2$ formation after irradiating liquid $(CH_3)_3CNH_2$. Either radical would give a triplet from $(CH_3)_3CND_2$ but neither would give a quintet for $(CH_3)_3CNH_2$. A possible assignment is the parent ion $(CH_3)_3C\overset{+}{N}H_2$ with $A_{^{14}N} \simeq A_H^{NH_2} \simeq 18$ G. Such a ^{14}N coupling, if isotropic, is similar to that in NH_3^+ (33, 36) and $\overset{+}{N}(CH_3)_3$ (29) (see Table 2). Although it would be surprising if this ion were stable at 190 °K in the solid, an identical radical was produced by γ-irradiation of *tert*-butylamine adsorbed on silica gel and in the latter case the parent ion is a not unreasonable assignment (see accompanying paper).

Conclusions

The radiolysis of aliphatic amines at 77 °K results in radicals formed by hydrogen atom loss from the amino or alkyl groups. The $R\dot{N}H$ radicals disappear on warming to give $R\dot{C}HNH_2$ radicals. (Neta and Fessenden (22) invoke such a reaction to explain some of their observations.) The relative proportion of these two types of radicals is considerably influenced by selective deuteration of the alkyl or amino groups, and (in the case of CH_3NH_2) also depends on whether the solid is glassy or polycrystalline. Some difficulties are anisotropy of $A_{^{14}N}$, the broadening of the $M_I(^{14}N) = \pm 1$ lines and the restricted rotation of alkyl groups in the solid amines at low temperatures.

We acknowledge the helpful criticism of the manuscript by Dr. F. P. Sargent.

1. G. V. Pukhal'skaya, A. G. Kotov, and S. Ya. Pshezhetskii. Proc. Acad. Sci. U.S.S.R. Phys. Chem. Sect. (English Transl.) **171**, 829 (1966).
2. G. V. Pukhal'skaya, A. G. Kotov, and S. Ya. Pshezhetskii. High Energy Chem. (English Transl.) **1**, 471 (1967).
3. S. G. Hadley and D. H. Volman. J. Am. Chem. Soc. **89**, 1053 (1967).
4. C. J. Ogle. A study of the rates and mechanisms of some ion–molecule reactions by high pressure mass spectrometry. Ph.D. Thesis, University of Leeds, England. 1968.
5. E. L. Cochran, F. J. Adrian, and V. A. Bowers. J. Chem. Phys. **36**, 1938 (1962).
6. J. Dewing, G. F. Longster, J. Myatt, and P. F. Todd. Chem. Commun. 391 (1965).
7. P. B. Ayscough and C. Thomson. Trans. Faraday Soc. **58**, 1477 (1962).
8. D. E. Wood and R. V. Lloyd. J. Chem. Phys. **52**, 3840 (1970); **53**, 3932 (1970).
9. R. Livingston and H. Zeldes. J. Chem. Phys. **44**, 1245 (1966).
10. L. Kevan. Radiation chemistry of frozen polar systems, chapter in Actions Chimiques et Biologiques des Radiations, 13ème série. *Edited by* M. Haissinsky, Masson et Cie, Paris. 1969. p. 57.
11. M. Katayama and W. Gordy. J. Chem. Phys. **35**, 117 (1961).
12. F. P. Sargent. Can. J. Chem. **46**, 1029 (1968).
13. A. Horsfield, J. R. Morton, and D. H. Whiffen. Mol. Phys. **5**, 115 (1962).
14. G. Smith and G. A. Swan. J. Chem. Soc. 886 (1962).
15. J. C. J. Thynne. Trans. Faraday Soc. **60**, 2207 (1964).
16. A. R. Ubbelohde and K. J. Gallagher. Acta Cryst. **8**, 71 (1955).
17. D. Smithies and A. J. Whitworth. J. Chem. Soc. A, 1987 (1969).
18. P. Gray and A. Jones. Trans. Faraday Soc. **62**, 112 (1966) and references therein.
19. D. J. Hyatt. Ph.D. Thesis, University of Leeds, England. 1967.
20. W. G. French and J. E. Willard. J. Phys. Chem. **72**, 4604 (1968) and references therein.
21. M. J. A. de Bie and R. Braams. Chem. Phys. Lett. **6**, 331 (1969).
22. P. Neta and R. W. Fessenden. J. Phys. Chem. **75**, 738 (1971).
23. W. C. Danen and T. T. Kensler. J. Am. Chem. Soc. **92**, 5235 (1970).
24. E. L. Cochran, F. J. Adrian, and V. A. Bowers. J. Chem. Phys. **51**, 2759 (1969).
25. D. R. Smith and W. A. Seddon. Can. J. Chem. **48**, 1938 (1970).
26. M. C. R. Symons. Adv. Chem. Ser. **82**, 1 (1968).
27. D. Cordischi and R. Di Blasi. Can. J. Chem. **47**, 2601 (1969).
28. K. N. Shrivastava and R. S. Anderson. J. Chem. Phys. **48**, 4599 (1968).
29. J. A. Brivati, K. D. J. Root, M. C. R. Symons, and D. J. A. Tinling. J. Chem. Soc. A, 1942 (1969).
30. S. Ya. Pshezhetskii and V. I. Tupikov. Russ. J. Phys. Chem. (Engl. Transl.) **38**, 1364 (1964).
31. S. Nagai, S. Ohnishi, and I. Nitta. Ann. Rep. Osaka Lab. for Radiat. Chem. J.A.E.R.I. 5022, 6 (1970).
32. J. R. Morton and D. R. Smith. Can. J. Chem. **44**, 1951 (1966).
33. M. Fujimoto and J. R. Morton. Can. J. Chem. **43**, 1012 (1965).
34. J. R. Morton. Chem. Revs. **64**, 453 (1964).
35. R. W. Fessenden and R. H. Schuler. J. Chem. Phys. **39**, 2147 (1963).
36. T. Cole. J. Chem. Phys. **35**, 1169 (1961).

Can. J. Chem. Downloaded from www.nrcresearchpress.com by 210.87.254.40 on 09/05/12
For personal use only.

Electron Spin Resonance Studies of the Radiolysis of Aliphatic Amines Adsorbed on Silica Gel[1]

P. WARDMAN[2] AND D. R. SMITH[3]

Physical Chemistry Branch, Atomic Energy of Canada Limited, Chalk River Nuclear Laboratories, Chalk River, Ontario

Received January 13, 1971

Several aliphatic amines have been adsorbed in sub-monolayer amounts on silica gel and γ-irradiated at 77 °K. The electron spin resonance (e.s.r.) spectra of the radicals trapped on the surface at 77 °K were similar, in most cases, to the spectra obtained after irradiating the corresponding polycrystalline solid amine at 77 °K. Methyl-, ethyl-, *n*-propyl, and *n*-butylamines all gave $R\dot{N}H$ radicals, and dimethylamine gave $(CH_3)_2\dot{N}$ radicals. The radical cation ($(CH_3)_3\dot{\overset{+}{N}}$) was observed in the case of trimethylamine. Adsorbed methoxy-amine and *t*-butyl amine have also been studied and the cation-radical of the latter tentatively identified. The results are discussed in terms of reaction of the adsorbed amine with a surface active site.

Plusieurs amines aliphatiques ont été absorbées sur le gel de silice pour donner des mono-couches et irradiées par des rayons-γ à 77 °K. Les spectres de résonance paramagnétique électronique (r.p.e.) des radicaux piégés à 77 °K sur la surface de l'absorbant sont semblables, dans la plupart des cas, aux spectres obtenus en irradiant la même amine à l'état polycristalline à 77 °K. Les méthyl-, éthyl-, *n*-propyl et *n*-butyl amines donnent tous les radicaux $R\dot{N}H$, et la diméthyl-amine donne les radicaux $(CH_3)_2\dot{N}$. Le cation radicalaire ($(CH_3)_3\dot{\overset{+}{N}}$) a été observé dans le cas de la triméthyl-amine. Aussi, methoxy-amine et *t*-butyl amine adsorbées ont été etudiées et le cation-radicalaire de ce dernier a été identifié provisoirement. Les résultats sont discutés en termes de réaction des amines absorbées sur un site actif à la surface de l'absorbant.

Canadian Journal of Chemistry, 49, 1880 (1971)

Introduction

Recent work has shown that when suitable scavengers are adsorbed on silica gel and the gel γ-irradiated, reactions with what are apparently migrating positive or negative charged species occur. Thus adsorbed benzene forms the benzene cation (1) and alkyl halides capture electrons dissociatively to produce alkyl radicals (2), both radicals being trapped on the surface.

Amines are adsorbed strongly on silica gel and are expected to have a low reactivity towards migrating electrons, but because of their low ionization potentials should trap positive charge very effectively. The use of silica gel as adsorbent therefore provides us with a means of investigating the radicals derived from ionization of amines. In contrast, we have found quite different radicals, not yet identified, by reaction of negative species (surface trapped electrons) with amines: these latter results are presented elsewhere, in our study of the radiolysis of amines adsorbed on magnesium oxide powder (3, 4).

[1]AECL No. 3871.

[2]NRCC Postdoctorate Fellow 1967–1969. Present address: Dept. of Chemistry, University of Manchester, Manchester M13 9PL, England.

[3]To whom correspondence should be addressed.

Experimental

The amines used, procedures for handling deuterated amines and irradiation and electron spin resonance (e.s.r.) spectroscopy have been described in the accompanying paper on irradiated polycrystalline or amorphous amines. Fisher 100–200 mesh (A.S.T.M.) silica gel was degassed with ~ 1 mm depth in a 2 cm diameter silica tube at 450 °C for 16 h at 10^{-5} Torr, cooled to 77 °K and a measured amount of amine distilled in. The tube, terminated by a length of 3 mm i.d. Spectrosil silica, was sealed off and the sample warmed to room temperature for 10 min with gentle shaking. The sample was irradiated at 77 °K in the wide end of the tube and tipped without warming into the Spectrosil end for e.s.r. observations. Amines deuterated in the amino group were adsorbed on silica gel which had been deuterated by first removing the bulk of the adsorbed H_2O by a preliminary degassing at 450 °C for 3 h, then exposing the cooled gel to 5 successive lots of D_2O for several minutes each, finally leaving the gel in contact with D_2O for 8 h before final degassing as above. The B.E.T. surface area of the gel was 635 $m^2 g^{-1}$. This was measured by nitrogen adsorption at 77 °K using an Aminco Sor-bet apparatus and the helium carrier technique. The area of the nitrogen molecule was assumed to be 16 $Å^2$.

Results

No e.s.r. absorption was observed in the sample prior to irradiation. We did not investigate the effects of variation of surface coverage with all the amines, but no qualitative differences were

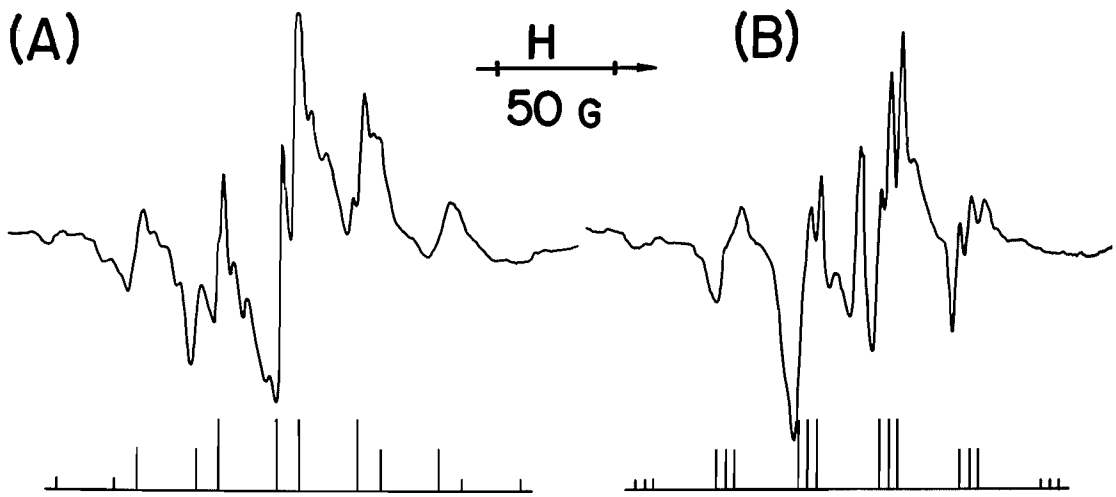

FIG. 1. First derivative e.s.r. spectra of γ-irradiated 10^{-3} mol g^{-1} methylamine on silica gel at 77 °K: (*A*), CH_3NH_2; (*B*) CH_3ND_2.

found for CH_3NH_2 between 2×10^{-4} and 2×10^{-3} mol g^{-1}. Most results were found for a coverage of 10^{-3} mol g^{-1}, which corresponds to $\sim$ 1 molecule/100 Å^2. The radicals disappeared in less than 1 min on warming to 300 °K. Support for our assignments, including better resolved spectra in some cases, is to be found in the accompanying paper.

(i) Methylamine

The spectrum of 10^{-3} mol g^{-1} CH_3NH_2 on silica gel after γ-irradiation at 77 °K is shown in Fig. 1(*A*), which has superior resolution to the similar spectrum observed in irradiated polycrystalline CH_3NH_2 and is assigned to $\dot{C}H_3\overset{+}{N}H$. The high field line of the outermost pair (total separation 200 G) is almost masked by the very broad line in this region which is characteristic of irradiated silica gel without adsorbent. The high field lines of several other spectra were also difficult to detect. The "stick" diagram gives satisfactory agreement with the position of the major lines for our assignment $A_H^{CH_3} = A_{^{14}N,\parallel} =$ 35 G and $A_N^{NH} = 25$ G, but additional splitting is observed. The most likely cause of at least part of this splitting is the perpendicular component of the ^{14}N anisotropic hyperfine tensor, the observed 35 G splitting corresponding to the parallel component (see preceding paper).

We may eliminate $\dot{C}H_2NH_2$ (5) or $\dot{C}H_2\overset{+}{N}H_3$ (6) as alternative assignments because these radicals would give quite different spectra only $\sim$ 64 and $\sim$ 132 G wide, respectively, assuming an $\sim$12 G ^{14}N principal splitting would be observed. The spectrum for $CH_3\overset{+}{N}H_2$ may be predicted by comparison with hyperfine (h.f.) parameters for $\overset{+}{N}H_3$ (7) and $(CH_3)_3\overset{+}{N}$ (8) (see also Table 2 of the preceding paper). For $CH_3\overset{+}{N}H_2$ we predict $A_H^{CH_3} \simeq 31$ G, $A_H^{NH_2} \simeq 26$ G, and $A_{^{14}N,\parallel} \geqslant 35$ G, which would result in a spectrum of 8 major groups of lines ($A_{av} \simeq 30$ G) spread over $\geqslant$215 G. This pattern would not be greatly affected by errors in the value of $A_{^{14}N,\parallel}$, the predicted proton splittings being fairly reliable and dominating the overall features of the spectrum because of broadening of the $M_I(^{14}N) = \pm 1$ lines. In particular, $CH_3\overset{+}{N}H_2$ is not expected to show a strong central line, as was observed and is predicted by our parameters for $CH_3\dot{N}H$.

The spectra from 10^{-3} mol g^{-1} $CH_3{}^{15}NH_2$, CD_3NH_2, and CD_3ND_2 on silica gel after γ-irradiation also resembled those found for the irradiated polycrystalline solid amines. One difference between the silica gel and solid systems (for CH_3NH_2 and $CH_3{}^{15}NH_2$ at least) is an increase in average hyperfine splitting of about 10% in the silica gel system. The difficulties in analyzing the spectra of radicals trapped on surfaces are illustrated by Fig. 1(*B*), which shows the spectrum of $CH_3\dot{N}D$ on silica gel. This shows the six h.f. lines ($A_{av} = 35$ G) but with additional 4–5 G splitting only resolved in the high field lines. Variation in line width is also observed for the $\dot{N}H_2$ radical on silica gel (9), and may be due to slow rotation of the radical on the surface.

Can. J. Chem. Downloaded from www.nrcresearchpress.com by 210.87.254.40 on 09/05/12
For personal use only.

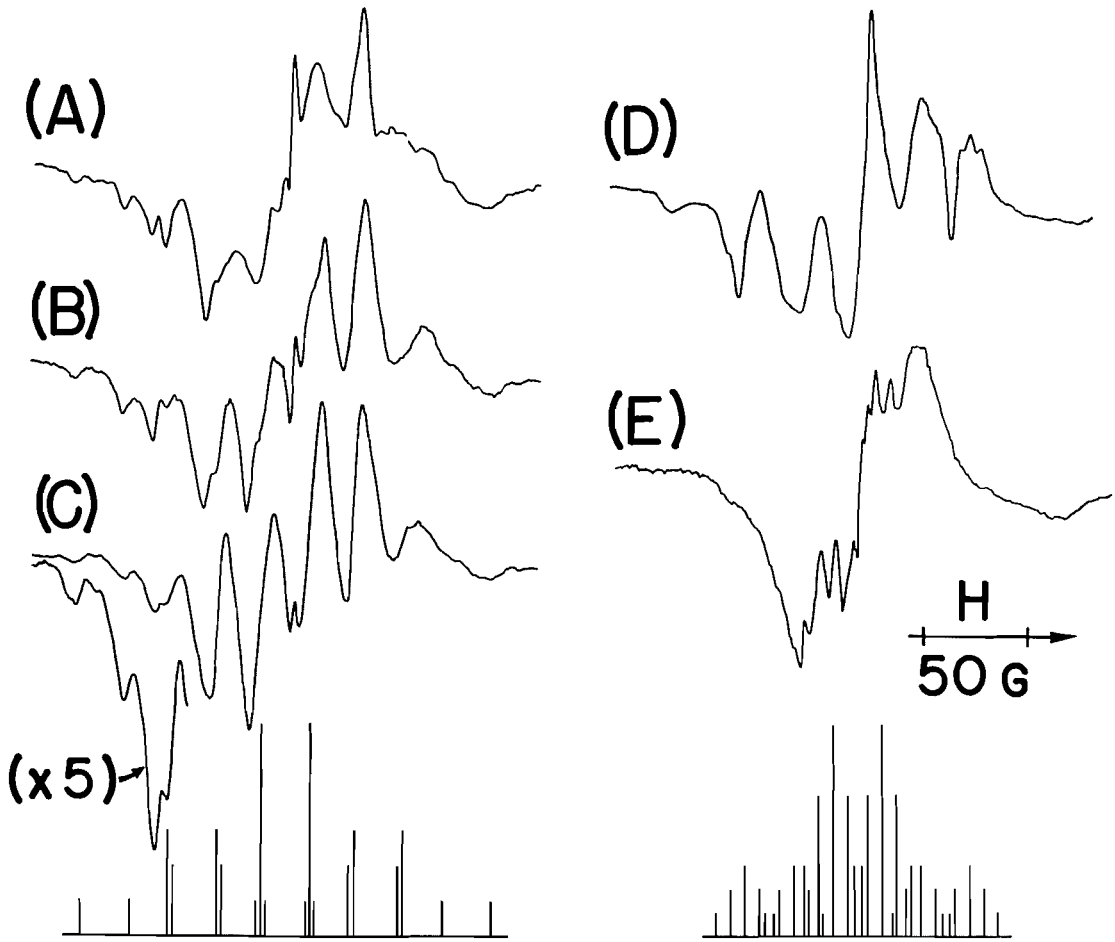

FIG. 2. First derivative e.s.r. spectra of γ-irradiated 10^{-3} mol g^{-1} *n*-alkyl amines on silica gel at 77 °K: (*A*), $C_2H_5NH_2$; (*B*), *n*-$C_3H_7NH_2$; (*C*), *n*-$C_4H_9NH_2$; (*D*), $C_2H_5ND_2$; (*E*), $CH_3CD_2NH_2$.

(ii) Ethyl-, n-Propyl-, and n-Butyl-amines

Poorer resolution of the $C_2H_5\dot{N}H$ radical was observed than in solid $C_2H_5NH_2$, but the results for the irradiation of these higher amines on silica gel support our assignment of $R\dot{N}H$ radicals. Similar spectra were observed for irradiated ethyl-, *n*-propyl-, and *n*-butyl-amines adsorbed on silica gel. In Fig. 2(*A*), (*B*), and (*C*) we see the spectra for γ-irradiated 10^{-3} mol g^{-1} $C_2H_5NH_2$, *n*-$C_3H_7NH_2$, and *n*-$C_4H_9NH_2$, respectively. The spectrum from *n*-butylamine is the best resolved of the three, but it is clear that the number of major lines and the line positions are identical in all three amines. This could only arise if the radicals are of the $R\dot{N}H$ (or $R\dot{N}H_2^+$) type, since neither $R\dot{C}HNH_2$ nor $\dot{C}H_2(CH_2)_nNH_2$ would give similar spectra for all three amines with lines up to 200 G total separation. The spectra from the ethylamines are not identical to those obtained from the γ-irradiated solids at 77 °K (see preceding paper) and in particular the total width from $C_2H_5NH_2$ is about 10% higher in the silica gel system than in the solid. By comparison with CH_3NH_2 and other amines, we might expect a small increase in alkyl proton couplings for $R\dot{N}H$ on silica gel compared to those in the solid phase, and our analysis agrees with this prediction.

In Fig. 2(*C*) the two outermost low-field lines, readily seen on higher gain, are characteristic of $M_I(^{14}N) = \pm 1$ lines that are broadened considerably relative to the $M_I = 0$ line. The separation between these lines is only ~ 23 G, too low for a ^{14}N parallel coupling in $R\dot{N}H$ or $R\dot{N}H_2^+$, suggesting that the 1st and 2nd lines (from low

Can. J. Chem. Downloaded from www.nrcresearchpress.com by 210.87.254.40 on 09/05/12
For personal use only.

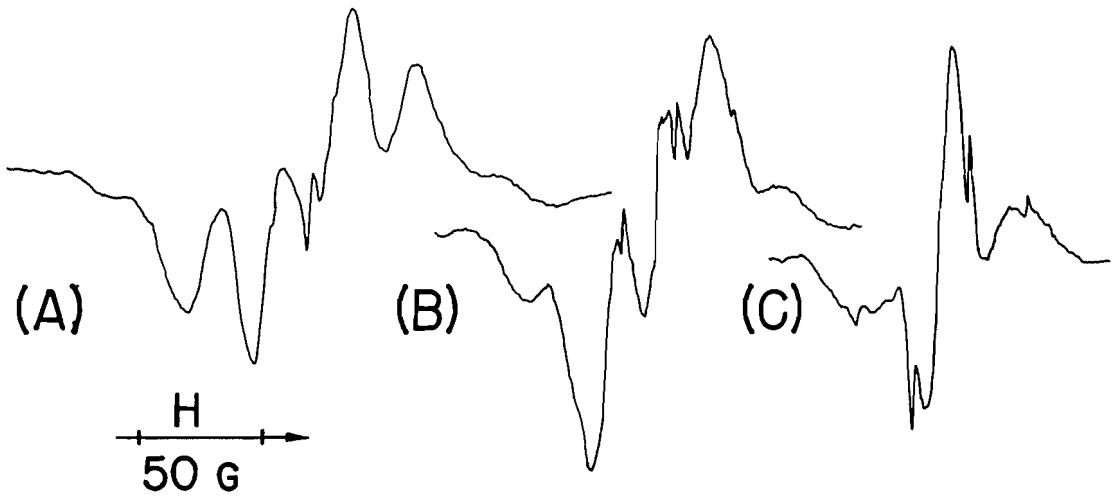

FIG. 3. First derivative e.s.r. spectra of γ-irradiated 10^{-3} mol g^{-1} isopropylamine or *t*-butylamine on silica gel at 77 °K: (*A*), $(CH_3)_2CHNH_2$; (*B*), $(CH_3)_3CNH_2$; (*C*), $(CH_3)_3CND_2$.

field) are both $M_I(^{14}N) = \pm 1$ lines and the 3rd and 4th lines the corresponding $M_I = 0$ lines with $A_{^{14}N,\parallel} = 43$ G. Thus as generally observed the proton couplings dictate the major spectral lines, which form a sextet with total separation of the outermost lines ~115 G and $A_{av} = 23$ G. The total width of the spectrum from $C_2H_5ND_2$ (Fig. 2(*D*)) is ~177 G, suggesting coupling with a single amino proton in $C_2H_5NH_2$ of ~ 25 G, *i.e.* that appropriate for A_H^{NH} in $RCH_2\dot{N}H$. With this coupling the total methylene proton coupling in the $RCH_2\dot{N}H$ radical must be (115–25) ≃ 90 G. The sextet of major lines from the total proton coupling in $RCH_2\dot{N}H$ must then arise from two equivalent methylene protons, $A_H^{CH_2} \simeq 45$ G and a single amino proton, $A_H^{NH} \simeq 25$ G. The "stick" diagram below Fig. 2(*C*) gives a best fit for our analysis for $RCH_2\dot{N}H$ with $A_H^{CH_2} = 45$ G, $A_H^{NH} = 24$ G, and $A_{^{14}N,\parallel} = 43$ G. There is excellent agreement with all three experimental spectra, apart from poor correspondence with line intensities due to line width variation. (Both "stick" spectra in Fig. 2 have been drawn with the $M_I(^{14}N) = \pm 1$ lines only one third the height of the $M_I = 0$ line to approximate this effect.)

The spectrum from $CH_3CD_2NH_2$ on silica gel (Fig. 2(*E*)) supports this analysis, an ~ 7 G deuterium splitting being resolved only on the $M_I(^{14}N) = 0$ line and the total width being that expected. The "stick" diagram is for the couplings above. Surprisingly, although the total width of the spectrum from $C_2H_5ND_2$ (Fig. 2(*D*)) is exactly that expected for $C_2H_5\dot{N}D$, the pattern of 5 major lines ($A_{av} \simeq 25$ G) is quite unlike the ~ 45 G triplet expected from the CH_2 splitting. Poor agreement with the computed spectrum was also obtained with γ-irradiated solid $C_2H_5ND_2$ (see preceding paper). It may be that an isotope effect is being observed in this case, producing a mixture of radicals with a radical other than $C_2H_5\dot{N}D$ dominating the center of the spectrum. The quintet with $A_{av} \simeq 25$ G is not unlike that found for $CH_3\dot{C}HND_2$ (see preceding paper).

Attempts to fit the sextet major spectrum arising from proton h.f. interaction from irradiated RCH_2NH_2 on silica gel to either $RCH_2\dot{N}H$ with inequivalent β protons or to $RCH_2\dot{N}H_2$ failed. In both cases reasonable values of the h.f. parameters failed to produce a sextet with the observed splittings; rather precise degeneracy is necessary to produce the relatively narrow lines seen in Fig. 2(*C*).

(iii) Isopropyl- and tert-Butylamines

The spectrum from irradiated 10^{-3} mol g^{-1} $(CH_3)_2CHNH_2$ on silica gel is shown in Fig. 3(*A*) and is similar to that observed in the irradiated solid at 77 °K but the central doublet (only partially resolved in the solid) is completely resolved on silica gel. The latter spectrum is approximately that expected from $(CH_3)_2CH\dot{N}H$ with the β proton coupling (40 G in the solid) increased to $A_H^{CH} \simeq 50$ G, with $A_H^{NH} \simeq 25$ G and $A_{^{14}N,\parallel} \simeq 35$ G.

The spectrum from irradiated $(CH_3)_3CNH_2$

Can. J. Chem. Downloaded from www.nrcresearchpress.com by 210.87.254.40 on 09/05/12
For personal use only.

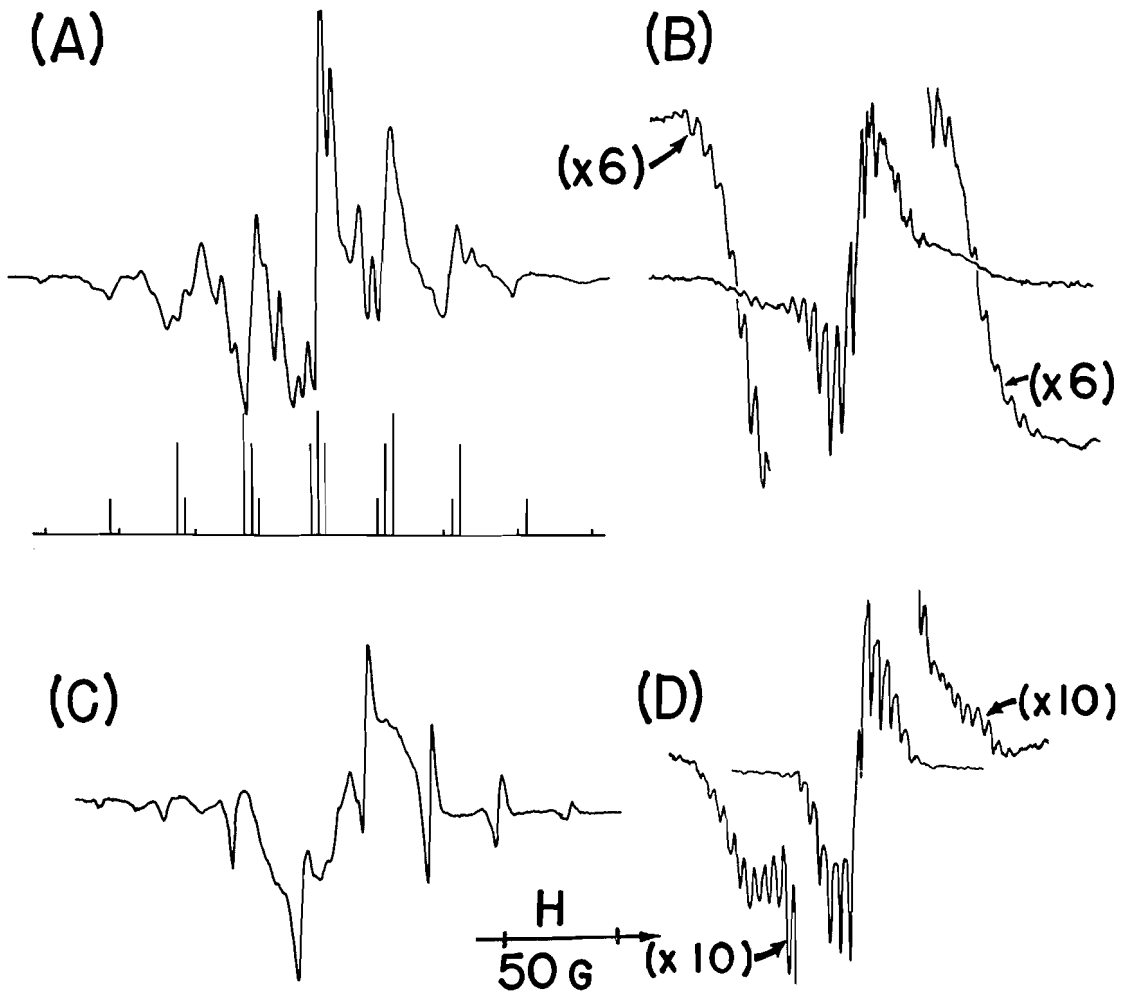

FIG. 4. First derivative e.s.r. spectra of γ-irradiated di- and tri-methylamines on silica gel at 77 °K: (*A*), 2×10^{-4} mol g^{-1} $(CH_3)_2NH$; (*B*), 2×10^{-4} mol g^{-1} $(CD_3)_2NH$; (*C*), 10^{-3} mol^{-1} $(CH_3)_3N$; (*D*), 10^{-3} mol g^{-1} $(CD_3)_3N$.

on silica gel (Fig. 3(*B*)) is seen to be *identical* to that observed from the solid amine after irradiation at 77 °K (see Fig. 7(*A*) of the preceding paper). A *very* small amount of $\dot{C}H_3$ radicals was also observed, the 23 G quartet being readily recognizable in the spectrum from $(CH_3)_3CND_2$ on silica gel (Fig. 3(*C*)). Again, the spectrum from $(CH_3)_3CND_2$ is very similar to that observed in the irradiated solid at 77 °K. We have tentatively attributed these spectra to the parent ion, $(CH_3)_3C\overset{+}{N}H_2$ ($(CH_3)_3C\overset{+}{N}D_2$) with $A_H^{NH_2} \simeq A_{^{14}N,iso} \simeq 18$ G in the solid (see preceding paper). The ^{14}N coupling may not be isotropic at 77 °K and is probably increased over the ~18 G value seen at ~175 °K in the solid. Poor resolution on silica gel prevents precise measurement of the anisotropic coupling.

(iv) Di- and Tri-methylamines

At a coverage of 2×10^{-4} mol g^{-1}, $(CH_3)_2NH$ on silica gel gave a well-resolved $(CH_3)_2\dot{N}$ spectrum after γ-irradiation (Fig. 4(*A*)). The seven major lines from the proton coupling give $A_H^{CH_3} = 29.5 \pm 1$ G and the low-field outermost line of the parallel component of the ^{14}N splitting, readily observed on high gain gives $A_{^{14}N,\parallel} = 33$ G. The "stick" spectrum is for this assignment. The additional splitting observed arises from the imprecise degeneracy of the proton coupling and the ^{14}N parallel coupling and probably also from

Can. J. Chem. Downloaded from www.nrcresearchpress.com by 210.87.254.40 on 09/05/12
For personal use only.

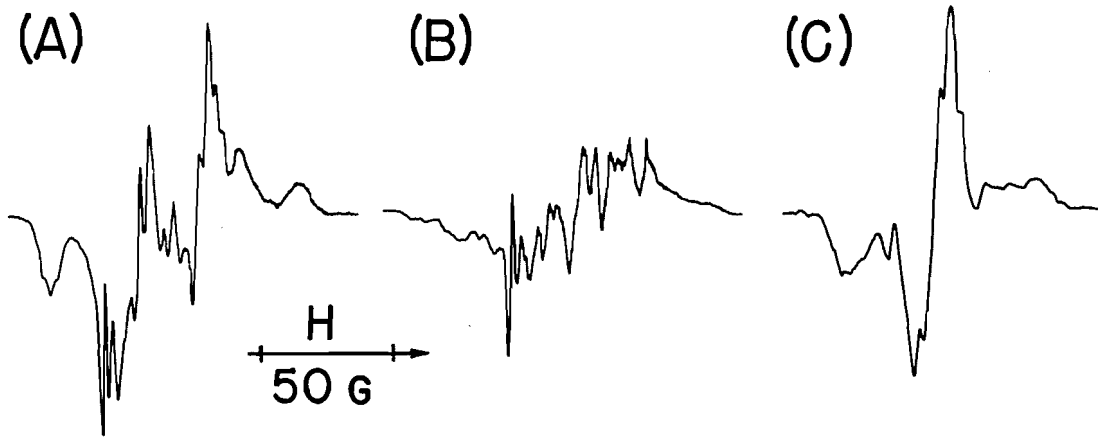

FIG. 5. First derivative e.s.r. spectra of γ-irradiated methoxyamine on silica gel at 77 °K: (*A*), 10^{-3} mol g^{-1} CH_3ONH_2; (*B*), 2×10^{-4} mol g^{-1} CH_3ONH_2; (*C*), 10^{-3} mol g^{-1} CH_3OND_2.

an $\sim$ 5 G ^{14}N perpendicular component. The spectrum from 2×10^{-4} *M* $(CD_3)_2NH$ on silica gel (Fig. 4(*B*)) illustrates clearly the broadening of the $M_I(^{14}N) = \pm 1$ lines also seen in $R\dot{N}H$ radicals. The $\sim$ 4.5 G D-splitting confirms the $\sim$ 30 G H-coupling. The spectrum for 10^{-3} mol g^{-1} $(CH_3)_2{}^{15}NH$ on silica gel, though somewhat asymmetric, was in accord with the results for $(CH_3)_2NH$.

The radical produced by irradiation of 10^{-3} mol g^{-1} $(CH_3)_3N$ on silica gel was not observed in irradiated solid trimethylamine. Figure 4(*C*) shows the spectrum for $(CH_3)_3N$ and Fig. 4(*D*) that for $(CD_3)_3N$. For both amines a central, broader absorption obscured the spectra, but the narrow lines (again of varying width) are ascribed to the $(CH_3)_3\overset{+}{\dot{N}}$ ($(CD_3)_3\overset{+}{\dot{N}}$) radical cation, the isotropic and anisotropic couplings of which are known (8, 11). For $(CH_3)_3\overset{+}{\dot{N}}$ we observed 8 of the 10 isotropic ($M_I(^{14}N) = 0$) lines arising from the proton coupling ($A_H = 29.5 \pm 1.0$ G) but the much weaker anisotropic $M_I(^{14}N) = \pm 1$ lines were too ill-resolved to extract the ^{14}N coupling. The broadening of the $M_I(^{14}N) = \pm 1$ lines is particularly well illustrated in the spectra for $(CD_3)_3\overset{+}{\dot{N}}$. We expect to detect at most only 13 of the 19 deuterium lines for each value of $I_N = 0$, ± 1 and on this basis the total separation should be less than $2A_{^{14}N} + 12A_D$. We observed 31 h.f. lines ($A_D = 4.5$ G) over 134 G, showing $A_{^{14}N,\parallel} >$ 40 G. This is in agreement with the 49 G parallel component of the ^{14}N coupling of $(CH_3)_3\overset{+}{\dot{N}}$ in solid betaine hydrochloride (11) and much larger than the 18 G isotropic ^{14}N splitting (8) of this radical.

(v) Methoxyamine

Quite different spectra were observed for CH_3ONH_2 on silica gel at coverages of 10^{-3} and 2×10^{-4} mol g^{-1}, Fig. 5(*A*) and (*B*), respectively. At the higher coverage, the major species was clearly the $CH_3O\dot{N}H$ radical, which we have observed in solid methoxyamine (preceding paper). We assign $A_H^{NH} \simeq 25$ G, $A_H^{CH_3} \simeq 0$, and $A_{^{14}N,\parallel} \simeq 35$ G. In addition to this major quartet feature, we see further splitting of the central portion of the spectrum. This does not arise from the $CH_3O\dot{N}H$ radical (*e.g.* from the methoxy protons) because at the lower coverage essentially only the spectrum of narrow lines is observed, with very little $CH_3O\dot{N}H$ spectrum underlying. We cannot analyze this latter spectrum because of the possibility of small contributions from $CH_3O\dot{N}H$ and/or $\dot{C}H_2ONH_2$ to an already weak spectrum. It may be due to $\dot{N}H_2$ radicals, as these lines were not observed in the CH_3OND_2/silica gel systems and in fact the marked variation in line shape and approximate positions of the major lines are similar to those found for $\dot{N}H_2$ on silica gel (9). Figure 5(*C*) shows the spectrum of irradiated 10^{-3} mol g^{-1} CH_3OND_2 on silica gel. The $\sim$30 G triplet of the $CH_3O\dot{N}D$ radical has additional lines superimposed, possibly some $\dot{C}H_2OND_2$ or $\dot{N}D_2$ radicals.

(vi) g-Values

Except those for $(CH_3)_3\overset{+}{\dot{N}}$ ($(CD_3)_3\overset{+}{\dot{N}}$), all our spectra had $g = 2.003 \pm 0.001$, which is that

Can. J. Chem. Downloaded from www.nrcresearchpress.com by 210.87.254.40 on 09/05/12
For personal use only.

Can. J. Chem. Downloaded from www.nrcresearchpress.com by 210.87.254.40 on 09/05/12
For personal use only.

expected for the radicals we have identified. Our measured $g = 2.0046 \pm 0.0006$ for $(CH_3)_3\dot{N}^+$ is in good agreement with published values (8, 11).

Discussion

(i) Formation of the Radicals

The nature of the adsorbed species when ammonia is adsorbed on silica gel has been studied extensively (for reviews see ref. 12), although less is known for monoamines other than ethylamine (13, 14) and for higher amines. Silica gel degassed at 450 °C retains little or no adsorbed bulk H_2O molecules but does retain large numbers of hydroxyl groups, perhaps ~0.5 monolayer (15). Adsorption of amines strongly perturbs these OH groups, the major reaction probably being [1] (13)

[1] $\equiv SiOH + RNH_2 \rightleftharpoons \equiv SiO^-R\dot{N}H_3^+$

resulting in a very high heat of adsorption (~15–20 kcal mol^{-1}).

Production of radicals originating from adsorbed species after irradiation of silica gel systems has been explained in terms of migrating surface electrons (2), energy tranfer (1) or reaction of the adsorbate with hydrogen atoms released from surface hydroxyl groups (16). Although the free amine molecules are expected to be unreactive towards migrating surface electrons, the conjugate acid produced in [1] may have higher reactivity. However, the ammonium ion has low reactivity towards solvated electrons in water (17), and the increased basicity of amines over ammonia is probably insufficient to affect the reactivity markedly. Hydrogen atoms are expected to be unreactive towards amines adsorbed on silica gel, since protonation of the amino group greatly deactivates protons on the α carbon towards abstraction reactions (5). (Amines are not protonated on adsorption on magnesium oxide, but we have been unable to observe radicals produced by bombardment with H atoms of MgO doped with methylamine, using the technique described by Smith and Tench (18). Large yields of radicals were observed by H abstraction from CH_3OH on MgO under the same conditions.[4])

It appears then that the more likely routes for production of radicals by irradiation of amines on silica gel are either by reaction with a migrating surface positive center (surface hole) or by ionization of the amine by direct energy transfer. Doping MgO powder with an adsorbed amine prevents the formation of surface holes (V_s^+ centers) upon γ-irradiation, but no $R\dot{N}H$ or $R\dot{N}H_2^+$ radicals are observed (3, 4). The most appropriate model for the formation of $R\dot{N}H$ or $R\dot{N}H_2^+$ radicals on silica gel may be represented by reactions 2 to 5

[2] $S \dashrightarrow S^*$

[3] $S^* + \equiv SiO^-R\dot{N}H_3^+ \rightarrow S + \equiv SiOR\dot{N}H_3^+ + e^-$

[4] $\equiv SiOR\dot{N}H_3^+ \rightarrow [\equiv SiOH\text{---}R\dot{N}H_2^+]$

[5] $[\equiv SiOH\text{---}R\dot{N}H_2^+] \rightleftharpoons [\equiv SiOH_2^+\text{---}R\dot{N}H]$

Following Kinell *et al.* (1) we denote S as a surface active site formed by migration of energy from the bulk solid to the surface.

Of course, reaction 5 is simply the acid–base dissociation of $R\dot{N}H$ radicals on the surface. The effective pK of this equilibrium will be greatly affected by the stability of the $R\dot{N}H_2^+$ parent ion. Such an ion may form $R\dot{N}H$ either by equilibrium 5 being to the right or by ion–molecule (proton transfer) reactions, [6],

[6] $R\dot{N}H_2^+ + RNH_2 \rightarrow R\dot{N}H_3^+ + R\dot{N}H$

with adjacent amine molecules. Nearest neighbors are ~10 Å away. In the case of trimethylamine (and probably *tert*-butylamine) the radical cation was stabilized on the surface of silica gel. The gas phase ion–molecule reaction analogous to reaction 6 is only slightly slower for trimethylamine than for the mono- and di-methylamines (19). A reasonable explanation of these differences is that the positive charge is more effectively delocalized (by hyperconjugation) in trimethylamine and *tert*-butylamine. The radical cations of these two amines are more stable and hence equilibrium 5 is further to the left than for the other amines studied.

(ii) The e.s.r. Parameters of the Radicals

The β proton splittings observed for $R\dot{N}H$ radicals on the surface of silica gel were ~ 35 G for $CH_3\dot{N}H$, ~ 45 G in $RCH_2\dot{N}H$ (R = CH_3,

[4] D. R. Smith and P. Wardman, unpublished observations.

C_2H_5, n-C_3H_7), ~ 50 G in $(CH_3)_2CH\dot{N}H$, and ~ 30 G in $(CH_3)_2\dot{N}$. The isotropic (solution) spectrum for $(CH_3)_2\dot{N}$ gives a β proton splitting of 27.4 G (20), an increase of 11% over that in the isoelectronic $(CH_3)_2\dot{C}H$ radical (10). We have seen in the preceding paper that β proton couplings in $R\dot{N}H$ radicals are some 10–20% higher than for the corresponding alkyl radicals. The β proton splittings for $R\dot{N}H$ on silica gel are further increased by ~ 10–20% over those in the solid, giving rather high values for proton couplings. The β proton splittings in $R_2\dot{N}$ radicals in solution are markedly affected by conformational factors (20) and we must assume a similar explanation.

It is interesting that Bobrovskii and Kholmogorov (21) observed 5–10% higher methyl proton couplings for the well-resolved $(CH_3)_2\dot{C}OH$ radical on silica gel than those observed in solution or the solid phase for this radical. The β proton splittings for $RCH_2\dot{N}H$ ($R \neq H$) on silica gel show equivalence of the methylene protons whereas inequivalence was inferred from the spectrum of $C_2H_5\dot{N}H$ in solid ethylamine. Evidently there is somewhat more rotational freedom of the alkyl groups in amines on silica gel than in the solid at 77 °K.

Conclusions

Radiolysis of sub-monolayer amounts of aliphatic amines adsorbed on silica gel produced $R\dot{N}H$ radicals from lower monoamines, $R_2\dot{N}$ radicals from dimethylamine and radical-cations from trimethylamine and probably t-butylamine.

The authors wish to thank Dr. F. P. Sargent for helpful criticism of the manuscript.

1. P. O. Kinell, A. Lund, and A. Shimizu. J. Chem. Phys. **46**, 3679 (1967); Adv. Chem. Ser. **82**, 311 (1968).
2. P. K. Wong and J. E. Willard. J. Phys. Chem. **72**, 2623 (1968).
3. Abstracts, 158th National Meeting of the American Chemical Society, New York, Sept. 8–12, 1969. Paper Phys. 095.
4. Atomic Energy of Canada Limited, Progress Report PR-CMa-10. (AECL 3477). Sept. 30, 1969. p. 56.
5. P. Neta and R. W. Fessenden. J. Phys. Chem. **75**, 738 (1971).
6. R. P. Kohin and P. G. Nadeau. J. Chem. Phys. **44**, 691 (1966).
7. T. Cole. J. Chem. Phys. **35**, 1169 (1961).
8. A. J. Tench. J. Chem. Phys. **38**, 593 (1963).
9. S. Nagai, S. Ohnishi, and I. Nitta. Ann. Rept. Osaka Lab. for Radiation Chem. (No. 2), J.A.E.R.I. 5022, p. 6.
10. P. B. Ayscough and C. Thomson. Trans. Faraday Soc. **58**, 1477 (1962).
11. J. A. Brivati, K. D. J. Root, M. C. R. Symons, and D. J. A. Tinling. J. Chem. Soc. A, 1942 (1969).
12. M. L. Hair. Infrared spectroscopy in surface chemistry. Marcel Dekker, Inc., New York. 1967. L. H. Little. Infrared spectra of adsorbed species. Academic Press, New York. 1966.
13. R. A. Ross and A. H. Taylor. The physics and chemistry of ceramic surfaces. Proc. Brit. Ceramic Soc. No. 5, 167 (1965).
14. R. A. Ross and A. H. Taylor. J. Catal. **9**, 104 (1967).
15. N. H. Sagert and P. J. Dyne. Can. J. Chem. **45**, 615 (1967).
16. V. V. Strelko and K. A. Suprunenko. High Energy Chem. Engl. Transl. **2**, 222 (1968).
17. M. Anbar and P. Neta. Int. J. Appl. Rad. Isot. **18**, 493 (1967).
18. D. R. Smith and A. J. Tench. Can. J. Chem. **47**, 1381 (1969).
19. M. S. B. Munson. J. Phys. Chem. **70**, 2034 (1966).
20. W. C. Danen and T. T. Kensler. J. Am. Chem. Soc. **92**, 5235 (1970).
21. A. P. Bobrovskii and V. E. Kholmogorov. Kinet. Catal. Engl. Transl. **9**, 752 (1968).

Can. J. Chem. Downloaded from www.nrcresearchpress.com by 210.87.254.40 on 09/05/12
For personal use only.

Can. J. Chem. Downloaded from www.nrcresearchpress.com by 210.87.254.42 on 09/05/12
For personal use only.

The Trifluoroacetic Acid Solvent System. Part I. Bases

M. G. Harriss and J. B. Milne
Department of Chemistry, University of Ottawa, Ottawa 2, Canada

Received September 28, 1970

Electrical conductivity has been used to study the ionic behavior of several simple solutes in 100% trifluoroacetic acid. Fuoss extrapolations have been used to evaluate the limiting equivalent conductivities and association constants of the ammonium and alkali metal trifluoroacetates. The dependence of ionic mobility upon cation radius is different from that in water and other solvents and suggests that solvation is much less important in 100% trifluoroacetic acid. On the basis of these results, a proton transfer mechanism of conductance for the trifluoroacetate ion appears unlikely.

On a utilisé la conductivité électrique pour étudier le comportement ionique de solutés simples dans l'acide trifluoroacétique à 100%. On a utilisé les extrapolations de Fuoss pour évaluer les conductivités équivalentes limites et les constantes d'association des trifluoroacétates d'ammonium et de métaux alcalins. On note que la dépendance de la mobilité ionique sur le rayon du cation est différente de celle observée dans l'eau ou les autres solvants et ces résultats suggéreraient que la solvatation est moins importante dans l'acide trifluoroacétique à 100%. En se basant sur ces données, on peut déduire qu'il semble peu probable que la mécanisme de la conductivité de l'ion trifluoroacétate implique un transfert de proton.

Canadian Journal of Chemistry, 49, 1888 (1971)

Trifluoroacetic acid is a moderately strong non-oxidizing acid with good solvent properties (1) and a convenient liquid range. It is an attractive reaction medium (2) and, principally because of its acid properties, it has been used as a solvent for the titration of weak bases (3). Before we can fully understand the chemical reactions which take place in this solvent a basic knowledge of the behavior of simple solutes is necessary. For this reason it was considered of interest to begin a basic study of the solvent. Such a study affords, in addition, an opportunity for comparison with acetic acid, which has been extensively studied (4), and contributes to what has been termed "a fertile field . . . for experimental research" (*5a*), that is electrical conductivity in solvents of low dielectric constant ($\varepsilon < 20$).

Electrical conductivity studies on solutions in pure trifluoroacetic acid were first carried out by Simons and Lorentzen (6). Since that time, the dielectric constant for this solvent has been firmly established as 8.20–8.40 at 25 °C (7–10). Bessière (11) has re-treated the results of Simons and Lorentzen for potassium trifluoroacetate by the Shedlovsky method (*5b*) using a dielectric constant of 7.8. From the dissociation constants of potassium trifluoroacetate and perchloric acid, the latter determined by the indicator method of Kolthoff and Bruckenstein (12), Bessière established a scale of dissociation constants for several acids and bases by a potentiometric method. In the present work electrical conductivity has been used to study the behavior of the ammonium and alkali metal trifluoroacetates and water at concentrations where simple ion-pairing is occurring and the concentration of higher ion-aggregates is negligible.

Experimental Section

Materials

Trifluoroacetic acid for conductivity experiments was prepared by a preliminary fractional distillation of acid, with 5% by weight of anhydride added, through a 40 cm column packed with glass helices followed by a double distillation in a one-piece double distillation apparatus. The best grade acid from Matheson, Coleman and Bell was used. A small quantity of trifluoroacetic acid anhydride was added in the first step and the receiving end of the apparatus was flamed out for both steps while dry nitrogen was passed through the apparatus. The acid was distilled directly into the conductivity cell. In both distillation steps the acid boiling at 71.0–72.0 °C was collected. Acid prepared in this way had a specific conductivity (K_{sp}) of 0.041–0.079 μmho cm^{-1}.

Trifluoroacetic acid anhydride was prepared by refluxing the acid over P_2O_5 and then distilling the product (b.p. 38–39 °C).

The trifluoroacetates were prepared from the parent carbonate or hydroxide and sufficient trifluoroacetic acid for neutralization. The salts were recrystallized from water except for the lithium salt which was too soluble in water for recrystallization and could only be obtained by pumping an exactly neutral solution to dryness under vacuum. All of the salts were found to be deliquescent, particularly those of Li and Na.

Procedure

Electrical conductivities were measured with a Beckman RC-18A conductivity bridge. The temperature for all measurements was maintained at 25 ± 0.010 °C by

TABLE 1. Analyses of trifluoroacetates

Compound $MOOCCF_3$	%M		%F	
	Obsd.	Calcd.	Obsd.	Calcd.
NH_4OOCCF_3	13.75	13.77	43.81	43.50
$LiOOCCF_3$	—	5.76	47.35	47.50
$NaOOCCF_3$	16.77	16.91	41.68	41.90
$KOOCCF_3$	25.82	25.68	37.14	37.43
$RbOOCCF_3$	43.22	43.10	28.59	28.71
$CsOOCCF_3$	53.45	53.90	23.47	23.18

means of an oil bath. Measurements were made in a glass conductivity cell similar to that described previously (13) with a cell constant of 0.0177 cm^{-1}. To ensure that the acid in the cell remained dry during the course of the additions of the electrolyte solution, a small quantity of anhydride (*ca.* 0.5% by weight) was added to this solution in the weight dropper used for solute additions. The amount necessary was estimated from the concentration of water present in the freshly distilled acid and the amount introduced during each solute addition as determined from the increase in conductivity caused by a dummy addition. All solutions were made up by weight and the solvent density was taken as 1.4775 g/cc (14) for the calculation of molarity. For the concentrations studied, 10^{-4}–10^{-5} m l^{-1}, the density of the solutions will differ little from that of pure acid. Solutions of the solutes were added to the cell, and the cell was shaken and readings taken until steady values were obtained.

The dielectric constant of the solvent was taken as 8.40, the value determined by Harris and O'Konski (9), since these authors took considerable precautions to ensure the purity of their acid. The viscosity used, 0.008565 P at 25 °C, has been interpolated from data given in reference (14). The limiting equivalent conductivity, Λ^0, and association constant, K_a, of electrolytes were determined by the Fuoss method (15) of 1935, using the extended Debye–Hückel expression for the activity coefficient, thereby allowing for ionic volume. The calculation and least mean squares extrapolation were carried out by computer and repeated until a Λ^0 was obtained, self consistent to within 1 part in 10^5. Initially Λ^0 was assumed to be 60 $ohms^{-1}$ cm^2 $equiv.^{-1}$ and the distance of closest approach, "a", was taken as 5×10^{-8} cm. The distance a was then calculated from the association constant by the Fuoss expression (5*c*) and the calculation of Λ^0 and K_a repeated.

Results and Discussion

Solutes, Water, and Trifluoroacetic Acid Anhydride

The results of the conductivity measurements for all solutes are given in Table 2. The results of an experiment in which several additions of anhydride were added to freshly distilled acid and then back titrated with water show that the freshly distilled acid contained some water ($[H_2O] \sim 0.005$ M). The addition of anhydride causes an initial steep decrease in the conductivity followed by a more gradual decrease with further additions. The conductivity curve was retraced upon addition of water. The intersection of the steep section, where excess water is present, and the more gradual section, where excess anhydride is present, fixes the 100% pure trifluoroacetic acid on the concentration scale. The initial steep decrease upon addition of anhydride is due to the presence of water in the freshly distilled acid. The difference in the positions of 100% acid and freshly distilled acid on the concentration scale gives the water concentration in freshly distilled acid.

Comparison of the specific conductivities of water and potassium trifluoroacetate in Table 2 shows that water is a very weak electrolyte. This rather surprising result confirms Simons and Lorentzen's (6) and shows the water molecule is indeed a weak base compared to bulk water since trifluoroacetic acid is a moderately strong acid in water. Water behaves similarly in nitric acid (16). Addition of anhydride to 100% pure trifluoroacetic acid causes the conductivity to decrease slightly. This is to be expected since the introduction of the anhydride molecules, which are less polar than the solvent molecules, would make ionization less favorable and the concentration of the solvent self-dissociation ions would be reduced. Randles *et al.* have also reported on the conductivity of water and anhydride in trifluoroacetic acid (17) but at solute concentrations an order of magnitude greater than ours. The results are essentially in agreement.

Solutes, Ammonium and Alkali Metal Trifluoroacetates

The dielectric constant of trifluoroacetic acid at 25 °C is 8.40 (9) and, consequently, ion association is expected to be important even at low concentrations. Both the Bjerrium and the Fuoss equations (5*c*) predict for an ionophore with a distance of closest approach of 5×10^{-8} cm, an ion-pair association constant of greater than 10^5 m^{-1} l. The limiting equivalent conductivity

Can. J. Chem. Downloaded from www.nrcresearchpress.com by 210.87.254.42 on 09/05/12
For personal use only.

TABLE 2. Specific conductances (K_{sp}) at 25 °C

Compound	10^3C ($m\,l^{-1}$)	10^6K_{sp} ($ohm^{-1}\,cm^{-1}$)
$(CF_3CO)_2O$ and H_2O (Initial $K_{sp} = 0.0949 \times 10^{-6}$ $ohm^{-1}\,cm^{-1}$)		
$(CF_3CO)_2O$ additions	21.85	0.0688
	40.25	0.0672
	58.70	0.0660
	81.02	0.0644
	99.59	0.0636
	122.59	0.0631
H_2O* additions	34.45	0.0641
	65.50	0.0661
	96.90	0.0686
	128.20	0.1320
	154.10	0.2610
	187.00	0.4364
	217.50	0.6240
$LiOOCCF_3$ (Initial $K_{sp} = 0.0428 \times 10^{-6}$ $ohm^{-1}\,cm^{-1}$)		
	0.01232	0.1306
	0.02359	0.1776
	0.04032	0.2315
	0.05119	0.2607
	0.06403	0.2918
	0.08172	0.3299
	0.1035	0.3721
	0.1249	0.4090
	0.1452	0.4417
	0.1797	0.4906
$NaOOCCF_3$ (Initial $K_{sp} = 0.0418 \times 10^{-6}$ $ohm^{-1}\,cm^{-1}$)		
	0.02480	0.2274
	0.04568	0.3152
	0.06738	0.3872
	0.9000	0.4522
	0.1133	0.5118
	0.1292	0.5487
	0.1479	0.5895
	0.1670	0.6286
$KOOCCF_3$ (Initial $K_{sp} = 0.0647 \times 10^{-6}$ $ohm^{-1}\,cm^{-1}$)		
	0.00961	0.2492
	0.02090	0.3852
	0.03695	0.5370
	0.05032	0.6423
	0.06129	0.7195
	0.07497	0.8075
	0.08999	0.8946
	0.1029	0.9654
	0.1142	1.025
	0.1356	1.129
	0.1541	1.212
	0.1707	1.284
$RbOOCCF_3$ (Initial $K_{sp} = 0.0821 \times 10^{-6}$ $ohm^{-1}\,cm^{-1}$)		
	0.01347	0.3546
	0.03204	0.6010
	0.05533	0.8374
	0.07573	1.007
	0.09489	1.150
	0.1166	1.297
	0.1381	1.431
	0.1574	1.544
	0.1741	1.637
$CsOOCCF_3$ No. 1 (Initial $K_{sp} = 0.0745 \times 10^{-6}$ $ohm^{-1}\,cm^{-1}$)		
	0.01838	0.5159
	0.05461	1.052
	0.08558	1.397
	0.1191	1.714
	0.1493	1.970
	0.1728	2.153

Can. J. Chem. Downloaded from www.nrcresearchpress.com by 210.87.254.42 on 09/05/12
For personal use only.

TABLE 2. (*Concluded*)

Compound	10^3C ($m\,l^{-1}$)	10^6K_{sp} ($ohm^{-1}\,cm^{-1}$)
$CsOOCCF_3$ No. 2 (Initial $K_{sp} = 0.0815 \times 10^{-6}$ $ohm^{-1}\,cm^{-1}$)		
	0.01902	0.5331
	0.03436	0.7889
	0.05869	1.114
	0.07627	1.315
	0.08778	1.431
	0.1016	1.568
	0.1184	1.726
	0.1304	1.831
	0.1481	1.982
	0.1597	2.076
	0.1741	2.184
NH_4OOCCF_3 (Initial $K_{sp} = 0.0646 \times 10^{-6}$ $ohm^{-1}\,cm^{-1}$)		
	0.01431	0.3551
	0.03062	0.5640
	0.05053	0.7631
	0.06757	0.9078
	0.09078	1.081
	0.1059	1.184
	0.1223	1.288
	0.1385	1.385
	0.1547	1.478
	0.1711	1.567

*Uncorrected for solvent produced by reaction with anhydride.

and ion-pair association constant of an electrolyte in a solvent of low dielectric constant may be calculated by means of a Fuoss (15) or a Shedlovsky (18) plot. Both methods yield the same Λ^0 and the difference in the association constants is less than 0.1% for a solvent of dielectric constant, 8.4 (19). The Fuoss extrapolation was used in this work with modification to allow for ionic volume in the activity function. The equations used were

$$\Lambda = \gamma(\Lambda^0 - (B_1\Lambda^0 + B_2)\sqrt{c\gamma})$$

$$\frac{1}{K_a} = \frac{cf^2\gamma^2}{1-\gamma}$$

$$\log f = -\frac{A\sqrt{c\gamma}}{1 + Ba\sqrt{c\gamma}}$$

The constants used here are defined as in ref. 20 and γ is the degree of dissociation.

According to Fuoss (5*d*), triple ion formation should become noticeable in electrical conductivity measurements in this solvent at 1.9×10^{-4} $m\,l^{-1}$. This should represent an upper limit for the treatment of data, assuming only a simple ion-pair equilibrium. A lower limit of applicability of the extrapolation would arise where the solvent contains an ion common to the solute. Such an ion may arise from solvent self-dissociation or from some extraneous electrolyte. If the equilibrium giving rise to such an ion were not completely repressed by the solute, the conductivity observed will not be due to solute ions alone and deviations from the Fuoss slope will be observed. Both the upper and lower limits of the extrapolation are expected to appear as negative deviations from the slope since the apparent Λ used in constructing the plot will be too large. Figure 1 shows an extrapolation for potassium trifluoroacetate. An abscissa value of 100 in the figure shows the upper limit for simple ion-pair behavior. However, from the plot it may be seen that the points lie on the straight line up to concentrations three times that of this limit. The inclusion of even higher concentration points in the extrapolation will result in a low Λ^0 and a small association constant. The lowest concentration point is seen to be below the line, indicating an additional contribution to the conductivity as discussed above.[1]

[1]The lowest pure solvent conductivity observed in this work was 0.041 μmho cm^{-1}. In subsequent studies of other electrolytes (Parts II and III, to be published), the first fractions of acid distillate were used to rinse the conductivity cell and then discarded. The pure acid collected after this procedure was carried out had conductivity one tenth of that reported here, which suggests that the residual conductivity was due to electrolyte leached from the apparatus by this strongly acid solvent. If such an electrolyte were solvolyzed to give trifluoroacetate ion in solution, this would be more likely to cause the low concentration deviation in the Fuoss plot than ions arising from solvent self-dissociation.

Can. J. Chem. Downloaded from www.nrcresearchpress.com by 210.87.254.42 on 09/05/12
For personal use only.

TABLE 3. Limiting equivalent conductivities (Λ^0) and association constants (K_a)

Salt	Λ^0 (ohm^{-1} cm^2 equiv.$^{-1}$)	% Standard error on Λ^0	$10^{-5}K_a$ (m l^{-1})	10^8 a† (cm)
$NaOOCCF_3$	73.79	1.7	25.1	4.04
$KOOCCF_3$	63.73	0.79	4.56	4.63
$KOOCCF_3$*	61.18	9.3	2.65	4.86
$RbOOCCF_3$	58.60	0.32	2.37	4.91
$CsOOCCF_3$ No. 1	51.76	0.12	0.99	5.36
$CsOOCCF_3$ No. 2	53.06	0.70	1.02	5.34
NH_4OOCCF_3	54.73	0.75	2.20	4.95

*Simons and Lorentzen's measurements (1).
†Distance of closest approach according to the Fuoss equation (ref. 5, p. 213).

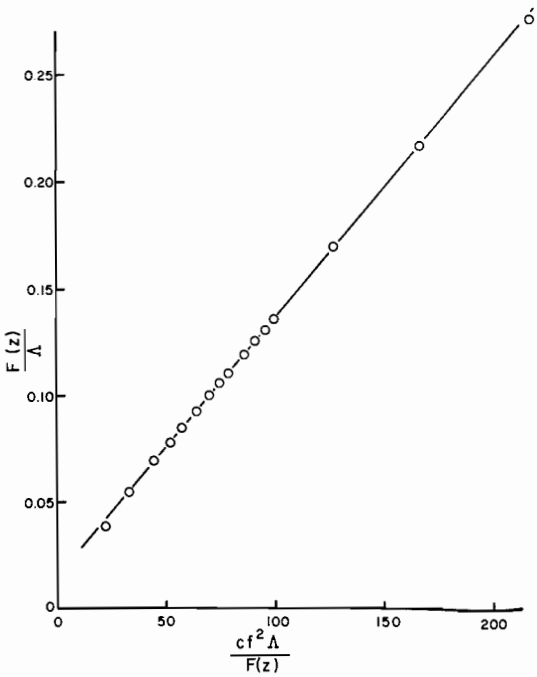

FIG. 1. Fuoss extrapolation of the potassium trifluoroacetate conductivities.

The results of extrapolation of measurements on ammonium and alkali metal trifluoroacetates, strong 1:1 bases in trifluoroacetic acid, are collected in Table 3. These values are arrived at by considering only those measurements below the triple-ion region (1.9×10^{-4} ml^{-1}) and eliminating the lowest concentration measurement (the lowest two in the case of potassium trifluoroacetate), which all lay below the extrapolation line and resulted in a greater Λ^0 and standard error on Λ^0. Included in Table 3 are the % standard error on Λ^0 and the "a" value, calculated from the theoretical Fuoss equation for the association constant. The results of the extrapolation of Simons and Lorentzen's data are given for comparison.

Considering the scatter of Simons and Lorentzen's measurements, reflected in the % standard error, the agreement between results obtained in this work and theirs is excellent. The results from two cesium trifluoroacetate runs are also in good agreement, showing the reproducibility of the experiments.

Bessière has used a Shedlovsky plot to evaluate Simons and Lorentzen's results (11). The association constant for potassium trifluoroacetate is 5×10^4 ml^{-1}, which is nearly an order of magnitude lower than the value reported here. Single hand extrapolations of Simons and Lorentzen's results below the triple-ion formation limit by both the Fuoss and Shedlovsky methods, assuming an initial Λ^0 of 60.0 ohm^{-1} cm^2 equiv.$^{-1}$, give Λ^0 and K_a values within 2% of each other. This order of discrepancy is within the variation which results from the subjective choice of the slope and thus Bessière's low K_a may well be due to the inclusion of some high concentration points above the simple ion-pairing concentration limit. For sodium trifluoroacetate the association constant reported here is 80× that reported by Bessière based on potentiometric measurements. Many of Bessière's measurements were carried out at concentrations where triple ion equilibria predominate and this may account for the discrepancy.

Lithium trifluoroacetate is an electrolyte in trifluoroacetic acid but extrapolation of the results gives a negative intercept. Examination of the association constants in Table 3 with changing alkali metal cation size shows that the association

Can. J. Chem. Downloaded from www.nrcresearchpress.com by 210.87.254.42 on 09/05/12
For personal use only.

Can. J. Chem. Downloaded from www.nrcresearchpress.com by 210.87.254.42 on 09/05/12
For personal use only.

constant for the lithium salt is expected to be very large. The competition between the solvent molecules (solvation) and the anion (ion association) for the cation presumably favors the latter due to low solvation energies. The trifluoroacetate ion concentration coming from the lithium salt appears to be too low to completely repress the equilibria contributing to the initial solvent conductivity and a steep slope, resulting in a negative intercept, arises as discussed above. Triple ions are formed before the solvent self-dissociation is repressed and the Fuoss plots for values of Λ^0, chosen between 50 and 200 ohms^{-1} cm^2 equiv.$^{-1}$, yield smooth curves with no flat portion as for the potassium salt in Fig. 1.

Trifluoroacetic acid is a non-electrolyte in sulfuric acid (21). It is a very weak base and, for this reason, cation solvation is expected to be weak. For solutions of alkali metal halides in solvents where solvation is important, ion association decreases with decreasing cation size since the anion is more readily displaced by solvent molecules (22). It has been argued that the opposite trend is present in solvents such as acetonitrile and nitromethane (24). While the trend is substantiated for quaternary ammonium compounds, Minc and Werblan's work on alkali metal perchlorates in acetonitrile (24, 25) suggests that solvation is important for small cations in this system also. Trifluoroacetic acid is, however, exceptional with a more than 20 fold decrease in K_a from the sodium to cesium trifluoroacetate. However, ammonium trifluoroacetate is less associated than the rubidium salt while, according to its crystal radius, it should lie between potassium and rubidium. There appears, in this case, to be some special stabilization of the ammonium ion in solution, perhaps by hydrogen bonding. The % standard error on Λ^0 for ammonium trifluoroacetate is larger than that for the other salts studied and the conductivity of solutions of this salt was observed to decrease very slowly. We have subsequently shown that bis(trifluoroacetyl)amide may be prepared by refluxing the anhydride with ammonium trifluoroacetate and this reaction occurring at 25 °C will affect the conductivity results for this electrolyte also, although the relative order of Λ^0 and K_a for this base among the others will not be affected.

The limiting equivalent conductivities of the electrolytes studied increase with decreasing cation size with the exception of the ammonium salt, where the ammonium cation in solution is apparently larger than that of rubidium. This suggests a greater degree of solvation as was indicated by the K_a for the ammonium salt. The general trend of change in Λ^0 with changing cation size is different from that generally observed (23, 26, 27). In water, alkali metal cations or any series of alkali metal salts with a common anion exhibit a maximum mobility at rubidium and Λ^0 decreases with decreasing cation radius from rubidium to lithium. The decrease in Λ^0 is attributed to increasing solvation and consequent greater effective size of the diffusing ion. The diffusion of the alkali metal cations in trifluoroacetic acid apparently depends upon ion size and solvation is not of primary importance as was indicated by the variation in K_a discussed above. The large spread of Λ^0 values for the 1:1 trifluoroacetates in the solvent indicates that the cation is making a large contribution to the conductivity and suggests that the anion conducts by diffusion, unlike the corresponding self-dissociation anions in water (20), sulfuric (20), and fluorosulfuric acids (28).

From the individual ionic mobilities listed in ref. 20 and Λ^0 for trifluoroacetic acid in water (14), Λ^0 for the alkali metal trifluoroacetates in water can be calculated. (Λ^0 for potassium trifluoroacetate is 115.5 ohms^{-1} cm^2 equiv.$^{-1}$.) By comparison the values in trifluoroacetic acid are low. These low ionic mobilities in trifluoroacetic acid cannot be accounted for by cation solvation, which appears to be weak in this solvent, and tunnelling of the ions between the much larger solvent molecules and consequent failure of Stoke's Law would lead to higher mobilities. Fuoss has shown that for large ions in some solvents ionic mobility may be retarded by a solvent dipole "relaxation effect" (29). This concept has been given a quantitative basis by Boyd (30) and Zwanzig (31). Application of Zwanzig's expression to the trifluoroacetic acid solvent system gives impossibly small mobilities for the trifluoroacetates. These low mobilities arise from an inordinately large contribution to the ion size from the "relaxation effect" compared to the ionic crystal radius. Moreover, the solvent dipole "relaxation effect" cannot have a predominant influence, since the mobilities are larger for the smaller cation; exactly the opposite trend to that predicted by the theory. Apparently no single concept may be used to account for the mobilities

in trifluoroacetic acid and detailed consideration of these effects at this time would be premature.

Unfortunately a comparison with the mobilities of the alkali metal acetates in acetic acid (32–36) is not possible for several reasons. Hopfgartner (32), Jones and Griswold (33), and Martin (34) worked at temperatures other than 25 °C and, apart from the work reported in refs. 33 and 34 the concentrations studied exceed the limit of simple ion-pair formation in this solvent (0.771×10^{-4} $m\,l^{-1}$). Jones and Griswold subtracted the pure solvent conductivity from their measurements for the acetates studied and evaluated Λ^0 and K_a from a Fuoss extrapolation. This correction for solvent self-dissociation ions is not justified, since the autoprotolysis equilibrium is undoubtedly repressed at the lowest solute concentrations studied and the observed conductivity arises from solute ions alone. Fuoss extrapolation of Jones and Griswold's data with pure solvent conductivity included leads to a negative intercept and the study of the conductivity of $NaOOCCH_3$ and $KOOCCH_3$ at 25 °C would bear further study for this reason.

The authors thank the National Research Council of Canada for generous financial support and M.G.H. thanks the Council for the award of a bursary.

1. R. Hara and F. H. Cady. J. Am. Chem. Soc. **76**, 4285 (1954).
2. H. C. Brown and R. A. Wirkkala. J. Am. Chem. Soc. **88**, 1447, 1453, 1456 (1966).
3. J. E. DeVries, S. Schiff, and E. S. Gantz. Anal. Chem. **27**, 1814 (1955); G. Kresze and V. Schmidt. Chem. Ber. **90**, 1687 (1957).
4. K. Heymann and H. Klaus. *In* Chemie in niederen Fettsauren und ihren Derivaten. Vol. IV of the series Chemie in nichtwässrigen ionisierenden Losungsmitteln. G. Jander, H. Spandau, and C. C. Addison (Editors). Vieweg, New York. 1963.
5. R. M. Fuoss and F. Accascina. Electrolytic conductance. Interscience, New York. 1959. (*a*) p. 250, (*b*) p. 230, (*c*) p. 213, and (*d*) p. 253.
6. J. H. Simons and Keith E. Lorentzen. J. Am. Chem. Soc. **74**, 4746 (1952).
7. W. Dannhauser and R. H. Cole. J. Am. Chem. Soc. **74**, 6105 (1952).
8. J. M. Tedder. J. Chem. Soc. 2646 (1954).
9. F. E. Harris and C. T. O'Konski. J. Am. Chem. Soc. **76**, 4317 (1954).
10. Yu. Ya. Borovikov and Yu. Ya. Fialkov. Soviet Electrochem. **1**(9), 989 (1965).
11. Jacques Bessière. Bull. Soc. Chim. Fr. 3353 (1969).
12. I. M. Kolthoff and S. Bruckenstein. J. Am. Chem. Soc. **78**, 1 (1956).
13. R. J. Gillespie, J. V. Oubridge, and C. Solomons. J. Chem. Soc. 1804 (1957).
14. Technical Information. Perfluorocarboxylic acid. 3M Company, St. Paul, Minnesota.
15. R. M. Fuoss. J. Am. Chem. Soc. **57**, 488 (1935).
16. R. J. Gillespie, E. D. Hughes, and C. K. Ingold. J. Chem. Soc. 2552 (1950).
17. J. E. B. Randles, J. C. Tatlow, and J. M. Tedder. J. Chem. Soc. 436 (1954).
18. T. Shedlovsky. J. Franklin Inst. **225**, 739 (1938).
19. R. M. Fuoss and T. Shedlovsky. J. Am. Chem. Soc. **71**, 1496 (1949).
20. R. A. Robinson and R. H. Stokes. Electrolyte solutions. Butterworths, London. 1965. p. 171.
21. J. Barr, R. J. Gillespie, and E. A. Robinson. Can. J. Chem. **39**, 1266 (1961).
22. Th. L. Fabry and R. M. Fuoss. J. Phys. Chem. **68**, 971, 974 (1964).
23. R. L. Kay. J. Am. Chem. Soc. **82**, 2099 (1960).
24. D. F. Evans, C. Zawoyski, and R. L. Kay. J. Phys. Chem. **69**, 3878 (1965).
25. J. Minc and L. Werblan. Electrochim. Acta, **7**, 256 (1961).
26. C. H. Springer, J. F. Coetzee, and R. L. Kay. J. Phys. Chem. **73**, 471 (1969).
27. T. C. Waddington (Editor). Non-aqueous solvent systems. Academic Press. 1965.
28. J. Barr, R. J. Gillespie, and R. C. Thompson. Inorg. Chem. **3**, 1149 (1964).
29. R. M. Fuoss. Proc. Nat. Acad. Sci. **45**, 807 (1959).
30. R. H. Boyd. J. Chem. Phys. **35**, 1281 (1961).
31. R. Zwanzig. J. Chem. Phys. **38**, 1603 (1963).
32. K. Hopfgartner. Monatsh. **33**, 123 (1912); **34**, 1313 (1913).
33. M. M. Jones and E. Griswold. J. Am. Chem. Soc. **76**, 3247 (1954).
34. R. J. L. Martin. Aust. J. Chem. **15**, 409 (1962).
35. I. M. Kolthoff and A. Willman. J. Am. Chem. Soc. **56**, 1007 (1934).
36. G. Maass and G. Jander. Fortschr. chem. Forsch. **2**, 619 (1953).

Can. J. Chem. Downloaded from www.nrcresearchpress.com by 210.87.254.42 on 09/05/12
For personal use only.

Can. J. Chem. Downloaded from www.nrcresearchpress.com by 210.87.254.42 on 09/05/12
For personal use only.

Sur quelques réactions acide–base dans les solvants fortement basiques anhydres. III. *n*-Butylamine

W. R. HEUMANN ET L. ŠAFAŘÍK[1]

Département de chimie, Université de Montréal, Montréal, Québec

Reçu le 7 decembre 1970

Le césium est le seul métal alcalin à réagir avec la *n*-butylamine, même à chaud. Les *n*-butylamidures de Na et de K ont été préparés par chauffage de l'amine avec les hydrures des deux métaux. Ces amidures forment des poudres cristallines blanches grisâtres, stables sous une atmosphère d'azote pur. La neutralisation par ces amidures, d'une série d'acides monobasiques de différentes forces dans la *n*-butylamine a été étudiée par potentiométrie au moyen d'une électrode indicatrice de platine. Les sauts de potentiel variaient entre 1550 mV pour l'acide chlorhydrique et environ 110 mV pour le diphénylméthane. Ce dernier composé était le moins acide ($pK^{H_2O} = 35$) à réagir avec les bases, tandis que le toluène ($pK^{H_2O} = 37$) ne réagit pas. Le pK^{H_2O} de la *n*-butylamine se situe probablement autour de 37 et 38. Plusieurs acides dibasiques et des mélanges d'acides ont également été neutralisés. Le pouvoir de différenciation du système *n*-butylamine/butylamidure est assez bon, mais la précipitation des sels formés rendait souvent difficiles les mesures potentiométriques. La neutralisation du triphénylméthane donne des solutions fortement colorées en orange rougeâtre. Ceci permettrait d'utiliser ce produit comme indicateur dans des titrages visuels d'acides faibles avec les *n*-butylamidures.

Cesium is the only alkali metal to react with *n*-butylamine, even at higher temperature. The *n*-butylamides of Na and K were prepared by heating the amine with the respective alkali hydrides. The amides were obtained as crystalline greyish white powders, which are stable when kept under pure nitrogen. The neutralization of a series of monobasic acids of various strength in *n*-butylamine by these amides was studied potentiometrically using a platinum indicating electrode. Potential jumps ranging from 1550 mV for hydrochloric acid to about 110 mV for diphenylmethane were obtained. The latter compound was the least acidic ($pK^{H_2O} = 35$) to react with the bases, while toluene ($pK^{H_2O} = 37$) did not react. The pK^{H_2O} value of *n*-butylamine should therefore be about 37 to 38. Several dibasic acids and mixtures of two acids were also neutralized. The power of differentiation of the *n*-butylamine/butylamide system is quite pronounced, but in many cases potentiometric measurements were difficult due to precipitation of the salts formed. The neutralization of triphenylmethane produces an intense reddish orange color, which could be used as an indicator in visual titrations of weak acids with the *n*-butylamides.

Canadian Journal of Chemistry, 49, 1895 (1971)

En 1951, la *n*-butylamine a été introduite dans l'analyse chimique comme solvant fortement basique pour les titrages d'acides très faibles en milieu non-aqueux (1). A en juger par les travaux qui ont été publiés depuis, cette amine semble avoir été acceptée comme une alternative pour l'éthylènediamine dans le domaine des titrages acide–base, bien que les propriétés fondamentales de ce système de solvant soient peu connues. La présente étude a été entreprise dans le but d'étudier quelques aspects fondamentaux du système *n*-butylamine/butylamidure en vue d'une évaluation objective des possibilités d'applications pratiques. Dans ce but, les *n*-butylamidures de sodium C_4H_9NHNa et de potassium ont été préparés. Leurs réactions dans la *n*-butylamine avec une serie d'acides ont été étudiées potentiométriquement, pour établir la gamme des acidités possibles dans ce solvant.

La préparation des n-butylamidures alcalins

Les métaux alcalins

Les alcalins réagissent difficilement avec la *n*-butylamine. Même à la température d'ébullition de l'amine, 78 °C, seul le césium réagit, bien que cette réaction est lente. Il s'est, en effet avéré nécessaire de chauffer ce métal dans l'amine pendant 5 h à ébullition pour qu'un gramme se dissolve dans 100 ml d'amine, en engendrant ainsi une solution d'amidure environ 0.07 *M*. Contrairement à l'ammoniac anhydre liquide, à l'éthylènediamine et à d'autres amines aliphatiques, la réaction du césium avec la *n*-butylamine ne conduit pas à la formation d'une solution bleue foncé d'électrons solvatés, comme stage intermédiaire de la formation de l'amidure. L'alliage

[1]Adresse permanente: Institut d'état pour le contrôle des médicaments, Šrobarová 48, Praha 10, Tchécoslovaquie.

Can. J. Chem. Downloaded from www.nrcresearchpress.com by 210.87.254.42 on 09/05/12
For personal use only.

liquide de 78% de potassium et 22% de sodium, qui, en général, est plus réactif que l'un ou l'autre des deux métaux seul, se montre également indifférent envers la *n*-butylamine.

L'amidure ammoniacal de sodium

$NaNH_2$ ne réagit pas avec la *n*-butylamine à la température ambiante. Des essais visant à aider la réaction par un abaissement de la pression pour enlever l'ammoniac formé par la réaction ont échoué en raison de la trop grande volatilité de la *n*-butylamine. Un procédé breveté pour la préparation de *n*-butylamidure de sodium à partir de l'amidure ammoniacal de sodium est la seule mention faite dans la littérature d'un *n*-butylamidure (2). D'après ce procédé, le butylamidure est obtenu en faisant bouillir pendant 63 h une solution de *n*-butylamine dans du toluène, contenant de l'amidure ammoniacal de sodium. L'amidure formé est recueilli par cristallisation du résidu après distillation de l'excès d'amine. Selon nos expériences, cette réaction est accompagnée de la formation d'un produit orange rougeâtre, soluble avec coloration rouge intense dans le pentane, le toluène ou l'éther. Au contact de l'humidité atmosphérique, ces solutions se décolorent et dégagent un précipité blanc de NaOH. Ces observations semblent indiquer que la coloration est due au benzylsodium $C_6H_5CH_2$-Na, produit de la réaction entre l'amidure ammoniacal et le toluène. Etant donné que dans ce procédé le rôle du toluène se limite apparemment à augmenter la température du mélange au-dessus du point d'ébullition de l'amine pure, 78 °C, il a été essayé de remplacer le toluène par le *n*-octane (p.éb. 114 °C). Cependant, le *n*-butylamidure de sodium n'est pas soluble dans les hydrocarbures aliphatiques et précipite lors de sa formation. De ce fait le produit est contaminé par de l'hydroxyde de sodium qui se forme à partir des traces d'eau toujours présentes et, éventuellement, aussi par de l'amidure ammoniacal n'ayant pas réagi.

Les hydrures alcalins

Les hydrures alcalins sous leurs formes commerciales, c'est-à-dire LiH comme poudre cristalline, NaH et KH comme dispersions à 50% dans de l'huile minérale, ne réagissent pas avec la *n*-butylamine à la température ambiante. Ils réagissent, cependant, à des températures plus élevées pour former leurs *n*-butylamidures. L'hydrure de lithium réagit le moins facilement. Une quantité de l'hydrure, suffisante pour former une solution 1.2 *M* de C_4H_9NHLi dans la *n*-butylamine, avait réagi si peu après 8 h d'ébullition de l'amine sous reflux (environ 78 °C), que la concentration de la solution d'amidure formée n'était que de 0.04 *M*. Par ailleurs, dans les mêmes conditions, la réaction de l'hydrure de sodium est considérablement plus vive; elle atteint son maximum de vitesse, qui se manifeste par un dégagement d'hydrogène, sitôt que le milieu atteint la température de l'ébullition et la réaction est complète après 4 h. L'amidure formé reste en solution. L'hydrure de potassium réagit encore plus facilement; sa réaction commence dès que la température dépasse 30 °C et elle est complète en moins de 2 h. C'est à partir des hydrures que les *n*-butylamidures de sodium et de potassium ont été préparés et isolés.

Partie expérimentale

Azote

L'azote pur, utilisé pour purger les récipients les appareils et la boîte à gants, passe par des colonnes contenant des tamis moléculaires "Linde Molecular Sieves 4A" ou "5A" pour éliminer l'eau et le CO_2, ainsi que par un tube de verre "Vycor" contenant du cuivre maintenu à 600 ± 20 °C pour éliminer les traces d'oxygène.

n-Butylamine anhydre

Le produit commercial contenant moins de 2% d'eau est d'abord traité avec de l'oxyde de barium poreux (Barium & Chemicals Inc., Willoughby, Ohio) à raison d'environ 200 g de BaO par litre d'amine. Le mélange est remué de temps à autre pendant 5 à 6 jours ou secoué continuellement durant 25 à 30 h, ce qui réduit la teneur en eau à moins de 500 p.p.m. Le liquide est transféré par décantation moyennant une pression d'azote en système clos dans un appareil à distillation. Celui-ci est muni d'un réfrigérant de reflux et d'un réfrigérant de distillation. Le récipient du distillat a deux tubulures, dont l'une est connectée au réfrigérant et l'autre à un petit barboteur contenant soit une huile de silicone pas trop visqueuse soit un hydrocarbure peu volatil tel que le *n*-dodécane. Cette barrière contre les contaminants atmosphériques est suivie d'un tube d'absorption contenant des "Linde Molecular Sieves 5A". Les deux connections du récipient comprennent des robinets, pour qu'il puisse être déconnecté sans danger de contamination. On ajoute à la *n*-butylamine de l'hydrure de sodium sous forme d'émulsion dans de l'huile à 50% à raison d'environ 1 g de NaH par litre. Le mélange est chauffé à l'ébullition (environ 78 °C) sous reflux pendant 1 à 2 h, avant de distiller sous pression ambiante. Si du *n*-butylamidure de sodium est disponible, 40 à 50 milli-équivalents (4 à 5 g), sous forme d'une solution dans la *n*-butylamine, peuvent être ajoutés par litre d'amine au lieu de NaH. Dans ce cas, le réfrigérant de reflux n'est pas nécessaire et la distillation peut être effectuée tout de suite. La *n*-butylamine préparée

Can. J. Chem. Downloaded from www.nrcresearchpress.com by 210.87.254.42 on 09/05/12
For personal use only.

ainsi ne contient pas plus que 10 p.p.m. d'eau, qui peut être titrée avec une solution étalonnée de *n*-butylamidure de sodium dans la *n*-butylamine suivant la technique décrite plus loin.

n-Butylamidures de sodium et de potassium

Un ballon à 3 tubulures est utilisé. Une tubulure est munie d'un robinet pour l'entrée de l'azote; une autre porte un tube, muni d'un robinet, qui descend jusqu'au fond du ballon, où il se termine par un petit filtre de verre fritté de porosité moyenne ou grossière. La troisième tubulure est surmontée d'un réfrigérant de reflux, dont la sortie est connectée avec un petit barboteur contenant du dodécane ou de l'huile de silicone. Le barboteur communique avec l'extérieur par un tube d'absorption chargé de "Linde Molecular Sieves 5A". Après avoir purgé l'appareil avec de l'azote pur, on charge le ballon à environ deux tiers de *n*-butylamine, qui a été séchée préalablement avec de l'oxyde de Ba et qui contient moins qu'environ 500 p.p.m. d'eau. La quantité voulue de dispersion huileuse de NaH à 50% est ajoutée, en tenant compte de la quantité nécessaire pour réagir avec l'eau. Des solutions allant jusqu'à 2 *M* peuvent être préparées ainsi. On chauffe le mélange à l'ébullition (environ 78 °C) en agitant avec une barre magnétique enrobée de polyéthylène ou de verre. La réaction, qui si manifeste par un courant d'hydrogène dans le barboteur, cesse après environ 4 h. On laisse alors refroidir, en faisant passer en même temps un courant d'azote.

Si la solution de l'amidure est utilisée comme telle, le ballon est transféré dans la boîte à gants et laissé au repos pendant la nuit. La solution est ensuite transférée à l'aide de pression d'azote par le tube muni du filtre de verre poreux, dans une bouteille ou, encore, dans le réservoir d'une burette automatique. Ces solutions peuvent être étalonnées potentiométriquement par le *p*-méthoxyphénol suivant la technique décrite par la suite.

Si la solution est destinée à la préparation de l'amidure solide, elle est transvasée, moyennant une pression d'azote en système clos, par le tube muni du filtre de verre dans un appareil de distillation sous vide. Le ballon de cet appareil, qui a été purgé préalablement avec de l'azote, a deux tubulures, dont une comporte un robinet pour l'entrée de la solution. L'autre tubulure doit être aussi large que possible pour faciliter le transfert sur le filtre de l'amidure solide qui cristallise après l'évaporation du solvant. Elle est connectée au réfrigérant par l'intermédiaire d'un robinet à grand diamètre intérieur. Le récipient du distillat est refroidi avec de la glace ou de la neige carbonique. On applique graduellement le vide, sans chauffage, en agitant avec une barre magnétique. On distille jusqu'à ce que le vide ait baissé à environ 20 mm et la cristallisation ait commencé. Le ballon est ensuite déconnecté et transféré dans la boîte à gants. Le lendemain le contenu est filtré par aspiration sur un filtre de verre de porosité moyenne. Le résidu est lavé avec de l'octane et séché dans un courant d'azote. Une poudre cristalline blanche grisâtre, devant être gardée sous azote pur, est ainsi recueillie.

Le *n-butylamidure de potassium* et ses solutions sont préparés de la même façon, mais la réaction avec l'hydrure de potassium est déjà terminée après 1½ à 2 h.

Les *solubilités des butylamidures* dans la *n*-butylamine furent déterminées comme suit: Le mélange de 5 ml d'amine et d'un excès d'amidure solide fut agité dans un pèse-tare fermé, pendant 5 à 6 h, puis laissé au repos jusqu'au lendemain. Un ml de la solution claire fut dilué à 30 ml avec de la *n*-butylamine et titré potentiométriquement avec une solution étalon 0.3 à 0.4 *M* de *p*-méthoxyphénol.

Acides

La préparation de la plupart des acides purs utilisés dans le présent travail a été décrite dans deux études antérieures (3, 4). L'acide chlorhydrique fut utilisé sous forme du chlorhydrate de *n*-butylammonium; le produit commercial fut purifié par précipitation à partir d'une solution alcoolique, par addition d'éther (5). L'acide carbonique a été utilisé sous forme de carbonate de *n*-butylammonium, obtenu par évaporation spontanée de l'amine pure dans une atmosphère enrichie de CO_2. De la masse cristalline qui en est résultée, les cristaux blancs du carbonate furent isolés par filtration avec aspiration, puis séchés dans une atmosphère d'azote. Ce produit se décompose et se volatilise assez facilement tant par l'action de la chaleur que par l'effet d'une réduction de pression.

Appareillage

L'appareil utilisé pour effectuer et suivre potentiométriquement les réactions de neutralisation, était le *titreur clos* aux électrodes de platine décrit dans un autre mémoire (6). Ce dernier donne aussi la description de la *boîte à gants*, dans laquelle le titreur était placé, et où toutes les autres opérations ont été effectuées à l'exception de celles qui nécessitaient l'application de chaleur. Le contrôle analytique de l'atmosphère de la boîte fut décrit dans le mémoire précédent (4).

Tous les joints rodés étaient secs et garnis de manchons de Teflon. Tous le robinets étaient également en Teflon. Puisque ni les manchons ni les robinets en Teflon sont parfaitement étanches, ils étaient scellés de l'extérieur par de la graisse "Silicone". Les butylamidures attaquent légèrement le Teflon. Dès lors, les robinets qui étaient en contact fréquent, voire même continu avec les solutions des amidures, devaient être remplacés de temps en temps.

Mode opératoire

De même que lors des deux études antérieures sur le système éthylènediamine/amino-2 éthylamidure (3, 4), le comportement des différents acides a été étudié en neutralisant toujours 25 ou 30 ml de solution d'acide 0.065 à 0.066 *N* par une solution étalonnée 0.195 à 0.200 *N* de l'amidure, de sorte qu'aux points d'équivalence les solutions étaient toujours 0.05 *N*.

Résultats et discussion

Les n-butylamidures

Les *n*-butylamidures de sodium et de potassium ont été obtenus sous forme de poudres cristallines blanches grisâtres, stables dans une atmosphère inerte, qui réagissent violemment avec l'eau. Ils ont été identifiés par la détermination de leurs poids moléculaires en titrant conductimétriquement par l'acide chlorhydrique des solutions aqueuses obtenues par décomposition des ami-

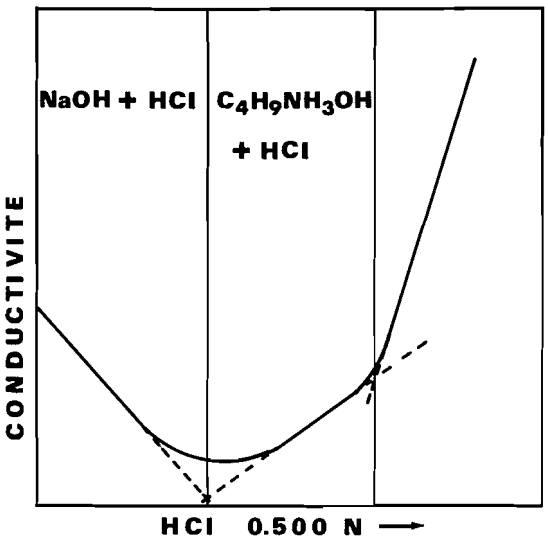

FIG. 1. Titrage conductimétrique du *n*-butylamidure de sodium. Environ 190 mg (2 méquiv) d'amidure dans 100 ml d'eau.

dures avec de l'eau. Une courbe de titrage obtenue à partir de l'amidure de sodium est reproduite dans la Fig. 1. Elle permet la distinction nette entre les hydroxydes de sodium et de *n*-butylammonium. Le poids moléculaire trouvé ainsi dans deux titrages fut 97 au lieu de 95.1. Dans le cas de l'amidure de potassium, la valeur trouvée fut 112 au lieu de 111.2. Comme les poids moléculaires des hydrures NaH et KH, respectivement 24.0 et 40.1, sont beaucoup plus petits que ceux des butylamidures correspondants, la présence, dans ces produits, d'hydrures qui n'auraient pas réagi lors de la préparation des amidures, pouvait être exclue avec certitude.

Les *solutions* de ces deux amidures *dans la n-butylamine* ont une coloration jaune pâle à faible concentration, tandis que les solutions concentrées sont colorées en brun foncé. Contrairement aux amino-2 éthylamidures (4) ni les *n*-butylamidures solides, ni leurs solutions, sont affectées de façon perceptible par des traces d'oxygène moléculaire; ils ne changent pas de couleur; la formation de produits de polymérisation foncés, goudronneux, même après des semaines, n'a pas été observée.

Les *solubilités* des deux *n*-butylamidures *dans la n-butylamine* sont de 4.5 à 5 mol/l de solution pour l'amidure de sodium et 1.5 à 1.6 mol/l pour celui de potassium. La solution saturée de l'amidure de sodium étant assez visqueuse, son analyse exacte est assez difficile.

Réactions acide–base

La Fig. 2 représente les courbes potentiométriques de la neutralisation de plusieurs acides monobasiques par le *n*-butylamidure de sodium. Ces courbes représentent les moyennes de 2 ou 3 expériences. Cependant, la reproductibilité des mesures, ainsi que la régularité des changements des f.e.m. laissaient parfois à désirer, surtout dans la partie des courbes comprise entre le début et l'inflexion autour du point d'équivalence. La raison principale, sinon la seule, était sans doute que, dans la plupart des cas, le sel de sodium formé précipitait de la solution. Avec l'acide chlorhydrique et avec l'eau, les précipités se formaient dès le début de la réaction. Dans le cas de l'eau, ceci s'avérait particulièrement gênant, en raison de la formation d'agglomérations gélatineuses, qui tendaient à boucher la pointe de la burette. La courbe de l'acide benzoïque n'a

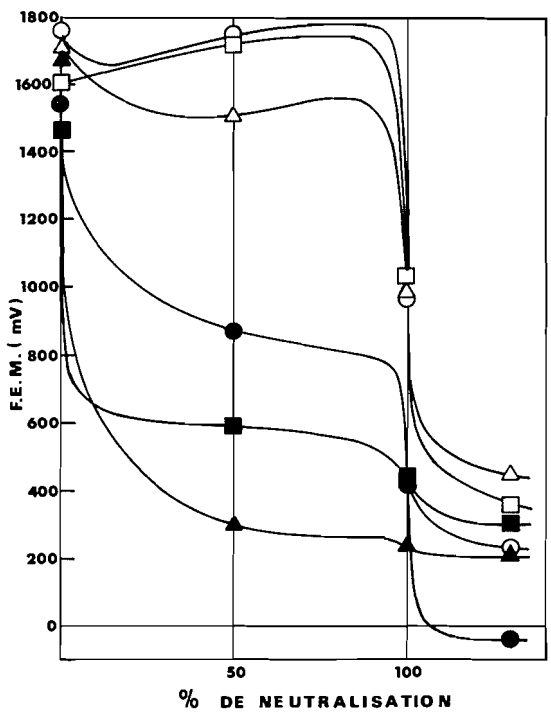

FIG. 2. Courbes potentiométriques de neutralisation d'acides monobasiques par le *n*-butylamidure de sodium. ○, acide chlorhydrique; □, *p*-méthoxyphénol; △, eau; ●, aminoéthanol; ■, triphénylméthane; ▲, diphénylméthane.

Can. J. Chem. Downloaded from www.nrcresearchpress.com by 210.87.254.42 on 09/05/12
For personal use only.

Can. J. Chem. Downloaded from www.nrcresearchpress.com by 210.87.254.42 on 09/05/12
For personal use only.

pas pu être établie, parce que le précipité volumineux rendait les mesures des f.e.m. trop irrégulières et instables. Le *p*-méthoxyphénol, le triphénylméthane et le diphénylméthane ne formaient pas de précipité. Ces deux hydrocarbures donnent des solutions fortement colorées, ce qui est vraisemblablement dû à la liaison carbone–sodium. La coloration des solutions de triphénylméthane sodique change avec la concentration croissante de jaune–orange jusqu'au rouge foncé brunâtre. Les solutions du diphénylméthane sodique sont colorées en orange foncé. Le diphénylméthane, dont le $pK_a^{H_2O}$ est d'environ 35 (7), était l'acide le plus faible de ceux qui ont réagi avec l'amidure. Le toluène ($pK^{H_2O} = 37$) ne réagit pas, ses solutions dans la *n*-butylamine se comportant comme le solvant seul. Par un raisonnement analogue à celui exposé au sujet de l'acidité de l'éthylènediamine (3), il semble raisonnable de conclure que la valeur du $pK_a^{H_2O}$ de la *n*-butylamine se situe vers 37–38.

La neutralisation de quelques *acides dibasiques* et de *mélanges de deux acides* a également été étudiée. Les trois acides hydroxybenzoïques se comportent comme des acides monobasiques, ils donnent, en effet, une seule inflexion potentiométrique, qui correspond à la somme des deux fonctions acides. Les courbes ressemblent à celles obtenues avec des phénols. Même les deux fonctions de l'acide *o*-hydroxybenzoïque (salicylique) ne se différencient pas malgré la différence numérique considérable entre les deux constantes d'acidité ($pK_2 - pK_1 = 13.4 - 3.0 = 10.4$). Il est à noter, que la même observation a été faite pour les solutions de ces mêmes acides dans l'éthylènediamine (3). D'un autre côté, l'acide carbonique, malgré la différence assez petite entre les deux acidités ($pK_2 - pK_1 = 3.9$) et nonobstant la formation d'un léger précipité pendant la réaction, donne une courbe nette avec deux inflexions, qui est présentée dans la Fig. 3. Quant aux mélanges d'acides, les acides suivants se différencient facilement dans leurs mélanges respectifs avec l'eau : acide chlorhydrique (malgré la formation de précipités), *p*-méthoxyphénol, aminoéthanol, triphénylméthane. Les mélanges de l'eau avec le phénol et l'acide carbonique ne permettent pas d'obtenir des courbes suffisamment nettes à cause de la formation de précipités. Le mélange eau–éthanol ne se différencie pas, d'une part probablement à cause de la petite différence entre leurs forces acides respectives et, d'autre part, parce que ces deux composés polaires peuvent facilement subir une interaction dans un milieu si peu polaire que la *n*-butylamine. Plusieurs exemples de différenciation sont illustrés dans la Fig. 3.

Les neutralisations avec le *n*-butylamidure de potassium donnent des courbes semblables à celles obtenues avec l'amidure sodique. Les forces électromotrices mesurées aux points de demi-neutralisation, ainsi que les sauts de potentiel autour des points d'équivalence, sont à peu près les mêmes avec les deux amidures. Les petites différences ne sont pas assez régulières ou significatives pour permettre une conclusion quant à une différence entre les forces basiques des deux amidures.

La différenciation entre le triphénylméthane et des acides plus forts tels que l'eau ou le *p*-méthoxyphénol, ainsi que l'apparition de la coloration jaune–orange foncé du triphénylméthane sodique, sont très nettes. Ceci devrait permettre l'utilisation du triphénylméthane comme indicateur dans des titrages visuels avec

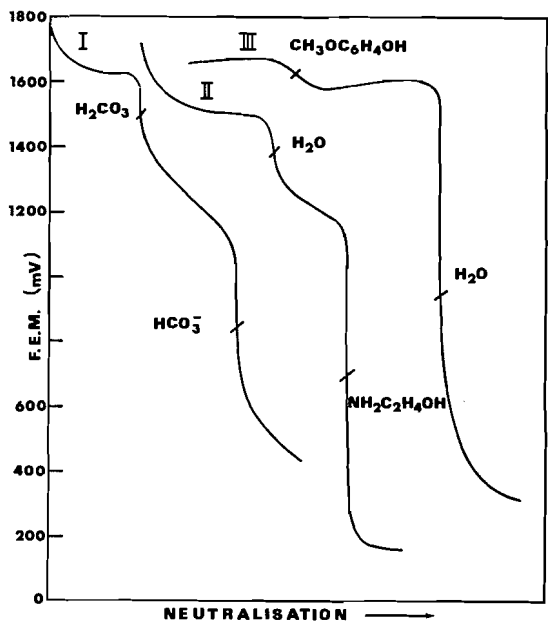

FIG. 3. Courbes de neutralisation de solutions à deux fonctions acides. Courbe *I*, acide carbonique; *II*, mélange d'eau et d'aminoéthanol; *III*, mélange de *p*-méthoxyphénol et d'eau. Les courbes *II* et *III* sont déplacées horizontalement afin de mieux les observer.

les *n*-butylamidures. En effet, des solutions d'eau dans la *n*-butylamine ont été titrées et par la méthode potentiométrique dans le titreur clos et visuellement avec cet indicateur de la manière conventionnelle dans une fiole conique ouverte, sans différence significative entre les résultats.

Dans une étude ultérieure, les résultats du présent mémoire seront comparés avec ceux obtenus avec d'autres systèmes de solvants fortement basiques.

Nous remercions sincèrement le Conseil National de Recherches du Canada de l'aide financière sous forme d'octrois de recherches (W.R.H.), qui a rendu possible ce travail.

1. J. S. FRITZ et N. M. LISICKI. Anal. Chem. **23**, 589 (1951).
2. D. D. HUMPHREYS. Sharples Chemicals Inc. U.S. 2 685 604, August 3, 1954; Chem. Abstr. 49, 10358c (1955).
3. W. R. HEUMANN, A. BOUCHARD, et G. TREMBLAY. Can. J. Chem. **45**, 3129 (1967).
4. W. R. HEUMANN, A. BOUCHARD et L. ŠAFAŘÍK. Can. J. Chem. **47**, 3509 (1969).
5. J. F. BUNNETT et G. T. DAVIS. J. Am. Chem. Soc. **82**, 665 (1960).
6. W. R. HEUMANN, A. BOUCHARD et F. D. ROCHON. Anal. Chem. **40**, 1529 (1968).
7. W. K. MCEWEN. J. Am. Chem. Soc. **58**, 1124 (1936).

Can. J. Chem. Downloaded from www.nrcresearchpress.com by 210.87.254.42 on 09/05/12
For personal use only.

Can. J. Chem. Downloaded from www.nrcresearchpress.com by 210.87.254.42 on 09/05/12
For personal use only.

The Crystal Structure of $[Rh(f_6fos)_2]^+[cis\text{-}(CO)_2RhCl_2]^-$

F. W. B. Einstein and C. R. S. M. Hampton
Department of Chemistry, Simon Fraser University, Burnaby 413, British Columbia

Received October 19, 1970

The crystal structure of di(1,2-bis(diphenylphosphino)hexafluorocyclopentene) rhodium(I) *cis*-dicarbonyldichlororhodate(I), $[Rh(f_6fos)_2][cis\text{-}Rh(CO)_2Cl_2]$ has been determined from three-dimensional X-ray scintillation counter data. The structure has been refined by full-matrix least-squares techniques to a conventional R factor of 8.8%. The salt crystallizes in the tetragonal space group $I4_1/a$ with eight formula units in a cell of dimensions $a = 17.722(1)$ Å and $c = 36.773(4)$ Å. Each ion is nearly square planar and has a crystallographic two-fold axis passing through the rhodium atom. The two independent Rh—P distances are 2.282(6) and 2.300(6) Å, and the bite of the chelating ditertiary phosphine, f_6fos, is 3.111(8) Å as measured by the intra-ligand P—P distance.

On a déterminé la structure cristalline du di(1,2-bis(diphenylphosphino)hexafluorocyclopentène) rhodium(I) *cis*-dicarbonyldichlororhodate(I), $[Rh(f_6fos)_2][cis\text{-}Rh(CO)_2Cl_2]$, à partir des données tridimensionelles de diffraction des rayons-X, mesurées par un compteur de scintillation. La structure a été affinée par moindrescarrés (matrice complète) jusqu'à un facteur d'accord $R = 8.8\%$. Ce sel cristallise dans le groupe d'espace $I4_1/a$ avec 8 unités dans la maille de dimensions $a = 17.722(1)$ et $c = 36.773(4)$ Å. Chaque ion est presque plan et l'atome de rhodium se trouve sur un axe cristallographique d'ordre 2. Les deux distances indépendantes Rh—P mesurent 2.282(6) et 2.300(6) Å tandis que la distance entre phosphores des ligands f_6fos est de 3.111(8) Å.

Canadian Journal of Chemistry, 49, 1901 (1971)

Introduction

As a part of a program to investigate the reactions of fluorocarbon-bridged tertiary diphosphines and diarsines with transition metals (1–9), the reactions between these ligands and chlorodicarbonyl rhodium dimer were studied. The intention was to prepare simple monocarbonyl complexes of the type LRh(CO)Cl (L is a chelating ditertiary diphosphine), and to study the ability of the ligands to stabilize these complexes with respect to oxidative addition (1). However, instead of simple monocarbonyl complexes, the type of product obtained from reacting 1,2-bis(diphenylphosphino) ethane with $[Rh(CO)_2Cl]_2$, Cullen *et al.* obtained salts containing cations of the type $[RhL_2]^+$ by reacting *cis*-1,2-bis(diphenylphosphino) ethylene with $[Rh(CO)_2Cl]_2$. We describe the crystal structure of one of these salts.

Experimental

Crystals were kindly provided by Dr. W. R. Cullen and their preparation is described elsewhere (1). The sample received was a mixture of crystals which had two different morphologies. The majority were small needles (of the order of 0.1 mm long) and much smaller fraction were approximately octahedral in shape. A crystal of the second type was used for the crystal structure determination. (The two types gave identical X-ray powder patterns.)

Crystal Data

$[Rh(f_6fos)_2][cis\text{-}Rh(CO)_2Cl_2]$ f.w. = 1421

Tetragonal, space group $I4_1/a$ (identified unambiguously from Laue group $4/m$ and systematic absences). $a = b = 17.722(1)$ Å, $c = 36.773(4)$ Å, $V = 11\,815$ Å^3, $1.60 < D_m < 1.63$ g/cc, $F_{(000)} = 5664$ and μ (Mo-Kα) = 8.2 cm^{-1}.

X-Ray Data Collection

Weissenberg photographs of the layers $h0l$–$h4l$ inclusive using Cr-Kα radiation, together with precession photographs of the zones $hk0$ and $h0l$ using Mo-Kα radiation, showed absences for hkl with $h + k + l$ = odd, for 001 with $l = 4n + 2$ and for $hk0$ with h = odd.

All counter data were collected using a crystal mounted with the "b" axis parallel to Φ. The crystal had the shape of a slightly tetragonally distorted octahedron. Distension was in the c direction of the crystal. In the apical directions a, b, and c the dimensions of the crystal were $0.36 \times 0.36 \times 0.28$ mm. However, one c apex was chipped off, and had that apex been complete it is estimated that the dimension in the c direction would have been 0.42 mm. Cell dimensions were determined by least-squares refinement of 13 accurately measured high-angle reflections at 19 °C ($\lambda K\alpha_1 = 0.70926$ Å). The standard errors were estimated from the internal consistency obtained by the least-squares procedure.

Reflection intensities for the unique set of data were measured using a Picker four-circle diffractometer equipped with our own semi-automation. Zirconium filtered Mo-Kα radiation was used in conjunction with a scintillation detector and pulse height analysis. The take-off angle was 1.3° and a symmetrical θ–2θ scan of 1.6° width was used. Background was measured by stationary counts lasting 12 s on either side of the 1.6°

Can. J. Chem. Downloaded from www.nrcresearchpress.com by 210.87.254.42 on 09/05/12
For personal use only.

scans. Any net intensity which was less than two standard deviations (*i.e.*, 2σ where $\sigma = \sqrt{N}$, and N is the sum of counts obtained for the scan plus both background counts) was treated as unobserved, and denoted as $-F_{obs}$ in Table 1. Of the 2934 intensities recorded in the range $0° < 2\theta < 40°$, 1628 were observed. Three measurements for each of two standard reflections were taken at intervals ranging from 1½ to 5 h, and the scale determined from them ranged over ±5% during the data collection. Because of the large size of the unit cell care had to be exercised in order to recognize cases of scans overlapping more than one reflection.

Lorentz and polarization factors were applied and the structure factors calculated in the usual way. No correction for absorption was made since the small size, regular shape, and low absorption coefficient suggested this would be negligible and nearly isotropic.

Structure Solution

From the unsharpened Patterson function (13)[1] it was possible to assign approximate positions on the two-fold axis to two crystallographically distinct rhodium atoms, and also to one other atom which was assumed to be a chlorine atom. One cycle of least-squares (12)[2] refinement varying the scale, together with coordinates and isotropic thermal parameters for four atoms yielded a conventional R factor of 46.2% (a misplaced chlorine atom was incorrectly included). The remainder of the structure was filled in as prominent features of successive difference maps and good chemical sense dictated.

With all non-hydrogen atoms allowed appropriate coordinates and isotropic thermal parameters, the structure was refined to a conventional R value of 11.5%. It was inferred from prominent features of a difference map at this point that the six fluorine atoms were all vibrating anisotropically, and after two further cycles of least-squares, varying anisotropic parameters for these atoms, the R factor dropped to 9.8% (weighted R, 10.1%). A difference map indicated the possibility that the anion was also vibrating anisotropically. After two cycles of least-squares varying the required anisotropic parameters, the R had dropped to 9.4% (weighted R, 9.7%).

Up to this point all reflections had received unit weights. Unobserved reflections were not included in the least-squares refinement at any stage. After introduction of the weighting scheme described below, and further refinement, the R factor dropped to 9.2% (weighted R, 11.1%). The weighting scheme was set up to approximate the condition $w = 1/\sigma_F^2$ where σ_F is the standard deviation of F_{obs}. The weighting function

$$w = \frac{1}{378 - 3.49|F_o| + 0.011|F_o|^2}$$

was chosen to make $w\Delta^2$ constant as a function of $|F_o|$; $\sin\theta/\lambda$, and the Miller indices (11) ($\Delta = |F_o| - |F_c|$). The standard deviation for an observation of unit weight, at the stage where the conventional R was 9.2% was 0.97.

The R factor dropped to its final value of 8.8% (weighted R, 10.5%) after three changes had been made: (*i*) anomalous dispersion corrections (10)[3] were applied to the rhodium scattering factor curve; (*ii*) the cationic rhodium atom and the carbon (C(6)) at the extreme end of the fluorocarbon moiety of the $f_6$fos ligand were allowed anisotropic thermal parameters; (*iii*) the phosphorus scattering factor curve was employed, in the calculations, for phosphorus atoms which had been mistakenly given chlorine scattering power.

In the last cycle of least squares refinement all elements of the full-matrix were varied except for the parameters of atoms (C(16)–C(21)). These parameters were varied in the previous cycle. Final positional and thermal parameters are listed in Table 2.

A final difference Fourier contained no peaks larger than 0.86 e/Å^3, which corresponds to about 29% of the height of the broad peak that was found for the carbonyl group. There was also a peak of 0.75 e/Å^3 remaining 1.49 Å from the cationic carbon atom. This corresponds to the position a fluorine atom would be expected to take for the alternative conformation of the fluorocyclopentenyl ring. This together with the extreme anisotropic motion of the fluorine atoms led us to consider the possibility of disorder involving another conformation for the fluorocyclopentenyl ring. Such a conformation, if it exists, must occur much less frequently in the crystal structure than the one which was selected. No refinement involving two conformations of

[1]This program was originally written by A. Zalkin, University of California.

[2]This program is based on versions of UCILS (Northwestern University and University of California, Irvine, but with additional features, notably as regarding weighting schemes and optional printed summaries.

[3]Both real ($\Delta F'$) and imaginary ($\Delta F''$) corrections were applied.

Can. J. Chem. Downloaded from www.nrcresearchpress.com by 210.87.254.42 on 09/05/12
For personal use only.

TABLE 2. Final positional and thermal parameters with standard deviations*

Atom	x	y	z†	B (in Å^2)
	Atoms with isotropic thermal parameters			
P(3)	0.0865(3)	0.8454(3)	0.1410(2)	3.2(1)
P(4)	0.1025(3)	0.6707(3)	0.1440(2)	3.5(1)
C(9)	0.252(1)	0.840(1)	0.1316(7)	4.8(5)
C(13)	0.268(2)	0.706(2)	0.1339(7)	5.3(6)
C(14)	0.186(1)	0.729(1)	0.1370(5)	2.8(4)
C(15)	0.180(1)	0.803(1)	0.1362(5)	3.1(5)
C(16)	0.096(1)	0.894(1)	0.1842(6)	4.4(5)
C(17)	0.062(1)	0.963(2)	0.1886(7)	5.5(6)
C(18)	0.065(2)	0.997(2)	0.2246(9)	8.0(8)
C(19)	0.099(2)	0.958(2)	0.2528(9)	7.5(7)
C(20)	0.130(2)	0.891(2)	0.2473(8)	6.7(7)
C(21)	0.132(1)	0.856(1)	0.2119(8)	5.3(6)
C(22)	0.085(1)	0.914(1)	0.1047(6)	3.8(4)
C(23)	0.054(1)	0.890(1)	0.0733(7)	5.0(6)
C(24)	0.055(2)	0.938(2)	0.0414(8)	7.0(7)
C(25)	0.086(2)	1.008(2)	0.0454(7)	6.1(6)
C(26)	0.116(1)	1.033(1)	0.0768(8)	6.1(6)
C(27)	0.118(1)	0.984(1)	0.1082(6)	4.2(5)
C(28)	0.119(1)	0.630(1)	0.1878(5)	3.3(4)
C(29)	0.078(1)	0.659(1)	0.2155(6)	4.2(5)
C(30)	0.090(2)	0.633(2)	0.2529(8)	6.4(7)
C(31)	0.147(1)	0.580(1)	0.2592(7)	5.6(6)
C(32)	0.183(2)	0.548(2)	0.2305(7)	6.0(7)
C(33)	0.174(1)	0.574(1)	0.1951(6)	4.2(5)
C(34)	0.116(1)	0.595(1)	0.1114(6)	3.5(5)
C(35)	0.099(1)	0.521(1)	0.1184(7)	4.6(5)
C(36)	0.110(2)	0.462(2)	0.0920(8)	6.3(7)
C(37)	0.132(2)	0.483(2)	0.0585(9)	7.6(8)
C(38)	0.144(2)	0.558(2)	0.0499(8)	7.1(7)
C(39)	0.138(1)	0.615(1)	0.0767(7)	5.7(6)
	Atoms with anisotropic thermal parameters			
Rh(1)	0.0	0.75	0.1410(1)	
Rh(2)	0.0	0.25	0.0389(1)	
C(6)	0.309(2)	0.778(2)	0.1330(9)	
F(5)	0.329(1)	0.780(1)	0.1716(9)	
F(7)	0.376(1)	0.786(1)	0.1225(7)	
F(8)	0.2668(8)	0.8977(9)	0.1546(5)	
F(10)	0.2598(8)	0.871(1)	0.0981(4)	
F(11)	0.291(1)	0.658(1)	0.154(1)	
F(12)	0.285(1)	0.687(2)	0.0986(8)	
Cl(40)	0.0888(7)	0.228(1)	−0.0059(4)	
C(41)	0.075(2)	0.242(2)	0.076(1)	
O(42)	0.112(2)	0.241(2)	0.0932(9)	

*Standard deviations in parentheses.
†The positional coordinates x, y, and z are fractions of the unit cell edges a, b, and c, respectively.

Atom	U_{11}*	U_{22}	U_{33}	U_{12}	U_{13}	U_{23}
Rh(1)	0.035(2)	0.038(2)	0.043(1)	−0.001(1)	0.0	0.0
Rh(2)	0.085(3)	0.088(3)	0.093(3)	−0.005(2)	0.0	0.0
C(6)	0.05(2)	0.09(2)	0.13(3)	−0.01(2)	−0.02(2)	0.02(2)
F(5)	0.16(2)	0.17(2)	0.25(3)	0.07(2)	−0.11(2)	−0.05(2)
F(7)	0.06(1)	0.09(1)	0.29(3)	0.002(9)	0.07(2)	0.03(2)
F(8)	0.05(1)	0.10(1)	0.13(2)	−0.028(9)	0.019(9)	−0.03(1)
F(10)	0.047(9)	0.14(2)	0.10(1)	−0.029(9)	0.016(9)	0.05(1)
F(11)	0.05(1)	0.14(2)	0.41(4)	0.01(1)	−0.02(2)	0.16(2)
F(12)	0.05(1)	0.34(4)	0.26(3)	0.03(2)	0.00(2)	−0.20(3)
Cl(40)	0.136(9)	0.30(2)	0.17(1)	−0.07(1)	0.023(9)	−0.09(1)
C(41)	0.09(3)	0.09(2)	0.08(3)	−0.03(2)	0.00(2)	0.00(2)
O(42)	0.08(2)	0.12(2)	0.16(3)	0.00(2)	−0.02(2)	−0.02(2)

*U's are in Å^2 and are obtained from the expression $\exp[-2\pi^2(a^{*2}h^2U_{11} + 2a^*b^*hkU_{12} + \cdots)]$.

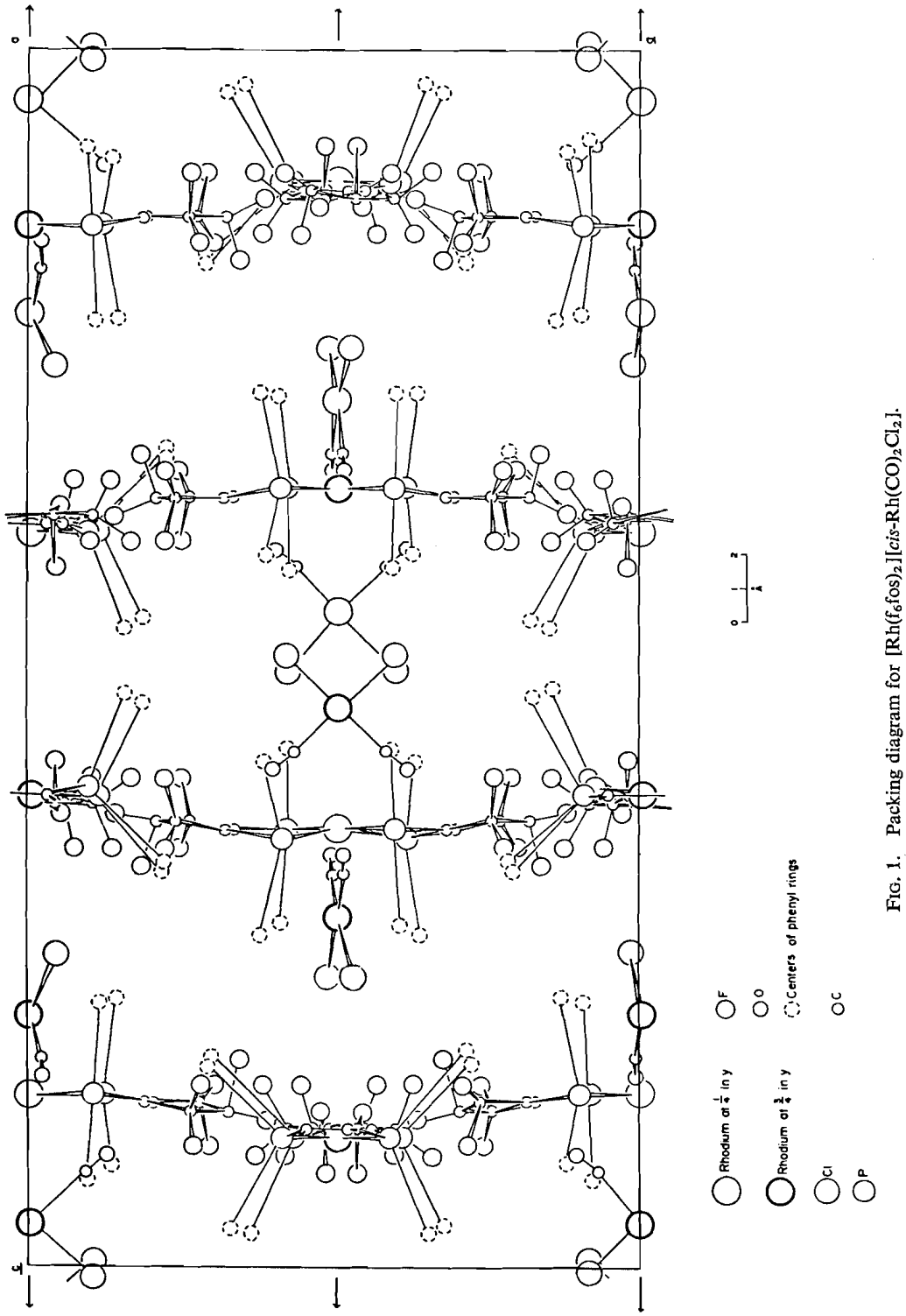

FIG. 1. Packing diagram for $[Rh(f_6fos)_2][cis\text{-}Rh(CO)_2Cl_2]$.

Can. J. Chem. Downloaded from www.nrcresearchpress.com by 210.87.254.42 on 09/05/12
For personal use only.

Can. J. Chem. Downloaded from www.nrcresearchpress.com by 210.87.254.42 on 09/05/12
For personal use only.

the ring was carried out since one conformation was predominant. Numerous smaller peaks appeared, many of them in likely hydrogen atom positions.

The function minimized was $\sum w(|F_o| - |F_c|)^2$ and the discrepancy factor R was $\sum(||F_o| - |F_c||)/\sum|F_o|$. The weighted R was $[\sum w(|F_o| - |F_c|)^2/\sum wF_o^2]^{1/2}$.

Scattering factors used for the rhodium atoms were those calculated on the basis of the TFD statistical model; for the other atoms, scattering factors were obtained from self-consistent or variational wave functions (14). Structure factors listed in Table 1 have the modulus of the structure amplitude with the sign of the real component.[4] All calculations are based on a cell with an origin at the center of symmetry. Interatomic distances and bond angles with standard deviations are given in Table 4.

Description and Discussion of the Crystal Structure

The crystal structure of $[Rh(f_6fos)_2][cis\text{-}Rh(CO)_2Cl_2]$ contains $[Rh(f_6fos)_2]^+$ ions and $[cis\text{-}Rh(CO)_2Cl_2]^-$ ions packed together in a body-centered tetragonal lattice (see Fig. 1). Interatomic distances and angles are listed in Table 4.

The asymmetric unit contains half a cation and half an anion. All rhodium atoms are on two-fold special positions so that both cation and anion possess crystallographic two-fold symmetry. The disposition of coordinating atoms about the rhodium in both cation and anion is approximately square planar. The bite of the ligand as measured by the intra-ligand P–P distance is 3.111(8) Å. Cation and anion are so packed together than the terminal atoms of the anion are directed toward the adjacent cation, as illustrated in Fig. 2. These terminal atoms are directed away from the P(3) and P(3)′ atoms and towards the P(4) and P(4)′ atoms. This is accommodated by a twist in the cation such that the P(4) and P(4)′ atoms are depressed relative to the anion. (In Fig. 2, the z-coordinate of P(3) is −0.1410(2), of Rh(1) is −0.1410(1), and of P(4) is −0.1440(2).) Consequently the cation is not superimposable on its mirror image;

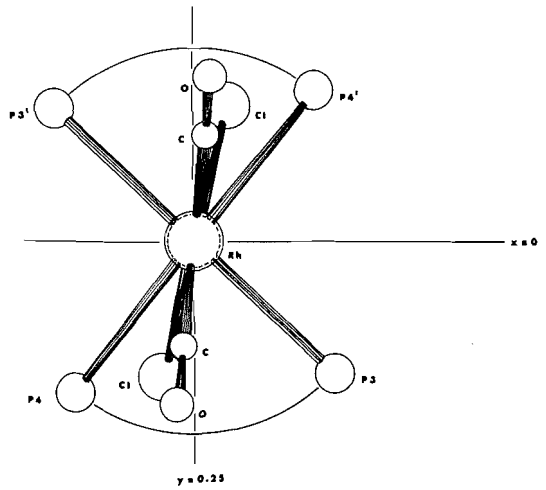

FIG. 2. View down a two-fold axis ($x = 0, y = 0.25$) illustrating the relation between cation and adjacent anion. Only the anion and the cationic rhodium atom (in dashed lines) with its phosphorus atoms are shown; arcs between phosphorus atoms represent the fluorocarbon bridge. The anion is above the cation, with chlorine atoms directed down towards the cation, and carbonyl groups directed upwards.

this means there are two distinct enantiomorphs in the crystal lattice, related to each other by either a center of symmetry or a glide plane operation.

Each half of the cation contains two puckered, five-membered rings (Fig. 3). Carbon atoms C(14) and C(15) are, respectively 0.28(2), and 0.26(2) Å out of the plane of the phosphorus atoms of the same ligand and the rhodium (Rh(1)) atom. The fluorocarbon ring is also significantly puckered. This can be seen by examination of the results in Table 3 for the weighted mean plane through four of the carbon atoms of this ring. C(6), the carbon atom farthest from the cationic rhodium atom, is significantly out of this plane (in fact by 0.10(3) Å). Featured in Fig. 4 are the conformations of the five-membered rings of the cation; the cyclopentenyl ring conformation is shown to be consistent with the orientation of the C—F bonds farthest from the rhodium atom. F(5) is in the axial position, F(7) in the equatorial. Discussion of the C—F bond lengths is precluded by the extreme thermal motion of the fluorine atoms (see Table 2) which may be further aggravated by the fractional presence of the other (flipped) conformation of the cyclopentene ring.

[4]Photocopies of Table 1 may be obtained, free of charge, upon request, from the Depository of Unpublished Data, National Science Library, National Research Council of Canada, Ottawa, Canada.

Can. J. Chem. Downloaded from www.nrcresearchpress.com by 210.87.254.42 on 09/05/12
For personal use only.

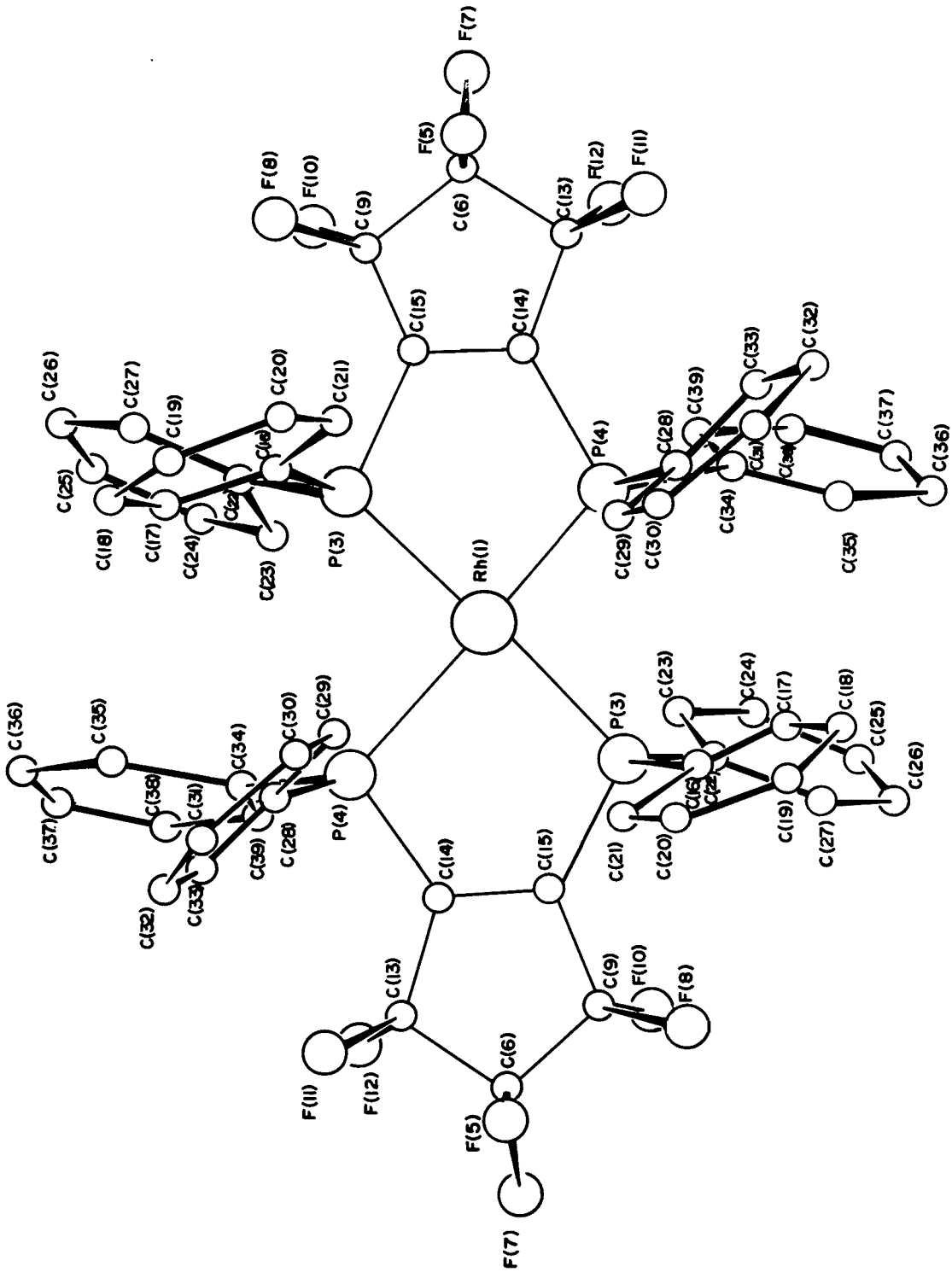

FIG. 3. The cation $[Rh(f_6fos)_2]^+$.

Can. J. Chem. Downloaded from www.nrcresearchpress.com by 210.87.254.42 on 09/05/12
For personal use only.

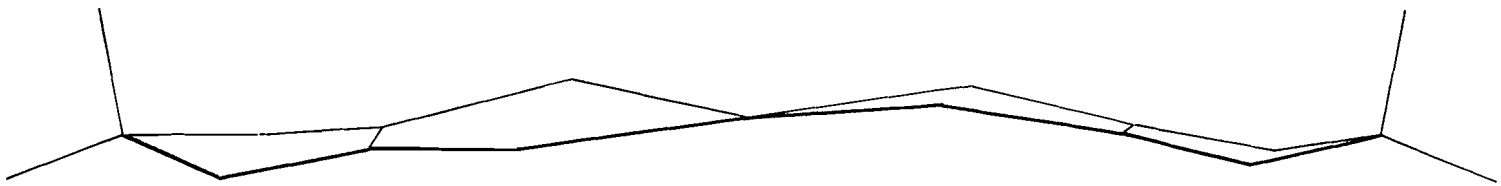

FIG. 4. Diagram featuring ring conformations of the cation. Lines protruding from the extreme ends of the cation indicate the approximate orientations of C—F bonds.

Can. J. Chem. Downloaded from www.nrcresearchpress.com by 210.87.254.42 on 09/05/12
For personal use only.

TABLE 3. Equations of best planes and distances of atoms from planes*

Anion

(1) Plane containing Rh(2) and its bonded Cl atoms

$0.2433x + 0.9699y - 8.5976 = 0$

Atom	Distance from plane (in Å)
C(41)	0.18(4)
C(41)′	−0.18(4)
C(42)	0.32(3)
O(42)′	−0.32(3)

Cation

(2) Plane through Rh(1), P(3), and P(3)′ and parallel to the xy plane

$-z + 5.185 = 0$

Atom	Distance from plane (in Å)
P(4)	−0.112(6)
P(4)′	−0.112(6)

(3) Plane containing Rh(1) and only the P atoms of one ligand

$0.0355x - 0.0321y - 0.9989z + 5.6055 = 0$

Atom	Distance from plane (in Å)
C(14)	0.28(2)
C(15)	0.26(2)

(4) Mean plane through C(9), C(13), C(14), and C(15) of the fluorocarbon ring

$-0.0999x - 0.0414y - 0.9941z + 5.8798 = 0$

Atom	Distance from plane (in Å)
C(9)	0.01(3)
C(13)	−0.01(3)
C(14)	0.01(2)
C(15)	−0.01(2)
C(6)	−0.10(3)

*The equations are given in Å coordinates. Planes (2) and (4) are weighted mean planes. The weight assigned to an atom is inversely proportional to the sum of the standard deviations for the positional coordinates of the atom.

In the anion the Rh–Cl and Rh–CO(midpoint) distances are identical. This fact coupled with the lower thermal motion of the light atoms, the high correlation coefficients (Table 5), and the unreasonable C—O bond length indicate that while the electron density may be approximately described, a more sophisticated model is needed. Disorder involving the Cl and CO groups could explain all the features mentioned.

Two structural features of the $[Rh(f_6fos)_2]$ cation have implications concerning other compounds containing the $f_6$fos ligand. Firstly, the bite of the ligand (3.111(8) Å) has a bearing on the structure proposed for $f_6$fosFe$(CO)_3$ (7). The nuclear magnetic resonance (n.m.r.) spectrum showed that the original symmetry of the $f_6$fos ligand was preserved in the latter complex. Cullen *et al.* have suggested two possible

TABLE 4. Interatomic distances and bond angles with standard deviations

Bonded distances

Bond	Distance* (Å)	Average
Cation		
Rh—P distances		
Rh(1)—P(3)	2.282(6)	
Rh(1)—P(4)	2.300(6)	2.291
P—C(phenyl) distances		
P(3)—phenyl(1)	1.81(2)	
P(3)—phenyl(2)	1.80(2)	
P(4)—phenyl(3)	1.79(2)	
P(4)—phenyl(4)	1.81(2)	1.80
P—C(fluorocarbon) distances		
P(3)—C(15)	1.83(2)	
P(4)—C(14)	1.82(2)	1.83
C=C(fluorocarbon double bond)		
C(14)—C(15)	1.30(3)	
C—C(fluorocarbon single bond)		
C(14)—C(13)	1.52(3)	
C(13)—C(6)	1.48(3)	
C(6)—C(9)	1.50(3)	
C(9)—C(15)	1.44(3)	1.49
C—C(phenyl)		1.39
C—F distances (uncorrected for thermal motion)†		
C(6)—F(5)	1.46(4)	1.33
C(6)—F(7)	1.26(3)	
C(9)—F(8)	1.35(3)	
C(9)—F(10)	1.36(3)	
C(13)—F(11)	1.20(3)	
C(13)—F(12)	1.37(3)	
Anion		
Rh(2)—Cl(40)	2.35(1)	
Rh(2)—C(41)	1.90(4)	
C(41)—O(42)	0.91(3)	

Non-bonded distances

Atom pair	Distance (Å)
Anion	
Cl(40)—Cl(40)′	3.24(3)
Cation	
P(4)—P(4)′	4.59(1)
Anion–cation	
Cl(40)—Rh(1)	5.23(1)
Shortest anion–cation distance	
Cl(40)—C(39)(Phenyl(4))	3.40(3)
Inter-anion	
O(42)—Rh(2)	4.77(3)
C(41)—C(41)	4.10(7)
O(42)—O(42)	3.66(6)

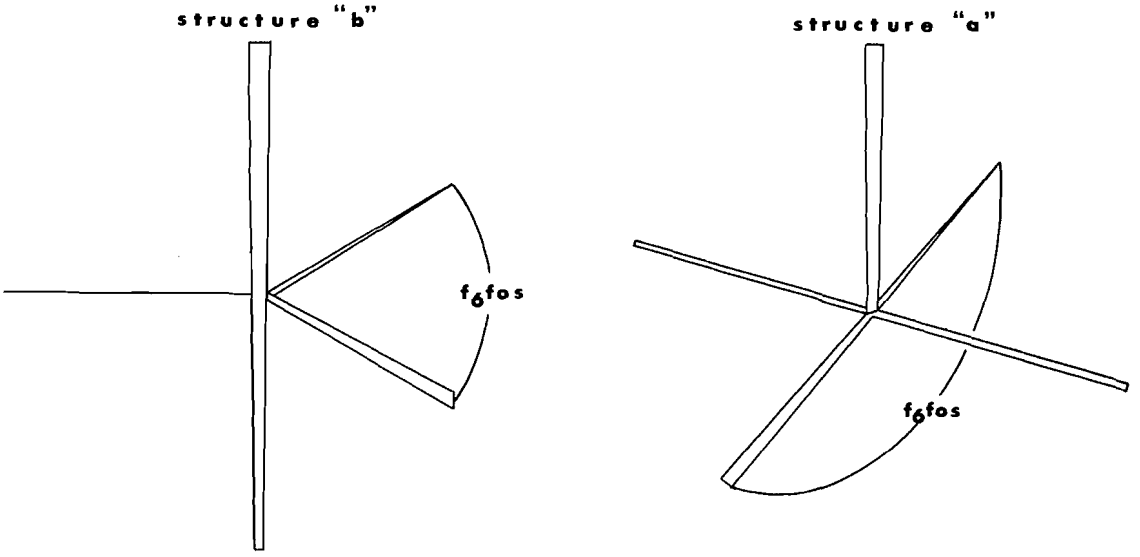

FIG. 5. Alternative structural proposals for $f_6fosFe(CO)_3$. Structure "a" is based on a square pyramidal arrangement; structure "b" is based on a trigonal bipyramidal arrangement. These alternatives were proposed by Cullen *et al.* (7).

TABLE 4. (*Concluded*)

Bond angles

Bonds	Angle (deg)
Cation	
P(3)—Rh(1)—P(4) (for one ligand)	85.5(2)
P(3)—Rh(1)—P(4) (inter-ligand)	94.5(2)
Phenyl(1)—P(3)—Phenyl(2)	109.4(7)
Phenyl(3)—P(4)—Phenyl(4)	106(1)
Rh(1)—P(4)—C(14)	106.4(6)
Rh(1)—P(3)—C(15)	107.6(7)
C(15)—C(14)—P(4)	121(2)
C(14)—C(15)—P(3)	119(2)
C(15)—C(14)—C(13)	110(2)
C(14)—C(15)—C(9)	113(2)
C(15)—C(9)—C(6)	104(2)
C(14)—C(13)—C(6)	104(2)
C(13)—C(6)—C(9)	108(2)
F(11)—C(13)—F(12)	109(3)
F(8)—C(9)—F(10)	104(2)
F(5)—C(6)—F(7)	94(3)
Anion	
Cl(40)—Rh(2)—Cl(40)′	89.2(7)
Cl(40)—Rh(2)—C(41)	91(1)
C(41)—Rh(2)—C(41)′	90(2)
Cl(40)—Rh(2)—C(41)′	175(1)
Rh(2)—C(41)—O(42)	177(6)

*Standard deviations in parentheses.
†The correction for thermal motion was not considered to be strictly applicable to the C—F bond situation. However, calculations based on the fluorine riding on the carbon atom indicated that corrections to the bond length are of the order of 0.1 Å.

TABLE 5. Correlation coefficients (δ) greater than 0.45 between parameters of the carbonyl atoms

Carbon atom parameter	Oxygen atom parameter	δ
x	z	0.54
x	B_{11}	0.48
y	B_{12}	0.56
y	B_{23}	0.59
z	x	0.52
z	B_{33}	0.60
B_{11}	B_{11}	0.56
B_{12}	B_{23}	0.58
B_{33}	B_{33}	0.50
B_{23}	B_{12}	0.48

regular arrangements (Fig. 5) and proposed that the true structure is one that is intermediate between these two possibilities.

Assuming that the Fe–P distance in f_6fos-$Fe(CO)_3$ is close to 2.2 Å (it is 2.18 Å in the compound $(\pi\text{-}C_5H_5)Fe(CO)(f_6fos)Sn(CH_3)_3$ where f_6fos is monodentate (15)) and also that the P–P distance is no greater than 3.1 Å in $f_6fosFe(CO)_3$, the angle subtended at the Fe atom by the Fe–P vectors would be 90°. This suggests that structure (**b**) is more likely.

Secondly, the conformations found for the cation suggest that other complexes shown to contain f_6fos (*e.g.*, $f_6fos(CO)_3$ and $f_6fosM(CO)_4$,

Can. J. Chem. Downloaded from www.nrcresearchpress.com by 210.87.254.42 on 09/05/12
For personal use only.

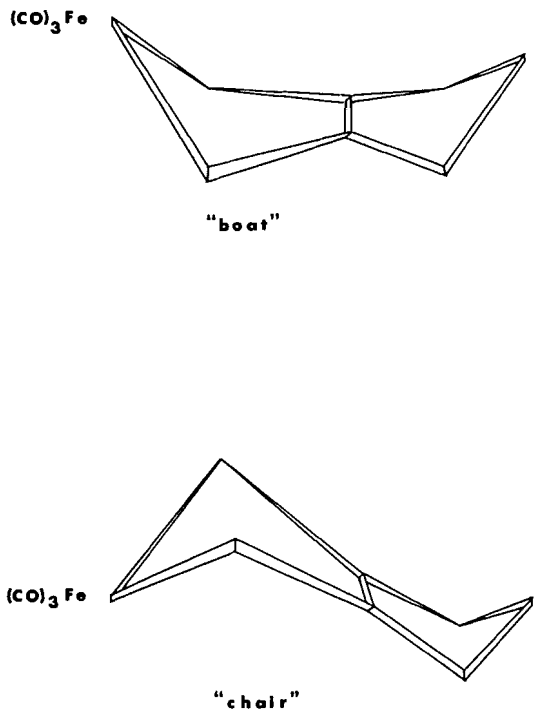

FIG. 6. Two possible isomers of $f_6fosFe(CO)_3$. The pucker of the five-membered rings has been much exaggerated to emphasize the difference between the two conformations.

M = Cr, Mo, W) also may contain puckered, five-membered rings. It is conceivable that two short-lived isomers might appear in solution. They might be loosely described as "boat" and "chair" forms. (See Fig. 6.) The carbonyl stretching (i.r.) spectrum of $f_6fosFe(CO)_3$ shows four bands, one more than the number expected for a compound with C_{2v} symmetry (5). Similarly in $f_6fosM(CO)_4$ complexes four bands are predicted yet five are observed. The evidence here adds credibility to the suggestion of Cullen and co-workers that this extra band could arise from the presence of two distinct isomers in solution which have a long enough lifetime to be detected by i.r. spectroscopy.

We wish to thank the National Research Council of Canada for providing the financial support which made this work possible.

1. W. R. CULLEN and J. A. J. THOMPSON. Can. J. Chem. **48**, 1730 (1970).
2. W. R. CULLEN, D. A. HARBOURNE, B. V. LIENGME, and J. R. SAMS. Inorg. Chem. **9**, 702 (1970).
3. W. R. CULLEN. Fluorine chemistry reviews. Vol. 3. *Edited* by Paul Tarrant. Marcel Dekker, Inc., New York. 1969.
4. W. R. CULLEN and D. A. HARBOURNE. Can. J. Chem. **47**, 3371 (1969).
5. W. R. CULLEN, D. F. DONG, and J. A. J. THOMPSON. Can. J. Chem. **47**, 4673 (1969).
6. W. R. CULLEN, D. A. HARBOURNE, B. V. LIENGME, and J. R. SAMS. Inorg. Chem. **8**, 95 (1969).
7. W. R. CULLEN, D. A. HARBOURNE, B. V. LIENGME, and J. R. SAMS. Inorg. Chem. **8**, 1469 (1969).
8. W. R. CULLEN, D. A. HARBOURNE, B. V. LIENGME, and J. R. SAMS. J. Am. Chem. Soc. **90**, 3293 (1968).
9. W. R. CULLEN, P. S. DHALIWAL, and C. J. STEWART. Inorg. Chem. **6**, 2256 (1967).
10. D. H. TEMPLETON. *In* International Tables for X-Ray Crystallography. Vol. 3. The Kynoch Press, Birmingham, England. 1962. p. 216.
11. P. W. R. CORFIELD. Ohio State University; University of Canterbury, New Zealand version.
12. Crystallographic structure factor and full-matrix least-squares program Bucils. University of Canterbury, New Zealand version.
13. Program Fordap: Crystallographic Fourier Summation with optional numeric or alphanumeric plotting and peak searching, University of Canterbury, New Zealand version.
14. International Tables for X-Ray Crystallography. Vol. 3. Kynoch Press, Birmingham, England. 1962. p. 201.
15. F. W. B. EINSTEIN and R. RESTIVO. To be published.

Can. J. Chem. Downloaded from www.nrcresearchpress.com by 210.87.254.42 on 09/05/12
For personal use only.

Can. J. Chem. Downloaded from www.nrcresearchpress.com by 210.87.254.5 on 09/05/12
For personal use only.

Indole Oxidation: the Dimer of 3-Hydroxy-2,3-dimethylindolenine[1]

VINOD DAVE AND E. W. WARNHOFF
Department of Chemistry, University of Western Ontario, London, Ontario

Received November 3, 1970

Chemical and spectroscopic evidence for the structure **1** of the dimer of 3-hydroxy-2,3-dimethylindolenine is presented. This evidence is based mainly on a comparison of the spectroscopic properties and reactions of both the dimer **1** and its hexadeutero analog **13**. The stereochemistry derived by consideration of n.m.r. shielding is that found by the X-ray analysis of other investigators. The various ways in which this dimer can arise are discussed critically.

Des données chimiques et spectroscopiques permettant d'attribuer la structure **1** au dimère de l'hydroxy-3 diméthyl-2,3 indolénine sont présentées. Les conclusions sont basées principalement sur une comparaison des réactions et des propriétés spectroscopiques du dimère **1** et de son analogue hexadeutéré **13**. La stéréochimie déduite par considération du blindage en r.m.n. est la même que celle trouvée par d'autres chercheurs à l'aide d'une analyse par rayons-X. Les diverses façons par lesquelles ce dimère peut se former sont discutées d'une façon critique.

Canadian Journal of Chemistry, 49, 1911 (1971)

Oxidation and rearrangement play a key role in the chemistry of indoles and indole alkaloids (1–3). The susceptibility of indoles to oxidation is well illustrated by 2,3-dimethylindole which gives rise to a dimeric oxidation product, $C_{20}H_{22}N_2O_2$ (m.p. variously reported as 213 (4), 214 (5), 222 (6), 224 (7), and 225° (8)), under a variety of conditions: simple recrystallization from petroleum ether (7), peroxide-catalyzed oxidation (8), and catalytic oxygenation–reduction (5). In an earlier investigation (5) Kershaw and Taylor suggested an imidazolidine formula **11** for this compound, but further work,[1] the details of which are now presented, definitely established the revised formula **1** as the correct structure of this product. Recently, on the basis of mechanistic considerations and spectroscopic data Berti *et al.* (7), have independently proposed this structure for the dimeric product without, however, providing unambiguous evidence to support it. Still more recently (9), an X-ray crystallographic analysis has been reported which confirms this structure and, moreover, provides the stereochemistry of this molecule.

The unusual feature of the dimer as a chemical structural problem was that spectroscopy was of limited utility, and this limitation obliged the use of supplementary chemical methods. The problem became more interesting during the course of obtaining the structural evidence when an intricate rearrangement sequence was discovered (10). In this paper is presented briefly the chemical proof for the dimer structure together with observations on its chemistry, and in the accompanying paper (10) a description of the acid-catalyzed rearrangements which it undergoes.

Structure

Since the same oxidation product has also been found to arise by dimerization of 3-hydroxy-2,3-dimethylindolenine (**5**) (5), the simplest interpretation[1] of its formation would be addition of the enamine tautomer **6** to the indolenine **5** followed by intramolecular addition of a tertiary hydroxyl group in the resulting imine **7** to yield the dimer **1**, as also suggested by Berti *et al.* (7) (see Scheme 1). This structure is in accord with the two indoline chromophores of the u.v. spectrum and the absence of carbonyl absorption in the i.r. region. As expected of structure **1**, only one nitrogen atom is titratable in the methylcellosolve–water (80:20) system, and the pK_a ~ 3.0 found[2] corresponds to an *N*-alkylaniline (*cf.* *N*-methylaniline pK_a 3.37 in the same solvent); the basicity of the nitrogen atom of the ring-closed carbinolamine ether is weakened by the oxygen atom (expected decrease: 2–3 pK_a units (11)) to the point that it is not titratable in this solvent system. Also in agreement with structure **1**, the n.m.r. spectrum (Fig. 1) consisted of three

[1]Presented in part at the 52nd Annual Conference of the Chemical Institute of Canada, Montreal, Quebec, May 25–29, 1969.

[2]We would like to thank Dr. W. Simon, E. T. H., Zürich, for this determination.

Can. J. Chem. Downloaded from www.nrcresearchpress.com by 210.87.254.5 on 09/05/12
For personal use only.

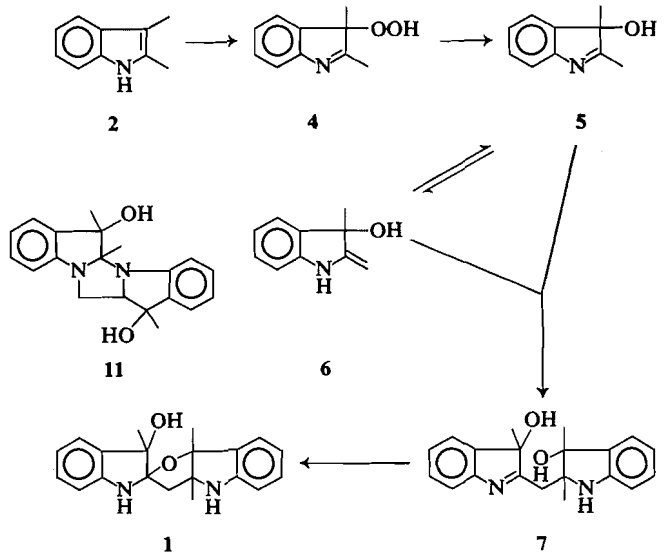

SCHEME 1

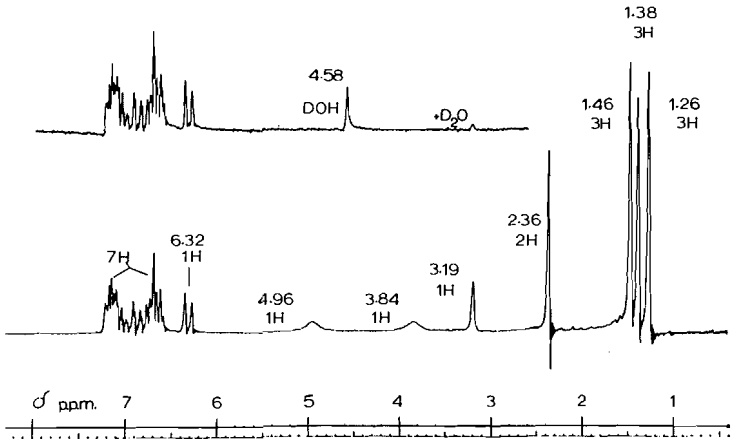

FIG. 1. The n.m.r. spectrum (100 MHz) of the dimer **1** of 3-hydroxy-2,3-dimethylindolenine in $CDCl_3$.

unsplit methyl peaks (δ 1.26, 1.38, and 1.46), a two-proton singlet (δ 2.36), a broad pattern from eight aromatic protons, and three separate broad one-proton peaks exchangeable with deuterium oxide (δ 3.19, 3.84, and 4.96).[3] The nature of these three exchangeable hydrogen atoms was determined by acetylation in mildly basic medium to mono-, di-, and triacetyl derivatives. The first acyl group was introduced onto the more basic indoline nitrogen atom even at room temperature,[4] but acetylation of the other two functions occurs at a convenient rate only at higher temperature. The mono- and diacetates **8** and **9** were both *N*-acyl compounds (i.r.), but the triacetate **10** was an *N,N,O*-triacyl compound (i.r.). Each of the acetates was saponified back to the dimer, and the spectra of

[3]Of course the shape and position of these peaks are solvent, temperature, and p*H* dependent. This fact and the appearance of a DOH peak corresponding to ~1H close to the lowest field peak after addition of D_2O are partly responsible for the original suggestion of the imidazolidine structure **11** (5).

[4]Evidence that the monoacetate is indeed **8** comes from its acid-catalyzed rearrangement described in the succeeding paper (10).

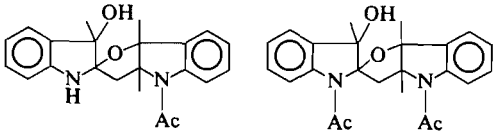

8 9

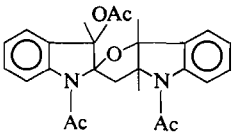

10

the acetates indicate the carbinolamine ether ring to be still intact.

That the two indolenine moieties were joined through the 2-methyl group of one was determined by preparing the dimer from 2-methyl-3-methyl-d_3-indole. The Fischer indole synthesis with butanone-4,4,4-d_3 (available from methyl iodide-d_3 and ethyl acetoacetate) and phenylhydrazine gave **12** whose n.m.r. spectrum had a single methyl peak at δ 2.28. Catalytic oxygenation–reduction to the 3-hydroxyindolenine and subsequent dimerization furnished the hexadeuterio dimer (later found to be **13**) whose n.m.r. spectrum was lacking only the two methyl peaks at δ 1.38 and 1.46 of the protio analog. The two-proton peak at δ 2.36, which is still present in the n.m.r. spectrum of the hexadeuterio dimer, must originate from the hydrogen atoms of the carbon bridge which joins the two hydroxyindolenines, and therefore this connecting carbon atom must have been a 2-methyl group.

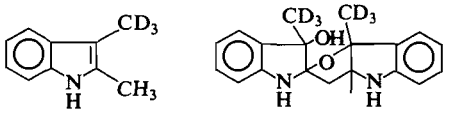

12 13

The question of whether the 2-methyl group of one indolenine unit was linked to the 2- or the 3-position of the other unit was answered by a dissolving metal reduction, a reaction considered unlikely to lead to skeletal rearrangement because of general experience with the method. The action of sodium and *t*-butyl alcohol on **1** gave six products of progressive reduction (**2** and **14–18**) two of which, desoxystereoisomers of partial formula **19**, could be used to decide between the alternative arrangements. In the n.m.r. spectrum of each of these epimeric products one methyl group was a doublet (J = 7 Hz) due to coupling with an adjacent methine hydrogen, but in the n.m.r. spectra of the analogous products from sodium–*t*-butyl alcohol reduction of the hexadeuterio dimer **13** this doublet was absent.[5] Therefore, the methyl group in **19** with an adjacent carbinyl hydrogen atom was the C-3 methyl group of the indolinyl moiety, and the desoxy compounds are the epimers **14** and **15** with the methylene bridge linking the C-2 position of each heterocyclic unit. Attachment of the two hydroxyl groups to this firmly established carbon–nitrogen skeleton in the only way possible gives **7** which would only undergo facile ring closure to **1**, the structure derived from the earlier mentioned mechanistic considerations.

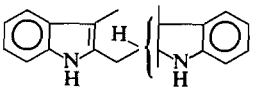

19

Stereochemistry

During the formation of the dimer, the addition of the enamine **6** to the imine **5** should occur mainly from the least hindered side opposite the C-3 methyl group to produce *cis* methyl groups at C-2 and -3 of the indoline, and certainly ring closure (reversible) of the carbinolamine ether ring would be expected only with the *cis* fusion of the two five-membered rings. The X-ray analysis (9) found that these methyl groups were indeed *cis*. The closure of the carbinolamine ether ring could occur in two senses to yield **20** or **21**,[6] and the actual arrangement **20** found by the X-ray determination is the only one in agreement with certain shielding effects in the n.m.r. spectra. One of the eight aromatic protons is so shielded (δ 6.32, $J \sim 7$ Hz) that it is separated from the other seven. From its position and coupling and by analogy with model indolines (12, 13) this proton is one of the two ortho to the nitrogen atom on a benzene ring. In the monoacetate of the dimer **8**, the strongly shielded proton is still present, but in the di- and triacetates **9** and **10**, this proton has been deshielded and moved back among the other seven aromatic hydrogen atoms, a known effect of acetylation on the C-7 proton of an indoline (12, 13). Therefore, this proton must be the one encircled in **20**, and the abnormal

[5]The peak from the indole methyl group was also missing.

[6]Only one of the racemic pair is shown.

Can. J. Chem. Downloaded from www.nrcresearchpress.com by 210.87.254.5 on 09/05/12
For personal use only.

Can. J. Chem. Downloaded from www.nrcresearchpress.com by 210.87.254.5 on 09/05/12
For personal use only.

shielding is attributed to the orientation of the other aromatic ring. The acetyl methyl on the basic indoline nitrogen atom is strongly deshielded ($\delta \sim 2.5$–2.6) in all three acetates, but the carbinolamine *N*-acetyl methyl group in the di- and triacetates is abnormally shielded ($\delta \sim 1.9$ instead of ~ 2.2 (12)), the latter observation being in agreement only with the stereochemistry in **20**. Finally, the reaction of the dimer with formaldehyde to produce a homo dimer in which the two nitrogen atoms are linked by a methylene group (10) is only possible with **20**.

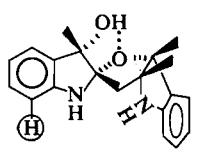

20

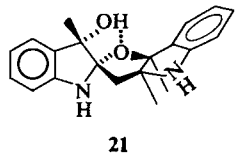

21

Formation in Other Reactions

The basic features of the mechanism leading to dimer from the 3-hydroxyindolenine **5** suggest that dimerization could also occur through the hydroperoxide **4** or a combination of **4** and **5** followed by reduction of any hydroperoxide linkages, and there is no evidence to exclude this possibility. Furthermore, thermal breakdown of the hydroperoxide regenerates some 2,3-dimethylindole which could react with more hydroperoxide to yield the hydroxyindolenine. As might then be expected, dimer is formed to some extent under a variety of conditions not initially involving the hydroxyindolenine: autoxidation of 2,3-dimethylindole in chloroform solution,[7] reaction of the indole and hydroperoxide at room temperature (8), and thermal decomposition of the hydroperoxide in boiling benzene.

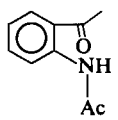

22

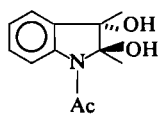

23

[7]This reaction shows an interesting dependence on agitation (see Experimental). If the solution is allowed to stand without stirring, oxygen absorption is slow. Consequently any hydroperoxide formed has time to react with the indole to yield hydroxyindolenine and finally dimer. However, if the solution is stirred so that oxygen absorption is rapid, most of the indole is converted to hydroperoxide before much reaction of the peroxide with excess indole can occur. In this case the major product is *o*-acetamidoacetophenone (**22**) from the usual decomposition of the hydroperoxide (8).

This last reaction was done according to the conditions of Ghosal and Dutta (6) who obtained a compound,[8] $(C_{10}H_{11}NO)_n$, m.p. 220–222°, which they formulated as the 2,3-epoxide of the indole **2**, but which is undoubtedly the dimer **1** (see Experimental).[9]

However, one reaction reported to lead to the dimer does not do so on re-investigation. Although saponification of *N*-acetyl-2,3-*trans*-dihydroxy-2,3-dimethylindoline (**23**) was reported (5) to yield 2,2-dimethylindoxyl (**25**) and dimer **1**,[10] only 2,2-dimethylindoxyl was formed in our repetition of the experiment. Nevertheless, variation of the ratio of indoxyl **25** to dimer **1** with experimental conditions is to be expected. For the two competing reactions (Scheme 2), the higher the concentration of hydroxide ion or other added base, the greater the proportion of indoxyl formed. On the other hand, the imine $\rightleftharpoons$ enamine tautomerization is fast relative to dimerization and, provided the reaction medium is basic enough to maintain the equilibrium, an increased concentration of base would have little effect on the dimerization rate. Moreover, the dimerization being bimolecular in hydroxyindolenine will be slowed by dilution.

This dimerization reaction should have some degree of generality, and provided that steric factors are not unfavorable, other 3-hydroxyindolenines and indoles should undergo the same reaction.

Addendum

The products of the sodium – *t*-butyl alcohol reduction are readily rationalized (Scheme 3). Whether the left hand aromatic ring of **1** or the imine group of **7** accepts electrons, the initial

[8]In our hands treatment of the compound (actually dimer **1**) with dilute hydrochloric acid did not give *o*-acetamidoacetophenone (**22**) as reported (6), but only the rearrangement products described in the accompanying paper (10). However, treatment of the hydroperoxide **4** with dilute hydrochloric acid does give *o*-acetamidoacetophenone (see footnote 7).

[9]The difference in products from the benzene and chloroform reactions (see footnote 7) is probably mainly a function of temperature. At higher temperatures the hydroperoxide breaks down to the indole **2** which reacts with additional hydroperoxide to produce dimer via the hydroxyindolenine. In the absence of this thermal regeneration of **2** the favored reaction path of hydroperoxide is formation of *o*-acetamidoacetophenone (see footnote 8).

[10]Dimer was found after recrystallization of chromatogram fractions having the same m.p. as hydroxyindolenine **5**.

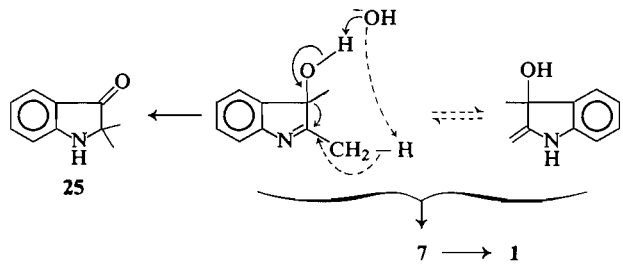

SCHEME 2

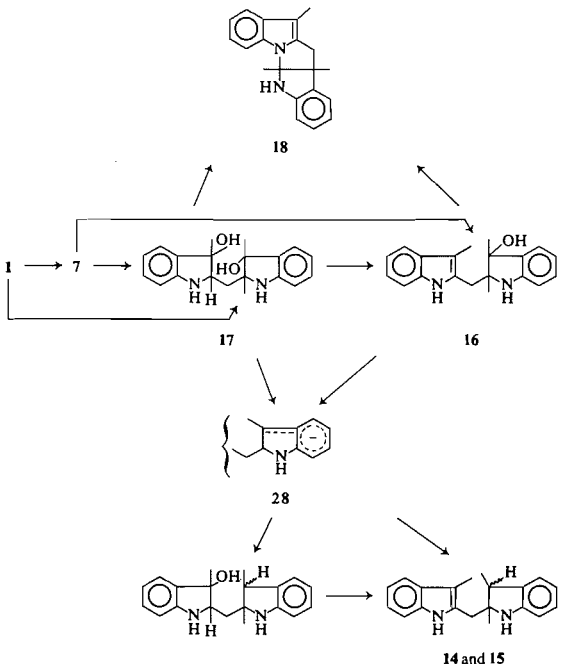

SCHEME 3

product could be diol **17**. Elimination of water would then produce the indole **16**, or possibly **7** is hydrogenolyzed directly to **16**. Similar electron addition to the aromatic ring on the right and hydroxyl elimination would remove the other oxygen function. Protonation of the carbanion **28** would occur from both sides of the benzylic carbon atom to produce both epimers **14** and **15**. 2,3-Dimethylindole could arise by reduction of the 3-hydroxyindolenine from retro Mannich scission of dimer (see footnote 12) or else by direct reductive cleavage, *e.g.*

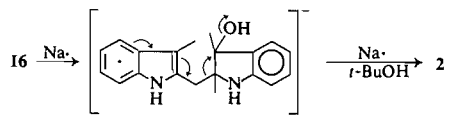

It is not surprising that both **16** and **17** should be extremely sensitive to acid, even the traces of hydrogen chloride present in chloroform, and undergo dehydration with rearrangement to **18**, thus explaining its presence in the reduction product (see the accompanying paper, ref. 10).

Experimental

General

Melting points were determined on a Reichert–Kofler microscope hot stage and are corrected.

The i.r. spectra were recorded on a Beckman IR-10 instrument with chloroform solutions. The n.m.r. spectra were recorded on Varian A-60, T-60 and HA-100 spectrometers with ~ 10–15% (w/v) solutions in deuteriochloroform solution containing tetramethylsilane as internal standard. In the few cases where a different solvent was used, it is specified. Aromatic n.m.r. absorptions are not reported. The u.v. spectra were recorded on a Cary model 14 spectrometer with methanol solutions. Mass spectra were obtained on a Varian M-66 instrument.

Silica gel GF_{254} (Merck, Germany) was used for thin and thick layer (20 g/20 × 20 cm plate) chromatography. Thin layer plates were sprayed with a 5% solution of phosphomolybdic acid in ethanol. On thick layer plates bands were detected under a u.v. lamp. Woelm neutral, Brockman grade IV alumina, or British Drug Houses silica gel was used for column chromatography. Petroleum ether refers to the fraction of b.p. 60–80°.

Organic layers from work-up of reactions were washed with saturated NaCl solution, dried over anhydrous $MgSO_4$, and then evaporated at reduced pressure on the rotary evaporator.

The n.m.r. data are given in Table 1.

2,3-Dimethylindole (2)

This starting material was either purchased from the Aldrich Chemical Co. or was made by the Fischer indole synthesis in which a solution of methyl ethyl ketone (50 g, 0.70 mol), phenylhydrazine hydrochloride (100 g, 0.70 mol), and glacial acetic acid (500 ml) was refluxed for 3 h. The cooled solution was diluted with water, filtered, washed with water, and dried. Percolation of a petroleum ether solution of the crude product through silica gel gave 71 g (70%) of white crystalline solid, m.p. 98–100° (lit. (14) 106°).

2,3-Dimethylindolenyl-3-hydroperoxide (4)

In our hands the procedure of Beer *et al.* (8) gave miserable yields of **4**. The major product obtained was

Can. J. Chem. Downloaded from www.nrcresearchpress.com by 210.87.254.5 on 09/05/12
For personal use only.

TABLE 1. The n.m.r. data exclusive of aromatic protons*

Compound	Absorption δ
2,3-Dimethylindole (**2**)	2.20 (s, 3-Me), 2.28 (s, 2-Me) *dilute* $CDCl_3$ (13 mg/0.25 ml) 2.19 (s, 3-Me), 2.28 (s, 2-Me) CD_3COOD
2-Methyl-3-methyl-d_3-indole (**12**)	2.28 (s, 2-Me) dilute $CDCl_3$ (15 mg/0.25 ml) 2.28 (s, 2-Me) CD_3COOD
3-Hydroperoxy-2,3-dimethylindolenine (**4**)	1.40 (s, 3-Me), 2.17 (s, 2-Me) 10.97 (s, OOH)
3-Hydroxy-2,3-dimethylindolenine (**5**)	1.39 (s, 3-Me), 1.89 (s, 2-Me)
2-Hydroxymethyl-3-methylindole (**24**)	2.28 (s, Me), 4.81 (s, CH_2), 1.68 (s, OH), 8.07 (b, NH)
2-Formyl-3-methylindole (**3**)	2.72 (s, Me), 9.03 (b, NH), 10.12 (s, CHO)
2,2-Dimethylindoxyl (**25**)	1.32 (s, diMe), 4.85 (s, NH)
N-Acetyl-2,3-dimethylindole	2.15 (s, Me) 2.50 (s, Me), 2.62 (s, NCOMe)
N-Acetyl-*trans*-2,3-dihydroxy-2,3-dimethylindoline (**23**)	1.72 (s, Me), 1.91 (s, Me), 2.03 (s, Me), 4.40 (OH)
N-Acetyl-*cis*-2,3-dihydroxy-2,3-dimethylindoline (?)	1.45 (s, Me), 1.56 (s, Me), 2.23 (s, NCOMe), 4.28 (OH)
2-Acetamidoacetophenone (**22**)	2.26 (s, Me), 2.70 (s, NCOMe), 11.69 (NH)
Dimer **1**	1.26 (s, 2-Me), 1.38 (s, 3-Me), 1.46 (s, 3-Me), 2.36 (s, CH_2), 3.19 (OH), 3.84 (NH), 4.96 (NH)
Dimer-d_6 **13**	1.26 (s, 2-Me) 2.36 (s, CH_2), 3.20 (OH), 3.84 (NH), 4.95 (NH)
Dimer monoacetate **8**	1.38 (s, Me), 1.52 (s, diMe), 2.54 (s, NCOMe), 3.05 (s, OH), 3.30 and 3.54 (AB of CH_2, J = 14), 3.88 (b, NH)
Dimer diacetate **9**	1.35 (s, Me), 1.51 (s, Me), 1.73 (s, Me), 1.95 (s, NCOMe), 2.55 (s, NCOMe), 4.27 center of AB of CH_2 of which only two strongest lines visible. [OH not apparent in this spectrum]
Dimer triacetate **10**	1.32 (s, Me), 1.73 (s, Me), 1.80 (s, Me), 1.88 (s, COMe), 2.47 (s, COMe), 2.51 (s, COMe), 3.50 and 3.84 (AB of CH_2, J = 16)
Reduction product **16**	1.07 (s, Me), 1.40 (s, Me), 2.27 (s, Me), 3.10 (s, CH_2)
Desoxy indolylindoline **14**	1.06 (s, Me), 1.19 (d, 3H, J = 7), 2.24 (s, Me), 2.94 (s, CH_2), 3.35 (indoline NH), 8.53 (indole NH)
Desoxy indolylindoline **15**	1.30 (s, Me), 1.34 (d, 3H, J = 7), 2.16 (s, Me), 2.58 and 2.88 (AB of CH_2, J = 14)

*Chemical shifts are given in p.p.m. from tetramethylsilane (δ) and coupling constants in Hz; $CDCl_3$ solutions unless otherwise specified; 2-Me and 3-Me signify that the methyl group giving rise to the absorption originated from a 2- or 3- methyl group of 2,3-dimethylindole, respectively; s = singlet, d = doublet, b = broad absorption.

the hydroxyindolenine dimer **1**. However, the hydroperoxide **4** was obtained in good yield by McCapra's procedure.[11] A solution of 2,3-dimethylindole (**2**) (0.50 g), which had been freshly crystallized from aqueous methanol, was dissolved in petroleum ether (50 ml) and cooled to ~ 0°. Oxygen was bubbled in with stirring at ~ 0°, and a white crystalline solid slowly precipitated. At the end of 12 h, t.l.c. showed the absence of **2** and the presence of a single spot more polar than **2**. The solid was filtered, washed once with petroleum ether, and dried to give 0.35 g (57%) of colorless hydroperoxide, m.p. 103–108° (dec.) (lit. (8) 113° (dec.)). The compound was used without further attempted purification. It tends to decompose within a day at room temperature, but it is stable for months in a refrigerator. It also turns brown on the t.l.c. plate.

[11]We would like to thank Dr. F. McCapra, University of Sussex, Brighton, England, for sending us his experimental details before publication.

3-Hydroxy-2,3-dimethylindolenine (5)

The procedure of Beer, Donavanik, and Robertson (8) was used. To a mixture of pure hydroperoxide **4** (200 mg), ether (6 ml) and 2 *N* NaOH (3.5 ml) was added sodium dithionite (0.4 g). The mixture was stirred (magnetic bar) at room temperature for 1.5 h, diluted with ether, and separated. The organic layer was washed with water, dried, and evaporated to leave 170 mg of crystalline solid which t.l.c. showed to be composed of ~ 90% of **5** and ~ 10% of dimer **1**. The n.m.r. spectrum agreed with this analysis. Attempts at further purification by recrystallization only increased the proportion of dimer **1**.

Reactions Leading to Dimer 1

(a) Oxygenation–Hydrogenation of 2,3-Dimethylindole (2) (5)

Platinum oxide (0.40 g) in ethyl acetate (200 ml) was reduced with hydrogen. The apparatus was flushed with nitrogen, and 2,3-dimethylindole (3.00 g) was added to the mixture which was stirred (magnetic bar) and oxy-

Can. J. Chem. Downloaded from www.nrcresearchpress.com by 210.87.254.5 on 09/05/12
For personal use only.

Can. J. Chem. Downloaded from www.nrcresearchpress.com by 210.87.254.5 on 09/05/12
For personal use only.

genated for 12 h (oxygen uptake ~ 400 ml). The t.l.c. showed the *complete absence* of 2,3-dimethylindole (**2**). The apparatus was flushed with nitrogen, and the mixture then hydrogenated for 30 min (hydrogen uptake ~ 400 ml). The t.l.c. at this stage revealed the *presence* of 2,3-dimethylindole (**2**) and more polar materials. The catalyst was removed by filtration, and the filtrate was evaporated at reduced pressure to leave 3.10 g of viscous brown liquid which was chromatographed on a column of 90 g of alumina.

(*i*) Petroleum ether eluted 0.70 g (23%) of **2,3-dimethylindole** (**2**), m.p. 98–100°, identical with starting material.

(*ii*) Petroleum ether – benzene (95:5) eluted 0.30 g (8.2%) of ***o*-acetamidoacetophenone** (**22**) which was recrystallized from chloroform – petroleum ether to give colorless needles, m.p. 74–75° (lit. (8) m.p. 77–78°), ν_{max} 3240 (NH), 1690 (ArC=O), and 1650 cm^{-1} ($CH_3C(=O)N$).

(*iii*) Petroleum ether – benzene (85:15) eluted 70 mg (2%) of **2-formyl-3-methylindole** (**3**) which on recrystallization from methanol gave colorless crystals, m.p. 137–139° (lit. (15) m.p. 139–140°), ν_{max} 3640 (NH) and 1650 cm^{-1} (conj. CH=O); *m/e* 159 (molecular ion).

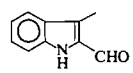

3

(*iv*) Petroleum ether – benzene (60:40) eluted 1.20 g (36%) of crude **dimer 1** which on recrystallization from methanol gave 0.70 g of colorless crystals, m.p. 195–225° (lit. (4–8) m.p. from 213 to 225°),[12] pK_a ~ 3.0 (80% methyl collosolve – 20% water), λ_{max} 245 (16 300) and 297 nm (7600); *m/e* 322 (molecular ion).

Anal. Calcd. for $C_{20}H_{22}N_2O_2$ (322.4): O, 9.92. Found: O, 10.41.

(*v*) Benzene eluted 0.15 g (4.5%) of crude yellowish **2-hydroxymethyl-3-methylindole** (**24**) which was purified by thick layer chromatography (ether–benzene (60:40) used for development) and subsequent recrystallization from chloroform – petroleum ether to give colorless crystals, m.p. 124–126° (lit. (15) m.p. 123–124°), undepressed on admixture with an authentic specimen, m.p. 125–127°, prepared by lithium aluminum hydride reduction of 2-formyl-3-methylindole (**3**), *m/e* 161 (molecular ion).

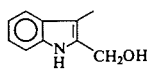

24

(b) Autoxidation of 2,3-Dimethylindole (2)

A solution of **2** (25 g) in reagent grade chloroform (400 ml) was allowed to stand undisturbed in an open beaker at room temperature for 4 days with chloroform being added occasionally to maintain the original volume. Concentration of the dark brown solution gave an oily solid which was recrystallized once from methanol and twice from chloroform – petroleum ether to yield 11 g (40%) of the dimer **1** identical in all respects with the compound obtained in section *a*.

[12]The wide m.p. range is due to thermal decomposition; see later experimental description.

If the chloroform solution of **2** in an open vessel was *stirred* (magnetic bar), the major product was *o*-acetamidoacetophenone (**22**) with only a minor amount (2–5%) of dimer **1**.

(c) Reaction of 2,3-Dimethylindole (2) and 2,3-Dimethylindolenyl-3-hydroperoxide (4)

A solution of **2** (35 mg) and **4** (35 mg) in chloroform (1 ml) was sealed under nitrogen in a tube and stored in the dark for 3 days. The t.l.c. of the reaction mixture showed the absence of hydroperoxide **4** and the presence of 2,3-dimethylindole (**2**) and dimer **1**. The n.m.r. spectrum of the mixture gave the proportion of **1**:**2** as 80:20.

When the hydroperoxide **4** alone was allowed to stand at room temperature in chloroform solution, *o*-acetamidoacetophenone (**22**) was the major product together with a minor amount of the dimer **1**.

(d) Thermal Decomposition of 2,3-Dimethylindolenyl-3-hydroperoxide (4)

The reaction was conducted according to the directions of Ghosal and Dutta (6). A solution of colorless hydroperoxide **4** (0.20 g, pure by t.l.c.) in reagent grade benzene (25 ml) was refluxed for 40 min, after which time the benzene was evaporated at reduced pressure to leave a brown oily solid. The t.l.c. (benzene–ether, 50:50) showed some remaining **4** and three other spots corresponding to **2**, **3**, and dimer **1**. Chromatography on alumina (6.0 g) yielded: (*i*) 75 mg of 2,3-dimethylindole (**2**) eluted by petroleum ether; (*ii*) 8 mg of 2-formyl-3-methylindole (**3**) eluted by petroleum ether – benzene (70:30); and (*iii*) 24 mg of dimer **1** eluted by petroleum ether – benzene (60:40). Recrystallization of the 24 mg of **1** from methanol gave colorless crystals, m.p. 195–225° (dec.)

(e) Basic Treatment of 3-Hydroxy-2,3-dimethylindolenine (5)

A solution of **5** (50 mg, 90% pure with 10% of dimer **1** as impurity) in 2 *N* aqueous NaOH (4 ml) was refluxed for 3 h. After extraction into ether, the product was washed with water and dried. Evaporation left 49 mg of yellowish solid whose t.l.c. (benzene–ether, 50:50) showed a major spot corresponding to dimer **1** and a minor spot corresponding to 2,2-dimethylindoxyl (**25**). From the n.m.r. spectrum the ratio of **1**:**25** was ~ 90:10.

Acidic Treatment of Hydroperoxyindolenine 4

A solution of the hydroperoxide **4** (100 mg) in 2 *N* HCl (1 ml) was stirred at room temperature for 1.5 h. The brownish black solution was diluted with chloroform, washed with water, dried, and concentrated to leave 38 mg of a dark brown oil. The t.l.c. in benzene–ether (50:50) gave a single significant spot of the same R_f as **22**. The n.m.r. spectrum of the crude product clearly showed it to contain about 85% of *o*-acetamidoacetophenone (**22**). No attempt was made to isolate **22**.

Acetylation of Dimer 1

(a) Monoacetate

A mixture of dimer **1** (0.50 g), anhydrous sodium acetate (0.10 g), pyridine (5.0 ml), and acetic anhydride (3.0 ml) was stirred (magnetic bar) at room temperature for 11 days. At this point t.l.c. showed the absence of starting material **1**. The reaction mixture was poured into chloroform, washed with water, dried, and concentrated to leave 0.48 g of viscous brown liquid. The t.l.c.

Can. J. Chem. Downloaded from www.nrcresearchpress.com by 210.87.254.5 on 09/05/12
For personal use only.

(benzene–ether, 50:50) gave a spot (R_f 0.71) corresponding to *O*-acetate **26** (absent in t.l.c. of the reaction mixture before work-up), a spot (R_f 0.49) corresponding to monoacetate **8**, and two minor spots due to di- and triacetates **9** and **10**. Separation by t.l.c. (benzene–ether, 1:1, used for development) gave 0.20 g (40%) of solid which after several recrystallizations from chloroform – petroleum ether gave 50 mg of *N*-monoacetate **8**, m.p. 175–177°, ν_{max} 3530 (OH), 3380 (NH), and 1650 cm^{-1} (amide C=O); λ_{max} 248 (16 700) and 280 nm (3600); *m/e* 364 (molecular ion).

Anal. Calcd. for $C_{22}H_{24}N_2O_3$ (364.4): C, 72.51; H, 6.64; N, 7.69. Found: C, 72.36; H, 6.61; N, 7.54.

From a less polar band of the t.l.c. separation was isolated 42 mg of yellow oily solid. One recrystallization from petroleum ether gave 30 mg of *O*-acetate **26** identical (m.p., t.l.c., i.r., n.m.r.) with the authentic specimen (10). This compound was an artifact formed at some stage of the work-up procedure. It was not present if the chloroform solution of the crude product was washed with $NaHCO_3$ solution.

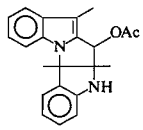

26

(b) Di- and Triacetates

To a stirred (magnetic bar) mixture of dimer **1** (0.30 g), anhydrous sodium acetate (0.1 g), and pyridine (2.0 ml) was added acetic anhydride (2.0 ml), and the reaction mixture was heated at 85° for 18 h. Dilution of the cooled reaction mixture with water and extraction with chloroform gave an organic layer which was washed with water, dried, and evaporated to leave 0.32 g of dark brown oil. Separation by t.l.c. (benzene–ether, 25:75, used for development) gave a band (R_f 0.34) from which 32 mg of crystalline ***N,N*-diacetate 9** was extracted. Recrystallization from ether – petroleum ether (b.p. 30–60°) gave colorless granules, m.p. 194–204°, ν_{max} 3535 (OH), and 1655 cm^{-1} (amide C=O); *m/e* 406 (molecular ion).

Anal. Calcd. for $C_{24}H_{26}N_2O_4$ (406.5): C, 70.92; H, 6.45. Found: C, 71.11; H, 6.74.

From a slightly more polar band (R_f 0.44) was extracted 48 mg of the ***N,N,O*-triacetate 10** which on recrystallization from chloroform – petroleum ether gave colorless granules, m.p. 165–188° (wide range due to stereoisomers?), ν_{max} no OH or NH absorption, 1730 (ester C=O) and 1650 cm^{-1} (amide C=O); *m/e* 448 (molecular ion).

Anal. Calcd. for $C_{26}H_{28}N_2O_5$ (448.5): C, 69.63; H, 6.29. Found: C, 69.18; H, 6.32.

Saponification of Dimer Acetates

A solution of the *N,N*-diacetate **9** (90 mg), KOH (2 pellets), and methanol (2 ml) was refluxed for 18 h. Dilution of the reaction mixture with water and extraction with chloroform gave an organic layer which was washed with water, dried, and evaporated at reduced pressure to leave 48 mg of yellowish solid. Two recrystallizations from chloroform – petroleum ether gave colorless crystals of the dimer **1**, m.p. 195–225° (dec.), undepressed on admixture with the authentic sample. The i.r. and n.m.r. spectra of the saponification product were also identical with those of authentic **1**.

The same procedure was used to saponify the *N*-monoacetate **8** and the *N,N,O*-triacetate **10**; in both cases the dimer **1** was the only product recovered.

2-Methyl-3-methyl-d_3-indole (12)

Methyl ethyl ketone-4,4,4-d_3 was prepared by modification of the *Organic Syntheses* procedure (16). To a solution of sodium (0.80 g) in absolute ethanol (17.5 ml) was added ethyl acetoacetate (4.4 g, 0.033 mol). After a 10 min reflux period, methyl iodide-d_3 (5.0 g, 0.034 mol, > 99% D) was added to the refluxing solution during 15 min. The reaction mixture was refluxed for 6 h at the end of which time it was neutral to p*H* paper. After additon of 5% aqueous NaOH (35 ml), the solution was stirred at room temperature for 5 h. Aqueous H_2SO_4 (1:1, 4 ml) was added and the acidic solution was stirred at room temperature for 15 min before refluxing for 2 h. The solution was distilled, and the fraction of b.p. 78–90° was collected. Redistillation from five pellets of NaOH gave the ketone accompanied by some ethyl alcohol. To this mixture of ketone and ethyl alcohol was added glacial acetic acid (20 ml) and phenylhydrazine hydrochloride (3.1 g, 0.021 mol). The resulting solution was refluxed for 3 h, then cooled and diluted with water. The precipitate was filtered, washed with water, dried, and percolated in petroleum ether solution through a column of 50 g of silica gel to give 1.8 g (37%) of colorless crystalline **12**, m.p. 90–96°, *m/e* 148 (molecular ion). The t.l.c. gave a single spot of the same R_f as **2**. The compound was used for subsequent reactions without further purification.

Hexadeuterio Dimer 13

The procedure of Kershaw and Taylor (5), described in section *a* under dimer preparation above, was used with 2-methyl-3-methyl-d_3-indole (590 mg). The dimer-d_6 (110 mg, 17%) obtained had identical m.p. and t.l.c. behavior as the non-deuterated material, *m/e* 328 (molecular ion corresponding to hexadeuteration).

Sodium–t-Butanol Reduction of Dimer 1

To a refluxing solution of the pure (t.l.c. and n.m.r.) dimer (4.50 g, 14.1 mmol) in *t*-butyl alcohol (150 ml) was added freshly cut sodium metal (15 g) during 0.5 h. Reflux was continued for 2.5 h. Methanol was added to the cooled solution to dissolve unreacted sodium. After the sodium had dissolved, water was added and the mixture was thoroughly extracted with ether. The ethereal solution was washed with water, dried, and evaporated to leave 4.38 g of clear brown oil composed of six compounds according to t.l.c. in benzene – petroleum ether (70:30). The crude product was chromatographed on 200 g of neutral alumina.

(*i*) Petroleum ether eluted 30 mg (1.4%) of colorless **2,3-dimethylindole (2)**, R_f 0.85.

(*ii*) Further elution with petroleum ether gave 55 mg (1.3%) of **Berti's desoxy compound 18**, R_f 0.67, which was recrystallized from chloroform – petroleum ether to give colorless crystals, m.p. 185–190°, whose n.m.r. spectrum was identical with that of the authentic synthetic specimen (see ref. 10).

(*iii*) Continued elution with petroleum ether gave a pale

Can. J. Chem. Downloaded from www.nrcresearchpress.com by 210.87.254.5 on 09/05/12
For personal use only.

yellow oil (660 mg) which was chromatographed again on six thick plates developed with benzene–ether (95:5). Extraction yielded 475 mg (11%) of colorless oil, R_f 0.54, which solidified (single t.l.c. spot). Recrystallization from chloroform – petroleum ether gave 330 mg of colorless crystals of the **indolylindoline 14**, m.p. 106–108°, ν_{max} 3480 and 3410 cm^{-1} (NH); λ_{max} 230 (33 500) and 288 nm (9900).

Anal. Calcd. for $C_{20}H_{22}N_2$ (290.4): C, 82.72; H, 7.64; N, 9.65. Found: C, 83.02; H, 7.68; N, 9.66.

(*iv*) The final petroleum ether eluates left 580 mg (14%) of colorless oily solid which on recrystallization from chloroform – petroleum ether gave 355 mg of colorless crystals of the **indolylindoline** stereoisomer **15**, m.p. 160–170°, R_f 0.44 ν_{max} 3440 and 3390 cm^{-1} (NH); λ_{max} 227 (31 900) and 285 nm (9500).

Anal. Calcd. for $C_{20}H_{22}N_2$ (290.4): C, 82.72; H, 7.64; N, 9.65. Found: C, 82.35; H, 6.92; N, 9.57.

(*v*) Elution with petroleum ether – benzene (60:40) gave 220 mg (5%) of colorless oil which was chromatographed again on four thick plates developed in petroleum ether–benzene (50:50). Extraction yielded 70 mg of colorless oil which solidified. On recrystallization from chloroform – petroleum ether the compound underwent dehydration and rearrangement to Berti's desoxy compound **18**, m.p. 178–183°, n.m.r., and u.v. spectrum identical with that of authentic synthetic **18** (see ref. 10).

(*vi*) Elution with chloroform gave 650 mg of a brown viscous mass which was chromatographed on four thick plates developed with ether–benzene (75:25). Extraction of the band at R_f 0.39 gave 55 mg of colorless solid, m.p. 162–174° (dec.) after recrystallization from methanol – petroleum ether. However, on standing in chloroform solution this product of unknown structure[13] was transformed into Berti's desoxy compound **18** before analysis.

N-Acetyl-2,3-dimethylindole

This compound was made according to a modification of the published procedure (17). A solution of 2,3-dimethylindole (4.0 g), camphor-10-sulfonic acid (40 mg), and acetic anhydride (40 ml) was refluxed for 9 h. The excess anhydride was distilled at reduced pressure, and the residue was percolated in benzene solution through a column of 100 g of silica gel. Evaporation of the eluate left 3.4 g (66%) of colorless crystalline amide which was used without further purification. A sample recrystallized from petroleum ether (b.p. 30–60°) had m.p. 68–70° (lit. (17) m.p. 74°), ν_{max} 1700 cm^{-1} (indole amide C=O); *m/e* 187 (molecular ion).

N-Acetyl-trans (and cis?) -2,3-dihydroxy-2,3-dimethylindoline (23)

The published procedure (18) was modified. To a stirred (magnetic bar) solution of *N*-acetyl-2,3-dimethylindole (2.0 g) in glacial acetic acid (3 ml) cooled in an ice–salt bath was added nitric acid (0.84 g) during 5 min. After being stirred for 1 h at room temperature, the reaction mixture was filtered to remove unreacted starting material. The filtrate was concentrated to one quarter of its volume at room temperature under reduced pressure. The residual viscous brown liquid was diluted with ether and allowed to stand overnight to complete the precipitation of solid. Filtration and washing with ether gave 0.66 g (28%) of yellowish **23** (single t.l.c. spot). Two recrystallizations from methanol gave 0.42 g of colorless crystals, m.p. 130–132° (lit. (18) m.p. 133–134°), ν_{max}(Nujol) 3420, 3300 (OH), and 1635 cm^{-1} (amide C=O); *m/e* 221 (molecular ion). The n.m.r. spectrum indicated the crystalline compound to be a mixture of the *trans* and *cis* stereoisomers. The mother liquors from the two recrystallizations were saved for the basic treatment described below.

Base Treatment of N-Acetyl-trans-2,3-dihydroxy-2,3-dimethylindoline (23)

The directions of Kershaw and Taylor (5) were followed. A mixture of 130 mg of **23**, m.p. 130–132° (single t.l.c. spot), in 1 *N* aqueous NaOH solution (5 ml) was refluxed. Within a few minutes a greenish-yellow fluorescent color had appeared. At the end of 1 h the reaction mixture was cooled and extracted with benzene. The organic layer was washed with water, dried, and evaporated to leave 85 mg (90%) of yellow **2,2-dimethyl indoxyl (25)**. The n.m.r. spectrum showed the absence of starting material **23** and dimer **1**, and t.l.c. gave a single spot corresponding to **25**. The n.m.r. spectrum of the crude product contained no peaks due to the dimer **1**. Recrystallization from petroleum ether gave yellow needles, m.p. 86–87.5° (lit. (8) m.p. 89–90°), ν_{max} 3420 (NH) and 1710 cm^{-1} (indoxyl C=O).

The mother liquors from the isolation of **23** in the experiment above were treated with refluxing sodium hydroxide as described above for pure **23**. The n.m.r. spectrum and t.l.c. of the crude product did show the presence of 5–10% of the dimer **1**, but no attempt was made to isolate it.

Thermal Decomposition of Dimer 1

Dimer (0.20 g) was heated at ~ 225° in a test tube for 1 h. The t.l.c. of the dark brown residue gave only one significant spot having the same R_f as the dimer. Chromatography on a thick plate developed with benzene–ether (50:50) gave a yellow band at R_f 0.59. Extraction of the band yielded 124 mg (62%) of yellow solid whose n.m.r. spectrum unambiguously showed it to be a mixture of 2,2-dimethylindoxyl (**25**) and the dimeric indoxyl **27** (see accompanying paper, ref. 10). No attempt was made to separate the mixture.

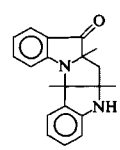

27

We would like to thank the National Research Council of Canada for financial support. We would also like to thank Dr. A. Taylor, NRCC Atlantic Regional Laboratory, Halifax, Nova Scotia, for his very helpful cooperation.

[13]The product had the same t.l.c. R_f as **17**, the $LiAlH_4$ reduction product (7) from **1**, but it was not investigated further.

1. W. C. SUMPTER and F. M. MILLER. *In* Heterocyclic compounds with indole and carbazole systems. *Edited by* A. Weissburger. Interscience Publishers, New York, N.Y., 1954.
2. W. I. TAYLOR. Indole alkaloids. Pergamon Press, Oxford, 1966.
3. E. W. WARNHOFF. *In* Molecular rearrangements. Part 2. *Edited by* P. de Mayo. Interscience Publishers, New York, N.Y., 1964. p. 841.
4. K. M. BISWAS and A. H. JACKSON. Tetrahedron, **24**, 1145 (1968).
5. J. W. KERSHAW and A. TAYLOR. J. Chem. Soc. 4320 (1964).
6. S. GHOSAL and S. K. DUTTA. Indian J. Chem. **7**, 135 (1969).
7. G. BERTI, A. DA SETTIMO, G. DI COLO, and E. NANNIPIERI. J. Chem. Soc. 2703 (1969).
8. R. J. S. BEER, T. DONAVANIK, and A. ROBERTSON. J. Chem. Soc. 4139 (1954).
9. S. MCLEAN, E. K. STRØM-GUNDERSEN, K. S. DICHMANN, J. K. FAWCETT, and S. C. NYBURG. Tetrahedron Lett. 2645 (1970).
10. V. DAVE and E. W. WARNHOFF. Chem. Commun. 919 (1970); Can. J. Chem. This issue.
11. J. F. KING. *In* Elucidation of structures by physical and chemical methods. Part 2. *Edited by* K. W. Bentley. Interscience Publishers, New York, N.Y., 1963. p. 347.
12. K. NAGARAJAN, M. D. NAIR, and P. M. PILLAI. Tetrahedron, **23**, 1683 (1967).
13. A. M. MONRO and M. J. SEWELL. Tetrahedron Lett. 595 (1969).
14. E. FISCHER. Ann. **236**, 129 (1886).
15. W. I. TAYLOR. Helv. Chim. Acta, **33**, 164 (1950).
16. C. S. MARVEL and F. D. HAGER. Org. Syn. **1**, 248 (1948); J. R. JOHNSON and F. D. HAGER. Org. Syn. **1**, 351 (1948).
17. S. G. P. PLANT and M. L. TOMLINSON. J. Chem. Soc. 955 (1933).
18. C. M. ATKINSON, J. W. KERSHAW, and A. TAYLOR. J. Chem. Soc. 4426 (1962).

Can. J. Chem. Downloaded from www.nrcresearchpress.com by 210.87.254.5 on 09/05/12
For personal use only.

Can. J. Chem. Downloaded from www.nrcresearchpress.com by 210.87.254.105 on 09/05/12
For personal use only.

Complex Rearrangements of the Dimer of 3-Hydroxy-2,3-dimethylindolenine[1]

VINOD DAVE AND E. W. WARNHOFF
Department of Chemistry, University of Western Ontario, London, Ontario

Received November 3, 1970

In the presence of acid the dimer **1** of 3-hydroxy-2,3-dimethylindolenine rearranges to **4**, and then via **6** to **7***a* which is cleaved to 2,3-dimethylindole (**2**) and 2-formyl-3-methylindole (**3**). If peroxides and oxygen are not excluded, two other products, **13** and **30**, are also formed. A rationalization of these reactions is offered which takes into account subtle differences in migratory aptitudes.

Le dimère **1** de l'hydroxy-3 diméthyl-2,3 indolénine se réarrange, en milieu acide, en **4** puis en **7***a* via **6**; **7***a* est scindé dans ces conditions en diméthyl-2,3 indole (**2**) et formyl-2 méthyl-3 indole (**3**). Si des précautions pour exclure les peroxydes et l'oxygène ne sont pas prises, deux autres produits, **13** et **30** sont aussi formés. La rationalisation proposée pour ces réactions fait appel à des différences subtiles dans les aptitudes migratrices des groupes.

Canadian Journal of Chemistry, 49, 1921 (1971)

During the accumulation of evidence for the structure **1** of the dimer ($C_{20}H_{22}N_2O_2$) of 3-hydroxy-2,3-dimethylindolenine presented in the preceding paper (1), the dimer was treated with acid (2). With hot hydrochloric acid in an organic co-solvent or with phosphoric acid the major products were 2,3-dimethylindole (**2**) and 2-formyl-3-methylindole (**3**), as noted by Berti *et al.* (3), with varying amounts of another crystalline compound ($C_{20}H_{20}N_2O_2$, m.p. 217°) formed if oxygen and/or traces of organic peroxides were present (see later).[2] In peroxide-free co-solvent and the absence of oxygen, the yield of equimolar amounts of **2** and **3** was nearly quantitative (t.l.c.). However, with dilute hydrochloric acid at room temperature, t.l.c. (benzene–ether 50:50) revealed intermediates (2). After about 1 h the only product detectable, **A** (R_f 0.34), was more polar than the dimer **1** (R_f 0.62). After longer periods (~3 h) another less polar compound **B** (R_f 0.46) appeared as well as the ultimate products **2** (R_f 0.81) and **3** (R_f 0.71). Compounds **A** and **B** are probably intermediates on the reaction path from the dimer **1** to **2** and **3** because pure **A** was shown to be transformed into **B**, **2** and **3** without any noticeable amount of dimer being reformed. Furthermore **B** was converted into **2** and **3** without any dimer or **A** becoming evident on t.l.c.

The structure of **B** was determined to be **7***a* in the following way. Initially it was a liquid which was purified through the crystalline *O*-acetate **7***b*, m.p. 175°, to obtain crystals, m.p. 169°, whose u.v. absorption contained both indole and indoline chromophores (Fig. 1). The compound was a secondary alcohol (δ_{CHOH} 5.00 → δ_{CHOAc} 6.31) with an indoline NH and three unsplit methyl groups, one of which (δ 2.35) was attached to the indole heterocyclic ring (Fig. 2*b*), thus accounting for all of its non-aromatic hydrogen atoms. Moreover, the n.m.r. spectrum of this alcohol prepared from the hexadeuterio dimer (1) lacked two methyl peaks, one being the indolic methyl. With this information plus the dual requirements that the action of acid on the dimer monoacetate **8** give *N*-acetyl indole and the aldehyde **3** (Scheme 1), and that acid treatment of the alcohol **B** yield **2** and **3**, there were only two reasonable structural possibilities, **7***a* or **15**. These isomers were distinguishable through their desoxy derivatives. Alcohol **B** could be converted by two different routes (Scheme 2) into its desoxy derivative, m.p. 126°, whose formation is, therefore, unlikely to have involved rearrangement. Firstly, sodium – *t*-butyl alcohol hydrogenolysis of alcohol **B** yielded the desoxy compound (either **10***a* or **18**) directly. Secondly, alcohol **B** was oxidized by the chromic acid – pyridine reagent to a pale yellow ketone, subsequently found to be **11**, m.p. 194°, which on mild Wolff–Kishner reduction at 155° gave, as the only product, the same desoxy compound, m.p. 126°. By direct comparison this desoxy derivative was *not* identical with a sample

[1]Presented in part at the 52nd Conference of the Chemical Institute of Canada, Montreal, Quebec, May 25–28, 1969.

[2]A fourth compound was occasionally isolated if peroxides were not excluded, and it is also discussed later.

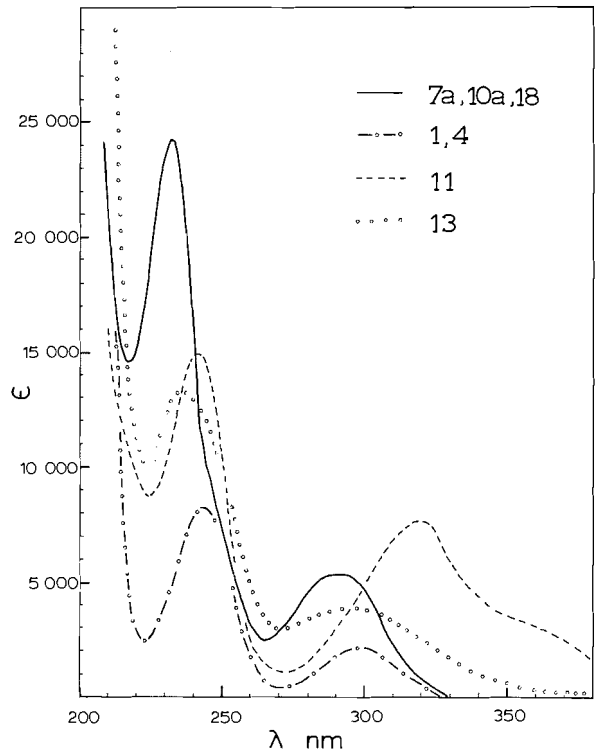

FIG. 1. The u.v. spectra of dimer **1** transformation products.

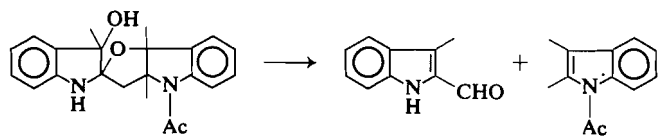

8 **3**

SCHEME 1

of **18**, m.p. 194°, prepared by the unambiguous synthesis of Berti *et al.* (4), which employs the Grignard reagent from 2,3-dimethylindole in a nucleophilic displacement of the pyridinium group of **16** (Scheme 3). (See Fig. 2*d* and *e* for the n.m.r. spectra of the two compounds.)

Although both **10***a* and **18** can exist as *cis* and *trans* racemates, the desoxy compound of m.p. 126° cannot differ from the synthetic compound **18** in stereochemistry alone. The formation of **18** occurs by closure of the central ring in a reversible reaction, amine addition to an imine, and results in the more stable, presumably *cis*, 5/5 ring fusion. If the alcohol precursor of the 126° desoxy compound, which alcohol is also formed by closure of the central ring, had had the structure **15**, it would also have been formed by the same reversible reaction and would necessarily have the same ring configuration as the synthetic desoxy compound **18**. Therefore, the 126° desoxy derivative must possess the other structure **10***a*. This assignment was confirmed by demonstrating that the 126° compound **10***a* did not undergo deuterium exchange under the same conditions that Berti's 194° compound **18** did incorporate deuterium into the methyl group (δ 1.79) adjacent to the potential imine (see **17**).

The initial, more polar compound **A** formed in acid is identical by direct comparison with the boron fluoride isomerization product of the dimer **1** reported by Berti *et al.* (3), whose procedure is the better preparative method. The u.v.

Can. J. Chem. Downloaded from www.nrcresearchpress.com by 210.87.254.105 on 09/05/12
For personal use only.

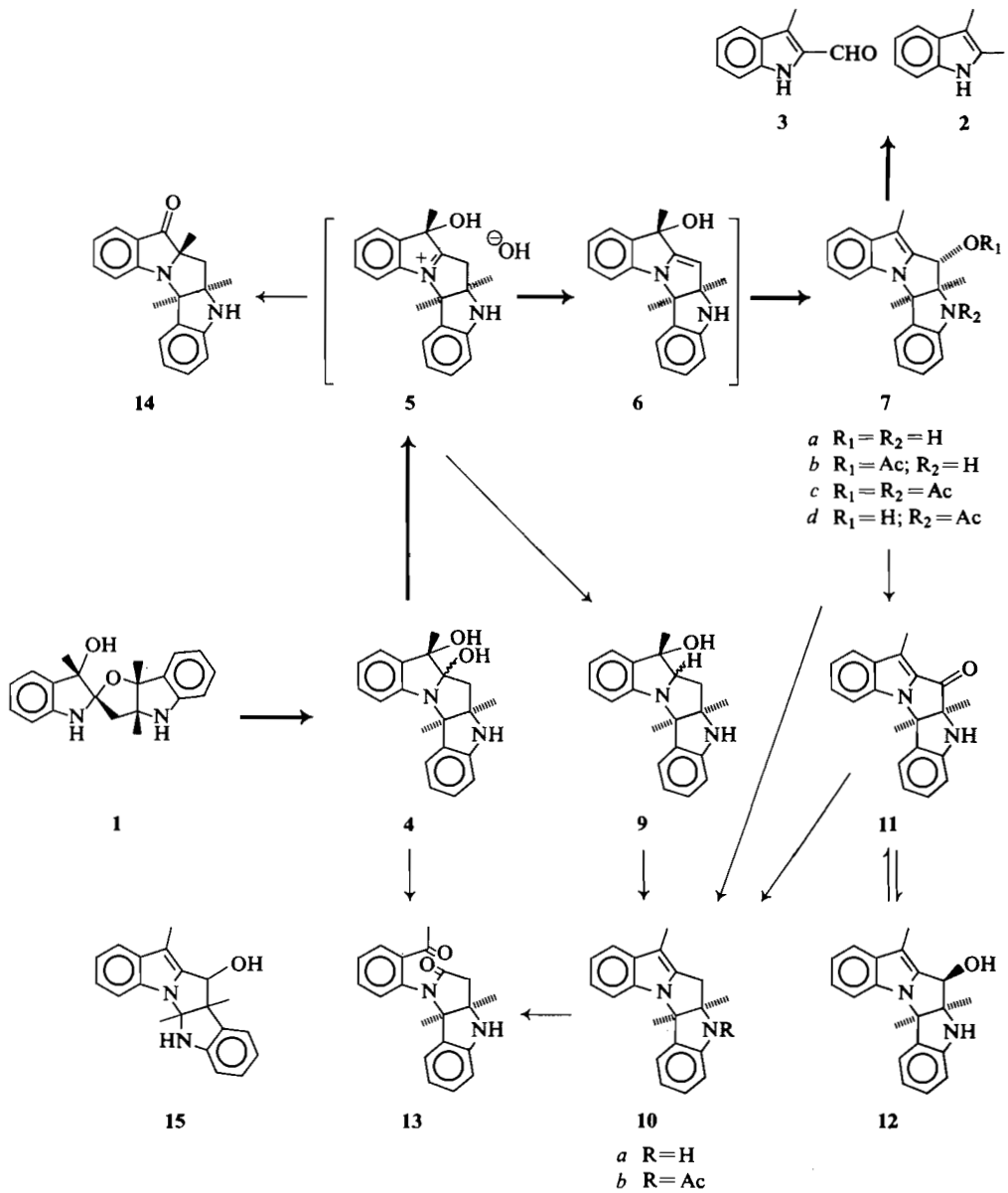

SCHEME 2

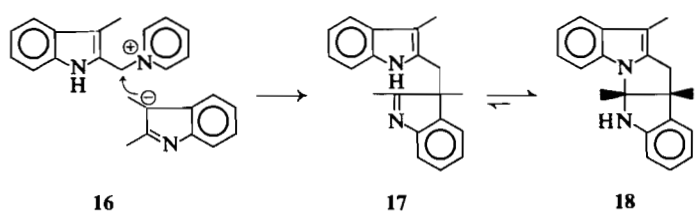

SCHEME 3

Can. J. Chem. Downloaded from www.nrcresearchpress.com by 210.87.254.105 on 09/05/12
For personal use only.

Can. J. Chem. Downloaded from www.nrcresearchpress.com by 210.87.254.105 on 09/05/12
For personal use only.

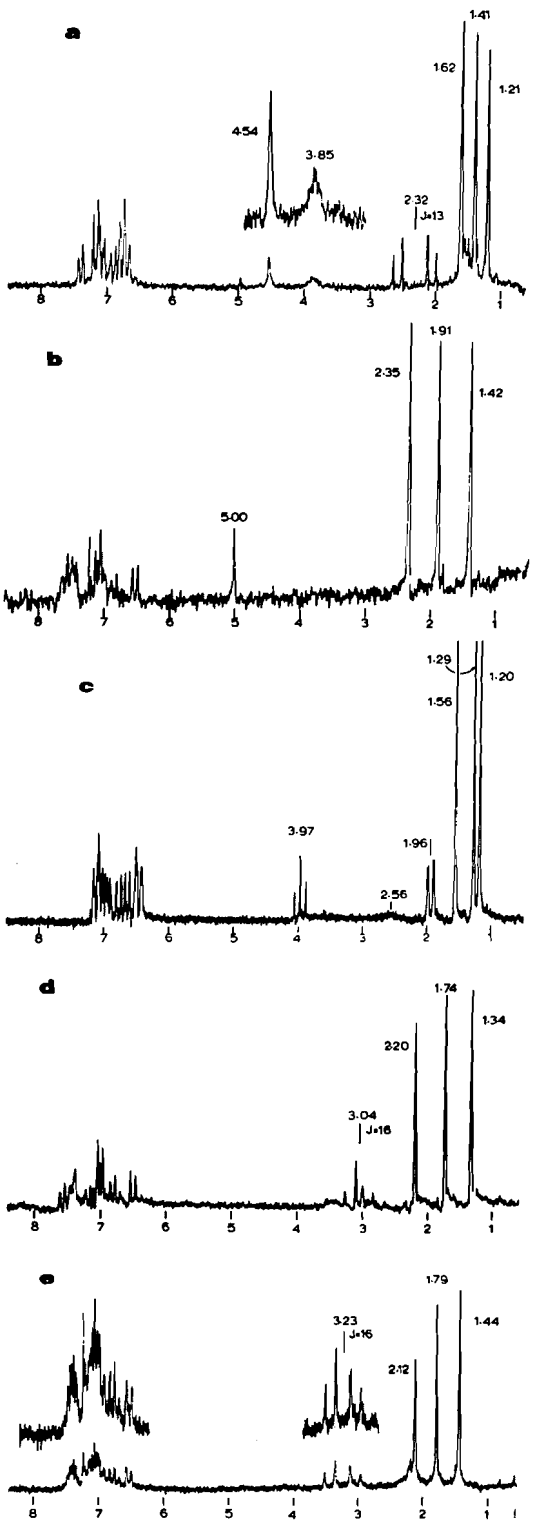

FIG. 2. The n.m.r. spectra ($CDCl_3$, 100 MHz) of diol **4** (*a*), alcohol **7***a* (*b*), sodium borohydride product **9** (*c*), 126° desoxy compound **10***a* (*d*), and Berti's 194° desoxy compound **18** (*e*).

spectrum (Fig. 1) contains two indoline chromophores while the n.m.r. spectrum (Fig. 2*a*) contains three unsplit methyl peaks and a methylene AB pattern. Intermediate **A** shows the properties of a carbinolamine in that it is readily reduced by sodium borohydride with loss of one oxygen atom. This borohydride product **9** (see Fig. 2*c* for the n.m.r. spectrum) is very sensitive to acid and readily loses a molecule of water to generate the 126° desoxy compound **10***a* encountered above. Acetylation of the borohydride product under mildly basic conditions also resulted in dehydration and formation of the *N*-acetyl derivative **10***b* of the 126° desoxy compound. It is unlikely that skeletal rearrangement occurred during the borohydride reduction or the acetylation,[3] and consequently the initial diol must be assigned structure **4** instead of the alternative **19** proposed by Berti *et al.* (3). It follows that the yellow indoxyl that is formed readily from diol **4** on heating or treatment with base must be **14** rather than **20** proposed by the same group (3).[4]

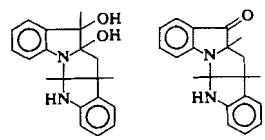

19 **20**

The vicinal relationship of the two hydroxyl groups in **4** was demonstrated by sodium periodate oxidation. Surprisingly, the same crystalline compound, $C_{20}H_{20}N_2O_2$, m.p. 217°, was obtained that was formed during acid treatment of the dimer in the presence of oxygen or peroxides (see above). Previously, the n.m.r. spectrum of this compound from the acid reaction had been very puzzling, but this second method of preparation provided the clue needed to realize that it must indeed be the ketone **13**. The i.r.

[3]However, acetylation of the diol **4**, which cannot be readily dehydrated to an indole, does proceed with rearrangement since the *O*,*N*-diacetate **7***c* of alcohol **B** was obtained.

[4]The structure of the indoxyl *N*-nitroso compound prepared by this group (3) must also be re-assigned; structure **14** with N–NO in place of NH would fit the reported n.m.r. effects on the methylene and (one) methyl groups.

Can. J. Chem. Downloaded from www.nrcresearchpress.com by 210.87.254.105 on 09/05/12
For personal use only.

spectrum contained both carbonyl (1680 cm^{-1})[5] and amino (3390 cm^{-1}) absorption. In the u.v. spectrum (Fig. 1) there were indoline and *o*-acylaminobenzoyl chromophores. The non-aromatic region of the n.m.r. spectrum in deuteriochloroform contained two narrow unsplit quaternary methyl signals (δ 1.35 and 1.52), a methylene AB pattern (δ 2.70 and 2.87, J = 17 Hz), an indoline NH (δ 4.18), but instead of a sharp three-proton singlet for the acetyl methyl group there was only a broad three-proton lump centered at δ 2.25. The explanation for this remarkable observation lies in rotation of the acetyl and heterocyclic groups being substantially hindered by their *o*-relationship. At 37° the deuteriochloroform solution is coincidentally near the coalescence point for conformations of the acetyl methyl group which have appreciably different chemical shifts due to varying anisotropic effects, and the absorption for this group is a broad ill-defined pattern. This signal is absent in the spectrum of **13** prepared from the hexadeuterio dimer in which the acetyl methyl is now a CD_3 group. A variable temperature study, the effects of various solvents, and the results of additional chemical experiments all fully confirm this interpretation.[6] Ketone **13** is also formed by periodate oxidation of the desoxyindole **10***a* according to Dolby's procedure (6). This transformation completes a web of reactions inter-relating compounds **4**, **7**, **9**, and **10** and providing assurance that they all have the same C, H, N skeleton.

The origin of the same ketone **13** during the acid-catalyzed rearrangement of the dimer is understandable after the first stage of the reaction sequence. The carbinolamine **4** on loss of hydroxide ion could then undergo addition of any hydroperoxide present (or formed by air oxidation during reaction) to form **21**. Breakdown as indicated would yield the keto pyrrolidone **13** just as Witkop and Patrick (5) have found for the reaction of hydroxyindolenines with peracid. In fact, when precautions were taken to exclude both oxygen and peroxides in the solvent, no **13** was formed in the acid-catalyzed reaction.

The evidence presented above strongly supports the probable sequence of reactions (Scheme 2) for the acid-catalyzed reaction to be rearrangement of the dimer **1** to diol **4**, dehydration of the carbinolamine to the enamine **6** (postulated) via **5**, allylic rearrangement of the enamine to the indole alcohol **7***a* (well precedented by the work of Taylor (7)), and finally cleavage of the alcohol as indicated in **31** to 2,3-dimethylindole (**2**) and 2-formyl-3-methylindole (**3**). This mechanism is

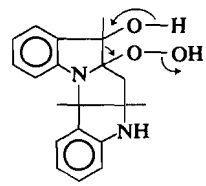

21

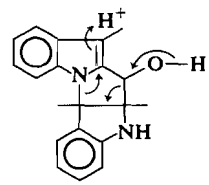

31

supported by the fact that rearrangement of the dimer in DCl–D_2O gives alcohol **7***a*-d_1 (see Scheme 4) with the deuterium atom on the carbon atom bearing the hydroxyl group, and this alcohol is further transformed by phosphoric acid into 2-formyl-3-methylindole-d_1 bearing the deuterium atom in the aldehyde function.

Although the overall driving force toward the cleavage products is the reformation of two stable indole systems from the dimer, it must be asked why, with such good grounds for divorce, the partners of this union choose this roundabout route (**1** → **4** → **5** → **6** → **7***a* → **2** + **3**) to sever relations when there is an apparently more direct way (**1** → **22** → **23** → **24** → **2** + **3**, Scheme 5) that does not involve formation of a new N–C bond. Part of the answer is that the carbinolamine ether ring is more reluctant to open and enolize than might be expected, perhaps due to the intramolecular hydrogen bonding of OH and NH groups (8). The dimer was not affected by sodium borohydride in refluxing methanol, although it was reduced to the dihydroderivative **26** by lithium aluminum hydride (3). The dimer slowly incorporates up to two *C*-deuterium atoms in refluxing methanol-*O*-d_1 containing sodium methoxide (~20% deuteration in 12 h, but with no rearrangement to indoxyl detectable by n.m.r.

[5]The carbonyl absorption of *N*-phenylpyrrolidone is at 1684 cm^{-1} and the ketone carbonyl absorption of *o*-acetamidoacetophenone is at 1650 cm^{-1}. The model compound **i** has a single carbonyl peak at *ca.* 1670 cm^{-1} (5).

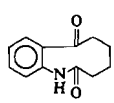

i

[6]Dave and Warnhoff, unpublished work to be submitted to Can. J. Chem.

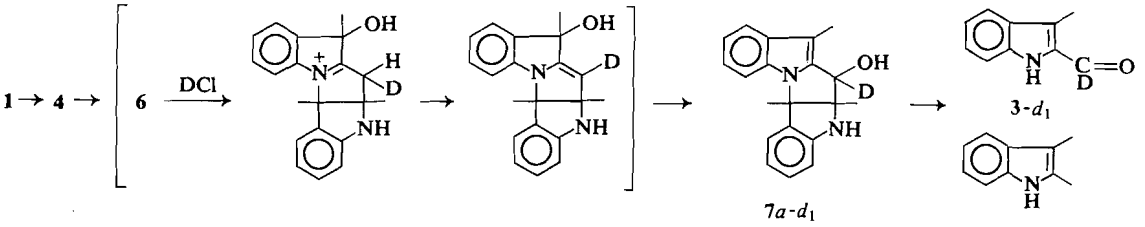

SCHEME 4

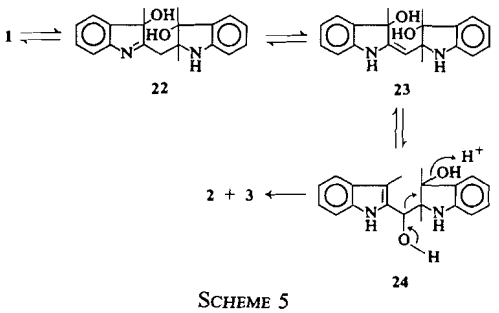

SCHEME 5

in this time).[7] In dilute deuteriochloric acid – acetone-d_6 solution when rearrangement was allowed to proceed part way, only 15% of the recovered dimer had incorporated *C*-deuterium atoms after ½ h at room temperature. The observed slow rates of the forward steps leading to **22** and **23** together with the fast back reactions (undetectable equilibrium concentration of **22** and **23** in n.m.r. solutions of **1**) and the slowness of the allylic rearrangement **23** → **24** (*cf.* the slow rate of **4** → **6** → **7***a*), all combine to allow the alternative rupture of one of the benzylic oxygen bonds to become a competitive process.

Loss of a protonated hydroxyl group from the dimer should lead by migration of the adjacent *trans*-situated methylene group to **29** (or a transformation product thereof) (Scheme 6), which was not found among the products of the acid treatment. However, in the absence of anchimeric

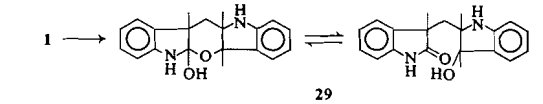

SCHEME 6

assistance the loss of this hydroxyl group might be slower than scission of the protonated benzylic ether bond because of the additional electronegative substituent in the β-position with respect to the hydroxyl group. Once the benzylic ether bond is broken, the subsequent attachment of nitrogen to form the five-membered ring of **4** is expected,[8] and the remainder of the route to **2** and **3** is thereby fixed. This ring closure takes place *without* migration of the methylene group from the 2- to the 3-position, probably because the migrating efficiency of the methylene group with an adjacent carbinolamine (or imine) function is reduced. Nevertheless, $C_2 \rightarrow C_3$ migration can occur when the methylene group has fewer electronegative groups nearby as in Berti's dihydrodimer **26** from lithium aluminum hydride reduction of **1**. On heating (3) or treatment with acid (see Experimental) this compound undergoes loss of water, rearrangement, and ring closure (**26** → **18**, Scheme 7). The migrating group is either the β-aminomethylene of **26** or, more likely, the methylene of **27** resulting from loss of the first molecule of water because this same indole **27** obtained in the sodium – *t*-butanol reduction of the dimer also undergoes dehydration with migration of the benzylic methylene group (**27** → **28** → **18**) on standing in chloroform solution (1).[9]

[7]However, heating the dimer to its melting point does result in rearrangement to a mixture of indoxyl **14** and the decomposition product 2,2-dimethylindoxyl (**25**) (1). The decomposition is presumably initiated by a retro Mannich reaction:

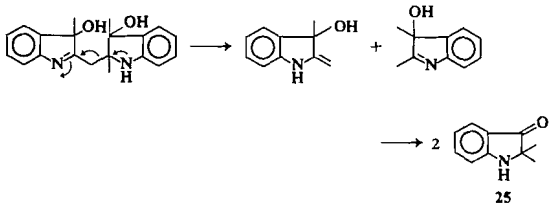

This behavior probably accounts for the dimer's wide and variable melting point.

[8]Ring formation cannot be a concerted S_N2 displacement of the protonated ether because inversion at the carbon atom undergoing displacement cannot occur so long as the carbinolamine ether is intact.

[9]Several of the compounds in the present work (**9**, **26**, **27**, and the most polar sodium – *t*-butanol reduction product from **1** (1)) were unstable in chloroform solution due to dehydration and rearrangement presumably catalyzed by hydrogen chloride formed either on exposure of these solutions to light or else from reaction of a basic nitrogen atom with the chloroform.

Can. J. Chem. Downloaded from www.nrcresearchpress.com by 210.87.254.105 on 09/05/12
For personal use only.

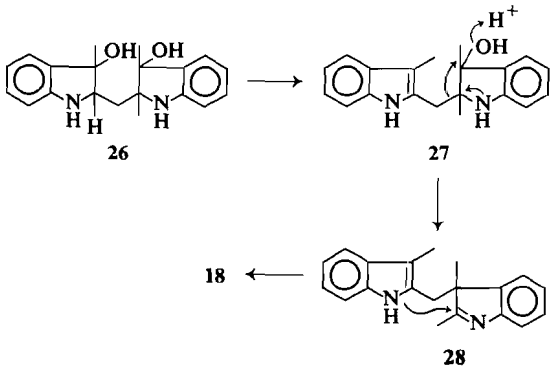

SCHEME 7

The relative stereochemistry of these compound can now be specified. When the dimer rearranges to **4**, only the *cis* stereochemistry of the fused pyrrolidine rings would be expected to result, and the all *cis* orientation of the methyl groups of **1** (8) would therefore become the *trans,trans,cis* arrangement shown in **4** after the required rotation of the right hand indoline moiety of **1**. For the two alcohol stereoisomers **7***a* and **12** which are epimeric only at the hydroxyl-bearing carbon atom, the stereochemistry depicted is assigned because formation of an alcohol by allylic rearrangement of **6** should occur by attack of water at the less hindered side of the carbon atom away from the fold of the molecule, while the hydroxyl group resulting from hydride reduction of ketone **11** should be in the more hindered position because hydride is donated to the less protected side.

The earlier mentioned second artifact found when peroxides were not excluded from the acid treatment of dimer in dioxane co-solvent proved to be **30**, a molecule of 2,3-dimethylindole and one of 2-formyl-3-methylindole joined at the nitrogen atoms by a methylene bridge presumably from formaldehyde or its precursor. Since treatment of these two indoles **2** and **3** with formaldehyde and acid gave no **30**, the two nitrogen atoms must have been joined earlier in the reaction sequence. When dimer **1** was treated with formaldehyde under the conditions for the acid-catalyzed rearrangement, it was changed completely into **30** within 15 min, much faster than the rearrangement sequence. However, under milder conditions (more dilute acid, shorter reaction time) the dimer was converted exclusively into the crystalline homo compound **32**. The formation of this product is not surprising in view of the stereochemistry of the dimer (8, 1). Acid treatment of **32** gave **30** quantitatively. Although the product is basically **2** + **3**, this latter rearrangement cannot take place by the path established for the dimer itself, and presumably occurs by some variation of it. The reaction was not investigated further.

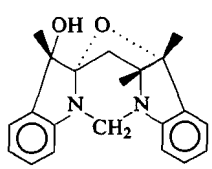

32

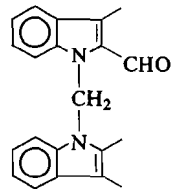

30

Experimental[10]

Cleavage of Dimer 1 by Phosphoric Acid

To a solution of the dimer (200 mg) in warm 95% ethanol (5 ml) was added 85% H_3PO_4 (3.5 ml). The solution, which immediately became a cherry red to dark brown color, was stirred at room temperature for 2.5 h. The reaction mixture was diluted with water and extracted with ether. Evaporation of the water-washed and dried ethereal solution left 193 mg (~100%) of yellowish solid whose t.l.c. (benzene–ether, 1:1) had only two spots corresponding to **2** and **3**. The crude product was chromatographed on alumina (5 g). Petroleum ether eluted 65 mg of colorless crystalline **2,3-dimethylindole** (**2**). Petroleum ether – benzene (1:1) eluted 85 mg of **2-formyl-3-methylindole** (**3**), m.p. 137–140° (lit. (9) m.p. 139–140°) after two recrystallizations from chloroform – petroleum ether; ν_{max} 3550 (NH) and 1650 cm^{-1} (conj. C=O); λ_{max} 241 (4000) and 315 nm (6500).

Preparation of the Diol 4

(a) By the Action of Hydrochloric Acid on Dimer 1

To a stirred solution of the dimer (1.00 g) in acetone (25 ml) was added a solution of 0.1 *N* HCl (2 ml) and acetone (5 ml). After 1 h at room temperature the yellow solution was diluted with water and extracted with ether. The organic layer was dried and concentrated to leave 1.10 g of a pale yellow liquid whose t.l.c. had only two spots corresponding to **4** and **1**. Chromatography on four thick layer plates developed in benzene–ether (50:50) and ether extraction of the band at R_f 0.33 gave 220 mg of pale yellow oil. Further purification of this material on three thick-layer plates gave 85 mg (8.5%) of almost colorless oil which solidified. Recrystallization from ether – petroleum ether (b.p. 30–60°) gave colorless crystals of the **diol 4**, m.p. 115–125° (dec.).

Anal. Calcd. for $C_{20}H_{22}O_2N_2$ (322.4): C, 74.51; H, 6.88; N, 8.69. Found: C, 75.15; H, 7.14; N, 8.54.

The i.r., u.v., and n.m.r. spectra were identical with those of the compound prepared with boron trifluoride in section *b* below.

A yellow band (R_f 0.58) on some of the t.l.c. plates was found to contain the indoxyl **14**, m.p. 190–196° (lit. (3) m.p. 200–210°) after recrystallization from chloroform –

[10]For general experimental methods see the preceding paper (1). The n.m.r. data are given in Table 1.

Can. J. Chem. Downloaded from www.nrcresearchpress.com by 210.87.254.105 on 09/05/12
For personal use only.

TABLE 1. The n.m.r. data exclusive of aromatic protons*

Compound	Absorption
Diol **4**	1.21 (s, 2-Me), 1.41 (s, 3-Me), 1.62 (s, 3-Me), 2.08 and 2.56 (AB of CH_2, J = 13), 3.85 (NH), 4.54 (OH)
Diol **4**-d_6	1.21 (s, 2-Me), 2.08 and 2.56 (AB of CH_2, J = 13) [spectrum too weak to see NH and OH]
$NaBH_4$ product **9**	1.20 (s, 2-Me), 1.29 (s, 3-Me), 1.56 (s, 3-Me), 1.96 (center of complex AB of CH_2), 2.56 (b, OH or NH), 3.65 (v.b, NH or OH), 3.97 (center of 1H 3-line pattern, 9Hz spacing)
Alcohol **7***a*	1.42 (s, 2-Me), 1.91 (s, 3-Me), 2.35 (s, indole Me), 5.00 (s, C*H*OH) [OH and NH too broadened to be noticeable]
Alcohol **7***a*-d_6	1.41 (s, 2-Me), 5.00 (s, C*H*OH)
Alcohol **7***a*-d_1	Same as spectrum of alcohol **7***a* except that the 1H peak at δ 5.00 missing
O-Acetate **7***b*	1.31 (s, 2-Me), 1.91 (s, 3-Me), 2.08 (s, OCOMe), 2.27 (s, indole Me), 4.00 (NH), 6.31 (s, C*H*OAc)
N-Acetate **7***d*	1.68 (s, 2-Me), 1.95 (s, 3-Me), 2.31 (s, indole Me), 2.42 (s, NCOMe) [spectrum too weak to locate C*H*OH]
O,*N*-Diacetate **7***c*	1.62 (s, 2-Me), 1.98 (s, 3-Me), 2.10 (s, OCOMe), 2.30 (s, indole Me or NCOMe), 2.35 (s, NCOMe or indole Me), [C*H*OAc indistinguishable among aromatic protons]
Alcohol **12**	1.35 (s, Me), 1.75 (s, Me), 2.33 (s, indole Me), 3.02 (2H, NH + OH), 5.00 (s, C*H*OH)
O-Acetate of **12**	1.47 (s, Me), 1.85 (s, Me), 2.05 (s, OCOMe), 2.23 (s, indole Me), 4.30 (NH), 6.12 (s, C*H*OAc)
Ketone **11**	1.49 (s, Me), 2.01 (s, Me), 2.54 (s, indole Me), 4.70 (NH)
126° Desoxy compound **10***a*	1.34 (s, 2-Me), 1.74 (s, 3-Me), 2.20 (s, indole Me), 2.96 and 3.12 (AB of CH_2, J = 16) [NH not observable]
N-Acetate of 126° compound **10***b*	1.62 (s, 2-Me), 1.75 (s, 3-Me), 2.18 (s, indole Me), 2.31 (s, NCOMe), 3.08 and 4.34 (AB of CH_2, J = 17)
194° Desoxy compound **18**	1.44 (s, 3-Me), 1.79 (s, 2-Me), 2.12 (s, indole Me), 3.06 and 3.42 (AB of CH_2, J = 16) [NH not observable]
Ketone **13**	1.35 (s, Me), 1.52 (s, Me), 2.25 (b.l. COMe), 2.70 and 2.87 (AB of CH_2, J = 17), 4.18 (NH)
Ketone **13**-d_6	1.35 (s, Me), 2.70 and 2.87 (AB of CH_2, J = 17), 4.18 (NH)
Indoxyl **14**	1.17 (s, Me), 1.41 (s, Me), 1.43 (s, Me), 2.02 and 2.16 (AB of CH_2, J = 13), 3.72 (b, NH)
Dihydrodimer **26** (Pyridine solution)	1.28 (s, Me), 1.41 (s, Me), 1.59 (s, Me), 2.16 and 2.74 (AB of CH_2, J = 13), 4.28 (1H, X of ABX, $J \sim 6$, ~ 6)
Homodimer **32**	1.21 (s, 2-Me), 1.50 (s, di-3-Me), 2.10 (s, CH_2), 3.30 (s, OH), 4.10 and 4.59 (AB of NCH_2N, J = 11)
The methylene bis indole **30**	2.13 (s, di Me), 2.61 (s, Me), 6.80 (s, NCH_2N) 10.00 (s, CHO)

*Chemical shifts are given in p.p.m. from tetramethylsilane (δ) and coupling constants in Hz; $CDCl_3$ solutions unless otherwise specified; 2-Me and 3-Me signify that the methyl group giving rise to the absorption originated from a 2- or 3-methyl group of 2,3-dimethylindole, respectively; s = singlet, d = doublet, b = broad absorption, l = lump.

petroleum ether. The i.r. and n.m.r. spectra were identical with those reported (3).

(b) By the Action of Boron Trifluoride on Dimer **1**

The procedure is that of Berti *et al.* (3), slightly modified. A solution of dimer (200 mg) in chloroform (20 ml) was chilled in an ice-salt bath and treated with a mixture of boron trifluoride etherate (0.2 ml) and chloroform (0.2 ml). After 5 min the yellow reaction mixture was diluted with 2 *N* Na_2CO_3 solution and extracted with ether. The pale yellow oil (185 mg) obtained after evaporation of the water-washed and dried organic layer was chromatographed on a thick plate developed with benzene–ether (50:50). Extraction of the band at R_f 0.32 gave 23 mg (11%) of almost colorless solid **4**. Recrystallization from ether – petroleum ether (b.p. 30–60°) gave colorless crystals, m.p. 114–125° (dec.) (lit. (3) m.p. 112–122° (dec.)); ν_{max} 3580, 3360, and 3340 (shoulder) cm^{-1} (NH and OH); λ_{max} 250 (8000) and 298 nm (3400).

(c) By the Action of Boron Trifluoride on Dimer **1**-d_6

The reaction was carried out on 54 mg of **1**-d_6 (1) as described in section *b*. There was obtained 53 mg of diol **4**-d_6 (90% pure by t.l.c.) whose n.m.r. spectrum was lacking the methyl peaks at δ 1.41 and 1.62 of the protio analog.

Borohydride Reduction of Diol **4**

A solution of the diol (35 mg), methanol (6 ml), and $NaBH_4$ (50 mg) was allowed to stand at room temperature for 4 h. The methanol was removed at reduced

Can. J. Chem. Downloaded from www.nrcresearchpress.com by 210.87.254.105 on 09/05/12
For personal use only.

Can. J. Chem. Downloaded from www.nrcresearchpress.com by 210.87.254.105 on 09/05/12
For personal use only.

pressure, and the residue was treated with water. Extraction with chloroform yielded 37 mg of colorless oily solid after evaporation of the water-washed and dried solution. The t.l.c. gave a single spot slightly more polar than **4**. Recrystallization from ether – petroleum ether (b.p. 30–60°) gave colorless crystals of **9**, m.p. 128–140°; ν_{max} 3575 (OH) and 3380 cm^{-1} (NH); λ_{max} 247 (8800) and 295 nm (5100).

Anal. Calcd. for $C_{20}H_{22}N_2O$ (306.4): C, 78.40; H, 7.24; N, 9.14. Found: C, 78.77; H, 7.31; N, 9.06.

When a chloroform solution of **9** was allowed to stand in an open vessel at room temperature for 3 days, it was found to have been dehydrated to **10***a*. The n.m.r. spectrum, m.p., mixed m.p., and t.l.c. behavior were identical with that of authentic **10***a*.

Acetylation of Borohydride Product **9**

A mixture of the borohydride reduction product (100 mg), sodium acetate (100 mg), and acetic anhydride (2.0 ml) was heated at 140° (bath temperature) for 12 h. The cooled mixture was added to 5% $NaHCO_3$ solution and extracted with chloroform. The organic layer was washed with water, dried, and evaporated to leave 104 mg (96%) of yellowish solid which was essentially pure (t.l.c.). Recrystallization from chloroform – petroleum ether gave colorless crystals of the **N-acetyl desoxy compound 10***b*, m.p. 273–275°; ν_{max} 1637 cm^{-1} (amide C=O); λ_{max} 232 (18 000), 285 (8900), and 290 nm (4400); *m/e* 330 (molecular ion).

Anal. Calcd. for $C_{22}H_{22}N_2O$ (330.4): C, 79.97; H, 6.71; N, 8.48. Found: C, 79.90; H, 6.31; N, 8.48.

Preparation of the Alcohol 7a

(a) From Dimer and Hydrochloric Acid

To a stirred (magnetic bar) solution of the dimer **1** (100 mg) in *p*-dioxane (2.5 ml Baker Analyzed freshly distilled from $LiAlH_4$) under a nitrogen atmosphere was added at room temperature a solution of 0.1 *N* HCl (0.2 ml) in the same dioxane (0.2 ml). The solution immediately became pale yellow changing successively to dark yellow, pale brown, and finally dark brown. After 5.5 h the reaction mixture was diluted with chloroform, washed once with water, dried, and concentrated at reduced pressure to leave 102 mg of brownish black viscous liquid. Chromatography on a thick plate developed with benzene–ether (75:25) gave a band (R_f 0.66) from which 15 mg of pale yellow oil was isolated. The n.m.r. spectrum of this fraction revealed it to be a mixture of the dimer **1**, 2-formyl-3-methylindole (**3**), and an unknown component. From a band with R_f 0.39 was extracted 51 mg (54%) of pure (t.l.c.) almost colorless liquid **alcohol 7***a*. Attempts to induce crystallization were unsuccessful. However, the crystalline compound was obtained by saponification of the crystalline *O*-acetate (see below) with sodium hydroxide in methanol at room temperature. The oily solid from the saponification was recrystallized from methanol to give colorless crystals of **7***a*, m.p. 162–169°; ν_{max} 3585 (OH) and 3380 cm^{-1} (NH); λ_{max} 232 (25 000) and 297 nm (6300); *m/e* 304 (molecular ion).

Anal. Calcd. for $C_{20}H_{20}N_2O$ (304.4): C, 78.92; H, 6.62; N, 9.20. Found: C, 78.77; H, 7.03; N, 9.09.

The n.m.r. and i.r. spectra as well as the t.l.c. behavior of the crystalline material were identical with those of the liquid alcohol obtained from the reaction with HCl.

Essentially the same results were obtained when acetone was used in place of dioxane as the organic cosolvent. If reagent grade *p*-dioxane was used without purification for the reaction, varying amounts of two other compounds were formed in addition to the alcohol **7***a* when the reaction was conducted under a nitrogen atmosphere. One of these appeared in the least polar t.l.c. band (R_f 0.85) whose extraction yielded a pale yellow solid which was recrystallized from petroleum ether to give very pale yellow clusters of needles of **30**, m.p. 146–147.5°; ν_{max} 1650 cm^{-1} (conj. C=O), NH absorption absent; λ_{max} 230 (25 000) and 315 nm (13 000); *m/e* 316 (molecular ion).

Anal. Calcd. for $C_{21}H_{20}N_2O$ (316.4): C, 79.72; H, 6.37; N, 8.85. Found: C, 79.15; H, 6.40; N, 8.69.

A second artifact, the ketone **13**, is described later.

(b) From Diol **4**

To a stirred (magnetic bar) solution of the diol (~90% pure by t.l.c.) (35 mg) in acetone (1.5 ml) was added a solution of 0.1 *N* HCl (0.2 ml) in acetone (0.5 ml). After 4 h at room temperature during which the color of the solution changed from yellow to pink to brown to almost black, most of the solvent was removed at reduced pressure on the rotary evaporator. A chloroform solution of the residue was washed with water, dried, and evaporated to leave 27 mg of clear amber liquid whose i.r. and n.m.r. spectra as well as t.l.c. behavior were identical with those of **alcohol 7***a* prepared in section *a* above.

(c) From Dimer **1** *and Deuteriochloric Acid*

To a stirred (magnetic bar) solution of the dimer **1** (80 mg) in dioxane (1 ml, freshly distilled from $LiAlH_4$) was added a solution of 0.1 *N* DCl in D_2O (0.25 ml). The solution was kept at room temperature for 3 h, then diluted with chloroform, washed with water, dried, and evaporated. The 72 mg of residual brown oil was chromatographed on a thick plate developed in benzene – petroleum ether (75:25). Extraction of the band at R_f 0.34 gave 18 mg (24%) of the liquid **alcohol 7***a*-d_1 whose n.m.r. spectrum lacked the carbinyl proton (< 5%) present at δ 5.00 in the protio compound. The crystalline acetate, m.p. 173–177° was prepared for mass spectroscopy; *m/e* 347 (molecular ion corresponding to monodeuteration).

Phosphoric Acid Cleavage of Alcohol 7a-d_1

To a stirred (magnetic bar) solution of monodeuterio alcohol **7***a*-d_1 (140 mg) in 95% ethanol (2 ml) was added 85% H_3PO_4 (1 ml), and the reaction mixture was kept at room temperature for 3 h. The solution was diluted with ether, washed twice with water, dried, and concentrated to 118 mg of brown oily solid. The t.l.c. in benzene–ether (50:50) gave only two spots which corresponded to **2** and **3** in about equal amounts. Chromatography on alumina (5 g) gave 20 mg of colorless 2,3-dimethylindole (**2**) from the petroleum ether eluates. Elution with petroleum ether – benzene (50:50) gave 52 mg (70%) of pale yellow solid 2-deuterioformyl-3-methylindole (**3**-d_1). Recrystallization gave colorless plates, m.p. 137–140°; *m/e* 160 (molecular ion corresponding to monodeuteration), whose n.m.r. spectrum lacked the formyl proton.

Elution with chloroform yielded 42 mg of brown oily solid whose t.l.c. behavior and n.m.r. spectrum showed it to be the dimer **1**, presumably formed by air oxidation of the 2,3-dimethylindole.

Can. J. Chem. Downloaded from www.nrcresearchpress.com by 210.87.254.105 on 09/05/12
For personal use only.

*Reaction of Dimer Monoacetate **8** with Acid*

A solution of **8** (200 mg), acetone (4 ml), and HCl (0.8 ml of 0.1 *N* aqueous HCl) was refluxed for 2 h. Evaporation of the acetone and partition of the residue between chloroform and water gave 180 mg of crude product which was chromatographed on two thick plates developed with benzene–ether (88:12). The band at R_f 0.71 yielded 15 mg of colorless crystalline *N*-acetyl-2,3-dimethylindole identical with an authentic specimen. The band at R_f 0.53 yielded 7 mg of colorless crystalline 2-formyl-3-methylindole (**3**) identical with an authentic specimen. More polar products (48 mg) on the base line had a complex n.m.r. spectrum and were not investigated further.

O-Acetate of Alcohol 7a

A solution of the liquid alcohol (55 mg), pyridine (0.5 ml), and acetic anhydride (0.5 ml) was allowed to stand at room temperature for 5 h. After the addition of chloroform, the reaction mixture was washed with water, dried, and concentrated to leave 72 mg of a brown viscous oil. Chromatography on alumina (3 g) gave a white solid on elution with petroleum ether – benzene (80:20). Recrystallization from methanol – petroleum ether gave 23 mg (38%) of colorless crystals of 7*b*, m.p. 172–175°; ν_{max} 3371 (NH), and 1732 cm^{-1} (*O*-acetate C=O); λ_{max} 230 (26 000) and 295 nm (7000); *m/e* 346 (molecular ion).

Anal. Calcd. for $C_{22}H_{22}N_2O_2$ (346.4): C, 76.28; H, 6.40; N, 8.09; O, 9.24. Found: C, 76.81; H, 6.26; N, 8.29; O, 9.22.

N-Acetate of Alcohol 7a

To a solution of the *O,N*-diacetate 7*c* (180 mg) in a mixture of methanol (3 ml) and dioxane (3 ml) was added sodium hydroxide (3 pellets) with stirring at room temperature. Within 15 min solid began to precipitate. After 30 min water was added, and the mass was extracted with chloroform. The organic layer was washed with water, dried, and concentrated to leave 135 mg of pale yellowish solid. Recrystallization from chloroform–methanol gave colorless crystals of pure 7*d*, m.p. 268–280°; ν_{max} (Nujol) 3280 (OH) and 1625 cm^{-1} (amide C=O); *m/e* 346 (molecular ion).

Anal. Calcd. for $C_{22}H_{22}N_2O_2$ (346.4): C, 76.28; H, 6.40; N, 8.09. Found: C, 76.53; H, 6.32; N, 7.89.

O,N-Diacetate of Alcohol 7a

*(a) From Diol **4***

A mixture of the diol (320 mg), pyridine (5 ml), sodium acetate (320 mg), and acetic anhydride (2 ml) was heated at 120° for 17 h. The cooled reaction mixture was added to 5% aqueous $NaHCO_3$ and extracted with chloroform. The organic layer was washed with water, dried, and evaporated to give 327 mg of a brown solid. Recrystallization from chloroform–methanol gave 78 mg of colorless crystals of the *O,N*-diacetate 7*c*, m.p. 245–252° (capillary sealed under vacuum); ν_{max} 1735 (*O*-acetate C=O) and 1650 cm^{-1} (amide C=O); *m/e* 388 (molecular ion).

Anal. Calcd. for $C_{24}H_{24}N_2O_3$ (388.5): C, 74.21; H, 6.23; N, 7.21. Found: C, 74.42; H, 6.33; N, 7.10.

(b) From Alcohol 7a

A mixture of alcohol (70 mg), pyridine (1 ml), sodium acetate (70 mg), and acetic anhydride (0.5 ml) was heated at 120° for 17 h. Work-up as in section *a* gave 68 mg of viscous brown oil which was chromatographed on a thick plate developed with benzene–ether (50:50). The band at R_f 0.60 yielded 31 mg (47%) of colorless solid. On recrystallization from chloroform – petroleum ether there was obtained 18 mg of colorless crystals of 7*c*, m.p. 245–250° (capillary sealed under vacuum), undepressed on admixture with the sample prepared from the diol **4** in section *a*. The two samples had identical i.r., n.m.r., and t.l.c. data.

(c) Saponification

A solution of the *O,N*-diacetate 7*c* (30 mg), NaOH (2 pellets), methanol (2 ml), and dioxane (2 ml) was refluxed for 4 days. After evaporation of solvent and addition of water, the product was extracted with chloroform. The organic solution was washed with water, dried, and evaporated to leave 24 mg of pale yellow oily alcohol 7*a*, whose t.l.c. behavior and n.m.r. spectrum were identical with those of authentic alcohol 7*a*.

*Ketone **11***

(a) From Liquid Alcohol 7a

To a stirred solution of the liquid alcohol 7*a* (200 mg, 0.66 mmol) in pyridine (2 ml) at room temperature was added CrO_3 (200 mg, 2.00 mmol) during 5 min. After the mixture was stirred at room temperature for 24 h, it was partitioned between water and chloroform. The organic layer was washed with water, dried, and evaporated to leave 183 mg of a violet oil which was chromatographed on alumina (3 g). Elution with petroleum ether – benzene (80:20) afforded 48 mg (25%) of yellow solid **ketone 11**. Recrystallization from methanol gave 17 mg of pale yellow crystals, m.p. 192–194°; ν_{max} 3370 (NH) and 1690 cm^{-1} (conj. ketone); λ_{max} 242 (15 000) and 322 nm (8500); *m/e* 302 (molecular ion).

Anal. Calcd. for $C_{20}H_{18}N_2O$ (302.4): C, 79.44; H, 6.00; N, 9.26. Found: C, 78.76; H, 5.81; N, 9.53.

*(b) From $LiAlH_4$ Alcohol **12***

A solution of alcohol **12** (150 mg, 0.49 mmol) in pyridine (3 ml) was oxidized at room temperature by addition of CrO_3 (150 mg, 1.5 mmol) in the same procedure used in section *a* above. There was obtained 12 mg of pale yellow ketone **11**, m.p. 188–194°, identical (i.r., t.l.c., n.m.r., mixed m.p.) with the ketone prepared by oxidation of 7*a*.

*Desoxy Compound **10a***

*(a) By Wolff–Kishner Reduction of Ketone **11***

A mixture of ketone **11** (45 mg), hydrazine hydrate (0.7 ml), and diethylene glycol (1 ml) was heated at 155° (bath temperature) for 2.5 h. Then NaOH (2 pellets) was added, and heating was continued for 1.5 h more. The reaction mixture was partitioned between water and ether. The organic layer was washed with water, dried, and evaporated to leave 40 mg of a colorless oil whose t.l.c. showed a single spot less polar than ketone **11**. Further purification on a thick layer plate gave 36 mg of an oil which crystallized on trituration with petroleum ether. Recrystallization from petroleum ether gave colorless rosettes of **10***a*, m.p. 125–126°, ν_{max} 3470 cm^{-1} (NH); λ_{max} 232 (24 000) and 295 nm (4600); *m/e* 288 (molecular ion).

Anal. Calcd. for $C_{20}H_{20}N_2$ (288.4): C, 83.30; H, 6.99. Found: C, 83.56; H, 7.08.

Can. J. Chem. Downloaded from www.nrcresearchpress.com by 210.87.254.105 on 09/05/12
For personal use only.

When the above reaction was carried out at 220°, the only product isolated was 2,3-dimethylindole (**2**).

(b) By Hydrogenolysis of Alcohol 7a

To a refluxing solution of alcohol **7***a* (160 mg) in *t*-butyl alcohol was added sodium metal (1 g). The mixture was refluxed for 9.5 h and then partitioned between water and ether. The ethereal extract was dried and concentrated to a brown oil (130 mg) which was chromatographed on a thick plate developed in benzene–ether (95:5). The band on the base line yielded 33 mg of recovered liquid alcohol **7***a*. Extraction of the band at R_f 0.55 gave 48 mg (32%) of almost colorless **desoxy compound 10***a*, m.p. 118–122° after recrystallization from ether – petroleum ether (b.p. 30–60°). The mixed m.p. with the specimen from the Wolff–Kishner reduction was 120–123°, undepressed. The i.r., n.m.r. and t.l.c. data were the same for both samples.

(c) By Saponification of the N-acetate 10b

A solution of the *N*-acetyl desoxy compound **10***b* (35 mg) and NaOH (2 pellets) in methanol (2 ml) – dioxane (2 ml) was refluxed for 12 h. After evaporation of the solvents, water was added and organic material was extracted with chloroform. The water-washed and dried organic solution was concentrated to leave 32 mg of a brown oil whose i.r. and n.m.r. spectra as well as t.l.c. behavior were identical with those of the desoxy compound **10***a*.

Deuteration of Desoxy Compounds

(a) Berti's 194° Desoxy Compound 18

A mixture of **18** (30 mg), methanol-*O*-d_1 (1.8 ml), and sodium methoxide (50 mg) protected from atmospheric moisture was refluxed for 10 h. The methanol was evaporated at reduced pressure and the residue was partitioned between chloroform and water to yield 30 mg of recovered **18** which was purified by recrystallization from chloroform – petroleum ether. In the n.m.r. spectrum the methyl peak at δ 1.79 had almost completely disappeared. Deuterium analysis by mass spectroscopy gave 2% d_0, 4% d_1, 15% d_2, 74% d_3, and 5% d_4.

(b) 126° Desoxy Compound 10a

The above reaction was carried out on 30 mg of **10***a* for 10 h. The crude product was recrystallized from ether – petroleum ether (b.p. 30–60°) to yield 18 mg of pure **10***a* whose n.m.r. spectrum showed no diminution of any peak. Deuterium analysis by mass spectroscopy gave 100% d_0, and no d_1 or d_2 species.

Epimeric Alcohol 12

A mixture of ketone **11** (50 mg), dry tetrahydrofuran (2 ml), and lithium aluminum hydride (50 mg) was stirred (magnetic bar) at room temperature for 5 h. Water was added and the reaction mixture was extracted with ether. The organic layer was washed with water, dried, and evaporated to leave 47 mg of colorless liquid epimeric alcohol **12** which crystallized on trituration with petroleum ether. Recrystallization from methanol and from chloroform – petroleum ether gave glistening granules, m.p. 189–193°; ν_{max} 3530 (OH) and 3360 cm^{-1} (NH); *m/e* 304 (molecular ion), whose R_f on t.l.c. was greater than that of alcohol **7***a*.

Anal. Calcd. for $C_{20}H_{20}N_2O$ (304.4): C, 78.92; H, 6.62; N, 9.20. Found: C, 78.39; H, 6.97; N, 9.07.

The ***O*-acetate** was prepared by treatment of **12** with acetic anhydride and pyridine at room temperature. Recrystallization from chloroform gave colorless crystals, m.p. 153–160°; ν_{max} 3395 (NH) and 1728 cm^{-1} (ester C=O); *m/e* 346 (molecular ion).

Anal. Calcd. for $C_{22}H_{22}N_2O_2$ (346.4): C, 76.28; H, 6.40. Found: C, 76.83; H, 6.51.

Preparation of Ketone 13

(a) During Treatment of Dimer 1 with Hydrochloric Acid

Treatment of the dimer with 0.1 *N* HCl in undistilled, unpurified Fisher *p*-dioxane (the n.m.r. spectrum showed only the *p*-dioxane peak) in a stoppered flask gave the liquid alcohol **7***a* (R_f 0.77, ether) in ~30% yield and in addition ~10% of a more polar (R_f 0.19, ether) compound which was separated by chromatography.[11] Recrystallization from chloroform – petroleum ether gave colorless crystals of the **ketone 13**, m.p. 214–217°, ν_{max} 3390 (NH) and 1680 cm^{-1} (Ar—C=O and pyrrolidone C=O); λ_{max} 235 (13 000) and 300 nm (3800); *m/e* 320 (molecular ion). The compound was identical with that prepared in section *b* below.

(b) By Periodate Oxidation of Diol 4

To a solution of the diol **4** (30 mg, 0.094 mmol) in methanol (3 ml) under a nitrogen atmosphere was added with stirring (magnetic bar) a solution of $NaIO_4$ (30 mg, 0.14 mmol) in water (1 ml) and methanol (0.5 ml). Within 5 min a white solid ($NaIO_3$) had precipitated. After 15 min water was added and the mixture was extracted with chloroform. The organic layer was washed with water, dried, and evaporated to leave 30 mg (100%) of an oily solid whose t.l.c. (chloroform–methanol, 87:13) showed the absence of starting material **4** and the presence of a single more polar spot of the same R_f as the ketone from section *a* above. Recrystallization from chloroform – petroleum ether gave colorless crystals of ketone **13**, m.p. 214–216°, undepressed on admixture with the compound from section *a* above. The n.m.r. and i.r. spectra of the two samples were identical.

Anal. Calcd. for $C_{20}H_{20}N_2O_2$ (320.4): C, 74.98; H, 6.29; N, 8.74; O, 9.99. Found: C, 74.51; H, 6.11; N, 8.72; O, 9.96.

(c) By Periodate Oxidation of Desoxy Compound 10a

A modification of Dolby's procedure (6) was used. To a solution of **10***a* (25 mg, 87 μmol) in methanol (2 ml) was added with stirring (magnetic bar) at room temperature a solution of $NaIO_4$ (60 mg, 280 μmol) in water (0.5 ml). Within 15 min solid had begun to precipitate. The mixture was stirred for 12 h, then diluted with water and extracted with chloroform. Evaporation of the washed and dried chloroform solution left 24 mg of light brown oily solid. Recrystallization from chloroform – petroleum ether gave 18 mg of buff colored solid, m.p. 208–217°. Sublimation (190° at 0.1 mm Hg) gave colorless crystalline **13**, m.p. 213–217°, undepressed on admixture with the sample from section *b* above. Their i.r. and n.m.r. spectra and t.l.c. behavior were also identical.

(d) By Periodate Oxidation of Diol 4-d_6

The reaction was carried out with 50 mg of **4**-d_6 and 36 mg of $NaIO_4$ according to the procedure described in section *b* above. The n.m.r. spectrum of the 50 mg of

[11]When oxygen was deliberately bubbled into the reaction mixture, the yield of ketone **13** increased markedly.

Can. J. Chem. Downloaded from www.nrcresearchpress.com by 210.87.254.105 on 09/05/12
For personal use only.

13-d_6 obtained was lacking the methyl peak at δ 1.52 and the three proton lump centered at δ 2.25. Recrystallization from chloroform – petroleum ether gave material of m.p. 214–216° whose t.l.c. behavior was identical with that of **13**; *m/e* 326 (molecular ion corresponding to hexadeuteration).

194° Desoxy Compound ***18***

(*a*) The procedure of Berti *et al.* (3) was used. The pyridinium salt **16** was prepared from 2,3-dimethylindole (1.0 g), *N*-bromosuccinimide (1.23 g), and pyridine (0.6 g). The crude salt obtained was treated with the Grignard reagent prepared from 2,3-dimethylindole (2.0 g). There was obtained 3.1 g of crude product which after two chromatograms and recrystallization from chloroform – petroleum ether yielded 28 mg of **18**, m.p. 178–183° (lit. (4) 186–194°).

(*b*) The low yields of **18** from section *a* and the difficulty of obtaining reproducible yields of **18** by thermal dehydration (3) of the dihydrodimer **26** led to the development of the following procedure.

A solution of **26** (480 mg) from $LiAlH_4$ reduction of **1** (3) in chloroform (35 ml) was refluxed for 36 h. The t.l.c. (benzene:ether, 50:50) showed the absence of starting material and the presence of a less polar product. Evaporation of the chloroform and recrystallization from ether – petroleum ether (b.p. 30–60°) gave 66 mg of colorless crystals of **18**. The residue from evaporation of the mother liquors was chromatographed on four thick plates developed with benzene – petroleum ether (63:37). The bands at R_f 0.36 yielded 70 mg more of **18** which after recrystallization amounted to 31 mg of **18** to bring the total yield of pure material to 97 mg (23%), m.p. 175–188°, identical with the compound prepared by the other two methods.

Deuteration of Dimer ***1***

(a) In Methanol-O-d_1 *with Sodium Methoxide*

A mixture of dimer (100 mg), sodium methoxide (100 mg), and methanol-*O*-d_1 (2 ml) was refluxed for 12 h with exclusion of atmospheric moisture. Evaporation of the methanol and partition between water and chloroform yielded 93 mg of recovered dimer which was recrystallized from methanol – petroleum ether. The 60 mg of **1** obtained was identical in melting point and t.l.c. behavior with starting material. Deuterium analysis by mass spectroscopy gave 78% d_0, 20% d_1, and 2% d_2 species.

(b) In Acetone-d_6 *with DCl*

To a solution of dimer **1** (100 mg) in acetone-d_6 (2 ml) was added a solution of 0.1 *N* DCl in D_2O (0.2 ml). The yellow solution was stirred at room temperature for 0.5 h and was then diluted with chloroform. Extraction with water, drying, and evaporation of chloroform left 105 mg of colorless oil. The t.l.c. showed the presence of **4** and **7***a* in addition to **1**. Separation on a thick plate developed in benzene–ether (75:25) gave 43 mg of recovered dimer which after recrystallization from methanol – petroleum ether was identical in melting point and t.l.c. behavior with **1**. Deuterium analysis by mass spectroscopy gave 85% d_0, 6% d_1, and 9% d_2.

Homodimer ***32***

To a stirred (magnetic bar) mixture of dimer **1** (400 mg), acetone (8 ml), and formaldehyde (1.6 ml of 37% aqueous solution) at room temperature was added a mixture of aqueous HCl (0.8 ml of 0.01 *N*) and acetone (0.5 ml). At the end of 5 min the pale yellow solution was added to ether, washed with water, dried, and concentrated to leave an amber oil. The t.l.c. in benzene–ether (50:50) showed the absence of **1** and the presence of a spot slightly more polar than **1** with considerable tailing. Chromatography on two thick plates developed in benzene–ether (75:25) yielded 280 mg (67%) of colorless crystalline solid from a band at R_f 0.43. Two recrystallizations from methanol – petroleum ether gave pure homodimer of m.p. 155–170° unchanged by further recrystallization; ν_{max} 3505 cm^{-1} (OH); λ_{max} 252 (6700) and 290 nm (1400); *m/e* 334 (molecular ion). This material was pure from its n.m.r. spectrum, and the wide melting point is due to decomposition to **30** during melting as demonstrated by t.l.c.

Anal. Calcd. for $C_{21}H_{22}N_2O_2$ (334.4): C, 75.42; H, 6.63; N, 8.38. Found: C, 75.11; H, 6.39; N, 8.49.

Treatment of the dimer with formaldehyde under the same conditions of concentration and acidity that allowed isolation of **4** gave only **30** and no **32**. Thus, from dimer (100 mg), acetone (2 ml), formaldehyde (0.5 ml of 37% aqueous solution), and aqueous HCl (0.2 ml of 0.1 *N*) after 15 min at room temperature there was obtained 103 mg (97%) of crude **30**. Thick layer chromatography and recrystallization from chloroform – petroleum ether gave 62 mg of pale yellow needles of 30, m.p. 146–147.5°, identical with the compound obtained from treatment of **1** with acid in dioxane.

Rearrangement of Homodimer ***32***

To a stirred (magnetic bar) solution of **32** (100 mg) in acetone (2 ml) at room temperature was added a solution of aqueous HCl (0.2 ml of 0.1 *N*) in a few drops of acetone. After 10 min the pale yellow solution was poured into ether, washed with water, dried, and concentrated to leave 93 mg (98%) of yellow solid. Two recrystallizations from chloroform – petroleum ether gave colorless **30**, m.p. 146–149°, identical with the artifact obtained by the action of acid on dimer **1** in dioxane.

We gratefully acknowledge the financial support of the National Research Council of Canada.

1. V. Dave and E. W. Warnhoff. Can. J. Chem. This issue.
2. V. Dave and E. W. Warnhoff. Chem. Commun. 919 (1970).
3. G. Berti, A. Da Settimo, G. Di Colo, and E. Nannipieri. J. Chem. Soc. 2703 (1969).
4. G. Berti, A. Da Settimo, and E. Nannipieri. J. Chem. Soc. 2145 (1968).
5. B. Witkop and J. B. Patrick. J. Am. Chem. Soc. **73**, 2196 (1951).
6. L. J. Dolby and D. L. Booth. J. Am. Chem. Soc. **88**, 1049 (1966).
7. W. I. Taylor. Proc. Chem. Soc. 247 (1962).
8. S. McLean, E. K. Strøm-Gundersen, K. S. Dichman, J. K. Fawcett, and S. C. Nyburg. Tetrahedron Lett. 2645 (1970).
9. W. I. Taylor. Helv. Chim. Acta, **33**, 164 (1950).

Can. J. Chem. Downloaded from www.nrcresearchpress.com by 210.87.254.6 on 09/05/12
For personal use only.

Etude par spectroscopie infrarouge de mélanges binaires de l'eau avec quelques accepteurs de protons dans la région des vibrations de valence OH

ANNE LE NARVOR, EMILIE GENTRIC, ET PIERRE SAUMAGNE

Laboratoire de Spectrochimie Moléculaire, Faculté des Sciences, 29N Brest, France

Reçu le 18 novembre, 1970

Les spectres i.r. de mélanges binaires de l'eau (HDO et H_2O) avec quatre cosolvants non ioniques: acétonitrile, dioxanne, diméthylsulfoxyde, et hexaméthylphosphorotriamide, ont été enregistrés entre 3700 et 3100 cm^{-1}, pour des concentrations en eau variant de 0 à 1 en fraction molaire. L'analyse de la région des bandes de valence OH de l'eau suggère la présence de différents types de complexes par liaison hydrogène et confirme en particulier l'existence de complexes bien définis de type I–II (une molécule d'eau liée à deux molécules de cosolvant) quand $X_{eau} < 0.1$. Dans le domaine de concentration $0.8 < X_{eau} < 1$ l'effet du cosolvant organique sur le spectre de l'eau est négligeable.

The i.r. spectra of binary mixtures of water (HDO and H_2O) and four non-electrolyte cosolvants: acetonitrile, dioxane, dimethylsulfoxide, and hexamethylphosphorotriamide have been recorded from 3700 to 3100 cm^{-1}, the mole fractions of water varying from 0 to 1. The investigation of the OH stretching bands of water suggests the presence of various types of hydrogen bonded complexes and confirms the existence of well-defined I–II complexes (one molecule of water bonded to two molecules of cosolvent) when $X_{water} < 0.1$. In the range $0.8 < X_{water} < 1$ the organic cosolvent has negligible effect on the spectrum of water.

Canadian Journal of Chemistry, 49, 1933 (1971)

Introduction

Les études sur la structure de l'eau liquide et sur les interactions eau-soluté ont fait l'objet de récentes mises au point (1–4).

Le problème de la structure de l'eau liquide n'est pas encore élucidé; la diversité des structures proposées reflète la difficulté de l'interprétation des résultats expérimentaux. On peut cependant classer les différents modèles de structure en deux types principaux. Le premier, ou "modèle discontinu" représente l'eau liquide comme un mélange en équilibre d'"agrégats fluctuants" comportant des molécules diversement liées. Le second modèle ou "modèle continu" décrit l'eau comme un réseau continu de molécules liées, les quatre liaisons hydrogène sur chaque molécule pouvant se courber ou se tordre et présentant une distribution continue d'énergies et de géométries. Les spectres i.r. et Raman de l'eau liquide ont donné lieu à des interprétations différentes s'appuyant sur l'un ou l'autre des modèles.

Il existe peu d'études concernant les solutions concentrées d'eau dans des solvants organiques accepteurs de protons. Très récemment, des mélanges eau–diméthylsulfoxyde ont été étudiés par spectroscopie i.r. pour des concentrations en eau de 1 à 0.8 en fraction molaire (5). En outre, Fratiello et coll. (6), Mavel (7), Holmes *et al.* (8) ont analysé par r.m.n. les spectres de quelques mélanges eau–solvant organique, tandis que la diffusion des neutrons lents par le mélange eau–diméthylsulfoxyde était suivie par Safford *et al.* (9). Enfin Kenttämaa et Lindberg (10) par des mesures thermodynamiques et diélectriques, Cowie et Toporowski (11) par des mesures de viscosité, et tout récemment Jung et Hyne (12) par des déterminations de compressibilité, ont discuté les structures des mélanges eau–diméthylsulfoxyde, tandis que le système eau–dioxanne était étudié par Rizk (13). Mais aucun de ces travaux ne paraît permettre une détermination précise des espèces présentes en solution.

Au contraire, il semble que la structure des solutions diluées d'eau dans les solvants organiques soit mieux connue à la suite des travaux de spectroscopie i.r. de Greinacher *et al.* (14), Saumagne (15–18), Sidorov (19), de Mohr *et al.* (20), et de Yuknevich *et al.* (21).

Dans ce mémoire, nous analyserons systématiquement les spectres de vibration de solutions contenant les molécules HDO et H_2O et les organiques suivants: acétonitrile, dioxanne, diméthylsulfoxyde, et hexaméthylphosphorotriamide.

Partie expérimentale

L'acétonitrile, le dioxanne, et l'hexaméthylphosphorotriamide sont d'origine Prolabo, tandis que le diméthylsulfoxyde provient du Laboratoire du Bois de Boulogne. Ces solvants ont été desséchés par contact prolongé avec

Can. J. Chem. Downloaded from www.nrcresearchpress.com by 210.87.254.6 on 09/05/12
For personal use only.

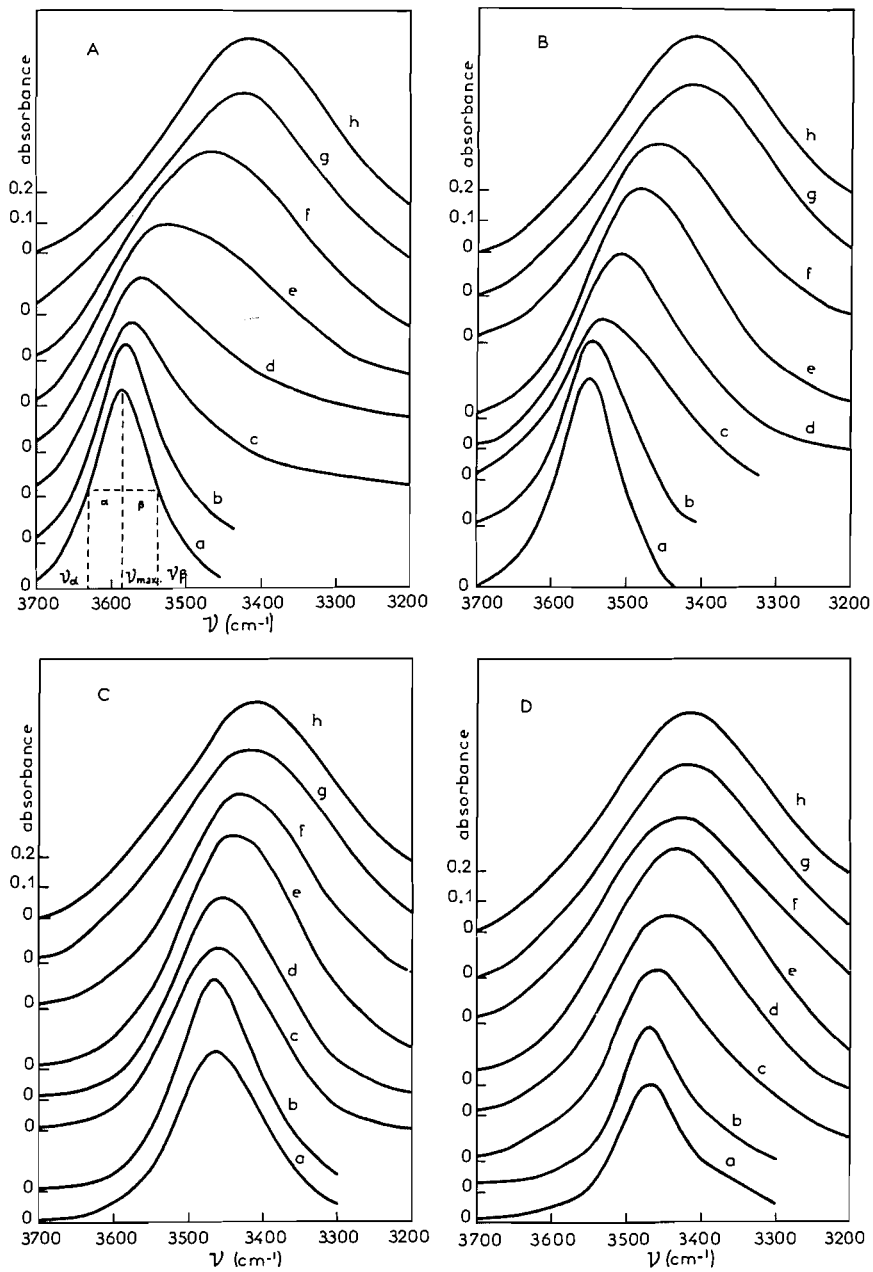

FIG. 1. Spectres de vibration de valence ν(OH) de HDO en mélange binaire avec A, acétonitrile; B, dioxanne; C, diméthylsulfoxyde (DMSO); D, hexaméthylphosphorotriamide (HMPT); concentrations, voir tableau 1. La courbe *h* est celle de HDO.

du tamis moléculaire Linde 4 Å. L'eau résiduelle a été dosée par la méthode de Karl Fisher: on a trouvé moins de 100 p.p.m. pour le diméthylsulfoxyde et moins de 50 p.p.m. pour les autres solvants. Les solvants anhydres ont été conservés et manipulés en boîte sèche. L'eau lourde titre 99.7% en D_2O et provient du Commissariat à l'Energie Atomique. Les solutions à faible teneur en eau ont été préparées en utilisant une micro-seringue Hamilton, et les autres par pesée directe. Les correspondances entre concentrations en mol l^{-1} et fractions molaires en eau pour les divers mélanges sont indiquées dans le tableau 1.

Les solutions jusqu'à 10 *M* en eau ont été étudiées dans une cuve à pas variable RIIC à fenêtres en CaF_2, le

TABLEAU 1. Concentrations en eau des solutions étudiées

Désignation de la courbe	Concentration en mol l^{-1} de l'eau dissoute dans les différents solvants	Fraction molaire en eau: X_{eau}			
		Acétonitrile	Dioxanne	DMSO	HMPT
a	0.05	0.0026	0.0042	0.0035	0.0087
b	0.5	0.026	0.041	0.035	0.081
c	2.5	0.12	0.18	0.16	0.31
d	5	0.22	0.32	0.28	0.49
e	10	0.39	0.51	0.46	0.68
f	20	0.62	0.73	0.69	0.84
g	40	0.88	0.92	0.91	0.99

produit concentration par épaisseur étant maintenu constant. L'eau pure ou les solutions plus concentrées ont été étudiées en film capillaire entre faces de CaF_2. Les spectres ont été enregistrés indifféremment sur un spectromètre Perkin–Elmer 225, équipé d'un réseau à 150 traits par mm travaillant dans le premier ordre, ou Beckman IR 9 muni d'un réseau à 150 traits par mm travaillant dans le second ordre. Quel que soit l'appareil, la précision de lecture sur les fréquences et les demi-largeurs est de $\pm 1\ cm^{-1}$ pour les bandes fines des solutions diluées, et de $\pm 3\ cm^{-1}$ pour les massifs les plus larges. Tous les spectres ont été enregistrés à température ambiante.

Résultats

Sur la fig. 1, nous avons représenté les spectres i.r. obtenus entre 3700 et 3100 cm^{-1} pour des solutions binaires d'eau HDO dans les solvants organiques cités, pour des valeurs de la fraction molaire X en eau totale variant de 1 à 0.005. L'eau HDO résulte de l'équilibre $H_2O + D_2O \rightleftarrows 2\ HDO$, dont la constante vaut 3.80 à 25 °C (22). Dans ce cas, les fractions molaires sont indiquées en eau "totale" ($[H_2O] + [D_2O] + [HDO]$), aux fins de comparaisons ultérieures avec le terme H_2O seul: dans les solutions utilisées, les concentrations à l'équilibre sont: $[H_2O] = 1.04$, $[HDO] = 17.91$, $[D_2O] = 81.04\%$ en volume. On admettra que la dilution par un solvant organique ne modifie pas l'équilibre.

Dans tous les cas, on constate un glissement vers les basses fréquences du maximum d'absorption et un élargissement du massif avec l'augmentation de la concentration en eau. Sur les figs. 2, 3, et 4, nous avons reporté respectivement le déplacement du maximum, la demi-largeur $\Delta\nu 1/2$ et la dissymétrie de la bande ν(OH) de HDO en fonction de la fraction molaire en eau.

Les spectres analogues de solutions d'eau H_2O sont reproduits sur la fig. 5. Bien que ces spectres soient compliqués par la présence de deux bandes de vibration de valence OH, l'allure générale du massif évolue de façon similaire à celle observée dans le cas précédent de l'eau HDO.

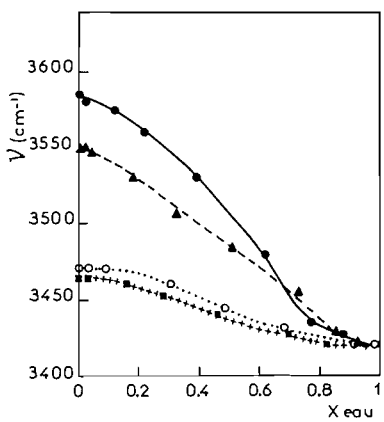

FIG. 2. Variation de la position du maximum de la bande ν(OH) de HDO en fonction de la fraction molaire en eau. ● acétonitrile; ▲ dioxanne; ▣ DMSO; ○ HMPT.

Discussion

Solutions très diluées en eau

L'interprétation des spectres de solutions à faible concentration d'eau ($0 < X_{eau} < 0.1$) dans

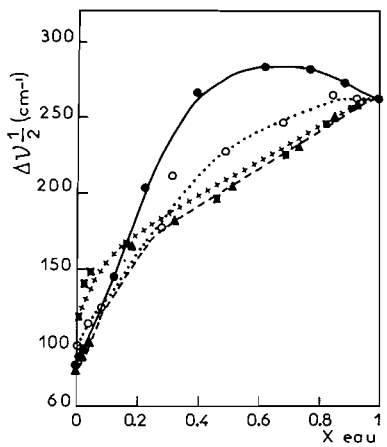

FIG. 3. Variation de la largeur à demi-absorbance ($\Delta\nu$ 1/2) de la bande ν(OH) de HDO en fonction de la fraction molaire en eau. ● acétonitrile; ▲ dioxanne; ▣ DMSO; ○ HMPT.

Can. J. Chem. Downloaded from www.nrcresearchpress.com by 210.87.254.6 on 09/05/12
For personal use only.

Can. J. Chem. Downloaded from www.nrcresearchpress.com by 210.87.254.6 on 09/05/12
For personal use only.

les solvants organiques découle de travaux antérieurs (15–21). En effet, les spectres de HDO présentent dans la région des vibrations de valence OH (fig. 1) une bande fine correspondant au vibrateur OH non couplé, dont la position varie en fonction du caractère basique plus ou moins marqué du solvant. Pour la molécule H_2O (fig. 5), nous retrouvons les deux maximums des vibrations symétrique ν_1 et antisymétrique ν_3, dont les nombres d'onde sont également fonction du solvant. Pour ces faibles concentrations en eau, les spectres s'interprètent par l'existence de complexes I–II comprenant une molécule d'eau liée par pont d'hydrogène à deux molécules de solvant (15, 17). Cependant, sur le spectre de l'eau H_2O dissoute dans l'hexaméthylphosphorotriamide (fig. 5D), on relève la présence d'une petite absorption vers 3690 cm^{-1}; on l'attribue à la vibration ν(OH) libre de complexes I–I contenant une molécule d'eau pour une molécule de solvant (16, 21, 23). Un phénomène d'empêchement stérique est vraisemblablement responsable de tels complexes en faible proportion dans le mélange.[1]

Solutions très concentrées en eau

A l'opposé, l'examen des spectres de la fig. 1 ou 5 montre que l'addition de petites quantités de soluté organique à l'eau modifie très peu l'allure générale des spectres tant que la concentration en eau reste supérieure à 0.8 en fraction molaire. Dans ce cas, on remarque que pour les solutions contenant HDO, la position du maximum de la bande ν(OH), sa demi-largeur et sa dissymétrie restent sensiblement inchangées en fonction de la concentration du soluté ou en fonction de sa nature (figs. 2, 3, et 4). Notons cependant que, parmi les quatre solvants étudiés, l'acétonitrile et le dioxanne ont une influence plus

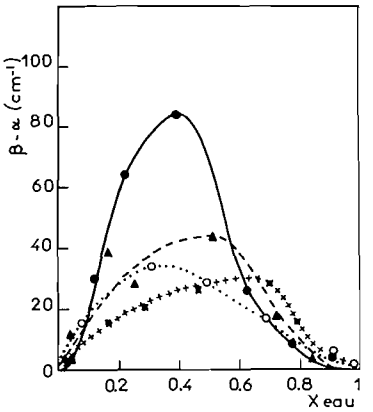

FIG. 4. Evolution de la dissymétrie (β-α) de la bande ν(OH) de HDO en fonction de la fraction molaire en eau. β et α sont respectivement définis par $\beta = \nu_{max} - \nu_\beta$ et $\alpha = \nu_\alpha - \nu_{max}$ (*cf.* fig. 1A, courbe *a*). On appelle ν_α et ν_β les nombres d'onde correspondant aux limites supérieure et inférieure de la largeur de la bande à demi-absorbance. ● acétonitrile; ▲ dioxanne; ✖ DMSO; ○ HMPT.

marquée sur le profil de la bande. En effet, pour une fraction molaire en eau de 0.8 ces composés élèvent d'environ 15 cm^{-1} la fréquence du maximum, en même temps qu'ils provoquent un élargissement égal au plus à 20 cm^{-1}, aux erreurs d'expérience près. Toutefois, ces modifications du spectre restent faibles et nos résultats dans leur ensemble confirment les observations récentes de Brink et Falk (5) sur le mélange eau–diméthylsulfoxyde.

L'absence de modification importante du spectre i.r. de l'eau contenant de petites quantités de soluté organique semble indiquer que les liaisons hydrogène présentes dans le milieu restent, en moyenne, de même force. Par ailleurs, lors d'une étude électrochimique de la solvatation du cation Ag^+ dans les mélanges eau–diméthylsulfoxyde, il a été montré que dans les milieux très riches en eau le rôle du soluté organique est négligeable (26). Dans ces conditions, on pourrait admettre que les molécules organiques sont piégées par l'eau et ne se manifestent pas. Il est donc vraisemblable que la structure de l'eau se conserve jusqu'à une fraction molaire de l'ordre de 0.9 à 0.8 en eau.

Solutions de concentrations intermédiaires

L'interprétation des courbes de variation de la fréquence, de la demi-largeur et de la dissymétrie pour les solutions d'eau HDO de concentrations

[1]Dans les complexes I–I (HOH...A) observés dans les mélanges eau–solvant accepteur de proton à faible concentration dans CCl_4, la symétrie C_{2v} de la molécule H_2O disparaît, tandis qu'elle se conserve dans le complexe I–II (A...HOH...A) correspondant à l'eau dans le solvant basique pur (24, 25). Le premier cas se traduit par une vibration de valence ν(OH) libre dont le nombre d'onde se situe dans la région 3700–3680 cm^{-1} et par une vibration ν(OH) associée dont la position dépend de la basicité du solvant. Par contre, pour une force croissante du pouvoir accepteur de proton du solvant, les fréquences ν_1 et ν_3 sont abaissées de façon parallèle, tandis que la différence $(\nu_3 - \nu_1)$ diminue et que le rapport des intensités $I(\nu_1)/I(\nu_3)$ augmente et tend vers 1.

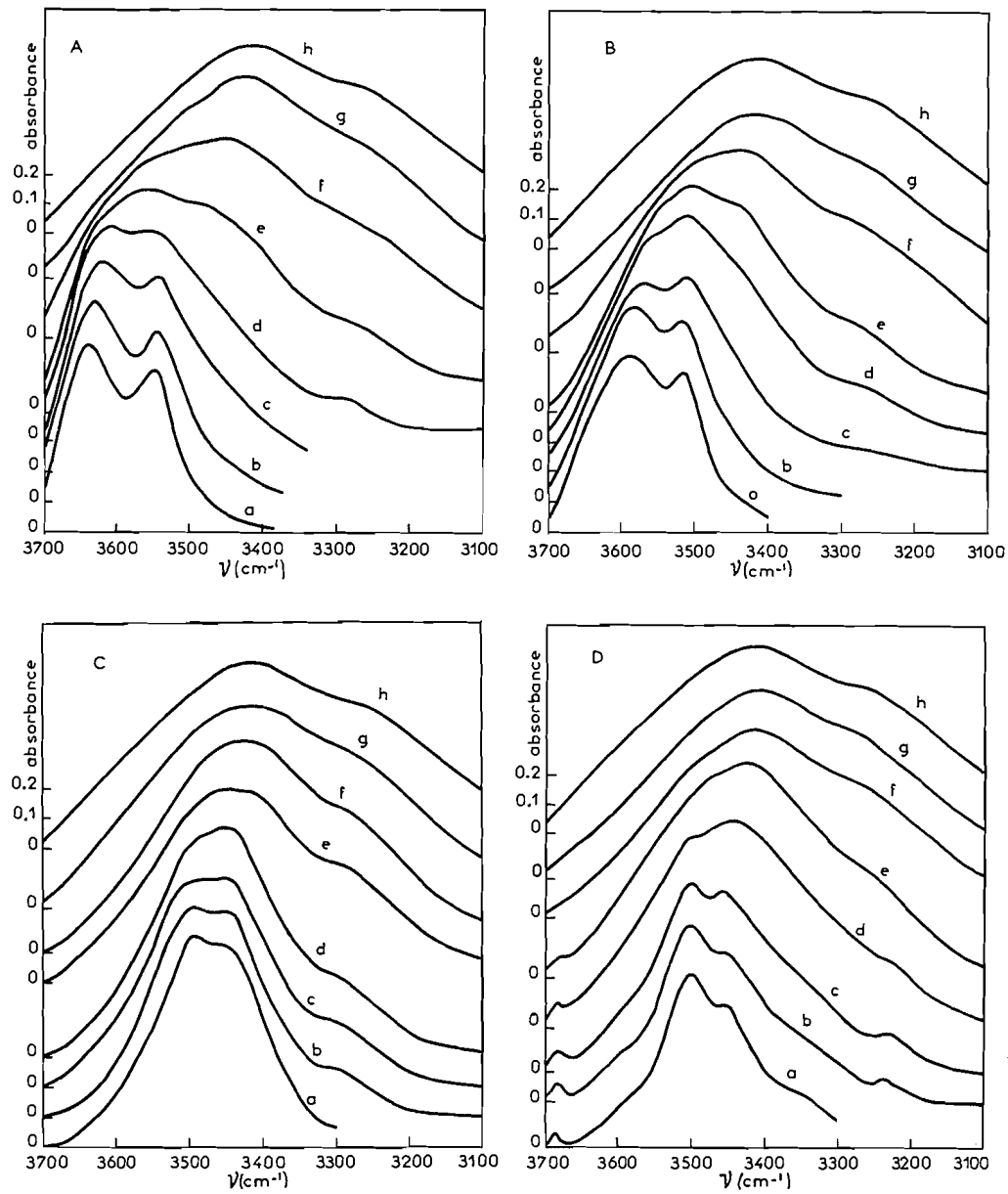

FIG. 5. Spectres de vibration de valence de H_2O en mélange binaire avec A, acétonitrile; B, dioxanne; C, DMSO; D, HMPT. La courbe *h* est celle de H_2O pure.

intermédiaires ($0.1 < X_{eau} < 0.8$) est délicate. La dissymétrie du massif passe par un maximum d'autant plus marqué que le cosolvant est moins basique et que l'écart entre les nombres d'onde du vibrateur OH complexé et autoassocié est grand (fig. 4). Au contraire, dans le même intervalle de concentration, la fréquence du maximum et la demi-largeur du massif varient continûment sans accident (figs. 2, 3).

Dans les études de certaines propriétés physico-chimiques du mélange eau–diméthylsulfoxyde (constante diélectrique et grandeurs thermodynamiques, viscosité, compressibilité isotherme ...), différents auteurs (10–12) ont observé, pour

Can. J. Chem. Downloaded from www.nrcresearchpress.com by 210.87.254.6 on 09/05/12
For personal use only.

une composition du mélange X_{eau} de l'ordre de 0.6 à 0.7, un extremum qu'ils relient à l'existence préférentielle d'un agrégat contenant une molécule de diméthylsulfoxyde pour deux molécules d'eau. Il ne semble pas que les maximums de dissymétrie observés précédemment puissent valablement être reliés à ces agrégats définis; ces maximums résultent plutôt sans doute d'une composition graphique très variable avec X d'un nombre élevé de bandes, souvent très larges, qui correspondent chacune à un type donné de complexe eau–solvant par liaison hydrogène.

L'interprétation des courbes similaires obtenues pour les solutions de H_2O dans le même intervalle de concentration est encore plus difficile. Par accroissement progressif de la teneur en eau dans les diverses solutions, on constate que les intensités relatives des bandes ν_3 et ν_1 varient, ainsi que leur position, ces bandes tendant à se rapprocher et à se confondre en un même massif. Cette évolution pourrait s'expliquer par un découplage progressif entre les deux vibrateurs OH d'une molécule d'eau, en raison des perturbations importantes auxquelles celle-ci est soumise dans ces solutions. Les vibrations ν_1 et ν_3 ne sont donc plus des vibrations purement symétrique et antisymétrique. Simultanément, dès $X_{eau} > 0.1$, apparaît sur tous les spectres une absorption notable centrée autour de 3420 cm^{-1}. Celle-ci augmente considérablement avec la concentration en eau et devient le maximum principal pour des fractions molaires en eau supérieures en moyenne à 0.5. Cette absorption a été attribuée à de l'eau autoassociée (16).[2]

En outre, sur tous les spectres de solutions de H_2O, lorsque l'absorption propre du solvant le permet, on remarque vers 3250 cm^{-1} une épaule dont l'intensité et la position restent sensiblement constantes dans toute la gamme de concentration étudiée. Ce sous-maximum correspond à l'harmonique de la vibration de déformation $2\nu_2$ (16).

[2]Une interprétation différente des spectres eau–acétonitrile pour des concentrations inférieures à 10 *M* a été donnée par Karetnikov et Golishnikova (27). Ces auteurs observent aux faibles concentrations deux bandes à 3620 et 3650 cm^{-1} qu'ils attribuent à ν_1 et ν_3. Ces deux maximums correspondent, selon nous, à l'acétonitrile lui-même. D'autre part, la bande située à 3540 cm^{-1} serait due d'après ces auteurs à une association eau–eau, ce qui n'est pas en accord avec la disparition progressive de ce massif pour des concentrations en eau supérieures à 10 *M*.

Conclusion

L'effet de concentration nous permet d'apporter quelques précisions concernant le spectre de l'eau H_2O liquide, qui confirment l'interprétation proposée précédemment par l'un de nous (16). Nous pensons que le maximum principal situé vers 3420 cm^{-1} contient les bandes de valence ν_3 et ν_1 des vibrateurs OH partiellement découplés tandis que l'épaule à 3250 cm^{-1} correspond à l'harmonique $2\nu_2$. Cette interprétation est en accord avec celles données récemment par Falk et Ford (28) Schiffer et Hornig (29).

Nous remercions Monsieur J. Lauransan, Maître de Conférences à la Faculté des Sciences de Brest, pour l'intérêt qu'il a porté à ce travail et pour les discussions dont il nous a fait bénéficier.

1. J. L. KAVANAU. Water and solute–water interactions. Holden-Day, Inc., San Francisco, California, 1964.
2. S. F. FRANK. Physico-chemical processes in mixed aqueous solvents. Heinemann Educational Books Ltd., London, 1967.
3. A. K. COVINGTON et P. JONES. Hydrogen-bonded solvent systems. Taylor and Francis Ltd., London, 1968.
4. D. EISENBERG et W. KAUZMANN. The structure and properties of water. Oxford University Press, New York, N.Y., 1969.
5. G. BRINK et M. FALK. J. Mol. Struct. **5**, 27 (1970).
6. A. FRATIELLO et D. C. DOUGLASS. J. Mol. Spectrosc. **11**, 465 (1963). A. FRATIELLO et J. P. LUONGO. J. Am Chem. Soc. **85**, 3072 (1963).
7. G. MAVEL. Thèse, Université, Paris, France, 1960.
8. J. R. HOLMES, D. KIVELSON, et W. C. DRINKARD. J. Am. Chem. Soc. **84**, 4677 (1962).
9. G. J. SAFFORD, P. C. SCHAFFER, P. S. LEUNG, G. F. DOEBBLER, G. W. BRADY, et E. F. X. LYDEN. J. Chem. Phys. **50**, 2140 (1969).
10. J. KENTTÄMAA et J. J. LINDBERG. Suomen Kemistilehti. **B33**, 32, 98, 104 (1960).
11. J. M. G. COWIE et P. M. TOPOROWSKI. Can. J. Chem. **39**, 2240 (1961).
12. K. H. JUNG et J. B. HYNE. Can. J. Chem. **48**, 2423 (1970).
13. H. A. RIZK. Z. Physik. Chem. Neue Folge. **66**, 257 (1969).
14. E. GREINACHER, W. LÜTTKE, et R. MECKE. Z. Elektrochem. **59**, 23 (1955).
15. P. SAUMAGNE et M. L. JOSIEN. Bull. Soc. Chim. 813 (1958).
16. P. SAUMAGNE. Thèse, Université, Bordeaux, France, 1961.
17. P. SAUMAGNE et M. L. JOSIEN. Disc. Faraday Soc. **43**, 142 (1967).
18. P. SAUMAGNE. J. Chem. Phys. **53** (9), 3768 (1970).
19. A. N. SIDOROV. Opt. i Specktr. **7**, 24 (1960).
20. S. C. MOHR, W. D. WILK, et G. M. BARROW. J. Am. Chem. Soc. **87**, 3048 (1965).

Can. J. Chem. Downloaded from www.nrcresearchpress.com by 210.87.254.6 on 09/05/12
For personal use only.

21. G. V. YUKNEVICH, A. V. KARYAKIN, et A. V. PETROV. Zhur. prikladnoi Spektroskopii, **3**, 142, (1965).
22. H. C. UREY. J. Chem. Soc. 569 (1947).
23. A. BURNEAU. Thèse 3ème cycle, Université, Paris, France, 1970; J. Chem. Phys. Sous presse.
24. E. GENTRIC, A. LE NARVOR, et P. SAUMAGNE. C. R. Acad. Sci. Paris. **270**C, 1053 (1970).
25. J. LAURANSAN, J. CORSET, et M. T. FOREL. Ann. Chim. **3**, 109 (1968).
26. J. COURTOT-COUPEZ, C. MADEC, et M. LE DEMEZET. C.R. Acad. Sci. **270**C, 1397 (1970).
27. G. S. KARETNIKOV et L. YA. GOLISHNIKOVA. Zhur. Fiz. Khim. **42**, 1885 (1968).
28. M. FALK et T. A. FORD. Can. J. Chem. **44**, 1699 (1966).
29. J. SCHIFFER et D. F. HORNIG. J. Chem. Phys. **49**, 4150 (1968).

Can. J. Chem. Downloaded from www.nrcresearchpress.com by 210.87.254.6 on 09/05/12
For personal use only.

Can. J. Chem. Downloaded from www.nrcresearchpress.com by 210.87.254.105 on 09/05/12
For personal use only.

Conformational Preference and Configurational Equilibria of the Methyl 3-Deoxy-3-nitro-pentopyranosides and their Nitronates[1]

HANS H. BAER AND JAN KOVÁŘ
Department of Chemistry, University of Ottawa, Ottawa, Canada

Received November 27, 1970

The conformations of four methyl 3-deoxy-3-nitropentopyranosides and their sodium nitronates in aqueous solution were examined by n.m.r. spectroscopy, and the results are explained by calculation of free energies of non-bonded interactions. It is shown that protonation of glycoside nitronates is a kinetically controlled process. The β-epimerization of nitronates was investigated, and relative thermodynamic stabilities of epimers were determined and correlated with conformations. The non-bonded interaction between the nitronate grouping and an adjacent, equatorial hydroxyl group ($A^{(1,3)}$ effect) must be associated with a free energy in excess of 2 kcal/mol. The influence of this effect upon conformational and configurational equilibria in glycoside nitronates and upon nitromethylene acidity is emphasized. The compounds were found to differ in their behavior during early stages of the β-epimerization reaction, which was linked to differential nitromethylene acidities. Mechanisms for the reaction are discussed.

On a déterminé en solution aqueuse et par r.m.n., les conformations de quatre méthyl déoxy-3 nitro-3 pentopyranosides et de leurs nitronates de sodium; on explique les résultats obtenus à l'aide de calculs d'énergie libre d'intéractions non liées. On démontre que la protonation des nitronates de glycosides est un processus contrôlé cinétiquement. On a de plus étudié l'épimérisation β des nitronates; on a déterminé les stabilités thermodynamiques relatives des épimères et établi une corrélation avec les conformations. On doit considérer que l'intéraction non liée entre le groupe nitronate et un groupe hydroxyle équatorial voisin (effet $A^{(1,3)}$) amène une contribution de plus de 2 kcal/mol à l'énergie libre. On met en relief l'influence de cet effet sur l'équilibre conformationnel et configurationnel des nitronates de glycosides et sur l'acidité des groupes nitrométhylènes. On a trouvé que, suivant l'acidité des groupes nitrométhylènes, la réactivité des divers composés varie dans les stades préliminaires de la réaction d'épimérisation β. On discute des mécanismes de la réaction.

Canadian Journal of Chemistry, 49, 1940 (1971)

Introduction

The nitromethane cyclization of L′-methoxydiglycolaldehyde (**1**) and its D′ enantiomer (**1***)[2] (1–3), and many further applications of this reaction which have recently been reviewed (4), have provided facile access to a large body of nitrogenous carbohydrates. In the course of these investigations a stereochemical rule has emerged that concerns the liberation of 3-deoxy-3-nitroaldopyranosides (and analogous 4-deoxy-4-nitro-ketopyranose derivatives) from their *aci* salts, in which process a new center of asymmetry is created. The configuration adopted, usually to the exclusion of the epimeric alternative, is that which possesses an equatorial nitro group in the favored chair conformation. Thus, for example, in methyl D-hexopyranosides with their innate preference for the C_1^4 chair, products having the D-*gluco*, D-*manno*, D-*galacto*, and D-*talo* configurations are obtained, whereas corresponding β-1,6-anhydro sugars locked in the C_4^1 conformation give rise to products having the D-*allo*, D-*altro*, D-*gulo*, and D-*ido* configurations (4). One puzzlement of long standing has been the seemingly exceptional behavior of methyl 3-deoxy-3-*aci*-nitro-β-D-*erythro*-pentopyranoside sodium (**2**), the main product in the nitromethane cyclization of **1**, which on acidification gave both 3-epimers, with methyl 3-deoxy-3-nitro-β-D-ribopyranoside (**6**) unexpectedly preponderating strongly over the β-D-*xylo* isomer **7** (2). Methyl 3-deoxy-3-*aci*-nitro-α-L-*threo*-pentopyranoside sodium (**3**) produced the α-L-arabinopyranoside **8**, whereas the β-D-*threo* nitronate **4** gave the β-D-arabinopyranoside **9**; in other words,

[1]Part XIX of a series on the reactions of nitro sugars. For part XVIII see ref. 22.

[2]Occasional reference is made herein to optical antipodes of some of the compounds depicted. They are indicated by starred numbers, and mirror image formulas are dispensed with. The conformational symbols used in this article are explained in ref. 23.

Can. J. Chem. Downloaded from www.nrcresearchpress.com by 210.87.254.105 on 09/05/12
For personal use only.

opposite configurations were engendered at C-3 in these two nitronates (3). The 3-epimers of **8** and **9**, *i.e.* the corresponding *lyxo* derivatives **10** and **11**, were not encountered.

In order to shed light on these stereochemical problems, and also to explore further the factors which govern epimeric product composition in the formation and base-catalyzed epimerization of sugar nitronates, we have now examined by n.m.r. spectroscopy the aforementioned methyl deoxynitropentosides and their sodium salts. For the purpose of this study the β-D-*xylo* isomer **7**, which had previously been shown to exist but had not been isolated, was prepared in crystalline form for the first time, as were also the β-L-*xylo* and β-L-*ribo* enantiomers **7*** and **6***.

Results and Discussion

Conformation of the Glycoside Nitronates

Contrary to earlier assumptions (2), which were based on the tenets of conformational analysis prevailing at a time when the importance of certain non-bonded interactions had not yet been realized and the benefits of n.m.r. spectroscopy were not widely available, we now have found that the β-D-*erythro* nitronate **2** does not prefer the C_1^4 chair conformation (**2***a*). All the coupling constants for the ring protons H-1, -2, and -4 are small (Table 1), indicating absence of vicinal, *trans*-diaxial orientations and therefore ruling out the C_1^4 form which would possess two pairs of protons so oriented. The spectral data are consistent with the inverted, C_4^1 chair conformation (**2***b*), which we believe describes best the molecule in its ground state even though three axial substituents are present.[3]

The α-L-*threo* isomer **3** possesses one pair of vicinal, *trans*-diaxial protons in either chair conformation (**3***a* and *b*). However, the n.m.r. spectrum shows only small couplings in the H-1, -2, and -4 proton signals (Table 1), thus ruling out both chair forms, and it therefore appears that we are dealing with one of the unusual cases where a skew conformation can be postulated for a monocyclic pyranoside. Inspection of models leaves little choice but the S_1^5 form (**3***c*), which is consistent with the spectrum.[4]

The spectrum of the β-D-*threo* isomer **4** also exhibits only small couplings in the H-1, -2, and -4 signals, indicating absence of vicinal *trans*-diaxial protons. While this feature eliminates conformation **4***a* from consideration, it is compatible with the inverted chair **4***b* but also with a skew form, S_1^5 (**4***c*).

Relative Thermodynamic Stabilities of the Glycoside Nitronates

As had earlier been shown (3), mainly by polarimetry and chromatography, the three sodium nitronates **2**, **3**, and **4** spontaneously equilibrate, in aqueous solution, by epimerizing at C-2 and -4. At equilibrium, which is reached at room temperature within several hours, the β-D-*erythro* isomer **2** was found to predominate strongly over the *threo* isomers **3** and **4**. We have now confirmed this by n.m.r. spectroscopy, the chemical shifts and intensities of the methoxyl proton signals affording a convenient means of differentiating components, and of determining their ratios, in mixtures of the isomers. As the equilibration reaction progressed, starting from whichever nitronate, a fourth methoxyl signal appeared, at lowest field. We assign it to the fourth possible stereoisomer, the α-L-*erythro* nitronate **5**, which had hitherto escaped detection. A typical spectrum of an equilibrium mixture is depicted in Fig. 1, and the results of various experiments are recorded in Table 2. The differences in free energy calculated from the equilibrium constants show that **2** is more stable than its stereoisomers by approximately 0.8–1.0 kcal/mol. The differences between the three less stable compounds are slight, but **5** quite consistently appears to have the lowest stability.

[3]The chair may be assumed to be slightly flattened due to the sp^2 hybridization of C-3, which relieves somewhat the *syn*-diaxial hydroxyl interaction strain. The molecule could thus *approach* the half-chair form **2***c* (which would still agree with our n.m.r. data), but there is no reason for assuming a very great departure from the C_4^1 chair.

[4]A referee has suggested that the n.m.r. data of **3** may be interpreted in terms of "a rather strongly distorted chair form". Strong distortion so as to approach the half-chair HC_4^5 would in fact be consistent, and a definitive assignment is not implied. However, the half-chair would suffer from eclipsing of the C-2 and -3 bonds whereas rotation about the $C_{(2)}$–$C_{(3)}$ axis produces **3***c*, in which these bonds are staggered, without very much affecting the positions of the hydroxyl groups relative to the nitronate group. We therefore believe the skew form to be more likely (see also footnote 6) but, in the subsequent discussion, the only point that really matters is the fact that the compound obviously does not assume one of the normal chair forms.

TABLE 1. The n.m.r. data of sodium nitronates in D_2O

Compound	Chemical Shifts (τ)*						Couplings (Hz)			
	H-1	H-2	H-4	H-5	H-5′	OCH_3	$J_{1,2}$	$J_{4,5}$	$J_{4,5'}$	$J_{5,5'}$
2	5.32	5.38	5.52	6.18	6.35	6.73	1.5	2	1.5	12
3	5.28	5.37	5.54	6.17	6.33	6.62	2	<1	<1	11
4	5.22	5.29	5.48	6.08	6.41	6.66	2.5	3	3	12.5
5						6.57				

*Measured with reference to acetone (τ = 7.91) as internal standard.

TABLE 2. Configurational equilibration of nitronates at room temperature, as determined by n.m.r. spectroscopy

Starting nitronate	Equilibrium mixture (percentage figures obtained from OCH_3 peak intensities)			
	2	**3**	**4**	**5**
2	65	14	14	7
	60	14	15	11
3	59	15	13.5	12.5
	57	17	15	11
4	64	14	11	11
Mean	61	14.8	13.7	10.5

$K_{2/3} = 4.12$, whence* $-\Delta G^\circ_{2/3} = 0.84$ kcal/mol
$K_{2/4} = 4.45$, $-\Delta G^\circ_{2/4} = 0.88$
$K_{2/5} = 5.80$, $-\Delta G^\circ_{2/5} = 1.04$

*From $-\Delta G^\circ = RT \ln K = 1.36 \log K$.

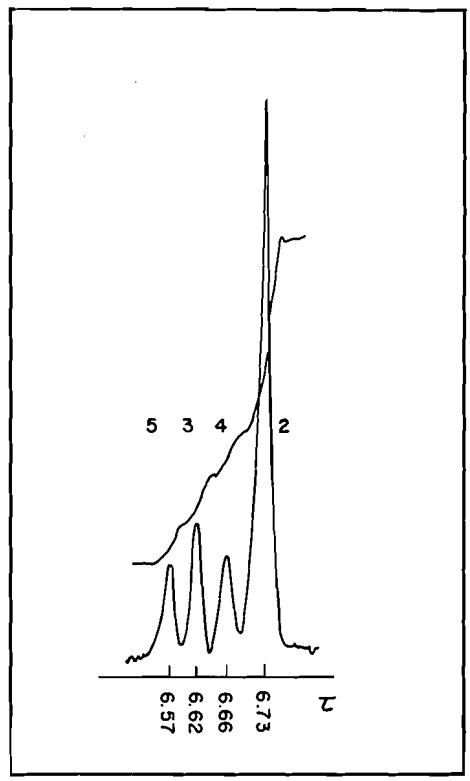

FIG. 1. The n.m.r. spectrum (60 MHz, with 100 Hz sweep width) of the methoxyl signal region of sodium nitronates at epimeric equilibrium in D_2O.

With this information on hand, the conformational preferences displayed by the nitronates may be discussed in terms of free energies of non-bonded interactions. Experimental values recorded for conformational free energies of substituents on six-membered rings show considerable scattering (5*a*, 6), and some arbitrariness is therefore inherent in the choice of certain parameters for calculations. Nevertheless, a reasonable picture has been presented of the conformational preferences in cyclitols, hexopyranosides, and pentopyranosides (5*b*, *c*). We are using the same approach and are adopting recent improvements which have been described in great detail by Angyal (7). Accordingly, we employ the following values (in kcal/mol) for non-bonded interactions: between an axial hydroxyl or methoxyl group and one *syn*-axial hydrogen, 0.45; between two *syn*-axial hydroxyl groups, 1.5; between adjacent, diequatorial hydroxyl (or methoxyl) groups, 0.35; for the anomeric effect of the methoxyl group in aqueous solution, 1.05; increment to the anomeric effect if 2-OH is axial, 0.45 (Δ2 effect). Unknown at the outset was the magnitude of the interaction between the nitronate grouping and an adjacent hydroxyl. When the latter is axial, its dihedral angle with the C=N bond is about 120°, and interaction can be assumed to be negligible; but when it is equatorial, the dihedral angle is close to 0°, and substantial strain will exist. This condition is an example of the more general $A^{(1,3)}$ effect (8), and an energy term (*A*) must be added whenever it occurs. Table 3 contains the calculated, total interaction energies for the two chair forms of each of the four nitronates, and by

Can. J. Chem. Downloaded from www.nrcresearchpress.com by 210.87.254.105 on 09/05/12
For personal use only.

Can. J. Chem. Downloaded from www.nrcresearchpress.com by 210.87.254.105 on 09/05/12
For personal use only.

TABLE 3. Calculated energies of non-bonded interaction in nitronates

Compound (Configuration)	Conformation	kcal/mol
2 (β-D-*erythro*)	**2***a*	1.4+2*A*
	b	1.95
3 (α-L-*threo*)	**3***a*	1.85+*A*
	b	0.9+*A*
4 (β-D-*threo*)	**4***a*	2.30+*A*
	b	1.25+*A*
5 (α-L-*erythro*)	**5***a*	3.35
	b	0.8+2*A*

relating these data with our experimental findings it became possible to derive at least a minimum estimate for the *A* term and to demonstrate the importance of the $A^{(1,3)}$ effect in the stereochemical behavior of nitro glycosides.

From the fact that compound **2** preponderantly exists in the conformation **2***b* one may deduce for **2***a* a relative energy excess of at least 1 kcal/mol, whence $1.4 + 2A \geqq 1.95 + 1$, or $A \geqq 0.8$ kcal/mol. More revealing is the observation that the free energy of **3** is 0.84 kcal/mol higher than that of **2** (Table 2). From this difference an interaction energy of 2.8 kcal/mol is computed for **3**, based on the value 1.95 for **2** in its prevailing form, **2***b*. Hence if **3** existed as an equilibrium mixture of conformers **3***b* and *a*, and the free energy of such a mixture were given[5] by the expression (0.8 + *A*) kcal/mol, *A* would equal 2.0 kcal/mol. However, the n.m.r. spectrum showed that **3** does not in fact occupy the chair forms, and therefore one has to conclude that *A* is even larger, perhaps 2.5 kcal/mol or more, causing the energy of **3***b* to exceed markedly that of the skew form **3***c* into which the molecule seems to escape on account of this strain. For although skew forms are not normally adopted by pyranosides, **3***c* is free from $A^{(1,3)}$ strain, thus offering an attractive choice for a molecule which would be severely hindered in either chair form.[6] A similar calculation for the isomer **4**, using the experimentally determined energy difference *vs.* **2** (0.9 kcal/mol, see Table 2) and assuming an equilibrium of conformers **4***b* and *a* in the ratio 86:14 (calculated from Table 3), would result in an *A* value of 1.70 kcal/mol. However a higher value, demanded by the conformational behavior of **3** as just discussed, should apply here too, on the premise that the $A^{(1,3)}$ effects are equal in the chair conformations of both isomers. Since any higher *A* value will make **4***b* (and *a*) less stable than the compound has actually been found to be, in relation to **2**, one is led to postulate that **4***b*, although allowed by the n.m.r. data, is not the preferred conformation but that a skew form, **4***c*, is adopted to a large extent.

These results can be viewed in yet another way. Considering that the calculated energy difference between the most favored chair forms **3***b* and **4***b* is 0.35 kcal/mol, one would expect the isomers to be present, at the epimeric equilibrium, in a ratio of about 2:1 if indeed the chair conformations prevailed. The ratio actually found is different (close to 1:1), suggesting that other conformations are involved.

Finally, the epimeric equilibrium between **2** and what is presumed to be the α-L-*erythro* isomer **5** (Table 2) corresponds to a free energy difference of 1.04 kcal/mol. The preferred conformation of **5** is not known, but in view of the magnitude of the $A^{(1,3)}$ effect it is safe to say that it should be **5***a* even though all the other steric factors work in favor of **5***b* (see Table 3). The difference in interaction energies calculated for the system **2***b* ⇌ **5***a* (1.4 kcal/mol, Table 3) is somewhat higher than the experimental value,[7] but calculation based on **5***b*, using any *A*- value consistent with the other findings, would give much too high a figure.

In summary, the studies have revealed that the $A^{(1,3)}$ effect is the most powerful factor determining preferred conformations and equilibria of epimerization in glycoside nitronates, the interaction energy associated with it certainly exceeding 2 kcal/mol. The order of thermodynamic stabilities, **2** > **3** > **4** > **5**, is as previously

[5]The difference (0.95 kcal/mol) in interaction energies calculated for **3***b* and *a* (Table 3) corresponds to an equilibrium ratio 83:17 for these conformers. By taking into account the entropy of mixing, one finds 0.8 + *A* as the calculated energy value for an equilibrium mixture **3***b* ⇌ **3***a*.

[6]In cyclohexanone, the energy difference between chair and flexible forms is only about one-half that in cyclohexane, allowing skew forms in substituted cyclohexanones to play a significant role (5*d*). A similar situation should pertain in our nitronates.

[7]Agreement would of course be achievable by taking the anomeric effect to contribute 0.35 kcal/mol less energy. Such arbitrary measure, when applied to the isomers **3** and **4**, would affect the results of the previous calculations somewhat but not significantly, in the direction of a higher *A* value.

TABLE 4. The n.m.r. data of nitro glycosides in D_2O

	Chemical Shifts (τ)*							Couplings (Hz)					
Compound	H-1	H-2	H-3	H-4	H-5	H-5′	OCH_3	$J_{1,2}$	$J_{2,3}$	$J_{3,4}$	$J_{4,5}$	$J_{4,5'}$	$J_{5,5'}$
6	5.14	5.52	5.13	5.68	6.14	6.21	6.67	3	3	3	1.5	1.5	12
7	5.70	5.98	5.45	6.26	6.54	6.68	6.58	9	11	8	1.5	10	9
8	5.75	5.90	5.27†	5.63	6.18	6.25	6.56	7.8	9.5	3.7	2	1.5	12
9	5.22	5.60	5.23	5.62	6.24	6.33	6.72	3.5	10.5	3.5	1.5	1.5	12.5

*Measured with reference to acetone (τ = 7.91) as internal standard.
†The H-3 signal is a quartet whose peaks are slightly broadened presumably because of the small shift between H-1 and -2 giving rise to virtual coupling.

suggested but must be interpreted in the light of this interaction. Whether the effect is primarily of steric or dipolar nature remains open.

Conformation of the Free Nitro Glycosides

Methyl 3-deoxy-3-nitro-β-D-ribopyranoside (**6**) and its β-D-*xylo* (**7**), α-L-*arabino* (**8**), and β-D-*arabino* (**9**) isomers were all found to prefer, in aqueous solution, that chair conformation in which the nitro substituent occupies the equatorial position. This is the C_1^4 conformation for the β-D-*xylo* compound (**7***a*), but the C_4^1 conformation for the others (**6***a*, **8***a*, **9***a*). The ring proton resonances leading to these conclusions are listed in Table 4. In agreement herewith, the signals given by the axial methoxyl groups in **6***a* and **9***a* occur at higher field than those of the equatorial methoxyl groups in **7***a* and **8***a*.

These findings remove the basis for regarding the formation of the β-D-riboside **6** from the β-D-*erythro* salt **2** as a peculiar exception to the general rule of equatorial placement of the nitro group, and this rule is now recognized to hold for the acidification of all known 3-deoxy-3-nitro-aldopyranosides and structurally analogous keto-pyranosides and sugar anhydrides. The conformations **7***a*, **8***a*, and **9***a* come as no surprise as they are the same as those preferred by the corresponding, non-nitro parent glycosides, but the case of **6***a* is worthy of special note. β-D-Ribopyranose favors the C_1^4 chair (9), although the inverted chair is populated to a considerable degree (7). Methyl β-D-ribopyranoside had long been assumed to exist in the C_1^4 chair form (10), but recent n.m.r. data indicate that the two chair forms have about equal stability (7), and this is ascribed to a somewhat greater anomeric effect of the methoxyl group compared to that of the hydroxyl group. An analogous situation pertains in β-D-ribopyranose tetraacetate in acetone solution (11). Only further enhancement of the anomeric effect, as experienced by tri-*O*-acetyl-β-D-ribopyranosyl halides in chloroform, causes strong predominance of the C_4^1 form (12). Substitution by a nitro group of the axial hydroxyl on C-3 in methyl β-D-ribopyranoside (in the C_1^4 form) evidently compels chair inversion with similar strength.[8] The conformational free energy of the nitro group in the nitrocyclohexane system has been determined (6) to be 1 kcal/mol, but this value (which refers to a nonaqueous medium) barely exceeds the 0.9 kcal/mol associated here with an axial hydroxyl, in opposition to two axial hydrogens, and would be unable to account for the observed effect.[9] An appreciably higher value must apply in our nitro glycosides in water, which could be due to increased bulk owing to hydration, or to dipolar interaction with the ring oxygen.

Stereochemistry of Acidification of Nitronates

At this point it is interesting to discuss, in the light of the preceding considerations, the stereochemical course of the acidification of the nitronates **2**, **3**, and **4**. Let us compare the relative, thermodynamic stabilities calculated for the two 3-epimeric nitro glycosides that can theoretically arise from each nitronate. The interaction energies for the favored conformers (*i.e.* those having an equatorial nitro group) are listed in Table 5.

[8]The n.m.r. spectra of **6** in D_2O (Table 4) and in $CDCl_3$ exhibited virtually identical splitting patterns, indicating that the predominant conformation (**6***a*) was, within observable limits, no less populated in the former solvent than in the latter. The extra stabilization that **6***a* may be afforded in a nonpolar solvent due to an increased anomeric effect and the possibility of intramolecular hydrogen bonding between the *syn*-axial hydroxyl groups is, therefore, not required for its preponderance.

[9]In fact, by equating the interaction of an axial nitro group and two opposing hydrogen atoms with 1 kcal/mol, one would obtain equal energies for the two chair forms of **6**, assuming that the *gauche*, nitro–hydroxyl interactions are the same.

Can. J. Chem. Downloaded from www.nrcresearchpress.com by 210.87.254.105 on 09/05/12
For personal use only.

Can. J. Chem. Downloaded from www.nrcresearchpress.com by 210.87.254.105 on 09/05/12
For personal use only.

TABLE 5. Calculated, partial* energies of non-bonded interaction in conformers having an equatorial nitro group

Compound (Configuration)	kcal/mol
6*a* (β-D-*ribo*)	2.4
7*a* (β-D-*xylo*)	1.75
8*a* (α-L-*arabino*)	2.20
10*a* (α-L-*lyxo*)	1.35
9*a* (β-D-*arabino*)	1.70
11*a* (β-D-*lyxo*)	2.65

*Less *gauche* nitro-hydroxyl interactions; see text.

Where applicable in these computations, the anomeric effect was assigned a value of 1.4 kcal/mol (rather than 1.05 kcal/mol as in Table 3), the higher value applying to methanolic solutions (5*e*).[10] The figures do not include the contributions by *gauche* interactions of the nitro group with its neighboring hydroxyls; the energy associated therewith is unknown but may be disregarded as it should be equal in any two 3-epimers and will therefore cancel in their free energy difference. Now it is seen that the β-D-riboside (**6***a*), the major product obtained from **2**, is considerably less stable than the β-D-xyloside (**7***a*) which was obtained as a minor product only. Similarly the α-L-arabinoside (**8***a*), which arose from the salt **3**, is less stable according to these calculations than its 3-epimer, the α-L-lyxoside (**10***a*), which has not been detected as a product. It is therefore concluded that the acidification of **2** and **3** is kinetically controlled. The same is presumably true for the acidification of **4**, although in this case the product, namely the β-D-arabinoside (**9***a*), represents the more stable epimer. Angyal and Luttrell have recently reported (14) that, in the analogous acidification of 2-*aci*-nitrocyclohexan-1,3-diol, kinetic control is not achievable because epimerization at the nitro carbon is too rapid. Obviously this does not apply to the nitro sugars, and as far as **6** and **7** are concerned we have noticed no mutual interconversion of these epimers in aqueous solution, neutral or acidic.

Evidently, the predominant path for protonation of the salt **2** is approach from the less hindered, upper side of the favored conformer **2***b*. Protonation of **2***b* from the opposite side, to give the minor product **7**, is disfavored for one or both of two reasons, namely, hindrance from the hydroxyl groups and resistance of the nitro group against being placed axially. Protonation of the conformer **2***a* should lead to **7** more readily, but since **2***a* can be present only in small proportion, **7** is relegated to the role of a by-product. As for the *threo* salts **3** and **4**, inspection of molecular models of the likely conformations **3***c* and **4***c* suggests that steric impediments to proton approach are not much different on either side, but it reveals that the direction which leads to the respective *arabino* configuration is that which avoids transitional placement of the nitro group in the unfavorable, axial position. One may thus infer, from the observed stereoselectivity in these protonations, that the structure of the transition state resembles the product and not the nitronate; for if it resembled the latter, appreciable selectivity would not be expected.[11]

Mechanism of β-*Epimerization*

To explain epimerizations at carbon atoms adjacent to the nitromethylene group, as well as some other base-catalyzed reactions involving those β-carbons, intermediate α-nitroalkene structures have been postulated, and the role of such intermediates has been substantiated by experimental evidence in several instances (16–20). Accordingly it is thought that $\Delta^{2,3}$- and $\Delta^{3,4}$-unsaturated nitro glycosides are intermediates in the epimerizations **2** ⇌ **3** ⇌ **4** ⇌ **5**. We have been able to isolate a small amount of an unsaturated material by column chromatography of the mixture of **6*** and **7*** that was obtained upon deionization of the β-L-*erythro* nitronate **2*** (see footnote 2). The i.r. spectrum of the syrupy material showed a strong peak at 1528 cm^{-1} indicating a nitroalkene grouping. The n.m.r.

[10]For preparative purposes the liberation of the nitro glycosides from their *aci* salts has been performed in this work and earlier (3, 13) by the action of a cation exchange resin in methanol, which superseded the original procedure (2) of acidification with potassium bisulfate in the dry state.

[11]During this writing there appeared extensive studies by Bordwell and Yee (15), presenting evidence for product-like transition states in the protonation of cycloalkanenitronates.

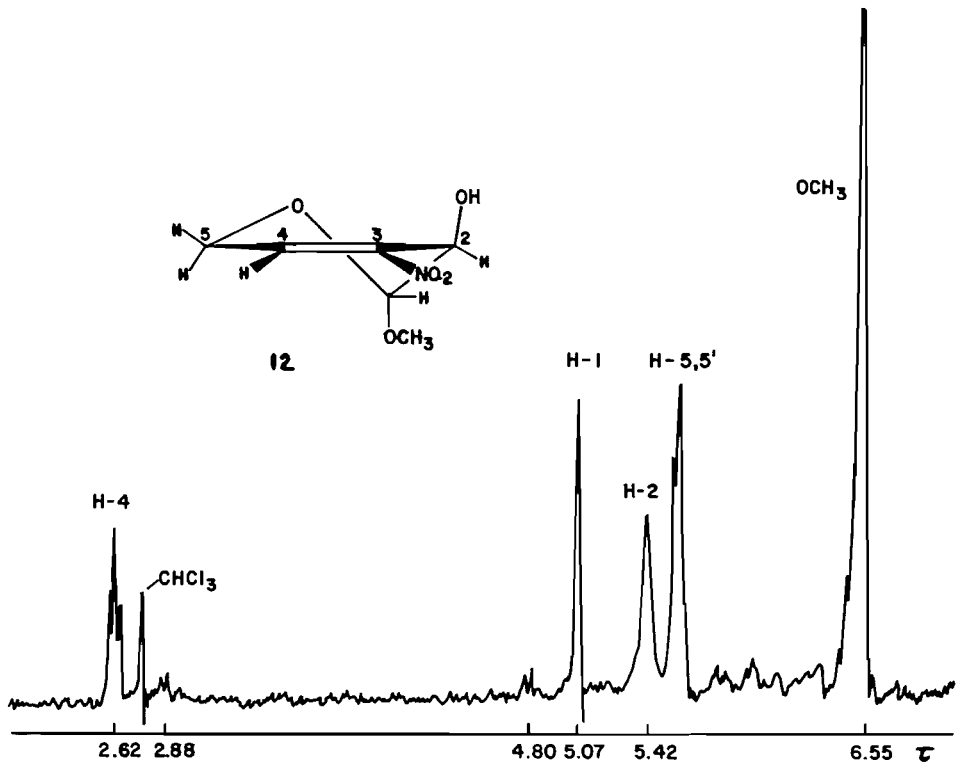

FIG. 2. The n.m.r. spectrum (100 MHz in $CDCl_3$) of nitro olefin **12**.

spectrum (Fig. 2) revealed that the product was not entirely uniform. The major component was characterized by a low-field triplet attributable to an olefinic proton which was coupled with two vicinal protons and must, therefore, be situated on C-4. The two one-proton signals assigned to H-1 and -2, respectively, appeared as singlets due to very small vicinal coupling. The spectrum fits the structure of methyl 3,4-dideoxy-3-nitro-β-L-*glycero*-pent-3-enopyranoside (**12**) in the conformation depicted. The weak doublets observed at τ 4.80 and 2.88 are probably due to the olefinic and anomeric protons of the corresponding, $\Delta^{2,3}$-unsaturated isomer. The minor component amounted to about 15% of the product.

The nitro olefins so obtained arose by acid-catalyzed dehydration of **6*** and(or) **7***, and it does not necessarily follow that they are involved in the epimerizations which occur in weakly basic medium. However, the fact that dehydration can take place under mild conditions, albeit to a limited extent, seems significant. It was shown, moreover, that **12** meets at least one requirement for being an intermediate in the epimerization. When placed in aqueous alkali (1 equiv), the olefin instantly added base to give nitronate, and the addition was found to be faster than the epimeric nitronate equilibration. An n.m.r. spectrum scanned from 1–5 min after the start of the reaction indicated that the olefin had already disappeared, giving mainly **2*** along with some **4*** (the latter presumably originating from the minor component in the olefin). There was only a trace of **3*** at this point, but its proportion increased with time as the proportion of **2*** decreased. These observations may be interpreted in terms of a rapid setting-up of a mobile equilibrium **2*** ⇌ **12** in which **2*** preponderates vastly (so that **12** is not seen in the spectrum), and through which **3*** is formed in a relatively slow reaction.

Whereas the findings just described lend support to the mechanism of reversible dehydration

Can. J. Chem. Downloaded from www.nrcresearchpress.com by 210.87.254.105 on 09/05/12
For personal use only.

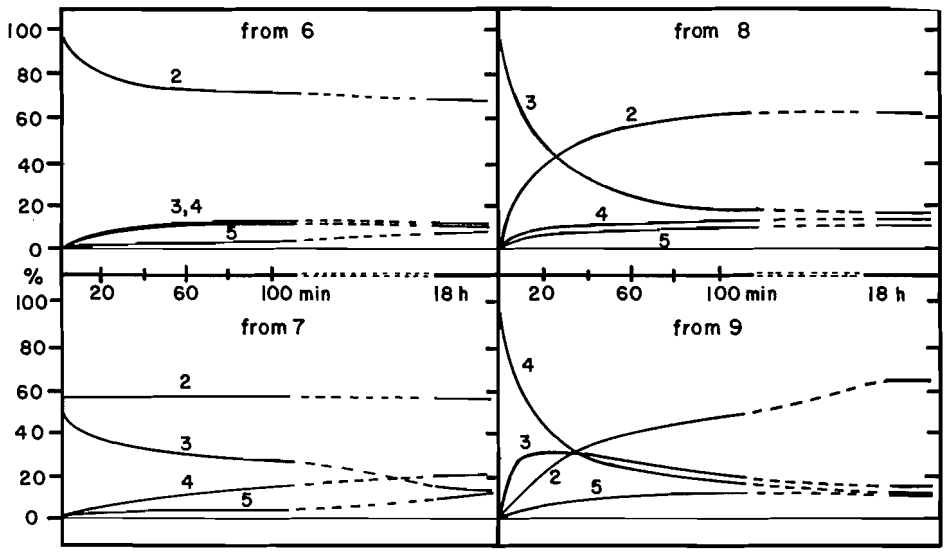

FIG. 3. Time-dependent change in composition of glycoside mixtures during alkaline epimerization.

for the β-epimerization of **2** (and hence, **6**), an unexpected behavior exhibited by the nitro xyloside **7** in alkaline solution requires that a second mechanism be assumed to operate, at least in part, in the epimerization of this compound. Even though the reaction eventually leads to the expected equilibrium mixture of nitronates, it differs in early stages from the alkaline epimerization of the nitro riboside **6**. Upon addition of an equivalent amount of alkali, **6** is rapidly converted into its salt **2**, and no other product is visible in the n.m.r. spectrum for several minutes until the epimeric salts slowly emerge (Fig. 3). Since the salt **2** is common to the 3-epimers **6** and **7**, it might have seemed obvious to expect precisely the same sequence of events to occur with **7**. Contrary to expectations, addition of alkali to **7** produced the salt **2** *and* the salt **3** practically simultaneously (*i.e.*, within the 2 min needed for recording a spectrum), in a ratio of about 1:1. Thereafter followed slow equilibration, with formation of the remaining nitronate epimers and with a final ratio of about 4:1 in respect of **2** and **3** (Fig. 3; compare also Fig. 1). The change in optical rotation during this reaction also was in agreement with an "initial" formation, not of **2** alone but of **2** and **3** in about equal amounts (Fig. 4). Clearly, the large proportion of **3** observed near the start of the reaction must be due to a fast epimerization that occurs in **7**

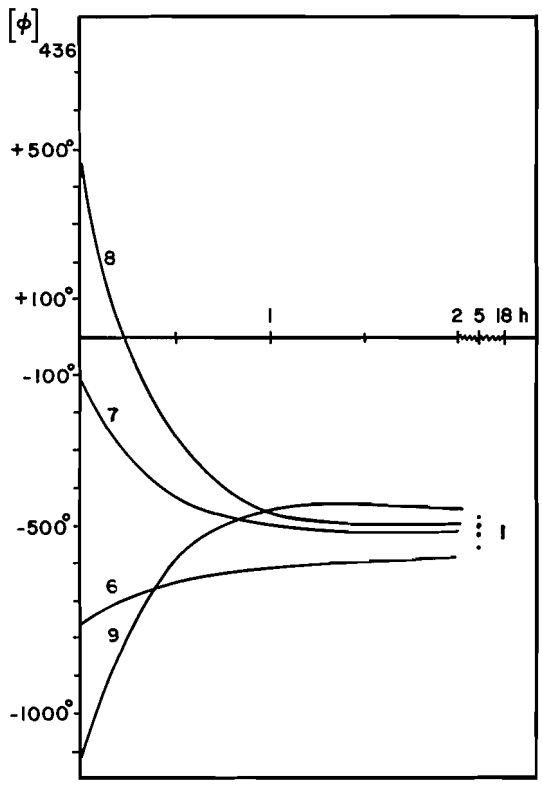

FIG. 4. Change of molecular rotations $[\Phi]_{436}$ of nitro glycosides in alkaline medium.

Can. J. Chem. Downloaded from www.nrcresearchpress.com by 210.87.254.105 on 09/05/12
For personal use only.

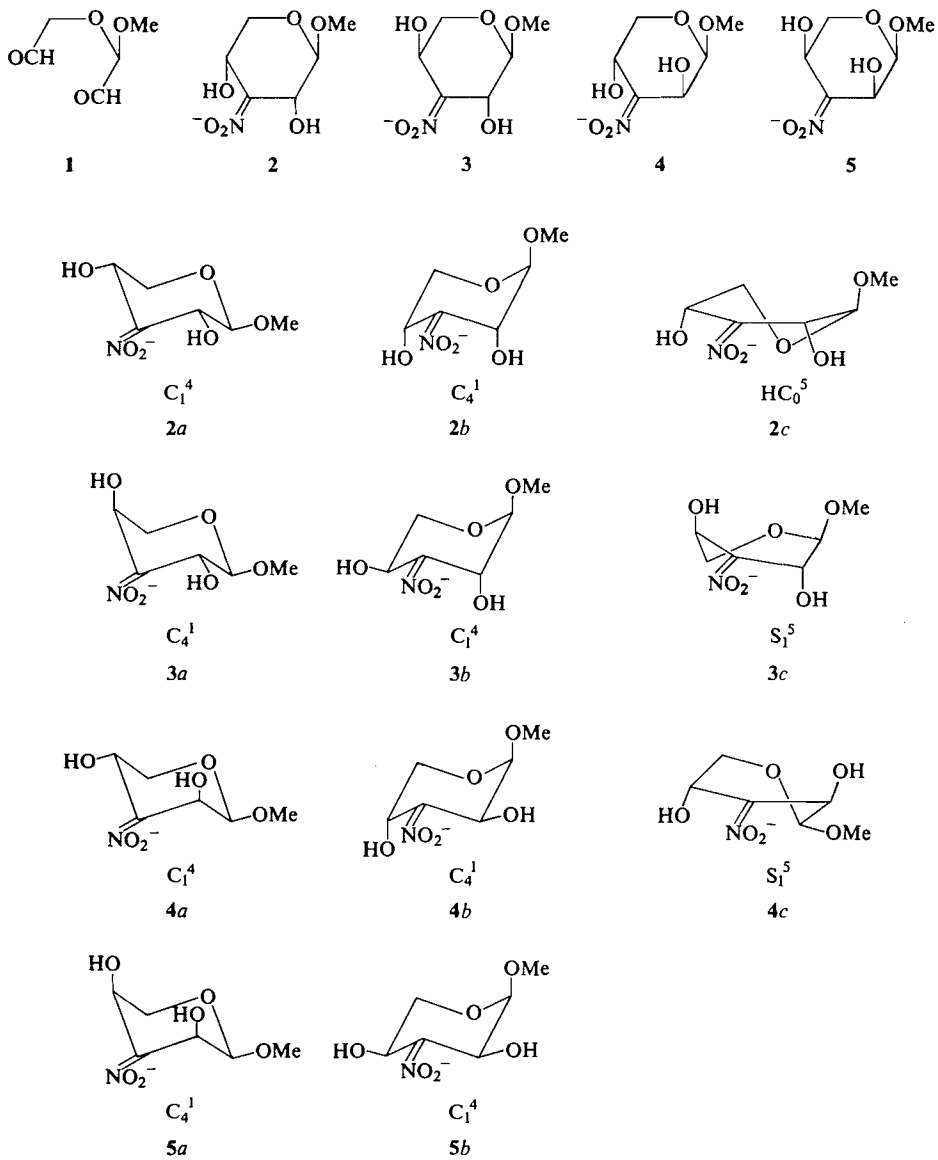

and does not proceed via **2**. Another phenomenon apparently related herewith was observed in the alkaline epimerization of the β-D-arabinoside **9**. In an early stage of this reaction, too, the nitronate **3** was produced in an amount larger than corresponded to the final equilibrium proportion. Its initial rate of formation was greater than that of **2** concurrently formed, but the rates then reversed, and that part of **3** which constituted a temporary excess over the equilibrium disappeared slowly (Fig. 3). It has thus become understandable that **9**, in the presence of alkali, displays a *complex* "mutarotation", a fact which had been recorded but not commented upon earlier (3). The results suggest that a mechanism other than the reversible dehydration to nitroalkene is involved at least in part of the over-all epimerization. For if only the dehydration mechanism were available, all **3** engendered from **9** (or its salt **4**) would of necessity have to arise via **2** (or via **5**), which evidently is not the case. A clue to an understanding of the epimerizations

Can. J. Chem. Downloaded from www.nrcresearchpress.com by 210.87.254.105 on 09/05/12
For personal use only.

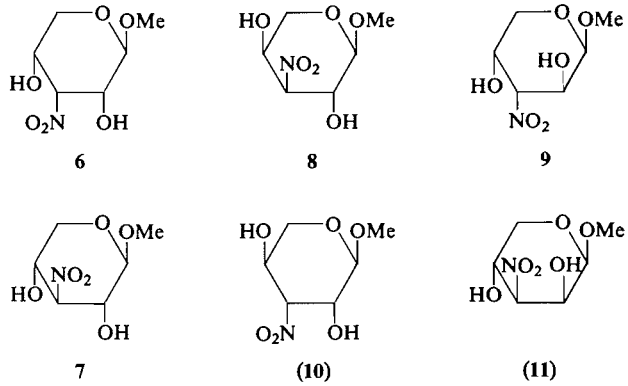

6 8 9

7 (10) (11)

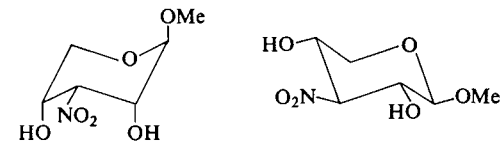

6*a* 7*a*

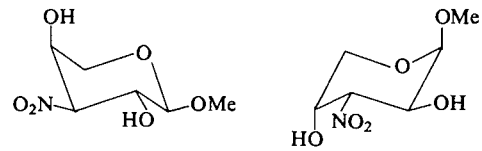

8*a* 9*a*

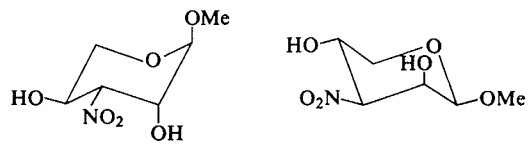

(10*a*) (11*a*)

Can. J. Chem. Downloaded from www.nrcresearchpress.com by 210.87.254.105 on 09/05/12
For personal use only.

came forth when the pK_a values of the nitro glycosides were compared. Table 6 shows p*H* values measured (at zero time) upon half-titration, and while some of these data may be apparent rather than true pK_a values,[12] they nevertheless reflect differential tendencies of nitronate formation. Most conspicuously, the xyloside **7** is a markedly weaker acid than the riboside **6**. This result is in harmony with the conformational free energies of **7***a*, **6***a*, and their common anion **2***b* which, on the basis of the preceding discussions, is expected to arise more readily from the latter than from the former. Now we suggest that **7***a*, having for stereochemical reasons a diminished nitromethylene acidity, is prone to competitive proton abstraction from its hydroxyl groups. Alkoxide formation at position 4 would initiate

TABLE 6. Acidities of nitro glycosides (by half-titration with NaOH in water)

Compound	p*H**
6	8.40
7	10.15
8	9.20
9	10.00

*Measured at room temperature with a glass electrode immediately after adding 1/2 equiv of base. Changes with time were insignificant within 15 min.

[12]A true value would be expected only if there existed, at the time of measurement, an equilibrium between the given nitro compound and the corresponding *aci* form, unadulterated by the presence of substantial amounts of epimers. This condition seems to be largely fulfilled for **6** and **8**, perhaps less so for **9**, but certainly not for **7**.

ring opening between C-4 and -3 (reverse Henry reaction), and subsequent recyclization would account for the formation of the epimeric nitronate **3** (Scheme 1). A similar if more complicated

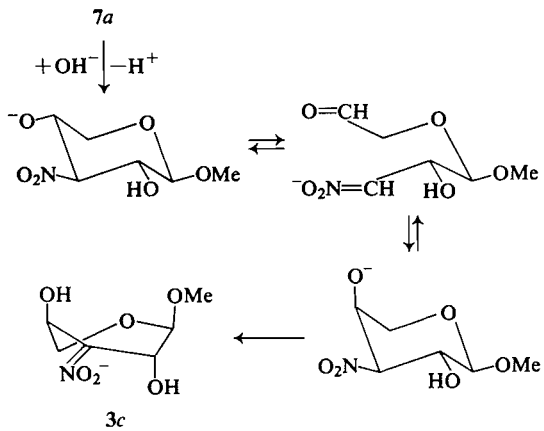

SCHEME 1

sequence could be written to explain the formation of **3** from the relatively weak acid **9** without intermediacy of **2** (Scheme 2). Although reversible ring opening was invoked by Grosheintz and Fischer (21) to explain epimerization in deoxynitroinositols, those investigators did not consider alternative pathways via nitroolefins, nor did they advance proof for the mechanism. The nitroolefin route is certainly available as long as the nitromethylene group, rather than a vicinal carbinol group, is the site of base-induced ionization. This condition can ordinarily be presumed to apply.[13] However, when steric factors reduce the nitromethylene acidity, as they do in **7**, the compound approaches in character a *tertiary*-nitro β-carbinol.[14] Such carbinols, in contrast to those having a primary or secondary nitro group, are known to undergo reverse Henry reaction with facility.

In the light of the results presented in this article, many observations regarding epimerizations and relative thermodynamic stabilities in the hexose analogs (4) become understandable. An example is the predominance of the α-D-*talo* configuration after nitronate equilibration followed by acidification. A comprehensive treatment of the hexose series is under way.

[13]The formation of $\Delta^{4,5}$-unsaturated 3-nitronate (18) is compelling evidence for the presence of $\Delta^{3,4}$-olefins in equilibrium with 3-nitronates.

[14]Other instances of steric diminution of nitromethylene acidity have been discovered by W. Rank in this laboratory and will be dealt with elsewhere.

Experimental

Nuclear Magnetic Resonance Spectra

The spectral data of Table 4 and Fig. 2 were measured on a Varian HA 100 instrument, and those of Tables 1 and 2 and of Figs. 1 and 3 were obtained on a Varian T60 instrument. The values for the nitronates **2**, **3**, and **4** in Table 1 were recorded within 2–3 min of adding an equivalent amount of sodium deuteroxide to solutions of the corresponding nitro glycosides **6**, **8**, and **9** in deuterium oxide. The spectra from which the points of Fig. 3 were derived by measuring methoxyl signal intensities were taken in similar fashion. Epimeric nitronate distributions at equilibrium (Table 2) were calculated from spectra that were taken 18–22 h after the start of the reaction; Fig. 1 is representative.

Optical Rotations

Optical rotations refer to aqueous solutions (*c* approximately 0.5 unless specified otherwise) at room temperature. They were determined in 1-dm tubes in a Perkin–Elmer automatic polarimeter, model 141. The specific rotations at various wavelengths of the free nitro glycosides are shown in Table **7**.

The molecular rotation curves of Fig. 4 were obtained from solutions which were made up by adding equal volumes of 0.02 *N* NaOH to 0.01 *M* solutions of the nitro glycosides. Hence the solutions were 0.05 *M* in nitronate (*c* approximately 0.1) and contained 1 equiv of excess NaOH. The wavelength 436 nm was chosen because large absolute rotations and optimal light intensity resulted in more accurate readings than at other wavelengths.

Materials

The sodium nitronates **2** and **2*** and the nitro glycosides **8** and **9** were prepared as previously described (refs. 2 and 3, respectively).

The nitronate **2** (0.62 g) was suspended in a mixture of methanol (36 ml) and nitromethane (4 ml), and the suspension was shaken for 5 min with 6 ml of methanol-washed Amberlite IR-120 (H^+), whereby the salt went in solution. Filtration and evaporation of the filtrate furnished a residue which was crystallized from ethyl acetate – petroleum ether (b.p. 30–60°) to give 0.27 g (48%) of *methyl 3-deoxy-3-nitro*-β-D-*ribopyranoside* (**6**), melting as reported (2) at 90–92°. The amorphous residue (0.31 g) obtained by evaporation of the mother liquor was chromatographed on 15 g of silica gel (Merck, 70–325 mesh) with carbon tetrachloride to which increasing amounts of ethyl acetate were added. At an eluent composition 2:1, a crystalline mixture of glycosides was obtained. Recrystallization from ethyl acetate – petroleum ether gave *methyl 3-deoxy-3-nitro*-β-D-*xylopyranoside* (**7**) as shiny needles, m.p. 186–187°, in a yield of 70 mg (13%).

Anal. Calcd. for $C_6H_{11}O_6N$ (193.2): C, 37.31; H, 5.74; N, 7.25. Found: C, 37.21; H, 5.62; N, 7.12.

An additional 17 mg (3%) of **6**, m.p. 92–94°, was obtained from the mother liquor.

In order to identify the product **7**, a sample (21 mg)

Can. J. Chem. Downloaded from www.nrcresearchpress.com by 210.87.254.105 on 09/05/12
For personal use only.

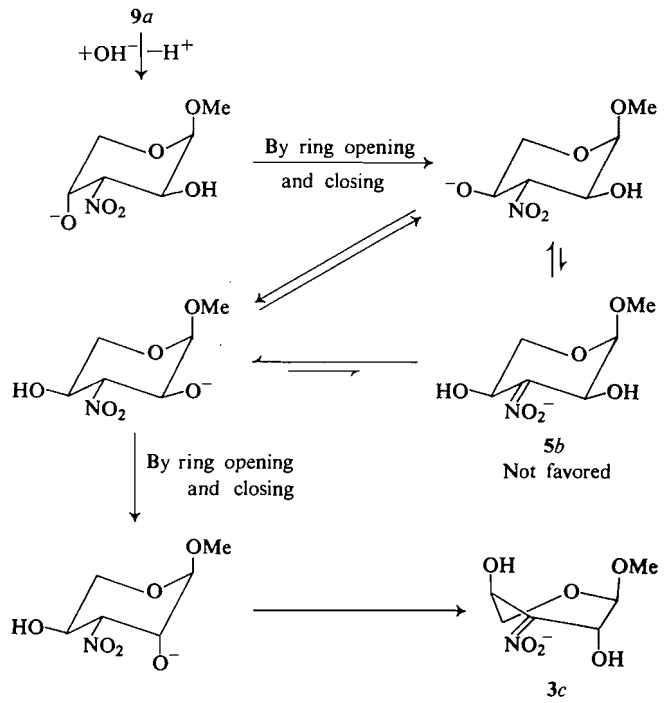

SCHEME 2

TABLE 7. Specific rotations of the free nitro glycosides

Compound	λ (nm)				
	589	578	546	436	365
6	−113.5	−118	−134	−226	−375
6*	+116	+120	+133	+227	+373
7	−46.7	−49.6	−57.0	−92.0	−124.3
7*	+48.0	+50.0	+55.5	+91.2	+123
8	+86	+87	+100	+155	+117
9	−273	−285	−323	−578	−635

was catalytically hydrogenated in 11 ml of 0.01 *N* hydrochloric acid in the presence of PtO_2 (30 mg), at 28° and ordinary pressure. Hydrogen consumption was 15 ml (required, 13.5 ml) after 2 h. The solution was then passed through a small column containing 0.5 ml of Dowex 1X2 (OH^-) resin, and was evaporated to give 16 mg of spontaneously crystallizing methyl 3-amino-3-deoxy-β-D-xylopyranoside. It melted at 195–197° after recrystallization from ethanol, undepressed upon admixture of a freshly recrystallized, authentic specimen (2).

The enantiomeric nitronate **2*** was deionized as described above for **2**. Work-up including column chromatography gave *methyl 3-deoxy-3-nitro-β-L-ribopyranoside* (**6***) as soft, granular crystals, m.p. 92–93°, and *methyl 3-deoxy-3-nitro-β-L-xylopyranoside* (**7***) as either feather-like crystals or hard prisms. Both kinds of crystals melted at 186–187°. A chromatographic fraction immediately preceding the fraction of **6*** and **7*** furnished a colorless oil which failed to crystallize although it showed a single spot on t.l.c. (CCl_4–EtOAc, 1:1). It had $[\alpha]_D$ +214, $[\alpha]_{578}$ +224, $[\alpha]_{546}$ +255, $[\alpha]_{436}$ +451° (*c*, 0.4 in water); ν_{max} in chloroform, 3200 (OH) and 1528 cm^{-1} (nitroalkene). The n.m.r. spectrum (Fig. 2) was in agreement with the structure of *methyl 3,4-dideoxy-3-nitro-β-L-glycero-pent-3-enopyranoside* (**12**).

Financial support of this work by the National Research Council of Canada is gratefully acknowledged.

1. H. H. BAER and H. O. L. FISCHER. Proc. Natl. Acad. Sci. **44**, 991 (1958).
2. H. H. BAER and H. O. L. FISCHER. J. Am. Chem. Soc. **81**, 5184 (1959).
3. H. H. BAER and A. AHAMMAD. Can. J. Chem. **41**, 2931 (1963).

Can. J. Chem. Downloaded from www.nrcresearchpress.com by 210.87.254.105 on 09/05/12
For personal use only.

4. H. H. BAER. Adv. Carbohydr. Chem. Biochem. **24**, 67 (1969).
5. E. L. ELIEL, N. L. ALLINGER, S. J. ANGYAL, and G. A. MORRISON. Conformational analysis. Interscience Publishers, New York, N.Y., 1965. (*a*) pp. 433–444; (*b*) pp. 355–357; (*c*) pp. 371–378; (*d*) pp. 115, 469–476; (*e*) p. 412.
6. F. R. JENSEN, C. H. BUSHWELLER, and B. H. BECK. J. Am. Chem. Soc. **91**, 344 (1969).
7. S. J. ANGYAL. Aust. J. Chem. **21**, 2737 (1968).
8. S. K. MALHOTRA and F. JOHNSON. J. Am. Chem. Soc. **87**, 5493 (1965). F. JOHNSON and S. K. MALHOTRA. J. Am. Chem. Soc. **87**, 5492 (1965).
9. R. U. LEMIEUX and J. D. STEVENS. Can. J. Chem. **44**, 249 (1966).
10. R. E. REEVES. Adv. Carbohydr. Chem. **6**, 107 (1951).
11. P. L. DURETTE and D. HORTON. Carbohydr. Res. **10**, 565 (1969).
12. D. HORTON and W. N. TURNER. J. Org. Chem. **30**, 3387 (1965).
13. H. H. BAER. Ber. **93**, 2865 (1960).
14. S. J. ANGYAL and B. M. LUTTRELL. Aust. J. Chem. **23**, 1485 (1970).
15. F. G. BORDWELL and K. C. YEE. J. Am. Chem. Soc. **92**, 5939 (1970).
16. H. O. L. FISCHER and H. H. BAER. Ann. **619**, 53 (1958).
17. H. H. BAER and W. RANK. Can. J. Chem. **43**, 3330 (1965).
18. H. H. BAER and F. KIENZLE. Ann. **695**, 192 (1966).
19. H. H. BAER and W. RANK. Can. J. Chem. **47**, 2811 (1969).
20. H. H. BAER and F. KIENZLE. Can. J. Chem. **47**, 2819 (1969).
21. J. M. GROSHEINTZ and H. O. L. FISCHER. J. Am. Chem. Soc. **70**, 1479 (1948).
22. H. H. BAER and M. BAYER. Can. J. Chem. **49**, 568 (1971).
23. L. HOUGH and A. C. RICHARDSON. *In* Rodd's chemistry of carbon compounds. Vol. I. Part F. *Edited by* S. Coffey. Elsevier Publishing Company, Amsterdam 1967. p. 90.

Can. J. Chem. Downloaded from www.nrcresearchpress.com by 210.87.254.105 on 09/05/12
For personal use only.

Gas–Solid Exchange Reactions: Zinc Vapor and Monocrystalline Zinc Telluride[1]

E. A. Secco and Richard Swee-Chye Yeo

Chemistry Department, St. Francis Xavier University, Antigonish, Nova Scotia

Received[2] July 28, 1970

The exchange reaction between radioactive zinc vapor and single crystals of zinc telluride was studied in a static system in the temperature range 760–860 °C and $P_{Zn} = 0.10$ atm.

The experimental rate data are consistent with a diffusion process which is interpreted in terms of a simple vacancy mechanism. The diffusion coefficient is given by

$$D = 2.34 \pm 0.37 \exp(-47.1 \pm 5 \text{ kcal}/RT)\ \text{cm}^2\ \text{s}^{-1}$$

Utilisant un système statique entre 760 et 860 °C et à $P_{Zn} = 0.10$ atm on a étudié la réaction d'échange entre de la vapeur de zinc radioactif et des cristaux uniques de tellurure de zinc.

Les résultats expérimentaux sont consistants avec un processus de diffusion qui peut être interprété en termes d'un mécanisme de cavités simples. Le coefficient de diffusion peut être exprimé par l'équation

$$D = 2.34 \pm 0.37 \exp(-47.1 \pm 5 \text{ kcal}/RT)\ \text{cm}^2\ \text{s}^{-1}$$

Canadian Journal of Chemistry, **49**, 1953 (1971)

Introduction

This study is a continuation of a program of research on heterogeneous isotopic exchange reaction involving a metallic vapor and its II–VI solid compound. The program is an attempt to understand the kinetics and mechanism of gas–solid interaction.

Previous studies reporting on the Zn–ZnO (1) and Zn–ZnS (2) systems have shown the exchange rate to be controlled by two processes, an initial first-order rate followed by a diffusion rate. On the other hand, the Zn–ZnSe (3) kinetic data showed the exchange reaction to be diffusion-controlled over the entire range investigated. The fact that ZnSe possesses a zinc blende cubic structure in contrast to the wurtzite hexagonal structure of ZnO and ZnS focussed attention on the crystal structure of the solid compound.

It was considered desirable, therefore, to probe the effect of the structural parameter by including the Zn–ZnTe system in this program; ZnTe is the fourth member in this family of compounds and possesses a cubic structure.

Experimental

The ZnTe single crystals used in this work were obtained from the laboratory of Prof. D. A. Stevenson, Dept. of Materials Science, Stanford University. The ZnTe was grown from Te rich solution, with Zn 6′9[3] and Te 6′9[3], and spectrosil quartz. A given crystal specimen was re-used for successive exchange experiments at the same temperature.

The exchange reaction was assumed to occur on one face, since the specimen geometry approximated a thin plate and the bottom face resting on the bucket floor was not exposed to the zinc vapor. The accessible depth for exchange is thus assumed to be the average thickness of the crystal. The crystal thickness was calculated from the projected area which was measured by an Olympus ECTR microscope.

The exchange runs were carried out in a static system with the use of quartz vessels, and the reaction fraction was determined by the uptake of radioactive zinc, as previously described (4, 5). All exchange experiments were done at a zinc pressure of 0.10 atm at the annealing temperature.

Results

The kinetic data for the Zn–ZnTe exchange reaction, although exhibiting exponential features, could not be fitted to a first-order rate expression. The alternative, that is, that the exchange process is a diffusion-controlled transport mechanism whose rate is a function of depth, was most probable.

The diffusion equation of interest in this case is that in which an infinite sheet of uniform material of thickness h is bathed in an atmosphere containing the diffusant. For the case of the lamina, to which the single crystal specimen is assumed to approximate quite well, the solution to the prob-

[1]This work represents a partial fulfillment of the requirements for the M.Sc. degree by R. S-C. Yeo.

[2]Revision received February 17, 1971.

[3]99.9999.

Can. J. Chem. Downloaded from www.nrcresearchpress.com by 210.87.254.40 on 09/05/12
For personal use only.

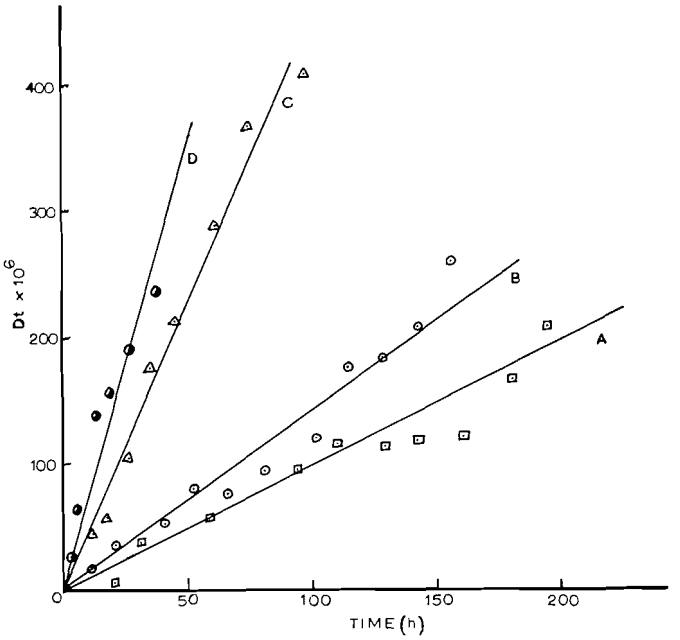

FIG. 1. Plot of Dt *vs.* time. *A*(769 °C); *B*(800 °C); *C*(820 °C); *D*(860 °C).

lem is given by Crank (6) in the form

$$[1]\quad \frac{M_t}{M_\infty} = 1 - \sum_{n=1}^{\infty} \frac{2\beta(\beta+1)}{1+\beta+\beta^2 q_n^2} \times \exp(-Dq_n^2 t/h^2)$$

This gives the total amount of M_t of tracer in the solid lamina at time t as a fraction of the amount M_∞ at equilibrium. β is the ratio of the moles of zinc in the vapor to the moles of zinc in the solid, *i.e.* n^g/n^s; D is the diffusion coefficient and h is the lamina thickness. The q_n's are the non-zero positive roots of

$$[2]\quad \tan q_n + \beta q_n = 0$$

In order to test the applicability of the diffusion equation and evaluate the diffusion coefficients, a theoretical plot is made of (M_t/M_∞) against $x = (Dt/h^2)^{1/2}$ and from this curve a value of x is read from each experimental value of (M_t/M_∞) and mole fraction, $S = n^s/(n^s + n^g)$. Eventually, a plot of $x^2h^2 = Dt$ against the reaction time $t = \sum_{i=1}^{n} t_i$ was made; t_i represents the individual reaction time intervals. If the diffusion equation is obeyed, the resulting graph should be a straight line through the origin, the slope of which is D. Figure 1 shows such plots of Dt as a function of time for ^{65}Zn exchange with ZnTe at different temperatures. The very good fit of the experimental data with the theoretical diffusion expression supports the interpretation that the exchange reaction is governed by a diffusion process at the outset.

The diffusion coefficients at the various temperatures were taken from the slope of the straight line in Fig. 1. The logarithm of the diffusion coefficients *vs.* $1/T$ °K yields a straight line, Fig. 2, corresponding to an activation energy of 47.1 ± 5 kcal. The diffusion equation is given as

$$[3]\quad D = 2.34 \pm 0.37 \exp(-47.1 \pm 5 \text{ kcal}/RT) \text{ cm}^2 \text{ s}^{-1}$$

Discussion

The fact that a single diffusion-controlled rate is observed in the cases of cubic ZnTe and ZnSe whereas two rate processes, first-order followed by diffusion, are observed in the hexagonal structures of ZnO and ZnS confirms the effect of the crystal structure parameter on the gas–solid exchange reaction. The rate-determining processes involved in our gas–solid exchange studies have been analyzed and interpreted (3) in terms of two limiting conditions: (*i*) the solid is relatively permeable and the exchange sites are readily accessible to the gas with a first-order rate pre-

Can. J. Chem. Downloaded from www.nrcresearchpress.com by 210.87.254.40 on 09/05/12
For personal use only.

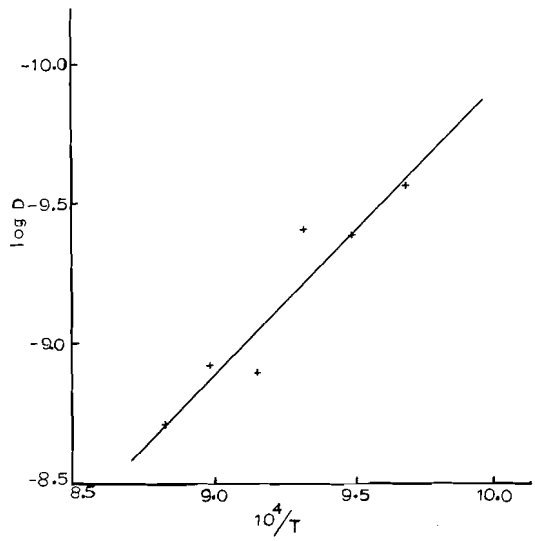

FIG. 2. Plot of log D *vs.* $1/T$ °K.

vailing, and (*ii*) the solid exchange sites are *not* readily accessible to the gas so that diffusion or transport step is rate-controlling. In the case of hexagonal structure conditions (*i*) and (*ii*) are operative in sequence whereas condition (*ii*) only is operative in the cubic structure.

Diffusion Mechanism in Zinc Telluride

Thomas and Sadowski (7) have reported results which are consistent with the vacancy model suggested by Aven and Segall (8); that is, doubly ionized zinc vacancies are the dominant native acceptor defect in undoped ZnTe in contact with zinc vapor. The equilibrium between lattice zinc atoms, Zn_i, zinc vacancies V_{Zn}, holes h, and zinc vapor Zn_g, may be written as

$$[4] \qquad Zn_i \rightarrow V_{Zn}^{2-} + 2h^+ + Zn_g$$

with the equilibrium constant K expressed as

$$[5] \qquad K = [V_{Zn}^{2-}]p^2P_{Zn} = \tfrac{1}{2}p^3P_{Zn}$$

where $[V_{Zn}^{2-}]$ is the concentration of V_{Zn}^{2-}, doubly ionized zinc vacancy, p is the concentration of holes h^+, and P_{Zn} is zinc vapor pressure. Rearranging [5], we have

$$[6] \qquad p = 2[V_{Zn}^{2-}] = (2K/P_{Zn})^{1/3}$$

which is the observed pressure dependence on the hole concentration (7),

$$[7] \quad p(\text{holes/cm}^3) = 3.73 \times 10^{23}P_{Zn}^{-1/3} \text{ (mm Hg) } \exp(-1.31 \text{ eV}/kT)$$

Assuming that zinc diffusion in zinc telluride crystal occurs via the vacancy mechanism, the diffusion coefficient is given by (9)

$$[8] \qquad D = \alpha\lambda^2\Gamma[V_{Zn}^{2-}]$$

where α is the geometry jump factor, that is, the number of possible jump vectors that give the same jump distance λ and still move in a particular direction; in the case of ZnTe, $\alpha = 4$. Γ is the jump frequency which is given as

$$[9] \qquad \Gamma = \nu \exp(-E_m/RT)$$

where ν is the atomic vibration frequency and E_m is the activation energy for mobility or the migration energy. The concentration of V_{Zn}^{2-} can be expressed as

$$[V_{Zn}^{2-}] = \exp(S_v^f/R)\exp(-E_v^f/RT)$$

where E_v^f and S_v^f are the energy and entropy change involved in the formation of the vacancy, respectively.

The zinc vacancy concentration in ZnTe in contact with zinc vapor at $P_{Zn} = 0.10$ atm can be calculated from [7] and [8] to yield

$$[10] \quad [V_{Zn}^{2-}] = 2.23 \exp(-30.2 \text{ kcal}/RT)$$

The diffusion coefficient normally expressed as $D = D_0 \exp(-Q/RT)$ now becomes

$$[11] \quad D = \alpha\lambda^2\nu \exp(S_v^f/R)\exp(-E_m - E_v^f/RT)$$

where

$$D_0 = \alpha\lambda^2\nu \exp(S_v^f/R) \quad \text{and} \quad Q = E_m + E_v^f$$

By assuming ν as the average between $\nu_{760\,°C}$ and $\nu_{860\,°C}$ which is calculated from Debye theory to be 9.639×10^{13} s^{-1} and taking λ as Zn–Zn jump distance in ZnTe to be 4.31×10^{-8} cm, D_0 is computed to be 1.67 cm^2 s^{-1} as compared to the experimental value of 2.34 ± 0.37 cm^2 s^{-1}. The agreement is to be considered excellent in view of the assumptions and the experimental errors involved.

The diffusion equation for self-diffusion of ^{65}Zn in ZnTe reported by Reynolds and Stevenson (10), $D = 14 \exp(-62.0 \text{ kcal}/RT)$ cm^2 s^{-1}, differs from our observed equation. They reported an enhanced self-diffusion of Zn in Al-doped (2×10^{19}/cm^3) ZnTe in the temperature interval 650–830 °C, $D = 10^{-4} \exp(-39.2 \text{ kcal}/RT)$ cm^{-2} s^{-1}, but observed no dependence of D on Zn partial pressure in undoped ZnTe crystals.

Can. J. Chem. Downloaded from www.nrcresearchpress.com by 210.87.254.40 on 09/05/12
For personal use only.

The authors are indebted to the National Research Council of Canada for financial support of this research program and to Prof. D. A. Stevenson, Stanford University, for the ZnTe single crystal.

1. E. A. SECCO. *In* Fourth International Symposium on Reactivity of Solids. *Edited by* J. H. deBoer. Elsevier Publishing Co., Inc., Amsterdam. 1960. p. 188.
2. E. A. SECCO. Can. J. Chem. **42**, 1396 (1964).
3. E. A. SECCO and CHIEN-HUO SU. Can. J. Chem. **46**, 1621 (1968).
4. E. A. SECCO and W. J. MOORE. J. Chem. Phys. **26**, 942 (1957).
5. E. A. SECCO. *In* Sixth International Symposium on Reactivity of Solids. *Edited by* J. W. Mitchell, R. C. DeVries, R. W. Roberts, and P. Cannon. Wiley-Interscience, Division of John Wiley & Sons, Toronto. 1968. p. 523.
6. J. CRANK. The mathematics of diffusion. Clarendon Press, Oxford. 1956. p. 53.
7. D. G. THOMAS and E. A. SADOWSKI. J. Phys. Chem. Solids, **25**, 395 (1964).
8. M. AVEN and B. SEGALL. Phys. Rev. **130**, 81 (1963).
9. L. A. GIRIFALCO. Atomic migration in crystals. Blaisdell Publishing Co., Division of Ginn & Co. 1964. pp. 49, 54, 64.
10. R. A. REYNOLDS and D. A. STEVENSON. J. Phys. Chem. Solids, **30**, 139 (1969).

Can. J. Chem. Downloaded from www.nrcresearchpress.com by 210.87.254.40 on 09/05/12
For personal use only.

Can. J. Chem. Downloaded from www.nrcresearchpress.com by 210.87.254.105 on 09/05/12
For personal use only.

Infrared Combination Frequencies in Coordination Complexes containing Nitrate Groups in various Coordination Environments. A Probe for the Metal–Nitrate Interaction

A. B. P. LEVER, E. MANTOVANI, AND B. S. RAMASWAMY
Department of Chemistry, York University, Downsview, Toronto, Ontario

Received November 30, 1970

The number and relative energies of nitrate combination frequencies in the 1700–1800 cm^{-1} region of the infrared spectrum may be used as an aid to distinguish the various coordination modes of the nitrate group. The data also provide an excellent probe for the strength of the metal–nitrate interaction.

Le nombre et les énergies relatives des combinaisons de fréquence des groupes nitrates dans la région de 1700–1800 cm^{-1} du spectre infrarouge peuvent être utilisés dans le but de déterminer les divers modes de coordination du groupe nitrate. Les résultats fournissent un outil excellent pour déterminer la force d'une intéraction métal–nitrate.

Canadian Journal of Chemistry, 49, 1957 (1971)

Introduction

It is well known that in a nitrato complex, the nitrate group may be present as a free ion, or as a coordinated ligand, bound in a unidentate or bidentate or intermediate fashion or may be bridging (1). Moreover, in complexes containing several nitrate groups, more than one coordination mode may be present. Many papers have appeared (2–21) in which attempts have been made to use the infrared spectra and Raman spectra of such complexes as a guide to the coordination mode present. It was initially proposed that the presence of an N=O stretching frequency above 1570 cm^{-1} (10) (or above 1600 cm^{-1} (9)) indicated the presence of a bidentately coordinated nitrate group, but many exceptions to these suggestions soon became apparent (3, 14, 15). Of more fundamental validity was the suggestion that the doubly degenerate asymmetric ν_3 stretching vibration (E' in the D_{3h} symmetry of the free nitrate ion (16)) should split upon coordination (8), since the symmetry of the nitrate species would be reduced to C_{2v}, and moreover that the extent of the splitting is a guide to the coordination mode (3, 7). Unfortunately this criterion is also highly unreliable (15).

Raman studies have been of greater utility in distinguishing monodentate from bidentate coordination since these give rise to different sequences of polarization of the fundamental stretching modes (19). However, for various reasons Raman data are not so routinely available as infrared spectra.

In 1965 Curtis and Curtis (7) concluded, on the basis of a very small amount of data, that bands in the infrared spectra near 1750 cm^{-1}, assigned to combination modes, could be used for structural diagnosis. In particular, an ionic nitrate group gives rise to one relatively strong and very sharp combination frequency, whilst coordinated nitrate groups give two frequencies with the bidentate coordination mode giving a wider separation of these two frequencies than the unidentate coordination mode. The intensities were shown to decrease in the order ionic > unidentate > bidentate. This correlation has rarely been referred to in subsequent studies despite the apparent usefulness of the criteria and the fact that this region of the spectrum is generally free from other absorption.

In this paper we have studied this region in the spectra of a large number of nitrato complexes and report our conclusions. Some typical spectra are shown in Fig. 1.

Experimental

Most of the compounds have been previously reported. They were prepared by the methods outlined in the literature according to the references. The new complexes listed in Table 1 were all prepared by reaction of the stoichiometric amounts of amine and metal nitrate in ethanol, followed by recrystallization from the same solvent where feasible. They were dried in a vacuum desiccator prior to analysis and the recording of spectra.

Analyses

$Cu(3\text{-}Pic)_2(NO_3)_2$
Anal. Calcd. for $C_{12}H_{14}CuN_4O_6$: Cu, 17.0; NO_3, 33.2. Found: Cu, 16.8; NO_3, 33.0.

$Co(3\text{-}Pic)_2(NO_3)_2$
Anal. Calcd. for $C_{12}H_{14}CoN_4O_6$: Co, 15.95; NO_3, 33.6. Found: Co, 15.9; NO_3, 33.25.

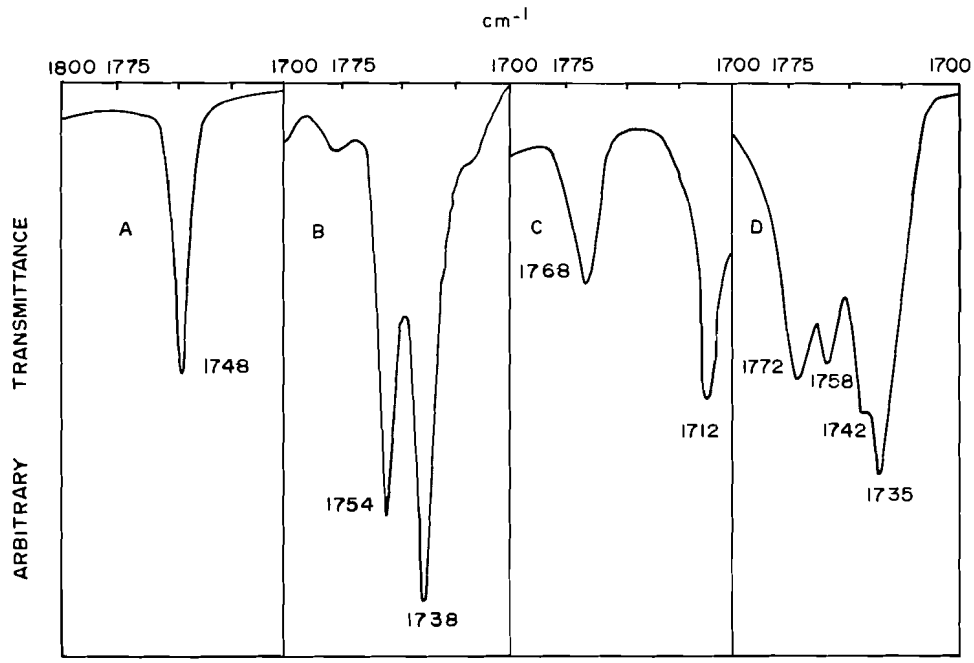

FIG. 1. Combination frequencies exhibited by (*A*) Cu(asym-$Et_2en)_2(NO_3)_2$ (red isomer), (*B*) Co(asym-$Me_2en)_2(NO_3)_2$, (*C*) $Ni(Py)_2(NO_3)_2$, and (*D*) $Co(3\text{-}Pic)_3(NO_3)_2$.

Co(4-Pic)$_4$(NO$_3$)$_2$
Anal. Calcd. for $C_{24}H_{28}CoN_6O_6$: Co, 10.6; NO_3, 22.3. Found: Co, 10.6; NO_3, 22.0.

Co(3-Pic)$_3$(NO$_3$)$_2$
Anal. Calcd. for $C_{18}H_{21}CoN_5O_6$: Co, 12.7; NO_3, 26.8. Found: Co, 12.6; NO_3, 26.5.

Ni(Py)$_2$(NO$_3$)$_2$
Anal. Calcd. for $C_{10}H_{10}N_4NiO_6$: Ni, 17.2; NO_3, 36.4. Found: Ni, 17.3; NO_3, 36.3.

Ni(Et$_4$dien)(NO$_3$)$_2$
Anal. Calcd. for $C_{12}H_{29}N_5NiO_6$: Ni, 14.7; NO_3, 31.15. Found: Ni, 14.7; NO_3, 30.9.

The nickel analysis employed the dimethylglyoxime complex, whilst the cobalt and copper analyses were by the pyridine thiocyanate method. Nitrate was analyzed as its Nitron salt. Infrared spectra were obtained as Nujol mulls between NaCl plates with a Beckman IR12 instrument. There was no evidence of any exchange of Cl^- for NO_3^- when using NaCl plates, since the nitrates under study were generally of low reactivity.

In order to correctly identify the combination bands the spectra of the complexes were compared with the spectra of corresponding complexes with other anions, in the 1700–1800 cm^{-1} region. Overtones from organic ligands are sometimes seen in this region.

Results and Discussion

Nitrate complexes are known (7, 11, 12) to give rise to combination frequencies near 1750 and near 2400 cm^{-1} and to an overtone (of the symmetric stretching vibration) near 2000 cm^{-1}. The bands near 1750 cm^{-1} are generally clearly defined and often relatively strong (see below), whilst those near 2000 and 2400 cm^{-1} are weaker, and often broad and sometimes very difficult to locate. For these reasons we are concerned here solely with the absorption near 1750 cm^{-1}. In this region the ionic nitrate group exhibits a single band which has been assigned (7, 11, 12) to a combination of the ν_1 symmetric stretch (A_1, in D_{3h}) and the doubly degenerate in-plane bending mode ν_4 (E' in D_{3h}). This combination is allowed by symmetry although of course combination frequencies are generally forbidden for an harmonic oscillator. The fact that it is observed implies some anharmonicity is present. When the nitrate group coordinates to a metal atom (in either a unidentate or bidentate fashion), then its local symmetry is reduced to C_{2v} (or perhaps lower (1)). As a consequence, the doubly degenerate in-plane bending mode splits into two components (A_1 and B_2 in C_{2v}). Combination of both of these modes with the symmetric stretch (A_1 in C_{2v}) is still allowed by symmetry and therefore two combination frequencies may be expected. These are observed and it is highly pertinent to their assignment that their separation

Can. J. Chem. Downloaded from www.nrcresearchpress.com by 210.87.254.105 on 09/05/12
For personal use only.

TABLE 1. Nitrato combination frequencies ($\nu_1 + \nu_4$)

Complexes*	Combination frequencies (cm^{-1})‖				Δ	Reference number
Bidentate nitrate derivatives						
$Cu(1,3\text{-DAP})(NO_3)_2$	1735	1757			22	43
$Cu(sym\text{-}Et_2en)(NO_3)_2$	1737	1769			32	43
$Cu(asym\text{-}Et_2en)(NO_3)_2$†	1715	1735			20	43
$Cu(sym\text{-}Me_2en)(NO_3)_2$	1740	1763			23	43
$Cu(2\text{-Pic})_2(NO_3)_2$	1721	1742			21	3
$Cu(3\text{-Pic})_2(NO_3)_2$	1721	1759			38	This work
$Cu(PS)(NO_3)_2$	1718	1765			47	24
$Co(2\text{-Pic})_2(NO_3)_2$	1718	1763			45	3
$Co(3\text{-Pic})_2(NO_3)_2$	1717	1769			52	This work
$Ni(Py)_2(NO_3)_2$	1712	1768			51	This work
$Ni(2\text{-Pic})_2(NO_3)_2$	1718	1774			56	3
$[Ph_3AsCH_3][Co(NO_3)_4]$	1725	1776			41	6, 22
$[Ph_3AsCH_3][Mn(NO_3)_4]$	1730	1775			45	6
$[Ph_3AsCH_3][Zn(NO_3)_4]$	1730	1779			49	6
$[Nien_2(NO_3)]ClO_4$	1725	1771			46	7
$[nBu_4N]_3[Sm(NO_3)_6]$	1749	1785			36	41
$[nBu_4N]_3[Nd(NO_3)_6]$	1747	1780			33	41
$Rb[UO_2(NO_3)_3]$	1727	1761			34	12, 26
$UO_2(NO_3)_2$	1785	1830			45	12, 26
$UO_2(NO_3)_2(TBP)_2$	1732	1778			46	20
$(NH_4)_2Ce(NO_3)_6$	1739	1780			41	This work
$Th(NO_3)_4(TBP)_2$	1724	1770			46	20
$Ln(NO_3)_3(TBP)_3$§	—	—			29–54	20
Monodentate nitrate derivatives						
$Cuen_2(NO_3)_2$	1753	1761			8	29
$Cu(1,3\text{-DAP})_2(NO_3)_2$	1752	1763			11	29
$Cu(sym\text{-}Et_2en)_2(NO_3)_2$	1745	1750			5	29
$Cu(1,2\text{-DAP})_2(NO_3)_2$	1751	1761			10	42
$Cu(sym\text{-}Me_2en)_2(NO_3)_2$	1753	1760			7	29
$Cu(asym\text{-}Me_2en)_2(NO_3)_2$	1753	1762			9	29
$Co(asym\text{-}Me_2en)_2(NO_3)_2$	1738	1754			16	43
$Co(sym\text{-}Me_2en)_2(NO_3)_2$	1750	1768			18	43
$Cu(4\text{-Pic})_4(NO_3)_2$	(1746)	1754			8	44
$Cu(Py)_4(NO_3)_2$	1746	1756			10	45
$Co(4\text{-Pic})_4(NO_3)_2$	1747	(1773)			26	This work
$Ni(4\text{-Pic})_4(NO_3)_2$	1748	(1773)			25	46
$Nien_2(NO_3)_2$	1741	1762			21	7
$Ni(1,3\text{-DAP})_2(NO_3)_2$	1752	1776			24	29
Mixed monodentate and bidentate						
$Co(3\text{-Pic})_3(NO_3)_2$	1735	1742	1758	1772	16, 37	This work
$Ni(Py)_3(NO_3)_2$	1699	1710	1747	1765	37, 66	31
$Cu(PE)(NO_3)_2$	1715	1729	1756	1782	14, 26	24
$(Ph_3AsCH_3)_2(Ni(NO_3)_4)$	1720	1742	1777br		35, 57	6
$Ni(dien)(NO_3)_2$	1734	1738	1748	1785	14, 47	7
$Ni(Et_4dien)(NO_3)_2$	1717	1730	(1735)	1774		This work
$[Ph_3AsCH_3][Cu(NO_3)_4]$	1724	1771br	(1787)		16, 47	6
Ionic						
$Ni(PE)_2(NO_3)_2$	1745				0	47
$Nien_3(NO_3)_2$	1750				0	7
$Cu(asym\text{-}Et_2en)_2(NO_3)_2$‡	1748				0	29
$Ca(NO_3)_2$	1810				0	39
$Pb(NO_3)_2$	1773				0	39
Bridging						
$Ni(NO_3)_2 2H_2O$	1797					31
β-$Cu(NO_3)_2$	(1733)	1792				11
$AgNO_3$	1754	1774				This work

*en = Ethylenediamine; 1,3-DAP = 1,3-propylenediamine; sym-Me_2en, sym-Et_2en, asym-Me_2en, and asym-Et_2en = symmetric and antisymmetric *N,N*-dimethyl and diethylethylenediamines; Py = pyridine; *n*-Pic = *n*-picoline, *n* = 2, 3, 4; PS = bis(2-pyridyl)disulfide; PE = 1,2-bis(2′-pyridyl)ethane; dien = diethylenetriamine; Et_4dien = 1,1,7,7-tetraethyldiethylenetriamine; and TBP = tri-*n*-butylphosphate.

†Purple isomer.

‡Red isomer.

§A series of different lanthanide ions.

‖Shoulders in parentheses.

Can. J. Chem. Downloaded from www.nrcresearchpress.com by 210.87.254.105 on 09/05/12
For personal use only.

Can. J. Chem. Downloaded from www.nrcresearchpress.com by 210.87.254.105 on 09/05/12
For personal use only.

corresponds closely to the splitting of the ν_4 fundamental mode (7).

Whilst coordination of the nitrate group will formally reduce its symmetry to C_{2v}, one may suppose that if the metal nitrate interaction is small the species may still be effectively D_{3h} and give rise to only a small splitting in ν_4 and, therefore, a small splitting in the combination frequency. Thus the separation in the combination frequencies is expected to be a guide to the degree of metal–nitrate interaction. It is expected that for a given metal, bidentate coordination involves a greater distortion from D_{3h} symmetry than unidentate coordination and, therefore, bidentate complexes should show a larger separation of $(\nu_1 + \nu_4)$; Curtis and Curtis (7) showed that this is indeed true.

The above discussion makes the tacit assumption that correlation coupling between one nitrate molecule and another in a polynitrato species (such as the ion $Ce(NO_3)_6^{2-}$) or between one molecule and another (solid state site symmetry phenomena) will not lead (if the nitrate groups within the molecule are equivalent by symmetry) to more than one set of combination bands. Curiously, and somewhat unexpectedly, this assumption does seem to be valid for all the complexes we have investigated to date. Thus even though the ν_1 and the components of the ν_4 fundamental bands in the spectrum of the hexanitratocerate(IV) ion show structure presumably arising through coupling phenomena, only two sharp bands, whose separation is typical of a bidentate coordination, are observed in the combination region near 1750 cm^{-1}. The only indication of any structure in this region is an almost imperceptible shoulder on the lower energy band.

It is worthwhile emphasizing at this point that the data to be discussed in this paper reflect the symmetry of the environment in which the nitrate finds itself and does not necessarily infer a covalent metal–nitrate interaction. If the nitrate group is asymmetrical as a consequence of monodentate or bidentate coordination to a metal ion, then there is clearly some degree of metal–nitrate interaction, and the nitrate electron density is clearly polarized by the metal ion. The polarization, however, may proceed by an ionic or covalent mechanism or mixture thereof.

With this background it is now useful to consider the various series of complexes studied in turn.

Complexes with Bidentate Nitrate Groups

The series $M(R\text{-}Py)_2(NO_3)_2$ (M = Co(II), Ni(II), and Cu(II), see Table 1) all possess bidentate nitrate groups (3, 13) and give rise to two fairly weak combination bands separated (with one exception, see below) by 38–56 cm^{-1}. These data agree well with those found (41–53 cm^{-1}) by Curtis and Curtis (7) for a series of mononitrato tetraammine complexes of nickel(II). The series $(Ph_3AsCH_3)_2\ M^{II}(NO_3)_4$ have varying structures depending upon the nature of M. The cobalt complex (with Ph_4As^+ as cation) was shown to be eight coordinate, with bidentate nitrate groups, by Cotton and Bergman (22). Very recently the manganese and zinc complexes were also shown (23) to be eight coordinate, analogous to the cobalt derivative (in the case of the zinc complex the structure was inferred from a limited amount of X-ray data). All three complexes exhibit a pair of combination frequencies separated by 45–51 cm^{-1}, in agreement with their structure. The nickel and copper complexes have different structures and different i.r. spectra and are referred to below. The complex dinitrato[bis(2-pyridyl)disulfide]copper(II) has been shown to be octahedral with bidentate nitrate groups (24) and exhibits two combination frequencies separated by 47 cm^{-1}. The complex $Cu_2(Py)_5(NO_3)_2$ has recently been shown by X-ray methods (25) to contain both bidentate and bridging nitrate groups. The presence of the bidentate nitrate groups is shown by two well defined bands at 1720 and 1741 cm^{-1} whilst the bridging bands appear only to give rise to weak absorption at higher energies (see below). If the interaction between the metal and the bidentate nitrate group is weakened for some reason, then, following the argument developed above, a decrease in the splitting may be expected. Such decreases are exhibited, for example, by $Rb(UO_2NO_3)_3$ and the salts of $Nd(NO_3)_6^{3-}$ and $Sm(NO_3)_6^{3-}$, presumably as a consequence of the more electropositive character of the lanthanides and actinides, which would form only weak metal oxygen bonds. The rubidium complex has been shown to contain bidentate nitrate groups (26, 27). Although X-ray structural data are not available for the lanthanide derivatives quoted, there are some X-ray data available for lanthanide nitrate complexes (28) and it is fairly safe to infer that the coordination polyhedron around these ions is 12 coordinate.

Can. J. Chem. Downloaded from www.nrcresearchpress.com by 210.87.254.105 on 09/05/12
For personal use only.

A series of lanthanide complexes of the formulae $Ln(NO_3)_3(TBP)_3$ (TBP = tri-*n*-butylphosphate) have been studied by Ferraro *et al.* (20) and are shown by Raman polarization studies (19) to contain bidentate nitrate groups. These exhibit a pair of combination bands near 1750 cm^{-1} separated by 29–54 cm^{-1}. Some uranium and thorium TBP complexes (shown in Table 1) contain bidentate nitrate groups as indicated by Raman studies (20) and give rise to combination band splittings near 45 cm^{-1}. The salt $(NH_4)_2Ce(NO_3)_6$ exhibits a separation of similar amount (*vide supra*) and X-ray evidence (28) indicates that the $[Ce(NO_3)_6]^{2-}$ ion contains bidentate nitrate.

The mono-diamine copper complexes also represent interesting members of this class. Because of the tetragonal distortion expected for d^9 Cu(II) complexes, it is very likely that these complexes have an in-plane CuN_2O_2 chromophore with long axial Cu—O bonds (29), such that the bidentate nitrate group is unsymmetrically bound with two different copper oxygen bond lengths. No X-ray data are available to confirm this supposition but it is significant that the splitting of the combination bands is decreased from the values observed with the cobalt and nickel complexes described above. It is also highly relevant that whilst the complex $Cu(3\text{-}Pic)_2(NO_3)_2$ has a band splitting of 38 cm^{-1} the more highly hindered $Cu(2\text{-}Pic)_2(NO_3)_2$ gives a splitting of only 21 cm^{-1}. In this last case a very recent X-ray structure has indeed revealed (30) the presence of a long and a short copper–oxygen interaction to the same nitrate group. The situation is intermediate between monodentate and bidentate coordination.

Complexes with Monodentate Nitrate Groups

Curtis and Curtis (7) had shown, on the basis of only three nickel compounds, that the splitting of the combination bands for a monodentately bound nitrate group, was of the order of 15–21 cm^{-1}. Our own data (Table 1) for cobalt and nickel complexes suggest a slightly larger range of 16–26 cm^{-1} for a strongly bound monodentate nitrate group. Once again, however, the copper complexes, in which the nitrate groups occupy the axial sites and will only be weakly bound, give rise to much smaller splittings, of the order of 5–11 cm^{-1}. There seems little doubt that *for a given metal* the splitting in complexes with monodentate nitrate complexes is smaller than that exhibited by the bidentate derivatives and that the size of the splitting for a given mode of bonding depends upon the strength of the interaction (*vide infra*).

Complexes with both Monodentate and Bidentate Nitrate Groups

Such complexes may be expected to show four combination bands because a pair of frequencies is generated from each coordination mode. In many cases four such bands are observed, although occasionally two may overlap. There is no simple way of identifying which bands belong to which coordination mode and the splitting values given in Table 1 are somewhat arbitrary in that the pairs are chosen to yield values of Δ consistent with the presence of the two coordination modes. If inter or intramolecular coupling between equivalently bonded nitrate groups can be excluded as a mechanism for introducing band multiplicity in the combination region, then the presence of multiple bands (more than two) in this region can be used as an indicator of the presence of inequivalently bound nitrate groups. As discussed above, such coupling might well be expected to introduce additional structure in the combination region, but our experiments to date indicate that this does not generally occur. Clearly however, care must be taken in deducing information from multiple combination bands, and solution data should be obtained if possible. Rosenthal and Drago (31) had previously proposed that the tris(pyridine) metal nitrates contained both monodentate and bidentate coordination and our results support this supposition. These data also support the structure previously suggested for the complex $Cu(PE)(NO_3)_2$ (24). The tetranitrato anions of nickel and copper have long been known to have structures different from their cobalt and manganese analogs, but the precise structures have remained unknown. The nickel complex is undoubtedly octahedral (6, 32) on the basis of its electronic spectrum. Our data support the previously inferred conclusion (32) that the coordination polyhedron is made up of both monodentate and bidentate nitrate groups, although it is not possible to unequivocally exclude the presence of bridging nitrate groups (see Note added in proof). Similar comments may be made about the structure of the $[Cu(NO_3)_4]^{2-}$ ion; in this case there is a

Can. J. Chem. Downloaded from www.nrcresearchpress.com by 210.87.254.105 on 09/05/12
For personal use only.

similarity between the spectrum of this compound in this region and that of the solid anhydrous $Cu(NO_3)_2$, which may favor a polymeric structure.

Bridging Nitrate Groups

Three kinds of bridging nitrate groups may generally be recognized. The first, through all oxygen atoms, is likely to occur in some simple anhydrous metal nitrates. Such structures may be seen as an extension of simple ionic structures, such as $NaNO_3$, when the alkali metal is replaced by a more covalent metal such as silver. Silver nitrate itself has an "ionic" lattice in which the nitrate ions are asymmetrically situated such that two oxygen atoms are similar to one another but different from the third in their environment (33). A separation of 20 cm^{-1} is observed in the combination bands which probably reflects the asymmetry of the nitrate group and does not necessarily reflect the presence of a covalent metal oxygen interaction. Whether such a lattice may be considered to contain bridging nitrate groups is perhaps debatable and a Raman study to locate silver–oxygen vibrations would be useful in this context. Certainly the combination spectra are not consistent with the presence of symmetric nitrate ions.

Bridging through two oxygen atoms to different metal atoms is exemplified by the α modification of copper nitrate (34). Finally one oxygen atom of the nitrate group may bridge two metal atoms as in the complex $Cu_2(Py)_5(NO_3)_2$ previously described (25).

Consideration of the combination frequencies of these and other bridging nitrate complexes does not, unfortunately, lead to any unequivocal relationships between the spectra and structure, or mode of bridging. Perhaps the only systematic observation is that complexes containing bridging nitrate groups almost invariably exhibit a combination band at a higher frequency (near 1800 cm^{-1}) than those generally observed in non-bridging systems. The presence of such a band may well imply bridging nitrate, but its absence does not convey the converse. The polymeric $Ni(NO_3)_2.2H_2O$ complex (35) absorbs at 1797 cm^{-1}, considerably higher than any other nickel complexes studied so far.

Similarly high energies were observed in some anhydrous metal nitrates reported by Addison and Gatehouse (11). Anhydrous copper nitrate (β form, which apparently has a similar structure to the α form (1)) also shows a band at 1792 cm^{-1} with a shoulder at 1733 cm^{-1}. The obvious relationship of this spectrum to that of the $[Cu(NO_3)_4]^{2-}$ ion suggests the latter might be polymeric. The data do not appear consistent with the recent suggestion (23) that this complex is similar to the $[Au(NO_3)_4]^-$ ion which possesses monodentate nitrate groups (36).

The complex $(Ph_3P)_2Ni(NO_3)_2$ described by Venanzi (37) has been an enigma for some time. Similar complexes with the halides were shown to be tetrahedral but the magnetic and electronic spectroscopic properties of the nitrate were inconsistent with this stereochemistry. The complex exhibits multiple absorption in the region 1700–1800 cm^{-1} but unfortunately so does the free triphenylphosphine ligand. The bands indicated in Table 1 were chosen on the assumption that the bands due to the ligand have not shifted much upon coordination; these were then subtracted from the spectrum. The band at 1798 cm^{-1} is consistent with the presence of a bridging nitrate group (although it is very weak) whilst the bands at 1765 and 1711 cm^{-1} (the latter being the strongest) represent the pair of bands arising from a bidentate nitrate group. The complex is then formulated as being a polymeric octahedral derivative with both bidentate and bridging nitrate groups.

Ionic Nitrate Complexes

Ionic nitrates when present with complex counterions, such as those in Table 1 give rise to a single sharp narrow band near 1750–1800 cm^{-1}. The absorption is strong relative to the absorption shown in this region by other types of nitrate group, and is quite distinctive. Simple salts such as $NaNO_3$ and $Sr(NO_3)_2$ generally exhibit a similar sharp narrow band, but somewhat weaker and at energies varying from 1750 to as high as 1800 cm^{-1} or a little above (38–40). Detailed studies of some anhydrous Group(II) metal nitrates have been reported (39, 40) in which the spectra were analyzed with correlation coupling of the nitrate groups (39, 40) taken into account. Although multiple combination bands are expected they are not generally observed (39) (Schutte finds evidence in some cases of a splitting of the order of 5 cm^{-1} or less (40)). Hydrated

Can. J. Chem. Downloaded from www.nrcresearchpress.com by 210.87.254.105 on 09/05/12
For personal use only.

nitrates, on the other hand, do not always show this absorption. Extensive hydrogen bonding may be responsible.

Conclusion

It is apparent that useful structural information can be derived from consideration of the combination bands exhibited by nitrato complexes in the 1700–1800 cm^{-1} region. Intermolecular or intramolecular correlation coupling of the nitrate groups does not seem to be an interfering factor although it may be responsible for minor shoulders in some of the spectra. The magnitude of the splitting depends on the metal–nitrate interaction and is generally larger for bidentate than for monodentate coordination *for a given metal and oxidation state*. With the fairly restricted range of polarizing cations in this study the separation for the monodentate nitrate group lies in the range 5–26 cm^{-1} whilst for the bidentate complexes it is 20–66 cm^{-1}. It is relevant that the Ce(III) complex $Ce(NO_3)_3(TBP)_3$ gives a separation of 54 cm^{-1} (20) whilst the Ce(IV) complexes $Ce(NO_3)_4(TBP)_2$ (20) and $(NH_4)_2Ce(NO_3)_6$ yield separations of 25 and 41 cm^{-1}, respectively. Clearly polarization alone cannot explain these differences and consideration must be taken of the number of nitrate groups attached to the metal ion and of the nature of any other coordinating ligands. With the very strongly polarizing Au(III) cation, in the complex ion $Au(NO_3)_4^-$ containing monodentate nitrate groups (36), the fundamental ν_4 band is split by as much as 80 cm^{-1} inferring that the combination band should be similarly split.[1] However, this complex does not exhibit combination absorption in the 1750 cm^{-1} region.[1]

Thus in conclusion the multiplicity and separation of the combination bands in the 1750 cm^{-1} region when observed can be used as additional support for structural diagnosis when used in conjunction with Raman studies or with information from the fundamental vibration region of the infrared spectrum. They may also provide information concerning the polarizing power of the cation but further studies with a wider range of cations are needed to confirm whether useful bonding information can be derived.

[1]We are grateful to a referee for providing this information.

NOTE ADDED IN PROOF: The combination frequencies of the $M(NO_3)_4^{2-}$ series (M = Mn, Co, Ni, Zn) in CH_2Cl_2 solution are essentially identical to the solid state spectra except for minor shifts in energy. Evidently the nickel complex is not polymeric.

We are indebted to the National Research Council of Canada and the Consiglio Nazionale delle Ricerche (Rome) for financial support.

1. C. C. ADDISON and D. SUTTON. Prog. Inorg. Chem. **8**, 195 (1967).
2. F. A. COTTON, D. M. L. GOODGAME, and R. H. SODERBERG. Inorg. Chem. **2**, 1162 (1963).
3. A. B. P. LEVER. Inorg. Chem. **4**, 1042 (1965) and references therein.
4. R. L. CARLIN and M. J. BAKER. J. Chem. Soc. 5008 (1964).
5. B. M. GATEHOUSE, S. F. LIVINGSTONE, and R. S. NYHOLM. J. Chem. Soc. 4222 (1957).
6. D. K. STRAUB, R. S. DRAGO, and J. T. DONOGHUE. Inorg. Chem. **1**, 848 (1962).
7. N. F. CURTIS and Y. M. CURTIS. Inorg. Chem. **4**, 804 (1965).
8. R. E. HESTER and W. E. L. GROSSMAN. Inorg. Chem. **5**, 1308 (1966).
9. C. C. ADDISON and W. B. SIMPSON. J. Chem. Soc. 598 (1965) and references therein.
10. B. O. FIELD and C. J. HARDY. Quart. Rev. **18**, 361 (1964).
11. C. C. ADDISON and B. M. GATEHOUSE. J. Chem. Soc. 613 (1960).
12. B. M. GATEHOUSE and A. E. COMYNS. J. Chem. Soc. 3965 (1958).
13. S. BUFFAGNI, L. M. VALLERINO, and J. V. QUAGLIANO. Inorg. Chem. **3**, 480 (1964).
14. N. LOGAN and W. B. SIMPSON. Spectrochim. Acta, **21**, 857 (1965).
15. D. W. JAMES and G. M. KIMBER. Aust. J. Chem. **22**, 2287 (1969).
16. K. NAKAMOTO. Infrared spectra of inorganic and coordination compounds. John Wiley, New York. 2nd ed. 1970.
17. K. NAKAMOTO and P. J. MCCARTHY. Spectroscopy and structure of metal chelate compounds. John Wiley, New York. 1968.
18. J. R. FERRARO and A. WALKER. J. Chem. Phys. **43**, 550 (1966); **43**, 2689 (1965); Can. J. Chem. **48**, 711 (1970).
19. C. C. ADDISON, D. W. AMOS, D. SUTTON, and W. H. H. HOYLE. J. Chem. Soc. 808 (1967).
20. J. R. FERRARO, C. CRISTALLINI, and I. FOX. J. Inorg. Nucl. Chem. **29**, 139 (1967).
21. J. R. FERRARO. J. Mol. Spectry. **4**, 99 (1960).
22. F. A. COTTON and J. G. BERGMAN. J. Am. Chem. Soc. **86**, 2941 (1964); Inorg. Chem. **5**, 1208 (1966).
23. J. DRUMMOND and J. S. WOOD. J. Chem. Soc. A, 226 (1970).
24. M. KEETON, A. B. P. LEVER, and B. S. RAMASWAMY. Can. J. Chem. **48**, 3185 (1970).

25. A. F. CAMERON, K. P. FORREST, R. H. NUTTALL, and D. W. TAYLOR. J. Chem. Soc. D, 210 (1970).
26. J. L. HOARD and J. D. STROUPE. U.S. ATOMIC Energy Comm. TID-5290, Book I, 323 (1958).
27. W. F. ZACHARIASEN. Acta Cryst. 7, 795 (1954).
28. A. ZALKIN, J. D. FORRESTER, and D. H. TEMPLETON. J. Chem. Phys. **39**, 2881 (1963).
29. A. B. P. LEVER and E. MANTOVANI. Inorg. Chem. **10**, 817 (1971).
30. A. F. CAMERON, R. H. NUTTALL, and D. W. TAYLOR. J. Chem. Soc. D, 865 (1970).
31. M. R. ROSENTHAL and R. S. DRAGO. Inorg. Chem. **4**, 840 (1965).
32. F. A. COTTON and T. B. DUNNE. J. Am. Chem. Soc. **84**, 2013 (1962).
33. A. NIGGLI. Z. Kryst. **111**, 269 (1959); P. F. LINDLEY and P. WOODWARD. J. Chem. Soc. A, 123 (1966).
34. S. C. WALLWORK and W. E. ADDISON. J. Chem. Soc. 2925 (1965).
35. L. BERGER and S. A. FRIEDBERG. Phys. Rev. **136A**, 158 (1964).
36. C. D. GARNER and S. C. WALLWORK. J. Chem. Soc. D, 108 (1969).
37. L. M. VENANZI. J. Chem. Soc. 719 (1958); J. Inorg. Nucl. Chem. **8**, 137 (1958).
38. Sadtler Standard Spectra, Sadtler Research Laboratories, Philadelphia.
39. H. M. BROOKER, D. E. IRISH, and G. E. BOYD. J. Chem. Phys. **53**, 1083 (1970).
40. C. J. H. SCHUTTE. Z. Phys. Chem. **39**, 241 (1963).
41. I. M. WALKER. Unpublished data.
42. R. UGGLA, J. VISTI, S. LUNDELL, and M. NASAKKALA. Suomen. Kem. B**43**, 124 (1970).
43. A. B. P. LEVER and E. MANTOVANI. To be published.
44. W. R. MCWHINNIE. J. Inorg. Nucl. Chem. **27**, 2578 (1970).
45. C. W. FRANK and L. B. ROGERS. Inorg. Chem. **5**, 615 (1966).
46. L. M. VALLERINO, W. E. HILL, and J. V. QUAGLIANO. Inorg. Chem. **4**, 1598 (1965).
47. M. KEETON and A. B. P. LEVER. Inorg. Chem. **10**, 47 (1971).

Can. J. Chem. Downloaded from www.nrcresearchpress.com by 210.87.254.105 on 09/05/12
For personal use only.

Can. J. Chem. Downloaded from www.nrcresearchpress.com by 210.87.254.40 on 09/05/12
For personal use only.

NOTES

Temperature Dependence of the Diffusion of 1,2-Dichloroethane, 1,1,1-Trichloroethane, Trichloroethylene, and Tetrachloroethylene in Air[1]

HARRY WATTS

Exploratory Research Laboratory, Dow Chemical of Canada Limited, Sarnia, Ontario

Received January 19, 1971

The diffusion coefficients in air of 1,1-dichloroethane, 1,1,1-trichloroethane, trichloroethylene, and tetrachloroethylene have been measured over a temperature range from room temperature to close to their boiling points by a rate of evaporation method.

Utilisant une méthode faisant appel à la vitesse d'évaporation, on a mesuré à différentes températures variant entre celle de la pièce et celle de leur point d'ébullition les coefficients de diffusion dans l'air du dichloro-1,1 éthane, du trichloro-1,1,1 éthane et du tétrachloroéthylène.

Canadian Journal of Chemistry, 49, 1965 (1971)

Introduction

The measurements reported in this paper constitute a continuation of a study of diffusion in air of chlorinated hydrocarbons of industrial importance. Previously, data obtained with some chloromethanes over a wide temperature range were reported (1). Earlier data on diffusion in air of a number of compounds have been collected by Fuller, Schettler, and Giddings (2). Lugg (3) recently published measurements of the diffusion coefficients of 147 compounds in air at 25 °C, while other measurements have been reported by the present author and co-workers (4, 5).

Experimental

The apparatus and procedure for measurements by the rate of evaporation method have been described previously (1). All of the chlorinated hydrocarbons were made by Dow Chemical of Canada, Limited and shown by gas chromatographic analysis to have the following purities: 1,2-dichloroethane 99.89%, 1,1,1-trichloroethane 99.96%, trichloroethylene 99.99%, tetrachloroethylene 99.99%.

Results

Measurements were made from 25 °C up to near the boiling point of each substance except tetrachloroethylene for which the vapor pressure at 25 °C was too low to permit measurements in a reasonable time and the boiling point was above the temperature range for which the present apparatus functioned satisfactorily. Diffusion coefficients were calculated both by assuming that vapor of the diffusing substance behaved as an ideal gas so that its concentration was proportional to its partial pressure and by making appropriate corrections for gas non-ideality using the McGlashan–Potter equation (6) to calculate second virial coefficients as before (1). Auxiliary data used in computing the diffusion coefficients are given in an appendix. All diffusion coefficients were corrected to 1 atm pressure by the usual method (1).

Diffusion coefficients were fitted to the equation

$$[1] \qquad \log D = \log D_0 + \nu \log T$$

where D is the diffusion coefficient, T is the absolute temperature, and D_0 and ν are constants. Values of D_0 and ν for each system are given in Table 1 together with the root mean square deviations of experimental diffusion coefficients from the fitted line which are given only for the data corrected for gas non-ideality; the corresponding deviations when the vapor was assumed ideal differ from these insignificantly.

Discussion

The precision of the results as measured by the root mean square deviations from the least squares fit to eq. 1 is 1–2% and comparable with that obtained in earlier work on the same apparatus. More significant is the difference between

[1]Contribution No. 186.

TABLE 1. Constants in eq. 1 for diffusion of stated component in air

Component	Number of data	Temperature range (°C)	Assumed ideal gas		Corrected for non-ideality		Root mean square deviation
			$D_0 \times 10^6$	v	$D_0 \times 10^6$	v	
1,1-Dichloroethane	36	25–65	0.46997	2.1346	0.77914	2.0426	0.0026
1,1,1-Trichloroethane	36	25–65	2.2733	1.8403	8.4615	1.6052	0.0017
Trichloroethylene	65	25–75	0.9797	1.9883	1.9387	1.8654	0.0012
Tetrachloroethylene	51	45–85	0.9439	1.9728	1.5231	1.8869	0.0012

TABLE 2. Comparison of diffusion coefficients in air

Substance	Temperature (°C)	Smoothed values			
		(Assumed ideal gas)	This work (corrected for non-ideality)	Lugg (3)	Theoretical from eq. 2
1,1-Dichloroethane	25	0.0899	0.0883	$0.0919 \pm 0.0007_7$	0.0891
	65	0.117_7	0.114_1		0.112_1
1,1,1-Trichloroethane	25	0.0814	0.0793	$0.0794 \pm 0.0008_1$	0.0812_6
	65	0.102_6	0.0971		0.102_3
Trichloroethylene	25	0.0815	0.0800	$0.0875 \pm 0.0002_3$	0.0829_1
	75	0.110_9	0.106_9		0.110
Tetrachloroethylene	25	0.0719	0.0711	$0.0797 \pm 0.0002_3$	0.0755_6
	45	0.0817	0.0803		0.0850
	85	0.103_2	0.100_4		0.104_6

diffusion coefficients calculated assuming the diffusing vapor is an ideal gas and those calculated making corrections for non-ideality. This difference is shown clearly by the smoothed values given in Table 2 and varies from 1 to 6%, depending on the system and temperature. The importance of correction for non-ideality of the vapor is again stressed. Diffusion coefficients so corrected are those that should be compared with theoretical values and with diffusion coefficients determined by other methods that measure the true concentration of diffusing gases. However, it is still desirable to publish diffusion coefficients uncorrected for non-ideality because in certain practical problems they may be required to calculate the amount of vapor diffusing when the partial pressure of it is known.

Diffusion in these systems at 25 °C has been studied by Lugg (3), and his results are quoted in Table 2. Lugg used the rate of evaporation method and did not correct for gas non-ideality, consequently his results must be compared with the uncorrected results of this study. Our results are in excellent agreement with 1,2-dichloroethane and 1,1,1-trichloroethane. However, the agreement between our results for trichloroethylene and tetrachloroethylene is not good. Admittedly the value at 25 °C for tetrachloroethylene in this work is extrapolated from data at higher temperatures, which can account for part of the discrepancy. Lugg does not give an analysis of purity of his materials but simply states that they were the purest available. Hence in view of the analysis of the materials used in this work it is suspected that the discrepancy between our results is due to impurities in his materials and the present results are to be preferred. In view of the close agreement between some of our results given here and elsewhere (1), it is unlikely that the discrepancy is due to differences in our experimental techniques.

Theoretical values of diffusion coefficients were also calculated using the equation (7)

[2]
$$D_{12} = \frac{2.628 \times 10^{-5}[T^3(M_1 + M_2)/2M_1M_2]^{1/2}}{p\sigma_{12}^2\Omega_{12}(T_{12}^*)}$$

where the subscripts 1 and 2 refer to the two components, D_{12} is the first approximation to the binary diffusion coefficient, M the molecular weight, T the absolute temperature, p the pressure in atmospheres, and Ω_{12} (T_{12}^*) is a collision integral at a reduced temperature of $T_{12}^* = kT/\varepsilon_{12}$, and σ_{12} and ε_{12}/k are molecular potential energy parameters characteristic of a 1–2 inter-

Can. J. Chem. Downloaded from www.nrcresearchpress.com by 210.87.254.40 on 09/05/12
For personal use only.

action expressed in units of nm and K, respectively. Values of the collision integral for a Lennard–Jones 6–12 potential function have been tabulated (7). Experimental values of σ_{11} and ε_{11}/k for the pure components were not available so values were estimated from the critical properties by the method of Stiel and Thodos (8). Where experimental values of the critical properties were not available, values were estimated by Lyderson's method and the method of García–Bárcena (8). The Hudson–McCoubrey combining rules (9) were used to calculate σ_{12} and ε_{12}/k from the corresponding values for the pure components. Comparison of the theoretical diffusion coefficients with the experimental values corrected for non-ideality shows agreement almost within experimental error for most systems. Even when some of the data required to use eq. 2 is not available, estimation of data by the best methods available can give values of the diffusion coefficient in accord with experiment.

1. H. WATTS. Can. J. Chem. **49**, 67 (1971).
2. E. N. FULLER, P. D. SCHETTLER, and J. C. GIDDINGS. Ind. Eng. Chem. **58**, 19 (1966).
3. G. A. LUGG. Anal. Chem. **40**, 1072 (1968).
4. M. COWIE and H. WATTS. Can. J. Chem. **49**, 74 (1971).
5. R. F. BARR and H. WATTS. Submitted for publication.
6. M. L. MCGLASHAN and D. J. B. POTTER. Proc. Roy. Soc. London, Ser. A. **267**, 478 (1962).
7. J. O. HIRSCHFELDER, C. F. CURTISS, and R. B. BIRD. Molecular theory of gases and liquids. John Wiley and Sons, Inc., New York. 1954.
8. R. C. REID and T. K. SHERWOOD. The properties of gases and liquids. 2nd Ed. McGraw-Hill Book Company, New York. 1966.
9. G. H. HUDSON and J. C. MCCOUBREY. Trans. Faraday Soc. **56**, 761 (1960).
10. A. P. KUDCHADKER, G. H. ALANI, and B. J. ZWOLINSKI. Chem. Rev. **68**, 659 (1968).
11. R. R. DREISBACH. Physical properties of chemical compounds. Vol. I. Adv. Chem. Ser. No. 15. Am. Chem. Soc. Washington, 1955; Vol. II. Adv. Chem. Ser. No. 22, Am. Chem. Soc. Washington, 1959. Vol. III. Adv. Chem. Ser. No. 29, Am. Chem. Soc. Washington, 1961.
12. G. HERZBERG. Molecular spectra and molecular structure. III. Electronic spectra and electronic structure of polyatomic molecules. D. VanNostrand Company, Inc., Princeton. 1966.
13. E. A. GUGGENHEIM and C. J. WORMALD. J. Chem. Phys. **42**, 3775 (1965).

Appendix

Data used in calculations

Property	Units	1,1-Dichloro-ethane	1,1,1-Trichloro-ethane	Trichloro-ethylene	Tetrachloro-ethylene
T_c	K	561[a]	548.5[b]	571.2[c]	613.2[c]
V_c	l mol^{-1}	0.22[a]	0.283[b]	0.256[c]	0.289[c]
$(PV/RT)_c$		0.26[a]	0.268[d]	0.265[a]	0.255[a]
Ionization potential	eV	9.4[e]	9.4[e]	9.47[f]	9.32[f]
Interaction parameters					
σ^g	nm	0.5673	0.5948	0.5835	0.6355
ε/k^g	K	286.9	312.9	312.9	292.5
n, parameter in McGlashan–Potter equation[h]		7.0	8.7	5.5	8.0
Antoine constants[c]					
a		7.18431	6.94983	7.02808	7.02003
b		1358.5	1217.0	1315.0	1415.5
c		232	225.0	230.0	221.0

[a]Kudchadker, Alani, and Zwolinski (10).
[b]Estimated by Lyderson's method (8).
[c]Dreisbach (11).
[d]Estimated by the method of García-Bárcena (8).
[e]Value assumed.
[f]Herzberg (12).
[g]Estimated by the method of Stiel and Thodos (8).
[h]Estimated by the method of Guggenheim and Wormald (13).

Can. J. Chem. Downloaded from www.nrcresearchpress.com by 210.87.254.40 on 09/05/12
For personal use only.

Synthesis of *N*-Methylamino Acid Derivatives from Amino Acid Derivatives using Sodium Hydride/Methyl Iodide[1]

JOHN R. COGGINS AND N. LEO BENOITON[2]

Department of Biochemistry, University of Ottawa, Ottawa 2, Canada

Received January 8, 1971

Reaction of *N*-acetyl-, *N*-benzoyl-, and *N*-carbobenzoxy derivatives of aliphatic amino acids with sodium hydride/methyl iodide in tetrahydrofuran containing dimethylformamide at 80° gave the corresponding *N*-methylamino acid methyl esters as oils in high yields. Saponification of these gave the *N*-protected-*N*-methylamino acids, and decarbobenzoxylation gave the *N*-methylamino acid methyl ester hydrobomides. The products are essentially optically pure and free of unmethylated amino acid derivative.

On fait réagir, à 80 °C dans le tétrahydrofuranne contenant de la diméthylformamide, les dérivés *N*-acétyle-, *N*-benzoyle-, ou *N*-carbobenzoxyle d'acides aminés avec de l'iodure de méthyle en présence d'hydrure de sodium et l'on obtient, avec d'excellents rendements, les esters méthyliques des dérivés *N*-méthylamino correspondants qui se présentent sous forme d'huile. La saponification de ces esters conduit aux acides aminés portant sur l'azote un groupe méthyle et un groupe protecteur; leur décarbobenzoxylation conduit aux bromhydrates des esters méthyliques des acides aminés *N*-méthylés. Les produits sont essentiellement optiquement purs et exempts de produits non méthylés.

Canadian Journal of Chemistry, 49, 1968 (1971)

The preparation of derivatives of optically active *N*-methylamino acids presents many obstacles. Optically pure *N*-methylamino acids are not readily accessible; no method has been described for establishing their optical purity; *N*-methylamino acids are difficult to determine because they react slowly with ninhydrin; and their derivatives are not easy to make because *N*-methylamino acids are generally less reactive than are amino acids. We report here a new and simple one or two step synthesis of optically pure *N*-methylamino acid derivatives from commercially available starting materials. The method involves the *N*-methylation of *N*-acyl- or *N*-carbobenzoxyamino acids with methyl iodide and sodium hydride.[3] The determination of *N*-methylamino acids and their optical purity has been described elsewhere (3).

Methylation of aromatic amides has been achieved using methyl iodide (4–7) or dimethyl sulfate (8) in the presence of alkali. Alkylation of aliphatic amides (7, 9) and lactams (9) has been similarly achieved. Methylation of sulfonamides (10) has provided a route to *N*-methylamino acids (11). The more recent permethylation of peptides using silver oxide/methyl iodide (12), a reagent previously used for the methylation of a lactam (13), suggested consideration of this reagent for an approach to the synthesis of *N*-methylamino acid derivatives. Sodium hydride, however, was investigated in preference on the basis of the reports of its use for the alkylation of amides (14) and urethanes (15).[4]

N-Carbobenzoxyleucine in tetrahydrofuran (THF) was treated with sodium hydride/methyl iodide under various conditions, and the reaction mixture was analyzed for amino acids with an amino acid analyzer[5] after suitable deprotection. Representative results of these and subsequent experiments with other leucine derivatives appear in Table 1. The best yield (96%) of *N*-methylleucine was obtained using the reactants in an 8:3:1 molar ratio (MeI/NaH/R-Leu) after 24 h at 80 °C

[1]Supported by a grant from the Medical Research Council of Canada. This investigation is dedicated to the memory of our colleague Dr. Jean Leclerc who died on December 31, 1969, at the age of 27.

[2]Associate of the Medical Research Council of Canada.

[3]A preliminary account of this work has been presented (1). Complete details of all aspects of this work are described in the Ph.D. thesis of J.R.C. Sodium hydride/methyl iodide has since been used for the permethylation of peptides for sequencing by mass spectrometry (2).

[4]A synthesis of *N*-methylamino acid derivatives using silver oxide/methyl iodide has since appeared (16).

[5]We have found that α-*C*-methyl- and *N*-methylamino acids can be determined satisfactorily with a Beckman amino acid analyzer if a half-normal eluting buffer flow rate is used. Under these conditions, the ninhydrin color constants are 10–30 times those obtained using the normal flow rate (3).

Can. J. Chem. Downloaded from www.nrcresearchpress.com by 210.87.254.40 on 09/05/12
For personal use only.

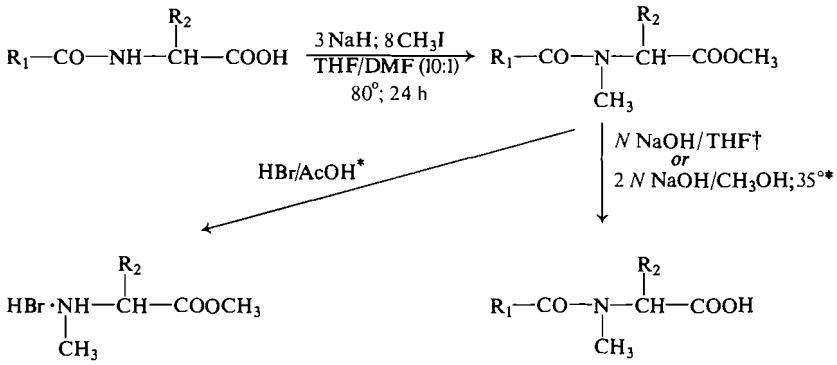

SCHEME 1. R_1 = CH_3, C_6H_5, $C_6H_5CH_2O$; R_2, corresponding to the amino acids in Table 2; (*) for R_1 = $C_6H_5CH_2O$; (†) for R_1 = CH_3, C_6H_5.

TABLE 1. Methylation of leucine derivatives with sodium hydride/methyl iodide*

Derivative	Amino acid recovered (yield, %)†		
	MeLeu	Leu	Total
Cbz	96	1.1	97
Cbz‡	46	39	85
Cbz§	32	0.6	33
Cbz‖	54	1.0	55
Boc	86	3.0¶	89
Boc**	37	28	65
Bz	96	0.1	96
Ac	88	0.7	89
For	95	4.0	99
Tos	61	4.0	65††

*Standard conditions: MeI/NaH/R-Leu (8:3:1 mol). NaH added to a solution of R-Leu (1 mmol) and MeI in THF/DMF (10:1). Mixture was placed on an oil bath at 80 °C for 24 h.
†Determined with an amino acid analyzer (3) after deprotection.
‡Reactant ratio: 4:2:1 mol.
§DMF replaced by dimethylsulfoxide as solvent.
‖MeI added after heating R-Leu and NaH for 10 min.
¶Same value obtained in a duplicate experiment.
**MeI added after leaving R-Leu and NaH at room temperature until hydrogen evolution had ceased.
††Low total believed due to difficulty with deprotection.

in the presence of dimethylformamide (DMF), and unexpectedly when the sodium hydride was added to the mixture after the methyl iodide had been added and not before.

In experiments on a preparative scale (Scheme 1), *N*-acetyl-, *N*-benzoyl-, and *N*-carbobenzoxy-amino acids were methylated to give the corresponding *N*-methylamino acid methyl esters whose i.r. curves were characterized by a sharp absorption band at 1735–1740 cm^{-1} (ester carbonyl), and the absence of bands at 3280 and 1520 cm^{-1} (—NH stretch and amide II bands, respectively). The esters were isolated as oils by extraction into ether and were therefore contaminated with the paraffin oil from the sodium hydride dispersion. Saponification of the *N*-acyl-*N*-methylamino acid esters in *N* NaOH/THF gave the *N*-acyl-*N*-methylamino acids in satisfactory yield. Similar treatment of the *N*-carbobenzoxy-*N*-methylamino acid esters gave very low yields of the corresponding acids. Good yields were finally obtained using warm 2 *N* NaOH/methanol. Removal of the carbobenzoxy group from the esters with hydrogen bromide in acetic acid gave the *N*-methylamino acid methyl esters as hydrobromides. After one recrystallization, these esters contained less than 0.1% of the unmethylated amino acid ester. An aliquot of one preparation of L-MeLeu-OMe·HBr was hydrolyzed before the crystallization step, and was shown to contain not more than 1% (the limit of detection) of the D-isomer by the method described elsewhere (3). Similarly, crystalline L-MePhe prepared from the carbobenzoxy derivative, and the hydrolysis product of Ac-L-MeLeu were also shown to be optically pure. However, preparations of Ac-MePhe were found to be partially or completely racemized. It is known that phenylalanine derivatives are more susceptible to base-catalyzed racemization than are most other amino acids (19). The properties of the derivatives prepared are recorded in Table 2. The i.r. curves of all compounds have been recorded.[3]

Experimental

Materials and Methods

Methyl iodide and DMF were obtained from Fisher Scientific Co. The DMF was purified by shaking over KOH pellets, then over CaO, followed by distillation (151–154°/753 mm) (20). The THF was the J. T. Baker product containing butylated hydroxytoluene as stabilizer.

Can. J. Chem. Downloaded from www.nrcresearchpress.com by 210.87.254.40 on 09/05/12
For personal use only.

Can. J. Chem. Downloaded from www.nrcresearchpress.com by 210.87.254.40 on 09/05/12
For personal use only.

TABLE 2. Properties of derivatives of *N*-methyl-L-amino acids

Compound*	Yield† (%)	Melting point (°C)	$[\alpha]_D^{25}$‡	Analysis							
				Formula	Molecular weight	Calculated			Found		
						C	H	N	C	H	N
Bz-MeAla	57	133	−31.7	$C_{11}H_{13}NO_3$	207.2	63.8	6.3	6.8	64.1	6.6	6.9
Bz-MeLeu	74	135–137	−54.8	$C_{14}H_{19}NO_3$	243.3	67.4	7.7	5.6	67.7	7.6	5.7
Ac-MeAla§	7	110–112	−50.0	$C_6H_{11}NO_3$	145.2	49.6	7.6	9.7	50.5	7.4	10.2
Ac-MeVal§	73	112–114	−144.3	$C_8H_{15}NO_3$	173.2	55.5	8.7	8.1	55.4	8.6	8.2
Ac-MeIle	39	121.5–122.5	−135.4	$C_9H_{17}NO_3$	187.2	57.7	9.2	7.5	58.0	8.7	7.4
Ac-MeLeu·H_2O	60	83–85‖	+34.5	$C_9H_{19}NO_4$	205.25	52.7	9.3	6.8	53.4	9.5	7.1
Ac-MePhe¶	50			$C_{12}H_{15}NO_3$	221.25	65.1	6.8	6.3	64.7	7.2	6.5
Cbz-MeAla§	65	65–66	−29.2	$C_{12}H_{15}NO_4$	237.25	60.7	6.4	5.9	61.2	6.5	5.8
Cbz-MeVal	65	semi-solid**									
Cbz-MeIle	55	oil									
Cbz-MeLeu	40	73–74	−26.1	$C_{16}H_{23}NO_4$	279.3	64.5	7.6	5.0	64.7	7.4	4.8
Cbz-MePhe	82	oil									
MeAla-OMe·HBr	82	109–109.5	−5.7	$C_5H_{12}NO_2Br$	198.1	30.3	6.1	7.1	29.6	6.0	6.8
MeVal-OMe·HBr	61	127–128	+17.0	$C_7H_{16}NO_2Br$	226.1	37.2	7.1	6.2	37.3	7.4	5.8
MeIle-OMe·HBr	56	126.5–127.5	+23.8	$C_8H_{18}NO_2Br$	240.15	40.0	7.6	5.8	40.2	7.6	5.8
MeLeu-OMe·HBr	65	105–106	+17.5	$C_8H_{18}NO_2Br$	240.15	40.0	7.6	5.8	40.3	7.7	5.8
MePhe-OMe·HBr	81	132–133	+37.3	$C_{11}H_{16}NO_2Br$	274.2	48.2	5.9	5.1	48.4	6.1	5.3

*Esters were crystallized once from methanol–ether; all other derivatives, from water except where indicated.
†Based on the *N*-protected amino acid used for the methylation.
‡In DMF; $c = 1$ for acetyl and benzoyl derivatives; $c = 2$ for others.
§Crystallized from ethyl acetate – petroleum ether. Literature m.p. 62–64.5°; $[\alpha]_D^{28}$ −31° (c, 2 in AcOH (16)).
‖The m.p. 107–108° after drying at 65°.
¶Racemized.
**Literature m.p. 69° (17, 18).

Can. J. Chem. Downloaded from www.nrcresearchpress.com by 210.87.254.40 on 09/05/12
For personal use only.

Sodium hydride was a 50% dispersion in oil obtained from BDH Chemicals. The amino acids were purchased from General Biochemicals, Chagrin Falls, Ohio. The *N*-carbobenzoxyamino acids were synthesized by the usual procedure of Bergmann and Zervas (21), with the phenylalanine derivative being purified as described (22). The *N*-benzoyl- and *N*-acetylamino acids were prepared by standard procedures as described for each amino acid in the treatise by Greenstein and Winitz (23). The optical purity of the *N*-acetylamino acids was verified.

The DMF and THF were dried immediately before use by adding sodium hydride dispersion (0.2 g/10 ml solvent) and filtering under suction after shaking for 2 min. Optical rotations were measured with a Perkin–Elmer model 141 polarimeter using a 1 dm tube. Melting points were taken by the capillary method and are uncorrected. All evaporations were carried out under reduced pressure using a rotary evaporator. Compounds melting above 100° were dried for analysis by heating at 65° under vacuum over P_2O_5 for 2 h.

N-Acyl- and N-Carbobenzoxy-N-methylamino Acid Methyl Esters

To a solution of *N*-acyl- or *N*-carbobenzoxyamino acid (0.020 mol) in THF/DMF (10:1; 55 ml)[6] were added methyl iodide (10.0 ml; 0.160 mol) and sodium hydride dispersion (2.88 g; 0.060 mol of NaH) (*caution*) *in that order*. A reflux condenser protected with a drying-tube (Drierite) was mounted on the flask which was then placed in an 80 °C wax-bath for 24 h. The solvent was removed under vacuum, ether (25 ml) was added, and the evaporation was repeated (to remove the methyl iodide). The residue was distributed between ether (100 ml) and water (25 ml). The ether layer was washed with water (25 ml), dried ($MgSO_4$), and evaporated to give two clear immiscible oils[7] (one is the oil from the sodium hydride dispersion). All products gave satisfactory i.r. analyses at this stage.

N-Acyl- and N-Carbobenzoxy-N-methylamino Acids

The suspension of oils described above was saponified by stirring in the presence of 80 ml of *N* NaOH/THF (1:1) for 30 min for the *N*-acyl derivatives and 60 ml of 2 *N* NaOH/methanol (1:2) at 35 °C for 3 h for the *N*-carbobenzoxy derivatives. The THF and methanol were evaporated off, the remaining aqueous solution was washed with ether (2 × 20 ml), cooled (0°), and brought to p*H* 2 with 4 *N* HCl. The product was extracted into ethyl acetate (3 × 40 ml), the combined extracts were dried ($MgSO_4$), and the solvent was removed by evaporation. The residue was crystallized as indicated in Table 2.

[6]This solvent volume was used for 0.01 to 0.03 mol quantities.

[7]The product is sometimes slightly colored due to the presence of iodine. We have recently found that washing with aqueous potassium iodide solution removes the color.

N-Methylamino Acid Methyl Ester Hydrobromides

To an *N*-carbobenzoxy-*N*-methylamino acid methyl ester obtained as described above was added 37% HBr in acetic acid and the mixture was left at room temperature for 2 h. The mixture was evaporated to an oil which was dissolved in water (25 ml). The solution was washed with ether (2 × 10 ml), and then evaporated to dryness. The residue was dried overnight under vacuum over P_2O_5, and crystallized from methanol–ether.

1. J. R. Coggins and N. L. Benoiton. Proc. 156th Meet. Am. Chem. Soc. Div. Biol. Chem. Abstr. 18 (1968).
2. (*a*) E. Lederer. Pure and Appl. Chem. **17**, 489 (1968); (*b*) D. W. Thomas. FEBS Lett. **5**, 53 (1969); (*c*) P. Roepstorpff, K. Norris, S. Severinsen, and K. Brunfeldt. FEBS Lett. **9**, 235 (1970); (*d*) W. O. Godtfedsen, S. Vangedal, and D. W. Thomas. Tetrahedron, **26**, 4931 (1970).
3. J. R. Coggins and N. L. Benoiton. J. Chromatogr. **52**, 251 (1970).
4. P. Hepp. Ber. **10**, 327 (1877).
5. A. Pictet and P. Crepieux. Ber. **21**, 1106 (1888).
6. I. J. Pachter and M. C. Kloetzel. J. Am. Chem. Soc. **74**, 1321 (1952).
7. R. A. W. Johnstone, D. W. Payling, and C. Thomas. J. Chem. Soc. C, 2223 (1969).
8. E. Thielepape and A. Fulde. Ber. **68**, 751 (1935).
9. R. E. Benson and T. L. Cairns. J. Am. Chem. Soc. **70**, 2115 (1948).
10. O. Hinsburg. Ann. **265**, 178 (1891).
11. E. Fischer and W. Lipschitz. Ber. **48**, 360 (1915).
12. B. C. Das, S. D. Gero, and E. Lederer. Biochem. Biophys. Res. Commun. **29**, 212 (1967).
13. P. Karrer, C. Granacher, and A. Schlosser. Helv. Chim. Acta, **5**, 139 (1922).
14. W. S. Jones. J. Org. Chem. **14**, 1099 (1949).
15. R. L. Dannley and M. Lukin. J. Org. Chem. **22**, 268 (1957).
16. R. K. Olsen. J. Org. Chem. **35**, 1912 (1970).
17. P. A. Plattner, K. Vogler, R. O. Studer, P. Quitt, and W. Keller-Schierlein. Helv. Chim. Acta, **46**, 927 (1963).
18. Y. A. Ovchinnikov, V. T. Ivanov, and A. A. Kiryushkin. Izv. Akad. Nauk SSSR, Otd. Khim. Nauk, 2046 (1932).
19. M. Bodanszky and M. A. Ondetti. Peptide synthesis. John Wiley and Sons, New York, N.Y., 1966. p. 148.
20. G. R. Leader and J. F. Gormley. J. Am. Chem. Soc. **73**, 5731 (1951).
21. M. Bergmann and L. Zervas. Ber. **65**, 1192 (1932).
22. W. Grassman and E. Wunsch. Ber. **91**, 462 (1958).
23. J. P. Greenstein and M. Winitz. Chemistry of the amino acids. John Wiley and Sons, New York, N.Y., 1962.

A Possible Relationship Between Oxidation Rates of Alcohols and Their Carbon-13 Chemical Shifts

A. S. PERLIN
Department of Chemistry, McGill University, Montreal, Quebec

Received November 9, 1970

Variations in the oxidation rates of alicyclic alcohols with chromate and of aldopyranoses with bromine, parallel variations in ^{13}C chemical shifts for the carbinols. Accepting that these shifts closely reflect electron densities, mechanisms for these oxidations are depicted in terms of the minimal change in electron configuration required on passage from the ground to the transition state. A net flow of electrons from H-1 to C-1 is visualized for the chromate reaction, and hence relief of strain is associated in the transition state, as well as in the ground state, with a relatively high electron density on carbon. In the bromine oxidations, a net flow of electrons from C-1 to H-1 is visualized, which thereby allows for a sterically-dependent contribution by the ring oxygen atom to resonance stabilization of the transition state. These patterns are consistent with chromate and bromine oxidation mechanisms that now find wide acceptance.

On a observé un parallèle entre d'une part les variations dans les vitesses d'oxydation chromique d'alcools alicycliques ou les vitesses d'oxydation d'aldopyranoses par le brome et d'autre par les variations des déplacements chimiques du ^{13}C des carbinols. Acceptant que ces déplacements permettent d'évaluer avec précision les densités électroniques au niveau de ces atomes de carbone, on représente les mécanismes de ces oxydations en terme d'un changement minimal de la configuration électronique pour passer de l'état fondamental à l'état de transition. Pour l'oxydation chromique on imagine un déplacement net d'électrons de H-1 à C-1; l'amoindrissement des tensions serait donc associé dans l'état de transition et dans l'état fondamental avec une densité électronique relativement grande au niveau du carbone. Dans les oxydations par le brome, on imagine que ce serait plutôt un déplacement net d'électrons de C-1 vers H-1 qui interviendrait; cette conception permettrait d'envisager que l'oxygène du cycle apporte une contribution, dépendante des facteurs stériques, à la stabilisation par résonance de l'état de transition. Ces propositions sont en accord avec les mécanismes d'oxydations chromiques ou par le brome qui sont le plus couramment acceptés.

Canadian Journal of Chemistry, 49, 1972 (1971)

Differences in the rate of oxidation of alcohols have been examined, perhaps most extensively, with reference to chromate oxidation of alicyclic alcohols and sterols, and bromine oxidation of aldoses. In both series, the observed variations in rate have been ascribed to specific steric factors. It is found, for example, that bromine oxidation of an aldose (which is highly selective in converting the hemiacetal to a lactone) takes place more rapidly when the anomeric hydroxyl group is equatorial than when axial; or that a sugar possessing the β-D-*xylo* or α-L-*arabino* configuration is oxidized at a faster rate than a conformationally less stable epimer of the β-D-*lyxo* or β-D-*ribo* configuration (1, 2). The situation is reversed for chromate oxidation of alicyclic alcohols: in this instance, an axial carbinol is more reactive than its equatorial epimer (3–8), and the greater the number of non-bonding interactions present in the alcohol the faster the oxidation rate (9, 10). Both the bromine and chromate reactions are characterized by a kinetic isotope effect (2, 11) which shows that rupture of the C-1 to hydrogen bond is a rate-determining process.

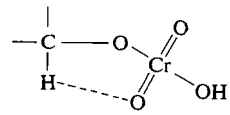

1

Most mechanisms proposed for chromate oxidation (7, 12, 13) invoke transient formation of an ester **1** and subsequent loss of the hydrogen to the medium as a proton (11, 14) or via a concerted process (5, 15) to an oxygen atom of ester **1** (broken line). It is generally accepted that rate differences between epimeric alcohols reflect variations in relief of strain on going from the ground state to the activated complex (3, 7, 8). Wilcox *et al.* (9) have shown additionally that among alicyclic alcohols and related sterols there is a close relationship between ground state free energy differences and differences in oxidation rate, which has led to the suggestion that transition states for the epimeric alcohols approach each other in energy (9, 10).

In the light of conformational and geometrical influences on the ^{13}C chemical shifts of cyclo-

Can. J. Chem. Downloaded from www.nrcresearchpress.com by 210.87.254.42 on 09/05/12
For personal use only.

TABLE 1. The ^{13}C chemical shifts and rates of chromate oxidation

	$\delta^{13}C$-1*	Δ†	$\Sigma\delta^{13}C$‡	Relative rate§	Ratio
Cyclohexanol					
cis-4-*t*-butyl-	127.8			2.5	
		5.4			3.1
trans-4-*t*-butyl-	122.4			0.8	
cis-2-methyl-	121.4‖		1117.6	4.6	
		5.5			3.8
trans-2-methyl-	115.9		1092.1	1.2	
trans-3-methyl-	126.0		1105.6	3.7	
		4.0			4.1
cis-3-methyl-	122.0		1085.2	0.9	
cis-4-methyl-	126.6		1109.9	2.4	
		3.8			3.0
trans-4-methyl-	122.8		1088.9	0.8	
Isoborneol	115.7¶			49.1	
		2.9			2.0
Borneol	112.8			25.0	
3-α-Cholestanol	123.0**			4.2	
		3.7			3.0
3-β-Cholestanol	119.3			1.4	

*In p.p.m. relative to *downfield* carbon disulfide.
†Value for *e,a* isomer minus the value for *e,e* isomer.
‡Sum of the chemical shifts (p.p.m.) reported for each compound in ref. 19.
§Relative to cyclohexanol. Data from refs. 7 and 9.
‖Values for the methylcyclohexanols are from ref. 19.
¶Values furnished by H. J. Koch.
**Values for the *O*-acetates, from ref. 35.

hexanes (16–19), we have noted recently (20) that the net shielding of ^{13}C nuclei of isomeric cyclohexane derivatives increases additively with an increase in repulsive non-bonding interactions. This applies equally for a number of cyclohexanols for which chromate oxidation rates have been measured (Table 1). As shown in Table 1, an increase in ^{13}C shielding for a given epimeric pair is accompanied by an increase in the oxidation rate. Moreover, differences between epimers are seen to be relatively constant. The sums of the chemical shifts (column 3) permit comparisons to be made of total shielding (20) of ^{13}C nuclei within the group of six isomeric methylcyclohexanols. Hence total shielding decreases in the order *cis*-2 > *cis*-4 > *trans*-3 > *trans*-2 > *trans*-4 > *cis*-3, which also is the general order of decreasing interaction energy and of decreasing oxidation rate. Since the ^{13}C chemical shift appears to be determined principally by electron density at the atom (21–25), the data of Table 1 express the rate *vs.* stability relationship of Wilcox *et al.* (9) in terms of charge density, rather than of non-bonding interaction. That is, with this class of molecules steric and electronic factors appear to be interconvertible, at least qualitatively.

From these and the earlier data, therefore, it is found that the charge density on carbon is increased when a destabilizing interaction is introduced, and we assume (20) that this arrangement of electron densities arises in response to the unfavorable interaction, as part of the energy-minimizing process. If a similar situation were to hold for the transition state, then relief of strain during the chromate oxidation also should be accompanied by a tendency to maintain a relatively high electron density on carbon.[1] Transfer of electrons within the ester **1** from carbon towards the chromium could then be compensated for by a flow of electrons from the hydrogen towards carbon. In this way, a proton would be released on rupture of the C—H bond (8, 12, 13), in contrast with the alternative possibility of abstraction of a hydride ion by the chromate (24). With the more reactive isomers, therefore, the arrangement of electrons in the ground state is closer to that anticipated for the transition state.

Isbell (1) has treated the bromine oxidation of aldoses in terms of a resonance-stabilized transition state resembling anion **2**. The latter is regarded as more easily attainable when the hydroxyl group in the ground state is equatorial rather than axial, because less reorganization would be required of the equatorial isomer.

[1]It may be noted also that chromate oxidations are characterized by negative rho values (14), an indication that these reactions are favored by high electron density at the reaction site.

Can. J. Chem. Downloaded from www.nrcresearchpress.com by 210.87.254.42 on 09/05/12
For personal use only.

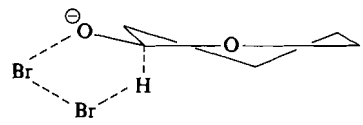

2

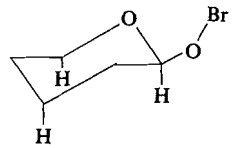

3

Another possibility (26) considers the relative ease of a base-catalyzed *trans*-elimination of hydrogen bromide from an intermediate such as **3**. This process can be visualized more readily for the equatorial product than for the axial one because in the latter, suitable orientation of the bromine atom would be relatively hindered by substituents at positions 3 and 5 (26).

Relief of strain can have only a minor bearing on the rate of bromine oxidation of aldoses, because the most reactive anomers are also the most thermodynamically stable ones (1, 2, 26). It is noteworthy, therefore, that ^{13}C chemical shifts and oxidation rates in this series appear to be related inversely, with respect to the chromate reactions just considered: *i.e.*, the rate of bromine oxidation decreases progressively as ^{13}C shielding increases (Table 2). An orderly progression is found also for the proton chemical shifts (Table 2), which emphasizes the differences in polarization of C—H bonds in these molecules[2] (27, 28).

Taking the anomeric forms of D-glucose as examples, the ^{13}C-1 nucleus of the β-isomer is the *less* shielded (by 3.9 p.p.m.) whereas its appended proton is the *more* shielded (by 0.58 p.p.m.), and the oxidation rate for β-D-glucose is 39 times that of the α-anomer (Table 2). If oxidation of these aldoses involves a flow of electrons from C towards H in the rate-determining step then, initially, the C—H bond of the β-anomer is more polarized in this same direction than is the C—H bond of the less reactive α-anomer. That is, a closer relationship between the ground and transition states may be visualized for the β-anomer than for the latter.

Turning to the transition states there is the possibility, suggested by Isbell (1), of resonance

[2]Although only anomeric centers are considered here, these differences apply broadly to the molecules themselves (27).

TABLE 2. The ^{13}C and ^{1}H chemical shifts and rates of bromine oxidation

Aldopyranose	^{13}C-1*	τ H-1†	Relative rates‡
α-L-Arabinose	95.3	5.40	52
β-D-Xylose	95.5	5.35	52
β-D-Galactose	95.8	5.32	50
β-D-Glucose	96.5	5.26	39
β-D-Mannose	98.2	5.03	24
β-D-Talose	—	5.12	22
β-D-Lyxose	98.2	5.06	14
β-D-Ribose	98.9	5.01	6.1
β-D-Allose	—	5.00	5.0
α-D-Lyxose	98.2	4.92	4.9
β-L-Arabinose	99.4	4.66	3.0
α-D-Xylose	100.0	4.74	2.8
α-D-Talose	—	4.63	2.4
α-D-Mannose	97.6	4.75	1.6
α-D-Galactose	100.0	4.66	1.3
α-D-Glucose	100.4	4.68	1.0

*In p.p.m. from *downfield* carbon disulfide (19, 36).
†In p.p.m. from *upfield* tetramethylsilane (37).
‡References 1, 2.

stabilization through involvement of the unshared electrons of the ring oxygen atom and the anomeric C—O bond (which offers a reasonable explanation of the greater reactivity of hemiacetal carbinol groups than of other kinds of carbinols towards bromine (1)). However, such stabilization could be relatively greater for the β-anomer. Thus, as pointed out by Snyder (29), the developing β-transition state appears to allow for more effective overlap between an orbital occupied by unshared electrons of the ring oxygen and an emerging vacant orbital of C-1, than would be permitted in the transition state for the α-anomer (compare **4** and **5**).

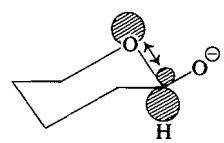

4

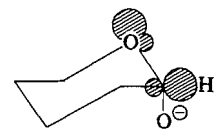

5

Accordingly, these overall characteristics favor more rapid oxidation of β- than of α-D-glucose, and apply similarly for several of the other anomeric pairs listed (arabinose, xylose, galactose). D-Mannose represents the most extreme departure from this pattern, since the anomers differ little in chemical shift but, nevertheless, the β- is oxidized 15 times more rapidly than the α-anomer. Accordingly, in this instance more facile stabilization of the β-transition state (as above) could be regarded as the overriding rate determinant.

In contrast to the aldopyranoses, *cis*- and *trans*-

Can. J. Chem. Downloaded from www.nrcresearchpress.com by 210.87.254.42 on 09/05/12
For personal use only.

Can. J. Chem. Downloaded from www.nrcresearchpress.com by 210.87.254.42 on 09/05/12
For personal use only.

4-*t*-butylcyclohexanol, or 3-α- and -β-cholestanol, are oxidized by bromine at nearly the same rate, their reactions are not base-catalyzed and, of course, are relatively very slow (30). A concerted type of mechanism involving **6** has been proposed (30),[3] simultaneous removal of the hydrogen atoms accounting for the lack of sensitivity to p*H*. Since resonance stabilization of the transition states is not a likely factor here, then there is no need to anticipate, as with the aldoses (above), that the favored direction of electron flow is from carbon towards hydrogen. Taking **6** as a model for the two transition states and noting the difference in electron density of C-1 of the epimers (based on the ^{13}C shifts, Table 1), a net flow of electrons in opposite directions may be visualized: from hydrogen towards carbon in the axial reaction, maintaining the relatively high charge density associated with C-1, and in the reverse direction (**7**) in the equatorial one. The overall tendency is to equalize the difference between the ground and transition states of the epimers, and hence minimize differences between their oxidation rates.

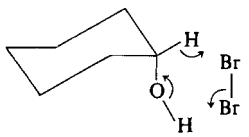

6

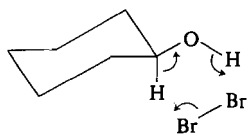

7

To summarize, variations in the oxidation rates of alcohols discussed above find close analogies with the manner in which ^{13}C chemical shifts, and hence C-1 electron densities, vary. The fact that chromate oxidation of alicyclic alcohols is more rapid with those epimers characterized by a relatively high charge density on carbon, appears to be compatible with the most widely-accepted view that a proton is abstracted in these oxidations. Thus, rate-determining rupture of the C_1—H bond would involve a minimal change of electronic configuration as the transition state is formed. It is suggested also that relief of strain due to non-bonding interactions may be associated both in the ground and transition states with a relatively high electron density on carbon. Because chemical shift and rate differences are reversed in the bromine oxidation of aldoses, rate-determining release of a hydride ion (1) rather than of a proton appears to be a plausible step. In addition, the incipient development of carbonium ion character on C-1 allows for a sterically dependant resonance stabilization of the transition state.

Many mechanisms that have been proposed for these different reactions are concerted, and involve cyclic transition states. Accordingly, the C—H bond-breaking process has been described here in terms of the direction of flow of electrons rather than of formation of a proton or hydride ion, *per se*. In these concerted routes the net flow in a given direction corresponds to the extent of change in electronic configuration between the ground and transition states. Hence, in the bromine oxidation of cyclohexanol derivatives, in which resonance stabilization becomes unimportant, charge density could be displaced in either direction, whichever is a minimal pathway.

It is not evident that the changes in electron distribution visualized above are related quantitatively to the energy changes that govern the oxidation rates (admittedly, in fact, the relationships that have been drawn may be coincidental). Nevertheless, the rate differences between epimers are not large: in the chromate oxidations the factor is 3–5 and in the bromine oxidation of aldopyranoses, a maximum of 50. Therefore, it is not unreasonable that they could be reflected in relatively small ground state epimeric differences in the polarization of C—H bonds, especially since these polarization differences could well be magnified in the transition states.

The author expresses his gratitude to P. G. Farrel, J. P. Snyder, and H. J. Koch for most helpful discussions.

[3]Other mechanistic possibilities for bromine oxidation of carbinols, involving either hydride (31–33) or proton (34) abstraction, have been described (also see ref. 12, p. 131–132).

1. H. S. Isbell. J. Res. Natl. Bur. Stand. **66A**, 233 (1962).
2. H. S. Isbell and L. T. Sniegoski. J. Res. Natl. Bur. Stand. **68A**, 145 (1964).
3. S. Winstein and N. J. Holness. J. Am. Chem. Soc. 77, 5562 (1955).
4. J. Schreiber and A. Eschenmoser. Helv. Chim. Acta, **38**, 1529 (1955).
5. H. Kwart and P. S. Francis. J. Am. Chem. Soc. **81**, 2116 (1959).
6. H. Favre and J. C. Richer. Can. J. Chem. **37**, 411 (1959).
7. K. B. Wiberg. *In* Oxidation in organic chemistry. Academic. New York, N.Y., 1965. p. 164–166.
8. E. L. Eliel. J. Am. Chem. Soc. **88**, 3327 (1966).
9. C. F. Wilcox, Jr., M. Sexton, and M. F. Wilcox. J. Org. Chem. **28**, 1079 (1963).
10. J. C. Richer and C. Gilardeau. Can. J. Chem. **43**, 538 (1965).

11. F. H. WESTHEIMER and N. NICOLAIDES. J. Am. Chem. Soc. **71**, 25 (1949).
12. R. STEWART. *In* Oxidation mechanisms: applications to organic chemistry. Benjamin. New York, N.Y., 1964. p. 37–46.
13. W. A. WATERS. *In* Mechanisms of oxidation of organic compounds. John Wiley and Sons, Inc., New York, N.Y., 1964. p. 58–64.
14. J. ROČEK, F. H. WESTHEIMER, A. ESCHENMOSER, L. MOLDOVANYI, and J. SCHREIBER. Helv. Chim. Acta, **45**, 2554 (1962).
15. R. STEWART and D. G. LEE. Can. J. Chem. **42**, 439 (1964).
16. D. M. GRANT and E. G. PAUL. J. Am. Chem. Soc. **86**, 2984 (1964).
17. G. W. BUCHANAN, D. A. ROSS, and J. B. STOTHERS. J. Am. Chem. Soc. **88**, 4301 (1966).
18. D. K. DALLING and D. M. GRANT. J. Am. Chem. Soc. **89**, 6612 (1967).
19. H. J. REICH, M. JAUTELAT, M. T. MESSE, F. J. WEIGERT, and J. D. ROBERTS. J. Am. Chem. Soc. **91**, 7445 (1969).
20. A. S. PERLIN and H. J. KOCH. Can. J. Chem. **48**, 2639 (1970).
21. P. C. LAUTERBUR. J. Am. Chem. Soc. **83**, 1838, 1846 (1961).
22. J. M. SICHEL and M. A. WHITEHEAD. Theor. Chim. Acta, **5**, 35 (1966).
23. T. YONEZAWA, I. MORISHIMA, and H. KATO. Bull. Chem. Soc. Jap. **39**, 1398 (1966).
24. V. CHENEY and D. M. GRANT. J. Am. Chem. Soc. **89**, 5319 (1967).
25. J. B. STOTHERS. Quart. Rev. **19**, 144 (1965).
26. I. R. L. BARKER, W. G. OVEREND, and C. W. REES. J. Chem. Soc. 3254 (1964).
27. A. S. PERLIN, B. CASU, and H. J. KOCH. Can. J. Chem. **48**, 2596 (1970).
28. H. J. KOCH and A. S. PERLIN. Carbohyd. Res. **15**, 403 (1970).
29. J. P. SNYDER. Private communication.
30. I. R. L. BARKER, W. G. OVEREND, and C. W. REES. J. Chem. Soc. 3263 (1964).
31. L. FARKAS, B. PERLMUTTER, and O. SCHACHTER. J. Am. Chem. Soc. **71**, 2829 (1949).
32. L. KAPLAN. J. Am. Chem. Soc. **80**, 2639 (1958).
33. C. G. SWAIN, R. A. WILES, and R. F. W. BADER. J. Am. Chem. Soc. **83**, 1945 (1961).
34. N. C. DENO and N. H. POTTER. J. Am. Chem. Soc. **89**, 3555 (1967).
35. J. D. ROBERTS, F. J. WEIGERT, J. I. KROSCHWITZ, and H. J. REICH. J. Am. Chem. Soc. **92**, 1338 (1970).
36. D. E. DORMAN and J. D. ROBERTS. J. Am. Chem. Soc. **92**, 1355 (1970).
37. R. U. LEMIEUX and J. D. STEVENS. Can. J. Chem. **44**, 249 (1966).

Can. J. Chem. Downloaded from www.nrcresearchpress.com by 210.87.254.42 on 09/05/12
For personal use only.

Alkaloids of Certain Oriental *Ormosia* Species

STEWART MCLEAN, P. K. LAU, S. K. CHENG, AND D. G. MURRAY
Department of Chemistry, University of Toronto, Toronto, Ontario

Received January 21, 1971

The basic extracts of five oriental *Ormosia* species (*O. sumatrana*, *O. emarginata*, *O. indurata*, *O. semicastrata*, and *O. pachycarpa*) have been examined and *N*-methylcytisine, *N*-methyltetrahydrocytisine, ormosanine, 18-epiormosanine, and *racemic* piptanthine have been isolated and identified. A further alkaloid of formula $C_{20}H_{33}N_3$, which does not appear to have been described previously, has been isolated from *O. semicastrata*.

On a étudié les extraits basiques de cinq espèces orientales d'*Ormosia* (*O. sumatrana*, *O. emarginata*, *O. indurata*, *O. semicastrata*, et *O. pachycarpa*) et l'on a ainsi pu isolé et identifié la présence de *N*-méthylcytisine, *N*-méthyltétrahydrocytisine, ormosanine, 18-epiormosanine, et de piptanthine racémique. Un autre alcaloïde de formule moléculaire $C_{20}H_{33}N_3$ qui ne semble pas avoir été décrit précédemment a aussi été isolé de *O. semicastrata*.

Canadian Journal of Chemistry, 49, 1976 (1971)

The genus *Ormosia* is comprised of about 100 species of woody legumes native to tropical regions of the Americas and South-East Asia (1). The geographical separation of these two areas and the absence of surviving members of the genus elsewhere indicate that genetic isolation of the two divisions could have been complete for 50 million years or more and that a comparison of their phytochemistry is of great potential interest. The alkaloids of occidental species, which have received a considerable amount of attention in recent years (2), fall into two main groups, both of which are substituted quinolizidines. Members of the first group appear to have

11. F. H. WESTHEIMER and N. NICOLAIDES. J. Am. Chem. Soc. **71**, 25 (1949).
12. R. STEWART. *In* Oxidation mechanisms: applications to organic chemistry. Benjamin. New York, N.Y., 1964. p. 37–46.
13. W. A. WATERS. *In* Mechanisms of oxidation of organic compounds. John Wiley and Sons, Inc., New York, N.Y., 1964. p. 58–64.
14. J. ROČEK, F. H. WESTHEIMER, A. ESCHENMOSER, L. MOLDOVANYI, and J. SCHREIBER. Helv. Chim. Acta, **45**, 2554 (1962).
15. R. STEWART and D. G. LEE. Can. J. Chem. **42**, 439 (1964).
16. D. M. GRANT and E. G. PAUL. J. Am. Chem. Soc. **86**, 2984 (1964).
17. G. W. BUCHANAN, D. A. ROSS, and J. B. STOTHERS. J. Am. Chem. Soc. **88**, 4301 (1966).
18. D. K. DALLING and D. M. GRANT. J. Am. Chem. Soc. **89**, 6612 (1967).
19. H. J. REICH, M. JAUTELAT, M. T. MESSE, F. J. WEIGERT, and J. D. ROBERTS. J. Am. Chem. Soc. **91**, 7445 (1969).
20. A. S. PERLIN and H. J. KOCH. Can. J. Chem. **48**, 2639 (1970).
21. P. C. LAUTERBUR. J. Am. Chem. Soc. **83**, 1838, 1846 (1961).
22. J. M. SICHEL and M. A. WHITEHEAD. Theor. Chim. Acta, **5**, 35 (1966).
23. T. YONEZAWA, I. MORISHIMA, and H. KATO. Bull. Chem. Soc. Jap. **39**, 1398 (1966).
24. V. CHENEY and D. M. GRANT. J. Am. Chem. Soc. **89**, 5319 (1967).
25. J. B. STOTHERS. Quart. Rev. **19**, 144 (1965).
26. I. R. L. BARKER, W. G. OVEREND, and C. W. REES. J. Chem. Soc. 3254 (1964).
27. A. S. PERLIN, B. CASU, and H. J. KOCH. Can. J. Chem. **48**, 2596 (1970).
28. H. J. KOCH and A. S. PERLIN. Carbohyd. Res. **15**, 403 (1970).
29. J. P. SNYDER. Private communication.
30. I. R. L. BARKER, W. G. OVEREND, and C. W. REES. J. Chem. Soc. 3263 (1964).
31. L. FARKAS, B. PERLMUTTER, and O. SCHACHTER. J. Am. Chem. Soc. **71**, 2829 (1949).
32. L. KAPLAN. J. Am. Chem. Soc. **80**, 2639 (1958).
33. C. G. SWAIN, R. A. WILES, and R. F. W. BADER. J. Am. Chem. Soc. **83**, 1945 (1961).
34. N. C. DENO and N. H. POTTER. J. Am. Chem. Soc. **89**, 3555 (1967).
35. J. D. ROBERTS, F. J. WEIGERT, J. I. KROSCHWITZ, and H. J. REICH. J. Am. Chem. Soc. **92**, 1338 (1970).
36. D. E. DORMAN and J. D. ROBERTS. J. Am. Chem. Soc. **92**, 1355 (1970).
37. R. U. LEMIEUX and J. D. STEVENS. Can. J. Chem. **44**, 249 (1966).

Can. J. Chem. Downloaded from www.nrcresearchpress.com by 210.87.254.6 on 09/05/12
For personal use only.

Alkaloids of Certain Oriental *Ormosia* Species

STEWART MCLEAN, P. K. LAU, S. K. CHENG, AND D. G. MURRAY
Department of Chemistry, University of Toronto, Toronto, Ontario

Received January 21, 1971

The basic extracts of five oriental *Ormosia* species (*O. sumatrana*, *O. emarginata*, *O. indurata*, *O. semicastrata*, and *O. pachycarpa*) have been examined and *N*-methylcytisine, *N*-methyltetrahydrocytisine, ormosanine, 18-epiormosanine, and *racemic* piptanthine have been isolated and identified. A further alkaloid of formula $C_{20}H_{33}N_3$, which does not appear to have been described previously, has been isolated from *O. semicastrata*.

On a étudié les extraits basiques de cinq espèces orientales d'*Ormosia* (*O. sumatrana*, *O. emarginata*, *O. indurata*, *O. semicastrata*, et *O. pachycarpa*) et l'on a ainsi pu isolé et identifié la présence de *N*-méthylcytisine, *N*-méthyltétrahydrocytisine, ormosanine, 18-epiormosanine, et de piptanthine racémique. Un autre alcaloïde de formule moléculaire $C_{20}H_{33}N_3$ qui ne semble pas avoir été décrit précédemment a aussi été isolé de *O. semicastrata*.

Canadian Journal of Chemistry, 49, 1976 (1971)

The genus *Ormosia* is comprised of about 100 species of woody legumes native to tropical regions of the Americas and South-East Asia (1). The geographical separation of these two areas and the absence of surviving members of the genus elsewhere indicate that genetic isolation of the two divisions could have been complete for 50 million years or more and that a comparison of their phytochemistry is of great potential interest. The alkaloids of occidental species, which have received a considerable amount of attention in recent years (2), fall into two main groups, both of which are substituted quinolizidines. Members of the first group appear to have

Can. J. Chem. Downloaded from www.nrcresearchpress.com by 210.87.254.6 on 09/05/12
For personal use only.

structures based on a tetracyclic $C_{15}H_{26}N_2$ parent or to be derived from it, at least nominally, by oxidation; the second group can be related in a similar way to a $C_{20}H_{35}N_3$ pentacyclic parent structure and a notable feature of the group is the occurrence of a diversity of stereoisomers differing in relative or absolute configuration or both. The C_{20} alkaloids ormosanine and panamine, found in American *Ormosia* species, have also been isolated from the stems of *O. emarginata* from Hong Kong (3), but otherwise the alkaloids of oriental species appear to have received little attention.

We have examined the bases isolated from five Asian species of *Ormosia* and found representatives of both main alkaloid groups in them. The seeds of *O. semicastrata* have been studied the most thoroughly and have yielded the most interesting results. Four alkaloids, all members of the C_{20} group, have been isolated from this source and, of these, one has been identified as (±)-ormosanine (**1***a*)[1] and another as (±)-piptanthine (**1***b*); although the occurrence of (−)-piptanthine and the elucidation of its complete structure are well documented (2, 4) and Liu *et al.* have very recently described the total synthesis of the racemic modification (2*d*), this appears to be the first time that the isolation of the *racemic* alkaloid from a natural source has been described. (We report a second case in the sequel.) An interesting feature, and one that initially caused us some difficulty, is that the melting point of the racemic base (220–221°) is substantially different from that of the optically active form (142–143°). Identification was secured by comparison with natural (−)-piptanthine by spectroscopy and behavior on t.l.c., and by direct comparison with (±)-piptanthine derived from (±)-ormosanine (2*c*).

The third alkaloid, m.p. 267° (dec.), also has the formula $C_{20}H_{35}N_3$ and reacts with phosgene to form a urea (referred to as the "homoxy" derivative (2*c*)) bridging the two secondary

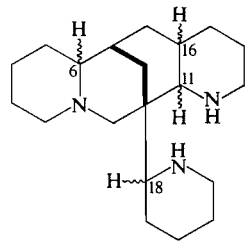

1

	6	11	16	18
a	α	β	α	α
b	β	β	α	α
c	α	β	α	β

(α indicates H below plane at position designated; β, H above plane at position designated)

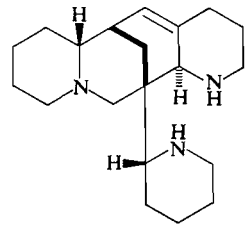

2

amine groups. This alkaloid has not been previously obtained from a natural source, but it has been shown by direct comparison of the bases and their homoxy derivatives to be identical with 18-epiormosanine (**1***c*) which has been synthesized and characterized by Liu *et al.* (2*d*). The fourth alkaloid, m.p. 263° (dec.), has the formula $C_{20}H_{33}N_3$, shows a doublet (J = 6 Hz) at τ 4.35 characteristic of one vinyl proton in its n.m.r. spectrum, and forms a homoxy derivative under standard conditions. It is not identical with dihydroormojanine (**2**) (2*c*), but is probably stereoisomeric with it, although the possibility that it may differ structurally, particularly with respect to the position of the double bond, has not been ruled out. Further investigation of this alkaloid is being undertaken at the present time.

The seeds of *O. sumatrana* afforded ormosanine (**1***a*) and representatives of the first group of alkaloids, *N*-methylcytisine and *N*-methyltetrahydrocytisine, were obtained from the seeds of *O. emarginata* and *O. indurata*, respectively. In each of the latter cases, t.l.c. provided evidence that the basic extract contained at least one more component, but shortage of material precluded further examination of its constitution.

[1]Despite an indication to the contrary in a review (2*a*), apparently arising from a misreading of the original literature, natural ormosanine has always been obtained as a racemic modification as far as we are aware. It should be noted further that, for purposes of illustration, one enantiomer has been drawn for each alkaloid discussed in this paper; however, no claim regarding the true absolute configuration of the molecules is implied and, in the case of racemic modifications, the description in the text makes the stereochemical situation clear.

Can. J. Chem. Downloaded from www.nrcresearchpress.com by 210.87.254.6 on 09/05/12
For personal use only.

The bark of *O. pachycarpa* afforded a single isolable alkaloid which was shown to be identical with the racemic piptanthine described above.

It is clear that the alkaloids obtained so far from Asiatic *Ormosia* species belong to the same structural classes as the alkaloids from American species and the differences which have been established are stereochemical and no greater than the differences that exist between alkaloids previously isolated from American species only.

Experimental

Melting points were determined on a Thomas–Kofler micro hot stage. Spectrometers used were: Perkin–Elmer model 257 infracord (i.r.), Varian A-60 and HA-100 (n.m.r.), and AEI MS902 (mass spectra). Plant identifications were made by the collectors (see Acknowledgements).

Extraction Procedures

Coarsely ground seeds (ground bark in the case of *O. pachycarpa*) were placed in a Soxhlet apparatus and extracted with light petroleum ether and then methanol. Extracts which, after evaporation of the solvent, gave a positive Dragendorff test (5) were partitioned between dilute hydrochloric acid and chloroform. The aqueous solution was made basic and then extracted with an organic solvent.

O. sumatrana Prain

Extraction with ether afforded a basic fraction (*ca.* 1.5%) which deposited crystals from the ether solution. Recrystallization afforded ormosanine, m.p. 178–179°; identity with an authentic sample was confirmed on the basis of m.p. and spectroscopic characteristics. The mother liquor (ether extract) afforded a material which showed two spots on t.l.c., one of which appeared to correspond to ormosanine.

O. emarginata Benth.

Extraction with chloroform afforded a basic fraction (*ca.* 0.5%) which was purified by preparative t.l.c. on silica gel with elution by ether containing a little diethylamine. *N*-Methylcytisine, m.p. 131–134°, identical with an authentic sample was obtained. Analytical t.l.c. indicated that the basic fraction contained at least one more component but this has not yet been characterized.

O. indurata Chen

Extraction with chloroform afforded a basic fraction (*ca.* 3.1%) which was fractionally crystallized from ether. The fraction which, on recrystallization from acetone, afforded crystals, m.p. 210°, was identified as *N*-methyltetrahydrocytisine. The mass spectrum was identical with that described by Schumann *et al.* (6). Catalytic hydrogenation of *N*-methylcytisine over pre-reduced platinum oxide produced material that was spectroscopically indistinguishable from the above material.

O. semicastrata Hance

Extraction with ether afforded a basic fraction (*ca.* 0.3%) consisting of one main component and several smaller components which appeared to be identical to alkaloids obtained in more substantial quantities by continuing the extraction with chloroform. The main component, after recrystallization from ethyl acetate, was identified as (±)-piptanthine, m.p. 220–221°; this formed a homoxy derivative (2*c*), m.p. 164–165°. Identification was made on the basis of comparison with material obtained by Valenta and co-workers (2*c* and *d*). The chloroform extract afforded, on fractional crystallization, ormosanine, an alkaloid, m.p. 267° (dec.), mol. wt. 317.2829 ($C_{20}H_{35}N_3$ requires 317.2831), and an alkaloid, m.p. 263° (dec.), mol. wt. 315.2665 ($C_{20}H_{33}N_3$ requires 315.2674). The $C_{20}H_{35}N_3$ alkaloid formed a homoxy derivative, m.p. 193–194°, and comparison of the free base and its derivative with material supplied by Valenta and co-workers allowed us to identify the alkaloid as 18-epiormosanine. The $C_{20}H_{33}N_3$ alkaloid, i.r. max ($CHCl_3$) 3.30, 6.25 μ; n.m.r. (τ; $CDCl_3$; HA-100) 3.62 (2H; removed by D_2O), 4.35 (1H; doublet, *J*, 6 Hz), 6.34 (1H; removed by D_2O), 6.56, 6.70 (together ≃2H), 6.90 (≃1H), 7.0–8.9 (remainder of protons; complex, 7.20 peak very prominent), formed a homoxy derivative m.p. 178–180°, i.r. max ($CHCl_3$) 3.50, 6.22 μ; n.m.r. (τ; $CDCl_3$; HA-100) 4.45 (1H; doublet, *J*, 6 Hz), 5.2–5.9 (6H; complex), 6.37 (1H; singlet), 6.7–9.2 (remaining protons; complex).

O. Pachycarpa Champ.

Extraction with ether afforded a basic fraction which, although it showed several spots on t.l.c., afforded predominantly (±)-piptanthine (*ca.* 0.14%) (*cf. O. semicastrata* Hance).

We thank the National Research Council of Canada for financial support of this research. Plant material was obtained through the courtesy of Mr. S. Azis, National Biological Institute, Indonesia, Mr. H. C. Tang, Hong Kong Herbarium, and Professor L. B. Thrower, Department of Botany, University of Hong Kong, to whom we express our sincere thanks. Professor J. L. Beal kindly supplied an authentic sample of *N*-methylcytisine. Professor Z. Valenta supplied a number of invaluable reference compounds and spectra, and we are additionally indebted to him for his frequent advice and encouragement.

1. V. E. Rudd. Contrib. U.S. Nat. Herb. **32**, 279 (1965).
2. (*a*) F. Bohlmann and D. Schumann. The alkaloids. *Edited by* R. H. F. Manske. Vol. 9. Academic Press Inc., New York, N.Y., 1967. Chapt. 5. (*b*) S. McLean, A. G. Harrison, and D. G. Murray. Can. J. Chem. **45**, 751 (1967). (*c*) Z. Valenta, P. Deslongchamps, M. H. Rashid, R. H. Wightman, and J. S. Wilson. Can. J. Chem. **44**, 2525 (1966). P. Deslongchamps, Z. Valenta, and J. S. Wilson. Can. J. Chem. **44**, 2539 (1966). (*d*) H. J. Liu, Z. Valenta, and T. T. J. Yu. Chem. Commun. 1116 (1970).
3. H. R. Arthur and S. N. Loo. Aust. J. Chem. **20**, 809 (1967).
4. U. Eisner and F. Sorm. Collect. Czech. Chem. Commun. **24**, 2348 (1959). R. A. Konovalova, B. S. Diskina, and M. S. Rabinovich. Zh. Obshch. Khim. **21**, 773 (1951); Chem. Abstr. **45**, 9548 (1951).
5. R. Munier and M. Macheboeuf. Bull. Soc. Chim. Biol. **31**, 1144 (1949).
6. D. Schumann, N. Neuner-Jehle, and G. Spiteller. Monatsh. **99**, 390 (1968).

On the Intermediate in the Reaction of Diethyl Malonate with 1-Fluoro-2,4-dinitrobenzene

K. T. LEFFEK AND P. H. TREMAINE[1]
Department of Chemistry, Dalhousie University, Halifax, Nova Scotia

Received October 28, 1970

No evidence has been found for a stable intermediate during the reaction of 1-fluoro-2,4-dinitrobenzene with diethyl malonate in the presence of triethylamine as has been reported in the literature. The spectral and chemical properties attributed by earlier work to the intermediate have been assigned to the final products of the reaction.

Aucune preuve n'a été trouvée pour la formation d'un intermédiaire stable pendant la réaction du dinitro-2,4-fluoro-1-benzène avec le malonate d'éthyle. Les propriétés spectrales et chimiques qu'attribuait un rapport dans la littérature à un intermédiaire ont été appliquées aux produits finals de la réaction.

Canadian Journal of Chemistry, 49, 1979 (1971)

Introduction

The aromatic nucleophilic displacement of halide from halonitrobenzenes has been thoroughly investigated (1) but little attention has been paid to carbanions as displacing nucleophiles in this reaction.

Baudet reported (2) the observation of an intermediate **1** during the reaction of 1-fluoro-2,4-dinitrobenzene with diethyl malonate in the presence of triethylamine.

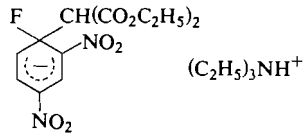

1

As part of a study of aromatic nucleophilic substitution by carbanions, we have repeated Baudet's preparation and found that the observed "intermediate" is in fact the anion of diethyl 2,4-dinitrophenylmalonate, the final product **3** of the reaction (eqs. 1 and 2).

Experimental

The u.v. and visible spectra were recorded on a Unicam SP800 spectrophotometer. The i.r. spectra were recorded on a Perkin–Elmer 237B, with frequency calibration at 1601 cm^{-1} from polystyrene film.

The sodium salt of diethyl malonate was prepared by allowing sodium metal to react overnight in an ether solution of excess diethyl malonate. After filtering and washing with ether, the white salt was pumped dry *in vacuo*.

Diethyl 2,4-dinitrophenylmalonate was prepared by the method of Zaheer and Sidhu (3), from the sodium salt of diethyl malonate and 1-chloro-2,4-dinitrobenzene in diethyl ether and recrystallized from ethanol–water (m.p. 48–49 °C; lit. 50 °C).

Diethyl 2,4-dinitrophenylmalonate was also prepared in dimethyl sulfoxide (DMSO) in a similar manner using 1-fluoro-2,4-dinitrobenzene. The product consisted of pale orange leaflets, m.p. 46–47 °C (mixed m.p. with authentic material 47–48 °C).

[1] 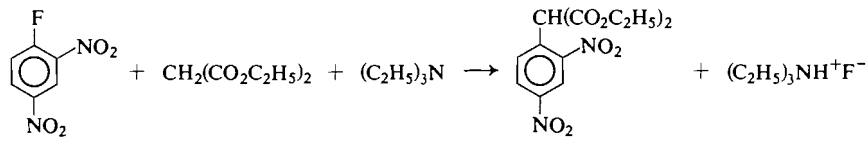

[2] 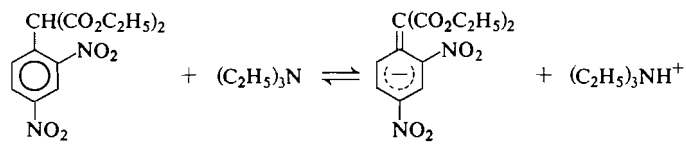

2 **3**

[1]NRCC Postdoctorate Fellow, 1970–1971.

Can. J. Chem. Downloaded from www.nrcresearchpress.com by 210.87.254.40 on 09/05/12
For personal use only.

Can. J. Chem. Downloaded from www.nrcresearchpress.com by 210.87.254.40 on 09/05/12
For personal use only.

The electronic spectra of the sodium salt of diethyl 2,4-dinitrophenylmalonate in mixtures of methanol–DMSO (0, 30, 60, 80, and 100% (v/v) methanol) showed respective λ_{max} (log ε) of 520 (4.38), 514 (4.28), 505 (4.21), 490 (4.14), and 480 nm (3.97).

Results and Discussion

Baudet (2) reported two absorption maxima of the intermediate **1** in solution in DMSO, one weak at 370 and one very strong at 520 nm. The spectrum of the sodium salt of the product **2** was reported in methanol (λ_{max} 475 nm; log ε 3.98), but not in DMSO.

We have found that the reaction of 1-fluoro-2,4-dinitrobenzene with an excess of the sodium salt of diethyl malonate in DMSO produced immediately a stable purple color (λ_{max} 520 nm; log ε 4.38). The only other feature of the spectrum is end-absorption near 275 nm. Acidification and subsequent work-up afforded a 55% yield of diethyl 2,4-dinitrophenylmalonate (**2**).

The addition of an excess of base to diethyl 2,4-dinitrophenylmalonate in DMSO produced immediately a spectrum identical with the one obtained above (λ_{max} 520 nm; log ε 4.38). On addition of methanol, this maximum decreased in wavelength and intensity, and in 100% methanol, the anion appeared orange (see Experimental), as Baudet observed.

The i.r. spectrum of the crude equimolar mixture of 1-fluoro-2,4-dinitrobenzene, diethyl malonate, and triethylamine exhibited an absorption peak at 1676–1680 cm^{-1}, in DMSO or in the absence of solvent (2). The triethylammonium salt of the product **2**, both in Nujol and in DMSO, showed a band at 1677 cm^{-1}. Exposure of any of these samples to air resulted in a rapid disappearance of the red color and of the i.r. band at 1676–1680 cm^{-1}. Both the red color and the i.r. band were restored by treatment of the sample with triethylamine vapor. It is apparent that the changing concentration of the volatile base affects the concentration of the anion **3** (eq. 2).

The reaction of an excess of both diethyl malonate and triethylamine with 1-fluoro-2,4-dinitrobenzene in DMSO gave rise to two absorption maxima, one at 500 and the other at 365 nm. The formation of both peaks was relatively slow at 25 °C (half-life ~100 s), and the relative intensities of the peaks depended on the relative concentrations of diethyl malonate and triethylamine. Triethylamine in the absence of diethyl malonate reacted with 1-fluoro-2,4-dinitrobenzene in DMSO to form a yellow solution (λ_{max} 380 nm). We have observed similar spectra on addition of 1-fluoro-2,4-dinitrobenzene to DMSO solutions of tri-*n*-butylamine (λ_{max} 370 nm) and tribenzylamine (λ_{max} 370 nm). The synthesis of a quaternary pyridinium salt by aromatic nucleophilic substitution of 1-chloro-2,4-dinitrobenzene in pyridine has been reported (4). There is a very early report (5) of the formation of a quaternary salt from triethylamine and *o*-bromonitrobenzene. Although it is most probable that the product of the reaction of triethylamine and 1-fluoro-2,4-dinitrobenzene in DMSO is the quaternary salt **4**, our attempts to isolate it have been unsuccessful. Cavell and Chapman (6) have mentioned the instability of similar quaternary products.

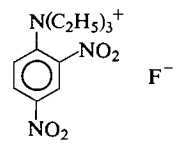

4

Thus, there is no evidence that compound **1** is a stable observable intermediate during the reaction of 1-fluoro-2,4-dinitrobenzene with diethyl malonate and triethylamine. The properties attributed by Baudet (2) to the intermediate **1** are more readily explained as those of a mixture of starting materials, end-product **3** and by-product **4**.

Although the reaction of the sodium salt of diethyl malonate with 1-fluoro-2,4-dinitrobenzene in DMSO is complete in seconds, the slower reaction of diethyl malonate in the presence of triethylamine is probably due to a lower concentration of the attacking nucleophile, the conjugate base of diethyl malonate. Further kinetic work is in progress on the detailed mechanism of this reaction.

The authors are grateful for financial assistance from the National Research Council of Canada.

1. J. MILLER. Aromatic nucleophilic substitution. Elsevier, New York, N.Y., 1968.
2. P. BAUDET. Helv. Chim. Acta, **49**, 545 (1966).
3. S. H. ZAHEER and G. S. SIDHU. J. Ind. Chem. Soc. **24**, 134 (1947).
4. N. I. FISHER and F. H. HAMER. J. Chem. Soc. 189 (1933).
5. N. N. NAGORNOFF. J. Russ. Chem. Ges. **29**, 699 (1898). (J. Chem. Soc. Abstr. **76**, Part 1, 425 (1899)).
6. E. A. CAVELL and N. B. CHAPMAN. J. Chem. Soc. 3392 (1953).

Studies on the Ethylation of Nucleosides with Triethyloxonium Fluoroborate[1]

F. J.-M. RAJABALEE[2] AND S. HANESSIAN
Department of Chemistry, University of Montreal, Montreal, Quebec

Received January 14, 1971

Alkylation of inosine and adenosine triacetates with triethyloxonium fluoroborate leads to selective *N*-ethylation. Inosine triacetate affords 7-ethylinosine as a major product, while adenosine triacetate is ethylated at the N-6 and -1 positions. Treatment with base affords the 6-ethyl analog by rearrangement.

L'alkylation des triacétates d'inosine et d'adénosine avec le fluoroborate du triéthyloxonium conduit à une *N*-éthylation sélective. Le triacétate d'inosine fournit l'éthyl-7 inosine comme produit majeur alors que l'éthylation de l'adénosine se fait aux positions 1 et 6. Le traitement avec des bases conduit, par réarrangement, aux analogues éthylés en position 6.

Canadian Journal of Chemistry, 49, 1981 (1971)

Can. J. Chem. Downloaded from www.nrcresearchpress.com by 210.87.254.5 on 09/05/12
For personal use only.

The isolation of various *N*-methylated purine (1, 2) and pyrimidine (3) nucleosides from biological sources in the past few years has prompted an interest in evaluating the methods of alkylation of nucleosides. The available procedures for purine nucleosides (1) in general utilize methyl iodide, dimethyl sulfate and methyl *p*-toluenesulfonate as methylating agents. Diazomethane, methyl iodide, and *N*,*N*-dimethylformamide dimethyl acetal among other reagents, have been used in the case of pyrimidine nucleosides (4). In all these methods, which involve a variety of conditions, the specificity of alkylation as well as the stability of the nucleosidic linkage are some important factors (4).

N-Alkylated nucleosides present various aspects of biological interest such as their potential inhibitory action on deaminating enzymes (5) and their role in t-RNA, ribosomal RNA, and DNA (6). Although the ultimate biological function of the methylated nucleosides in nucleic acids remains obscure, their presence imparts significant biological characteristics to these vital substances. For example, methylation of homologous RNA from lost cells induces complete resistance to subsequent viral infection to the cells (7). On the other hand the action of alkylating agents on nucleic acid components might lead to mutagenesis and a perturbation of the normal base–pair sequences (6).

We report on the ethylation of certain nucleoside *O*-acetates with triethyloxonium fluoroborate (8) in organic solvents. While our work was in progress, a communication (9) was published on the ethylation of certain heterocyclic bases and nucleosides with the same reagent in aqueous buffers. Although our results differ significantly from those of the Japanese workers (9)[3] the two methods could be considered as being complementary to each other.

Reaction of inosine triacetate with a slight excess of triethyloxonium fluoroborate in dichloromethane solution at 0° during 3 h, followed by treatment with aqueous sodium bicarbonate and processing gave a mixture of ethylated inosine triacetates as a syrup (*ca.* 90%). Deacetylation of the product in methanolic ammonia gave crystalline 7-ethylinosine (**1**, 59%) which

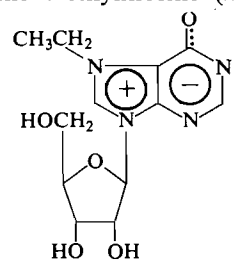

1

crystallized from solution. It exhibited a blue fluorescence on paper chromatograms, characteristic of 7-substituted inosines (1). Authentic 7-ethylinosine was prepared by the method of Jones and Robins (1) for the corresponding methyl analog and found to be identical (m.p., mixed m.p., R_f, u.v.) with the deacetylated sample. The mother liquors of deacetylation con-

[1]Reactions of carbohydrates with oxonium salts. II. For Part I, see ref. 20.

[2]Postdoctoral Fellow, 1969–1970.

[3]Unfortunately, details of the alkylation as well as physical constants of the products and their method of identification were not given in ref. 9. References to known compounds for purposes of comparison were also omitted.

Can. J. Chem. Downloaded from www.nrcresearchpress.com by 210.87.254.5 on 09/05/12
For personal use only.

tained, in addition to some 7-ethylinosine, a faster-moving ethylated component which was isolated by column chromatography on Avicel, as a syrup (18%). This product was different from 1-ethylinosine (10) and is tentatively assigned a 3-ethylinosine structure based on spectrophotometric data on the corresponding ethylhypoxanthine obtained by acid hydrolysis, λ_{max} 266 (p*H* 7), 254 (p*H* 2), and 266 mμ (p*H* 12) and comparative data on 1-ethylhypoxanthine (10) and 3-methylhypoxanthine (11). The major product of ethylation of inosine triacetate with triethyloxonium fluoroborate is therefore the 7-ethyl derivative in agreement with the predictions of quantum calculations and electron density considerations (12). The patterns of alkylation of inosine with oxonium salts is the same as in the alkylation with methyl iodide in dimethylsulfoxide (1).

Treatment of adenosine triacetate with triethyloxonium fluoroborate in dichloromethane solution (0°, 2.5 h) followed by processing with aqueous bicarbonate gave a mixture of *N*-ethyladenosine triacetates as a syrup (*ca.* 90%). Deacetylation in methanolic ammonia followed by evaporation gave a crystalline product (40%) which consisted of two components on paper chromatograms. The mother liquors were evaporated to a syrup (38%) which also consisted of the same two components in addition to some adenosine and a third component. Fractional crystallization of the solid portion from small volumes of water gave crystalline 6-ethyladenosine (**2**) (20%). The product was identical (mixed

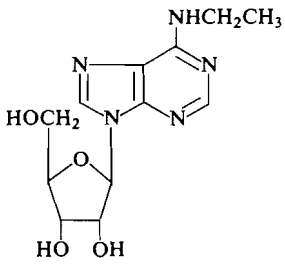

2

m.p., u.v., R_f) with an authentic sample prepared from ethylamine and 9-(β-D-ribofuranosyl)-6-chloropurine (13). Treatment of a mixture of the three components with aqueous NH_4OH at 90° for 3 h (14) gave only two of the original components from which the 6-ethyl derivative could be obtained crystalline. It follows from this experiment that one of the components (slowest-moving) in the mixture must correspond to 1-ethyladenosine which like other N-1 alkylated adenosines (1, 14, 15) rearranges to the N-6 analog. The minor component in the alkylation could correspond to 3-ethyladenosine (16).

Reaction of adenosine triacetate with triethyloxonium fluoroborate occurs even at −50° but at a much slower rate, to give the N-6 ethylated product selectively. The alkylation procedure was also adapted to the direct preparation of 6-ethyladenosine in 55–60% overall yield without isolation of intermediates, by sequential alkylation, rearrangement and crystallization. It is of interest that methylation of adenosine with methyl *p*-toluenesulfonate in DMF or with methyl iodide in DMAC at room temperature leads to selective N-1 methylation. This result is in agreement with predictions based on electron density considerations of adenine and its simple analogs. Alkylation with trialkyloxonium salts differs from all other methods in the case of adenosine, in that appreciable alkylation occurs on the N-6 nitrogen atom, which is perhaps a reflection of the extreme reactivity of alkyloxonium type reagents.

Uridine triacetate reacted very sluggishly at 0° even in the presence of a large excess of reagent. Thus, with 10 equiv at 0° only a 25–30% conversion to 3-ethyluridine could be realized as evidenced by paper chromatography and u.v. spectral data of the deacetylated mixture. According to the Japanese workers (9), uridine is ethylated nearly quantitatively with 2 mol of the reagent at p*H* 9 in aqueous buffer. Under the same conditions, adenosine, cytidine, and guanosine resist ethylation (9). Furthermore, treatment of an aqueous mixture of adenosine, cytidine, and uridine with the reagent (3 equiv) is reported to effect exclusive ethylation of uridine only (9). We have observed the opposite behavior when a mixture of uridine acetate and adenosine acetate was treated with an equimolar amount or an excess of triethyloxonium fluoroborate in methylene chloride. Preliminary experiments indicate that cytidine tetraacetate and 2-deoxy adenosine diacetate are also ethylated under mild conditions (0°, 2–4 h). These and related results will be reported at a later date.

Experimental

Melting points are uncorrected. The n.m.r. spectra were obtained in deuteriochloroform (unless otherwise stated) at 60 or 100 MHz using tetramethylsilane as internal standard. The i.r. spectra were recorded on a Beckman IR-8 instrument. The u.v. spectra were recorded on a Beckman DK recording spectrophotometer. Paper

Can. J. Chem. Downloaded from www.nrcresearchpress.com by 210.87.254.5 on 09/05/12
For personal use only.

chromatography was performed on Whatman No. 1 paper using the solvent system methanol–water (7:3) and spots were revealed with u.v. light.

Ethylation of Inosine Triacetate with Triethyloxonium Fluoroborate

To a suspension of inosine triacetate (17, 18) (5 g, 12.7 mmol) in 100 ml of dichloromethane was added triethyloxonium fluoroborate (8) (2.90 g, 15.3 mmol) with stirring at 0°. After a few minutes, the reaction mixture became homogeneous and the solution was stirred at 0° for 3 h. The t.l.c. (chloroform–methanol, 5:1) indicated the virtual absence of starting material. The solution was treated with aqueous sodium bicarbonate, the organic layer was separated, washed, and evaporated to a foam (yield, 5.42 g). An n.m.r. spectrum of this product showed incorporation of the ethyl group. The product was dissolved in 80 ml of methanol previously saturated with ammonia and the solution was left at room temperature for 6–8 h at which time a crystalline product had separated out. After storing at 0° overnight, the solution was filtered, the product was washed with cold methanol and dried; yield 1.345 g, m.p. 153–155° (dec.); a further crop afforded a total quantity of 1.8 g (46%) of product. The mother liquors (1.8 g) showing two spots (R_f 0.69, 0.83) on paper chromatograms, was chromatographed on a column containing Avicel[4] using methanol–water (7:3) as developer. Fractions containing the faster-moving component (R_f 0.83) were combined and evaporated to a syrup (0.7 g, 18%) which failed to crystallize. Fractions containing the slower-moving component (R_f 0.69) were combined and evaporated to give a crystalline product, m.p. 152–154°, yield 0.43 g, identical with the crystalline product obtained above; combined yield 2.3 g (59%); m.p. 159–161°. Recrystallization from methanol–water afforded *7-ethylinosine* (**1**), m.p. 173–174°; λ_{max} 262 (p*H* 7), 252 (p*H* 2), 256 mμ (p*H* 12); R_f 0.69 (blue fluorescence); identical with an authentic sample (22 g),[5] mixed m.p. 168–170°.

Anal. Calcd. for $C_{12}H_{17}N_4O_5$: C, 48.60; H, 5.44; N, 18.88. Found: C, 48.53; H, 5.22; N, 18.91.

The syrup corresponding to the R_f 0.83 component was an *N*-ethylinosine as shown by the presence of an ethyl group in the n.m.r. spectrum. This product was different from 1-ethylinosine (10) and is designated as 3-ethylinosine based on the u.v. spectral properties of the corresponding *N*-ethylhypoxanthine obtained by acid hydrolysis with *N* HCl (2 h at 100°); λ_{max} 266 (p*H* 7), 254 (p*H* 2), and 266 mμ (p*H* 12). These values are in agreement with u.v. data on 3-methylhypoxanthine (11) but not 1-ethylhypoxanthine (10).

Ethylation of Adenosine Triacetate with Triethyloxonium Fluoroborate

Procedure a

A solution containing 4.5 g (11.3 mmol) of adenosine triacetate (18) in 100 ml of dichloromethane was treated with 2.85 g (15 mmol) of triethyloxonium fluoroborate at 0°. After stirring for 2.5 h in the cold, t.l.c. (chloroform–methanol, 5:1) indicated a small amount of starting material and the appearance of a slow-moving elongated spot. The solution was treated with aqueous sodium bicarbonate and the organic phase was processed to a syrup; yield 4.75 g. The n.m.r. spectrum of this product showed the incorporation of an ethyl group in the adenine portion.

The syrup was dissolved in 75 ml of methanol, previously saturated with ammonia, and the solution was left standing at 0° overnight. The solution was evaporated to dryness, the residue was taken up in methanol, and the solution was chilled. Successive crops of crystalline material could be recovered by repeating the procedure; total yield, 1.36 g (40%). On paper chromatograms, this product consisted of two spots with R_f 0.72 and 0.65. Fractional crystallization of this product from small volumes of water gave *6-ethyladenosine* (**2**) (20%), m.p. 186–188° (dec.); λ_{max} 266 (p*H* 7), 261 (p*H* 1), 265 mμ (p*H* 12); R_f 0.72. The product was identical (mixed m.p., u.v., R_f) with an authentic sample prepared from ethylamine and 9-(β-D-ribofuranosyl)-6-chloropurine (13). The n.m.r. spectrum of 6-ethyladenosine in DMSO-d_6 showed the expected patterns, particularly the triplet at τ 2.2 due to the NH proton. This triplet was diagnostic of N-6 ethylation.

The mother liquor from the original crystallization was evaporated to a syrup (1.135, 38%) which showed three spots on paper chromatograms, R_f 0.80, 0.72, and 0.65, in addition to some adenosine, R_f 0.45. The syrup was dissolved in aqueous NH_4OH (10 ml) and the solution was heated at 90° for 2.5 h. Evaporation to a small volume afforded crystalline 6-ethyladenosine (0.5 g, 14%). The final mother liquors contained small amounts of adenosine and the R_f 0.8 component which was not investigated further.

Procedure b

In another experiment the preparation of 6-ethyladenosine was carried out without the isolation of intermediates. A solution containing 0.5 g (1.3 mmol) of adenosine triacetate and 350 mg (1.8 mmol) of triethyloxonium fluoroborate in 15 ml of dichloromethane was stirred at 0° for 2.5 h. The slightly acidic solution was neutralized with a drop of dilute ammonium hydroxide solution and evaporated to dryness. The resulting foam was dissolved in 4 ml of water, containing 0.5 ml of concentrated ammonium hydroxide and the solution was heated at 80–90° with stirring for 2 h, with periodic addition 0.1 ml of base. The solution was evaporated to a crystalline residue which was triturated with methanol and filtered. This product was inorganic and was discarded. The mother liquors were evaporated to give a crystalline residue which was triturated with cold water, filtered and washed well with the same to give 6-ethyladenosine (180 mg, 48%), m.p. 181–184°. The mother liquors were evaporated to dryness and extracted with boiling ethyl acetate to give a syrup consisting of the expected product and minor quantities of adenosine and the R_f 0.8 component.

Ethylation of Adenosine with Ethyl Iodide in N,N-Dimethylacetamide

The same procedure was used as for the methylation of

[4]A product of American Viscose Corporation, Marcus Hook, Pennsylvania.

[5]This product was obtained by ethylation of inosine with ethyl iodide in DMSO as described for the methyl analog (1). A small amount of pure product was recovered for comparison purposes and optimum yields were not pursued.

Can. J. Chem. Downloaded from www.nrcresearchpress.com by 210.87.254.5 on 09/05/12
For personal use only.

adenosine (1). A suspension of adenosine (0.4 g) in 7 ml of DMAC containing 0.5 ml of ethyl iodide was left at room temperature in the dark for 6 days. The slightly colored solution was diluted with a large volume of acetone and ether. The precipitate was allowed to settle and the supernatant was decanted. The residue, consisting of unreacted adenosine and the hydroiodide salt of 1-ethyladenosine was dissolved in 5 ml of water and adjusted to p*H* 8 with aqueous ammonium hydroxide. The solution was diluted with acetone–ether and the precipitate allowed to settle at 5° overnight. Decantation, washing, and drying afforded 0.45 g of a white crystalline solid which consisted of substantial amounts of adenosine (R_f 0.46) and another product (R_f 0.66), presumably 1-ethyladenosine as evidenced by paper chromatography. An n.m.r. spectrum showed the presence of an ethyl group, but the characteristic NH triplet was absent. This product was heated in aqueous ammonia at 90° for 2 h and the solution evaporated to dryness. Trituration of the crystalline residue with water and filtration gave 215 mg (47%) of 6-ethyladenosine, m.p. 182–184°.

Ethylation of Uridine Triacetate with Triethyloxonium Fluoroborate

Uridine triacetate (19) (0.37 g, 1 mmol) was dissolved in 30 ml of dichloromethane and the solution was treated with triethyloxonium fluoroborate (1.9 g, 10 mmol) at 0°. After stirring at 0° overnight, approximately 40% conversion to another component was evidenced by t.l.c. The solution was treated with aqueous sodium bicarbonate and the organic phase was processed as usual to give a syrup which was deacetylated in methanolic ammonia to give another syrup (0.26 g). This product showed the presence of unreacted uridine (R_f 0.62) and 3-ethyluridine (R_f 0.74) on paper chromatograms. The latter was isolated as a syrup (25–30%) by column chromatography on Avicel; λ_{max} 277 (p*H* 1), 268 (p*H* 7), 268 mμ (p*H* 12); n.m.r. data (D_2O): τ 8.6 (center of a triplet, CH_3—CH_2), 2.23 (doublet, H-5), 2.6 (doublet, H-6), etc. The product obtained was identical (R_f, u.v., n.m.r.) with 3-ethyluridine obtained from the reaction of uridine with triethyloxonium fluoroborate (9) in aqueous solution at p*H* 9. Complete ethylation, as claimed by the Japanese workers (9) could not be achieved in our experiments.

Ethylation of a Mixture of Uridine Triacetate and Adenosine Triacetate with Triethyloxonium Fluoroborate

The two nucleosides (0.5 mmol each) were dissolved in 30 ml of dichloromethane and treated at 0° with 0.5 mmol of triethyloxonium fluoroborate. After 6 h at 0°, t.l.c. indicated that only the adenosine triacetate had reacted. The solution was treated with aqueous sodium bicarbonate and the organic phase was processed to give a syrup. Deacetylation with methanolic ammonia followed by paper chromatography indicated traces of 3-ethyluridine and considerable *N*-ethyladenosine formation. In the presence of an excess of reagent (6 mmol/mmol of nucleoside), a preferential reaction with adenosine triacetate was still observed.

The generous financial assistance of the National Research Council of Canada is gratefully acknowledged.

1. J. W. Jones and R. K. Robins. J. Am. Chem. Soc. **85**, 193 (1963), and references therein.
2. B. H. Rizkalla, R. K. Robins, and A. D. Broom. Biochim. Biophys. Acta, **195**, 285 (1969).
3. R. H. Hall. Biochem. **4**, 661 (1965); see also K.-I. Miura. Prog. Nucleic Acid Res. Mol. Biol. **6**, 39 (1967).
4. A. Holy and J. Zemlicka. Collection Czech. Chem. Commun. **34**, 3383 (1969).
5. L. N. Simon, R. J. Bauer, R. L. Tolman, and R. K. Robins. Biochem. 9, 573 (1970).
6. P. R. Srinivasan and E. Borek. Sci. **145**, 548 (1964).
7. J.-P. Ebel, J.-H. Weil, G. Beck, C. Bollak, L. Colobert, and P. Louisot. Biochem. Biophys. Res. Com. **30**, 148 (1968).
8. H. Meerwein, G. Hinz, P. Hofman, E. Kroning, and E. Pfiel. J. Prakt. Chem. **147**, 257 (1937); H. Meerwein. Org. Synth. **46**, 113 (1966).
9. Y. Kanaoka, E. Sato, M. Aiura, O. Yonemitsu, and Y. Mizuno. Tetrahedron Lett. 3361 (1969).
10. R. W. Balsiger, A. L. Fikes, T. P. Johnston, and J. A. Montgomery. J. Org. Chem. **26**, 3446 (1961).
11. F. Bergmann, G. Levin, A. Kalmus, and H. Kwietny-Govrin. J. Org. Chem. **26**, 1504 (1961).
12. B. Pullman and A. Pullman. Progr. Nucleic Acid Res. Mol. Biol. 9, 327 (1969).
13. H. Lettré and H. Ballweg. Ann. **656**, 158 (1962).
14. M. H. Fleysher, A. Bloch, M. T. Hakala, and C. A. Nichol. J. Med. Chem. **12**, 1056 (1969).
15. W. Grimm, T. Fujii, and N. J. Leonard. Synth. Proced. Nucleic Acid Chem. **1**, 213 (1968) and references cited therein.
16. B. C. Pal. Biochem. **1**, 558 (1962).
17. H. Bredereck. Ber. **80**, 401 (1947).
18. M. Ikehara. Chem. Pharm. Bull. Jap. **8**, 367 (1960).
19. D. M. Brown, A. R. Todd, and S. Vakadarajan. J. Chem. Soc. 2388 (1956).
20. S. Hanessian. Tetrahedron Lett. 1549 (1967); J. Org. Chem. **34**, 675 (1969).

Can. J. Chem. Downloaded from www.nrcresearchpress.com by 210.87.254.5 on 09/05/12
For personal use only.

Déplacement induit par un lanthanide en résonance magnétique nucléaire. Une application à un problème stéréochimique

P. BÉLANGER
Laboratoires de recherches isotopiques, Merck, Sharp & Dohme Canada, Limited, Montréal, Québec

ET

C. FREPPEL, D. TIZANÉ, ET J.-C. RICHER
Département de chimie, Université de Montréal, Montréal, Québec

Reçu le 11 février, 1971

Nous avons poursuivi l'étude de déplacements induits par le tris(dipivalométhanato) praséodyme (III) en r.m.n. Des déplacements vers des champs plus élevés que le tétraméthylsilane ont été observés de même qu'une relation linéaire entre le déplacement chimique induit et l'inverse du cube de la distance métal–hydrogène. Cette relation sert de base à la détermination de la stéréochimie de paires d'épimères et les résultats y sont rapportés pour les *tert*-butyl-4 trimethyl-1,2,2 cyclohexanols *cis* et *trans*.

Shifts induced by tris(dipivalomethanato) praseodymium (III) have been applied to the determination of the stereochemistry of *cis* and *trans* 4-*tert*-butyl 1,2,2-trimethyl cyclohexanols. Observed shifts were at higher field than tetramethylsilane and a linear relationship has been established between the induced shifts and the cube of reciprocal distance metal–hydrogen.

Canadian Journal of Chemistry, 49, 1985 (1971)

La découverte de Hinckley (1) et de Sanders et Williams (2) sur l'utilisation du tris (dipivalométhanato) europium (III), $Eu(dpm)_3$, a été suivie de nombreuses publications sur certaines applications de ce réactif (3–6). Jusqu'à présent, il n'existe que très peu de publications sur le tris (dipivalométhanato) praséodyme (III), $Pr(dpm)_3$, bien que ce réactif est légèrement supérieur à $Eu(dpm)_3$ quant aux déplacements chimiques induits (7–9). A cause de la relation linéaire typique aux déplacements chimiques induits de cette façon, qui relie le déplacement chimique et l'inverse du cube de la distance métal–hydrogène (10), il devenait intéressant d'examiner l'utilisation possible de ces réactifs à la solution de certains problèmes stéréochimiques, un peu à la manière de Yonezawa *et al.* (11) qui ont utilisé des complexes du nickel et du cobalt pour déduire la stéréochimie de méthyl pipéridines.

Au cours de nos travaux sur la stéréochimie des produits dérivés de la *tert*-butyl-4 diméthyl-2,2 cyclohexanone (**1**), les *tert*-butyl-4 triméthyl-1,2,2 cyclohexanols *cis* (**2**) et *trans* (**3**) furent obtenus et caractérisés (12).

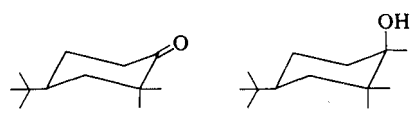

1 **2**

3

La stéréochimie des deux alcools tertiaires **2** et **3** étant bien établie, les spectres de r.m.n. furent déterminés en présence de $Pr(dpm)_3$ dans le but de déterminer les différents déplacements paramagnétiques et de voir l'effet de la stéréochimie des deux alcools tertiaires **2** et **3** sur les déplacements observés.

Les meilleurs résultats sont obtenus lorsque 50 mg de **1**, **2**, ou **3** et 50 mg de $Pr(dpm)_3$ sont dissous dans 0.5 ml de tétrachlorure de carbone et que la solution résultante est filtrée pour enlever les quelques particules en suspension. Les résultats sur **1**, **2** et **3** sont compilés dans le tableau 1 pour les différents groupements méthyles.

TABLEAU 1. Déplacement induit par le tris(dipivalométhanato) praséodyme (III) sur la cétone **1** et sur les deux alcools tertiaires **2** et **3**

	$-\Delta\delta$*			
Produit†	$(CH_3)_3C$—	CH_3 1	CH_3 2*a*	CH_3 2*e*
1	1.14	—	5.95	9.35
2	2.07	10.80	5.12	8.02
3	1.35	10.35	8.00	9.10

*$\Delta\delta = \delta_{Pr=100\,mg} - \delta_{Pr=0\,mg}$ exprimé en p.p.m.
†La concentration en produit est 1.28×10^{-4} mol dans 0.5 ml CCl_4.

Les observations suivantes peuvent être facilement notées à partir des valeurs contenues dans le tableau 1. Dans le cas de la cétone **1**, les deux groupements méthyles sont entièrement différents l'un de l'autre et le spectre obtenu le montre clairement. Le méthyle équatorial, qui se trouve dans le plan du carbonyle, est le plus rapproché de l'ion métallique et se trouve à être le plus déplacé. Par contre, le méthyle axial est plus faiblement déplacé vers les champs élevés à cause de son éloignement beaucoup plus considérable.

L'alcool *cis* **2** montre dans le spectre de r.m.n. des groupements méthyles déplacés de 5.12, 8.02, et de 10.80 p.p.m. pour les méthyles 2*a*, 2*e* et 1 respectivement. L'isomère *trans*, **3**, au contraire, montre une différence beaucoup moins marquée pour les deux groupements méthyles axiaux et équatoriaux de la position 2. Dans le cas de l'isomère **2**, la distance entre le méthyle axial et équatorial de la position 2 d'une part et l'ion métallique complexant d'autre part est grandement différente, ce qui n'est pas le cas pour l'alcool **3** où les deux groupes méthyles se trouvent de part et d'autre du plan comportant le groupement hydroxyle. Il est aussi à noter que le méthyle de la position 1 est déplacé de façon à peu près identique, car la distance demeure constante pour les deux isomères.

Il faut aussi remarquer que le groupement *tert*-butyle, facilement identifié dans le spectre, est beaucoup plus déplacé lorsque la fonction hydroxyle est axiale.

Une relation linéaire existe entre le déplacement chimique et l'inverse du cube de la distance oxygène portant le métal et les hydrogènes déplacés. Cette relation linéaire est aussi observée pour les complexes du praséodyme et il devient alors possible de prédire le déplacement chimique de certains hydrogènes dans des molécules cycliques simples. D'autres exemples permettront d'augmenter la précision de ces prédictions, rendant alors possible de préciser certaines conformations.

Ce travail préliminaire montre donc qu'il est facile de déterminer la stéréochimie d'une paire d'épimères par la simple détermination de quelques spectres de r.m.n. Ces déterminations sont d'autant plus aisées qu'il y a toujours une partie de la molécule qui est facilement identifiable et qui servira de base pour une telle détermination. Ce travail démontre aussi que le complexe du praséodyme est aussi utile que celui de l'europium pour des études de ce genre.

Il devient possible, à partir des conclusions de ce travail, de déterminer la stéréochimie d'une série d'alcools alicycliques où des doutes subsistent actuellement au cours d'études faites actuellement dans nos laboratoires.

Les auteurs tiennent à remercier monsieur A. T. Morse du département de production de la compagnie Merck, Sharp & Dohme Canada, Limited pour un don généreux de $Pr(dpm)_3$. Des remerciements vont aussi au Conseil National de Recherches du Canada pour l'aide financière apportée.

1. C. C. HINCKLEY. J. Am. Chem. Soc. **91**, 5160 (1969).
2. J. K. M. SANDERS et D. H. WILLIAMS. Chem. Commun. 422 (1970).
3. P. V. DEMARCO, T. K. ELZEY, R. B. LEWIS, et E. WENKERT. J. Am. Chem. Soc. **92**, 5734 (1970).
4. C. C. HINCKLEY. J. Org. Chem. **35**, 2834 (1970).
5. G. H. WAHL, JR. et M. R. PETERSEN, JR. Chem. Commun. 1167 (1970).
6. J. K. M. SANDERS et D. H. WILLIAMS. J. Am. Chem. Soc. **93**, 641 (1971), et les références compris dans cet article.
7. J. BRIGGS, G. H. FROST, F. A. HART, G. P. MOSS, et M. L. STANIFORTH. Chem. Commun. 749 (1970).
8. D. R. CRUMP, J. K. M. SANDERS, et D. H. WILLIAMS. Tetrahedron Lett. 4419 (1970).
9. J. BRIGGS, F. A. HART, et G. P. MOSS. Chem. Commun. 1506 (1970).
10. D. R. EATON et W. D. PHILIPS. Advan. Magn. Resonance, **1**, 103 (1965).
11. T. YONEZAWA, I. MORISHIMA, et Y. OHMORI. J. Am. Chem. Soc. **92**, 1267 (1970).
12. J.-C. RICHER et C. LAMARRE. Can. J. Chem. **47**, 2349 (1969).

Can. J. Chem. Downloaded from www.nrcresearchpress.com by 210.87.254.5 on 09/05/12
For personal use only.

Can. J. Chem. Downloaded from www.nrcresearchpress.com by 210.87.254.6 on 09/05/12
For personal use only.

Canadian Journal of Chemistry

Published by THE NATIONAL RESEARCH COUNCIL OF CANADA

VOLUME 49 JUNE 15, 1971 NUMBER 12

The Rates of Some Reactions of Aqueous Hypobromous Acid and Hypobromite Ions

M. W. LISTER AND P. E. MCLEOD

Department of Chemistry, University of Toronto, Toronto 181, Ontario

Received October 21, 1970

The reactions of hypobromite ions, or of hypobromous acid, with iodate, nitrite, and formate ions have been investigated, together with the decomposition of hypobromite ions. The p*H* dependence of the rate show that the reactions with formate and nitrite ions are presumably reactions of hypobromous acid. The kinetic parameters for these reactions are reported, and show some similarities to the analogous reactions of hypochlorite ions or hypochlorous acid.

On a étudié la décomposition des ions hypobromites de même que leurs réactions, ou celles de l'acide hypobromeux, avec les ions iodate, nitrite ou formiate. Le fait que les vitesses de ces réactions dépendent du p*H* indique que les réactions des ions nitrites ou formiates se font probablement avec l'acide hypobromeux. On rapporte les paramètres cinétiques de ces réactions et ils sont similaires à ceux des réactions impliquant les ions hypochlorites ou l'acide hypochloreux.

Canadian Journal of Chemistry, **49**, 1987 (1971)

Numerous studies have been made of rates of a series of somewhat similar reactions in order to detect regularities of trends in the rate constants, and hence to throw light on the mechanisms of the reactions. In particular, oxidations by the hydrogen peroxide and related peroxides (1, 2), and by hypochlorous acid or the hypochlorite ion (3, 4) with a series of reducing agents, mostly fairly simple oxidizable anions, have shown somewhat parallel trends. Some empirical relations of the rate constants with other properties of the reagents have been deduced (see also ref. 5). The present paper describes an extension of this work to hypobromous acid and hypobromite ions. In addition some work on the decomposition of aqueous sodium hypobromite is briefly reported. This decomposition has already been studied (6, 7), but it was necessary to extend somewhat the range of conditions used, in order to have rate constants which could be applied to correct for the effects of decomposition in the study of other reactions. The decomposition is itself an oxygen transfer reaction, similar to the others under study.

Experimental

The reactions reported in this paper are those between sodium hypobromite and sodium iodate, nitrite, and formate. As the experimental procedures were fairly similar in each case (this also applies to the decomposition of sodium hypobromite), the experimental aspects will be outlined first.

Sodium hypobromite was prepared in the usual way by adding bromine slowly to cold sodium hydroxide solution. Sodium bromide or sodium nitrate was in general added to adjust ionic strength. Analytical reagent grade samples of these substances, and of the reducing agents, were used throughout.

Runs were carried out by immersing the appropriate mixture in a thermostat held constant to ± 0.02 °C. Samples were removed at known times, rapidly cooled, and analyzed.

Bromine oxyions were mostly estimated spectrophotometrically, but the results were checked (*i*) by titration with arsenious oxide in a bicarbonate solution, which measures hypobromite plus bromite, and (*ii*) by addition of potassium iodide and acid, followed by titration with sodium thiosulfate. Attempts to destroy hypobromite ions by phenol, followed by titration of the residual bromite with arsenious oxide, as recommended by Chapin (8), gave rather erratic results. A similar method of Hashmi and Ayaz (9) using ammonium sulfate to destroy hypobromite also seemed not to be sufficiently

Can. J. Chem. Downloaded from www.nrcresearchpress.com by 210.87.254.6 on 09/05/12
For personal use only.

accurate, a result which agrees with that of Andersen and Madsen (10).

The spectrophotometric analyses involved determining the extinction coefficients of sodium hypobromite and bromite. For the latter a sample of sodium bromite ($NaBrO_2.3H_2O$) was prepared by the method of La Societe d'Etudes Chimique pour l'Industrie et l'Agriculture (Argenteuil, France) (11), which also kindly supplied us with samples of the material. The extinction coefficients found were

	Extinction coefficient (M^{-1} cm^{-1}) at wavelength (mμ)			
Compound	380	355	333	296
NaBrO	56.6	192.2	304.8	113.2
$NaBrO_2$	19.4	53.3	81.4	115.3

Measurements on samples were usually made at two of the above wavelengths, except with sodium nitrite as reducing agent, as this also absorbs appreciably at these wavelengths. For these solutions, measurements were made at 355, 333, and 296 mμ.

Other analyses used were as follows. The concentration of hydroxide ions was found by treating a sample with hydrogen peroxide to destroy hypobromite and bromite, followed by titration with HCl. In the reaction with sodium iodate, sodium periodate precipitates out. It was filtered off, washed, and dried, and analyzed by adding potassium iodide at a pH regulated by excess sodium bicarbonate, followed by titration with arsenious oxide. The analysis agreed with the formula $Na_3H_2IO_6$, which is that to be expected from the phase diagram (12). It was checked that, before precipitation of sodium periodate, the total oxidizing normality did not change, as measured by the iodine liberated by potassium iodide plus acid. In the reaction with sodium formate, analyses for sodium formate were made as follows. Hypobromite ions were destroyed in a sample by adding excess hydrogen peroxide, the excess being then destroyed by boiling; excess standardized potassium permanganate was added, and the excess potassium permanganate remaining after oxidation of the formate was determined by adding potassium iodide and sulfuric acid, and titrating the iodine.

Evaluation of Rate Constants

It was found that the reactions studied followed similar rate laws (with minor differences arising from dependence on hydroxide concentration), and consequently a general method was used to determine the rate constants, which will be outlined here. Firstly, a correction had to be made for the decomposition of sodium hypobromite, and for this reason measurements of the rate of this reaction were made under conditions comparable to those used in the other experiments. It was known from the work of Perlmutter-Hayman and Stein (7) that this was a second order reaction, so the mechanism presumably is

$$2BrO^- \xrightarrow{k_1} BrO_2^- + Br^-$$

$$BrO^- + BrO_2^- \xrightarrow{k_2} BrO_3^- + Br^-$$

k_2 is larger, but not immensely larger, than k_1. If k_2 were immensely larger than k_1, then a plot of $[BrO^-]^{-1}$ against time would give a straight line of slope $3k_1$. For fairly large values of k_2, the limiting slope would be

$$3k_1\left\{\frac{1 + 2R - \sqrt{1 - 8R + 4R^2}}{6R}\right\}$$

where $R = k_1/k_2$. This assumes that the concentration of bromite has adjusted itself so that a plot of $[BrO^-]^{-1}$ against time is linear. A similar equation is given by Perlmutter-Hayman and Stein. If R is small, the slope approximates to $3k_1(1 + R + 4R^2)$, and Perlmutter-Hayman and Stein quote values of R of 0.05 to 0.08 under different conditions. However, if the differential equations corresponding to the reaction mechanism are solved numerically, with the assumption that the bromite concentration is initially zero, it is found that the limiting slope is established somewhat slowly, and that the mean slope over the range from roughly 10 to 40% decomposition is within 2–3% of $3k_1$. Accordingly k_1 was calculated from this.

The rate laws for the reaction of sodium hypobromite with the reducing agents were the same, except for the dependence on hydroxide concentration. The effective rate law was always

$$\frac{dx}{dt} = -kxy - 3k_1x^2 \quad \frac{dy}{dt} = -kxy$$

where $x = [BrO^-]$, and y is the concentration of reducing agent. These equations allow for the simultaneous spontaneous decomposition of sodium hypobromite. As we could not integrate these equations completely, approximate rate constants were calculated for each time interval with the use of average values of the concentrations. The first equation was rearranged to

$$k = \frac{-\Delta[\ln x]/\Delta t - 3k_1\bar{x}}{\bar{y}}$$

where the bar indicates an average value. It was found that the average rate constants, obtained from this equation, did not drift during a run, in some cases up to 80% reaction of the hypobromite ions.

The size of the error introduced by use of the approximate equation was investigated by integrating the above equations numerically with rate constants of approximately the size actually found. The equations were integrated numerically over small intervals, and the concentrations so obtained were then used to generate a second, and better, approximation. It was found that a third repetition of this procedure produced virtually no

TABLE 1. Percentage error in approximate rate constant

	% error for % drop in x =		
k_1/k	10	20	30
0.33	0.5	1.8	3.1
0.17	0.2	1.0	2.4

TABLE 2. Decomposition of sodium hypobromite

Run	T (°C)	Ionic strength	$[OH^-]$ (M)	$10^5 k_1$ (M^{-1} s^{-1})
1	60.0	0.66	0.166	2.48
2	60.0	0.80	0.257	2.59
3	60.0	0.96	0.551	2.96
4	60.0	0.95	0.549	2.96
5	60.0	1.96	0.271	3.38
6	60.0	1.96	0.271	3.18 (Na_2SO_4 used)
7	25.0	1.40	1.130	0.113
8	25.0	0.70	0.560	0.104
9	50.0	1.03	0.553	1.25
10	50.0	1.04	0.433	1.28
11	69.6	1.00	0.243	7.73
12	69.6	1.02	0.542	8.36
13	69.6	1.04	0.816	8.72
14	76.1	0.26	0.127	11.6
15	76.1	0.31	0.106	12.1
16	76.1	0.51	0.231	12.9

TABLE 3. Reaction constants for reaction of sodium hypobromite and sodium iodate

Run	T (°C)	Ionic strength	$[OH^-]$ (M)	$[BrO^-]_0$ (M)	$[IO_3^-]_0$ (M)	$10^4 k$ (M^{-1} s^{-1})
1	60.0	0.77	0.102	0.171	0.0600	5.80
2	60.0	0.78	0.065	0.115	0.0799	6.02
3	60.0	0.97	0.255	0.118	0.0617	5.55
4	60.0	0.98	0.169	0.0796	0.171	5.75
5	60.0	0.98	0.173	0.0777	0.171	5.72
6	60.0	0.97	0.549	0.0756	0.175	6.33
7	60.0	0.97	0.551	0.0757	0.175	6.51
8	60.0	0.97	0.239	0.108	0.0984	5.67
9	60.0	0.96	0.239	0.105	0.0984	5.47
10	60.0	2.35	0.267	0.158	0.0596	5.87
11	50.0	1.11	0.634	0.0834	0.171	1.78
12	50.0	1.16	0.759	0.102	0.171	1.70
13	69.6	0.96	0.553	0.0688	0.170	17.8
14	69.6	0.96	0.554	0.0689	0.170	17.6
15	69.6	0.98	0.242	0.160	0.0594	15.8
16	69.6	0.97	0.243	0.153	0.0594	18.6

further change. These concentrations were then used to give approximate values of k by the method outlined above. The error depends on the ratios k_1/k and x_0/y_0, and the calculated rate constants were low by an amount given in Table 1, in which the initial concentrations are assumed equal. Consequently under the conditions of experiments, the error introduced by use of the approximate equation for k was always well under 2%.

Results

Decomposition of Sodium Hypobromite

The values of k_1 (defined above) obtained are given in Table 2. A few comments may be made on these results. There is a slight upward drift in the rate constant with ionic strength, and also with hydroxide concentration. The ionic strength was adjusted by adding sodium bromide, except in Run 6, when sodium sulfate was used, and this gave a somewhat lower rate constant. The initial sodium hypobromite was between 0.19 and 0.07 M in various runs. From runs under similar conditions the activation energy was calculated to be 19.4 kcal/mol; hence at 60 °C $\Delta H^{\ddagger}$ is 18.8 kcal/mol, and $\Delta S^{\ddagger}$ is -21 cal/deg mol.

Oxidation of Sodium Iodate

The reaction here is

$$NaBrO + NaIO_3 + 2NaOH \rightarrow NaBr + Na_3H_2IO_6$$

The analogous oxidation by sodium hypochlorite has already been investigated (3). The rate constants obtained as described above showed no dependence on hydroxide ion concentration. They are given in Table 3. From the average rate

Can. J. Chem. Downloaded from www.nrcresearchpress.com by 210.87.254.6 on 09/05/12
For personal use only.

TABLE 4. Rate constants for reaction of sodium hypobromite and sodium nitrite

Run	T (°C)	Ionic strength	$[OH^-]_0$ (M)	$[BrO^-]_0$ (M)	$[NO_2^-]_0$ (M)	$10^5k'$ (s^{-1})
1	48.0	1.00	0.053	0.0859	0.274	1.38
2	48.0	1.07	0.105	0.180	0.304	1.25
3	48.0	1.00	0.040	0.0917	0.276	1.67 ($NaNO_3$ used)
4	48.0	1.05	0.089	0.203	0.254	1.22
5	48.0	0.82	0.214	0.037	0.290	1.37
6	48.0	1.29	0.293	0.378	0.111	1.20
7	76.3	1.02	0.120	0.064	0.144	6.22
8	76.3	0.82	0.096	0.068	0.107	6.08
9	76.3	0.81	0.096	0.068	0.107	6.37
10	76.3	1.02	0.276	0.128	0.128	5.92
11	76.3	1.01	0.282	0.103	0.167	5.73
12	76.3	1.01	0.471	0.111	0.168	5.53
13	76.3	0.98	0.325	0.057	0.141	6.05
14	76.3	1.95	0.322	0.041	0.130	6.00

TABLE 5. Rate constants for reaction of sodium hypobromite and sodium formate

Run	T (°C)	Ionic strength	$[OH^-]_0$ (M)	$[BrO^-]_0$ (M)	$[HCO_2^-]$ (M)	$10^4k'$ (s^{-1})
1	59.9	0.91	0.121	0.075	0.072	1.87
2	59.9	0.97	0.123	0.072	0.072	1.79
3	59.9	0.97	0.124	0.069	0.072	1.93
4	59.9	1.12	0.421	0.072	0.072	2.29
5	59.9	2.12	0.416	0.068	0.072	2.57
6	59.9	1.03	0.471	0.073	0.036	2.28
7	59.9	1.00	0.223	0.110	0.036	2.07
8	59.9	0.99	0.217	0.056	0.036	2.07
9	70.4	1.00	0.115	0.070	0.074	3.14
10	70.4	1.01	0.122	0.068	0.074	3.42
11	70.4	0.95	0.222	0.084	0.037	3.07
12	70.4	0.98	0.226	0.048	0.037	3.02
13	49.7	1.00	0.228	0.057	0.036	0.69
14	49.7	1.01	0.109	0.078	0.074	0.79
15	49.7	1.01	0.109	0.079	0.074	0.73

constant at each temperature, the activation energy is 25.9 kcal/mol; whence $\Delta H^{\ddagger}$ is 25.2 kcal/mol and $\Delta S^{\ddagger}$ is 4 cal/deg mol.

Oxidation of Sodium Nitrite

Here the reaction is

$$NaBrO + NaNO_2 \rightarrow NaBr + NaNO_3$$

and the analogous oxidation by sodium hypochlorite has also been investigated (3). The rate constants, obtained as described above, were inversely proportional to the hydroxide ion concentration. Hence the rate constants, which are given in Table 4, allow for this and are defined by

$$\frac{-d[BrO^-]}{dt} = k'\frac{[BrO^-][NO_2^-]}{[OH^-]} + 3k_1[BrO^-]^2$$

The values for k_1 were taken from the measurements on the decomposition of sodium hypobromite, although they could in theory be obtained directly from the present runs. The apparent activation energy obtained from k' is 11.5 kcal/mol.

Oxidation of Sodium Formate

Here the reaction is

$$NaBrO + NaHCO_2 + NaOH \rightarrow NaBr + Na_2CO_3 + H_2O$$

As with sodium nitrite, the rates fitted the equation

$$\frac{-d[BrO^-]}{dt} = k'\frac{[BrO^-][HCO_2^-]}{[OH^-]} + 3k_1[BrO^-]^2$$

The rate constants, k', are given in Table 5. The main group of runs at 60 °C show a slight increase in the rate constant with hydroxide concentration, and with the ionic strength. The mean values of

Can. J. Chem. Downloaded from www.nrcresearchpress.com by 210.87.254.6 on 09/05/12
For personal use only.

TABLE 6. A comparison of the kinetic parameters for analogous reactions of hypochlorite and hypobromite

Reducer	Oxidizer	log k (25 °C)	$\Delta H^{\ddagger}$	$\Delta S^{\ddagger}$	Oxidizer	log k (25 °C)	$\Delta H^{\ddagger}$	$\Delta S^{\ddagger}$
ClO^-	ClO^-	−7.63	24.2	−9.7	BrO^-	—	—	—
BrO^-	ClO^-	—	—	—	BrO^-	−5.53	18.8	−21
IO_3^-	ClO^-	−6.58	25.5	9.2	BrO^-	−5.23	25.2	4
NO_2^-	HOCl	0.82	5.85	−31.0	HOBr	−0.05	2.5	−49
HCO_2^-	HOCl	−1.40	6.1	−40.4	HOBr	0.45	6.7	−34
$HC_2O_4^-$	HOCl	1.2	14.4	−4.7	HOBr	2.5	14.7	2

the rate constants at an ionic strength of about 1.0 and $[OH^-]$ about 0.1 M are 0.76×10^{-4} (49.7 °C), 1.83×10^{-4} (59.9 °C), and 3.28×10^{-4} (70.4 °C). These do not give a good straight line plot of log k' against $1/T$; the activation energy appears to be about 15 kcal/mol. This may in part be connected with the degree of protonation of hypobromite ions at various temperatures, and will be discussed further.

Discussion

Some of the reactions are dependent on $[OH^-]$, and in similar cases this has usually been interpreted as involving reaction of the acid molecule, in this case HOBr, rather than the ion. The reaction could, of course, be one involving the conjugate acid of the reducing ion. However, if we consider these as reactions of hypobromous acid, the true rate constants can be evaluated from the hydrolysis constants of hypobromite ions. Data are available on the ionization constants of hypobromous acid (13), and these combined with the ionization constants of water make pK_h (where $K_h = [HOBr][OH^-]/[BrO^-]$), 5.52 (15 °C), 5.40 (25 °C), 5.21 (35 °C), and 5.03 (45 °C). These values must be extrapolated for the higher temperatures used in some runs, and it should be noted that the calculated ΔH° for the hydrolysis reaction over various temperature intervals is not very constant: $\Delta H^\circ = 4.7$ kcal (15 to 25 °C), 8.0 (25 to 35 °C), and 8.1 (35 to 45 °C). It seemed best therefore to take ΔH° as increasing by 0.1 kcal for each 10° interval above these values. This gives extrapolated pK_h values of 4.86 (55 °C), 4.70 (65 °C), and 4.54 (75 °C), and values at other temperatures were interpolated from these.

If we define the rate constant, k_3, in terms of hypobromous acid by

$$\text{Rate of reaction} = k_3[HOBr][X^-]$$

then when X^- is the nitrite ion, k_3 is 1.29 $M^{-1}\,s^{-1}$ at 48 °C and 1.92 $M^{-1}\,s^{-1}$ at 76.3 °C. The values make $\Delta H^{\ddagger} = 2.5$ kcal/mol and $\Delta S^{\ddagger} = -49$ cal/deg mol. Extrapolation to 25 °C makes log $k_3 = -0.05$ at this temperature.

When X^- is the formate ion, k_3 is 6.9 (49.7 °C), 10.5 (59.9 °C), and 13.8 (70.4 °C); from which $\Delta H^{\ddagger}$ is 6.7 kcal/mol and $\Delta S^{\ddagger}$ is −34 cal/deg mol. By extrapolation log k_3 at 25 °C is 0.45.

The dependence on $[OH^-]$ is the same for the analogous reactions of sodium hypochlorite. This suggests that this aspect depends on the properties of the reducing agent. However, presumably both reactions can occur; *i.e.*, HOBr + X^- and BrO^- + HX. At present this property cannot be related to the structure of the reducing agent, X^-.

Various regularities have been observed in the rate constants of reactions of this type. In particular, Edwards (1, 2, 5) related rate constants for oxidations by peroxides to the standard electrode potential for X^-/X_2, and pK_a of HX, and later he proposed that a better correlation could be found with polarizability instead of standard electrode potential. Similarly rate constants for a single reducing agent with a series of peroxides, ROOH, gave a linear relation with pK_a of ROH. These ideas were applied to hypochlorite oxidations (3, 4), which showed some similar regularities, though not as precisely. The correlation with pK_a of ROH is only to be expected if the RO—OH bond breaks about equally easily as the Cl—OH bond. In aqueous solution the relative ΔH°_{298} of $AOH + X^- \rightarrow XOH + A^-$ are very nearly equal for A = OH or Cl, but are about 9 kcal more endothermic for A = Br. Hence if this is a factor in the rates of reaction, hypochlorous acid might be expected to fit in with the peroxides (as it seems to), but not hypobromous acid.

A comparison of the kinetic parameters for analogous reactions of hypochlorite and hypobromite ions is given in Table 6, which includes data on oxalate ions (14). The ionic strengths are approximately 1.0. The results do not follow a

Can. J. Chem. Downloaded from www.nrcresearchpress.com by 210.87.254.6 on 09/05/12
For personal use only.

very regular pattern, but some comments can be made. The rate constants of hypobromite are generally larger, except for the reaction with nitrite, where a very large negative $\Delta S^{\ddagger}$ occurs. Correlations with standard electrode potentials (either for the complex X^-/X_2 or X^-/XO^-) do not seem to hold for hypobromites, and the same applies to correlations with pK_a of HX.

The similar trends in the rates of hypobromite and hypochlorite reactions mean that the correlation of $\Delta H^{\ddagger}$ and the enthalpy of the reaction, which was found earlier for hypochlorites (4), holds to some extent for hypobromite. In both cases, the more exothermic reactions are faster. It had also been noted earlier that $\Delta H^{\ddagger}$ plotted against $\Delta S^{\ddagger}$ gave a rough straight line for reactions of a particular peroxide species, and less accurately for hypochlorites. For hypobromites, the three reactions of hypobromous acid fall fairly close to a line of slope $d\Delta H^{\ddagger}/d\Delta S^{\ddagger} = 240\ °K$, with the points for the reactions of hypobromite ion not on this line. More reactions would have to be investigated to discover if any extensive regularity of this sort exists. The general conclusion must be that the regularities of various sorts found for peroxides or hypochlorites are (so far) scarcely observable for hypobromites.

1. J. O. EDWARDS. J. Am. Chem. Soc. **76**, 1540 (1954).
2. J. O. EDWARDS. J. Am. Chem. Soc. **78**, 1819 (1956).
3. M. W. LISTER and P. ROSENBLUM. Can. J. Chem. **39**, 1645 (1961).
4. M. W. LISTER and P. ROSENBLUM. Can. J. Chem. **41**, 2727, 3013 (1963).
5. J. O. EDWARDS. Peroxide reaction mechanisms. Interscience Publishers, New York. 1962.
6. P. ENGEL, A. OPLATKA, and B. PERLMUTTER-HAYMAN. J. Am. Chem. Soc. **76**, 2010 (1954).
7. B. PERLMUTTER-HAYMAN and G. STEIN. J. Phys. Chem. **63**, 734 (1959).
8. R. M. CHAPIN. J. Am. Chem. Soc. **56**, 2211 (1934).
9. M. H. HASHMI and A. A. AYAZ. Anal. Chem. **35**, 908 (1963).
10. T. ANDERSEN and H. E. HUNDAGER MADSEN. Anal. Chem. **37**, 49 (1965).
11. British Patent 843558 (1960).
12. A. E. HILL. J. Am. Chem. Soc. **50**, 2678 (1928).
13. C. M. KELLEY and H. V. TARTAR. J. Am. Chem. Soc. **78**, 5752 (1956).
14. R. O. GRIFFITH, A. MCKEOWN, and A. G. WINN. Trans. Faraday Soc. **28**, 107 (1932).

Can. J. Chem. Downloaded from www.nrcresearchpress.com by 210.87.254.6 on 09/05/12
For personal use only.

Can. J. Chem. Downloaded from www.nrcresearchpress.com by 210.87.254.6 on 09/05/12
For personal use only.

The Proton Magnetic Resonance Spectra of some Chlorinated Polycyclodiene Pesticide Metabolites. Rapid Assessment of Stereochemistry[1]

J. D. McKinney, L. H. Keith,[2] A. Alford,[2] and C. E. Fletcher[3]

National Institute of Environmental Health Sciences, National Institutes of Health, Public Health Service, and Department of Health, Education, and Welfare, Research Triangle Park, North Carolina 27709

The rapid and accurate determination of the relative stereochemistry of some postulated chlorinated polycyclodiene pesticide metabolites without excessive dependence on chemical methods is described. Proton assignments were made employing the new nuclear magnetic resonance (n.m.r.) shift reagent, $Eu(DPM)_3$, which effected the separation of superimposed signals in these systems. The assignments based on coupling constant information and requiring spin decoupling equipment are in good agreement with those obtained from the $Eu(DPM)_3$ studies. The data presented establishes the relative stereochemistry of these biologically important compounds and demonstrates the utility of one or both approaches in elucidating their overall structures.

On décrit une méthode rapide et précise de déterminer sans dépendre d'une façon excessive sur des méthodes chimiques la stéréochimie relative de quelques métabolites postulés de pesticides de polycyclodiènes chlorés. On a assigné les différents protons en utilisant, en r.m.n., le réactif $Eu(DPM)_3$ qui permet de séparer les signaux qui seraient par ailleurs superposés dans ce système. Les attributions faites en se basant sur des constantes de couplage ou nécessitant l'utilisation d'équipement pour le découplage des spins sont en bon accord avec celles découlant des études faites avec $Eu(DPM)_3$. Les données présentées permettent d'établir la stéréochimie relative de ces composés biologiquement importants et démontrent l'utilité de chacune des méthodes dans l'élucidation des structures.

Canadian Journal of Chemistry, 49, 1993 (1971)

The chlorinated polycyclodiene pesticides have received considerable attention in the past few years since they are among the most stable and persistent insecticides that can contaminate our environment. Although these compounds have been studied extensively both chemically (1) as well as in living organisms (2–7), their mechanism(s) and mode(s) of action on a molecular level still remain, to a large extent, enigmatic. Metabolic studies of these pesticides have been complicated by difficulties in the unequivocal identification of the biotransformation products which in most cases also require proof of stereochemical structures since stereospecific as well as stereoselective transformations are possible. Detailed elucidation and elimination of metabolic possibilities are necessary in illuminating the possible differences in toxicity due to stereochemical factors (3). This paper describes the use of n.m.r. spectroscopy to more rapidly and accurately determine the stereochemical structures of some postulated chlorinated polycyclodiene pesticide metabolites by establishing patterns of identification in their spectra. The use of n.m.r. data in assigning the stereochemistry of analogous compounds without excessive dependence on chemical methods has been previously reported (8, 9).

A representative series of compounds were obtained for the most part by stereoselective syntheses as outlined in Scheme 1: *trans*-4,5-dihydroxy-4,5-dihydroaldrin (**1**), *cis-exo*-4,5-dihydroxy-4,5-dihydroaldrin (**2**), *exo*-4-hydroxy-4,5-dihydroaldrin (**3**), 4-oxo-4,5-dihydroaldrin (**4**), *endo*-4-hydroxy-4,5-dihydroaldrin (**5**), and *cis-exo*-4,5-dihydroxy-4,5-dihydroisodrin (**6**). All of these compounds, with the exception of **6**, have been implicated as metabolites or degradation products in diverse metabolism studies. However, in some cases the authenticity of standards used for obtaining comparison data with metabolites is not corroborated by a description of the synthetic methodology. Delta-keto endrin (**7**) was commercially available[4] and was examined primarily for any similarities its proton magnetic resonance (p.m.r.) spectra had with those of 4-oxo-4,5-dihydroaldrin (**4**).

[1]Presented at the Regional S.E.S.W. A.C.S. Meeting in New Orleans, La., December, 1970.

[2]Present address: Southeast Water Laboratory, WQO, Environmental Protection Agency, Athens, Ga. 30601.

[3]Present address: School of Dentistry, Emory University, Atlanta, Ga. 30333.

[4]The δ-keto endrin (7) used in this study was obtained from Shell Development Co., a Division of Shell Oil Co., Modesto, Calif.; however, it can also be obtained from thermal degradation of endrin (10).

Can. J. Chem. Downloaded from www.nrcresearchpress.com by 210.87.254.6 on 09/05/12
For personal use only.

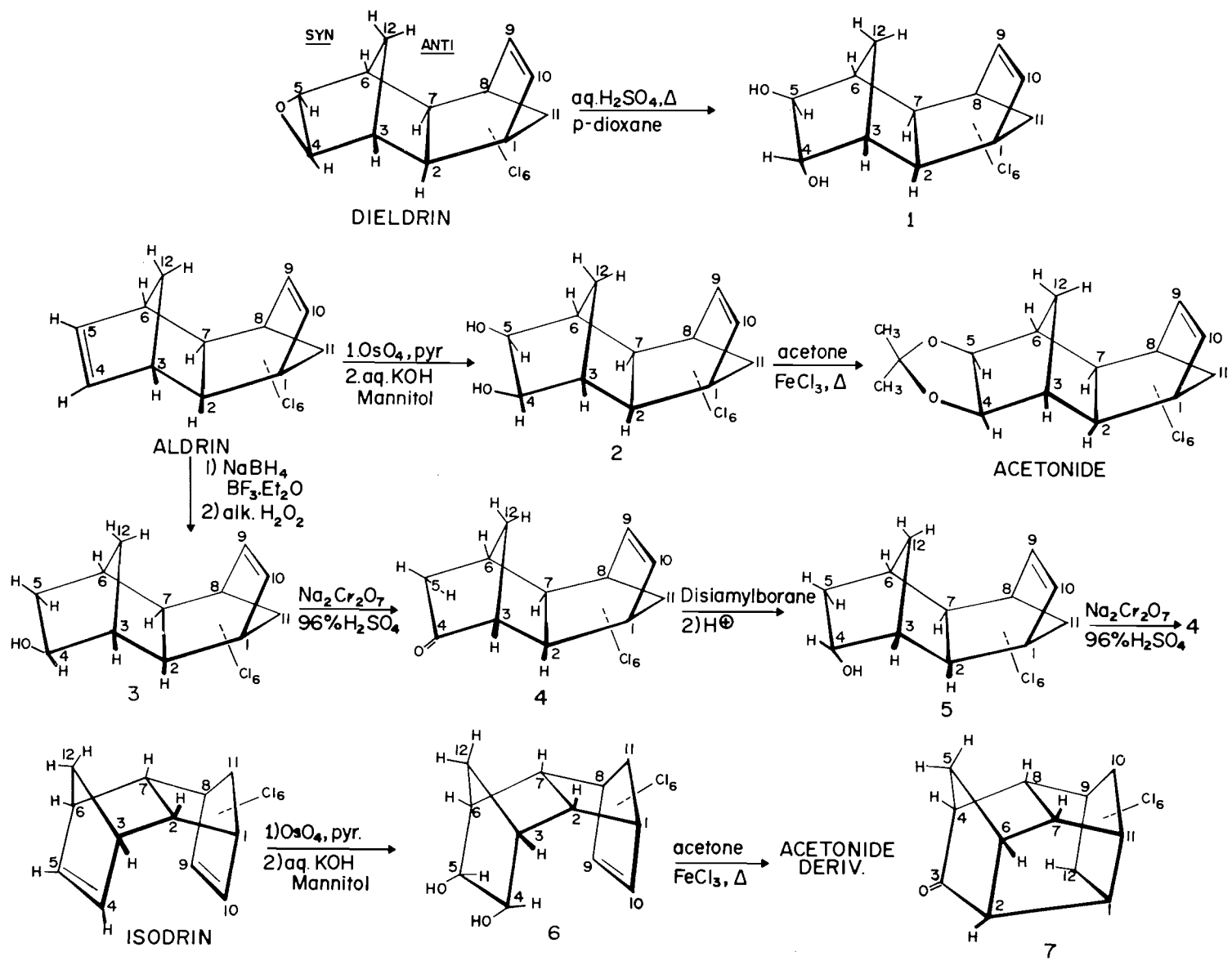

Can. J. Chem. Downloaded from www.nrcresearchpress.com by 210.87.254.6 on 09/05/12
For personal use only.

The preparation of *cis*-diols (**2** and **6**) was accomplished via hydrolysis of their osmic acid esters (11) and gave somewhat higher yields than the previously reported method employing potassium permanganate as an oxidant. The *cis*-diols had identical properties to those obtained by the permanganate procedure [*cis*-dihydroaldrin diol (13); *cis*-dihydroisodrin diol (12)]. Both diols **2** and **6** formed their corresponding acetonides when treated with acetone in the presence of ferric chloride according to the literature method (12), and the facile formation of these acetonides confirms the *cis*-relationship of the two hydroxyl groups. The *trans*-diol (**1**) was prepared according to the literature synthesis (13); however, the yield was significantly increased by the addition of 1,4-dioxane to enhance homogeneity.

The *exo*-alcohol (**3**) was synthesized by hydroboration–oxidation of aldrin. Hydroboration–oxidation of the *endo-exo* octahydrodimethanonaphthalene system is known (14) to give the *exo*-alcohol. Oxidation of alcohol **3** with sodium dichromate in sulfuric acid gave 4-oxo-4,5-dihydroaldrin (**4**), a Lewis acid rearrangement product (15) of the parent pesticide dieldrin. The stereoselective reduction of ketone **4** with disiamylborane (16) afforded the *endo*-alcohol (**5**) which could be reconverted to ketone **4** by oxidation with chromic acid. Alcohols **3** and **5** have been previously characterized (17) as solid materials melting at 125 and 131°, respectively; however, in our hands these compounds, even though chromatographically pure, had no precise melting points. This anomaly has been previously observed (1) for other adducts of hexachlorocyclopentadiene.

The 100 MHz p.m.r. spectra of compounds **1**–**7** were analyzed with the aid of spin decoupling techniques and by addition of the n.m.r. shift reagent (18), *tris*(dipivalomethanato)europium [$Eu(DPM)_3$], which induces paramagnetic shifts in protons via association with lone-pair electron bearing functional groups. The magnitude of the shift is primarily dependent on the distance of each proton from the center of the europium atom (19). A variety of solvents, including chloroform-*d*, acetone-d_6, benzene-d_6, and acetonitrile-d_3, were employed in establishing indentification patterns. Comparison spectra reported in this paper for untreated and $Eu(DPM)_3$ treated samples were obtained in chloroform-*d*. Although the $Eu(DPM)_3$ was normally added to the chloroform solutions of the compounds in approximately one millimolar increments with spectra recorded with each addition, the data from the spectrum which gave the best separation of the protons involved was used for tabulative comparison with the normal spectrum. In almost all cases the p.m.r. data was obtained on 10 mg or less of sample.

A study of the effects of varied concentrations of $Eu(DPM)_3$ on the p.m.r. spectra of some of the parent chlorinated polycyclodiene pesticides has been made (20). The objective of our study was to obtain, for the most part, qualitative information which would permit a rapid and at the same time accurate stereochemical description of these types of compounds. In elaborating the p.m.r. data of these representative compounds, three comparative analyses were made, *i.e.*, dihydroxy compounds (**1**, **2**, and **6**), monohydroxy compounds (**3** and **5**), and ketonic compounds (**4** and **7**).

The chemical shifts obtained for the dihydroxy compounds and derivatives with and without the presence of $Eu(DPM)_3$ are given in Table 1. Examination of the data shown for compound **1** reveals the non-equivalency of all protons except the methylene bridge protons (12a, 12s).[5] The most reasonable explanation for this result would be the presence of both an *endo*- and *exo*-hydroxyl group in the molecule at positions C-4 and C-5 destroying the plane of symmetry present in the parent compound. The *trans*-1,2-relationship[6] of the hydroxyls at C-4 and C-5 is supported by the observed coupling constants of $J_{3,4} = 4.5$, $J_{5,6} < 0.5$, and $J_{4,5} = 1.5$ Hz which conform well to the measured dihedral angles of about 35, 80, and 120°, respectively.[7] The presence of the "W effect"[8] coupling ($J_{5n,12a} = 2.0$ Hz) of the C-5 *endo*-proton with the C-12 *anti*-proton and the absence of such a coupling with the C-4 proton, as deduced from decoupling experiments on various combinations of protons, confirm

[5]The p.m.r. spectrum of **1** in acetonitrile-d_3 also demonstrated the non-equivalency of the C-12 protons (H_{12a} τ 8.66, H_{12s} τ 8.41; where *a* and *s* refer to *anti* and *syn* configurations relative to the C-4, C-5 positions).

[6]It was necessary to confirm the 1,2-relationship of these groups since rearrangement equilibria (21) of the bridged norbornyl cation formed during the synthesis of **1** could have led to other isomers.

[7]A study of the variation of coupling constants with dihedral angle in the p.m.r. spectra of the camphane-2,3-diols has been made (22).

[8]Meinwald's "W-letter rule" (23).

TABLE 1. Chemical shifts (τ in $CDCl_3$) for dihydroxy compounds and derivatives

H	**1** (< 0.1 *M*)	**1** + 0.2 *M* Eu(DPM)$_3$	**2**	Acetonide of **2**	Acetonide of **2** + excess Eu(DPM)$_3$	**6** (< 0.1 *M*)	**6** + 0.06 *M* Eu(DPM)$_3$	Acetonide of **6**
2	6.67	1.87	7.47	7.55	7.53	6.82	5.74	6.79
7	7.38	3.42						
3	7.51	*ca.* 3.36	7.66	7.56	6.35	7.47	5.00	7.37
6	7.71	0.94						
4	6.13	−6.32	6.31	6.02	4.77	5.93	2.22	5.65
5	6.64	−5.62						
12a	8.52	4.83	8.66	8.72	8.46	8.61	7.02	8.71
12s	8.52	1.20	8.35	8.40	7.28	7.84	4.11	7.88
OH	7.56	—	8.73	—	—	7.18	—	—
CH_3	—	—	—	8.56	7.30	—	—	8.58
CH_3	—	—	—	8.72	7.79	—	—	8.74

the *trans*-stereochemistry of the hydroxyl groups. Eu(DPM)$_3$ treatment of the *trans*-diol (**1**) is complicated by the presence of two different associable oxygen atoms which produce a cumulative and unequal deshielding of the various protons since they are not equidistant from the two europium complexes. However, the C-2 and C-7 protons which are distant (4 bonds away) from both hydroxyl groups show comparatively larger deshielding of the C-2 proton by the C-4 *endo*-hydroxyl than that observed for the C-7 proton ($J_{2,7}$ = 8.0 Hz). On the other hand, H_{12s} experiences larger deshielding than H_{12a} by the *exo*-hydroxyl group at C-5 (see Fig. 1) thus corroborating the H_2, H_7, H_4, H_5, H_{12s}, and H_{12a} signal assignments as well as the *trans*-stereochemistry of the diol. Likewise, the two bridgehead protons experience unequal deshielding; H_6 is shifted downfield 6.77 p.p.m. while H_3 is shifted 4.15 p.p.m. downfield. This confirms the H_3 and H_6 signal assignments since Dreiding models show that the bridgehead protons are spatially closer to the *exo*-hydroxyl oxygen (2.6 Å), and hence to the europium complex, than to the *endo*-hydroxyl oxygen (2.9 Å). The extremely large deshielding observed for the H_4 and H_5 signals would be expected since contact as well as pseudocontact interactions of these protons with the complex are possible.

Since the *cis*-relationship of the hydroxyl groups in diols **2** and **6** has been established on chemical grounds *via* acetonide formation, it was only necessary to verify that the expected *exo*-addition to the double bond had occurred. Although *endo*-attack is unlikely chemically,[9] it is a reasonable possibility in studying the metabolism of these compounds. The occurrence of the equivalent pairs of protons H_2–H_7, H_3–H_6, and H_4–H_5 is consistent with the presence of a plane of symmetry generated by two *cis*-oriented hydroxyl groups at positions C-4 and C-5. The *exo*-stereochemistry of these hydroxyl groups is in agreement with the small difference ($\Delta\delta$ 0.09) in the value of the chemical shift obtained for the C-2–C-7 protons of **2** with the value of the C-7 proton proximal to an *exo*-hydroxyl group in **1**. The "W effect" coupling (J = 2.0 Hz) of H_{12a} with $H_{4,5}$ is also present since $H_{4,5}$ collapses to an apparent singlet on irradiation of 12a, thereby confirming the absence of appreciable coupling (J < 0.5 Hz) for $H_{3,4}$ and $H_{5,6}$. The *cis*-diol (**2**) was not amenable to n.m.r. analysis in the presence of Eu(DPM)$_3$ due to its insolubility in suitable solvents. The more soluble acetonide derivative of **2** might be expected to associate with the europium complex *via* association with the ether type oxygens of the dimethylmethylenedioxy ring system. However, a large excess (saturated solution) of Eu(DPM)$_3$ was required to produce significant deshielding of protons in this compound. Since this has been shown (19) to be an equilibrium association, the weaker association of this acetonide can be attributed to the poorer Lewis base character of the ether type oxygens

[9]An *endo*-epoxide has been isolated as an epoxidation product of norbornene which was attributed to *endo*-attack on the system (24).

Can. J. Chem. Downloaded from www.nrcresearchpress.com by 210.87.254.6 on 09/05/12
For personal use only.

Can. J. Chem. Downloaded from www.nrcresearchpress.com by 210.87.254.6 on 09/05/12
For personal use only.

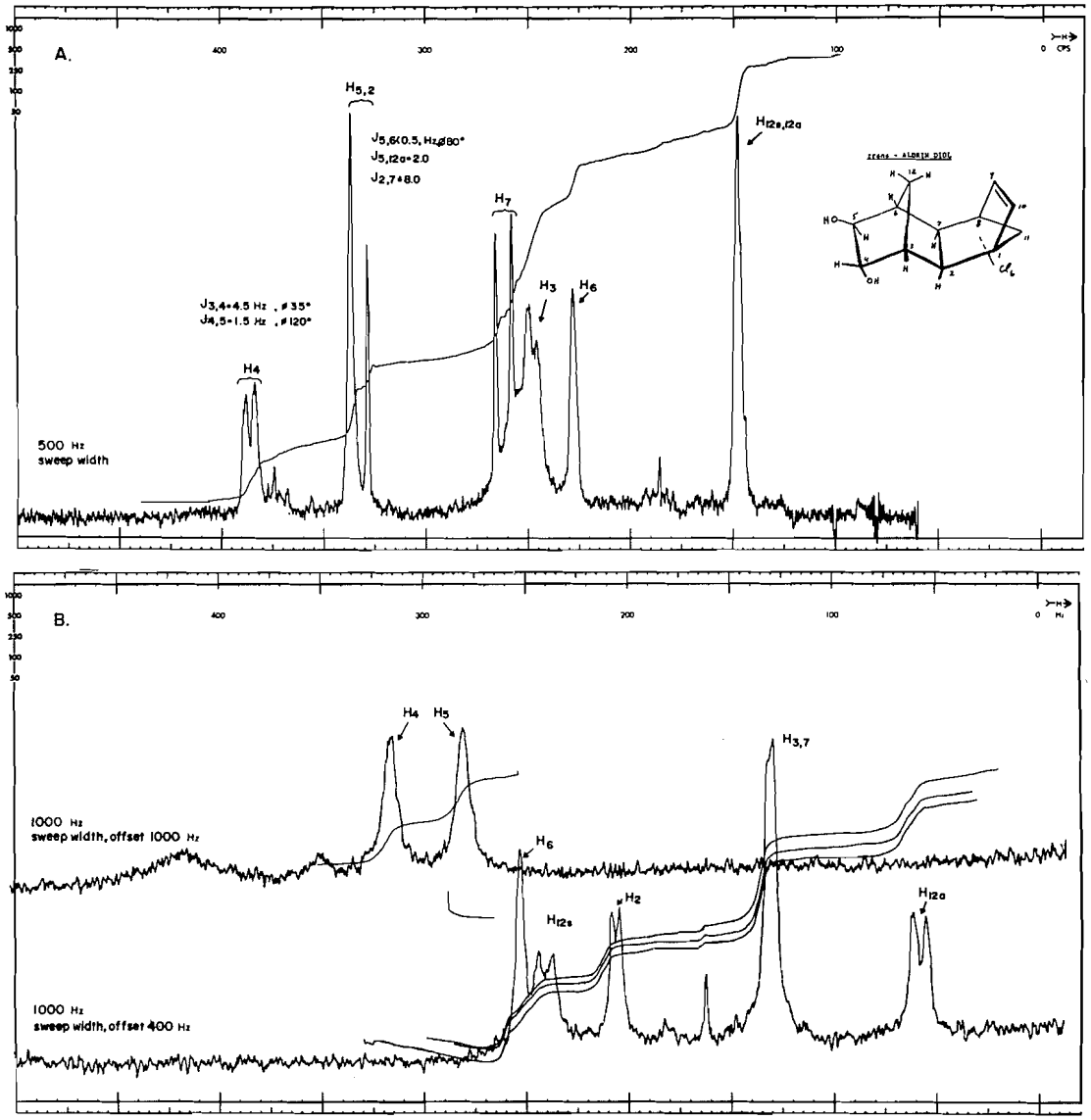

FIG. 1. (*A*) *trans*-Aldrin diol (< 0.1 *M*) without $Eu(DPM)_3$ and (*B*) with 0.2 *M* $Eu(DPM)_3$ in $CDCl_3$ at 100 MHz; 1000 Hz sweep width; sweep offset (*a*) 400 Hz, (*b*) 100 Hz.

as well as the steric requirements of the *gem* dimethyl groups. Nevertheless, the comparatively large deshielding of the H_{12s} signal ($\Delta\delta$ H_{12s} = 1.12 p.p.m.; $\Delta\delta$ H_{12a} = 0.26 p.p.m.) was noted and confirmed the *cis-exo*-stereochemistry of diol **2**.

The formation of the acetonide of diol **6** which is derived from isodrin (*endo–endo* skeleton) not only establishes the *cis*-relationship of the hydroxyl groups but also supports the *exo*-configuration of these groups since such a derivative of the *endo*-isomer of **6**, if it could be formed at all, would have severe steric interactions. The equivalency of protons is also characteristic of this diol as well, with marked differences in chemical shifts for the H_{12s}, $H_{2,7}$, and $H_{4,5}$ signals due to significant differences in the magnetic anisotropy of these protons in the *endo–endo* skeleton. As in diol **2**, the "W effect" coupling (J = 1.8 Hz) of H_{12a} and $H_{4,5}$ and

Can. J. Chem. Downloaded from www.nrcresearchpress.com by 210.87.254.6 on 09/05/12
For personal use only.

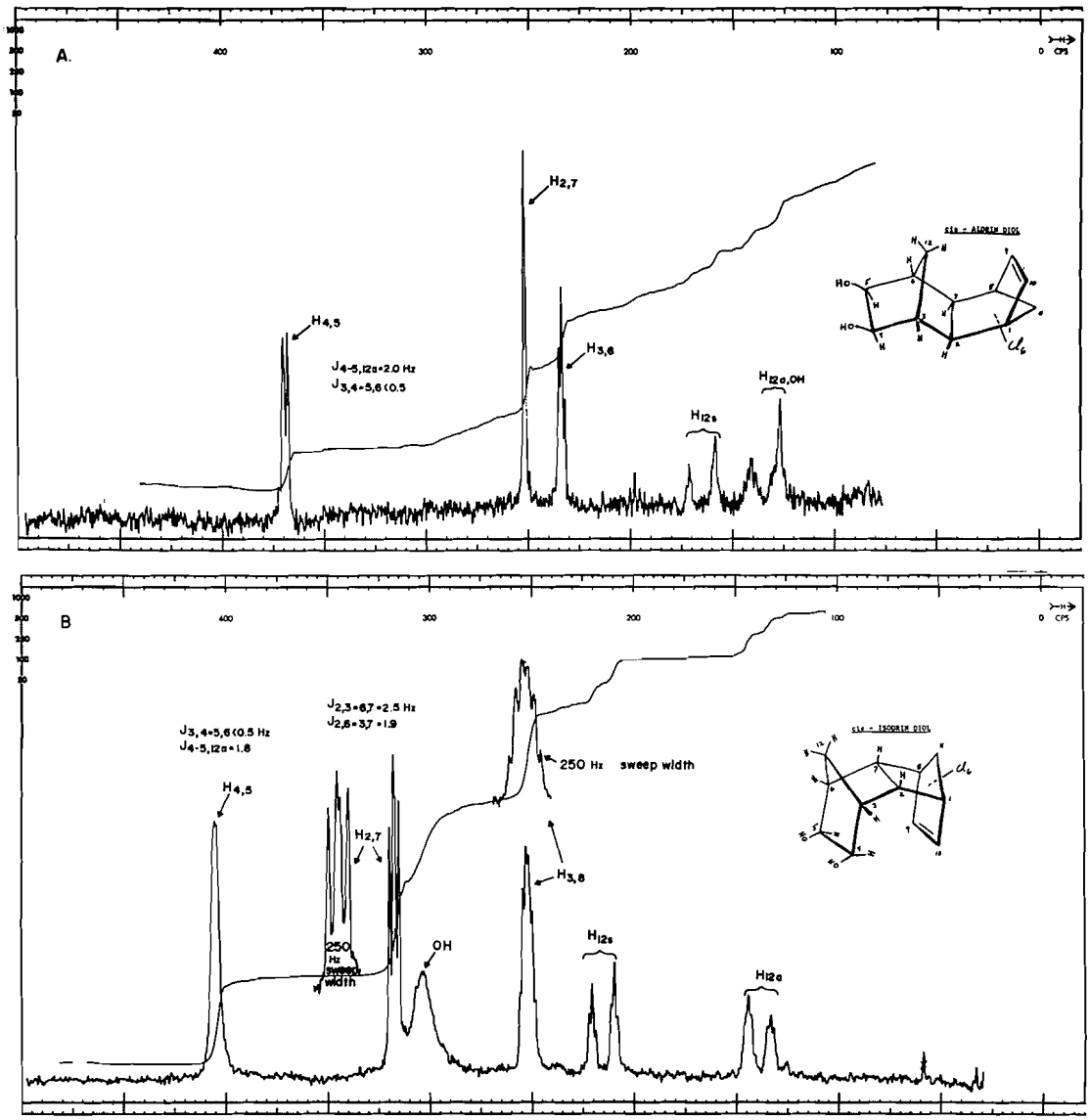

FIG. 2. (*A*) *cis*-Aldrin diol and (*B*) *cis*-isodrin diol in $CDCl_3$ at 100 MHz.

small couplings ($J < 0.5$ Hz) of $H_{3,4}$ and $H_{5,6}$ are characteristic. The most salient difference in the p.m.r. spectrum of diol **6** is the expected pair of doublets for $H_{2,7}$ due to vicinal coupling ($J_{2,3} = J_{6,7} = 2.5$ Hz) with the adjacent bridgehead proton and long-range coupling ($J_{2,6} = J_{3,7} = 1.9$ Hz) with the distant bridgehead proton (Fig. 2) *via* a somewhat distorted "W" (26). As previously reported (25), the presence of these couplings is characteristic of compounds possessing the *endo–endo* skeleton since the $H_{2,7}$ signal in symmetrical compounds possessing the *endo–exo* skeleton appears uniformly as a singlet. In unsymmetrical compounds of the *endo–exo* type such as **1**, **3**, and **5**, the $H_{2,7}$ signals occur as an easily recognizable pair of doublets ($J = 7.5$–8.0 Hz). Addition of $Eu(DPM)_3$ to the chloroform solution of diol **6** produced the larger deshielding of H_{12s} ($\Delta\delta\ H_{12s} = 3.73$ p.p.m.; $\Delta\delta\ H_{12a} = 1.49$ p.p.m.) and completes delineation of the *cis-exo* stereochemistry of the hydroxyl groups.

In light of the information acquired from the dihydroxy compounds, the spectra of the less

Can. J. Chem. Downloaded from www.nrcresearchpress.com by 210.87.254.6 on 09/05/12
For personal use only.

TABLE 2. Chemical shifts (τ in $CDCl_3$) for monohydroxy compounds

H	3 (exo)	3 + excess Eu(DPM)$_3$	5 (*endo*)	5 + excess Eu(DPM)$_3$
2	7.44	6.56	6.46	4.76
7	7.56	6.70	7.20	6.58
3	7.60	5.73	*ca.* 7.5	6.76
6	7.70	6.12	*ca.* 7.6	7.28
4	6.24	2.56	5.77	4.20
5*n*	8.38	6.89	7.93	7.36
5x	*ca.* 8.5	6.37	9.12	7.83
12*a*	8.56	7.51	8.51	8.15
12s		5.93	8.82	8.64
OH	8.00	5.46	7.80	—

discernible monohydroxy compounds **3** and **5** were obtained. The proton chemical shifts of these alcohols are given in Table 2. The most diagnostic observations in rapidly differentiating between *exo*-alcohol **3** and *endo*-alcohol **5** are the appreciable deshieldings of H_2 in the *endo*-alcohol and H_{12s} in the *exo*-alcohol which are markedly increased by the addition of Eu(DPM)$_3$ and the ostensible doublet-character of the H_4 signal in **3** as compared to the octet multiplicity produced by the same proton in **5** (see Fig. 3). The multiplicity differences can be ascribed to large couplings ($J_{4,5x}$ = 10.0 Hz, $J_{4,5n}$ = 3.5 Hz, and $J_{4,3}$ = 5.0 Hz) of H_{4x} in the *endo*-alcohol and comparatively smaller couplings ($J_{4,5x}$ = 1.5 Hz, $J_{4,5n}$ = 6.0 Hz, and $J_{4,3} < 0.5$ Hz) of H_{4n} in the *exo*-alcohol. These couplings are also in good agreement with coupling constants calculated on the basis of dihedral angles. Comparison of $J_{4,5x}$ of **3** and $J_{4,5n}$ of **5** shows the effect of the angle of the hydroxyl substituent to the coupling path and reflects greater distortion of bond angles in the *endo*-alcohol. Greater shielding of H_{5x} by the pseudoaxial hydroxyl substituent in the *endo*-alcohol was also notable. This shielding effect would be consistent with earlier observations (27) on the effect of an axial alkyl substituent on the adjacent equatorial proton in cyclohexane compounds. Although the "W effect" coupling of H_{4n} with H_{12a} was not resolvable in the *exo*-alcohol **3**, the relatively large deshielding of H_{12s} on treatment with Eu(DPM)$_3$ is also in accord with the *exo*-configuration of the hydroxyl group.

The $H_{3,6}$ signals for both alcohols appeared for the most part as broad singlets except for H_3 in the *endo*-alcohol which had doublet character due to its relatively large coupling with H_4 previously described. Decoupling experiments of both alcohols involving H_4 permitted resolution of the H_5 ($J_{5x,5n}$ *exo* and *endo* cpds. = 13 Hz) and H_{12} ($J_{12a,12s}^{exo}$ = 12.5 Hz, $J_{12a,12s}^{endo}$ = 13 Hz) couplings as well as chemical shift assignments of these protons. Addition of Eu(DPM)$_3$ to these alcohols further facilitated the assignment of chemical shifts. The position and configuration of the hydroxyl group in compounds **3** and **5** are consistent both with the p.m.r. spectral data and the methods of preparation.

The p.m.r. spectral characteristics of 4-oxo-4,5-dihydroaldrin (**4**) were investigated as a reference compound for comparing the effects of the carbonyl group on the proton environments of the *endo-exo* skeletal system. *Delta*-keto endrin (**7**) provided less relevant data as a ketonic compound of the *endo–endo* type skeleton. (See Table 3.) The expected non-equivalency of protons at H_2 and H_7 ($J_{2,7}$ = 7.5 Hz) and of H_3 and H_6 in **4** was present but was not as perceptible as in the hydroxy compounds. Double decouplings of $H_{5x,5n}$, $H_{3,6}$, and of $H_{12a,12s}$ provided the most interpretative data for assigning chemical shifts; however, the smaller coupling constants of these protons remained undecipherable. Eu(DPM)$_3$ studies confirmed the assignments and were helpful in revealing the multiplicities of some protons; in particular the characteristic four pairs of doublets produced by the C-5 methylene protons from the large geminal coupling of $H_{5n,5x}$ ($J_{5x,5n}$ = 18.0 Hz) and the smaller vicinal couplings of the $H_{5,6}$ ($J_{5n,6}$ = 5.0 Hz, $J_{5x,6}$ = 4.5 Hz) signals (see Fig. 4). Table 4 summarizes the decoupling experiments employed in establishing the major coupling constants of all compounds discussed thus far. Other decoupling experiments were helpful in some cases to confirm our signal assignments.

The assignments given for δ-keto endrin (**7**) are to some degree tenuous since neither decoupling experiments nor Eu(DPM)$_3$ treatment produced adequate changes in its spectra. The H_2, H_4, and H_6 signals were differentiated primarily on the basis of the expected larger deshielding of H_2 by the proximal C-1 chlorine and the presence of the large vicinal coupling ($J_{2,6}$ = 7.0 Hz) suspected of H_2 and H_6 which conforms well to the dihedral angle of 25° as measured from a Dreiding model. The vicinal coupling of $H_{6,7}$ and $H_{4,8}$ ($J_{6,7} = J_{4,8}$ = 2.0 Hz) and the long-range coupling of $H_{4,7}$ and $H_{6,8}$ ($J_{4,7} = J_{6,8}$ = 1.3 Hz) characteristic of compounds possessing

Can. J. Chem. Downloaded from www.nrcresearchpress.com by 210.87.254.6 on 09/05/12
For personal use only.

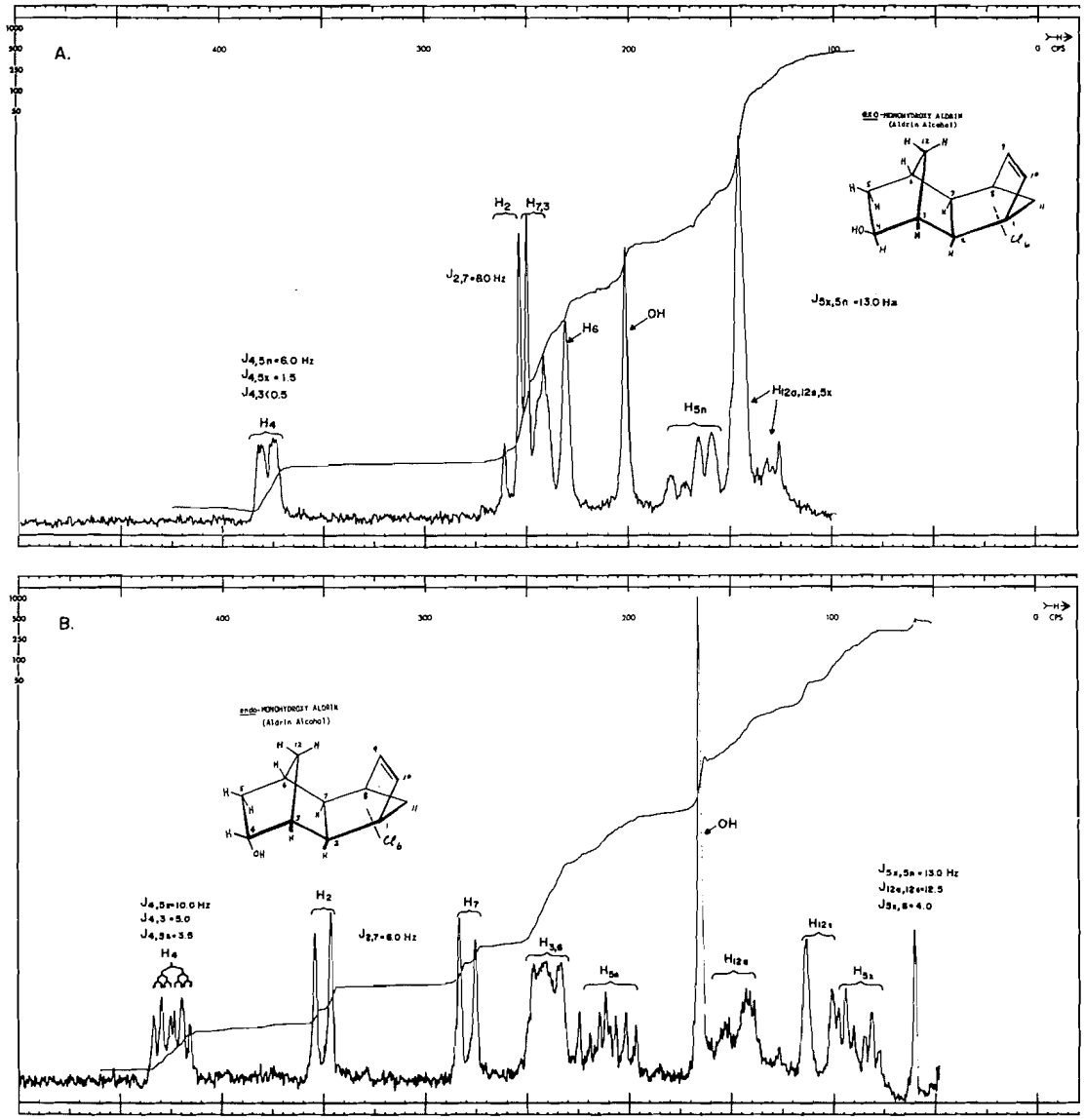

FIG. 3. (*A*) *exo*-Monohydroxy aldrin and (*B*) *endo*-monohydroxy aldrin in $CDCl_3$ at 100 MHz.

the *endo–endo* skeleton were also resolvable. These couplings are smaller in magnitude than those observed (25) for unbridged *endo–endo* systems due to the distortion of bond angles which is a manifestation of the half-cage system. Addition of $Eu(DPM)_3$ to **7** did not provide more substantial data for confirming our signal assignments since sufficient deshielding of protons to resolve all the signals was still not achieved.

In general, addition of $Eu(DPM)_3$ to the keto compounds produced paramagnetic shifts of smaller magnitude than those observed for the hydroxy containing compounds. This finding is consistent with earlier observations (18) and with the stronger associating properties which might be expected for the hydroxyl group on electronic grounds.

The results presented demonstrate that, in rigid systems such as these, a great deal of structural information can be obtained from their p.m.r. spectra. Such information will permit

TABLE 3. Chemical shifts (τ in $CDCl_3$) for keto compounds

H	4 (< 0.1 *M*)	4 + 0.14 *M* Eu(DPM)$_3$	H	7 (< 0.1 *M*)	7 + 0.06 *M* Eu(DPM)$_3$
2	7.04	6.18	2	6.67	6.40
3	7.22	5.38	3	—	—
4	—	—	4	7.11	6.98
5x	8.08	6.47	5a	8.31	8.24
5*n*	7.71	6.07	5s	8.18	8.13
6	*ca.* 7.2	6.60	6	6.91	6.67
7	7.14	6.42	7	6.66	*ca.* 6.6
9	—	—	8	6.66	*ca.* 6.6
12a	*ca.* 8.1	7.46	12	4.98	4.81
12s	8.51				

rapid assessment of the stereochemistry as well as other structural characteristics of these systems whether they be of theoretical or metabolic interest. In addition, the deshielding effects of Eu(DPM)$_3$ were shown to be useful as a confirmatory technique of signal assignments without the requirement of spin decoupling equipment and as a selective shift reagent enabling superimposed signals in these systems to be separated from one another.

Experimental

Melting points were taken on a Fisher–John melting point apparatus and are uncorrected. The n.m.r. studies were made with a Varian HA-100 spectrometer with spin decoupling accessories using tetramethylsilane (TMS) as an internal reference. The Eu(DPM)$_3$ used in these studies was obtained from Alfa Inorganics, Beverly, Massachusetts, and the chloroform-*d* employed in obtaining spectra of Eu(DPM)$_3$ treated samples was stored over anhydrous sodium carbonate. The i.r. spectra were obtained with a Perkin–Elmer Model 337 spectrophotometer, and the low resolution mass spectra were obtained with a Perkin–Elmer Model 270 gas chromatograph-mass spectrometer. The preparative thin layer chromatography (t.l.c.) was done on Uniplate, Silica Gel GF plates 250 microns in thickness. The bands were detected with u.v. light.

Preparation of Dihydroxy Compounds

The *trans*-diol **1** was prepared by a modification of Korte and Arent (13) procedure. To a solution of 243 mg (0.61 mmol) of dieldrin (from Shell Development Co.) in 25 ml of 1,4-dioxane was added 22 ml of water and 3.5 ml of concentrated H_2SO_4. The resulting solution was refluxed for 72 h in oil bath. After cooling, the reaction mixture was diluted with an equal volume of H_2O extracted with two 50-ml portions of ethyl acetate. The combined extracts were washed with sodium carbonate, water and then dried over anhydrous sodium sulfate. Evaporations of these extracts gave a residue which was redissolved and streaked on t.l.c. plates. Elution of the plates with benzene – ethyl acetate (3 to 1) followed by removal of the largest band as detected by u.v. light gave 117 mg (49%) of solid material. Recrystallization from hexane afforded crystalline material melting at 132–134°. Spectral properties were characteristic of *trans*-4,5-dihydroxy-4,5-dihydroaldrin (2).

The *cis*-diols **2** and **6** were prepared according to the following general procedure: To solution of 719 mg (2.1 mmol) of the olefinic compound (aldrin or isodrin) in 10 ml of absolute ether and 1 ml of pyridine was added 500 mg (1.97 mmol) of osmium tetroxide in 50 ml of absolute ether, resulting in the immediate formation of a creamy brown precipitate. The reaction mixture was stirred magnetically for 1 h and allowed to stand overnight unexposed to any light. The light brown precipitate was removed by filtration and dissolved in 50 ml of methylene chloride. The hydrolysis of the olefin–OsO_4–

TABLE 4. Coupling constants (J) obtained from specified decoupling experiments for compounds **1**–**6**

Compound	Irradiated at	J (Hz)
1	2	$J_{2,7}$ = 8.0
	3	$J_{3,4}$ = 4.5
	4,6	$J_{5n,12a}$ = 2.0
	5,12a	$J_{5,6}$ < 0.5
	6,12a	$J_{4,5}$ = 1.5
2	3,6	$J_{4,5-12a}$ = 2.0
	12a	$J_{3,4=5,6}$ < 0.5
3	3,12a	$J_{4,5x}$ = 1.5
	5x	$J_{5x,5n}$ = 13
	5x,12a	$J_{4n,5n}$ = 6.0
	12a*	$J_{12a,12s}$ = 12.5
	12a,12s*	$J_{4,3}$ < 0.5
4	6	$J_{5x,5n}$ = 18
		$J_{5n,6}$ = 5.0
		$J_{5x,6}$ = 4.5
	7*	$J_{2,7}$ = 7.5
	12a	$J_{12a,12s}$ = 12.5
5	3,5*n*	$J_{4,5x}$ = 10.0
	3,5x	$J_{4,5n}$ = 3.5
	4	$J_{5x,6}$ = 4.0
	4,6	$J_{5x,5n}$ = 13
	5*n*,5x	$J_{4,3}$ = 5.0
	12a	$J_{12a,12s}$ = 13
6	3,6	$J_{4,5-12a}$ = 1.8
		$J_{2,3=6,7}$ = 2.5
		$J_{2,6=3,7}$ = 1.9
	12a	$J_{3,4=5,6}$ < 0.5

*Decoupling experiments were done on a sample of compound to which Eu(DPM)$_3$ had been added to separate superimposed signals.

Can. J. Chem. Downloaded from www.nrcresearchpress.com by 210.87.254.6 on 09/05/12
For personal use only.

Can. J. Chem. Downloaded from www.nrcresearchpress.com by 210.87.254.6 on 09/05/12
For personal use only.

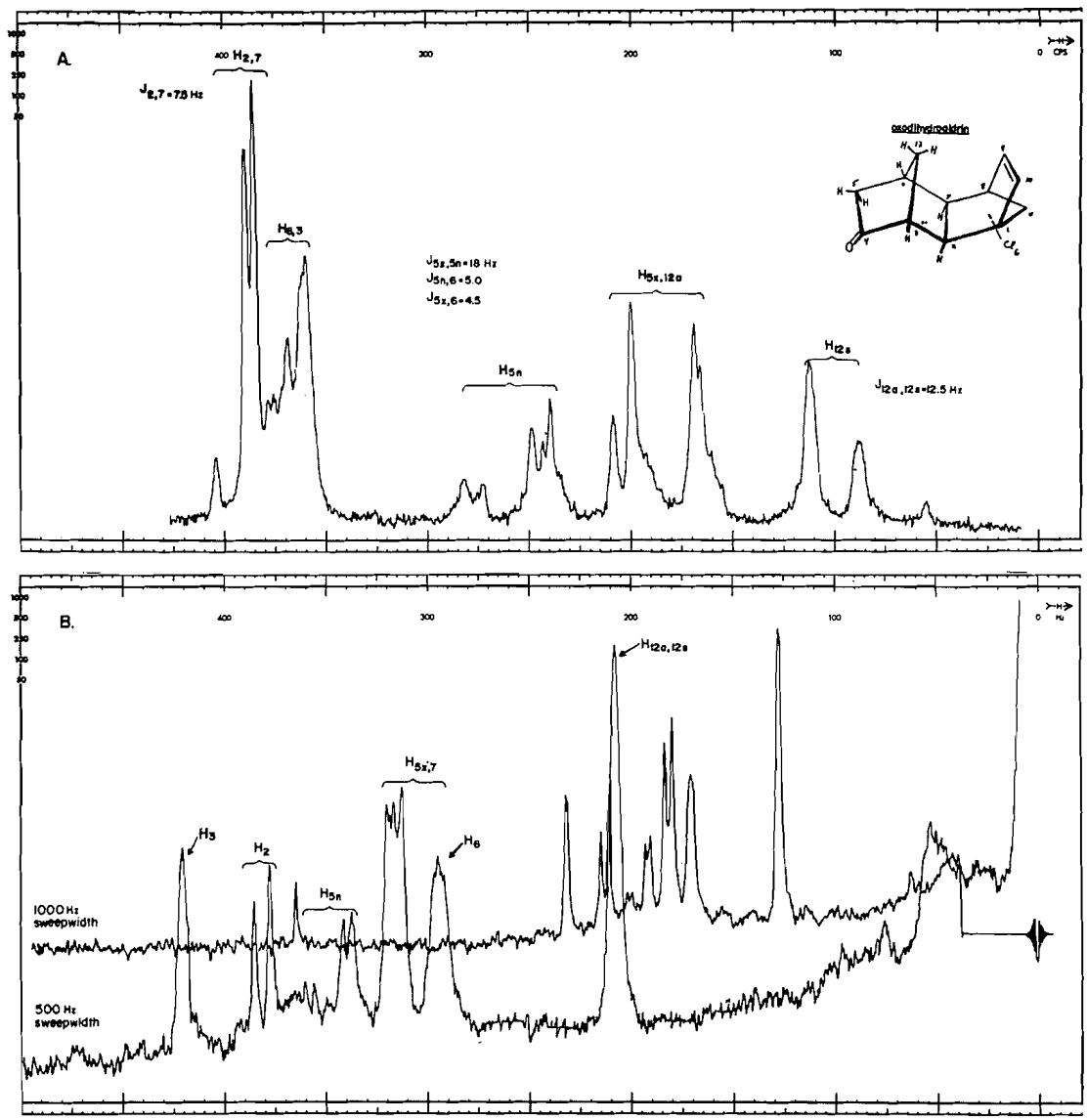

FIG. 4. (*A*) Oxodihydroaldrin (<0.1 *M*) in $CDCl_3$ at 100 MHz; sweep width 250 Hz and (*B*) with 0.14 *M* $Eu(DPM)_3$; sweep width 500 Hz.

pyridine adduct was accomplished by shaking the methylene chloride solution with 65 ml of water containing KOH (11.6 mmol) and mannitol (34.9 mmol) for 2 h or until the brown methylene chloride layer becomes relatively colorless while the aqueous phase acquires a deep reddish brown color. The methylene chloride layer is removed, washed with an equal volume of water, and dried over anhydrous sodium sulfate. Evaporation of this layer left a brown residue from which the *cis*-diol could be obtained by dissolving in hot benzene, decolorizing the resulting solution with charcoal, filtering and cooling the filtrate. Successive recrystallizations afforded 60–75% yields of pure material. The *cis-exo*-4,5-dihydroxy-4,5-dihydroaldrin (**2**) melted at 218–219 °C (m.p. 217 °C (13)) and *cis-exo*-4,5-dihydroxy-4,5-dihydroisodrin (**6**) melted at 201–203 °C (m.p. 199–201 °C (12)). The acetonides of these materials, which were prepared according to the method of Soloway *et al.* (12) in refluxing acetone in the presence of ferric chloride hexahydrate, melted at 151–153 °C (from **2**) and 136–138 °C (from **6**), and had the expected spectral properties for the dimethylmethylenedioxy ring system.

Preparation of Monohydroxy and Keto Compounds

To a solution of 145 mg (3.8 mmol) of sodium borohydride and 1.62 ml of boron trifluoride etherate in 10 ml

Can. J. Chem. Downloaded from www.nrcresearchpress.com by 210.87.254.6 on 09/05/12
For personal use only.

of tetrahydrofuran (THF) was added dropwise a 10 ml solution of 2.88 g (7.9 mmol) of aldrin. The resulting solution was stored for 70 h at room temperature and then 1.4 ml of 3 *N* NaOH solution was added followed by 1.4 ml of 30% hydrogen peroxide. The mixture was stirred at room temperature for 3 h and then diluted with 50-ml portions of ether. The combined extracts were washed with water, dried over anhydrous sodium sulfate, and evaporated under vacuum. The residue was transferred to preparative t.l.c. plates which were eluted with a mixture of chloroform – ethyl acetate (9 to 1). Two major bands were detected with u.v.-light. The material in the band nearest the solvent front was cochromatographical with aldrin. The material in the band nearest the origin was removed and repeatedly chromatographed until pure. Solid material (1.19 g, 39%) obtained from crystallization of the latter purified material from *n*-hexane had no precise melting point but had the expected mass spectral properties ($C_{12}H_{10}O^{35}Cl_{4.5}{}^{37}Cl_{1.5}$, *m/e* 383, 347, 329, 311, and 301) of the *exo*-alcohol (**3**).

A solution of 1.15 g (3.0 mmol) of (**3**) in 10 ml of ether was added dropwise to 10 ml of water containing 880 mg (3.0 mmol) of sodium dichromate and 0.66 ml of 96% H_2SO_4 over a 15-min period while maintaining the temperature below 20 °C. The solution was stirred for 3 h and allowed to reach room temperature followed by stirring for an additional 22 h. The ether layer was separated and the aqueous phase extracted with three 25-ml portions of ether. The combined ether extracts, including the initial ether phase, were washed twice with 50-ml portions of saturated sodium bicarbonate solution, water, and then dried over anhydrous sodium sulfate. A white solid was obtained on evaporation of the extracts to dryness under vacuum and recrystallization from hot *n*-hexane afforded 1.03 g (90% yield) of 4-oxo-4,5-dihydroaldrin (**4**). The material melting at 136–137 °C was chromatographically pure and had the expected spectral properties (i.r., (KBr), C=O, 5.72 μ; MS, $C_{12}H_8O^{35}Cl_{4.5}{}^{37}Cl_{1.5}$, *m/e* 381, 339).

Anal. Calcd. for $C_{12}H_8OCl_6$: C, 37.82; H, 2.10; O, 4.20; Cl, 55.89. Found: C, 37.93; H, 2.26; O, 5.05; Cl, 55.32.

The *endo*-alcohol (**5**) was prepared from (**4**) by the following procedure. Ketone **4** (130 mg, 0.34 mmol) was dissolved in 10 ml of 1 *M* disiamylborane in THF and stirred at room temperature for 20 h. The excess disiamylborane was destroyed by the cautious addition of 0.5 ml of water followed by stirring for 4 h. The reaction was then diluted further with 20 ml of water and extracted with two 15-ml portions of ethyl acetate. The combined dried extracts were taken to dryness and the residue was dissolved in 1 ml of 1,4-dioxane to which was added 0.1 ml of concentrated HCl. (The organoborane had resisted earlier attempts at hydrolysis *in situ* with acetic acid.) The resulting solution was heated at 85 °C for 0.5 h. The reaction solution was diluted to 5 ml with water and extracted with two 4-ml portions of ether. The combined ethers were washed with water, dried, and evaporated to dryness under vacuum. The residue was transferred to preparative t.l.c. plates and developed with a mixture of chloroform – ethyl acetate (9 to 1). Two major bands were detectable with u.v.-light. The band nearest the solvent front was identified as starting ketone **4**. The material in the band nearest the origin was repeatedly chromatographed until pure and crystallized from *n*-hexane. The pure solid (40 mg, 30%) had no precise melting point, but appeared to melt over a long range. This material had the expected mass spectral properties ($C_{12}H_{10}O^{35}Cl_{4.5}{}^{37}Cl_{1.5}$, *m/e* 383, 347, 329, 301) of the *endo*-alcohol (**5**) and was reconverted, in part, to ketone **4** using the dichromate oxidation procedure. The oxidation product had identical gas-chromatographic retention time and superimposable mass spectrum to an authentic sample of **4**.

1. R. RIEMSCHNEIDER. Wld. Rev. of Pest Control, **2**(4), 29 (1963).
2. S. B. SOLOWAY. Adv. Pest Control Res. **6**, 85 (1965).
3. G. T. BROOKS. Wld. Rev. of Pest Control, **5**(2), 62 (1966).
4. A. R. SOTO and W. B. DEICHMANN. Environ. Res. **1**, 307 (1967).
5. J. N. DAMICO, JO-YUN T. CHEN, C. E. COSTELLO, and E. O. HAENNI. J. Assoc. Official Anal. Chem. **51**(1), 48 (1968).
6. F. MATSUMURA, G. M. BOUSH, and AKIRA TAI. Nature, **219**, 965 (1968).
7. M. R. BALDWIN, J. ROBINSON, and R. A. G. CARRINGTON. Chem. Ind. London, 595 (1970).
8. A. M. PARSONS and D. J. MOORE. J. Chem Soc. C, 2026 (1966).
9. C. H. M. ADAMS and K. MACKENZIE. J. Chem. Soc. C, 480 (1969).
10. D. D. PHILLIPS, G. E. POLLARD, and S. B. SOLOWAY. J. Agr. Food Chem. **10**(3), 217 (1962).
11. R. CRIEGEE, B. MARCHAND, and H. WANNOWIUS. Ann. der Chem. **550**, 99 (1942).
12. S. B. SOLOWAY, A. M. DAMIANA, J. W. SIMS, H. BLUESTONE, and R. E. LIDOV. J. Am. Chem. Soc. **82**, 5377 (1960).
13. F. KORTE and H. ARENT. Life Sci. **4**, 2017 (1965).
14. J. K. STILLE and D. R. WITHERELL. J. Am. Chem. Soc. **86**, 2188 (1964).
15. E. J. SKERRETT and E. A. BAKER. Analyst, **84**, 376 (1959); **85**, 184 (1960).
16. H. C. BROWN. *In* Hydroboration. W. A. Benjamin, Inc., New York, N.Y. Chap. 18, 1962.
17. G. T. BROOKS and A. HARRISON. Biochem. Pharmacol. **18**(3), 557 (1969).
18. J. K. M. SANDERS and D. H. WILLIAMS. Chem. Commun. D, 422 (1970).
19. C. C. HINCKLEY. J. Am. Chem. Soc. **91**, 5160 (1969); J. Org. Chem. **35**, 2834 (1970).
20. L. H. KEITH. Tetrahedron Lett. No. 1, 3 (1971).
21. ANDREW STREITWIESER, JR. Chem. Rev. **56**, 571 (1956).
22. F. A. L. ANET. Can. J. Chem. **39**, 789 (1961).
23. J. MEINWALD and A. LEWIS. J. Am. Chem. Soc. **83**, 2769 (1961).
24. H. KWART and T. TAKESHITA. J. Org. Chem. **28**, 670 (1963).
25. L. H. KEITH, A. L. ALFORD, and J. D. MCKINNEY. Tetrahedron Lett. No. 28, 2489 (1970).
26. E. D. BECKER. *In* High resolution NMR, Academic Press, New York, N. Y. 1969. p. 163.
27. H. BOOTH. Tetrahedron, **22**, 615 (1966).

Can. J. Chem. Downloaded from www.nrcresearchpress.com by 210.87.254.105 on 09/05/12
For personal use only.

Conductance Mechanism in the Solid Phase

PUSHTI PRAKASH RASTOGI
Department of Chemistry, Lucknow University, Lucknow, India

Received October 9, 1970

From the conductance measurements, the effect of solidification of solvent on the mobility of common ions (*e.g.*, Na^+, K^+, Cs^+, Cl^-, Br^-, I^-), in *N*-methylacetamide (NMA) solutions has been studied and the energy of activation for the conduction of electrolytes in both solid and liquid states calculated from Arrhenius plots. The conductance behavior in solid phase (or better in solid solutions) has been indicated to be through the "hole-formation mechanism".

On a étudié, à l'aide de mesures de conductivité, l'effet de la solidification du solvant sur la mobilité d'ions communs (par exemple, Na^+, K^+, Cs^+, Cl^-, Br^-, I^-) en solution dans la *N*-méthylacétamide; on a de plus calculé, à partir de diagrammes d'Arrhenius, l'énergie d'activation pour la conduction d'électrolytes soit à l'état liquide soit à l'état solide. On interprête les résultats de conductivité en phase solide (ou mieux en solutions solides) par le "mécanisme de la formation de trous".

Canadian Journal of Chemistry, 49, 2004 (1971)

Introduction

The variation of specific conductance and viscosity with temperatures near the freezing point of water has been the subject of recent critical studies (1–3). The studies aimed, mainly, at checking the mechanisms of conductance and viscous flow in the region where abnormal structural changes occur in water. Glasstone, Laidler, and Eyring (4) have suggested that "the mechanism of ionic conduction, in water, is through the formation of a 'hole' followed by the jump of a nearby 'solvent molecule' or 'solvated ion' into the 'hole'," a contention supported by Horne and co-workers (1, 2). This prompted us to study the effect of solidification of solvent on the mobility of common ions, and to investigate the mechanism of conductance in solid phase *N*-methylacetamide solutions as this solvent freezes at a very convenient temperature (≈29.8 °C) and is fairly stable.

Experimental

N-methylacetamide (NMA), obtained from Eastman Organic Chemicals Co., Rochester, N.Y., was twice fractionally recrystallized, treated with freshly ignited quicklime, and kept overnight. It was distilled under reduced pressure (b.p. 60–70 °C) and the middle fraction of the distillate collected. The process of purification was repeated until the specific conductance of the distillate was reduced to about 10^{-7} ohm^{-1} cm^{-1} (about 6×10^{-7} ohm^{-1} cm^{-1} at 35 °C and 1×10^{-9} ohm^{-1} cm^{-1} at 0 °C). This was stored in a colored bottle, kept inside a dry nitrogen box, and was always used immediately after distillation.

Et_4NI supplied by Eastman Organic Chemicals Co., Rochester, N.Y. was dissolved in a minimum amount of absolute alcohol, precipitated from the solution with ether, and dried in a vacuum desiccator. The KI and CsI were Merck's A.G. reagents and were used without further purification. Reagent grade NaI and KCl were recrystallized from conductivity water and dried in an air oven.

Cell resistance measurements were made at 1000-cycles with a Kohlrausch bridge assembly. Considerable attention was paid during the measurements of conductance at low temperatures, especially near the freezing point of solvent. Data were only taken when the cells containing solid had attained the thermostatic bath temperature (ascertained by the constant values of cell resistance, which were recorded after long intervals). A closed conductivity cell with arrangements for passing dry nitrogen, when desired, was used in the experiments. The cell constant (0.6858 cm^{-1}) was determined with 0.02 *N* KCl solution and checked after every experiment, and was found to be unchanged. The system was observed to be opaque in solid phase. The temperature variation in thermostatic bath was ±0.01° near room temperature and ±0.03° in ranges 0–10 and 40–50 °C.

Results

The specific conductance, Λ, of decinormal solution of KCl, KBr, NaI, KI, CsI, and Et_4NI in *N*-methylacetamide obtained at different temperatures (0–50 °C) are given in Table 1[1]. The Λ values are plotted against temperature. The plots are almost linear above the temperature of crystallization and the Λ can be related to t as $\Lambda = \Lambda_0 (1 + \alpha t)$. The values of Λ *vs.* t are in increasing order in the series Et_4NI, CsI, KI, and NaI in the solid phase, and quite the opposite to that in the liquid phase where the curves become regular, *i.e.* without any hysteresis over the temperature range 0–25 °C, as shown in Figs. 1*a* and 1*b*.

TABLE 1. The specific conductance data for 0.1 *N* solution of alkali halides and Et_4NI in NMA between 0 and 50 °C

	$\Lambda \times 10^2$, $ohm^{-1}\ cm^{-1}$					
t (°C)	Et_4NI	CsI	KI	NaI	KBr	KCl
0	0.0715	0.1174	0.3262	0.3765	0.1913	0.0565
5	0.0932	0.1898	0.5055	0.5598	0.2980	0.0905
10	0.1257	0.3271	0.7538	0.8021	0.4445	0.1351
15	0.2795	0.7146	1.146	1.256	0.6756	0.2043
20	0.7705	1.395	1.884	2.000	1.234	0.6046
25	2.984	3.730	4.112	4.437	3.181	2.250
30	14.74	14.42	14.14	14.00	12.42	11.36
35	16.71	16.45	16.27	15.96	14.31	12.84
40	18.80	18.54	18.31	17.94	16.10	14.40
45	21.01	20.66	20.38	19.97	17.96	15.94
50	22.92	22.70	22.49	21.98	19.81	17.44

Calculations

The energy of activation, E_a, for the conduction of electrolytes in both the liquid and solid phases of solvent has been calculated from the usual $\log \Lambda$ *vs.* $1/T$ plots based on Arrhenius equation, namely,

$$\Lambda = A\, e^{-E_a/RT}$$

or

$$\log \Lambda = \log A - \frac{E_a}{4.576}\frac{1}{T}$$

and been summarized in Table 2.

TABLE 2. The activation energy for the conduction of various electrolytes in liquid and solid states of NMA

	E_a in kcal/mol	
Electrolytes	Liquid state E_a^l	Solid state E_a^s
KCl	4.57	14.19
KBr	4.12	13.73
KI	3.66	13.16
NaI	4.45	12.82
KI	4.40	13.16
CsI	4.29	16.48
Et_4NI	4.18	9.15

Discussion

It has been suggested by Bonner *et al.* (5) that solute–solvent interaction accounts for solvation in such solvents. The solvation of cation arises from an electrostatic interaction between the positively charged cation and the negatively charged oxygen-atom of carbonyl group of associated *N*-methylacetamide molecule, whereas hydrogen bonding is responsible for the solvation of anions. Such specific solvation of cations *vs.* anions in NMA could be best demonstrated by plotting the limiting ionic equivalent conductances (λ_0^+ and λ_0^-) reported by Dawson *et al.* (6) against their crystal ionic radii determined by Robinson and Stokes (7) as shown in Fig. 2. A linear plot is obtained for anions whereas cations show no specific behavior. This supports the view that at least in NMA the anions and cations are definitely solvated in different ways. The linearity of the solvation of anions may be questioned and the relative order of anionic mobilities are difficult to explain.

(1) Liquid Phase (30–50 °C)

The higher the charge density, the greater the

[1]The reported values in Table 1 do not represent the specific conductances due to crystal radii, which, of course, are of a very low order. Moreover, the concentrated 0.5 *N* KI solution was found to be highly conducting in the solid state region, ruling out the separation of solute from the frozen solvent. These observations suggest the formation of a solid solution, which is further supported by the following evidence. (*a*) Precautions were taken to exclude atmospheric moisture from the system when measuring depressions of freezing points; yet a continuous depression was observed. There was also a range of temperature over which frozen solvent NMA melted, and this range was extended in the case of solutions. Thus a long melting range, instead of a sharp melting point, very strongly supports the formation of a solid solution (10). (*b*) A 100 ml 0.1 *N* KI solution was prepared and was frozen while stirring in a clean and dry beaker. About six samples were taken from the frozen solution. They were each melted, and a measured amount of 10 ml from each was put into a conical flask. The amount of iodide present in each flask was estimated gravimetrically as AgI, which was found almost to be the same in all the cases as well as very close to the calculated amount. The estimated amounts of AgI were found to be within the maximum deviation of 0.5%. This observation not only suggests the formation of a "solid solution", but very strongly supports the formation of a "homogeneous solid solution". The products of partial freezing were also analyzed and the results were found to support the same conclusion.

Can. J. Chem. Downloaded from www.nrcresearchpress.com by 210.87.254.105 on 09/05/12
For personal use only.

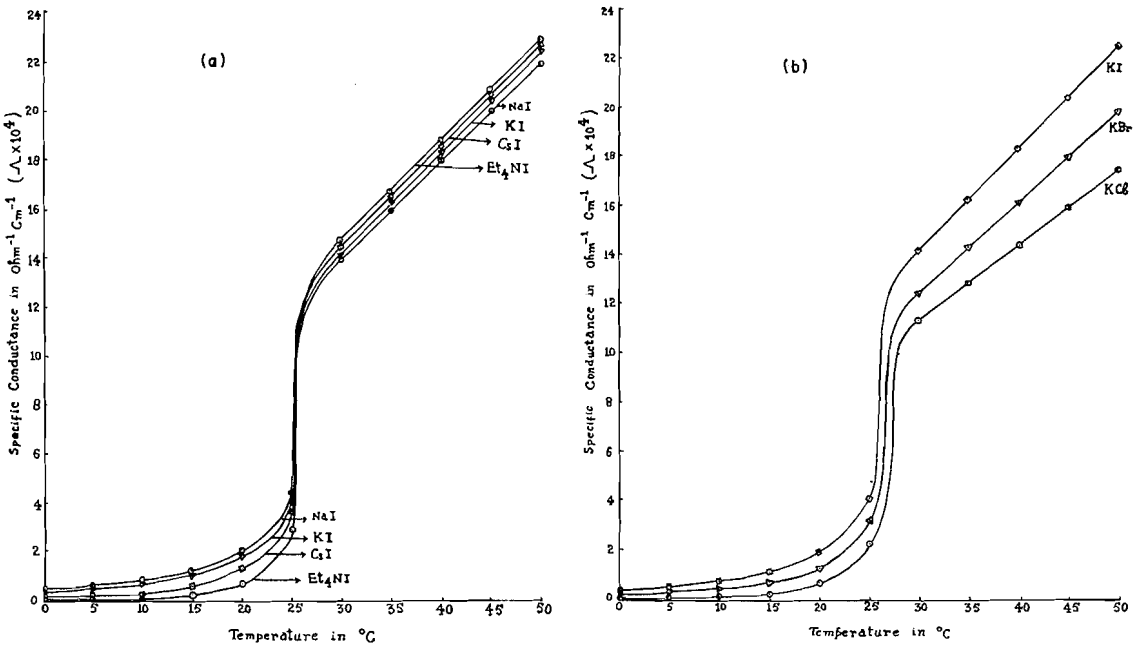

FIG. 1. Plot of specific conductance *vs.* temperature.

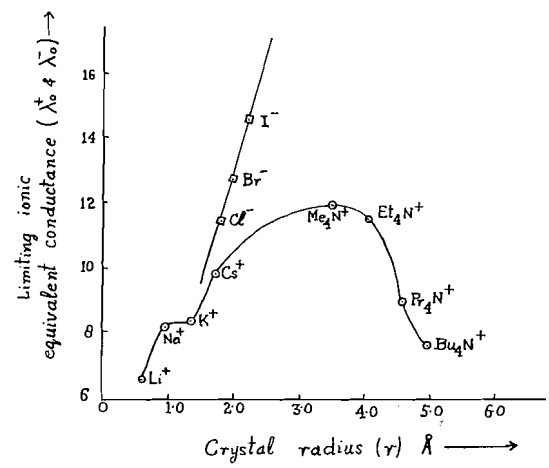

FIG. 2. Plot of limiting ionic equivalent conductance *vs.* crystal radius.

electrostatic interaction, which accounts for the higher solvation and consequently the smaller mobilities[2] of the ions. The absolute mobilities of the ions cannot be calculated from the present data, but the relative order of magnitudes is the same as reported by French and Glover (8) and Dawson *et al.* (9), *i.e.*, $\lambda_0^l(I^-) > \lambda_0^l(Br^-) > \lambda_0^l(Cl^-)$ and $\lambda_0^l(Et_4N^+) > \lambda_0^l(Cs^+) > \lambda_0^l(K^+) > \lambda_0^l(Na^+)$.

(2) Crystallization Phase (25–30 °C)

The sharp inflexion in Λ–t curves around the temperature of crystallization is due to an abnormal increase in the viscosity of solvent as it solidifies on freezing, which hampers the free movement of the ions and consequently accounts for the corresponding sharp decrease in conductance.

(3) Solid Phase (0–25 °C)

It may be noted from Figs. 1*a* and 1*b* that there is an inversion of order in the mobility of cations going into the solid phase but not for the anions; Na^+ conducts more than Et_4N^+ in the solid phase but not in the liquid phase. This leads to a conclusion of "desolvation" in mobility of cations going into solid phase or the speculation of a jumping mechanism in the solid phase that reflects the relative radii of the bare ions. On the contrary the anions seem to retain their relative mobility trend (Fig. 1*b*), an indication either of constant solvation or lack of it. However, anion solvation is supported by Fig. 2, showing the larger ion I^- moving faster. Thus the effect of

[2]Where μl, μf, and μs represent the conductance of liquid, crystallization, and solid phase or solid solutions and that their corresponding ionic mobility is indicated by λ_0^l, λ_0^f, and λ_0^s.

Can. J. Chem. Downloaded from www.nrcresearchpress.com by 210.87.254.105 on 09/05/12
For personal use only.

Can. J. Chem. Downloaded from www.nrcresearchpress.com by 210.87.254.105 on 09/05/12
For personal use only.

solidification of solvent on the solvated ions is that the bare cations are trapped out in the solvent lattices, whereas the anions are left still solvated in solid solutions. The data presented in Table 1 indicate that the relative order of ionic mobility in solid solutions decreases in the increasing order of solvated anionic and bare cationic sizes, *i.e.*, $\lambda_0^s(I^-) > \lambda_0^s(Br^-) > \lambda_0^s(Cl^-)$ and $\lambda_0^s(Na^+) > \lambda_0^s(K^+) > \lambda_0^s(Cs^+) > \lambda_0^s(Et_4N^+)$. It has therefore been tentatively suggested that the smaller the size of solvated anion or bare cation the more conducting it would be in solid solution. The same behavior was also represented with other alkali halides like LiCl, NaCl, and KCl.

It may be noted from Table 2 that the activation energy for the conduction of electrolytes is, in general, about three- to four-fold higher in solid state as compared to that in liquid state; which very strongly maintains an easier ionic conduction in the liquid phase than in the solid phase. It may be noted further that the E_a decreases, in general, with an increase of the size of anion w.r.t. common cation in liquid state, whereas E_a for the cations w.r.t. common anion also decreases in liquid state in contrast to its regular increase in solid state (except for Et_4N^+); suggesting thereby that the phenomenon of ionic conduction in solid phase is through the bare cationic lattices in the case of cations and through the solvated anionic lattices in the case of anions, solely depending upon their sizes, and appears to follow the jumping of ion into the "hole" as suggested earlier (4) in case of H_2O. However, a comparatively smaller value of E_a for bare Et_4N^+ ion in solid state, despite its larger size in comparison to bare Na^+, K^+, and Cs^+ ions may be on account of its organic origin or otherwise remains unexplained.

In conclusion, the reported results appear to indicate that the behavior of ionic conduction in solid phase of NMA solutions (or in solid solutions) occurs through the "hole-formation mechanism". This observation, although it needs a wider study, seems to have a very potential applicability in determining the relative size of the ions.

The financial assistance given by the Society of Sigma Xi of America for carrying out the research project is gratefully acknowledged.

1. R. A. HORNE and R. A. COURANT. J. Phys. Chem. **68**, 1258 (1964).
2. R. A. HORNE, R. A. COURANT, D. S. JOHNSON, and F. F. MARGOSIAN. J. Phys. Chem. **69**, 3988 (1965).
3. R. A. HORNE and R. A. COURANT. J. Geophys. Res. **69**, 1152 (1964).
4. S. GLASSTONE, K. J. LAIDLER, and H. EYRING. The theory of rate processes. McGraw-Hill Book Co., Inc., New York, N.Y. 1941. pp. 505, 520, 523, 557, 562.
5. O. D. BONNER, K. W. BUNZL, and G. B. WOOLSEY. J. Phys. Chem. **70**, 778 (1966).
6. L. R. DAWSON, E. D. WILHOIT, R. R. HOLMES, and P. G. SEARS. J. Am. Chem. Soc. **79**, 3004 (1957).
7. R. A. ROBINSON and R. H. STOKES. Electrolyte solutions. Butterworths Scientific Publications, London. 1959. pp. 124–126.
8. C. M. FRENCH and K. H. GLOVER. Trans. Faraday Soc. **61**, 1427 (1955).
9. L. R. DAWSON, E. D. WILHOIT, and P. G. SEARS. J. Am. Chem. Soc. **78**, 1569 (1956).
10. HERMANN SCHILDKNECHT. Zone melting. Verlag Chemie, GambH Weinhein/Bergstr. Academic Press, New York and London. 1966. pp. 6–10.

Can. J. Chem. Downloaded from www.nrcresearchpress.com by 210.87.254.6 on 09/05/12
For personal use only.

Near Infrared Spectra of Water in Aqueous Solutions of Organic Salts. A Solvation Study of Bu_4NBr, ϕ_4AsCl, and $NaB\phi_4$

C. JOLICOEUR[1]

Department of Chemistry, State University of New York at Stony Brook, Stony Brook, Long Island, N.Y. 11790

AND

NGUYEN DINH THE AND A. CABANA

Département de chimie, Université de Sherbrooke, Sherbrooke, Québec

Received December 29, 1970

The near-infrared spectrum of water at various temperatures and in aqueous solutions of Bu_4NBr, $NaB\phi_4$, and ϕ_4AsCl is studied in the region 0.8–1.2 μ. The spectra are recorded differentially with respect to water by varying the cell lengths as to take into account density changes or the volume occupied by the solutes. A simple analysis of these spectra illustrates the qualitative similarity between the effects of the Bu_4N^+ ion and that of a temperature decrement on the spectrum of water. On the other hand striking differences are observed in the differential spectra obtained with Bu_4NBr and the phenyl substituted salts. Further differences are exhibited in the relative solute–solvent interactions of $B\phi_4^-$ and ϕ_4As^+.

Les spectres de l'eau à diverses températures et de quelques solutions aqueuses de Bu_4NBr, $NaB\phi_4$ et ϕ_4AsCl ont été examinés dans la région 0.8–1.2 μ. Le spectre différentiel (solution *vs.* eau pure) de l'eau est obtenu directement en compensant les variations de densité ou le volume occupé par l'électrolyte en solution par une variation de la longueur des cellules. Une analyse qualitative des spectres démontre que l'effet de l'ion Bu_4N^+ sur le spectre de l'eau est semblable à celui d'un abaissement de température. Par ailleurs une différence marquée apparaît entre les spectres différentiels obtenus pour Bu_4NBr et ceux pour les sels contenant des noyaux benzéniques. On observe également une différence dans les interactions soluté-solvant des ions $B\phi_4^-$ et ϕ_4As^+.

Canadian Journal of Chemistry, 49, 2008 (1971)

Introduction

One of the major contemporary advances of solution chemistry is the recognition of solvent structural changes in aqueous solutions of hydrocarbon-like solutes. Hydrophobic solutes, such as the larger tetraalkylammonium ions, are believed to promote in water a three dimensional structure (1). The nature of the structure induced by the hydrocarbon chains still remains to be elucidated: whether the hydrophobic groups simply enhance the short range structure already present in liquid water (2), or promote a new type of structure, is still unknown. We report here a simple differential analysis of the near-infrared spectra of aqueous solutions, which provides a sensitive method for comparing the effect of temperature to that of hydrophobic solutes on the solvent spectrum. Near-infrared spectroscopy has often been employed as a means of studying solvent modifications in aqueous solutions (3–13). Discussion of the methods can be found in several recent papers and review articles (14, 15). In essence, these investigations consist in following changes in either the absorption intensity of bands assigned to distinctly bonded water molecules (or —OH— oscillators) or in following the shifts of an absorption maximum when the temperature is changed or when solutes are added. In practice, the interpretation of such results in terms of the structural influence of an organic ion is often complicated by (*1*) absorption due to the ion itself (overtones and combination bands of the organic ions), (*2*) the volume occupied by the salt which in some cases will reduce the solvent concentration by more than 25%, (*3*) the effect of the co-ion on the water spectra and for combination modes involving ν_2, (*4*) the opposite shifts caused by hydrogen bonding on the bending (ν_2) and stretching (ν_1, ν_3) normal modes. Finally, investigations based upon measurements of integrated absorption intensity always suffer from the fact that the absorption coefficients of the

[1]NRCC Postdoctorate Fellow, 1969–1971.

Can. J. Chem. Downloaded from www.nrcresearchpress.com by 210.87.254.6 on 09/05/12
For personal use only.

postulated species are unknown. (In the near-infrared, the integrated intensity usually decreases upon hydrogen-bonding (14, 16).)

In our work, suitable corrections will be applied in order to eliminate the first three difficulties listed above. Although we do not know how to account for the last two drawbacks mentioned above, these will be circumvented by the use of a phenomenological approach. Thus our results are not subjected to the usual criticisms. The method is applied to solutions of Bu_4NBr in order to compare specifically the effect of the Bu_4N^+ ion to that of a temperature decrement on the water spectrum. Similar studies of ϕ_4AsCl and $NaB\phi_4$ are also carried out to help solve the current question regarding the relative solution behavior of alkyl and aryl substituted salts in water (17, 18).

Experimental

The differential spectra of water at various temperatures and of the aqueous solutions were recorded in the 0.8–1.2 μ region. The choice of this particular band over other near-infrared components of the spectra seems desirable for the following reasons: (*1*) This combination mode assigned to $2\nu_1 + \nu_3$ (4) or $3\nu_3$ (19) probably does not involve the bending vibrational mode at all. (*2*) The absorption intensity of the mode is such that a cell of ~5 cm is required to produce one full scale of absorbance; therefore, good accuracy on the cell lengths is easily achievable. (*3*) In this region, the solute absorption is rather weak; thus it can be corrected without introducing large uncertainties (absorption due to $NaB\phi_4$ and ϕ_4AsCl is negligibly small). (*4*) Since D_2O absorbs only very faintly, it can be used to record the spectrum of the salt in conditions very similar to their aqueous environment.

The solutions were prepared volumetrically with water doubly distilled over alkaline permanganate or from 99.7% D_2O purchased from Merck, Sharp and Dohme of Canada Ltd. Alkali halides (Baker Reagent quality) were used without further purifications. Bu_4NBr, ϕ_4AsCl, and $NaB\phi_4$ were purchased from K & K Laboratories Inc. and purified with standard methods. To the extent possible, manipulations were carried out under dry nitrogen atmosphere.

The spectra were recorded on a Cary-14 spectrometer; the length of the reference cell containing H_2O or D_2O was fixed at 10.00 cm for most spectra, while the length of the sample cell was adjusted to provide an equivalent quantity of water molecules in both beams. The sample cell was made of two concentric tubes; a fine pitch thread which served as a micrometric adjustment was machined on the outside of the smaller tube and, over a short length, inside the larger tube. The remaining portion of the larger tube provided space for an O-ring seal (Viton).

Optical quartz was used as window material. The cell length was measured with an accuracy of 0.01 cm. Both cells were thermostated by water jackets to ±0.3 °C. With 10 cm of water in each compartment the baseline was reasonably straight up to 1.15 μ, the stability being better than 0.01 absorbance unit; at longer wavelengths, so little energy is transmitted that the results become unreliable.

Results and Discussion

The absorption of liquid water at 25 °C in the region 0.8–1.1 μ is shown in Fig. 1*a* for a cell thickness of 0.5 cm. The differential spectrum obtained with 10 cm cells when the reference cell is kept at room temperature (28.0 ± 0.3 °C), while the temperature of the sample cell is varied from 2 to 50 °C, is shown in Fig. 1*b*. The absorbance at 0.96 μ increases with temperature while that observed at 1.02 μ decreases. The occurrence of isobestic points, respectively, near 1.0 and 1.1 μ agrees well with similar observations by Luck (14)

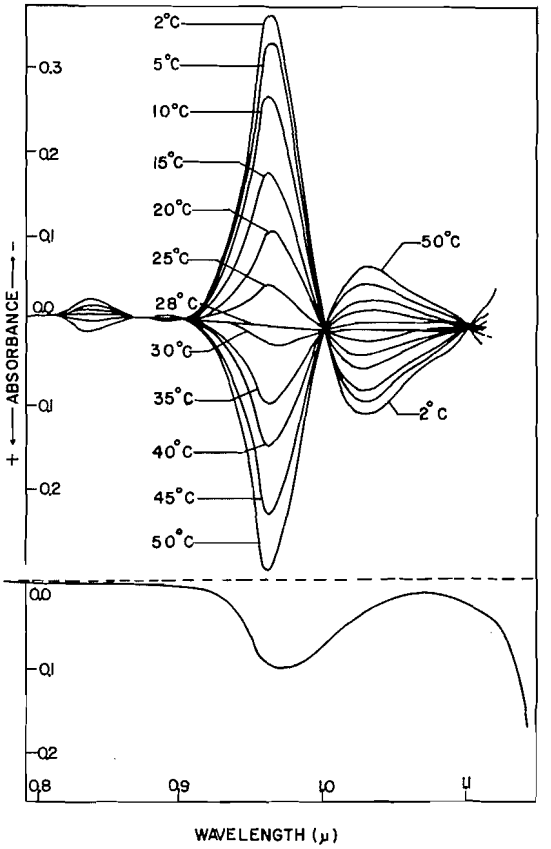

FIG. 1. (*a*) Spectrum of liquid water at 25 °C; cell thickness: 0.5 cm. (*b*) Differential spectra of water at various temperatures; the reference cell is kept at 28 °C and its length is 10.00 cm. The length of the sample cell is varied to correct for density changes.

Can. J. Chem. Downloaded from www.nrcresearchpress.com by 210.87.254.6 on 09/05/12
For personal use only.

for non-differential spectra. It has been shown through detailed analysis (20) that the existence of such points strongly supports the idea of an equilibrium mixture of at least two widely different types of OH oscillators *e.g.* those strongly coupled (hydrogen-bonded) absorbing at the longer wavelengths (1.02 μ) and those un- or weakly coupled responsible for the higher frequency component (0.96 μ). The relative intensities of these two components is consistent with the usual behavior of combination modes. How the two sets of species involved in this equilibrium interact with their neighbors is hard to specify (21); nonetheless, the thermal differential spectra can be used as a basis for comparing the effects of solutes on the water–water interactions.

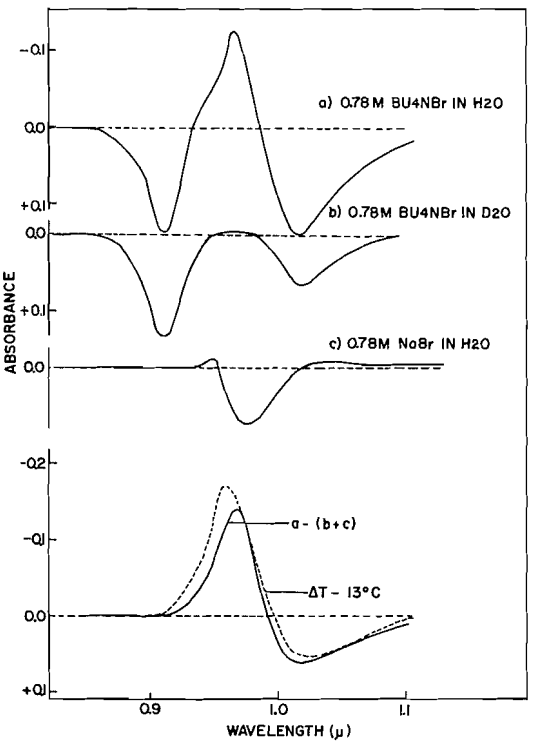

FIG. 2. Differential spectra at 25 °C of solutions against pure H_2O or D_2O; reference cell length: 10.00 cm. (*a*) 0.78 *M* Bu_4NBr in H_2O; cell length: 13.00 cm. (*b*) 0.78 *M* Bu_4NBr in D_2O; cell length: 13.00 c.m. (*c*) 0.78 *M* NaBr in H_2O; cell length: 10.18 cm. Bottom curves: the full line shows spectrum *a* after subtraction of spectra *b* and *c*; the dotted line is the differential spectrum recorded for water at 15 °C against water at 28 °C. In these and following differential spectra, the uncertainty at maximum absorption ranges between ±0.01 to ±0.02 absorbance units, depending on the number of operations performed on the original recordings. Note that the absorbance scale of the trace labelled $a - (b + c)$ applies to all traces of this figure.

The differential spectra of a 0.78 *M* solution of Bu_4NBr is reproduced in Fig. 2*a*; Fig. 2*b* illustrates the salt absorbance recorded in D_2O and the effect of NaBr on the water spectra is shown in Fig. 2*c*. For these and all following solutions, the cell length required to provide the equivalent of 10.00 cm of water in the reference cell was calculated[2] from known apparent molal volumes.[3] The differential spectra observed for NaBr is believed to be mostly due to the presence of the bromide ion. It has been known for some time that the anions have a much greater influence than cations on the spectrum of water (4) simply because anions can interact with the hydrogens of the water molecules. In fact we have observed that the differential spectra of NaBr, KBr, and CsBr are all very similar below 1.0 *M*, the difference being small compared to the effects sought here. With the assumption that the ionic influences on the spectra are additive, the effect of Bu_4N^+ on the water spectrum can be obtained by subtracting spectra *2b* and *2c* from spectrum *2a*. The resultant curve is plotted in the lower part of Fig. 2 (full line). The dotted lines show one of the temperature effects from Fig. 1*b* with $\Delta T = -13$ °C. The striking resemblance of these two curves indicates that the effect of the hydrophobic ion on the hydrogen-bonding equilibrium of water is similar to a decrease in temperature. The discrepancies are of the order of the overall uncertainty and no new absorption is found to confirm the existence of widely different hydrogen bonds in the solution.

The spectra obtained at several concentrations of Bu_4NBr are reported in Fig. 3; comparing these with the thermal differential spectra (Fig. 1), one can evaluate a molar "structural" ΔT (ΔT_{str}) for the Bu_4N^+ ion. The structural temperature idea has been introduced in an early paper by Bernal and Fowler (24). Over the concentration range studied, $\Delta T_{str} = -13 \pm 2$ °C;

[2]From the density, concentration, and solute molecular weight we can calculate the number of moles of solvent per unit volume. The volume of the sample cell can then be varied (at constant cross-section) to contain the same number of moles of water as the reference cell. Since the relevant cross-section is that of the light beam, only the cell lengths need to be considered.

[3]For alkyl halides, see ref. 22*a*; Bu_4NBr, ref. 22*b*; $NaB\phi_4$ and ϕ_4AsCl, ref. 23.

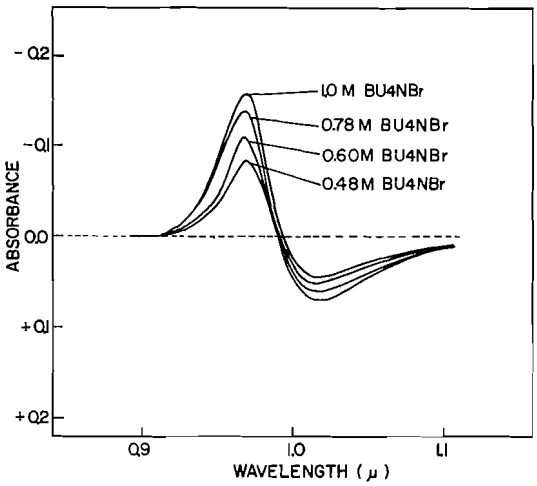

FIG. 3. Differential spectra at 25 °C of Bu_4NBr solutions at various concentrations against H_2O, corrected for solute absorption and for the effect of Br^-.

within the accuracy of the present results, no concentration dependence could be ascertained. This ΔT_{str} is of the same order of magnitude as that estimated by Bunzl (8) from shifts of the 0.97 μ band. Because of unaccounted solute absorption in the latter work (see Fig. 2*b*) and the effect of the bromide ion (Fig. 2*c*), good agreement would be fortuitous. The present results apparently disagree with those of Worley and Klotz (7) who report a ΔT_{str} of ~ -1.0 °C for an experimental temperature of 5 °C. However, from their spectra and the data given on absorption ratios at 25 °C, it can be seen that ΔT_{str} should be much more negative near room temperature.

It is interesting to compare the observed ΔT_{str} with the effect of this salt on the viscosity. The magnitude of the *B*-coefficient of the viscosity equation depends on the size of the solute and its local effects on the solvent (24, 25). Knowing the radii of the ions, the size effect can be estimated and Kay *et al.* (25) found that in MeOH the calculated *B*-coefficient agrees quite well with the experimental one (respectively 0.81 and 0.85). In water, *B* is equal to 1.24 (25); if one pictures the ΔB, $B_{CH_3OH} - B_{H_2O} = 0.39$, as a measure of the change in the local viscosity of water around the solute, this increase in viscosity is equivalent to a temperature increment of -14 °C. The agreement with the present estimate is certainly better than what can be expected.

A more formal comparison of the effect of a decrease in temperature and the structural changes promoted by the Bu_4N^+ ions can be devised through the following scheme. Let us assume that the absorption maximum (λ_I) and minimum (λ_{II}) observed on the differential spectra in Fig. 2*c* characterize the two species involved in the hydrogen-bonding equilibrium of water: II $\rightleftarrows$ I; so defined, form II would be the more structured component. The changes in absorbance (A) at λ_I and λ_{II} with temperature or solute concentration are related to the changes in concentration of the two species. The variation of the mole fraction of species I (x_I) with temperature is given by

$$[1] \quad \frac{dx_I}{dT} = \left[\frac{A_{\lambda I}}{dA_{\lambda I}/dT} - \frac{A_{\lambda II}}{dA_{\lambda II}/dT}\right]^{-1}$$

where A_{λ_I} and $A_{\lambda_{II}}$ are measured on a non-differential spectrum. Neglecting the small differences between the two curves in Fig. 2*c*, a similar expression can be written for dx_I/dc where c is the molar concentration of the solute added.

To picture the significance of dx_I/dc in terms of the solvent co-sphere of the Bu_4N^+ ion, we can write that the number of moles of species I, n_I, in a solution containing a given weight of solvent is

$$[2] \quad n_I = n_I^0 + n_i \int_{r_i}^{r_s} [c_I(r) - c_I^0]\, d^3r$$

Here, n_I^0 is the number of moles of species I before the addition of solute and n_i is the number of solute particles of species i. r_i is the radius of particle i while r_s is the radius of the co-sphere of solvent available to it. c_I^0 and $c_I(r)$ are, respectively, the equilibrium concentration of species I in pure water at 25 °C and the local concentration of I in the solution as a function of distance from the surface of the solute particle. This leads to an expression for dx_I/dc

$$[3] \quad \frac{dx_I}{dc} = \frac{N}{10^{27}} \int_{r_i}^{r_s} [x_I(r) - x_I^0]\, d^3r$$

where N is Avogadro's number and the factor of 10^{27} allows r to be in Å. Since we do not know how x_I varies with r, we can try setting $x_I(r)$ constant at $x_I(r) = x_I(0\ °C)$ in a co-sphere between r_i and r_c. Evaluating dx_I/dT, dx_I/dc, and $x_I(0\ °C) - x_I°$, we find that for $r_i = 4.5$ Å, $r_c = 7.0$ Å. Thus, according to such calculations, if the water in the co-sphere of Bu_4N^+ ion is like water at 0 °C, the co-sphere extends out to approximately 7 Å. It follows that in a solution of Bu_4NBr the

Can. J. Chem. Downloaded from www.nrcresearchpress.com by 210.87.254.6 on 09/05/12
For personal use only.

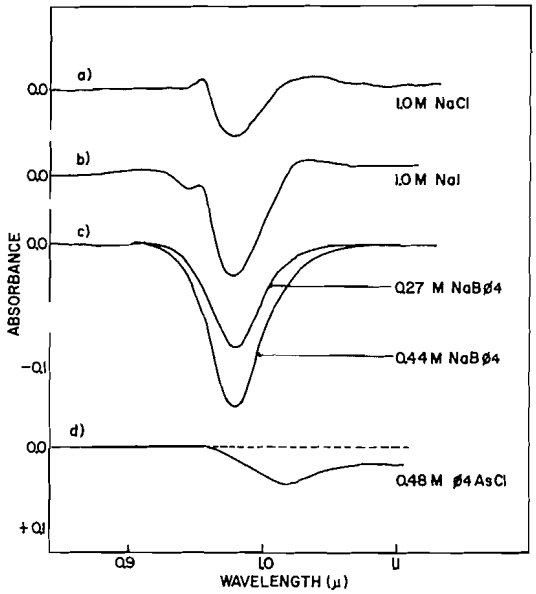

FIG. 4. Differential spectra at 25 °C of various solutions against pure water: (*a*) 1.0 *M* NaCl, (*b*) 1.0 *M* NaI, (*c*) 0.27 and 0.44 *M* $NaB\phi_4$, (*d*) 0.48 *M* ϕ_4AsCl. *c* and *d* were corrected for solute absorption which is very weak around 1.0 μ. The spectrum given for ϕ_4AsCl was also corrected for the effect of Cl^- by subtracting spectrum *a*.

co-spheres of the hydrophobic ions would be forced to overlap at concentrations greater than 0.6 *M*. Though this result is the end product of many assumptions, it may provide some measure of the extent of solvent structural rearrangement around hydrophobic solutes.

The differential spectra of $NaB\phi_4$ (0.27, 0.44 *M*) and ϕ_4AsCl (0.48 *M*) are reported in Fig. 4 along with those of NaCl and NaI (1.0 *M*). In spite of some similarities between the properties of aqueous solutions of $NaB\phi_4$ and Bu_4NBr, *e.g.* partial molal heat capacities (27), the two salts exhibit very different effects on the water spectrum. The main feature of the differential spectrum obtained with $NaB\phi_4$ suggests that the interactions of the water molecules with $B\phi_4^-$ are similar to those occurring with Cl^-, Br^-, and I^-. For the latter ions, the composite nature of the differential band might suggest that part of it is due to structure-breaking, *i.e.* analogous to an increase in temperature on the pure water spectrum. The greater changes of the water spectrum induced by NaI compared to NaCl or NaBr has often been interpreted as resulting from the greater structure-breaking ability of the I^- ion (3, 5, 7). Apart from a slight asymmetry of the differential band, there is no indication that $B\phi_4^-$ stabilizes hydrogen bonds in water as does Bu_4NBr. If such an effect is present, it is totally obscured by the stronger absorption which occurs at 0.98 μ (slightly lower than the "unbonded" —OH groups discussed previously). The structure-breaking character of $B\phi_4^-$ suggested by the spectral results does not agree with conclusions drawn from heat capacity measurements. The large partial molal heat capacity of $NaB\phi_4$ had been explained on the basis of the structure promoting effect on the $B\phi_4^-$ ion due to its hydrophobic properties (27).

The influence of ϕ_4As^+ on the water spectrum was obtained by subtracting the differential spectrum of NaCl from that of ϕ_4AsCl (Fig. 2*d*); this influence is much smaller than that observed for Bu_4N^+ or $B\phi_4^-$. Only a weak and broad absorption band is seen at 1.02 μ and again, there is no direct correlation between the effect of the organic ion with that of a temperature increment. Similar results are found for ϕ_4P^+. Compared to Bu_4N^+, ϕ_4As^+ does not appear to be hydrophobic and its interactions with water are different from those of $B\phi_4^-$. The hydrogen-bonding between water and the phenyl rings of ϕ_4As^+, suggested by other workers from osmotic coefficient measurements (18), is not apparent in the present observations.

It cannot be excluded, however, that in the case of ϕ_4As^+ (or ϕ_4P^+) the differential spectra results from two or more contributions, the effect of which could partly cancel out (*e.g.* a curve similar to those in Fig. 3 added to curve *4e* could yield a spectrum resembling Fig. 4*d*).

The spectral results, on the other hand, confirm the conclusions derived from heats of transfer studies (17, 28). The different behavior of alkyl and aryl substituted ions was emphasized from opposite signs in their heat of transfer from H_2O to D_2O (17). Similar inferences were also possible from heats of solution in water, propylene carbonate, and dimethyl sulfoxide (28). The different interaction of water with $B\phi_4^-$ and ϕ_4As^+ illustrated by the spectra may cast doubt on the assumption of equal heats of hydration for these two ions (28), which is crucial in the assignment of ionic contributions. Recent heat of solution measurements[4] also tend to discredit the equal-heat assumption.

[4]C. V. Krishnan, private communication.

Can. J. Chem. Downloaded from www.nrcresearchpress.com by 210.87.254.6 on 09/05/12
For personal use only.

Can. J. Chem. Downloaded from www.nrcresearchpress.com by 210.87.254.6 on 09/05/12
For personal use only.

Conclusion

The simple method of analysis of the near-infrared spectra outlined above and its applications to selected problems lead to the following conclusions: (*a*) the influence of large tetraalkylammonium ions on the hydrogen-bonding equilibrium of water is similar to the effect observed upon lowering the temperature. (*b*) the nature of solute–solvent interactions for the alkyl and aryl substituted salts studied is quite different; the aryl substituted salts do not exhibit a marked hydrophobic character. As in the case of simple 1:1 electrolytes, the influence of an anion on the water spectra is much greater than that of a cation. By comparison with alkali halides, the spectra suggest that $B\phi_4^-$ acts mainly as a structure breaker while ϕ_4As^+ has little specific effect on the water structure.

The sensitivity of the method seems greater than that which can be obtained from the fundamental stretching modes (29, 30). It thus appears justified to apply it to broader categories of solutes of actual interest.

Financial assistance from the National Research Council of Canada and from the "Ministère de l'Education du Québec" is gratefully acknowledged. We would like to thank H. L. Friedman, R. L. Kay, and J. E. Desnoyers for stimulating discussions.

1. H. S. Frank and W. Y. Wen. Discuss. Faraday Soc. **24**, 133 (1957).
2. A. H. Narten, M. D. Dandord, and H. A. Levy. Discuss. Faraday Soc. **43**, 97 (1967).
3. K. Buijs and G. R. Choppin. J. Chem. Phys. **39**, 2035, 2042 (1963).
4. H. Yamatera, B. Fitzpatrick, and G. Gordon. J. Mol. Spectry. **14**, 268 (1964).
5. M. R. Thomas, H. A. Scheraga, and E. E. Schrier. J. Phys. Chem. **69**, 3722 (1965).
6. W. A. P. Luck. Ber. Bunsenges Phys. Chem. **69**, 626 (1965).
7. J. D. Worley and I. M. Klotz. J. Chem. Phys. **45**, 2868 (1966).
8. K. W. Bunzl. J. Phys. Chem. **71**, 1358 (1967).
9 E. U. Franck and K. Roth. Discuss. Faraday Soc. **43**, 108 (1967).
10. O. D. Bonner and G. B. Woolsey. J. Phys. Chem. **72**, 899 (1968).
11. O. D. Bonner. J. Phys. Chem. **72**, 2512 (1968).
12. R. Cohen and J. Peretz. Israel J. Chem. **7**, 667 (1969).
13. W. C. McCabe and H. F. Fisher. J. Phys. Chem. **74**, 2990 (1970).
14. W. A. P. Luck. *In* Physico-chemical processes in mixed aqueous solvents. (Editor) F. Franks. Elsevier, New York. 1967. p. 11.
15. J. E. Desnoyers and C. Jolicoeur. *In* Modern aspects of electrochemistry. *Edited by* J. O'M. Bockris and B. E. Conway. Plenum Press, New York. 1969. p. 1.
16. G. C. Pimentel and A. L. McClellan. The hydrogen bond. Reinhold, New York. 1960. p. 80.
17. C. V. Krishnan and H. L. Friedman. J. Phys. Chem. **74**, 2356 (1970).
18. C. Kalfoglou and L. H. Bowen. J. Phys. Chem. **73**, 2728 (1969).
19. W. A. P. Luck. Fortschr. Chem. Forsch. **4**, 653 (1964).
20. W. A. Senior and R. E. Verrall. J. Phys. Chem. **73**, 4242 (1969).
21. H. S. Frank. Sci. **169**, 635 (1970).
22. (*a*) J. E. Desnoyers, M. Arel, G. Perron, and C. Jolicoeur. J. Phys. Chem. **73**, 3346 (1969). (*b*) W. Y. Wen and S. Saito. **68**, 2639 (1964).
23. C. Jolicoeur. Unpublished results.
24. J. D. Bernal and R. H. Fowler. J. Chem. Phys. **1**, 515 (1933).
25. H. S. Frank. *In* Chemical physics of ionic solutions. *Edited by* B. E. Conway and R. G. Barradas. John Wiley and Sons, Inc., New York. 1966. p. 53.
26. R. L. Kay, T. Vituccio, C. Zawoyski, and D. F. Evans. J. Phys. Chem. **70**, 2336 (1966).
27. S. Subramanian and J. C. Ahluwali. J. Phys. Chem. **72**, 2525 (1968).
28. C. V. Krishnan and H. L. Friedman. J. Phys. Chem. **73**, 3934 (1969).
29. K. A. Hartman. J. Phys. Chem. **70**, 270 (1966).
30. M. Falk and T. A. Ford. Can. J. Chem. **44**, 1699 (1966).

Can. J. Chem. Downloaded from www.nrcresearchpress.com by 210.87.254.5 on 09/05/12
For personal use only.

The Determination of Calcium Carbide and its Dissociation Products in Fused Calcium Chloride

C. AKSARANAN, V. DOSAJ, D. R. MORRIS, AND S. H. WHITE[1]

Department of Chemical Engineering, University of New Brunswick, Fredericton, New Brunswick

Received October 30, 1970

The principal constituents in molten solutions of calcium carbide in calcium chloride have been determined. The analytical results were generally within order of magnitude agreement with calculations from thermodynamic data based upon a model in which the calcium carbide is thought to be dissociated according to the equation

$$CaC_{2\,(soln)} \rightleftharpoons Ca_{(soln)} + 2C_{(s)}$$

On a établi la nature des principaux constituants des solutions fondues de carbure de calcium dans le chlorure de calcium. Les résultats analytiques sont généralement en accord à l'intérieur d'une ordre de grandeur-avec les données thermodynamiques basées sur un modèle dans lequel on croyait que le carbure de calcium est dissocié suivant l'équation

$$CaC_{2\,(soln)} \rightleftharpoons Ca_{(soln)} + 2C_{(s)}$$

Canadian Journal of Chemistry, 49, 2014 (1971)

Introduction

Electrochemical and physico-chemical studies of solutions of calcium carbide in molten calcium chloride require an accurate knowledge of the concentration of calcium carbide and its probable decomposition products. Thermodynamic arguments (*vide infra*) predict that a small but significant concentration of calcium metal will be in equilibrium with calcium carbide dissolved in molten calcium chloride and a known activity of carbon (usually fixed by the crucible material). The form taken by the calcium metal in solution in calcium chloride is uncertain but "F centers" or lower valent forms of calcium ions have been suggested for calcium chloride – calcium (1, 2) and calcium fluoride – calcium melts (3).

The analytical procedure to determine the concentration of the principal constituents of the solution was a development of the method described by Edwards (4) and used later by Morris and Harry (5). A weighed sample of the solidified calcium carbide – calcium chloride solution was hydrolyzed in a closed system. A sample of the gases thus liberated was analyzed with a gas partitioner which was calibrated previously with hydrogen–acetylene mixtures. This method was preferred to those of Barber and Sloan (6) and Mitchell (7) because it permitted the direct, independent analysis of the calcium metal content, at the same time as the determination of the carbide content. Total chloride and free oxide were determined by conventional analysis of the hydrolyzed sample.

In this paper we report a model for calcium carbide – calcium chloride melts based on thermodynamic arguments and data obtained with the improved analytical procedure.

[1]Post Doctoral Fellow 1968–1970.

Experimental

(1) Apparatus

(a) Gas Generation Equipment

The equipment consisted of a 150-ml flask which was fitted with a rubber septum through which gas samples could be withdrawn by means of a Hamilton gas syringe. The flask could be connected by glass stopcocks to a manometer and a vacuum pump, or a source of dry argon. The flask was capped by a reservoir from which the hydrolyzing solution could be introduced. The glass lines in the system were kept to a minimum length to ensure their volume was small compared with the total volume of the apparatus. The total volume of the apparatus was determined by weighings using distilled water.

(b) Gas Analysis

A model 25V Fisher Gas Partitioner fitted with two columns was used for the acetylene–hydrogen analysis. The first column, 5 ft long, was packed with hexamethyl phosphoramide, the second 7 ft long was packed with 13X molecular sieve.

The partitioner was calibrated using mixtures of acetylene and hydrogen. Acetylene was generated in the gas apparatus from calcium carbide synthesized from the elements (8) using excess carbon to ensure the absence of free calcium. Analysis of the gas derived by hydrolysis from such material was found to be H_2-free. The mixtures were prepared by back-filling the apparatus to 1 atm

TABLE 1. Duplicate sample analysis, effect of sampling method

Sample designation	Composition				Sampling method
	Ca		CaC_2		
	Mole fraction	% Error	Mole fraction	% Error	
CCA-19	0.00027 0.00023	16	0.0107 0.0125	18	Drilling
CCA-1	0.00027 0.00026	4	0.0424 0.0455	7	Crucible

pressure with hydrogen (99.99% purity). Replicate samples of the mixtures (0.6 ml) were injected into the partitioner using a Hamilton gas syringe. A plot of peak height *vs.* composition was prepared and checked at frequent intervals.

Typical operating conditions for the gas partitioner were: argon flow rate, 100 ml/min; thermistor current, 5 mA; sensitivity, 50%; recorder span, 2 mV; operating temperature, ambient. The retention times were found to be: hydrogen, 1.8 min; acetylene, 14.0 min. The output from the gas partitioner was recorded continuously. Air contamination which occasionally occurred due to faulty loading of the instrument was immediately detected by the presence of oxygen and nitrogen peaks on the chromatogram.

(2) Analytical Procedure

Samples of the calcium carbide – calcium chloride solution equilibrated in a graphite crucible were obtained in two ways.

(*a*) A small graphite crucible supported inside the particular apparatus being used for the physico-chemical studies was dipped into the melt and quenched by quickly withdrawing the crucible to the cool part of the apparatus.

(*b*) Samples were drilled from the solidified melt after the experiment. When possible, this procedure was carried out in a dry box.

The sample of the calcium carbide – calcium chloride solidified melt (approximately 4 to 8 g) was accurately weighed in the dry box and transferred to the dried reaction flask which was quickly connected to the gas generation equipment. The apparatus was evacuated and the temperature and pressure noted. Twenty-five ml of distilled water were then added from the reservoir to completely hydrolyze the sample. The steady-state temperature and pressure were recorded (after about 1 h). The apparatus was brought to atmospheric pressure by filling with argon. Replicate samples (0.6 ml) of the gas mixture were transferred with a Hamilton gas syringe to the gas partitioner and the peak heights for hydrogen and acetylene recorded. The weights of calcium carbide and calcium metal in the sample were calculated from the measured gas composition, corrected to an argon free basis, and the known total volume of dry gases at N.T.P. A correction for the solubility of acetylene in water was made, based on the data given by Miller (9). The liquid in the reaction flask was acidified with 50 ml 1.0 *N* nitric acid and the solution diluted to 500 ml in a volumetric flask. The total basicity was obtained by back-titration of 10-ml aliquots with 0.1 *N* sodium hydroxide using methyl orange as indicator. The total oxide content was calculated from the difference between total basicity and the basicity due to hydrolysis of calcium metal and calcium carbide determined previously.

A further 10-ml sample was treated with a known excess of 0.1 *N* silver nitrate. The silver chloride was filtered off and the excess silver nitrate was determined volumetrically with 0.1 *N* ammonium thiocyanate and ferric ion as indicator. From this information the total chloride was determined.

Free carbon was separated by filtration from the residual solution, dried, and weighed.

Results and Discussion

The total errors of 3%, 3%, and 1% were estimated from the individual errors in the analytical procedure for CaC_2, Ca, and $CaCl_2$, respectively. The error in the reported figures of CaO content was estimated at 10%. Duplicate analyses are given (Table 1) for samples obtained by the two methods. The drilling was *not* carried out in a dry box, and the large errors probably result from hydrolysis of the sample by the damp air. Much more reasonable agreement between results was obtained from the crucible sampling technique and it is to be preferred.

A consideration of the available thermodynamic data relating to the solution equilibrium

$$CaC_2 \text{ (soln in } CaCl_2) \rightleftharpoons Ca \text{ (soln in } CaCl_2) + 2C \text{ (solid)}$$

will show that calcium metal in the dissolved state is an important species in solutions of calcium carbide dissolved in molten calcium chloride.

The standard free energy change for the above reaction, $\Delta G_{T_1}^0$, is related to the equilibrium constant K by the usual relations

$$[1] \quad \Delta G_{T_1}^0 = -RT \ln K = -RT \ln (\gamma_{Ca} N_{Ca} / \gamma_{CaC_2} N_{CaC_2})$$

where γ is the activity coefficient and N is the mole fraction of the respective species, R and T have their usual meanings. The standard state is

Can. J. Chem. Downloaded from www.nrcresearchpress.com by 210.87.254.5 on 09/05/12
For personal use only.

TABLE 2. Typical analytical results and calculated equilibrium calcium metal concentrations

Sample designation	Composition mole fraction CaC_2 ±3%	CaO ±10%	$CaCl_2$ ±1%	Ca metal By analysis ±3%	Ca metal By calculation	Equilibration temperature (°C)
SHW	0.0037	—	—	3.0×10^{-5}	$(5 \pm 4) \times 10^{-7}$	800*
VDL10	0.012	0.007	0.981	1.65×10^{-6}	$(4 \pm 2) \times 10^{-6}$	950
VDL2	0.023	0.002	0.974	9.81×10^{-5}	$(7 \pm 5) \times 10^{-6}$	950
CCA 15	0.045	—	—	2.20×10^{-3}	$(9 \pm 6) \times 10^{-6}$	850
VD 72	0.046	0.006	0.947	4.96×10^{-5}	$(1.5 \pm 1) \times 10^{-5}$	950
VD 313	0.085	0.013	0.902	3.61×10^{-5}	$(3 \pm 2) \times 10^{-5}$	975
VD 612	0.088	0.005	0.907	2.41×10^{-4}	$(2 \pm 1.5) \times 10^{-5}$	900
VD 44	0.102	0.001	0.896	2.00×10^{-4}	$(4 \pm 3) \times 10^{-5}$	1000

*Sample taken by drilling solidified melt; all others by graphite sampling crucible.

chosen as the pure liquid at the particular temperature, such that $\gamma \rightarrow 1$ as $N \rightarrow 1$. Graphite is assumed to be insoluble in the melt, and the container.

In order to calculate ΔG_{T1}^0, equations describing the standard free energy changes accompanying the processes

[2] $CaC_{2\,(s)} \rightarrow Ca_{(g)} + 2C_{(s)}$ ΔG_{T2}^0

[3] $Ca_{(g)} \rightarrow Ca_{(l)}$ ΔG_{T3}^0

[4] $CaC_{2\,(s)} \rightarrow CaC_{2\,(l)}$ ΔG_{T4}^0

as a function of temperature were obtained from the literature. At temperatures below the melting point of calcium metal (840 °C), the free energy change of the process $Ca_{(s)} \rightarrow Ca_{(l)}$ should be taken into account. However, this quantity is small compared to other uncertainties and is neglected.

Measurements of the calcium metal vapor pressure over calcium carbide in the temperature range 1300 to 1900 °K by Faircloth, Flowers, and Pummery (10) give

[5] $\Delta G_{T2}^0 = (49\,000 \pm 950) - (13.3 \pm 0.6)T$ cal/mol

The calcium vapor pressure data compiled by Hultgren *et al.* (11) give

[6] $\Delta G_{T3}^0 = [-37\,390 + 21.37T] \pm 400$ cal/mol

For process 4, Schlumberger (12) gives the heat of fusion of calcium carbide as 7680 cal/mol and Juza and Bunzen (13) give the melting point at 2140 °C. No data are available for ΔC_p, accordingly this was taken as 1.2 ± 0.5 cal/mol °K, the average of the various data listed by Janz (14) for a number of halides. These data give

[7] $\Delta G_{T4}^0 = [4790 + 7.35T - 2.76T \log T] \pm 200$ cal/mol

Combination of eqs. 5, 6, and 7 leads to

[8] $\Delta G_{T1}^0 = [6820 + 0.7T + 2.76T \log T] \pm 2000$ cal/mol

In order to calculate N_{Ca} (eq. 1) the activity coefficients γ_{CaC_2} and γ_{Ca} must be known. Barber and Sloan (6) reported the solubility of CaC_2 in $CaCl_2$ to be 10.4 mol% at 820 °C, hence $\gamma_{CaC_2} \simeq 10$. A value of γ_{Ca} may be estimated from the phase diagram for the Ca–$CaCl_2$ system (15). This neglects any effect due to the presence of CaC_2. The change of γ_{CaC_2} with temperature and composition has been neglected and the change of γ_{Ca} with composition has been neglected.

The results of some typical analyses determined by the experimental procedures outlined are presented in Table 2 together with the concentrations of calcium metal calculated from eqs. 1 and 8.

In most instances, the agreement between the calculated calcium metal concentration and that obtained by analysis is satisfactory. The analyses confirm the thermodynamic prediction that a small but significant concentration of calcium metal is in solution in molten calcium chloride when calcium carbide is dissolved in this solvent. The chemistry and electrochemistry of these solutions are more clearly understood using this model.

Can. J. Chem. Downloaded from www.nrcresearchpress.com by 210.87.254.5 on 09/05/12
For personal use only.

Thanks are due to the American Iron and Steel Institute, and the National Research Council of Canada for financial support and to the University of New Brunswick for a Fellowship for S. H. White.

1. A. S. DWORKIN, H. R. BRONSTEIN, and M. A. BREDIG. J. Phys. Chem. **70**, 2384–2388 (1966).
2. A. S. DWORKIN, H. R. BRONSTEIN, and M. A. BREDIG. Discuss. Faraday Soc. **32**, 188–196 (1961). See also, M. A. Bredig. **32**, 257 (1961).
3. P. S. ROGERS, J. W. TOMLINSON, and F. D. RICHARDSON. Phys. Chem. of Process Metallurgy Pt 2 pp. 909–924. Met. Soc. Conf. Vol. 8. (Editor) G. R. St. Pierre. Interscience Publ., New York. 1961.
4. A. H. EDWARDS. Anal. **71**, 521 (1946).
5. D. R. MORRIS and J. R. HARRY. Proc. Inter. Conf. Industrial Carbon and Graphite. Soc. Chem. Ind. London. 1965. pp. 36–47.
6. W. A. BARBER and C. L. SLOAN. J. Phys. Chem. **65**, 2026–28 (1961).
7. A. MITCHELL. Trans. TMS AIME **242**, 2507–2511 (1968).
8. C. AKSARANAN. M.Sc. Thesis. Univ. of New Brunswick. 1969.
9. S. A. MILLER. Acetylene, its properties, manufacture and uses. Ernest Benn Ltd. 1965.
10. R. L. FAIRCLOTH, R. H. FLOWERS, and F. C. W. PUMMERY. J. Inorg. Nucl. Chem. **29**, 311–315 (1967).
11. R. HULTGREN, R. L. ORR, P. D. ANDERSON, and K. K. KELLEY. Selected values of thermodynamic properties of metals and alloys. J. Wiley and Sons Inc. p. 60.
12. E. SCHLUMBERGER. Z. Agnew Chem. **40**, 141 (1927).
13. R. JUZA and K. BUNZEN. Z. Phys. Chem. II, 82–99 (1958).
14. G. J. JANZ. Molten salts handbook. Academic Press, New York. 1967. p. 201.
15. L. I. STAFFANSON. Ph.D. Thesis. Univ. of London. 1960. See B. R. Sundheim. Fused salts. McGraw-Hill Book Co., New York. 1964. p. 355.

Can. J. Chem. Downloaded from www.nrcresearchpress.com by 210.87.254.5 on 09/05/12
For personal use only.

Can. J. Chem. Downloaded from www.nrcresearchpress.com by 210.87.254.40 on 09/05/12
For personal use only.

Studies on Some 2,1-Benzisoxazole Derivatives

D. M. McKINNON AND J. Y. WONG
Chemistry Department, University of Manitoba, Winnipeg, Manitoba

Received January 26, 1971

7-Acetyl-3-methyl-2,1-benzisoxazole has been synthesized by reduction of 2,6-diacetylnitrobenzene. While the chemical properties of the compound indicate that it undergoes valency-tautomerism, spectroscopic studies indicate that this is a relatively slow process. Comparisons with other heterocyclic systems having similar properties are noted.

La réduction du diacétyl-2,6 nitrobenzène conduit à l'acétyl-7 méthyl-3 benzizoxazole-2,1. Alors que les propriétés chimiques de ce composé indiquent qu'il est sujet à une tautomérie de valence, les études spectroscopiques suggèrent que ce processus est relativement lent. Par comparaisons avec d'autres systèmes hétérocycliques on note qu'ils ont des propriétés semblables.

Canadian Journal of Chemistry, 49, 2018 (1971)

Theories of bonding in 6*a*-thiathiophthenes **1** have invoked the use of sulfur d-orbitals (1, 2) in the bonding of the central sulfur atom to explain their symmetry in solution as established by n.m.r. (3) and present evidence (4) indicates that they are in fact best represented by structure **1***a* rather than structures of type **1***b*. Similar considerations also appear to hold for an isothiazole derivative **2***a* (5) and for a benzo-1,2-thioxole derivative **2***b* (6). However, it is of interest to examine related compounds in which the central atom is incapable of valency shell expansion to determine to what extent their properties approach those of the 6*a*-thiathiophthenes **1**. These should possibly exhibit valency-tautomerism which has been proposed (7) to explain the properties of the thiathiophthenes. A suitable compound for examination is 7-acetyl-3-methyl-2,1-benzisoxazole (**3***a*), which has a structure of the required potential symmetry for n.m.r. examination and possesses similar electronic and structural features to some benzo-1,2-dithiolium derivatives (8) of the thiathiophthene system.

1*a* **1***b*

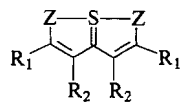

2

a $R_1 = H; R_2 = Me; Z = NMe$

b $R_1, R_2 = CH{:}C(OMe){\cdot}CH{:}CH; Z = O$

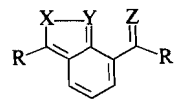

3

a R = Me; X = Z = O; Y = N
b R = Me; X = S; Y = N; Z = O
c R = Me; X = O; Y = N; Z = S
d R = Me; X = Z = S; Y = N
e R = Me; X = NMe; Y = N; Z = O
f R = Me; X = NPh; Y = N; Z = O
g R = Me; X = O; Y = N; Z = NMe
h R = Me; X = O; Y = N; Z = NPh
i R = Me; X = Z = NMe; Y = N
j R = Me; X = Z = NPh; Y = N
k R = NHMe; X = Z = O; Y = N

2-Nitroisophthaloyl chloride (**4***a*) reacted with ethyl ethoxymagnesiummalonate to provide the tetracarboxylic ester **4***b*. This was not isolated but provided, after acid hydrolysis, 2,6-diacetylnitrobenzene (**4***c*). This method is reported to be the most satisfactory for the preparation of *o*-nitroacetophenones (9). When the nitro compound was reduced, using stannous chloride in hydrochloric acid, 7-acetyl-3-methyl-2,1-benzisoxazole (**3***a*) and 2,6-diacetylaniline (**4***d*) were obtained after separation by chromatography. 2,6-Diacetylaniline (**4***d*) was obtained as the sole product when the reaction was performed at a higher temperature.

Although the ^1H n.m.r. spectrum of the 2,1-benzisoxazole **3***a* in deuterochloroform solution at 0° to 20° gave only one peak, indicating that

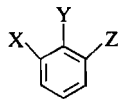

4

a X = Z = COCl; Y = NO_2
b X = Z = $COCH(CO_2Et)_2$; Y = NO_2
c X = Z = COMe; Y = NO_2
d X = Z = COMe; Y = NH_2
e X = Z = CONHMe; Y = NO_2
f X = Z = CSNHMe; Y = NO_2
g X = Z = CONHMe; Y = NH_2
h X = CONHMe; Y = NH_2; Z = CO_2^-; NH_3^+Me

the two methyl groups were equivalent, at other temperatures two peaks were obtained, indicating that the equivalence of the methyl groups was merely coincidental. The n.m.r. spectrum in hexadeuterobenzene, on the other hand, because of its aromatic solvent effects (10), gave a wide separation of the two methyl groups. Increasing the temperature by 150° brought these two methyl singlets together by only 0.32 τ, indicating that there is a rather high energy barrier to interconversion of the two identical valency tautomers. Similar results were obtained in perdeuterotoluene. Under no circumstances were we able to obtain an AB_2 type pattern from the protons on the aromatic ring. Only ABX types were evident.

Treatment of the 2,1-benzisoxazole **3***a* with phosphorus pentasulfide in carbon disulfide or pyridine gave another compound in which one oxygen had been replaced with sulfur. Examination of the i.r. spectrum indicated that a carbonyl group was present, hence the compound is probably the acyl-2,1-benzisothiazole **3***b* rather than the thioacyl-2,1-benzisoxazole **3***c*. The isolation of this can be rationalized by initial formation of the thioacyl compound **3***c* which under the conditions of the reaction undergoes valency-tautomerism to **3***b*. Although it has been demonstrated above that such tautomerism in these compounds is not detectable by n.m.r. this is not inconsistent with interconversion under the conditions of the chemical reaction. This reaction is related to the conversion of a 2,1-benzisoxazole into an acetylfuroxan (11) and some furoxan interconversions (12). Some 4-thioacyl-1,2-dithiole-3-thiones (8) also appear to undergo such tautomerism, and it has been recently demonstrated (13) that some 1,2,3-benzothiadiazole diazonium salts give rearranged products by such interconversions. The failure to demonstrate suitable symmetry in the 2,1-benzisoxazole **3***a* suggests that valency-tautomerism is inadequate in explaining the special properties of thiathiophthenes. Likewise, doubt is also cast on the existence of single-bond – no-bond resonance (3) in this system.

The 2,1-benzisothiazole **3***b* should be further sulfurized under the conditions of the reaction to 3-methyl-7-thioacetyl-2,1-benzisothiazole (**3***d*), but this is probably readily hydrolyzed back to **3***b* during the isolation procedure. Certain thiones are reported to undergo such hydrolyses (14). Compounds without substituents capable of interacting with the heterocyclic ring were not sulfurized under the conditions used. Thus 3-methyl-2,1-benzisoxazole was not converted to 3-methyl-2,1-benzisothiazole and was recovered when carbon disulfide was used as a solvent. Attempted sulfurization in pyridine caused extensive decomposition.

Reaction of the 2,1-benzisoxazole **3***a* with methylamine and aniline provided the benzopyrazoles **3***e* and *f* respectively, which, like the sulfurization above, could have been formed via the imines, **3***g* and *h*, followed by tautomerism to the acetylbenzopyrazoles. These compounds **3***e* and *f* might also have reacted with more imine to form imines **3***i* and *j* respectively but under the conditions of the work-up, hydrolysis of these to **3***e* and *f* would have occurred. These compounds exhibited C=O absorption in the i.r., indicating that they exist as acetylbenzopyrazoles rather than the isomeric imino-2,1-benzisoxazoles.

Attempts were also made to synthesize the amino-2,1-benzisoxazole derivative **3***k*. 2-Nitroisophthaloyl chloride reacted with methylamine to give *N,N'*-dimethyl-2-nitroisophthalamide (**4***e*). This was readily converted into the bis-thioamide **4***f*, but attempts to convert it directly to the 2,1-benzisoxazole **3***k* failed. Synthesis via the aminodiamide **4***g* was attempted, but no satisfactory method of reduction of the nitro group was found. Hydrogenation over Raney nickel in methanol gave an aromatic amine, but this was probably the compound **4***h* in which one amide function had been hydrolyzed, since it readily dissolved in water and effervesced on treatment with sodium bicarbonate.

Can. J. Chem. Downloaded from www.nrcresearchpress.com by 210.87.254.40 on 09/05/12
For personal use only.

Can. J. Chem. Downloaded from www.nrcresearchpress.com by 210.87.254.40 on 09/05/12
For personal use only.

Experimental

The i.r. spectra were performed on a Perkin–Elmer model 337 spectrophotometer in liquid paraffin mulls. The n.m.r. spectra were obtained on a Varian model 56/60A spectrometer and, unless otherwise stated, in deuterochloroform at 40°, using tetramethylsilane as an internal standard. The t.l.c. was performed using "Camag" silica-gel type D.S.F.5 supplied by Mondray Ltd. Development of plates, unless otherwise stated, was carried out using benzene with increasing proportions of chloroform. Melting points were obtained on a Fisher–Johns melting point apparatus.

2-Nitroisophthaloyl Chloride (4a)

2-Nitroisophthalic acid (25 g, 0.12 mol) (15, 16) was suspended in benzene (100 ml) and treated with thionyl chloride (30 ml). The mixture was refluxed until homogeneous then evaporated under reduced pressure. The crude material was recrystallized from benzene and was used for further reactions. Yield was almost quantitative.

2,6-Diacetylnitrobenzene (4c)

Magnesium turnings (9.3 g, 0.39 atoms), in a three-necked flask equipped with a magnetic stirrer and a reflux condenser, were treated with a mixture of anhydrous ethanol (10 ml) and carbon tetrachloride (1 ml). The mixture was warmed gently to start the reaction then anhydrous ether (300 ml) was added. A mixture of anhydrous ether (50 ml), ethyl malonate (60 g, 0.375 mol), and anhydrous ethanol (100 ml) was added at such a rate that rapid boiling was maintained. The mixture was heated under reflux for 3 h, when all the magnesium had dissolved.

To the solution was added dropwise over 15 min a solution of 2-nitroisophthaloyl chloride (45 g, 0.18 mol) in anhydrous ether (100 ml). Reflux was maintained for 4 h until the mixture became too viscous to stir. The cooled reaction mixture was treated with dilute sulfuric acid and the mixture extracted with ether. The dried extract on evaporation gave the tetracarboxylic ester **4b** as a viscous yellow oil. This was refluxed 4 h with a mixture of glacial acetic acid (120 ml) and concentrated sulfuric acid (15 ml), and water (80 ml). The cooled mixture was thrown on ice and the colorless precipitate was washed with water and recrystallized from ethanol, m.p. 160° (89%).

Anal. Calcd. for $C_{10}H_9NO_4$: C, 57.97; H, 4.35; N, 6.76. Found: C, 57.87; H, 4.54; N, 6.86.

The i.r. spectrum: 1700 (C=O), 1555, 1370 cm^{-1} (NO_2). The n.m.r. spectrum: τ 7.68 (6H singlet, two equivalent CH_3 groups), 2.84, 2.75, 2.63, 2.50 (3H bands, three aromatic protons, AB_2 pattern).

Reduction of 2,6-Diacetylnitrobenzene (3a)

Diacetylnitrobenzene (2.07 g, 0.01 mol) was added to a stirred solution of stannous chloride (8.2 g) in concentrated hydrochloric acid (21 ml) at 5°. A pale yellow precipitate was initially formed, but dissolved after 3 h. After 5 h the mixture was diluted with water (100 ml) and extracted with ether (3 × 50 ml). The dried ether extracts on evaporation gave a pale yellow solid which was examined by t.l.c. Three bands were evident under u.v. examination.

The first on elution gave 2,6-diacetylaniline as yellow crystals, m.p. 144° (8%).

Anal. Calcd. for $C_{10}H_{11}NO_2$: C, 67.79; H, 6.22; N, 7.91. Found: C, 67.73; H, 6.36; N, 8.09.

The i.r. spectrum: 1668 (C=O); 3310, 3450 cm^{-1} (NH_2). The n.m.r. spectrum: τ 7.48 (6H singlet, two equivalent CH_3 singlets), 2.01, 2.18, 3.37, 3.48, 3.60 (3H bands, protons on aromatic ring, AB_2 pattern). A better synthesis of this compound is described below.

The second band on elution gave the 2,1-benzisoxazole **3a** as colorless needles, m.p. 97° (38%).

Anal. Calcd. for $C_{10}H_9NO_2$: C, 68.77; H, 5.15; N, 8.00. Found: C, 68.37; H, 5.04; N, 7.94.

The i.r. spectrum: 1650 (tentatively C=N), 1695 cm^{-1} (C=O). The n.m.r. spectrum is described below.

A third band on elution gave only traces of material and was not further examined.

Nuclear Magnetic Resonance Spectral Data of 7-Acetyl-3-methyl-2,1-benzisoxazole (3a)

These were performed in degassed, sealed tubes. In deuterochloroform at 20°, τ 7.13 (6H singlet, two superimposed singlets), 3.11–1.83 (3H bands, protons on the aromatic ring, ABX pattern).

In hexadeuterobenzene at 20°, τ 7.95 (3H singlet, methyl protons on the heterocyclic ring), 7.10 (3H singlet, methyl protons on the acetyl group). At 0° the two methyl singlets were separated by τ 0.88, at 160° they were separated by 0.56.

In perdeuterotoluene at 20°, τ 7.84 (3H singlet, methyl protons on the heterocyclic ring), 7.19 (3H singlet, methyl protons on the acetyl group), 3.61–1.89 (3H bands, protons on the aromatic ring, ABX pattern). At −20° the methyl singlets were separated by τ 0.80, at 160° they were separated by 0.43.

The peaks at higher τ values in deuterobenzene and toluene were assigned to the methyl group on the heterocyclic ring since an n.m.r. spectrum of 3-methyl-2,1-benzisoxazole (17) in hexadeuterobenzene gave τ 7.74 (3H singlet, methyl group), 3.55–2.42 (4H bands, protons on the aromatic ring).

2,6-Diacetylaniline (4d)

2,6-Diacetylnitrobenzene (7.24 g, 0.035 mol) stannous chloride (30 g) and concentrated hydrochloric acid (80 ml) were heated at 90° for 2½ h. The orange mixture was neutralized with solid sodium carbonate and extracted with ether (3 × 100 ml). The ether extracts were washed with dilute sodium carbonate, with water, and dried over sodium sulfate. Evaporation gave a yellow powder which was recrystallized from water as yellow needles, m.p. 144° (76%).

Sulfurization of 7-Acetyl-3-methyl-2,1-benzisoxazole to form 7-Acetyl-3-methyl-2,1-benzisothiazole (3d)

The benzisoxazole (5 g, 0.0285 mol) in pyridine (80 ml) was refluxed with phosphorus pentasulfide (8 g) for 8 h. The mixture was cooled, poured into water, and extracted with chloroform (3 × 50 ml). The extract was washed with water (5 × 20 ml), dried, and evaporated to give a yellow oil which crystallized on standing, and was further purified by t.l.c. using chloroform as a developing solvent. Yellow crystals were obtained, m.p. 79° (75%).

Can. J. Chem. Downloaded from www.nrcresearchpress.com by 210.87.254.40 on 09/05/12
For personal use only.

Anal. Calcd. for $C_{10}H_9NOS$: C, 62.83; H, 4.71; N, 7.33; S, 16.76. Found: C, 62.67; H, 4.84; N, 7.15; S, 16.76.

The i.r. spectrum: 1725 (C=O), 1635 cm^{-1} (tentatively C=N). The n.m.r. spectrum: τ 7.15, 7.17 (6H, two methyl singlets), 3.12–1.80 (3H bands, protons on the aromatic ring).

Similar results, but with lower yields (~15%), were obtained when sulfurization was performed in carbon disulfide.

Reaction of 7-Acetyl-3-methyl-2,1-benzisoxazole with Aniline. Preparation of 7-Acetyl-3-methyl-2-phenylbenzo[c]pyrazole (3f)

The benzisoxazole (0.5 g, 0.00285 mol) and aniline (0.6 g, 0.00645 mol) in glacial acetic acid (50 ml) were refluxed 16 h. The mixture was poured onto ice and extracted with ether (3 × 50 ml). The ether extracts were washed with saturated sodium carbonate solution, with water, and dried over anhydrous sodium sulfate. Evaporation gave a crude solid which was purified by t.l.c. Using a 5% solution of diethyl ether in chloroform as a developer. A band with a blue fluorescence in the u.v. was eluted and gave a pale yellow solid on evaporation, m.p. 120–122° (27%).

Anal. Calcd. for $C_{16}H_{14}N_2O$: C, 76.80; H, 5.60; N, 11.20. Found: C, 76.93; H, 5.75; N, 11.00.

The i.r. spectrum: 1698 cm^{-1} (C=O str). The n.m.r. spectrum, τ 7.31 (3H singlet, methyl group on the heterocyclic ring), 7.00 (3H singlet methyl on acetyl group), 2.42 (5H singlet, protons on phenyl group), 2.98–1.81 (3H bands, protons on the "benzo" ring, ABX pattern).

Reaction of 7-Acetyl-3-methyl-2,1-benzisoxazole with Methylamine. Preparation of 7-Acetyl-2,3-dimethylbenzo[c]pyrazole (3e)

The benzisoxazole (0.5 g, 0.00285 mol) and 40% aqueous methylamine solution (10 ml) in methanol (25 ml) were refluxed 16 h. The mixture was poured into ice, and extracted with ether (3 × 25 ml). The combined ether extracts were washed with water, dried, and evaporated to give a solid product. Purification was effected by t.l.c. using 16% diethyl ether in chloroform as a developer. A band with a blue fluorescence in the u.v. was eluted and gave on evaporation pale yellow crystals, m.p. 110–114° (34%).

Anal. Calcd. for $C_{11}H_{12}N_2O$: C, 70.21; H, 6.38; N, 14.89. Found: C, 69.97; H, 6.60; N, 14.67.

The i.r. spectrum: 1701 cm^{-1} (C=O str). The n.m.r. spectrum: τ 7.35 (3H singlet, methyl group on the heterocyclic ring), 7.09 (3H singlet, methyl on acetyl group), 5.82 (3H singlet, methyl on nitrogen), 3.01–1.92 (3H bands, protons on the aromatic ring, ABX pattern).

N,N'-Dimethyl-2-nitroisophthalamide (4e)

2-Nitroisophthaloyl chloride (16 g, 0.06 mol) in benzene (100 ml) was treated with 40% methylamine solution in water (200 ml). After the immediate vigorous reaction, the mixture was allowed to stand 1 h, then filtered. The precipitate was washed with cold water, dried, and recrystallized from dimethylformamide. Small colorless prisms were obtained, m.p. 273–275°, subliming above 250° (61%).

Anal. Calcd. for $C_{10}H_{11}N_3O_4$: C, 50.61; H, 4.64; N, 17.72. Found: C, 50.85; H, 4.61; N, 17.62.

The i.r. spectrum: 1636 (C=O), 3205 cm^{-1} (NH str).

N,N'-Dimethyl-2-nitroisothiophthalamide (4f)

N,N'-Dimethyl-2-nitroisophthalamide (5 g, 0.021 mol) in pyridine (60 ml) was refluxed with phosphorus pentasulfide (15 g) for 3 h. The mixture was poured into water and extracted with benzene (3 × 150 ml). The dried benzene extracts on evaporation gave a yellow oil which crystallized on standing. The crude product was recrystallized from methanol as lemon-yellow prisms, m.p. 204–206° (81%).

Anal. Calcd. for $C_{10}H_{11}N_2O_2S_2$: C, 44.65; H, 4.09; N, 16.61; S, 23.83. Found: C, 44.90; H, 4.36; N, 16.29; S, 23.93.

The i.r. spectrum: 1193 (tentatively C=S), 3191 cm^{-1} (NH str).

Reduction of N,N'-Dimethyl-2-nitroisophthalamide

The amide (2 g, 0.0084 mol) suspended in methanol (50 ml) was hydrogenated over Raney nickel (0.5 g) at 600 p.s.i. at 60° for 48 h in a pressure vessel with a glass liner. A yellow solution was obtained which on evaporation gave a yellow solid, which was crystallized from methanol. Colorless needles with a blue fluorescence in the u.v. were obtained. The compound partly melted at 158°, resolidified about 180°, and completely melted at 212°.

Anal. Calcd. for $C_{10}H_{15}N_3O_4$: C, 53.22; H, 6.66; N, 18.22. Found: C, 53.21; H, 6.71; N, 18.47.

Hydrogenation at lower temperatures, pressures, or shorter times gave erratic yields and products were contaminated with starting materials. Other methods of reduction, *e.g.* dissolving metal, hydride, were also tried but the extreme solubility of the products in polar or aqueous solvents made isolation unsatisfactory.

Attempted Sulfurization of 3-Methyl-2,1-benzisoxazole

3-Methyl-2,1-benzisoxazole (1 g) (17) and phosphorus pentasulfide (5 g) in carbon disulfide (10 ml) were refluxed for 6 h. Work-up provided only starting material.

When the reaction was performed in pyridine, extensive decomposition was evident. Examination of the products by t.l.c. gave only ill-defined bands which could not be properly separated.

We wish to thank Mr. R. Dickinson for the preparation of n.m.r. spectra, and the National Research Council of Canada for financial support. We also wish to thank Dr. T. Schaefer for helpful suggestions and advice.

1. R. GLEITER and R. HOFFMAN. Tetrahedron, **24**, 5899 (1968).
2. K. MAEDA. Bull. Chem. Soc. Jap. **33**, 1466 (1960); **34**, 785, 1166 (1961).
3. H. G. HERTZ, G. TRAVERSO, and W. WALTER. Ann., **625**, 43 (1959).
4. E. I. G. BROWN, D. LEAVER, and D. M. MCKINNON. J. Chem. Soc. C, 1202 (1970).
5. D. H. REID and J. D. SYMON. Chem. Commun. 1314 (1969).

6. (*a*) I. H. POMERANTZ and L. J. MILLER. Q. Rev. Sulfur Chem. **5**, 233 (1970). (*b*) I. POMERANTZ, L. MILLER, E. LUSTIG, D. MASTBROOK, E. HANSEN, R. BARRON, N. OATES, and J. Y. CHEN. Tetrahedron Lett. 5307 (1969).
7. D. LEAVER and D. M. MCKINNON. Chem. and Ind., 461 (1964).
8. E. I. G. BROWN, D. LEAVER, and T. J. RAWLINGS. Chem. Commun. 83 (1969).
9. G. A. REYNOLDS and C. R. HAUSER. Org. Synth. **30**, 70 (1950).
10. R. WASYLISHEN, T. SCHAEFER, and R. SCHWENK. Can. J. Chem. **48**, 2885 (1970) and references therein.
11. A. J. BOULTON, I. J. FLETCHER, and A. R. KATRITZKY. Chem. Commun. **62**, (1968).
12. A. J. BOULTON, A. C. GRIPPER-GRAY, and A. R. KATRITZKY. J. Chem. Soc. B, 909 (1967).
13. E. HADDOCK, P. KIRBY, and A. W. JOHNSON. J. Chem. Soc. C, 2514 (1970).
14. R. MAZER, J. MORGENSTEIN, and J. FABIAN. Angew. Chem. Int. Edn. Engl. **3**, 277 (1964).
15. E. NOELTING and C. GACHOT. Ber. **39**, 73 (1906).
16. A. WOHL. Ber. **43**, 3480 (1910).
17. R. CAMPS. Arch. Pharm. **240**, 423 (1902).

Can. J. Chem. Downloaded from www.nrcresearchpress.com by 210.87.254.40 on 09/05/12
For personal use only.

Can. J. Chem. Downloaded from www.nrcresearchpress.com by 210.87.254.105 on 09/05/12
For personal use only.

Benzodiazocines. II.[1] The Synthesis of Some Hexahydro-1,4-benzodiazocines

J. M. MUCHOWSKI
Bristol Laboratories of Canada, Limited, Candiac, Quebec

Received January 14, 1971

The synthesis of some hexahydro-1,4-benzodiazocine derivatives by the dicyclohexylcarbodiimide (DCC) induced cyclization of the appropriate *N*-2-(2-aminophenyl)ethyl glycines is described. An analogous synthetic approach was used to prepare a hexahydro-1*H*-1,5-benzodiazonine derivative.

On rapporte la synthèse de quelques dérivés de l'hexahydrobenzodiazocine-1,4 qui sont obtenus par la cyclisation, induite par la dicyclohexylcarbodiimide (DCC), des *N*-[(amino-2 phényl)-2 éthyl] glycines appropriées. On a utilisé une méthode de synthèse analogue pour préparer un dérivé de l'héxahydro 1*H*-benzodiazonine-1,5.

Canadian Journal of Chemistry, 49, 2023 (1971)

The synthesis of a simple derivative of hexahydro-1,4-benzodiazocine was recently published (1). This paper describes an alternative, potentially more flexible, route to several members of the title ring system.

In the above connection, 2-(2-nitrophenyl)-ethyl bromide (**1**; see Scheme 1 and Table 1) was aminated with methylamine, and the secondary amine **4***a* thus produced was alkylated (see Scheme 2) with ethyl bromoacetate. Hydrolysis of the ester **5***a* was effected with hot hydrobromic acid, and the carboxylic acid **6***a* so produced was catalytically reduced to the diamino acid **7***a* which, without purification, was cyclized with DCC in pyridine. The use of solvents other than pyridine (*e.g.*, acetonitrile or dimethyl formamide) for this cyclization, did not result in the formation of significant amounts of the 1,4-benzodiazocine (**8***a*).

The ester **5***b* (Scheme 2) was prepared from ethyl bromoacetate and the sodium salt of the benzenesulfonamide **4***b*, which in turn was readily obtained from **1** via 2-(2-nitrophenyl)-ethyl azide (**2**, Scheme 1). Saponification of **5***b* gave the carboxylic acid **6***b* which was converted to the amino acid **7***b* in the usual manner. The DCC promoted cyclization of **7***b* proceeded readily in acetonitrile, but not in pyridine. We have no explanation for the pronounced influence of the solvent on the above cyclization reactions.

The structures of **8***a* and *b* were supported by the correct elemental analyses and molecular weights (Rast) and by i.r. and n.m.r. spectral data (see Table 2).

Whereas the lactam **8***a* was easily reduced by lithium aluminum hydride to the diamine **9**, no basic product was produced under the same conditions from **8***b*. Furthermore, attempts to prepare the parent (**8**, R = H, $n = 1$) system from **8***b*, by reductive removal of the benzenesulfonyl group with disodium naphthalenide (2), or by elimination of benzenesulfinic acid with sodium hydride (3) followed by borohydride reduction of the anticipated imine, were not

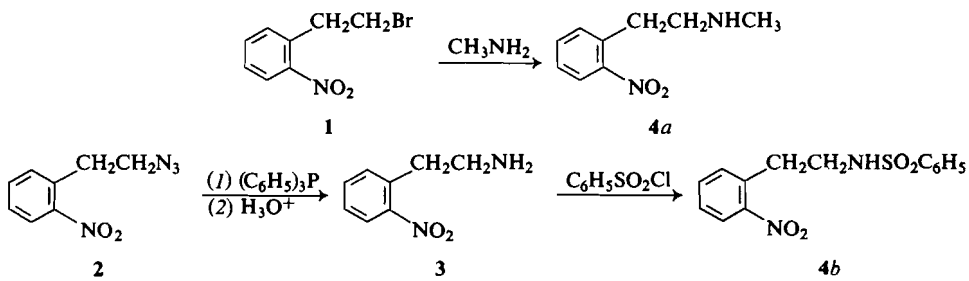

SCHEME 1

[1]For Part I see ref. 1.

Can. J. Chem. Downloaded from www.nrcresearchpress.com by 210.87.254.105 on 09/05/12
For personal use only.

TABLE 1. Yields and properties of some 1,4-benzodiazocines and related compounds

Compound	Yield (%)[a]	Melting point (°C) or boiling point (°C/mm)[a]	Crystallization solvent	% Calculated			% Found		
				C	H	N	C	H	N
1	84	35–37[b]	Petroleum ether (b.p. 60–90°)	41.77	3.51	6.09[c]	41.70	3.60	5.81
3	81[d]	159–161[e]	Acetonitrile	38.88	4.49	—	39.15	4.69	—
4*a*	68[f]	171–173[e]	Acetonitrile	41.39	5.02	11.43	41.52	5.04	11.31
4*b*	92	85–86	Cyclohexane:benzene(1:1)	55.64	4.67[g]	—	55.63	4.70	—
5*a*	76	120/0.005[h]	—	58.64	6.81	—	58.59	6.82	—
5*c*	98[i]	134–136[j]	Ethanol	51.86	5.99	—	52.17	6.24	—
6*a*	97[k]	170–172	Acetonitrile	41.39	4.74	8.78	41.29	4.76	8.99
6*b*	49	145–147	Ethanol:water(1:1)	52.70	4.43	7.80	52.95	4.43	7.86
6*c*	91[k]	184–186	Acetonitrile	43.26	5.14	8.41	43.39	5.11	8.58
8*a*[l]	59	104–105	Cyclohexane:benzene(1:1)	69.44	7.42	14.73	69.57	7.44	14.95
8*b*[m]	78	173–174	Benzene	60.70	5.10	8.86	60.96	5.17	9.12
8*c*[n]	30	103–105	Cyclohexane	70.56	7.90	13.72	70.58	8.00	13.96
9	82	100/0.005[h]	—	74.96	9.15	15.89	75.11	9.18	15.71[o]

[a]Yields refer to once crystallized or once distilled products. The melting points and boiling points are those of the analytical specimens.
[b]Literature (4), m.p. 36–38°.
[c]Anal. Calcd. for $C_8H_8BrNO_2$: Br, 34.74. Found: Br, 34.84.
[d]Crude yield of the known (5) undistilled base.
[e]Melting point and analysis of the hydrobromide salt.
[f]Yield of base evaporatively distilled at 110–115°/0.25 mm.
[g]Anal. Calcd. for $C_{14}H_{14}N_2O_4S$: 1/12 C_6H_6. See Experimental.
[h]Evaporative distillation.
[i]Yield of base evaporatively distilled at 125°/0.005 mm.
[j]Melting point and analysis of the acid oxalate.
[k]Yield, m.p., and analysis of the hydrobromide salt.
[l]Molecular Wt. Calcd. for $C_{11}H_{14}N_2O$: 190.2. Found (Rast): 183.
[m]Molecular Wt. Calcd. for $C_{16}H_{16}N_2O_3S$: 316.4. Found (Rast): 327.
[n]Molecular Wt. Calcd. for $C_{12}H_{16}N_2O$: 204.3. Found (Rast): 219.
[o]% N found by difference.

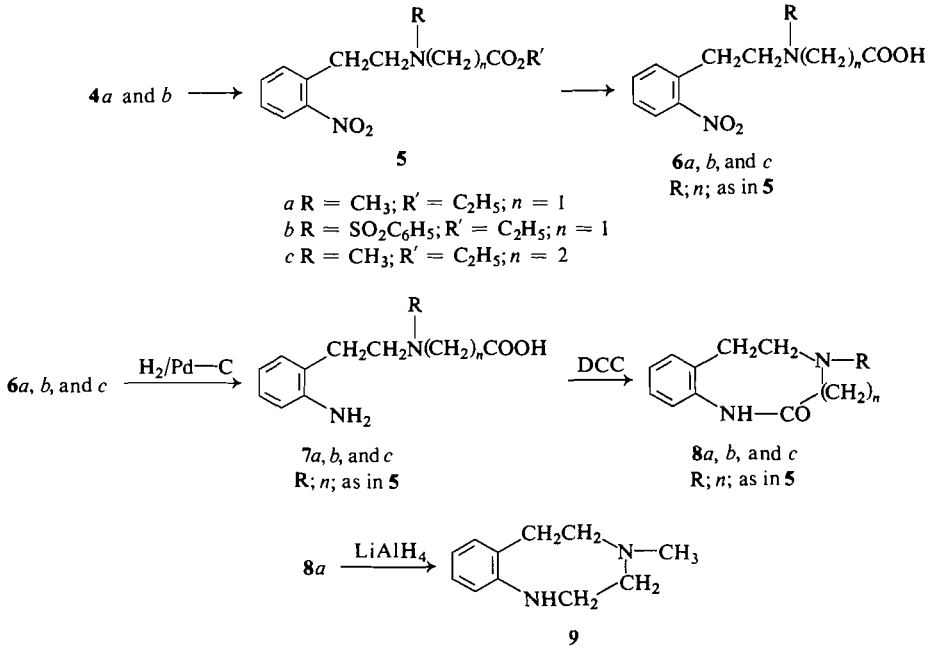

SCHEME 2

TABLE 2. Spectral properties of some 1,4-benzodiazocines and 1,5-benzodiazonines

Compound	Number	Infrared (cm^{-1})[a]	Nuclear magnetic resonance δ (p.p.m.)[b]
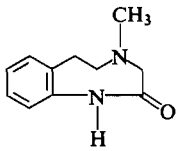	**8***a*	3377, 1665	2.45(s, 3H), 2.82(s, 4H), 3.13(s, 2H), 7.20(s, 4H), 9.13(s, 1H)
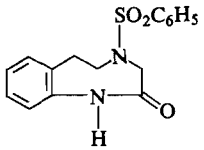	**8***b*	3376, 1670	3.14(m, 4H)[c], 3.98(s, 2H), 7.39(m, 9H), 8.81(s, 1H)
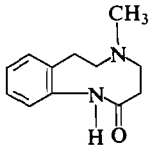	**8***c*	3385, 1664	2.43(s, 3H), 2.54(m, 8H), 7.23(m, 4H), 7.88(s, 1H)
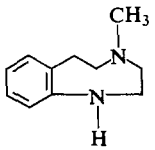	**9**	3400, 3320[d]	2.38(s, 3H), 2.81(m, 8H), 3.41(s, 1H), 7.03(m, 4H)

[a]Recorded in chloroform with a Perkin–Elmer 237B grating spectrophotometer.
[b]Recorded with a Varian A-60A spectrometer in deuteriochloroform containing internal tetramethylsilane.
[c]Two skewed quintets with fine structure centered at δ 2.88 and 3.40. The spectrum was unchanged at 100 °C.
[d]Liquid film.

Can. J. Chem. Downloaded from www.nrcresearchpress.com by 210.87.254.105 on 09/05/12
For personal use only.

promising. The first procedure gave only a small amount[2] of a basic product, the second resulted in the formation of a stable insoluble (in dimethyl formamide) sodium salt. Further synthetic efforts in this area were discontinued.

The synthetic principles described above were extendable to the preparation of the first known 1,5-benzodiazonine derivative **8***c*, the structure of which was apparent from its elemental analysis, molecular weight, and spectral properties (see Tables 1 and 2).

Experimental

The melting points were determined in a Gallenkamp m.p. apparatus and are not corrected. 2-Nitrophenylacetic acid was purchased from the Aldrich Chemical Company.

2-(2-Nitrophenyl)ethanol

Ethyl-2-nitrophenylacetate (6), prepared from 2-nitrophenylacetic acid and ethanol containing sulfuric acid, was reduced to 2-(2-nitrophenyl)ethanol with sodium borohydride and aluminum chloride (7) in 80–85% yield (b.p. 105–110°/0.04 mm; lit. (8), b.p. 136°/2 mm). This alcohol can now be readily prepared in one step from 2-nitrotoluene and formaldehyde (9, 10).

2-(2-Nitrophenyl)ethyl Bromide (1)

2-(2-Nitrophenyl)ethanol (25.0 g, 150 mmol) and concentrated hydrobromic acid (125 ml, 47–49%) were maintained at gentle reflux for 2 h. The cooled mixture was diluted with water, the organic phase was separated, and combined with a dichloromethane extract of the aqueous phase. This solution was washed well with water, dried over sodium sulfate, and evaporated *in vacuo*. The residue was distilled *in vacuo* and the fraction (28.9 g, 84%), b.p. 85–93°/0.025 mm, was collected. The oil solidified spontaneously; it could be recrystallized from petroleum ether (b.p. 60–90°) at low temperature to give a solid m.p. 35–37° (lit. (4) m.p. 36–38°).

2-(2-Nitrophenyl)ethyl Azide (2)

Solutions of the above bromo compound (23.0 g, 100 mmol) in dimethyl sulfoxide (400 ml) and sodium azide (19.5 g, 300 mmol) in water (100 ml), were combined and heated on a steam bath for 6 h. The solution was diluted with water and extracted with benzene. The extract was washed well with water, dried over sodium sulfate, and evaporated *in vacuo*. The residual oil (18.3 g, 95%; i.r. spectrum (neat), 2100 cm^{-1}) was used without purification.

2-(2-Nitrophenyl)ethyl Amine (3)

The conditions for this reduction were similar to those described by Horner and Gross (11).

A solution of the crude nitro azide (10.59 g, 55.1 mmol) and triphenylphosphine (14.43 g, 55.1 mmol) in anhydrous benzene (600 ml) containing several marble chips, was stirred at room temperature for 1 h, at 50° for 1 h, and at reflux temperature for 1 h. The solvent was removed *in vacuo*, acetic acid (180 ml) and concentrated hydrobromic acid (180 ml, 47–49%) were added to the residue, and the solution was heated at reflux temperature for 2 h. The solution was evaporated to a small volume *in vacuo*, water was added to the residue, and the mixture was extracted with dichloromethane. The aqueous phase was made basic with 2 *N* sodium hydroxide, the mixture was extracted with benzene, the extract was dried over sodium sulfate, and evaporated *in vacuo*. The residual, carbon dioxide sensitive, oil (7.42 g, 81%) gave a hydrobromide salt which had m.p. 159–161° after crystallization from acetonitrile.

N-Benzenesulfonyl-2-(2-nitrophenyl)ethyl Amine (4b)

To a stirred cooled solution of the crude nitro amine (7.42 g, 44.6 mmol) in dry pyridine (100 ml) was added benzenesulfonyl chloride (8.66 g, 49.1 mmol) at a rate such that the reaction temperature did not exceed 10°. After 14 h at 5° and 1 h at room temperature ice (10 g) was added to the solution and after an additional 1/2 h the solution was diluted with water and extracted with benzene. The extract was washed with water, dried over sodium sulfate, and evaporated *in vacuo*. The residue was crystallized from 1:1 benzene:cyclohexane to give a solid, m.p. 85–86° (12.55 g, 92%) which contained a small amount of benzene of crystallization as shown by n.m.r. After drying for 24 h *in vacuo* at room temperature the sample still contained the same amount (1/12 mol) of benzene as shown by the n.m.r. spectrum and elemental analysis.

N-Methyl-2-(2-nitrophenyl)ethyl Amine (4a)

A solution of methylamine (31.0 g, 910 mmol) and 2-(2-nitrophenyl)ethyl bromide (23.0 g, 100 mmol) in acetonitrile (100 ml) contained in a pressure bottle, was maintained at 65 ± 5° for 21 h. The solvent was removed *in vacuo*, the residue was diluted with water, acidified with hydrochloric acid (10%), and then extracted with dichloromethane. The aqueous phase was made basic with sodium carbonate solution (200 g/l), the mixture was extracted with dichloromethane, the extract was dried over sodium sulfate and evaporated *in vacuo*. Evaporative distillation of the residue at 110–115°/0.25 mm gave a yellow oil (12.2 g, 68%). The hydrobromide salt was prepared in ether, and after crystallization from acetonitrile it had m.p. 171–173°.

Ethyl-N-2-(2-nitrophenyl)ethyl Sarcosinate (5a)

A solution of the secondary amine **4***a* (7.21 g, 40 mmol) and ethyl bromoacetate (6.70 g, 40.1 mmol) in acetonitrile (300 ml) containing anhydrous potassium carbonate (2.80 g, 20.3 mmol) was stirred at room temperature for 65 h. The mixture was evaporated *in vacuo*, water was added to the residue, this mixture was made basic with sodium carbonate solution (200 g/l) and then extracted with dichloromethane. The extract was shaken with 10% hydrochloric acid, the acid phase was made basic with sodium carbonate solution, and the liberated base was extracted into dichloromethane. The extract was dried over sodium sulfate, evaporated *in vacuo*, and the residual oil was evaporatively distilled at 120°/0.005 mm to give the product (8.04 g, 76%).

N-2-(2-nitrophenyl)ethyl Sarcosine Hydrobromine (6a)

A solution of the ester **5**a (8.04 g, 30 mmol) in concentrated hydrobromic acid (160 ml, 47–49%) was

[2]A basic substance (*ca.* 5%, m.p. 148–149°), which had i.r. absorptions ($CHCl_3$) at 3520, 3458, 3420, and 1686 cm^{-1}, was obtained. It was not investigated further.

Can. J. Chem. Downloaded from www.nrcresearchpress.com by 210.87.254.105 on 09/05/12
For personal use only.

Can. J. Chem. Downloaded from www.nrcresearchpress.com by 210.87.254.105 on 09/05/12
For personal use only.

heated at gentle reflux for 16 h, and then reduced to a small volume *in vacuo*. The residual oil was taken up in acetonitrile and the solution was evaporated *in vacuo*. This procedure was repeated until the water was removed and a crystalline residue remained. The solid was crystallized from acetonitrile to give the product with m.p. 155–170° (dec.) (9.39 g, 92%). In spite of the wide melting range this material did not require further purification for use in the next step. Two crystallizations of this solid from acetonitrile raised the melting point to 170–172° (dec.).

4-Methyl-1,2,3,4,5,6-hexahydro-1,4-benzodiazocin-2-one (8a)

The above amino acid salt (9.39 g, 29.5 mmol) in ethanol (200 ml) containing palladium-on-charcoal (900 mg, 10%) was hydrogenated at room temperature and an initial hydrogen pressure of 45 p.s.i.g. After 1 h, the catalyst was removed by filtration through Celite, and the filtrate was evaporated to dryness *in vacuo*. The residue was dissolved in dry pyridine (900 ml), the solution was cooled with stirring to 0°, and a solution of DCC (6.1 g, 29.6 mmol) in pyridine (40 ml) was added all at once. After 1 h at 0° and 48 h at room temperature, the mixture was filtered, the filtrate was evaporated *in vacuo*, the residue thus obtained was slurried with 10% hydrochloric acid and filtered. The filtrate was extracted with ether, the aqueous phase was made basic with sodium carbonate solution (200 g/l), and the base was extracted into dichloromethane. The extract was dried over sodium sulfate, evaporated *in vacuo*, and the residue was crystallized from cyclohexane containing a small amount of benzene. A white solid m.p. 103–105° (3.33 g, 59%) was obtained.

N-Benzenesulfonyl-N-2-(2-nitrophenyl)ethyl Glycine (6b)

Sodium hydride (1.92 g of a 55% dispersion in mineral oil) was washed free of the carrier with hexane and layered with dry dimethylformamide (125 ml). The solid benzenesulfonamide **4***b* (12.25 g, 40 mmol) was added portionwise over a 10 min period at 0° and then the solution was stirred at room temperature until hydrogen evolution was slow. Ethyl bromoacetate (6.68 g, 40 mmol) was then added at a rate such that the reaction temperature did not exceed 10°. The solution was then stirred at room temperature for 1 h, diluted with water, and extracted with benzene. The extract was washed with water, dried over sodium sulfate, and evaporated *in vacuo*. The oily ester (15.2 g, i.r. spectrum (neat) 1748 cm^{-1}) was saponified without purification.

A solution of the crude ester (4.95 g, 12.62 mmol) in 50% aqueous methanol (50 ml), which was 0.5 *N* in sodium hydroxide, was heated at reflux temperature for 4.5 h, the methanol was removed *in vacuo*, and the residue was diluted with water and extracted with benzene. The aqueous phase was made acidic with concentrated hydrochloric acid, extracted with dichloromethane, the extract was washed with water, dried over sodium sulfate, and evaporated *in vacuo*. The residue on crystallization from 50% aqueous ethanol gave 2.24 g (49%) of a solid, m.p. 145–147°.

4-Benzenesulfonyl-1,2,3,4,5,6-hexahydro-1,4-benzodiazocin-2-one (8b)

The above nitro acid (5.12 g, 14.1 mmol) was hydrogenated as before and the crude dried amino acid was dissolved in 800 ml of dry acetonitrile. Dicyclohexylcarbodiimide (2.90 g, 14.1 mmol) was added all at once to the stirred solution and after 18 h at room temperature the mixture was filtered and the filtrate was evaporated *in vacuo*. The residue was slurried with acetonitrile (50 ml) filtered, the filtrate was evaporated *in vacuo* and the residue was crystallized from benzene. The product, m.p. 95–100° then solidifying and remelting at 172–173°, crystallized as the mono benzene solvate (4.32 g, 78%) as shown by n.m.r. A sample which was dried at 100° *in vacuo* for 18 h had m.p. 173–174° and was shown to be solvent free by n.m.r.

Ethyl-N-methyl-N-2-(2-nitrophenyl)ethyl-β-alanate (5c)

Ethyl acrylate (3.5 g, 35 mmol) was added at 0° to a solution of the methyl secondary amine **4***a* (6.13 g, 34 mmol) in absolute ethanol (35 ml). The solution was then left at room temperature for 65 h, the solvent was removed *in vacuo* and the residue was evaporatively distilled at 125°/0.005 mm to give a clear yellow oil (9.37 g, 98%). The acid oxalate was prepared in ethanol, and after crystallization from the same solvent it had m.p. 134–136°.

N-Methyl-N-2-(2-nitrophenyl)ethyl-β-alanine Hydrobromide (6c)

The amino ester (2.67 g, 9.53 mmol) in concentrated hydrobromic acid (55 ml, 47–49%) was heated at gentle reflux for 13 h. The amino acid hydrobromide was isolated in the manner described for **6***a*. Upon crystallization from acetonitrile, a solid, m.p. 183–186°, was obtained (2.85 g, 91%). Two crystallizations gave material with m.p. 184–186°.

5-Methyl-2,3,4,5,6,7-hexahydro-1H-1,5-benzodiazonin-2-one (8c)

The above amino acid hydrobromide (9.62 g, 28.8 mmol) was hydrogenated in the usual manner and a solution of the crude diamine in dry pyridine (900 ml) was treated at 0° with DCC (6.0 g, 29.1 mmol) in pyridine (100 ml) as before. After 1 h at 0° and 70 h at room temperature the reaction was worked-up as for **8***a*. A thick oil, which solidified on standing, was obtained. This material was extracted with boiling cyclohexane (2 × 100 ml), the hot solution was treated with charcoal, filtered, and evaporated *in vacuo*. The residue was crystallized from cyclohexane to give a solid (1.57 g), m.p. 99–102°. The cyclohexane insoluble residue from above and the mother liquor from the above crystallization were combined, evaporated to dryness *in vacuo*, and the residue was sublimed at 90–100°/0.001 mm. The sublimate (0.49 g) had m.p. 99–102°. The total yield of product was 29.5% of the theoretical.

4-Methyl-1,2,3,4,5,6-hexahydro-1,4-benzodiazocine (9)

A solution of the lactam **8***a* (1.193 g, 6.27 mmol) in anhydrous ether (250 ml) was added dropwise during a 1/2 h period to a stirred suspension of lithium aluminum hydride (1.2 g) in ether (50 ml). After 17 h at reflux temperature the excess hydride was destroyed at 0° by the cautious addition of water. The ether was decanted, combined with two ether washings of the solids, dried over sodium sulfate and evaporated *in vacuo*. The residue was evaporatively distilled at 95–105°/0.001 mm to give a colorless oil (0.902 g, 82%).

The high temperature (100°) n.m.r. spectrum of **8***b* was measured at the Chemistry Department, McGill University, Montreal, Quebec. We are grateful to Dr. K. Valentin for providing us with this service.

1. J. M. MUCHOWSKI. Can. J. Chem. **48**, 1946 (1970).
2. SUNGCHUL JI, L. B. GORTLER, A. WARING, A. BATTISTI, S. BANK, W. D. CLOSSON, and P. WRIEDE. J. Am. Chem. Soc. **89**, 5311 (1967).
3. E. NEGISHI and A. R. DAY. J. Org. Chem. **30**, 43 (1965).
4. E. L. FOREMAN and S. M. MCELVAIN. J. Am. Chem. Soc. **62**, 1435 (1940).
5. A. JAENISCH. Chem. Ber. **56B**, 2448 (1923).
6. A. REISSERT and J. SCHERK. Chem. Ber. **31**, 395 (1898).
7. H. C. BROWN and B. C. SUBBA RAO. J. Am. Chem. Soc. **78**, 2582 (1956).
8. G. M. BENNET and M. M. HAFEZ. J. Chem. Soc. 287 (1941).
9. B. WESSLEN. Acta Chem. Scand. **21**, 718 (1967).
10. (*a*) J. BAKKE. Acta Chem. Scand. **21**, 1967 (1967); (*b*) **23**, 3055 (1969).
11. L. HORNER and A. GROSS. Ann. **591**, 117 (1955).

Can. J. Chem. Downloaded from www.nrcresearchpress.com by 210.87.254.105 on 09/05/12
For personal use only.

11-Hydroxy-*trans*-8-dodecenoic Acid Lactone, a 12-Membered-Ring Compound from a Fungus

R. F. VESONDER, F. H. STODOLA, L. J. WICKERHAM, J. J. ELLIS, AND W. K. ROHWEDDER

Northern Regional Research Laboratory, Agricultural Research Service, United States Department of Agriculture, Peoria, Illinois 61604

Received January 26, 1971

The 12-membered lactone of 11-hydroxy-*trans*-8-dodecenoic acid is formed when the fungus *Cephalosporium recifei* NRRL 5161 is grown on glucose solution.

On a observé que la lactone à douze chaînons de l'acide hydroxy-11 dodécèn-8-*trans*-oïque se forme lorsque l'on fait croître les champignons du *Cephalosporium recifei* NRRL 5161 dans des solutions de glucose.

Canadian Journal of Chemistry, 49, 2029 (1971)

Naturally occurring large-ring lactones were first described by Kerschbaum (1) in 1927. Since that time many more examples of this class of compounds have appeared, most of them macrolides. We now report the isolation of the monocyclic lactone **1** from a fungus.

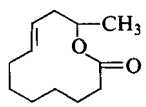

1

The organism appears to belong to the group *Cephalosporium recifei*, based on morphological studies and production of yellow pigment. The fungus was grown for 35 days on a shaken malt–glucose medium. Ether extraction of the whole culture liquor gave an average of 1.7 g of a viscous yellow oil *A* per liter of culture liquor. Hexane extraction of *A* at room temperature gave a 14% yield of nonpolar oil *B*, silicic acid column purification of which yielded a colorless mobile liquid *C* (77%), shown by g.l.c. to be 95% **1**. Pure lactone **1** was obtained from fraction *C* in about 50% yield by preparative g.l.c.

The structure of **1** was established as follows: elementary analyses and the molecular ion peak of *m/e* 196 corresponded to a formula of $C_{12}H_{20}O_2$. The i.r. spectrum showed a band at 1735 cm^{-1}, indicative of either a lactone or an ester, and a band at 975 cm^{-1}, characteristic of a *trans* double bond. That the double bond was unconjugated was evident from the u.v. spectrum (end absorption only). Chemical studies are summarized in Scheme 1.

It was first established that **1** is a lactone, rather than an ester, by saponification to **3**, which was shown to be a 12-carbon acid by elementary analysis of its phenacyl derivative **4**.

Next, the size of the lactone ring was determined. The optical activity of **1** ($[\alpha]_D^{25}$ + 73.2°) required substitution on the lactone ring. The nature and the position of the substituent were arrived at by CrO_3 oxidation of **5** to the keto acid **6**, which gave iodoform and the acid **7** on treatment with hypoiodite.

Finally, the position of the double bond in **1** was ascertained by oxidation procedures (ozonolysis and $KMnO_4$–HIO_4), which led to 3-hydroxy-butyric acid (**8**) and suberic acid (**9**), both characterized as their benzhydrylamine salts.

Information on the mass spectra of simple large-ring lactones appears to be meagre, the only two compounds studied so far being cyclopentadecanolide and 12-stearolactone (2). In our work the fragmentation patterns appear to be compatible with the assigned structures. The low resolution spectra of **1** (Fig. 1) and its dihydro derivative **2** (Fig. 2) are plotted along with the atomic compositions (determined by high resolution peak matching). Large peaks occur in the spectrum of **1** at 152 and 98, due probably to rearrangements involving opening of the lactone ring and cleavage at the C_{10}—C_{11} bond to form the 152 peak and cleavage at the C_6—C_7 bond to give the 98 peak.

The 152 peak of **1** also shifts two mass units higher to 154 in **2**, while the 98 peak of **1** at the carbonyl end of the molecule remains at 98 in **2**.

Can. J. Chem. Downloaded from www.nrcresearchpress.com by 210.87.254.42 on 09/05/12
For personal use only.

Can. J. Chem. Downloaded from www.nrcresearchpress.com by 210.87.254.42 on 09/05/12
For personal use only.

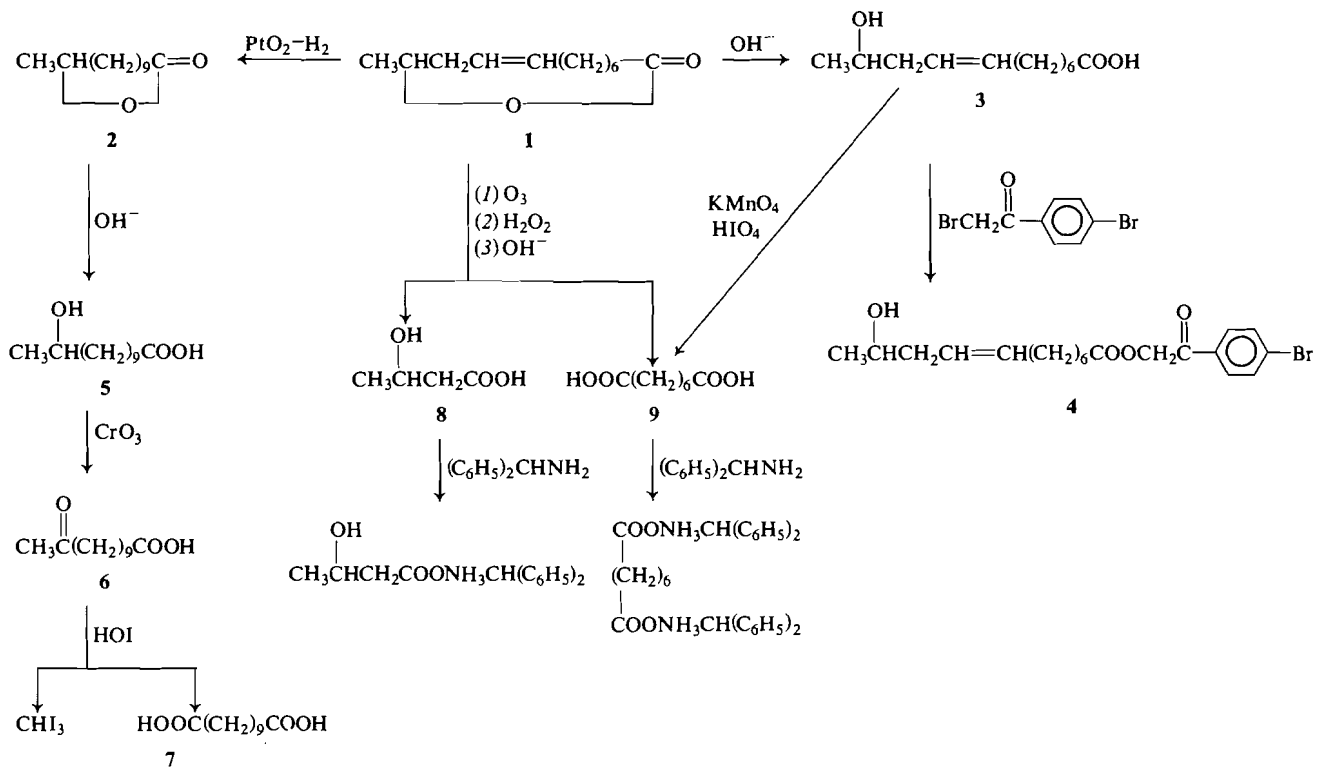

SCHEME 1

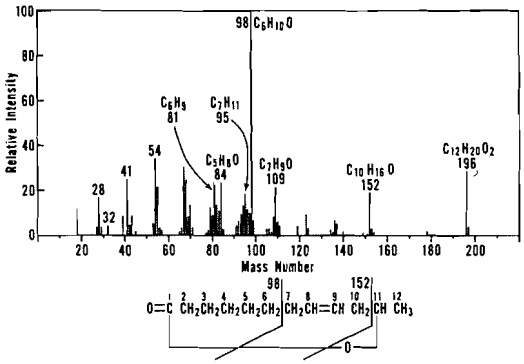

FIG. 1. Mass spectrum of lactone of 11-hydroxy-*trans*-8-dodecenoic acid (**1**).

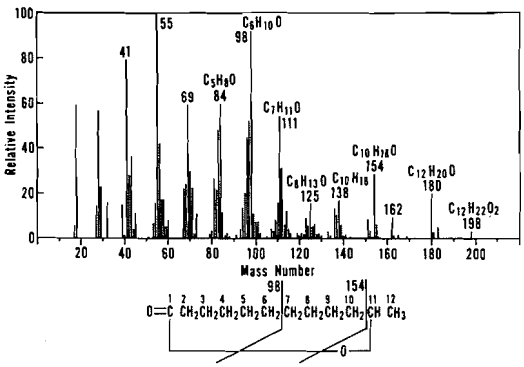

FIG. 2. Mass spectrum of lactone of 11-hydroxydodecanoic acid (**2**).

The 98 peak is the most intense peak in **1**, being three times the next highest peak; it is due to the weakening of the C_6—C_7 bond beta to the C_8—C_9 double bond. When the double bond is reduced, this cleavage is less selective and peaks appear at 84, 98, and 112 in **2**.

The mass spectrum, not shown, of the methyl ester of **3** had peaks at mass 74, 88%, and 87, 52%, characteristic of methyl esters. The molecular weight of the methyl ester is 228, but its spectrum did not show a molecular ion peak. Peaks were found at 210, 9%, due to loss of water; 184, 20%, due to loss of C_2H_4O; and at 152, 62%, due to further loss of methanol from the 184 peak. The loss of water, cleavage at the carbon-to-carbon bond adjacent to the OH, and the further loss of methanol from the chain cleavage fragment are all well-characterized fragmentations of methyl hydroxy esters, and these particular mass numbers indicate that the OH is on C-11 (3).

The simple large-ring lactones have found commercial application as fixatives in perfumes; this usage has stimulated considerable interest in their synthesis and properties (4).

Experimental

Melting points were determined on a Fisher–Johns[1] apparatus and are uncorrected. The i.r. spectra were recorded on Perkin–Elmer (Model 137) and Beckman (Model IR8) spectrophotometers. The g.l.c. analyses were carried out in a Packard 7401 gas chromatograph equipped with dual columns and independent flame-ionization detectors. Two columns were used: (*1*) 12 ft × 1/4 in.; 5% LAC-2-R 446 on Chromosorb W AW-DMCS; (*2*) 4 ft × 1/4 in., 5% Apiezon L on Chromosorb W AW-DMCS. The temperature of the inlet was 200 °C and that of the column oven was 190 °C. An Aerograph (Model 1520) gas chromatograph, equipped with a thermoconductivity detector, was used for preparative g.l.c. The column (6 ft × 1/4 in. stainless steel) was packed with 20% DEGS on 60/80 AW firebrick, and the temperature was maintained at 150 °C.

Mass spectra were measured on a Nuclide 1290 DF double focusing, high-resolution mass spectrometer operated with a 4460 V accelerating potential and at 70 V electron energy. The high-resolution mass determinations were made with a peak matching system based on using perfluorokerosene as an internal standard. The samples were run in an all-glass inlet at 200 °C.

The n.m.r. spectra were measured in a Varian HA-100 spectrometer and the u.v. was recorded with a Cary 14 spectrophotometer.

The Organism

The fungus was isolated in August 1960 from frass taken from the inside of a dead deciduous tree on the Livingston Ranch near Walker, Louisiana. It is designated as NRRL 5161 in the ARS Culture Collection here, and is judged to be a strain of *Cephalosporium recifei* on the basis of the following cultural characteristics: colonies on wheat germ agar and Czapek agar were white with a faintly pink center; on synthetic mucor agar the colonies became golden yellow with a white margin, and on malt extract agar and potato dextrose agar their color was dull yellow–orange. Long tapering phialides typically formed on the substrate hyphae. On most media small synnema were present, from which phialides also arose. Phialides were usually single or branched, and less frequently were verticillate. Conidia were borne in moist, colorless heads and were typically ellipsoidal and curved. They measured (2) 3–7 μ (9) in length and 1–3 μ (4) in width. Because of the yellow color, the strain is assigned to the *Cephalosporium recifei* group, as described by Sukapure and Thirumalachar (5).

Production of Crude Lactone A

The stock culture of the fungus was maintained on YM

[1]Mention of firm names or trade products does not imply that they are endorsed or recommended by the Department of Agriculture over other firms or similar products not mentioned.

Can. J. Chem. Downloaded from www.nrcresearchpress.com by 210.87.254.42 on 09/05/12
For personal use only.

Can. J. Chem. Downloaded from www.nrcresearchpress.com by 210.87.254.42 on 09/05/12
For personal use only.

agar slants (1% glucose, 0.5% peptone, 0.3% yeast extract, 0.3% malt extract, and 2% agar). A sterilized liquid medium (200 ml), consisting of 5% commercial glucose hydrate and 2% malt extract contained in 500-ml Erlenmeyer flasks, was inoculated with 0.1 ml of a cell suspension prepared from a 4-day-old YM slant culture and 1 ml of sterile distilled water. The flasks were incubated at 25 °C on a Gump shaker (180 r.p.m.; 1 in. radius). After 35 days growth the culture liquor was extracted with ether to give about 1.7 g of yellow viscous oil *A* per liter of medium.

*Isolation of Lactone of 11-Hydroxy-trans-8-dodecenoic Acid (**1**)*

Hexane extraction of oil *A* (10.0 g) at room temperature yielded 1.4 g of oil *B*, a portion (506 mg) of which was chromatographed on silicic acid (Bio-Sil A, 20 g), the eluting solvent being hexane–ether (95:5). The main fraction *C* (391 mg) was shown by g.l.c. to be 95% **1**; preparative g.l.c. of 167 mg *C* gave 88 mg of pure lactone of 11-hydroxy-*trans*-8-dodecenoic acid (**1**), a colorless mobile liquid, $[\alpha]_D^{25}$ +73.2° (*c*, 7.5, $CHCl_3$).

Anal. Calcd. for $C_{12}H_{20}O_2$: C, 73.43; H, 10.27. Found: C, 73.7; H, 10.4.

The u.v. spectrum: end absorption only. The i.r. spectrum (neat): 3010 (sh), 2978 (s), 2935 (s), 2850 (s), 1735 (s), 1450 (m), 1365 (m), 1225 (s), 975 cm^{-1} (s). The n.m.r. spectrum: doublet at δ 1.2 (methyl group attached to a carbon with one proton), 5.3 (two vinyl protons). Mass spectrum (Fig. 1): *m/e* 196 ($C_{12}H_{20}O_2$; found 196.1450, calcd. 196.1463).

*$KMnO_4$–HIO_4 Oxidation of 11-Hydroxy-trans-8-dodecenoic Acid (**3**)*

Fraction *C* (122 mg) refluxed 3 h with alcoholic KOH yielded 91 mg of hydroxy acid **3**, 47 mg of which was subjected to a von Rudloff (6) oxidation. The main product (26 mg) was shown by g.l.c. to consist of about 80% suberic acid. Identity was further established by conversion of 14 mg to the bisbenzhydrylamine salt (7) (28 mg; m.p. 172–174 °C), which was indistinguishable from an authentic sample.

*Ozonolysis of Lactone of 11-Hydroxy-trans-8-dodecenoic Acid (**1**)*

Ozone was passed for 45 s through a solution of fraction *C* (115 mg) in 5 ml ethanol and 1 ml ethyl acetate at 0 °C. The reaction mixture was taken to dryness, heated for 1 h at 95° with formic acid (98%, 3 ml) and H_2O_2 (30%, 0.2 ml), and kept overnight at room temperature. After additional heating (95 °C) for 35 min, the mixture was concentrated to 149 mg of oil, which was refluxed for 1 h with alcoholic KOH. Acidification and continuous ether extraction gave a first fraction of crude suberic acid (**9**) (44 mg; m.p. 133–138 °C). (Recrystallization: 26 mg, m.p. 140–142 °C; identity established by i.r. and mixture m.p.).

The second ether extract gave 65 mg of a semisolid. The third extract left 15 mg of oil ($[\alpha]_D^{25}$ −32° (*c*, 1, $CHCl_3$)), which was converted to the benzhydrylamine salt of **8** (m.p. 139–140 °C) the i.r. of which was identical with that of the corresponding salt prepared from *d,l*-3-hydroxybutyric acid.

*Hypoiodite Oxidation of 11-Ketododecanoic Acid (**6**)*

On hydrogenation (PtO_2; ethyl acetate), fraction *C* (101 mg) gave 67 mg of pure (g.l.c.) **2** (mass spectrum (Fig. 2): *m/e* 198 ($C_{12}H_{22}O_2$; found 198.1589; calcd. 198.1619). Saponification yielded 58 mg of hydroxy acid **5**, which was oxidized in 1 ml acetic acid with 0.56 ml of 0.53 *N* CrO_3–CH_3COOH for 1 h. When the resulting keto acid (57 mg) was subjected to the haloform reaction, it yielded 20 mg of iodoform, m.p. 123–124 °C. Ether extraction of the acidified reaction mixture gave 56 mg of solid, which g.l.c. analysis showed to be 48% 1,9-nonanedicarboxylic acid (**7**) and 62% unreacted 11-ketododecanoic acid (**6**).

*p-Bromophenacyl-11-hydroxy-trans-8-dodecenoate (**4**)*

11-Hydroxy-*trans*-8-dodecenoic acid (**3**) (18.5 mg) was converted to the *p*-bromophenacyl ester in acetone (15 min at 95°) by the dicyclohexylethylamine procedure (8). The crude product (22 mg; m.p. 60–68 °C) on crystallization from acetone–hexane gave 12 mg of *p*-bromophenacyl-11-hydroxy-*trans*-8-dodecenoate (**4**) (m.p. 73–74 °C).

Anal. Calcd. for $C_{20}H_{27}BrO_4$: C, 58.39; H, 6.61. Found: C, 58.5; H, 6.6.

1. M. KERSCHBAUM. Ber. **60B**, 902 (1927).
2. W. H. MCFADDEN, E. A. DAY, and M. J. DIAMOND. Anal. Chem. **37**, 89 (1965).
3. R. RYHAGE and E. STENHAGEN. *In* Mass spectrometry of organic ions. *Edited by* F. W. McLafferty. Academic Press, Inc. New York, N.Y., 1963. Chapt. 9.
4. K. ZIEGLER. *In* Methoden der Organischen Chemie (Houben–Weyl). *Edited by* E. Müller. George Thieme Verlag, Stuttgart, West Germany, 1955. Chapt. 9.
5. R. S. SUKAPURE and M. J. THIRUMALACHAR. Mycologia, **58**, 351 (1966).
6. E. VON RUDLOFF. Can. J. Chem. **34**, 1413 (1956).
7. A. F. WAGNER, E. WALTON, G. E. BOXER, M. P. PRUSS, F. W. HOLLY, and K. FOLKERS. J. Am. Chem. Soc. **78**, 5080 (1956); F. H. STODOLA, R. F. VESONDER, and L. J. WICKERHAM. Biochem. **4**, 1390 (1965).
8. F. H. STODOLA. Microchem. J. **7**, 389 (1963).

Can. J. Chem. Downloaded from www.nrcresearchpress.com by 210.87.254.105 on 09/05/12
For personal use only.

Proton Magnetic Resonance Studies of Rotational Isomerism in Halotoluenes VIII. Stereospecific ^1H–^{19}F Coupling Constants and Conformations of some Fluoro and Chloro Derivatives of Benzalchloride

H. M. HUTTON, J. B. ROWBOTHAM, B. H. BARBER, AND T. SCHAEFER
Chemistry Department, University of Manitoba, Winnipeg, Manitoba

Received January 26, 1971

In solution the 2-fluoro-5-chloro-, 2-fluoro-6-chloro-3-nitro-, 2-fluoro-6-chloro-5-nitro-, and 2,4,5-trichloro-benzalchlorides prefer conformations in which the C—H bond of the side-chain lies in the plane of the aromatic ring. This C—H bond eclipses that ortho C—X bond (X = H, F, Cl) in which X is smaller than Y = H, F, Cl in the C—Y bond, also ortho to the dichloromethyl group. The long-range spin–spin coupling constants between the proton in the side-chain and the ring protons or fluorine nucleus are stereospecific. In particular, the coupling over four bonds between the side-chain proton and the ring fluorine is −0.3 Hz when the C—H and C—F bonds are arranged *cis* to each other but is −2.5 Hz when these bonds have a *transoid* planar arrangement.

En solution, la conformation privilégiée des fluoro-2 chloro-5, fluoro-2 chloro-6 nitro-3, fluoro-2 chloro-6 nitro-5 et trichloro-2,4,5 dichlorométhylbenzènes correspond à celle dans laquelle le lien C—H de la chaîne latérale est dans le plan du noyau aromatique. Ce lien C—H éclipsera plutôt le lieu ortho C—X (X = H, F, Cl) dans lequel X sera plus petit que Y = H, F, Cl du lien C—Y aussi ortho au groupe dichlorométhyle. Les constantes de couplage à longue distance entre le proton de la chaîne latérale et les protons ou les fluors du cycle sont stéréospécifiques. En particulier on peut noter que le couplage à travers quatre liaisons entre le proton de la chaîne latérale et le fluor du cycle est de −0.3 Hz quand le C—H et le C—F sont *cis* l'un par rapport à l'autre alors que cette constante est de −2.5 Hz quand ces liens sont dans un arrangement planaire *transoïde*.

Canadian Journal of Chemistry, 49, 2033 (1971)

Introduction

The primary purpose of this paper is the demonstration of **1***a*, **2***a*, **3***a*, and **4***a*, as opposed to **1***b*, **2***b*, **3***b*, and **4***b*, as the stable conformations in solution of 2-fluoro-α,α,5-trichlorotoluene (**1**), of 2-fluoro-3-nitro-α,α,6-trichlorotoluene (**2**), of 2-fluoro-5-nitro-α,α,6-trichlorotoluene (**3**), and of α,α,2,4,5-pentachlorotoluene (**4**), respectively. The demonstration depends mainly on the observed magnitudes of the long-range spin-spin coupling constants over five bonds between the methine proton and the ring protons, $J_m^{H,CHCl_2} \equiv {}^5J_m(\alpha,H)$. Semiempirical barrier calculations based on modified Buckingham and on van der Waals potential functions are compared with the conformational data. In addition, the four-bond couplings, $J_o^{F,CHCl_2}$, are shown to be negative and highly stereospecific.

Experimental

(1) Preparation of Compounds

Compound **1** was prepared by free radical chlorination of 2-fluoro-5-chlorobenzylchloride in a manner described previously (1) for the preparation of α,α,2,4,6-pentachlorotoluene. Compounds **2** and **3** were prepared by nitration under mild conditions of 2-chloro-6-fluorobenzalchloride. Compounds **2** and **3** were not separated but were isolated as a mixture by distillation, following separation from the aqueous layer.

(2) Proton Magnetic Resonance Spectra

Degassed samples of **1** as a 30 mol % solution in toluene-d_8, of an approximately 5:1 mixture of **2** and **3** as a 30 vol % solution in toluene-d_8, and of **4** as a 25 vol % solution in carbon disulfide, also contained internal TMS as internal reference. Spectra were calibrated by period-averaging techniques on a DA-60I spectrometer operated in the frequency sweep mode. In solution the proton spectra of **2** and **3** overlap but the transitions do not coincide so that their spectra can be analyzed reliably.[1] In addition the methine proton resonance of a 20 mol % solution of 2-fluoro-α,α,6-trichlorotoluene in toluene-d_8 was examined between −105 and 60 °C on an HA100-D spectrometer.

Relative sign determinations were made by the usual double and triple resonance experiments.

Results and Discussion

(1) Analysis of Spectra

Spectral analyses by LAOCOON3 (2) gave the values in Table 1. In an attempted evaluation of

[1]As mooted by a referee, problems in separating **2** and **3** forced the use of the mixture.

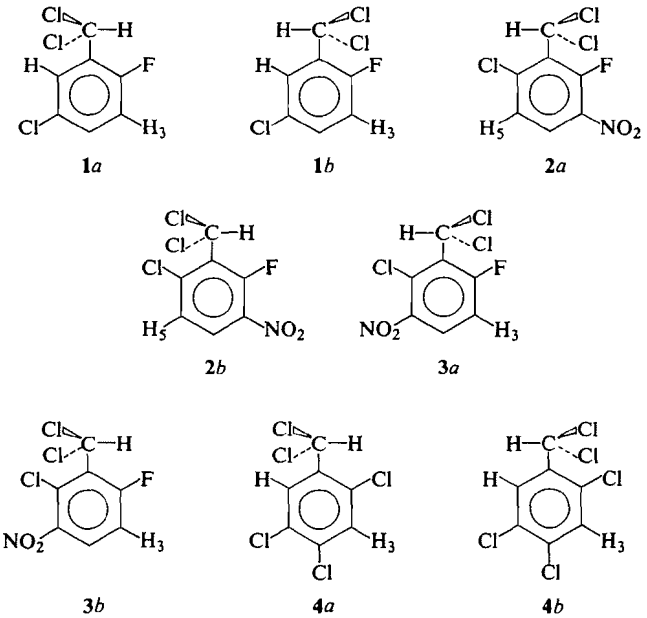

1*a* 1*b* 2*a* 2*b* 3*a* 3*b* 4*a* 4*b*

TABLE 1. Chemical shifts* and coupling constants† of some halotoluene derivatives

	Compound‡			
Parameter	**1**	**2**§	**3**§	**4**¶
ν_α	395.69	422.19(.13)	423.70(.61)	400.64
ν_3	388.52	—	396.68(.61)	413.80
ν_4	409.73	447.37(.29)	436.48(.40)	—
ν_5	—	405.13(.13)	—	—
ν_6	455.32	—	—	465.33
$^4J(\alpha,F)$‖	−0.30	−2.48(.50)	−2.58(.52)	—
$^4J(\alpha,6)$	−0.44	—	—	(−)0.35
$^5J(\alpha,3)$	0.05	—	0.38(.38)	0.05
$^5J(\alpha,5)$	—	0.00(.00)	—	—
$^6J(\alpha,4)$	−0.16	0.00(.00)	−0.01(.01)	—
$^3J_o(3,F)$	9.56	—	9.44(.41)	—
$^4J_m(4,F)$	4.43	7.77(.78)	4.90(5.00)	—
$^4J_m(6,F)$	6.32	—	—	—
$^5J_p(5,F)$	—	−1.83(−1.93)	—	—
$^3J_o(H,H)$	8.82	8.98(9.03)	9.09(.13)	—
$^4J_m(H,H)$	2.66	—	—	—
$^5J_p(H,H)$	0.34	—	—	0.35

*In Hz at 60 MHz to low field of internal TMS.
†In Hz, errors well within 0.05 Hz in most cases.
‡At concentrations in toluene-d_8 as given in the text. Compound **4** is in carbon disulfide.
§The parameters in brackets give the results from an independent analysis on the same sample performed at a different time.
‖α refers to the proton on the side-chain, while numbers in brackets refer to the protons at the relevant position in the rings depicted in the text.
¶The same coupling constants were found in solution in carbon tetrachloride and in carbon disulfide.

the accuracy of the parameters in Table 1 the spectra of **2** and **3** were calibrated twice, during different weeks, and the results in Table 1 suggest an accuracy of about 0.05 Hz in general and a higher accuracy in the coupling constants of particular interest in this study. In **2** and **3** the ring protons were somewhat broadened by incomplete relaxation of the coupling to the quadrupolar nitrogen (linewidths of up to 0.4 Hz), thereby increasing the uncertainty in peak positions. In the analyses of all compounds the r.m.s. error varied from 0.004 to 0.019 while the probable

Can. J. Chem. Downloaded from www.nrcresearchpress.com by 210.87.254.105 on 09/05/12
For personal use only.

errors in the parameters, as given by LAOCOON3, lay between 0.001 and 0.014 Hz.

(2) The Long-range Coupling $^5J(\alpha,H)$ and Conformations

Potential energy calculations (3, 4) demonstrate that **5** and **6** are the stable conformers of these molecules and p.m.r. measurements (1, 5)

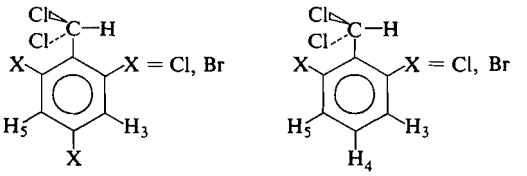

5 6

show that $^5J(\alpha,5) = 0.5$ Hz while $^5J(\alpha,3) \leq 0.1$ Hz (stereospecific couplings of similar magnitude over five bonds involving aldehydic (6), hydroxyl (7), and amino protons (8, 9) in aromatic systems demonstrate their preponderant dependence on geometry instead of on hybridization or on the nature of the side-chain atoms). Now $^5J(\alpha,H) \leq 0.05$ Hz in **1**, **2**, and **4** but $^5J(\alpha,H) = 0.4$ Hz in **3** (see Table 1). Therefore the *a* forms of these molecules are more stable than the *b* forms.

(3) Potential Energy Calculations

Potential energy calculations based on a van der Waals function (3, 4) predict that **2***a* and **3***a* are more stable than **2***b* and **3***b* by about 3 kcal/mol. Consequently the absence of any observable coupling from the side-chain proton to the meta proton in **2** is entirely reasonable. Similar conclusions hold for **4***a* and *b*. Calculations (3) based on a modified Buckingham potential suggest that **1***a* is more stable than **1***b* by about 1 kcal/mol, in only qualitative agreement[2] with the observed $^5J(\alpha,H) = 0.05$ Hz.

(4) Torsional Oscillations and $^4J(\alpha,H)$, $^6J(\alpha,H)$

The potential energy computations also indicate that torsional oscillation about the equilibrium position (C—H_α in plane) is largest for **1***a* and smallest for **2***a* and **3***a*. It is generally accepted (10, 11) that negative π electron contributions to $^4J(\alpha,H)$ and $^6J(\alpha,H)$ are smallest when the C—H_α bond lies in the plane of the ring and are largest when this bond lies parallel to the pπ orbital on the bonded ring carbon atom. The value for $^6J(\alpha,H)$ is -0.16 Hz in **1** but is undetectably small in **2** or **3**. These facts are in agreement with the potential energy calculations, which indicate substantially larger torsion angles about the sp^2–sp^3 carbon–carbon bond in **1** than in **2** or **3**. Because the difference in coupling constants is small and because the two substituents on the side-chain can affect (10) the magnitude of the π contribution to $^6J(\alpha,H)$ in a complex way, a quantitative treatment of the torsion angles will not be attempted.

The $^4J(\alpha,H)$ value is -0.4 Hz in **1** and **4**, suggesting a negative σ contribution to this coupling in conformations **1***a* and **4***a* because the negative π contribution should not differ by more than 0.1 Hz (12–15) for $^4J(\alpha,H)$ and $^6J(\alpha,H)$.

(5) The Stereospecificity of $^4J(\alpha,F)$

In *cis*-1-fluoropropene (16), pentafluorobenzaldehyde (17), pentafluorotoluene (17), 2-fluoro-4-iodo-5-nitrotoluene (18), and 2-fluoro-3-methylpyridine (19), the coupling over four bonds, $^4J(\alpha,F)$, lies between $+1$ and $+3$ Hz. Previous work (18, 19) indicates a positive π electron contribution to this coupling. In contrast to the above molecules, $^4J(\alpha,F) = -0.3$ Hz in **1***a* with a *cisoid* arrangement of the C—H_α and the C—F bonds while $^4J(\alpha,F) = -2.5$ Hz in **2***a* and **3***a* where the two bonds are in a planar transoid arrangement.

In the planar configuration the π contribution is small (10) so that a negative σ electron contribution to $^4J(\alpha,F)$ remains as the explanation for the large negative value observed in **2***a* and **3***a*. Scale drawings based on standard geometries give an internuclear H_α—F distance of 2.35 Å for a planar arrangement in **1***a*, indicating an overlap of 0.2 Å of the H_α and F atoms. It is therefore possible that in **1***a* there is a substantial positive "through-space" component (20–23) in $^4J(\alpha,F)$, thereby accounting for its smaller magnitude in this molecule. Alternative rationalizations would invoke a difference in the negative σ contribution to $^4J(\alpha,F)$ in the *cisoid* and *transoid* coupling path or an appreciably larger torsion angle in **1***a* with a larger positive π contribution to $^4J(\alpha,F)$ in this molecule.

[2]Calculations (3) using a van der Waals potential suggest the opposite and are presumably wrong. Mannschreck and Ernst, in a private communication, demonstrate that optimization of the molecular geometry for each rotational angle about the sp^2–sp^3 carbon–carbon bond yields reliable ground state energy differences between conformers.

Can. J. Chem. Downloaded from www.nrcresearchpress.com by 210.87.254.105 on 09/05/12
For personal use only.

(6) Temperature Studies on 2-Chloro-6-fluorobenzalchloride

The p.m.r. spectrum is very complex even in toluene-d_8 solution at 100 MHz. But a 2.6 Hz splitting of the H_α resonance, arising from coupling to fluorine over four bonds as in **2** or **3**, is evident in this solution (in contrast to other solvents where the H_α resonance occurs in the ring proton region). This splitting remains constant at 2.6 $\pm$ 0.2 Hz between -105 and 60 °C at 100 MHz. Comparison with the data for **2** and **3** suggests that the conformation analogous to **2***a* and **3***a* is the predominant one over this temperature range and, by comparison with $^4J(\alpha,F)$ for **1**, that the calculated energy difference of 3 kcal/mol between the two planar conformations of **2** and **3** is at least semiquantitatively correct.

(7) Chemical Shifts and Coupling Constants in the Ring

The spectra were taken in toluene-d_8 where the aromatic solvent induced shifts resulted in spectra amenable to analysis and to unequivocal multiple resonance experiments. The observed proton chemical shifts are similar to those discussed recently for numerous benzene derivatives dissolved in benzene-d_6 (24). The coupling constants between ring protons and between ring protons and the fluorine nuclei follow the regularities summarized by Wasylishen and Schaefer (25).

We are grateful to the National Research Council of Canada for financial support.

1. B. J. Fuhr, B. W. Goodwin, H. M. Hutton, and T. Schaefer. Can. J. Chem. **48**, 1558 (1970).
2. S. Castellano and A. A. Bothner-By. J. Chem. Phys. **41**, 3863 (1964).
3. B. H. Barber. M.Sc. Thesis. University of Manitoba, Winnipeg, Manitoba, 1970.
4. B. H. Barber and T. Schaefer. Can. J. Chem. **49**, 789 (1971).
5. J. Peeling, T. Schaefer, and C. M. Wong. Can. J. Chem. **48**, 2839 (1970).
6. G. J. Karabatsos and F. M. Vane. J. Am. Chem. Soc. **85**, 3886 (1963).
7. S. Forsén and R. A. Hoffman. J. Mol. Spectrosc. **20**, 168 (1966).
8. J. A. Weil, A. Blum, A. H. Heiss, and J. K. Kinnaird. J. Chem. Phys. **46**, 3132 (1967).
9. T. Schaefer and R. Wasylishen. Can. J. Chem. **48**, 1343 (1970).
10. A. F. Janzen and T. Schaefer. Can. J. Chem. **49**, 1818 (1971).
11. D. J. Blears, S. S. Danyluk, and T. Schaefer. Can. J. Chem. **46**, 564 (1968) and references therein.
12. M. P. Williamson, R. J. Kostelnik, and S. M. Castellano. J. Chem. Phys. **49**, 2218 (1968).
13. M. Barfield and B. Chakrabarti. J. Am. Chem. Soc. **91**, 4346 (1969).
14. M. Barfield and J. J. Read. J. Chem. Phys. **51**, 3039 (1969).
15. C. J. Macdonald and W. F Reynolds. Can. J. Chem. **48**, 1002 (1970).
16. R. A. Beaudet and J. D. Baldeschwieler. J. Mol. Spectrosc. **9**, 30 (1962).
17. R. R. Dean and W. McFarlane. J. Chem. Soc. B, 509 (1969).
18. D. J. Blears, S. S. Danyluk, and T. Schaefer. J. Chem. Phys. **47**, 5037 (1967).
19. T. Schaefer, S. S. Danyluk, and C. L. Bell. Can. J. Chem. **47**, 5107 (1969).
20. G. W. Gribble and J. R. Douglas, Jr. J. Am. Chem. Soc. **92**, 5764 (1970) and references therein.
21. R. D. Chambers, L. H. Sutcliffe, and G. J. T. Tiddy. Trans. Faraday Soc. **66**, 1025 (1970).
22. M. Barfield and B. Chakrabarti. Chem. Rev. **69**, 757 (1969).
23. P. C. Myhre, J. W. Edmonds, and J. D. Kruger. J. Am. Chem. Soc. **88**, 2459 (1966).
24. R. Wasylishen, T. Schaefer, and R. W. Schwenk. Can. J. Chem. **48**, 2885 (1970).
25. R. Wasylishen and T. Schaefer. Can. J. Chem. **49**, 94 (1971).

Can. J. Chem. Downloaded from www.nrcresearchpress.com by 210.87.254.105 on 09/05/12
For personal use only.

Can. J. Chem. Downloaded from www.nrcresearchpress.com by 210.87.254.40 on 09/05/12
For personal use only.

A Semi-theoretical van der Waals Equation for Calculation of Vapor–Liquid Equilibria at High Pressures

J. H. VERA[1] AND J. M. PRAUSNITZ

Department of Chemical Engineering, University of California, Berkeley, California

Received January 12, 1971

An equation of the van der Waals type is derived and applied to the calculation of vapor–liquid equilibria at elevated pressures. For the hard-sphere part of the equation the theoretical relation of Carnahan–Starling is used. The effect of intermolecular forces is represented by the usual van der Waals term but the "constant a" is permitted to vary with temperature and density as dictated by the experimental PVT data for argon; this variation of the "constant a" is generalized for other simple fluids through corresponding states. While this treatment is of little interest for representing the configurational properties of pure fluids, it is useful for calculating the properties of simple fluid mixtures. Illustrative vapor–liquid equilibrium calculations are performed for binary and ternary mixtures of nitrogen, argon, and oxygen at 6 and 18 atm.

On déduit une équation de type van der Waals qu'on applique au calcul des équilibres liquide–vapeur aux pressions élevées. Pour la partie sphère rigide de l'équation, on utilise la relation théorique de Carnahan–Starling. L'effet des forces intermoléculaires est représenté par le paramètre habituel de van der Waals, mais la "constante a" est ajustable en fonction de la température et de la densité comme l'exigent les données PVT expérimentales pour l'argon; par les états correspondants on généralise aux autres fluides simples cette variation de la "constante a". Le présent traitement présente peu d'intérêt pour la représentation des propriétés configurationnelles des fluides purs, par contre il est utile pour le calcul des propriétés des mélanges de fluides simples. A titre d'exemple, on a effectué des calculs d'équilibre liquide–vapeur pour des mélanges binaires et ternaires d'azote, d'argon et d'oxygène, à 6 et 18 atm.

Canadian Journal of Chemistry, 49, 2037 (1971)

In recent years extensive work has been done on the theory of simple fluids (1–6). It has been shown that the structure of a real fluid is similar to that of a hard-sphere fluid; that is, the distribution of molecules in space is determined primarily by the molecule's repulsive forces while the attractive forces may be considered to produce a uniform potential field which holds the molecules together. This view is remarkably similar to that proposed by van der Waals 100 years ago and therefore several modern theories of fluids and fluid mixtures are called "augmented" or "modified" van der Waals theories.

In this work we discuss a semi-theoretical treatment of simple mixtures which extends the work of Snider and Herrington (7). Unlike most previous work, our treatment is not limited to liquids at low pressures but is applicable also to high pressure vapor–liquid equilibria, including the critical region. Further, our treatment is in analytical form which is useful for implementation on an electronic computer.

[1]Present address: Universidad Técnica del Estado, Santiago, Chile.

Equation of State and Chemical Potential

Pure Component

The compressibility factor z of a pure fluid is given by an expression of the van der Waals type

$$[1] \qquad z = \frac{Pv}{RT} = z^{HS} - \frac{a}{RTv}$$

where z^{HS} is the compressibility factor of a hard-sphere fluid at temperature T and molar volume v. The van der Waals a is a constant only in the zeroth approximation (8); it depends on both temperature and volume.

For z^{HS} we use the theoretical expression of Percus and Yevick as modified by Carnahan and Starling (9)

$$[2] \qquad z^{HS} = \frac{1 + \xi + \xi^2 - \xi^3}{(1 - \xi)^3}$$

with

$$[3] \qquad \xi = b/4v$$

and $b = (2/3)\pi N_A \sigma^3$, where N_A is Avogadro's number and σ is the molecular diameter.

To find a, we use a reduced version of a highly accurate empirical equation of state proposed by

Can. J. Chem. Downloaded from www.nrcresearchpress.com by 210.87.254.40 on 09/05/12
For personal use only.

Strobridge for nitrogen (10) and used also by Gosman for argon (11). This equation is of the form

$$[4] \qquad z^{SG} = z(T_R, v_R)$$

where the reduced temperature $T_R = T/T_c$ and the reduced volume is v/v_c; subscript c stands for critical and superscript SG for Strobridge–Gosman. Details of the reduced equation of state (based on the properties of argon) are given in Appendix 1. From eq. 1 we have

$$[5] \qquad a = RTv[z^{HS} - z^{SG}]$$

where z^{SG} is found from eq. 4 and z^{HS} from eq. 2.

Since eq. 5 has not incorporated any new information, for a pure component z calculated from eq. 1 is identical to z^{SG} calculated from eq. 4. Consequently the chemical potential of the pure component is just the one obtained from the generalized Strobridge–Gosman expression, eq. 4, and given in Appendix 1. The main practical advantage of eq. 5 as a complement to eq. 1 follows from extension to mixtures as discussed in the next section.

For a fluid at a particular T and v, the value of the van der Waals a depends on the value of σ as used in eq. 2. It is not at all obvious how to obtain the best, or most representative, value of σ from reduction of experimental data.

Our purpose is to write equations in terms of macroscopic parameters suitable for practical mixture calculations. We therefore define a proportionality factor L

$$[6] \qquad b = b/4 = Lv_c$$

Equation 3 then becomes

$$[7] \qquad \xi = L/v_R$$

Unfortunately, the value of a is very sensitive to the value chosen for L. Using the values of σ reported by Snider and Herrington (7) for simple fluids in the dense region, we obtain values for L in the range 0.15 to 0.18.

These values are about 40% larger than that obtained by Dymond and Alder (12, 13) from high-density, high-temperature volumetric data for argon. The results of Dymond and Alder suggest that $L = 0.116$. We find that when $L = 0.116$, we obtain smooth behavior of the van der Waals a when plotted against reduced density and reduced temperature as shown in Fig. 1. At very high densities a is negative, suggesting that

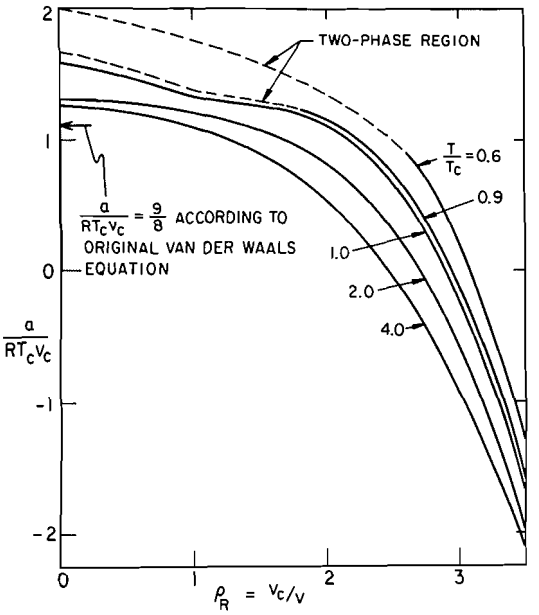

FIG. 1. Reduced van der Waals a as determined from Carnahan–Starling equation for z^{HS} and properties of argon (σ = 3.02 Å).

our value of L may be too low. However, larger values of L tend to give erratic plots of van der Waals a.

The large effect of the numerical value of L on the van der Waals a is illustrated in Fig. 2 which presents reduced values of a for argon at two temperatures. We see that the qualitative as well as quantitative variation of a with density is changed when L is increased from 0.116 to 0.150.

Mixtures

For a multicomponent mixture, following the original van der Waals suggestion, we write

$$[8] \qquad z_m = z_m^{HS} - \frac{\sum_{j,l} x_j x_l a_{jl}}{RTv_m}$$

where subscript m stands for mixture and x_j is the mole fraction of component j in the mixture.

The summation in the attractive term extends for both subindices from 1 to the number of components; for example, for a binary mixture eq. 8 becomes

$$[9] \qquad z_m = z_m^{HS} - \frac{a_{11}x_1^2 + 2a_{12}x_1x_2 + a_{22}x_2^2}{RTv_m}$$

The expression for z_m^{HS}, given by Carnahan and Starling (9), is

$$[10]\quad z_m^{HS} = \frac{1 + \xi_m + \xi_m^2}{(1-\xi_m)^3} - \frac{\xi_m\left(\sum_k x_k b_k^{2/3}\right)^3}{v_m^2(1-\xi_m)^3} - \frac{3}{v_m(1-\xi_m)^3}\sum_{j,l} x_j x_l (b_j^{1/3} - b_l^{1/3})^2 \left[2b_{jl}^{1/3} + \frac{b_j^{1/3} b_l^{1/3}}{v_m}\sum_k x_k b_k^{2/3}\right]$$

where

$$[11]\quad \xi_m = \frac{1}{v_m}\sum_k x_k b_k$$

Equation 10 differs from that derived by Lebowitz and Rowlinson (14) (Percus–Yevick compressibility equation) only in the second term; in Lebowitz and Rowlinson's expression this term does not appear.

Generalizing eq. 6 we write

$$[12]\quad b_{jl} = L v_{c_{jl}}$$

where $v_{c_{jl}}$ is given by

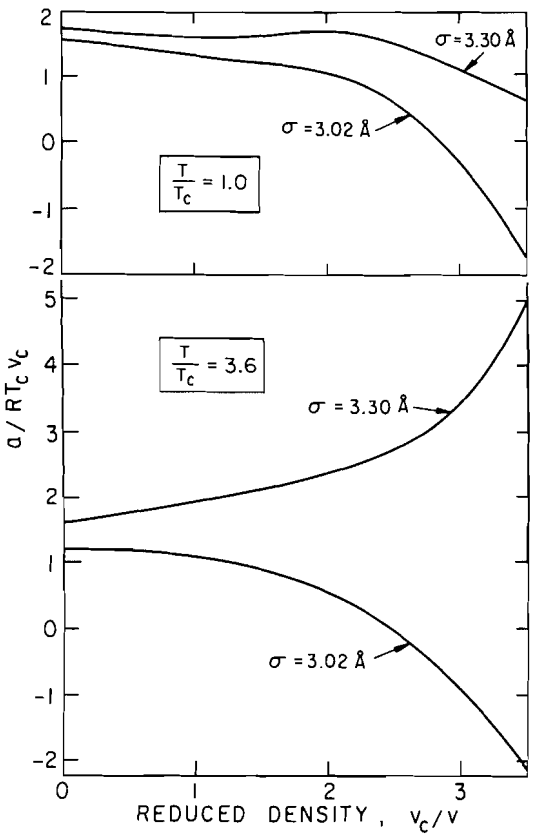

FIG. 2. Reduced van der Waals a for argon at two temperatures for different values of σ. When σ = 3.02 Å, L = 0.116; when σ = 3.30 Å, L = 0.150.

$$[13]\quad v_{c_{jl}}^{1/3} = \left(\frac{v_{c_j}^{1/3} + v_{c_l}^{1/3}}{2}\right)[1 - s_{jl}]$$

In eq. 13, s_{jl} is a dimensionless binary distance parameter characterizing the j–l interaction; s_{jl} may be positive or negative but its magnitude is small compared to unity.

The van der Waals coefficient a_{jl} is obtained from a generalization of eq. 5

$$[14]\quad a_{jl} = RTv_m[z_{jl}^{HS} - z_{jl}^{SG}]$$

where z_{jl}^{HS} is given by eq. 2 with $\xi_{jl} = b_{jl}/v_m$; z_{jl}^{SG} is given by eq. 4 with $T_{R_{jl}} = T/T_{c_{jl}}$ and $v_{R_{jl}} = v_m/v_{c_{jl}}$.

$T_{c_{jl}}$ is given by

$$[15]\quad T_{c_{jl}} = (T_{c_j}T_{c_l})^{1/2}[1 - k_{jl}]$$

where k_{jl} is a dimensionless energy parameter characteristic of the j–l potential; k_{jl} is usually a positive number small compared to unity.

The chemical potential of a component i in a multicomponent mixture can be written in the form

$$[16]\quad \mu_i = \mu_i^{ig} + \mu_i^{HS} + \mu_i^{F}$$

As described by Lebowitz and Rowlinson (14), μ_i^{ig} is the ideal-gas contribution to μ_i and μ_i^{HS} is the work of putting one mole of species i into a hard-sphere fluid. The chemical potential μ_i^F represents the effect of intermolecular forces.

For a Carnahan–Starling hard-sphere fluid the term μ_i^{HS} was obtained by just adding to the equivalent expression derived by Lebowitz and Rowlinson (14) the corrections due to the extra term in eq. 10.

The chemical potential μ_i^F was obtained using the standard thermodynamic relations

$$[17]\quad \mu_i^F = \left(\frac{\partial A^F}{\partial n_i}\right)_{T,V,n_j}$$

and

$$[18]\quad P^F = -\left(\frac{\partial A^F}{\partial V}\right)_{T,n}$$

where A^F is the contribution to the Helmholtz energy and P^F is the contribution to the total

Can. J. Chem. Downloaded from www.nrcresearchpress.com by 210.87.254.40 on 09/05/12
For personal use only.

TABLE 1. Calculated and experimental vapor–liquid equilibria for the binary system nitrogen–argon*

	T, °K		y_{N_2}	
x_{N_2}	Calcd.	Obsd.	Calcd.	Obsd.
$P = 6$ atm				
0.145	105.8	106.0	0.268	0.266
0.376	102.5	102.7	0.555	0.558
0.622	99.6	99.9	0.774	0.768
0.741	98.3	98.8	0.858	0.851
0.937	96.3	97.1	0.970	0.966
$P = 18$ atm				
0.167	125.1	124.8	0.240	0.250
0.271	123.5	123.2	0.367	0.373
0.458	120.8	120.4	0.569	0.576
0.620	118.6	118.2	0.719	0.715
0.871	115.3	115.4	0.915	0.911

*$s = -0.025$; $k = 0.005$.

pressure arising from intermolecular forces between real, rather than hard-sphere molecules. From eq. 18

$$[19] \qquad P^F = -\frac{\sum_{j,l} x_j x_l a_{jl}}{v_m^2}$$

The expressions for μ_i^{HS} and μ_i^F are given in Appendix 2.

There are two important differences between our equations and those of Snider and Herrington (7). As they use the Longuet–Higgins and Widom equation of state, the hard-sphere part in their treatment is that corresponding to the Percus–Yevick compressibility equation (2), and their van der Waals a is independent of volume. In our treatment we use the hard-sphere expression of Carnahan–Starling (9) which gives results remarkably close to the "exact" molecular-dynamics results of Alder (13). Further, we allow the "constant a" to depend on both temperature and volume as dictated by the empirical, reduced Strobridge–Gosman equation (11). Therefore, mainly as a result of the volume and temperature dependence of a, our equations can be used for calculation of vapor–liquid equilibria for mixtures of simple fluids at high pressures while those of Herrington and Snider are essentially restricted to the calculation of excess properties of liquid mixtures at low or modest pressures.

Results

Using the expressions developed in the previous section, vapor–liquid equilibrium calculations have been made for three binary systems and for one ternary system. The calculations are tedious but they can be made quickly with an electronic computer.

In this work we performed "bubble-point" calculations; that is, given the total pressure and the liquid-phase composition we find, by iteration, the equilibrium temperature and the vapor-phase composition. The three binary systems studied were nitrogen–argon, nitrogen–oxygen, and argon–oxygen.

Table 1 gives experimental and calculated results for the binary system nitrogen–argon; similar results were obtained for the binary systems nitrogen–oxygen and oxygen–argon. Values of the binary parameters s and k were obtained by fitting the bubble temperatures of each system. Table 2 gives experimental and calculated results for the ternary system nitrogen–argon–oxygen; all experimental values were reported by Wilson *et al.* (15). Agreement between calculated and experimental results is satisfactory but not outstanding. Failure to achieve better agreement is probably due to the fact that, contrary to our assumption in calculating a_m, these three fluids do not conform to two-parameter corresponding states with sufficient accuracy. Unfortunately, vapor–liquid equilibria are extremely sensitive to small changes in the constants a and b, in particular to small changes in a_{ij}.

While the van der Waals model is attractive because of its simplicity, the form of eq. 8 has a serious disadvantage for performing accurate calculations of the pressure; the two terms on the right-side of eq. 8 are often large and nearly equal and, as a result, a small error in either term can

Can. J. Chem. Downloaded from www.nrcresearchpress.com by 210.87.254.40 on 09/05/12
For personal use only.

TABLE 2. Calculated and experimental vapor–liquid equilibria for the ternary system nitrogen–argon–oxygen*

		T, °K		y_{N_2}		y_{O_2}	
x_{N_2}	x_{O_2}	Calcd.	Exptl.	Calcd.	Exptl.	Calcd.	Exptl.
$P = 6$ atm							
0.874	0.011	97.0	97.6	0.938	0.933	0.005	0.005
0.771	0.166	98.3	98.7	0.888	0.884	0.077	0.078
0.515	0.296	101.4	101.5	0.699	0.707	0.172	0.163
0.229	0.596	105.7	105.9	0.398	0.412	0.447	0.428
0.019	0.824	109.9	110.4	0.046	0.044	0.777	0.761
$P = 18$ atm							
0.858	0.020	115.5	115.4	0.907	0.904	0.012	0.013
0.762	0.053	116.9	116.5	0.837	0.839	0.034	0.033
0.403	0.441	122.7	122.1	0.523	0.522	0.343	0.347
0.262	0.643	125.3	124.8	0.368	0.380	0.543	0.527
0.017	0.875	129.9	129.8	0.029	0.030	0.853	0.846

*Characteristic binary parameters were obtained from binary-data reduction: nitrogen–argon: $s = -0.025, k = 0.005$; nitrogen–oxygen: $s = -0.035$, $k = 0.005$; argon–oxygen: $s = -0.012$, $k = 0.015$.

lead to a large error in the calculated pressure. If attention is confined to low-pressure fluids it is convenient to set $P = 0$ and to find constant values of a and b from experimental liquid-phase volumetric data as was done by previous workers. However, parameters obtained in this manner are not useful for calculations of vapor–liquid equilibria at advanced pressures. It appears then, that for accurate high-pressure phase-equilibrium calculations with an equation of the van der Waals type, primary attention must be given to a meaningful method for reducing pure-component experimental data to yield physically significant parameters.

The authors are grateful to the National Science Foundation, the donors of the Petroleum Research Fund, and to Universidad Técnica del Estado, Chile, for financial support and to the Computer Center, University of California, Berkeley, for the use of its facilities.

1. J. S. ROWLINSON. Rep. Progr. Phys. **28**, 169 (1965).
2. P. A. EGELSTAFF. An introduction to the liquid state. Academic Press, London. 1967.
3. J. S. ROWLINSON. Liquids and liquid mixtures. Butterworths, London. 1969.
4. M. RIGBY. Quart. Rev. London, **24**, 416 (1970).
5. S. A. RICE and P. GRAY. The statistical mechanics of simple liquids. John Wiley and Sons, Inc., New York. 1965.
6. G. A. MANSOORI and F. B. CANFIELD. Ind. Eng. Chem. **62**, No. 8, 12 (1970).
7. N. S. SNIDER and T. M. HERRINGTON. J. Chem. Phys. **47**, 2248 (1967).
8. R. W. ZWANZIG. J. Chem. Phys. **22**, 1420 (1954).
9. N. F. CARNAHAN and K. E. STARLING. J. Chem. Phys. **51**, 635 (1969); **53**, 472 (1970); **53**, 600 (1970), and private communication.
10. T. R. STROBRIDGE. NBS Technical Note No. 129 (1962).
11. A. L. GOSMAN, R. D. MCCARTHY, and J. G. HURST. National Standard Reference Data Series (NBS) No. 27 (March 1969).
12. J. H. DYMOND and B. J. ALDER. J. Chem. Phys. **45**, 2061 (1966).
13. B. J. ALDER, W. G. HOOVER, and S. YOUNG. J. Chem. Phys. **49**, 3693 (1968).
14. J. L. LEBOWITZ and J. S. ROWLINSON. J. Chem. Phys. **41**, 133 (1964).
15. G. M. WILSON, P. M. SILVERBERG, and M. G. ZELLNER. International Advances in Cryogenic Engineering. *Edited by* K. Timmerhaus. Plenum Press. 1965. p. 192.

Appendix 1

A. Reduced Form of Strobridge–Gosman Equation of State

$$[I.1] \qquad z^{SG} = 1 + \frac{C_{1T}}{v_R} + \frac{C_{2T}}{v_R^2} + \frac{C_{3T}}{v_R^5} + \frac{C_{4T}}{v_R^2} e^{-C_{16}/v_R^2} + \frac{C_{5T}}{v_R^4} e^{-C_{16}/v_R^2} + \frac{C_8}{v_R^3}$$

where

$$C_{1T} = C_1 + \frac{C_2}{T_R} + \frac{C_3}{T_R^2} + \frac{C_4}{T_R^3} + \frac{C_5}{T_R^5}$$

$$C_{2T} = C_6 + \frac{C_7}{T_R}$$

Can. J. Chem. Downloaded from www.nrcresearchpress.com by 210.87.254.40 on 09/05/12
For personal use only.

$$C_{3T} = \frac{C_{15}}{T_R}$$

$$C_{4T} = \frac{C_9}{T_R^3} + \frac{C_{10}}{T_R^4} + \frac{C_{11}}{T_R^5}$$

$$C_{5T} = \frac{C_{12}}{T_R^3} + \frac{C_{13}}{T_R^4} + \frac{C_{14}}{T_R^5}$$

The sixteen dimensionless constants are:

i	C_i	i	C_i
1	0.42455068	9	0.30728890
2	−0.97209685	10	0.27318478
3	−0.48307469	11	−0.32212511
4	−0.12610889	12	−0.07442445
5	0.02041906	13	0.35400823
6	0.15445801	14	0.05514637
7	−0.06794006	15	0.02432729
8	0.06653963	16	0.86320302

B. Chemical Potential for a Pure Component from Strobridge–Gosman Reduced Equation

$$\frac{\mu - \mu^{ig}}{RT} = \frac{2C_{1T}}{v_R} + \frac{3}{2}\frac{C_{2T}}{v_R^2} + \frac{4}{3}\frac{C_8}{v_R^3} + \frac{6}{5}\frac{C_{3T}}{v_R^5} + \frac{1}{v_R^2}\left(C_{4T} + \frac{C_{5T}}{v_R^2} - \frac{C_{5T}}{2C_{16}}\right) e^{-C_{16}/v_R^2} + \frac{1}{2C_{16}}\left(C_{4T} + \frac{C_{5T}}{C_{16}}\right)(1 - e^{-C_{16}/v_R^2})$$

where μ^{ig} is the chemical potential of the ideal gas at the same temperature and volume and the constants are those given in Part *A*.

Appendix 2

A. The hard-sphere chemical potential of component i in a multicomponent mixture is

$$\frac{\mu_i^{HS}}{RT} = -\ln(1 - \xi_m) + z_m^{HS}\left(\frac{b_i}{v_m}\right) + \frac{9}{2}\frac{b_i^{2/3}A_1^2}{(1 - \xi_m)^2} + \frac{3(b_i^{2/3}A_2 + b_i^{1/3}A_1)}{(1 - \xi_m)} + \frac{\xi_m b_i A_1^3}{(1 - \xi_m)^3} - \frac{b_i A_1^3}{\xi_m^2(1 - \xi_m)} + \left(\frac{3\xi_m A_1^2 b_i^{2/3} - 2A_1^3 b_i}{\xi_m^3}\right)\ln(1 - \xi_m) + \frac{A_1^3(1 - 3\xi_m)b_i}{2\xi_m(1 - \xi_m)^3} + \frac{(2 - 3\xi_m)(3\xi_m A_1^2 b_i^{2/3} - A_1^3 b_i)}{2\xi_m^2(1 - \xi_m)^2}$$

where

$$\xi_m = \frac{1}{v_m}\sum_k x_k b_k$$

$$A_1 = \frac{1}{v_m}\sum_k x_k b_k^{2/3}$$

$$A_2 = \frac{1}{v_m}\sum_k x_k b_k^{1/3}$$

and z_m^{HS} is defined by eq. 10 in the text. The fourth term has been introduced in order to correct z_m^{HS} (from Percus–Yevick compressibility equation) to the Carnahan–Starling form. The last four terms are the correction to the expression of Lebowitz and Rowlinson (14) originated by the extra term in eq. 10.

Can. J. Chem. Downloaded from www.nrcresearchpress.com by 210.87.254.40 on 09/05/12
For personal use only.

B. The contribution of intermolecular forces to the chemical potential of a component i in a multicomponent mixture is designated by μ_i^F

When the "constant a" is volume dependent as in this work

$$\frac{\mu_i^F}{RT} = 2\sum_k x_k F_{ik} - \sum_{j,l} x_j x_l \left(F_{jl} + v_m \frac{\partial F_{jl}}{\partial v_m} \right)$$

where

$$F_{jl} = n_T \int_\infty^V \frac{a_{jl}}{RTV^2}\, dV = \int_\infty^V \frac{(z_{jl}^{HS} - z_{jl}^{SG})}{V}\, dV; \quad [V = n_T v_m]$$

using eq. I-1 to determine a_{jl}, we obtain

$$F_{jl} = \frac{\xi_{jl}(3\xi_{jl} - 4)}{(1 - \xi_{jl})^2} + \frac{C_{1T_{jl}}}{v_{R_{jl}}} + \frac{C_{2T_{jl}}}{2v_{R_{jl}}^2} + \frac{C_{3T_{jl}}}{5v_{R_{jl}}^5} + \frac{C_8}{3v_{R_{jl}}^3} - \frac{C_{5T_{jl}}}{2C_{16}} \frac{1}{v_{R_{jl}}^2} e^{-C_{16}/v_{R_{jl}}^2} + \frac{1}{2C_{16}} \left(C_{4T_{jl}} + \frac{C_{5T_{jl}}}{C_{16}} \right) (1 - e^{-C_{16}/v_{R_{jl}}^2})$$

and

$$v_m \frac{\partial F_{jl}}{\partial v_m} = \frac{2\xi_{jl}(2 - \xi_{jl})}{(1 - \xi_{jl})^2} - \left[\frac{C_{1T_{jl}}}{v_{R_{jl}}} + \frac{C_{2T_{jl}}}{v_{R_{jl}}^2} + \frac{C_{3T_{jl}}}{v_{R_{jl}}^5} + \frac{C_8}{v_{R_{jl}}^3} + \frac{1}{v_{R_{jl}}^2} \left(C_{4T_{jl}} + \frac{C_{5T_{jl}}}{v_{R_{jl}}^2} \right) e^{-C_{16}/v_{R_{jl}}^2} \right]$$

where

$$\xi_{jl} = b_{jl}/v_m$$

$$v_{R_{jl}} = v_m/v_{c_{jl}}$$

The coefficients $C_{iT_{jl}}$ are those defined in Part *A* of Appendix 1, evaluated with $T_{R_{jl}} = T/T_{c_{jl}}$.

C. Equations of Section B, Appendix 2, in the special case where a is independent of volume

$$F_{jl} = n_T \int_\infty^V \frac{a_{jl}}{RTV^2}\, dV = -\frac{a_{jl}}{RTv_m}$$

Then

$$v_m \frac{\partial F_{jl}}{\partial v_m} = \frac{a_{jl}}{RTv_m}$$

and

$$\sum_{j,l} x_j x_l \left[F_{jl} + v_m \frac{\partial F_{jl}}{\partial v_m} \right] = 0$$

As a result of this simplification, we obtain

$$\frac{\mu_1^F}{RT} = -\frac{2\sum_k x_k a_{ik}}{RTv_m}$$

For a binary system

$$\frac{\mu_i^F}{RT} = -2\left(\frac{x_1 a_{11} + x_2 a_{12}}{RTv_m} \right)$$

Can. J. Chem. Downloaded from www.nrcresearchpress.com by 210.87.254.40 on 09/05/12
For personal use only.

Can. J. Chem. Downloaded from www.nrcresearchpress.com by 210.87.254.6 on 09/05/12
For personal use only.

Thermoelectric Studies of Silver Nitrate in Sodium Nitrate – Potassium Nitrate Eutectic Melt

L. G. BOXALL[1] AND K. E. JOHNSON

Department of Chemistry, University of Saskatchewan, Regina, Saskatchewan

Received[2] July 22, 1970

The Seebeck coefficient, ε_T, of the thermocell $Ag(T)/AgNO_3$ in $NaNO_3$–KNO_3/Ag $(T + \Delta T)$ was measured as a function of silver nitrate concentration and temperature. Extrapolation of the results to unit mole fraction, N, of $AgNO_3$ gave the value $\varepsilon_T^0 = -277.5 - 0.136T$ °C (μV deg^{-1}).

For several mixed melts of $AgNO_3$ and an alkali nitrate the function $P = \varepsilon_T - \varepsilon_T^0 - (R/F) \ln N + \Delta\bar{S}^E$ was calculated and shown to be linear in N. P was extrapolated to finite values for the pure alkali nitrates.

Le coefficient de Seebeck ε_T de la thermopile $Ag(T)/AgNO_3$ dans $NaNO_3$–KNO_3/Ag $(T + \Delta T)$ a été mesuré en fonction de la concentration en nitrate d'argent et de la température. La valeur $\varepsilon_T^0 = -277.5 - 0.136T$ °C (μV deg^{-1}) est trouvée par extrapolation des résultats à la fraction moléculaire N de $AgNO_3$ égale à l'unité.

La fonction $P = \varepsilon_T - \varepsilon_T^0 - (R/F) \ln N + \Delta\bar{S}^E$ a été calculée pour plusieurs mélanges fondus de $AgNO_3$ et d'un nitrate d'alcalin; cette fonction varie de façon linéaire avec N. Par extrapolation on trouve des valeurs finies de P pour les nitrates d'alcalins purs.

Canadian Journal of Chemistry, 49, 2044 (1971)

The Seebeck coefficient, ε_T^0, for the pure fused silver nitrate thermocell has been measured by several workers (1–6) and others have studied the Seebeck coefficient, ε_T, of thermocells based on binary mixtures of silver nitrate with lithium nitrate (3, 7, 8), sodium nitrate (1, 6, 8–10), potassium nitrate (8, 11), rubidium nitrate (11), and thallium nitrate (12) and dilute solutions of silver nitrate in alkali nitrate eutectics and mixtures (13).

In this paper we report measurements of ε_T for silver nitrate in $NaNO_3$–KNO_3 eutectic and discuss these and similar data in terms of Dupuy's (5) derived relationship between ε_T and ε_T^0.

Experimental Procedure

Measurements were carried out with the furnace illustrated in Fig. 1, based on a U-shaped piece of glass tubing with each limb wrapped with separately controlled heating tapes. Two sintered glass discs were incorporated in the tubing to retard the thermal diffusion of the ions in the melt and a central tube facilitated the filling of the cell. To eliminate a.c. interference, the glass of the cell was wrapped with aluminum foil before attaching the heating tapes. The temperature of each limb of the cell could be varied independently by the use of two proportional controllers (Cole-Parmer), a maximum temperature gradient of 100 °C being possible.

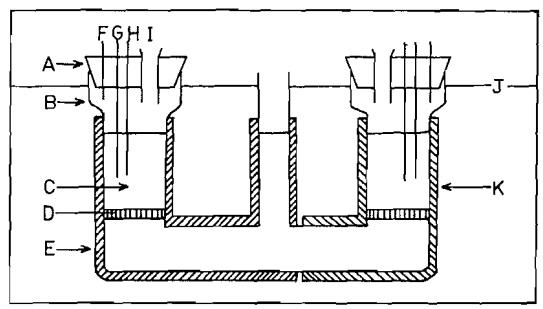

FIG. 1. Cell for thermoelectric studies; *A*, foil-wrapped rubber stopper; *B*, foil (earthed) wrapped Pyrex cell; *C*, melt; *D*, 20 mm, fine fritted disk; *E*, heating tape connected to left temperature controller, *F*, N_2 inlet; *G*, probe for melt temperature controller; *H*, thermocouple; *I*, glass-lined inlet for electrode compartment; *J*, upper level of insulation; *K*, heating tape connected to right temperature controller.

Thermal stability in each half cell was obtained 15 to 60 min after a temperature change. For each mixture a given temperature profile was applied with first the left-hand half of the cell and then the right-hand half the hotter of the two. Each run consisted of taking ΔT through the cycle $0 \rightarrow +50 \rightarrow 0 \rightarrow -50 \rightarrow 0$ °C. The average temperature of the cell was maintained to ± 2 °C and temperature and e.m.f. were recorded only after they had remained stable at ± 0.5 °C and 0.05 mV, respectively, for 15 min. Eight to ten points were recorded per run.

Sodium and potassium nitrates (Fisher Scientific, reagent grade) were twice recrystallized from water and dried *in vacuo* at 120 °C. Silver nitrate (Fisher Scientific, reagent grade) was dried *in vacuo* at 100 °C.

[1]Present address: Department of Chemistry, Colorado State University, Fort Collins, Colorado.

[2]Revision received February 22, 1971.

Can. J. Chem. Downloaded from www.nrcresearchpress.com by 210.87.254.6 on 09/05/12
For personal use only.

Results

The results for two runs at 275 ± 2 °C with a mole fraction of silver nitrate of 0.2 are combined in Fig. 2. The least squares fit of the data has a slope of -315 μV deg^{-1} and a standard deviation in the measured e.m.f. of 0.62 μV. ε_T values for seven different concentrations of silver nitrate were measured at four temperatures and the ε_T^0 values obtained by extrapolation to unit mole fraction of silver nitrate, N, were as follows

Temperature ±2 °C	$-\varepsilon_T^0$ ±5 μV deg^{-1}
275	314
300	320
325	321
350	325

The variation may be written as

$$\varepsilon_T^0 = -(277.5 \pm 0.7) - (0.136 \pm 0.025)T\ °C\ (\mu V\ deg^{-1})$$

with a standard deviation of 1.4 μV deg^{-1}. The increase in $|\varepsilon_T^0|$ of (0.042 ± 0.08)% deg^{-1} agrees with previous work (7).

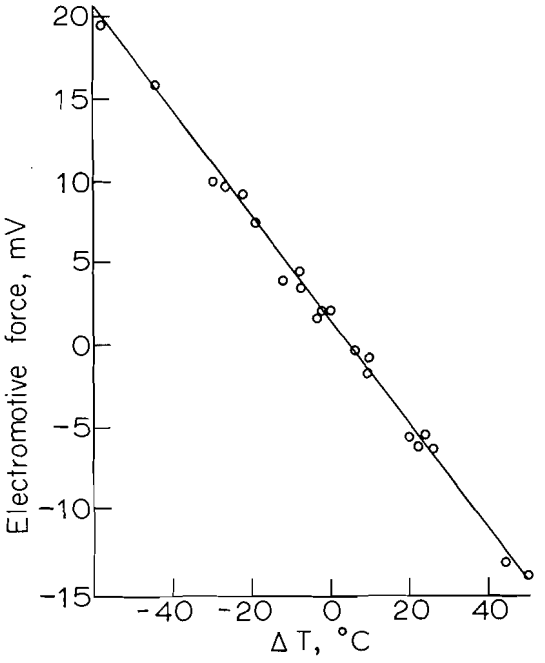

FIG. 2. Electromotive force of dilute silver nitrate thermal cell; mole fraction $AgNO_3$ = 0.20, solvent = (Na, K)NO_3, average temperature = 275 ± 2 °C.

Discussion

The relationship derived between ε_T and ε_T^0 has the form (5)

$$[1]\quad \varepsilon_T - \varepsilon_T^0 - \frac{R}{F}\ln N\gamma + \frac{\Delta\bar{H}^M}{FT} = \frac{1}{F}\Delta\left\{-\sum_i \frac{t_i s_i}{Z_i}\right\} = P$$

where γ is the activity coefficient of silver nitrate on the mole fraction scale, $\Delta\bar{H}^M$ is the partial molar excess enthalpy, t_i is the transport number of species i, Z_i is the valence of species i, s_i is the entropy of transport of species i, and the right-hand term is the difference between the summation for the mixture and that for pure silver nitrate. The expression may be rewritten

$$[2]\quad P = \varepsilon_T - \varepsilon_T^0 - \frac{R}{F}\ln N + \frac{\alpha}{F}(1-N)^2$$

where $\alpha(1-N)^2$ is the partial molar excess entropy, $\Delta\bar{S}^E$ (14).

Now $\Delta\bar{H}^M$ is obtainable for $LiNO_3$, $NaNO_3$, KNO_3, and $RbNO_3$ from the calorimetric measurements of Kleppa *et al.* (15) while the γ and α values may be derived from e.m.f. measurements (14, 16, 17). For the single alkali nitrates we have used both methods of calculating P for each mole fraction, N; $-\Delta\bar{H}^M$ from calorimetry (15) and γ from e.m.f. measurements (16, 17) or α from e.m.f. measurements (16, 17).[3] Since the α values came from studies involving only limited temperature variation, the former method which gave P values a few μV deg^{-1} more negative, seems preferable; except for $LiNO_3$ the difference is small. For $NaNO_3$–KNO_3 containing $AgNO_3$, $\Delta\bar{H}^M$ data are not available so that total reliance on e.m.f. measurements was necessary.

The resulting functions, P, appear to follow a linear dependence (Fig. 3) on alkali nitrate mole fraction; thus $P = x + (1-N)y$ with the values of x and y given in Table 1. We note that the variation for $NaNO_3$–KNO_3 is practically the same as for $NaNO_3$. The question remains as to the interpretation of x and $(x+y)$, the values of P for pure silver and alkali nitrate, respectively.

[3]We have shown for these systems (16) that $\gamma \to \gamma_{N=0}$ at low N in which case the variation of $\gamma_{N=0}$ with T yields α, thus $RT\ln\gamma_{N=0} = a - \alpha T$.

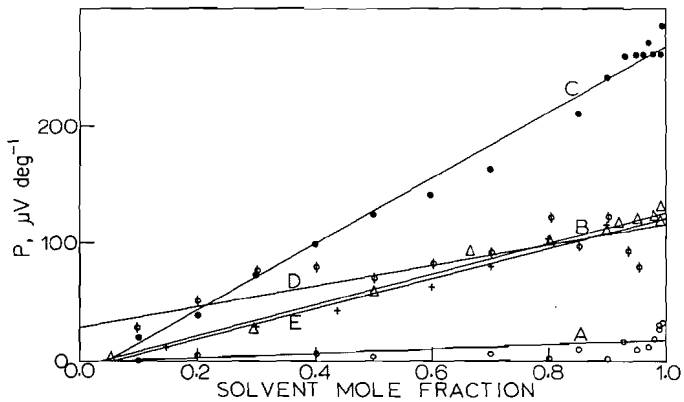

FIG. 3. The function $P = \varepsilon_T - \varepsilon_T^0 - (R/F) \ln N\gamma + \Delta\bar{H}^M/FT$ *vs.* $(1 - N)$ for the solvent systems *A* (○), $LiNO_3$ at 340 °C; *B* (△), $NaNO_3$ at 340 °C; *C* (●), KNO_3 at 360 °C; *D* (ϕ), $RbNO_3$ at 310 °C; *E* (+), $NaNO_3$–KNO_3 at 350 °C.

TABLE 1. Values of *P* according to its functional dependence

		$P = x + (1 - N)y$			$P = (1 - N)y^1$		
System	T °C	x	y	σ	y^1	σ	Reference
$LiNO_3$	340	−3.7±2.2	20.3± 6.6	8.9	16.0±2.8	8.8	8
$NaNO_3$	340	−6.6±1.7	133.0± 4.7	5.8	125.4±2.4	6.4	8
KNO_3	360	−14.5±2.8	283.9± 8.1	11.3	266.5±4.2	12.9	8
$RbNO_3$	310	27.3±5.1	90.0±16.0	18.4	127.0±9.8	22.6	11
(Na, K)NO_3	350	−8.6±3.0	132.3±10.2	8.5	119.4±5.8	9.2	This work

Equation 1 implies that x should be zero and its departure from this is clearly a measure of inconsistencies in the data. On the other hand, $(x + y)$ can be equated to the difference between the entropies of transport summations for pure alkali nitrate and pure silver nitrate, provided there is no parallel heterogeneous thermoelectric power (18). It is possible to write $x = 0$ with consequent changes in the errors and with the new y alone (y') then having the former significance of $(x + y)$. Table 1 carries the details of this formulation and the derived quantities $(x + y)$ and y' compare as follows

System	$x + y$	y'
$LiNO_3$	16.6	16.0
$NaNO_3$	126.4	125.4
KNO_3	269.4	266.5
$RbNO_3$	117.3	127.0
(Na, K)NO_3	123.7	119.4

The linearity in N of P may be fortuitous but could reflect the simplicity of interactions in the systems. It may be instructive to perform comparable measurements on a solvent system in which more than one metal ion/metal system is reversible.

This work was supported by the Defence Research Board of Canada under Contract No. 5412-07 and by the National Research Council of Canada through a Scholarship (to L.G.B.). We much appreciate discussions and clarification of the theoretical aspects of this study with A. R. Allnatt.

1. R. SCHNEEBAUM and B. R. SUNDHEIM. Discuss. Faraday Soc. **32**, 197 (1961).
2. R. H. DETIG and D. H. ARCHER. J. Chem. Phys. **32**, 661 (1963).
3. R. CONNAN, J. DUPUY, and J. BRENET. Compt. Rend. **C262**, 1120 (1966).
4. B. R. SUNDHEIM and J. ROSENSTREICH. J. Phys. Chem. **63**, 419 (1959).
5. J. DUPUY. Compt. Rend. **C262**, 8 (1966).
6. J. DUPUY, Y. NAKAMURA, S. BRILLANT, and J. BRENET. J. Chim. Phys. **63**, 886 (1966).
7. K. WALLIN and A. LUNDEN. Z. Naturforsch. **a22**, 591 (1967).
8. C. SINISTRI. Z. Naturforsch. **a21**, 753 (1966).
9. B. R. SUNDHEIM and J. D. KELLNER. J. Phys. Chem. **69**, 1204 (1965).
10. V. BACKLUND, J. DUPUY, S. GUSTAFSSON, and A. LUNDEN. Z. Naturforsch. **a22**, 471 (1967).

Can. J. Chem. Downloaded from www.nrcresearchpress.com by 210.87.254.6 on 09/05/12
For personal use only.

11. R. CONNAN. Electrochim. Acta, **15**, 821 (1970).
12. M. BAKES, S. BRILLANT, J. BRENET, J. DUPUY, J. GUION, Y. NAKAMURA, and J. RUCH. J. Chim. Phys. **63**, 1491 (1966).
13. C. SINISTRI and E. PEZZATI. Ric. Sci. **37**, 111 (1967).
14. J. A. A. KETELAAR and A. DAMMERS-DEKLERK. Proc. Kon. Ned. Akad. Wetensch. Ser. B. **68**, 169 (1965).
15. O. J. KLEPPA, R. B. CLARKE, and L. S. HERSCH. J. Chem. Phys. **35**, 175 (1961).
16. L. G. BOXALL and K. E. JOHNSON. Trans. Faraday Soc. In press.
17. M. BAKES, J. GUION, and J. P. BRENET. Electrochim. Acta, **10**, 1001 (1965).
18. A. R. ALLNATT and P. W. M. JACOBS. Proc. Roy. Soc. London, **A260**, 350 (1961).

Can. J. Chem. Downloaded from www.nrcresearchpress.com by 210.87.254.6 on 09/05/12
For personal use only.

Can. J. Chem. Downloaded from www.nrcresearchpress.com by 210.87.254.6 on 09/05/12
For personal use only.

Flash Photolysis with Kinetic Mass Spectrometry

O. P. STRAUSZ, S. C. BARTON, W. K. DUHOLKE, H. E. GUNNING, AND P. KEBARLE
Department of Chemistry, University of Alberta, Edmonton, Alberta

Received December 14, 1970

A flash photolysis apparatus coupled with a fast response conventional sector field mass spectrometer for the rapid time resolved detection of short-lived neutral transients is described. The utility of the apparatus is illustrated by the detection of the $Fe(CO)(NO)_3$ intermediate with a half-life of ~ 0.1 s in the flash photolysis of $Fe(CO)_5$ in the presence of NO.

On décrit un appareil susceptible de détecter les intermédiaires dans les expériences de photolyse éclair. Cet appareil résulte du couplage d'un système de photolyse éclair à un spectromètre de masse conventionnel. Le spectromètre, à analyseur magnétique, permet d'effectuer des balayages ultra rapides et possède un système de détection qui permet de mesurer le temps de vie de l'entité mesurée.

La détection de l'intermédiaire $Fe(CO)(NO)_3$, dont le temps de demi-vie est ~ 0.1 s, dans la photolyse de $Fe(CO)_5$ en présence de NO démontre les possibilités de l'appareil.

Canadian Journal of Chemistry, 49, 2048 (1971)

Introduction

Fast response kinetic mass spectrometry offers a useful technique complementary to kinetic absorption and emission spectroscopy for the detection and time-resolved kinetic study of short-lived intermediates of flash photochemical reactions. This application of kinetic mass spectrometry was first attempted but not pursued by Kistiakowsky and Kydd (1). More recently Meyer reported studies utilizing a flash photolysis – kinetic mass spectrometric apparatus (2).

The apparatus of Kistiakowsky and Meyer utilized a time-of-flight mass spectrometer with which mass scans could be obtained every 50 μs. Such rapid mass scanning allows in principle the time-resolved detection of reaction intermediates and reactants with half-lives which are considerably less than 1 ms. Unfortunately the very rapid scanning leads to an extremely large drop in detection sensitivity which in practice (*i.e.* with the detection devices used by the authors) limited the usefulness of the method.

The present apparatus was designed with more modest instrumental objectives. Time resolved ion detection was obtained by following the intensity of only one ion mass per photoflash. The much larger effective detection sensitivity obtained in this manner has to be paid for, by the fairly large number of repetitive flashes required to cover the pertinent ions.

The usefulness of the present instrument has been demonstrated through a number of preliminary reports dealing with the flash photolysis of COSe (3) in the presence of olefins, paraffins, and oxygen; COS (4) in the presence of olefins and acetylenes; cyclobutadiene–irontricarbonyl (5); and others (6).

The present article gives a detailed description of the apparatus and reports the detection of a novel transient nitrosyl iron carbonyl, $FeCO(NO)_3$.

Experimental

The apparatus, shown schematically in Fig. 1, consisted of a flash photolysis cell coupled to the specially constructed ion source of an Atlas CH4 spectrometer. Changes in the concentration of species of interest were monitored by photographically recording the oscilloscopic display of ion signal intensities at appropriate *m/e* values.

Photolysis Cell

The geometry of the coaxial flash lamp and photolysis cell and their attachment to the ion source of the mass spectrometer are shown in Fig. 2. The concentric walls of the photolysis cell were constructed from two standard glass-to-metal tubulations fitted with stainless steel O-ring seal flanges. Interchangeable quartz, Vycor or Pyrex inner walls were employed as required. The effective reaction zone was a volume of ~ 10 cc between the inner wall and the sampling orifice. The sampling orifice was a circular opening (~ 0.005 in. diameter) in a 0.002 in. thick disc of tantalum foil cemented over a small hole (~ 2 mm diameter) in the curved end of the outer wall. The vacuum side of the outer wall was silvered to provide a reflective and conductive surface.

Flash Lamp

The coaxial flash lamp was supported on the recess of the photolysis cell by a protective, coarse wire grid. The flash lamp circuitry consisted of a high voltage transformer, capacitors (one 10 μF and one 5 μF), and a triggering circuit. The capacitors were normally charged to 8000 V and the flash set off by triggering an ignitron (General Electric GL-7703) in series with the capacitor

Can. J. Chem. Downloaded from www.nrcresearchpress.com by 210.87.254.6 on 09/05/12
For personal use only.

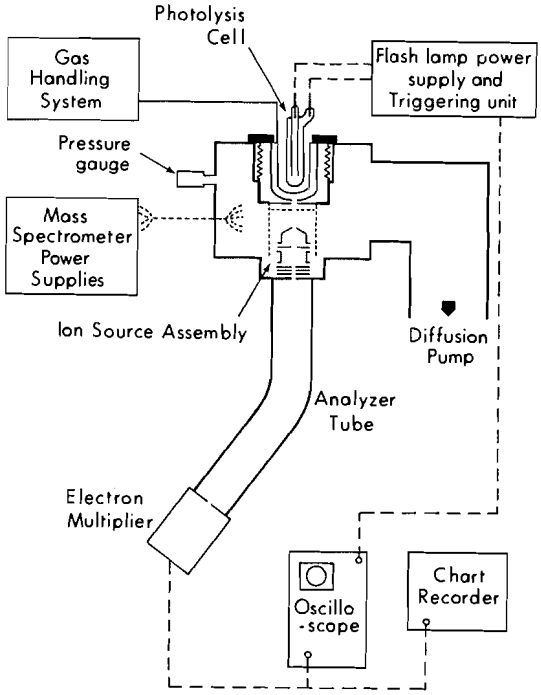

FIG. 1. Schematic illustration of apparatus.

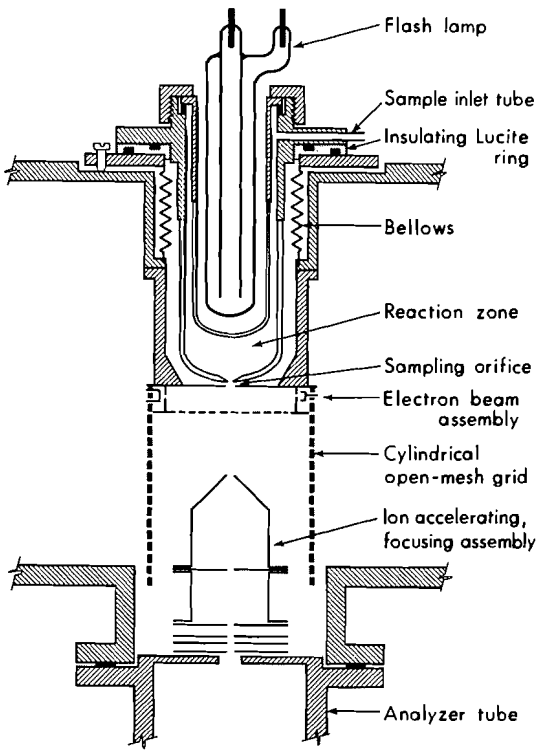

FIG. 2. Photolysis cell – ion source assembly.

and the lamp. The duration of the flash was approximately 60 μs.

Mass Spectrometer

The mass spectrometer was a conventional 60° sector magnetic deflection Atlas CH4 instrument, and only the specially constructed ion source need be described here. In order to provide a representative mass spectrum a sampling orifice should be sufficiently large to assure hydrodynamic flow, and ions should be formed predominantly from molecules just leaving the sampling orifice rather than from those which have suffered collisions with the wall or other molecules in the ion source. The ion source was designed with these criteria in mind.

As shown in Figs. 1 and 2, the photolysis cell – ion source assembly was enclosed in a large stainless steel chamber mounted on the analyzer tube of the mass spectrometer and evacuated by a 6 in. NRC oil diffusion pump fitted with a 6 in. NRC water-cooled baffle. The short 8 in. diameter pumping lead to the 10 in. diameter ion source vacuum chamber, combined with the above pumping units gives an estimated pumping speed of 500 l/s at the ion source. A flexible bellows attached to the flange supporting the photolysis cell permitted optimum adjustment of the sampling orifice relative to the ion source. The sampling orifice was located ~ 4 mm away from the ionizing electron beam directly above a 1 cm diameter mesh-covered hole in the repeller plate.

The ion source of the mass spectrometer operated at an accelerating voltage of 2 kV and the photolysis cell was also maintained at this voltage in order to prevent electrical discharges in the vicinity of the sampling orifice. The complete bottom of the ion source was made of an 80% transmission nickel grid. The tip of the first (conically shaped) electrode was placed 3 cm below the bottom of the ion source. This open ion source and electrode construction gives a large (gas) conductance (~ 500 l/s) out of the ion source.

A series of accelerating and focusing slits and deflection plates mounted on the analyzer tube completed the ion source assembly. The relative voltages of these electrodes were chosen to optimize sensitivity and mass resolution

Data Recording

Subsequent to magnetic separation of the ions, the ion current was amplified (~ 10^5) by an electron multiplier and then oscillographically displayed and recorded in one of two ways. Generally, a time-resolved ion intensity plot of a single *m/e* value was obtained by adjusting the mass spectrometer to the *m/e* value of interest prior to commencing the experiment. Alternatively a single scan of a preselected portion of the mass spectrum could be recorded within 200 ms after the flash occurred. In both modes of operation the oscilloscope was externally triggered by a signal from an induction coil on a lead of the flash lamp. The response time of the output circuitry was approximately 200 μs.

Gas Sampling

The open configuration of the ion source in conjunction with the large pumping system resulted in rapid removal of the sampled gas from the ionization region. This, and the proximity of the sampling orifice to the electron beam, resulted in ions being formed predominantly from molecules coming directly from the photolysis cell.

The approximate ratio of "beam molecules" to

Can. J. Chem. Downloaded from www.nrcresearchpress.com by 210.87.254.6 on 09/05/12
For personal use only.

"scattered molecules" being ionized was determined as follows. With $\sim 10^{-2}$ Torr of argon diluted with some 10–20 Torr helium in the photolytic cell, the $m/e = 40$ ion intensity (I_1) and the pressure measured by the ionization gauge were recorded. The pressure measured by the ionization gauge corresponds to the pressure in the large vacuum housing containing the ion source. Because of the completely open construction of the ion source this pressure is also essentially equal to the pressure due to diffusely scattered molecules in the ion source since the geometry is such that practically no beam molecules are scattered by the walls of the ion source. In a second experiment with the reaction cell evacuated the same gas mixture was admitted by means of a valve directly to the ion source vacuum housing. The observed $m/e = 40$ ion intensity (I_2) was again recorded for an ion gauge pressure equal to that of the previous experiment. Then,

$$\frac{P_b + P_{s,1}}{P_{s,2}} = \frac{I_1}{I_2}$$

where P_b and P_s refer to partial pressures of beam and scattered background molecules, respectively, and I_1 and I_2 refer to $m/e = 40$ ion intensities. P_b/P_s was determined to be ~ 60, indicating that over 90% of the ions were formed from molecules coming directly from the photolytic cell.

With 20 Torr of helium in the photolysis cell the pressure measured on the ionization gauge was about 10^{-5} Torr. Between experiments the apparatus was evacuated to about 10^{-7} Torr.

Experimental Procedure

All reaction mixtures were prepared in the stainless steel gas handling system of the mass spectrometer. The reaction mixtures normally consisted of about 10 μ of $Fe(CO)_5$ (or other reactants) and 2.5 Torr of NO diluted to a total pressure of 20 Torr with helium to assure approximately isothermal conditions during the reaction. (Additional reactive substances were added in varying amounts in some experiments.) The purity of the reactants and the occurrence of any dark reaction prior to photolysis was checked mass spectrometrically.

After thorough mixing, the reaction mixture was allowed to flow through the photolysis cell, final adjustment of the instrument made, and the flash experiment performed. The validity of all experimental observations were confirmed by repeating the experiments with appropriate "blank" mixtures.

Results and Discussion

The observations included both time-resolved ion intensity plots of single m/e values and single scans of preselected portions of the mass spectrum of the gas mixture. The relatively simple spectra were readily interpreted without ambiguity in the assignment of mass peaks. Peak heights were assumed proportional to gas concentrations and because of the qualitative nature of the study a knowledge of absolute concentrations was not required.

Figures 3 to 5 are single scan records of the mass spectrum in the region of the $(Fe(CO)_4)^+$ fragment ion peak of $Fe(CO)_5$. Comparison of the intensity of m/e 166 $(Fe^{54}(CO)_4)^+$ before and after the flash (Figs. 3 and 4) indicates $\sim 75\%$ decomposition of the $Fe(CO)_5$ during flash photolysis of the gas mixtures. Upon photolysis of the $Fe(CO)_5$/NO mixture, new mass peaks appeared at m/e 172 and 174 (Figs. 3 and 4) but no new peaks resulted from photolyzing $Fe(CO)_5$ in the absence of NO (Fig. 5). Similar observations were made in the region of the parent peak (m/e 196), but no new peaks were detected here or at higher masses and so the mass peaks at m/e 172 and 174 were interpreted as parent peaks.

The mass peaks at m/e 172 and 174 can be

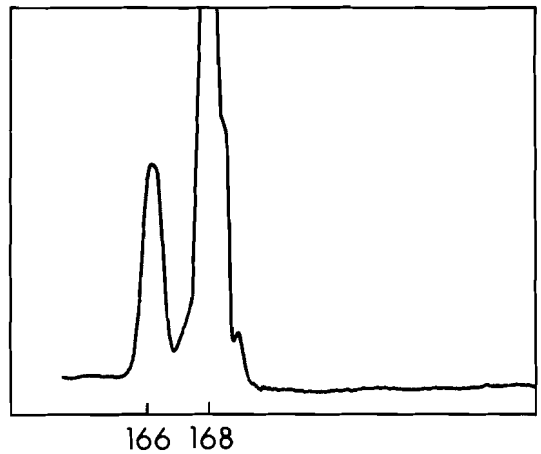

FIG. 3. Single scan, showing m/e 168 $(Fe(CO)_4)^+$ as largest peak, before flash; 500 mV full scale deflection, 100 ms full scale deflection, $Fe(CO)_5$/NO/He mix.

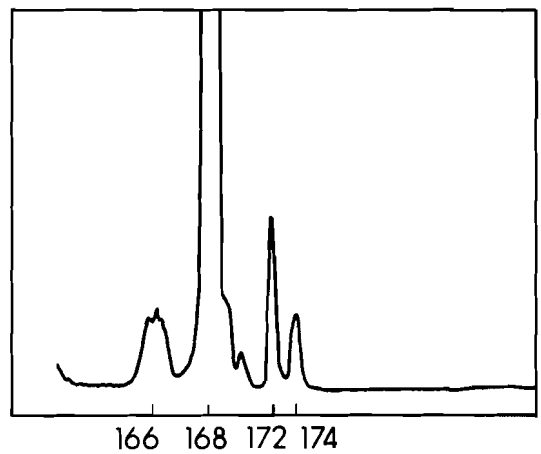

FIG. 4. As in Fig. 3, but immediately after flash. Note new peaks at 172 and 174; 500 mV, 100 ms, $Fe(CO)_5$/NO/He mix.

Can. J. Chem. Downloaded from www.nrcresearchpress.com by 210.87.254.6 on 09/05/12
For personal use only.

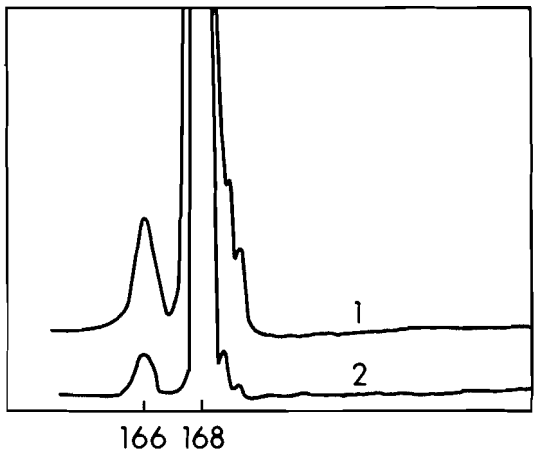

FIG. 5. As in Figs. 3 and 4 but without NO. Trace *1*, before flash; trace *2*, after flash; 500 mV, 100 ms.

unambiguously attributed to $Fe(CO)_2(NO)_2$ and $Fe(CO)(NO)_3$, respectively, and no other products were detected. $Fe(CO)_2(NO)_2$ is a known stable compound (7). The unstable $Fe(CO)(NO)_3$, however, is a novel structure whose composition seems to violate the noble gas rule for predicting the formulae of stable known coordination complexes (7). In these complexes nitric oxide forms a three-electron bond to the metal atom. Since CO is regarded as a two-electron donor, two NO are equivalent with three CO molecules as in $Fe(CO)_2(NO)_2$.

The stability of the two products was investigated by recording time-resolved ion intensities for $m/e = 172$ and 174. As seen from Fig. 6, $Fe(CO)_2(NO)_2$ shows no decay being a stable molecule whereas $Fe(CO)(NO)_3$, as shown in Fig. 7, decays with a half-life of ~75 ms.

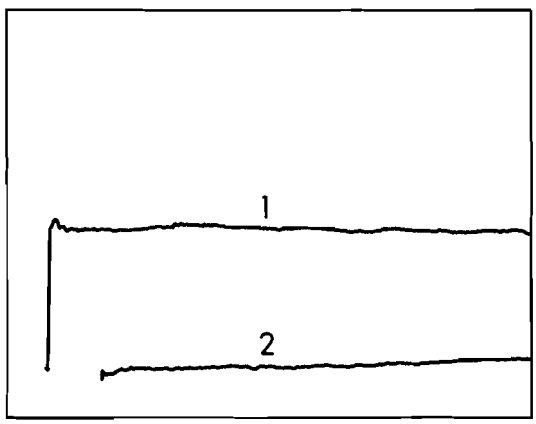

FIG. 6. *I m/e* 172 $(Fe(CO)_2(NO)_2)^+$ *vs.* time; 500 mV, 500 ms. Trace *1*, $Fe(CO)_5$/NO/He; Trace *2*, $Fe(CO)_5$/He.

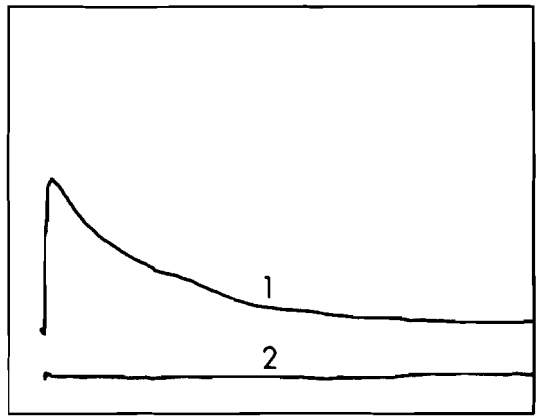

FIG. 7. *I m/e* 174 $(Fe(CO)(NO)_3)^+$ *vs.* time; 200 mV, 500 ms. Trace *1*, $Fe(CO)_5$/NO/He; trace *2*, $Fe(CO)_5$/He.

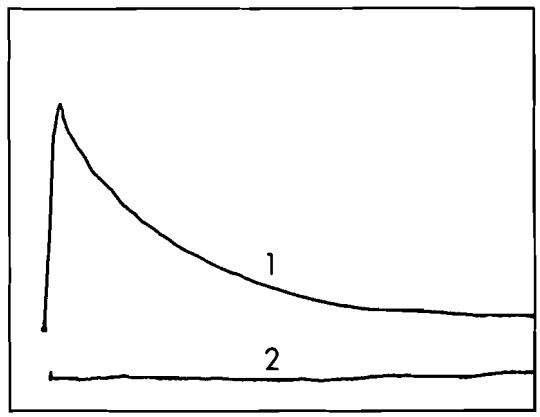

FIG. 8. *I m/e* 146 $(Fe(NO)_3)^+$ *vs.* time; 1 V, 500 ms. Trace *1*, $Fe(CO)_5$/NO/He; trace *2*, $Fe(CO)_5$/He.

Decay patterns of some of the fragment ions were also investigated. The decay curve for $m/e = 146$, $(Fe(NO)_3)^+$, shown in Fig. 8 gives a half-life of ~75 ms, in agreement with the decay of the parent molecule $Fe(CO)(NO)_3$. The temporal variation of another fragment ion $(Fe(CO)(NO)_2)^+$ at $m/e = 144$ depicted in Fig. 9 shows an initial decay after which it tends to level off at a fairly high residual value, indicating that it is a fragment common to both the $Fe(CO)(NO)_3$ and $Fe(CO)_2(NO)_2$ molecules.

The effect of varying the concentration of nitric oxide on the relative yield of the two product molecules was examined in one experiment; Fig. 10, in which the nitric oxide concentration was decreased by a factor of ten. This caused a decrease in the parent ion intensity ratio, $I(Fe(CO)(NO)_3)/I(Fe(CO)_2(NO)_2)$, by about a

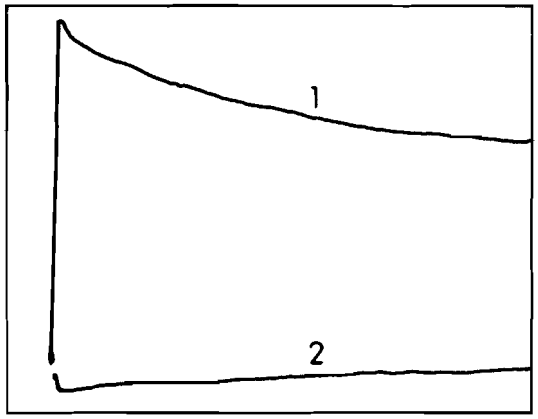

FIG. 9. *I m/e* 144 $(Fe(CO)(NO)_2)^+$ *vs.* time; 500 mV, 500 ms. Trace *1*, $Fe(CO)_5/NO/He$; trace *2*, $Fe(CO)_5/He$.

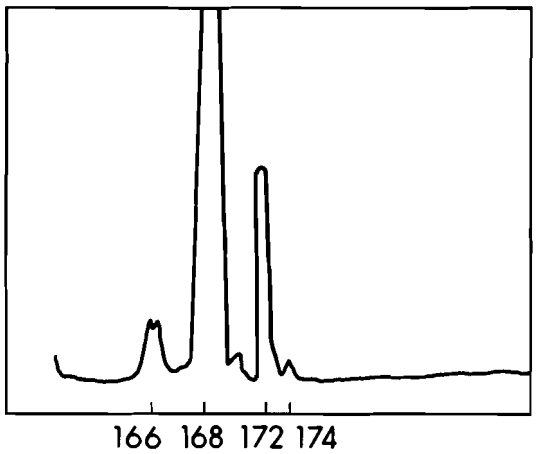

FIG. 10. As in Fig. 4 but NO concentration decreased by 10. Note change in 172/174 ratio.

factor of four. The trend is certainly in the right direction since the rate of the corresponding product molecules formation should be a linear function of nitric oxide concentration. The deviation from linearity, and the nearly equal yields of the $Fe(CO)_2(NO)_2$ complex at 0.25 and 2.5 Torr NO pressures suggest that the rate constant for the formation of this product is considerably higher than that for $Fe(CO)(NO)_3$ formation and that even at the lower nitric oxide pressure the scavenging of the $Fe(CO)_2$ intermediate is complete.

Finally, the possibility that the $Fe(CO)(NO)_3$ complex forms not as a neutral molecule, but as an ion, via ion–molecule reactions in the ion source was also explored. Experiments in which NO was admitted directly to the ion source have conclusively shown that $Fe(CO)(NO)_3$ does not form in the ion source and consequently it must form in the photolysis cell as a neutral entity.

The mode of decay of the unstable $Fe(CO)(NO)_3$ complex could not be established in the present study. A search for products such as CO_2, NO_2, or a dimeric form of the complex indicated that these molecules were not present and consequently it is assumed that decomposition occurs via dissociation to form Fe, CO, and NO.

Reports on the detection of additional novel inorganic molecules using the technique of flash photolysis – kinetic mass spectrometry will be forthcoming at a later date.

The authors thank the National Defence Board and the National Research Council of Canada for financial support and Mr. R. Kadlecz for helpful assistance.

1. G. B. KISTIAKOWSKY and P. H. KYDD. J. Am. Chem. Soc. **79**, 4825 (1957).
2. R. T. MEYER. J. Chem. Phys. **46**, 967 (1967); J. Phys. Chem. **72**, 1583 (1968).
3. W. J. R. TYERMAN, W. B. O'CALLAGHAN, P. KEBARLE, O. P. STRAUSZ, and H. E. GUNNING. J. Am. Chem. Soc. **88**, 4277 (1966).
4. O. P. STRAUSZ, J. FONT, E. L. DEDIO, P. KEBARLE, and H. E. GUNNING. J. Am. Chem. Soc. **89**, 4805 (1967).
5. W. J. R. TYERMAN, M. KATO, P. KEBARLE, S. MASAMUNE, O. P. STRAUSZ, and H. E. GUNNING. Chem. Commun. 497 (1967); J. FONT, S. C. BARTON, and O. P. STRAUSZ. Chem. Commun. 499 (1970).
6. J. CONNOR, G. GREIG, and O. P. STRAUSZ. J. Am. Chem. Soc. **91**, 5695 (1969).
7. F. A. COTTON and G. WILKINSON. Advanced inorganic chemistry. 2nd Ed. John Wiley & Sons, New York. 1967. p. 747.

Can. J. Chem. Downloaded from www.nrcresearchpress.com by 210.87.254.6 on 09/05/12
For personal use only.

Can. J. Chem. Downloaded from www.nrcresearchpress.com by 210.87.254.42 on 09/05/12
For personal use only.

The Excited Singlet State of Chloropentafluoroacetone; Quenching by Unsaturated Hydrocarbons

H. S. SAMANT AND A. J. YARWOOD
Department of Chemistry, McMaster University, Hamilton, Ontario

Received January 8, 1971

The fluorescence of chloropentafluoroacetone in the gas phase at 23 °C is quenched by the addition of certain olefins. The quenching rate constants of 17 unsaturated hydrocarbons for the first excited singlet state of chloropentafluoroacetone are reported. The molecules are divided into two classes on the basis of their quenching abilities, (*a*) olefins with only electron-withdrawing substituents and (*b*) olefins with electron-donating substituents. It is shown that the quenching by molecules in the latter group can be quantitatively correlated with the ionization potential (i.p.) of the quenching molecule. The relation is $\log k = 18.0 - 0.79$ (i.p.), *i.e.* a type of linear free energy relation is obeyed. This implies that the quenching by molecules containing only electron-donating substituents involves a charge-transfer complex.

La fluorescence de la chloropentafluoroacetone en phase gazeuse à 23 °C est inhibée par l'addition de certains hydrocarbures insaturés. On rapporte les constantes de désactivation de 17 hydrocarbures insaturés pour le premier singulet excité de la chloropentafluoroacétone. Les molécules sont classifiées en deux catégories selon leur efficacité de désactivation: (*a*) celles qui possèdent seulement des substituants attracteurs d'électrons et (*b*) celles avec des substituants donneurs d'électrons. On montre que la désactivation par les molécules du groupe *b* peut être reliée quantitativement au potentiel d'ionisation de la molécule désactivante, *i.e.* $\log k = 18.0 - 0.79$ (p.i.). Ceci semble indiquer que la désactivation par les molécules qui contiennent uniquement des substituants donneurs d'électrons se ferait par l'intermédiaire d'un complexe ou il y aurait transfert de charge.

Canadian Journal of Chemistry, 49, 2053 (1971)

Electronically excited molecules can be deactivated in bimolecular collisions with added quenching molecules, and the quenching effect on the singlet and triplet states of aromatic compounds has been extensively studied (1–4). Carbonyl compounds, particularly ketones and diketones, have also been investigated, and the quenching of the triplet states of alkyl ketones is an active research area at present (5–7). The quenching of the triplet states of ketones by olefins has been interpreted in various ways (5, 6) and can involve either energy transfer or deactivation (with or without the formation of a stable product).

The excited singlet states of ketones can also transfer energy to quenching molecules, *e.g.*, alkyl ketones can sensitize diketone fluorescence (8, 9). They can also be deactivated by olefins, and again the formation of a stable product depends on the nature of the quenching molecule (10–13).

We have recently reported (14, 15) luminescence studies of chloropentafluoroacetone and determined the rate constants for the processes removing the excited singlet state in the gas phase at room temperature. In this paper we report on the quenching effect of a series of unsaturated hydrocarbons on the excited singlet state of chloropentafluoroacetone in the gas phase and discuss the mechanism of the quenching.

Experimental

Material

Chloropentafluoroacetone (Allied Chemical) was purified by low temperature distillation and stored in the dark at 77 °K. The following olefins (C.P. grade) were supplied by Matheson Co. and were used after distillation at appropriate low temperatures: ethylene, propylene, but-1-ene, 2-methylpropene, and *cis*-but-2-ene. The Matheson Co. also supplied the 1,1-difluoroethylene, perfluorobut-2-ene, and the chloroethylene, which were also distilled at low temperature. Tetrachloroethylene (Eastman Organic Chemicals) was used after distillation at low temperature that removed inhibitor. The cyclohexene (Eastman Organic Chemicals) and hex-1-ene (Aldrich Co.) were passed through an alumina column and distilled under nitrogen. 2,3-Dimethylbut-2-ene (Chemical Samples Co.), trichloroethylene (Allied Chemical), and 1,3-cyclohexadiene (Aldrich) were distilled at low temperature. 1,3-Pentadiene (Matheson, Coleman and Bell) and benzene (Baker spectrophotometric grade) were deaerated.

Fluorescence Apparatus

The excitation source was a medium pressure mercury lamp (Hanovia #673A) used with a third order 313 nm interference filter (Baird Atomic). Fluctuations in the light intensity were monitored by reflecting a portion of the incident light from a Vycor plate onto a photocell

Can. J. Chem. Downloaded from www.nrcresearchpress.com by 210.87.254.42 on 09/05/12
For personal use only.

(RCA 935). The quartz cell was 1 cm long and was connected to a grease-free vacuum system that was saturated with mercury, since the pressures were measured on mercury manometers. The light passed through the cell and was condensed by a quartz lens onto a photocell (RCA 935). The emitted light passed through a glass filter (Corning 0-52) and was condensed by a quartz lens onto a photomultiplier (RCA 1P28) which operated at 800 V. The output of the photomultiplier was monitored by an electrometer (Keithley 610B). The relative fluorescence yield Q is defined as $(I_f - I_f^\circ)/(I_t^\circ - I_t)$ where I_t and I_f are the transmitted and emitted light intensities; the superscript indicates that the ketone was absent.

In the early studies the ketone and olefin diffused to reach equilibrium, while in some later experiments they were mixed using a magnetically driven double action glass pump.

Results

The chloropentafluoroacetone pressure in each quenching experiment was 200 ± 5 Torr and the temperature was 23 °C. The quenching ability of each olefin was investigated by adding increasing quantities of the olefin and noting the decrease in the fluorescence of the ketone. Figures 1–5 show plots of Q_0/Q *vs.* concentration of quenching olefin for the molecules studied, except perfluorobut-2-ene and cyanoethylene, which were very inefficient quenchers. None of the quenching molecules is expected to absorb 313 nm so no correction to the absorbed light intensity is necessary.

The lines shown on the figures are the best lines through the data points that include the data for the pure ketone.

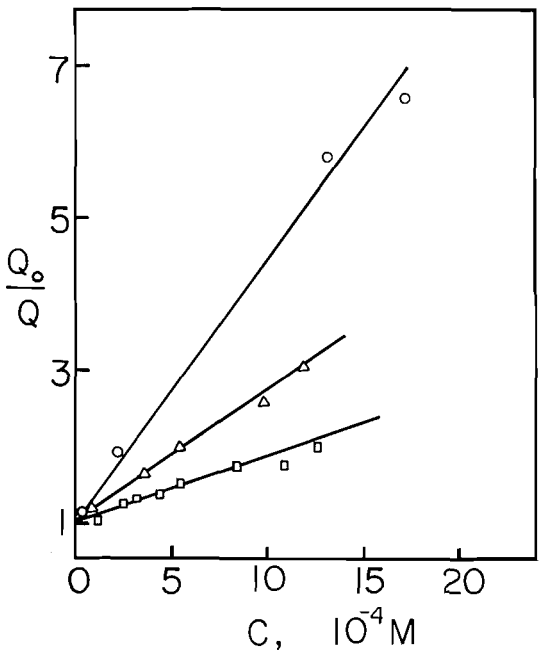

FIG. 1. Quenching of fluorescence of chloropentafluoroacetone; Q_0/Q *vs.* concentration of quencher. ○, 1,3-pentadiene; △, 2-methylpropene; □, propylene.

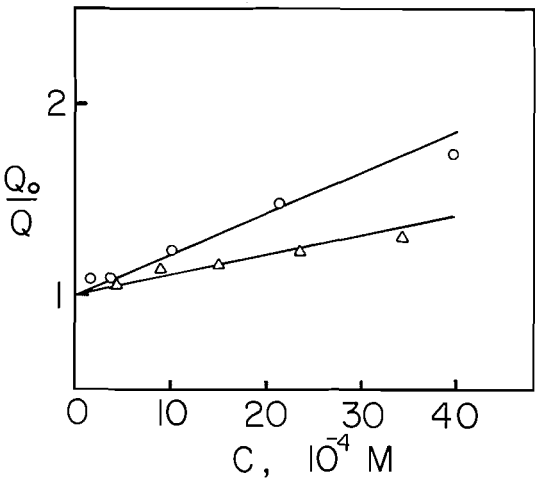

FIG. 2. Quenching of fluorescence of chloropentafluoroacetone; Q_0/Q *vs.* concentration of quencher. ○, chloroethylene; △, ethylene.

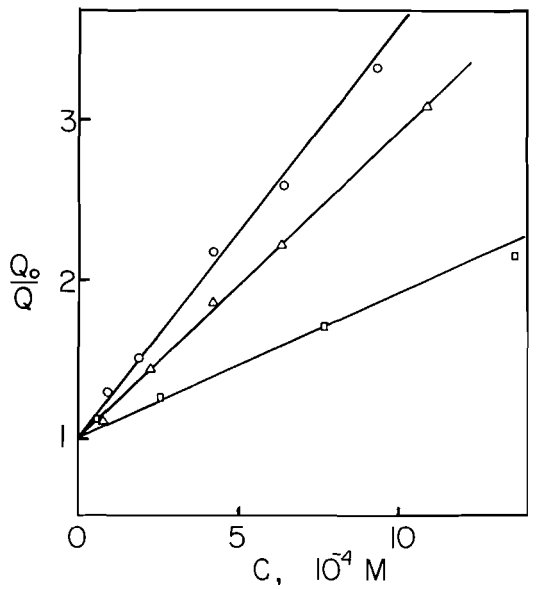

FIG. 3. Quenching of fluorescence of chloropentafluoroacetone; Q_0/Q *vs.* concentration of quencher. ○, cyclohexene; △, *cis*-but-2-ene; □, but-1-ene.

Can. J. Chem. Downloaded from www.nrcresearchpress.com by 210.87.254.42 on 09/05/12
For personal use only.

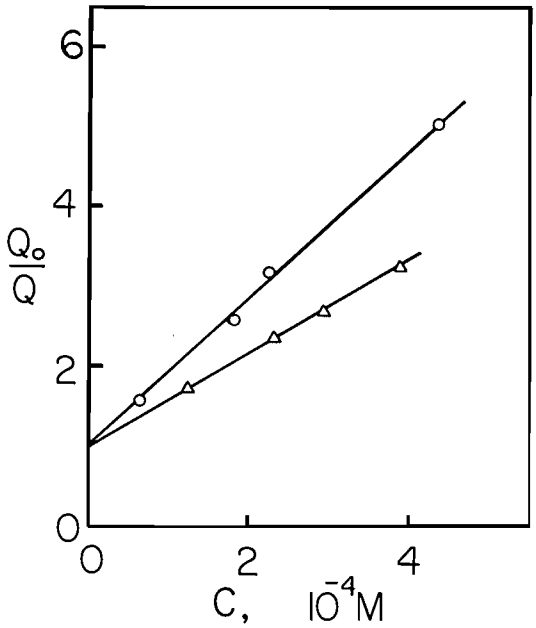

FIG. 4. Quenching of fluorescence of chloropentafluoroacetone; Q_0/Q *vs.* concentration of quencher. ○, 1,3-cyclohexadiene; △, 2,3-dimethylbut-2-ene.

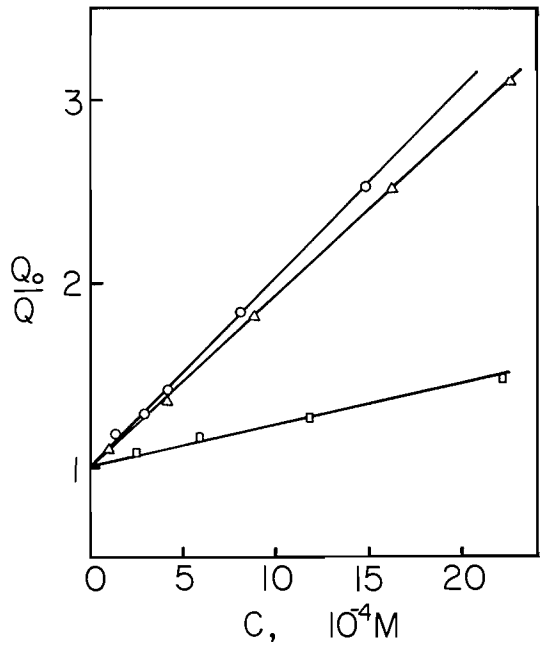

FIG. 5. Quenching of fluorescence of chloropentafluoroacetone: Q_0/Q *vs.* concentration of quencher. ○, hex-1-ene; △, benzene; □, 1,1-difluoroethylene.

Discussion

Chloropentafluoroacetone fluoresces but does not phosphoresce in the gas phase at room temperature (14) when excited in the π^*–n band. Thus, when chloropentafluoroacetone is excited at 313 nm and the total luminescence passed through a Corning 0-52 glass filter is monitored, this corresponds to direct measurement of the fluorescence. The mechanism proposed (14) to explain the fluorescence behavior of chloropentafluoroacetone is

[1]	$A + h\nu \rightarrow {}^1A_n$	I_a
[2]	${}^1A_n + A \rightarrow {}^1A_0 + A$	k_2
[3]	${}^1A_n \rightarrow$ Removal	k_3
[4]	${}^1A_0 \rightarrow A + h\nu_f$	k_4
[5]	${}^1A_0 \rightarrow$ Removal	k_5

It was shown that under appropriate conditions enhancement of the fluorescence could occur when high pressures of an added gas were present. However, in this study the ketone pressure was maintained at 200 Torr and this pressure corresponds to essentially complete deactivation of any vibrationally excited singlet states before emission occurs. So the quenching of electronically excited singlet state chloropentafluoroacetone molecules in low vibrational levels is discussed in this paper.

If the process

$$ {}^1A_0 + Q \rightarrow \text{Removal} \qquad k_6 $$

is added to the mechanism then a steady state treatment of the kinetics yields

$$ Q_0/Q = 1 + k_6\tau[G] $$

where τ is the actual lifetime of the excited singlet state in the absence of the olefin quencher, G, and is the reciprocal of the sum of the unimolecular processes removing the singlet ($k_4 + k_5$). Since τ has been determined experimentally to be 3.5×10^{-8} s (14), the quenching rate constant k_6 for each olefin can be determined from the slopes of the lines of Figs. 1–5.

Table 1 lists the quenching rate constants for the olefin quenchers and also shows the adiabatic ionization potentials of the quenching molecules. The rate constants reported are probably precise to about 5%. The errors are larger for those molecules which are inefficient quenchers or relatively involatile (so that only a restricted pressure range could be studied).

TABLE 1. Rate constants and ionization potential of quencher for ketone fluorescence

Quencher	k_6 (M^{-1} s^{-1})	Ionization potential (eV)
1,3-Pentadiene	9.7×10^{10}	8.68*
Ethylene	2.9×10^{9}	10.51†
Propylene	2.3×10^{10}	9.70‡
But-1-ene	2.4×10^{10}	9.65‡
Hex-1-ene	2.9×10^{10}	9.46*
2-Methylpropene	4.8×10^{10}	8.95‡
cis-But-2-ene	5.6×10^{10}	9.24‡
2,3-Dimethylbut-2-ene	1.7×10^{11}	8.30*
1,1-Difluoroethylene	6.0×10^{9}	10.31†
Perfluorobut 2-ene	$< 10^{7}$	
Chloroethylene	6.3×10^{9}	10.00†
Trichloroethylene	5.9×10^{9}	9.48†
Tetrachloroethylene	$\sim 2\times10^{9}$	9.34†
Cyclohexene	7.1×10^{10}	9.20§
1,3-Cyclohexadiene	2.7×10^{11}	8.40*
Benzene	2.7×10^{10}	9.24‡

*Reference 20.
†Reference 21.
‡Reference 22.
§Reference 23.

Consider now the relative values of the quenching rate constants. In their study of the quenching of the fluorescence of hexafluoroacetone in the gas phase Ware and Lee (10) found that 1,3-pentadiene had the largest quenching rate constant with a value of 8.0×10^{10} M^{-1} s^{-1}. In comparison a rate constant of 9.7×10^{10} M^{-1} s^{-1} is observed for the quenching by 1,3-pentadiene of chloropentafluoroacetone fluorescence. The quenching behavior of the diolefin is similar in hexafluoro and chloropentafluoroacetone photolysis.

The straight chain mono-olefins that are unsaturated in the 1 position are an interesting series of molecules. The first comment concerns the much smaller value of k_6 for ethylene (2.9×10^9) as compared to that of the diolefin (9.7×10^{10}). There is a sharp increase in k_6 for propylene (2.3×10^{10}) as compared to ethylene and this is presumably due to the inductive effect of the methyl group on the double bond. However, further increase in the side chain only increases k_6 for but-1-ene to 2.4×10^{10} and for hex-1-ene to 2.9×10^{10}. This further emphasizes that a methyl group as a substituent on the double bond is almost as effective as an ethyl, or butyl group. Again the quenching of chloropentafluoroacetone fluorescence is similar to that of hexafluoroacetone fluorescence, since Ware and Lee found that the quenching constants for ethylene (4.1×10^9) and propylene (1.6×10^{10}) also differed significantly.

The effect of successive substitution of a hydrogen atom in ethylene by a methyl group can also be clearly seen in the sequence ethylene, propylene, 2-methylpropene, and 2,3-dimethyl-but-2-ene. The k_6 value for 2-methyl propene (4.8×10^{10}) is about twice that for propylene (2.3×10^{10}), while the value for 2,3-dimethyl-but-2-ene (1.7×10^{11}) is about 3.5 times larger than that of 2-methylpropene, so the effect of methyl substitution is not just additive.

The value of k_6 for 2-methylpropene (4.8×10^{10}) differs from that for *cis*-but-2-ene (5.6×10^{10}) by little more than the combined experimental error; again compatible with the quenching data for hexafluoroacetone, where 2-methylpropene and *cis*-but-2-ene were both found to be 3.5×10^{10} M^{-1} s^{-1}. However, the quenching of chloropentafluoroacetone fluorescence by but-1-ene (2.4×10^{10}) is much smaller and shows that not all butenes are equally efficient in deactivating the excited singlet state of the ketone.

The following mechanisms might explain the quenching effect of the olefins on the excited singlet state of chloropentafluoroacetone. They are similar to those suggested by Gandini and Kutschke (7) to explain the quenching effect of hydrocarbons on the triplet state of hexafluoroacetone.

(*1*) The ketone molecule transfers energy to the olefin to promote it to its first excited singlet state. However, the singlet state energy of chloropentafluoroacetone is about 83 kcal (14) and the first excited π^*,π singlet states of the olefins are at much higher energies (16). The probability of energy transfer with a very large endothermicity is negligible.

(*2*) The deactivation of the ketone is due to intersystem crossing to the triplet state of the ketone that is collisionally induced by the olefin. This, too, is unlikely as not all olefins, see below, are efficient quenchers of the ketone singlet state.

(*3*) The ketone molecule interacts with the olefin and a stable product may or may not be formed. This is the most likely explanation of the quenching behavior of the olefins and it is also compatible with the effect of methyl substitution on the quenching rate constant that was noted above. However, the most notable correlation is between the quenching constant of an olefin and its ionization potential. As the ionization potential of the quencher molecule decreases, its quenching rate constant in general is found to increase. A qualitative correlation of this type was also noted by Ware and Lee (10) in their

Can. J. Chem. Downloaded from www.nrcresearchpress.com by 210.87.254.42 on 09/05/12
For personal use only.

Can. J. Chem. Downloaded from www.nrcresearchpress.com by 210.87.254.42 on 09/05/12
For personal use only.

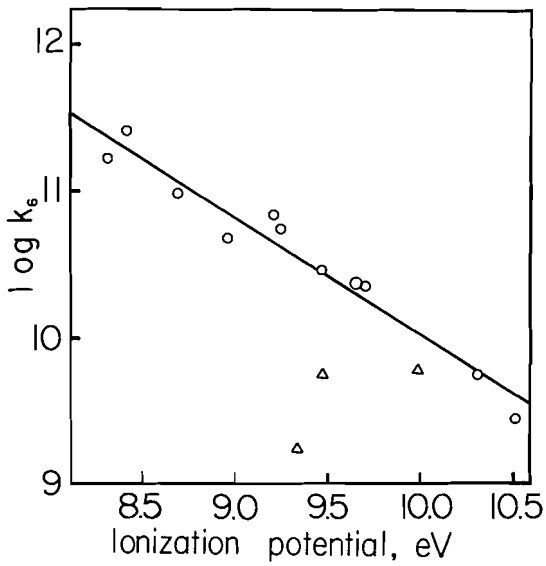

FIG. 6. Plot of logarithm of the quenching rate constant *vs.* ionization potential of quenching molecule. △, chlorinated ethylenes; ○, all other olefins.

study of the effect of olefin quenching on the first excited singlet of hexafluoroacetone. However, in the present study a larger number of quenching olefins has been studied and this allows a quantitative comparison between quenching rate constant and the ionization potential of the olefin. Figure 6 shows a plot of the logarithm of the quenching rate constant *vs.* the ionization potential of the olefin. It includes not only the data on the unsubstituted mono-olefins discussed above, but also the data on substituted olefins that are to be discussed below. If one restricts attention for the moment to the eight unsubstituted mono-olefins discussed above, then it is found that there is a linear relation between (log k_6) and the ionization potential (i.p.) of the olefin of the form $\log k_6 = 17.6 - 0.76$ (i.p.). The correlation factor for the line is 0.974 and the sigma values of the intercept and slope are 0.7 and 0.07, respectively.

In an attempt to confirm or reject the hypothesis the series of substituted olefins was investigated. The quenching rate constant for 1,1-difluoroethylene is compatible with the hypothesis. However, it was found that perfluorobut-2-ene is a very inefficient quencher. The ionization potential of perfluorobut-2-ene is not available but this molecule could well be an exception to the above hypothesis. The next series of molecules to be considered are the chlorinated olefins and the data for these molecules are shown by the triangles on Fig. 6. The data for both tetrachloroethylene and trichloroethylene are not in agreement with the above hypothesis. It was found that cyanoethylene was also an inefficient quencher. The exceptions to the hypothesis are molecules that have strong electron-withdrawing groups attached directly to the double bond and clearly the correlation between $\log k_6$ and the ionization potential is not valid for these molecules. This includes the behavior of perfluorobut-2-ene where the trifluoromethyl groups have a strong effect, but not 1,1-difluoroethylene which seems to obey the hypothesis. This could be due to the "back-bonding" effect by the fluorine lone pair electrons that allows the fluorine atom to act as a weak π electron donor (17) when it is substituted directly on the double bond.

Other unsubstituted unsaturated molecules were investigated to further test the hypothesis. The molecules chosen were cyclohexene, 1,3-cyclohexadiene, and benzene to check the effect of increasing the unsaturation. It can be seen from Table 1 that the quenching increases from cyclohexene (7.1×10^{10}) to cyclohexadiene (2.7×10^{11}) and decreases to 2.7×10^{10} M^{-1} s^{-1} for benzene. This behavior is in excellent accord with the ionization potentials of the quenching molecules. It confirms that there is a linear relation between the logarithm of the quenching rate constant and the ionization potential of the quenching molecule for unsubstituted olefins that do not contain electron-withdrawing groups. If one excludes the data for perfluorobut-2-ene, cyanoethylene, and chlorinated ethylenes then $\log k_6 = 18.0 - 0.79$ (i.p.) with sigma values of the intercept and slope of 0.6 and 0.06, respectively (the correlation factor is 0.97).

A similar correlation has been observed by Swarc and co-workers (18, 19) in the addition of the strongly electrophilic trifluoromethyl radical to mono-olefins and substituted benzenes. They also proposed that a charge-transfer interaction was involved in the process.

The electronically excited singlet state of the ketone interacts with the unsubstituted mono-olefins, cyclohexene, 1,3-cyclohexadiene, and benzene via a charge transfer mechanism. The correlation implies that there are only small changes in the pre-exponential factors for the different quenching molecules that obey the correlation. It also implies that the activation energy of the quenching reaction is linearly related to the

ionization potential of the quenching molecule. Note that 1,3-cyclohexadiene quenches the singlet state at practically every collision.

Ware and Lee (10) showed that there was a qualitative correlation between the rate constant for quenching hexafluoroacetone fluorescence and the ionization potential of the quenching molecule. However, they noted that the quenching rate constant decreased with increasing temperature. They introduced a mechanism that involved a collision complex that could either cause quenching or revert to an electronically excited ketone molecule and the ground state quencher molecule. The present data suggests that the collision complex in the quenching of chloropentafluoroacetone is removed mostly by the process that involves quenching.

It has been suggested (10) that similar mechanisms operate in the olefin quenching of the singlet and triplet states of hexafluoroacetone. So a correlation might exist between the ionization potential and the quenching rate constant of a quencher for the triplet states of hexafluoroacetone and chloropentafluoroacetone. The available data (7) on the quenching of the triplet of hexafluoroacetone are not inconsistent with such a correlation.

We thank Dr. K. O. Kutschke for communicating his results and the National Research Council of Canada for financial support.

1. F. WILKINSON. Adv. Photochem. **3**, 241 (1964).
2. P. J. WAGNER and G. S. HAMMOND. Adv. Photochem. **5**, 21 (1968).
3. E. K. C. LEE, M. W. SCHMIDT, R. G. SHORTRIDGE, JR., and G. A. HANINGER, JR. J. Phys. Chem. **73**, 1805 (1969).
4. G. A. HANINGER, JR. and E. K. C. LEE. J. Phys. Chem. **73**, 1815 (1969).
5. J. S. DALTON and N. J. TURRO. Ann. Rev. Phys. Chem. 499 (1970).
6. I. H. KOCHEVAR and P. J. WAGNER. J. Am. Chem. Soc. **92**, 5742 (1970).
7. A GANDINI and K. O. KUTSCHKE. Can. J. Chem. **44**, 1720 (1966).
8. J. T. DUBOIS and M. COX. J. Chem. Phys. **38**, 2536 (1963).
9. J. S. E. MCINTOSH and G. B. PORTER. J. Chem. Phys. **48**, 5475 (1968).
10. W. R. WARE and S. K. LEE. J. Chem. Phys. **49**, 217 (1968).
11. N. J. TURRO and R. ENGEL. J. Am. Chem. Soc. **91**, 7113 (1969).
12. N. J. TURRO and P. A. WRIEDE. J. Am. Chem. Soc. **92**, 320 (1970).
13. J. C. DALTON, P. A. WRIEDE, and N. J. TURRO. J. Am. Chem. Soc. **92**, 1318 (1970).
14. H. S. SAMANT and A. J. YARWOOD. Can. J. Chem. **48**, 2611 (1970).
15. H. S. SAMANT and A. J. YARWOOD. Can. J. Chem. **48**, 2937 (1970).
16. M. ITOH and R. S. MULLIKEN. J. Phys. Chem. **73**, 4332 (1909).
17. J. A. POPLE and D. L. BEVERIDGE. Approximate molecular orbital theory. McGraw-Hill, New York. 1970. p. 121.
18. A. P. STEFANI, L. HERK, and M. SWARC. J. Am. Chem. Soc. **83**, 4732 (1961).
19. I. M. WHITTEMORE, A. P. STEFANI, and M. SWARC. J. Am. Chem. Soc. **84**, 3799 (1962).
20. D. W. TURNER. Adv. Phys. Org. Chem. **4**, 31 (1966).
21. R. F. LAKE and H. THOMPSON. Proc. Roy. Soc. Ser. A. **315**, 323 (1970).
22. W. C. PRICE. Chem. Rev. **41**, 257 (1947).
23. K. WATANABE. J. Chem. Phys. **26**, 542 (1957).

Can. J. Chem. Downloaded from www.nrcresearchpress.com by 210.87.254.42 on 09/05/12
For personal use only.

Can. J. Chem. Downloaded from www.nrcresearchpress.com by 210.87.254.40 on 09/05/12
For personal use only.

Electron Spin Resonance Spectra of Azine – Alkali Metal Triple Ions in Ethereal Solvents

S. A. AL-BALDAWI AND T. E. GOUGH[1]

Department of Chemistry, University of Waterloo, Waterloo, Ontario

Received February 5, 1971

Electron spin resonance spectroscopy has been used to study triple ions formed between pyrazine and tetramethylpyrazine and the cations Li^+, Na^+, K^+ in dimethoxyethane, tetrahydrofuran, and 2-methyltetrahydrofuran. Differential line-broadening effects are reported within the hyperfine splitting patterns of the alkali metals incorporated into the triple ions, and a possible application of such effects to the study of ionic association is described.

La résonance paramagnétique électronique a été utilisée pour étudier les ions triples formés entre la pyrazine et la tétraméthyl-pyrazine et les cations Li^+, Na^+, K^+ dans le diméthoxyéthane. Des effets de largeur de raies différentielles sont observés parmi les écarts hyperfins des métaux alcalins incorporés dans les ions triples et une application possible de ces effets pour l'étude de l'association ionique est décrite.

Canadian Journal of Chemistry, 49, 2059 (1971)

Introduction

Recently, electron spin resonance (e.s.r.) spectroscopy has been used to demonstrate the existence, in ethereal solvents, of triple ions of the general formula Na_2A^+ where A may be *p*-benzosemiquinone, pyrazine or their methylated derivatives (1–3). From the hyperfine splitting patterns of the e.s.r. spectra it has been deduced that these triple ions have symmetrical structures, one cation associating with each electronegative site of the anion. A particularly interesting feature of such spectra is that the differential line-broadening effects, caused by molecular tumbling modulating the line-positions through anisotropies in the **g** and hyperfine tensors, are extremely pronounced. From these line-broadening effects it has been found possible, following the theory of Freed and Fraenkel (4, 5), to characterize the form of the hyperfine tensor of the sodium counter ions, and thence to deduce that these counter ions occupy positions along the O–O or N–N axes of the anions. In the present work we extend the range of counter ions to include lithium, potassium and, unsuccessfully, cesium, and indicate further information available from semi-quantitative analyses of line-width variations within the spectra.

Experimental

Pyrazine (P), tetramethylpyrazine (TMP), and sodium tetraphenylboride were purchased commercially and used without further purification. Lithium, potassium, and cesium tetraphenylborides were prepared by metathetical reactions between sodium tetraphenylboride and the appropriate alkali halide, following standard literature procedures (6). Dimethoxyethane (DME), tetrahydrofuran (THF), and 2-methyltetrahydrofuran (MeTHF) were purified by fractional distillation, dried by refluxing over sodium, and stored *in vacuo* in the presence of the sodium ketyl of benzophenone. Apparatus for the production of triple ions and the recording of their e.s.r. spectra were as described previously (3). Reduction by lithium was performed using lithium chips, introduced into the reduction apparatus in an argon-filled dry-box, and normally took a few hours to reach completion. Potassium tetraphenylboride was relatively insoluble in the ethereal solvents used, and so triple ions containing potassium were prepared by contacting a solution of the azine with a potassium film in the presence of a milky suspension of the tetraphenylboride. Overnight, the suspension cleared leaving a yellow solution having an intense e.s.r. spectrum. Cesium films were prepared in the reduction apparatus by heating mixtures of calcium filings and powdered cesium chloride *in vacuo*, and driving the cesium vapor through a sintered glass frit.

Results

The preparation and e.s.r. spectra of Na_2P^+ and Na_2TMP^+ in THF and in MeTHF have been reported previously (3). Using the techniques described in the experimental section the following additional triple ions were successfully observed: Li_2P^+ and Li_2TMP^+ in DME, THF, and MeTHF, K_2P^+ and K_2TMP^+ in THF. Attempts to produce Cs_2P^+ and Cs_2TMP^+ were unsuccessful in all three solvents; small additions of cesium tetraphenylboride to solutions of cesium–azine ion-pairs collapsed the cesium hyperfine structure and larger additions destroyed the e.s.r. signal completely. Figure 1

[1]To whom all correspondence should be addressed.

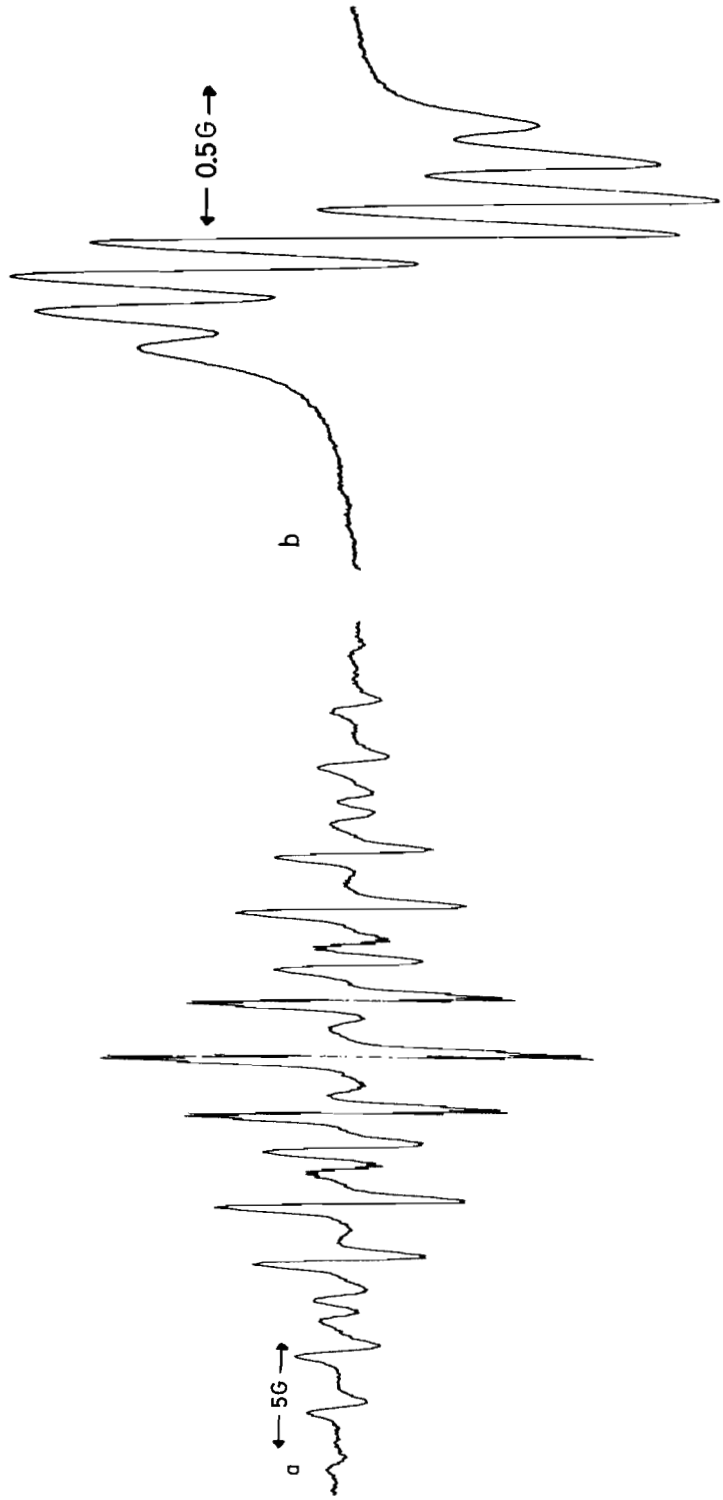

FIG. 1. Electron spin resonance spectra at −40 °C of K_2P^+ in THF: (*a*) complete spectrum; (*b*) expanded center septet.

Can. J. Chem. Downloaded from www.nrcresearchpress.com by 210.87.254.40 on 09/05/12
For personal use only.

Can. J. Chem. Downloaded from www.nrcresearchpress.com by 210.87.254.40 on 09/05/12
For personal use only.

TABLE 1. Hyperfine splitting constants of hydrogen and nitrogen for azine triple ions at 20 °C*

		M_2P^+		M_2TMP^+	
Solvent	M	a_H (G)	a_N (G)	a_H (G)	a_N (G)
DME	Li	2.79	6.90	1.77	6.11
THF	Li	2.75	6.80	1.77	6.11
MeTHF	Li	2.78	6.89	—	—
THF	Na	2.70	7.12	1.78	6.19
MeTHF	Na	2.69	7.13	1.77	6.10
THF	K	2.65	7.13	1.79	6.10

*All values are accurate to ±0.03 G.

shows the e.s.r. spectrum of K_2P^+ in THF recorded at a sample temperature of −40 °C. The hyperfine septets generated by the two equivalent potassium nuclei are clearly visible on the $\tilde{M}_N = 0$ lines of spectrum, and just visible on the $\tilde{M}_N = -1$ components. Line broadening effects obscure the potassium hyperfine structure in the remainder of the spectrum.

For all the azine triple ion systems studied in the present work, the nitrogen and proton hyperfine splitting constants were, within the experimental error of ±0.03 G, independent of temperature. Measured values of these splitting constants are given in Table 1. However, alkali metal hyperfine splitting constants were found to be temperature dependent; to facilitate comparison between the various alkali metals, in Fig. 2 we have plotted observed metal hyperfine splitting constant divided by the appropriate atomic hyperfine splitting constant as a function of temperature for the triple ions M_2P^+ and M_2TMP^+ (M = Li, Na, K) in THF, the only solvent in which all these species are stable.

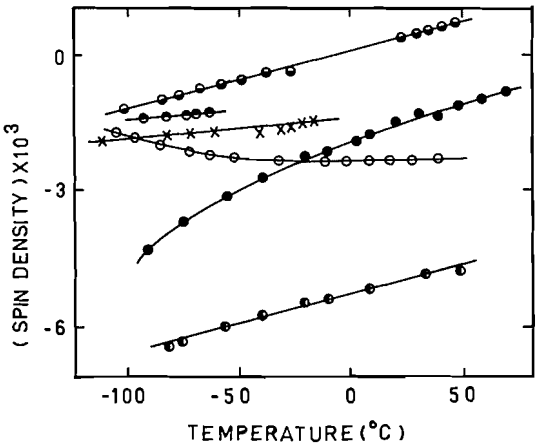

FIG. 2. Alkali metal hyperfine splitting constants in G divided by the corresponding atomic hyperfine coupling constants and given as a function of temperature for the following systems in THF: ◒, Na_2TMP^+; ◓, K_2TMP^+; ×, K_2P^+; ●, Li_2TMP^+; ○, Na_2P^+; ◐, Li_2P^+.

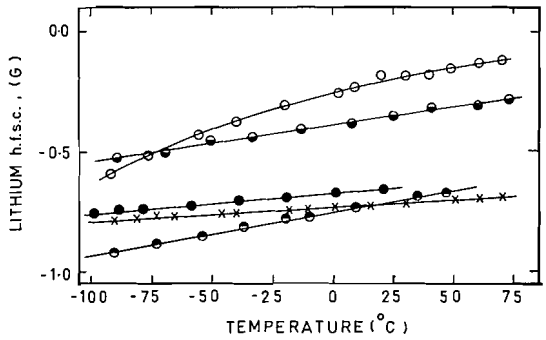

FIG. 3. Lithium hyperfine splitting constants in G as a function of temperature for the following systems: ○, Li_2TMP^+ in THF; ◒, Li_2TMP^+ in DME; ●, Li_2P^+ in DME; ×, Li_2P^+ in MeTHF; ◓, Li_2P^+ in THF.

The effect of solvent upon the alkali metal hyperfine splitting constants is shown for the lithium triple ions in Fig. 3; only Li_2P^+ could be formed in all three solvents used. The choice of signs for the metal hyperfine splitting constants follows from arguments previously listed (2, 3).

As had been previously observed, differential line-broadening effects were found to be very pronounced in the e.s.r. spectra of azine triple ions. In Fig. 4 the widths of the principle nitrogen lines (lines having spectral indices for all nuclei other than nitrogen equal to zero) relative to the width of the central $\tilde{M}_N = 0$ line are plotted as a function of $\tilde{M}_N$. The curves drawn through the data represent the least-squares fits of the data to equations of the form [1] proposed empirically by Barton and Fraenkel (7).

$$[1] \qquad W = 1.00 + A_N\tilde{M}_N + B_N\tilde{M}_N^2$$

Relative widths were determined by the stan-

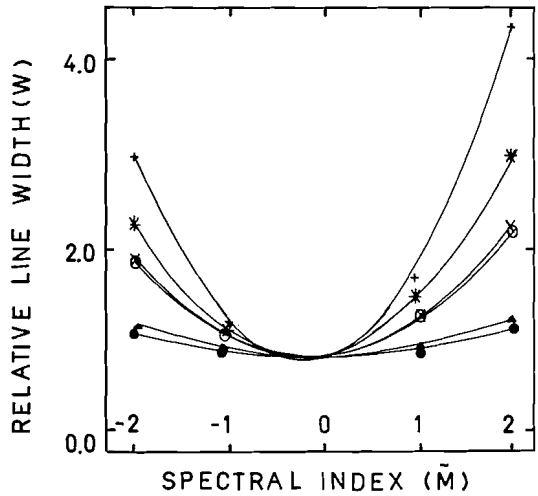

FIG. 4. The least-square fit of the experimental linewidths of the principle nitrogen lines relative to the center line ($\tilde{M} = 0$) to the equation $W = 1 + A\tilde{M}_N + B\tilde{M}_N^2$ for the following systems in THF at 10 °C: ▲ K_2TMP^+; ●, K_2P^+; ○, Na_2P^+; ×, Li_2P^+; ★, Na_2TMP^+; +, Li_2TMP^+. For the significance of A and B see text and Table 2.

dard method of measuring relative amplitudes of the first derivative presentation: values of A_N and B_N obtained from the least-squares fitting are given in Table 2. Values are not given for the potassium species because the unresolved potassium hyperfine structure prevents the determination of reliable values for A_N and B_N. Table 3 contains values of A_N, B_N, A_{Li}, and B_{Li} determined for Li_2P^+ at 10 °C in DME, THF, and MeTHF. For the MeTHF sample, overlapping lines at 10 °C prevented a direct accurate determination of the A and B values. Therefore, measurements were made at more favorable temperatures and interpolated to values at 10 °C; the interpolations were made by plotting the measured line-width parameters as functions of solvent viscosity/temperature, such plots being linear as predicted by the theory of Freed and Fraenkel (4). Values for the viscosity were taken from tables published by Szwarc (8).

TABLE 2. A_N and B_N values for azine triple ion at 10 °C in THF calculated by least square fit of the experimental relative line widths to the equation $W = 1 + A_N\tilde{M}_N + B_N\tilde{M}_N^2$

Triple ion	A	B
Li_2P^+	0.0854	0.2768
Li_2TMP^+	0.2863	0.6376
Na_2P^+	0.0767	0.2659
Na_2TMP^+	0.1632	0.4062

TABLE 3. Values of A_N, B_N, A_{Li}, and B_{Li} for Li_2P^+ in THF, MeTHF, and DME obtained from the equation $W = 1 + A\tilde{M} + B\tilde{M}^2$; sample temperature 10 °C

Solvent	A_N	B_N	A_{Li}	B_{Li}
DME	0.0792	0.1123	0.0157	0.0074
THF	0.0854	0.2768	0.0158	0.0164
MeTHF	0.0767	0.2659	0.0164	0.0260

Discussion

The isotropic metal hyperfine splitting constants for the lithium and sodium azine triple ions in Fig. 2 deserve little comment since they follow the expectations of our previous discussion (2, 3); a more negative value is obtained for the unsubstituted pyrazine because the counter-ion can approach closer to the molecular plane of the anion. Similarly, in spin density units, the lithium splitting is more negative than the sodium splitting, suggesting that the lithium cation forms a "tighter" triple ion than does sodium. This tighter character of the lithium triple ion is reflected in the nitrogen and hydrogen hyperfine splitting constants of Na_2P^+ and Li_2P^+; in the tighter associate more charge is localized into the $2p_z$ orbital of nitrogen thereby repelling spin into the $2p_z$ carbon orbitals, causing a decrease in a_N and an increase in a_H (see Table 1). This decrease in a_N has also been observed by Carrington (9); the situation is analogous to the behavior of the carbonyl groups of semiquinones (10–12) and ketyls (13, 14) under the influence of ionic association.

The potassium hyperfine splitting constant of K_2P^+ fits into the overall description of these systems with the assumption (*cf.* refs. 2 and 3) that da_K/dT is positive which means a_K must be negative. As can be seen from Fig. 1(b) any broadening of the central septet linear in $\tilde{M}_K$ is undetectable and so no check on the sign of a_K is available. However, for K_2TMP^+ in THF, pronounced high field broadening of the central septet was detected, thereby establishing (2, 3) that a_K is indeed negative for this system. It can be seen that the amount of spin density on the counter ion decreases smoothly with increasing M^+ radius for M_2P^+ which is as expected if one correlates the strength of the ionic interaction with the extent of spin transfer. However, such a correlation does not hold for the M_2TMP^+ species, indicating the difficulties inherent in the

Can. J. Chem. Downloaded from www.nrcresearchpress.com by 210.87.254.40 on 09/05/12
For personal use only.

Can. J. Chem. Downloaded from www.nrcresearchpress.com by 210.87.254.40 on 09/05/12
For personal use only.

interpretation of metal splitting constants. To interpret the data in Fig. 3 in terms of the effect of solvent upon the strength of the lithium–pyrazine interaction is obviously impossible.

The B_M values reported in Table 3 are a potential source of information concerning the strength of the lithium pyrazine interaction. B_M is a measure of the strength of the anisotropic dipolar interaction between lithium and the unpaired electron. Because the lithium nucleus is close to the N–N axis, this dipolar interaction is dominated (> 95%) by the spin density on nitrogen, and hence the magnitude of the lithium–electron dipolar interaction is an indication of the lithium–nitrogen distance and hence of the strength of the lithium–pyrazine interaction. However, B_M is also a function of the correlation time for molecular tumbling τ_R, and so to make comparisons between systems as to the strength of the lithium–pyrazine interaction it is first necessary to eliminate the effects of variations in τ_R. This is most readily done by dividing B_M by B_N, since both terms are linearly dependent upon τ_R provided (as is normally assumed (4)) that electronic non-secular terms may be neglected, and provided that the spin density on nitrogen is the same among the systems under comparison. Therefore, within these limitations, as the strength of the lithium–pyrazine interaction increases, so should the value of B_M/B_N. The data given in Table 3 allow an evaluation of this approach for Li_2P^+ in DME, THF, and MeTHF at 10 °C; values of B_M/B_N, calculated from this data, are plotted in Fig. 5 against the reciprocal of the dielectric constant of the solvent, taken from data compiled by Szwarc (8). The number of points in Fig. 5 is too few to prove a linear dependence of B_M/B_N upon $1/D$, but would seem to demonstrate the expected increase in the lithium–pyrazine interaction as the polarity of the solvent is decreased. Thus measurements of counter ion line-width broadening patterns can be a useful approach to the study of the strength of ionic interactions.

It should be noted that both the nitrogen and proton hyperfine splitting constants of the tetramethylpyrazine species are appreciably smaller than the corresponding values of the pyrazine species. This would seem to indicate that the value of Q_{Me} normally used for methyl substituted hydrocarbon radicals is not suitable for azine radical anions. However, more methyl substituted azine anions need to be studied before more quantitative conclusions can be arrived at.

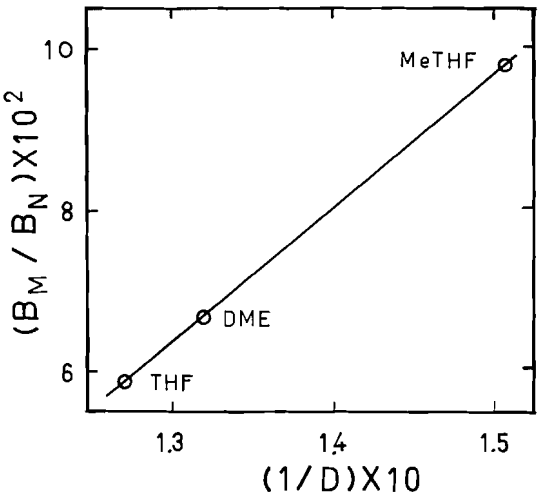

FIG. 5. The function B_M/B_N for the triple ion Li_2P^+ at 10 °C plotted as a function of the inverse dielectric constant of the solvent.

We thank the National Research Council of Canada for operating funds, and the Gulbenkian Foundation, through the Iraqi Government, for a scholarship to S. A. Al-B.

1. T. E. GOUGH and P. R. HINDLE. Can. J. Chem. **47**, 1698 (1969).
2. T. E. GOUGH and P. R. HINDLE. Can. J. Chem. **47**, 3393 (1969).
3. S. A. AL-BALDAWI and T. E. GOUGH. Can. J. Chem. **48**, 2798 (1970).
4. J. H. FREED and G. K. FRAENKEL. J. Chem. Phys. **39**, 326 (1963).
5. J. H. FREED and G. K. FRAENKEL. J. Chem. Phys. **40**, 1815 (1964).
6. D. N. BHATTACHARYYA, C. L. LEE, J. SMID, and M. SZWARC. J. Phys. Chem. **69**, 608 (1965).
7. B. L. BARTON and G. K. FRAENKEL. J. Chem. Phys. **41**, 695 (1964).
8. M. SZWARC. Carbanions, living polymers and electron transfer processes. Interscience Publishers, New York. Chap. IV, pp. 160–161.
9. A. CARRINGTON and J. DOS SANTOS-VEIGA. Mol. Phys. **5**, 21 (1962).
10. P. S. GILL and T. E. GOUGH. Trans. Faraday Soc. **64**, 1997 (1968).
11. P. S. GILL and T. E. GOUGH. Can. J. Chem. **45**, 2112 (1967).
12. P. S. GILL and T. E. GOUGH. Can. J. Chem. **46**, 656 (1968).
13. N. HIROTA. J. Am. Chem. Soc. **89**, 32 (1967).
14. K. NAKAMURA and N. HIROTA. Chem. Phys. Lett. **3**, 137 (1969).

Can. J. Chem. Downloaded from www.nrcresearchpress.com by 210.87.254.105 on 09/05/12
For personal use only.

Reaction of *trans*-2-Acylaminocyclanols with Thionyl Chloride[1]

R. A. B. BANNARD, N. C. C. GIBSON, AND J. H. PARKKARI
Defence Research Establishment Ottawa, Ottawa, Canada

Received December 23, 1970

trans-2-Acetamidocyclohexanol (**1**; $n = 2$, R = CH_3) on addition to thionyl chloride in chloroform at 0° was converted rapidly and quantitatively to D,L-2-methyl-4,5-*cis*-cyclohexanoöxazoline hydrochloride (**2**; $n = 2$, R = CH_3) judging from shifts in the methyl proton resonances of the n.m.r. spectra of the amide and the reaction solution. The intermediate chlorosulfinate was estimated to have a half-life of less than 2.25 min. The oxazoline salt was isolated in 98% yield by sublimation of the crude product *in vacuo* and was identified by its i.r. and n.m.r. spectra and by its facile and almost quantitative hydrolysis to *cis*-2-aminocyclohexanol hydrochloride. The oxazoline salts **2** ($n = 1$, R = CH_3, C_6H_4-*p*NO_2 and $n = 2$, R = C_6H_5, C_6H_4-*p*NO_2) were readily obtained in 95% yield or better by the same general method and it was shown that the *trans*-2-acetamidocyclanols are the preferred starting materials for conversion to *cis*-2-aminocyclanol derivatives by the thionyl chloride inversion reaction. The oxazoline bases **4** ($n = 1$, R = CH_3, C_6H_4-*p*NO_2 and $n = 2$, R = CH_3, C_6H_4-*p*NO_2) were readily obtained in high yield from the corresponding salts and differences in the i.r. and n.m.r. spectral characteristics of the salts and bases are reported.

La D,L-méthyl-2 cyclohexano-4,5-*cis* oxazoline (**2**; $n = 2$, R = CH_3) est rapidement et quantitativement produite en ajoutant le chlorure de thionyle à 0 °C à l'acétamido-2 cyclohexanol-*trans* (**1**; $n = 2$, R = CH_3) dans du chloroforme. On estime que le demi temps de vie du chlorosulfinate intermédiaire est moins que 2.25 min. Ce résultat est mis en évidence par un glissement dans le signal des protons du groupement méthyle dans les spectres r.m.n., de l'amide et de la solution réactionnelle. Le chlorhydrate de l'oxazoline est isolé avec un rendement de 98% par la sublimation sous vide du produit brut. On a établi la structure du composé en se servant de données obtenues par spectroscopie i.r. et r.m.n. et on l'a vérifiée par une méthode d'hydrolyse simple qui conduit avec un rendement pratiquement quantitatif au chlorhydrate de l'amino-2 cyclohexanol-*cis*. On obtient facilement les chlorohydrates des oxazolines **2** ($n = 1$, R = CH_3, C_6H_4-*p*NO_2 et $n = 2$, R = C_6H_5, C_6H_4-*p*NO_2) avec des rendements d'au moins 95% en utilisant la même méthode générale et on a démontré que les acétamido-2 cyclanols-*trans* sont les produits de départ les plus utiles pour obtenir les dérivés d'aminocyclanol-2-*cis* par la réaction d'inversion à l'aide du chlorure de thionyle. On obtient facilement les bases oxazolines **4** ($n = 1$, R = CH_3, C_6H_4-*p*NO_2 et $n = 2$, R = CH_3, C_6H_4-*p*NO_2) avec de bons rendements à partir des sels correspondants et on décrit des différences dans les spectres r.m.n. et i.r. des sels et des bases.

Canadian Journal of Chemistry, 49, 2064 (1971)

In 1950, Johnson and Schubert (1) and McCasland and Smith (2) reported simultaneously and independently studies on the reaction between *trans*-2-benzamidocyclanols **1** ($n = 1, 2$, R = C_6H_5, C_6H_4-*p*NO_2) and thionyl chloride, which led by an inversion process to D,L-2-phenyl-4,5-*cis*-cycloalkanoöxazoline hydrochlorides **2** ($n = 1, 2$, R = C_6H_5, C_6H_4-*p*NO_2). Hydrolysis of the latter with aqueous hydrochloric acid proceeded with retention of configuration to provide low over-all yields (40–50%) of *cis*-2-aminocyclanol hydrochlorides **3** ($n = 1, 2$). These two groups of workers considered the oxazoline salts, which they found to be unstable and difficult to isolate in a pure condition, to arise by the internal S_N2 displacement of a hydroxyl or chlorosulfinate group by the oxygen atom of the amide carbonyl group. This viewpoint was strengthened by Winstein and Boschan's (3) classic study of the participation of the benzamido group in neighboring displacements in which they showed, among other things, that *trans*-2-benzamidocyclohexyl *p*-toluenesulfonate was converted almost quantitatively to the corresponding oxazoline tosylate in refluxing glacial acetic acid in 6 min. They also examined the reaction between *trans*-2-benzamidocyclohexanol and thionyl chloride at 0°, ultimately isolating *cis*-2-benzamidocyclohexanol in high yield by hydrolysis of the intermediate oxazoline hydrochloride **2** ($n = 2$, R = C_6H_5), which they considered to result by internal displacement of a chlorosulfinate group which had been introduced into the molecule by a rapid initial reaction of the hydroxyl group with thionyl chloride. These workers also determined the rate of displacement

[1]Issued as DREO Report No. 638.

Can. J. Chem. Downloaded from www.nrcresearchpress.com by 210.87.254.105 on 09/05/12
For personal use only.

of the tosyl group from *trans*-2-benzamidocyclohexyl tosylate under solvolytic conditions in anhydrous ethanol at 74°, from which it was clear that the half-life of the substrate under these conditions is approximately 6.5 min at 74° or 1060 h at 0°. No effort was made, however, to study the rate of conversion of *trans*-2-acylaminocyclanols to the oxazoline salts by thionyl chloride.

We first became interested in the acylaminocyclanol – thionyl chloride reaction several years ago when one of us (4) briefly examined the conversion of *trans*-2-acetamidocyclohexanol (**1**; $n = 2$, R = CH_3) to *cis*-2-aminocyclohexanol and its derivatives by this means. The yields obtained at that time were significantly better than those reported by Johnson and Schubert (1) starting from the benzamido analogue but not nearly as good as that reported by Winstein and Boschan (3). Because of our continuing interest in the conversion of *trans*-2-acylaminocyclanols to their *cis*-analogues we decided to reexamine the reaction from two standpoints, firstly to attempt to develop it into a useful synthetic method, and secondly to attempt to obtain an approximate measure of the rate of the reaction. It occurred to us in the latter connection that it should be possible, in principle at least, to follow the rate of the reaction by observing either the rate of appearance of D,L-2-methyl-4,5-*cis*-cyclohexanoöxazoline hydrochloride (**2**; $n = 2$, R = CH_3), or the rate of disappearance of *trans*-2-acetamidocyclohexanol or the intermediate chlorosulfinate by looking for shifts in the methyl resonances in the n.m.r. spectrum of the reaction mixture.

We first examined the addition of *trans*-2-acetamidocyclohexanol (1 mol) dissolved in anhydrous chloroform to thionyl chloride (3.85 mol) at 0°.[2] Because of the exothermicity of the reaction even when moderated by the presence of the solvent, addition of the amide required 20 min. A sample taken immediately thereafter for n.m.r. examination revealed no trace of the starting material, judging from the complete absence of an acetamido methyl proton resonance

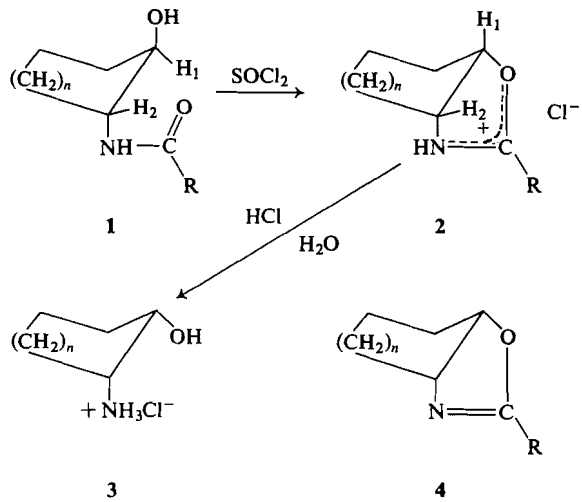

at τ 8.01, (Fig. 1*a*) and the presence of a new methyl resonance equivalent to three protons at τ 7.41, together with broad methine resonances at τ 4.90 and 5.91 and methylene resonances from τ 7.8–8.6 in the reaction solution (Fig. 1*b*). The spectrum was measured at intervals for a period of 48 h and although the solution, which was originally pale pink, gradually became deep red in color, there was no change in the appearance of the spectrum. The oxazoline hydrochloride **2** ($n = 2$, R = CH_3) could be isolated in quantitative crude yield, m.p. 98.5–100.5°, as described in the Experimental, 2 h after the addition of the amide had been completed and it was therefore concluded that the n.m.r. spectrum obtained within 5 min of completion of the addition indicated that the reaction had proceeded to completion within 25 min.

Subsequent experiments conducted on a semimicro scale at 0° in which the addition of the amide was completed in 1.25 min established that the reaction had proceeded to completion in less than 9 min from the start of addition of the amide, judging from the fact that the n.m.r. spectrum of the reaction solution was identical with that of Fig. 1*b*. Assuming that the formation of chlorosulfinate is virtually instantaneous and that four half-lives of the chlorosulfinate would be required to produce a spectrum of oxazoline salt apparently free of contaminants, it is concluded that the half-life of the chlorosulfinate cannot exceed 2.25 min at 0°. Thus the rate of oxazoline salt formation from the chlorosulfinate of the hydroxyamide **1** ($n = 2$, R = CH_3)

[2]These conditions represented the best features of procedures due to Winstein and Boschan (3) (temperature and molar proportions) and Elliott (5) (addition of amide in solvent). Most other workers (1–3, 6–8) have used portionwise addition of the amide to neat thionyl chloride.

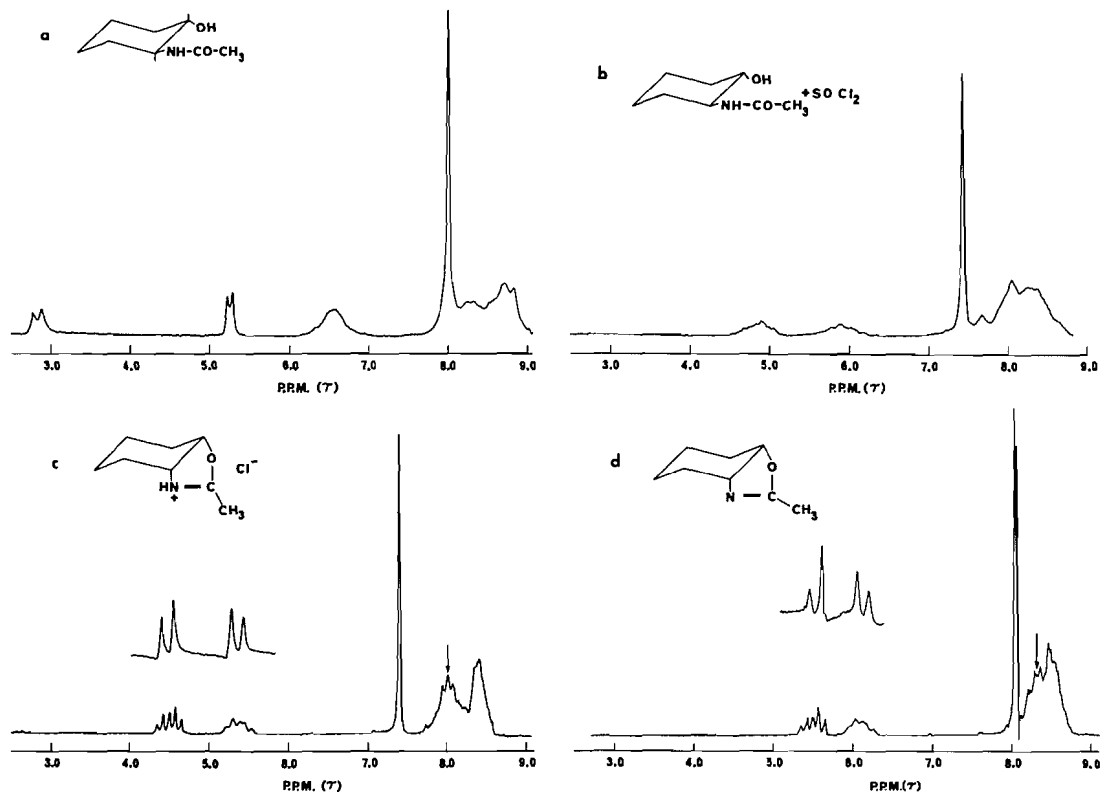

FIG. 1. (*a*) The 60 MHz n.m.r. spectrum of *trans*-2-acetamidocyclohexanol in chloroform.
(*b*) The 60 MHz n.m.r. spectrum of *trans*-2-acetamidocyclohexanol + excess thionyl chloride in chloroform (recorded 25 min after initiation of the reaction).
(*c*) The 60 MHz Spectrum of D,L-2-methyl-4,5-*cis*-cyclohexanoöxazoline hydrochloride in chloroform (insert shows methine proton resonances resulting from irradiation of H-3 and -6 at τ 8.01).
(*d*) The 60 MHz n.m.r. spectrum of D,L-2-methyl-4,5-*cis*-cyclohexanoöxazoline in chloroform (insert shows methine proton resonances resulting from irradiation of H-3 and -6 at τ 8.30).

in chloroform – thionyl chloride is at least 2.8×10^4 times faster than by solvolysis of the hydroxyamide *p*-toluenesulfonate in ethanol at 0°.

The oxazoline salt **2** ($n = 2$, $R = CH_3$) is extremely hygroscopic and on attempted recrystallization from anhydrous chloroform – ether or absolute ethanol – ether decomposes with the formation of a difficultly separable mixture of D,L-*cis*-1-acetoxy-2-aminocyclohexane hydrochloride (**5**) and D,L-*trans*-1-chloro-2-acetamidocyclohexane (**6**). The *O*-acetylamine hydrochloride **5** probably results from a simple acidic partial hydrolysis of the oxazoline salt by traces of moisture in the solvents, with concomitant N → O acyl migration (9–12) and the chloroamide **6** is likely formed by opening of the ring by backside displacement of the oxazoline oxygen

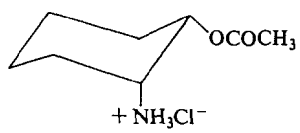

5

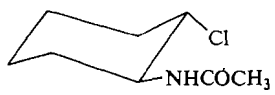

6

by the chloride ion present in hot solutions of the salt (3, 5, 13). The crude oxazoline hydrochloride was readily purified by sublimation *in vacuo* and was obtained in 98% yield as a colorless crystalline solid, which was readily hydrolyzed quantitatively to *cis*-2-aminocyclo-

Can. J. Chem. Downloaded from www.nrcresearchpress.com by 210.87.254.105 on 09/05/12
For personal use only.

Can. J. Chem. Downloaded from www.nrcresearchpress.com by 210.87.254.105 on 09/05/12
For personal use only.

hexanol hydrochloride **3** ($n = 2$), by brief heating with 10% aqueous hydrochloric acid (*cf.* 1, 2, 4). This two-step reaction sequence thus provides an almost quantitative conversion of *trans*-2-acetamidocyclohexanol to *cis*-2-aminocyclohexanol hydrochloride.

The isolated oxazoline salt **2** ($n = 2$, R = CH_3) gave a much sharper spectrum (Fig. 1*c*) than that obtained directly from the reaction solution and some shifts in the positions of the resonances were noted presumably because of the removal of the thionyl chloride from the system.[3] For example, the methine resonances were now seen to be sharp (H-1) and broad (H-2) multiplets at τ 4.50 and 5.38 respectively. A sharp methylene triplet was now evident at τ 8.01, which decoupling experiments clearly indicated to be due to H-3*a*,*e* and -6*a*,*e* (see below).[4] The methyl resonance had shifted slightly to τ 7.40 and was now clearly seen to be a doublet ($J \approx 0.5$–0.8 Hz). Irradiation of H-2 caused this doublet to collapse to a singlet. Similarly, irradiation of the methyl doublet caused the broad multiplet at τ 5.38 to sharpen, confirming the long range coupling between H-2 and the methyl group. Irradiation of H-3*a*,*e* and -6*a*,*e* at τ 8.01 caused the methine multiplets at τ 4.50 and 5.38 to collapse to an AB quartet ($J_{1,2} = 8.5$–9.0 Hz).

The n.m.r. spectrum of the oxazoline free base **4** (R = CH_3, $n = 2$) (Fig. 1*d*) shows some significant differences (see Table 1) from that of the oxazoline hydrochloride **2** (R = CH_3, $n = 2$) from which it was readily prepared, *e.g.* the oxazoline methyl proton doublet is shifted upfield to τ 8.03 ($J \approx 1.5$ Hz). Irradiation of H-2, which is shifted upfield to τ 6.10, caused the methyl doublet to collapse to a sharp singlet, again indicating long range coupling between H-2 and the oxazoline methyl protons. The signal for H-1 is also shifted upfield to τ 5.50 and now appeared as a double triplet. Irradiation of the H-3*a*,*e* and -6*a*,*e* triplet at τ 8.30 caused the methine multiplets from H-1 and -2 to collapse to an AB quartet ($J_{1,2} \approx 8.5$ Hz).

The long range coupling between H-2 and the oxazoline methyl protons agrees with the observations of Weinberger and Greenhalgh (14) on the occurrence of long range coupling between methyl protons and methylene or methine protons attached to the carbon atom which is also attached to nitrogen in monocyclic oxazolines and thiazolines. Also, the change in chemical shift in the oxazoline methyl proton resonance observed for **2** and **4** (R = CH_3, $n = 2$)[5] is characteristic for such compounds (14). The magnitude of $J_{1,2}$ observed in the salt and free base is not at variance with the assignment of a *cis*-fused oxazoline–cyclohexane structure to **2** ($n = 2$, R = CH_3) since several heterocyclic ring systems (15–19), including 2-oxazolidine–cyclohexane (18) have recently been reported in which $J_{cis} > J_{trans}$ due to a combination of substituent electronegativity effects and dihedral angular variation between the protons.

Assuming a flexible *cis* cyclohexane–oxazoline ring fusion and free inversion of the cyclohexane ring, average coupling constants were assigned to the interacting methine and adjacent methylene protons. The chemical shifts of the methine protons and $J_{1,2}$ (8.5 Hz) were obtained from the experimental spectrum. Substitution of these values in a modified LAOCOON-2 computer program (20) resulted in a spectrum drawn by a Calcomp plotter which showed good correspondence with the methine resonance pattern of the experimental spectrum, thus supporting the *cis*-fused ring structure. Assumption of a rigid *trans*-fused ring structure with appropriate values for the coupling constants and chemical shifts in a similar analysis gave poor correspondence with the methine resonances of the experimental spectrum.[6]

[3]Removal of the excess reagent and solvent *in vacuo* from the reaction mixture immediately after completion of the amide addition gave, on reconstitution in deuterochloroform, a spectrum identical with Fig. 1*c*.

[4]The approximate coincidence of the signals due to the methylene protons H-3 and -6 in 1,2-disubstituted cyclohexanes and cyclopentanes is not generally observed. However, this behavior was noted for such protons in all the cyclopentano- and cyclohexano-oxazolines examined herein.

[5]In structure **2** a proton is shown attached to the nitrogen atom, following the designation used for oxazolinium salts used in refs. 1–3. A referee has pointed out that the occurrence of long range coupling between methyl and H-2 in both the salt **2** and in the base **4**, the comparable sizes of the J values for these compounds and the circumstance that the signal for H-1 moves further upfield than does the signal for H-2 during the change from compound **2** to compound **4** may indicate that the proton is attached to oxygen rather than to nitrogen. Consequently, the location of the proton in the oxazoline ring is not certain, but in the absence of conclusive evidence to the contrary we prefer to use the protonated nitrogen structure.

[6]We are indebted to Prof. R. Y. Moir and Mr. R. S. Reeve, Department of Chemistry, Queen's University, Kingston, Ontario, for performing this analysis.

Can. J. Chem. Downloaded from www.nrcresearchpress.com by 210.87.254.105 on 09/05/12
For personal use only.

TABLE 1. Chemical shifts (τ) of acetamidocyclanols,* oxazoline salts, and bases†

Compound											
No.	*n*	R	Aromatic H	NH	OH	H-1	H-2	N*H*Ac	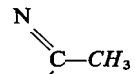	$(CH_2)_4$	$J_{1,2}$(Hz)‡
1	2	CH_3	—	2.87 d	5.34 d	6.55 m	6.55 m	8.01 s	—	7.8–9.0 m	—
1	1	CH_3	—	2.85 d	4.90 s	6.12 m	6.12 m	8.02 s	—	7.7–8.7 m	—
2	2	CH_3	—	—	—	4.50 m	5.38 m	—	7.40 d	7.8–8.6 m	8.5
2	2	C_6H_5	2.37, 3.20	—	—	5.20 m	6.03 m	—	—	8.5–9.4 m	8.5
2	2	C_6H_4-*p*NO_2	2.08, 2.54	—	—	5.29 m	6.05 m	—	—	8.5–9.4 m	8.5
2	1	CH_3	—	—	—	4.20 m	5.03 m	—	7.45 d	7.3–8.3 m	8.0
2	1	C_6H_4-*p*NO_2	1.37	—	—	4.00 m	4.75 m	—	—	7.3–8.2 m	7.5
4	2	CH_3	—	—	—	5.50 m	6.10 t	—	8.03 d	8.1–8.7 m	8.5
4	2	C_6H_4-*p*NO_2	2.67	—	—	6.11 m	6.67 m	—	—	8.8–9.5 m	8.5
4	1	CH_3	—	—	—	5.10 m	5.50 m	—	8.06 d	8.1–8.6 m	8.0
4	1	C_6H_4-*p*NO_2	1.78	—	—	4.78 m	5.17 m	—	—	7.7–8.4 m	7.5

*Only the acetamidocyclanols were sufficiently soluble in $CDCl_3$ to give good spectra (10–20% solutions).
†d, Doublet; m, multiplet; s, singlet; t, triplet.
‡By decoupling from methylene protons.

TABLE 2. Principal infrared absorption (cm^{-1}) of acetamidocyclanols,* oxazoline salts, and bases

Compound														
No.	*n*	R	OH		NH	Imine salt	Oxazoline salt	C=O	N=C—O	Amide II	NO_2		C—O	
1	2	CH_3	3590 w	3438 s	3315 m	—	—	1660 s	—	1500 m	—		1260 m†	1066 m
1	1	CH_3	3590 w	3442 s	3310 sh	—	—	1655 s	—	1497 m	—		1258 m†	1060 m
2	2	CH_3	—	—	—	2100–2800 m	1810 w	—	1667 s	—	—		1270 m†	965 s
2	2	C_6H_5	—	—	—	2100–2888 m	1780 w	—	1640 s	—	—		1270 m†	980 w
2	2	C_6H_4-*p*NO_2	—	—	—	1940–2740 m	1790 w	—	1650 s	—	1525 s	1365 s	—	970 w
2	1	CH_3	—	—	—	2100–2800 m	1810 w	—	1670 s	—	—		1254 m†	970 w
2	1	C_6H_4-*p*NO_2	—	—	—	1940–2800 m	1790 w	—	1650 s	—	1535 s	1350 s	1255 m†	970 w
4	2	CH_3	—	—	—	—	—	—	1665 s	—	—		1220 s†	960 s
4	2	C_6H_4-*p*NO_2	—	—	—	—	—	—	1645 s	—	1525 s	1365 s	—	960 m
4	1	CH_3	—	—	—	—	—	—	1667 s	—	—	—	1237 m†	950 m
4	1	C_6H_4-*p*NO_2	—	—	—	—	—	—	1645 s	—	1525 s	1342 s	1258 m†	1010 m

*Only the acetamidocyclanols were sufficiently soluble in chloroform to provide good spectra (0.05 *M* solutions).
†A 0.05 *M* solution in $CDCl_3$.

Can. J. Chem. Downloaded from www.nrcresearchpress.com by 210.87.254.105 on 09/05/12
For personal use only.

The i.r. spectra of the oxazoline salt **2** and free base **4** ($n = 2$, R = CH_3) also showed some characteristic features (see Table 2). The salt has a very strong absorption at 1667 cm^{-1} and the base a strong band at 1665 cm^{-1} which are undoubtedly due to the 2-oxazoline N=C—O group (21, 22). The salt also has strong imine salt absorption at 2100–2800 cm^{-1} and a medium intensity salt band at 1810 cm^{-1}, both of which are, of course, absent from the base. The i.r. spectrum of the pure oxazoline salt **2** ($n = 2$, R = CH_3) could be readily observed on samples removed from the reaction solution 5 min after completion of the addition of the amide to the thionyl chloride when they were treated as described in the Experimental to eliminate the excess reagent. The i.r. spectrum of the oxazoline salt is markedly different from that of *trans*-2-acetamidocyclohexanol, the latter containing free and bonded hydroxyl absorptions at 3590 and 3438 cm^{-1}, NH absorption at 3315 cm^{-1}, and amide II absorption at 1500 cm^{-1}, all of which are absent from the spectrum of the oxazoline salt (see Table 2).

The influence of reaction conditions on the yield of oxazoline salt **2** ($n = 2$, R = CH_3) was examined. Control of the reaction temperature at 18–20° caused the yield to fall to 92%, whereas addition of thionyl chloride to a slurry of the amide in chloroform at 5–10° gave a 96% yield. Addition of the amide via a worm-feed addition-tube (23) to a solution of thionyl chloride in chloroform at 0° provided a 98% yield.

The behavior of *trans*-2-acetamidocyclopentanol **1** ($n = 1$, R = CH_3) in the reaction was completely analogous to that of the corresponding cyclohexyl derivative, furnishing D,L-2-methyl-4,5-*cis*-cyclopentanoöxazoline hydrochloride **2** ($n = 1$, R = CH_3) in 95% yield. The latter substance was also readily purified by sublimation *in vacuo* and was hydrolyzed quantitatively to *cis*-2-aminocyclopentanol hydrochloride **3** ($n = 1$) in the usual manner.

The aryloxazoline salts **2** ($n = 2$, R = C_6H_5, C_6H_4-*p*NO_2 and $n = 1$, R = C_6H_4-*p*NO_2) were prepared in yields of 95% or better by the same method.[7] These compounds were not amenable to purification by recrystallization or by sublimation *in vacuo*, but were obtained analytically pure directly from the reaction if proper precautions for the exclusion of moisture were observed. They were also readily convertible to the corresponding free bases **4** ($n = 2$, R = C_6H_5, C_6H_4-*p*NO_2 and $n = 1$, R = C_6H_4-*p*NO_2) in high yield but did not provide yields of *cis*-2-aminocycloalkanol hydrochlorides above 91% by acidic hydrolysis, presumably owing to complications introduced by the formation of the more difficultly separable benzoic and *p*-nitrobenzoic acids as by-products. Consequently, the *trans*-2-acetamidocyclanols are the preferred intermediates for the synthesis of *cis*-2-aminocyclanol derivatives and can provide the latter readily in almost quantitative yield. Nuclear magnetic resonance spectroscopy was not as useful a tool for following the formation of the 2-aryloxazoline salts as it was for the 2-methyloxazoline salts because of the absence of the 2-methyl group, the i.r. spectra of the aryl compounds being more useful in this connection. The chemical shifts of the protons in the 60 MHz n.m.r. spectra of the 2-substituted oxazoline salts and bases examined in this work are given in Table 1 together with those of the *trans*-2-acetamidocyclanols. The principal i.r. absorption frequencies of the *trans*-2-acetamidocyclanols, oxazoline salts, and bases are shown in Table 2.

Experimental[8, 9]

The i.r. spectra were measured as 0.05–0.10 *M* solutions in chloroform on a Perkin–Elmer Model 221 spectrophotometer. When spectra were required of oxazoline salts present in reaction mixtures containing excess thionyl chloride, a sample of the reaction solution (0.1 ml) was distilled to dryness three times at room temperature or below with 1 ml of chloroform or deuterochloroform at water pump pressure, taking precautions to prevent access of water vapor to the sample.

The n.m.r. spectra were measured on a Varian V-4300C spectrometer (60 MHz) using a Varian V-5321 integrator for base-line stabilization. Solutions were 10–20% in chloroform or deuterochloroform and were calibrated with reference to internal tetramethylsilane by the usual side-band technique.

D,L-*trans*-2-Aminocyclohexanol and Derivatives

trans-2-Aminocyclohexanol, m.p. 67.5–68.5°, *trans*-2-aminocyclohexanol hydrochloride, m.p. 180–181°, and *trans*-2-acetamidocyclohexanol, m.p. 126.5–127.5°, were prepared following methods described by Hawkins and Bannard (24), *cf.* McCasland *et al.* (26). *trans*-2-Benzamidocyclohexanol, m.p. 171–172°, was prepared by application of the acylation procedure of Leffler and Adams (25) as reported by Johnson and Schubert (1).

[7]Because of solubility restrictions, these acylaminocyclanols were added *via* a worm-feed addition-tube (23) to thionyl chloride – chloroform solutions at 0°.

[8]All melting points are uncorrected.

[9]Microanalyses by J. G. Helie of these laboratories.

Can. J. Chem. Downloaded from www.nrcresearchpress.com by 210.87.254.105 on 09/05/12
For personal use only.

Anal. Calcd. for $C_{13}H_{17}O_2N$: C, 71.20; H, 7.82; N, 6.39. Found: C, 71.03; H, 7.76; N, 6.56.

trans-2-*p*-Nitrobenzamidocyclohexanol, m.p. 211–211.5°, was prepared similarly (*cf.* McCasland and Smith (2)).

Anal. Calcd. for $C_{13}H_{16}O_4N_2$: C, 59.08; H, 6.10; N, 10.60. Found: C, 59.08; H, 6.00; N, 10.70.

D,L-*2-Methyl-4,5-cis-cyclohexanoöxazoline Hydrochloride (2; n = 2, R = CH_3)*

A solution of *trans*-2-acetamidocyclohexanol (3.92 g, 0.025 mol) in anhydrous chloroform (12 ml, Fisher spectro grade dried over silica gel) was added dropwise with stirring at −5 to 0° over a period of 20 min to thionyl chloride (7.0 ml, *ca.* 0.095 mol) in an apparatus protected against the entry of moisture. The dropping funnel used for the addition was rinsed with an additional 2 ml of chloroform. The temperature of the resultant colorless opalescent solution was allowed to rise to 21° over a period of 30 min while stirring was continued, following which stirring was continued at the same temperature for a further 2 h. The excess thionyl chloride and chloroform were removed from the pale pink solution by distillation at a pressure of 50–60 mm, leaving a viscous pink oil. Chloroform (2 ml) was added and the solution was added dropwise to vigorously stirred anhydrous ether (450 ml) at room temperature. A colorless oil separated and the ether layer became yellow. The mixture was kept overnight at 0° during which the oil crystallized. The ether was decanted and retained and the pale yellow crystals were collected, washed with anhydrous ether (5 × 25 ml), taking care to keep them covered with ether until washing was complete, and then were dried *in vacuo*; wt. 4.17 g, m.p. 98.5–100.5°. A second small crop of crystals, 0.15 g, was recovered by extraction of the residual material in the flask and funnel with chloroform, followed by removal of the solvent *in vacuo*. Evaporation of the ether decanted from the crystals gave 0.289 g of dark evil-smelling oil, which on hydrolysis with 10% hydrochloric acid, furnished 70 mg of *cis*-2-aminocyclohexanol hydrochloride (equivalent to 81 mg of oxazoline salt). Total yield of crude oxazoline hydrochloride, 4.40 g (100%). Sublimation of 200 mg of the crude salt at 50° at 0.001 mm furnished 196 mg (98.0%) of colorless hygroscopic crystals of D,L-2-methyl-4,5-*cis*-cyclohexanoöxazoline hydrochloride, m.p. 104–106°.[10]

Anal. Calcd. for $C_8H_{14}ONCl$: C, 54.69; H, 8.03; N, 7.98; Cl, 20.18. Found: C, 54.70; H, 8.20; N, 8.04; Cl, 20.10.

D,L-*cis-1-Acetoxy-2-aminocyclohexane Hydrochloride (5) and* D,L-*trans-1-Chloro-2-acetamidocyclohexane (6)*

Attempted recrystallization of the oxazoline salt (500 mg) from ethanol–ether or chloroform–ether resulted in decomposition and furnished 314 mg (55%) of D,L-*cis*-1-acetoxy-2-aminocyclohexane hydrochloride, as colorless needles, m.p. 213–213.5° (dec.).

Anal. Calcd. for $C_8H_{16}O_2NCl$: C, 49.60; H, 8.33; N, 7.23; Cl, 18.30. Found: C, 49.51; H, 8.61; N, 7.13; Cl, 18.25.

This substance gave a positive ionic halogen test and its i.r. spectrum (0.1 *M* in chloroform) showed prominent bands at 3300–2400 (NH^+), 1728 (ester carbonyl), 1595 (N—H deformation), 1220, and 1013 cm^{-1} (C—O acetate). In addition, 64 mg (12.8%) of D,L-*trans*-1-chloro-2-acetamidocyclohexane[11] was recovered as fine colorless needles, m.p. 130–132°.

Anal. Calcd. for $C_8H_{14}ONCl$: C, 54.69; H, 8.03; N, 7.98; Cl, 20.18. Found: C, 54.55; H, 7.94; N, 7.77; Cl, 20.07.

This substance did not contain ionic halogen and its i.r. spectrum (0.1 *M* in chloroform) had prominent bands at 3445 (N—H, free), 3330 (N—H, bonded) 1665 (amide carbonyl), and 1503 cm^{-1} (amide II).

D,L-*2-Methyl-4,5-cis-cyclohexanoöxazoline (4, n = 2, R = CH_3)*

2-Methyl-4,5-*cis*-cyclohexanoöxazoline hydrochloride (2.69 g, 0.0153 mol) was shaken with 15 ml of 5% sodium hydroxide and 30 ml of ether. The ether layer was decanted and the aqueous phase was extracted with ether (4 × 30 ml). The ether solutions were combined, dried over anhydrous magnesium sulfate, decanted, and the ether was removed *in vacuo* The pale brown residue was fractionated in a micro-distillation apparatus at 13 mm pressure and furnished 1.90 g (89.3%) of colorless mobile liquid b.p. 75.5–76.5°, n_D^{25} 1.4698, with a very penetrating odor.

Anal. Calcd. for $C_8H_{13}ON$: C, 69.03; H, 9.41; N, 10.06. Found: C, 69.01; H, 9.17; N, 10.02.

D,L-*cis-2-Aminocyclohexanol Hydrochloride (3, n = 2)*

Hydrolysis of the crude oxazoline hydrochloride (2.00 g) by heating it under reflux for 1 h with 10% hydrochloric acid (35 ml) gave, after evaporation to dryness and recrystallization from ethanol–ether, 1.69 g (97.7%) of D,L-*cis*-2-aminocyclohexanol hydrochloride as colorless platelets, m.p. 190–191.5°, alone, and in admixture with an authentic sample (4).

D,L-*2-Phenyl-4,5-cis-cyclohexanoöxazoline Hydrochloride (2, n = 2, R = C_6H_5)*

A stirred slurry of *trans*-2-benzamidocyclohexanol (2.74 g, 0.0125 mol) and anhydrous chloroform (100 ml) was kept at 0–8° in an apparatus protected against the entry of moisture while thionyl chloride (3.5 ml, 0.0483 mol) was added over a period of 21 min. The temperature of the resultant clear solution was allowed to rise to 21° over a period of 45 min and the solution was stirred at room temperature for an additional 2¾ h. The chloroform and excess thionyl chloride were removed by distillation at a pressure of 50–60 mm, leaving a very viscous pale yellow residue which was transferred quantitatively in 10 ml of chloroform to 250 ml of stirred anhydrous ether. The turbid mixture began to deposit colorless crystals almost immediately and was kept overnight at 0°. The crystals were collected, washed with anhydrous ether, and dried *in vacuo*; wt. 2.96 g (99.3%) m.p. 102–105°. Johnson and Schubert (1) report m.p 96.5–101° but no analytical data on the hydrochloride.

Anal. Calcd. for $C_{13}H_{17}ONCl$: C, 65.40; H, 7.18;

[10]If the crude oxazoline salt is allowed to stand for a prolonged period prior to further purification by sublimation, it slowly decomposes, *e.g.* after standing for 2 months 252 mg of crude oxazoline salt furnished only 222 mg (88.0%) of colorless sublimate.

[11]The structure of this compound was confirmed by measurement of the coupling constant (J = 10 Hz) between the methine protons in $CDCl_3$–C_6H_6 solution. We are indebted to Dr. R. R. Fraser for this measurement.

Can. J. Chem. Downloaded from www.nrcresearchpress.com by 210.87.254.105 on 09/05/12
For personal use only.

N, 5.87; Cl, 14.86. Found: C, 65.28; H, 6.99; N, 5.92; Cl, 14.87.

Hydrolysis of D,L-2-phenyl-4,5-*cis*-cyclohexanoöxazoline hydrochloride with 10% aqueous hydrochloric acid as described for the methyl analogue furnished 91.0% of D,L-*cis*-2-aminocyclohexanol hydrochloride, m.p. 189–190° (4) and 96.5% of benzoic acid, m.p. 121.5–122°.

D,L-*2-p-Nitrophenyl-4,5-cis-cyclohexanoöxazoline Hydrochloride (2, n = 2, R = C_6H_4-pNO_2)*

The procedure was identical with that given above for D,L-2-phenyl-4,5-*cis*-cyclohexanoöxazoline hydrochloride except that *trans*-2-*p*-nitrobenzamidocyclohexanol (3.30 g, 0.0125 mol) was used. The oxazoline salt separated as a solid during the removal of the excess chloroform and thionyl chloride *in vacuo* but was taken up in anhydrous chloroform (10 ml) and precipitated by addition to anhydrous ether as described for the methyl and phenyl analogues. The salt was collected, washed with ether, and dried *in vacuo*; wt. 3.34 g (94.4%), m.p. 144–145°[12] and again at 175–179°, *cf.* McCasland and Smith (2).

Anal. Calcd. for $C_{13}H_{15}O_3N_2Cl$: C, 55.24; H, 5.35; N, 9.91; Cl, 12.54. Found: C, 55.08; H, 5.28; N, 9.64; Cl, 12.50.

Hydrolysis of the oxazoline salt in the usual manner gave a 90% recovery of D,L-*cis*-2-aminocyclohexanol hydrochloride, m.p. 189–190°, and 91% of *p*-nitrobenzoic acid, m.p. 241–242.5°.

D,L-*2-p-Nitrophenyl-4,5-cis-cyclohexanoöxazoline (4, n = 2, R = C_6H_4-pNO_2)*

The oxazoline hydrochloride (731 mg) was shaken with a mixture of 18 ml of 5% sodium hydroxide and 25 ml of ether. The ether layer was decanted and the aqueous phase was extracted with ether (3 × 25 ml). The ether solutions were combined, dried over anhydrous magnesium sulfate, decanted, and taken to dryness *in vacuo* leaving a pale yellow solid, which was recrystallized from absolute ethanol and furnished 460 mg (72.5%) of pale yellow crystals. m.p. 120–121°. McCasland and Smith (2) report m.p. 120–121°.

D,L-*trans-2-Aminocyclopentanol*

D,L-*trans*-2-Aminocyclopentanol was prepared by the ammonolysis of 1,2-epoxycyclopentane (27) following the method used by Hawkins and Bannard (24) for preparation of the cyclohexane analogue, except that it was found necessary to extend the heating period to 4 h. The substance was obtained as a colorless oil, b.p. 65° at 1.5 mm, n_D^{25} 1.4920, in 81.5% yield.

Anal. Calcd. for $C_5H_{11}ON$: C, 59.37; H, 10.96; N, 13.85. Found: C, 59.14; H, 11.21; N, 13.98.

The identity of the compound was confirmed by conversion to the hydrochloride, m.p. 193–194°, after recrystallization from ethanol–ether. McCasland and Smith (2) report m.p. 193–194°.

D,L-*trans-2-Acetamidocyclopentanol*

This substance was prepared according to the method described by Bannard and Hawkins (28) for the preparation of *N*-acetyl derivatives of the alkoxyaminocyclohexanols, and was obtained in 90% yield as a very viscous colorless oil, b.p. 118–120° at 0.02 mm, n_D^{25} 1.4995.

Anal. Calcd. for $C_7H_{13}O_2N$: C, 58.72; H, 9.15; N, 9.78. Found: C, 58.59; H, 9.27; N, 9.96.

D,L-*trans-2-Benzamidocyclopentanol*

This compound was prepared in 77.5% yield in the same manner as its cyclohexyl analogue, and had m.p. 120–121°. McCasland and Smith (2) report m.p. 120–121°.

Anal. Calcd. for $C_{12}H_{15}ON_2$: C. 70.21; H, 7.38; N, 6.83. Found: C, 70.03; H, 7.29; N, 6.82.

D,L-*trans-2-p-Nitrobenzamidocyclopentanol*

This substance was prepared in 75% yield in the same manner as its cyclohexyl analogue as reported by McCasland and Smith (2), m.p. 158–159°.

Anal. Calcd. for $C_{12}H_{14}O_4N_2$: C, 57.58; H, 5.65; N, 11.19. Found: C, 57.50; H, 5.64; N, 11.27.

D,L-*2-Methyl-4,5-cis-cyclopentanoöxazoline Hydrochloride (2, n = 1, R = CH_3)*

The procedure was identical with that given in detail for the preparation of D,L-2-methyl-4,5-*cis*-cyclohexanoöxazoline hydrochloride except that *trans*-2-acetamidocyclopentanol (3.58 g, 0.0250 mol) was used. The crude oxazoline salt (red oil) failed to crystallize on standing in anhydrous ether. The ether was decanted, the oil was taken up in anhydrous chloroform (10 ml), treated with decolorizing charcoal at room temperature, filtered through celite, and the solvent was removed *in vacuo* yielding 4.09 g of brown solid. The latter material was sublimed at 50° at 0.001 mm pressure and furnished 3.87 g (94.7%) of colorless crystals, m.p. 94.5–96.5°.

Anal. Calcd. for $C_7H_{12}ONCl$: C, 52.02; H, 7.49; N, 8.67; Cl, 21.95. Found: C, 51.98; H, 7.26; N, 8.78; Cl, 22.11.

D,L-*2-Methyl-cis-4,5-cyclopentanoöxazoline (4, n = 1, R = CH_3)*

The procedure was identical with that described for the preparation of the cyclohexyl homologue except that D,L-2-methyl-*cis*-4,5-cyclopentanoöxazoline hydrochloride (2.59 g, 0.016 mol) was used. The oxazoline base was obtained as a colorless mobile oil with a very penetrating odor. Yield. 1.75 g (87.7%), b.p. 57.0–57.5° at 13 mm, n_D^{25} 1.4619.

Anal. Calcd. for $C_7H_{11}ON$: C, 67.17; H, 8.86; N, 11.19. Found: C, 66.96; H, 9.06; N, 11.27.

D,L-*cis-2-Aminocyclopentanol Hydrochloride*

2-Methyl-4,5-*cis*-cyclopentanoöxazoline hydrochloride (1.19 g, 0.00617 mol) was hydrolyzed in the usual manner and furnished 1.01 g (100%) of colorless platelets, m.p. 181–183°, after recrystallization from absolute ethanol and ethanol–ether. McCasland and Smith (2) report m.p. 179–180°.

Anal. Calcd. for $C_5H_{12}ONCl$: C, 43.64; H, 8.79; N, 10.18; Cl, 25.77. Found: C, 43.60; H, 8.75; N, 9.92; Cl, 25.56.

D,L-*cis-2-Aminocyclopentanol*

A solution of *cis*-2-aminocyclopentanol hydrochloride (6.88 g, 0.05 mol) and sodium hydroxide (4.0 g, 0.10 mol) in water (90 ml) was continuously extracted with ether for 3 days. The ether was removed *in vacuo* and the colorless residue was recrystallized from ether yielding 4.66 g (92.4%) of colorless needles, m.p. 71.0–73.0°.

[12]If the sample was placed in the capillary m.p. apparatus at a temperature below 135°, only the higher m.p. was observed, *cf.* Fry (13).

Anal. Calcd. for $C_5H_{11}ON$: C, 59.37; H, 10.96; N, 13.85. Found: C, 59.09; H, 10.78; N, 13.64.

D,L-*2-p-Nitrophenyl-4,5-cis-cyclopentanoöxazoline Hydrochloride (2, n = 1, R = C_6H_4-pNO_2)*

trans-2-*p*-Nitrobenzamidocyclopentanol (3.07 g, 0.0123 mol) was added portionwise at −5 to 0° over a period of 8 min via a worm-feed addition tube to a magnetically-stirred solution of thionyl chloride (3.5 ml, 0.0483 mol) in deuterochloroform (9.0 ml) in an apparatus protected against the entry of moisture. The temperature of the clear yellow solution was allowed to rise to 29° over a period of 45 min and two 0.1 ml aliquots were removed for i.r. examination. The solution was stirred at room temperature for a further 2.5 h, following which the solution was transferred quantitatively with deuterochloroform (5 ml) to a round-bottom flask and the excess reagent and solvent were removed at 13 mm pressure, taking precautions to prevent the access of moisture. The crystalline residue 3.04 g (99.1%), had m.p. 153.5–155°. McCasland and Smith (2) report m.p. 150–151°, and Fodor and Kiss (29) report m.p. 159–161° for this compound.

Anal. Calcd. for $C_{12}H_{13}O_3N_2Cl$: C, 53.64; H, 4.88; N, 10.43; Cl, 13.20. Found: C, 53.55; H, 5.11; N, 10.40; Cl, 13.02.

This compound decomposes on attempted recrystallization from ethanol.

D,L-*2-p-Nitrophenyl-4,5-cis-cyclopentanoöxazoline (4, n = 1, R = C_6H_4-pNO_2)*

D,L-2-*p*-Nitrophenyl-4,5-*cis*-cyclopentanoöxazoline hydrochloride (1.05 g, 0.00391 mol) was converted to the free base in the usual manner, and, after removal of the ether *in vacuo*, was obtained as a pale yellow crystalline solid, 882 mg (96.9%), m.p. 138.5–140°. McCasland and Smith (2) report m.p. 139–140° for this compound.

Anal. Calcd. for $C_{12}H_{12}O_3N_2$: C, 62.06; H, 5.21; N, 12.06. Found: C, 62.03; H, 4.88; N, 12.16.

This compound is best purified by recrystallization from ethanol.

Thanks are extended to Dr. M. A. Weinberger and Miss P. M. Lutley for measurement of the majority of the n.m.r. spectra reported herein. We are also indebted to Dr. R. R. Fraser, Mr. F. McClusky, and Mr. A. E. Castagne for n.m.r. spectral measurements made during the final stages of the investigation.

1. W. S. Johnson and E. N. Schubert. J. Am. Chem. Soc. **72**, 2187 (1950).
2. G. E. McCasland and D. A. Smith. J. Am. Chem. Soc. **72**, 2190 (1950).
3. S. Winstein and R. Boschan. J. Am. Chem. Soc. **72**, 4669 (1950).
4. R. A. B. Bannard. Can. J. Chem. **42**, 744 (1964).
5. D. F. Elliott. J. Chem. Soc. 589 (1949).
6. J. Weijlard, K. Pfister, E. F. Swanezy, C. A. Robinson and M. Tishler. J. Am. Chem. Soc. **73**, 1216 (1951).
7. K. Pfister, C. A. Robinson, A. C. Shabica, and M. Tishler. J. Am. Chem. Soc. **71**, 1101 (1949).
8. J. Attenburrow, D. F. Elliott, and G. F. Penny. J. Chem. Soc. 310 (1948).
9. R. H. Wiley and L. L. Bennett. Chem. Rev. **44**, 447 (1949).
10. A. A. Goldberg and W. Kelly. J. Chem. Soc. 1919 (1948).
11. E. M. Fry. J. Org. Chem. **15**, 802 (1950).
12. R. Greenhalgh, R. M. Heggie, and M. A. Weinberger. Can. J. Chem. **41**, 1662 (1963).
13. E. M. Fry. J. Org. Chem. **14**, 887 (1949).
14. M. A. Weinberger and R. Greenhalgh. Can. J. Chem. **41**, 1038 (1963).
15. I. Fleming and D. H. Williams. Spectroscopic methods in organic chemistry. McGraw-Hill Book Co. Inc., New York, N.Y., 1966. p. 109.
16. S. L. Manatt, D. D. Elleman, and S. J. Brois. J. Am. Chem. Soc. **87**, 2220 (1965).
17. S. J. Brois and G. P. Beardsley. Tetrahedron Lett. 5113 (1966).
18. J. E. Herweh, T. A. Foglia, and D. Swern. J. Org. Chem. **33**, 4029 (1968).
19. C. V. Pittman and S. P. McManus. J. Org. Chem. **35**, 1187 (1970).
20. S. Castellano and A. A. Bothner-By. J. Chem. Phys. **41**, 3863 (1964).
21. A. R. Katritzky. Physical methods in heterocyclic chemistry. Vol. II. Academic Press, New York, N.Y., 1963. p. 218.
22. D. Tomalia, N. D. Ojha, and B. P. Thill. J. Org. Chem. **34**, 1400 (1969).
23. R. A. B. Bannard. Can. J. Technology, **32**, 68 (1954).
24. L. R. Hawkins and R. A. B. Bannard. Can. J. Chem. **36**, 220 (1958).
25. M. T. Leffler and R. Adams. J. Am. Chem. Soc. **59**, 2256 (1937).
26. G. E. McCasland, R. K. Clark, and H. E. Carter. J. Am. Chem. Soc. **71**, 637 (1949).
27. R. A. B. Bannard, A. A. Casselman, E. J. Langstaff, and R. Y. Moir. Can. J. Chem. **45**, 2605 (1967).
28. R. A. B. Bannard and L. R. Hawkins. Can. J. Chem. **36**, 1241 (1958).
29. G. Fodor and J. Kiss. J. Chem. Soc. 1589 (1952).

Can. J. Chem. Downloaded from www.nrcresearchpress.com by 210.87.254.105 on 09/05/12
For personal use only.

Can. J. Chem. Downloaded from www.nrcresearchpress.com by 210.87.254.5 on 09/05/12
For personal use only.

Metal – Aminopolycarboxylic Acid Complexes. I. Studies of Lead(II) and Cadmium(II) Complexes with Diethylenetriaminepentaacetic Acid in Aqueous Solution by Proton Magnetic Resonance Spectroscopy

P. LETKEMAN
Department of Chemistry, Brandon University, Brandon, Manitoba

AND

J. B. WESTMORE
Department of Chemistry, University of Manitoba, Winnipeg, Manitoba

Received June 29 1970[1]

Lead(II) and cadmium(II) each form a 1:1 complex with DTPA. Nuclear magnetic resonance (n.m.r.) spectroscopy was used to show that each complex has three metal–nitrogen bonds and labile metal–oxygen bonds to terminal acetate groups. The latter lead to proton equivalence for the methylene protons of the terminal acetate groups of the lead complex, and near equivalence for those of the cadmium complex. The central carboxylate group is coordinated to the lead but not to the cadmium. Protonation occurs below p*H* 5.5 for the lead complex and occurs predominantly at a terminal nitrogen atom with consequent breaking of the metal–nitrogen bond. In the cadmium complex protonation occurs below p*H* 5 at the terminal nitrogen, breaking the metal–nitrogen bond, and also to almost the same extent at the central, uncoordinated carboxylate group. These differences in behavior of the lead and cadmium complexes are attributed to differences in ionic size. Possible structures are proposed and allowances are made for the possibility of coordination number greater than six. In the protonated complexes, structures and interconversion of protonated forms are discussed in the light of the observed simplification of the n.m.r. spectra.

Le plomb(II) et le cadmium(II) forment chacun un complexe 1:1 avec le DTPA. La spectroscopie r.m.n. a été utilisée pour montrer que chaque complexe possède trois liaisons métal–azote et des liaisons labiles métal–oxygène aux groupes acétates terminaux. Ces dernière rendent équivalent les protons du groupe méthylène situés sur les groupes acétates terminaux dans le complexe avec le plomb. Une quasi-équivalence est obtenue pour le complexe avec le cadmium. Le groupe carboxylate central est coordonné au plomb mais pas au cadmium. Dans le cas d'un complexe avec le plomb, la protonation se fait pour un p*H* inférieur à 5.5 et de préférence sur un atome d'azote terminal avec pour conséquence la rupture de la liaison métal–azote. Avec le complexe du cadmium, la protonation se situe en dessous de p*H* 5 sur l'atome d'azote terminal, provoquant la rupture de la liaison métal–azote, et avec la même importance sur le groupe carboxylate central non coordonné. Ces différences de comportement entre le complexe du plomb et celui du cadmium sont attribuables à des différences de grosseurs ioniques. Des structures possibles sont proposées et il est tenu compte de la possibilité de nombres de coordination supérieurs à six. Dans les complexes protonés, les structures et l'interconversion des formes protonées sont discutées à la lumière de la simplification observée dans les spectres r.m.n.

Canadian Journal of Chemistry, 49, 2073 (1971)

Introduction

The use of proton magnetic resonance (p.m.r.) spectroscopy for the study of aqueous solutions of aminopolycarboxylic acids (1–5) and their diamagnetic complexes with metal ions (5–16) is well-established. In this paper we describe a systematic study of the behavior of the aqueous systems: lead(II)–DTPA and cadmium(II)–DTPA, where DTPA represents diethylenetriaminepentaacetic acid. The pentaanion of DTPA is conveniently represented (1) by

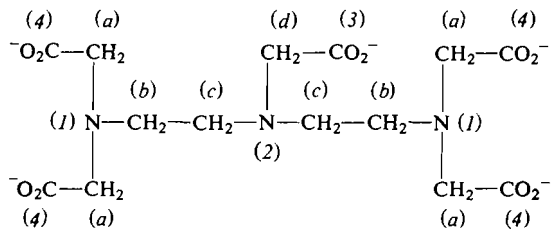

in which there are eight equivalent acetate protons labelled (*a*), two equivalent acetate protons labelled (*d*), four equivalent ethylenic protons labelled (*b*), and four equivalent ethylenic protons labelled (*c*). The equivalent terminal nitrogen

[1]Revision received March 12, 1971.

Can. J. Chem. Downloaded from www.nrcresearchpress.com by 210.87.254.5 on 09/05/12
For personal use only.

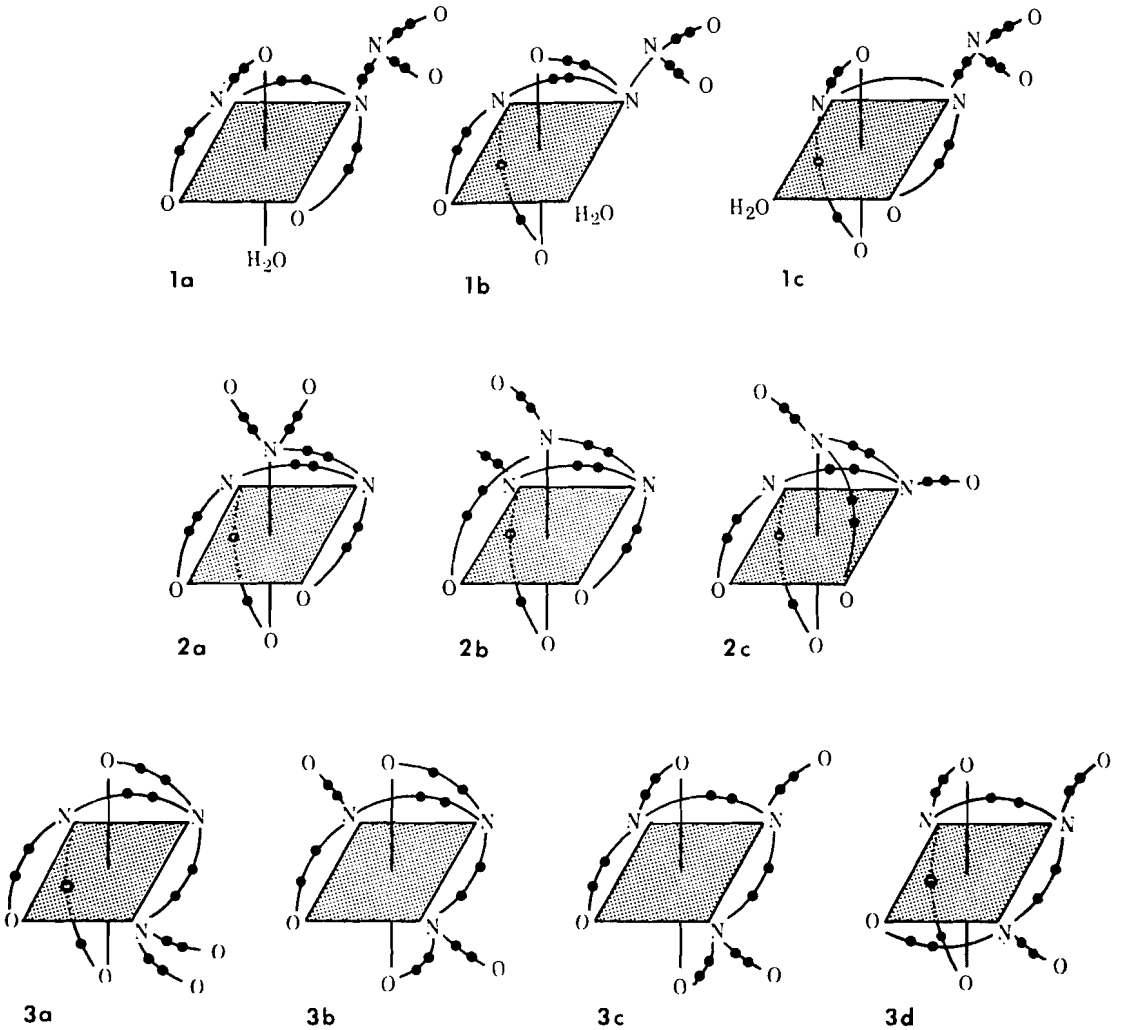

FIG. 1. Possible instantaneous configurations, based on octahedral coordination, for a metal–DTPA complex. In each case, only one of the equivalent forms is shown.

atoms are labelled (*1*) and the unique center nitrogen atom is labelled (*2*). The unique carboxyl group is labelled (*3*) and the four equivalent terminal carboxyl groups are labelled (*4*).

A survey of the coordination chemistry of divalent metal – aminopolycarboxylate complexes revealed evidence for preferred octahedral coordination (17–21) but the X-ray crystallographic studies of Hoard and co-workers (22–30) indicate that this is a simplification and some principles for prediction of coordination number were proposed. DTPA is a potentially octadentate ligand. In this introductory section we have assumed octahedral coordination for the sake of convenience, but as will be shown in the Discussion section, for the most part, the conclusions drawn do not depend upon this assumption. Even assuming octahedral coordination, DTPA can wrap itself around a metal ion in many different ways. The different possible instantaneous configurations, ignoring the consequences of ring strain and steric interference, are shown in Fig. 1. These are also possible configurations for non-labile complexes. It does not seem reasonable to consider configurations in which less than two nitrogen atoms (of which one must be the center nitrogen atom)

Can. J. Chem. Downloaded from www.nrcresearchpress.com by 210.87.254.5 on 09/05/12
For personal use only.

are coordinated, or where carboxylate groups are coordinated but not the associated nitrogen atom. Furthermore, in an instantaneous configuration, different conformations of the ethylenic rings are possible. The different possibilities of optical isomerism are not considered since this will have no bearing on the n.m.r. spectra. Also not shown are configurations in which DTPA acts as less than a sexadentate ligand (except in configurations *1a–1c*) although in labile complexes partially unwrapped structures may make a greater than negligible contribution. For labile complexes the molecule will exist in various stages of unwrapping with the more complete stages of unwrapping being less prevalent. Such unwrapping would be expected to occur from the end of the molecule so that the metal–oxygen (*4*) bonds will form and break more quickly than the metal–nitrogen bonds, *i.e.* all the metal–nitrogen bonds will have longer lifetimes than the metal–oxygen (*4*) bonds. Two characteristic metal–nitrogen bond lifetimes can be distinguished since unwrapped states like *1a, 1b*, and *1c* are possible. The lifetime of the metal–nitrogen (*1*) bond is thus shorter than that of the metal–nitrogen (*2*) bond, which has the longest lifetime of all metal–ligand bonds. The metal–oxygen (*3*) bond lifetime must be shorter than that of the metal–nitrogen (*2*) bond but can be either longer or shorter than those of the other metal–ligand bonds. Thus, the following sequences of relative bond lifetimes are possible:

$$\text{M—N}(2) > \text{M—N}(1) > \text{M—O}(3) > \text{M—O}(4)$$

$$\text{M—N}(2) > \text{M—N}(1) > \text{M—O}(4) > \text{M—O}(3)$$

$$\text{M—N}(2) > \text{M—O}(3) > \text{M—N}(1) > \text{M—O}(4)$$

In a p.m.r. study of metal–DTPA complexes, examples may be encountered in which all metal–ligand bonds have long lifetimes, have short lifetimes, or have some bonds with long lifetimes and others with short lifetimes. Day and Reilley (8) have discussed the effect of the lability of metal–ligand bonds in metal–ethylenediaminetetraacetic acid (EDTA) complexes on their n.m.r. spectra. In the latter part of this paper these discussions have been extended to metal–DTPA complexes.

Experimental

The proton nuclear magnetic resonance spectra were recorded with a Varian A56/60A spectrometer. Most of the spectra were recorded at temperatures (± 1°) of 0, 39, and 70°. The spectral data obtained were average readings of several recordings with a reproducibility of ±0.4 Hz. The values of the chemical shifts were measured with respect to *t*-butyl alcohol (TBA) but reported with respect to DSS (3-trimethylsilylpropanesulfonic acid, sodium salt). The advantage of using TBA is that its signal is independent of p*H* and ionic strength (5) and it has a single resonance close to the region under investigation. One percent by volume of TBA was sufficient to yield a good reference signal at 1.233 p.p.m. downfield from DSS. Prior to recording the spectra of some of the solutions of the metal complexes nitrogen was passed through them, but, as found previously (4) little improvement was achieved by deoxygenation of the solutions.

Stock solutions of DTPA were prepared from the acid (J. T. Baker Chemical Company) after recrystallization from hot water. To 1.000 mol (394.4 g) of the acid suspended in 800 ml of water were added 3 mol of solid potassium hydroxide pellets and the resulting solution was diluted to 1.000 l. Stock solutions (1.000 *M*) of lead(II) and cadmium(II) were prepared from their nitrate salts (reagent grade). From these stock solutions various metal–ligand solutions were prepared in which the ligand concentration was 0.10 to 0.50 *M* since a relatively high concentration of ligand was necessary to obtain a satisfactory n.m.r. signal.

A Radiometer type PH28 p*H* meter, which had been calibrated at p*H* = 6.86, 4.01, and 2.00 (Beckman buffers), was used to determine the p*H* of all the solutions. The p*H* was adjusted by the addition of potassium hydroxide since the metal–DTPA solutions were initially acidic (sometimes the p*H* was as low as 1.5). For the concentrated solutions required to obtain satisfactory n.m.r. spectra no additional buffer was necessary, *i.e.* DTPA served as its own buffer.

Results and Discussion

Our studies on the p.m.r. spectra of aqueous solutions of DTPA as a function of p*H* were in close agreement with those reported previously by other workers (1, 2) and hence are not presented here.

The assignments of the various resonances in the spectra of the metal complexes were made from their relative peak areas, dependence upon p*H*, and from expectations based on earlier work (8).

Lead(II)–DTPA Solutions

Representative n.m.r. spectra obtained for 1:1 ratios of Pb(II):DTPA for a 0.50 *M* concentration over the p*H* range 2–10 and at temperatures of 0, 39, and 72° are presented in Figs. 2–4. In Fig. 2 are recorded the spectra obtained at 39° at p*H* values of 2.0, 5.0, and 7.0. Figure 3 shows the effect of temperature on the spectra at p*H* 8.0. Figure 4 shows a spectrum obtained at p*H* = 9.0 where the spectra are sharper than at lower p*H* values.

The position and form of the resonance due to the (*a*) protons depends upon the p*H* of the solu-

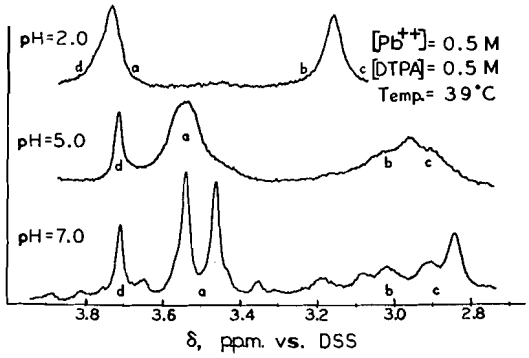

FIG. 2. Nuclear magnetic resonance spectra of Pb–DTPA complex at 39° at selected p*H* values.

tion. All four (*a*)-type carboxyl groups are equivalent throughout the p*H* range. At p*H* values $\geqslant 6$ the (*a*) protons give superimposed *AB* and *ABX* patterns (see Fig. 4) in the approximate ratio required for the relative abundances of lead isotopes having zero spin to one-half spin; ^{207}Pb, the only lead isotope with spin, has a spin of one-half and a relative abundance of 21% (31). From the *AB* spectrum it was found that $\nu_0\delta_{AB} = 12.1$ Hz and the absolute value of $J_{AB} = 16.2$ Hz. The sign of the coupling constant was assumed to be negative since this is close to the value expected for geminal protons adjacent to a keto group (32). Only the inner four peaks of the *AB* part of the *ABX* pattern can be distinguished. Within experimental error (± 0.2 Hz) these are symmetrically displaced with respect to the center of the *AB* multiplet. This is an example of a simple spectrum obtained when $J_{AX} = J_{BX}$ and the coupling constants were calculated from equations derived by Abraham and Bernstein (33, 34). The parameters obtained from the *AB* spectrum were used in the *ABX* spectrum to show that $J_{AX} = J_{BX}$ within 0.5 Hz. The lead-to-acetate proton coupling constant was equal to 12.8 Hz. Metal-to-proton coupling has previously been reported for some EDTA complexes (8) and the coupling constants found were: lead-to-acetate proton = 21.5 Hz, lead-to-ethylenic proton = 19.0 Hz, cadmium-to-acetate proton = 17.2 Hz.

As the p*H* is lowered below 6 the position of the resonance due to the (*a*) protons shifts to lower field and simultaneously the *AB* and *ABX* peaks broaden, then collapse to a common singlet. The p*H* dependence of the chemical shift is shown in Fig. 5, where for values of the p*H* above 6, the chemical shifts shown are for the center of the *AB* multiplet. Above p*H* values of 6 there is little dependence of chemical shifts upon p*H*. Starting from alkaline solution, as the p*H* is lowered, significant protonation of the complex, manifested by movement of chemical shifts towards lower field, does not begin until p*H* values of about 5.5 are reached, the extent of protonation increasing as the p*H* is lowered and reaching a steady value at about 3.5 (see Fig. 5). Allowing for differences in concentration and ionic strength, this is in agreement with studies of the protonation of Pb–DTPA complexes (35) for which it was found that

$$PbA^{3-} + H^+ \rightleftharpoons PbHA^{2-} \qquad \log K = 4.52$$

where A^{5-} represents the pentaanion of DTPA.

The (*d*) protons gave a simple spectrum throughout the entire study. No evidence was found for an *AB* spectrum (expected for unsymmetrical configurations) although broadening of the resonance did occur at $\sim 0°$. Evidence for metal–proton coupling was given by a small peak at a constant displacement of 10.5 Hz on the low field side of the (*d*) proton singlet. This was attributed to one half of an *AX* pattern, the high-field half being lost in resonances due to other protons. A lead-to-acetate proton coupling constant of 21 Hz was obtained, close to the value given above for the EDTA complex. A simple singlet can arise for the (*d*) protons in complexes in which the metal–oxygen(*4*) bonds are labile since rapid interconversion of configurations can give a time-averaged state in which there is a plane of symmetry through the (*d*)-type acetate group. This is consistent with the simplicity of the spectra due to the (*a*) protons which indicates that the lead–oxygen bonds are labile since the four terminal acetate groups show equivalent spectra under all conditions used in this study. Reference to Fig. 1 shows that there is no instantaneous structure in which this is possible so that a rapid exchange between coordinated and non-coordinated acetate groups is occurring. Since an *AB* pattern is observed for these acetate groups for p*H* $\geqslant 6$ the complex has an average configuration based on one or more configurations of type *2a*, *2b*, *3a*, or *3b* with relatively non-labile metal–nitrogen bonds. The contribution of configurations based on *1a*, *1b*, or *1c* to the average configuration must be small for p*H* $\geqslant 6$ since in these configurations inversion at the nitrogen atom is permitted and the (*a*) proton resonance would appear as a singlet. This conclusion is supported by the p*H* de-

Can. J. Chem. Downloaded from www.nrcresearchpress.com by 210.87.254.5 on 09/05/12
For personal use only.

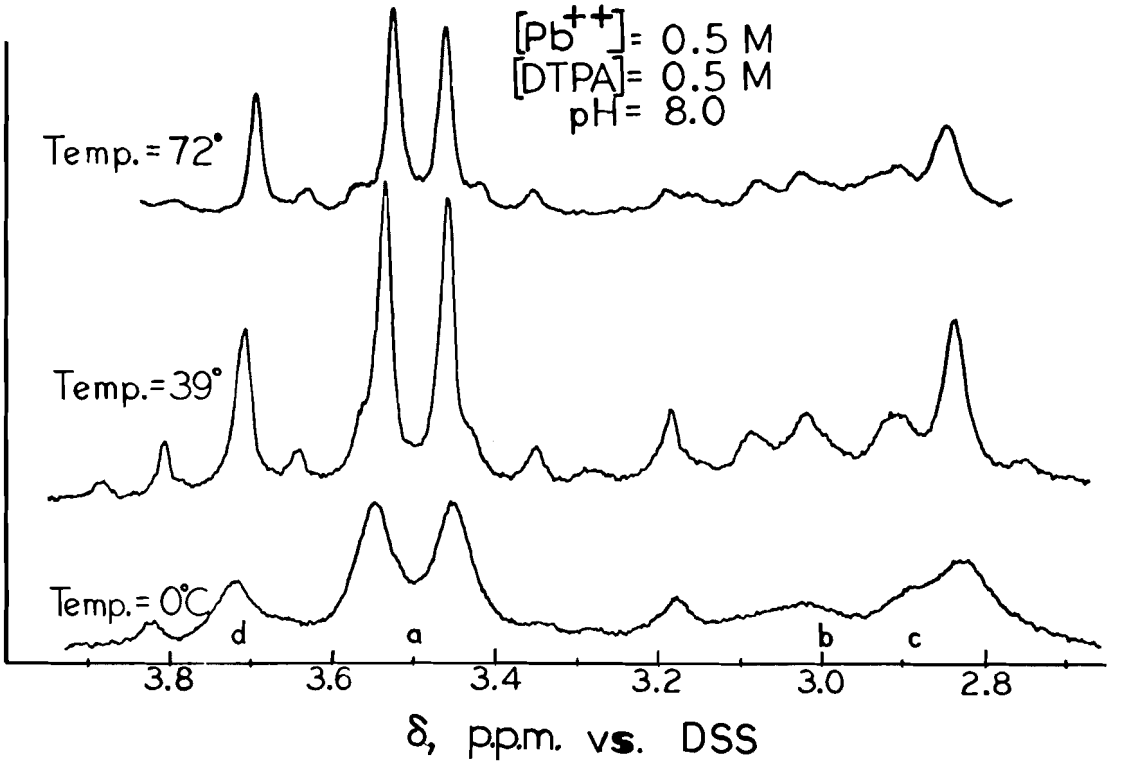

FIG. 3. Nuclear magnetic resonance spectra of Pb–DTPA complex at pH = 8 at selected temperatures.

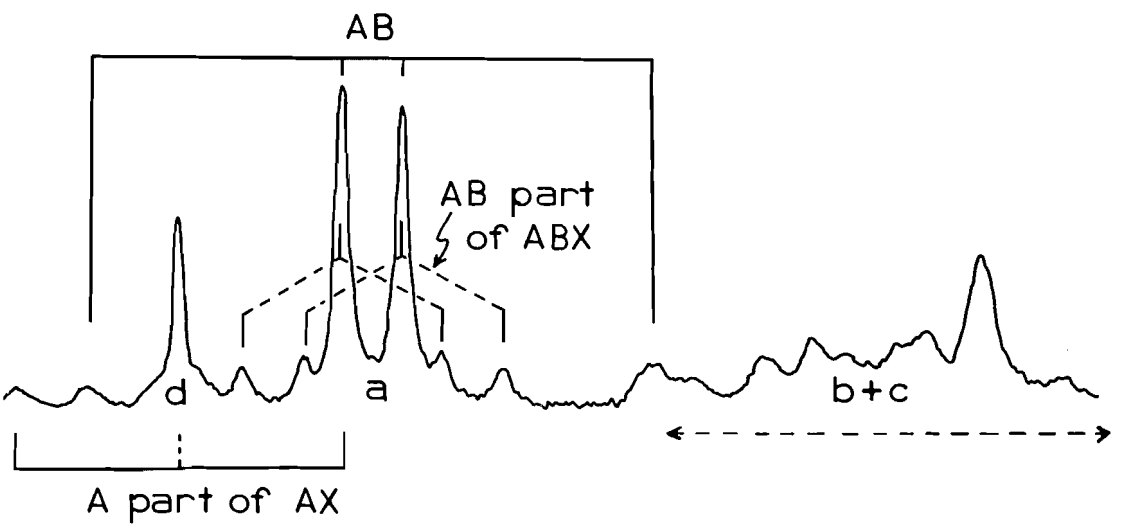

FIG. 4. Nuclear magnetic resonance spectrum of Pb–DTPA complex at pH = 9, and 72° showing metal–proton coupling.

Can. J. Chem. Downloaded from www.nrcresearchpress.com by 210.87.254.5 on 09/05/12
For personal use only.

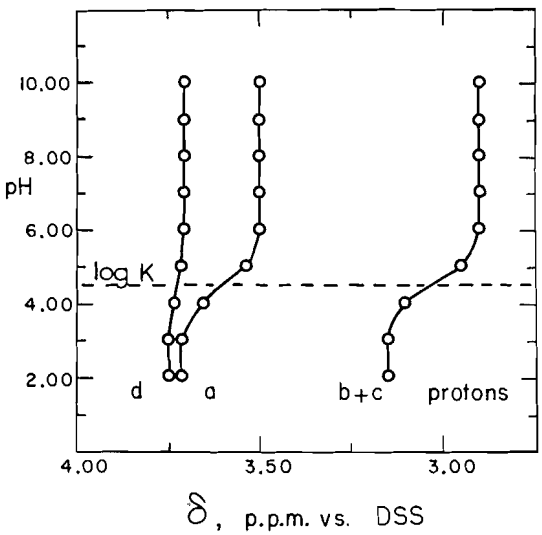

FIG. 5. Variation with pH of chemical shifts of non-labile protons for the Pb–DTPA complex, at 39°. Log K relates to the equilibrium constant for the protonation reaction (35): $PbA^{3-} + H^+ \rightleftharpoons PbHA^{2-}$.

pendence of the chemical shifts. For the free DTPA anion protonation begins when the pH is lowered to ~ 11 and as the pH is further lowered between 10 and 7 the preferred protonation sites are the terminal nitrogen atoms (1, 2). Complexes having average configurations with large contributions from *1a*, *1b*, and *1c* would show evidence (from variation of chemical shifts) of protonation at similar pH values to the free DTPA anion. Since little pH dependence of the chemical shifts is observed between pH = 10 and pH = 6 then contributions to the average configuration from *1a*, *1b*, and *1c* can play no significant part. Thus, all three nitrogen atoms are bonded to the metal atom, but a decision between a planar or non-planar arrangement of the nitrogen atoms cannot be made from the n.m.r. data.

The (*d*) protons show very little change in chemical shift as the pH is lowered from 10 to 3, indicating little change in the extent of protonation at the center nitrogen atom or center carboxylate group. Little protonation at the center nitrogen atom is expected without extensive unwrapping of the complex, but a carboxylate group free for a large fraction of time would surely show some protonation at pH values as low as 2. It seems likely that, irrespective of whether the metal–oxygen bond is labile, the center carboxylate group remains coordinated for an extensive fraction (nearly 100%) of the time throughout the complete range of conditions used in this study.

As the pH is lowered below 5.5, protonation of the complex occurs and the AB pattern of the (*a*) protons collapses to a singlet. This observation, together with the pH dependence of the chemical shifts is consistent with protonation predominantly at a terminal nitrogen atom and rapid interconversion between configurations in which one of the terminal nitrogen atoms is alternately coordinated or non-coordinated as in rapid interchange between one or more configurations of type *1a*, *1b*, *1c* (see Fig. 9). This conclusion is based mainly on the magnitude of the pH dependence of the chemical shift of the (*a*) protons. It is necessary to make the following assumptions: (*i*), in a configuration such as *1a* or *1b* or *1c* the non-coordinated aminodiacetate group shows a similar affinity for protonation both at its nitrogen and carboxylate sites as it does in free DTPA, *i.e.* we are not concerned with the actual extent of protonation at each site, though it is known that the nitrogen site is preferred (1, 2) (this assumption also requires the reasonable condition that proton transfer reactions are very much faster than the making and breaking of the metal–nitrogen bond); (*ii*), the chemical shift of the (*a*) protons is insensitive to whether the center nitrogen atom is protonated, or coordinated to the metal; (*iii*), when one of the terminal nitrogen atoms and its associated acetate groups are not coordinated to the metal the competition for coordination sites by the remaining carboxylate groups is reduced. If the terminal carboxylate groups are now coordinated to the metal ion for a greater percentage of the time that the terminal nitrogen atom is coordinated then a movement of chemical shift toward lower field (higher δ values) will occur. It was assumed that the correction for this effect was negligible; (*iv*), the chemical shift of the (*a*) protons depends directly upon the fraction of time that they spend in a given chemical environment. With these assumptions we can write

$$\delta_a = f\delta_c + (1 - f)\delta_l$$

where δ_a is the chemical shift of the (*a*) protons in the complex at a given pH, δ_l is the chemical shift of the (*a*) protons in free DTPA at the same pH, δ_c is the chemical shift of the (*a*) protons in the unprotonated complex (value at pH 10 used where it is assumed that the nitrogen atoms are co-ordi-

Can. J. Chem. Downloaded from www.nrcresearchpress.com by 210.87.254.5 on 09/05/12
For personal use only.

TABLE 1. Estimation of the extent of coordination of a terminal nitrogen atom, as a fraction of time (f) for which the nitrogen atom is coordinated, in lead(II) and cadmium(II) complexes with DTPA at 40°

		Lead(II)		Cadmium(II)	
pH	$\nu_0\delta_l$ (Hz)	$\nu_0\delta_a$ (Hz)	f (%)	$\nu_0\delta_a$ (Hz)	f (%)
10	199.0	209.0	100	197.0	100
7	227.7	209.8	96	196.8	100
6	228.8	210.5	93	196.8	100
5	228.8	212.4	83	197.5	99
4	229.5	219.5	49	199.5	92
3	231.5	223.0	37	204.0	80
2	233.5	223.3	42	217.4	44

nated 100% of the time), f is the fraction of time for which a terminal nitrogen atom is coordinated to the metal. Thus

$$f = (\delta_l - \delta_a)/(\delta_l - \delta_c)$$

Values of f, together with the required data for their calculation are given in Table 1. These values, though approximate, indicate that, on lowering the pH to 3 or 2 a single protonation of the complex occurs, with each terminal nitrogen atom becoming free about 50% of the time, *i.e.* either one or the other of the terminal nitrogen atoms becomes free nearly 100% of the time. A single protonation of the complex is indicated since, in free DTPA in this approximate pH range (p$H \simeq 4$) each aminodiacetate group is associated with one proton (1), and is confirmed by the protonation constant of the complex determined potentiometrically (35) (see above). The approximate nature of the results arises mainly from weaknesses in assumptions (*i*) and (*iii*) above. It has been shown that the extent of protonation of a given site in DTPA and other ligands is not independent of the condition of other sites (1, 2) though the extent of error is difficult to evaluate. The failure to apply a correction for weaknesses in assumption (*iii*) tends to make the f values in Table 1 too low. There can be little doubt that for the pH range 2 to 4 f values close to 50% would be obtained if adequate corrections could be applied and that the f values cited for p$H = 3$ and p$H = 2$ are equal within the accuracy of this approximate treatment.

The (*b*) and (*c*) protons gave a broad unresolved resonance at p$H = 5$. For p$H = 6$ a complex pattern of peaks involving many components resulted. Depending upon the rate of interconversion of configurations of the complex a complicated spectrum of the type $ABCD$ or $AA'BB'$ is to be expected. Lead-to-proton coupling for the ethylenic protons is also to be expected but components attributable to this could not be distinguished in the complex spectrum. No attempt was made to obtain quantitative information from the chemical shifts of the ethylenic protons owing to the complexity of their spectra and their poor resolution. The chemical shifts for the individual (*b*) and (*c*) protons were not obtained but the approximate center of gravity of the chemical shifts of the (*b*) and (*c*) pattern is plotted in Fig. 5. Although it is difficult to evaluate the chemical shifts of the (*b*) and (*c*) protons protonation of a terminal nitrogen atom should cause bigger variations in chemical shift for the (*b*) than for the (*c*) protons. Since protonation causes a narrowing of the width of the (*b*) + (*c*) resonance the (*b*) protons are initially at higher field (lower δ values). For the non-protonated complex, for p$H \geqslant 6$, the high field region of the (*b*) + (*c*) resonances contains higher, less broad peaks, than the low field region. Such asymmetry can be observed for an $ABCD$ type spectrum (36) and can readily be explained for the present case. The (*c*) protons are adjacent to the least labile metal–nitrogen bond in the complex. As far as the (*c*) protons are concerned, this quaternary nitrogen atom has three other substituents which are all different. The (*b*) protons are adjacent to a relatively more labile metal–nitrogen bond. To this quaternary nitrogen atom are bonded two acetate groups which have been shown to become equivalent by rapid exchange of coordination sites in the complex. Thus, the chemical environments of the type (*b*) geminal protons are more similar than those of type (*c*). Consequently the part of the (*b*) + (*c*) spectrum due to the (*b*) protons should be higher and less broad than that due to the (*c*) protons, in agreement with experimental observations.

Can. J. Chem. Downloaded from www.nrcresearchpress.com by 210.87.254.5 on 09/05/12
For personal use only.

Can. J. Chem. Downloaded from www.nrcresearchpress.com by 210.87.254.5 on 09/05/12
For personal use only.

Temperature changes alter the appearance of some of the spectra of solutions for which conditions are otherwise identical. This is due to alterations in labilities of metal to ligand bonds; these labilities may control the width of some of the resonances. Changes in chemical shift with temperature are small. On reducing the temperature from 70 to 0° the resonances of the (*a*) and (*d*) protons both move to lower field by 2–3 Hz, relative to the internal references, over the p*H* range studied.

Cadmium(II)–DTPA Solutions

The n.m.r. spectra of aqueous solutions of Cd(II) and DTPA were studied from p*H* = 2.0 to p*H* = 10.0. Representative spectra obtained for 1:1 ratios of Cd(II):DTPA are presented in Figs. 6 and 7. Figure 6 shows the spectra obtained at 40° at p*H* = 3.0, 4.5, and 6.0. Figure 7 shows the effect of temperature at p*H* = 10.0.

The position and form of the resonance due to the (*a*) protons depends upon the p*H* of the solution. At p*H* $\leqslant$ 3.0 all four (*a*)-type carboxyl groups are equivalent and give rise to a single n.m.r. peak. As the p*H* is raised, the peak broadens (p*H* $\simeq$ 4.5) and splits into two components (p*H* $\geqslant$ 6). These components are almost, though not quite, symmetrical and identical, and are not as sharp as the resonance for the *d* protons. They were interpreted as the center peaks of the *AB* spectra of chemically very similar, though not identical, (*a*) type, carboxymethyl groups where the outer peaks are lost in the background noise level so that J_{AB} could not be determined. As before metal–proton coupling is to be expected

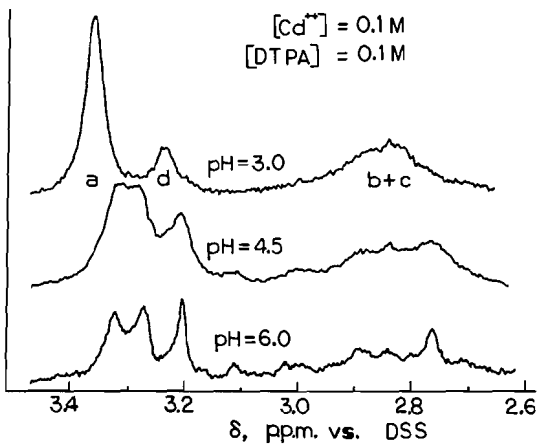

FIG. 6. Nuclear magnetic resonance spectra of Cd–DTPA complex at 40° at selected p*H* values.

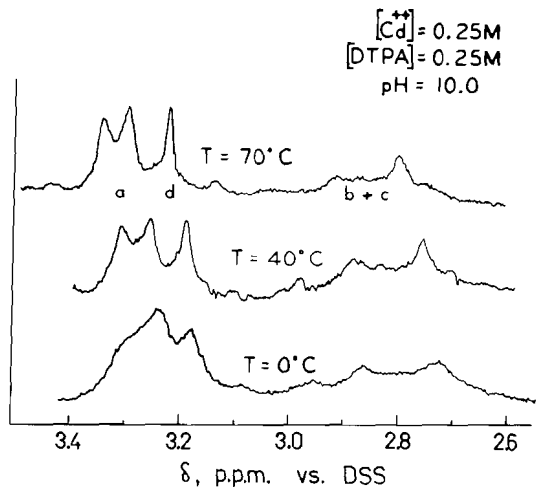

FIG. 7. Nuclear magnetic resonance spectra of Cd–DTPA complex at p*H* = 10 at selected temperatures.

since cadmium isotopes 111 and 113, with spin one-half, have together a relative abundance of approximately 25% (31). We were unable to observe the expected *ABX* pattern, probably because of the broadness of the spectra obtained. At high p*H* (see Fig. 7), as the temperature is lowered, the resonances due to the (*a*) protons broaden and become more unsymmetrical. This may be attributable to decreasing lability of the metal–oxygen bonds as the temperature is lowered, with the result that some of the "instantaneous" configurations of Fig. 1 have lifetimes which are significant in terms of the n.m.r. experiment. The chemical shift of the (*a*) protons as a function of p*H* is shown in Fig. 8. The p*H* region in which the chemical shift changes (p*H* = 2 to p*H* = 5) corresponds to the region in which the resonance changes from a singlet to an *AB* spectrum. For the *AB* spectrum the chemical shift is taken as the center of the twin inner peaks.

The (*d*) protons gave a singlet peak throughout the study. We were unable to detect the expected metal–proton coupling possibly because the small peaks anticipated for an *AX* spectrum overlapped the resonances for the (*a*) or (*b*) + (*c*) protons. An *AB* pattern expected for unsymmetrical configurations was not detected for the (*d*) protons but, at low temperatures, significant broadening of the resonance occurred. This is consistent with the decreasing metal–oxygen(*4*) bond lability suggested by the spectra of the (*a*) protons. The p*H* dependence of the chemical shift of the (*d*) protons is shown in Fig. 8.

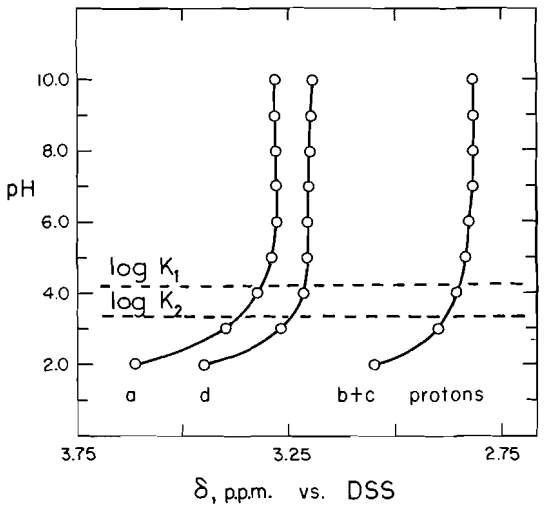

FIG. 8. Variation with pH of chemical shifts of non-labile protons for the Cd–DTPA complex, at 40°. Log K_1 and log K_2 relate to the respective equilibrium constants for the protonation reactions (37): $CdA^{3-} + H^+ \rightleftharpoons CdHA^{2-}$; $CdHA^{2-} + H^+ \rightleftharpoons CdH_2A^-$.

For p$H \geqslant 5$ there is little dependence of the chemical shifts of the (*a*) and (*d*) protons upon pH. Starting from alkaline solution, as the pH is lowered significant protonation of the complex, measured by movement of chemical shifts towards lower field, does not occur until the pH has reached approximately 4.5 (see Fig. 8) and the extent of protonation increases as the pH is lowered to pH = 2.0 and possibly lower. Allowing for differences in concentration and ionic strength, this is in agreement with studies of the protonation of Cd–DTPA complexes, where for the following equilibria the results obtained (37, 38) were

$$CdA^{3-} + H^+ \rightleftharpoons CdHA^{2-} \qquad \log K = 4.17 \text{ or } 4.09$$
$$CdHA^{2-} + H^+ \rightleftharpoons CdH_2A^- \qquad \log K = 3.32$$

where A^{5-} represents the pentaanion of DTPA. These results indicate that double protonation of the Cd(II)–DTPA complex will occur at sufficiently low pH values and will be extensive, *i.e.* greater than 50% of the complexes are doubly protonated, when p$H \leqslant 3.3$.

The (*a*) and (*d*) protons show closely similar dependencies of chemical shift upon the pH of the solution. Closer examination reveals that protonation of the complex causes bigger changes in chemical shift for the (*a*) protons than for the (*d*) protons. Furthermore, the variation in chemical shift on acidifying the solution occurs at slightly higher values of pH for the (*a*) protons than for the (*d*) protons.

When the spectra shown in Fig. 7 are compared with those of Pb–DTPA complexes under similar conditions (see Fig. 3), it is seen that the metal–ligand bonds are less labile for the cadmium than for the lead complexes. (Note the generally broader resonances for the (*a*) and (*d*) protons for the Cd—DTPA complexes than for the Pb–DTPA complexes.) It has also been reported that cadmium–ligand bonds are less labile than lead–ligand bonds in EDTA complexes (2). These observations allow a decision as to whether the (*d*)-type carboxyl group is coordinated to cadmium in the complex with DTPA. Thus, if the (*d*)-type carboxyl group were coordinated to cadmium it would be unlikely to protonate readily, since protonation of the (*d*)-type carboxyl group did not occur for the Pb–DTPA complex (1). In this latter complex, the (*d*)-type carboxyl group was shown to be coordinated to lead and protonation occurred preferentially at the terminal nitrogen atoms. Since the (*d*) protons suffer a significant change in chemical shift as the pH is lowered below 5, protonation of a non-coordinated (*d*)-type carboxyl group is indicated. The magnitude of the change (14.5 Hz between pH = 5.0 and pH = 2.0) is in agreement with that expected for protonation of a carboxyl group adjacent to a methylene group in an aminopolycarboxylic acid (5). Further support for the non-coordination of the (*d*)-type carboxyl group in the Cd complex is given by comparing the chemical shifts of the (*a*) and (*d*) protons in the Cd(II)–DTPA complex with those in the Pb(II)–DTPA complex.

Although the pH dependence of the chemical shift of the (*a*) protons parallels that of the (*d*) protons, a similar interpretation of the cause is not possible. That is, it is not due to protonation of the (*a*)-type carboxyl groups. The four (*a*)-type carboxyl groups are equivalent and even one proton per carboxyl group would be insufficient to produce the observed downfield movement of chemical shift of the (*a*) protons with pH, even assuming that the upfield shift produced by breaking a metal–oxygen bond is small. Furthermore, protonation of the (*a*)-type carboxyl groups would not produce changes in chemical shift of the magnitude observed for the (*b*) + (*c*) protons, nor cause collapse of the *AB* pattern for the spectra of the (*a*) protons. The results, in fact, are consistent with protonation occurring pre-

Can. J. Chem. Downloaded from www.nrcresearchpress.com by 210.87.254.5 on 09/05/12
For personal use only.

Can. J. Chem. Downloaded from www.nrcresearchpress.com by 210.87.254.5 on 09/05/12
For personal use only.

dominantly at one of the terminal nitrogen atoms and rapid interconversion between complexes in which first one, then the other, terminal nitrogen atom is coordinated to the metal. The breaking of the metal–nitrogen bond permits rapid umbrella inversion at the nitrogen atom and the (*a*) proton spectrum collapses to a singlet (2). Support for this view is given by the magnitude of the p*H* dependence of the chemical shifts of the (*a*) protons. These data were used to calculate *f*, the fraction of time for which a terminal nitrogen atom is coordinated, as described earlier for the Pb(II)–DTPA complex. Values of *f*, together with the data required for their calculation are given in Table 1. These approximate values, subject to the errors described earlier, indicate that as the p*H* is lowered to 2 each terminal atom becomes free about 50% of the time, *i.e.* either one or the other of the terminal nitrogen atoms is free nearly 100% of the time.

The (*b*) and (*c*) protons gave a broad, unresolved resonance at p$H \leqslant 4$ and for p$H \geqslant 5$ a complex pattern of peaks involving many components resulted, consistent with predictions from earlier discussion. The spectrum was asymmetric, the peaks to higher field being higher and less broad than those to lower field. However, the resolution was too poor for us to identify all the components of the assumed *ABCD* type spectrum, or to detect metal–proton coupling. No attempt was made to obtain quantitative information from the chemical shifts of the ethylenic protons but in Fig. 8 the chemical shift dependence of the approximate center of gravity of the resonances due to the (*b*) + (*c*) protons is shown. As with the Pb(II)–DTPA complex the width of the (*b*) + (*c*) resonance pattern decreases upon protonation and a similar interpretation of the spectrum is possible.

As with the lead complexes, temperature changes alter the labilities of metal to ligand bonds with consequent modification of the spectra. Changes in chemical shift with temperature are again small. On reducing the temperature from 70 to 0° the resonances of the (*a*) and (*d*) protons both move to lower field by 3–4 Hz, relative to the internal reference, over the p*H* range studied.

Comparison between the DTPA Complexes of Pb(II) and Cd(II)

The interpretations of the experimental results are summarized in the schemes of Fig, 9.

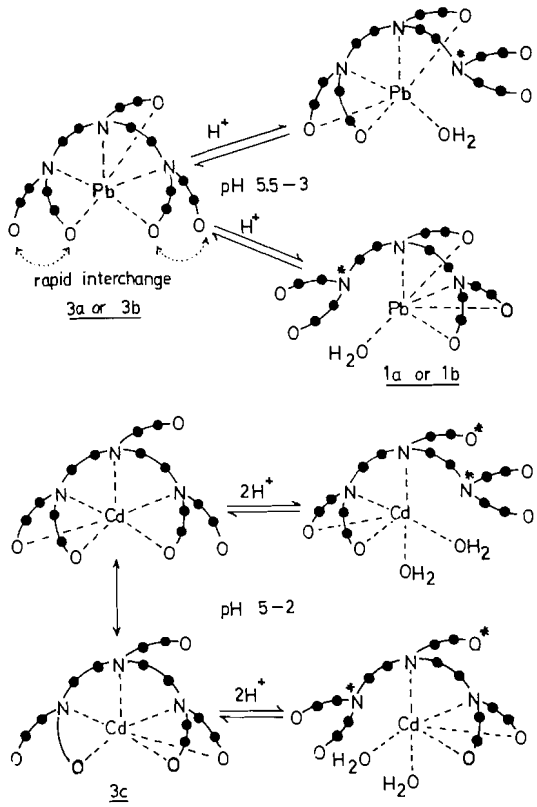

FIG. 9. Schematic representation of equilibria in Pb–DTPA solutions and Cd–DTPA solutions. Six-coordinate complexes are shown though seven or eight-coordinate complexes are considered probable. The more likely octahedral configurations are identified by reference to Fig. 1. (* = preferred protonation site).

The Pb(II)–DTPA complex has labile metal-to-oxygen bonds which permit the terminal carboxyl groups to become equivalent, or at least not detectably different, in the coordination polyhedron. For p$H \geqslant 6$ the complex is not protonated. At lower p*H* values, protonation of the complex occurs predominantly at one of the terminal nitrogen atoms. Rapid interconversion then occurs between protonated complexes in which first one, then the other, terminal nitrogen atom is coordinated to the metal. The center carboxyl group remains coordinated in the p*H* range 2–10.

The Cd(II)–DTPA complex has labile metal-to-oxygen bonds which permit the terminal carboxyl groups to become nearly equivalent in the coordination polyhedron. However, the metal-to-ligand bonds are less labile than those of the lead–DTPA complexes and at low temperatures, at high p*H*, the lability decreases sufficiently to

Can. J. Chem. Downloaded from www.nrcresearchpress.com by 210.87.254.5 on 09/05/12
For personal use only.

show that non-equivalent carboxyl groups are present. For $pH \geqslant 5$ the complex is not protonated. As the pH is lowered, protonation occurs preferentially at two non-equivalent sites, namely, at the non-coordinated center carboxyl group and also at one of the terminal nitrogen atoms. Of these two sites the proton seems to show a slight preference for the nitrogen atom. Since the two pairs of terminal carboxyl groups remain equivalent, interconversion between protonated complexes having first one, then the other, nitrogen atom coordinated, occurs.

The difference in behavior between the lead and cadmium complexes is attributed mainly to the difference in size between the lead(II) and cadmium(II) ions, though the different electronic structures ($d^{10}s^2$ and $d^{10}s^0$, respectively) may be a contributing factor. In both complexes the metal-to-ligand bonds will be predominantly ionic and it is to be expected that the bonds formed by the smaller Cd(II) ion will be less labile than those formed by the larger Pb(II) ion (17, 20), as found experimentally. Further deductions were made from a study of molecular models, with the result that the conclusions drawn will be indicative rather than conclusive.

First, the octahedral configurations of Fig. 1 were considered. Configurations *2a–2c* and *3a–3d* are fundamentally different in that in *2a–2c* the nitrogen atoms occupy adjacent positions in the coordination octahedron whereas in *3a–3d* the three nitrogen atoms and the metal atom lie in the same plane. The models predict that ring strain in the acetate rings is less when the carboxymethyl groups attached to the same nitrogen atom adopt *cis* rather than *trans* positions in the coordination octahedron and thus configurations *1c* and *3d* are considered less probable than other configurations. The models further predict very considerable steric interference between the methylene groups of the terminal carboxymethyl groups in configurations *2a–2c*, even when the central metal ion is very large. Although the center carboxyl group is sterically readily accessible to the metal none of the configurations *2a–2c* seem probable for metal–DTPA complexes. Furthermore, in these configurations, for relatively non-labile metal–nitrogen bonds, it is not possible for the terminal carboxyl groups to become equivalent by rapid exchange of coordination positions. Of the pair of carboxyl groups at either end of the DTPA molecule one can coordinate only at a position *trans* to the center nitrogen atom. The other carboxyl group of this pair can coordinate either at this position or at a position *cis* to the center nitrogen atom. Thus, for the terminal carboxymethyl groups to have nearly equivalent n.m.r. spectra would imply that they were in fact coordinated to the metal ion for a small, nearly equal, fraction of time. This seems unlikely in view of the very high stability constants of metal–DTPA complexes.

When the metal and three nitrogen atoms are coplanar, as in configurations *3a–3d*, steric interference is much less. Even when the metal ion is small, none of the terminal acetate groups interfere with each other. However, the steric accessibility of the center carboxyl group to the metal depends upon the size of the metal ion. For small metal ions, interference between the center and terminal carboxymethyl groups will occur. This interference decreases as the size of the central ion increases. It is to be anticipated that there will be a critical size below which steric interference becomes a major factor in determining the nature of the coordination of metal–DTPA complexes. Possibly this is the main reason why the center carboxyl group is coordinated in the lead–DTPA complex but not in the smaller cadmium–DTPA complex.

When the center carboxyl group is not coordinated, as in configurations *3c* and *3d* then each of the terminal carboxyl groups can coordinate either *cis* or *trans* to the center nitrogen atom. The two *cis* positions (one above, one below, the plane shown in configurations *3c* and *3d*) are not strictly equivalent since only one *cis* position is on the same side of the plane as the uncoordinated center carboxymethyl group. The difference between them is probably very small and in rapidly interconverting structures the four terminal acetate groups can become essentially equivalent. This could be an adequate, though not necessarily correct description of the Cd(II)–DTPA complex. The center carboxyl group can only coordinate at a position *cis* to the center nitrogen atom, as in configurations *3a* and *3b* and in these cases the terminal carboxymethyl groups should not become strictly equivalent by rapid interconversion of structures. Thus, so far, an adequate description of the structure of the Pb(II)–DTPA complex has not been found.

The foregoing discussion has assumed octahedral coordination for the metal ions. The possibility of the trigonal prism as an alternative basis for six-coordination was considered and rejected.

Can. J. Chem. Downloaded from www.nrcresearchpress.com by 210.87.254.5 on 09/05/12
For personal use only.

In view of the conclusions of Hoard and coworkers (22–30) the assumption of six-coordination is doubtful. They found the coordination numbers in aminopolycarboxylate complexes of the following ions were: Mn(II), seven (25); Fe(III), seven (26, 30); Zr(IV), eight (27); Ln(III), eight to ten (28, 29). Coordination numbers of seven and eight for Fe(III) in aminopolycarboxylate complexes have also been proposed on the basis of Mössbauer studies (39, 40). For large metal ions the strain in the ethylenic chelate ring increases rapidly with increasing size of the central ion. The stress is expected to be relieved mainly by distortions in the coordinate bonds. Bond angles at the metal may be reduced from the usual 90°. Consequently, the ethylenic chelate rings do not extend as far around the central ion as in a regular octahedral complex. This leaves more room for carboxyl groups to coordinate on the opposite hemisphere of the metal. A coordination number greater than six is therefore to be expected for large ions.

It is difficult to estimate the coordinate bond lengths in the DTPA complexes studied here but the Pauling ionic radii of Cd^{2+} (0.97 Å) and Pb^{2+} (1.21 Å) are larger than those of Mn^{2+}, Fe^{3+}, and Zr^{4+} whereas the radius of La^{3+} is 1.15 Å (17). In comparison with Hoard's results discussed above, and considering the scant tabulated data (41) for the appropriate metal–nitrogen and metal–oxygen coordinate bonds, it is probable that for Cd(II) and Pb(II) complexes (particularly the latter) seven or eight coordination can occur though this conclusion must await experimental confirmation. Configurations in which the metal and the three nitrogen atoms are approximately coplanar are anticipated since these should have minimal steric interference. Even without the restricting assumption of octahedral coordination the equivalence (or apparent equivalence) of the n.m.r. spectra of the four terminal carboxymethyl groups in the Pb–DTPA complex is difficult to explain. The four terminal carboxyl groups cannot coordinate at exactly equivalent positions. Differences between these positions are likely to be smaller than for regular octahedral coordination, however, and in rapidly interconverting structures they may not be large enough to cause noticeable differences in n.m.r. spectra.

The most basic sites in the DTPA molecule are the nitrogen atoms. In a metal complex the nitrogen atoms are free only for a very small fraction of the time and do not protonate extensively until $[H^+]$ becomes relatively high. When one of the terminal nitrogen atoms is not coordinated the stress in the ligand is reduced and the other terminal nitrogen atom is expected to coordinate more strongly. Thus only one terminal nitrogen atom is protonated at one time. The basicity of its associated carboxyl groups is reduced, and the center carboxyl group, if not coordinated, should protonate more readily than these. This is thought to be the case for the Cd(II)–DTPA complex.

We thank the National Research Council of Canada for financial support of this work.

1. J. L. Sudmeier and C. N. Reilley. Anal. Chem. **36**, 1698 (1964)
2. R. J. Kula and D. T. Sawyer. Inorg. Chem. **3**, 458 (1964).
3. J. L. Sudmeier and C. N. Reilley. Anal. Chem. **36**, 1707 (1964).
4. D. Chapman, D. R. Lloyd, and R. H. Prince. J. Chem. Soc. 3645 (1963).
5. R. J. Kula, D. T. Sawyer, C. I. Chan, and C. M. Finley. J. Am. Chem. Soc. **85**, 2930 (1963).
6. R. J. Kula. Anal. Chem. **37**, 989 (1965).
7. J. L. Sudmeier and C. N. Reilley. Inorg. Chem. **5**, 1047 (1966).
8. R. J. Day and C. N. Reilley. Anal. Chem. **36**, 1073 (1964).
9. C. N. Reilley. Anal. Chem. **37**, 1298 (1965).
10. Y. A. Aochi and D. T. Sawyer. Inorg. Chem. **5**, 2085 (1966).
11. L. V. Haynes and D. T. Sawyer. Inorg. Chem. **6**, 2146 (1967).
12. B. B. Smith and D. T. Sawyer. Inorg. Chem. **7**, 922 (1968).
13. B. B. Smith and D. T. Sawyer. Inorg. Chem. **7**, 1526 (1968).
14. B. B. Smith and D. T. Sawyer. Inorg. Chem. **8**, 1154 (1969).
15. B. B. Smith and R. H. Betts. J. Am. Chem. Soc. **91**, 7749 (1969).
16. A. Bryson and G. H. Nancollas. Chem. Ind. 654 (1965).
17. F. A. Cotton and G. Wilkinson. Advanced inorganic chemistry. 2nd ed. Interscience, New York. 1968.
18. S. Kirschner. (Editor) Advances in the chemistry of the coordination compounds. Macmillan, New York. 1961.
19. J. Lewis and R. G. Wilkins. (Editors) Modern coordination chemistry. Interscience. New York. 1960.
20. F. Basalo and R. G. Pearson. Mechanisms of inorganic reactions. 2nd Ed. John Wiley, New York. 1960.
21. A. E. Martell and M. Calvin. Chemistry of the metal chelate compounds. Prentice-Hall, Inc., Englewood Cliffs, N.J. 1952.

22. H. A. WEAKLIEM and J. L. HOARD. J. Am. Chem. Soc. **81**, 549 (1959).
23. G. S. SMITH and J. L. HOARD. J. Am. Chem. Soc. **81**, 556 (1959).
24. J. L. HOARD, G. S. SMITH, and M. LIND. *In* Advances in the chemistry of the coordination compounds. MacMillan, New York. 1961. pp. 296–302.
25. S. N. RICHARDS, B. PEDERSEN, J. V. SILVERTON, and J. L. HOARD. Inorg. Chem. **3**, 27 (1964).
26. M. D. LIND, M. J. HAMOR, T. A. HAMOR, and J. L. HOARD. Inorg. Chem. **3**, 34 (1964).
27. J. L. HOARD, E. WILLSTADTER, and J. V. SILVERTON. J. Am. Chem. Soc. **87**, 1610 (1965).
28. M. D. LIND, B. LEE, and J. L. HOARD. J. Am. Chem. Soc. **87**, 1611 (1965).
29. J. L. HOARD, B. LEE, and M. D. LIND. J. Am. Chem. Soc. **87**, 1612 (1965).
30. G. H. COHEN and J. L. HOARD. J. Am. Chem. Soc. **88**, 3228 (1966).
31. J. W. EMSLEY, J. FEENEY, and L. H. SUTCLIFFE. High resolution nuclear magnetic resonance spectroscopy. Vol. 2, Appendix A. Pergamon Press, Oxford. 1966.
32. J. A. POPLE and A. A. BOTHNER-BY. J. Chem. Phys. **42**, 1339 (1965).
33. R. J. ABRAHAM and H. J. BERNSTEIN. Can. J. Chem. **39**, 216 (1961).
34. J. A. POPLE, W. G. SCHNEIDER, and H. J. BERNSTEIN. High resolution nuclear magnetic resonance. McGraw-Hill, New York. 1959. p. 132.
35. G. ANDEREGG, P. NÄGELI, F. MÜLLER, and G. SCHWARZENBACH. Helv. Chim. Acta, **42**, 827 (1959).
36. C. A. REILLY and J. D. SWALEN. J. Chem. Phys. **34**, 980 (1961).
37. S. CHABAREK, A. E. FROST, M. A. DORAN, and N. J. BICKNELL. J. Inorg. Nucl. Chem. **11**, 184 (1959).
38. E. J. DURHAM and D. P. RYSKIEWICH. J. Am. Chem. Soc. **80**, 4812 (1958).
39. J. J. SPIJKERMAN, L. H. HALL, and J. L. LAMBERT. J. Am. Chem. Soc. **90**, 2039 (1968).
40. L. H. HALL, J. J. SPIJKERMAN, and J. L. LAMBERT. J. Am. Chem. Soc. **90**, 2044 (1968).
41. Tables of Internuclear Distances. Special Publication Nos. 11 and 18. The Chemical Society, London, 1958 and 1965.

Can. J. Chem. Downloaded from www.nrcresearchpress.com by 210.87.254.5 on 09/05/12
For personal use only.

Can. J. Chem. Downloaded from www.nrcresearchpress.com by 210.87.254.5 on 09/05/12
For personal use only.

Metal – Aminopolycarboxylic Acid Complexes. II. Studies of Triethylenetetraaminehexaacetic Acid and its Lead(II) Complexes in Aqueous Solution by Proton Magnetic Resonance Spectroscopy

P. LETKEMAN

Department of Chemistry, Brandon University, Brandon, Manitoba

AND

J. B. WESTMORE

Department of Chemistry, University of Manitoba, Winnipeg, Manitoba

Received June 29, 1970[1]

Nuclear magnetic resonance (n.m.r.) spectroscopy was used to determine the preferred protonation sites in TTHA. For its 1:1 complex with Pb(II) the following equilibrium constants for protonation were obtained (triethylenetetraaminehexaacetic acid ≡ H_6A)

$$PbA^{4-} + H^+ \rightleftharpoons PbHA^{3-} \qquad \log K = 8.25 \pm 0.2$$
$$PbHA^{3-} + H^+ \rightleftharpoons PbH_2A^{2-} \qquad \log K = 4.25 \pm 0.25$$

The non-protonated complex is considered to have four coplanar (or nearly coplanar) metal–nitrogen bonds with the center carboxylate groups coordinated above and below this plane, and with the terminal carboxylate groups playing only a small part in the coordinate bonding. The first and second protonations of the complex occur preferentially at the terminal and center nitrogen atoms, respectively, on the same side of the complex, accompanied by breaking of the respective metal–nitrogen bonds. This causes partial unwrapping of the complex from one side. Rapid interconversion between configurations in which unwrapping and rewrapping occurs first from one side of the molecule and then from the other leads to simplified n.m.r. spectra.

La spectroscopie r.m.n. a été utilisée pour déterminer les sites préférentiels de protonation dans le TTHA. Dans le cas d'une complexation 1:1 avec le Pb(II) les constantes d'équilibre suivantes ont été obtenues pour la protonation (acide triéthylènetétraaminehéxaacétique ≡ H_6A)

$$PbA^{4-} + H^+ \rightleftharpoons PbHA^{3-} \qquad \log K = 8.25 \pm 0.2$$
$$PbHA^{3-} + H^+ \rightleftharpoons PbH_2A^{2-} \qquad \log K = 4.25 \pm 0.25$$

Dans le complexe non protoné, on considère que les quatre liaisons métal–azote sont coplanaires (ou presque coplanaires), que les groupes carboxylates centraux sont coordonnés au-dessus et en dessous du plan et que les groupes carboxylates terminaux n'interviennent que très peu dans les liaisons coordonnées. La première et la seconde protonation du complexe se font préférentiellement et respectivement sur les atomes d'azote terminaux et centraux et sur le même côté du complexe provoquant ainsi la rupture respective des liaisons métal–azote. Ceci provoque un déroulement du complexe à partir d'un côté. L'interconversion rapide entre les configurations ou l'enroulement et le déroulement se fait d'abord d'un côté de la molécule puis de l'autre, conduit à simplifier les spectres r.m.n.

Canadian Journal of Chemistry, 49, 2086 (1971)

Introduction

The application and background of proton magnetic resonance (p.m.r.) in the study of aqueous solutions of aminopolycarboxylic acids and their diamagnetic complexes have been discussed in the first paper in this series (see ref. 1 and references therein). These discussions may be readily extended to aminopolycarboxylic acids and their complexes other than those described in Part I.

In this paper we report the results of a study of aqueous solutions containing triethylenetetraaminehexaacetic acid (TTHA) and Pb(II), using p.m.r. spectroscopy. The hexaanion of TTHA is represented as

[1]Revision received March 12, 1971.

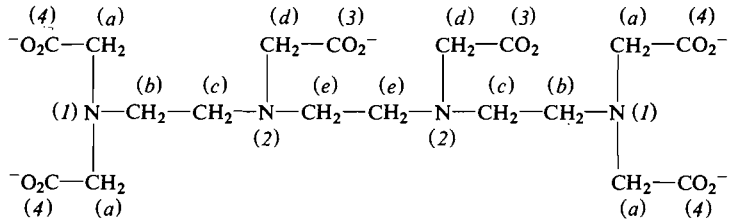

in which donor sites are labelled as (*1*), (*2*), (*3*), and (*4*) and non-labile protons by (*a*), (*b*), (*c*), (*d*), and (*e*). Donor sites or non-labile protons which are equivalent by symmetry have the same label.

Since it was first reported in 1956 (2) TTHA has been used as a titrimetric reagent for metal ions (3) and formation constants of its complexes with a few metal ions have also been determined (4–8). Of particular interest from a theoretical viewpoint is its ability to form 1:1, 2:1, and 3:1 complexes with metal ions (5–7) and also to form mixed complexes (9–11). Its acid dissociation constants have also been determined (2, 4, 5). Infrared (11) and polarographic (12, 13) studies of some of its metal complexes have been reported as well. Since a p.m.r. study of TTHA has not appeared to date this was undertaken by us and since the results are important in the interpretation of the spectra of the 1:1 Pb–TTHA complexes studied here they are also reported in this paper.

Experimental

The proton magnetic resonance spectra were recorded with Varian A56/60A and A-60D spectrometers. The spectra were recorded at temperatures (±1°) of 0, 40, and 72 °C. The spectral data obtained were average readings of three or more recordings with a reproducibility of ±0.4 Hz. Tertiary-butyl alcohol (TBA) was used as an internal reference, though the values of the chemical shifts are reported with respect to sodium trimethylsilylpropane sulfonate (DSS) as previously described (1).

Triethylenetetraaminehexaacetic acid (TTHA) was obtained through the courtesy of the Geigy Chemical Co., Basel, Switzerland. The compound was purified by recrystallization from water. A 0.20 *M* solution of free ligand (TTHA) was prepared by adding 4.945 g of the acid to 40 ml of water, the suspension stirred and potassium hydroxide pellets added until the acid was dissolved. The solution was then diluted to 50.00 ml with the addition of distilled water. Similarly, the Pb–TTHA solutions were prepared by first dissolving the acid (TTHA) in water (made basic with KOH) and later adding the appropriate amount of reagent grade lead nitrate to make a 1:1 mole ratio of metal to ligand at 0.20 *M*. The p*H* of the various solutions was adjusted by the addition of potassium hydroxide or nitric acid and recorded as previously described (1).

Results and Discussion

TTHA

The p.m.r. spectra of TTHA were studied over the p*H* range 1–12. Representative spectra for 0.2 *M* solutions are shown in Figs. 1 and 2. Figure 1 shows the effect of varying p*H* at a temperature of 40° while Fig. 2 shows the effect of varying temperature when the p*H* = 12.0. The assignments of the various resonances in the spectra were made from their relative peak areas, dependence upon p*H* and from expectations based on earlier work (14, 15). Symmetry requires that (*i*) the eight (*a*) protons be equivalent, (*ii*) the four (*d*) protons be equivalent, (*iii*) the four (*e*) protons be equivalent. As anticipated, these groups of protons each give single peaks throughout the entire p*H* range of the study. The (*b*) and (*c*) protons are non-equivalent but their chemical shift difference is likely to be relatively small. This is borne out by the experimental results in which individual (*b*) and (*c*) resonances were not observed. Instead a multi-

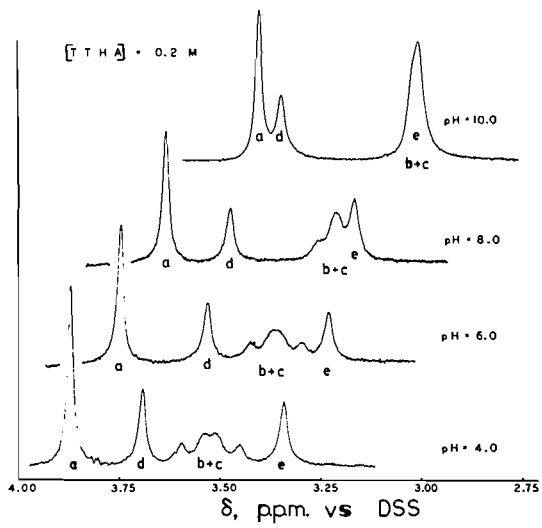

FIG. 1. Proton magnetic resonance spectra of TTHA at 40° at selected p*H* values.

Can. J. Chem. Downloaded from www.nrcresearchpress.com by 210.87.254.5 on 09/05/12
For personal use only.

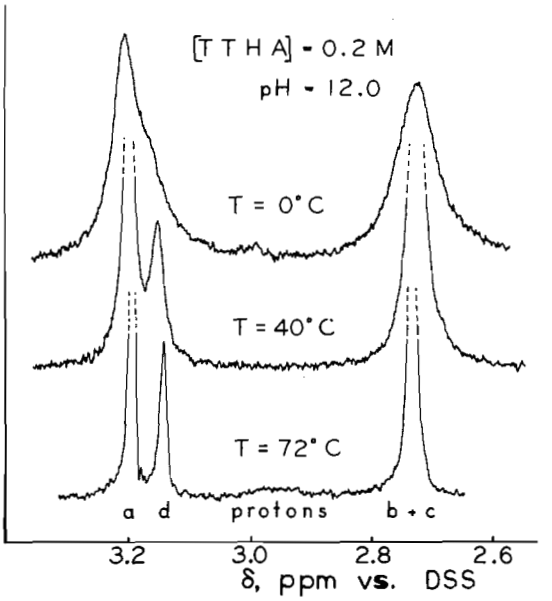

FIG. 2. Proton magnetic resonance spectra of TTHA at pH = 12 at selected temperatures.

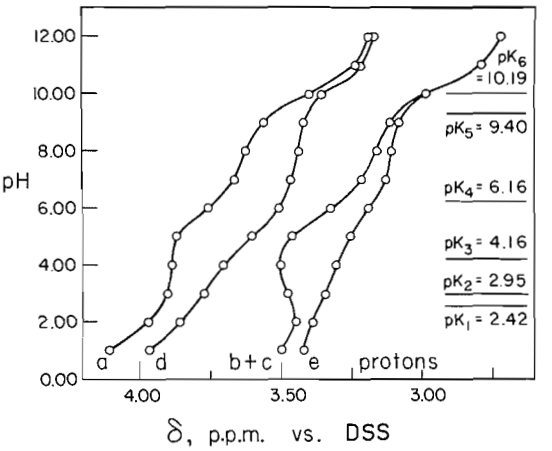

FIG. 3. Variation of chemical shifts of non-labile protons of TTHA with pH.

plet (presumably an unresolved $AA'BB'$ spectrum) is observed, comprising two equivalent sets of four protons. Thus, the only possible source of ambiguity concerns the resonances attributable to the (*d*) and (*e*) protons. Fortunately, it has been shown (14) that, for aminopolycarboxylic acids, resonances due to acetate protons occur at significantly lower field than those due to ethylenic protons. In fact, any other assumption than this is irreconcilable with the pH dependencies of the chemical shifts observed in this work.

The pH dependencies of the chemical shifts of the various resonances are shown in Fig. 3 (for the (*b*) and (*c*) protons the mean chemical shift is given). Also shown are pK values for TTHA (2, 4, 5). At pH = 12, TTHA exists in solution as the hexaanion. As the pH is lowered to *ca.* 8.5 the chemical shifts of all protons move toward lower field. Between pH = 8.5 and pH = 7.0, further movement of chemical shift toward lower field is small indicating that little protonation occurs in this region. This is in agreement with the large difference between pK_4 and pK_5 ($\Delta pK \simeq 3.2$). The pK values indicate that when the pH is lowered from pH = 12 to pH = 8 two protons are added to the TTHA hexaanion. The magnitude of the change in chemical shifts supports this view (see below). When the pH is lowered below pH = 7, further pH regions within which the chemical shifts of all protons remain approximately constant are not apparent. This is to be expected since only small differences exist between successive values of pK_1, pK_2, pK_3, and pK_4 (*i.e.* $pK_n - pK_{n-1} \leq 2$).

It is of importance to the results discussed in the latter part of this paper to determine the preferred protonation sites, and extent of protonation of these sites, in the TTHA anions. This can be done by a method similar to that used by Sudmeier and Reilley (14) if certain rather approximate assumptions are made. In a molecule such as the hexaanion of TTHA, which has several different sites which can accept a proton, the change in chemical shift of a given type of non-labile proton upon varying the pH will depend upon the proximity of the non-labile proton to the site, or sites, at which protonation occurs, and also the fractions of time for which the site or sites, are protonated. It is assumed that the contributions to the chemical shift changes from protonation of different sites are perfectly additive, and linearly related to the fractions of time for which the sites are protonated (14). For TTHA the chemical shifts of the various protons are given by

$$[1] \quad \delta_a = \delta_a^0 + f_1 C_N + f_4 C_0$$
$$[2] \quad \delta_b = \delta_b^0 + f_1 C_N + f_2 C_N'$$
$$[3] \quad \delta_c = \delta_c^0 + f_2 C_N + f_1 C_N'$$

Can. J. Chem. Downloaded from www.nrcresearchpress.com by 210.87.254.5 on 09/05/12
For personal use only.

Can. J. Chem. Downloaded from www.nrcresearchpress.com by 210.87.254.5 on 09/05/12
For personal use only.

$$[4] \quad \delta_{bc} = \delta_{bc}^{0} + \tfrac{1}{2}(f_1 + f_2)(C_N + C_N')$$

$$[5] \quad \delta_d = \delta_d^{0} + f_2 C_N + f_3 C_0$$

$$[6] \quad \delta_e = \delta_e^{0} + f_2(C_N + C_N')$$

where δ_a, δ_b, δ_c, δ_d, and δ_e are the chemical shifts of the (*a*), (*b*), (*c*), (*d*), and (*e*) protons, respectively, at a given p*H*; δ_a^{0}, δ_b^{0}, δ_c^{0}, δ_d^{0}, and δ_e^{0} are the chemical shifts of the corresponding protons in the TTHA hexaanion (values at p*H* = 12 were used); f_1, f_2, f_3, and f_4 are the fractions of time for which each equivalent site of types (*1*), (*2*), (*3*), and (*4*), respectively, are protonated; C_N is the change in chemical shift produced in the methylene protons, either acetate or ethylenic, upon protonation of the adjacent nitrogen; C_N' is the change in chemical shift produced in an ethylenic proton separated by one CH_2 group from the nitrogen at which protonation occurs; C_0 is the change in chemical shift produced in the acetate protons upon protonation of the carboxylate group; δ_{bc} and δ_{bc}^{0} are the average values of δ_b and δ_c, and δ_b^{0} and δ_c^{0}, respectively, introduced because these values are more readily determined than the individual chemical shifts which are not accurately determinable from the experimental data.

A further important relationship is

$$2f_1 + 2f_2 + 2f_3 + 4f_4 = n$$

where *n* is the number of equivalents of acid added to one mole of TTHA hexaanion and the coefficients arise from the number of equivalent sites of each type.

If C_N, C_N' and C_0 are known then, in principle, f_1, f_2, f_3, and f_4 can be determined since all other quantities are experimentally observable. The first task is to calculate C_N, C_N' and C_0. Values of C_0 and C_N' were obtained by assuming that at p*H* = 7.4 two equivalents of acid have been added to one mole of TTHA hexaanion. Since carboxyl groups are negligibly protonated at such high p*H* values then $f_3 = f_4 = 0$ and therefore $2f_1 + 2f_2 = 2$. Equations 1, 4, 5, and 6 may be used to determine C_N and C_N'. There are more equations than necessary and slight differences in values of C_N and C_N' arise depending upon which equations are used. These variations are not serious and arise because of the simplifying assumptions made. It is apparent that $C_N \simeq 45 \pm 5$ Hz (0.75 p.p.m.) and $C_N' \simeq 15 \pm 5$ Hz (0.25 p.p.m.). Since these values agree favorably with those obtained by Sudmeier and Reilley (C_N = 0.75 p.p.m., C_N' = 0.35 p.p.m.) for similar though different systems (14), they were used for subsequent calculations.

Values of f_1 and f_2 can be calculated as a function of p*H*. The δ_e values can be used to determine values of f_2, using eq. 6. The δ_{bc} values may be used to determine values of $f_1 + f_2$, using eq. 4, and hence f_1. We estimate that the error in the values obtained for f_2 are probably not larger than $\pm 10\%$ and for f_1 not larger than $\pm 20\%$, of the calculated values. Values of f_3 and f_4 are more difficult to calculate. In principle, these can be obtained from δ_d and δ_a, respectively, if f_1, f_2, and C_0 are known. In fact, because C_0 is relatively small (0.2 p.p.m. according to Sudmeier and Reilley (14)), the relatively small errors in f_1, f_2, C_N, or C_N' can cause large errors in f_3 and f_4. Instead, we have assumed (rather arbitrarily, though with probably small error) that at p*H* = 2, *n* = 6; *i.e.* $2f_1 + 2f_2 + 2f_3 + 4f_4 = 6$ and have calculated that C_0 = 17 Hz. Finally f_3 and f_4 were calculated from δ_d and δ_a though the error could be as much as twice as high as those in f_2 and f_1, respectively. The results given in Fig. 4 show that initially all the nitrogen sites are approximately equally basic but when $f_2 \geq 0.3$ the preferred protonation sites are the terminal nitrogen atoms. Somewhat less preferred are the center nitrogen atoms where repulsions between protons would be greater. The center carboxylate groups protonate more readily than the terminal

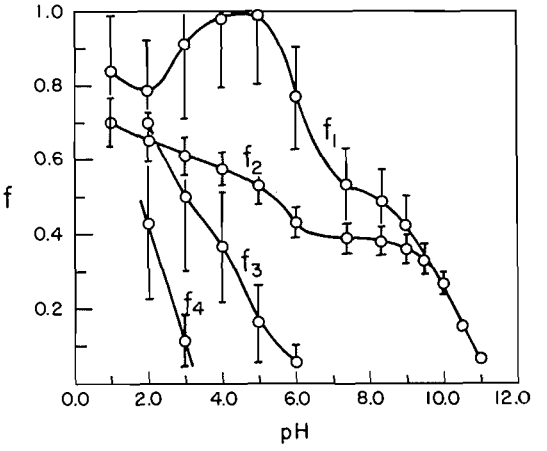

FIG. 4. Extent of protonation of various sites in TTHA as a function of p*H*, expressed as the fraction, *f*, of the time for which a site is protonated.

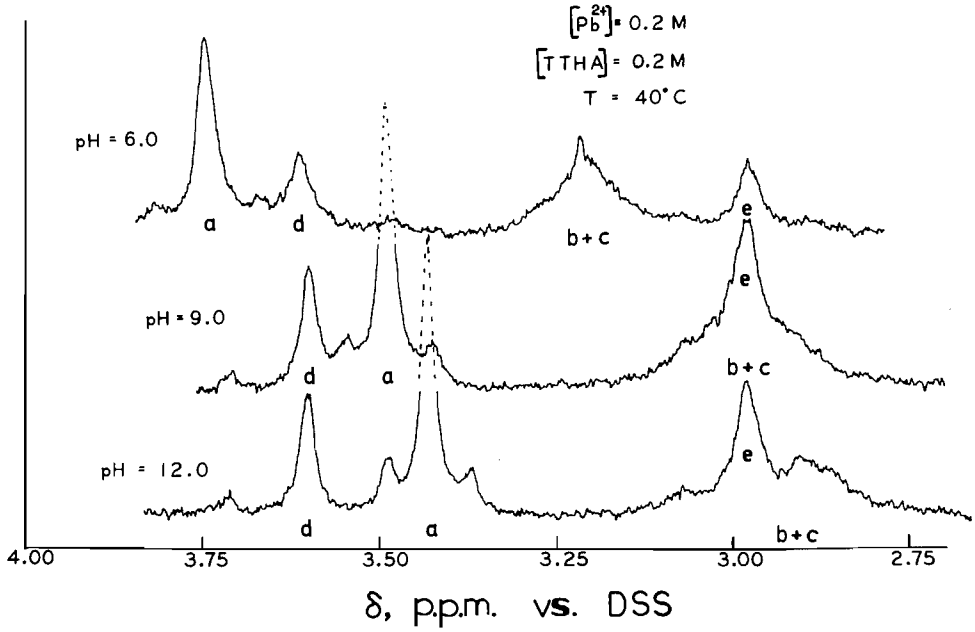

FIG. 5. Proton magnetic resonance spectra of the Pb–TTHA complex at 40° at selected pH values.

carboxylate groups, readily explained by the less extensive protonation of the center nitrogen atoms. Similar behavior has previously been observed for diethylenetriaminepentaacetic acid (DTPA) (3). Interestingly, when the terminal carboxylate groups do eventually protonate there is some deprotonation of the terminal nitrogen atoms. These findings may be compared with earlier discussions, based on potentiometric studies of the species present in aqueous solutions of TTHA (5).

Pb–TTHA

The proton n.m.r. spectra obtained for 1:1 ratios of Pb:TTHA, at a concentration of 0.2 M, were studied over the range pH = 2 to pH = 13. Representative spectra at selected pH values at 40 °C are shown in Fig. 5. Figure 6 gives the pH dependence of the chemical shifts of the various resonances. Assignments of the various resonances in the spectra were made from their relative peak areas, dependence upon pH, and from expectations based on previous discussions (1).

The variations in chemical shift indicate that there are two pH ranges in which protonation of the complex occurs, namely between pH = 10 and pH = 7, and also between pH = 5 and pH = 2.

All four (a)-type carboxyl groups give equivalent spectra throughout the entire pH range of the study, the spectrum of the (a) protons being a simple singlet containing eight protons. At high pH, *i.e.* p$H \geq 9$, the peak is sufficiently far removed from other resonances that two smaller satellite peaks can be distinguished. These are of the approximate intensity required for an AX pattern due to coupling between the (a) protons and the lead isotope 207, which has a spin of one-half and a relative intensity of 21% (15). Lead–proton coupling has been previously reported in EDTA (17) and DTPA (1) complexes. In the TTHA complex the lead–proton coupling constant for the (a) protons is determined to be 3.6 Hz. As the pH is lowered from pH = 9 to pH = 7 the chemical shift of the (a) protons moves to lower field and for p$H \leq 7$ an AX pattern caused by metal–proton coupling is no longer detectable.

The two (d)-type carboxyl groups also give equivalent spectra (simple singlets). For p$H \geq 9$ a satellite peak which can be attributed to one half of an AX pattern due to metal–proton coupling in those molecules containing the ^{207}Pb isotope was detected. The lead–proton coupling constant for the (d) protons was measured to be 6.5 Hz. For both the (a) and (d) protons the lead–proton coupling constants are much smaller than

Can. J. Chem. Downloaded from www.nrcresearchpress.com by 210.87.254.5 on 09/05/12
For personal use only.

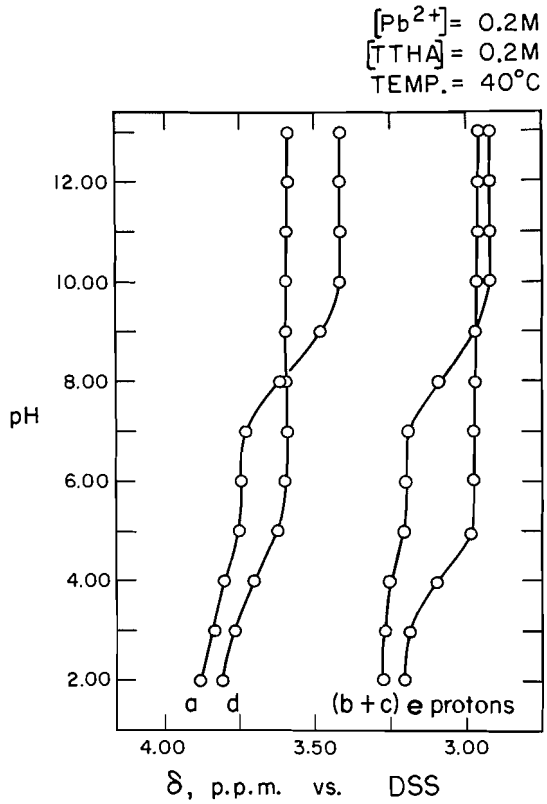

FIG. 6. Variation of chemical shifts of non-labile protons in the Pb–TTHA complex with p*H*.

reported for other lead(II) complexes with aminopolycarboxylic acids (1, 17).

The (*b*) + (*c*) ethylenic protons gave a broad, unresolved resonance throughout the complete p*H* range. Earlier discussions (1) have revealed that a complex spectrum involving many components is to be expected for ethylenic protons in aminopolycarboxylate complexes of this type. Metal–proton coupling could not be detected among the unresolved resonances. The mean chemical shift of the (*b*) + (*c*) protons was taken as the center of the spectral pattern. The results for the (*a*) and (*d*) protons indicate that the two sets of (*b*) + (*c*) protons are equivalent. At p*H* = 12 the (*b*) + (*c*) spectrum appears asymmetric. As the p*H* is lowered to p*H* = 7 the resonance moves downfield and becomes narrower in width, indicating that one end of the ethylenic linkage is more sensitive to protonation changes than the other.

The ethylenic (*e*) protons give a simple singlet throughout the study. Although the (*e*) protons are all equivalent by symmetry in the uncomplexed ligand, there are many instantaneous configurations of a metal–TTHA complex in which they are not. However, the foregoing results indicate that the average configuration of the Pb–TTHA complex is one in which rapid interconversion between non-equivalent configurations produces four equivalent (or not detectably different) (*a*)-type carboxyl groups, and two equivalent (or not detectably different) (*d*)-type carboxyl groups. Thus, the two halves of the TTHA ligand are equivalent in the complex and the four (*e*) protons are also expected to be equivalent.

The n.m.r. spectrum of an aminopolycarboxylate complex will depend upon the labilities of the various metal–ligand bonds, and also upon the fraction of time for which the bond exists, as has been previously shown for EDTA (17) and DTPA (1) complexes. These discussions can be readily extended to diamagnetic metal - TTHA complexes.

In non-labile complexes there are many possible configurations which a metal–TTHA complex can adopt. The p.m.r. spectra of such complexes will be very complicated, as consideration of the various possibilities for the simpler metal - DTPA complexes will show (1). These possibilities will not be discussed here since the comparative simplicity of the Pb(II)–TTHA spectra obtained in aqueous solution shows that the Pb–TTHA complexes are relatively labile in terms of the n.m.r. experiment.

In labile complexes the molecule will exist in various stages of unwrapping with the more complete stages of unwrapping being less prevalent. Such unwrapping would be expected to occur from the ends of the molecule so that the metal–oxygen (*4*) bonds will form and break more quickly than the metal–nitrogen bonds, *i.e.* all the metal–nitrogen bonds will have longer lifetimes than the metal–oxygen (*4*) bonds. Two characteristic metal–nitrogen bond lifetimes can be distinguished since breaking of the metal–nitrogen (*2*) bond corresponds to the formation of a more completely unwrapped complex than does breaking of the metal–nitrogen (*1*) bond. The metal–nitrogen (*2*) bond has the longest lifetime of all metal–ligand bonds in the molecule. The metal–oxygen (*3*) bond lifetime must be shorter than that of the metal–nitrogen (*2*) bond but can be either longer or shorter than those of

Can. J. Chem. Downloaded from www.nrcresearchpress.com by 210.87.254.5 on 09/05/12
For personal use only.

Can. J. Chem. Downloaded from www.nrcresearchpress.com by 210.87.254.5 on 09/05/12
For personal use only.

the other metal–ligand bonds. Thus the following sequences of relative bond lifetimes are possible

M—N(*2*) > M—N(*1*) > M—O(*3*) > M—O(*4*)

M—N(*2*) > M—N(*1*) > M—O(*4*) > M—O(*3*)

M—N(*2*) > M—O(*3*) > M—N(*1*) > M—O(*4*)

In the following discussion the lifetimes are regarded as "long" or "short" with respect to the n.m.r. experiment.

TTHA is potentially a decadentate ligand and consequently not all donor sites can be coordinated at one time. Even for very large cations with very high coordination numbers steric interference probably prevents complete coordination of all donor sites (1). In fact, the terminal carboxyl groups may be coordinated in the Pb(II)–TTHA complex only a small percentage of the time even though the coordination number is probably greater than six (1). The n.m.r. spectra show the four terminal carboxyl groups to be equivalent and the two center carboxyl groups to be equivalent. Since there is no instantaneous configuration in which this can be true then all metal–oxygen bonds must have short lifetimes so that carboxyl groups can rapidly interchange positions in the coordination polyhedron.

The lifetimes of the metal–nitrogen (*1*) bonds are also relatively short. For a long lifetime an *AB* pattern would be expected for the (*a*) protons, as observed for similar protons in Pb–DTPA complexes (1). However, when the lifetime of the metal–nitrogen (*1*) bond is short then the (*a*) protons can become equivalent by rapid umbrella inversion at the N(*1*) atom, and a singlet rather than an *AB* pattern is expected. Even though a singlet is observed for the (*a*) protons here, for p$H \geq 9$ coupling is still observed between the (*a*) protons and the ^{207}Pb isotope because the metal–nitrogen bond reforms to the same metal ion (17).

The (*d*) protons might be expected to exhibit an *AB* pattern instead of the observed singlet. There are two possibilities why a singlet may be observed; first, the metal–nitrogen (*2*) bond has a short lifetime so that rapid umbrella inversion at the N(2) atom can occur; or second, the (*d*) protons may not see very much difference between the ethylenic bridges connected to the nitrogen (*2*) atoms, irrespective of whether the (*d*)-type carboxyl groups are coordinated, or free to rotate. The first possibility seems unlikely since it requires a high proportion of almost completely unwrapped complexes. The second possibility seems more reasonable; in fact, the magnetic environments of the two protons on a given (*d*)-type acetate group would be expected to be very similar.

When the p$H \geq 10$ the Pb–TTHA complex is non-protonated and the chemical shifts, and their pH dependence at lower pH, indicate that when p$H \geq 10$ all four nitrogen atoms are coordinated to the metal (see below). As the pH is lowered to p$H = 7$ the chemical shifts of the (*a*) and (*b*) + (*c*) protons show significant movement toward lower fields whereas those of the (*d*) and (*e*) protons are hardly affected. Furthermore, the metal–proton coupling exhibited by the (*a*) proton spectra is destroyed.

The magnitudes of the changes of chemical shift of the (*a*) and (*b*) + (*c*) protons indicate that the preferred protonation sites are the terminal nitrogen atoms (carboxyl groups do not protonate in this pH range). The quantitative treatment applied to determine the extent of protonation of Pb–DTPA and Cd–DTPA (1) complexes from the chemical shifts of the non-labile protons does not work well here because (*i*) in the range p$H = 10$ to p$H = 7$ the proton affinity of the terminal nitrogen atom is significantly smaller in free TTHA than a non-coordinated terminal nitrogen atom in the lead complex (the results shown in the earlier part of this paper indicate that, in TTHA, protonation of the center nitrogen atoms reduces the proton affinity of the terminal nitrogen atoms, and vice-versa); (*ii*) study of molecular models suggests that when one of the metal–N(1) bonds breaks some strain in the ligand is relieved and steric interference between terminal carboxyl groups is reduced; the other metal–N(1) bond is expected to gain strength, and as a consequence of this the chemical shifts of the (*a*) and (*b*) protons should move to higher δ values (perhaps approaching those of (*d*) and (*e*), respectively. In spite of these difficulties it is possible to ascertain that only one proton is added to the complex when the pH is lowered from 10 to 7 since the chemical shifts of the (*a*) protons in the complex between p$H = 7$ and p$H = 5$ are close to the value expected for complexes in which a given terminal nitrogen atom is coordinated about 50% of the time, and protonated about 50% of the time, *i.e.* either one or the other terminal nitrogen atoms is co-

Can. J. Chem. Downloaded from www.nrcresearchpress.com by 210.87.254.5 on 09/05/12
For personal use only.

ordinated nearly 100% of the time. Double protonation of the complex would correspond to values of $f_1 = 1$ for the uncomplexed ligand; from Figs. 3 and 4 a value of 3.9 p.p.m. is predicted for the value of δ_a in the complex. For single protonation the value predicted for δ_a is the mean of this latter value and the chemical shift expected for acetate protons adjacent to a coordinated nitrogen atom. In the non-protonated complex, Fig. 6 shows the extremes for these chemical shifts are $\simeq$ 3.4 and $\simeq$ 3.6 p.p.m. (in the range pH = 12 to pH = 10). Use of the value 3.6 p.p.m. gives a predicted value for δ_a in the complex of 3.75 p.p.m., close to the observed value between pH = 7 and pH = 5. (This result suggests strengthening of one metal–N(1) bond as the other N(1) atom is protonated.) Though the values of the chemical shifts of the (*b*) + (*c*) protons are less precise they also support single, rather than double, protonation of the complex in this step. From the pH variation of the chemical shifts it is determined that for the reaction

$$PbA^{4-} + H^+ \rightleftharpoons PbHA^{3-}$$

where triethylenetetraaminehexaacetic acid $\equiv H_6A$,

$$\log K = 8.25 \pm 0.2$$

The protonation of the complex thus occurs at approximately 2 pH units lower than does the first protonation of the free TTHA hexaanion, strongly suggesting that all four nitrogen atoms can coordinate to the lead ion at the same time, though the terminal nitrogen atoms will be bound less strongly than the center ones. (A non-coordinated terminal nitrogen atom should have approximately the same proton affinity in the lead complex as in the free ligand. For the terminal nitrogen atoms to be coordinated only 50% of the time would lead to protonation of the complex at pH values only about 0.3 pH unit lower than in the free TTHA hexaanion.)

When the pH is lowered from pH = 5 to pH = 2 all proton chemical shifts move downfield (towards higher δ values) but the movements of the (*a*) and (*b*) + (*c*) protons are relatively small. This is only possible if, in this pH range, the preferred coordination sites are the center nitrogen atoms. The magnitude of the movement of the shifts of the (*e*) protons indicates that the N(2) atoms are coordinated 50% of the time and protonated 50% of the time; *i.e.* at pH = 2 the chemical shift ($\simeq$ 3.2 p.p.m.) of the (*e*) protons is the average of $\simeq$ 2.95 p.p.m. expected when N(2) is coordinated (Fig. 6), and $\simeq$ 3.5 p.p.m. expected when N(2) is fully protonated (Fig. 3). Rapid interconversion between forms in which first one, then the other, center nitrogen atom is coordinated, occurs. Further information about the structure of the complex can be deduced by noting the following considerations: (*i*) Fig. 4 and the earlier Cd(II)–DTPA results (1) indicate that non-coordinated carboxymethyl groups attached to coordinated nitrogen atoms will show increasing protonation as the pH starts to decrease below *ca.* 5, whereas carboxymethyl groups attached to protonated nitrogen atoms have a much smaller tendency to protonate; (*ii*) the movements of the chemical shifts of the (*b*) + (*c*) and (*d*) protons in the range pH = 5 to pH = 3 are smaller than anticipated from 50% protonation at each N(2) atom, though the movement for the (*e*) protons is close to that expected (see above). The following reasoning can be applied. The movement of the (*b*) + (*c*) resonance is small because some deprotonation of the N(1) atoms occurs as the N(2) atoms protonate, a coulombic repulsion effect which has already been observed in aminopolycarboxylate anions (17). The change in position of the (*a*) resonance will be the resultant of that produced by the partial deprotonation at N(1) and that produced by partial protonation of terminal carboxyl groups during the 50% of the time N(1) is coordinated. The second contribution predominates. The smallness of the movement of the (*d*) proton resonance (8.8 Hz compared with 14.0 Hz for the (*e*) protons) indicates that when N(2) is coordinated its attached carboxymethyl group is also coordinated. If this were not so then substantial protonation of the carboxyl group would occur, producing a much larger movement of the (*d*) proton resonance than observed.

In the range pH = 5 to pH = 2 there is more than one type of potential protonation site so that protonation constants determined from variations in chemical shifts will not be precise. However, it is apparent that for the reaction

$$PbHA^{3-} + H^+ \rightleftharpoons PbH_2A^{2-}$$

$$\log K = 4.25 \pm 0.25$$

To summarize, the results can be most readily reconciled in terms of a Pb–TTHA complex having labile bonds. At p$H \geq$ 10, all four

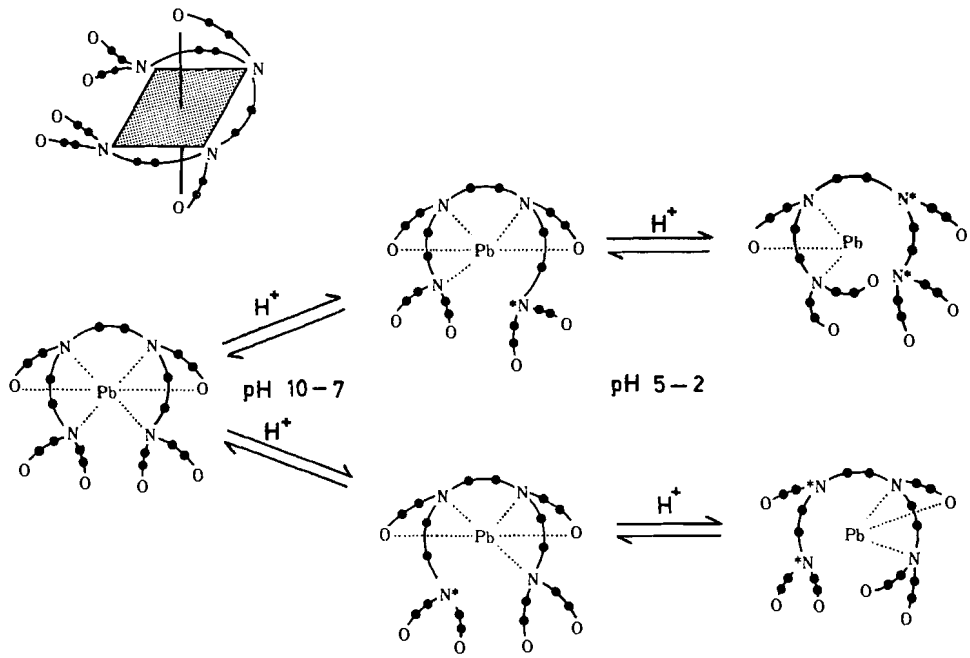

FIG. 7. Schematic representation of the equilibria in 1:1 Pb(II)–TTHA solutions. (* = preferred protonation site).

nitrogen atoms are coordinated to the metal. Since the lifetimes of the terminal oxygen–metal bonds must be shorter than those of the terminal nitrogen–metal bonds the terminal carboxylate groups probably play only a little part in the coordinate bonding in the complex. The remaining places in the coordination polyhedron are taken by the center carboxylate groups. Study of molecular models, using similar considerations to those outlined previously (1), shows that for large ions the least strained and least congested configuration has the four nitrogen atoms and the metal approximately coplanar. Sterically, the center carboxylate groups can then readily coordinate above and below this plane. This is shown diagrammatically in Fig. 7 in which octahedral coordination is assumed. However, the coordination number for lead(II) is probably greater than six, with water molecules or possibly terminal carboxyl groups also participating in the coordinate bonding.

The Pb–TTHA complex protonates in two stages, represented schematically in Fig. 7. In the first stage the Pb–TTHA complex protonates much more readily than the Pb–DTPA complex (1). Two reasons may be advanced for this: first, the proposed small participation in coordinate bonding by the terminal carboxylate groups means that partial unwrapping of the complex at the terminal nitrogen atom can occur more readily in the TTHA complex; second, the TTHA complex is more sterically crowded than the DTPA complex and this crowding can be reduced by breaking the metal–nitrogen bond. The former reason arises possibly because of steric crowding and also because the terminal carboxyl groups are unfavorably situated to compete for the limited number of coordination positions around the metal. The second protonation stage causes further unwrapping of the complex from the same side of the molecule as the first, rather than from the other side. This situation resembles that proposed (5) for the 1:1 Ca(II)–TTHA complex, though for the Pb(II)–TTHA complex the n.m.r. results show that the center nitrogen–metal bond is not broken until the second proton is added (otherwise a downfield shift of the (*d*) proton, resonances would be observed between pH = 10 and pH = 7). It is to be expected that such a complex would readily bind a second metal ion, as, in fact, potentiometric studies have shown (5, 6, 9). This is confirmed also by the n.m.r. spectra of solutions containing Pb(II) and TTHA in the ratio 2:1. At pH = 5 very broad resonances

Can. J. Chem. Downloaded from www.nrcresearchpress.com by 210.87.254.5 on 09/05/12
For personal use only.

are obtained indicating exchanging roles of the lead ions in the complexes, and further studies of this system are required.

We thank the National Research Council of Canada for financial support of this work.

1. P. LETKEMAN and J. B. WESTMORE. Can. J. Chem. This issue.
2. A. E. FROST. Nature, **178**, 322 (1956).
3. R. PRIBIL and V. VESELY. Talanta, **9**, 939 (1962); **10**, 879 (1963); **11**, 1319 (1964); **12**, 475 (1965); **12**, 925 (1965); Chem.–Anal. **53**, 12 (1964); **53**, 44 (1964); **53**, 77 (1964).
4. J. H. GRIMES, A. J. HUGGARD, and S. P. WILFORD. J. Inorg. Nucl. Chem. **25**, 1225 (1963).
5. T. A. BOHIGIAN and A. E. MARTELL. Inorg. Chem. **4**, 1264 (1965).
6. K. H. SCHRODER. Acta Chem. Scand. **19**, 1797 (1965); **20**, 881 (1966).
7. L. HARJN and A. RINGBOM. Anal. Chim. Acta, **49**, 205, 221 (1970).
8. D. A. SOUCEK, K. L. CHENG, and H. A. DROLL. Talanta, **15**, 849 (1968).
9. T. A. BOHIGIAN and A. E. MARTELL. J. Inorg. Nucl. Chem. **29**, 453 (1967).
10. T. A. BOHIGIAN and A. E. MARTELL. J. Am. Chem. Soc. **89**, 812 (1967).
11. R. S. SIEVERS and J. C. BAILAR. Inorg. Chem. **1**, 174 (1962).
12. G. CONRADI and M. KOPANICA. Coll. Czech. Chem. Commun. **28**, 1600 (1963); **29**, 1952 (1964).
13. G. CONRADI, M. KOPANICA, and J. KORYTA. Coll. Czech. Chem. Commun. **30**, 2029 (1965).
14. J. L. SUDMEIER and C. N. REILLEY. Anal. Chem. **36**, 1698 (1964).
15. R. J. KULA and D. T. SAWYER. Inorg. Chem. **3**, 458 (1964).
16. J. W. EMSLEY, J. FEENEY, and L. H. SUTCLIFFE. High resolution nuclear magnetic resonance spectroscopy. Vol. 2. Pergamon Press, Oxford. 1966. Appen. A.
17. R. J. DAY and C. N. REILLEY. Anal. Chem. **36**, 1073 (1964).

Can. J. Chem. Downloaded from www.nrcresearchpress.com by 210.87.254.5 on 09/05/12
For personal use only.

Can. J. Chem. Downloaded from www.nrcresearchpress.com by 210.87.254.40 on 09/05/12
For personal use only.

Metal – Aminopolycarboxylic Acid Complexes. III. Studies of Lead(II) – Tetraethylenepentaaminehеptaacetic Acid in Aqueous Solution by Proton Nuclear Magnetic Resonance Spectroscopy

PETER LETKEMAN[1] AND DONALD T. SAWYER

Department of Chemistry, University of California, Riverside, California 92502

Received August 28, 1970

Proton nuclear magnetic resonance (n.m.r.) spectroscopy and the p*H* dependence of the chemical shifts of the nonlabile protons have been used to determine the preferred protonation sites in tetraethylenepentaaminehеptaacetic acid (TPHA). The nitrogen atoms are protonated more readily than the carboxylate groups with the sequence of protonation dependent on electrostatic interactions. The 1:1 Pb(II)–TPHA complex which is not protonated for solution conditions from p*H* 10 to 14, has five metal–nitrogen bonds. The coordinate bonds are labile so that rapid interconversion between nonequivalent configurations produces an average configuration in which the protons of the acetate groups exhibit single n.m.r. peaks. Protonation of the complex probably occurs in three stages. From p*H* 10 to p*H* 8 the preferred protonation sites are the terminal nitrogen atoms with the attendant elimination of the metal–nitrogen bonds. Increasing the acidity to p*H* 4 causes all but the central nitrogen site to be protonated. Below p*H* 4 the central nitrogen atom becomes protonated and causes further unwrapping of the complex.

La spectroscopie r.m.n. et la dépendance du p*H* avec les déplacements chimiques des protons non labiles ont été utilisées pour déterminer les sites de protonation préférentiels dans l'acide tétraéthylénepentaaminehеptaacétique (TPHA). Les atomes d'azote sont protonés plus rapidement que les groupes carboxylates; la séquence de protonation dépendant des interactions électrostatiques. Le complexe 1:1 Pb(II)–TPHA qui n'est pas protoné pour des solutions ayant un p*H* compris entre 10 et 14, possède cinq liaisons métal–azote. Les liaisons coordonnées sont labiles et de ce fait, l'interconversion rapide entre des configurations non équivalente, produit une configuration moyenne dans laquelle les protons des groupes acétates ne montrent que des singulets. La protonation du complexe se fait probablement en trois étapes. Entre p*H* 10 et p*H* 8 les sites de protonation préférentiels sont les atomes d'azote terminaux; ceci se faisant avec rupture subséquente des liaisons métal–azote. L'augmentation de l'acidité jusqu'à p*H* 4 provoque la protonation de tous les sites à l'exception de l'atome d'azote central. En dessous de p*H* 4 l'atome d'azote central se protone et provoque le déroulement ultérieur du complexe.

Canadian Journal of Chemistry, 49, 2096 (1971)

Introduction

The application of proton nuclear magnetic resonance to the study of aqueous solutions of aminopolycarboxylic acids and their diamagnetic complexes have been discussed in the previous papers of this series (1, 2). The heptaanion of tetraethylenepentaaminehеptaacetic acid (TPHA) can be represented as

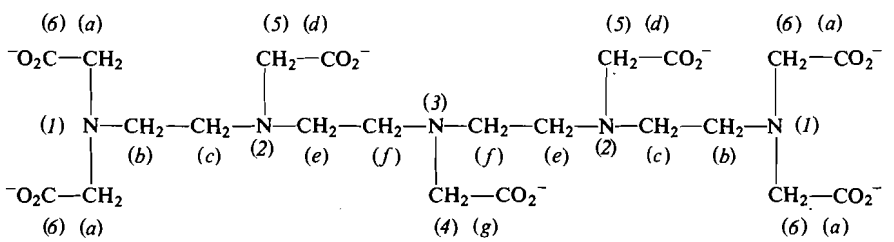

in which donor sites are labelled as (*1*)–(*6*) and nonlabile protons by (*a*)–(*g*). Donor sites or nonlabile protons which are equivalent by symmetry have the same label.

Unlike triethylenetetraaminehexaacetic acid (TTHA) (2), TPHA is a relatively new complexing agent. It was first prepared in 1960 by the Geigy Chemical Company, Basel, Switzerland, using a modified Strecker synthesis (3). Later a method based on a chloroacetic acid – amine reaction was developed using ion exchange techniques to

[1]Currently on a sabbatical leave (1970) from Brandon University, Brandon, Manitoba, Canada.

Can. J. Chem. Downloaded from www.nrcresearchpress.com by 210.87.254.40 on 09/05/12
For personal use only.

separate the acid from the reaction mixture (4), the latter being similar to Frost's preparation of TTHA (5). The new ligand was first used in the removal of internally deposited radionuclides from rats (6, 7). This study as well as a 1965 review paper (8) conclude the complexing ability of TPHA is slightly weaker than that of TTHA, which in turn was less than diethylenetriaminepentaacetic acid (DTPA). Such a trend has been attributed to the increased steric hindrance and inability to use all of the carboxyl groups when forming metal complexes (8).

A recent spectrophotometric study of Am(III)–TPHA indicates that 2:1, 1:1, and 1:2 complexes are formed (9). The complexes of Mg(II), Ca(II), Sr(II), and Ba(II) have a metal–ligand ratio of 2:1, while those for Co(II), Ni(II), Cu(II), Zn(II), and Pb(II) have ratios of 3:2 (8).

The present paper summarizes the results of a protonation study of TPHA and its Pb(II) complexes in aqueous solutions using proton n.m.r. spectroscopy. The results of the free TPHA study are important in the interpretation of the spectra of Pb–TPHA complexes.

Experimental

The proton nuclear magnetic resonance spectra were recorded with a Varian A-60D spectrometer at temperatures of 40 and 80 °C (±1°). The spectral data obtained were average readings of several recordings with a reproducibility of ±0.4 c.p.s. The values of the chemical shifts were measured with respect to *t*-butyl alcohol (TBA) but reported with respect to sodium trimethylsilylpropane sulfonate (DSS).

A sample of purified TPHA was obtained through the courtesy of the Geigy Chemical Company, Basel, Switzerland, and was used without further purification. A 0.20 *M* stock solution of free ligand was prepared by adding 1.192 g of the acid to 8 ml of D_2O, the suspension stirred with subsequent addition of potassium hydroxide pellets until the acid had dissolved, and finally diluting the solution to 10.00 ml with D_2O. The presence of K^+ ions caused the ligand to be soluble down to p*H* 1.0. The p*H* of the stock solution was adjusted by the addition of potassium hydroxide or nitric acid as needed. The individual n.m.r. samples (p*H* 1.0–13.0) were obtained by adjusting the p*H* of the stock solution to the required value and transferring 0.5 ml of that solution into an n.m.r. tube. Such additions caused dilution of the stock solution, but this could not be avoided due to the limited amount of TPHA available.

Similarly, the metal–ligand (Pb–TPHA) solutions were prepared by first dissolving the acid in D_2O (basic with KOH) and then adding the appropriate amount of reagent grade lead nitrate to make a 1:1 mole ratio of lead to TPHA at 0.20 *M*. Again the concentration of individual Pb–TPHA solutions (p*H* 2.0–12.0) was slightly less than 0.20 *M* due to the dilution caused by adding base or acid in the p*H* adjustments. The p*H* of the various solutions was recorded with a Leeds and Northrup p*H* meter (Cat. #7664) equipped with micro-electrodes and calibrated at p*H* 4.00, 7.00, and 10.00 (Sargent buffers).

Results and Discussion

TPHA

The proton n.m.r. spectra of TPHA have been studied from p*H* 1 to p*H* 13 in D_2O solutions; representative spectra for 0.2 *M* solutions are shown in Fig. 1. Increasing the temperature of the sample solution from 40 to 80 °C at a given p*H* sharpens the spectra in a fashion similar to the TTHA system. The assignments of the various resonances in the spectra have been made from their relative peak areas, dependence on p*H*, and from expectations based on earlier work with DTPA (10, 11) and TTHA (2). Symmetry requires that (*i*) the eight (*a*) protons be equivalent, (*ii*) the four (*d*) protons be equivalent, and (*iii*) the two (*g*) protons be equivalent. These groups of protons each give single peaks throughout the entire p*H* range of the study. The (*b*) and (*c*) protons, as well as the (*e*) and (*f*) protons, are nonequivalent, but their chemical shift differences are likely to be relatively small. This is borne out by the experimental results in which at high p*H* the whole group ((*b*), (*c*), (*e*), and (*f*)) appeared as a single broad peak, and at low p*H* as an unresolved A_2B_2 spectrum (see Fig. 1). The areas of these peaks (at p*H* 10 and p*H* 4) correspond to sixteen protons, which relieves any ambiguity about the proton labelling.

The p*H* dependencies of the chemical shifts of the various resonances are illustrated by Fig. 2 (for the (*b*), (*c*), (*e*), and (*f*) protons the mean chemical shift is given). The reported p*K* values of TPHA (8) are: $pK_1 = —$, $pK_2 = 2.73$, $pK_3 = 3.82$, $pK_4 = 5.56$, $pK_5 = 8.88$, $pK_6 = 9.95$, and $pK_7 = —$; which provide some help in explaining the protonation of the acid. At p*H* 12, TPHA exists in solution as the heptaanion. As the p*H* is lowered to p*H* 9.0, the chemical shifts of all protons move toward lower field with the (*d*) protons showing a pronounced shift. Using the p*K* values ($\frac{1}{2}pK_5 + \frac{1}{2}pK_6 \approx 9.0$), p*H* 9.0 would correspond to the addition of two moles of protons per mole of ligand. Hence, the main sites of protonation are the nitrogen(*2*) positions; *i.e.*, a compromise between basicity of nitrogen atoms and proton–proton repulsion on adjacent nitrogens. Adding another mole of H^+ causes a deprotonation of the nitrogen(*2*) positions as seen from Fig. 2. Hence, the three moles of H^+ mainly occupy positions on nitrogen(*1*), nitro-

Can. J. Chem. Downloaded from www.nrcresearchpress.com by 210.87.254.40 on 09/05/12
For personal use only.

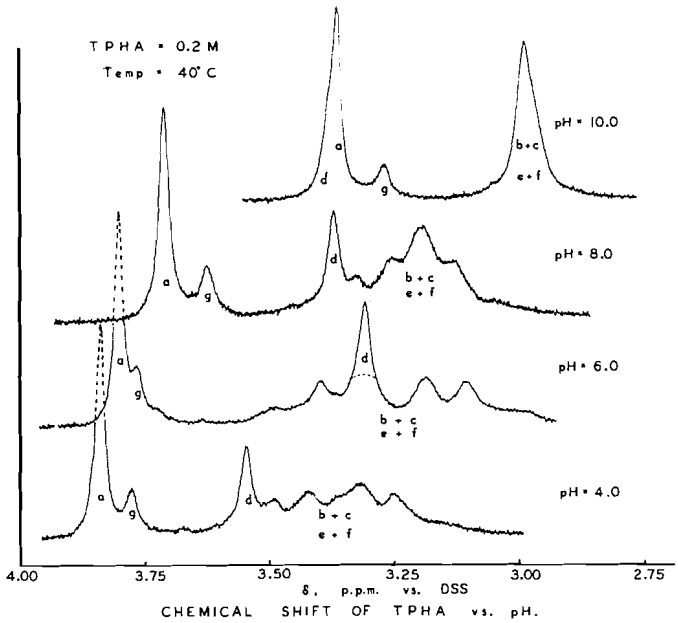

FIG. 1. Proton n.m.r. spectra of TPHA at 40 °C at selected pH values.

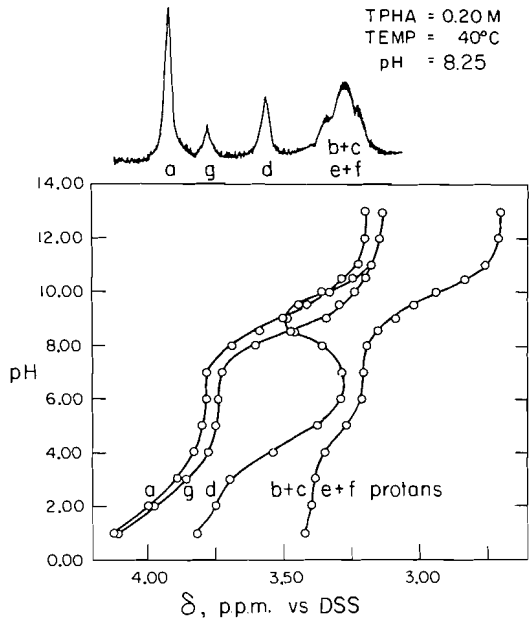

FIG. 2. Variation of the chemical shifts of the nonlabile protons of TPHA with pH.

gen(*3*), and nitrogen(*1*), at approximately pH 6.5. This arrangement of protons is expected because it minimizes proton–proton repulsion on adjacent nitrogen sites. Close inspection of Fig. 2 indicates that little or no protonation occurs between pH 7.5 and pH 5.5. This is in agreement with the large difference between pK_4 and pK_5 ($\Delta pK \cong 3.3$). Upon the addition of a fourth mole of H^+, the (*d*) protons move toward lower field faster than the other protons, indicating the protonation of nitrogen(*2*) sites in preference to protonation of the carboxylate groups.

When the pH is lowered below pH 4.0, the chemical shifts of all protons shift in a constant fashion due to the small differences between successive values of pK_2, pK_3, and pK_4 (*i.e.*, $pK_n - pK_{n-1} \leqslant 2$).

Using a method similar to one described previously (2), the preferred protonation sites and the extent of protonation can be determined quantitatively for the TPHA anion. Again, the contributions to the chemical shift changes from protonation of different sites are assumed to be additive and to be linearly related to the fractions of time for which the sites are protonated (10). For TPHA the chemical shifts, δ, of the various protons are given by

$$[1] \qquad \delta_a = \delta_a^0 + f_1 C_N + f_6 C_0$$

$$[2] \qquad \delta_b = \delta_b^0 + f_1 C_N + f_2 C_N'$$

$$[3] \qquad \delta_c = \delta_c^0 + f_2 C_N + f_1 C_N'$$

$$[4] \qquad \delta_{bc} = \delta_{bc}^0 + 1/2(f_1 + f_2)(C_N + C_N')$$

$$[5] \qquad \delta_d = \delta_d^0 + f_2 C_N + f_5 C_0$$

TABLE 1. Estimation of the extent of protonation of the various nitrogen atoms of TPHA in terms of the fraction of time (f), the nitrogen atoms are protonated at a given pH value

pH	$\nu_0\delta_a$ (c.p.s.)	$\nu_0\delta_g$ (c.p.s.)	$\nu_0\delta_d$ (c.p.s.)	$\nu_0\delta_{(b+c)}$ $_{(e+f)}$ (c.p.s.)	f_1 (%)	f_2 (%)	f_3 (%)
6.0	226.5	224.5	197.0	193.0	81	21	85
7.0	226.0	223.7	197.4	192.0	80	22	83
8.0	221.5	216.5	201.5	192.0	67	32	66
9.0	209.1	199.0	209.7	185.0	40	50	25
10.0	200.8	194.5	201.5	176.0	21	31	15
11.0	193.5	190.5	190.5	165.0	4	5	5
12.0	192.0	188.5	188.5	163.0	~1	~1	~1
13.0	191.7	188.2	188.2	162.0	—	—	—

$$[6] \qquad \delta_e = \delta_e^0 + f_2C_N + f_3C_N'$$

$$[7] \qquad \delta_f = \delta_f^0 + f_3C_N + f_2C_N'$$

$$[8] \qquad \delta_{ef} = \delta_{ef}^0 + 1/2(f_2 + f_3)(C_N + C_N')$$

$$[9] \qquad \delta_g = \delta_g^0 + f_3C_N + f_4C_0$$

where f represents the fraction of a proton on a given nitrogen or carboxylate site and C the chemical shift due to protonation of the adjacent site. The δ^0 values are for the ligand at pH 13.0. A further important relationship is

$$2f_1 + 2f_2 + f_3 + f_4 + 2f_5 + 4f_6 = n$$

where n is the number of equivalents of acid added to one mole of TPHA heptaanion and the coefficients arise from the number of equivalent sites of each type. Values of C_N and C_N' are obtained by assuming that at pH 7.0 three equivalents of acid have been added to one mole of TPHA heptaanion. Because at such high pH values the carboxyl groups are negligibly protonated, $f_4 = f_5 = f_6 = 0$ and therefore $2f_1 + 2f_2 + f_3 = 3$. Equations 1, 2, 5, 6, and 9 have been used to give values for C_N and C_N' of 0.72 and 0.30 p.p.m., respectively. These values agree favorably with those obtained by Sudmeier and Reilley ($C_N = 0.75$ p.p.m. and $C_N' = 0.35$ p.p.m.) (10) and have been used to calculate f_1, f_2, and f_3 from pH 6 to pH 12. Table 1 summarizes the f values as a function of pH and parallels the qualitative protonation sequence presented.

The values of C_0, f_4, f_5, and f_6 are much more difficult to determine. An attempt to calculate C_0 has been made by assuming that at pH 2.0

$$2f_1 + 2f_2 + f_3 + f_4 + 2f_5 + 4f_6 = 7$$

Furthermore, because (*b*), (*c*), (*e*), and (*f*) protons all appear under one broad A_2B_2 spectrum, eqs. 2, 3, 4, 6, 7, and 8 indicate that $f_1 = f_2 = f_3 \approx 2/3$ at pH < 6. This gives an approximate value for C_0 of 0.5 p.p.m., which is high compared to Sudmeier and Reilley's value of 0.2 p.p.m. (10). However, calculation does predict extensive protonation of all nitrogen atoms as well as of the terminal and central carboxyl groups with little protonation for the (*d*) type carboxyl groups. A possible explanation for this is the high congestion of carboxyl groups in the TPHA molecule with an attendant high degree of proton–proton repulsion for neighboring carboxyl groups. No further attempt has been made to determine quantitatively the extent of protonation of the carboxyl groups.

Pb–TPHA

The proton n.m.r. spectra for 1:1 ratios of 0.2 *M* Pb:TPHA have been studied from pH 2.0 to pH 12.0. Representative spectra are illustrated in Fig. 3. Figure 4 summarizes the pH dependence of the chemical shifts for the various resonances. Assignments have been made on the basis of relative peak areas, pH dependence, and expectations based on the behavior of the free ligand.

The variations in chemical shift (see Fig. 4)

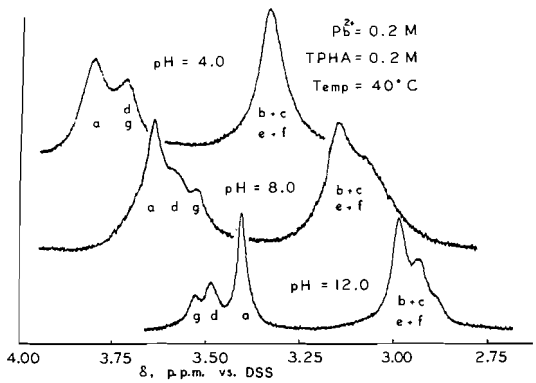

FIG. 3. Proton n.m.r. spectra of the Pb–TPHA complex at 40 °C at selected pH values.

Can. J. Chem. Downloaded from www.nrcresearchpress.com by 210.87.254.40 on 09/05/12
For personal use only.

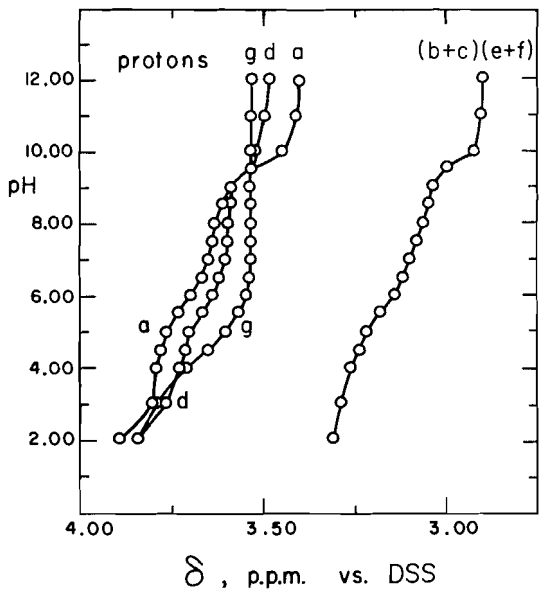

FIG. 4. Variation of the chemical shifts of the nonlabile protons in the Pb–TPHA complex with p*H*.

indicate that there are three p*H* ranges in which protonation of the complex occurs; namely, between p*H* 10–8, p*H* 6–4, and p*H* 4–2. Figure 4 indicates a clear distinction between the first and second stage of protonation with a somewhat less defined distinction between the second and third stage of protonation. This behavior, however, is reasonable when one considers the stability of protonated aminopolycarboxylic acid complexes (12–17); *i.e.*, the stability constants of MH_2Y and MH_3Y differ by approximately one p*K* unit or less, whereas the difference between the stability constants of MHY and MH_2Y is usually five p*K* units or more.

All four (*a*)-type carboxyl groups are equivalent throughout the entire p*H* range of the study; their spectrum is a singlet containing eight protons. The two (*d*)-type carboxyl groups are equivalent and give a singlet as does the (*g*)-type carboxyl group. There is no evidence for any coupling between (*a*), (*d*), or (*g*) protons and the ^{207}Pb isotope, in contrast to earlier studies (1, 2). This probably is due to the lability of Pb–TPHA complex and the resulting poorly resolved spectra. Furthermore, the metal–proton coupling constants follow the sequence Pb–EDTA ≈ Pb–DTPA > Pb–TTHA (1, 2). Thus, metal–proton coupling probably is quite small for Pb–TPHA.

In Fig. 3 the (*b*), (*c*), (*e*), and (*f*) ethylenic protons exhibit a broad, unresolved resonance throughout the complete p*H* range. Earlier discussions (1) have revealed that a complex spectrum is to be expected for ethylenic protons in aminopolycarboxylate complexes of this type. The chemical shift of the (*b*), (*c*), (*e*), and (*f*) protons has been taken as the center of the spectral pattern. At p*H* 12 the (*b*), (*c*), (*e*), and (*f*) spectrum appears asymmetric, which may indicate a slightly different chemical shift for the (*b*) + (*c*) protons compared to the (*e*) + (*f*) protons. Judging from previous work on Pb–TTHA (3) such an explanation is reasonable. As the p*H* is lowered to p*H* 4.0, the resonance moves downfield and becomes a narrower symmetrical peak, indicating that any difference in chemical shifts (between (*b* + *c*) and (*e* + *f*)) has disappeared upon protonation of the complex. The symmetrical peak corresponds to 16 protons.

The n.m.r. spectrum of an aminopolycarboxylate complex will depend upon the labilities of the various metal–ligand bonds, and also upon the fraction of time for which the bond exists, as has been previously shown for EDTA (18), DTPA (1), and TTHA (2) complexes. These discussions can readily be extended to the Pb–TPHA complex, which is relatively labile in terms of the n.m.r. experiment (judging from the simple n.m.r. spectra obtained).

In labile complexes the molecule will exist in various stages of unwrapping with the more complete stages of unwrapping being less prevalent. Such unwrapping is expected to occur from the ends of the molecule so that the metal–oxygen(*6*) bonds will form and break more quickly than the metal–nitrogen bonds, *i.e.*, all metal–nitrogen bonds will have longer lifetimes than the metal–oxygen(*6*) bonds. Three characteristic metal–nitrogen bond lifetimes can be distinguished because breakage of the metal–nitrogen(*3*) bond corresponds to a more completely unwrapped complex than does breakage of the metal–nitrogen(*2*) bond, which in turn is more unwrapped than when the metal–nitrogen(*1*) bond is broken. Thus, the metal–nitrogen(*3*) bond must have the longest lifetime of all of the metal–ligand bonds in the complex. The metal–oxygen(*5*) bond lifetime must be shorter than the metal–nitrogen(*2*) bond.

TPHA is potentially a dodecadentate ligand and consequently not all donor sites can be coordinated at one time in a 1:1 mole ratio solution

Can. J. Chem. Downloaded from www.nrcresearchpress.com by 210.87.254.40 on 09/05/12
For personal use only.

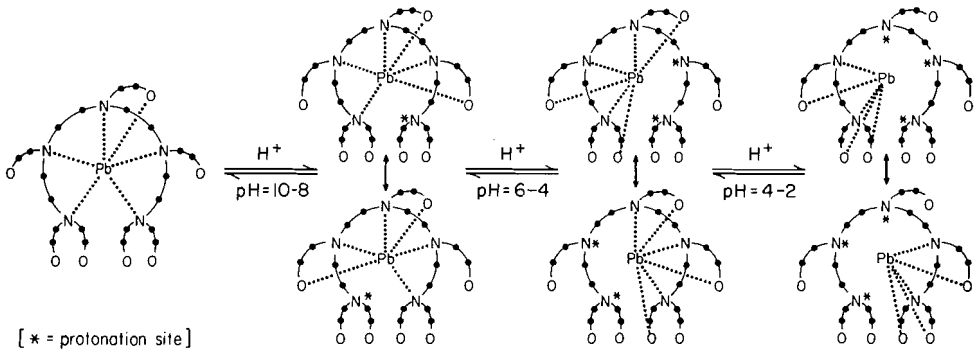

FIG. 5. Possible instantaneous configurations (at various p*H* values) of the Pb–TPHA complex.

of Pb–TPHA. In fact, the terminal carboxylate and nitrogen groups may be coordinated in the Pb(II)–TPHA complex only a small percentage of the time. The n.m.r. spectra indicate that the four terminal carboxyl groups are equivalent and that the two (*d*)-type carboxylate groups also are equivalent. Because there is no instantaneous configuration in which this is possible, all of the metal–oxygen bonds must have short lifetimes so that the carboxylate groups rapidly interchange positions in the coordination polyhedron.

The lifetimes of the metal–nitrogen(*1*) and nitrogen(*2*) bonds also must be relatively short. Otherwise, an *AB* pattern would be expected for the (*a*) and (*d*) protons, as is observed for similar protons in the Pb–DTPA (1) and Pb–TTHA (2) complexes. However, when the lifetime of a metal–nitrogen bond is short, then the (*a*) and (*d*) protons can become equivalent by rapid umbrella inversion at the nitrogen, and a singlet rather than an *AB* pattern is expected. This would involve unwrapping of the complex first from one side of the molecule and then from the other side, with the metal ion continuously attached *via* the central nitrogen(*3*) atom. Experiment indicates that the central nitrogen(*3*) and carboxyl(*4*) groups are coordinated to Pb(II) from p*H* 12 to p*H* 6 (see Fig. 4).

At p*H* > 10 the Pb–TPHA complex is not protonated and all five nitrogen atoms appear to be coordinated to the metal. As the p*H* is lowered to p*H* 8, all protons show significant movement toward lower fields except the (*g*) protons. The magnitudes of the changes of chemical shift of the (*a*), (*b*), (*c*), (*d*), (*e*), and (*f*) protons indicate that the preferred protonation sites are the nitrogen(*1*) and nitrogen(*2*) positions (the carboxylate groups do not protonate in this p*H* range). When the p*H* is lowered from p*H* 6.0 to p*H* 2, all proton chemical shifts move downfield with the (*g*) protons exhibiting the largest change. This is only possible if, in this p*H* range, the preferred protonation site is the central nitrogen(*3*) atom.

In conclusion, the results can be most readily reconciled in terms of a Pb–TPHA complex having labile bonds. At p*H* > 10 all five nitrogen atoms are involved in the coordination of the Pb(II) ion, although the lifetimes of the metal–nitrogen(*1*) and nitrogen(*2*) bonds probably are short. This short lifetime permits these nitrogen atoms to rapidly change positions in the coordination polyhedron, thus producing an averaged configuration which is symmetric through the middle of the complex. The metal–oxygen(*6*) bonds, which have shorter lifetimes than the metal–nitrogen bonds, must play an insignificant role in the coordinate bonding of the Pb–TPHA complex. The central carboxylate groups (types (*4*) and (*5*)) probably occupy the remaining places in the coordination polyhedron when some of the nitrogen atoms are protonated. The Pb–TPHA complex protonates much more readily than the Pb–DTPA complex (1), probably for the same reasons as for the Pb–TTHA complex (2).

The Pb–TPHA complex protonates in three stages, represented schematically in Fig. 5. The second protonation stage causes further unwrapping of the complex from the same side of the molecule as the first, rather than from the other side. The n.m.r. results establish that the central nitrogen–metal bond is not broken until the second and third proton are added (otherwise a downfield shift of the (*g*) proton resonance would be observed between p*H* 10 and p*H* 6). A large ligand such as TPHA should be capable of bond-

Can. J. Chem. Downloaded from www.nrcresearchpress.com by 210.87.254.40 on 09/05/12
For personal use only.

ing two or three metal ions, as recent studies have indicated (8, 9). Hence, a large number of possible metal–TPHA complexes remain to be investigated in the future.

Financial support for this work was provided by the National Research Council of Canada (P.L.) and the National Science Foundation (D.T.S.) under Grant No. GP-16114. One of us (P.L.) would like to thank Brandon University for a sabbatical leave.

1. P. LETKEMAN and J. B. WESTMORE. Can. J. Chem. This issue (Part I).
2. P. LETKEMAN and J. B. WESTMORE. Can. J. Chem. This issue (Part II).
3. A. KREBSER. Geigy Chemical Co., Basel, Switzerland. Private communication.
4. V. G. YASHUMSKII and O. I. SAMOILOVA. Zh. Uses. Khim. Obschchestva in D. I. Mendeleeva **8** (3), 360 (1963).
5. A. E. FROST. Nature, **178**, 322 (1956).
6. A. CATSCH and D. SCHINDEWOLF-JORDAN. Experentia, **17**, 205 (1961).
7. A. CATSCH and D. SCHINDEWOLF-JORDAN. Nature, **191**, 715 (1961).
8. N. M. DYATLOVA and R. P. LASTOVKI. Russ. Chem. Rev. **34**, 481 (1965).
9. A. D. SITE and R. D. BAYBARZ. J. Inorg. Nucl. Chem. **31**, 2201 (1969).
10. J. L. SUDMEIER and C. N. REILLEY. Anal. Chem. **36**, 1968 (1964).
11. R. J. KULA and D. T. SAWYER. Inorg. Chem. **3**, 458 (1964).
12. L. HARJU and A. RINGBOM. Anal. Chim. Acta, **49**, 205 (1970); **49**, 221 (1970).
13. S. CHABEREK, A. E. FROST, M. A. DORAN, and N. J. BICKNELL. J. Inorg. Nucl. Chem. **11**, 184 (1959).
14. S. CHABEREK and R. HARDER. J. Inorg. Nucl. Chem. **11**, 197 (1959).
15. S. CHABEREK, J. VANDEGAER, and A. E. FROST. J. Inorg. Nucl. Chem. **11**, 210 (1959).
16. J. H. GRIMES, A. J. HUGGARD, and S. P. WILFORD. J. Inorg. Nucl. Chem. **25**, 1225 (1963).
17. G. ANDEREGG and G. SCHWARZENBACH. Helv. Chim. Acta, **42**, 827 (1959).
18. R. J. DAY and C. N. REILLEY. Anal. Chem. **36**, 1073 (1964).

Can. J. Chem. Downloaded from www.nrcresearchpress.com by 210.87.254.40 on 09/05/12
For personal use only.

Can. J. Chem. Downloaded from www.nrcresearchpress.com by 210.87.254.6 on 09/05/12
For personal use only.

Sesquiterpene Lactones from Pyrethrum Flowers

RAYMOND W. DOSKOTCH, FAROUK S. EL-FERALY, AND CHARLES D. HUFFORD
Division of Natural Products Chemistry, College of Pharmacy, The Ohio State University, Columbus, Ohio 43210

Received January 4, 1971

Three new sesquiterpene lactones, dihydro-β-cyclopyrethrosin (**3**), chrysanin (**4**), and chrysanolide (**5**) were isolated from the flowers of *Chrysanthemum cinerariaefolium* and their structures determined by physical and chemical methods. The configuration at C-1 of pyrethrosin (**2**) was established as *R* by its conversion to dihydro-β-cyclopyrethrosin (**3**), a hydrogenation product of β-cyclopyrethrosin (**1**), which had the C-1 hydroxyl group assigned by the Horeau procedure and Brewster's benzoate method. The preparation and properties of the C-11 epimers, **12** and **17**, of dihydropyrethrosin are reported and their stereochemistry established.

L'extraction des fleurs du *Chrysanthemum cinerariaefolium* permet d'isoler trois nouvelles lactones sesquiterpéniques: la dihydro β-cyclopyréthrosine (**3**) la chrysanine (**4**), et la chrysanolide (**5**); leur structure a pu être déduite grâce à des méthodes physiques et chimiques. Grâce à une corrélation avec la dihydro β-cyclopyréthrosine (**3**), un produit d'hydrogénation de la β-cyclopyrethrosine (**1**) pour laquelle la configuration de l'hydroxyle en position 1 a pu être attribuée par les méthodes de Horeau et de Brewster, on a pu établir que la configuration en C-1 de la pyréthrosine (**2**) est *R*. On rapporte aussi la préparation, les propriétés et la façon de déterminer la stéréochimie des épimères **12** et **17** en C-11.

Canadian Journal of Chemistry, 49, 2103 (1971)

In a previous publication (1), we reported the isolation of β-cyclopyrethrosin (**1**) from the flowers of *Chrysanthemum cinerariaefolium* Visiani. Prior to this, pyrethrosin (**2**), the first recognized germacranolide was the only sesquiterpene lactone obtained from this source (2). By careful chromatography of a fraction of the pyrethrum flower extract, three additional sesquiterpene lactones, dihydro-β-cyclopyrethrosin (**3**), chrysanin (**4**), and chrysanolide (**5**) were isolated.

The isolated dihydro-β-cyclopyrethrosin (**3**) was identical (m.p., i.r., n.m.r., and specific rotation) with the hydrogenation product of β-cyclopyrethrosin (**1**). The stereochemistry at C-11 was determined from the value of the n.m.r. coupling constant between H-7 and -11, and the application of the relationship of Narayanan and Venkatasubramanian (3). The C-11 proton in the 100 MHz spectrum appears as six peaks at δ 2.64, the X of an A_3MX pattern, where $J_{H_7-H_{11}}$ = 12.0 and $J_{H_{11}-H_{13}}$ = 6.8 Hz. The C-11 proton is, therefore, pseudo-axial as shown in the Newman projection **6**. The preparation of desacetyldihydro-β-cycloisopyrethrosin (**7**), a hydrolysis product of dihydro-β-cyclopyrethrosin (**3**), in which the lactone is to C-6 confirmed the assignment. The C-11 proton becomes pseudo-equatorial as in **8** and the pattern[1] changes to five peaks located at δ 2.80, $J_{H_7-H_{11}}$ = 7.7 Hz.

The assignment of stereochemistry at C-1 in β-cyclopyrethrosin (**1**) and its dihydro-derivative **3** has yet to receive unambiguous experimental support. Iriuchijima and Tamura (2*d*) in their study of the α- and β-dihydrocyclopyrethrosin mixture, derived from pyrethrosin by cyclization, utilized the coupling constant values (J = 5 and 10.5 Hz) for the H-1 pattern to assign that proton an axial position, if a chair conformation (**9**) is assumed (4). The boat conformation as shown in **10** (C-2 and -5 being the "flagpole" carbons) in which the hydroxyl is pseudo-equatorial would give similar J values. Consequently, the n.m.r. pattern for H-1 is unable to provide a unique answer for the C-1 configuration.

Utilization of Brewster's benzoate method (5) for this purpose resulted in a large negative shift (−344°) in the molecular rotation between the alcohol **1** and the benzoate ester **11**, signifying an *R* configuration according to the sequence rule

[1]These results are from the n.m.r. spectrum taken in MeOH-d_4, for reasons of solubility. A spectrum in $CDCl_3$ was obtained with aid of a time-averaging computer and after 293 scans a clear five-peak pattern was observed at δ 2.88.

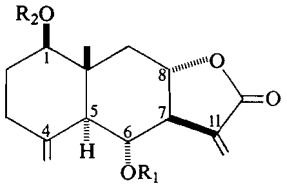

1 $R_1 = Ac$; $R_2 = H$

4 $R_1 = -OC(CH_3)=CHCH_3$ (tiglate); $R_2 = H$

11 $R_1 = Ac$; $R_2 = Benzoyl$

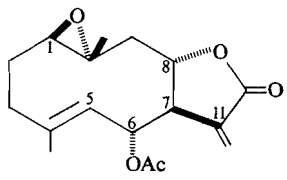

2

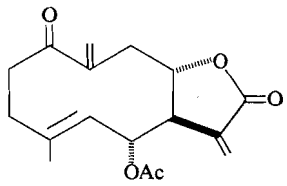

5

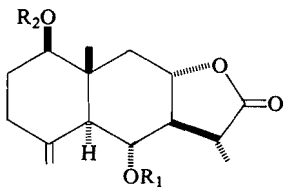

3 $R_1 = Ac$; $R_2 = H$

13 $R_1 = Angeloyl$; $R_2 = H$

14 $R_1 = R_2 = H$

18 $R_1 = R_2 = Ac$

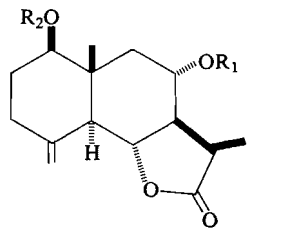

7 $R_1 = R_2 = H$

19 $R_1 = R_2 = Ac$

(6). The Horeau method (7) of "partial resolution" gave the same result[2] since the recovered α-phenylbutyric acid was positive in an optical yield of 46%.

To relate C-1 of pyrethrosin to β-cyclopyrethrosin a mixture of dihydrocyclopyrethrosins was prepared from dihydropyrethrosin (**12**) (*vide infra*) by acid cyclization. Careful chromatography of the mixture on $AgNO_3$-impregnated silica gel yielded dihydro-β-cyclopyrethrosin (**3**) identical with the material isolated from the flowers. The configuration of C-1 in pyrethrosin is, therefore, also *R*.[3]

[2]In assigning the stereochemistry for certain C-8 alcohols of the eudesmanolide sesquiterpene lactones, the two methods gave opposite results (8). Studies on a closely related substance (asperilin) with a C-1 hydroxyl are found in ref. 9.

[3]In a publication on the biosynthesis of santonin, Barton *et al.* (10) mention the results of an X-ray study of pyrethrosin reported to them by Professor C. E. Nordman. The drawing of pyrethrosin as given there can lead to the erroneous conclusion of a *cis* epoxide and an *S* configuration at C-1. Professor Nordman informed us that this work is still unpublished but that both C-1 and -10 have the *R* configuration and our results are in agreement.

Chrysanin, (**4**) m.p. 202–204° (dec.), gave a mass spectrum with a molecular ion peak at 346.1792 (0.26%) which corresponds to the formula $C_{20}H_{26}O_5$. The i.r. spectrum showed peaks for a hydroxyl group, an α,β-unsaturated γ-lactone, an α,β-unsaturated ester, and two double bonds. The u.v. spectrum supported the α,β-unsaturated lactone and ester functions, showing only intense end absorption (log ε_{210} 4.22). The n.m.r. spectrum had many features identical with the spectrum of β-cyclopyrethrosin (see ref. 1 for a reproduction). It differed in that an acetate peak was lacking, but instead two additional olefinic methyl groups were present at δ 1.95 and 1.88. The former appeared as a doublet ($J \sim 8$) that was further weakly split ($J = 1$) into at least four peaks, while the latter appeared as a broadened singlet. Chrysanin was, therefore, formulated as desacetyl-β-cyclopyrethrosin esterified by an unsaturated five-carbon plant acid. The complex one-proton pattern at δ 6.12 was consistent with the olefinic proton of angelic acid (11), which was obtained on hydrolysis of chrysanin (**4**) and characterized as the *p*-phenylphenacyl derivative.

Can. J. Chem. Downloaded from www.nrcresearchpress.com by 210.87.254.6 on 09/05/12
For personal use only.

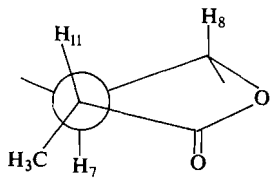

6

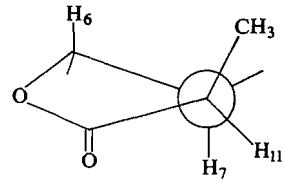

8

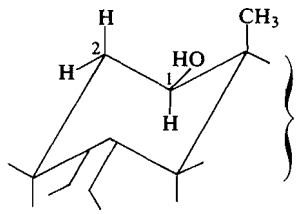

9

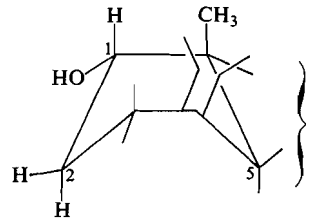

10

The alcohol portion of chrysanin (**4**) was characterized by the hydrolysis products of dihydrochrysanin (**13**); namely desacetyldihydro-β-cyclopyrethrosin (**14**) and its isomer **7**. The hydroxyl group in chrysanin must be located at C-1 since the H-1 pattern (pair of doublets) is found at δ 3.61 and shows a considerable sharpening after D_2O exchange. The lactone must close to C-8 for the six-peak pattern for H-8 shows a smaller chemical shift (δ 4.12) than the three-peak pattern for the proton on the ester bearing carbon (δ 5.64). Additional support for the *trans* lactone structure came from the circular dichroism curve of chrysanin with a maxima for the $n \rightarrow \pi^*$ transition of the α,β-unsaturated lactone at 262 mμ, [θ] +1420 (12). β-Cyclopyrethrosin showed a similar maxima at 253 mμ, [θ] +2340.

Chrysanolide, m.p. 204–205°, $[\alpha]_D^{25}$ −52°, analyzed for $C_{17}H_{20}O_5$, showed a molecular ion at *m/e* 304 in the mass spectrum and exhibited strong i.r. bands for an α,β-unsaturated γ-lactone, an acetate, an α,β-unsaturated ketone, and medium intensity peaks for three olefins, one of which is *trans*. The u.v. spectrum consisted of high intensity end absorption ($\log \varepsilon_{210}$ 4.40) with a weak shoulder at 300 mμ (ε 23). The n.m.r. spectrum showed a pair of one-proton doublets at δ 6.36 (J = 2.9 Hz) and 5.88 (J = 2.4 Hz), that were further weakly split (J = 0.8 Hz), for the H-13 protons; a sharp three-proton singlet at δ 2.07 for an acetate and a slightly split three-proton singlet at δ 1.76 (J = 0.9 Hz) for an olefinic methyl. A two-proton complex between δ 4.8–5.4 was analyzed as a modified AB pattern, δ_A 4.98 and δ_B 5.13 (J = 9.8 Hz, $J_{AB}/\Delta\nu$ = 1.02), where H_B is further split by H_X (J = 8.6 Hz) and H_A is broadened by long-range coupling, a characteristic of the grouping **15** (8). The latter coupling value (J = 8.6 Hz) supports the *trans* arrangement of protons H_B and H_X. A one-proton pattern of eight peaks at δ 4.05 (J = 11.1, 5.3, and 3.1 Hz) is the same as that for the H-8 proton (δ 4.16) of pyrethrosin.

Chrysanolide (**5**) lacks the three-proton singlet for the C-10 methyl group (δ 1.31 in pyrethrosin). Instead a two-proton, partially split and broadened, singlet between δ 5.3–5.9 is present. The 100 MHz spectrum more clearly shows this region to be a pair of doublets at δ 5.83 and 5.87 (J = 2.0 Hz) consistent with an exocyclic methylene. Chrysanolide was, therefore, proposed as a dehydropyrethrosin with the possible structure **5**.

Double irradiation experiments established the partial structure for chrysanolide from C-4 through -8. Irradiation at δ 3.0, the position[4] for H-7, results in the collapse of the split doublets at δ 6.36 and 5.88 to split singlets (C-13 protons), the H-5 and -6 complex (δ 4.98 and 5.13) changed to a simple AB pattern (J = 9.8) with one branch broadened, and the H-8 octet became a broadened doublet (J = 11.2). The latter result establishes the J value for H-7 and -8 as 5.3 Hz, a figure comparable to 6.4 Hz which occurs for pyrethrosin and indicates a *trans* lactone. When the

[4]At 60 MHz this proton pattern is unclear, being obscured by other peaks, but at 100 MHz it is unobstructed and appears at δ 2.95. The spectrum of pyrethrosin at 60 MHz gives a clean pattern at δ 3.06.

Can. J. Chem. Downloaded from www.nrcresearchpress.com by 210.87.254.6 on 09/05/12
For personal use only.

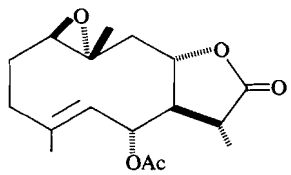

12

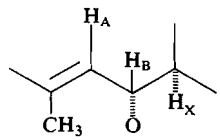

15

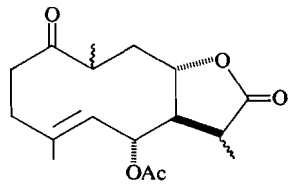

16

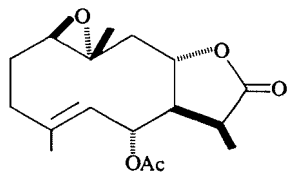

17

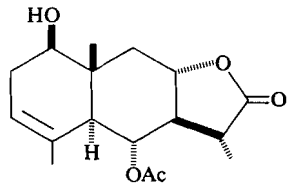

20

olefinic methyl doublet at δ 1.76 (J = 0.8 Hz) was irradiated, the broadened uneven doublet at δ 4.98 (H-5) was considerably sharpened, while the reverse process sharpened the methyl peak.

The c.d. curve of chrysanolide showed a maxima at 246 mμ with [θ] −6170, while pyrethrosin shows a maxima at 249 mμ and [θ] −3620. This is opposite in sign to the general rules as established by W. Stöcklin *et al.* (12) for C-8 *trans* lactones. These lactones are to be added to the few exceptions already known.

The presence of two conjugated exocyclic methylenes in chrysanolide was confirmed by the preparation, with diazomethane, of a crystalline dipyrazoline which in the n.m.r. spectrum lacked the four olefinic methylene protons. Hydrogenation of chrysanolide gave a tetrahydro-product **16** which lacked in the n.m.r. spectrum the methylene protons, but instead showed two three-proton doublets for secondary methyl groups at δ 1.08 (J = 6.8 Hz) and 1.38 (J = 6.9 Hz). Reduction of the remaining olefin group in tetrahydrochrysanolide (**16**) to a substance previously derived from pyrethrosin (*2a*) could not be accomplished under the reported (platinum oxide and ethyl acetate), as well as more drastic (platinum oxide and perchloric acid in ethyl acetate, or glacial acetic acid) conditions. Sodium borohydride reduction of tetrahydrochrysanolide (**16**) gave an alcohol. The scarcity of chrysanolide prevented further study of this product.

Attempts to show a direct relationship between pyrethrosin (**2**) and chrysanolide (**5**) by first opening of the oxirane ring over activated alumina (13) to the corresponding α-methylene allylic alcohol and then oxidation of the hydroxyl group to the ketone failed at the first step. Apparently only cyclization products (judged by n.m.r.) formed. Attempted openings of the epoxide by lithium diethylamide (14) were also unsuccessful.

As an adjunct to our study, we have re-examined the reduction products of pyrethrosin. Barton and de Mayo (*2b*) on hydrogenation over Pd on C obtained two dihydro- derivatives which were separated (but their purity not established) into a major (dihydropyrethrosin), m.p. 156–159°, and a minor (isodihydropyrethrosin) product, m.p. 205–208°. The latter was first reported by Rose and Haller (15) as the hydrogenation product of chrysanthin (pyrethrosin) using Adams' platinum catalyst. A study of the n.m.r. spectrum of the total mixture of dihydro- products from both reductions showed that the palladium catalyst furnished the two isomers in an approximate ratio (dihydro- to isodihydro-) of 4:1, while platinum gave, 1:4. Pure samples of

Can. J. Chem. Downloaded from www.nrcresearchpress.com by 210.87.254.6 on 09/05/12
For personal use only.

TABLE 1. Fractions from chromatography of pyrethrum flower extract

Fraction	Weight in g	Constituents
1–72	13.7	Taraxasterol, 4.11 g
73–83	0.98	Green oil
84–88	2.55	(+)-Sesamin, 0.209 g
89–99	2.01	Chrysanolide, 0.031 g
100–113	2.20	Green oil
114–121	1.41	Chrysanin, 0.023 g
122–125	0.50	Oil
126–140	1.06	β-Cyclopyrethrosin, 0.693 g
141–143	0.13	Resin oil
144–148	0.27	Dihydro-β-cyclopyrethrosin, 0.102 g
149–153	0.22	Oil
MeOH wash	11.9	Dark brown gum

both isomers were obtained, as evidenced by their n.m.r. spectra.[5] The major product (m.p. 168–170°) from Pd on C hydrogenation has structure **12** with the C-11 methyl positioned α, since it was possible to isolate dihydro-β-cyclopyrethrosin (**3**) and dihydro-α-cyclopyrethrosin (**20**) from the mixture of cyclization products formed on treatment of **12** with acid. Sodium borohydride reduction of pyrethrosin gives solely epimer **12**. The major product (isodihydropyrethrosin) formed using Adams' platinum catalyst is the C-11 epimer **17**. We prefer to call it epidihydropyrethrosin leaving the prefix iso- for the isomers possessing the reverse lactone closing.

Experimental

Melting points are uncorrected. Elemental analyses were determined by A. Bernhardt, West Germany, or by the Scandinavian Microanalytical Laboratory, Denmark. The i.r. spectra were obtained in chloroform or as KBr pellets on a Perkin–Elmer Infracord 237 or 257 instrument. The u.v. spectra were taken in methanol on a Cary Model 15 spectrophotometer. The n.m.r. spectra were obtained in deuterochloroform or stated otherwise, with tetramethylsilane as internal standard using a Varian A-60A or T-60 spectrometer and signals reported in δ (p.p.m.) units, *J* in Hz and the following abbreviations for spin patterns; s = singlet, d = doublet, t = triplet, q = quartet, m = multiplet and br = broad. Spin decoupling was performed with frequency sweep on the latter instrument. The c.d. curves and optical rotations were taken on a Jasco spectropolarimeter with c.d. attachment. Mass spectra were performed on an A.E.I. MS-9 double-focusing instrument via a direct inlet probe.

Isolation of Constituents

Powdered dried flowers of *Chrysanthemum cinerariaefolium* (2 kg, lot no. LHC-680, S. B. Penick and Co., New York) were percolated to exhaustion at room temperature with ethanol. The residue (457 g), left after evaporation of the solvent at reduced pressure, was partitioned between 1 l of chloroform and three 200-ml portions of water. The chloroform residue (193 g) was partitioned between 600 ml of 10% aqueous methanol and six 200-ml portions of petroleum ether, b.p. 60–68°. The aqueous methanol residue weighed 63 g.

A chromatographic column poured as a slurry in chloroform from 800 g of silicic acid (Mallinckrodt, 100 mesh) was loaded with 45 g of the aqueous methanol fraction. The chloroform effluent was discarded until a positive $KMnO_4$ test was obtained and then 80 ml fractions were collected, evaporated at reduced pressure, and residue weights determined. The results of the column separation are summarized in Table 1.

Taraxasterol, a previously reported common triterpene constituent (2*c*, 16) obtained in the early fractions was not further studied. Results on (+)-sesamin and β-cyclopyrethrosin have already been reported (1). The new compounds have the following properties.

Chrysanolide (5)

The column fraction 89–99 yielded from ethanol – isopropyl ether 31 mg of chrysanolide (**5**) as needles; m.p. 204–205 °C, $[\alpha]_D^{25}$ – 52° (*c*, 0.315 in methanol); u.v. end absorption log ε 4.40 at 210 with a shoulder at 300 mμ (ε 23); i.r. ν_{max} 1765 (γ-lactone), 1737 (acetate), 1680 (α,β-unsaturated ketone), 1665 and 1630 cm^{-1} (olefins); and the mass spectrum showed a parent ion at *m/e* 304.1306 (2%) (calculated for $C_{17}H_{20}O_5$, *m/e* 304.1311). The c.d. curve showed Cotton effect maxima at 310 [θ] −1540; 246, [θ] −6170; and 215 mμ, [θ] +119 000.

Anal. Calcd. for $C_{17}H_{20}O_5$: C, 67.09; H, 6.62. Found: C, 66.94; H, 6.61.

Chrysanin (4)

Column fraction 114–121 when treated with ethanol – isopropyl ether gave 23 mg of chrysanin (**4**); m.p. 202–204° (dec.); $[\alpha]_D^{25}$ +80° (*c*, 0.15 in methanol); u.v. end adsorption log ε 4.22 at 210 mμ; i.r. ν_{max} 3590 and 3450 (hydroxyl), 1770 (γ-lactone), 1710 (ester), 1675 and 1655 cm^{-1} (olefins); and the mass spectrum showed a molecular ion at 346.1792, $C_{20}H_{26}O_5$ requires 346.1780. The c.d. showed $[\theta]_{262}$ +1420, $[\theta]_{224}$ −3530, and $[\theta]_{208}$ +19 300.

Anal. Calcd. for $C_{20}H_{26}O_5$: C, 69.34; H, 7.57. Found: C, 69.20; H, 7.59.

[5]Our experience with these and other sesquiterpenes (8) has been that the n.m.r. spectrum is often the only analytical method that will allow distinguishing of these closely related substances.

Can. J. Chem. Downloaded from www.nrcresearchpress.com by 210.87.254.6 on 09/05/12
For personal use only.

Can. J. Chem. Downloaded from www.nrcresearchpress.com by 210.87.254.6 on 09/05/12
For personal use only.

Dihydro-β-cyclopyrethrosin (3)

Column fraction 144–148 yielded 102 mg of dihydro-β-cyclopyrethrosin (**3**) on treatment with ethanol – isopropyl ether in the form of needles, m.p. 212–213°. The physical constants were identical with the compound produced by hydrogenation of β-cyclopyrethrosin (**1**) (1) and the i.r. spectra were superimposable.

Dihydro-β-cyclopyrethrosin Acetate (18)

Dihydro-β-cyclopyrethrosin (0.1 g) was dissolved in a mixture of 1 ml of acetic anhydride and 1 ml of pyridine. After 16 h, 2 g of ice were added and the solution extracted with three 50-ml portions of ether. The ether solution was extracted with water, 1 *N* H_2SO_4, 5% $NaHCO_3$, and water. The dried ether (Na_2SO_4) solution left an oily residue (0.11 g) that crystallized from ethanol – isopropyl ether to give 81 mg of acetate **18**; m.p. 191–192°; $[\alpha]_D^{25}$ +69° (*c*, 0.195 in methanol); i.r. ν_{max} 1775 (γ-lactone), 1730 and 1240 cm^{-1} (acetate) with no absorption around 3500 cm^{-1}, and n.m.r. peaks at δ 2.05 and 2.08 (singlets, 3H, acetate methyl).

Anal. Calcd. for $C_{19}H_{26}O_6$: C, 65.12; H, 7.48. Found: C, 65.20; H, 7.42.

Hydrolysis of Dihydro-β-cyclopyrethrosin (3)

A 0.6 g sample of dihydro-β-cyclopyrethrosin (**3**) was dissolved in 6 ml of ethanol and mixed with 40 ml of 0.8 *N* aqueous NaOH. After refluxing for 1 h, the solution was acidified with 1 *N* H_2SO_4 and extracted the following day, first with seven 50-ml portions of ether and then with three 50-ml portions of ethyl acetate. The combined and dried (Na_2SO_4) extracts yielded 214 mg of a heavy oil after evaporation of the solvent. The t.l.c. on silica gel G (Merck) with ether as solvent showed two spots, R_f 0.30 and 0.04 (0.3% $KMnO_4$ as detecting reagent).

The mixture was separated on a column (1.0 × 13.5 cm) of silica gel G (14 g) with 10% chloroform in ether as solvent. The eluting solvent was changed to ether after 30 ml. The colorless oil (71 mg) from fractions (2 ml) 32–60 was crystallized from ethyl acetate – chloroform to give fine needles of desacetyldihydro-β-cyclopyrethrosin (**14**); m.p. 155–156°; $[\alpha]_D^{25}$ +79° (*c*, 0.165 in methanol); i.r. ν_{max} 3580 and 3470 (hydroxyl), 1770 (γ-lactone), and 1648 cm^{-1} (olefin); and lacking the peak in the n.m.r. spectrum at δ 2.03 (s, 3H) for acetate.

Anal. Calcd. for $C_{15}H_{22}O_4$: C, 67.64; H, 8.33. Found: C, 67.32; H, 8.28.

Acetylation of this material with acetic anhydride in pyridine gave a diacetate identical with dihydro-β-cyclopyrethrosin acetate (**18**).

The 500 ml of ether effluent, after column fraction 91, left 61 mg of an oily residue that yielded from ethyl acetate – isopropyl ether, 33 mg of desacetyldihydro-β-cycloisopyrethrosin (**7**); m.p. 196–197° with softening at 112°; $[\alpha]_D^{25}$ +184° (*c*, 0.125 in methanol); i.r. ν_{max} (Nujol) 3440 (hydroxyl) and 1750 cm^{-1} (γ-lactone); and the n.m.r. spectrum lacked the peak at δ 2.03 (s, 3H).

Anal. Calcd. for $C_{15}H_{22}O_4$: C, 67.64; H, 8.33. Anal. Calcd. for $C_{15}H_{22}O_4 \cdot \frac{1}{2}$ EtOAc: C, 65.78; H, 8.44. Found: C, 65.73; H, 8.47.

Dihydro-β-cycloisopyrethrosin Acetate (19)

A 50 mg sample of dihydro-β-cycloisopyrethrosin (**7**) was treated with 1 ml of pyridine and 1 ml of acetic anhydride. After 24 h the solution was treated with 10 ml of water, extracted with ether, and the extract washed with dilute aqueous acid, $NaHCO_3$, and water. The residue crystallized from isopropyl ether to give prisms; m.p. 148–149°; $[\alpha]_D^{25}$ +270° (*c*, 0.215 in methanol); i.r. ν_{max} 1780 (γ-lactone), 1730 and 1250 cm^{-1} (acetate, double-intensity); and n.m.r. peaks at δ 2.06 (s, 6H, acetate methyl).

Anal. Calcd. for $C_{19}H_{26}O_6$: C, 65.12; H, 7.48. Found: C, 65.02; H, 7.41.

β-Cyclopyrethrosin Benzoate (11)

β-Cyclopyrethrosin (**1**, 50 mg) dissolved in 0.6 ml of dry pyridine was treated with 0.1 ml of benzoyl chloride. After 2 h at room temperature, 5 ml of water was added and the reaction mixture extracted with ether. The ether extract was washed with dilute acid, $NaHCO_3$ solution and water, and the solvent evaporated. The residue (76 mg) crystallized from ethanol, after chromatography on silica gel G (5 g) with $CHCl_3$–ether (1:1) as the solvent. The yield was 35 mg of **11** as needles; m.p. 240° (dec.); i.r. ν_{max} 1725 cm^{-1} (double intensity, acetate and benzoyl); n.m.r. δ 7.2–7.7. (m, 3H) and 7.9–8.2 (m, 2H) for protons of the aromatic ring; and $[\alpha]_D^{25}$ −40.4° (*c*, 0.68 in methanol), $[M]_D$ −166. The alcohol **1** showed $[M]_D$ +178 resulting in $\Delta[M]_D$ (benzoate–alcohol) of −344°.

Anal. Calcd. for $C_{24}H_{26}O_6$: C, 70.23; H, 6.39. Found: C, 70.27; H, 6.49.

Determination of C-1 Configuration in β-Cyclopyrethrosin (1) by Horeau's Method (8)

A 48.9 mg sample of β-cyclopyrethrosin (**1**) and 158.1 mg of α-phenylbutyric anhydride were dissolved in 2.5 ml of dry pyridine. After 18 h at room temperature, 1 ml of water was added, and 6 h later the reaction mixture was extracted with ether and the extract washed with water, 5% $NaHCO_3$, and water. The ether solution residue (68 mg) showed no starting material by t.l.c. The combined aqueous and $NaHCO_3$ solutions left 114 mg of α-phenylbutyric acid, $[\alpha]_D^{25}$ +8.3° (*c*, 1.14 in benzene) corresponding to an optical yield of 46% positive and indicating an *R* configuration.

Dihydrochrysanin (13)

Chrysanin (**4**) (100 mg) was hydrogenated over 60 mg of 5% Pd on C at ambient temperature and pressure. After the rapid uptake of 1 equiv of hydrogen the reaction was stopped. The crude dihydro- derivative crystallized from ethanol – isopropyl ether as needles of **13** (65 mg); m.p. 201–202°; $[\alpha]_D^{25}$ +106° (*c*, 0.1 in methanol); and n.m.r. peak δ 1.10 (d, J = 6.8, 3H, secondary methyl).

Anal. Calcd. for $C_{20}H_{28}O_5$: C, 68.94; H, 8.10. Found: C, 68.52; H, 7.86.

Hydrolysis of Chrysanin (4)

A 70 mg sample of chrysanin was hydrolyzed at room temperature for 3 days in 2.5 ml of 0.3 *N* NaOH in 60% ethanol. The acidified reaction mixture was extracted with ether. The ether extract was back-extracted with 5% $NaHCO_3$ solution which was acidified with 1 *N* H_2SO_4 and extracted with ether. The ether residue (55 mg) was triturated with petroleum ether to remove the crude angelic acid (13 mg).

The sodium salt of the crude acid was treated with 50 mg of *p*-phenylphenacyl bromide in 5 ml of ethanol. After refluxing 1 h, the filtered solution was concentrated

Can. J. Chem. Downloaded from www.nrcresearchpress.com by 210.87.254.6 on 09/05/12
For personal use only.

and diluted with water to give 27 mg of pale yellow needles, m.p. 86–87°, identical (i.r., mixed m.p.) with authentic *p*-phenylphenacyl ester of angelic acid (11*a*).

Hydrolysis of Dihydrochrysanin (13)

Dihydrochrysanin (**13**) (60 mg) was refluxed for 2 h in about 8 ml of 0.8 *N* NaOH. The reaction solution was acidified with 1 *N* H_2SO_4 and allowed to stand overnight for relactonization and then extracted with ether and ethyl acetate. The combined extract was washed with water, 5% $NaHCO_3$, and water. The residue (45 mg) showed two spots R_f 0.04 and 0.30 (t.l.c. silica gel G, ether) and was separated on a column of silica gel G (7 g) by eluting with ether. The first 23 ml of effluent (fraction I) contained R_f 0.30 material and after a 5 ml fraction with no residue the next 100 ml (fraction II) contained the lower R_f substance. Fraction I gave 18 mg of desacetyldihydro-β-cyclopyrethrosin (**14**), m.p. 155–156°, identical (i.r., mixed m.p., and t.l.c.) with the sample obtained from dihydro-β-cyclopyrethrosin (**3**), while fraction II yielded 14 mg of desacetyldihydro-β-cycloisopyrethrosin (**7**).

Chrysanolide Dipyrazoline

Chrysanolide (**5**, 21 mg) was suspended in 10 ml of ether and mixed with ethereal diazomethane (9 ml) generated from 0.17 g of *N*-methyl-*N*-nitroso-*p*-toluenesulfonamide. The solution was kept at 0° for 16 h and on evaporation of the solvent deposited a silky mass of crystals (24 mg). Recrystallization from chloroform–methanol gave the dipyrazoline, m.p. 155–156° (dec.), with gas evolution.

Anal. Calcd. for $C_{19}H_{24}N_4O_5$: N, 14.43. Found: N, 14.30.

Tetrahydrochrysanolide (16)

Chrysanolide (80 mg) was hydrogenated in absolute ethanol over 5% Pd on C at ambient temperature and pressure. Hydrogen uptake was rapid and ceased after 2 equiv. The residue (85 mg) crystallized readily from ethanol – isopropyl ether to give 57 mg of tetrahydrochrysanolide (**16**) as needles; m.p. 159.5–160.0°; $[\alpha]_D^{25}$ +14° (*c*, 0.10 in methanol); u.v. end absorption log ε 4.67 at 210 mμ and λ_{max} 285 mμ (ε 54); i.r. ν_{max} 1765 (γ-lactone), 1730 (acetate), 1710 (ketone), and 1670 cm^{-1} (weak, olefin); n.m.r. δ 1.08 (d, 3H, J = 6.8) and 1.38 (d, 3H, J = 6.7) for two secondary methyl groups and 1.94 (d, 3H, J = 1.3) for olefinic methyl; and the mass spectrum showed a molecular ion at *m/e* 308.1636 ($C_{17}H_{24}O_5$ requires *m/e* 308.1624).

Hexahydrochrysanolide

Tetrahydrochrysanolide (**16**, 40 mg) in 5 ml of absolute ethanol was stirred with 7 mg of $NaBH_4$ for 1.5 h. The mixture was evaporated, two drops of HOAc were added, and the residue was dissolved in 10 ml of chloroform and then extracted with water and dried (Na_2SO_4). Removal of solvent left 39 mg of an oil which on t.l.c. examination (silica gel G, 1% ethanol in ether) showed a major spot at R_f 0.33. Column chromatography on 7 g of the same adsorbent and with the same solvent gave 17 mg of hexahydrochrysanolide as an oil, i.r. ν_{max} 3600 and 3460 (hydroxyl), 1755 (γ-lactone) and 1730 (acetate), and lacking the ketone band at 1710 cm^{-1}. The n.m.r. spectrum indicated a mixture of isomers.

Dihydropyrethrosin (12)

(A) Hydrogenation over Pd on C

Pyrethrosin (**2**, 1.0 g) was hydrogenated over 200 mg of 5% Pd on C in 30 ml of ethanol. Hydrogenation ceased after 1 equiv was absorbed at ambient temperature and pressure. The crude residue crystallized upon addition of ether to give 827 mg of a mixture (4:1 by n.m.r.) of dihydro- and epidihydropyrethrosin,[6] m.p. 152–190°. Recrystallization three times from ethanol gave 263 mg of pure (n.m.r.) dihydropyrethrosin, m.p. 168–170°, $[\alpha]_D^{25}$ −173° (*c*, 0.048 in methanol) which showed in the n.m.r. spectrum a 3H doublet (J = 6.7) at δ 1.38 for the secondary methyl.

Anal. Calcd. for $C_{17}H_{24}O_5$: C, 66.21; H, 7.85. Found: C, 65.87; H, 7.79.

(B) $NaBH_4$ Reduction

A 1.0 g sample of pyrethrosin was suspended in 50 ml of absolute ethanol and while stirring 200 mg of $NaBH_4$ was added portionwise. After about 30 min, the solution was acidified with 10% acetic acid to p*H* 6.0 and the ethanol removed by evaporation at reduced pressure. The concentrate was diluted with 30 ml of chloroform and extracted with water, 1% $NaHCO_3$, and water. The dried chloroform (Na_2SO_4) residue (1.13 g) contained only one isomer (dihydropyrethrosin) by n.m.r. examination. Chromatography of the residue over 70 g of silica gel G with chloroform–ether as eluant to remove other impurities yielded 686 mg of dihydropyrethrosin (**12**), m.p. 168–170°, identical (i.r., n.m.r., and mixed m.p.) with the major isomer from Pd on C hydrogenation.

Epidihydropyrethrosin (Isodihydropyrethrosin) (17)

Pyrethrosin (**2**, 500 mg) and platinum oxide (45 mg) were suspended in 20 ml of ethanol and hydrogenated under ambient conditions. The reaction was stopped after 1 equiv of hydrogen was absorbed. The residue (516 mg) crystallized when treated with ether. The crystalline product (420 mg), m.p. 169–190°, by n.m.r. analysis was a mixture of dihydro- and epidihydropyrethrosin (1:4).[6] Three recrystallizations from ethanol gave 143 mg of pure epidihydropyrethrosin (**17**) which softens at 195° and melts at 205–207°, $[\alpha]_D^{25}$ −117° (*c*, 0.064 in methanol). The n.m.r. spectrum shows a 3H doublet (J = 7.2) at δ 1.23 for the secondary methyl.

Anal. Calcd. for $C_{17}H_{24}O_5$: C, 66.21; H, 7.85. Found: C, 66.23; H, 7.84.

Cyclization of Dihydropyrethrosin (12)

To a 500 mg sample of **12** dissolved in 4 ml of chloroform and 2 ml of ether was added three drops of concentrated HCl and the mixture stirred for ½ h. Chromatography of 100 mg of the reaction mixture on 50 g of silica gel G impregnated with 10% $AgNO_3$ and elution with 1 l of benzene followed by 200 ml each of 1, 5, 10, and 40% ether in benzene gave with the last solvent a bell-shaped elution curve (dry-weight analysis of 5-ml fractions) from which pure isomers were obtained at each end. The α-isomer was isolated from fractions 1–4 (37 mg) and the β-isomer from fractions 14–20 (20 mg). The

[6]Although we have not systematically studied the effect of the ratio of catalyst to starting material, it was, however, observed that the product ratio varied when such a change was made.

β-isomer recrystallized from ethanol–pentane was identical with (m.p., mixed m.p., i.r., and n.m.r.) dihydro-β-cyclopyrethrosin (**3**).

Recrystallization of dihydro-α-cyclopyrethrosin (**20**) from ether–pentane gave 24 mg of needles; m.p. 169–170°; $[\alpha]_D^{25}$ +78 (*c*, 0.058 in methanol); i.r. ν_{max} 3620 and 3490 (hydroxyl), 1780 (γ-lactone), 1735 (ester) and 1240 cm^{-1} (acetate); and n.m.r. peaks at δ 5.40 (m, 1H, H-3), 5.27 (t, J = 10.5, 1H, H-6), 4.18 (octet, 3.9, 11.2, 12.1, 1H, H-8), 3.74 (q, 6.8, 9.4, 1H, H-1), 2.11 (s, 3H, acetate), 1.68 (br s, 3H, olefinic methyl), 1.18 (d, 6.8, 3H, secondary methyl), and 0.95 (s, 3H, tertiary methyl).

Anal. Calcd. for $C_{17}H_{24}O_5$: C, 66.21; H, 7.85. Found: C, 66.22; H, 7.81.

This study was supported by Public Health Service Research Grant No. CA-08133 from the National Cancer Institute and a National Institute of Health Predoctoral Fellowship to one of us (C.D.H.) during 1969–1970. We thank Dr. R. W. Price of S. B. Penick and Company, New York for the pyrethrum flowers and Mr. D. R. Maciver of The Pyrethrum Bureau, Kenya, for a supply of pyrethrosin. The mass spectra determined by Dr. R. L. Foltz of Battelle Memorial Institute, Columbus, Ohio, and by Mr. R. Weisenberger of the Chemistry Department, Ohio State University are gratefully acknowledged.

1. R. W. Doskotch and F. S. El-Feraly. Can. J. Chem. **47**, 1139 (1969).
2. (*a*) D. H. R. Barton, O. C. Böckman, and P. de Mayo. J. Chem. Soc. 2263 (1960). (*b*) D. H. R. Barton and P. de Mayo. J. Chem. Soc. 150 (1957). (*c*) A. Castille. Ann. Pharm. Fr. **25**, 121 (1967). (*d*) S. Iriuchijima and S. Tamura. Tetrahedron Lett. 1965 (1967).
3. C. R. Narayanan and N. K. Venkatasubramanian. J. Org. Chem. **33**, 3156 (1968).
4. F. A. Bovey. Nuclear magnetic resonance. Academic Press, New York, N.Y. 1969. pp. 132–141; 363–364.
5. J. H. Brewster. Tetrahedron, **13**, 106 (1961) and references therein.
6. R. S. Cahn, C. Ingold, and V. Prelog. Angew. Chem. Int. Ed. **5**, 385 (1966).
7. A. Horeau and H. B. Kagan. Tetrahedron, **20**, 2431 (1964).
8. R. W. Doskotch and F. S. El-Feraly. J. Org. Chem. **35**, 1928 (1970).
9. W. Herz and H. B. Kagan. J. Org. Chem. **32**, 216 (1967).
10. D. H. R. Barton, G. P. Moss, and J. A. Whittle. J. Chem. Soc. C, 1813 (1968).
11. (*a*) K. Naya, I. Takagi, Y. Kawaguchi, Y. Asada, Y. Hirose, and N. Shinoda. Tetrahedron, **24**, 5871 (1968). (*b*) W. Herz and M. V. Lakshmikantham. Tetrahedron, **21**, 1711 (1965). (*c*) R. R. Fraser. Can. J. Chem. **38**, 549 (1960).
12. W. Stöcklin, T. G. Waddell, and T. A. Geissman. Tetrahedron, **26**, 2397 (1970).
13. V. S. Joshi, N. P. Damodaran, and S. Dev. Tetrahedron, **24**, 5817 (1968).
14. J. K. Crandall and L.-H. C. Lin. J. Org. Chem. **33**, 2375 (1968).
15. W. G. Rose and H. L. Haller. J. Org. Chem. **2**, 484 (1937).
16. W. Herz and R. N. Mirrington. J. Pharm. Sci. **55**, 104 (1966).

Can. J. Chem. Downloaded from www.nrcresearchpress.com by 210.87.254.6 on 09/05/12
For personal use only.

Can. J. Chem. Downloaded from www.nrcresearchpress.com by 210.87.254.5 on 09/05/12
For personal use only.

Long-range Spin–Spin Coupling in Pyrimidine Nucleosides

FRANK E. HRUSKA

Departments of Chemistry, The University of Winnipeg and the University of Manitoba,[1] *Winnipeg, Manitoba*

Received December 15, 1970

A study has been made of the 100 MHz p.m.r. spectra of a number of pyrimidine nucleosides in aqueous solution. Long-range five-bond spin–spin coupling interactions between the H-5 and H-1′ hydrogens were noted in uridine, 2′-deoxyuridine, 6-azauridine, and 6-azacytidine and rationalized by a predominantly *anti* conformation for each nucleoside. The absence of a detectable five-bond coupling in orotidine suggested that the *syn* conformation is preferred in this instance. The relative magnitudes of the four-bond and five-bond interactions in uridine and pseudouridine were shown to be consistent with the calculated mobile π-bond orders of the C_6—N_1 and C_6—C_5 bonds of the uracil base.

Les spectres de r.m.n. à 100 MHz d'un certain nombre de nucléosides pyrimidiniques en solution aqueuse, ont été étudiés. Une intéraction de couplage spin–spin à longue distance à travers cinq liaisons entre les hydrogènes H-5 et H-1′ a été mise en évidence dans l'uridine, la 2′-déoxyuridine, la 6-azauridine, et la 6-azacytidine et rationalisée en invoquant une conformation *anti* prédominante pour chacun des nucléosides. L'absence d'un tel couplage dans l'orotidine, suggère que dans ce cas, la conformation *syn* est privilégiée. L'amplitude relative des intéractions sur quatre liaisons et cinq liaisons dans l'uridine est consistante avec les ordres calculés pour les électrons π-mobiles des liaisons C_6—N_1 et C_6—C_5 de l'uracile.

Canadian Journal of Chemistry, 49, 2111 (1971)

Introduction

To facilitate discussion of the orientation of the heterocyclic base relative to the ribose (or deoxyribose) ring in purine and pyrimidine nucleosides Donohue and Trueblood (1) have defined the sugar-base torsion angle about the *N*-glycosyl bond (ϕ) and its *syn* and *anti* ranges. Considerable spectroscopic evidence (1–11) has now been accumulated and indicates that the major nucleoside components of transfer RNA, as well as modified components such as pseudouridine, exist preferentially in their *anti* conformations in the crystalline state as well as in solution. Recent evidence points to a *syn* conformation for orotidine (6-carboxyuridine) in aqueous solution (12) and crystalline 6-thiouridine (13). The p.m.r. studies have been particularly useful for conformational studies in solution. Three-dimensional models have been derived through consideration of the observed base– and ribose – ring proton chemical shifts and via Karplus treatments (14) of the three-bond interactions between hydrogens on bonded carbons. Long-range coupling interactions[2] as well are known to be dependent upon molecular conformation and a number of useful structural correlations have been proposed. These have been considered in a number of reviews (15–18). However, this long-range phenomenon has seldom been observed in nucleosides. Hruska, Grey, and Smith (7, 10) have noted a four-bond benzylic type of interaction in α- and β-pseudouridine and suggested its potential for monitoring perturbations in ϕ. Cushley *et al.* (19) reported a five-bond interaction between fluorine and hydrogen and proposed on this basis the *anti* conformation of 5-fluorouridine.

In this report I wish to present evidence for a five-bond coupling between the H-5 and H-1′ hydrogens of uridine (U), 2′-deoxyuridine (dU), 6-azauridine (6-aU), and 6-azacytidine (6-aC). (Fig. 1). Although p.m.r. spectra of U and dU have appeared on several occasions, these interactions have not been reported. The observed coupling constants are discussed in terms of established correlations of $^5J_{HH'}$,[3] with molecular geometry and their magnitudes are taken as evidence that the *anti* ranges of ϕ are favored in U, dU, 6-aU, and 6-aC. The *syn* range is suggested to be favored in orotidine (O, Fig. 1) since in this instance no $^5J_{51'}$ interaction was detected.

[1]Present address of the author.

[2]Between nuclei separated by more than three bonds.

[3]The coupling constants are henceforth denoted by $^nJ_{HH'}$ where the superscript refers to the number of intervening bonds in the coupling path between the coupled nuclei H and H′.

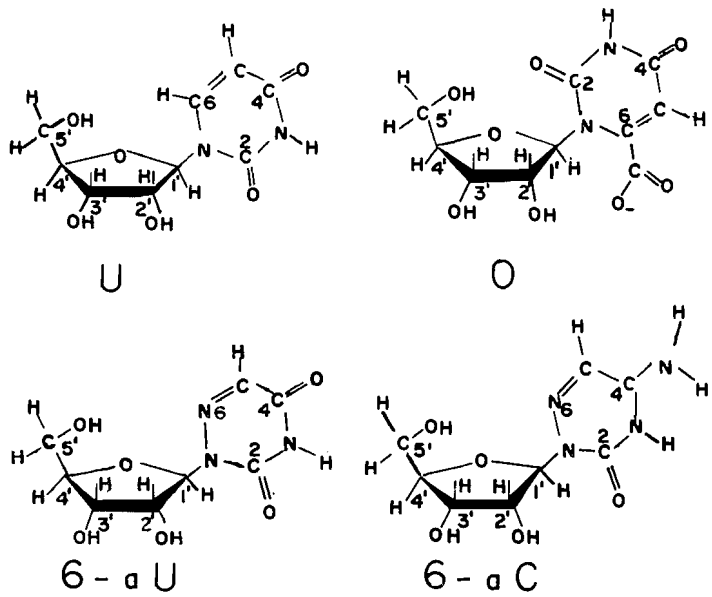

FIG. 1. Structural formulae of uridine (U), 6-azauridine (6-aU), 6-azacytidine (6-aC), and orotine (O).

The absence of any observable four-bond coupling between the H-6 and -1′ hydrogens of U and dU is shown to be consistent with their *anti* conformations and the theoretically calculated mobile π-bond orders of the uracil base. The previously reported (7, 10) four-bond interactions in the pseudouridines are reconsidered in the light of the present study.

Experimental

The nucleosides (A grade) were obtained from Calbiochem and used without further purification. The D_2O solutions containing 0.12 *M* nucleoside and 0.12 *M* DSS (3-trimethylsilylpropanesulfonic acid for internal referencing) were freeze-dried three times to reduce the HDO concentration. The p*D* of the solution[4] was adjusted with DCl and NaOD. Spectra were obtained at 30 °C on a Varian HA-100 spectrometer. Line positions relative to internal DSS were reproducible to within 0.05–0.1 Hz depending on their linewidth. The various bands were assigned by comparison with previously reported data (7–11) of U, dU, and the pseudouridines.

Results

In an earlier report (8) we discussed the spectral analysis of U in neutral solution. Under these conditions there is considerable overlap between the H-5 and -1′ spectral bands and no $^5J_{51'}$ interaction was noted. In this study measurements were carried out in a weakly basic solution such that the nucleoside is in fact present as the monoanion formed by dissociation of the N—H hydrogen at the 3-position of the base (pK_a = 9.4). This dissociation and the associated electronic changes in the uracil moiety produce a shielding of H-5 relative to H-1′ and the two spectral regions become well separated. Data for the other nucleosides were obtained under similar conditions. In Fig. 2 the H-6, -5, and -1′ resonances are shown for U (p*D* 11.2). The doublet centered at 7.660 p.p.m. was assigned to H-6 which is magnetically coupled to H-5 ($^3J_{56}$ = 7.70 Hz). The H-5 resonances are centered at 5.796 p.p.m. and comprise a doublet of doublets with a large splitting ($^3J_{56}$) and a smaller splitting of 0.41 Hz. Centered at 5.906 is a somewhat broader doublet assigned to H-1′ which is coupled to H-2′ ($^3J_{1'2'}$ = 4.4 Hz).

The source of the extra splitting of 0.41 Hz present in the H-5 region was readily established by double-resonance experiments. In Fig. 2 (inverted) is shown the H-5 region obtained with simultaneous irradiation in the H-1′ portion of the spectrum and shows clearly the disappearance of the small spacing. A 0.41 Hz splitting is not, however, apparent in the H-1′ region. That this spacing is present, but unresolved, was demon-

[4]p*D* = p*H* meter reading + 0.4. See Glascoe and Long, ref. 32.

Can. J. Chem. Downloaded from www.nrcresearchpress.com by 210.87.254.5 on 09/05/12
For personal use only.

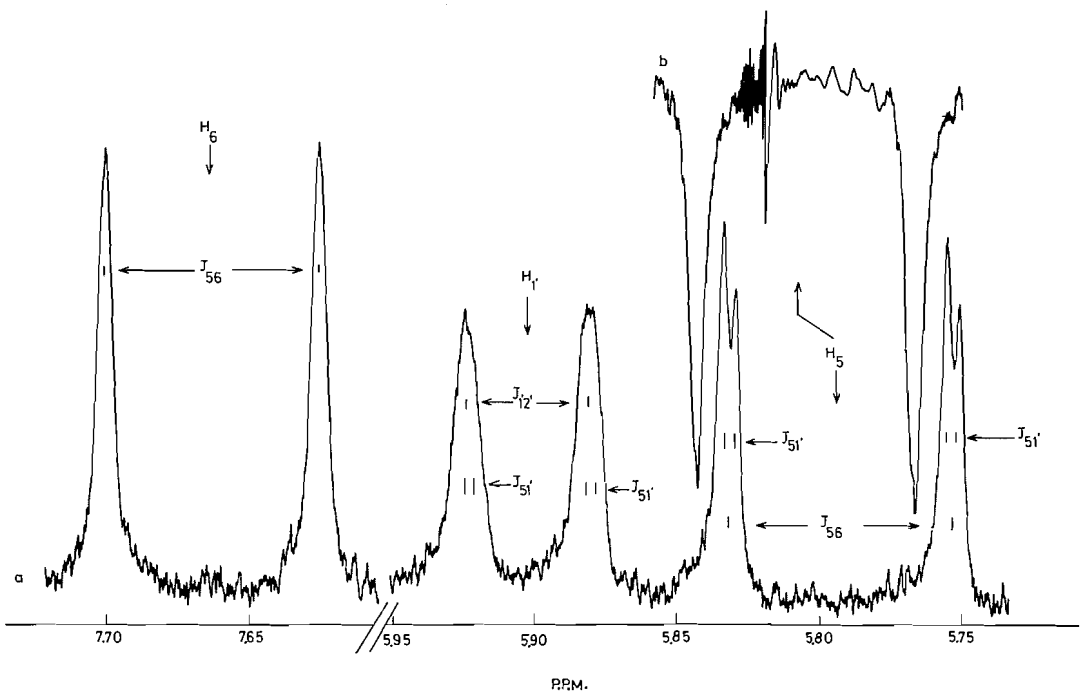

FIG. 2. (*a*) The H-6, -5, and -1′ regions of the 100 MHz p.m.r. spectrum of 0.12 *M* uridine in D_2O (p*D* = 11.2, 30 °C). Chemical shifts in p.p.m. are relative to internal 3-(trimethylsilyl) propanesulfonic acid. (*b*) Inverted H-5 region obtained under double resonance conditions with a second field applied at the frequency of the low-field H-1′ band. Sweep width 50 Hz.

strated by irradiation of the H-5 doublets. Under these double resonance conditions considerable enhancement (15–20%) in peak height as well as line narrowing was observed in the H-1′ lines.[5] No extra splitting is noted in the H-6 region and thus it is safe to conclude that any $^4J_{61'}$ interaction must be less than about 0.2 Hz.

In Fig. 3 are shown the H-5 and -1′ regions of 6-aU (p*D* 10.0). The H-5 region comprises a doublet with a 0.61 Hz splitting; H-1′ appears as a broader doublet at 6.113 p.p.m. ($^3J_{1'2'}$ = 3.6 Hz). Also shown (inverted) is the single H-5 line obtained through irradiation in the H-1′ region. Collapse of H-5 doublet under these decoupling conditions clearly establishes the presence of a 0.61 Hz $^5J_{51'}$ interaction in 6-aU.

Spectra of dU and 6-aC are not shown but in these instances $^5J_{51'}$ interactions of 0.45 and 0.52 Hz respectively were manifest in their H-5 multiplet patterns and confirmed by double resonance experiments.

[5]Other sources of line broadening in the H-1′ region could be unresolved coupling to H-6 and -3′ as well as virtual coupling to H-3′ and nitrogen quadrupolar effects.

In an earlier report (12) a discussion of the p.m.r. data of O was presented but no attention to possible long-range interactions was given at that time. Displayed in Fig. 4 are the H-5 and -1′ regions of this nucleoside (p*D* 12.0). The 3.7 Hz splitting in the latter region was readily attributed to coupling with H-2′ (12). No splitting, however, is evident in the H-5 region. In view of the narrow linewidth of this single resonance (0.35 Hz at half height), any $^5J_{51'}$ interaction, if present, is safely estimated to be less than about 0.1 Hz.

The p.m.r. data of the H-6 and -5 hydrogens are presented in Table 1. The $^5J_{51'}$ couplings are listed as positive numbers although no sign determinations were carried out. However, the signs of the coupling constants between protons separated by five bonds along an extended zig–zag path (*vide infra*) have been shown to be positive in a wide variety of compounds (15–18).

Discussion

(A) Benzylic Coupling

Numerous observations of long-range H–H couplings are now compiled in a number of

Can. J. Chem. Downloaded from www.nrcresearchpress.com by 210.87.254.5 on 09/05/12
For personal use only.

TABLE 1. Proton chemical shifts and coupling constants*: H-6 and H-5 regions of uridine(U), 2′-deoxyuridine(dU), 6-azauridine (6-aU), 6-azacytidine (6-aC), and orotidine (O)

Compound	Chemical shifts (p.p.m.)		Coupling constants (Hz)		
	H-6	H-5	$^5J_{51'}$	$^4J_{61'}$	$^3J_{56}$
U(p*D* 11.2)	7.660	5.796	0.41	<0.2	7.70
dU(p*D* 12.2)	7.666	5.801	0.45	<0.2	7.6
6-aU(p*D* 10.0)	—	7.403	0.61	—	—
6-aC(p*D* 10.4)	—	7.719	0.52	—	—
O(p*D* 12.0)	—	5.751	<0.1	—	—

*The chemical shifts relative to DSS are estimated to be accurate to within 0.002 Hz. The $^5J_{HH'}$ interactions were reproducible to within 0.05 Hz.

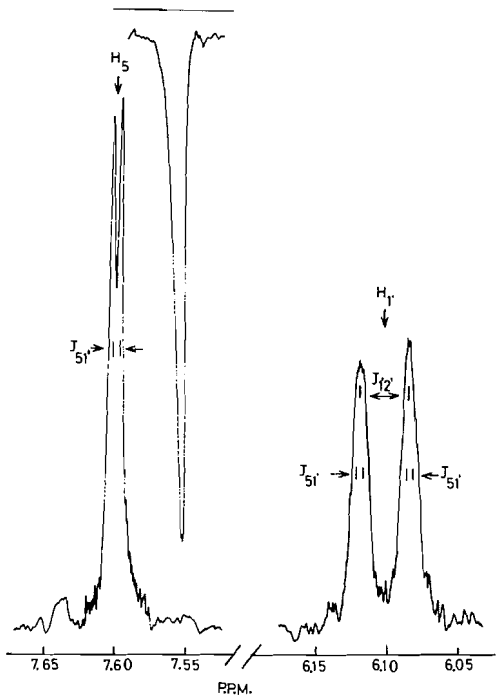

FIG. 3. (*a*) The H-5 and -1′ regions of the 100 MHz p.m.r. spectrum of 0.12 *M* 6-azauridine in D_2O (p*D* = 10.0, 30 °C). Chemical shifts in p.p.m. are relative to internal 3-(trimethylsilyl) propanesulfonic acid. (*b*) Inverted H-5 singlet obtained under double resonance conditions with a second field applied at the frequency of the low-field H-1′ band. Sweep width 100 Hz.

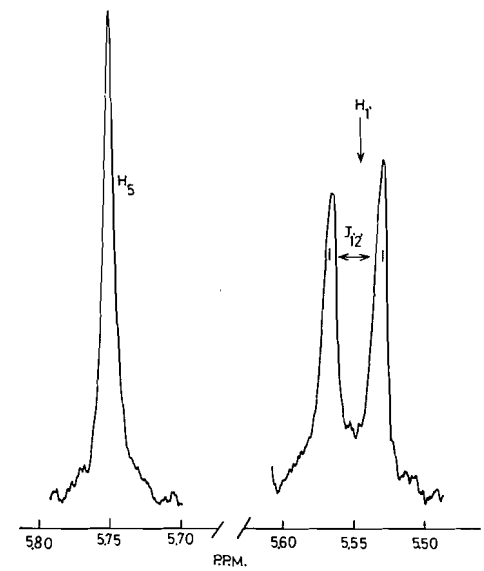

FIG. 4. The H-5 and -1′ regions of the 100 MHz p.m.r. spectrum of 0.12 *M* orotidine in D_2O (p*D* = 12.0, 30 °C). The chemical shifts are in p.p.m. relative to internal DSS. Sweep width 50 Hz.

reviews (15–18). Particularly relevant to the present discussion are the benzylic type of interactions noted in aromatic and heteroaromatic molecules. Three types may be distinguished, the four-, five-, and six-bond interactions of the side chain (α) proton with hydrogens at the ortho (*o*), meta (*m*), and para (*p*) positions of a six-membered ring system. The $^5J_{51'}$ couplings are examples of *m*-benzylic interactions. Although the absolute magnitudes of *m*-benzylic interactions are generally small (<1.0 Hz), a critical dependence on molecular geometry is evident. The dependence is such that coupling is favored when the α- and meta-hydrogens are separated by an extended "zig–zag" path. This steric requirement has been particularly well demonstrated by studies on halogenated toluenes. Schaefer *et al.* (20) for instance, argue that at −40 °C the proton spectrum of α,α,2,6-tetrachlorotoluene (Fig. 5) was consistent with highly-hindered rotation of the side chain and a locked conformation of the molecule with H_α located preferentially in the plane of the benzene ring.

Can. J. Chem. Downloaded from www.nrcresearchpress.com by 210.87.254.5 on 09/05/12
For personal use only.

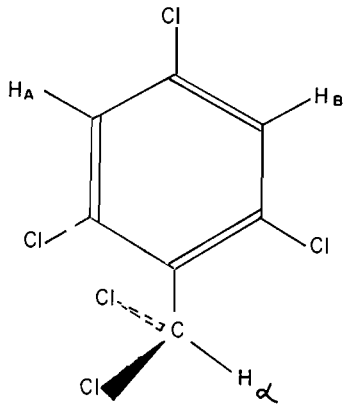

FIG. 5. Structural formula of α,α,2,6-tetrachlorotoluene. The H_α is coplanar with the ring and connected to H_A via a zig–zag route.

The H_α region appeared as a doublet with a splitting of 0.5 Hz attributable to coupling with H_A which is connected to H_α via a zig–zag route. Coupling to the other meta position (H_B) was not detected at this temperature. This zig–zag restriction on $^5J_{HH'}$ interactions is not peculiar to toluene-like molecules but has been noted in heterocyclic, polycyclic, and acyclic systems.

In subsequent paragraphs arguments are presented in support of the zig–zag restriction on the $^5J_{51'}$ interactions. On this basis predictions are made regarding the favored conformations of 6-aU, 6-aC, and O about their respective *N*-glycosyl bonds.

(B) Uridine and 2′-Deoxyuridine

The evidence that the *anti* conformations of U and dU are favored over *syn* in the solid state as well as in solution is not disputed (1–11). That *syn* conformations are not present to any detectable extent is generally agreed to be a consequence of unfavorable steric interactions (between the 2-keto oxygen and the *endo* ribose substituents) not present when the molecules are *anti*. X-Ray data (21) for a number of uridine derivatives indicates a preference for the φ values from −40 to −60° in the *anti* range. Examination of Drieding models shows clearly that when the uracil base is rotated into this range the $C_{1'}$—$H_{1'}$ bond approaches an orientation coplanar with the base plane and that an extended zig–zag path connects H-5 and -1′. Thus in the *anti* conformation of U and dU H-5 and -1′ bear a steric relationship similar to that of H_A and H_α in Fig. 5. Since the magnitudes of their $^5J_{51'}$ are comparable to the observed values in a large number of toluene derivatives, it is reasonable to assume that the electronic and steric factors governing five-bond interactions in pyrimidine nucleosides are similar to those suggested to be operative in toluene-like molecules.

(C) 6-Azauridine and 6-Azacytidine

The 6-azaderivatives have been the center of interest in a number of laboratories because of their potential as chemotherepeutic agents (22). As yet little detailed information regarding their three-dimensional conformations in aqueous solutions is available. The i.r. studies (23, 24) have shown that the diketo and amino forms of 6-aU and 6-aC (*i.e.* those shown in Fig. 1) predominate in nonpolar solvents. I propose as evidence that an extended zig–zag path connects their H-5 and -1′ hydrogens (*i.e.* that their *anti* range is favored over the *syn*) the magnitudes of the observed $^5J_{51'}$. This conclusion is very reasonable on a steric basis since there appear to be no close contacts present in the azaderivatives which could significantly alter their conformations about the *N*-glycosyl bond.

(D) Orotidine

If an extended zig–zag path is a structural requirement for a detectable five-bond interaction in O, then I propose that its absence is evidence that such a path *does not* connect the 5- and 1′-hydrogens and therefore this nucleoside must exist in its *syn* range of torsion angles. In the *syn* range H-5 and -1′ bear a spatial relationship similar to that between H_B and H_α in Fig. 5 where H_B is the meta hydrogen not coupled to the α-position. That the *syn* range should be favored is very reasonable on steric grounds. Locking O into its *anti* range requires placement of the bulky carboxyl group (rather than the 2-keto oxygen) above the sugar in close proximity with its *endo* substituents. In molecular models of O rotation of the 6-substituent is virtually impossible and the torsional freedom of the furanose ring (7–8) severely restricted when the molecule is *anti*. These librational motions are less restricted when the molecule is *syn*.

Thus the present work supports earlier conclusions (12) regarding the conformation of O based on trends in the observed proton chemical shifts and the $^3J_{HH'}$ coupling constants of the ribose ring.

Can. J. Chem. Downloaded from www.nrcresearchpress.com by 210.87.254.5 on 09/05/12
For personal use only.

Can. J. Chem. Downloaded from www.nrcresearchpress.com by 210.87.254.5 on 09/05/12
For personal use only.

(E) Ortho Benzylic Interactions

Newsoroff and Sternhell (25) have noted that in cases where the α-carbon is sp^3-hybridized the four-bond *o*-benzylic coupling constants are generally larger (in absolute magnitude) than the five-bond *m*-benzylic coupling constants. In toluene itself values of −0.75 and 0.36 Hz have been reported for the *o*-benzylic and *m*-benzylic interactions, respectively (26). It is clear from Fig. 2, however, that any $^4J_{61'}$ interaction, if present in U, is smaller than $^5J_{51'}$ and probably less than about 0.2 Hz. This apparent anomaly in the trends can be readily understood if the (*i*) electronic and (*ii*) steric differences between U and toluene are considered in the light of current theoretical formulations of long-range coupling mechanisms. These have been clearly summarized in the recent review by Barfield and Charabarti (18).

(i) Electronic

Theory suggests that *o*-benzylic couplings may be adequately discussed in terms of σ–π configuration interaction between the benzylic proton (H_α in toluene, H-1′ in U) and the 2pπ orbital on the ring atom to which the benzylic carbon is bonded (C-1 in toluene, N-1 in U).[6] Furthermore, the theoretical treatment predicts a dependence of the four-bond interaction on the square of the mobile π-bond order (P^2) of the C_1—C_{ortho} linkage (N_1—C_6 is the analogous linkage in U). Reasonable correlations between P^2 and *o*-benzylic couplings have appeared in the literature to substantiate these predictions (27, 28). A number of theoretical evaluations of the π-structure of the pyrimidine bases have appeared (29, 30). Pullman and Pullman (29), for instance, list a value of 0.479 for $P(N_1—C_6)$ in uracil which is considerably smaller than the 0.667 value for C_1—C_{ortho} in toluene (26). One factor, therefore, which accounts for the anomalously diminutive $^4J_{61'}$ in U (and dU) must be the attenuated capacity in this nucleoside for σ–π interactions, attributable to the reduced π-density in the N_1—C_6 linkage.

[6]A contribution to the *o*-benzylic coupling from a mechanism involving only the σ network might also be considered in view of the numerous examples of ^4J interactions in saturated systems. It is generally found, however, that such contributions are unimportant unless the bonds form a planar "W". This arrangement between the α- and *o*-hydrogens is not possible since the C_{ortho}—H and C_1—C_α bonds are *cis* across the C_1—C_{ortho} linkage.

(ii) Steric

Theory predicts further that the magnitude of the σ–π interaction between the sp^3 side chain orbital and the adjacent 2pπ orbital bears a $\sin^2\theta$ relationship where θ is the angle between the C_α—H_α bond and the plane of the aromatic ring. The contribution is expected to be maximal when C_α—H_α is perpendicular to the aromatic ring and vanishing small in a coplanar orientation. In toluene free rotation of the methyl group is possible allowing the α-hydrogens to sample coplanar and perpendicular orientations. Since the average value of $\sin^2\theta$ is 0.5 over one complete rotation of the methyl group, the observed magnitude of the four-bond interaction is probably near to 50% of its maximal value at $\theta = 90°$. In U motion about the *N*-glycosyl bond is restricted to a narrower range of θ. The perpendicular orientations ($\theta = \pm 90°$) required for maximal σ–π interactions correspond to sterically unfavorable values of φ (+30 and −15°) and may be discounted. Thus $\sin^2\theta$ averaged over the torsional motion is expected to be less than 0.50. Therefore, insofar as σ–π configuration interaction and *o*-benzylic coupling are concerned the steric as well as electronic properties of U are less favorable than those of toluene.

Contributions to the *m*-benzylic coupling, on the other hand, apparently arise from both the σ–π mechanism as well as from a mechanism involving only the intervening σ-network. The former contribution is maximal for the perpendicular orientation ($\theta = 90°$); the latter is maximal for the planar zig–zag orientation. Thus the observation that in U $^5J_{51'} > {}^4J_{61'}$ whereas in toluene $^5J_{m\alpha} < {}^4J_{o\alpha}$ is readily rationalized on a theoretical basis if the nucleoside is assumed to be *anti* with an essentially planar zig–zag connection between H-5 and -1′.

(F) The Pseudouridines

β-Pseudouridine (β-ψ) is a unique component of all *t*-RNA in that it is a *C*-glycoside (Fig. 6) the point of attachment of the ribose being to the C-5 carbon of the base. At the two meta positions are found N_3—H_3 and N_1—H_1. Thus detection of a $^5J_{51'}$ interaction is precluded in aqueous solution due to rapid exchange of the hydrogens with the solvent. However, we did detect a $^4J_{61'}$ interaction of 0.8 Hz and discussed it briefly (7, 10). In these reports a comparison of the ribose chemical shifts and $^3J_{HH'}$ interaction of U

Can. J. Chem. Downloaded from www.nrcresearchpress.com by 210.87.254.5 on 09/05/12
For personal use only.

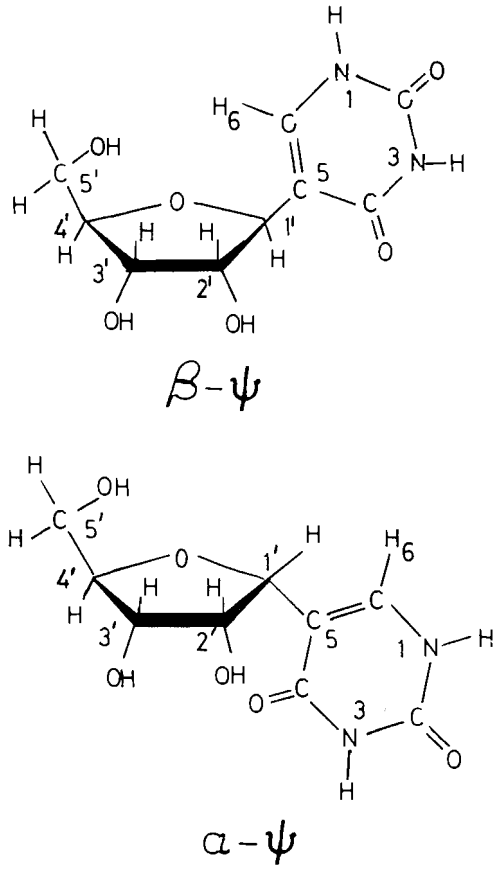

FIG. 6. Structural formula of β-pseudouridine (*anti*) and α-pseudouridine (*syn*).

and β-ψ was made and it was concluded that their three dimensional conformations were similar. In view of the distinctive stereochemical dependence of *o*-benzylic coupling and the absence of a detectable $^4J_{61'}$ in U our conclusions regarding the structural similarity of this isomeric pair may seem invalid. However, the apparent inconsistency is understood if comparison of the coupling paths in U and β-ψ is made.

In U the four-bond coupling proceeds via the segment $H_6—C_6—N_1—C_{1'}—H_{1'}$, whereas in β-ψ the relevant path involves the segment $H_6—C_6—C_5—C_{1'}—H_{1'}$. The σ–π interaction which is thought to be of fundamental importance for *o*-benzylic coupling should be related therefore to the mobile π-bond order of the $C_6—C_5$ and $C_6—N_1$ bonds of β-ψ and U respectively. Pullman and Pullman (29) estimate, however, $P(C_6—C_5)$ to be 0.82 in uracil, considerably larger than their value of 0.48 for $P(C_6—N_1)$. Thus the larger $^4J_{61'}$ interaction in β-ψ is readily interpreted in terms of an enhanced potential (relative to U) for σ–π interaction involving the H-1′ sp^3 orbital, without invoking gross conformational differences for the two nucleosides.

A slightly larger four-bond interaction ($^4J_{61'}$ = 1.2 Hz) was noted for α-ψ, the α-anomer of pseudouridine. This larger coupling is presumably a reflection of larger σ–π contributions in the α-anomer. Since the mobile π-bond order of the uracil base is not expected to be significantly dependent on the anomeric configuration of the molecule their magnitudes must reflect differences in the average values of θ (and therefore φ). Arguments were presented in a previous study (10) supporting a predominantly *anti* conformation for both anomers. However, if it is assumed that the conformations approaching the perpendicular orientation (θ = 90°, φ = 30°) are more favorable in α- than in β-ψ, then the relative magnitudes of their $^4J_{51'}$ couplings can be understood. Recently Rohrer and Sundaralingam (31) have reported a value of +3.2° for φ(θ = 63°) for crystalline α-ψ. The corresponding value is not yet known for β-ψ but if it were to be in the range centered at about −60° which is observed for most β-nucleosides, then the above assumption would be very reasonable.

Conclusions

This study demonstrates the potential usefulness of long-range coupling measurements in the determination of pyrimidine nucleoside conformations. The five-bond couplings in uridine, 2-deoxyuridine, 6-azauridine, and 6-azacytidine were shown to be consistent with their *anti* conformations. The absence of the analogous interaction in orotidine suggested a predominantly *syn* orientation in this case. The relative magnitudes of the *o*- and *m*-benzylic interactions in uridine, 2′-deoxyuridine, and the pseudouridines were shown to be in qualitative agreement with current theoretical formulations of long-range couplings and theoretically determined mobile π-bond orders of the uracil base.

I am grateful to Mr. Rod Wasylishen and Professor T. Schaefer for helpful discussions on the long-range phenomenon and to Drs. H. Dugas, B. Blackburn, R. K. Robins, and I. C. P. Smith for communicating their results on β-CAR prior to publication. This work was made possible through financial aid from The

National Research Council of Canada and The Faculty of Graduate Studies of the University of Manitoba. The work was initiated at The University of Winnipeg and I thank Professor Lawrence Swyers of this institution for his constant encouragement.

1. J. DONOHUE and K. N. TRUEBLOOD. J. Mol. Biol. **2**, 363 (1960).
2. A. E. V. HASCHMEYER and A. RICH. J. Mol. Biol. **27**, 369 (1967).
3. T. R. EMERSON, R. J. SWAN, and T. L. V. ULBRICHT. Biochem. **6**, 843 (1967).
4. D. W. MILES, W. H. INSKEEP, M. J. ROBINS, M. W. WINKLEY, R. K. ROBINS, and H. EYRING. J. Am. Chem. Soc. **92**, 3872 (1970).
5. S. S. DANYLUK and F. E. HRUSKA. Biochem. **7**, 1038 (1968).
6. M. P. SCHWEIZER, A. D. BROOM, P. O. P. Ts'O, and D. P. HOLLIS. J. Am. Chem. Soc. **90**, 1042 (1968).
7. F. E. HRUSKA, A. A. GREY, and I. C. P. SMITH. J. Am. Chem. Soc. **92**, 214, 4088 (1970).
8. B. J. BLACKBURN, A. A. GREY, I. C. P. SMITH, and F. E. HRUSKA. Can. J. Chem. **48**, 2866 (1970).
9. H. DUGAS, B. J. BLACKBURN, R. DESLAURIERS, R. K. ROBINS, and I. C. P. SMITH. J. Am. Chem. Soc. In press.
10. A. A. GREY, I. C. P. SMITH, and F. E. HRUSKA. J. Am. Chem. Soc. **93**, 1765 (1971).
11. J. H. PRESTEGARD and S. I. CHAN. J. Am. Chem. Soc. **91** 2843 (1969).
12. F. E. HRUSKA. J. Am. Chem. Soc. **93**, 1795 (1971).
13. W. SAENGER and K. SCHEIT. Angew. Chemie, Int. Ed. **8**, 139 (1969).
14. M. KARPLUS. J. Chem. Phys. **30**, 11 (1959).
15. S. STERNHELL. Rev. Pure and Appl. Chem. **14**, 15 (1964).
16. L. M. JACKMAN and S. STERNHELL. Applications of nuclear magnetic resonance spectroscopy in organic chemistry. Vol. 5. Pergamon Press Ltd., London, 1969. Chapt. 4–4.
17. S. STERNHELL. Quart. Rev. (London), **23**, 236 (1969).
18. M. BARFIELD and B. CHAKRABARTI. Chem. Rev. **69**, 757 (1969).
19. R. J. CUSHLEY, I. WEMPEN, and J. J. FOX. J. Am. Chem. Soc. **90**, 709 (1968).
20. T. SCHAEFER, R. SCHWENK, C. J. MACDONALD, and W. F. REYNOLDS. Can. J. Chem. **46**, 2187 (1968).
21. M. SUNDARALINGAM. Biopolymers, **7**, 821 (1969).
22. J. SKODA. *In* Prog. Nucl. Acid Res. **2**, 197 (1963).
23. J. PITHA and J. ZEMLICKA. Coll. Czech. Chem. Commun. **29**, 31 (1964).
24. J. PITHA and J. BERANEK. Coll. Czech. Chem. Commun. **28**, 1507 (1963).
25. G. P. NEWSOROFF and S. STERNHELL. Aust. J. Chem. **21**, 747 (1968).
26. M. P. WILLIAMSON, R. J. KOSTELNIK, and S. M. CASTELLANO. J. Chem. Phys. **49**, 2218 (1968).
27. D. J. BLEARS, S. S. DANYLUK, and T. SCHAEFER. Can. J. Chem. **46**, 654 (1968).
28. K. D. BARTLE, D. W. JONES, and R. S. MATHEWS. Rev. Pure and Appl. Chem. **19**, 191 (1969).
29. B. PULLMAN and A. PULLMAN. Quantum biochemistry. John Wiley and Sons, New York, N.Y., 1963. p. 225.
30. J. I. FERNANDEZ-ALONSO. Adv. Chem. Phys. **7**, 1 (1964).
31. D. C. ROHRER and M. SUNDARALINGAM. J. Am. Chem. Soc. **92**, 4950 (1970).
32. P. K. GLASCOE and F. A. LONG. J. Phys. Chem. **64**, 188 (1960).

Can. J. Chem. Downloaded from www.nrcresearchpress.com by 210.87.254.5 on 09/05/12
For personal use only.

Can. J. Chem. Downloaded from www.nrcresearchpress.com by 210.87.254.105 on 09/05/12
For personal use only.

Surface Effects in Cationic Polymerizations[1]

V. C. ARMSTRONG,[2] Z. KATOVIC,[2] AND A. M. EASTHAM
National Research Council of Canada, Ottawa, Canada

Received February 11, 1971

β-Methylstyrene dimerizes in the presence of boron fluoride. The rate of dimerization is very erratic under the usual conditions of high vacuum operation but becomes reproducible when reactors are baked out for a few hours at 500 °C under vacuum. In baked reactors reaction still occurs without added cocatalyst, and the rate seems to depend in part on the temperature and length of time of baking. The results suggest the existence of a surface reaction whose rate is of the first order in both monomer and boron fluoride.

Le β-méthylstyrène se dimérise en présence de fluorure de bore. La vitesse de dimérisation est excessivement changeante sous forte pression et dans des conditions standards. Celle-ci devient cependant reproductible lorsque les réacteurs sont calcinés à 500 °C sous vide pendant quelques heures. Dans ces réacteurs calcinés, la réaction se fait encore sans l'adjonction d'un catalyseur et la vitesse semble alors dépendre en partie de la température et de la durée de la calcination. Les résultats suggèrent l'existence d'une réaction de surface dont la vitesse est du premier ordre pour le monomère et le fluorure de bore.

Canadian Journal of Chemistry, 49, 2119 (1971)

In spite of considerable effort, there has been little real progress in our understanding of cationic polymerizations since the classic work of Evans, Polanyi, and coworkers nearly thirty years ago (1). This situation is due, at least in part, to the great difficulty in obtaining precise experimental measurements for the classical cationic systems, so we have sought alternative systems from which accurate kinetic and other data might be obtained. In principle the aliphatic monomers (olefins) should be the simplest and hence most desirable for investigation, but unfortunately they are also the monomers which present the greatest difficulty in analysis, so we have been forced to consider the substituted olefins. The dimerization of β-methylstyrene offers some possibility of serving as a model for the processes occurring in a cationic polymerization and can be followed accurately, at useful concentrations, under rigorous conditions by spectrographic methods. We are aware that results obtained with such a system are not necessarily suitable for direct comparison with our previous data on aliphatic systems, but we do not subscribe to the view that it should be possible to generalize in a simple scheme the reactions of all the monomers and catalysts employed in cationic polymerizations. In this paper we report the results of some studies of the boron fluoride - catalyzed dimerization of β-methylstyrene.

In preliminary experiments the boron fluoride - catalyzed isomerization of allylbenzene to β-methylstyrene was evaluated as a possible model of a protonation (initiation) reaction but was found to be too rapid for satisfactory measurement. It was observed that the isomerization overlapped a consecutive but slower dimerization of the product (β-methylstyrene) so we selected this dimerization as the starting point for our studies. The techniques used were generally similar to those developed earlier in studies of aliphatic systems, but were modified as necessary. Methanol and ethylene dichloride were selected as cocatalyst and solvent respectively.

Despite our most careful efforts the reproducibility of the early experiments was poor, much worse than we had experienced in our studies of aliphatic monomers. Materials were repeatedly purified and dried, vacuum techniques were improved, and analyses refined without improving the quality of the data. Conclusions drawn were necessarily limited but seemed generally similar to those reported in our earlier studies; reaction did not occur in the presence of a 1:1 catalyst–cocatalyst complex but took place immediately if excess boron fluoride were present. Curiously, the initial rates seemed considerably higher if, instead of adding all the boron fluoride at once, the 1:1 complex was left in contact with monomer for a short time before adding the excess boron fluoride. The initial rate of dimerization was found to be dependent on the concentrations of

[1]Issued as NRCC No. 11933.
[2]NRCC Postdoctorate Fellows.

Can. J. Chem. Downloaded from www.nrcresearchpress.com by 210.87.254.105 on 09/05/12
For personal use only.

monomer, free boron fluoride, and catalyst–cocatalyst complex but accurate orders could not be obtained. The temperature dependence was small and negative.

In the presence of boron fluoride alone ('blanks', *i.e.* no added cocatalyst) the initial rates were usually slow but were never zero, and were erratic. The blanks reached their lowest rates when the reactor was pumped and flamed for one or two days, then thoroughly flushed with dry solvent, before filling with reactants; behavior of this kind is, according to conventional views, most probably due to the presence in the reactor of random traces of cocatalytic impurities. It was also observed, however, that the method of cleaning the reactor had a marked effect on the rate of the blanks. Vessels which had been thoroughly cleaned with chromic acid gave consistently higher rates than those cleaned by washing with acetone–water, and a reduced but high rate persisted through a subsequent series of runs in which the reactor was simply washed out after use and pumped out for about a day. Treating the reaction flask with methylsilylchlorides was the only technique which seemed to reduce the rate of the blanks (see below). Because of these observations we are now of the opinion that in our earlier work the walls of the flask may have developed a thin layer of polymeric material during the reactions, which was not removed by washing, and which helped to improve reproducibility. It was our practice at that time to burn out the reaction flask at red heat in a stream of air after a series of experiments; after this treatment it usually took two or three runs, despite prolonged pumping, before the flask returned to its original condition (as judged by the rate data), presumably because polymer had to redeposit on the glass. In the present system, polymer is not formed so perhaps the reaction is less reproducible.

Because of these observations the apparatus was rebuilt so that (*a*) the reaction flask could be pumped out under vacuum at controlled temperature, up to 500 °C, (*b*) bellows-sealed stainless steel valves with Teflon seats replaced all stopcocks, and (*c*) separate lines were provided for evacuating those parts of the system (*e.g.* the reactor) which were occasionally opened to the atmosphere. There was no obvious way in which the whole system could be baked out for each run and still permit us to do a reasonable number of experiments, but on the basis of our previous experience we think that once a system has been well pumped out and flushed with solvent vapor, there is very little mobility of such residual cocatalytic impurities as may be adsorbed on the walls. The reaction vessel itself is thus the primary concern in attempting to obtain rigorous drying of the apparatus.

Rates in the new smaller reactors could not be compared with those from the earlier reactors because, under seemingly identical conditions, they were found to be about three times faster. The source of the difference is not clear since the surface is smaller in the new reactors and furthermore, the difference persists after treatment with silyl chloride.

We were surprised to find that baking-out the reaction vessel actually increased the rate of the blanks (Fig. 1). The rate first fell off, presumably due to drying of the glass surface, then increased again with increase in either time or temperature of baking. Obviously if this is the effect of heating, then the usual techniques of pumping and flaming the reactor can only lead to erratic blanks such as those observed. As an arbitrary reference point for these experiments we carried out reactions in a vessel which had been pumped out under high vacuum for 1 h, then pumped for a further 16 h at liquid nitrogen temperature.

Rate increases in cationic systems always raise a question as to whether they are due to removal of inhibitors or to formation of accelerators, and the present example is no exception. We have concluded, *very* tentatively, that the initial decrease in rate with heating results from removal of cocatalytic material from the glass surface and that the subsequent increase is due to the formation on the glass surface of some sort of active centers which combine with boron fluoride to catalyze reaction. Admission of air to any of these slow reactions causes immediate acceleration (Fig. 2), presumably because of the moisture in the air, but can also stop the reaction if the amount of moisture is in excess of the boron fluoride.

Attempts to clarify and define the surface effect were not very successful but gave some interesting results. Reproducibility in the baked-out systems, though much improved over earlier reactions still left something to be desired. Thus it was found difficult, after major repairs to the vacuum system, to return to the rates obtained prior to the repairs. A mixing problem exists but we have not been able to trace its origin. It is probably due to several factors and leads to a

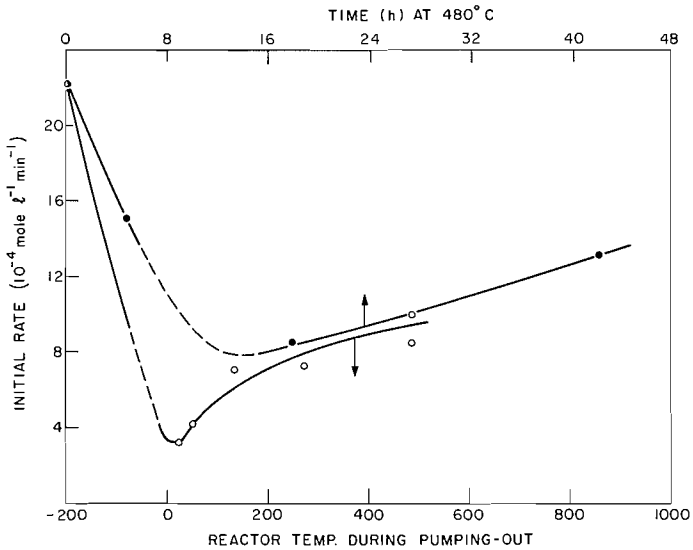

FIG. 1. Effect of time and temperature of bake-out on initial rate: upper curve, bake-out time at 480 °C before filling reactor; lower curve, temperature of bake-out for 22 h prior to filling reactor. ◑ Reference point, cell pumped out at liquid nitrogen temperature (−186°, see text).

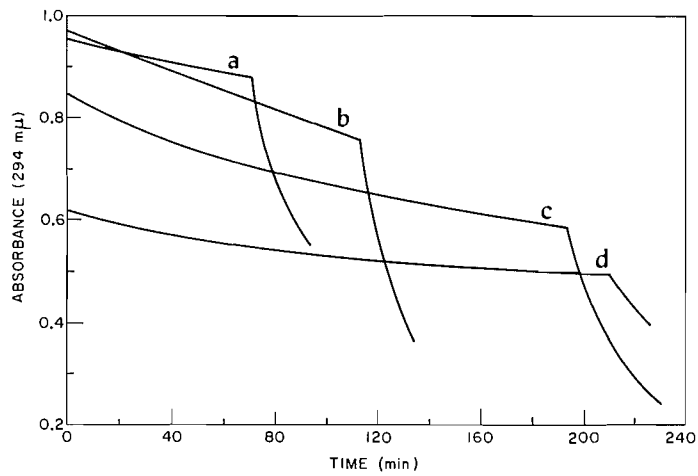

FIG. 2. Effect of admitting air to the reactors. *a*, Reactor (type *a*) treated with dimethylsilyl chloride; *b*, reactor (type *a*) pumped two days at 200 °C; *c*, reactor (type *a*) treated with dimethylsilyl chloride at elevated temperature; *d*, reactor (type *b*) pumped out at 480 °C (initial absorbance = 1.8, curve starts at 200 min).

difference in rates in the optical cell and in the bulk of the solution. We do not think it is due to temperature differences or to variations in the concentration of BF_3. The difference persists when the light is cut off between readings so is not photochemical in origin. It is not due to the difference in composition of the cell and reactor (quartz *vs.* pyrex) since an all-quartz reactor failed to produce marked rate change. One might perhaps expect a higher rate in the cell due to the higher surface/volume ratio and a consequently higher contribution from the surface reaction, but the difference is often in the opposite direction. The effect of this problem on the rate measurements was minimized by frequent mixing (by tipping the contents of the cell into the bulk of the solution) but it is nevertheless disturbing.

The initial rate of reaction in reactors baked out at 500 °C for 18 h was found to be of the first order in both monomer and boron fluoride (Fig.

Can. J. Chem. Downloaded from www.nrcresearchpress.com by 210.87.254.105 on 09/05/12
For personal use only.

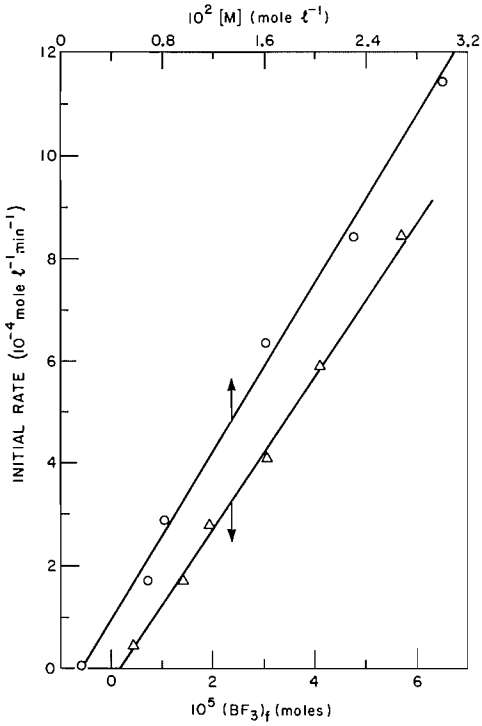

FIG. 3. Variation of initial rate with the concentration of free BF_3 (lower curve, [M] = 2.3×10^{-2} mole l^{-1}), and with the concentration of β-methylstyrene (upper curve, $(BF_3)_f = 5.7 \times 10^{-5}$ moles), in type *b* reactors pumped out for 18 h at 480 °C.

3). The results are generally similar to but more self-consistent than those from unbaked systems, but a small unexplained intercept is to be seen in each plot. The internal rate (the rate at which monomer disappears during the course of the run) does not follow first-order kinetics but falls off much more rapidly, suggesting a consumption of the active centers postulated above. The effect of added cocatalyst has not been examined but admission of air produces a marked rate increase which we attribute to cocatalysis by moisture in the air. All reactions go to completion but the slower ones may take a few days to do so.

Treatment of the unbaked reactors with trimethylsilylchloride or dimethylsilyldichloride causes a marked decrease in the rate of the blanks. The actual rate seems independent of the previous treatment of the cell (annealing, washing with solvent, or cleaning with chromic acid) or of the method of applying the silane (as silylchloride vapor at room temperature or at 200 °C, as the pure liquid, or as a solution in carbon tetrachloride). However, treatment of the vessel with the silylchloride for 4 h at 500 °C, followed by 2 h of pumping, gave no further reduction in rate. Interpretation of these results is not simple. According to the literature two types of reactions at the glass surface must be considered and can be represented by [1] and [2]. Reaction 1 is to be

$$[1] \quad (CH_3)_3SiCl + H_2O \rightarrow (CH_3)_3SiOH + HCl$$

$$[2] \quad (CH_3)_3SiCl + \underset{|}{\overset{|}{SiOH}} \rightarrow \underset{|}{\overset{|}{SiOSi(CH_3)_3}} + HCl$$

regarded as a simple dehydrating process with the products being pumped off, but reaction 2 or some similar process converts surface hydroxyl or siloxy groups to an organic coating on the surface of the glass. It seems to be generally believed that the latter process occurs only at elevated temperatures (*ca.* 400 °C) whereas reaction 1 takes place at ordinary temperatures (2, 3). However, it is also claimed that a dense hydrophobic coating is formed on the glass at ordinary temperatures if the silylchloride is applied in CCl_4 solution (3).

The silane treatment may prove useful but at present we are wary of it. We observed that reactors treated with silane vapors at room temperature were not wetted by solvent–monomer solutions but were wetted completely when the methanol – boron fluoride complex was present. Vessels treated at high temperature were not wetted in either case. These differences may be simple physical phenomena and hence unimportant, but they may indicate reaction between the catalyst and the treated surface in which case they lead to uncertainty concerning the catalytic species.

It is difficult to estimate the importance of this surface effect. The reaction is slow, as is very clear from the marked acceleration which occurs on opening the reactors to the atmosphere (Fig. 2), but it is also true that the product is only a dimer and that we know nothing about the kinetic chain lengths of the reaction. It is therefore conceivable that the surface reaction could be important in the formation of high molecular weight polymer at low cocatalyst concentrations. There seems little doubt that the surface reaction is responsible for the poor reproducibility encountered in the early stages of the present work, and it is possible too, that the strange results reported by Sigwalt and his coworkers (4) may have a similar origin, although their most recent results (7) suggest

Can. J. Chem. Downloaded from www.nrcresearchpress.com by 210.87.254.105 on 09/05/12
For personal use only.

Can. J. Chem. Downloaded from www.nrcresearchpress.com by 210.87.254.105 on 09/05/12
For personal use only.

otherwise. A surface reaction could also explain the odd shape of the rate curves we observe in the blanks for olefin polymerization; the shape of these curves suggests a two-component rate in which one part falls off rapidly while the other continues steadily to completion. Perhaps the falling off in the initial rate is due to consumption of adventitious cocatalyst leaving the surface reaction to go to completion.

While the slowness of the surface reaction may mean that this process cannot make an important contribution to the overall reaction, nevertheless the mere existence of the heterogeneous reaction is of some interest since it suggests the possibility of an alternative to the classic concept of proton initiation. Our evidence indicates that a catalyst is formed by interaction of boron fluoride with the baked-out glass surface. It has been suggested to us (5) that at temperatures up to about 500 °C, strained, and hence highly reactive silylether groups, may be formed on the glass by reaction 3.

[3] 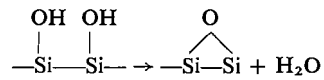

At higher temperatures the activity of these ether bonds will tend to disappear because the bond strain is relieved by adjustments in the body of the glass. Reaction of these siloxy groups with boron fluoride might lead to the formation of some sort of silicon–fluoborate compound not unlike the silicon–perchlorate or silicon – acid sulfate catalyst described by Kucera and coworkers (6) and used in the polymerization of trioxane.

Experimental

Materials

β-Methylstyrene (Aldrich) was fractionally distilled, then purified further by preparative g.l.c. on Carbowax 20M. It was dried over silica gel, degassed, and stored on the vacuum line over neutral alumina. When freshly prepared the product contained about 95% *trans*-isomer and very little impurity, but on storage, even though frozen when not in use, the amount of *cis*-isomer increased and some low-boiling impurity appeared.

Purification of solvent ethylene dichloride by our usual treatment with concentrated sulfuric acid was not satisfactory, apparently because of a change in the supply leading to a change in the impurities. The most important contaminant was isolated and identified as trichloroethylene which forms a close-boiling azeotrope with the solvent. We were unable to find a ternary azeotrope which would permit removal of this impurity by distillation, nor could we remove it by treatment with hot H_2SO_4, HCl–$AlCl_3$, ICl, alkali, or adsorption on molecular sieves. The only successful treatments were (*a*) washing with mixtures of concentrated nitric and sulfuric acids or (*b*) treating with a mixture of sulfuryl chloride and aluminum chloride, followed by washing with water; of these, the former method was easier to use. With these methods the major impurity in the solvent could be reduced below 0.01%, other contaminants below the level of detection on a Carbowax g.l.c. column. The purified ethylene dichloride was stored on the vacuum system in a darkened flask over phosphorus pentoxide; for each run, sufficient solvent was transferred to a separate flask and stirred overnight with neutral alumina before use. No difference was observed in the behavior of different batches of solvent.

Boron fluoride was dried by repeated evaporation from freshly prepared sodium mirrors and was stored at liquid nitrogen temperature. Its concentration has been expressed in moles of free boron fluoride; in a type *b* reactor containing 10 ml of solvent, 10^{-5} moles $(BF_3)_f$ is approximately equivalent to 5×10^{-4} mole l^{-1} in solution.

Methanol was used only in the preliminary experiments and was purified and handled as previously described.

Dimethyldichlorosilane and trimethylchlorosilane were purified by distillation, care being taken to exclude atmospheric moisture. The center fractions were stored on the vacuum line at −78 °C, and dispensed as needed through a stopcock lubricated with Kel-F grease.

Apparatus

The usual vacuum system capable of evacuation to a pressure of about 10^{-5} mm Hg was employed. In the later stages of the work most of the glass stopcocks were replaced with Hoke 4251 N6Y bellows-sealed valves attached to the glass system with Kovar seals. These valves proved very satisfactory and eliminated many problems associated with stopcocks and greases.

Reactions were carried out in vessels, shown in Fig. 4, which could be filled under vacuum and then sealed off. For type *a*, a 1 × 1 cm quartz cell containing a quartz spacer block to reduce the light path to a suitable length, usually 0.5 mm, was attached to the body of the pyrex vessel through a graded seal. The spacer could be moved in and out of the cell by means of an attached glass-enclosed magnet to serve as a mixing device. A furnace permitted the reactor to be heated to about 180 °C. Boron fluoride was contained in a separate chamber and was admitted to the reaction zone through a break seal after the remainder of the reactants had been brought to temperature (25 °C) and their initial optical absorbance determined. The temperature of the cell compartment was maintained at 25 °C throughout the run. Volume of the reactor was approximately 60 ml. The decrease in absorbance at 294 mμ was recorded automatically with a Cary Model 14 spectrophotometer and the initial rate obtained directly from the resulting curve since preliminary experiments had shown a good Beer's law dependence. No integrated rate expression was found to fit the curves.

To facilitate baking-out, the reactor was modified as shown at Fig. 4*b*. The 1 × 1 cm cell was replaced with a 1 mm cell and the spacer block was eliminated. The whole assembly, having a volume of about 22 ml, was designed to fit easily into a combustion tube furnace having a 1″ × 12″ heating zone, and was baked-out for every

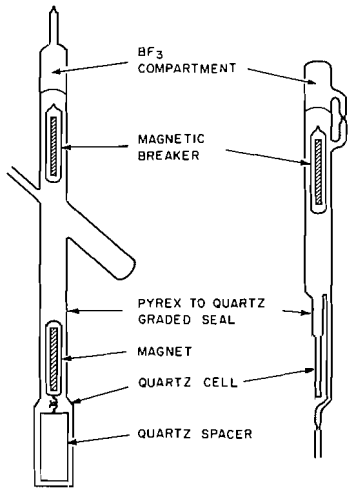

FIG. 4. Reaction vessels; *a*, with spacer block in 1 cm optical cell; *b*, with 1 mm quartz cell for baking-out at 500 °C.

experiment. No difficulty was experienced with the reactors at temperatures up to 500 °C, but as a precaution they were annealed before being attached to the vacuum system. The BF_3 was introduced into the chamber of the baked-out reactor through a by-pass which was then sealed off. A mixing problem (mentioned above) caused difficulty in estimating the initial rates of the faster reactions.

Reaction Products

All experiments showed the same u.v. spectrum at the end of reaction; loss of the long wavelength absorption (*ca.* 300 nm) corresponded to loss of the external conjugated double bond. Reaction products at 15, 50, and 100% reaction were identical according to g.l.c., but attempts to isolate the pure products by this method were unsuccessful. Mass spectrometry showed that the product had a molecular weight of 236, corresponding to a dimer of β-methylstyrene, and further, showed that there were no products of slightly higher weight resulting from incorporation of solvent, catalyst, etc., or from fragmentation of higher molecular weight species. From the mass, n.m.r., and u.v. spectra, it is clear that the product is an indane derivative of the type frequently found in styrene reactions, and is a mixture of approximately equal amounts of two geometric forms of compound **1**.

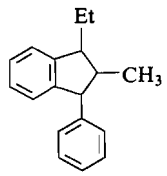

1

1. A. G. EVANS and G. W. MEADOWS. Trans. Faraday Soc. **46**, 327 (1950); A. G. EVANS and M. POLANYI. J. Chem. Soc. 252 (1947).
2. L. H. LITTLE. Infrared spectra of adsorbed species. Academic Press, London, 1967.
3. T. E. WHITE. Proc. Anniv. Tech. Conf. Soc. Plast. Ind. Reinforced Plastics Division, Chicago, Illinois, 1965; Sec. 3–13. p. 1.
4. H. CHÉRADAME and P. SIGWALT. C. R. Acad. Sci. Paris, **259**, 4273 (1964); **260**, 159 (1965).
5. C. CLARK-MONKS. Private communication.
6. M. KUCERA and E. SPOUSTA. J. Chem. Soc. 1478 (1965), and related papers.
7. H. CHÉRADAME and P. SIGWALT. Bull. Soc. Chim. Fr. 843 (1970); H. CHÉRADAME, NGUYEN ANH HUNG, P. BONNET, and P. SIGWALT. Bull. Soc. Chim. Fr. 849 (1970).

Can. J. Chem. Downloaded from www.nrcresearchpress.com by 210.87.254.105 on 09/05/12
For personal use only.

Can. J. Chem. Downloaded from www.nrcresearchpress.com by 210.87.254.5 on 09/05/12
For personal use only.

Mécanisme de la décomposition photosensibilisée au mercure du méthylvinyléther à 2537 Å

J. Castonguay et Y. Rousseau

Département de Chimie, Université de Montréal, Montréal, Québec

Reçu le 27 janvier 1971

La décomposition du méthylvinyléther par les atomes Hg6($^3P_1$) a été étudiée dans un système statique à des pressions variant de 10 à 800 Torr. Les résultats obtenus suggèrent que le processus primaire, la rupture de la liaison O—CH_3, procède d'un intermédiaire excité dont la décomposition n'est inhibée qu'à 50% à 800 Torr. L'addition d'oxide nitrique au système a permis de mettre en évidence la formation radicalaire de tous les produits sauf l'éthylène; celle de CH_3SH a permis de confirmer le rendement quantique quasi unitaire des produits primaires.

The study of the mercury 6($^3P_1$) photosensitized decomposition of methyl vinyl ether has been studied in a static system at substrate pressures from 10 to 800 Torr. The excited precursor proposed has a calculated lifetime of 1.18×10^{-10} s and its decomposition proceeds almost exclusively through the rupture of the O—CH_3 bond. A second primary process is the intramolecular formation of ethylene but it accounts only for 2% of the total ether decomposition. The major products are shown to be formed by free radical reactions and the overall reactivity appears to be very similar to that of the olefins. The results obtained with CH_3SH added to the system indicate that the primary radicals are formed with a quantum yield close to unity.

Canadian Journal of Chemistry, **49**, 2125 (1971)

Introduction

La similitude qui existe entre les réactions des atomes Hg6($^3P_1$) avec les éthers et les hydrocarbures saturés était déjà apparente à la suite des travaux de Steacie sur le diméthyléther (1). Les ouvrages plus récents (2–4) ont confirmé cette similarité entre les deux classes de composés, tant du point de vue du processus primaire impliquant dans les deux cas la rupture d'une liaison C—H, que du point de vue de la formation des produits de réaction: hydrogène moléculaire par abstraction d'un atome d'hydrogène et dimère par recombination radicalaire. La différence la plus grande se situe au niveau de l'efficacité de désactivation des atomes de mercure excités; la plus grande efficacité des éthers étant d'ailleurs expliquée en termes d'effet inductif du groupe alkoxy adjacent au radical alkyle (5, 2). D'autre part, les ressemblances qui peuvent exister entre les alcènes et les éthers insaturés ne sont pas connues mais on s'attend à ce que la similarité soit encore plus grande puisque la liaison π est généralement considérée comme le site du transfert d'énergie dans le cas des alcènes (6). De plus, les sections efficaces de désactivation des alcènes et des éthers insaturés sont très voisines (ref. 7, ref. 8 pp. 74–75): $\sigma_q{}^2$MVE = 31.5 Å^2 (7), $\sigma_q{}^2CH_2CHCH_3$ = 29.8 Å^2 (5).

Toutefois, lors d'une étude récente de la décomposition du méthylvinyléther (MVE) photosensibilisé au Hg6($^3P_1$) (7), on n'a pu mettre en évidence la formation d'un intermédiaire excité dans l'étape primaire comme le laisse supposer le parallélisme réactionnel avec les alcènes. Bien que les processus importants aient été établis, les rendements quantiques mesurés sont très faibles et peuvent difficilement être expliqués uniquement en termes d'addition de radicaux sur la double liaison de l'éther (9). Il semble donc désirable d'étudier le système dans des conditions expérimentales qui permettront de mettre en évidence l'intermédiaire excité, s'il existe, et de vérifier les rendements quantiques maxima des produits primaires.

Partie expérimentale

Le méthylvinyléther, obtenu de Matheson, fut purifié par distillation fractionnée "in vacuo" entre −115 et −130 °C et conservé à la température de la pièce dans un ballon noir. Les seules impuretés décelées par analyses au spectromètre de masse et au chromatographe en phase gazeuse sont l'acétaldéhyde (~ 0.035%) et le méthanol (0.015%). Une procédure semblable a servi à purifier et analyser les autres substances utilisées.

La décomposition du MVE fut étudiée en système statique dans une cellule cylindrique de quartz (4.4 cm de diamètre intérieur × 9.1 cm de longueur). L'enceinte réactionnelle contenant la cellule et la source lumineuse

TABLEAU 1. Variations des rendements quantiques de formation en fonction du temps de photolyse*

Temps (min)	ϕ (Produits)						
	CH_4	CO	C_2H_4	C_2H_6	Éthanal	Propanal	Produits lourds
0.5	0.007	0.027	0.014	0.190	—	—	0.146
1.0	0.006	0.024	0.013	0.158	—	—	0.158
2.0	0.007	0.029	0.013	0.187	0.040	0.271	0.147
4.0	0.008	0.033	0.013	0.190	0.036	0.317	0.124
8.0	0.012	0.041	0.014	0.193	0.034	0.290	0.074
16.0	0.014	0.046	0.012	0.172	0.034	0.268	0.068

*Pression de MVE = 50 Torr.

était maintenue à 26 ± 0.5 °C par une circulation d'air adéquate. Une lampe à basse pression de mercure Hanovia SC 2537 contenue dans une boîte séparée, a servi de source lumineuse. Cet ensemble était muni d'une fenêtre Vycor et d'une ventillation indépendante. Pour les expériences à 2.0 μE min^{-1}, 10 cm d'air entre la cellule et la source lumineuse servait de filtre pour la lumière de λ = 1849 Å. Les intensités lumineuses absorbées (I_a) furent mesurées par l'actinomètre N_2O–propylène (6, 10), et vérifiées fréquemment.

La photolyse terminée, les produits de réaction furent séparés par distillation simple sur une rampe à vide conventionnelle équipée de valves au Hg. L'analyse proprement dite s'effectuait à l'aide d'une burette à gaz et d'un chromatographe en phase gazeuse. Une colonne de Porapak Q (10 ft × 0.25 in.) utilisée à diverses températures, a servi à séparer tous les produits recueillis au-dessous de −64 °C et a permis leur analyse quantitative.

La nature de tous ces constituants avait auparavant été déterminée par spectrométrie de masse et en chromatographie par l'étude comparative de leur temps de rétention en regard de celui des substances pures. La fraction condensable à −64 °C avait une tension de vapeur trop faible (~ 0.2 Torr) pour en permettre une analyse précise.

Résultats et discussion

Les produits de réaction suivants furent identifiés et dosés: le méthane, le monoxyde de carbone, l'éthylène, l'éthane, l'éthanal et le propanal. Une étude du rendement de chacun de ces produits en fonction du temps d'irradiation permet de différencier, tout au moins partiellement, entre les produits primaires et secondaires. En effet, comme on peut le constater au tableau 1, l'éthylène, l'éthane, le propanal et l'éthanal semblent issus de réactions primaires tandis que le méthane et le monoxyde de carbone semblent surtout formés par des processus secondaires. Les très faibles rendements des aldéhydes n'en permettent pas une mesure quantitative précise à des temps de réaction courts.

Les produits de réaction identifiés sont en accord avec ceux trouvés par Filseth et le mécanisme qu'il propose peut en expliquer la formation (7).

[1] $Hg6(^3P_1) + MVE \rightarrow CH_3: + CH_2CHO\cdot + Hg6(^1S_0)$

[2] $2CH_2CHO\cdot \rightarrow CH_3CHO + CH_2CO$

[3] $CH_2CHO\cdot \rightarrow \cdot CH_2CHO$

[4] $CH_3\cdot + \cdot CH_2CHO \rightarrow CH_3CH_2CHO$

[5] $CH_3\cdot + CH_3\cdot \rightarrow C_2H_6$

[6] $Hg^* + CH_3CH_2CHO \rightarrow CH_3CH_2\cdot + \cdot CHO + Hg$

[7] $CH_3CH_2\cdot + \cdot CH_2CHO \rightarrow n\text{-}C_3H_7CHO$

[8] $CH_3CH_2\cdot + \cdot CH_3 \rightarrow C_3H_8$

[9] $\cdot CHO + \cdot CH_3 \rightarrow CO + CH_4$

[10] $\cdot CH_2CHO + \cdot CHO \rightarrow CO + CH_3CHO$

Les rendements quantiques observés par Filseth à des pressions beaucoup plus faibles que les nôtres (0.82 Torr comparé à 50) sont du même ordre de grandeur que ceux que l'on peut voir au tableau 1. Cependant, nous n'avons pas mesuré quantitativement les rendements du propane et du butanal, ceux-ci étant trop faibles. La présence de cétène n'a pu être mise en évidence qu'indirectement.

Le mécanisme proposé implique la formation dans l'étape primaire de radicaux $CH_3\cdot$ et $CH_2CHO\cdot$. Si tous les produits de réaction sont issus de ces radicaux primaires, l'addition d'oxyde nitrique (au système) devrait inhiber la formation de tous les produits. Au tableau 2, on peut voir que les rendements quantiques de l'éthanal, du propanal et de l'éthane sont considérablement diminués tandis que celui de l'éthylène n'est pas affecté. On peut remarquer aussi que l'oxyde nitrique semble catalyser la décomposition du MVE en acétylène, méthanol, éthylène et éthanal; cette décomposition se fait même sans irradiation.

Afin d'éviter les inconvénients de l'oxyde

Can. J. Chem. Downloaded from www.nrcresearchpress.com by 210.87.254.5 on 09/05/12
For personal use only.

TABLEAU 2. Variation des rendements quantiques en fonction de la concentration d'oxyde nitrique ajoute*

NO (%)	ϕ (Produits)						
	CH_4	CO	C_2H_2†	C_2H_4	C_2H_6	Éthanal	Propanal
0	0.012	0.052	‡	0.014	0.275	0.055	0.174
1	0.012	0.042	0.015	0.014	0.138	0.044	0.093
4	‡	‡	0.034	0.065	0.008	0.042	‡

*P (MVE) = 50 Torr, I_a = 2.0 μE min^{-1}, t = 6 min.
†NO a catalysé la décomposition du MVE, principalement en C_2H_2 et MeOH.
‡Trop faible pour être mesuré.

nitrique et pour mieux caractériser les radicaux piégés, le méthanethiol fut utilisé. En présence du mercaptan, le rendement quantique du méthane et de l'éthanal a considérablement augmenté; ceci, en accord avec les réactions suivantes

[11] $CH_3\cdot + CH_3SH \rightarrow CH_4 + CH_3S\cdot$

[12] $(CH_2CHO)\cdot + CH_3SH \rightarrow CH_3CHO + CH_3S\cdot$

La Fig. 1 montre la variation linéaire de $\phi(CH_4)$ en fonction de $[CH_3SH]$. Cependant, il semble qu'à cette intensité lumineuse (4.74 μE min^{-1}), les concentrations radicalaires soient trop grandes pour permettre un piégeage quantitatif; les bilans de $CH_3\cdot$ et $(CH_2CHO)\cdot$ sont moindres qu'en l'absence de méthanethiol. Ceci peut être expliqué par les réactions [13] et [14]. Les produits des trois réactions suivantes ont d'ailleurs été identifiés par spectrométrie de masse.

[13] $CH_3\cdot + CH_3S\cdot \rightarrow CH_3SCH_3$

[14] $(CH_2CHO)\cdot + CH_3S\cdot \rightarrow (CH_3SCH_2CHO)$

[15] $CH_3S\cdot + CH_3S\cdot \rightarrow CH_3SSCH_3$

La diminution de I_a de deux ordres de grandeur a permis un titrage presque complet des radicaux méthyles. Les résultats de ces expériences sont résumés au tableau 3. Ils mettent clairement en évidence le rendement quantique quasi unitaire de la rupture O—CH_3. En effet, on a mesuré des rendements quantiques de radicaux $CH_3\cdot$ atteignant 0.95. Ils suggèrent aussi la formation intramoléculaire d'éthylène comme mode concurrent de la décomposition du MVE. Ce processus n'aurait cependant qu'une probabilité maximale de 2%.

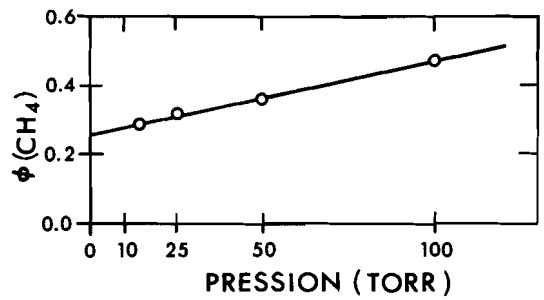

FIG. 1. Variation du rendement quantique de CH_4 en fonction de la concentration de CH_3SH; I_a = 4.74 μE min^{-1}, $[CH_3SH]$ = 5%.

[16] $Hg6(^3P_1) + MVE \rightarrow C_2H_4 + H_2CO + Hg6(^1S_0)$

Le comportement des radicaux $CH_3\cdot$ en présence de méthanethiol est conforme aux observations de Greig et Thynne (11).

Le taux de formation d'éthane est réduit d'un facteur 13 (tableau 3, résultats à 50 Torr) alors que le bilan des radicaux CH_3 recueillis subit une majoration de 25%. Le titrage du radical formylméthyle semble, pour sa part, moins favorisé. Même en profitant d'une augmentation de près de 20%, il demeure qu'environ la moitié de cet espèce manque à l'analyse. La réaction [14] peut être partiellement responsable de cette différence, étant donné la stabilité du radical $(CH_2CHO)\cdot$, [3]. Néanmoins, considérant (*a*) la vitesse de la réaction [15], $k_{15} = 10^{10.3}$ l mol^{-1} s^{-1} (12), (*b*) le fait que la recombinaison des $CH_3\cdot$ est défavorisée, $k_5 \simeq 10^{10.5}$ l mol^{-1} s^{-1} et (*c*) le parallélisme existant entre $\phi(C_2H_6)$ et ϕ(propanal), il semble qui ni [13] ni [14] ne soient très importants dans notre système.

Dans ces conditions, on peut se demander quelles réactions peuvent être responsables du faible rendement quantique observé pour le radical $(C_2H_3O)\cdot$. En effet, la réaction [17] est endothermique de 18 kcal mol^{-1} (13) et enthropiquement défavorisée. De plus, ni l'oxyde d'éthylène ni l'oxyde de propylène n'ont été détectés. On pourrait considérer une isomérisation du radical $(CH_2CHO)\cdot$ en CH_3CO selon [20]. Cependant, le rendement quantique de CO

Can. J. Chem. Downloaded from www.nrcresearchpress.com by 210.87.254.5 on 09/05/12
For personal use only.

TABLEAU 3. Variation des rendements quantiques en fonction de CH_3SH ajouté*

P_{totale} (Torr)	% CH_3SH	$(CH_2CHO)\cdot$ piégé	CH_4	CO	C_2H_4	C_2H_6	Éthanal	Propanal	$(CH_3\cdot)$ piégé
			$I_a = 0.037$ μE min^{-1}						
25	0	0.340	0.016	0.040	0.013	0.235	0.043	0.210	0.700
25	5	0.280	0.752	0.054	0.014	0.028	0.191	0.043	0.857
25	10	0.550	0.900	0.046	0.019	0.020	0.504	0.020	0.960
50	0	0.382	0.017	0.052	0.013	0.240	0.069	0.188	0.685
50	5	0.526	0.876	0.047	0.016	0.018	0.463	0.032	0.944
100	5	0.567	0.836	0.037	0.014	0.013	0.508	0.037	0.900
			$I_a = 1.0$ μE min^{-1}						
25	0	0.373	0.008	0.030	0.013	0.200	0.043	0.232	0.661
25	5	0.219	0.502	0.027	0.012	0.048	0.144	0.060	0.658
50	0	0.356	0.007	0.028	0.011	0.183	0.040	0.253	0.705
50	5	0.204	0.565	0.030	0.010	0.026	0.138	0.046	0.664
100	5	0.168	0.551	0.027	0.009	0.014	0.093	0.056	0.584
			$I_a = 4.74$ μE min^{-1}						
14	5	0.207	0.280	0.026	0.010	0.085	0.115	0.046	0.454
32	5	0.170	0.316	0.026	0.007	0.060	0.107	0.043	0.479
50	0	0.376	0.007	0.029	0.013	0.187	0.040	0.271	0.652
50	5	0.161	0.354	0.022	0.006	0.050	0.100	0.045	0.499
100	5	0.132	0.470	0.021	0.006	0.025	0.098	0.017	0.537

Les valeurs ci-dessus sont corrigées pour la désactivation du Hg produite par CH_3SH. Le % de conversion n'a jamais excédé 2%.

est très bas, et selon Benson (13) l'isomérisation ne peut qu'être suivie de la décomposition ($\Delta H = 10$ kcal mol^{-1}).

[17] $(CH_2CHO)\cdot \rightarrow CH_2\text{—}CH\cdot$ (O)

[18] $CH_2\text{—}CH\cdot + CH_3SH \rightarrow CH_2\text{—}CH_2 + CH_3S\cdot$ (O) (O)

[19] $(CH_2CHO)\cdot \xrightarrow{\text{parois}}$ polymère

[20] $(CH_2CHO)\cdot \rightarrow (CH_3CO)\cdot$

[21] $(CH_3CO)\cdot \rightarrow CH_3\cdot + CO$

Vu la faible réactivité de $(CH_2CHO)\cdot$, ainsi que l'influence minime de CH_3SH sur la vitesse de formation de CO, la réaction [19] semble être principalement responsable du faible $\phi(CH_2CHO)\cdot$ observé. D'ailleurs, le fait de doubler (CH_3SH) (tableau 3: 25 Torr à 10% de CH_3SH *vs.* 100 Torr à 5% de CH_3SH) ne modifie que peu le rendement quantique d'éthanal, même si l'une ou l'autre des formes de résonnance [3] de $(C_2H_3O)\cdot$ conduit à sa formation.

De ce même tableau 3, on observe qu'une augmentation de la pression totale diminue légèrement le taux des radicaux CH_3 collectés. Ce phénomène peut s'expliquer soit par l'addition de $CH_3\cdot$ sur la double liaison de l'éther [22], soit par la désactivation par collision d'un intermédiaire excité [25].

[22] $CH_3\cdot + MVE \rightarrow R_1\cdot$

[23] $Hg^* + MVE \rightarrow (MVE)^* + Hg$

[24] $(MVE)^* \rightarrow CH_3\cdot + CH_2CHO\cdot$

[25] $(MVE)^* + M \rightarrow MVE + M$

[26] $(MVE)^* \rightarrow C_2H_4 + H_2CO$

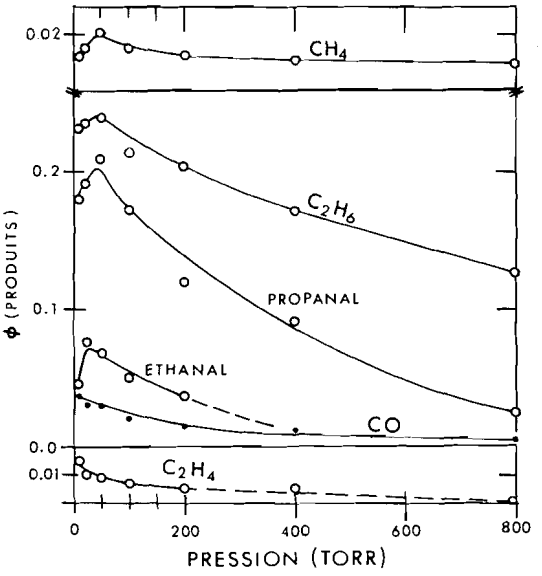

FIG. 2. Variation des rendements quantiques en fonction de la pression totale. C_3F_8 ajouté à 22 Torr de MVE (sauf à 10 Torr); $I_a = 0.037$ μE min^{-1}.

Can. J. Chem. Downloaded from www.nrcresearchpress.com by 210.87.254.5 on 09/05/12
For personal use only.

Can. J. Chem. Downloaded from www.nrcresearchpress.com by 210.87.254.5 on 09/05/12
For personal use only.

Les résultats obtenus en variant la pression totale et qui sont représentés à la Fig. 2 indiquent la présence d'une molécule d'éther excitée [23]. Au cours de ces expériences, la pression de MVE fut maintenue à 22 Torr et C_3F_8 fut utilisé comme gaz inerte. Dans ces conditions, la réaction [22] peut être négligée, et d'ailleurs, les expériences utilisant le MVE pur (Fig. 4) confirment cette hypothèse. La diminution observée enfin pour les rendements quantiques à des pressions inférieures à 50 Torr est compatible avec celle obtenue par Filseth (7) entre 10 et 0.21 Torr. La raison en est vraisemblablement la désactivation incomplète des atomes $Hg6(^3P_1)$, ou encore une absorption lumineuse différente.

On peut constater, toujours au tableau 3, que le rendement quantique d'éthylène ne varie pas avec l'intensité lumineuse absorbée. Ceci est compatible avec le mécanisme déjà proposé pour sa formation. Sans mercaptan (50 Torr, 0% CH_3SH), cette très faible variation est observée pour les taux de titrage des radicaux primaires. La réaction [27], certainement responsable de cet effet, aurait alors une probabilité de 0.25, calculée de la différence des $\phi(\cdot CH_3)$, avec et sans le thiol.

[27] $CH_3\cdot + CH_2CHO\cdot \rightarrow MVE$

[28] $CH_3\cdot + CH_2CHO\cdot \rightarrow CH_4 + CH_2CO$

[29] $2\cdot CH_2CHO \rightarrow CHOCH_2CH_2CHO$

De plus, seul le rendement quantique de propanal varie dans le même sens que l'intensité lumineuse. Un calcul simple, utilisant ϕ(éthane) et ϕ(propanal), montre ainsi que l'accroissement des concentrations stationnaires de $(CH_3)\cdot$ et $(C_2H_3O)\cdot$ est respectivement de 10 et 18 lorsque leur taux de formation est 130 fois accéléré. Alors, ou les radicaux méthyles sont consommés plus rapidement par d'autres réactions [27], [28] ou encore la disparition de $(CH_2CHO)\cdot$ implique une étape relativement plus lente que les procédés biradicalaires. Ces derniers, [2] et [29], peuvent être négligés devant [19]. L'accumulation de $(CH_2CHO)\cdot$ est aussi un signe de sa stabilité et de sa faible réactivité. Ainsi, à faible I_a, la diffusion de ce radical devient sensiblement plus compétitive vis-à-vis des autres réactions en phase gazeuse.

Enfin, si les réactions [28] et [29] étaient de quelques importance, on devrait observer une augmentation des rendements de méthane et de succénaldéhyde avec une augmentation de I_a. Comme on peut le voir au tableau 3, en l'absence de CH_3SH, $\phi(CH_4)$ qui est très faible de toute façon n'est pas favorisé par une telle augmentation. Quant au succénaldéhyde, même si on a cru le déceler à quelques reprises, au spectromètre de masse, on n'a pu l'identifier d'une façon positive.

Un traitement cinétique basé sur les réactions [2] à [5] et [23] à [29] indique une dépendance linéaire entre l'inverse du rendement quantique d'éthane et la pression totale.

$$[30]\quad \frac{1}{\phi(C_2H_6)} = (1 + ka) + \frac{k_{25}}{k_{24}}(1 + ka)[M]$$

où

$$ka = \frac{k_4 + k_{28} + k_{27}}{\sqrt{k_5(k_2 + k_{29})}}$$

En utilisant l'équation précédente et les paramètres de la droite de la Fig. 3, le rapport k_{25}/k_{24} fut estimé à environ 4.4×10^{-2} mol l^{-1}. En conséquence, à 800 Torr, la désactivation [25] devient aussi importante que la décomposition. On trouve alors: $k_{24} = k_{25}[M] = 8.5 \times 10^9\ s^{-1}$, et de là, $k_{25} = 1.93 \times 10^{11}\ l\ mol^{-1}\ s^{-1}$.

Le temps de vie calculé de (MVE)* apparaît ainsi quelques 50 fois plus court que celui mesuré par Cvetanović et Doyle (14) pour le butène-1. Ces homologues isoélectroniques montrent un parallélisme réactionnel postérieur à la rupture initiale. Ni le MVE, ni le butène-1 ne semblent subir l'addition de $CH_3\cdot$, ni même l'abstraction d'hydrogène de la part de ce radical. La courbe

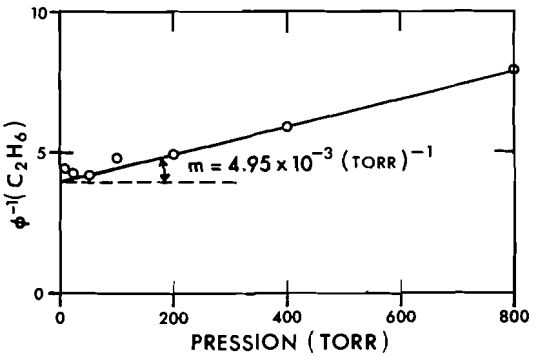

FIG. 3. Inverse du rendement quantique d'éthane en fonction de la pression totale (C_3F_8 ajouté à 22 Torr d'éther); $I_a = 0.037\ \mu E\ min^{-1}$.

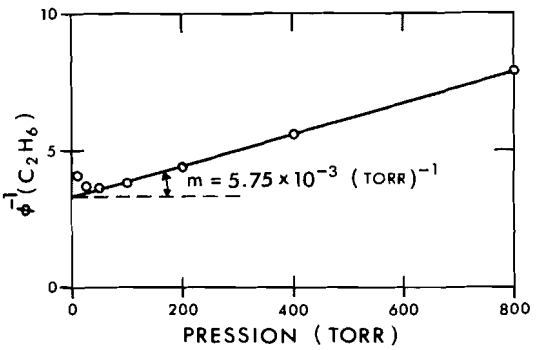

FIG. 4. Inverse du rendement quantique d'éthane en fonction de la pression d'éther. $I_a = 2.0$ μE min^{-1}.

TABLEAU 4. Variation de $\phi(CH_4)$ en fonction de la concentration de MVE*

P(MVE)(Torr)	$\phi(CH_4)$
10	0.0211
25	0.0121
50	0.0118
100	0.0095
200	0.0092
400	0.0085
800	0.010

*$I_a = 2.0$ μE min^{-1}, $t = 10$ min.

de la Fig. 4 et le tableau 4 vérifient ces observations pour l'éther.

Discussion

Le présent travail a principalement mis en évidence la grande similitude des systèmes (Hg6($^3P_1$)–éther insaturé) et (Hg6($^3P_1$)–alcène).

(*a*) L'activation initiale produit, semble-t-il, un état triplet vibrationnellement excité. C'est d'ailleurs le propre des alcènes.

(*b*) L'efficacité du MVE à désactiver Hg6($^3P_1$) est identique à celle du propylène (tableau 5). La présence d'oxygène, ou encore le remplacement de CH_3 par CH_3O ne cause pas, à priori, d'activation particulière comme nous l'observons chez les homologues saturés (2, 3).

(*c*) La décomposition dans les deux cas s'effectue presqu'exclusivement par la rupture β, et le radical de type alkyle ainsi créé est stabilisé par résonnance (9, 15). L'énergie du lien C—CH_3, 64 kcal mol^{-1}, suggérée par Lossing, Marsden et Farmer (16) se compare avantageusement à 65 ± 2 kcal mol^{-1}, calculée pour O—CH_3 à l'aide des valeurs suivantes

TABLEAU 5. Réactivité relative du MVE et du propylène en competition avec N_2O*

$\frac{[RH]}{[N_2O]}$	$d[N_2]/dt$	
	C_3H_6	MVE
1	1.39	1.40
3	3.21	3.20
σ_q^2(Å)^2	29.8†	34.0‡

*$I_a = 2.0$ μE min^{-1}, $t = 7.5$ min, $P_{totale} = 200$ Torr.
†Processus I, référence (5).
‡Filseth (7) mesure 31.5 Å^2 en se servant de la valeur "physique" de $\sigma q^2 N_2O$. Cette méthode de calcul conduirait à: σq^2MVE ≃ 47 Å^2.

$$\Delta H_f(\text{MVE}) = -26.2 \text{ kcal mol}^{-1} \quad \text{(ref. 17)}$$

$$\Delta H_f(CH_3\cdot) = 32 \text{ kcal mol}^{-1} \quad \text{(ref. 8, p. 819)}$$

$$\Delta H_f(CH_3O\cdot) = -0.5 \text{ kcal mol}^{-1} \quad \text{(ref. 8, p. 819)}$$

$$\Delta H_f(CH_2{=}CH\cdot) = 65 \text{ kcal mol}^{-1} \quad \text{(ref. 8, p. 819)}$$

$$\text{p.i.}(CH_3\cdot) = 9.83 \text{ eV} \quad \text{(ref. 8)}$$

$$\text{p.a.}(CH_3^+) = 12.7 \text{ eV}^1$$

$$\text{p.a.}(CH_2CHO^+) = 11.6 \text{ eV}^1$$

p.i. = potentiel d'ionisation; p.a. = potentiel d'apparition

(*d*) La très grande majorité des composés stables analysés résultent de réactions radicalaires impliquant uniquement $CH_3\cdot$ et $(CH_2CHO)\cdot$. Les réactions d'abstraction d'hydrogène et d'addition à la double liaison semblent grandement défavorisées.

Il est concevable que ces ressemblances trouvent leur origine dans la similarité de structure de l'état fondamental: cis-planaire (19, 20). Même la barrière de rotation du groupe vinyle a la même hauteur chez l'un et chez l'autre (21).

Néanmoins, il existe chez le MVE une conjugaison interne "$n\pi$" (20) qui ne saurait avoir lieu dans le butène-1. Elle est sûrement responsable de la stabilité inhabituelle de la liaison éther O-vinyl: d'après les données thermodynamiques

[1]Mesuré à l'aide d'un spectromètre de masse CEC 21–104 non modifié, par la méthode d'extrapolation directe. Les gaz suivants, Ne, Xe, Kr ont servi de références internes (18).

Can. J. Chem. Downloaded from www.nrcresearchpress.com by 210.87.254.5 on 09/05/12
For personal use only.

précédentes, $\Delta H(CH_2CH—OCH_3) = 90.5$ kcal mol^{-1}.

De ce fait, il est raisonnable d'observer la décomposition de (MVE)* par le procédé quasi exclusif [24], de même que le temps de vie relativement court de cet espèce.

Enfin, un transfert 1,4 d'hydrogène, semblable à celui menant à la formation de méthylcyclopropane (14), conduirait chez le MVE à l'oxyde de propylène. Cependant, faute de désactivation, le (C_3H_6O)* s'isomériserait surtout en propanal (13). Toutefois, la série d'expériences faites en fonction de la pression a montré la formation progressive d'acétone (ϕ à 400 Torr = 0.046, ϕ à 800 Torr = 0.072).

Aucune expérience à plus de 800 Torr ne fut tentée, vu les difficultés d'analyse déjà encourrues: impossibilité de séparer les produits oxygénés du substrat de départ à cause de la grande ressemblance de ces composés dont au moins quatre s'identifient à la formule C_3H_6O.

Finalement, le transfert de H· entre les positions 1 et 3 est suggéré pour la formation intramoléculaire de C_2H_4 et H_2CO.

Les auteurs tiennent à remercier particulièrement le Conseil National de Recherches du Canada pour l'aide financière qu'il leur a accordée. Ils remercient également Monsieur Gabriel Sanchez pour son assistance lors des analyses chromatographiques.

1. R. A. Marcus, B. de B. Darwent, and E. W. R. Steacie. J. Chem. Phys. **16**, 987 (1948).
2. R. Payette, M. Bertrand, and Y. Rousseau. Can. J. Chem. **46**, 2693 (1968).
3. S. V. Filseth. J. Phys. Chem. **73**, 793 (1969).
4. (*a*) L. F. Loucks and K. J. Laidler. Can. J. Chem. **45**, 2763 (1967). (*b*) L. F. Loucks and K. J. Laidler. Can. J. Chem. **45**, 2767 (1967).
5. Y. Rousseau, O. P. Strausz, and H. E. Gunning. J. Chem. Phys. **39**, 962 (1963).
6. Y. Rousseau and H. E. Gunning. Can. J. Chem. **41**, 465 (1963).
7. R. V. Morris and S. V. Filseth. Can. J. Chem. **48**, 924 (1970).
8. J. N. Pitts and J. G. Calvert. Photochemistry. John Wiley and Sons Inc., New York, 1966.
9. E. Murad. J. Am. Chem. Soc. **83**, 1327 (1961).
10. R. Payette, M. Bertrand, and Y. Rousseau. J. Am. Chem. Soc. **90**, 5341 (1968).
11. G. Greig and J. C. J. Thynne. Trans. Faraday Soc. **62**, 379 (1966).
12. R. P. Steer and A. R. Knight. J. Phys. Chem. **72**, 2145 (1968).
13. Sidney W. Benson. J. Chem. Phys. **40**, 105 (1964)
14 R. J. Cvetanović and L. C. Doyle. J. Chem. Phys. **37**, 543 (1962).
15. R. Gomer and W. A. Noyes, Jr. J. Am. Chem. Soc. **72**, 101 (1950).
16. F. P. Lossing, D. G. H. Marsden, and J. B. Farmer. Can. J. Chem. **34**, 701 (1956).
17. F. R. Cruickshank and S. W. Benson. J. Am. Chem. Soc. **91**, 2487 (1969).
18. Robert W. Kiser. Introduction to mass spectrometry and its application. Prentice Hall, London. 1965. p. 319.
19. N. L. Owen and N. Sheppard. Trans. Faraday Soc. **60**, 634 (1964).
20. P. D. Foster, V. M. Rao, and R. F. Curl. J. Chem. Phys. **43**, 1064 (1965).
21. P. Cahill and L. P. Gold. J. Chem. Phys. **48**, 1620 (1968).

Can. J. Chem. Downloaded from www.nrcresearchpress.com by 210.87.254.5 on 09/05/12
For personal use only.

Can. J. Chem. Downloaded from www.nrcresearchpress.com by 210.87.254.105 on 09/05/12
For personal use only.

Total Synthesis of Several Monodeoxy and Dideoxy-DL-hexopyranoses from 6,8-Dioxabicyclo[3.2.1]oct-2-ene and 6,8-Dioxabicyclo[3.2.1]oct-3-ene

T. P. MURRAY,[1] U. P. SINGH,[1] AND R. K. BROWN
Department of Chemistry, University of Alberta, Edmonton, Alberta

Received January 18, 1971

Reaction of osmic acid with 6,8-dioxabicyclo[3.2.1]oct-3-ene (**1**) gave 1,6-anhydro-4-deoxy-β-DL-*ribo*-hexopyranose (**3**, R = H) which was hydrolyzed to 4-deoxy-α,β-DL-*ribo*-hexopyranose (**4**, R = H). Conversion of **1** to 1,6:2,3-dianhydro-4-deoxy-β-DL-*ribo*-hexopyranose (**5**) followed by treatment of **5** with lithium aluminum hydride, gave 1,6-anhydro-3,4-dideoxy-β-DL-*erythro*-hexopyranose (**6**, R = H), and this in turn was hydrolyzed to 3,4-dideoxy-α,β-DL-*erythro*-hexopyranose (**7**, R = H).

Reaction of osmic acid with 6,8-dioxabicyclo[3.2.1]oct-2-ene (**2**) gave 1,6-anhydro-2-deoxy-β-DL-*ribo*-hexopyranose (**8**, R = H), which was hydrolyzed to 2-deoxy-DL-*ribo*-hexopyranose (**9**, R = H). Compound **2** was converted to 1,6:3,4-dianhydro-2-deoxy-β-DL-*ribo*-hexopyranose (**10**) which was hydrolyzed by aqueous base to 1,6-anhydro-2-deoxy-β-DL-*arabino*-hexopyranose (**12**) and this in turn was hydrolyzed by dilute hydrochloric acid to 2-deoxy-α,β-DL-*arabino*-hexopyranose (2-deoxy-DL-glucose) (**13**). The reaction of **10** with lithium aluminum hydride gave 1,6-anhydro-2,3-dideoxy-β-DL-*erythro*-hexopyranose (**14**).

Yields were good to excellent in each of the above reactions.

La réaction de l'acide osmique avec le dioxa-6,8 bicyclo[3.2.1] octène-3 (**1**) conduit à l'anhydro-1,6 désoxy-4 β-DL-*ribo*-hexapyranose (**3**, R = H) qui par hydrolyse fournit le désoxy-4 α,β-DL-*ribo*-hexapyranose (**4**, R = H). Le composé **1** peut être transformé successivement en dianhydro-1,6:2,3 désoxy-4 β-DL-*ribo*-hexapyranose (**5**), puis par traitement par $LiAlH_4$ en anhydro-1,6 didésoxy-3,4 β-DL-*erythro*-hexapyranose (**6**, R = H) et finalement, par hydrolyse, en didésoxy-3,4 α,β-DL-*erythro*-hexapyranose (**7**, R = H).

Par ailleurs l'action de l'acide osmique sur le dioxa-6,8 bicyclo[3.2.1] octène-2 (**2**) fournit l'anhydro-1,6 désoxy-2 β-DL-*ribo*-hexapyranose (**8**, R = H) qui conduit, par hydrolyse, au désoxy-2 DL-*ribo*-hexapyranose (**9**, R = H). On peut aussi transformer le composé **2** pour obtenir successivement le dianhydro-1,6:3,4 désoxy-2 β-DL-*ribo*-hexapyranose (**10**), puis par hydrolyse en milieu basique en anhydro-1,6 désoxy-2 β-DL-*arabino*-hexapyranose (**12**) et finalement par hydrolyse en milieu acide chlorhydrique dilué en désoxy-2 α,β-DL-*arabino*-hexapyranose (désoxy-2 DL-glucose) (**13**). La réaction de **10** avec $LiAlH_4$ fournit l'anhydro-1,6 didésoxy-2,3 β-DL-*erythro*-hexapyranose (**14**).

Dans chacune des réactions décrites ci-haut les rendements sont excellents.

Canadian Journal of Chemistry, 49, 2132 (1971)

Introduction

Recent reports from this laboratory have described the total synthesis of 1,6-anhydro-4-deoxy-β-DL-*xylo*-hexopyranose (1) and α,β-DL-chalcose (2) from 6,8-dioxabicyclo[3.2.1]oct-3-ene (**1**), a compound in turn readily prepared from acrolein dimer (1). We now report the preparation of several monodeoxy and dideoxy-hexopyranoses from the bicyclic olefin **1** and its isomer 6,8-dioxabicyclo[3.2.1]oct-2-ene (**2**), a compound recently described (3).

Results and Discussion

The reactions performed with olefin **1**, and the products so obtained, are shown in Scheme 1. Those involving olefin **2** are portrayed in Scheme 2.

[1]Postdoctoral Fellow.

The reaction of **1** with osmic acid in dioxane or pyridine, following published directions (4–6), gave a nearly quantitative yield of crude material which showed only one spot on a t.l.c. Distillation provided pure 1,6-anhydro-4-deoxy-β-DL-*ribo*-hexopyranose (**3**, R = H) in 96% yield. The elemental analysis and the 100 MHz p.m.r. spectrum of **3** (R = H) as well as those of its diacetate **3** ($R = CH_3CO$) were in complete agreement with the structure shown by **3**. The previous observation (6) that the direction of attack by osmic acid on the double bond of such substituted cyclic olefins is strongly subject to steric influence also provides support for the structure **3**. Acid-catalyzed hydrolysis of **3** (R = H or CH_3CO) in aqueous dioxane gave 4-deoxy-α,β-DL-*ribo*-hexopyranose (**4**) (R = H) as a syrup in 85% yield. The 100 MHz p.m.r. spectrum of **4** (R = H) in D_2O, as well as that

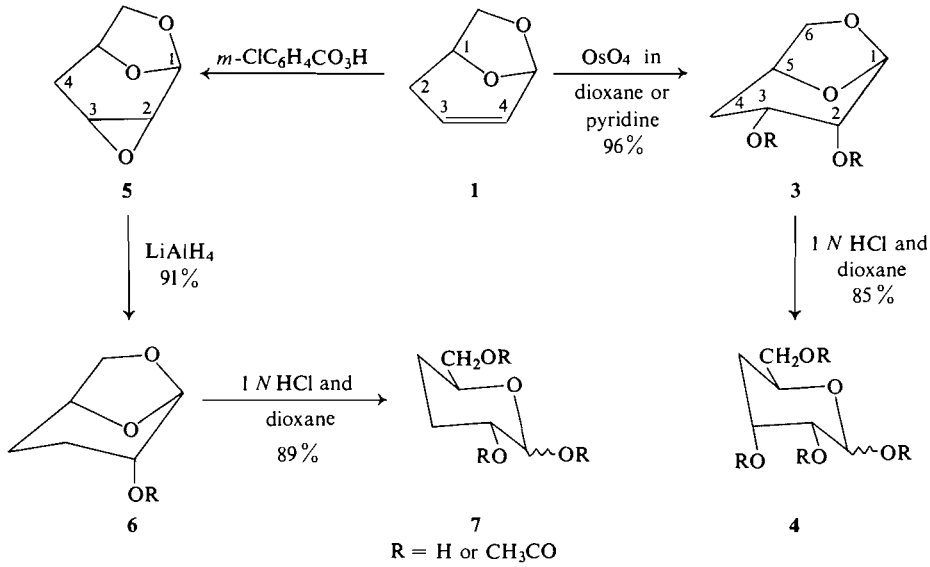

SCHEME 1

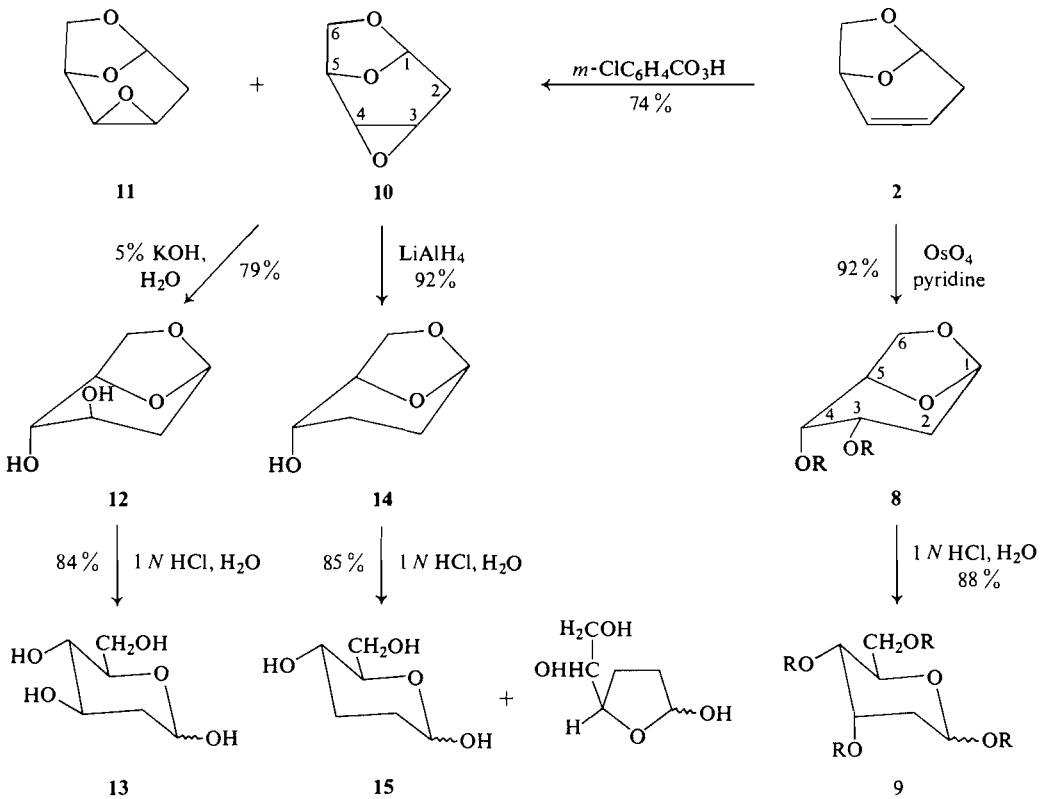

SCHEME 2

Can. J. Chem. Downloaded from www.nrcresearchpress.com by 210.87.254.105 on 09/05/12
For personal use only.

Can. J. Chem. Downloaded from www.nrcresearchpress.com by 210.87.254.105 on 09/05/12
For personal use only.

of its tetraacetate (**4**, R = CH_3CO) in $CDCl_3$, showed that this substance possessed the configuration and conformation shown by **4**, and that it was present in D_2O as a mixture of the α and β isomers in the ratio 1:3 respectively.

When 1,6:2,3-dianhydro-4-deoxy-β-DL-*ribo*-hexopyranose (**5**), prepared from **1** according to published directions (1, 2), was treated with lithium aluminum hydride in diethyl ether, the compound obtained in 91% yield was **6** (R = H). This was the product expected from preferential cleavage of the O—C_3 bond (7) as well as preferential formation of the chair structure obtained by cleavage of the oxirane ring so that the attacking agent and the leaving group are *trans* diaxially disposed (8–10). The 100 MHz p.m.r. spectra of both **6** (R = H) and its acetate **6** (R = CH_3CO) clearly showed that the product of lithium aluminum hydride reduction of **5** was indeed structure **6**. Acid-catalyzed hydrolysis of **6** (R = H) provided 3,4-dideoxy-α,β-DL-*erythro*-hexopyranose (**7**, R = H). The 100 MHz p.m.r. spectrum of **7** (R = H) as well as that of its triacetate (**7**, R = CH_3CO) completely supported the structure and conformation shown by **7**. The integrated areas of the two anomeric proton signals for **7** (R = H) of the spectrum in D_2O, showed that the α and β isomers were present in the ratio 1:4 respectively.

Treatment of olefin **2** with osmic acid in pyridine gave 1,6-anhydro-2-deoxy-β-DL-*ribo*-hexopyranose (**8**, R = H) in 92% yield. Here again most if not all of the reaction with osmic acid had occurred from the least hindered side of the double bond of **2**. The structure was supported by its 100 MHz p.m.r. spectrum, since upon irradiation of the nucleus of the anomeric proton (H-1), a collapsed high field multiplet was obtained for the two protons on C-2 which contained a large coupling of ~10 Hz. A coupling of such magnitude can occur only if the H-3 proton and one of the C-2 protons are *trans* diaxially disposed. The elemental analysis and 100 MHz p.m.r. spectrum of the diacetate **8** (R = CH_3CO) also supported the structure designated by **8**. Hydrolysis of **8** (R = H) or its diacetate with 1 *N* aqueous hydrochloric acid gave 2-deoxy-DL-*ribo*-hexopyranose (**9**, R = H) in 88% yield. The 100 MHz p.m.r. spectrum of **9** (R = H) was identical to that of an authentic sample of 2-deoxy-D-*ribo*-hexopyranose (11, 12) kindly provided by Dr. K. V. Bhat. The elemental analysis and 100 MHz p.m.r. spectrum of the tetraacetate **9** (R = CH_3CO) agreed completely with the assigned structure.

Treatment of **2** with *m*-chloroperoxybenzoic acid gave a 74% yield of an oil whose analysis by g.l.c. showed only two symmetrical peaks in the area ratio of 49:1. The major compound, 1,6:3,4-dianhydro-2-deoxy-β-DL-*ribo*-hexopyranose (**10**), was readily separated in the pure state by g.l.c. The elemental analysis, and the i.r. and 100 MHz p.m.r. spectral data clearly supported structure **10**. The minor component, **11**, could not be obtained free of **10** because of the tailing from **10** during attempted g.l.c. separation. However, the mixture finally isolated was sufficiently enriched in **11** to obtain a 100 MHz p.m.r. spectrum which confirmed that the compound had the structure shown by **11**. The reaction of aqueous potassium hydroxide with **10** gave crystalline 1,6-anhydro-2-deoxy-β-DL-*arabino*-hexopyranose (**12**) in 79% yield. The 100 MHz p.m.r. spectrum agreed completely with the structure assigned and this structure was confirmed by hydrolysis of **12** with 1 *N* aqueous hydrochloric acid to 2-deoxy-α,β-DL-*arabino*-hexopyranose (**13**), whose 100 MHz p.m.r. spectrum in D_2O was identical to that of authentic 2-deoxy-D-glucose.

Lithium aluminum hydride in ether reacted with the oxirane **10** to give, after sublimation, the solid 1,6-anhydro-2,3-dideoxy-β-DL-*erythro*-hexopyranose (**14**) as the only isolable product. Here again cleavage of the oxirane ring gave that product which was the chair form obtainable by opening of the three-membered ring so that the attacking and leaving groups are *trans* diaxially oriented (8–10). The 100 MHz p.m.r. spectrum's pattern of high field signals equivalent to four protons could be accounted for only if these protons were aliphatic and on two adjacent carbon atoms as shown by **14**.

Hydrolysis of **14** with 1 *N* hydrochloric acid gave a viscous syrup whose t.l.c. showed only one spot but the p.m.r. spectrum indicated it to be a mixture, presumably of pyranose and furanose structures. Several attempts to resolve this mixture were unsuccessful.

Experimental

Melting points and boiling points are uncorrected. Elemental analyses were made by Mrs. Darlene

Can. J. Chem. Downloaded from www.nrcresearchpress.com by 210.87.254.105 on 09/05/12
For personal use only.

Mahlow and Miss A. Dunn in our microanalytical laboratory.

The i.r. absorption spectra were obtained by Mr. R. Swindlehurst of this Department using a Perkin–Elmer Model 421 spectrometer.

The 60 MHz p.m.r. spectra were made by Mr. R. Swindlehurst using a Varian A-60 instrument. The 100 MHz p.m.r. spectra and spin decoupling experiments were carried out by Mr. Glen Bigam and his associates. Tetramethylsilane was the internal reference. Signal assignments were made with the aid of double irradiation spin decoupling. The coupling constants were estimated from the signal spacings where this was possible, and accordingly are approximate values.

Column and t.l.c. was carried out using Silica Gel G (E. Merck and Co.) as absorbent. Solvents were removed by rotary evaporator under vacuum unless otherwise stated.

*6,8-Dioxabicyclo[3.2.1]oct-3-ene (**1**)*

Compound **1** was prepared according to the modification (2) of the published procedure (1).

*6,8-Dioxabicyclo[3.2.1]oct-2-ene (**2**)*

Compound **2** was prepared in good yield by using directions previously described (3).

*1,6-Anhydro-4-deoxy-β-DL-ribo-hexopyranose (**3**, R = H)*

Osmic acid (1.0 g, 3.93 mmol) in 5 ml of dry pyridine (4–6) was added slowly to a solution of 0.44 g (3.90 mmol) of **1** in 5 ml of pyridine at room temperature. The solution was then kept at room temperature and stirred for 15 h. The reaction mixture was treated with a solution of 1.8 g of sodium bisulfite in 20 ml of pyridine and 30 ml of water and the resulting mixture stirred for 1 h. The orange solution was extracted continuously for 24 h with 250 ml of chloroform. The chloroform extract was dried (Na_2SO_4), filtered, and freed from solvent at 45°. The syrupy residue showed only one spot on t.l.c. (solvent, 2% methanol in dichloromethane). The 60 MHz p.m.r. spectrum in deuteriochloroform showed only one anomeric proton signal and no signals in the olefinic proton region. The syrup was distilled at 120–121° at 0.05 mm to provide a low-melting colorless solid (~ 30°), yield, 0.55 g (96%); lit. m.p. of D isomer 105–107° (108–110° after sublimation) (13).

Anal. Calcd. for $C_6H_{10}O_4$: C, 49.31; H, 6.90. Found: C, 49.12; H, 7.06.

The i.r. spectrum in chloroform showed a band at 3560 with a shoulder at 3610 cm^{-1} (OH).

The 100 MHz p.m.r. spectrum in deuteriochloroform showed signals at τ 4.51 for H-1 (doublet, $J_{1,2} \sim 2.5$ Hz); 5.98–6.40 (multiplet for H-2, -3, -6*exo*, and -6*endo*); 7.8–8.4 (multiplet for H-4*exo* and -4*endo*); 5.47 (broad singlet $w/2 = 10$ Hz for H-5); and 7.82 (singlet for OH). Irradiation of H-5 at τ 5.47 simplified the multiplet at 7.8–8.4 for H-4*exo* and -4*endo* to two quartets showing geminal coupling of ~ 14, $J_{3,4exo} \sim 10$, and $J_{3,4endo} \sim$ 6.5 Hz which can occur only if the C-3 proton is *endo* to the bicyclic structure.

When a mixture of 0.88 g of **1** and 2.0 g of osmic acid in 10 ml of dry dioxane was stirred at room temperature for 24 h as described in published directions (4–6), and then treated with dry hydrogen sulfide, followed by removal of the black precipitate, there was obtained after isolation and distillation as above, 1.0 g (87%) of the low melting (~ 30°) solid boiling at 120–123° at 0.05 mm. This was identical in every respect to **3** (R = H) described immediately above.

*1,6-Anhydro-2,3-di-O-acetyl-4-deoxy-β-DL-ribo-hexopyranose (**3**, R = CH_3CO)*

Compound **3** (R = H) (100 mg) was treated with acetic anhydride (5 ml) in pyridine (5 ml) at 60° for 0.5 h, and gave 130 mg (82.5%) of the crude diacetate **3** (R = CH_3CO). Distillation at 137–139° at 0.1 mm provided a viscous syrup.

Anal. Calcd. for $C_{10}H_{14}O_6$: C, 52.17; H, 6.13. Found: C, 52.43; H, 5.93.

The i.r. spectrum in chloroform showed strong absorption at 1750 cm^{-1} (C=O).

The 100 MHz p.m.r. spectrum in deuteriochloroform showed signals at τ 4.61 for H-1 (doublet, $J_{1,2} \sim 2.5$ Hz); 4.95 for H-2 (quartet showing some long range coupling (< 1.0 Hz) with H-4*endo*, $J_{2,3} \sim 4.5$ Hz); 4.75 for H-3 (multiplet $J_{3,4endo} \sim 6.5$, $J_{3,4exo} \sim 11$ Hz); 8.8 for H-4*exo* and -4*endo* (multiplet masked by acetyl protons); 5.39 for H-5 (multiplet, $J_{5,6endo} \sim 1.5$, $J_{5,6exo} \sim 5.0$ Hz); 6.08 for H-6*endo* (doublet of doublets, $J_{6exo,6endo} \sim$ 7.0 Hz); 6.28 for H-6*exo* (quartet of doublets, $J_{4,6exo} \sim$ 1.7 Hz long range coupling); 7.91 and 8.04 (each a singlet due to two CH_3CO).

*4-Deoxy-α,β-DL-ribo-hexopyranose (**4**, R = H)*

A mixture of 275 mg of **3** (R = H), 5 ml of dioxane, and 10 ml of 1 *N* aqueous hydrochloric acid was heated at ~ 80° for 5 h. The mixture was then cooled, neutralized with Amberlite IRA 400 ($OH^{\ominus}$), and filtered. The solvent was removed and the residue freeze-dried. The yellow syrup obtained was passed twice through a short column of Silica Gel G using a 1:1 mixture of methanol and chloroform as eluent. The solvent was removed and the residue distilled at 110–115° at 0.01 mm and gave 261 mg (85%) of a colorless viscous oil; lit. m.p. of D isomer 89–93° (13).

Anal. Calcd. for $C_6H_{12}O_5$: C, 43.90; H, 7.37. Found: C, 43.75; H, 7.92.

The 100 MHz p.m.r. spectrum in D_2O obtained after the solution had stood for 24 h to permit completion of mutarotation, showed signals at τ 4.06 for H-1 of the α anomer (doublet, $J_{1,2} \sim 3.0$ Hz); 4.64 for H-1 of the β anomer (doublet, $J_{1,2} \sim 8.0$ Hz). Signal area ratio H-1α: H-1β was 1.0:3.0. Other signals were at τ 5.20–6.30 for H-2, -3, -5, and —CH_2— (complex multiplet); 7.40–7.92 for H-4*e* and -4*a* (multiplet); and 4.82 for OH (singlet).

*1,2,3,6-Tetra-O-acetyl-4-deoxy-α,β-DL-ribo-hexopyranose (**4**, R = CH_3CO)*

Treatment of 100 mg of **4** (R = H) with a mixture of 5 ml of acetic anhydride and 5 ml of pyridine at 60° for 0.5 h and then at room temperature overnight gave a syrup from which **4** (R = CH_3CO) was obtained as a colorless oil boiling at 141–143° at 0.1 mm; yield, 165 mg (79%).

Anal. Calcd. for $C_{14}H_{20}O_9$: C, 50.60; H, 6.07. Found: C, 50.68; H, 6.17.

The i.r. spectrum in chloroform showed strong absorption at 1755 cm^{-1} (C=O).

Can. J. Chem. Downloaded from www.nrcresearchpress.com by 210.87.254.105 on 09/05/12
For personal use only.

The 100 MHz p.m.r. spectrum in deuteriochloroform showed signals at τ 3.80 for H-1 of the α anomer (doublet, $J_{1,2} \sim 4.0$ Hz); 4.01 for H-1 of the β anomer (doublet, $J_{1,2} \sim 8.5$ Hz). Signal area ratio α:$\beta \sim 1.0$:3.0. Other signals were at τ 5.19 for H-2 of the β anomer (quartet, $J_{2,3} \sim 3.0$ Hz); 4.98 for H-2 of the α anomer (triplet, $J_{2,3} \sim J_{1,2} \sim 4.0$ Hz); 4.40–4.70 for H-3 of α and β anomers (multiplet); 7.8–8.3 for H-4*e* and -4*a* masked by the four CH_3—CO (multiplet); 5.60–5.95 for H-5 and —CH_2— (multiplet); 7.90, 7.92, 7.94, and 8.02 (four singlets, each CH_3CO).

*1,6-Anhydro-3,4-dideoxy-*β-DL*-erythro-hexopyranose (**6**, R = H)*

A solution of 1.28 g (0.01 mol) of 1,6:2,3-dianhydro-4-deoxy-β-DL-*ribo*-hexopyranose (**5**) (1, 2) in 20 ml of dry ether was added slowly, dropwise, to a stirred solution of lithium aluminum hydride (0.88 g, 0.01 mol) in 25 ml of dry ether at room temperature. This was stirred for 12 h at room temperature. The aluminum complex was then decomposed by gradual addition of 15 ml of ether saturated with water, then further addition of 1 ml of 15% aqueous sodium hydroxide. The granular precipitate was separated by gravity filtration and the colorless solid was washed with ether (3 × 20 ml). The combined ether solutions from the washings and filtrate were dried (Na_2SO_4) and freed from solvent at 40° under vacuum (50 mm). The residual solid was sublimed under vacuum (50–55° at 0.01 mm) and provided **6** (R = H) as colorless needles; m.p. 81–82°; yield, 1.18 g (~91%).

Anal. Calcd. for $C_6H_{10}O_3$: C, 55.37; H, 7.74. Found: C, 55.25; H, 7.80.

The i.r. spectrum in chloroform showed absorption at 3517 cm^{-1} (OH).

The 100 MHz p.m.r. spectrum in deuteriochloroform showed signals at τ 4.67 for H-1 (narrow triplet, $w/2 \sim 4$, $J_{1,2} \sim 1.0$, $J_{1,3} \sim 1.0$ Hz due to long range coupling); 6.40 for H-2 (multiplet, $w/2 \sim 7$; $J_{2,3} \sim 2.0$ Hz); 7.60–8.20 for H-3*exo* and -3*endo* (multiplet); 8.20–8.70 for H-4*exo* and -4*endo* (multiplet $J_{4endo,5} \sim 2.0$; $J_{4exo,6exo} \sim 1.2$ Hz due to long range coupling); 5.50 for H-5 (multiplet, $w/2 \sim 10$, $J_{5,6endo} \sim 1.5$, $J_{5,6exo} \sim 5.0$ Hz); 6.00–6.13 for H-6*endo* (doublet of doublets, $J_{6exo,6endo} \sim 7.0$ Hz); 6.13–6.30 for H-6*exo* (multiplet); τ 7.41 for OH (singlet).

*2-O-Acetyl-1,6-anhydro-3,4-dideoxy-*β-DL*-erythro-hexopyranose (**6**, R = CH_3CO)*

The reaction of 300 mg of **6** (R = H) with acetic anhydride (5 ml) in pyridine (5 ml) for 1 h at 60° gave the crude monoacetate as a pale yellow liquid. Distillation provided a colorless oil boiling at 55–59° at 0.01 mm; yield, 370 mg (93%).

Anal. Calcd. for $C_8H_{12}O_4$: C, 55.81; H, 7.02. Found: C, 55.66; H, 6.96.

The i.r. spectrum in chloroform showed a strong absorption band at 1725 cm^{-1} (C=O).

The 100 MHz p.m.r. spectrum in deuteriochloroform showed signals at τ 4.61 for H-1 (narrow quartet, $J_{1,2} \sim 2.0$, $J_{1,3} \sim 1.0$ Hz); 5.30–5.53 for H-2 and -5 (overlapping multiplets, $J_{2,3} \sim 2.0$, $J_{5,6exo} \sim 5.0$, $J_{5,6endo} \sim 1.0$ Hz); τ 8.0–8.35 for H-4*exo* and -4*endo* (multiplet, $J_{4endo,5} \sim 2.0$, $J_{4exo,6exo} \sim 1.2$ Hz long range coupling); 8.35–8.70 for H-3*exo* and -3*endo* (multiplet); 6.07 for H-6*endo* (doublet of doublets, $J_{6exo,6endo} \sim 7.0$ Hz), 6.12–6.30 for H-6*exo* (multiplet); 7.96 for CH_3CO (singlet).

*3,4-Dideoxy-*α,β-DL*-erythro-hexopyranose (**7**, R = H)*

A solution of 500 mg of **6** (R = H) in a mixture of 10 ml of 1 *N* aqueous hydrochloric acid and 5 ml of dioxane was heated at 80° for 5 h in an oil bath. The mixture was cooled and then neutralized with Amberlite IRA 400 ($OH^{\ominus}$) and filtered. The solvent was removed and the residue freeze-dried to give a pale yellow syrup. This was purified by column chromatography using a 3:2 mixture (by volume) of chloroform and methanol as eluent. The first fraction (50 ml) gave a gum which was discarded. The second fraction (150 ml) provided a syrup which was distilled at 130–135° at 0.4 mm to give 7 (R = H) as a viscous colorless oil; yield, 505 mg (89%).

Anal. Calcd. for $C_6H_{12}O_4$: C, 48.64; H, 8.16. Found: C, 48.46; H, 7.73.

The 100 MHz p.m.r. spectrum in deuterium oxide, obtained after the solution has stood for 24 h to complete mutarotation, showed signals at τ 4.59 for H-1 of the α anomer (doublet, $J_{1,2} \sim 3.5$ Hz); 5.22 for H-1 of the β anomer (doublet, $J_{1,2} \sim 8.0$ Hz). Signal area ratio H-1α:H-1β was 1.0:4.0. Other signals appeared at τ 6.31 for H-2 of β anomer (multiplet); 7.75–8.40 for two H-3 and two -4 (complex multiplet); 5.05 for OH (singlet); 6.15 for —CH_2— and H-5 (multiplet).

*3,4-Dideoxy-*α,β-DL*-erythro-hexopyranose Triacetate (**7**, R = CH_3CO)*

Treatment of 150 mg of 7 (R = H) with a mixture of 5 ml of acetic anhydride and 5 ml of pyridine at 60° for 30 min and then at room temperature overnight gave a syrup which distilled at 95–97° at 0.2 mm to give 7 (R = CH_3CO) as a viscous oil; yield, 265 mg (90%).

Anal. Calcd. for $C_{12}H_{18}O_7$: C, 52.55; H, 6.62. Found: C, 52.81; H, 6.50.

The i.r. spectrum in chloroform showed strong absorption at 1735 cm^{-1} (C=O).

The 100 MHz p.m.r. spectrum in deuteriochloroform showed signals at τ 3.79 for H-1 of α anomer (doublet $J_{1,2} \sim 3.5$ Hz); 4.34 for H-1 of β anomer (doublet, $J_{1,2} \sim 8.0$ Hz). Signal area ratio H-1α:H-1$\beta \sim 1$:3. Other signals appeared at τ 4.90–5.40 for H-2 (broad multiplet); 7.50–8.70 for two H-3 and two -4 (multiplets); 7.87, 7.90, and 7.93 each a singlet for CH_3CO.

*1,6-Anhydro-2-deoxy-*β-DL*-ribo-hexopyranose (**8**, R = H)*

The reaction of osmic acid with **2** (3) was carried out essentially as described above for the reaction of osmic acid with **1** to form **3** (R = H). From 0.44 g (0.0039 mol) of **2**, treated with 1.0 g (0.0039 mol) of osmic acid was obtained a colorless syrup which was sublimed at 80° at 1.0 mm to provide 0.52 g (92%) of **8** (R = H) melting at 28–31°; lit. m.p. for D isomer, 98–99° (14). The t.l.c. analysis (3% methanol in chloroform) showed only one spot. A satisfactory elemental analysis could not be obtained, carbon being generally low. The diacetate **8** (R = CH_3CO) gave satisfactory analysis (see below).

The i.r. spectrum (neat) showed a broad band at 3300–3500 cm^{-1} (OH).

The 100 MHz p.m.r. spectrum in $CDCl_3$ showed signals at τ 4.55 for H-1 (broad singlet $w/2 \sim 5$ Hz); 5.46 for H-5 (multiplet $w/2 \sim 11$ Hz); 5.94–6.50 for H-3,

Can. J. Chem. Downloaded from www.nrcresearchpress.com by 210.87.254.105 on 09/05/12
For personal use only.

-4, -6*exo*, -6*endo* (overlapping multiplets); 6.30 for two OH (singlet); 8.00 for H-2*endo* (quartet $J_{2exo,2endo} \sim 14$, $J_{2endo,3} \sim 6.5$ Hz); 8.42 for H-2*exo* (quartet, $J_{2exo,3} \sim 10$ Hz).

3,4-Di-O-acetyl-1,6-anhydro-2-deoxy-β-DL-*ribo-hexopyranose (**8**, R = CH_3CO)*

A mixture of 12 ml of acetic anhydride, 10 ml of pyridine, and 1.05 g (0.0072 mol) of **8** (R = H) was stirred at room temperature for 72 h. The excess of acetic anhydride and pyridine was removed and the residual brown oil was neutralized with 10 ml of 6 *N* ammonium hydroxide. The mixture was then extracted with chloroform (6 × 15 ml) and the solution dried ($MgSO_4$). Removal of solvent gave a light brown syrup which formed crystals from hexane. Yield of **8** (R = CH_3CO), 1.24 g (93%), m.p. 80–81°.

Anal. Calcd. for $C_{10}H_{14}O_6$: C, 52.17; H, 6.13. Found: C, 52.19; H, 5.95.

The i.r. spectrum in chloroform showed a strong band at 1755 cm^{-1} (C=O).

The 100 MHz p.m.r. spectrum in $CDCl_3$ showed signals at τ 4.37 for H-1 (narrow multiplet, $w/2 \sim 5$ Hz); 4.50–5.00 for H-3 and -4 (multiplet); 5.30–5.40 for H-5 (multiplet); 6.05 for H-6*endo* (quartet, $J_{6endo,6exo} \sim 7.5$, $J_{5,6endo} \sim 1.5$ Hz); 6.23 for H-6*exo* (quartet, $J_{5,6exo} \sim 5$ Hz); 7.70–8.20 for H-2*exo* and -2*endo* (multiplet); 7.82 and 7.96, each a singlet for CH_3CO.

2-Deoxy-DL-*ribo-hexopyranose (**9**, R = H)*

A solution of 0.3 g (0.0021 mol) of **8** (R = H) in 15 ml of 1 *N* hydrochloric acid was stirred at 55° for 12 h. The solution was then diluted with 100 ml of water and neutralized with Amberlite IRA-400 resin ($OH^{\ominus}$). The resin was removed by filtration and washed with water. The water was removed from the filtrate and washings at reduced pressure to give a colorless syrup. Crystallization from absolute ethanol gave 0.29 g (88%) of solid **9** (R = H), melting at 138–140°; lit. m.p. of 2-deoxy-D-*ribo*-hexopyranose, 140–142° (12).

The 100 MHz p.m.r. spectrum in D_2O was identical to that of authentic 2-deoxy-D-*ribo*-hexopyranose (12). The two quartets for H-1 at τ 4.00 and 4.40 showed that the α and β anomers were present in the approximate ratio of 1:2 as shown by the integrated areas.

2-Deoxy-DL-*ribo-hexopyranose Tetraacetate (**9**, R = CH_3CO)*

Acetylation was accomplished by the same procedure as that used to prepare **8** (R = CH_3CO) above. From 0.1 g (0.0006 mol) of **9** (R = H) there was obtained 0.17 g (88%) of **9** (R = CH_3CO), a syrup, after sublimation of the crude viscous oil at 95° at 0.75 mm. Attempts to crystallize this were unsuccessful. A t.l.c. analysis using 4% methanol in chloroform showed only one spot.

Anal. Calcd. for $C_{14}H_{19}O_9$: C, 50.76; H, 5.78. Found: C, 50.49; H, 6.08.

The i.r. spectrum (neat) showed a strong band at 1775 cm^{-1} (C=O).

The 100 MHz p.m.r. spectrum in $CDCl_3$ showed two anomeric proton signals, at τ 3.64 for H-1 of the α anomer (quartet), $J_{1,2e \text{ or } a} \sim 3.0$, $J_{1,2a \text{ or } e} \sim 5.0$ Hz) and at 3.99 for H-1 of the β anomer (quartet, $J_{1,2a} \sim 7.5$, $J_{1,2e} \sim 3.5$ Hz).

2-Deoxy-1,6:3,4-dianhydro-β-DL-*ribo-hexopyranose (**10**)*

To a stirred solution of 11.2 g (0.01 mol) of **2** in 200 ml of methylene chloride kept at room temperature, was added 21.5 g (0.10 mol) of 87% *m*-chloroperoxybenzoic acid. The resulting mixture was stirred at room temperature for an additional 24 h then filtered to remove precipitated *m*-chlorobenzoic acid. The precipitate was washed with 50 ml of methylene chloride. The combined washings and filtrate were washed with water, then with saturated aqueous sodium carbonate (2 × 50 ml). The aqueous washings were extracted with methylene chloride. The combined methylene chloride solutions were dried ($MgSO_4$) and freed from solvent to provide a light amber oil which was distilled at 55–56° at 1.0 mm to give 9.5 g (74%) of 2-deoxy-1,6:3,4-dianhydro-β-DL-*ribo*-hexopyranose (**10**) containing the *lyxo* isomer **11** to the extent of 2%. The g.l.c. analysis of this distillate with a column of 20% butanediol succinate on Gas-Chrom P at 185°, showed two distinct symmetrical peaks in the area ratio 49:1. A 12′ × 1/4″ preparative g.l.c. column of 20% butanediol succinate on Gas-Chrom P, 60–80 mesh, separated the major component **10**. Reinjection of this separated material showed only one peak.

The minor component **11** could not be freed from the isomer **10** because of tailing from the major peak but was obtained as a mixture of **10** and **11** in the ratio 1:2 respectively as measured by the areas of the signals of the H-5 protons in the 100 MHz p.m.r. spectrum and by the g.l.c. analysis.

Anal. Calcd. for $C_6H_8O_3$ for **10**: C, 56.25; H, 6.29. Found: C, 56.38; H, 6.56.

The i.r. spectrum of **10** (neat) showed no absorption band in the double bond region.

The 100 MHz p.m.r. spectrum of **10** in $CDCl_3$ showed signals at τ 4.65 for H-1 (narrow multiplet, $J_{1,2exo} \sim J_{1,2endo} \sim 1$, $J_{1,3} \sim 1.5$ Hz for long range coupling); 5.35 for H-5 (doublet of narrow quartets, $J_{5,6exo} \sim 4.5$, $J_{5,6endo} \sim 1$, $J_{4,5} \sim 1.5$ Hz); 5.95 for H-6*endo* (quartet, $J_{6exo,6endo} \sim 8$ Hz); 6.27 for H-6*exo* (quartet); 6.85–7.05 for H-3 and -4 (narrow multiplet); 7.87 for H-2*exo* (quartet, $J_{2exo,2endo} \sim 16$, $J_{1,2exo} \sim 2.7$ Hz); 8.20 for H-2*endo* (quartet of triplets, $J_{2endo,3} \sim 3.5$, $J_{1,2endo} \sim 1$ Hz).

2-Deoxy-1,6:3,4-dianhydro-β-DL-*lyxo-hexopyranose (**11**)*

The 100 MHz p.m.r. spectrum of this mixture showed the signals found for isomer **10** above. In addition the following signals were perceived. τ 4.60 for H-1 overlapping H-1 of isomer **10** (narrow multiplet $w/2 \sim 6$ Hz); 5.20 for H-5 (triplet $J_{5,6exo} \sim 5$, $J_{4,5} \sim 5$, $J_{5,6endo} < 1$ Hz); 5.97 for H-6*endo* (doublet, $J_{6endo,6exo} \sim 6.5$ Hz); 6.37–6.58 for H-6*exo* and -4 (multiplet); 6.80–7.20 for H-3 overlapping H-3 and -4 of the isomer **10** (multiplet); 7.28–8.23 for H-2*exo* and -2*endo* overlapping the signals for these protons of the isomer **10** (multiplet).

1,6-Anhydro-2-deoxy-β-DL-*arabino-hexopyranose (**12**)*

A mixture of 1.46 g (0.014 mol) of **10** in 5% aqueous potassium hydroxide was stirred and heated under reflux for 24 h. It was then cooled, neutralized with dilute hydrochloric acid to p*H* 8, saturated with sodium chloride, and then extracted continuously for 65 h with chloroform. The chloroform extract was dried ($MgSO_4$), filtered, and freed from solvent to provide a syrup.

This was sublimed at 78–85° at 0.2 mm to give 1.6 g (79%) of the diol **12** as colorless needles melting at 98–101°. The t.l.c. of this material (on silica gel with 20% methanol in chloroform) showed only one spot; lit. m.p. of D isomer 156–153° (14).

Anal. Calcd. for $C_6H_{10}O_4$: C, 49.31; H, 6.89. Found: C, 49.38; H, 6.81.

The i.r. spectrum in $CHCl_3$ showed a broad band at 3420 and a narrower band at 3580 cm^{-1} (OH).

The 100 MHz p.m.r. spectrum in $CDCl_3$ showed signals at τ 4.40 for H-1 (narrow multiplet $w/2 \sim 4$ Hz); τ 5.48 for H-5 (multiplet, $J_{5,6exo} \sim 6$ Hz); 5.61 for H-6*endo* (doublet of doublets, $J_{6endo,6exo} \sim 7$, $J_{5,6endo} \sim 1$ Hz); 6.05–6.35 for H-3, -4, and -6*exo* (multiplet); 7.02 for two OH (broad singlet $w/2 \sim 6$ Hz); 7.81 for H-2*exo* (doublet of quartets, $J_{2exo,2endo} \sim 14$; $J_{2exo,3} \sim 5$, $J_{1,2exo} \sim 2$ Hz); 8.17 for H-2*endo* (complicated doublet).

2-Deoxy-α,β-DL-arabino-hexopyranose (13)

A stirred solution of 1.12 g (0.0077 mol) of **12** in 50 ml of 1 *N* hydrochloric acid was heated at 55° for 12 h. The mixture was then diluted to 200 ml with distilled water and neutralized with Amberlite IRA-400 ($OH^{\ominus}$). The resulting water solution was treated with animal charcoal and the excess water removed under reduced pressure to afford 1.06 g (84%) of **13**. The t.l.c. analysis (50% methanol in chloroform) showed a single spot with slight tailing. Therefore, the sugar was chromatographed over a short column of Silica Gel G (eluting with 50% methanol in chloroform) to afford a colorless syrup which crystallized as white needles from methanol–ether (m.p. 125–126°). The p.m.r. is identical with that of an authentic sample of the D isomer.

Anal. Calcd. for $C_6H_{12}O_5$: C, 43.90; H, 7.37. Found: C, 44.04; H, 7.32.

1,6-Anhydro-2,3-dideoxy-β-DL-erythro-hexopyranose (14)

A solution of the oxirane **10** (0.73 g, 0.0057 mol) in 25 ml of dry ether was added dropwise with stirring, over a 45 min period, to a slurry of 0.23 g (0.006 mol) of lithium aluminum hydride in 35 ml of dry ether. The resulting mixture was then stirred for 20 h and subsequently treated slowly with 15 ml of ether saturated with water, then with 1 ml of 15% aqueous sodium hydroxide. The colorless precipitate was removed by filtration and washed with ether (3 × 10 ml). The combined ether washings and filtrate were dried ($MgSO_4$). Removal of the drying agent and solvent gave a hygroscopic solid which was sublimed at 60° at 0.3 mm to afford 0.68 g (92%) of **14**, melting at 79–81°.

Anal. Calcd. for $C_6H_{10}O_3$: C, 55.37; H, 7.75. Found: C, 55.07; H, 7.62.

The i.r. spectrum in chloroform showed a band at 3580 cm^{-1} (OH).

The 100 MHz p.m.r. spectrum in deuteriochloroform showed signals at τ 4.48 for H-1 (broad singlet $w/2 \sim 4$ Hz, $J_{1,2endo} \sim 1.5$, $J_{1,6exo} \sim 1$ Hz); 5.53 for H-5 (narrow multiplet $w/2 \sim 10$ Hz); 6.04–6.30 for H-6*exo* and -6*endo* (multiplets); 6.33 for H-4 (narrow multiplet $w/2 \sim 8$ Hz); 6.65 for one OH (singlet); 7.78–8.60 for H-3*exo*, -3*endo*, -2*exo*, -2*endo* (multiplets).

Hydrolysis of 14

A solution of 0.37 g (0.00285 mol) of **14** in a mixture of 10 ml of water and 10 ml of 1 *N* hydrochloric acid was kept at 55° for 24 h and then diluted with 50 ml of water. The acid was neutralized with Amberlite IRA-400 ($OH^{\ominus}$). The water was removed from the filtrate under reduced pressure. The residual syrup was chromatographed through a short column of silica gel (eluent, 20% methanol in chloroform) and gave 0.36 (85%) of a viscous syrup. The t.l.c. analysis (20% methanol in chloroform) showed a single spot.

Anal. Calcd. for $C_6H_{12}O_4$: C, 48.63; H, 8.10. Found: C, 47.90; H, 8.12.

The i.r. spectrum (neat) had a broad band at 3390 cm^{-1} (OH).

The 100 MHz p.m.r. spectrum in DMSO-d_6 showed a broad unresolved signal over the range τ 8.00–8.80 for the two methylene aliphatic groups, and broad unresolved multiplets over the range τ 4.90–5.50 in the anomeric proton region.

We thank the National Research Council of Canada for their financial assistance in this work.

We are grateful to Dr. V. K. Bhat, Gulf South Research Institute, P.O. Box 117, New Iberia, Louisiana 70561, for the sample of 2-deoxy-D-*ribo*-hexose.

1. F. Sweet and R. K. Brown. Can. J. Chem. **46**, 2289 (1968).
2. R. M. Srivastava and R. K. Brown. Can. J. Chem. **48**, 830 (1970).
3. T. P. Murray, C. S. Williams, and R. K. Brown. J. Org. Chem. **36**, 1311 (1971).
4. J. S. Baran. J. Org. Chem. **25**, 257 (1960).
5. D. H. R. Barton and Dov Elad. J. Chem. Soc. 2085 (1955).
6. U. P. Singh and R. K. Brown. Can. J. Chem. **49**, 1179 (1971).
7. F. Sweet and R. K. Brown. Can. J. Chem. **46**, 707 (1968).
8. H. B. Henbest and R. A. L. Wilson. J. Chem. Soc. 1958 (1957).
9. A. Furst and Pl. A. Plattner. Int. Congr. Pure and Appl. Chem. 12th Congr. New York, N.Y., 1951. Abstr. of Pap. p. 405.
10. A. S. Hallsworth and H. B. Henbest. J. Chem. Soc. 3571 (1960).
11. C. C. Bhat, K. V. Bhat, and W. W. Zorbach. Chem. Commun. 808 (1968).
12. W. W. Zorbach and A. P. Ollapally. J. Org. Chem. **29**, 1790 (1964).
13. M. Cerny, J. Stanek, Jr., and J. Pacak. Collect. Czechoslov. Chem. Commun. **34**, 1750 (1969).
14. P. A. Seib. J. Chem. Soc. C, 2552 (1969).

Can. J. Chem. Downloaded from www.nrcresearchpress.com by 210.87.254.105 on 09/05/12
For personal use only.

Can. J. Chem. Downloaded from www.nrcresearchpress.com by 210.87.254.42 on 09/05/12
For personal use only.

Reactions of 1-Substituted 5-Tetrazolyllithium Compounds; Preparation of 5-Substituted 1-Methyltetrazoles

R. RAAP

R & L Molecular Research Ltd., 8045 Argyll Road, Edmonton 82, Alberta

Received January 29, 1971

1-Methyl-5-tetrazolyllithium undergoes fragmentation to nitrogen and lithium methylcyanamide at temperatures exceeding −50°. Below −60° it is however fairly stable and a useful reagent for the preparation of various 5-substituted 1-methyltetrazoles. It reacts readily with halogens, cyanogen bromide, sulfur, aldehydes, ketones, and acid chlorides but not appreciably with benzyl bromide and benzonitrile. With methyl benzoate it forms a labile addition compound which can be hydrolyzed to 5-benzoyl-1-methyltetrazole.

1-Phenyl-5-tetrazolyllithium rapidly decomposes to lithium phenylcyanamide at temperatures as low as −65 to −70°.

Le méthyl-1 tétrazolyl-5 de lithium se décompose en azote et en méthylcyanamide de lithium pour une température dépassant −50 °C. En dessous de −60° il demeure peu stable et est un réactif utile pour la préparation de divers méthyl-1 tétrazoles substitués en position-5. Il réagit rapidement avec les halogènes, le bromure de cyanogène, les sulfures, les aldéhydes, les cétones, et chlorures d'acide; il est cependant peu réactif vis-à-vis du bromure de benzyle et du benzonitrile. Avec le benzoate de méthyle il forme un composé d'addition labile qui peut être hydrolysé en benzoyl-5 méthyl-1 tétrazole.

Le phényl-1 tétrazolyl-5 de lithium se décompose rapidement en lithium et phénylcyanamide pour une température aussi basse que −65 à −70 °C.

Canadian Journal of Chemistry, 49, 2139 (1971)

Over the past few years we had the opportunity to investigate the reactions of various five-membered heteroaryllithium compounds (1–4). In the course of this work it was discovered that ring fragmentation occurs with 5-(1,2,3-thiadiazolyl)lithium compounds (at −60°) and 5-(1,2,3-triazolyl)lithium compounds (at or above room temperature) to lithium alkynylthiolates and lithium alkynylamides respectively (1, 4) (eq. 1).

[1] 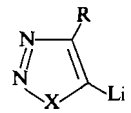 $\longrightarrow N_2 + R{-}C{\equiv}C{-}X^{\ominus}Li^{\oplus}$

X = S, NR′

1-Substituted tetrazoles constitute another group of compounds where lithiation can result in a ring fragmentation of this type. Kauer and Sheppard (5) have already demonstrated that the reaction of 5-chloro-1-phenyltetrazole with magnesium or *n*-butyllithium results in the formation of phenylcyanamide. An elegant synthesis of carbodiimides, developed by Zimmerman and Olofson (6), involves the ring cleavage of 1,4-disubstituted tetrazolium salts with a weak base. 1-Methyl-5-tetrazolyllithium on the other hand is reportedly stable at −50° (7). In order to gain some insight into their degree of usefulness in organic syntheses we studied the reactions of 1-methyl- and 1-phenyl-5-tetrazolyllithium.

1-Methyl-5-tetrazolyllithium (**2**) was prepared by the careful addition of a solution of 1-methyltetrazole (**1**) in tetrahydrofuran (THF) to *n*-butyllithium at −60 to −65°, conditions similar to the ones employed by Garber and Brubaker (7) for the preparation of di(1-methyl-5-tetrazolyl)-nickel. Although **2** was found to be considerably more prone to ring opening than 1,2,3-triazolyllithium compounds (4) it is sufficiently stable at −60° to permit its use for the preparation of a large variety of 5-substituted 1-methyltetrazoles. The various reactions performed with **2** are outlined in Scheme 1.

When a THF suspension of **2** was left with benzyl bromide at −60° for 1 h, little or no reaction took place. When the temperature was allowed to rise, an exothermic reaction (with gas evolution) started at approximately −50° and the only product isolated was benzylmethylcyanamide (**4**), indicating that **2** had undergone fragmentation to nitrogen and lithium methylcyanamide (**3**). Bromine and iodine however reacted readily with **2** at −60° to give 5-bromo-1-methyltetrazole (**5***a*) and 5-iodo-1-methyltetrazole (**5***b*). In an attempt to prepare the 5-cyano derivative, cyanogen bromide was added to **2**;

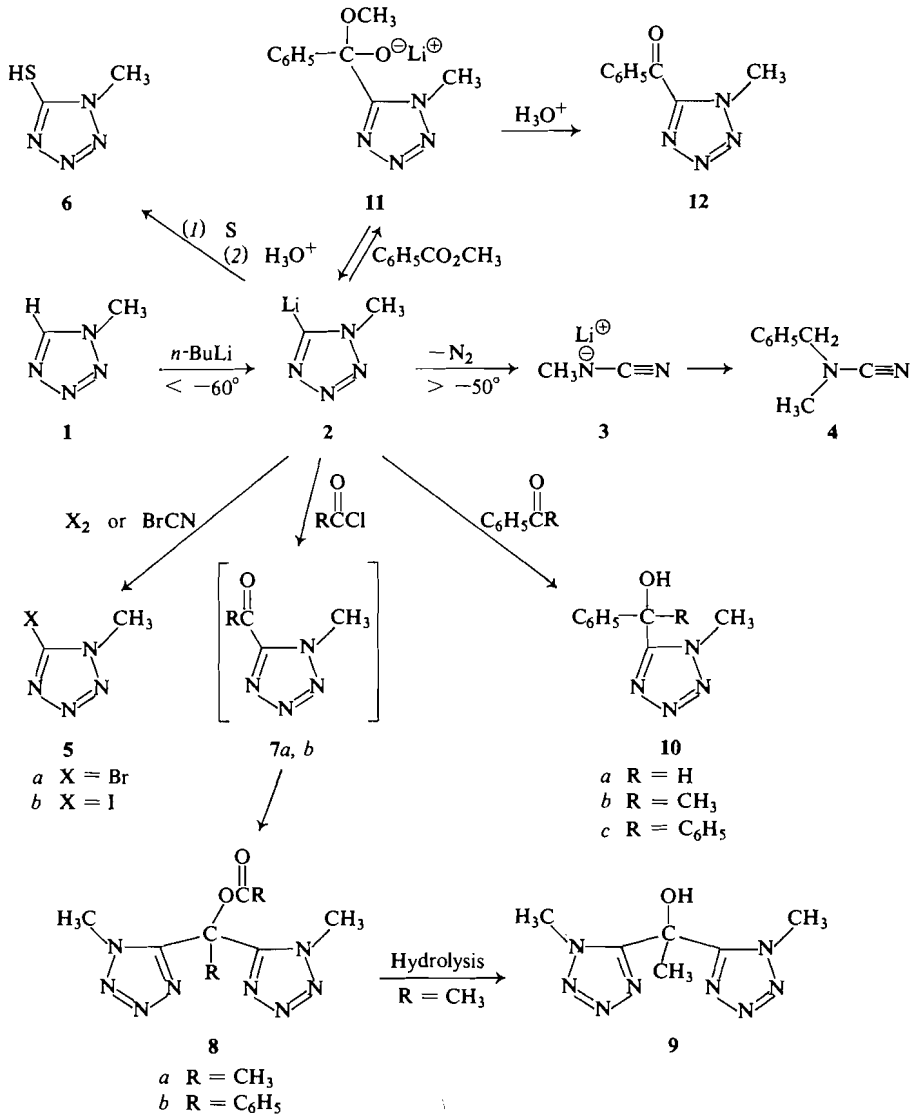

SCHEME I

however the attack took place at the bromine as **5***a* was the only product isolated. 5-Mercapto-1-methyltetrazole (**6**) became readily available in good yield by reaction of **2** with sulfur, followed by acidification of the lithium thiolate. The reaction product of **2** with acetyl chloride was 1,1-di(1′-methyl-5′-tetrazolyl)ethyl acetate (**8***a*). The structure of **8***a* was indicated by the i.r. and n.m.r. spectra (see Experimental) and by the formation of 1,1-di(1′-methyl-5′-tetrazolyl)-ethanol (**9**) by reaction with sodium hydroxide. Apparently **2** reacts immediately with the initially formed 5-acetyl-1-methyltetrazole (**7***a*) followed by acylation of the addition product with acetyl chloride. A similar reaction occurred with benzoyl chloride, and **8***b* was obtained. Whereas **2** did not react with benzonitrile at −60°, it reacted readily with benzaldehyde, acetophenone, and benzophenone, thereby providing a good route to the diaryl and triaryl hydroxy compounds **10**.

The affinity of **2** towards carbonyl groups was also indicated by its reaction with methyl benzoate to give **11**, a very labile addition product which rapidly undergoes fragmentation at −50°.

Can. J. Chem. Downloaded from www.nrcresearchpress.com by 210.87.254.42 on 09/05/12
For personal use only.

[2] 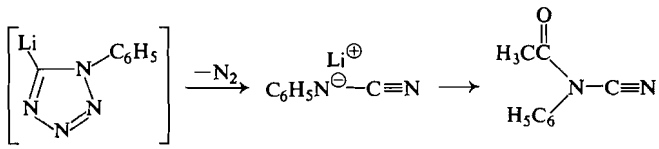

13 14

When a suspension of **11** was quenched with dilute hydrochloric acid 5-benzoyl-1-methyltetrazole (**12**) was obtained in 41% yield.

Analogous to the results obtained in the triazole series (4), 1-phenyl-5-tetrazolyllithium (**13**) decomposed at a lower temperature than **2**. When a solution of 1-phenyltetrazole in THF was added to *n*-butyllithium at −65 to −70° an immediate gas evolution occurred and subsequent addition of acetyl chloride resulted in the formation of *N*-cyanoacetanilide (**14**), which was isolated in 80% yield (eq. 2).

Experimental

All melting points and boiling points are uncorrected. The i.r. spectra were recorded on a Perkin–Elmer Model 137 "Infracord" spectrophotometer. The n.m.r. spectra were measured using a Varian Associates Model A-60 spectrometer with tetramethylsilane as a reference. Microanalyses were performed by Dr. F. B. Strauss, Microanalytical Laboratory, Oxford, England.

1-Methyltetrazole (1)

This compound was prepared from hydrazoic acid and methyl isocyanide by a modification of the procedure of Oliveri-Mandalà (8). A solution of methyl isocyanide (23.4 g, 0.57 mol) (9) in 50 ml of benzene was added to a solution of hydrazoic acid, prepared from 71.1 g (1.1 mol) of sodium azide (10), in 450 ml of benzene. The reaction mixture was heated at 75–80° (in pressure bottles) for 30 h. Removal of the solvent followed by crystallization of the residue from *n*-hexane yielded 36.6 g (77%) of pale yellow solid, m.p. 39–41°; reported m.p. 36–37° (8).

1-Methyl-5-tetrazolyllithium Reactions

A solution of 1-methyltetrazole (2.52 g, 0.030 mol) in 10 ml of THF was added dropwise in 15–30 min to a stirred mixture of 15 ml of a 2.0 *M* solution of *n*-butyllithium in *n*-hexane and 25 ml of THF at −60 to −65° in a N_2 atmosphere. An exothermic reaction took place and the lithium compound **2** precipitated as a pale yellow solid. Next a solution of either benzyl bromide, bromine, cyanogen bromide, iodine, acetyl chloride, benzoyl chloride, benzaldehyde, acetophenone, or benzophenone in 10 ml of THF was added dropwise at −60 to −65°. The reaction mixture was maintained at this temperature for an additional 30 min. In the reactions with benzaldehyde, acetophenone, and benzophenone, the temperature was allowed to rise to −30° followed by the addition of 25 ml of 2 *N* hydrochloric acid, drying, and removal of the solvent of the organic layer and recrystallization of the solid residue. In all other instances the temperature was allowed to rise to 0°, followed by removal of the solvent and treatment of the residue with a mixture of ether and water. Compounds **8***a* and **8***b* were isolated by filtration at this stage. For the isolation of **4**, **5***a*, and **5***b* the ether layer was dried, concentrated, and the residue distilled *in vacuo*. The following products were thus prepared.

Benzylmethylcyanamide (**4**) (71%), b.p. 91–95° (0.5 mm); reported b.p. 139–142° (12 mm) (11). At −65° **2** did not react with benzyl bromide. At approximately −50° an exothermic reaction started with concomitant gas evolution. The decomposition of **2** became vigorous at approximately −30° and had to be moderated by cooling. The structure of the product was confirmed by the n.m.r. and i.r. spectra and by the elemental analysis.

5-Bromo-1-methyltetrazole (**5***a*), b.p. 80–82° (0.3 mm), m.p. 72–74° (C_6H_6 – *n*-C_6H_{14}); reported m.p. 72–74° (12); n.m.r. ($CDCl_3$): τ 5.88; yield: 41% (from Br_2), 55% (from BrCN).

Anal. Calcd. for $C_2H_3BrN_4$: C, 14.74; H, 1.86; Br, 49.02; N, 34.38. Found: C, 14.92; H, 1.79; Br, 48.62; N, 34.61.

5-Iodo-1-methyltetrazole (**5***b*) (36%), m.p. 94–96° (C_6H_6 – *n*-C_6H_{14}); n.m.r. ($CDCl_3$): τ 5.86.

Anal. Calcd. for $C_2H_3IN_4$: C, 11.44; H, 1.44; I, 60.44; N, 26.68. Found: C, 11.73; H, 1.40; I, 60.02; N, 26.68.

1,1-Di(1′-methyl-5′-tetrazolyl)ethyl acetate (**8***a*) (35%), m.p. 171–172° (MeOH); ν_{max} (Nujol) 1740 cm^{-1}; n.m.r. (DMSO-d_6): singlets at τ 5.89, 7.49, and 7.65 with an integrated area ratio of 2:1:1 respectively.

Anal. Calcd. for $C_8H_{12}N_8O_2$: C, 38.09; H, 4.80; N, 44.43. Found: C, 38.23; H, 4.93; N, 44.68.

Di(1-methyl-5-tetrazolyl)phenylmethyl benzoate (**8***b*) (68%), m.p. 238–240° (dec.) (acetone); ν_{max} (Nujol) 1730 cm^{-1}; n.m.r. (DMSO-d_6): τ 1.7–2.8 (m, 5H) and 6.14 (s, 3H).

Anal. Calcd. for $C_{18}H_{16}N_8O_2$: C, 57.44; H, 4.29; N, 29.77. Found: C, 57.55; H, 4.09; N, 30.11.

(1-Methyl-5-tetrazolyl)phenylmethanol (**10***a*) (63%), m.p. 103–104° (EtOAc–*n*-C_6H_{14}); n.m.r. ($CDCl_3$): τ 2.67 (s, 5H), 3.64 (s, 1H), 4.64 (broad singlet, 1H), and 6.12 (s, 3H).

Anal. Calcd. for $C_9H_{10}N_4O$: C, 56.83; H, 5.30; N, 29.46. Found: C, 56.98; H, 5.42; N, 29.97.

1-(1′-Methyl-5′-tetrazolyl)-1-phenylethanol (**10***b*) (67%), m.p. 121–122° (C_6H_6 – *n*-C_6H_{14}); n.m.r. ($CDCl_3$): τ 2.64 (s, 5H), 4.53 (s, 1H), 6.20 (s, 3H) and 7.89 (s, 3H).

Anal. Calcd. for $C_{10}H_{12}N_4O$: C, 58.80; H, 5.93; N, 27.44. Found: C, 58.93; H, 5.86; N, 27.67.

Diphenyl(1-methyl-5-tetrazolyl)carbinol (**10***c*) (75%), m.p. 110–111° (C_6H_6 – *n*-C_6H_{14}); n.m.r. ($CDCl_3$): τ 2.73 (s, 10H), 5.28 (s, 1H), and 6.26 (s, 3H).

Anal. Calcd. for $C_{15}H_{14}N_4O$: C, 67.64; H, 5.30; N, 21.04. Found: C, 67.93; H, 5.32; N, 21.40.

Can. J. Chem. Downloaded from www.nrcresearchpress.com by 210.87.254.42 on 09/05/12
For personal use only.

Can. J. Chem. Downloaded from www.nrcresearchpress.com by 210.87.254.42 on 09/05/12
For personal use only.

5-Mercapto-1-methyltetrazole (6)

A solution of 1-methyltetrazole (15.1 g, 0.18 mol) in 60 ml of THF was dropwise added in 30 min to a stirred mixture of 2 *M* *n*-butyllithium in *n*-hexane (90 ml) and THF (150 ml) at −65 to −70° in a N_2 atmosphere. After 15 min sulfur (6.4 g, 0.20 g at.) was added in one portion at −70°, resulting in a very mildly exothermic reaction. The reaction mixture was stirred at −70° for 1 h and was then allowed to warm to 0° and concentrated to dryness. The residue was treated with 60 ml of water and some sulfur was removed by filtration. The filtrate was cooled, acidified, and extracted with two 60 ml portions of ether. The ether extracts were dried, concentrated, and the solid residue (18 g) recrystallized from $CHCl_3$–CCl_4 (3:1) to give 13.9 g (67%) of white crystals, m.p. 124–126°; reported m.p. 126° (13); n.m.r. (DMSO-d_6): singlet at τ 6.17.

Anal. Calcd. for $C_2H_4N_4S$: C, 20.68; H, 3.47; N, 48.24; S, 27.61. Found: C, 20.34; H, 3.46; N, 48.45; S, 27.27.

5-Benzoyl-1-methyltetrazole (12)

A solution of methyl benzoate (4.1 g, 0.030 mol) in 10 ml of THF was added to a suspension of **2**, prepared in the usual manner from 2.52 g (0.030 mol) of 1-methyltetrazole, in THF at −60 to −70°. The reaction mixture was stirred at this temperature for an additional 30 min and then poured into a stirred mixture of 2 *N* hydrochloric acid (60 ml), ice (40 g), and ether (50 ml). The organic layer was washed with a saturated aqueous sodium chloride solution, dried, and concentrated. The residue, consisting of methyl benzoate and **12**, was treated with 10 ml of ether and cooled. The white crystals, 2.3 g (41%), were collected by filtration and could be recrystallized from a mixture of EtOAc – *n*-C_6H_{14}; m.p. 80–82°; reported m.p. 83–83.5° (14); ν_{max} (Nujol) 1660 cm^{-1} (carbonyl); n.m.r. ($CDCl_3$): phenyl signals at τ 1.4–1.65 (2H) and 2.2–2.5 (3H) and a methyl singlet at 5.63.

Anal. Calcd. for $C_9H_8N_4O$: C, 57.44; H, 4.28; N, 29.77. Found: C, 57.16; H, 4.31; N, 29.64.

1,1-Di(1'-methyl-5'-tetrazolyl)ethanol (9)

A solution of **8***a* (0.76 g, 0.003 mol) was treated with 2 ml of 3 *N* methanolic NaOH. The mixture was left at room temperature for 15 min, then the solvent was removed and the residue dissolved in 5 ml of water. The product was extracted with five 15 ml portions of ethyl acetate. The combined extracts were dried and the solvent removed giving 0.25 g (38%) of solid residue, m.p. 120–123°. When recrystallized from ethyl acetate the material melted at 116–118°, then resolidified and melted at 126–128°. The i.r. spectrum confirmed the presence of a hydroxyl group. The n.m.r. spectrum (DMSO-d_6) consisted of singlets at τ 2.36 (1H), 5.91 (6H), and 7.86 (3H).

Anal. Calcd. for $C_6H_{10}N_8O$: C, 34.29; H, 4.80; N, 53.32. Found: C, 34.29; H, 4.68; N, 53.63.

N-Cyanoacetanilide (14)

A solution of 1-phenyltetrazole (2.92 g, 0.020 mol) (5) in 15 ml of THF was added dropwise in 1 h to a stirred mixture of 10 ml of a 2 *M* solution of *n*-butyllithium in *n*-hexane and 30 ml of THF at −65 to −70° in a N_2 atmosphere. A strongly exothermic reaction (with gas evolution) took place instantaneously. A solution of acetyl chloride (1.73 g, 0.022 mol) in 10 ml of THF was added and the solution was allowed to warm to 0°. The solvent was removed and the residue treated with ether and water. The ether solution was dried, concentrated, and distilled to give 2.6 g (80%) of colorless liquid, b.p. 90–94° (0.1 mm), which solidified and could be recrystallized from CCl_4; m.p. 48–50°; ν_{max} (Nujol) 2240 and 1720 cm^{-1}; n.m.r. ($CDCl_3$): τ 2.56 (s, 5H) and 7.57 (s, 3H).

Anal. Calcd. for $C_9H_8N_2O$: C, 67.48; H, 5.03; N, 17.56. Found: C, 67.46; H, 5.01; N, 17.97.

The author thanks Mr. P. K. Wolfert for his capable technical assistance and Professor R. U. Lemieux, Director of Research, for his interest in this work.

1. R. Raap and R. G. Micetich. Can. J. Chem. **46**, 1057 (1968).
2. R. G. Micetich and C. G. Chin. Can. J. Chem. **48**, 1371 (1970).
3. R. G. Micetich. Can. J. Chem. **48**, 2006 (1970).
4. R. Raap. Can. J. Chem. **49**, 1792 (1971).
5. J. C. Kauer and W. A. Sheppard. J. Org. Chem. **23**, 3580 (1967).
6. D. M. Zimmerman and R. A. Olofson. Abstracts of the 158th National Meeting of the American Chemical Society, New York, N.Y., September 7–12, 1969, paper ORGN 133; Tetrahedron Lett. 3453 (1970).
7. L. L. Garber and C. H. Brubaker, Jr. J. Am. Chem. Soc. **88**, 4266 (1966).
8. E. Oliveri-Mandalà. Atti R. Accad. dei Lincei, Roma [5] **19**, I, 228; Chem. Zentr., 1794 (1910).
9. J. Cassanova, R. E. Schuster, and N. D. Werner. J. Chem. Soc. 4280 (1963).
10. H. Wolff. Org. React. Vol. III. p. 327.
11. J. von Braun and H. Engel. Ann. **436**, 299 (1924).
12. K. Hattori, E. Lieber, and J. P. Horwitz. J. Am. Chem. Soc. **78**, 411 (1956).
13. R. Stollé and Fr. Henke-Stark. J. Prakt. Chem. **124**, 261 (1930).
14. P. Yates and D. G. Farnum. J. Am. Chem. Soc. **85**, 2967 (1963).

Can. J. Chem. Downloaded from www.nrcresearchpress.com by 210.87.254.42 on 09/05/12
For personal use only.

Syntheses of 3,3-Disubstituted 2-Arylacrylic Acids

R. RAAP, C. G. CHIN, AND R. G. MICETICH
R & L Molecular Research Ltd., 8045 Argyll Road, Edmonton 82, Alberta

Received February 1, 1971

The syntheses of several 3,3-disubstituted 2-arylacrylic acids are described. The Wittig reaction between arylglyoxylic esters and isopropylidenetriphenylphosphorane provides an efficient route to 2-aryl-3-methylcrotonic esters. Bromination of these esters with *N*-bromosuccinimide gives a mixture of the 3-bromomethyl-2-arylcrotonic esters and -2-arylisocrotonic esters. The 3-bromomethylcrotonic esters upon heating cyclize to lactones. Also prepared were 2-aryl-3-azidomethylisocrotonic acids and 3-aminomethyl-2-phenylisocrotonic acid. A stereospecific route to 3-azidomethyl-2-phenylisocrotonic acid and *cis*-3-azidomethyl-2-phenyl-2-pentenoic acid has been developed starting from α-methyl- and α-ethylcinnamic esters.

La synthèse de plusieurs acides aryl-2 acryliques disubstitués en position-3,3 est décrite. La réaction de Wittig effectuée entre des esters arylglyoxyliques et l'isopropylidènetriphénylphosphorane conduit avec un bon rendement aux esters de l'acide aryl-2 méthyl-3 crotonique. La bromuration de ces esters avec le *N*-bromosuccinimide conduit à un mélange des esters de l'acide bromoéthyl-3 aryl-2 crotonique et de l'acide aryl-2 isocrotonique. Les esters de l'acide bromoéthyl-3 crotonique se cyclisent en lactones par chauffage. Il a également été préparé les acides aryl-2 azidométhyl-3 isocrotoniques et aminoéthyl-3 phényl-2 isocrotonique. Une synthèse stéréospécifique des acides azidométhyl-3 phényl-2 isocrotonique et azidométhyl-3 *cis* phényl-2 pentenoique-2 a été développée en partant des esters des acides α-méthyl et α-éthylcinnamique.

Canadian Journal of Chemistry, **49**, 2143 (1971)

The syntheses described in the literature for 3,3-disubstituted 2-arylacrylic acids of the general formula **1** include the dehydration of the corresponding saturated β-hydroxy acids (*1*) and the rearrangement of 2,2-dimethyl-3-hydroxy-3-phenylpropionic esters under the influence of P_2O_5 (*2*). In a recent program directed towards the synthesis of penicillins with broad-spectrum activity we synthesized various hindered acids of this type. This paper reports these syntheses and some reactions of these compounds.

The methods employed for the syntheses of the acids **1** are outlined in Scheme 1. The rather curious P_2O_5 rearrangement of 2,2-dimethyl-3-hydroxy-3-phenylpropanoic esters (**2**, R = C_6H_5), first demonstrated by Blaise and Courtot (*2*), could be extended to halogen substituted phenyl derivatives to give the esters **3** in 20–50% yield. The Wittig reaction between an arylglyoxylic ester and isopropylidenetriphenylphosphorane was found to represent a much more versatile method, also applicable to heteroaryl derivatives, to give the esters **3** in fair to good yields. The esters prepared by one of these two methods are listed

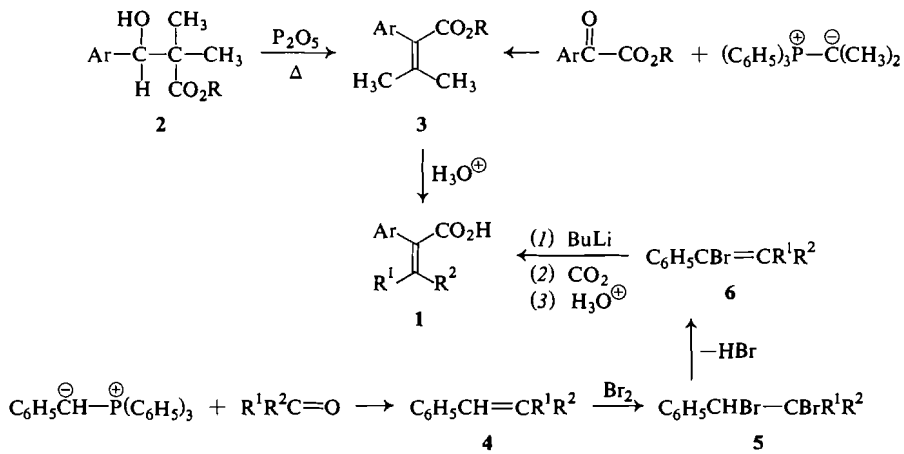

2 **3** **1** **6** **4** **5**

SCHEME 1

Can. J. Chem. Downloaded from www.nrcresearchpress.com by 210.87.254.42 on 09/05/12
For personal use only.

TABLE 1. 2-Aryl-3-methylcrotonic esters

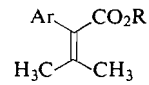

Ar	R	Boiling point (mm Hg) °C	% Yield: Wittig reaction	% Yield: P_2O_5 rearrangement
C_6H_5	CH_3	70–72 (0.4)*	72	36
C_6H_5	C_2H_5	73–75 (0.4)†	—	25
C_6H_5	t-C_4H_9	73–75 (0.1)	73	—
o-ClC_6H_4	CH_3	86–88 (0.5)	52	28
m-ClC_6H_4	CH_3	91–92 (0.7)	60	—
p-ClC_6H_4	C_2H_5	118–119 (2.0)	72	48
2,4-$Cl_2C_6H_3$	CH_3	99–101 (0.1)	—	41
2,4-$Cl_2C_6H_3$	C_2H_5	100–105 (0.5)	55	—
2,6-$Cl_2C_6H_3$	CH_3	121–124 m.p.	—	17
3,4-$Cl_2C_6H_3$	C_2H_5	115–118 (0.5)	58	52
o-F C_6H_5	C_2H_5	80–83 (0.7)	—	43
o-$CH_3C_6H_4$	CH_3	83–85 (0.5)	42	—
p-$CH_3C_6H_4$	CH_3	80–82 (0.1)	74	—
p-$CH_3OC_6H_4$	CH_3	106–112 (0.4)	81	—
1-Naphthyl	C_2H_5	133–134 (0.5)	40	—
2-Thienyl	CH_3	74–78 (0.1)	40	0
5-Cl-2-thienyl	C_2H_5	118–119 (2.5)	59	—
2,5-Cl_2-3-thienyl	C_2H_5	94–95 (0.4)	57	—
3,5-Br_2-2-thienyl	C_2H_5	115–120 (1.0)	19	—
3-CH_3-2-thienyl	C_2H_5	86–88 (0.5)	35	—
2-Thiazolyl	C_2H_5	94–95 (0.5)	50	—
5-Isothiazolyl	C_2H_5	76–78 (0.1)	10	—
N-CH_3-2-pyrrolyl	CH_3	80–85 (0.8)	33	—

*Reported b.p. 142° (26 mm) (2).
†Reported b.p. 132° (13 mm) (2).

in Table 1. The third approach involved the Wittig reaction between the commercially available benzyltriphenylphosphonium chloride and a ketone. The thus obtained β,β-disubstituted styrenes **4** could subsequently be brominated, dehydrobrominated, lithiated, and carboxylated to give the acids **1** in good overall yield. This method, particularly useful for the preparation of 3-methyl-2-phenylcrotonic acid (**1**, R = C_6H_5, $R^1 = R^2 = CH_3$) and 3-ethyl-2-phenyl-2-pentenoic acid (**1**, R = C_6H_5, $R^1 = R^2 = C_2H_5$), has the added advantage of avoiding the hydrolysis step. The Wittig reaction between ethyl phenylglyoxylate and dichloromethylenetriphenylphosphorane provided ethyl 3,3-dichloro-2-phenylacrylate (**1**, R = C_6H_5, $R^1 = R^2$ = Cl) in 36% yield. The latter ylid was prepared *in situ* by heating triphenylphosphine with carbon tetrachloride by the procedure of Rabinowitz and Marcus (3).

The esters **3** were hydrolyzed by heating under reflux in a mixture of 6 *N* hydrochloric acid and acetic acid for 4–16 h except for ethyl 3-methyl-2-thiazolylcrotonate and methyl 3-methyl-2-(1-methyl-2-pyrrolyl)crotonate which could be hydrolyzed in good yield with refluxing methanolic sodium hydroxide, whereas acid hydrolysis resulted in decomposition. In most other instances base hydrolysis led to extensive decomposition. The acids thus prepared are listed in Table 2.

The 2-aryl-3-methylcrotonic esters and acids could readily be brominated with *N*-bromosuccinimide in carbon tetrachloride. Bromination of the esters **3** with an equivalent amount of NBS gave a mixture of the isocrotonic ester **7** and crotonic ester **8** (Scheme 2); the isomer ratio could be determined from the n.m.r. spectra.[1] Upon distillation of a mixture of **7** and **8** only the isocrotonic esters **7** distilled, whereas **8** cyclized to the lactones **9** with the loss of alkyl bromide. The

[1]For the phenyl and phenyl-substituted derivatives **7** and **8**, the chemical shift (in CCl_4) of the allylic methyl protons are in the regions τ 7.65–7.87 and 8.16–8.25 respectively, for the allylic methylene protons in the regions 6.24–6.35 and 5.38–5.65 respectively. When Ar = 5-chloro-2-thienyl the differences in chemical shifts between isomers **7** and **8** are less pronounced, with the methyl signals at τ 7.87 and 7.98 and the methylene signals at 6.03 and 5.74 respectively.

Can. J. Chem. Downloaded from www.nrcresearchpress.com by 210.87.254.42 on 09/05/12
For personal use only.

TABLE 2. 3,3-Disubstituted 2-arylacrylic acids

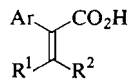

Ar	R^1	R^2	Melting point °C	Recrystallizing solvent[a]	% Yield hydrolysis[b] (h of reflux)	The n.m.r. chemical shifts (τ)[c] CH_3	CH_2	Formula	Analysis[d]
C_6H_5	CH_3	CH_3	150–153[e]	B–H	33(16)[f]	7.79, 8.32	—	$C_{11}H_{12}O_2$	—
o-ClC_6H_4			136–138	B–H	48(16)	7.68, 8.35	—	$C_{11}H_{11}ClO_2$	CHCl
m-ClC_6H_4			105–106	H	62(16)	7.77, 8.31	—	$C_{11}H_{11}ClO_2$	CHCl
p-ClC_6H_4			143–144	B–H	47(16)	7.77, 8.32	—	$C_{11}H_{11}ClO_2$	CHCl
2,4-$Cl_2C_6H_3$			133–135	H	24(16)	7.74, 8.28	—	$C_{11}H_{10}Cl_2O_2$	CHCl
2,6-$Cl_2C_6H_3$			175–178	H	61(30)	7.60, 8.33	—	$C_{11}H_{10}Cl_2O_2$	CHCl
3,4-$Cl_2C_6H_3$			133–134	H	39(16)	7.75, 8.29	—	$C_{11}H_{10}Cl_2O_2$	CHCl
o-FC_6H_4			148–149	B–H	60(16)	7.68, 8.26	—	$C_{11}H_{11}FO_2$	CHF
o-$CH_3C_6H_4$			104–105	H	71(16)	7.73, 7.82, 8.40	—	$C_{12}H_{14}O_2$	CH
p-$CH_3C_6H_4$			139–140	B–H	54(16)	7.67, 7.82, 8.32	—	$C_{12}H_{14}O_2$	CH
p-$CH_3OC_6H_4$			123–125	H	50(17)	7.82, 8.31	—	$C_{12}H_{14}O_3$	CH
2-Thienyl			126–128	H	69(4.5)	7.77, 8.15	—	$C_9H_{10}O_2S$	CHS
5-Cl-2-thienyl			144–146	H	40(16)	7.78, 8.13	—	$C_9H_9ClO_2S$	CHClS
2,5-Cl_2-3-thienyl			137–139	H	56(16)	7.72, 8.21	—	$C_9H_8Cl_2O_2S$	CHClS
3,5-Br_2-2-thienyl			131–132	H	23(24)	7.66, 8.14	—	$C_9H_8Br_2O_2S$	CHBrS
3-CH_3-2-thienyl			166–167	H	43(5)	7.72, 7.95, 8.24	—	$C_{10}H_{12}O_2S$	CHS
2-Thiazolyl			123(dec.)	CCl_4	62(2)[g]	7.66, 8.00	—	$C_8H_9NSO_2$	CHNS
N-CH_3-2-pyrrolyl			129–130	B–H	67(16)[g]	6.56, 7.74, 8.25	—	$C_{10}H_{13}NO_2$	CHN
1-Naphthyl			187–188	B–H	79(16)	7.69, 8.49	—	$C_{15}H_{14}O_2$	CH
C_6H_5	CH_2N_3		103–105	H	32(2.5)[h]	7.77	6.33	$C_{11}H_{11}N_3O_2$	CHN
o-ClC_6H_4			100–101.5	H	36(2 × 6)	7.64	6.35	$C_{11}H_{10}ClN_3O_2$	CHClN
p-$CH_3C_6H_4$			60–65	H	16(2 × 2)	7.64, 7.77	6.29	$C_{12}H_{13}N_3O_2$	CHN
C_6H_5	CH_2OH		134–135	EtOEt	—	7.94[i]	6.16[i]	$C_{11}H_{12}O_3$	CH
C_6H_5	CH_2OAc		111–112	EtOAc—H	—	7.84, 7.97	5.52	$C_{13}H_{14}O_4$	CH
C_6H_5	CH_2NH_2		213–214 (dec.)	H_2O	—	7.67[j]	6.10(q)[j]	$C_{11}H_{13}NO_2$	CHS
C_6H_5	CH_2NH-NO_2Cbo		132–133	EtOAc—H	—	—	—	$C_{19}H_{18}N_2O_6$	CHN
C_6H_5	CH_2Br	CH_2Br	127–128	CCl_4	—	—	5.33, 5.96	$C_{11}H_{10}Br_2O_2$	—
C_6H_5	CH_2N_3	CH_2N_3	75–77	CCl_4	10(2 × 3)	—	5.63, 6.16	$C_{11}H_{10}N_6O_2$	CHN
C_6H_5	Cl	Cl	128–130	B–H	64(20)	—	—	$C_9H_6Cl_2O_2$	CHCl
C_6H_5	C_2H_5	C_2H_5	104–106[l]	H	—	8.84, 9.09(t)[k]	7.42, 8.02(q)[k]	$C_{13}H_{16}O_2$	CH
C_6H_5	CH_2N_3	C_2H_5	80–81	H	—	8.83(t)	7.38(q), 6.28	$C_{12}H_{13}N_3O_2$	CHN
C_6H_5	CH_2OH	C_2H_5	164.5–165	Et_2O	—	8.83(t)[m]	7.40(q), 6.00[m]	$C_{12}H_{14}O_3$	CH
C_6H_5	CH_2Cl	C_2H_5	113–114	H	—	8.82(t)	7.33(q), 6.09	$C_{12}H_{13}ClO_2$	CHCl

[a]B, benzene; H, *n*-hexane.
[b]The methyl and ethyl esters were hydrolyzed by heating under reflux in a mixture of 6 *N* hydrochloric acid and acetic acid, unless indicated otherwise.
[c]The spectra were taken of $CDCl_3$ solutions, unless indicated otherwise.
[d]See footnote 3.
[e]Reported m.p. 151° (2).
[f]A 70% yield was obtained from the *t*-butyl ester by 1 h reflux in a mixture of trifluoroacetic acid and benzene.
[g]These hydrolyses were carried out in methanol with 3 *N* methanolic NaOH.
[h]A 46% yield was obtained from the *t*-butyl ester (15 min reflux).
[i]In DMSO-d_6.
[j]In trifluoroacetic acid.
[k]In CCl_4.
[l]Reported m.p. 105–106° (1).
[m]In acetone-d_6.

Can. J. Chem. Downloaded from www.nrcresearchpress.com by 210.87.254.42 on 09/05/12
For personal use only.

TABLE 3. 2-Aryl-3-bromomethylisocrotonic esters and 2-aryl-3-hydroxymethylcrotonic acid lactones*

		7			9				
Ar	R	% Yield	Boiling point (mm Hg) °C	7/8	% Yield	Boiling point (mm Hg) °C	Melting point °C	Formula	Analysis
C_6H_5	CH_3	37	107–112(0.8)	2.7	16	134–152(0.7)	84–86	$C_{11}H_{10}O_2$	CH
o-ClC_6H_4	CH_3	28	123–126(0.8)	1.3	21	167–174(1.5)	111.5–112.5	$C_{11}H_9ClO_2$	CHCl
p-ClC_6H_4	C_2H_5	43	125–127(0.4)	1.7	25	164–166(0.4)	85–87	$C_{11}H_9ClO_2$	CHCl
2,4-$Cl_2C_6H_3$	C_2H_5	45	130–150(0.4)	—	22	150–175(0.4)	103–105	$C_{11}H_8Cl_2O_2$	CHCl
3,4-$Cl_2C_6H_3$	C_2H_5	46	135–150(0.5–0.8)	1.5	27	150–190(0.8–1.5)	125–127	$C_{11}H_8Cl_2O_2$	CHCl
p-$CH_3C_6H_4$	CH_3	35	128–130(1.2)	1.8	12	149–154(1.5)	95–96	$C_{12}H_{12}O_2$	CH
5-Cl-2-thienyl	C_2H_5	—	—	1.7	24	170–174(0.5)	75–77	$C_9H_7ClO_2S$	CHClS

3 7 8 9

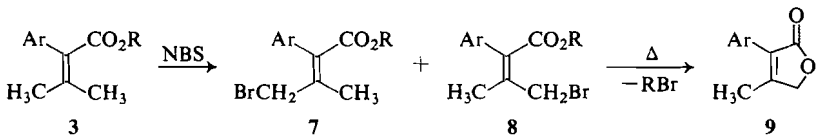

SCHEME 2

lactones **9** could be isolated by distillation and purified by recrystallization from carbon tetrachloride. Table 3 gives the isolated yields and some physical constants of the isocrotonic esters **7** and lactones **9**,[2] that were prepared. The bromine in **7** could be replaced by azide by reaction with sodium azide in aqueous acetone and subsequent acid hydrolysis provided the azido acids **10**. The bromination of 2-aryl-3-methylcro-

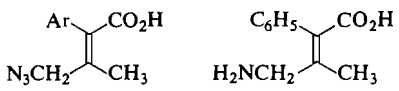

10 **11**

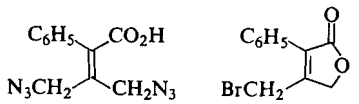

12 **13**

tonic acids with 1 equiv of NBS again gave rise to a mixture of the isomeric monobromo acids. When this mixture was treated with sodium azide a mixture of **10** and **9** was obtained, the latter compound arising presumably by cyclization of sodium 2-aryl-3-bromomethylcrotonate. This opened a route to the synthesis of 3-aminomethyl-2-phenylisocrotonic acid (**11**) by treatment of the mixture of isomeric monobromo acids with ammonium hydroxide. The bromination of methyl 3-methyl-2-phenylcrotonate or the acid with 2 equiv of NBS resulted in the formation of a quantitative amount of methyl 4-bromo-3-bromomethyl-2-phenylcrotonate or the dibromo acid. From the dibromo ester, upon reaction with sodium azide, was obtained the diazido ester which could be hydrolyzed, in low yield, to the diazido acid **12**. The dibromo acid upon brief treatment with aqueous sodium bicarbonate cyclized to the lactone **13**.

In order to establish unambiguously the structural assignment for **10** and to obtain homologs of these acids, a synthetic route was devised in which the stereochemistry was controlled throughout and which should lead to only one of the two possible geometrical isomers. Scheme 3 outlines the sequence of reactions that were successfully carried out to synthesize 3-azidomethyl-2-phenylisocrotonic acid (**21***a*) and *cis*-3-azidomethyl-2-phenyl-2-pentenoic acid (**21***b*) starting from the α-methyl and α-ethyl cinnamic esters **14**. When α-methyl-β-bromoisocinnamyl alcohol (**16***a*) was lithiated and then treated with carbon dioxide, only 3-hydroxymethyl-2-phenylcrotonic acid lactone (**9**, Ar = C_6H_5) was isolated after the work-up, indicating that isomerization had taken place in the lithiation step. This isomerization could be avoided by using the tetrahydropyranyl ether **17**. The azido acid **21***a* was identical with the azido acid **10** prepared from 3-methyl-2-phenylcrotonic ester. The hydroxy acid **19***a* was also obtained (in low yield) by acid hydrolysis of methyl 3-bromomethyl-2-phenylisocrotonate. The hydrolysis of these bromo esters however resulted in considerable isomerization as evident from the formation of the lactone.

The various crystalline 3,3-disubstituted 2-arylacrylic acids prepared in this program are listed in Table 2.

Experimental[3]

All melting points and boiling points are uncorrected. The i.r. spectra were recorded on a Perkin–Elmer Model 137 "Infrared" spectrophotometer. The n.m.r. spectra were measured using a Varian Associates Model A-60 spectrometer with tetramethylsilane as a reference. Microanalyses[3] were performed by Dr. F. B. Strauss, Microanalytical Laboratory, Oxford, England.

t-Butyl Phenylglyoxylate

To a solution of phenylglyoxylic acid (54.0 g, 0.36 mol) in 300 ml of anhydrous ether, cooled in an ice–salt mixture, was carefully added with stirring 30 ml of concentrated sulfuric acid. The mixture was cooled in Dry

[2]The n.m.r. chemical shifts (in $CDCl_3$) of the allylic methyl and methylene protons of the lactones **9** in Table 3 were in the region τ 7.74–7.99 and 5.17–5.30 respectively.

[3]Elemental analyses were only performed on the 3,3-disubstituted 2-arylacrylic acids (Table 2) and the lactones **9** (Table 3) and **13**, for the elements indicated. They were all within ±0.4% of the calculated values and are filed in the Depository of Unpublished Data, National Science Library, National Research Council of Canada, Ottawa, Canada.

Can. J. Chem. Downloaded from www.nrcresearchpress.com by 210.87.254.42 on 09/05/12
For personal use only.

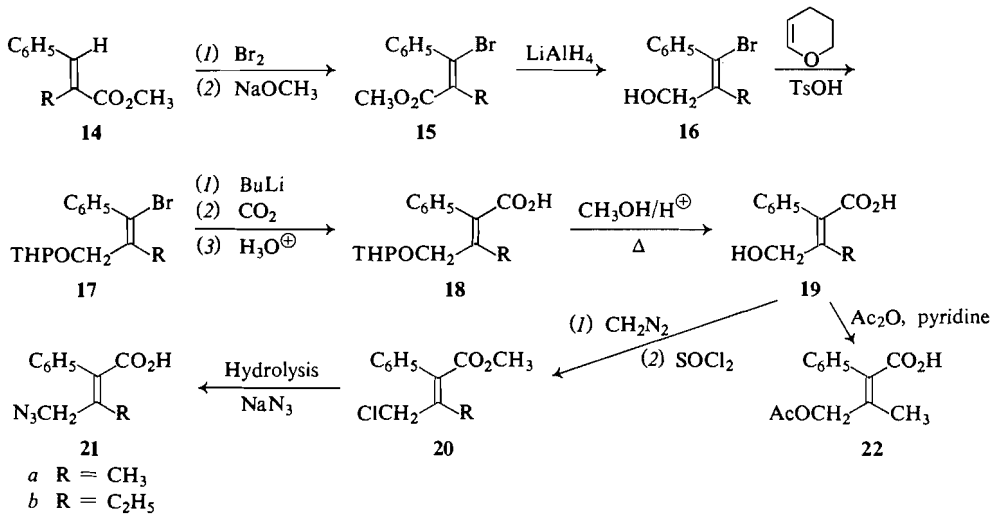

SCHEME 3

Ice – acetone and isobutylene (45.0 g, 0.80 mol) was added. The reaction mixture was allowed to warm slowly to 0° and kept at 0° for 1 day. It was then poured into 200 ml of ice-water. The ether layer, after washing with water and 2 *N* aqueous sodium carbonate, was dried, concentrated, and the residue distilled *in vacuo* to give 51.7 g (70%) of product, b.p. 86–93° (0.5–0.8 mm).

2-Aryl-3-methylcrotonic Esters. General Procedures

(a) From 3-Aryl-3-hydroxy-2,2-dimethylpropanoic Esters with P_2O_5

A solution of the hydroxypropanoic ester (0.10 mol) (2, 4) in 20 ml of benzene was added dropwise in approximately 5 min under vigorous stirring to a suspension of P_2O_5 (0.09 mol) in 40 ml of benzene. The reaction mixture was heated and the benzene distilled off at atmospheric pressure. The last traces of benzene were removed under reduced pressure. The reaction flask was then connected to a vacuum pump and immersed in an oil bath heated at approximately 200°. All volatile material was collected by distillation *in vacuo*. The product was purified by a fractional distillation.

(b) From Arylglyoxylic Esters by a Wittig Reaction

In a N_2 atmosphere a 1.6 *M* solution of *n*-butyllithium in *n*-hexane (64 ml, 0.10 mol of butyllithium) was dropwise added in 15–30 min to a stirred suspension of isopropyltriphenylphosphonium bromide (38.5 g, 0.10 mol) (5) in 200 ml of anhydrous tetrahydrofuran, cooled at 0°. The mixture was stirred at 0° for an additional 30 min, then a solution of the arylglyoxylic ester (0.10 mol) (6–9) in 50 ml of tetrahydrofuran was added in one portion. The cooling bath was removed and the reaction mixture left at room temperature for approximately 3 h (frequently the mixture was left overnight). The solvent was removed, the residue treated with water (100 ml), and the organic material extracted with ether (2 × 100 ml). The ether extract was dried and the ether removed. The residue was treated with *n*-hexane (sometimes a small amount of benzene was added as well) and, after cooling, triphenylphosphine oxide was removed by filtration. Removal of the solvent and distillation of the residue *in vacuo* provided the desired product.

The compounds prepared by either one of the two outlined procedures are listed in Table 1.

Ethyl 3,3-Dichloro-2-phenylacrylate

A mixture of triphenylphosphine (26.2 g, 0.10 mol), ethyl phenylglyoxylate (17.8 g, 0.10 mol), and carbon tetrachloride (75 ml) was heated under reflux for 7 h. To the mixture was added 100 ml of *n*-hexane and the triphenylphosphine oxide removed by filtration. The filtrate was concentrated and the residue distilled *in vacuo* to give 17.7 g of distillate, b.p. 92–102° (1.0 mm), a mixture of product and ethyl phenylglyoxylate. The two components were separated by a fractional distillation using a spinning-band column. Ethyl 3,3-dichloro-2-phenylacrylate, 8.9 g (36%), was obtained as a clear liquid, b.p. 71° (0.1 mm).

2-Aryl-3-methylcrotonic Acids. General Procedure

The ester (1.0 g) was heated under reflux in a mixture of acetic acid (10 ml) and 6 *N* hydrochloric acid (5–10 ml, depending on the solubility of the ester) for the time indicated in Table 2. Generally the acid precipitated by diluting the mixture with 50 ml of water and cooling. In other instances the acetic acid was removed under reduced pressure, the residue diluted with water and the product extracted with ether. The acids are listed in Table 2 together with their melting points and n.m.r. chemical shifts of the methyl groups.

β,β-*Diethylstyrene*

Benzyltriphenylphosphonium chloride (194 g, 0.5 mol) (Carlisle Chemical Works Inc., Reading, Ohio) was added in portions, at room temperature, to a solution of sodium methoxide, prepared from 11.5 g (0.5 g at) of sodium, in 250 ml of methanol in a N_2 atmosphere. An endothermic reaction occurred and an orange color developed. For completion of the reaction the mixture was stirred for an additional 30 min, then 3-pentanone (64.5 g, 0.75 mol) was added and the mixture heated

Can. J. Chem. Downloaded from www.nrcresearchpress.com by 210.87.254.42 on 09/05/12
For personal use only.

Can. J. Chem. Downloaded from www.nrcresearchpress.com by 210.87.254.42 on 09/05/12
For personal use only.

under reflux for 6 h. After cooling, the mixture was filtered and the solvent removed from the filtrate. The oily residue was triturated with cold *n*-hexane and the precipitated triphenylphosphine oxide removed by filtration. Removal of the solvent and distillation of the residue *in vacuo* gave 44.8 g (56%) of product, b.p. 92° (9 mm).

β,β-*Dimethylstyrene* (83%) b.p. 64° (9 mm), was prepared in the same manner using acetone instead of 3-pentanone; reported b.p. 76–77° (11 mm) (10).

α-Bromo-β,β-diethylstyrene

A solution of bromine (20.5 g, 0.128 mol) in CCl_4 (25 ml) was added dropwise with stirring to an ice-cooled solution of β,β-diethylstyrene (20.0 g, 0.125 mol) in 25 ml of CCl_4. The resulting dibromo compound (40.0 g, 0.125 mol) was isolated by removal of the solvent and added to a suspension of sodium hydride (3.4 g, 0.14 mol) in 200 ml of benzene. The mixture was stirred and heated under reflux for 12 h with periodic addition of small amounts of methanol (0.5 ml every 30 min). After cooling, the mixture was washed with water and the benzene solution dried. Removal of the solvent, followed by distillation of the residue *in vacuo* gave 18.3 g (64%) of product, b.p. 64–68° (0.3 mm).

α-*Bromo-β,β-dimethylstyrene* (85%), b.p. 52–58° (0.3 mm), was prepared similarly.

3-Ethyl-2-phenyl-2-pentenoic Acid

In a N_2 atmosphere a 1.6 *M* solution of *n*-butyllithium in *n*-hexane (9.4 ml, 0.015 mol of butyllithium) was added dropwise with stirring to a solution of α-bromo-β,β-diethylstyrene (2.9 g, 0.012 mol) in 100 ml anhydrous THF, at −65°. The reaction mixture was cooled at −65° for 1 h, and then poured into a large excess of solid carbon dioxide. When the mixture had reached room temperature, the solvent was removed, the residue dissolved in 30 ml of water, and this solution washed with ether. The aqueous solution was acidified and the product extracted with ether. Drying and removal of the solvent gave 1.9 g (76%) of white solid which could be recrystallized from *n*-hexane; m.p. 104–106°; reported m.p. 105–106° (1). The acid is further described in Table 2.

3-Methyl-2-phenylcrotonic acid (61%), m.p. 151–153°, was prepared in the same manner from α-bromo-β,β-dimethylstyrene; reported m.p. 151° (2).

2-Aryl-3-bromomethylisocrotonic Esters (7) and 2-Aryl-3-hydroxymethylcrotonic Acid Lactones (9). General Procedure

A mixture of 2-aryl-3-methylcrotonic ester (0.10 mol), *N*-bromosuccinimide (17.8 g, 0.10 mol), benzoylperoxide (0.2–0.4 g), and CCl_4 (250 ml) was heated under reflux for 1 h. The succinimide was filtered off and the solvent removed leaving a residue which, according to the n.m.r. spectra, primarily consisted of the two isomeric monobromo compounds but also contained small amounts of the dibromo compound and starting material. The residue was slowly heated *in vacuo*. At approximately 100–120° a decomposition took place as was evident from the increase in pressure. When the decomposition was complete the bath temperature was raised further and the 2-aryl-3-bromomethylisocrotonic ester was distilled. A higher boiling distillation fraction consisted of the lactone which solidified upon cooling and was recrystallized from CCl_4. In the case of ethyl 2-(5-chloro-2-thienyl)-3-methylcrotonate the bromomethylisocrotonic ester decomposed upon distillation and only the lactone could be isolated. The bromomethylisocrotonic esters and lactones prepared in this way are described in Table 3.

Monobromination of 2-Phenyl- and 2-p-Methoxyphenyl-3-methylcrotonic Acid with N-Bromosuccinimide

A mixture of 3-methyl-2-phenylcrotonic acid (36.4 g, 0.206 mol), NBS (36.7 g, 0.206 mol), benzoyl peroxide (0.5 g), and CCl_4 (600 ml) was heated under reflux for 1 h. The mixture was cooled, filtered, and the filtrate concentrated to dryness giving 58 g (100%) of white solid residue, m.p. 92–96°. The n.m.r. spectrum indicated the product to be a mixture of 3-bromomethyl-2-phenylisocrotonic acid, 3-bromomethyl-2-phenylcrotonic acid, 4-bromo-3-bromomethyl-2-phenylcrotonic acid, and starting material in relative amounts of 6:3:1:1 respectively. In the bromination of 2-*p*-methoxyphenyl-3-methylcrotonic acid the ratio of the corresponding products was 6:2:1:1 respectively.

2-Aryl-3-azidomethylisocrotonic Esters

A mixture consisting of 2-aryl-3-bromomethylisocrotonic ester **7** (0.050 mol), sodium azide (3.6 g, 0.055 mol), water (10 ml), and acetone (90 ml) was stirred at room temperature for 3 h. The acetone was removed and water and ether were added to the residue. The ether solution was dried and the solvent removed giving a quantitative amount of the 2-aryl-3-azidomethylcrotonic ester as a liquid residue.

*2-Aryl-3-azidomethylisocrotonic Acids (**10**)*

(a) By Hydrolysis of the Ester

The 2-aryl-3-azidomethylisocrotonic esters (0.050 mol) were heated under reflux in a mixture of acetic acid (100 ml) and 6 *N* hydrochloric acid (50–75 ml) for 2–6 h. The mixture was concentrated to dryness and water and ether added to the residue. The acidic material was extracted from the ether solution with 2 *N* aqueous Na_2CO_3 followed by acidification of the carbonate extract and extraction of the product with ether. Drying and removal of the ether gave the crude azido acid. The recovered neutral material consisted mainly of starting material and was generally subjected again to the same hydrolysis procedure. The azido acids were generally obtained as oils (containing some of the other geometrical isomer resulting from partial isomerization in the hydrolysis) and could be purified by chromatography on silica gel by elution with 10% ether in benzene. The azidomethylisocrotonic acids that were obtained crystalline are described in Table 2.

(b) From 2-Aryl-3-bromomethylisocrotonic Acid

The crude product (38.3 g, 0.15 mol) from the monobromination of 3-methyl-2-phenylcrotonic acid was dissolved in 360 ml of acetone and treated with a solution of sodium azide (9.8 g, 0.15 mol) in 40 ml of water. The mixture was stirred overnight at room temperature, then the acetone was removed and the residue, after dilution with 100 ml of water, extracted with ether. The aqueous solution was cooled and acidified, resulting in a precipitate of 3-azidomethyl-2-phenylisocrotonic acid; 3.2 g, m.p. 96–100°. The ether solution was extracted with two 50 ml portions of 2 *N* aqueous Na_2CO_3. The carbonate

Can. J. Chem. Downloaded from www.nrcresearchpress.com by 210.87.254.42 on 09/05/12
For personal use only.

extract was cooled and acidified to give an additional 12.2 g of the azido acid after recrystallization from 1:2 mixture of CCl_4 and *n*-hexane, m.p. 87–90°; total yield 15.4 g (47%). The low m.p. was due to some contamination with 3-methyl-2-phenylcrotonic acid. The neutral material (9.1 g) obtained by drying and removal of the ether consisted mainly of the lactone.

3-Azidomethyl-2-*p*-methoxyphenylisocrotonic acid was prepared in the same manner from the crude bromo acid and was obtained as a pale yellow oil (50% yield): ν_{max} (Nujol) 2100 and 1685 cm^{-1}; n.m.r. ($CDCl_3$): τ – 1.4 (s, CO_2H), 2.97 (AB quartet, phenyl protons), 6.22 (s, overlapping OCH_3 and N_3CH_2), and 7.81 (s, CH_3).

3-Aminomethyl-2-phenylisocrotonic Acid (11)

The crude product (56.0 g, 0.2 mol) from the monobromination of 3-methyl-2-phenylcrotonic acid was added in portions in 20 min, with stirring, to 600 ml of concentrated ammonium hydroxide cooled in ice. The mixture was kept at 15–20° for an additional 1.5 h, then it was concentrated under reduced pressure to half its original volume and extracted with ether. From the ether extract was obtained, after recrystallization from CCl_4, 5.5 g (16%) of 3-hydroxymethyl-2-phenylcrotonic acid lactone, m.p. 73–82°. The aqueous solution was further concentrated to a volume of approximately 75 ml and cooled at 0° overnight. The white solid was filtered off, washed with ice-water, and dried; 7.2 g (19%), m.p. 222–223° (dec.). An analytical sample, m.p. 213–214° (dec.), prepared by recrystallization from water and drying *in vacuo* at 60° over P_2O_5, still contained some water.

Anal. Calcd. for $C_{11}H_{13}NO_2 \times 0.5\ H_2O$: C, 65.97; H, 7.05; N, 7.00. Found: C, 66.21; H, 7.21; N, 7.32.

The amino acid was further characterized as its *p*-nitrocarbobenzoxy derivative, m.p. 132–133°, prepared by reaction with *p*-nitrobenzyl chloroformate in aqueous THF at p*H* 7–9 (76% yield). More information on these acids is given in Table 2.

Dibromination of 3-Methyl-2-phenylcrotonic Acid with NBS

A mixture of 3-methyl-2-phenylcrotonic acid (14.5 g, 0.0825 mol), NBS (29.4 g, 0.165 mol), benzoyl peroxide (0.2 g), and CCl_4 (400 ml) was heated under reflux for 1.5 h. The mixture was cooled, filtered, and the filtrate concentrated to a volume of approximately 150 ml. Upon cooling *4-bromo-3-bromomethyl-2-phenylcrotonic acid* crystallized from the solution as fine white needles; 23.9 g (87%), m.p. 116–119° (dec.). By recrystallization from CCl_4 the decomposition point could be raised to 127–128°. Although no impurities could be detected in the n.m.r. spectrum (Table 2), the elemental analyses were unsatisfactory and not reproducible. A small sample (2.7 g, 0.008 mol) was added in portions with stirring to 40 ml of 1 *N* aqueous $NaHCO_3$ at room temperature. The white precipitate of *4-bromo-3-hydroxymethyl-2-phenylcrotonic acid lactone* (**13**) (1.2 g, 60%) was collected by filtration and recrystallized from CCl_4; m.p. 94–96°; ν_{max} (Nujol) 1750 cm^{-1}; n.m.r. ($CDCl_3$): τ 2.50 (s, 5H), 5.00 (s, 2H), and 5.70 (s, 2H). Anal. $C_{11}H_9BrO_2$: CHBr.

4-Azido-3-azidomethyl-2-phenylcrotonic Acid (12)

A mixture of methyl 3-methyl-2-phenylcrotonate (19.0 g, 0.104 mol), NBS (37.0 g, 0.208 mol), benzoyl peroxide (0.5 g), and CCl_4 (350 ml) was heated under reflux for 2 h, resulting in the formation of a quantitative amount of methyl 4-bromo-3-bromomethyl-2-phenylcrotonate as a yellow oil; ν_{max} (neat) 1720 cm^{-1}; n.m.r. (CCl_4): sharp singlets at τ 2.67 (phenylprotons), 5.47 (CH_2 *trans* to phenyl), 6.00 (CH_2 *cis* to phenyl), and 6.32 (OCH_3). This dibromo ester (36.0 g, 0.104 mol) was stirred with sodium azide (13.5 g, 0.21 mol) in a mixture of water (40 ml) and acetone (360 ml) for 3 h at room temperature, giving the diazido ester as a yellow oil in quantitative amount (28.5 g); ν_{max} (neat) 2100 and 1730 cm^{-1}. This ester could be hydrolyzed to the diazido acid (ν_{max} (Nujol) 2100 and 1685 cm^{-1}) by heating under reflux with a 2:3 mixture of 6 *N* hydrochloric acid and acetic acid. The acid, which had to be purified by chromatography on silica gel, was obtained in low yield and is further described in Table 2.

Methyl β-Bromo-α-methylisocinnamate (15a) and Methyl β-Bromo-α-ethylisocinnamate (15b)

The methyl ester of α-methylcinnamic acid (300 g, 1.7 mol) (11) in CH_2Cl_2 (300 ml) was treated with bromine (287 g, 1.8 mol) at 25–30°, followed by removal of the solvent. A mixture of the crude dibromo compound, sodium hydride (45.6 g, 1.9 mol), and benzene (300 ml) was treated with methanol, in portions, until the further addition of methanol did not result in any more gas evolution. The mixture was heated under reflux for 5 h, then stirred at room temperature overnight and washed with water. The benzene solution was dried, concentrated, and the residue fractionally distilled *in vacuo* to give 291 g (67%) of product, b.p. 106–111° (1.0 mm).

Compound **15***b* (79%), b.p. 100–110° (0.25–0.5 mm), was prepared in the same manner from the methyl ester of α-ethylcinnamic acid (12).

α-Methyl- and α-Ethyl-β-bromoisocinnamyl Alcohol (16a, b)

A solution of **15***a* (114.8 g, 0.45 mol) in ether was added dropwise to a stirred suspension of lithium aluminum hydride (17.1 g, 0.45 mol) in 200 ml of anhydrous ether, at 0–5°. When the addition was completed the mixture was stirred at this temperature for an additional 1 h, then very carefully water was added, followed by 6 *N* sulfuric acid. The ether solution was dried, concentrated, and distilled *in vacuo* to give 90 g (88%) of **16***a*, b.p. 118–122° (1.5 mm); n.m.r. (CCl_4): τ 2.8 (s, 5H), 6.16 (s, 2H), 6.60 (s, 1H) and 7.98 (s, 3H).

Compound **16***b*, b.p. 112–117° (0.7 mm), was prepared in the same way (88%).

Tetrahydropyranyl Ethers of 16 (17a, b)

To a solution of **16***a* (137.4 g, 0.60 mol) in freshly distilled dihydropyran (94 g, 1.12 mol) at 0°, a few crystals of *p*-toluenesulfonic acid monohydrate were added. The mixture was stirred at 0° for 1 h, at 20° for an additional 1 h and was concentrated under reduced pressure. The residue was dissolved in ether and this solution was washed with an aqueous sodium bicarbonate solution and water, then dried and concentrated to dryness to give a quantitative amount of **17***a*. In the same manner was prepared **17***b*. Attempted distillation of these compounds resulted in decomposition and regeneration of the alcohols.

Can. J. Chem. Downloaded from www.nrcresearchpress.com by 210.87.254.42 on 09/05/12
For personal use only.

*Tetrahydropyranyl Ethers of 3-Hydroxymethyl-2-phenylisocrotonic Acid and cis-3-Hydroxymethyl-2-phenyl-2-pentenoic Acid (**18***a*, *b*)*

In a N_2 atmosphere a 1.6 *M* solution of *n*-butyllithium in *n*-hexane (194 ml, 0.31 mol of butyllithium) was dropwise added to a stirred solution of **17***a* (87.1 g, 0.28 mol) in 700 ml of ether at −65 to −70°. Towards the end of the addition some THF was added to redissolve the precipitate. The reaction mixture was stirred at −70° for an additional 1 h, then poured on solid CO_2, and left overnight. The solvent was removed, the residue was dissolved in water, and this solution, after washing with ethyl acetate, acidified. The product was extracted with ethyl acetate. The extract was dried, the solvent removed, and the solid residue washed with *n*-hexane to give 51 g (66%) of off-white solid, m.p. 90–97°, which was not further purified.

Compound **18***b* was prepared by the same procedure (40%).

*3-Hydroxymethyl-2-phenylisocrotonic Acid (**19a**) and cis-3-Hydroxymethyl-2-phenyl-2-pentenoic Acid(**19b**)*

A mixture of **18***a* (2.8 g, 0.010 mol), *p*-toluenesulfonic acid monohydrate (0.10 g), and methanol (40 ml) was heated under reflux for 8 h. The mixture was concentrated, the residue dissolved in ethyl acetate, and this solution extracted with aqueous sodium bicarbonate. A small amount (0.4 g) of a lactone was isolated from the ethyl acetate solution. The bicarbonate extract was cooled, acidified, and the precipitated solid recrystallized from ethyl acetate to give 1.5 g (78%) of **19***a*, m.p. 126–129°. The acid **19***b*, m.p. 160–164°, was prepared analogously (55%). The acids **19** are further described in Table 2.

*3-Acetoxymethyl-2-phenylisocrotonic Acid (**22**)*

The hydroxy acid **19***a* (4.0 g, 0.021 mol), acetic anhydride (8 ml), and pyridine (10 ml) were allowed to stand at room temperature overnight. The mixture was poured into ice-water (25 ml), cooled, and acidified. The product was collected by filtration and recrystallized from ethyl acetate – *n*-hexane to give 3.0 g (61%) of **22**, m.p. 110–111°; neutralization equivalent 232 (calcd. 234); ν_{max} (Nujol) 1740, 1670, 1620, 1210, and 1012 cm^{-1}. See also Table 2.

*3-Azidomethyl-2-phenylisocrotonic Acid (**21a**)*

An excess of ethereal diazomethane was added to a solution of **19***a* (9.4 g, 0.049 mol) in 10 ml of methanol at 0°. The crude hydroxy ester (10 g, 0.049 mol), obtained by removal of the solvent, was treated at 0° with 30 ml of thionyl chloride, resulting in an immediate reaction. The excess of thionyl chloride was removed and the residual chloro ester **20***a* (11.1 g, 0.049 mol) was stirred for 23 h at 25° with sodium azide (3.9 g, 0.06 mol), water (16 ml), and acetone (160 ml), then worked-up in the usual manner to give 11.15 g (99%) of the azido ester as a yellow oil; ν_{max} (neat) 2100, 1720, 1210 and 1060 cm^{-1}; n.m.r. ($CDCl_3$): τ 2.65 (m, 5H), 6.30 (s, 2H) and 7.85 (s, 3H). The hydrolysis of the azido ester has been described. The acid obtained was identical in all respects with the azido acid prepared via bromination of 3-methyl-2-phenylcrotonic acid or methyl 3-methyl-2-phenylcrotonate.

cis-3-Chloromethyl-2-phenyl-2-pentenoic Acid

The chloro ester **20***b* (7.9 g, 0.033 mol), prepared from **19***b* by the same procedure as **20***a*, was treated with 40 ml of concentrated sulfuric acid at 0°. The mixture was stirred at 0° overnight, then poured on ice and the product extracted with ethyl acetate. Drying and removal of the ethyl acetate gave 6.0 g (80%) of acid, m.p. 113–114°, after recrystallization from *n*-hexane (*cf.* Table 2).

*cis-3-Azidomethyl-2-phenyl-2-pentenoic Acid (**21b**)*

This acid, m.p. 80–81°, was prepared by reaction of the chloro acid with sodium azide in aqueous acetone by the procedure described above for the bromo acids; yield, 68%. The material is further described in Table 2.

The authors are grateful to Professor R. U. Lemieux, Director of Research, for advice and to Messrs. V. R. Baker, S. Cherwonka, R. A. Fortier, R. R. Thomas, A. Vanson, and P. K. Wolfert for technical assistance.

1. Loevens Kemiske Fabrik Productionsaktiesalskab. Belgian Patent 633 397, November 4, 1963; Chem. Abstr. **60**, 15878 (1964).
2. E. E. Blaise and A. Courtot. Bull. Soc. Chim. Paris, **35** (3), 589 (1906).
3. R. Rabinowitz and R. Marcus. J. Am. Chem. Soc. **84**, 1312 (1962).
4. A. I. Vogel. Practical organic chemistry. Longmans, Green and Co. Ltd., London, 1956. p. 875.
5. U. H. M. Fagerlund and D. R. Idler. J. Am. Chem. Soc. **79**, 6473 (1957).
6. M. Julia and M. Baillargé. Bull. Soc. Chim. Fr. 850 (1959).
7. T. S. Oakwood and C. A. Weisgerber. Org. Synth. Coll. Vol. III. p. 112.
8. R. G. Micetich. Org. Preps. Proc. **2**, 249 (1970).
9. R. G. Micetich and R. Raap. Org. Preps. Proc. In press.
10. J. Lévy and A. Tabart. Bull. Soc. Chim. Fr. **49**, 1776 (1931).
11. J. R. Johnson. Org. React. Vol. 1. p. 251.
12. W. J. Gensler and E. Berman. J. Am. Chem. Soc. **80**, 4949 (1958).

Can. J. Chem. Downloaded from www.nrcresearchpress.com by 210.87.254.40 on 09/05/12
For personal use only.

Nuclear Magnetic Resonance Studies. XXIII. Long-range ^1H–^1H Couplings (J_{HCCOCH}) in some Methyl Bicyclo[2.2.1]heptane-2-carboxylates[1]

H. BROUWER[2] AND J. B. STOTHERS
Department of Chemistry, University of Western Ontario, London 72, Ontario

Received February 3, 1971

The methoxyl proton signals of several 3-substituted 2-carbomethoxybicyclo[2.2.1]hept-5-enes and -heptanes appear as doublets because of ^1H–^1H coupling over five σ-bonds (^5J). The dependence of these long-range coupling constants on the nature and orientation of 2- and 3- substituents is discussed in terms of the probable conformations of the 2-carbomethoxyl groups.

Les signaux des protons du groupe méthoxy de quelques carbométhoxy-2 bicyclo[2.2.1]heptènes-5 et heptanes substitués en position-5 apparaissent sous forme de doublets par suite du couplage ^1H–^1H à travers cinq liaisons σ (^5J). La relation entre ces constantes de couplage à longue distance et la nature et l'orientation des substituants en position-2 et -3 est discutée à la lumière des conformations probables des groupes carbométhoxy-2.

Canadian Journal of Chemistry, 49, 2152 (1971)

Long-range proton–proton coupling interactions over five bonds, ^5J, have been reported for a variety of systems (1) but the majority of these occur through an unsaturated bonding network. There are relatively few reports of coupling constants between protons separated by five σ-bonds. One of the first reported examples, however, is the long-range coupling observed in the spectra of formic acid esters (2) between the formyl proton and the protons on the β-carbon of the alkyl group, **1**. Other carboxylic acid esters were expected to exhibit similar interactions since the nearest protons are separated by five bonds, **2**, and Hayamizu and Yamamoto (3) subsequently reported measurements of these couplings for a series of 14 saturated aliphatic esters as well as for three unsaturated systems. These compounds exhibit a small, but readily resolved, ^5J splitting either in the methoxyl signals of the methyl esters or in the α-proton absorption of the substituted acetates with values in the range, 0.1–0.25 Hz. Although the signs are not easily determined, the authors assumed these to be positive by analogy with the results for several saturated formic acid esters (4); in the latter series the five-bond couplings are $+0.52 \pm 0.1$ Hz (4). A few additional examples have been reported more recently by Riggs and Verma (5) who ascribed the couplings to transmission through planar "extended-W" σ-bond systems (**1** and **2**) with

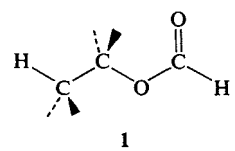

1

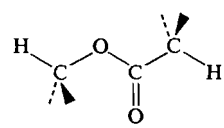

2

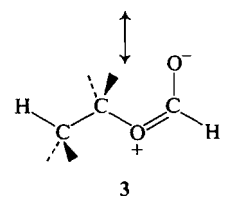

3

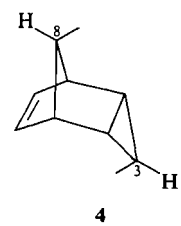

4

the ester group serving to maintain "the necessary degree of planarity". It had been suggested earlier (6), however, that the contribution of resonance forms such as **3** may be a factor although five-bond couplings are known in systems in which such resonance forms cannot contribute. Examples of the latter include $^5J_{14}$ and $^5J_{25}$ for the equatorial protons in pyranose

[1]For Part XXII, see Stothers *et al.* (13).
[2]Holder of NRCC scholarships, 1966–1970.

Can. J. Chem. Downloaded from www.nrcresearchpress.com by 210.87.254.40 on 09/05/12
For personal use only.

derivatives (7), similarly, $^5J_{25}$ for 1,3-dioxane (8) and $^5J_{3_{x8_s}}$ in **4** (9). According to Barfield and Chakrabarti (1), the indirect mechanism for coupling over five bonds in a fragment of σ-bonds, *e.g.* **5**, leads to a dependence on dihedral angles specified as in eq. 1; where ϕ and ϕ′ are

$$[1]\quad {}^5J_{HH} = (A\cos^2\phi + B\cos\phi + C)(A\cos^2\phi' + B\cos\phi' + C)$$

dihedral angles involving the terminal C—H bonds (see **6**); maximum coupling occurs for $\phi = \phi' = 180°$, but $^5J_{HH}$ is independent of the dihedral angle about the central C_2—C_3 bond in **5**. In the course of an investigation of the ^1H and ^{13}C spectra of an extensive series of 3-substituted norbornene- and norbornane-2-carboxylic acid derivatives, **7** and **8**, we have observed five-bond coupling constants in several methyl esters between the methoxyl protons and the C-2 methine proton, *i.e.* J_{HCCOCH}, which we wish to report here.

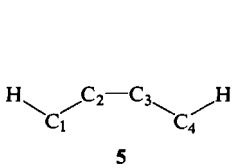

5

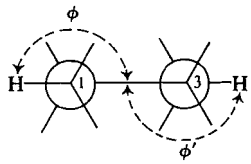

6

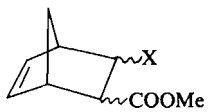

7

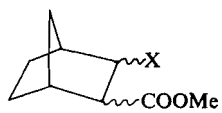

8

The data are listed in Table 1 for a series of 22 norbornene-2-carboxylic methyl esters and 20 methyl norbornane-2-carboxylates. Most of these were obtained by measurements of the wiggle-beat patterns (10) produced by rapid scanning through the methoxyl signals. Although the methoxyl absorption appears as a closely spaced doublet in the normal spectrum, more precise measurements of the spacing are possible with the wiggle-beat technique; the precision of the tabulated data is judged to be ±0.02 Hz.

It is apparent that the long-range coupling in the *exo*-esters is independent of the nature of the *endo*-3-substituents and is slightly attenuated by increasingly bulky *exo*-3-substituents. As expected these ^5J values are independent of the nature of the 5,6 bond; ^5J is essentially the same in both

TABLE 1. Long-range J_{HCCOCH} values* for some 2-carbomethoxynorbornenes **7** and -norbornanes **8**

C-3 Substitution	*endo*-2-COOMe		*exo*-2-COOMe	
	7	**8**	**7**	**8**
endo-OCH_3	0.18	—	0.19	0.19
endo-Cl	0.18	0.15†	0.18	0.18
endo-Br	0.17	0.17	0.19	0.18
endo-I	0.16	<0.1‡	0.19	0.18
endo-CH_3	0.21	0.18	0.18	0.20
Nil	0.27	0.24	0.18	0.19
exo-OCH_3	0.29	0.23	0.17	—
exo-Cl	0.28	0.23	0.16	0.17
exo-Br	0.28	0.24	0.16	0.14
exo-I	0.28	0.24	0.14	0.13
exo-CH_3	0.27	0.24	0.15	0.14

*In Hz, for CCl_4 solutions.
†By direct measurement of spacing in methoxyl absorption.
‡No wiggle-beat observed, splitting of methoxyl signal not resolved.

the norbornene and norbornane derivatives. Greater variations in ^5J are found for the *endo*-esters, with the largest values exhibited by the *exo*-3-substituted compounds, averaging 0.27 Hz in the norbornenes. The coupling appears to be slightly smaller in the corresponding norbornanes while ^5J for the *endo*-3-substituted *endo*-2 esters is comparable to that found for the *exo*-esters. There is no marked trend attributable to substituent polarity, but all ^5J values are equal to or smaller than the ^5J for the corresponding unsubstituted esters.

These results may be compared with the previously reported values for various acetates (3, 5) as well as with the data for the methyl *cis*- and *trans*-4-*t*-butylcyclohexanecarboxylates, 0.30 and 0.16 Hz, respectively. The latter value is comparable to ^5J of 0.19 Hz for methyl isobutyrate, an acyclic analog for the cyclic systems. Since the methoxyl group is essentially unhindered in each of the cyclic systems and consequently ϕ can be the same in each, the variation in ^5J must arise from differences in the relative orientation of the carbonyl group with respect to the α-methine proton. There is a general tendency for carbonyl groups to eclipse one of the bonds to the α-carbon (11). Thus the two nonequivalent rotamers available to the cyclohexanecarboxylates may be represented as **9** and **10**, of which **9** will be destabilized in the *cis*-4-*t*-

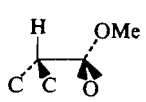

9

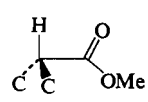

10

Can. J. Chem. Downloaded from www.nrcresearchpress.com by 210.87.254.40 on 09/05/12
For personal use only.

butylcyclohexyl systems because of nonbonded interactions between the carbonyl oxygen and the axial 3-(5-)proton. In **10**, $\phi = 180°$ (*vs.* 60° in **9**); consequently the increase in ^5J for an axial carbomethoxyl relative to that for the equatorial group is readily rationalized. The difference in ^5J values for *exo*- and *endo*-carbomethoxyl groups bonded to the norbornenyl and norbornyl skeletons without 3-substituents may be explained similarly since the rotamer in which the carbonyl bond of an *endo*-COOMe eclipses the C_1—C_2 bond is destabilized by interaction with C-6. The fact that, relative to the unsubstituted cases, ^5J is essentially unaffected by *trans*-vicinal substitution, *i.e.* by *endo*-3 and *exo*-3-substituents in the *exo*- and *endo*-esters, respectively, is consistent with this view. In each series, however, *cis*-vicinal substitution tends to decrease ^5J. This tendency suggests that the decrease results from a steric effect which reduces the relative population in the rotamer corresponding to **10** but dipolar repulsion between electronegative atoms at C-3 and the carbonyl oxygen produces the same effect. In addition, there may be an attractive interaction between the 3-substituents and the ethereal oxygen because of resonance forms corresponding to **3**. In any event the dependence of these five-bond couplings on molecular geometry appears to be qualitatively consistent with eq. 1 as predicted earlier (1).

Experimental

Spectra

All spectra were determined with a Varian HA-100 spectrometer equipped with a Sanborn 151 recorder for the wiggle-beat measurements, using 5 mol % solutions in carbon tetrachloride. The precision of the data is estimated to be ± 0.02 Hz, although repeated measurements showed less scatter for individual cases. The beat frequency of the wiggles produced by rapidly scanning through the methoxyl absorption gives the separation directly. Decoupling experiments confirmed the origins of the observed coupling.

Materials

All of the methyl esters were prepared from the carboxylic acids by reaction with diazomethane in ether. The carboxylic acids are, for the most part, known compounds and were prepared by the Diels–Alder reaction of freshly distilled cyclopentadiene with the appropriate substituted acrylic acid except for the 3-methoxy derivatives (see below). In each case both isomers formed, with the *endo*-acid as the major product; the *exo*-acid was readily separated from the *endo*-isomer using the iodolactone method. Hydrogenation in ethyl acetate over platinum oxide furnished the norbornanecarboxylic acids. Three of the 3-iodo derivatives have not been described previously; their melting points and elemental analyses are as follows.

exo-3-Iodo-*endo*-bicyclo[2.2.1]hept-5-ene-2-carboxylic acid; m.p. 136–138°.

Anal. Calcd. for $C_8H_9O_2I$: C, 36.38; H, 3.44; I, 48.06. Found: C, 36.43; H, 3.44; I, 48.21.

exo-3-Iodo-*endo*-bicyclo[2.2.1]heptane-2-carboxylic acid; m.p. 139–141°.

Anal. Calcd. for $C_8H_{11}O_2I$: C, 36.11; H, 4.17; I, 47.70. Found: C, 36.09; H, 3.90; I, 48.05.

endo-3-Iodo-*exo*-bicyclo[2.2.1]hept-5-ene-2-carboxylic acid; m.p. 105–106°.

Anal. Calcd. for $C_8H_9O_2I$: C, 36.38; H, 3.44; I, 48.06. Found: C, 36.26; H, 3.70; I, 48.13.

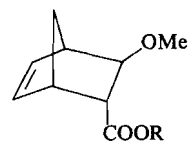

11

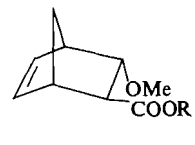

12

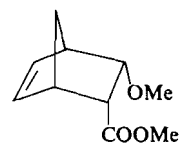

13

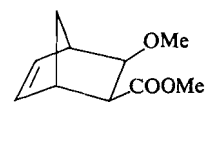

14

3-Methoxybicyclo[2.2.1]hept-5-ene-2-carboxylic Acid Esters ***11–14***

These isomers were prepared using a modification of the method described by Miller (12). Propynoic acid (60 g) was added to freshly distilled cyclopentadiene (100 g) at such a rate that the temperature was maintained below 45°, after which the mixture was stirred for 2 h at 40°. Excess cyclopentadiene was removed by evaporation under vacuum and the residue refluxed with methanol (400 ml) containing concentrated H_2SO_4 (2 ml). Polymeric material was removed by filtration and excess methanol evaporated under vacuum. The residue was poured into ice-water and the product (130 g) extracted with methylene chloride which, after removal of solvent, appeared to contain *ca.* 25% of the desired 3-methoxyl substituted esters while the remainder was 2-carbomethoxybicyclo[2.2.1]hepta-2,5-diene. This mixture was dissolved in methanol (250 ml) and benzyltrimethylammonium methoxide (5 g; 40% solution in methanol) was added before the solution was refluxed for 9 h. After removal of methanol, the residue was dissolved in CH_2Cl_2, extracted twice with water, and dried over Na_2SO_4. Fractional distillation of the residue obtained after evaporation of solvent yielded a major fraction containing the *trans* isomers, b.p. 46°/0.4 mm consisting of 94% **11** and 6% **12**. Hydrolysis with 10% Na_2CO_3 solution (200 ml) afforded, by CH_2Cl_2 extraction, a solid residue from which the *endo*-acid (**11**, R = H) was recrystallized from ethyl acetate to yield 22 g, m.p. 109–110°.

Anal. Calcd. for $C_{10}H_{12}O_3$: C, 64.32; H, 7.19. Found: C, 64.19; H, 7.13.

Neutralization of the mother liquors with 20% NaOH solution, followed by the reaction with I_2/KI solution permitted isolation of 3.5 g of the minor component (**12**, R = H) *ca.* 95% pure; the contaminant was **11**. Repeated attempts to crystallize **12** failed and the product was esterified to give **12** (R = Me) which was employed for the spectral study. Gas chromatography on a column of diethylene glycol succinate (5% on Chromosorb P, 80/100 mesh) and the proton spectrum showed that **11** (R = Me) was the only contaminant. The higher boiling fractions 48–69°/0.4 mm, shown by gas chromatography to contain varying amounts of **11** and **12** (R = Me) as well as the *cis*-isomers **13** and **14**, were combined and dissolved in pentane. At Dry Ice temperatures, **13** slowly crystallized from solution and, after several recrystallizations, 1.69 g, m.p. 28–30° was obtained. A small sample of **14** (0.1 g) was isolated by preparative gas chromatography on a 15′ × 3/8″ column of diethylene glycol succinate (15% on Chromosorb P, 80/100 mesh) at 180°. The retention times (min) for the four isomers were **11**, 34; **12**, 39.5; **14**, 41.5; **13**, 57.5, at a helium flow rate of 120 ml/min. Analytical g.l.c. indicated that the sample of **14** was at least 97% pure.

We thank the National Research Council of Canada for generous support of this work.

1. M. Barfield and B. Chakrabarti. Chem. Rev. **69**, 757 (1969).
2. D. G. Kowalewski and V. J. Kowalewski. Mol. Phys. **8**, 93 (1964).
3. K. Hayamizu and O. Yamamoto. J. Mol. Spectrosc. **22**, 119 (1967).
4. K. Hayamizu and O. Yamamoto. J. Mol. Spectrosc. **23**, 121 (1967).
5. N. V. Riggs and S. M. Verma. Tetrahedron Lett. 3767 (1968).
6. F. Hruska, H. M. Hutton, and T. Schaefer. Can. J. Chem. **43**, 1942 (1965).
7. L. D. Hall, J. F. Manville, and A. Tracey. Carbohyd. Res. **4**, 514 (1967).
8. K. C. Ramey and J. Messick. Tetrahedron Lett. 4423 (1965); J. Delmau and J. Duplan. Tetrahedron Lett. 559 (1966).
9. K. Tori and M. Ohtsuru. Chem. Commun. 886 (1966).
10. N. Bloembergen, E. M. Purcell, and R. V. Pound. Phys. Rev. **73**, 679 (1948).
11. A. J. Bowles, W. O. George, and D. B. Cunliffe-Jones. Chem. Commun. 103 (1970).
12. L. A. Miller. U.S. Patent 3 053 882 (1962).
13. M. Gordon, W. C. Howell, C. H. Jackson, and J. B. Stothers. Can. J. Chem. **49**, 143 (1971).

Preparation of 5-Aminomethyl-2-thienylacetic Acid from 1-Methylthio-2-(2′-thienyl)ethyne

R. Raap

R & L Molecular Research Ltd., 8045 Argyll Road, Edmonton, Alberta

Received January 29, 1971

A five-step synthesis of 5-aminomethyl-2-thienylacetic acid is described starting from a 2-thienylethynyl thioether.

On décrit une synthèse qui permet de transformer en cinq étapes le méthylthio-1 (thiényl-2)-2 éthyne en acide aminométhyl-5 thiényl-2 acétique.

Canadian Journal of Chemistry, **49**, 2155 (1971)

In a recent program we required 5-aminomethyl-2-thienylacetic acid. After several unsuccessful attempts to obtain this material via chloromethylation or amidomethylation of 2-thienylacetic acid (or ester) we investigated the use of 1-methylthio-2-(2′-thienyl)ethyne (**1**) as possible starting material. Compound **1** was readily available from 4-(2′-thienyl)-1,2,3-thiadiazole by treatment with *n*-butyllithium at −60° followed by reaction of the resulting lithium 2-thienylethynethiolate with methyl iodide (1).

Lithiation of **1** with *n*-butyllithium at −60° and subsequent reaction with formaldehyde provided the 5-hydroxymethyl thiophene derivative **2** which gave the chloromethyl compound **3** by reaction with thionyl chloride and triethylamine in methylene chloride (Scheme 1). Reaction of **3** with potassium phthalimide in dimethylformamide gave **4**, which could be hydrolyzed to 5-phthalimidomethyl-2-thienylacetic acid (**5**). The hydrolysis was carried out in two stages; **4** was first heated under reflux with dilute sulfuric acid and methanol to give the methylester of **5** which was

Can. J. Chem. Downloaded from www.nrcresearchpress.com by 210.87.254.40 on 09/05/12
For personal use only.

Neutralization of the mother liquors with 20% NaOH solution, followed by the reaction with I_2/KI solution permitted isolation of 3.5 g of the minor component (**12**, R = H) *ca.* 95% pure; the contaminant was **11**. Repeated attempts to crystallize **12** failed and the product was esterified to give **12** (R = Me) which was employed for the spectral study. Gas chromatography on a column of diethylene glycol succinate (5% on Chromosorb P, 80/100 mesh) and the proton spectrum showed that **11** (R = Me) was the only contaminant. The higher boiling fractions 48–69°/0.4 mm, shown by gas chromatography to contain varying amounts of **11** and **12** (R = Me) as well as the *cis*-isomers **13** and **14**, were combined and dissolved in pentane. At Dry Ice temperatures, **13** slowly crystallized from solution and, after several recrystallizations, 1.69 g, m.p. 28–30° was obtained. A small sample of **14** (0.1 g) was isolated by preparative gas chromatography on a 15′ × 3/8″ column of diethylene glycol succinate (15% on Chromosorb P, 80/100 mesh) at 180°. The retention times (min) for the four isomers were **11**, 34; **12**, 39.5; **14**, 41.5; **13**, 57.5, at a helium flow rate of 120 ml/min. Analytical g.l.c. indicated that the sample of **14** was at least 97% pure.

We thank the National Research Council of Canada for generous support of this work.

1. M. Barfield and B. Chakrabarti. Chem. Rev. **69**, 757 (1969).
2. D. G. Kowalewski and V. J. Kowalewski. Mol. Phys. **8**, 93 (1964).
3. K. Hayamizu and O. Yamamoto. J. Mol. Spectrosc. **22**, 119 (1967).
4. K. Hayamizu and O. Yamamoto. J. Mol. Spectrosc. **23**, 121 (1967).
5. N. V. Riggs and S. M. Verma. Tetrahedron Lett. 3767 (1968).
6. F. Hruska, H. M. Hutton, and T. Schaefer. Can. J. Chem. **43**, 1942 (1965).
7. L. D. Hall, J. F. Manville, and A. Tracey. Carbohyd. Res. **4**, 514 (1967).
8. K. C. Ramey and J. Messick. Tetrahedron Lett. 4423 (1965); J. Delmau and J. Duplan. Tetrahedron Lett. 559 (1966).
9. K. Tori and M. Ohtsuru. Chem. Commun. 886 (1966).
10. N. Bloembergen, E. M. Purcell, and R. V. Pound. Phys. Rev. **73**, 679 (1948).
11. A. J. Bowles, W. O. George, and D. B. Cunliffe-Jones. Chem. Commun. 103 (1970).
12. L. A. Miller. U.S. Patent 3 053 882 (1962).
13. M. Gordon, W. C. Howell, C. H. Jackson, and J. B. Stothers. Can. J. Chem. **49**, 143 (1971).

Preparation of 5-Aminomethyl-2-thienylacetic Acid from 1-Methylthio-2-(2′-thienyl)ethyne

R. Raap
R & L Molecular Research Ltd., 8045 Argyll Road, Edmonton, Alberta

Received January 29, 1971

A five-step synthesis of 5-aminomethyl-2-thienylacetic acid is described starting from a 2-thienylethynyl thioether.

On décrit une synthèse qui permet de transformer en cinq étapes le méthylthio-1 (thiényl-2)-2 éthyne en acide aminométhyl-5 thiényl-2 acétique.

Canadian Journal of Chemistry, **49**, 2155 (1971)

In a recent program we required 5-aminomethyl-2-thienylacetic acid. After several unsuccessful attempts to obtain this material via chloromethylation or amidomethylation of 2-thienylacetic acid (or ester) we investigated the use of 1-methylthio-2-(2′-thienyl)ethyne (**1**) as possible starting material. Compound **1** was readily available from 4-(2′-thienyl)-1,2,3-thiadiazole by treatment with *n*-butyllithium at −60° followed by reaction of the resulting lithium 2-thienylethynethiolate with methyl iodide (1).

Lithiation of **1** with *n*-butyllithium at −60° and subsequent reaction with formaldehyde provided the 5-hydroxymethyl thiophene derivative **2** which gave the chloromethyl compound **3** by reaction with thionyl chloride and triethylamine in methylene chloride (Scheme 1). Reaction of **3** with potassium phthalimide in dimethylformamide gave **4**, which could be hydrolyzed to 5-phthalimidomethyl-2-thienylacetic acid (**5**). The hydrolysis was carried out in two stages; **4** was first heated under reflux with dilute sulfuric acid and methanol to give the methylester of **5** which was

Can. J. Chem. Downloaded from www.nrcresearchpress.com by 210.87.254.5 on 09/05/12
For personal use only.

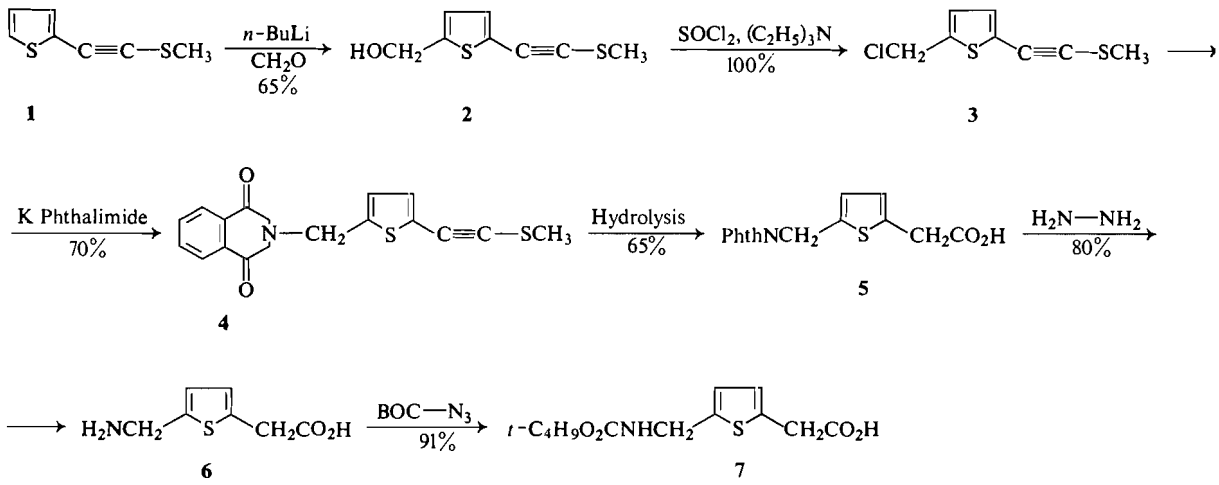

SCHEME 1

then hydrolyzed at room temperature in a mixture of 6 *N* hydrochloric acid and acetic acid.[1] Hydrazinolysis of **5** in refluxing methanol provided the desired amino acid **6** in good yield. Compound **6** behaved as a normal amino acid and could readily be converted to the BOC-protected amino acid **7** by reaction with *t*-butoxycarbonyl (BOC) azide and triethylamine in aqueous tetrahydrofuran at room temperature.

The successful synthesis of **6** further exemplifies the synthetic value of acetylenic thioethers (3) and indicates that 2-thienylethynyl thioethers may provide useful starting materials for other 5-substituted 2-thienylacetic acids as well.

Experimental

All melting points and boiling points are uncorrected. The i.r. spectra were recorded on a Perkin-Elmer model 137 "Infracord" spectrophotometer. The n.m.r. spectra were measured using a Varian Associates model A-60 spectrometer, with tetramethylsilane as a reference. Microanalyses were performed by Dr. F. B. Strauss, Microanalytical Laboratory, Oxford, England.

[1]When, instead of sulfuric acid, hydrochloric acid was employed in the first stage, the main product was that resulting from the addition of HCl across the triple bond. On the basis of spectral and analytical data and from mechanistic considerations (2) this product was assigned structure **8**.

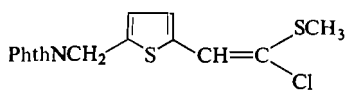

8

1-Methylthio-2-(2′-thienyl)ethyne (1)

This compound was prepared from 4-(2′-thienyl)-1,2,3-thiadiazole (87.1 g, 0.52 mol) (1), *n*-butyllithium (260 ml of a 2 *M* solution in *n*-hexane), and methyl iodide (110.8 g, 0.78 mol) by the procedure described previously (1). There was obtained 68.7 g (86%) of the product as a pale yellow liquid, b.p. 72–74° (0.2 mm). The i.r. spectrum of the neat liquid contained a weak acetylene band at 2160 cm^{-1}; n.m.r. spectrum (CCl_4): τ 2.7–3.3 (m, 3H), 7.60 (s, 3H).

Anal. Calcd. for $C_7H_6S_2$: C, 54.51; H, 3.92; S, 41.59. Found: C, 54.23; H, 3.87; S, 42.00.

1-Methylthio-2-(5′-hydroxymethyl-2′-thienyl)ethyne (2)

A 2 *M* *n*-butyllithium solution in *n*-hexane (110 ml, 0.22 mol of butyllithium) was added dropwise with stirring, in a nitrogen atmosphere, to a solution of **1** (30.8 g, 0.20 mol) in 200 ml of anhydrous tetrahydrofuran cooled at −60 to −65°. A solution of formaldehyde (8 g, 0.24 mol) in 100 mol of anhydrous THF, prepared immediately before use by thermal depolymerization of paraformaldehyde and collection of the formaldehyde in THF at −60°, was added in one portion at −60°. The reaction mixture was allowed to warm to 0° and treated with 200 ml of 2 *N* hydrochloric acid. The layers were separated and the aqueous layer extracted with ether. The combined organic layers were dried, concentrated, and the residue fractionally distilled *in vacuo* to give 23.7 g (65%) of pale yellow liquid, b.p. 135–140° (0.2 mm). The product solidified upon cooling and could be recrystallized to pale yellow fine needles from a 1:3 mixture of carbon tetrachloride – *n*-hexane; m.p. 34–36°. The i.r. spectrum (Nujol mull) contained a strong OH band at 3100–3500 and a very weak acetylene band at 2150 cm^{-1}. The n.m.r. spectrum (CCl_4) contained two one-proton doublets (J = 3.5 Hz) of an AB quartet at τ 3.01 and 3.27 and singlets at 5.42 (CH_2), 6.64 (OH), and 7.56 (CH_3).

Anal. Calcd. for $C_8H_8OS_2$: C, 52.14; H, 4.38; S, 34.81. Found: C, 51.87; H, 4.19; S, 34.36.

Can. J. Chem. Downloaded from www.nrcresearchpress.com by 210.87.254.5 on 09/05/12
For personal use only.

Can. J. Chem. Downloaded from www.nrcresearchpress.com by 210.87.254.5 on 09/05/12
For personal use only.

1-Methylthio-2-(5'-chloromethyl-2'-thienyl)ethyne (3)

A solution of thionyl chloride (6.4 g, 0.054 mol) in 35 ml of methylene chloride was added dropwise in 30 min to a stirred solution of **2** (10.0 g, 0.054 mol) and triethylamine (5.5 g, 0.054 mol) in 115 ml of methylene chloride at 0°. The reaction mixture was kept at 0° for an additional 30 min and then treated with 75 ml of water. The methylene chloride solution was dried and the solvent removed giving a quantitative amount (10.9 g) of the chloromethyl compound as a slightly colored liquid residue, which was used for the next step without further purification. In a separate experiment the chloromethyl compound was distilled *in vacuo* (with slight decomposition); b.p. 113–118° (0.4 mm); n.m.r. spectrum (CCl_4): τ 3.04 (q, 2H), 5.33 (s, 2H), and 7.56 (s, 3H).

1-Methylthio-2-(5'-phthalimidomethyl-2'-thienyl)ethyne (4)

A mixture of **3** (10.9 g, 0.054 mol), potassium phthalimide (12.4 g, 0.067 mol), and dimethylformamide (80 ml) was stirred at 40–50° for 5 h, followed by removal of the solvent under reduced pressure. The residue was treated with ethyl acetate (100 ml) and water (50 ml). The ethyl acetate solution was dried, concentrated to a volume of approximately 50 ml and cooled. The pale yellow crystals were collected by filtration; yield 11.8 g (70%), m.p. 131–133°; n.m.r. spectrum (DMSO-d_6): τ 2.06 (s, 4H), 2.85 (AB q, 2H), 5.06 (s, 2H), and 7.53 (s, 3H).

Anal. Calcd. for $C_{16}H_{11}NO_2S_2$: C, 61.32; H, 3.54; S, 20.47. Found: C, 61.42; H, 3.20; S, 20.10.

5-Phthalimidomethyl-2-thienylacetic Acid (5)

A mixture of **4** (17.4 g, 0.0556 mol), methanol (400 ml), and 3 *N* sulfuric acid (60 ml) was heated under reflux for 3 h. The mixture became homogeneous after approximately 2 h. Most of the solvent was removed and the residue treated with ethyl acetate. The ethyl acetate solution was washed with water, dried, and concentrated to dryness, leaving the crude methyl ester as a solid residue (18.5 g, m.p. 77–81°). This was dissolved in 350 ml of acetic acid followed by the addition of 75 ml of 6 *N* hydrochloric acid. The resultant solution was stirred at room temperature for 64 h. After cooling, the white solid precipitate was collected by filtration, washed with water, and taken up in 50 ml of 2 *N* aqueous sodium carbonate. The carbonate solution, after washing with ethyl acetate, was cooled and acidified. The white solid was filtered off, dried, and recrystallized from ethyl acetate to give 8.9 g of white needles, m.p. 180–182°. By concentrating the original filtrate, followed by the same purification procedure, an additional 2.0 g of product, m.p. 180–182°, was obtained. Total yield 10.9 g (65%); ν_{max} (Nujol) 1720 and 1695 cm^{-1}; n.m.r. (DMSO-d_6): τ 2.10 (s, 4H), 3.08 (AB q, 2H), 5.07 (s, 2H), and 6.22 (s, 2H).

Anal. Calcd. for $C_{15}H_{11}NO_4S$: C, 59.79; H, 3.68; N, 4.65; S, 10.64. Found: C, 59.86; H, 3.83; N, 5.02; S, 10.35.

When, instead of 3 *N* sulfuric acid, the same amount of 6 *N* hydrochloric acid was used, yellow crystals of compound **8** precipitated from the reaction mixture in approximately 50% yield; m.p. 135–137° (ethyl acetate); ν_{max} (Nujol) 1700 cm^{-1}; n.m.r. spectrum (DMSO-d_6): τ 2.13 (s, 4H), 2.74 (s, 1H), 2.92 (q, 2H), 5.07 (s, 2H), and 7.55 (s, 3H).

Anal. Calcd. for **8**, $C_{16}H_{12}ClNO_2S_2$: C, 54.93; H, 3.46; Cl, 10.14; S, 18.33. Found: C, 55.05; H, 3.76; Cl, 10.40; S, 18.58.

5-Aminoethyl-2-thienylacetic Acid (6)

5-Phthalimidomethyl-2-thienylacetic acid (7.3 g, 0.0242 mol) was dissolved in 125 ml of refluxing methanol followed by the addition of 97% hydrazine (0.80 g, 0.0242 mol). The reaction mixture was heated under reflux for 16 h, then cooled. The white solid precipitate (6.8 g) was filtered off, treated with 75 ml of water, and this mixture filtered again. The aqueous filtrate was concentrated to dryness and the residue dried to give 3.3 g (80%) of the amino acid, m.p. 228–230° (dec.); n.m.r. spectrum (CF_3CO_2H): τ 2.92 (AB quartet superimposed on broad singlet, 5H), 5.39 (q, 2H), and 5.98 (s, 2H). An elemental analysis was performed on the BOC-amino acid.

5-t-Butoxycarbonylaminomethyl-2-thienylacetic Acid (7)

A solution of *t*-butoxycarbonyl azide (1.43 g, 0.010 mol) in 20 ml of THF was added to a solution of 5-aminomethyl-2-thienylacetic acid (1.38 g, 0.008 mol) and triethylamine (2.0 g, 0.020 mol) in 25 ml of water. The mixture was stirred at room temperature for 16 h, then washed with ether. The aqueous solution was layered with 75 ml of ether and, with ice-cooling and stirring, acidified to p*H* 3. The ether layer was dried and the solvent removed to give 2.0 g (91%) of the BOC-amino acid as a white solid, m.p. 115–117°, which could be recrystallized from an ethylacetate – *n*-hexane mixture; m.p. 116–117°, ν_{max} (Nujol) 3300, 1710, and 1645 cm^{-1}; n.m.r. spectrum ($CDCl_3$): τ 1.53 (s, 1H), 3.21 (s, 2H), 5.59 (d, 2H), 6.19 (s, 2H), and 8.54 (s, 9H).

Anal. Calcd. for $C_{12}H_{17}NO_4S$: C, 53.11; H, 6.32; N, 5.16; S, 11.82. Found: C, 53.30; H, 5.86; N, 5.35; S, 12.17.

The author is grateful to Mr. P. K. Wolfert for his capable technical assistance and to Professor R. U. Lemieux, Director of Research, for his interest in this work.

1. R. Raap and R. G. Micetich. Can. J. Chem. **46**, 1057 (1968).
2. W. Drenth. Properties of 1-alkynyl thioethers. *In* The chemistry of organic sulfur compounds. Vol. 2. *Edited by* N. Kharasch and C. Y. Meyers. Pergamon Press, New York, N.Y. 1966. Chapt. 7.
3. For a recent review on acetylenic thioethers, see: L. Brandsma, H. J. T. Bos, and J. F. Arens. Chemistry of acetylenic ethers and thioethers. *In* Chemistry of acetylenes. *Edited by* H. G. Viehe. Marcel Dekker Publishers, New York, N.Y., 1969.

Synthesis of β-Poly-α-ethyl-L-aspartate[1]

S. E. MOSCHOPEDIS AND C. MUMFORD[2]
Research Council of Alberta, 11315—87 Avenue, Edmonton, Alberta

Received June 11, 1970[3]

A simple procedure is described for the preparation of *N*-carboxy-L-aspartic anhydride α-esters, and the confirmation of the six-membered ring by i.r. and n.m.r. spectroscopic studies. The polymerization of *N*-carboxy-α-ethyl-L-aspartate to the corresponding β-poly-α-ethyl-L-aspartate is also described.

Un moyen simple de préparation des α-esters de l'anhydride de l'acide *N*-carboxy L-aspartique est décrite. La présence d'un cycle à six chaînons est confirmée par des études i.r. et de r.m.n. La polymérisation du *N*-carboxy L-aspartate d'α-éthyle en β-poly L-aspartate d'α-éthyle correspondant est également décrite.

Canadian Journal of Chemistry, 49, 2158 (1971)

In attempting to synthesize β-poly-α-ethyl-L-aspartate by polymerization of the corresponding *N*-carboxy-L-aspartic anhydride α-ester, we observed that the conventional procedures for the synthesis of the latter (1, 2) are beset with difficulties and lead mainly to unwanted by-products.[4] Furthermore, Birkofer and Modic (3) have shown that β-amino acids do not readily form *N*-carboxy anhydrides by phosgenation.

We have successfully modified the procedure by adding all of the phosgene, as a solution, to the amino acid suspension **1**, since this favors the formation of the carbamyl chloride **2**, and then adding 2 equiv of triethylamine. Addition of triethylamine results in the formation of the triethylammonium salt of the carbamyl chloride **3**, which may promote the nucleophilic attack on the carbonyl group, which subsequently will eliminate the chlorine anion and result in ring closure, as in Scheme 1.

The formation of the six-membered ring anhydride has been confirmed by i.r. and n.m.r. spectroscopic studies. The i.r. spectra of the *N*-carboxy anhydride **4** ($CHCl_3$ and dioxane solutions) showed very prominent absorption bands at 1810 and 1760 cm^{-1}. The five-membered ring Leuch anhydrides exhibit absorptions at 1860 and 1790 cm^{-1} (4). The i.r. spectra failed to show clearly the carbonyl absorption of the esterified α-carboxyl group, which appeared as a shoulder at approximately 1740 cm^{-1}, because it was masked by the strong absorption at 1760 cm^{-1} of the *N*-carboxy anhydride. Therefore, the n.m.r. spectra ($CDCl_3$ solution) of the *N*-carboxy anhydride **4** (R = ethyl) was studied; this further confirmed the presence of the ethyl ester group by exhibiting a quadruplet absorption centered at 5.73 τ and a triplet absorption centered at 8.65 τ, which were assigned to the protons of the ethyl ester group. The presence of the ethyl ester group in the structure of the *N*-carboxy anhydride strongly confirms the formation of a six-membered ring *N*-carboxy anhydride via ring closure by the β-carboxyl group of the α-ethyl aspartate.

Upon heating of the *N*-carboxy-L-aspartic anhydride α-ester above its m.p. at atmospheric and 0.1–0.5 mm pressures for 2 and 5 h, respectively, carbon dioxide was evolved and a polymeric glass-like white material was obtained. The i.r. spectrum of the polymeric product **5** (KBr pellet), besides exhibiting the carbon–hydrogen stretching vibrations at frequencies of 2900 to 3000 cm^{-1}, exhibited absorptions at 3300, 1740, 1650, and 1540 cm^{-1}, which are characteristic of these types of compounds (5). This, combined with the presence of ethoxy groups in the polymer **5**, strongly indicates that the amide bands in the i.r. spectra (absorptions at 1650 and 1540 cm^{-1}) were due to formation of amide bonds from the β-carboxyl group of aspartic acid. Molecular weight determinations have shown that the polymer is a nonamer. Higher molecular weight polymers may be obtained by polymerization of *N*-carboxy-L-aspartic anhydride α-esters in solution (5).

[1]Contribution No. 522 from the Research Council of Alberta, Edmonton, Alberta.

[2]Present address: E. I. DuPont de Nemours and Co. Ltd., Electrochemical Division, The Experimental Station, Wilmington, Delaware.

[3]Revision received March 16, 1971.

[4]Isocyanates are predominant in the product mixture (the i.r. spectra show strong absorption at 2250 cm^{-1}).

Can. J. Chem. Downloaded from www.nrcresearchpress.com by 210.87.254.5 on 09/05/12
For personal use only.

Can. J. Chem. Downloaded from www.nrcresearchpress.com by 210.87.254.5 on 09/05/12
For personal use only.

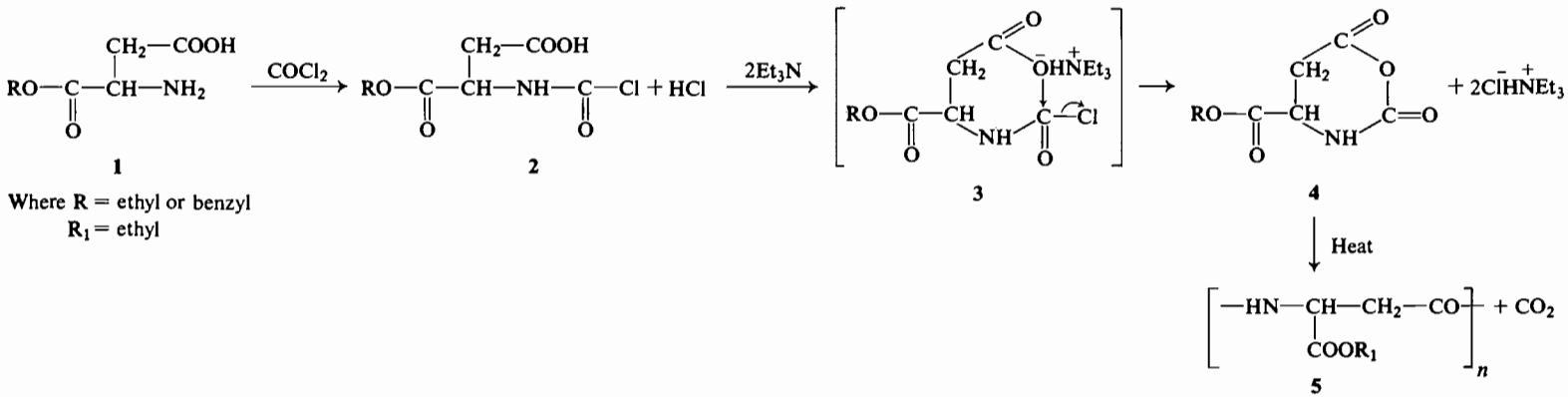

Where R = ethyl or benzyl
R_1 = ethyl

SCHEME 1

Can. J. Chem. Downloaded from www.nrcresearchpress.com by 210.87.254.5 on 09/05/12
For personal use only.

Experimental

Melting points were determined on a Buchi, Dr. Tottoli m.p. apparatus and are uncorrected. The i.r. spectra were recorded on a Beckman IR8 i.r. spectrophotometer. The n.m.r. spectra were taken in deuteriochloroform solutions with a Hitachi Perkin–Elmer R20 high resolution n.m.r. spectrometer using tetramethylsilane as internal standard. Optical rotations were obtained with a Perkin–Elmer polarimeter, Model 141. Elemental analyses were carried out by Alfred Bernhardt Microanalytical Laboratory, West Germany, and Schwarzkopf Microanalytical Laboratory, U.S.A. Molecular weights, determined by the Alfred Bernhardt Microanalytical Laboratory, were measured osmotically in dimethylformamide solution. All apparatus was oven dried at 110 °C for at least 1 h. Solvents were purified and dried by conventional methods.

Preparation of α-Esters of L-*Aspartic Acid (1)*

The method of Kovacs *et al.* (6) was used. For R = ethyl: m.p. 180.5–181° (dec.), $[\alpha]_D^{26}$ +25.5° (*c*, 2.1 water); lit. (6) m.p. 181–183°, $[\alpha]_D^{26}$ +24.2° (*c*, 2.1 water). For R = benzyl: m.p. 168–169.5°, $[\alpha]_D^{26}$ −15.5° (*c*, 5.1 1 *N* hydrochloric acid); lit. (6) m.p. 174–175°.

*Preparation of N-Carboxy-*L-*aspartic Anhydride α-Esters (4)*

Method A

Phosgene (1.18 g, 0.012 mol) dissolved in 10 ml tetrahydrofuran, and triethylamine (2.02 g, 0.02 mol) in 10 ml tetrahydrofuran were added simultaneously, from separate dropping funnels (15 min), to a stirred suspension of dry α-ester of L-aspartic acid (0.01 mol) in 10 ml tetrahydrofuran at 0–5 °C. The resulting slurry was filtered under suction and exclusion of moisture and the precipitate was washed with 10 ml dry ether. The combined filtrates were evaporated at 40° on a rotary evaporator, and further dried under high vacuum. A viscous yellow oil remained which solidified on standing at room temperature. After two crystallizations from chloroform – petroleum ether, the *N*-carboxy anhydride α-ester was obtained in the form of white crystals.

For R = ethyl: yield 0.54 g (≈29%), m.p. 85–86° (dec.), $[\alpha]_D^{26}$ +18.9° (*c*, 1.06 dioxane).

Anal. Calcd. for $C_7H_9N_1O_5$ (mol. wt. 187.15): C, 44.92; H, 4.85; N, 7.48. Found: C, 45.04; H, 4.69; N, 7.66.

For R = benzyl: yield 0.57 g (≈23%), m.p. 101–102° (dec.), $[\alpha]_D^{26}$ +19.8° (*c*, 2.05 dioxane).

Anal. Calcd. for $C_{12}H_{11}N_1O_5$ (mol. wt. 249.21): C, 57.83; H, 4.45; N, 5.62. Found: C, 57.43; H, 4.66; N, 5.41.

Method B

Dry α-ethyl-L-aspartate (3.22 g, 0.02 mol) was suspended in 40 ml tetrahydrofuran. The stirred mixture was cooled to 0–5 °C and 25 ml of tetrahydrofuran containing 1.98 g (0.02 mol) of phosgene was added. The mixture was stirred for 30 min, under cooling, and then 4.05 g (0.04 mol) of triethylamine in 25 ml tetrahydrofuran was added dropwise. The mixture was then filtered and further treated as described in method A. The residue was crystallized from chloroform – petroleum ether. Yield 2.20 g (59%), m.p. 85–86° (dec.), $[\alpha]_D^{26}$ +18.5° (*c*, 1.06 dioxane).

*Preparation of β-Poly-α-ethyl-*L-*aspartate (5)*

(*a*) The *N*-carboxy anhydride of α-ethyl-L-aspartate (0.953 g) obtained under method A or B was slowly heated in a silicone-oil bath at 95 to 100 °C at atmospheric pressure in a flask fitted with a drying tube containing anhydrous calcium chloride. After 2 h, the gas evolution, which had begun at approximately 80°, came to a stop. The white glassy residue (0.624 g), after cooling, could be crushed to a white powder. The substance gave a positive ninhydrin test, and the i.r. spectrum (KBr pellet) showed absorptions centered at 3300, 3080, 2980, 2940, 1740, 1650, and 1540 cm^{-1}. The molecular weight determined osmotically in dimethylformamide was found to be 1247, and the calculated, from the amino-nitrogen (van Slyke) which corresponds to nonapeptide, is 1306; m.p. (dec.) above 240°, melts 253–256°, $[\alpha]_D^{27}$ −2.0° (*c*, 1.0 90% w/w phenol–water).

Anal. Calcd. for $(C_6H_9N_1O_3)_9 \cdot OH_2$ (mol. wt. 1306.27): C, 49.64; H, 6.40; N, 9.65; C_2H_5O, 31.04; H_2N–N, 1.07. Found:[5] C, 49.43; H, 6.55; N, 9.73; C_2H_5O, 30.81; H_2N–N, 1.03.

(*b*) The *N*-carboxy anhydride (2.1 g) was slowly heated in a silicone-oil bath under high vacuum to 95–100 °C and kept at this temperature for 5 h. The white glassy residue (1.48 g), after cooling, was crushed to a fine powder. The polymer gave a positive ninhydrin test and the i.r. spectrum (KBr) pellet was identical to the spectrum of the polymer obtained from section *a*. The molecular weight (osmotically DMF) was found to be 1255, m.p. (dec.) above 240°, 250–253° melts, $[\alpha]_D^{27}$ −2.9° (*c*, 1.0 90% w/w phenol–water).

Anal. Calcd. for $(C_6H_9N_1O_3)_9 \cdot OH_2$ (mol. wt. 1306.27): C, 49.64; H, 6.40; N, 9.65; C_2H_5O, 31.04; H_2N–N, 1.07. Found:[5] C, 49.41; H, 6.19; N, 9.47; C_2H_5O, 30.54; H_2N–N, 1.08.

The authors are indebted to Drs. H. Habgood, S. M. Creighton, and J. G. Speight for commenting on the manuscript, to Miss M. Vetter for valuable assistance, and to Mr. M. Anderson for recording the i.r. and n.m.r. spectra.

1 V. Bruckner, T. Vajda, and J. Kovacs. Naturwiss, **41**, 449 (1954).
2. V. Bruckner, T. Vajda, and J. Kovacs. Acta Chim. Acad. Sci. Hung. **6**, 209 (1955).
3. L Birkofer and R. Modic. Ann. **628**, 162 (1960).
4. M. Idelson and E. R. Blout. J. Am. Chem. Soc. **79**, 3948 (1957).
5. E. Katchalski. Advances in protein chemistry. Academic Press Inc., New York, N.Y. **6**, 172 (1951).
6. J. Kovacs, H. N. Kovacs, and R. Ballina. J. Am. Chem. Soc. **85**, 1839 (1963).

[5]Attempts to purify the polymers by precipitation with water from a solution in hot DMF resulted in a compound having practically the same m.p. and elemental composition.

A Study of the Pfeiffer Effect in Systems containing Trisoxalatometallate(III) Complexes and Cinchonine Hydrochloride

K. T. KAN AND D. G. BREWER

Department of Chemistry, University of New Brunswick, Fredericton, New Brunswick

Received August 4, 1970[1]

The Pfeiffer effect was studied in systems containing cinchonine hydrochloride and trisoxalatometallate(III) complexes of Al, Fe, Cr, Co, and Ir. The Pfeiffer rotatory dispersion curves of the Cr and Co complexes show Cotton effects analogous to that observed in the optical rotatory dispersion (o.r.d.) curves of the respective complexes. The source of the Pfeiffer effect in all these systems is attributed either to an association between the complex ion and the optically active species in solution alone, as in the case of the Ir(III) complex, or to a combination of this association and an "equilibrium shift" between the two enantiomers in solution in favor of one of them, as in the case of the other complexes under investigation.

On a étudié l'effet Pfeiffer dans des systèmes contenant du chlorhydrate de cinchonine et des complexes trisoxalatométallates de Al, Fe, Cr, Co et Ir. On observe que ces courbes de dispersion rotatoire Pfeiffer des complexes du Cr et du Co montrent des effets Cotton analogues à ceux observés dans les courbes de d.c.o. des complexes respectifs. On attribue la source de l'effet Pfeiffer dans tous ces systèmes soit à une association de l'ion complexe avec l'espèce optiquement active seulement en solution (cas du complexe de Ir(III)) ou à une combinaison de cette association et d'un "déplacement d'équilibre" entre les deux énantiomères en solution en faveur de l'un d'eux (cas des autres complexes examinés).

Canadian Journal of Chemistry, 49, 2161 (1971)

Introduction

In 1939, Pfeiffer *et al.* (1–3) observed that the optical rotation of a solution of an optically active compound was altered upon the addition of racemic mixtures of certain optically active complex compounds. A detailed review of the studies of the "Pfeiffer effect" was given by Kirschner, Ahmad, and Magnell (4) and by Kirschner and Ahmad (5).

Early work by Pfeiffer and Nakutsuka (3) proposed that there was a shift in the equilibrium existing between the optical isomers of the compound in solution, resulting in one of the isomers being present in greater quantity. Dwyer *et al.* (6) concluded that the activity coefficients of the optical isomers were different in an asymmetric environment due to "configurational activity" and explained the Pfeiffer effect in terms of this. The controversy was virtually settled when Brasted and his students proved that an association of the enantiomers with the environment compound was the prime source of the Pfeiffer effect in aqueous solution and in methanol, this kind of association being attributed to a combination of van der Waal's force, Debye–Hückel interionic force, and particularly, hydrophobic bonding (7–10).

In this work, we observed that trisoxalatometallate(III) complexes with the formula $K_3M(C_2O_4)_3 \cdot xH_2O$ (M = Al, Fe, Cr, Co, and Ir), exhibit the Pfeiffer effect in cinchonine hydrochloride solution. Since this series of complexes consists of compounds of different lability, the investigation might lead to some further understanding of the Pfeiffer effect.

Experimental

The trisoxalato complexes were prepared by the procedure given in the literature (11, 12). The resolution of the chromium(III), cobalt(III), and iridium(III) complexes was carried out by the method of Dwyer and Sargeson (13).

Cinchonine hydrochloride was obtained from Koch-Light Laboratories, Ltd., and was recrystallized twice from hot water. Analytical grade menthol was used without further purification.

The u.v.–visible spectra were obtained using a Hitachi Ratio Recording spectrophotometer, Model EPS-3T. Optical rotations were determined on a Rudolph Model 200A Photoelectric Polarimeter equipped with a 200 W Mercury Xenon lamp. A Honeywell Electronik 19 Recorder was used to help obtain the polarimeter reading. The optical rotatory dispersion curves were measured with the Rudolph Polarimeter, and subsequently checked with a Durum-Jasco, ORD/UV-5 Recording Spectro-

[1]Revision received March 1, 1971.

Can. J. Chem. Downloaded from www.nrcresearchpress.com by 210.87.254.40 on 09/05/12
For personal use only.

Can. J. Chem. Downloaded from www.nrcresearchpress.com by 210.87.254.40 on 09/05/12
For personal use only.

polarimeter. When using the latter instrument, the large rotation of cinchonine hydrochloride solution under investigation required the expansion of the sensitivity scale and hence reduced the sensitivity. To overcome this, a solution of 1-menthol of suitable concentration in a 1 cm cell was placed in series with the cell containing cinchonine hydrochloride solution. This allowed us to obtain in all the experiments a sensitivity of $\pm 0.002°$. Solutions were studied at a constant temperature of 23 ± 0.5 °C.

Results and Discussion

It was found that the trisoxalato–metal complexes of aluminum(III), iron(III), chromium(III), cobalt(III), and iridium(III) all exhibited the Pfeiffer effect in aqueous solution containing cinchonine hydrochloride. The choice of the concentrations used was a compromise between the strong absorptivity of the chromium and cobalt complexes, and the formation of insoluble diastereoisomers of the complexes and cinchonine hydrochloride at higher concentrations. In all systems studied, the Pfeiffer rotations attain their maximum readings immediately upon the mixing of the complexes with the environment. For the systems containing $Al(C_2O_4)_3^{3-}$ and $Ir(C_2O_4)_3^{3-}$ anion, the rotation remained unchanged for a week. However, the instability of the $Fe(C_2O_4)_3^{3-}$, $Cr(C_2O_4)_3^{3-}$, and $Co(C_2O_4)_3^{3-}$ anions towards heat and light limited our observation to 24 h, during which no change in rotation was noted.

The lability of the tris(oxalato) complexes of trivalent metals follows the trend of Al > Fe > Cr > Co > Ir, which has been established by stability constant, rate of racemization, and ligand exchange measurements (14). The lack of such an analogous trend indicates that the mechanism of the Pfeiffer effect in these systems may be quite complicated. Also, the presence of a magnetic-dipole-allowed d–d transition in complexes of chromium(III) and cobalt(III) contributes greatly to the relatively large Pfeiffer rotations of their complexes at this particular wavelength.

In the systems of trisoxalato complexes with cinchonine hydrochloride, a nearly linear relationship was observed between the Pfeiffer rotation and the concentration of either the complex or the environment compound if the other is held constant, and would suggest that there is no well-defined association (compound formation) between the complex and the environment compound in solution (15, 16). Also, Kirschner and Magnell (16) have used the similar shapes of the o.r.d. curve of the resolved ion and the Pfeiffer rotatory dispersion (P.r.d.) curve of the same cation in the solution of the environment compound to conclude that there was an equilibrium shift between the two enantiomers.

Figures 1 and 2 show the rotatory dispersion curves of solutions containing $M(C_2O_4)_3^{3-}$ ion in cinchonine hydrochloride, and solutions containing the same amount of environment compound alone. The Pfeiffer rotation of $Al(C_2O_4)_3^{3-}$, $Fe(C_2O_4)_3^{3-}$, and $Ir(C_2O_4)_3^{3-}$ shown in Figs. 3 and 4 varies smoothly with respect to the wavelength, whereas a Cotton effect was observed in both the Pfeiffer rotatory dispersion curves of $Cr(C_2O_4)_3^{3-}$ and $Co(C_2O_4)_3^{3-}$ in the wavelength range corresponding to their $^4A_{2g} \rightarrow {}^1T_{2g}$ and $^1A_{1g} \rightarrow {}^1T_{1g}$ magnetic-dipole-allowed d–d transition, respectively. A comparison of the o.r.d. curves of the resolved D(+)-$[Cr(C_2O_4)_3]^{3-}$ and D(−)-$[Co(C_2O_4)_3]^{3-}$ with the Pfeiffer rotatory dispersion curves of the corresponding anions is shown in Figs. 5 and 6. The o.r.d. of the resolved D(+)-$[Ir(C_2O_4)_3]^{3-}$ shows a Cotton effect near 475 mμ. However, the Pfeiffer rotatory dispersion curve of the same ion

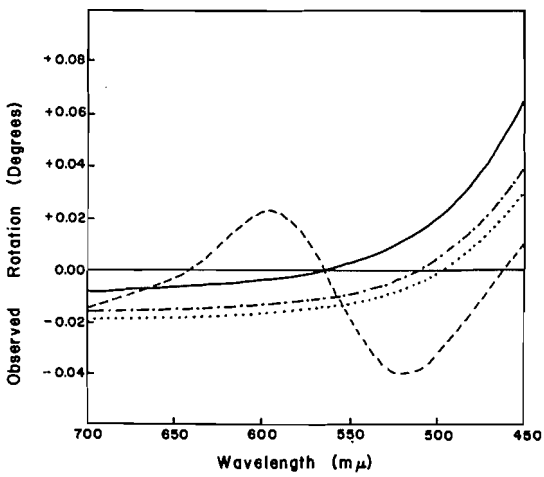

FIG. 1. Comparison of o.r.d. curves of $Al(C_2O_4)_3^{3-}$, $Fe(C_2O_4)_3^{3-}$, and $Cr(C_2O_4)_3^{3-}$ in cinchonine hydrochloride (CH) in a 5 cm cell at 23 °C. (A 9.16×10^{-4} *M* alcoholic solution of 1-menthol was placed in series with the 5 cm cell.) —, 2×10^{-2} *M* CH; ·····, 2×10^{-2} *M* $Al(C_2O_4)_3^{3-}$ + 2×10^{-2} *M* CH; ····, 1.5×10^{-2} *M* $Fe(C_2O_4)_3^{3-}$ + 2×10^{-2} *M* CH; ---, 5×10^{-3} *M* $Cr(C_2O_4)_3^{3-}$ + 2×10^{-2} *M* CH.

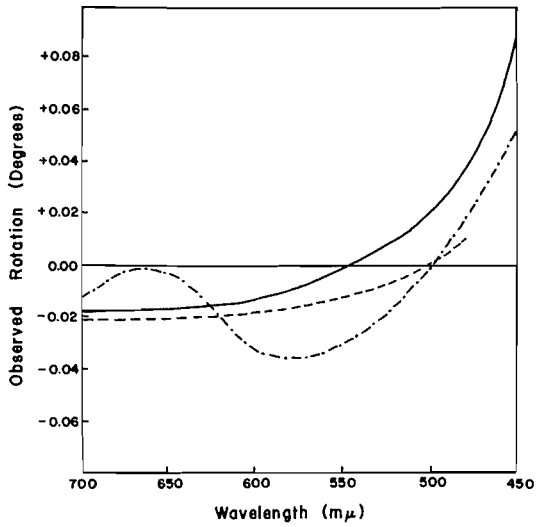

FIG. 2. Comparison of the o.r.d. curves of $Co(C_2O_4)_3^{3-}$ and $Ir(C_2O_4)_3^{3-}$ in cinchonine hydrochloride (CH) in a 5 cm cell at 23 °C. (A 1.34×10^{-3} *M* alcoholic solution of l-menthol in a 1 cm cell was placed in series with the 5 cm cell.) —, 3×10^{-2} *M* CH; ·····, 2×10^{-3} *M* $Co(C_2O_4)_3^{3-}$ + 3×10^{-2} *M* CH; ---, 5×10^{-3} *M* $Ir(C_2O_4)_3^{3-}$ + 1.5×10^{-2} *M* CH.

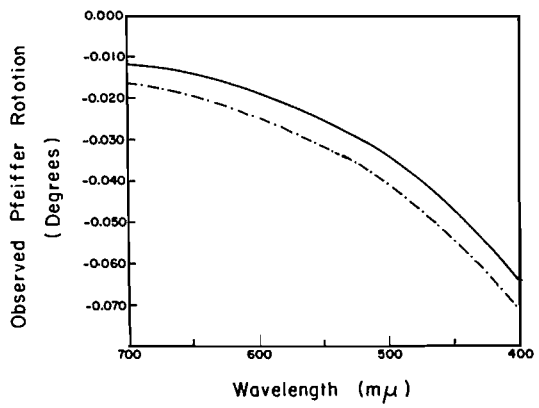

FIG. 3. Pfeiffer rotatory dispersion curves of 2×10^{-2} *M* cinchonine hydrochloride with: —, 2×10^{-2} *M* $Al(C_2O_4)_3^{3-}$, and ·····, 1.5×10^{-2} *M* $Fe(C_2O_4)_3^{3-}$ in a 1 dm cell at 23 °C.

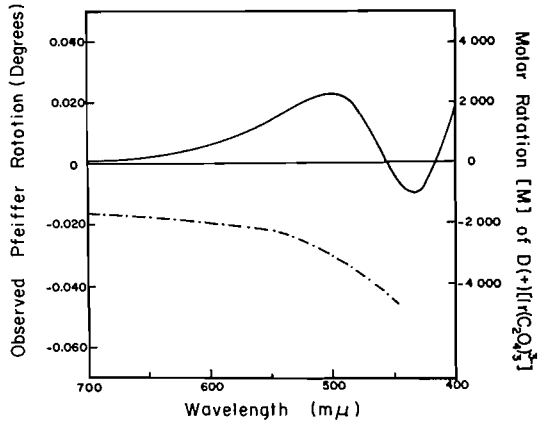

FIG 4. Comparison of the o.r.d. and Pfeiffer rotatory dispersion (P.r.d.) curves of $Ir(C_2O_4)_3^{3-}$. —, o.r.d. curve of D(+)-$[Ir(C_2O_4)_3^{3-}]$. ·····, P.r.d. curve of 5×10^{-3} *M* $Ir(C_2O_4)_3^{3-}$ + 1.5×10^{-2} *M* CH in a 1 dm cell at 23 °C.

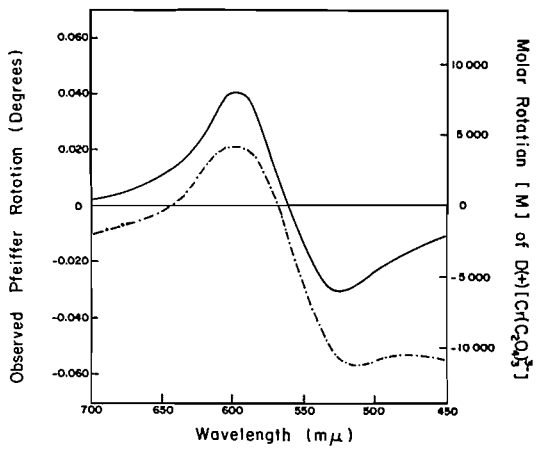

FIG. 5. Comparison of the o.r.d. and the Pfeiffer rotatory dispersion (P.r.d.) curves of $Cr(C_2O_4)_3^{3-}$. —, o.r.d. curve of D(+)-$[Cr(C_2O_4)_3^{3-}]$. ·····, P.r.d. curve of 5×10^{-3} *M* $Cr(C_2O_4)_3^{3-}$ + 2×10^{-2} *M* CH in a 5 cm cell at 23 °C.

does not indicate such an effect, as can be seen in Fig. 4. This is a strong indication that the occurrence of the Pfeiffer effect in systems containing the different trisoxalatometallate(III) complexes does not result from the same source.

In the case of trisoxalatoiridate(III) anion, the inertness of the compound makes the equilibrium shift very unlikely. In view of the stability of the optical isomers of this anion (17), we compared the Pfeiffer rotation of D-, L-, and DL-$[Ir(C_2O_4)_3]^{3-}$ with the same amount of cinchonine hydrochloride and found that the Pfeiffer rotations of all three species were equal within experimental error. This result, together with the absence of a Cotton effect in the Pfeiffer rotatory dispersion curve, rules out any shift in equilibrium between the two enantiomers in solution for the

Can. J. Chem. Downloaded from www.nrcresearchpress.com by 210.87.254.40 on 09/05/12
For personal use only.

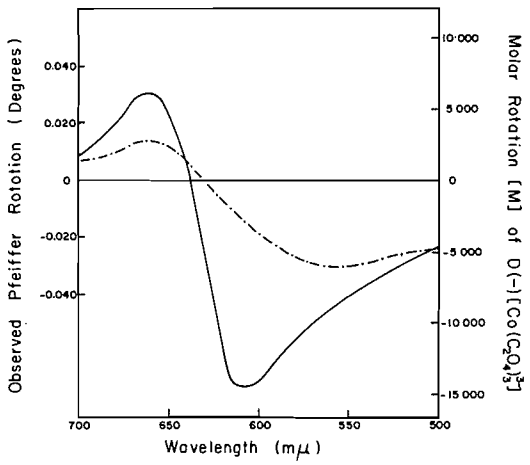

FIG. 6. Comparison of the o.r.d. and the Pfeiffer rotatory dispersion (P.r.d.) curves of $Co(C_2O_4)_3^{3-}$. —, o.r.d. curve of D(−)-$[Co(C_2O_4)_3^{3-}]$. ·····, P.r.d. curve of 2×10^{-3} *M* $Co(C_2O_4)_3^{3-}$ + 3×10^{-2} *M* CH in a 5 cm cell at 23 °C.

iridium system and leaves association as the operative mechanism.

Cinchonine hydrochloride, dissolved in aqueous solution, exists mainly as monoprotonated and diprotonated ions (18). At a p*H* of 6, the monoprotonated cinchonium ion is predominant and it is quite probable that there is an association between this positively charged cinchoninium ion and the negatively charged complex ion in solution (19). In addition, there is also a probability that hydrogen bonding occurs between the cinchoninium ion and the oxalate ligands surrounding the metal.

Experimentally, we found no change in the two d–d transition bands of either the $Co(C_2O_4)_3^{3-}$ or the $Cr(C_2O_4)_3^{3-}$ ion upon the addition of cinchonine hydrochloride. Yet the absorption coefficient of the first charge transfer band of the cinchoninium ion at 315.5 mμ increased from 3.50×10^3 to 3.61×10^3 upon the addition of 1.5×10^{-3} *M* $Al(C_2O_4)_3^{3-}$ to 5×10^{-4} *M* of cinchonine hydrochloride. Therefore, considering association only, the Pfeiffer rotation is likely due to a perturbation of the cinchoninium ion energy levels, not to any distortions of the complex. Unfortunately, the studies on the effect of the d–d transition cannot be extended to the other trisoxalato complexes in the series because they do not have a well-defined absorption band in the visible region. On the other hand, $Al(C_2O_4)_3^{3-}$ is the only choice for the investigation of the variation of the first charge transfer band of the cinchonine hydrochloride, since the other complexes absorb strongly near 135 mμ.

In metal complexes containing optically active ligands, Larsen and Olsen tentatively proposed that an induced Cotton effect in a d–d transition of a transition metal complex will only be of measurable magnitude if the asymmetric ligand is a chelate (20). (Exceptional results of some induced optical activity using monodentate ligands has been reported (21).) Mason and Norman speculated that chelate hydrogen bonding between an optically inactive complex and an optically active ion can induce a Cotton effect (22). It is not very likely, in view of the structure of cinchonine, that this optically active species can act as a chelate. Association alone, therefore, will not likely explain the origin of the induced Cotton effect observed in the trisoxalatochromate(III) ion in aqueous cinchonine hydrochloride solution. In the case of the labile trisoxalatochromate(III) and trisoxalatocobaltate(III) complexes, a first order equilibrium shift between the dextro and levo enantiomers appears to take place through an association of the complex ion with the cinchoninium ion in solution, in agreement with the conclusions reached by Bosnich (23), Kirschner and Ahmad (24), and Brasted *et al.* (10).

Both trisoxalatochromate(III) and trisoxalatocobaltate(III) anion show a positive Pfeiffer rotatory dispersion curve, indicating that the equilibrium shift is in favor of the D-enantiomer. A closer comparison of the resolved o.r.d. curve of the D(+)-$[Cr(C_2O_4)_3]^{3-}$ to the Pfeiffer rotatory dispersion curve of the same anion (Fig. 5) reveals that, besides the striking similarity in shape of these two curves, the ratio of the peak-to-trough for the o.r.d. curve is not the same as that for the P.r.d. curve, so that the whole P.r.d. curve seems to shift down to the negative side. The crossover wavelength (at which the optical rotation is zero) for the P.r.d. curve is higher than that for the o.r.d. curve. Moreover, at shorter wavelengths (below 525 mμ), the P.r.d. curve tends to level off. If an association between the Cr(III) complex anion and the cinchoninium ion does occur in addition to the equilibrium shift, we would expect that the contribution of the association alone will yield a Pfeiffer rotatory dispersion curve

Can. J. Chem. Downloaded from www.nrcresearchpress.com by 210.87.254.40 on 09/05/12
For personal use only.

similar to the one observed in the iridium(III) case (Fig. 4). When we subtracted this contribution from the observed P.r.d. curve, we were able to obtain a partial P.r.d. curve due to equilibrium shift alone, which was more similar in shape to the resolved o.r.d. curve, and in this way accounted for the differences observed between the o.r.d. and the P.r.d. curve mentioned above.

This similarity between the o.r.d. curve of the resolved D(−)-$[Co(C_2O_4)_3]^{3-}$ and the Pfeiffer rotatory dispersion curve of the same anion is not as good, and the amplitude of the Cotton effect is smaller (Fig. 6), probably because there is a lesser degree of equilibrium shift owing to the greater inertness of the system. This, together with the high absorptivity of the complex, reduces the accuracy of the measurement. Moreover, the two different forms of the trisoxalatocobaltate anion known to exist in aqueous solution (25, 26) may interact differently with the environment. The same arguments may also be applied to the trisoxalatoaluminate(III) and trisoxalatoferrate-(III) systems. However, the lack of a compatibly strong magnetic-dipole-allowed d–d transition in these two complexes minimizes the influence of the equilibrium shift contribution to the Pfeiffer rotatory dispersion curve, so that the P.r.d. curves of the $Al(C_2O_4)_3^{3-}$, $Fe(C_2O_4)_3^{3-}$, and $Ir(C_2O_4)_3^{3-}$ are similar in shape.

In summary, it seems that the combination of an association and an equilibrium shift can successfully be used to account for the observed Pfeiffer rotation in these systems, as concluded by Brasted *et al.* (10), and most recently by Doron *et al.* (27).

The authors wish to thank Dr. D. Idler and Mr. D. Ellis of the Fisheries Research Board in Halifax for the use of their Durum-Jasco Spectropolarimeter and the National Research Council of Canada for financial support.

1. P. Pfeiffer and K. Quehl. Ber. **64**, 2667 (1931).
2. P. Pfeiffer and K. Quehl. Ber. **65**, 560 (1932).
3. P. Pfeiffer and Y. Nakatsuka. Ber. **66**, 415 (1933).
4. S. Kirschner, N. Ahmad, and K. Magnell. Coord. Chem. Rev. **3**, 201 (1968).
5. S. Kirschner and N. Ahmad. *In* Coordination chemistry. *Edited by* S. Kirschner. Plenum Press, N.Y. 1969. pp. 42ff.
6. F. P. Dwyer, E. C. Gyarfas, and M. F. O'Dwyer. Nature, **167**, 1036 (1951).
7. R. C. Brasted. Ph.D. Thesis. University of Minnesota Duluth, Minnesota. 1942.
8. V. J. Landis. Ph.D. Thesis. University of Minnesota Duluth, Minnesota. 1957.
9. P. Nordquist, Jr. Ph.D. Thesis. University of Minnesota Duluth, Minnesota. 1964.
10. R. C. Brasted, V. J. Landis, E. J. Kuhajek, P. E. R. Nordquist, Jr., and L. Mayer. *In* Coordination chemistry. S. Kirschner (*Editor*) Plenum Press, N.Y. 1969. pp. 64ff.
11. H. S. Booth (*Editor-in-Chief*). Inorganic synthesis. Vol. 1. McGraw-Hill Inc., New York and London. 1939. pp. 35–37.
12. K. Jorgensen. Acta Chem. Scand. **10**, 500 (1956).
13. F. P. Dwyer and A. M. Sargeson. J. Phys. Chem. **60**, 1331 (1956).
14. K. V. Krishnamurty and G. M. Harris. Chem. Rev. **61**, 213 (1961).
15. E. J. Kuhajek. Ph.D. Thesis. University of Minnesota Duluth, Minnesota. 1962.
16. S. Kirschner and K. R. Magnell. Adv. Chem. **62**, 366 (1966).
17. M. Billardon. J. Chem. Phys. **61**, 1070 (1964).
18. E. B. R. Prideaux and F. T. Winfield. J. Chem. Soc. 1587 (1930).
19. M. T. Beck. Coord. Chem. Rev. **3**, 91 (1968).
20. E. Larsen and I. Olsen. Acta Chem. Scand. **18**, 1025 (1964).
21. C. J. Hawkins and P. J. Lawson. Inorg. Chem. **9**, 6 (1970).
22. S. F. Mason and B. J. Norman. Chem. Commun. 335 (1965).
23. B. Bosnich. J. Am. Chem. Soc. **89**, 6143 (1967).
24. S. Kirschner and N. Ahmad. J. Am. Chem. Soc. **90**, 1910 (1968).
25. A. J. McCaffery and S. F. Mason. Proc. Chem. Soc. 388 (1962).
26. R. D. Gillard, S. H. Laurie, and P. R. Mitchell. J. Chem. Soc. A, 3006 (1969).
27. V. Doron, W. Durham, and D. Frazier. Inorg. Nucl. Chem. Lett. **7**, 91 (1971).

Can. J. Chem. Downloaded from www.nrcresearchpress.com by 210.87.254.40 on 09/05/12
For personal use only.

The Number of Hydride Ions in AlH_2Cl Available for Hydrogenolysis of 1,3-Dioxolanes[1]

H. A. DAVIS AND R. K. BROWN
Department of Chemistry, University of Alberta, Edmonton, Alberta

Received January 22, 1971

2-Methyl-1,3-dioxolane (**1**) in ether is hydrogenolyzed completely to 2-ethoxyethanol by an equimolar proportion of AlH_2Cl, whereas a 1/2 mol of AlH_2Cl hydrogenolyzes 1 mol of **1** only to the extent of 50%. In the latter case, the intermediate compound 2-ethoxyethoxyhydridoaluminum chloride ($C_2H_5OCH_2CH_2OAlHCl$) formed with half of the 2-methyl-1,3-dioxolane, even though it contains a hydride ion, fails to react with the remainder of the dioxolane. This is believed due to the preference of $C_2H_5OCH_2CH_2OAlHCl$ to form an internal Lewis acid–base complex rather than form a similar complex with **1**, a step essential to facilitate the hydrogenolysis of **1**.

La réaction dans l'éther entre le méthyl-2 dioxolane-1,3 (**1**) et une proportion molaire de AlH_2Cl conduit à l'éthoxy-2 éthanol provenant d'une hydrogénolyse complète; par ailleurs l'action d'une demi-mole de AlH_2Cl sur une mole de **1** conduit à une hydrogénolyse de 50% de ce composé. Dans ce cas, le composé intermédiaire ($C_2H_5OCH_2CH_2OAlHCl$) formé avec la moitié du dioxolane **1** contient encore un ion hydrure mais il ne réagit toutefois pas avec le restant du dioxolane. On croit que ce phénomène est dû à la préférence de l'intermédiaire à former un complexe de Lewis interne plutôt que de former avec **1** un complexe semblable qui est essentiel pour faciliter l'hydrogénolyse de **1**.

Canadian Journal of Chemistry, 49, 2166 (1971)

In connection with a study of the $LiAlH_4$–$AlCl_3$ (mixed hydride) reductive cleavage of 1,3-dioxolanes in this laboratory, we have found that 2-methyl-1,3-dioxolane (**1**, Scheme 1) is converted completely to 2-ethoxyethanol **4** in less than 30 min by an *equimolar* proportion of dihydridoaluminum chloride, AlH_2Cl.[2] However, no more than 50% conversion of **1** to **4** could be obtained if a *half molar* proportion of AlH_2Cl was used, even if the reaction time was extended to 48 h. In accordance with the views concerning the course of the reductive cleavage of 1,3-dioxolanes (1, 2), the reaction of AlH_2Cl with **1** first involves formation of a complex **2** due to the Lewis acidity of AlH_2Cl, and this complex subsequently forms an alkoxyhydridoaluminum chloride **3** (Scheme 1).

Although alkoxyaluminum hydrides have been postulated as intermediates in the ring cleavage of epoxides by the mixed hydride (3, 4) and alkoxyaluminum hydrides have been prepared and used to hydrogenolyze epoxides (5), it appears from our work that **3** cannot hydrogenolyze **1**. That this is so has been shown by the failure to observe any reductive cleavage when an ether solution of **1** was treated for as long as 48 h with **3**, prepared separately by the reaction of AlH_2Cl with an equimolar amount of 2-ethoxyethanol according to directions (5) which describe the preparation of alkoxyaluminum hydrides.

The complete conversion of benzaldehyde to benzyl alcohol by **3** in less than 1 h shows that the single hydride unit in **3** is available for reduction of carbonyl compounds and it is not the *bulk* of reagent **3** which causes its failure to react with **1**. Furthermore, we have also shown that **1** is converted to 2-ethoxyethanol **4** in less than 30 min by the reagent ethoxyhydridoaluminum chloride.

It is known that 1,3-dioxolanes are hydrogenolyzed by $LiAlH_4$ much more readily, and in most cases only, if a Lewis acid is present (ref. 1 and references therein, 6). It is clear that both ethoxyhydridoaluminum chloride and **3** are Lewis acids and thus should be able to form a complex with **1** which would initiate the process of reductive cleavage of **1** to **4**. The fact that ethoxyhydridoaluminum chloride rapidly hydrogenolyzes **1** to **4** while **3** apparently fails to do so strongly suggests that the internal structure of **3** is responsible for

[1]Taken from the thesis of H. A. Davis, presented to the Faculty of Graduate Studies at the University of Alberta in partial fulfilment of the requirements for the Ph.D. degree, 1970.

[2]That the reducing species present in the ether solutions obtained by mixing equimolar quantities of $AlCl_3$ and $LiAlH_4$ was AlH_2Cl and not $AlHCl_2$ or AlH_3 was shown by the infrared spectrum of the resulting solution which showed an absorption band only at 5.39 μ characteristic of Al–H_2 stretching frequency. The bands at 5.59 and 5.23 μ characteristic of AlH_3 and $AlHCl_2$ were not detected (3, 6).

Can. J. Chem. Downloaded from www.nrcresearchpress.com by 210.87.254.40 on 09/05/12
For personal use only.

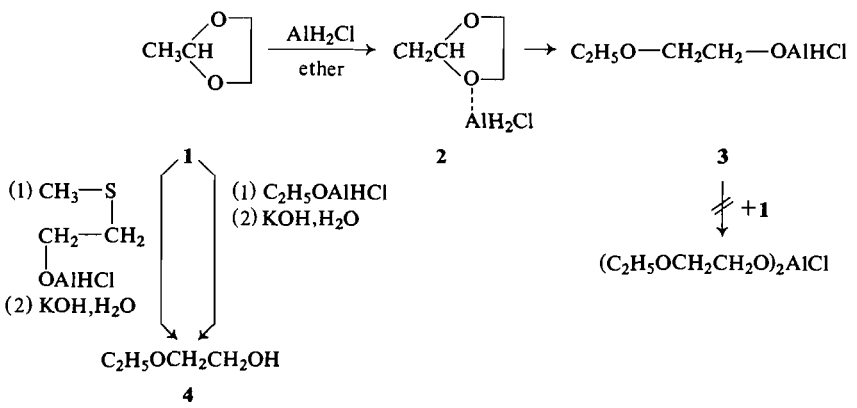

SCHEME 1

the latter's failure to react with **1** and that it is not due to the tendency to form polymeric structures as has been found to occur with alkoxyaluminum hydrides (5). Our view is that **3** forms an internal complex such as **A**(X = O) in preference to the formation of a complex such as **2** with **1**. In support of this proposal, it is found that **1** is converted

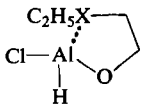

to **4** to the extent of 50% in 1 h by reaction with an equimolar proportion of (2-methylthio)ethoxyhydridoaluminum chloride, the homolog and sulfur analog of **3**. On the basis of the finding that 1,3-oxathiolanes are reductively cleaved at the C—O but not the C—S bond by mixed hydrides (7, 8) presumably because of the great preference of the Lewis acid to complex with the oxygen rather than the sulfur atom (8), the reagent (2-methylthio)ethoxyhydridoaluminum chloride is believed to prefer complex formation with the oxygen atom of **1** rather than with its own sulfur atom to form an internal complex such as **A**(X = S).

Experimental

Boiling points are uncorrected.

Elemental analyses were made by Mrs. Darlene Mahlow of this Department.

Infrared spectra were recorded on a Perkin–Elmer Model 21 instrument.

Proton magnetic resonance (p.m.r.) spectra were recorded on a Varian Associates A-60 instrument by Mr. R. Swindlehurst of this Department. All spectra were referred to tetramethylsilane.

Gas liquid chromatographic (g.l.c.) analyses were made with an F and M Model 700 instrument equipped with a 12 ft × 1/8 in. column packed with butanediol succinate, 20% on Gas Chrom P (60–80 mesh) or silicone rubber SE30, 20% on Gas Chrom P (60–80 mesh). Helium was the carrier gas at a flow rate of ~ 40 ml/min. The column temperature depended upon the boiling point of the compounds analyzed. For some cases the temperature was linearly programmed to achieve better resolution, the temperature being increased at the rate of 7.5°/min starting from 80°.

Solvents were removed by rotary evaporator under vacuum. Ether solutions were dried with anhydrous magnesium sulfate.

2-Ethoxyethanol was obtained from Eastman Kodak Co.

2-Methyl-1,3-dioxolane (1) was prepared by the procedure of Hibbert and Timm (9). B.p. 72° at 700 mm; η_D^{25} 1.3962. Lit. b.p., 83–85° at 700 mm (9).

2,Methylthioethanol

To a solution of 39 g (0.5 mol) of 2-mercaptoethanol in 300 ml of dry 1,2-dimethoxyethane (DME) was added 12 g (0.5 mol) of sodium hydride. The resulting mixture was stirred at room temperature for 2 h whereupon methyl iodide (71 g, 0.5 mol) was added slowly. The mixture was stirred overnight at room temperature and then the solids removed by filtration and the filtrate dried and freed from solvent. The residue was dissolved in 200 ml of ether, the solution separated from precipitated solids and the filtrate freed from ether. Distillation of the residue gave 25 g (54%) of colorless liquid, b.p., 78° at 30 mm, η_D^{24} 1.4869. Lit. b.p., 61° at 10 mm, η_D^{20} 1.4930 (10).

Hydrogenolysis of 2-Methyl-1,3-dioxolane (1) with AlH_2Cl

The procedure employed was that described by Diner (11).

Lithium aluminum hydride (0.57 g, 0.015 mol) was dissolved in 15 ml of dry ether and the solution cooled to 5° in an ice bath. To this was added, dropwise, an ether solution of aluminum chloride prepared by adding anhydrous aluminum chloride (1.99 g, 0.015 mol) in small portions to 15 ml of dry ether at 5°. The resulting mixed hydride (AlH_2Cl) solution (3, 6) was stirred at room temperature for 15 min and then 0.03 mol of **1** was added. The reaction mixture was stirred at room tem-

Can. J. Chem. Downloaded from www.nrcresearchpress.com by 210.87.254.40 on 09/05/12
For personal use only.

perature for 30 min and then treated dropwise with a 15% aqueous solution of potassium hydroxide until no further reaction occurred. The colorless solid (lithium aluminate) was separated by filtration under suction, and the ether removed from the filtrate. The residue was analyzed by g.l.c. Only 2-ethoxyethanol was found in the product, in a yield of at least 90%, according to g.l.c. retention time and signal area compared with those of an authentic sample.

Hydrogenolysis of **1** *with Alkoxyhydridoaluminum Chloride*

The same procedure as that above, using AlH_2Cl, was employed except that before the addition of the dioxolane **1**, one molar equivalent of the requisite alcohol was added dropwise to the solution of AlH_2Cl in ether and the mixture then stirred for 15 min. Compound **1** was then added and the remainder of the procedure above was followed.

Hydrogenation of **1** was carried out using the following anhydrous alcohols (*a*) ethanol, (*b*) 2-ethoxyethanol, (*c*) 2-methylthioethanol.

The authors wish to thank the National Research Council of Canada for their financial assistance in this work. One of us, H.A.D., thanks the National Research Council of Canada for the award of a bursary for the academic year 1969–1970.

1. B. E. LEGGETTER and R. K. BROWN. Can. J. Chem. **42**, 990 (1964).
2. B. E. LEGGETTER and R. K. BROWN. Can. J. Chem. **43**, 1030 (1965).
3. E. C. ASHBY and J. PRATHER. J. Am. Chem. Soc. **88**, 729 (1966).
4. P. T. LANSBURY, D. J. SCHARF, and V. A. PATTISON. J. Org. Chem. **32**, 1748 (1967).
5. B. COOKE, E. C. ASHBY, and J. LOTT. J. Org. Chem. **33**, 1132 (1968).
6. U. E. DINER, H. A. DAVIS, and R. K. BROWN. Can. J. Chem. **45**, 207 (1967).
7. E. L. ELIEL, V. G. BADDING, and L. A. PILATO. J. Am. Chem. Soc. **84**, 2377 (1962).
8. B. E. LEGGETTER and R. K. BROWN. Can. J. Chem. **41**, 2671 (1963).
9. H. HIBBERT and J. A. TIMM. J. Am. Chem. Soc. **46**, 1286 (1924).
10. M. SELIM-DORGANS, M. SELIM, and H. GAULT. Compt. rend. **244**, 1047 (1957). Chem. Abstr. **51**, 1206a (1957).
11. U. E. DINER. Ph.D. Thesis. University of Alberta, Edmonton, Alberta, Canada. 1967. p. 169.

Reaction of Xenon Difluoride with Organosilicon Compounds

J. A. GIBSON[1] AND A. F. JANZEN

Department of Chemistry, University of Manitoba, Winnipeg, Manitoba

Received September 22, 1970

The reaction of xenon difluoride in acetonitrile solution with some organosilicon compounds is reported.

On rapporte les résultats obtenus lors de la réaction du difluorure de Xenon en solution dans l'acétonitrile avec quelques composés organiques du silicium.

Canadian Journal of Chemistry, **49**, 2168 (1971)

Xenon difluoride was recently found to be a useful reagent for aromatic substitution reactions in the liquid phase, in the presence of hydrogen fluoride as catalyst (1), as well as in the vapor phase at temperatures 100–200° (2).

We are currently studying the reaction of xenon difluoride with organometallic compounds and wish to report reactions with organosilicon compounds containing Si—Cl, Si—H, Si—C-(allyl), and Si—O bonds. Reactions were carried out with approximately 0.5 *M* solutions of XeF_2 in acetonitrile. These solutions were stable indefinitely at −78° but decomposed slowly at room temperature (see Experimental).

The reaction of xenon difluoride with organosilicon chlorides occurred readily, within 3 to 9 min, to give organosilicon fluorides.

[1] $2R_3SiCl + XeF_2 \rightarrow 2R_3SiF + Cl_2 + Xe$
$R_3Si = (CH_3)_3Si, (C_2H_5)_3Si, C_6H_5(CH_3)_2Si$

[2] $(CH_3)_2SiCl_2 + XeF_2 \rightarrow (CH_3)_2SiF_2 + Cl_2 + Xe$

Organosilicon fluorides were identified by their characteristic ^{19}F and ^{1}H nuclear magnetic resonance (n.m.r.) spectra, xenon by mass

[1]Holder of Alcan Fellowship, 1970.

Can. J. Chem. Downloaded from www.nrcresearchpress.com by 210.87.254.40 on 09/05/12
For personal use only.

perature for 30 min and then treated dropwise with a 15% aqueous solution of potassium hydroxide until no further reaction occurred. The colorless solid (lithium aluminate) was separated by filtration under suction, and the ether removed from the filtrate. The residue was analyzed by g.l.c. Only 2-ethoxyethanol was found in the product, in a yield of at least 90%, according to g.l.c. retention time and signal area compared with those of an authentic sample.

Hydrogenolysis of **1** *with Alkoxyhydridoaluminum Chloride*

The same procedure as that above, using AlH_2Cl, was employed except that before the addition of the dioxolane **1**, one molar equivalent of the requisite alcohol was added dropwise to the solution of AlH_2Cl in ether and the mixture then stirred for 15 min. Compound **1** was then added and the remainder of the procedure above was followed.

Hydrogenation of **1** was carried out using the following anhydrous alcohols (*a*) ethanol, (*b*) 2-ethoxyethanol, (*c*) 2-methylthioethanol.

The authors wish to thank the National Research Council of Canada for their financial assistance in this work. One of us, H.A.D., thanks the National Research Council of Canada for the award of a bursary for the academic year 1969–1970.

1. B. E. LEGGETTER and R. K. BROWN. Can. J. Chem. **42**, 990 (1964).
2. B. E. LEGGETTER and R. K. BROWN. Can. J. Chem. **43**, 1030 (1965).
3. E. C. ASHBY and J. PRATHER. J. Am. Chem. Soc. **88**, 729 (1966).
4. P. T. LANSBURY, D. J. SCHARF, and V. A. PATTISON. J. Org. Chem. **32**, 1748 (1967).
5. B. COOKE, E. C. ASHBY, and J. LOTT. J. Org. Chem. **33**, 1132 (1968).
6. U. E. DINER, H. A. DAVIS, and R. K. BROWN. Can. J. Chem. **45**, 207 (1967).
7. E. L. ELIEL, V. G. BADDING, and L. A. PILATO. J. Am. Chem. Soc. **84**, 2377 (1962).
8. B. E. LEGGETTER and R. K. BROWN. Can. J. Chem. **41**, 2671 (1963).
9. H. HIBBERT and J. A. TIMM. J. Am. Chem. Soc. **46**, 1286 (1924).
10. M. SELIM-DORGANS, M. SELIM, and H. GAULT. Compt. rend. **244**, 1047 (1957). Chem. Abstr. **51**, 1206a (1957).
11. U. E. DINER. Ph.D. Thesis. University of Alberta, Edmonton, Alberta, Canada. 1967. p. 169.

Reaction of Xenon Difluoride with Organosilicon Compounds

J. A. GIBSON[1] AND A. F. JANZEN

Department of Chemistry, University of Manitoba, Winnipeg, Manitoba

Received September 22, 1970

The reaction of xenon difluoride in acetonitrile solution with some organosilicon compounds is reported.

On rapporte les résultats obtenus lors de la réaction du difluorure de Xenon en solution dans l'acétonitrile avec quelques composés organiques du silicium.

Canadian Journal of Chemistry, **49**, 2168 (1971)

Xenon difluoride was recently found to be a useful reagent for aromatic substitution reactions in the liquid phase, in the presence of hydrogen fluoride as catalyst (1), as well as in the vapor phase at temperatures 100–200° (2).

We are currently studying the reaction of xenon difluoride with organometallic compounds and wish to report reactions with organosilicon compounds containing Si—Cl, Si—H, Si—C-(allyl), and Si—O bonds. Reactions were carried out with approximately 0.5 *M* solutions of XeF_2 in acetonitrile. These solutions were stable indefinitely at −78° but decomposed slowly at room temperature (see Experimental).

The reaction of xenon difluoride with organosilicon chlorides occurred readily, within 3 to 9 min, to give organosilicon fluorides.

[1] $2R_3SiCl + XeF_2 \rightarrow 2R_3SiF + Cl_2 + Xe$
$R_3Si = (CH_3)_3Si, (C_2H_5)_3Si, C_6H_5(CH_3)_2Si$

[2] $(CH_3)_2SiCl_2 + XeF_2 \rightarrow (CH_3)_2SiF_2 + Cl_2 + Xe$

Organosilicon fluorides were identified by their characteristic ^{19}F and ^{1}H nuclear magnetic resonance (n.m.r.) spectra, xenon by mass

[1]Holder of Alcan Fellowship, 1970.

Can. J. Chem. Downloaded from www.nrcresearchpress.com by 210.87.254.40 on 09/05/12
For personal use only.

Can. J. Chem. Downloaded from www.nrcresearchpress.com by 210.87.254.40 on 09/05/12
For personal use only.

spectrometry, and chlorine by reaction with cyclohexene and styrene.

The products $(CH_3)_3SiF$ and $(C_2H_5)_3SiF$ were formed in quantitative yield and no evidence was found for reaction of XeF_2 with Si—C or C—H bonds.

Lower yields were found for $(CH_3)_2SiF_2$ (70%) and $C_6H_5(CH_3)_2SiF$ (50%) suggesting side reactions and, in each case, chloromethyl derivatives $CH_3(CH_2Cl)SiF_2$ and $C_6H_5(CH_3)(CH_2Cl)$-SiF were formed in about 25% yield. Reaction of chlorine with C—H bonds in organosilicon compounds is well known (3) and the reactivity of chlorine must be taken into account in any reaction of XeF_2 with Si—Cl bonds.

When the reaction of XeF_2 was extended to compounds containing Si—H, Si—C(allyl), and Si—O bonds, no reaction was apparent within about 1 h. After considerably longer reaction times organosilicon fluorides were formed, but additional experiments suggested that XeF_2 was not reacting directly with these bonds.

For example, xenon difluoride did not react appreciably within 1 h when reactions with trimethylsilane, triphenylsilane, allyltrimethylsilane, and dimethyldiethoxysilane were attempted. On the other hand, if a Si—Cl bond was present in similar compounds, reaction occurred within several minutes. Thus reaction of methylphenylchlorosilane, $C_6H_5(CH_3)SiHCl$, and XeF_2 gave $C_6H_5(CH_3)SiF_2$ within 3 min in quantitative yield. It seems reasonable that a stepwise reaction is occurring in which Cl_2, produced as in reaction 1, converts the Si—H to a Si—Cl bond (ref. 3, p. 209) and the Si—Cl bond reacts further with XeF_2.

$$[3]\quad \overset{H}{\underset{|}{R_2Si}}Cl \xrightarrow{XeF_2} \overset{H}{\underset{|}{R_2Si}}F \xrightarrow{Cl_2} \overset{Cl}{\underset{|}{R_2Si}}F \xrightarrow{XeF_2} R_2SiF_2$$

In support of stepwise reaction 3 it is found that increasing the ratio $C_6H_5(CH_3)SiHCl:XeF_2$ to 6:1 permits formation of intermediate C_6H_5-$(CH_3)SiHF$ in 60% yield. In this case any Cl_2 produced could react with excess starting material rather than with the intermediate.

When allyldimethylchlorosilane, $(CH_3)_2Si(Cl)$-$CH_2CH{=}CH_2$, was allowed to react with XeF_2, dimethyldifluorosilane was quantitatively formed within 6 min and at the same time allyl chloride was formed in 60% yield. Reaction again appears to go stepwise, as in eq. 4, since it was found that

$$[4]\quad (CH_3)_2\overset{Cl}{\underset{|}{Si}}CH_2CH{=}CH_2 \xrightarrow{XeF_2} (CH_3)_2\overset{F}{\underset{|}{Si}}CH_2CH{=}CH_2 \xrightarrow{Cl_2} (CH_3)_2\overset{F}{\underset{|}{Si}}Cl \xrightarrow{XeF_2} (CH_3)_2SiF_2$$

allyltrimethylsilane and XeF_2 did not react within 1 h. If chlorine is bubbled through a 10% solution of allyldimethylchlorosilane in acetonitrile, cleavage occurs readily at 0–20° to give allyl chloride and dimethyldichlorosilane. Chlorine may also add to allylsilanes under different conditions (ref. 3, pp. 141, 390).

Xenon difluoride and dimethyldiethoxysilane, $(CH_3)_2Si(OC_2H_5)_2$, did not react within 1 h. After 4 days dimethyldifluorosilane was quantitatively produced, but during this time decomposition of XeF_2 in acetonitrile becomes significant and the decomposition product hydrogen fluoride is known to cleave Si—O bonds and give silicon fluorides (4).

In conclusion, xenon difluoride in acetonitrile solution readily converts Si—Cl to Si—F bonds but does not appear to react directly with Si—H, Si—C(allyl), or Si—O bonds. However, end products or decomposition products such as chlorine, hydrogen fluoride or hydrogen chloride may lead to further reaction.

Experimental

General

Organosilicon compounds were purchased from Peninsular Chemresearch with the exception of trimethylsilane which was prepared by reduction of trimethylchlorosilane with lithium tetrahydridoaluminate in dioxane (5) and purified by trap-to-trap distillation. Fluorine (Matheson of Canada) was passed over potassium fluoride to remove traces of hydrogen fluoride and handled in a metal vacuum system. Xenon difluoride was prepared photochemically (6) and dissolved in dried (P_2O_5) and distilled acetonitrile to give approximately 0.5 *M* solutions. These solutions were standardized by reacting aliquots with mercury and weighing the xenon gas produced.

Nuclear magnetic resonance spectra were obtained on a Varian A-56/60A spectrometer using 56.4 and 60 MHz for fluorine and proton, respectively. ^{19}F and ^{1}H chemical shifts are relative to internal trichlorofluoromethane and internal tetramethylsilane in dilute acetonitrile. Mass spectra were determined on a Hitachi Perkin–Elmer RMU-6D mass spectrometer.

Stability of Xenon Difluoride in Acetonitrile

Solutions of xenon difluoride in acetonitrile (0.5 *M*) were stored under vacuum at −78° and appeared stable

indefinitely. Slow decomposition occurred at room temperature in daylight and xenon difluoride was consumed within 10 days, as indicated by ^{19}F n.m.r.

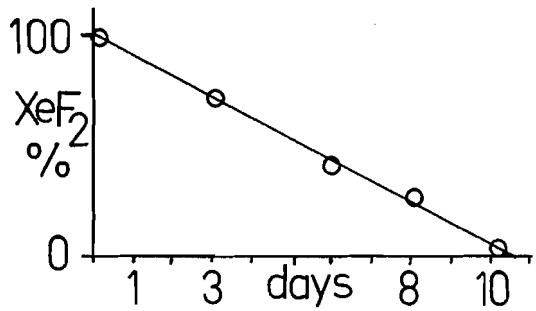

Reaction of Xenon Difluoride in Acetonitrile with Trimethylchlorosilane

In a typical reaction xenon difluoride (0.15 mmol) in 0.30 ml acetonitrile solution was syringed into a standard n.m.r. tube and cooled to −10°. Trimethylchlorosilane (80 mg, 0.74 mmol) was added and the reaction mixture allowed to warm to 40° in the sample probe of the n.m.r. spectrometer. The solution turned light brown and reaction was followed by monitoring the disappearance of XeF_2 (and $^{129}XeF_2$) and appearance of product in the ^{19}F n.m.r. spectrum.

After 3 min all XeF_2 had reacted and trimethylfluorosilane, identified by ^{19}F and ^1H n.m.r. (7, 8), was formed in quantitative yield (based on XeF_2).

The other products were xenon, identified by mass spectrometry, and chlorine, identified by reaction with cyclohexene and styrene.

A similar procedure was used in the reactions described below.

Reaction with Triethylchlorosilane

Xenon difluoride (0.12 mmol) and triethylchlorosilane (43 mg, 0.29 mmol) reacted within 9 min to give triethylfluorosilane, identified by ^{19}F and ^1H n.m.r. (7, 9), in 90% yield.

Reaction with Dimethyldichlorosilane

Xenon difluoride (0.15 mmol) and dimethyldichlorosilane (16 mg, 0.13 mmol) reacted within 4 min to give dimethyldifluorosilane, identified by ^{19}F and ^1H n.m.r. (7, 8), in 70% yield.

Another product was formed in 25% yield. The ^{19}F n.m.r. showed a multiplet at +139 p.p.m. which appeared to be a quartet of triplets, assigned to $CH_3(CH_2Cl)SiF_2$.

Reaction with Dimethylphenylchlorosilane

Xenon difluoride (0.12 mmol) and dimethylphenylchlorosilane (49 mg, 0.29 mmol) reacted within 6 min to give dimethylphenylfluorosilane in 50% yield. Nuclear magnetic resonance spectra could not be found in the literature. The ^{19}F n.m.r. showed a septet at +159 p.p.m., $J_{F-CH_3} = 7.5$ Hz and the ^1H n.m.r. showed a doublet at −0.5 p.p.m., $J_{CH_3-F} = 7.5$ Hz, and phenyl peaks, consistent with the assigned structure.

Another product was formed in 30% yield. The ^{19}F n.m.r. showed a multiplet at +164 p.p.m., which appeared to be a quartet of triplets, assigned to $C_6H_5(CH_3)(CH_2Cl)SiF$.

Reaction with Methylphenylchlorosilane

Xenon difluoride (0.15 mmol) and methylphenylchlorosilane (25 mg, 0.16 mmol) reacted within 3 min to give methylphenyldifluorosilane in quantitative yield. Suitable n.m.r. spectra could not be found in the literature (10). ^{19}F n.m.r. showed a quartet at +136 p.p.m., $J_{F-CH_3} = 6$ Hz and the ^1H n.m.r. showed a triplet at −0.70 p.p.m., $J_{CH_3-F} = 6$ Hz, and phenyl peaks, consistent with the assigned structure.

When the reaction was carried out with a 6:1 molar excess of methylphenylchlorosilane, methylphenyldifluorosilane was formed in only 35% yield. Another product, formed in 60% yield, was identified as the intermediate phenylmethylfluorosilane on the basis of its ^{19}F n.m.r. spectrum which showed a doublet of quartets at +170.8 p.p.m., $J_{F-Si-H} = 58$ Hz and $J_{F-CH_3} = 8$ Hz.

Reaction with Trimethylsilane

Xenon difluoride (0.12 mmol) and trimethylsilane (30 mg, 0.41 mmol) were kept in a sealed n.m.r. tube at room temperature. Examination of the ^{19}F n.m.r. spectrum revealed that approximately 30% of XeF_2 had reacted after 1 h, 70% after 4 h, and 100% after 24 h. At the end of this time trimethylfluorosilane (75%) and unreacted trimethylsilane (0.23 mmol) remained.

Reaction with Triphenylsilane

Xenon difluoride (0.12 mmol) and triphenylsilane (60 mg, 0.25 mmol) did not react within 1 h. After 2 days about 50% of XeF_2 had reacted but products could not be positively identified.

Reaction with Allyldimethylchlorosilane

Xenon difluoride (0.15 mmol) and allyldimethylchlorosilane (19 mg, 0.14 mmol) reacted within 6 min to give dimethyldifluorosilane in quantitative yield. Allyl chloride was formed in at least 60% yield and identified by comparing its ^1H n.m.r. spectrum to that of an authentic sample.

When chlorine was bubbled through a 10% solution of allyldimethylchlorosilane in acetonitrile at 0–20° cleavage occurred readily to give allyl chloride and dimethyldichlorosilane, identified by ^1H n.m.r.

Reaction with Allyltrimethylsilane

Xenon difluoride (0.12 mmol) and allyltrimethylsilane (23 mg, 0.20 mmol) did not react within 1 h. After 4 days all XeF_2 had reacted and trimethylfluorosilane (0.10 mmol, 42%) was identified. The yield varied and seemed to be affected by light. Other products could not be identified.

Reaction with Dimethyldiethoxysilane

Xenon difluoride (0.15 mmol) and dimethyldiethoxysilane (27 mg, 0.18 mmol) did not react within 1 h. After 4 days dimethyldifluorosilane was produced in quantitative yield. Ethanol was also identified by ^1H n.m.r.

Reaction with Hexaphenyldisilane

Hexaphenyldisilane (100 mg, 0.19 mmol) is insoluble in acetonitrile and shaking with XeF_2 solution (0.15 mmol) at room temperature for 3 days gave no products containing Si—F bonds.

We wish to thank Dr. L. Stein, Argonne National Laboratories, for valuable advice concerning techniques of handling fluorine compounds. We also thank the

Can. J. Chem. Downloaded from www.nrcresearchpress.com by 210.87.254.40 on 09/05/12
For personal use only.

National Research Council of Canada for financial assistance.

1. M. J. SHAW, H. H. HYMAN, and R. FILLER. J. Am. Chem. Soc. **91**, 1563 (1969); **92**, 6498 (1970); M. J. SHAW, J. A. WEIL, H. H. HYMAN, and R. FILLER. J. Am. Chem. Soc. **92**, 5096 (1970).
2. D. R. MACKENZIE and J. FAJER. J. Am. Chem. Soc. **92**, 4994 (1970).
3. C. EABORN. Organosilicon compounds. Butterworths, London. 1960. pp. 124, 379–382.
4. C. EABORN. J. Chem. Soc. 2846 (1952).
5. S. TANNENBAUM, S. KAYE, and G. F. LEWENZ. J. Am. Chem. Soc. **75**, 3753 (1953).
6. J. H. HOLLOWAY. J. Chem. Educ. **43**, 202 (1966).
7. E. A. V. EBSWORTH. Volatile silicon compounds. Pergamon, New York. 1963. p. 56.
8. H. SCHMIDBAUR. Chem. Ber. **98**, 83 (1965); F. KLANBERG and E. L. MUETTERTIES. Inorg. Chem. **7**, 155 (1968).
9. H. SCHMIDBAUR and F. SCHINDLER. J. Organomet. Chem. **2**, 466 (1964).
10. V. A. PESTUNOVICH, A. N. EGOROCHKIN, M. G. VORONKOV, V. F. MIRINOV, and YU. I. KORIK. Zh. Strukt. Khim. **6**, 915 (1965); Chem. Abstr. **64**, 9551 (1966).

Trimethylgermanium Nitrate

D. POTTS AND A. WALKER

Department of Chemistry, Scarborough College, University of Toronto, 1265 Military Trail, West Hill, Ontario

Received December 21, 1970

The spectroscopic and solution properties of trimethylgermanium nitrate have been determined and compared with those of other known Group IV alkyl nitrates. The vibrational spectra show that the nitrato group is covalently bound to the germanium atom in a unidentate manner. Ultraviolet spectra and conductivity measurements indicate that the compound behaves as a 1:1 electrolyte in water and dimethylsulfoxide, but is a non-electrolyte in methyl cyanide, nitromethane, and ethyl acetate. Attempts to prepare methylgermanium trinitrate are also described.

On a déterminé les propriétés spectroscopiques et celles des solutions du nitrate de triméthylgermanium; on les a ensuite comparé à celles d'autres nitrates connus de dérivés alkylés d'éléments du groupe IV. Le spectre de vibration montre que le groupe nitrate est lié à l'atome de germanium d'une manière covalente et n'impliquant qu'un site de coordination. Le spectre u.v. et les mesures de conductivité indiquent que le composé se comporte comme un électrolyte (1:1) en solution dans l'eau ou le DMSO mais comme un non-électrolyte dans l'acétonitrile, le nitrométhane et l'acétate d'éthyle. On décrit aussi des essais de préparer le trinitrate de méthylgermanium.

Canadian Journal of Chemistry, **49**, 2171 (1971)

The preparation of trimethylgermanium nitrate has been reported previously (1), but as a recent nitrate review points out (2) concerning the compound, more work must be done before it can be said to be adequately characterized. This note describes the solution and spectroscopic properties of the compound and compares them with those reported recently (3) for dimethylgermanium dinitrate. The effects of increased alkylation are compared to similar trends found for analogous tin nitrato complexes (4, 5).

Results and Discussion

In agreement with Schmidt and Ruidisch (1), we found that trimethylgermanium nitrate, a colorless liquid, is soluble in water and in many polar and non-polar organic solvents. These solubility properties are very similar to those found for $Me_2Ge(NO_3)_2$ (3). The lack of reactivity of Me_3GeNO_3 towards diethyl ether, acetone, and Nujol argues against the presence of a symmetrically bound bidentate nitrate group, and in this respect is consistent with the Raman spectroscopic data which indicates a unidentate nitrate group (6).

Vibrational Spectra

The observed infrared and Raman spectra together with suggested assignments are presented in Table 1. The appearance of a medium intensity Raman nitrato band in the 1300 cm^{-1}

Can. J. Chem. Downloaded from www.nrcresearchpress.com by 210.87.254.40 on 09/05/12
For personal use only.

National Research Council of Canada for financial assistance.

1. M. J. SHAW, H. H. HYMAN, and R. FILLER. J. Am. Chem. Soc. **91**, 1563 (1969); **92**, 6498 (1970); M. J. SHAW, J. A. WEIL, H. H. HYMAN, and R. FILLER. J. Am. Chem. Soc. **92**, 5096 (1970).
2. D. R. MACKENZIE and J. FAJER. J. Am. Chem. Soc. **92**, 4994 (1970).
3. C. EABORN. Organosilicon compounds. Butterworths, London. 1960. pp. 124, 379–382.
4. C. EABORN. J. Chem. Soc. 2846 (1952).
5. S. TANNENBAUM, S. KAYE, and G. F. LEWENZ. J. Am. Chem. Soc. **75**, 3753 (1953).
6. J. H. HOLLOWAY. J. Chem. Educ. **43**, 202 (1966).
7. E. A. V. EBSWORTH. Volatile silicon compounds. Pergamon, New York. 1963. p. 56.
8. H. SCHMIDBAUR. Chem. Ber. **98**, 83 (1965); F. KLANBERG and E. L. MUETTERTIES. Inorg. Chem. **7**, 155 (1968).
9. H. SCHMIDBAUR and F. SCHINDLER. J. Organomet. Chem. **2**, 466 (1964).
10. V. A. PESTUNOVICH, A. N. EGOROCHKIN, M. G. VORONKOV, V. F. MIRINOV, and YU. I. KORIK. Zh. Strukt. Khim. **6**, 915 (1965); Chem. Abstr. **64**, 9551 (1966).

Trimethylgermanium Nitrate

D. POTTS AND A. WALKER

Department of Chemistry, Scarborough College, University of Toronto, 1265 Military Trail, West Hill, Ontario

Received December 21, 1970

The spectroscopic and solution properties of trimethylgermanium nitrate have been determined and compared with those of other known Group IV alkyl nitrates. The vibrational spectra show that the nitrato group is covalently bound to the germanium atom in a unidentate manner. Ultraviolet spectra and conductivity measurements indicate that the compound behaves as a 1:1 electrolyte in water and dimethylsulfoxide, but is a non-electrolyte in methyl cyanide, nitromethane, and ethyl acetate. Attempts to prepare methylgermanium trinitrate are also described.

On a déterminé les propriétés spectroscopiques et celles des solutions du nitrate de triméthylgermanium; on les a ensuite comparé à celles d'autres nitrates connus de dérivés alkylés d'éléments du groupe IV. Le spectre de vibration montre que le groupe nitrate est lié à l'atome de germanium d'une manière covalente et n'impliquant qu'un site de coordination. Le spectre u.v. et les mesures de conductivité indiquent que le composé se comporte comme un électrolyte (1:1) en solution dans l'eau ou le DMSO mais comme un non-électrolyte dans l'acétonitrile, le nitrométhane et l'acétate d'éthyle. On décrit aussi des essais de préparer le trinitrate de méthylgermanium.

Canadian Journal of Chemistry, **49**, 2171 (1971)

The preparation of trimethylgermanium nitrate has been reported previously (1), but as a recent nitrate review points out (2) concerning the compound, more work must be done before it can be said to be adequately characterized. This note describes the solution and spectroscopic properties of the compound and compares them with those reported recently (3) for dimethylgermanium dinitrate. The effects of increased alkylation are compared to similar trends found for analogous tin nitrato complexes (4, 5).

Results and Discussion

In agreement with Schmidt and Ruidisch (1), we found that trimethylgermanium nitrate, a colorless liquid, is soluble in water and in many polar and non-polar organic solvents. These solubility properties are very similar to those found for $Me_2Ge(NO_3)_2$ (3). The lack of reactivity of Me_3GeNO_3 towards diethyl ether, acetone, and Nujol argues against the presence of a symmetrically bound bidentate nitrate group, and in this respect is consistent with the Raman spectroscopic data which indicates a unidentate nitrate group (6).

Vibrational Spectra

The observed infrared and Raman spectra together with suggested assignments are presented in Table 1. The appearance of a medium intensity Raman nitrato band in the 1300 cm^{-1}

Can. J. Chem. Downloaded from www.nrcresearchpress.com by 210.87.254.40 on 09/05/12
For personal use only.

region compared to only a weak Raman nitrato band in the 1600 cm^{-1} region is characteristic of the pattern observed for compounds known to contain unidentate nitrato groups, and quite unlike that observed for those compounds containing known symmetrically bidentate nitrato groups (7). Consequently, the nitrate bands are assigned in accordance with Addison and Logan (8) assuming a unidentate nitrato group. The Ge—methyl vibrations are assigned following Griffiths (9).

When the infrared spectrum of trimethylgermanium nitrate is compared to that reported for dimethylgermanium dinitrate (3), it can be seen that the value Δ (the difference in asymmetric and symmetric NO_2 stretching frequencies) is smaller for the mononitrate. Furthermore the symmetric N—O stretching frequency is higher for the mononitrate. Both these observations indicate a less covalently bound unidentate nitrato group in the mononitrate than those in the dinitrate. Thus the effect of increasing alkylation is to produce a less polarizing germanium atom. In support of this conclusion the observed germanium–oxygen stretching frequencies for the mononitrate are some 20 cm^{-1} lower than those seen for the dinitrate (3), indicating weaker germanium–nitrate bonding in the mononitrate. Likewise the degeneracy weighted Ge—C stretching frequencies are lower for the mononitrate.

It should be noted that the structure of Me_3GeNO_3 must be quite different to the analogous tin compound, for which the infrared evidence (10, 11) has been interpreted as containing planar Me_3Sn groups possibly linked together by bridging nitrate groups. The presence of the symmetric Ge—C stretch in the infrared spectrum of Me_3GeNO_3, however, rules out planar Me_3Ge groups and the nitrate group is probably unidentate. The molecule is likely pseudo-tetrahedral.

Nuclear Magnetic Resonance Spectra

The nuclear magnetic resonance spectra of Me_3GeNO_3 and $Me_2Ge(NO_3)_2$ have been determined in chloroform and exhibit single peaks at $\tau = 9.28$ and $\tau = 8.63$, respectively. Under the same conditions, tetramethylgermane shows a peak at $\tau = 9.87$. These results indicate that the germanium atom becomes increasingly electron-deficient (compared to its state in tetramethylgermane) as the number of nitrate groups attached to the germanium atom increases. These conclusions are consistent with the changes in germanium–carbon stretching frequencies observed in the infrared spectra of Me_3GeNO_3 and $Me_2Ge(NO_3)_2$. Similar observations have been made for methyltin nitrato complexes (4) and, as in the case of the tin complexes, the shift to lower field is greater for the nitrato compounds than analogous chloride complexes. (The nuclear magnetic resonance (n.m.r.) spectrum of dimethylgermanium dichloride measured in $CHCl_3$ shows a peak at $\tau = 8.79$.)

TABLE 1. Vibrational spectra of trimethylgermanium nitrate*

Frequency (cm^{-1})		
Infrared	Raman	Assignment
2995w		C—H stretching
2920w		
2858w		(2 × 1417)
1786m		
1585s, sp	1565w, br	Asym. NO_2 stretching
1417w	1412w, br	Asym. CH_3 deformation
1290s, sp	1288m, sp	Sym. NO_2 stretching
1248m, sp	1247m, br	Sym. CH_3 deformation
1162w, sp		
1043w, sp	1041vw	
940s, sp	949m, sp	N—O stretching
827s, br		CH_3 rocking
778w		NO_3 out-of-plane rocking
760w	761w	CH_3 rocking
698w	700w	Sym. NO_2 bending
632s, sp	630s, sp	Deg. Ge—C_2 stretching
581w	578vs, sp	Sym. Ge—C stretching
373s, sp	357m, br	Ge—O stretching
224m	191s, br	Ge—C bending
208m		

*s = strong, m = medium, w = weak, v = very, sp = sharp, br = broad.

Ultraviolet Spectra

The ultraviolet spectra of solutions of trimethylgermanium nitrate in water and dimethylsulfoxide exhibit peaks at 302.5 mμ ($\varepsilon = 6.90$) and 312.5 mμ ($\varepsilon = 4.41$), respectively, which correspond to dissociation of the molecule yielding one nitrate ion per mol in these solvents (12).

The ultraviolet solution spectra of trimethylgermanium nitrate in methyl cyanide, ethyl acetate, and methanol are typical of those obtained for solutions of many covalent metal nitrates in these solvents (3, 6, 12), indicating considerable metal nitrate interaction (12). In methyl cyanide ε_{max} is 6.38 at 277.5 mμ, in ethyl acetate ε_{max} is 6.14 at 275.0 mμ, and in methanol ε_{max} is 8.40 at 270.0 mμ.

Can. J. Chem. Downloaded from www.nrcresearchpress.com by 210.87.254.40 on 09/05/12
For personal use only.

Can. J. Chem. Downloaded from www.nrcresearchpress.com by 210.87.254.40 on 09/05/12
For personal use only.

TABLE 2. Molar conductivities of Me_3GeNO_3 in various solvents at 25 °C

H_2O		DMSO		MeOH		MeCN		$MeNO_2$	
Conc. ($M \times 10^3$)	Cond. (ohm^{-1} cm^2)	Conc. ($M \times 10^3$)	Cond. (ohm^{-1} cm^2)	Conc. ($M \times 10^3$)	Cond. (ohm^{-1} cm^2)	Conc. ($M \times 10^3$)	Cond. (ohm^{-1} cm^2)	Conc. ($M \times 10^3$)	Cond. (ohm^{-1} cm^2)
1.33	363	2.10	33.9	1.31	86.4	2.34	0.232	1.01	5.28
5.25	363	7.69	32.1	6.99	51.1	13.8	0.165	4.58	2.44
10.9	361	15.7	30.2	15.0	38.7	20.1	0.170	9.64	1.68
20.5	356	29.7	28.2	28.5	30.6	27.4	0.171	18.1	1.15
25.8	351	37.4	27.3	35.8	28.0	33.0	0.170	22.7	0.95

Can. J. Chem. Downloaded from www.nrcresearchpress.com by 210.87.254.40 on 09/05/12
For personal use only.

Conductivities

The molar conductivities of trimethylgermanium nitrate in water, dimethylsulfoxide, methanol, methyl cyanide, and nitromethane are listed in Table 2. The low conductivity of methyl cyanide and nitromethane solutions indicate that Me_3GeNO_3 is virtually a non-electrolyte in these solvents (13). The molar conductivities of aqueous solutions exceed the expected value for 1:1 electrolytes (~ 130 ohm^{-1} cm^2), but as these solutions are quite acidic, the high conductivities can be attributed to hydrolysis similar to that encountered with $Me_2Ge(NO_3)_2$ (3). The conductivities of Me_3GeNO_3 in dimethylsulfoxide are typical of values obtained for a 1:1 electrolyte in this solvent (14). The values obtained in methanol show concentration dependence typical of weak electrolyte behavior. Thus, as was found for methanol solutions of $Me_2Ge(NO_3)_2$ (3), while in very dilute solutions (0.001 *M*) the conductivity indicates some degree of ionization ($AgNO_3$ in MeOH has a molar conductivity of 94.20 ohm^{-1} cm^2 at a concentration of 0.00168 *M* (15)), at the concentration used for the u.v. spectrum (0.0730 *M*) considerable association is evident.

Molecular Weight

The molecular weight of Me_3GeNO_3 was determined cryoscopically in nitrobenzene and found to be 179.2 for a 0.195 *M* solution. (Calcd. value for Me_3GeNO_3 is 179.6.)

Reactions of Dinitrogen Pentoxide with Methylgermanium Trichloride

As a result of our work on alkyl nitrato complexes of lead (5), tin (4), and germanium (3), it has become apparent that monomethyl and dimethyl derivatives of these metals may be reacted with dinitrogen pentoxide without removal of methyl groups. Since dinitrogen pentoxide is known to react with chloride complexes of these metals, it was hoped that the reaction between dinitrogen pentoxide and methylgermanium trichloride would yield methylgermanium trinitrate. However, it was found that when $MeGeCl_3$ was reacted with either pure N_2O_5, or solutions of N_2O_5 in carbon tetrachloride, the product was always a viscous unstable oil which liberated NO_2 above 0 °C. The infrared spectrum of the product confirms the presence of a methyl group and two strong bands at 1620 and 1290 cm^{-1} are indicative of covalently bound nitrate. The region between 800–900 cm^{-1} consists of three strong bands suggesting the presence of a Ge—O—Ge species (16). It is probable that the highly polarizing nature of germanium in monomethylgermanium compounds is sufficient to make $MeGe(NO_3)_3$ unstable with respect to nitrogen dioxide and methylgermanium oxide species.

Experimental

Trimethylgermanium nitrate was prepared by the literature method (1). Dinitrogen pentoxide was prepared by a gas phase reaction between dinitrogen tetroxide and ozone.

Infrared spectra were recorded using a Beckman I.R. 12 spectrophotometer. The spectra were taken in carbon tetrachloride and carbon disulfide using variable path length cells with silver chloride windows. Far infrared spectra (200–400 cm^{-1}) were taken in carbon tetrachloride using 0.1 mm polyethylene liquid cells.

Raman spectra of pure liquid Me_3GeNO_3 were obtained on a Spex Raman Instrument using the red line of a Krypton laser.

Nuclear magnetic resonance spectra were run on a Varian T-60 spectrophotometer. Spectra were obtained as 10% solutions in chloroform using either tetramethylsilane or the proton peak of chloroform as standards.

Ultraviolet spectra were recorded on a Cary #14 spectrophotometer using fused silica cells and dried spectroscopic solvents.

Conductivities were recorded with a Beckman model RC-18 bridge system, and a cell following the design of Greiner (17).

We wish to thank the National Research Council of Canada for supporting this work and for a Studentship to D.P.

1. M. Schmidt and I. Ruidisch. Chem. Ber. **95**, 1434 (1962).
2. C. C. Addison and D. Sutton. Prog. Inorg. Chem. **8**, 195 (1967).
3. D. Potts and A. Walker. Can. J. Chem. **49**, 202 (1971).
4. J. R. Ferraro, D. Potts, and A. Walker. Can. J. Chem. **48**, 711 (1970).
5. D. Potts and A. Walker. Can. J. Chem. **47**, 1621 (1969).
6. C. C. Addison and W. B. Simpson. J. Chem. Soc. 598 (1965).
7. G. S. Brownlee. Ph.D. Thesis. Nottingham University, Nottingham, England. 1969.
8. C. C. Addison and N. Logan. Advances in inorganic and radiochemistry. Vol. 4. Academic Press. 1964. p. 72.
9. J. E. Griffiths. Spectrochim. Acta, **20**, 1335 (1964).
10. K. Yasuda and R. Okawara. J. Organometal. Chem. **3**, 76 (1965).
11. H. C. Clark, R. J. O'Brien, and A. L. Pickard. J. Organometal. Chem. **4**, 43 (1965).

12. C. C. ADDISON and D. SUTTON. J. Chem. Soc. A, 1524 (1966).
13. C. C. ADDISON, B. J. HATHAWAY, N. LOGAN, and A. WALKER. J. Chem. Soc. 4308 (1960).
14. P. G. SEARS, G. R. LESTER, and L. R. DAWSON. J. Phys. Chem. **60**, 1433 (1956).
15. R. E. BUSBY and V. S. GRIFFITHS. J. Chem. Soc. 902 (1963).
16. T. D. GOLDFARB and S. SUJISHI. J. Am. Chem. Soc. **86**, 1679 (1964).
17. R. H. GREINER. Fusion. p. 11 Nov. (1960).

Can. J. Chem. Downloaded from www.nrcresearchpress.com by 210.87.254.40 on 09/05/12
For personal use only.

Nuclear Recoil Reactions in Organo-Manganese Compounds. V. —$Mn(CO)_5$ Target Compounds

H. JAKUBINEK, S. C. SRINIVASAN,[1] AND D. R. WILES
Chemistry Department, Carleton University, Ottawa, Canada

Received January 28, 1971

$HMn(CO)_5$, $DMn(CO)_5$, $CH_3Mn(CO)_5$, and $C_6H_5Mn(CO)_5$ have been irradiated with neutrons and the product spectrum of ^{56}Mn-containing molecules determined. The results show that $H^{56}Mn(CO)_5$ is formed in all cases: 21.0%, 23.6% from $HMn(CO)_5$ and $DMn(CO)_5$ targets, respectively, and 6.9% and 2.1% from $CH_3Mn(CO)_5$ and $C_6H_5Mn(CO)_5$, respectively. Thus the yields are not in accord with the number of H atoms per target molecule. Preliminary experiments show that $\cdot{}^*Mn(CO)_5$ exchanges rapidly with $HMn(CO)_5$ and $DMn(CO)_5$ and very slowly with $CH_3Mn(CO)_5$ and $C_6H_5Mn(CO)_5$. It is deduced that the very high yield of $H^{56}Mn(CO)_5$ in $HMn(CO)_5$ and $DMn(CO)_5$ targets could arise from the rapid exchange, while the lower yields of $H^{56}Mn(CO)_5$ in other targets must likely come from radical reactions following thermal dissociation of the target molecule.

On a irradié le $HMn(CO)_5$, le $DMn(CO)_5$, le $CH_3Mn(CO)_5$ et le $C_6H_5Mn(CO)_5$ avec des neutrons et l'on a déterminé le spectre des molécules contenant du ^{56}Mn. On observe que le $H^{56}Mn(CO)_5$ se forme dans tous les cas: 21.0% et 23.6% respectivement lorsque le $HMn(CO)_5$ et le $DMn(CO)_5$ sont utilisés comme cibles et 6.9% et 2.1% respectivement à partir du $CH_3Mn(CO)_5$ et $C_6H_5Mn(CO)_5$. Les rendements ne sont donc pas en accord avec le nombre d'atome d'hydrogène par molécule-cible. Des expériences préliminaires ont permis de mettre en évidence que $\cdot{}^*Mn(CO)_5$ s'échange rapidement avec $HMn(CO)_5$ et $DMn(CO)_5$ et très lentement avec $CH_3Mn(CO)_5$ et $C_6H_5Mn(CO)_5$. On en conclut que les rendements élevés de $H^{56}Mn(CO)_5$ obtenus lorsque $HMn(CO)_5$ et $DMn(CO)_5$ sont utilisés proviendraient de l'échange rapide alors que les faibles rendements de $H^{56}Mn(CO)_5$ obtenus lorsque l'on utilise d'autres cibles seraient dus à des réactions radicaliques qui seraient subséquentes à la dissociation thermique de la cible.

Canadian Journal of Chemistry, 49, 2175 (1971)

Introduction

In earlier publications of this series, we have described studies of the chemical behavior of manganese atoms following neutron bombardment of various manganese carbonyl compounds. In particular it has been found (1) that in cyclopentadienylmanganese tricarbonyl ($CpMn(CO)_3$) and its methyl homolog ($CH_3CpMn(CO)_3$), a surprisingly large fraction of the organically bound ^{56}Mn atoms are found as various —$Mn(CO)_5$ compounds. It has also been shown that, in Mn_2CO_{10}, the radioactive free radical $\cdot Mn(CO)_5$ is formed and reacts or decomposes only on dissolution.

It became evident from studies of $CH_3CpMn(CO)_3$ (2) that competitive radical reactions were involved, as in reaction 1.

$$[1] \qquad \left.\begin{matrix}\cdot H \\ \cdot CH_3\end{matrix}\right\} + Mn(CO)_5 \longrightarrow \begin{matrix}HMn(CO)_5 \\ CH_3Mn(CO)_5\end{matrix}$$

While it was not sure whether the hydrogen atoms were abstracted from nearby molecules, or were made available for reaction by radiolysis or local

[1]Present address: Chemistry Department, University of Wisconsin, Madison, Wisconsin.

12. C. C. ADDISON and D. SUTTON. J. Chem. Soc. A, 1524 (1966).
13. C. C. ADDISON, B. J. HATHAWAY, N. LOGAN, and A. WALKER. J. Chem. Soc. 4308 (1960).
14. P. G. SEARS, G. R. LESTER, and L. R. DAWSON. J. Phys. Chem. **60**, 1433 (1956).
15. R. E. BUSBY and V. S. GRIFFITHS. J. Chem. Soc. 902 (1963).
16. T. D. GOLDFARB and S. SUJISHI. J. Am. Chem. Soc. **86**, 1679 (1964).
17. R. H. GREINER. Fusion. p. 11 Nov. (1960).

Can. J. Chem. Downloaded from www.nrcresearchpress.com by 210.87.254.105 on 09/05/12
For personal use only.

Nuclear Recoil Reactions in Organo-Manganese Compounds. V. —$Mn(CO)_5$ Target Compounds

H. JAKUBINEK, S. C. SRINIVASAN,[1] AND D. R. WILES
Chemistry Department, Carleton University, Ottawa, Canada

Received January 28, 1971

$HMn(CO)_5$, $DMn(CO)_5$, $CH_3Mn(CO)_5$, and $C_6H_5Mn(CO)_5$ have been irradiated with neutrons and the product spectrum of ^{56}Mn-containing molecules determined. The results show that $H^{56}Mn(CO)_5$ is formed in all cases: 21.0%, 23.6% from $HMn(CO)_5$ and $DMn(CO)_5$ targets, respectively, and 6.9% and 2.1% from $CH_3Mn(CO)_5$ and $C_6H_5Mn(CO)_5$, respectively. Thus the yields are not in accord with the number of H atoms per target molecule. Preliminary experiments show that $\cdot{}^*Mn(CO)_5$ exchanges rapidly with $HMn(CO)_5$ and $DMn(CO)_5$ and very slowly with $CH_3Mn(CO)_5$ and $C_6H_5Mn(CO)_5$. It is deduced that the very high yield of $H^{56}Mn(CO)_5$ in $HMn(CO)_5$ and $DMn(CO)_5$ targets could arise from the rapid exchange, while the lower yields of $H^{56}Mn(CO)_5$ in other targets must likely come from radical reactions following thermal dissociation of the target molecule.

On a irradié le $HMn(CO)_5$, le $DMn(CO)_5$, le $CH_3Mn(CO)_5$ et le $C_6H_5Mn(CO)_5$ avec des neutrons et l'on a déterminé le spectre des molécules contenant du ^{56}Mn. On observe que le $H^{56}Mn(CO)_5$ se forme dans tous les cas: 21.0% et 23.6% respectivement lorsque le $HMn(CO)_5$ et le $DMn(CO)_5$ sont utilisés comme cibles et 6.9% et 2.1% respectivement à partir du $CH_3Mn(CO)_5$ et $C_6H_5Mn(CO)_5$. Les rendements ne sont donc pas en accord avec le nombre d'atome d'hydrogène par molécule-cible. Des expériences préliminaires ont permis de mettre en évidence que $\cdot{}^*Mn(CO)_5$ s'échange rapidement avec $HMn(CO)_5$ et $DMn(CO)_5$ et très lentement avec $CH_3Mn(CO)_5$ et $C_6H_5Mn(CO)_5$. On en conclut que les rendements élevés de $H^{56}Mn(CO)_5$ obtenus lorsque $HMn(CO)_5$ et $DMn(CO)_5$ sont utilisés proviendraient de l'échange rapide alors que les faibles rendements de $H^{56}Mn(CO)_5$ obtenus lorsque l'on utilise d'autres cibles seraient dus à des réactions radicaliques qui seraient subséquentes à la dissociation thermique de la cible.

Canadian Journal of Chemistry, 49, 2175 (1971)

Introduction

In earlier publications of this series, we have described studies of the chemical behavior of manganese atoms following neutron bombardment of various manganese carbonyl compounds. In particular it has been found (1) that in cyclopentadienylmanganese tricarbonyl ($CpMn(CO)_3$) and its methyl homolog ($CH_3CpMn(CO)_3$), a surprisingly large fraction of the organically bound ^{56}Mn atoms are found as various —$Mn(CO)_5$ compounds. It has also been shown that, in Mn_2CO_{10}, the radioactive free radical $\cdot Mn(CO)_5$ is formed and reacts or decomposes only on dissolution.

It became evident from studies of $CH_3CpMn(CO)_3$ (2) that competitive radical reactions were involved, as in reaction 1.

$$[1] \qquad \left.\begin{matrix}\cdot H \\ \cdot CH_3\end{matrix}\right\} + Mn(CO)_5 \longrightarrow \begin{matrix}HMn(CO)_5 \\ CH_3Mn(CO)_5\end{matrix}$$

While it was not sure whether the hydrogen atoms were abstracted from nearby molecules, or were made available for reaction by radiolysis or local

[1]Present address: Chemistry Department, University of Wisconsin, Madison, Wisconsin.

Can. J. Chem. Downloaded from www.nrcresearchpress.com by 210.87.254.105 on 09/05/12
For personal use only.

thermal effects ("pyrolysis"), it seemed clear that the $-CH_3$ came from the ring substituent, likely by pyrolysis.

A most important question emerging in these studies is that of the origin of the hydrogen atom. There seem to be two extreme possibilities, that of abstraction [2] and that of radiolytic or thermal productions of hydrogen atoms [3]. These would result in reactions such as the following

$$[2] \quad [R, Ar, etc.]H + \cdot Mn(CO)_5 \rightarrow [R, Ar, etc.]\cdot + HMn(CO)_5$$

$$[3a] \quad [R, Ar, etc.]H \rightarrow [R, Ar, etc.]\cdot + H\cdot$$

$$[3b] \quad H\cdot + \cdot Mn(CO)_5 \rightarrow HMn(CO)_5$$

Since in these $-Mn(CO)_3$ systems the formation of the $-Mn(CO)_5$ group is an additional complication, it seemed reasonable to study cases in which $-Mn(CO)_5$ forms part of the initial matrix, so that other differences might perhaps stand out more clearly. (It is not here implied that the $Mn(CO)_5$ group remains intact following nuclear activation; indeed evidence is very strong that activated molecules are largely, if not totally, dissociated.) We are now able to report the results from a study on neutron-irradiated $HMn(CO)_5$, $DMn(CO)_5$, $CH_3Mn(CO)_5$, and $C_6H_5Mn(CO)_5$.

Experimental

The target compounds were made by procedures similar to known methods, starting with $NaMn(CO)_5$, and using the "nitrogen glove" technique (3) for the manipulations.

$HMn(CO)_5$

$NaMn(CO)_5$ was treated with glacial H_3PO_4, and the product purified by vacuum distillation at low temperature (4). $DMn(CO)_5$ was similarly prepared from D_3PO_4.

$CH_3Mn(CO)_5$

$NaMn(CO)_5$ in THF solution was treated with CH_3I. After 2 h at -22 °C, the product was distilled to a cold trap and was subsequently purified by vacuum sublimation (5).

$C_6H_5Mn(CO)_5$

$NaMn(CO)_5$ in THF was treated with benzoyl chloride to produce $C_6H_5COMn(CO)_5$. This intermediate was heated, without purification, at 90 °C for 1 h to remove CO. The product was purified by vacuum sublimation (6).

Separation of Products

Carriers were added for all compounds other than the parent compound.

$HMn(CO)_5$ was converted to $IMn(CO)_5$ by one or more of the following steps

(*a*) Reaction with I_2

$$[4] \quad HMn(CO)_5 + I_2 \rightarrow IMn(CO)_5 + HI$$

(*b*) Exchange with $IMn(CO)_5$

$$[5] \quad H^*Mn(CO)_5 + IMn(CO)_5 \rightleftharpoons I^*Mn(CO)_5 + HMn(CO)_5$$

(*c*) Vacuum distillation followed by (*a*).

Reaction 4 has been shown to be quantitative and fast (7). Reaction 5 has been found to be complete within the time of the experiment (see below). Reactions 4 and 5 have been shown not to occur with $CH_3Mn(CO)_5$ or $C_6H_5Mn(CO)_5$ during the time of the experiment, and since the amount of $IMn(CO)_5$ used in this case was very much larger than the amount of $HMn(CO)_5$, reaction 5 can be considered to go completely to the right. $IMn(CO)_5$ was purified by column chromatography.

$CH_3Mn(CO)_5$ and $C_6H_5Mn(CO)_5$ were separated from the $IMn(CO)_5$ remaining from [4] or [5] by vacuum transfer, and were subsequently purified by further vacuum sublimation. It was assumed that $CH_3Mn(CO)_5$ and $C_6H_5Mn(CO)_5$ were not found in the same experiment and thus did not require to be separated from each other.

Neutron Irradiations

Neutron irradiations were done with the Sb–Be neutron sources at Commercial Products Division, A.E.C.L., and at Carleton University. The flux of thermal neutrons was of the order of 10^8 cm^{-2} s^{-1} and the γ-ray dose rate about 1 Mrad h^{-1}. The irradiations were carried out at Dry Ice temperature.

Analytical Measurements

Determination of the chemical recovery of the purified target compounds and carriers was done gravimetrically. $HMn(CO)_5$ was weighed after conversion to $IMn(CO)_5$. Since the quantities recovered were 20 mg or more, the analytical uncertainties are $\leq 1\%$ on individual determinations.

Radioactivity measurements were done using a 3 in. × 3 in. NaI scintillation counter coupled to a 100 channel pulse height analyzer. Numerical integration was done over the 0.84 Mev γ peak from ^{56}Mn. The radioactivity reference was in most cases a sample of crystalline $CpMn(CO)_3$ counted without chemical processing.

Exchange Measurements

Exchange of the $-Mn(CO)_5$ group between $IMn(CO)_5$ and $HMn(CO)_5$, $DMn(CO)_5$, $CH_3Mn(CO)_5$, and $C_6H_5Mn(CO)_5$ has been studied, and a fuller report will be published separately (8). A radioactive species taken to be the radical $\cdot Mn(CO)_5$ (9) is formed by the neutron irradiation of $Mn_2(CO)_{10}$. This species has been found to react rapidly with I_2 in petroleum ether solution or (10) to exchange rapidly with $IMn(CO)_5$ by the assumed reaction

$$[6] \quad \cdot^*Mn(CO)_5 + IMn(CO)_5 \rightleftharpoons \cdot Mn(CO)_5 + I^*Mn(CO)_5$$

Radioactive $I^*Mn(CO)_5$ prepared by direct neutron irradiation of $IMn(CO)_5$ was purified and mixed with either $HMn(CO)_5$, $CH_3Mn(CO)_5$, or $C_6H_5Mn(CO)_5$ in

TABLE 1. Distribution of ^{56}Mn-labelled products

Target	Yield of ^{56}Mn			
	$HMn(CO)_5$	$CH_3Mn(CO)_5$	$C_6H_5Mn(CO)_5$	$Mn_2(CO)_{10}$
$HMn(CO)_5$[a]	21.0	—	—	4.3
$DMn(CO)_5$[b]	23.6	—	—	3.7
$CH_3Mn(CO)_5$[a]	6.9	3.5	—	2.3
$C_6H_5Mn(CO)_5$[b]	2.1	—	2.5	3.6
$CpMn(CO)_3$[c]	7.0	0.0	—	0.9
$CH_3CpMn(CO)_3$[c]	10.0	1.7	—	—

[a]Five irradiations.
[b]Two irradiations.
[c]Taken from ref. 1.

tetrahydrofuran solution. The components of the mixture were separated in vacuo and their specific radioactivity measured. It is found that in the space of 3 min, the exchange with $HMn(CO)_5$ is complete.

[5a] $$HMn(CO)_5 + I^*Mn(CO)_5 \rightleftharpoons H^*Mn(CO)_5 + IMn(CO)_5$$

Exchange with $DMn(CO)_5$ is likewise very fast. With $CH_3Mn(CO)_5$ and $C_6H_5Mn(CO)_5$, no exchange is observed after 10 min.

Results and Discussion

The results of the experiments are given in Table 1.

It is clear from the data in Table 1 that the yield of $HMn(CO)_5$ is not related to the number of hydrogen atoms in the target molecules; in fact, quite the reverse.

The value 25.3% for the sum of the yields of radioactive $Mn_2(CO)_{10}$ and $HMn(CO)_5$ gives a lower limit for the radiochemical production of $—^{56}Mn(CO)_5$ in $HMn(CO)_5$ targets. Similar values are to be expected in the other two target compounds.

To identify the reactions occurring and establish their sequence is not easy, although some important indications can be found. It had been concluded before (1) that $\cdot Mn(CO)_5$ does not abstract hydrogen from hydrocarbons, such as those found in petroleum ether. It is apparent then that in $CH_3Mn(CO)_5$ and $C_6H_5Mn(CO)_5$ targets, the $HMn(CO)_5$ produced must be constituted from hydrogen atoms formed by collision-induced thermal dissociation.

Regarding the parent yields, it seems from the exchange results given above that $HMn(CO)_5$ can likely be formed in $HMn(CO)_5$ targets by an exchange mechanism, while parallel reactions in the other targets are not possible. The very much higher parent yield in $HMn(CO)_5$ than in the other targets lends support to this exchange as the dominant mechanism for parent reformation in $HMn(CO)_5$. Inertial effects (11) cannot be responsible for this high yield of $HMn(CO)_5$, since the parent yield in $DMn(CO)_5$ is so nearly equal to that in $HMn(CO)_5$.

The inertness of $CH_3Mn(CO)_5$ and $C_6H_5Mn(CO)_5$ to exchange with $IMn(CO)_5$ suggests that the $\cdot CH_3$ and $\cdot C_6H_5$ radical may not be transferred by simple chemical reactions. It was observed earlier (1) that in mixed $CH_3CpMn(CO)_3$–isooctane targets the availability of $—CH_3$ appeared to control the amount of $CH_3Mn(CO)_5$ produced. The same must hold for the present case, and likely for the phenyl compound as well.

It thus seems reasonable to conclude that for $CH_3Mn(CO)_5$ and $C_6H_5Mn(CO)_5$ targets, the reformation of the radioactive $RMn(CO)_5$ (where R = H, CH_3, or C_6H_5) is through the recombination of radicals produced from neighboring molecules by the nuclear event. Whether the radicals are produced by direct collision or more diffusely by local thermal effects is not yet known. If the radicals were produced by extensive Auger ionization (12), instead of by thermal dissociation, the methyl and phenyl radicals would themselves not likely have survived (13). In such cases too, the number of hydrogen atoms produced would be in the ratio of 5:3, while our results indicate a ratio of approximately 2:7 for the yields of $H^*Mn(CO)_5$. The general reaction, then, appears to be one of massive radical production followed by a rapid reaction or perhaps more coalescence, reminiscent of the mechanism suggested some years ago by Willard (14) for similar reactions in alkyl halides.

We wish to express our gratitude to Mrs. I. de Jong for experimental assistance, to the Commercial Product, Division, A.E.C.L. for the use of their Sb–Be neutron facility, and to the National Research Council of Canada for financial support.

Can. J. Chem. Downloaded from www.nrcresearchpress.com by 210.87.254.105 on 09/05/12
For personal use only.

1. I. G. DE JONG, S. C. SRINIVASAN, and D. R. WILES. Can. J. Chem. **47**, 1327 (1969).
2. I.-C. YANG and D. R. WILES. Can. J. Chem. **45**, 1357 (1967).
3. S. C. SRINIVASAN and D. R. WILES. J. Chem. Ed. In press.
4. R. B. KING. Organometallic syntheses. Vol. I. Academic Press, New York. 1965. p. 158.
5. S. C. SRINIVASAN. Ph.D. Thesis. Carleton University, Ottawa, Canada. 1970.
6. R. D. CLOSSON, J. KOZIKOWSKI and T. H. COFFIELD. J. Org. Chem. **22**, 598 (1957).
7. I. G. DE JONG, S. C. SRINIVASAN, and D. R. WILES. J. Organometal. Chem. **26**, 119 (1971).
8. H. JAKUBINEK, S. C. SRINIVASAN, and D. R. WILES. To be published.
9. I. G. DE JONG and D. R. WILES. Chem. Commun. 519 (1968).
10. I. G. DE JONG and D. R. WILES. To be published.
11. H. E. SUESS. Z. Phys. Chem. **B45**, 312 (1940).
12. P. R. GEISSLER and J. E. WILLARD. J. Phys. Chem. **67**, 1675 (1963).
13. T. A. CARLSON and R. M. WHITE. J. Chem. Phys. **48**, 5191 (1968).
14. J. E. WILLARD. Ann. Revs. Nucl. Science, **3**, 193 (1953).

Absolute Rate Constants for Hydrocarbon Autoxidation. Part XX. Oxidation of Some Organic Sulfides[1]

J. A. HOWARD AND S. KORCEK[2]

Division of Chemistry, National Research Council of Canada, Ottawa, Canada

Received January 22, 1971

Absolute rate constants for the liquid phase autoxidation of some organic sulfides at 30 °C have been measured. The reactivities of organic sulfides towards *t*-butylperoxy radicals are equal to or somewhat less than the reactivities of structurally analogous ethers. The α-alkylthiylalkylperoxy radicals appear to be about 3–5 times more reactive in hydrogen atom abstraction than the α-alkoxyalkylperoxy radicals.

La constante de vitesse absolue pour l'autoxydation en phase liquide de quelques sulfures organiques a été mesurée à 30 °C. Les réactivités des sulfures organiques vis à vis des radicaux *t*-butylpéroxy sont égales ou un peu inférieures aux réactivités des éthers de structure analogue. Les radicaux α-alkylthiylalkylpéroxy semblent 3 à 5 fois plus réactifs pour l'abstraction d'atome d'hydrogène que les radicaux α-alkoxyalkylpéroxy.

Canadian Journal of Chemistry, 49, 2178 (1971)

Introduction

Previous publications in this series have reported absolute propagation and termination rate constants for liquid-phase autoxidations of hydrocarbons, aldehydes, ethers, and α-monosubstituted toluenes at atmospheric pressure and 30 °C (1). An attempt has been made to extend this work to the autoxidation of organic sulfides.

Saturated alkyl, aralkyl, and aryl mono- and disulfides do not react spontaneously with molecular oxygen at temperatures below about 100 °C. Unsaturated sulfides, however, absorb oxygen autocatalytically at first and faster than comparable mono-olefins but the rate soon begins to slow down and may cease before 0.1 mol of oxygen per mole of sulfide has been absorbed. This autoretardation is a feature of sulfide autoxidation and is indicative of the formation of oxidation inhibitors.

The reaction of many sulfides with molecular oxygen can be accelerated by the addition of typical free radical initiators, *e.g.* α,α′-azobisisobutyronitrile, upon irradiation with near ultraviolet light and can be retarded by the addition of free-radical inhibitors.

Unlike hydrocarbons and their oxygenated derivatives, organic sulfides give little or no hydroperoxidic material upon autoxidation. The principal reaction products appear to be a sulfoxide, water, and products resulting from scission of the weaker C—S bond. The reaction of organic sulfides with molecular oxygen at ambient temperatures has been described by the following reaction scheme (2)

[1]NRCC No. 11908.
[2]NRCC Postdoctorate Fellow 1968–1970.

Can. J. Chem. Downloaded from www.nrcresearchpress.com by 210.87.254.105 on 09/05/12
For personal use only.

1. I. G. DE JONG, S. C. SRINIVASAN, and D. R. WILES. Can. J. Chem. **47**, 1327 (1969).
2. I.-C. YANG and D. R. WILES. Can. J. Chem. **45**, 1357 (1967).
3. S. C. SRINIVASAN and D. R. WILES. J. Chem. Ed. In press.
4. R. B. KING. Organometallic syntheses. Vol. I. Academic Press, New York. 1965. p. 158.
5. S. C. SRINIVASAN. Ph.D. Thesis. Carleton University, Ottawa, Canada. 1970.
6. R. D. CLOSSON, J. KOZIKOWSKI and T. H. COFFIELD. J. Org. Chem. **22**, 598 (1957).
7. I. G. DE JONG, S. C. SRINIVASAN, and D. R. WILES. J. Organometal. Chem. **26**, 119 (1971).
8. H. JAKUBINEK, S. C. SRINIVASAN, and D. R. WILES. To be published.
9. I. G. DE JONG and D. R. WILES. Chem. Commun. 519 (1968).
10. I. G. DE JONG and D. R. WILES. To be published.
11. H. E. SUESS. Z. Phys. Chem. **B45**, 312 (1940).
12. P. R. GEISSLER and J. E. WILLARD. J. Phys. Chem. **67**, 1675 (1963).
13. T. A. CARLSON and R. M. WHITE. J. Chem. Phys. **48**, 5191 (1968).
14. J. E. WILLARD. Ann. Revs. Nucl. Science, **3**, 193 (1953).

Absolute Rate Constants for Hydrocarbon Autoxidation. Part XX. Oxidation of Some Organic Sulfides[1]

J. A. HOWARD AND S. KORCEK[2]

Division of Chemistry, National Research Council of Canada, Ottawa, Canada

Received January 22, 1971

Absolute rate constants for the liquid phase autoxidation of some organic sulfides at 30 °C have been measured. The reactivities of organic sulfides towards *t*-butylperoxy radicals are equal to or somewhat less than the reactivities of structurally analogous ethers. The α-alkylthiylalkylperoxy radicals appear to be about 3–5 times more reactive in hydrogen atom abstraction than the α-alkoxyalkylperoxy radicals.

La constante de vitesse absolue pour l'autoxydation en phase liquide de quelques sulfures organiques a été mesurée à 30 °C. Les réactivités des sulfures organiques vis à vis des radicaux *t*-butylpéroxy sont égales ou un peu inférieures aux réactivités des éthers de structure analogue. Les radicaux α-alkylthiylalkylpéroxy semblent 3 à 5 fois plus réactifs pour l'abstraction d'atome d'hydrogène que les radicaux α-alkoxyalkylpéroxy.

Canadian Journal of Chemistry, 49, 2178 (1971)

Introduction

Previous publications in this series have reported absolute propagation and termination rate constants for liquid-phase autoxidations of hydrocarbons, aldehydes, ethers, and α-monosubstituted toluenes at atmospheric pressure and 30 °C (1). An attempt has been made to extend this work to the autoxidation of organic sulfides.

Saturated alkyl, aralkyl, and aryl mono- and disulfides do not react spontaneously with molecular oxygen at temperatures below about 100 °C. Unsaturated sulfides, however, absorb oxygen autocatalytically at first and faster than comparable mono-olefins but the rate soon begins to slow down and may cease before 0.1 mol of oxygen per mole of sulfide has been absorbed. This autoretardation is a feature of sulfide autoxidation and is indicative of the formation of oxidation inhibitors.

The reaction of many sulfides with molecular oxygen can be accelerated by the addition of typical free radical initiators, *e.g.* α,α′-azobisisobutyronitrile, upon irradiation with near ultraviolet light and can be retarded by the addition of free-radical inhibitors.

Unlike hydrocarbons and their oxygenated derivatives, organic sulfides give little or no hydroperoxidic material upon autoxidation. The principal reaction products appear to be a sulfoxide, water, and products resulting from scission of the weaker C—S bond. The reaction of organic sulfides with molecular oxygen at ambient temperatures has been described by the following reaction scheme (2)

[1]NRCC No. 11908.
[2]NRCC Postdoctorate Fellow 1968–1970.

Can. J. Chem. Downloaded from www.nrcresearchpress.com by 210.87.254.5 on 09/05/12
For personal use only.

TABLE 1. Rate data for the oxidation of tetrahydrothiophene at 30°

Concentration (M)	Oxygen pressure (mm Hg)	$R_i \times 10^7$ ($M\,s^{-1}$)	$R_s \times 10^6$ ($M\,s^{-1}$)	$k_p/(2k_t)^{1/2} \times 10^3$ ($M^{-1/2}\,s^{-1/2}$)
11.3	95	0.97	4.8	1.4
11.3	150	0.97	4.8	1.4
11.3	396	0.97	4.3	1.2
11.3	700	0.97	4.5	1.3
4.54	700	0.40	1.04	1.2
11.3	700	0.18	1.85	1.2
11.3	700	0.88	3.5	1.1
11.3	700	2.75	7.5	1.3

Initiation

[1] Production of free radicals

Propagation

[2] $R\dot{C}HSR' + O_2 \rightarrow RCH(OO^{\cdot})SR'$

[3] $RCH(OO^{\cdot})SR' + RCH_2SR' \xrightarrow{k_p} RCH(OOH)SR' + R\dot{C}HSR'$

Hydroperoxide decomposition

[4] $RCH(OOH)SR' + RCH_2SR' \rightarrow RCH(OH)SR' + RCH_2SOR'$

[5] $RCH(OOH)SR' + RCHSOR' \rightarrow R_2'S_2 + H_2O +$ other products

Monothioacetal decomposition

[6] $RCH(OH)SR' \rightarrow RCHO + R'SH$

[7] $RCH(OH)SR' + R'SH \rightarrow H_2O +$ complex sulfides

where RCH_2SR' represents the organic sulfide, $R\dot{C}HSR'$ the carbon radical formed by abstraction of an α-hydrogen atom, and $RCH(OO^{\cdot})SR'$ the corresponding peroxy radical. Reactions 1, 2, and 3 are the initiation and propagation steps usually used to describe the autoxidation of other organic compounds. Reaction 4 accounts for the absence of hydroperoxides and the high yields of sulfoxides at low conversions. Reactions 5, 6, and 7 represent secondary reactions which are believed to be responsible for the complex nature of the autoxidation of organic sulfides. Although a termination step was not included in this reaction scheme it can be assumed that the chain reaction would be terminated (at least initially), at oxygen pressures above about 100 mm Hg, by the self-reaction of two peroxy radicals to give non-radical products.

[8] $RCH(OO^{\cdot})SR' + RCH(OO^{\cdot})SR' \rightarrow$ non-radical products

We have attempted to measure absolute rate constants for reactions 3 and 8, the rate controlling propagation and termination steps, for the autoxidation of some cyclic and acyclic organic sulfides and the results are reported below.

Experimental

Materials

Tetrahydrothiopyran, tetrahydrothiophene, α-toluenethiol, and cyclohexene were dried and distilled before use. Dibenzyl sulfide, dibenzyl disulfide, and benzyl phenyl sulfide were purified by recrystallization. Benzyl *t*-butyl sulfide was prepared from isobutylene and α-toluenethiol (3). Isopropyl sulfide was purified to better than 99.9% by preparative gas–liquid chromatography using a F & M Prepmaster Jr. 776 instrument, equipped with a 3/4 in. column packed with silicone gum rubber on Chromosorb W at 70°. Nitrogen was used as the carrier gas at a flow rate of 200 cc/min. Tetrahydrothiophene-α-d_4 and cyclohexene-d_{10} were obtained from Merck, Sharpe and Dohme of Canada Limited.

Kinetic Procedure

Measurement of rates of oxidation and chain initiation have been described previously (4). Absolute rate constants were measured at 30° using the rotating sector method. Autoxidations were initiated with either α,α′-azobisisobutyronitrile or α,α′-azobiscyclohexylnitrile and inhibited by 2,6-di-*t*-butyl-4-methoxyphenol.

Results and Discussion

Cyclic Sulfides

Rates of oxidation of tetrahydrothiophene at various partial pressures of oxygen, rates of chain initiation, and substrate concentrations are summarized in Table 1. These results imply that the overall rate of oxidation of this organic sulfide is given by

[9] $$R_s = k_p[RH]R_i^{1/2}/(2k_t)^{1/2}$$

which is the kinetic expression used to describe the autoxidation of many hydrocarbons and their oxygenated derivatives. In this expression R_s represents the rate of oxidation, R_i the rate of chain initiation, [RH] the concentration of tetrahydrothiophene, and k_p and $2k_t$ the rate

Can. J. Chem. Downloaded from www.nrcresearchpress.com by 210.87.254.5 on 09/05/12
For personal use only.

TABLE 2. Absolute propagation and termination rate constants for the oxidation of tetrahydrothiophene at 30°

Concentration (M)	$R_i \times 10^7$ ($M\,s^{-1}$)	$R_s \times 10^6$ ($M\,s^{-1}$)	$k_p/(2k_t)^{1/2} \times 10^3$ ($M^{-1/2}\,s^{-1/2}$)	k_p ($M^{-1}\,s^{-1}$)	$2k_t \times 10^{-7}$ ($M^{-1}\,s^{-1}$)
11.3	0.18	1.85	1.2	6.8	3.2
11.3	0.88	3.5	1.05	5.3	2.6
11.3	2.75	7.5	1.27	7.1	3.1

controlling propagation and termination rate constants.

Photochemically initiated rates of oxidation of tetrahydrothiophene were found to be reasonably constant over the length of time necessary to measure the following four rates of oxidation: (*i*) the rate of an oxidation illuminated continuously, R_s; (*ii*) the rate at a very high speed of sector rotation, R_∞; (*iii*) the rate at a sector speed where the rate was most sensitive to the length of the dark period; and (*iv*) a second value of R_s. The ratio of R_∞/R_s for tetrahydrothiophene was found to equal 0.5. Absolute propagation and termination rate constants were determined at three different rates of chain initiation and are summarized in Table 2.

The average propagation and termination rate constants for the oxidation of tetrahydrothiophene are $k_p = 6.4\ M^{-1}\ s^{-1}$ and $2k_t = 3.0 \times 10^7\ M^{-1}\ s^{-1}$. These rate constants are very similar to the propagation and termination rate constants we have previously obtained for the oxidation of the structurally analogous ether, tetrahydrofuran (see Table 4).

Tetrahydrothiophene-α-d_4 oxidizes about one tenth as fast as tetrahydrothiophene, *i.e.* $(k_p/(2k_t)^{1/2})_H/(k_p/(2k_t)^{1/2})_D = 10$. We have previously reported a deuterium isotope effect for the rate constants for the self reaction of secondary alkylperoxy radicals, $(2k_t)_H/(2k_t)_D$ equal to 1.37 (5). Using this isotope effect and the relative rates of oxidation of the deuterated and undeuterated tetrahydrothiophenes, a value of k_p equal to $0.58\ M^{-1}\ s^{-1}$ has been calculated for tetrahydrothiophene-α-d_4 and a propagation deuterium isotope effect equal to about 11. This isotope effect can be compared with the relative reactivities of tetralin and perdeuterotetralin towards *t*-butylperoxy radicals, $(k_p)_H/(k_p)_D = 16$ (6) and diphenylmethane and diphenylmethane-α-d_2 towards the diphenylmethylperoxy radical, $(k_p)_H/(k_p)_D = 5.1$ (7). While the work on the oxidation of organic sulfides was in progress we carefully checked the reactivities of cyclohexene and perdeuterocyclohexene towards *t*-butylperoxy radicals. Cyclohexene gave a value of $k_p = 1.5\ M^{-1}\ s^{-1}$ and perdeuterocyclohexene gave a value of $k_p = 0.13\ M^{-1}\ s^{-1}$ and an isotope effect of 11.5, in excellent agreement with the value for tetrahydrothiophene.

Tetrahydrothiopyran oxidizes about one fifth as fast as tetrahydrothiophene since the ratio $k_p/(2k_t)^{1/2}$ is equal to $2.7 \times 10^{-4}\ M^{-1}\ s^{-1}$. Because of the similarity between termination rate constants for the oxidation of tetrahydrothiophene, tetrahydrofuran, and tetrahydropyran a value of $2k_t$ equal to $3.0 \times 10^7\ M^{-1}\ s^{-1}$ has been assumed for tetrahydrothiopyran. This means that k_p for this six-membered cyclic sulfide is about $1.5\ M^{-1}\ s^{-1}$.

Acyclic Sulfides

The rate constant ratio, $k_p/(2k_t)^{1/2}$, and individual values of k_p and $2k_t$ could not be measured for the autoxidation of diisopropyl sulfide, dibenzyl sulfide, dibenzyl disulfide, benzyl *t*-butyl sulfide or α-toluenethiol. This was because the overall rates of oxidation of these sulfides were close to first order in light intensity and hence close to first order in the rate of chain initiation. For example, oxidation rates for the photochemically initiated autoxidation of diisopropyl sulfide gave a value of 0.25 for the ratio R_∞/R_s.

Benzyl phenyl sulfide was the only acyclic sulfide which gave a ratio of R_∞/R_s close to 0.5 and the individual rate constants for this compound were found to be $k_p/(2k_t)^{1/2} = 1.2 \times 10^{-3}\ M^{-1/2}\ s^{-1/2}$, $k_p = 9.5\ M^{-1}\ s^{-1}$, and $2k_t = 5.6 \times 10^7\ M^{-1}\ s^{-1}$. This sulfide appears to oxidize about four times faster than benzyl phenyl ether because of a larger propagation rate constant (see Table 4).

Autoxidation of Organic Sulfides in the Presence of t-Butyl Hydroperoxide

Previous publications in this series have reported rate constants for the reaction of organic compounds with *t*-butylperoxy radicals

Can. J. Chem. Downloaded from www.nrcresearchpress.com by 210.87.254.5 on 09/05/12
For personal use only.

TABLE 3. Oxidation of some organic sulfides in the presence of *t*-butyl hydroperoxide at 30°

Sulfide	Concentration (M)	Hydroperoxide concentration (M)	$R_i \times 10^7$ ($M\,s^{-1}$)	$R_s \times 10^7$ ($M\,s^{-1}$)	$k_p/(2k_t)^{1/2} \times 10^3$ ($M^{-1/2}\,s^{-1/2}$)	k_p^{br*} ($M^{-1}\,s^{-1}$)
Tetrahydrothiophene	9.04	2.0	0.13	2.95	2.84	0.1
Tetrahydrothiophene	9.04	2.0	3.0	8.3	1.7	0.06
Benzyl *t*-butyl sulfide	6.8	2.0	0.2	0.28	0.3	0.01
Dibenzyl disulfide	0.8	2.0	2.8	1.67	4.0	0.14
Dibenzyl disulfide	0.6	4.0	2.8	1.52	4.8	0.17
Benzyl phenyl sulfide	0.8	2.0	4.4	2.6	4.8	0.17
Benzyl phenyl sulfide	0.6	4.0	3.2	1.45	4.3	0.15
Dibenzyl sulfide	0.8	2.0	3.5	4.7	10	0.35
Dibenzyl sulfide	0.6	4.0	4.3	4.23	11	0.38

*Calculated from $k_p/(2k_t)^{\frac{1}{2}}$ using $2k_t = 1.2 \times 10^3\ M^{-1}\,s^{-1}$ for the mutual reaction of *t*-butylperoxy radicals.

TABLE 4. Propagation and termination rate constants for autoxidation of organic sulfides and ethers at 30°

Substrate	$k_p/(2k_t)^{1/2} \times 10^3$ ($M^{-1/2}\,s^{-1/2}$)	k_p ($M^{-1}\,s^{-1}$)	$2k_t \times 10^{-7}$ ($M^{-1}\,s^{-1}$)	k_p^{br} ($M^{-1}\,s^{-1}$)
Tetrahydrothiopyran	0.27	1.5	(3.0)†	0.02
Tetrahydropyran*	0.12	0.55	2.1	0.024
Tetrahydrothiophene-α-d_4	0.12	0.58	(2.2)†	0.015
Tetrahydrothiophene	1.2	6.4	3.0	0.1
Tetrahydrofuran*	0.78	4.4	3.1	0.34
Benzyl phenyl sulfide	1.3	9.5	5.65	0.16
Benzyl phenyl ether*	0.31	1.5	2.4	0.2
Dibenzyl sulfide	—	—	—	0.35
Dibenzyl ether*	—	—	—	1.3
Benzyl *t*-butyl sulfide	—	—	—	0.1
Benzyl *t*-butyl ether*	—	—	—	1.1

*Reference 8.
†Values in parentheses are estimated rate constants.

determined from oxidations in the presence of *t*-butyl hydroperoxide (usually > 1.0 M). Hydroperoxides are, however, believed to be unstable in the presence of organic sulfides. For example, no titratable hydroperoxide is formed during the oxidation of tetrahydrothiophene or the co-oxidation of tetrahydrothiophene and tetralin at 30°. *t*-Butyl hydroperoxide is, however, stable enough in the presence of some organic sulfides for rate constants to be measured for their reaction with the *t*-butylperoxy radical, k_p^{br}

$$[10]\quad BOO\cdot + RCH_2SR' \xrightarrow{k_p^{br}} BOOH + R\dot{C}HSR'$$

where BOO· represents the *t*-butylperoxy radical.

Table 3 summarizes rate and rate constant data for the oxidation of benzyl *t*-butyl sulfide, tetrahydrothiophene, dibenzyl disulfide, benzyl phenyl sulfide and dibenzyl sulfide in the presence of *t*-butylhydroperoxide (2–4 M). In all cases R_∞/R_s was close to or equal to 0.5 and the termination rate constant was about $1.2 \times 10^3\ M^{-1}\,s^{-1}$, our best value of the termination rate constant for *t*-butylperoxy radicals (8).[3]

Rates of oxidation of α-toluenethiol in the presence of *t*-butyl hydroperoxide were too autoretarding to give a meaningful value of $k_p/(2k_t)^{1/2}$ while the ratio R_∞/R_s for the oxidation of diisopropyl sulfide in the presence of *t*-butyl hydroperoxide was less than 0.3.

Tetrahydrothiophene-α-d_4 ($k_p^{br} = 0.015\ M^{-1}\,s^{-1}$) is less reactive towards *t*-butylperoxy radicals than tetrahydrothiophene and the deuterium isotope effect, $(k_p^{br})_H/(k_p^{br})_D$, is about 7, close to the value obtained from the oxidation of the pure sulfides.

In conclusion, propagation and termination rate constants for the oxidation of organic

[3]The oxidation of most sulfides in the presence of *t*-butyl hydroperoxide developed a large thermal rate of chain initiation after the absorption of a small quantity of oxygen. This implies that an oxidation product may be inducing the decomposition of *t*-butyl hydroperoxide by a free-radical process.

Can. J. Chem. Downloaded from www.nrcresearchpress.com by 210.87.254.5 on 09/05/12
For personal use only.

sulfides are summarized in Table 4 and are compared with the rate constants for the oxidation of structurally analogous ethers. It can be seen that towards the *t*-butylperoxy radical the sulfides are of equal or lower reactivity than the corresponding ethers. Furthermore, all three of the sulfides for which absolute rate constants have been determined are more reactive towards their own peroxy radical than the corresponding ethers are towards their own peroxy radical. Tetrahydrothiophene and tetrahydrofuran exhibit the mildest difference in k_p values, but for this pair the k_p^{br} values indicate a 3-fold higher reactivity for tetrahydrofuran. If allowance is made for this factor the measured rate constants suggest that α-alkylthiylalkylperoxy radicals are about 3–5 times more reactive in hydrogen atom abstractions than α-alkoxyalkylperoxy radicals.

1. J. A. HOWARD. Adv. Free Radical Chem. In press.
2. D. BARNARD, L. BATEMAN, and J. I. CUNEEN. Organic sulphur compounds. Vol. 1. *Edited by* N. Kharasch. Pergamon Press, New York. 1961. Chap. 21.
3. V. N. IPATIEFF, H. PINES, and B. S. FREDMAN. J. Am. Chem. Soc. **60**, 2731 (1938).
4. J. A. HOWARD and K. U. INGOLD. Can. J. Chem. **47**, 3809 (1969).
5. J. A. HOWARD and K. U. INGOLD. J. Am. Chem. Soc. **90**, 1058 (1968).
6. J. A. HOWARD and K. U. INGOLD. Can. J. Chem. **46**, 1017 (1968).
7. J. A. HOWARD and K. U. INGOLD. Can. J. Chem. **44**, 1119 (1966).
8. J. A. HOWARD and K. U. INGOLD. Can. J. Chem. **48**, 873 (1970).

Can. J. Chem. Downloaded from www.nrcresearchpress.com by 210.87.254.5 on 09/05/12
For personal use only.

4-9
2183-3074

Canadian Journal of Chemistry

Published by THE NATIONAL RESEARCH COUNCIL OF CANADA

VOLUME 49 JULY 1, 1971 NUMBER 13

Can. J. Chem. Downloaded from www.nrcresearchpress.com by 210.87.254.105 on 09/05/12
For personal use only.

The Acetone – Acetic Anhydride – Carbon Disulfide System: Surface Tension, Viscosity, and Total and Partial Vapor Pressures

A. N. CAMPBELL, E. M. KARTZMARK, AND S. C. ANAND

Department of Chemistry, University of Manitoba, Winnipeg

Received February 5, 1971

The surface tensions, viscosities, and vapor pressures, total and partial, have been determined as functions of concentration for the following systems: (*a*) acetone – acetic anhydride; (*b*) acetone – carbon disulfide; (*c*) acetic anhydride – carbon disulfide; and (*d*) pseudo-binary mixtures of (*a*) and (*b*), whose compositions lie on a straight line tangential to the plait point of the ternary system.

The general behavior of ideal and non-ideal systems, in regard to surface tension and viscosity is discussed. For the system acetone – carbon disulfide, whose vapor phase can be considered ideal, the activities, activity coefficients, excess free energies, enthalpies and entropies of mixing have been obtained from the vapor pressures. The vapor phase of the other three systems contains acetic anhydride which is associated in the vapor state, and for these systems the experimental data are reported without further calculation.

Les tensions superficielles, les viscosités et les pressions de vapeur, totales et partielles, ont été déterminées en fonction de la concentration pour les systèmes suivants: (*a*) acétone – anhydride acétique; (*b*) acétone – disulfure de carbone; (*c*) anhydride acétique – disulfure de carbone; et (*d*) des pseudo-mélanges binaires de (*a*) et (*b*), dont les compositions se trouvent sur une droite tangente au point de plissement du système ternaire.

Le comportement général des systèmes idéaux et non idéaux est discuté en fonction de la tension superficielle et de la viscosité. Pour le système acétone – disulfure de carbone, dont la phase vapeur peut être considérée comme idéale, les activités, les coéfficients d'activité, l'excès d'énergie libre, les enthalpies et les entropies de mélanges ont été obtenus des pressions de vapeur. La phase vapeur des trois autres systèmes contient de l'anhydride acétique qui existe à l'état associé en phase vapeur; pour ces systèmes les données expérimentales sont rapportées sans calculs ultérieurs

Canadian Journal of Chemistry, **49**, 2183 (1971)

Introduction

The acetone – acetic anhydride – carbon disulfide system has been the subject of extended research in this laboratory because the acetic anhydride – carbon disulfide binary system forms two layers over a composition range of about 35 mol% at 25°, the critical solution temperature being 52.8° (1–4), but the heterogeneity is destroyed by the addition of about 4 mol% acetone. It is therefore possible, by studying the properties of mixtures whose compositions lie on a straight line tangential to the plait point, to examine isothermally the behavior of solutions just outside the critical condition. The line tangential to the plait point was obtained by drawing a straight line through the plait point, parallel to the tie-lines in the heterogeneous region. The compositions corresponding to the intersection of this line with the two binary systems acetic anhydride – acetone and carbon disulfide – acetone were described as solutions *A* and *B*. Large volumes of these solutions were made up. Mixtures in various proportions of these two solutions gave solutions lying on this straight line. The properties we have previously studied both for the ternary system and its component binary systems are: congruent compositions, excess volumes, and dielectric constants (1) and heats of mixing (2). In the present paper, we report on the surface tensions, viscosities, and total and partial vapor pressures, all at 25°.

Experimental

The purification of materials and experimental methods have all been described before (1–4 and particularly ref.

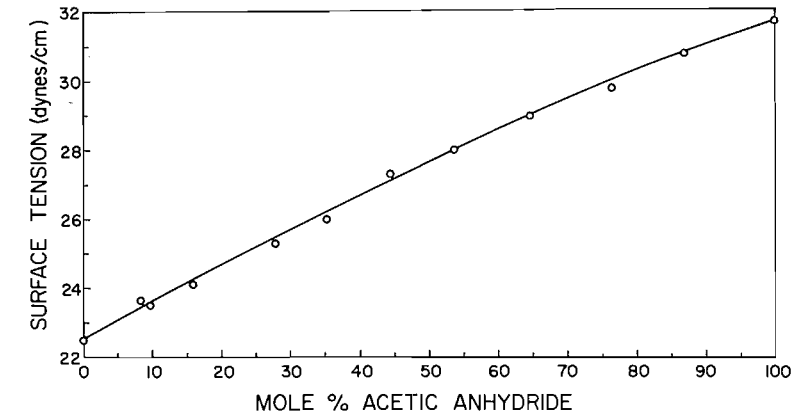

FIG. 1. Surface tension of the acetone – acetic anhydride system at 25°.

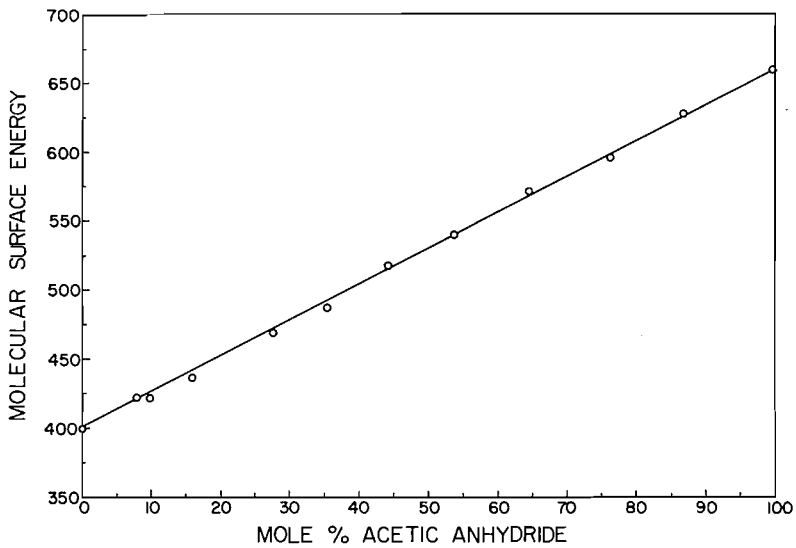

FIG. 2. Molecular surface energy of the acetone – acetic anhydride system at 25°.

5), with the exception of total and partial vapor pressures. The total pressure was determined using a wide bore manometer containing mercury. Solutions were repeatedly frozen in liquid nitrogen and exhausted for several hours, before establishing communication with the manometer. With solutions rich in carbon disulfide, a peculiar phenomenon was observed. Such solutions frequently exploded on warming up, after cooling to liquid nitrogen temperatures. Experiment in an open vessel with pure carbon disulfide showed that the warming up is accompanied by a pronounced crackling sound, which seems to indicate a phase change in the solidified carbon disulfide, with consequent rupture of the containing vessel. This problem was solved by using vessels with very thick walls containing short lengths of sealed Teflon tubing to take up the expansion. Composition of the equilibrium liquid was checked refractometrically. The compositions of the vapors in equilibrium with liquid mixtures of given composition were determined by the air-saturation method, using what was essentially the apparatus of Bichowsky and Storch (6). For the one system whose vapor may be said to behave ideally, *viz.* acetone – carbon disulfide, partial pressures were calculated.

Results

Surface Tension

All numerical results are to be found in the Depository of Unpublished Data of the National Research Council of Canada, but for the benefit of the general reader we express our results

Can. J. Chem. Downloaded from www.nrcresearchpress.com by 210.87.254.105 on 09/05/12
For personal use only.

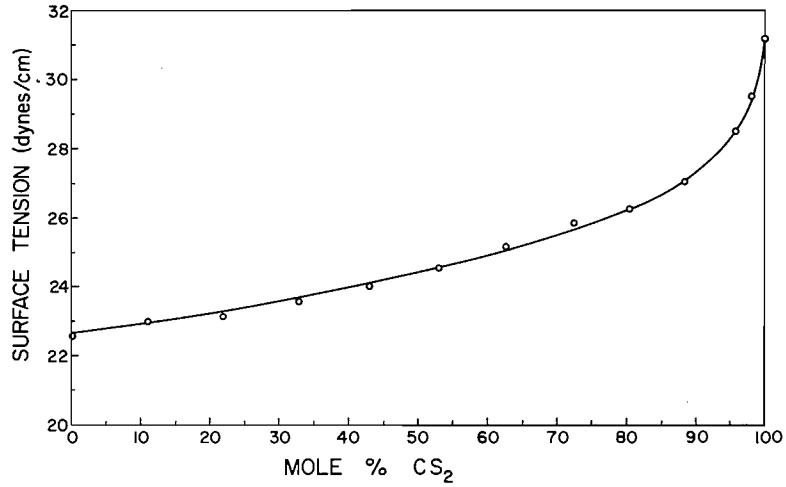

FIG. 3. Surface tension of the acetone – carbon disulfide system at 25°.

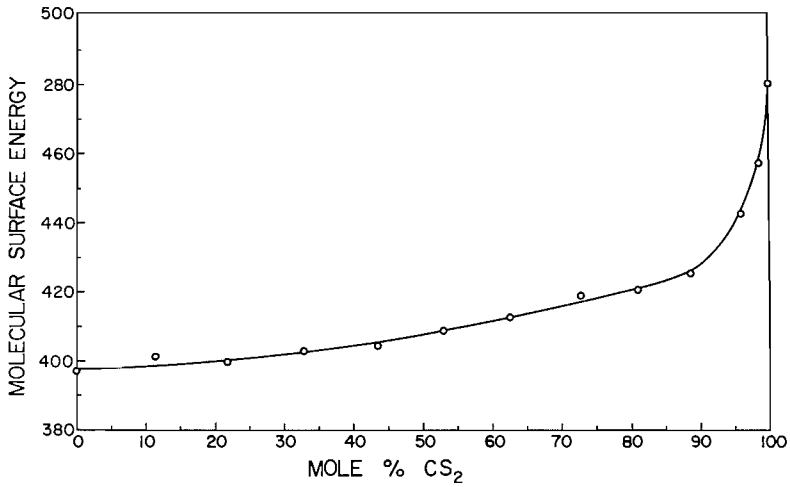

FIG. 4. Molecular surface energy of the acetone – carbon disulfide system at 25°.

graphically.[1] Although the old-fashioned molecular surface energy ($\gamma(Mv)^{2/3}$) no longer has any exact meaning, it still serves as a method of comparison and we have also represented this graphically. Figure 1 expresses the surface tension and Fig. 2 the molecular surface energy (m.s.e.) of the acetone – acetic anhydride system, *vs.* mol% acetic anhydride. Figures 3 and 4 represent the same data for acetone – carbon disulfide. There seem to be some discrepancies in the literature as to the surface tension of pure carbon disulfide. Our own figure for 25° is 31.78 dyn/cm. Figures 5 and 6 show the surface tensions and m.s.e.'s of the acetic anhydride – carbon disulfide system on both sides of the miscibility gap.

The same data were obtained for the pseudo-binary system and are represented graphically in Figs. 7 and 8, where the compositions are calculated to absence of acetone.

Viscosity

The viscosities (water = 1) of all systems are represented graphically in Figs. 9, 10, 11, and 12.

[1]Photocopies may be obtained free of charge, upon request, from the Depository of Unpublished Data, National Science Library, National Research Council of Canada, Ottawa, Canada.

Can. J. Chem. Downloaded from www.nrcresearchpress.com by 210.87.254.105 on 09/05/12
For personal use only.

Can. J. Chem. Downloaded from www.nrcresearchpress.com by 210.87.254.105 on 09/05/12
For personal use only.

TABLE 1. Total and partial pressure and thermodynamic quantities of the acetone–CS_2 system

Composition of liquid (mol% CS_2)	Total pressure manometric (mm of Hg calculated at 0 °C)
0.0	230.4
4.54	292.4
9.98	339.5
19.6	397.4
31.3	425.4
42.5	440.0
64.4	449.7
76.4	449.8
83.0	444.0
92.2	425.6
100	361.1

Liquid comp'n		Vapor Comp'n											
m.f. CS_2	m.f. acetone	m.f. CS_2	m.f. acetone	Interpolated total P	P_{CS_2}	$P_{acetone}$	a_{CS_2}	$a_{acetone}$	γ_{CS_2}	$\gamma_{acetone}$	G^E	H^E	TS^E
0.0740	0.926	0.286	0.714	322	92.0	230	0.255	0.998	3.446	1.078	95.6	54.6	−41.0
0.114	0.886	0.390	0.610	356	139	217	0.390	0.944	3.376	1.065	115.4	76.9	−38.5
0.214	0.786	0.500	0.500	404	202	202	0.559	0.877	2.612	1.116	172.8	116.8	−56.0
0.336	0.664	0.584	0.416	430	251	179	0.695	0.777	2.068	1.170	206.7	146.0	−60.7
0.425	0.575	0.616	0.384	440	271	169	0.750	0.734	1.765	1.277	226.5	160.0	−66.5
0.648	0.352	0.675	0.325	450	304	146	0.842	0.634	1.299	1.801	223.4	174.4	−49.0
0.766	0.234	0.710	0.290	450	320	130	0.886	0.564	1.157	2.410	187.7	158.7	−29.0
0.828	0.172	0.736	0.264	444	327	117	0.906	0.508	1.094	2.953	154.6	136.7	−17.9
0.915	0.085	0.806	0.194	423	341	82	0.944	0.357	1.032	4.201	89.3	85.6	−3.7

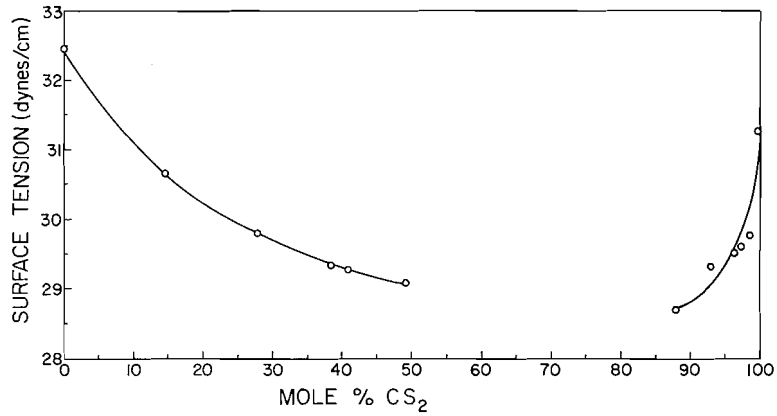

FIG. 5. Surface tension of the acetic anhydride – carbon disulfide system at 25°.

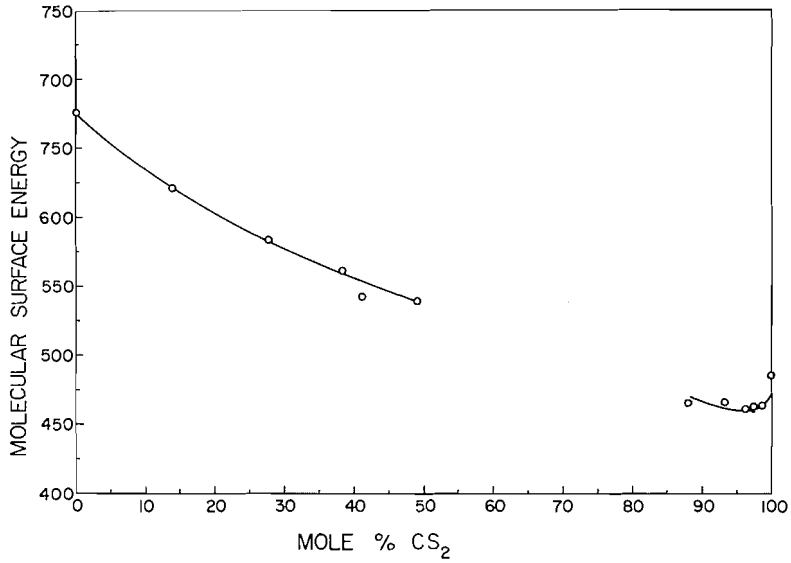

FIG. 6. Molecular surface energy of the acetic anhydride – carbon disulfide system at 25°.

Vapor Pressure

Tables 1, 2, 3, and 4 give the total pressures and vapor compositions of all four systems. For the acetone – carbon disulfide system, the partial pressures and derived thermodynamic quantities have also been calculated and are given in Table 1. The partial pressures yield the activities directly and from these and the concentrations, the activity coefficients. The excess free energy of mixing is then obtained from

$$G^E = X_1 RT \ln \gamma_1 + X_2 RT \ln \gamma_2$$

A previous paper (3) enabled us to calculate H^E ($= \Delta H_m$), using the constants of the Redlich and Kister equation given in that paper. From these

TABLE 2. Vapor pressures and vapor composition of acetone – acetic anhydride system at 25 °C

Mole fraction of acetic anhydride in		
Liquid phase	Vapor phase (interpolated)	Total pressures (mm of Hg)
0.000	0.000	230.4
0.0920	0.004	207.9
0.1725	0.005	184.8
0.2430	0.009	172.4
0.3734	0.014	142.6
0.4903	0.020	116.5
0.6007	0.032	91.8
0.7360	0.070	63.4
0.8620	0.156	36.8
0.9480	0.293	18.9
1.000	1.000	7.1

Can. J. Chem. Downloaded from www.nrcresearchpress.com by 210.87.254.105 on 09/05/12
For personal use only.

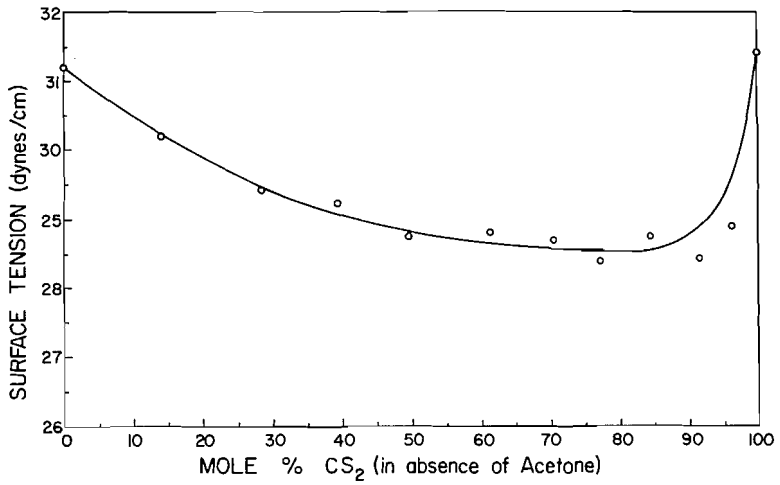

FIG. 7. Surface tension of the acetone – acetic anhydride – carbon disulfide (pseudo-binary system) at 25°.

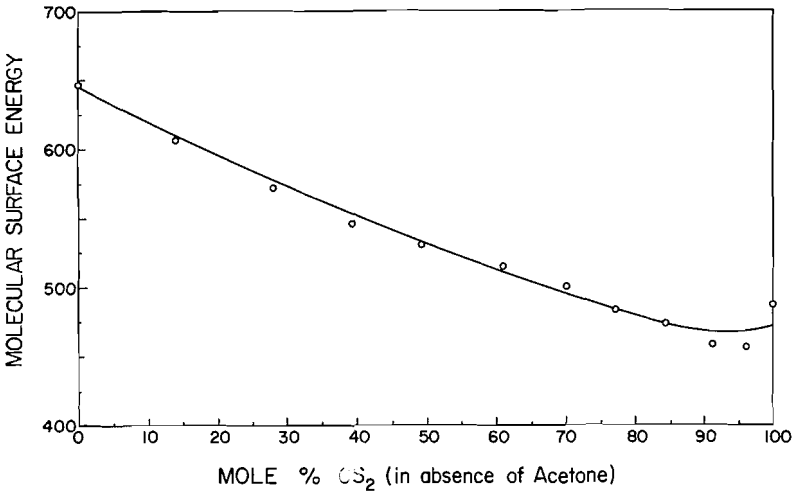

FIG. 8. Molecular surface energy of the acetone – acetic anhydride – carbon disulfide (pseudo-binary system) at 25°.

TABLE 3. Total pressures (mm of Hg) and vapor compositions for the carbon disulfide – acetic anhydride system at 25 °C

Mol% CS_2 in		
Liquid phase	Vapor phase (interpolated)	Total pressure (mm of Hg)
0.00	0.00	7.1
11.30	97.80	192.5
21.89	98.30	285.0
27.20	98.50	309.1
35.30	98.60	336.4
88.20	98.70	350.4
97.48	99.28	356.4
100.00	100.00	361.1

data, S^E or TS^E results in the usual manner. The results are expressed graphically as Fig. 13. The vapor pressures of the system, carbon disulfide – acetone were first determined by Zawidsky (7) at 35.17° and later by Hirschberg (8) at 29.2°.

Thermodynamic quantities have not been derived for the remaining systems, because the vapor of acetic anhydride is associated (11) and it is therefore not possible to obtain the true partial pressures or activities by any simple method, although no great error would be made in making the calculations for the more volatile constituents, since the vapor pressure of acetic

Can. J. Chem. Downloaded from www.nrcresearchpress.com by 210.87.254.105 on 09/05/12
For personal use only.

Can. J. Chem. Downloaded from www.nrcresearchpress.com by 210.87.254.105 on 09/05/12
For personal use only.

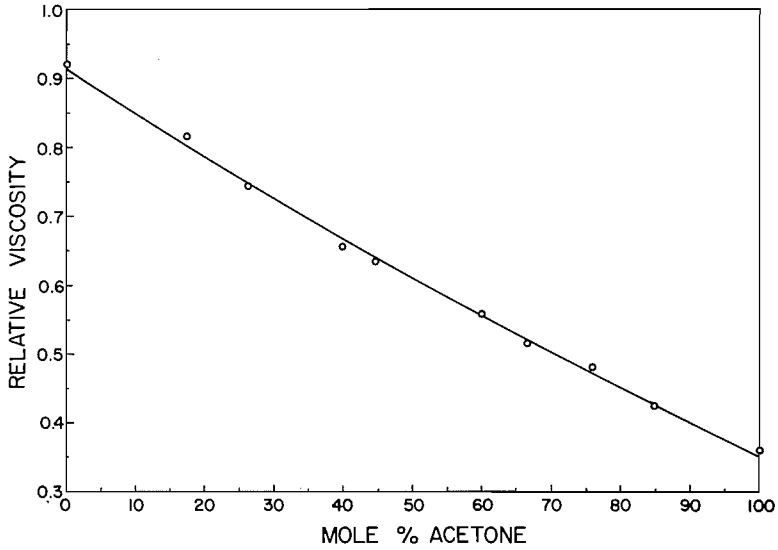

FIG. 9. Viscosity of the acetone – acetic anhydride system at 25°.

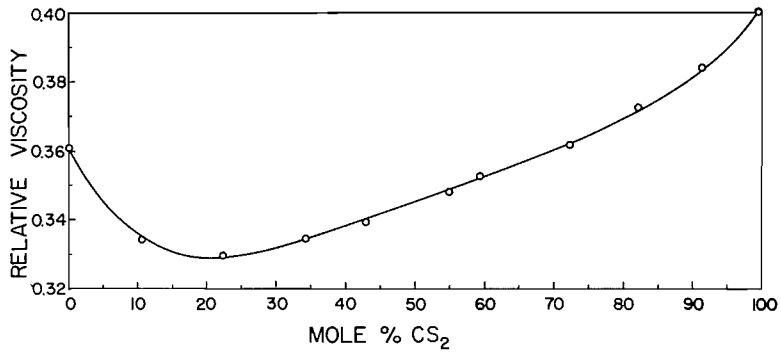

FIG. 10. Viscosity of the acetone – carbon disulfide system at 25°.

TABLE 4. Vapor–liquid equilibria and total pressure data for the acetic anhydride – carbon disulfide – acetone ternary system at 25 °C*

Liquid composition (mol%)			Vapor composition (mol%)			
Acetic anhydride	CS_2	Acetone	Acetic anhydride	CS_2	Acetone	Total pressure (mm Hg)
0.00	98.50	1.50	0.00	93.20	6.80	392.8
7.47	90.63	1.90	0.95	95.20	3.85	363.8
23.50	73.80	2.70	1.30	95.60	3.10	357.8
27.02	70.02	2.96	1.30	95.60	3.10	357.8
35.03	61.50	3.47	1.40	95.70	2.90	357.9
51.60	44.12	4.28	1.70	95.20	3.10	354.1
71.46	22.87	5.37	1.90	94.40	3.70	295.7
93.46	0.00	6.54	26.20	0.00	73.80	21.0

*The liquid phase lies on the pseudo-binary line but this, of course, is not true of the vapor composition.

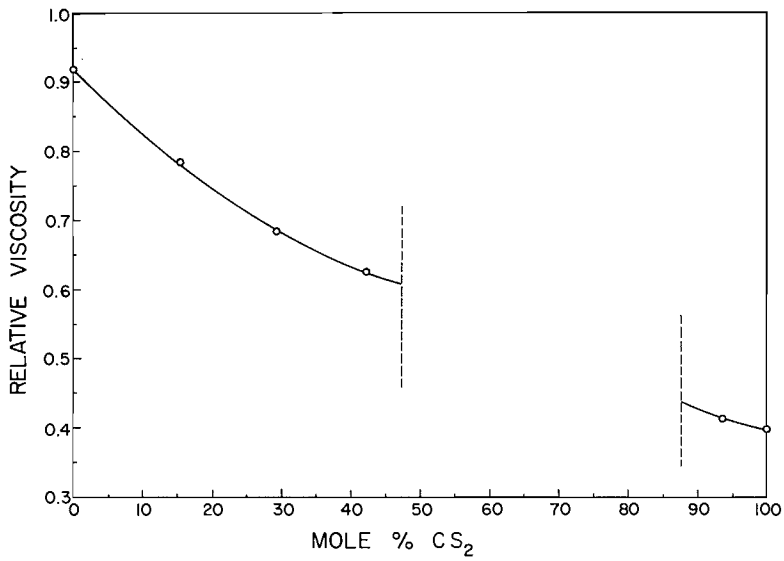

FIG. 11. Viscosity of the acetic anhydride – carbon disulfide system at 25°.

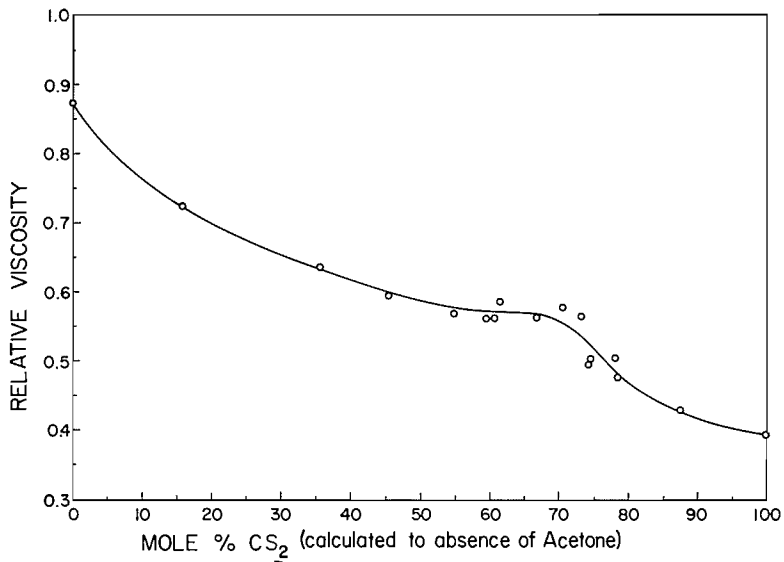

FIG. 12. Viscosity of the acetone – acetic anhydride – carbon disulfide system at 25°.

anhydride is quite low (= 7 mm at 25°). If it is desired to take into account the dimerization of one component in the vapor phase, this can be done, if, as in the present paper, the equilibrium compositions of liquid and vapor are known (10–12).

Discussion

In Fig. 1 the surface tensions of acetone – acetic anhydride mixtures show slight positive deviation from linearity. The m.s.e., however (Fig. 2), gives a practically straight line plot. We have previously pointed out (1, 2) that the acetone – acetic anhydride system is practically ideal. The acetone – carbon disulfide system shows very strong negative deviation from straight line behavior of the surface tension and m.s.e. plots, and it is well known that this system is very non-ideal. Indeed, at a sufficiently low temperature

Can. J. Chem. Downloaded from www.nrcresearchpress.com by 210.87.254.105 on 09/05/12
For personal use only.

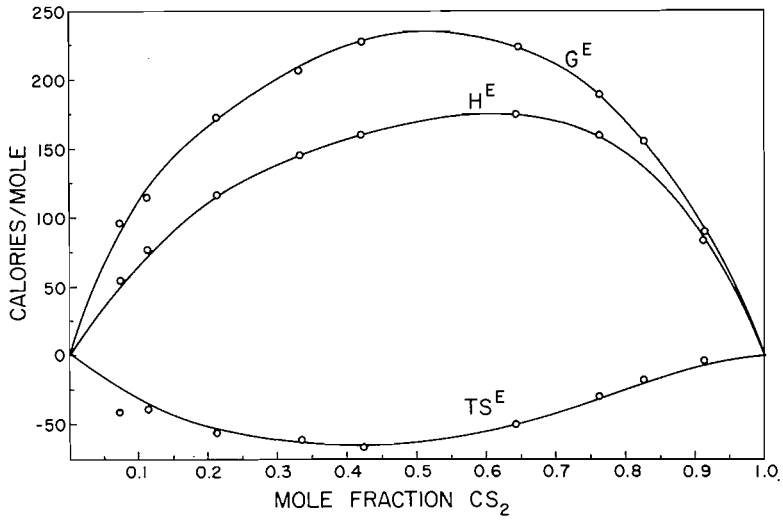

FIG. 13. Thermodynamic quantities *vs.* mole fraction of the acetone – carbon disulfide system at 25°.

(−73 °C), the system forms two layers (2). Figures 5 and 6 show similar non-ideal behavior for the acetic anhydride – carbon disulfide system, as of course is to be expected, since this system forms two layers at 25°. The pseudo-binary system, *A–B*, while also showing negative deviation from ideality, is not so markedly non-ideal as the two other non-ideal systems. The application of the Gibbs adsorption equation to this is obvious.

A general scrutiny of these non-ideal systems indicates that the surface tension of the non-polar substance (carbon disulfide) is rapidly reduced by small additions of the polar substance (acetic anhydride or acetone). On the other hand, the surface tension of the polar substance, though also reduced, follows an almost linear relation for small additions of the non-polar substance. It is not necessary, where partial miscibility occurs, that the congruent layers should have the same surface tension (9).

The behavior of these systems with respect to viscosity seems not unlike that with respect to surface tension. The viscosities of the acetic anhydride – acetone system show almost straight line behavior, as a function of molar composition. The other three (non-ideal) systems show pronounced negative deviation from additivity. Concerning the system showing a gap at 25° (acetic anhydride – carbon disulfide), it is noteworthy that the viscosities of the congruent layers are far from being the same. The pseudo-binary system, however, seems to show a region of roughly constant viscosity in the neighborhood of the plait point. This region of constant viscosity is a manifestation of the "anomalous viscosity", commonly observed in the neighborhood of critical points, *i.e.*, the viscosity is greater than what would correspond to the smooth curve. This again is a manifestation of the colloidal, or semi colloidal, nature of solutions close to the critical state.

An extended discussion of the vapor pressure and thermodynamic measurements seems to us out of place. We have applied the equations of Margulese and of van Laar and obtained the usual 5% discrepancy between calculated and observed activity coefficients of acetone and of carbon disulfide.

Table 4, which gives total pressures and liquid and vapor compositions in the pseudo-binary system, is of particular interest. If total pressure is plotted against mol% carbon disulfide (calculated to absence of acetone), it is seen to be practically constant over the range 23 to 51 mol% acetic anhydride. The same must be true of the partial pressures, since the vapor composition changes hardly at all. Since all compositions of the pseudo-binary system lie on a straight line tangential to the curve of congruent compositions at the plait point, it appears that the (isothermal) thermodynamic requirement that two liquid layers in equilibrium must possess the same total and partial pressures persists in the homogeneous region in the immediate neighborhood of the plait point.

Can. J. Chem. Downloaded from www.nrcresearchpress.com by 210.87.254.105 on 09/05/12
For personal use only.

1. A. N. CAMPBELL and E. M. KARTZMARK. Can. J. Chem. **48**, 904 (1970).
2. A. N. CAMPBELL, E. M. KARTZMARK, and S. C. ANAND. Can. J. Chem. **48**, 1579 (1970).
3. A. N. CAMPBELL and E. M. KARTZMARK. Can. J. Chem. **47**, 619 (1969).
4. A. N. CAMPBELL and E. M. KARTZMARK. Can. J. Chem. **45**, 2433 (1967).
5. A. N. CAMPBELL, E. M. KARTZMARK, S. C. ANAND, Y. CHENG, H. P. DZIKOWSKI, and S. M. SKRYNYK. Can. J. Chem. **46**, 2399 (1968).
6. F. R. V. BICHOWSKY and H. V. STORCH. J. Am. Chem. Soc. **37**, 2696 (1915).
7. J. VON ZAWIDSKY. Z. Phys. Chem. **35**, 129 (1900).
8. J. HIRSCHBERG. Bull. Soc. Chim. Belg. **41**, 163 (1932).
9. J. H. HILDEBRAND and R. L. SCOTT. Solubility of nonelectrolytes. Dover Publications, Inc., New York. 1964. p. 416.
10. M. B. KING. Phase equilibria in mixtures. Pergamon Press, Toronto. 1969. p. 356.
11. A. N. CAMPBELL, E. M. KARTZMARK, and J. M. GIESKES. Can. J. Chem. **41**, 407 (1963).
12. S. D. CHRISTIAN. J. Phys. Chem. **64**, 764 (1960).

Can. J. Chem. Downloaded from www.nrcresearchpress.com by 210.87.254.105 on 09/05/12
For personal use only.

Can. J. Chem. Downloaded from www.nrcresearchpress.com by 210.87.254.5 on 09/05/12
For personal use only.

Production of $O(^1D_2)$ Atoms in the Photolysis of CO_2 at close to 1600 Å[1]

L. M. QUICK[2] AND R. J. CVETANOVIĆ

Division of Chemistry, National Research Council of Canada, Ottawa, Canada

Received March 4, 1971

Photolysis of CO_2/neopentane mixtures with a bromine lamp was studied at room temperature to obtain chemical evidence for primary formation of $O(^1D_2)$ atoms in the photolysis of CO_2 at close to 1600 Å. The trends in the effects of various added gases on the yield of neopentanol agreed well with those reported in the literature for the rates of deactivation of $O(^1D_2)$ atoms. This agreement demonstrated $O(^1D_2)$ formation in the photolysis of CO_2 at the wavelength used.

On a étudié la photolyse de mélanges CO_2/neopentane à la température de la pièce et à l'aide d'une lampe à brome afin de détecter des preuves chimiques concernant la formation primaire d'atomes $O(^1D_2)$ lors de la photolyse du CO_2 autour de 1600 Å. Les effets produits par l'addition de divers gaz sur le rendement de néopentanol sont en accord avec ceux rapportés dans la littérature pour les taux de désactivation des atomes $O(^1D_2)$. Cette concordance démontre que des atomes $O(^1D_2)$ sont formés lors de la photolyse du CO_2 à la longueur d'onde utilisée.

Canadian Journal of Chemistry, **49**, 2193 (1971)

Introduction

Photolysis of carbon dioxide takes place in the vacuum ultraviolet spectral region at wavelengths shorter than about 1700 Å. It is a process of importance for understanding of the photochemical balances of some planetary atmospheres and although it has been studied extensively in recent years (1–9), some aspects of its detailed mechanism are still quite controversial and uncertain. Primary formation of the excited oxygen atoms $O(^1D_2)$ is generally postulated but their direct observation by spectroscopic methods is difficult because of their great reactivity and quite long radiative life time. On the other hand, their indirect observation by chemical methods is now well established and is responsible for much of the current knowledge of their chemical and physical behavior.

In the present work an attempt is made to use the relatively simple reaction of $O(^1D_2)$ atoms with neopentane (10, 11) as a chemical probe for the production of $O(^1D_2)$ atoms in the photolysis of CO_2 at about 1600 Å. In this reaction neopentanol is formed by insertion of $O(^1D_2)$ into the CH bonds of neopentane with an efficiency of about 65% and the "hot" alcohol is completely stabilized at moderate pressures (100–200 Torr). The known effects (10, 12–16) of various additive gases are used in conjunction with the yield of neopentanol as qualitative evidence for the presence of $O(^1D_2)$ atoms. The quantum yield of neopentanol provides a quantitative indication of the primary quantum yield of $O(^1D_2)$ atoms. The present study is a continuation of an earlier investigation (17) of CO_2 photolysis at close to 1600 Å.

Experimental

Photolyses were carried out at room temperature (25 ± 1 °C) in a semispherical reaction vessel of about 250 ml in volume, incorporated in a circulating system containing a piston type circulating pump and connected to a bromine lamp through a thin semispherical Suprasil window. A lamp and reactor of the same construction were designed and used in the earlier study of CO_2 photolysis and are described in greater detail elsewhere (17). The lamp itself was an adaptation of the bromine lamp of Harteck and co-workers (18). The main output is at 1633 Å and also there are two smaller lines at around 1575 Å and some low background continuum extending to the 2100 Å region. The circulating pump was used to achieve efficient mixing of the reactants before the photolysis and to assure after the photolysis complete condensation at −196 °C of the condensable products in a U-bend of the reaction system immersed in liquid nitrogen. The non-condensable gases were collected through a liquid nitrogen trap into a combined Toepler pump-gas burette. The condensables were warmed up and the above procedure repeated to collect any residual non-condensables trapped in the frozen products. The non-condensables were analyzed on a 20 ft 13X molecular sieve column at room temperature, using helium as the carrier gas and a thermistor detector.

A known amount of toluene was added as an internal standard to the condensable products in a vessel provided with a magnetically operated stirrer. After thorough mixing, these products were analyzed at room temperature on a 300 ft 0.015 in. i.d. stainless steel capillary column coated with β,β′thiodipropionitrile, using helium as the

[1]NRCC No. 11934.
[2]NRCC Postdoctorate Fellow 1968–1970.

Can. J. Chem. Downloaded from www.nrcresearchpress.com by 210.87.254.5 on 09/05/12
For personal use only.

carrier gas and a hydrogen flame detector. Mass spectrometric identification of the individual gas chromatographic peaks was carried out on a fast scanning CH4 Atlas mass spectrometer connected so to scan directly the column eluents. Hydrocarbon products were analyzed on a 300 ft squalane capillary column at 25 °C and a 300 ft dinonyl phthalate capillary column at 0 °C.

The main emphasis was on a quantitative analysis of the neopentanol/CO ratios. These ratios were time dependent at larger conversions, decreasing at longer irradiation times, and the initial values were then obtained by extrapolation to zero time. In later work, analyses were carried out at small conversions and extrapolations to zero time were found to be unnecessary.

Matheson Research Grade carbon dioxide was used after degassing at −196 °C and several bulb-to-bulb distillations from −78 to −196 °C with retention of the middle cut. Phillips Research Grade neopentane was treated with concentrated H_2SO_4 and then passed over KOH pellets to remove traces of olefins. This was followed by several bulb-to-bulb distillations from −78 to −196 °C, with degassing. However, a sample of neopentane not treated with H_2SO_4 and KOH gave results similar to those obtained with a treated sample.

Matheson Research Grade xenon was degassed from solid nitrogen. Matheson carbon monoxide (stated purity 99.5%) was passed through a trap at −78 °C to remove iron carbonyl. Matheson Research Grade nitrogen was used without further purification and Matheson Ultra High Purity hydrogen was expanded into its vacuum reservoir through a liquid nitrogen trap. Matheson sulfur hexafluoride was degassed at −140 °C to remove carbon tetrafluoride and subjected to two bulb-to-bulb distillations with retention of the middle cut. Phillips Research grade ethane and propane were used after degassing and several bulb-to-bulb distillations from −78 to −196 °C.

At the wave lengths of 1633 and 1575 Å from the bromine lamp used no photolysis of sulfur hexafluoride was observed, in agreement with the fact that SF_6 begins to absorb at 1520 Å and peaks at 1050 Å.

Results

Chemical evidence for $O(^1D)$ atom formation in the photolysis of CO_2 was sought in the present work in the type of products formed in the photolysis of CO_2/neopentane mixtures. An obvious complication arises from the fact that the bromine lamp used photolyzes not only CO_2 but also neopentane and some of the primary reaction products. However, although this complication was troublesome it did not interfere with the primary objective of the work to obtain evidence for the presence of $O(^1D)$ atoms. Photolysis of neopentane at about 1600 Å was found to produce H_2, CH_4, C_2H_6 and various higher paraffins and olefins (hexamethylethane, 2,2,4-trimethylpentane, and 2,4,4-trimethylpentene-1 were identified). Some of these products were also found in the photolysis of CO_2/neopentane mixtures but they did not interfere with the study of the yields of oxygen-containing products, notably of neopentanol, the major product of reaction of $O(^1D)$ with neopentane. Hydrocarbons higher than C_2H_6 were therefore not measured quantitatively. Photolysis of neopentanol alone at about 1600 Å formed a variety of products, including pivalaldehyde, acetone, tert-butanol, methanol, and isobutyraldehyde. Pivalaldehyde was the main product. These products were formed also in the neopentane/CO_2 system but were not measured quantitatively. Initial yield of neopentanol was determined by extrapolation to zero reaction time, as will be described below.

Photolysis of CO_2 alone at pressures up to about 1 atm has been recently investigated in some detail in this laboratory (17). Our experiments at 100, 220, and 600 Torr CO_2 show similar O_2/CO values and do not require further discussion.

With CO_2/neopentane mixtures the main attention was focused on the neopentanol/CO ratio. As already indicated, this ratio was time dependent mainly as a result of the secondary photolysis of neopentanol. Figure 1 shows examples of decreasing neopentanol/CO ratios at longer reaction times. Steeper decrease is observed at larger

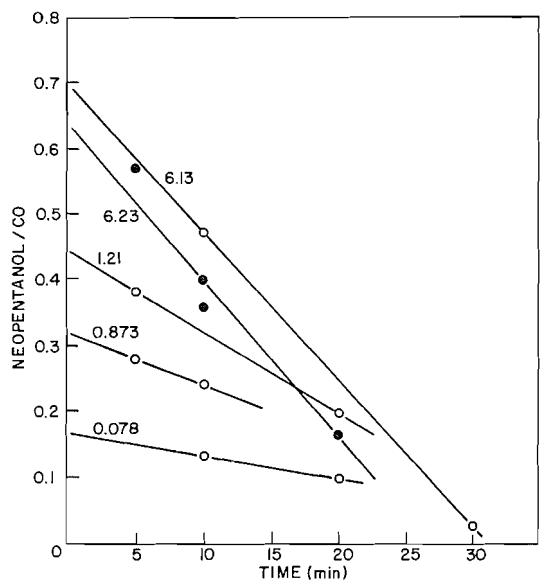

FIG. 1. Variation of the neopentanol/CO yields as a function of time at different [neopentane]/[CO_2] ratios (indicated on the lines).

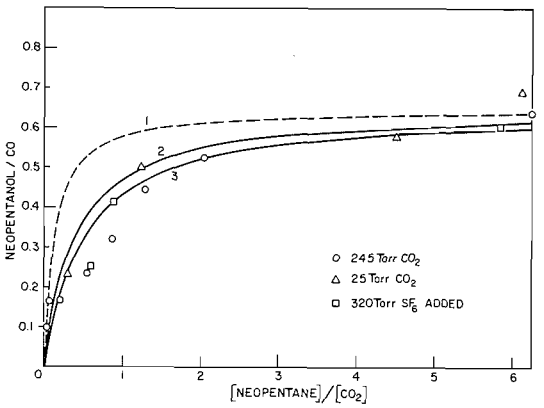

FIG. 2. Variation of the neopentanol/CO yields as a function of the [neopentane]/[CO_2] ratio. (The meaning of the broken and solid curves is explained in the text).

neopentane/CO_2 ratios (indicated by the numbers on the lines). Linear extrapolations to zero time were used to determine approximately the initial values of the neopentanol/CO ratios and these are plotted in Fig. 2 for a number of experiments. The ratios increase with increasing neopentane/CO_2, tending to a plateau value between 0.6 and 0.7. Because of errors in extrapolations to zero time and possible slight changes in the character of lamp emission, there is considerable scatter of points, but within this uncertainty there does not seem to be a difference between experiments with 25 and 245 Torr CO_2. Furthermore, as shown in Fig. 2, addition of approximately 320 Torr SF_6 in some of these experiments had no effect on the neopentanol/CO ratios. The significance of the solid and the interrupted curves in Fig. 2 will be discussed later.

In order to test directly whether O(^{1}D) atoms are involved in the process, the effect of various added gases on the relative yield of neopentanol has been investigated. Since Fig. 2 shows that for neopentane/$CO_2 \geqslant 6.5$ the neopentanol yield was at the plateau value, such mixtures were used (with about 11 Torr CO_2) in the presence of different pressures of added gases (SF_6, Xe, C_2H_6, C_3H_8, CO, N_2, and H_2). The ratios of the initial rates of formation of CO and neopentanol (r_{CO}/r_{ROH}) were determined and plotted as a function of the ratio of concentrations of the added gas (A) and neopentane (RH). At the very small conversions used in some of the systems studied extrapolations to zero time were found to be unnecessary and were not made. Slope to intercept ratios of the linear r_{CO}/r_{ROH} plots gave ratios of rate constants for the over-all (chemical plus physical) reaction of O($^1D_2$) atoms with the added gas (k_A) and with neopentane (k_{np}), since, as will be shown later, under conditions of these experiments

$$[1] \qquad \frac{r_{CO}}{r_{ROH}} = \frac{1}{\alpha}\left(1 + \frac{k_A}{k_{np}}\frac{[A]}{[RH]}\right)$$

The constant α is the fraction of O($^1D_2$) atoms interacting with neopentane which insert into the CH bonds to form neopentanol.

Plots of eq. 1 for SF_6, Xe, C_2H_6, and C_3H_8 are shown in Fig. 3. There is an appreciable scatter of points but the expected pronounced increase in reactivity in going from SF_6 to Xe, C_2H_6, and C_3H_8 is clearly shown. Least-square values and the corresponding standard deviations of k_A/k_{np} are given in Table 1 and are compared with the literature values obtained in vastly different systems.

The values of k_A/k_{np} for CO, N_2, and H_2 have been obtained in somewhat similar manner and are also included in Table 1. However, in the presence of large amounts of these non-condensable gases it was not feasible to measure directly the yield of CO and it was assumed that the lamp intensity remained approximately constant. Under such conditions and at constant concentrations of CO_2 and neopentane, plots of $1/r_{ROH}$ against [A]/[RH] would be expected to be

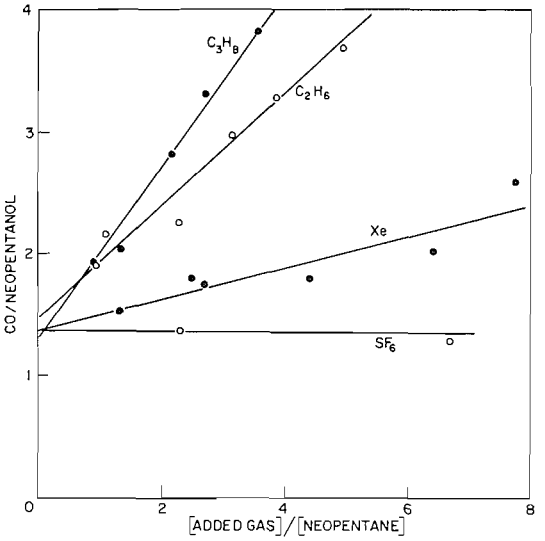

FIG. 3. Plot of eq. 1 for SF_6, Xe, C_2H_6, and C_3H_8. (CO_2 pressure 11 Torr, neopentane pressure 78 Torr.)

Can. J. Chem. Downloaded from www.nrcresearchpress.com by 210.87.254.5 on 09/05/12
For personal use only.

TABLE 1. Comparison of over-all* relative rates of reaction of $O(^1D_2)$ from different sources†

Reactant	CO_2 present work	N_2O 2139 Å ref. 10	NO_2 2288 Å ref. 13	N_2O 1849 Å ref. 12	O_3 2537 Å ref. 15	O_3, flash photolysis ref. 14	O_2 1470 Å ref. 16
Neopentane	1.0	1.0	1.0	1.0	1.0	1.0	1.0
SF_6	0	0	0	0	—	0	—
Xe	0.10	0.127	0.098	0.104	—	0.138	—
CO	0.08	0.075	—	—	0.052	—	0.035
N_2	0.035	0.039	0.030	0.033			0.03
H_2	0.1	0.25	—	—	0.25	—	0.13
C_2H_6	0.30	—	—	—	—	—	—
C_3H_8	0.60	—	0.59	—	0.62	—	—
CH_4	–	0.32	—	—	—	—	0.14
CO_2	—	0.127	—	—	—	0.127	—

*Chemical reaction plus physical deactivation.
†All expressed relative to neopentane ≡ 1.0, using either directly determined relative rates when available or calculated indirectly from the relevant data in the literature, in particular ref. 10.

linear and the intercept to be independent of the gas added. The lamp intensity was kept constant by (*a*) using the same current in the microwave generator and (*b*) by adjusting the visible output of the lamp so that it just filled the Suprasil window between the lamp and the reactor. Scatter of points showed that the u.v. output of the lamp remained constant to better than ±20%. Moreover, the least squares intercepts for the three gases were the same within ±10%. The least squares k_A/k_{np} values compare again quite well with the corresponding literature values although the standard deviations are appreciably larger.

Discussion

Discussion of the results of this work may be based on the following reaction scheme

[2]	$CO_2 + h\nu$	$\rightarrow CO_2^*$
[2*a*]	CO_2^*	$\rightarrow CO + O(^1D_2)$
[2*b*]		$\rightarrow CO + O(^3P)$
[3]	$O(^1D_2) + CO_2$	$\rightarrow O(^3P) + CO_2$
[4*a*]	$O(^1D_2) + RH$	$\rightarrow ROH^*$
[4*b*]		$\rightarrow R + OH$
[4*c*]		$\rightarrow RH + O(^3P)$
[5*a*]	$O(^1D_2) + A$	$\rightarrow A + O(^3P)$
[5*b*]		$\rightarrow$ Products
[6]	ROH^*	$\rightarrow$ Fragmentation
[7]	$ROH^* + M$	$\rightarrow ROH + M$

Some other reactions will be mentioned later. RH stands for neopentane, ROH for neopentanol, A is a "quencher" of $O(^1D_2)$ atoms, and M stands for any molecules present which can collisionally deactivate the "hot" neopentanol (ROH^*). Steady state treatment gives

$$[8]\quad \frac{r_{ROH}}{r_{CO}} = \frac{k_{2a}}{k_{2a}+k_{2b}} \cdot \frac{1}{1+\dfrac{k_6}{k_7[M]}} \cdot \frac{k_{4a}/k_4}{1+\dfrac{k_3[CO_2]}{k_4[RH]}+\dfrac{k_5[A]}{k_4[RH]}}$$

The constant k_4 stands for $(k_{4a} + k_{4b} + k_{4c})$, *i.e.* for $(k_{4a} + k_{4b})$ since k_{4c} has been shown (10) to be very small or zero. Similarly, k_5 stands for $(k_{5a} + k_{5b})$.

At pressures higher than about 100 to 200 Torr $k_7[M] \gg k_6$ and when also $[CO_2]/[RH]$ is small enough so that $k_3[CO_2]/k_4[RH] \ll (1 + k_5[A]/k_4[RH])$, eq. 8 reduces to eq. 1, with $\alpha = \{k_{2a}/(k_{2a}+k_{2b})\}\{k_{4a}/k_4\}$, $k_{np} = k_4$, and $k_A = (k_{5a} + k_{5b})$. The present values of k_A listed in Table 1 are based on the use of eq. 1 derived in this manner. Their good agreement with the corresponding literature values clearly shows the presence of $O(^1D_2)$ atoms in the reaction system studied. The primary objective of the present work has been to obtain such information and the experimental accuracy is evidently adequate for this purpose in spite of the considerable scatter of experimental points. At the same time, the overall experimental uncertainty of present determinations is appreciable and we therefore feel that they should not be used to refine the corresponding k_A values in the literature.

The neopentanol/CO trend in Fig. 2 is qualitatively predicted by eq. 8 with [A] = 0. However, it is now known (10, 14) that $k_3/k_4 = 0.127$ and the expected trend calculated using this value is

Can. J. Chem. Downloaded from www.nrcresearchpress.com by 210.87.254.5 on 09/05/12
For personal use only.

Can. J. Chem. Downloaded from www.nrcresearchpress.com by 210.87.254.5 on 09/05/12
For personal use only.

shown by curve *1* (interrupted curve) in Fig. 2. In these calculations it was assumed that $k_6/k_7[M] \ll 1$ and $\alpha = 0.65$. The latter figure is identical with the experimental value of k_{4a}/k_4 for neopentane determined recently in this laboratory (10) and is also approximately equal to the "plateau" value of r_{ROH}/r_{CO} in Fig. 2. The approximate validity of the assumption that $k_6/k_7[M] \ll 1$ is shown by the insensitivity of the data in Fig. 2 to variation in CO_2 pressure and addition of 320 Torr SF_6.

The exact reasons for the deviations in Fig. 2 of the observed $r_{neopentanol}/r_{CO}$ values from those expected (curve *1*) are not known. It is important to note that deviations become negligible at higher neopentane/CO_2, where also $r_{neopentanol}/r_{CO}$ coincides with the experimental k_{4a}/k_4 value of 0.65. It could be argued that the deviations are only due to an error in the value $k_3/k_4 = 0.127$ used to compute curve *1*. Alternative curves (curves *2* and *3* in Fig. 2) have been computed with k_3/k_4 values which are, respectively, 3 and 4 times larger than 0.127 and they are indeed reasonably close to the experimental points. Nevertheless, such an explanation of the deviations must be rejected, in particular because it would also lead to a k_{CO_2}/k_{Xe} value 3 to 4 times larger than the well established literature values of close to unity (10, 12–14).

The deviations in $r_{neopentanol}/r_{CO}$ at lower neopentane/CO_2 in Fig. 2 appear therefore to be real. No doubt they are at least partly due to inaccurate extrapolations to zero time and it is in fact possible that such extrapolations may be inadequate in some cases. Such would be the case, for example, if in the very early stages of the reaction a preferential attack on neopentanol occurred by some reactive intermediates which are scavenged efficiently later in the reaction by other reaction products (olefins, free radicals), especially so at higher neopentane/CO_2 ratios. Alternatively, at larger CO_2/neopentane there could be some attack on CO_2 to form extra CO (in addition to the CO formed in reaction 2) by some active intermediates, as for example "hot" hydrogen atoms formed in the photolysis of neopentane. Additional assumptions would then be required to explain the trend with neopentane/CO_2. However, it would not be feasible at present to obtain a direct experimental evidence for or against such hypotheses and further discussion is not warranted. An attack of OH* ("hot" OH radicals formed in reaction 4*b*) on CO_2 to produce excess CO seems to be ruled out by the experiments with N_2O/CO_2/neopentane mixtures at 2139 Å (10) in which a substantial increase in CO was not observed under conditions conducive to an appreciable interaction of OH* with CO_2.[3] An interaction of CO_2* formed in reaction 2 with CO_2 to produce CO

$$CO_2^* + CO_2 \rightarrow CO + O(^3P) + CO_2$$

may appear at first sight to provide a feasible explanation of the deviations (excess CO) in Fig. 2 at larger CO_2/neopentane. However, since $r_{neopentanol}/r_{CO}$ is not a function of $[CO_2]$ but of $[CO_2]/[neopentane]$, it would be necessary to postulate also that

$$[CO_2^*] + RH \rightarrow CO + O(^1D_2) + RH$$

while other gases, such as SF_6 etc., should have no effect on CO_2*. Such a behavior would be difficult to understand.

While these various possible explanations of the deviations at lower $[neopentane]/[CO_2]$ ratios cannot be resolved at this time, the overall agreement in the quenching rates (Table 1) with the corresponding literature values shows that under conditions used in their determinations, *i.e.* at $[neopentane]/[CO_2] \geqslant 6.5$, such complications are negligible.

The overall agreement in the trends found in the present and the literature determinations of k_A in Table 1 shows clearly that $O(^1D_2)$ atoms are generated in the photolysis of CO_2 at close to 1600 Å and are responsible for the formation of neopentanol when neopentane is added. Furthermore, the observation in this work of a plateau value for $r_{neopentanol}/r_{CO}$ of about 0.65, which is the same as observed in N_2O photolysis (10), suggests that the quantum yield of $O(^1D_2)$ atom production in the photolysis of CO_2 is close to unity. However, the appreciable experimental scatter weakens the quantitative aspect of this conclusion.

1. B. H. MAHAN. J. Chem. Phys. **33**, 959 (1960).
2. P. WARNECK. Discuss. Faraday Soc. **37**, 57 (1964); J. Chem. Phys. **41**, 3435 (1964).
3. A.-Y. UNG and H. I. SCHIFF. Can. J. Chem. **44**, 1981 (1966).
4. T. G. SLANGER. J. Chem. Phys. **45**, 4127 (1966).

[3]The authors are grateful to Dr. G. Paraskevopoulos for an additional experiment verifying this conclusion.

5. L. J. STIEF, V. J. DECARLO, and W. A. PAYNE. J. Chem. Phys. **51**, 3336 (1969).
6. J. F. NOXON. J. Chem. Phys. **52**, 1852 (1970).
7. L. J. STIEF, W. A. PAYNE, V. J. DECARLO, R. GORDEN, JR., and P. AUSLOOS. J. Chem. Phys. **53**, 475 (1970).
8. T. G. SLANGER and G. BLACK. J. Chem. Phys. **54**, 1889 (1971).
9. M. CLERC and F. BARAT. J. Chim. Phys. **63**, 1525 (1966); J. Chem. Phys. **46**, 107 (1967).
10. G. PARASKEVOPOULOS and R. J. CVETANOVIĆ. J. Am. Chem. Soc. **91**, 7572 (1969).
11. G. PARASKEVOPOULOS and R. J. CVETANOVIĆ. J. Chem. Phys. **52**, 5821 (1970).
12. H. YAMAZAKI and R. J. CVETANOVIĆ. J. Chem. Phys. **39**, 1902 (1963); **40**, 582 (1964); **41**, 3703 (1964).
13. K. F. PRESTON and R. J. CVETANOVIĆ. J. Chem. Phys. **45**, 2888 (1966).
14. P. M. SCOTT and R. J. CVETANOVIĆ. J. Chem. Phys. **54**, 1440 (1971).
15. W. B. DEMORE. J. Phys. Chem. **73**, 391 (1969).
16. R. A. YOUNG, G. BLACK, and T. G. SLANGER. J. Chem. Phys. **49**, 4758 (1968).
17. L. LOUKS and R. J. CVETANOVIĆ. To be published.
18. B. A. THOMPSON, R. R. REEVES, JR., and P. HARTECK. J. Phys. Chem. **69**, 3964 (1965).

Can. J. Chem. Downloaded from www.nrcresearchpress.com by 210.87.254.5 on 09/05/12
For personal use only.

Can. J. Chem. Downloaded from www.nrcresearchpress.com by 210.87.254.42 on 09/05/12
For personal use only.

Mechanism of the Pyrolysis of Acetylene

M. H. BACK
Chemistry Department, The University of Ottawa, Ottawa, Canada

Received January 28, 1971

A free radical chain mechanism is presented to describe the kinetics of the pyrolysis of acetylene over the temperature range 700–2400 °K. The mechanism is based on the following initiation reaction

$$2\,C_2H_2 \rightarrow {}^{\bullet}C_2H + {}^{\bullet}C_2H_3$$

and subsequent addition, abstraction, and decomposition reactions of the radicals involved are shown to account for the products observed and for the kinetic characteristics of the reaction.

Pour décrire la cinétique de la pyrolyse de l'acétylène entre 700 et 2400 °K, on propose un mécanisme en chaîne impliquant des radicaux libres et qui serait basé sur la réaction d'initiation suivante

$$2\,C_2H_2 \rightarrow {}^{\bullet}C_2H + {}^{\bullet}C_2H_3$$

des réactions subséquentes d'addition, d'abstraction et de décomposition des radicaux impliqués permettent de rendre compte des produits obtenus et de la cinétique caractéristique de la réaction.

Canadian Journal of Chemistry, 49, 2199 (1971)

Introduction

The mechanism of the pyrolysis of acetylene is not well established, partly because of the analytical difficulties involved in obtaining reliable data with highly reactive products and also because of the variable effects of heterogeneous reactions. Modern analysis has largely overcome many of these problems and in particular the work of Cullis and Franklin (1) over the range 700–1200 °K and of Gay *et al.* (2) in the range 1600–2400 °K has clearly distinguished the primary from the secondary products. In the lower temperature region, below about 1200 °K, vinyl acetylene, C_4H_4, is the sole initial product, while in the high temperature region diacetylene, C_4H_2, is the primary molecular product. Benzene is an important secondary product, particularly in the lower temperature range, and methane, hydrogen, ethylene, and butadiene are also formed in varying yields depending on temperature and conversion.

A remarkable feature of the acetylene system is that the second-order rate constants for the reaction of acetylene obtained by many different workers covering the temperature range 620–2450 °K apparently lie on a single linear plot of $\log k$ against $1/T$ (3) and may be represented by the Arrhenius expression (2)

$$\log k\ (\text{l mol}^{-1}\text{s}^{-1}) = 10.8 - 41\,600/2.3RT$$

This suggests that the mechanism involves the same rate-controlling steps over the entire temperature range.

In several respects the kinetics of the acetylene pyrolysis bear a strong resemblance to those observed in the pyrolysis of ethylene (4). The activation energy of the reaction is low, between 40 and 45 kcal/mol, and induction periods are observed. Both the initial rates and the maximum rates after the induction period are second order in acetylene (5). The activation energy is too low to allow initiation by unimolecular fission of bonds in the acetylene molecule and many authors have favored a bimolecular reaction of acetylene to give an excited molecule of acetylene in the triplet state (6, 7) or a triplet or biradical species C_4H_4* (8, 9). The rate of formation of excited molecules in thermal systems is, however, somewhat uncertain; the frequency factor may be very low. In the ethylene system initiation was suggested to occur by the bimolecular disproportionation reaction of two ethylene molecules to form an ethyl and a vinyl radical. Such a reaction appeared reasonable in the acetylene system also, and had been suggested (8), but was not followed up with a complete mechanism. With this initiation a series of radical addition, abstraction and decomposition reactions may occur which will lead to the formation of the observed products over a wide temperature range.

The Mechanism

Reactions 1–17 represent an outline of the most probable reactions and may be considered a framework for the building of a complete mechanism.

The products formed depend on the tempera-

Can. J. Chem. Downloaded from www.nrcresearchpress.com by 210.87.254.42 on 09/05/12
For personal use only.

[1]	$C_2H_2 + C_2H_2 \rightarrow {}^{\bullet}C_2H + {}^{\bullet}C_2H_3$	
[2]	${}^{\bullet}C_2H_3 \rightarrow C_2H_2 + H^{\bullet}$	
[3]	${}^{\bullet}C_2H + C_2H_2 \rightarrow {}^{\bullet}C_4H_3$	
[4]	${}^{\bullet}C_4H_3 \rightarrow C_4H_2 + H^{\bullet}$	High temperature
[5]	$H^{\bullet} + C_2H_2 \rightarrow H_2 + {}^{\bullet}C_2H$	
[6]	$2{}^{\bullet}C_2H \rightarrow C_4H_2$	
[7]	${}^{\bullet}C_2H_3 + C_2H_2 \rightarrow {}^{\bullet}C_4H_5$	
[8]	${}^{\bullet}C_4H_5 \rightarrow C_4H_4 + H^{\bullet}$	
[9]	${}^{\bullet}C_2H_3 + C_2H_2 \rightarrow C_2H_4 + {}^{\bullet}C_2H$	
[10]	${}^{\bullet}C_4H_3 + C_2H_2 \rightarrow C_4H_4 + {}^{\bullet}C_2H$	
[11]	${}^{\bullet}C_4H_3 + C_2H_2 \rightarrow {}^{\bullet}C_6H_5$	Intermediate temperature
[12]	$2{}^{\bullet}C_4H_3 \rightarrow C_8H_6$	
[13]	$2{}^{\bullet}C_2H_3 \rightarrow C_4H_6$	
[14]	${}^{\bullet}C_4H_5 + C_2H_2 \rightarrow {}^{\bullet}C_6H_7$	
[15]	${}^{\bullet}C_6H_7 \rightarrow C_4H_2 + {}^{\bullet}C_2H_3$	
[16]	${}^{\bullet}C_6H_7 + C_2H_2 \rightarrow {}^{\bullet}C_8H_9$	Low temperature
[17]	${}^{\bullet}C_nH_{n+1} + C_2H_2 \rightarrow {}^{\bullet}C_{n+2}H_{n+3}$	

ture region where the reaction occurs. At high temperatures, as found in shock tubes, the vinyl radical will be largely dissociated and the chain will be carried by hydrogen atoms and C_2H radicals. Decomposition of the C_4H_3 radical will compete with addition and C_4H_2 will be the primary product. This region is illustrated by the work of Gay *et al.* (2). At lower temperatures reactions of the vinyl radical will become important and vinyl acetylene, ethylene, and butadiene are products. At still lower temperatures further addition reactions will build up higher molecular weight products.

Rate Expressions

Assuming a long chain reaction with a steady state concentration of radicals, the rates of formation of the products may be expressed as follows:

(a) High Temperature Region

$$\text{Rate } C_4H_2 = k_3(k_1/k_6)^{\frac{1}{2}}(C_2H_2)^2$$

(b) Intermediate Temperature Region

Vinyl acetylene may be formed by either of the sequences [3] followed by [10] or [7] followed by [8], depending on the relative concentration of C_2H_3 and C_2H radicals. If C_2H radicals are dominant the rate may be expressed as

$$\text{Rate } C_4H_4 = k_3(k_1/k_6)^{\frac{1}{2}}(C_2H_2)^2$$

while if C_2H_3 radicals are dominant the rate becomes

$$\text{Rate } C_4H_4 = k_7(k_1/k_{13})^{\frac{1}{2}}(C_2H_2)^2$$

The relative concentration of C_2H_3 and C_2H radicals is a complex function of a number of competing reactions. High temperatures favor the formation of C_2H, which is formed by abstraction from acetylene, while the addition reaction to form C_2H_3, either of hydrogen atoms or of larger radicals followed by decomposition, having a lower activation energy, will make an increasing contribution as the temperature is lowered. It is possible that the changes in the product distribution with temperature follow the change in the relative concentration of C_2H and C_2H_3, but this cannot be ascertained without a more exact knowledge of the rate constants for the elementary reactions involved.

(c) Low Temperature Region

The primary products in this region are somewhat more uncertain but a general expression similar to those for the other regions may be written,

$$\text{Rate polymer} = k_a(k_1/k_t)^{\frac{1}{2}}(C_2H_2)^2$$

where k_a is an average rate constant for addition and k_t represents the termination rate constant for the radicals involved.

TABLE 1. Thermodynamic quantities used in the estimation of rate constants

Radical	$\Delta H_f°$(298 °K) kcal/mol	Reference	$S°$(298 °K)* Gibbs/mol	Reference
C_2H_2	54.3	31	48.0	31
C_2H_3	64	16	56.3	32
C_2H	114	†	52.0	‡
H	52.1	16	27.4	32

*Standard state 1 atm of ideal gas at 298 °K.
†Estimated assuming D(C_2H—H) = 112 kcal/mol.
‡Estimated.

Thus the rate expressions covering a wide temperature range differ only insofar as the rate constants for addition of radicals to acetylene and for combination of radicals vary with the size of the radical. Neither of these rate constants would be expected to change very much as the size of the radical is increased, keeping in mind that because of the ease of C—C bond fission in larger radicals, the chain is probably carried by low molecular weight radicals even in the lower temperature region. An Arrhenius plot linear within the error limits involved in the measurements of the acetylene pyrolysis would therefore be consistent with the radical mechanism.

A quantitative comparison between these rate expressions and the experimental rate measurements may be made by making reasonable estimates of the rate constants involved. The equilibrium constant for the initiation reaction may be estimated using the thermodynamic quantities listed in Table 1. The rate constant for reaction 1 may then be calculated by making some assumptions about the reverse disproportionation reaction of vinyl and ethynyl radicals. Holroyd and Klein (10) have shown that the relation proposed by Bradley (11) between the ratio of the rate constants for disproportionation and combination and the difference in entropy of the products of the disproportionation and combination reactions is applicable for a large number of alkyl radicals. On this basis k_d/k_c for ethynyl and vinyl radicals would have the low value of 0.03. Measurements of the ratio k_d/k_c for methyl and vinyl radicals and for vinyl radicals themselves, however, gave values of 2.3 and 1.1 respectively (12), although from the relation with the entropy difference the value should also be low in both cases. It seems that the transfer of the hydrogen atom from the vinyl radical may be very facile, leading to a larger ratio for k_d/k_c than would be predicted from the corresponding entropy difference between the disproportionation and combination products of alkyl radicals. A reasonable estimate for k_d/k_c for the ethynyl–vinyl radical pair may be 1.0 and if the rate constant for combination of these radicals is assumed equal to that for two ethyl radicals (13) then

$$\log k_{-1}(\text{l mol}^{-1}\text{s}^{-1}) = 10.04$$

The rate constant for reaction 1 may then be written as

$$\log k_1(\text{l mol}^{-1}\text{s}^{-1}) = 12.7 \pm 0.5 - (70\,000 \pm 3000)/2.3RT$$

An average rate constant for addition of low molecular weight radicals to acetylene may be estimated by comparison of values for addition of radicals to olefins (14) and from values reported by Dominguez and Trotman–Dickenson (15) for the addition of saturated radicals to acetylene. The rate constant for addition of unsaturated radicals to acetylene is probably somewhat faster than the corresponding value for the saturated radicals and the following value is suggested,

$$\log k_a(\text{l mol}^{-1}\text{s}^{-1}) = 8.8 \pm 0.5 - (6500 \pm 1000)/2.3RT$$

Very few rate constants have been reported for reactions of radicals with alkynes and the experimental difficulties involved make the wide error limits necessary. The rate constant for termination may be taken equal to that for two ethyl radicals (13),

$$\log k_t(\text{l mol}^{-1}\text{s}^{-1}) = 10.3$$

The composite rate constant may therefore be expressed as

$$\log k(\text{l mol}^{-1}\text{s}^{-1}) = 10.0 - 41\,500/2.3RT$$

This expression is shown as the dashed line in

Can. J. Chem. Downloaded from www.nrcresearchpress.com by 210.87.254.42 on 09/05/12
For personal use only.

Can. J. Chem. Downloaded from www.nrcresearchpress.com by 210.87.254.42 on 09/05/12
For personal use only.

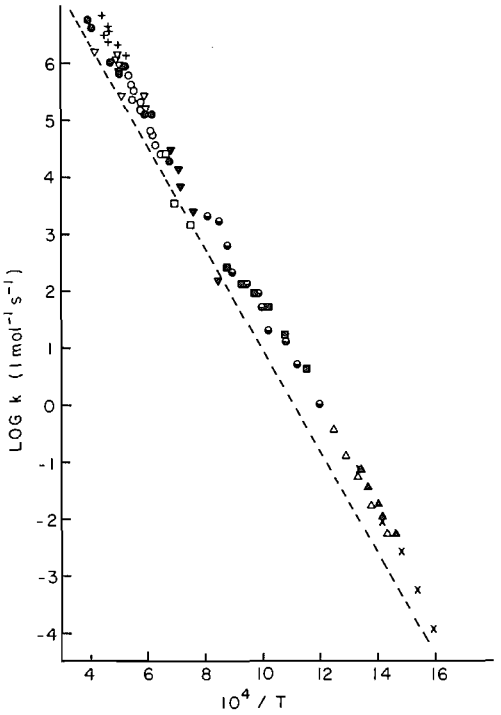

FIG. 1. Arrhenius plot of the second-order rate constants for the pyrolysis of acetylene: ○, ref. 27; △, ref. 26; ▼, ref. 28; ▲, ref. 5; ▽, ref. 29; ×, ref. 30; ●, ref. 3; □, ref. 9; ■, ref. 22; ◒, ref. 1; +, ref. 2; broken line, calculated from the rate expressions derived from the mechanism.

Fig. 1 together with rate constants obtained by 11 different investigators. The uncertainties in these estimated rate constants could easily allow for an uncertainty of a factor of 10 and perhaps as much as 50 in the composite rate constant. The correspondence of the calculated rate with the measurements is therefore as close as may be reasonably expected.

The mechanism depends on the assumption that the addition of radicals is the rate-controlling step in the chain propagation. The rate of addition of C_4H_3 radicals to acetylene may be compared to their rate of decomposition taking the value for k_a used in the preceding calculation and assuming the following value for k_4,

$$\log k_4(s^{-1}) = 14 - (40\,000 \pm 4000)/2.3RT$$

The activation energy for dissociation of the C—H bond in the C_4H_3 radical would be expected to be very similar to that for dissociation of the C—H bond in the vinyl radical (16). Although the substitution of the C_2H radical for the hydrogen atom in the vinyl radical would act to increase the strength of the C—H bond through conjugation, the stability of the molecule formed by the loss of the hydrogen atom would be correspondingly increased and the two effects would probably cancel. Thus a value of 40 kcal/mol is a reasonable estimate. This value is lower than the endothermicity of 61 kcal/mol suggested by Cowperthwaite and Bauer (17) from a consideration of the heats of formation of various C_4H_3 and C_4H_2 species. Their C_4H_3 radical, however, did not have the same structure as the radical formed by addition of C_2H to acetylene.

$$\frac{\text{Rate (4)}}{\text{Rate (a)}} = \frac{k_4}{k_a(C_2H_2)}$$

Thus at 1200 °K and a pressure of 100 Torr of acetylene,

$$\frac{\text{Rate (4)}}{\text{Rate (a)}} \sim 100$$

Thus at temperatures above 1200 °K, C_4H_2 may be the main primary product with addition being the rate-determining step. If vinyl radicals are somewhat more stable than the C_4H_3 radicals, C_4H_5 radicals may be formed in appreciable amounts below 1200 °K and vinyl acetylene may become the main initial product. Dissociation of C_4H_5 to vinyl acetylene may still compete successfully with addition down to about 1000 °K. Palmer and Dormish (9) observed that the more prominent C_4 product at 1333 °K was vinyl acetylene while at 1528 °K it was diacetylene. These regions are essentially in agreement with the present rough estimate.

As addition of radicals to acetylene becomes important at lower temperatures, radicals of molecular weight C_6 or C_8 may be formed. From these radicals lower molecular weight products may be formed by C—C fission and this process, having a lower activation energy than that for C—H dissociation, will remain faster than addition down to fairly low temperatures. Vinyl acetylene could be formed by such a route at lower temperatures, for example as follows,

$$\dot{C}H{=}CH{-}CH{=}CH_2 + C_2H_2 \rightarrow \dot{C}H{=}CH{-}CH{=}CH{-}CH{=}CH_2$$

$$\dot{C}H{=}CH{-}CH{=}CH{-}CH{=}CH_2 \rightarrow CH_2{=}CH{-}CH{=}\dot{C}{-}CH{=}CH_2$$

$$CH_2{=}CH{-}CH{=}\dot{C}{-}CH{=}CH_2 \rightarrow CH_2{=}\dot{C}H + CH{\equiv}C{-}CH{=}CH_2$$

Can. J. Chem. Downloaded from www.nrcresearchpress.com by 210.87.254.42 on 09/05/12
For personal use only.

There is some evidence (18) that in the addition of radicals to ethylene, low molecular weight molecules are formed by C—C dissociation of larger radicals rather than by C—H fission of a parent radical. Formation of vinyl acetylene by this route would not affect the kinetics as long as addition is the rate-controlling process.

Over small ranges of temperature, deviation from the simple mechanism, where addition is rate-controlling, may occur as different decomposition mechanisms become important. This may account for the fact that certain sets of data obtained over a narrow temperature range give Arrhenius parameters rather different from the average. Palmer and Dormish (9) in fact suggested that the Arrhenius plot of the data showed a transition region in the neighborhood of 1000 °K where a change in mechanism must occur. The errors involved in obtaining rate constants from the acetylene system are, however, probably sufficiently large to account for the scatter observed and it is probably not possible to fix with any certainty the region of temperature where a change in mechanism occurs. Indeed several changes in mechanism must occur over such a wide temperature range and the radical chain mechanism allows such changes without altering the main kinetic characteristics.

An alternative initiation step, kinetically indistinguishable from reaction 1 was suggested by Gay *et al.* (2) and by Cullis and Read (19).

$$2C_2H_2 \rightarrow C_4H_3 + H$$

It seems more probable however, that this reaction would occur by the series of reactions 1, 2, and 3 of the present mechanism.

Other Features of the Acetylene System

The mechanism as outlined thus accounts for the major kinetic characteristics of the acetylene pyrolysis, in particular the second order rate dependence and the low activation energy. In addition several other features of the acetylene system are explained by this type of radical chain reaction. The rather erratic effects of surfaces observed (20) may be expected in a long chain reaction where the propagation reactions of radicals may occur following adsorption on surface sites. Because the over-all rate is second order the initiation step is probably homogeneous. The formation of methane and of compounds containing an odd number of carbon atoms may be most easily accounted for by isomerization and dissociation of radicals. For example, a 1,5 hydrogen shift may occur in the C_6H_7 radical in a similar way to that shown to occur in the hexyl radical (21):

$$C_4H_5 + C_2H_2 \rightarrow CH_2{=}CH{-}CH{=}CH{-}CH{=}\dot{C}H$$

$$CH_2{=}CH{-}CH{=}CH{-}CH{=}\dot{C}H \rightarrow CH_3{-}\dot{C}H{-}CH{=}CH{-}C{\equiv}CH$$

The terminal methyl radical may split off and form methane by abstraction. Similar isomerizations may occur with larger radicals, and other radicals containing an odd number of carbon atoms may be formed. The radical mechanism also accounts adequately for the products formed when halogens are added to the reacting acetylene (22). The isotope exchange observed at very high temperatures (2) would occur rapidly by the dissociation and formation of vinyl radicals by reactions 2 and -2. Cyclization processes giving benzene and higher molecular weight aromatic ring compounds are important reactions in the acetylene system (23). Such processes may occur through biradical intermediates (5, 24) or from monoradicals, or, as has been suggested recently, through a Diels–Alder condensation (25). The kinetics of formation of the higher products has not been sufficiently well established to favor one particular mode.

The Induction Period

Induction periods have been observed in the acetylene pyrolysis by most investigators. The kinetics are second order both in the initial stages and in the region of maximum rate (5). The bimolecular reaction of acetylene is therefore very likely the main initiation step in both regions. The increase in rate after a period of time may be the result of an increase in the rate of the propagation steps which may occur if the rate of addition of radicals to the products is faster than to acetylene itself. This is possible because the maximum rate is only 2–4 times the initial rate (5, 26) and a large factor is not involved. If the increase in rate were due to secondary initiation caused by dissociation of the products, the kinetic characteristics would be expected to alter more drastically.

In summary, the radical chain process outlined here is intended to show that there is no need to suggest the formation of excited molecules of acetylene as a kinetically important step in the reaction. The rates of such processes are difficult

to assess particularly when a change of multiplicity is involved. On the other hand the rate of the simple bimolecular disproportionation reaction of two molecules of acetylene may be estimated with fair accuracy and together with the addition, abstraction, and decomposition reactions of the resulting radicals may account for the main features of the acetylene pyrolysis.

The author thanks Dr. R. A. Back of the National Research Council of Canada for helpful suggestions concerning the manuscript.

1. C. F. CULLIS and N. H. FRANKLIN. Proc. R. Soc. A**280** 139 (1964).
2. I. D. GAY, G. B. KISTIAKOWSKY, J. V. MICHAEL, and H. NIKI. J. Chem. Phys. **43**, 1720 (1965).
3. C. F. ATEN and E. F. GREENE. Combust. and Flame, **5**, 55 (1961).
4. M. L. BOYD, T.-M. WU, and M. H. BACK. Can. J. Chem. **46**, 2415 (1968).
5. C. F. CULLIS, G. J. MINKOFF, and M. A. NETTLETON. Trans. Faraday Soc. **58**, 1117 (1962).
6. G. J. MINKOFF. Can. J. Chem. **36**, 131 (1958).
7. G. J. MINKOFF and C. F. H. TIPPER. Chemistry of combustion reactions. Butterworths, London, 1962.
8. F. C. STEHLING, J. D. FRAZEE, and R. C. ANDERSON. 8th Int. Symp. on Combust. Cal. Inst. Tech., 1960. p. 775.
9. H. B. PALMER and F. L. DORMISH. J. Phys. Chem. **68**, 1553 (1964).
10. R. A. HOLROYD and G. W. KLEIN. J. Phys. Chem. **67**, 2275 (1963).
11. J. N. BRADLEY. J. Chem. Phys. **35**, 748 (1961).
12. N. A. WEIR. J. Chem. Soc. 6870 (1965).
13. A. SHEPP and K. O. KUTSCHKE. J. Chem. Phys. **26**, 1020 (1957).
14. S. W. BENSON and H. E. O'NEAL. Kinetic data on gas phase unimolecular reactions, NSRDS–NBS. 21 (1970).
15. J. A. G. DOMINGUEZ and A. F. TROTMAN–DICKENSON. J. Chem. Soc. 940 (1962).
16. J. A. KERR. Chem. Rev. **66**, 465 (1966).
17. M. COWPERTHWAITE and S. H. BAUER. J. Chem. Phys. **36**, 1743 (1962).
18. A. S. GORDON, S. R. SMITH, and J. R. MCNESBY. 7th Int. Symp. on Combust. London and Oxford, 1958. p. 317.
19. C. F. CULLIS and I. A. READ. Trans. Faraday Soc. **66**, 920 (1970).
20. C. F. CULLIS and M. A. NETTLETON. Trans. Faraday Soc. **59**, 361 (1963).
21. V. B. SEFTON and D. J. LEROY. Can. J. Chem. **34**, 41 (1956).
22. M. S. B. MUNSON and R. C. ANDERSON. J. Phys. Chem. **67**, 1582 (1963).
23. J. R. ARTHUR, B. T. COMMINS, J. A. S. GILBERT, A. J. LINDSEY, and D. H. NAPIER. Combust. and Flame, **2**, 267 (1958).
24. M. S. B. MUNSON and R. C. ANDERSON. Carbon, **1**, 55 (1963).
25. E. K. FIELDS and S. MEYERSON. Tetrahedron Lett. 571 (1967).
26. G. J. MINKOFF, D. M. NEWITT, and P. RUTLEDGE. J. Appl. Chem. **7**, 406 (1957).
27. G. B. SKINNER and E. M. SOKOLOSKI. J. Phys. Chem. **64**, 1952 (1960).
28. G. D. TOWELL and J. J. MARTIN. A.I.Ch. E.J. **7**, 693 (1961).
29. E. F. GREENE, R. L. TAYLOR, and W. L. PATTERSON. J. Phys. Chem. **62**, 238 (1958).
30. C. G. SILCOCKS. Proc. R. Soc. A**242**, 411 (1957).
31. Selected values of physical and thermodynamic properties of hydrocarbons. American Petroleum Institute Research Project. Carnegie Press, Carnegie Inst. of Tech., Pittsburgh, Pa., 1953.
32. S. W. BENSON. Thermochemical Kinetics. John Wiley and Sons, Inc., New York, N.Y., 1968.

Can. J. Chem. Downloaded from www.nrcresearchpress.com by 210.87.254.42 on 09/05/12
For personal use only.

Can. J. Chem. Downloaded from www.nrcresearchpress.com by 210.87.254.6 on 09/05/12
For personal use only.

Nuclear Charge Dispersion in the Fission of ^{235}U by Protons of Energy 20–85 MeV[1]

G. B. SAHA,[2] I. TOMITA,[3] AND L. YAFFE

Radiochemistry Laboratory, Department of Chemistry, McGill University, Montreal, Quebec

Received January 14, 1971

Independent formation cross sections of ^{129}Cs, ^{130}Cs, ^{131}Cs, $^{134}Cs^{m}$, $^{134}Cs^{m+g}$, ^{136}Cs, ^{139}Ce, and cumulative formation cross sections of ^{141}Ce and ^{143}Ce were obtained when ^{235}U was caused to fission with protons of energies varying between 20 and 85 MeV. The energies at which the excitation functions reached their maxima were related to the neutron-to-proton ratio of the fission products. These were compared with other fissioning systems. Charge dispersion curves were obtained from the cross section data. The variation of $(Z_A - Z_p)$ with energy, both in magnitude and in trend, agrees extremely well with predictions made by Saha and Yaffe for nuclides in this mass range. Calculations for Z_p show that good agreement is obtained with the unchanged charge division hypothesis. An estimate has been made of the total number of neutrons emitted in fission at these energies.

On a obtenu des sections efficaces de formation indépendante de ^{129}Cs, ^{130}Cs, ^{131}Cs, $^{134}Cs^{m}$, $^{134}Cs^{m+g}$, ^{136}Cs, ^{139}Ce, et des sections efficaces de formation cumulative de ^{141}Ce et de ^{143}Ce, par la réaction de fission de ^{235}U sous l'action de protons d'énergie variant de 20 à 85 MeV. Les énergies auxquelles les fonctions d'excitation atteignent leur maxima ont été reliées au rapport neutron-à-proton des produits de fission. Celles-ci ont été comparées à d'autres systèmes où il y a réaction de fission. Des courbes de dispersion de charge ont été obtenues d'après les valeurs des sections efficaces. L'allure et la grandeur de la variation de $(Z_A - Z_p)$ avec l'énergie sont tout à fait conformes aux prédictions de Saha et Yaffe pour les nucléides de masse comparable. Des calculs de Z_p sont tout à fait en accord avec l'hypothèse de la division de la charge inchangée. On a fait un estimé du nombre total de neutrons émis lors de la fission se passant à ces énergies.

Canadian Journal of Chemistry, 49, 2205 (1971)

Introduction

A number of studies on nuclear charge dispersion in the fission of heavy-mass targets by protons of energies 20–85 MeV have been reported (1–10). In all these studies the displacement of the most probable charge, Z_p, from the charge, Z_A, corresponding to stability for mass A has been measured. In addition the full-widths at half-maximum (FWHM) of the charge dispersion curves have been determined. All the above-mentioned studies (with the exception of refs. 2, 6, and 10) have dealt with fission products with masses A in the range 129–144. The others have concerned themselves with the lighter fragment.

In all cases, as the bombarding energy is increased, the most probable charge, Z_p, shifts towards stability. It has been shown by Tomita and Yaffe (8) and Saha and Yaffe (9) that the values of $(Z_A - Z_p)$ can be correlated with the neutron-to-proton ratio, N/Z, of the target. Thus, for fission products in the mass range A = 129–144, and in the energy range 20–85 MeV the most probable charge, Z_p, can be predicted from the nuclear composition (protons and neutrons) of the target. A recent summary (11) correlates the information obtained from the various targets. This summary, for completeness, included some preliminary information about ^{235}U which had not yet been published. Since some of these data are being used by others (particularly those who use mass spectrometry as a measuring device and thus obtain only relative yields) as calibration and reference points, and because of the intrinsic interest in this area of research, the original and amended data on ^{235}U are now being published.

In the present work we report the study of the nuclear charge dispersion of fission products in the mass range A = 129–143 formed in the fission of ^{235}U by protons of energies 20–85 MeV.

Experimental

(1) Targets and Irradiations

The targets were foils of ^{235}U (94% enrichment) having a superficial density of about 122 mg/cm^2. Prior

[1]This research was supported by the National Research Council of Canada.

[2]Present address: Division of Nuclear Medicine, 2nd Floor Medical Wing, Royal Victoria Hospital, Montreal, Quebec.

[3]Present address: Department of Chemistry, Tokyo Kyoiku University, Otsuka, Tokyo, Japan.

Can. J. Chem. Downloaded from www.nrcresearchpress.com by 210.87.254.6 on 09/05/12
For personal use only.

to irradiation the foils were cleaned with nitric acid, washed with water, then acetone, dried and the superficial density of each foil determined by obtaining the weight of a measured area. The $^{65}Cu(p,pn)^{64}Cu$ reaction was used to monitor the proton beam. The monitor copper foil had a superficial density of 21.4 mg/cm^2. The target foil was sandwiched between two aluminum foils (20 μm thick) which served as guard foils for fission products recoiling out of the target. The copper foil, guarded in a similar manner by two other copper foils, was placed upstream to the protons with respect to the target. The target and monitor foils were properly aligned and wrapped with a thin aluminum cover foil. The entire stack was then fastened to the target holder which was in turn attached to the cyclotron probe. The target assembly was then placed inside the cyclotron at a fixed radius corresponding to the desired energy.

All irradiations were performed in the internal circulating beam of the McGill proton synchrocyclotron. Irradiations, for a period of about 10 min, at a beam current of about 1 μA, were made at 10-MeV intervals in the energy range 20–70 MeV, at 77, and 85 MeV. The energy spread was ±2 MeV and the degradation of the beam in the target was calculated to be negligible compared to this.

(2) Chemical Separations

After irradiation the respective foils were dissolved in suitable acids and the different elements separated. The uranium and its aluminum guard foils were dissolved together in concentrated hydrochloric acid, to which a few drops of nitric acid had been added, in the presence of cesium, cerium, lanthanum, barium, strontium, yttrium, and rubidium carriers. The solution was made up to a standard volume and aliquots were taken for the chemical separation of cesium and cerium. The copper monitor foil was dissolved in concentrated hydrochloric acid and a few drops of hydrogen peroxide.

(i) Cesium

The details of the purification of cesium have been given elsewhere (9). These consisted of precipitation of cesium as silicotungstate, as bismuth iodide, and finally as chloroplatinate. The final precipitate was filtered on a glass-fiber disc, dried, weighed, and mounted for activity measurements.

(ii) Cerium

The procedure for chemical separation of the cerium was adapted from those of Glendenin *et al.* (12) and Barnes (13). The aliquot for cerium separation was evaporated to near dryness. Four ml of concentrated nitric acid and 2 ml of 2.5 *M* sodium bromate were added to make the solution 9–10 molar in nitric acid. The solution was heated for about 1 min to complete the oxidation of Ce^{3+} to Ce^{4+}, cooled, and extracted into 50 ml of methyl isobutyl ketone. The organic phase was washed three times with 1 ml of 9 *M* nitric acid containing a few drops of 2.5 *M* sodium bromate, and cerium was back-extracted into 5 ml water containing a few drops of 30% hydrogen peroxide. Cerium oxalate was precipitated with saturated oxalic acid, washed with water, alcohol, and ignited to CeO_2 at 800 °C for about 30 min. The oxide was powdered, slurried with alcohol, filtered on a small glass-fiber disc, dried at 110 °C, weighed, and mounted for activity measurements.

(iii) Copper

The copper was chemically separated by using the procedure of Kraus and Moore (14). The copper solution was adsorbed on a Dowex-1 anion exchange column and copper was eluted with 1.5 *M* hydrochloric acid. The copper was reduced to Cu^+ by heating with sodium bisulfite, and cuprous thiocyanate was precipitated with ammonium thiocyanate. The precipitate was filtered, washed with alcohol and ether, dried, weighed, and mounted for activity measurements.

(3) Activity Measurements

The pertinent decay characteristics of the nuclides of interest are shown in Table 1. They have been taken from the compilation by Lederer *et al.* (15).

Three instruments were used for the activity measurements. A 7.6 cm × 7.6 cm NaI(Tl) crystal coupled to a 400-channel pulse-height analyzer was used to measure the γ-radiations and K X-rays emitted by the different nuclides. An end-window gas-flow proportional counter was used to measure the β-radiation from ^{136}Cs. The annihilation radiation from the decay by positron emission of ^{130}Cs was measured by two NaI(Tl) crystals at 180 °C to each other coupled to a γ–γ coincidence unit gated to receive the 511-keV photopeak. The details of this unit and the determination of its operating characteristics have been described elsewhere (9).

The decay of 2.9-h $^{134}Cs^m$ and 2.05-year $^{134}Cs^g$ was followed by measuring the activity due to the 127-keV and 796-keV photopeaks, respectively. In order to reduce the background due to Compton scattering of the high-energy γ-rays, $^{134}Cs^m$ was measured after the complete decay of 32.2 min ^{138}Cs, and $^{134}Cs^g$ after the essentially complete decay of 12.9-day ^{136}Cs.

The activities of 32-h ^{129}Cs, 9.7-day ^{131}Cs, 6.5-day ^{132}Cs were measured by detecting their characteristic X-rays. The composite curve resulting from the X-ray activities was resolved by the CLSQ least-squares computer program of Cumming (16). The K X-ray emission rates were converted to K electron-capture decay rates using a fluorescence yield of 0.87 (17) and a value of 0.12 (18) for the L/K capture ratio. The activity due to the 2.05-year $^{134}Cs^g$ was resolved from that of the 12.9-day ^{136}Cs in the gross β^--decay by the CLSQ program. However, the uncertainty in the $^{134}Cs^g$ component was too large to enable the β^--activity to be used in the cross-

TABLE 1. Decay characteristics (15) of nuclides

Nuclides	Half-life	Radiation measured	Abundance
^{129}Cs	32.2 h	K X-ray	1.0
^{130}Cs	30.0 min	β^+	0.46
^{131}Cs	9.7 day	K X-ray	1.0
^{132}Cs	6.5 day	K X-ray	1.0
$^{134}Cs^m$	2.9 h	127-keV γ	0.14
$^{134}Cs^g$	2.05 year	796-keV γ	0.99
^{136}Cs	12.9 day	β^-	1.0
^{139}Ce	140 day	165-keV γ	0.80
^{141}Ce	32.5 day	145-keV γ	0.48
^{143}Ce	33.0 h	293-keV γ	0.46
^{64}Cu	12.8 h	β^+ (511-keV annihilation)	0.19

Can. J. Chem. Downloaded from www.nrcresearchpress.com by 210.87.254.6 on 09/05/12
For personal use only.

section calculation and this was done from the γ-ray data as indicated above. A small correction for the self-absorption in the source of the β^--radiations from ^{136}Cs was made.

The ^{64}Cu activity was measured by detecting the 511-keV annihilation radiation with the NaI spectrometer. The activity of ^{143}Ce was measured by following the decay of the photopeak due to the 293-keV γ-ray on the NaI spectrometer. The resolution of the NaI crystal was not good enough to resolve completely the 145-keV and 166-keV γ-rays due to 32.5-day ^{141}Ce and 138-day ^{139}Ce, respectively. These were measured as a composite photopeak and the activities resolved by the CLSQ program.

The efficiency of the annihilation radiation coincidence counter was determined with a standard source of ^{22}Na. The efficiency of the NaI(Tl) detector was determined with the aid of several γ-ray standards, while the end-window proportional counter was calibrated against a 4πβ-counter (9).

The counting rates of the different nuclides at the end of bombardment were converted to disintegration rates by correcting for chemical yields, branching ratios, and counter efficiencies. Disintegration rates were then used to calculate the formation cross sections of the different nuclides using well-known equations (19). The cross sections for the $^{65}Cu(p,pn)^{64}Cu$ reaction at different energies were those of Meghir (20) and are given in Table 2.

Results

The measured formation cross sections of the nuclides are given in Table 3 and the excitation functions are shown in Figs. 1–4. The errors shown in the table and the figures were estimated from the uncertainties in activity measurements, chemical yields, counting efficiencies, and target thicknesses. The energy spread (±2 MeV) in the proton beam is not shown in the diagrams.

The formation cross section of 2.2-h ^{129}Ba, even at a proton energy of 85 MeV, is very small, as evidenced from the charge dispersion curves and the low yield of ^{129}Cs. The separation time from end of bombardment was only 30 min and so the contribution from the decay of ^{129}Ba to the formation of ^{129}Cs can be considered to be negligible. The yields of ^{129}Cs were thus considered to be independent. Similarly the rapid separation time precluded a large contribution to the yield of ^{131}Cs from its relatively long-lived parent, 11.6-day ^{131}Ba, and the yields of the former could be considered as independent.

It can be noted from Table 3 and Fig. 3 that the cross sections for formation of $^{134}Cs^m$ are greater than those for $^{134}Cs^g$ and that the isomer ratios

TABLE 2. Cross sections for the $^{65}Cu(p,pn)^{64}Cu$ reaction (20)

Proton energy (MeV)	σ (mb)
20	260
30	390
40	260
50	210
60	180
70	160
77	150
85	140

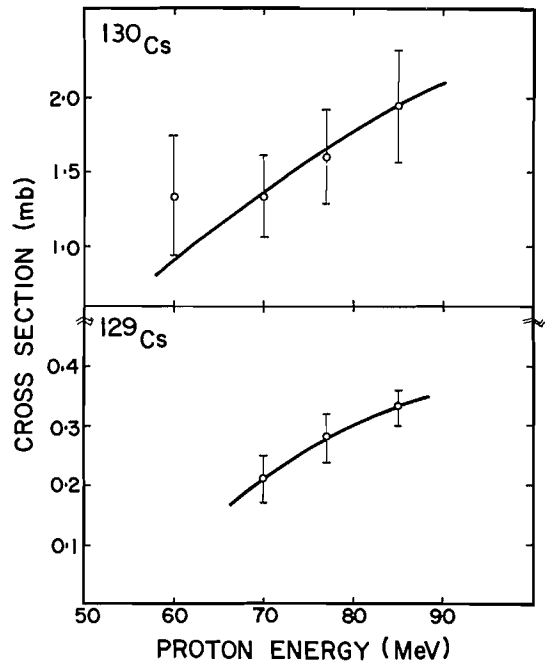

FIG. 1. Excitation functions of the independent yields of ^{129}Cs and ^{130}Cs.

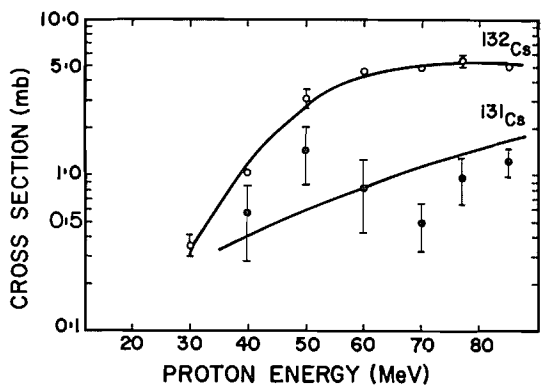

FIG. 2. Excitation functions of the independent yields of ^{131}Cs and ^{132}Cs.

Can. J. Chem. Downloaded from www.nrcresearchpress.com by 210.87.254.6 on 09/05/12
For personal use only.

TABLE 3. Experimental cross sections of different nuclides in ^{235}U fission

Proton energy (MeV)	Cross sections (mb)									
	^{129}Cs(I)	^{130}Cs(I)	^{131}Cs(I)	^{132}Cs(I)	$^{134}Cs^{m}$(I)	$^{134}Cs^{m+g}$(I)	^{136}Cs(I)*	^{139}Ce(I)	^{141}Ce(C)*	^{143}Ce(C)
20	—	—	—	—	1.9±0.2	3.0†	12±1	—	35±3	—
30	—	—	—	0.4±0.1	4.2±0.5	6.1±1.2	24±2	—	41±4	24±2
40	—	—	0.6±0.3	1.0±0.2	6.9±0.8	9.8±2.0	16±2	2.3±0.4	36±4	26±3
50	—	—	1.5±0.6	3.1±0.4	11 ±1	16 ±3	18±2	3.4±0.5	45±4	31±3
60	—	1.3±0.4	0.8±0.4	4.7±0.4	9.1±1.1	12 ±2	13±1	2.9±0.4	34±3	22±2
70	0.21±0.04	1.3±0.3	0.5±0.2	5.0±0.4	8.5±1.0	12 ±2	11±1	3.5±0.5	33±3	21±2
77	0.28±0.04	1.6±0.3	1.0±0.3	5.5±0.4	8.2±1.0	11 ±2	11±1	3.8±0.6	31±3	20±2
85	0.33±0.03	2.0±0.4	1.2±0.2	5.0±0.4	7.7±0.9	9.5±1.9	11±1	3.4±0.5	26±3	16±2

*I and C refer to independent and cumulative cross sections.
†Extrapolated from excitation function.

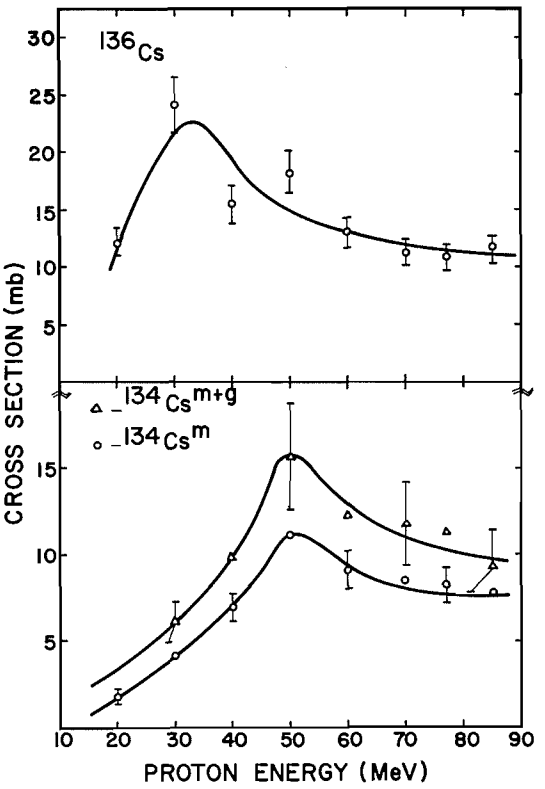

FIG. 3. Excitation functions of the independent yields of $^{134}Cs^{m}$, $^{134}Cs^{m+g}$, and ^{136}Cs.

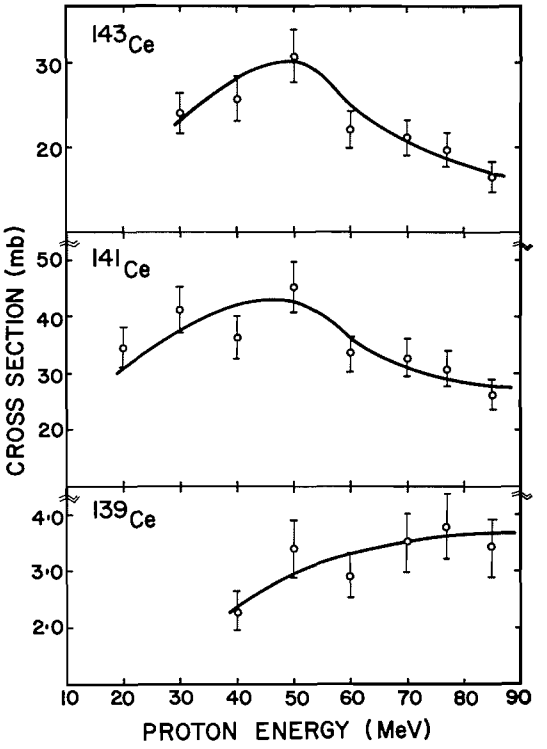

FIG. 4. Excitation functions of the independent yields of ^{139}Ce and the cumulative yields of ^{141}Ce and ^{143}Ce.

are insensitive to energy. Interpretation of the relative formation probabilities of these isomers in terms of the average spins of the primary fragments has been presented in a separate publication (21). The cross sections for ^{133}Cs, ^{135}Cs, and ^{137}Cs have been interpolated from the charge dispersion curves (see section 2 of Discussion). The excitation functions are shown in Fig. 5 without error bars.

In Fig. 4 are shown the cumulative yields of ^{141}Ce and ^{143}Ce, and the independent yields of ^{139}Ce. The formation cross sections of the latter are judged to be independent because the yields of ^{139}Pr in this energy region are very small. When the formation yields of ^{141}Ce and ^{143}Ce were being determined, the chemical separations were made after complete decay of the precursors to ensure that the yields determined would indeed be cumulative.

Discussion

(1) Excitation Functions

The excitation functions shown in Figs. 1–5 exhibit the trends expected at these bombarding energies. The excitation functions of the relatively neutron-deficient nuclides increase with increasing bombarding energy, while those of the neutron-rich products show maxima in this energy region. Also the formation cross sections of the neutron-deficient nuclides are relatively smaller than those of the neutron-richer products. Qualitatively these results can be explained in terms of increasing energy deposition leading to increasing neutron evaporation, either prior to or after fission, as the bombarding energy is increased. Because of this one would expect the charge dispersion curves to broaden with increasing energy as the contribution from the neutron-deficient components becomes larger. Thus the independent yield of any member of a chain will increase with increasing excitation energy, pass through a maximum and then decrease. The initial increase in the cumulative yields of ^{141}Ce and ^{143}Ce thus results from the increasing contribution of the various members of the chain. The nuclides contributing to these products are produced in good yield early in the

Can. J. Chem. Downloaded from www.nrcresearchpress.com by 210.87.254.6 on 09/05/12
For personal use only.

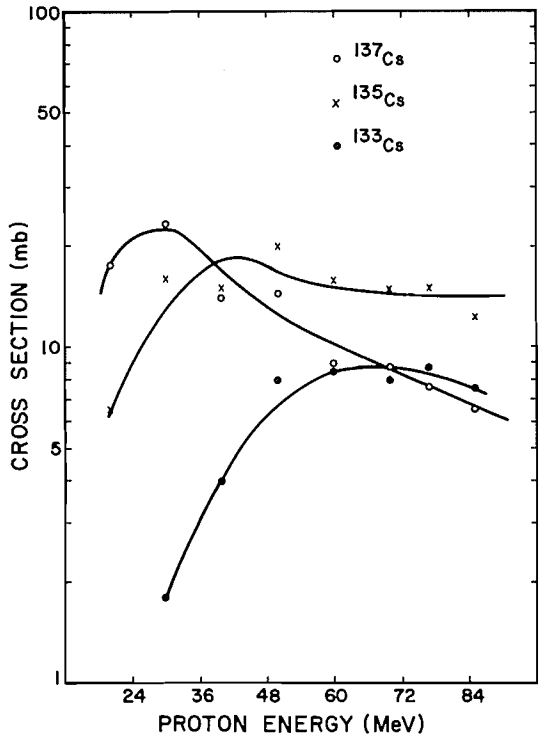

FIG. 5. Excitation functions of independent yields of ^{133}Cs, ^{135}Cs, and ^{137}Cs interpolated from charge dispersion curves.

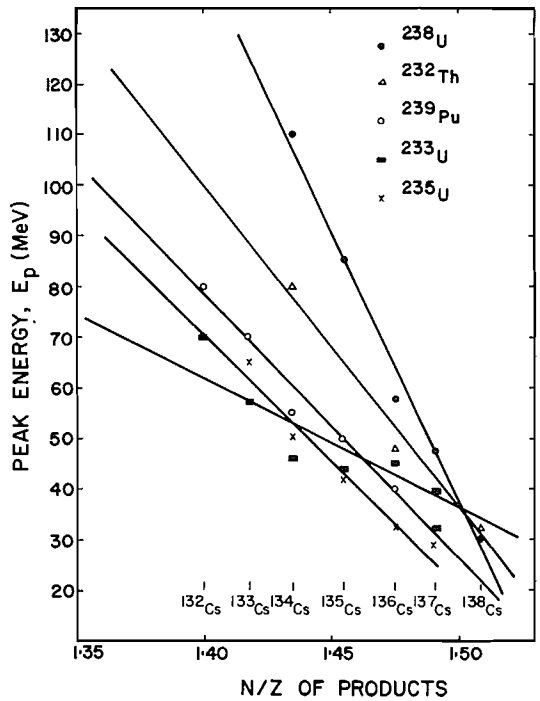

FIG. 6. Energies at which excitation functions in the fission of ^{238}U, ^{232}Th, ^{239}Pu, ^{233}U, and ^{235}U reach their maxima as a function of N/Z of the fission product.

chain at low excitation energies and lower yield at higher energies. This is confirmed from the charge dispersion curves, their broadening and shift of Z_p towards Z_A with increasing bombardment energy.

The excitation functions of ^{134}Cs and ^{136}Cs (experimentally determined) and of ^{133}Cs, ^{135}Cs, and ^{137}Cs (interpolated from charge dispersion curves) show well-defined maxima. As was first done by Friedlander *et al.* (19), the energies at which these excitation functions reach their peak are plotted against the neutron-to-proton (N/Z) ratio of the fission product and are shown in Fig. 6. Also included for comparison are data for ^{238}U (3), ^{232}Th (7), ^{239}Pu (9), and ^{233}U (8) by other workers. The determination of the peak energy may, as is evident from many of the excitation functions, involve an error of anywhere between 10 and 20 MeV, depending on the prominence of the maximum of the excitation function. It is also obvious that the ^{233}U data are very sparse and more data are obviously needed. However, all the data show an approximately linear decrease of the energy at which the fission product has its greatest probability of occurrence with an increase in N/Z of the products, although the slopes of the lines are different for different targets and some curvature may be occurring. It is obvious from the data that the same fission product has its greatest probability of occurrence at a relatively lower energy in the fission of a target of lower N/Z. This is shown graphically in Fig. 7 for ^{129}Cs, ^{132}Cs, ^{134}Cs, and ^{136}Cs. This conclusion lends support to the earlier observation made by Tomita and Yaffe (8) and Saha and Yaffe (9), who pointed out the importance of the role of the neutron-to-proton ratio of the target in the fission process. The lines in Fig. 6, despite the uncertainty of the slopes, converge on the N/Z axis at a value of about 1.55. This means that such a fission product, *e.g.* ^{140}Cs, would have a maximum formation probability with very low energy expenditure in all of these fissioning systems.

(2) Charge Dispersion

The cross sections were used to construct charge dispersion curves, according to the

Can. J. Chem. Downloaded from www.nrcresearchpress.com by 210.87.254.6 on 09/05/12
For personal use only.

TABLE 4. Parameters of charge dispersion curves in ^{235}U fission

Proton energy (MeV)	Full-width at half-maximum		Peak position		
	N/Z	ΔZ	N/Z	Z_p for $A = 136$	$Z_A - Z_p$
20	0.067	1.46	1.500	54.4	1.8
30	0.068	1.52	1.484	54.8	1.4
40	0.073	1.62	1.473	55.0	1.2
50	0.078	1.75	1.463	55.2	1.0
60	0.080	1.78	1.459	55.3	0.9
70	0.083	1.82	1.458	55.3	0.9
77	0.083	1.83	1.454	55.4	0.8
85	0.084	1.86	1.450	55.5	0.7

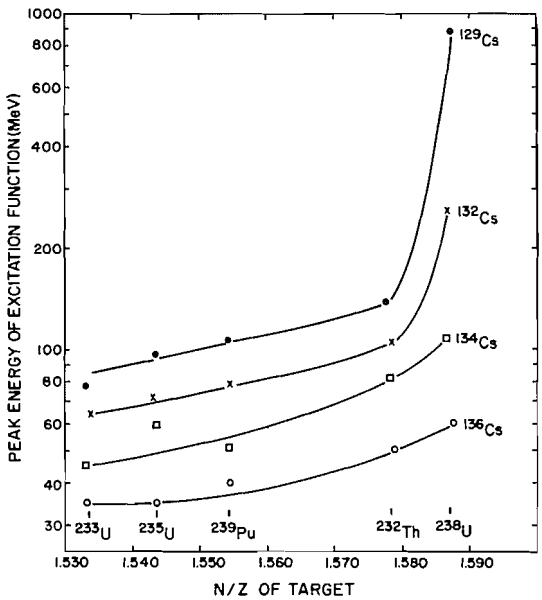

FIG. 7. Energies at which various cesium isotopes have their greatest probability of production as a function of N/Z of the target.

method suggested by Friedlander *et al.* (19) and since then used by many other workers. The independent formation cross sections were plotted against the neutron-to-proton ratio (N/Z) of the products. The dotted portion of the curve was so drawn that the sum of the independent yields read from the curve of the individual members of chains giving ^{141}Ce and ^{143}Ce equalled the experimentally-determined cumulative yields of ^{141}Ce and ^{143}Ce. It has been shown (1, 19) that this restriction uniquely determines the shape of the curve, provided that there are no discontinuities. Underlying the above is the assumption that, in the energy range 20–85 MeV, the mass–yield curve is flat in the region A = 129–143. This enables one to plot cross sections rather than fractional yields. The charge dispersion curve at 70 MeV is shown in Fig. 8 as a typical example of the curves obtained in this fashion.

The most probable charge, Z_p, was calculated for each curve from the value of N/Z corresponding to the maximum of the curve for the mass number nearest the peak. The full-widths at half-maximum (FWHM) of the curves were also calculated, in Z units for the same mass number, from the values of N/Z at half-maximum.[4] These parameters of the charge dispersion curves are given in Table 4. Values of Z_A used are those of Coryell (23). The variations of the FWHM and of $Z_A - Z_p$ with proton bombarding energy are given in Figs. 9 and 10, respectively, along with data obtained by other workers.

From Fig. 9 it can be seen that the FWHM of the charge dispersion curves increases with increasing bombarding energy for all the systems shown. In the case of ^{238}U (3) and ^{232}Th (7) the values of FWHM are almost constant up to 40–45 MeV and then increase at higher energies. This is not the case with the targets of lower values of N/Z, where there is a regular increase with energy. In Fig. 10 the variation of $(Z_A - Z_p)$ for the same fissioning systems is shown. The dotted line gives the prediction made by Saha and Yaffe (9) for the variation of $(Z_A - Z_p)$ with bombarding energy for fission products with A = 129–140 in the fission of ^{235}U. The agreement

[4]Hogan and Sugarman (22) have shown that such an analysis for the FWHM values in Z units is valid only if Z_p is constant with A. Work in this laboratory (unpublished) has shown that while this is important at higher bombarding energies, the correction for this effect in this energy region is small, of the order of 0.2 Z units.

Can. J. Chem. Downloaded from www.nrcresearchpress.com by 210.87.254.6 on 09/05/12
For personal use only.

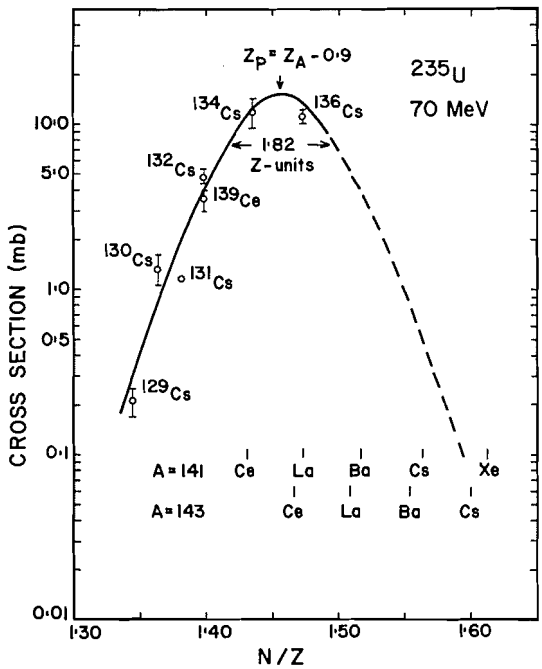

FIG. 8. Charge dispersion at 70 MeV.

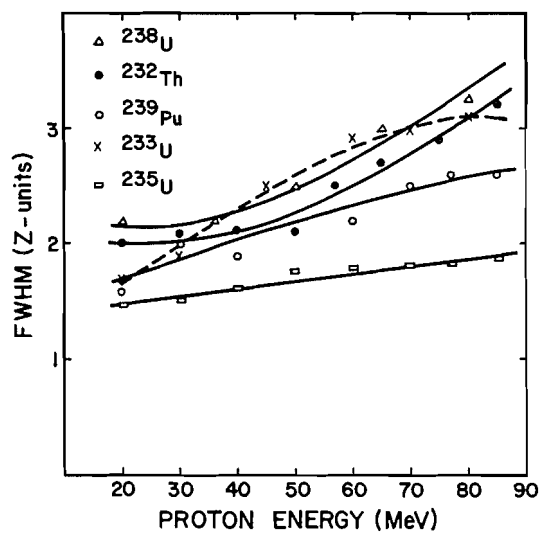

FIG. 9. Full-width at half-maximum of charge dispersion curves in the fission of ^{238}U, ^{232}Th, ^{239}Pu, ^{233}U, and ^{235}U.

between prediction and experiment is excellent. It should be emphasized that these predictions, made in the mass region $A = 129$–140, only hold for this region. Khan *et al.* (10) have shown that the behavior of the light-mass region, in the

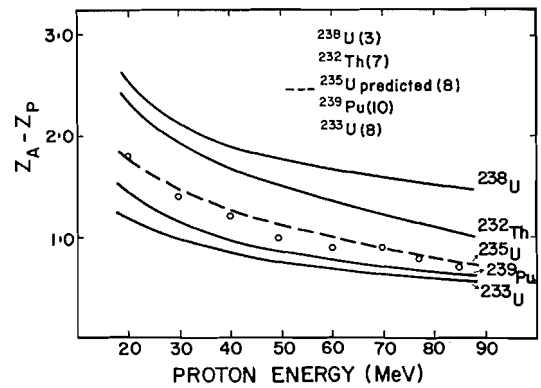

FIG. 10. Variation of $Z_A - Z_p$ as a function of energy in the fission of ^{238}U, ^{232}Th, ^{235}U, ^{239}Pu, and ^{233}U.

vicinity of $A = 96$, is totally different. One cannot, for example, differentiate $(Z_A - Z_p)$ as a function of energy between ^{235}U and ^{238}U as one can easily do in the present study. Thus one cannot regard the light-mass fragment merely as the accompanying partner of the heavy-mass fragment, but the different neutron-emission characteristics of the two fragments must be considered.

The above predictions were made on the basis of plots of $(Z_A - Z_p)$ *vs.* N/Z of the *target* by Tomita and Yaffe (8) and Saha and Yaffe (9). The data of the other workers have been supplemented in Fig. 11 by the present data. It is rather interesting to note that the values, for example, of $(Z_A - Z_p)$ for fission of ^{233}U at 25 MeV (interpolated) are the same as those at 80 MeV for ^{238}U, leading one to suspect that the average fissioning nucleus is the same in both cases.

As can be seen from Figs. 10 and 11 the values of $(Z_A - Z_p)$ remain almost constant for each system at higher energies. As pointed out by Saha and Yaffe (9), this indicates a direct interaction where only part of the bombarding energy is transferred to the fissioning nucleus and thus the fission process takes place as though induced at lower energies.

It would indeed have been more rigorous not to use N/Z of the target, but to consider the variation of $(Z_A - Z_p)$ as a function of N/Z of the *average* fissioning nucleus for each target at each energy. This has been done, as shown in Fig. 12, using the calculated values of N/Z of the average fissioning nucleus. This calculation is outlined in the following section. It is apparent

Can. J. Chem. Downloaded from www.nrcresearchpress.com by 210.87.254.6 on 09/05/12
For personal use only.

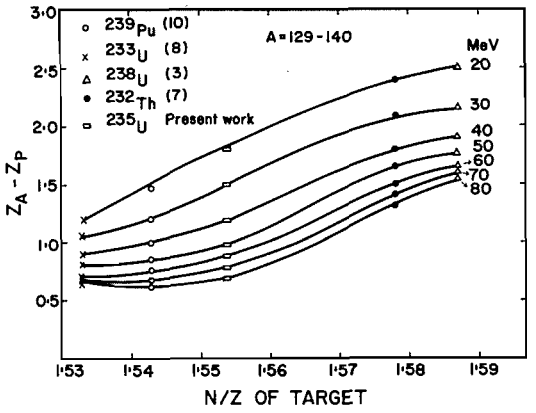

FIG. 11. Variation of $Z_A - Z_p$ as a function of N/Z of the target for various bombarding energies.

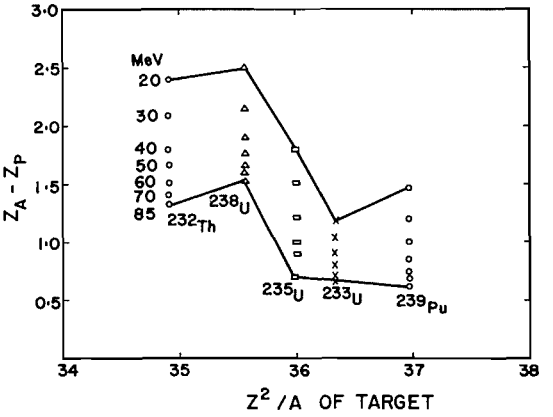

FIG. 13. Variation of $Z_A - Z_p$ as a function of the fissionability parameter, Z^2/A, of the target.

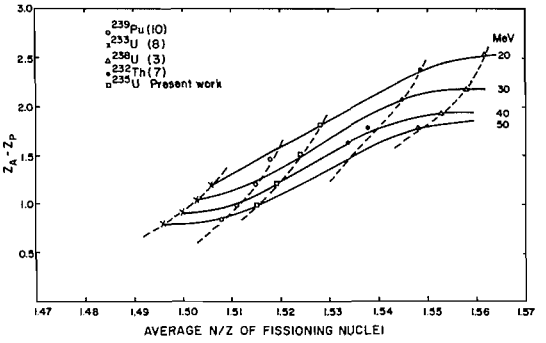

FIG. 12. Variation of $Z_A - Z_p$ as a function of N/Z of the average fissioning nucleus for various bombarding energies.

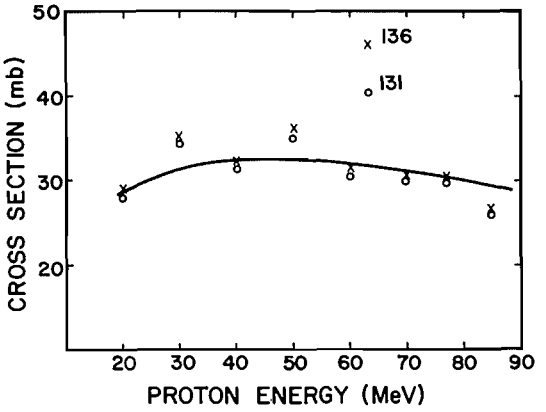

FIG. 14. Excitation function of the isobaric yields of masses 131 and 136 in the fission of ^{235}U.

that, at these energies, this gives no better correlation than with N/Z of the original target.

An attempt was made to correlate $(Z_A - Z_p)$ with the fissionability parameter Z^2/A of the target. As can be seen from Fig. 13 no ready correlation exists, although here again the *average* fissioning target might be a more useful parameter. However, it is questionable whether Z^2/A is itself a very meaningful parameter at these energies. The parameter owes its origin to the liquid-drop model, a model which has proved to be very useful at much lower energies.

The total isobaric yields of chains $A = 131$ and $A = 136$ were obtained from the charge dispersion curves and are plotted as a function of energy in Fig. 14. The excitation functions are almost energy-invariant in this region and are indistinguishable. The latter confirms the assumption that the mass–yield curve is sensibly flat in this energy region in the narrow mass range studied.

(3) Comparison of Experimental Z_p Values with Those Calculated

Unfortunately no reasonable theory for the distribution of nuclear charge in fission has yet been proposed. The experimental values for Z_p have been compared with those calculated on the basis of equal charge displacement (e.c.d.) and unchanged charge division (u.c.d.) postulates. The details of the calculation have been given elsewhere (8, 9). Compound nucleus formation was assumed at bombarding energies, of 30, 40, and 50 MeV and calculations made at these energies for $A = 136$.

The compound nucleus was considered to undergo fission or neutron evaporation. The

Can. J. Chem. Downloaded from www.nrcresearchpress.com by 210.87.254.6 on 09/05/12
For personal use only.

TABLE 5. Parentage of primary fragments leading to fission product of mass 136 and the calculated Z_p in ^{235}U-fission

Proton energy (MeV)	Fissioning nucleus	Primary fragments	Z_p e.c.d.	Z_p u.c.d.	Z_p Experimental
30	236, 235, 234, 233	139, 139,138, 138, 137	53.9	54.8	54.8
40	236, 235, 234, 233, 232	140, 139, 139, 138, 137	54.2	55.0	55.0
50	236, 235, 234, 233, 232, 231	141, 140, 139, 139, 138, 137	54.6	55.4	55.2

neutrons were assumed to carry off energy equal to $B_n + 2T$ where B_n is the binding energy of the neutron, and $2T$ is the average kinetic energy of the emitted neutron. T, the nuclear temperature, is calculated from $U = aT^2 - 4T$ (24), where U is the excitation energy of the residual nucleus and a, the level-density parameter, was taken to be 10.5 MeV^{-1} (25). Corresponding to each fissioning nucleus a number of primary fragments were obtained with values of $A = 136$–142. The total excitation energy was assumed to be shared between the two complementary fragments in the ratio of their masses. Each fragment was then allowed to evaporate neutrons, once again assuming that each neutron carries away energy equal to $B_n + 2T$. Only those final fragments were chosen which gave rise to products of mass 136. Values of Z_p were then calculated according to the e.c.d. and u.c.d. postulates for each fragment corresponding to each fissioning nucleus. Finally the average value of Z_p was obtained by weighting each calculated Z_p value with the fission branching ratio of each fissioning nucleus $G = \Gamma_f/(\Gamma_f + \Gamma_n)$, obtained from Huizenga and Vandenbosch (25). These data are summarized in Table 5. The u.c.d. values are in excellent agreement with the experimental results, whereas the e.c.d. values are 0.6–0.9 Z units lower than the experimental values. Similar results have been found in the fission of ^{233}U (8) and ^{239}Pu (9).

(4) Total Number of Neutrons Emitted

McHugh and Michel (26) have shown that the total number of neutrons, ν_T, emitted in fission can be calculated from the variation of Z_p with excitation energy. The relevant equation is

$$[1] \qquad d\nu/dE = (dZ_p/dE)/0.38$$

where dZ_p/dE, the variation of the most probable charge with excitation energy, is available from the present data. These are shown in Fig. 15 along with the data for ^{238}U (3) for $A = 136$. Compound nucleus formation has been assumed up to a bombarding energy of 50 MeV in the calculation of excitation energy. Table 6 shows the values for $d\nu_h/dE$, where h refers to the heavy fragments in fission, derived in this fashion. Khan *et al.* (10) have determined Z_p values in the mass range $A = 96$ in the fission of ^{235}U and ^{238}U and these, as a function of excitation energy

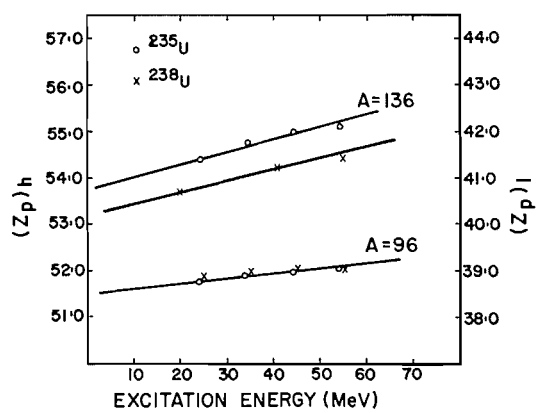

FIG. 15. dZ_p/dE for masses 96 and 136 in the fission of ^{235}U and ^{238}U.

Can. J. Chem. Downloaded from www.nrcresearchpress.com by 210.87.254.6 on 09/05/12
For personal use only.

Can. J. Chem. Downloaded from www.nrcresearchpress.com by 210.87.254.6 on 09/05/12
For personal use only.

TABLE 6. Neutron emission during fission

Parameter	Value (MeV^{-1})				
	^{235}U	^{238}U	^{232}Th	^{239}Pu	^{233}U
$(dZ_p/dE)_h$	0.0274	0.0250	0.030	0.024	0.013
$(dZ_p/dE)_l$	0.0111	0.0111	—	—	—
$d\nu_h/dE$	0.072	0.066	0.080	0.063	0.034
$d\nu_l/dE$	0.029	0.029	0.040	0.031	0.017
$d\nu_T/dE$	0.101	0.095	0.120	0.094	0.051

for the light fragments, l, are also shown in Fig. 15. The values for $d\nu_l/dE$ are also given in Table 6. Since

$$[2] \qquad d\nu_l/dE + d\nu_h/dE = d\nu_T/dE$$

the summation yields the total number of neutrons emitted both prior to and after fission for two fragments in these mass ranges. It may of course be that $A = 136$ and $A = 96$ may not arise from complementary fragments, but there is no reason to expect great variation in a very narrow mass region for either $d\nu_l/dE$ or $d\nu_h/dE$.

Saha and Yaffe (9) have made a similar calculation, but lacking the data of Khan *et al.* (10), they had assumed that $d\nu_l/dE = d\nu_h/dE$. The present treatment is of course more reliable. McHugh and Michel (26) and Nethaway and Levy (27) also concluded that the heavy fragments emit more neutrons than the light fragments. The data for fissioning systems other than ^{235}U and ^{238}U have been recalculated on the basis of $d\nu_h/dE = 2d\nu_l/dE$, although this is obviously an assumption, and the data are also given in Table 6.

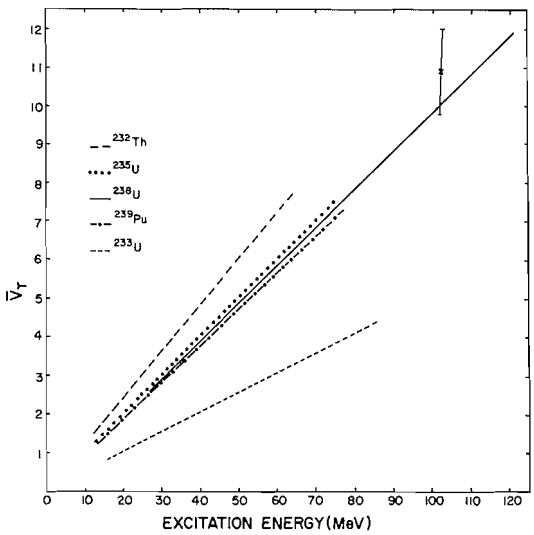

FIG. 16. Variation of the average number of neutrons, $\bar{\nu}_T$, emitted during fission from ^{232}Th, ^{235}U, ^{238}U, ^{239}Pu, and ^{233}U.

The total number of neutrons, ν_T, has been obtained by multiplying $d\nu_T/dE$ with excitation energy and is shown as a function of excitation energy in Fig. 16. These data are of course representative of these two mass regions only. Cheifetz *et al.* (28) have studied the emission of both pre-fission and post-fission neutrons in the fission of ^{238}U by 155-MeV protons. Their value, $\nu_T = 10.9 \pm 1.1$, has been plotted at the appropriate average excitation energy, 102 MeV.[5] The results are in very good agreement with the present data.

1. B. D. PATE, J. S. FOSTER, and L. YAFFE. Can. J. Chem. **36**, 1691 (1958).
2. A. KJELBERG, H. TANIGUCHI, and L. YAFFE. Can. J. Chem. **39**, 635 (1961).
3. J. H. DAVIES and L. YAFFE. Can. J. Phys. **41**, 762 (1963).
4. J. H. FORSTER, N. T. PORILE, and L. YAFFE. Can. J. Chem. **44**, 2951 (1966).
5. S. S. PARIKH, D. A. MARSDEN, N. T. PORILE, and L. YAFFE. Can. J. Chem. **45**, 1863 (1967).
6. A. H. KHAN, G. B. SAHA, and L. YAFFE. Can. J. Chem. **46**, 3565 (1968).
7. P. P. BENJAMIN, D. A. MARSDEN, N. T. PORILE, and L. YAFFE. Can. J. Chem. **47**, 301 (1969).
8. I. TOMITA and L. YAFFE. Can. J. Chem. **47**, 2921 (1969).
9. G. B. SAHA and L. YAFFE. J. Inorg. Nucl. Chem. **32**, 745 (1970).
10. A. H. KHAN, G. B. SAHA, and L. YAFFE. Can. J. Chem. **48**, 1924 (1970).
11. L. YAFFE. Symposium on the Physics and Chemistry of Fission. International Atomic Energy Agency, Vienna, Austria, paper SM-122/3. 1969. p. 701.
12. L. E. GLENDENIN, K. F. FLYNN, R. F. BUCHANAN, and E. P. STEINBERG. Anal. Chem. **27**, 59 (1955).
13. J. W. BARNES. Collected radiochemical procedures. 2nd ed. Los Alamos Scientific Laboratory, University of California, LA-1721. 1966.
14. K. A. KRAUS and G. E. MOORE. J. Am. Chem. Soc. **75**, 1460 (1953).
15. C. M. LEDERER, J. M. HOLLANDER, and I. PERLMAN. Table of isotopes. 6th ed. John Wiley and Sons Inc., New York. 1967.
16. J. B. CUMMING. Nat. Acad. Sci., Nat. Res. Council, Nucl. Sci. Series, NAS-NS-3107. 1962. p. 25.
17. A. H. WAPSTRA, G. J. NIJGH, and R. VAN LEISHOUT.

[5]We are grateful to Dr. G. Friedlander for extracting this value from the Vegas data. The above value refers to the step calculation with refraction. Stepno would yield a value some 15% lower.

Nuclear spectroscopy tables. Interscience, New York. 1950.
18. H. BRYSK and M. E. ROSE. Rev. Mod. Phys. **30**, 1169 (1958).
19. G. FRIEDLANDER, L. FRIEDMAN, B. GORDON, and L. YAFFE. Phys. Rev. **129**, 1809 (1963).
20. S. MEGHIR. Ph.D. Thesis. McGill University, Montreal, Quebec. 1962.
21. G. B. SAHA, I. TOMITA, and L. YAFFE. J. Inorg. Nucl. Chem. **31**, 3731 (1969).
22. J. J. HOGAN and NATHAN SUGARMAN. Phys. Rev. **182**, 1210 (1969).
23. C. D. CORYELL. Ann. Rev. Nucl. Sci. **2**, 305 (1953).
24. H. K. VONACH, R. VANDENBOSCH, and J. R. HUIZENGA. Nucl. Phys. **60**, 70 (1964).
25. J. R. HUIZENGA and R. VANDENBOSCH. Nuclear reactions. *Edited by* P. M. Endt and P. B. Smith. North-Holland Publ. Co., Amsterdam. 1962. p. 42.
26. J. A. MCHUGH and M. C. MICHEL. Phys. Rev. **172**, 1160 (1968).
27. D. R. NETHAWAY and H. B. LEVY. Phys. Rev. **139**, B1505 (1965).
28. E. CHEIFETZ, Z. FRAENKEL, J. GALIN, M. LEFORT, J. PÉTER, and X. TARRAGO. Phys. Rev. **C2**, 256 (1970).

Can. J. Chem. Downloaded from www.nrcresearchpress.com by 210.87.254.6 on 09/05/12
For personal use only.

Can. J. Chem. Downloaded from www.nrcresearchpress.com by 210.87.254.105 on 09/05/12
For personal use only.

Ion–Molecule Reactions in Methyl Fluoride and Methyl Chloride

A. A. HEROD,[1] A. G. HARRISON,[2] AND N. A. MCASKILL[3]
Department of Chemistry, University of Toronto, Toronto 181, Ontario

Received January 22, 1971

The reactions of the molecular ion have been studied as a function of the ion kinetic energy for methyl fluoride and methyl chloride. The following reactions are observed

[*a*] $CH_3X^+ + CH_3X \rightarrow C_2H_4X^+ + (H_2X)$

[*b*] $\rightarrow CH_4X^+ + CH_2X$

[*c*] $\rightarrow CH_2X^+ + (CH_4X)$

[*d*] $\rightarrow CH_3^+ + (CH_3X_2)$

For methyl fluoride (X = F) reactions *c* and *d* have kinetic energy thresholds and become significant at high ion energies. For CH_3Cl (X = Cl) reaction *a* is not observed and reactions *c* and *d* are of only minor importance at high ion energies. Rate coefficients for the molecular ions and a number of fragment ions as well as rate coefficients for further reaction of CH_4X^+ are reported.

On a étudié les réactions de l'ion moléculaire des fluorure et chlorure de méthyle en fonction de l'énergie cinétique de l'ion. On a observé les réactions suivantes

[*a*] $CH_3X^+ + CH_3X \rightarrow C_2H_4X^+ + (H_2X)$

[*b*] $\rightarrow CH_4X^+ + CH_2X$

[*c*] $\rightarrow CH_2X^+ + (CH_4X)$

[*d*] $\rightarrow CH_3^+ + (CH_3X_2)$

Les réactions *c* et *d*, dans le cas du fluorure de méthyle (X = F), ont des énergies cinétiques minima et ne deviennent importantes qu'à hautes énergies des ions. Dans le cas du chlorure de méthyl (X = Cl) on n'observe pas la réaction *a* et l'importance des réactions *c* et *d* est négligeable à hautes énergies des ions. On rapporte les coefficients de vitesse des ions moléculaires et d'un certain nombre d'ions fragmentés ainsi que les coefficients de vitesse d'autres réactions de l'ion CH_4X^+.

Canadian Journal of Chemistry, 49, 2217 (1971)

Introduction

The ion–molecule reactions forming CH_4Cl^+ in CH_3Cl have been studied previously at low electron energies both by the zero-field pulsing technique (1) and by pressure variation (2). More recently McAskill (3) has reported a detailed study of the ionic reactions in methyl chloride at 70–85 eV ionizing energy and ion exit energies ranging from 0.2 to 2.0 eV. In this pressure study the major reactions occurring have been elucidated and the energy dependence of the reactions investigated. A similar, but briefer, study of the methyl fluoride system also has been reported by McAskill (4), while the reactions of the molecular ion have been studied at thermal ion energies using ion cyclotron resonance techniques by Marshall and Buttrill (5).

The present study of the ionic reactions in methyl fluoride and methyl chloride can be divided into three parts. Pressure studies at 50–70 eV electron energy have been carried out; the results from these studies confirm the earlier results of McAskill (3, 4). In each system the reactions of the molecular ion have been studied in detail at low electron energies and the product distribution determined as a function of ion energy. Finally, the ionic reactions have been investigated using the ion-trapping technique reported recently (6).

Experimental

The pressure studies, both at low and high electron energies, were carried out using the medium pressure instrument described previously (2, 7). The ionizing electron beam was pulsed and ion source residence times were measured directly by the deflection technique (2).

[1]Present address: British Coal Utilization Research Association, Leatherhead, Surrey, England.

[2]To whom correspondence should be addressed.

[3]Present address: Australian Atomic Energy Commission, Lucas Heights, NWS, Australia.

Can. J. Chem. Downloaded from www.nrcresearchpress.com by 210.87.254.105 on 09/05/12
For personal use only.

At low electron energies, pressure studies were made at various repeller voltages covering the range of ion exit energies detailed in the following. In each run the electron energy was adjusted to give the maximum possible fractional yield of the molecular ion at low pressures. For methyl chloride CH_3Cl^+ was >95% of the total ionization at low pressures, however, for methyl fluoride the CH_2F^+ fragment ion amounted to ~20% of the total ionization at low pressures since a.p.(CH_2F^+) = 13.25 eV (8) is relatively close to i.p.(CH_3F) = 12.85 eV (9) (where a.p. = appearance potential, i.p. = ionization potential). The remaining pressure studies were carried out at 50 or 70 eV electron energy and ion exit energies as detailed in the following. Source pressures were measured directly using an MKS Baratron micromanometer.

The ion-trapping studies were carried out using the instrument and techniques previously described (6) and source concentrations in the region of 1×10^{13} molecule cm^{-3}. The source pressure was not measured directly but was related to the measured sample system inlet pressure through a study of the reaction $CH_4^+ + CH_4$ in methane. Consequently the rate coefficients reported for the ion-trapping experiments are relative to the value of 1.20×10^{-9} cm^3 $molecule^{-1}$ s^{-1} (2) for the methane reaction.

Methyl chloride was obtained from Matheson and Co. while methyl fluoride was obtained from Columbia Organic Chemical Co. In each case samples were distilled bulb-to-bulb *in vacuo* and a middle fraction retained for use. The mass spectra showed no detectable impurities.

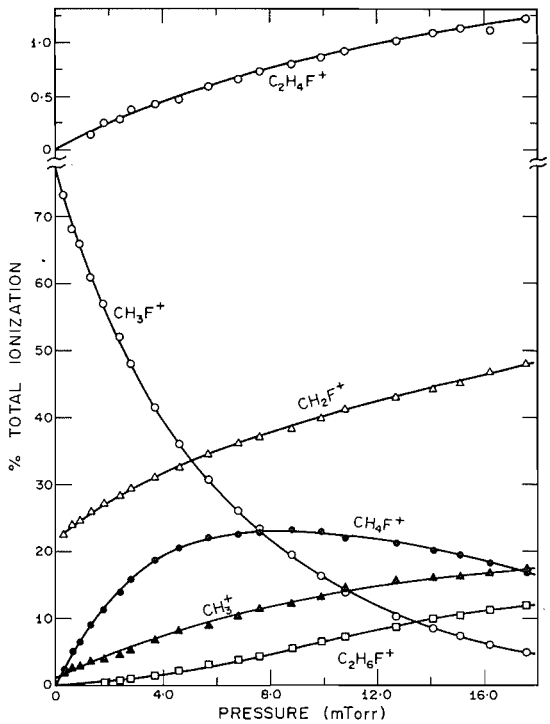

FIG. 1. Pressure plot for CH_3F at low electron energy.

Results and Discussion

Methyl Fluoride

A typical pressure plot obtained at 3.3 eV ion exit energy and low electron energy is shown in Fig. 1. It is evident that at this ion energy CH_3^+, CH_2F^+, CH_4F^+, and $C_2H_4F^+$ are products of the reaction of CH_3F^+ while $C_2H_6F^+$ is a higher-order product originating from the reaction

[1] $$CH_4F^+ + CH_3F \rightarrow C_2H_6F^+ + HF$$

The reaction of CH_3F^+ to produce both $C_2H_4F^+$ and CH_4F^+ as well as the subsequent reaction of CH_4F^+ by reaction 1 have been reported previously (4, 5). At higher conversions some of the CH_2F^+ also may originate from reaction of CH_4F^+ as suggested previously (4).

From Δ plots (7, 10) we have obtained the initial fractional yields at ion exit energies ranging from 0.73 to 3.3 eV. These fractional yields are plotted in Fig. 2 as a function of the average ion energy $\bar{E} = E_{e/3}$ (11) where E_e is the ion exit energy. Also shown in Fig. 2 are the fractional yields at thermal energies reported by Marshall and Buttrill (5) and the yields obtained from the ion-trapping studies at low electron energies (see below).

The yields of CH_4F^+ and $C_2H_4F^+$, both formed in presumably exothermic reactions, decrease with increasing ion energy while the yields of CH_2F^+ and CH_3^+ increase with ion energy and have an apparent kinetic energy threshold (ill-defined for CH_2F^+) consistent with formation of these products by endothermic reactions. Reactions 2 to 4 are possible reactions for formation of CH_2F^+.

[2] $$CH_3F^+ + CH_3F \rightarrow CH_2F^+ + H + CH_3F \qquad \Delta H = +15 \text{ kcal/mol}$$

[3] $$\rightarrow CH_2F^+ + H_2 + CH_2F \qquad \Delta H = +3 \text{ kcal/mol}$$

[4] $$\rightarrow CH_2F^+ + HF + CH_3 \qquad \Delta H = -9 \text{ kcal/mol}$$

Although the energy threshold for formation of CH_2F^+ is low this product is not observed at thermal ion energies indicating that the reaction must have a significant energy barrier and suggesting reaction 2 as the most probable reaction. This reaction is analogous to the collision-induced decomposition of CH_4^+ responsible for CH_3^+ formation in methane at higher ion kinetic energies (12).

TABLE 1. Rate coefficients in methyl fluoride system

Average ion energy (eV)	Rate coefficient (cm^3 $molecule^{-1}$ s^{-1}) × 10^9							Reference
	C^+	CH^+	CH_2^+	CF^+	CHF^+	CH_3F^+	CH_4F^+	
0.24						1.5_3		This work
0.33						1.6_5		This work
0.57						1.9_1		This work
0.73						2.1_0		This work
1.1						2.2_7		This work
0.24	1.7_7	1.7_2	1.2_1	0.4_7	1.2_1	2.2_0		This work
0.65	2.9_5	2.7_1	1.7_4	0.4_8	1.1_0	2.5_1		This work
~0.45*				0.3_4	1.1_9	1.8_7	0.90	This work
0.2	1.9	2.0	1.1	0.56	1.6	2.2		4
Thermal						1.4_6	0.80	5

*Trapped-ion experiments.

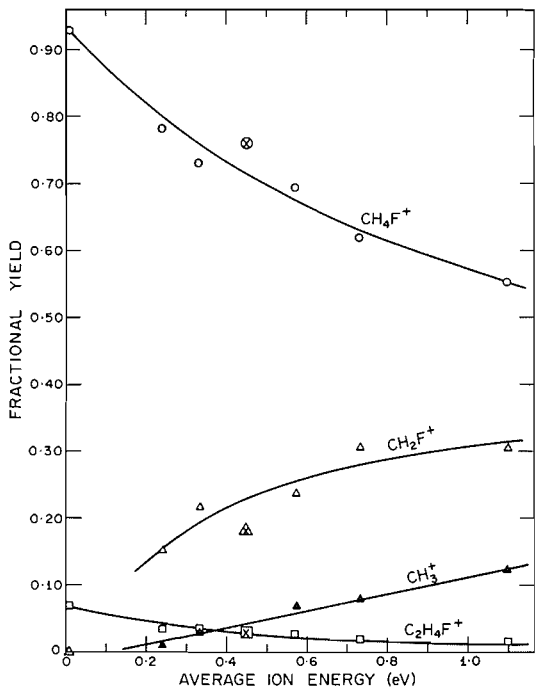

FIG. 2. Fractional yield *vs.* ion energy for CH_3F system.

Reactions 5 to 7 are possible reactions leading to CH_3^+ formation. Although reaction 7 is essentially thermoneutral, the threshold behavior

[5] $CH_3F^+ + CH_3F \rightarrow CH_3^+ + F + CH_3F$
$\Delta H = +45$ kcal/mol

[6] $\rightarrow CH_3^+ + F_2 + CH_3$
$\Delta H = +119$ kcal/mol

[7] $\rightarrow CH_3^+ + HF + CH_2F$
$\Delta H = +1$ kcal/mol

indicates that there is a significant energy barrier in the reaction forming CH_3^+. No clear decision concerning the reaction occurring can be made.

The rate coefficients for disappearance of the CH_3F^+ primary ion obtained from the pressure studies at low electron energy are recorded as the first five entries in Table 1. Pressure studies were also carried out at 70 eV electron energy and ion exit energies of 0.78 and 1.9_5 eV. The results obtained with respect to the reactions occurring were in agreement with the conclusions reached by McAskill (4). The disappearance rate coefficients for the molecular ion and several fragment ions are listed in Table 1.

Figure 3 shows typical results obtained in the study of the methyl fluoride system at low electron energies using the ion-trapping technique. The fractional yields of the products, with the exception of CH_3^+, are shown in Fig. 2 as the data points at 0.45 eV ion energy. Because of mass discrimination effects the low yield of CH_3^+ could not be determined with any accuracy. The CH_4F^+ ion reacts quite rapidly, primarily to produce $C_2H_6F^+$ but may also produce CH_2F^+ as suggested by McAskill (4). Both $C_2H_6F^+$ and $C_2H_4F^+$ are unreactive with CH_3F at the pressures used while CH_2F^+ reacts only very slowly to produce CHF_2^+ and $C_2H_5F_2^+$.

Difficulties were encountered in studying the reactions of fragment ions by the trapping technique because it was observed that several of the fragment ions (C^+, CH^+, CH_2^+, CH_3^+) were not completely trapped, presumably because they are formed with initial kinetic energy. Consistent with this reasoning was the observation that these ions also had broad shallow ion source residence time profiles on the medium pressure instrument. The kinetic data which could be obtained reliably from the trapping experiments is summarized as entry 8 in Table 1.

Can. J. Chem. Downloaded from www.nrcresearchpress.com by 210.87.254.105 on 09/05/12
For personal use only.

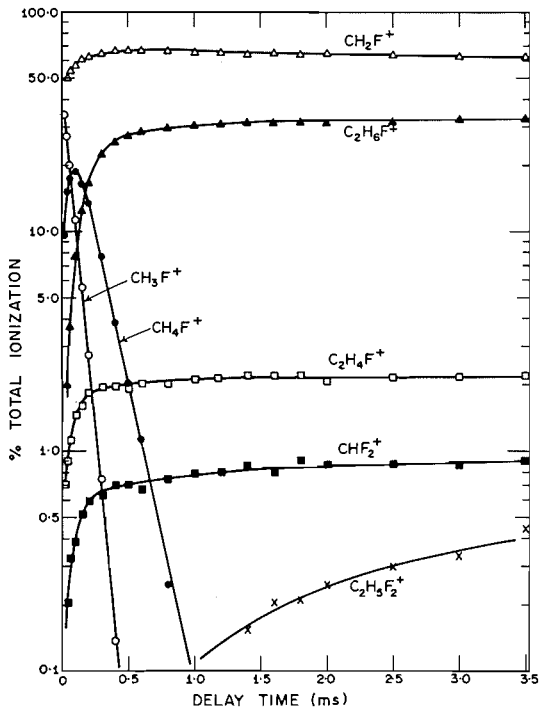

FIG. 3. Normalized ion intensities *vs.* reaction time for CH_3F system.

The final two entries in Table 1 present the kinetic data obtained by McAskill (4) from pressure studies at 70 eV electron energy and the thermal energy results of Marshall and Buttrill (5). The agreement between the present results and the earlier data is quite satisfactory; it is particularly encouraging to note the excellent agreement between the trapped-ion results and the i.c.r. results for reaction of CH_4F^+.

The rate coefficient for disappearance of CH_3F^+ clearly increases with increasing ion energy in contrast to the results for many simple systems (2) where the rate coefficient is independent of energy and in contrast to theoretical predictions. For an ion-induced dipole interaction as for an ion-averaged dipole interaction the collision rate coefficient should be independent of ion energy, while for an ion "locked-in" dipole interaction the collision rate coefficient should decrease with increasing ion energy (2). It should be noted that the experimental rate coefficient is considerably less than the calculated rate constant of 3.3×10^{-9} cm^3 molecule^{-1} s^{-1} (4) based on ion-averaged dipole interaction model (3), indicating that an appreciable fraction of the collisions lead to no detectable chemical change (*i.e.* no reaction or charge transfer). The increase of the disappearance rate coefficient undoubtedly reflects the effect of the ion kinetic energy on the competition between the reactive and the non-reactive or charge-transfer reaction channels. Several of the fragment ions, notably C^+, CH^+, and CH_2^+, also appear to have rate coefficients which are energy dependent.

Methyl Chloride

Figure 4 shows a typical pressure plot obtained at low electron energy and 3.3 eV ion exit energy. The major reaction of CH_3Cl^+ results in formation of CH_4Cl^+ which subsequently reacts to form $C_2H_6Cl^+$. CH_2Cl^+ and CH_3^+ are formed in low yield only in contrast to the methyl fluoride system at the same ion exit energy (*cf.* Fig. 1) where the analogous products are formed in substantial yield. No $C_2H_4Cl^+$ product, comparable to $C_2H_4F^+$ in methyl fluoride, was observed.

Table 2 records the fractional yields obtained from Δ plots as a function of the average reactant ion energy. Comparison of the results with those obtained for methyl fluoride (Fig. 2) clearly shows the much lower yield of the CH_2X^+ and CH_3^+ products. This undoubtedly results from the fact that the possible reactions producing these species in the methyl chloride system, reactions 8 to 13, are much more endothermic than the analogous reactions 2 to 7 in the methyl fluoride system.

[8] $CH_3Cl^+ + CH_3Cl \rightarrow CH_2Cl^+ + H + CH_3Cl$
$\Delta H = +41$ kcal/mol

[9] $\rightarrow CH_2Cl^+ + HCl + CH_3$
$\Delta H = +21$ kcal/mol

[10] $\rightarrow CH_2Cl^+ + H_2 + CH_2Cl$
$\Delta H = +25$ kcal/mol

[11] $\rightarrow CH_3^+ + Cl + CH_3Cl$
$\Delta H = +52$ kcal/mol

TABLE 2. Fractional yields for reaction of CH_3Cl^+

Average ion energy (eV)	Fractional yield		
	CH_3^+	CH_2Cl^+	CH_4Cl^+
0.21	0	0	0.99_7
0.36	0	0.01_5	0.98_9
0.58	0.00_3	0.02_1	0.98_2
0.78	0.00_5	0.02_9	0.96_9
0.91	0	0.03_4	0.95_0
1.1_3	0.02_8	0.04_8	0.91_1

Can. J. Chem. Downloaded from www.nrcresearchpress.com by 210.87.254.105 on 09/05/12
For personal use only.

TABLE 3. Rate coefficients in methyl chloride system

Average ion energy (eV)	Rate coefficient (cm^3 $molecule^{-1}$ s^{-1}) × 10^9									
	C^+	CH^+	CH_2^+	CH_3^+	Cl^+	HCl^+	CCl^+	$CHCl^+$	CH_3Cl^+	CH_4Cl^+
0.21	2.1	1.8	1.3	0.9_7	0.5_3	1.2	0.1_2	0.6_1	1.5_1	
0.46	2.7	2.2	1.4	0.4_2	0.2_7	1.5	0.1_7	0.4_4	1.6_2	
0.65	3.1	2.4	1.6	0.4_0	0.4_9	1.6	0.2_1	0.3_3	1.5_5	
1.1	3.0	2.1	0.9_7		0.2_7	1.4	0.1_4	0.3_2	1.4_7	
~0.45*				0.8_6				0.7_1	1.5_3	0.10

*Trapped-ion experiments.

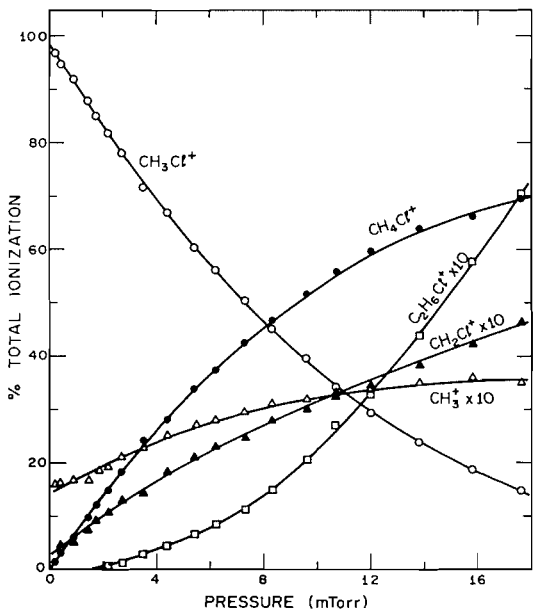

FIG. 4. Pressure plot for CH_3Cl at low electron energy.

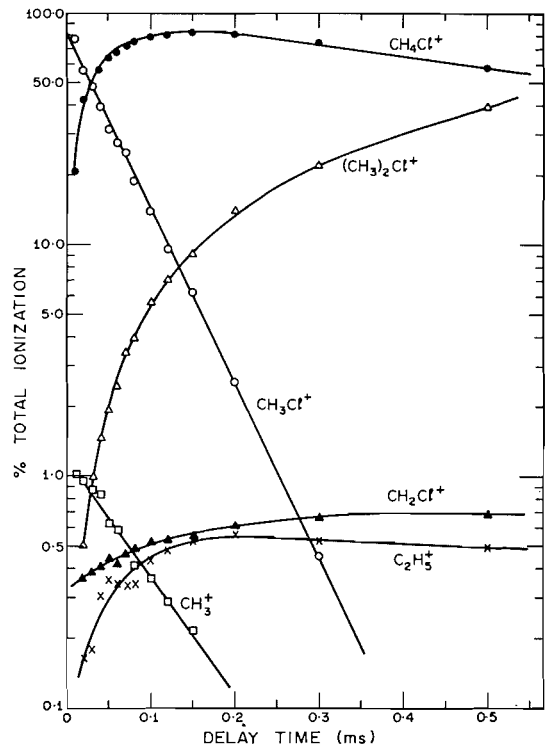

FIG. 5. Normalized ion intensities *vs.* reaction time for CH_3Cl system.

[12] $\rightarrow CH_3^+ + Cl_2 + CH_3$
$\Delta H = +73$ kcal/mol

[13] $\rightarrow CH_3^+ + HCl + CH_2Cl$
$\Delta H = +49$ kcal/mol

Pressure plots were also carried out at 50 eV electron energy and ion exit energies in the range 0.63 to 3.3 eV. The general features of these plots and the reaction assignments are in agreement with those reported earlier by McAskill (3). The disappearance rate coefficients obtained for a number of ions are summarized in Table 3. The rate coefficient for disappearance of CH_3Cl^+ was found to be independent of ion energy, in contrast to the CH_3F results, and yielded an average value of $1.5_3 \times 10^{-9}$ cm^3 $molecule^{-1}$ s^{-1} in good agreement with the CH_3Cl^+ decay rate of 1.66×10^{-9} cm^3 $molecule^{-1}$ s^{-1} obtained by McAskill (3). The low electron energy pressure plots yielded rate constants in agreement with the high electron energy data.

As in the methyl fluoride system we observed that several of the low mass ions were formed with initial kinetic energy and were not completely trapped in the electron space charge. Consequently rate coefficients for disappearance of only a few ions could be determined. Figure 5 shows a typical plot obtained at 12 eV nominal electron energy, while the rate coefficients obtained from the trapping experiments are shown as the final entry in Table 3.

Several points should be noted concerning the

Can. J. Chem. Downloaded from www.nrcresearchpress.com by 210.87.254.105 on 09/05/12
For personal use only.

methyl chloride results. At the ion energies of the trapping experiments the yield of CH_2Cl^+ is very low and can be accounted for almost entirely by reaction of CH_3^+. This indicates that the reaction

[14] $CH_4Cl^+ + CH_3Cl \rightarrow CH_2Cl^+ + HCl + CH_4$

suggested by McAskill (3) is not significant at these energies. McAskill has presented evidence that reaction 14 is endothermic with the rate increasing with ion energy. Our Δ plots at high ion energies indicated a tertiary formation of CH_2Cl^+ which supports this conclusion. Neither in the pressure studies nor the trapped-ion studies was there any evidence that CH_2Cl^+ reacted to form CH_4Cl^+. This result is in agreement with McAskill but in disagreement with earlier ratio plot studies (1) in this laboratory which must be considered erroneous.

The authors are indebted to the National Research Council of Canada for continued financial support.

1. A. G. HARRISON and J. C. J. THYNNE. Trans. Faraday Soc. **64**, 1287 (1968).
2. S. K. GUPTA, E. G. JONES, A. G. HARRISON, and J. J. MYHER. Can. J. Chem. **45**, 3107 (1967).
3. N. A. MCASKILL. Aust. J. Chem. **22**, 2275 (1969).
4. N. A. MCASKILL. Aust. J. Chem. **23**, 2301 (1970).
5. A. G. MARSHALL and S. E. BUTTRILL, JR. J. Chem. Phys. **52**, 2752 (1970).
6. A. A. HEROD and A. G. HARRISON. Int. J. Mass Spectrom. Ion Phys. **4**, 415 (1970).
7. A. A. HEROD and A. G. HARRISON. J. Phys. Chem. **73**, 3189 (1969).
8. R. H. MARTIN, F. W. LAMPE, and R. W. TAFT. J. Am. Chem. Soc. **88**, 1353 (1966).
9. D. C. FROST and C. A. MCDOWELL. Proc. Roy. Soc. London, **A241**, 194 (1957).
10. J. J. MYHER and A. G. HARRISON. J. Phys. Chem. **72**, 1905 (1968).
11. P. WARNECK. J. Chem. Phys. **46**, 513 (1967).
12. F. P. ABRAMSON and J. H. FUTRELL. J. Chem. Phys. **45**, 1925 (1966).

Can. J. Chem. Downloaded from www.nrcresearchpress.com by 210.87.254.105 on 09/05/12
For personal use only.

Can. J. Chem. Downloaded from www.nrcresearchpress.com by 210.87.254.5 on 09/05/12
For personal use only.

Reactions of Norbornen-7-one with Organolithium Reagents

F. R. S. CLARK AND J. WARKENTIN[1]
Chemistry Department, McMaster University, Hamilton, Ontario

Received December 15, 1970

Alkyllithium reagents (RLi: R = methyl, *n*-butyl, *t*-butyl) add to norbornen-7-one either without stereochemical preference (R = *n*-butyl) or with *syn* attack favored. This addition selectivity is qualitatively the same as that shown by corresponding alkylmagnesium reagents but competition from reduction is much less important in the case of alkyllithium reagents.

Phenyllithium and vinyllithium add preferentially from the *anti* face, although the corresponding Grignard reagents add selectively from the *syn* face. Possible causes of the stereoselectivities are considered. Solvent effects on the stereochemistry of addition are small.

L'addition des alkyl-lithium (RLi ou R = Me, *n*-Bu, *t*-Bu) à la norbornèn-7 one se fait soit sans préférence stéréochimique (R = *n*-Bu) soit avec une attaque *syn* favorisée. La sélectivité de cette addition est qualitativement la même que celle observée lors de l'action des organomagnésiens correspondants mais la compétition des réactions de réduction est beaucoup moins importante avec les organo-lithiens.

Quoique les organomagnésiens correspondants s'additionnent sélectivement par la face *syn*, le phényllithium et le vinyl-lithium s'additionnent préférentiellement par la face *anti*. On considère les causes possibles de ces stéréosélectivités. Les effets de solvants sur la stéréochimie de ces additions sont faibles.

Canadian Journal of Chemistry, 49, 2223 (1971)

Introduction

The treatment of norbornen-7-one (1) (**1**), with alkyl Grignard reagents gives mainly the corresponding 7-alkylnorbornen-7-*anti*-ols (2). Reduction of the ketone to *syn*- and *anti*-norbornen-7-ol accompanies the addition and in cases where the number of β-hydrogens of the Grignard reagent is large, reduction dominates.

The alternative synthesis of 7-R-norbornen-7-ols (R = alkyl, aryl), from organolithium reagents, has been used to prepare 7-methylnorbornen-7-ol of both *syn* and *anti* configurations (3). At 0–5 °C, in diethyl ether as solvent, *syn* attack was favored by a factor of 1.5:1. Similarly, Gassman and coworkers (4) have prepared a series of 7-arylnorbornen-7-ols by the reaction of **1** with aryllithium compounds.

In view of the marked difference in stereoselectivity of reactions of organolithium reagents and Grignard reagents with **1** (3, 5) and also the lesser importance of reduction by the former (6), a more systematic study of the reactions of organolithium compounds with **1** was undertaken.

Results and Discussion

Norbornen-7-one was reacted with three alkyllithium reagents in which the extent of β-branching varied (RLi: R = methyl, *n*-butyl, *t*-butyl), and with two unsaturated organolithium reagents, phenyllithium and vinyllithium. To a mimimum of 81% of a material balance, the only products obtained, in general, were the two isomeric 7-R-norbornen-7-ols. *t*-Butyllithium, which has the maximum number of β-hydrogens, gave a maximum of 20% reduction. In all other cases, reduction was not detectable.

The assignment of stereochemistry at C-7 of the alcohols has been approached in several ways. Relative retention times in g.l.p.c. and intramolecular hydrogen bonding in *syn*-ols (3, 4, 7) have served as criteria of configuration. Warkentin (2) used the g.l.p.c. criterion, backed by conversion to the isomer of a known bromide. The bromide from material thought to be 7-methylnorbornen-7-*anti*-ol was shown (p.m.r.) to be isomeric with 7-methyl-7-*syn*-bromonorbornene, the structure of which had been assigned on the basis of its slow solvolysis (8).

In the present work, analogy with the known members of the series was used; the p.m.r. spectra and, in particular, the chemical shifts of the vinyl protons and the bridgehead protons provided good evidence for stereochemistry at C-7 (Table 1). Relative g.l.p.c. retention times on Carbowax were also consistent with those previously established, "*syn*-ols" eluting before "*anti*-ols" (2, 3, 7). A further criterion of

[1]Author to whom correspondence may be addressed.

TABLE 1. 7-R-Norbornen-7-*anti*-ols (**1**) and 7-R-norbornen-7-*syn*-ols (**2**)

Compound R	%C*	%H*	The p.m.r. (δ, CCl_4, internal TMS)†·‡ H_1	H_2	H_5	H_6	H_R
1 CH_3§			2.27	5.92	2.00	0.92	1.25
2 CH_3§			2.42	6.12	1.80	0.95	1.13
1 *n*-C_4H_9	79.46 78.45	10.92 10.90	2.34	5.92	—	—	—
2 *n*-C_4H_9	79.46 79.16	10.92 10.90	2.50	6.11	1.80	0.90	1.40
1 *t*-C_4H_9	79.46 79.50	10.92 10.90	2.50	5.82	2.00	1.00	0.90
2 *t*-C_4H_9	79.46 78.65	10.92 10.99	2.75	6.20	2.00	1.00	1.08
1 *t*-C_4H_9—CH_2CH_2	80.41 80.29	11.34 11.79	2.33	5.90	—	—	0.80‖
2 *t*-C_4H_9—CH_2CH_2	80.41 80.27	11.34 11.90	2.49	6.08	1.75	0.92	0.85‖
1 CH_2=CH¶			2.40	5.95	2.06	0.92	**
2 CH_2=CH¶			2.62	6.20	1.85	1.00	††
1 C_6H_5‡‡			2.85	5.82	—	—	7.20
2 C_6H_5‡‡			3.16	6.23	—	—	7.32

*Calculated figures in the upper rows; analytical results in the lower rows. Analyses by Chemalytics, Inc., Tempe, Arizona.

†The numbering system is $H_1 = H_4$ = bridgehead, $H_2 = H_3$ = vinyl, H_5 = *exo*, H_6 = *endo*, H_R = chemical shift of C-7 substituent (R). Signals from the hydroxyl group are not tabulated.

‡Blanks indicate that the exact chemical shift could not be obtained because of severe overlap.

§Previously reported. See ref. 3.

‖*t*-Butyl signal.

¶Previously reported. See ref. 9.

**The H_8 signal: four lines centered at 6.35 δ, $J_t = 17$, $J_c = 11$ Hz, relative area 1. The H_9 signal: complex triplet centered at 5.12 δ, $J_t = 17$, $J_c = 11$, $J_g = 2$ Hz, relative area 2. These are observed parameters, obtained by first-order analysis. Relative intensities indicated that the spectrum is of higher order.

††The H_8 signal: four lines centered at 6.02 δ, $J_t = 15$, $J_c = 9.5$ Hz, relative area 1. The H_9 signal: complex triplet, 5.04, 5.26, and 5.58 δ, $J_t = 15$, $J_c = 9.5$, $J_g = 3$ Hz, relative area 2. The qualification in footnote ** applies here also.

‡‡Previously reported. See ref. 4.

stereochemistry is the O—H stretching pattern in the i.r. spectrum. Intramolecular hydrogen bonding to the etheno bridge leads to absorption near 3575 cm^{-1} in the spectra of "*syn*-ols" (3, 5). All "*syn*-ols" reported in this paper showed such absorption while "*anti*-ols" showed a free O—H stretching band above 3600 cm^{-1}. These criteria were sufficient for all alkylnorbornenols studied.

The products from phenyllithium were not separable on the Carbowax g.l.p.c. column used for the alkylnorbornenols. On a SE-30 column, the isomer assigned "*anti*-ol" by p.m.r. had the shorter, rather than the longer, retention time. To confirm the structures, the two 7-phenylnorbornen-7-ols were separated (g.l.p.c.) and each was partially acetylated in conditions unlikely to cause isomerization (acetyl chloride in excess pyridine). Changes in the bridgehead and vinyl proton resonances resulting from acetylation could then be studied with the best possible internal references. Erman (3) has prepared 7-*syn*- and 7-*anti*-acetoxy-7-methylnorbornene and these, together with the corresponding alcohols, were used as model compounds. The results are summarized in Table 2. Acetylation of 7-methylnorbornen-7-*anti*-ol causes a downfield shift of the bridgehead resonance but leaves the chemical shift of the vinyl hydrogens unchanged. A comparable shift of the bridgehead resonance occurs on acetylation of 7-methylnorbornen-7-*syn*-ol, but here the vinyl proton resonance moves upfield by 0.12 δ. Similar effects are observed for the phenyl compounds. In both isomers, bridgehead resonances move downfield, while in one isomer the vinyl resonance remains constant on acetylation and in the other it moves upfield by 0.17 δ. The former was therefore assigned the "*anti*-ol" structure and the latter the "*syn*-ol" structure. Thus, as with the 7-alkylnorbornen-7-ols, the phenyl compound with the vinyl proton resonance at lower field is that with the "*syn*-ol" stereochemistry.

The 7-vinylnorbornenols, like the 7-alkylnor-

Can. J. Chem. Downloaded from www.nrcresearchpress.com by 210.87.254.5 on 09/05/12
For personal use only.

TABLE 2. Bridgehead and vinyl shifts of norbornenes*

	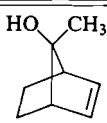	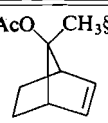	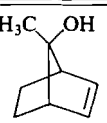	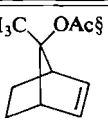	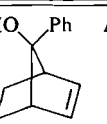	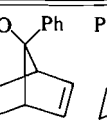	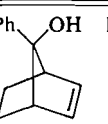	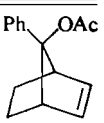
Bridgehead	2.30	2.88	2.42	3.03	2.92	3.40	3.16	3.68
Vinyl	5.97	5.95	6.12	6.00	5.83	5.83	6.23	6.06
Δδ, Bridgehead†	0.58		0.61		0.48		0.52	
Δδ, Vinyl‡	0.02		0.12		0.00		0.17	

*All numbers are chemical shifts expressed in p.p.m. downfield from TMS.
†The difference in chemical shift between the bridgehead protons of the acetate and the corresponding alcohol.
‡The difference in chemical shift between the vinyl protons of the acetate and the corresponding alcohol.
§Reference 3.

TABLE 3. Product ratios from norbornen-7-one and RLi*

R of RLi	Ether/ether†	Ether/*n*-hexane†	Hydrocarbon/ether†	Hydrocarbon/*n*-hexane†
CH_3	1:2.9	1:4.0	1:2.2‡	1:2.4‡
CH_3	1:1.9§			
n-C_4H_9	1:1.0	1:1.1	1:1.0	1:1.0
n-C_4H_9			1:1.3‖	
t-C_4H_9	¶	¶	1:6.3	1:2.0
CH_2=CH	2.4:1	—	—	—
C_6H_5	2.6:1	2.0:1	4.3:1	2.5:1

*The ratios are expressed as *syn*-7-ol: *anti*-7-ol. The error involved, estimated from the spread of a minimum of two runs, is at least 10% of the stated ratio.
†The solvents are given in the order: solvent of RLi/solvent of ketone.
‡Methyllithium is only partly soluble in *n*-hexane. These runs were conducted with slurries of methyllithium in diethyl ether and excess *n*-hexane.
§BF_3 present; see Experimental.
‖NaOEt present; see Experimental.
¶*t*-Butyl addition was observed in variable yield and ratio in these cases.

bornenols, were separable on the Carbowax column. Elution order and i.r. and p.m.r. spectra were consistent criteria of configuration. Moreover these criteria pointed to the solid isomer, m.p. 56–56.5°, as 7-vinylnorbornen-7-*anti*-ol, in agreement with a previous assignment, lit. (9), m.p. 58.2–59.8°.[2]

With the C-7 configuration of the products established the sense of attack of organolithium compounds on **1** could be investigated. In a series of experiments the solvents of both ketone and organolithium reagent were varied from diethyl ether to saturated hydrocarbon. Thus, for example, methyllithium, which is commercially available in diethyl ether solution, was added to the ketone, itself dissolved in diethyl ether or *n*-hexane. A similar pair of results was obtained by adding a large excess of *n*-hexane to the sample of methyllithium in diethyl ether; this was also reacted with the ketone in the two solvents. Phenyllithium is supplied commercially in benzene – diethyl ether (70:30). The reagent is insoluble in *n*-hexane and was used undiluted (in benzene – diethyl ether 70:30) and also with excess diethyl ether. *t*-Butyllithium was used in *n*-pentane and in *n*-pentane – ether solutions. *n*-Butyllithium was used in hexane and in ether–hexane solutions. Vinyllithium in tetrahydrofuran was added to the ketone in diethyl ether. A summary of the results of the solvent dependence of addition ratio appears in Table 3, together with results of experiments in which BF_3 and LiOEt were also present.

t-Butyllithium reacted to form expected addition products in *n*-hexane, but when diethyl ether was present, other alcohols were formed, assigned by p.m.r. and by relative retention time (g.l.p.c.) as 7-(3′,3′-dimethylbutyl)-norbornen-7-ols. In a series of experiments in which the mole ratio of *t*-butyllithium, relative to **1**, was varied from 1 to 10, only 3,3-dimethylbutyl addition products were observed until the ratio exceeded 8:1; at 10:1, *t*-butyl addition was also observed. The stereochemistry of attack at C-7 of **1**, in both *t*-butyl and 3,3-dimethylbutyl addition varied considerably over a number of runs. Unreacted ketone **1** was always present in product mixtures containing 7-(3′,3′-dimethyl-

[2]Melting points are corrected.

Can. J. Chem. Downloaded from www.nrcresearchpress.com by 210.87.254.5 on 09/05/12
For personal use only.

[1] $$t\text{-BuLi} + CH_3CH_2{-}OEt \longrightarrow H_2C{=}CH_2 + LiOEt + (CH_3)_3CH$$

[2] 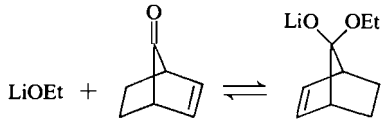

[3] $$t\text{-BuLi} + H_2C{=}CH_2 \longrightarrow (CH_3)_3CCH_2CH_2Li$$

[4] 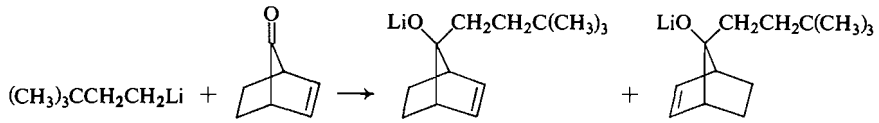

butyl)-norbornen-7-ols. A rationale for these observations is illustrated with eqs. 1–4. There is precedent for addition of *t*-butyllithium to ethylene (10). Evidently some of the norbornen-7-one is protected as the hemiketal anion.

Of particular note is the *anti* addition preference shown by phenyllithium and vinyllithium. In view of the pronounced *syn* preference shown by Grignard reagents (2, 5, 9), phenyl Grignard reagent was added to the ketone in diethyl ether. A 2.8:1 preference for *syn* attack was observed. Vinyl Grignard reagent shows a still higher (4:1) preference for *syn* attack (9). Thus, either isomer of the 7-phenylnorbornen-7-ols and 7-vinylnorbornen-7-ols can be prepared in excess of the other isomer simply by choosing the appropriate reagent.

The stereochemical preferences shown by the different organolithium reagents are not likely to be caused by impurities. Two equivalents of BF_3, for example, altered the *syn*:*anti* attack ratio of methyllithium from 2.9 to 1.9. In the presence of 10 equiv of LiOEt, addition of *n*-butyllithium to **1** gave a product ratio of 1.3, in favor of *syn* attack, as compared to 1.0 without LiOEt. Phenyllithium from a new bottle gave the same product ratio as that which had been stored for 3 years. In view of the fact that neither an electrophilic reagent nor a nucleophilic impurity present in copious amount changed the ratios drastically it is unlikely that unknown impurities in the reagents are responsible for observed differences.

Although the reasons for the dependence of product stereochemistry on reagent structure or solvent composition are not clear, some potential factors are worthy of brief discussion. A change in the sense of the stereochemical preference indicates that there are at least two opposing factors involved and that they are nearly balanced. Which side, *syn* or *anti*, is the more hindered has not been rigorously established. Two studies of equilibrated systems indicate that the larger of two substituents at C-7 prefers the *syn* position (4, 11), suggesting that the *syn* face is less hindered. Preliminary studies of equilibria involving mixed ketals of **1** lend support to that conclusion (12).

The preferred course of alkyllithium addition may therefore be the result of a dominating steric factor and the magnitude of the selectivity may be related to the effective steric requirements of the alkyllithium. Alkyllithium reagents tend to be associated in solution (13, 14); methyllithium, for example, being tetrameric in ether, tetrahydrofuran, and triethylamine (13). This means that the effective steric requirement of such a reagent is not easily predicted from the formula of the monomer.

In the case of phenyllithium and vinyllithium, both of which are more polar than alkyllithium reagents (15), a polar factor may be dominant. A possible destabilizing polar interaction in transition states for *syn*-addition is that between carbanion-like reagent and the double bond (**2**).

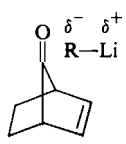

2

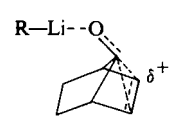

3

Can. J. Chem. Downloaded from www.nrcresearchpress.com by 210.87.254.5 on 09/05/12
For personal use only.

Can. J. Chem. Downloaded from www.nrcresearchpress.com by 210.87.254.5 on 09/05/12
For personal use only.

A similar interaction may be responsible for the lower acidity of norbornene-*syn*-7-carboxylic acid ($pK_a = 4.66$) relative to that of the *anti* acid ($pK_a = 4.50$) (16).[3] Qualitatively, this picture can accommodate the *syn* preference of the Grignard reagents which, being less polar than corresponding organolithium reagents (15) would be controlled primarily by the steric factor.

The alternative that must be considered is a factor stabilizing transition states for *anti* addition. A well-known process in which *anti* attack is greatly favored is capture of nonclassical 7-norbornenyl cations (18). However, such an analogy would require that phenyllithium and vinyllithium can behave primarily as electrophiles capable of inducing nonclassical cation character into the ketone, as in **3**. Such behavior is quite unlikely, especially in view of the fact that BF_3 did not overcome the *syn* preference of methyllithium.

Small variations in attack ratio with solvent are readily accommodated in the general scheme. Both the steric factor and the polar factor can be expected to depend on structural detail, which includes solvation.

Experimental

Chemicals

Methyllithium, *t*-butyllithium, vinyllithium, and phenyllithium were supplied by Alpha Inorganics Inc. *n*-Butyllithium was a product of Foote Mineral Co. Limited.

Product Analyses

Crude product mixtures were analyzed by g.l.p.c. using a 10′ × 3/8″ column packed with 15% Carbowax 20M on 60–80 mesh Chromosorb W (7-alkyl-norbornen-7-ols) and a 5′ × 1/4″ column packed with 20% SE30 on the same support (7-phenyl-norbornen-7-ols). Analytical samples were obtained by preparative g.l.p.c. employing a freshly prepared 10′ × 1/4″ column packed with 15% Carbowax 20M on the same support. An Aerograph 90P-3 instrument, with thermal conductivity detector, was used throughout.

Product ratios were determined both by measuring areas under peaks from the g.l.p.c. traces by triangulation[4] and by repeated integration of the vinyl proton absorptions in the p.m.r. spectra. All p.m.r. data were obtained with a Varian T60 instrument.

Organolithium Reagents

The concentration of the reagents was obtained by titration against hydrochloric acid (2.44 *M*) using phenolphthalein as indicator. This analysis relies on the insolubility of lithium hydroxide in the solvents present.

The following description is typical of all experiments. *n*-Butyllithium (1.6 *M* in *n*-hexane, 2.0 ml, 3.2 mmol) was dissolved in *n*-hexane (5.0 ml) and stirred magnetically. The *n*-butyllithium solution was added dropwise to the ketone solution, at −75°, over 2 min and the resulting mixture was stirred for a further 15 min at −75°. The reaction was quenched by pouring onto water at room temperature (approximately 75 ml). The ether layer was separated, washed twice with water (2 × 75 ml) and dried over $MgSO_4$ before concentrating with a rotary evaporator. Product ratios were accepted only if the last traces of ether were not removed, as the products are quite volatile.

In a similar experiment employing methyllithium in ether (the products of which were the most volatile encountered) and norbornen-7-one (1.06 g, 9.82 mmol) in *n*-hexane the yield of ether-free 7-methylnorbornen-7-ols was 0.98 g (81%). In all other cases the yields were higher.

Effect of Boron Trifluoride

To norbornen-7-one (50 mg, 0.46 mmol) in dry diethyl ether (10 ml) was added freshly-distilled boron trifluoride etherate (144 mg, 1.01 mmol) and the solution was stirred for 5 min at 22° before it was cooled to −70°. Methyllithium (1.83 *M* in ether, 2.6 ml, 4.6 mmol) was added during 3 min. Work-up analogous to that described above gave a colorless oil which crystallized on standing (60 mg). Analysis by g.l.p.c. showed that the ratio, *anti*-ol : *syn*-ol, of 7-methylnorbornen-7-ols was 1.9.

Effect of Sodium Ethoxide

n-Butyllithium (1.78 *M* in hexane, 5.2 ml, 9.3 mmol) was added to ethanol (0.43 g, 9.3 mmol) in diethyl ether (10 ml) at −78°. The mixture was stirred for 5 min before norbornen-7-one (100 mg, 0.93 mmol) was added, followed, after 5 min, by *n*-butyllithium (5.2 ml, 9.3 mmol). After 15 min of stirring at −78° the mixture was worked-up, resulting in a colorless oil (0.090 g). Analysis by g.l.p.c. showed this to consist of norbornen-7-one (7%) and 7-*n*-butylnorbornen-7-ols in the ratio 1.3 (*anti*-ol : *syn*-ol) compared to about 1.0 (Table 3) without lithium ethoxide.

Phenyl Grignard Reagent

Dry bromobenzene (7.60 g, 46.0 mmol) was added through a serum cap to a stirred mixture of heat-dried, Grignard-grade magnesium turnings (2.0 g, 0.082 g-atom) in sodium-dried diethyl ether (25 ml) under a N_2 atmosphere. The reaction was initiated with gentle heating, and after 1 h reflux the solution was brown in color. Norbornen-7-one (0.50 g, 4.6 mmol) was added dropwise and the mixture was held at reflux temperature for 1 h. The reaction was quenched by pouring onto saturated aqueous NH_4Cl solution. This hydrolysis was highly exothermic, indicating the presence of excess Grignard reagent. Drying the ether layer over K_2CO_3 and evaporation of ether left a yellow oil (1.0 g). This was shown to contain 7-phenylnorbornen-7-*anti*-ol (44 parts) and 7-phenylnorbornen-7-*syn*-ol (16 parts) (70% yield) by spectral and g.l.p.c. comparison with authentic samples. The third product, biphenyl, was identified from its p.m.r. spectrum and m.p. (70–71°, lit (19) 70°).

[3]The order of these acidities has been confirmed (17).

[4]Thermal conductivities of products were assumed to be the same.

1. P. G. GASSMAN and J. L. MARSHALL. Organic syntheses. *Edited by* P. Yates. **48**, 25 (1968).
2. J. WARKENTIN. Can. J. Chem. **48**, 1391 (1970).
3. W. F. ERMAN. J. Org. Chem. **32**, 765 (1967).
4. P. G. GASSMAN, J. ZELLER, and J. T. LUMB. Chem. Commun. 69 (1968).
5. R. K. BLY and R. S. BLY. J. Org. Chem. **28**, 3165 (1963).
6. P. D. BARTLETT and E. B. LEFFERTS. J. Am. Chem. Soc. 77, 2804 (1955).
7. R. S. BLY, R. K. BLY, A. O. BEDENBAUGH, and O. R. VAIL. J. Am. Chem. Soc. **89**, 880 (1967).
8. L. SKATTEBOL. Tetrahedron. **23**, 1107 (1967).
9. J. A. BERSON and M. JONES, JR. J. Am. Chem. Soc. **86**, 5019 (1964).
10. R. E. DESSY and W. KITCHING. Advances in organometallic chemistry. *Edited by* F. G. A. Stone and R. West. **4**, 277 (1966).
11. R. R. SAUERS. Chem. and Ind. 176 (1960).
12. S. R. KORN and J. WARKENTIN. Unpublished work.
13. L. D. MCKEEVER, R. WAACK, M. A. DORAN, and E. B. BAKER. J. Am. Chem. Soc. **91**, 1057 (1969).
14. G. E. COATES and K. WADE. Organometallic compounds. *Edited by* G. E. Coates, M. L. H. Green, and K. Wade. 3rd Ed., Vol. 1. Methuen, London, 1967. p. 32.
15. (*a*) H. F. EBEL. Tetrahedron, **21**, 699 (1965); (*b*) **24**, 459 (1968).
16. R. K. BLY and R. S. BLY. J. Org. Chem. **31**, 1577 (1966).
17. E. ZADOR and J. WARKENTIN. Unpublished work.
18. (*a*) S. WINSTEIN, A. H. LEWIN, and K. C. PANDE. J. Am. Chem. Soc. **85**, 2324 (1963); (*b*) A. DIAZ, M. BROOKHART, and S. WINSTEIN. J. Am. Chem. Soc. **88**, 3133 (1966); (*c*) M. BROOKHART, A. DIAZ, and S. WINSTEIN. J. Am. Chem. Soc. **88**, 3135 (1966).
19. Handbook of chemistry and physics. *Edited by* R. C. Weast. 49th Ed. The Chemical Rubber Company, Cleveland, Ohio, 1968–1969.

Can. J. Chem. Downloaded from www.nrcresearchpress.com by 210.87.254.5 on 09/05/12
For personal use only.

Can. J. Chem. Downloaded from www.nrcresearchpress.com by 210.87.254.5 on 09/05/12
For personal use only.

Normal Coordinate Calculations of the Vibrations of Methylene Cyclopropane-h_6 and -d_6

J. E. BERTIE AND M. G. NORTON
Department of Chemistry, The University of Alberta, Edmonton, Alberta

Received March 1, 1971

Normal coordinate calculations for methylene cyclopropane-h_6 and -d_6 have been carried out using two models. In the first model 31 internal coordinates were used, and in the second model 25 internal coordinates were used. The force constants were, in each case, refined to the 40 frequencies observed for the two molecules. Using the first model 26 force constants, of which four were constrained, fitted the frequencies with an average error of 1.2% for C_4H_6 and 2.8% for C_4D_6. Using the second model 24 force constants, of which two were constrained, fitted the frequencies with an average error of 1.4% for C_4H_6 and 2.8% for C_4D_6.

The very low isotopic shift of the C═C stretching mode can be explained by an interaction with the ethylenic CH_2 deformation, which is best assigned at 1047 cm^{-1}, rather than at 1139 cm^{-1}, in C_4D_6. The calculations indicate that the experimental assignment for the A_1 ring breathing mode and the A_1 methylenic wag in C_4H_6 should probably be reversed. For the A_1 and the B_1 modes with frequencies between 500 and 1300 cm^{-1}, the normal coordinates change considerably on deuteration. The symmetry coordinates are mixed in the normal modes of C_4D_6 to a much greater extent than in those of C_4H_6.

Des calculs en coordonnées normales ont été effectués pour le méthylène cyclopropane-h_6 et -d_6 utilisant deux modèles. Dans le premier modèle 31 coordonnées internes ont été utilisées et dans le second modèle 25 coordonnées internes ont été utilisées. Les constantes de force ont été, dans chaque cas, raffinées aux 40 fréquences observées pour les deux molécules. En utilisant le premier modèle comprenant 26 constantes de force, parmi lesquelles quatre étaient contraintes, les fréquences coincidèrent avec une erreur moyenne de 1.2% pour C_4H_6 et 2.8% pour C_4D_6. En utilisant le second modèle comprenant 24 constantes de force, parmi lesquelles deux étaient contraintes, les fréquences coincidèrent avec une erreur moyenne de 1.4% pour C_4H_6 et 2.8% pour C_4D_6.

Le déplacement isotopique très faible du mode de valence C═C peut être expliqué par une interaction avec la déformation CH_2 éthylénique, qui est mieux attribuée à 1047 cm^{-1}, plutôt qu'à 1139 cm^{-1}, dans C_4D_6. Les calculs indiquent que l'attribution expérimentale pour le mode A_1 de pulsation du cycle et le balancement (wag) A_1 méthylénique dans C_4H_6 devrait probablement être inversée. Pour les modes A_1 et B_1 de fréquences entre 500 et 1300 cm^{-1}, les coordonnées normales changent considérablement avec la deutération. Les coordonnées de symétrie sont mélangées dans les modes normaux de C_4D_6 de façon beaucoup plus importante que ceux du C_4H_6.

Canadian Journal of Chemistry, 49, 2229 (1971)

I. Introduction

The vibrational assignments reported in an earlier paper (1) imply surprisingly small isotopic shifts of certain vibrations. In particular, the C═C stretching mode, ν_3, appears to shift from 1742.2 to 1727.7 cm^{-1} on deuteration, instead of to about 1650 cm^{-1} as would be expected on simple grounds. The frequency shift on deuteration of the ethylenic CH_2 deformation, ν_5, is uncertain between 1411.0 to 1139 cm^{-1}, (assignment I) and 1411.0 to 1047 cm^{-1} (assignment II). The former appears to be more reasonable in relation to the shifts of the methylenic CH_2 deformations, but the latter is required to fit the product rule reasonably. Further, the B_1 methylenic wag, ν_{17}, shifts on deuteration from 1125 to 1017 cm^{-1}, yielding an isotopic frequency ratio of only 1.11, compared to 1.27 found for the A_1 wag, ν_7. On the other hand, the B_1 ring deformation, ν_{18}, shifts on deuteration from 895 to 735 cm^{-1}, yielding a surprisingly high isotopic frequency ratio of 1.22. Without normal coordinate calculations one would ascribe these peculiarities to the different modes coupling to a different extent in the different isotopic molecules. It is desirable to carry out the calculations and determine which of these peculiarities can be accounted for by the mass changes and the geometry of the molecule alone, *i.e.* by kinetic coupling, and which of them require specific force constants to account for interactions between certain internal coordinates for their explanation, *i.e.* potential energy coupling. And further, to determine whether a harmonic force field can account for

Can. J. Chem. Downloaded from www.nrcresearchpress.com by 210.87.254.5 on 09/05/12
For personal use only.

the observed frequencies in both molecules at all. These calculations were undertaken, also, to see if the apparently high frequency, 1354.4 cm^{-1} in C_4H_6 and 1073 cm^{-1} in C_4D_6 of the ethylenic rock, ν_{16}, could arise from interaction with other modes of vibration, or merely from a high force constant. Further, the force field of cyclopropane has been investigated by several authors (2–4) and it is of interest to extend this work to include methylene cyclopropane, in which the C_3 ring is thought to be under greater strain due to the presence of the ethylenic group.

Blau (5) and Loewenstein (6) solved the secular equation for C_4H_6 to assist in the assignment of the normal modes, but did not attempt a convergent solution to the problem. No calculations have been reported for C_4D_6.

We have therefore used the results of the vibrational assignment of C_4H_6 and C_4D_6 described in a previous paper (1) to carry out normal coordinate analyses of these molecules. In the calculations we have used two sets of coordinates: (*a*) the 31 internal valence coordinates which introduce 7 redundancies and (*b*) a set of 25 internal coordinates which do not require consideration of redundancy in the ring, but which do include one redundancy by the use of the two C—C=C angles. Set *b* is directly comparable with those used in the previous work on cyclopropane (2–4). Modified valence force fields were used for each case.

These two treatments will be discussed in Sections III and IV, respectively.

II. Computer Programs

The calculations were carried out on the I.B.M. model 360/67 computer at the University of Alberta. The **G** matrices were calculated from the **X** matrix via the **B** matrix using Schachtschneider's (7) GMAT program. The **X** matrix was constructed from the microwave data of Laurie and Stigliani (8).

Two programs were used to calculate the normal modes and their frequencies, and to refine the force constants. A program originally written by Smith (9), and translated into PL/1 for the University of Alberta computer by M. G. Norton, was used for the majority of the work, including the development of the force-field. This program is similar in method to Schachtschneider's program FPERT (7), but allows greater flexibility in input. Towards the end of the work all of the results of the PL/1 program were checked using the widely-used FPERT, to confirm the results obtained.

Both programs were checked out using the methyl fluoride data of Schachtschneider (7). Our implementation of FPERT reproduced Schachtschneider's solutions exactly, and has satisfactorily reproduced other published data. The PL/1 program reproduced Schachtschneider's frequencies for normal and heavy methyl fluoride to better than 1 cm^{-1}, and reproduced his force constants well, the worst disagreement being about 2% on an interaction constant. Because the two programs converged to slightly different solutions, and because FPERT converged at times when the PL/1 program led to a slightly oscillatory solution, the final force constants and frequencies presented are those obtained with FPERT. The potential energy distribution was obtained, using the force constants presented, from the PL/1 program, without allowing it to refine the force constants further, because this program yields the potential energy distribution in a rather more convenient form for our purpose than does FPERT. The PL/1 program also yields the potential energy distribution in the same form as FPERT, and these agreed very closely when the same force constants were used in both programs.

The criteria for accepting a solution were the following. The calculation must converge to a repeatedly consistent solution. The singularity test ratio (10) must be examined, because when this is very near to zero false potential energy minima may be entered. Solutions for which the potential energy distribution among the symmetry coordinates was consistent with the original assignments (1) were sought.

III. Calculation Including all Internal Coordinates

This calculation was carried out because it seemed to be a more rigorous approach to the problem than the method described in Section IV, which is the more usual one (2–4). After constructing the symmetry coordinates, we proceeded in two stages. First the best solution for C_4H_6 alone was sought. Then this force field was applied to C_4D_6, without refinement, to see how serious the discrepancies were. They were serious, and so the force field was re-refined, and modified

TABLE 1. Redundancy conditions

(1) $\delta\alpha_{12} + \delta\alpha_{27} + \delta\alpha_{17} = 0$

(2) $\delta\alpha_{78} + \delta\alpha_{79} + \delta\alpha_{89} = 0$

(3) $\delta\alpha_{89} + \delta\alpha_{810} + \delta\alpha_{910} = 0$

(4) $0.46538\delta R_{10} - 0.24615(\delta R_8 + \delta R_9) + 0.57544(\delta\alpha_{810} + \delta\alpha_{910}) = 0$

(5) $0.16043(\delta\alpha_{810} + \delta\alpha_{910}) + 0.44081(\delta\alpha_{34} + \delta\alpha_{56}) + 0.26455(\delta\alpha_{38} + \delta\alpha_{310} + \delta\alpha_{48} + \delta\alpha_{410} + \delta\alpha_{59} + \delta\alpha_{510} + \delta\alpha_{69} + \delta\alpha_{610}) = 0$

(6) $0.52348(\delta R_8 - \delta R_9) + 0.47536(\delta\alpha_{810} - \delta\alpha_{910}) = 0$

(7) $0.16043(\delta\alpha_{810} - \delta\alpha_{910}) + 0.44081(\delta\alpha_{34} - \delta\alpha_{56}) + 0.26455(\delta\alpha_{38} + \delta\alpha_{310} + \delta\alpha_{48} + \delta\alpha_{410} - \delta\alpha_{59} - \delta\alpha_{69} - \delta\alpha_{510} - \delta\alpha_{610}) = 0$

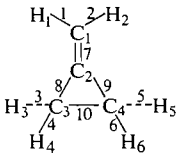

FIG. 1. The bond numbering scheme upon which the definition of the internal coordinates is based.

by the inclusion of new force constants, using the data for C_4H_6 and C_4D_6 together.

The 31 internal coordinates are defined with reference to Fig. 1. The bond stretching coordinates are δR_i, using the i appropriate to each bond as shown in Fig. 1, *e.g.* $\delta R_{C_1H_1}$ is δR_1 etc. The angle deformation coordinates are $\delta\alpha_{ij}$, where i and j are the numbers assigned in Fig. 1 to the bonds forming the angle, *e.g.* $\delta\alpha_{410}$ is the change in the angle H_4—C_3—C_4. The torsional coordinate τ is the dihedral angle between the planes $H_1C_1H_2$ and $C_3C_2C_4$. β_{712} is the angle between the double bond and the $H_1C_1H_2$ plane, and β_{789} is the angle between the double bond and the $C_3C_2C_4$ plane.

(a) Construction of Symmetry Coordinates

Seven relationships between these internal displacement coordinates arise from the geometry of the molecule, and are given in Table 1. Conditions *1* and *2* relate the coplanar angles about C_1 and about C_2, conditions *3*, *4*, and *6* represent the *3* ring redundancy conditions, and conditions *5* and *7* are symmetric and asymmetric combinations, respectively, of the relation between the six angles about C_3 with that between the angles about C_4. The relation between the six angles about a point through which one symmetry plane passes that we used is

$$\delta\alpha_{12} + \frac{\tan(\alpha_{34}/2)}{\tan(\alpha_{12}/2)} \cdot \delta\alpha_{34} + \frac{\sin\alpha_{13}}{2\sin(\alpha_{12}/2)\cos(\alpha_{34}/2)}(\delta\alpha_{13} + \delta\alpha_{14} + \delta\alpha_{23} + \delta\alpha_{24}) = 0$$

where R_i, $i = 1$ to 4, designate the 4 bonds, and α_{ik} designates the angle between bond i and bond k.

The redundancy conditions, *1*, *2*, *3*, *4*, and *5* transform according to representation A_1 of C_{2v}, while *6* and *7* transform according to the B_1 representation. The redundancy relations belonging to a given representation were made orthonormal to each other by the Schmidt method (11). The remainder of the symmetry coordinates were then made orthonormal to the redundant set and to each other. The final set of 31 symmetry coordinates is given in Table 2. The seven redundant or "null" coordinates were found to give zero roots upon solving the secular equation and were removed from the **U** matrix to give a 24 × 31 **U** matrix.

(b) Calculation and Results for C_4H_6 Alone

In order to simplify the development of a force field which would serve as a starting approximation for the whole, two molecule, problem, we first considered the C_4H_6 molecule alone. Before even the simplest force field is used, two diagonal force constants must be constrained. The ethylenic torsional mode has not been observed, and the torsional force constant was given the value 0.15 mdyn Å which gives a calculated frequency for this mode of around 740 cm^{-1}, close to the torsional frequency in asymmetrically disubstituted ethylenes (12). With our present set of internal coordinates, the C_3 ring has 4 diagonal force constants, $F(R_8) = F(R_9)$, $F(R_{10})$, $F(\alpha_{89})$, $F(\alpha_{810}) = F(\alpha_{910})$, to contribute to 3 degrees of

Can. J. Chem. Downloaded from www.nrcresearchpress.com by 210.87.254.5 on 09/05/12
For personal use only.

TABLE 2

(*a*) Redundancy conditions after orthonormalization

A_1

(1) $0.57735(\delta\alpha_{12} + \delta\alpha_{27} + \delta\alpha_{17}) = 0$

(2) $0.16043(\delta\alpha_{810} + \delta\alpha_{910}) + 0.44081(\delta\alpha_{34} + \delta\alpha_{56}) + 0.26455(\delta\alpha_{38} + \delta\alpha_{310} + \delta\alpha_{48} + \delta\alpha_{410} + \delta\alpha_{59} + \delta\alpha_{510} + \delta\alpha_{69} + \delta\alpha_{610}) = 0$

(3) $0.58751\delta\alpha_{89} + 0.55727(\delta\alpha_{810} + \delta\alpha_{910}) - 0.08310(\delta\alpha_{34} + \delta\alpha_{56}) - 0.0497(\delta\alpha_{38} + \delta\alpha_{310} + \delta\alpha_{48} + \delta\alpha_{410} + \delta\alpha_{59} + \delta\alpha_{510} + \delta\alpha_{69} + \delta\alpha_{610}) = 0$

(4) $0.62491\delta R_{10} - 0.33052(\delta R_8 + \delta R_9) - 0.50601\delta\alpha_{89} + 0.25300(\delta\alpha_{810} + \delta\alpha_{910}) - 0.03763(\delta\alpha_{34} + \delta\alpha_{56}) - 0.02269(\delta\alpha_{38} + \delta\alpha_{310} + \delta\alpha_{48} + \delta\alpha_{410} + \delta\alpha_{59} + \delta\alpha_{510} + \delta\alpha_{69} + \delta\alpha_{610}) = 0$

(5) $0.20415\delta R_{10} - 0.10797(\delta R_8 + \delta R_9) + 0.25748\delta\alpha_{89} - 0.12874(\delta\alpha_{810} + \delta\alpha_{910}) + 0.64564(\delta\alpha_{78} + \delta\alpha_{79}) + 0.01925(\delta\alpha_{34} + \delta\alpha_{56}) + 0.01145(\delta\alpha_{38} + \delta\alpha_{310} + \delta\alpha_{48} + \delta\alpha_{410} + \delta\alpha_{59} + \delta\alpha_{510} + \delta\alpha_{69} + \delta\alpha_{610}) = 0$

B_1

(6) $0.52968(\delta R_8 - \delta R_9) + 0.45623(\delta\alpha_{810} - \delta\alpha_{910}) - 0.06803(\delta\alpha_{34} - \delta\alpha_{56}) - 0.04083(\delta\alpha_{38} + \delta\alpha_{48} + \delta\alpha_{310} + \delta\alpha_{410} - \delta\alpha_{59} - \delta\alpha_{69} - \delta\alpha_{510} - \delta\alpha_{610}) = 0$

(7) $0.16043(\delta\alpha_{810} - \delta\alpha_{910}) + 0.44081(\delta\alpha_{34} - \delta\alpha_{56}) + 0.26455(\delta\alpha_{38} + \delta\alpha_{48} + \delta\alpha_{310} + \delta\alpha_{410} - \delta\alpha_{59} - \delta\alpha_{69} - \delta\alpha_{510} - \delta\alpha_{610}) = 0$

(*b*) Symmetry coordinates after orthonormalization

A_1

$S_1 = 0.70711(\delta R_1 + \delta R_2)$

$S_2 = \delta R_7$

$S_3 = 0.5(\delta R_3 + \delta R_4 + \delta R_5 + \delta R_6)$

$S_4 = 0.56623(\delta R_8 + \delta R_9) + 0.59897\delta R_{10}$

$S_5 = 0.24244(\delta R_8 + \delta R_9) - 0.4576\delta R_{10} - 0.58387\delta\alpha_{89} + 0.27691(\delta\alpha_{810} + \delta\alpha_{910}) - 0.04127(\delta\alpha_{34} + \delta\alpha_{56}) + 0.29194(\delta\alpha_{78} + \delta\alpha_{79}) - 0.02478(\delta\alpha_{38} + \delta\alpha_{310} + \delta\alpha_{48} + \delta\alpha_{410} + \delta\alpha_{59} + \delta\alpha_{510} + \delta\alpha_{69} + \delta\alpha_{610})$

$S_6 = 0.40824(2\delta\alpha_{12} - \delta\alpha_{27} - \delta\alpha_{17})$

$S_7 = 0.35356(\delta\alpha_{310} + \delta\alpha_{410} + \delta\alpha_{510} + \delta\alpha_{610} - \delta\alpha_{38} - \delta\alpha_{48} - \delta\alpha_{59} - \delta\alpha_{69})$

$S_8 = 0.5433(\delta\alpha_{34} + \delta\alpha_{56}) - 0.2263(\delta\alpha_{38} + \delta\alpha_{310} + \delta\alpha_{48} + \delta\alpha_{410} + \delta\alpha_{59} + \delta\alpha_{510} + \delta\alpha_{69} + \delta\alpha_{610})$

A_2

$S_9 = 0.5(\delta R_3 - \delta R_4 - \delta R_5 + \delta R_6)$

$S_{10} = 0.35356(\delta\alpha_{38} + \delta\alpha_{69} - \delta\alpha_{48} - \delta\alpha_{59} - \delta\alpha_{310} - \delta\alpha_{610} + \delta\alpha_{410} + \delta\alpha_{510})$

$S_{11} = 0.35356(\delta\alpha_{38} + \delta\alpha_{69} - \delta\alpha_{48} - \delta\alpha_{59} + \delta\alpha_{310} + \delta\alpha_{610} - \delta\alpha_{410} - \delta\alpha_{510})$

$S_{12} = \delta\tau$

B_1

$S_{13} = 0.70711(\delta R_1 - \delta R_2)$

$S_{14} = 0.5(\delta R_3 + \delta R_4 - \delta R_5 - \delta R_6)$

$S_{15} = 0.46844(\delta R_9 - \delta R_8) + 0.51587(\delta\alpha_{810} - \delta\alpha_{910}) + 0.07692(\delta\alpha_{56} - \delta\alpha_{34}) + 0.04617(\delta\alpha_{59} + \delta\alpha_{69} + \delta\alpha_{510} + \delta\alpha_{610} - \delta\alpha_{38} - \delta\alpha_{310} - \delta\alpha_{48} - \delta\alpha_{410})$

$S_{16} = 0.70711(\delta\alpha_{78} - \delta\alpha_{79})$

$S_{17} = 0.70711(\delta\alpha_{17} - \delta\alpha_{27})$

$S_{18} = 0.35356(\delta\alpha_{59} + \delta\alpha_{69} + \delta\alpha_{310} + \delta\alpha_{410} - \delta\alpha_{48} - \delta\alpha_{38} - \delta\alpha_{510} - \delta\alpha_{610})$

$S_{19} = 0.5433(\delta\alpha_{34} - \delta\alpha_{56}) - 0.2263(\delta\alpha_{38} + \delta\alpha_{48} + \delta\alpha_{310} + \delta\alpha_{410} - \delta\alpha_{59} - \delta\alpha_{69} - \delta\alpha_{510} - \delta\alpha_{610})$

B_2

$S_{20} = 0.5(\delta R_3 - \delta R_4 + \delta R_5 - \delta R_6)$

$S_{21} = 0.35356(\delta\alpha_{38} - \delta\alpha_{48} + \delta\alpha_{59} - \delta\alpha_{69} - \delta\alpha_{310} + \delta\alpha_{610} + \delta\alpha_{410} - \delta\alpha_{510})$

$S_{22} = 0.35356(\delta\alpha_{38} - \delta\alpha_{48} + \delta\alpha_{59} - \delta\alpha_{69} + \delta\alpha_{310} - \delta\alpha_{610} - \delta\alpha_{410} + \delta\alpha_{510})$

$S_{23} = \delta\beta_{712}$

$S_{24} = \delta\beta_{789}$

Can. J. Chem. Downloaded from www.nrcresearchpress.com by 210.87.254.5 on 09/05/12
For personal use only.

Can. J. Chem. Downloaded from www.nrcresearchpress.com by 210.87.254.5 on 09/05/12
For personal use only.

freedom. $F(\alpha_{89})$ was, therefore, arbitrarily constrained to 0.9 mdyn Å. The two methylenic H—C—C force constants were assumed to be equal, *e.g.* $F(\alpha_{38}) = F(\alpha_{310})$.

This diagonal force field allowed only two modes to converge to the correct frequencies, the ethylenic wag at 890.5 cm^{-1} and the C—C=C out-of-plane bend at 279.6 cm^{-1}. These two modes are uniquely determined, *i.e.*, they interact very little with other modes. The other frequencies did not converge to their observed values, and even the order of the methylenic deformation frequencies was calculated incorrectly. In particular the methylenic twist was calculated to low frequency of the methylenic rock.

The following interaction constants were then introduced:

(*1*) To improve the fit of the C—H stretching modes the constants F(CH,CH')(eth), *i.e.*, $F(R_1,R_2)$, and F(CH,CH')(meth), *i.e.*, $F(R_3,R_4) = F(R_5,R_6)$, were introduced.

(*2*) To improve the calculated frequencies for the methylenic deformation modes the following constants were introduced: $F^a(\alpha,\alpha)$, H—C—C H—C—C angle interaction, with bonds R_3, R_4, R_5 or R_6 common, *e.g.* $F(\alpha_{38},\alpha_{310})$; $F^b(\alpha,\alpha)$, H—C—C H—C—C angle interaction, with bonds R_8, R_9 or R_{10} common, *i.e.* $F(\alpha_{38},\alpha_{48}) = F(\alpha_{59},\alpha_{69})$ and $F(\alpha_{310},\alpha_{410}) = F(\alpha_{510},\alpha_{610})$. For simplicity $F(\alpha_{38},\alpha_{48})$ was assumed equal to $F(\alpha_{310},\alpha_{410})$, thus introducing only one parameter.

(*3*) To improve upon the agreement in the ring modes F(C—C,C—C) interactions were used. $F(R_9,R_{10})$ equals $F(R_8,R_{10})$ by symmetry, and we assumed for simplicity that these two also equal $F(R_8,R_9)$, and used these three constants, set equal to each other. The introduction of this extra parameter again overdetermines the ring frequencies, and $F(\alpha_{810})$ and $F(\alpha_{910})$ were constrained to 0.5 mdyn Å to overcome this.

This force field allowed complete convergence of the C—H stretches and gave a more accurate description of the methylenic deformations. The methylenic twist converged to 1073 cm^{-1} and the methylenic rock converged to 748 cm^{-1}. However, the three ring frequencies were still poorly determined, and an oscillatory solution involving F(C—C) and F(C=C) resulted.

Because of the ring redundancies, no unique solution can be obtained for the ring force constants. Therefore we tried three different approximations to seek the best fit.

(*1*) The F(C—C,C—C) interaction constants were all constrained at the value −0.15 mdyn/Å found in cyclopropane (3). No further constants were introduced and no constraints were released, and thus $F(R_8) = F(R_9)$, and $F(R_{10})$ were the only ring constants allowed to vary. This did not improve the frequency fit and gave an oscillatory solution involving F(C=C) and F(C—C).

(*2*) An interaction constant of the type F(C—C,C=C) was introduced, with the constraints above maintained, thus leaving three parameters varying to fit the three ring frequencies. There are two constants of this type, $F(R_7,R_8) = F(R_7,R_9)$, and $F(R_7,R_{10})$. The latter was found to be more helpful than the former, with the PL/1 program, and was used. Including $F(R_7,R_{10})$ then, an oscillatory solution resulted with the value of F(C=C) around 8 mdyn/Å and $F(R_7,R_{10})$ around 1 mdyn/Å. In order to allow further experiments with the ring force constants, $F(R_7,R_{10})$ was constrained at this value, 1 mdyn/Å.

(*3*) Because the F(C—C,C—C) interaction constants $F(R_9,R_{10}) = F(R_8,R_{10})$ might be expected to approximate more closely to the value found in cyclopropane for this type of constant than would $F(R_8,R_9)$, $F(R_9,R_{10}) = F(R_8,R_{10})$ were kept constrained at −0.15 mdyn/Å, while $F(R_8,R_9)$ was released to seek its preferred value. At this stage the ring constants $F(\alpha_{89})$, $F(\alpha_{810})$, $F(\alpha_{910})$, and the F(C—C,C=C) interaction constant, were still constrained, leaving $F(R_8) = F(R_9)$, $F(R_{10})$, and $F(R_8,R_9)$ as the only ring constants allowed to adjust to their optimum values. This improved the ring frequency fit, the best being obtained with $F(R_8,R_9) = 0.2$ mdyn/Å. However, this did not represent a stable solution, and $F(R_8,R_9)$ converged to a value more consistent with $F(R_8,R_{10})$, even though this gave a poorer fit to the ring frequencies. This arose because of interactions between the ring modes and the methylenic deformations, in particular, between the A_1 ring stretch and the A_1 methylenic deformation, and between the A_1 ring deformation and the A_1 methylenic wag.

The convergent solution obtained from approximation *3* just described gave the most satisfactory description of the ring modes, but the calculated frequency difference between the A_1 and B_1 methylenic wags was still smaller than that required by the assignment, being calculated at 1065 and 1097 cm^{-1} and assigned at 1003 and 1125 cm^{-1}, respectively. To correct this a further H—C—C, H—C—C angle interaction constant

TABLE 3. Optimum force field for C_4H_6 and C_4D_6: assignment I

	Frequency*			
	C_4H_6		C_4D_6	
Mode	Observed	Calculated	Observed	Calculated
ν_1	3008.3	3020.5	2241.7	2242.6
ν_2	2999.3	3001.3	2202.3	2197.8
ν_3	1742.2	1766.7	1727.7	1703.0
ν_4	1436.5	1465.5	1168	1149.4
ν_5	1411.0	1416.2	1139	1083.6
ν_6	1037.4	1053.2	895	925.4
ν_7	1002.6	998.2	804.2	810.1
ν_8	723.8	682.1	637.0	571.1
ν_{13}	3086.2	3086.2	2321.1	2314.1
ν_{14}	2996.0	2996.2	2179.0	2182.2
ν_{15}	1410	1421.4	1122	1159.3
ν_{16}	1354.4	1341.7	1073	1041.3
ν_{17}	1125.3	1149.8	1017	964.7
ν_{18}	895	905.6	735	764.6
ν_{19}	355	354.2	304	304.7
ν_{20}	3069.5	3077.2	2315.2	2297.0
ν_{21}	1073.0	1063.0	835.5	854.3
ν_{22}	890.5	889.3	705.0	704.2
ν_{23}	748.6	746.0	537.5	537.5
ν_{24}	279.6	278.8	240	242.3

Force constant†	Value	Force constant†	Value
F(C=C)	9.059	F(C—C=C)	0.3700
F(C—H) (eth)	5.064	$F(\alpha_{89})$	0.9000‡
F(C—H) (meth)	5.037	$F(\alpha_{810})$	0.5000‡
F(C—C) (R_8)	3.474	$F(\tau)$	0.1500‡
F(C—C) (R_{10})	3.418	$F(\beta_{789})$	0.2415
F(CH,CH′) (eth)	0.0397	$F(\beta_{712})$	0.2373
F(CH,CH′) (meth)	0.0257	$F(\alpha_{38},\alpha_{310})$	−0.3525
F(C—C,C—C′)	−0.15‡	$F(\alpha_{38},\alpha_{48})$	0.0039
$F(R_7,R_{10})$	0.9012	$F(\alpha_{310},\alpha_{510})$	−0.0993
F(HCH) (eth)	0.2830	$F(\alpha_{34},\alpha_{56})$	0.0441
F(HCH) (meth)	0.4081	$F(R_7,\alpha_{17})$	0.1575
F(HC=C)	0.8529	$F(R_8,\alpha_{38})$	0.0463
F(HC—C)	0.6673	$F(R_{10},\alpha_{310})$	0.1934

*The frequencies are in cm^{-1} units.
†The force constants are in units of mdyn $Å^{-1}$, mdyn, or mdyn Å, for constants of the type $F(R)$ and $F(RR')$, $F(R\alpha)$, or $F(\alpha)$ and $F(\alpha\alpha')$, respectively.
‡The force constant was constrained at the value shown.

was introduced $F(\alpha_{310},\alpha_{510}) = F(\alpha_{410},\alpha_{610})$, and a more acceptable frequency difference for the wags was obtained.

At this stage no further development was possible using C_4H_6 frequencies only, and the force-field developed above was used as a starting approximation for calculations using C_4H_6 and C_4D_6 frequencies together.

(c) *Calculation and Results for C_4H_6 and C_4D_6 Combined*

The force field described above, when allowed to refine to fit the combined C_4H_6 and C_4D_6 data, was unable to calculate an isotopic shift near to that observed (1) for the C=C stretching mode, ν_3. The smallest shift calculated was 105 cm^{-1} compared to the observed shift of 14.5 cm^{-1}. This force field also failed to explain the small shift of the B_1 methylenic wag, which was assigned as 1125.3 to 1017 cm^{-1} and calculated as 1135 to 950 cm^{-1}.

The additional data allowed further experimenting with the force field. In an attempt to improve the fit of the ring frequencies, $F(R_7,R_{10})$ and $F(R_8,R_{10}) = F(R_9,R_{10})$ were released from constraint, but this field failed to converge. Reconstraint of $F(R_8,R_{10}) = F(R_9,R_{10})$ at −0.15 mdyn/Å did not improve the calculation, and a convergent solution could only be obtained with all of the F(C—C,C—C) constants constrained at

Can. J. Chem. Downloaded from www.nrcresearchpress.com by 210.87.254.5 on 09/05/12
For personal use only.

Can. J. Chem. Downloaded from www.nrcresearchpress.com by 210.87.254.5 on 09/05/12
For personal use only.

TABLE 4. Optimum force field for C_4H_6 and C_4D_6: assignment II

	Frequency*			
	C_4H_6		C_4D_6	
Mode	Observed	Calculated	Observed	Calculated
ν_1	3008.3	3019.4	2241.7	2238.6
ν_2	2999.3	3001.0	2202.3	2196.8
ν_3	1742.2	1759.0	1727.7	1711.6
ν_4	1436.5	1446.8	1168	1141.0
ν_5	1411.0	1414.3	1047	1041.2
ν_6	1037.4	1034.0	895	925.8
ν_7	1002.6	997.1	804.2	816.7
ν_8	723.8	686.4	637.0	573.2
ν_{13}	3086.2	3086.2	2321.1	2314.1
ν_{14}	2996.0	2996.2	2179.0	2182.1
ν_{15}	1410	1421.3	1122	1158.1
ν_{16}	1354.4	1341.5	1073	1041.3
ν_{17}	1125.3	1156.1	1017	972.2
ν_{18}	895	905.1	735	763.2
ν_{19}	355	354.1	304	304.6
ν_{20}	3069.5	3077.3	2315.2	2297.2
ν_{21}	1073.0	1060.0	835.5	854.4
ν_{22}	890.5	888.9	705.0	704.1
ν_{23}	748.6	747.5	537.5	536.5
ν_{24}	279.6	278.9	240	242.4

Force constant†	Value	Force constant	Value
F(C=C)	9.541	F(C—C=C)	0.3700
F(C—H) (eth)	5.064	$F(\alpha_{89})$	0.9000‡
F(C—H) (meth)	5.037	$F(\alpha_{810})$	0.5000‡
F(C—C) (R_8)	3.485	$F(\tau)$	0.1500‡
F(C—C) (R_{10})	3.272	$F(\beta_{789})$	0.2420
F(CH,CH′) (eth)	0.0397	$F(\beta_{712})$	0.2370
F(CH,CH′) (meth)	0.0257	$F(\alpha_{38},\alpha_{310})$	−0.3285
F(C—C,C—C′)	−0.15‡	$F(\alpha_{38},\alpha_{48})$	0.0162
$F(R_7,R_{10})$	0.8530	$F(\alpha_{310},\alpha_{510})$	−0.1250
F(HCH) (eth)	0.2327	$F(\alpha_{34},\alpha_{56})$	0.0658
F(HCH) (meth)	0.3855	$F(R_7,\alpha_{17})$	0.4378
F(HC=C)	0.8522	$F(R_8,\alpha_{38})$	0.0338
F(HC—C)	0.6796	$F(R_{10},\alpha_{310})$	0.2098

*The frequencies are in cm^{-1} units.
†The force constants are in units of mdyn $Å^{-1}$, mdyn, or mdyn Å, for constants of the type $F(R)$ and $F(RR')$, $F(R\alpha)$, or $F(\alpha)$ and $F(\alpha\alpha')$, respectively.
‡The force constants were constrained at the value shown.

−0.15 mdyn/Å, and $F(R_7,R_{10})$ varying. In a successful attempt to improve the fit of the A_1 and B_1 methylenic deformations, an interaction constant of the type F(H—C—H,H—C′—H) was also introduced, $F(\alpha_{34},\alpha_{56})$. To improve the isotopic shift for the C=C stretching mode, the constant $F(R_7,\alpha_{17}) = F(R_7,\alpha_{27})$ was introduced. In order to help further to account for the interactions between the ring modes and the methylenic deformations (including wag, rock, and twist), two further bond-angle interaction constants were introduced: F^a(C—C,α) *i.e.*, $F(R_8,\alpha_{38}) = F(R_8,\alpha_{48}) = F(R_9,\alpha_{59}) = F(R_9,\alpha_{69})$; F^b(C—C,α) *i.e.*, $F(R_{10},\alpha_{310}) = F(R_{10},\alpha_{410}) = F(R_{10},\alpha_{510}) = F(R_{10},\alpha_{610})$.

The results of this force-field are given in Tables 3 and 4, and represent the best agreement with the observed frequencies that we have been able to obtain. The assignment of ν_5 was uncertain between 1139 and 1047 cm^{-1} (or 1043 cm^{-1}) from experimental data (1). Table 3 shows the results obtained by refining ν_5 to 1139 cm^{-1} (assignment I), and Table 4 presents the results obtained by refining ν_5 to 1047 cm^{-1} (assignment II).

It is apparent that this force field has improved the fit of the C=C stretching mode by reducing the isotopic shift to about 60 cm^{-1} in Table 3 and about 50 cm^{-1} in Table 4. This is accomplished primarily by $F(R_7,\alpha_{17}) = F(R_7,\alpha_{27})$ and is neces-

TABLE 5. Distribution of the potential energy for each normal mode among the symmetry coordinate force constants*

	H	3008	2999	1742	1437	1411	1037	1003	724
A_1	(D)	(2242)	(2202)	(1727)	(1168)	(1047)	(895)	(804)	(637)
S_1		98(48)		(10)					
S_2		(6)		78(64)			5(4)	(5)	16(6)
S_3			98(51)						
S_4				10(10)	5(24)		17(19)	60(15)	8(4)
S_5				12(12)		0(5)	27(29)	5(4)	53(22)
S_6					11(5)	90(46)		0(4)	
S_7							73(21)	16(22)	11(26)
S_8					89(37)	11(6)	0(11)	3(13)	

	H	3086	2996	1410	1354	1125	895	355
B_1	(D)	(2321)	(2179)	(1122)	(1073)	(1017)	(735)	(304)
S_{13}		104(58)						
S_{14}			99(52)					
S_{15}				3(16)	5	7(8)	55(20)	
S_{16}				(4)	4		5	11(8)
S_{17}				(18)	74(12)	(4)	8(13)	
S_{18}						60(34)	5(12)	
S_{19}				59(6)	4(38)		(8)	

	H	3069	1073	890.5	748	280
B_2	(D)	(2315)	(835)	(705)	(538)	(240)
S_{20}		104(58)				
S_{21}			9(5)		8(5)	
S_{22}					23(12)	
S_{23}				25(15)		
S_{24}						4(3)

*Figures in parentheses are those for C_4D_6, others for C_4H_6; values less than 3 not recorded.

sarily accompanied by an increase in the shift of the ethylenic deformation, ν_5.

It is seen that the larger isotopic shift required for ν_5 in assignment II is more consistent with the calculations. The overall agreement between calculated and observed frequencies is better for assignment II than for assignment I. This suggests that ν_5 in C_4D_6 should be assigned to 1047 cm^{-1}, not 1139 cm^{-1}, if the other A_1 modes are correctly assigned. The combination of the reasonably good agreement obtained by calculation for the A_1 frequencies and assignments, plus the lack of viable alternative assignments, leads us to believe that assignment II is correct for methylene cyclopropane. We have therefore only given the calculated assignments, as potential energy distributions (p.e.d.), for assignment II. The potential energy distribution of the normal modes among the symmetry coordinates was calculated from the expression

$$\text{p.e.d.}\ (i,j) = \frac{100 \times \mathbf{L}_s^2(i,j) \times \mathbf{F}_s(i,i)}{\lambda_j}$$

where $\mathbf{L}_s$ is the symmetrized eigenvector matrix, $\mathbf{F}_s$ is the symmetrized force constant matrix, and λ_j is the eigenvalue for mode j, and is given for assignment II in Table 5.

The omission of the potential energy distribution for assignment I makes it necessary to point out one further argument against assignment I. In Table 3, ν_4 and ν_5 are shown to be calculated for C_4H_6 at 1465.5 and 1416.2 cm^{-1}, respectively. But the potential energy distribution shows that it is the ethylenic deformation that is calculated at 1465.5 cm^{-1} and the methylenic deformation at 1416.2 cm^{-1}. This is the reverse of the assignment, and the evidence presented for the assignment in ref. 1 makes it extremely unlikely that the ethylenic deformation can be to high frequency of the methylenic deformation in the molecule. In assignment II the ethylenic deformation is calculated at 1414.3 cm^{-1} and the methylenic deformation at 1446.8 cm^{-1}, both for C_4H_6, in agreement with the assignment.

The results in Table 4 show that the calculations have reproduced the observed frequencies for both molecules reasonably well, and the data in Table 5 show that the calculated assignments are consistent with the assignments made in ref. 1.

It is perhaps worth briefly stating that various attempts to improve the frequency fit were made,

Can. J. Chem. Downloaded from www.nrcresearchpress.com by 210.87.254.5 on 09/05/12
For personal use only.

Can. J. Chem. Downloaded from www.nrcresearchpress.com by 210.87.254.5 on 09/05/12
For personal use only.

unsuccessfully. These included: (*a*) releasing the approximation $F(\alpha_{38}) = F(\alpha_{310})$; (*b*) setting $F(R_8,\alpha_{38}) = F(R_{10},\alpha_{310})$ to be consistent with the assumption that $F(\alpha_{38}) = F(\alpha_{310})$; (*c*) raising the value of $F(\alpha_{89})$ relative to that of $F(\alpha_{810})$. Attempt *c* was intended to improve the fit of the symmetric ring deformation, ν_8, and it did raise ν_8, but not by far enough to be useful. To raise it to the observed frequency by this method would require $F(\alpha_{89})$ to be about 10 times, or more, $F(\alpha_{810})$ which is unreasonable. Any other attempt to raise ν_8 harmed the fit of the other ring modes.

IV. Calculations Using a Set of Coordinates Ignoring Redundancy of the Ring

In order to make meaningful comparisons with the work reported on cyclopropane (2, 3), we also carried out a normal coordinate analysis using a set of 25 internal coordinates involving no redundancy in the ring and using group coordinates to describe the methylenic deformational modes. The 25 internal coordinates were obtained by ignoring α_{34}, α_{56}, α_{89}, α_{810}, α_{910}, and α_{12}, in the original set of 31 (Section III). The methylenic group coordinates are as follows:

Deformation on C_3

$$\zeta_1 = \tfrac{1}{2}(\delta\alpha_{38} + \delta\alpha_{48} + \delta\alpha_{310} + \delta\alpha_{410})$$

Deformation on C_4

$$\zeta_2 = \tfrac{1}{2}(\delta\alpha_{59} + \delta\alpha_{69} + \delta\alpha_{510} + \delta\alpha_{610})$$

Wag on C_3

$$\eta_1 = \tfrac{1}{2}(\delta\alpha_{38} + \delta\alpha_{48} - \delta\alpha_{310} - \delta\alpha_{410})$$

Wag on C_4

$$\eta_2 = \tfrac{1}{2}(\delta\alpha_{59} + \delta\alpha_{69} - \delta\alpha_{510} - \delta\alpha_{610})$$

Twist on C_3

$$\theta_1 = \tfrac{1}{2}(\delta\alpha_{38} - \delta\alpha_{48} - \delta\alpha_{310} + \delta\alpha_{410})$$

Twist on C_4

$$\theta_2 = \tfrac{1}{2}(\delta\alpha_{59} - \delta\alpha_{69} - \delta\alpha_{510} + \delta\alpha_{610})$$

Rock on C_3

$$\xi_1 = \tfrac{1}{2}(\delta\alpha_{38} - \delta\alpha_{48} + \delta\alpha_{310} - \delta\alpha_{410})$$

Rock on C_4

$$\xi_2 = \tfrac{1}{2}(\delta\alpha_{59} - \delta\alpha_{69} + \delta\alpha_{510} - \delta\alpha_{610})$$

The 24 non-trivial symmetry coordinates used are shown in Table 6. The twenty-fifth symmetry coordinate, $(1/\sqrt{2})(\alpha_{78} + \alpha_{79})$, was carried through the calculation and yielded a zero frequency.

The most successful force field was found to be analogous to that given in Table 4, and it was possible to obtain good frequency agreement in all modes for assignment II. As with the first force field model, reduction in the ν_3 isotopic shift was accompanied by an increase in ν_5's isotopic shift, supporting assignment II. The results of this calculation are given in Table 7 for assignment II. The force constants equivalent to the bond-angle interaction constants F^a(C—C,α) and F^b(C—C,α) of Section III were F(C—C,ζ) and F(C—C,η), using the approximations $F(R_8,\zeta_1) = F(R_9,\zeta_2) = F(R_{10},\zeta_1) = F(R_{10},\zeta_2)$ and $F(R_8,\eta_1) = F(R_9,\eta_2) = F(R_{10},\eta_1) = F(R_{10},\eta_2)$.

TABLE 6. Symmetry coordinates in terms of 24 internal coordinates ignoring redundancies

A_1 Block

$S_1 = (1/\sqrt{2})(\delta R_1 + \delta R_2)$
$S_2 = \delta R_7$
$S_3 = (1/2)(\delta R_3 + \delta R_4 + \delta R_5 + \delta R_6)$
$S_4 = (1/\sqrt{3})(\delta R_8 + \delta R_9 + \delta R_{10})$
$S_5 = (1/\sqrt{6})(2\delta R_{10} - \delta R_9 - \delta R_8)$
$S_6 = (1/\sqrt{2})(\delta\alpha_{17} + \delta\alpha_{27})$
$S_7 = (1/\sqrt{2})(\eta_1 + \eta_2)$
$S_8 = (1/\sqrt{2})(\zeta_1 + \zeta_2)$

A_2 Block

$S_9 = (1/2)(\delta R_3 - \delta R_4 - \delta R_5 + \delta R_6)$
$S_{10} = (1/\sqrt{2})(\theta_1 - \theta_2)$
$S_{11} = (1/\sqrt{2})(\xi_1 - \xi_2)$
$S_{12} = \delta\tau$

B_1 Block

$S_{13} = (1/\sqrt{2})(\delta R_1 - \delta R_2)$
$S_{14} = (1/2)(\delta R_3 + \delta R_4 - \delta R_5 - \delta R_6)$
$S_{15} = (1/\sqrt{2})(\delta R_8 - \delta R_9)$
$S_{16} = (1/\sqrt{2})(\delta\alpha_{78} - \delta\alpha_{79})$
$S_{17} = (1/\sqrt{2})(\delta\alpha_{17} - \delta\alpha_{27})$
$S_{18} = (1/\sqrt{2})(\eta_1 - \eta_2)$
$S_{19} = (1/\sqrt{2})(\zeta_1 - \zeta_2)$

B_2 Block

$S_{20} = (1/2)(\delta R_3 - \delta R_4 + \delta R_5 - \delta R_6)$
$S_{21} = (1/\sqrt{2})(\theta_1 + \theta_2)$
$S_{22} = (1/\sqrt{2})(\xi_1 + \xi_2)$
$S_{23} = \delta\beta_{712}$
$S_{24} = \delta\beta_{789}$

V. Discussion

Arguments have been presented in Section III *c* that favor assignment II over assignment I. In this section the discussion is restricted to the results obtained for assignment II by the two force fields. Model I refers to the calculation using 31 internal coordinates, and model II to that using 25 internal coordinates. The potential energy distribution for model II is not presented in a table. For C_4H_6 it gives essentially the same assignments as indicated by Table 5, except that it assigns ν_4 to the ethylenic CH_2 deformation and ν_5 to the methylenic CH_2

TABLE 7. Force field for C_4H_6 and C_4D_6 using 24 internal coordinates: assignment II

	Frequency*			
	C_4H_6		C_4D_6	
Mode	Observed	Calculated	Observed	Calculated
ν_1	3008.3	3017.9	2241.7	2236.6
ν_2	2999.3	3003.8	2202.3	2203.9
ν_3	1742.2	1764.7	1727.7	1706.6
ν_4	1436.5	1435.9	1168	1160.2
ν_5	1411.0	1403.0	1047	1051.1
ν_6	1037.4	1054.7	895	917.1
ν_7	1002.6	1000.1	804.2	824.3
ν_8	723.8	672.0	637.0	553.1
ν_{13}	3086.2	3086.1	2321.1	2313.9
ν_{14}	2996.0	2996.1	2179.0	2181.9
ν_{15}	1410	1425.5	1122	1168.2
ν_{16}	1354.4	1344.7	1073	1058.0
ν_{17}	1125.3	1148.2	1017	954.9
ν_{18}	895	891.4	735	747.8
ν_{19}	355	351.4	304	301.8
ν_{20}	3069.5	3076.9	2315.2	2296.2
ν_{21}	1073.0	1065.1	835.5	847.3
ν_{22}	890.5	890.7	705.0	704.4
ν_{23}	748.6	743.6	537.5	542.8
ν_{24}	279.6	278.5	240	241.6

Force constant†	Value	Force constant†	Value
F(C=C)	8.621	F(C—C=C)	0.3664
F(C—H) (eth)	5.064	$F(\theta)$	1.042
F(C—H) (meth)	5.037	$F(\xi)$	0.2393
F(C—C) (R_8)	4.370	$F(\tau)$	0.1500‡
F(C—C) (R_{10})	3.864	$F(\beta_{789})$	0.2420
F(CH,CH′) (eth)	0.040	$F(\beta_{712})$	0.2370
F(CH,CH′) (meth)	0.026	$F(\eta_1\eta_2)$	0.0049
F(C—C,C—C′)	−0.150‡	$F(\zeta_1\zeta_2)$	−0.0188
$F(R_7,R_{10})$	−0.4314	$F(\alpha_{17},\alpha_{27})$	0.2400
$F(\zeta)$	0.9114	$F(R_7,\alpha_{17})$	0.3856
F(HC=C)	1.086	$F(R_8,\zeta_1)$	0.0463
$F(\eta)$	0.9538	$F(R_8,\eta_1)$	−0.1982

*Frequency units are cm^{-1}.
†Force constants are in units of mdyn $Å^{-1}$, mdyn, or mdyn Å for constants of the type $F(R)$ and $F(RR')$, $F(R\alpha)$, or $F(\alpha)$ and $F(\alpha\alpha')$, respectively.
‡The force constant was constrained at the value shown.

deformation. As discussed above, this is unlikely on experimental grounds and must be considered a defect of model II. For C_4D_6 model II provides essentially the same assignments as model I. The calculations indicate a large degree of mixing of the symmetry coordinates in the normal vibrations of A_1 and B_1 symmetry. This mixing is greater in C_4D_6 than in C_4H_6, as expected from the smaller frequency separations in C_4D_6, and this explains some of the rather unusual isotopic shifts found for this molecule.

The calculations have been partly successful in explaining the low isotopic shift of ν_3 and, as has been pointed out, in doing so have strongly indicated that ν_5 in C_4D_6 should be assigned at 1047 cm^{-1} rather than at 1139 cm^{-1}. An examination of the potential energy distribution for both models shows that there is no major difference in the normal coordinate for ν_3 between C_4H_6 and C_4D_6, ν_3 involving interactions between C=C stretch and ring stretch in both molecules, with slight interaction with the ethylenic C—D stretch in C_4D_6. Thus the low isotopic shift is not a product of major changes in the form of the ν_3 vibration between C_4H_6 and C_4D_6. As discussed above, the isotopic shift of ν_3 was reduced by the introduction of the interaction between the C=C stretch and the HC=C angles, leading to a 1 to 2% admixture of the ethylenic deformation in ν_3.

In our experimental assignment (1) we postu-

Can. J. Chem. Downloaded from www.nrcresearchpress.com by 210.87.254.5 on 09/05/12
For personal use only.

Can. J. Chem. Downloaded from www.nrcresearchpress.com by 210.87.254.5 on 09/05/12
For personal use only.

lated that ν_4, the symmetric methylenic deformation, gains Raman intensity in C_4D_6 by coupling with the ring modes. The calculations support this suggestion, and further indicate some mixing with the A_1 ethylenic deformation in both molecules. ν_5 is clearly indicated as the ethylenic deformation, with about 12% of the methylenic deformation in both molecules. ν_6 was assigned as the ring stretching mode because of its high Raman intensity. The calculations assign it as predominantly methylenic wag plus some ring stretch in C_4H_6, and a fairly even mixture of the methylenic wag plus ring stretch, plus some methylenic deformation, in C_4D_6. ν_7, assigned previously (1) as the methylenic wag, is calculated to be mainly ring stretch in C_4H_6, and a mixture of ring stretch plus methylenic wag plus methylenic deformation in C_4D_6. Similarly the contribution of the methylenic wagging motion to ν_8 increases drastically on deuteration. In C_4D_6, ν_6, ν_7, and ν_8 cannot be usefully classified by a single symmetry coordinate at all, but are all heavy mixtures of ring motion and methylenic wag, with the methylenic deformation contributing significantly to ν_6 and ν_7.

Similar changes in the normal coordinates upon deuteration are indicated by the calculations for the B_1 modes, ν_{15} to ν_{18}. In C_4H_6 they are calculated to be as assigned experimentally, rather pure methylenic deformation, ethylenic rock, methylenic wag, and the ring deformation, respectively. In C_4D_6, ν_{15} is calculated as an even mixture of ethylenic rock and ring deformation, with some methylenic deformation involved, ν_{16} as mainly methylenic deformation with some ethylenic rock, ν_{17} as mainly the methylenic wag with some ring deformation and ethylenic rock included, and ν_{18} as a fairly even mixture of the ring deformation, the ethylenic rock and the methylenic wag, with some methylenic deformation included. It is clear that in C_4D_6 no one symmetry coordinate is an adequate description of ν_{15} to ν_{18}.

The calculations from both models reverse the experimental assignment for ν_6 and ν_7 in C_4H_6. One must consider whether the calculated assignment is to be preferred. It is clear that the calculation of the modes involving the ring must be subject to a certain amount of arbitrariness because of the large number of redundancies and the correspondingly large number of force constants, some of which must be constrained. However, the two models gave the same assignment in spite of the force fields being quite different. In each model the interactions in the ring are accounted for by use of interaction constants that undoubtedly cannot truly represent the forces acting in the ring but which combine to achieve much the same effect. But the way in which this is achieved differs in the two models. This is perhaps most clearly indicated by the interaction constant between the ring basal bond and the C=C stretch, $F(R_7,R_{10})$ which is of different sign in the two models. It seems clear that the observed frequencies have been reasonably well reproduced by each model, yet the way in which the ring interactions achieve this result differs significantly between the two models. Yet the calculated assignments are the same in the two models, except for ν_4 and ν_5. This makes us conclude that the calculated assignments for ν_6 and ν_7 are likely correct.

The calculations have reproduced the frequencies reasonably well. The average errors are: model I, for C_4H_6 1.2%, for C_4D_6 2.8%; model II, for C_4H_6 1.4%, for C_4D_6 2.8%. For model I the worst agreement is for ν_8, which is calculated 37.4 cm^{-1} low for C_4H_6 and 63.8 cm^{-1} low for C_4D_6. As discussed in Section III no reasonable change in the force field would raise these values. The observed isotope shift of ν_{17} could not be reproduced by model I, the calculation being 30.8 cm^{-1} high for C_4H_6 and 44.8 cm^{-1} low for C_4D_6. ν_{15} and ν_{16} were calculated reasonably well for C_4H_6 but were 36.1 cm^{-1} high and 31.7 cm^{-1} low, respectively, for C_4D_6. This appears to indicate errors in the degree of mixing of the motions involved, but no improvement could be found. Model II had its greatest errors in the frequencies of the same modes, being worse than model I for ν_8, ν_{15}, and ν_{17}, and better for ν_{16}. Bearing in mind the somewhat different force fields of the two models, one is tempted to assign these considerable errors, found in the same modes in both models, to the influence of anharmonicity.

A few observations can be made from the magnitudes of the force constants. Both models show that the high C=C stretching frequency is due entirely to the kinetic effects of the $\sim 60°$ $C_3C_2C_4$ angle. Indeed, comparison with F(C=C) in ethylene (13) (9.57 mdyn/Å) shows that the distortion in the sp^2 hybridization needed to accommodate the ring structure has resulted in weakening the C=C stretching force constant by 0.3 to 0.6 mdyn/Å depending on the model employed. In model II (Section IV), which is more com-

TABLE 8. Thermodynamic functions for C_4H_6 and C_4D_6 at 1 atm pressure and for the ideal gaseous state*

T (°K)	$(H_0 - E_0^0)/T$		$-(G_0 - E_0^0)/T$		S_0		C_p	
	C_4H_6	C_4D_6	C_4H_6	C_4D_6	C_4H_6	C_4D_6	C_4H_6	C_4D_6
150	8.62	9.10	46.89	48.18	55.51	57.28	10.3	12.3
200	9.31	10.46	49.45	50.97	58.76	61.43	12.6	17.0
250	10.29	12.31	51.63	53.49	61.92	65.81	16.0	22.5
300	11.57	14.47	53.62	55.92	65.19	70.40	20.1	27.9
350	13.09	16.75	55.51	58.33	68.60	75.08	24.3	32.8
400	14.76	19.03	57.37	60.71	72.12	79.74	28.5	37.0
450	16.50	21.24	59.20	63.08	75.70	84.32	32.3	40.7
500	18.25	23.35	61.03	65.43	79.28	88.78	35.7	43.9

*Using the observed frequencies of assignment II and the A_2 mode frequencies of model 1; units are cal mol^{-1} deg^{-1}.

parable to work on cyclopropane, the C—C stretching force constants are 4.25 and 4.03 mdyn/Å. In Duncan and Burn's (3) work the primary force constant was 4.29 mdyn/Å and in Cyvin's work (2) 4.22 mdyn/Å. As the latter used frequencies that were supposedly corrected for anharmonicity, we consider Duncan and Burn's value more useful from our point of view. It is seen that no significant change has occurred in the strength of the two C—C bonds adjacent to the C=C bond, but that, in keeping with its greater length, the third C—C bond is slightly weaker.

The frequencies of the A_2 modes were calculated, using both models, and the A_2 modes, if they could be located, would be extremely helpful for deciding between these two force fields. For C_4H_6 the A_2 modes were calculated at 3086.1, 1176.3, 908.1, and 790.5 cm^{-1} using model I, and at 3081.6, 1013.4, 860.6, and 751.1 cm^{-1} using model II. For C_4D_6 they were at 2318.8, 938.7, 646.3, and 561.1 using model I, and at 2307.7, 785.0, 631.3, and 534.7 using model II. For each model the assignment was C—H stretch, methylenic twist, methylenic rock, and ethylenic torsion, respectively, with some mixing of motions, particularly in C_4D_6. The main difference between the two models is the frequency of the A_2 methylenic twist, and its experimental location would indicate which, if either, of these two models is correct.

It is difficult to predict the relative order of the A_2 and B_2 twists and rocks using data from other molecules. Cyclopropane is the only molecule which is reasonably similar and for which reasonably definitive data exist, yet cyclopropane is not similar enough to methylene cyclopropane for one to be sure of one's analogy. The A_1'' twist in cyclopropane is expected to relate to the A_2 twist in methylene cyclopropane while the E'' twist relates to the B_2 twist. The A_2'' rock in cyclopropane relates to the B_2 rock in methylene cyclopropane while the E'' rock relates to the A_2 rock. But the relation is not as straightforward as is desirable. In cyclopropane the E'' twist is 62 cm^{-1} higher in frequency than the A_1'' twist, suggesting that the B_2 twist in methylene cyclopropane should be higher in frequency than the A_2 twist. This favors the result of model II. The A_2'' rock in cyclopropane is 115 cm^{-1} higher than the E'' rock, suggesting that the B_2 rock in methylene cyclopropane should be higher than the A_2 rock. Neither model predicts this result. The picture is, thus, confused, and no strong indication of the correct relative frequencies of the A_2 and B_2 twists can be obtained. We distrust the suggestion obtained by the analogy with cyclopropane, and believe that the best indication of the frequencies of the A_2 modes in methylene cyclopropane is the result calculated by model I. The force field used for the motions of the methylenic group in model I is quite general and has reasonably well reproduced all of the observed frequencies and can therefore be reasonably expected to yield the unobserved frequencies correctly. The corresponding force field for model II is far more specific, and is, we believe, less likely to correctly yield the unobserved frequencies. However, it is clear that a good deal of uncertainty exists as to the correct A_2 mode frequencies.

VI. Thermodynamic Functions

The vibrational plus rotational plus translational contributions to the enthalpy ($(H_0 - E_0^0)/T$), the Gibbs free energy ($(G_0 - E_0^0)/T$), the entropy, S_0, and the heat capacity, C_p, for

Can. J. Chem. Downloaded from www.nrcresearchpress.com by 210.87.254.5 on 09/05/12
For personal use only.

C_4H_6 and C_4D_6 were calculated twice. In each case the observed frequencies for assignment II were used, and in one case the A_2 mode frequencies from model I were used, and in the second case the A_2 mode frequencies from model II were used. In Table 8 the results obtained with the A_2 mode frequencies from model I are tabulated. Some uncertainty is associated with these values because of the uncertainty in the A_2 mode frequencies. An indication of this uncertainty can be obtained by comparing Table 8 with the results obtained when the A_2 mode frequencies obtained from model II are used. In the latter case we find for C_4H_6 and C_4D_6 (in parentheses) that: $(H_0 - E_0^0)/T$ is the same at 150 °K, is greater by 0.1 (0.13) at 300 °K, and by 0.17 (0.20) at 500 °K; $-(G_0 - E_0^0)/T$ is the same at 150 °K, is greater by 0.02 (0.06) at 300 °K, and by 0.09 (0.14) at 500 °K; S_0 is the same at 150 °K, is greater by 0.1 (0.18) at 300 °K, and by 0.26 (0.33) at 500 °K; C_p is the same at 150 °K (greater by 0.1), is greater by 0.2 (0.3) at 300 °K, and by 0.3 (0.2) at 500 °K.

This work was supported by the National Research Council of Canada.

1. J. E. Bertie and M. G. Norton. Can. J. Chem. **48**, 3889 (1970).
2. S. J. Cyvin. Spectrochim. Acta, **16**, 1022–30 (1960).
3. J. L. Duncan and G. R. Burns. J. Mol. Spectrosc. **30**, 253–265 (1969).
4. Hs. W. Gunthard, R. C. Lord, and T. K. McCubbin, Jr. J. Chem. Phys. **25**, 768–774 (1956).
5. E. J. Blau. Ph.D. Thesis. Ohio State University, Columbus, Ohio. 1953. Univ. Microfilms, L.C. Card No. Mic. 58–730.
6. W. B. Loewenstein. Ph.D. Thesis. Ohio State University, Columbus, Ohio. 1954; Univ. Microfilms, L.C. Card No. Mic. 60–82.
7. J. H. Schachtschneider. Technical report No. 57–65, Project Number 31450, Shell Development Company, Emeryville, California.
8. V. W. Laurie and W. M. Stigliani. J. Am. Chem. Soc. **92**, 1485 (1970).
9. J. G. Smith. Ph.D. Thesis. University of Bristol. Bristol, England. 1968.
10. J. Aldous and I. M. Mills. Spectrochim. Acta, **18**, 1073 (1962).
11. H. Margenau and G. M. Murphy. The mathematics of physics and chemistry. New York, Van Nostrand Co. 1967. p. 312.
12. N. Sheppard and D. M. Simpson. Quart. Revs. **6**, 1 (1952).
13. G. Herzberg. Infrared and Raman spectra. D. Van Nostrand Co. Inc., New York. 1959. p. 184.

Can. J. Chem. Downloaded from www.nrcresearchpress.com by 210.87.254.5 on 09/05/12
For personal use only.

Can. J. Chem. Downloaded from www.nrcresearchpress.com by 210.87.254.40 on 09/05/12
For personal use only.

Studies on Hydrogen–Oxygen Systems in the Electrical Discharge. V. Raman Spectra of the Trapped Products

XAVIER DEGLISE[1] AND PAUL A. GIGUÈRE

Centre de Recherches sur les Atomes et les Molécules, Université Laval, Québec, Québec

Received February 12, 1971

The condensed products (at −180 °C) of electrically dissociated water vapor and other related systems were examined by means of laser Raman spectroscopy. A new type of total reflection cell had to be developed for the study of metastable species trapped in an amorphous matrix. Besides the characteristic O—O stretching band of hydrogen peroxide at 878 cm^{-1}, always the strongest, another fairly strong band at 500 cm^{-1}, and a third one at about 760 cm^{-1} were present in all cases. A couple of weaker bands around 820–830 cm^{-1} and 430–440 cm^{-1} occurred only in oxygen-rich system (H_2O_2 vapor or H_2O–O_2 mixtures). In the latter, the presence of condensed ozone was confirmed by a band at 1025 cm^{-1}, and occasionally another faint one around 1120 cm^{-1}. The relative intensities of the bands varied locally in a given sample, indicating uneven composition.

Isotopic shifts with ^{18}O confirmed that these Raman bands arise from vibrations of oxygen atoms. Essentially the same results were obtained in hydrogen as in deuterium systems, except that in the latter case the new bands were appreciably stronger and sharper. The present results support the assignment of previous infrared spectra to hydrogen polyoxides, H_2O_3 and H_2O_4.

On a étudié par spectroscopie Raman à laser les produits piégés à −180 °C de la vapeur d'eau et autres systèmes connexes dissociés dans une décharge électrique. La préparation des échantillons a nécessité la construction d'un nouveau type de cellule spécialement adapté à l'examen de molécules instables piégées dans une matrice amorphe. Outre la bande caractéristique du peroxyde à 878 cm^{-1}, de beaucoup la plus forte, on a observé dans tous les cas une seconde bande assez forte à 500 cm^{-1} ainsi qu'une troisième, vers 760 cm^{-1}. Une couple de bandes plus faibles vers 820–830 cm^{-1} et 430–440 cm^{-1} apparaissaient seulement dans les systèmes riches en oxygène (vapeur de H_2O_2 ou mélanges de H_2O et O_2). Dans ces derniers, également, la présence d'ozone condensé se manifestait par une bande à 1025 cm^{-1}, et parfois une seconde, très faible, vers 1120 cm^{-1}. Les intensités relatives des bandes semblaient varier d'un point à l'autre dans le même échantillon dû, sans doute, à des gradients de composition.

Grâce au décalage isotopique avec ^{18}O on a vérifié que toutes ces bandes proviennent de vibrations des atomes d'oxygène dans le matériau piégé. Les systèmes deutériés ont donné essentiellement les mêmes résultats que les systèmes hydrogénés, sauf que dans ces derniers les nouvelles bandes étaient sensiblement moins fortes et moins nettes. Ces résultats renforcent notre interprétation récente des spectres infrarouges des polyoxydes H_2O_3 et H_2O_4.

Canadian Journal of Chemistry, 49, 2242 (1971)

Introduction

Following our recent identification (1) by infrared spectroscopy of the polyoxide molecules H_2O_3 and H_2O_4 (more exactly D_2O_3 and D_2O_4) trapped in a frozen ice–peroxide matrix, it was felt desirable to secure further direct evidence from another source. Now, diffraction techniques did not seem suitable because the preparation method of that material (by trapping electrically dissociated vapors) yields a vitreous, nonhomogeneous deposit with relatively low concentrations (less than 10% mol) of the new molecular species. For the same reason conventional Raman spectroscopy is not easily applicable. In fact we have made, without success, a number of preliminary attempts using combined Raman cells – liquid nitrogen traps of various designs in a mercury arc spectrometer (Cary, Model 81). However, the advent of laser excitation has made possible the Raman study of such optically imperfect material. A considerable advantage of Raman spectroscopy in the present case comes from the fact that the region where the characteristic bands of the polyoxide molecules occur is virtually free, in contrast with the infrared.

Experimental

The design and construction of the low temperature Raman cell presented a difficult problem. The multiple reflection technique described by Devlin (2) for investiga-

[1]Postdoctorate Research Fellow, 1968–1970. Present address: Faculté des Sciences, Université de Nancy, Nancy, France.

Can. J. Chem. Downloaded from www.nrcresearchpress.com by 210.87.254.40 on 09/05/12
For personal use only.

tion of thin films deposited on a metal strip was later found unsuitable. Likewise, it was not possible to get any spectra by condensing the dissociated gas stream on a Pyrex flat sealed at the bottom of a liquid nitrogen trap. The only arrangement that gave satisfactory results incorporated the device described by Levin (3). Basically the cell (Fig. 1) resembled that used for the infrared (1), except that the inlet and outlet tubes entered through the top part. Condensation of the deposit took place, not on a salt window, but on a stainless steel mirror at the bottom of the coolant well. It was found by trial that fairly thick deposits (0.2 to 0.4 mm) were needed for a good spectrum. This meant rather long deposition times (3 to 8 h) with input rates of the order of 0.5 g/h. Because of the low trapping efficiency of the Raman cell at least 20% of the input was evacuated as permanent gases.

For recording the spectra the whole cell assembly was disconnected from the vacuum system and mounted in the sample compartment of the spectrometer. The laser beam entered the cell vertically through a glass flat at the bottom. After reflection at 90° on the cold mirror it was focussed *directly onto* the entrance slit of the monochromator. Only with such an arrangement was it possible to get any spectra. The optical lining-up, a rather delicate operation, required positioning the whole cell, both vertically and laterally, by means of micrometer screws. A suitable spot on the sample was located using the strong 878 cm^{-1} band of hydrogen peroxide as a monitor. Only the significant region, from 400 to 1500 cm^{-1}, was scanned.

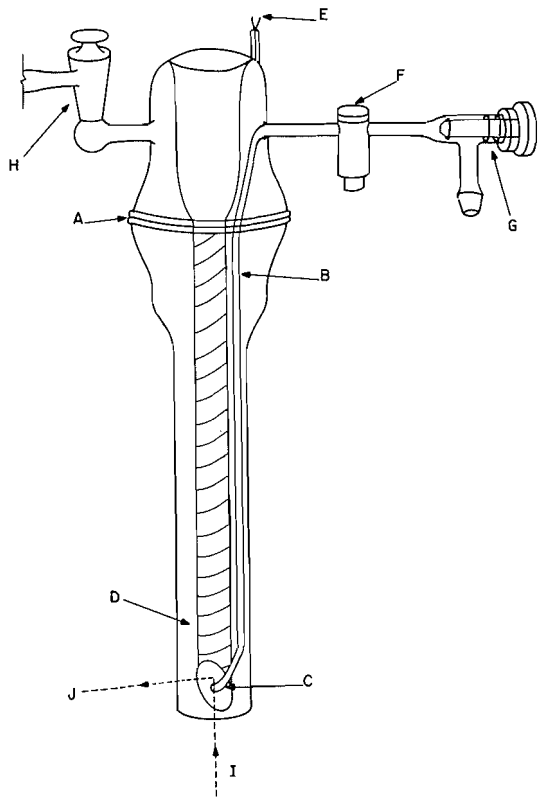

FIG. 1. Combined low temperature Raman cell and discharge tube. *A*, Large size (10 cm diam.) O-ring joint; *B*, injector tube, 8 mm o.d., 40 cm long; *C*, oval shaped stainless steel mirror silver soldered to Kovar seal, *D*; *E*, outlet for the copper–constantan thermocouple located at *D*; *F*, microwave discharge cavity; *G*, greaseless vacuum stopcock with Teflon plug and Viton O-rings; *H*, large stopcock leading to the vacuum line; *I*, *J*, incident and reflected laser beam.

The Raman spectrometer comprised a Spex, Model 14-II monochromator, and a Coherent Radiation, He–Ne laser. The other components have been described elsewhere (4). The samples of heavy water and concentrated hydrogen peroxide were the same as for the infrared work. The deuterium peroxide was prepared by the electrical discharge process (5). By repeated fractional distillations the peroxide concentration of the end product (about 60%) was brought up to near 99%. As for the mixed isotopic water sample (Bio-Rad Laboratories), the ^{18}O content was stated to be 66.4% and the deuterium content, 19.7%.

Results

Due to the poor optical quality of the condensed films and the low power (50 mW max.) of the laser source it was necessary to work with rather wide slits (0.1 to 0.3 mm), and a high amplifier gain. This reduced the signal-to-noise ratio and, consequently, the accuracy in evaluating the band contour as well as the location of the maximum; specially for the weaker bands (Fig. 2). For clarity the original tracings were smoothed out in drawing Fig. 3.

The New Bands

The most conspicuous among the new features of the present spectra (Table 1) is the band at exactly 500 cm^{-1} found in all cases, and with an intensity about one tenth that of the peroxide band at 878 cm^{-1}. Blank runs made by condensing water–peroxide vapor mixtures of roughly equimolar composition in the same cell, but without electrical dissociation, confirmed that the new band was genuine of the discharge products. Since the infrared spectra gave no indication of a corresponding band, albeit the conditions there are not at all favorable, a number of tests were carried out to insure that it was not spurious. For instance, it remained unaltered whether the microwave discharge was located before or after the vacuum stopcock and ring seal, in the case of the long discharge tube; also whether the latter was made of some different material, *e.g.* quartz, or coated with phosphoric acid as described before (6). Incidentally, the

TABLE 1. Principal bands in the Raman spectra of the condensed products from electrically dissociated systems*

H_2O	H_2O_2	D_2O	D_2O_2	$H_2{}^{16/18}O$
	1120 vw		1120 vw	
	1022 w		1025 w	
878 s	878 vs 820 w	878 vs 830 vw	878 vs 830 w	880 855 } m 830
755 m	755 m	765 m	755 m	760 sh 740 m 720 m
500 m	500 m	500 m	500 m	490 m 470 m 440 sh
430 vw	430 m	430 w	430 m	430 w

*Frequencies in cm^{-1}; s = strong, m = medium, w = weak, sh = shoulder, v = very.

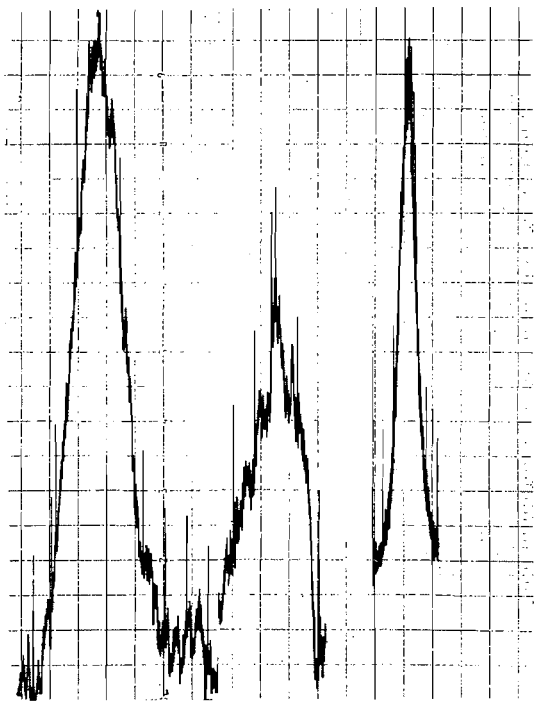

FIG. 2. Actual tracing of sections of a Raman spectrum showing, from left to right, the bands at 760, 830, and 878 cm^{-1}. For the latter the amplifier gain was reduced tenfold, and the slit width, halved.

presence of nitrogen oxides resulting from minute leaks in the vacuum system could be readily monitored from a few sharp peaks in the 1270–1290 cm^{-1} region. Another band, generally less intense than that at 500 cm^{-1}, was also found in all systems at about 760 cm^{-1}, the same frequency as the main infrared band of the polyoxides. Lastly, two other weaker bands could be seen, also at frequencies corresponding to those in infrared, namely 430 and 820 cm^{-1}. They were barely detectable, especially the latter, in the products from dissociated water alone. In some spectra there were indications of a third low-frequency component bridging the gap between the main bands at 500 and 430 cm^{-1}.

The Isotope Effects

Since identification of the polyoxides by infrared rested almost exclusively on the study of deuterated systems, it was desirable to confirm that the corresponding hydrogen species are also produced under the same conditions. As may be judged from spectra *A* and *B* in Fig. 3, there was no essential difference between the spectra of the two systems as far as the frequency of the new bands is concerned. In particular the lower frequency band in the region of 430 cm^{-1}, which is badly obscured in infrared by libration and lattice modes, in both the hydrogen and deuterium systems, is hereby confirmed definitely as an oxygen atom vibration. On the other hand it was observed consistently that the new bands were weaker and more diffuse in the hydrogen than in the deuterium compounds. Accordingly thicker deposits were required (*e.g.* 15 h for *B*, Fig. 3), or else wider slits, for recording the spectra. This implies that the hydrogen polyoxides are somewhat less stable, and therefore less readily produced than their deuterium counterparts. A similar, although very much larger (about 6 times), isotope effect was reported

Can. J. Chem. Downloaded from www.nrcresearchpress.com by 210.87.254.40 on 09/05/12
For personal use only.

Can. J. Chem. Downloaded from www.nrcresearchpress.com by 210.87.254.40 on 09/05/12
For personal use only.

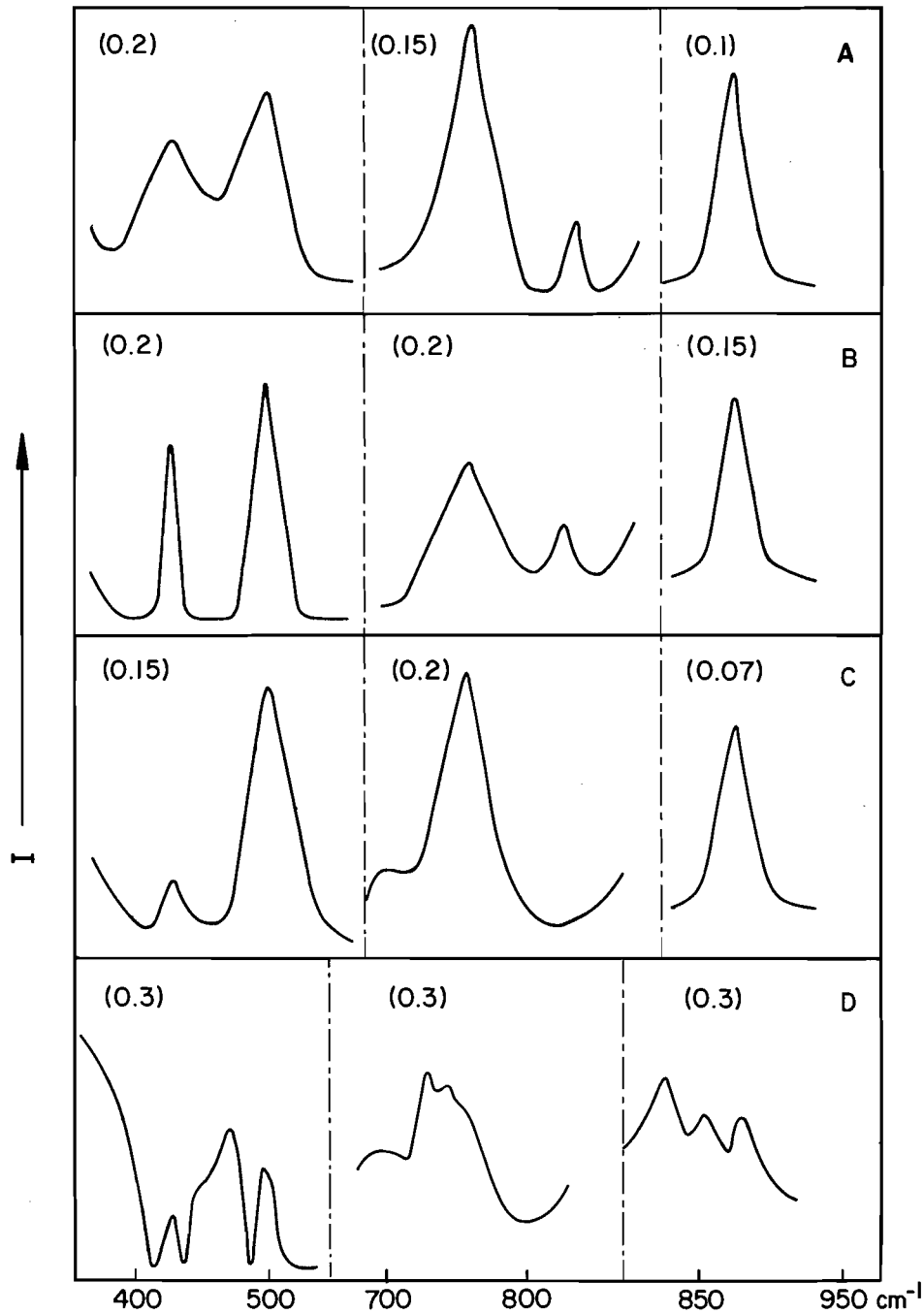

FIG. 3. Laser Raman spectra of the trapped products from electrically dissociated systems: *A*, D_2O_2; *B*, H_2O_2; *C*, H_2O; *D*, $H_2{}^{18/16}O$. Slit widths (in brackets) shown in mm. Sensitivity of detector reduced tenfold in the 800 to 900 cm^{-1} range.

Can. J. Chem. Downloaded from www.nrcresearchpress.com by 210.87.254.40 on 09/05/12
For personal use only.

recently (7) in the half-life of a metastable intermediate, presumably the trioxide, produced in the radiolysis of aqueous acid solutions.

As for the ^{18}O experiments, only two were carried out to confirm qualitatively that all the new bands, and specially that at 500 cm^{-1}, involve oxygen atom vibrations. Since ^{18}O content of the sample was only of the order of two thirds the resulting spectra were somewhat complex. Exceptionally the O—O band of the peroxide gave rise to three distinct peaks as in infrared. The 760 cm^{-1} band evolved into a broad group with maximum at 730 cm^{-1} and a couple of minor components; that at 500 cm^{-1} was mostly shifted to 470 cm^{-1}. Unfortunately, it was not possible to confirm the shift of the weak band around 430 cm^{-1}, expected to occur near 400 cm^{-1}. This was below the lower limit of our observations set by the excessive width of the exciting line in our unusual optical line-up.

The Band Intensities

For obvious reasons the experimental conditions did not allow accurate intensity measurements, even on a relative basis. From the results of some 20 different runs the following generalizations emerge: (*a*) The strongest of the new bands, at 500 cm^{-1}, was in all cases, and within narrow limits, about one tenth as intense as the peroxide band. (*b*) The other bands showed much wider intensity variations depending, among others, on the chemical composition of the system. (*c*) The new bands tended to grow weaker away from the impact point of the dissociated gas stream. This fractionation follows from the very fast recombination reactions. Also, since the latter are exothermic, thermal conductivity of the cold surface is an important factor. (*d*) Slow diffusion of the trapped species at $-180°$ was noticeable. For instance, the yellow color visible in freshly condensed samples, and generally ascribed to trapped free radicals, faded away and was completely bleached after 10–12 h.

The Bands of Condensed Ozone

In the glassy deposits from oxygen-rich systems the dark blue color characteristic of liquid ozone was usually noticeable. Accordingly the Raman spectra revealed a medium intensity band at 1020–1030 cm^{-1} and, in two instances, a weaker one near 1120 cm^{-1}. As in the case of infrared (1) the trapping was certainly a matrix effect. Indeed, at the temperature of our cold surface ($-180°$) the vapor pressure of ozone (1 Torr) is greater, by about an order of magnitude, than the operating pressure in our plasma. In view of the close agreement with the frequencies of the infrared bands (8), which could hardly be a coincidence, the present bands are therefore ascribed to condensed ozone. However, this interpretation meets with a serious difficulty because the intensities are in the same order as in infrared, instead of the normal reversed order. It is also at variance with the Raman spectrum of gaseous ozone (9) which shows only two highly polarized bands; $\nu_1 = 1103.3$ cm^{-1}, $\nu_2 = 702.1$ cm^{-1}. *A priori* it is not clear why the antisymmetric stretching mode should be stronger than the symmetric one in the Raman effect of condensed ozone. On the other hand there is no other obvious explanation for the band at 1030 cm^{-1}. It must belong to an oxygen vibration as it appears both in hydrogen and deuterium systems. Other species, such as $(O_2)_2$, seem much less probable than O_3. We intend to investigate this question further, in particular by means of isotopically pure ^{18}O compounds.

Conclusion

The present study adds substantial evidence to the infrared detection of metastable intermediates in the hydrogen–oxygen reactions. In addition to confirming three of the four oxygen vibrations of the polyoxide species already discovered, it has revealed a fifth mode apparently inactive in infrared. Except for the latter, the intensity pattern of the new bands resembles that in infrared. This must arise from overlapping of different bands from two distinct species; namely H_2O_3 and H_2O_4, as in the case of the analogous hydrogen polysulfides (10). Likewise, all the O—O stretching frequencies of the polyoxides are seen to lie *lower* than that of the peroxide. This is contrary to recent calculations (11) which yielded values ranging from 900 up to 1250 cm^{-1} for various models of the H_2O_4 molecule. Lastly, a frequency of 500 cm^{-1} seems a little high for the bending of single-bonded oxygen atoms. Hydrogen bonds in the matrix may be partly responsible for this. Also in agreement are the results of a recent *a priori* calculation of the electronic structure of the H_2O_3 molecule (12) which indicate a slightly shorter O—O distance (1.438 Å) than in H_2O_2 (1.48 Å). Clearly, there is a great need for more experimental data on the structure of these molecules.

The authors would like to thank the National Research Council of Canada for financial assistance. They are also grateful to Messers. F. Bouchard and G. Robert, glassblowers, and G. Marier, mechanic, for their skillful assistance in constructing the laser Raman cell. The junior author (X.D.) benefited from a teaching assistantship in the Department of Chemistry while carrying out this research work.

1. P. A. GIGUÈRE and K. HERMAN. Can. J. Chem. **48**, 3473 (1970).
2. J. P. DEVLIN. Raman Newsletter, **10**, 34 (1969).
3. I. W. LEVIN. Spectrochim. Acta, **25A**, 1157 (1969).
4. R. E. MILLER, D. L. ROUSSEAU, and G. E. LEROI. Tech. Rept. No. 22, ONR Contract 1858 (27), May 1967, DDC Accession No. AD651646.
5. P. A. GIGUÈRE, E. A. SECCO et R. S. EATON. Discuss. Faraday Soc. **14**, 104 (1953).
6. P. E. BRUNET, X. DEGLISE, and P. A. GIGUÈRE. Can. J. Chem. **48**, 2042 (1970).
7. B. H. J. BIELSKI. J. Phys. Chem. **74**, 3213 (1970).
8. K. B. HARVEY and A. M. BASS. J. Mol. Spectry. **2**, 405 (1958).
9. H. SELIG and H. H. CLAASSEN. Israel J. Chem. **6**, 499 (1968).
10. H. WIESER, P. J. KRUEGER, E. MULLER, and J. B. HYNE. Can. J. Chem. **47**, 1633 (1969).
11. T. V. YAGODOVSKAYA and L. I. NEKRASOV. Russ. J. Phys. Chem. **44**, 965 (1970).
12. J. D. NEWTON. Private communication.

Can. J. Chem. Downloaded from www.nrcresearchpress.com by 210.87.254.40 on 09/05/12
For personal use only.

Can. J. Chem. Downloaded from www.nrcresearchpress.com by 210.87.254.105 on 09/05/12
For personal use only.

Free-ion Yield in the Radiolysis of Dimethylsulfoxide

T. K. Cooper and D. C. Walker

Chemistry Department, University of British Columbia, Vancouver, British Columbia

Received January 27, 1971

Dimethylsulfoxide is a dipolar aprotic solvent of high basicity having a large dielectric constant ($\varepsilon = 48$) but very low solvating power for negative ions. The radiation yield of "free ions" in this liquid is in accord with the dielectric constant, G(free ions) $= 1.8 \pm 0.2$, but these "free ions" do not resemble the strongly solvated electrons found in other polar media such as water and aliphatic alcohols. Evidence for this conclusion is based principally on competitive reactions involving a wide range of scavengers in competition with nitrous oxide. The radiation yields of gaseous products from pure liquid dimethylsulfoxide are $G(H_2) = 0.20 \pm 0.01$, $G(CH_4) = 3.3 \pm 0.1$, and $G(C_2H_6) = 0.49 \pm 0.03$.

Le diméthylsulfonyle est un solvant dipolaire aprotique de haute basicité, ayant une constante diélectrique élevée ($\varepsilon = 48$) mais un pouvoir de solvatation très faible pour les ions négatifs. Le rendement d"ions libres" obtenus par radiation dans ce liquide, G(ions libres) $= 1.8 \pm 0.2$, est en accord avec la constante diélectrique mais ces ions libres ne ressemblent pas du tout aux électrons hautement solvatés trouvés dans des milieux polaires comme l'eau ou les alcools aliphatiques. Les preuves supportant cette conclusion sont basées principalement sur les réactions compétitives impliquant un grand nombre de scavangers en compétition avec l'oxyde nitreux. Les rendements de produits gazeux obtenus par radiation de DMSO pur à l'état liquide sont $G(H_2) = 0.20 \pm 0.01$, $G(CH_4) = 3.3 \pm 0.1$ et $G(C_2H_6) = 0.49 \pm 0.03$.

Canadian Journal of Chemistry, 49, 2248 (1971)

Introduction

The yield of solvated electrons in the radiolysis of a pure liquid has implications for chemistry in general because it gives some indication of the ability of the solvent to stabilize these species and thus permit their involvement in certain reactions, such as Birch reductions. There is little doubt that the yield of solvated electrons in general increases systematically with increasing static dielectric constant (1–4), but one might expect the solvating power of the solvent also to be a crucial factor.

Dimethylsulfoxide $(CH_3)_2SO$, referred to as DMSO for brevity, is an aprotic polar solvent that is widely used in organic and inorganic chemistry because of its inability to solvate negative ions; consequently bases appear exceptionally strong in this medium. We have endeavored to establish the radiation yield of "free ions" in DMSO and to determine whether or not solvated electrons are formed. It is evident from a recent study on liquid formamide (3) that some systems may show "free ion" yields which are consistent with a high dielectric constant, but that the chemical species formed, although strongly reducing, are neither solvated electrons nor hydrogen atoms and are too long-lived to be quasi-free electrons.

Some recent studies on aspects of the radiolysis of DMSO have been reported including pulse radiolysis absorption spectroscopy using various solutes to scavenge electrons and cations produced (4, 5). The only other report (6) on the radiolysis of DMSO concerns a study of DMSO containing 0.4 M H_2SO_4 where the chemistry seems to be rather different, since neither solvated electrons nor solvent anions can be involved in secondary reactions.

Experimental

The dimethylsulfoxide (Matheson, Coleman and Bell, spectroscopic grade) was stirred in a closed vessel over calcium hydride for at least 2 days and then distilled under reduced pressure (~1 Torr at 48–50 °C). Only the middle 50% was collected and stored over a layer of Linde 4 A molecular sieve and sealed in an atmosphere of pure nitrogen. Prior to use it was redistilled and the samples immediately prepared. Nitrous oxide was purified by trap-to-trap distillation and other chemicals used were reagent grade or better and not purified further.

Irradiations were performed in a 4000 curie ^{60}Co Gammacell at a dose rate of approximately 5.0×10^3 rads min^{-1} with total doses up to 1.7×10^6 rads. The experiments were performed using a sample cell similar to the one described previously (3) but containing an additional side-arm with a standard tapered joint. Dosimetry was established using the Fricke solution, taking for Fe^{3+} ions $\varepsilon(304) = 2174$ M^{-1} cm^{-1} and $G(Fe^{3+}) = 15.5$. The dose rate in DMSO was then obtained by multiplying by 0.971, the ratio of the electron densities of the DMSO and Fricke solution.

DMSO samples were prepared by adding the liquid

Can. J. Chem. Downloaded from www.nrcresearchpress.com by 210.87.254.105 on 09/05/12
For personal use only.

through the B10 cone and then deoxygenated by bubbling high purity argon through the sintered disk for 30 min prior to the irradiation which was conducted at 23 ± 2 °C. After irradiation, the cell was attached to the gas chromatograph (Varian Aerograph Series 1700) and the volatile gaseous products flushed directly into the chromatograph. A Poropak-Q pre-column at 23 °C was used to prevent DMSO vapor from saturating the 20 ft × 1/4 in. stainless steel 13X molecular sieve chromatograph column. Argon was used as the carrier gas, detection was made using WX thermal conductivity detectors and the detector and column temperatures used were 125 and 55 °C, respectively. Ethane was measured by temperature programming, after the other gas products were detected, by heating the column to 130 °C at a rate of 20 °C per min. With a flow rate of 30 ml a minute, it was found that over 95% of the volatile gases (CH_4, N_2, H_2, and C_2H_6) were extracted in the first 3 min so that tailing of the peaks was very small. However, the bubbling was continued throughout the analysis (except for ethane) to avoid a pressure change during analysis. Under such conditions the response factors ($cm^2/\mu mol$ gas) for hydrogen, nitrogen, methane, and ethane were 59.5, 4.85, 15.2, and 12.7, respectively. Non-volatile products were not analyzed for. For the DMSO – nitrous oxide solutions, the DMSO was deoxygenated by flushing the sample with argon, degassed on a vacuum line, and equilibrated with nitrous oxide. The solubility of nitrous oxide in DMSO was found to be $1.10 \pm 0.05 \times 10^{-4}$ M $Torr^{-1}$ at 23 °C.

Results

The gaseous products obtained under γ-radiolysis of pure DMSO were hydrogen, methane, and ethane. Hydrogen and ethane were formed with yields of $G(H_2) = 0.20 \pm 0.01$ and $G(C_2H_6) = 0.49 \pm 0.03$, which were independent of dose up to at least 1.3×10^6 rads. However, methane formation was not linear with dose, in contrast to some previously reported results (6), and the data suggest that some non-volatile radiation product was being built up which scavenges the precursor of part of the methane. This can be seen in Fig. 1 in which the volatile gases were removed after each irradiation and the total accumulated yield plotted as a function of dose. Three different series were carried out; one in which all the doses were the same, another in which each dose was different, and a third in which a small dose was followed by a large dose and then followed by the same small dose. As can be seen, all the points fall on a smooth curve but the methane yield is only linear up to about 1.8×10^5 rads. Consequently, all scavenging studies with various added solutes were carried out with doses less than 1.8×10^5 rads so that the real effect of these on the methane yield could be seen. By taking the slope at various portions of the curve, it was found that $G(CH_4)$ falls from 3.3 ± 0.1 to 2.1 ± 0.1 over the dose range studied.

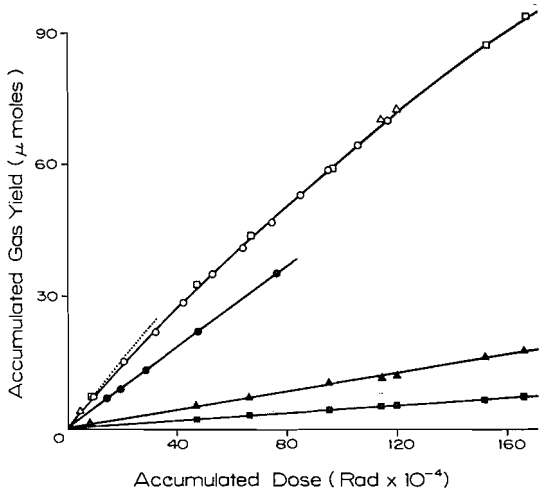

FIG. 1. Accumulated gas yields as a function of accumulated dose: ○, □, △, CH_4 at various doses; ▲, C_2H_6; ■, H_2; and ●, N_2 yield when 0.054 M N_2O added.

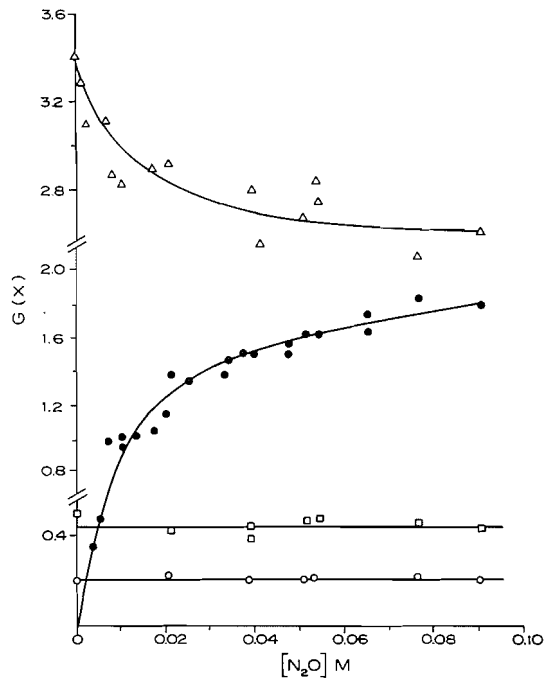

FIG. 2. Radiation yields as a function of N_2O concentration: △, CH_4; □, C_2H_6; ○, H_2 and ●, N_2. In the case of CH_4, all doses were $< 1.8 \times 10^5$ rads.

The addition to DMSO of various concentrations of nitrous oxide affects these gas yields in the manner shown in Fig. 2. Methane was found

TABLE 1. Radiation yields from irradiated DMSO containing 0.05 M N_2O plus the second scavenger indicated in column 1 at concentration given in column 2

Second scavenger	Concentration (M)	$G(N_2)$	$G(CH_4)$	$G(H_2)$	$G(C_2H_6)$
Water	0.22	1.7	3.1	0.21	0.46
Methanol	0.098	1.7	3.0	0.23	0.42
	0.196	1.7	3.0	0.23	0.43
	0.196*	—	3.6	0.24	0.46
Isopropanol	0.103	1.8	2.8	0.26	0.45
	0.103*	—	3.1	0.25	0.46
Acetone	0.107	1.7	2.8	0.23	0.45
	0.264	1.8	2.6	0.23	0.44
$AgNO_3$	0.00947	1.4	2.6	0.21	0.40
	0.0249	1.2	2.4	0.21	0.42
	0.0516	0.95	2.3	0.20	0.41
	0.102	0.65	2.1	0.19	0.41
	0.158	0.57	2.1	0.20	0.41
$CHCl_3$	0.0124	1.2	2.3	0.20	0.36
	0.0696	0.68	2.2	0.21	0.41
	0.0990	0.63	2.2	0.19	0.39
	0.197	0.43	2.1	0.21	0.40
	0.304	0.38	1.9	0.20	0.37
Iodine	0.00652	1.5	0.32	0.22	0.42
	0.0208	1.1	0.26	0.21	0.29
	0.0300	0.99	0.25	0.22	0.28
	0.0941	0.59	0.20	0.20	0.25
	0.126	0.45	0.21	0.19	0.26
CCl_4	0.0179	1.11	2.2	0.21	0.45
	0.0490	0.74	1.8	0.21	0.38
	0.0685	0.68	1.7	0.21	0.37
	0.0740	0.65	1.7	0.20	0.36
	0.103	0.45	1.5	0.20	0.36
Anhydrous sulfuric acid	0.00918	1.4	2.4	0.20	0.41
	0.0195	1.2	2.5	0.20	0.45
	0.0295	1.1	2.7	0.21	0.45
	0.0377	1.0	2.8	0.20	0.47
	0.0559	0.80	2.7	0.19	0.47
	0.0895	0.68	3.0	0.20	0.50
	0.114	0.63	3.0	0.20	0.53
	0.137	0.55	3.2	0.20	0.50
	0.0718†	0.78	2.8	0.23	

*No N_2O added.
†0.5 M methanol added.

to decrease by about 20% (from 3.3 to 2.6) while hydrogen and ethane were unaffected. At $[N_2O] = 0.054$ M, the nitrogen yield was independent of dose up to at least 7.5×10^5 rads (Fig. 1) suggesting that whatever the non-volatile product is which inhibits the methane, it does not affect the nitrogen yield. From the slope of Fig. 1, $G(N_2) = 1.6 \pm 0.1$ at this concentration. Figure 2 shows the steady increase in $G(N_2)$ as the nitrous oxide concentration is increased up to 0.09 M. No simple plateau is evident and $G(N_2)$ increases from 1.4 to 1.8 over the range 0.03 to 0.09 M.

In order to test the nature of the chemical species with which the nitrous oxide was reacting, various second scavengers were added to compete with it. Several of the scavengers, such as carbon tetrachloride, hydrogen ions, silver nitrate, chloroform, acetone, and iodine are known to react rapidly with solvated electrons in various polar liquids whereas methanol and isopropanol react rapidly only with hydrogen atoms. Data on the effect of these scavengers in competition with 0.05 M N_2O are given in Table 1.

The effect of iodine and hydrogen ions on the gaseous products is shown in Figs. 3 and 4. The addition of water was also tested because DMSO is quite hygroscopic and there could have been a trace of water in the sample despite the precau-

Can. J. Chem. Downloaded from www.nrcresearchpress.com by 210.87.254.105 on 09/05/12
For personal use only.

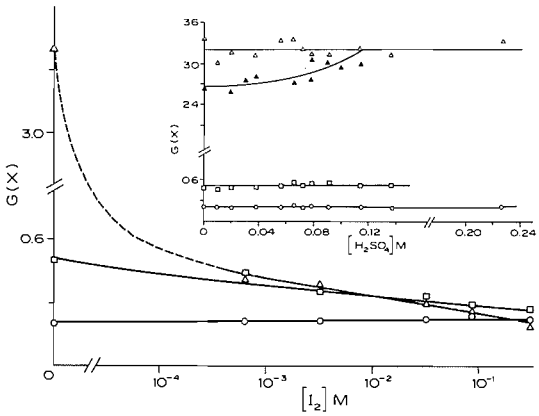

FIG. 3. Radiation yields of CH_4, C_2H_6, and H_2 as a function of I_2 and H^+ concentration: △, CH_4; □, C_2H_6 and ○, H_2; ▲ corresponds to the yield of CH_4 when 0.05 *M* N_2O is added to the corresponding acid solution of DMSO. In the case of CH_4 yields, all doses were $< 1.8 \times 10^5$ rads. For the I_2 solutions, the doses were $< 5 \times 10^4$ rads.

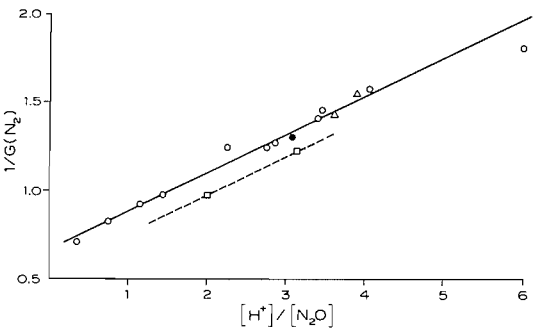

FIG. 4. Plot of $1/G(N_2)$ as a function of $[H^+]/[N_2O]$ in which ○, □, and △ correspond to different N_2O concentrations; ○, 0.05 *M* N_2O; △, 0.04 *M* N_2O and □, 0.07 *M* N_2O. ● corresponds to 0.5 *M* methanol added to acid solution containing 0.05 *M* N_2O.

tions taken to eliminate it. As can be seen from Table 1 the added water had no appreciable effect on any of the gas yields, so that either all samples contained enough adventitious water for its effect to be fully felt or water cannot compete with the precursors of the gaseous products, including nitrogen.

Discussion

Since the original work with nitrous oxide in aqueous solutions by Dainton and Peterson (7), nitrous oxide has been widely used as a specific scavenger for solvated electrons in many liquids. However, this solute may give nitrogen by reactions with other types of strongly reducing species formed in the radiolysis and strong inferences have to be drawn from competition studies with other scavengers. In DMSO solvated electrons, hydrogen atoms, free radicals (R), and solvent anions could yield nitrogen in reactions 1, 2, 3, and 4 if their alternate fates were comparatively slow.

[1] $$e_s^- + N_2O \rightarrow N_2 + O_s^-$$

[2] $$H\cdot + N_2O \rightarrow N_2 + \cdot OH$$

[3] $$R\cdot + N_2O \rightarrow N_2 + RO\cdot$$

[4] $$DMSO^- + N_2O \rightarrow N_2 + DMSO_2^-$$

In this scheme $DMSO^-$ is to be regarded as a solvent anion formed by electron attachment or solvent decomposition from free or solvated electrons.

It is evident from Table 1 that addition of methanol or isopropanol to a nitrous oxide solution did not alter the nitrogen yield. Since these alcohols are generally much better scavengers of hydrogen atoms than is nitrous oxide these results imply that reaction 2 is not contributing significantly to the nitrogen yield. Furthermore $G(H_2)$ changes only from 0.21 to 0.25 by the addition of alcohols to DMSO in both the presence and absence of nitrous oxide suggesting that hydrogen atoms are produced in only low yield. Involvement of reaction 3 can likewise be disregarded by analogy with similar competition studies and because iodine, which in other systems is a much better radical scavenger than nitrous oxide, competed almost on an equal basis with nitrous oxide for the precursor of nitrogen in DMSO. This inference is supported by the data in Fig. 3 where it is evident that iodine, even at 0.006 *M*, virtually eliminates the methane. This suggests that methane arises from methyl radicals which abstract a hydrogen atom from DMSO. Nevertheless, N_2O decreases the CH_4 yield somewhat and evidently can interfere with a minor reaction leading to the formation of methane. Iodine also cuts down the ethane yield somewhat indicating that it too is partly formed by radical reactions. On the other hand iodine does not affect the hydrogen yield implying that all the hydrogen is formed in "molecular processes" or by a fast reaction of thermal hydrogen atoms with DMSO. About half of the ethane

Can. J. Chem. Downloaded from www.nrcresearchpress.com by 210.87.254.105 on 09/05/12
For personal use only.

Can. J. Chem. Downloaded from www.nrcresearchpress.com by 210.87.254.105 on 09/05/12
For personal use only.

and 10% of the methane may also originate from direct or non-thermal radical reactions.

With regard to the formation of N_2 from N_2O solutions, there are several reasons for believing that any solvated electrons formed in DMSO do not resemble in reactivity the strongly-solvated electrons found in other highly polar solvents such as water. Firstly, although H^+, Ag^+, $CHCl_3$, CCl_4, and I_2 compete effectively with N_2O, acetone does not. Secondly, when these competitions are analyzed the relative rate constants obtained differ markedly from the relative rates of these scavengers with hydrated electrons. The following relationship was applied to the competitions between nitrous oxide and the second scavenger (S) for the precursor (P) of nitrogen

$$\frac{1}{G(N_2)} = \frac{1}{G(P)}[1 + k_s[S]/k_{N_2O}[N_2O]]$$

where k_s is the rate constant of P with S and k_{N_2O} is the rate constant for the reaction of P with N_2O. The data is plotted in Figs. 4 and 5 and appear to follow the simple competition relationship. The slopes of these plots give values for k_s/k_{N_2O} which are recorded in Table 2 and compared with the published values of this ratio for reaction with e_{aq}^-. It should be noted that the intercept of these plots gives the value of $G(P) = 1.6 \pm 0.2$ but because $G(N_2)$ does not show a plateau value at high nitrous oxide concentrations (see Fig. 2), the yield of $G(P)$ depends on the nitrous oxide concentrations used above 0.03 M. This is evident in Fig. 4, the H^+ competition, in which two lines having the same slope but different intercepts were obtained from two different but high values of nitrous oxide. Therefore, in the competitions in Fig. 5, the nitrous oxide concentration was held constant at 0.05 M and the concentration of the second scavenger varied.

The third argument against involvement of a solvated electron stems from the competition between H^+ and N_2O with 0.5 M methanol also added to the solution (Table 1). If the reaction 1 was in competition with [5] then the hydrogen

[5] $$e_s^- + H_s^+ \rightarrow H\cdot$$

yield would be increased by the presence of methanol in an acidic solution of DMSO. No such increase was found. In fact hydrogen ions do not affect the gaseous yields of pure DMSO at all (Fig. 3), in agreement with the results of Pujo and Berthou (6), and counteract the slight effect nitrous oxide has on the methane yield. However, it is possible that hydrogen atoms

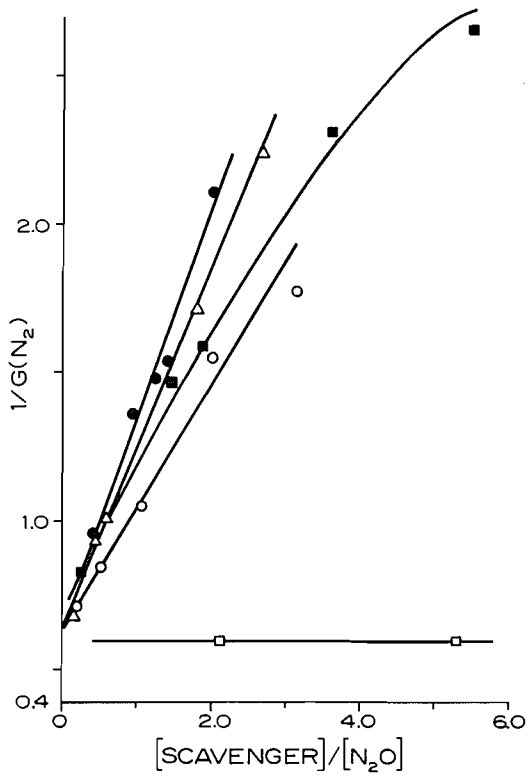

FIG. 5. Plot of $1/G(N_2)$ as a function of [scavenger]/[N_2O]. The N_2O concentration was 0.05 M and the second scavenger concentration was varied. The data were taken from Table 1. ● CCl_4, △ I_2, ■ $CHCl_3$, ○ Ag^+, and □ acetone.

TABLE 2. Ratio of k_s/k_{N_2O} obtained for the precursor of N_2 in DMSO with various second scavengers (S) added to a 0.05 M solution of N_2O. Column headed water refers to the published rate constant ratio for the hydrated electron

S	k_s/k_{N_2O} (DMSO)	k_s/k_{N_2O} (water)*
CCl_4	0.85±0.09	5.4
I_2	0.60±0.06	9.1
$CHCl_3$	0.45±0.05	3.6
Ag^+	0.40±0.04	5.7
H^+	0.25±0.03	3.9
$(CH_3)_2CO$	<0.01	1.1

*Data taken from the compilation of rate constants (12).

Can. J. Chem. Downloaded from www.nrcresearchpress.com by 210.87.254.105 on 09/05/12
For personal use only.

react rapidly with DMSO to give non-gaseous products.

Additional evidence against thermodynamically stable solvated electrons in DMSO comes from the fact that irradiated polycrystalline DMSO at 77 °K (only partially transparent) does not show any coloration nor does it yield an electron spin resonance (e.s.r.) signal corresponding to a trapped electron (8), despite the fact that it has a high dipole moment (3.9 D). Furthermore metallic sodium does not dissolve to generate hydrogen gas but rather decomposes DMSO, producing a mixture of sodium mesityl, methane sulfenate, dimethyl sulfide, and methane (9).

In a recent pulse radiolysis study of pure liquid DMSO (10), there are strong indications of very short-lived (τ = 10–20 ns) solvated electrons having an optical absorption band maximum at $\lambda > 1500$ nm and produced in low yield ($G < 1$). These species are incompletely scavenged by 0.08 M N_2O. Such data suggest that the solvation energy is very small (comparable to hydrocarbons) and that these weakly-solvated electrons react with the solvent or very rapidly with trace impurities. These observations corroborate the notion that the solvating power of the solvent is more important than the dielectric constant in stabilizing electrons in liquids (10).

The curvature of $G(N_2)$ at $[N_2O] > 0.03$ is difficult to interpret without knowledge of the absolute rates of the reactions involved and the alternative fates of the N_2 precursor(s). Perhaps some solvated electrons may be scavenged by N_2O at high concentrations but that the major part of $G(N_2) = 1.8$ (the total free-ion yield) corresponds to another reducing species such as a solvent anion or decomposition product formed therefrom.

Pulse radiolysis studies on DMSO have yielded similar values for the free ion yield. Kemp *et al.* (5) obtained $G = 1.7$ for the yield of radical cations of TMPD in DMSO which they attribute to the "free ion" yield. Hayon (4) has also recently reported $G = 1.62$ as the yield of anthracene anions produced from solvated electrons in DMSO. However, as with H^+, I_2, $CHCl_3$, CCl_4, and Ag^+ in this study, perhaps anthracene can undergo charge transfer with a solvent anion just as easily as it scavenges a solvated electron. The available d orbital on the sulfur atom of DMSO perhaps favors electron attachment there but the product may well be quite reactive towards these other "electron" scavengers. Meissner *et al.* (11) have studied the absorption spectra of species produced during the pulse radiolysis of a dilute solution of DMSO in water and have assigned an absorption band centered at 350 nm to a DMSO radical anion.

The authors wish to acknowledge the generous financial support of the National Research Council of Canada. T.K.C. wishes to thank the F. J. Nicholson Family and the National Research Council for graduate scholarships during part of this work.

1. R. A. Holroyd. *In* Fundamental processes in radiation chemistry. *Edited by* P. Ausloos. Interscience Publishers. 1968. p. 413.
2. G. R. Freeman and J. M. Fayadh. J. Chem. Phys. **43**, 86 (1965).
3. D. A. Head and D. C. Walker. Can. J. Chem. **48** 1657 (1970).
4. E. Hayon. J. Chem. Phys. **53**, 2353 (1970).
5. T. J. Kemp, J. P. Roberts, G. A. Salmon, and G. F. Thompson. J. Phys. Chem. **72**, 1464 (1968).
6. A. M. Koulkes-Pujo and M. Berthou. J. Chim. Phys. **66**, 1178 (1969).
7. F. S. Dainton and D. B. Peterson. Proc. Roy. Soc. London, Ser. A. **267**, 443 (1962).
8. T. K. Cooper. Unpublished data.
9. D. E. O'Conner and W. I. Lyness. J. Org. Chem. **30**, 1620 (1965).
10. H. A. Gillis, N. V. Klassen, and D. C. Walker. To be published.
11. G. Meissner, A. Henglein, and G. Beck. Z. Naturforsch, **22***b*, 13 (1967).
12. M. Anbar and P. Neta. Int. J. Appl. Rad. Isot. **18**, 493 (1967).

Can. J. Chem. Downloaded from www.nrcresearchpress.com by 210.87.254.40 on 09/05/12
For personal use only.

Etude des spectres de vibration de l'isothiazole et des spectres infrarouges de trois mono et dideutério isothiazoles

JEAN-LOUIS MEYER, GISELE DAVIDOVICS, ET JACQUES CHOUTEAU

Centre Technique de Spectroscopie Infrarouge, Département de Chimie Organique, Faculté des Sciences, 13 Marseille, France

ET

JEAN-CLAUDE POITE ET JEAN ROGGERO

Laboratoire de Chimie Organique, C.S.U., 33 rue Louis Pasteur, 84 Avignon, France

Reçu le 14 décembre, 1970

Les deutério-4, deutério-5, et dideutério-4,5 isothiazoles ont été synthétisés et leurs spectres i.r. enregistrés sous différents états, vapeur notamment.

L'étude du spectre Raman de l'isothiazole a permis de rectifier l'attribution de deux modes fondamentaux de cet hétérocycle. Une interprétation des spectres i.r. des trois deutério isothiazoles est discutée.

The 4- and 5-monodeuterio and 4,5-dideuterio isothiazoles were prepared and their i.r. spectra recorded in different states, vapor particularly.

The Raman spectrum of isothiazole was also measured; its analysis leads to the modification of the assignment of two of the fundamental modes previously described for this compound. The analysis of the i.r. spectra of the three deuterio isothiazoles is discussed.

Canadian Journal of Chemistry, **49**, 2254 (1971)

Introduction

Dans le cadre de recherches d'ensemble sur la structure et la réactivité de composés hétérocycliques, nous avons été amenés à examiner les spectres i.r. et Raman de l'isothiazole ainsi que

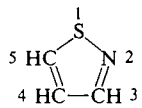

les spectres i.r., sous différents états (vapeur en particulier), des dérivés mono et dideutériés de l'isothiazole en positions -4, -5, et -4,5.

Une étude du spectre i.r. de l'isothiazole a déjà été publiée par Califano *et al.* (1), mais l'analyse du spectre Raman de cette molécule apportant de nouvelles données, il nous a paru intéressant de rediscuter les attributions. Celles-ci ont été étendues aux dérivés deutériés et leur validité confirmée à l'aide des structures de vibration rotation i.r. à l'état vapeur et des règles isotopiques.

Nous donnerons d'abord nos conditions expérimentales. Après un court chapitre consacré au dénombrement des vibrations dans l'isothiazole et ses dérivés deutériés, nous indiquerons nos résultats expérimentaux qui seront suivis de l'analyse des spectres.

Conditions expérimentales

La synthèse de l'isothiazole C_3H_3NS étudié dans ce travail a été exécutée par la méthode de Wille *et al.* (2), modifiée par Raap (3); celle du deutério-4 isothiazole a nécessité l'emploi de D_2O, CH_3CO_2D, et $S_2O_3Na_2$ anhydre.

Les deutério-5 et dideutério-4,5 isothiazoles ont été obtenus à partir, respectivement, d'isothiazole et de deutério-4 isothiazole, par réaction d'échange dans un mélange D_2O, CH_3OD, en présence de NaOD à température ambiante, la position 3 étant, dans ces conditions, très peu affectée (4, 5).

L'isothiazole a été purifié par formation du complexe mercurique C_3H_3NS, $HgCl_2$, dont la décomposition a été effectuée à 80 °C, sous un vide de 10^{-4} mm Hg.

Les impuretés isotopiques décelées par spectroscopie i.r. dans les échantillons d'isothiazoles deutériés sont indiquées dans les tableaux 3 à 5. Leurs pourcentages, quand ils ont pu être évalués par r.m.n. ou spectroscopie i.r. sont les suivants: dans le deutério-4 isothiazole, D-4,5 isothiazole ~0.8–1.5% (i.r.), isothiazole, moins de 3% (r.m.n.); dans le deutério-5 isothiazole, isothiazole ~0.6% (r.m.n.); dans le dideutério-4,5 isothiazole, D-4 isothiazole ~4.5% (r.m.n.),

TABLEAU 1. Moments principaux d'inertie et paramètres moléculaires*

	I_x (uma Å^2)	I_y (uma Å^2)	I_z (uma Å^2)
(7) Isothiazole	61.087	86.471	147.634
Isothiazole	59.8	87.6	147.4
D-4 Isothiazole	61	92.9	153.9
D-5 Isothiazole	65.2	87.7	152.9
D-4,5 Isothiazole	66.2	92.9	159.1

Longueurs (Å): $C_3H = C_4H = 1.079$ (9); $C_5H = 1.083$ (10)
[SN = 1.631; $NC_3 = 1.327$; $C_3C_4 = 1.420$] (8, 9); [$C_4C_5 = 1.355$; $C_5S = 1.719$] (10)
Angles (d°): [$C_3C_4C_5 = 111.7$; $C_3C_4H = 123.5$] (11)
[$SNC_3 = 106.5$; $NC_3C_4 = 113.7$; $C_4C_3H = 126.2$] (9);
[$C_4C_5S = 119.6$; $SC_5H = 128$] (10)

*Les différents paramètres sont accompagnés, entre parenthèses, de la référence bibliographique du travail dont ils sont tirés.

~1.1–2.3% (i.r.), D-5 isothiazole ~1.4% (r.m.n.), ~1–2.2% (i.r.). Les deux taux d'impuretés calculés à partir des spectres i.r. correspondent, respectivement, à des mesures de densité optique effectuées avec et sans correction d'ailes.

L'étude des spectres de masse des deutério isothiazoles n'a pu être faite à des énergies suffisamment proches du potentiel d'ionisation pour que les puretés isotopiques des différents échantillons puissent être déterminées par cette méthode. Il semblerait, cependant, que la proportion d'isothiazole non deutérié soit deux fois plus élevée dans le deutério-5 que dans le deutério-4 isothiazole, d'après leurs spectres de masse. L'existence d'un pic $M = 76$ susceptible d'être dû à CS_2 dans le spectre de masse des quatre isothiazoles (5), permet de penser que les bandes d'absorption faibles et sensibles à la température observées, vers 1515 cm^{-1}, dans les spectres i.r. de ces hétérocycles, proviennent de traces de sulfure de carbone.

Les conditions d'enregistrement des spectres i.r. et Raman sont identiques à celles indiquées dans un précédent mémoire (6).

Dénombrement des vibrations

Les moments principaux d'inertie de l'isothiazole, déduits des constantes rotationnelles (7), vérifient très sensiblement la planéité de cet hétérocycle (*cf.* tableau 1). Ils sont en assez bon accord avec les valeurs calculées en adoptant certains des paramètres moléculaires du -1,2,5 thiadiazole (8, 9), du thiazole (10), et du thiophène (11) (*cf.* tableau 1).

L'isothiazole et ses dérivés deutériés admettant la symétrie C_s, leurs 18 vibrations normales se décomposent en 13 modes de classe A′ et cinq modes de classe A″ (12).

Dans l'approximation des vibrations de groupe, on attend neuf oscillations (6A′ + 3A″) des liaisons CX (X = H ou D) et neuf mouvements (7A′ + 2A″) du squelette.

Il est possible de distinguer les vibrations de classe A″ et A′ qui doivent, le grand axe d'inertie de ces molécules étant normal au plan du noyau, donner lieu, respectivement, à des bandes de vibration rotation de type C d'une part, et A, B, ou hybride A + B d'autre part, dans les spectres i.r. des composés à l'état vapeur (13, 14).

Dans le spectre Raman on s'attend, en outre, à ce que les oscillations de symétrie A″ se manifestent par des raies Raman faibles et dépolarisées (15), celles de symétrie A′, par des raies plus intenses et polarisées (12).

Dans une même classe de symétrie, l'exactitude des attributions peut être vérifiée, pour chacune des molécules isotopiques, à l'aide de la règle du produit des fréquences de Teller–Redlich (16, 17) et, pour l'ensemble des quatre molécules, en appliquant la règle de la somme des carrés des fréquences expérimentales (16).

Résultats expérimentaux

Les spectres i.r. des deutério-4, deutério-5, et dideutério-4,5 isothiazoles à l'état liquide sont reproduits dans la fig. 1. Les fréquences i.r. observées dans les spectres de ces composés et dans celui de l'isothiazole en solution dans des solvants inertes et à l'état vapeur, sont, ainsi que les coefficients d'extinction molaire apparents et les structures des bandes de vibration rotation, indiqués dans les tableaux 2 à 5. Le tableau 2 comporte également les fréquences, intensités relatives et les facteurs de dépolarisation, des raies de diffusion du spectre Raman de l'isothiazole.

Can. J. Chem. Downloaded from www.nrcresearchpress.com by 210.87.254.40 on 09/05/12
For personal use only.

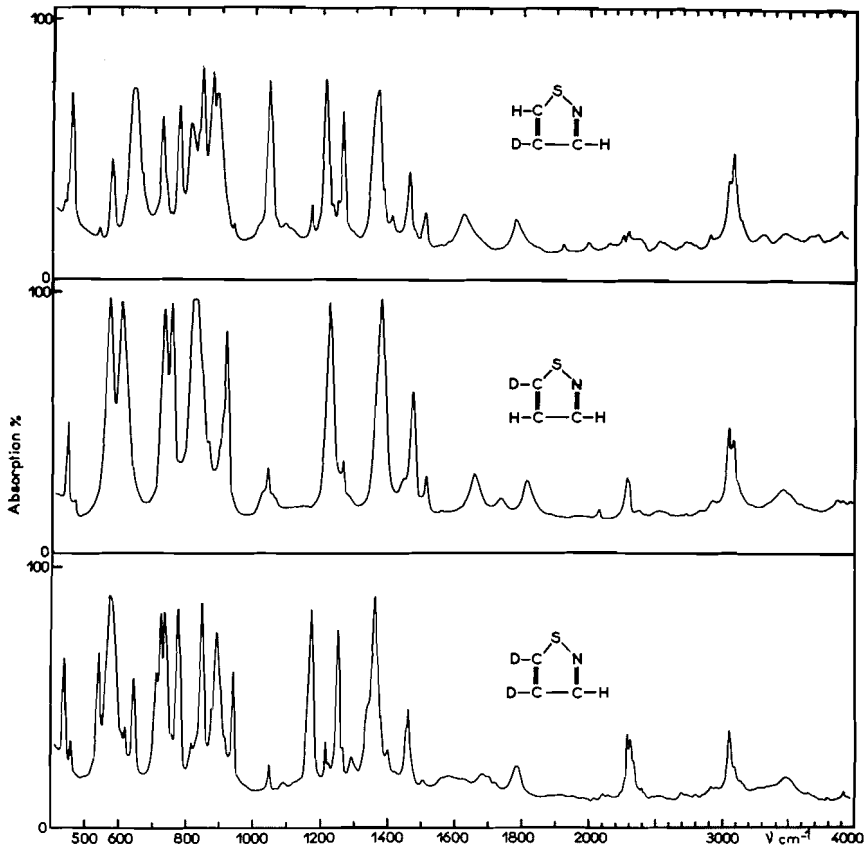

FIG. 1. Spectres i.r. entre 400 et 4000 cm^{-1} des deutério-isothiazoles à l'état liquide.

TABLEAU 2. Spectres i.r. et Raman de l'isothiazole*

Infrarouge†				Raman‡	Attributions		
Vapeur		Solution		Liquide			
ν cm^{-1}	Structure	ν cm^{-1}		ν cm^{-1}	Référence 1	Présent travail	Symétrie
3130 3120 3111	P Q R	3105	8	~3105e	ν_1, ν(CH)	ν(CH)	A′
3101	Q	3086	5	~3088e	ν_2, ν(CH)	ν(CH)	A′
3083 3073 3063	P Q R	3056	9	~3056e	ν_3, ν(CH)	ν(CH)	A′
1824 1814 1802	P Q R	1812	5		$\nu_8 + \nu_{13}$	$2\gamma_1$	
1768 1752	P R	1760	4			$\gamma_1 + \gamma_2$	A′
		1714	3			$2\gamma_2$	
1588 1580 1572	P Q R	1585	6		$\nu_{15} + \nu_{16}$	$\gamma_2 + \gamma_3$	A′
		~1505e				CS_2 ?	

Can. J. Chem. Downloaded from www.nrcresearchpress.com by 210.87.254.40 on 09/05/12
For personal use only.

TABLEAU 2. (*Conclu*)

Infrarouge†				Raman‡			Attributions		
Vapeur		Solution		Liquide					
ν cm^{-1}	Structure	ν cm^{-1}		ν cm^{-1}			Référence 1	Présent travail	Symétrie
1496 1488 1474	P Q R	1484	17	1484	(3/2)	0.30	ν_4, cycle	ω_1	A′
1456	Q	1455	5				$2\nu_{16}$	$2\gamma_3$	
1400 1392 1381	P Q R	1390	105	1392	(6)	0.57	ν_5, cycle	ω_2	A′
1338 1322	Q R	1335 1316	3 3	1342	(2)	0.44	ν_6, cycle $\nu_{17} + \nu_{16}$	$\gamma_2 + \Gamma_2$ $\gamma_3 + \Gamma_1$	A′
		1295	1	1296	(10)	0.31	$\nu_{18} + \nu_{12}$	ω_3	A′
1246 1234	P R	1236	57	1237	(4)	0.27	ν_7, δ(CH)	δ(CH)	A′
		1175f *1110ff*						$2\Gamma_1$ $\omega_7 + \Gamma_2$	A′
1074 1069 1068	P Q Q	1066	24	1071	(5)	0.38	ν_8, δ(CH)	δ(CH)	A′
1065 1060 1056 1051	P Q Q R	1056	29	~1060e			ν_9, cycle	$\Gamma_1 + \Gamma_2$	
1042 1032	Q Q	1040	9	1045	(7)	0.26	ν_8, δ(CH)	δ(CH)	A′
		950	1				$2\nu_{18}$	$2\Gamma_2$	
925 915 908	P Q Q	908	12				ν_{14}, γ(CH)	γ(CH):γ_1	A″
879 871 864	P Q R	869	41	871	(2)	0.27	ν_{11}, cycle	ω_4	A′
858	Q	858	24				ν_{15}, γ(CH)	γ(CH):γ_2	A″
826 818 806	P Q R	815	82	815	(10)	0.27	ν_{12}, cycle	ω_5	A′
768	P	758	44	757	(7)	0.48	ν_{13}	ω_6	A′
740 726 710	P Q R	728	365				ν_{16}, γ(CH)	γ(CH):γ_3	A′
650 636	P R	639	4	639	(8)	0.31	ν_5–ν_{13}	ω_7	A′
606 589 582 573	P Q Q R	587	31				ν_{17}, cycle	Γ_1	A″
493 477 459	P Q R	474	35	476	(1)	0.75	ν_{18}, cycle	Γ_2	A″

*Dans les tableaux 1 à 4, les nombres en italiques correspondent à des fréquences observées à l'état liquide. m, Moyenne; f, faible; ff, très faible; e, épaulement.
†Les fréquences infrarouges à l'état dissous sont accompagnées du coefficient d'extinction molaire apparent.
‡Les fréquences Raman sont suivies de l'intensité relative des raies entre parenthèses et du facteur de dépolarisation.

Analyse des spectres

Nous examinerons, en premier lieu, les vibrations de symétrie A′, puis celles de symétrie A″. Nous dirons ensuite quelques mots sur les vibrations de combinaison.

Les attributions relatives aux vibrations fondamentales des quatre hétérocycles sont réunies dans le tableau 6, et sont aussi mentionnées, ainsi qu'une interprétation possible des principales bandes de combinaison, dans les tableaux 2 à 5.

Can. J. Chem. Downloaded from www.nrcresearchpress.com by 210.87.254.40 on 09/05/12
For personal use only.

TABLEAU 3. Spectres i.r. du deutério-4 isothiazole

Vapeur		Solution			
ν cm^{-1}	Structure	ν cm^{-1}		Attributions	Symétrie
		~3156e			
		3105	4	ν(CH)	A′
3082	P				
3073	Q	3060	8	ν(CH)	A′
3063	R				
2305		*2305*		ν(CD)	A′
2267	P				
2250	R	*2250f*		$\delta_1 + \delta_2$	A′
1788	P				
1778	Q	1782	5	$2\gamma_1$	A′
1770	R				
1615	P				
1598	R	1616	4	$2\gamma_2$	A′
		1515m		CS_2 ?	
		~1511e			
1478	P				
1470	Q	*~1480e*		isothiazole	
1460	Q	1468	9	ω_1	A′
		1416	2	$\omega_5 + \gamma$CD	
		~1390e		isothiazole	
1382	P				
1373	Q	1372	65	ω_2	A′
1371	Q	*~1365e*		D-4,5 isothiazole	
1363	R				
1354	Q	1354	18	$\gamma_1 + \Gamma_2$	A′
~1344e	R				
1280	P				
1272	Q	1268	14	ω_3	A′
1260	R				
		~1252e		D-4,5 isothiazole	
		~1234e		isothiazole	
1223	P				
1210	R	1215	53	δ(CH):(δ_1)	A′
~1180e					
1166		1172	2	D-4 5 isothiazole	
~1115e					
1096		*1095ff*		$\gamma_{CD} + \Gamma_2$	
1054	P				
1046	Q	1046	37	δ(CH):δ_2	A′
1036	R				
		~1015ff			
~954	P				
~940	R	*944f*		D-4,5 isothiazole	
908	Q	~908e		isothiazole	
891	Q	891	57	γ(CH):γ_1	A″
879	Q	878	57	ω_4	A′
868	R				
~858e	P				
849	Q	849	49	ω_5	A′
838	R ?				
~826e					
~818e					
806	Q	809	59	γ(CH):γ_2	A″
795	P				
787	Q	782	61	δ(CD)	A′
777	R				
743	Q	~740e		D-4,5 isothiazole	
~740e	P	731	30	ω_6	A′
~730e	R				

Can. J. Chem. Downloaded from www.nrcresearchpress.com by 210.87.254.40 on 09/05/12
For personal use only.

TABLEAU 3. (*Conclu*)

Vapeur		Solution				
ν cm^{-1}	Structure	ν cm^{-1}			Attributions	Symétrie
726	Q	*~728e*			isothiazole	
709	Q				D-4,5 isothiazole	
~668e		~668e				
659	P					
644	Q	644	279		γ(CD)	A''
629	R Q				ω_7	A'
~592e	P					
589	Q					
584	Q					
577	Q	576	16		Γ_1	A''
560	R					
541	Q	542	1		D-4,5 isothiazole	
477	P					
462	Q	462	44		Γ_2	A''
444	R					

TABLEAU 4. Spectres i.r. du deutério-5 isothiazole

Vapeur		Solution				
ν cm^{-1}	Structure	ν cm^{-1}			Attributions	Symétrie
3116	P					
3106	Q	~3085e			ν(CH)	A'
3083	P					
3073	Q	3058	6		ν(CH)	A'
3062	R					
		2320			ν(CD)	A'
		2290f			$\omega_3 + \delta_2$	
2090	P					
2082	Q	*2080ff*			$2\delta_2$	A'
2070	R					
1812	P					
1803	Q	1804	5		$2\gamma_1$	A'
1794	R					
		1730	1		$\gamma_1 + \omega_5$	
~1654	P					
1644	Q	1651	4		$2\omega_5$	A'
~1634	R					
1536	P					
1519	R	1517			CS_2 ?	
		~1512e				
1485	P					
1470	R	1479	8		ω_1	A'
1434	Q	1432			$\gamma_2 + \gamma$(CD)	
1392	P					
1383	Q	1380	85		ω_2	A'
1373	R					
		~1358e			$\gamma_1 + \gamma_2$	
~1280e						
~1271e		1268	4		ω_3	A'
1232	P					
1218	R	1224	68		δ(CH):δ_1	A'
		~1152ff			$2\Gamma_1$	
1050	P					
1040	Q	1040	6		δ(CH):δ_2	A'
1030	Q				$\Gamma_1 + \Gamma_2$	
~934e						

Can. J. Chem. Downloaded from www.nrcresearchpress.com by 210.87.254.40 on 09/05/12
For personal use only.

TABLEAU 4. (*Conclu*)

Vapeur		Solution			
ν cm^{-1}	Structure	ν cm^{-1}		Attributions	Symétrie
929	P	922	38	ω_4	A′
919	R				
904	Q	904	15	γ(CH):γ_1	A″
		~870e			
~858e				γ(CH):γ_2 ?	
832	P				
826	Q	825	155	ω_5 (et γ_2 ?)	A′
820	Q				
815	R				
775	P				
768	Q	761	61	δ(CD)	A′
~762e	R				
751	P				
739	Q	737	46	ω_6	A′
~732e	R				
726	Q	~728e		isothiazole	
645	Q				
~632e	P?				
622	Q?	626	9	ω_7	A′
620	P				
606	Q	606	82	γ(CD)	A″
603	Q				
590	P R				
~581e					
576	Q	575	160	Γ_1	A″
~571	Q				
561	R				
		476f		isothiazole	
451	Q	450	10	Γ_2	A″

TABLEAU 5. Spectres i.r. du dideutério-4,5 isothiazole

Vapeur		Solution			
ν cm^{-1}	Structure	ν cm^{-1}		Attributions	Symétrie
		~3100e		isothiazole	
3084	P				
3074	Q	3058	10	ν(CH)	A′
3064	R				
		~2340e		2δCH	
		2318m		ν(CD)	A′
		~2310e		$\omega_1 + \omega_5$	
		2295m		ν(CD)	A′
1790	P				
1780	Q	1777	6	$2\gamma_1$	A′
1770	R				
		~1725e			
		~1685ff		$2\omega_5$	
		1510ff		CS_2	
~1466	P				
1457	Q	1465	10	ω_1	A′
		~1455e		$2\omega_6$	
		~1425e			
		1405	3	$2\gamma_2$	
		1384	4	$\omega_5 + \Gamma_1$	
1374	P				
1365	Q	1365	75	ω_2	A′
1355	R				

Can. J. Chem. Downloaded from www.nrcresearchpress.com by 210.87.254.40 on 09/05/12
For personal use only.

TABLEAU 5. (*Conclu*)

Vapeur		Solution			
ν cm^{-1}	Structure	ν cm^{-1}		Attributions	Symétrie
		1332	6	$\gamma_1 + \Gamma_2$	
		1284	5	$\gamma_2 + \gamma_3$	
~1270e		~1265e		D-4 isothiazole	
1254	Q	1254	23	ω_3	A′
~1225e		1225		D-5 isothiazole	
~1214e		1215		D-4 isothiazole	
1180	P	1171	45	δ(CH)	A′
1169	R				
		~1150e		$2\gamma_3$	
		1085ff		$2\Gamma_1$	
~1055	P	1045		D-4 isothiazole	
1048	Q				
~1035	R				
952	P	944	16	ω_4	A′
942	R				
~920e		920		D-5 isothiazole	
907	P	890	48	γ(CH):γ_1	A″
893	Q				
891	Q				
888	Q				
884	Q				
880	Q	~878e		D-4 isothiazole	
861	P	850	54	ω_5	A′
852	Q				
843	R				
826	Q	826		D-5 isothiazole	
808	Q	808		D-4 isothiazole	
796	P	780	39	δ(CD)	A′
788	Q				
786	Q				
784	Q				
782	Q				
776	R				
		~762e		D-5 isothiazole	
752	P	740	42	δ(CD)	A′
743	Q				
~736e					
732	Q	728	31	ω_6	A′
726	?				
709	Q	707	18	γ(CD):γ_2	A″
660	P	644		D-4 isothiazole	
645	Q				
632	R				
		624	5	ω_7	A′
~606e		~606e		D-5 isothiazole	
593	P	576	162	γ(CD):γ_3	A″
578	Q				
562	R				
541	Q	541	29	Γ_1	A″
~526	R				
		460		D-4 isothiazole	
443	Q	441	15	Γ_2	A″

Le tableau 7 contient les rapports de Teller–Redlich observés et théoriques et les sommes des carrés des fréquences expérimentales.

Vibrations de symétrie A′

Nous analyserons successivement les mouvements de valence ν(CX) et de déformation δ(CX) (X = H ou D), puis les oscillations de noyau qui seront notées ω_1 à ω_7.

(1) Vibrations de valence ν(CX)

Oscillations ν(CH)

Les trois bandes d'absorption à 3105, 3086, et 3056 cm^{-1} du spectre i.r. de l'isothiazole ont été

Can. J. Chem. Downloaded from www.nrcresearchpress.com by 210.87.254.40 on 09/05/12
For personal use only.

TABLEAU 6. Fréquences i.r. des vibrations fondamentales de l'isothiazole et des deutério isothiazoles en solution dans des solvants inertes*

Attributions (X = H ou D)	Isothiazole	D-4 Isothiazole	D-5 Isothiazole	D-4,5 Isothiazole
$\nu(C_5X)$	3105 (8)	3105 (4)	2320†	2318†
$\nu(C_4X)$	3086 (5)	2305†	3085 (2)	2295†
$\nu(C_3H)$	3056 (9)	3060 (8)	3058 (6)	3058 (10)
ω_1	1484 (17)	1468 (9)	1479 (8)	1465 (10)
ω_2	1390 (105)	1372 (65)	1380 (85)	1365 (75)
ω_3	1296 (1) et R	1268 (14)	1268 (4)	1254 (23)
$\delta(CH)$	1236 (57)	1215 (53)	1224 (68)	1171 (45)
$\delta(CX)$	1066 (24)	782 (61)	1040 (6)	780 (39)
$\delta(CX)$	1040 (9)	1046 (37)	761 (61)	740 (42)
ω_4	869 (41)	878 (57)	922 (38)	944 (16)
ω_5	815 (82)	849 (49)	**825** (155)	850 (54)
ω_6	758 (44)	731 (30)	737 (46)	728 (31)
ω_7	639 (4) et R	629‡	626 (9)	624 (5)
$\gamma(CH)$	908 (12)	891 (57)	904 (15)	890 (48)
$\gamma(CX)$	858 (24)	644 (279)	858‡ ou **825**	707 (18)
$\gamma(CX)$	728 (365)	809 (59)	606 (82) ou 575	576 (162)
Γ_1	587 (31)	576 (16)	575 (160) ou 606	541 (29)
Γ_2	474 (35)	462 (44)	450 (10)	441 (15)

*Les nombres entre parenthèses sont les coefficients d'extinction molaire apparents. Les nombres en caractères gras correspondent à des fréquences attribuées deux fois. C_iX désigne la liaison CX en position i; R, Raman.
†A l'état liquide.
‡A l'état gazeux.

TABLEAU 7. Rapports de Teller–Redlich et sommes des carrés des fréquences expérimentales*

Symétrie	Rapports de Teller–Redlich	Expérimental	Théorique	Sommes des carrés des fréquences ($S = 10^{-6}\ \Sigma\nu^2$)	
A′	$\pi_{it}/\pi_{D\text{-}4}$	1.95	1.95		
	$\pi_{it}/\pi_{D\text{-}5}$	1.91	1.94	$S_{it} + S_{D\text{-}4,5}$	71.162
	$\pi_{it}/\pi_{D\text{-}4,5}$	3.69	3.76	$S_{D\text{-}4} + S_{D\text{-}5}$	71.148
A″	$\pi_{it}/\pi_{D\text{-}4}$	1.29	1.35		
	$\pi_{it}/\pi_{D\text{-}5}$	1.30† 1.35‡	1.34	$S_{it} + S_{D\text{-}4,5}$	4.786
				$S_{D\text{-}4} + S_{D\text{-}5}$	4.862† 4.808‡
	$\pi_{it}/\pi_{D\text{-}4,5}$	1.81	1.82		

*it, Isothiazole; π, produit de Teller–Redlich.
†Produit et somme calculés avec la fréquence 858 cm^{-1}.
‡Avec la fréquence 826 cm^{-1}.

affectées aux vibrations de valence ν(CH) (1); les raies Raman correspondantes sont faibles (*cf.* tableau 2).

Des bandes i.r. qui, en raison de leurs positions proches de celles des fréquences précédentes, peuvent également être rattachées à des mouvements ν(CH) sont observées, vers 3060 cm^{-1}, dans les spectres des trois dérivés deutériés et vers 3095 ± 10 cm^{-1}, dans ceux des composés monodeutériés (*cf.* tableaux 3 à 5 et fig. 1).

Les résultats expérimentaux sembleraient indiquer que les vibrateurs CH ne sont que faiblement couplés dans les oscillations de valence ν(CH). En effet, le maximum vers 3060 cm^{-1} qui subsiste lors d'une double substitution sur les carbones 4 et 5, paraît appartenir à la vibration mettant plus particulièrement en jeu la liaison CH en 3. Par ailleurs, les mouvements de valence des vibrateurs CH en 4 et en 5 paraissent, respectivement, donner lieu aux sommets vers 3090 et 3110 cm^{-1}, que l'on retrouve dans les spectres des dérivés monodeutériés en position 5 ou 4 (*cf.* tableau 6 et fig. 1).

Ceci n'est, cependant, qu'une première approximation qui devra être vérifiée lorsque, la géométrie de l'isothiazole étant parfaitement

Can. J. Chem. Downloaded from www.nrcresearchpress.com by 210.87.254.40 on 09/05/12
For personal use only.

Can. J. Chem. Downloaded from www.nrcresearchpress.com by 210.87.254.40 on 09/05/12
For personal use only.

connue, il sera possible de comparer les structures prévues et observées des bandes de vibration rotation dues aux oscillations ν(CH). On doit, du reste, remarquer que l'ordre expérimental des fréquences: $\nu(C_5H) > \nu(C_4H) > \nu(C_3H)$, ne coïncide pas avec celui: $\nu(C_3H) > \nu(C_5H) > \nu(C_4H)$, que laisseraient prévoir les valeurs calculées des charges π des atomes de carbone (18).

Oscillations ν(CD)

Dans les spectres i.r. des deutério-4 et dideutério-4,5 isothiazoles à l'état liquide, on peut affecter une bande d'absorption vers 2300 cm^{-1} à la vibration $\nu(C_4D)$, tandis qu'un maximum vers 2320 cm^{-1}, existant à la fois dans les spectres des deutério-5 et dideutério-4,5 isothiazoles, paraît attribuable au mouvement $\nu(C_5D)$ (*cf.* tableau 6).

(2) Vibrations de déformation δ(CX)

Vibrations δ(CH)

Califano *et al.* (1) assignent les vibrations de déformation δ(CH) à 1236, 1066, et 1040 cm^{-1}, dans l'isothiazole. L'intensité et les facteurs de dépolarisation des raies Raman correspondantes, confirment qu'il s'agit bien de modes fondamentaux de symétrie A′ (*cf.* tableau 2). L'interprétation des deux maximums vers 1050 cm^{-1} se trouve justifiée par l'examen des spectres i.r. des trois isothiazoles deutériés. Le spectre du dérivé dideutérié ne présente, en effet, aucune bande i.r. au voisinage de cette fréquence (*cf.* tableau 5 et fig. 1) tandis que celui de chacun des dérivés monodeutériés en comporte une seulement, de type AB à l'état vapeur, qui peut, par conséquent, être rattachée à un mouvement δ(CH) (*cf.* tableaux 3 et 4).

Soulignons, en faveur de l'attribution de la fréquence 1236 cm^{-1} à une vibration de déformation δ(CH), dans le spectre de l'isothiazole, que l'oscillation δ(CH) la plus élevée de nombreux dérivés hétérocycliques pentagonaux, est observée vers 1250 ± 20 cm^{-1} (19–31). Par analogie, nous relions aussi à un mouvement δ(CH), la suite vers 1200 cm^{-1}, composée de bandes i.r. présentant, dans les spectres des deutério isothiazoles à l'état vapeur, des enveloppes de type B (*cf.* tableaux 3 à 5).

Vibrations δ(CD)

Nous affectons à des vibrations de déformation δ(CD), une absorption vers 780 cm^{-1}, dans les spectres des deutério-4 et dideutério-4,5 isothiazoles et vers 750 cm^{-1}, dans ceux de ce dernier composé et du deutério-5 isothiazole (*cf.* tableau 6 et fig. 1). Les contours de type A ou AB de ces bandes, dans les spectres i.r. des dérivés à l'état vapeur, indiquent qu'elles sont bien dues à des vibrations de symétrie A′.

(3) Vibrations de noyau

Isothiazole

Les sept vibrations de noyau dans le plan ont, pour l'isothiazole, été situées par Califano *et al.* (1) à 1484, 1390, 1335, 1056, 869, 815, et 758 cm^{-1} (*cf.* tableau 2).

Or, le spectre Raman de l'isothiazole montre encore, outre des raies plus ou moins intenses, correspondant aux sept fréquences précédentes, deux autres raies de diffusion, fortes et polarisées, à 1296 et 639 cm^{-1}. Celles-ci appartenant incontestablement à des mouvements de noyau dans le plan, l'attribution de Califano *et al.* (1) est incorrecte pour deux des oscillations de noyau de symétrie A′.

Le choix des maximums à 1390, 815, et 758 cm^{-1} doit être maintenu, en raison de leur structure de vibration rotation, dans les spectres i.r. des composés à l'état vapeur et de leur forte activité en i.r. et en Raman. De plus, par comparaison avec le thiazole (19, 20) et le thiophène (21), on peut rattacher les enveloppes de type A, plus faibles, et les deux raies Raman peu intenses, à 1484 et 869 cm^{-1}, aux deux vibrations de noyau de classe A′ restantes.

Quant aux fréquences 1335 et 1056 cm^{-1}, elles doivent être reliées à des oscillations de combinaison (*cf.* tableau 2). La plus élevée n'apparaît, en effet, que très faiblement à la fois en Raman et en i.r. La plus basse se manifeste par une raie Raman faible et par une bande i.r. assez forte, mais dont l'intensité pourrait s'expliquer par un phénomène de résonance de Fermi avec le niveau δ(CH) adjacent à 1040 cm^{-1}.

Deutério isothiazoles

Des suites de bandes i.r. ayant des positions assez voisines de celles des vibrations ω_1 à ω_7 de l'isothiazole, dont on peut, pour cette raison, les rapprocher, peuvent être constituées pour les trois isothiazoles deutériés (*cf.* tableau 6).

Du fait de recouvrements, ou de leur faible intensité, les enveloppes des bandes à 849, 731, et 629 cm^{-1}, à 1268, 737, et 626 cm^{-1} et à 728 et 624 cm^{-1}, ne sont pas bien observées dans les spectres respectifs des deutério-4, deutério-5, et dideutério-4,5 isothiazoles. Par contre, la symétrie A′ de toutes les autres vibrations faisant l'objet des suites ω_1 à ω_7 est bien vérifiée par les structures de type A, B, ou AB des bandes de vibration

Can. J. Chem. Downloaded from www.nrcresearchpress.com by 210.87.254.40 on 09/05/12
For personal use only.

rotation i.r. correspondantes, dans les spectres des composés à l'état vapeur (*cf.* tableaux 3 à 5).

Soulignons que les fréquences rattachées à des oscillations de mode A′ (*cf.* tableau 6), vérifient, de façon satisfaisante, à la fois la règle du produit de Teller–Redlich et celle de la somme des carrés des fréquences expérimentales (*cf.* tableau 7), ce qui justifie l'ensemble des attributions, dans cette classe de symétrie.

Vibrations de symétrie A″

Nous envisagerons d'abord les vibrations de noyau hors du plan, dans l'isothiazole et ses dérivés deutériés, successivement, puis les mouvements de déformation γ(CX).

(1) Vibrations de noyau

Les vibrations de noyau hors du plan sont observées, dans l'isothiazole, à 587 et 474 cm^{-1} (1), nous les avons notées, respectivement, Γ_1 et Γ_2: la plus basse, seule, donne lieu, dans le spectre Raman, à une faible raie dépolarisée (*cf.* tableau 2).

Une suite, formée de bandes de vibration rotation i.r. de type C peut être reliée, dans les spectres des trois dérivés deutériés à l'état vapeur, à une vibration analogue au mouvement Γ_2. Les spectres des trois composés à l'état vapeur montrant deux bandes de type C entre 610 et 540 cm^{-1}, l'oscillation Γ_1 ne peut pas être assignée avec certitude, particulièrement dans le deutério-5 isothiazole, où elle doit être responsable de l'une des deux fréquences 606 ou 576 cm^{-1}. Toutefois, dans les spectres du dideutério-4,5 isothiazole, pour les raisons qui seront discutées par la suite, l'un des mouvements γ(CD) pouvant, vraisemblablement, être situé à 578 cm^{-1}, nous préférons affecter à la vibration de noyau Γ_1 la bande de type C à 541 cm^{-1}.

Dans le cas du deutério-4 isothiazole, la difficulté vient de ce que les deux enveloppes de type C à 577 et 541 cm^{-1} ont des positions identiques à celles observées dans le spectre du dideutério-4,5 isothiazole. Or ce composé constitue, précisément, l'une des impuretés contenues dans l'échantillon de deutério-4 isothiazole examiné (*cf.* tableau 3). Mais, tandis que les intensités relatives des autres bandes i.r. dues au dideutério-4,5 isothiazole d'une part, et du maximum à 541 cm^{-1}, d'autre part, indiquent que dans le spectre du deutério-4 isothiazole, ce dernier sommet provient uniquement de l'impureté, il ne semble pas en être de même pour l'absorption à 576 cm^{-1} dont le coefficient d'extinction molaire est trop important. Comme, par ailleurs, les deux bandes à 576 cm^{-1} n'ont, dans les spectres i.r. du deutério-4 et du dideutério-4,5 isothiazole, ni même profil à l'état liquide (*cf.* fig. 1), ni même structure de vibration rotation à l'état vapeur, on peut envisager que l'absorption à 576 cm^{-1} recouvre, dans le spectre du deutério-4 isothiazole, la vibration γ(CD) du dideutério-4,5 isothiazole et l'oscillation de noyau Γ_1 du deutério-4 isothiazole.

(2) Vibrations de déformation hors du plan γ(CX)

Les vibrations γ(CH) ont été attribuées par Califano *et al.* (1) à 908, 858, et 728 cm^{-1}, dans l'isothiazole; elles ne se manifestent pas dans le spectre de diffusion.

Les spectres i.r. de tous les dérivés deutériés de l'isothiazole, montrent une forte branche Q vers 900 cm^{-1}, appartenant certainement à une bande de vibration–rotation de type C, et pouvant donc être rapprochée de la vibration γ(CH) la plus élevée de l'isothiazole (*cf.* tableau 6).

Dans le spectre i.r. du deutério-4 isothiazole en phase vapeur, on observe deux fortes branches Q à 806 et 726 cm^{-1}, caractéristiques de bandes de type C et une enveloppe de type C, de contour nettement défini, à 644 cm^{-1}. Tandis que ce dernier sommet peut être relié à une oscillation hors du plan γ(CD), la branche Q à 726 cm^{-1}, dont la position est semblable à celle de l'un des mouvements γ(CH) de l'isothiazole, est certainement due à la présence de ce composé à l'état d'impureté. C'est donc l'absorption à 806 cm^{-1} qui doit être affectée à la deuxième vibration hors du plan γ(CH) du deutério-4 isothiazole. Cette interprétation est confirmée par le bon accord entre le produit de Teller–Redlich expérimental, faisant intervenir cette fréquence, et le produit théorique (*cf.* tableau 7).

En ce qui concerne le dideutério-4,5 isothiazole, le spectre i.r. de cet hétérocycle à l'état gazeux montre deux branches Q à 709 et 645 cm^{-1} et une bande de type C à 578 cm^{-1}, résultant de mouvements de symétrie A″. Le maximum à 645 cm^{-1} étant manifestement dû à la présence de deutério-4 isothiazole (*cf.* tableaux 3 et 5), nous affectons les deux autres aux vibrations γ(CD). La bonne concordance entre le produit de Teller–Redlich théorique et celui, calculé avec ces valeurs, justifie cette attribution (*cf.* tableau 7). On note que la bande vers 580 cm^{-1}, assignée à la vibration γ(CD), est large et

Can. J. Chem. Downloaded from www.nrcresearchpress.com by 210.87.254.40 on 09/05/12
For personal use only.

dissymétrique dans le spectre du composé à l'état liquide, (*cf.* fig. 1) et devient fine, symétrique et beaucoup plus intense, dans celui du dideutério-4,5 isothiazole à l'état dissous dans un solvant neutre. C'est ce comportement, analogue à celui de certaines absorptions γ(CH) dans les hétérocycles thiazoliques (19–20), qui nous a incités à choisir, pour la vibration γ(CD), cette fréquence plutôt que celle, plus basse, à 541 cm^{-1}, qui a été rattachée à l'oscillation de noyau Γ_1.

La méthode précédente ne peut servir à reconnaître si la vibration γ(CD) du deutério-5 isothiazole doit être située à 606 ou 576 cm^{-1}, en raison de la trop grande intensité et de la forme mal définie de ces deux bandes i.r. dans le spectre du composé à l'état liquide (*cf.* fig. 1). Par ailleurs, aucune autre enveloppe de type C, susceptible de correspondre au deuxième mouvement γ(CH), n'est observée dans le spectre du deutério-5 isothiazole à l'état vapeur. Toutefois, la position de quatre vibrations de symétrie A'' étant connue, celle de la cinquième peut être déterminée, approximativement, en appliquant les règles isotopiques qui fournissent les fréquences 813 et 830 cm^{-1} (*cf.* tableau 7). On peut, par suite, envisager de relier au deuxième mouvement γ(CH) du deutério-5 isothiazole, soit un fort épaulement à 858 cm^{-1}, vu seulement dans le spectre du composé à l'état vapeur, soit la très forte bande de vibration rotation de type A à 826 cm^{-1}, qui résulterait alors de la superposition de deux mouvements (*cf.* tableau 6).

Vibrations de combinaison

Califano *et al.* (1) ont assigné quelques unes des vibrations de combinaison de l'isothiazole: certaines de ces attributions, principalement en ce qui concerne les combinaisons mettant en jeu les mouvements γ(CH), ne concordent pas avec celles que nous indiquons dans le tableau 2. D'une manière générale, lorsque les bandes i.r., dues aux combinaisons des mouvements γ(CX) ont été mesurées à l'état liquide et à l'état dissous dans un solvant neutre, on constate un glissement de fréquence de même sens que celui observé pour les oscillations γ(CX) (32), ce qui est en faveur de notre interprétation.

1. S. Califano, F. Piacenti, et G. Sbrana. Spectrochim. Acta, **20**, 339 (1964).
2. F. Wille, L. Capeller, et A. Steiner. Angew. Chem. Intern. Ed. Engl. **1**, 335 (1962).
3. R. Raap. Can. J. Chem. **44**, 1324 (1966).
4. R. A. Olofson, J. M. Landesberg, K. N. Houk, et J. S. Michelman. J. Am. Chem. Soc. **88**, 4265 (1966).
5. J.-C. Poite, L. Vivaldi, A. Bonzom, et J. Roggero. C.R. Acad. Sci. **268C**, 12 (1969).
6. J. C. Panizzi, G. Davidovics, R. Guglielmetti, G. Mille, J. Metzger, et J. Chouteau. Can. J. Chem. **49**, 956 (1971).
7. J. H. Griffiths, A. Wardley, V. E. Williams, N. L. Owen, et J. Sheridan. Nature, **216**, 1301 (1967).
8. R. A. Bonham et F. A. Momany. J. Am. Chem. Soc. **83**, 4475 (1961).
9. V. Dobyns, Sr. et L. Pierce. J. Am. Chem. Soc. **85**, 3553 (1963).
10. E. J. Vincent. Thèse Sciences. Marseille, France, 1966.
11. B. Bak, D. Christensen, J. Rastrup-Andersen, et E. Tannenbaum. J. Chem. Phys. **25**, 892 (1956).
12. J. P. Mathieu. Spectres de vibration et symétrie des molécules et des cristaux. Hermann et Cie, Paris, 1945.
13. R. M. Badger et L. R. Zumwalt. J. Chem. Phys. **6**, 711 (1938).
14. W. A. Seth Paul et G. Dijkstra. Spectrochim. Acta, **23A**, 2861 (1967).
15. J. Lecomte. Licht und Materie, Handbuch der physik. XXVIII. Springer, Berlin, 1958. p. 246.
16. E. B. Wilson, J. C. Decius, et P. C. Cross. Molecular vibrations. McGraw-Hill Book Company Inc., New York, N.Y. 1955.
17. G. Herzberg. Infrared and Raman spectra of polyatomic molecules. D. Van Nostrand, New York, N.Y. 1945.
18. R. Phan Tan Luu, L. Bouscasse, E. J. Vincent, et J. Metzger. Bull. Soc. Chim. 3283 (1967).
19. G. Davidovics, C. Garrigou-Lagrange, J. Chouteau, et J. Metzger. Spectrochim. Acta, **23A**, 1477 (1967).
20. G. Davidovics. Thèse Sciences. Marseille, France, 1969.
21. M. Rico, J. M. Orza, et J. Morcillo. Spectrochim. Acta, **21**, 689 (1965).
22. R. C. Lord et F. A. Miller. J. Chem. Phys. **10**, 328 (1942).
23. J. Morcillo et J. M. Orza. Anal. Real. Soc. Espan. Fis. y Quim. **B56**, 253 (1960).
24. P. Mirone. Gazz. Chim. Ital. **86**, 165 (1956).
25. C. Perchard, A. M. Bellocq, et A. Novak. J. Chim. Phys. **62**, 1344 (1965).
26. M. I. V. Soares. Rev. Portug. de Quim. **6**, 112 (1964).
27. M. Rico, M. Barrachina, et J. M. Orza. J. Mol. Spectrosc. **24**, 133 (1967).
28. E. Benedetti, G. Sbrana, et V. Bertini. Gazz. Chim. Ital. **97**, 379 (1967).
29. G. Sbrana, E. Castellucci, et M. Ginanneschi. Spectrochim. Acta, **23A**, 751 (1967).
30. G. Sbrana, M. Ginanneschi, et M. P. Marzocchi. Spectrochim. Acta, **23A**, 1757 (1967).
31. E. Benedetti et V. Bertini. Spectrochim. Acta, **24A**, 57 (1968).
32. J.-L. Meyer. Thèse Doctorat de spécialité. Marseille, France, 1970.

Can. J. Chem. Downloaded from www.nrcresearchpress.com by 210.87.254.42 on 09/05/12
For personal use only.

Solubility of Bromine in Molten Silver Bromide

A. Block-Bolten and S. N. Flengas
Department of Metallurgy and Materials Science, University of Toronto, Toronto 5, Ontario

Received March 8, 1971

The solubility of bromine vapor in molten silver bromide has been measured gravimetrically. At 950 °K the solubility is about 0.4×10^{-4} g-mol of Br_2 per ml of salt, or 14.6×10^{-4} g-mol of bromine per g-mol of salt. At 760 °K the solubility of bromine is about 1.1×10^{-4} mol per ml of salt, or 36.6×10^{-4} g-mol per g-mol of salt.

The solutions were also investigated spectrophotometrically and absorption spectra were compared with the gravimetric results to provide calibration curves. The results indicate that bromine vapor dissolves in the molten AgBr predominantly in the form of Br_3^- anions. Possible molecular solubility is small and cannot be detected by the gravimetric technique. The thermodynamic properties of the solutions are reported, and indicate an exothermic partial molar heat of mixing and negative excess entropies.

On a mesuré gravimétiquement la solubilité des vapeurs de brome dans le bromure d'argent fondu. A 950 °K, la solubilité est approximativement de 0.4×10^{-4} g-mol de Br_2 par ml de sel ou 14.6×10^{-4} g-mol par g-mol de sel. A 760 °K la solubilité du brome est approximativement de 1.1×10^{-4} mol par ml de sel ou 36.6×10^{-4} g-mol par g-mol de sel.

On a aussi étudié les solutions par des méthodes spectrophotométriques et les spectres d'absorption ont été comparés aux résultats gravimétriques afin d'obtenir des courbes de calibration. Les résultats indiquent que le brome à l'état vapeur se dissout dans le bromure d'argent fondu principalement sous forme d'anions Br_3^-. La solubilité moléculaire possible est faible et ne peut être mise en évidence par la technique gravimétrique. Les propriétés thermodynamiques des solutions rapportées indiquent que la chaleur de mélange molaire partielle est endothermique et que les entropies d'excès sont négatives.

Canadian Journal of Chemistry, 49, 2266 (1971)

Introduction

In spite of the large amount of work which is now available on the physical chemical properties of molten salt systems, information regarding the solubility and behavior of reacting gases in molten salts is still scarce. This information is important from the theoretical point of view, and also for the practical purpose of understanding metal–salt corrosion reactions in high temperature electrochemical systems, gas–melt chemical reactions, and also for understanding the limits of purification of salts by degassing techniques.

Previous work in this field includes the work of Flengas and associates on the solubility of the reactive gases $TiCl_4$, $ZrCl_4$, and $HfCl_4$ in molten salts (1–4), and of Morozov and Sun-In-Chzu (5) on the solubility of hafnium and zirconium tetrachlorides in molten alkali chlorides. Other papers on reactive gases in the molten salts are those of Wartenberg (6) on the halogen gases in their alkali and alkaline earth-halides, of Winsor and Cady (7) on HF solubility in CsF, of Burkhardt and Corbett (8) on water vapor solubility in alkali chlorides, of Greenberg and Sundheim (9) on halogen gases in halide eutectic melts, of Shaffer, Grimes, and Watson (10) on HF solubility in molten fluoride mixtures, of Pearce (11) on CO_2 in sodium borate melts, Sachetto, Bombi, and Fiorani (12) on the iodine–iodide system in molten (Li,K) nitrate, of Van Norman and Tivers (13) on chlorine and bromine solubility in lithium, potassium, lead, and silver halides, and that of Ryabuchin (14) on chlorine solubility in alkali chlorides.

In the present work the solubilities of gaseous bromine in molten AgBr have been investigated by both gravimetric and spectrophotometric methods.

Experimental

The solubility of bromine in molten silver bromide was investigated gravimetrically. For the measurements a quartz spring thermobalance, and the Ruska-Worden torsion quartz-fiber type microbalance were used. The experimental apparatuses are shown in Fig. 1. Both designs included a sliding resistance furnace, and an all glass reaction cell which was connected to a liquid bromine reservoir by means of a side-arm glass tube. As the wax in the ground glass joints could not stand the bromine vapors a completely sealed system was used in all the experiments. For measurements the temperature in the reaction cell in the sliding furnace was varied between 742 and 952 °K. To start an experiment a disc of silver metal of known weight of about 5 mm diameter

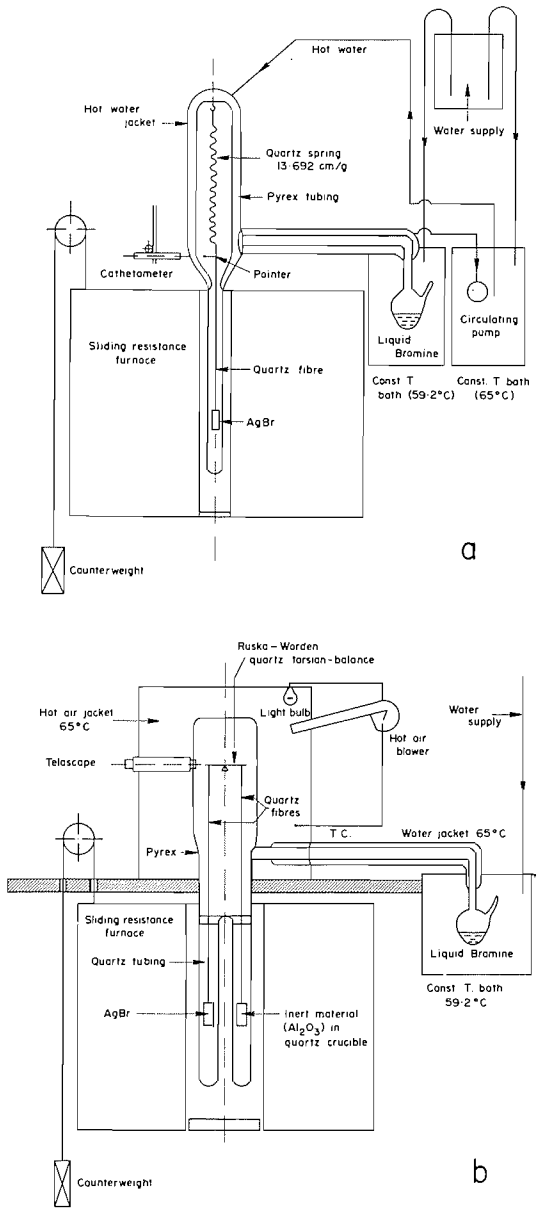

FIG. 1. (*a*) Spring balance apparatus, (*b*) torsion balance apparatus.

was placed at the bottom of the crucible containing the silver bromide, and the apparatus was assembled as shown in Fig. 1. To evacuate the system liquid bromine in its container was frozen using liquid nitrogen. The filling side arm was then flame-sealed under vacuum. The part of the balance containing the crucible was then heated and when temperature equilibrium had been established the temperature of the bromine bath was raised to 59 °C, at which temperature a Br_2 pressure of 1 atm was created throughout the entire system. To prevent the condensation of liquid bromine on the exposed cooler parts of the glass apparatus the double-jacket glass tube shown in the diagram was connected to a recirculating hot water pump, its water temperature being about 65 °C. In the case of the torsion balance a hot air bath replaced the hot water jacket to serve the same purpose. The disc of silver metal was placed inside the AgBr melt used for the solubility measurements for the purpose of promoting the diffusion of bromine into the melt through counter-diffusion of dissolved silver and dissolved bromine. Thus, the overall solubility process may be described by two stages. In the first stage, bromine dissolves in the AgBr melt and then it reacts with the silver metal in solution to produce more silver bromide. When all the silver has been consumed in this manner, excess bromine will dissolve until its solubility limit in the melt is reached. In the actual weight-gain measurement the true solubility was calculated from the total weight gain after subtracting the weight of bromine required to react with all the metallic silver present. In the case of the quartz spring balance, buoyancy corrections were made whilst the Ruska torsion balance did not require any corrections.

Each experimental point was accepted as an equilibrium value after a rest period of at least 24 h, during which numerous intermediate readings were also taken.

The visible spectra of the AgBr–Br_2 system were measured using a Hitachi–Perkin–Elmer 139, u.v.–visible light spectrophotometer modified for high temperature work, as described by Brookes and Flengas (15). The design of the spectrophotometric cell and its attachments was based on the same principle as that for the gravimetric work described above. The quartz optical cell had its optical path reduced through the insertion of precision quartz inserts of 10 mm thickness, and was placed into the furnace of the modified Hitachi–Perkin–Elmer spectrophotometer. The cell was connected by a quartz tube to a heart shaped bromine reservoir, immersed in a controlled-temperature bath. The side-arm tube connecting the spectrophotometric cell to the bromine reservoir was always kept at a temperature higher than the dew point of bromine, as during the gravimetric measurements. Absorption spectra were measured at various cell temperatures and bromine pressures.

Prior to use, the spectrophotometric cells filled with the silver bromide salt were kept under vacuum for several hours at temperatures above the melting point of AgBr, and then the system was sealed under vacuum.

For purposes of comparison the spectra of aqueous solutions of bromine were also obtained. The saturated solutions of Br_2 in aqueous KBr were created directly in an optical cell sealed at the top. The Br_2 pressure inside this system and the bromine solubility was directly dependent upon the temperature of the furnace which was controlled between 15 and 75 °C. This low temperature cell was not supplied with quartz inserts and its light path was 10 mm.

All values of $\ln \tau$, where τ is the transmittance, are given only corrected to a constant sensitivity. For all measurements the spectrophotometer slit was set at 0.5 mm. In the case of the solution of bromine in molten silver bromide the light path was only 0.0425 mm. The wavelength scale of the spectrophotometer was calibrated by means of the 656.1 mμ line of the deuterium u.v. lamp

Can. J. Chem. Downloaded from www.nrcresearchpress.com by 210.87.254.42 on 09/05/12
For personal use only.

Can. J. Chem. Downloaded from www.nrcresearchpress.com by 210.87.254.42 on 09/05/12
For personal use only.

TABLE 1. Solubility measurements of Br_2 in molten AgBr and thermodynamic properties of the solutions (P_{Br_2} = 1 atm)

T (°K)	$\frac{10^4}{T}$	Density* of AgBr (g/ml)	[Br_2] dissolved in AgBr: g-mol/ml $\times 10^4$	[Br_2] dissolved in AgBr: g-mol/g-mol $\times 10^3$	ΔH_{vap} of Br_2 at T (cal/mol)	ΔH_{total}, exp (cal/mol)	$\overline{\Delta H}_{Br_2} = (\Delta H_{total} - \Delta H_{evap})$	ΔG_{evap} of Br_2 at T (cal/mol)	log γ_{Br_2} (Henry)	$\overline{\Delta S}_{Br_2}^{xs}$ (e.u.)	ΔS_{evap} of Br_2 at T (e.u.)	ΔS_{mix} (e.u.)
Spring balance												
862±2	11.61	5.414	0.639	2.22	1858	8270 ±600	−6410	−8940	0.409	−9.3	+12.55	−9.6
897±1	11.15	5.378	0.491	1.71	1542		−6730	−9380	0.475	−9.7	+12.18	−9.2
950±2	10.52	5.323	0.414	1.46	1065		−7210	−10 000	0.513	−10.1	+11.67	−8.8
Torsion balance												
760±2	13.16	5.521	1.076	3.66	2777	8270 ±600	−5490	−7600	0.253	−8.4	+13.69	−10.9
790±1	12.67	5.489	0.985	3.38	2507		−5760	−8010	0.259	−8.5	+13.33	−10.5
810±2	12.35	5.469	0.865	2.97	2326		−5940	−8280	0.319	−8.8	+13.10	−10.2
860±1	11.64	5.418	0.645	2.24	1875		−6400	−8910	0.391	−9.2	+12.57	−9.6
885±1	11.30	5.392	0.543	1.89	1650		−6620	−9230	0.448	−9.5	+12.31	−9.3

*The densities used for the calculation are those of pure liquid AgBr given by Janz (17).

Can. J. Chem. Downloaded from www.nrcresearchpress.com by 210.87.254.42 on 09/05/12
For personal use only.

provided with the instrument. For all other measurements the visible-light tungsten lamp was used. The absorption band for quartz limited the range of those measurements, as below the wavelength of 620 mμ there was considerable interference, and the measured absorptivities had to be corrected for this effect.

Results and Discussion

(a) Solubility Measurements

The results of the solubility measurements are given in Table 1, and plotted in Fig. 2. It may be seen that at 950 °K bromine dissolves in AgBr to the extent of 1.46×10^{-3} g per g-mol of molten silver bromide, and that at 760 °K the solubility increases to 3.66×10^{-3}.

The corresponding concentrations in g-mol/ml salt are 0.414×10^{-4} and 1.076×10^{-4}, respectively.

For the reaction

$$[1] \qquad |Br_2|_{\substack{\text{gas phase}\\ \text{at 1 atm, } T}} = |Br_2|_{\substack{\text{liquid phase}\\ \text{at 1 atm, } T}}$$

the reference states are chosen as follows. For gaseous bromine its standard state represents the state of gaseous Br_2 at 1 atm pressure and any temperature T. For bromine in solution the standard state is taken as the state of pure liquid Br_2 under a pressure of 1 atm and all temperatures.

For reaction 1,

$$\Delta G_R = 0$$

and

$$G^0_{\substack{Br_2,\ \text{gas}\\ 1\ \text{atm},\ T}} = G^0_{\substack{Br_2,\ \text{liquid}\\ 1\ \text{atm},\ T}} + RT \ln a_{Br_2}$$

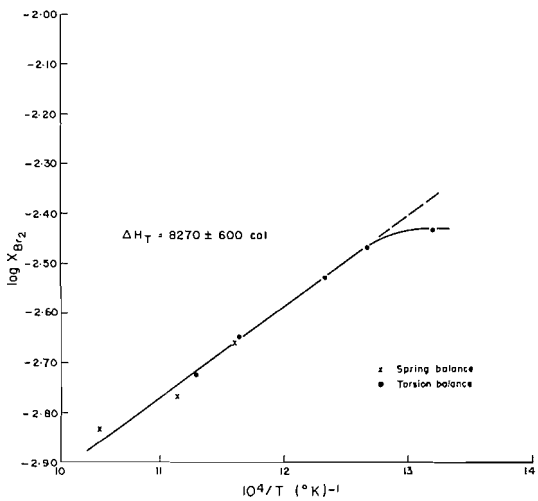

FIG. 2. Plot of log X_{Br_2} *vs.* $1/T$.

where

$$\Delta G^0_{Br_2} = -\Delta G_V{}^0$$

Accordingly

$$[2] \qquad \left[\frac{d \ln a_{Br_2}}{d\left(\frac{1}{T}\right)}\right]_P = \frac{\Delta H_V{}^0}{R}$$

where $\Delta H_V{}^0$ and $\Delta G_V{}^0$ are the heat and the free energy of vaporization of liquid bromine at any temperature. If it assumed that for dilute solutions the activity coefficients are independent of composition and depend only on temperature (Henrian behavior), then this equation may be written as

$$[3] \qquad \left[\frac{d \ln X}{d\left(\frac{1}{T}\right)}\right]_P = \frac{\Delta H_T}{R}$$

where

$$[4] \qquad \Delta H_T = \Delta H_V{}^0 - \overline{\Delta H}_{Br_2}$$

and $\overline{\Delta H}_{Br_2}$ is the limiting heat of mixing of liquid bromine in molten AgBr. Hence, the plot of log x *vs.* $1/T$ should yield a curve having a slope equal to $\Delta H_T/R$.

The plot is presented in Fig. 2. It may be seen that it is linear over the temperature range 950 to 790 °K. Excluding the point at 760 °K, the calculated least-squares slope represent a heat term equal to 8270 ± 600 cal/mol. This uncertainty includes the effect of uncertainty of ±2 °K in the temperature measurements. The solubility measurement at 760 °K, which is close to the melting point of silver bromide, lies outside the least-square curve.

To calculate the partial molar heats of mixing $\overline{\Delta H}_{Br_2}$, the heat of vaporization at each temperature was calculated from tabulated data given in JANAF thermodynamic tables (16). These calculations are included in Table 1. The partial molar heats of mixing which are obtained from eq. 4 are also given in Table 1. It is readily seen that the limiting heats of mixing are exothermic and indicate a slight temperature dependence.

All measurements presented in Table 1 refer to a pressure of 1 atm. Solubilities were also measured at lower pressures, and indicated a pronounced decrease in solubility. Because of the large relative error of these measurements at low solubilities, those values were not too conclusive and shall not be reported. It appears,

Can. J. Chem. Downloaded from www.nrcresearchpress.com by 210.87.254.42 on 09/05/12
For personal use only.

however, that the apparent heat of mixing is independent of pressure.

Considering the mixing reaction to proceed in two steps, *e.g.*

(*a*) $Br_{2\ \underset{1atm,\ T}{gas}} \rightarrow Br_{2\ \underset{1\ atm,\ T}{Pure\ liquid}}$ $\quad \Delta S_1 = -\Delta S_V$

(*b*) $Br_{2\ \underset{1\ atm,\ T}{Pure\ liquid}} \rightarrow (Br_2)_{\ In\ solution}$ $\quad \Delta S_2 = \overline{\Delta S}_{Br_2}$

the total entropy for the solubility process (reaction 1) may be described as

$$[5] \qquad \Delta S_{mix} = -\Delta S_V + \overline{\Delta S}_{Br_2}$$

when ΔS_V is the entropy of vaporization of Br_2 at a temperature T, and $\overline{\Delta S}_{Br_2}$ is the partial molar entropy of mixing of liquid bromine. The excess partial molar entropy of mixing is given as

$$\overline{\Delta S}_{Br_2}{}^{XS} = \overline{\Delta S}_{Br_2} - \overline{\Delta S}_{ideal}$$

where, $\overline{\Delta S}_{ideal}$ is the configurational component of the entropy of mixing based on the mole fraction concentration scale.

The excess partial molar entropy of mixing may be calculated directly from the expression

$$[6] \qquad \overline{\Delta S}_{Br_2}{}^{XS} = (\overline{\Delta H}_{Br_2} - RT \ln \gamma_{Br_2})/T$$

and may be taken to represent vibrational contributions. Values for the excess entropies and for the total entropy of mixing for reaction 1, as calculated from eqs. 5 and 6, are also listed in Table 1.

From these calculations, the partial molar heats of mixing between 760 and 950 °K, are exothermic and change from about $-5\,500$ to $-7\,200$ cal/mol, respectively. The corresponding excess entropies of mixing are also negative and also vary from -8.4 to -10.1 e.u.

The exothermic heats and the negative excess entropies of solution indicate that the solution process involves strong interactions between Br_2 and bromide ions in the melt. The magnitude of solubility of bromine found in the present study is in agreement with the predictions by Greenberg and Sundheim (9), and by Wartenberg (6). By analogy with the mechanism of solubility in the other reactive halogen gases, the solubility of bromine may be described by the reaction

$$[7] \qquad Br_{2\ (gas)} + Ag^+Br^-{}_{liquid} \rightarrow Ag^+Br_3^-{}_{liquid}$$

where the Br_3^- anion is thought (9, 18) to represent a triplet resulting from an ion–dipole type interaction of the structure $Br^-(Br^+ \ldots Br^-)$

(b) Spectrophotometric Measurements

The observed absorption spectra are limited by the absorption band for quartz. The wavelength range below 620 mμ is dominated by the absorption of the quartz cells. Above this range the spectra characteristic of the solutions are evident and may be described by a single peak, the position of which depends upon temperature and the concentration of the bromine species which is taken to be pressure dependent. The transition between transmission and absorption is rather abrupt as it occurs over a wavelength change of less than 50 to 60 mμ. As quartz still shows some absorbance in this range, all observed spectrograms had to be corrected for the corresponding quartz absorbance at each wavelength. In fused salt spectra of this type the reported characteristic wavelengths are usually those representing the transition between absorption and transmission. In this paper, because of the observed short range for this transition, only maximum transmittance wavelengths shall be reported.

The absorption spectrum of pure molten AgBr has been reported by Sundheim and Greenberg (19). At 454 °C, it is characterized by a single peak which rises rather abruptly. The wavelength λ_0, representing the mid-point between peak absorption and peak transmission, depends on temperature and at 454 °C, it is given as 600 mμ. Spectra of this kind have been interpreted as due to a change transfer between Br^- anions and the surrounding cations. The spectra of the solutions of bromine in molten AgBr are similar and the maximum transmission occurs at slightly higher wavelengths: λ_0 as well as peak transmittance are shifted towards higher wavelengths as the temperature is increased. In the present system the shift of λ_0 with temperature is about 55 mμ per 200 °C. The pressure effect is less consistent. As the pressure is increased the concentration of bromine in the liquid increases. However, at temperatures between 760 and 820 °K, an increase in pressure shifts the peak transmittance towards shorter wavelengths. At higher temperatures, between 820 and 950 °K, an increase in pressure has no significant influence on the wavelength of peak transmittance. The pressure–temperature dependence of peak transmittance for those solutions is given in Fig. 3. The curve at $P = 1$ atm in this figure corresponds to the solubility measurements de-

Can. J. Chem. Downloaded from www.nrcresearchpress.com by 210.87.254.42 on 09/05/12
For personal use only.

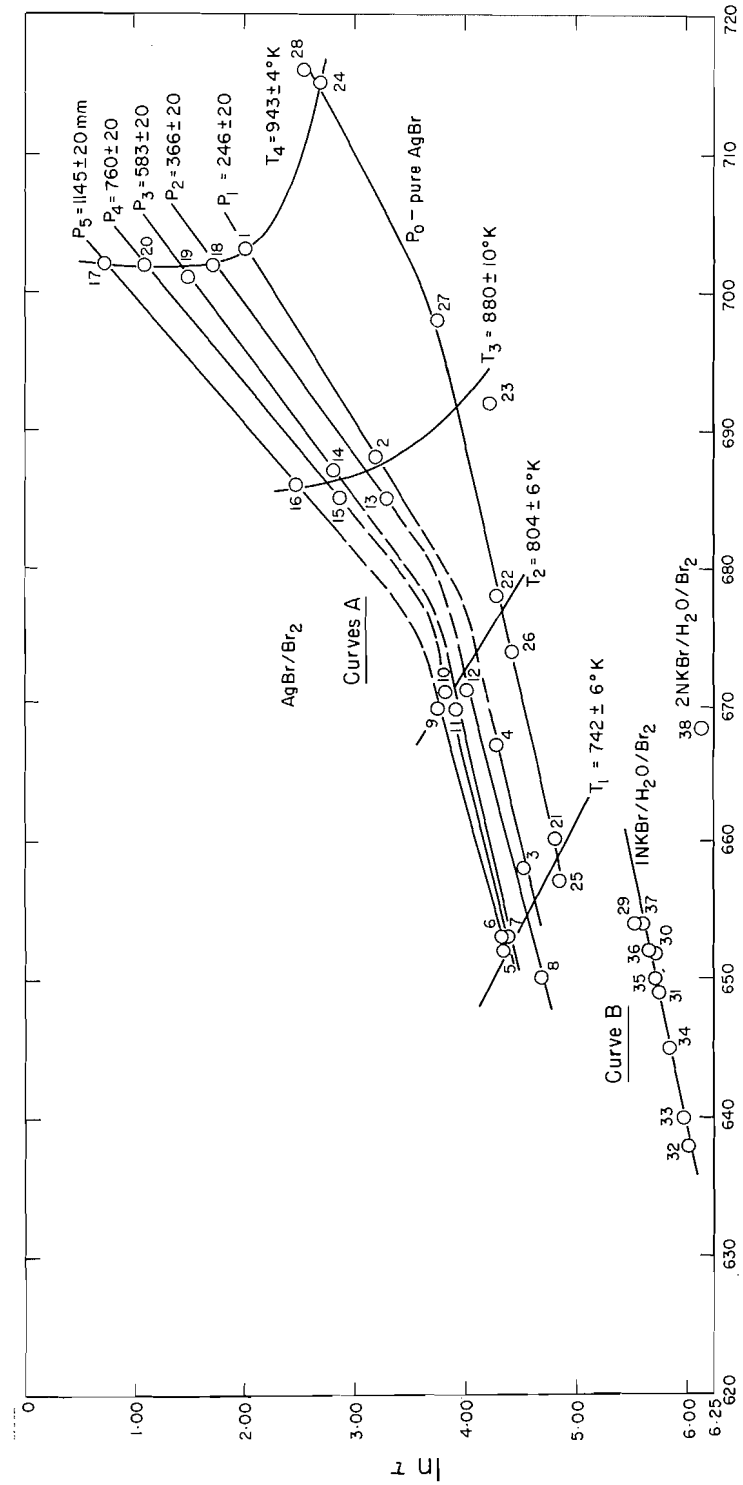

FIG. 3. Shift of transmittance maxima with changing temperature and bromine pressure.

Can. J. Chem. Downloaded from www.nrcresearchpress.com by 210.87.254.42 on 09/05/12
For personal use only.

TABLE 2. Transmittance maxima

Run No.	P_{Br_2} (mm Hg)	T (°K)	Wavelength (±1 mμ)	ln τ
AgBr–Br₂				
1	234 p_1	945 T_4	703	2.027
2	234 p_1	871 T_3	688	3.199
3	266 p_1	740 T_1	658	4.544
4	246 p_1	804 T_2	667	4.293
5	1140 p_5	737 T_1	652	4.380
6	760 p_4	736 T_1	653	4.406
7	570 p_3	734 T_1	653	4.420
8	370 p_2	739 T_1	650	4.696
9	1140 p_5	808 T_2	670	3.770
10	740 p_4	809 T_2	671	3.837
11	570 p_3	807 T_2	670	3.940
12	383 p_2	810 T_2	671	4.033
13	346 p_2	873 T_3	685	3.300
14	603 p_3	873 T_3	687	2.821
15	760 p_4	870 T_3	685	2.886
16	1145 p_5	870 T_3	686	2.485
17	1164 p_5	944 T_4	702.5	0.744
18	386 p_2	943 T_4	702	1.741
19	577 p_3	943 T_4	701	1.504
20	900 p_4	947 T_4	702	1.099
21	— p_0	748 T_1	660	4.820
22	— p_0	798 T_2	678	4.288
23	— p_0	889 T_3	692	4.228
24	— p_0	940 T_4	715	2.701
25	— p_0	747 T_1	657	4.887
26	— p_0	799 T_2	674.5	4.431
27	— p_0	890 T_3	698	3.752
28	— p_0	939 T_4	716	2.549
1 N KBr – Water – Bromine				
29	1140	345	654	5.578
30	760	331	652	5.721
31	537	322	649	5.774
32	140	289	638	6.022
33	147	290	640	5.983
34	380	312.5	645	5.852
35	576	324.5	650	5.728
36	770	332	652	5.693
37	1140	345	654	5.603
2 N KBr – Water – Bromine				
38	576	324.5	668	6.170

scribed earlier. The detailed data are summarized in Table 2.

Figure 3 also contains the shift in peak transmittance for aqueous solutions of bromine in 1 and 2 *N*, KBr, respectively. The temperature behavior is similar as in the fused salt systems. However, peak transmittances for the aqueous solutions are shifted towards slightly shorter wavelengths. The increase of concentration of KBr from 1 to 2 *N*, which is expected to increase the solubility of bromine as Br_3^-, shifts further the peak transmittance to longer wavelengths and higher transmittances. However, it is significant that in both systems transmittance occurs in a wavelength range which varies only between 640 and 720 mμ, indicating the similarity of the two processes.

It should be noted that u.v. spectra in aqueous solutions (20) have indicated that a very small proportion of the total solubility may be attributed to the presence of molecularly dissolved Br_2. However, this amount is usually three to four orders of magnitude lower than the ionic solubility as Br_3^- and cannot be detected in macroscopic gravimetric measurements. In a molten bromide salt where the activity of Br^- is higher than in any possible aqueous solutions, the equilibrium favors the formation of Br_3^- ions, particularly at low temperatures, and the molecular solubility should be expected to decrease further.

It appears, therefore, that the shift in the transmittance curves in the present system, as compared to that occurring in pure molten silver bromide, indicates that the charge transfer between the Br_3^- triplet and the surrounding Ag^+ is requiring lower energies at higher temperatures.

At low temperature, between 740 and 800 °K, the solubilities are high and the solutions have an orange-reddish color. This color changes to deep red at the higher temperatures up to 950 °K, for which the total solubilities of bromine have decreased considerably. The transmittance isobars appear to indicate differences in the absorption mechanisms at temperatures below and above about 820 °K. At a given bromine pressure the shift in transmittance peaks with temperature indicates that the solution becomes more opaque as the temperature is increased. The two possible absorption mechanisms indicated by the change in slope in the transmittance curves, could be attributed to the existence of two kinds of soluble Br_2 in these melts. At low temperatures the higher energy charge transfer type transition should correspond to bromine dissolved in its ionic form as Br_3^-.

At temperatures higher than 820 °K where the solubilities are lower, the higher absorptivity could indicate the presence of some molecularly dissolved bromine.

The molecular and ionic mechanism for the solubility of halogens in molten salts is also supported by recent electrochemical measurements on an iodine–iodide electrode in molten salts by Sachetto, Bombi, and Fiorani (12).

However, it should be understood that the thermodynamic evidence from the gravimetric measurements indicates that the Br_3^- type inter-

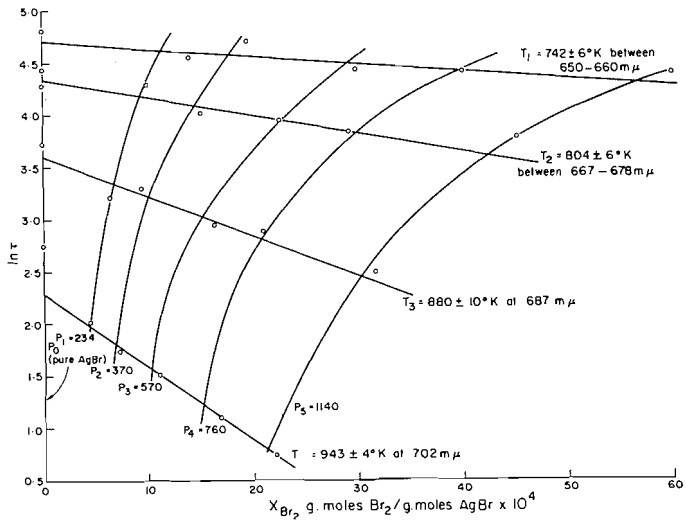

FIG. 4. Calibration curves based on peak transmittance for bromine solubility at various temperatures and bromine pressures.

action is probably the main effect determining the solubility in this system.

The transmittance curves in Fig. 3 may be used as a calibration method for the purpose of calculating the solubility of bromine in molten AgBr at various pressures of bromine.

Thus from the transmittance isobar at P_{Br_2} = 1 atm and various temperatures, Henry's law may be written as

$$X_{Br_2} = KP$$

where, X_{Br_2} is the mole fraction of soluble bromine and K is Henry's law solubility constant which is only temperature dependent. From the measured solubility at P = 1 atm pressure and various temperatures, the solubility at other pressures may be calculated as

$$(X_{Br_2})_{P,T} = (X_{Br_2})_{1\ atm,\ T}P$$

The calibration plot of ln τ *vs.* mole fraction of soluble bromine at various pressures for four isotherms is given in Fig. 4. It may be seen that ln τ is a linear relation of X, as expected, and the isotherms intercept zero solubility at transmittance values close to those representing pure silver bromide. In a sense this limiting value represents the solubility of bromine in silver bromide at a pressure P_0 equal to the bromine decomposition pressure of the salt.

In conclusion, the combined solubility and spectrophotometric measurements support the existence of Br_3^- species in these solutions and that the solubility reaction is exothermic and accompanied by a decrease in entropy. It is obvious that when a gaseous molecule dissolves in a liquid it must loose its vibrational and translational degrees of freedom and by necessity acquire the vibrational characteristics of the form in which it appears in the liquid phase.

However, the calculation of excess entropies is based on the assumption that the configurational component of the entropy of mixing is totally random. If the species in solutions are not randomly distributed then the excess entropy cannot be identified entirely with vibrational contributions.

We express our gratitude to Mr. R. H. Chappell for his considerable effort and time in preparing the glass components of our apparatus.

1. S. N. FLENGAS. Ann. N.Y. Acad. Sci. **79**, 853 (1960).
2. R. L. LISTER and S. N. FLENGAS. Can. J. Chem. **43**, 2947 (1965).
3. J. E. DUTRIZAC and S. N. FLENGAS. Can. J. Chem. **45**, 2317 (1967).
4. S. N. FLENGAS and P. PINT. Can. Met. Quart. **8**, 151 (1969).
5. I. S. MOROZOV and SUN-IN-CHZU. Russ. J. Inorg. Chem. **4**, 307 (1959); **4**, 1176 (1959).
6. V. H. WARTENBERG. Zft. f. Electrochem. **32**, 330 (1926).
7. R. V. WINSOR and G. H. CADY. J. Am. Chem. Soc. **70**, 1500 (1948).
8. W. J. BURKHARD and J. D. CORBETT. J. Am. Chem. Soc. **794**, 6361 (1957).

Can. J. Chem. Downloaded from www.nrcresearchpress.com by 210.87.254.42 on 09/05/12
For personal use only.

9. J. GREENBERG and B. R. SUNDHEIM. J. Chem. Phys. **29**, 1029 (1958).
10. J. H. SHAFFER, W. R. GRIMES, and G. M. WATSON. J. Phys. Chem. **63**, 1999 (1959).
11. M. L. PEARCE. J. Am. Ceram. Soc. **48**, 175 (1965).
12. G. A. SACHETTO, G. G. BOMBI, and M. FIORANI. J. Electroanal. Chem. **20**, 89 (1969).
13. J. D. VAN NORMAN and R. J. TIVERS. Molten salts. *Edited by* Gleb Mamantov. M. Dekker, New York, London. 1969. pp. 509–527.
14. Y. M. RYABUKHIN. Russ. J. Inorg. Chem. Engl. Transl. **7**, 565 (1962).
15. H. C. BROOKES and S. N. FLENGAS. Can. J. Chem. **48**, 55 (1970).
16. JANAF Thermochemical Tables. National Bureau of Standards.
17. G. J. JANZ. Molten salts handbook. Academic Press, New York. 1967.
18. G. ZIMMERMAN and F. C. STRONG. J. Am. Chem. Soc. **79**, 2063 (1957).
19. B. R. SUNDHEIM and J. GREENBERG. J. Chem. Phys. **28**, 439 (1958).
20. L. I. KATZIN. J. Chem. Phys. **20**, 1165 (1952).

Can. J. Chem. Downloaded from www.nrcresearchpress.com by 210.87.254.42 on 09/05/12
For personal use only.

Can. J. Chem. Downloaded from www.nrcresearchpress.com by 210.87.254.40 on 09/05/12
For personal use only.

Production of Electrons by Reaction of Sodium with Methanol and Ethanol: Kinetics of their Formation and Subsequent Reactions[1]

J. W. FLETCHER AND P. J. RICHARDS

Physical Chemistry Branch, Atomic Energy of Canada Limited, Chalk River Nuclear Laboratories, Chalk River, Ontario

Received December 3, 1970

In the reaction of sodium with alcohols an electron is generated without the formation of other reactive products. This, therefore, provides an excellent system to study the reactions of the electrons with themselves, with the solvent, and with added scavengers. A mathematical treatment for such formation and reaction has been derived.

Evidence for a bimolecular electron reaction was investigated by observing the formation of D_2 in the reaction of sodium with ethanol-d_1 or methanol-d_1, via reaction

$$e_{ROD}^- + e_{ROD}^- \rightarrow D_2 + 2RO^-$$

A calculated rate constant for this reaction in ethanol at 25 °C, $k = (5 \pm 4) \times 10^9\ M^{-1}\ s^{-1}$, similar to that observed for the equivalent reaction in water, is obtained. An isotope effect ($\alpha = 2$) for the above reaction in both ethanol and methanol is observed. This would indicate the formation of an electron dimer $(e^-)_2$ as an intermediate in the formation of hydrogen as has been suggested for the equivalent reaction in water.

Lors de la réaction entre le sodium et des alcools, un électron est engendré sans formation d'autres produits réactifs. Ceci fournit ainsi un excellent système pour étudier les réactions des électrons entre eux, avec le solvant et avec des agents capteurs ajoutés. Un traitement mathématique pour de telles formations et réactions en a été déduit.

La preuve d'une réaction des électrons bimoléculaire a été recherchée en observant la formation de D_2 dans la réaction entre le sodium et l'éthanol-d_1, ou le méthanol-d_1, au moyen de la réaction

$$e_{ROD}^- + e_{ROD}^- \rightarrow D_2 + 2RO^-$$

Une constante de vitesse calculée est obtenue pour cette réaction dans l'éthanol à 25 °C $k = (5 \pm 4) \times 10^9\ M^{-1}\ s^{-1}$, et il apparaît que celle-ci est très semblable à celle observée pour la même réaction dans l'eau. Un effet isotopique ($\alpha = 2$) pour la réaction ci-dessus est observé à la fois dans l'éthanol et le méthanol; ceci prouverait la formation d'un électron dimère $(e^-)_2$ en tant qu'intermédiaire dans la formation d'hydrogène, comme cela a été suggéré pour la même réaction dans l'eau.

Canadian Journal of Chemistry, 49, 2275 (1971)

Introduction

Bennett *et al.* (1) have observed the electron as an intermediate in the reaction of sodium with solid alcohol, both optically and by electron spin resonance (e.s.r.) in a rotating cryostat experiment. Shaede and Walker (2) have obtained chemical evidence that the electron is an intermediate in the reaction of sodium with liquid water. Therefore it would be expected that the electron would also be formed in liquid alcohols

[1] $$Na + ROD \rightarrow e_{ROD}^- + Na^+$$

where ROD represents an alcohol deuterated in the oxy position.

The formation of the electron is demonstrated by the addition of an electron scavenger such as N_2O with the resultant formation of N_2, as has been observed in the aqueous system (2). In the absence of electron scavengers two modes of electron decay are possible, *i.e.* either pseudo first order decay or bimolecular recombination. Using pure alcohol deuterated in the oxy position the former can be represented by reaction 2 to produce HD.

[2*a*] $$e_{ROD}^- + ROD \rightarrow RO^- + D$$

[2*b*] $$D + ROD \rightarrow (R - 1)CHOD + HD$$

A bimolecular electron decay reaction has been shown to occur in aqueous solutions (3, 4). Formation of deuterium in isotopic studies (4) has been used as evidence for the occurrence of the bimolecular reaction in the aqueous system and by analogy it can be assumed that in oxy deuterated alcohol the deuterium would be

[1]AECL No. 3896.

TABLE 1. Reaction of sodium with alcohol: production of hydrogen

Alcohol	Temperature (°C)	Products (%) D_2	Products (%) HD	N_A (mol s^{-1} cm^{-2})
CH_3CH_2OD	25	96±1	4±1	4×10^{-6}
	−78	82±2	18±2	4×10^{-8}
CH_3OD	25	96±1	4±1	10×10^{-6}

formed by the bimolecular electron reaction 3.

[3] $$e_{ROD}^- + e_{ROD}^- \rightarrow 2RO^- + D_2$$

The assumption is consistent with the results given in the paper. In this work the relative importance of reactions 2 and 3 have been investigated by measurement of the ratio of HD to D_2.

In the sodium alcohol system the sodium ion produced does not react with the electron whereas the radiolytically produced acetaldehyde and positive ion (ROH_2^+) do.

[4] $$e_{ROD}^- + ROD_2^+ \rightarrow D + ROD$$

Thus the electron disappears only by the pseudo first order reaction 2 and the bimolecular reaction 3, in competition with each other. The relative importance of reaction 2 can be increased by dilution with ether, which is unreactive towards sodium in alcohol, to decrease the rate of electron formation and hence the electron concentration. Electron scavengers can also be added to compete with reactions 2 and 3.

It is observed that the reactions involved in this system do not obey simple homogeneous kinetics as a result of high electron concentration gradients originating at the surface of the sodium. In this paper a mathematical treatment of the system using a combination of homogeneous and diffusion kinetics has been developed to explain the experimental results.

Experimental

The sodium was handled in an inert atmosphere dry box. A clean piece of sodium was placed in a sodium press and extruded in wire form as required. In most experiments a 1 cm length of 0.006 in. diameter sodium wire was used. It was placed in a double valved side arm of a reaction vessel to which 5 ml of alcohol had previously been added and degassed. The side arm was evacuated and the measured amount of sodium added to the alcohol and allowed to completely react. The resulting hydrogen was pumped off, after freezing the alcohol, and analyzed by a CEC 21-130 mass spectrometer. The rate of dissolution of sodium was obtained from the rate of weight loss from a flat piece of sodium of known surface area.

Reagents

The anhydrous ethanol was obtained from Commercial Alcohols and purified by distillation through a spinning band column (5). Shawinigan Chemical Reagent grade methanol was vacuum distilled with only the middle fraction being used. The ethanol-d_1 and methanol-d_1 were used as received from Merck, Sharpe and Dohme and were stated to be better than 99% deuterium. Nuclear magnetic resonance (n.m.r.) analysis of one lot of ethanol gave >99.5%. Fisher anhydrous ether was dried with and stored over sodium. J. T. Baker Analyzed Reagent dry sodium was used as received.

Results

In pure ethanol-d_1 and methanol-d_1, the reaction of sodium with the alcohol at room temperature leads to the formation of hydrogen which is mainly D_2 (Table 1). When the reaction temperature is lowered to −78 °C the percentage D_2 is lowered (Table 1). The lowering of the reaction temperature to Dry Ice temperature also decreases the rate of dissolution (N_A) of the sodium and hence the rate of formation of the electron in ethanol from 4×10^{-6} to 4×10^{-8} mol s^{-1} cm^{-2} as shown in Table 1.

Dilution of the alcohol-d_1 with undeuterated alcohol increases the relative proportion of HD and H_2 in the hydrogen produced as shown in Fig. 1.

The addition of N_2O to the pure ethanol-d_1 before reaction with the sodium results in N_2 being formed. The amount of N_2 formed is a function of the N_2O concentration as is given in Table 2. The total gas yield was 0.7 ± 0.3 mol of gas per mol of sodium added and remained relatively constant over the N_2O concentration studied. The large errors in the absolute yield arise from the difficulty in determining the exact amount of sodium added, however, the relative amounts of hydrogen and nitrogen can be accurately determined. The addition of electron scavengers which compete with the N_2O for the electrons, leads to a reduction in the percentage N_2 yield. For example a solution of 0.2 *M* hydrogen chloride and 0.2 *M* N_2O leads to an

Can. J. Chem. Downloaded from www.nrcresearchpress.com by 210.87.254.40 on 09/05/12
For personal use only.

TABLE 2. Reaction of sodium with alcohol: formation of nitrogen in the presence of nitrous oxide

		% N_2 in gas collected		
	$[N_2O]$, M	Experimental	Computer calculation	Simple homogeneous reaction kinetics
Pure Ethanol				
	10^{-4}	1±1	2.4	30
	10^{-3}	7±3	10	80
	10^{-2}	16±4	45	98
	10^{-1}	40±5	59	99.7
	10^{-0}	75±5	75	100
90% Ether				
	1.3×10^{-3}	98±2	92	
	1.4×10^{-2}	98±2	99.4	

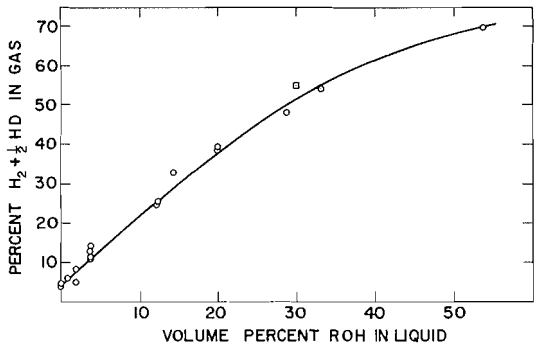

FIG. 1. Atom percent hydrogen as a function of added alcohol-OH: ○, methanol, individual experimental observations; □, ethanol, individual experimental observations. The curve is calculated by first subtracting the hydrogen yield from the competing 1st order decay, then using a value of $\alpha = 2$. In pure alcohol-d_1 the hydrogen formed is $<1\%$ H_2.

experimental yield of 2% nitrogen and 98% hydrogen, while a solution of 0.2 M N_2O yields 45% nitrogen. The addition of C_6F_{12} to an ethanolic N_2O solution also reduces the nitrogen yield. The percentage nitrogen yield at a given N_2O concentration is increased by the addition of an inert solvent (diethyl ether) to the ethanol. In 90% ether solution N_2O is $\geqslant 10^3$ times as effective in scavenging the electron as it is in pure ethanol (Table 2).

Discussion

The results obtained using N_2O as an electron scavenger, both by itself and in competition with a second electron scavenger (Table 2), indicate that the electron is formed as an intermediate in the reaction of sodium with alcohols to give hydrogen.

In pure alcohol the yield of hydrogen from reaction 3 should be one half mole per mole of sodium reacted, while in N_2O solutions the yield of N_2 from reaction 5 should tend towards unity with increasing N_2O concentration

$$[5] \qquad N_2O + e_{ROD}^- \rightarrow N_2 + O^-$$

However, due to the large errors in the absolute yield measurements noted in the Results section this could not be quantitatively demonstrated.

(1) Bimolecular Reaction

The large percentage of D_2 obtained in pure ethanol-d_1 (Table 1) can by analogy with the aqueous system (4) be assumed to be due to the bimolecular decay of the electron (reaction 3), and indicates that this reaction is more important than the pseudo first order decay (reaction 2) which produces HD.

$$[2] \qquad e_{ROD}^- + ROD \xrightarrow{k_2} HD + (R-1)CHOD$$

$$[3] \qquad e_{ROD}^- + e_{ROD}^- \xrightarrow{k_3} D_2 + 2RO^-$$

Knowing the rate of reaction 2 an estimate can be made of k_3, the rate constant for reaction 3.

The formation and decay reactions 1, 2, and 3 involve spacial inhomogeneity, since they occur at or near the surface of the sodium. Hence calculation of the reaction rate must include the diffusion of the electron from the surface. Before this can be done a mathematical model must be developed. It is postulated that the electron is formed at the surface of the sodium which for purposes of calculation is assumed to be flat. The electron subsequently diffuses away and ultimately reacts. Since the reaction distances are very small (Fig. 2), thermally induced convection currents can be neglected. The use of elementary

Can. J. Chem. Downloaded from www.nrcresearchpress.com by 210.87.254.40 on 09/05/12
For personal use only.

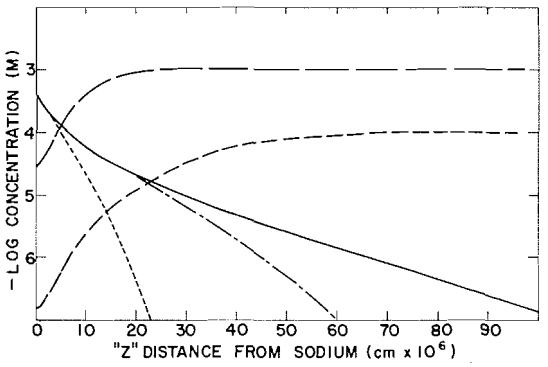

FIG. 2. Electron and N_2O concentration as a function of distance from the sodium surface. Electron concentration profile: ——, $[N_2O] = 0$; ----, $[N_2O] = 10^{-4}$; ------, $[N_2O] = 10^{-3}$. N_2O concentration profile: – –, $[N_2O] = 10^{-4}$; — —, $[N_2O] = 10^{-3}$.

diffusion theory combined with homogeneous chemical reaction kinetics (6), leads to eqs. 6 and 7 at steady state.

$$[6] \quad (dN_A/dZ) \times 10^3 + k_2C_A + (2k_3)C_A^2 = 0$$

The concentration gradient established by diffusion is related to a molar flux (N_A) as follows

$$[7] \quad N_A = -D_A(dC_A/dZ) \times 10^{-3}$$

where N_A = molar flux for electrons produced from Na reaction (mol s^{-1} cm^{-2}), D_A = diffusion constant (cm^2 s^{-1}), C_A = electron concentration (M), k_2 = rate constant for reaction 2 (s^{-1}), k_3 = rate constant for reaction 3 (M^{-1} s^{-1}), Z = distance from sodium surface (cm).

Combining eqs. 6 and 7 gives

$$[8a] \quad -D_A \frac{d^2C_A}{-dZ^2} + k_2C_A + (2k_3)C_A^2 = 0$$

and solving for the first differential gives

$$[8b] \quad \frac{dC_A}{dZ} = -\left(\frac{k_2}{D_A} C_A^2 + \frac{(2k_3)}{D_A}\frac{2}{3} C_A^3\right)^{\frac{1}{2}}$$

The experimentally observed HD-to-D_2 ratio can be expressed in terms of the electron concentration as follows

$$[9a] \quad \frac{[HD]}{[D_2]} = \frac{\int_0^\infty k_2C_A\,dZ}{\int_0^\infty (2k_3)C_A^2\,dZ}.$$

Substituting dZ from eq. 8b in eq. 9a and integrating gives

$$[9b] \quad \frac{[HD]}{[D_2]} = \frac{\frac{3k_1^{3/2}D_A^{1/2}}{(2k_2)}[(b+1)^{\frac{1}{2}} - 1]}{\frac{1}{2}\frac{3k_1^{3/2}D_A^{1/2}}{(2k_2)}[2 - (2-b)(1+b)^{\frac{1}{2}}]} = \frac{2((b+1)^{\frac{1}{2}} - 1)}{2 - (2-b)(1+b)^{\frac{1}{2}}}$$

where

$$[9c] \quad b \text{ (dimensionless parameter)} = \frac{2}{3}\frac{(2k_3)}{k_2} C_{A_0}$$

C_{A_0} represents the electron concentration at the surface of the sodium. A second independent eq. 10 is obtained by combining eqs. 8 and 7 as $Z \to 0$

$$[10] \quad \frac{2}{3}(2k_3)C_{A_0}^3 + k_2C_{A_0}^2 = \frac{N_A^2}{D_A} \times 10^6$$

At 25 °C the empirical "b" value (Table 3) was calculated to be 30 from eq. 9b using the experimental HD to D_2 ratio in Table 1.

Can. J. Chem. Downloaded from www.nrcresearchpress.com by 210.87.254.40 on 09/05/12
For personal use only.

TABLE 3. Reaction of sodium with alcohol: constants used in computer calculations

	Value		
	CH_3CH_2OD		CH_3OD
Constants	25 °C	−78 °C	25 °C
$D_A(cm^2\ s^{-1})^a$	3×10^{-5}	0.12×10^{-5}	5×10^{-5}
b	30	3	30
$C_{A_0}(M)$	4.2×10^{-4} 3.8×10^{-4}	5.1×10^{-4}	7.7×10^{-4}
$k_2(s^{-1})$	9×10^{4c} 1.2×10^{5b}	1.2×10^{3d}	1.1×10^{5c}
$k_3(M^{-1}\ s^{-1})$	$(5\pm4)\times10^9$ $(7\pm3)\times10^9$	$(5.3\pm2)\times10^6$	$(3.3\pm2)\times10^9$
$k_{3\ aq}(M^{-1}\ s^{-1})$	6.3×10^{9e}		
$D_{N_2O}(cm^2\ s^{-1})$	1×10^{-5f}		
$k_5(M^{-1}\ s^{-1})$	8×10^{9g}		

[a]Calculated from the value obtained in water 4.7×10^{-5} cm^2 s^{-1} (ref. 3 using the Wilke Stoke Einstein eq. ref. 6 which is the same as a value by Russell and Freeman (9)).
[b]Reference 5.
[c]In alkaline solution ref. 10. This independent value at room temperature makes a useful comparison.
[d]Value calculated using E_a = 4.8 kcal/mol for [2] (10) which is similar to a value of 4.6 ± 1 estimated by Freeman (12) and 4.5 ± 1 obtained for the aqueous system (11).
[e]Aqueous system ref. 7.
[f]Estimated from data in ref. 6.
[g]J. W. Fletcher, unpublished data; obtained by steady state γ-radiolysis relative to $k_{(e^-+H^+)} = 2\times10^{10}\ M^{-1}\ s^{-1}$. This value is similar to that obtained by other authors $7\times10^9\ M^{-1}\ s^{-1}$ ref. 12.

The values of k_3 and C_{A_0} given in Table 3 are calculated from eqs. 9*c* and 10 using the values of b, N_A, D_A, and k_2 given in Tables 1 and 3. The value of $k_3 = (5 \pm 4) \times 10^9\ M^{-1}\ s^{-1}$ is similar to the value obtained $k_{3\ aq} = 6.3 \times 10^9\ M^{-1}\ s^{-1}$ obtained in radiolysis of aqueous solutions (7).

The results obtained at −78 °C were calculated in the same way using the experimental numbers in Table 1 and the constants in Table 3. The derived values for $k_3 = (5 \pm 2) \times 10^6\ M^{-1}\ s^{-1}$ at −78 °C and $(5 \pm 4) \times 10^9\ M^{-1}\ s^{-1}$ at 25 °C lead to an activation energy $E_A = 7.6 \pm 2$ kcal/mol for the bimolecular reaction in ethanol which is slightly higher than the value of 5.2 ± 0.3 kcal/mol obtained for water (7).

(2) Isotope Effects Arising from the Bimolecular Decay of the Electron

Similar results were obtained for the isotopic composition of the gas evolved in both methanol and ethanol, shown in Fig. 1. The isotope effect α is defined as the ratio of the (H/D) in the hydrogen product to the oxy (H/D) in the solvent mixture. A comparison of the uncorrected values of α (Table 4), for alcohol with results obtained in aqueous solutions (8), show a similar trend as a function of %D, but the value of α is one half that in water. When a correction is made for the HD formed in pure alcohol-d_1 due to the first order decay, the value of α is decreased slightly and becomes a constant value $\alpha = 2 \pm 0.1$. The curve in Fig. 1 is calculated using this correction and assuming $\alpha = 2$.

The rates of the aqueous analogue of reaction 3 in H_2O and D_2O are comparable (3)

$$e_{H_2O}^- + e_{H_2O}^- \rightarrow H_2 + 2OH^-$$

$$e_{D_2O}^- + e_{D_2O}^- \rightarrow D_2 + 2OD^-$$

Since they are comparable no isotope effect would be expected from these reactions in H_2O–D_2O solutions. We have estimated in this paper that the rate of reaction 3 in alcohol is similar to that in water. It can therefore be assumed that the rate of reaction 3 in oxy-deuterium and oxy-hydrogen alcohol would also be similar and that no isotope effect would arise from reaction 3 in ROD–ROH solutions.

It has been suggested (8) that the relatively large isotope effect found in water could arise from the decomposition of the dimer intermediate $(e_{aq}^-)_2$, formed by the diffusion controlled reaction 11

[11] $$e_{aq}^- + e_{aq}^- \rightarrow (e_{aq}^-)_2$$

where aq can represent both deuterated and undeuterated water in the solvent shell. The dimer intermediate would have to have a lifetime long enough to allow preferential cleavage of the OH over the OD bonds of the molecules in the solvation shell to take place. The isotope effect arising from the direct decomposition of the solvated dimer should be similar in alcohol and water.

Since the isotope effect in alcohol is observed to be less than in water there must be a second source of the isotope effect in the aqueous system.

Can. J. Chem. Downloaded from www.nrcresearchpress.com by 210.87.254.40 on 09/05/12
For personal use only.

TABLE 4. Reaction of sodium with alcohol: H/D isotope effects

Atom % oxy-hydrogen	"α" aqueous (8)[a]	"α" alcoholic[a]	
		Uncorrected	Corrected
25	5.5±0.2	2.4±0.4	2.0±0.2
50	4.7±0.2	2.0±0.3	2.0±0.2

[a] $\alpha = (H/D)_{\text{hydrogen product}}/(H/D)_{\text{solvent oxy-hydrogen}}$.

This second isotope effect could arise from each electron within the dimer (reaction 12) becoming associated with a specific molecule $(H_2O^-)_2$ before the formation of hydrogen (reaction 13),

[12] $$(e_{aq}^-)_2 \rightarrow (H_2O^-)_2$$

[13] $$(H_2O^-)_2 \rightarrow H_2 + 2OH^-$$

where H_2O represents both deuterated and undeuterated water. If this occurred, then no further isotope effect would arise from the decomposition of the desolvated dimer by a reaction analogous to reaction 13 in the ROH–ROD alcohol system since there are only two available hydrogens per dimer. However, in the aqueous H_2O–D_2O system an isotope effect in addition to that in reaction 12 would be observed from reaction 13 since there are four available hydrogens per dimer. This additional isotope effect in water could account for the larger value of α in the aqueous system than in alcohol.

The desolvation process [12] would require time and this could account for the finite lifetime of the solvated dimer $(e_{aq}^-)_2$ as an intermediate and thus the observed isotope effect. The lifetime and the concentration of the dimer is still small in comparison with that of the electron and would not affect the mathematical treatment in this paper.

(3) Scavenger Kinetics

The electron formed in reaction 1

[1] $$Na + ROD \rightarrow e_{ROD}^- + Na^+$$

can react with N_2O to give N_2 by reaction 5

[5] $$N_2O + e_{ROD}^- \xrightarrow{k_5} N_2 + O^-$$

in competition mainly with reaction 3

[3] $$e_{ROD}^- + e_{ROD}^- \rightarrow D_2 + 2RO^-$$

Calculations based on the assumption that reactions 3 and 5 obey simple homogeneous reaction kinetics, give much higher N_2 yields than the experimental values (Table 2). A more exact solution is required, which takes into account the rates of diffusion and concentration gradients of both the electron and the scavenger.

An exact solution of the equations is not possible so an iterative solution has been developed using a computer for the calculations. This solution makes use of the diffusion and reaction terms of the electron and nitrous oxide in eqs. 14 and 15, respectively.

[14] $$-D_A \frac{d^2C_A}{dZ^2} + k_2C_A + (2k_3)C_A^2 + k_5[N_2O]C_A = 0$$

[15] $$-D_{N_2O} \frac{d^2[N_2O]}{dY^2} + k_5[N_2O]C_A = 0$$

The solution is a mixed boundary value problem in which Z is a measure of the distance the electron has diffused away from the sodium surface and Y is a measure of the distance the N_2O has diffused toward the surface from a point Y_0 where the N_2O has a constant concentration. The first step is to calculate an electron concentration gradient equation assuming no nitrous oxide has been added and for this case the differential eq. 7*b* can be solved in the form

[16] $$Z = \left(\frac{D_A}{K}\right)^{\frac{1}{2}}\left[\ln\left(\frac{(1 + B_0)^{\frac{1}{2}} - 1}{(1 + B_0)^{\frac{1}{2}} + 1}\right) - \ln\left(\frac{(1 + B)^{\frac{1}{2}} - 1}{(1 + B)^{\frac{1}{2}} + 1}\right)\right]$$

Can. J. Chem. Downloaded from www.nrcresearchpress.com by 210.87.254.40 on 09/05/12
For personal use only.

where

$$B_0 = \frac{4}{3}\left(\frac{k_3 C_{A_0}}{K}\right)$$

$$B = \frac{4}{3}\left(\frac{k_3 C_A}{K}\right)$$

$$K = k_2$$

The calculated electron concentration as a function of distance from the sodium surface is shown in Fig. 2 for $[N_2O] = 0$.

A first estimate of the N_2O concentration profile can then be made using the electron concentration obtained from the profile calculated above. This is done using eq. 17 which is a solution of eq. 15 assuming a constant electron concentration in an interval ΔY.

$$[17] \qquad [N_2O]_n = [N_2O]_{n-1} \frac{\cosh(BA(1 - \Delta Y/L))}{\cosh(BA)}$$

where ΔY = the distance interval, $Y_1 - Y_0, \cdots, Y_n - Y_{n-1}$ etc., $BA = (k_5 E/D_{N_2O})^{1/2} L$, k_5 = rate of reaction of electron with N_2O, E = average electron concentration over ΔY, D_{N_2O} = rate of diffusion of N_2O, L = effective distance from Y_n to the surface of the sodium.[2]

Equation 17 is used to calculate the N_2O concentration $[N_2O]_1$ a distance ΔY from Y_0, the point where the N_2O concentration $[N_2O]_0$ is the same as the bulk concentration. The value ΔY is chosen such that the electron concentration is relatively constant over the interval. Taking $Y_1 = Y_0 + \Delta Y$ as a new starting point this process is repeated until the concentration profile of the N_2O has been calculated to the surface of the sodium. The equation for the N_2O profile can then be obtained.

The first approximation of the N_2O concentration as a function of distance from the sodium surface can be used to calculate a better estimate of the electron concentration gradient from the solution of the electron diffusion eq. 14. Equation 14 can be solved only for constant N_2O concentration. The solution obtained is the same as eq. 16 except that

$$K = k_2 + k_5[N_2O]$$

The distance Z must be small enough that the N_2O concentration does not vary within the interval. Therefore a step-by-step process is again used to calculate a distance for each decreasing electron concentration. The N_2O concentration used is that calculated from the N_2O concentration gradient equation.

The electron concentration profile above is used to obtain a better estimate of the N_2O concentration, which in turn is used to calculate a more accurate electron concentration profile. The process is repeated until convergence to a constant value is obtained. The calculated N_2O and electron concentrations (in the presence of N_2O) are also shown in Fig. 2. From these values the percentage N_2 is calculated. The calculated values (Table 2) do not give an exact fit with the experimental values but are in much better agreement than that obtained by simple competitive kinetic calculations. No attempt was made to vary the rate or diffusion constants in order to obtain a better fit. It was felt that the mathematical treatment was not exact enough to merit this fitting procedure.

(4) Scavenger Kinetics with Added Inert Solvent

The addition of ether, which reacts at a negligible rate with sodium, decreased the rate of formation and thus the concentration of the electron; this made it easier for the N_2O to scavenge electrons, reaction 5, in competition with reaction 3. The expected N_2 yields can be calculated using the same equations as in

[2]The parameter L arises from the boundary conditions that there is no diffusion of N_2O through the sodium surface. At a constant electron concentration, L is equivalent to the distance from Y_0 to the surface of the sodium. Since the electron concentration is greater near the sodium surface, more N_2O will be removed than if the electron concentration were constant. Parameter L takes this into consideration and hence has a value larger than the actual distance from Y_0 to the surface of the sodium. Hence, the larger value of L is related to the concentration gradient and to a first approximation

$$L = \left(\int_{Y_0}^{\text{Na surface}} C_A \, dY\right)/C_A.$$

Can. J. Chem. Downloaded from www.nrcresearchpress.com by 210.87.254.40 on 09/05/12
For personal use only.

section 3 and are given in Table 2. These calculations indicate that N_2O should be greater than 10^3 times as effective in scavenging the electron when an inert solvent has been added, which confirms the effect observed experimentally (Table 2).

Conclusions

The reaction of sodium with alcohol to produce hydrogen involves the electron as an intermediate. The electron in pure alcohol reacts mainly bimolecularly with another electron to produce hydrogen. It is suggested that an electron dimer is formed prior to the production of hydrogen. A comparison of the isotope effect in alcohol ($\alpha = 2$) and water suggests that this dimer is desolvated before the formation of hydrogen and this desolvation contributes to the finite lifetime of the dimer.

We wish to thank Drs. W. A. Seddon and D. R. Smith for their helpful suggestions.

1. J. E. BENNETT, B. MILE, and A. THOMAS. J. Chem. Soc. A, 1393 (1967).
2. E. A. SHAEDE and D. C. WALKER. Chem. Soc. London Spec. Publ. **22**, 277 (1967).
3. E. J. HART. Acc. Chem. Res. **2**, 161 (1969).
4. L. M. DORFMAN and I. A. TAUB. J. Am. Chem. Soc. **85**, 2370 (1963).
5. J. W. FLETCHER, P. J. RICHARDS, and W. A. SEDDON. Can. J. Chem. **48**, 1645 (1970).
6. R. B. BIRD, W. E. STEWART, and E. N. LIGHTFOOT. Transport phenomena. John Wiley and Sons, New York. 1960.
7. W. C. GOTTSCHALL and E. J. HART. J. Phys. Chem. **71**, 2102 (1967).
8. M. ANBAR and D. MEYERSTEIN. Radiation chemistry of aqueous solutions. *Edited by* G. Stein. The Weizmann science press of Israel. Jerusalem, 1968. P. 109ff specifically section II D, p. 139.
9. J. C. RUSSELL and G. R. FREEMAN. J. Phys. Chem. **71**, 755 (1967).
10. P. WARDMAN. Private communication.
11. E. M. FIELDEN and E. J. HART. Trans. Faraday Soc. **64**, 3158 (1968).
12. G. R. FREEMAN. Actions chemiques et biologiques des radiations. *Edited by* M. Haissinsky. **14**, 73 (1970).
13. K. H. SCHMIDT and W. L. BUCK. Science, **151**, 70 (1966).

Can. J. Chem. Downloaded from www.nrcresearchpress.com by 210.87.254.40 on 09/05/12
For personal use only.

Can. J. Chem. Downloaded from www.nrcresearchpress.com by 210.87.254.105 on 09/05/12
For personal use only.

A Re-examination of the Yields in the High Dose Rate Radiolysis of Gaseous Ammonia[1]

A. W. BOYD, C. WILLIS, AND O. A. MILLER

Physical Chemistry Branch, Chalk River Nuclear Laboratories, Atomic Energy of Canada Limited, Chalk River, Ontario

Received January 14, 1971

Eyre and Smithies have recently obtained radical yields of $G_{NH_2} = G_H = 10.4$ in the radiolysis of gaseous ammonia. The consistency of these with N_2, H_2, and N_2H_4 yields obtained in the high dose rate radiolysis of NH_3 and NH_3–C_3H_6 mixtures has been shown by numerical integration of the rate expressions in a simple radical mechanism. These calculations give a value of $2.1 \pm 0.5 \times 10^{10}\ M^{-1}\ s^{-1}$ for the reaction of H atoms and NH_2 radicals and a ratio of recombination to disproportionation of 6:1.

Eyre et Smithies ont récemment obtenu les rendements radicalaires de $G_{NH_2} = G_H = 10.4$ lors de la radiolyse d'ammoniaque gazeux. Ces résultats sont consistants avec les rendements de N_2, H_2 et N_2H_4 obtenus lors de la radiolyse de NH_3 et de mélanges NH_3–C_3H_6 aux débits de dose trés éleves; ceci a pu être mis en évidence par intégration numérique des expression de vitesse dans un mécanisme radicalaire simple. Ces calculs conduisent à une valeur de $2.1 \pm 0.5 \times 10^{10}\ M^{-1}\ s^{-1}$ pour la réaction d'atomes d'hydrogène et de radicaux NH_2, et à un rapport recombinaison sur disproportionation de 6:1.

Canadian Journal of Chemistry, 49, 2283 (1971)

Introduction

In a recent paper (1) we gave values for the yields of H_2, N_2, and N_2H_4 in the radiolysis of gaseous ammonia and ammonia–propene mixtures with intense electron pulses at a dose rate of 2×10^{27} eV g^{-1} s^{-1}. Minimum primary radical yields of $G_{NH_2} = G_H = 4.8$ were derived from the yields in NH_3–C_3H_6 mixtures by extrapolating to zero C_3H_6 concentration and assuming for these extrapolated values that reactions of NH_2 with propene, propyl radicals, and residual H atoms could be neglected.

Nishikawa *et al.* (2) using NH_3–C_3H_8 mixtures at low dose rates reported a value of $G_H = 5.1$. This is lower than the yield of $G_H = 7.2$ obtained by Johnson and Simic (3) from the same system. Jones and Sworski (4) using both NH_3–N_2H_4 and NH_3–D_2 mixtures obtained a value of $G_H = 12.5$. A paper just published by Eyre and Smithies (5) reports $G_{NH_2} = G_H = 10.4$ from a very careful study using a variety of additives. They suggest that the low values reported in refs. 2 and 3 are due to the build-up of propene in NH_3–C_3H_8 mixtures.

It is clearly of interest to determine, then, if our product yields at high dose rates are consistent with the higher and apparently most reliable primary yields of Eyre and Smithies. To do this we have assumed the simplest mechanism, taken experimentally measured values for the rate constants of some of the reactions and derived the values of the other rate constants by numerical integration of the rate expression (using the computer program of Schmidt (6)). We have also measured the yield of propylamine in NH_3–C_3H_6 mixtures at 2×10^{27} eV g^{-1} s^{-1} at room temperature and the yields of N_2, H_2, and N_2H_4 from room temperature to 460 °C in pure NH_3 at one tenth this dose rate and determined the consistency of these new data.

Experimental

Irradiation Procedure and Analysis

The irradiations of NH_3 and NH_3–C_3H_6 mixtures and the analyses for H_2, N_2, and N_2H_4 were as described in (1).

Propylamine was analyzed by gas chromatography using Chromasorb 103. To obtain consistent results with the propylamine it was found necessary to use Teflon plug stopcocks as both neoprene O-ring or greased stopcocks gave irreproducible results.

The pyrolysis corrections in the irradiation of pure NH_3 above 400 °C were 10–20%. These are less than would be inferred from the corrections at the higher dose rate in ref. 1. This reduction in the magnitude of the corrections was obtained by reducing the time the sample was in the furnace before irradiation. It was found that the sample gas reached thermal equilibrium within 5 min.

Dosimetry

In the previous work (1) and in the irradiations of NH_3–C_3H_6 mixtures in the present work the window of the quartz cell was placed ~3 cm from the Febetron

[1]AECL No. 3894.

Can. J. Chem. Downloaded from www.nrcresearchpress.com by 210.87.254.105 on 09/05/12
For personal use only.

tube window. In this position the dose in the gas is 1.6 Mrads per pulse. A dose rate one tenth of this was obtained by putting a 0.005 cm Ta scattering foil 2 cm from the tube window and placing the cell window 5 cm from the foil. The irradiations of pure NH_3 at temperatures from room temperature to 450 °C in ref. 1 were repeated with this lower dose rate.

The dosimetry at both dose rates is based on the yield of nitrogen of $G(N_2) = 12.4$ in N_2O radiolysis (7, 8). This value was established by calorimetry at the higher dose rate. It is expected to be the same at the lower dose rate (8) and this has been confirmed by measurement of the ozone yield in oxygen radiolysis. At both dose rates $G(O_3) = 12.8 \pm 0.6$ relative to $G(N_2) = 12.4 \pm 0.4$. The value of the ozone yield in single pulse irradiations should be constant down to at least 10^{25} eV g^{-1} s^{-1} (9).

Results

(a) Propylamine in the Radiolysis of NH_3–C_3H_6 Mixtures

The yields of propylamine in NH_3–C_3H_6 mixtures at room temperature and a pressure of 760 Torr are compared with the hydrazine yields in these mixtures in Fig. 1. These yields were obtained at a dose rate of 2×10^{27} eV g^{-1} s^{-1}.

(b) Hydrazine, Hydrogen, and Nitrogen in Pure Ammonia

The yields of N_2H_4, H_2, and N_2 in pure NH_3 at 760 Torr at temperatures to 460 °C and a dose rate of 2×10^{26} eV g^{-1} s^{-1} are compared with the yields reported in ref. 1 at 2×10^{27} eV g^{-1} s^{-1} in Fig. 2.

In ref. 1 we reported an increase in yields with decreasing pressure below 700 Torr at room temperature. We have since determined the effect of decreasing pressure at 300 °C and 2×10^{27} eV g^{-1} s^{-1}. The relative increase is not noticeably different at this higher temperature from that observed at 25 °C.

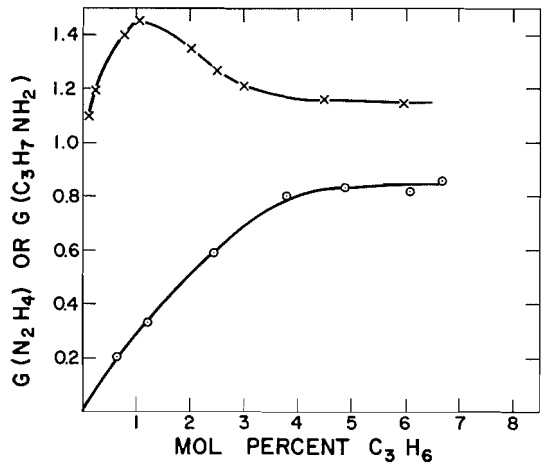

FIG. 1. Yields of $C_3H_7NH_2$ and N_2H_4 from the radiolysis of NH_3–C_3H_6 mixtures at 700 Torr, 25 °C at 2×10^{27} eV g^{-1} s^{-1}. ○, $C_3H_7NH_2$; ×, N_2H_4.

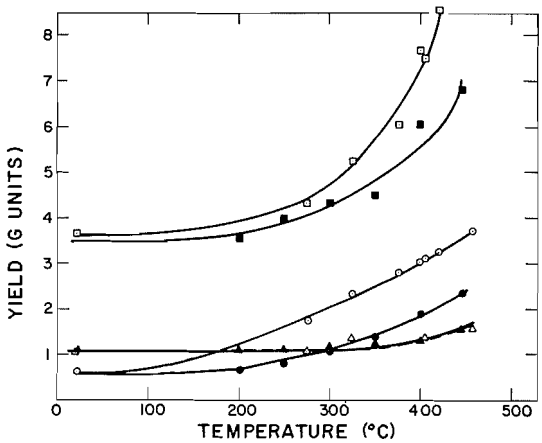

FIG. 2. Yields of N_2H_4, H_2, and N_2 from the radiolysis of NH_3 at 700 Torr *vs.* temperature. ○, N_2H_4 from NH_3 at 2×10^{26} eV g^{-1} s^{-1}; ●, N_2H_4 from NH_3 at 2×10^{27} eV g^{-1} s^{-1} (1); □, H_2 from NH_3 at 2×10^{26} eV g^{-1} s^{-1}; ■, H_2 from NH_3 at 2×10^{27} eV g^{-1} s^{-1} (1); △, N_2 from NH_3 at 2×10^{26} eV g^{-1} s^{-1}; ▲, N_2 from NH_3 at 2×10^{27} eV g^{-1} s^{-1} (1).

Discussion

The consistency of our data with the yields of Eyre and Smithies will be discussed under three headings: NH_3 at room temperature, NH_3–C_3H_6 mixtures at room temperature, and NH_3 at high temperatures.

As discussed in ref. 1 the reactions producing radicals should not be different at $\sim 10^{27}$ eV g^{-1} s^{-1} from those at low dose rates. These are assumed to be

[1] $NH_3 \rightsquigarrow NH_3^*$

[2] $NH_3^* \rightarrow NH_2 + H$

[3] $NH_3^* \rightarrow NH + H_2$

[4] $NH_3 \rightsquigarrow NH_3^+ + e$

[5] $NH_3^+ + NH_3 \rightarrow NH_4^+ + NH_2$

[6] $NH_4^+ + e \rightarrow NH_3 + H$

The yield of reaction 3 is taken to be 0.74 G units (2–5).

The radical yields, then, at our dose rates should be those measured by Eyre and Smithies. The subsequent mechanism for high dose rate

Can. J. Chem. Downloaded from www.nrcresearchpress.com by 210.87.254.105 on 09/05/12
For personal use only.

radiolysis, as discussed below, will be simpler than the low dose rate mechanism due to the absence of back reactions of the radicals with the products (1).

NH_3 at 25 °C

At 2×10^{27} eV g^{-1} s^{-1} in pure NH_3 from 1 to 5 atm and for doses from 1×10^{20} to 5×10^{20} eV g^{-1}, $G(H_2) = 3.6 \pm 0.1$, $G(N_2) = 1.0 \pm 0.05$, and $G(N_2H_4) = 0.58 \pm 0.05$ (1).

In order to satisfactorily explain these yields we must assume the following set of reactions, 7–12.

[7] $NH_2 + NH_2 \rightarrow N_2H_4$

[8] $NH_2 + NH_2 \rightarrow NH + NH_3$

[9] $NH_2 + H \rightarrow NH_3$

[10] $NH_2 + H \rightarrow NH + H_2$

[11] $H + H \rightarrow H_2$

[12] $NH + NH \rightarrow N_2 + H_2$

As well as recombination of NH_2 radicals to form hydrazine, reaction 7, it is known (10) that these radicals can also disproportionate to give NH and NH_3, reaction 8. The difference between our product yields and the high primary radical yields can only be explained by a back reaction, reaction 9, and this must be accompanied by reaction 10 to explain the relatively high hydrogen yield we observe. Reaction 11 is well known and removes the residual hydrogen atoms and reaction 12 has been observed directly by Meaburn and Gordon (11) and may account for the removal of NH radicals from the system.

Another possible reaction is 13 presumably (12) followed by reaction 14.

[13] $NH + NH_2 \rightarrow N_2H_3$

[14] $N_2H_3 + N_2H_3 \rightarrow N_2 + 2NH_3$

On the basis of the value of 7×10^{11} M^{-1} s^{-1} reported (11) for k_{12} NH radicals should disappear by reaction 12 provided k_{13} is much smaller, of the order of k_7. In any event the primary yield of NH is less than 10% that of NH_2 and the mode of NH disappearance will not greatly affect reactions 7 to 11.

Hanes and Bair (13) from work with discharges in NH_3 at low pressures give a value of 2.3×10^9 M^{-1} s^{-1} for the second order disappearance of NH_2 at the high pressure limit (above 0.85 Torr) and this can be equated to $k_7 + k_8$. The value of k_{11} is 1.6×10^8 M^{-1} s^{-1} (at 1 atm) (14).

Experimental values for reactions 9 and 10 have not been reported though Hanes and Bair (13) have calculated a value of $\sim 1.3 \times 10^{10}$ M^{-1} s^{-1} for the high pressure limit above 1000 Torr.

In our calculations we have taken the yields of Eyre and Smithies, set $k_7 + k_8 \approx 2.3 \times 10^9$ M^{-1} s^{-1} and then determined, using a computer program based on that of Schmidt (6), $G(N_2H_4)$, $G(H_2)$, and $G(N_2)$ for various values of k_7/k_8 and k_9, k_{10}, k_{11}, and k_{12}. The results for these calculations are given in Table 1.

It is evident from Table 1 that the yield of N_2H_4 is mainly dependent on k_7 and k_9 as changes in the other rate constants have little effect on this yield. Similarly the yield of hydrogen for fixed values of k_7 and k_9 is largely dependent on k_{10}. Assuming the mechanism given in the table and taking $k_7 = 1.8 \times 10^9$ M^{-1} s^{-1} and $G_{NH_2} = G_H = 10.4$, k_9 must be equal to 1.8×10^{10} M^{-1} s^{-1} and k_{10} to 2.9×10^9 M^{-1} s^{-1} within $\pm 20\%$. Since the rate constants of the other reactions can be changed by a factor of 2 or more without any significant change in the yields our results give little information as to their values.

The calculated values for the concentrations of NH_2, H, NH, N_2H_4, H_2, and NH_3 formed by recombination of $NH_2 + H$ as a function of time following a Febetron pulse are shown in Fig. 3. The initial rapid decrease in the H atom

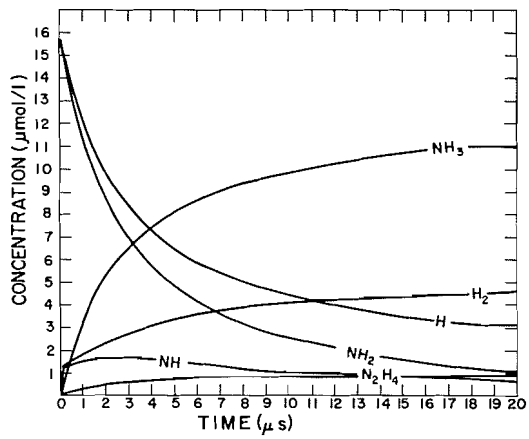

FIG. 3. Calculated concentrations of NH_2, H, NH, N_2H_4, and H_2 *vs.* time following 1.6 Mrads 60 ns electron pulse in NH_3 at 700 Torr and 25 °C at a maximum dose rate of 1.5×10^{27} eV g^{-1} s^{-1}. The calculated concentration of NH_3 formed by reaction 9 is also shown. The shape of the curve for NH is dependent largely on the value assumed for reaction 12.

TABLE 1. Calculated yields of N_2H_4, H_2, and N_2 in the radiolysis of NH_3 at 2×10^{27} eV g^{-1} s^{-1}*

Reaction	Rate constant (M^{-1} s^{-1})	$G(N_2H_4)$	$G(H_2)$	$G(N_2)$
[7] $NH_2 + NH_2 \rightarrow N_2H_4$	1.8×10^9			
[8] $NH_2 + NH_2 \rightarrow NH + NH_3$	5×10^8			
[9] $NH_2 + H \rightarrow NH_3$	1.8×10^{10}	0.59	3.57	1.07
[10] $NH_2 + H \rightarrow NH + H_2$	2.9×10^9			
[11] $H + H \rightarrow H_2$	1.6×10^8			
[12] $NH + NH \rightarrow N_2 + H_2$	5×10^{10}			
†$k_7 = 1.5 \times 10^9$		0.51	3.54	1.08
$= 2.1 \times 10^9$		0.66	3.60	1.06
†$k_8 = 2.5 \times 10^5$		0.61	2.50	1.04
$= 1 \times 10^9$		0.56	3.70	1.13
†$k_9 = 1.5 \times 10^{10}$		0.66	3.93	1.17
$= 2.1 \times 10^{10}$		0.53	3.29	0.99
†$k_{10} = 2.5 \times 10^9$		0.60	3.36	0.99
$= 3.5 \times 10^9$		0.58	4.88	1.18
†$k_{11} = 1 \times 10^8$		0.59	3.49	1.07
$= 4 \times 10^8$		0.60	3.70	1.07
†$k_{12} = 5 \times 10^9$		0.59	3.57	1.07
$= 1 \times 10^{11}$		0.59	3.57	1.07

*Assumed primary radical yields: $G_{NH_2} = G_H = 10.4$; $G_{NH} = G_{H_2} = 0.74$.
†In each of these cases the other rate constant values are as listed in the first section of the table.

concentration is due mainly to reaction with NH_2 radicals, reaction 9. As NH_2 radicals are also disappearing by reactions 7 and 8, there is an excess of H atoms which disappear relatively slowly by reaction 11. It is obvious from the figure that the major reaction is reformation of NH_3.

NH_3–C_3H_6 Mixtures

The increase in the N_2H_4 yield with the addition of C_3H_6 shown in Fig. 1 is primarily due to the removal of H atoms by reaction 15

[15] $$H + C_3H_6 \rightarrow C_3H_7$$

thus reducing the occurrence of reactions 9 and 10, and favoring reactions 7 and 8. The calculated fit to our experimental results for these mixtures using the yields in ref. 5 will be largely dependent on the value of the ratio k_{15}/k_8 at low propene concentrations. Reported values of k_{15} range from 10^7 M^{-1} s^{-1} to 6×10^8 M^{-1} s^{-1} (15) and we have calculated yields using values of k_{15} in this range.

Propylamine will be formed by reaction 16

[16] $$NH_2 + C_3H_7 \rightarrow C_3H_7NH_2$$

The calculations predicted that the amount of $C_3H_7NH_2$ from this reaction would reach a plateau value at ~1 mol% C_3H_6. To account for the increase observed at higher C_3H_6 concentrations in Fig. 1*a*, reaction of the form

[17] $$NH_2 + C_3H_6 \rightarrow X \rightarrow C_3H_7NH_2$$

must be occurring. This will give a linear dependence of the $C_3H_7NH_2$ yield on C_3H_6 concentration. The reduction in N_2H_4 at propene concentrations above 1% is presumably due to reaction of NH_2 with propene as in reaction 17 or to form other products as in reaction 18.

[18] $$NH_2 + C_3H_6 \rightarrow P$$

The rate constant for reaction 18 will also have a marked effect on the calculated yields as is shown in Table 2.

The calculated values for the yields of N_2H_4, H_2, N_2, and $C_3H_7NH_2$ for the range of C_3H_6 concentrations used are compared with the experimental values in Fig. 4. The overall fit is satisfactory. The rise and fall in the N_2H_4 yields are predicted quite well by the mechanism and the fit to both the N_2 and $C_3H_7NH_2$ is probably within the experimental error. The experimental hydrogen yields above 2% propene are considerably higher than the calculated curve. This is to be expected as contributions from direct radiolysis of propene and from disproportionation reactions of H atoms with hydrocarbon radicals were neglected. As well as

Can. J. Chem. Downloaded from www.nrcresearchpress.com by 210.87.254.105 on 09/05/12
For personal use only.

TABLE 2. Calculated yields of N_2H_4, H_2, N_2, and $C_3H_7NH_2$ in the radiolysis of a NH_3–1 mol% C_3H_6 mixture at 2×10^{27} eV g^{-1} s^{-1}*

Reaction	Rate constant (M^{-1} s^{-1})	$G(N_2H_4)$	$G(H_2)$	$G(N_2)$	$G(C_3H_7NH_2)$
[7] to [12] as in Table 1					
[15] $H + C_3H_6 \rightarrow C_3H_7$	8.5×10^8				
[16] $NH_2 + C_3H_7 \rightarrow C_3H_7NH_2$	8.0×10^7				
[17] $NH_2 + C_3H_6 \rightarrow X \rightarrow C_3H_7NH_2$	3.0×10^6	1.45	2.15	0.84	0.32
[18] $NH_2 + C_3H_6 \rightarrow P$	3.0×10^7				
[19] $H + C_3H_7 \rightarrow C_3H_8$	1×10^{10}				
[20] $C_3H_7 + C_3H_7 \rightarrow C_3H_6 + C_3H_8$	1×10^9				
†k_{15} =	4×10^8	1.09	2.39	0.88	0.26
	6×10^8	1.28	2.26	0.86	0.29
	1×10^9	1.53	2.10	0.83	0.34
†k_{16} =	4×10^7	1.46	2.15	0.84	0.28
	1.5×10^8	1.44	2.15	0.84	0.39
	3×10^8	1.41	2.14	0.84	0.52
†k_{17} =	1.5×10^6	1.47	2.15	0.85	0.21
	4.5×10^6	1.43	2.15	0.84	0.43
†k_{18} =	1.5×10^7	1.72	2.19	0.88	0.42
	4.5×10^7	1.27	2.12	0.82	0.27
	6×10^7	1.13	2.10	0.80	0.23
†k_{19} =	5×10^9	1.42	2.17	0.84	0.32
	2×10^{10}	1.49	2.12	0.84	0.32

*Assumed primary radical yields: $G_{NH_2} = G_H = 10.4$; $G_{NH} = G_{H_2} = 0.74$.
†In each of these cases the other rate constant values are as listed in the first part of the table.

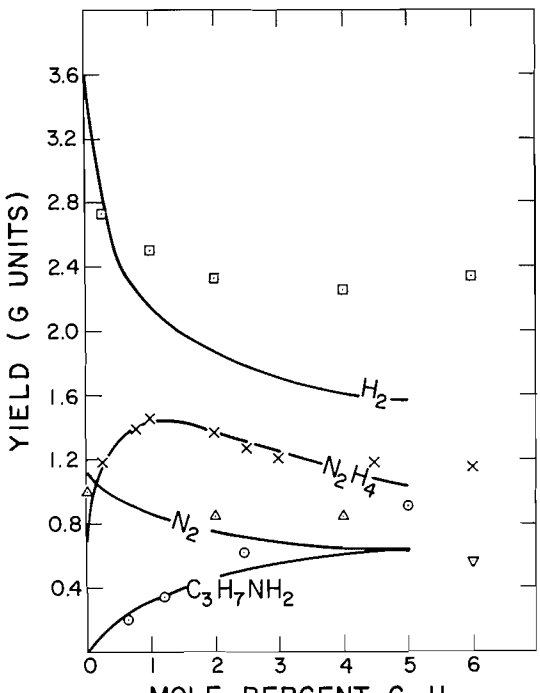

FIG. 4. Calculated and experimental yields from the radiolysis of NH_3–C_3H_6 mixtures at 700 Torr, 25 °C at a dose rate of 2×10^{27} eV g^{-1} s^{-1}. Solid lines, calculated values.

the product yields, the contributions of each of the reactions of NH_2 and H have been calculated. The importance of these various reactions as a function of C_3H_6 concentration is shown in Table 3. It is evident that at any propene concentration, less than 30% of the NH_2 radicals form N_2H_4. As the reaction of these with H atoms is suppressed their reaction with C_3H_6 increases. The simple extrapolation made in ref. 1 could then give only minimum values for the primary radical yields.

The value of $k_{15} = 8.5 \times 10^8$ M^{-1} s^{-1} used in these calculations is necessary to give the observed dependence of the N_2H_4 yield on the propene concentration. The decrease in $G(N_2H_4)$ above 1 mol% C_3H_6 must be due to removal of NH_2 by propene and this in turn requires a high value of k_{15}. This value of k_{15} is at the high end of the reported values (15) but is consistent with the value of 5.5×10^8 M^{-1} s^{-1} reported recently for the high pressure limit of $H + C_2H_4$ (16).

NH_3 at High Temperatures

It was proposed in ref. 1 that the increase in the yields with temperature shown in Fig. 2 is due to reaction 20.

[20] $H + NH_3 \rightarrow H_2 + NH_2$

A value of $k_{20} = 4 \pm 2 \times 10^9 \exp(-10\,000 \pm$

Can. J. Chem. Downloaded from www.nrcresearchpress.com by 210.87.254.105 on 09/05/12
For personal use only.

TABLE 3. Calculated importance of various reactions in NH_3–C_3H_6 mixtures as a function of C_3H_6 concentration*

Reaction	% of NH_2 reacting when C_3H_6 mol% = 0	0.5	1	2	3	5
$NH_2 + NH_2 \rightarrow N_2H_4$	11.4	26.2	27.9	26.6	24.1	20.0
$NH_2 + NH_2 \rightarrow NH + NH_3$	3.1	7.3	7.7	7.3	6.7	5.6
$NH_2 + H \rightarrow NH_3$	73.7	43.3	32.7	22.6	17.4	11.9
$NH_2 + H \rightarrow H_2 + NH$	11.8	7.0	5.3	3.7	2.8	1.9
$NH_2 + C_3H_7 \rightarrow C_3H_7NH_2$	—	0.6	0.8	0.8	0.8	0.7
$NH_2 + C_3H_6 \rightarrow X \rightarrow C_3H_7NH_2$	—	1.4	2.3	3.6	4.4	5.5
$NH_2 + C_3H_6 \rightarrow P$	—	14.2	23.4	35.6	43.8	54.4

Reaction	% of H reacting when C_3H_6 mol% = 0	0.5	1	2	3	5
$H + NH_2 \rightarrow NH_3$	73.7	43.3	32.7	22.6	17.4	11.9
$H + NH_2 \rightarrow H_2 + NH$	11.8	7.0	5.3	3.7	2.8	1.9
$H + H \rightarrow H_2$	14.5	0.6	0.4	0.3	0.2	0.1
$H + C_3H_6 \rightarrow C_3H_7$	—	42.0	55.2	68.5	75.4	82.7
$H + C_3H_7 \rightarrow C_3H_8$	—	7.2	6.4	5.1	4.2	3.1

*Assuming $G_{NH_2} = G_H = 10.4$, $G_{NH} = G_{H_2} = 0.74$ and the rate constants in the first sections of Tables 1 and 2.

1500 cal/RT) M^{-1} s^{-1} was derived from the observed increases in product yields assuming the primary yields of $G_{NH_2} = G_H = 4.8$. The relative rates of k_{20} were estimated from the total NH_2 formed at the different temperatures. To find the absolute value it was assumed that at ~380 °C, k_{20} [NH_3] = ($k_9 + k_{10}$) [NH_2] *i.e.* k_{20} [4×10^{-2} M] = 1.1×10^{10} [$\sim 5 \times 10^{-6}$ M], see Fig. 3.

Using the values for the rate constants of reactions 6 to 12 in the first part of Table 1, values for k_{20} to give the experimental yields at the higher dose rate were calculated with the computer program. These values give an activation energy of 10.5 kcal mol^{-1} and a pre-exponential factor of 3.6×10^9 M^{-1} s^{-1} in good agreement with the rate constant in ref. 1 However, treating the experimental yields at the lower dose rate in the same way gives an activation energy of 7.2 kcal mol^{-1} and a pre-exponential factor of 8×10^7 M^{-1} s^{-1}. For both dose rates the derived rate expression gave a very good fit to the experimental values. This inconsistency in values for k_{20} indicates that the rate constants for some or all of reactions 6 to 12 change with temperature and that a precise value of k_{20} cannot be estimated. The most probable changes in these reactions are in the ratios of disproportionation to combination for $NH_2 + NH_2$ and $H + NH_2$. Figure 5 compares the experimental N_2H_4 yields for both dose rates with values calculated setting k_{20} equal to the intermediate value of 4×10^8 exp (−8500/cal/RT) M^{-1} s^{-1}. This clearly shows the effect of the uncertainty in k_{20} and further, that no single value can give agreement with both dose rates.

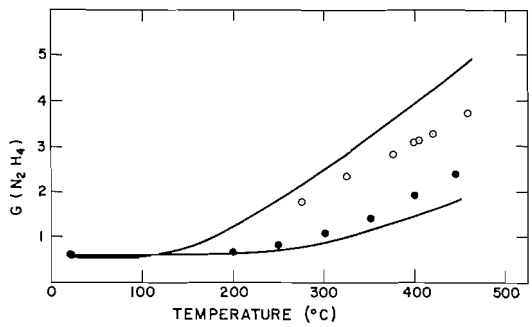

FIG. 5. Calculated and experimental yields of N_2H_4 from the radiolysis of NH_3 at 700 Torr *vs.* temperature. Upper solid line, calculated values at 2×10^{26} eV g^{-1} s^{-1}; lower solid line, calculated values at 2×10^{27} eV g^{-1} s^{-1}. ○, experimental yields at 2×10^{26} eV g^{-1} s^{-1}; ●, experimental yields at 2×10^{27} eV g^{-1} s^{-1}.

Conclusions

The yields of N_2H_4, H_2, and N_2 obtained in irradiations of NH_3 and NH_3–C_3H_6 mixtures at 2×10^{27} eV g^{-1} s^{-1} are consistent with the primary radical yields of $G_{NH_2} = G_H = 10.4$ reported by Eyre and Smithies (5). Assuming that reactions of NH with NH_2 or H are not significant at these dose rates and that the rate constant for NH_2 recombination is 1.8×10^9 M^{-1} s^{-1}, the rate

Can. J. Chem. Downloaded from www.nrcresearchpress.com by 210.87.254.105 on 09/05/12
For personal use only.

constants for recombination and disproportionation of H with NH_2, k_9 and k_{10} are $1.8 \pm 0.4 \times 10^{10}$ and $2.9 \pm 0.7 \times 10^9$ M^{-1} s^{-1}, respectively. The results in NH_3–C_3H_6 mixtures are consistent with $k_{NH_2 + C_3H_6} = 3 \times 10^7$ M^{-1} s^{-1}.

Comparison of the product yields from 200–450° at 2×10^{27} and 2×10^{26} eV g^{-1} s^{-1} indicates that a precise derivation for the rate expression for reaction 20 cannot be obtained from our data.

[20] $$H + NH_3 \rightarrow H_2 + NH_2$$

The rate constants we have derived are clearly dependent upon the mechanism we have assumed. Although it is difficult to assess the uniqueness of this mechanism, it seems clear that the back reaction must be an order of magnitude faster than the reaction between NH_2 radicals.

1. C. WILLIS, A. W. BOYD, and O. A. MILLER. Can. J. Chem. **47**, 3007 (1969).
2. M. NISHIKAWA, K. KURODA, and N. MATSUURA. Bull. Chem. Soc. Japan, **41**, 1276 (1968).
3. G. R. A. JOHNSON and M. SIMIC. Adv. Chem. **82**, 197 (1968).
4. F. T. JONES and T. J. SWORSKI. Trans. Faraday Soc. **63**, 241 (1967).
5. J. A. EYRE and D. SMITHIES. Trans. Faraday Soc. **66**, 2199 (1970).
6. K. H. SCHMIDT. USAEC Report ANL-7199 (1966).
7. C. WILLIS, O. A. MILLER, A. E. ROTHWELL, and A. W. BOYD. Adv. Chem. **81**, 539 (1959).
8. C. WILLIS, A. W. BOYD, and D. A. ARMSTRONG. Can. J. Chem. **47**, 3783 (1969).
9. C. WILLIS, A. W. BOYD, M. J. YOUNG, and D. A. ARMSTRONG. Can. J. Chem. **48**, 1505 (1970).
10. J. D. SALZMAN and E. J. BAIR. J. Chem. Phys. **41**, 3654 (1964).
11. G. M. MEABURN and S. GORDON. J. Phys. Chem. **72**, 1592 (1968).
12. L. J. STIEF. J. Chem. Phys. **52**, 4841 (1970).
13. M. H. HANES and E. J. BAIR. J. Chem. Phys. **38**, 672 (1963).
14. K. SCHOFIELD. Planet. Space Sci. **15**, 643 (1967).
15. B. A. THRUSH. Prog. React. Kinet. **3**, 63 (1965).
16. J. A. EYRE, T. HIKIDA, and L. M. DORFMAN. J. Chem. Phys. **53**, 1281 (1970).

Can. J. Chem. Downloaded from www.nrcresearchpress.com by 210.87.254.105 on 09/05/12
For personal use only.

Can. J. Chem. Downloaded from www.nrcresearchpress.com by 210.87.254.6 on 09/05/12
For personal use only.

Thermal Decomposition of di-*tert*-Butyl Peroxide in Binary Mixtures near the Critical Point

C. K. YIP AND H. O. PRITCHARD

Centre for Research in Experimental Space Science, York University, Downsview, Ontario

Received December 24, 1970

The thermal decomposition of di-*tert*-butyl peroxide has been studied in the presence of high pressures of cyclopropane; the rate constant for the decomposition was determined from the sum of the rates of formation of *tert*-butanol and acetone. In the temperature range 125–160 °C, *i.e.* above the critical point of cyclopropane, concentrations of cyclopropane of between 2.6 and 3.6 mol/l (60–80 amagats) were used; in the temperature range 100–124 °C, *i.e.* below the critical point of cyclopropane, an equivalent mean (liquid + gas) cyclopropane concentration was used. An Arrhenius plot of the rate constants for the peroxide decomposition is continuous through the critical point of the cyclopropane, and is indistinguishable from the best Arrhenius line representing all previous work on the reaction.

However, an Arrhenius plot of the ratio of the rates of formation of *tert*-butanol and acetone shows a marked discontinuity at the critical point, but further investigation shows that this results from the unequal distribution of the reactant peroxide between the two phases which are present below the critical point of the cyclopropane.

Less extensive series of experiments using propane, isobutane, cyanogen, and carbon dioxide as pressurizing gases confirm the pressure-independence of the rate of decomposition of di-*tert*-butyl peroxide: the experiments with propane and isobutane confirm the phase-independence of the rate; the propane experiments also exhibit the same apparent kinetic discontinuity at the critical point. Finally, rate-constant data are obtained for the reactions of the *tert*-butoxy radical with cyclopropane and isobutane, and for the addition of methyl radicals to cyanogen.

La décomposition thermique du péroxyde di-*tert*-butylique a été étudiée en présence de fortes pressions de cyclopropane; la constante de vitesse de décomposition a été déterminée à partir de la somme des vitesses de formation du *tert*-butanol et de l'acétone. Dans un intervalle de température de 125–160 °C, *i.e.* au-dessus du point critique du cyclopropane, des concentrations de cyclopropane entre 2.6 et 3.6 mol/l (60–80 amagate) ont été utilisées; dans l'intervalle de température 100–124 °C, *i.e.* en-dessous du point critique du cyclopropane, une moyenne équivalente (liquide + gaz) de concentration de cyclopropane a été utilisée. Un graphe d'Arrhénius des constantes de vitesse pour la décomposition du péroxyde est continu en passant par le point critique du cyclopropane, et est indiscernable de la meilleure ligne d'Arrhénius représentant tous les travaux antécédents sur la réaction.

Cependant, un graphe d'Arrhénius du rapport des vitesses de formation du *tert*-butanol et de l'acétone montre une discontinuité marquée au point critique, mais des recherches ultérieures montrent que ceci résulte d'une distribution inégale du réactif péroxyde entre les deux phases qui sont présentes au-dessous du point critique du cyclopropane.

Des séries d'expériences moins étendues utilisant le propane, l'isobutane, le cyanogène et le dioxyde de carbone comme gas pour pressuriser confirment que la vitesse de décomposition du péroxyde di-*tert*-butylique est indépendante de la pression. Les expériences avec le propane et l'isobutane confirment que la vitesse est indépendante de la phase; les expériences avec le propane montrent également la même discontinuité cinétique apparente au point critique. Enfin, les données de constante de vitesse sont obtenues pour les réactions du radical *tert*-butoxyle avec le cyclopropane et l'isobutane et pour l'addition des radicaux méthyles au cyanogène.

Canadian Journal of Chemistry, 49, 2290 (1971)

The purpose of the work described in this paper is two-fold, (*i*) to extend the study of the thermal decomposition of di-*tert*-butyl peroxide (DTBP) to higher pressures of added gases than have been used before, with a view to eliminating the concept of "induced decomposition" from the terminology of unimolecular reaction theory; and (*ii*) to study the decomposition in both liquid and gaseous phases, keeping as far as possible all other system parameters constant, possibly to throw light on the apparent difference between the rate of this reaction in the gas phase and in solution.

(*i*) We have already emphasized the importance of studying this thermal decomposition in the presence of high pressures of added gases, but in our earlier study, we were only able to perform satisfactory experiments using, at most, 10–15

Can. J. Chem. Downloaded from www.nrcresearchpress.com by 210.87.254.6 on 09/05/12
For personal use only.

atm of pressurizing gas (1). Improvements in our analytical procedures (2) now enable us to use ten times as much of certain pressurizing gases, in particular propane, cyclopropane, and carbon dioxide. Much of the preliminary work was done using propane, but for reasons explained below, the most extensive series of experiments was performed with cyclopropane as the pressurizing gas. Because the hydrocarbons used have high compressibility factors in the experimental temperature range, the absolute pressure is, however, much less than that of an ideal gas at the same molar concentration; it is therefore convenient to use the amagat unit of density where 1 amagat is equivalent to 0.0446 mol l^{-1}. These experiments still reside in the concentration range where normal unimolecular reaction theories remain adequate and volume effects which have been observed in this reaction (3) and other first order reactions (4) at still higher pressures are not in question.

(*ii*) The thermal decomposition of di-*tert*-butyl peroxide has been studied in both the gaseous and liquid phases by Raley, Rust, and Vaughan (5). They found that in each of the three solvents they used, the rate of decomposition was about 50% greater than it was in the gas phase, throughout their experimental temperature range. We (2) have recently studied some aspects of this reaction in the gas phase using high pressures of added propane, and we decided to extend these measurements down below the critical temperature of propane to see if any change in kinetic behavior could be detected; the liquid-phase results of Raley, Rust, and Vaughan (5) would indicate that we might find a discontinuity or a curvature in the Arrhenius plot of the rate constant for the decomposition of the peroxide, at or near the critical point of the solvent.

Experimental

The preparation and/or purification of di-*tert*-butyl peroxide, carbon dioxide, and propane have been described previously (1, 2). Cyclopropane was supplied by Matheson of Canada Ltd: the principal impurities were stated to be air and cyclopropyl chloride; the latter would be expected to have a marked catalytic effect on the peroxide decomposition (1). After conventional degassing procedures with rejection of tail-fractions, the material was found to be free of any impurity that could be detected by mass-spectrographic or gas-chromatographic techniques, and can safely be assumed to have been cyclopropane, perhaps containing traces of other C_3 hydrocarbons. Isobutane was of research grade, supplied by Phillips Petroleum Company, and was similarly treated; cyanogen was supplied by Matheson of Canada Ltd.

Two stainless-steel reaction vessels were used, and their volumes were both determined to be in the range 11.90 ± 0.05 cc. The remainder of the experimental procedures have been described in detail (1, 2): in each of the main series of experiments, a total of 10^{-4} mol of peroxide was used, together with a propane or cyclopropane concentration of 3.1 ± 0.5 mol l^{-1}; departures from these standard conditions are noted below as they arise.

Results and Discussion

(a) Exploratory Experiments using Propane

The accepted reaction scheme (see refs. 1 and 2 for further discussion) for the thermal decomposition of di-*tert*-butyl peroxide is

[1] $$\text{DTBP} \rightarrow 2t\text{-BuO}$$

[2] $$t\text{-BuO} \rightarrow \text{CH}_3 + \text{CH}_3\text{COCH}_3$$

[3] $$t\text{-BuO} + \text{RH} \rightarrow t\text{-BuOH} + \text{R etc.}$$

The decomposition of the peroxide was studied between 90 and 104 °C at propane densities of about 70–75 amagats. Rate constants k_1 were established by measuring the rate of formation of acetone + *tert*-butanol as described previously (2), and when plotted in Arrhenius form, whether obtained at temperatures above or below the critical point, were consistent with those obtained previously (1). Since the critical temperature of propane (6) is 96.7 °C, and the reaction becomes too slow (1) for convenient study below 90 °C, the accessible liquid range is somewhat limited; in fact, at our propane concentrations, the gas density is such (7) that two phases would only be present in pure propane below about 93 °C. At the same time, whilst the sum of acetone + *tert*-butanol formation did not appear to show anomalies at 90 °C, the ratio of acetone/*tert*-butanol was only about 50% of that expected by extrapolating the previous gas-phase data (2); unfortunately, at 90 °C, these ratios are quite small, and probably not very reliable. On both counts, therefore, the decisive experiment would need an added hydrocarbon having a higher critical temperature. The next hydrocarbon in the series is isobutane, with a critical temperature (6) of 135 °C, but this is a little too near the top of the accessible temperature range (1) for a reliable Arrhenius plot to be established in gas-phase experiments carried out above the critical temperature; also, the analytical problems are more severe because the boiling point of isobutane

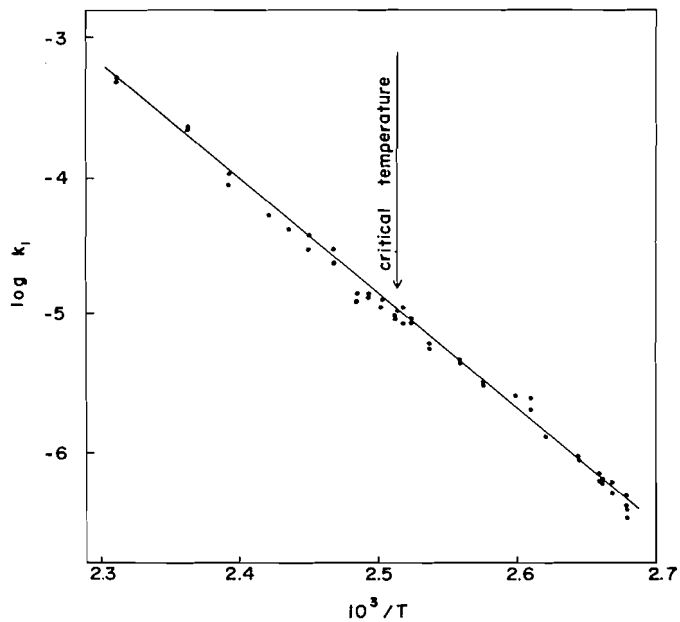

FIG. 1. Thermal decomposition of di-*tert*-butyl peroxide in the presence of 60–80 amagats of cyclopropane; the line shown in the diagram is not fitted to the points, but is the line selected for k_1 in our earlier review of the published data (1).

is too close to that of acetone. Two choices remain. One is to use suitable mixtures of propane and isobutane (or indeed other pairs of gases) tailored to a chosen critical temperature (8); the disadvantages of this approach are an increase in the complexity of the analytical procedure and the continual need to make up gas mixtures reliably conforming to the chosen critical temperature. The other is to use cyclopropane, which has a more convenient critical temperature (6) of 124.6 °C: the principal disadvantage of using cyclopropane was that its liquid and gas densities have not been measured near the critical point, so that one could not calculate reliably whether liquid should be present under any given conditions; it turned out subsequently that the presence of liquid could be inferred from the acetone/*tert*-butanol ratio.

(b) Experiments using Cyclopropane

Forty-seven experiments were carried out at cyclopropane densities between 60 and 80 amagats in the temperature range 100–160 °C. The results of these experiments are shown in Arrhenius form in Fig. 1: note that the line shown is *not* the best line drawn through these points, but is the "best" line (1) representing all previous work on this reaction, almost all of which was carried out at sub-atmospheric pressures. This, in our view, establishes[1] much more convincingly than our earlier work (1, 2) the absence of any pressure dependence in reaction 1; thus our previous comments about induced decomposition (1) are strongly reinforced.

Comparison between the Arrhenius parameters for the previously selected line (1) and the present results is[2]: for the selected line, log A_1 (s^{-1}) = 15.80 ± 0.03, E_1 (kcal/mol) = 37.78 ± 0.06; Fig. 1 (47 points), log A_1 (s^{-1}) = 15.62 ± 0.23, E_1 (kcal/mol) = 37.51 ± 0.42. The coincidence of our high-pressure experiments with earlier work is very satisfactory.

[1]Incidentally, using an analytical method somewhat different to any used previously: a slight variant of this method would be to use the methyl radical balance, *i.e.*, *tert*-butanol + methane + 2(ethane) as a measure of the extent of reaction; this proved to be more time-consuming and less reproducible, and was abandoned.

[2]Least-squares treatments of results reported in this paper use the method of York as noted previously (1) with the following assumed uncertainties in the temperature and rate constant, respectively: cyclopropane data: ±0.2 °C and ±10%; other data: ±0.2 °C and ±20%; data from refs. 13 to 15: ±0.1 °C and ±5% (for sake of consistency with other values quoted in ref. 1); errors quoted for the calculated A and E are standard deviations.

Can. J. Chem. Downloaded from www.nrcresearchpress.com by 210.87.254.6 on 09/05/12
For personal use only.

Can. J. Chem. Downloaded from www.nrcresearchpress.com by 210.87.254.6 on 09/05/12
For personal use only.

Further inspection of Fig. 1 shows that 26 of the 47 experiments were conducted below the critical temperature of cyclopropane. In the absence of gas and liquid density for cyclopropane[3] and of dew- and bubble-point data for peroxide–cyclopropane mixtures, it is impossible to predict whether liquid is present in any experiment, and if so, how much. However, by comparison with other hydrocarbons, it seems likely that at our cyclopropane concentrations, phase separation in pure cyclopropane would occur below about 119 °C; thus, in 20 of the 26 experiments carried out below T_c, liquid must have been present to a greater or lesser extent, and in all probability, at the lowest temperature (100 °C) the distribution would be of the order of half liquid – half gas. However, from evidence presented in Appendices 1 and 2, it is clear that liquid onset occurs in our binary mixtures at, or very close to, the critical temperature of the hydrocarbon. Thus, our evidence is that the rate of reaction 1 is completely independent of phase in light hydrocarbon substrates. The cause of the acceleration observed by Raley, Rust, and Vaughan (5) is not obvious, but the possibility that each of the three solvents they used could have contained *traces* of halogenated impurity, which would catalyze (1) reaction 1, should not be overlooked.

The main conclusions, therefore, in respect of the two objectives defined at the beginning of this paper are (*i*) that there is no anomalous pressure dependence at high pressures in the thermal decomposition of di-*tert*-butyl peroxide; and (*ii*) that the rate of decomposition of the peroxide is the same in light hydrocarbon solutions as it is in the gas phase. Appendices 1 to 3 below describe other features of these binary systems containing di-*tert*-butyl peroxide, and Appendix 4 brings up to date our earlier review of the work on the thermal decomposition of this molecule.

The authors are indebted to Professor J. S. Rowlinson, F.R.S., for helpful correspondence.

Appendix 1

The Reaction of tert-BuO with Cyclopropane

In Fig. 2 we show, in Arrhenius form, a plot of the ratio

$$\frac{k_2}{k_3} = \frac{[\mathrm{RH}]R_{\text{acetone}}}{R_{\textit{tert}\text{-butanol}}}$$

and it is clear that there is a marked break at the critical point of cyclopropane, similar to that indicated by the preliminary propane experiments; in this expression [RH] is simply the total number of moles of cyclopropane present in the vessel divided by the volume of the vessel. Hence, above T_c, the activation energy difference $(E_2 - E_3)$ is about 11 kcal/mol, but below T_c, there is an apparent difference of about 17 kcal/mol between E_2 and E_3; the figure of 11 kcal is consistent with previous data on the reaction of the *tert*-butoxy radical with toluene (2), propane (2), butane (10), and isobutane (10). A change in slope of this magnitude is much too large, in our view, to be caused by any cage or diffusion effects which may be present (3). We believe the explanation to be the following, and in the Appendix 2 below, we describe experiments which support this contention. The (approximately 400 to 1) cyclopropane–peroxide mixtures we use are such that two phases appear whenever the temperature is below T_c of the hydrocarbon, the liquid/gas ratio of course increasing as the temperature decreases. The concentrations of both hydrocarbon and peroxide will be different in each phase, each giving rise to its own characteristic acetone and *tert*-butanol production rates. It is a simple matter to write down expressions for the rates of formation of each product in either phase, and to show that the ratio of acetone/*tert*-butanol is different in the two phases; it is not quite so simple to show that the overall (*i.e.* gas + liquid) rate ratio is *less* than the gas-phase rate ratio would be at *the same mean* hydrocarbon concentration.

A least-squares treatment of the 21 points in Fig. 2, corresponding to experiments carried out above the critical point of cyclopropane gives

$$E_2 - E_3 = 10.96 \pm 0.47 \text{ kcal/mol}$$

$$\log \frac{A_2}{A_3} = 7.06 \pm 0.25 \text{ (mol/l)}$$

the rate of attack of the *tert*-butoxy radical on cyclopropane is just about a factor of ten slower than on propane (for example, at 124 °C, the values of k_2/k_3 are 12 and 1.2, respectively), although the activation energies are very similar (2).

Appendix 2

Attempts to Detect the Dew Point

If only one phase is present, a plot of the ratio of acetone/*tert*-butanol formation against $[\mathrm{RH}]^{-1}$, at fixed temperature, is a straight line of slope k_2/k_3 passing through the origin (2). Thus, starting at low hydrocarbon concentrations, one should find acetone/*tert*-butanol ratios lying on a straight line when plotted against $[\mathrm{RH}]^{-1}$: the straight line should point toward the origin, and should have a slope equal to the value of k_2/k_3 which can be determined by extrapolation of the gas-phase data in Fig. 2; as soon as phase separation occurs, the acetone/*tert*-butanol ratios should fall below the line. With this in mind, a series of 33 experiments was carried out at 115 °C, at cyclopropane densities ranging from 1 to 64 amagats. That these experiments were reliable was judged from the acetone + *tert*-butanol formation, which of

[3]Since this paper was written, these data have become available (9) and our estimate of liquid onset is confirmed: 119 °C for the highest and 116 °C for the lowest densities used in the subcritical temperature range.

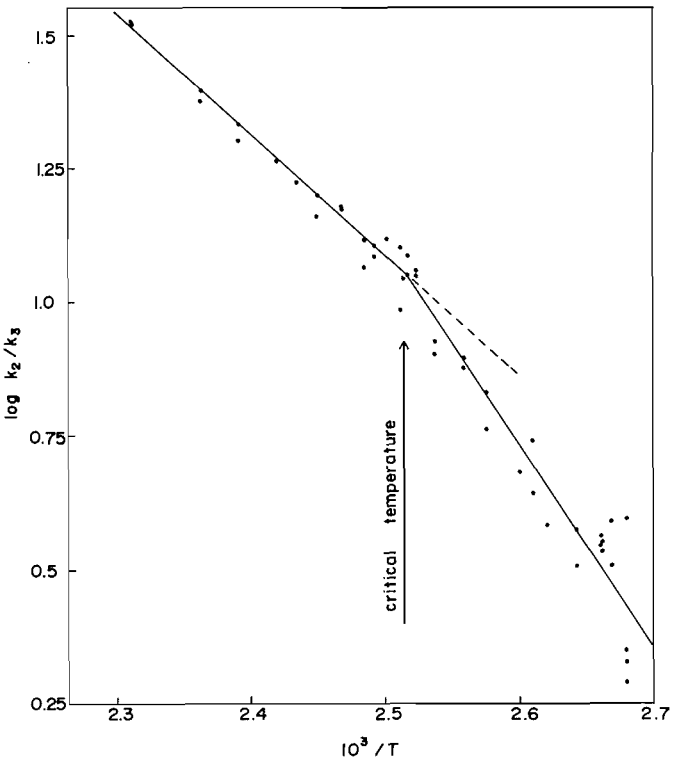

FIG. 2. Arrhenius plot of k_2/k_3 in the presence of 60–80 amagats of cyclopropane.

course gives k_1, and the mean of the 33 values of k_1 is shown in Fig. 4. At high pressures, the acetone/*tert*-butanol ratio was below the theoretical line as expected, but as the cyclopropane concentration was reduced, the ratios, instead of coming up to the predicted line, fell further and further below it! It was found, however, that if the vessel was packed with steel balls, lower acetone/*tert*-butanol ratios were obtained than at the same gas density in an unpacked vessel. It appears that reaction 3 has a heterogeneous component, which shows up because the reaction of *tert*-butoxy radicals with cyclopropane is so slow that some of the radicals scavenge hydrogen atoms from the metal surface to form *tert*-butanol; thus, a demonstration of the effect of liquid onset would need a much more reactive hydrocarbon, and preferably also a higher temperature.

Consequently, a similar series of experiments was performed using isobutane as the hydrocarbon; these experiments were carried out at 118.3 °C, the highest temperature at which accurate density data is available for isobutane (11). The results are shown in Fig. 3 for the acetone/*tert*-butanol formation ratio, and the values of k_1 derived from acetone + *tert*-butanol, used as a reliability check, are shown in Fig. 4. The low-pressure data in Fig. 3 do lie on a reasonable straight line having zero intercept and a slope k_2/k_3 of about 0.40 mol/l, indicating that the rate of reaction of the *tert*-butoxy radical with isobutane is about twice as fast as with propane at 118 °C. The high-pressure data in Fig. 3 do seem to fall below this line, and would suggest that the dew

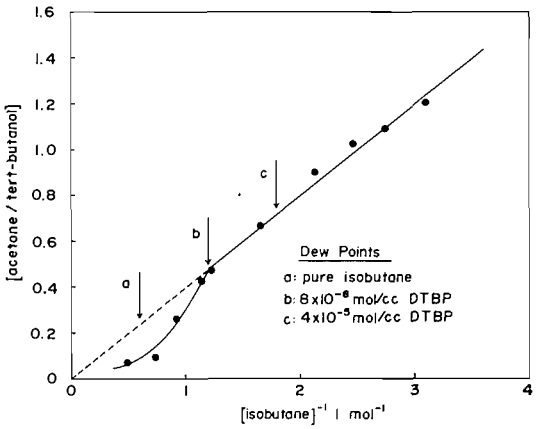

FIG. 3. Illustration of liquid onset in isobutane/di-*tert*-butyl peroxide mixtures at 118.3 °C.

point occurs near [isobutane]$^{-1} \approx 1.2$ l/mol, *i.e.* [isobutane] ≈ 0.8 mol/l ≈ 18.5 amagats; the dew point in *pure* isobutane (11) is at much higher densities (1.6 mol/l ≈ 36.6 amagats), also shown on Fig. 3. All the measurements plotted in Fig. 3 were made in the same reaction vessel. A second set, made in the other reaction vessel were distinguishable from them, having a slightly higher slope of 0.43 mol/l, but with the break at about the same

Can. J. Chem. Downloaded from www.nrcresearchpress.com by 210.87.254.6 on 09/05/12
For personal use only.

Can. J. Chem. Downloaded from www.nrcresearchpress.com by 210.87.254.6 on 09/05/12
For personal use only.

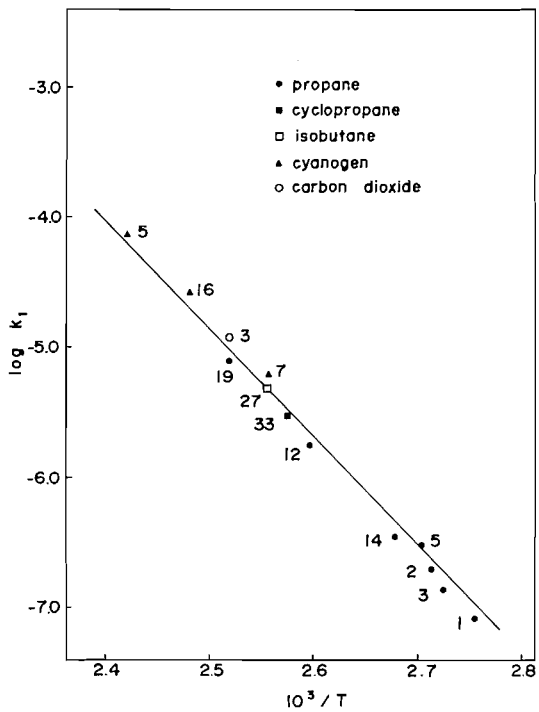

FIG. 4. Thermal decomposition of di-*tert*-butyl peroxide in the presence of high pressures of propane, cyclopropane, isobutane, cyanogen, and carbon dioxide: the line shown in the diagram is not fitted to the points, but is the line selected for k_1 in our earlier review of the published data (1); the integer adjacent to each point indicates the number of experiments the point represents.

density; presumably this slight difference in behavior is due to the heterogeneous effects already described above.

In a further attempt to confirm our hypothesis, this series of experiments was repeated in one reaction vessel using five times as much peroxide per filling (*i.e.* 5×10^{-4} mol). The dew point should now occur at even lower isobutane concentrations (8), and in fact a break similar to that shown in Fig. 3 occurred at about 0.55 mol/l (12.5 amagats). Unfortunately, this latter experiment is not absolutely conclusive because at low density, a falling-off in the acetone/*tert*-butanol ratio was observed, presumably as the result of abstraction from the wall; at the same time, the limiting high pressure gas phase rate-constant ratio k_2/k_3 appeared to be a little low, 0.35 mol/l, presumably for the same reason. Thus, we feel that our explanation of the break which occurs in Fig. 2 at the critical point of cyclopropane (and the similar one found for propane) is moderately well substantiated; hence, one has the possibility that in some system uncomplicated by wall effects and given somewhat more reproducible analytical procedures, dew-point curves could be deduced from kinetic observations.

Appendix 3

Experiments with Carbon Dioxide and Cyanogen

A few experiments were performed with carbon dioxide and with cyanogen as pressurizing gases. Virtually no *tert*-butanol was formed in these cases, and in this sense the values of k_1 shown in Fig. 4 more nearly resemble those determined previously (1) in experiments where only the rate of formation of acetone was measured.

The cyanogen experiments are interesting in several respects. In the first place, there is a very rapid removal of methyl radicals by cyanogen, to the extent that ethane could be detected only at sub-atmospheric pressures; on the other hand, no volatile nitrogen-containing products were found, only a brown coloration on the (glass) vessel walls, which was not paracyanogen. We postulate the reaction

$$[4] \qquad CH_3 + C_2N_2 \rightarrow [?] \rightarrow \text{solid products}$$

and will proceed to deduce its rate. Apart from forming ethane

$$[5] \qquad CH_3 + CH_3 \rightarrow C_2H_6$$

all the methyl radicals formed by reaction 2 must abstract from DTBP or acetone to form methane, or react with cyanogen. Thus, the rate of reaction 4 can be obtained from the methyl-radical balance *i.e.*

$$R_4 = R_{\text{acetone}} - R_{\text{methane}} - 2R_{\text{ethane}}$$

and in Fig. 5 we show a plot of $R_4/R_{\text{ethane}}^{1/2}$ against $[C_2N_2]$, the slope of which gives $k_4/k_5^{1/2} \approx 20$ mol$^{-1/2}$ cm$^{3/2}$ s$^{-1/2}$ at 130 °C; similar values of $k_4/k_5^{1/2}$ were obtained at 118 and at 140 °C, suggesting that reaction 4 has virtually zero activation energy, but rather a low frequency factor.

Second, the consistency of k_1 with the other data for reaction 1 means that even at the highest cyanogen concentrations (34 amagats), the *tert*-butoxy radical does not react with cyanogen to any detectable extent. And third, that at high cyanogen pressures, some methyl cyanide is formed: it can be detected in all experiments using more than 5 amagats of cyanogen; it is rather

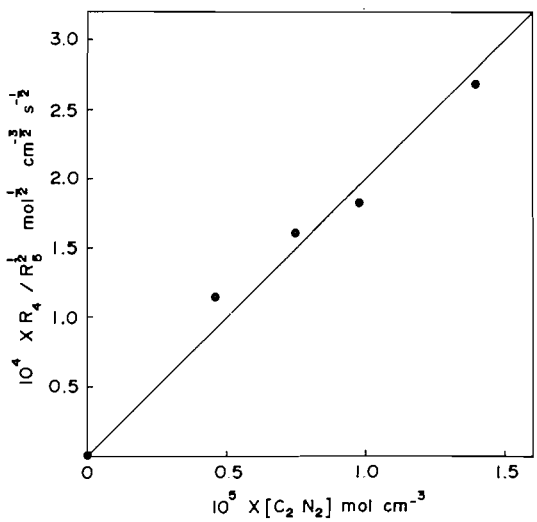

FIG. 5. The reaction of methyl radicals with cyanogen at 130 °C.

variable, but accounts for about 5% of the methyl radicals at these pressures, rising to more than 50% of the methyl radicals above 30 amagats. The reaction

[6] $$R + C_2N_2 \rightarrow RCN + CN$$

has been postulated in the liquid phase (12), and clearly reaction 4 as written is an oversimplification.

Appendix 4

Tabulated Data

In our previous review of the thermal decomposition of di-*tert*-butyl peroxide (1), we lodged a list of 272 values of k_1 with the National Science Library in Ottawa. One set of data obtained by Brinton and Volman (13) was inadvertently omitted from this list, and two new sets of data have been published (14, 15) since, as follows:

Temperature range (°C)	Number of points	E (kcal/mol)	log A (s^{-1})	Reference
130–167	7	37.44±1.05	15.56±0.55	13
231–254	8	39.46±0.41	16.59±0.17	14
140–165	6	37.77±0.48	15.82±0.25	15

Whilst the Arrhenius slopes of two of these sets of data differ somewhat from our selected value, the points lie very close to our selected line, and their inclusion would not alter perceptibly our selected values (1) of the Arrhenius parameters for k_1. As part of this paper, we now lodge a further list of 219 values of k_1, the 21 mentioned above, and 198 values obtained in this work,[4] and in ref. 2. Only one point merits comment here, a caveat on the use of least squares with inconsistent sets of data. We have separated the data in Fig. 1 and Fig. 4 on the basis of reproducibility[2]: the cyclopropane analyses were the cleanest of the whole set; the propane experiments were performed at a much earlier date and relatively poor for that reason; in the isobutane experiments, the closeness of the boiling point to that of acetone is a problem; the cyanogen and carbon dioxide experiments were only exploratory in nature, and the analytical procedure was not optimized. The following data illustrate our point.

Data set	Temperature range (°C)	Number of points	E (kcal/mol)	log A (s^{-1})
Cyclopropane	100–160	80	38.12±0.53	15.94±0.29
Propane	90–124	56	38.31±0.59	15.99±0.34
Cyanogen	118–140	28	36.37±0.71	15.14±0.38
All three sets	90–160	164	40.31±0.41	17.17±0.23

In our view, the importance of this kind of averaging on the discussion of anomalous Arrhenius parameters needs to be well appreciated, for it can arise not only, as in this case, when data having different systematic errors in different temperature ranges are combined (see Fig. 4), but when there is a variation of reliability with temperature within one set of data; we refer again to footnote 2 of ref. 1, and to the recent discussions by Thorn of this problem in another context (16).

1. D. H. Shaw and H. O. Pritchard. Can. J. Chem. **46**, 2721 (1968).
2. C. K. Yip and H. O. Pritchard. Can. J. Chem. **47**, 4708 (1969).
3. C. Walling and G. Metzger. J. Am. Chem. Soc. **81**, 5365 (1959).
4. J. Aspden, N. A. Khawaja, J. Reardon, and D. J. Wilson. J. Am. Chem. Soc. **91**, 7580 (1969).
5. J. H. Raley, F. F. Rust, and W. E. Vaughan. J. Am. Chem. Soc. **70**, 88 (1948).
6. A. P. Kudchadker, G. H. Alani, and B. J. Zwolinski. Chem. Rev. **68**, 659 (1968).
7. W. V. Stearns and E. J. George. Ind. Eng. Chem. **35**, 602 (1943).
8. J. S. Rowlinson. Liquids and liquid mixtures. Butterworths, London. 1959. Chap. 6.
9. D. C-K. Lin, I. H. Silberberg, and J. J. McKetta. J. Chem. Eng. Data, **15**, 483 (1970).
10. J. L. Brokenshire, A. Nechvatal, and J. M. Tedder. Trans. Faraday Soc. **66**, 2029 (1970).
11. B. H. Sage and W. N. Lacey. Ind. Eng. Chem. **30**, 673 (1938).
12. D. D. Tanner and N. J. Bunce. J. Am. Chem. Soc. **91**, 3028 (1969).
13. R. K. Brinton and D. H. Volman. J. Chem. Phys. **20**, 25 (1952).
14. D. G. Retzloff, B. M. Coull, and J. Coull. J. Phys. Chem. **74**, 2455 (1970).
15. D. E. Hoare, T-M. Li, and A. D. Walsh. Proceedings of the Twelfth Symposium (International) on Combustion, 357 (1969).
16. R. J. Thorn. J. Chem. Phys. **52**, 474 (1970).

[4]This list of rate constants can be obtained free of charge upon request from: The Depository of Unpublished Data, National Science Library, National Research Council of Canada, Ottawa, Canada.

Can. J. Chem. Downloaded from www.nrcresearchpress.com by 210.87.254.6 on 09/05/12
For personal use only.

Can. J. Chem. Downloaded from www.nrcresearchpress.com by 210.87.254.105 on 09/05/12
For personal use only.

New Syntheses of Demethylsuberosin, Xanthyletin, (±)-Decursinol, (+)-Marmesin, (−)-Nodakenetin, (±)-Decursin, and (±)-Prantschimgin[1]

WARREN STECK

National Research Council of Canada, Prairie Regional Laboratory, Saskatoon, Saskatchewan

Received February 25, 1971

The title compounds, natural coumarins or their racemic modifications, were synthesized via malonic acid condensations with appropriate salicylaldehydes. Oxidation of 2,4-dihydroxy-5-(3-methyl-2-butenyl)benzaldehyde with DDQ, peracid, and acid–peracid gave the aldehydes for xanthyletin, marmesin, and decursinol, respectively. Some ^{14}C-labelled coumarins were prepared similarly. The n.m.r. spectral data for the products are presented.

Les produits mentionnés dans le titre qui sont des coumarines naturelles ou des modifications racémiques ont été synthétisées en faisant appel à la condensation malonique sur les salicaldéhydes appropriés. Les aldéhydes nécessaires pour la préparation de la xanthylétine, de la marmésine et du décursinol ont respectivement été obtenus par oxydation du dihydroxy-2,4 (méthyl-3 butén-2 yl)-5 benzaldéhyde à l'aide du DDQ, de péracide et d'acide péracide. On a préparé de la même manière quelques coumarines contenant du ^{14}C. On rapporte les spectres de r.m.n. des produits.

Canadian Journal of Chemistry, 49, 2297 (1971)

Introduction

The synthesis of coumarins can be achieved in several ways, of which the most widely used are the Pechmann reaction (1), the Perkin reaction (2), and condensation with malonic acid derivatives. The latter reactions require salicylaldehydes as starting materials, and encounter difficulties when applied to the synthesis of natural coumarins: for example, the malonate route has as the final step decarboxylation of the 3-carboxycoumarin, which may affect other functional groups present; the severe conditions of the Perkin reaction may be similarly deleterious. But in practice the most immediate problem in most cases lies in obtaining the suitably substituted salicylaldehydes to begin with, especially when isoprenoid coumarins are desired.

I have solved this problem for a number of natural products by chemical manipulation of 2,4-dihydroxy-5-(3-methyl-2-butenyl)benzaldehyde, have converted the aldehydes to coumarins, and have demonstrated the application of these sequences to radiochemical labelling. Some biogenetic-type syntheses of natural coumarins have been carried out similarly.

Results and Discussion

2,4-Dihydroxy-5-(3-methyl-2-butenyl)benzaldehyde (**1***a* in Scheme 1) was prepared from 2,4-dihydroxybenzaldehyde and 3-hydroxy-3-methyl-1-butene as previously reported (3). It was condensed with malonic acid under a variety of conditions, producing a number of products. Under vigorous reaction conditions cyclization of the initially formed product (3-carboxy-6-[3-methyl-2-butenyl]-7-hydroxycoumarin, **2***a*) usually occurred, affording 3-carboxydihydroxanthyletin (4). Only under very mild conditions of condensation was **2***a* obtained, but in such cases the yields were excellent, and the product could be decarboxylated satisfactorily to **3***a* (demethylsuberosin) by controlled heating in copper–quinoline. The final product was compared directly with natural material isolated from *Chloroxylon swietenia* wood. This is a more convenient synthetic method for this coumarin than that involving the Perkin reaction (5).

The aldehyde **1***a* was oxidatively cyclized in three ways to provide salicylaldehyde derivatives for the synthesis of marmesin, decursinol, and xanthyletin. With 2,3-dichloro-5,6-dicyano-1,4-benzoquinone (DDQ) as oxidant, the chromene **1***b* was obtained in good yield, m.p. 95–96°. Its conversion to 3-carboxyxanthyletin and xanthyletin (**3***b*) was straightforward. With *m*-chloroperoxybenzoic acid/*p*-toluenesulfonic acid as an oxidant system the chromanol **1***c* was obtained in good yield, m.p. 97.5–99°; from it was prepared (±)-decursinol (**3***c*). With neutral *m*-chloroperoxybenzoic acid, **1***a* gave a mixture of **1***c* and **1***d* which was most easily separated by column chromatography on silicic acid. In

[1]NRCC No. 11943.

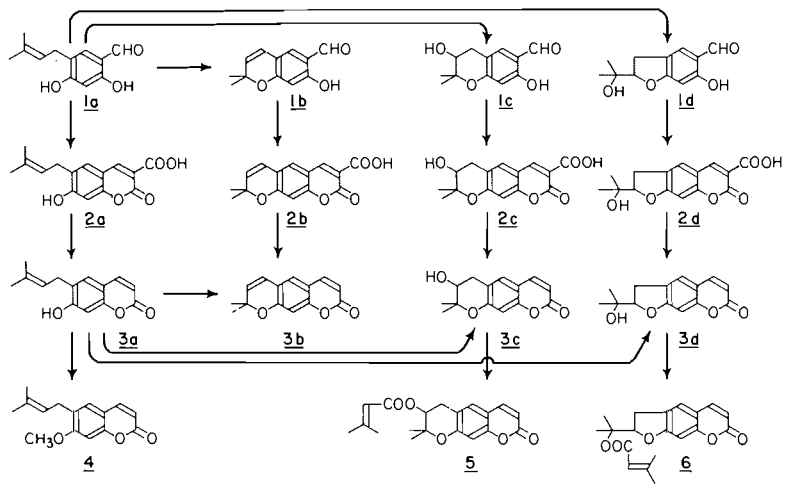

SCHEME 1. Transformations of 2,4-dihydroxy-5-(3-methyl-2-butenyl)-benzaldehyde (**1***a*).

chloroform **1***d* always predominated in at least a 2:1 ratio, and the formation of **1***c* could be suppressed entirely by using a trace of triethylamine in the reaction or by using acetone as the solvent. (±)-Marmesin (**3***d*) was synthesized from **1***d*; the intermediate acid has been optically resolved, and the isomers decarboxylated, previously (6). In my hands the reported alkaline bisulfite decarboxylation method was unsatisfactory, so that here again, copper–quinoline proved a better method. Condensations of **1***d* with [2-^{14}C]malonic acid were also successful, leading to (+)-, (−)-, and (±)-[3-^{14}C]marmesin.

Demethylsuberosin (**3***a*), oxidized in the same ways as **1***a*, gave directly xanthyletin (**3***b*) with DDQ, and (±)-decursinol (**3***c*) and (±)-marmesin with peracid. This last reaction is a biogenetic-type synthesis which undoubtedly proceeds through an epoxide intermediate, as suggested for the *in vivo* formation of the products (7). Both (+)- and (−)-marmesin as well as (+)- and (−)-decursinol occur naturally and many of their esters have also been isolated from plants. For example (−)-marmesin angelate (8), (−)-prantschimgin (**6**) (9), and (−)-marmesin benzoate (10) have been isolated from umbellifers, and (+)-decursinol angelate (11) and (+)-decursin (**5**) (12) are also known. Warming 5 mg each of (±)-marmesin and senecioyl chloride in a few drops of pyridine gave an excellent yield of (±)-prantschimgin, m.p. 145–147°, readily identified by its n.m.r. spectrum. Similar reaction of (±)-decursinol and senecioyl chloride gave (±)-decursin as a glassy substance, its n.m.r. spectrum superimposable on that of natural decursin.

Aldehydes **1***a* and *d* were used as starting materials for the preparation of ^{14}C-labelled coumarins. From **1***a* about 30% [3-^{14}C]demethylsuberosin was obtained. From **1***d* both (+)-[3-^{14}C]marmesin and (−)-[3-^{14}C]nodakenetin (= (−)-[3-^{14}C]marmesin) were prepared by resolving the intermediate ^{14}C-carboxylic acid with brucine (6) and thermally decarboxylating each isomer. Besides the yield of each pure isomer (24 and 32%) a further 20% of racemic (±)-[3-^{14}C]marmesin also resulted from work-up of combined mother liquors.

The difficulty of introducing a 3-methyl-2-butenyl type group into the 6-position of preformed 7-hydroxycoumarins is well known (13, 14); consequently the synthesis of linear three-ring coumarins has usually been launched from natural coumarins in which the necessary substituents are already in place (11). Rearrangements of 7-alkoxycoumarins favor 8-alkylation (15). The methods described above give linear compounds readily and in generally good yields, and seem to represent an improvement over existing methods of synthesis.

Experimental

All melting points are uncorrected. The n.m.r. spectra were obtained with a Varian HA-100 instrument using tetramethylsilane as an internal reference standard and are summarized for nine coumarins in Table 1.

Authentic 7-demethylsuberosin and xanthyletin were obtained by extraction of ground *Chloroxylon swietenia* wood (16).

Can. J. Chem. Downloaded from www.nrcresearchpress.com by 210.87.254.105 on 09/05/12
For personal use only.

Can. J. Chem. Downloaded from www.nrcresearchpress.com by 210.87.254.105 on 09/05/12
For personal use only.

TABLE 1. The n.m.r. spectral data for some synthetic coumarin derivatives (Scheme 1)*

Compound	Solvent	H-3	H-4	H-5	H-8	H-a	H-b	*gem*-CH_3's	Other
2*a*	d_6-DMSO	—	8.66 s	7.57 s	6.77 s	3.24 d^7 (CH_2)	5.28 t^7	1.68, 1.70 s	7-OH 11.1; COOH 12.8
2*b*	$DCCl_3$	—	8.79 s	7.28 s	6.81 s	6.39 d^{10}	5.78 d^{10}	1.52 s	COOH 12.2
2*c*	$DCCl_3$	—	8.78 s	7.43 s	6.87 s	3.15 d^5d^{16} 2.89 d^6d^{16}	3.93 d^5d^6	1.41, 1.44 s	OH 1.95; COOH 12.2
2*d*	d_6-DMSO	—	8.66 s	7.66 s	6.82 s	4.75 t^8	3.19 d^8	1.14, 1.17 s	OH 4.70; COOH 12.6
3*a*	$DCCl_3$	6.23 $d^{9.5}$	7.65 $d^{9.5}$	7.44 s	7.07 s	3.38 d^7 (CH_2)	5.32 t^7	1.75, 1.80 s	OH 7.20
3*b*	$DCCl_3$	6.19 $d^{9.5}$	7.56 $d^{9.5}$	7.03 s	6.71 s	6.33 d^{10}	5.67 d^{10}	1.46 s	
3*c*	$DCCl_3$	6.19 $d^{9.5}$	7.54 $d^{9.5}$	7.15 s	6.76 s	3.07 d^5d^{16} 2.80 d^6d^{16}	3.86 d^5d^6	1.35, 1.38 s	OH 1.86
3*d*	d_6-DMSO	6.21 $d^{9.5}$	7.93 $d^{9.5}$	7.48 s	6.79 s	3.18 d^8 (CH_2)	4.71 t^8	1.16 s	OH 4.66
3*d*	$DCCl_3$	6.16 $d^{9.5}$	7.56 $d^{9.5}$	7.19 s	6.70 s	3.20 d^8 (CH_2)	4.72 5^8	1.24, 1.36 s	OH 1.96
4	$DCCl_3$	6.21 $d^{9.5}$	7.60 $d^{9.5}$	7.17 s	6.76 s	3.30 d^7 (CH_2)	5.28 t^7	1.70, 1.76 s	OCH_3 3.89

*δ-Values. s, Singlet; d, doublet; t, triplet; m, multiplet; superscripts are *J* values in Hz. H-a is the proton or protons of the sidechain carbon next to the aromatic ring; H-b is the proton of the carbon beyond.

Can. J. Chem. Downloaded from www.nrcresearchpress.com by 210.87.254.105 on 09/05/12
For personal use only.

3-Carboxy-6-(3-methyl-2-butenyl)-7-hydroxycoumarin (2a)

Malonic acid and **1***a* (1.0 g each) were dissolved in 5.5 ml pyridine containing 0.5 ml aniline, and the solution, after 24 h at 22°, was poured into 80 ml ice-cold 10% HCl. The yellow precipitate was washed with cold water to remove mineral acid, then air dried. Yield 1.3 g (100%), m.p. 205–215°, raised to 218–224° on recrystallization from EtOAc–MeOH–hexane [2:1:2]. λ_{max} (EtOH) 261, 363 nm. For n.m.r. data see Table 1.

6-(3-Methyl-2-butenyl)-7-hydroxycoumarin (Demethylsuberosin, 3a)

Crude **2***a* (0.23 g) in 2 ml quinoline containing 0.4 g Cu powder was held 3 min at 215–220° in an oil bath, cooled and diluted with 30 ml chloroform. The decanted solution was shaken with 2 × 30 ml 10% HCl then with 30 ml water. The dried chloroform solution was evaporated, leaving a tacky orange solid which was chromatographed on a small amount of silicic acid (developed with 50 up to 100% EtOAc–hexane) to afford 0.12 g (62%) cream crystals of **3***a*, m.p. 129–133° (lit. m.p. 133–134° (16)). The product co-chromatographed (paper chromatography, t.l.c., g.l.c.) with authentic material and had identical u.v. and n.m.r. spectra. λ_{max} (EtOH) 247, 257, 333 nm.

2H-2,2-Dimethyl-7-hydroxychromen-6-aldehyde (1b)

Compound **1***a* (0.60 g) was oxidized with 0.6 g DDQ (2,3-dichloro-5,6-dicyanobenzoquinone) in 15 ml benzene (5 min boiling). The filtrate was freed of solvent and the residue chromatographed on silicic acid (ether–hexane, 1:1), giving 0.44 g (75%) colorless crystals of **1***b*, m.p. 95–96° from hexane.

Anal. Calcd. for $C_{12}H_{12}O_3$: C, 70.6; H, 5.9. Found: C, 70.4; H, 6.0.

The n.m.r. signals ($DCCl_3$) at δ 1.46 (singlet, CH_3's); 5.58 and 6.26 (doublets, J = 9.5 Hz, H-3 and -4); 7.10 and 6.33 (singlets, H-5 and -8); 9.67 (singlet, CHO), and 11.4 (singlet, 7-OH).

Xanthyletin (3b)

The procedure for **2***a* gave, from 0.40 g **1***b* and 0.7 g malonic acid, 0.4 g crude and 0.21 g (40%) purified **2***b*, m.p. 193–195° from alcohol. λ_{max} (EtOH) 263, 280, 374 nm. Decarboxylation in copper–quinoline (235–240° for 5 min) gave, after work-up, 50% yield of **3***b*, m.p. 128–130° (lit. m.p. 128–131° (16)).

(±)-2,2-Dimethyl-3,7-dihydroxychroman-6-aldehyde (1c)

A mixture of 0.50 g **1***a*, 0.50 g *m*-chloroperoxybenzoic acid, 0.02 g *p*-toluenesulfonic acid, and 60 ml chloroform were kept overnight at room temperature, then the solution was washed with dilute aqueous $NaHCO_3$ and H_2O. Evaporation of the chloroform left crystals, m.p. 97.5–99°, from benzene–hexane. Yield 0.4 g (75%).

Anal. Calcd. for $C_{12}H_{14}O_4$: C, 64.8; H, 6.3. Found: C, 64.5; H, 6.5.

The n.m.r. signals ($DCCl_3$) at δ 1.36 and 1.38 (CH_3's), 6.36 (H-8), 7.21 (H-5), 9.65 (CHO), and 11.0 (7-OH), all singlets; 2.05 (broad, 3-OH). The presence of a six-membered ring was indicated by a —CH_2CH— ABX system, δ 2.73 and 3.02 (doublets of doublets, J_{AB} = 16 Hz, CH_2), 3.82 (doublet of doublet, J_{AX} = 5, J_{BX} = 6 Hz, CH).

(±)-Decursinol (3c)

The procedure for **2***a* gave, from 1.6 g **1***c* and 2.5 g malonic acid, 1.5 g (72%) **2***c*, m.p. 191.5–193° from methanol. λ_{max} (EtOH) 358 nm.

Anal. Calcd. for $C_{15}H_{14}O_6$: C, 62.0; H, 4.9. Found: C, 61.7; H, 5.0.

This product (0.10 g) was decarboxylated in copper–quinoline (230° for 10 min) to give about 0.05 g **3***c*, m.p. 166–168° from benzene (lit. m.p. 167.5–168.5° (11)). λ_{max} (EtOH) 248, 258, 329 nm.

(±)-2,3-Dihydro-2-(1-hydroxy-1-methylethyl)-6-hydroxybenzofuran-5-aldehyde (1d)

Aldehyde **1***a* was oxidized as in the preparation of **1***c* above but omitting *p*-toluenesulfonic acid. The crude product was chromatographed on a small column of silicic acid (developed with 1:1 ether–hexane) to obtain first a small amount of **1***c*, then **1***d* (65–85% yield), m.p. 116–118° from benzene:hexane (lit. m.p. 117–118°) (6)). The n.m.r. signals ($DCCl_3$) at δ 1.23 and 1.35 (CH_3's), 1.75 (*t*-OH), 6.36 (H-7), 7.26 (H-5), 9.65 (CHO) and 11.7 (6-OH), all singlets. A five-membered ring was indicated by the coupled signals at δ 3.11 (doublet, CH_2) and 4.71 (triplet, CH, J = 8.5 Hz).

(±)-Marmesin (3d)

This was made from **1***d* by the reported method (6). From 0.20 g malonic acid and 0.12 g aldehyde kept 24 h in 2 ml pyridine containing a drop of aniline was obtained 0.15 g (95%) **2***d*, m.p. 217–222° (lit. 222–223°). The decarboxylation with bisulfite and alkali (6) gave poor yields and was replaced by the copper–quinoline method (50–80% yields).

[3-^{14}C]Demethylsuberosin

A solution of 100 mg **1***a* and 52 mg [2-^{14}C]malonic acid in 0.5 ml 9:1 pyridine:aniline was kept 4 h, then a further 50 mg non-labelled malonic acid was added. After yet another 18 h the solution was acidified with ice – 3 *N* HCl and the precipitated yellow solid was filtered, washed thoroughly with cold water, and air-dried to give 140 mg (107%) crude [3-^{14}C]-**1***b*. It was decarboxylated by heating 3.5 min at 214–218° in 1.5 ml quinoline containing 0.3 g copper powder. Work-up as described above gave a tacky orange product which was purified by chromatography on silicic acid followed by chromatography on Polyclar AT powder (development with 2:1 methanol–water). Yield of [3-^{14}C]demethylsuberosin was 38 mg (33%) after recrystallization from ethyl acetate – hexane. A further 6 mg (5%) was recovered from the mother liquors. The material was radiochemically pure and melted at 131.5–133° (lit. m.p. 133–134° (16)).

(+)-[3-^{14}C]Marmesin and (−)-[3-^{14}C]Nodakenetin

A solution of 0.45 g **1***d* and 0.21 g [2-^{14}C]malonic acid in 3 ml pyridine and 0.2 ml aniline was kept overnight at room temperature, then 0.40 g non-labelled malonic acid was added. After a further 24 h the solidified reaction mixture was stirred with 30 ml ice – 3 *N* HCl and the yellow solid was filtered, washed with water, and air

Can. J. Chem. Downloaded from www.nrcresearchpress.com by 210.87.254.105 on 09/05/12
For personal use only.

dried. The yield of (±)-3-carboxy[3-^{14}C]marmesin was 0.49 g (84% based on aldehyde). This was boiled 2 min with 0.70 g (−)-brucine in 10 ml methanol, then the solvent was evaporated and the residue crystallized overnight from 30 ml water. Hydrolysis (6) of crystals and mother liquors gave, respectively, 0.23 g crude (+)-3-carboxy[3-^{14}C]marmesin and 0.20 g crude (−)-3-carboxy[3-^{14}C]nodakenetin. Recrystallization from methanol (150 ml per g acid) gave 0.18 and 0.12 g of pure materials, both m.p. 240–244° (lit. m.p. 241,° 236–237° (6)). Each isomer was decarboxylated in 2 ml quinoline containing 0.2 g Cu powder (7 min at 230–232°), and the products, isolated in the way described above, were recrystallized from benzene (about 100 ml/g coumarin). Overall yield of (+)-[3-^{14}C]marmesin, m.p. 178–186° (lit. m.p. 186.5–187° (6)), was 0.08 g (32% of theoretical); yield of (−)-[3-^{14}C]nodakenetin, m.p. 186–189° (lit. m.p. 188–189° (6)) was 0.06 g (24%). Both products gave only one radioactive spot on paper chromatograms.

(±)-[3-^{14}C]Marmesin

All the mother liquors from the above crystallizations were combined and concentrated to give a crystalline mixture of labelled marmesin and 3-carboxymarmesin which was decarboxylated to provide 0.10 g (20% based on aldehyde) (±)-[3-^{14}C]marmesin, m.p. 150–152° (lit. m.p. 153–154° (6)).

Derivatives of 3a

(±)-Marmesin and (±)-Decursinol

Oxidation of **3a** with 1 equiv of *m*-chloroperoxybenzoic acid gave (±)-marmesin and a small amount of (±)-decursinol, which were separated by column chromatography on silicic acid (development with 1:3 EtOAc–hexane). (±)-Decursinol was eluted first, m.p. 166–168° from CH_2Cl_2–ether (lit. m.p. 167.5–168.5° (11)), and was identified by g.l.c., n.m.r. spectrum, and by comparison with **3c** prepared as described above. (±)-Marmesin was eluted next, m.p. 152–154° from benzene (lit. m.p. 153–154° (6)), and was identified similarly.

Xanthyletin

Oxidation of **3a** with DDQ in boiling benzene gave a 50% yield of xanthyletin, m.p. 128–130° (lit. m.p. 128–131° (16)) which was identical with xanthyletin as prepared earlier and with xanthyletin isolated from *Chloroxylon swietenia*.

Suberosin (4)

A solution of 0.1 g **3a** in 3 ml 1:1 methanol–methylene chloride was treated with 3 ml fresh diazomethane solution. Evaporation of the solvent left a viscous yellow syrup which on chromatography gave mostly suberosin, m.p. 84–86° (lit. m.p. 86–87° (5)), whose identity was confirmed by n.m.r.

(±)-Prantschimgin (6)

A solution of about 5 mg (±)-marmesin in 0.1 ml pyridine was treated with 1 drop of senecioyl chloride (3-methyl-2-butenoyl chloride) and warmed a few minutes. After dilution with CH_2Cl_2 and work-up as for decarboxylation reactions, 6 mg yellow syrup was obtained. Gas chromatography showed one major peak. The product from a five-fold reaction was crystallized from ethyl acetate – hexane to needles, m.p. 145–147°, and identified by n.m.r. spectroscopy. Besides appropriate signals for the marmesin nucleus, senecioate peaks were seen at δ 5.53 (quartet $J \sim 1$ Hz, = CH), 2.09 (doublet, $J \sim 1$ Hz, *trans*-CH_3) and 1.85 (doublet, $J \sim 1$ Hz, *cis*-CH_3).

(±)-Decursin (5)

This was prepared from (±)-decursinol and senecioyl chloride in the same manner as (±)-prantschimgin, and was isolated pure by gas chromatography. It was obtained as a glassy product and was characterized by n.m.r. (signals, assigned as above, at δ 5.67, 2.14, and 1.88). The same spectrum and gas chromatographic behavior was exhibited by a specimen of natural decursin.

I thank Mr. B. K. Bailey for skillful technical assistance, Mr. W. Haid for microanalyses, and Mr. M. Mazurek for measurement of n.m.r. spectra. A specimen of natural decursin was kindly supplied by Prof. K. Hata (Osaka College of Pharmacy, Osaka, Japan); *Chloroxylon swietenia* wood was the generous gift of Robert Bury & Co., Toronto, Ontario. I am also indebted to Drs. D. J. Austin and S. A. Brown for their interest and assistance in problems of synthesis.

1. S. Sethna and R. Phadke. *In* Organic reactions. **7**, 1 (1953).
2. J. R. Johnson. *In* Organic reactions. **1**, 210 (1942).
3. W. Steck. Can. J. Chem. **49**, 1197 (1971).
4. J. C. Bell, W. Bridge, and A. Robertson. J. Chem. Soc. 1542 (1937).
5. P. W. Austin and T. R. Seshadri. Indian J. Chem. **6**, 412 (1968).
6. M. Nakajima, J. Oda, and H. Fukami. Agric. Biol. Chem. **27**, 695 (1963).
7. S. A. Brown, M. El-Dakhakhny, and W. Steck. Can. J. Biochem. **48**, 863 (1970).
8. G. K. Nikonov. Dokl. Acad. Nauk SSSR **156**, 1210 (1964).
9. G. A. Kuznetsova and L. M. Belenovskaya. Khim. Prir. Soedin. **2**, 235 (1966).
10. I. Ognyanov and D. Botcheva. Z. Naturforsch. **22b**, 1231 (1967).
11. J. Lemmich, E. Lemmich, and B. E. Nielsen. Acta Chem. Scand. **20**, 2497 (1966).
12. K. Hata and K. Sano. Tetrahedron Lett. 1461 (1966).
13. F. M. Dean. Naturally occurring oxygen ring compounds. Butterworths, London, 1963.
14. J. Hlubucek, E. Ritchie, and W. C. Taylor. Tetrahedron Lett. 1369 (1969).
15. R. D. H. Murray, M. M. Ballantyne, and K. P. Mathai. Tetrahedron Lett. 243 (1970).
16. F. E. King, J. R. Housley, and T. J. King. J. Chem. Soc. 1392 (1954).

Can. J. Chem. Downloaded from www.nrcresearchpress.com by 210.87.254.5 on 09/05/12
For personal use only.

Further Investigations on the Chemistry of Fulvic Acid, a Soil Humic Fraction[1]

S. U. KHAN[2] AND M. SCHNITZER
Soil Research Institute, Canada Department of Agriculture, Ottawa, Canada

Received March 1, 1971

The fractionation scheme described in this and in an earlier paper resulted in the isolation and identification of about 2.0 g of pure components from 100 g of fulvic acid. About 28% of these compounds were phenolic acids, 19% benzenecarboxylic acids, 13% alkanes and fatty acids, and 40% dialkyl phthalates. The isolation of appreciable amounts of dialkyl phthalates was somewhat surprising but their presence was shown not be an artifact. The $KMnO_4$ oxidation of the same fractions increased the yields of methylated phenolic and benzenecarboxylic acids by between 3 and 11 times.

Following $KMnO_4$ oxidation of methylated but unfractioned fulvic acid, the yield of phenolic and benzenecarboxylic acids increased substantially. The increased yields, after oxidation, of the same compounds as those that were separated without oxidation indicate that either these compounds originated from more complex structures or that they came from a structure of the type proposed earlier, which consists of phenolic and benzenecarboxylic acids joined by hydrogen-bonds, on which alkanes, fatty acids, and dialkyl phthalates are adsorbed.

Le schéma de fractionnement dans cette note et dans une note précédente résulte de la séparation et de l'identification d'à peu près 2.0 g de constituants purs à partir de 100 g d'acide fulvique. Environ 28% de ces composés sont des acides phénoliques, 19% des acides benzènecarboxyliques, 13% des alcanes et des acides gras, et 40% de dialkylphtalates. L'isolement de quantités appréciables de dialkylphtalates avait quelque chose de surprenant mais il a été montré que leur présence était due à la réaction. L'oxydation par $KMnO_4$ des mêmes fractions a accru entre 3 et 11 fois les rendements d'acides phénoliques et benzènecarboxyliques méthylés.

Après une oxydation par $KMnO_4$ d'acide fulvique méthylé mais non fractionné, le rendement en acides phénoliques et benzènecarboxyliques est accru de façon notable. Les rendements accrus, après oxydation, des mêmes composés que ceux qui avaient été séparés sans l'oxydation indiquent soit que ces composés proviennent de structures plus complexes ou qu'ils sont issus d'une structure du type proposé précédemment. Cette structure est faite d'acides phénoliques et benzènecarboxyliques reliés par des liaisons hydrogène au sein desquelles les alcanes, les acides gras et les phtalates dialkylés sont adsorbés.

Canadian Journal of Chemistry, 49, 2302 (1971)

Introduction

In 1963, Barton and Schnitzer (1) proposed a new approach to unravelling the chemical structure of fulvic acid, a water-soluble, relatively low-molecular weight humic fraction. The fulvic acid was first exhaustively methylated so as to make it soluble in benzene. The benzene-soluble methyl esters and ethers were then separated over Al_2O_3 with the aid of solvents of increasing polarity into chromatographically homogeneous fractions which differed in molecular weights, oxygen-containing functional groups, and spectroscopic properties. In a recent communication (2) from this laboratory, an extension and modification of this approach was reported. Following preliminary separation over Al_2O_3, each fraction was further separated by t.l.c. and preparative gas-chromatography into relatively pure components which were identified by matching their mass and micro-i.r. spectra and gas chromatographic retention times with those of standards of known structures. Using this approach, over 20 phenolic and benzenecarboxylic acids were isolated as methyl ethers and esters from two fractions eluted from the Al_2O_3 column with mixtures of benzene and ethyl acetate.

The present report deals with the isolation from the same fulvic acid of major components from fractions of greater molecular complexity, that is, fractions that were eluted from the Al_2O_3 column with more polar solvents such as ethyl acetate and methanol. The major components of the fractions were identified by the same techniques that had been used in the previous investigation (2). We were especially interested

[1]Contribution No. 367, Soil Research Institute.

[2]On interdepartmental transfer of work from the Research Station, Canada Department of Agriculture, Lacombe, Alberta.

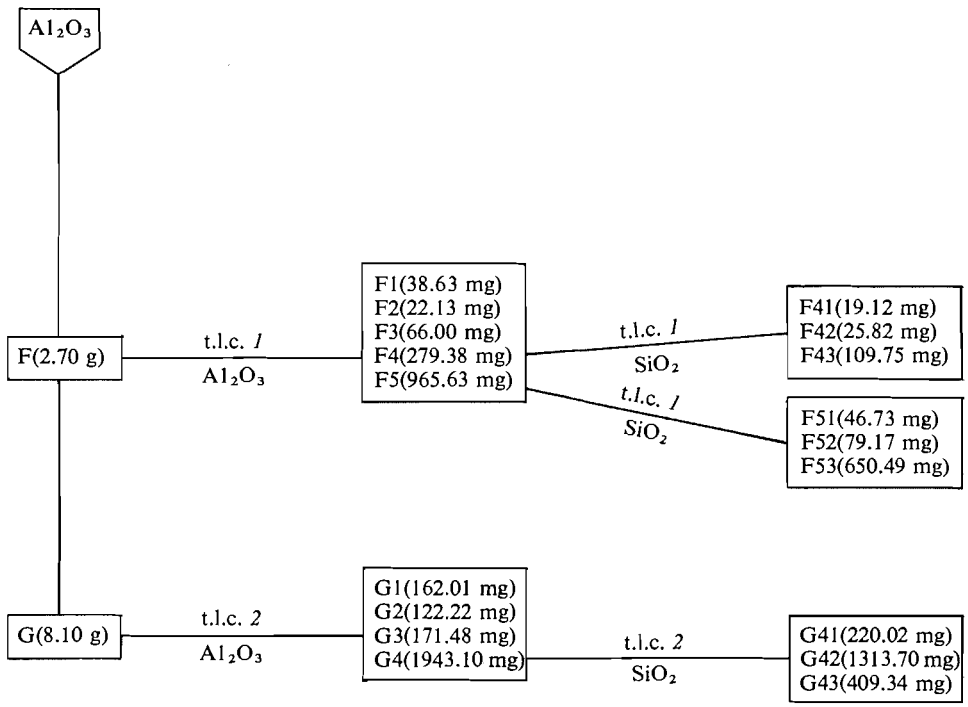

FIG. 1. Fractionation scheme (t.l.c. 1: toluene – ethyl acetate (1:1); t.l.c. 2: toluene – ethyl acetate (2:1)).

in finding out how our approach, which does not involve any chemical degradation, would work with the chemically more complex fractions. To obtain additional information on the main components of the two fractions, we oxidized each fraction with alkaline $KMnO_4$ and identified the oxidation products.

Experimental

Extraction, Purification, Methylation, and Separation of Fulvic Acid

The origin of the fulvic acid, methods of extraction, purification, methylation, and separation over Al_2O_3 were identical to those described previously (2).

Briefly, 100 g of fulvic acid yielded 75.0 g of methylated fulvic acid. Of the latter, 41.3 g was soluble in benzene. Chromatography of the benzene-soluble material over neutral Al_2O_3 (2000 g) with 3 l of each of the following solvents: hexane, benzene, benzene – ethyl acetate (9:1), benzene – ethyl acetate (1:1), and an additional 3 l of benzene – ethyl acetate (1:1) yielded fractions A, B, C, D, and E, weighing 0.07, 0.02, 0.04, 0.50, and 0.61 g, respectively. Fraction A contained only alkanes (3), whereas fractions B and C were found to contain both alkanes and fatty acid methyl esters in addition to small amounts of dialkyl phthalates (4). Fractions D and E consisted mainly of phenolic and benzenecarboxylic acid methyl ethers and esters (2). Elution with 3 l of ethyl acetate and 3 l of methanol afforded fractions F and G, weighing 2.70 and 8.10 g, respectively. Fraction F contained 60.8% C, 5.4% H, and 33.0% OCH_3; fraction G analyzed 60.1% C, 5.2% H, and 29.6% OCH_3. This paper deals with the separation of fractions F and G, which were quantitatively the major fractions that we were able to separate from the fulvic acid.

Analytical Methods

Following chromatography over the Al_2O_3 column, fraction F was further separated by preparative t.l.c. on Al_2O_3 (activated at 150 °C for 18 h, thickness of sorbent coating, 0.5 mm) with toluene – ethyl acetate (1:1) as solvent. The t.l.c. plate was inspected under a u.v. lamp and five subfractions (F1 to F5) were marked out, scraped off the plate, and extracted with ethyl acetate. Subfractions F4 to F5 were further separated by t.l.c. on SiO_2 (activated at 150 °C for 18 h, thickness of sorbent coating, 0.5 mm) with toluene – ethyl acetate (1:1) to afford additional subfractions F41 to F43 and F51 to F53. Fraction G was separated first by t.l.c. on Al_2O_3 with toluene – ethyl acetate (2:1) to yield the four subfractions G1 to G4. Subfraction G4 was further separated by t.l.c. on SiO_2 with toluene – ethyl acetate (2:1) into subfractions G41 to G43. The fractionation scheme, including the yield of each fraction and subfraction, is shown in Fig. 1. The R_f values for the main fractions separated by t.l.c. are given in Table 1.

Each subfraction was then separated by preparative

Can. J. Chem. Downloaded from www.nrcresearchpress.com by 210.87.254.5 on 09/05/12
For personal use only.

TABLE 1. The R_f values of main fractions separated by t.l.c. on Al_2O_3 with toluene – ethyl acetate (1:1) and (2:1)

Fraction	F1	F2	F3	F4	F5	G1	G2	G3	G4
R_f value	0.87	0.66	0.47	0.38	0.08	0.79	0.44	0.23	0.09

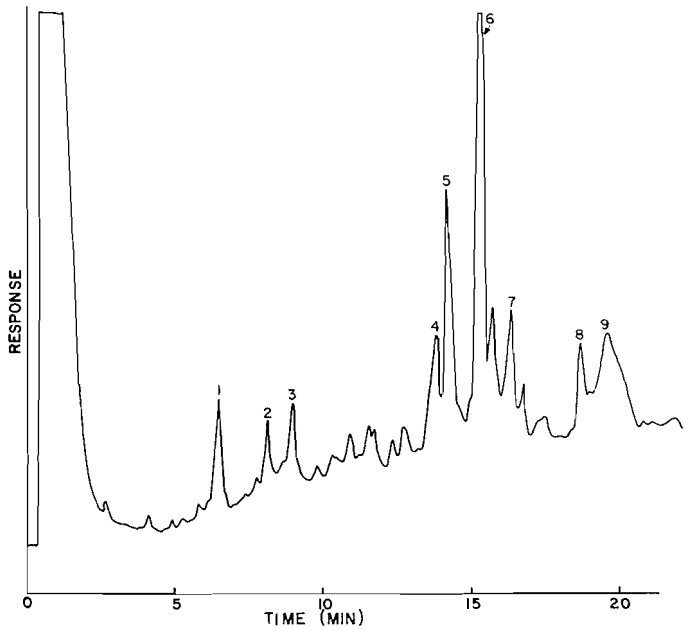

FIG. 2. Gas chromatographic separation of fraction G1

Peak	Compound
1	1,2,3-benzenetricarboxylic acid trimethyl ester
2	2-methoxy-1,3,5-benzenetricarboxylic acid trimethyl ester
3	Dibutyl phthalate
4	Dicyclohexyl phthalate
5	Methoxy-benzenepentacarboxylic acid pentamethyl ester
6	Bis(2-ethylhexyl)phthalate
7	Dioctyl phthalate
8	Dialkyl phthalate (not identified)
9	Dialkyl phthalate (not identified)

gas chromatography and the material in each major peak was analyzed by i.r. spectrophotometry and mass spectrometry. The gas chromatographic conditions (except that the support was coated with 5% SE-30 instead of 3% OV-17), methods of collection of gas chromatographic peaks, of preparation of micro-i.r. pellets, as well as of mass spectrometric analysis were the same as those employed in the earlier investigation (2). The gas chromatographic separation of subfraction G1 is illustrated in Fig. 2.

The origins and preparations of the known compounds used as standards for the mass spectrometric and i.r. spectrophotometric identification of the unknowns were identical to those described previously (2).

Alkaline $KMnO_4$ Oxidation

Samples (1.0 g) of fractions F and G were refluxed for 8 h with 250 ml of 4% (w/v) aqueous $KMnO_4$ solution. Following oxidation, the excess $KMnO_4$ was destroyed by careful addition of small volumes of CH_3OH. The insoluble MnO_2 was removed by filtration and washed with small aliquots of hot water. The filtrate (p*H* 9.9) plus washings were acidified to p*H* 2 with 6 *N* H_2SO_4 solution, transferred to a liquid–liquid extractor, and extracted with 500 ml of ethyl acetate for 48 h. The extract was dried and dissolved in a small volume of CH_3OH and methylated with an ether solution of diazomethane, generated from Diazald. The methylated oxidation product was first analyzed by analytical gas

Can. J. Chem. Downloaded from www.nrcresearchpress.com by 210.87.254.5 on 09/05/12
For personal use only.

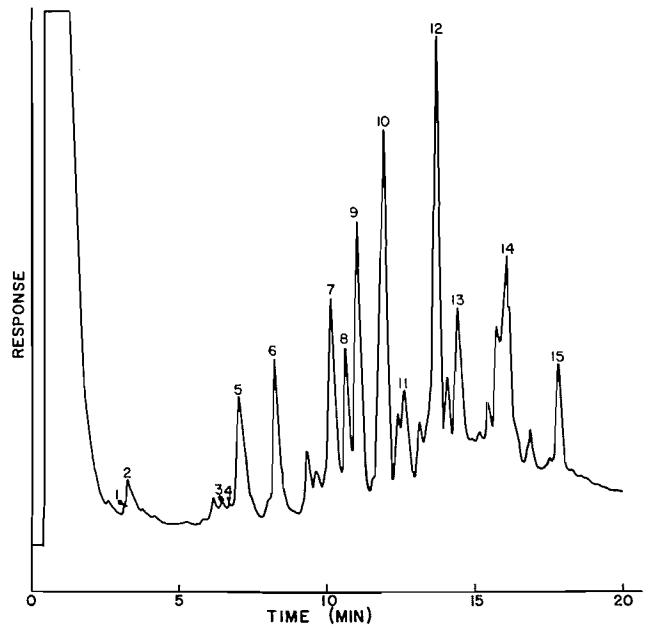

FIG. 3. Gas chromatographic separation of products resulting from the permanganate oxidation of fraction G

Peak	Compound
1	1,2-Benzenedicarboxylic acid dimethyl ester
2	1,4-Benzenedicarboxylic acid dimethyl ester
3	1,2,3-Benzenetricarboxylic acid trimethyl ester
4	1,2,4-Benzenetricarboxylic acid trimethyl ester
5	1,3,5-Benzenetricarboxylic acid trimethyl ester
6	2-Methoxy-1,3,5-benzenetricarboxylic acid trimethyl ester
7	1,2,3,4-Benzenetetracarboxylic acid tetramethyl ester
8	1,2,4,5-Benzenetetracarboxylic acid tetramethyl ester
9	1,2,3,5,-Benzenetetracarboxylic acid tetramethyl ester
10	5-Methoxy-1,2,3,4-benzenetetracarboxylic acid tetramethyl ester
11	Methoxy-1,2,3,5-benzenetetracarboxylic acid tetramethyl ester
12	Benzenepentacarboxylic acid pentamethyl ester
13	Methoxy-benzenepentacarboxylic acid pentamethyl ester
14	Benzenehexacarboxylic acid hexamethyl ester
15	Dehydrodiveratric acid dimethyl ester

chromatography (Fig. 3). The major peaks were then collected by preparative gas-chromatography and identified by comparing their chromatographic retention times, mass and micro-i.r. spectra with those of authentic specimens, and by co-chromatography with the latter.

Results and Discussion

Compounds Isolated from Fractions G and F

Three types of compounds were found (Table 2): (*a*) fully methylated phenolic acids; (*b*) benzenecarboxylic acid methyl esters, and (*c*) dialkyl phthalates. The chemical structures of all compounds identified are shown in Fig. 4. In view of the low OCH_3-content of the unmethylated fulvic acid (2), it is likely that most of the phenolic and benzenecarboxylic acids were methylated in the laboratory and that they occurred as phenols and acids in the untreated fulvic acid.

The most prominent component isolated from fraction F was **13**. Next in abundance were **18**, **19**, and **11**.

After oxidation (Table 2), the yields of all compounds except that of **13** and of the dialkyl phthalates increased substantially. Also, a number of additional benzenecarboxylic acid methyl

Can. J. Chem. Downloaded from www.nrcresearchpress.com by 210.87.254.5 on 09/05/12
For personal use only.

Can. J. Chem. Downloaded from www.nrcresearchpress.com by 210.87.254.5 on 09/05/12
For personal use only.

TABLE 2. Compounds isolated from fractions F and G without and after $KMnO_4$ oxidation

Component no.*	Compounds	Fraction F (mg)		Fraction G (mg)	
		Without oxidation	After oxidation	Without oxidation	After oxidation
6	2-Methoxy-1,3,5-benzenetricarboxylic acid trimethyl ester	2.3	25.9	17.6	28.8
	Dimethoxy-benzenetricarboxylic acid trimethyl ester	8.2	—	—	—
14	2-Methoxy-1,3,4,5-benzenetetracarboxylic acid tetramethyl ester	10.0	—	—	—
10	5-Methoxy-1,2,3,4-benzenetetracarboxylic acid tetramethyl ester	2.9	54.1	—	76.1
	Methoxy-1,2,3,5-benzenetetracarboxylic acid tetramethyl ester	—	8.6	—	10.7
12	Methoxy-benzenepentacarboxylic acid pentamethyl ester	11.2	22.2	13.3	32.5
15	Dehydrodiveratric acid dimethyl ester	9.4	47.3	—	12.1
1	1,2-Benzenedicarboxylic acid dimethyl ester	—	1.3	—	1.7
2	1,4-Benzenedicarboxylic acid dimethyl ester	—	11.9	—	16.5
3	1,2,3-Benzenetricarboxylic acid trimethyl ester	—	0.8	—	0.8
4	1,2,4-Benzenetricarboxylic acid trimethyl ester	—	0.7	—	0.2
5	1,3,5-Benzenetricarboxylic acid trimethyl ester	—	8.5	8.0	13.9
7	1,2,3,4-Benzenetetracarboxylic acid tetramethyl ester	—	12.7	—	23.3
8	1,2,4,5-Benzenetetracarboxylic acid tetramethyl ester	—	9.2	—	19.4
9	1,2,3,5-Benzenetetracarboxylic acid tetramethyl ester	—	16.6	—	39.4
11	Benzenepentacarboxylic acid pentamethyl ester	12.0	46.1	—	78.7
13	Benzenehexacarboxylic acid hexamethyl ester	46.2	49.5	—	82.5
16	Dibutyl phthalate	—	—	2.6	—
17	Dicyclohexyl phthalate	9.6	—	3.8	—
18	Bis(2-ethylhexyl)phthalate	28.0	—	282.5	—
19	Dioctyl phthalate	12.1	—	11.8	—
	Dialkyl phthalate (not identified)	4.0	—	42.8	—
	Total	155.9	315.4	382.4	436.7

*Refers to chemical structures shown in Fig. 4.

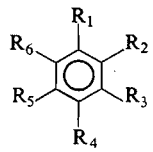

1 $R_1 = R_2 = CO_2CH_3$; $R_3 = R_4 = R_5 = R_6 = H$
2 $R_1 = R_4 = CO_2CH_3$; $R_2 = R_3 = R_5 = R_6 = H$
3 $R_1 = R_2 = R_3 = CO_2CH_3$; $R_4 = R_5 = R_6 = H$
4 $R_1 = R_2 = R_4 = CO_2CH_3$; $R_3 = R_5 = R_6 = H$
5 $R_1 = R_3 = R_5 = CO_2CH_3$; $R_2 = R_4 = R_6 = H$
6 $R_1 = R_3 = R_5 = CO_2CH_3$; $R_2 = OCH_3$; $R_4 = R_6 = H$
7 $R_1 = R_2 = R_3 = R_4 = CO_2CH_3$; $R_5 = R_6 = H$
8 $R_1 = R_2 = R_4 = R_5 = CO_2CH_3$; $R_3 = R_6 = H$
9 $R_1 = R_2 = R_3 = R_5 = CO_2CH_3$; $R_4 = R_6 = H$
10 $R_1 = R_2 = R_3 = R_4 = CO_2CH_3$; $R_5 = OCH_3$; $R_6 = H$
11 $R_1 = R_2 = R_3 = R_4 = R_5 = CO_2CH_3$; $R_6 = H$
12 $R_1 = R_2 = R_3 = R_4 = R_5 = CO_2CH_3$; $R_6 = OCH_3$
13 $R_1 = R_2 = R_3 = R_4 = R_5 = R_6 = CO_2CH_3$
14 $R_1 = R_3 = R_4 = R_5 = CO_2CH_3$; $R_2 = OCH_3$; $R_6 = H$

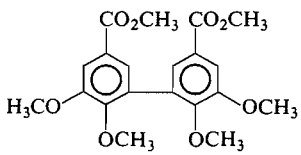

15

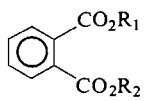

16 $R_1 = R_2 = C_4H_9$
17 $R_1 = R_2 =$ 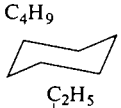
18 $R_1 = R_2 = CH_2CH(C_2H_5)—C_4H_9$
19 $R_1 = R_2 = C_8H_{17}$

FIG. 4. Chemical structures of compounds isolated.

esters (**1–5** and **7–9**) were isolated. Since more than 90% of **13** was isolated without degradation, it is likely that most of this compound occurred in this fulvic acid fraction as the free acid.

From fraction G we were able to isolate only small amounts of methylated phenolic and benzenecarboxylic acids; most of the components that could be identified were dialkyl phthalates. While the identifiable components in fraction F consisted of about 65% fully methylated phenolic and benzenecarboxylic acids and of 35% dialkyl phthalates, those in fraction G consisted of only 10% phenolic and benzenecarboxylic acid esters but of 90% dialkyl phthalates (Table 2).

The alkaline $KMnO_4$ oxidation of fraction G yielded increased amounts of **5**, **6**, and **12** aside from substantial quantities of **10**, **11** and **13**. For fractions F and G the yields of fully methylated phenolic and benzenecarboxylic acids after oxidation were between 3 and 11 times higher than those obtained without degradation.

Most of the fully methylated phenolic and benzenecarboxylic acids listed in Table 2 were the same as those isolated from fractions D and E in the earlier investigation (2). Small amounts of dialkyl phthalates were also found in fractions B and C (4). The occurrence in fractions F and G of significant amounts of dialkyl phthalates, especially *bis*(2-ethylhexyl)phthalate, was quite unexpected. Dialkyl phthalates are used in industry as plasticizers, lubricants, and in the manufacture of alkyd resins and dyes (4). We first suspected that the phthalates were contaminants that had interacted with the fulvic acid during the extraction and purification procedure. Hot toluene washings of a polyethylene bottle, used for the extraction of fulvic acid from the soil, did not contain any dialkyl phthalates. Prolonged extraction of 50 g of ovendry Rexyn-101 H-resin, used for lowering the ash content of the fulvic acid, with 300 ml of hot toluene yielded no dialkyl phthalates. A hot toluene extract of silicone grease, used occasionally to grease the ground-glass joint of the inlet tube of the rotary evaporator, was free of phthalates. To check on possible air contamination, we exposed 250 ml of toluene in a 20 l glass flask, with the mouth loosely covered with aluminum foil, to air in the laboratory for 24 h. Gas chromatographic analysis of the exposed toluene failed to show any dialkyl phthalates. Similarly, repeated checks for column-bleeding indicated that the liquid phase (SE-30) in our gas chromatographic columns was not the source of any measureable amounts of dialkyl phthalates. In view of all these checks, and considering the fact that small amounts of dialkyl phthalates were found earlier (4), we believe that the dialkyl phthalates are components of the fulvic acid. In connection with this, it is noteworthy that Cifrulak (5) reported the occurrence of unidentified phthalates in organic extracts of soil samples.

Can. J. Chem. Downloaded from www.nrcresearchpress.com by 210.87.254.5 on 09/05/12
For personal use only.

TABLE 3. Summary of compounds isolated from 100 g of fulvic acid without and after $KMnO_4$ oxidation

Compounds	Without oxidation (mg)	After $KMnO_4$ oxidation (mg)
Dimethoxy-benzoic acid methyl esters	7.5	—
Trimethoxy-benzoic acid methyl esters	3.2	—
Methoxy-benzenedicarboxylic acid dimethyl esters	7.7	—
Dimethoxy-benzenedicarboxylic acid dimethyl esters	23.1	—
Methoxy-benzenetricarboxylic acid trimethyl esters	54.1	1191.0
Dimethoxy-benzenetricarboxylic acid trimethyl esters	14.4	—
Methyl-dimethoxy-benzenetricarboxylic acid trimethyl esters	4.6	—
Methoxy-benzenetetracarboxylic acid tetramethyl esters	64.9	4755.0
Dimethoxy-benzenetetracarboxylic acid tetramethyl esters	7.6	—
Methoxy-benzenepentacarboxylic acid pentamethyl esters	100.3	2455.0
Dehydrodiveratric acid dimethyl esters	10.5	546.0
Benzenedicarboxylic acid dimethyl esters	6.0	256.0
Benzenetricarboxylic acid trimethyl esters	10.5	330.0
Benzenetetracarboxylic acid tetramethyl esters	25.9	3170.0
Benzenepentacarboxylic acid pentamethyl esters	34.7	4465.0
Benzenehexacarboxylic acid hexamethyl esters	117.3	3268.0
Dibutyl phthalate	6.1	—
Dicyclohexyl phthalate	15.4	—
Bis(2-Ethylhexyl) phthalate	315.9	—
Dioctyl phthalate	25.9	—
Dialkyl phthalates (not identified)	46.7	—
C_{14}–C_{36} Alkanes	78.0	—
C_{14}–C_{36} Fatty acids	50.0	—
Total	1030.3	20436.0

Dialkyl phthalates have also been found to occur in plants, petroleum and in fungal metabolites (4), so that a biosynthetic origin cannot be excluded.

Recent work in our laboratory showed that aqueous fulvic acid solutions reacted readily with dialkyl phthalates. One number-average molecular weight (951 g) of fulvic acid was found to solubilize 4 mol of **18** (1560 g) but only 1 mol of **16** (278 g), whereas two number-average molecular weights of fulvic acid (1902 g) were found to solubilize 3 mol of **17** (990 g). The i.r. spectra of untreated fulvic acid, dialkyl phthalates, and fulvic acid – dialkyl phthalate complexes failed to provide evidence for the occurrence of chemical reactions between fulvic acid and the phthalates. The latter appeared to be solubilized by the fulvic acid molecule. We also found that while the $KMnO_4$ oxidation of 600 mg of **18** in the absence of fulvic acid yielded no *o*-phthalic acid, that of the same amount of **18** in the presence of 366 mg of fulvic acid produced 12.0 mg of *o*-phthalic acid (or 14.0 mg of **1**). Since 100 g of fulvic acid contained approximately 300 mg of **18** plus about 90 mg of the other phthalates (see Table 3), one would expect the $KMnO_4$ oxidation of these compounds to yield about 9.0 mg of **1**. We found that the $KMnO_4$ oxidation of 100 g of fulvic acid produced 159.0 mg of **1**, which is ample to account for any *o*-phthalic acid that may have originated from the dialkyl phthalates.

Summary of Compounds Isolated from All Fractions

Table 3 lists the compounds that were isolated from all fractions of the fractionation scheme including those reported in the earlier investigation (2). *In toto*, the compounds isolated from 100 g of fulvic acid weighed 1.03 g. Since preliminary experiments with known fully methylated phenolic and benzenecarboxylic acids showed that at least 50% of the starting material was lost during the fractionation and purification procedure, it is likely that the compounds listed in Table 3 may account for up to 2.0% of the original fulvic acid.

It should be borne in mind that these compounds were isolated from the fulvic acid without degradation by chemical methods in the laboratory. About 28% of the material identified consisted of fully methylated phenolic acids, 19% of benzenecarboxylic acid methyl esters, 40% of dialkyl phthalates, and 13% of alkanes and fatty

Can. J. Chem. Downloaded from www.nrcresearchpress.com by 210.87.254.5 on 09/05/12
For personal use only.

acid methyl esters. Compounds **12** and **13** accounted for about 45% of the fully methylated phenolic- and benzene-carboxylic acids, respectively. Following $KMnO_4$ oxidation of methylated but unfractionated fulvic acid, the yields of phenolic and benzenecarboxylic acids increased by between 20 and 125 times (Table 3). Many of the compounds listed in Table 3 have been reported to arise from the $KMnO_4$ oxidation of lignin (6), thus indicating a lignin origin for the fulvic acid.

It was suggested earlier (2) on the basis of i.r. studies that in fulvic acid, benzenecarboxylic and phenolic acids were joined by hydrogen-bonding to form a polymeric structure of considerable stability on which alkanes, fatty acids and dialkyl phthalates were adsorbed. This structure could be weakened by methylation which is known to reduce hydrogen-bonding (2). Thus, the increased release of the same phenolic and benzenecarboxylic acids after oxidation as those that were isolated without oxidation indicates that either these compounds originated from more complex structures or that they came from a structure of the type mentioned above, in which the components are held together relatively loosely. Additional work is needed to shed light on this point.

We thank S. I. M. Skinner for mass spectrometric analyses and J. G. Desjardins for technical assistance.

1. D. H. R. Barton and M. Schnitzer. Nature, **198**, 217 (1963).
2. G. Ogner and M. Schnitzer. Can. J. Chem. **49**, 1053 (1971).
3. G. Ogner and M. Schnitzer. Geochim. et Cosmochim. Acta, **34**, 921 (1970).
4. (*a*) M. Schnitzer and G. Ogner. Israel J. Chem. **8**, 505 (1970). (*b*) G. Ogner and M. Schnitzer. Sci. **170**, 317 (1970).
5. S. D. Cifrulak. Soil Sci. **107**, 63 (1969).
6. K. Freudenberg and A. C. Neish. Constitution and biosynthesis of lignin. Springer Verlag, New York, N.Y., 1968. p. 79.

Can. J. Chem. Downloaded from www.nrcresearchpress.com by 210.87.254.5 on 09/05/12
For personal use only.

Can. J. Chem. Downloaded from www.nrcresearchpress.com by 210.87.254.40 on 09/05/12
For personal use only.

Metal Oxide Trialkylsilyloxide Polymers. Part VI. Aluminum Oxide Trimethylsilyloxides[1]

D. C. Bradley,[2] J. W. Lorimer,[3] and C. Prevedorou-Demas

Department of Chemistry, The University of Western Ontario, London 72, Ontario

Received February 19, 1971

Tris(trimethylsilyloxy)aluminum, $[Al(OSiMe_3)_3]_2$, was hydrolyzed under controlled conditions in dioxane at 25 °C. The soluble initial products $[AlO_x(OH)_z(OSiMe_3)_{3-2x-z}]_n$, with $x = 0.03$–0.65, underwent disproportionation when heated at 120–150 °C under vacuum to give final products with $x = 0.8$–1.1. Molecular weights were determined by cryoscopy in cyclohexane, and the linear dependence of $1/n$ on x was combined with an extension of the theory of regular polymer series to show that the number of OH groups, z, was small compared to the number of bridging oxygen atoms, x, per Al atom. The initial products consist of dimeric units, each linked to an adjacent unit by one or two oxygen bridges between aluminum atoms. The degree of polymerization is 1 to 4, based on the dimer unit. The final products have much higher degrees of polymerization (10–40, based on the dimer), and appear to contain a higher proportion of Al—O—Al bridges.

Le tris(triméthylsilyloxy)aluminium, $[Al(OSiMe_3)_3]_2$, a été hydrolysé dans le dioxane à 25 °C et dans des conditions définies. Les produits initiaux solubles $[AlO_x(OH)_z(OSiMe_3)_{3-2x-z}]_n$, avec $x = 0.03$–0.65, subissent une disproportionation lorsqu'ils sont chauffés à 120–150 °C sous vide, pour donner des produits finaux avec $x = 0.8$–1.1. Les masses moléculaires ont été déterminées par cryoscopie dans le cyclohexane, et la dépendance linéaire de $1/n$ sur x a été combinée avec une extension de la théorie des séries des polymères réguliers, afin de montrer que le nombre de groupes OH, z, était petit comparé au nombre d'atomes d'oxygène servant de pont, x, par atome d'Al. Les produits initiaux sont des unités dimériques, chacune étant liée à une unité adjacente par un ou deux ponts oxygène entre les atomes d'aluminium. Le degré de polymérisation, fondé sur l'unité dimérique, est de 1 à 4. Les produits finaux ont des degrés de polymérisation bien plus élevés (10–40, fondé sur le dimère) et semblent contenir une plus grande proportion de ponts Al—O—Al.

Canadian Journal of Chemistry, 49, 2310 (1971)

Introduction

Previous papers in this series (1–5) have described the hydrolysis of the trialkylsilyloxides of some group IV B and V B metals to form the metal oxide trialkylsilyloxides, or poly(trialkylsiloxanometalloxanes). Of these, the titanium oxide triethylsilyloxides (4, 5), the tantalum oxide trimethylsilyloxides (3, 6), and the zirconium oxide trimethylsilyloxides (before disproportionation) (2, 6) could be described with the aid of the theory of regular polymer series (6) as simple repeating units containing one or two metal atoms joined through metal–oxygen–metal bridges. By contrast, the oxide trimethylsilyloxides of titanium (1, 6) and zirconium (after disproportionation) (2, 6) could be described successfully only in terms of octameric repeating units, each containing twelve metal–oxygen–metal bridges, and linked together by one or two such bridges.

It is of interest to extend these observations to compounds containing metal atoms with different possibilities of coordination. This paper describes the products of the hydrolysis of tris(trimethylsilyloxy)aluminum (III) (aluminum trimethylsilyloxide, $[Al(OSiMe_3)_3]_2$), the thermal disproportionation of these products, and the interpretation of the data according to the theory of regular polymer series (6).

Experimental

Aluminum trimethylsilyloxide has been prepared by the reaction of anhydrous aluminum chloride with sodium trimethylsilanolate in ether solution (7). Here, the general method of Bradley and Thomas (8) was used, in which trimethylsilanol was added slowly to a refluxing solution of aluminum isopropoxide in benzene, and the alcohol liberated was distilled off as an azeotrope with benzene as the reaction proceeded. The solid product was purified by sublimation under vacuum. Analysis by general methods (8) gave Al 9.16%, Si 28.6%; calcd. for

[1]The research for this paper was supported, in part, by the Defence Research Board of Canada, Grant number 7583-04, and the National Research Council of Canada.

[2]Present address: Queen Mary College, Mile End Road, London E.1, England.

[3]Address for the academic year 1970–1971: Department of Chemistry, The University, Southampton, England.

TABLE 1. Initial hydrolysis products of aluminum trimethylsilyloxide

Moles water per mole Al	Wt.% Al		Wt.% Si		Molecular weight $\bar{M}_n$	Degree of hydrolysis $\bar{x}'_n$	Degree of polymerization $\bar{n}'_n$
	Obsd.	Calcd.	Obsd.	Calcd.			
0.05	9.3	9.33	28.4	28.5	601	0.033	2.08
0.10	9.4	9.50	28.1	28.4	604	0.064	2.13
0.15	9.5	9.63	27.9	28.3	658	0.089	2.35
0.20	9.7	9.80	27.9	28.2	643	0.118	2.36
0.25	9.9	9.88	28.2	28.1	675	0.132	2.47
0.27	10.0	9.96	28.2	28.1	645	0.146	2.38
0.30	10.1	10.2	27.7	27.9	730	0.183	2.76
0.35	10.2	10.4	27.4	27.8	704	0.210	2.70
0.40	10.4	10.6	27.1	27.7	766	0.248	3.01
0.50	10.6	10.9	26.7	27.5	796	0.291	3.22
0.80	10.7	11.1	26.5	27.4	857	0.310	3.51
0.85	10.9	11.2	26.4	27.2	878	0.337	3.66
0.90	11.5	11.8	26.3	26.9	902	0.402	3.93
1.00	12.1	12.3	26.2	26.6	980	0.460	4.46
1.15	12.2	12.5	25.8	26.4	1270	0.484	5.88
1.25	12.4	12.8	25.4	26.2	1290	0.516	6.12
1.50	12.8	13.4	24.7	25.8	1400	0.573	6.95
1.75	13.5	14.2	24.0	25.3	1380	0.646	7.28
2.00	14.2	15.2	23.0	24.6	1110	—	6.26
3.00	14.7	16.4	21.4	23.9	1380	—	8.39
Standard deviation		0.54		0.93			

$Al(OSiMe_3)_3$, Al 9.16%, Si 28.6%. Molecular weight 587 (by cryoscopy in cyclohexane); calcd. molecular weight for dimer (7), 589.1.

Hydrolysis was carried out in dioxane which had been refluxed over sodium for several hours and fractionally distilled. A weighed amount of the silyloxide (2.0–2.5 g) was dissolved in dioxane (30 g) at room temperature, and a weighed amount of water (h mole per mole metal atoms) was added to the stirred solution. After 1 h of further stirring, the volatile products and solvent were evaporated under vacuum at room temperature. Analysis of these volatile products by gas chromatography showed the presence of dioxane and trimethylsilanol, and quantitative determination of trimethylsilanol indicated that hydrolysis was complete. The residues from this procedure constitute the initial hydrolysis products (I). These were heated under vacuum at 120–150 °C to give the final hydrolysis products (II). $[Al(OSiMe_3)_3]_2$ was identified as a volatile product on heating.

All hydrolysis products were analyzed for aluminum and silicon (8) and their molecular weights were determined by cryoscopy in cyclohexane. Infrared spectra were recorded for several products at concentrations of 3.0, 4.0, 5.0, and 6.0 wt.% in cyclohexane, using KBr cells of path length 0.1 mm and a Beckman IR-7 spectrophotometer. Comparative analyses for hydroxyl groups were obtained from spectra showing absorbance as a function of frequency. A baseline was interpolated from the strong background absorption adjoining the band between 3450 and 3800 cm^{-1}, and the area under this band was measured by planimeter.

Results and Discussion

Tables 1 and 2 give the number of moles of water added per mole of aluminum, the percentages by weight of aluminum and silicon, and the number average molecular weight, $\bar{M}_n$, for the initial (I) and final (II) polymers, respectively. Above $h = 1.50$, the hydrolysis products are not completely soluble. The products remaining after removal of the insoluble portion by filtration gave the same analyses for Al and Si as before filtration. Analyses of the insoluble portions were impracticable because of their small volumes. For a given mass concentration of polymer (3, 4, 5, or 6 wt.%), the OH infrared bands could be superposed for all the initial products (I) that were examined (h = 0.4, 1.15, 1.75 mole H_2O per mole Al). This was also true for the final products (II) (h = 0.3, 0.8) but the band intensities were higher. For products I, the ratio of band area (cm^{-1}) to concentration (wt.%) was 0.10, standard error 0.02, while for products II this ratio was 0.15, standard error 0.02. No correlation between these ratios and percent Si (see Tables 1, 2), degree of hydrolysis $\bar{x}_n$ (see below) or degree of polymerization (related to $\bar{M}_n$) is found. From Tables 1 and 2, the percent Al varies from 10.4 to 13.5 (average 12.0) for products I with h = 0.4, 1.14, 1.75, and has the value 22.8 for products II. The ratio of these values lies between 1.7 and 2.2, which is equal to the ratios of the band areas per unit concentration for the two products, within experimental error. A consistent interpretation

Can. J. Chem. Downloaded from www.nrcresearchpress.com by 210.87.254.40 on 09/05/12
For personal use only.

TABLE 2. Final hydrolysis products of aluminum trimethylsilyloxide

Moles water per mole Al	Wt.% Al		Wt.% Si		Molecular weight $\bar{M}_n$	Degree of hydrolysis $\bar{x}'_n$	Degree of polymerization $\bar{n}'_n$
	Obsd.	Calcd.	Obsd.	Calcd.			
0.20	23.8	21.0	23.7	20.9	2770	1.022	21.5
0.27	21.8	20.0	23.5	21.5	2960	0.982	21.9
0.30	22.8	22.1	20.8	20.2	4700	1.062	38.5
0.35	21.0	20.2	22.2	21.4	4060	0.992	30.4
0.50	20.4	19.0	23.9	22.2	1870	0.937	13.1
0.80	22.5	21.1	22.1	20.8	5260	1.028	41.2
0.85	23.7	21.6	22.4	20.4	5580	1.046	44.7
1.25	16.8	16.3	24.7	23.9	2110	0.794	12.7
1.50	22.8	20.8	23.1	21.0	4810	1.013	37.0
2.00	20.1	20.0	21.6	21.5	—	0.985	—
3.00	25.1	22.7	21.9	19.8	9780	1.081	82.2
Standard deviation		1.75		1.76			

of these data is that the ratio of OH groups to Al atoms is roughly constant for all hydrolysis products. No satisfactory standard is available for estimation of the actual concentration of OH groups, but the band intensities are very small compared to the intensity of the neighboring aliphatic C—H band centered at 2980 cm^{-1}.

The effect of OH groups on the general relations of the theory of regular polymer series (6) will not be examined. The hydrolysis reaction may be written

$$[1]\quad n\mathrm{Al(OSiMe_3)_3} + n(x+z)\mathrm{H_2O} \rightarrow [\mathrm{AlO}_x(\mathrm{OH})_z(\mathrm{OSiMe_3})_{3-2x-z}]_n + n(2x+z)\mathrm{Me_3SiOH}$$

where x is the ratio of bridging oxygen atoms to metal atoms, z is the ratio of hydroxyl groups to metal atoms, and n is the number of metal atoms per mole, or the degree of polymerization. In general n, x, and z are not integral, and are written as the number averages $\bar{n}_n$, $\bar{x}_n$, and $\bar{z}_n$.

Consider a polymer chain i of degree of polymerization n_i, with x_i bridging oxygens and z_i OH groups per metal atom, and containing q metal–oxygen–metal bridges between successive repeating units. If r is an integer, the basic equations for the chain are, according to eq. 1,

$$[2]\qquad n_i = pr, \quad r = 1,2,\cdots$$

for the degree of polymerization, where p is the number of metal atoms per repeating unit, and

$$[3]\qquad n_i(x_i + z_i) = q(r-1) + n_i z_i$$

or

$$[4]\qquad n_i x_i = q(r-1)$$

for the degree of hydrolysis. Equations 2 and 4 are identical with the usual case $z_i = 0$ (6), if calculations of n_i and the degree of hydrolysis $x_i + z_i$ are carried out properly. The equations for the four general models of the theory of regular polymer series (6) are, therefore, unchanged by the presence of hydroxyl groups.

From eq. 1, the mole ratios of Si to Al and of OH to Al are, respectively,

$$[5]\quad N_{\mathrm{Si}}/N_{\mathrm{Al}} = 3 - 2\bar{x}_n - \bar{z}_n, \quad N_{\mathrm{OH}}/N_{\mathrm{Al}} = \bar{z}_n$$

from which the average degree of hydrolysis is

$$[6]\quad \bar{x}_n + \bar{z}_n = (3 - N_{\mathrm{Si}}/N_{\mathrm{Al}} + N_{\mathrm{OH}}/N_{\mathrm{Al}})/2$$

As an approximation $\bar{x}'_n$ to the true value of $\bar{x}_n$, set $\bar{z}_n = 0$ in eq. 5 to give $N_{\mathrm{Si}}/N_{\mathrm{Al}} = 3 - 2\bar{x}'_n$. Substitute this value and $N_{\mathrm{OH}}/N_{\mathrm{Al}} = \bar{z}_n$ in eq. 6 to give

$$[7]\qquad \bar{x}'_n = \bar{x}_n + \bar{z}_n/2$$

If P_{Al}, P'_{Al} and $\bar{n}_n$, $\bar{n}'_n$ are the true values and approximate values (with $\bar{z}_n = 0$) for the percent Al and the degree of polymerization, respectively,

$$[8]\quad P'_{\mathrm{Al}}/P_{\mathrm{Al}} = (1/\bar{n}'_n)/(1/\bar{n}_n) = [\mathrm{Al(OX)_3} - (\mathrm{O}+2\mathrm{X})\bar{x}_n - (\mathrm{X}-\mathrm{H})\bar{z}_n]/[\mathrm{Al(OX)_3} - (\mathrm{O}+2\mathrm{X})\bar{x}_n] = 1 + \bar{z}_n/(A - B\bar{x}'_n)$$

where each chemical symbol represents 1 mole, X is $SiMe_3$, and the constants have the values $A = \mathrm{Al(OX)_3}/(\mathrm{O}/2 + \mathrm{H}) = 32.70$, $B = (\mathrm{O}+2\mathrm{X})/(\mathrm{O}/2 + \mathrm{H}) = 18.02$. Equation 8 may also be written

$$[9]\quad (P'_{\mathrm{Al}} - P_{\mathrm{Al}})/P'_{\mathrm{Al}} = \bar{z}_n/(A - B\bar{x}'_n + \bar{z}_n)$$

The approximate value of the percent Al will always be greater than the true value, since $A > B\bar{x}'_n$ in general.

Can. J. Chem. Downloaded from www.nrcresearchpress.com by 210.87.254.40 on 09/05/12
For personal use only.

Can. J. Chem. Downloaded from www.nrcresearchpress.com by 210.87.254.40 on 09/05/12
For personal use only.

Values of $\bar{x}'_n$ can be calculated from eq. 5 and the analytical data, and calculated values of P'_{Al} can then be found from the formula weights. The degrees of polymerization $\bar{n}'_n$ (approximate) can then be found from the formula weights and the number average molecular weights. These values are also given in Tables 1 and 2. As predicted by eq. 9, the calculated values of the percent Al for products I are greater than the observed values, although any solvent or trimethylsilanol not removed from the products would give a similar effect. The percentage difference between the calculated and observed values of the percent Al may be used, with eq. 9, to give a rough estimate of $\bar{z}_n \sim 1$. In view of the very small infrared OH intensity and the analysis given below, this value is almost certainly much too high. For products II, the calculated percent Al is smaller than the observed value, possibly because of a systematic error in analysis. For this reason, it is believed that the small differences in the observed and calculated values of the percent Al are not significant in terms of eq. 9.

The theory of regular polymer series (6) yields the general relation $1/\bar{n}_n = a + b\bar{x}_n$ for many metal oxide trialkylsilyloxides over a large range of $\bar{x}_n$. If this equation holds for the present case, eqs. 7 and 8 give

$$[10] \quad 1/\bar{n}'_n = [a - b\bar{z}_n/2 + b\bar{x}'_n]/[1 + \bar{z}_n/(A - B\bar{x}'_n)]$$

Figure 1 is a plot of $1/\bar{n}'_n$ against $\bar{x}'_n$ for both sets of hydrolysis products, and Table 3 contains the results of a least-square analysis (6). The slope and intercept in the general relation $y = 1/\bar{n}'_n = a' + b'\bar{x}'_n$ are given, together with the ratio $a'/|b'|$, the corresponding standard errors in a' and b', the standard error $\sigma(y)$ and the correlation coefficients $\rho(x,y)$ for the variables and $\rho(a',b')$ for the parameters.

TABLE 3. Hydrolysis products of $[Al(OSiMe_3)_3]_2$
$y = 1/\bar{n}'_n = a' + b'\bar{x}'_n$

	Value		
	Initial products (I)	Final products (II)	
		(*a*)	(*b*)
Range of $\bar{x}'_n$	0.03–0.57	0.79–1.08	0.94–1.08
No. of points	17	10	9
Intercept, a'	0.496	0.281	0.425
$\sigma(a')$	0.006	0.046	0.078
Slope, b'	−0.635	−0.243	−0.384
$\sigma(b')$	−0.019	−0.046	−0.077
Ratio, $a'/\|b'\|$	0.781	1.157	1.109
$\sigma(a'/b')$	0.016	0.034	0.020
$\rho(x,y)$	−0.993	−0.880	−0.884
$\rho(a,b)$	−0.855	−0.997	−0.999
$\sigma(y)$	0.013	0.011	0.009

For products I, the first 17 entries in Table 1 yield a good straight line. The intercept is equal to the reciprocal degree of polymerization of the dimer to within experimental error, and the theory of regular polymer series indicates that the polymers are made up of dimeric repeating units, presumably containing 4-coordinated Al atoms as in the pure dimer $[Al(OSiMe_3)_3]_2$. With the help of eq. 10, the data for products I indicate that $\bar{z}_n$ must be considerably smaller than 0.01; *i.e.*, the effect of OH groups on the properties of the polymers can be disregarded.

Since the degree of polymerization is $p = 2$ for products I, the four general models which result from a systematic application of the theory of regular polymer series (6) can be simplified considerably. Cyclic species are improbable, since the reciprocal of the slope b' is neither integral nor infinite (6). Only one of the general equations applies

$$[11] \quad 1/\bar{n}_n = 1/p - \bar{x}_n/\bar{q}$$

where $\bar{n}_n = \bar{n}'_n$, $\bar{x}_n = \bar{x}'_n$, $p = 2$, and $\bar{q} = \alpha q_A + (1 - \alpha)q_B$; q_A, q_B are the bridge multiplicities (numbers of metal–oxygen–metal bridges between adjacent repeating units). The parameter α is either the fraction of metal atoms in homo-

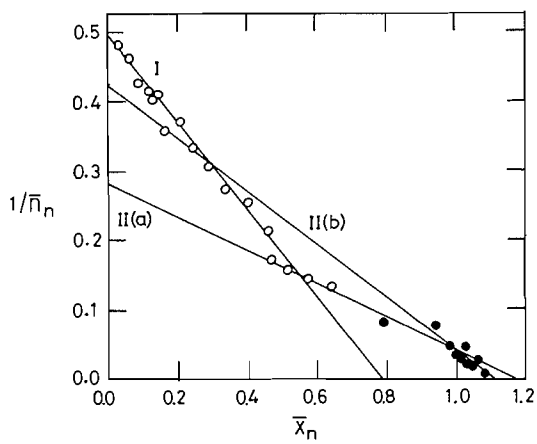

FIG. 1. Dependence of reciprocal degree of polymerization on degree of hydrolysis for aluminum oxide trimethylsilyloxides: ○, before thermal disproportionation; ●, after thermal disproportionation. The lines are the least-square equations with parameters given in Table 3.

Can. J. Chem. Downloaded from www.nrcresearchpress.com by 210.87.254.40 on 09/05/12
For personal use only.

geneous chains with bridge multiplicity α, or the fraction of bridges of multiplicity q_A within a single heterogeneous chain. No distinction can be made between these two cases on the basis of the available experimental evidence. The values $q_A = 1$, $q_B = 2$, $\alpha = 0.43$, standard error in $\alpha = 0.05$, fit the data, indicating that the polymers may be considered to be dimeric units linked by one or two metal–oxygen–metal bridges. This mixture could arise by disproportionation, as outlined previously for the titanium oxide triethylsilyloxides (5). The first member of either a p_2q_1 or a p_2q_2 series is the unhydrolyzed dimer, and a mixture of this dimer (p_2q_0) and p_2q_2 chains, with $\alpha = 0.43$, will also satisfy the data, as will a mixture $p_2q_0 + p_2q_1 + p_2q_2$. The polymer thus may contain the unhydrolyzed dimer. A mixture of p_2q_1 and p_2q_3 chains will also satisfy the data, but the combination p_2q_3 is highly improbable. Figure 2 indicates the nature of chains of the p_2q_1 and p_2q_2 types.

Table 3 gives two sets of parameters for the final products II. In the second set, the point with $\bar{x}'_n = 0.79$ has been omitted (see also Fig. 1). Clearly, the range of $\bar{x}'_n$ for the products II is too narrow and the errors are too large to justify a systematic application of theory. However, it will be noted that products I contain only a few dimer units at low values of $\bar{x}'_n$. At higher values, the points appear to lie on a curved extension to the line for products I that includes the points for products II. This suggests that high values of the apparent degree of hydrolysis and thermal disproportionation have similar effects, namely, to increase the degree of polymerization and to increase the degree of hydrolysis. Thermal disproportionation is a more rapid process, however, and may occur by the mechanism suggested for the disproportionation of the titanium oxide triethylsilyloxides (5). Since the number of OH groups per Al atom appears to be more or less constant, deviations from the linear plot at higher values of $\bar{x}'_n$ can be attributed to increases in the average bridge multiplicity, and possible decomposition of the dimeric repeating units. This would increase both the intercept and slope, which, despite the values in Table 3, could account for the data at high values of $\bar{x}'_n$. For example, a p_2q_2 series will fit products II within 95% confidence levels based on the standard errors given in column (*b*) of Table 3. The values of $\bar{x}_n$ show a small but significant variation with $\bar{n}_n$, so that a mixture of cyclic species, or a pure cyclic species, is improbable (6). A mixture of a linear and a cyclic species will not give a reasonable value of α for the values $p = 3$ or 4 suggested by the experimental data and the appropriate model (6). A more precise description of products II would require preparation of samples with a wider range of $\bar{x}_n$, but this has not been possible using the present techniques.

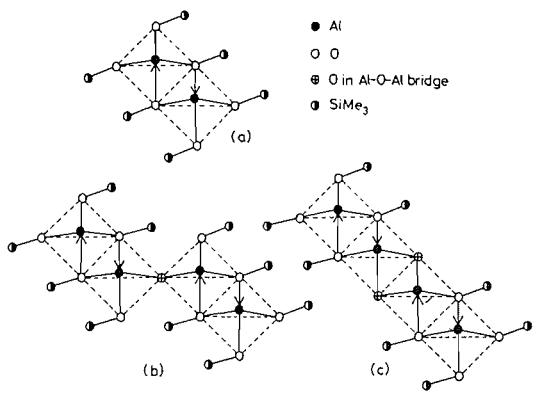

FIG. 2. (*a*) $[Al(OSiMe_3)_3]_2$ dimer, (*b*) $Al_4O(OSiMe_3)_{10}$, a p_2q_1 polymer, (*c*) $Al_4O_2(OSiMe_3)_8$, a p_2q_2 polymer.

H. H. Afifi and A. Wong assisted with some of the infrared measurements. One of us (J.W.L.) wishes to thank the British Council for a travel grant.

1. D. C. BRADLEY and C. PREVEDOROU-DEMAS. Can. J. Chem. **41**, 629 (1963).
2. D. C. BRADLEY and C. PREVEDOROU-DEMAS. J. Chem. Soc. 1580 (1964).
3. D. C. BRADLEY and C. PREVEDOROU-DEMAS. J. Chem. Soc. 1139 (1966).
4. D. C. BRADLEY and C. PREVEDOROU-DEMAS. J. Chem. Soc. A, 43 (1967).
5. D. C. BRADLEY, J. W. LORIMER, and C. PREVEDOROU-DEMAS. Can. J. Chem. **47**, 4113 (1969).
6. J. W. LORIMER and D. E. G. JONES. Can. J. Chem. **47**, 4101 (1969).
7. H. SCHMIDBAUR. Ber. **96**, 2696 (1964).
8. D. C. BRADLEY and I. M. THOMAS. J. Chem. Soc. 3404 (1959).

Can. J. Chem. Downloaded from www.nrcresearchpress.com by 210.87.254.105 on 09/05/12
For personal use only.

Reaction of Phenyllithium with Some *N,N*-Disubstituted Cyanamides

HUGH J. ANDERSON, NAM-CHIANG WANG, AND (IN PART) E. T. P. JWILI
Department of Chemistry, Memorial University of Newfoundland, St. John's, Newfoundland

Received February 15, 1971

Phenyllithium adds to *N,N*-dialkylcyanamides **1** to form, successively, the metal salts of the amidines **3** and the guanidinylamidines **5** followed by further addition and ring closure to give the phenyl-1,3,5-triazines **8**. This proposed course of the reaction is supported by the isolation of intermediates, and compounds derived from them, as well as by determination of product yields with varying ratio of reactants. It appears that 2-thienyllithium reacts similarly with dimethylcyanamide. The reaction of phenyllithium with *N*-methyl-*N*-phenylcyanamide gives mostly the tetrasubstituted cyanoguanidine **10**.

Le phényl-lithium s'additionne aux *N,N*-dialkylcyanamides **1** pour former successivement les sels métalliques des amidines **3** et les guanidinylamidines **5**; des additions supplémentaires peuvent se produire pour conduire, après cyclisation aux phényltriazines-1,3,5 **8**. Cette séquence de réaction est supportée (*a*) par le fait que les intermédiaires ont pu être isolés et transformés en produits et (*b*) en se basant sur les rendements en produits obtenus à partir de diverses quantités de réactifs. Il semble que le thiényl-2 lithium réagit de la même manière avec la diméthyl-cyanamide. La réaction du phényl-lithium avec la *N*-méthyl *N*-phénylcyanamide fournit principalement la cyanoguanidine tétrasubstituée **10**.

Canadian Journal of Chemistry, **49**, 2315 (1971)

Some organometallics, such as phenyllithium, are known to react with *N*-methyl-*N*-phenylcyanamide to give nitriles (1). It was found however that when 2-thienyllithium reacted with dimethylcyanamide a solid was obtained instead of the desired nitrile. Microanalysis and spectral properties suggested the product to be 2,4-bis-(dimethylamino)-6-(2-thienyl)-1,3,5-triazine. To support this identification the reaction was repeated using phenyllithium and the expected 2,4-bis(dimethylamino)-6-phenyl-1,3,5-triazine (2) obtained. In addition, a second solid precipitated from the aqueous layer overnight. Subsequently it was identified as 1,1-dimethyl-2-benzoylguanidine (3).

As these results differed from those using the other cyanamide (1) and from the reaction of dimethylcyanamide with phenylmagnesium halide (4) it was decided to examine the reaction of phenyllithium with several disubstituted cyanamides varying the concentrations and solvent.

Scheme 1 shows the types of compounds obtained from the reactions of phenyllithium with dimethylcyanamide (**1***a*) and with tetramethylenecyanamide (*N*-cyanopyrrolidine) (**1***b*). It will be seen that additions of successive organometallic reagents to molecules of the cyanamide formed the salt of the amidine **2**, the salt of the guanidinylamidine **4**, and then, probably, the intermediate **7** which cyclized to the triazine **8**.

The amidine **3***a* and the triazine **8***a* obtained from dimethylcyanamide and phenyllithium were known compounds. The liquid amidine **3***a* (4) was characterized as its *p*-toluenesulfonyl derivative (5). The 2,4-bis(dimethylamino)-6-phenyl-1,3,5-triazine (**8***a*) (2) was separated from a small amount of 2,4,6-tris(dimethylamino)-1,3,5-triazine (**9***a*) (hexamethylmelamine) (6) by chromatography on silica gel.

The triazine **9** probably arose from the addition of the eliminated dialkylamide ion to further molecules of dialkylcyanamide. When lithium dimethylamide was mixed with an excess of dimethylcyanamide in ether the symmetrical triazine **9***a* was obtained in poor yield.

The guanidinylamidine type compounds **5** were characterized as their *p*-toluenesulfonyl derivatives. On the basis of analysis, spectral properties, and the conversion by base solution to the corresponding benzoylguanidine **6**, structure **5** was assigned to these compounds. The known benzoylguanidine **6***a* (3) was synthesized and was identical to the hydrolysis product from **5***a*.

The structures of the "*b*" series of compounds were assigned on the basis of analysis, spectral data, and by analogy to the "*a*" series of products. Only **9***b* had been reported before (7).

It was observed that a small phenyllithium/dialkylcyanamide ratio gave more triazine while a higher ratio gave more amidine. When the solvent was a hydrocarbon, where phenyllithium has a very low solubility, triazine **9** was the major product with phenyltriazine **8** an impurity.

Observing that Lettré *et al.* had obtained a very low yield of benzonitrile when phenyllithium re-

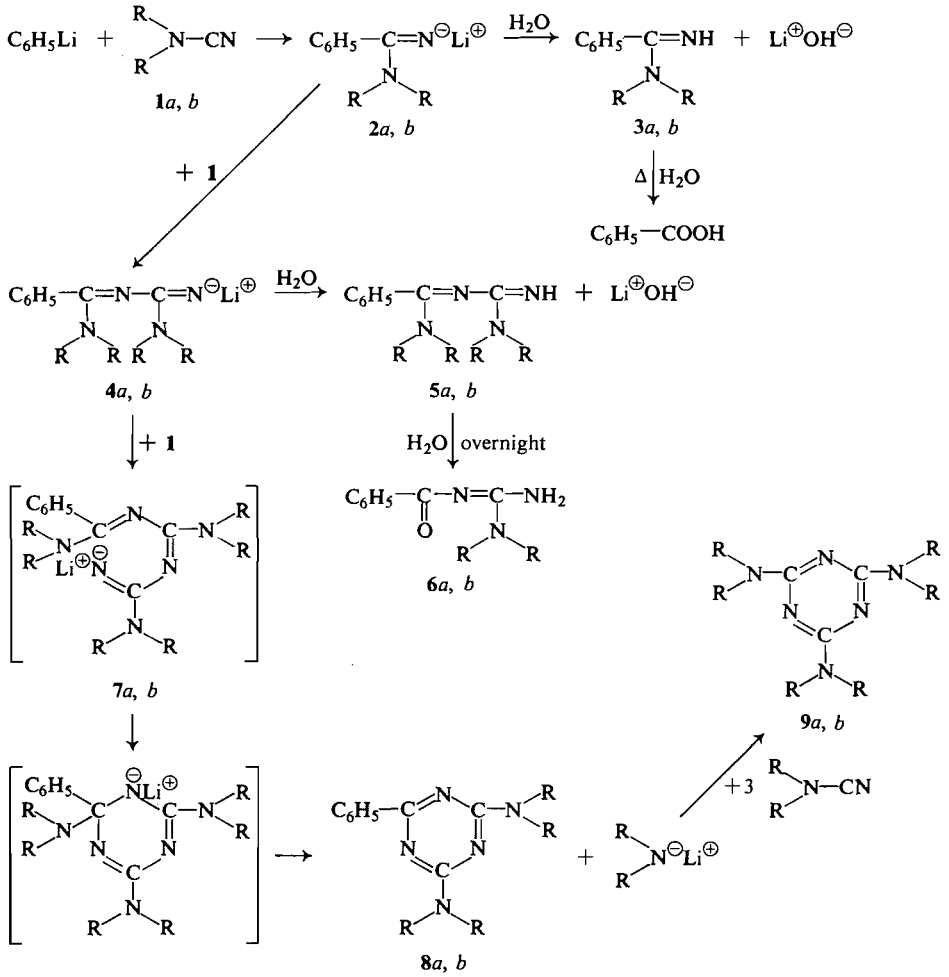

SCHEME 1

acted with *N*-methyl-*N*-phenylcyanamide at room temperature (1) we decided to examine the residues of this reaction. A small amount of benzonitrile was obtained, together with some methylaniline. The rather insoluble substance **10** was formed in about 60% yield, based on the cyanamide. The i.r. indicated a C≡N at 2170 cm^{-1}, while the parent cyanamide value is 2225 cm^{-1}. Substance **10** was gently hydrolyzed in acid to an amide **11**, while prolonged acid hydrolysis gave 1,3-dimethyl-1,3-diphenylguanidine (**12**). The i.r. spectrum of the latter compound was identical to that recorded by Meek *et al.* (8).[1]

The 1,3-dimethyl-1,3-diphenylguanidine **12** was then hydrolyzed in base to the corresponding urea **13** which was identical to an authentic specimen (9). These reactions showed that **10** was 1,3-dimethyl-1,3-diphenyl-2-cyanoguanidine.[2] The probable mode of formation of **10** is shown in Scheme 2. To support it, lithium methyl-

[1]We thank Dr. P. M. Daugherty, Director, Chemicals Research of Scripto, Inc., for further experimental details and physical constants.

[2]The known 1,1,3,3-tetramethyl-2-cyanoguanidine (10) shows a similar C≡N peak at 2173 cm^{-1}, and in the C=N region it had two peaks at 1564 and 1546 cm^{-1}. The first was assigned to C=N stretch and the second to asymmetric CN_2 stretch. McCarty *et al.* (11) prepared *N*-substituted-*N'*-cyano-*S*-methylisothioureas. These showed the C≡N at 2160–2180 and the C=N at 1520–1550 cm^{-1}. In our cyanoguanidine the aromatic bands overlap the C=N region. There is a broad band with strong maximum at 1535, a shoulder about 1555, as well as a weak peak at 1580 cm^{-1}.

Can. J. Chem. Downloaded from www.nrcresearchpress.com by 210.87.254.105 on 09/05/12
For personal use only.

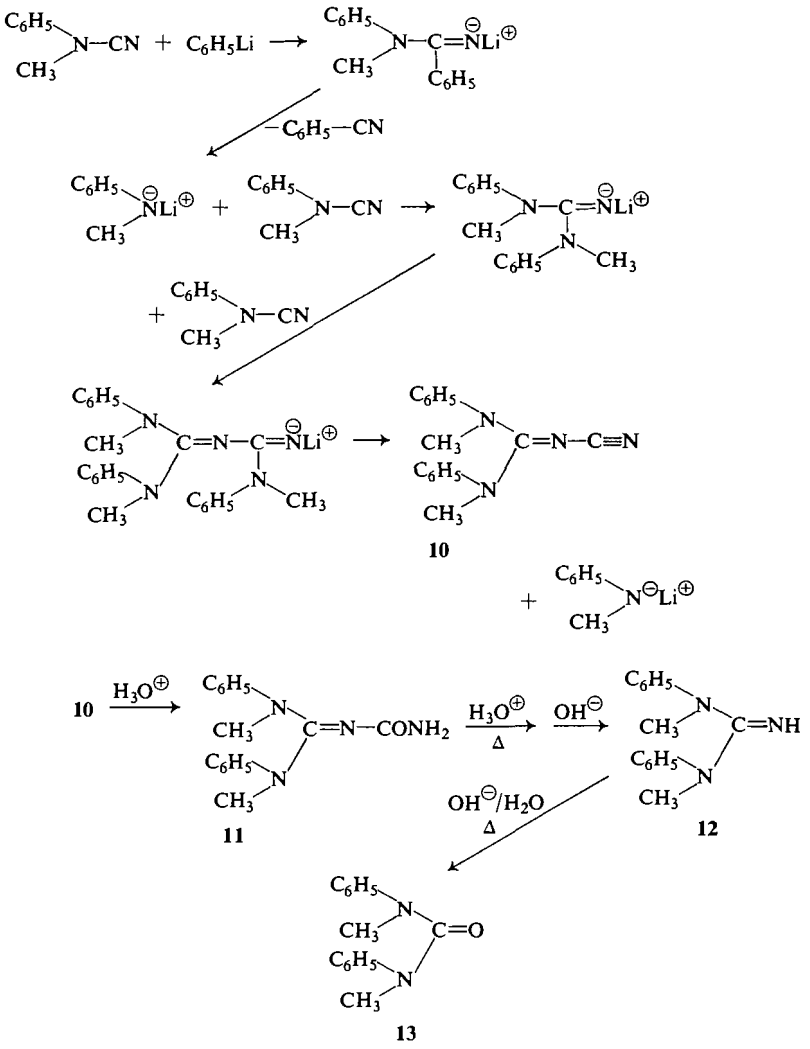

SCHEME 2

phenylamide was reacted with methylphenylcyanamide to give an 80% yield of the cyanoguanidine **10**. It will be seen that the significant difference in Scheme 2 is the splitting out of the methylphenylamide ion.

These results led to us to consider the reaction of phenyllithium with diphenylcyanamide. However, the yield of benzonitrile was small and most of the cyanamide was recovered unchanged.

The mass spectra of the triazines are consistent with those observed previously for triazines which possess the alkylamino group (12). All the triazines showed a strong molecular ion. For the bis- and tris-pyrrolidinyltriazines the base peak was M-28, representing the loss of ethylene. In the dimethylamino series loss of CH_3 was important as was loss of 43(CH_3—N=CH_2). There were strong peaks at 71($(CH_3)_2$N—$\overset{+}{C}$NH) and 96($(CH_3)_2$N—$\overset{+}{C}$N—CN). Corresponding peaks occurred in the pyrrolidinyl series. Mechanisms may be drawn for the formation of these ions in the manner of Ross and Tweedy (12).

Experimental

Melting points (uncorrected) were determined on a Fisher–Johns apparatus. Elemental analyses were by Alfred Bernhardt, West Germany. The i.r. spectra were recorded on a Perkin–Elmer 237B grating spectrophotometer using potassium chloride discs, while u.v. spectra were recorded on a Perkin–Elmer 202 spectrophotometer. The p.m.r. spectra were determined using a Varian A-60 or HA100 instrument. Values are given using the τ scale

Can. J. Chem. Downloaded from www.nrcresearchpress.com by 210.87.254.105 on 09/05/12
For personal use only.

Can. J. Chem. Downloaded from www.nrcresearchpress.com by 210.87.254.105 on 09/05/12
For personal use only.

with tetramethylsilane as internal reference. Mass spectra were recorded on a Hitachi–Perkin–Elmer RMU-6E spectrometer using the direct inlet system. Spectra were normalized when the variation of total ion current was less than 6%. Peak intensities are given as a percentage of the base peak.

Reaction of Phenyllithium with Dimethylcyanamide

Phenyllithium (2.1 g, 0.025 mol) in 40 ml dry ether (13) was transferred under dry nitrogen into a 1-l three-necked flask equipped with dropping funnel, stirrer, and condenser. A solution of dimethylcyanamide (7 g, 0.1 mol) (14) in 40 ml dry ether was added, under nitrogen and with stirring, at a rate to maintain gentle reflux. After 15 min reflux the solution was cooled and cold water (80 ml) was added. Some solid separated, but redissolved. The layers were separated and the aqueous one extracted twice again with ether. After drying ($MgSO_4$) the combined ether layer was flashed down and the residue distilled in vacuum to remove unreacted materials. The remaining solid was extracted with isopropyl alcohol and chromatographed on silica gel using chloroform as eluant to give two pure products.

2,4-Bis(dimethylamino)-6-phenyl-1,3,5-triazine (**8***a*), 2.29 g (38%) m.p. 103–103.5° from isopropyl alcohol, lit. (2) m.p. 105–106°; λ_{max} (ethanol) 235 nm (ε 40 500); ν_{max} 1595s, 1550s, 1520s, 1460w, 1385s, and 1215m cm^{-1}; n.m.r. τ 1.50 (m, 2H), 2.58 (m, 3H), 6.78 (s, 12H); mass spectrum M^+ 243 (100%), major fragments at *m/e*, 228(62), 214(28), 200(53), 96(26), and 71(34).

2,4,6-Tris(dimethylamino)-1,3,5-triazine (**9***a*), 1.02 g (14%) m.p. 172.5–173° from dimethylformamide, lit. (6) m.p. 172–174°; λ_{max} (ethanol) 226 nm (ε 49 400); ν_{max} 1625m, 1545s, 1525s, 1450m, 1385s, and 1215m cm^{-1}; n.m.r. τ 6.90(s); mass spectrum M^+ 210(100%) major fragments at *m/e* 195(62), 167(37), 152(30), 96(57), and 71(19).

The distillate from an experiment where the ratio of reactants was 1:1 was dissolved in ether (80 ml) and extracted with an equal volume of 3 *N* hydrochloric acid. The extract was cooled and made basic. An ether extract of the basic solution was washed with water and dried ($MgSO_4$). After removal of the solvent vacuum distillation gave *N,N*-dimethylbenzamidine (**3***a*) b.p. 76–78°/1 mm (yield about 28%), lit. b.p. 118°/11 mm (4). The i.r. spectrum was identical to that of an authentic specimen. *p*-Toluenesulfonyl derivative, m.p. 161–162° lit. (5) m.p. 161–162°.

The aqueous layer from the original separation was then treated in one of two ways:

(*a*) From a reaction where the ratio of dimethylcyanamide to phenyllithium was 1.5:1 the aqueous layer was immediately extracted twice with chloroform and dried ($MgSO_4$). After removal of the chloroform the residue, **5***a*, was dissolved in acetone and a solution of *p*-toluenesulfonyl chloride was added followed by 50% sodium hydroxide solution and, after stirring, ice-water (100 ml). The precipitate was 1-(α-dimethylaminobenzylidene)-3,3-dimethyl-2-*p*-toluenesulfonylguanidine, m.p. 168–170° from isopropyl alcohol; λ_{max} (methanol) 239 nm (ε 20 800); ν_{max} 1585s, 1570s; n.m.r. τ 2.50 (m, 9H), 7.02 (s, 6H), 7.22 (s, 6H), 7.65 (s, 3H); mass spectrum M^+ 372(9%).

Anal. Calcd. for $C_{19}H_{24}N_4O_2S$: C, 61.27; H, 6.49; N, 15.04; S, 8.61. Found: C, 61.40; H, 6.35; N, 15.26; S, 8.41.

(*b*) The aqueous layer from a reaction where the ratio of reactants was 2:1 was allowed to stand overnight. 1,1-Dimethyl-2-benzoylguanidine (**6***a*) precipitated, m.p. 163–164°, from benzene (yield 17%). Identical to an authentic sample prepared by the method of Bredereck and Richter (3), as determined by comparison of i.r. spectra and mixture m.p.

Reaction of Lithium Dimethylamide with Dimethylcyanamide

A solution of lithium dimethylamide (0.05 mol) was prepared in 100 ml absolute ether (15). Dimethylcyanamide (14 g, 0.20 mol) in 20 ml ether was then added at a rate which kept the mixture at reflux. After a further 30 min reflux, it was cooled and an equal volume of cold water added. The layers were separated and the aqueous layer extracted twice with ether. From the residue of the dried ether extract about 8% of 2,4,6-tris(dimethylamino)-1,3,5-triazine (**9***a*) was obtained, m.p. 172.5–173°. Most of the cyanamide was recovered unreacted. No crystals precipitated from the aqueous layer overnight.

Reaction of Phenyllithium with Tetramethylenecyanamide

The procedures used were identical to those described above but using a 2.5:1 mol ratio of tetramethylenecyanamide (*N*-cyanopyrrolidine) (16) to phenyllithium. Evaporation of the combined, dried ether extracts produced a solid which was chromatographed on silica gel, eluting with a 15:1 mixture of chloroform and acetone. This gave 2,4-bis(1-pyrrolidinyl)-6-phenyl-1,3,5-triazine (**8***b*), m.p. 179–180°, from dimethylformamide; λ_{max} (methanol) 237 nm (ε 46 500); ν_{max} 1590m, 1580m, 1550s, 1520s, 1490m, 1475s, 1460s, 1385m, 1350m cm^{-1}; n.m.r. τ 1.55 (m, 2H), 2.58 (m, 3H), 6.34 (t, 8H), 8.08 (m, 8H); mass spectrum M^+ 295(94%) major fragments at *m/e* 268(62), 267(100), 266(33), 239(31), 226(43), 70(30), 55(26).

Anal. Calcd. for $C_{17}H_{21}N_5$: C, 69.12; H, 7.17; N, 23.71. Found: C, 69.02; H, 7.37; N, 23.54.

Also eluted was 2,4,6-tris(1-pyrrolidinyl)-1,3,5-triazine (**9***b*), m.p. 184.5–187°, from dimethoxyethane and a little water, lit. (7) m.p. 186.6–189.8°; λ_{max} (ethanol) 230 nm (ε 58 000); ν_{max} 1525s, 1490m, 1475m, 1450s, 1350m, 1330m, 810m cm^{-1}; n.m.r. τ 6.45 (t, 12H), 8.10 (m, 12H); mass spectrum M^+ 288(78%) major fragments at *m/e* 260(100), 232(40), 219(41), 122(28), 55(28).

After standing overnight, the aqueous layer precipitated 1,1-tetramethylene-2-benzoylguanidine (**6***b*), m.p. 167–168°, from benzene; λ_{max} (methanol) 246 (sh ε 9200) 271 nm (ε 17 000); ν_{max} 3290m, 1625m, 1590s, 1560s, 1525s, 1445s, 1425m, 1340s, 1325s cm^{-1}; n.m.r. τ 1.75 (m, 2H), 2.35 (s, broad, 2H), 2.62 (m, 3H), 6.48 (m, 4H), 8.08 (m, 4H); mass spectrum M^+ 217(31%) major fragments at 140(26), 105(27), 77(32), 70(100).

Anal. Calcd. for $C_{12}H_{15}N_3O$: C, 66.34; H, 6.96; N, 19.34. Found: C, 66.21; H, 6.89; N, 19.51.

From an experiment where the mole ratio of tetramethylenecyanamide to phenyllithium was 1:1 the corresponding amidine **3***b* and guanidinylamidine **5***b* were obtained from the ether and aqueous layers by the procedures described earlier and isolated as their *p*-toluenesulfonyl derivatives.

N,N - Tetramethylene - *N'* - *p* - toluenesulfonylbenzamidine, m.p. 150–151° from ethyl acetate; λ_{max} (methanol) 248 nm (ε 19 000); ν_{max} 1575w, 1525s, 1450s, 1440s,

Can. J. Chem. Downloaded from www.nrcresearchpress.com by 210.87.254.105 on 09/05/12
For personal use only.

1275s, 1140s, 1075s, 830s, 690m; n.m.r. τ 2.70 (m, 9H), 6.28 (t, 2H); 6.94 (t, 2H), 7.62 (s, 3H), 8.10 (m, 4H); mass spectrum M^+ 328(3%) major fragments at *m/e* 173(31), 91(30), 70(100).

Anal. Calcd. for $C_{18}H_{20}N_2O_2S$: C, 65.83; H, 6.14; N, 8.53; S, 9.75. Found: C, 65.92: H, 6.00; N, 8.37; S, 9.60.

1-[α-(1-Pyrrolidinyl)benzylidene]-3,3-tetramethylene-2-*p*-toluenesulfonylguanidine, m.p. 221–223° (dec.) from methanol; λ_{max} (methanol) 237 nm (ε 21 950); ν_{max} 1610m, 1590s, 1575s, 1495s, 1450s, 1400s, 1145s cm^{-1}; n.m.r. τ 2.40 (m, 9H); 6.70 (m, 8H), 7.62 (s, 3H), 8.08 (m, 4H), 8.32 (m, 4H); mass spectrum M^+ 424(4%) major fragments at *m/e* 354(34), 269(57), 200(100), 104(32), 97(61), 91(62), 70(84), 44(48).

Anal. Calcd. for $C_{23}H_{28}N_4O_2S$: C, 65.07; H, 6.65; N, 13.20; S, 7.55. Found: C, 65.03; H, 6.52; N, 13.25; S, 7.45.

Reaction of 2-Thienyllithium with Dimethylcyanamide

2-Thienyllithium (17) (0.1 mol) was prepared in ether (100 ml), and was added to dimethylcyanamide (0.1 mol) in ether (50 ml) with stirring and cooling. After stirring a further 2 h at room temperature the solution was poured onto ice, acidified with 3 *N* hydrochloric acid, and the layers separated. The combined dried ether extract of the aqueous layer was removed and some low boiling material distilled off under vacuum. The black crystalline residue was crystallized from isopropyl alcohol. 2,4-Bis(dimethylamino)-6-(2-thienyl)-1,3,5-triazine, m.p. 95–96°; λ_{max} (ethanol) 233 (ε 30 400), 285 nm (16 800); ν_{max} 1595m, 1550s, 1535s, 1505s, 1395s; n.m.r. (CCl_4) τ 2.12 (q, 1H), 2.71 (q, 1H), 3.03 (q, 1H), 6.88 (s, 12H); mass spectrum M^+ 249(100%) major fragments at *m/e* 234(47), 220(25), 206(35), 96(24), 71(23).

Anal. Calcd. for $C_{11}H_{15}N_5S$: C, 52.99; H, 6.06; N, 28.09; S, 12.86. Found: C, 52.98; H, 6.54; N, 27.91; S, 12.85.

Reaction of Phenyllithium with Phenylmethylcyanamide

Following the method of Lettré *et al.* (1) a solution of phenyllithium (0.1 mol) in 100 ml absolute ether was added to *N*-phenyl-*N*-methylcyanamide (32.5 g, 0.24 mol) in 35 ml absolute ether. A white solid separated which persisted during a 30 min reflux and appeared at the interface when an equal volume of water was added to the reaction mixture. It was filtered and the two layers separated. After two extractions the combined ether extract was washed with dilute hydrochloric acid, water, and dried. Following evaporation of ether the benzonitrile and unreacted material were distilled under reduced pressure. A pure sample of benzonitrile was obtained by passing the mixture through a column of neutral alumina, eluting with 5 parts petroleum (60–80°) to 3 parts benzene; yield 4%. Recrystallization of the residue from distillation yielded more of the insoluble material above (yield 58%). 1,3-Dimethyl-1,3-diphenyl-2-cyanoguanidine (**10**), m.p. 126–126.5°, from carbon tetrachloride; λ_{max} (methanol) 258 nm (ε 21 000); ν_{max} 2170s, 1535s, 1480s; n.m.r. τ 2.92 (m, 6H), 3.25 (m, 4H), 6.64 (m, 6H); mass spectrum M^+ 264(30%) major fragments at *m/e* 158(23), 147(100), 132(24), 117(24), 106(30), 77(57).

Anal. Calcd. for $C_{16}H_{16}N_4$: C, 72.70; H, 6.10; N, 21.20. Found: C, 72.60; H, 6.08; N, 21.30.

The dilute hydrochloric acid wash solution was allowed to stand overnight, cooled, and made basic with 6 *N* sodium hydroxide solution. It was extracted and the ether layer was washed with water, dried ($MgSO_4$), and removed. A thick liquid, 1,3-dimethyl-1,3-diphenylguanidine, distilled at 105–110°/0.05 mm, lit. (8) 124°/0.07 mm. The i.r. spectrum was identical to that reported by these authors for 1,3-dimethyl-1,3-diphenylguanidine (**12**).

The hydrogen halide salts were prepared by bubbling the appropriate dried gas into an ether solution of the guanidine **12**. 1,3-Dimethyl-1,3-diphenylguanidinium chloride, sintered 238° (blue color), m.p. 242–243° (dec.) from methanol/ether, lit. (8) m.p. 238°. 1,3-Dimethyl-1,3-diphenylguanidinium bromide, sintered 237°, m.p. 243–244° (dec.), lit. (8) m.p. 244–245°.

Reaction of Methylphenylcyanamide with Lithium Methylphenylamide

A solution of lithium methylphenylamide was prepared from *N*-methylaniline (16 g, 0.15 mol) and phenyllithium (0.1 mol) in about 80 ml absolute ether. The solution was refluxed 30 min, cooled, and a solution of methylphenylcyanamide (26.4 g, 0.2 mol) in 20 ml absolute ether was added slowly. After a further 30 min reflux the white solid was filtered and a second crop was recovered from the ether layer. After recrystallization the solid was proved to be 1,3-dimethyl-1,3-diphenyl-2-cyanoguanidine (**10**) (75%) by comparison of i.r. spectra and mixture m.p.

Hydrolyses of 1,3-Dimethyl-1,3-diphenyl-2-cyanoguanidine

(*a*) 1,3-Dimethyl-1,3-diphenyl-2-cyanoguanidine (2.0 g, 0.0076 mol) was warmed with 60 ml 6 *N* hydrochloric acid until clear, was cooled in ice, neutralized with 6 *N* sodium hydroxide, and the solid filtered. 1,3-Dimethyl-1,3-diphenyl-2-carbamylguanidine (**11**), m.p. 154–155°, from pyridine, yield 80%; λ_{max} (methanol) 256 nm (ε 19 100); ν_{max} 3300m (broad), 1675m, 1600m, 1585w, 1560s, 1495m, 1365s; n.m.r. (d_6DMSO) τ 3.00 (m, 10H), 3.82 (s, broad, 2H), 6.90 (s, 6H); mass spectrum M^+ 282(3%), major fragments at *m/e* 238(41), 133(30), 107(100), 106(77), 77(34), 43(41).

Anal. Calcd. for $C_{16}H_{18}N_4O$: C, 68.06; H, 6.43; N, 19.85. Found: C, 68.19; H, 6.39; N, 20.01.

(*b*) The cyanoguanidine (4 g, 0.015 mol) was refluxed in 6 *N* hydrochloric acid for 24 h. The solution was cooled, made strongly basic with 6 *N* sodium hydroxide, and extracted with ether. The ether layer was washed with water, dried ($MgSO_4$), and flashed down in vacuum. A thick liquid distilled at 105–110°/0.05 mm identical with 1,3-dimethyl-1,3-diphenylguanidine (**12**) (80%) above.

(*c*) The cyanoguanidine was refluxed in 3 *N* sodium hydroxide solution for 48 h, cooled, and extracted with chloroform. The extract was washed with water and dried ($MgSO_4$). After distillation the residue was recrystallized from ether to give *N,N'*-dimethyl-*N,N'*-diphenylurea (**13**) m.p. 118–119°, lit. (9) m.p. 121°. Shown by i.r. spectra and mixture m.p. to be identical to an authentic specimen (9).

Reaction of Phenyllithium and Diphenylcyanamide

Following the procedure for the reaction with phenylmethylcyanamide the reaction of phenyllithium and

N,N-diphenylcyanamide was found to give about a 10% yield of benzonitrile and unreacted starting material.

The authors gratefully acknowledge the continued financial support of the National Research Council of Canada. They also thank Miss Carol Cohen for technical assistance and Dr. B. Gregory for useful comments.

1. H. Lettré, P. Jungmann, and J. C. Salfeld. Chem. Ber. **85**, 397 (1952).
2. D. Sheehan, A. P. Bentz, and J. C. Petropoulos. J. Appl. Polymer Sci. **6**, 47 (1962).
3. K. Bredereck and R. Richter. Chem. Ber. **99**, 2454 (1966).
4. L. Vuylsteke. Bull. Sci. Acad. Roy. Belg. **12**, 535 (1926).
5. V. L. Dubina, S. I. Burmistrov, and N. I. Levochenko. Zh. Org. Khim. **3**, 2024 (1967). Chem. Abstr. **68**, 68585 (1968).
6. D. N. Kaiser, J. T. Thurston, J. R. Dudley, F. C. Schaffer, I. Hechenbleikner, and D. H. Hansen. J. Am. Chem. Soc. **73**, 2984 (1951).
7. W. K. Detweiler and E. D. Amstutz. J. Am. Chem. Soc. **74**, 1483 (1952).
8. R. L. Meek, C. E. Feazel, P. M. Daugherty, F. L. Mallory, and E. P. Cofield, Jr. U.S. Pat. 3 278 486 (Cl.260–47). Chem. Abstr. **66**, 19262 (1967).
9. W. Michler. Ber. **9**, 716 (1876). W. Michler and R. Zimmermann. Ber. **12**, 1166 (1879).
10. E. Allenstein and P. Quis. Chem. Ber. **96**, 2918 (1963).
11. C. G. McCarty, J. E. Parkinson, and D. M. Wieland. J. Org. Chem. **35**, 2067 (1970).
12 J. A. Ross and B. G. Tweedy. Org. Mass Spectrom. **3**, 219 (1970).
13. R. G. Jones and H. Gilman. Organic syntheses Coll. Vol. II. *Edited by* A. H. Blatt. John Wiley and Sons, Inc., New York, 1950, p. 150.
14. M. Kuhn and R. Mecke. Chem. Ber. **93**, 618 (1960).
15. A. C. Cope and B. D. Tiffany. J. Am. Chem. Soc. **73**, 4158 (1951).
16. W. L. Garbrecht and R. M. Herbst. J. Org. Chem. **18**, 1003 (1953).
17. H. Gilman and D. A. Shirley. J. Am. Chem. Soc. **71**, 1870 (1949).

Can. J. Chem. Downloaded from www.nrcresearchpress.com by 210.87.254.105 on 09/05/12
For personal use only.

Can. J. Chem. Downloaded from www.nrcresearchpress.com by 210.87.254.42 on 09/05/12
For personal use only.

Base-catalyzed Dehydrobromination of Several α-Bromoacetals[1]

H. A. Davis and R. K. Brown
Department of Chemistry, University of Alberta, Edmonton, Alberta

Received February 18, 1971

Base-catalyzed dehydrohalogenation with potassium *t*-butoxide in *t*-butyl alcohol of the acetals obtained from homologues of α-bromoacetaldehyde and ethylene glycol[2-(α-bromoalkyl)-1,3-dioxolanes] or 1,3-propanediol[2-(α-bromoalkyl)-1,3-dioxane] provides the corresponding ketene acetal, in some cases exclusively and in others as the major product along with a smaller proportion of the α,β-unsaturated acetal. In contrast, similar dehydrohalogenation conditions convert the acetals obtained from homologues of α-bromoacetaldehyde and monohydroxy alcohols, to the α,β-unsaturated acetals, in some cases exclusively, and in others as the major product accompanied by a smaller proportion of the corresponding ketene acetal.

The preference for the ketene acetal formation from the 2-(α-bromoalkyl)-1,3-dioxolanes (the ethyleneacetals) is believed due to greater ease of approach by base to the methine proton as a result of the restricted shape of the 1,3-dioxolane ring. Approach by base to the methine proton of the α-bromoalkyl dialkylacetals is more hindered by the two alkoxy groups, which cause preferred attack by base at the β proton to provide the α,β-unsaturated acetal.

The proportion of α,β-unsaturated acetal obtained from base-catalyzed dehydrohalogenation of 2-(α-bromoalkyl)-1,3-dioxolanes can be greatly increased if the reaction is carried out in dimethyl sulfoxide. This marked change in proportion of products is thought to be due to a change in mechanism occasioned by the dimethyl sulfoxide.

La déhydrohalogénation baso-catalysée avec le *t*-butoxyde de potassium dans l'alcool *t*-butylique, des acétals obtenus à partir des homologues de l'α-bromoacétaldéhyde et des [(α-bromoalkyl)-2 dioxolanes-1,3] éthylène glycol ou [(α-bromoalkyl)-2 dioxanes-1,3] propanediol-1,3, conduit aux acétals cétène correspondants; et ceci exclusivement dans certains cas et dans d'autres cas en tant que produits majoritaires avec une plus petite proportion d'acétal α–β insaturé. Au contraire, les mêmes conditions de déhydrohalogénation transforment les acétals obtenus à partir des homologues de l'α-bromoacétaldéhyde et des alcools monohydroxy, en acétals α–β insaturés, exclusivement dans certains cas, et en tant que produits majoritaires dans d'autres cas, accompagnés par une petite proportion de l'acétal cétène correspondant.

La formation préférentielle de l'acétal cétène à partir des (α-bromoalkyl)-2 dioxolanes-1,3 (les éthylèneacétals) est probablement due à une plus grande facilité d'approche du proton méthyne par la base et ceci probablement par suite de la forme restreinte du cycle du dioxolane-1,3. L'approche par une base du proton méthyne des α-bromoalkyl dialkylacétals est plus empêchée par les deux groupes alkoxy qui provoquent l'attaque préférentielle par une base sur le proton β pour conduire à un acétal α–β insaturé.

Le proportion d'acétal α–β insaturé obtenu par déhydrohalogénation baso-catalysée des (α-bromoalkyl)-2 dioxolanes-1,3 peut être de beaucoup augmentée si la réaction est effectuée dans le diméthyl sulfoxyde. Cette modification importante dans la proportion des produits obtenus est probablement due à un mecanisme différent provoqué par le diméthyl sulfoxyde.

Canadian Journal of Chemistry, 49, 2321 (1971)

Introduction

For a part of our general study of the hydrogenolysis of acetals and ketals, several α,β-unsaturated ethyleneacetals were required. The preparation of a few α,β-unsaturated dialkylacetals has been described by McElvain *et al.* (1–4) in reports of their extensive investigations of ketene acetals. They found that base-catalyzed dehydrohalogenation of α-haloacetals containing only hydrogen, aryl, or halogen substituents on the α carbon, gave only ketene acetals (**1** in eq. *a*, Scheme 1). However, if the α carbon had attached to it a carbon atom bearing one or more hydrogen atoms, then only the α,β-unsaturated acetal was produced (**2** in eq. *b*, Scheme 1). They also showed that authentic alkylketene acetals (*e.g.* **3**, R, R′ = H or alkyl in eq. *b*, Scheme 1) were not converted to α,β-unsaturated acetals under the dehydrobromination conditions. They did pre-

[1]From the thesis of H. A. Davis, submitted to the Faculty of Graduate Studies, University of Alberta, Edmonton, Alberta, 1970 in partial fulfilment of the requirements for the Ph.D. degree.

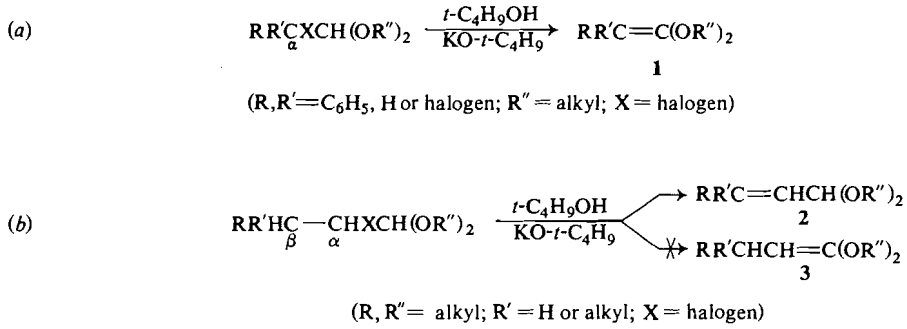

SCHEME 1

pare some α-bromo acetals from diols, but none of these had an alkyl group attached to the α carbon, hence on dehydrohalogenation these could produce only the ketene acetals (4).

This paper describes the results of our experiments concerning the base-catalyzed dehydrobromination of several α-bromoacetals derived from the combination of some higher homologues of α-bromoacetaldehyde with dihydroxy alcohols as well as with some monohydroxy alcohols.

Results and Discussion

When α-bromo-*n*-valeraldehyde ethyleneacetal was dehydrohalogenated with potassium *t*-butoxide in *t*-butyl alcohol and the product isolated and purified by the procedure of McElvain *et al.* (3) (procedure IIIA, Experimental), only the ketene acetal was produced. There was no evidence whatsoever, either by g.l.c., t.l.c., or the p.m.r. spectrum of the crude product obtained by distillation, that the α,β-unsaturated acetal had been formed even in small amount (experiment 3, Table 1). Similar treatment of α-bromo-*iso*-valeraldehyde ethyleneacetal provided primarily the ketene acetal, but in this case the α,β-unsaturated acetal was also formed, though only to the extent of 14% of the product (experiment 7, Table 1). These results are contrary to those expected on the basis of the previous work (1–4). Accordingly, the dehydrohalogenation of several homologues of these α-bromoaldehyde ethyleneacetals (experiments 1, 2, 4, 8, 11) and of the acetal obtained from α-bromo-*n*-valeraldehyde and 1,3-propanediol (experiment 12) was investigated. As well, a number of α-bromoaldehyde dialkylacetals were also dehydrohalogenated (experiments 13–17) and the products examined by modern techniques.

Since we had found in several cases that the α,β-unsaturated acetal and ketene acetal products of an experiment had nearly the same g.l.c. retention time and also that some of the ketenes decomposed on the g.l.c. column, the isolation procedure was modified by treating the reaction mixture, after the heating period was completed, with water followed by extraction of the products and subsequent purification (procedure IIIB, Experimental). This addition of water trapped the ketene product by quantitative conversion to an ester (4) which was stable on the g.l.c. column. Because the g.l.c. retention time was considerably greater than that of the α,β-unsaturated acetal, the relative quantity of the ester, and hence of the ketene acetal precursor, could be estimated by g.l.c. The results are shown in Table 1.

It is seen that base-catalyzed dehydrohalogenation of our 2-(α-bromoalkyl)-1,3-*dioxolanes* (the ethyleneacetals) and of 2-(α-bromoalkyl)-1,3-*dioxane* generally provides the ketene acetal in greater proportion, and in several cases exclusively (experiments 1–4, 7, 8, 12). The only one which does not follow this general course is the tetramethylated 1,3-dioxolane of experiment 11, and this goes to the other extreme in giving only the α,β-unsaturated acetal. In contrast, the dehydrohalogenation of our di*alkyl*acetals provides the α,β-unsaturated acetals, in some cases exclusively (experiments 13, 16) and in other cases as the major product along with a smaller proportion (6–26%) of the ketene acetal (experiments 14, 15, 17).

The reduction of the percentage of ketene acetal obtained from the α-bromo-*n*-valeraldehyde dialkylacetals from 26 to 12 to 0% when the alkyl group is changed from methyl to ethyl, to isopropyl respectively (experiments 14–16) could be

Can. J. Chem. Downloaded from www.nrcresearchpress.com by 210.87.254.42 on 09/05/12
For personal use only.

Can. J. Chem. Downloaded from www.nrcresearchpress.com by 210.87.254.42 on 09/05/12
For personal use only.

TABLE 1. Base-catalyzed dehydrobromination of α-bromoacetals

Experiment	Acetal	Reaction* procedure III	Time (h)	Product	Relative amount, %	% Reaction	Total recovery, %
1	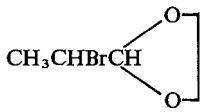	B	3	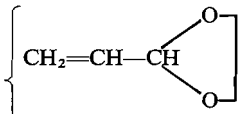 $C_2H_5CO_2C_2H_4OH$	0 100	50	85
2	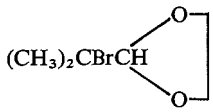	B	5	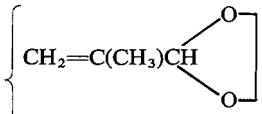 $(CH_3)_2CHCO_2C_2H_4OH$	0 100	40	90
3	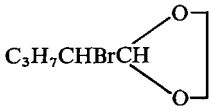	A	5	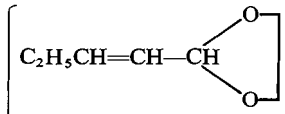 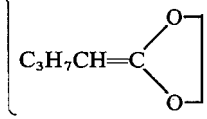	0 100	70	70
4	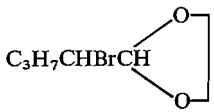	B	5	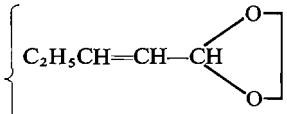 $C_4H_9CO_2C_2H_4OH$	0 100	42	90
5	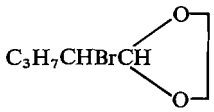	C	1 or 20	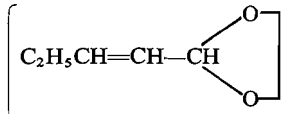 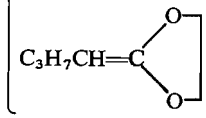	70 30	95	90

Can. J. Chem. Downloaded from www.nrcresearchpress.com by 210.87.254.42 on 09/05/12
For personal use only.

TABLE 1 (*Continued*)

Experiment	Acetal	Reaction* procedure III	Time (h)	Product	Relative amount, %	% Reaction	Total recovery, %
6	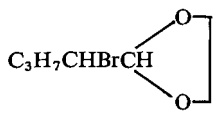	D	1	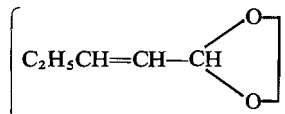	33	100	90
				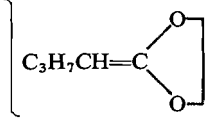	67		
7	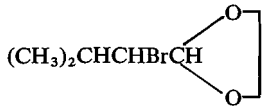	A	5	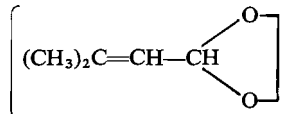	14†	70	70
				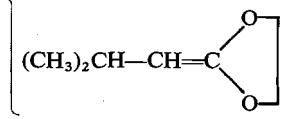	86†		
8	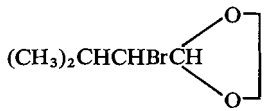	B	5	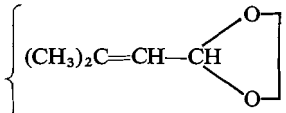	15	49	75
				$(CH_3)_2CH—CH_2CO_2C_2H_4OH$	85		
9	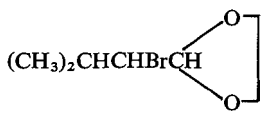	C	1 or 20	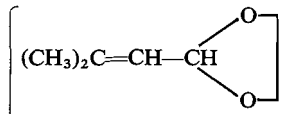	98	100	90
				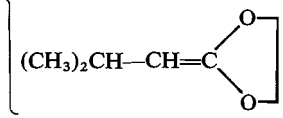	2		

Can. J. Chem. Downloaded from www.nrcresearchpress.com by 210.87.254.42 on 09/05/12
For personal use only.

TABLE 1 (*Concluded*)

Experiment	Acetal	Reaction* procedure III	Time (h)	Product	Relative amount, %	% Reaction	Total recovery, %
10	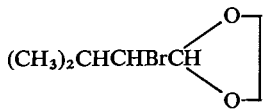	D	1	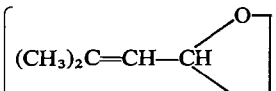	72	100	90
				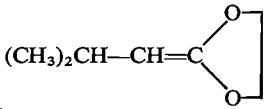	28		
11	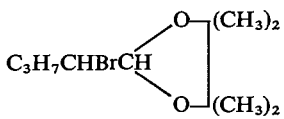	B	24	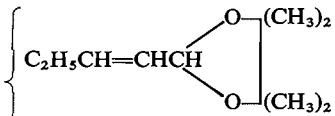	100	20	90
				$C_4H_9CO_2C(CH_3)_2C(CH_3)_2OH$	0		
12	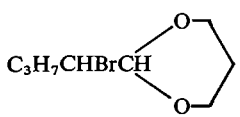	B	20	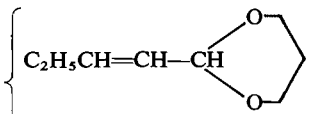	40	53	90
				$C_4H_9CO_2(CH_2)_3OH$	60		
13	$CH_3CHBrCH(OC_2H_5)_2$	B	20	$CH_2{=}CHCH(OC_2H_5)_2$	100	48	80
				$C_2H_5CO_2C_2H_5$	0		
14	$C_3H_7CHBrCH(OCH_3)_2$	B	20	$C_2H_5CH{=}CHCH(OCH_3)_2$	74	53	85
				$C_4H_9CO_2CH_3$	26		
15	$C_3H_7CHBrCH(OC_2H_5)_2$	B	20	$C_2H_5CH{=}CHCH(OC_2H_5)_2$	88	45	90
				$C_4H_9CO_2C_2H_5$	12		
16	$C_3H_7CHBrCH[OCH(CH_3)_2]_2$	B	20	$C_2H_5CH{=}CHCH[OCH(CH_3)_2]_2$	100	42	85
				$C_4H_9CO_2CH(CH_3)_2$	0		
17	$(CH_3)_2CHCHBrCH(OC_2H_5)_2$	B	20	$(CH_3)_2C{=}CHCH(OC_2H_5)_2$	94	40	90
				$(CH_3)_2CHCH_2CO_2C_2H_5$	6		

*(A) Heated to 80° in *t*-butyl alcohol containing KO-*t*-butoxide, then purified by fractional distillation. (B) Heated to 80° in *t*-butyl alcohol containing KO-*t*-butoxide, cooled to 50°, then treated with water to trap the ketene as the ester, extracted with ether, and subsequently worked-up. (C) Heated at 40° in dimethyl sulfoxide containing sodium methoxide, then worked-up as in A. (D) Heated at 40° in dimethyl sulfoxide containing KO-*t*-butoxide, then worked-up as in A.

†The relative amounts were determined from the relative integrated areas of the signals for the methyl groups in the 60 MHz n.m.r. spectrum of a mixture of the two products, since g.l.c. failed to separate them.

Can. J. Chem. Downloaded from www.nrcresearchpress.com by 210.87.254.42 on 09/05/12
For personal use only.

due to either an electronic effect following the views of McElvain *et al.* (2) or to an increasing steric opposition to approach of the methine hydrogen by the base as the alkyl group becomes larger. The exclusive formation of the ketene acetal from 2-(α-bromo-*n*-butyl)-1,3-dioxolane (experiment 4) strongly supports the view that it is the steric approach to the methine hydrogen rather than the difference in electronic properties of the alkyl groups, which is the feature which determines the proportion of ketene acetal obtained, since the small difference in electron donor properties of the methyl groups (experiment 14) and the ethylene group (experiment 4) would not account for the marked change in the proportion of ketene acetal obtained in these two cases. Models of the dialkylacetals of α-bromo-*n*-valeraldehyde show that the freely rotating alkoxy groups offer much steric opposition to approach to the methine hydrogen. On the other hand, models of the ethyleneacetals show that the restricted shape and position of the 1,3-dioxolane ring permits easy access by base to the methine hydrogen. When this approach is blocked, as in the case of 2-(α-bromo-*n*-butyl)-4,4,5,5-tetramethyl-1,3-dioxolane (experiment 11), then the α,β-unsaturated acetal rather than the ketene acetal is produced. The chair conformation of the 2-(α-bromo-*n*-butyl)-1,3-dioxane ring (5) provides some steric opposition to approach of the base to the methine hydrogen due to interaction of the two remaining axial protons (1,3-diaxial interaction) and hence the proportion of ketene to α,β-unsaturated acetal obtained in this case is as low as 60:40 (experiment 12).

The results described above clearly show that the methine hydrogen of acetals (the "anomeric" hydrogen) can be removed by base if an halogen atom is attached to the α carbon, and that this appears to occur more readily than does the alternate path of dehydrohalogenation involving removal of hydrogen from the β carbon of α-halogenated acetals, providing that the methine hydrogen is readily accessible to the base. The formation of only the ketene acetal from both α-bromopropionaldehyde ethyleneacetal (experiment 1) and α-bromo-*iso*-butyraldehyde ethyleneacetal (experiment 2) also supports this view. We have found that *n*-valeraldehyde ethyleneacetal, when subjected to the dehydrohalogenation conditions with potassium *t*-butoxide in *t*-butyl alcohol-OD (procedure IIIA, Experimental), was unchanged, containing no deuterium on the methine carbon. Furthermore, α-bromo-*n*-valeraldehyde ethyleneacetal, heated in *t*-butyl alcohol-OD with a half-molar equivalent of potassium *t*-butoxide (procedure IIIA, Experimental), provided the ketene acetal along with recovered α-bromo-*n*-valeraldehyde ethyleneacetal which contained no deuterium. These results strongly suggest that the elimination of the halogen acid to form the ketene acetal does not involve initial removal of the methine hydrogen as a proton by an ElcB process, but rather that the loss of the proton and the halogen occurs by a concerted process under the conditions employed.

The observation that as much as 15% of α,β-unsaturated acetal is obtained from the dehydrohalogenation of α-bromo-*iso*-valeraldehyde ethyleneacetal (experiment 8), while only the ketene acetal is obtained by similar dehydrohalogenation of α-bromo-*n*-valeraldehyde ethyleneacetal (experiment 4) suggests that the transition state leading to the formation of the α,β-unsaturated acetal in experiment 8 is stabilized by the two methyl groups (6), and this counteracts to some extent the ease of access to and removal of the methine hydrogen by base to cause preferential formation of the ketene acetal. The same phenomenon could explain the greater proportion (94%) of α,β-unsaturated acetal formed from α-bromo-*iso*-valeraldehyde diethylacetal (experiment 17) than from α-bromo-*n*-valeraldehyde diethylacetal (88%, experiment 15).

It has been possible to increase markedly the proportion of α,β-unsaturated acetals obtained from the α-bromoaldehyde ethyleneacetals by changing the solvent from *t*-butyl alcohol to dimethyl sulfoxide (DMSO). Dehydrohalogenation of α-bromo-*n*-valeraldehyde ethyleneacetal (experiment 5) and α-bromo-*iso*-valeraldehyde ethyleneacetal (experiment 9) with sodium methoxide in DMSO (procedure IIIC, Experimental) provides the corresponding α,β-unsaturated acetals to the extent of 70 and 98% respectively. If the base employed in DMSO is potassium *t*-butoxide (procedure IIID, Experimental), the proportion of α,β-unsaturated acetal obtained is decreased to 33 and 72% respectively (experiments 6 and 10), but this is still much more than is obtained by using *t*-butyl alcohol as solvent (0 and 14% respectively, experiments 3 and 7). The difference in results obtained by the two bases in DMSO may be due to their differences in size.

The pronounced increase in proportion of

Can. J. Chem. Downloaded from www.nrcresearchpress.com by 210.87.254.42 on 09/05/12
For personal use only.

α,β-unsaturated ethyleneacetal to ketene acetal obtained by changing the solvent from *t*-butyl alcohol to DMSO is believed due to a change in mechanism. It is known that the basicity of metal alkoxides is enhanced in DMSO and this is thought to result in a greater degree of C—H bond stretching as compared with C—Br bond stretching in the transition state (7, 8). The following explanation is suggested to account for the results obtained.

In *t*-butyl alcohol, association of the solvent with the bromine atom as well as with the oxygen atom(s) of the 1,3-dioxolane ring would encourage C—Br bond stretching in the former situation, while in the latter, the methine hydrogen would tend to become more acidic. If one assumes a considerable extent of both C—Br and C—H bond breaking along with a substantial degree of double bond formation in the transition state, then steric or "*cis*" effects become important (9 and references therein). Because of the shape of the 1,3-dioxolane ring, one would expect these steric effects to be much less important in the transition state leading to the ketene acetal than in the transition state leading to the α,β-unsaturated acetal. On this basis the preference for the formation of the ketene acetal (100% from α-bromo-*n*-valeraldehyde ethyleneacetal, experiment 3; 85% from α-bromo-*iso*-valeraldehyde ethyleneacetal, experiment 8) becomes understandable. The formation of the α,β-unsaturated acetal to the extent of 15% from α-bromo-*iso*-valeraldehyde ethyleneacetal may be a reflection of electronic effects due to the two methyl groups.

In DMSO, such association of the solvent with the bromine and oxygen atoms does not occur. In this situation, C—H bond breaking is considered to be much more important than is C—Br breaking (7, 8). Accordingly, the transition state does not involve substantial double bond formation and hence the "*cis*" effects noted above would not hinder the attainment of the transition state. Of importance is the ease of C—H bond stretching with consequent development of carbanion character. Development of a negative charge on the methine ("anomeric") carbon of the ring would be opposed by the partial negative charge on the adjacent oxygen atom(s), a charge which is not reduced by solvation, as was suggested above for the solvent *t*-butyl alcohol. Hence attainment of the transition state leading to the ketene acetal becomes more difficult. The greater extent of α,β-unsaturated acetal formation from the α-bromo-*iso*-valeraldehyde ethyleneacetal than from the α-bromo-*n*-valeraldehyde ethyleneacetal (experiments 10 and 6 respectively) may be the result of electronic effects due to the alkyl substituents, while the greater effectiveness of sodium methoxide (experiments 5 and 9) over that of potassium *t*-butoxide (experiments 6 and 10) may be due to steric requirements of the base.

In agreement with the findings of McElvain *et al.* (1–4) we have found that ketene acetals were not converted to the corresponding α,β-unsaturated acetals either in *t*-butyl alcohol containing sodium methoxide or potassium *t*-butoxide, or in DMSO containing either of these two bases. In addition it was established that α,β-unsaturated acetals were not converted to ketene acetals under the conditions of dehydrohalogenation noted immediately above. However, the α,β-unsaturated acetals are slowly converted, at least in part, to the β,γ-unsaturated acetals. For example, when 2-pentenal ethyleneacetal was heated in refluxing *t*-butyl alcohol containing potassium *t*-butoxide, very little isomerization to the β,γ-unsaturated acetal was observed. Extension of the reflux period to ~25 h resulted in 25% conversion. Dehydrohalogenation reactions in DMSO, however, had to be carried out at temperatures no greater than 40°, since at higher temperatures, the conversion of the α,β- to the β,γ-unsaturated acetal was much more readily achieved. Table 2 shows the results of isomerization experiments carried out with several unsaturated acetals in DMSO at 80°, and containing either sodium methoxide or potassium *t*-butoxide. These support the statements above, and show also that the β,γ-unsaturated acetals under these conditions are also converted in part to the α,β-isomer. But neither is isomerized to the ketene acetal. The proportion of α,β- to β,γ-unsaturated acetal obtained apparently depends upon the relative stability of these two isomers under the reaction conditions. Experiments 5 and 9 in Table 1 also illustrate the stability of the ketene acetals and as well that the α,β-unsaturated acetals are not converted to the ketene acetals.

Experimental

Boiling points and melting points are uncorrected. The g.l.c. analyses were made with an F and M Model 700 instrument, equipped with 12′ × 1/8″ columns packed with either (*a*) butanediol succinate, 20% on Gas Chrom P (60–80 mesh), (*b*) silicone rubber SE30, 20% on Gas Chrom P (60–80 mesh) or, (*c*) Carbowax 20M, 20% on Gas Chrom P (60–80 mesh). Helium was the

Can. J. Chem. Downloaded from www.nrcresearchpress.com by 210.87.254.42 on 09/05/12
For personal use only.

TABLE 2. Base-catalyzed isomerization of several unsaturated acetals in DMSO*

Compound	Base	Reaction time (h)	Material recovery, %	Product(s)	Relative amount, %
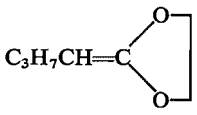	$NaOCH_3$ or KO-*t*-C_4H_9	18	90	$C_4H_9CO_2C_2H_4OH$	100
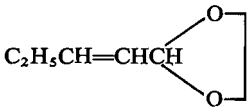	$NaOCH_3$ or KO-*t*-C_4H_9	12	80	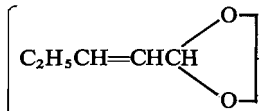	2
				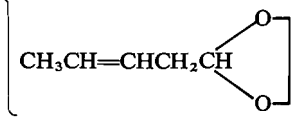	98
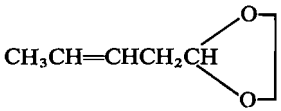	$NaOCH_3$	12	85	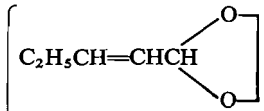	2
				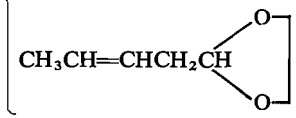	98
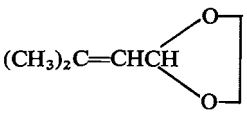	$NaOCH_3$	20	80	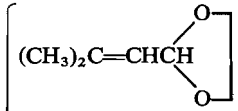	45
				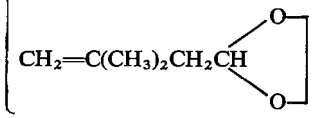	55
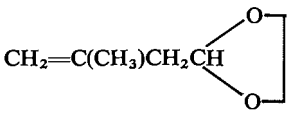	$NaOCH_3$	20	80	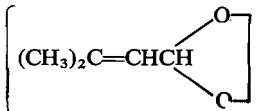	50
				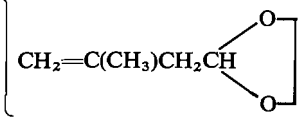	50

*All reactions were done at 80° and then treated with water and worked-up as in procedure IIIB, (Table 1) as described for the dehydrohalogenation reactions (see Experi-

Can. J. Chem. Downloaded from www.nrcresearchpress.com by 210.87.254.42 on 09/05/12
For personal use only.

carrier gas at a flow rate of ~40 ml/min. For preparative g.l.c., an Aerograph Autoprep Model A-700 was employed and this was equipped with a column 12′ × 1/4″ packed with butanediol succinate, 20% on Gas Chrom P (60–80 mesh). The column temperature and type of column used was dependent on the boiling points of the compounds. For some analytical work on the F and M Model 700, the temperature was linearly programmed to achieve better resolution. The temperature was increased at the rate of 7.5°/min starting from 80–100°, while the terminal temperature depended on the column stability. Quantitative analyses were made by measuring the areas of the peaks. In many cases, these areas were compared with those obtained from known artificial mixtures. It was found that equimolar mixtures of the products obtained from dehydrohalogenation gave peaks that were very nearly equal, if not equal in area, the difference being well within 10%.

The i.r. spectra were recorded with a Perkin–Elmer Model 21 instrument.

The p.m.r. spectra were recorded on either a Varian Associates A-60 instrument or Varian Associates A-56/60A instrument operated by Mr. R. Swindlehurst and assistants. All spectra were referred to tetramethylsilane and carried out in carbon tetrachloride solution. Signal positions were located in many cases by spin decoupling, using a 100 MHz Varian instrument. These were carried out by Mr. Glen Bigham and his associates of this Department.

The p.m.r. and i.r. spectra were obtained for all compounds, and found to be consistent with the assigned structure.

Elemental analyses were made by Mrs. Darlene Mahlow of this Department.

The drying agent for solutions was anhydrous magnesium sulfate unless otherwise stated. Solvents were removed by rotary evaporator under vacuum unless otherwise stated.

(I) Preparation of Saturated Acetals

n-Valeraldehyde Dimethylacetal

This compound was prepared by the following modification of the procedure used by Bachman for the preparation of hexanal diethylacetal (10).

To a stirred suspension of magnesium turnings (22.6 g, 0.94 mol) in 100 ml of anhydrous ether, was added dropwise 20 ml of a solution of 129 g (0.94 mol) of *n*-butyl bromide in 100 ml of anhydrous ether. The addition was carried out cautiously at first until the Grignard reaction was well started, then at such a rate as to maintain the ether at gentle reflux. After the 20 ml of the solution of *n*-butyl bromide had been added, the reaction mixture was diluted with a further quantity (400 ml) of anhydrous ether, and then the remainder of the *n*-butyl bromide solution was added dropwise. After the addition was completed, the ether solution was heated under gentle reflux for 4 h, then cooled to room temperature and 100 g (0.94 mol) of trimethyl orthoformate added dropwise and then the solution was heated under reflux overnight.

The solution, cooled to room temperature, was poured onto 500 ml of a stirred ice-water mixture. The ether layer was separated and the aqueous layer extracted with ether (2 × 200 ml). The combined ether solutions were washed first with 100 ml of water, then with 100 ml of saturated aqueous sodium chloride solution. The ether layer was dried, filtered free of solid, and the filtrate freed from ether. The residue was distilled to give a colorless liquid (45 g, 36%) boiling at 51–53° at 30 mm; η_D^{24} 1.3969 (lit. b.p. 120–129° at 760 mm (11)).

The Following Three Acetals were Prepared by the Method Used to Prepare n-Valeraldehyde Dimethylacetal Described Above

n-Valeraldehyde diethylacetal from *n*-butyl bromide and triethyl orthoformate in 80% yield. Colorless liquid, b.p. 60° at 11 mm; η_D^{23} 1.4019 (lit. b.p. 162.5–163.5°; η_D^{20} 1.4021 (12)).

iso-Valeraldehyde diethylacetal from 1-bromo-2-methylpropane and triethyl orthoformate in 75% yield. The b.p. 71° at 50 mm; η_D^{24} 1.3974 (lit. b.p. 156–158° (2)).

Propionaldehyde diethylacetal from ethyl bromide and triethyl orthoformate in 73% yield. The b.p. 121–124° at 704 mm; η_D^{26} 1.3861 (lit. b.p. 123° at 760 mm; η_D^{20} 1.3897 (13)).

(II) Preparation of α-Bromoacetals

α-Bromo-n-valeraldehyde Dimethylacetal

This compound was prepared by the following modification of the literature procedure (14).

To a stirred solution of *n*-valeraldehyde dimethylacetal (42 g, 0.32 mol) in 300 ml of dry chloroform was added, dropwise, 51 g (0.32 mol) of bromine at such a rate as to maintain the temperature of the reaction mixture at 30–35°. When the addition was complete, the solution was stirred at room temperature for 2 h and then cooled to −10°. Potassium hydroxide (18 g, 0.32 mol) in 150 ml of methanol was then added dropwise and the resulting solution then stirred while it reached room temperature. The precipitated potassium bromide was separated and the solvents removed from the filtrate by fractional distillation at atmospheric pressure through a 4-in Vigreux column. An ether (400 ml) solution of the residue was washed first with saturated aqueous sodium carbonate solution (4 × 100 ml) and then with 100 ml of saturated aqueous sodium chloride solution. The ether layer was dried, filtered, and freed from ether. The residue when distilled gave 40 g (59%) of colorless liquid, b.p. 78–80° at 12 mm; η_D^{23} 1.4559.

Anal. Calcd. for $C_7H_{15}BrO_2$: C, 39.80; H, 7.12; Br, 37.90. Found: C, 39.58; H, 7.04; Br, 38.08.

The 60 MHz p.m.r. spectrum showed a doublet centered at τ 5.70 (1H, $J \sim 6$ Hz for the methine hydrogen); a multiplet between 6.0–6.32 (1H); two singlets at 6.66 and 6.68 (6H); and a multiplet between 8.0–9.25 (7H).

The Following Three α-Bromoaldehyde Acetals were Prepared by the Same Method Used to Make α-Bromo-n-valeraldehyde dimethylacetal Above

α-Bromo-n-valeraldehyde diethylacetal from *n*-valeraldehyde diethylacetal in 70% yield. Colorless liquid, b.p. 80° at 7 mm; η_D^{23} 1.4453 (lit. b.p. 92–96° at 12 mm (15)).

α-Bromo-iso-valeraldehyde diethylacetal from *iso*-valeraldehyde diethylacetal in 60% yield, b.p. 90° at 15 mm; η_D^{23} 1.4426 (lit. b.p. 92–93° at 14 mm; η_D^{25} 1.4438 (2)).

α-Bromopropionaldehyde diethylacetal from propionaldehyde diethylacetal in 65% yield, b.p. 76–79° at 19 mm; η_D^{23} 1.4375 (lit. b.p. 82–85° at 30 mm; η_D^{20} 1.4371 (16)).

α-Bromo-n-valeraldehyde ethyleneacetal

This compound was prepared by the *trans*-acetalization of α-bromo-*n*-valeraldehyde diethylacetal with ethylene

Can. J. Chem. Downloaded from www.nrcresearchpress.com by 210.87.254.42 on 09/05/12
For personal use only.

glycol by the following modification of the procedure of McElvain and Curry (4).

α-Bromo-*n*-valeraldehyde diethylacetal (41 g, 0.17 mol) was added to a solution of ethylene glycol (11 g, 0.17 mol) in 200 ml of dry toluene. The flask was set up for fractional distillation through a 4-in. Vigreux column. *p*-Toluene sulfonic acid (0.1 g) was added to the reaction mixture which was then heated. A mixture of toluene and ethanol distilled between 75–110°. The distillation was continued until the temperature reached 110° at which only toluene was collected. The solution was cooled, washed with saturated aqueous sodium carbonate solution (2 × 100 ml), and then with 100 ml of saturated aqueous sodium chloride solution. The toluene layer was dried, filtered, and freed from solvent. The residue distilled to give 30 g (85%) of liquid, b.p. 81° at 5 mm; η_D^{24} 1.4734.

Anal. Calcd. for $C_7H_{13}BrO_2$: C, 40.02; H, 6.23; Br, 38.25. Found: C, 40.13; H, 6.10; Br, 38.15.

The 60 MHz p.m.r. spectrum showed a doublet at τ 5.15 (1H, $J \sim 4$ Hz for the methine proton); a multiplet centered at 6.1 (5H); a multiplet between 8.0–8.75 (4H); and a multiplet between 8.91–9.25 (3H).

The Following Four α-Bromoaldehyde Acetals were Prepared by the Same Method Used Above to Synthesize α-Bromo-n-valeraldehyde Ethyleneacetal

α-Bromo-iso-valeraldehyde ethyleneacetal from α-bromo-*iso*-valeraldehyde diethylacetal and ethylene glycol in 75% yield, b.p. 75° at 4.5 mm; η_D^{24} 1.4747.

Anal. Calcd. for $C_7H_{13}BrO_2$: C, 40.02; H, 6.23; Br, 38.25. Found: C, 40.09; H, 6.22; Br, 38.39.

The 60 MHz p.m.r. spectrum showed a doublet at τ 5.08 (1H, $J \sim 5$ Hz for the methine proton); a multiplet centered at 6.10 (5H); a broad multiplet between 7.70 and 8.24 (1H); and two doublets centered at 8.98 and 9.00 (6H, $J \sim 2.5$ Hz).

α-Bromopropionaldehyde ethyleneacetal from α-bromopropionaldehyde diethylacetal and ethylene glycol in 67% yield, b.p. 72° at 10 mm; η_D^{22} 1.4769.

Anal. Calcd. for $C_5H_9BrO_2$: C, 33.15; H, 4.97; Br, 44.10. Found: C, 33.49; H, 5.03; Br, 43.87.

The 60 MHz p.m.r. spectrum showed a doublet at τ 5.18 (1H, $J \sim 4$ Hz for the methine proton); a multiplet centered at 6.1 (5H); and a doublet at 8.38 (3H, $J \sim 7$ Hz).

α-Bromo-n-valeraldehyde tetramethylethyleneacetal from α-bromo-*n*-valeraldehyde diethylacetal and dry pinacol. The pinacol was prepared from pinacol hydrate (17) which was dried by the method described by Vogel (18). Yield of acetal, 75%, b.p. 84–88° at 2 mm; η_D^{24} 1.4626.

Anal. Calcd. for $C_{11}H_{21}BrO_2$: C, 49.80; H, 7.93: Br, 30.07. Found: C, 49.94; H, 7.52; Br, 30.02.

The 60 MHz p.m.r. spectrum showed a doublet at τ 5.08 (1H, $J \sim 6.5$ Hz for the methine proton); a multiplet at 6.37 (1H); a multiplet between 8.08 and 9.17 (7H); and two closely spaced singlets (12H).

2-(α-Bromo-n-butyl)-1,3-dioxane from α-bromo-*n*-valeraldehyde diethylacetal and 1,3-propanediol in 90% yield, b.p. 89–91° at 4.5 mm; η_D^{23} 1.4770.

Anal. Calcd. for $C_8H_{15}BrO_2$: C, 43.09; H, 6.73; Br, 35.83. Found: C, 43.06; H, 7.15; Br, 35.75.

The 60 MHz p.m.r. spectrum showed a doublet at τ 5.43 (1H, $J \sim 4$ Hz for the methine proton); a multiplet between 5.68 and 6.53 (5H); a multiplet between 7.52 and 9.24 (9H).

α-Bromo-n-valeraldehyde Diisopropylacetal

α-Bromo-n-valeraldehyde was made by the following modification of the procedure of Erlenmeyer and Yung (19). To a stirred solution of *n*-valeraldehyde (86 g, 1 mol) in 300 ml of chloroform, kept at −15° by means of a Dry Ice – acetone bath, was added dropwise 160 g (1 mol) of bromine. After addition of the bromine, the stirred solution was allowed to come to room temperature and then left overnight, by which time the solution's color had changed from red to yellow. Sodium bicarbonate (90 g, 1.07 mol) was added in 10 g portions so as to control the evolution of carbon dioxide. The solution was then stirred for 1 h and filtered. The chloroform was removed from the filtrate by fractional distillation at atmospheric pressure, and the residue was then distilled under vacuum from 10 g of solid sodium carbonate. Yield of colorless liquid which yellowed on standing, 49.5 g (30%), b.p. 52–56° at 15 mm; η_D^{24} 1.4702 (lit. b.p. 53–54° at 13 mm (19); η_D^{20} 1.4640 (20)).

To a stirred solution of α-bromo-*n*-valeraldehyde (66 g, 0.4 mol) in 200 ml of *iso*-propyl alcohol was added 100 g of anhydrous magnesium sulfate and 0.5 g of *p*-toluenesulfonic acid. The mixture was heated under reflux for 24 h and then cooled to room temperature and filtered free of solid. The excess *iso*-propyl alcohol was removed by fractional distillation at atmospheric pressure and the residue was distilled to give 35 g (34%) of colorless α-bromo-*n*-valeraldehyde di-*iso*-propylacetal, b.p. 85° at 8 mm; η_D^{23} 1.4398.

Anal. Calcd. for $C_{11}H_{23}BrO_2$: C, 49.44; H, 8.61; Br, 29.96. Found: C, 49.23; H, 8.31; Br, 29.67.

The 60 MHz p.m.r. spectrum showed a doublet at τ 5.40 (1 H, $J \sim 3.5$ Hz for the methine proton); a multiplet between 5.94 and 6.44 (3H), and a multiplet between 8.00 and 9.15 (19H).

α-Bromo-iso-butyraldehyde Ethyleneacetal

To a stirred solution of *iso*-butyraldehyde (43 g, 0.5 mol) in 400 ml of dry chloroform, maintained at 0° by means of an ice bath, was added dropwise 80 g (0.5 mol) of bromine. After complete addition, the solution was stirred for 1 h at room temperature whereupon sodium bicarbonate (42 g, 0.5 mol) was added to the reaction mixture in 5 g portions to control the evolution of carbon dioxide. The resulting mixture was stirred overnight and then filtered free of solid. The filtrate was washed with saturated aqueous sodium bicarbonate solution (2 × 100 ml) and then with 100 ml of saturated aqueous sodium chloride solution. The chloroform layer was dried, filtered, and freed from solvent.

To a dry benzene solution (200 ml) of the residue, was added 31 g (0.5 mol) of ethylene glycol and 0.5 g of *p*-toluenesulfonic acid. The mixture was heated under reflux for 16 h in an apparatus equipped with a water trap. The solution, cooled to room temperature, was washed with saturated aqueous sodium carbonate solution (2 × 100 ml), and then with 100 ml of saturated aqueous sodium chloride solution. The benzene layer was dried, filtered, and freed from solvent. The residue distilled to give 35 g (36%) of colorless liquid, b.p. 66° at 8 mm; η_D^{23} 1.4731.

Anal. Calcd. for $C_6H_{11}BrO_2$: C, 36.90; H, 5.74; Br, 41.00. Found: C, 36.52; H, 5.95; Br, 41.00.

The 60 MHz p.m.r. spectrum showed a singlet at τ 5.18 (1H, for the methine proton); a multiplet at 6.0 (4H); and a singlet at 8.35 (6H).

TABLE 3. Physical constants of products isolated from dehydrobromination of some α-bromo acetals

Products	Boiling point (°C/mm)	$\eta_D(T°C)$	Analysis Calculated C H	Analysis Found C H
$(CH_3)_2C{=}CHCH(OC_2H_5)_2$	65/14	1.4196 (22)	68.31 11.47	68.50 11.02
$C_2H_5CH{=}CHCH(OC_2H_5)_2$	54/13	1.4175 (22)	68.31 11.47	68.05 11.67
$C_2H_5CH{=}CHCH(OCH_3)_2$	67/55	1.4156 (22)	64.58 10.84	64.58 11.11
$C_2H_5CH{=}CHCH[OCH(CH_3)_2]_2$	74/10	1.4172 (26)	70.92 11.90	70.98 11.90
$CH_2{=}CHCH(OC_2H_5)_2$	120/720	1.4002 (24)	64.58 10.84	64.44 10.67
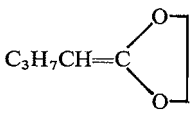	66/16	1.4850 (23)	65.60 9.44	65.61 9.23
$C_4H_9COOC_2H_4OH$	92/4	1.4315 (25)	57.51 9.65	57.78 9.80
$(CH_3)_2CHCH_2COOC_2H_4OH$	75/2	1.4298 (25)	57.51 9.65	57.41 9.41
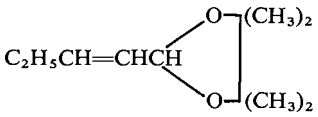	64–66/5.5	1.4422 (22)	71.70 10.94	71.46 10.82
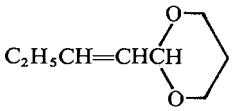	78–80/12	1.4503 (24)	67.57 9.92	67.33 9.74
$C_4H_9COO(CH_2)_3OH$	88–90/2	1.4324 (25)	59.98 10.07	60.27 10.07
$C_2H_5COOC_2H_4OH$	87/10	1.4328 (27)	50.84 8.53	51.05 8.78
$(CH_3)_2CHCOOC_2H_4OH$	78–79/8	1.4224 (25)	54.53 9.15	54.13 9.17
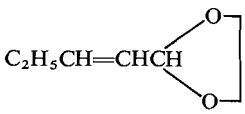	64–67/14	1.4442 (22)	65.60 9.44	65.82 9.33
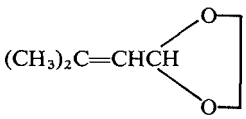	63/10	1.4494 (23)	65.60 9.44	65.42 9.27
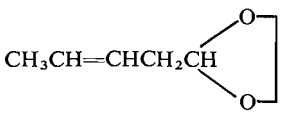	57/14	1.4434 (24)	65.60 9.44	65.77 9.57

(III) Dehydrobrominations of α-Bromoaldehyde Acetals

Procedure A

This followed in detail the published procedure (3).

Procedure B

Dehydrobromination followed by addition of water to trap the ketene acetal. This is illustrated as follows for the dehydrohalogenation of *α-bromo-iso-butyraldehyde ethyleneacetal.*

To a stirred solution of potassium *t*-butoxide (2.87 g, 0.0256 mol) in 25 ml of dry *t*-butyl alcohol was added 5 g (0.0256 mol) of α-bromo-*iso*-butyraldehyde ethyleneace-

Can. J. Chem. Downloaded from www.nrcresearchpress.com by 210.87.254.42 on 09/05/12
For personal use only.

Can. J. Chem. Downloaded from www.nrcresearchpress.com by 210.87.254.42 on 09/05/12
For personal use only.

TABLE 4. Pertinent spectral data for compounds reported in Table 3

Compound	Proton magnetic spectra				Infrared	
	Proton	Multiplicity	Chemical shift τ	Coupling (Hz)	Absorption (cm^{-1})	Assignment
$(CH_3)_2C{=}CHCH(OR)_2$	H-1, H-2	multiplet	4.68–5.08		1680(w)	C=C
3 2 1	H-3	broad singlet	8.28	$w/2 \sim 5$		
$CH_3CH_2CH{=}CHCH(OR)_2$	H-1	doublet	5.29	$J_{1,2} \sim 4$	1685(w)	C=C
4 3 2 1	H-2, H-3	multiplet	4.12–4.57			
(R=alkyl)	H-4	multiplet	7.96			
$CH_3CH_2CH{=}CHCH(OCH_3)_2$	H-1, 2, 3, and 4	Same as above			1680(w)	C=C
4 3 2 1 5	H-5	singlet	6.82			
$CH_3CH_2CH{=}CHCH[OCH(CH_3)_2]_2$	H-1, 2, 3, and 4	Same as above			1680(w)	C=C
4 3 2 1 5 6	H-5	multiplet	6.18			
	H-6	two doublets	8.89	$J_{5,6} \sim 6.5$		
$CH_2{=}CHCH(OR)_2$	H-1	doublet	5.20	$J_{1,2} \sim 3.5$		
3 2 1	H-2, H-3	multiplet	4.0–4.95			
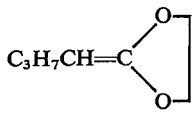	H-1	singlet	5.92	$w/2 \sim 2$		
	H-2	triplet	6.51	~ 7.5		
3 2 1	H-3	multiplets	7.90–9.30		1720(s)	C=C
$C_3H_7CH_2COOCH_2CH_2OH$	H-1, H-2	multiplet	6.12–6.52		3650–3100	O—H
4 3 2 1	H-3	triplet	5.84	$J_{3,2} \sim 5.5$	1740	C=O
	H-4	multiplet	7.50–7.84			
$(CH_3)_2CHCH_2CO_2CH_2CH_2OH$	H-1	multiplet	6.26		3650–3150	O—H
5 4 3 2 1	H-2	multiplet	5.87		1750	C=O
	H-3, H-4	multiplet	7.80			
	H-5	doublet	9.00	$J_{5,4} \sim 6.5$		
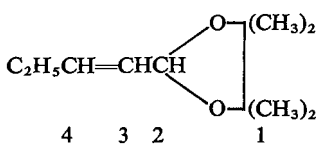	H-1	singlet	8.85		1680(w)	C=C
	H-2	multiplet	4.82			
4 3 2 1	H-3, H-4	multiplet	4.20–4.63			

Can. J. Chem. Downloaded from www.nrcresearchpress.com by 210.87.254.42 on 09/05/12
For personal use only.

TABLE 4 (*Concluded*)

Compound	Proton magnetic spectra				Infrared	
	Proton	Multiplicity	Chemical shift τ	Coupling (Hz)	Absorption (cm^{-1})	Assignment
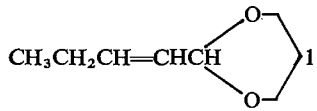	H-1, H-6	multiplet	7.58–8.52		1680(w)	C═C
6 5 4 3 2	H-2	multiplet	5.78–6.18			
	H-3	doublet	5.25	$J_{3,4}\sim 4.5$		
	H-4, H-5	multiplet	3.97–4.97			
$C_3H_7CH_2CO_2CH_2CH_2CH_2OH$	H-1	singlet	7.05		3650–3150	O—H
6 5 4 3 2 1	H-2	triplet	6.44	$J_{2,3}\sim 6$	1730	C═O
	H-4	triplet	5.85	$J_{4,3}\sim 6.5$		
	H-3, 5, and 6	multiplet	7.60–9.28			
$CH_3CH_2CO_2CH_2CH_2OH$	H-1	singlet	6.67		3650–3100	O—H
5 4 3,3′ 2 1	H-2	two doublets	6.32	$J_{2,3}\sim 5; J_{2,3'}\sim 7$	1740(s)	C═O
	H-3, H-3′	two doublets	5.87, 5.94	$J_{3,2}\sim 5; J_{3',2}\sim 7$		
	H-4	quartet	7.67	$J_{4,5}\sim 7.5$		
	H-5	triplet	8.90	$J_{5,4}\sim 7.5$		
$(CH_3)_2CHCO_2CH_2CH_2OH$	H-1	singlet	7.10		3650–3100	O—H
5 4 3,3′ 2 1	H-2	two doublets	6.31	$J_{2,3}\sim 5.5; J_{2,3'}\sim 6.5$	1735(s)	C═O
	H-3, H-3′	two doublets	5.85, 5.90	$J_{3,2}\sim 5.5; J_{3',2}\sim 6.5$		
	H-4	multiplet	7.46	$J_{4,5}\sim 7$		
	H-5	doublet	8.85	$J_{5,4}\sim 7$		
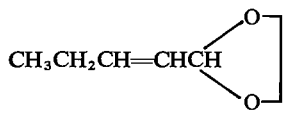	H-1	multiplet	6.20		1685(w)	C═C
6 5 4 3 2 1	H-2	doublet	4.95	$J_{2,3}\sim 5.5$		
	H-3, H-4	multiplet	3.90–4.65			
	H-5	multiplet	7.92	$J_{5,4}\sim J_{5,6}\sim 7$		
	H-6	triplet	8.97	$J_{6,5}\sim 7$		
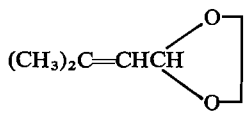	H-1	multiplet	6.18		1680(w)	C═C
4 3 2 1	H-2, H-3	multiplet	4.54–4.85			
	H-4	singlet	8.27			

Can. J. Chem. Downloaded from www.nrcresearchpress.com by 210.87.254.42 on 09/05/12
For personal use only.

tal. The mixture was heated at 80° for 5 h (or for the time indicated in Table 1) then cooled to 50° and 50 ml of water added. This mixture was stirred for a short time, then extracted continuously for 12 h with ether. The ether layer was dried, filtered and the filtrate freed from ether and *t*-butyl alcohol by fractional distillation through a 4-in. Vigreux column. A g.l.c. analysis of the residue showed only two peaks, one due to the unreacted starting material and the other due to β-hydroxyethyl *iso*-butyrate. Comparison of the retention time of authentic methacrolein ethyleneacetal with the g.l.c. spectrum of the crude residue showed no evidence that this α,β-unsaturated acetal had been produced.

The residue was then distilled to provide unreacted α-bromo-*iso*-butyraldehyde ethyleneacetal and a 40% yield of β-hydroxyethyl-*iso*-butyrate, b.p. 78–79° at 8 mm; η_D^{20} 1.4224.

Anal. Calcd. for $C_6H_{12}O_2$: C, 54.53; H, 9.15. Found: C, 54.13; H, 9.17.

Procedure B was used in all dehydrobromination reactions involving the use of water during the work-up procedure. Products were identified either by comparison of the retention times of authentic samples with those of the peaks obtained from a g.l.c. analysis of the crude residue, or by isolation of the products and their characterization by means of their p.m.r. and i.r. spectra as well as their elemental analysis. Physical constants and elemental analysis of the products isolated from these reactions are given in Table 3. Their spectral data are shown in Table 4.

Procedure C

Dehydrobromination in DMSO followed by addition of water to trap the ketene acetal.

The procedure used was the same as that of procedure *B* except that (*a*) the solvent was DMSO and the base was sodium methoxide; (*b*) the bromoacetal was added slowly and the temperature was kept at ~40° for the requisite time (1 or 20 h); (*c*) the water was added as a saturated aqueous solution of sodium chloride to decrease the solubility of the products in the DMSO–water mixture. Products were identified by comparison of their g.l.c. retention times with those of authentic materials.

Procedure D

This was identical to procedure C except that the base was potassium *t*-butoxide.

(IV) Preparation of Some Authentic Dehydrobromination Products

Methyl n-Valerate

To a stirred solution of *n*-valeric acid (25 g, 0.245 mol) in 100 ml of anhydrous methanol was added 1 ml of concentrated sulfuric acid, and the solution heated under reflux for 2 h and then left overnight. The mixture was poured into 200 ml of saturated aqueous sodium chloride solution and this was extracted with ether (2 × 100 ml). The ether extract was washed with saturated aqueous sodium carbonate solution (3 × 50 ml) and then with 100 ml of saturated aqueous sodium chloride solution. The ether layer was dried, filtered, and the filtrate freed of solvent by fractional distillation at atmospheric pressure. The residue when distilled gave 20 g (70%) of colorless liquid, b.p. 122–123° at 705 mm; η_D^{24} 1.3952 (lit. b.p. 130° at 760 mm; η_D^{20} 1.4003 (21)).

The Following Two Esters were Prepared by the Procedure Used for the Synthesis of Methyl n-Valerate Above

Ethyl iso-valerate from *iso*-valeric acid and ethanol. Yield, 50%, b.p. 120–121° at 700 mm; η_D^{25} 1.3939 (lit. b.p. 134.7° at 760 mm; $\eta_D^{18.35}$ 1.39738 (21)).

Isopropyl n-valerate from *iso*-propyl alcohol and *n*-valeric acid. Yield, 57%, b.p. 60° at 20 mm; η_D^{24} 1.3988 (lit. b.p. 153.5° at 760 mm; η_D^{20} 1.4009 (22)).

Acrolein Ethyleneacetal

This compound was prepared by the following modification of the procedure of Fischer and Smith (23).

To a mixture of 300 ml of pentane and 100 ml of anhydrous ether was added 123.3 g (2.2 mol) of acrolein, 126 g (2.0 mol) of ethylene glycol, and 1 g of *p*-toluenesulfonic acid. The mixture was then heated under reflux in an apparatus equipped with a water trap. Vigorous stirring was required to ensure mixing of the two phases. After a 50-h reflux period, 29 ml of water was collected whereupon the mixture was allowed to cool, and then was treated with 20 g of anhydrous sodium carbonate and stirred for 1 h. Solid material was removed by suction filtration, and the filtrate freed of solvent. The residue was distilled to give 45 g (23%) of colorless oil, b.p. 62° at 110 mm; η_D^{28} 1.4260 (lit. b.p. 114–116° at 760 mm; η_D^{20} 1.4327 (23)).

Methacrolein Ethyleneacetal

This compound was prepared by published general directions (24).

From 70 g (1.0 mol) of methacrolein and 62 g (1.0 mol) of ethylene glycol there was obtained 18 g (15%) of colorless oil, b.p. 61° at 50 mm; η_D^{26} 1.4338.

Anal. Calcd. for $C_6H_{10}O_2$: C, 63.14; H, 8.83. Found: C, 63.34; H, 9.04.

The 60 MHz p.m.r. spectrum showed a multiplet centered at τ 4.92 (2H, olefinic); a triplet at 5.10 (1H, $J \sim 1.5$ Hz methine proton); a multiplet centered at 6.17 (4H); and a doublet at 8.31 (3H, $J \sim 1.5$ Hz).

The authors thank the National Research Council of Canada for financial support for a part of this work. One of us, H.A.D., is grateful for the award of a National Research Council of Canada bursary.

1. S. M. McElvain. Chem. Rev. **45**, 453 (1949).
2. S. M. McElvain, R. L. Clarke, and G. D. Jones. J. Am. Chem. Soc. **64**, 1966 (1942).
3. P. R. Johnson, H. M. Barnes, and S. M. McElvain. J. Am. Chem. **62**, 964 (1940).
4. S. M. McElvain and M. J. Curry. J. Am. Chem. Soc. **70**, 3781 (1948).
5. E. L. Eliel and Sr. M. C. Knoeber. J. Am. Chem. Soc. **90**, 3444 (1968).
6. M. L. Dahr, E. D. Hughes, C. K. Ingold, A. M. M. Mandour, G. A. Maw, and L. I. Woolf. J. Chem. Soc. 2093 (1948).
7. D. H. Froemsdorf and M. E. McCain. J. Am. Chem. Soc. **87**, 3983 (1965).
8. D. H. Froemsdorf, M. E. McCain, and W. W. Wilkinson. J. Am. Chem. Soc. **87**, 3984 (1965).
9. D. J. Cram, F. D. Greene, and C. H. DePuy. J. Am. Chem. Soc. **78**, 790 (1956).

10. G. B. BACHMAN. Organic synthesis. Coll. Vol. II. John Wiley and Sons, Inc., New York, N.Y., 1963. p. 323.
11. A. C. J. OPFERMANN. Brit. Pat. 691 820; Chem. Abstr. **48**, 7050 (1954).
12. YA. L. GOL'DFARB and P. A. KONSTANTINOV. Izvest. Akad. Nauk SSSR Otdel. Khim. Nauk, 217 (1957); Chem. Abstr. **51**, 10474 (1957).
13. J. DESCHAMPS, M. PATY, and P. PINEAU. C.R. **238**, 911 (1954); Chem. Abstr. **49**, 3001 (1955).
14. W. H. HARTUNG and H. ADKINS. J. Am. Chem. Soc. **49**, 2520 (1927).
15. R. KUHN and C. GRUNDMANN. Chem. Ber. **70**, 1894 (1937).
16. E. N. MARVELL and M. J. JONCICH. J. Am. Chem. Soc. **73**, 973 (1951).
17. R. ADAMS and E. W. ADAMS. Organic syntheses. Coll. Vol. I. John Wiley and Sons, Inc., New York, N.Y., 1964 p. 459.
18. A. I. VOGEL. A textbook of practical organic chemistry. Longmans, Green and Co., New York, N.Y., 1948 p. 348.
19. H. ERLENMEYER and J. P. YUNG. Helv. Chim. Acta, **32**, 37 (1949).
20. A. KIRRMANN. C.R. **184**, 525 (1927); Chem. Abstr. **21**, 1796 (1927).
21. Dictionary of organic compounds. Vol. 5. Eyre and Spottiswoode, London, 1965. p. 3234.
22. Handbook of chemistry and physics. 48th Ed. *Edited by* R. C. Weast. Chemical Rubber Co., Cleveland, Ohio, 1967–1968.
23. R. F. FISCHER and C. W. SMITH. J. Org. Chem. **25**, 319 (1960).
24. D. L. HEYWOOD and B. PHILLIPS. J. Org. Chem. **25**, 1699 (1960).

Can. J. Chem. Downloaded from www.nrcresearchpress.com by 210.87.254.42 on 09/05/12
For personal use only.

Can. J. Chem. Downloaded from www.nrcresearchpress.com by 210.87.254.5 on 09/05/12
For personal use only.

Electronic Raman Spectra. VII. Raman Spectra of the Lanthanides[1]

J. A. KONINGSTEIN[2] AND P. GRUNBERG[3]
Chemistry Department, Carleton University, Ottawa, Canada

Received November 16, 1970

Additional experimental data are reported on electronic Raman scattering of trivalent lanthanides, making the observation of this effect of the series nearly complete. The bulk of the information now available points to the fact that the intensity of electronic Raman transition is strongest for the rare earth ions in the middle of the series. The most profound differences of polarization features of electronic transitions and phonons is observed in the situation where the lanthanide ions have an odd number of 4f electrons. Antisymmetric scattering tensors play a less important role.

Des données expérimentales supplémentaires sont rapportées sur la dispersion électronique Raman des lanthanides trivalents. Ceci rend l'observation de cet effet dans les séries à peu prés complète. Le volume de l'information maintenant disponible met en évidence le fait que l'intensité de la transition électronique Raman est très importante pour les ions des terres rares dans le milieu des séries. Les différences très grandes de traits de polarisation des transitions électroniques et de phonons sont observées quand les ions lanthanidiques ont un nombre impair d'électrons 4f. Les tenseurs de dispersion antisymétriques jouent un rôle moins important.

Canadian Journal of Chemistry, 49, 2336 (1971)

Introduction

The interest in exciting the electronic Raman effect of trivalent lanthanide ions mainly stems from the fact that it can be used as a technique to determine the position and symmetry species of low lying electronic levels. Only in a few isolated cases in the pre-laser period was Raman scattering detected in which electronic levels were involved (4–6) but experimental data now available suggest that the intensity of the electronic effect of lanthanide ions in crystals is in some cases comparable to the intensity of phonons of those crystals. In this regard it may be remarked that direct transitions between the electronic states of the same configuration are parity forbidden, but they become weakly allowed as a result of crystal field or vibronic coupling effects. The intensity of these direct electronic transitions is, however, much weaker than the intensity of the phonons of the host lattice and as we shall see later this situation is sometimes reversed in the Raman spectra.

In this paper scattering of some of the ions is reported for the first time making the observation of this effect almost complete throughout the series. In other cases results of new rare earth compounds are given. Some previous results will also be mentioned where it helps to enlighten the discussion. All new results are collected in Table 1.

Up to now the following rare earth compounds have been investigated; rare earth aluminum and gallium garnets (ref. 1 and other papers of this series), chlorides (2, 7) and fluorides (3), ethyl sulfates and oxides (8), and rare earth aluminates (25).[4] One has not always been successful in exciting the electronic Raman effects. For instance, the rare earth ethyl sulfate crystals have a rather complicated phonon spectrum and the position of phonon and electronic transitions may coincide, but also the percentage of lanthanide ions in this compound is much smaller than for the rare earth aluminates and garnets. Apart from the concentration effects there is the width of the transitions. For chlorides and ethylsulfates it is necessary to study the spectra at low temperature of the samples but even then, as a result of local heating effects, due to the laser radiation, the widths of the transitions are so large that they have escaped detection (7).

The most pronounced differences of the polarization properties of phonon and electronic transitions of the same rare earth doped crystal occurs in the situation of lanthanide ions having an odd number of electrons. Examples are given

[1]Research supported by the National Research Council and Defence Research Board of Canada.

[2]Visiting Professor at the National Research Council of Canada.

[3]NRCC Postdoctorate Fellow, 1969–1971.

[4]Electronic Raman effect of $NdAlO_3$ was first observed by J. Scott (private communication).

TABLE 1. Raman shifts of the electronic transitions reported in this paper

Ion	Host	Transition	Temperature (°K)	Shift (cm^{-1})
Yb^{3+}	YbAlG	$^2F_{7/2}$	77 and 4.2	586
				610
				750
Tm^{3+}	TmAlG	$^3H_6$	77 and 4.2	228
Er^{3+}	ErAlG	$^4I_{15/2}$	77 and 4.2	24
				56
				76
				426
				444
	ErGaG	$^4I_{15/2}$	77 and 4.2	44
				55
				75
				436
Dy^{3+}	DyAlG	$^6H_{15/2}$	77 and 4.2	69
				115
				195
				441
		$^6H_{15/2}$–$^6H_{13/2}$		3567
				3596
				3790
				3953*
Eu^{3+}	EuGaG	$^7F_0$–$^7F_1$	4.2	306
				329
				411
		$^7F_0$–$^7F_2$		819
				824
				857
				1324
				1341
		$^7F_0$–$^7F_3$		2834
				2927
				3077
				3089
				3103
Sm^{3+}	$SmAlO_3$	$^6H_{5/2}$	77 and 4.2	159
				284
		$^6H_{5/2}$–$^6H_{4/2}$		1053
				1111
				1293
				1488
		$^6H_{5/2}$–$^6H_{9/2}$		2247
				2301
				2463
				2520
Pr^{3+}	PrF_3	$^3H_4$	4.2 and 20	68
				98
				248
				460
				539
		$^3H_4$–$^3H_5$	4.2	2194
				2288*
Ce	$CeMg(NO_3)_6H_2O$	$^2F_{5/2}$	4.2	26

*The electronic nature is uncertain.

in Experimental section. These differences are related to the fact that extended groups (double groups) have to be employed to determine the selection rules and thus the polarization features.

Experimental Procedure

Good quality Raman spectra of single crystals of rare earth compounds were photo-electrically recorded. The apparatus has been described elsewhere (1). Some Raman spectra are shown in Figs. 1–8. The spectra were obtained from polished single crystals (4 × 2 × 4 mm) and the orientation of the crystals was in most cases known. They were cooled to 4.2 or 77 °K and several excitation frequencies were used. This was sometimes necessary to distinguish fluorescence lines from Raman bands but the routine was normally adopted to make sure that the observed spectrum was a Raman spectrum. At low temperatures of the sample the intensity of the anti-Stokes lines is very weak and a comparison of Stokes and anti-Stokes lines cannot be made.

Can. J. Chem. Downloaded from www.nrcresearchpress.com by 210.87.254.5 on 09/05/12
For personal use only.

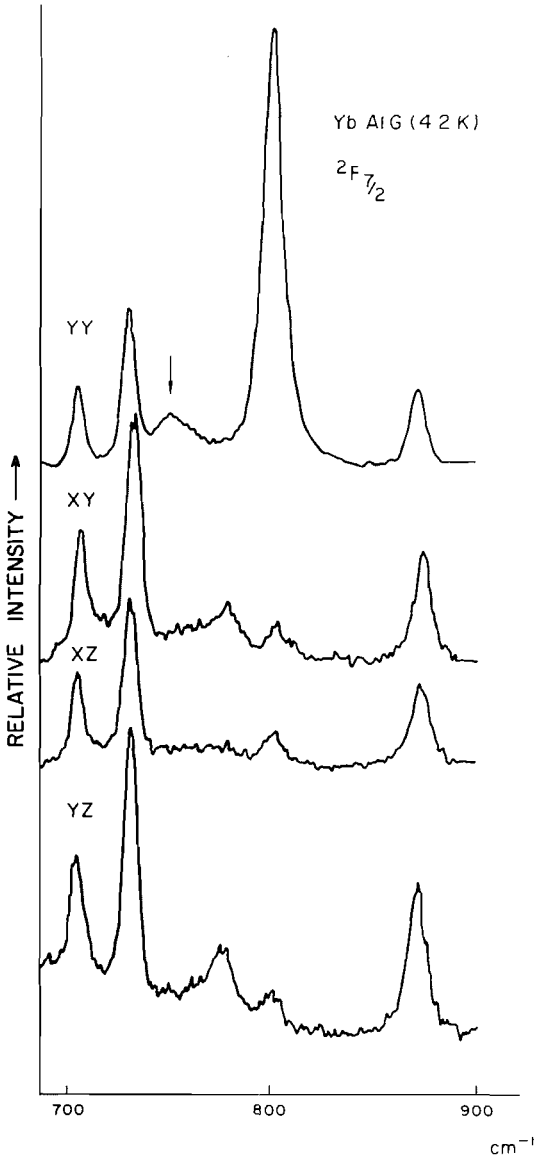

FIG. 1. Phonons and electronic (↓) Raman effects of the compound YbAlG. Temperature of the sample was 4.2 °K, slit width of 4 cm^{-1}. Indicated are the tensor components of the various Raman transitions. λ_0 = 4880 Å.

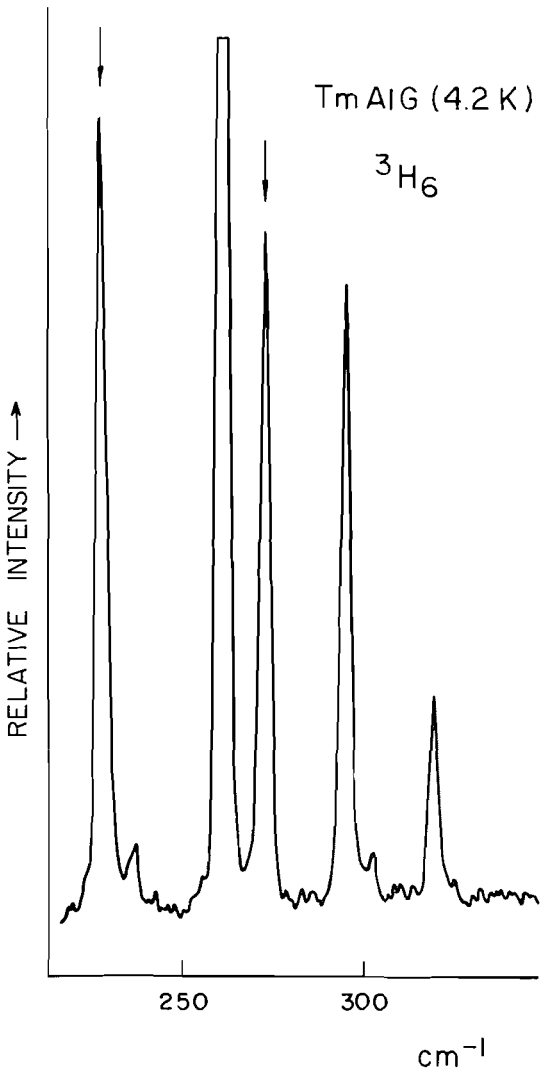

FIG. 2. Part of the low temperature Raman spectrum of an oriented crystal of TmAlG. The electronic effects are indicated. The symmetry of the Raman lines of 274 (electronic) and 296 cm^{-1} (phonon) is T_{2g}. Slit width 3 cm^{-1}, λ_0 = 5154 Å.

Discussion of the Experimental Data

(a) Scattering of Yb^{3+}

The ground state $^2F_{7/2}$ of the Yb^{3+} ion contains a maximum of 4 Kramers degenerate crystal field levels. The crystal field components of the other 4f state $^2F_{5/2}$ are at about 10 000 cm^{-1}. The case of Yb (and also Tm) in the aluminum garnet crystals may serve as an example that electron Raman spectroscopy can be employed as a tool to find low lying electronic states. Although the selection rules do not forbid the observation of the $^2F_{7/2} \rightarrow {}^2F_{5/2}$ transitions, Raman lines with shifts of 10 000 cm^{-1} are weaker by a factor of eight if compared to the intensities of transition with shifts of $\Delta\tilde{\nu} \approx 1000$ cm^{-1}, assuming $\tilde{\nu}_0 = 20\,000$ cm^{-1}. The sensitivity of detectors is

Can. J. Chem. Downloaded from www.nrcresearchpress.com by 210.87.254.5 on 09/05/12
For personal use only.

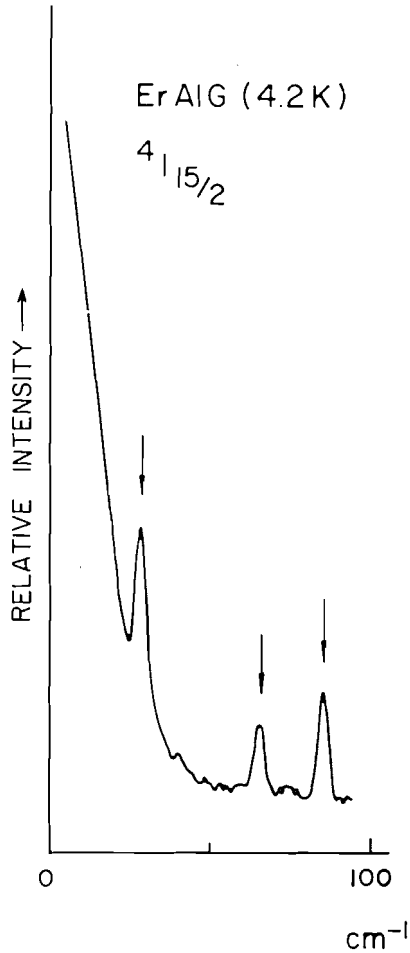

FIG. 3. Electronic Raman scattering of Er in ErAlG. All the elements of the scattering tensor for the electronic transitions are different from zero and independent of the orientation of the crystal, all three transitions are observed.

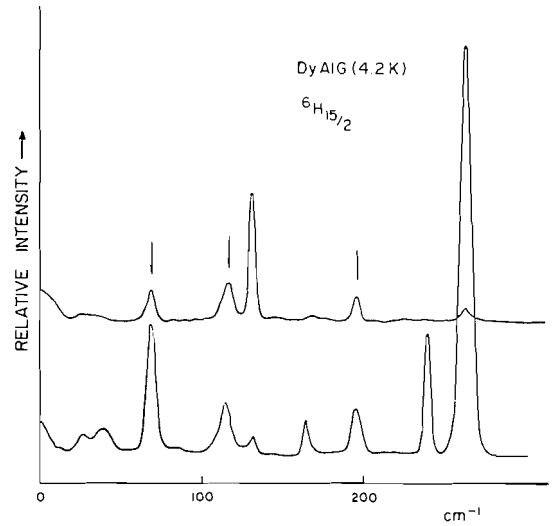

FIG. 4. Polarized Raman spectrum of cubic DyAlG (arbitrarily oriented in space). The intensity of T_{2g} phonons modes in the upper trace is about 1/30 of the intensity of the modes in the lower trace, for an E_g mode this ratio is 7/1 (compare lines at 260 and 135 cm^{-1}). The electronic transitions (↓) have different polarization features because the Dy^{3+} ion has 4f electrons and all levels and parts of the tensor belong to representatives of a double group.

also lower in the region of 1 μ and consequently from an experimental point of view it is more convenient to try to find scattering to crystal field states of the $^2F_{7/2}$ ground manifold. For YbAlG there are four Kramers pairs (9) because the site symmetry for the rare earth ion is D_2.

Fluorescence, absorption, and Raman measurement all point to the existence of a state at ~610 cm^{-1} above the ground state. Due to the occurrence of strong vibronic coupling in the fluorescence and absorption spectrum (9) a clear way to pin down the pure electronic transitions does not exist. It has been shown that such vibronic coupling effects are very weak in electronic Raman scattering (10) and that the intensity of pure electronic transition is at least one order of magnitude stronger than the intensity of vibroelectronic Raman bands. The position of phonon bands of the cubic aluminum, gallium, and also ytterbium iron garnet crystals is known in great detail (11–15). Vibrational and electronic Raman transitions differ in their polarization features (14) and usually in their line width and this allowed the assignment of Raman lines of YbAlG with shifts of 586 and 610 cm^{-1} as due to electronic transitions of the Yb^{3+} ion. The third transition was found in a similar way but due to the presence of close lying phonons its position was more difficult to locate. In Fig. 1 the Raman spectrum with shifts of 700 to 900 cm^{-1} is shown. The symmetry of the phonons are as follows: 710, 735, and 870 cm^{-1} belong to the species T_{2g}, 775 cm^{-1} is of species E_g, and the shift on 806 cm^{-1} is of type A_{1g} of the group O_h. The position of the third electronic transition is indicated in Fig. 1 and it is seen that the polarization features are different from those of the phonons.

The case of Yb in YbAlG may serve as a good

Can. J. Chem. Downloaded from www.nrcresearchpress.com by 210.87.254.5 on 09/05/12
For personal use only.

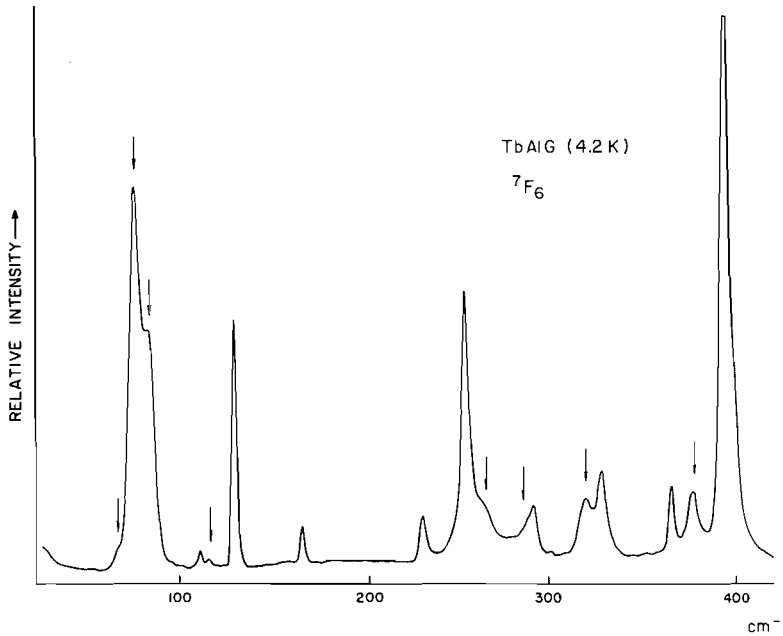

FIG. 5. Electronic effects (↓) of Tb^{3+} in TbAlG. Slit width 3 cm^{-1}. The tensor components are $\alpha_{xx} + \alpha_{xz}$. The electronic Raman line at 373 cm^{-1} is a case of pure isotropic scattering.

example if a comparison is made of the results of electronic Raman scattering and fluorescence and absorption spectra. The electronic levels of the $^2F_{7/2}$ manifold of Yb^{3+} in YbAlG could be determined from the polarization measurement of the Raman lines. Apart from the occurrence of vibronic bands it was not possible to find all the electronic levels from the fluorescence or absorption spectra because direct-electric dipole transitions do not show polarization features in the cubic garnet crystals but the Raman lines of such a crystal do have definite polarization features. The results of recent work on the Yb^{3+} ion are collected in Table 1.

(b) Scattering between Levels of the Tm^{3+} Ion

The excited states $^3H_4$ and $^3H_5$ of the free Tm^{3+} ion are ~6000 and ~8000 cm^{-1} above the ground state ($^3H_6$), respectively. Only Raman transitions from the lowest to higher crystal field components of $^3H_6$ have been observed.

In the garnets the crystal field states of the Tm^{3+} ion belong to the representations A, B_1, B_2, B_3 of the single group D_2. Raman tensors of transitions at the site belong necessarily to these representations. The effect of all rare earth sites in the primitive cell should be considered to explain the polarization properties of Raman transitions of the whole crystal (16). In the cubic symmetry of the crystal, space group O_h^{10}, a transition of type A at the sites is observed as $A_{1g} + E_g + T_{2g}$. B_1 goes to $E_g + T_{1g}$, B_2 and B_3 go to $T_{2g} + T_{1g}$.

Strong vibronic coupling has been observed in the absorption or phonon spectrum of TmAlG or Tm in YAlG and therefore again the electronic Raman effect has been used successfully in finding new electronic levels. In Fig. 2 part of the 4.2 °K Raman spectrum of TmAlG is shown and from a knowledge of the position of phonons the electronic effects could be assigned. Additional electronic Raman transitions were observed in other parts of the spectrum and all data are brought together in Table 1. Although twelve electronic Raman transitions can in principle be expected from the lowest to other crystal field states of the $^3H_6$ ground manifold a maximum of only four transitions have been observed for TmAlG and only one of TmGaG. Two of the four transitions of the former crystal are, however, very strong (see Fig. 2). The tensor could be determined and the electronic Raman transition with a shift of 228 cm^{-1} is of species $A_{1g} + E_g + T_{2g}$ and the transition at 274 cm^{-1} belongs to

Can. J. Chem. Downloaded from www.nrcresearchpress.com by 210.87.254.5 on 09/05/12
For personal use only.

Can. J. Chem. Downloaded from www.nrcresearchpress.com by 210.87.254.5 on 09/05/12
For personal use only.

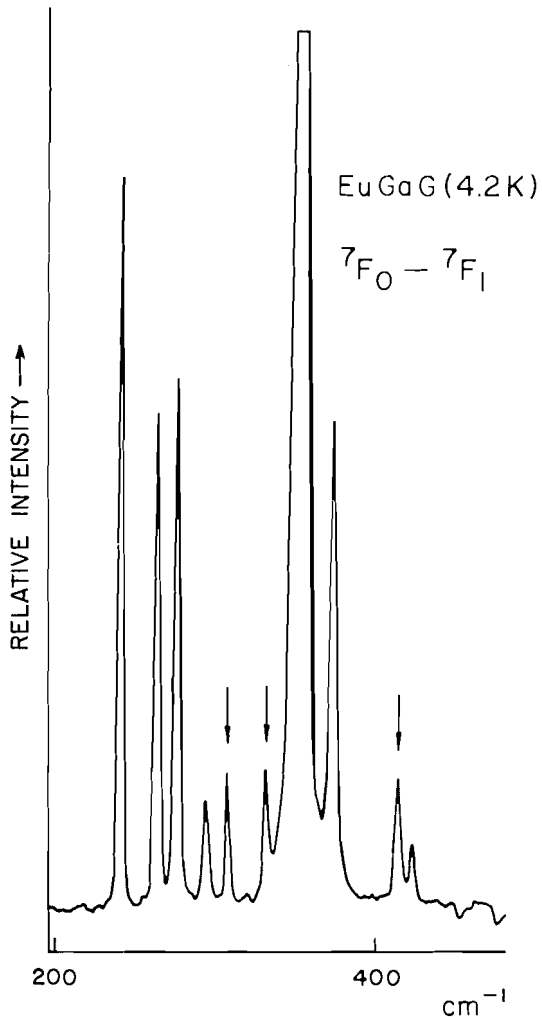

FIG. 6. Electronic Raman effects of EuGaG. The asymmetry of the transition is believed to be present, although part of the intensity is the result of crystal field mixing effects of wave functions of $^7F_1$ and $^7F_2$ states.

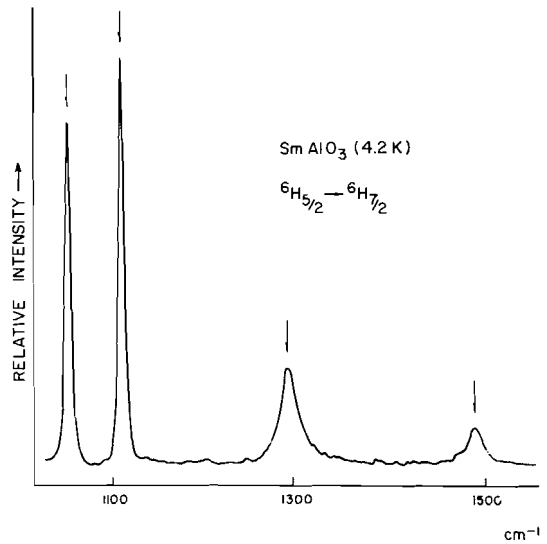

FIG. 7. Low temperature electronic Raman transitions of a small crystal of $SmAlO_3$. $\lambda_0 = 5154$ Å, slit width 2 cm^{-1}. The position of all four Kramers pairs of $^6H_{7/2}$ can be directly obtained from the spectrum.

the species T_{2g}. Thus, the former Raman line is associated with a transition between states of the same symmetry and the latter is one of $A \rightarrow B_3$; $B_1 \rightarrow B_2$; $B_2 \rightarrow B_3$ or $B_1 \rightarrow B_3$. The amount of T_{2g} character of the Raman line at 228 cm^{-1} is larger than the amount of $A_{1g} + E_g$ combined. This is an indication that the components α_{xx}, α_{yy}, and α_{zz} for the tensor at one site are quite different. If the symmetry of the surrounding of the Tm^{3+} ion would be described by the point group D_{4h} then $\alpha_{xx} = \alpha_{yy} \neq \alpha_{zz}$. It can therefore be concluded that the local symmetry of Tm^{3+} in TmAlG cannot be approximated by D_{4h}. Evidence of an electronic transition of TmGaG has already been presented (16) but the search for electronic effects of this lanthanide ion in other crystals was negative.

(c) Scattering of Er^{3+} Levels

Electronic transitions of Er^{3+} were detected in ErAlG and ErGaG crystals but the main difference with the data of Yb^{3+} and Tm^{3+} in garnets is that the position of the crystal field states of the ground manifold and excited manifolds have already been determined from low temperature absorption and fluorescence spectra (17–19). To a certain degree the position of these excited states interfere with the excitation of the Raman spectrum in that near resonance occurs of some of the states and the energy of the radiation of either the He–Ne or Argon ion laser. As a result of this resonance, for some exciting lines, fluorescence is excited in the same spectral region where Raman transitions occur and the intensity of the fluorescence transitions being much more intense than the electronic Raman transitions makes it difficult to observe the latter. Electronic Raman scattering was, however, observed at 4.2 °K in ErAlG and ErGaG employing the 4965 Å line of argon ion laser. The transitions are shown in Fig. 3 and the frequency shifts are given in Table 1. The width of higher lying

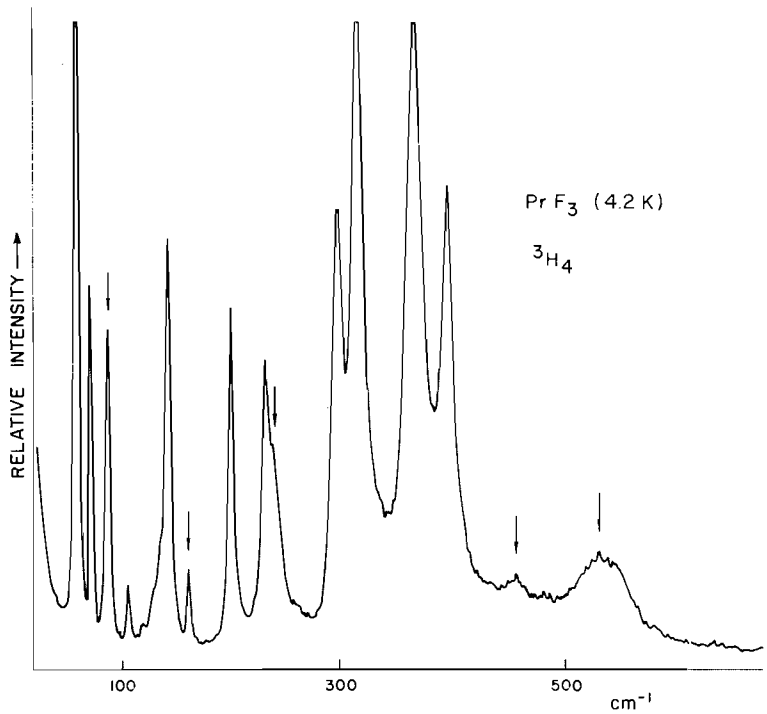

FIG. 8. Low temperature Raman spectrum of PrF_3. The tensor is α_{xx} and all electronic Raman effects are indicated. $\lambda_0 = 5154$ Å and the slit width is 2 cm^{-1}.

crystal field levels of the $^4I_{15/2}$ manifold of Er^{3+} is considerably more than the width of the ground state and as a result, the Raman lines representing a transition from the ground state to such higher lying states are rather broad. On the other hand, the peak height of transitions with small shifts is large and this allows the detection of the Raman transitions to very low lying electronic states in a straightforward way. Figure 3 suggests that it is quite easy to detect levels with a shift of >25 cm^{-1}.

Raman spectra of other erbium compounds have also been investigated but electronic transitions there escaped detection, partly due to sample size or due to the excitation of strong fluorescence which obscured electronic Raman effects. In the course of the experiments we have been unable to detect electronic effects of the Holmium ion.

(d) Scattering of the Dy^{3+} Ion

The levels of the $^6H_{13/2}$ manifold are approximately 3600 cm^{-1} above the ground state. $^6H_{15/2}$, and other electronic states are at energies >6000 cm^{-1}. Transitions within $^6H_{15/2}$ and to the components of $^6H_{13/2}$ have been observed. Some of the electronic Raman transitions of DyAlG are shown in Fig. 4. They could be assigned because of (*i*) their temperature dependence and (*ii*) their polarization features. The data obtained from the Raman measurements of DyAlG are of interest in that the positions of the levels of $^6H_{13/2}$ could not be determined (20) from either absorption of fluorescence measurements of this compound.

All frequency shifts are given in Table 1. Due to increasing widths of electronic states several electronic Raman transitions escaped detection. It is perhaps worthwhile to note that the percentage of rare earth ions in garnet structures is smaller than in rare earth aluminate compounds and experimental data are available which show that the electronic effect of rare earth aluminates is much stronger than those of garnet crystals. On the other hand, the transitions of DyAlG which were observed were so strong that detailed polarization studies could be made and in Fig. 4 is shown an example of the fact that electronic

Can. J. Chem. Downloaded from www.nrcresearchpress.com by 210.87.254.5 on 09/05/12
For personal use only.

Can. J. Chem. Downloaded from www.nrcresearchpress.com by 210.87.254.5 on 09/05/12
For personal use only.

transitions between Kramers pairs differ very much in their polarization properties if compared to the phonons of the crystal.

Although only scattering to the lower lying states of $^6H_{15/2}$ and $^6H_{13/2}$ manifolds could be detected, the intensity of the transitions is comparable to the intensity of the phonon modes of the garnet crystal. Many hot bands were also observed while studying the 77 °K Raman spectrum of this crystal. The population of the lower lying levels at 77 °K is apparently large enough so that transitions originating in levels situated at 69 and 112 cm^{-1} appear in the spectrum.

Other rare earth compounds containing the Dy ion have not been studied yet but in view of the fact that the Dy ion scatters more intensely than Er, Tm, and Yb ions, there is no reason to assume that the observation of electronic transitions should be limited to DyAlG only.

(e) Scattering of the Tb^{3+} and Eu^{3+} Ion

The low lying states of the Tb^{3+} and Eu^{3+} ion are the almost pure Russell–Saunders multiplet components of ^7F, in reversed order for Tb^{3+} and Eu^{3+}. The splitting of the levels by the crystal field can in most cases not be considered to be small compared to the distances between the free ion levels and strong *J*-mixings of the states occurs. This has a strong influence on the intensities and polarization features of the electronic Raman transitions. For TbAlG very strong electronic effects have been observed from the ground state to the crystal field levels of the $^7F_6$ split manifold. Some of the electronic transitions are shown in Fig. 5. Detailed measurements have been made of the polarization properties and magnetic field dependence of the Raman shifts (21) and at least one of the Raman transitions is related to a tensor which contains asymmetry. The case of TbAlG is of importance in that many of the electronic transitions have a larger intensity than the phonons and it thus appears that the Tb ion is an excellent example for strong electronic Raman spectroscopy, the reader is referred to other publications for details (22). This, to a certain degree, is also true for the europium ion. Transitions between $^7F_0$ and the components of $^7F_1$ have been observed in the spectral range of $250\ cm^{-1} < \Delta\nu < 450\ cm^{-1}$ for Eu^{3+} in YAlG, YGaG, and YVO_4 (1, 23, 24). For Eu in EuGaG transitions of medium intensity have now also been observed (1). Some are shown in Fig. 6. The tensors have been measured and in agreement with theory (1), the antisymmetric tensors do contribute to these intensities.

(f) Scattering of Sm^{3+}

The low lying energy levels of Sm^{3+} are the multiplet components of ^6H. We succeeded in exciting Raman transitions between the lowest crystal field components of $^6H_{5/2}$ and the components of $^6H_{7/2}$ and $^6H_{9/2}$. The Raman shifts are given in Table 1. They agreed with the level positions obtained from fluorescence spectra, only the highest component of $^6H_{9/2}$ was not found in the Raman spectrum. The absorption spectrum of $SmAlO_3$ contains a great number of lines in the area between 4600 and 5050 Å, the occurrence of a resonance Raman effect has some probability. In particular the laser line at 4965 sits in the wing of a broad absorption line and some indication of resonance was found in the Raman spectrum excited with the 4965 line. Like Dy^{3+} also, Sm^{3+} seems to be a fairly good scatterer.

(g) Scattering of Pr^{3+} and Ce^{3+}

Low lying manifolds of Pr^{3+} in crystals are the components of $^3H_{4,5,6}$. Electronic scattering in $PrCl_3$ was already reported before the advent of the laser. Hougen and Singh (26) found scattering from the ground state to other crystal field levels of $^3H_4$, and also $^3H_4 \rightarrow {}^3H_5$ and $^3H_4$–$^3F_2$ transitions. We have repeated the experiments with an argon ion laser and could only detect $^3H_4$ intermanifold transitions. Bauman and Porto (3) studied the Raman spectrum of PrF_3. Electronic effects were observed with shifts of 66, 94, and 537 cm^{-1} whilst the temperature of the sample was 20 °K (see Table 1). In Fig. 9 the 4.2 °K Raman spectrum of PrF_3 is shown and the electronic effects at 68, 243, and 539 cm^{-1} are indicated. Apparently there is a drastic change in the positions of the $^3H_4$ states of PrF_3 and Pr^{3+} in LaF_3. (Note also the ten-fold increase in line width of the 539 cm^{-1} band compared to the Raman line shift of 68 cm^{-1}.) Other weak electronic effects were observed with shifts $>2000\ cm^{-1}$. They have been assigned to $^3H_4$–$^3H_5$ transitions. Only one electronic Raman transition of $CeMg(NO_3)_6H_2O$ could be observed. The transition terminates on the lowest level of the split $^2F_{5/2}$ state situated at 27 cm^{-1}

but due to strong phonon bands the search for electronic effects in the 150–200 cm^{-1} region was negative. Good spectra were, however, recorded by Kiel *et al.* (2) of a single crystal of $CeCl_3$. Asymmetry in some of the tensors which was predicted (27) was verified experimentally.

Conclusions

Comparing the electronic Raman spectra of the lanthanide ions in different crystals some general considerations can be made. It is for instance obvious that the strongest spectra have been obtained from the ions in the middle of a series, *i.e.*, Eu and Tb. Ce at the beginning and Yb at the end of the series show the weakest effects.

The width of the first excited state configuration (that is the energy difference of highest and lowest electronic level of this configuration) is larger for the ions in the middle than for the ions at the beginning and end of the series (28). It may very well be that this change in width is related to the observed intensity pattern. Unfortunately, such large widths are responsible for the fact that the theory to compute the intensities is not valid anymore. More experimental data are required to arrive at a better understanding of the intensity problem.

The authors wish to thank Drs. L. G. Van Uitert and J. Scott of the Bell Telephone Laboratories, Inc. for supplying rare earth garnet and rare earth aluminate crystals. Thanks are also due to Dr. G. Schaack of the T. H. Darmstadt, Germany for information on the rare earth ethyl sulfates, rare earth chlorides, and rare earth oxides crystals and their suitability for exciting the electronic spectra.

1. J. A. KONINGSTEIN. J. Chem. Phys. **51**, 1163 (1969).
2. A. KIEL, T. DAMEN, S. P. S. PORTO, S. SINGH, and F. VARSANYI. Phys. Rev. **170**, 1518 (1969).
3. R. P. BAUMAN and S. P. S. PORTO. Phys. Rev. **161**, 842 (1967).
4. J. HOUGEN and S. SINGH. Phys. Rev. Lett. **10**, 406 (1963).
5. J. Y. H. CHAU. J. Chem. Phys. **44**, 1700 (1966).
6. F. RASETTI. Z. Phys. **66**, 646 (1930).
7. G. SCHAACK and J. A. KONINGSTEIN. J. Phys. Chem. Solids. In press.
8. G. SCHAACK and J. A. KONINGSTEIN. J. Opt. Soc. Am. **60**, 1110 (1970).
9. R. A. BUCHANAN *et al.* Phys. Rev. **159**, 245 (1967).
10. O. S. MORTENSEN and J. A. KONINGSTEIN. Chem. Phys. Lett. **1**, 409 (1968).
11. J. P. HURRELL, S. P. S. PORTO, I. F. CHANG, S. S. MITRA, and R. P. BAUMAN. Phys. Rev. **173**, 851 (1968).
12. N. T. MCDEVITT. J. Opt. Soc. Am. **59**, 1240 (1969).
13. G. MACE, G. SCHAACK, TOANING NG, and J. A. KONINGSTEIN. Z. Phys. **230**, 391 (1970).
14. J. A. KONINGSTEIN. Phys. Rev. **174**, 477 (1968).
15. G. MACE and J. A. KONINGSTEIN. Chem. Phys. Lett. **3**, 343 (1969).
16. TOANING NG and J. A. KONINGSTEIN. Can. J. Chem. **47**, 1395 (1969).
17. K. H. HELLWEGE, S. HÜFNER, M. SCHINKMANN, and H. SCHMIDT. Phys. Kond. Materie, **4**, 397 (1966).
18. E. ORLICH, S. HÜFNER, and P. GRÜNBERG. Z. Phys. **231**, 144 (1970).
19. H. M. CROSSWHITE and H. W. MOOS. Optical properties of ions in crystals. Interscience Publ. Inc., New York. 1967. S. 3.
20. P. GRÜNBERG, S. HÜFNER, E. ORLICH, and J. SCHMITT. Phys. Rev. **184**, 285 (1969).
21. J. A. KONINGSTEIN and G. SCHAACK. J. Opt. Soc. Am. **60**, 755 (1970).
22. J. A. KONINGSTEIN and G. SCHAACK. Phys. Rev. **2B**, 1242 (1970).
23. J. A. KONINGSTEIN and O. S. MORTENSEN. Nature, **217**, 445 (1968).
24. J. A. KONINGSTEIN and O. S. MORTENSEN. Phys. Rev. Lett. **18**, 831 (1967).
25. J. SCOTT. Private communication.
26. J. T. HOUGEN and S. SINGH. Proc. Roy. Soc. London, **277A**, 243 (1964).
27. J. A. KONINGSTEIN and O. S. MORTENSEN. Chem. Phys. Lett. **1**, 695 (1968).
28. G. H. DIEKE. Spectra and energy levels of rare earth ions in crystals. John Wiley and Sons, Inc. 1968.

Can. J. Chem. Downloaded from www.nrcresearchpress.com by 210.87.254.5 on 09/05/12
For personal use only.

Can. J. Chem. Downloaded from www.nrcresearchpress.com by 210.87.254.40 on 09/05/12
For personal use only.

Orientation of Solute Molecules in Nematic Liquid Crystal Solvents

J. C. ROBERTSON, C. T. YIM,[1] AND D. F. R. GILSON
Department of Chemistry, McGill University, Montreal 110, Quebec

Received February 1, 1971

The tendency of solute molecules to align with their longest dimension parallel to the optic axis of a nematic liquid crystal solvent can be explained by a simple model, based on dispersion force interactions, relating *S*-values obtained from nuclear magnetic resonance measurements, to molecular dimensions.

Les molécules de soluté ont tendance à s'aligner suivant leur plus grande dimension parallèlement à l'axe optique du solvant constitué de cristaux liquides nématiques. Ceci peut être expliqué par un modèle simple en invoquant des interactions de forces de dispersion, qui relient les valeurs de *S* obtenues des mesures de résonance magnétique nucléaire, aux dimensions moléculaires.

Canadian Journal of Chemistry, 49, 2345 (1971)

Nematic liquid crystals provide a means of partially orienting solute molecules in nuclear magnetic resonance experiments (1–4). The degree of solute alignment can be described either by the order matrix {**S**} due to Saupe (5), or in terms of the motional constants given by Snyder (6); the two approaches are simply related (6). The number of elements of the **S**-matrix required to describe the degree of orientation depends upon the symmetry of the molecule and can be minimized by a proper choice of axes. If the molecule has two perpendicular planes of symmetry, but a less than three-fold symmetry axis, two elements suffice. The *S*-value of a given axis lies between -0.5 and $+1.0$ for alignment ranging between perpendicular and parallel to the applied magnetic field and, unless a high degree of parallel alignment occurs, *i.e.* $S > 0.5$, the sign of *S* is not immediately determined. It is generally observed, however, that a solute molecule is preferentially oriented with the longest molecular dimension parallel to the optic axis of the liquid crystal.

Saupe has shown that, except in the case of specific interactions such as hydrogen bonding, dispersion forces are primarily responsible for the alignment of solute molecules and permanent electric dipole moments are of minor importance. Using a statistical treatment, the interaction potential energy has been correlated with localized contributions from substituent bonds in chloro- and fluoro-substituted benzene derivatives (7, 8). Since dispersion forces are involved, a dependence on polarizability anisotropies and thus on molecular size is not unexpected. In the present work, a simple treatment relating *S*-values to molecular dimensions is developed.

The average potential energy of a solute molecule is, as a function of its orientation (8),

$$[1]\quad \bar{V}(\theta,\phi) = -a_1 \sin^2\theta\cos^2\phi - a_2 \sin^2\theta\sin^2\phi - a_3\cos^2\theta$$

where θ and ϕ are the usual polar angles relating the molecule-fixed *1*, *2*, *3* axial system to the optic axis of the solvent and a_i is the potential energy of interaction along the *i*th molecular axis. It is assumed in the subsequent discussion that the longest molecular feature lies along the *2*-direction with the shortest along the *3*-direction. Equation 1 is conveniently rewritten as

$$[2]\quad \bar{V}(\theta,\phi) = -a_3 - (a_1 - a_3)\sin^2\theta\cos^2\phi - (a_2 - a_3)\sin^2\theta\sin^2\phi$$

Saupe (7) has shown that according to classical Boltzmann statistics, the two *S*-values required for molecules possessing two perpendicular planes of symmetry but a less than three-fold symmetry axis can be described by

$$[3a]\quad S_{11} = \frac{3}{2}\frac{\int_0^{\pi/2}\int_0^{\pi/2}\sin^2\theta\cos^2\phi\exp\{-\bar{V}(\theta,\phi)/kT\}\sin\theta\,d\theta\,d\phi}{\int_0^{\pi/2}\int_0^{\pi/2}\exp\{-\bar{V}(\theta,\phi)/kT\}\sin\theta\,d\theta\,d\phi} - \frac{1}{2}$$

[1]Present address: Department of Chemistry, Dawson College, Westmount 215, Quebec.

and

$$[3b] \qquad S_{22} = \frac{3}{2} \frac{\int_0^{\pi/2} \int_0^{\pi/2} \sin^2\theta \sin^2\phi \exp\{-\bar{V}(\theta, \phi)/kT\} \sin\theta \, d\theta \, d\phi}{\int_0^{\pi/2} \int_0^{\pi/2} \exp\{-\bar{V}(\theta, \phi)/kT\} \sin\theta \, d\theta \, d\phi} - \frac{1}{2}$$

Clearly, the term $-a_3$ in eq. 2 cancels in the exponentials of eqs. 3. Thus the two elements of the S-matrix are dependent only on the differences $(a_1 - a_3)$ and $(a_2 - a_3)$.

If only the dispersion forces are considered and a dipole–dipole approximation used, the orientational potential energy may be expressed in terms of polarizability anisotropies (9). For certain specific orientations of the molecular axial system with respect to the optic axis of the liquid crystal, it is found that

$$[4a] \qquad \bar{V}\left(\frac{\pi}{2}, 0\right) = -a_1 \propto (\alpha_1\alpha_\parallel + \alpha_2\alpha_\perp + \alpha_3\alpha_\perp)$$

$$[4b] \qquad \bar{V}\left(\frac{\pi}{2}, \frac{\pi}{2}\right) = -a_2 \propto (\alpha_1\alpha_\perp + \alpha_2\alpha_\parallel + \alpha_3\alpha_\perp)$$

$$[4c] \qquad \bar{V}\left(0, \frac{\pi}{2}\right) = -a_3 \propto (\alpha_1\alpha_\perp + \alpha_2\alpha_\perp + \alpha_3\alpha_\parallel)$$

where α_1, α_2, and α_3 are the semi-axes of the solute molecule polarizability ellipsoid while $\alpha_\parallel$ and $\alpha_\perp$ are the polarizabilities of the liquid crystal solvent parallel and perpendicular to the optic axis (it is assumed that the optic axis has C_∞ symmetry). Defining the ratio of differences between interaction energies,

$$[5] \qquad R = \frac{a_2 - a_3}{a_1 - a_3}$$

then substitution of eqs. 4 leads to

$$[6] \qquad R = \frac{\alpha_2 - \alpha_3}{\alpha_1 - \alpha_3}$$

This ratio is a function of the properties of the solute molecule only and is independent of the mesophase properties and of temperature. Anisotropic polarizability ellipsoids are known for relatively few molecules of interest in the present context. However, Le Fèvre and Le Fèvre (10) have noted that the ratio of the semi-axes $\alpha_1:\alpha_2:\alpha_3$ approximates the ratio of the corresponding molecular dimensions $L_1:L_2:L_3$ and thus eq. 6 can be replaced by

$$[7] \qquad R = \frac{L_2 - L_3}{L_1 - L_3}$$

The dependence of S_{11} and S_{22} on the ratio R as computed from eqs. 3 is shown for a range of values $(a_1 - a_3)/kT$ in Fig. 1 (*a*) and (*b*), respectively. Clearly it is not possible to predict S-values unambiguously from molecular dimensions alone. An estimate of $(a_1 - a_3)/kT \propto (\alpha_1 - \alpha_3)$-$(\alpha_\parallel - \alpha_\perp)/kT$ is required. In Fig. 2, the curves demonstrate the calculated dependence of the ratio S_{11}/S_{22} on R for the same range in $(a_1 - a_3)/kT$. It is observed that for a given R, S_{11}/S_{22} should fall within rather narrow limits irrespective of the value of $(a_1 - a_3)/kT$. S_{11}/S_{22} is a measure of the extent to which a solute molecule is aligned and it is expected that a plot of the observed S_{11}/S_{22} ratio against R, calculated from molecular dimensions (eq. 7), should exhibit the same trend. For $S_{11}/S_{22} = 1.0$, there is no alignment, while for $S_{11}/S_{22} = -0.5$, alignment is complete.

For a number of solute molecules possessing C_{2v} or D_{2h} symmetry, Table 1 compares the observed S_{11}/S_{22} ratio with R. In Table 2, the nematic liquid crystals used are listed. The molecular dimensions L_1 and L_2 are calculated by superposition of Stuart's "Wirkungsradien" (11) upon nuclear positions (12) as suggested by Le Fèvre and Le Fèvre (10). The "thickness", L_3, of the ethylenic and aromatic molecules is taken to be 3.70 Å (13); in no case would the "Wirkungsradius" of a substituent atom lead to a larger L_3.

The data of Table 1 are plotted on Fig. 2. The

Can. J. Chem. Downloaded from www.nrcresearchpress.com by 210.87.254.40 on 09/05/12
For personal use only.

Can. J. Chem. Downloaded from www.nrcresearchpress.com by 210.87.254.40 on 09/05/12
For personal use only.

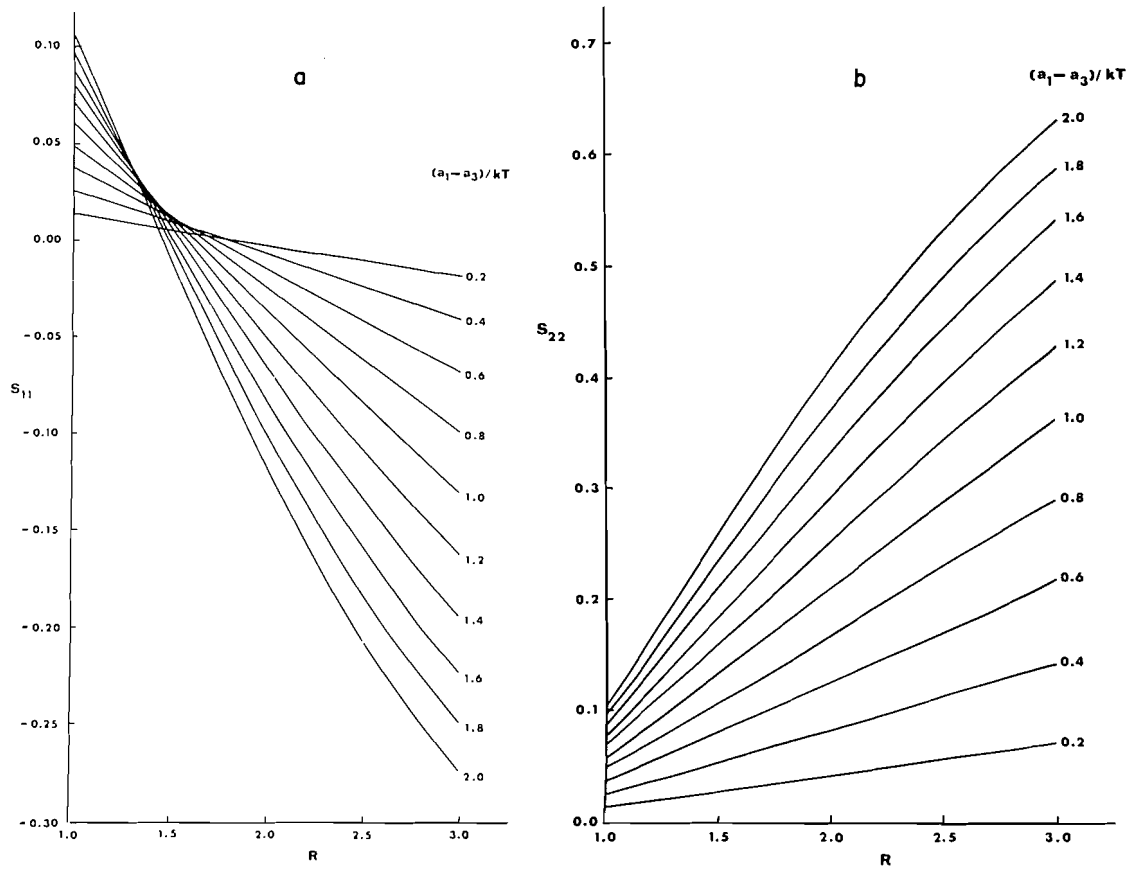

FIG. 1. The calculated dependence of (*a*), S_{11} and (*b*), S_{22} on the dimension ratio R for a range of values of $(a_1 - a_3)/kT$.

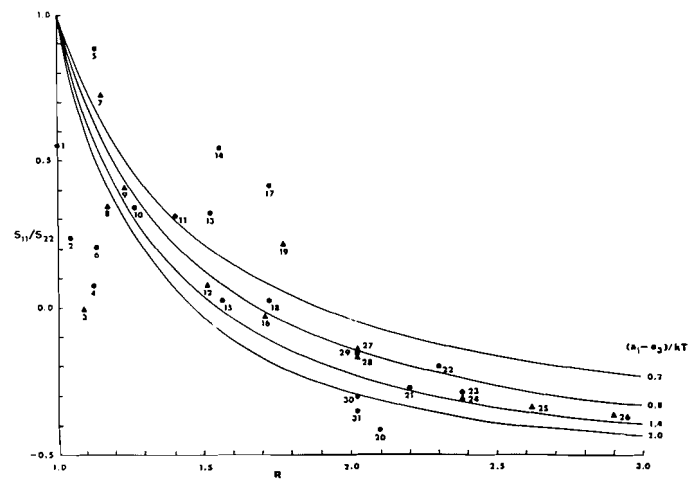

FIG. 2. The calculated dependence of S_{11}/S_{22} on the dimension ratio R for a range of values of $(a_1 - a_3)/kT$ (curves). Experimental points are numbered as in Table 1, the triangles representing solutes in solvent VI.

TABLE 1. Calculated R and observed S_{11}/S_{22} ratios

	Solute	Solvent[a]	L_1 (Å)	L_2 (Å)	R[b]	S_{11}/S_{22}[c]
(1)	Pyridine	VII	5.79	5.79	1.00	0.548[d]
(2)	*o*-Difluorobenzene	3.5% IV, 34.8% V, 61.7% VI	6.67	6.80	1.04	0.238[e]
(3)	1,2,4,5-Tetrafluorobenzene	VI	6.82	7.10	1.09	−0.001[f]
(4)	*m*-Difluorobenzene	3.5% IV, 34.8% V, 61.7% VI	6.81	7.18	1.12	0.070[e]
(5)	1,4-Cyclohexadiene	40% I, 60% II	5.92	6.20	1.13	0.883[g]
(6)	1,1-Difluoroethylene	40% I, 60% II	4.68	4.81	1.13	0.207[h]
(7)	Pyrazine	VI	5.52	5.80	1.15	0.726[i]
(8)	*o*-Dichlorobenzene	VI	6.80	7.33	1.17	0.350[j]
(9)	Thiophene	VI	5.88	6.38	1.23	0.415[k]
(10)	*o*-Dibromobenzene	VII	6.80	7.60	1.26	0.340[j]
(11)	*o*-Dicyanobenzene	VII	6.70	7.90	1.40	0.311[j]
(12)	Fluorobenzene	VI	6.12	7.35	1.51	0.082[l]
(13)	Furan	VII	5.15	5.90	1.52	0.322[m]
(14)	Pyridazine	40% I, 60% II	5.56	6.59	1.55	0.539[n]
(15)	*m*-Dichlorobenzene	X	6.81	8.56	1.56	0.024[o]
(16)	*p*-Benzoquinone	VI	6.16	7.90	1.71	−0.027[l]
(17)	Tetrafluoroethylene	40% VIII, 60% IX	4.68	5.39	1.72	0.416[p]
(18)	*m*-Dibromobenzene	X	6.81	9.05	1.72	0.027[o]
(19)	2,6-Dibromopyridine	VI	6.70	9.00	1.77	0.220[q]
(20)	*p*-Chlorofluorobenzene	3.5% IV, 34.8% V, 61.7% VI	6.00	8.52	2.10	−0.413[r]
(21)	*p*-Bromofluorobenzene	3.5% IV, 34.8% V, 61.7% VI	6.00	8.76	2.20	−0.272[r]
(22)	*p*-Nitrofluorobenzene	3.5% IV, 34.8% V, 61.7% VI	6.00	9.00	2.30	−0.201[r]
(23)	*p*-Cyanofluorobenzene	3.5% IV, 34.8% V, 61.7% VI	6.00	9.18	2.38	−0.287[r]
(24)	*p*-Dichlorobenzene	VI	6.00	9.18	2.38	−0.310[f]
(25)	*p*-Dibromobenzene	VI	6.00	9.72	2.62	−0.338[f]
(26)	*p*-Diiodobenzene	VI	6.00	10.38	2.90	−0.363[f]
(27)	*p*-Difluorobenzene	VI	6.00	8.34	2.02	−0.144[f]
(28)		VI				−0.167[s]
(29)		3.5% IV, 34.8% V, 61.7% VI				−0.154[e]
(30)		40% II, 60% III				−0.300[s]
(31)		XI				−0.347[t]

[a] Table 2.
[b] Equation 7, L_3 is taken to be 3.70 Å.
[c] S-values are either taken directly from published work, as referenced below, or calculated from the motional constants with the assumption that the optic axis of the liquid crystal is parallel to the magnetic field.
[d] Reference 15.
[e] Reference 16.
[f] Reference 17.
[g] Reference 18.
[h] Reference 19.
[i] Reference 20.
[j] Reference 21.
[k] Reference 22.
[l] Reference 6.
[m] Reference 23.
[n] Reference 24.
[o] Reference 25.
[p] Reference 26.
[q] Reference 27.
[r] Reference 28.
[s] Reference 8.
[t] Reference 29.

TABLE 2. The nematic liquid crystals

No.	Name
I	4-*n*-Pentanoyloxy-4′-ethoxyazobenzene
II	4-*n*-Hexanoyloxy-4′-ethoxyazobenzene
III	4-*n*-Heptanoyloxy-4′-ethoxyazobenzene
IV	4,4′-di-*n*-Butoxyazoxybenzene
V	4,4′-di-*n*-Pentyloxyazoxybenzene
VI	4,4′-di-*n*-Hexyloxyazoxybenzene
VII	Anisole azophenyl-*n*-capronate
VIII	4-Capronyloxy-4′-ethoxyazobenzene
IX	O-Carbobutoxy-*p*-oxybenzoic acid *p*-ethoxyphenyl ester
X	4-Methoxybenzylidene-4-amino-α-methyl cinnamic acid-*n*-propyl ester
XI	*N*-(*p*-Ethoxybenzylidine)-*p*-*n*-butylaniline

Can. J. Chem. Downloaded from www.nrcresearchpress.com by 210.87.254.40 on 09/05/12
For personal use only.

general trend of the theoretical curves is followed but with considerable scatter, particularly at low R values. A part of the deviation can be attributed to errors in the values of R due to uncertainties in the "Wirkungsradien" and the molecular thickness which may be accurate only to 0.05 to 0.10 Å, leading to errors in R of up to 10%. The more serious errors in this treatment result from the assumed independence from solvent properties and from solute concentration. The potential energy function, eq. 1, should properly include dependence on the molar volume and solvent order (14). Such an enlarged function can be employed with relative facility in electron paramagnetic resonance studies where solute mole fractions of less than 10^{-3} can be used; thus the molar volume and solute order are essentially the same for the dilute solution and the pure liquid crystal. The high solution concentrations required in n.m.r. studies preclude an exactly analogous treatment. The variation in the ratio S_{11}/S_{22} for the same solute molecule in different nematic solvents is shown in Table 1 for *p*-difluorobenzene. The range of values of S_{11}/S_{22} clearly indicates the involvement of a solvent-dependent term in the potential energy function.

Compounds which have been examined in the most commonly used solvent VI (triangles, Fig. 2) show much better agreement with the theoretical curves, the notable exceptions being 1,2,4,5-tetrafluorobenzene and 2,6-dibromopyridine. The latter molecule is almost triangular in shape making it difficult to approximate the length-to-width ratio. The reason for the poor agreement for tetrafluorobenzene is difficult to rationalize. Molecules which possess large dipole moments do not appear to show large deviations, supporting the assumption that dipole interactions are relatively unimportant (7).

The authors thank Dr. B. C. Eu for helpful discussions. This work was supported by grants from the National Research Council of Canada.

1. A. D. BUCKINGHAM and K. A. MCLAUCHLAN. Progress in NMR spectroscopy. Vol. 2. *Edited by* J. W. Emsley, J. Feeney, and L. H. Sutcliffe. Pergamon Press, Oxford. 1967. p. 63.
2. A. SAUPE. Angew. Chem. Int. Ed. 7, 97 (1968).
3. S. MEIBOOM and L. C. SNYDER. Science, **162**, 1337 (1968).
4. P. DIEHL and C. L. KHETRAPAL. NMR basic principles and progress. Vol. 1. *Edited by* P. Diehl, E. Fluck, and R. Kosfeld. Springer Verlag, Berlin. 1969. p. 1.
5. A. SAUPE. Z. Naturforsch. **19***a*, 161 (1964).
6. L. C. SNYDER. J. Chem. Phys. **43**, 4041 (1965).
7. A. SAUPE. Mol. Cryst. **1**, 527 (1966).
8. J. NEHRING and A. SAUPE. Mol. Cryst. Liquid Cryst. **8**, 403 (1969).
9. K. S. PITZER. Advances in chemical physics. Vol. 2. *Edited by* I. Prigogine. Interscience Publishers, Inc., New York. 1959. p. 59.
10. C. G. LE FÈVRE and R. J. W. LE FÈVRE. Rev. Pure Appl. Chem. **5**, 261 (1955).
11. H. A. STUART. Z. Phys. Chem. **27B**, 350 (1935).
12. L. E. SUTTON (*Editor*). Interatomic Distances. Chem. Soc. Spec. Publ. No. 11, 1958, and No. 18, 1965.
13. R. C. WEAST (*Editor*). Handbook of chemistry and physics. 50th ed. The Chemical Rubber Co., Cleveland. 1969.
14. D. H. CHEN, P. G. JAMES, and G. R. LUCKHURST. Mol. Cryst. Liquid Cryst. **8**, 71 (1969).
15. P. DIEHL, C. L. KHETRAPAL, and H. P. KELLERHALS. Mol. Phys. **15**, 333 (1968).
16. C. T. YIM and D. F. R. GILSON. Can. J. Chem. **47**, 1057 (1969).
17. J. BULTHUIS, J. GERRITSEN, C. W. HILBERS, and C. MACLEAN. Rec. Trav. Chim. **87**, 417 (1968).
18. A. D. BUCKINGHAM, E. E. BURNELL, and C. A. DE LANGE. Mol. Phys. **16**, 521 (1969).
19. A. D. BUCKINGHAM, E. E. BURNELL, and C. A. DE LANGE. Mol. Phys. **16**, 299 (1969).
20. P. DIEHL and C. L. KHETRAPAL. Mol. Phys. **14**, 327 (1968).
21. P. DIEHL and C. L. KHETRAPAL. Mol. Phys. **15**, 201 (1968).
22. P. DIEHL and C. L. KHETRAPAL. Can. J. Chem. **46**, 2645 (1968).
23. P. DIEHL, C. L. KHETRAPAL, and H. P. KELLERHALS. Helv. Chim. Acta, **51**, 529 (1968).
24. E. E. BURNELL and C. A. DELANGE. Mol. Phys. **16**, 95 (1969).
25. P. DIEHL and C. L. KHETRAPAL. Mol. Phys. **15**, 633 (1968).
26. H. SPIESECKE and A. SAUPE. Mol. Cryst. Liquid Cryst. **6**, 287 (1970).
27. P. DIEHL, C. L. KHETRAPAL, and U. LIENHARD. Mol. Phys. **14**, 465 (1968).
28. C. T. YIM and D. F. R. GILSON. J. Am. Chem. Soc. **91**, 4360 (1969).
29. J. C. ROBERTSON and D. F. R. GILSON. Unpublished results.

Can. J. Chem. Downloaded from www.nrcresearchpress.com by 210.87.254.40 on 09/05/12
For personal use only.

Can. J. Chem. Downloaded from www.nrcresearchpress.com by 210.87.254.40 on 09/05/12
For personal use only.

The Electron Spin Resonance Spectra of the Photochemically Produced Perfluorobenzophenone Ketyl and Anion Radicals[1]

F. P. SARGENT AND M. G. BAILEY

Materials Science Branch, Atomic Energy of Canada Limited, Whiteshell Nuclear Research Establishment, Pinawa, Manitoba

Received February 25, 1971

The electron spin resonance spectra of the ketyl and radical anion of perfluorobenzophenone were generated in alcoholic solution by means of a photochemical method. The radical anion was prepared in alkaline solutions by means of a flow system to prevent nucleophillic degradation of the perfluorobenzophenone prior to photolysis. A comparison is made of the fluorine nuclear hyperfine coupling constants to those reported for partially fluorinated radical anions.

Grâce à une méthode photochimique, on a généré en solution alcoolique le spectre r.p.e. du cétyle et de l'anion-radical de la perfluorobenzophénone. L'anion-radical a été préparé dans un système continu pour éviter la dégradation nucléophile de la perfluorobenzophénone avant sa photolyse. On a établi une comparaison entre les constantes de couplage hyperfines du fluor et celles rapportées pour les anion-radicaux partiellement fluorés.

Canadian Journal of Chemistry, 49, 2350 (1971)

In recent years there has been much interest in the electron spin resonance (e.s.r.) spectra of fluorinated radicals (for example, see ref. 1). In the case of benzophenone, only partly fluorinated radicals have been reported. There have been several attempts to prepare the radical ion of perfluorobenzophenone (PFB) but each has led to partly fluorinated species usually via removal of the para fluorines. Brown and Williams (2) attempted to prepare the PFB radical anion by means of a photochemical method (3) in a basic alcohol solution but found that their spectra were due to the *pp'*-dialkoxy PFB anion. Attempts by both Fischer and Zimmermann (4) and by Kulkarni and Trapp (5) to produce the PFB anion electrochemically were not successful and in the former case removal of the two para fluorines was postulated. We believe that we have been successful in producing both the ketyl, $(C_6F_5)_2\dot{C}OH$, and the radical anion of PFB in alcohol solution by a photochemical method. These species have recently been detected in a pulse radiolysis and flash photolysis study (6).

Solutions of PFB in various alcohols were photolyzed *in situ* in a Varian V4500 e.s.r. spectrometer by a medium pressure mercury arc lamp. The e.s.r. spectra were calibrated by means of a dual cavity and the standard aqueous solutions of Fremy's salt, taking $\alpha_N = 13.0$ G. The e.s.r. spectra were simulated by means of a computer together with a plotter. The spectra obtained at room temperature during continuous photolysis were often poorly resolved but on raising the temperature the resolution improved considerably. The spectrum from PFB in isopropanol at 80 °C is shown in Fig. 1(*a*). This was interpreted in terms of hyperfine interaction with two sets of four equivalent fluorine nuclei of 4.66 and 1.77 G, two equivalent fluorines of 8.23 G, and a doublet splitting of 2.42 G. The simulated spectrum based on these values together with a linewidth of 0.25 G and a Lorentzian line shape is shown in Fig. 1(*b*). From expanded charts we were able to obtain an almost perfect fit of the experimental and computed spectra. From additional studies such as the variation of these values with temperature and solvent, molecular orbital calculations, and the absence of the doublet in deuterated alcohols, we feel confident that this species is the ketyl radical of PFB with fluorine coupling constants assigned as in Table 1,

[1]AECL No. 3889.

TABLE 1. Fluorine coupling constants in various fluorinated benzophenone radicals

Radical	Position			Reference
	Ortho	Meta	Para	
Perfluorobenzophenone ketyl	4.66	1.77	8.23	This work
Perfluorobenzophenone anion	4.80	1.06	8.36	This work
4,4′-Difluorobenzophenone anion			7.42	5
			7.50	4
4-Fluorobenzophenone anion			7.27	5
2-Fluorobenzophenone anion	4.63			4
2,2′,6,6′-Tetrafluorobenzophenone anion	4.12			5
2,3,4,5,6-Pentafluorobenzophenone anion	4.08	1.14	5.88	5
4,4′-Dimethoxy-perfluorobenzophenone anion	4.60	1.14		2

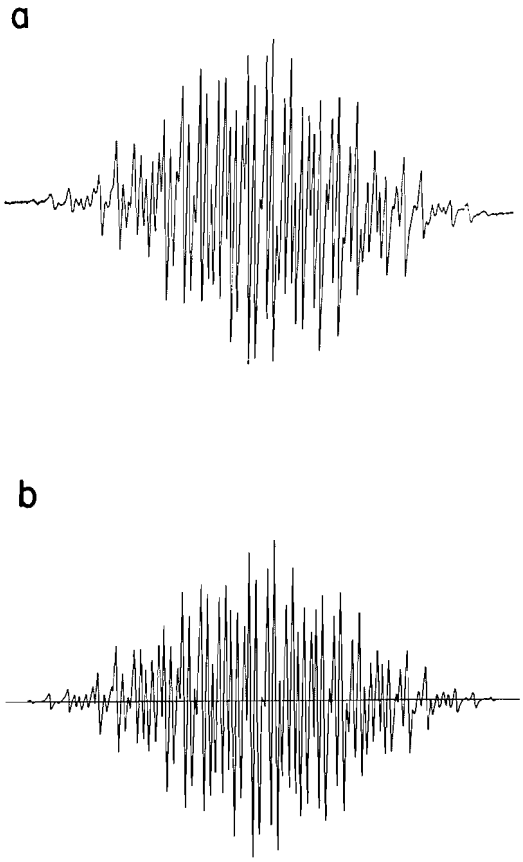

FIG. 1. The e.s.r. of the perfluorobenzophenone ketyl radical in 2-propanol at 80 °C. (*a*) The experimental spectrum, (*b*) the computer simulated spectrum.

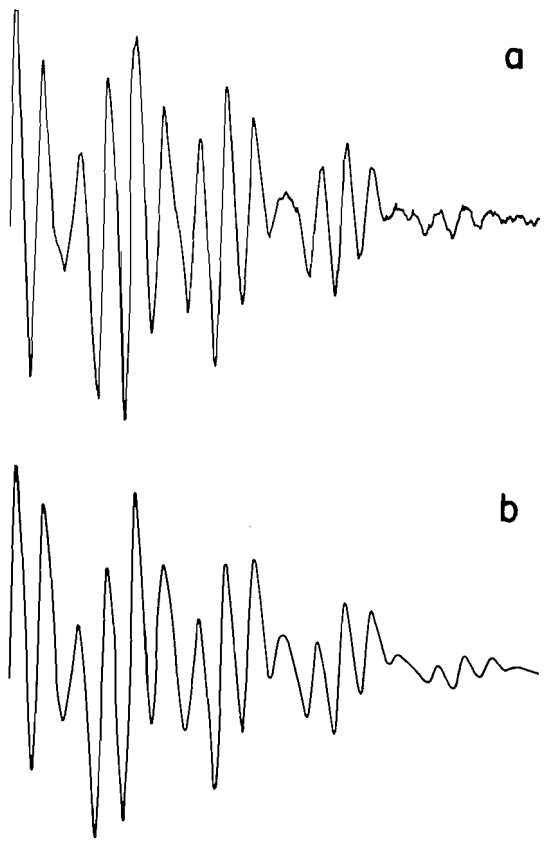

FIG. 2. One half of the e.s.r. spectrum of the perfluorobenzophenone radical anion observed in basic methanol at room temperature: (*a*) the experimental spectrum (*b*) the computer simulated spectrum.

together with a proton coupling of 2.42 G due to the ketyl OH group.

When two solutions, one of PFB in methanol and the other of 0.05 *M* sodium methoxide in methanol, were flowed together and mixed just prior to entering the e.s.r. cavity, *i.e.* the photolysis zone, quite different spectra were observed. These spectra were a function of the absolute and relative flow rates of the two components. With no base flow the ketyl radical was observed but as the base flow was increased this was replaced by the spectrum shown in Fig. 2(*a*).

Can. J. Chem. Downloaded from www.nrcresearchpress.com by 210.87.254.40 on 09/05/12
For personal use only.

This was interpreted in terms of nuclear hyperfine interaction with two sets of four equivalent fluorines of 4.80 and 1.06 G and two equivalent fluorines of 8.36 G. The simulated spectrum based on these values together with a linewidth of 0.58 G and a Lorentzian line shape is shown in Fig. 2(*b*). From expanded charts a good fit of the computed and experimental spectra was possible. We attribute this spectrum to the radical anion of PFB and on the basis of molecular orbital calculations, make the positional assignments of Table 1.

We wish to draw attention to the magnitude of the fluorine splitting in the perfluorinated ketyl and the anion. From Table 1 it is seen that these are substantially larger than those observed for the partly fluorinated species. We are at present attempting to explain these differences by means of molecular orbital calculations. From preliminary calculations it has become obvious that a general revision of the usual parameters is required.

We thank Dr. R. E. D. McClung of the University of Alberta and K. H. Witzke of W.N.R.E. for assistance with the development of the computer simulation program. Dr. A. Singh of W.N.R.E. is gratefully acknowledged for constructive discussions and for suggesting the problem.

1. P. H. H. Fischer and J. P. Colpa. Z. Naturforsch, **24**A, 1980 (1969). A. Hudson and J. W. E. Lewis. Mol. Phys. **19**, 241 (1970).
2. J. K. Brown and W. G. Williams. Trans. Faraday Soc. **64**, 298 (1968).
3. G. A. Russell and E. J. Geels. Tetrahedron Lett. **20**, 1333 (1963). P. B. Ayscough and F. P. Sargent. Chem. Commun. 94 (1963).
4. P. H. H. Fischer and H. Zimmermann. Z. Naturforsch. **23**A, 1339 (1968).
5. S. V. Kulkarni and C. Trapp. J. Am. Chem. Soc. **92**, 4809 (1970).
6. A. Singh. To be published.

Compressibilities of Porous Glass

W. B. Kipkie[1] and R. McIntosh
Department of Chemistry, Queen's University, Kingston, Ontario

Received February 18, 1971

Partial extension isotherms have confirmed earlier results that polar adsorbates cause greater extensions than non-polar adsorbates. Data now found for ethyl chloride are in disagreement with those reported by Quinn and McIntosh (3) which are presumed to be in error. Support of this view is provided by consistent values of β', the compressibility of the glass–adsorbate system, based upon studies with four adsorbates. The consistency now revealed suggests that the mechanism postulated by Quinn and McIntosh is valid for the reversible adsorption along the top of a desorption loop.

Les extensions partielles isothermes ont confirmé les résultats précédents d'après lesquels les produits polaires adsorbés provoquent une extension plus grande que les produits non polaires adsorbés. Les données actuellement trouvées pour le chlorure d'éthyle sont en désaccord avec celles rapportées par Quinn et McIntosh (3), ces dernières étant probablement fausses. Les valeurs consistantes obtenues pour β', la compressibilité du système verre–adsorbé, provenant des études effectuées avec quatre produits adsorbés, sont en accord avec le point de vue proposé. Ces résultats suggèrent que le mécanisme postulé par Quinn et McIntosh est valable pour l'adsorption réversible le long du sommet d'une boucle de désorption.

Canadian Journal of Chemistry, 49, 2352 (1971)

In the past there have been numerous studies of adsorption and the hysteresis phenomenon utilizing the measurement of dimensional changes of the adsorbent on adsorption to aid in the analysis of the findings (1–5). In ref. 1 the authors used a linear variable differential transducer, incorporated into a cell of a dead space of 25.9 ml, for their investigations into the influence of meniscus curvature on the detection of solidification of adsorbates in porous glass (1).

Several partial extention isotherms were

[1]Present address: Process Technology, The International Nickel Company of Canada Limited, Copper Cliff, Ontario.

Can. J. Chem. Downloaded from www.nrcresearchpress.com by 210.87.254.40 on 09/05/12
For personal use only.

This was interpreted in terms of nuclear hyperfine interaction with two sets of four equivalent fluorines of 4.80 and 1.06 G and two equivalent fluorines of 8.36 G. The simulated spectrum based on these values together with a linewidth of 0.58 G and a Lorentzian line shape is shown in Fig. 2(*b*). From expanded charts a good fit of the computed and experimental spectra was possible. We attribute this spectrum to the radical anion of PFB and on the basis of molecular orbital calculations, make the positional assignments of Table 1.

We wish to draw attention to the magnitude of the fluorine splitting in the perfluorinated ketyl and the anion. From Table 1 it is seen that these are substantially larger than those observed for the partly fluorinated species. We are at present attempting to explain these differences by means of molecular orbital calculations. From preliminary calculations it has become obvious that a general revision of the usual parameters is required.

We thank Dr. R. E. D. McClung of the University of Alberta and K. H. Witzke of W.N.R.E. for assistance with the development of the computer simulation program. Dr. A. Singh of W.N.R.E. is gratefully acknowledged for constructive discussions and for suggesting the problem.

1. P. H. H. Fischer and J. P. Colpa. Z. Naturforsch, **24**A, 1980 (1969). A. Hudson and J. W. E. Lewis. Mol. Phys. **19**, 241 (1970).
2. J. K. Brown and W. G. Williams. Trans. Faraday Soc. **64**, 298 (1968).
3. G. A. Russell and E. J. Geels. Tetrahedron Lett. **20**, 1333 (1963). P. B. Ayscough and F. P. Sargent. Chem. Commun. 94 (1963).
4. P. H. H. Fischer and H. Zimmermann. Z. Naturforsch. **23**A, 1339 (1968).
5. S. V. Kulkarni and C. Trapp. J. Am. Chem. Soc. **92**, 4809 (1970).
6. A. Singh. To be published.

Compressibilities of Porous Glass

W. B. Kipkie[1] and R. McIntosh
Department of Chemistry, Queen's University, Kingston, Ontario

Received February 18, 1971

Partial extension isotherms have confirmed earlier results that polar adsorbates cause greater extensions than non-polar adsorbates. Data now found for ethyl chloride are in disagreement with those reported by Quinn and McIntosh (3) which are presumed to be in error. Support of this view is provided by consistent values of β', the compressibility of the glass–adsorbate system, based upon studies with four adsorbates. The consistency now revealed suggests that the mechanism postulated by Quinn and McIntosh is valid for the reversible adsorption along the top of a desorption loop.

Les extensions partielles isothermes ont confirmé les résultats précédents d'après lesquels les produits polaires adsorbés provoquent une extension plus grande que les produits non polaires adsorbés. Les données actuellement trouvées pour le chlorure d'éthyle sont en désaccord avec celles rapportées par Quinn et McIntosh (3), ces dernières étant probablement fausses. Les valeurs consistantes obtenues pour β', la compressibilité du système verre–adsorbé, provenant des études effectuées avec quatre produits adsorbés, sont en accord avec le point de vue proposé. Ces résultats suggèrent que le mécanisme postulé par Quinn et McIntosh est valable pour l'adsorption réversible le long du sommet d'une boucle de désorption.

Canadian Journal of Chemistry, 49, 2352 (1971)

In the past there have been numerous studies of adsorption and the hysteresis phenomenon utilizing the measurement of dimensional changes of the adsorbent on adsorption to aid in the analysis of the findings (1–5). In ref. 1 the authors used a linear variable differential transducer, incorporated into a cell of a dead space of 25.9 ml, for their investigations into the influence of meniscus curvature on the detection of solidification of adsorbates in porous glass (1).

Several partial extention isotherms were

[1]Present address: Process Technology, The International Nickel Company of Canada Limited, Copper Cliff, Ontario.

Can. J. Chem. Downloaded from www.nrcresearchpress.com by 210.87.254.40 on 09/05/12
For personal use only.

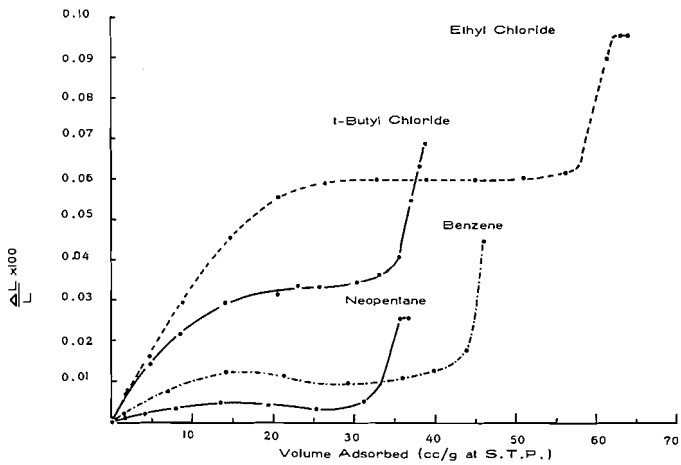

FIG. 1. Extension isotherms of ethyl chloride, *t*-butyl chloride, benzene, and neopentane.

obtained for neopentane, *t*-butyl chloride, benzene, and ethyl chloride in order to compare the performance of this extensometer with others of the parallel-plate version (2–5). It was found that ethyl chloride exhibited the largest extension followed by *t*-butyl chloride, benzene, and neopentane (Fig. 1). These results were consistent with the results of Quinn and McIntosh (2) for ethyl chloride and butane. In general, polar adsorbates tended to exhibit greater expansions than non-polar adsorbates.

However, the magnitude of the dimensional changes for ethyl chloride in this study over the whole extension isotherm was approximately one-third of that found by Quinn and McIntosh (3). In fact, Quinn and McIntosh found extensions for ethyl chloride that were considerably greater than those for water. On the other hand, the magnitude of the dimensional changes for benzene in the present work were almost identical to those observed by Hodgson and McIntosh (4).

In an effort to clarify this discrepancy, it was considered worthwhile to calculate the compressibility coefficient β' of the porous glass – adsorbate system, using the steep desorption branch of both the ethyl chloride and neopentane isotherms, to compare them with those obtained by Quinn and McIntosh (3), Amberg and McIntosh (5), and Hodgson and McIntosh (4). The procedure has been outlined previously by Quinn and McIntosh and the results are seen in Table 1.

It is immediately obvious that results of Quinn and McIntosh on ethyl chloride are approximately four times greater than the present ones. Also, there is reasonably close agreement among all values of β', except for that of Quinn and McIntosh even though the adsorbate molecules are all very dissimilar. The results obtained by Quinn and McIntosh cannot be due to a difference in adsorbents, as the porous glass used, and its treatment before use, were identical in all respects to that used in this study, so far as is known. It would appear that they may be in error although it is impossible to determine the cause, other than a possible error in calibration.

On the basis of the data available at that time, Sereda and Feldman (6) suggested that the discrepancy in the values obtained by Quinn and McIntosh may have been due to the difficulty in evaluating correctly such quantities as wetting angles, capillary radius, and molar volume, or more seriously, that the concept of changing radius of curvature of meniscus was invalid. The relatively close agreement now found for all the

TABLE 1. Compressibility of porous-glass adsorbate system

Adsorbate	$\beta' \times 10^7$ (p.s.i.)$^{-1}$	Reference
Ethyl chloride at 6.0 °C	25	3
Butane	14	3
Water	4.0	*
Benzene at 9.0 °C	4.4	4
Benzene at −3.8 °C	3.5	4
Ethyl chloride at −21.4 °C	5.1	This work
Ethyl chloride at −30.0 °C	6.2	This work
Neopentane at −1.0 °C	4.7	This work

*Calculation of the Amberg and McIntosh data by Quinn and McIntosh.

Can. J. Chem. Downloaded from www.nrcresearchpress.com by 210.87.254.40 on 09/05/12
For personal use only.

compressibility data, exclusive of that of Quinn and McIntosh, would tend to refute this suggestion.

1. W. B. KIPKIE, R. MCINTOSH, and B. A. KELLY. J. Coll. Interface Sci. To be published.
2. H. W. QUINN and R. MCINTOSH. Can. J. Chem. **35**, 745 (1957).
3. H. W. QUINN and R. MCINTOSH. Congress of Surface Activity. April 8–12, 1957. Butterworths Publications, London, England.
4. C. HODGSON and R. MCINTOSH. Can. J. Chem. **38**, 958 (1960).
5. C. H. AMBERG and R. MCINTOSH. Can. J. Chem. **30**, 1012 (1952).
6. P. J. SEREDA and R. F. FELDMAN. The Solid–Gas Interface. 2. Marcel Dekker, New York. 1967. Chap. 24, p. 729.

Can. J. Chem. Downloaded from www.nrcresearchpress.com by 210.87.254.40 on 09/05/12
For personal use only.

Selected Catalytic Decompositions of Indole-2-diazoketone[1]

KULDIP S. BHANDARI AND VICTOR SNIECKUS
Department of Chemistry, University of Waterloo, Waterloo, Ontario

Received February 15, 1971

Whereas Wolff rearrangement of indole-2-diazoketone (**1**) in the presence of silver benzoate led to the indolyl-2-acetic esters **2***a* and *b* in low yields, the reaction of **1** in methanol with copper powder or with acidic resin gave methoxymethyl-2-indolyl ketone (**3**) in 65–80% yields. Chloromethyl 2-indolyl ketone (**4**) was prepared and converted to the α-aminoketone hydrochloride salts **5***a* and *b*. Treatment of **1** with cuprous iodide in acetonitrile–methanol gave **2***a*, iodomethyl 2-indolyl ketone (**6**), and methyl 2-indolylglyoxalate (**7**). Compound **6** was converted to *N*-(2-(2-indolyl)-2-oxoethyl)pyridinium iodide (**8**) and to 2-acetylindole (**9**) while **7** was degraded *via* indole-2-glyoxylic acid (**10**) to indole-2-carboxylic acid (**11**). Compound **7** represents a type of product not previously observed in diazoketone chemistry. The mechanism of its formation is discussed.

Alors que le réarrangement de Wolff de l'indole diazocétone-2 (**1**) en présence de benzoate d'argent conduit avec de mauvais rendements aux esters **2***a* et *b* de l'acide indolyl-2 acetique, on observe que la réaction de **1**, en solution dans le méthanol, avec de la poudre de cuivre ou une résine acide, forment la méthoxyméthyl indolyl-2 cétone (**3**) avec des rendements de 65 à 80%. On a préparé la chlorométhyl indolyl-2 cétone (**4**) qui par transformation conduit aux chlorhydrates **5***a* et *b* de l'α-amino-cétone. Le traitement de **1** par de l'iodure cuivreux dans un mélange d'acétonitrile/méthanol fourni l'ester **2***a*, l'iodométhyl indolyl-2 cétone (**6**) et l'indolyl-2 glyoxylate de méthyle (**7**). Le composé **6** peut être transformé en iodure de *N*-[(indolyl-(2)-2 oxo-2 éthyl] pyridinium (**8**) et en acétyl-2 indole (**9**) alors que **7** peut être dégradé pour conduire successivement à l'acide indole-2 glyoxylique (**10**) et à l'acide indole-2 carboxylique (**11**). Le composé **7** représente un type de composés qui n'avait pas été observé anterieurement en chimie des diazocétones; on discute de son mécanisme de formation.

Canadian Journal of Chemistry, 49, 2354 (1971)

As an outgrowth of our interest in the synthesis of the relatively unexplored 2-substituted indole derivatives (1), we studied some metal and acid-promoted decompositions of indole-2-diazoketone (**1**).[2] This study has led to the preparation of new indole derivatives (**3**, **4**, **5**, **6**, **7**, and **10**) and a type of reaction (**1** → **7**) not previously observed in diazoketone chemistry. These results may have synthetic utility and mechanistic interest.

Matell's lack of success (3) in effecting the Wolff rearrangement (4) of diazoketone **1** by the use of silver oxide led us to attempt the reaction in the presence of silver benzoate, a prescribed superior reagent for such a transformation (4). In the event, no reaction was observed at room temperature in methanol or ethanol solution but at reflux the indole-2-acetic esters, **2***a* and *b* respectively, were isolated in low yields. In view of the high yields of **2***a* and *b* obtained by the photochemical method (2), further study of these conditions was not warranted.

In harmony with the general observation that α-diazoketones undergo insertion reactions in the presence of copper powder (5, 6), diazoketone

[1]This work represents part of the Ph.D. Thesis of K.S.B. presented to the University Graduate Council of the University of Waterloo, Waterloo, Ontario, 1971.

[2]For studies on the photochemical decomposition of **1**, see ref. 2.

compressibility data, exclusive of that of Quinn and McIntosh, would tend to refute this suggestion.

1. W. B. KIPKIE, R. MCINTOSH, and B. A. KELLY. J. Coll. Interface Sci. To be published.
2. H. W. QUINN and R. MCINTOSH. Can. J. Chem. **35**, 745 (1957).
3. H. W. QUINN and R. MCINTOSH. Congress of Surface Activity. April 8–12, 1957. Butterworths Publications, London, England.
4. C. HODGSON and R. MCINTOSH. Can. J. Chem. **38**, 958 (1960).
5. C. H. AMBERG and R. MCINTOSH. Can. J. Chem. **30**, 1012 (1952).
6. P. J. SEREDA and R. F. FELDMAN. The Solid–Gas Interface. 2. Marcel Dekker, New York. 1967. Chap. 24, p. 729.

Selected Catalytic Decompositions of Indole-2-diazoketone[1]

KULDIP S. BHANDARI AND VICTOR SNIECKUS
Department of Chemistry, University of Waterloo, Waterloo, Ontario

Received February 15, 1971

Whereas Wolff rearrangement of indole-2-diazoketone (**1**) in the presence of silver benzoate led to the indolyl-2-acetic esters **2***a* and *b* in low yields, the reaction of **1** in methanol with copper powder or with acidic resin gave methoxymethyl-2-indolyl ketone (**3**) in 65–80% yields. Chloromethyl 2-indolyl ketone (**4**) was prepared and converted to the α-aminoketone hydrochloride salts **5***a* and *b*. Treatment of **1** with cuprous iodide in acetonitrile–methanol gave **2***a*, iodomethyl 2-indolyl ketone (**6**), and methyl 2-indolylglyoxalate (**7**). Compound **6** was converted to *N*-(2-(2-indolyl)-2-oxoethyl)pyridinium iodide (**8**) and to 2-acetylindole (**9**) while **7** was degraded *via* indole-2-glyoxylic acid (**10**) to indole-2-carboxylic acid (**11**). Compound **7** represents a type of product not previously observed in diazoketone chemistry. The mechanism of its formation is discussed.

Alors que le réarrangement de Wolff de l'indole diazocétone-2 (**1**) en présence de benzoate d'argent conduit avec de mauvais rendements aux esters **2***a* et *b* de l'acide indolyl-2 acetique, on observe que la réaction de **1**, en solution dans le méthanol, avec de la poudre de cuivre ou une résine acide, forment la méthoxyméthyl indolyl-2 cétone (**3**) avec des rendements de 65 à 80%. On a préparé la chlorométhyl indolyl-2 cétone (**4**) qui par transformation conduit aux chlorhydrates **5***a* et *b* de l'α-amino-cétone. Le traitement de **1** par de l'iodure cuivreux dans un mélange d'acétonitrile/méthanol fourni l'ester **2***a*, l'iodométhyl indolyl-2 cétone (**6**) et l'indolyl-2 glyoxylate de méthyle (**7**). Le composé **6** peut être transformé en iodure de *N*-[(indolyl-2)-2 oxo-2 éthyl] pyridinium (**8**) et en acétyl-2 indole (**9**) alors que **7** peut être dégradé pour conduire successivement à l'acide indole-2 glyoxylique (**10**) et à l'acide indole-2 carboxylique (**11**). Le composé **7** représente un type de composés qui n'avait pas été observé anterieurement en chimie des diazocétones; on discute de son mécanisme de formation.

Canadian Journal of Chemistry, 49, 2354 (1971)

As an outgrowth of our interest in the synthesis of the relatively unexplored 2-substituted indole derivatives (1), we studied some metal and acid-promoted decompositions of indole-2-diazoketone (**1**).[2] This study has led to the preparation of new indole derivatives (**3**, **4**, **5**, **6**, **7**, and **10**) and a type of reaction (**1** → **7**) not previously observed in diazoketone chemistry. These results may have synthetic utility and mechanistic interest.

Matell's lack of success (3) in effecting the Wolff rearrangement (4) of diazoketone **1** by the use of silver oxide led us to attempt the reaction in the presence of silver benzoate, a prescribed superior reagent for such a transformation (4). In the event, no reaction was observed at room temperature in methanol or ethanol solution but at reflux the indole-2-acetic esters, **2***a* and *b* respectively, were isolated in low yields. In view of the high yields of **2***a* and *b* obtained by the photochemical method (2), further study of these conditions was not warranted.

In harmony with the general observation that α-diazoketones undergo insertion reactions in the presence of copper powder (5, 6), diazoketone

[1]This work represents part of the Ph.D. Thesis of K.S.B. presented to the University Graduate Council of the University of Waterloo, Waterloo, Ontario, 1971.

[2]For studies on the photochemical decomposition of **1**, see ref. 2.

1 gave **3** in 65% yield using this catalyst in methanol solution under reflux. However, contrary to previous results (6), **1** did not give the corresponding α-aminoketones **5** when treated with secondary amines. This failure may be largely attributed to the instability of the expected products (*vide infra*).

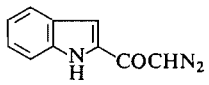

1

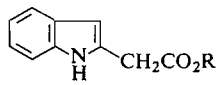

2

a R = CH_3
b R = C_2H_5
c R = $CH_2C_6H_5$

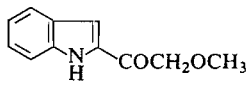

3

Numerous examples of acid-catalyzed decompositions of α-diazoketones to α-alkoxy-, and α-haloketones are known (7). Thus, not surprisingly, **1** furnished **3** in 70–80% yields when treated with hydrogen chloride gas or Dowex-50 acidic resin in methanol. The reaction of **1** in anhydrous ether in the presence of hydrogen chloride gas gave the α-chloroketone **4** in 89% yield. Compound **4** was readily converted into the α-aminoketones **5***a* (42%) and *b* (40%) by treatment with piperidine and pyrrolidine respectively. These new 2-substituted indole derivatives were unstable but were isolated and characterized as the corresponding hydrochloride salts.

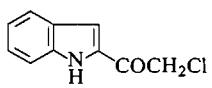

4

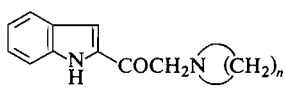

5

a *n* = 5
b *n* = 4

Among the copper salts, cuprous iodide is the only one reported to be an efficient catalyst for the Wolff rearrangement (6, 8) and, for the sake of a complete study, it became of interest to test this reagent in reaction with the diazoketone **1**.[3] When the reaction was carried out in acetonitrile–methanol solution there were isolated, in addition to the expected ester **2***a*, two other compounds which are assigned structures **6** and **7** on the basis of spectral and chemical evidence. Compound **6** exhibited a u.v. spectrum characteristic of a 2-acyl indole chromophore and i.r. absorption at 3400 (NH) and 1665 (C=O) cm^{-1}. The n.m.r. spectrum showed, in addition to the indole-NH and four aromatic protons, a two-proton singlet at τ 5.65, typical of a $COCH_2X$ (X = halogen) function (9). Chemical confirmation was obtained by conversion of **6** to the known pyridinium iodide salt **8** (10) and by its reduction to 2-acetylindole (**9**) which was prepared from diazoketone **1** (Scheme 1).

On the basis of the 2-acyl indole u.v. spectrum and i.r. absorption at 1740 (ester C=O) and 1650 (C=O) cm^{-1}, the third product from the reaction of **1** with cuprous iodide was formulated as **7**. In agreement with this structure, the n.m.r. spectrum showed a three-proton singlet at τ 6.05 (CO_2CH_3). Mild hydrolysis of **7** gave the glyoxylic acid **10** which could be reesterified to **7**. Finally, basic hydrogen peroxide treatment of **7** gave the known indole-2-carboxylic acid (**11**) (11) thus fully confirming the assigned structure.

A search of the literature revealed that Russian workers have claimed the synthesis of **7** by reaction of indolyl magnesium bromide with methyl glyoxalate (12).[4] However, the reported physical and spectral data are identical with those observed for the isomeric methyl indole-3-glyoxalate (**12**) (14). These experimental facts, theoretical considerations (15), and now our chemical evidence for **7** leave no doubt that the Russian workers had in fact prepared compound **12** by their method.

Mechanistically, the formation of **6** may be explained by an insertion of iodide ion into the ketocarbene–copper complex (6, 16) resulting from **1**. Since compound **7** represents a type of product not previously encountered in diazoketone chemistry, brief examination of the mode of its formation was undertaken. *A priori*, any one of the compounds **2***a*, **3**, and **6** could act as a precursor for **7**. However, when each of these was subjected to the identical reaction conditions, no **7** was formed. Alternatively, by analogy with previous observation (17), the ketocarbene–copper complex could undergo oxygen insertion to give **13** which, in turn, could yield the product (**7**) via oxidation of its methyl hemiacetal derivative.[5] That **7** was produced as a result of aerial

[3]Cupric acetate failed to promote decomposition of **1** (6).

[4]Recently, the *N*-methyl analogue of **7** has been synthesized, see ref. 13.

[5]For an analogous oxidation with chromium trioxide, see ref. 18.

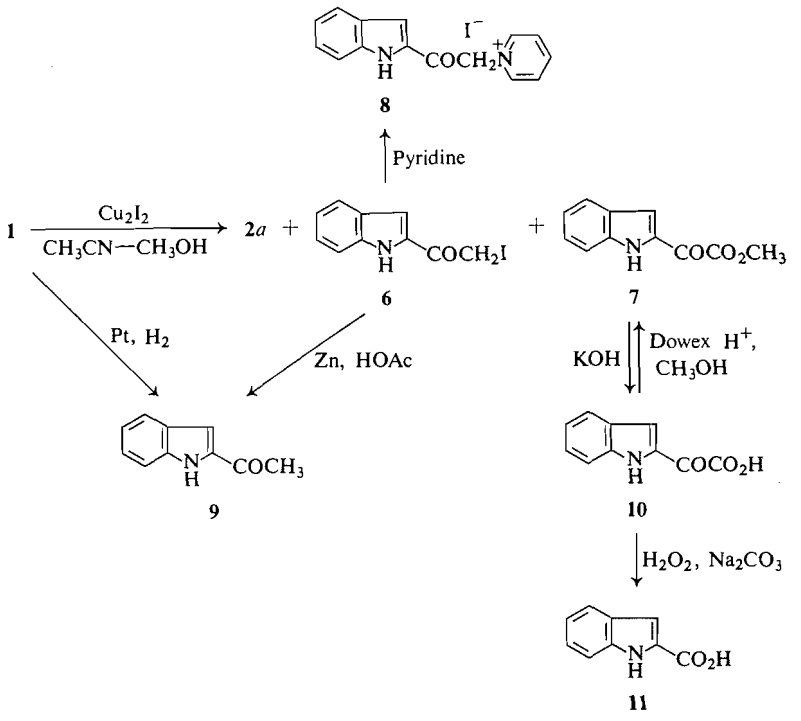

SCHEME 1

oxidation was shown by the following experiments. When the reaction was carried out at room temperature under nitrogen, only **2***a* (10–15%) and **6** (8–10%) were obtained and **7** was not detected. In contrast, in the presence of an atmosphere of oxygen but otherwise identical conditions, **7** was produced in 8–12% yield in addition to **6** (8–12%) and only a trace of **2***a* was obtained. Unfortunately, the proposal that **13** is an intermediate in the reaction could not be tested since it could not be prepared from **4** under the standard conditions for α-ketoaldehyde synthesis (19).

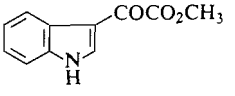

12

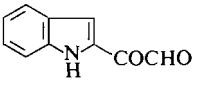

13

It may be expected that the presumed ketocarbene–copper complex would tend to be unstable with respect to Wolff rearrangement at higher reaction temperatures. The observed product distribution (**2***a* (25%), very low yields of **3** and **6**, and no **7**) when diazoketone **1** was treated with cuprous idide in acetonitrile–methanol at reflux temperature was in agreement with this expectation. Compound **7** was found to be stable to these reaction conditions. Similarly, the decomposition of **1** in acetonitrile–ethanol and acetonitrile – benzyl alcohol solutions in the presence of cuprous iodide at reflux temperatures gave the ethyl and benzyl esters **2***b* and *c* respectively together with trace amounts of **3** and **6** but no ethyl or benzyl glyoxalate ester corresponding to **7** was detected in each case.

The mechanism of the reaction may subtly involve the (**1**) + $Cu^+ \leftrightarrows Cu^{2+}$ + (products) redox system (20) but no further mechanistic information is presently available.

Experimental

Analyses were performed by Micro-Tech Laboratories, Inc., Skokie, Illinois, Chemalytics, Inc., Tempe, Arizona, and A. B. Gygli, Toronto, Ontario. Melting points were determined on a Fisher–Johns apparatus and are uncorrected. The i.r. spectra were recorded on a Beckman IR-5 spectrophotometer in chloroform solution unless otherwise stated. The u.v. spectra were measured on Beckman DB-G and Coleman EPS-3T spectrophotometers in methanol solution. The n.m.r. spectra were recorded on JEOL-C60 and Varian T-60 spectrometers in deuteriochloroform solution unless otherwise indicated with tetramethylsilane (TMS) as internal standard. Spectra

listed follow the order: chemical shift, multiplicity (s = singlet, d = doublet, t = triplet, q = quartet, and m = multiplet), number of protons, coupling constant (Hz), and assignment. Mass spectra were determined with a Hitachi–Perkin Elmer RMU-6E single focussing mass spectrometer. Column chromatography was performed with silical gel (0.05–0.20 mm) obtained from Brinkmann (Canada) Ltd. Acetonitrile was reagent grade as supplied by Allied Chemical Co. and cuprous iodide was obtained from Fisher Scientific Co.

*Reaction of Indole-2-diazoketone (**1**) with Silver Benzoate – Triethylamine*

(a) In Methanol Solution

To a solution of 100 mg (0.54 mmol) of **1** in 20 ml of absolute methanol at reflux was added dropwise a solution of 124 mg (0.56 mmol) of freshly prepared dry silver benzoate (**4**) in 5 ml of dry triethylamine. The mixture was refluxed and stirred under nitrogen in the dark for 15 h. After removal of the solvent *in vacuo*, the resulting residue was thoroughly shaken with ether (30 ml). The solid was removed by filtration and the filtrate was evaporated to yield a brown oil which was purified by chromatography (benzene) to give 9.5 mg (9%) of *methyl 2-indolylacetate* (**2***a*) as pale yellow crystals, m.p. 71–73°; i.r. ν_{max} 3405 (NH), 1736 (C=O) cm^{-1}; n.m.r. τ 1.48 (s, 1, NH), 2.28–3.11 (m, 4, aromatics), 3.68 (s, 1, indole-3H), 6.19 (s, 2, CH_2), 6.30 (s, 3, OCH_3).

Anal. Calcd. for $C_{11}H_{11}NO_2$: C, 69.83; H, 5.86; N, 7.40. Found: C, 69.99; H, 5.80; N, 7.25.

(b) In Ethanol Solution

Using the procedure described above, 100 mg (0.54 mmol) of **1** in ethanol at reflux afforded 11 mg (10%) of *ethyl 2-indolylacetate* (**2***b*) as a colorless oil, b.p. 119–122°/0.003 mm (lit. (21): b.p. 118–120°/0.003 mm); i.r. ν_{max} (neat) 3390 (NH), 1734 (C=O) cm^{-1}; n.m.r. τ 1.34 (s, 1, NH), 2.31–3.33 (m, 4, aromatics), 3.69 (s, 1, indole-3H), 5.58 (q, 2, J = 6, $CO_2C\underline{H}_2CH_3$), 6.30 (s, 2, CH_2), 8.59 (t, 3, J = 6, $CO_2CH_2C\underline{H}_3$).

*Preparation of Methoxymethyl 2-Indolyl Ketone (**3**)*

(a) Copper Powder

To a solution of 200 mg (1.08 mmol) of indole-2-diazoketone (**1**) in 40 ml of absolute methanol at reflux there was added 68 mg (1.08 mmol) of copper powder in small portions. After refluxing for 8 h, a precipitate was removed by filtration and the filtrate was treated with activated carbon. Evaporation to dryness *in vacuo* yielded 133 mg (65%) of **3** which was recrystallized from cyclohexane – methylene chloride to give colorless needles, m.p. 92–93°; i.r. ν_{max} 3250 (NH), 1650 (C=O) cm^{-1}; u.v. λ_{max} 310 (13 000), 235 (8240) mμ; n.m.r. τ 0.40 (s, 1, NH), 2.22–2.81 (m, 4, aromatics), 5.35 (s, 2, $COCH_2$), 6.45 (s, 3, OCH_3).

Anal. Calcd. for $C_{11}H_{11}NO_2$: C, 69.83; H, 5.86; N, 7.40. Found: C, 69.87; H, 5.83; N, 7.33.

(b) Hydrogen Chloride

Hydrogen chloride gas was bubbled through a solution of 200 mg (1.08 mmol) of **1** in 60 ml of absolute methanol at room temperature for 5–7 s and the reaction mixture was stirred for 10 min. It was then basified with excess of solid sodium carbonate and subjected to filtration. The filtrate was treated with activated carbon and evaporated to dryness *in vacuo* to yield 147 mg (72%) of crystalline **3**.

(c) Dowex Resin

A solution of 100 mg (0.54 mmol) of **1** in 30 ml of absolute methanol was stirred at room temperature with 250 mg of Dowex 50 W-X2 resin (200–400 mesh, H^+ Form) for about 10 min. Some solid was removed by filtration and the filtrate was evaporated to dryness *in vacuo* to leave a solid which was crystallized from cyclohexane – methylene chloride to yield 85 mg (83%) of ketone **3**.

*Preparation of Chloromethyl 2-Indolyl Ketone (**4**)*

A slow stream of dry hydrogen chloride gas was passed for 15–20 s through a suspension of 300 mg (1.62 mmol) of **1** in 30 ml of anhydrous ether at room temperature. After 15 min, gas evolution ceased and some solid was removed by filtration. The filtrate was evaporated to dryness *in vacuo* at room temperature to leave 280 mg (89%) of **4** which was characterized as its pyridinium chloride salt, m.p. 208–210° (lit. (10): m.p. 210°).

*N-Piperidinomethyl 2-Indolyl Ketone (**5***a*)

The freshly prepared chloro ketone **4** (316 mg, 1.63 mmol) was immediately dissolved in 15 ml of anhydrous ether and mixed with a solution of 275 mg (3.24 mmol) of piperidine in 10 ml of anhydrous ether. The reaction mixture was set aside under nitrogen for 24 h at room temperature. Evaporation to dryness under reduced pressure in a cold water bath left a crude residue which was washed twice with 10 ml portions of petroleum ether (35–60°) to remove traces of piperidine. The hydrochloride salt of **5***a* was prepared by the standard procedure and crystallized from ethanol – ethyl acetate to yield 190 mg (42%) of colorless crystals, m.p. 250–255° (dec.); i.r. ν_{max} (Nujol) 3100 (indole-N*H*), 2540 ($\overset{+}{N}H$), 1665 (C=O) cm^{-1}; u.v. λ_{max} 314 (14 560), 235 (9320) mμ; n.m.r. (D_2O) τ 2.00–2.84 (m, 5, aromatics), 5.30 (s, 2, $COCH_2$), 6.62 (broad s, 4, α-CH_2 of piperidine ring), 8.11 (broad s, 6, β- and γ-CH_2 of piperidine ring).

Anal. Calcd. for $C_{15}H_{19}N_2OCl$: C, 64.62; H, 6.82; N, 10.05. Found: C, 64.44; H, 6.74; N, 9.96.

*N-Pyrrolidinomethyl 2-Indolyl Ketone (**5***b*)

The hydrochloride salt of **5***b* was prepared in the same manner as described for compound **5***a*. From 300 mg (1.54 mmol) of **4** and 230 mg (3.24 mmol) of pyrrolidine there was obtained 172 mg (40%) of **5***b* hydrochloride as colorless crystals, m.p. 245–250° (dec.); i.r. ν_{max} (Nujol) 3200 (indole-NH), 2550 ($\overset{+}{N}H$) and 1666 (C=O) cm^{-1}; n.m.r. (D_2O) τ 2.04–2.92 (m, 5, aromatics), 5.15 (s, 2, $COCH_2$), 6.02–6.91 (m, 4, α-CH_2 of pyrrolidine ring), and 7.60–8.00 (m, 4, β-CH_2 of pyrrolidine ring).

Anal. Calcd. for $C_{14}H_{17}N_2OCl$: C, 63.51; H, 6.42; N, 10.58; Cl, 13.42. Found: C, 63.38; H, 6.74; N, 10.80; Cl, 13.59.

*Reaction of Indole-2-diazoketone (**1**) with Cuprous Iodide in Acetonitrile–Methanol Solution*

(a) At Room Temperature

A mixture of 500 mg (2.7 mmol) of **1**, 1.0 g (2.7 mmol) of cuprous iodide, 50 ml of acetonitrile, and 40 ml of absolute methanol was stirred at room temperature for 15 h. Evaporation to dryness *in vacuo* gave a reddish

brown residue which was triturated with 50 ml of ether. A precipitate was removed by filtration and washed thoroughly with ether until the filtrate remained colorless. Evaporation of the combined filtrates left a brown gum which was chromatographed (benzene) to give three products in the following order of elution which were purified and characterized individually:

Iodomethyl 2-indolyl ketone (**6**) was crystallized from cyclohexane – methylene chloride to give 60 mg (8%) of pale yellow crystals, m.p. 160°; mass spectrum: M^+ 285; i.r. ν_{max} 1645 (C=O) cm^{-1}; u.v. λ_{max} 312 (12 740) and 235 (8000) mμ; n.m.r. τ 0.45 (s, 1, NH), 2.21–2.83 (m, 5, aromatics), and 5.65 (s, 2, $COCH_2I$). The pyridinium iodide salt (**8**) was prepared in benzene and showed m.p. 245–246° (dec.) [lit. (10): m.p. 245–246° (dec.)].

Methyl 2-indolylacetate (**2***a*) was crystallized from petroleum ether (35–60°) to give 85 mg (17%) of pale yellow crystals identical by m.p. and mixture m.p. determinations with an authentic sample as prepared above.

Methyl 2-indolylglyoxylate (**7**) was crystallized from cyclohexane – methylene chloride to give 55 mg (10%) of orange–yellow crystals, m.p. 132–133°; mass spectrum: M^+ 203; i.r. ν_{max} 3400 (NH), 1740 (ester C=O), 1650 (C=O) cm^{-1}; u.v. λ_{max} 327 (13 850), and 240 (9000) mμ; n.m.r. τ 0.75 (s, 1, NH), 2.31–2.82 (m, 5, aromatics) and 6.05 (s, 3, OCH_3).

Anal. Calcd. for $C_{11}H_9NO_3$: C, 65.02; H, 4.43; N, 6.89. Found: C, 64.77; H, 4.44; N, 6.75.

(b) At Reflux Temperature

The above reaction was carried out using identical quantities of reactants at reflux for 13 h and the following compounds were isolated after chromatography: **2***a* (25%), **3** (7%), and **6** (4%).

*Conversion of Iodomethyl 2-Indolyl Ketone (**6**) to 2-Acetylindole (**9**)*

A mixture of compound **6** (57 mg, 0.2 mmol) and zinc dust (65 mg, 1 mmol) was refluxed in 15 ml of ethanol for 24 h. The inorganic precipitate was removed by filtration and the filtrate was evaporated to leave a gummy residue which was crystallized from cyclohexane – methylene chloride to give 25 mg (79%) of 9 as colorless needles, m.p. 147–148°, shown to be identical to authentic material by m.p. and mixture m.p. determinations as prepared below.

*Preparation of 2-Acetylindole (**9**)*

A solution of indole-2-diazoketone (**1**) (185 mg, 1 mmol) in 50 ml of ethanol was hydrogenated in the presence of 30 mg of platinum oxide under standard conditions. Normal isolation procedure gave a gummy material which was crystallized from cyclohexane – methylene chloride to yield 121 mg (76%) of colorless needles of 9, m.p. 147–148° [lit. (22): m.p. 148–149°].

*Indole-2-glyoxylic Acid (**10**)*

Compound 7 (120 mg, 0.59 mmol) was suspended in 10 ml of 1.0 *N* aqueous potassium hydroxide and the mixture was stirred at room temperature for 20 min. A small amount of solid was removed by filtration. The filtrate was cooled to 0° and acidified with 2 ml of concentrated hydrochloric acid. The resulting orange–yellow precipitate was collected, washed with minimum of cold water, and dried to yield 102 mg (92%) of **10**. Recrystallization from acetone–water furnished orange–yellow feathery needles, m.p. 160–161°; i.r. ν_{max} (CH_2Cl_2) 3400 (NH), 2900–3100 (OH), 1780 (acid C=O), and 1640 (C=O) cm^{-1}; u.v. λ_{max} 315 (14 000), 235 (9100) mμ; n.m.r. (polysol-*d*) τ −1.40 (s, 1, COOH), 0.51 (s, 1, NH), and 2.21–3.18 (m, 5, aromatics).

Anal. Calcd. for $C_{10}H_7NO_3$: C, 63.49; H, 3.73. Found: C, 63.50; H, 3.88.

*Esterification of Indole-2-glyoxylic Acid (**10**)*

A solution of 100 mg (0.53 mmol) of **10** in methanol was stirred in contact with 200 mg of Dowex 50 W-X2 resin (200–400 mesh, H^+ Form) at room temperature for 15.h. The resin was removed by filtration and the filtrate was evaporated to dryness *in vacuo*. The residue was crystallized from cyclohexane – methylene chloride to give 93 mg (86%) of orange–yellow needles, identical with 7 as shown by n.m.r. spectral, m.p., and mixture m.p. determinations.

*Conversion of Indole-2-glyoxylic Acid (**10**) to Indole-2-carboxylic Acid (**11**)*

To a solution of 15 mg (0.08 mmol) of **10** in 5 ml of 10% aqueous sodium carbonate solution, was added 5 drops of hydrogen peroxide and the reaction mixture was left overnight at room temperature. Acidification with hydrochloric acid followed by extraction with ether provided 9 mg (70%) of a solid which was recrystallized from acetone–water to give colorless needles of **11**, identical with an authentic sample (m.p. and mixture m.p. determinations) prepared by a literature method (11).

*Reaction of Indole-2-diazoketone (**1**) with Cuprous Iodide*

(a) In Acetonitrile–Ethanol Solution at Reflux

The procedure was essentially that described for the reaction of **1** in acetonitrile–methanol solution except that the mixture was refluxed for 1 h. From 100 mg of **1** there was obtained 28.5 mg (28%) of *ethyl 2-indolylacetate* (**2***b*) which was shown to be identical to a sample prepared as above.

(b) In Acetonitrile – Benzyl Alcohol Solution at Reflux

The above procedure was used. From 100 mg of **1** there was obtained 35 mg (24%) of *benzyl 2-indolylacetate* (**2***c*), m.p. 85–86° [lit. (23): m.p. 86°]; i.r. ν_{max} 3385 (NH), 1733 (C=O) cm^{-1}; n.m.r. τ 0.42 (s, 1, NH), 2.62–3.20 (m, 9, aromatics), 3.78 (s, 1, indole-3H), 4.85 (s, 2, $CO_2C\underline{H}_2C_6H_5$), and 6.25 (s, 2, CH_2).

Financial support of this work by the National Research Council of Canada and by Bristol Laboratories is gratefully acknowledged. We are indebted to Professor D. B. MacLean for the mass spectra and to Professor Potts for an authentic sample of compound **8**. We also thank Professor S. McLean for discussion and Dr. F. X. Garneau for correspondence regarding the mechanism of formation of 7.

1. J. A. Eenkhoorn, O. S. de Silva, and V. Snieckus. Chem. Commun. 1095 (1970).
2. V. Snieckus and K. S. Bhandari. Tetrahedron Lett. 3375 (1969); A. R. Battersby and A. K. Bhatnagar. Chem. Commun. 193 (1970).
3. M. Matell. Ark. Kemi, **10**, 179 (1956).

4. Y. YUKAWA, Y. TSUNO, and T. IBATA. Bull. Chem. Soc. Jap. **40**, 2613 (1967).
5. L. L. RODINA and I. K. KOROBITSYANA. Russ. Chem. Rev. **36**, 260 (1967).
6. P. YATES. J. Am. Chem. Soc. **74**, 5376 (1952).
7. H. DAHN and M. BALLENEGGER. Helv. Chim. Acta, **52**, 2417 (1969) and refs. therein.
8. P. YATES and J. FUGGER. Chem. Ind. London, 1511 (1957).
9. R. SILVERSTEIN and G. BASSLER. Spectrometric identification of organic compounds. 2nd Ed. John Wiley and Sons, Inc., New York, N.Y. 1967. p. 142.
10. K. T. POTTS and H. G. SHIN. Chem. Commun. 857 (1966).
11. W. J. BREHM. J. Am. Chem. Soc. **71**, 3541 (1949); R. H. CORNFORTH and R. ROBINSON. J. Chem. Soc. 680 (1942).
12. I. I. LAPKIN and YU. P. DORMIDONTOV. Khim. Geterotsikl. Soedin. 857 (1967).
13. F. E. ZIEGLER and E. B. SPITZNER. J. Am. Chem. Soc. **92**, 3492 (1970).
14. W. REEVE, R. S. HUDSON, and C. W. WOODS. Tetrahedron, **19**, 1243 (1963).
15. R. A. HEACOCK and S. KASPAREK. Advan. Heterocycl. Chem. **10**, 43 (1969).
16. W. R. MOSER. J. Am. Chem. Soc. **91**, 1135 (1969) and refs. therein.
17. I. K. KOROBITSYANA, L. L. RODINA, and L. M. STASHKOVA. Khim. Geterotsikl. Soedin. 843 (1966).
18. E. E. VAN TAMELEN, M. SHAMMA, A. W. BURGSTAHLER, J. WOLINSKY, R. TAMM, and P. E. ALDRICH. J. Am. Chem. Soc. **91**, 7315 (1969).
19. N. KORNBLUM, J. W. POWERS, G. J. ANDERSON, W. J. JONES, H. O. LARSON, O. LEVAND, and W. M. WEAVER. J. Am. Chem. Soc. **79**, 6562 (1957).
20. F. A. COTTON and G. WILKINSON. Advanced inorganic chemistry. 2nd Ed. Interscience Publ., New York, N.Y. 1966, p. 894.
21. W. SCHINDLER. Helv. Chim. Acta, **41**, 1441 (1958).
22. M. C. CHANG, C. I. HSING, and T. S. HO. Hua Hsueh Hsueh Pao. **32**, 64 (1966); Chem. Abstr. **65**, 10554g (1966).
23. R. GULIANO and M. L. STEIN. Ann. Chim. Rome, **48**, 1284 (1958).

Calcium(II) and Magnesium(II) Binding by L-Serine Orthophosphate in Aqueous Solutions

C. W. CHILDS[1]

Department of Medical Chemistry, Institute of Advanced Studies, Australian National University, Canberra, Australia

Received February 3, 1971

The dissociation of L-serine orthophosphate (H_3L) and its complexation reactions with calcium(II) and magnesium(II) have been studied by potentiometric titration at 37 °C in the 0.15 mol l^{-1} potassium nitrate medium and (with the exception of calcium(II) complexation) in the 0.15 mol l^{-1} tetraethylammonium bromide medium. A least squares interpretation of the data has yielded dissociation constants for H_3L and equilibrium constants for the formation of the 1:1 metal–ion complexes MH_2L^+, MHL, and ML^-. In addition the dimeric species $H_5L_2^-$, $MH_3L_2^-$, and $M_2H_2L_2$ are consistent with the data and equilibrium constants for their formation have been determined.

On a étudié, par titrage potentiométrique à 37 °C dans des milieux contenant 0.15 mol l^{-1} de nitrate de potassium et (à l'exception de la complexation du Ca(II)) 0.15 mol l^{-1} de bromure de tétraéthylammonium, la dissociation de l'orthophosphate de L-sérine (H_3L) et ses réactions de complexation avec le calcium(II) et le magnésium(II). Utilisant la méthode des moindres carrés, il est possible d'évaluer les constantes de dissociation de H_3L et les constantes d'équilibre pour la formation des complexes 1:1 ion–métal $MH_2L^{\oplus}$, MHL, et ML^-. De plus les données sont en accord avec les quantités d'espèces dimériques $H_5L_2^-$, $MH_3L_2^-$, et $M_2H_2L_2$ présentes et les constantes d'équilibre pour leur formation ont été déterminées.

Canadian Journal of Chemistry, **49**, 2359 (1971)

Introduction

Knowledge of the properties of serine orthophosphate (H_2O_3P—O—CH_2—$CH(NH_2)$—$COOH \equiv H_3L$) possibly offers insight into the metabolic role of phosphoproteins in physiological systems. One property, that of metal–ion binding in solution, has been studied once before by Österburg (1), who reported the dissociation constants of the ligand and the stability constants

[1]Present address: Canada Centre for Inland Waters, Box 5050, Burlington, Ontario.

4. Y. YUKAWA, Y. TSUNO, and T. IBATA. Bull. Chem. Soc. Jap. **40**, 2613 (1967).
5. L. L. RODINA and I. K. KOROBITSYANA. Russ. Chem. Rev. **36**, 260 (1967).
6. P. YATES. J. Am. Chem. Soc. **74**, 5376 (1952).
7. H. DAHN and M. BALLENEGGER. Helv. Chim. Acta, **52**, 2417 (1969) and refs. therein.
8. P. YATES and J. FUGGER. Chem. Ind. London, 1511 (1957).
9. R. SILVERSTEIN and G. BASSLER. Spectrometric identification of organic compounds. 2nd Ed. John Wiley and Sons, Inc., New York, N.Y. 1967. p. 142.
10. K. T. POTTS and H. G. SHIN. Chem. Commun. 857 (1966).
11. W. J. BREHM. J. Am. Chem. Soc. **71**, 3541 (1949); R. H. CORNFORTH and R. ROBINSON. J. Chem. Soc. 680 (1942).
12. I. I. LAPKIN and YU. P. DORMIDONTOV. Khim. Geterotsikl. Soedin. 857 (1967).
13. F. E. ZIEGLER and E. B. SPITZNER. J. Am. Chem. Soc. **92**, 3492 (1970).
14. W. REEVE, R. S. HUDSON, and C. W. WOODS. Tetrahedron, **19**, 1243 (1963).
15. R. A. HEACOCK and S. KASPAREK. Advan. Heterocycl. Chem. **10**, 43 (1969).
16. W. R. MOSER. J. Am. Chem. Soc. **91**, 1135 (1969) and refs. therein.
17. I. K. KOROBITSYANA, L. L. RODINA, and L. M. STASHKOVA. Khim. Geterotsikl. Soedin. 843 (1966).
18. E. E. VAN TAMELEN, M. SHAMMA, A. W. BURGSTAHLER, J. WOLINSKY, R. TAMM, and P. E. ALDRICH. J. Am. Chem. Soc. **91**, 7315 (1969).
19. N. KORNBLUM, J. W. POWERS, G. J. ANDERSON, W. J. JONES, H. O. LARSON, O. LEVAND, and W. M. WEAVER. J. Am. Chem. Soc. **79**, 6562 (1957).
20. F. A. COTTON and G. WILKINSON. Advanced inorganic chemistry. 2nd Ed. Interscience Publ., New York, N.Y. 1966, p. 894.
21. W. SCHINDLER. Helv. Chim. Acta, **41**, 1441 (1958).
22. M. C. CHANG, C. I. HSING, and T. S. HO. Hua Hsueh Hsueh Pao. **32**, 64 (1966); Chem. Abstr. **65**, 10554g (1966).
23. R. GULIANO and M. L. STEIN. Ann. Chim. Rome, **48**, 1284 (1958).

Calcium(II) and Magnesium(II) Binding by L-Serine Orthophosphate in Aqueous Solutions

C. W. CHILDS[1]

Department of Medical Chemistry, Institute of Advanced Studies, Australian National University, Canberra, Australia

Received February 3, 1971

The dissociation of L-serine orthophosphate (H_3L) and its complexation reactions with calcium(II) and magnesium(II) have been studied by potentiometric titration at 37 °C in the 0.15 mol l^{-1} potassium nitrate medium and (with the exception of calcium(II) complexation) in the 0.15 mol l^{-1} tetraethylammonium bromide medium. A least squares interpretation of the data has yielded dissociation constants for H_3L and equilibrium constants for the formation of the 1:1 metal–ion complexes MH_2L^+, MHL, and ML^-. In addition the dimeric species $H_5L_2^-$, $MH_3L_2^-$, and $M_2H_2L_2$ are consistent with the data and equilibrium constants for their formation have been determined.

On a étudié, par titrage potentiométrique à 37 °C dans des milieux contenant 0.15 mol l^{-1} de nitrate de potassium et (à l'exception de la complexation du Ca(II)) 0.15 mol l^{-1} de bromure de tétraéthylammonium, la dissociation de l'orthophosphate de L-sérine (H_3L) et ses réactions de complexation avec le calcium(II) et le magnésium(II). Utilisant la méthode des moindres carrés, il est possible d'évaluer les constantes de dissociation de H_3L et les constantes d'équilibre pour la formation des complexes 1:1 ion–métal $MH_2L^{\oplus}$, MHL, et ML^-. De plus les données sont en accord avec les quantités d'espèces dimériques $H_5L_2^-$, $MH_3L_2^-$, et $M_2H_2L_2$ présentes et les constantes d'équilibre pour leur formation ont été déterminées.

Canadian Journal of Chemistry, **49**, 2359 (1971)

Introduction

Knowledge of the properties of serine orthophosphate (H_2O_3P—O—CH_2—$CH(NH_2)$—$COOH \equiv H_3L$) possibly offers insight into the metabolic role of phosphoproteins in physiological systems. One property, that of metal–ion binding in solution, has been studied once before by Österburg (1), who reported the dissociation constants of the ligand and the stability constants

[1]Present address: Canada Centre for Inland Waters, Box 5050, Burlington, Ontario.

Can. J. Chem. Downloaded from www.nrcresearchpress.com by 210.87.254.42 on 09/05/12
For personal use only.

Can. J. Chem. Downloaded from www.nrcresearchpress.com by 210.87.254.42 on 09/05/12
For personal use only.

of the metal–ion complexes MHL and ML (where M represents calcium(II), magnesium(II), manganese(II), copper(II), and iron(III)) and, in addition, ML_2, (for copper(II) and iron(III)) at 25 °C for the 0.15 mol l^{-1} potassium chloride medium.

It is likely that H_3L in solution is mostly in the zwitterionic form with one proton removed from the phosphate segment and an extra one located on the amino nitrogen (1). Correlation with the dissociation constants of orthophosphate and serine (2) then suggests that the successive dissociations of H_3L would yield a ligand with metal–ion binding properties derived from the following combinations:

H_3L : —O—PO_3H^-

H_2L^- : —O—PO_3H^- and —COO^-

HL^{2-} : —O—PO_3^{2-} and —COO^-

L^{3-} : —O—PO_3^{2-} and —$HC(\dot{N}H_2)$—COO^-

Previous work on orthophosphate solution equilibria (3) and metal–ion orthophosphate complexes (4) indicated the possibility of dimeric species existing in solutions of serine orthophosphate.

All of these possibilities have been considered in deriving the equilibrium constants in the present paper for the dissociation of L-serine orthophosphate and the complexation reactions with calcium(II) and magnesium(II) in 0.15 mol l^{-1} potassium nitrate, and (calcium(II) complexation excepted) in 0.15 mol l^{-1} tetraethylammonium bromide at 37 °C. The results have been derived from potentiometric titration data in the pH range 3 to 10, where the species H_4L^+ can safely be neglected.

Experimental

L-Serine orthophosphate (Calbiochem A grade) was dried at 20 °C over anhydrous magnesium perchlorate and was used without purification as analysis for C, H, N, and P indicated close to 100% purity.[2] Freshly prepared solutions were always used in the experiments. Tetraethylammonium bromide (BDH Laboratory Reagent) was recrystallized from a chloroform–ether mixture and dried at 20 °C under reduced pressure for several weeks. The other materials and solutions were obtained as described previously (4).

AnalaR potassium hydrogen phthalate and sodium tetraborate were used without further purification for the preparation of 0.05 mol l^{-1} standard buffer solutions (pH values 4.029 and 9.082 respectively (5) at 37 °C). The potentiometric measurements were made at 37 ± 0.05 °C with the apparatus and procedure described previously (4). The precision of all of the pH measurements was estimated from duplicate titrations to be about ±0.005 pH unit. In all cases the standard buffer readings after a titration agreed within 0.005 pH unit with the initial settings.

The complete pH titration data are on file with the Depository of Unpublished Data.[3] There were five sets of three titrations; in each set the L-serine orthophosphate concentrations were close to 3×10^{-3}, 6×10^{-3}, and 9×10^{-3} mol l^{-1}. In three sets calcium(II) nitrate or magnesium(II) nitrate were included at concentrations close to 2×10^{-3}, 7×10^{-3}, and 5×10^{-3} mol l^{-1} respectively. The average number of readings in a titration was 33, the minimum number was 27, and each titration covered the pH range 3 to 10. The titrant was always potassium hydroxide solution close to 1.0 mol l^{-1}. In three sets of titrations (H_3L, Ca(II)–H_3L, and Mg(II)–H_3L) the medium was 0.15 mol l^{-1} potassium nitrate, and in two (H_3L and Mg(II)–H_3L) it was 0.15 mole l^{-1} tetraethylammonium bromide.

Interpretation of Data

The data were interpreted with the aid of the computer program SCOGS (6) as previously described (3, 4, 7). This program uses an iterative least squares method to find the best match between the observed and calculated volumes of titrant by refining the estimated values of the equilibrium constants for a postulated set of equilibria.

For the solution of mass balance equations the hydrogen ion concentrations were estimated from the pH values by eq. 1 (4). For the 0.15 mol

$$[1] \qquad p[H^+] = pH + \log F$$

l^{-1} potassium nitrate medium and the apparatus used in this work F has been shown (4) to lie in the range 0.80–0.85. For the 0.15 mol l^{-1} tetraethylammonium bromide medium the same range of F was used and this was consistent with the best least squares fit obtained as F was varied, a criterion which has proved useful before (3, 4, 7).

The ionic activity product of water was taken to be $10^{-13.62}$ at 37 °C (8).

The equilibrium constants are defined in eqs.

[2] I am grateful to Dr. J. E. Fildes of the Microanalytical Laboratory, John Curtin School of Medical Research, Canberra, Australia, for these analyses.

[3] Photocopies may be obtained free-of-charge, upon request, from: Depository of Unpublished Data, National Science Library, National Research Council of Canada, Ottawa, Canada.

TABLE 1. Equilibrium constants for reactions between hydrogen ions and L-serine orthophosphate anions

Medium*	KNO_3†		$(C_2H_5)_4NBr$†		KCl‡
	$F = 0.80$	$F = 0.85$	$F = 0.80$	$F = 0.85$	
pK_{a1}	2.04 ±0.07	2.17 ±0.05	2.01 ±0.09	2.14 ±0.07	2.08±0.08
pK_{a2}	5.771±0.005	5.771±0.005	5.892±0.007	5.892±0.008	5.64±0.01
pK_{a3}	9.655±0.002	9.653±0.002	9.700±0.003	9.698±0.003	9.74±0.02
log $K(H_5L_2^-)$	2.05 ±0.20	1.71 ±0.27	1.88 ±0.28	1.48 ±0.43	—
10^4SDT (ml)	17.1	17.6	23.7	24.8	—

*All 0.15 mol l^{-1}.
†This work, 37 °C.
‡Reference 1, 25 °C. Note that these results are for racemic serine orthophosphate.

2–11 in forms which involve $(H^+) = 10^{-pH}$, and the concentrations (denoted by square brackets) of all other species.

$$[2] \quad K_{a1} = [H_2L^-](H^+)/[H_3L]$$

$$[3] \quad K_{a2} = [HL^{2-}](H^+)/[H_2L^-]$$

$$[4] \quad K_{a3} = [L^{3-}](H^+)/[HL^{2-}]$$

$$[5] \quad K(H_5L_2^-) = [H_5L_2^-]/[H_3L][H_2L^-]$$

$$[6] \quad {}^*K_1 = [MOH^+](H^+)/[M^{2+}]$$

$$[7] \quad K_{m,1} = [MH_2L^+]/[M^{2+}][H_2L^-]$$

$$[8] \quad K_{m,2} = [MHL]/[M^{2+}][HL^{2-}]$$

$$[9] \quad K_{m,3} = [ML^-]/[M^{2+}][L^{3-}]$$

$$[10] \quad K_{m1,2} = [MH_3L_2^-]/[MH_2L^+][HL^{2-}]$$

$$[11] \quad K_{m2.m2} = [M_2H_2L_2]/[MHL]^2$$

Values for the equilibrium constants [2] to [5] were determined in the first two sets of experiments. By analogy with results obtained earlier from similar measurements on orthophosphate (3) the dimeric species $H_4L_2^{2-}$, $H_3L_2^{3-}$, and H_6L_2 were also tried in the interpretation, but their inclusion (individually or together) failed to produce an improvement in least squares fit to the data and the estimated values of the equilibrium constants were progressively decreased in the iteration process until the calculated concentrations of the species became negligible. The values obtained for equilibrium constants [2] to [5] are given in Table 1. The limits shown in Tables 1 and 2 for this work are the sums of the standard deviations of the cumulative equilibrium constants (as refined by the computer) used in obtaining the values. The standard deviation in volume of titrant (SDT) is a measure of the ability of the refined values to reproduce the experimental data.

The small amount of metal–ion hydrolysis occurring in the solutions was accounted for by the use of ${}^*K_1$ values given previously (4) with the exception of the formation of $MgOH^+$ in the 0.15 mol l^{-1} tetraethylammonium bromide medium; in this case the value of ${}^*K_1$ was determined simultaneously with the equilibrium constants for the magnesium(II) – L-serine orthophosphate species, and was found to be $10^{-10.5\pm0.1}$ for both $F = 0.80$ and 0.85.

The last three sets of experiments, when calcium(II) or magnesium(II) ions were included, were used to determine the values for equilibrium constants [7] to [11]. Initially MH_3L^{2+}, MH_2L^+, MHL, and ML^- were the metal–ion complexes included in the interpretations, but MH_3L^{2+} proved inconsistent with the data and was omitted from further calculations. Subsequently all of the possible 1:2 and 2:1 metal–ion – L-serine orthophosphate species were added successively to the interpretations, but of these only $MH_3L_2^-$ and $M_2H_2L_2$ were consistent with the data for each system, the inclusion of each of these species produced an improvement in the least squares fit to the data and the estimates of the corresponding equilibrium constants converged to apparently reasonable values. Table 2 lists the refined values of the equilibrium constants for species involving calcium(II) or magnesium(II). The same results were obtained with $F = 0.80$ as with $F = 0.85$.

Discussion

It should be noted that in this work the medium (0.15 mol l^{-1} potassium nitrate or tetraethylammonium bromide) has been treated as a 'solvent' in the sense that Rossotti and Rossotti

Can. J. Chem. Downloaded from www.nrcresearchpress.com by 210.87.254.42 on 09/05/12
For personal use only.

TABLE 2. Equilibrium constants for metal–ion L-serine orthophosphate complexes

	Calcium(II) complexes		Magnesium(II) complexes		
Medium*	KNO_3†	KCl‡	KNO_3†	$(C_2H_5)_4NBr$†	KCl‡
log $K_{m,1}$	1.34±0.14	—	1.35±0.12	1.97±0.10	—
log $K_{m,2}$	1.65±0.11	1.43±0.05	1.82±0.08	2.34±0.08	1.60±0.07
log $K_{m,3}$	2.23±0.04	2.19±0.08	2.55±0.02	2.89±0.04	2.48±0.04
log $K_{m1,2}$	2.1 ±0.3	—	2.0 ±0.3	1.4 ±0.3	—
log $K_{m2,m2}$	2.4 ±0.4	—	2.2 ±0.3	1.4 ±0.3	—
10^4SDT(ml)	20.2	—	15.3	8.7	

*All 0.15 mol l^{-1}.
†This work, 37 °C.
‡Reference 1, 25 °C. Note that these results are for racemic serine orthophosphate.

(9) and Sillén (10) have enunciated. Hence the formulas for the various species include an unknown number of water molecules and medium ions, and it is necessary to specify with the results both the nature and the ionic strength of the medium. It is not assumed that the medium ions do not form complexes with the reactants of interest. The results determined with this approach are sometimes referred to as 'apparent' equilibrium constants. The necessity for specifying the nature of the medium can be seen by comparing the results for the potassium nitrate medium with those for the tetraethylammonium bromide medium in Tables 1 and 2.

The agreement between the values of $K_{m,2}$ and $K_{m,3}$ obtained in this work for the potassium nitrate medium and those obtained by Österburg for the potassium chloride medium (see Table 2) is surprisingly close considering that the measurements were made at different temperatures and that the data have been interpreted in somewhat different ways. The differences between the results for the potassium nitrate medium and those for the tetraethylammonium bromide medium (see Tables 1 and 2) tend to be greater, probably due to the relative inertness of tetraethylammonium bromide in the systems studied.

The evidence for the dimeric species $H_5L_2^-$, $MH_3L_2^-$, and $M_2H_2L_2$ is partly dependent upon the decrease of a least squares parameter when each species is included in the interpretation. Such evidence is always open to question on the basis that the improvement in fit may be fortuitous. On the other hand, several other species tried did not improve the fit, and the values obtained for the equilibrium constants are of the same order as those obtained earlier for dimeric phosphates in solution (3, 4). Possible structures for $H_5L_2^-$, $MH_3L_2^-$, and $M_2H_2L_2$ in solution are shown in **1**, **2**, and **3** respectively. These are similar to those described earlier for orthophosphate complexes (3, 4). Note that if H_3L is zwitterionic in solution as $^-HO_3P—O—CH_2—CH(NH_3^+)—COOH$ then in $H_5L_2^-$ only two hydrogen bonds may exist between the two phosphate segments as against three in the corresponding orthophosphate dimer. With L-serine orthophosphate there is also the possibility of the existence of inter- or intra-molecular hydrogen bonds which involve the carboxylate and amino groups (11).

Table 3 lists the calculated compositions of solution containing 0.006 mol l^{-1} magnesium(II) and 0.009 mol l^{-1} L-serine orthophosphate as the p*H* varies from 3 to 10. The values in Tables 1 and 2 for the potassium nitrate medium have been

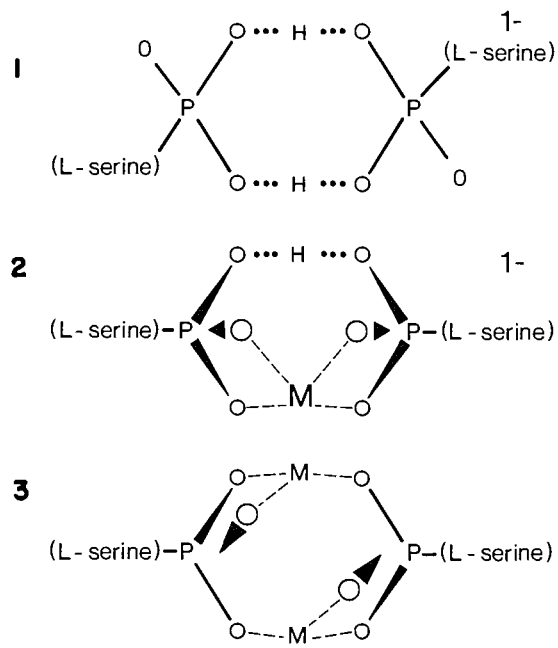

Can. J. Chem. Downloaded from www.nrcresearchpress.com by 210.87.254.42 on 09/05/12
For personal use only.

Can. J. Chem. Downloaded from www.nrcresearchpress.com by 210.87.254.42 on 09/05/12
For personal use only.

TABLE 3. Calculated compositions of a solution containing 0.009 mol l^{-1} of L-serine orthophosphate and 0.006 mol l^{-1} of magnesium(II)*

p*H*	$[Mg^{2+}]$	$[H_3L]$	$[H_2L^-]$	$[HL^{2-}]$	$[L^-]$	$[H_5L_2^-]$†	$[MgH_2L^+]$	[MgHL]	$[MgL^-]$	$[MgH_3L_2^-]$†	$[Mg_2H_2L_2]$†
3.0	523	71	647	‡	‡	104	76	‡	‡	‡	‡
4.0	507	8	769	13	‡	15	88	‡	‡	‡	‡
5.0	481	‡	659	112	‡	‡	71	35	‡	17	‡
6.0	406	‡	258	437	‡	‡	24	116	‡	23	42
7.0	369	‡	37	628	1	‡	‡	152	‡	‡	72
8.0	359	‡	4	641	14	‡	‡	151	18	‡	71
9.0	324	‡	‡	511	113	‡	‡	108	130	‡	37
10.0	243	‡	‡	170	376	‡	‡	27	325	‡	‡

*Concentrations $\times 10^5$ in mol l^{-1}; concentration less than 5×10^{-5} mol l^{-1} are shown by a double dagger (‡); medium: 0.15 mol l^{-1} potassium nitrate; 37 °C.
†Concentration as L-serine orthophosphate.

used in the calculations. For none of the pH values shown was $[MgOH^+]$ greater than 5×10^{-5} mol l^{-1}.

1. R. Österburg. Arkiv Kemi, **13**, 393 (1959). Preliminary communication, R. Österburg. Nature, **179**, 476 (1957).
2. L. G. Sillén and A. E. Martell. Stability constants of metal–ion complexes. Chem. Soc. Spec. Publ. No. 17, London, 1964.
3. C. W. Childs. J. Phys. Chem. **73**, 2956 (1969).
4. C. W. Childs. Inorg. Chem. **9**, 2465 (1970).
5. D. J. Alner, J. J. Greczek, and A. G. Smeeth. J. Chem. Soc. A, 1205 (1967).
6. I. G. Sayce. Talanta, **15**, 1397 (1968).
7. C. W. Childs and D. D. Perrin. J. Chem. Soc. A, 1039 (1969).
8. H. S. Harned and R. A. Robinson. Trans. Faraday Soc. **36**, 973 (1940).
9. F. J. C. Rossotti and H. Rossotti. The determination of stability constants. McGraw-Hill, London, 1961. pp. 17–27.
10. L. G. Sillén. *In* Equilibrium concepts in natural water systems. Advances in chemistry. Series 67. American Chemical Society, Washington, D.C., 1967. pp. 47–50.
11. G. H. McCallum, J. Monteath Robinson, and G. A. Sim. Nature, **184**, 1863 (1959).

Alkylammonium Ions: Chemical Shifts and Interactions with Solvent in Aqueous Acid Solutions

J. T. Edward

Department of Chemistry, McGill University, Montreal, Quebec

Received January 19, 1971

The difference between the chemical shifts of the α and β hydrogens of the mono-, di-, tri-, and tetraethylammonium ions changes as the concentration of the solvent sulfuric acid is increased from 0 to 94%. A tentative explanation based on hydration of the ions is presented.

La différence entre les déplacements chimiques des hydrogènes α et β des ions mono-, di-, tri-, et tetraéthylammonium change par rapport à la concentration de l'acide sulfurique employé comme solvant. On propose une explication basée sur l'hydratation des ions.

Canadian Journal of Chemistry, **49**, 2364 (1971)

In the past nine years several investigators (cited in ref. 1) have followed the protonation of organic molecules in increasing concentrations of sulfuric acid by observing changes in their n.m.r. chemical shifts. It accordingly becomes important to know how the chemical shift varies with acid concentration when the degree of protonation of the molecule is not changing. For this reason we have measured the difference Δδ (previously symbolized by δ_i (2)) between the chemical shifts of the α and β hydrogens of the ethyl groups in the mono-, di-, tri-, and tetraethylammonium ions in 0–80% sulfuric acid. The results are shown in Fig. 1 and are included in Table 1.

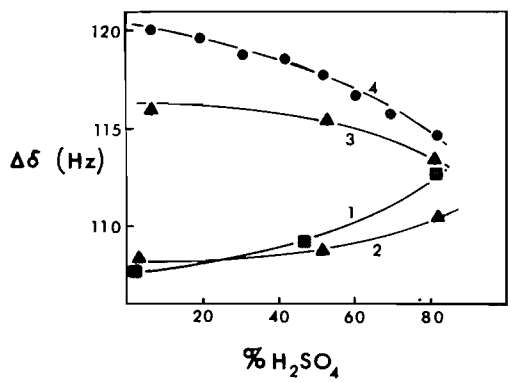

FIG. 1. Effect of acid concentration on Δδ of (*1*) monoethylammonium; (*2*) diethylammonium; (*3*) triethylammonium; and (*4*) tetraethylammonium ions.

The Δδ of the ethyl group is known to be proportional to the electronegativity of the group attached to it (3), so that it is evident (Fig. 1) that in aqueous solution the positive nitrogen of the tetraethylammonium ion attracts electrons more strongly than the positive nitrogen of the ethylammonium ion. This may be plausibly attributed to hydrogen-bonding of water molecules to the $-NH_3^+$ group, as shown in **1** (see ref. 4 for documentation). The negative ends of

Can. J. Chem. Downloaded from www.nrcresearchpress.com by 210.87.254.42 on 09/05/12
For personal use only.

used in the calculations. For none of the pH values shown was $[MgOH^+]$ greater than 5×10^{-5} mol l^{-1}.

1. R. Österburg. Arkiv Kemi, **13**, 393 (1959). Preliminary communication, R. Österburg. Nature, **179**, 476 (1957).
2. L. G. Sillén and A. E. Martell. Stability constants of metal–ion complexes. Chem. Soc. Spec. Publ. No. 17, London, 1964.
3. C. W. Childs. J. Phys. Chem. **73**, 2956 (1969).
4. C. W. Childs. Inorg. Chem. **9**, 2465 (1970).
5. D. J. Alner, J. J. Greczek, and A. G. Smeeth. J. Chem. Soc. A, 1205 (1967).
6. I. G. Sayce. Talanta, **15**, 1397 (1968).
7. C. W. Childs and D. D. Perrin. J. Chem. Soc. A, 1039 (1969).
8. H. S. Harned and R. A. Robinson. Trans. Faraday Soc. **36**, 973 (1940).
9. F. J. C. Rossotti and H. Rossotti. The determination of stability constants. McGraw-Hill, London, 1961. pp. 17–27.
10. L. G. Sillén. *In* Equilibrium concepts in natural water systems. Advances in chemistry. Series 67. American Chemical Society, Washington, D.C., 1967. pp. 47–50.
11. G. H. McCallum, J. Monteath Robinson, and G. A. Sim. Nature, **184**, 1863 (1959).

Alkylammonium Ions: Chemical Shifts and Interactions with Solvent in Aqueous Acid Solutions

J. T. Edward

Department of Chemistry, McGill University, Montreal, Quebec

Received January 19, 1971

The difference between the chemical shifts of the α and β hydrogens of the mono-, di-, tri-, and tetraethylammonium ions changes as the concentration of the solvent sulfuric acid is increased from 0 to 94%. A tentative explanation based on hydration of the ions is presented.

La différence entre les déplacements chimiques des hydrogènes α et β des ions mono-, di-, tri-, et tetraéthylammonium change par rapport à la concentration de l'acide sulfurique employé comme solvant. On propose une explication basée sur l'hydratation des ions.

Canadian Journal of Chemistry, **49**, 2364 (1971)

In the past nine years several investigators (cited in ref. 1) have followed the protonation of organic molecules in increasing concentrations of sulfuric acid by observing changes in their n.m.r. chemical shifts. It accordingly becomes important to know how the chemical shift varies with acid concentration when the degree of protonation of the molecule is not changing. For this reason we have measured the difference Δδ (previously symbolized by δ_i (2)) between the chemical shifts of the α and β hydrogens of the ethyl groups in the mono-, di-, tri-, and tetraethylammonium ions in 0–80% sulfuric acid. The results are shown in Fig. 1 and are included in Table 1.

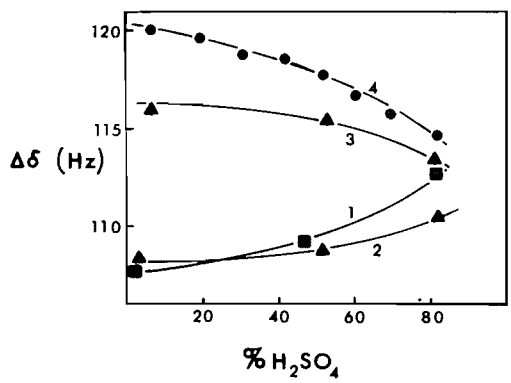

FIG. 1. Effect of acid concentration on Δδ of (*1*) monoethylammonium; (*2*) diethylammonium; (*3*) triethylammonium; and (*4*) tetraethylammonium ions.

The Δδ of the ethyl group is known to be proportional to the electronegativity of the group attached to it (3), so that it is evident (Fig. 1) that in aqueous solution the positive nitrogen of the tetraethylammonium ion attracts electrons more strongly than the positive nitrogen of the ethylammonium ion. This may be plausibly attributed to hydrogen-bonding of water molecules to the $-NH_3^+$ group, as shown in **1** (see ref. 4 for documentation). The negative ends of

Can. J. Chem. Downloaded from www.nrcresearchpress.com by 210.87.254.6 on 09/05/12
For personal use only.

TABLE 1. Effect of acid concentration on Δδ of different ethylammonium ions

Ion	% H_2SO_4	Δδ	Ion	% H_2SO_4	Δδ	Ion	% Acid	Δδ
$EtNH_3^+$	0.03	107.8	Et_4N^+	5.5	120.0	Et_4N^+	7.8*	119.9
$EtNH_3^+$	46.4	109.3	Et_4N^+	19.1	119.5	Et_4N^+	30.2*	118.3
$EtNH_3^+$	80.6	112.7	Et_4N^+	30.0	118.7	Et_4N^+	11.0†	119.9
$Et_2NH_2^+$	3.6	108.4	Et_4N^+	40.8	118.5	Et_4N^+	30.9†	118.4
$Et_2NH_2^+$	50.9	108.8	Et_4N^+	51.4	117.7	Et_4N^+	60.3†	117.8
$Et_2NH_2^+$	81.2	110.5	Et_4N^+	60.0	116.7	Et_4N^+	10.0‡	119.0
Et_3NH^+	6.2	116.0	Et_4N^+	68.8	115.7	Et_4N^+	27.9‡	118.3
Et_3NH^+	52.2	115.0	Et_4N^+	81.4	114.7	Et_4N^+	51.7‡	116.5
Et_3NH^+	80.6	113.6	Et_4N^+	94.0	113.8	Et_4N^+		

*HCl.
†HNO_3.
‡$HClO_4$.

the bonded water dipoles neutralize slightly the partial positive charges of the hydrogen atoms attached to N^+, and so effectively decrease the positive charge of the $—NH_3^+$ group. The $—NEt_3^+$ group, where this effect is absent, should accordingly be expected to be more strongly electron-pulling. Fraenkel and Kim (5) observed a similar difference for primary and quaternary anilinium ions dissolved in methanol.

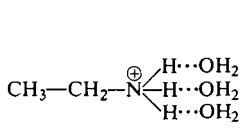

1

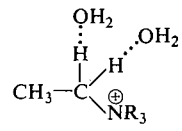

2

The $—NH_3^+$ may be expected progressively to lose its bonded water molecules as the concentration of sulfuric acid increases from 0 to 80%, and the activity of water decreases from 1.00 to 0.005 (6). This explains satisfactorily the increase in Δδ of the ethylammonium ion with acid concentration, as shown in Fig. 1; similar increases have been noted in Δδ of other protonated species (1, 2). However, it does not explain the *decrease* of Δδ of the tetraethylammonium ion as the acid concentration is increased (Table 1 and Fig. 1); it might have been expected that Δδ of this ion would remain constant. Any explanation of this result must be highly tentative: shifts of ionic species are poorly understood, and may be due to many factors. A possible explanation may be weak hydrogen-bonding of the methylenic protons, known to be slightly acidic (7), to water molecules as pictured in **2**.[1] Such hydrogen bonding would shift the resonance of the methylenic hydrogens downfield (9), and increase Δδ; the effect would diminish with the decreasing water activity accompanying increase of acid concentration. Deno and co-workers (10) have noted that the chemical shift of the methyl protons of the tetramethylammonium ion (referred to the methyl protons of $(CH_3)_3Si(CH_2)_3SO_3H$) moves downfield as the concentration of sulfuric acid is increased from 0 to 96%, and a similar explanation would apply.

Some support for this interpretation comes from the fact that Δδ of the tetraethylammonium ion in water decreases from 120.1 ± 0.3 Hz at 31° to 118.6 ± 0.2 Hz at 86.5 ± 2°; hydrogen bonding would be expected to diminish at higher temperatures.

Other explanations, based on a specific interaction between tetraethylammonium and bisulfate ions, are made less likely by the fact that a wide variety of other solutes (*e.g.* calcium chloride and sodium hydroxide) lower Δδ, the extent of the lowering depending on the solute concentration. The general similarity of the behavior of the ion in different strong acids is shown in Fig. 2: Δδ is roughly linear with $-H_0$ (11) between 0 and +8 for solutions in aqueous sulfuric, perchloric, nitric and hydrochloric acids. The increase in $-H_0$ with acid concentration is known to be related to the decreasing water activity in different acid solutions (12).

In summary, chemical shift data seem to indicate that even the tetraethylammonium ion (regarded as the "ideal" cation (13)) shows some interaction with solvent.

Experimental

Measurements were made with a Varian HR-60 spectrometer at a probe temperature of about 39°

[1]Ko and Leffek (8) have recently reported a variation of isotope effect with solvent in the decomposition of benzyl-α-d_2-phenyldimethylammonium bromide and have given a similar rationalization in terms of a specific solvent interaction with methylenic protons or deuterons.

Can. J. Chem. Downloaded from www.nrcresearchpress.com by 210.87.254.6 on 09/05/12
For personal use only.

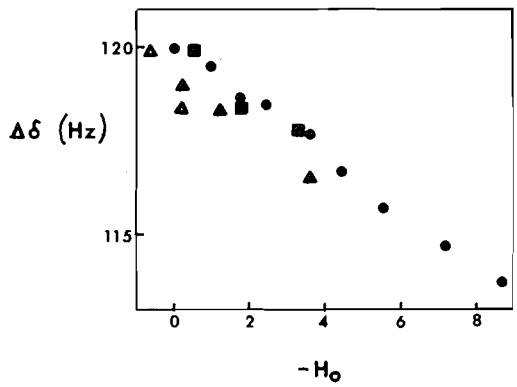

FIG. 2. Variation of Δδ of tetraethylammonium ion with acidity function H_0 of: sulfuric (●), hydrochloric (△), nitric (■), and perchloric (▲), acids.

(unless otherwise noted); Δδ was generally reproducible to within 1 Hz. Each of the three peaks of the methyl triplet of tetraethylammonium were further split into three peaks of equal intensity (J = 3.8 Hz) by coupling with the ^{14}N nucleus. Acid concentrations were determined by titration of the solutions.

I am grateful to Prof. F. A. L. Anet for discussion and for the measurement of spectra at high temperatures, to Drs. H. Baikowitz, O. J. Chin, and C. Stammer for experimental assistance, and to the National Research Council of Canada for financial support.

1. D. G. LEE. Can. J. Chem. **48**, 1919 (1970). D. G. LEE and R. CAMERON. J. Am. Chem. Soc. In press.
2. J. T. EDWARD, J. B. LEANE, and I. C. WANG. Can. J. Chem. **40**, 1521 (1962).
3. B. P. DAILEY and J. N. SHOOLERY. J. Am. Chem. Soc. **77**, 3477 (1955).
4. E. M. ARNETT and J. J. BURKE. J. Am. Chem. Soc. **88**, 2340 (1966).
5. G. FRAENKEL and J. P. KIM. J. Am. Chem. Soc. **88**, 4203 (1966).
6. C. J. O'CONNOR. J. Chem. Educ. **46**, 686 (1969).
7. D. J. CRAM. Fundamentals of carbanion chemistry. Academic Press, New York, N.Y., 1965. p. 71.
8. E. C. F. KO and K. T. LEFFEK. Can. J. Chem. **49**, 129 (1971).
9. J. A. POPLE, W. G. SCHNEIDER, and H. J. BERNSTEIN. High-resolution nuclear magnetic resonance. McGraw-Hill, New York, N.Y., 1959. p. 407.
10. N. C. DENO, H. G. RICHEY, N. FRIEDMAN, J. H. DODGE, J. J. HOUSER, and C. U. PITTMAN. J. Am. Chem. Soc. **85**, 2991 (1963).
11. M. A. PAUL and F. A. LONG. Chem. Rev. **57**, 1 (1957).
12. K. N. BASCOMBE and R. P. BELL. Discuss. Faraday Soc. **24**, 158 (1957). P. A. H. WYATT. Discuss. Faraday Soc. **24**, 162 (1957). K. YATES and H. WAI. J. Am. Chem. Soc. **86**, 5408 (1964).
13. R. H. BOYD. J. Am. Chem. Soc. **85**, 1555 (1963). K. W. BUNZL. J. Phys. Chem. **71**, 1358 (1967). R. H. WOOD and H. L. ANDERSON. J. Phys. Chem. **71**, 1871 (1967). J. T. EDWARD. *In* Intestinal absorption of metal ions, trace elements, and radionuclides. *Edited by* S. C. Skoryna and D. Waldron-Edward. Pergamon Press, Oxford, 1970. p. 3.

Can. J. Chem. Downloaded from www.nrcresearchpress.com by 210.87.254.6 on 09/05/12
For personal use only.

The Mode of Formation and some Reactions of 2,3,6,7-Tetramethoxy-9,10-dimethylphenanthrene

KARL H. WEISGRABER[1] AND ULRICH WEISS

National Institute of Arthritis and Metabolic Diseases, National Institutes of Health, Bethesda, Maryland 20014

Received January 12, 1971

Reaction of veratrole and biacetyl in 70% aqueous H_2SO_4 very rapidly yields 3,3-bis-(3,4-dimethoxyphenyl)-2-butanone (**3**), which is slowly converted further to 2,3,6,7-tetramethoxy-9,10-dimethylphenanthrene (**1**). The reaction sequence leading to **1** is interpreted on the basis of this finding, and some new reactions of **1** are described.

La réaction du vératrole et du biacétyle dans H_2SO_4 à 70% dans l'eau conduit rapidement à la bis-(diméthoxy-3,4 phényl)-3,3 butanone-2 (**3**) qui se transforme lentement en tétraméthoxy-2,3,6,7 diméthyl-9,10 phénanthrène (**1**). On interprête la suite de réaction conduisant à **1** en se basant sur les résultats obtenus ici; on décrit aussi quelques réactions nouvelles de **1**.

Canadian Journal of Chemistry, **49**, 2366 (1971)

As part of a program aimed at the synthesis of certain polycyclic quinones, we have investigated the formation of the phenanthrene **1** from veratrole and biacetyl in 70% v/v sulfuric acid, and certain transformations of **1**. Since this part of the program is not being pursued any further, and is not likely to be taken up again in the foreseeable

[1]Present address: United States Department of Agriculture, Fruit and Vegetable Chemistry Laboratory, Pasadena, California 91106.

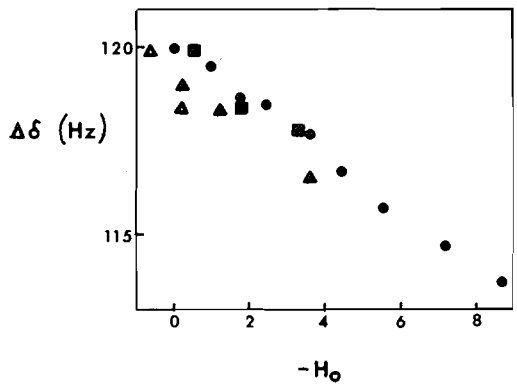

FIG. 2. Variation of Δδ of tetraethylammonium ion with acidity function H_0 of: sulfuric (●), hydrochloric (△), nitric (■), and perchloric (▲), acids.

(unless otherwise noted); Δδ was generally reproducible to within 1 Hz. Each of the three peaks of the methyl triplet of tetraethylammonium were further split into three peaks of equal intensity (J = 3.8 Hz) by coupling with the ^{14}N nucleus. Acid concentrations were determined by titration of the solutions.

I am grateful to Prof. F. A. L. Anet for discussion and for the measurement of spectra at high temperatures, to Drs. H. Baikowitz, O. J. Chin, and C. Stammer for experimental assistance, and to the National Research Council of Canada for financial support.

1. D. G. LEE. Can. J. Chem. **48**, 1919 (1970). D. G. LEE and R. CAMERON. J. Am. Chem. Soc. In press.
2. J. T. EDWARD, J. B. LEANE, and I. C. WANG. Can. J. Chem. **40**, 1521 (1962).
3. B. P. DAILEY and J. N. SHOOLERY. J. Am. Chem. Soc. **77**, 3477 (1955).
4. E. M. ARNETT and J. J. BURKE. J. Am. Chem. Soc. **88**, 2340 (1966).
5. G. FRAENKEL and J. P. KIM. J. Am. Chem. Soc. **88**, 4203 (1966).
6. C. J. O'CONNOR. J. Chem. Educ. **46**, 686 (1969).
7. D. J. CRAM. Fundamentals of carbanion chemistry. Academic Press, New York, N.Y., 1965. p. 71.
8. E. C. F. KO and K. T. LEFFEK. Can. J. Chem. **49**, 129 (1971).
9. J. A. POPLE, W. G. SCHNEIDER, and H. J. BERNSTEIN. High-resolution nuclear magnetic resonance. McGraw-Hill, New York, N.Y., 1959. p. 407.
10. N. C. DENO, H. G. RICHEY, N. FRIEDMAN, J. H. DODGE, J. J. HOUSER, and C. U. PITTMAN. J. Am. Chem. Soc. **85**, 2991 (1963).
11. M. A. PAUL and F. A. LONG. Chem. Rev. **57**, 1 (1957).
12. K. N. BASCOMBE and R. P. BELL. Discuss. Faraday Soc. **24**, 158 (1957). P. A. H. WYATT. Discuss. Faraday Soc. **24**, 162 (1957). K. YATES and H. WAI. J. Am. Chem. Soc. **86**, 5408 (1964).
13. R. H. BOYD. J. Am. Chem. Soc. **85**, 1555 (1963). K. W. BUNZL. J. Phys. Chem. **71**, 1358 (1967). R. H. WOOD and H. L. ANDERSON. J. Phys. Chem. **71**, 1871 (1967). J. T. EDWARD. *In* Intestinal absorption of metal ions, trace elements, and radionuclides. *Edited by* S. C. Skoryna and D. Waldron-Edward. Pergamon Press, Oxford, 1970. p. 3.

Can. J. Chem. Downloaded from www.nrcresearchpress.com by 210.87.254.6 on 09/05/12
For personal use only.

The Mode of Formation and some Reactions of 2,3,6,7-Tetramethoxy-9,10-dimethylphenanthrene

KARL H. WEISGRABER[1] AND ULRICH WEISS

National Institute of Arthritis and Metabolic Diseases, National Institutes of Health, Bethesda, Maryland 20014

Received January 12, 1971

Reaction of veratrole and biacetyl in 70% aqueous H_2SO_4 very rapidly yields 3,3-bis-(3,4-dimethoxyphenyl)-2-butanone (**3**), which is slowly converted further to 2,3,6,7-tetramethoxy-9,10-dimethylphenanthrene (**1**). The reaction sequence leading to **1** is interpreted on the basis of this finding, and some new reactions of **1** are described.

La réaction du vératrole et du biacétyle dans H_2SO_4 à 70% dans l'eau conduit rapidement à la bis-(diméthoxy-3,4 phényl)-3,3 butanone-2 (**3**) qui se transforme lentement en tétraméthoxy-2,3,6,7 diméthyl-9,10 phénanthrène (**1**). On interprête la suite de réaction conduisant à **1** en se basant sur les résultats obtenus ici; on décrit aussi quelques réactions nouvelles de **1**.

Canadian Journal of Chemistry, **49**, 2366 (1971)

As part of a program aimed at the synthesis of certain polycyclic quinones, we have investigated the formation of the phenanthrene **1** from veratrole and biacetyl in 70% v/v sulfuric acid, and certain transformations of **1**. Since this part of the program is not being pursued any further, and is not likely to be taken up again in the foreseeable

[1]Present address: United States Department of Agriculture, Fruit and Vegetable Chemistry Laboratory, Pasadena, California 91106.

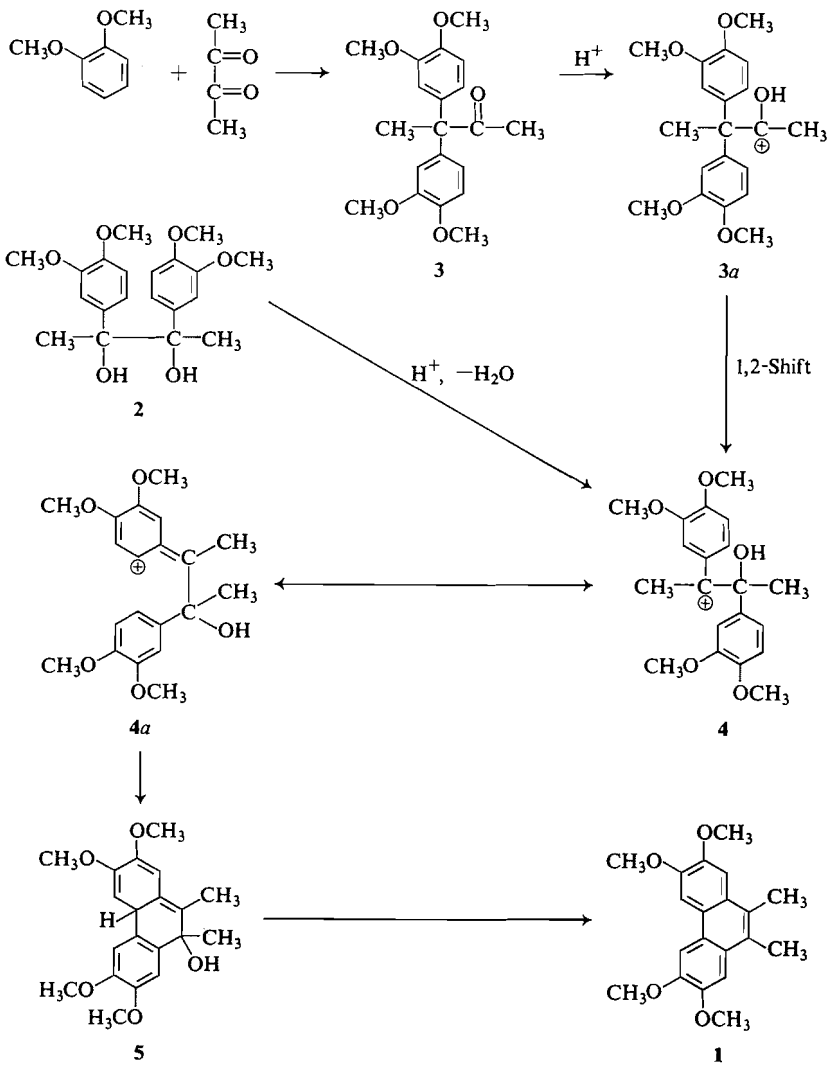

SCHEME 1

future, we wish to present some observations made, in the hope that they may be of interest for synthetic approaches to biologically active phenanthrene derivatives (*e.g.* the alkaloids of the tylophorine and cryptopleurine types).

The reaction of veratrole with biacetyl in 70% v/v aqueous sulfuric acid at room temperature to give the phenanthrene **1** has been reported by Manson and Musgrave (1), who suggested that the reaction proceeds through 2,3-bis-(3,4-dimethoxyphenyl)butane-2,3-diol (**2**), since this diol gave **1** in 75% v/v aqueous sulfuric acid. It was later claimed (2) that 3,3-bis-(3,4-dimethoxyphenyl)butane-2-one (**3**) was not converted to **1** in this medium.

Attempting to define the conditions for formation of **1** more clearly, we have monitored the reaction by t.l.c.[2] The results show that veratrole and biacetyl react very rapidly to give an intermediate which is slowly (2–4 days) converted to **1**.[3] By quenching the reaction with water within 20 min of mixing the reactants, and extracting with chloroform, the intermediate was isolated in 75% yield; m.p. 88.5–90 °C from methanol. Spectral data are completely consistent with 3,3-bis-(3,4-dimethoxyphenyl)butane-2-

[2]Silica gel, Merck, developed with 2% methanol in chloroform.

[3]The aqueous sulfuric acid was prepared by adding 700 ml of 97.9% sulfuric acid to 300 ml of water.

Can. J. Chem. Downloaded from www.nrcresearchpress.com by 210.87.254.6 on 09/05/12
For personal use only.

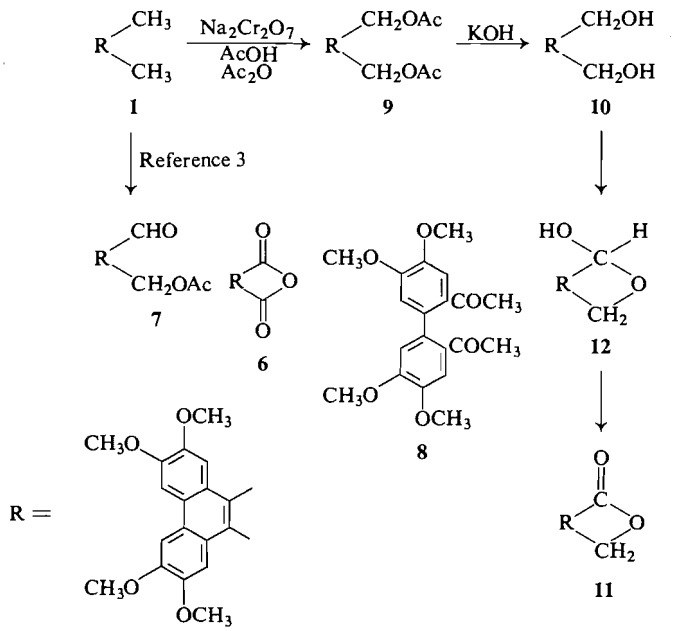

SCHEME 2

one (**3**) (2). Contrary to earlier results (2), this ketone was converted in 50% yield to **1** in aqueous sulfuric acid.

In view of the many possible equilibria involving the pinacol–pinacolone pair **2** and **3**, no definite statement about the actual reaction sequence leading to **1** can be made. However, the observed rapid appearance of **3**, and its further conversion to **2**, suggest the sequence shown in Scheme 1 as the most straightforward interpretation of the formation of **1**.

The oxidation of **1** has been examined by Edwards and Weiss (3), who obtained, depending upon conditions, the phenanthrene dicarboxanhydride **6**, the monoacetoxy aldehyde **7**, and the diacetyl-tetramethoxybiphenyl **8**. In extension of this work, we have now found that oxidation of **1** with $Na_2Cr_2O_7$ in Ac_2O–AcOH directly gives the diacetate **9** which had previously (3) been obtained on hydride reduction of **7**, followed by acetylation (see Scheme 2). Attempts to convert the parent diol **10** (3) to the dialdehyde with pyridine–CrO_3 were unsuccessful; the only product isolable was the phthalide **11** which was presumably formed through the hemiacetal **12**, a well-known side reaction in this type of oxidation (4). The structure of **11** rests on chemical and spectroscopic evidence. Compound **11**, $C_{20}H_{18}O_6$, does not form a dinitrophenylhydrazone; the i.r. absorption at 1735 cm^{-1} is indicative of an ester carbonyl rather than an aromatic aldehyde. The n.m.r. did not reveal any aldehydic protons and from its pattern, the compound is clearly not symmetrical (see Experimental). In view of this non-symmetrical structure, and of the versatile reactivity of phthalides in general, **11** may be a useful intermediate in the synthesis of a variety of polycyclic compounds.

Experimental

Melting points, determined on a Reichert hot-stage microscope, are uncorrected. The i.r. spectra were recorded in $CHCl_3$ on an Perkin–Elmer 257 instrument; u.v. spectra in absolute methanol or chloroform were recorded on a Cary 14 spectrophotometer; and n.m.r. spectra in deuteriochloroform or deuteriodimethyl sulfoxide on a Varian Associates A-60 instrument. Mass spectra were obtained on an L.K.B. 7000 mass spectrometer through the courtesy of Mr. W. E. Comstock.

3,3-Bis-(3,4-dimethoxyphenyl)butane-2-one (3)

To a stirred solution of veratrole (3.2 g, 23.2 mmol) in 40 ml 70% aqueous H_2SO_4, biacetyl (1 g, 11.6 mmol) was added dropwise. After 20 min the mixture was poured into water, (300 ml), and extracted with $CHCl_3$. The extracts were washed with water, dried ($MgSO_4$), and concentrated. The residue was crystallized from methanol to give **3** in 74% yield; m.p. 85–87° (lit. (2) 83.5–84.5°); ν_{max} 1725 cm^{-1} (ketone); δ ($CDCl_3$) 6.82 (multiplet, 6H),

Can. J. Chem. Downloaded from www.nrcresearchpress.com by 210.87.254.6 on 09/05/12
For personal use only.

aromatic protons, 3.90 (singlet, 6H), and 3.82 (singlet, 6H), OCH_3, 2.12 (singlet, 3H), CH_3—C=O, 1.86 (singlet, 3H), CH_3—C; λ_{max} (ethanol) 282 nm (log ε 3.80); mol. wt. 344 (mass spectrometry) (calcd. 344).

2,3,6,7-Tetramethoxy-9,10-dimethylphenanthrene (1)

(*a*) Compound **1** was prepared in 50% yield by the method of Manson and Musgrave (1); m.p. 226.5–227° (lit. (1) 222–223°).

(*b*) The intermediate **3** (1 g) was dissolved in 12 ml 70% H_2SO_4 and kept at room temperature for 4 days. The mixture was filtered, the solid dissolved in ethanol, treated with charcoal, and crystallized to give **1** in 50% yield; m.p. 226.5–227°. The m.p. was not depressed on admixture with a sample prepared by method *a*, and the i.r. spectra of the two samples were identical.

2,3,6,7-Tetramethoxy-9,10-diacetoxymethylphenanthrene (9)

A solution of $Na_2Cr_2O_7 \cdot 2H_2O$ (9.4 g, 31 mmol) in acetic acid (75 ml) was added dropwise over a period of 20 min to a refluxing solution of **1** (10 g, 31 mmol) in 150 ml acetic anhydride – acetic acid (1:1). The hot solution was poured into ice water (750 ml) and kept overnight. Crude **9** was obtained in 65% yield by filtration; m.p. 224–226°, after recrystallization from MeOH–$CHCl_3$; (lit. (3) 226–228°). This compound was spectroscopically identical with **9** prepared earlier in this laboratory.

Compound **10** was prepared by a saponification of **9** with KOH; m.p. 223–225° (lit. (3) 225–227°). Again this compound was identical with the **10** previously prepared.

2′,3′,6′,7′-Tetramethoxyphenanthro-[3,10-c]-(5H)-furan-2-one (11)

CrO_3 (6 g, 60 mmol) was slowly added to stirred pyridine (60 ml) cooled in an ice bath. After the addition was complete, a solution of **10** (3.58 g, 10 mmol) in pyridine (25 ml) was added. The mixture was stirred for 30 min and allowed to stand overnight. It was next poured into water (200 ml) and extracted with $CHCl_3$. The extracts were washed with 10% HCl, water, 10% $NaHCO_3$, and water, dried ($MgSO_4$), and evaporated. The residue was crystallized from $CHCl_3$ to give **11** in 63% yield; yellow crystals of m.p. 254–256°; ν 1735 cm^{-1} (phthalide C=O); δ (DMSO) 7.94, (1H), 7.43, (1H) 7.39, (1H), and 6.66 (1H), singlets, aromatic protons, 5.13 (singlet, 2H), benzylic protons, and 4.09, (3H), 4.06, (3H), 3.98 (3H), and 3.92 (3H), singlets, OCH_3; λ_{max} ($CHCl_3$) 372, 352, 333, 325 sh, 288 and 280 sh. nm (log ε 3.72, 3.74, 4.15, 4.09, 4.46, and 4.43).

Anal. Calcd. for $C_{20}H_{18}O_6$ (mol. wt. 354): C, 67.79; H, 5.12. Found (354 (mass spectrometry)): C, 67.68; H, 5.24.

1. D. L. Manson and O. C. Musgrave. J. Chem. Soc. 1011 (1963).
2. I. M. Davidson, O. C. Musgrave, and D. L. Manson. J. Chem. Soc. 3040 (1965).
3. J. M. Edwards and U. Weiss. Can. J. Chem. **48**, 1785 (1970).
4. H. O. House. Modern synthetic reactions. W. A. Benjamin, Inc., New York and Amsterdam, 1965. pp. 87.

Synthesis of (RS)-Abscisic Acid

J. A. Findlay and W. D. MacKay
Chemistry Department, University of New Brunswick, Fredericton, New Brunswick

Received February 18, 1971

New approaches to the abscisic acid synthetic precursor **4** and the abscisic acid analog **6** are reported.

On rapporte de nouvelles approches pouvant conduire au composé **4** et **6** qui sont respectivement un précurseur synthétique et un analogue de l'acide absicique.

Canadian Journal of Chemistry, **49**, 2369 (1971)

Syntheses of the plant hormone abscisic acid **1** have been reported previously (1–3). The three-step synthesis of Roberts *et al.* (3) involves the conversion of α-ionone into 1-hydroxy-4-keto-α-ionone (**4**) in 23–27% yield by the agency of *t*-butyl chromate. The compound **4** is subsequently converted into (RS)-abscisic acid and its *trans,trans* isomer in two steps by routine methods.

We have now prepared the key intermediate **4** from β-ionone in 43% yield, thus providing an alternate synthetic approach to (RS)-abscisic acid. Tungsten lamp irradiation of a carbon tetrachloride solution containing β-ionone and *N*-bromosuccinimide afforded 3,4-dehydro-β-ionone (**2**) in 91% yield (4). This material was oxidized with *m*-chloroperbenzoic acid to the known (5) epoxide **3** which was treated directly with Jones' reagent, yielding the crystalline abscisic acid precursor **4** (m.p. 109–112°) in 48% yield from **2**.

Can. J. Chem. Downloaded from www.nrcresearchpress.com by 210.87.254.6 on 09/05/12
For personal use only.

aromatic protons, 3.90 (singlet, 6H), and 3.82 (singlet, 6H), OCH_3, 2.12 (singlet, 3H), CH_3—C=O, 1.86 (singlet, 3H), CH_3—C; λ_{max} (ethanol) 282 nm (log ε 3.80); mol. wt. 344 (mass spectrometry) (calcd. 344).

2,3,6,7-Tetramethoxy-9,10-dimethylphenanthrene (1)

(*a*) Compound **1** was prepared in 50% yield by the method of Manson and Musgrave (1); m.p. 226.5–227° (lit. (1) 222–223°).

(*b*) The intermediate **3** (1 g) was dissolved in 12 ml 70% H_2SO_4 and kept at room temperature for 4 days. The mixture was filtered, the solid dissolved in ethanol, treated with charcoal, and crystallized to give **1** in 50% yield; m.p. 226.5–227°. The m.p. was not depressed on admixture with a sample prepared by method *a*, and the i.r. spectra of the two samples were identical.

2,3,6,7-Tetramethoxy-9,10-diacetoxymethylphenanthrene (9)

A solution of $Na_2Cr_2O_7 \cdot 2H_2O$ (9.4 g, 31 mmol) in acetic acid (75 ml) was added dropwise over a period of 20 min to a refluxing solution of **1** (10 g, 31 mmol) in 150 ml acetic anhydride – acetic acid (1:1). The hot solution was poured into ice water (750 ml) and kept overnight. Crude **9** was obtained in 65% yield by filtration; m.p. 224–226°, after recrystallization from MeOH–$CHCl_3$; (lit. (3) 226–228°). This compound was spectroscopically identical with **9** prepared earlier in this laboratory.

Compound **10** was prepared by a saponification of **9** with KOH; m.p. 223–225° (lit. (3) 225–227°). Again this compound was identical with the **10** previously prepared.

2′,3′,6′,7′-Tetramethoxyphenanthro-[3,10-c]-(5H)-furan-2-one (11)

CrO_3 (6 g, 60 mmol) was slowly added to stirred pyridine (60 ml) cooled in an ice bath. After the addition was complete, a solution of **10** (3.58 g, 10 mmol) in pyridine (25 ml) was added. The mixture was stirred for 30 min and allowed to stand overnight. It was next poured into water (200 ml) and extracted with $CHCl_3$. The extracts were washed with 10% HCl, water, 10% $NaHCO_3$, and water, dried ($MgSO_4$), and evaporated. The residue was crystallized from $CHCl_3$ to give **11** in 63% yield; yellow crystals of m.p. 254–256°; ν 1735 cm^{-1} (phthalide C=O); δ (DMSO) 7.94, (1H), 7.43, (1H) 7.39, (1H), and 6.66 (1H), singlets, aromatic protons, 5.13 (singlet, 2H), benzylic protons, and 4.09, (3H), 4.06, (3H), 3.98 (3H), and 3.92 (3H), singlets, OCH_3; λ_{max} ($CHCl_3$) 372, 352, 333, 325 sh, 288 and 280 sh. nm (log ε 3.72, 3.74, 4.15, 4.09, 4.46, and 4.43).

Anal. Calcd. for $C_{20}H_{18}O_6$ (mol. wt. 354): C, 67.79; H, 5.12. Found (354 (mass spectrometry)): C, 67.68; H, 5.24.

1. D. L. Manson and O. C. Musgrave. J. Chem. Soc. 1011 (1963).
2. I. M. Davidson, O. C. Musgrave, and D. L. Manson. J. Chem. Soc. 3040 (1965).
3. J. M. Edwards and U. Weiss. Can. J. Chem. **48**, 1785 (1970).
4. H. O. House. Modern synthetic reactions. W. A. Benjamin, Inc., New York and Amsterdam, 1965. pp. 87.

Synthesis of (RS)-Abscisic Acid

J. A. Findlay and W. D. MacKay
Chemistry Department, University of New Brunswick, Fredericton, New Brunswick

Received February 18, 1971

New approaches to the abscisic acid synthetic precursor **4** and the abscisic acid analog **6** are reported.

On rapporte de nouvelles approches pouvant conduire au composé **4** et **6** qui sont respectivement un précurseur synthétique et un analogue de l'acide absicique.

Canadian Journal of Chemistry, **49**, 2369 (1971)

Syntheses of the plant hormone abscisic acid **1** have been reported previously (1–3). The three-step synthesis of Roberts *et al.* (3) involves the conversion of α-ionone into 1-hydroxy-4-keto-α-ionone (**4**) in 23–27% yield by the agency of *t*-butyl chromate. The compound **4** is subsequently converted into (RS)-abscisic acid and its *trans,trans* isomer in two steps by routine methods.

We have now prepared the key intermediate **4** from β-ionone in 43% yield, thus providing an alternate synthetic approach to (RS)-abscisic acid. Tungsten lamp irradiation of a carbon tetrachloride solution containing β-ionone and *N*-bromosuccinimide afforded 3,4-dehydro-β-ionone (**2**) in 91% yield (4). This material was oxidized with *m*-chloroperbenzoic acid to the known (5) epoxide **3** which was treated directly with Jones' reagent, yielding the crystalline abscisic acid precursor **4** (m.p. 109–112°) in 48% yield from **2**.

Can. J. Chem. Downloaded from www.nrcresearchpress.com by 210.87.254.105 on 09/05/12
For personal use only.

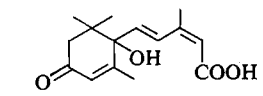
1

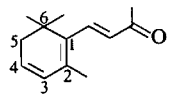
2

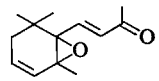
3

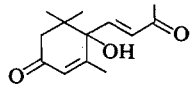
4

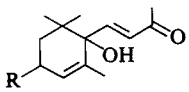
5 R = H
5*a* R = OH

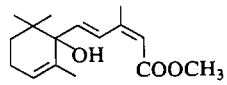
6

The spectral and physical characteristics of **4** were in agreement with the reported data (3).

The location of the oxide bridge in **3** was readily ascertained from its n.m.r. spectrum which shows no signal corresponding to a vinylic methyl group but an appropriate sharp singlet at τ 8.72 assigned to the C-2 methyl. The vinylic protons of the side chain display a simple AB pattern, hence the ether linkage must span C-1 and -2. The oxidation of **3** to **4** probably proceeds via the intermediate **5***a*, a hydration product of the epoxide **3**.

The racemic ester **6**, made via **5** by Tamura and Nagao (6), was found to be a biologically potent analog of abscisic acid. In preparing the synthetic precursor **5** these authors employed the two-step procedure of Roberts (2) which gives it in less than 5% yield from β-ionone. We have recently prepared the key intermediate 1-hydroxy-α-ionone (m.p. 89–90°) in 31% yield by direct oxidation of α-ionone with selenium dioxide in refluxing ethanol. The mass spectrum of this product displays a prominent molecular ion (*m/e* 208) corresponding to $C_{13}H_{20}O_8$ and appropriate hydroxylic absorption (3600, 3450 cm^{-1}) in the i.r. Its n.m.r. spectrum confirms formulation **5** by displaying a simple AB pattern for the signals of the vinyl protons of the side chain and a doublet for the C-2 vinylic methyl group, completely parallel with features of the n.m.r. spectrum of **4**. Hence the tertiary hydroxyl group is located at C-1.

Experimental

The i.r. spectra were recorded on a Perkin–Elmer model 237B spectrophotometer. The mass spectra were determined with an Hitachi Perkin–Elmer model RMU-6D spectrometer. The n.m.r. were recorded with a Varian T-60 instrument and using tetramethylsilane as internal standard. A Kofler hot stage apparatus was employed to determine melting points which are uncorrected. All compounds described proved homogeneous on a variety of t.l.c. systems and their n.m.r. spectra showed them to be devoid of detectable amounts of impurities.

3,4-Dehydro-β-ionone (2)

A refluxing solution of β-ionone (1.92 g) and *N*-bromosuccinimide (2.30 g) in dry carbon tetrachloride (100 ml) contained in a Pyrex vessel was irradiated with a tungsten lamp (100 W) for 30 min. After cooling to room temperature and filtering, anhydrous sodium carbonate (2.5 g) and dimethylformamide (25 ml) were added and the bulk of the carbon tetrachloride was distilled off. The mixture was cooled to room temperature, diluted with ether (200 ml), filtered, washed with 5% aqueous HCl (2 × 50 ml), washed with a dilute solution of sodium chloride, dried ($MgSO_4$), and evaporated yielding a brown liquid (2.9 g) which was chromatographed on a silica gel column giving 3,4-dehydro-β-ionone (1.73 g, 91%) as a yellow liquid; ν_{max} ($CHCl_3$) 1665, 1660 cm^{-1}; λ_{max} (EtOH) 226 (ε, 8500), 233 (ε, 6800); τ ($CDCl_3$) 2.66 (1H, broad d, *J* 16 Hz), 3.80 (1H, d, *J* 16 Hz), 6.12 (2H, m), 7.68 (3H, s), 7.88 (2H, m), 8.08 (3H, s), 8.90 (6H, s); M (mass spectrometry) 190.

3,4-Dehydro-1,2-epoxy-β-ionone (3)

A solution of 3,4-dehydro-β-ionone (**2**) (1.7 g) and *m*-chloroperbenzoic acid (2.0 g) in anhydrous ether (35 ml) was stirred at room temperature for 5 h. Excess acid was decomposed with sodium bisulfite solution (10%) and the mixture diluted to 100 ml with ether, washed with 5% aqueous sodium bicarbonate (2 × 20 ml), washed with saturated sodium chloride solution (2 × 20 ml), dried ($MgSO_4$), filtered, and evaporated yielding the crude 3,4-dehydro-1,2-epoxy-β-ionone (**3**) (1.78 g) which was used without further purification to prepare **4**. A sample of compound **3** was chromatographed on silica gel for spectral characterization; ν_{max} ($CHCl_3$) 1680, 1640 cm^{-1}; λ_{max} 242 (ε, 7700); τ ($CDCl_3$) 2.88 (1H, d, *J* 16 Hz), 3.68 (1H, d, *J* 16 Hz), 4.18 (2H, m), 7.69 (3H, s), 7.8–8.5 (2H, m), 8.72 (3H, s), 8.87 (3H, s), 8.97 (3H, s); M (mass spectrometry) 206.

1-Hydroxy-4-keto-α-ionone (4)

The crude epoxide **3** (1.78 g) prepared as above, was dissolved in 95% aqueous acetone (35 ml) and cooled to 0°. Jones' reagent was added dropwise until an orange color persisted and the mixture was allowed to come to room temperature slowly and was stirred overnight. The bulk of the acetone was evaporated, water (100 ml) was added and the mixture extracted with ether (4 × 20 ml). The ether layer was dried ($MgSO_4$) and evaporated yielding a light orange oil (1.59 g) which was chromatographed on a silica gel column using benzene as eluant yielding white crystalline 1-hydroxy-4-keto-α-ionone (**4**), m.p. 109–112° (lit. 112–113°) (0.961 g, 48% from **2**); ν_{max} ($CHCl_3$) 3560 (broad), 1670, 1620 cm^{-1}; ν_{max} (KBr) 3509, 1661, 1629, 1429, 1366, 1292, 1266, 1178, 1122, 1025, 994, 978, 918, 883 cm^{-1}; λ_{max} 237 (ε, 13 500); τ ($CDCl_3$) 3.08 (1H, d, *J* 16 Hz), 3.53 (1H, d, *J* 16 Hz), 4.02 (1H, s, broad), 7.25 (s, broad, exchanges with D_2O), 7.58 (2H, s, broad), 7.64 (3H, s), 8.08 (3H, d, *J* 2 Hz), 8.86 (3H, s), 8.95 (3H, s); M (mass spectrometry) 222.

Anal. Calcd. for $C_{13}H_{18}O_3$: C, 70.24; H, 8.16. Found: C, 70.38; H, 8.21.

Can. J. Chem. Downloaded from www.nrcresearchpress.com by 210.87.254.105 on 09/05/12
For personal use only.

1-Hydroxy-α-ionone (5)

Selenium dioxide (1.11 g) in 95% ethanol (400 ml) was added dropwise over 5 h to a refluxing solution of α-ionone (2.5 g) in 95% ethanol (100 ml). After allowing the mixture to reflux for a further 16 h, it was filtered and evaporated yielding a dark brown oil (3.4 g) which was chromatographed on silica gel using ether/petroleum ether (1:1) as eluant. A light brown oil (1.64 g) was thus obtained which after two recrystallizations from petroleum ether furnished pure 1-hydroxy-α-ionone (**5**) (0.65 g, 31%), m.p. 89–90° (lit. 82–83°); ν_{max} ($CHCl_3$) 3600, 3450, 1675, 1625 cm^{-1}; τ ($CDCl_3$) 3.13 (1H, d, *J* 16 Hz), 3.67 (1H, d, *J* 16 Hz), 4.43 (1H, broad), 7.70 (3H, s), 7.98 (2H, m), 8.40 (3H, d, *J* 2 Hz) superimposed on 8.45 (2H, m), 9.00 (3H, s), 9.33 (3H, s); M (mass spectrometry) 208.

This work was supported, in part, by a grant from the National Research Council of Canada.

1. J. W. Cornforth, B. V. Hilborrow, and G. Ryback. Nature **206**, 715 (1965). M. Mousseron-Canet, J. C. Mani, J. P. Dalle, and J. L. Olive. Bull. Soc. Chim. Fr. 3874 (1966). J. W. Cornforth, W. Draber, B. V. Hilborrow, and G. Ryback. Chem. Commun. 114 (1967).
2. D. L. Roberts. U.S. Patent, 3 400 158 (1968). (C.A. **69** 9085, (1968)).
3. D. L. Roberts, R. A. Heckman, Bonita P. Hege, and Stuart A. Bellin. J. Org. Chem. **33**, 3566 (1968).
4. H. B. Henbest. Nature, **161**, 481 (1948). G. Buchi, K. Seitz, and O. Jeger. Helv. Chim. Acta, **32**, 39 (1949).
5. T. Oritani and K. Yamashita. Agr. Biol. Chem. **34**, 1821 (1970).
6. S. Tamura and M. Nagao. Agr. Biol. Chem. **33**, 1357 (1969).

Reaction of Trialkylboranes with Cyclic α-Diazo Ketones. A New Synthesis of α-Alkyl Cycloalkanones

John Hooz, Donald M. Gunn,[1] and Hiromichi Kono[2]

Department of Chemistry, University of Alberta, Edmonton, Alberta

Received March 9, 1971

An efficient procedure has been developed for the alkylation of cyclic ketones, based on the reaction of trialkylboranes with cyclic α-diazo ketones. The reaction proceeds under mild conditions, affords high yields of α-alkylated cycloalkanones, and circumvents certain difficulties inherent in previous alkylation methods.

On a développé une procédure efficace pour alkyler des cétones cycliques; cette méthode fait appel à la réaction de trialkylboranes avec des α-diazocétones cycliques. La réaction se fait dans des conditions douces et conduit à des rendements élevés de cycloalcanones α-alkylées et permet d'éviter certaines difficultés inhérentes aux méthodes d'alkylation précédentes.

Canadian Journal of Chemistry, **49**, 2371 (1971)

Two general schemes have previously been designed to offset the traditional problems (polyalkylation, self-condensation) encountered in typical base-catalyzed ketone alkylation procedures, involving prior modification of the α-methylene group: (*i*) activation (path *a*, A = activating group, eq. 1), and (*ii*) the use of blocking groups (path *b*, B = blocking group, eq. 1) the latter being employed particularly for alkylation at angular positions. However, either former approach necessitates the discrete removal (occasionally requiring several independent steps) of the activating/protecting group, and the pursuant problems frequently lead to but modest yields of the desired alkylate (1).

It was previously observed that trialkylboranes react with a variety of functional diazo compounds to provide numerous synthetically useful derivatives (aldehydes (2), ketones (3, 4), diketones (5), nitriles (6), esters (6)). Moreover, these transformations usually occurred in high yields and under mild conditions, and of special consideration is the fact that the homologated functionalized organoborane intermediate[3]

[1]University of Alberta Postdoctoral Research Fellow, 1967–1969.

[2]University of Alberta Postdoctoral Research Fellow, 1969–Present.

[3]The initial suggestions regarding mechanism (3) have been of considerable value for exploratory synthetic studies. Subsequent work (2, 4) has suggested the intermediacy of enol borinates, and this additional subtlety is in accord with the recent isolation of vinyloxyboranes (7). However, the presence of transient B—C bonded species cannot at present be rigorously eliminated.

Can. J. Chem. Downloaded from www.nrcresearchpress.com by 210.87.254.105 on 09/05/12
For personal use only.

1-Hydroxy-α-ionone (5)

Selenium dioxide (1.11 g) in 95% ethanol (400 ml) was added dropwise over 5 h to a refluxing solution of α-ionone (2.5 g) in 95% ethanol (100 ml). After allowing the mixture to reflux for a further 16 h, it was filtered and evaporated yielding a dark brown oil (3.4 g) which was chromatographed on silica gel using ether/petroleum ether (1:1) as eluant. A light brown oil (1.64 g) was thus obtained which after two recrystallizations from petroleum ether furnished pure 1-hydroxy-α-ionone (**5**) (0.65 g, 31%), m.p. 89–90° (lit. 82–83°); ν_{max} ($CHCl_3$) 3600, 3450, 1675, 1625 cm^{-1}; τ ($CDCl_3$) 3.13 (1H, d, *J* 16 Hz), 3.67 (1H, d, *J* 16 Hz), 4.43 (1H, broad), 7.70 (3H, s), 7.98 (2H, m), 8.40 (3H, d, *J* 2 Hz) superimposed on 8.45 (2H, m), 9.00 (3H, s), 9.33 (3H, s); M (mass spectrometry) 208.

This work was supported, in part, by a grant from the National Research Council of Canada.

1. J. W. Cornforth, B. V. Hilborrow, and G. Ryback. Nature **206**, 715 (1965). M. Mousseron-Canet, J. C. Mani, J. P. Dalle, and J. L. Olive. Bull. Soc. Chim. Fr. 3874 (1966). J. W. Cornforth, W. Draber, B. V. Hilborrow, and G. Ryback. Chem. Commun. 114 (1967).
2. D. L. Roberts. U.S. Patent, 3 400 158 (1968). (C.A. **69** 9085, (1968)).
3. D. L. Roberts, R. A. Heckman, Bonita P. Hege, and Stuart A. Bellin. J. Org. Chem. **33**, 3566 (1968).
4. H. B. Henbest. Nature, **161**, 481 (1948). G. Buchi, K. Seitz, and O. Jeger. Helv. Chim. Acta, **32**, 39 (1949).
5. T. Oritani and K. Yamashita. Agr. Biol. Chem. **34**, 1821 (1970).
6. S. Tamura and M. Nagao. Agr. Biol. Chem. **33**, 1357 (1969).

Reaction of Trialkylboranes with Cyclic α-Diazo Ketones. A New Synthesis of α-Alkyl Cycloalkanones

John Hooz, Donald M. Gunn,[1] and Hiromichi Kono[2]

Department of Chemistry, University of Alberta, Edmonton, Alberta

Received March 9, 1971

An efficient procedure has been developed for the alkylation of cyclic ketones, based on the reaction of trialkylboranes with cyclic α-diazo ketones. The reaction proceeds under mild conditions, affords high yields of α-alkylated cycloalkanones, and circumvents certain difficulties inherent in previous alkylation methods.

On a développé une procédure efficace pour alkyler des cétones cycliques; cette méthode fait appel à la réaction de trialkylboranes avec des α-diazocétones cycliques. La réaction se fait dans des conditions douces et conduit à des rendements élevés de cycloalcanones α-alkylées et permet d'éviter certaines difficultés inhérentes aux méthodes d'alkylation précédentes.

Canadian Journal of Chemistry, **49**, 2371 (1971)

Two general schemes have previously been designed to offset the traditional problems (polyalkylation, self-condensation) encountered in typical base-catalyzed ketone alkylation procedures, involving prior modification of the α-methylene group: (*i*) activation (path *a*, A = activating group, eq. 1), and (*ii*) the use of blocking groups (path *b*, B = blocking group, eq. 1) the latter being employed particularly for alkylation at angular positions. However, either former approach necessitates the discrete removal (occasionally requiring several independent steps) of the activating/protecting group, and the pursuant problems frequently lead to but modest yields of the desired alkylate (1).

It was previously observed that trialkylboranes react with a variety of functional diazo compounds to provide numerous synthetically useful derivatives (aldehydes (2), ketones (3, 4), diketones (5), nitriles (6), esters (6)). Moreover, these transformations usually occurred in high yields and under mild conditions, and of special consideration is the fact that the homologated functionalized organoborane intermediate[3]

[1]University of Alberta Postdoctoral Research Fellow, 1967–1969.

[2]University of Alberta Postdoctoral Research Fellow, 1969–Present.

[3]The initial suggestions regarding mechanism (3) have been of considerable value for exploratory synthetic studies. Subsequent work (2, 4) has suggested the intermediacy of enol borinates, and this additional subtlety is in accord with the recent isolation of vinyloxyboranes (7). However, the presence of transient B—C bonded species cannot at present be rigorously eliminated.

Can. J. Chem. Downloaded from www.nrcresearchpress.com by 210.87.254.105 on 09/05/12
For personal use only.

[1] 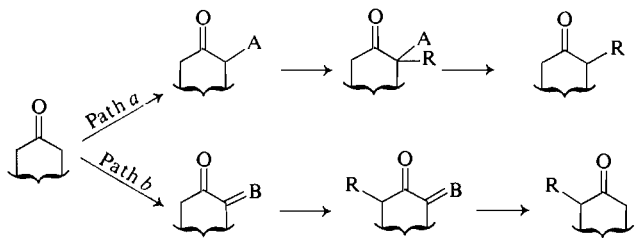

underwent rapid *in situ* hydrolysis when the reaction was conducted in the presence of water (2, 4, 6).

Since such processes may be regarded as conceptually analogous[4] to the previous "activating- or blocking-group approach" toward constructing 2-alkylcycloalkanones (eq. 1), it was of interest to explore some reactions of representative cyclic α-diazo ketones with trialkylboranes (eq. 2) in the hope that this method could circumvent the aforementioned difficulties.

[2] 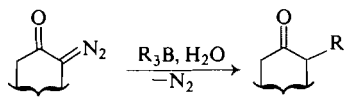

In the event, we employed (for convenience) triethylborane[5] as alkylating agent and observed that in the presence of water, a variety of cyclic α-diazo ketones reacted with smooth evolution of nitrogen to furnish excellent yields (82–100%) of the corresponding 2-ethylcycloalkanones.

Equations 3–9 summarize the scope and yields[6] of the transformations accomplished using triethylborane; in a single experiment 2-diazocyclohexanone was alkylated with tripentylborane and provided a 96% yield of 2-*n*-pentylcyclohexanone. In all instances the products were analyzed by g.l.p.c., isolated, and characterized by i.r., p.m.r., and mass spectroscopy, and (in the case of new products), corroborative combustion analyses.

Since neither the organoborane nor diazo substrate react with water appreciably under the experimental conditions, the reactions are conveniently performed by adding water to a solution of the organoborane in tetrahydrofuran at *ca.* 25°; subsequent addition of the diazo ketone results in smooth liberation of nitrogen and the concurrent alkylation, *in situ* hydrolysis

[3] 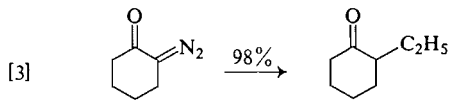

[4] 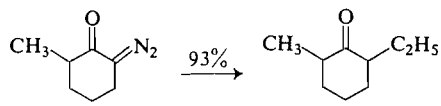

[5] 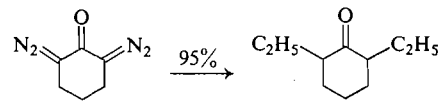

[6] 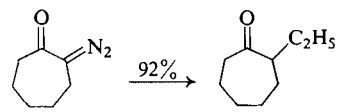

[7] 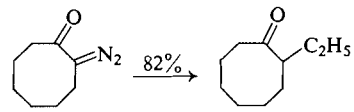

[8] 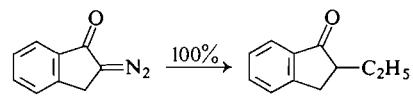

[9] 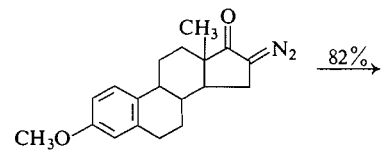

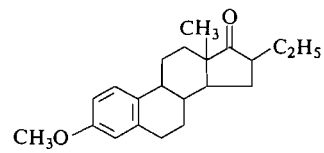

[4]The diazo function serves the interesting dual purpose (in terms of previous methodology) of acting as both an activating group (eq. 1, path *a*, A = N_2), as well as a blocking group (eq. 1, path *b*, B = N_2).

[5]Obtained from Alfa Inorganics Inc.

[6]By g.l.p.c. analysis. Yields of isolated product (with no special attention to avoid handling losses) were *ca.* 15–20% lower.

Can. J. Chem. Downloaded from www.nrcresearchpress.com by 210.87.254.105 on 09/05/12
For personal use only.

Can. J. Chem. Downloaded from www.nrcresearchpress.com by 210.87.254.105 on 09/05/12
For personal use only.

of the functionalized organoboron intermediate. The results for a variety of structural types (eqs. 3–9) indicate the method to be general for ring sizes 5 through 8. Interestingly, this procedure may also be employed for the concurrent α,α′-dialkylation of *bis*-diazo ketones, as exemplified by the high yield of 2,6-diethylcyclohexanone (eq. 5). However, it is to be anticipated that concurrent dialkylations are of preparative value for the exclusive introduction of two identical alkyl groups (9).

There has been considerable effort devoted to devising and improving synthetic routes to cyclic α-diazo ketones (8). The present development illustrates that in instances where the diazo substrate is readily accessible, this method provides a useful and unique, high-yield abridgment of prior approaches (1) by obviating the necessity of multi-step, yield-lowering removal of activating/protecting groups. Owing to the structural stringencies imposed on the requisite diazo ketone, however, this process is obviously intrinsically inapplicable to angular alkylations.

Experimental

General Considerations

All boiling points and melting points are uncorrected. Microanalyses were performed by the Microanalytical Laboratory, Department of Chemistry, University of Alberta, Edmonton, Alberta. Mass spectra were measured by Dr. A. M. Hogg and his associates using an A.E.I. MS-9 spectrometer at an ionization potential of 70 eV; n.m.r. spectra were recorded on a Varian A-60 spectrometer using TMS as internal standard and $CDCl_3$ as solvent.

In all cases the molar ratio of diazo ketone:trialkylborane:water was 1:1.5:10, although it was not established that this stoichiometry is optimal. In cases where products were isolated, the yields (based on diazo ketone) were *ca.* 15–20% lower than the quoted g.l.p.c. yields; since no special precautions were observed to minimize handling losses, however, this yield could doubtless be improved. The stereochemistry of the products derived from eqs. 4, 5, and 9 were not established.

The procedure described in detail for the preparation of 2-ethyl-1-indanone (eq. 8) is representative, except that the reactions with 2-diazocyclooctanone and 16-diazoestrone methyl ether require a brief reflux period before nitrogen evolution ceases.

2-Ethyl-1-indanone

In a 100-ml three-necked flask fitted with a dropping funnel, a thermometer, a reflux condenser connected to an azotometer, and a magnetic stirring bar, were placed triethylborane[5] (30 mmol), 20 ml of tetrahydrofuran, and water (200 mmol). To this stirred mixture was added (2 h) a solution of 2-diazo-1-indanone (19.5 mmol) (8*a*) in 30 ml THF at 27°. After stirring an additional hour at 27° nitrogen evolution was quantitative. At this stage g.l.p.c. analysis indicated a 100% yield of 2-ethyl-1-indanone. The mixture was treated with 15 ml of 3 *N* sodium acetate solution and 15 ml of 30% hydrogen peroxide, maintaining the temperature below 60°. The organic layer was poured into water and extracted with ether (three 30-ml portions). The yellow oil which remained after removal of solvent from the combined, dried (Na_2SO_4) extracts was distilled to afford 2-ethyl-1-indanone (78%), b.p. 65.5–67.0° (0.05 mm); n_D^{25} 1.5449; i.r. (liquid film) 1714 cm^{-1}; n.m.r. ($CDCl_3$) 2.58 (4H, multiplet, aromatic protons), 6.97 (2H, multiplet, benzylic protons), 7.48 (1H, multiplet, methine), 8.30 (2H, multiplet, methylene), 9.03 τ (3H, triplet methyl); mass spectrum (70 eV) M^+ 160.0886 (calcd. 160.0888).

Anal. Calcd. for $C_{10}H_{20}O$: C, 82.46; H, 7.55. Found: C, 82.66; H, 7.67.

Other new compounds prepared in this study were:

2-Ethylcycloheptanone, n_D^{25} 1.4610; mass spectrum (70 eV), M^+ 140.1194 (calcd. 140.1201).

Anal. Calcd.: C, 77.09; H, 11.50. Found: C, 77.07; H, 11.80.

2-Ethylcyclooctanone, b.p. 56–57° (0.4 mm); n_D^{25} 1.4615; mass spectrum (70 eV), M^+ 154.1358 (calcd. 154.1358).

Anal. Calcd.: C, 77.89; H, 11.76. Found: C, 77.99; H, 11.63.

16-Ethyldiazoestrone methyl ether, m.p. 77–78°; mass spectrum (70 eV), M^+ 313.2121 (calcd. 313.2127).

Anal. Calcd.: C, 80.73; H, 9.04. Found: C, 80.94; H, 9.44.

We wish to thank the National Research Council of Canada for financial support of this work, and the University of Alberta for the award of Postdoctoral Fellowships (D.M.G. and H.K.).

1. H. O. House. Modern synthetic reactions. W. A. Benjamin, Inc., New York, N.Y., 1965. Chapt. 7, provides a summary of this problem.
2. J. Hooz and G. F. Morrison. Can. J. Chem. **48**, 868 (1970).
3. J. Hooz and S. Linke. J. Am. Chem. Soc. **90**, 5936 (1968).
4. J. Hooz and D. M. Gunn. J. Am. Chem. Soc. **91**, 6195 (1969).
5. J. Hooz and D. M. Gunn. Chem. Commun. 139 (1969).
6. J. Hooz and S. Linke. J. Am. Chem. Soc. **90**, 6891, (1968).
7. D. J. Pasto and P. W. Wojtkowski. Tetrahedron Lett. 215 (1970).
8. (*a*) M. P. Cava, R. L. Litle, and D. R. Napier. J. Am. Chem. Soc. **80**, 2257 (1958); (*b*) M. P. Cava and E. Moroz. J. Am. Chem. Soc. **84**, 115 (1962); (*c*) J. Meinwald, G. G. Curtis, and P. G. Gassman. J. Am. Chem. Soc. **84**, 116 (1962); (*d*) M. Rosenberger, P. Yates, J. B. Hendrickson, and W. Wolf. Tetrahedron Lett. 2285 (1964); (*e*) R. Tasovac, M. Stefanovic, and A. Stojiljkovic. Tetrahedron Lett. 2729 (1967).
9. J. Hooz and D. M. Gunn. Chem. Commun. 139 (1969).

Can. J. Chem. Downloaded from www.nrcresearchpress.com by 210.87.254.6 on 09/05/12
For personal use only.

Cyclic Alkoxyoxosulfonium Ions in the Chlorination of Hydroxy Sulfoxides

T. DURST AND K.-C. TIN

Department of Chemistry, University of Ottawa, Ottawa 2, Canada

Received March 5, 1971

Chlorination of β-, γ-, and δ-hydroxy sulfoxides with SO_2Cl_2 in CH_2Cl_2 at −78° resulted in the formation of the corresponding β-, γ-, and δ-chloro sulfones. Stereochemical evidence is presented that cyclic alkoxyoxosulfonium salts (*O*-alkylated sulfones) are intermediates in these transformations.

La chloration des β-, γ-, et δ-hydroxy sulfoxydes avec SO_2Cl_2 dans CH_2Cl_2 a −78° conduit aux β-, γ-, et δ-chloro sulfones correspondantes. Des preuves stéréochimiques permettent de montrer que des sels d'alcoxyoxosulfonium cycliques (sulfones *O*-alcoylées) sont des intermédiaires dans ces réactions.

Canadian Journal of Chemistry, 49, 2374 (1971)

Recently we reported the α-chlorination of sulfoxides with sulfuryl chloride in CH_2Cl_2 at −78 or 0° (1). In addition to α-chloro sulfoxides we generally observed the formation of sulfones as by-product. We now propose Scheme 1 to explain the formation of both types of products and present evidence supporting various intermediates.

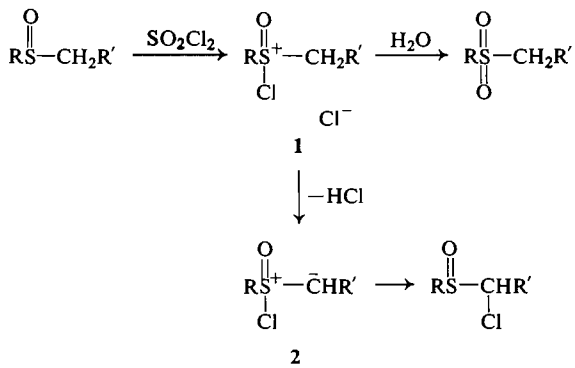

SCHEME 1

Chlorination of sulfoxides could occur either at carbon or at sulfur (2, 3), the latter pathway leading to chloro-oxosulfonium ions, *e.g.* **1**. α-Chloro sulfoxides can be obtained from **1** via the ylid **2** (3) either by a concerted rearrangement (3) or by an elimination–addition sequence.[1] Displacement of chloride from **1** by H_2O results, after proton transfer, in sulfone formation. In agreement with this, the presence of water in the reaction mixture greatly increased the ratio of sulfone to α-chloro sulfoxide.

In order to obtain further evidence regarding **1** and to examine some of its chemistry we have carried out the chlorination of a number of sulfoxides bearing hydroxyl functions β, γ, or δ to the sulfoxide grouping. In all of these reactions we obtained, in high yield, products in which the sulfur had been oxidized from sulfoxide to sulfone and the remote hydroxyl group replaced by chlorine; the production of α-chlorosulfoxide was completely suppressed. The formation of the chloro sulfones **6** is rationalized as involving intramolecular displacement of chloride ion from **4**, forming cyclic alkoxyoxosulfonium ions (oxygen-alkylated sulfones), *e.g.* **5**, followed by ring cleavage, Scheme 2. Bromination of **3** ($n = 2$) in the presence of pyridine (required) gave the bromo sulfone **7** and the pyridinium salt **8**,[2] both of which are readily explained as the products of the ring opening

[1]The rearrangement **1** to α-chloro sulfoxides can be considered analogous to Pummerer-type rearrangement, T. Durst, ref. 4.

[2]All new compounds had the expected spectroscopic properties (i.r. and n.m.r.) and satisfactory analysis.

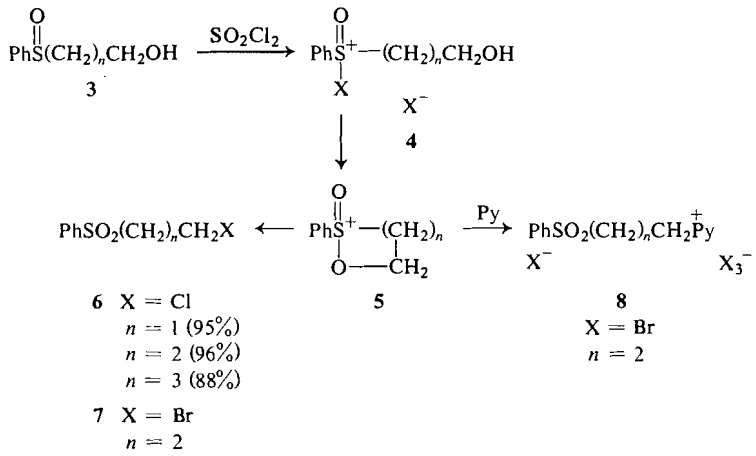

3

4

6 X = Cl
n = 1 (95%)
n = 2 (96%)
n = 3 (88%)

7 X = Br
n = 2

5

8
X = Br
n = 2

SCHEME 2

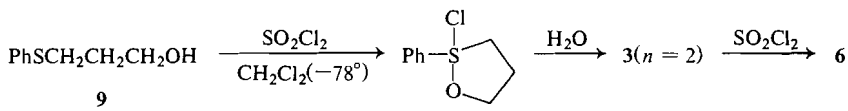

9

10

SCHEME 3

of **5** ($n = 2$) by bromide ion and pyridine respectively.

Alkoxyoxosulfonium derivatives such as **5** have previously not been considered as potential intermediates in the oxidation of sulfoxides to sulfones. The closely related aryloxosulfonium salts have recently been isolated from the thermal decomposition of aryldiazonium salts in the presence of sulfones (5). Other species which have a structural similarity to **5** are the (dialkylamino)oxosulfonium salts (6) and, more distantly, the trialkyloxosulfonium salts (2, 7).

Chlorination of hydroxy sulfides, *e.g.* **9** at −78°, in contrast to the hydroxy sulfoxides, gave an intermediate formulated as **10** (8) which is stable enough to be observed by n.m.r. at room temperature. Addition of water resulted in hydrolysis and formation of the hydroxy sulfoxide **3** ($n = 2$). With 2 equiv of sulfuryl chloride, **9** is converted to the chloro sulfone **6** ($n = 2$), presumably via **10** and **3** ($n = 2$), Scheme 3.

Stereochemical evidence supporting the intermediacy of species such as **5** was provided from a study of the sulfoxides **11** and **14** (Scheme 4). Chlorination of **11**, prepared from cyclohexene oxide and $PhS(O)CH_2Li$, proceeded rapidly in CH_2Cl_2 at −78° and gave the chloro sulfone **13** in 77% yield. The *cis* stereochemistry in **13** was established by n.m.r. The hydrogen on carbon bearing chlorine which occurred at $\delta = 4.53$ with a width at half-height of less than 7 Hz is consistent with the equatorial assignment in **13**. The formation of the *cis*-sulfone **13** from the *trans*-hydroxy sulfoxide **11** requires inversion at the carbon initially bearing the hydroxyl group, in agreement with the intermediacy of the alkoxyoxosulfonium ion **12**. In contrast, chlorination of the *trans*-hydroxy sulfoxide **14** gave a complex mixture containing at least five components which we have not been able to separate. The n.m.r. inspection of the total mixture indicated the absence of significant amounts of the chloro sulfone **16**. The failure to obtain **16** is not unexpected since its formation requires the intermediacy of **15** which contains the highly strained 6,4-*trans* fused ring system.

Extension of these results to systems involving

Can. J. Chem. Downloaded from www.nrcresearchpress.com by 210.87.254.6 on 09/05/12
For personal use only.

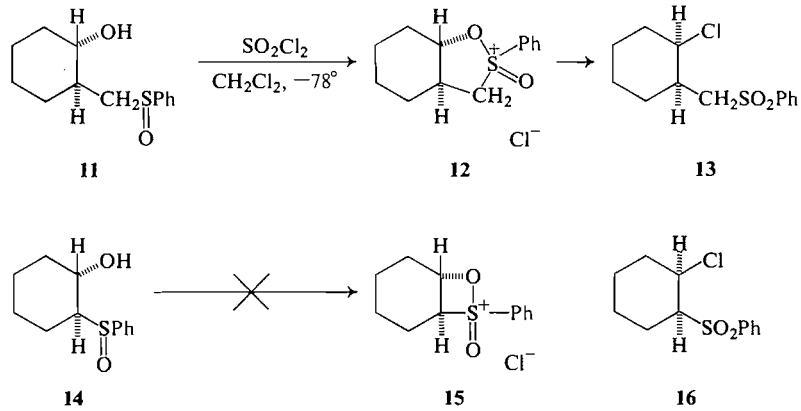

SCHEME 4

the interaction of other functional groups such as acids, amides, amines, *etc.* with chlorooxosulfonium ions is in progress.

Financial support by the National Research Council of Canada is gratefully acknowledged.

1. K.-C. TIN and T. DURST. Tetrahedron Lett. 4643 (1970).
2. In analogy with the alkylation of sulfoxides. *c.f.* S. G. SMITH and S. WINSTEIN. Tetrahedron, **3**, 317 (1958).
3. M. CINQUINI, S. COLONNA, and F. MONTANARI. Chem. Commun. 1442 (1970), and references therein.
4. T. DURST. *In* Advances in organic chemistry. Vol. 6. E. C. Taylor and H. Wynberg, *editors*. J. Wiley and Sons, Inc., New York, N.Y. 1969. pp. 356–365.
5. G. R. CHALKLEY, D. J. SNODIN, G. STEVENS, and M. C. WHITING. J. Chem. Soc. C, 682 (1970).
6. C. R. JOHNSON, M. HAAKE, and C. W. SCHROEK. J. Am. Chem. Soc. **92**, 6594 (1970).
7. Reference 4. pp. 318–320.
8. C. R. JOHNSON and J. J. RIGAU. J. Am. Chem. Soc. **91**, 5398 (1969).

Erratum: Biosynthesis of Lobinaline

R. N. GUPTA AND IAN D. SPENSER
Department of Chemistry, McMaster University, Hamilton, Ontario

Received April 26, 1971

(Ref. Can. J. Chem. **49**, 384 (1971))

Canadian Journal of Chemistry, **49**, 2376 (1971)

The editors regret that an unfortunate error was introduced into the dedication (footnote 1) of this article during editing. The correct version of footnote 1 is as follows. "This paper is dedicated to Professor Kurt Mothes, Director Emeritus of the Institute of Plant Biochemistry, German Academy of Sciences, Halle, D.D.R., on the occasion of his 70th birthday."

Can. J. Chem. Downloaded from www.nrcresearchpress.com by 210.87.254.6 on 09/05/12
For personal use only.

Can. J. Chem. Downloaded from www.nrcresearchpress.com by 210.87.254.5 on 09/05/12
For personal use only.

Canadian Journal of Chemistry

Published by THE NATIONAL RESEARCH COUNCIL OF CANADA

VOLUME 49 JULY 15, 1971 NUMBER 14

Structure and Nuclear Magnetic Resonance Spectrum of *N*-Nitrosocamphidine

J. W. APSIMON AND J. D. COONEY[1]

Department of Chemistry, Carleton University, Ottawa, Canada

Received March 11, 1971

The 220 MHz n.m.r. spectrum of *N*-nitrosocamphidine is interpreted in terms of a 1:1 *syn–anti* isomer mixture. Benzene solvent-induced shifts and the spectrum of the tris(dipivalomethanato)europium(III) – nitrosocamphidine complex are used to assign the methyl resonances.

On interprète le spectre à 220 MHz de la *N*-nitrosocamphidine en termes d'un mélange 1:1 d'isomères *syn–anti*. On a utilisé les déplacements chimiques induits par le butène ainsi que le spectre du complexe *N*-nitrosocamphidine – Eu $(DPM)_3$ pour attribuer les résonances des groupes méthyles.

Canadian Journal of Chemistry, 49, 2377 (1971)

The three methyl groups of *N*-nitrosocamphidine **1** (*N*-nitroso-1,8,8-trimethyl-3-azabicyclo-[3.2.1] octane) were reported (1) to exhibit a 60 MHz n.m.r. spectrum with four unsplit peaks in

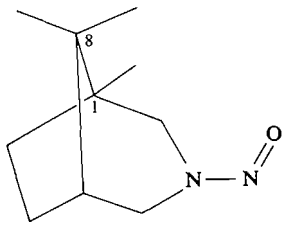

1

the methyl region at 1.09, 1.01, 0.96, and 0.91 δ from TMS with intensity ratios 3.0:2.0:2.7:1.4, respectively. Marburg (1) suggested the presence of either a *syn–anti* isomerism of the nitroso group or a chair–boat equilibrium of the ring system as an explanation for the four methyl peaks since one of the methyl groups would experience different shielding in the two forms. In this paper the *N*-nitrosocamphidine 220 MHz n.m.r. spectrum is analyzed for the CH_2—N region and an argument in favor of *syn–anti* isomerism is presented. Specific assignments of the methyl peaks are also included.

Before analyzing the *N*-α-methylene n.m.r. splitting pattern it is necessary to know both the geometry and the long-range shielding effects of the *N*-nitroso group. A large ionic resonance contribution to the *N*-nitroso group is well supported by i.r. spectroscopy (2); a large barrier to N—NO bond rotation (20–25 kcal/mol) (3); a large dipole moment (4.01 D) (4); electron diffraction studies (5); and molecular orbital theory (6). The best depiction of this group should therefore show a planar CCNNO unit as in **2**.

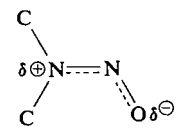

2

The long range n.m.r. diamagnetic shielding effect of the *N*-nitroso group was described by Harris and Spragg (7) and illustrated by Chow and Colón (8) as shown in **3**. The shielding cones derived from the C_α—N single bond and the N===N===O partial double bond are regarded as

[1]Taken in part from the M.Sc. thesis of J. D. Cooney, Carleton University, Ottawa, Canada, April, 1970. Present Address: Textile Chemistry Section, Division of Chemistry, National Research Council of Canada, Ottawa, Canada.

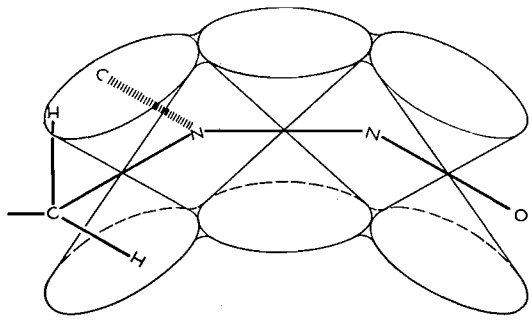

3

being fused together to form a semicircular shielding zone curved towards the *cis* side. The shielding zone extends perpendicularly above and below the C_α—N=N=O plane. This results in a greater shielding environment on the *cis* side than on the *trans* side. The deshielding zone is located in the C_α—N=N=O plane and studies on conformationally "frozen" 4-substituted *N*-nitrosopiperidines (9) indicated a slightly stronger deshielding zone on the *cis* side.

The possibility of a *syn–anti* isomerism of the *N*-nitroso group and a chair–boat equilibrium of the nitrogen containing ring could give a mixture of the four structures **4–7**.

Application of the Karplus expression (10) to the vicinal coupling constants J_{CE} and J_{DE} immediately eliminates the possibility of a boat conformation since the n.m.r. spectrum of **1** (Fig. 1) shows values of 1.3 and 2.5 Hz, respectively. Examination of molecular models would suggest approximate values of J_{DE} 1.2, J_{CE} 2.5 Hz for **4** or **5** and J_{DE} 6.8, J_{CE} 0.2 Hz for **6** or **7**. Presumably the 8-methyl to N—N bond interaction aids in destabilization of the boat conformations (**6** and **7**).

The 220 MHz spectrum of **1** is shown in Fig. 1, together with the assignments given to the *N*-α-methylene resonances based on the following reasons (using the proton designations in **4** and **5**):

(*i*) The spectrum is a composite of the spectra of **4** and **5**, showing normal coupling for AB, A′B′, CD, C′D′, DE, D′E′.

(*ii*) The *cis*-α-equatorial hydrogens, H_A and $H_{C'}$ are furthest downfield since they are *cis* and lie almost in the NNO plane.

(*iii*) The *trans*-α-equatorial hydrogens $H_{A'}$ and H_C should resonate approximately 0.4 p.p.m.

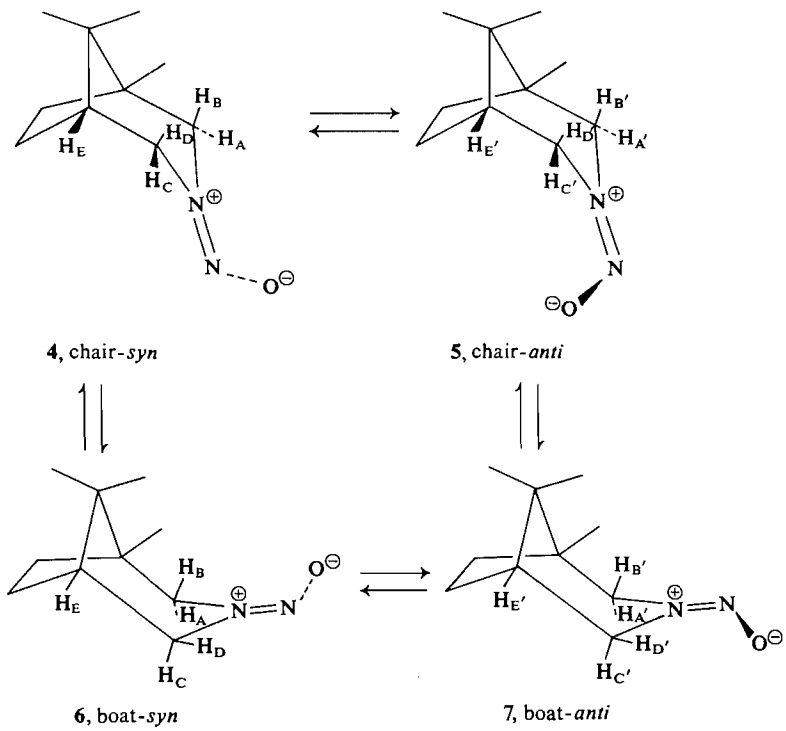

4, chair-*syn* **5**, chair-*anti*

6, boat-*syn* **7**, boat-*anti*

Can. J. Chem. Downloaded from www.nrcresearchpress.com by 210.87.254.5 on 09/05/12
For personal use only.

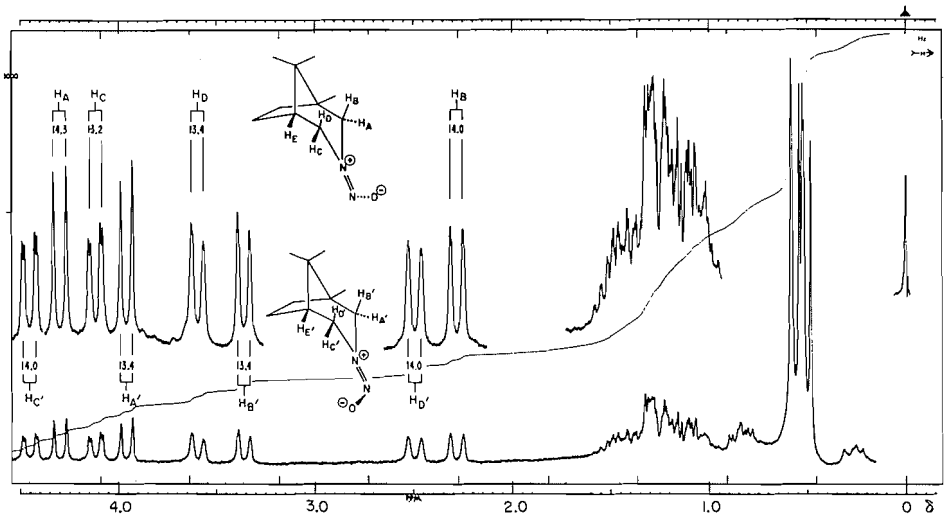

FIG. 1. The 220 MHz n.m.r. spectrum of *N*-nitrosocamphidine in C_6D_6, 1000 Hz sweep width.

TABLE 1. Methyl resonances of *N*-nitrosocamphidine at 100 MHz (δ from TMS)

Solvent	*cis*-8-Me *syn* and *anti*	1-Me *anti*	*trans*-8-Me *syn* and *anti*	1-Me *syn*	Relative peak heights
CCl_4 + $Eu(DPM)_3$	2.584*	2.028	1.903*	2.321	
CCl_4	1.092	1.008	0.951	0.910	2.8:2.0:3.0:2.2
C_6H_6	0.565	0.523	0.538	0.487	2.5:2.3:3.0:2.3
CCl_4–C_6H_6 Solvent shifts (Hz)	52.7	48.5	41.3	42.3	
$Eu(DPM)_3$ Shifts (Hz)	149.2	102.0	95.2	141.1	
Relative Eu to Me distances	1.00	1.12	1.25	1.03	

*Average of *syn* and *anti* resonances.

upfield (9) from H_A and $H_{C'}$ since they are *trans* to, and almost in the plane of, the NNO group.

(*iv*) The *trans*-α-axial hydrogens H_D and $H_{B'}$ should be upfield from the H_A and H_C resonances since they are outside the deshielded region.

(*v*) The *cis*-α-axial hydrogens, H_B and $H_{D'}$ should be in the shielding cones of the *N*-nitroso group (see **3**) and will therefore resonate at higher fields.

Spin decoupling (100 MHz) confirmed the coupling $J_{AB}, J_{C'D'}$. Only partial spin decouplings of $J_{A'B'}$ and J_{CD} were observed because of the promixity of the resonances. Integration suggests a *syn–anti* isomer ratio of 1:1.

The 100 MHz n.m.r. spectra of *N*-nitrosocamphidine exhibited the expected four methyl resonances (see Table 1). The use of benzene-induced shifts in the n.m.r. spectrum of *N*-nitrosoamines (11) enabled assignment of the methyl resonances. Thus, in the case of the chair-*syn* isomer, **4**, a benzene molecule would be oriented close to C-4 and would induce an upfield shift in the *cis*-8-methyl[2] resonance by comparison to its resonance in carbon tetrachloride. In the case of the chair-*anti* isomer, **5**, a benzene molecule would be oriented close to C-2 and both the 1-methyl and the *cis*-8-methyl groups would experience a shielding effect. The *trans*-8-methyl[3] group in both isomers and the 1-methyl group in the *syn* isomer experience much smaller solvent upfield shifts since the associated benzene molecule is further away. This rationale suggested the methyl assignments presented in Table 1. The

[2]*cis*-8-Methyl ≡ 8-methyl closest to the ring nitrogen.
[3]*trans*-8-Methyl ≡ 8-methyl furthest from the ring nitrogen.

Can. J. Chem. Downloaded from www.nrcresearchpress.com by 210.87.254.5 on 09/05/12
For personal use only.

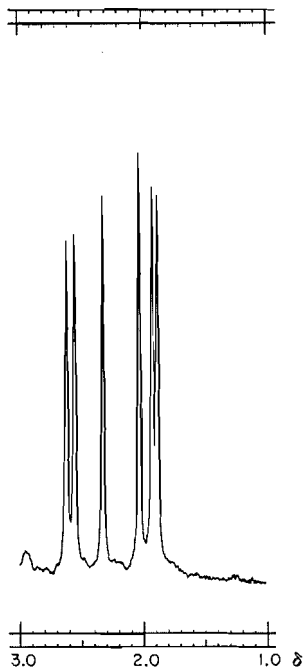

FIG. 2. The 100 MHz n.m.r. spectrum of the methyl resonances of *N*-nitrosocamphidine-tris(dipivalomethanato)-europium(III) complex (2:1 molar mixture) in CCl_4 solution.

1-methyl group experiences slightly different environments in the *syn* and *anti* isomers and is responsible for the appearance of a fourth methyl resonance.

The 100 MHz n.m.r. spectrum of the *N*-nitrosocamphidine - tris(dipivalomethanato)europium-(III) complex (12) shows six *N*-nitrosocamphidine methyl peaks (Fig. 2) *i.e.* one for each methyl in the *syn* and *anti* isomers, **8** and **9**, respectively. The $Eu(DPM)_3$ induced pseudocontact methyl shifts listed in Table 1 support the methyl assignments deduced from benzene solvent shift data. The methyl shifts increased with decreasing methyl to europium distances (R) and an approximate $1/R^3$ relationship was observed.[4]

Addition of $Eu(DPM)_3$ shifted the *N*-nitrosocamphidine α-methylene resonances 2 p.p.m. downfield but line broadening prevented unambiguous assignment.

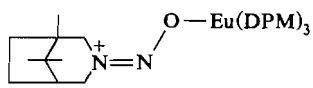

8

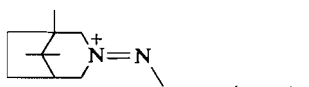

9

Experimental

The n.m.r. spectra were recorded at 220 and 100 MHz on Varian HR-220 and HR-100 spectrometers using TMS as an internal standard.

N-Nitrosocamphidine

N-Nitrosocamphidine was prepared by a three step synthesis. Camphoric anhydride was converted to camphorimide by heating with concentrated ammonium hydroxide (13). Camphorimide was reduced to camphidine by $LiAlH_4$ (14). The *N*-nitrosocamphidine, formed by nitrosation of camphidine (1), showed all requisite spectral and analytical properties (15).

Eu(DPM)$_3$

The $Eu(DPM)_3$ was synthesized according to the procedure of Eisentraut and Sievers (16).

J. D. C. thanks the National Research Council of Canada for study leave. We thank Dr. A. A. Grey, Canadian 220 MHz NMR Centre for his free introductory offer of a spectrum and Mr. J. Bornais, Division of Chemistry, National Research Council of Canada, for the 100 MHz n.m.r. spectra.

1. S. MARBURG. J. Org. Chem. **30**, 2834 (1965).
2. (*a*) R. N. HASZELDINE and J. JANDER. J. Chem. Soc. 691 (1954). (*b*) R. L. WILLIAMS, R. J. PACE, and G. J. JEACOCKE. Spectrochim. Acta, **20**, 225 (1964). (*c*) J. W. LINNETT and R. M. ROSENBURG. Tetrahedron, **20**, 53 (1964).
3. (*a*) C. E. LOONEY, W. D. PHILLIPS, and E. L. REILLY. J. Am. Chem. Soc. **79**, 6136 (1957). (*b*) C. L. BUMGARDNER, K. S. MCCALLUM, and J. P. FREEMAN. J. Am. Chem. Soc. **83**, 4417 (1961). (*c*) D. J. BLEARS. J. Chem. Soc. 6256 (1964). (*d*) K. H. ABRAMSON, P. T. INGLEFIELD, E. KRAKOWER, and L. W. REEVES. Can. J. Chem. **44**, 1685 (1966). (*e*) R. K. HARRIS and R. A. SPRAGG. Chem. Commun. 362 (1967). (*f*) Y. L. CHOW, C. J. COLÓN, and J. N. S. TAM. Can. J. Chem. **46**, 2821 (1968).
4. E. G. COWLEY and J. R. PARTINGTON. J. Chem. Soc. 1255 (1933).
5. (*a*) P. RADEMACHER and R. STØLEVIK. Acta Chem. Scand. **23**, 660 (1969). (*b*) P. RADEMACHER, R. STØLEVIK, and W. LUTTKE. Angew. Chem. Int. Ed. Engl. **7**, 806 (1968).
6. (*a*) P. RADEMACHER and R. STØLEVIK. Acta Chem. Scand. **23**, 660 (1969). (*b*) J. TANAKA. J. Chem. Soc. Jap. **78**, 1647 (1957). (*c*) W. D. PHILLIPS. Ann. N. Y. Acad. Sci. **70**, 817 (1958).

[4]An n.m.r. study of the series of cyclic *N*-nitrosamines from C-4 to -8 with $Eu(DPM)_3$ is in progress.

Can. J. Chem. Downloaded from www.nrcresearchpress.com by 210.87.254.5 on 09/05/12
For personal use only.

7. R. K. HARRIS and R. A. SPRAGG. J. Mol. Spectrosc. **23**, 158 (1967).
8. Y. L. CHOW and C. J. COLÓN. Can. J. Chem. **46**, 2827 (1968).
9. Y. L. CHOW. Angew. Chem. Int. Ed. Engl. **6**, 75 (1967).
10. J. R. DYER. Applications of absorption spectroscopy of organic compounds. Prentice-Hall, Inc., Englewood Cliffs, N. J., 1965. p. 116, 117.
11. G. J. KARABATSOS and R. A. TALLER. J. Am. Chem. Soc. **86**, 4373 (1964).
12. J. K. M. SANDERS and D. H. WILLIAMS. J. Am. Chem. Soc. **93**, 641 (1971).
13. N. R. HUNTER. M.Sc. Thesis. Carleton University, Ottawa, Canada, 1968. p. 63.
14. W. R. HERTLER and E. J. COREY. J. Org. Chem. **24**, 572 (1959).
15. J. D. COONEY. M.Sc. Thesis. Carleton University, Ottawa, Canada, 1970. p. 154.
16. K. J. EISENTRAUT and R. E. SIEVERS. Inorg. Syn. **11**, 94 (1968).

Can. J. Chem. Downloaded from www.nrcresearchpress.com by 210.87.254.5 on 09/05/12
For personal use only.

Can. J. Chem. Downloaded from www.nrcresearchpress.com by 210.87.254.40 on 09/05/12
For personal use only.

Radiation-induced Rearrangement of Ethylene Glycol in Aqueous Solution[1]

C. E. BURCHILL AND K. M. PERRON
Department of Chemistry, University of Manitoba, Winnipeg 19, Manitoba

Received March 8, 1971

Under γ-irradiation, aqueous solutions of ethylene glycol containing hydrogen peroxide form acetaldehyde as a major product via a free-radical chain rearrangement. The yield of acetaldehyde is essentially unchanged when hydrogen peroxide is replaced by N_2O or $HClO_4$. A mechanism is proposed in which the glycol radical, $\dot{C}HOHCH_2OH$, rearranges to the acetaldehyde precursor, $\dot{C}H_2CHO$, followed by the hydrogen atom transfer reaction;

$$\dot{C}H_2CHO + (CH_2OH)_2 \rightarrow CH_3CHO + \dot{C}HOHCH_2OH$$

thus propagating a chain reaction.[2]

The rearrangement is also induced by the photo-dissociation of H_2O_2 in aqueous solutions of ethylene glycol.

Sous une γ-irradiation, des solutions aqueuses d'éthylène glycol contenant du peroxyde d'hydrogène produisent de l'acétaldéhyde comme produit principal par une transposition radicalaire en chaîne. Le rendement en acétaldéhyde n'est pas modifié lorsque le peroxyde d'hydrogène est remplacé par N_2O ou $HClO_4$. Un mécanisme est proposé ou le radical glycol, $\dot{C}HOHCH_2OH$, se transpose en un précurseur, $\dot{C}H_2CHO$, de l'acétaldéhyde suivi par une réaction de transfert d'atome d'hydrogène;

$$\dot{C}H_2CHO + (CH_2OH)_2 \rightarrow CH_3CHO + \dot{C}HOHCH_2OH$$

il en résulte une réaction de propagation en chaîne.[2]

Dans des solutions aqueuses d'éthylène glycol, la transposition peut également être induite par la photo-dissociation de H_2O_2.

Canadian Journal of Chemistry, 49, 2382 (1971)

During a recent investigation of the radiation-induced oxidation of aliphatic alcohols by hydrogen peroxide (1) it was observed that irradiation of deaerated aqueous solutions of ethylene glycol (2.0 *M*) containing hydrogen peroxide resulted in the formation of acetaldehyde as a major product. The yield of acetaldehyde ($G \sim 15$) suggested that a chain reaction was involved but it was the nature of this product which evoked our curiosity. Acetaldehyde cannot be represented as a product of the oxidation of ethylene glycol. If acetaldehyde is written as the hydrate, $CH_3CH(OH)_2$, its formation from ethylene glycol may be represented as a rearrangement or, alternatively, the reaction may be considered as a dehydration. By analogy with the pinacol–pinacolone reaction we have chosen to refer to the formation of acetaldehyde from ethylene glycol as a rearrangement.

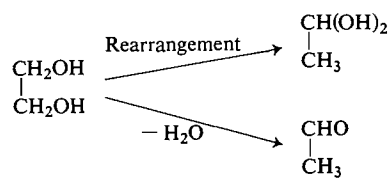

The study reported here was undertaken in an attempt to establish a plausible mechanism for the rearrangement. Shortly after this work was begun Seidler and von Sonntag (2) reported the formation of acetaldehyde on irradiation of dilute aqueous solutions of ethylene glycol saturated with nitrous oxide. More recently Scherz (3) has reported the formation of deoxy products (perhaps better termed *dehydro* products) in the radiolysis of dilute aqueous solutions of carbohydrates and polyalcohols. In neither case was the effect of varying the concentration of the organic substrate investigated and a chain mechanism for the rearrangement of ethylene glycol was inferred only at high temperature (100 °C).

[1]This work was supported in part by the Defence Research Board of Canada, Grant No. 9530-78, and in part by the National Research Council of Canada.

[2]After this paper was submitted for publication a note appeared by von Sonntag and Thoms (26) in which a similar conclusion was reached regarding the nature of the chain process for the formation of acetaldehyde by γ-irradiation of N_2O-saturated aqueous solutions of ethylene glycol.

Can. J. Chem. Downloaded from www.nrcresearchpress.com by 210.87.254.40 on 09/05/12
For personal use only.

Experimental

The general techniques of sample preparation and irradiation were identical to those previously employed in the study of the radiation-induced oxidation of alcohols (4). Samples, of 10-ml volume, were degassed under vacuum by the freeze–pump–thaw technique and irradiated in a Gammacell 220 ^{60}Co radiation facility. The average dose-rate was 1.45×10^{19} eV l^{-1} s^{-1} estimated by ferrous sulfate dosimetry, assuming $G(Fe^{3+}) = 15.6$ (5). Lower dose rates were achieved by the use of a cylindrical lead attenuator in the sample chamber. Irradiations were carried out at the ambient temperature of the Gammacell (35 without and 40 °C with the attenuator).

Photo-initiation of the reaction employed a Hanovia Z 1500-108 low pressure mercury arc with a Vycor envelope. The reaction cells and experimental assembly were the same as those used by Burchill and Wolodarsky (6). The intensity of the 2537 Å light at the cell face was estimated by ferri-oxalate actinometry (7, 6) and the fraction of the incident light absorbed by H_2O_2 in the solution was calculated from its measured concentration and a molar absorbancy of 19.6 l mol^{-1} cm^{-1} at 2537 Å (8).

Acetaldehyde was determined by vapor-phase chromatography using a 6 ft column of Chromosorb 102 with flame-ionization detection. Hydrogen peroxide was determined by the tri-iodide method (9). Glycolic acid was measured by reaction with chromotropic acid (10).

Ethylene glycol (Fisher Certified Reagent) and hydrogen peroxide (Fisher Certified Reagent, 30%, unstabilized) were used to prepare solutions in triply-distilled water. Acid solutions were prepared with $HClO_4$ (Baker and Adamson, 70% A.C.S.). Nitrous oxide (Matheson, anaesthetic grade) was passed through a column of KOH pellets and freed of permanent gases by freezing, pumping, and thawing on a vacuum line. Aqueous solutions were equilibrated with this gas at a particular pressure and its concentration in the solution was calculated from the data of Markham and Kobe (11).

Results

Under γ-irradiation, deaerated aqueous solutions of ethylene glycol containing H_2O_2 formed acetaldehyde in a dose-independent yield, as shown in Fig. 1. The G(acetaldehyde) value, determined from similar linear yield–dose plots, increased linearly with increasing glycol concentration, as shown in Fig. 2. The reduction of H_2O_2 under irradiation was approximately first-order in H_2O_2 (see Fig. 3) and the apparent first-order rate constant for this reduction increased with increasing glycol concentration although the apparent linear relationship did not extrapolate to the origin (see Fig. 4).

That the yield of acetaldehyde is independent of H_2O_2 concentration was demonstrated by the fact that the acetaldehyde formation yield remained independent of dose, as in Fig. 1, despite the reduction of more than one-half the initial hydrogen peroxide. This is further demonstrated by the data of Table 1. For solutions whose concentration of ethylene glycol was 1.78 M, varying the initial concentration of H_2O_2 from 0.02 to

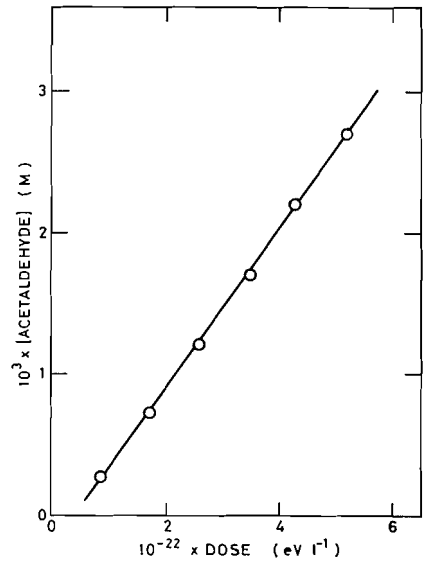

FIG. 1. Yield–dose plot for a deaerated aqueous solution 0.54 M in ethylene glycol and 0.01 M in H_2O_2; dose-rate = 1.45×10^{19} eV l^{-1} s^{-1}.

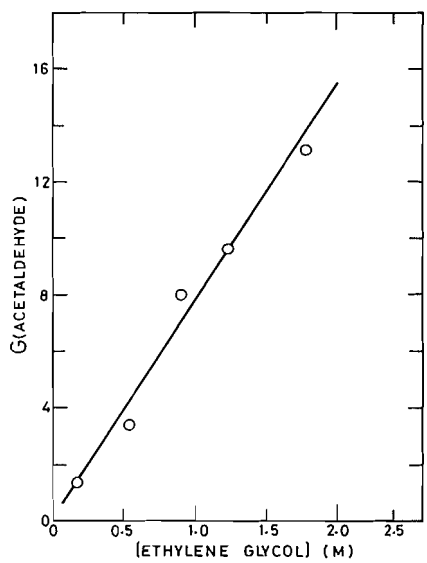

FIG. 2. Variation of G(acetaldehyde) with [ethylene glycol] for solutions 0.01 M in H_2O_2; dose-rate = 1.44×10^{19} eV l^{-1} s^{-1}.

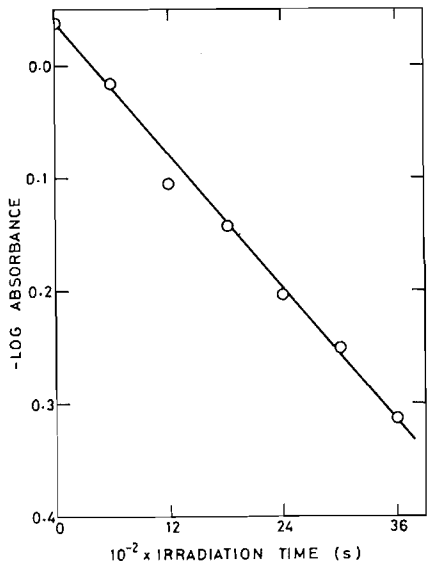

FIG. 3. First-order plot for H_2O_2 reduction in an aqueous solution 0.54 M in ethylene glycol. $[H_2O_2]_0$ = 0.01 M; dose rate = 1.45×10^{19} eV l^{-1} s^{-1}.

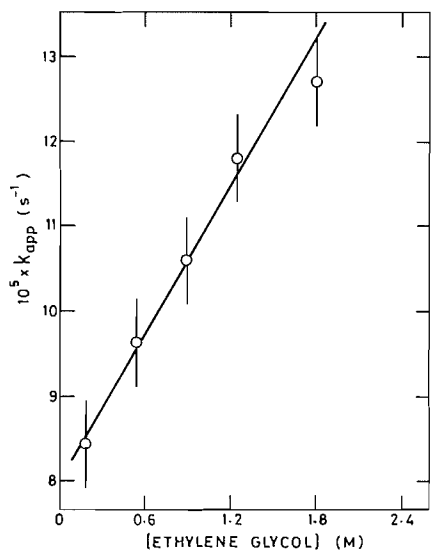

FIG. 4. Variation of the apparent first-order rate constant for peroxide reduction with glycol concentration. $[H_2O_2]_0$ = 0.01 M; dose-rate = 1.44×10^{19} eV l^{-1} s^{-1}.

1.5×10^{-4} M did not markedly affect G(acetaldehyde).

When solutions containing 0.01 M H_2O_2 and 1.78 M ethylene glycol were acidified with $HClO_4$, the yield of acetaldehyde was only slightly affected whereas the consumption of H_2O_2 was reduced almost to zero in 0.1 M acid. When H_2O_2 was omitted from a solution 0.1 M in acid the yield of acetaldehyde was somewhat greater than that with H_2O_2 present. This information is presented in Table 2.

When neutral solutions of ethylene glycol containing nitrous oxide were irradiated, acetaldehyde was formed in a yield which increased with increasing glycol concentration. The reproducibility of the results was somewhat poorer than when H_2O_2 was present, but for solutions containing 0.01 M N_2O the yields of acetaldehyde were similar to those obtained from solutions with 0.01 M H_2O_2 at the same glycol concentrations. The yields are tabulated for comparison in Table 3.

TABLE 1. Effect of initial $[H_2O_2]$ on G(acetaldehyde)*

$[H_2O_2]$(initial) (M)	$10^4 \times k_{app}(-H_2O_2)$ (s^{-1})	G(acetaldehyde)
0.02	0.92±0.08	13.6±0.7
0.01	1.27±0.10	13.2±0.7
3×10^{-4}	5.3±0.4	17.0±1.5
1.5×10^{-4}	4.4±0.4	12.8±1.5
Zero	—	4.3±0.4

*[Ethylene glycol] = 1.78 M, dose rate = 1.42×10^{19} eV l^{-1} s^{-1}.

TABLE 2. Effect of varying acid ($HClO_4$) concentration on the radiolysis of solutions 0.01 M in H_2O_2 and 1.78 M in ethylene glycol*

$[H_3O^+]$ (M)	$10^4 \times k_{app}(-H_2O_2)$ (s^{-1})	G(acetaldehyde)
Neutral	1.27±0.10	13.2±0.7
10^{-3}	0.67±0.10	14.5±0.7
10^{-2}	0.59±0.10	9.6±0.7
10^{-1}	0.19±0.05	10.4±0.7
10^{-1}	$[H_2O_2]$ = zero initially	16.1±0.7

*Dose rate = 1.42×10^{19} eV l^{-1} s^{-1}.

TABLE 3. Comparison of acetaldehyde yields for solutions containing N_2O and H_2O_2*

[Ethylene glycol] (M)	G(acetaldehyde)	
	0.01 M N_2O	0.01 M H_2O_2
0.18	1.60±0.15	1.37±0.15
0.54	—	3.4±0.3
0.88	5.8±0.6	8.0±0.6
1.23	9.2±0.7	9.6±0.6
1.77	9.2±1.0	13.2±0.7

*Average dose-rate = 1.40×10^{19} eV l^{-1} s^{-1}.

Can. J. Chem. Downloaded from www.nrcresearchpress.com by 210.87.254.40 on 09/05/12
For personal use only.

TABLE 4. Variation of G(acetaldehyde) with attenuation of dose rate. All solutions 1.77 M in ethylene glycol

Solution	G(acetaldehyde)	
	$D = 1.42 \times 10^{19}$ eV l^{-1} s^{-1}	$D = 3.76 \times 10^{18}$ eV l^{-1} s^{-1}
0.01 M H_2O_2, neutral	13.2±0.7	38±2
0.01 M H_2O_2, 0.1 M $HClO_4$	16.1±0.7	51±3
0.01 M N_2O, neutral	10.2±0.8	38±2

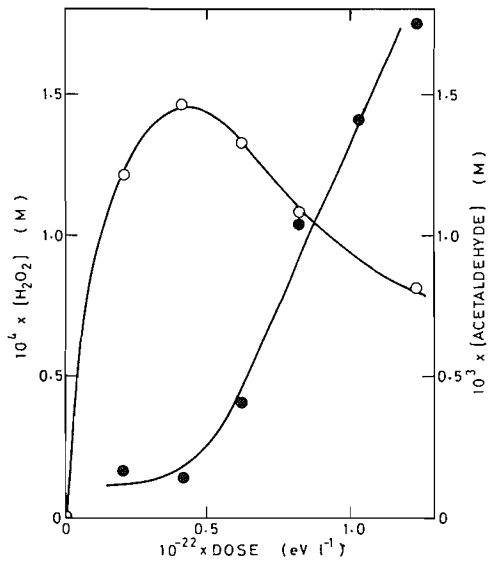

FIG. 5. Yield–dose profile for an aerated solution 1.78 M in ethylene glycol. ○, H_2O_2; ●, acetaldehyde.

The effect of dose-rate on the yield of acetaldehyde was investigated for a variety of initial conditions. In all cases G(acetaldehyde) increased considerably with a decrease in dose-rate as shown in Table 4.

Air saturation, of aqueous solutions containing only ethylene glycol, initially inhibited the formation of acetaldehyde. As shown in Fig. 5, H_2O_2 was formed as a net product at low dose, reaching a maximum concentration of 1.5×10^{-4} M after a dose of 5×10^{21} eV l^{-1}, after which its concentration decreased. The formation of acetaldehyde was inhibited until this same dose had been delivered, after which G(acetaldehyde) was essentially equal to that from a deaerated solution containing H_2O_2 initially. Saturation with O_2 increased the induction dose and the maximum concentration of H_2O_2 formed.

To demonstrate that the formation of acetaldehyde from ethylene glycol was not merely an artifact of γ-irradiation the rearrangement was initiated by photo-dissociation of H_2O_2. With a light path length of 1.0 cm the absorption by 0.01 M H_2O_2 of 2537 Å light was approximately 35%, giving reasonably homogeneous initiation. For neutral solutions 1.78 M in ethylene glycol ϕ(acetaldehyde) was 8.0 ± 0.5 with $I_a = 1.41 \times 10^{-7}$ einstein l^{-1} s^{-1}. When such a solution was made 0.1 M in $HClO_4$ the yield of acetaldehyde increased slightly, although probably not significantly, to $\phi = 9.6 \pm 0.6$.

In neutral solutions containing ethylene glycol and H_2O_2, the peroxide is reduced in a chain reaction initiated by γ-irradiation or photodissociation of the peroxide. This reductive process must necessarily be accompanied by an equivalent oxidation but the nature of the oxidized product was not established unequivocally. When hydrogen peroxide is reduced under γ-irradiation in the presence of aliphatic primary or secondary alcohols the major oxidized product is the corresponding aldehyde or ketone (4, 12). The analogous product from ethylene glycol would be glycolaldehyde but attempts to find this product in the irradiated solutions were unsuccessful. If glycolaldehyde were formed it is possible that it could undergo a further thermal oxidation by H_2O_2 to glycolic acid. Reaction with chromotropic acid gave a violet color (10) but this test is not specific for glycolic acid, being a test for formaldehyde, and gives the same reaction with any other species decomposing to formaldehyde (13). Vasudeva and Wasif (14) have reported glycolic acid and oxalic acid as products of the oxidation of ethylene glycol by peroxydisulfate. In that study no glycolaldehyde was found as a product, nor was acetaldehyde reported, although the authors did not specifically mention having looked for it. In this work the yield of the product reacting with chromotropic acid, and assumed to be glycolic acid, was less than half that required by the stoichiometry $2H_2O_2 + (CH_2OH)_2 \rightarrow 3H_2O + CH_2OHCOOH$.

Can. J. Chem. Downloaded from www.nrcresearchpress.com by 210.87.254.40 on 09/05/12
For personal use only.

Can. J. Chem. Downloaded from www.nrcresearchpress.com by 210.87.254.40 on 09/05/12
For personal use only.

Discussion

The major features of the formation of acetaldehyde from ethylene glycol under γ-irradiation may be summarized as follows:

(*a*) It is a chain reaction, as demonstrated by the large *G* values (up to 50 in one case).

(*b*) The *G*(acetaldehyde) value is linearly dependent upon glycol concentration in solutions containing H_2O_2 but it is independent of the concentration of H_2O_2.

(*c*) The concurrent reduction of H_2O_2 occurs by an independent chain reaction since it is apparently first-order in H_2O_2.

(*d*) H_2O_2 may be replaced by N_2O or H_3O^+ without a major effect on *G*(acetaldehyde) but if none of these is present initially the yield of acetaldehyde is significantly reduced.

Seidler and von Sonntag (2) attributed the formation of acetaldehyde from ethylene glycol to the disproportionation of a radical produced by the rearrangement of the primary ethylene glycol radical (eq. 1).

[1] $$\dot{C}HOHCH_2OH \xrightarrow{-H_2O} \dot{C}H_2CHO$$

A similar mechanism was proposed by Scherz (3) to account for the formation of deoxy products from sugars and polyalcohols. The rearrangement, or dehydration, of the radical was observed by Buley *et al.* (15) using e.s.r. detection of intermediates in a flowing system of Ti(III) – H_2O_2 – ethylene glycol. The rearrangement was represented as

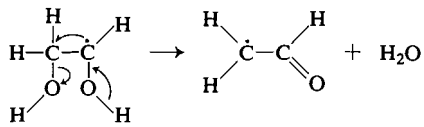

and was said to be acid-catalyzed since the broad triplet spectrum of the rearranged radical was observed only at high acid concentrations while with a minimum acid concentration a 24 line spectrum was observed, characteristic of the primary radical. Livingston and Zeldes (16) also observed this transformation by e.s.r. in a flow system with initiation by photolysis of H_2O_2. In pure ethylene glycol only the spectrum of the primary glycol radical, $\dot{C}HOHCH_2OH$, was observed but as the glycol was diluted with water the intensity of the 24 line spectrum was reduced and broader lines were observed. When acid was added, only the broad triplet spectrum of the rearranged radical was observed, again suggesting that the rearrangement was acid-catalyzed.

We propose that this rearrangement occurs and is acid-catalyzed but that it also occurs at a significant rate in neutral solution. The rearranged radical was not observed at higher p*H* in the e.s.r. flow systems because of a relatively high rate of initiation. If the radicals in these systems undergo bimolecular termination their average lifetime before termination is a function of their steady-state concentration and hence the rate of initiation. At the higher rates of initiation typical of the e.s.r. experiments described there may be insufficient time for the primary glycol radicals to undergo a first-order rearrangement before termination. With acid present to increase the rate of rearrangement, or at the lower rates of initiation such as those of the radiation–chemical experiments described here, the situation may be reversed and the rearranged radical may be the dominant form.

If the primary radical from ethylene glycol can rearrange in neutral solution to $\dot{C}H_2CHO$, the rearranged radical may be considered as a substituted methyl radical. As such it may be expected to be capable of abstracting an α hydrogen from an alcohol or glycol as has been demonstrated for similar radicals with 2-propanol and ethanol (4, 12), eq. 2. This would provide the propagating step for a chain rearrangement of the glycol.

[2] $$\dot{C}H_2CHO + (CH_2OH)_2 \rightarrow CH_3CHO + \dot{C}HOHCH_2OH$$

At the same time the primary glycol radical, being an α-hydroxyalkyl radical, would be expected to be capable of reducing H_2O_2 to propagate an oxidative chain reaction, eq. 3.

[3] $$\dot{C}HOHCH_2OH + H_2O_2 \rightarrow CHOCH_2OH + H_2O + \dot{O}H$$

This oxidative chain reaction need not, however, affect the rearrangement chain reaction since $\dot{C}HOHCH_2OH$ is immediately replaced via reaction 4. Glycolaldehyde was not found in the

[4] $$\dot{O}H + (CH_2OH)_2 \rightarrow H_2O + \dot{C}HOHCH_2OH$$

irradiated solutions containing H_2O_2 but it may undergo further oxidation in such solutions.

The overall reaction mechanism proposed for the irradiation of aqueous solutions of ethylene

Can. J. Chem. Downloaded from www.nrcresearchpress.com by 210.87.254.40 on 09/05/12
For personal use only.

glycol and H_2O_2 is summarized in the following equations:

$$H_2O \rightsquigarrow e_{aq}^-,\ H,\ OH,\ H_2O_2,\ H_2,\ H_3O^+$$

[5] $$e_{aq}^- + H_2O_2 \rightarrow OH^- + \dot{O}H$$

[6] $$H + (CH_2OH)_2 \rightarrow H_2 + \dot{C}HOHCH_2OH \qquad \dot{C}HOHCH_2OH = \mathbf{1}$$

[4] $$\dot{O}H + (CH_2OH)_2 \rightarrow H_2O + \mathbf{1}$$

[1] $$\mathbf{1} \rightarrow H_2O + \dot{C}H_2CHO \qquad \dot{C}H_2CHO = \mathbf{2}$$

[1c] $$\mathbf{1} + H^+ \rightarrow H_3O^+ + \mathbf{2}$$

[2] $$\mathbf{2} + (CH_2OH)_2 \rightarrow CH_3CHO + \mathbf{1}$$

[3] $$\mathbf{1} + H_2O_2 \rightarrow CHOCH_2OH + H_2O + \dot{O}H$$

[7] $$CHOCH_2OH + n\,H_2O_2 \rightarrow \text{Other oxidized products}$$

[8] $$\mathbf{2} + \mathbf{2} \rightarrow \text{Termination}$$

On the basis of this mechanism and the usual steady-state assumptions, expressions for the radiation chemical yields, eqs. 9 and 10, may be derived; D is the dose-rate in units of 6.023×10^{25} eV l^{-1} s^{-1}.

[9] $$G(\text{acetaldehyde}) = k_2\left(\frac{G_{e_{aq}^-} + G_{OH} + G_H}{2k_8 D}\right)^{1/2}[\text{glycol}]$$

[10] $$\frac{-d[H_2O_2]}{dt} = (G_{e_{aq}^-} - G_{H_2O_2})D + A[H_2O_2]$$

$$A = \frac{(n+1)k_3}{k_1 + k_{1c}[H^+]} \times \left[k_2\left\{\frac{(G_{e_{aq}^-} + G_{OH} + G_H)D}{2k_8}\right\}^{1/2} \times [\text{glycol}] + (G_{e_{aq}^-} + G_{OH} + G_H)D\right]$$

The yield of acetaldehyde predicted by this mechanism is seen to be directly proportional to the glycol concentration and independent of peroxide concentration, as observed experimentally. Extrapolation of the straight line in Fig. 2 gives an intercept of very nearly zero which suggests that acetaldehyde is not a significant product of the termination step. Termination by processes other than reaction 8, such as combination of radicals **1** or cross-combination of **1** and **2**, would lead to some dependence of the acetaldehyde yield on $[H_2O_2]$, which was not observed. This supports the suggestion made earlier that, at the dose rates used here, the rearranged radical, **2**, is the predominant radical intermediate species. Equation 9 predicts a reciprocal square-root dependence of the acetaldehyde yield on the dose rate. As shown in Table 4 the acetaldehyde yield increased by more than the predicted amount on attenuation of the dose rate to ~25%. This excess increase in the acetaldehyde yield on attenuation may perhaps be accounted for by the higher temperature in the Gammacell with the attenuators in place. Seidler and von Sonntag (2) noted that the acetaldehyde yield increased with increasing temperature.

If this mechanism is accepted it is possible to estimate the magnitude of k_2 for the hydrogen atom transfer from ethylene glycol to the rearranged radical. It may be seen that the coefficient of [glycol] in eq. 9 is the slope of the line in Fig. 2. Taking $G_{e_{aq}^-} + G_H = 3.18$ and $G_{OH} = 2.72$ (17), and $2k_8 = 2 \times 10^9$ l mol^{-1} s^{-1} as representative of the rate of bimolecular reaction of simple organic radicals in aqueous solution (18), leads to a value of $k_2 = 75 \pm 5$ l mol^{-1} s^{-1}. This is of the same order as the rate constants for similar reactions with 2-propanol and ethanol (4, 12).

Equation 10, derived from the above mechanism, is in fair agreement with the observed kinetics of the reduction of H_2O_2 under irradiation in the presence of ethylene glycol. If the first term, $(G_{e_{aq}^-} - G_{H_2O_2})D$, is small compared to the rest, eq. 10 is seen to represent a process first order in H_2O_2, with the whole coefficient of $[H_2O_2]$, A, being $k_{app}(-H_2O_2)$. The k_{app} value may be seen to be linearly dependent on the concentration of glycol (as observed experimentally) and also to involve a term independent of glycol concentration (corresponding to the extrapolated non-zero intercept of Fig. 4). The increase in $k_{app}(-H_2O_2)$ at low peroxide concentrations (Table 1) is a consequence of the failure of the approximation above, $(G_{e_{aq}^-} - G_{H_2O_2})D$ being of the same order as the chain term for peroxide reduction at these low concentrations. Without a better knowledge of the stoichiometry of the peroxide reduction any attempt to estimate the values of the individual rate constants is highly speculative. However, the extrapolated intercept of Fig. 4 is $\sim 8 \times 10^{-5}$ s^{-1} and this may be equated with $(n+1)k_3/k_1(G_{e_{aq}^-} + G_H + G_{OH})D$ for neutral

Can. J. Chem. Downloaded from www.nrcresearchpress.com by 210.87.254.40 on 09/05/12
For personal use only.

solutions. Assuming $n = 1$, and $(G_{e_{aq}^-} + G_H + G_{OH}) = 5.9$ (17) gives $k_3/k_1 = 28 \pm 2$ mol^{-1} for the dose rate involved. If k_3 is of the same order as the rate constant for the reduction of H_2O_2 by the hydroxymethyl radical (4×10^4 l mol^{-1} s^{-1} (12)) this suggests that the rate constant for reaction 1 is of the order of 10^3 s^{-1}. Such a value for this rate constant is consistent with the unrearranged radical being the dominant species at high rates of initiation, as in the e.s.r. experiments (15, 16), but the rearranged radical being dominant at low rates of initiation.

If the rearrangement is also acid-catalyzed, [1*c*], eq. 10 predicts a decrease in $k_{app}(-H_2O_2)$ with increasing acid concentration. Such a decrease was observed (Table 2).

When H_2O_2 is replaced by N_2O, reaction 5 is replaced by reaction 11, and no oxidative chain would be anticipated since α-hydroxyalkyl radicals from simple alcohols do not reduce N_2O (19).

[11] $$e_{aq}^- + N_2O + H_2O \rightarrow N_2 + OH^- + \dot{O}H$$

The remaining reactions are unchanged and the yield of acetaldehyde should be given by eq. 9, and unchanged from that with H_2O_2 present.

With neither N_2O nor H_2O_2 in solution, but in the presence of a mineral acid, e_{aq}^- will be converted to H by reaction 12 and, via reaction 6, give the same initial radical from ethylene glycol.

[12] $$e_{aq}^- + H^+ \rightarrow H$$

The yield of acetaldehyde should again be unchanged from that with N_2O or H_2O_2 present, except as it reflects any change in the primary radical yields.

Under the experimental conditions used here the yield of acetaldehyde was generally somewhat smaller when N_2O was used in place of H_2O_2 and somewhat greater when replaced with $HClO_4$ (Tables 3 and 4). However the continuance of the chain reaction and the similarity of the yield under these changed conditions lead us to believe that the proposed mechanism is a reasonable representation of the overall reaction.

With none of H_2O_2, N_2O, or $HClO_4$ present in the solution the yield of acetaldehyde was significantly less (Table 1). Under these circumstances the only scavenger for e_{aq}^- is the acetaldehyde formed as a product.

[13] $$e_{aq}^- + CH_3CHO + H_2O \rightarrow OH^- + CH_3\dot{C}HOH$$

The hydroxyethyl radical so formed would not enter into the rearrangement chain reaction nor is there sufficient H_2O_2 formed as a primary product to oxidize it to generate ȮH as in the chain oxidation of ethanol (12). Thus the number of free radicals initiating the rearrangement chain is reduced and a portion of the product acetaldehyde is consumed as an electron scavenger.

When a deaerated aqueous solution of ethylene glycol and H_2O_2 is subjected to irradiation by 2537 Å light the peroxide dissociates into ȮH radicals, eq. 14 (8) (Φ_a represents the primary

[14] $$H_2O_2 \xrightarrow{h\nu} 2\Phi_a\dot{O}H$$

quantum yield for peroxide homolysis). The remaining reactions would be the same as for the radiation initiation, and the quantum yield of acetaldehyde formation would be given by eq. 15.

[15] $$\Phi(\text{acetaldehyde}) = k_2(\Phi_a/k_8\, I_a)^{1/2}[\text{glycol}]$$

The effects of light intensity and glycol concentration on the acetaldehyde yield were not investigated but the addition of 0.1 *M* $HClO_4$ did not significantly affect the yield. The photochemical and radiation chemical yields may be compared by taking the ratio of eqs. 15 and 9 for identical glycol concentrations.

[16] $$\frac{\Phi(\text{acetaldehyde})}{G(\text{acetaldehyde})} = \left(\frac{2\Phi_a D}{(G_{e_{aq}^-} + G_H + G_{OH})I_a}\right)^{1/2}$$

Using the results for solutions 1.78 *M* in glycol and 0.01 *M* in H_2O_2, $I_a = 1.41 \times 10^{-7}$ einstein l^{-1} s^{-1}, $D = 1.45 \times 10^{19}$ eV l^{-1} s^{-1}

$$\frac{\Phi(\text{acetaldehyde})}{G(\text{acetaldehyde})} = \frac{8.0 \pm 0.5}{13.2 \pm 0.7} = 0.60 \pm 0.05$$

Assuming $2\Phi_a = 1.0$ for peroxide photolysis (8) and $(G_{e_{aq}^-} + G_H + G_{OH}) = 5.9$ (17) a value of 0.54 is predicted for this ratio for the dose rate and light intensity involved. The yield of acetaldehyde is thus somewhat greater in the photochemical experiment than would be predicted from the radiation chemical results. This may, in part, be a result of the uncertainty in the appropriate values for the primary free-radical yields in these systems. Once again the fair correlation of the radiation-induced with the photochemical initiation serves to confirm the major features of the proposed mechanism.

Can. J. Chem. Downloaded from www.nrcresearchpress.com by 210.87.254.40 on 09/05/12
For personal use only.

The inhibition of the rearrangement by oxygen may be explained by the very fast reaction of radical **1** with O_2 and the net yield of H_2O_2 by the disproportionation of the product peroxy radicals (20).

[17] $\mathbf{1} + O_2 \rightarrow CH_2OHCHO + HO_2$

[18] $2HO_2 \rightarrow O_2 + H_2O_2$

The rate of reaction of α-hydroxyalkyl radicals with O_2 is sufficiently rapid (21) to scavenge all of **1** prior to rearrangement or oxidation by H_2O_2 until essentially all O_2 is consumed, whereupon the chain rearrangement, as previously described, follows and with it the chain reduction of H_2O_2. (A similar concentration-dose profile is observed for H_2O_2 with a wide variety of organic solutes in aerated aqueous solution (22).)

A number of observations suggest that the rearrangement of vicinal glycols to the corresponding carbonyl compound via a free-radical mechanism is a general phenomenon. Preliminary experiments in this laboratory demonstrated the formation of acetone from 1,2-propanediol and methyl ethyl ketone from 2,3-butanediol on γ-irradiation of their aqueous solutions saturated with N_2O (23). The formation of deoxy products on irradiation of aqueous solutions of sugars and polyalcohols (3) suggests a similar mechanism. The rearrangement of the intermediate free radicals has been observed by Norman and co-workers (15, 24) using the flow-e.s.r. technique for a number of vicinal glycols, including one cyclic glycol, chlorhydrins, sugars, and for mesoinositol. Livingston and Zeldes (25) have suggested a similar rearrangement for the fragment ĊHOHCHOHCOOH formed in the photolysis of tartaric acid.

The rearrangement or dehydration of polyhydroxy compounds may be of considerable significance in systems containing high concentrations of carbohydrates or carbohydrate residues, particularly under anoxic conditions. The fact that the overall rearrangement may proceed by a chain mechanism would make it particularly important at low dose rates. The implications of such processes in biological systems may be considerable.

1. I. S. Ginns. Ph.D. Thesis. University of Manitoba, Winnipeg, Manitoba, 1970.
2. F. Seidler and C. von Sonntag. Z. Naturforsch. **24***b*, 780 (1969).
3. H. Scherz. Radiat. Res. **43**, 12 (1970).
4. C. E. Burchill and I. S. Ginns. Can. J. Chem. **48**, 1232 (1970).
5. H. A. J. Battaerd and G. W. Tregear. Rev. Pure and Appl. Chem. **16**, 83 (1966).
6. C. E. Burchill and W. H. Wolodarsky. Can. J. Chem. **48**, 2955 (1970).
7. C. G. Hatchard and G. A. Parker. Proc. Roy. Soc. A**235**, 518 (1956).
8. J. H. Baxendale and J. A. Wilson. Trans. Faraday Soc. **53**, 344 (1957).
9. A. O. Allen, C. J. Hochanadel, J. A. Ghormley, and T. W. Davis. J. Phys. Chem. **56**, 575 (1952).
10. F. D. Snell and C. T. Snell. Colorimetric methods of analysis. Vol. IIIA. Van Nostrand, Princeton, N.J., 1957. p. 317.
11. A. E. Markham and K. A. Kobe. J. Am. Chem. Soc. **63**, 449 (1941).
12. C. E. Burchill and I. S. Ginns. Can. J. Chem. **48**, 2628 (1970).
13. C. E. Bricker and H. R. Johnson. Ind. and Eng. Chem. (Anal. Ed.), **17**, 400 (1945).
14. W. C. Vasudeva and S. Wasif. J. Chem. Soc. B, 960 (1970).
15. A. L. Buley, R. O. C. Norman, and R. J. Pritchett. J. Chem. Soc. B, 849 (1966).
16. R. Livingston and H. Zeldes. J. Am. Chem. Soc. **88**, 4333 (1966).
17. I. G. Dragonic, M. T. Nedadovic, and Z. D. Dragonic. J. Phys. Chem. **73**, 2564 (1969).
18. M. Simic, P. Neta, and E. Hayon. J. Phys. Chem. **73**, 3794 (1969).
19. G. Scholes, M. Simic, and J. J. Weiss. Discuss. Faraday Soc. **36**, 214 (1963).
20. W. M. Garrison. Curr. Top. in Radiat. Res. **4**, 43 (1968).
21. G. E. Adams and R. L. Willson. Trans. Faraday Soc. **63**, 2981 (1969).
22. Mary E. Van Buskirk. M.Sc. Thesis. University of Manitoba, Winnipeg, Manitoba, 1969.
23. K. M. Perron. M.Sc. Thesis. University of Manitoba, Winnipeg, Manitoba, 1970.
24. R. O. C. Norman and R. J. Pritchett. J. Chem. Soc. B, 1329 (1967).
25. R. Livingston and H. Zeldes. J. Chem. Phys. **53**, 1406 (1970).
26. C. von Sonntag and E. Thoms. Z. Naturforsch, **25***b*, 1405 (1970).

Nucleophilic Reactivity of 4,4′-Disubstituted Diphenyl Sulfides Towards *trans*-Dichlorobis(pyridine)platinum(II)

J. R. GAYLOR AND C. V. SENOFF
Department of Chemistry, University of Guelph, Guelph, Ontario

Received March 12, 1971

The kinetics of the reaction of *trans*-$[PtCl_2py_2]$ with a series of 4,4′-disubstituted diphenyl sulfides, $XC_6H_4SC_6H_4Y$, have been studied at 30° in methanol. A linear free energy correlation has been obtained between the logarithm of the second order rate constant and the sum of the Hammett substituent parameters for X and Y. This result is consistent with the notion that bond making is the driving force when divalent sulfur functions as a nucleophile towards platinum(II) substrates and is consistent with the inability of 4,4′-dinitrodiphenyl sulfide to coordinate to platinum(II).

Les cinétiques des réactions entre le $[PtCl_2py_2]$-*trans* et une série de diphénylsulfures disubstitués en -4,4′, $XC_6H_4SC_6H_4Y$, ont été étudiées à 30 °C dans le méthanol. Une corrélation linéaire de l'énergie libre a été obtenue entre le logarithme de la constante de vitesse du second ordre et la somme des paramètres de Hammett pour les substituants X et Y. Ce résultat est consistant avec la notion d'après laquelle l'établissement d'une liaison est la force directive lorsqu'un soufre divalent fonctionne en tant que nucléophile envers le platine(II); ce résultat est également cohérent avec le fait que le dinitro-4,4′ diphénylsulfure ne se coordonne pas avec le platine(II).

Canadian Journal of Chemistry, 49, 2390 (1971)

Substitution reactions of square planar d^8 metal complexes, especially those of platinum(II) have been well documented (1–3). Previous investigations have utilized *trans*-$[PtCl_2py_2]$ as a representative substrate in order to investigate the reactivity of a variety of nucleophiles towards platinum(II) complexes (4, 5). As part of a general interest in the donor properties of ligands containing a sulfur donor atom, we have undertaken a kinetic study of reaction 1 where Ar_2S = a 4,4′-disubstituted diphenyl sulfide and py = pyridine. It was also anticipated that this study

[1] *trans*-$[PtCl_2py_2] + 2Ar_2S \rightarrow$ *trans*-$[Pt(Ar_2S)_2py_2]^{2+} + 2Cl^-$

would provide a quantitative indication of the ability of divalent sulfur in a diaryl sulfide to transmit the electronic effect of a para-substituent. The results of this study are reported at this time.

Results and Discussion

The rates of reaction between *trans*-$[PtCl_2py_2]$ and $XC_6H_4SC_6H_4Y$ (= Ar_2S) follow the usual two term rate law which is common to substitution reactions of square planar platinum(II) complexes, *viz.* eq. 2, where k_1 is a first order rate constant associated with solvolysis of the complex and k_2 is a second order rate constant associated with direct nucleophilic displacement at the complex (1). The two term rate law is consistent with the reaction scheme, [3] and [4].

[2] $\text{Rate} = k_1[\text{Complex}] + k_2[\text{Complex}][XC_6H_4SC_6H_4Y]$

[3] *trans*-$[PtCl_2py_2] + Ar_2S \xrightarrow[\text{slow}]{k_2}$ *trans*-$[PtCl(Ar_2S)py_2]^+ + Cl^-$

[4] *trans*-$[PtCl(Ar_2S)py_2]^+ + Ar_2S \xrightarrow{\text{fast}}$ *trans*-$[Pt(Ar_2S)_2py_2]^{2+} + Cl^-$

The experimental pseudo first order rate constants, k_{obs}, are related to k_1 and k_2 by [5].

[5] $$k_{obs} = k_1 + k_2[XC_6H_4SC_6H_4Y]$$

Typical plots of k_{obs} *vs.* $[XC_6H_4SC_6H_4Y]$ are shown in Fig. 1. The slopes of these linear plots correspond to the various k_2's and the common intercept to k_1. The kinetic data are tabulated in Table 1 together with the calculated values of the nucleophilic reactivity constant, n_{Pt}^0, and the sum of the Hammett substituent parameters for each nucleophile. The nucleophilic reactivity constant has been defined by eq. 6. In order to

[6] $$n_{Pt}^0 = \log(k_2/k_1)$$

render n_{Pt}^0 a dimensionless quantity, k_1 has been divided by 26, the molar concentration of methanol (4). A fairly good linear free energy

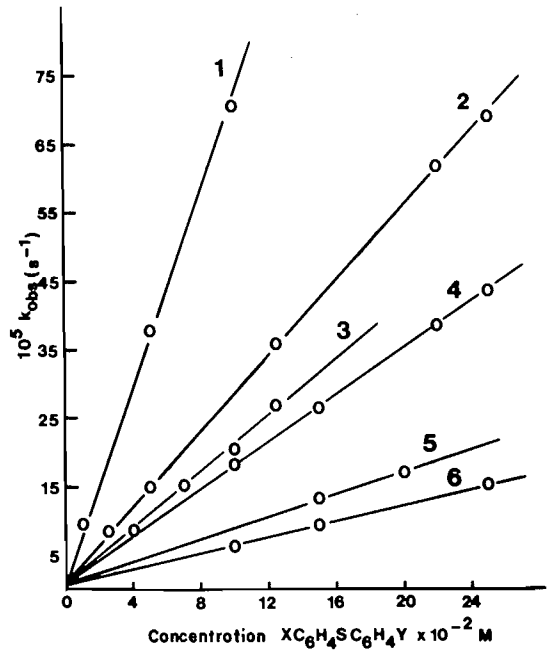

FIG. 1. Typical plots of k_{obs} *vs.* the concentration of nucleophile. **1**, X = Y = NH_2; **2**, X = Y = OH; **3**, X = Y = CH_3O; **4**, X = CH_3O Y = H; **5**, X = Y = F; **6**, X = Y = H.

TABLE 1. Kinetic data for the reaction: *trans*-$[PtCl_2py_2]$ + $2Ar_2S \rightarrow$ *trans*-$[Ptpy_2(Ar_2S)_2]^{2+}$ + $2Cl^-$ in methanol at 30°

$XC_6H_4SC_6H_4Y$				
X	Y	$k_2 \times 10^3$ ($s^{-1} M^{-1}$)	n_{Pt}^0	$\Sigma\sigma_p$*
NH_2	NH_2	7.25	4.27	−1.32
OH	OH	2.72	3.85	−0.74
CH_3O	CH_3O	2.06	3.73	−0.54
CH_3	CH_3	1.84	3.68	−0.34
CH_3O	H	1.70	3.64	−0.27
H	H	0.64	3.22	0
F	F	0.77	3.30	+0.12
NH_2	NO_2	0.78	3.31	+0.12
Cl	H	0.69	3.25	+0.23
Cl	Cl	0.63	3.21	+0.45
NO_2	NO_2	0.096†	2.4	+1.56

*Values obtained from ref. (18).
†Extrapolated from Fig. 2.

relation is obtained when log k_2 is plotted *vs.* $\Sigma(\sigma_p)$ where σ_p is the Hammett substituent parameter for X and Y (see Fig. 2). This linear correlation indicates that the para-substituents make a significant contribution to the nucleophilic reactivity of the diaryl sulfide towards the substrate. This may be readily attributed to a change in "basicity" (σ donor capability) of the sulfur donor atom as a direct consequence of the inductive and mesomeric effects of the substituents, X and Y. Hence, nucleophilic reactivity is lessened when electron withdrawing substituents are present and vice versa for electron releasing substituents. The kinetic results reported herein also lend further support to the suggestion that bond making is the driving force in the intimate mechanism when divalent sulfur functions as a nucleophile towards a platinum(II) substrate (6).

From a synthetic point of view, the kinetic data given in Table 2 are of some interest since it has been observed that 4,4′-dinitrodiphenyl sulfide will not readily react with K_2PtCl_4 to form *trans*-$[PtCl_2(Ar_2S)_2]$ as does diphenyl sulfide and other 4,4′-disubstituted diphenyl sulfides (7–9). The data plotted in Fig. 2 are consistent with this observation. Extrapolation of this linear plot to $\Sigma(\sigma_p) = 1.54$ (X = Y = NO_2) gives $k_2 = 9.6 \times 10^{-5} M^{-1} s^{-1}$ and a value of 2.4 for the nucleophilic reactivity constant. This small value of n_{Pt}^0 catalogues 4,4′-dinitrodiphenyl sulfide as a very poor nucleophile for platinum(II). Hence it is not surprising that this particular sulfide does not readily coordinate to platinum(II).

The calculated values of n_{Pt}^0 listed in Table 2 may be taken as an overall relative measure of the "nucleophilicity" of organic sulfides of the type, $XC_6H_4SC_6H_4Y$ towards *trans*-$[PtCl_2py_2]$. Presumably, this order of reactivity applies to other square planar complexes of platinum(II) as well.

Experimental

(1) Materials

trans-Dichlorobis(pyridine)platinum(II)

This complex was prepared according to the procedure of Kauffman (10).

4,4′-Dihydroxydiphenyl Sulfide

A generous sample of this nucleophile was provided by Dr. Karl H. Heller, Farbenfabriken Bayer A-G, West Germany.

4,4′-Dimethoxydiphenyl Sulfide

This was prepared by the methylation of 4,4′-dihydroxydiphenyl sulfide with dimethyl sulfate (11), m.p. 41–43° (lit. (11), m.p. 42–45°).

4,4′-Dimethyldiphenyl Sulfide

This nucleophile was prepared by reacting the Grignard reagent formed from 4-methyl-4′-bromobenzene in tetrahydrofuran with sulfur monochloride (12), m.p. 55–57° (lit. (13), m.p. 56.6–56.9°).

4-Methoxydiphenyl Sulfide

This was prepared according to the method outlined in the literature (14).

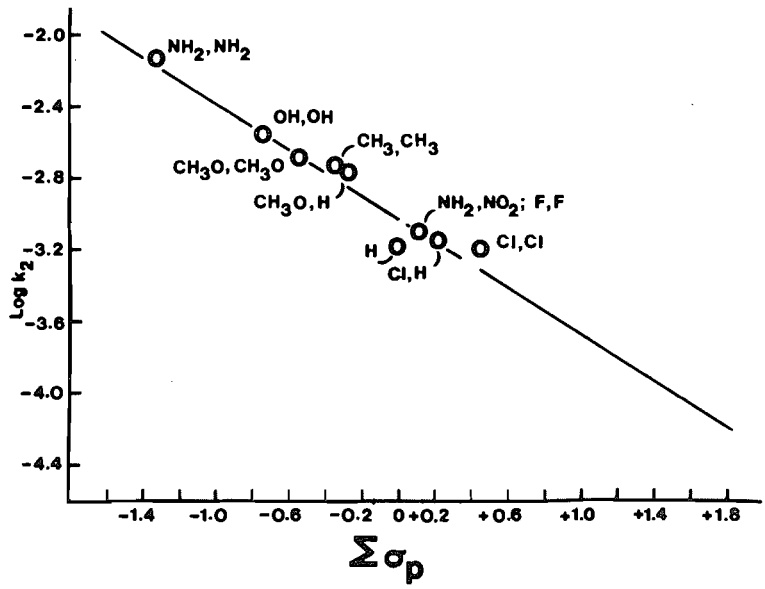

FIG. 2. Hammett plot of $\log k_2$ *vs.* $\Sigma\sigma_p$.

Anal. Calcd. for $C_{13}H_{12}OS$: C, 72.22; H, 5.55. Found: C, 71.42; H, 5.46.

4,4′-Difluorodiphenyl Sulfide

This was prepared by following the procedure of Leonard and Sutton (15), b.p. 134–138° (10 mm) (lit. (15), b.p. 136–137° (9 mm)).

4,4′-Dichlorodiphenyl Sulfide

This was prepared by reduction of the corresponding sulfoxide with zinc in acetic acid (16).

4-Chlorodiphenyl Sulfide

This nucleophile was isolated from the reaction of sodium thiophenolate with *para*-dichlorobenzene in DMF (17), b.p. 156–160° (2 mm) (lit. (17), b.p. 155–158° (2.5 mm)).

The following nucleophiles were obtained from Eastman Organic Chemicals, Inc. or Aldrich Organic Chemicals, Inc. and were purified by fractional distillation or recrystallization from ethanol: 4,4′-diaminodiphenyl sulfide, diphenyl sulfide, and 4-amino-4′-dinitrodiphenyl sulfide.

(2) Kinetic Measurements

The rates of reaction of the diaryl sulfides with *trans*-$[PtCl_2py_2]$ were determined at 30 ± 0.1° in methanol by monitoring the change in electrical conductivity with a Beckman Model RC16B1 conductivity meter at 1000 Hz. The platinum electrodes of the conductivity cell were coated with platinum black. Pseudo first order kinetics were maintained during the course of a kinetic run where the concentration of the substrate, *trans*-$[PtCl_2py_2]$, was 5.0×10^{-5} *M* and the concentration of the nucleophile was varied from 4.5×10^{-3} to 2.5×10^{-1} *M* (at least a 90-fold excess). Pseudo first order rate plots of $\ln R_t/R_t - R_\infty$ *vs.* time, where R_t, R_∞ are the electrical resistances at time, *t*, and at infinite time respectively, were linear for at least 50–60% reaction. The pseudo first order rate constants (k_{obs}) were calculated from the slopes of these linear plots using a least squares analysis. The pseudo first order rate constants were reproducible to within ± 5%.

(3) Isolation of Reaction Products

The following general procedure based on the outline of Pearson *et al.* (5) was used to obtain several of the reaction products. Stoichiometric amounts of *trans*-$[PtCl_2py_2]$, the appropriate nucleophile, and silver para-toluenesulfonate (silver tosylate) were allowed to react in methanol at 25° for approximately 24 h with the exclusion of light. The AgCl which precipitated from the reaction mixture was filtered off and the filtrate evaporated to dryness. The product was washed with water, ether, and recrystallized from methanol.

Anal. Calcd. for $[Ptpy_2(Ph_2S)_2](tosylate)_2$: C, 53.96; H, 4.12; Pt, 18.26. Found: C, 51.64; H, 4.57, Pt, 17.62.

Anal. Calcd. for $[Ptpy_2(CH_3OC_6H_4SC_6H_4OCH_3)_2](tosylate)_2$: C, 52.57; H, 4.38; Pt, 16.42. Found: C, 51.45; H, 4.53; Pt, 15.36.

Anal. Calcd. for $[Ptpy_2(CH_3OC_6H_4SC_6H_5)_2](tosylate)_2$: C, 53.23; H, 4.25; Pt, 17.29. Found: C, 51.23; H, 4.20; Pt, 16.85.

Anal. Calcd. for $[Ptpy_2(CH_3C_6H_4SC_6H_4CH_3)_2](tosylate)_2$: C, 55.57; H, 4.63; Pt, 17.35. Found: C, 53.54; H, 4.38; Pt, 17.02.

Microanalyses were determined by A. B. Gygli, Toronto, Ontario. Platinum was determined by reduction to the metal in an atmosphere of hydrogen at *ca.* 700°.

The authors wish to thank the National Research Council of Canada for financial support.

1. L. CATTALINI. Prog. Inorg. Chem. **13**, 295 (1970).
2. F. BASOLO and R. G. PEARSON. Mechanism of inorganic reactions. 2nd Ed. John Wiley and Sons, Inc., New York, N.Y., 1967.
3. C. H. LANGFORD and H. B. GRAY. Ligand sub-

stitution processes. W. A. Benjamin, Inc., New York, N.Y., 1965.
4. U. BELLUCO, L. CATTALINI, F. BASOLO, R. G. PEARSON, and A. TURCO. J. Am. Chem. Soc. **87**, 241 (1965).
5. R. G. PEARSON, H. SOBEL, and J. SONGSTAD. J. Am. Chem. Soc. **90**, 319 (1968).
6. L. CATTALINI, M. MARTELLI, and G. KIRSCHNER. Inorg. Chem. **7**, 1488 (1968).
7. C. V. SENOFF. Can. J. Chem. **46**, 3287 (1968).
8. W. A. SPOFFORD, E. L. AMMA, and C. V. SENOFF. Submitted for publication.
9. C. V. SENOFF. Unpublished results.
10. G. B. KAUFFMAN. Inorg. Synth. **7**, 251 (1963).
11. H. J. SHINE, M. RAHMAN, H. SEEGER, and G. S. WU. J. Org. Chem. **32**, 1901 (1967).
12. H. E. RAMSDEN. U.S. Pat. 2 921 964. Chem. Abstr. **55**, 64416 (1961).
13. G. C. HAMPSON, R. H. FARMER, and L. E. SUTTON. Proc. Roy. Soc. London **143A**, 147 (1933).
14. G. E. HILBERT and T. B. JOHNSON. J. Am. Chem. Soc. **51**, 1526 (1929).
15. N. J. LEONARD and L. E. SUTTON. J. Am. Chem. Soc. **70**, 1564 (1948).
16. H. RHEINBOLT and E. GIESBRECHT. J. Am. Chem. Soc. **68**, 973 (1946).
17. J. H. UHLENBROEK. Rec. Trav. Chim. **80**, 1057 (1961).
18. D. H. MCDANIEL and H. C. BROWN. J. Org. Chem. **23**, 420 (1958).

Can. J. Chem. Downloaded from www.nrcresearchpress.com by 210.87.254.5 on 09/05/12
For personal use only.

The Pseudo Thermodynamics of Solvolysis. A Detailed Study of the Pressure and Temperature Dependence of Benzyl Chloride Solvolysis in *t*-Butyl Alcohol – Water Mixtures

S. J. DICKSON AND J. B. HYNE

Department of Chemistry, University of Calgary, Calgary, Alberta

Received March 15, 1971

The pseudo first order rate constants for the solvolysis of benzyl chloride in aqueous *t*-butyl alcohol (*t*-BuOH) are reported at 40.00, 50.25, and 60.50 °C at various pressures up to 4084 atm. From these data the first temperature derivatives (ΔH^* and ΔS^*), the first (ΔV^*) and second pressure derivatives, $\partial\Delta V^*/\partial P$, and the mixed second derivative, $\partial\Delta V_0^*/\partial T$, of the rate are evaluated. These activation parameters exhibit extremum behavior in the highly aqueous solvent region. This behavior is discussed in terms of solvent structure variation. The signs of the pressure dependence of ΔH^* and ΔS^* are shown to be consistent with those required by the Maxwell type relationships for classical thermodynamic systems.

Les constantes de vitesse du pseudo premier ordre pour la solvolyse du chlorure de benzyle dans l'alcool tertiobutyllique (*t*-BuOH) sont rapportées à 40.00, 50.25, et 60.50 °C pour différentes pressions supérieures à 4084 atm. A partir de ces données, les dérivées premières de la vitesse par rapport à la température (ΔH^* et ΔS^*), ses dérivées première (ΔV^*) et seconde par rapport à la pression, $\partial V^*/\partial P$, et sa dérivée seconde $\partial\Delta V_0^*/\partial T$ sont calculées. Ces paramètres d'activation montrent un comportement extrême dans la région des solvants fortement aqueux. Ce comportement est analysé en fonction de la variation de structure du solvant. On montre que les signes de ΔH^* et ΔS^* dépendant de la pression sont compatibles avec ceux requis par les relations du type relations de Maxwell pour des systèmes thermodynamiques classiques.

Canadian Journal of Chemistry, 49, 2394 (1971)

Introduction

In recent years a number of researchers (1–3) have investigated the behavior of the first derivative pseudo thermodynamic activation parameters. Their efforts have demonstrated that many interesting phenomena are concealed in free energy parameters by the compensatory behavior of enthalpy and entropy. More recently the extremum behavior exhibited by ΔH^* and ΔS^* in aqueous binary solvent mixtures has been observed for the volume, ΔV^*, (4–6) and the heat capacity, ΔC_p^*, (7) of activation. The particular sensitivity of ΔC_p^*, the second derivative of the rate with respect to temperature, to variation of the binary solvent composition suggests that the parameter may be even more valuable than ΔH^* or ΔS^* for the investigation of solvent effects on reaction rates. This increased sensitivity of a second derivative parameter also prompts investigation of the second *pressure* derivative of the rate, $\partial\Delta V^*/\partial P$.

A major difficulty in understanding the solvent dependence of the various pseudo thermodynamic parameters has arisen because no single system has been examined exhaustively to obtain values for all of the accessible activation parameters. Accordingly, it was decided to examine the solvolysis of benzyl chloride in *t*-butyl alcohol – water binary solvent mixtures with a view to determining ΔH^*, ΔS^*, ΔV^*, $\partial\Delta V^*/\partial P$, $\partial\Delta V^*/\partial T$, $\partial\Delta H^*/\partial P$, and $\partial\Delta S^*/\partial P$. A summary of the relationship between the various derivatives is demonstrated in Fig. 1. The ΔC_p^* value was not included in this study since the accurate determination of this parameter requires that the rate be measured at many more than the three temperatures used in this work.

The technique of dissecting the differential pseudo thermodynamic parameters of activation into their component initial and transition state parts has been previously employed (4, 8). In this study the enthalpy and volume of activation were so dissected by determining the partial molal enthalpies and volumes of solution of the initial state benzyl chloride as a function of binary solvent composition. Such dissections establish whether the initial state or transition state is primarily responsible for the observed behavior of the differential activation parameter.

The Maxwell relationships shown in eqs. 1 and

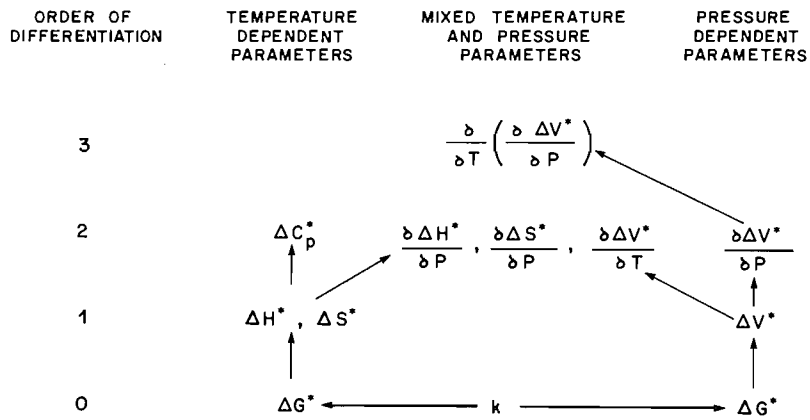

FIG. 1. Inter-relationship of pseudo thermodynamic parameters of activation.

2 can also be tested for a pseudo thermodynamic

$$[1] \qquad (\partial \Delta S/\partial P)_T = -(\partial \Delta V/\partial T)_P$$

$$[2] \qquad (\partial \Delta H/\partial P)_T = \Delta V - T(\partial \Delta V/\partial T)_P$$

system since the parameters $\partial \Delta S^*/\partial P$, $\partial \Delta V^*/\partial T$, $\partial \Delta H^*/\partial P$, and ΔV^* are available from the rate–pressure–temperature data.

The solvolysis of benzyl chloride in aqueous *t*-butyl alcohol solvent mixtures was chosen for this investigation for the following reasons. The solvolysis of benzyl chloride has been extensively investigated (4–6, 9–11) in other solvent media and a wide range of other activation parameters are available. The solvolysis reaction velocity is also convenient for the precision rate determinations required in second derivative rate studies. In addition, aqueous *t*-butyl alcohol solvent mixtures are known to display the most marked extremum behavior of any aqueous binary mixture both in activation parameters and other physical properties (12). Consequently, it was hoped that large changes in the parameters studied might be observed with variation of the composition of this aqueous binary.

Experimental

Kinetics

All rate constants were determined by following the change of conductance of the reaction mixture due to HCl formation as a function of time. With the exception of the conductivity cells, the high pressure apparatus and techniques employed in this work have been described previously (13). Some comments on the types of conductance cell employed are, however, justified. The three different types of conductivity cells which were used to determine the reaction rates are illustrated in Fig. 2. For the majority of the slower reactions studied the cell shown in Fig. 2A was used. This cell had a capacity of about 10 ml. Occasionally during the course of a slow reaction the teflon rods moved to the end of the precision bore glass tubing and into the electrode compartment changing the cell characteristics and producing discontinuities in the rate data plots. In order to reduce the risk of this happening the cells shown in Fig. 2B were employed for the slowest reactions. These cells had the advantage of having a longer length of precision bore tubing and removed the danger of the pistons dropping into the cell compartment between the electrodes.

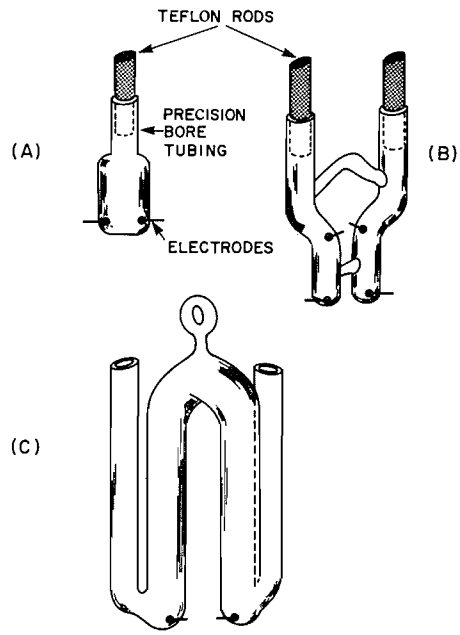

FIG. 2. Conductivity reaction cells.

Can. J. Chem. Downloaded from www.nrcresearchpress.com by 210.87.254.5 on 09/05/12
For personal use only.

TABLE 1. Rate constants for the solvolysis of benzyl chloride at 40.00 °C as a function of *t*-BuOH – H_2O solvent composition and pressure

Pressure (atm)	$k \times 10^5$ s^{-1}		$k \times 10^6$ s^{-1}		$k \times 10^7$ s^{-1}	
	Mol fraction *t*-BuOH		Mol fraction *t*-BuOH		Mol fraction *t*-BuOH	
	0	0.025	0.05	0.10	0.20	0.30
1	7.538±0.005	4.88±0.04	15.27±0.02	2.323±0.004	6.150±0.004	2.96±0.06
341	8.33 ±0.09	5.44±0.02	21.68±0.01	—	—	—
681	9.64 ±0.03	6.28±0.04	28.63±0.05	4.528±0.003	9.99 ±0.02	4.75±0.08
1021	10.74 ±0.06	—	—	—	—	—
1362	12.3 ±0.2	7.86±0.10	43.6 ±0.1	7.827±0.007	15.49 ±0.01	7.47±0.06
2042	14.94 ±0.08	9.76±0.10	58.7 ±0.4	11.8 ±0.1	22.3 ±0.1	10.52±0.02
2722	18.86 ±0.07	11.67±0.06	74.3 ±0.2	17.4 ±0.1	29.8 ±0.2	13.9 ±0.2
3403	23.9 ±0.3	—	—	—	—	17.7 ±0.2
4084	—	—	102.2 ±0.9	31.53 ±0.35	51.98 ±0.09	—

TABLE 2. Rate constants for the solvolysis of benzyl chloride at 50.25 °C as a function of *t*-BuOH – H_2O solvent composition and pressure

Pressure (atm)	$k \times 10^5$ s^{-1}		$k \times 10^6$ s^{-1}		$k \times 10^7$ s^{-1}	
	Mol fraction *t*-BuOH		Mol fraction *t*-BuOH		Mol fraction *t*-BuOH	
	0*	0.025	0.05	0.10	0.20	0.30
1	21.35±0.04	12.23±0.06	38.4 ±0.7	6.79±0.06†	18.68±0.02†	9.10±0.05†
341	24.3 ±0.1	14.67±0.01	54.44±0.06	—	—	—
681	28.1 ±0.3	17.5 ±0.1	69.8 ±0.9	13.03±0.03	32.3 ±0.2	15.2 ±0.3
1021	31.3 ±0.2	—	—	—	—	—
1362	35.54±0.01	22.3 ±0.3	110.8 ±0.4	21.1 ±0.5	47.5 ±1.3	22.1 ±0.5
2042	46.6 ±0.7	28.2 ±0.2	155.9 ±0.8	31.8 ±0.4	70.6 ±0.1	32.53±0.08
2722	61.0 ±1.1	35.5 ±0.3	203 ±2	44.5 ±0.2†	95.0 ±0.3	43.4 ±0.1
4084	—	—	—	77.9 ±0.3†	157 ±1	69.2 ±0.8†

*Temperature recorded for rates in pure water was 50.10 not 50.25 °C.
†Data taken from ref. 4.

The cell used for the fastest ($k = 10^{-3}$ to 10^{-4} s^{-1}) solvolysis reactions in pure water had a capacity of 25 ml and is shown in Fig. 2C. It was found that if the small cells were employed to measure the fast reaction rates, the differences in successive resistance values were close to zero after thermal and pressure equilibration had been attained. The larger cells, having a path length about 20 times greater than the smaller cells, were preferred because of the increased differences in successive resistance values and hence increased experimental sensitivity.

Duplicate kinetic runs carried out in the three different types of conductivity cells yielded rates which agreed within the maximum experimental uncertainty of ±1%.

Enthalpy and Volume of Solution

The modified dilatometric technique employed in this study for the measurement of the partial molal volume ($\bar{V}^s$) of the benzyl chloride as a function of solvent composition has been discussed previously (4). The partial molal heat of solution of the initial state, $\Delta\bar{H}_s^s$, was determined using the method described by Arnett and coworkers (8). As reported by Arnett, limited solubility of benzyl chloride in highly aqueous solvent systems precluded enthalpy determinations in this composition region.

Results

Rates

The pseudo first order rate constants for the solvolysis of the benzyl chloride (10^{-3} *M* maximum concentration) under various conditions of temperature, pressure, and solvent composition were obtained by analyzing the conductance–time data by the method of Guggenheim (14) using a computerized least mean squares calculation (13). Rate constants and associated uncertainties are presented in Tables 1–3. In all cases the rate constants are the average of a minimum of three duplicate runs. The deviations listed are the average deviations of the individual rate determinations from the mean value and in general represent an uncertainty of less than ±1%. In some instances the rate *vs.* pressure data are incomplete; although it was desirable, it was not always possible to record rate data over the entire pressure range (1–4084 atm). The rate of reaction increased as the temperature and

Can. J. Chem. Downloaded from www.nrcresearchpress.com by 210.87.254.5 on 09/05/12
For personal use only.

TABLE 3. Rate constants for the solvolysis of benzyl chloride at 60.50 °C as a function of *t*-BuOH – H_2O solvent composition and pressure

Pressure (atm)	$k \times 10^5$ s^{-1}		$k \times 10^6$ s^{-1}		$k \times 10^7$ s^{-1}	
	Mol fraction *t*-BuOH		Mol fraction *t*-BuOH		Mol fraction *t*-BuOH	
	0	0.025	0.05	0.10	0.20	0.30
1	58.75±0.08	30.3 ±0.1	92.1±0.5	18.88±0.1	53.56±0.01	26.1±0.3
171	62.5 ±0.1	—	—	—	—	—
341	66.4 ±0.7	36.88±0.09	130.9±0.5	26.3 ±0.3	—	33.5±0.1
511	71.5 ±0.3	—	—	—	—	—
681	74.9 ±0.4	45.0 ±0.2	170.7±0.9	33.96±0.08	89.7±1.5	42.5±0.5
851	81.09±0.09	—	—	—	—	—
1021	86.3 ±0.5	50.6 ±0.9	—	43.7 ±0.2	—	—
1191	94.3 ±1.1	—	—	—	—	—
1362	100.2 ±0.3	59.5 ±0.2	259.7±0.7	53.9 ±0.1	137 ±1	63.1±0.9
1532	106.7 ±0.1	—	—	—	—	—
1702	112.6 ±0.4	—	—	66.7 ±0.8	—	—
1872	122.6 ±1.5	—	—	—	—	—
2042	—	79.8 ±0.7	365 ±1	81.3 ±0.1	202.1±0.2	92.8±1.2
2382	—	—	—	97.75±0.08	—	—
2722	—	—	493 ±1	113.0 ±0.9	258 ±5	125 ±1
3062	—	—	—	128.9 ±0.2	—	—
3403	—	—	—	151.3 ±0.7	—	—
3742	—	—	—	173 ±1	—	—
4084	—	—	—	189 ±1	373 ±6	184.8±0.3

pressure increased, and consequently at the higher temperatures and pressures the rate could not always be measured with the conventional apparatus employed. For each system studied the rate was determined at a minimum of six pressures.

Golinkin *et al.* (4) have reported rate constants for the solvolysis of benzyl chloride in aqueous *t*-butyl alcohol mixtures at 50.25 °C. It will be noted that some of the data used here have been measured by Golinkin (5). The general effects studied by Golinkin *et al.* required less accurate data than was considered essential for this study. Consequently, if the uncertainty in Golinkin's rate constants was greater than ±1%, or if the data did not lie on a smooth ln *k vs.* pressure curve, it was redetermined in this study. In the majority of instances in which repetition was deemed necessary the data lay within the limits of uncertainty claimed by the earlier workers.

The solvolysis of benzyl chloride in 0.10 mol fraction of *t*-butyl alcohol at 60.50 °C was examined in considerable detail as a specific test of the adequacy of the rate–pressure relationship used in this work. The ln *k vs.* pressure plot for this system is shown in Figure 3A. Two important points should be noted. Firstly, this plot indicates that ln *k* is a smooth monotonic function of pressure. Secondly, because the uncertainties in

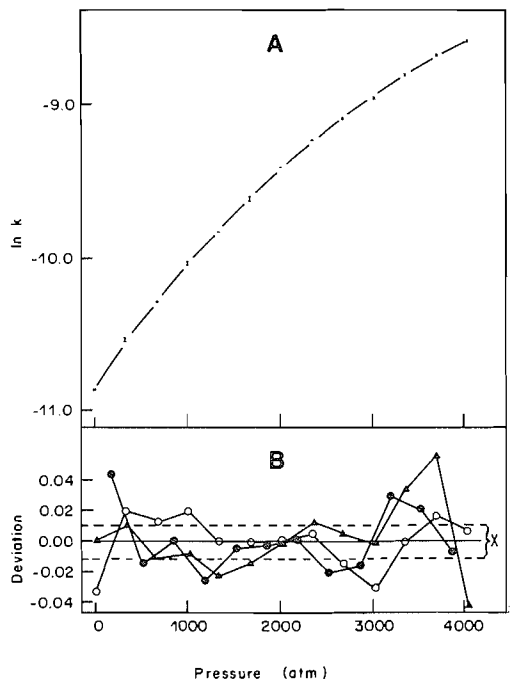

FIG. 3. Solvolysis of benzyl chloride in 0.10 mol fraction aqueous *t*-butyl alcohol at 60.50 °C. (A) Pressure dependence of rate (ln *k*); (B) deviation between ln $k_{obs.}$ and ln $k_{calc.}$ for various expressions. ○, Quadratic; ▲, Benson–Berson; ●, incremental; ×, experimental uncertainty.

Can. J. Chem. Downloaded from www.nrcresearchpress.com by 210.87.254.5 on 09/05/12
For personal use only.

TABLE 4. Dependence of ΔH^* (ΔS^*) on pressure and solvent composition

Pressure (atm)	ΔH^* kcal mol^{-1} (ΔS^* cal deg^{-1} mol^{-1})† Mol fraction *t*-BuOH 0	0.025	0.05	0.10	0.20	0.30
1	20.1±0.2 (13.1±0.7)	17.9±0.1 (21.4±0.4)	17.6±0.2 (24.6±0.7)	20.6±0.2 (18.7±0.6)	21.3±0.2 (19.1±0.6)	21.4±0.1 (20.1±0.4)
341	20.4±0.2 (12.2±0.6)	18.7±0.2 (18.3±0.5)	17.6±0.2 (23.9±0.7)	—	—	—
681	20.1±0.2 (12.7±0.7)	19.3±0.2 (16.2±0.6)	17.4±0.2 (23.8±0.7)	19.8±0.2 (19.9±0.7)	21.6±0.3 (17.1±1.0)	21.5±0.2 (18.7±0.5)
1021	20.5±0.2 (11.4±0.7)	—	—	—	—	—
1362	20.6±0.1 (10.8±0.1)	19.9±0.1 (14.0±0.4)	17.4±0.2 (22.9±0.6)	18.9±0.2 (21.7±0.7)	21.5±0.3 (16.7±0.9)	21.0±0.3 (19.8±0.9)
2042	—	20.6±0.2 (11.1±0.6)	17.9±0.1 (20.9±0.4)	18.9±0.1 (20.9±0.4)	21.7±0.2 (15.2±0.6)	21.4±0.3 (17.6±0.9)
2722	—	—	18.5±0.3 (18.3±1.1)	18.3±0.2 (22.0±0.6)	21.2±0.3 (16.0±1.1)	21.6±0.2 (16.3±0.5)
4084	—	—	—	17.5±0.1 (23.4±0.3)	19.3±0.3 (21.0±1.1)	—

†All entropies negative.

the rate determinations are extremely small, it is possible to establish with confidence the magnitude of the curvature in these plots, *i.e.* $\partial \Delta V^*/\partial P$.

The Enthalpy and Entropy of Activation

The enthalpies of activation used in this work were all calculated using eq. 3.

$$[3] \qquad \Delta H^* = -R\left(\frac{\ln k_2/T_2 - \ln k_1/T_1}{1/T_2 - 1/T_1}\right)$$

The temperatures, T_2 and T_1, in this case are 60.50 and 40.00 °C respectively. The extracted enthalpies of activation can then be associated with the mean temperature of 50.25 °C (15). The values obtained for ΔH^* in pure water are in excellent agreement with the results of other researchers (15–17). The uncertainties associated with each ΔH^* value listed in Table 4 are shown.

The entropies of activation used in this work were calculated by substituting the rate constant k at 50.25 °C, and the corresponding ΔH^* value into eq. 4, where k_b is Boltzmann's constant, and

$$[4] \qquad \Delta S^* = R \ln k - R \ln k_b T/h + \Delta H^*/T$$

h is Planck's constant.

It should be noted that the hydrolyses in water were carried out at 40.00, 50.10 (not 50.25), and 60.50 °C. The difference between this intermediate temperature, 50.10 °C, and that at which ΔH^* was calculated, 50.25 °C, is sufficiently small to render any correction insignificant compared with the experimental uncertainty.

The Volume of Activation

According to the transition state theory (18) the volume of activation, ΔV^*, for a reaction is related to the pressure dependence of the rate constant by eq. 5.

$$[5] \qquad \Delta V^* = -RT(\partial \ln k/\partial P)_T$$

Before the evaluation of ΔV^* from a set of rate constants is possible, the functional dependence of ln k on pressure must be established. The four main algebraic expressions that have been employed are given by eqs. 6–9 (19).

$$[6] \qquad \text{Linear: } \ln k = A + BP$$

$$[7] \qquad \text{Quadratic: } \ln k = A + BP + CP^2$$

$$[8] \qquad \text{Benson–Berson: } \frac{\ln k/k_0}{P} = A + BP^{0.523}$$

$$[9] \qquad \text{Incremental: } \frac{\ln k_{n+1}/k_n}{P_{n+1} - P_n} = A + B\left(\frac{P_{n+1} + P_n}{2}\right)$$

Golinkin *et al.* (19) have examined the relative merits of these empirical equations, and con-

Can. J. Chem. Downloaded from www.nrcresearchpress.com by 210.87.254.5 on 09/05/12
For personal use only.

TABLE 5. Activation volume parameters for the solvolysis of benzyl chloride in aqueous *t*-butyl alcohol as a function of temperature

Mol fraction *t*-BuOH	ΔV_0^* (ml mol^{-1})		
	40.00 °C	50.25 °C	60.50 °C
0.0000	−9.09±0.01	−9.9 ±0.1	−10.3 ±0.2
0.0250	−10.07±0.06	−13.0 ±0.1	−15.20±0.04
0.0500	−21.54±0.05	−24.7 ±0.6	−24.5 ±0.05
0.1000	−24.7 ±0.1	−23.97±0.01	−23.1 ±0.1
0.2000	−18.66±0.06	−20.22±0.03	−22.03±0.04
0.3000	−19.8 ±0.5	−19.5 ±0.2	−20.71±0.01

Mol fraction *t*-BuOH	$(\partial\Delta V^*/\partial P)_T \times 10^3$ (ml atm^{-1} mol^{-1})		
	40.00 °C	50.25 °C	60.50 °C
0.0000	0.2 ±0.2	−0.3 ±0.2	−0.6 ±0.2
0.0250	1.27±0.04	2.09±0.02	2.36±0.01
0.0500	4.92±0.06	6.4 ±0.4	6.0 ±0.5
0.1000	4.2 ±0.1	4.12±0.02	3.88±0.06
0.2000	2.62±0.03	3.21±0.01	4.44±0.07
0.3000	3.7 ±0.3	3.15±0.07	3.70±0.02

cluded that for the solvolysis of benzyl chloride in aqueous alcohol mixtures the quadratic (eq. 7) gives the best representation of the data. Nevertheless, it was considered necessary to recheck these expressions to determine which one gave a best fit for the present data. The linear eq. 6 was eliminated because of the obvious non-linear pressure dependence of ln k (see Fig. 3A). The constants A, B, and C in the other three equations were evaluated by fitting the 0.1 mol fraction alcohol rate data to each expression in turn using a computer programmed least mean squares technique. The deviations between ln $k_{(\text{observed})}$ and ln $k_{(\text{calculated})}$ for each equation were determined as previously reported (13). These deviations are shown in Fig. 3B as a function of experimental pressure for each of the three equations tested. Similar analyses were performed on all the rates at the several temperatures and solvent compositions employed. The deviations for the quadratic equation, when taken for all mol fractions of solvent, at all temperatures, were considered to be more random functions of pressure than those obtained by using the other two expressions. The standard deviations were smaller for the quadratic equation than for the other functions. On this basis the quadratic form was preferred to the other relationships.

A possibility which deserves consideration is whether or not the data could be better represented by a polynomial of higher than second order (see ref. 20). In view of the fact that most of the deviations shown in Fig. 3B are of the same order of magnitude as the experimental uncertainty (±1%), the extension of the polynomial to powers higher than two seems unjustified in this particular instance.

Substitution of the quadratic expression (eq. 7) into eq. 5 produces eq. 10 and enables ΔV^* to be evaluated.

$$[5] \qquad \Delta V^* = -RT(\partial \ln k/\partial P)_T$$

$$[10] \qquad = -RT\,\partial(A + BP + CP^2)/\partial P$$

$$[11] \qquad = -RT(B + 2CP)$$

The volume of activation at atmospheric pressure (zero applied pressure) is therefore given by eq. 12.

$$[12] \qquad \Delta V_0^* = -RTB$$

The pressure dependence of ΔV^* is given by differentiation of eq. 11 with respect to pressure.

$$[13] \qquad \partial\Delta V^*/\partial P = -2RTC$$

The uncertainties in ΔV_0^* and $\partial\Delta V^*/\partial P$ were calculated using eqs. 14 and 15 respectively,

$$[14] \qquad \delta\Delta V_0^* = -RT\delta B$$

$$[15] \qquad \delta\partial\Delta V^*/\partial P = -2RT\delta C$$

where δB and δC are the uncertainties in the B and C coefficients of eq. 7 given by the least squares analysis. The values of ΔV_0^* and $\partial\Delta V^*/\partial P$ and their limits of uncertainty are shown in Table 5.

Can. J. Chem. Downloaded from www.nrcresearchpress.com by 210.87.254.5 on 09/05/12
For personal use only.

Can. J. Chem. Downloaded from www.nrcresearchpress.com by 210.87.254.5 on 09/05/12
For personal use only.

TABLE 6. The partial molal volume ($\bar{V}^g$) and partial molal heat of solution ($\Delta\bar{H}^s$) of the benzyl chloride initial state

Mol fraction *t*-BuOH	$\bar{V}^g$ (ml mol^{-1}) (50.25 °C)	$\Delta\bar{H}_s^g$ (kcal mol^{-1}) (25.0 °C)
0	115*	—
0.05	135.1±0.9	7.21±0.10
0.075	—	7.41±0.11
0.10	137.7±0.6	5.16±0.06
0.20	132.5±0.6	3.15±0.01
0.30	126.5±0.6	2.65±0.02

*Reference 4.

Enthalpies and Volumes of the Initial State

The partial molal volumes, $\bar{V}^g$, and the partial molal heats of solution, $\Delta\bar{H}_s^g$, of benzyl chloride in aqueous *t*-butyl alcohol mixtures are listed in Table 6. The values of $\Delta\bar{H}_s^g$ were determined at 25.0 °C (not 50.25 °C) to minimize solvolysis of the reacting solute. The determination of the solvent dependence of the partial molal heat of solution of the benzyl chloride transition state in the following section is therefore based on the difference between two enthalpies determined at two different temperatures. While this may have a small effect on absolute magnitude of the transition state enthalpies, it is unlikely to effect the general form of the solvent dependence.

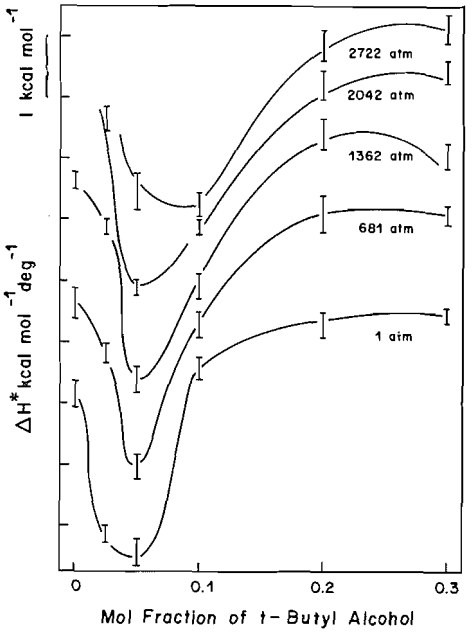

FIG. 4. Solvent dependence of activation enthalpy at various pressures.

Discussion

The Temperature Derivatives of the Rate, ΔH^* and ΔS^*

The enthalpies and entropies of activation are plotted against binary solvent composition in Figs. 4 and 5 respectively. The main feature of both plots is the appearance of deep minima in the range 0.05–0.10 mol fraction *t*-butyl alcohol.

Arnett (21) has offered the most comprehensive explanation of this extremum behavior. For the solvolysis of *t*-butyl chloride in aqueous ethyl alcohol, Arnett was able to demonstrate that the minimum in ΔH^* was due, in large part, to the variation of the partial molal heat of solution of the *initial state* with solvent composition.

In Fig. 6 the solvent dependences of ΔH^*, at atmospheric pressure, and the partial molal heat of solution of the initial state ($\Delta\bar{H}_s^g$) across the same solvent composition range are compared for the solvolysis of benzyl chloride in aqueous *t*-butyl alcohol. This data permits the extraction of the solvent dependence of the enthalpy of the transition state, $\delta\Delta\bar{H}_s^t$, using eq. 16.

$$[16] \qquad \delta\Delta\bar{H}_s^t = \delta(\Delta H^* + \Delta\bar{H}_s^g)$$

The solubility of benzyl chloride in highly aqueous *t*-butyl alcohol was insufficient to permit measurement of $\Delta\bar{H}_s^g$ at compositions containing

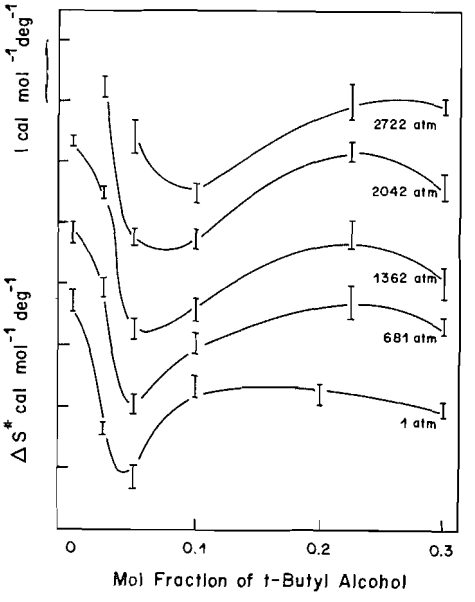

FIG. 5. Solvent dependence of activation entropy at various pressures.

Can. J. Chem. Downloaded from www.nrcresearchpress.com by 210.87.254.5 on 09/05/12
For personal use only.

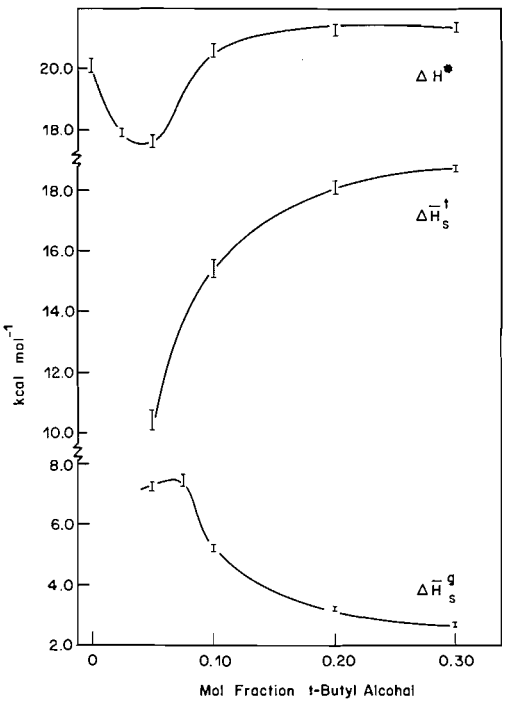

FIG. 6. Dissection of activation enthalpy. Solvent dependence of activation (ΔH^*) and initial ($\Delta \bar{H}_s^g$) and transition state ($\Delta \bar{H}_s^t$) enthalpies at 50.25 °C.

less than 0.05 mol fraction alcohol. For this reason one cannot be dogmatic about concluding that the extremum in ΔH^* is due to a corresponding extremum in the enthalpy behavior of the initial state $\Delta \bar{H}_s^g$. However, there is every indication in the limited data available at 0.05 and 0.075 mol fraction *t*-butyl alcohol that this may indeed be so.

In Figs. 4 and 5 the positions of minima in ΔH^* and ΔS^* appear to be pressure dependent and move to higher alcohol compositions as the pressure is increased. If the extremum in ΔH^* is due to the difference in the structure making and breaking abilities of the initial and transition states, as Arnett has suggested (21), then this observation is not surprising. The application of pressure itself is known to influence the structure of aqueous binary solutions (22) and hence presumably the additional structural influence of solute molecules, such as benzyl chloride, would be expected to vary with pressure.

The concurrent shift of the position of the extremum in ΔS^* is in keeping with the generally observed compensatory behavior of enthalpy and entropy changes, but also suggests that the order–disorder phenomena which produce the observed extrema have their optimum effect at higher alcohol compositions at higher pressures.

The Pressure Derivatives of the Rate, ΔV^* and $\partial \Delta V^*/\partial P$

The volumes of activation obtained in this work are plotted against solvent composition in Fig. 7. The negative values of ΔV_0^* are characteristic for solvolyses of alkyl halides in aqueous binary solvents (4–6). The negative sign corresponds to increased electrostriction of the kinetically important immediate solvent environment around the more polar transition state compared with the initial state (23–25).

The volume of activation is defined by eq. 17 and thus can be "dissected" in a similar manner to enthalpy. Values of $\bar{V}^t$ were calculated from

$$\Delta V_0^* = \bar{V}^t - \bar{V}^g \qquad [17]$$

the measured values of ΔV_0^* and $\bar{V}^g$. The solvent dependences of these three parameters at 50.25 °C are shown in Fig. 8. It is apparent that the minimum in the behavior of the activation parameter, ΔV_0^*, is primarily, but not exclusively, the result of a maximum in $\bar{V}^g$ rather than in the extremum behavior of the transition state volume, $\bar{V}^t$, as a function of solvent composition.

The extremum behavior of $\bar{V}^t$ of benzyl chlo-

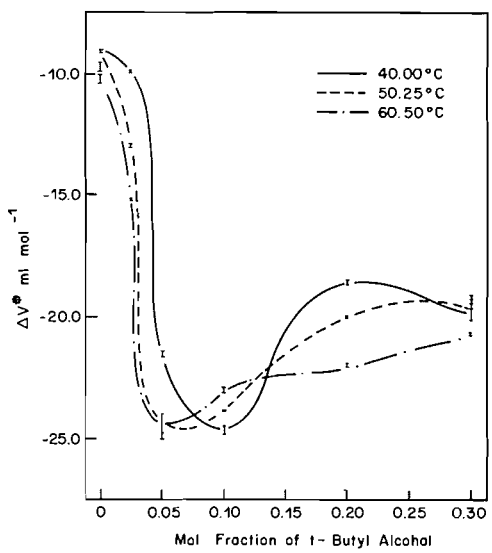

FIG. 7. Solvent dependence of activation volume at three temperatures.

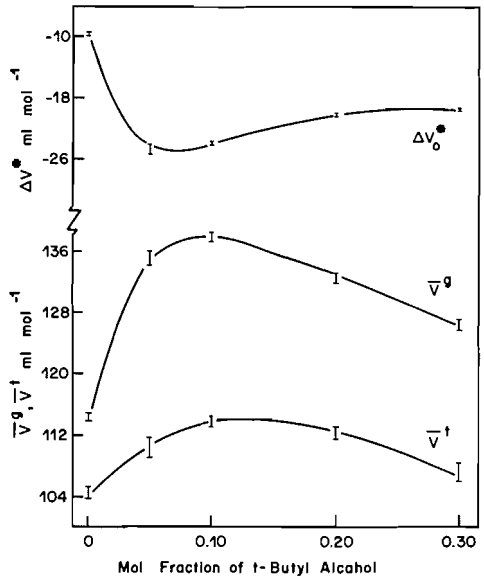

FIG. 8. Dissection of activation volume. Solvent dependence of activation (ΔV_0^*) and initial ($\overline{V}^g$) and transition state ($\overline{V}^t$) volumes at 50.25 °C.

ride in aqueous *t*-butyl alcohol is actually typical of several other non-electrolytes in aqueous alcohol mixtures. In aqueous ethyl alcohol, for example, benzyl fluoride, benzyl chloride and *p*-chloro benzyl chloride all pass through a maximum in $\overline{V}^g$ near 0.3 mol fraction alcohol (26). These maxima occur at a solvent composition which has been suggested to possess minimum structuredness (27). *If* it is valid to draw an analogy between the behavior of the benzyl chloride initial state in aqueous ethyl alcohol and in aqueous *t*-butyl alcohol, then the maximum in $\overline{V}^g$ in the latter solvent may indicate that the solvent possesses a minimum of structuredness at 0.1 mol fraction of alcohol. The observed minima in ΔV_0^* in the 0.05–0.10 mol fraction alcohol region would then be largely attributed to solvent structural changes.

Since 0.1 mol fraction *t*-butyl alcohol corresponds to 30% alcohol by volume it is hardly surprising that relatively little water-like open structuredness remains in such a binary and hence non-electrostricting solutes such as benzyl chloride must *displace* solvent molecules on dissolution resulting in a maximization of partial molal volume of solution.

In Fig. 7 it is apparent that an increase in temperature from 40.00 to 50.25 °C causes the minimum in ΔV_0^* to move to a less alcoholic composition. Whether the further increase in temperature from 50.25 to 60.50 °C produces any further shift in the extremum is not conclusive. An increase in temperature also causes the minimum in the partial molal volume of *t*-butyl alcohol in aqueous *t*-butyl alcohol mixtures, $\overline{V}_{t\text{-BuOH}}$, to move to lower alcohol compositions (12). Since $\overline{V}_{t\text{-BuOH}}$ presumably reflects the solvent structure, the parallel effect of temperature on the extremum in ΔV_0^* and $\overline{V}_{t\text{-BuOH}}$ strengthens the argument that this activation parameter reflects solvent structural changes.

Figure 9 illustrates the effect of solvent and temperature variation on $\partial\Delta V^*/\partial P$ the second pressure derivative of the rate. The values of $\partial\Delta V^*/\partial P$ are generally positive and exhibit a pronounced maximum at about 0.05 mol fraction of *t*-butyl alcohol.

The pressure dependence of ΔV^* is defined by eq. 18. This dissection is analogous to the Arnett

$$[18] \qquad \partial\Delta V^*/\partial P = \partial\overline{V}^t/\partial P - \partial\overline{V}^g/\partial P$$

et. al. (8) and Golinkin *et al.* (4) dissections of ΔH^* and ΔV_0^* respectively.

In pure water $\partial\Delta V^*/\partial P$ is approximately zero indicating that the partial molal volumes of the initial and transition states responded similarly to pressure, *i.e.* $\partial\overline{V}^t/\partial P \doteqdot \partial\overline{V}^g/\partial P$. This appar-

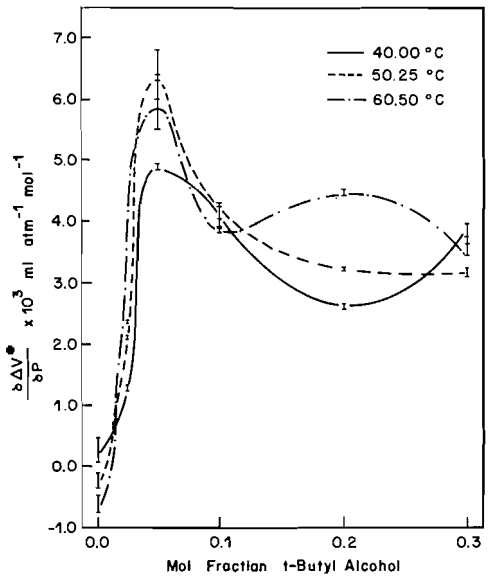

FIG. 9. Pressure dependence of activation volume as a function of solvent composition at three temperatures.

Can. J. Chem. Downloaded from www.nrcresearchpress.com by 210.87.254.5 on 09/05/12
For personal use only.

TABLE 7. The relative signs of $\partial\Delta V_0^*/\partial T$, $\partial\Delta S^*/\partial P$, $(\Delta V_0^* - T\partial\Delta V_0^*/\partial T)$ and $\partial\Delta H^*/\partial P$ at 50.25 °C and atmospheric pressure

Mol fraction *t*-BuOH	ΔV_0^*	$-T\partial\Delta V_0^*/\partial T$	$\partial\Delta S^*/\partial P$	$\partial\Delta H^*/\partial P$	$(\Delta V_0^* - T\partial\Delta V_0^*/\partial T)$
0	−9.9	+20	+	+	+10
0.025	−13.0	+75	+	+	+60
0.05	−24.7	?	+	0	?
0.10	−24.0	−25	−	−	−50
0.20	−20.2	+50	+	+	+30
0.30	−19.5	?	+	0	?
		Maxwell relationship		Maxwell relationship	

ently equal "compressibility" of the transition state and initial state solvent shells is particularly interesting since it implies that the *electrostricted* solvent shell around the strongly dipolar transition state is no "harder" than the solvation shell around the initial state which presumably is primarily the result of *hydrophobic* type interactions.

Until experimental techniques are developed to enable the transition and initial state contributions to $\partial\Delta V^*/\partial P$ to be determined, any interpretation of the solvent dependence of this parameter is perhaps premature. It is nonetheless interesting to note that the compression of aqueous *t*-butyl alcohol passes through a minimum at 0.03 mol fraction alcohol (28), close to the composition possessing a maximum in $\partial\Delta V^*/\partial P$. This must surely be yet a further indication that the extremum behavior of these activation parameters primarily reflects changes in solvent structure.

The sharp extremum behavior of $\partial\Delta V^*/\partial P$, a *second pressure derivative* of the rate, for the solvolysis of benzyl chloride in aqueous *t*-butyl alcohol, is remarkably similar to the solvent dependence of the second temperature derivative of the rate, ΔC_p^*, for the solvolysis of *t*-butyl chloride in the same solvent mixtures as reported by Robertson and Sugamori (7). It would appear that the extremum behavior of such second derivative pseudo thermodynamic parameters of activation is both more pronounced and more complex than is the case for the corresponding first derivative parameters (ΔH^*, ΔS^*, ΔV^*) where single extrema of modest amplitude are more characteristic.

Mixed Temperature and Pressure Derivatives, $\partial\Delta S^*/\partial P$, $\partial\Delta H^*/\partial P$, and $\partial\Delta V_0^*/\partial T$

It should be recognized at once that the parameters under consideration in this section are second derivatives of the measured rate and are subject to the accumulated errors of rate, pressure, and temperature measurements. It is, therefore, hardly surprising that the errors associated with such mixed second derivatives are sizeable. The values shown in Table 7 should therefore be viewed primarily as indications of the sign of the parameter (*i.e.* the slope, positive or negative, of the plots in Figs. 10 and 11) with little significance being attached to the numerical values where these are shown.

The entropy and enthalpy of activation are plotted against pressure in Figs. 10 and 11. The plots indicate that both these activation parameters are pressure dependent and at some compositions the dependence is non-linear. This non-linearity presents difficulties in obtaining numerical values of the pressure dependence of the entropy, $\partial\Delta S^*/\partial P$, and the enthalpy, $\partial\Delta H^*/\partial P$. Because of these difficulties the signs, as obtained from the *initial* slopes of Figs. 10 and 11, but not the magnitudes of $\partial\Delta S^*/\partial P$ and $\partial\Delta H^*/\partial P$ are reported in Table 7.

Examination of Figs. 10 and 11 and also the signs in Table 7 reveals that the solvent dependence of $\partial\Delta S^*/\partial P$ and $\partial\Delta H^*/\partial P$ are very similar. This would tend to suggest that the well known compensatory behavior of ΔH^* and ΔS^* (27) is still in evidence when the second derivatives are compared. This is in fact to be expected. The differences in the intermolecular interactions, of the initial state and the transition state with the solvent environment, that resulted in the compensatory behavior of the first derivative parameters are still operative in the second derivatives.

The volumes of activation for the solvolysis of benzyl chloride in aqueous *t*-butyl alcohol mixtures were determined at 40.00, 50.25, and

Can. J. Chem. Downloaded from www.nrcresearchpress.com by 210.87.254.5 on 09/05/12
For personal use only.

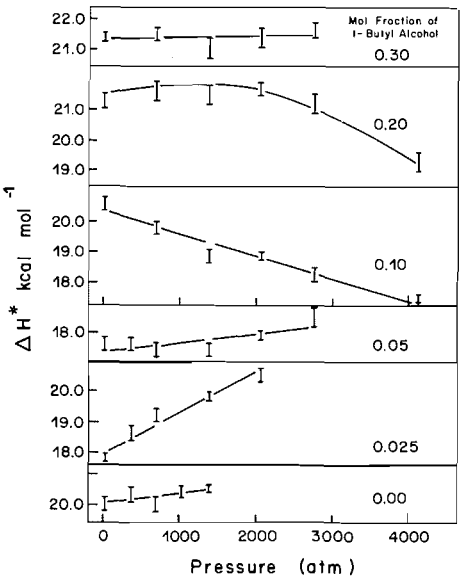

FIG. 10. Pressure dependence of activation enthalpy at various *t*-butyl alcohol mol fractions.

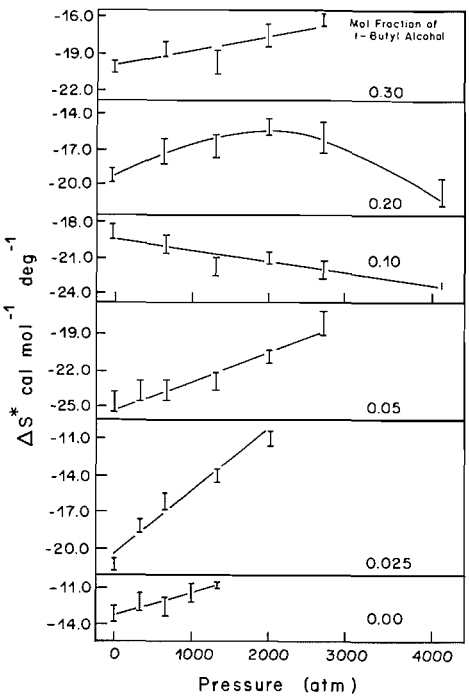

FIG. 11. Pressure dependence of activation entropy at various *t*-butyl alcohol mol fractions.

60.50 °C (Table 5). The temperature dependence, $\partial\Delta V_0^*/\partial T$, can thus be evaluated. Values of $\partial\Delta V_0^*/\partial T$ are not reported for 0.05 or 0.30 mol fraction of *t*-butyl alcohol since it appears that at these solvent compositions the dependence of ΔV_0^* on temperature is markedly non-linear. The values of $\partial\Delta V_0^*/\partial T$ obtained at other solvent compositions are listed in Table 7, and it is apparent that this second derivative of the rate is extremely sensitive to solvent composition changes.

The solvent dependence of $\partial\Delta V_0^*/\partial T$ is due to the different responses of the temperature dependence of the volume of the component initial and transition states to solvent changes. The solvent dependence of the initial and transition state contributions, and hence of the activation parameter itself, may well be a reflection of the changing structural stability of the solvent medium as cosolvent is added to water.

Maxwell Type Pseudo Thermodynamic Relationships

The availability of a large number of temperature and pressure derived pseudo thermodynamic parameters of activation for the single system examined in this work permits the application of classical thermodynamic identity tests to these "kinetic" parameters. In particular the following well established thermodynamic relationships may be tested using the pseudo thermodynamic parameters obtained in this work.

$$[19] \qquad (\partial\Delta S^*/\partial P)_T = -(\partial\Delta V^*/\partial T)_P$$

$$[20] \qquad (\partial\Delta H^*/\partial P)_T = \Delta V^* - T(\partial\Delta V^*/\partial T)_P$$

The high experimental accuracy required to obtain meaningful values of the mixed second derivative parameters in eq. 19 has limited the testing of this identity to establishing that the parameters have indeed opposite signs in the case of the Menshutkin reaction (29) and some hydrolyses (30).

The present work offers the opportunity of examining this Maxwell relationship as a function of solvent composition. Unfortunately, as was noted above, the determination of a numerical value of $\partial\Delta S^*/\partial P$ was not possible. It was possible, however, to determine the sign of $\partial\Delta S^*/\partial P$. The signs of both $\partial\Delta S^*/\partial P$ and $\partial\Delta V_0^*/\partial T$ are shown in Table 7 and demonstrate again that these parameters have opposite signs as required by eq. 19.

The present data also enables eq. 20 to be tested. The numerical evaluation of $\Delta V_0^* - T\partial\Delta V_0^*/\partial T$ is shown in Table 7. Numerical values of $\partial\Delta H^*/\partial P$ could not be obtained but again its

Can. J. Chem. Downloaded from www.nrcresearchpress.com by 210.87.254.5 on 09/05/12
For personal use only.

Can. J. Chem. Downloaded from www.nrcresearchpress.com by 210.87.254.5 on 09/05/12
For personal use only.

sign could be determined. It is apparent, from the results listed in Table 7, that the signs of $\partial\Delta H^*/\partial P$ and $\Delta V_0^* - T\partial\Delta V_0^*/\partial T$ are in agreement with eq. 20.

Although it is not presently justifiable to extract numerical values which would permit rigorous checks of the validity of eqs. 19 and 20 for pseudo thermodynamic parameters, the agreement of signs obtained in these complex second derivative relationships serves to establish further the credibility and reality of the mixed second derivative parameters obtained from exhaustive examination of the temperature and pressure dependence of the rate of this solvolytic reaction.

Conclusion

(*1*) The extremum behavior exhibited by the activation parameters, as a function of solvent composition, holds clues to our understanding of kinetic solvent effects. Explanation of these extrema requires knowledge of both the initial and transition state solvent dependences.

(*2*) The extrema observed in ΔH^*, ΔS^*, and ΔV^* are also present in the second derivative parameters. These latter exhibit more pronounced extremum behavior and, as in the study of ΔH^* and ΔS^* behavior, may further aid our comprehension of these systems.

(*3*) The analogous behavior of the activation parameters and non-kinetic properties of the solvent itself indicate that the extrema in the former are related to solvent structure.

(*4*) The validity of Maxwellian type relationships in this pseudo thermodynamic system supports the application of real state thermodynamics to kinetic systems.

(*5*) The evaluation of a third derivative of the rate, the temperature dependence of $\partial\Delta V^*/\partial P$ is at present premature. Figure 9 suggests that $\partial\Delta V^*/\partial P$ is temperature dependent, but this dependence is small. This demonstrates that, in spite of the extreme accuracy of the data, still greater reproducibility will be necessary to permit the determination of third derivative pseudo thermodynamic parameters.

The authors would like to acknowledge the assistance of Dr. Moyra Mackinnon and Mrs. Margaret Estep who determined the partial molal volumes and the partial molal heats of solution respectively. Financial assistance for this research was provided by the National Research Council of Canada.

1. S. Winstein and A. H. Fainberg. J. Am. Chem. Soc. **79**, 5937 (1957).
2. E. Tommila, A. Koivisto, J. P. Lyyra, K. Antell, and S. Heimo. Ann. Acad. Sci. Fenn. Ser. A, II, 47 (1959).
3. J. B. Hyne and R. E. Robertson. Can. J. Chem. **34**, 931 (1956).
4. H. S. Golinkin, I. Lee, and J. B. Hyne. J. Am. Chem. Soc. **89**, 1307 (1967).
5. H. S. Golinkin. Ph.D. Thesis. The University of Calgary, Calgary, Alberta, 1966.
6. D. D. Macdonald. Ph.D. Thesis. The University of Calgary, Calgary, Alberta, 1969.
7. R. E. Robertson and S. E. Sugamori. J. Am. Chem. Soc. **91**, 7254 (1969).
8. E. M. Arnett, W. G. Bentrude, J. J. Burke, and P. McC. Duggebly. J. Am. Chem. Soc. **87**, 1541 (1965).
9. B. Bensley and G. J. Kohnstam. J. Chem. Soc. 4747 (1957).
10. E. Tommila, E. Paakkala, U. K. Vintaneau, A. Erva, and S. Varila. Ann. Acad. Sci. Fenn. AII (91), 1 (1959).
11. E. Tommila. Acta Chem. Scand. **20**, 923 (1966).
12. F. Franks and D. J. G. Ives. Quart. Rev. **20**, 1 (1966).
13. J. B. Hyne, H. S. Golinkin, and W. G. Laidlaw. J. Am. Chem. Soc. **88**, 2140 (1966).
14. E. A. Guggenheim. Phil. Mag. **2**, 538 (1926).
15. H. S. Golinkin and J. B. Hyne. Can. J. Chem. **46**, 125 (1968).
16. J. B. Hyne, R. Wills, and R. E. Wonkka. J. Am. Chem. Soc. **84**, 2914 (1962).
17. R. E. Robertson, R. L. Heppolette, and J. M. W. Scott. Can. J. Chem. **37**, 803 (1959).
18. M. G. Evans and M. Polanyi. Trans. Faraday Soc. **31**, 875 (1935).
19. H. S. Golinkin, W. G. Laidlaw, and J. B. Hyne. Can. J. Chem. **44**, 2193 (1966).
20. B. T. Baliga and E. Whalley. Can. J. Chem. **48**, 528 (1970).
21. E. M. Arnett. *In* Physico chemical processes in mixed aqueous solvents. *Edited by* F. Franks. Heinemann, London, 1967.
22. A. W. Lawson and A. J. Hughes. *In* High pressure physics and chemistry. *Edited by* A. S. Bradley. Academic Press, London, 1963.
23. S. D. Hamaan. Physico-chemical effects of pressure. Butterworths Scientific Publications, London, 1957.
24. E. Whalley. *In* Advances in physical organic chemistry. Vol. 2. *Edited by* V. Gold. Academic Press Inc., New York, N.Y., 1964.
25. K. E. Weale. Chemical reactions at high pressures. *Edited by* M. B. Donald. Spon's Chemical Engineering Series, London, 1967.
26. M. J. Mackinnon. Private communication.
27. J. B. Hyne. *In* Hydrogen bonded solvent systems. *Edited by* A. K. Covington and P. Jones. Taylor and Francis Ltd., London, 1968.
28. J. E. Stutchbury. Aust. J. Chem. **9**, 536 (1956).
29. K. E. Weale. J. Chem. Soc. 2959 (1954).
30. B. T. Baliga and E. Whalley. J. Phys. Chem. **73**, 654 (1969).

Can. J. Chem. Downloaded from www.nrcresearchpress.com by 210.87.254.6 on 09/05/12
For personal use only.

Permeation of Electrolytically Generated Hydrogen and Tritium Atoms through Lead[1]

BANSI L. MUJU AND FRANK R. SMITH[2]
Chemistry Department, Memorial University, St. John's, Newfoundland

Received February 26, 1971

Radiochemical and electrochemical evidence is presented that electrochemically generated tritium and hydrogen atoms permeate through lead foil at measureable rates at room temperature. The permeation process is controlled by diffusion through the metal lattice, Fick's First Law being obeyed by both H and ^{3}H atoms. Using earlier measurements of the diffusivity of H in Pb, H and ^{3}H concentrations of 4×10^{-7} and 9×10^{-13} g-atom cm^{-3} are computed for a current density of 53 mA cm^{-2} at the Pb cathode surface.

The overall hydrogen–tritium separation factor, S_T is apparently 0.3 ± 0.15, in contrast to Bockris and Srinivasan's 6.7 and 7.2 for cathodic gas evolution from acidic and alkaline media, respectively. Reasons are suggested for this large difference.

Une preuve radiochimique et électrochimique est donnée pour montrer que des atomes d'hydrogène et de tritium, engendrés d'une façon électrochimique, traversent à la température de la pièce et à vitesse mesurable un feuille de plomb. Le processus de passage est contrôlé par la diffusion à travers le réseau métallique; la première loi de Fick étant observée à la fois pour les atomes H et ^{3}H En se servant des mesures antérieures sur la diffusion de H dans le Pb, les concentrations de 4.10^{-7} et 9.10^{-13} pour H et ^{3}H sont calculées dans le but d'avoir une densité de courant de 53 mA cm^{-2} à la surface de la cathode en Pb.

Le facteur de séparation global, S_T, hydrogène–tritium semble être de 0.3 ± 0.15; valeur très différente de celles de Bockris et Srinivasan (6.7 et 7.2) pour le dégagement de gaz à la cathode à partir d'un milieu respectivement acide et basique. Des raisons pour cette grande différence sont suggérées.

Canadian Journal of Chemistry, **49**, 2406 (1971)

In earlier work, Ives and Smith (1) presented evidence of long-term overpotential changes in electrolytic hydrogen evolution at lead electrodes under conditions of high purity. During periods of electrolysis of several days, overpotential decreases of hundreds of mV were observed and attributed to activation of the lead by continuous accumulation in the lattice of electro-generated H atoms. The possibility that the effects were caused by impurities was discounted (*i*) by the observation that little change of overpotential occurred when experimental conditions were not optimal and (*ii*) because of the use in the work of proven methods of attaining high surface cleanliness, namely anodic polishing, cathodic preelectrolysis, and continuous adsorptive cleaning with activated carbon.

The argument for hydrogen entry into the lead lattice was based largely on grounds of plausibility, although some earlier (2) and some more recent work (3, 4) was unfavorable to this hypothesis. However, the atomic H uptake experiments of Wells and Roberts (5) in 1964 with evaporated and sintered Pb films were encouraging. The H uptake was far more than could be accounted for by *adsorption* on the measured surface. This work, recently extended by Roberts and Young (6), led to a proposal that a solid lead hydride exists, and is of composition $PbH_{0.19}$ at 0 °C. This hydride has considerably more stability than such transient entities as Paneth's assumed gaseous PbH_4 (7).

Recently, we have shown by an electrochemical method (8) that electrolytic permeation of hydrogen through lead foils of 0.15 mm thickness does indeed occur (9), in contrast to earlier negative findings (3, 4), and that the diffusivity at 25 °C lies between 10^{-7} and 10^{-6} cm^2 s^{-1}. We now present radiochemical and electrochemical evidence that the electrolytic permeation rate of tritium and of hydrogen is governed by diffusion in the solid phase. The radiochemical method has

[1]This research was supported, in part, by the Defence Research Board of Canada, Grant Number 5401-09.

[2]To whom correspondence should be addressed.

Can. J. Chem. Downloaded from www.nrcresearchpress.com by 210.87.254.6 on 09/05/12
For personal use only.

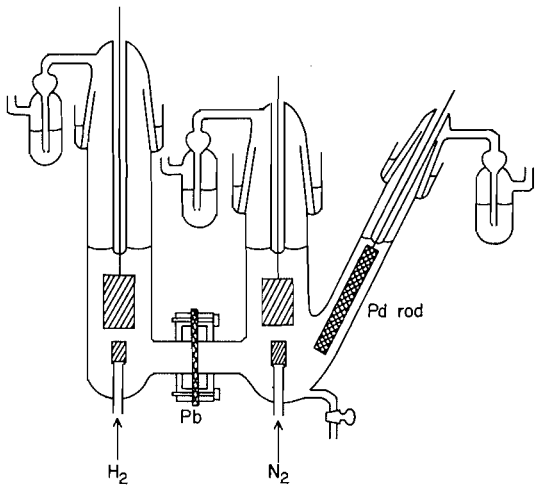

FIG. 1. Electrolysis permeation cells. Left hand side, cathodization cell with Ptized Pt anode and cathode side of Pb in H_2-saturated 1 *M* $HClO_4$; right hand side, diffusion side cell with Ptized Pt cathode, Pd hydride reference and diffusion side of Pb in N_2-saturated 0.2 *M* KOH.

not previously been reported. It is likely to have wide applicability to metals having low hydrogen solubilities, hitherto little studied.

Experimental

Goodfellow Metals Ltd. 99.9% pure lead foils were degreased in refluxing benzene (4 h), washed with ethanol and with 3× distilled water. They were chemically polished in 60% $HClO_4$ in contact with Pt, washed in 3× distilled water and mounted in the cell (Fig. 1) with thin polyethylene gaskets between the flat flanges. Thicknesses were determined with a micrometer.

The cathode side had a 3 cm^2 platinized platinum counter electrode, supplied with H_2 from an Elhygen generator. This H_2 passed through copper and Pyrex tubing, a liquid N_2-cooled trap and a 3× distilled water-filled presaturator. $HClO_4$ (7 ml of 1.0 *M*, 70% double vacuum distilled $HClO_4$ from G. F. Smith and Co., diluted with 3× distilled water) with a ^{3}H concentration of 2 mCi ml^{-1} (diluted from 100 mCi ml^{-1} Tracerlab tritiated water) was used as catholyte.

The diffusion side had a similar counter electrode supplied with Matheson prepurified N_2, passing through a similar gas train, except that the trap was cooled with solid CO_2 and ethanol. N_2 was deoxygenated by prereduced BTS catalyst Badische Anilin- und Soda-Fabrik maintained in a furnace at 140 °C. The reference electrode was a 3 mm diameter × 4 cm long palladium rod, first palladized in 2% aqueous $PdCl_2$ in 1 *M* HCl for 5 min (10) and then potentiostatically hydrogen-charged during 16 h at +50 mV *vs.* H_2 reference, both in H_2 saturated 0.2 *M* KOH. Charging was accomplished in the absence of the lead foil. As diffusion side electrolyte, 15 ml of 0.2 *M* KOH in 3 × distilled water was normally used.

The diffusion side of the Pb foil was potentiostatted at +136 to +140 mV *vs.* PdH with the inexpensive circuit of Fig. 2. Floating current measurements were made with a Keithley 150B Microvolt-Ammeter, the output of which was attenuated and recorded by a Heath EUW20A Servo Recorder, isolated from the ammeter by a Fluke A88 amplifier.

A Heath EUW15 Power Supply used at 300 V, a Simpson ammeter and make-before-break switchable resistors enabled cathodic currents of 30 μA up to tens of mA to be applied to the cathode side of the foil. With a protection current of 30 μA, the diffusion side background current was 1 to 2 μA anodic, apparently Pb dissolution.

Preliminary work by Cadersky *et al.*[3] established that H atom oxidation occurs on lead with high efficiency at potentials ⩾ 190 mV *vs.* H_2 in 0.2 *M* KOH. This potential is close to +136 mV *vs.* α/β PdH since the steady state plateau potential of the Pd–H system was found to lie in the range +50 to +60 mV, the potential being more positive during ionization of the absorbed H, in agreement with Barton and Lewis (11). Stability of reference potential was established experimentally to be ±1 mV over a 40 h period with continuous N_2 stirring.

After 4 h electrolysis at the desired current density, a cathodic protection current was reapplied and the diffusion side electrolyte run out via the 1 mm bore tap into a flask, from which twenty 0.25 ml samples were pipetted out. Fifteen ml of a scintillation cocktail of composition (12): naphthalene (80 g l^{-1}), 2,5-diphenyloxazole (5 g l^{-1}), and 1,4-bis-[2-(5-phenyloxazolyl)]benzene (50 mg l^{-1}) in xylene (38.5%), 1,4-dioxane (38.5%) and ethanol (23.1%), was used at −15 °C for each sample in a polyethylene vial. Fresh cocktail was prepared for each experiment and its efficiency (21.0 to 27.3%) determined with a standard 20 000 disintegrations per minute ^{3}H sample together with 0.25 ml 0.2 *M* KOH. A counting time of 40 min in a Nuclear Chicago Model 6860 Mark I liquid scintillation computer refrigerated to 0–5 °C was adopted as standard, the background count rate of 13 to 39 counts per minute being deducted or discriminated in the measurements. Sample count rates of 80 to 490 counts per minute were observed in the experiments reported.

Thorough cleaning and testing of the diffusion side glassware was essential for the success of this work. Initial cleaning was with hot concentrated HNO_3, followed by water washing, steaming and drying in an oven. Since glassware was blown onto the gas lines, subsequent cleaning was effected *in situ*. This always included steaming. The palladium hydride electrode was allowed to degas in 0.2 *M* KOH after each experiment. This also freed it of possible ^{3}H contamination.

Experiments were conducted at 25 ± 3 °C in a thermostatted room.

Results

In Figs. 3 and 4 are presented steady state permeation rates of H and ^{3}H atoms, respectively, as

[3]I. Cadersky, B. L. Muju, and F. R. Smith, unpublished work.

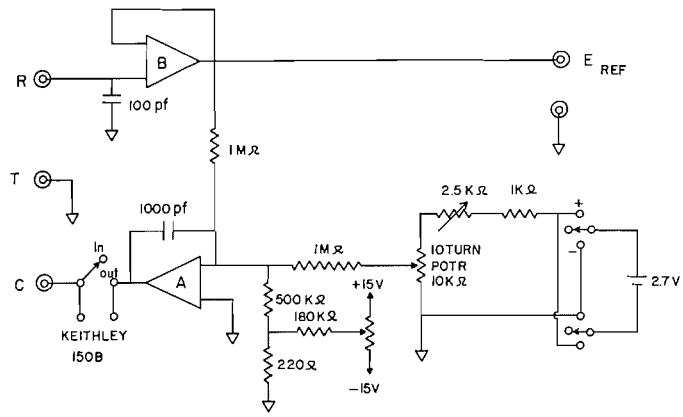

FIG. 2. Potentiostat circuit for diffusion side of Pb. R, T, and C are reference, test (Pb), and counter electrode inputs. Amplifiers A and B are Analog Devices Inc. Models 183K and 146K, respectively, powered from a ±15 V power supply (Model 904). Features are high common mode rejection, low drift and noise, and a 5 mA output capability at ±10 V. Potentials measured at E_{ref} equal R–T electromotive force within ±0.7 mV; input impedance of B is 10^{11} ohm.

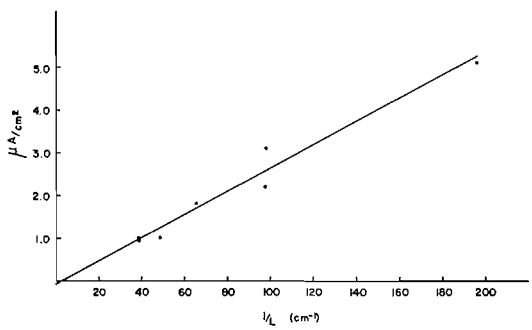

FIG. 3. Steady state H atom permeation current density (ordinate) *vs.* reciprocal thickness (abscissa) of chemically polished Pb foil.

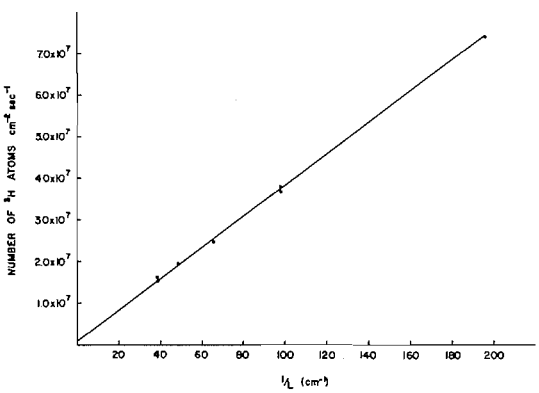

FIG. 4. Mean permeation rate of tritium (ordinate) *vs.* reciprocal thickness (abscissa) of chemically polished Pb foil.

functions of the reciprocal thickness ($1/L$) of the lead foils for L values 0.05 to 0.25 mm. These permeation rates apply to an assumed constant cathodic H atom surface coverage (^{3}H coverage) maintained for 4 h by cathodic polarization of 53 mA cm^{-2} in 1 M $HClO_4$ of 2 mCi ml^{-1} ^{3}H activity. The relatively short duration of the transient (*ca.* 0.1 h) is included in the 4 h electrolysis period.

The linearity of the plots and their zero intercepts indicate that Fick's First Law is obeyed

$$[1] \qquad J_H = D_H \frac{(C_H)_{cath} - (C_H)_{diff}}{L}$$

and

$$[1a] \qquad J_T = D_T \frac{(C_T)_{cath} - (C_T)_{diff}}{L}$$

where J_H and J_T are H and ^{3}H fluxes, respectively, and the C's are the H and ^{3}H atom concentrations *within* the metal on the cathode and diffusion sides, as indicated by the subscripts. It is assumed that the atom concentrations are determined solely by the prevailing electrochemical conditions: constant cathodic current density on the cathode side of the foil and constant potential on the diffusion side, sufficiently positive to ensure rapid ionization of diffusing atoms as they arrive. This last condition implies

$$[2] \qquad (C_H)_{diff} = (C_T)_{diff} = 0$$

Can. J. Chem. Downloaded from www.nrcresearchpress.com by 210.87.254.6 on 09/05/12
For personal use only.

Can. J. Chem. Downloaded from www.nrcresearchpress.com by 210.87.254.6 on 09/05/12
For personal use only.

and enables estimates to be made of $(C_H)_{cath}$ and $(C_T)_{cath}$ if D_H and D_T, respectively, are known.

Least squares values of the slopes of Figs. 3 and 4 are 0.027 μA cm^{-1} and 3.73 × 10^5 ^{3}H atoms cm^{-1} s^{-1}. Corresponding intercepts at $1/L = 0$ are −0.036 μA cm^{-2} and +1.01 × 10^6 ^{3}H atoms cm^{-2} s^{-1}, *i.e.* zero, within experimental error.

Consideration of errors is appropriate at this point. From the number of sample counts and background counts, assuming a Poisson distribution, the relative standard deviation calculated is in no case greater than 1.8%. Relative standard deviations of the sampling (20 samples of 0.25 ml) were between 5.3 and 9.05%, probably because a graduated 0.5 ml pipette was used. Disintegration rates of ^{3}H for the entire diffusion side electrolyte were calculated from the mean count rates, excluding in one experiment an extremely deviant count, and from the scintillation cocktail efficiency. Knowledge of the decay constant λ for tritium (13) enabled calculation of the ^{3}H concentration in the diffusion side electrolyte at the end of the electrolysis period and hence the average permeation rate (J_T).

The electrochemical permeation rates are the measured currents, the overall ammeter/recorder system accuracy being about ±2%.

Foil thicknesses were precise to ±5% or better.

It is evident from the very satisfactory linear plot of Fig. 4, in particular, that the above assessment of errors is probably pessimistic. The special difficulties of the electrochemical permeation measurements will be considered later.

Assuming that $D_H \approx 7 \times 10^{-7}$ cm^2 s^{-1}, from our previous work (9), an H atom concentration of 4 × 10^{-7} g-atom cm^{-3} just inside the cathode surface is calculated from eq. 1 and the slope of Fig. 3. This compares favorably with our earlier result (9) of 10^{-6} g-atom cm^{-3}, again at *ca.* 50 mA cm^{-2} in 1 *M* $HClO_4$.

In the absence of a measured diffusivity for tritium in lead, the value for hydrogen must be considered a fair approximation, judging by deuterium isotope effects on diffusivities of hydrogen in Pd and its alloys (14). From eq. 1*a* and the slope of Fig. 4, $(C_T)_{cath}$ is calculated to be 9 × 10^{-13} g-atom ^{3}H cm^{-3} for the present experimental conditions (^{3}H catholyte concentration of 6.85 × 10^{-8} g-atom cm^{-3}).

The data permit calculation of an overall separation factor for hydrogen and tritium originating in the catholyte, entering the metal and being ionized into the diffusion side electrolyte

$$[3] \qquad S_T = \frac{(J_H/J_T)_{diff\ side}}{(N_H/N_T)_{catholyte}}$$

where N_H and N_T are the H and ^{3}H atomic concentrations, respectively, in the cathode side electrolyte and J_H and J_T are the measured atom fluxes (expressed in the same units). S_T values range from 0.20 to 0.44, the mean of seven experiments being 0.28. S_T values less than unity have not previously been reported for electrolytic isotope separation. Thus, Bockris and Srinivasan (15) using Pb wires in 0.25 *M* H_2SO_4 and 0.5 *M* NaOH, each containing only 6 μCi ml^{-1} of tritium, obtained $S_T = 6.7 \pm 0.7$ and 7.2 ± 0.8, respectively, from the H_2 and HT evolved at the cathode.

Discussion

Hydrogen Diffusion and Hydrogen Overpotential

Ives and Smith (1) estimated the upper and lower limits for the diffusivity of hydrogen atoms in lead as 10^{-6} and 2.5 × 10^{-11} cm^2 s^{-1} (the value for interstitial Au diffusion in Pb) at 300 °K. Cadersky, Muju, and Smith (9) obtained values of 1.2 to 8.7 × 10^{-7} cm^2 s^{-1} from electrochemical permeation measurements at cathode current densities of 10 to 50 mA cm^{-2}, *i.e.* close to Ives and Smith's upper estimate.

The present work conclusively proves that H transport through Pb with these diffusivities is a bulk phenomenon, the rate of which is controlled by lattice diffusion for all foil thicknesses so far examined. This is to be expected for the chosen conditions of electrochemical generation of H atoms at the cathode side and ionization of H atoms at the diffusion side of the foil. Nothing can be said about H atom recombination at lead as a result of this work; processes of this type have occupied the attention of Roberts and Young (6).

The question arises whether the hypothesis of Ives and Smith (1) concerning the mechanism of the long term fall of hydrogen overpotential and of overshoot hysteresis effects upon step changes of current density is correct. It was assumed that both types of observation were manifestations of the same phenomenon, *i.e.* the accumulation of H atoms in the bulk of the metal during cathodic

Can. J. Chem. Downloaded from www.nrcresearchpress.com by 210.87.254.6 on 09/05/12
For personal use only.

electrolysis and its redistribution when the current was changed. The present observations may be used to comment on the velocity of the redistribution process.

If the radiochemical observations are taken as correct, the electrochemical ones being set aside for reasons to be given below, it is possible to calculate a more reasonable upper limit for the hydrogen concentration in the cathode surface layer of lead based on the more realistic separation factor ($S_T = 7$) of Bockris and Srinivasan (15). This would have a composition of $PbH_{0.0002}$ in contrast to the $PbH_{0.00002}$ of Cadersky, Muju, and Smith (9) and the $PbH_{0.2}$ of Roberts and Young (6). For a 2 mm diameter cylinder of lead, assuming a central core 1 mm deep free of hydrogen, the mean hydrogen gradient of 0.0001 g-atom cm^{-3} cm^{-1} and diffusivity of 7×10^{-5} cm^2 s^{-1} would result in a flux density of 7×10^{-11} g-atom cm^{-2} s^{-1} or a current of 7 μA cm^{-2}, which is appreciable. Correspondingly, with the thinnest foils examined (0.005 cm) in the work now reported the hydrogen permeation current should have been about 140 μA on this basis, whereas only 5.1 μA was observed. It must be emphasized that these calculations refer to a cathodic current density of *ca.* 50 mA cm^{-2}, at least five times larger than the largest steady current in Ives and Smith's investigation!

The evidence of the present work is therefore favorable to the views expressed by Ives and Smith, but it remains to clarify this matter further. Recent capacity measurements by Cadersky *et al.*[4] seem likely to provide the needed breakthrough; hydrogen adsorption pseudocapacities indicating $\theta_H \approx 0.05$ have been observed using Pb in $HClO_4$.

Hydrogen–Tritium Separation Factors

In discussing our abnormally low S_T results it may be helpful to indicate that the separation of H from ^3H according to eq. 3 is believed to involve the following stages

[4] $H_2O + H_{aq}^+ \rightleftharpoons H_3O_{aq}^+$

[4*a*] $HTO + H_{aq}^+ \rightleftharpoons H_2TO_{aq}^+$

[5] $H_3O_{aq}^+ + Pb + e_{metal}^- = H_2O + Pb\text{–}H_{ads}$

[5*a*] $H_2TO_{aq}^+ + Pb + e_{metal}^- = H_2O + Pb\text{–}T_{ads}$

[6] Diffusion of H atoms from cathode to diffusion side of Pb

[6*a*] Diffusion of ^3H atoms from cathode to diffusion side of Pb

[7] $Pb\text{–}H_{ads} + OH_{aq}^- = Pb + H_2O + e_{metal}^-$

[7*a*] $Pb\text{–}T_{ads} + OH_{aq}^- = Pb + HTO + e_{metal}^-$

Steps 4 and 5 occur in the catholyte and on the cathode side of the Pb foil, respectively, while step 7 occurs on the diffusion side. The S_T data of Bockris and Srinivasan (15) refer to steps 4 and 5, followed by H_{ads} and T_{ads} desorption as H_2 and HT, respectively. Their S_T value of 7 in acidic solution is consistent with cathodic H–D separation factors obtained on Pb, and on Hg, which is generally held to have a similar electrolytic hydrogen evolution mechanism to that of Pb (16).

In considering expected S_T values for steps 4 to 7 inclusive, it is necessary to estimate the additional separation attributable to steps 6 and 7, the values of ref. 15 being thought to be due to the equilibria of steps 4 and 4*a*, and the H_2- and HT-evolution rate-controlling steps 5 and 5*a*.

Recent work on H–D separation on cathode and diffusion sides of Ag–Pd alloy foils (17) suggests that additional separation by steps 6 and 7 is *unlikely* to result in $S_T > 15$. Under the chosen potentiostatic conditions, steps 7 and 7*a* should have rates determined solely by the diffusion steps 6 and 6*a*. The diffusivities of D and H in other metals and alloys (14, 17) are not markedly different from one another. Appreciable separation of H from ^3H is, therefore, not expected from steps 6 and 6*a* and it is extremely improbable that $D_T \approx 25\ D_H$, the relationship needed to bring our S_T's into conformity with those of ref. 15.

It is thought that our low S_T's arise from experimental difficulties associated with the complete elimination of O_2 from the system. The results of Cadersky and Smith,[5] who observed considerable sensitivity of electrochemical permeation currents to the experimental conditions, are in accord with this view. It is suggested that the H atom concentrations and permeation rates reported here and earlier (9) may be low by several orders of magnitude. To account for low S_T values, however, requires not merely that H and ^3H atoms be removed by a scavenger such as O_2 in proportion to their concentrations, but that

[4] I. Cadersky, G. M. Rao, and F. R. Smith, in preparation.

[5] I. Cadersky and F. R. Smith, unpublished work.

H atoms be removed *preferentially*. It can be argued that weakly adsorbed H and ^{3}H atoms on the cathode surface are both likely to react rapidly with O_2 and that these processes may well be diffusion-controlled. But preferential removal of H atoms would be likely only if the nature of the adsorbed species were fundamentally different in the two cases, an improbable hypothesis.

A possible explanation is that H and ^{3}H atoms, diffusing through the foil (steps 6 and 6*a*) to the diffusion side, may interact as above with O_2 and enter the solution without undergoing steps 7 and 7*a*. No error would result in the radiochemical counting method but the electrochemically measured permeation current would be diminished, since *only* those H atoms undergoing ionization (step 7) would be counted in this manner.

It is obvious that the water-sealed apparatus with its flanges and the tap on the diffusion side cannot be as gas-tight as, for instance, the high vacuum system used by Wells, Roberts, and Young (5, 6) in their gas phase adsorption studies with H atoms. This highlights one of the main difficulties of electrochemical studies of the adsorption of air-sensitive atoms and molecules.

. Finally, it may be commented that a surface phase composition of $PbH_{0.00001}$ seems very dilute for a current density of 50 mA cm^{-2}. When it is recalled that cathodic disintegration of lead in acid solution has been observed by Salzberg *et al.* (18) at 100 mA cm^{-2} and attributed by them to PbH_2 gas formation and decomposition, it is difficult to accept that even the more concentrated $PbH_{0.0002}$ is realistic. According to Bockris and Devanathan (19), surface H coverages are calculable from electrolytic permeation measurements but it is our view that this can be done only if the electrolyte composition is the same on both sides of the metal membrane. This prevents such a calculation being validly made here and is unfortunate since it is anticipated that a surface coverage approaching 100% would be found at current densities in the cathodic disintegration range.

We must emphasize, however, that we do not accept the view of the Russian (20) and Polish (21) schools that cathodic disintegration of lead and other metals is caused *solely* by alkali metal penetration into the cathode and subsequent decomposition of the alkali alloy. Experiments by Salzberg *et al.* (18) and Ives and Smith (1) have clearly shown that alkali ions are not essential in such disintegration processes.

We wish to thank Dr. W. H. Marshall and other members of the Memorial University Medical School for the use of the liquid scintillation facilities, Dr. I. Cadersky for his initial investigations of this problem and Mr. D. Seymour for glassware construction. The support of the Defence Research Board and the National Research Council of Canada is gratefully acknowledged.

1. D. J. G. Ives and F. R. Smith. Trans. Faraday Soc. **63**, 217 (1967).
2. D. P. Smith. Hydrogen in metals. University of Chicago Press, Chicago, Ill. 1948. p. 286.
3. H. R. Heath. Br. J. Appl. Phys. **3**, 13 (1952).
4. H. B. Wahlin and V. O. Naumann. J. Appl. Phys. **24**, 42 (1953).
5. B. R. Wells and M. W. Roberts. Proc. Chem. Soc. 173 (1964).
6. M. W. Roberts and N. J. Young. Trans. Faraday Soc. **66**, 2636 (1970).
7. F. Paneth. Ber. **53**, 1693 (1920).
8. M. A. V. Devanathan and Z. O. J. Stachurski. Proc. Roy. Soc. Ser. A. **270**, 90 (1962). M. A. V. Devanathan and Z. O. J. Stachurski. J. Electrochem. Soc. **111**, 619 (1964).
9. I. Cadersky, B. L. Muju, and F. R. Smith. Can. J. Chem. **48**, 1789 (1970).
10. T. B. Flanagan and F. A. Lewis. Trans. Faraday Soc. **55**, 1409 (1959).
11. J. C. Barton and F. A. Lewis. Talanta, **10**, 237 (1963).
12. F. E. Kinard. Rev. Sci. Instrum. **28**, 293 (1957).
13. G. Friedlander and J. W. Kennedy. Nuclear and radiochemistry. John Wiley, New York. 1955. p. 415.
14. F. A. Lewis. The palladium/hydrogen system. Academic Press, London. 1967. W. Jost. Diffusion in solids, liquids, gases. Academic Press, New York. 1960. p. 304 *et seq.* H. Brodowsky and E. Wicke. Engelhard Industries Tech. Bull. **7**, 41 (1966).
15. J. O'M. Bockris and S. Srinivasan. Electrochim. Acta, **9**, 31 (1964).
16. A. N. Frumkin. *In* Advances in electrochemistry and electrochemical engineering. Vol. 1. *Edited by* P. Delahay. John Wiley, New York. 1961. p. 65; Vol. 3. 1963. p. 287.
17. F. R. Smith and M. Hammerli. Z. phys. Chem. N.F. In press.
18. H. W. Salzberg. J. Electrochem. Soc. **100**, 146 (1953); H. W. Salzberg and L. W. Gastwirt. J. Electrochem. Soc. **104**, 701 (1957).
19. J. O'M Bockris and M. A. V. Devanathan. Tech. Rept. No. 4 to Office of Naval Research, Contract Nonr 551(22) NRO 36-028, 1961. p. 28.
20. B. N. Kabanov. Electrochim. Acta, **13**, 19 (1968); Electrokhim. **6**, 429 (1970). A. N. Frumkin. *In* Advances in electrochemistry and electrochemical engineering. Vol. 3. *Edited by* P. Delahay. John Wiley, New York. 1963. p. 287.
21. H. Angerstein. Bull. Acad. Polon. Sci. **3**, 447 (1955).

Can. J. Chem. Downloaded from www.nrcresearchpress.com by 210.87.254.6 on 09/05/12
For personal use only.

Can. J. Chem. Downloaded from www.nrcresearchpress.com by 84.22.46.98 on 09/08/12
For personal use only.

An Electron Spin Resonance Investigation of the Mechanism of the Intramolecular Cation Migration of Alkali Metal Semiquinone Ion-pairs

T. E. GOUGH[1] AND P. R. HINDLE

Department of Chemistry, University of Waterloo, Waterloo, Ontario

Received March 11, 1971

A systematic survey of the kinetic characteristics of the intramolecular cation exchange reactions of semiquinone ion-pairs is described. A linear correlation exists between the free energy of activation for the exchange and the strength of the ionic interaction within the ion pair; however, this correlation does not extend to the enthalpy of activation. The significance of the kinetic parameters is discussed in terms of the role solvation plays in determining the course of the exchange process.

Une analyse systématique des caractéristiques cinétiques des réactions d'échange par cation intramoléculaire des paires d'ions de la sémiquinone est faite. Il existe une corrélation linéaire entre l'énergie libre d'activation de l'échange et la force de l'interaction ionique dans une paire d'ions; toutefois, cette corrélation ne s'étend pas à l'enthalpie d'activation. La signification de paramètres cinétiques est discutée en fonction du rôle que la solvatation joue dans la détermination de l'évolution du procédé d'échange.

Canadian Journal of Chemistry, 49, 2412 (1971)

Introduction

The phenomenon of line-width alternation in an electron spin resonance spectrum is now well understood; a recent review article indicates the necessary conditions for its occurrence and the variety of systems which can exhibit the effect (1). Line-width alternation in the electron spin resonance spectra of semiquinone ion-pairs has been reported by a number of workers; the majority of these results have been collated by Oakes and Symons (2) and thus are not given separate reference here. It is now generally agreed that, for these systems, the alternation in line-widths is the result of an intramolecular migration of the cation of the ion-pair between the oxygens of the semiquinone. However, the mechanistic details remain uncertain because of the lack of quantitative data concerning the rates of cation exchange. Three previous papers (3–5) have reported E_a and $\log_{10} A$ values for a number of semiquinone ion-pairs but at least one of these (3) should no longer be regarded as more than an exploratory semi-quantitative series of measurements. Thus the literature contains insufficient data from which to draw general conclusions concerning the quantitative aspects of the exchange. Accordingly, we have performed kinetic studies on a series of semiquinone ion-pairs in ethereal solvents in order to generate consistent data with which to evaluate and interpret trends in the measured kinetic parameters.

[1]To whom all correspondence should be addressed.

Experimental

Experimental procedures for the purification of reagents and the production of the ion-pairs have been described (3). Cesium mirrors were prepared by heating cesium chloride/calcium mixtures *in vacuo* and driving the resultant cesium vapor through a sintered disc and onto a cool glass surface within the reduction vessel. The spectra were recorded on a Varian E-3 spectrometer equipped with a Varian E4540 variable temperature unit. The sample temperature for each spectrum was recorded using a copper–constantan thermocouple in conjunction with a Hewlett–Packard 3420 A voltmeter. Simulations of the experimental spectra, using the Bloch equations appropriately modified to include the 2-site cation exchange (6) were performed on an IBM 360/75 computer in conjunction with a Calcomp plotter.

Results

Electron spin resonance spectra of each system studied were recorded at 10° intervals over as wide a range of temperatures as possible. The spectra were fully in accord with expectation showing static configurations of the ion-pairs at low temperatures, and the effects of intramolecular cation migration at higher temperatures.

Sodium Durosemiquinone, NaD

Satisfactory concentrations of NaD were obtained in 1:2 dimethoxyethane, DME, and in tetrahydrofuran, THF, but not in 2-methyltetrahydrofuran, MeTHF. The methyl hyperfine splitting constants of NaD in DME and THF were found to be temperature dependent; Δa_{Me}, the difference between the two observed methyl splittings of the static configuration, increased as the temperature was increased, but the mean of

Can. J. Chem. Downloaded from www.nrcresearchpress.com by 84.22.46.98 on 09/08/12
For personal use only.

TABLE 1. Arrhenius parameters for the intramolecular migration of cations within semiquinone ion-pairs

System number	Ion pair	Solvent	E_a (kcal)	A (s^{-1})
1	NaD	DME	3.57 ± 0.20	1.2×10^9
2	NaD	THF	5.61 ± 0.23	4.7×10^9
*3**	KD	DME	5.27	1.4×10^{11}
4	KD	THF	7.39 ± 0.52	4.7×10^{12}
5	CsD	DME	4.46 ± 0.27	5.4×10^{11}
6	CsD	THF	4.82 ± 0.28	6.6×10^{12}
7	CsD	MeTHF	3.70 ± 0.25	6.9×10^{10}
8	KD	DME	5.05 ± 0.34	5.2×10^{11}
9	KD	THF	6.20 ± 0.70	2.7×10^{12}

*Data taken from ref. 5.

the two splittings remained constant (1.94 ± 0.03 G). In Fig. 1, Δa_{Me} is plotted as a function of temperature from -80 to $+20$ °C above which temperature exchange effects preclude measurement of the individual splitting constants. It is important when evaluating the kinetics of the exchange reaction to include the temperature dependence of Δa_{Me}. If this effect is neglected, as was done previously (3), then the Arrhenius plots become S shaped. Arrhenius plots for the intramolecular exchange of sodium for NaD in DME and THF are given in Fig. 2; values of E_a and A are given in Table 1. The Arrhenius plot for NaD in THF covered slow, intermediate, and fast exchange regions, while that for DME covered slow and intermediate regions.

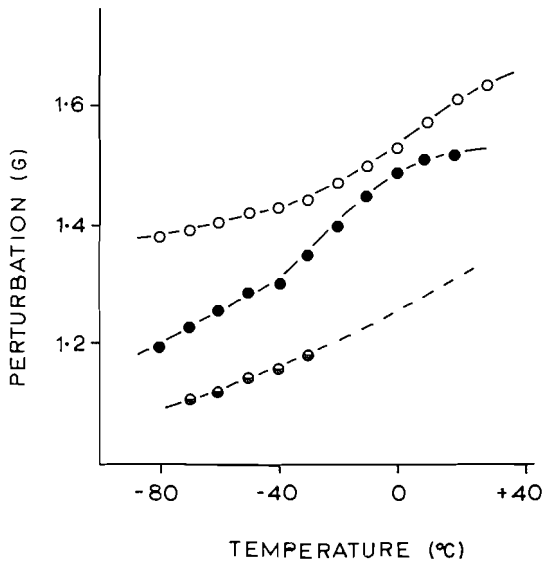

FIG. 1. Δa_{Me}, the perturbation of the hyperfine splitting constants of durosemiquinone produced by ionic association plotted as a function of temperature for ○, NaD in THF; ●, NaD in DME; ◒, KD in THF.

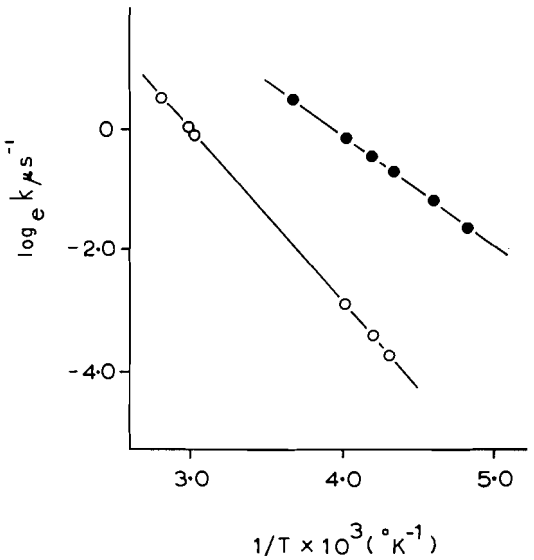

FIG. 2. Arrhenius plots for the intramolecular migration of sodium within the ion pair NaD in ○, THF; ●, DME.

Potassium Durosemiquinone, KD

KD was prepared in THF, and studied through the slow, intermediate, and fast exchange regions. The temperature dependence of Δa_{Me} could only be measured from -80 to -30 °C, exchange effects becoming too severe above this temperature range; as shown in Fig. 1, the results for NaD were used to guide the extrapolation of Δa_{Me} values for KD to $+20$ °C. Values of E_a and A for KD in THF are given in Table 1. Das and co-workers (5) have published an excellent linear Arrhenius plot for KD in DME and their results for E_a and A are incorporated into Table 1.

Cesium Durosemiquinone, CsD

CsD spectra were detectable in THF and

Can. J. Chem. Downloaded from www.nrcresearchpress.com by 84.22.46.98 on 09/08/12
For personal use only.

MeTHF only after 8 h reduction, though the ion-pair formed quite readily in DME. The initial solutions were light brown (DME) and wine-red (THF and MeTHF) but these colorations gradually settled out leaving pale green solutions having strong electron spin resonance spectra. Locked-in configurations of the ion-pairs were not observable over a sufficient temperature range to evaluate the temperature dependence of Δa_{Me} for CsD and so temperature independent values of 0.98 G in DME, 0.88 G in THF, and 1.12 G in MeTHF were used when evaluating E_a and A. Larger amounts of free D^- were present in the CsD solutions than in the NaD and KD solutions; the relative amount of free ion decreased in the series DME > THF > MeTHF. The spectrum of the ion-pair occurred to high field of the free ion, the separation being 0.15 G in DME, 0.13 G in THF, and 0.18 G in MeTHF. Figure 3 shows the variation with temperature of the cesium hyperfine interaction expressed as a percentage of the atomic interaction.

Potassium p-Benzosemiquinone, KB

The intramolecular exchange of potassium within the KB ion-pair was examined in DME and THF over the temperature range −30 to +40 °C,

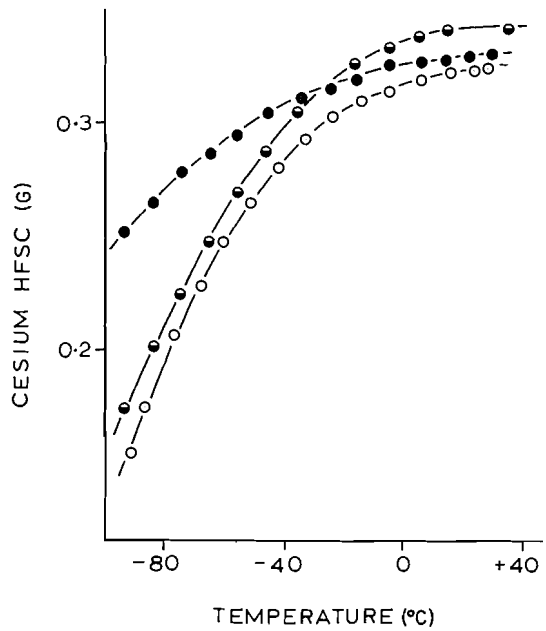

FIG. 3. Cesium hyperfine splitting constant of CsD plotted as a function of temperature in ○, THF; ●, DME; ◒, MeTHF.

including the slow intermediate, and fast exchange regions. Arrhenius parameters are listed in Table 1.

Discussion

Analysis of the line-widths of magnetic resonance spectra in terms of kinetic parameters has been attempted much more frequently for nuclear than for electronic resonances; hence the problems inherent in the analysis have been realized and discussed more fully by nuclear magnetic resonance (n.m.r.) spectroscopists (7, 8). Systematic errors have been shown to be particularly important when determining E_a and A, or in terms of the thermodynamic formulation of reaction rates, when determining $\Delta H^{\ddagger}$ and $\Delta S^{\ddagger}$ the enthalpy and entropy of activation. The principle systematic errors considered have been in the measurement of temperature and in the limitations of any approximations involved in the formulation of the spectra. It has been observed that, where several workers have studied a system, although the values reported for $\Delta H^{\ddagger}$ and $\Delta S^{\ddagger}$ vary considerably, they may be combined to give consistent values for $\Delta G^{\ddagger}$, the free energy of activation. The reason for this compensation of errors is readily seen from the Arrhenius formulation: a too high value of the slope necessarily leads to a too high value of the intercept. The electron spin resonance (e.s.r.) experiment offers some advantages over the n.m.r. experiment when determining kinetic parameters; because the E_a values of processes typically studied *via* e.s.r. are lower than those studied *via* n.m.r., meaningful measurements can be made over wider temperature ranges, thereby reducing the effects of systematic errors in the measurement of temperature; magnet homogeneity does not play a critical role in determining line-shape and so need not be frequently readjusted; the spectra are normally (*i*) first order, so that a complete and simple description is readily available, and (*ii*) contain many lines, so that many cross checks on the results are available. The most important sources of potential error in the present work are temperature measurement, contributions to the spectrum from small amounts of unassociated semiquinone anion, assignment of a value for the electronic transverse relaxation time, and correction for anisotropic broadening mechanisms. The last three factors were treated in subjective fashion,

TABLE 2. Kinetic parameters for the intramolecular migration of cations within semiquinone ion-pairs. System number code as for Table 1

System number	Temperature (°K)	Δa (G)	$\Delta G^{\ddagger}$ (kcal)	$\Delta H^{\ddagger}$ (kcal)	$\Delta S^{\ddagger}$ (e.u.)
1	200	1.22	6.83	3.17	−18.3
1′	300	1.52	8.70	2.97	−19.1
2	200	1.39	8.33	5.21	−15.6
2′	300	1.63	9.93	5.01	−16.4
3	200	0.98	6.63	4.87	−8.8
4	200	1.08	7.34	6.99	−1.8
5	200	0.98	5.28	4.06	−6.1
6	200	0.88	4.64	4.42	−1.1
7	200	1.12	5.34	3.30	−10.2
8	200	0.96	5.88	4.65	−6.2
9	200	1.16	6.37	5.80	−2.9

input parameters to the simulation programme being varied until it was judged that optimum agreement between experimental and computed spectra had been obtained. The decision as to when optimum agreement was reached was made by measuring the amplitudes of all lines having satisfactory signal-to-noise ratios, relative to the amplitude of the central line. When the r.m.s. difference between the relative amplitudes of the experimental and computed lines was a minimum, it was taken that optimum agreement had been obtained.

The measured rate constants were fitted to the Arrhenius equation, partly to extract E_a and $\log_{10} A$ values and partly to check the internal consistency of each temperature run. From the optimum least squares fit straight line through the data values of k_{200} and k_{300}, the rate constant at 200 and 300 °K were determined from which $\Delta G^{\ddagger}_{200}$ and $\Delta G^{\ddagger}_{300}$ were obtained *via* the relationship.

$$k_T = \frac{kT}{h} \exp(-\Delta G^{\ddagger}/RT)$$

The enthalpy of activation is most readily obtained (9) for a unimolecular reaction from

$$E_a = \Delta H^{\ddagger} + RT$$

and may be combined with the free energy of activation to give the entropy of activation. Results of these computations are given in Table 2.

A number of systematic trends within the data are noticeable and worthy of comment. Previous empirical calculations have shown (3, 10) that Δa_{Me}, the difference between the methyl hyperfine splitting constants of a durosemiquinone ion-pair, locked into a "static" configuration, is a direct measure of the strength of the perturbation applied to the anion. In Fig. 4, Δa_{Me} measured at 200 °K is plotted against $1/r$, the reciprocal of the radius of the cation incorporated into the ion-pair. Except for the Cs/DME point, a system which Swarc and co-workers have already demonstrated to be exceptional with respect to cation solvation (11) and which also appears anomalous in Fig. 3, an excellent correlation exists between Δa_{Me} and $1/r$ indicating, as intuitively expected, that the perturbation of durosemiquinone produced by a cation is proportional to the polarizing

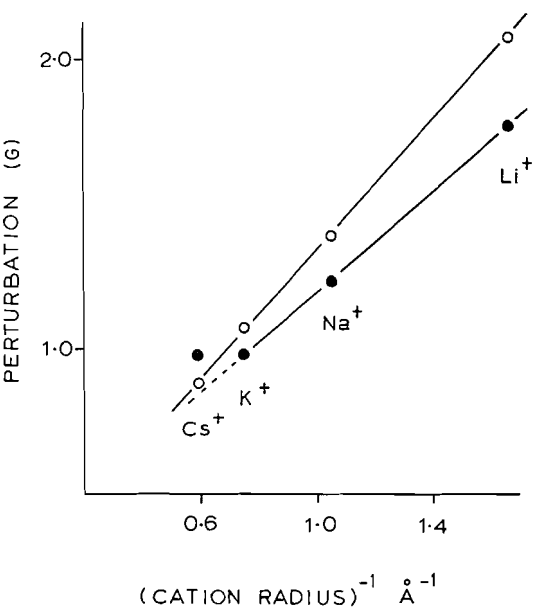

FIG. 4. Δa_{Me}, the perturbation of the hyperfine splitting constants of durosemiquinone produced by ionic association plotted as a function of inverse cation radius for ○ THF and ● DME. Sample temperature 200 °K; Li^+ data taken from (2).

Can. J. Chem. Downloaded from www.nrcresearchpress.com by 84.22.46.98 on 09/08/12
For personal use only.

Can. J. Chem. Downloaded from www.nrcresearchpress.com by 84.22.46.98 on 09/08/12
For personal use only.

power of the cation, and that Δa_{Me} may be used as a linear experimental parameter with which to estimate the strengths of the ionic interactions within the various ion-pairs examined.

In Fig. 5, $\Delta G^{\ddagger}$ measured as described above is plotted as a function of Δa; the data are for a temperature of 200 °K, with the exception of points *1'* and *2'* which are for 300 °K, only these sodium ion-pairs allowing a measurement of Δa_{Me} at 200 and 300 °K. Bearing in mind that the data in Fig. 5 cover three solvents, three cations, and two anions, the correlation between $\Delta G^{\ddagger}$ and Δa is very satisfactory, the r.m.s. error to the line drawn (0.63 kcal/mol) being comparable to those involved in fitting the raw data to the Arrhenius equation. The solid line in Fig. 5 has been drawn through the origin indicating that a hypothetical cation too large to perturb the anion will have a zero $\Delta G^{\ddagger}$ for the intramolecular exchange process. An increase in the strength of the ionic interaction, as measured by Δa, is accompanied by a linear increase in the free energy necessary to remove the cation from its equilibrium position close to one of the oxygens, and place it into the configuration of the activated complex, which must be symmetrical with respect to the two oxygens of the semiquinone.

Using the literature values (2) of Δa_{Me} for LiD in DME and THF, Fig. 5 may be used to estimate $\Delta G^{\ddagger}_{300}$ for LiD $\simeq$ 14 kcal mol^{-1}, corresponding to $k_{300} \simeq 10^3$ s^{-1}, a value compatible with the reported "static" geometry of the lithium ion-pair in these solvents.

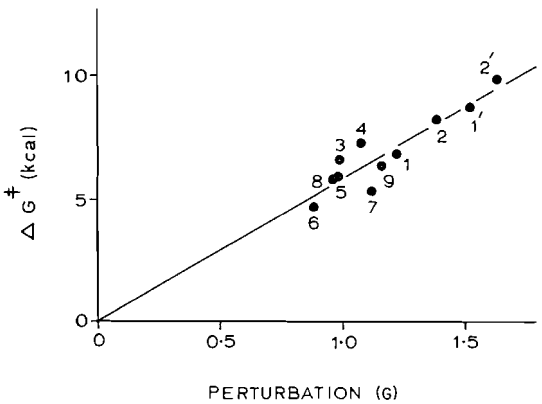

FIG. 5. Free energy of activation for intramolecular cation migration plotted as a function of the perturbation of the anion. Sample temperature 200 °K except *1'* and *2'* at 300 °K; numerals correspond to system numbers of Table 1.

The correlation found between $\Delta G^{\ddagger}$ and Δa indicates that the present measurements of the rates of intramolecular migration are at least internally consistent, and permits further speculation concerning the significance of E_a and A or, equivalently, of $\Delta H^{\ddagger}$ and $\Delta S^{\ddagger}$. Inspection of Table 2 shows that no correlation equivalent to Fig. 5 exists between $\Delta H^{\ddagger}$ and Δa. For example, in a given solvent $\Delta H^{\ddagger}$ for NaD is smaller than for KD even though Δa_{Me} is larger for the former species, but, for each of these ion-pairs, if Δa_{Me} is increased by changing the solvent from DME to THF then $\Delta H^{\ddagger}$ also increases. Conversely, the reverse trend is shown by the CsD ion-pair, $\Delta H^{\ddagger}$ being larger in the solvents where Δa_{Me} is smaller. Evidently, $\Delta H^{\ddagger}$ is not solely determined by the strength of the ionic interaction.

In Fig. 6 $\Delta H^{\ddagger}_{200}$ is plotted as a function of $\Delta S^{\ddagger}_{200}$ for all the systems studied; lines have been drawn to emphasize the relationship between data points for each of the ion-pairs. For any ion-pair, changing the solvent so as to increase $\Delta H^{\ddagger}$ also increases $\Delta S^{\ddagger}$ providing an example of the isokinetic principle discussed by Leffler (12). When $\Delta H^{\ddagger}$ and $\Delta S^{\ddagger}$ are combined to form $\Delta G^{\ddagger}$ the contributions common to $\Delta H^{\ddagger}$ and $\Delta S^{\ddagger}$ are cancelled out.

Some of the negative $\Delta S^{\ddagger}$ values observed are remarkably large when it is remembered that they apply to an elementary first order reaction, and can only mean that solvation plays an important role in determining the kinetics of these intramolecular migrations. In support of this statement there appears to be a rough correlation between the size of $\Delta S^{\ddagger}$ and the anticipated

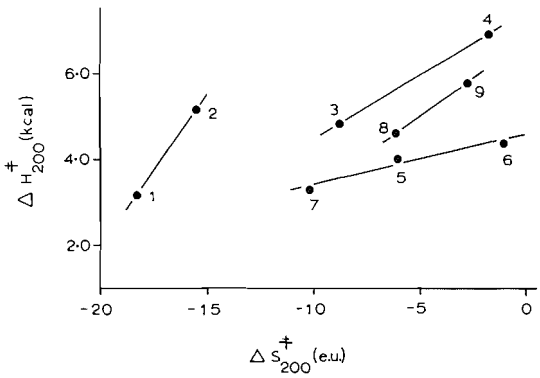

FIG. 6. Enthalpy of activation plotted as a function of entropy of activation for the intramolecular cation migration within semiquinone ion pairs at 200 °K: numerals correspond to system numbers of Table 1.

amount of cationic solvation in a system, the more negative values of $\Delta S^{\ddagger}$ being found for smaller cations and more polar solvents, though the cesium results are perhaps not as anticipated.

A negative entropy of activation indicates that there is a higher degree of order in the activated complex than in the reactants, which for the present systems must mean that the activated complex is more solvated than the reactant ion-pair. The higher degree of solvation postulated for the activated complex is in keeping with the greater charge separation in the symmetrical activated complex. Concurrent with the entropy change due to differential solvation of the reactant and the activated complex there will be an enthalpy change. The greater degree of solvation of the activated complex will decrease the value of $\Delta H^{\ddagger}$ and so, when discussing $\Delta H^{\ddagger}$, two factors must be considered; the difference in the enthalpy of ionic association between activated complex and reactant (positive) and the corresponding difference in solvation enthalpy (negative). Thus $\Delta H^{\ddagger}$ is not expected to be a linear function of Δa for a series of ion-pairs in differing environments because it is determined by the difference between larger terms of opposite sign, which, although related are not expected to be linearly dependent on one another. However, when $\Delta H^{\ddagger}$ and $\Delta S^{\ddagger}$ are combined to form $\Delta G^{\ddagger}$, the effects of the differential solvation are cancelled out leaving only the effects of the ionic association.

The above interpretation of the kinetic parameters allows further speculation concerning the details of the mechanism of the migration, particularly for systems where $\Delta S^{\ddagger}$ is very negative and $\Delta H^{\ddagger}$ correspondingly smaller than expected, *e.g.* NaD in DME. Solvation of the activated complex provides a lower energy path for the reaction to follow; however, in order for this solvation to facilitate the reaction, because of the rapidity of the actual transfer it is necessary that the reaction proceeds only when the solvent adopts, by chance, a favorable configuration. The more developed and organized the solvation shell of the activated complex the less likely is this configuration to occur, hence the more negative is $\Delta S^{\ddagger}$. It should be noted that this description of the migration is in conflict with that of Claxton who treats the solvent as a time-independent continuum (13).

The quantitative agreement between the data in Table 1 and the available literature data is not impressive as far as the Arrhenius parameters are concerned. For KD in THF Das and co-workers (5) report $E_A = 5.96$ kcal $A = 4.3 \times 10^{11}$ s^{-1}; for KB in DME values of $E_A = 3.40$ kcal $A = 3.2 \times 10^{9}$ s^{-1} have been given (4). However, these parameters when converted to $\Delta G^{\ddagger}_{200}$ produce values of 6.87 and 6.72 kcal, respectively, each within 0.5 kcal of the appropriate number in Table 2.

This work was supported by an operating grant from the National Research Council of Canada and by a Province of Ontario Graduate Fellowship to P.R.H.

1. J. R. Bolton and P. D. Sullivan. Adv. Mag. Res. **4**, 39 (1970).
2. J. Oakes and M. C. R. Symons. Trans. Faraday Soc. **66**, 10 (1970).
3. P. S. Gill and T. E. Gough. Trans. Faraday Soc. **64**, 1997 (1968).
4. J. C. Chippendale and E. Warhurst. Trans. Faraday Soc. **64**, 2332 (1968).
5. B. S. Prabhananda, M. P. Khakhar, and M. R. Das. J. Ind. Chem. Soc. **56**, 659 (1969).
6. H. M. McConnell. J. Chem. Phys. **28**, 430 (1958).
7. A. Allerhand, H. S. Gutowsky, J. Jonas, and R. A. Meinyer. J. Am. Chem. Soc. **88**, 3185 (1966).
8. W. E. Stewart and J. H. Siddall. Chem. Rev. **70**, 517 (1970).
9. K. J. Laidler. Chemical kinetics. McGraw-Hill. 1965. p. 90.
10. T. A. Claxton, T. E. Gough, and M. C. R. Symons. Trans. Faraday Soc. **62**, 279 (1966).
11. C. Carvajal, K. J. Töble, J. Smid, and M. Swarc. J. Am. Chem. Soc. **87**, 5548 (1965).
12. J. E. Leffler. J. Org. Chem. **20**, 1202 (1955).
13. T. A. Claxton. Trans. Faraday Soc. **65**, 2289 (1969).

Can. J. Chem. Downloaded from www.nrcresearchpress.com by 84.22.46.98 on 09/08/12
For personal use only.

Can. J. Chem. Downloaded from www.nrcresearchpress.com by 210.87.254.40 on 09/05/12
For personal use only.

Steroidal Acetals of Formaldehyde

J. E. HERZ, J. LUCERO, AND YOLANDA SANTOYO

Department of Chemistry, Centro de Investigación y de Estudios Avanzados del Instituto Politécnico Nacional, AP 14-740, México, 14, D.F. México

AND

E. S. WAIGHT

Department of Chemistry, Imperial College of Science and Technology, London S.W. 7, England

Received September 15, 1970[1]

The anodic oxidation of cholesterol yields 3β,3′β-(methylenedioxy)-dicholest-5-ene. A new method for the preparation of methoxymethyl ethers of steroids is described. The n.m.r. and mass spectra of these compounds is reported.

L'oxydation anodique du cholestérol conduit au (méthylènedioxy)-3β,3′β dicholestene-5. On décrit une nouvelle méthode pour la préparation des éthers méthoxyméthylés des stéroides. On rapporte les spectres de r.m.n. et de masse de ces composés.

Canadian Journal of Chemistry, 49, 2418 (1971)

In order to confirm the identity of the main anodic oxidation product of cholesterol in aqueous acidic methanol as 3β,3′β-(methylenedioxy)-dicholest-5-ene (**1**) direct comparison with an authentic specimen was necessary.

Compound **1** was prepared by reaction of cholesterol and chloromethyl methyl ether in the presence of sodium hydride (1) and shown to be identical in all respects with the anodic oxidation product. Reaction of 5α-cholestan-3β-ol under the same conditions however gave a mixture of 3β,3′β-(methylenedioxy)-5α-cholestane (**2**) and 3β-(methoxymethoxy)-5α-cholestane (**3**) in poor yield.

As an alternative method for preparing compound **1**, the reaction of cholesterol and dimethoxymethane in the presence of acidic catalysts was investigated. The product thus obtained was 3β-(methoxymethoxy)-cholest-5-ene (**4**), the structure of which was confirmed by its n.m.r. (Table 1) and mass spectra (see below). This method was also used to prepare compound **3** and seems of general applicability. Methoxymethyl ethers have also been prepared by Kupchan *et al.* (1) by a modification of the method employing chloromethyl methyl ether.

The mass spectrum of compound **1** differs from that of cholesterol only in the greater abundance of the ions *m/e* 368 and 353 relative to 386 (the molecular ion of cholesterol). Higher mass ions cannot be detected and no metastable transition can be found in the first field-free region of the spectrometer (2) for the decomposition of the parent molecular ion (M^+, *m/e* 784) to either 386 or 368. Evidently a very ready fragmentation, either thermal or electron impact induced, results in the formation of the molecular ions of cholesterol and cholestadiene. The mass spectrum of 3β-(methoxymethoxy)-cholest-5-ene (**4**) is also very similar to that of cholesterol and shows no parent molecular ion (*m/e* 430). Higher mass ions are very weak in the spectrum of compound **2** but the decomposition 788 (M^+) → 402 can be detected in the first field-free region. The latter together with a fairly intense ion at *m/e* 386 suggests a fragmentation producing (nominally) the molecular ion of methoxycholestane and of cholestanone. The mass spectrum of 3β-(methoxymethoxy)-5α-cholestane is remarkable. The molecular ion (*m/e* 432) is one of the strongest in the spectrum while another (370) is derived from it by loss of methoxymethanol. Such an intense molecular ion appears to be without precedent for an acetal (3).

TABLE 1. Partial proton magnetic spectra of steroidal acetals of formaldehyde

Compound	—OCH_2O— δ, p.p.m.	CH_3O— δ, p.p.m.
1	4.81	—
2	4.79	—
3	4.70	3.40
4	4.66	3.77

[1]Revision received March 30, 1971.

Can. J. Chem. Downloaded from www.nrcresearchpress.com by 210.87.254.40 on 09/05/12
For personal use only.

Experimental

The n.m.r. spectra were determined for deuteriochloroform solutions with tetramethylsilane as an internal reference using a Varian A-60 spectrometer. Mass spectra were determined using an A.E.I. MS9 instrument, samples being inserted directly into the ion source at the lowest possible temperature.

Anodic Oxidation of Cholesterol

Cholesterol (1 g) was partially dissolved in methanol (40 ml), water (40 ml), and 20% sulfuric acid (5 ml), and electrolyzed (4) for 5 h on a lead dioxide electrode (30 V, 2 A) with agitation and external cooling (ice–water). The mixture was extracted with methylene chloride and the extract washed free of acid. The residue on evaporation was crystallized several times from methylene chloride – acetone giving 3β,3′β-(methylenedioxy)-dicholest-5-ene, m.p. 191°, $[\alpha]_D$ −36° (lit. (1) m.p. 190.5°, $[\alpha]_D$ −30.8°).

Anal. Calcd. for $C_{55}H_{92}O_2$ (mol. wt. 785): C, 84.12; H, 11.81. Found (770 (Rast)): C, 83.93; H, 12.01.

Reaction of 5α-Cholestan-3β-ol with Chloromethyl Methyl Ether

5α-Cholestan-3β-ol (3.14 g) was added to a suspension of 50% sodium hydride (0.24 g NaH) in dry benzene (50 ml) and the mixture refluxed for 30 min. Chloromethyl methyl ether (1.1 g) was added dropwise to the cooled mixture which was then agitated for 18 h. Water was added and the organic layer separated and evaporated to dryness. The residue was separated on a dry silica gel column using methylene chloride as a solvent giving 3β-(methoxymethoxy)-5α-cholestane (243 mg), m.p. 61°, after crystallization from ethyl acetate – methanol, $[\alpha]_D$ +17° ($CHCl_3$).

Anal. Calcd. for $C_{29}H_{52}O_2$: C, 80.49; H, 12.11. Found: C, 80.64; H, 12.21.

Later fractions yielded 3β,3′β-(methylenedioxy)-di-5α-cholestane (100 mg), m.p. 206–207°, after crystallization from ethyl acetate, $[\alpha]_D$ +1° ($CHCl_3$).

Anal. Calcd. for $C_{55}H_{96}O_2$: C, 83.69; H, 12.36. Found: C, 83.47; H, 12.19.

3β-(Methoxymethoxy)-cholest-5-ene

To cholesterol (1 g), dimethoxymethane (10 ml), and dry tetrahydrofuran (10 ml) was added perchloric acid (70%, 5 drops). After agitation for 24 h at room temperature, solid Na_2CO_3 was added, the solids removed by filtration, and the filtrate evaporated to dryness. Chromatography of the residue on neutral alumina in hexane gave the title compound (265 mg), m.p. 76–78°, after crystallization from methylene chloride – methanol, $[\alpha]_D$ −23° (in $CHCl_3$) (lit. (1) m.p. 85–86°).

Anal. Calcd. for $C_{29}H_{50}O_2$: C, 80.87; H, 11.70. Found: C, 80.94; H, 11.70.

3β-(Methoxymethoxy)-5α-cholestane

This was prepared from 5α-cholestan-3β-ol and dimethoxymethane as described above. It was purified by chromatography on basic alumina (Bio Rad A 10) and crystallization from ethyl acetate – methanol, yield 41%, m.p. 62°, $[\alpha]_D$ +20° (in $CHCl_3$).

One of us (J.E.H.) thanks the Royal Society of Great Britain for a travel grant. We thank Mr. J. N. Bilton for assistance in measuring the mass spectra.

1. S. M. KUPCHAN, A. F. CASY, and J. W. SWINTOSKY. J. Pharm. Sci. **54**, 514 (1965).
2. M. BARBER and R. M. ELLIOTT. 12th A.S.T.M. Meeting on mass spectrometry. E-14. Montreal, Quebec, 1964; K. R. JENNINGS. J. Chem. Phys. **43**, 4176 (1965).
3. H. BUDZIKIEWICZ, C. DJERASSI, and D. H. WILLIAMS. Mass spectrometry of organic compounds. Holden–Day, San Francisco, California, 1967. p. 258.
4. M. J. ALLEN. Organic electrode processes. Chapman and Hall, London, 1958. p. 119.

Can. J. Chem. Downloaded from www.nrcresearchpress.com by 210.87.254.105 on 09/05/12
For personal use only.

Steroids and Steroidases. XI.[1] Synthetic Approaches to C-17 Bis(2-hydroxyethyl)-amino Compounds as Potential Precursors of 17-Hydroxyandrostane Nitrogen Mustards[2]

J. Bryan Jones and Jeffrey D. Leman

Lash Miller Chemical Laboratories, Department of Chemistry, University of Toronto, Toronto 181, Ontario

Received March 1, 1971

The synthesis of some potential nitrogen mustard precursor 17α-bis(2-hydroxyethyl)aminomethyl androst-17β-ol derivatives has been achieved by two routes. During the investigation, unequivocal proof was obtained that addition of cyanide to 17-keto steroids gives predominantly 17β-hydroxy-17α-cyano epimers.

On rapporte la synthèse par deux voies différentes de quelques dérivés de bis(hydroxy-2 éthyl) aminométhyl-17α-androstol-17β qui sont possiblement actifs comme moutardes azotés. Au cours de ces travaux, on a pu obtenir des preuves sans équivoques que l'addition du cyanure sur les 17-cétastéroïdes conduit principalement aux épimères hydroxy-17β cyano-17α.

Canadian Journal of Chemistry, 49, 2420 (1971)

In the search for anti-tumor effective nitrogen mustards many compounds in which a steroid molecule has been used as a carrier for the bis(2-chloroethyl)amino group have been examined.[3] We have previously synthesized and evaluated some androstane C-17 mustard compounds in which hormonally important ring A functional groups were present (2) and this communication describes our attempts to extend the investigation to androstane mustards in which *both* the ring A Δ^4-3-keto and ring D 17β-hydroxyl functions of 17β-hydroxyandrost-4-en-3-one (testosterone) were retained.

The compound selected as the initial target was the 17α-bis(2-chloroethyl)aminomethyl testosterone (**1***a*). The reservations expressed (2) regarding the usefulness of aliphatic nitrogen mustards in cancer chemotherapy owing to their high reactivity potential do not necessarily apply to hydroxy mustards of this type since for such compounds formation of a five-membered hydrogen bonded ring (3) should prolong the physiological activity by retarding the formation of the active ethylenimmonium ion species (4, 7–9).[4]

Our earlier studies (2) had indicated syntheses involving chlorination of bis(2-hydroxyethyl)-amino precursors in the final step to be the most satisfactory for the preparation of steroid mustards. Similar pathways to **2***a* were therefore examined and, as summarized in Schemes 1 and 3, two routes to the precursor triol **2***b* proved satisfactory. In the cyanohydrin approach (Scheme 1), 5α-androstan-17-one (**3**) was found to react smoothly with potassium cyanide in acetic acid to give in 87% yield a mixture of the C-17 cyanohydrin epimers in which the 17β-hydroxy compound **4** predominated to a large extent.[5] Reduction of **4** with lithium aluminum hydride followed by reaction with ethylene oxide gave the 2-hydroxyethylamino compound **2***b* in 38% overall yield.

The synthesis of the analogous bis(2-hydroxyethyl)amino precursor **1***b* of androst-4-en-3-one was also achievable via cyanohydrin routes and the two pathways followed are outlined in Scheme 2. The sequence **6** → **7** → **8** → **9** was explored first and although ketalization of testosterone (**6**) followed by Sarett oxidation of the C-17 hydroxyl group proceeded smoothly to give the 17-keto-3-ketal **8** in good yield, the presence of the ketal function posed problems with regard to the subsequent C-17 cyanohydrination reaction. The use of the acidic potassium

[1]For Part X see ref. 2.

[2]Abstracted from ref. 1. First presented in part at the C.I.C. Conferences, Montreal, Quebec, May 1969 and Toronto, Ontario, May 1970.

[3]A comprehensive review of nitrogen mustards is included in ref. 1 and the most relevant steroid literature is cited and discussed in ref. 2.

[4]It has been pointed out by Ross (4) and others (5, 6) that competition with chlorine for the lone pair of electrons on nitrogen produces modifications of biological actions of nitrogen mustards.

[5]That the desired 17β-hydroxy-17α-cyano compound would be the major product was expected from a consideration of the known preference for α-attack of the 17-carbonyl group by the cyanide ion in closely related steroids (10).

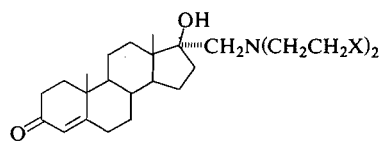

1

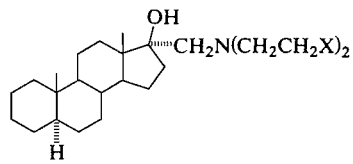

2

a X = Cl
b X = OH

cyanide conditions found to be satisfactory in the case of the model compound **3** was precluded by the acid sensitivity of the 3-ketal of **8** and it was found necessary to employ *trans*-cyanohydrination with acetone cyanohydrin. Again one epimer predominated in the mixture produced and this was assigned the 17β-hydroxy configuration shown in **9** for the reasons cited above for the 5α-androstane analogue.

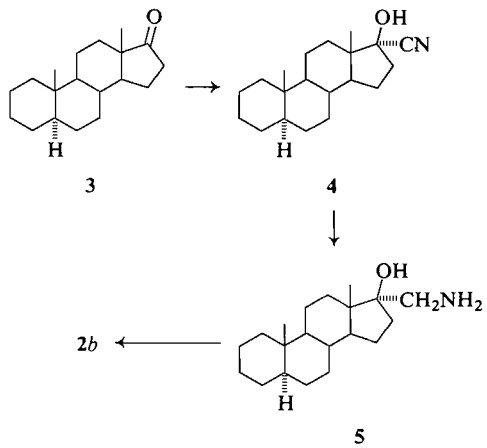

SCHEME I

Since the yields obtained of **9** in the last step of the above sequence were influenced quite markedly by minor variations in the *trans*-cyanohydrination reaction conditions, the alternative route to **9** via intermediates **10** and **11** was also investigated. On treatment of **10** with acetone cyanohydrin, selective reaction (11) at C-17 was achieved to give the 17β-hydroxy epimer **11** in 74% yield. Its subsequent ketalization was readily accomplished to give samples of **9** of superior purity and in higher overall yield (53% as opposed to 38%) than obtained by the initial route.

The subsequent transformations of **9** into the bis(2-hydroxyethyl)amino ketal **12** by lithium aluminum hydride reduction followed by ethylene oxide alkylation were accomplished in 46 and 73% yields respectively and preliminary experiments showed that acid-catalyzed deketalization of **12** to give the Δ^4-3-keto compound **1***b* could be readily achieved when required.

The cyanohydrin routes discussed above suffer from the disadvantage that the final yields obtained of the desired mustard precursors are rather low owing to the problems encountered in the cyanohydrin reduction steps where partial dissociation of the hydroxynitriles to the corresponding ketones during reduction could not be prevented even when the cyanohydrin acetates were used (12). A further cause for dissatisfaction with the cyanohydrin routes was that although the C-17 configurational assignments made were felt to be fairly secure on the basis of their analogy with earlier work in similar steroidal systems (10) no physical or chemical data had been obtained which would permit the C-17 stereochemistries of the cyanohydrins and their derivatives to be accepted unequivocally. Therefore, in an attempt to improve the yields of **1***b* and **2***b* and in order to remove all ambiguity from the assignment of their C-17 geometries, the alternative approaches involving the oxiranes **13** and **17** outlined in Schemes 3 and 4 were investigated.

5α-Androstan-17-one (**3**) was converted stereospecifically[6] by reaction with dimethylsulfonium methylide to give spiro-17β-oxiranyl-5α-androstane (**13**) in 84% yield. The 17β-configuration of the epoxide group was verified by reduction of **13** with lithium aluminum hydride to 17α-methyl-5α-androstan-17β-ol (**14**, 70% yield) which showed peaks in the p.m.r. spectrum for the C-17 proton, and C-18 and -19 methyl groups at chemical shifts characteristic of 17β-hydroxy-17α-methyl steroids (13, 14) and which was identical in all respects with an authentic sample prepared unambiguously from 17α-methyltestos-

[6]That a single C-17 epimer only was formed was confirmed by the p.m.r. spectrum which showed the C-18 methyl protons as a sharp *singlet* at δ 0.86 p.p.m. only.

Can. J. Chem. Downloaded from www.nrcresearchpress.com by 210.87.254.105 on 09/05/12
For personal use only.

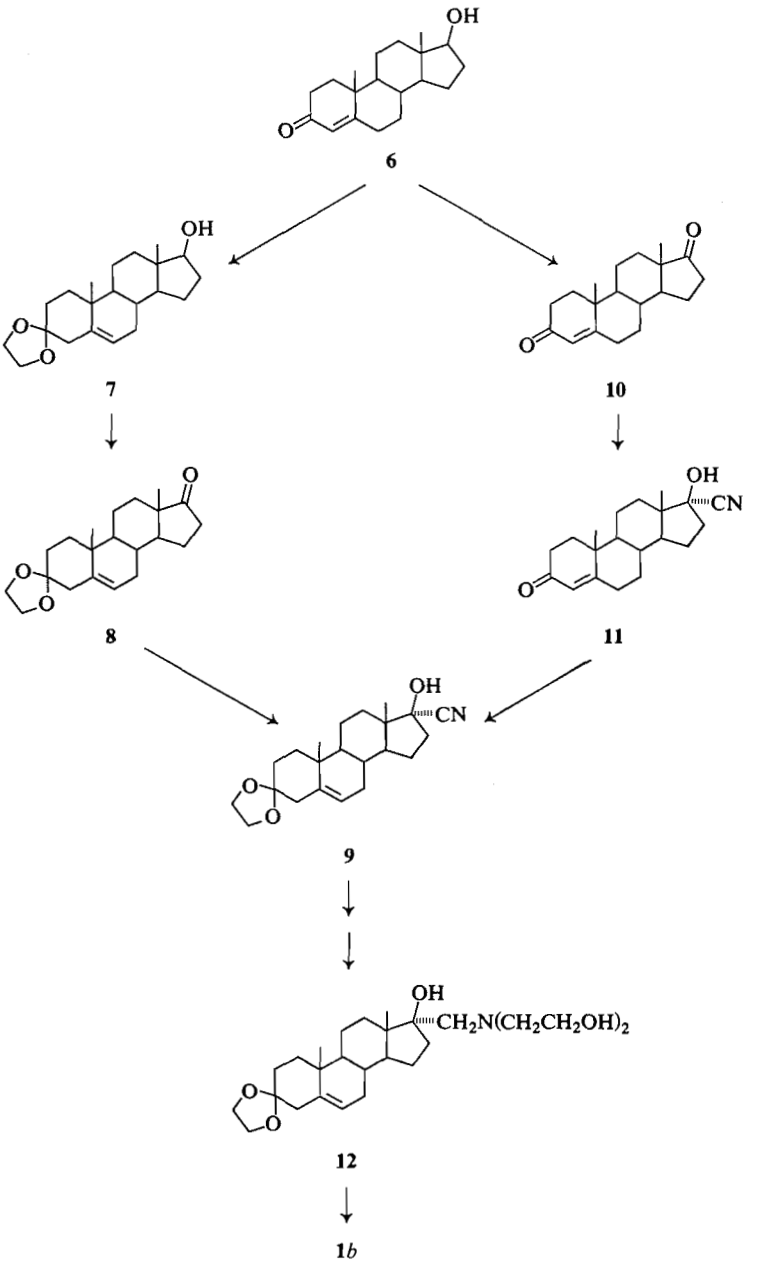

SCHEME 2

terone (**15**). The oxirane **13** was condensed with bis(2-hydroxyethyl)amine in ethylene glycol at 160° (15) and 92% of the mustard precursor triol **2***b* was obtained directly as the sole product.[7] A comparison of this sample of **2***b* of chemically verified C-17 stereochemistry with that obtained by the cyanohydrin route of Scheme 1 showed both to be identical in all respects. This therefore established unambiguously that the major products of cyanide ion addition to the C-17 carbonyl group of **3**, and by analogy to those of **8** and **10**,

[7]When water was used as a catalyst (16), a 42% yield only was obtained.

Can. J. Chem. Downloaded from www.nrcresearchpress.com by 210.87.254.105 on 09/05/12
For personal use only.

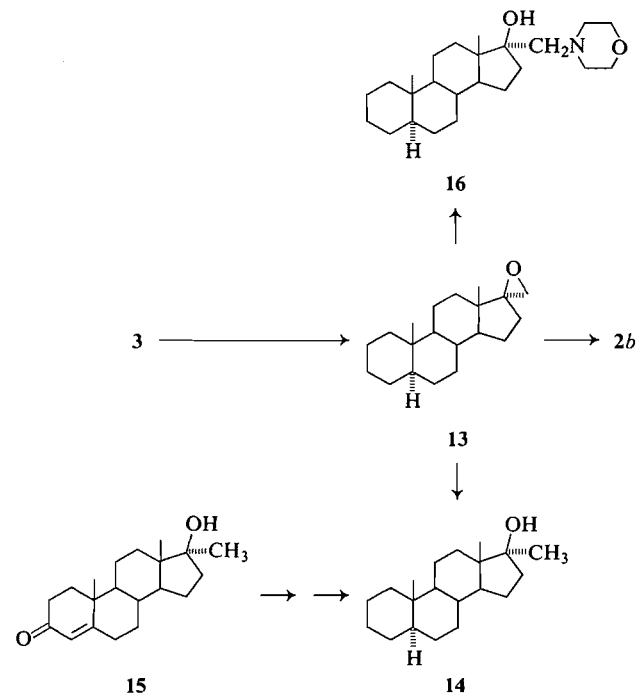

SCHEME 3

were the cyanohydrins **4**, **9**, and **11** respectively as had been predicted from steric considerations.[5] The overall yield (80%) of the triol **2*b*** from the starting ketone **3** by the oxirane route was much higher than that obtained via the cyanohydrin intermediates (38%) and thus was much the preferred synthetic method. Unfortunately, the preparation of the Δ^4-3-keto mustard precursor **1*b*** via reaction of the oxirane **17** with bis(2-hydroxyethylamine to give the ketal **12** (Scheme 4), followed by mild hydrolysis, turned out to be less satisfactory than for the analogous route described above for the model series (Scheme 3) the overall yield of **12** from testosterone (**6**) being only 15%.

Disappointingly, all attempts to effect the conversion of the mustard precursors **1*b***, **2*b***, and **12** into the corresponding bis(2-chloroethyl)amino derivatives were unsuccessful. Application of such reagents as thionyl chloride, phosphoryl chloride, and methane sulfonyl chloride under the conditions delineated previously (2) for other sensitive androstane compounds afforded extensively decomposed, complex, reaction mixtures in which none of the desired or related mustards could be detected even by the sensitive p.m.r. and mass spectral diagnostic methods (2). Major difficulties in achieving the desired selective chlorinations had, of course, been anticipated but surprisingly the products of the expected competitive reactions, such as $\Delta^{16,17}$, perhydrooxazino, and morpholino[8] derivatives, were not formed in isolable quantities either. Direct conversion of the oxiranes **13** and **17** to the corresponding nitrogen mustards by condensation with bis(2-chloroethyl)amine (17) was also attempted under a variety of conditions but in most cases the starting oxiranes were recovered quantitatively. Under forcing conditions (130° in alcoholic solvents in sealed tubes) multiple reactions occurred but in no instance was any steroid mustard detectable. The marked instability of nitrogen mustard itself to elevated tempera-

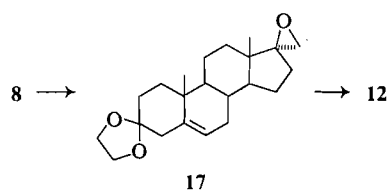

SCHEME 4

[8]For reference purposes a sample of one such possible product, **16**, was prepared by the phenol-catalyzed reaction of the oxirane **12** with morpholine.

Can. J. Chem. Downloaded from www.nrcresearchpress.com by 210.87.254.105 on 09/05/12
For personal use only.

Can. J. Chem. Downloaded from www.nrcresearchpress.com by 210.87.254.105 on 09/05/12
For personal use only.

tures (18) was presumably a major factor in the failure of this approach.

In view of the discouraging results encountered in the final stages it is considered unlikely that the approaches described above can be modified sufficiently to provide satisfactory syntheses of the mustards **1***a* and **2***a* and alternative routes to these latter compounds are now being explored.

Experimental

Melting points were determined on a Fisher–Johns block and are corrected. The i.r. spectra were recorded on a Perkin–Elmer 237 B or 257 spectrometer. The p.m.r. spectra were determined in deuteriochloroform with tetramethylsilane as the internal standard on a Varian A-60 or HA-100 instrument. Column chromatographic separations were effected with Fisher Scientific Co. Florisil or neutral alumina deactivated with 2% w/w of water. The t.l.c. and preparative layer chromatography was performed on silica gel G and the compounds were visualized with iodine vapor or under u.v. light. Unless otherwise stated, all compounds described were purified until they were homogeneous to t.l.c. analysis.

17α-Bis(2-hydroxyethyl)aminomethyl-5α-androstane (2b)

(a) Cyanohydrin Route

A solution of 5α-androstan-17-one (1 g, 3.7 mmol) in absolute ethanol (125 ml) was added to a solution of potassium cyanide (11 g) in water (50 ml). The mixture was cooled in an ice bath and glacial acetic acid (15 ml) was added dropwise with stirring. The resulting solution was stirred for 1 h, and was then diluted with water (200 ml) and filtered to give the *17α-cyano-5α-androstan-17β-ol* (**4**, 0.96 g, 87%), m.p. 120–124°; i.r. (KBr) 3448, 2232, and 1730 cm^{-1} (C-17 carbonyl impurity).[9]

A solution of the above cyanohydrin (2.50 g, 8.3 mmol) in anhydrous benzene–ether (1:1, 500 ml) was added dropwise during 1 h at 0° to a well-stirred slurry of lithium aluminum hydride (0.48 g, 12.5 mmol) in anhydrous ether (250 ml). The mixture was then refluxed 18 h, and water (50 ml) followed by 10% aqueous sodium hydroxide (50 ml) were added dropwise in the presence of Celite. The resulting mixture was filtered, and the filtrate dried ($MgSO_4$) and evaporated. The residual solid (1.3 g) was combined with the material (0.95 g) obtained by Soxhlet extraction[10] of the filter cake with chloroform–methanol (1:1). The product so obtained was shown by g.l.c., t.l.c., and p.m.r. analyses to contain 18% of 5α-androstan-17β-ol[11] and 82% of the desired *17α-aminomethyl-5α-androstan-17β-ol* (**5**) which was used without further purification.

A solution containing the aminomethyl alcohol **5** (0.5 g, 1.27 mmol) in the minimum amount of chloroform (*ca.* 15 ml) was added rapidly to a stirred solution of ethylene oxide (10 ml) in methanol (20 ml), at 0°. The reaction flask was tightly stoppered and stirring was continued for a further 1 h at 0°. The solution was then kept at 20° for a further 2 days and was then refluxed for 8 h using an acetone – Dry Ice coating system to condense the remaining ethylene oxide. The solvent was removed by rotary evaporation at 20° and the yellow residue obtained (0.45 g) was purified by chromatography on Florisil. Elution with chloroform removed the 5α-androstan-17β-ol (35 mg) impurity and subsequent elution with chloroform–methanol–ammonia (90:15:1) afforded a colorless solid (0.39 g) which was recrystallized from methylene chloride to give *17α-bis(2-hydroxyethyl)-aminomethyl-5α-androstan-17β-ol* (**2***b*) (0.37 g, 58%),[12] m.p. 182–183°; i.r. ($CHCl_3$) 3448 cm^{-1}; p.m.r. ($CDCl_3$) δ 0.78 (3H, s, C-19 CH_3), 0.85 (3H, s, C-18 CH_3), 2.68 (2H, midpoint of AB quartet superimposed on signal centered at 2.78 p.p.m., C-17 CH_2N), 2.78 (4H, 't', J = 4.8 Hz, NCH_2CH_2OH), 3.35 (3H, m, partially exchangeable with D_2O, OH), and 3.62 p.p.m. (4H, 't', J = 4.8 Hz, $NCHCH_2OH$).

(b) Oxirane Route

A mixture of spiro-17β-oxiranyl-5α-androstane (**13**, 60 mg, 0.21 mmol), bis(2-hydroxyethyl)amine (1 ml), and ethylene glycol (2 ml) was heated in a sealed tube at 160° for 5 h. The mixture was then poured into water and filtered. The solid obtained was dissolved in the minimum amount of anhydrous ether (20 ml) and hydrogen chloride was bubbled into the solution. The precipitate produced was filtered, washed with anhydrous ether, and dried *in vacuo* to give the hydrochloride (76 mg) which was resuspended in ether (50 ml) and then stirred with saturated aqueous sodium hydrogen carbonate (50 ml) for 1 h. The ether layer was then separated, washed with water (2 × 15 ml), and dried ($MgSO_4$). Evaporation of the solvent and recrystallization of the residue from methylene chloride gave the bis(2-hydroxyethyl)amino alcohol **2***b* (75 mg, 92%) which was identical in all respects to the material obtained above from the cyanohydrin route.

The analogous preparation of **2***b* using water as a solvent gave a 42% yield only.

Spiro-17β-oxiranyl-5α-androstane (13)

A 53.8% suspension of sodium hydride in mineral oil (0.65 g, 14.6 mmol) was washed with tetrahydrofuran by

[9]Recrystallization of this material from methanol did not remove the trace of the starting ketone **3** and attempted purification via column chromatography on alumina afforded 5α-androstan-17-one only. Accordingly the cyanohydrin **4** was used in its initially isolated form for the subsequent reaction.

[10]Several groups have observed that the filter cakes obtained during metal hydride reduction of cyanohydrins retain a considerable proportion of the desired amines (10, 19).

[11]The formation of the relatively large amount of this compound arises from the significant disproportionation which occurs during reduction of the cyanohydrin to the original C-17 ketone and cyanide ion (12).

[12]In spite of the application of various purification procedures satisfactory analytical data could not be obtained for this compound, nor for its hydrochloride. Analytical difficulties with steroid mustard compounds and intermediates have also been encountered previously (2, 20).

Can. J. Chem. Downloaded from www.nrcresearchpress.com by 210.87.254.105 on 09/05/12
For personal use only.

decantation. Dry dimethyl sulfoxide (10 ml) was added and the mixture was stirred for 45 min at 70° under nitrogen. Tetrahydrofuran (10 ml) was then added, the mixture cooled to −5°, and solution of trimethylsulfonium iodide (30 g, 14.6 mmol) in dimethyl sulfoxide (23 ml) added rapidly with stirring (13). During this addition the reaction mixture solidified and the addition of further tetrahydrofuran (14 ml) became necessary. 5α-Androstan-17-one (**3**) (1.0 g, 3.65 mmol) in tetrahydrofuran (30 ml) was then added to the mixture and after being kept at 20° for 15 h the whole was poured into water (150 ml) and extracted with ether (4 × 75 ml). The combined ether extracts were washed with water (2 × 25 ml), dried ($MgSO_4$), and evaporated. The residue (0.93 g) was purified by chromatography on alumina and elution with petroleum ether (60–70°). Recrystallization from acetone gave *spiro-17β-oxiranyl-5α-androstane* (**13**) as feathery plates (0.88 g, 84%), m.p. 160–161°; p.m.r. ($CDCl_3$) δ 0.78 (3H, s, C-19 CH_3), 0.86 (3H, s, C-18 CH_3), and 2.71 p.p.m. (2H, midpoint of AB quartet, δ_A 2.82, δ_B 2.52, J_{AB} = 5.0 Hz, C-17 CH_2).

Anal. Calcd. for $C_{20}H_{32}O$: C, 83.27; H, 11.18. Found: C, 83.22; H, 11.31.

17α-Methyl-5α-androstan-17β-ol (**14**)

(a) From the Oxirane (**13**)

Spiro-17β-oxiranyl-5α-androstane (**13**) (300 mg, 1.04 mmol) was refluxed for 4 h with lithium aluminum hydride (0.30 g, 7.8 mmol) in tetrahydrofuran (50 ml). Ethyl acetate (50 ml) was then carefully added to the cooled reaction mixture following which it was poured into aqueous hydrochloric acid (5%, 150 ml). The mixture was extracted with benzene (3 × 40 ml) and the combined extracts were washed with water and dried ($MgSO_4$). Evaporation gave a colorless solid (225 mg) which recrystallized from acetone to produce *17α-methyl-5α-androstan-17β-ol* (**14**) as plates (210 mg, 70%), m.p. 165–166°; i.r. ($CHCl_3$) 3597 and 3472 cm^{-1}; p.m.r. ($CDCl_3$) δ 0.79 (3H, s, C-19 CH_3), 0.82 (3H, s, C-18 CH_3), and 1.18 p.p.m. (3H, s, C-17 CH_3).

Anal. Calcd. for $C_{20}H_{34}O$: C, 82.69; H, 11.80. Found: C, 82.45; H, 11.95.

(b) From 17β-Hydroxy-17α-methylandrost-4-en-3-one (**15**)

17β-Hydroxy-17α-methylandrost-4-en-3-one (**15**, 4 g, 13.2 mmol) was converted, via lithium in liquid ammonia, followed by Wolff–Kishner reductions (21) into authentic 17α-methyl-5α-androstan-17β-ol (**14**, 1.95 g, 50%) which was identical in all respects with the material obtained above.

17α-Bis(2-hydroxyethyl)aminomethyl-3,3′-ethylenedioxyandrost-5-en-17β-ol (**12**)

(a) Cyanohydrin Routes

3,3′-Ethylenedioxy-17β-hydroxyandrost-5-ene (**7**) m.p. 183–184° (lit. (22) m.p. 182–184°) was obtained from testosterone (**6**) in 46% yield (22). Oxidation of **7** with chromium trioxide in pyridine (22) proceeded smoothly to give 3,3′-ethylenedioxyandrost-5-en-17-one (**8**) m.p. 196–197° (lit. (22) m.p. 197–198°) in 80% yield. Freshly prepared (23) acetone cyanohydrin (1 ml) was added to the ketal **8** (200 mg, 0.61 mmol) dissolved in the minimum quantity of warm methanol. The resulting solution was heated on a steam bath for 3 min and a few drops of a methanolic solution containing 2% w/w of potassium cyanide were added. After keeping for 4 h at 20° the crystalline precipitate was filtered off, washed with water, and then dried *in vacuo* to give 3,3′-ethylenedioxyandrost-5-ene-17-cyanohydrin (**9**, 180 mg, 83%), m.p. 205–209° (lit. (11) m.p. 185°); i.r. (KBr) 3390 and 1739 cm^{-1} (C-17 carbonyl impurity). This material was not further purified but was used directly in subsequent experiments (*cf.* footnote 9).

Alternatively, the cyanohydrin **9** could be prepared from androst-4-ene-3,17-dione (**10**).

Androst-4-ene-3,17-dione (2 g, 7.0 mmol) was dissolved by gentle warming and swirling in freshly prepared (23) acetone cyanohydrin (3 ml). The solution was allowed to stand for 2 h at 20° and was then diluted with water (15 ml) and extracted with ether (4 × 40 ml). The combined ether extracts were washed with water and the ether solution was then cooled in an ice bath. The precipitated crystalline mass was filtered and dried *in vacuo* to give crude androst-4-en-3-one-17-cyanohydrin (**11**) (1.62 g, 74%), m.p. 174–180° (lit. (11) m.p. 176–178°); i.r. (KBr) 2279, 2237, 1656, and 1739 cm^{-1} (C-17 C=O impurity). No attempt was made to further purify this material (*cf.* footnote 9).

A suspension of the above cyanohydrin **11** (1.0 g, 3.2 mmol) in benzene (65 ml) and ethylene glycol (1.30 ml) with toluene-*p*-sulfonic acid (0.1 g) was refluxed for 16 h in a Soxhlet extractor with the water formed during the reaction being removed with molecular sieves. Evaporation of the solvent and recrystallization of the residue from methanol containing a few drops of pyridine produced the cyanohydrin ketal **9** (0.91 g, 80%), m.p. 205–208°. The i.r. spectrum of this material indicated that less C-17 carbonyl impurity was present than in the previous material, m.p. 205–209°, obtained above.

3,3′-Ethylenedioxyandrost-5-ene-17-cyanohydrin (**9**) (1.20 g, 34 mmol) was treated with lithium aluminum hydride (0.19 g, 5.1 mmol) and the reaction mixture worked-up as described for the synthesis of the 5α-androstane analogue **5**. The product obtained by extraction of the filter cake[10] (0.51 g) was combined with the material obtained by evaporation of the supernatant (0.66 g) and the whole chromatographed on Florisil. Elution with chloroform gave 3,3′-ethylenedioxyandrost-5-en-17β-ol[9] (0.30 g) and elution with chloroform – methanol – ammonium hydroxide (90:15:1) produced the amino-carbinol **12** (0.56 g, 46%) which was recrystallized from benzene as prisms, m.p. 240°; i.r. (KBr) 3778, 3300, 3175, 1107, and 1093 cm^{-1}; p.m.r. ($CDCl_3$) δ 0.90 (3H, s, C-18 CH_3), 1.02 (3H, s, C-19 CH_3), 2.70 (2H, midpoint of AB quartet superimposed on other H signals, δ_A 2.90, δ_B 7.50, J_{AB} = 12.8 Hz, C-17 CH_2N), 3.90 (4H, s, OCH_2CH_2O), and 5.31 p.p.m. (1H, m, vinyl H). Mass spectrum (70 eV) *m/e* 361 (parent ion).

3,3′-Ethylenedioxy-17β-hydroxy-17α-aminomethylandrost-5-ene (**12**) (0.30 g, 0.83 mmol) and ethylene oxide (6 ml) were reacted and worked-up as described above for the synthesis of the model compound **2***b*. Recrystallization of the product from methylene chloride gave *17α-bis(2-hydroxyethyl)aminomethyl-3,3′-ethylenedioxyandrost-5-en-17β-ol* (**12**) as plates (270 mg, 72%), m.p. 199–201°; i.r. ($CHCl_3$) 3425, 1663, and 1096 cm^{-1}; p.m.r. ($CDCl_3$) δ 0.90 (3H, s, C-18 CH_3), 1.03 (3H, s,

C-19 CH_3), 2.69 (2H, m, superimposed on signal centered at 2.77 p.p.m., C-17 CH_2N), 3.40 (3H, m, partially exchangeable with D_2O, OH), 3.61 (4H, 't', $J = 5.5$ Hz, NCH_2CH_2OH), 3.90 (4H, s, OCH_2CH_2O), and 5.29 p.p.m. (1H, m, vinyl H). Mass spectrum (70 eV) *m/e* 449 (parent ion).

Anal. Calcd. for $C_{26}H_{43}NO_5$: C, 69.45; H, 9.64; N, 3.11. Found: C, 69.13; H, 9.48; N, 3.47.

(b) Oxirane Route

3,3′-Ethylenedioxyandrost-5-en-17-one (**8**, 1 g, 3 mmol) was reacted with dimethylsulfonium methylide as described above in the preparation of the oxirane **13**. 3,3′-Ethylenedioxy-spiro-17β-oxiranylandrost-5-ene (**17**) was obtained as feathery plates (0.88 g, 88%) from acetone, m.p. 185–190°; i.r. ($CHCl_3$) 1096 cm^{-1}; p.m.r. ($CDCl_3$) δ 0.94 (3H, s, C-18 CH_3), 1.09 (3H, s, C-19 CH_3), 2.78 (2H, midpoint of AB quartet, δ_A 2.78, δ_B 2.63, $J_{AB} = 4.9$ Hz, oxiranyl CH_2), 3.97 (4H, s, OCH_2CH_2O) and 5.40 p.p.m. (1H, m, vinyl H).

Anal. Calcd. for $C_{22}H_{32}O_3$: C, 76.65; H, 9.36. Found: C, 76.75; H, 9.43.

A mixture of the spiro-17β-oxiranyl-3-ketal **17** (0.50 g, 1.45 mmol), bis(2-hydroxyethyl)amine (25 ml), and water (6 ml) was reacted and worked-up by the procedure described above for the conversion of the oxirane **13** into **2***b*. Recrystallization of the product from methylene chloride yielded 0.31 g (48%) of the aminotriol **12** identical in all respects with the material obtained via the cyanohydrin route.

17α-(N-Morpholinomethyl)-5α-androstan-17β-ol (16)

A solution of spiro-17β-oxiranyl-5α-androstane (**13**, 125 mg, 0.44 mmol) in morpholine (5 ml) containing phenol (55 mg) was refluxed for 24 h. The solution was then poured into water (25 ml) and extracted with ether (3 × 20 ml). The combined ether extracts were washed with aqueous sodium hydroxide (10%, 3 × 10 ml), then with water (2 × 15 ml), and dried ($MgSO_4$). Evaporation of the solvent and recrystallization of the residue (130 mg) from methanol gave *17α-(N-morpholinomethyl)-5α-androstan-17β-ol* (**16**, 108 mg, 66%), m.p. 160–161.5°; i.r. ($CHCl_3$) 3425 cm^{-1}; p.m.r. ($CDCl_3$) δ 0.78 (3H, s, C-19 CH_3), 0.87 (3H, s, C-18 CH_3), 2.24–2.68 (6H, m, NCH_2CH_2O and C-17 CH_2N), 3.48 (1H, s, OH), and 3.71 p.p.m. (4H, 't', NCH_2CH_2O, $J = 4.4$ Hz).

Anal. Calcd. for $C_{24}H_{41}NO_2 \cdot \frac{1}{2}H_2O$: C, 74.95; H, 11.07; N, 3.64. Found: C, 75.27; H, 10.98; N, 3.78.

We thank the National Cancer Institute of Canada for generous financial support and the National Research Council of Canada for the award (to J.D.L.) of a Scholarship.

1. J. D. Leman. Ph.D. Thesis. University of Toronto, Toronto, Ontario, 1969.
2. J. B. Jones, D. J. Adam, and J. D. Leman. J. Med. Chem. In press, and references therein.
3. H. H. Friedman. J. Am. Chem. Soc. **83**, 2900 (1961).
4. W. C. J. Ross. Biological alkylating agents. Butterworths, London, 1962.
5. I. Niculescu-Duvaz, M. Ionescu, A. Cambanis, M. Vitan, and V. Feyns. J. Med. Chem. **11**, 500 (1968) and references therein.
6. F. D. Popp. J. Med. Chem. 7, 210 (1964).
7. C. Weatherbee, R. Temple, and W. J. Burke. J. Org. Chem. **21**, 1138 (1956).
8. R. C. Elderfield, M. Israel, J. H. Ross, and J. A. Waters. J. Org. Chem. **26**, 2827 (1961).
9. G. R. Pettit and A. K. Das Gupta. Chem. and Ind. 1016 (1962).
10. H. Heusser, P. T. Herzig, A. Furst, and P. A. Plattner. Helv. Chim. Acta, **33**, 1093 (1950).
11. P. De Ruggieri and C. Ferrari. J. Am. Chem. Soc. **81**, 5725 (1959) and previous papers.
12. J. D. Roberts and W. F. Gorham. J. Am. Chem. Soc. **74**, 2278 (1952).
13. C. E. Cook, R. C. Corley, and M. E. Wall. J. Org. Chem. **33**, 2789 (1968).
14. D. Bertin and L. Nedelec. Bull. Soc. Chim. Fr. 2140 (1964).
15. E. Batres, G. Monroy, and H. J. Ringold. J. Org. Chem. **26**, 878 (1961).
16. C. L. Hewett and D. S. Savage. J. Chem. Soc. C, 1134 (1968) and references therein.
17. C. L. Browne and R. E. Lutz. J. Org. Chem. **17**, 1187 (1952).
18. *cf.* G. R. Pettit and J. A. Settepani. J. Org. Chem. **27**, 2962 (1962) and references therein.
19. H. R. Nace and B. B. Smith. J. Am. Chem. Soc. **74**, 1861 (1952).
20. R. M. Peck, R. K. Preston, and H. H. Creech. J. Am. Chem. Soc. **76**, 3984 (1959).
21. *cf.* F. V. Brutcher and W. B. Bauer. J. Am. Chem. Soc. **84**, 2236 (1962).
22. H. J. Dauben, B. Loken, and H. J. Ringold. J. Am. Chem. Soc. **76**, 1359 (1954).
23. R. F. B. Cox and R. I. Stormont. Organic syntheses. Coll. Vol. 2. *Edited by* A. H. Blatt. J. Wiley and Sons, Inc., New York, N.Y., 1943. p. 7.

Can. J. Chem. Downloaded from www.nrcresearchpress.com by 210.87.254.105 on 09/05/12
For personal use only.

Can. J. Chem. Downloaded from www.nrcresearchpress.com by 210.87.254.105 on 09/05/12
For personal use only.

Pyrrole Chemistry. Part XIII. New Syntheses of 3-Alkylpyrroles

J. K. GROVES, HUGH J. ANDERSON, AND (IN PART) H. NAGY
Department of Chemistry, Memorial University of Newfoundland, St. John's, Newfoundland

Received March 22, 1971

3-*n*-Alkylpyrroles are prepared in good yield by a combined Wolff–Kishner reduction and hydrolysis and decarboxylation of 4-acyl-2-pyrrolethiolcarboxylates. Methyl 4-isopropyl-2-pyrrolecarboxylate and 4-*t*-butyl-2-pyrrolecarbonitrile are prepared by alkylation of methyl 2-pyrrolecarboxylate and 2-pyrrolecarbonitrile respectively. Hydrolysis and decarboxylation of these disubstituted compounds afford the corresponding 3-alkylpyrroles. Mass spectral data for some 1-, 2-, and 3-alkylpyrroles are reported.

Les alkyl-3-*n* pyrroles sont préparés avec un bon rendement par réduction de Wolff–Kishner, hydrolyse et décarboxylation des acyl-4 pyrrolethiolcarboxylates-2. L'isopropyl-4 pyrrolecarboxylate-2 de méthyle et le *t*-butyl-4 pyrrolecarbonitrile-2 sont préparés par alkylation respectivement du pyrrolecarboxylate-2 de méthyle et du pyrrolecarbonitrile-2. L'hydrolyse et la décarboxylation de ces composés disubstitués conduit aux alkyl-3 pyrroles correspondants. On rapporte les données de spectrométrie de masse pour des alkyl-1, -2, et -3 pyrroles.

Canadian Journal of Chemistry, 49, 2427 (1971)

Although numerous monoalkylpyrroles are known good synthetic routes to the 3-alkylpyrroles, with the possible exception of 3-methylpyrrole (1–6), are notably absent. Skell and Bean (7) have prepared numerous 3-alkylpyrroles by the alkylation of pyrrylmagnesium bromide. The low yields of 3-isomer so obtained (5–18%) together with the necessity of effecting separation from relatively large amounts (10–32%) of 2-alkylpyrrole have prompted us to devise new synthetic routes to the former compounds.

We have previously shown (8) that a 2-ethylthiolcarboxylate substituent at the pyrrole nucleus directs Friedel–Crafts acylation and formylation almost exclusively to the 4-position. We now report that the resulting 2,4-substituted pyrroles are readily converted to the corresponding 3-alkylpyrroles by a combined Wolff–Kishner reduction of the acyl substituent and hydrolysis and decarboxylation of the thiolester group (Scheme 1). Yields for the reaction were

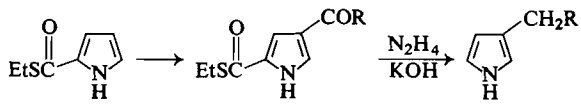

SCHEME 1

in the range 44–91% representing yields of 15–31% from pyrrole itself. The preparations of 3-methyl-, 3-ethyl-, and 3-benzylpyrrole are described but the method should prove to be quite general for the synthesis of 3-*n*-alkylpyrroles. A 2-methylcarboxylate substituent appears equally satisfactory in directing substitution to the 4-position thus methyl 2-pyrrolecarboxylate readily afforded 4-benzoyl-2-pyrrolecarboxylate which was subsequently converted to 3-benzylpyrrole by reduction and decarboxylation.

The aluminum chloride - catalyzed isopropylation (9) and *t*-butylation (10) of methyl 2-pyrrolecarboxylate afford the corresponding 4-alkyl-2-esters as the major kinetically controlled alkylation product. However these compounds exhibit a pronounced tendency to isomerize to the 5-alkyl-2-esters under these conditions preventing the use of these reactions as a convenient route to the corresponding 3-alkylpyrroles. Such rearrangement is largely avoided in the gallium trichloride - catalyzed isopropylation of the 2-ester (11) and by this method an 80% yield of methyl 4-isopropyl-2-pyrrolecarboxylate is obtained. This is readily separated from the small amount (*ca.* 8%) of 5-isopropyl-2-ester and hydrolysis and decarboxylation of the former affords 3-isopropylpyrrole in high yield (78%).

Rearrangement of the *t*-butyl group from the 4- to the 5-position of the alkylated 2-ester is more facile than for the corresponding isopropylated compound, thus the aluminum chloride - catalyzed *t*-butylation of methyl 2-pyrrolecarboxylate affords a 95:5 mixture of the 5- and 4-*t*-butyl-2-esters respectively (10). We find that the use of gallium trichloride as catalyst markedly increases the proportion of 4-*t*-butyl-2-ester (62% of the alkylation product) but still does not provide a sufficiently specific method

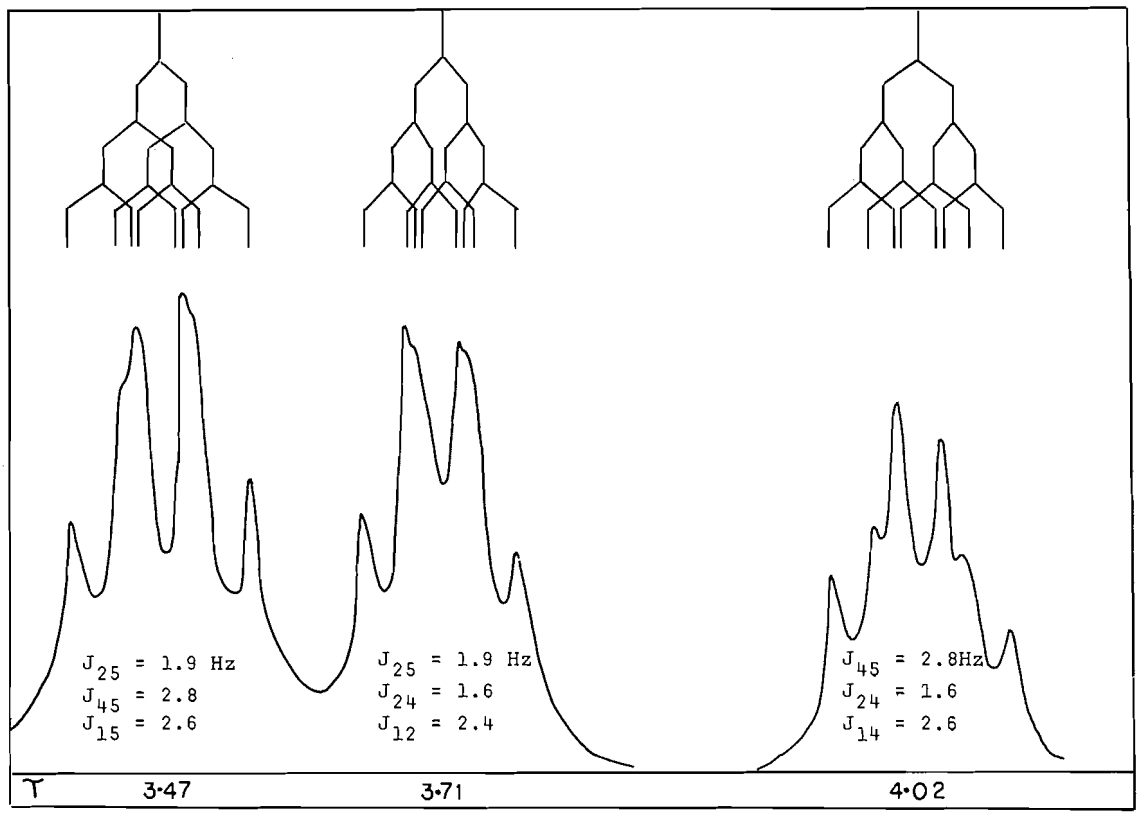

FIG. 1. Ring proton absorptions in the n.m.r. spectrum of 3-*t*-butylpyrrole.

of introducing a β-*t*-butyl substituent. A more strongly electron-withdrawing substituent at the 2-position should not only direct electrophilic attack more exclusively to the 4-position but should also suppress protonation of the product so obtained, hence reducing the extent of rearrangement. The cyano group might be expected to act in this way and should also permit a single stage hydrolysis and decarboxylation of the 4-*t*-butyl-2-pyrrolecarbonitrile to 3-*t*-butylpyrrole. Aluminum chloride - catalyzed *t*-butylation of 2-pyrrolecarbonitrile afforded a 13:87 mixture of the 5- and 4-alkylated products and the use of gallium trichloride as catalyst improved this ratio to 2:98. Purification and subsequent hydrolysis and decarboxylation of the 4-*t*-butylated product afforded pure 3-*t*-butylpyrrole (64%).

The structures of the alkylpyrroles were confirmed by their n.m.r. spectra. In all cases a separate signal was observed in the aromatic region for each of the three ring protons. Chemical shift data are given in Table 1. An analysis of the spectrum of 3-*t*-butylpyrrole is shown in Fig. 1. The various coupling constants were determined by deuteration and subsequent double irradiation. The spectra of the other 3-alkylpyrroles are further complicated by coupling between the ring protons and those of the alkyl substituent.

TABLE 1. The n.m.r. chemical shifts of 3-alkylpyrroles*

Substituent	H-2	H-4	H-5	3-Substituent
Me	3.71	4.12	3.57	8.93
Et	3.68	4.09	3.55	7.55 8.84
CH_2Ph	3.70	3.96	3.51	2.78 6.20
$CHMe_2$	3.65	4.05	3.53	7.21 8.82
CMe_3	3.71	4.02	3.47	8.79

*Values refer to *ca.* 10% solutions in CCl_4 and are quoted on the τ scale using TMS as an internal standard.

Mass spectral data for the 3-alkylpyrroles are reported in Table 2 along with those of some

Can. J. Chem. Downloaded from www.nrcresearchpress.com by 210.87.254.105 on 09/05/12
For personal use only.

Can. J. Chem. Downloaded from www.nrcresearchpress.com by 210.87.254.105 on 09/05/12
For personal use only.

TABLE 2. Mass spectral data for substituted pyrroles

Substituent	1-Me	2-Me	3-Me	2-Et	3-Et	1-Pr^i	2-Pr^i	3-Pr^i	1-Bu^t	2-Bu^t	3-Bu^t	1-CH_2Ph	2-CH_2Ph	3-CH_2Ph
[Parent]$^+$	100	76	72	57	78	86	53	58	38	50	47	50	100	100
[P-H]$^+$	66	100	100	9	15	2	4	9	0*	2	0	6	92	67
[P-Me]$^+$	0	0	0	100	100	60	100	100	5	100	100	—	—	—
[P-Ph]$^+$	—	—	—	—	—	—	—	—	—	—	—	1	100	91
	0	0	0	0	0	100	24	23	100	5	5	0	0	0
	29	24	24	21	19	4	6	6	2	4	4	1	13	9
	4	2	1	5	7	35	17	16	17	9	8	2.0	0	0
	20	5	4	8	8	16	17	13	10	7	5	6	5	6
[Substituent]$^+$	4	0	0	0	0	10	0	0	10	0	0	100	8	5

*Ions of < 1% abundance are entered in the table as zero.

Can. J. Chem. Downloaded from www.nrcresearchpress.com by 210.87.254.105 on 09/05/12
For personal use only.

1- and 2-alkylpyrroles. High resolution mass spectrometry was not available and hence assignments of the fragment structures are tentative.

The base peak for all the *C*-alkylpyrroles involves loss of a hydrogen or methyl radical to afford the azafulvene ions (*i* or *ii*) or their rearrangement products (Scheme 2). Such fragmentation might proceed with concurrent rearrangement to a pyridinium ion (12, 13). The very marked similarity of the spectra of the *C*-methylpyrroles both with each other and with those of the *C*-ethylpyrroles are consistent with the involvement of a mutual stable ion of $m/e = 80$ (Scheme 3). In the formation of *i*, *ii*, or their rearrangement products from *C*-alkylpyrroles loss of methyl is preferred to loss of hydrogen. The *C*-benzylpyrroles differ in that loss of phenyl and hydrogen are about equally favorable, doubtless because of the extensive charge delocalization that can occur in the ions *iii* or *iv* or their rearrangement products.

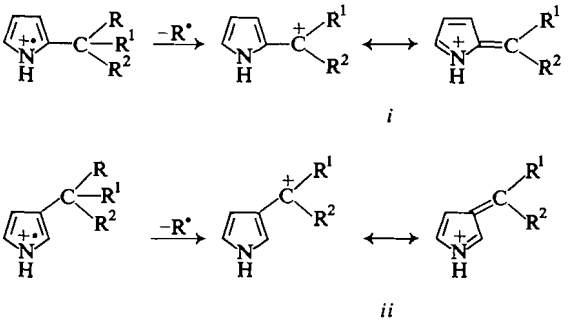

i

ii

SCHEME 2

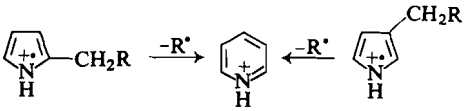

m/e 80

SCHEME 3

The mass spectra of the *C*-*t*-butylpyrroles also exhibit an ion of $m/e = 80$ of appreciable abundance (10%). Involvement of a cyclopropane intermediate, such as occurs in the fragmentation of *t*-butylbenzene (14), provides one possible explanation (Scheme 4).

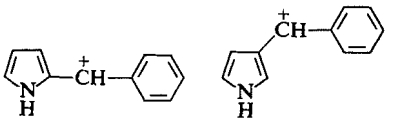

iii *iv*

Whilst the mass spectra of the isomeric 2- and 3-substituted pyrroles are very similar those of the 1-substituted pyrroles differ substantially. The base peak in the spectrum of 1-benzylpyrrole arises by decomposition of the parent ion to a pyrrolyl radical and tropylium ion. Analogous but less abundant fragmentation occurs for the branched alkylpyrroles, however the major fragmentation for these compounds involves loss of a molecule of alkene with concurrent hydrogen transfer (*cf.* refs. 15 and 16) (Scheme 5). The extent of formation of immonium ions or their rearrangement products (*cf.* ref. 17) varies from being the major fragmentation process for 1-methylpyrrole to being relatively insignificant for 1-*t*-butylpyrrole.

Experimental

Melting points were determined on a Fisher–Johns m.p. block and are uncorrected. The n.m.r. spectra were determined on a Varian HA 100 spectrometer at 100 MHz and i.r. spectra were determined on a Perkin–Elmer 237B spectrophotometer. Mass spectra were determined on a Hitachi Perkin–Elmer RMU 6E instrument using an ionization energy of 70 eV. An indirect inlet system maintained at 60° was used throughout and total ion current variation was maintained at $< 5\%$. The g.l.c. analyses of 2,4-substituted pyrroles were carried out on a Beckman GC 2A chromatograph fitted with a 30″ column (no. 70007) packed with Carbowax 4000 dioleate on firebrick and operating at 190°. The 3-alkylpyrroles were purified by preparative g.l.c. on a Wilkens Aerograph 1520 fitted with an 8 ft column packed with OV17 (methyl phenyl silicone) on Chromosorb G and operating between 80–130°.

Benzoylation of Ethyl 2-Pyrrolethiolcarboxylate

Ethyl 2-pyrrolethiolcarboxylate (465 mg), aluminum chloride (800 mg), and dichloromethane (20 ml) were stirred and heated under reflux during the dropwise addition of benzoyl chloride (420 mg) in dichloromethane

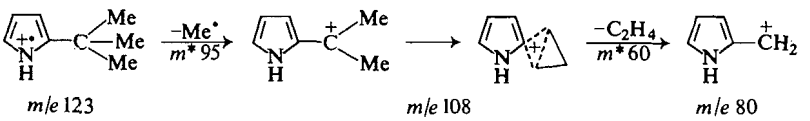

m/e 123 *m/e* 108 *m/e* 80

SCHEME 4

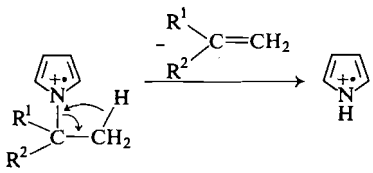

SCHEME 5

(5 ml). After 3 h the mixture was poured onto ice–HCl and extracted with chloroform. The extracts were washed with $NaHCO_3$ solution, dried ($MgSO_4$), and the solvents removed to afford an oily solid. Recrystallization from CCl_4 afforded ethyl 4-benzoyl-2-pyrrolethiolcarboxylate (435 mg, 56%); m.p. 103.5°; n.m.r. bands at τ 1.9–2.7 (complex, Ar—H), 6.90 (q, CH_2CH_3, *J* 7Hz), 8.64 (t, CH_2CH_3, *J* 7Hz).

Anal. Calcd. for $C_{14}H_{13}NO_2S$: C, 64.9; H, 5.1. Found: C, 65.1; H, 5.2.

Benzoylation of Methyl 2-Pyrrolecarboxylate

Analogous reaction of methyl 2-pyrrolecarboxylate (500 mg) with aluminum chloride (1.68 g) and benzoyl chloride (843 mg) afforded methyl 4-benzoyl-2-pyrrolecarboxylate (430 mg, 48%), m.p. 145–146° (from aqueous 2-propanol); n.m.r. bands at τ 2.05–2.73 (complex, Ar—H) and 6.14 (s, CO_2CH_3).

Anal. Calcd. for $C_{13}H_{11}NO_3$: C, 68.1; H, 4.8. Found: C, 68.4; H, 4.8.

Hydrolysis in methanolic KOH gave the corresponding acid m.p. 223.5–224° (dec.) (lit. (18) 224–225° (dec.)).

General Procedure for Alkylations

The 2-substituted pyrrole, catalyst (1.1 equiv), and carbon disulfide (40 ml) were stirred and heated at 40° for 30 min prior to the rapid addition of alkyl halide (1.1 equiv). After further stirring at 40° for the set time the reaction mixture was poured onto ice–HCl and extracted with chloroform. The extracts were washed with $NaHCO_3$ solution, dried ($MgSO_4$), and the solvent removed.

The t-Butylation of Methyl 2-Pyrrolecarboxylate

Methyl 2-pyrrolecarboxylate (1.50 g), gallium chloride, and *t*-butyl chloride were allowed to react for 40 min prior to isolation of the product (2.18 g, 91%) which was shown (g.l.c.) to contain two components in 38:62 ratio. Chromatography on neutral activity I alumina using 1:1 petroleum – diethyl ether effected separation and the major component was shown to be methyl 4-*t*-butyl-2-pyrrolecarboxylate, m.p. and mixture m.p. 121–122°; n.m.r. bands ($CDCl_3$) at τ 7.10 (m, 3H and 5H), 6.10 (s, CO_2CH_3), and 8.72 (s, *t*-Bu). The minor component was methyl 5-*t*-butyl-2-pyrrolecarboxylate, m.p. and mixture m.p. 127–128°; n.m.r. bands ($CDCl_3$) at τ 3.08 (q, 3H, J_{34} 3.8, J_{13} 2.5 Hz), 3.90 (q, 4H, J_{34} 3.8, J_{14}, 2.5 Hz), 6.10 (s, CO_2CH_3), and 8.65 (s, *t*-Bu).

The t-Butylation of 2-Pyrrolecarbonitrile

(*A*) 2-Pyrrolecarbonitrile (19) (950 mg), aluminum chloride, and *t*-butyl chloride were allowed to react for 30 min prior to isolation of the product (1.407 g, 95%) which was shown (g.l.c.) to contain two components in 13:87 ratio. These were shown to be 5-*t*-butyl-2-pyrrolecarbonitrile and 4-*t*-butyl-2-pyrrolecarbonitrile respectively since hydrolysis and subsequent methylation (CH_2N_2) of the mixture afforded the corresponding alkylated 2-esters which were identified by g.l.c. comparison with the authentic esters.

(*B*) 2-Pyrrolecarbonitrile (1.12 g), gallium chloride, and *t*-butyl chloride were allowed to react for 30 min whilst the reaction mixture was flushed with nitrogen. Isolation gave a product (1.62 g, 93%) shown by g.l.c. to contain 4-*t*-butyl-2-pyrrolecarbonitrile contaminated by < 2% of the 5-*t*-butyl isomer. Distillation, b.p. 125–128°/0.05 mm and subsequent crystallization from petroleum afforded pure 4-*t*-butyl-2-pyrrolecarbonitrile m.p. 56–57°; n.m.r. bands (CCl_4) at τ 3.2 (d, 3H and 5H, $J_{13} \approx J_{15} = 2.6$), ν_{CN} (Nujol) 2220 cm^{-1}.

Anal. Calcd. for $C_9H_{12}N_2$: C, 73.0; H, 8.1; N, 18.9. Found: C, 72.9; H, 8.0; N 19.0.

3-Methylpyrrole

Ethyl 4-formyl-2-pyrrolethiolcarboxylate (8) (500 mg), potassium hydroxide (500 mg), hydrazine (500 mg of 64%), and triethylene glycol (5 ml) were stirred at 125° for 90 min. The temperature was then raised to 220° for 4 h prior to pouring into ice–water and extracting with ether. The extract was washed with water, dried ($MgSO_4$), and chromatographed on neutral activity I alumina to remove tarry material. Subsequent distillation afforded 3-methylpyrrole (122 mg, 44%), b.p. 142–144° (lit. (1) b.p. 143–143.5°).

3-Ethylpyrrole

Ethyl 4-acetyl-2-pyrrolethiolcarboxylate (8) (500 mg) was similarly converted into 3-ethylpyrrole (20) (135 mg, 53%), b.p. 86–88°/20 mm.

3-Benzylpyrrole

(*A*) Ethyl 4-benzoyl-2-pyrrolethiolcarboxylate (330 mg) was similarly converted to 3-benzylpyrrole (182 mg, 91%).

Anal. Calcd. for $C_{11}H_{11}N$: C, 84.0; H, 7.1. Found: C, 84.1; H, 7.2.

(*B*) Methyl 4-benzoyl-2-pyrrolecarboxylate (425 mg) similarly afforded 3-benzylpyrrole (270 mg, 92%).

3-Isopropylpyrrole

Methyl 4-isopropyl-2-pyrrolecarboxylate (200 mg), prepared by the gallium chloride - catalyzed isopropylation of methyl 2-pyrrolecarboxylate (11), was heated at 230° for 5 h with KOH (250 mg), water (250 mg), and triethylene glycol (3 ml). The mixture was then poured onto ice–HOAc, extracted with ether, washed with $NaHCO_3$ solution, and dried ($MgSO_4$). Removal of the solvent afforded 3-isopropylpyrrole (7) (101 mg, 78%).

3-t-Butylpyrrole

4-*t*-Butyl-2-pyrrolecarbonitrile (200 mg) was similarly hydrolyzed and decarboxylated to afford 3-*t*-butylpyrrole (7) (126 mg, 64%).

1-Alkylpyrroles

The 1-alkylpyrroles were prepared from 2,5-dimethoxytetrahydrofuran and the appropriate amine according to the method of Elming and Clauson–Kaas (21, 22).

2-Alkylpyrroles

The 2-*n*-alkylpyrroles (23) and 2-benzylpyrrole (24) were prepared by Wolff–Kishner reduction of the corresponding 2-acylpyrrole. 2-Isopropylpyrrole (7) and 2-*t*-

Can. J. Chem. Downloaded from www.nrcresearchpress.com by 210.87.254.105 on 09/05/12
For personal use only.

butylpyrrole (7) were prepared by hydrolysis and decarboxylation of the methyl 5-alkyl-2-pyrrolecarboxylates by the method described above for the preparation of the corresponding 3-alkylpyrroles.

The authors gratefully acknowledge financial support from the National Research Council of Canada.

1. R. L. HINMAN and S. THEODOROPULOS. J. Org. Chem. **28**, 3052 (1963).
2. H. PLIENINGER, H. BAUER, W. BUEHLER, J. KURZE, and U. LERCH. Ann. Chem. **680**, 69 (1964).
3. R. E. LANCASTER and C. A. VANDERWERF. J. Org. Chem. **23**, 1208 (1958).
4. G. M. BADGER, R. L. N. HARRIS, and R. A. JONES. Aust. J. Chem. **17**, 1022 (1964).
5. J. ELGUERO, R. JAQUIER, and B. SHIMIZU. Bull. Soc. Chim. Fr. 2996 (1967).
6. J. W. CORNFORTH and M. E. FIRTH. J. Chem. Soc. 1091 (1958).
7. P. S. SKELL and G. P. BEAN. J. Am. Chem. Soc. **84**, 4665 (1962).
8. C. E. LOADER and H. J. ANDERSON. Tetrahedron, **25**, 3879 (1969).
9. H. J. ANDERSON and L. C. HOPKINS. Can. J. Chem. **42**, 1279 (1964).
10. H. J. ANDERSON and C. W. HUANG. Can. J. Chem. **48**, 1550 (1970).
11. H. J. ANDERSON and L. C. HOPKINS. Can. J. Chem. **44**, 1831 (1966).
12. A. BUDZIKIEWICZ, C. DJERASSI, A. H. JACKSON, G. W. KENNER, D. J. NEWMAN, and J. M. WILSON. J. Chem. Soc. 1949 (1964).
13. R. A. JONES. Adv. Heterocycl. Chem. **11**, 383 (1970).
14. H. BUDZIKIEWICZ, C. DJERASSI, and D. H. WILLIAMS. Mass spectrometry of organic compounds. Holden Day, San Francisco, California, 1967.
15. A. PADWA, R. GRUBER, D. PASHAYAN, M. BURSEY, and L. DUSOLD. Tetrahedron Lett. 3659 (1968).
16. A. M. DUFFIELD, R. BEUGELMANS, H. BUDZIKIEWICZ, D. A. LIGHTNER, D. H. WILLIAMS, and C. DJERASSI. J. Am. Chem. Soc. **90**, 678 (1968).
17. M. MARX and C. DJERASSI. J. Am. Chem. Soc. **90**, 678 (1968).
18. A. GOMEZ SANCHEZ, M. GOMEZ GUILLEN, V. SCHEIDEGGER. Carbohydr. Res. **3**, 486 (1967).
19. C. E. LOADER and H. J. ANDERSON. Can. J. Chem. **49**, 45 (1971).
20. H. FISCHER and W. ROSE. Ann. Chem. **519**, 1 (1935). G. P. BEAN. Anal. Chem. **37**, 756 (1965).
21. N. ELMING and N. CLAUSON-KAAS. Acta. Chem. Scand. **6**, 867 (1952).
22. H. GROSS. Chem. Ber. **95**, 2270 (1962).
23. H. FISCHER and H. ORTH. Die Chemie des Pyrrols. Vol. 1. Akad. Verlagsgesellschaft, Leipzig, 1934.
24. C. F. HOBBS, C. K. MCMILLIN, E. P. PAPADOPOULOS, and C. A. VANDERWERF. J. Am. Chem. Soc. **84**, 43 (1962).

Can. J. Chem. Downloaded from www.nrcresearchpress.com by 210.87.254.105 on 09/05/12
For personal use only.

The Aqueous Chemistry of Chromium(III) above 100 °C: Hydrothermal Synthesis of Chromium Spinels

T. W. SWADDLE, J. H. LIPTON, AND G. GUASTALLA
Department of Chemistry, The University of Calgary, Calgary 44, Alberta

AND

P. BAYLISS
Department of Geology, The University of Calgary, Calgary 44, Alberta

Received December 22, 1970

The hydrothermal deposition of CrO(OH) from aqueous chromium(III) chloride, nitrate, and perchlorate, and of $Cr_3(SO_4)_2(OH)_5.H_2O$ and $Cr(OH)SO_4.2H_2O$(?) from aqueous chromium(III) sulfate, has been investigated. Aqueous chromium(III) is oxidized to chromium(VI) by 0.4 *M* perchloric acid above 225 °C, and by molecular oxygen above 250 °C. Aqueous chromium(III) can react at 300 °C with iron or steel, cobalt, and copper to produce $FeCr_2O_4$, $CoCr_2O_4$, and $Cu_2Cr_2O_4$, respectively. CrO(OH) reacts with type 316 stainless steel at 440 °C in supercritical water of density 0.7 g cm^{-3} to yield (Fe,Ni)-Cr_2O_4, which is the "cubic Cr_2O_3" of Laubengayer and McCune. The spinels MCr_2O_4 (M = Mg, Mn, Fe, Co) can be made hydrothermally at *ca.* 300 °C from $Cr(OH)_3$ and $M(OH)_2$. This information is relevant to corrosion phenomena, and the possible hydrothermal origin of chromite deposits in serpentinized rocks.

Le dépot hydrothermique de CrO(OH) à partir d'une solution aqueuse de chlorure, nitrate et perchlorate de chrome(III) ainsi que le dépot de $Cr_3(SO_4)_2(OH)_5.H_2O$ et $Cr(OH)SO_4.2H_2O$(?) à partir d'une solution aqueuse de sulfate de chrome(III), ont été étudiés. Une solution aqueuse de chrome(III) est oxydée en chrome(VI) au-dessus de 225 °C par l'acide perchlorique 0.4 *M* et par de l'oxygène moléculaire au-dessus de 250 °C. Une solution aqueuse de chrome(III) peut réagir à 300 °C avec du fer ou de l'acier, du cobalt, et du cuivre pour donner respectivement du $FeCr_2O_4$, $CoCr_2O_4$ et $Cu_2Cr_2O_4$. Le CrO(OH) réagit à 440 °C avec l'acier inoxydable du type 316, dans de l'eau supracritique de densité 0.7 g cm^{-3} pour donner le (Fe,Ni)Cr_2O_4, qui est le "Cr_2O_3 cubique" de Laubengayer et McCune. Les spinelles MCr_2O_4 (M = Mg, Mn, Fe, Co) peuvent être formés d'une façon hydrothermique à 300 °C à partir de $Cr(OH)_3$ et $M(OH)_2$. Cette information correspond au phénomène de la corrosion et à l'origine hydrothermique possible de dépots de chromites dans les roches serpentinisées.

Canadian Journal of Chemistry, **49**, 2433 (1971)

Introduction

Chromium(III) offers several advantages as a model ion for studies intended to elucidate aqueous metal–ion chemistry at high temperatures. Much information is now available on its aqueous chemistry below 100 °C (1); the ion is not easily oxidized or reduced; and its complexes and hydrolytic polymers undergo substitution reactions sufficiently slowly at room temperature that it may be possible to characterize individual solute species formed at high temperatures after rapid quenching. Therefore a preliminary study of the qualitative solution chemistry of chromium(III) was undertaken; as it pertains to future experiments where the spectroscopic properties, hydrolysis, and complex formation of chromium(III) may be investigated quantitatively.

Experimental

Materials

The chemicals used were Fisher Certified reagents. Distilled water was passed through both Barnstead organic removal and de-ionizer cartridges before use. Chromium(III) hydroxide was prepared by precipitation from 1 *M* $CrCl_3$ solution with 0.1 *M* aqueous ammonia, followed by centrifugation and re-suspension in fresh ammonia; this process was repeated until no detectable chloride ion remained; then the product was dried under vacuum at 20 °C. Chromium(III) perchlorate was prepared by reducing chromium(VI) oxide in aqueous perchloric acid with hydrogen peroxide; the produce was recrystallized from 0.1 *M* perchloric acid.

Equipment

The pressure vessels used are of four types as follows: (*a*) a small vessel of capacity 87 cm^3 (Fig. 1) constructed from ATL-40 titanium with 0.2% palladium (Atlas Titanium, Welland, Ontario) for service up to 180 bars at 350 °C; the sealing gasket is Teflon contained between two rings constructed from titanium with 0.2% palladium

as recommended by Gill and Marshall (2). (*b*) Similar to the above vessel (type *a*) but with a smaller diameter to reduce the capacity to 62 cm^3. (*c*) A vessel constructed from type 316 stainless steel for service up to 420 °C at 150 bars; the sealing gasket is a commercial asbestos gasket shod with type 304 stainless steel rings (Flexitallic Type R3-25D, Canadian Gasket Co. Ltd., Fort Erie, Ontario). (*d*) A high-pressure vessel of capacity 50 cm^3 constructed from 316 stainless steel from the design by H.L.Barnes; the seal is a 90° delta-ring seated in 60° countersinks in the body and cap. A silica liner with a loose-fitting cap for the low-pressure vessels (types *a*, *b*, and *c*) or a mild steel liner (AISI C1020) for a low-pressure stainless steel vessel (type *c*) was used in some experiments.

The vessels were heated in either a Blue M Conwate CW-160HF-1 forced-convection oven, or a Thermolyne type 1700 electric furnace with a Barber–Coleman Capacitrol Model 292 temperature controller. The temperatures recorded are accurate to within ±5 °C.

Concentrations throughout this article are expressed as molarities valid at 20 °C. The atmospheres within the vessel prior to reaction unless otherwise specified were pure nitrogen at 1 bar pressure, and in no case did the pressure of nitrogen at higher temperatures exceed 3 bars.

Analyses

Aqueous chromium was estimated spectrophotometrically as CrO_4^{2-} after oxidation with alkaline H_2O_2; other chemical analyses followed standard practice (3). Solids were identified from X-ray diffraction powder patterns obtained from an X-ray diffractometer with Cu–Kα radiation. The letters ASTM followed by numbers in the following text refer to the data in the X-Ray Diffraction Powder File.

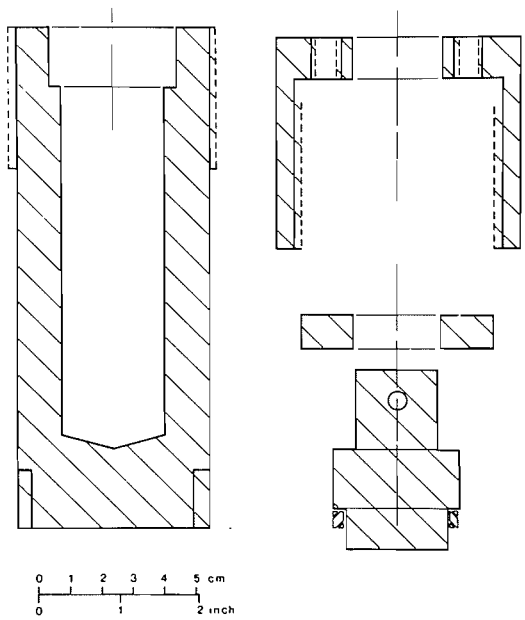

FIG. 1. Pressure vessel. The cap (top right) and the bearing ring (center right) are type 316 stainless steel, and the sealing ring is Teflon; the remaining parts are titanium with 0.2% palladium.

Results

Precipitation Reactions

Chromium(III) Nitrate

At 300 °C, $Cr(NO_3)_3$ solutions (0.05 *M*) deposited well-crystallized rhombohedral CrO(OH) (4) (ASTM 9-331) quantitatively in 24 h with the evolution of heavy nitrogen(IV) oxide fumes. These results are the same whatever the vessel type, although the final p*H* was 1.5 in a titanium vessel and 5 in a stainless steel vessel with a mild steel liner. Partial deposition of CrO(OH) from 1.05 *M* $Cr(NO_3)_3$ occurs below 150 °C. Table 1 summarizes the percentage of CrO(OH) deposited in a titanium vessel after 24 h as a function of temperature. At 200 °C, 1.05 *M* $Cr(NO_3)_3$ deposited a similar amount of CrO(OH) in 4 days as in 24 h, so these data in Table 1 represents equilibrium conditions. Nitrogen(IV) oxide fumes were only observed as a reaction product at 300 °C. None of the products contained $Cr(OH)_3$.

Chromium(III) Chloride

Chromium(III) chloride solutions were less extensively decomposed than their nitrate analogues when heated in an inert vessel. Thus 0.8 *M* $CrCl_3$ deposited in 24 h 86% of well-crystallized CrO(OH) (ASTM 9–331) at 300 °C, only 4% amorphous material at 250 °C, and none at 200 °C, in a titanium vessel. A 250 °C, 49% CrO(OH) was deposited in 48 h in a titanium vessel with silica liner, and 59% in 4 days in a stainless steel vessel with silica liner. Therefore the precipitation process is slow at 250 °C and is favored by silica surfaces. At 300 °C in an unlined stainless steel vessel, 0.05 *M* $CrCl_3$ reacted with the vessel walls to produce a near quantitative precipitate of $FeCr_2O_4$ and ferrous iron in solution.

Chromium(III) Sulfate

At a low acidity and above 250 °C, chromium-

TABLE 1. Percentage precipitation of CrO(OH) from aqueous chromium(III) nitrate (1.05 *M*)

Temperature (°C)	Duration (h)	% CrO(OH)
150	24	9
175	24	16
200	24	65
200	91	62
223	24	87
250	24	95
300	24	100

TABLE 2. Percentage deposition of $Cr_3(SO_4)_2(OH)_5.H_2O$ from aqueous chromium(III) sulfate

[Cr(III)] (M)	Vessel/liner	[H_2SO_4] added (M)	Temperature (°C)	Duration (h)	% yield $Cr_3(SO_4)_2(OH)_5.H_2O$
0.042	Ti/SiO_2	0.0	300	24	96
0.30	s.s./SiO_2†	0.0	300	30	100
0.30	s.s./SiO_2	0.1	300	24	94
0.30	Ti/SiO_2	0.5	300	24	71
0.30	Ti	1.0	300	19	0
0.30	Ti/SiO_2	0.0	275	24	95
0.30	Ti/SiO_2	0.4	275	24	47
0.56	Ti/SiO_2	0.4	275	24	58
0.23	Ti/SiO_2	0.0	250	24	47
0.30	Ti/SiO_2	0.2	250	24	46
0.30	Ti/SiO_2	0.2	250	64	68
0.30	Ti/SiO_2	0.5	250	24	0
0.30	Ti/SiO_2	0.2	230	24	0
0.30	Ti	0.0	200	24	0
2.31	Ti	0.0	300	24	79*
2.31	Ti	0.0	250	24	0
2.31	Ti	0.0	200	24	0

*SO_2 evolved.
†s.s. = stainless steel.

(III) sulfate solutions deposited a green, well-crystallized solid with an X-ray diffraction powder pattern similar to carphosiderite, $Fe_3(SO_4)_2(OH)_5.H_2O$ (ASTM 18-644 and ref. 5). The conditions of precipitation are summarized in Table 2. The solid is almost insoluble in water or mineral acids including aqua regia even on heating, but it dissolved in water after fusion with NaOH. The alkaline solution was heated with excess H_2O_2 and the chromium content estimated as CrO_4^{2-}. Then the sulfate content was determined gravimetrically as $BaSO_4$ following acidification and reduction of the chromium(VI) to chromium(III) with further H_2O_2.

Anal. Calcd. for $Cr_3(SO_4)_2(OH)_5.H_2O$: Cr, 34.6; SO_4, 42.6. Found: Cr, 33.5; SO_4, 42.5.

This compound is the same as that obtained by Lecerf *et al.* (6) from chromium(III) sulfate solutions at 300 °C under somewhat different conditions. Its X-ray diffraction powder pattern agrees with that of Lecerf *et al.* (ASTM 18–381), but its observed chemical composition is in better accordance than theirs with the formula $Cr_3(SO_4)_2(OH)_5.H_2O$.

In all the experiments listed in Table 2, the sole crystalline product is $Cr_3(SO_4)_2(OH)_5.H_2O$; ion-exchange chromatography of the quenched supernatant solutions indicated the presence of $Cr(H_2O)_5SO_4^+$ and $Cr(H_2O)_2(SO_4)_2^-$. However, at 300 °C, a solution 0.13 M in chromium(III) and 0.88 M in H_2SO_4 yielded no precipitate in 24 h, but after 5 days yielded 18% of a green powder, which was mainly $Cr_3(SO_4)_2(OH)_5.H_2O$. It also showed additional X-ray diffraction reflections at the d-spacings and relative intensities as follows: 5.76 Å (30), 5.06 Å (50), and 3.15 Å (100). Analogy with $Fe(OH)SO_4.2H_2O$ (parabutlerite, ASTM 16–939) suggests it is $Cr(OH)SO_4.2H_2O$.

When a high concentration (2.31 M) of $Cr_2(SO_4)_3$ was heated at 300 °C, a considerable amount of sulfur dioxide was produced. A similar effect was noted with 1.25 M H_2SO_4 in the absence of chromium(III); after 4 days at 300 °C in a titanium vessel with silica liner, 1.4% of the sulfur appeared as SO_2 as measured by iodometric titration. Even more SO_2 (4.8%) was produced in 3 days when an unlined titanium vessel was used. Aqueous Na_2SO_4 was not significantly changed by similar treatment.

Chromium(III) Perchlorate

A dilute (0.0167 M) chromium(III) perchlorate solution was examined for both hydrolytic precipitation and oxidation of chromium(III) in the presence of various concentrations of excess $HClO_4$ and $NaClO_4$ (total $[H^+] + [Na^+] = 0.4$ M) on heating for 24 h in a titanium vessel with silica liner. At 200 °C a small quantity of CrO(OH) (ASTM 9–331) was precipitated from solutions containing initially 0.02 M $HClO_4$ and also 0.05 M $HClO_4$, whereas all the chromium was precipitated as CrO(OH) when no $HClO_4$ was originally present, but no precipitation occurred with 0.4 M $HClO_4$. Each solution was passed through a Dowex 50W-X8 ion-exchange column to remove chromium(III) species; the issuing solution was tested for chromium(VI) both spectrophotometrically and with diphenyl-

carbazide solution with a negative result. Above 225 °C oxidation of chromium(III) by 0.4 *M* $HClO_4$ to chromium(VI) was essentially complete in 24 h, with the concomitant formation of 0.39 mol of chloride ion per mole chromium(III) originally present.

Chromium(III) Sulfate with Oxygen

In hydrothermal experiments at 300 °C, some chromium(VI) was often produced from chromium(III), if the original atmosphere in the vessel was air rather than nitrogen. This phenomenon was investigated using a silica-lined titanium vessel in which an oxygen atmosphere was generated by thermal decomposition of a measured amount of 8 *M* H_2O_2 placed in the vessel *outside* the silica liner; the chromium(III) sulfate solution was kept inside the capped liner. Any chromium(VI) in the products was detected as described under the previous section *Chromium(III) Perchlorate.*

At 250 °C after 24 h, 0.23 *M* chromium(III) as sulfate yielded approximately 40% $Cr_3(SO_4)_2(OH)_5.H_2O$ (ASTM 18–381) in a nitrogen atmosphere. In the presence of excess oxygen at 4.2 bars pressure, 3.7% aqueous chromium(VI) was also formed, but both precipitation and oxidation were completely suppressed by the addition of 0.63 *M* H_2SO_4 prior to heating. At 300 °C under 16 bars of excess oxygen pressure, 0.23 *M* chromium(III) sulfate yielded 13% chromium(VI), while the remainder was precipitated as $Cr_3(SO_4)_2(OH)_5.H_2O$. When 1.5 *M* H_2SO_4 was present initially, there was no precipitate, but 4.2% chromium(VI) was still produced. Similar results were obtained when the H_2O_2 was placed in the chromium(III) solution rather than outside the liner prior to heating.

Chromium(III) Solutions with Metals

Aqueous chromium(III) sulfate (0.111 *M* in chromium(III)) was heated for 24 h at 300 °C in a new unlined type 316 stainless steel vessel. It reacted completely with the vessel walls to yield a brown-black, feebly-magnetic spinel of unit cell $a_0 = 8.36$ Å; the remaining solution was found by dichromate titration to be 0.084 *M* in iron(II), *i.e.*, 3 mol of aqueous iron(II) were produced for every 4 mol chromium(III) originally present. The brown-black solid was identified as chromite, $FeCr_2O_4$ (ASTM 4–0759), however this X-ray diffraction powder pattern and those of other spinels did not include the strong 331 reflection reported in ASTM 4–0759. Similar results were obtained when 0.04 to 0.06 *M* chromium(III) sulfate solutions were heated for 24 h at 300 °C in a stainless steel vessel with a mild steel liner or with iron strips inside a titanium vessel except that in this last case the spinel formed was shown by X-ray fluorescence analysis to have the composition $(Fe(II)_{0.6}\ Fe(III)_{0.4})\ (Cr(III)_{1.6}\ Fe(II)_{0.4})O_4$. On the other hand, relatively concentrated chromium(III) sulfate solutions of 1 *M* in chromium(III) yielded mainly $Cr_3(SO_4)_2(OH)_5.H_2O$ (ASTM 18–381) after 24 h at 300 °C in a stainless steel vessel with mild steel liner; after 4 days at 250 °C, some $FeSO_4.H_2O$ (szomolnokite, ASTM 12–226) was also formed. Reaction of dilute $Cr_2(SO_4)_3$ solutions at 300 °C with small excesses of fine iron wire in a stainless steel vessel with silica liner produced green $Cr_3(SO_4)_2(OH)_5.H_2O$ and a red-brown solid of composition $Fe_{0.95}Cr_{1.05}O_3$ (X-ray fluorescence analysis), with an X-ray diffraction powder pattern similar to that of $FeCrO_3$ (ASTM 2–1357), *i.e.*, it is essentially a solid solution of α-Fe_2O_3 in α-Cr_2O_3.

Chromium chloride solutions (0.05 *M*) also produced $FeCr_2O_4$ after 24 h at 300 °C in a stainless steel vessel with mild steel liner, but CrO(OH) (ASTM 9-331) was also present and accounted for 30% of the total chromium content as determined by X-ray fluorescence analysis; CrO(OH) became the major product under the same conditions when the solution was heated in an unlined stainless steel vessel. At 235 °C, 0.73 *M* $CrCl_3$ precipitated only poorly-crystalline CrO(OH) in 4 days, whether in contact with mild steel or stainless steel. Chromium(III) nitrate solutions deposited CrO(OH) in all circumstances at temperatures above 150 °C.

Solid CrO(OH) did not react with a mild steel liner in water at 300 °C over a 24 h period. When $Cr(OH)_3$ (5 mmol) was heated for 11 days at 440 °C with 35.2 g water under nitrogen in a stainless steel Barnes high-pressure vessel, the product was a brown spinel with a unit cell of 8.37_4 Å and approximate composition $(Fe_{0.5}Ni_{0.4}Cu_{0.06})Cr_2O_4$ as determined by X-ray fluorescence analysis. The water vapor pressure at 440 °C is approximately 1.4 kbars in this experiment (7). This experiment was repeated several times with similar results; however, in one case all of the water was lost through malfunction of the sealing ring, and the product was then

α-Cr_2O_3 (ASTM 6-504). When α-Cr_2O_3 was exposed to supercritical water in a stainless steel vessel at 440 °C and 1.4 kbars for 10 days, no change was observed.

Chromium(III) sulfate solutions (0.042 *M*) in chromium(III) were heated for 24 h at 300 °C in a titanium vessel with a polished strip or sphere of a selected metal in excess. Cobalt yielded dark-green $CoCr_2O_4$ (ASTM 1-1122) and aqueous cobalt(II); no $Cr_3(SO_4)_2(OH)_5.H_2O$, α-$Co(OH)_2$, β-$Co(OH)_2$, or rhombohedral CrO(OH) was detected by X-ray diffraction, although a weak reflection at 3.29 Å may indicate the less familiar orthorhombic CrO(OH) (8) (ASTM 17-268). Nickel yielded well-crystallized $NiSO_4.H_2O$ (ASTM 1-659) but no spinel; weak reflections in the X-ray diffraction powder pattern match those of γ-NiO(OH) (ASTM 6-75), but this is unlikely to have been a reaction product. Copper yielded the olive-green cuprous compound, $Cu_2Cr_2O_4$ (ASTM 5-668), which is not a spinel (9). In the above cases, most of the metal was recovered. However, manganese reacted almost completely with the water to yield Mn_3O_4 (hausmannite, ASTM 16-154), and zinc to yield ZnO (zincite, ASTM 5-664); magnesium reacts quantitatively with water to yield $Mg(OH)_2$ (brucite, ASTM 7-239).

Hydrothermal Synthesis of Chromium Spinels

Magnesium oxide (4.25 mmol) and $Cr(OH)_3$ (8.5 mmol) in 60 g water reacted at 250 °C in 24 h to give $Mg(OH)_2$ (brucite, ASTM 7-239) and CrO(OH) (ASTM 9-331) only. The product after 24 h at 300 °C showed no $Mg(OH)_2$ or MgO reflections in its X-ray diffraction powder pattern, and the CrO(OH) reflections were much more diffuse and less intense than in similar experiments where MgO was omitted. In addition a new diffuse reflection appeared at 2.5 Å to indicate formation of $MgCr_2O_4$ (picrochromite, ASTM 10-351). On repeating the experiment at 300 °C for 12 days, a brown powder was produced with all the reported X-ray diffraction reflections greater than intensity 10 of $MgCr_2O_4$. In addition a reflection at 1.49 Å indicates MgO (periclase, ASTM 4-829; the principal MgO reflection at 2.11 Å is obscured by the 400 reflection of $MgCr_2O_4$), and also weak reflections due to CrO(OH) persisted.

Nickel hydroxide which was made by precipitation with NaOH from aqueous $Ni(NO_3)_2$ did not react with $Cr(OH)_3$ at 250 °C in 24 h, and the products recovered were $Ni(OH)_2$ (ASTM 14-117) and CrO(OH); at 300 °C the products were only well-crystallized NiO (bunsenite, ASTM 4-835) and CrO(OH) even after 12 days.

$MnCl_2.4H_2O$ (12.7 mmol) and NaOH (25.0 mmol) reacted with 25 mmol $Cr(OH)_3$ in 40 g water at 300 °C over 10 days to yield a brown spinel, $MnCr_2O_4$ with the typical 111, 220, 331 (strongest), 400, 333 and/or 511, and 440 X-ray diffraction reflections. The unit cell is 8.42 ± 0.02 Å, *cf.* 8.437 Å reported (10) for authentic $MnCr_2O_4$. Similarly when $CoCl_2.6H_2O$ replaced $MnCl_2.4H_2O$, a bottle-green spinel, $CoCr_2O_4$ (ASTM 1-1122), was produced with a unit cell of 8.34 ± 0.02 Å, *cf.* 8.319 Å reported (11) for $CoCr_2O_4$; all the X-ray diffraction reflections reported with intensities greater than 20 were observed, although the reflections were diffuse.

Iron(II) hydroxide oxidized water slowly to give hydrogen and magnetite, Fe_3O_4 (ASTM 19-629). Thus stoichiometric amounts of aqueous $FeSO_4$ and NaOH in the absence of oxygen were heated for 5 days at 200 °C to produce yellow-green particles, which were observed under the microscope to have a pale-colored center encased by a black, rhombic dodecahedral shell of magnetite, Fe_3O_4. The hand-picked yellow-green center had X-ray diffraction reflections at 7.4 Å (strong, diffuse), 3.8 Å (strong, diffuse), 2.82 Å (strong, sharp), 2.52 Å (weak, coincident with the 311 reflection of Fe_3O_4), and 1.63 Å (weak); these match the pattern (ASTM 13-90) cited for a "green rust" of composition $Fe(II)_{3.6}Fe(III)_{0.9}(OH,O,SO_4)_9$, but sulfate was present only in trace amounts in this product. Therefore the oxidation to Fe_3O_4 was much less than half complete in this experiment.

In contrast when 10 mmol aqueous $FeSO_4$ and 20 mmol chromium(III) sulfate were treated with 80 mmol aqueous NaOH to give a total liquid volume of 30 ml (20 °C) and then heated for 3 days at 200 °C; the sole product was 2.2 g of a brown-black, feebly magnetic, poorly crystalline powder with rather diffuse X-ray diffraction reflections at 2.97 Å (30), 2.53 Å (100), and 2.09 Å (40). No reflections due to CrO(OH) and so forth could be detected. These facts indicate that the product was $FeCr_2O_4$ (ASTM 4-0759) in essentially quantitative yield; the alternative possibility, that the solid was Fe_3O_4 intimately mixed with amorphous

CrO(OH) or $Cr(OH)_3$, cannot be ruled out, but this would require that CrO(OH) or $Cr(OH)_3$ catalyze the reaction of $Fe(OH)_2$ with water.

A similar experiment of only 24 h duration yielded a seemingly homogeneous but amorphous brown-black powder, and another experiment at 300 °C yielded once again a poorly crystalline brown-black spinel of unit cell 8.30 Å. However, at 150 and 175 °C mixtures of green and black powders resulted, and substantial pressures of gas (evidently H_2) were created. The p*H* of the solution (20 °C) rose from 7 to 12; a spinel was present in the products, but this may be Fe_3O_4. The chromium-containing products were CrO(OH) and some $Cr(OH)_3$ (ASTM 12-241). Experiments in which 4 *M* NaCl was present produced mixtures of insoluble, amorphous green and black solids. Other experiments using a deficiency of NaOH at various temperatures from 150 to 300 °C produced only amorphous or poorly-crystalline powders, or brown powders in which CrO(OH) was the only identifiable component.

Attempts to make $MgAl_2O_4$ from MgO and $Al(OH)_3$ under hydrothermal conditions in a titanium vessel at 300 °C were unsuccessful, the aluminium-containing products being mainly boehmite, AlO(OH) (ASTM 17-940) and tucanite $Al_2(OH)_6.H_2O$ (ASTM 18-32); when a silica liner was used, the main products were serpentine, $Mg_6Si_4O_{10}(OH)_8$ (ASTM 9-444) and boehmite.

Discussion

Hydrolytic Precipitation Reactions

Many of the phenomena reported may be explained with the sequential aqueous reactions 1 through 4.

[1] $$Cr(H_2O)_6^{3+} \rightleftarrows Cr(H_2O)_5OH^{2+} + H^+$$

[2] $$Cr(H_2O)_5OH^{2+} \rightleftarrows Cr(H_2O)_4(OH)_2^{+} + H^+$$

[3] $$Cr(H_2O)_4(OH)_2^{+} \rightleftarrows Cr(OH)_3(s) + H^+$$

[4] $$Cr(OH)_3(s) \rightleftarrows CrO(OH)(s)$$

Reaction 4 occurs above 55 °C in aqueous systems (12); CrO(OH) can exist in a grey-brown rhombohedral form (4) or a green orthorhombic form (8), but with one possible exception, the CrO(OH) in these experiments has the rhombohedral form. Reaction 1 and also presumably reactions 2 and 3 are markedly endothermic and slightly favored by pressure (13), so that these equilibria will lie increasingly to the right as the temperature is increased; the equilibrium constant for reaction 1 is probably about 0.14 *m* at 200 °C and near 1.0 *m* at 300 °C (14).

Furthermore nitric acid, which may not be completely dissociated in its more concentrated aqueous solutions even at room temperature, becomes an increasingly weak acid as the temperature is increased (15). This will force the equilibria even further to the right in chromium(III) nitrate solutions, so that CrO(OH) precipitates at temperatures as low as 150 °C. However, this precipitation occurs at higher temperatures than in the analogous iron(III) nitrate system (16), because hexaaquochromium(III) ion is a markedly weaker acid than hexaaquoiron(III).

In contrast, $CrCl_3$ solutions precipitated CrO(OH) only at temperatures above 200 °C. This shift of the equilibria to the left is ascribed partly to the greater acid strength of HCl (15), and partly to the greater ability of chloride (as compared with nitrate) to complex chromium(III) (17). The importance of this complex formation factor is stressed by the observation that CrO(OH) precipitates from unacidified $Cr(ClO_4)_3$ solutions at 200 °C; $HClO_4$ is a stronger acid than either HCl or HNO_3, but ClO_4^- is a weaker complexing agent than either Cl^- or NO_3^-. On the basis of the Bjerrum theory of ion pairing (18), complex formation between aqueous anions and cations will become increasingly important at high temperatures, because the product of the absolute temperature and the dielectric constant of water decreases as the temperature increases. The greater precipitation of CrO(OH) in a stainless steel vessel with silica liner as compared with a titanium vessel with silica liner can be ascribed to loss of molecular HCl in the vapor phase, either through reaction with the steel or by leakage through the relatively inefficient asbestos gaskets.

Aqueous HSO_4^- ion becomes progressively less acidic up to 300 °C, and it is neither appreciably acidic nor basic between 300 and 400 °C (19). Thus hydrolysis of chromium(III) sulfate at high temperatures is aided by protonation of SO_4^{2-} only as far as HSO_4^-, and the observed complexing of chromium(III) by SO_4^{2-} will suppress further hydrolysis. The limiting factor in the high-temperature solubility of chromium(III) sulfate is the precipitation of $Cr_3(SO_4)_2(OH)_5.H_2O$, which like the isomorphous iron(III)

compound (5), has a favorable crystal structure (6).

Data in Table 2 verify that $Cr_3(SO_4)_2(OH)_5.H_2O$ precipitates at temperatures above 250 °C and it is suppressed by the addition of H_2SO_4. The more concentrated chromium(III) sulfate solutions are markedly less susceptible to the precipitation of $Cr_3(SO_4)_2(OH)_5.H_2O$, presumably because of the extensive formation of di- and perhaps tri-sulfato complexes. This precipitation may not have reached equilibrium in some of the cases listed in Table 2. The evolution of SO_2 from a very concentrated solution, where extensive precipitation had occurred, evidently originated in the thermal decomposition of the H_2SO_4 generated by hydrolytic precipitation.

The precipitation of a new compound along with $Cr_3(SO_4)_2(OH)_5.H_2O$, from a relatively acidic solution near the borderline of solubility at 300 °C, is consistent with its tentative identification as $Cr(OH)SO_4.2H_2O$, which is more acidic than $Cr_3(SO_4)_2(OH)_5.H_2O$. The Cr_2O_3–H_2O–SO_3 system is similar to its iron(III) analogue (5), except that once again the lower acidity of aqueous chromium(III) *vis-à-vis* iron(III) leads to precipitation at significantly higher temperatures in the chromium system.

Oxidation of Aqueous Chromium(III)

The oxidation of chromium(III) to chromium(VI) by 0.4 *M* aqueous perchloric acid above 225 °C must occur by the direct interaction of $HClO_4$ and chromium(III), since the rate of spontaneous decomposition of 0.04 *M* aqueous $HClO_4$ is negligible at 250 °C (20). The yield of chloride ion and the absence of chlorine gas in the reaction products are consistent with the stoichiometry

$$[5] \quad 8Cr^{3+} + 3ClO_4^- + 2OH_2O \rightleftarrows 8HCrO_4^- + 3Cl^- + 32H^+$$

It is apparent that physical measurements on chromium(III) species in perchlorate media are feasible up to 200 °C.

The oxidation of chromium(III) to chromium(VI) by oxygen in acidic solution is not quite thermodynamically favored under standard state conditions at 25 °C; the standard potential for reaction 6 is −0.10 V.

$$[6] \quad 3O_2 + 4Cr^{3+} + 8H_2O \rightleftharpoons 2Cr_2O_7^{2-} + 16H^+$$

However, at high temperatures, with departures from standard conditions, changes in the nature of the chromium(III) species, and the breakdown of kinetic barriers, reaction 6 apparently becomes important enough to require the exclusion of oxygen from chromium(III) solutions. Reaction 6 indicates suppression of the oxidation by O_2 with the addition of substantial excess acid, at least at 250 °C.

Reaction of Aqueous Chromium(III) with Metals

The precipitation of $FeCr_2O_4$ when a chromium(III) solution reacts with a steel is explained by the hydrolytic reactions 1 to 3. The liberated hydrogen ion probably reacts with the metal to produce $Fe^{2+}(aq)$ and maintains the relatively high p*H*; then at about 300 °C, hydrolyzed iron(II) and chromium(III) species precipitate together as $FeCr_2O_4$ or a related compound. This sequence of events is most well-defined with chromium(III) sulfate solutions, because they retain relatively high concentrations of chromium(III) at high temperatures and deposit $Cr_3(SO_4)_2(OH)_5.H_2O$ only slowly. Recalling that 3 mol of iron(II) were found in solution after total precipitation of 4 mol of chromium(III) as $FeCr_2O_4$, and that aqueous HSO_4^- is neither acidic nor basic at 300 °C (19), reaction 7 is conceived as

$$[7] \quad 5Fe(s) + 2Cr_2(SO_4)_3(aq) + 8H_2O(l) \rightleftharpoons 2FeCr_2O_4(s) + 3Fe(HSO_4)_2(aq) + 5H_2(g)$$

The occurrence of iron(III) in some products suggests the reduction of either water or H^+ by Fe^{2+} in high-temperature water; certainly $Fe(OH)_2$ reduces water at a significant rate even at 150 °C. Aqueous $CrCl_3$ tends to deposit CrO(OH) by reactions 1 to 4 concomitantly with $FeCr_2O_4$ production. CrO(OH) does not react with steels in aqueous media or with aqueous Fe^{2+} in 24 h at 300 °C, so the formation of $FeCr_2O_4$ from chromium(III) solutions and steels evidently involves reactions 1 to 3 directly.

In supercritical water of density 0.7 g cm^{-3} at 440 °C, CrO(OH) reacts with stainless steel to produce a spinel $(Fe,Ni)Cr_2O_4$ (a trace of copper was also present in this spinel, because the strongly adhesive copper–graphite lubricant used on the threaded parts apparently accidentally contaminated the internal vessel walls). This experiment suggests that the "cubic Cr_2O_3" of Laubengayer and McCune (21), which was produced in the same way except that the CrO(OH) was contained in a platinum thimble, is probably $FeCr_2O_4$ or $(Fe,Ni)Cr_2O_4$. Certainly

their X-ray diffraction pattern (21) agrees closely with our pattern. Their failure to detect much iron in their "cubic Cr_2O_3" may result from the difficulty of dissolving $(Fe,Ni)Cr_2O_4$, which in any event contains only *ca.* 10% iron and furthermore the Laubengayer–McCune sample was contaminated with CrO(OH). The incomplete reaction of CrO(OH) in the Laubengayer–McCune (21) and Shafer–Roy (12) experiments is ascribed to its limited chemical contact with the stainless steel vessel walls, via the supercritical aqueous fluid through leaks or openings in the platinum container. The reported conversion of the "cubic Cr_2O_3" to α-Cr_2O_3 by heating in air at 800 °C (21) may result from aerial oxidation of $FeCr_2O_4$ to a solid solution of α-Fe_2O_3 in α-Cr_2O_3 (22), whose X-ray diffraction pattern is similar to that of α-Cr_2O_3.

Corrosion of Stainless Steel by High-Temperature Water

The chief corrosion product of stainless steel by water in the temperature range 200–350 °C is the mixed spinel $(Fe,Ni)(Cr,Fe)_2O_4$, in which the chromium content increases with the reaction temperature (23). This suggests that the metal surface reacts with water to produce $Fe(OH)_2$, which can react slowly with liquid water at 200 °C to produce Fe_3O_4. However, the concomitant aqueous oxidation of the chromium and nickel components in the stainless steel to produce CrO(OH) and $Ni(OH)_2$ will be followed (especially at the higher temperatures) by reaction with $Fe(OH)_2$ to produce $FeCr_2O_4$, and above 300 °C to produce $(Fe,Ni)Cr_2O_4$.

This insoluble chromite may be largely responsible for the passivity of stainless steel in contact with water above 200 °C. However, the oxidation of aqueous chromium(III) by molecular oxygen, at low acidities and above 250 °C, to soluble chromium(VI) suggests that the passivity of stainless steel in high-temperature aqueous environments may be destroyed by the presence of molecular oxygen in the system; the iron(II) content would yield iron(III) oxides which may be non-protective.

Hydrothermal Synthesis of Chromium Spinels

The results indicate that chromium spinels can form hydrothermally from the appropriate hydrolyzed metal species (*i.e.*, $M(OH)_2$ and $Cr(OH)_3$ or CrO(OH)) above 300 °C. The reaction of $Fe(OH)_2$ with CrO(OH) may be complicated by the slower reaction of $Fe(OH)_2$ with liquid water to produce Fe_3O_4 and hydrogen, but the main product is $FeCr_2O_4$ above 200 °C. This complication is avoided when the unstable $Fe(OH)_2$ is replaced by $Mn(OH)_2$, $Co(OH)_2$, $Mg(OH)_2$, and $Ni(OH)_2$. The manganese, cobalt and magnesium hydroxides produced a spinel after several days at 300 °C. The order of entry into the M(II) sites of MCr_2O_4 is $Fe^{2+} > Mn^{2+}$, $Co^{2+} > Mg^{2+} \gg Ni^{2+}$. This sequence is generally consistent with the thermodynamic data (24) for the formation of MCr_2O_4 from Cr_2O_3 and MO.

The failure to produce $NiCr_2O_4$ hydrothermally may be due to the conversion of $Ni(OH)_2$ into NiO between 250 and 300 °C. Ligand field theory predicts that Ni^{2+} will not readily leave the octahedral site in NiO, which has the NaCl structure, for a tetrahedral site in $NiCr_2O_4$; and it is unlikely to compete with Cr^{3+} for the octahedral sites. On the other hand, Mn^{2+} (d^5, high spin) and especially Co^{2+} (d^7, high spin) should enter tetrahedral sites readily.

Possible Hydrothermal Origin of Certain Chromite Mineral Deposits

Most major deposits of the mineral chromite, $(Fe,Mg)(Cr,Al,Fe)_2O_4$, were formed by magmatic segregation in ultrabasic rocks. Indeed chromite is one of the first minerals to separate from a cooling rock magma. However, several authors (25) have argued that chromite grains, which occur in hydrothermally altered ultrabasic rocks such as serpentinites, may have been deposited by the hydrothermal solutions themselves.

These views have not gone unchallenged (26), and it is not intended to review critically the mineralogical evidence for and against a hydrothermal origin of chromite in serpentinized rocks. The results in this paper show that $FeCr_2O_4$ and $MgCr_2O_4$, and therefore presumably $(Fe,Mg)Cr_2O_4$, may be deposited from aqueous solutions at near-neutral p*H* values, even in geologically short times and at temperatures of 300 °C and probably less. The few attempts to produce spinel ($MgAl_2O_4$) hydrothermally were unsuccessful, but it is expected that Al^{3+} like Fe^{3+} could be incorporated into the octahedral sites of a hydrothermally formed chromite in serpentinized rocks.

It is apparent that complexing of chromium(III)

by sulfate or chloride is necessary to effect large-scale transport of chromium(III) by aqueous solutions at temperatures about 300 °C into the regions where serpentinization occurs. It is noted that high concentrations of alkali metal chlorides and perhaps less commonly sulfates are evidently present in typical hydrothermal ore-forming fluids (27).

We thank Atomic Energy of Canada, Ltd., for financial support of this work through Whiteshell Nuclear Research Establishment, and Mr. D. Harvey for the X-ray fluorescence analyses.

1. J. E. Earley and R. D. Cannon. Transition metal chemistry. *Edited by* R. L. Carlin. M. Dekker, Inc., New York. 1965. Vol. 1. p. 33*ff*.
2. J. S. Gill and W. L. Marshall. Rev. Sci. Instrum. **32**, 1060 (1961).
3. A. I. Vogel. A textbook of quantitative inorganic analysis. 3rd ed. J. Wiley and Sons, Inc., New York. 1961.
4. B. J. Thamer, R. M. Douglass, and E. Staritzky. J. Am. Chem. Soc. **79**, 547 (1957).
5. E. Posnjak and H. E. Merwin. J. Am. Chem. Soc. **44**, 1965 (1922).
6. A. Lecerf, A. Bonnin, and A. Hardy. Comptes Rendus, **262**C, 353 (1966).
7. N. E. Dorsey. Properties of ordinary water substance. Reinhold Publishing Corp., New York. 1940.
8. C. Nørlund Christensen. Inorg. Chem. **5**, 1452 (1966).
9. J. D. Stroupe. J. Am. Chem. Soc. **71**, 569 (1949).
10. P. M. Raccah, R. J. Bouchard, and A. Wold. J. Appl. Phys. **37**, 1436 (1966).
11. S. Holgersson. Lunds Univ. Årsskr. **23**, 88 (1927).
12. M. W. Shafer and R. Roy. Z. anorg. allgem. Chem. **276**, 275 (1954).
13. T. W. Swaddle and P.-C. Kong. Can. J. Chem. **48**, 3223 (1970).
14. C. M. Criss. Ph.D. Thesis. Purdue University 1961. p. 110*ff*.
15. H. C. Helgeson. J. Phys. Chem. **71**, 3121 (1967).
16. R. G. Robins. J. Inorg. Nucl. Chem. **29**, 431 (1967).
17. T. W. Swaddle and G. Guastalla. Inorg. Chem. **7**, 1915 (1968).
18. H. S. Harned and B. B. Owen. The physical chemistry of electrolytic solutions. 2nd ed. Reinhold Publishing Corp., New York. 1950. pp. 42–44.
19. A. S. Quist, W. L. Marshall, and H. R. Jolley. J. Phys. Chem. **69**, 2726 (1965).
20. M. P. Henderson, V. I. Miasek, and T. W. Swaddle. Can. J. Chem. To be published.
21. A. W. Laubengayer and H. W. McCune. J. Am. Chem. Soc. **74**, 2363 (1952).
22. P. E. Wretblad. Z. anorg. Chem. **189**, 329 (1930).
23. T. Maekawa and M. Terada. Nippon Kinzoku Gakkaishi, **29**, 421 (1965); Chem. Abstr. **63**, 12763*f* (1965); T. Yanagihara, G. Shimaoka, S. Ikeda, and K. Tomita. Trans. Natl. Research Inst. Metals (Tokyo), **1**, 126 (1959); Chem. Abstr. **54**, 11916*b* (1960).
24. J. D. Tretjakow and H. Schmalzried. Ber. Bunsenges. Phys. Chem. **69**, 396 (1965).
25. E. Sampson. Econ. Geol. **24**, 632 (1929); C. S. Ross. Econ. Geol. **24**, 641 (1929); J. T. Singewald, Jr. Econ. Geol. **24**, 645 (1929); L. W. Fisher. Econ. Geol. **24**, 691 (1929); F. E. Keep. Econ. Geol. **25**, 425 (1930); C. S. Ross. Econ. Geol. **26**, 540 (1931); E. Sampson. Econ. Geol. **26**, 622 (1931); E. Sampson. Econ. Geol. **26**, 833 (1931); P. Eskola. Comptes Rendus Soc. Geol. Finlande, **7**, 33 (1933); A. C. Skerl. Econ. Geol. **37**, 153 (1942); M. S. Amin. Econ. Geol. **43**, 133 (1948).
26. F. E. Keep. Econ. Geol. **25**, 219 (1930); N. M. Shukri. Econ. Geol. **43**, 427 (1948); L. L. Fermor Geol. Mag. **89**, 39 (1952); T. P. Thayer. *In* Chromium. vol. 1. Am. Chem. Soc. Monograph Series No. 132. *Edited by* M. J. Udy. Reinhold Publishing Corp., New York. 1956. pp. 14–52; E. D. Jackson. Econ. Geol. **61**, 777 (1966).
27. H. C. Helgeson. Complexing and hydrothermal ore deposition. The Macmillan Co., New York. 1964. p. 80.

Can. J. Chem. Downloaded from www.nrcresearchpress.com by 210.87.254.42 on 09/05/12
For personal use only.

The Hydrothermal Chemistry of some Common Transition Metal Compounds

PI-CHANG KONG AND T. W. SWADDLE
Department of Chemistry, The University of Calgary, Calgary 44, Alberta

AND

P. BAYLISS
Department of Geology, The University of Calgary, Calgary 44, Alberta

Received December 22, 1970

The stabilities of aqueous solutions of typical salts of manganese(II), iron(II), cobalt(II), cobalt(III), nickel(II), and copper(II) at temperatures up to 300 °C have been investigated. At 200 to 300 °C, hydrolysis of the metal ions can lead to the partial precipitation of metal oxides, or silicates in the cases of nickel(II) and cobalt(II) when a silica vessel is used; except for the M(II) sulfates, which precipitate as $MSO_4.H_2O$ (M = Mn, Fe, Co, and Ni) and $Cu_3SO_4(OH)_4$. Manganese(II), iron(II), and cobalt(II) tend to be oxidized at 250 to 300 °C in neutral or acidic solutions, while cobalt(III) in aqueous ammonia is reduced. Aqueous $CuCl_2$ is in equilibrium with CuCl and Cl_2 at 300 °C. Hydrolytic precipitation is suppressed by the addition of small concentrations of hydrogen ion or larger concentrations of chloride ion, if oxidation–reduction processes do not interfere.

Les stabilités des solutions aqueuses de quelques sels caractéristiques de manganèse(II), fer(II), cobalt(II), cobalt(III), nickel(II) et cuivre(II) ont été étudiées jusqu'à des températures de 300 °C. Entre 200 et 300 °C, l'hydrolyse des ions métalliques peut provoquer une précipitation partielle d'oxydes métalliques, ou de silicates dans le cas du nickel(II) et cobalt(II) et ceci lorsque des récipients en silice sont utilisés; exception faite pour les sulfates de M(II) qui précipitent en tant que $MSO_4.H_2O$ (M = Mn, Fe, Co et Ni) et $Cu_3SO_4(OH)_4$. Le manganèse(II), le fer(II) et le cobalt(II) ont tendance à être oxydés entre 250 et 300 °C dans des solutions neutres ou acides, alors que le cobalt(III) est réduit dans l'ammoniaque aqueux. Une solution aqueuse de $CuCl_2$ est en équilibre à 300 °C avec du CuCl et du Cl_2. La précipitation hydrolytique peut être supprimée par l'addition d'ions hydrogène en petite concentration ou d'ions chlorure en concentration plus élevée, à condition que le processus d'oxydo-réduction n'interfère pas.

Canadian Journal of Chemistry, 49, 2442 (1971)

Introduction

The experiments reported herein were undertaken primarily to determine the feasibility of spectroscopic and other physicochemical studies of aqueous ions of the more common transition elements (manganese, iron, cobalt, nickel, and copper) at temperatures in the 100 to 300 °C range. Such studies are relevant to the corrosion processes and the transport of radioactive material in boiling or pressurized-water nuclear power reactors, and also the geochemistry of certain mineral deposits which have a hydrothermal origin. In any event the extension of our knowledge of the chemistry of aqueous solutions to temperatures beyond their normal boiling points is highly desirable (1).

Experimental

The chemicals used were Fisher Certified reagents with the exceptions of perchloric acid (Baker Analyzed) and $Co(ClO_4)_2.6H_2O$ (Alfa Inorganics). Perchlorate salts were prepared by precipitation of the corresponding metal hydroxide from a solution of the nitrate or chloride, followed by dissolution in dilute perchloric acid; precipitation and redissolution were repeated until the original anion could not be detected in the solution. Some of the $Co(ClO_4)_2.6H_2O$ used was also prepared in this manner with identical results as the commercial chemical.

The equipment and techniques have been described previously (2). The vessels are type 316 stainless steel, or titanium with 0.2% palladium. The solutions were contained in loosely-capped silica liners within the pressure vessels in all cases, to facilitate observation of small amounts of precipitate and to prevent interaction of the solutions with the metal of the vessel walls. In all experiments, the atmosphere in the vessels prior to heating was nitrogen at 1 bar pressure, and in no case did the partial pressure of nitrogen at high temperatures exceed 3 bars. Most experiments were duplicated to ensure reproducibility of the observations.

Concentrations are expressed in molar units valid at 20 °C, and the percentage decompositions quoted are the decreases in metal ion concentration in the solutions, measured spectrophotometrically. The letters ASTM followed by numbers refer to the data in the X-Ray Diffraction Powder File.

Results

Manganese

Manganese(II) perchlorate (0.05 *M*) maintained at 300 °C for 24 h in either a titanium or stainless steel vessel deposited 4% of a brown–

Can. J. Chem. Downloaded from www.nrcresearchpress.com by 210.87.254.42 on 09/05/12
For personal use only.

black solid (probably MnO(OH) or MnO_2). The same result was obtained after repeating the experiment with the addition of 0.012 *M* $HClO_4$. Manganese(II) nitrate (0.2 *M*) decomposed completely in 24 h at 300 °C in a titanium vessel to yield well-crystallized MnO_2 (pyrolusite, ASTM 12-716). At 250 °C, 0.2 *M* manganese(II) nitrate in a stainless steel vessel again decomposed completely in 24 h, but the products were mainly β-MnO(OH) (teitknechtite, ASTM 18-804) and γ-MnO(OH) (manganite, ASTM 18-805) and some MnO_2.

Manganese(II) chloride solution (0.05 *M*) in a stainless steel vessel lost about 9% of its manganese content (as determined by EDTA titration) at 300 °C in 24 h as a brown precipitate and suspension; the addition of 0.75 *M* NaCl prior to heating reduced this loss of manganese content to 4%. More concentrated $MnCl_2$ (0.2 *M*) similarly yielded a black precipitate (probably MnO(OH) or MnO_2) at 300 °C in 24 h; and at 250 °C a small quantity of a brown precipitate appeared as a light suspension, whether the solution was heated for either 1 day or 6 days. Manganese(II) sulfate (0.2 *M*) at 300 °C for 24 h yielded a well-crystallized white solid, $MnSO_4.H_2O$ (szmikite, ASTM 14-166).

Iron

Iron(II) chloride (0.05 *M*) at 300 °C for 24 h in a titanium vessel yielded well-crystallized α-Fe_2O_3 (hematite, ASTM 13-534) and a substance with a strong reflection at 4.92 Å and a weak reflection at 1.60 Å; the solution was colorless. No precipitate other than a slight turbidity is observed when 0.2 *M* $FeCl_2$ is heated with 0.1 *M* HCl at 300 °C for 24 h, although this iron(II) solution is slightly cloudy at the outset, presumably because of failure to remove the last traces of oxygen. Iron(II) sulfate solution (0.2 *M*) in H_2SO_4(0.1 *M*) at 300 °C in a stainless steel vessel for 24 h yielded $FeSO_4.H_2O$ (szomolnokite, ASTM 12-226) and a small amount of α-Fe_2O_3.

Cobalt

At 300 °C for 24 h in a stainless steel vessel 1.17 *M* cobalt(II) perchlorate yielded Co_3O_4 (ASTM 9-418) whether $NaClO_4$ is present or not, but 0.05 *M* $Co(ClO_4)_2$ in 0.01 *M* $HClO_4$ yielded 25% of black, highly-crystalline solid, whose X-ray diffraction pattern is similar to that of CoO(OH) (heterogenite, ASTM 7-169). At 250 °C for 24 h, the brown product obtained in absence of $HClO_4$ contained both cobalt and silicon in approximately a 2:5 atomic ratio as determined by X-ray fluorescence analysis; its X-ray diffraction pattern was diffuse, but the main reflections coincided with those of synthetic cobalt talc, $Co_3Si_4O_{10}(OH)_2$ (ASTM 15-187). This cobalt silicate is evidently the synthetic cobalt talc of Pistorius (3) intermixed with amorphous silica. At 200 °C for 24 h in a stainless steel vessel only a trace of a black precipitate (probably Co_3O_4) formed from 1.17 *M* $Co(ClO_4)_2$.

Cobalt(II) nitrate (0.025 to 0.01 *M*) at 300 °C for 24 h yielded black Co_3O_4 in major quantities. The Co_3O_4 yield is slightly greater when 1.0 *M* $NaNO_3$ is present. Approximately 8% of a similar black precipitate was obtained at 250 °C in 24 h with a titanium vessel, but the yield was 40% with a stainless steel vessel; the discrepancy probably originated through loss of HNO_3 in the vapor phase, either by leakage through the asbestos gasket or by reaction with the stainless steel.

Cobalt(II) chloride solutions (0.05 *M*) at 300 °C in either a titanium or stainless steel vessel yielded a black precipitate (probably Co_3O_4); the yield was only 10% after 7 days. This precipitation was suppressed completely by the addition of 0.01 *M* HCl or 0.25 *M* (or more) NaCl for cobalt concentrations from 0.045 to 0.18 *M* at least. At 250 °C in a titanium vessel $CoCl_2$ solutions without either HCl or NaCl added deposited a black precipitate (probably Co_3O_4) of less than 1% in 24 h and 5% in 6 days. Even at 200 °C a trace of a black residue was noticed. Cobalt(II) bromide solution (0.05 *M*) in a stainless steel vessel at 300 °C deposited a similar quantity of a black solid (probably Co_3O_4), and this precipitation was entirely suppressed by the addition of 0.01 *M* HBr but not by 1.0 *M* NaBr, which yielded 3% insoluble cobalt compounds.

Cobalt(II) sulfate solutions (0.09 *M*) in either a titanium or stainless steel vessel yielded in 24 h a trace of a black precipitate (probably Co_3O_4) even at 150 °C; but at 200, 250, and 300 °C, 0.05 to 0.4 *M* $CoSO_4$ solutions yielded a pink solid which is mainly $CoSO_4.H_2O$ (ASTM 15-701). It could be dissolved on prolonged contact with fresh water to give a red solution of Co^{2+} (aq) and a blue residue which is mainly poorly-crystalline α-$Co(OH)_2$ (ASTM 2-925). Thus typically a 0.4 *M* $CoSO_4$ solution deposited 42% of the pink solid at 300 °C in 24 h; the soluble component was shown spectroscopically to con-

Can. J. Chem. Downloaded from www.nrcresearchpress.com by 210.87.254.42 on 09/05/12
For personal use only.

tain 32% cobalt (*cf.* 33% for authentic $CoSO_4.H_2O$), and the residue after 24 h contact with water at 20 °C contained α-$Co(OH)_2$ and 6% sulfur, *i.e.* it contained 4 mol $Co(OH)_2$ to 1 mol of $CoSO_4.H_2O$. Addition of H_2SO_4 to the $CoSO_4$ solution prior to heating prevented deposition of $Co(OH)_2$, so that $CoSO_4$ (0.1 *M*) in H_2SO_4 (0.09 *M*) produced a 25% yield of pure $CoSO_4.H_2O$ at 300 °C in 24 h.

Hexaaminecobalt(III) chloride (0.128 *M*) in water and 1.4 *M* ammonia or 2.7 *M* ammonia decomposed completely at 300 °C in 24 h to yield mainly black Co_3O_4 and blue α-$Co(OH)_2$. A pink solid (probably $CoSO_4.H_2O$) was also present in the product from water at 300 °C.

Nickel

Nickel(II) perchlorate (0.05 *M*) at 300 °C in a titanium vessel for 24 h yielded 5% of a fibrous green precipitate, synthetic nickel talc ($Ni_3Si_4O_{10}(OH)_2$, ASTM 15-384) with some poorly crystalline synthetic nickel serpentine ($Ni_3Si_2O_5(OH)_4$, ASTM 11-98) (3). However, in the presence of 0.012 *M* $HClO_4$ at 300 °C for 24 h, no precipitate formed and the solution remained clear. Similarly nickel(II) nitrate (0.05 *M*) at 300 °C for 24 h yielded $Ni_3Si_4O_{10}(OH)_2$ with some $Ni_3Si_2O_5(OH)_4$, but these yields were greater than with the perchlorate salt at 70% for 0.025 *M* Ni(II), and 14% for 0.2 *M* Ni(II); the same products were obtained in lesser yields at 250 °C for 24 h. Again nickel(II) chloride (0.05 *M*) in 24 h gave the same silicates at 300 °C in yields of 10%. This occurred even in the presence of 0.5 *M* NaCl, and also to a minor extent at 200 °C. Nickel(II) sulfate solutions (0.05 *M*) in 24 h yielded 72% at 300 °C and 32% at 250 °C of the green solid, $NiSO_4.H_2O$ (ASTM 1-659).

Copper

Copper(II) perchlorate solutions (0.05 *M*) to 0.2 *M* yielded 4 to 6% of black CuO (tenorite, ASTM 5-661) at 300 °C in 24 h in a stainless steel vessel but this precipitation was prevented completely by the presence of 0.012 *M* $HClO_4$. A more dilute 0.02 *M* $Cu(ClO_4)_2$ solution remained homogeneous at 300 °C after 24 h even in the absence of $HClO_4$, so that the copper(II) concentration is an important variable. Copper(II) nitrate (0.05 *M*) produced well-crystallized CuO at 300 °C in a stainless steel vessel with a 5% yield in 24 h and a 10% yield after 5 days.

Copper(II) chloride (0.05 *M*) at 300 °C for 24 h in a stainless steel vessel yielded 22% of white, highly-crystalline CuCl (nantokite, ASTM 6-344), but no precipitate formed and the solution remained clear when the experiment was repeated at 300 or 250 °C in a titanium vessel. However, when the experiment was repeated at 300 °C using a titanium vessel in which the silica liner was wound on the outside with iron wire, CuCl was again precipitated and the wire was severely corroded. Copper sulfate solution (0.02 *M*) produced a large yield of well-crystallized $Cu_3SO_4(OH)_4$ (antlerite, ASTM 7-407) at 300 °C in 24 h.

Discussion

Many of the above results can be understood if it is recognized that the "hydrolysis" (acid dissociation) reactions 1 and 2 of divalent metal aquo ions is significant at 200 °C and of major importance at 300 °C.

$$[1] \quad M(H_2O)_6^{2+} \overset{K_1}{\rightleftharpoons} M(H_2O)_5OH^+ + H^+$$

$$[2] \quad M(H_2O)_5OH^{2+} \overset{K_2}{\rightleftharpoons} M(OH)_2(s) + H^+ + 4H_2O$$

Criss (4) has predicted that when M is manganese, pK_1 should fall sharply with temperature from 10.6 at 25 °C to 5.3 at 200 °C; further extrapolation suggests that pK_1 is less than 4 at 300 °C. It is expected that the other metal ions considered in this article (M = Fe, Co, Ni, and Cu) will be more acidic than Mn^{2+}(aq) (5).

M(II) Perchlorates

The deposition of CuO from aqueous $Cu(ClO_4)_2$ at 300 °C involves the dehydration of $Cu(OH)_2$, as this is known to occur in the presence of water above 77 °C (6). Similarly $Ni(ClO_4)_2$ at 300 °C probably formed some $Ni(OH)_2$, which would react with the silica dissolved from the liner to form $Ni_3Si_4O_{10}(OH)_2$ and $Ni_3Si_2O_5(OH)_4$; addition of a small amount of perchloric acid prevented this, just as it prevented deposition of CuO from aqueous $Cu(ClO_4)_2$. Therefore silica equipment is not inert with these aqueous solutions at 200–300 °C. Silica is quite soluble in superheated water (7) with solubilities of 900 p.p.m. at 200 °C and 1400–1500 p.p.m. at 300 °C (8). Cobalt(II) perchlorate solutions at 250 °C reacted similarly to their nickel analogues to form $Co_3Si_4O_{10}(OH)_2$, but at 300 °C partial oxidation of cobalt(II) occurred with the pre-

Can. J. Chem. Downloaded from www.nrcresearchpress.com by 210.87.254.42 on 09/05/12
For personal use only.

cipitation of Co_3O_4. In the presence of added $HClO_4$ but not $NaClO_4$, the precipitate was entirely cobalt(III) in the form of CoO(OH), which is also obtained from aqueous suspensions of $Co(OH)_2$ by boiling in air or by aerial oxidation at 20 °C (9).

Only a small concentration of added acid will suppress hydrolytic precipitation at 300 °C. This is consistent with Criss' predicted K_1 values (4) which show that reaction 1 though important at high temperatures favors the unhydrolyzed aquo-ion at 300 °C unless other factors intervene.

M(II) Nitrates

Whereas perchlorate ion is probably not appreciably basic at 300 °C, nitric acid is incompletely dissociated in aqueous solutions at high temperatures (10), so that hydrolytic precipitation from nitrate solutions is significantly greater than that from the perchlorate analogues, *cf.* chromium(III) nitrate (2). Cobalt(II) nitrate like the perchlorate precipitated Co_3O_4 at 300 °C. The formation of β-MnO(OH), γ-MnO(OH), and MnO_2 from $Mn(NO_3)_2$ solutions at 250 °C may involve oxidation by HNO_3 or its decomposition products. The mixture, hydrohausmannite, has been made (11) by aerial oxidation of an aqueous suspension of $Mn(OH)_2$ at 25 °C, but at 350 °C a reducing environment (hydrogen gas) is apparently necessary to prevent the oxidation of $Mn(OH)_2$ by liquid water (12). Criss (4) predicted that potential reducing agents are unstable in water at high temperatures, and this agrees with the observed oxidation of $Fe(OH)_2$ (2) and the formation of cobalt(III) from cobalt(II) in hydrothermal experiments. Aqueous nitric acid decomposes to oxygen and nitrogen(IV) oxide above 250 °C (2, 13), and at 300 °C a manganese(II) nitrate solution yields manganese(IV) oxide exclusively in accordance with the development of more strongly oxidizing conditions.

M(II) Chlorides

The precipitation of small quantities of various metal oxides or silicates from manganese(II), iron(II), cobalt(II), and nickel(II) solutions is suppressed by the addition of a little HCl, and also by a large concentration of NaCl. Chloride ion has been shown (14) to complex the metal ion at high temperatures and so displaces the reactions 1 and 2 further toward the left. This is particularly effective with cobalt(II), which gives comparatively stable tetrahedral halo-complexes. Bromide is markedly less effective than chloride in the suppression of precipitation, despite its lower basicity towards protons, and this reflects the lower ligand-field strength of bromide. The increasing importance of anion–cation complexing in aqueous solutions as one goes to higher temperatures is a consequence of the decreasing numerical value of the product of the solvent dielectric constant and the absolute temperature (2, 14).

Aqueous $CuCl_2$ at 300 °C yielded crystalline CuCl if the vapor phase was in contact with iron or stainless steel, which was then heavily corroded. This phenomenon suggests that the reaction

$$[3] \quad Cu^{2+}(aq) + 2Cl^{-}(aq) = CuCl(s) + \tfrac{1}{2}Cl_2(g)$$

which is very unlikely at 25 °C ($E^0 = -0.82$ V (15)), may become sufficiently favored at 300 °C that continuous removal of chlorine from the gas phase by reaction with iron would reduce significant amounts of copper(II) to CuCl. Indeed the available thermodynamic data (16) enable one to calculate $\Delta H^0 = +11$ kcal for reaction 3 at 25 °C, *i.e.*, it is favored by high temperatures.

Hydrothermal precipitation from solutions of $CrCl_3$, $MnCl_2$, $FeCl_2$, $CoCl_2$, $NiCl_2$, $CuCl_2$, $ZnCl_2$, and $AlCl_3$ has been reported by Fischer (17) to occur at 210 °C in ordinary sealed glass tubes, but these reactions would certainly be influenced by the presence of silicates and alkali leached from the glass. Katsurai and Sone (18) on the other hand found that solutions of several cobalt(II), nickel(II), and copper(II) salts remained visibly homogeneous up to at least 200 °C.

M(II) Sulfates

Solutions of manganese(II), iron(II), cobalt(II), and nickel(II) sulfates all yielded the monohydrates, $MSO_4.H_2O$, which are isomorphous with kieserite, $MgSO_4.H_2O$, which has a known structure (19). The insolubility of these and certain other basic sulfates (2, 20) under hydrothermal conditions may reflect the fact that sulfate ion exists almost exclusively as HSO_4^- in water between 300 and 400 °C (21), so that aqueous MSO_4 at 300 °C exists as MOH^+ and HSO_4^-. These components form $MSO_4.H_2O$ in the solid state.

The $NiO–SO_3–H_2O$ system at high temperatures has received detailed attention by previous workers (22), as has the $CuO–SO_3–H_2O$ system

(23). Our results with these solutions agree with the published data.

M(III) Salts

The total decomposition of aqueous $Co(NH_3)_6^{3+}$ to Co_3O_4 and α-$Co(OH)_2$ at 300 °C, even in the presence of large excesses of ammonia, was predictable; since at 20 °C the $Co(H_2O)_6^{3+}$ ion is slowly but completely reduced by water to cobalt(II), reaction 4, and the kinetic barriers which prevent aquation of $Co(NH_3)_6^{3+}$ at 20 °C would be overcome at high temperatures.

[4] $$4Co^{3+} + 2H_2O = 4Co^{2+} + 4H^+ + O_2$$

On the other hand, the partial reduction of cobalt(III) to cobalt(II) in these basic solutions contrasts with the tendency of cobalt(II) to be oxidized to cobalt(III) in acidic environments at high temperatures. These facts are reconciled by supposing that reaction 4 is freely reversible at high temperatures; oxygen may have been present in our experimental systems in small amounts as a contaminant, or in greater quantity as a decomposition product of HNO_3 or $HClO_4$.

The high-temperature aqueous chemistry of chromium(III) and iron(III) has been dealt with elsewhere(2, 20, 24).

We thank the Atomic Energy of Canada, Ltd., for financial support of this work through Whiteshell Nuclear Research Establishment and Mr. D. Harvey for the X-ray fluorescence analyses.

1. J. W. COBBLE. Science, **152**, 1479 (1966).
2. T. W. SWADDLE, P. BAYLISS, J. H. LIPTON, and G. GUASTALLA. Can. J. Chem. To be published.
3. C. W. F. T. PISTORIUS. Neues Jahrb. Mineral. Monatsh. 30 (1963).
4. C. M. CRISS. Ph.D. Thesis. Purdue University, Illinois. 1961. p. 110*ff*.
5. L. G SILLÉN and A. E. MARTELL. Stability constants. Special Publication No. 17. The Chemical Society, London. 1964.
6. J. W. MELLOR. Comprehensive treatise on inorganic and theoretical chemistry. Vol. 3. Longmans Green and Co., London. 1923. p. 144.
7. G. C. KENNEDY. Econ. Geol. **45**, 629 (1950).
8. W. A. J. MAHON. N.Z.J. Sci. **10**, 206 (1967).
9. N. V. SIDGWICK. The chemical elements and their compounds. Oxford University Press, Oxford, England. 1950. p. 1377.
10. H C. HELGESON. J. Phys. Chem. **71**, 3121 (1967).
11. O. BRICKER. Am. Mineral. **50**, 1296 (1965). G. C. KENNEDY. Econ. Geol. **45**, 1284 (1950).
12. C. KLINGSBERG and R. ROY. Am. Mineral. **44**, 819 (1959).
13. W. C. WAGGENER, A. J. WEINBERGER, and R. W. STOUGHTON. Appl. Spectr. **22**, 545 (1968).
14. H.-D. LÜDEMANN and E. U. FRANCK. Ber. Bunsenges. Phys. Chem. **71**, 455 (1967); H.-D. LÜDEMANN and E. U. FRANCK. Ber. Bunsenges. Phys. Chem. **72**, 514 (1968).
15. R. PARSONS. Handbook of electrochemical constants. Butterworths Scientific Publications, London. 1959. pp. 62–63.
16. D. D. WAGMAN, W. H. EVANS, V. B. PARKER, I. HALOW, S. M. BAILEY, and R. H. SCHUMM. Selected values of chemical thermodynamic properties. N.B.S. Technical Notes 270-3 and 270–4, Washington, D.C. 1968 and 1969.
17. H. W. FISCHER. Z. Anorg. Chem. **66**, 37 (1910).
18. T. KATSURAI and K. SONE. Kolloid. Z. **163**, 70 (1959).
19. J. LEONHARDT and R. WEISS. Naturwiss. **44**, 339 (1957).
20. E. POSNJAK and H. E. MERWIN. J. Am. Chem. Soc. **44**, 1965 (1922). A. LECERF, A. BONNIN, and A. HARDY. C.R. **262C**, 352 (1966).
21. A. S. QUIST, W. L. MARSHALL, and H. R. JOLLEY. J. Phys. Chem. **69**, 2726 (1965).
22. W. L. MARSHALL, J. S. GILL, and R. SLUSHER. J. Inorg. Nucl. Chem. **24**, 889 (1962).
23. E. POSNJAK and G. TUNELL. Am. J. Sci. **218**, 1 (1929). W. L. MARSHALL and J. S. GILL. J. Inorg. Nucl. Chem. **22**, 115 (1961).
24. R. G. ROBINS. J. Inorg. Nucl. Chem. **29**, 431 (1967). T. KATSURAI. Kolloid. Z. **170**, 58 (1960).

Can. J. Chem. Downloaded from www.nrcresearchpress.com by 210.87.254.42 on 09/05/12
For personal use only.

Can. J. Chem. Downloaded from www.nrcresearchpress.com by 210.87.254.42 on 09/05/12
For personal use only.

NOTES

Oxidation of 1,4-Cyclohexadiene Dioxide with Dimethyl Sulfoxide

B. McKAGUE

Orchem Research, 3650 Wesbrook Crescent, Vancouver 167, British Columbia

Received March 17, 1971

The oxidation of 1,4-cyclohexadiene dioxide with dimethyl sulfoxide and boron trifluoride etherate catalysis yields catechol in 70–75% yield.

L'oxydation du dioxyde du cyclohexanediène-1,4 par le diméthyl sulfoxyde, catalysée par l'éthérate de trifluorure de bore, conduit au cathécol avec un rendement de 70–75%.

Canadian Journal of Chemistry, **49**, 2447 (1971)

The use of dimethyl sulfoxide as an oxidizing agent in organic chemistry has recently been reviewed (1). The boron trifluoride etherate catalyzed oxidation of epoxides with dimethyl sulfoxide provides a useful synthesis of α-hydroxyaldehydes and α-hydroxyketones and the oxidation of cyclohexene oxide gives 2-hydroxycyclohexanone in good yield (2, 3). The reaction has been demonstrated as proceeding through an intermediate alkoxysulfonium salt which decomposes to the hydroxyketone and dimethyl sulfide (4).

The boron trifluoride etherate catalyzed oxidation of 1,4-cyclohexadiene dioxide (5, 6) with dimethyl sulfoxide yields catechol in 70–75% yield. Presumably after the oxidation of one epoxide ring the reaction intermediates decompose as shown in Scheme 1, dimethyl sulfide being a readily identifiable product.

The decomposition of the intermediate epoxyketol to catechol rather than resorcinol or hydroquinone would appear reasonable on the basis of the known severity of conditions usually required to eliminate hydroxyl groups next to ketone functions (7, 8) and the expected ease of epoxide opening due to the adjacent active methylene group (9).

The reaction was carried out using dimethyl sulfoxide as solvent, 0.025 to 0.1 mol of boron trifluoride etherate per mol of diepoxide, and a temperature of 90 to 130 °C. Under these conditions the time required for reaction was 3 to 12 h depending on the aforementioned variables. The reaction was also performed with tetramethylene sulfoxide, tetramethylene sulfide being isolated and identified.

The reaction was generally performed on the *trans*-diepoxide (5, 6) since the favored method of preparation was the *t*-butyl hydroperoxide – molybdenum trioxide method (10) which gave nearly exclusively the highly crystalline *trans*-isomer. However, when the diepoxide is prepared by an extension of the halohydrin method for cyclohexene oxide (11) a nearly equal mixture of both isomers is obtained which can also be used. Separation of the *cis*-isomer (6) by column chromatography on alumina and reaction separately also gave catechol in similar yield. Various

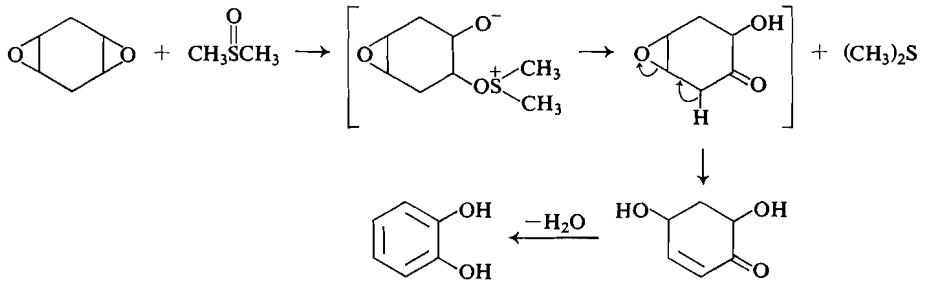

SCHEME 1

Can. J. Chem. Downloaded from www.nrcresearchpress.com by 210.87.254.42 on 09/05/12
For personal use only.

per-acids may also be used to prepare the diepoxides (6).

Experimental

Melting points were determined on a Fisher–Johns apparatus and are uncorrected. The i.r. spectra were run on a Perkin–Elmer Model 521 Grating Infrared Spectrophotometer. Gas chromatography was carried out on a Varian Aerograph Model 1200. The n.m.r. spectra were determined in deuteriochloroform at 60 MHz on a Varian T-60 spectrometer. Column chromatography was performed on standard silica gel and neutral activity II alumina.

Mixture of cis- and trans-1,4-Cyclohexadiene Dioxide

Calcium hypochlorite (19.0 g, 0.13 mol) was added to water (250 ml), and treated with glacial acetic acid (15.8 g, 0.26 mol). The resultant solution was added dropwise with stirring to 1,4-cyclohexadiene (8.4 g, 0.105 mol) over 45 min maintaining the temperature at 15–20 °C by cooling in a cold water bath. After the addition was complete the solution was stirred 10 min, then saturated with salt, and extracted with five 50-ml portions of ether. The combined extracts were washed with saturated salt solution, dried over anhydrous sodium sulfate, and evaporated to give a crude mixture of colorless solid chlorohydrins (17.3 g). This mixture was crushed and suspended in water (20 ml) then added to a solution of sodium hydroxide (8.0 g, 0.2 mol) in water (30 ml). The resultant mixture was stirred for 1½ h then saturated with salt and extracted with five 50-ml portions of dichloromethane. The combined extracts were washed with saturated salt solution and dried over anhydrous sodium sulfate. The solvent removed by distillation through a 40-cm Vigreux column at slightly reduced pressure to yield a crude residual mixture of *trans*- and *cis*-1,4-cyclohexadiene dioxides (10.9 g, 93% yield). Gas chromatography on 5% SE 30, 1/8″ × 5′, at 90 °C indicated the *trans*:*cis* ratio was about 6:4. This procedure could easily be scaled up to large quantities.

Column chromatography of a small amount of this mixture on alumina allowed an easy separation of the two isomers. Elution with benzene gave the pure *trans*-isomer, recrystallized from ether–hexane, m.p. 107.5–108.5 °C (lit. (6) 106.5–107.5 °C) and elution with benzene–ether (9:1) gave the *cis*-isomer, recrystallized from ether–hexane, m.p. 58–60 °C (lit. (6) 60–61 °C). The n.m.r. spectra of each isomer agreed with the reported data (6).

trans-1,4-Cyclohexadiene Dioxide

A solution of 1,4-cyclohexadiene (10 g, 0.125 mol) in benzene (20 ml) was refluxed with 90% *t*-butyl hydroperoxide (37.5 g, 0.375 mol) and molybdenum trioxide (1.0 g) for 12 h. The catalyst was filtered and the solution concentrated to a small volume by vacuum distillation through a 10-cm Vigreux column. The semi-solid crude diepoxide was triturated with hexane, filtered, and crystallized from ether–hexane to give long needles of the pure *trans*-diepoxide (7.5 g) m.p. 107.5–108.5 °C. This procedure could also be scaled up to larger quantities.

Oxidation of trans-1,4-Cyclohexadiene Dioxide with Dimethyl Sulfoxide

A solution of *trans*-1,4-cyclohexadiene dioxide (1.0 g, 8.93 mmol) in dry dimethyl sulfoxide (10 ml) containing boron trifluoride etherate (0.028 ml) was heated in an oil bath at 125 °C for 3 h. Dimethyl sulfide and most of the excess dimethyl sulfoxide were distilled under reduced pressure, the dimethyl sulfide being collected in a Dry Ice – acetone trap and identified by i.r. comparison with an authentic sample. The dark residue was extracted with five 10-ml portions of ether. The combined extracts were washed twice with a small amount of water, then the washes were back-extracted twice with ether. The combined ether extracts were dried over anhydrous sodium sulfate and evaporated to give crude yellow crystalline catechol (920 mg). This was chromatographed on silica gel (20 g) and elution with chloroform – ethyl acetate (5:1) gave pure catechol (740 mg, 75% yield) identical in all respects with an authentic sample.

A number of variations in quantities of the reactants were tried and a similar yield obtained. For example heating the *trans*-diepoxide (1.0 g), dimethyl sulfoxide (15 ml), and boron trifluoride etherate (0.057 ml) at 100–105 °C for 7 h gave catechol in 73% yield. Temperatures lower than 90 °C or smaller amounts of catalyst lowered the yield or made the reaction time unduly long. A mixture of *cis*- and *trans*-diepoxides, as obtained by the chlorohydrin route, or the pure *cis*-isomers could also be used with similar results.

Oxidation of trans-1,4-Cyclohexadiene Dioxide with Tetramethylene Sulfoxide

A solution of the *trans*-diepoxide (1.0 g, 8.93 mmol) in dry tetramethylene sulfoxide (15 ml) containing boron trifluoride etherate (0.028 ml) was heated at 125 °C for 5½ h. Work-up as described above gave tetramethylene sulfide identified by i.r. comparison with an authentic sample and catechol in 50–60% yield.

The author is grateful to Mr. C. E. Van Winckel Sr. for assistance in preparation of starting materials.

1. T. Durst. Advances in organic chemistry. Vol. 6. *Edited by* E. C. Taylor and H. Wynberg. John Wiley and Sons Inc., New York, N.Y., 1969. p. 285.
2. T. Cohen and T. Tsuji. J. Org. Chem. **26**, 1681 (1961).
3. T. Tsuji. Tetrahedron Lett. 2413 (1966).
4. T. M. Santosusso and D. Swern. Tetrahedron Lett. 4261 (1968).
5. N. D. Zelinsky and A. N. Titowa. Ber. **64**, 1399 (1931).
6. T. W. Craig, G. R. Harvey, and G. A. Berchtold. J. Org. Chem. **32**, 3743 (1967).
7. L. F. Fieser and M. Fieser. Advanced organic chemistry. Reinhold Publishing Corp., London, 1961. p. 140.
8. P. D. Bartlett and G. F. Woods. J. Am. Chem. Soc. **62**, 2933 (1940).
9. K. K. Maheshwari, P. de Mayo, and D. Wiegand. Can. J. Chem. **48**, 3265 (1970).
10. R. Landau, D. Brown, J. L. Russell, and J. Kollar. 7th World Petroleum Congress Proceedings. Vol. 5. Elsevier Publishing Co., Essex, England, 1967. p. 67.
11. Org. Synth. Coll. Vol. 1, 158, 185 (1941).

Molecular Conformation of 4-Thiouridine in Aqueous Solution

F. E. HRUSKA, K. K. OGILVIE, A. A. SMITH,[1] AND H. WAYBORN
Department of Chemistry, The University of Manitoba, Winnipeg 19, Manitoba

Received February 18, 1971

β-4-Thiouridine is a component of several tRNA molecules. A recent X-ray study has shown that this pyrimidine nucleoside favors the *syn* conformation in the crystalline state. The 100 and 220 MHz p.m.r. data and a comparison with those of uridine are presented here. A long-range five-bond spin–spin coupling interaction between the H-5 and -1′ hydrogens is noted. The results are consistent with an *anti* conformation for 4-thiouridine in an aqueous solution.

La β-thiouridine-4 est un composant de plusieurs molécules de tRNA. Il a été démontré récemment à l'aide d'une étude par rayons-X que ce nucléoside pyrimidinique existe préférentiellement, à l'état cristallin, dans la conformation *syn*. On a présenté les spectres de r.m.n. à 100 et 220 MHz et une comparaison de ces résultats avec ceux de l'uridine. On note un couplage à longue distance répartie sur cinq liens entre les protons H-5 et -1′. Les résultats sont consistants avec une conformation *anti* pour la thiouridine-4 en solution aqueuse.

Canadian Journal of Chemistry, 49, 2449 (1971)

We report here complete analyses of the 100 and 220 MHz spectra of β-4-thiouridine (4-SU). 4-SU is a sulfur analog of β-uridine (U) and is known to occur in a number of *E. coli* tRNA molecules (1). A recent X-ray study (2) has shown 4-SU to be the first pyrimidine nucleoside to favor the *syn* conformation in the crystalline state. The o.r.d. (3) and n.m.r. (4–7) studies, however, argue for a predominantly *anti* conformation for U and its phosphate derivatives in aqueous solution. Green *et al.* (8) have reported an *anti* conformation for U in the solid state as well. In view of the experimental evidence that the *anti* conformation for pyrimidine (and purine) nucleoside di- and triphosphates is required for enzymic incorporation into polynucleotides (9), we have carried out this study to determine the conformation of 4-SU in solution.

The n.m.r. spectra were obtained on Varian HA100 and 220 MHz spectrometers. Samples were freeze-dried three times using 99.8% D_2O. DSS was used as an internal reference. Spectra were analyzed using LAOCOON III (10).

The H-6, -5, and -1′ resonances of 4-SU (obtained at 100 MHz) are shown in Fig. 1. The H-6 doublet ($^3J_{56}$ = 7.7 Hz)[2] is centered at

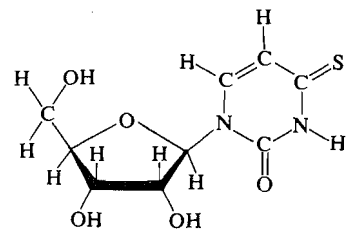

4-SU *anti*

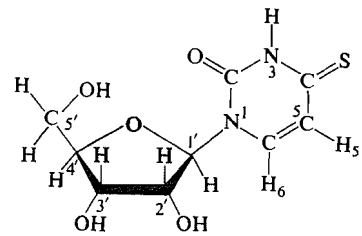

4-SU *syn*

7.75 p.p.m. from internal DSS. The H-5 region centered at 6.56 p.p.m. is a quartet with a $^3J_{56}$ splitting and a small splitting of 0.35 Hz. Double resonance experiments demonstrated that the 0.35 Hz separation was a consequence of a five-bond long-range spin–spin coupling interaction between the H-5 and -1′ hydrogens. The H-1′ portion of the spectrum consists of a broad doublet ($^3J_{1'2'}$ = 3.9 Hz) at 5.86 p.p.m. No 0.35 Hz splitting is evident in this region, presumably a consequence of the line broadening effect of unresolved long range interactions

[1]Postdoctoral Fellow, Faculty of Graduate Studies and Research, University of Manitoba, Winnipeg, Manitoba.

[2]The coupling constants are denoted by $^nJ_{HH'}$ where the superscript refers to the number of intervening bonds in the coupling path between the coupled nuclei H and H′.

Can. J. Chem. Downloaded from www.nrcresearchpress.com by 210.87.254.42 on 09/05/12
For personal use only.

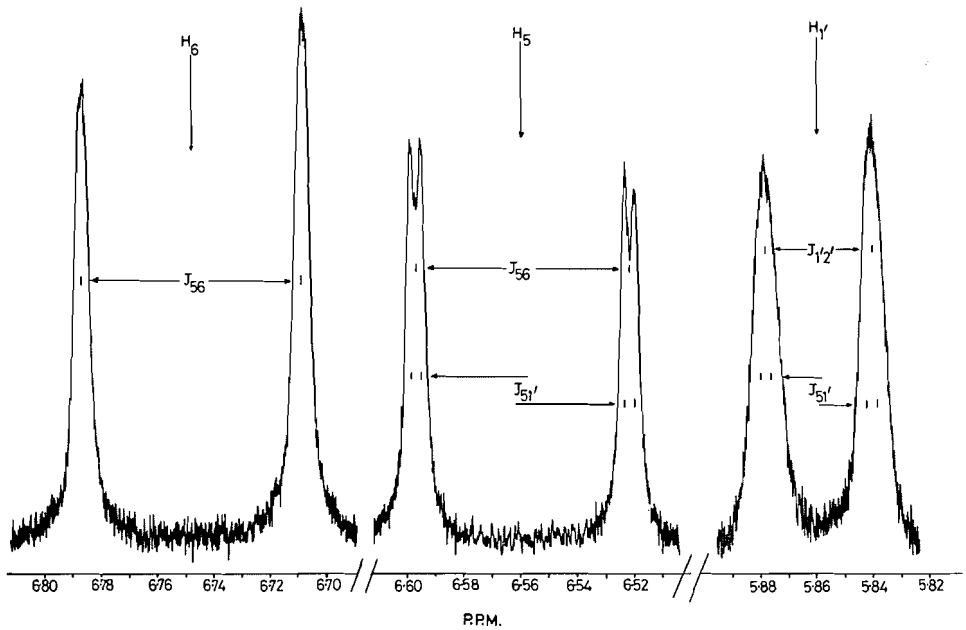

FIG. 1. The H-6, -5, and -1′ portions of the 100 MHz p.m.r. spectrum of a 0.12 *M* aqueous solution of 4-thiouridine (D_2O, p*D* = 6.9, 30 °C). In p.p.m. from internal DSS.

between H-1′ and the H-3′, -4′, and -5′ hydrogens of the ribose ring (11).[3]

The 220 MHz spectrum of the 2′ to 5′ regions is shown in Fig. 2. The assignment of the bands was carried out by comparison with published data for U(4) and confirmed by computer analysis. The calculated spectrum is also shown in Fig. 2.

The chemical shift and coupling constant data are presented in Table 1. For comparison, the 220 MHz data of U taken from ref. 4 are included.

Comparison of the tabulated ribose data reveals a striking similarity for the two nucleosides which is consistent with the existence of 4-SU in the *anti* conformation. First, all the corresponding ^3J and ^2J values differ by 0.1 Hz or less (except for the $^3J_{1'2'}$ values which differ by 0.5 Hz). Furthermore all corresponding ribose chemical shifts are identical to within 0.04 p.p.m. Recent studies, particularly on 1-β-D-ribofuranylcyanuric acid, by Schweizer *et al.* (12) and Dugas *et al.* (5) are relevant in this regard. In this nucleoside a keto group is found at both positions *ortho* to the *N*-glycosyl linkage and hence one keto oxygen must be located above the furanose ring. In this manner the authors have demonstrated that the magnetic anisotropy and steric effects of such a keto group lead to large and specific changes in the chemical shift and coupling constants of the ring. Thus, the similarity in the ribose data must be taken as evidence that 4-SU assumes the *anti* conformation in which the C_6—H_6 (rather than the C_2=O_2) moiety is located above the ribose.

Further evidence for the *anti* conformation of 4-SU is afforded by the long range $^5J_{51'}$ interactions. These interactions are examples of meta benzylic spin–spin coupling (13). Theory (substantiated by considerable experimental data) predicts a critical stereochemical dependence of ^5J couplings. The dependence is such that coupling is favored when the side-chain (H-1′) hydrogen and the meta substituent on the ring are connected by an "extended zig–zag" coupling path (14). Such a path connects the H-1′ and -5 hydrogens of a pyrimidine nucleoside and H-1′ and F-5 of 5-fluoropyrimidine nucleosides in the *anti* (but not the *syn*) conformation. The question of the $^5J_{HF}$ coupling and its relationship to the *syn–anti* structural problem in the latter group of molecules has been thoroughly discussed by Cushley *et al.* (15). Recently Hruska (16) has correlated observed $^5J_{51'}$ H–H couplings in a

[3]Another source of broadening of the H-1′ resonances could be N-1 quadrupolar relaxation.

Can. J. Chem. Downloaded from www.nrcresearchpress.com by 210.87.254.42 on 09/05/12
For personal use only.

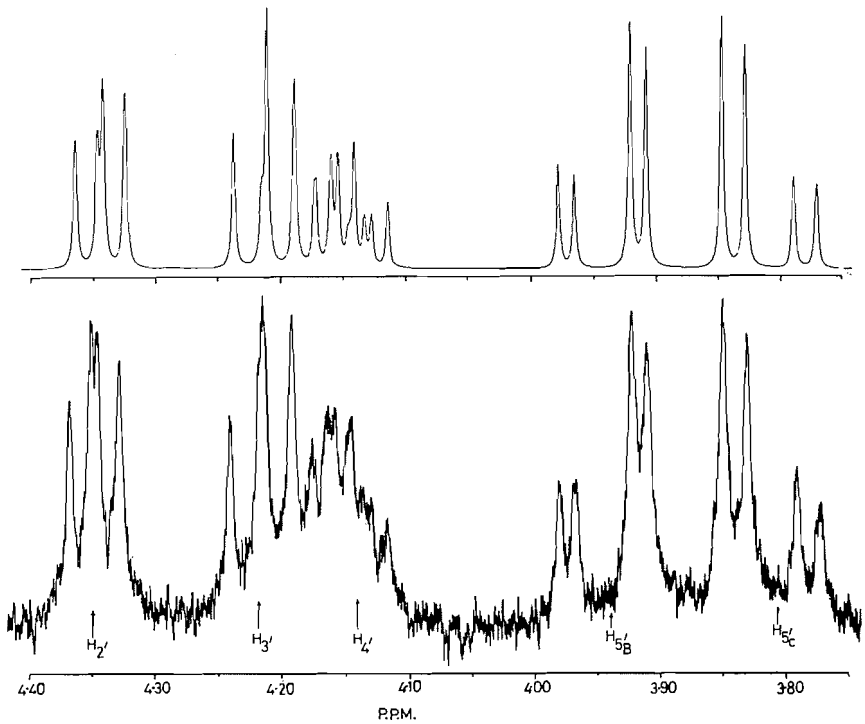

FIG. 2. The H-2′ to -5′ portions of the 220 MHz p.m.r. spectrum of a 0.12 *M* aqueous solution of 4-thiouridine (D_2O, p*D* = 6.9, 25 °C). The computer-simulated spectrum is shown above the Experimental. In p.p.m. from internal DSS.

TABLE 1. Proton chemical shifts and coupling constants of 4-thiouridine* (4-SU) and uridine† (U)

	Chemical shifts (p.p.m.)		Coupling constants (Hz)		
H	4-SU	U		4-SU	U
−6	7.75	7.86	$^3J_{56}$	7.7	8.0
−5	6.56	5.89	$^5J_{51'}$	0.35	0.41‡
−1′	5.86	5.90	$^3J_{1'2'}$	3.9	4.4
−2′	4.35	4.34	$^3J_{2'3'}$	5.4	5.3
−3′	4.22	4.22	$^3J_{3'4'}$	5.6	5.5
−4′	4.14	4.13	$^3J_{4'5'B}$	3.0	3.0
−5′B	3.94	3.91	$^3J_{4'5'C}$	4.3	4.4
−5′C	3.81	3.80	$^2J_{5'B5'C}$	−12.7	−12.7

*This work. Synthesized by procedure K. H. Scheit. ref. 20.
†Reference 4 except $^5J_{51'}$ from ref. 12.
‡p*D* 10.2.

number of nucleosides with their *anti* forms. No such coupling was detected for orotidine (6-carboxyuridine) which is known to prefer the *syn* form in aqueous solution (17). The interactions of 0.41 and 0.35 Hz for U and 4-SU respectively are, therefore, taken as evidence that a zig–zag path connects the H-5 and -1′ hydrogens in each instance, and, therefore, that 4-SU is *anti* in aqueous solution.

A more detailed consideration of the ribose conformation can be made via a Karplus equation of the vicinal ^3J coupling constant in the manner discussed in earlier reports (4, 18). In view of the similarity in the ^3J values for 4-SU

Can. J. Chem. Downloaded from www.nrcresearchpress.com by 210.87.254.42 on 09/05/12
For personal use only.

and U we may conclude that the conformation of the ribose ring of 4-SU is best described by a rapid equilibrium between various puckered forms (2′-*endo*, etc.). Furthermore, both U and 4-SU exhibit a preference for the *gauche–gauche*[4] rotamer about the $C_{4'}$—$C_{5'}$ bond, the conformation preferred by crystalline β-nucleosides in the *anti* conformation (19).

During the course of our work that of Schweizer *et al.* (12) appeared. The emphasis of their work was on the anisotropy effect of the 2-keto group on the ribose chemical shifts. By comparison of the shifts for a number of molecules the authors concluded that 4-SU existed mostly *anti* in solution. Our present study which involves comparison of the shift and coupling data of U and 4-SU is in agreement with their conclusion.

The financial support of the National Research Council of Canada is gratefully acknowledged. A.A.S. and F.E.H. thank the Faculty of Graduate Studies and Research of the University of Manitoba for support.

1. H. G. Zachau. Angew, Chem. Intern. Edit. **8**, 711 (1969).
2. W. Saenger and K. H. Scheit. J. Mol. Biol. **50**, 153 (1970).
3. T. R. Emerson, R. J. Swan, and T. L. V. Ulbricht. Biochem. **6**, 843 (1967).
4. B. J. Blackburn, A. A. Grey, I. C. P. Smith, and F. E. Hruska. Can. J. Chem. **48**, 2866 (1970).
5. H. Dugas, B. J. Blackburn, R. K. Robins, R. Deslauriers, and I. C. P. Smith. J. Am. Chem. Soc. In press.
6. S. I. Chan and J. H. Nelson. J. Am. Chem. Soc. **91**, 168 (1969).
7. P. O. P. Ts'O, N. S. Kondon, M. P. Schweizer, and D. P. Hollis. Biochem. **8**, 997 (1969).
8. F. A. Green, R. Shiono, and R. D. Rosenstein. Chem. Commun. **53**, (1971).
9. A. M. Kapuler, C. Monny, and A. M. Michelson. Biochim. Biophys. Acta. **217**, 18 (1970).
10. S. Castellano and A. A. Bothner-By. J. Chem. Phys. **41**, 3863 (1964).
11. J. Dalton, F. E. Hruska, and K. K. Ogilvie. Unpublished results.
12. M. P. Schweizer, J. T. Witkowski, and R. K. Robins. J. Am. Chem. Soc. **93**, 277 (1971).
13. L. M. Jackman and S. Sternhell. Applications of nuclear magnetic resonance spectroscopy in organic chemistry. Vol. 5. Pergamon Press, 1969. p. 330.
14. S. Sternhell. Quart. Rev. London, **23**, 236 (1969).
15. R. J. Cushley, I. Wempen, and J. J. Fox. J. Am. Chem. Soc. **90**, 709 (1968).
16. F. E. Hruska. Can. J. Chem. **49**, 2111 (1971).
17. F. E. Hruska. J. Am. Chem. Soc. **93**, 1795 (1971).
18. F. E. Hruska, A. A. Grey, and I. C. P. Smith. J. Am. Chem. Soc. **92**, 214, 4088 (1970).
19. M. Sundaralingam and L. H. Jenzen. J. Mol. Biol. **13**, 930 (1965).
20. K. H. Scheit. Ber. **101**, 1141 (1968).

[4]In the *gauche–gauche* rotamer $C_{5'}$–$O_{5'}$ is *gauche* to both the $C_{4'}$—$O_{1'}$ and $C_{4'}$—$C_{3'}$ bonds.

On the Triplet Energies of the Trifluorobenzenes and of *cis*-Butene-2

G. P. Semeluk and R. D. S. Stevens
Department of Chemistry, University of New Brunswick, Fredericton, New Brunswick

Received October 19, 1970

Evans' method of high pressure oxygen induced singlet–triplet absorption spectra were used to estimate the triplet energies of the title compounds. Phosphorescent emission spectra from EPA glassy matrix at 77 °K were taken for the trifluorobenzenes. The 0–0 bands of the T ← S absorption indicate that the triplet energy of *cis*-butene-2 is lower than that of all three trifluorobenzenes.

La méthode d'induction des spectres d'absorption singulet–triplet par l'oxygène sous pression décrite par Evans a été utilisée pour estimer l'énergie des niveaux triplets des composés mentionnés dans le titre. Les spectres d'émission de phosphorescence des trifluorobenzènes en solution dans une matrice de EPA à 77 °K ont été enregistrés. Les bandes 0–0 obtenues du spectre d'absorption T ← S indiquent que l'énergie de l'état triplet du *cis*-butène-2 est inférieure à celles des trois trifluorobenzènes.

Canadian Journal of Chemistry, 49, 2452 (1971)

Introduction

The methods of sensitized biacetyl emission (1) and of butene-2 *cis–trans* isomerization (2) in the detection of triplet states are commonly used techniques. A method which combines the two approaches (3) has been in use in this laboratory for some time. The success of these diagnostics depends primarily on three factors: (*i*) The triplet state energy of the donor relative to that of the acceptor. In solution for example, it appears that

Can. J. Chem. Downloaded from www.nrcresearchpress.com by 210.87.254.42 on 09/05/12
For personal use only.

and U we may conclude that the conformation of the ribose ring of 4-SU is best described by a rapid equilibrium between various puckered forms (2′-*endo*, etc.). Furthermore, both U and 4-SU exhibit a preference for the *gauche–gauche*[4] rotamer about the $C_{4'}$—$C_{5'}$ bond, the conformation preferred by crystalline β-nucleosides in the *anti* conformation (19).

During the course of our work that of Schweizer *et al.* (12) appeared. The emphasis of their work was on the anisotropy effect of the 2-keto group on the ribose chemical shifts. By comparison of the shifts for a number of molecules the authors concluded that 4-SU existed mostly *anti* in solution. Our present study which involves comparison of the shift and coupling data of U and 4-SU is in agreement with their conclusion.

The financial support of the National Research Council of Canada is gratefully acknowledged. A.A.S. and F.E.H. thank the Faculty of Graduate Studies and Research of the University of Manitoba for support.

1. H. G. Zachau. Angew, Chem. Intern. Edit. **8**, 711 (1969).
2. W. Saenger and K. H. Scheit. J. Mol. Biol. **50**, 153 (1970).
3. T. R. Emerson, R. J. Swan, and T. L. V. Ulbricht. Biochem. **6**, 843 (1967).
4. B. J. Blackburn, A. A. Grey, I. C. P. Smith, and F. E. Hruska. Can. J. Chem. **48**, 2866 (1970).
5. H. Dugas, B. J. Blackburn, R. K. Robins, R. Deslauriers, and I. C. P. Smith. J. Am. Chem. Soc. In press.
6. S. I. Chan and J. H. Nelson. J. Am. Chem. Soc. **91**, 168 (1969).
7. P. O. P. Ts'O, N. S. Kondon, M. P. Schweizer, and D. P. Hollis. Biochem. **8**, 997 (1969).
8. F. A. Green, R. Shiono, and R. D. Rosenstein. Chem. Commun. **53**, (1971).
9. A. M. Kapuler, C. Monny, and A. M. Michelson. Biochim. Biophys. Acta. **217**, 18 (1970).
10. S. Castellano and A. A. Bothner-By. J. Chem. Phys. **41**, 3863 (1964).
11. J. Dalton, F. E. Hruska, and K. K. Ogilvie. Unpublished results.
12. M. P. Schweizer, J. T. Witkowski, and R. K. Robins. J. Am. Chem. Soc. **93**, 277 (1971).
13. L. M. Jackman and S. Sternhell. Applications of nuclear magnetic resonance spectroscopy in organic chemistry. Vol. 5. Pergamon Press, 1969. p. 330.
14. S. Sternhell. Quart. Rev. London, **23**, 236 (1969).
15. R. J. Cushley, I. Wempen, and J. J. Fox. J. Am. Chem. Soc. **90**, 709 (1968).
16. F. E. Hruska. Can. J. Chem. **49**, 2111 (1971).
17. F. E. Hruska. J. Am. Chem. Soc. **93**, 1795 (1971).
18. F. E. Hruska, A. A. Grey, and I. C. P. Smith. J. Am. Chem. Soc. **92**, 214, 4088 (1970).
19. M. Sundaralingam and L. H. Jenzen. J. Mol. Biol. **13**, 930 (1965).
20. K. H. Scheit. Ber. **101**, 1141 (1968).

[4]In the *gauche–gauche* rotamer $C_{5'}$–$O_{5'}$ is *gauche* to both the $C_{4'}$—$O_{1'}$ and $C_{4'}$—$C_{3'}$ bonds.

On the Triplet Energies of the Trifluorobenzenes and of *cis*-Butene-2

G. P. Semeluk and R. D. S. Stevens
Department of Chemistry, University of New Brunswick, Fredericton, New Brunswick

Received October 19, 1970

Evans' method of high pressure oxygen induced singlet–triplet absorption spectra were used to estimate the triplet energies of the title compounds. Phosphorescent emission spectra from EPA glassy matrix at 77 °K were taken for the trifluorobenzenes. The 0–0 bands of the T ← S absorption indicate that the triplet energy of *cis*-butene-2 is lower than that of all three trifluorobenzenes.

La méthode d'induction des spectres d'absorption singulet–triplet par l'oxygène sous pression décrite par Evans a été utilisée pour estimer l'énergie des niveaux triplets des composés mentionnés dans le titre. Les spectres d'émission de phosphorescence des trifluorobenzènes en solution dans une matrice de EPA à 77 °K ont été enregistrés. Les bandes 0–0 obtenues du spectre d'absorption T ← S indiquent que l'énergie de l'état triplet du *cis*-butène-2 est inférieure à celles des trois trifluorobenzènes.

Canadian Journal of Chemistry, 49, 2452 (1971)

Introduction

The methods of sensitized biacetyl emission (1) and of butene-2 *cis–trans* isomerization (2) in the detection of triplet states are commonly used techniques. A method which combines the two approaches (3) has been in use in this laboratory for some time. The success of these diagnostics depends primarily on three factors: (*i*) The triplet state energy of the donor relative to that of the acceptor. In solution for example, it appears that

Can. J. Chem. Downloaded from www.nrcresearchpress.com by 210.87.254.105 on 09/05/12
For personal use only.

Can. J. Chem. Downloaded from www.nrcresearchpress.com by 210.87.254.105 on 09/05/12
For personal use only.

the donor triplet energy must exceed that of the acceptor by up to 3 kcal (4). (*ii*) The lifetime of the donor triplet state relative to the mean period between collisions with the acceptor. If processes competitive with the rate of collisions are very fast, then energy transfer may be difficult to observe in a conveniently accessible pressure range. (*iii*) The efficiency of energy transfer from triplet donor to acceptor during a collision. A useful and illuminating discussion of this factor has been given recently by Schmidt and Lee (5).

In a previous study (6), it was speculated that the triplet energy of 1,2,4-trifluorobenzene (1,2,4-F_3B) was lower than that of *cis*-butene-2 (*c*-B-2), based on the result that the addition of up to 50 Torr *c*-B-2 failed to noticeably decrease the biacetyl phosphorescent yield sensitized by triplet 1,2,4-F_3B. Recent work (7) with a number of fluorinated benzenes indicates that pressures of *c*-B-2 as high as 1000 Torr may not completely quench the donor triplet, even though energy considerations ((*i*) above) appear to be favorable. In this respect, triplet energy transfer from these compounds to biacetyl appears to be more efficient than to *c*-B-2. In view of these considerations, we felt it would be useful to determine the triplet state energies by the relatively straightforward method of Evans (8), and to obtain confirmation by examining phosphorescent emission from low temperature matrices, in an attempt to clarify these energy relationships.

Experimental

1,3,5-F_3B and 1,2,4-F_3B were obtained from Peninsular Chemresearch Inc., with a second sample of 1,2,4-F_3B being obtained from Bristol Organics Ltd. 1,2,3-Trifluorobenzene (1,2,3-F_3B) was a gift from Donald R. Dickerson of the Illinois State Geological Survey, Urbana. *c*-B-2 was Philips Research grade and was used without further purification. Chloroform solvent was A.C.S. reagent grade from Allied Chemical Company and was found to be transparent in the spectral region of interest.

The trifluorobenzenes were purified by temperature programmed preparative chromatography using carbowax 20M and di-isodecylphthalate columns with helium carrier.

Two Research and Industrial Instruments Company high pressure u.v. cells (number F-076) were used; one for reference which contained chloroform solvent alone, and one for sample, which contained an optimum concentration of the compound of interest in chloroform solution. Both cells contained equal pressures, typically 50 to 150 atm of oxygen. In the case of gas phase measurements the reference cell contained only oxygen at the same pressure as the sample cell, which in addition contained an optimum partial pressure of the compound. The absorption spectra were recorded on a Hitachi-Colemen model EPS-3T spectrophotometer.

EPA glassy matrix studies at 77 °K were carried out with a modified Aminco-Bowman spectrophotofluorometer. The modifications include a light condensing system and adjustable slits at the entrance to the excitation monochromator, provision for nitrogen flushing of the monochromator cases, for cooling of the emission monochromator photomultiplier housing, and for voltages up to 2500 V across photomultiplier dynode resistor networks.

Results and Discussion

($T \leftarrow S$) absorption spectra were obtained by the ingenious method developed by Evans (8). The (0–0) bands observed in this study, along with that previously reported for benzene (8*c*), are given in Table 1. Also included are the short wavelength limits of the phosphorescent emission from EPA glassy matrices at 77 °K. Not included in Table 1 are the several additional vibrational bands, having no greater diffuseness than observed for benzene, which were clearly evident for all three trifluorobenzenes. The highest of these were 5.9, 5.9, and 6.4 kcal mol^{-1} above the 0–0 bands for 1,3,5-F_3B, 1,2,3-F_3B, and 1,2,4-F_3B, respectively.

The value of 78.2 kcal mol^{-1} for the gas phase triplet energy of *c*-B-2 is higher than the value 76 kcal mol^{-1} obtained by the electron scattering method, but within the stated uncertainty of ± 0.2 eV (9). The data indicate the triplet energy of 1,2,4-F_3B to be greater than that of *c*-B-2 apparently by more than 5 kcal mol^{-1} in the gas phase, and to be only slightly smaller than that of benzene. Triplet–triplet energy transfer ought, therefore, to be energetically possible. Since *c*-B-2 readily quenches the triplet of benzene (2), the apparent "non-effect" of *c*-B-2 on the triplet 1,2,4-F_3B sensitized BiA emission yield may be due to a shorter triplet lifetime, an inefficient energy transfer on collision, to a combination of these factors, or to the experimental limitation noted in the previous article (6). A brief discussion of these considerations is therefore in order.

There is no direct evidence regarding transfer efficiency or triplet lifetimes, but there are reasons to suspect that the lifetimes of fluorinated benzenes may be considerably shorter than the lifetime of triplet benzene (10). As one example we may cite the data already reported (6), which show that 15 and 10 (estimated) Torr of BiA must be used for 1,2,4-F_3B and 1,3,5-F_3B triplets, respectively, to obtain a maximum sensitized

TABLE 1. Triplet energies of trifluorobenzenes and *cis*-butene-2

	From (T ← S) spectra				From (T → S) spectra	
	Vapor		$CHCl_3$ solution		EPA glassy matrix*	
Compound	cm^{-1}	kcal mol^{-1}	cm^{-1}	kcal mol^{-1}	cm^{-1}	kcal mol^{-1}
1,3,5-F_3B	30 120	86.12	30 080	85.99	29 890	85.47
1,2,3-F_3B	29 590	84.59	29 500	84.34	29 150	83.35
1,2,4-F_3B	29 320	83.84	29 280	83.72	29 450	84.21
c-B-2	27 360	78.22	~ 27 800†	79.4†		
Benzene	29 510‡	84.37‡	29 440	84.17	29 400	84.0

*The experimental arrangement did not allow the location of the (0–0) bands in (T → S) emission. The wave numbers noted are the shor wavelength limit of the observed phosphorescent emission.
†It was not possible to locate the (0–0) band precisely since the vibrational structure was very weak and diffuse.
‡Reference 8*c*. Confirmed in this laboratory.

emission yield compared with only 0.12 Torr of BiA for the case of benzene sensitized emission (1). These data suggest that the lifetime of triplet 1,3,5-F_3B is 1.2×10^{-2} times shorter than that of triplet benzene, and that the lifetime of triplet 1,2,4-F_3B is 1.5 times shorter than that of triplet 1,3,5-F_3B, if we assume that triplet energy transfer efficiency from the triplets of these molecules to biacetyl is the same as that from benzene triplet to biacetyl. This assumption is justified in part by two considerations, both supported by experimental observations. Thus, in spite of the wide differences in constitution, symmetry, and polarity between benzene and acetone, the rate of triplet energy transfer from acetone to biacetyl is not much different (less than a factor of two) from that of benzene to biacetyl (Table III, ref. 5). Because of the closer similarity of the trifluorobenzenes to benzene than of acetone to benzene (experimentally supported by a comparison of phosphorescent emission spectra), it may be expected that the triplet transfer efficiency of the substituted benzenes will be closer to that of benzene than to acetone.

Triplet energy transfer efficiency is most conveniently discussed in terms of an "exchange integral" used by Dexter (11) to discuss sensitized luminescence in solid phosphors. This integral may be approximated by the expression

$$K^2 \exp(-2R/L) \int_0^\infty F_d(\bar{\nu}) F_a(\bar{\nu})\, d\bar{\nu}$$

where the "spectral overlap integral" contains $F_d(\bar{\nu})$, the *normalized* donor luminescence (the shape of the phosphorescent emission spectrum), $F_a(\bar{\nu})$, the *normalized* acceptor absorption (the shape of the T ← S spectrum). $\bar{\nu}$ is the wave number, L is an effective average radius of the excited donor and unexcited acceptor molecules, R is the distance between excited donor and acceptor molecules which may be thought of as the donor–acceptor distance in the collision complex, and K^2 is a constant made up of the fundamental quantities relating to the energy transfer process.

Using *c*-B-2 as the acceptor common to 1,2,4-F_3B and 1,3,5-F_3B triplets as donors, we estimate

$$\frac{\int F_{1,2,4\text{-}F_3B} F_{c\text{-}B\text{-}2}\, d\bar{\nu}}{\int F_{1,3,5\text{-}F_3B} F_{c\text{-}B\text{-}2}\, d\bar{\nu}} = 0.93$$

Thus, the spectral overlap difference and the triplet lifetime difference indicate that a *c*-B-2 pressure 1.6 times as great would be required to produce the same extent of quenching of 1,2,4-F_3B triplet as for 1,3,5-F_3B triplet. Qualitatively, then, both factors predict a lesser triplet quenching efficiency of *c*-B-2 with 1,2,4-F_3B. We may therefore conclude tentatively, that the limited pressure range which was experimentally accessible to us in the previous study (6) probably prevented us from observing a *c*-B-2 quenching effect.

A final comment may be useful. It may be suggested that the triplet state which is detected in the spectrofluorometric studies is not the same as is observed in the (T ← S) studies: that there is a rapid crossover from the optically accessible triplet to another not optically accessible *lower* energy $n\pi^*$ triplet. This possibility seems unlikely in view of the existence of a potential well at least 5 kcal in depth in these triplet states, and the apparent absence of diffuseness in the (T ← S) spectra.

Financial support of this work by the National Research Council of Canada is gratefully acknowledged. We wish to acknowledge our indebtedness to Mr. Donald Dickerson, who kindly provided us with a sample of

Can. J. Chem. Downloaded from www.nrcresearchpress.com by 210.87.254.105 on 09/05/12
For personal use only.

1,2,3-trifluorobenzene. Thanks are due to Miss S. Lem and Mr. M. Grossman for assistance in collecting the phosphorescent emission data. We are grateful to Drs. F. Grein and I. Unger of this department for many helpful and stimulating discussions.

1. H. ISHIKAWA and W. A. NOYES, JR. J. Chem. Phys. **37**, 583 (1962).
2. R. B. CUNDALL, F. J. FLETCHER, and D. G. MILNE. Trans. Faraday Soc. **60**, 1146 (1964).
3. I. UNGER. J. Phys. Chem. **69**, 4284 (1965).
4. (*a*) G. PORTER and F. WILKINSON. Proc. Roy. Soc. **264**A, 1 (1961). (*b*) G. PORTER and M. R. WRIGHT. Discuss. Faraday Soc. **27**, 18 (1959).
5. M. W. SCHMIDT and E. K. C. LEE J. Am. Chem. Soc. **92**, 3579 (1970).
6. G. P. SEMELUK, R. D. S. STEVENS, and I. UNGER. Can. J. Chem. **47**, 589 (1969).
7. S. H. NG. Ph.D. Thesis. University of New Brunswick, Fredericton, New Brunswick. October 1970.
8. (*a*) D. F. EVANS. Nature, **178**, 534 (1956). (*b*) D. F. EVANS. J. Chem. Soc. 1351 (1957). (*c*) D. F. EVANS. J. Chem. Soc. 3885 (1957). (*d*) D. F. EVANS. J. Chem. Soc. 2753 (1959).
9. H. H. BRONGERSMA, J. A. V.D. HART, and L. J. OSTERHOFF. Fast reactions and primary processes in chemical kinetics. *Edited by* S. Claesson. Interscience, New York. 1967. p. 213. S. MCGLYNN, T. AZUMI, and M. KINOSHITA. Molecular spectroscopy of the triplet state. Prentice Hall, Englewood Cliffs, N.J. 1969. p. 60.
10. R. B. CUNDALL. The triplet state. *Edited by* A. B. Fahlan. Cambridge University Press, London. 1967. p. 183.
11. D. L. DEXTER. J. Chem. Phys. **21**, 836 (1953).

Acid-catalyzed Solvolysis of Isonitriles. I

Y. Y. LIM AND A. R. STEIN[1]

Department of Chemistry, Memorial University of Newfoundland, St. John's, Newfoundland

Received February 16, 1971

The acid-catalyzed hydrolysis of methyl isonitrile has been examined. The initial hydrolysis product is *N*-methylformamide which is further hydrolyzed to methyl amine and formic acid at a much slower rate. The hydrolysis to *N*-methylformamide is pseudo-first order in methyl isonitrile and shows a linear rate dependence on concentration of general (buffer) acid at fixed p*H*. The significance of general acid-catalysis in terms of the mechanism of the hydrolysis is considered and taken as evidence for carbon protonation rather than nitrogen protonation as the initiating step.

L'hydrolyse acido-catalysée du méthylisonitrile a été examinée. Le produit initial de l'hydrolyse est la *N*-méthylformamide qui est hydrolysée ultérieurement en méthylamine et en acide formique selon une vitesse beaucoup plus lente. L'hydrolyse en *N*-méthylformamide est du pseudo-premier ordre en méthylisonitrile et montre une relation linéaire entre la vitesse et la concentration en acide général (tampon) à p*H* déterminé. La signification d'une catalyse acide générale en terme de mécanisme d'hydrolyse est envisagée et constitue la preuve d'une protonation sur le carbone plutôt que sur l'azote, dans l'étape initiale.

Canadian Journal of Chemistry, **49**, 2455 (1971)

There have been numerous studies of the thermal rearrangement of isonitriles to nitriles, especially of methyl isonitrile in the vapor phase (1) and of the more complex reactions of isonitriles, most of which permit the synthesis of otherwise difficultly accessible nitrogen heterocyclic compounds (2). There is, however, a dearth of studies of the simpler chemistry of this fascinating if odoriferous class of compounds, the acid-catalyzed solvolysis being a case in point. Consequently, we have commenced such a study with an examination of the acid-catalyzed hydrolysis of methyl isonitrile to *N*-methylformamide.

Two mechanisms for the hydrolysis of isonitriles have on occasion been suggested, the first involving initial protonation on nitrogen, the other on carbon (3), eqs. 1 and 2 respectively.

Isonitriles are well known to give stable coordination compounds, especially with the softer metal cations (4) and to form strong hydrogen bonds with, for example, chloroform, alcohols, phenols, and water (5). Bonding in both cases is to the carbon of the isonitrile group. Consequently, the initial reversible formation of a hydrogen

[1]To whom correspondence should be addressed.

Can. J. Chem. Downloaded from www.nrcresearchpress.com by 210.87.254.105 on 09/05/12
For personal use only.

1,2,3-trifluorobenzene. Thanks are due to Miss S. Lem and Mr. M. Grossman for assistance in collecting the phosphorescent emission data. We are grateful to Drs. F. Grein and I. Unger of this department for many helpful and stimulating discussions.

1. H. ISHIKAWA and W. A. NOYES, JR. J. Chem. Phys. **37**, 583 (1962).
2. R. B. CUNDALL, F. J. FLETCHER, and D. G. MILNE. Trans. Faraday Soc. **60**, 1146 (1964).
3. I. UNGER. J. Phys. Chem. **69**, 4284 (1965).
4. (*a*) G. PORTER and F. WILKINSON. Proc. Roy. Soc. **264**A, 1 (1961). (*b*) G. PORTER and M. R. WRIGHT. Discuss. Faraday Soc. **27**, 18 (1959).
5. M. W. SCHMIDT and E. K. C. LEE J. Am. Chem. Soc. **92**, 3579 (1970).
6. G. P. SEMELUK, R. D. S. STEVENS, and I. UNGER. Can. J. Chem. **47**, 589 (1969).
7. S. H. NG. Ph.D. Thesis. University of New Brunswick, Fredericton, New Brunswick. October 1970.
8. (*a*) D. F. EVANS. Nature, **178**, 534 (1956). (*b*) D. F. EVANS. J. Chem. Soc. 1351 (1957). (*c*) D. F. EVANS. J. Chem. Soc. 3885 (1957). (*d*) D. F. EVANS. J. Chem. Soc. 2753 (1959).
9. H. H. BRONGERSMA, J. A. V.D. HART, and L. J. OSTERHOFF. Fast reactions and primary processes in chemical kinetics. *Edited by* S. Claesson. Interscience, New York. 1967. p. 213. S. MCGLYNN, T. AZUMI, and M. KINOSHITA. Molecular spectroscopy of the triplet state. Prentice Hall, Englewood Cliffs, N.J. 1969. p. 60.
10. R. B. CUNDALL. The triplet state. *Edited by* A. B. Fahlan. Cambridge University Press, London. 1967. p. 183.
11. D. L. DEXTER. J. Chem. Phys. **21**, 836 (1953).

Acid-catalyzed Solvolysis of Isonitriles. I

Y. Y. LIM AND A. R. STEIN[1]

Department of Chemistry, Memorial University of Newfoundland, St. John's, Newfoundland

Received February 16, 1971

The acid-catalyzed hydrolysis of methyl isonitrile has been examined. The initial hydrolysis product is *N*-methylformamide which is further hydrolyzed to methyl amine and formic acid at a much slower rate. The hydrolysis to *N*-methylformamide is pseudo-first order in methyl isonitrile and shows a linear rate dependence on concentration of general (buffer) acid at fixed p*H*. The significance of general acid-catalysis in terms of the mechanism of the hydrolysis is considered and taken as evidence for carbon protonation rather than nitrogen protonation as the initiating step.

L'hydrolyse acido-catalysée du méthylisonitrile a été examinée. Le produit initial de l'hydrolyse est la *N*-méthylformamide qui est hydrolysée ultérieurement en méthylamine et en acide formique selon une vitesse beaucoup plus lente. L'hydrolyse en *N*-méthylformamide est du pseudo-premier ordre en méthylisonitrile et montre une relation linéaire entre la vitesse et la concentration en acide général (tampon) à p*H* déterminé. La signification d'une catalyse acide générale en terme de mécanisme d'hydrolyse est envisagée et constitue la preuve d'une protonation sur le carbone plutôt que sur l'azote, dans l'étape initiale.

Canadian Journal of Chemistry, **49**, 2455 (1971)

There have been numerous studies of the thermal rearrangement of isonitriles to nitriles, especially of methyl isonitrile in the vapor phase (1) and of the more complex reactions of isonitriles, most of which permit the synthesis of otherwise difficultly accessible nitrogen heterocyclic compounds (2). There is, however, a dearth of studies of the simpler chemistry of this fascinating if odoriferous class of compounds, the acid-catalyzed solvolysis being a case in point. Consequently, we have commenced such a study with an examination of the acid-catalyzed hydrolysis of methyl isonitrile to *N*-methylformamide.

Two mechanisms for the hydrolysis of isonitriles have on occasion been suggested, the first involving initial protonation on nitrogen, the other on carbon (3), eqs. 1 and 2 respectively.

Isonitriles are well known to give stable coordination compounds, especially with the softer metal cations (4) and to form strong hydrogen bonds with, for example, chloroform, alcohols, phenols, and water (5). Bonding in both cases is to the carbon of the isonitrile group. Consequently, the initial reversible formation of a hydrogen

[1]To whom correspondence should be addressed.

Can. J. Chem. Downloaded from www.nrcresearchpress.com by 210.87.254.5 on 09/05/12
For personal use only.

TABLE 1. Acidity and the rate constant for the acid-catalyzed hydrolysis of CH_3NC

p*H*	$a_{H_3O^\oplus}$ ($\times 10^{-4}$)	Number of runs	Average rate constant ($\times 10^{-4}$ s^{-1})
3.57	2.70	5	4.65 ± 0.18
3.78	1.66	3	3.53 ± 0.15
3.99	1.02	6	2.62 ± 0.12
4.18	0 66	6	1.96 ± 0.12
4.37	0.43	6	1.64 ± 0.09
4.59	0.26	6	1.18 ± 0.10
4.77	0.17	6	0.859 ± 0.042
4.97	0.11	6	0.656 ± 0.025

[1] $$RNC + H_3O^\oplus \rightleftharpoons R{-}\overset{H}{N}{=}C \; (\oplus) + H_2O \longrightarrow \longrightarrow RN(H){-}C(=O){-}H$$

[2] $$RNC + H_3\overset{\oplus}{O} \rightleftharpoons R{-}N{\equiv}CH \; (\oplus) + H_2O \longrightarrow \longrightarrow RN(H){-}C(=O){-}H$$

bond to carbon might be expected if the second mechanistic sequence were followed. Such hydrogen bonding – proton transfer should show general acid-catalysis since any acidic species present could take part.

For initial protonation on nitrogen (eq. 1), protonation would be much more difficult, requiring a stronger acid and might be expected to show little reversibility in aqueous medium. Here specific acid-catalysis should be observed. This mechanism would be somewhat analogous to the hydration of alkenes, for example isobutylene, where general acid-catalysis is absent and specific acid-catalysis alone is observed (6).

Experimental

Methyl isonitrile was prepared by a procedure slightly modified from that of Ugi *et al.* (7) and redistilled through an 8-in. Vigreux column, b.p. 58.5–59.5 °C, until no impurities were detectable by i.r. or gas chromatography. The product was stored in the dark in a refrigerator, with aliquots being removed as required.

The reaction solutions were made with doubly distilled deionized water. Aqueous stock solutions of reagent grade citric acid and potassium hydroxide were mixed to give the desired p*H* (Radiometer p*H* meter 4d, glass electrode) and concentration and potassium chloride added to give the constant ionic strength (1.333 *M* in potassium ion). After 5 ml of the solution in a thin-walled 10-ml flask fitted with a gum rubber septum had equilibrated in a water bath controlled to 30.00 °C by a Sargent Thermonitor, Model ST, 10 μl of methyl isonitrile was injected, the flask shaken, and the timer started. At time intervals such that 12–20 points could be obtained, 2-μl aliquots were removed with a Hamilton 10-μl syringe and injected directly onto the column of an Aerograph Model 1520B Gas Chromatograph equipped with an all glass system and a flame ionization detector. The column was a 5 ft × $\frac{1}{8}$ in. glass column packed with 0.2% OV-17 on 100–120 mesh glass beads operated at approximately 60 °C.

The area of the methyl isonitrile peak varied linearly with concentration and was used directly as a measure of the relative methyl isonitrile concentration. The p*H* of the reaction solution was the same prior to and after reaction.

Additional experimental detail will appear in a later paper.

Results

The hydrolysis of isonitriles is a two step process:

$$RNC + H_2O \xrightarrow{H^\oplus} RNHCOH$$

$$RNHCOH + H_3O^\oplus \longrightarrow \overset{\oplus}{R}NH_3 + HCO_2H$$

Both reactions or stages are acid-catalyzed but in acidic media, a proton is incorporated in the product of the second. Despite the fact that the first reaction is several orders of magnitude faster than the second and that in following the rate of disappearance of methyl isonitrile, only the first reaction need be considered, the fact that the second reaction incorporates a proton necessitated the use of a rather high buffer concentration to ensure that no detectable change in p*H* occurred, especially in the later stages of the reaction.

In Table 1 are presented the results of a study of the rate constant for the acid-catalyzed hydrolysis of methyl isonitrile as a function of the p*H* and

Can. J. Chem. Downloaded from www.nrcresearchpress.com by 210.87.254.5 on 09/05/12
For personal use only.

Can. J. Chem. Downloaded from www.nrcresearchpress.com by 210.87.254.5 on 09/05/12
For personal use only.

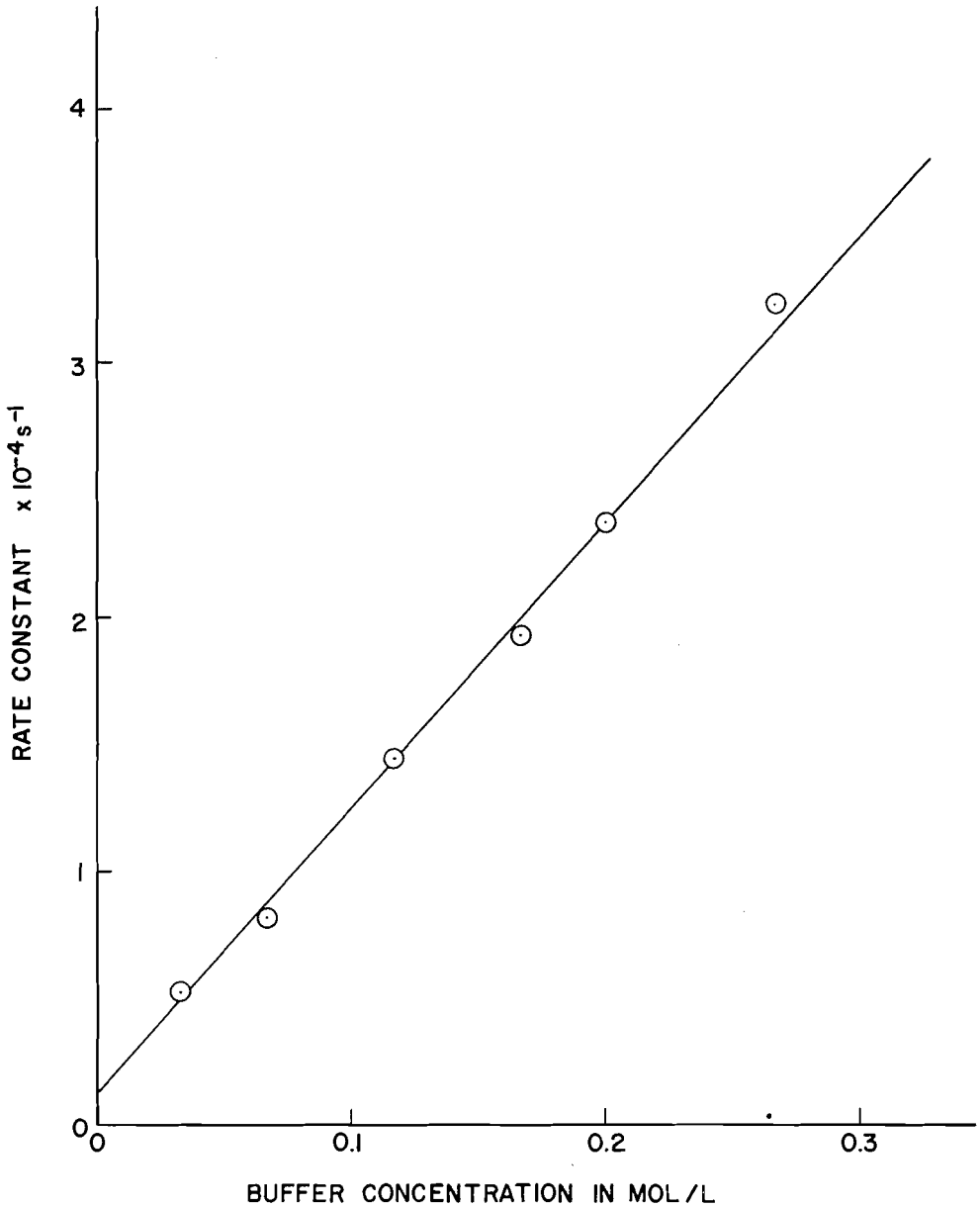

FIG. 1. Effect of citrate buffer concentration on the rate constant for the acid-catalyzed hydrolysis of methyl isonitrile; pH = 4.18; T = 30 °C; ionic strength = 1.33 M.

hydronium ion activity. Throughout this study, the ionic strength was maintained at 1.33 M in potassium ion, the buffer concentration at 0.167 M, and the temperature at 30.00 °C. When plotted as a function of pH, the catalytic rate constant approaches zero asymptotically at high pH and below a pH of 4.5 or 5, increases rapidly with decreasing pH.

Plotting the catalytic rate constant as a function of hydronium ion activity as determined with a glass electrode also gives a curve. Extrapolation to zero hydronium ion activity gives an intercept of zero or slightly greater but the rate of increase in the catalytic rate constant falls off with increasing hydronium ion activity. The acid-catalyzed hydrolysis of methyl isonitrile is then clearly not a

Can. J. Chem. Downloaded from www.nrcresearchpress.com by 210.87.254.5 on 09/05/12
For personal use only.

specific acid-catalyzed process. That the reaction is general acid-catalyzed was confirmed by varying the buffer concentration at constant p*H*.

The results of a study of the rate constant as a function of citrate buffer concentration are presented in Fig. 1. The p*H* was adjusted to 4.18 at each buffer concentration and the ionic strength and temperature were as before. Only at the lowest concentration was any change noted in the p*H* after the reaction period and this was only 0.01–0.02 p*H* unit. Taking the slope of the rate constant *vs.* p*H* curve at p*H* = 4.18, such a change would represent a maximum error in the rate constant of approximately 10%. The actual error from this source, however, should be much less since only in the later stages of the reaction would the concentration of *N*-methylformamide and hence its hydrolysis be significant and so affect the activity of the hydronium ion appreciably. Also no consistent curvature of the plots of the log of methyl isonitrile concentration *vs.* time for two and one half to three half lives was noted and the standard deviation in the least squares treatment of the data was not excessive, being about ±3.5% on the average of six runs at the lowest buffer concentration.

Discussion

The observation that the reaction shows general acid-catalysis means that the observed or experimental rate of disappearance of methyl isonitrile, equating activity and concentration, will be given by eq. 3.

$$[3] \qquad \frac{d[RNC]}{dt} = \{k_{H_3O^\oplus}[H_3O^\oplus] + k_{H_2O}[H_2O] + k_{HA}[HA] + k_{HA'}[HA'] + k_{HA''}[HA''] + \ldots\}[RNC]$$

By the Brønsted catalysis relationship, the log of the individual rate constants will be proportional to the log of the K_a of the acid in question. The values of the appropriate rate constants then will be:

$$k_{H_3O^\oplus} \gg k_{\text{citric I}} > k_{\text{citric II}} > k_{\text{citric III}} > k_{H_2O}$$

Since the study of $k_{obs.}$ *vs.* p*H* was done with fixed total buffer concentration, that is a constant initial amount of citric acid was used and potassium hydroxide solution added to give the desired p*H*, the concentration of citric acid is not constant at the different p*H*'s. Hence the contribution to the observed rate from the acid-catalysis by citric acid and the "bicitrates" would decrease as the activity of the hydronium ion decreased. At "zero" hydronium ion activity, the activities of the various citric acids would also be "zero" so that extrapolation of the $a_{H_3O^\oplus}$ *vs.* $k_{obs.}$ curve to zero hydronium ion activity should give an intercept of zero or, more accurately, at the catalytic rate constant for the only remaining acid, water. (The actual intercept is zero or slightly above but the extrapolation is not sufficiently accurate to assign a value to the water catalytic rate constant.)

The experimental observations are consistent with an acid-catalyzed hydrolysis in which there is a reversible initial hydrogen bonding between a general acid and the isonitrile carbon followed by a rate determining nucleophilic attack, also at carbon, by water. The mechanistic Scheme 1 is

$$RNC + HA \underset{}{\overset{K}{\rightleftharpoons}} RNC\cdots HA$$

$$RNC\cdots HA + H_2O \overset{k}{\rightleftharpoons} RN{=}C\begin{matrix}H\\OH\end{matrix} + HA$$

$$RN{=}C\begin{matrix}H\\OH\end{matrix} \overset{K}{\rightleftharpoons} RNHCOH$$

SCHEME 1

proposed. It must be emphasized that the alternate mechanism with initial protonation at nitrogen has not yet been ruled out but is unlikely in light of the present work. Subsequent papers will report additional results and elaborate upon the mechanistic conclusions presented here.

Financial support from the National Research Council of Canada and Memorial University of Newfoundland is gratefully acknowledged.

1. (*a*) D. SHAW, B. K. DUNNING, and H. O. PRITCHARD. Can. J. Chem. **47**, 669 (1969). (*b*) G. W. VAN DINE and R. HOFFMANN. J. Am. Chem. Soc. **90**, 3227 (1968). (*c*) J. CASANOVA JR., N. D. WERNER, and R. E. SCHUSTER. J. Org. Chem. **31**, 3473 (1966). (*d*) F. W. SCHNEIDER and B. S. RABINOVITCH. J. Am. Chem. Soc. **87**, 158 (1965).
2. See for example: (*a*) I. UGI. *In* Newer methods of preparative organic chemistry. *Edited by* W. Foerst. Verlag Chemie GMBH Weinheim/Bergstr. **4**, 1 (1968). (*b*) K. SJÖBERG. Sven. Kem. Tidskr. **75**, 493 (1963).
3. See for example: (*a*) T. SAEGUSA and Y. ITO. *In* Isonitrile chemistry. *Edited by* I. Ugi. Academic Press, New York, N.Y., 1971. p. 73. (*b*) M. KHALIFA. J. Pharm. Sci. U. Arab. Repub. **6**, 133 (1965).
4. See for example: (*a*) L. MALATESTA and F. BONATI. Isocyanide complexes of metals. John Wiley and Sons,

New York, N.Y., 1969. (*b*) F. A. COTTON and G. WILKINSON. Advanced inorganic chemistry. 2nd ed. Interscience Publishers, New York, N.Y., 1966. pp. 744–745.
5. (*a*) A. ALLERHARD and P. VON R. SCHLEYER. J. Am. Chem. Soc. **85**, 866 (1963). (*b*) L. L. FERSTANDIG. J. Am. Chem. Soc. **84**, 3553 (1962).
6. F. G. CIAPETTA and M. KILPATRICK. J. Am. Chem. Soc. **70**, 639 (1948).
7. (*a*) I. UGI *et al.* Agnew. Chem. Int. Ed. **4**, 472 (1965). See also: (*b*) E. J. COREY, *editor*. Organic synthesis. John Wiley and Sons, New York, N.Y. **46**, 75 (1966). (*c*) I. UGI. Reference 2*a*. pp. 52–53.

Far-infrared and Raman Spectra of Crystalline ICN

R. SAVOIE AND M. PÉZOLET

Centre de recherches sur les atomes et les molécules et Département de Chimie, Université Laval, Québec, Québec

Received March 25, 1971

The Raman and far-infrared spectra of crystalline cyanogen iodide have been recorded. High-frequency shoulders alongside the Raman bands confirm the piezoelectric nature of this solid and allow an estimate to be made of the frequencies of the longitudinal modes associated to the fundamental vibrations. Dipole derivatives calculated from these frequencies agree qualitatively with those obtained from infrared band intensity measurements.

Les spectres Raman et infrarouge lointain de l'iodure de cyanogène ont été enregistrés. Des épaulements à plus haute fréquence sur certaines bandes en Raman indiquent que le cristal est piézoélectrique et permettent d'estimer les fréquences des modes longitudinaux associés aux vibrations fondamentales. Les variations du moment dipolaire calculées à partir de ces fréquences sont qualitativement en accord avec les valeurs déduites de la mesure des intensités des bandes infrarouges.

Canadian Journal of Chemistry, **49**, 2459 (1971)

Introduction

The cyanogen iodide molecule, ICN, is known from electron diffraction (1) and microwave studies (2, 3) to be linear, with C—I and C—N bond lengths of 1.995 and 1.159 Å, respectively. The infrared spectra of the crystal reported by Freitag and Nixon (4), and the recent infrared intensity measurements by Bandy *et al.* (5), were found to be consistent with the reported crystal structure of this compound. An X-ray diffraction study (6) of crystalline cyanogen iodide has shown this solid to be built of parallel linear chains, the molecules being located on sites of C_{3v} symmetry. The crystal belongs to the trigonal system (space group C_{3v}^5-$R3m$), with one molecule per primitive cell.

Although ICN exists as a colorless solid at room temperature and seems well suited for Raman investigations, no such study has hitherto been reported. The only available Raman spectrum of cyanogen iodide was obtained with a photographic instrument, from a solution of ICN in methanol (7). Our main interest in this solid stemmed from the fact that it has a crystal structure somewhat similar to that of HCN, the Raman spectrum of which revealed anomalous dispersion on the high-frequency side of the fundamental bands (8). It has already been pointed out that such anomalies should occur in Raman spectra of non centro-symmetric crystals only (9). It was therefore expected that the fundamental bands in the Raman spectrum of crystalline ICN would be complicated by high-frequency shoulders, whereas such an effect was not detected in the spectra of ClCN and BrCN because of their centro-symmetric crystal structure (10).

Experimental

The cyanogen iodide used in our experiments was obtained by the reaction of an aqueous solution of NaCN with solid iodine, as described by Bak and Hillebert (11). The ICN thus produced was extracted with ether and recrystallized several times, first with cold water, and then with cold chloroform until a completely colorless solid was obtained. Purification was also accomplished by vacuum sublimation, but the final product then consisted of silky needles which proved very difficult to handle and gave poorer spectra.

The Raman spectrum was recorded on both a Cary 81 spectrometer with Toronto arc source and on a Spex

Can. J. Chem. Downloaded from www.nrcresearchpress.com by 210.87.254.5 on 09/05/12
For personal use only.

New York, N.Y., 1969. (*b*) F. A. COTTON and G. WILKINSON. Advanced inorganic chemistry. 2nd ed. Interscience Publishers, New York, N.Y., 1966. pp. 744–745.
5. (*a*) A. ALLERHARD and P. VON R. SCHLEYER. J. Am. Chem. Soc. **85**, 866 (1963). (*b*) L. L. FERSTANDIG. J. Am. Chem. Soc. **84**, 3553 (1962).
6. F. G. CIAPETTA and M. KILPATRICK. J. Am. Chem. Soc. **70**, 639 (1948).
7. (*a*) I. UGI *et al.* Agnew. Chem. Int. Ed. **4**, 472 (1965). See also: (*b*) E. J. COREY, *editor*. Organic synthesis. John Wiley and Sons, New York, N.Y. **46**, 75 (1966). (*c*) I. UGI. Reference 2*a*. pp. 52–53.

Far-infrared and Raman Spectra of Crystalline ICN

R. SAVOIE AND M. PÉZOLET

Centre de recherches sur les atomes et les molécules et Département de Chimie, Université Laval, Québec, Québec

Received March 25, 1971

The Raman and far-infrared spectra of crystalline cyanogen iodide have been recorded. High-frequency shoulders alongside the Raman bands confirm the piezoelectric nature of this solid and allow an estimate to be made of the frequencies of the longitudinal modes associated to the fundamental vibrations. Dipole derivatives calculated from these frequencies agree qualitatively with those obtained from infrared band intensity measurements.

Les spectres Raman et infrarouge lointain de l'iodure de cyanogène ont été enregistrés. Des épaulements à plus haute fréquence sur certaines bandes en Raman indiquent que le cristal est piézoélectrique et permettent d'estimer les fréquences des modes longitudinaux associés aux vibrations fondamentales. Les variations du moment dipolaire calculées à partir de ces fréquences sont qualitativement en accord avec les valeurs déduites de la mesure des intensités des bandes infrarouges.

Canadian Journal of Chemistry, **49**, 2459 (1971)

Introduction

The cyanogen iodide molecule, ICN, is known from electron diffraction (1) and microwave studies (2, 3) to be linear, with C—I and C—N bond lengths of 1.995 and 1.159 Å, respectively. The infrared spectra of the crystal reported by Freitag and Nixon (4), and the recent infrared intensity measurements by Bandy *et al.* (5), were found to be consistent with the reported crystal structure of this compound. An X-ray diffraction study (6) of crystalline cyanogen iodide has shown this solid to be built of parallel linear chains, the molecules being located on sites of C_{3v} symmetry. The crystal belongs to the trigonal system (space group C_{3v}^5-$R3m$), with one molecule per primitive cell.

Although ICN exists as a colorless solid at room temperature and seems well suited for Raman investigations, no such study has hitherto been reported. The only available Raman spectrum of cyanogen iodide was obtained with a photographic instrument, from a solution of ICN in methanol (7). Our main interest in this solid stemmed from the fact that it has a crystal structure somewhat similar to that of HCN, the Raman spectrum of which revealed anomalous dispersion on the high-frequency side of the fundamental bands (8). It has already been pointed out that such anomalies should occur in Raman spectra of non centro-symmetric crystals only (9). It was therefore expected that the fundamental bands in the Raman spectrum of crystalline ICN would be complicated by high-frequency shoulders, whereas such an effect was not detected in the spectra of ClCN and BrCN because of their centro-symmetric crystal structure (10).

Experimental

The cyanogen iodide used in our experiments was obtained by the reaction of an aqueous solution of NaCN with solid iodine, as described by Bak and Hillebert (11). The ICN thus produced was extracted with ether and recrystallized several times, first with cold water, and then with cold chloroform until a completely colorless solid was obtained. Purification was also accomplished by vacuum sublimation, but the final product then consisted of silky needles which proved very difficult to handle and gave poorer spectra.

The Raman spectrum was recorded on both a Cary 81 spectrometer with Toronto arc source and on a Spex

Can. J. Chem. Downloaded from www.nrcresearchpress.com by 210.87.254.6 on 09/05/12
For personal use only.

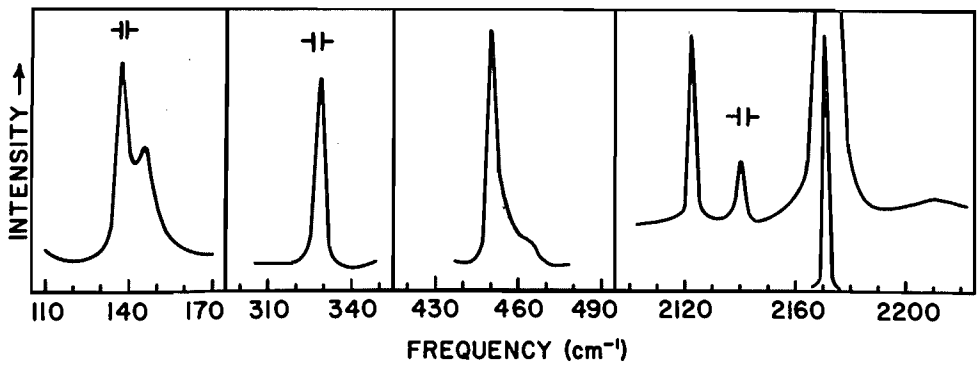

FIG. 1. Raman spectrum of crystalline ICN at −195 °C. Spectral slit widths in the 450 and 2170 cm^{-1} regions are 0.7 and 0.5 cm^{-1}, respectively.

(model 1400) monochromator with He–Ne laser source (Spectra Physics, model 125). These instruments were calibrated with a neon discharge lamp and the frequencies cited later are believed to be accurate to ± 1 cm^{-1}. Best results on the Cary spectrometer were obtained by using a conical cell (12) filled with very small crystals. With the laser instrument, a large polycrystalline needle, obtained by slow evaporation of a chloroform solution, was studied in a sealed capillary tube. The low-temperature spectra were recorded with the sample cells placed inside flat-end Dewar and cooled by a flow of cold nitrogen gas.

The far-infrared spectrum was recorded on a model FS-720 RIIC interferometer coupled to a Fourier transform computer (RIIC, model FTC-100/7). The theoretical resolution of this instrument in the 20–200 cm^{-1} region is 1.25 cm^{-1} and the frequency accuracy is estimated at 1 cm^{-1}. A conventional cryostat with polyethylene external windows was used to obtain the low-temperature spectrum. Samples were deposited from the vapor onto a wedge-shaped silicon plate cooled to −100 °C. Annealing, which in most cases resulted in partial loss of the deposited film, was done by raising the temperature to about −30 °C.

Results and Discussion

The Raman spectrum of crystalline ICN at liquid nitrogen temperature is reproduced in Fig. 1 and observed frequencies are given in Table 1. The far-infrared spectrum is not reproduced here since it contains a single band, with a half-width of about 15 cm^{-1}, located at 136 cm^{-1}.

Using standard group-theoretical procedures (13), it can be predicted that both the infrared and Raman spectra of crystalline ICN should be extremely simple. The correlation diagram (Table 2) indicates no splitting of the bands from either the site or coupling effect. As for the lattice vibrations, only one doubly degenerate (R_{xy}) librational mode is predicted, the three translations becoming acoustic modes with zero limiting frequency in the crystal. Coincidence of the Raman and infrared frequencies is also expected, the same vibrations being active in both types of spectra.

Although the main features of the Raman spectrum of crystalline ICN are in agreement with the above predictions, it is clear that many of the fundamental bands are complicated by anomalous high-frequency shoulders, as was the case in HCN (8). The effect is slight in the C—N stretching (ν_3) region where only an asymmetry of the band is seen. In the C—I stretching (ν_1) region however, a shoulder extending about 20 cm^{-1} from the main peak is clearly visible. In the region of the librational mode, this shoulder is of such proportion as to make the band appear as a well defined doublet.

We have already pointed out (9) that such features, related to the splitting of vibrations into transverse and longitudinal components, are likely to occur in Raman spectra of piezoelectric molecular crystals whenever a large variation of the electric dipole moment results from a particular vibration. To verify this interpretation in the present case, we have estimated the dipole derivatives for the fundamental vibrations using the formula of Haas and Hornig (14). In this calculation, the crystal density was taken as 3.1 g/cm^3 (6) and the refractive index as 1.64 (15). Calculated values for the $\partial\mu/\partial Q$ (see Table 1) agree qualitatively with those obtained from infrared band intensity measurements (5), which indicates that our explanation for the shoulders alongside the Raman fundamentals is most likely correct.

Can. J. Chem. Downloaded from www.nrcresearchpress.com by 210.87.254.6 on 09/05/12
For personal use only.

TABLE 1. Vibrational frequencies and dipole derivatives in crystalline ICN

Frequencies (cm^{-1})				$\partial\mu/\partial Q$ (e.s.u. $g^{-1/2}$)	
Infrared (~ -190 °C)	Raman 35 °C	Raman -195 °C	Assignment	Calcd.	Reference 5
136*	127	136 151‡	R_{xy} ν_t, ν_l	33	—
327†	330	329 <330‡	ν_2 ν_t, ν_l	<13	11.1
451†	456	449 465‡	ν_1 ν_t, ν_l	61	73.3
2125†	2122	2124	$\nu_3(^{13}C)$		
2142†	2139	2141	$\nu_3(^{15}N)$		
2172.5*	2169	2172 ~2175‡	ν_3 ν_t, ν_l	~58	65.7
	2200	2210	ν_3 + ν(lattice)		

*Present results.
†Reference 4.
‡Cutoff frequency of the shoulder alongside the fundamental band.

TABLE 2. Symmetry correlation diagram for crystalline ICN

Modes	Free molecule $C_{\infty v}$	Site C_{3v}	Crystal C_{3_1}	Activity
(ν_1, ν_3, T_z)	A_1	A_1	A_1	Raman, i.r.
(ν_2, R_{xy}, T_{xy})	E_1	E	E	Raman, i.r.

There is an apparent discrepancy between the reported infrared frequencies (4) of the fundamentals of crystalline ICN and the measured Raman frequencies. The difference in the ν_1 and ν_2 regions is not serious since it is within the probable combined experimental error on frequency measurements ($\pm 2\ cm^{-1}$). The reported ν_3 infrared frequency ($2176\ cm^{-1}$), however, differs significantly from that in the Raman spectrum ($2172\ cm^{-1}$). In order to clarify this point, we have reinvestigated the infrared spectrum in this region. (Experiments were performed on a Perkin–Elmer model 621 spectrometer.) We found that the ν_3 peak frequency was located at 2172–2173 cm^{-1}, which means that there is indeed coincidence of the Raman and infrared frequencies. A somewhat different behavior was observed in our far-infrared study, the frequency of the librational mode taking different values ranging from 136 to 141 cm^{-1}. When well-annealed very thin films were studied, however, peak frequencies were in most cases almost identical to the corresponding Raman frequency. It seems that as the film thickness is increased reflection, which should extend approximately to the longitudinal frequency (16), causes an apparent blue shift of this band maximum.

An interesting feature in the Raman spectrum of crystalline ICN is the weak band at 2200 cm^{-1}, which we tentatively assign to a combination of ν_3 and a lattice vibration. It is clear that this transition then has to occur at $\boldsymbol{k} \neq 0$, which is rather uncommon, although it is not theoretically forbidden (17). A similar phenomenon has been found to occur in solid OCS (18).

The authors gratefully acknowledge financial support of this work by the National Research Council of Canada. One of us (M.P.) is also indebted to this organization for a graduate fellowship.

1. J. Y. BEACH and A. TURKEVICH. J. Am. Chem. Soc. **61**, 299 (1939).
2. C. H. TOWNES, A. N. HOLDEN, and F. R. MERRITT. Phys. Rev. **74**, 1113 (1948).
3. W. LOW. Phys. Rev. **97**, 1664 (1955).
4. W. O. FREITAG and E. R. NIXON. J. Chem. Phys. **24**, 109 (1956).

Can. J. Chem. Downloaded from www.nrcresearchpress.com by 210.87.254.6 on 09/05/12
For personal use only.

5. A. R. BANDY, H. B. FRIEDRICH, and W. B. PERSON. J. Chem. Phys. **53**, 674 (1970).
6. J. A. A. KETELAAR and J. W. ZWARTSENBERG. Rec. Trav. Chim. **58**, 448 (1939).
7. W. WEST and M. FARNSWORTH. J. Chem. Phys. **1**, 402 (1933).
8. M. PÉZOLET and R. SAVOIE. Can. J. Chem. **47**, 3041 (1969).
9. R. SAVOIE and M. PÉZOLET. J. Chem. Phys. **50**, 2781 (1969).
10. M. PÉZOLET and R. SAVOIE. J. Chem. Phys. To be published.
11. B. BAK and A. HILLEBERT. Org. Synth. **32**, 29 (1952).
12. R. H. BUSEY and O. L. KELLER, JR. J. Chem. Phys. **41**, 215 (1964).
13. D. F. HORNIG. J. Chem. Phys. **16**, 1063 (1948). H. WINSTON and R. S. HALFORD. J. Chem. Phys. **17**, 607 (1949).
14. C. HAAS and D. F. HORNIG. J. Chem. Phys. **26**, 707 (1957).
15. A. R. BANDY. Ph.D. Thesis. University of Florida, Gainesville, 32601. 1968.
16. J. A. A. KETELAAR, C. HAAS, and J. FAHRENFORT. Physica, **20**, 1259 (1954).
17. S. S. MITRA. J. Chem. Phys. **39**, 3031 (1963).
18. J. E. CAHILL, K. L. TREUIL, R. E. MILLER, and G. E. LEROI. J. Chem. Phys. **49**, 3320 (1968).

The Removal of Oxide Impurities from Alkali Metal Fluoride Melts by Additions of Silver Halide

SYDNEY H. WHITE

Department of Chemical Engineering, University of New Brunswick, Fredericton, New Brunswick

Received September 2, 1970[1]

Electrochemical and chemical studies have shown that AgF and AgCl react quantitatively with oxide ions and hydroxide ions present as residual impurities in molten FLiNaK. This reaction offers a method for the simultaneous determination and removal of oxide containing impurities in fluoride melts.

Les études chimiques et électrochimiques ont montré que AgF et AgCl réagissent quantitativement avec les ions oxydes et les ions hydroxydes qui se trouvent à l'état d'impuretés résiduelles dans le FLiNaK fondu. Cette réaction permet d'avoir une méthode simultanée de détermination et d'élimination des impuretés contenant des oxydes dans des fluorures fondus.

Canadian Journal of Chemistry, 49, 2462 (1971)

The necessity of high purity, oxide-free, alkali metal fluoride melts for electrochemical studies has been emphasized (ref. 1, p. 529). Pizzini *et al.* (2) estimated that melts purified by conventional molten salt techniques (ref. 1, p. 532) contain oxygen impurities in the form of hydroxide at 10^{-2} to 10^{-1} formal concentration. In this note, a reaction is reported which leads to a method by which oxide impurities may be determined and removed simultaneously from alkali metal fluoride melts.

A chronopotentiometric study of silver halide dissolved in molten FLiNaK (lithium fluoride–sodium fluoride–potassium fluoride eutectic mixture) at 500 °C showed that small additions say 50–100 mg of AgCl or AgF gave transition times which were time dependent (Fig. 1). The con-

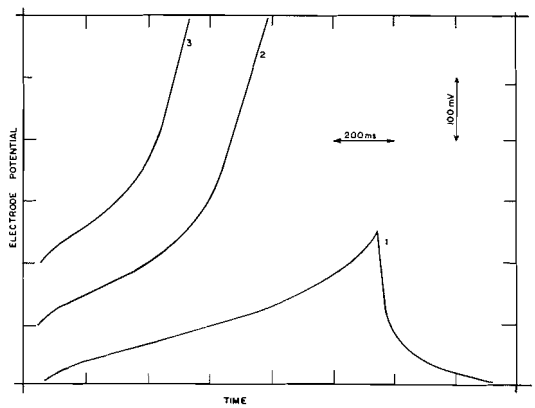

FIG. 1. Time dependence of the transition time for the initial addition of AgCl to a FLiNaK melt. mV/cm = 100, ms/cm = 200. (*1*) 7 min after addition of AgCl. (*2*) 13 min after addition of AgCl. (*3*) 26 min after addition of AgCl.

[1]Revision received April 19, 1971.

Can. J. Chem. Downloaded from www.nrcresearchpress.com by 210.87.254.6 on 09/05/12
For personal use only.

5. A. R. BANDY, H. B. FRIEDRICH, and W. B. PERSON. J. Chem. Phys. **53**, 674 (1970).
6. J. A. A. KETELAAR and J. W. ZWARTSENBERG. Rec. Trav. Chim. **58**, 448 (1939).
7. W. WEST and M. FARNSWORTH. J. Chem. Phys. **1**, 402 (1933).
8. M. PÉZOLET and R. SAVOIE. Can. J. Chem. **47**, 3041 (1969).
9. R. SAVOIE and M. PÉZOLET. J. Chem. Phys. **50**, 2781 (1969).
10. M. PÉZOLET and R. SAVOIE. J. Chem. Phys. To be published.
11. B. BAK and A. HILLEBERT. Org. Synth. **32**, 29 (1952).
12. R. H. BUSEY and O. L. KELLER, JR. J. Chem. Phys. **41**, 215 (1964).
13. D. F. HORNIG. J. Chem. Phys. **16**, 1063 (1948). H. WINSTON and R. S. HALFORD. J. Chem. Phys. **17**, 607 (1949).
14. C. HAAS and D. F. HORNIG. J. Chem. Phys. **26**, 707 (1957).
15. A. R. BANDY. Ph.D. Thesis. University of Florida, Gainesville, 32601. 1968.
16. J. A. A. KETELAAR, C. HAAS, and J. FAHRENFORT. Physica, **20**, 1259 (1954).
17. S. S. MITRA. J. Chem. Phys. **39**, 3031 (1963).
18. J. E. CAHILL, K. L. TREUIL, R. E. MILLER, and G. E. LEROI. J. Chem. Phys. **49**, 3320 (1968).

The Removal of Oxide Impurities from Alkali Metal Fluoride Melts by Additions of Silver Halide

SYDNEY H. WHITE

Department of Chemical Engineering, University of New Brunswick, Fredericton, New Brunswick

Received September 2, 1970[1]

Electrochemical and chemical studies have shown that AgF and AgCl react quantitatively with oxide ions and hydroxide ions present as residual impurities in molten FLiNaK. This reaction offers a method for the simultaneous determination and removal of oxide containing impurities in fluoride melts.

Les études chimiques et électrochimiques ont montré que AgF et AgCl réagissent quantitativement avec les ions oxydes et les ions hydroxydes qui se trouvent à l'état d'impuretés résiduelles dans le FLiNaK fondu. Cette réaction permet d'avoir une méthode simultanée de détermination et d'élimination des impuretés contenant des oxydes dans des fluorures fondus.

Canadian Journal of Chemistry, 49, 2462 (1971)

The necessity of high purity, oxide-free, alkali metal fluoride melts for electrochemical studies has been emphasized (ref. 1, p. 529). Pizzini *et al.* (2) estimated that melts purified by conventional molten salt techniques (ref. 1, p. 532) contain oxygen impurities in the form of hydroxide at 10^{-2} to 10^{-1} formal concentration. In this note, a reaction is reported which leads to a method by which oxide impurities may be determined and removed simultaneously from alkali metal fluoride melts.

A chronopotentiometric study of silver halide dissolved in molten FLiNaK (lithium fluoride–sodium fluoride–potassium fluoride eutectic mixture) at 500 °C showed that small additions say 50–100 mg of AgCl or AgF gave transition times which were time dependent (Fig. 1). The con-

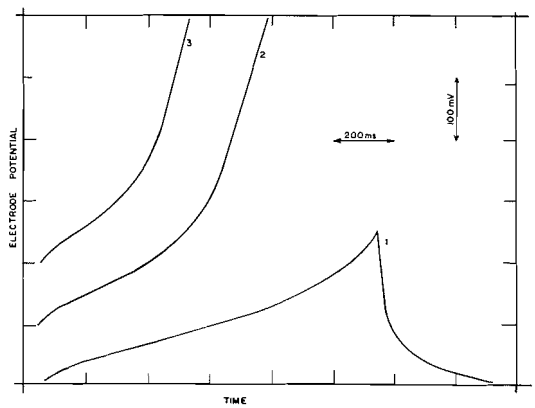

FIG. 1. Time dependence of the transition time for the initial addition of AgCl to a FLiNaK melt. mV/cm = 100, ms/cm = 200. (*1*) 7 min after addition of AgCl. (*2*) 13 min after addition of AgCl. (*3*) 26 min after addition of AgCl.

[1]Revision received April 19, 1971.

Can. J. Chem. Downloaded from www.nrcresearchpress.com by 210.87.254.105 on 09/05/12
For personal use only.

TABLE 1. Calculated thermodynamic data relating to reaction 4 at 1000 °K*

	Fluorides			Chlorides		
Oxide	$(\Delta G_R°)^{1000}$ (kcal/mol)	K oxide	a_{M_2O}	$(\Delta G_R°)^{1000}$ (kcal/mol)	K oxide	a_{M_2O}
Li_2O	−57.9	4.6×10^{12}	5.4×10^{-17}	+4.5	0.96×10^{1}	2.6×10^{-5}
Na_2O	−77.4	8.9×10^{16}	2.8×10^{-21}	−44.6	5.5×10^{9}	4.5×10^{-14}
K_2O	−86.0	6.5×10^{18}	3.9×10^{-23}	−68.6	1.0×10^{15}	2.5×10^{-19}

*Thermodynamic data on which the calculations are based were taken from ref. 5. It was assumed that $a_{Ag} = 1$, $a_{MX} = 0.5$, $a_{AgX} = 0.001$, and $p_{O2} = 10^{-18}$ atm, which might be typical values encountered under experimental conditions.

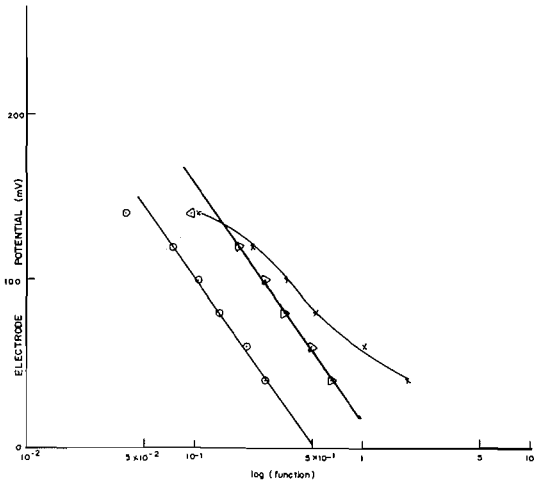

FIG. 2. Electrode potential *vs.* (*a*) $\log(\tau^{1/2} - t^{1/2})$ ○, (*b*) $\log 1 - (t/\tau)^{1/2}$ ▽, (*c*) $\log(\tau/t)^{1/2} - 1$ ×. Slope (*a*) = 143 mV (n = 1.08).

tinued addition of the silver halide finally resulted in a stable time independent transition time for silver ions. The transition time τ was determined, using a silver wire microelectrode, as a function of applied current i for the stabilized solution of silver ions. The product $i\tau^{1/2}$ was found to be a constant in accord with the Sand's equation

$$[1] \qquad i\tau^{1/2} = \frac{nF\pi^{1/2}D^{1/2}CA}{2}$$

for a diffusion controlled process (3) where the symbols have their usual meaning. A potential time analysis is shown in Fig. 2. The best fit is obtained using the equation for a reversible reduction process involving the formation of a solid product (4). This is supported by current reversal experiments (see Fig. 1 (*1*)). The number of electrons, n, involved in the overall reduction process was found from the slope in Fig. 2 to be equal to unity, *i.e.*

$$[2] \qquad Ag^+ + e \rightarrow Ag \text{ (solid)}$$

These observations suggest that the silver ions initially added to the FLiNaK melt were removed quantitatively by a reaction with oxygen containing impurities in the melt, *e.g.*

$$[3] \quad 2AgF(soln) + Li_2O(soln) \rightleftharpoons 2Ag(solid) + 2LiF(soln) + \tfrac{1}{2}O_2(gas)$$

Small beads of a silvery metal, determined chemically to be silver, were found in the base of a solidified ingot of FLiNaK in which time dependent transition times had been observed. This reaction between silver ions and oxide impurities is supported by the following experiment. A small pellet (24.5 mg) of sodium hydroxide was added to a stabilized solution of silver ions in FLiNaK melt. Transition time measurements before and after the addition of NaOH show that silver ions were removed quantitatively from the melt (Fig. 3).

Further confirmation for the proposed reaction 3 can be obtained from thermodynamic data calculated for the reaction

$$[4] \quad 2AgX(liq) + M_2O(solid) \rightleftharpoons 2Ag(solid) + 2MX(solid) + \tfrac{1}{2}O_2(gas)$$

where $X^- = F^-$, Cl^- and $M^+ = Li^+$, Na^+,

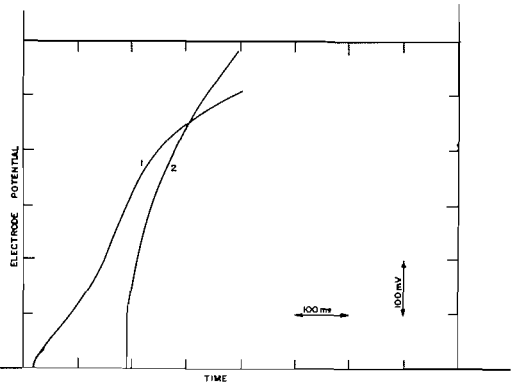

FIG. 3. Chronopotentiograms (*1*) before (*2*) after addition of NaOH to FLiNaK containing Ag^+ ions. mV/cm = 100, ms/cm = 100, i = 0.8 mA.

Can. J. Chem. Downloaded from www.nrcresearchpress.com by 210.87.254.105 on 09/05/12
For personal use only.

K^+. The results of these calculations are summarized in Table 1. The equilibrium activity of oxide a_{M_2O} is found to be very small in the case of the fluorides. The calculations although based on thermodynamic data for the pure substances (5), indicate that reactions such as [3] should be quantitative for dilute solutions in molten alkali metal fluorides and their mixtures. These predictions for fluoride melts are contrasted with those for chloride melts in Table 1.

The oxide ion impurity was found to be between 2 and 3×10^{-2} M in the melts used in this work.

1. G. MAMANTOV. *In* Molten salts. *Edited by* G. Mamantov. M. Dekker, New York. 1969.
2. S. PIZZINI, R. MORLOTTI, and E. ROEMER. J. Electrochem. Soc. **113**, 1305 (1966).
3. H. F. S. SAND. Phil. Mag. **1**, 45 (1901). P. DELAHAY and G. MAMANTOV. Anal. Chem. **27**, 478 (1955).
4. P. DELAHAY. New instrumental methods in electrochemistry. Interscience Inc., New York. 1954. Chap. 8.
5. C. J. SMITHELLS. Metals reference book. Vol. 2. Butterworths, London. 1962. p. 633.

Can. J. Chem. Downloaded from www.nrcresearchpress.com by 210.87.254.105 on 09/05/12
For personal use only.

Can. J. Chem. Downloaded from www.nrcresearchpress.com by 210.87.254.42 on 09/05/12
For personal use only.

Ozonolysis of Acetals. (*1*) Ester Synthesis, (*2*) THP Ether Cleavage, (*3*) Selective Oxidation of β-Glycoside, (*4*) Oxidative Removal of Benzylidene and Ethylidene Protecting Groups[1]

PIERRE DESLONGCHAMPS[2] AND CLAUDE MOREAU
Laboratoire de synthèse organique, Département de chimie, Université de Sherbrooke, Sherbrooke, Québec

Received April 20, 1971

Ozone reacts very smoothly with acetals to give the corresponding esters. Tetrahydropyranyl ethers, β-glycopyranosides, ethylidene, or benzylidene derivatives are also oxidized whereas the α-glycopyranosides are inert.

Les acétals se transforment facilement en esters correspondants sous l'action de l'ozone. Les éthers de tétrahydropyrannyle, les β-glucopyrannosides, les dérivés éthylidéniques et benzylidéniques sont facilement oxydés tandis que les α-glucopyrannosides résistent à l'ozone.

Canadian Journal of Chemistry, 49, 2465 (1971)

We wish to report the discovery that ozone reacts in essentially quantitative yield and in a complete specific manner with the acetal function to give the corresponding ester.

For example, acetal **1** dissolved in dichloromethane or ethyl acetate reacts quantitatively within 10 min at −78 °C with ozone to give the ester **2**.[3] Similarly, acetal **3** gives the methyl ester **4**[4] (90% yield) but the rate of this reaction is considerably slower (15 h at −78 °C or more conveniently 1.5 h at room temperature).

The generality of this reaction has been confirmed by obtaining similar results with acetals made from different aldehydes (*n*-heptanal, cyclohexanecarboxaldehyde, and benzaldehyde) and different types of alcohol (methanol, ethanol, ethylene glycol, 1,3-propanediol, and 2,2-dimethyl-1,3-propanediol). The cyclic acetals react readily at −78 °C within 2 h while the acyclic ones require approximately the same period of time, but at room temperature.

This new reaction constitutes a novel method for converting an aldehyde into an ester.

It is assumed that this reaction proceeds via insertion of ozone in the C—H bond of the acetal to give a hydrotrioxide intermediate such as **5** which then gives the corresponding ester and alcohol functions. Such an insertion reaction has been shown to be operative in the reaction of ozone with simple ether (1).

Ozone reacts with **6** (ethyl acetate, −78 °C, 1.5 h, 97% yield) in a complete specific manner to give exclusively **7**.[3] No trace of lactone **8** could be detected. A similar result was obtained with **9**. Thus, this reaction constitutes also a new highly efficient method for the cleavage of the tetrahydropyranyl protecting group.

Some conformationally rigid tetrahydropyranyl ethers were also investigated. Methyl 2,3,4,6-tetra-*O*-acetyl-β-D-glucopyranoside (**10**) dissolved in acetic anhydride – sodium acetate[5] reacts with ozone (room temperature, 15 h) to give methyl 2,3,4,5,6-penta-*O*-acetyl-gluconate (**11***b*, 95% yield, (2)). *The corresponding α anomer*

[1]Support for this work by the National Research Council of Canada, the Alfred P. Sloan Foundation, and by the "Ministère de l'Education" Québec, is gratefully acknowledged.

[2]A. P. Sloan Fellow, 1970–1972. To whom inquiries should be addressed.

[3]The corresponding acetate derivative gave satisfactory analytical data.

[4]This compound was identified by comparison with an authentic sample.

[5]The reaction proceeds at a similar rate in CH_2Cl_2 or ethyl acetate. The Ac_2O–AcONa system is used to trap **11***a* *in situ* (**11***a* being a secondary alcohol, it slowly reacts with ozone at room temperature).

Can. J. Chem. Downloaded from www.nrcresearchpress.com by 210.87.254.42 on 09/05/12
For personal use only.

1 2

3 4

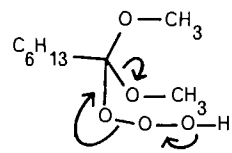

5

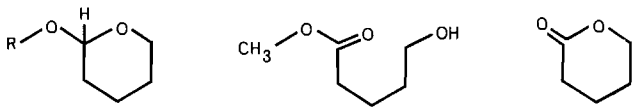

6 R = Methyl
9 R = Cyclohexyl 7 8

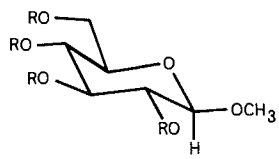

10 R = CH_3CO

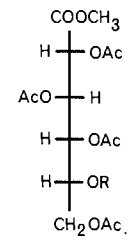

11a R = H
11b R = CH_3CO

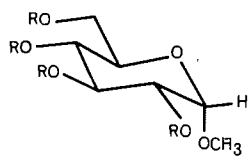

12 R = CH_3CO

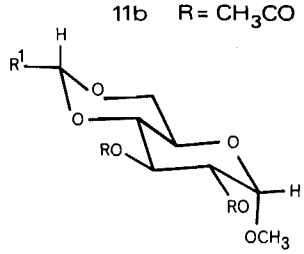

13 R = CH_3CO $R^1 = CH_3$
14 R = CH_3CO $R^1 = C_6H_5$

12, however, was shown to be completely unaffected under the same condition.[6,7]

Furthermore, methyl 4,6-*O*-ethylidene-2,3-di-*O*-acetyl-α-D-glucopyranoside (**13**) (5), dissolved in acetic anhydride – sodium acetate, was treated with an excess of ozone during 1 h at room temperature. The resulting mixture was then heated to reflux for 1 h to complete the acetylation and gave after usual work-up a quantitative yield of **12**.[4] Ozonolysis of methyl 4,6-*O*-benzylidene-2,3-di-*O*-acetyl-α-D-glucopyranoside (**14**) (6) gave **12**[4] (acetic acid, 1 h) after hydrolysis (triethylamine in 70% aqueous methanol (7)) and acetylation (Ac_2O–AcONa, reflux, 1 h). Ozone can therefore be used for the removal of ethylidene and benzylidene protecting group.[8,9]

The preceding results clearly indicate that this new ozonolysis reaction should find many important applications in the carbohydrate field. Ozone could in principle be used as a method of purification of α anomer from an α and β anomeric mixture by selective chemical transformation of the β isomer. These results also suggest that this ozonolysis reaction works only if the acetal function can assume a conformation in which both oxygens of the acetal can have one of their lone-pair orbitals oriented *trans*-antiparallel to the C—H bond. Such arrangement is impossible for the α-glycosides.

An investigation of the mechanism as well as the scope and limitation of this new reaction is under active study.

[6]Similarly, methyl 3,4,6-tri-*O*-acetyl-2-deoxy-β-D-glucopyranoside (3) was rapidly ozonized (1 h, room temperature), while the corresponding α anomer (3) was completely inert.

[7]It should be noted that Angyal and James (4) have recently shown that **10** and **12** are oxidized with chromium trioxide in glacial acetic acid. The β anomer (**10**) gave a keto ester while the α anomer (**12**) suffered oxidation of the methoxyl group.

[8]The regioselectivity for the oxidation cleavage of **13**, **14** (8, 9), and related compounds are being studied.

[9]It should be noted that Marvel and Joncich (10) have reported the oxidation of benzaldehyde diethyl acetal into ethyl benzoate by *N*-bromosuccinimide (NBS). The oxidation of benzylidene derivatives of cyclohexane-1,2-diols with molecular oxygen and NBS has also been reported (11). The NBS oxidation reaction has also been carried out on various types of acetals (12) and extended to benzylidene derivatives of the carbohydrates (8 and 9).

1. C. C. PRICE and A. L. TOMOLO. J. Am. Chem. Soc. **86**, 4691 (1964); R. E. ERICKSON, R. T. HANSEN, and J. HARKINS. J. Am. Chem. Soc. **90**, 6777 (1968).
2. R. T. MAJOR and E. W. COOK. J. Am. Chem. Soc. **58**, 2474 (1936); G. B. ROBBINS and F. W. UPSON. J. Am. Chem. Soc. **62**, 1074 (1940).
3. G. R. INGLIS, J. C. P. SCHWARZ, and L. MCLAREN. J. Chem. Soc. 1014 (1962).
4. S. J. ANGYAL and K. JAMES. Chem. Commun. 617 (1969) and Aust. J. Chem. **23**, 1209 (1970).
5. J. HONEYMAN and J. W. W. MORGAN. J. Chem. Soc. 3660 (1955); J. HONEYMAN and T. C. STENING. J. Chem. Soc. 3316 (1957).
6. D. S. MATHERS and G. J. ROBERTSON. J. Chem. Soc. 696 (1933).
7. T. L. NAGABHUSHAN. Can. J. Chem. **48**, 383 (1970).
8. S. HANESSIAN. Carbohydr. Res. **2**, 86 (1966); S. HANESSIAN and N. R. PLESSAS. J. Org. Chem. **34**, 1035, 1045, 1053 (1969).
9. D. L. FAILLA, T. L. HULLAR, and S. B. SISKIN. Chem. Commun. 716 (1966).
10. E. N. MARVEL and M. J. JONCICH. J. Am. Chem. Soc. **73**, 973 (1951).
11. A. RIECHE, E. SCHMITZE, W. SCHADE, and E. BEYER. Chem. Ber. **94**, 2926 (1961).
12. J. D. PRUGH and W. C. MCCARTHY. Tetrahedron Lett. 1351 (1966).

Can. J. Chem. Downloaded from www.nrcresearchpress.com by 210.87.254.42 on 09/05/12
For personal use only.

Thermal Conductivity, Anomaly in Temperature-dependence for Liquids[1]

J. E. S. VENART[2] AND N. MANI
Department of Mechanical Engineering, The University of Calgary, Calgary 44, Alberta

Received December 30, 1970

Most empirical equations express the thermal conductivity of normal simple liquids as linear functions of temperature. The majority of measurements to date, except water, support such a description. Very precise new measurements on toluene over the complete liquid range at 1 atm ($0.299 < T_r < 0.645$) show a substantial pre-freezing anomaly. At the freezing point (t_f) there is a depression of the expected conductivity of 7.9×10^{-3} W/m °K. This t_f behavior is attributed to cluster formation.

La plupart des équations empiriques expriment la conductivité thermique de liquides simples et normaux comme des fonctions linéaires de la température. Jusqu'à présent la majorité des mesures, excepté pour l'eau, sont en accord avec ce point de vue. De nouvelles mesures très précises avec le toluène, sur tout l'intervalle liquide et à une atmosphère ($0.299 < T_r < 0.645$), montrent un certain degré d'anomalie au point de précongélation. Au point de congélation (t_f) il y a une dépression par rapport à la conductivité attendue de 7.9×10^{-3} W/m °K. Ce comportement à la t_f est attribué à la formation d'agrégat.

Canadian Journal of Chemistry, 49, 2468 (1971)

Introduction

It is well known in viscometry that deviations from the usual Arrhenius type expression can occur as the freezing point is approached. This behavior is explained on the basis of the formation of multi-molecular clusters in the liquid state (1). Since it seems likely (2) that liquids conduct heat mainly through vibrational transfers, other methods of transfer such as molecular convection and radiation contribute on a small scale. It could thus be expected that for liquids formed of complex molecules, the formation of clusters near the freezing point would appreciably increase the scattering of phonons and hence decrease the conductivity over that normally expected (3).

Experimental difficulties, to date, have precluded any completely definitive attribution to this effect and for most simple normal liquids the thermal conductivity is generally characterized as decreasing linearly with increasing temperature;

$$[1] \qquad \lambda = A' - B't$$

Attempts to interpret the coefficients A' and B' are few (2) and it can only be stated that this type of behavior has been experimentally confirmed for simple liquids (Ar, Kr, Xe) (4) and other fluids. Even for some complex liquids at *sufficiently high temperature* the linear law seems to follow over a portion of the liquid range. Experimental evidence for the above mentioned anomaly and linear behavior is reported here for toluene.

Experimental

A modification of the absolute transient line source apparatus (5) was employed using A.R. grade toluene (99.96% pure conforming to ACS specifications: S < 0.003%, H_2O < 0.03%, residue after evaporation < 0.001%).[3] The measurements shown in Fig. 1 are

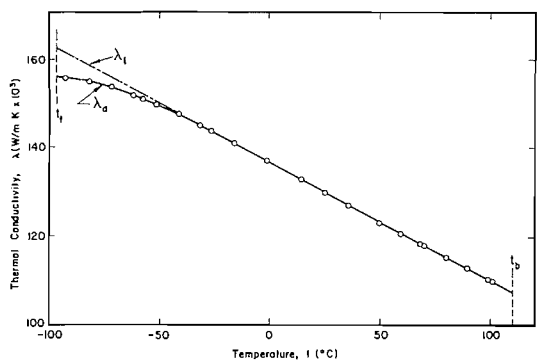

FIG. 1. Thermal conductivity of toluene at atmospheric pressure.

[1]Work supported by the National Research Council of Canada, under Grant Number NRC A2788.

[2]Present address: Visiting Fellow, School of Applied Sciences, University of Sussex, Falmer, Brighton, England.

[3]Checks on gross impurities were made by examination of the i.r. spectra and refractive index of samples before and after the experiments.

Can. J. Chem. Downloaded from www.nrcresearchpress.com by 210.87.254.6 on 09/05/12
For personal use only.

obtained with a precision of about 4000 p.p.m. by measuring the voltage–time behavior of a 25 μm platinum line source immersed in the fluid and pulsed with a constant current sufficient to produce temperature rises of 1 to 2 °C in 5 s. Experimental procedure is such that convection and radiation effects can be minimized.

Discussion

For toluene *sufficiently high temperature*, that is, the temperature range wherein conduction can be treated as consisting of the contributions of single molecules, was observed to occur between −25 and 101 °C; over this range a value of $A' = (136.7_7 \pm 0.25_3)$ mW/m °K and $B' = (0.295_2 \pm 0.7_4 \times 10^{-3})$ mW/m °K^2 were found. Letting this expression yield the *normal* or expected value λ_i by extrapolation to t_f, we can now consider the experimental deviations of the actual values λ_a. If the deviations near t_f were due to cluster formation, it would be expected that these deviations might follow a rate process and thus be governed by the Arrhenius type expression

$$\lambda_a/\lambda_i = 1 - A \exp(B/\sqrt{T^*})$$

where

$$T^* = (T - T')/(T_f - T)$$

Analysis of the data by the above expression yields the establishment of a t_f depression of 7.9×10^{-3} W/m °K with $A = 0.07144$ and $B = -1.74936$. The temperature T' at which the anomaly has been observed to vanish is numerically estimated as 148 °K. The data analysis further suggests that the pre-freezing anomalous behavior is dependent more upon $B/\sqrt{T^*}$ rather than B/T^*. This latter implication may thus advocate a scaling of the property (6).

Conclusion

A substantial pre-freezing anomaly has been shown to exist in the thermal conductivity of toluene. It is postulated that this pre-freezing behavior is due to cluster formation. This behavior emphasizes the need for further study with a great variety of liquids of more complex molecular structure and for exhaustive study on liquids suggested for thermal conductivity standards.

1. E. McLaughlin and A. R. Ubbelohde. Trans. Faraday Soc. **84**, 1804 (1958).
2. J. Horrocks and E. McLaughlin. Trans. Faraday Soc. **59**, 1702 (1963).
3. A. R. Ubbelohde. Melting and crystal structure. Clarendon Press. Oxford. 1965. p. 256.
4. L. D. Ikenberry and S. A. Rice. J. Chem. Phys. **39**, 1561 (1963).
5. N. Mani and J. E. S. Venart. Proc. 9th Conf. on Thermal Conductivity. U.S.A.E.C. Conf. 691002, 1969. p. 241.
6. J. V. Sengers and P. H. Keyes. Phys. Rev. Lett. **26**, 70 (1971).

Can. J. Chem. Downloaded from www.nrcresearchpress.com by 210.87.254.6 on 09/05/12
For personal use only.

Can. J. Chem. Downloaded from www.nrcresearchpress.com by 210.87.254.105 on 09/05/12
For personal use only.

Canadian Journal of Chemistry

Published by THE NATIONAL RESEARCH COUNCIL OF CANADA

VOLUME 49 AUGUST 1, 1971 NUMBER 15

Kinetics and Thermodynamic Data for the Hydrogen Fluoride Addition to Vinyl Fluoride

LEONARD O. MOORE

Research and Development Department, Chemicals and Plastics, Union Carbide Corporation, South Charleston, West Virginia 25303

Received February 22, 1971

The kinetics of the addition of hydrogen fluoride to vinyl fluoride have been measured in the vapor phase at temperatures of 100 and 150 °C and under pressures of 170, 308, and 446 N/m². The rate equation was found to be a typical second order expression, $-dx/dt = k\,[CHF{=}CH_2]\,[HF]$. The energy of activation was calculated to be 17 ± 2 kcal/mol, and the frequency factor, log A (l/mol s) was 6 ± 1. Based on reaction data from the literature, equilibrium constants and a value for ΔH_{298} were calculated. For this reaction, ΔH_{298} is about −12 kcal/mol.

Les cinétiques de l'addition du fluorure d'hydrogène au fluorure de vinyle ont été mesurées en phase vapeur à des températures de 100 et 150 °C et sous des pressions de 170, 308 et 446 N/m². L'équation de vitesse est une expression typique du second ordre, $-dx/dt = k[CHF{=}CH_2][HF]$. L'énergie d'activation calculée est de 17 ± 2 kcal/mol, et le facteur fréquence, log A (1 mol^{-1} s^{-1}), est de 6 ± 1. A partir des données de la littérature, les constantes d'équilibre et une valeur pour ΔH_{298} ont été calculées. Pour cette réaction, ΔH_{298} est environ de −12 kcal/mol.

Canadian Journal of Chemistry, 49, 2471 (1971)

Introduction

Although the patent literature is replete with examples of the addition of hydrogen fluoride to olefins, there is little experimental information on the kinetics of this reaction (1). In lieu of this, data have been compiled based on the R.R.K. and R.R.K.M. calculations starting from data of dehydrohalogenations of chemically activated molecules.

Sun and Sze (2) estimated the activation energy for the addition of hydrogen fluoride to ethylene from Morse curves and predicted that the reaction would not take place. Benson and Haugen (3), in discussion of the reactions of "hot" fluorinated ethanes, stated that calculations indicated the addition of hydrogen fluoride to ethylene or vinyl fluoride would have an activation energy of 54 ± 3 kcal/mol. Recent measurements using the shock-tube method have indicated that the activation energy for the elimination of hydrogen fluoride from 1,1-difluoroethane is 61.9 ± 1.8 kcal/mol, and that the earlier estimation of the energy of activation for the reverse reaction may be high by 8 to 13 kcal/mol (4).

In an attempt to study this reaction we have measured the rate of heterogeneous addition of hydrogen fluoride to vinyl fluoride.

Experimental

The equipment used is shown schematically in Fig. 1. Vinyl fluoride was fed through a Watts regulator to provide a constant pressure, a rotameter, and a Moore regulator with a needle valve to control the feed rate. Hydrogen fluoride was fed as a vapor from a heated cylinder through a Moore regulator with a needle valve. Check valves before the mixing tee prevented back flow into the feed lines. A portion of each of the feed lines was in the constant temperature bath to bring the reactants to temperature before mixing. Feed rates were sufficient to provide turbulent flow through the reactor. The reactor was a nickel pipe coil of 500 cc volume, ending at a motor valve mounted just after the pipe emerged from the bath. The water quench followed immediately and was backed by a calcium chloride drying tower and Dry Ice-cooled traps to collect the products.

Unreacted hydrogen fluoride was determined by titra-

Can. J. Chem. Downloaded from www.nrcresearchpress.com by 210.87.254.105 on 09/05/12
For personal use only.

TABLE 1. Hydrogen fluoride addition to vinyl fluoride; kinetic runs

Run No.	Pressure × 10^{-3} (N/m^2)	Contact time (s)	Concentrations (mol/l) Initial HF	Initial $CHF{=}CH_2$	Final HF	Final $CHF{=}CH_2$	CHF_2CH_3 × 10^4	k × 10^4 (l/mol s)
				100°				
1	170	159.4	0.0487	0.0058	0.0487	0.0058	0.082	1.83
2	308	47.3	0.0736	0.0211	0.0736	0.0211	0.11	1.49
3	308	59.2	0.0783	0.0164	0.0783	0.0164	0.10	1.32
4	308	87.1	0.0716	0.0231	0.0716	0.0231	0.21	1.44
5	308	202.2	0.0338	0.0610	0.0337	0.0609	0.79	1.91
							Average $k = 1.6 \pm 0.2 \times 10^4$	
				150°				
6	170	111.1	0.0347	0.0134	0.0346	0.0133	1.4	26.9
7	170	155.9	0.0331	0.0150	0.0330	0.0149	1.4	18.7
8	308	48.3	0.0501	0.0372	0.0499	0.0372	2.2	24.9
9	308	57.0	0.0578	0.0295	0.0576	0.0293	2.0	21.1
10	308	65.6	0.0676	0.0197	0.0674	0.0195	1.8	20.7
11	308	65.8	0.0667	0.0206	0.0665	0.0204	1.8	18.6
12	308	66.2	0.0554	0.0319	0.0552	0.0317	2.3	19.7
13*	308	72.3	0.0673	0.0200	0.0671	0.0198	2.3	24.2*
14	308	82.9	0.0584	0.0289	0.0581	0.0286	3.4	24.1
15	308	134.2	0.0552	0.0321	0.0544	0.0313	7.6	32.5
16	308	164.8	0.0636	0.0237	0.0632	0.0233	4.3	17.7
17	308	172.3	0.0646	0.0227	0.0641	0.0222	4.8	19.2
18	446	62.1	0.0699	0.0566	0.0690	0.0557	8.6	35.5
19	446	71.6	0.0999	0.0266	0.0995	0.0262	4.0	21.2
20	446	106.6	0.0654	0.0611	0.0640	0.0597	14.5	34.8
21	446	111.5	0.0543	0.0722	0.0532	0.0711	10.8	25.1
							Average $k = 24 \pm 4 \times 10^4$	

*Air was fed with the vinyl fluoride, 5%.

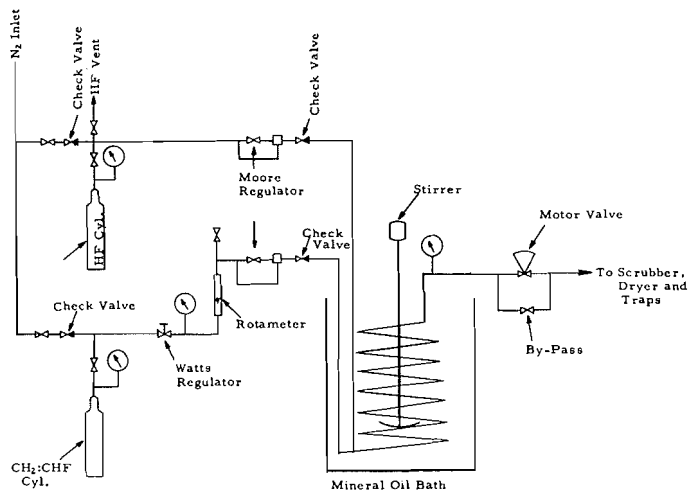

FIG. 1. Apparatus for measuring kinetics parameters.

tion with base, and the organic products were analyzed by gas chromatography and mass spectroscopy. The initial concentrations of reactants were calculated from the amounts of products.

$$[HF]_{initial} = [HF]_{final} + [CHF_2CH_3]_{final}$$

$$[CHF{=}CH_2]_{initial} = [CHF{=}CH_2]_{final} + [CHF_2CH_3]_{final}$$

Results and Discussion

Kinetics

The results from the kinetic runs fit a second order equation, $-d[CHF{=}CH_2]/dt = k[CHF{=}CH_2][HF]$. The numerical values are given in Table 1, and use of the Arrhenius equation, $\log k = \log A - E_{act}/2.303RT$, provides an energy of activation of 17 ± 2 kcal/mol and a frequency factor, log A (l/mol s) of 6 ± 1. This value for the activation energy is considerably lower than the 54 ± 3 kcal/mol predicted by Benson and Haugen (3) or even that predicted based on the results of Tschuikow-Roux *et al.* (4).

These results represent the kinetic expression for a surface catalyzed reaction since the data available for hydrogen fluoride elimination reactions from "hot" fluorinated ethanes (3–5) can be used in the R.R.K.M. calculation to predict the approximate energetics of the addition reactions (6, 7). It is known, for example, that the dehydrochlorination of ethyl chloride follows first order kinetics with either an activation energy of 24 or 56 kcal/mol depending on whether the system is surface catalyzed or not.

In our system, early experiments were erratic until the reactor wall was conditioned at 150 to 200 °C with vinyl fluoride. It was hoped that the conditioning would eliminate the surface catalyzed reaction, but it apparently did not.

In an experiment air was fed with the vinyl fluoride to detect radical mechanism (8). No acceleration was noted. The reaction is believed to be ionic or polar, probably a four-center reaction, rather than radical and the transition state therefore involves some degree of charge separation. This inductive effect of the fluorine (9) in vinyl fluoride is the major influence for the direction of addition, but, to what extent it affects the transition state cannot yet be stated. Tschuikow-Roux *et al.* (4), Pritchard and Perona (10), and Carlton *et al.* (11) have pointed out the pitfalls in trying to apply the point-dipole model of Benson *et al.* (12–14) to olefins with polar ground states. It will be of interest to compare the results reported here with similar ones for the reaction of hydrogen fluoride with ethylene and vinylidene fluoride when they are available.

It is also hoped that a system can be designed for the measurement of the homogeneous rates of addition of hydrogen fluoride to olefins.

Hydrogen fluoride posed certain problems not normally encountered in the type of study described here. Glass, because of its reactivity with hydrogen fluoride, had to be kept completely out of the system and the metal surfaces had to be conditioned.

Another possible problem was that hydrogen fluoride exists as an equilibrium mixture of

Can. J. Chem. Downloaded from www.nrcresearchpress.com by 210.87.254.105 on 09/05/12
For personal use only.

TABLE 2. Thermodynamic values for equilibrium calculations

Compound	$-\Delta H^0_{f\,298}$ kcal/mol	$-\Delta F_f$ 298 °K	$-\Delta F_f$ 600 °K	S^0_{298} kcal/mol	C_p 298 °K	C_p (t °K)	Reference
CHF_2CH_3	119.4			67.3*			17
	121.0			64.3			17
	115.7*						16
					16.1		21
	109.4				16.78*	25.94* (600)	19
		114.0	110.6				Calcd.
$CHF{=}CH_2$	28.0						22
	36.3*						16
				60.19*	12.33*	24.18* (1000)	18
				60.50	12.33		18
		38.3	39.8				Calcd.
HF	64.80	65.3	65.76	41.51	6.964	6.986 (600)	20

*Values used in calculation.

monomeric and polymeric forms (15). Consideration of this equilibrium under the conditions used in this study, however, indicated that the error in hydrogen fluoride monomer concentration would be less than 0.5% in the worst case. Erratic results at 100 °C and 446 N/m^2 apparently were due to partial condensation of hydrogen fluoride in the feed line preventing constant feed to the reactor.

Equilibrium Constant and Heat of Reaction

A discrepancy was noted when equilibrium constants for the reaction of hydrogen fluoride and vinyl fluoride were calculated using the thermodynamic values for the compounds involved and compared with the equilibrium constants estimated from experimental results in the literature. The values based on the thermodynamic functions are too large.

The thermodynamic values reported in the literature vary over a considerable range as indicated in Table 2. Use of $-\Delta H^0_{f\,298}$ values for vinyl fluoride and 1,1-difluoroethane from Vitvitskii (16) with the available values for S^0_{298} (17, 18) and C_p (18, 19) and the values of $-\Delta F_{f\,298}$ for hydrogen fluoride from the JANAF tables (20) led to values for log K_{eq} of 3.7 at 600 °K and 7.6 at 298 °K. These are compared with values of 0.9 at 600 °K based on experimental data from the literature and a derived value of 6.0 at 298 °K assuming that the values of C_p for the compounds involved are valid. The plots of these values are presented in Fig. 2.

The heat of reaction is derived from the values

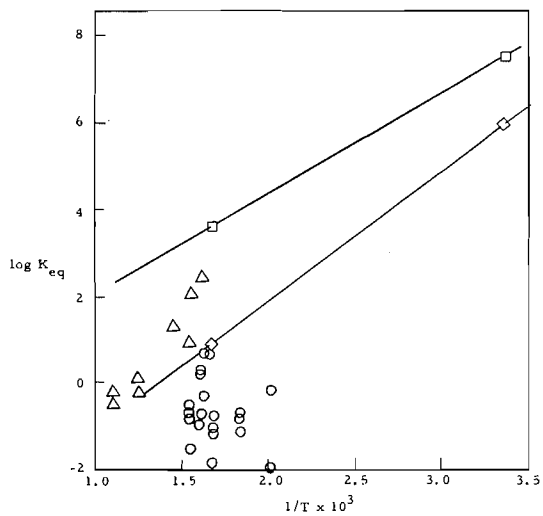

FIG. 2. Arrhenius plot. △, reaction data, maxima; ○, reaction data, minima; □, calculated constant, see text; ◇, corrected constants, $\Delta H_{298} = -12$ kcal/mol.

of the equilibrium constants by standard thermodynamic calculations assuming that the values of both S^0_{298} and C_p are valid. The heat of reaction is

$$\log K_{eq} = -\Delta F/2.303RT$$

$$\Delta F = \Delta H - T\Delta S$$

-12 kcal/mol. This compares to -14.6 kcal/mol based on the reported thermodynamic functions.

Benson *et al.* (23) have developed a method of estimating thermodynamic properties based on group contributions. Use of this method gives a

Can. J. Chem. Downloaded from www.nrcresearchpress.com by 210.87.254.105 on 09/05/12
For personal use only.

heat of reaction of -23.3 kcal/mol. These authors point out, however, that there are certain contradictions because of the differences of polarity and suggest that caution should be used in combining groups with large differences in polarity. The source of the group contribution of =CHF is CF_2=CHF. Further, Benson and Haugen (3) have estimated the heat of reaction for $HF + C_2FH_3 \rightarrow C_2F_2H_4$ to be -8 kcal/mol.

The literature data available for the reaction of vinyl fluoride and hydrogen fluoride are of two types. The formation of vinyl fluoride from thermal dehydrofluorination of 1,1-difluoroethane (24, 25) approaches the equilibrium from the high side and the formation of 1,1-difluoroethane from the addition of hydrogen fluoride to vinyl fluoride (24, 26–28) approaches it from the low side. The correct value should lie between these sets of values. The results of calculating equilibrium constants from the literature reaction data are plotted in Fig. 2.

The error in the thermodynamic functions could not be further defined, but the values of $-\Delta H^0_f$ for the organic compounds are most suspect because of the lack of good values for comparison and the major influence on the values of $-\Delta F^0_f$ and K_{eq}.

1. A. MACCOLL. Chem. Revs. **69**, 33 (1969).
2. C. E. SUN and C. H. SZE. J. Chin. Chem. Soc. **4**, 98 (1936). Quoted in Tables of chemical kinetics, homogeneous reactions. United States Department of Commerce, National Bureau of Standards, Circular 510, N. Thon, ed., September 28, 1951. pp. 563–4.
3. S. W. BENSON and G. R. HAUGEN. J. Phys. Chem. **69**, 3898 (1965).
4. E. TSCHUIKOW-ROUX, W. J. QUIRING, and J. M. SIMMIE. J. Phys. Chem. **74**, 2449 (1970).
5. M. DAY and A. F. TROTMAN-DICKENSON. J. Chem. Soc. (A), 233 (1969).
6. A. MACCOLL and P. J. THOMAS. *In* Progress in reaction kinetics. *Edited by* G. Porter. Pergamon Press, New York. 1967. pp. 119–148.
7. H. E. O'NEAL and S. W. BENSON. J. Phys. Chem. **71**, 2903 (1967).
8. CHEN WEN-CHI and HUANG PAO-TUNG. Sci. Sin. **13**, 1516 (1964); Chem. Abstr. **61**, 10566*a* (1964).
9. A. STREITWIESER, JR. and D. HOLTZ. J. Am. Chem. Soc. **89**, 692 (1967); A. STREITWIESER, JR., A. P. MARCHARD, and A. H. PUDJAATMAKA. J. Am. Chem. Soc. **89**, 693 (1967).
10. G. O. PRITCHARD and M. J. PERONA. Int. J. Chem. Kinet. **2**, 281 (1970).
11. T. S. CARLTON, A. B. HARKER, W. K. NATALE, R. E. NEEDHAM, R. L. CHRISTENSEN, and J. L. ELLENSON. J. Am. Chem. Soc. **91** 555 (1969).
12. S. W. BENSON and G. R. HAUGEN. J. Am. Chem. Soc. **87**, 4036 (1965).
13. S. W. BENSON and A. N. BOSE. J. Chem. Phys. **39**, 3463 (1963).
14. S. W. BENSON and G. R. HAUGEN. J. Phys. Chem. **70**, 3336 (1966).
15. J. W. ARMITAGE, P. GRAY, and P. G. WRIGHT. J. Chem. Soc. 1796 (1963).
16. A. I. VITVITSKII. J. Org. Chem. USSR, **3**, No. 8, 1316 (1967).
17. A. S. RODGERS. J. Phys. Chem. **71**, 1996 (1967).
18. W. F. BECKWITH and R. W. FAHIEN. Chem. Eng. Prog. Symp. Ser. **59**, 75 (1963).
19. W. L. CALHOUN. Private communication.
20. JANAF Thermochemical Data, December 31, 1963.
21. D. C. SMITH, R. A. SAUNDERS, J. R. NIELSON, and E. E. FERGUSON. J. Chem. Phys. **20**, 847 (1952).
22. P. G. MASLOV and YU. P. MASLOV. Khim. i Teknol, Topliv i Masel, **3**, No. 10, 50 (1958); Chem. Abstr. **53**, 1910h (1959).
23. S. W. BENSON, F. R. CRUICKSHANK, D. M. GOLDEN, G. R. HAUGEN, H. E. O'NEAL, A. S. RODGERS, R. SHAW, and R. WALSH. Chem. Revs. **69**, 279 (1969).
24. B. F. SKILES. U.S. Patent 2,716,142. August 23, 1955.
25. Imperial Chemical Industries, Ltd., Brit. Patent 619,394. March 8, 1949.
26. J. C. HILLYER and J. F. WILSON. U.S. Patent 2,471,525. May 31, 1949.
27. B. F. SKILES. U.S. Patent 2,716,143. August 23, 1955.
28. B. F. SKILES. U.S. Patent 2,892,000. June 23, 1959.

Can. J. Chem. Downloaded from www.nrcresearchpress.com by 210.87.254.105 on 09/05/12
For personal use only.

Can. J. Chem. Downloaded from www.nrcresearchpress.com by 210.87.254.105 on 09/05/12
For personal use only.

The Hydrocarbon-induced Fluorescence of Atoms in Flames[1]

A. T. BLADES
Research Council of Alberta, Edmonton, Alberta

Received February 8, 1971

The phenomenon of chemiluminescent emission from atoms introduced into hydrocarbon flames has been studied in a basic hydrogen–oxygen diffusion flame at low hydrocarbon concentrations. Emissions from several atoms are first order in methane concentration and examination of the relative populations of the excited states of arsenic suggests a single excitation mechanism with available energy in excess of 8.5 eV. Previously proposed mechanisms are discussed and the available evidence favors the process

$$CH + O \rightarrow CHO$$

as the origin of the energy of excitation.

Le phénomène de l'émission par chimioluminescence à partir d'atomes introduits dans une flamme d'hydrocarbure a été étudié dans une flamme de diffusion hydrogène–oxygène à faible concentration en hydrocarbure. Les émissions de différents atomes sont du premier ordre par rapport à la concentration en méthane et l'examen des populations relatives dans les états excités de l'arsenic, suggère un mécanisme d'excitation unique avec un excès d'énergie disponible de 8.5 eV. On discute des mécanismes proposés antérieurement ainsi que de la preuve qui existe en faveur du processus:

$$CH + O \rightarrow CHO$$

qui est à l'origine de l'énergie d'excitation.

Canadian Journal of Chemistry, 49, 2476 (1971)

Atomic emissions may be observed from both the primary reaction zone and the outer combustion zone of hydrocarbon–oxygen flames seeded with compounds of some of the elements. In the outer zone the emission arises from atoms previously excited either thermally or by the reactions (1)

$$H + H + M \rightarrow M^* + H_2$$

and

$$H + OH + M \rightarrow M^* + H_2O$$

the energy limit of excitation being determined by the exothermicity of the latter process, 5.2 eV. The spectrum observed in the primary reaction zone is commonly more extensive, including emissions from much higher energy levels, the extreme case being a zinc level at 9.0 eV (2). Since these emissions arise from the region of the flame defined by the blue and green emissions from CH and C_2, it may be assumed that the energy for the atomic excitation arises in the oxidation of these, or similar, hydrocarbon species. Thus, while the excitation of the atoms is probably of little consequence in itself, its occurrence provides a further source of information on the mechanism of hydrocarbon combustion. Unfortunately, although a number of mechanisms for the atom excitations have been proposed (1, 3–7), no clear preference exists for any one process. We have recently found that it is possible to observe chemi-ionization and CH emission when low concentrations of hydrocarbons are present in a hydrogen-in-oxygen diffusion flame on a commercial flame spectrophotometry burner. This same technique has now been applied to a study of the atomic emissions which arise when volatile inorganic compounds are added to the system.

Experimental

The apparatus consisted of a Beckman DU-2 spectrophotometer wherein the IP 28 photomultiplier was replaced by an RCA 7200 to facilitate measurements at short wavelength. The burner mount of the flame emission attachment was replaced with a Teflon holder and a spiral electrode was mounted above the primary reaction zone of the flame for rate of ion formation determination. The burner was modified by removing the axial aspirator capillary. Hydrogen (1 l/min) containing the gaseous additive and the hydrocarbon entered through the axial hole while oxygen (4 l/min) was supplied through the annular orifice. The luminous primary reaction zone so formed was about 1 mm in diameter and 4 mm high, and did not change appreciably with hydrocarbon concentrations up to 1%. The additive compounds, arsine, stibine, germanium hydride, tin tetramethyl, silicon tri-*n*-propyl and chromium, iron, nickel, and molybdenum carbonyl were diluted with hydrogen for convenient introduction to the hydrogen stream. The gaseous hydrocarbon additives, better than 99% pure grades, were introduced continuously into the hydrogen stream and their concentrations monitored by thermal conductivity.

[1]Contribution No. 535 from the Research Council of Alberta, Edmonton, Alberta.

Can. J. Chem. Downloaded from www.nrcresearchpress.com by 210.87.254.105 on 09/05/12
For personal use only.

Results

Chemiluminescence was observed from arsenic, antimony, tin, iron, nickel, chromium, molybdenum, germanium, and silicon. Some previously unrecorded emissions from high energy levels were observed, notably from (*a*) the $4p^4\ ^2D$ level of arsenic (8.5 eV), (*b*) the $7d\ ^3D^0$ level of tin (6.7 eV), (*c*) the $4d\ ^1F^0$ level of germanium (6.5 eV), and (*d*) the $3d\ ^1F^0$ level of silicon (6.6 eV). An attempt was made to correlate the population of excited states of arsenic with the excitation energies, as has been described by Brennen and Kistiakowsky (8). These data are plotted in Fig. 1, where the line drawn through the points corresponds to a flame "temperature" of 4500 °K. The emissions from the levels at 53 156 K (6.6 eV) and 54 605 K (6.8 eV) do not fit the line at all well, but similar population anomalies were observed in the emission from an arsenic hollow cathode lamp, and it would seem most probable that this arises from incorrect "*gA*" values, as have been observed by Brennen and Kistiakowsky (8).

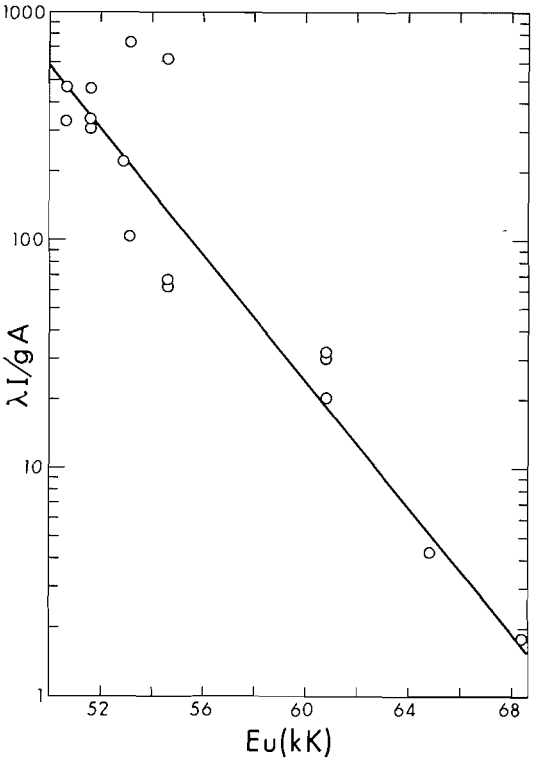

FIG. 1. Apparent relative populations ($\lambda I/gA$) of arsenic levels in the flame *vs.* excitation energy (1 kK = 0.124 eV).

The effect of the additive concentration in the flame was examined for arsenic emission at 197.2 nm and was found to be linear up to 0.01% arsenic in hydrogen, but exhibited some self-absorption at higher concentrations. The effect of hydrocarbon concentration on the atomic emission was determined for chromium, molybdenum, tin, antimony, and arsenic emissions, and was invariably found to be linearly dependent at low concentration. Some typical data are shown in Fig. 2 *a*, *b*, *c*. The maximum energy of excitation for which this relationship was established was 6.8 eV (As 228.8 nm).

Molecular emission of an additive compound was observed only for SnO; the intensity was linearly dependent on the tin concentration in the flame, and was independent of the presence of hydrocarbon. An electric field had no effect on the atomic emission intensities. It was, however, possible to observe the chemi-ionization due to hydrocarbons in the flame; this shows a similar behavior to the atomic emissions (Fig. 2 *e*). The CH emission at 431.5 nm (Fig. 2 *d*), while paralleling the atomic emission and chemi-ion formation at low concentrations, shows a declining

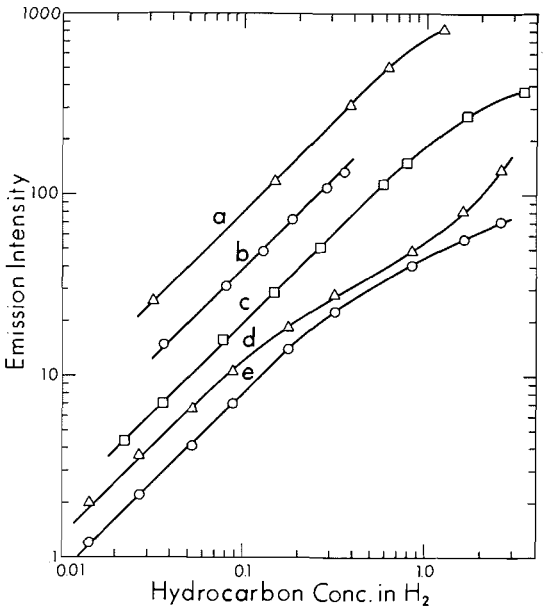

FIG. 2. Emission intensity (*a*, *b*, *c*, *d*) and rate of ion formation (*e*) variation with hydrocarbon concentration in the flame. (*a*), arsenic emission at 197.2 nm with C_2H_4; (*b*), antimony emission at 231.1 nm with C_2H_6; (*c*), arsenic emission at 228.8 nm with CH_4; (*d*), CH emission at 431.5 nm with CH_4; (*e*), ion formation with CH_4.

dependence below 1% hydrocarbon but an increasing dependence above this concentration.

Discussion

A major aspect of this research is the observation of a unit order dependence of the rate of ion formation, CH emission, and some atomic emissions on the concentration of hydrocarbon in a hydrogen–oxygen diffusion flame. Concern has been expressed (9) that even at very low concentrations, hydrocarbons may so alter the flame chemistry that apparent kinetic orders would be meaningless. Chemi-ion formation in such flames has been found proportional to the hydrocarbon concentration over several decades of concentration (10). Ions are formed from the interaction of CH and oxygen atoms (11), and their first order dependence may therefore be interpreted as evidence that CH arises by a series of processes first order in hydrocarbon fragments. But it also implies that the presence of the hydrocarbon has a negligible effect on the oxygen atom concentration in that region of the flame where ions are formed. Chemi-ionization is first order in hydrocarbon in the spectrophotometer flame where CH emission is also observed to be first order. If the electronically excited CH arises from the process

$$CH + H + OH \rightarrow CH^* + H_2O$$

as has recently been suggested for low concentration conditions (12), this order in emission must also be kinetically significant. Similar conclusions follow from the observation of second order dependence of the emission from C_2 (12) and S_2 (13) in this and other flame systems when methane and hydrogen sulfide are added to the flame.

On this basis, it seems reasonable to assume that the kinetic orders of the atomic emissions also have relevance to the mode of formation of the electronically excited emitter and discussion is based on this premise. The proportionality between the AsH_3 concentration in the flame and the arsenic emission at 197.2 nm at low concentrations is in keeping with similar observations in conventional flame photometry (3) and confirms that the mechanism involves a species with one arsenic or other additive atom. Similarly, the first order dependence of the atomic emission intensity on the methane concentration implies the participation of a single carbon species or a derivative. The parallel behavior of the rate of ion formation, the CH emission and the atomic emissions at low concentrations suggests that both $CH(X^2\Pi)$ and $CH(A^2\Delta)$ may be involved in the atomic excitation reaction. The discrepancy between the atomic emission and the CH emission, Fig. 2, at higher concentrations tends to exclude $CH(A^2\Delta)$ as a reactant, but it is uncertain whether the enhanced $CH(A^2\Delta)$ formation, presumably by (14)

$$C_2 + OH \rightarrow CH^* + CO$$

arises in the same zone of the flame as that excited by energy transfer. Further evidence against the involvement of this species is provided by studies of an acetylene–oxygen flame by Dean and Carnes (15) where the CH and atomic emission reach maxima in different regions of the flame.

The other feature of the excitation mechanism of major consequence is the maximum available energy. Buell (2) has reported emission from zinc at 9.0 and 8.5 eV, and a value of 8.5 eV is reported herein for arsenic. Unfortunately it was not possible to determine the order in methane concentration for the emission from this high energy state and hence it has not been proven that the order and energy conditions apply to the same process. The arsenic emission intensity data in Fig. 1, however, indicate a monotonous decline of the population of excited states with energy up to the energy limit of 8.5 eV. This is to be contrasted with the behavior of mercury excited by active nitrogen (8) where the population of the excited species declines more rapidly as the maximum energy is approached. It would therefore seem reasonable to assume that in hydrocarbon flames, a single atomic excitation reaction is operative, which is more exothermic than 8.5 eV.

The recombination of ions and electrons has been suggested as a potential source of the excitation energy of atoms in hydrocarbon flames (1, 2). Ions (and electrons) are formed in the flame by a process first order in hydrocarbon concentration; their recombination on the other hand is first order in the concentration of each, or second order in either, and hence the atomic emission would be expected to be second order in hydrocarbon concentration. The rigorous first order observed hence provides strong kinetic evidence against this type of excitation. This conclusion is

Can. J. Chem. Downloaded from www.nrcresearchpress.com by 210.87.254.105 on 09/05/12
For personal use only.

Can. J. Chem. Downloaded from www.nrcresearchpress.com by 210.87.254.105 on 09/05/12
For personal use only.

further justified by the failure of the electric field to influence the emission, and by previous objections on energetic grounds (1).

Mechanisms of excitation involving additive monoxides have been criticized on chemical and energetic grounds. The process

$$C + MO \rightarrow M^* + CO$$

was found to release insufficient energy to excite certain tin lines (1), and similar observations can be cited in the present studies on germanium, arsenic, and silicon, where energy deficiencies of 2.3, 2.3 and 3.8 eV exist. Uncertainty in the concentration of carbon atoms is an additional concern (1). The reaction

$$CO^* + MO \rightarrow M^* + CO_2$$

satisfies the energy requirements if the CO is in the $A^1\Pi$ or $a^3\Pi$ electronic states which have minimum energies of 8.0 and 6.0 eV. Nevertheless, for the maximum excitation energies herein observed for tin, germanium, arsenic, and silicon, energies of excitation of the CO of 7.0, 7.9, 7.9, and 9.5 eV would be required. While CO excitation up to 9.1 eV is known to occur in flames, it is attributed to the reaction (16)

$$C_2O + O \rightarrow 2CO$$

and this process is excluded from consideration by the "first order in methane" observation. Other processes for CO excitation

$$CH + O \rightarrow CO + H$$

or

$$CH_2 + O \rightarrow CO + H_2$$

are exothermic to the extent of 7.7 eV and hence fall far short of the energy requirement for silicon excitation.

Direct energy transfer from excited molecules to the atom has most frequently been suggested as the source of excitation. Prime consideration has been given to CO, particularly in the $a^3\pi$ state (4, 7, 17) as the excited molecule, since it might reasonably be expected to arise in the above reactions with energies of 7.7 eV plus a thermal contribution and yet satisfy the "first order in methane" requirement. While it is difficult to judge with certainty from the present data, indications are that the thermal contribution is not adequate to explain the intensity of the highest energy arsenic emission, or the observation of zinc emission from an upper state at 9.0 eV (2).

Energy transfer from CHO* formed in the process

$$CH + O \rightarrow CHO^*$$

has been proposed by Sugden (1) as the source of excitation energies up to 8.9 eV. While little is known of the energy states of this molecule, it is known from its emission to be formed in hydrocarbon flames (18). Cummings and Hutton (5) have discredited this mechanism on the grounds that the CHO* would have a lifetime too short for energy transfer, but this decision is premature in the absence of extensive knowledge of the excited states of CHO. As an alternative, Cummings and Hutton propose excitation by OH* formed in the process (14)

$$CH + O_2 \rightarrow CO + OH$$

which is exothermic by 7.0 eV and they attribute iron excitations above this energy to thermal contributions. There are, however, no known stable states of OH in the energy interval from 6.35 to 8.65 eV, and hence the thermal contribution for excitation to 7.6 eV is 1.25 eV rather than the superficially expected 0.6 eV. This mechanism is therefore extremely improbable as described; the basic oxidation process could, however, be a source of CO with excitation up to 7.0 eV.

Mechanistic difficulties associated with the existence and lifetime of vibronic states of the energy transferring molecule are obviated if the atom is excited in a termolecular reaction, *e.g.*

$$CH + O + M \rightarrow CHO + M^*$$

Broida and Shuler (17) pointed out that the low additive atom concentration made it an unlikely participant in a termolecular reaction, and they suggested the intermediacy of a major flame constituent such as H_2O or CO_2 as an energy transfer agent. A simple steady state treatment for such a process reveals that an intermediate is of consequence with regard to the atom concentration only under the circumstance that the energy transfer agent is quenched exclusively by the atom. This requires the emission to be zero order in additive atoms, which is not true. In any case, the distinction between a termolecular and two consecutive bimolecular reactions loses significance in the present context if there is almost complete energy retention between the occurrence of the first and second bimolecular

reactions. This fact, and the observation of SnO and other monoxide emissions (4) in flames, suggest an alternative mechanism to the termolecular reaction above, which may be generalized as

$$M + O \rightarrow MO^*$$

$$MO^* + CH \rightarrow CHO + M^*$$

where MO* is the electronically and (or) vibrationally excited additive monoxide.

Thus, while the available kinetic and energetic evidence favors the interaction of CH, O, and the additive atom as the source of atomic emissions from the primary reaction zone of hydrocarbon flames, the sequence of reactions leading to the excitation is still uncertain. Recent studies of the quenching of these emissions (7), however, suggest that resolution of the mechanism is possible and further studies are projected along these lines.

1. T. M. SUGDEN. *In* Annual reviews of physical chemistry. Annual Reviews, Palo Alto, California, 1962. p. 369.
2. B. E. BUELL. Anal. Chem. **35**, 372 (1963).
3. P. T. GILBERT, JR. Proc. Xth Colloq. Spectros. Intern. Spartan Books, Washington, 1963. p. 171.
4. R. MAVRODINEANU. Flame spectroscopy. John Wiley and Sons, New York. 1965.
5. G. A. MCD. CUMMINGS and E. HUTTON. Combust. Flame, **10**, 195 (1966).
6. D. T. COKER and J. M. OTTAWAY. Nature, **227**, 831 (1970).
7. J. F. ALDER, K. C. THOMPSON, and T. S. WEST. Anal. Chim. Acta, **50**, 383 (1970).
8. W. R. BRENNEN and G. B. KISTIAKOWSKY. J. Chem. Phys. **44**, 2695 (1966).
9. W. A. LOSSER. IX Intern. Symp. on Combustion. Academic Press, New York. 1963. p. 618.
10. J. C. STERNBERG, W. S. GALLAWAY, and D. T. L. JONES. Gas chromatography. Academic Press, New York. 1962. p. 231.
11. J. A. GREEN and T. M. SUGDEN. IX Intern. Symp. on Combustion. Academic Press, New York. 1963. p. 607.
12. J. PEETERS, J. F. LAMBERT, P. HERTOGHE, and A. VAN TIGGELEN. XIII Intern. Symp. on Combustion. In press.
13. R. M. DAGNALL, K. C. THOMPSON, and T. S. WEST. Analyst, **92**, 506 (1967).
14. A. G. GAYDON. The spectroscopy of flames. Chapman and Hall, London. 1957. p. 160.
15. J. A. DEAN and W. J. CARNES. Analyst, **87**, 743 (1962).
16. K. H. BECKER and K. D. BAYES. J. Chem. Phys. **45**, 396 (1966).
17. H. P. BROIDA and K. E. SHULER. J. Chem. Phys. **27**, 933 (1957).
18. W. M. VAIDYA. Proc. Roy. Soc. London, **147**, 513 (1934); **279**, 572 (1964).

Can. J. Chem. Downloaded from www.nrcresearchpress.com by 210.87.254.105 on 09/05/12
For personal use only.

Can. J. Chem. Downloaded from www.nrcresearchpress.com by 210.87.254.6 on 09/05/12
For personal use only.

Excess Thermodynamic Properties of Cyclopentane – Isomeric Decalin Systems at 25 °C[1]

D. E. G. Jones,[2] I. A. Weeks,[3] and G. C. Benson

Division of Chemistry, National Research Council of Canada, Ottawa, Canada

Received March 17, 1971

Molar excess enthalpies and volumes of the systems cyclopentane – *cis*-decalin and cyclopentane – *trans*-decalin at 25 °C were determined by direct calorimetric and dilatometric measurements. Excess Gibbs free energies, also at 25 °C, were obtained from a study of the vapor–liquid equilibria. The excess properties of these cyclopentane systems are compared with those of their cyclohexane counterparts, and are interpreted in terms of the theory of Flory.

On a mesuré par calorimétrie et par dilatométrie les enthalpies et les volumes molaires d'excés des systèmes cyclopentane-*cis*-décaline et cyclopentane – *trans*-décaline, à 25 °C. Les énergies libres d'excès de Gibbs furent tirées d'une étude des équilibres liquide–vapeur. Les propriétés d'excès de ces systèmes cyclopentaniques sont comparées à celles des systèmes cyclohexaniques équivalents et l'interprétation en est faite en termes de la théorie de Flory.

Canadian Journal of Chemistry, **49**, 2481 (1971)

Introduction

Comparisons of the excess properties of binary systems formed by mixing *cis*-decalin and *trans*-decalin with a common second component are of interest since they must reflect the structural and energetic differences between the isomeric decalins. Measurements of the excess enthalpies and volumes of cyclohexane – isomeric decalin mixtures at 25 °C were described recently (1). The results of similar calorimetric and dilatometric studies of the systems cyclopentane – *cis*-decalin and cyclopentane – *trans*-decalin are reported in the present paper, along with their vapor–liquid equilibria determined by the static method.

Experimental

The methods used in our laboratory for studying the excess thermodynamic properties of binary mixtures have been described previously (2–4). Reference should be made to these earlier publications for details of the equipment and operating techniques.

Calorimetric Measurements

The isothermally-jacketed calorimeter described by Murakami and Benson (2) was used to determine the change in enthalpy when cyclopentane was mixed with *cis*-decalin and with *trans*-decalin. All measurements were made at 25.00 ± 0.01 °C and the accuracy of the results is believed to be better than ±0.5% over most of the concentration range.

Volumetric Measurements

The volume changes associated with the formation of cyclopentane – isomeric decalin mixtures at 25.00 ± 0.01 °C were derived from direct dilatometric measurements (3). The uncertainty of the results for equimolar mixtures is estimated to be ±0.0015 $cm^3\ mol^{-1}$.

Vapor–Liquid Studies

Static vapor pressures of mixtures of known total composition and known total volume (*i.e.* liquid + vapor phases) were measured in a cell and vacuum system similar to that used by Singh and Benson (4). The equilibrium cell and sample manifold were thermostated at 25.000 ± 0.003 °C; pressures were measured to ±0.005 mm Hg with a calibrated quartz spiral gauge (Texas Instruments).

Materials

The component liquids were obtained by chromatographic purification of commercial reagents. Cyclopentane (pure grade reagent from Phillips Petroleum Co.) was pas ed through a column packed with Chromosorb W (30/60 mesh) containing 20% squalane. The *cis* and *trans* isomers of decalin were separated from a practical grade decalin mixture as described in ref. 1.

During the course of the investigation, samples from several preparations of each component were employed. In general, values of the densities, refractive indices, and vapor pressures of material from different preparations agreed well, and were in reasonable agreement with data from the literature (5, 6). This is shown in Table 1, where average values of the physical properties at 25 °C are listed, along with indications of the range of variation encountered.

All samples of the component liquids used in the vapor–liquid studies were thoroughly degassed. A vacuum sublimation technique (7) was used to degas initial charges

[1]NRCC No. 11972.

[2]NRCC Postdoctorate Fellow, 1969–1971. Present address: Department of Chemistry, University of Otago, Dunedin, New Zealand.

[3]NRCC Postdoctorate Fellow, 1969–1971.

TABLE 1. Properties of the pure component liquids at 25 °C

Component	Density d^{25}(g cm^{-3})		Refractive index n_D^{25}		Vapor pressure p^0(25)(mm Hg)	
	Experimental	Literature	Experimental	Literature	Experimental	Literature
Cyclopentane	0.74034 (±0.00005)	0.74045*	1.40360 (±0.00003)	1.40363*	317.49 (±0.06)	317.46*
cis-Decalin	0.89288 (±0.00005)	0.89291†	1.47883 (±0.00003)	1.47878†	0.83 (±0.01)	0.78†
trans-Decalin	0.86596 (±0.00005)	0.86592†	1.46716 (±0.00003)	1.46715†	1.48 (±0.01)	1.23†

*Reference 5.
†Camin and Rossini (6), values of vapor pressures were calculated from Antoine coefficients obtained from experimental results measured above 90 °C.

for the equilibrium cell; other samples, prepared in small ampuls, were repeatedly frozen and thawed while about half the sample was pumped away.

Results

The experimental results for the molar excess enthalpies, H^E, and molar excess volumes, V^E, of the two cyclopentane – isomeric decalin systems at 25.00 °C are summarized in Table 2. In both cases, x_1 indicates the mole fraction of cyclopentane. Figures 1 and 2 provide graphical presentations of these data.

Each set of results was fitted with a Redlich–Kister form of the type

$$[1] \quad X^E = x_1(1 - x_1)\sum_j^n a_j(1 - 2x_1)^{j-1}$$

where X^E represents the excess property under consideration. The method of least-squares was used to determine the values of the coefficients a_j. In each case, the optimum number of coefficients was ascertained from an examination of the variation with n, of the standard error of estimate

$$[2] \quad \sigma_x = [\sum(X_{obs.}^E - X_{calcd.}^E)^2/(n_{obs.} - n)]^{\frac{1}{2}}$$

where the sum was taken over the $n_{obs.}$ results.

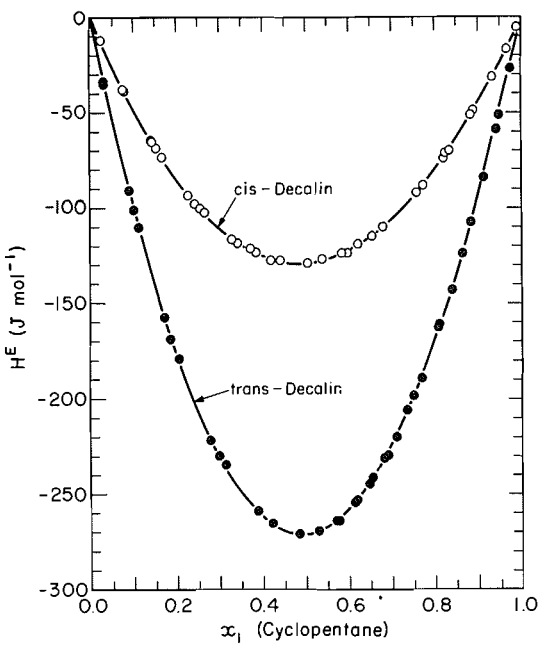

FIG. 1. Molar excess enthalpies at 25 °C. Experimental results: ○, cyclopentane – *cis*-decalin; ●, cyclopentane – *trans*-decalin. Solid curves are least-squares representations by eq. 1.

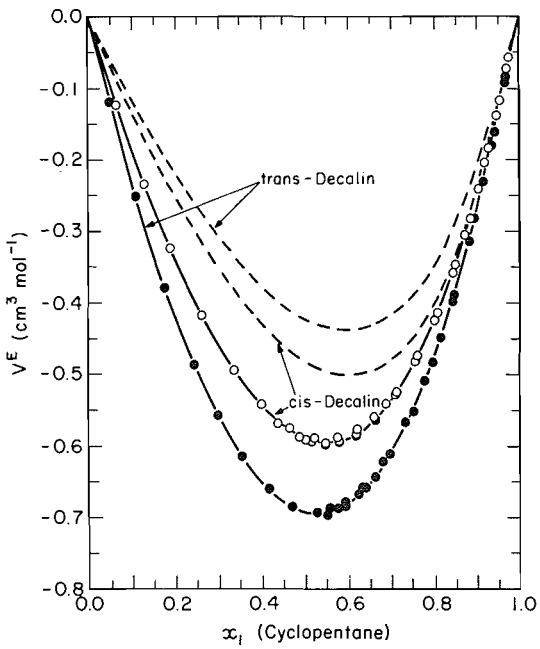

FIG. 2. Molar excess volumes at 25 °C. Experimental results: ○, cyclopentane – *cis*-decalin; ●, cyclopentane – *trans*-decalin. Solid curves are least-squares representations by eq. 1. Broken curves were calculated from the theory of Flory.

Can. J. Chem. Downloaded from www.nrcresearchpress.com by 210.87.254.6 on 09/05/12
For personal use only.

Can. J. Chem. Downloaded from www.nrcresearchpress.com by 210.87.254.6 on 09/05/12
For personal use only.

TABLE 2. Experimental values of the molar excess enthalpy H^E (J mol^{-1}) and molar excess volume V^E (cm^3 mol^{-1}) at 25 °C

Cyclopentane(*1*) – *cis*-decalin(*2*)				Cyclopentane(*1*) – *trans*-decalin(*2*)			
x_1	H^E	x_1	V^E	x_1	H^E	x_1	V^E
0.0232	−12.23	0.0660	−0.1237	0.0307	−34.06	0.0498	−0.1196
0.0760	−37.76	0.1304	−0.2340	0.0319	−35.37	0.1107	−0.2523
0.0779	−38.94	0.1897	−0.3237	0.0890	−90.94	0.1775	−0.3795
0.1403	−65.10	0.2622	−0.4176	0.0986	−101.01	0.2439	−0.4859
0.1438	−65.42	0.3365	−0.4945	0.1123	−110.13	0.2958	−0.5569
0.1499	−68.78	0.4004	−0.5420	0.1706	−157.14	0.3530	−0.6153
0.1653	−73.41	0.4359	−0.5694	0.1846	−168.79	0.4145	−0.6606
0.2251	−93.64	0.4627	−0.5746	0.2043	−179.11	0.4694	−0.6860
0.2411	−97.65	0.4867	−0.5883	0.2791	−221.76	0.5270	−0.6942
0.2535	−100.36	0.5007	−0.5911	0.2986	−229.74	0.5519	−0.6974
0.2633	−102.46	0.5144	−0.5938	0.3145	−234.73	0.5573	−0.6886
0.3261	−116.68	0.5220	−0.5900	0.3864	−258.78	0.5759	−0.6883
0.3419	−118.63	0.5444	−0.5976	0.4221	−265.00	0.5930	−0.6798
0.3708	−121.59	0.5454	−0.5968	0.4831	−270.56	0.5940	−0.6859
0.3852	−123.53	0.5741	−0.5895	0.5288	−268.89	0.6238	−0.6697
0.4190	−127.48	0.5785	−0.5948	0.5703	−263.69	0.6334	−0.6604
0.4408	−127.84	0.5794	−0.5940	0.5779	−263.52	0.6421	−0.6604
0.5044	−129.14	0.6169	−0.5851	0.6139	−254.49	0.6627	−0.6453
0.5379	−127.27	0.6183	−0.5832	0.6175	−252.88	0.6803	−0.6247
0.5826	−124.02	0.6199	−0.5784	0.6478	−244.29	0.6972	−0.6145
0.5963	−123.57	0.6580	−0.5617	0.6545	−241.21	0.7329	−0.5690
0.6204	−119.10	0.6601	−0.5649	0.6807	−231.23	0.7509	−0.5543
0.6528	−114.45	0.6624	−0.5631	0.6898	−229.53	0.7764	−0.5117
0.6791	−109.89	0.6883	−0.5430	0.7099	−219.94	0.7958	−0.4865
0.7563	−91.79	0.7086	−0.5302	0.7334	−205.83	0.8152	−0.4514
0.7723	−88.41	0.7132	−0.5266	0.7485	−198.14	0.8436	−0.4000
0.8190	−74.04	0.7562	−0.4839	0.7677	−189.12	0.8468	−0.3923
0.8215	−71.62	0.7617	−0.4775	0.8071	−162.47	0.8830	−0.3166
0.8320	−69.71	0.8013	−0.4271	0.8095	−160.63	0.8963	−0.2848
0.8814	−51.02	0.8091	−0.4171	0.8386	−142.93	0.9189	−0.2337
0.8818	−51.26	0.8439	−0.3608	0.8613	−123.88	0.9374	−0.1827
0.8894	−48.79	0.8510	−0.3492	0.8824	−107.22	0.9449	−0.1638
0.9314	−31.30	0.8727	−0.3089	0.9119	−83.81	0.9694	−0.0944
0.9318	−30.94	0.8846	−0.2852	0.9400	−58.46	0.9718	−0.0862
0.9647	−16.57	0.9056	−0.2431	0.9478	−51.29		
0.9653	−16.55	0.9207	−0.2073	0.9736	−26.63		
0.9894	−5.01	0.9303	−0.1863				
		0.9486	−0.1400				
		0.9571	−0.1195				
		0.9735	−0.0748				
		0.9787	−0.0604				

The resulting values of the coefficients are given in Table 3 along with the corresponding standard errors of estimate for the representations. The continuous curves for H^E and V^E, in Figs. 1 and 2 were calculated from eq. 1, using these values for the coefficients.

Molar excess energies at constant volume were obtained from the relation

$$[3] \qquad U_V^E = H^E - T(\alpha/\beta)V^E$$

using the smoothed representations of the excess enthalpies and volumes. Values of α, the coefficient of thermal expansion, and of β, the isothermal compressibility, were estimated for the mixture, from data for the pure components (1, 8) by assuming both properties to be additive on a volume fraction basis. Coefficients for the Redlich–Kister forms representing the results for U_V^E are included in Table 3.

A modified form of Barker's analysis (9) was used to calculate the distribution of material between the vapor and liquid phases from a series of observations of the equilibrium pressure p for known amounts of the two components contained in a known total volume. The molar excess Gibbs free energy of the liquid phase is related to the vapor–liquid equilibrium by the equation

$$[4] \quad G^E = \sum_i^2 x_i[RT\ln(y_i p/x_i p_i^0) + (B_{ii} - V_i^0)(p - p_i^0) + (2B_{12} - B_{11} - B_{22})(1 - y_i)^2 p]$$

TABLE 3. Values of the coefficients for eq. 1 determined by the method of least squares

System	Function	a_1	a_2	a_3	σ
Cyclopentane(*1*) – *cis*-decalin(*2*)	H^E(J mol^{-1})	−516.00	−31.07	0.941	0.49
	V^E(cm^3 mol^{-1})	−2.3546	0.4694	−0.1211	0.0021
	G^E(J mol^{-1})	−29.53	−71.29		1.6
	$U_V{}^E$(J mol^{-1})	257.77	−101.80	31.25	0.84
Cyclopentane(*1*) – *trans*-decalin(*2*)	H^E(J mol^{-1})	−1082.30	−46.51	7.06	1.01
	V^E(cm^3 mol^{-1})	−2.7700	0.3067	−0.0893	0.0024
	G^E(J mol^{-1})	−305.45	−117.99		3.4
	$U_V{}^E$(J mol^{-1})	−203.11	−83.61	30.02	1.26

where R is the gas constant, T is the absolute temperature, x_i and y_i are the mole fractions of component i in the liquid and vapor phases, respectively, and p_i^0 and V_i^0 are the vapor pressure and molar volume of pure liquid i. It is implicit in eq. 4 that the imperfection of the vapor phase can be described adequately for the present purpose by the equation of state

$$[5] \quad V^g = RT/p + y_1{}^2B_{11} + 2y_1y_2B_{12} + y_2{}^2B_{22}$$

where V^g is the molar volume of the vapor and the quantities B_{ij} are the second virial coefficients.

The Barker treatment assumes that at constant temperature G^E can also be represented by a Redlich–Kister form similar to eq. 1. The values of the coefficients a_γ are determined by an iterative calculation which minimizes the sum of the squares of the deviations between observed and calculated values of the pressure. In the present application, the composition of the liquid phase was computed for each iteration from the total amounts of the components by using eq. 5 to correct for the material present in the vapor phase. A value of $B_{11} = -1054$ cm^3 mol^{-1} (10) was adopted for cyclopentane. The empirical correlation developed by O'Connell and Prausnitz (11) was used to estimate B_{12} and B_{22} from critical point data (12–14). The values obtained were $B_{12} = -2825$ and $B_{22} = -8322$ cm^3 mol^{-1} for the *cis*-decalin system, and $B_{12} = -2599$ and $B_{22} = -6826$ cm^3 mol^{-1} for the *trans*-decalin system; these estimates are subject to fairly large uncertainties, not only because of the empirical nature of the correlation, but also due to the meager (and somewhat inconsistent) critical point data available for the decalins. Fortunately, the effects of these uncertainties are negligible since the terms in B_{12} and B_{22} make relatively minor contributions to G^E for the present systems.

The results of the vapor–liquid equilibrium studies at 25.000 °C are summarized in Table 4, where the experimental pressures and the corresponding values of x_1, y_1, and G^E calculated from the Barker analysis are given. Coefficients for the Redlich–Kister representation of G^E are included in Table 3. The experimental values of G^E and their representations by eq. 1, are plotted in Fig. 3.

The contribution of the molar excess entropy S^E to G^E is

$$[6] \quad TS^E = H^E - G^E$$

Curves for TS^E computed from this relation,

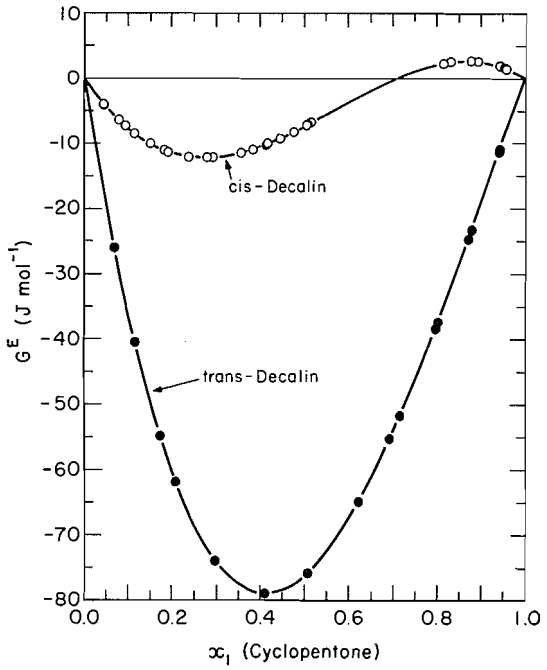

FIG. 3. Molar excess Gibbs free energies at 25 °C. Experimental results: ○, cyclopentane – *cis*-decalin; ●, cyclopentane – *trans*-decalin. Solid curves are least-squares representations by eq. 1.

Can. J. Chem. Downloaded from www.nrcresearchpress.com by 210.87.254.6 on 09/05/12
For personal use only.

TABLE 4. Vapor–liquid equilibria at 25 °C*

Cyclopentan(*1*) – *cis*-decaline(*2*)				Cyclopentane(*1*) – *trans*-decalin(*2*)			
x_1	p	y_1	G^E	x_1	p	y_1	G^E
0.0451	14.53	0.9448	−4.1	0.0687	20.72	0.9310	−26.0
0.0474	15.08	0.9474	−4.3	0.1156	33.61	0.9607	−40.5
0.0777	24.43	0.9684	−6.4	0.1734	51.41	0.9757	−54.8
0.0933	29.33	0.9740	−7.4	0.2093	61.12	0.9809	−61.9
0.1143	35.59	0.9792	−8.6	0.3000	88.78	0.9884	−74.0
0.1504	46.92	0.9848	−10.1	0.4120	126.11	0.9931	−79.0
0.1811	56.73	0.9878	−11.1	0.5081	157.47	0.9954	−75.9
0.1903	59.19	0.9885	−11.3	0.6236	195.74	0.9972	−64.8
0.2377	74.22	0.9913	−12.1	0.6927	218.83	0.9979	−55.3
0.2792	87.21	0.9930	−12.3	0.7162	225.87	0.9982	−51.7
0.2918	91.78	0.9935	−12.2	0.7955	251.86	0.9988	−38.3
0.3553	111.97	0.9951	−11.5	0.8006	253.28	0.9988	−37.4
0.3826	120.27	0.9956	−10.9	0.8699	275.36	0.9993	−24.7
0.4107	129.80	0.9961	−10.2	0.8776	278.53	0.9994	−23.2
0.4172	132.21	0.9962	−10.0	0.9403	298.08	0.9997	−11.3
0.4443	140.38	0.9966	−9.3	0.9422	299.01	0.9997	−11.0
0.4757	150.25	0.9970	−8.2				
0.5064	160.51	0.9974	−7.1				
0.5107	162.04	0.9974	−7.0				
0.5167	163.83	0.9975	−6.8				
0.8147	257.49	0.9994	2.3				
0.8313	263.49	0.9994	2.5				
0.8759	278.19	0.9996	2.6				
0.8947	283.32	0.9997	2.5				
0.9417	298.61	0.9998	1.8				
0.9532	302.59	0.9999	1.6				
0.9580	303.84	0.9999	1.4				

*Units: p, mm Hg; G^E, J mol.$^{-1}$

using the smoothed results for H^E and G^E are shown in Figs. 4 and 5.

Discussion

Comparison with Cyclohexane – Isomeric Decalin Systems

A direct comparison of our results with independent data from the literature is not possible since the excess properties of cyclopentane – isomeric decalin systems do not appear to have been studied previously. However, a qualitative comparison with the properties of cyclohexane – isomeric decalin systems (1, 15, 16) reveals some interesting differences.

At 25 °C, the excess enthalpies of cyclopentane – isomeric decalin systems are negative over the whole concentration range and the H^E curve for *trans*-decalin lies below that for *cis*-decalin. The excess enthalpies of cyclohexane – isomeric decalin systems (1) exhibit changes of sign at 25 °C but again the curve for *trans*-decalin is always lower than that for *cis*-decalin. Assuming the variations of H^E in these systems are qualitatively similar to those found in binary *n*-alkane systems (17, 18) it appears for both pairs of isomeric decalin systems that replacement of the *cis*-isomer by the *trans* is roughly equivalent to an increase in temperature or to an enhancement of the dissimilarity between the component molecules.

The volume changes for the four cycloalkane – isomeric decalin systems are all negative and the contractions for those formed from cyclopentane are considerably larger than for their cyclohexane counterparts (1). Qualitatively, this is in line with the greater disparity in the size of the component molecules in the cyclopentane systems. On the same basis, the relative positions of the V^E curves for *cis*-decalin and *trans*-decalin appear to be normal for the cyclopentane mixtures and reversed for the cyclohexane mixtures. Thus it is evident that other factors, apart from molecular size, are of importance in determining the volume behavior of these systems.

It was pointed out for the cyclohexane systems (1) that the volume correction needed to obtain U_V^E from H^E was relatively large. This is also true for the present cyclopentane systems. However, the values of U_V^E are positive for cyclopentane – *cis*-decalin and negative for

Can. J. Chem. Downloaded from www.nrcresearchpress.com by 210.87.254.6 on 09/05/12
For personal use only.

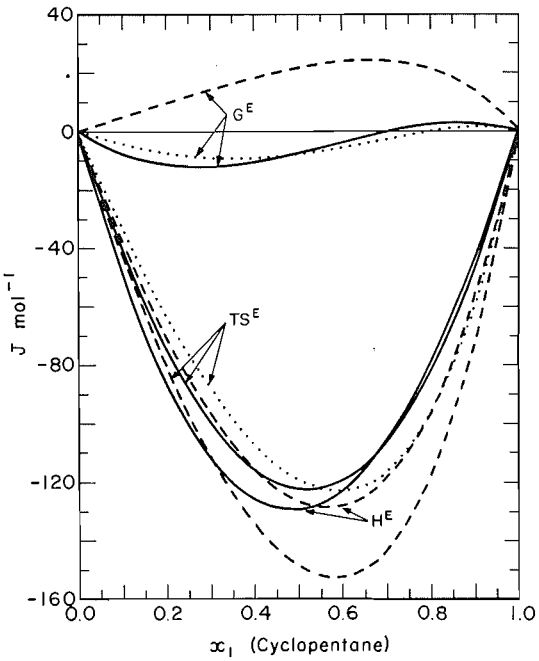

FIG. 4. Molar excess thermodynamic properties of cyclopentane – *cis*-decalin mixtures at 25 °C. Solid curves are least-squares representations of experimental results. Broken and dotted curves were calculated from the theory of Flory with $Q_{12} = 0$ and 0.00464 J cm^{-3} K^{-1}, respectively.

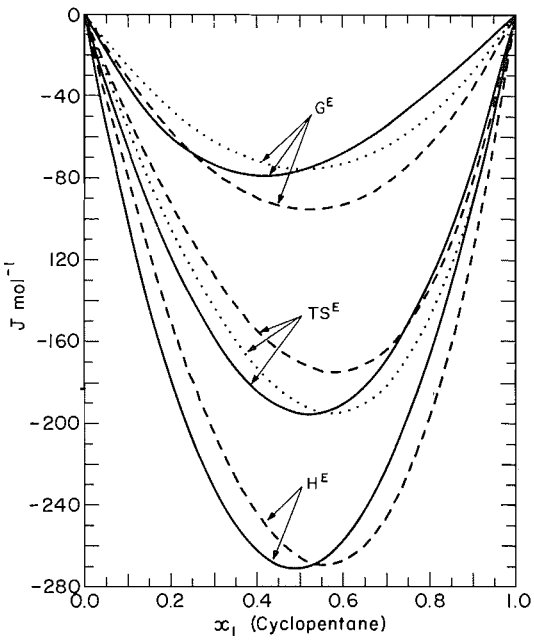

FIG. 5. Molar excess thermodynamic properties of cyclopentane – *trans*-decalin mixtures at 25 °C. Solid curves are least-squares representations of experimental results. Broken and dotted curves were calculated from the theory of Flory with $Q_{12} = 0$ and -0.00306 J cm^{-3} K^{-1}, respectively.

cyclopentane – *trans*-decalin, in contrast to the positive values found for both of the cyclohexane systems.

The excess Gibbs free energies of cyclopentane – isomeric decalin systems are relatively small at 25 °C and indicate a cancellation between the enthalpic and entropic contributions. The values of G^E for the *trans*-decalin systems are negative over the whole concentration range; those for the *cis*-decalin system change sign but the positive values observed are of the same magnitude as the experimental uncertainty. Unpublished vapor–liquid equilibria for the system cyclohexane – *cis*-decalin (15) indicate that the Gibbs free energy is small and positive at 25 °C. At higher temperatures (in the range 80–120 °C) Dutta (16) has reported G^E curves for cyclohexane with *cis*-decalin and with *trans*-decalin; both systems exhibit changes in the sign of G^E and a rather complicated variation with temperature.

Flory Theory of Mixtures

The theory of Flory (19) provided a fairly reasonable correlation (1) between the excess enthalpies and volumes of the cyclohexane – isomeric decalin mixtures and the properties of their pure components. It is therefore of interest to consider a similar treatment of the present results.

The Flory theory leads to the following formulae for the molar excess enthalpy, volume, and Gibbs free energy.

$$[7]\quad H^E = \sum_1^2 x_i p_i^* v_i^* (\tilde{v}_i^{-1} - \tilde{v}^{-1}) + x_1 v_1^* \theta_2 X_{12} \tilde{v}^{-1}$$

$$[8]\quad V^E = (x_1 v_1^* + x_2 v_2^*)(\tilde{v} - \phi_1 \tilde{v}_1 - \phi_2 \tilde{v}_2)$$

and

$$[9]\quad G^E = \sum_i^2 x_i p_i^* v_i^* \left[(\tilde{v}_i^{-1} - \tilde{v}^{-1}) + \tilde{T}_i \ln \left(\frac{\tilde{v}_i^{1/3} - 1}{\tilde{v}^{1/3} - 1} \right) \right] + x_1 v_1^* \theta_2 (X_{12} \tilde{v}^{-1} - Q_{12} T)$$

Derivations of these relations can be found in the original works of Flory and co-workers (19–21). The notation employed above is the same as in

Can. J. Chem. Downloaded from www.nrcresearchpress.com by 210.87.254.6 on 09/05/12
For personal use only.

Can. J. Chem. Downloaded from www.nrcresearchpress.com by 210.87.254.6 on 09/05/12
For personal use only.

our previous publications (1, 8) and will not be described in detail. It will suffice to note that the superscript asterisk and tilde are used, respectively, to label characteristic values and reduced values of the temperature, pressure, and volume. The reduced temperature of a mixture is

$$[10]\quad \tilde{T} = (\phi_1 p_1^* \tilde{T}_1 + \phi_2 p_2^* \tilde{T}_2)/(\phi_1 p_1^* + \phi_2 p_2^* - \phi_1 \theta_2 X_{12})$$

At low pressures, the reduced temperature and volume satisfy the equation of state

$$[11]\quad \tilde{T}\tilde{v}^{4/3} - \tilde{v}^{1/3} + 1 = 0$$

By hypothesis each molecule consists of a number of segments (isometric portions) and each segment carries a number of sites which may interact with sites on adjacent molecules. Segment fractions ϕ_i and site fractions θ_i are defined by the expressions

$$[12]\quad \phi_2 = 1 - \phi_1 = x_2/(x_2 + x_1 v_1^*/v_2^*)$$

and

$$[13]\quad \theta_2 = 1 - \theta_1 = \phi_2/(\phi_2 + \phi_1 s_1/s_2)$$

where s_1/s_2 is the ratio of the numbers of intermolecular contact sites per segment for the two species. Abe and Flory (20) showed that

$$[14]\quad s_1/s_2 = (v_2^*/v_1^*)^{1/3}$$

on the assumption that the number of sites on each molecule is proportional to the surface area of a sphere having a volume equal to the characteristic volume.

The quantity X_{12} in eq. 7 is treated as an empirical parameter and its value is usually adjusted to give the best fit between theoretical and experimental values of the excess enthalpy. It is assumed in eq. 9 that the combinatorial entropy is ideal; this is reasonable for molecules not differing excessively in size. The term with Q_{12} did not appear in the original formulation of the excess Gibbs free energy (19) but was added later (21). Q_{12}, like X_{12}, is treated as an adjustable parameter and its value is selected to give the best fit between theoretical and experimental values of G^E.

The characteristic temperatures, pressures, and volumes estimated previously for cyclopentane (8) and *cis*- and *trans*-decalin (1) were used in applying the Flory theory to the present systems. For convenience, the former estimates are listed again in Table 5. Assuming the validity of eq. 7, values of $X_{12} = -3.618$ and -9.949 J cm^{-3} gave least-squares fits of the smoothed excess enthalpies for the *cis*-decalin and *trans*-decalin systems, respectively. The broken curves for H^E in Figs. 4 and 5 were calculated with these values of X_{12}; the corresponding predictions for V^E, calculated from eq. 8, are plotted in Fig. 2.

TABLE 5. Characteristic values for the pure liquids at 25 °C

Component	T^* (°K)	p^* (J cm^{-3})	v^* (cm^3 mol^{-1})
Cyclopentane	4531	509.0	72.28
cis-Decalin	5739	542.6	127.30
trans-Decalin	5683	504.6	130.93

Two calculations of G^E and TS^E were carried out for each system. The first assumed $Q_{12} = 0$ for both systems; the second used the values of Q_{12} determined to give a least-squares fit of G^E for each system. The results of the calculations are shown as broken and dotted curves in Figs. 4 and 5.

Theoretical values of the excess functions for equimolar mixtures are compared with experimental results in Table 6. Also listed in this table are the standard deviations between the calculated and smooth experimental curves over the whole concentration range.

It can be seen from Figs. 2, 4, and 5, and from Table 6 that the Flory theory is fairly successful in correlating the excess properties of the cyclopentane – isomeric decalin systems. In some respects the correlation is better than that achieved previously for the cyclohexane – isomeric decalin systems (1). In order to approximate the sigmoid-shaped H^E curves of the latter systems, it was necessary to adjust not only X_{12}, but also the ratio s_1/s_2, and to use values of s_1/s_2 which were physically unrealistic.

The minima of H^E calculated for the cyclopentane – isomeric decalin systems are of the correct depth, but the curves are skewed to slightly larger mole fractions of cyclopentane than found experimentally. In contrast to the cyclohexane – isomeric decalin systems, the values of X_{12} are negative for the present systems. This is unusual for non-polar components, and it appears that the contributions to H^E arising from volume effects (1) are insufficient to account for the negative excess enthalpies observed experimentally. It is evident from Fig. 2 that the theory underestimates the contractions

Can. J. Chem. Downloaded from www.nrcresearchpress.com by 210.87.254.6 on 09/05/12
For personal use only.

TABLE 6. Comparison of results of Flory calculations with experimental values at 25 °C

System	Flory parameters		Molar excess property for equimolar mixture*							
			H^E (J mol^{-1})		V^E (cm^3 mol^{-1})		G^E (J mol^{-1})		TS^E (J mol^{-1})	
	X_{12} (J cm^{-3})	$10^3 Q_{12}$ (J cm^{-3} K^{-1})	Theory	Expt.	Theory	Expt.	Theory	Expt.	Theory	Expt.
Cyclopentane – *cis*-decalin	−3.618	0.0	−126.3 (11.6)	−129.0	−0.4830 (0.0754)	−0.5887	21.8 (21.8)	−7.4	−148.1 (23.7)	−121.6
	−3.618	4.64					−7.9 (2.3)	−7.4	−118.4 (9.5)	−121.6
Cyclopentane – *trans*-decalin	−9.949	0.0	−265.8 (20.6)	−270.6	−0.4221 (0.1937)	−0.6925	−95.6 (17.0)	−76.4	−170.2 (18.7)	−194.2
	−9.949	−3.06					−75.9 (9.0)	−76.4	−189.9 (11.8)	−194.2

*Entries in parentheses are standard deviations between theoretical and experimental values over the whole concentration range *i.e.* $[\int_0^1 (X_{\text{Flory}}{}^E(x_1) - X_{\text{Expt}}{}^E(x_1))^2 dx_1]^{1/2}$.

associated with the mixing process and that the relative positions of the *cis* and *trans* curves are reversed from those found experimentally. Whether this is due to inadequacies of the theoretical treatment or to uncertainties in the primary data for the component liquids is not clear.

The values of G^E and TS^E calculated for $Q_{12} = 0$ are of the right magnitude, however, there is a significant improvement in the agreement between theoretical and experimental values when Q_{12} is adjusted. The difference in sign of the least squares values of Q_{12} for the two systems follows directly from the calculations for $Q_{12} = 0$, which led to excess Gibbs free energies which were too positive for the *cis*-decalin system and too negative for the *trans*-decalin system.

We are indebted to Mr. P. J. D'Arcy and Mr. C. J. Halpin for their capable assistance in all phases of the experimental work.

1. G. C. Benson, S. Murakami, V. T. Lam, and J. Singh. Can. J. Chem. **48**, 211 (1970).
2. S. Murakami and G. C. Benson. J. Chem. Thermodynamics, **1**, 559 (1969).
3. H. D. Pflug and G. C. Benson. Can. J. Chem. **46**, 287 (1968).
4. J. Singh and G. C. Benson. Can. J. Chem. **46**, 1249 (1968).
5. American Petroleum Institute. Research Project 44. Selected values of properties of hydrocarbons and related compounds. Chemical Thermodynamics Properties Center, A. and M. College of Texas, College Station, Texas.
6. D. L. Camin and F. D. Rossini. J. Phys. Chem. **59**, 1173 (1955).
7. T. N. Bell, E. L. Cussler, K. R. Harris, C. N. Pepela, and P. J. Dunlop. J. Phys. Chem. **72**, 4693 (1968).
8. G. C. Benson and J. Singh. J. Phys. Chem. **72**, 1345 (1968).
9. J. A. Barker. Aust. J. Chem. **6**, 207 (1953).
10. R. W. Hermsen and J. M. Prausnitz. Chem. Eng. Sci. **18**, 485 (1963).
11. J. P. O'Connell and J. M. Prausnitz. Ind. Eng. Chem. Process Des. Develop. **6**, 245 (1967).
12. R. R. Dreisbach. Adv. Chem. Ser. No. 15 (1955).
13. R. C. Reid and T. K. Sherwood. The properties of gases and liquids. 2nd ed. McGraw-Hill Co., New York. 1966.
14. A. P. Kudchadker, G. H. Alani, and B. J. Zwolinski. Chem. Rev. **68**, 659 (1968).
15. T. Boublík. Unpublished results.
16. M. Dutta. Ph.D. Thesis. Ohio State University 1969; see also Dis. Abst. **30**, 1654B (1969).
17. M. L. McGlashan and K. W. Morcom. Trans. Faraday Soc. **57**, 581 (1961).
18. Th. Holleman. Physica, **31**, 49 (1965); see also Ph.D. Thesis. University of Amsterdam. 1964.
19. P. J. Flory. J. Am. Chem. Soc. **87**, 1833 (1965).
20. A. Abe and P. J. Flory. J. Am. Chem. Soc. **87**, 1838 (1965).
21. R. A. Orwoll and P. J. Flory. J. Am. Chem. Soc. **89**, 6822 (1967).

Can. J. Chem. Downloaded from www.nrcresearchpress.com by 210.87.254.6 on 09/05/12
For personal use only.

Can. J. Chem. Downloaded from www.nrcresearchpress.com by 210.87.254.5 on 09/05/12
For personal use only.

Kinetic and Equilibrium Studies of σ-Complex Formation Reactions Between 1,3,5-Trinitrobenzene and the Lyate Ions of Water, Methanol, Ethanol, *n*- and *i*-Propanol, and *n*-, *i*-, and *t*-Butanol in their Respective Solvents

L. H. GAN AND A. R. NORRIS
Department of Chemistry, Queen's University, Kingston, Ontario

Received March 16, 1971

Kinetic and thermodynamic parameters have been determined for the σ-complex formation reactions between 1,3,5-trinitrobenzene and the lyate ions of water, methanol, ethanol, *n*- and *i*-propanol and *n*-, *i*-, and *t*-butanol in their respective solvents. Trends in these values are interpreted in terms of specific solvation effects associated with both the base and the σ-complex. Solvent and kinetic isotope effects associated with the σ-complex formation reactions of ethoxide with 1,3,5-trinitrobenzene and 1,3,5-trinitrobenzene-d_3 in ethanol and ethanol-*O*-*d* have also been evaluated.

On a déterminé les paramètres cinétiques et thermodynamiques pour les réactions de formation de σ-complexes entre le trinitro-1,3,5 benzène et les ions lyates de l'eau, du méthanol, de l'éthanol, des propanols-1 et -2 et des *n*-, *i*-, et *t*-butanol dans leurs solvants respectifs. On interprête les tendances dans ces valeurs internes d'effets spécifiques de solvatation associés et avec la base et avec le σ-complexe. On a évalué les effets de solvant et les effets isotopiques cinétiques associés avec les réactions de formation de σ-complexe de l'éthylate avec le trinitro-1,3,5 benzène et le trinitro-1,3,5 benzène-d_3 dans l'éthanol et l'éthanol-*O*-*d*.

Canadian Journal of Chemistry, 49, 2490 (1971)

Introduction

As part of a comprehensive study of the effects of solvent and base in the reactions of bases with nitroaromatics we have looked at the reactions of a range of alkoxide ions with 1,3,5-trinitrobenzene (TNB) and 2,4,6-trinitrotoluene (TNT). Initially we determined at 25.0 °C specific rate constants only for the reactions of these two substrates with a wide range of alkoxide ions in the corresponding alcohols.[1] While the collection of rate data at a number of different temperatures was still in progress, but before studies had been extended to include the lower alcohols, Bernasconi (1) reported full kinetic data for the reactions of TNB with hydroxide ion in water, methoxide ion in methanol, and ethoxide ion in ethanol. We wish to report here kinetic and thermodynamic data for the reactions of TNB with a series of lyate ions derived from the higher alcohols together with some observations on the kinetics of the reactions of TNB and TNB-d_3 with ethoxide ion in ethanol and ethanol-*O*-*d*.

[1]The results of these studies were presented, in part, at the International Conference on the Mechanisms of Reactions in Solution held in Canterbury, England July 20–24, 1970. Paper B-11.

Experimental

Materials

Eastman 1,3,5-trinitrobenzene was recrystallized several times from an ethanol–water mixture and dried *in vacuo* over silica gel, m.p. 122 °C (uncorrected). 1,3,5-Trinitrobenzene-d_3 was prepared as described by Buncel and Symons (2), recrystallized from ethanol–water, and dried to constant weight *in vacuo*, m.p. 120.5–121.5° (uncorrected). Analysis of the compound using an i.r. technique described by Symons (3) indicated 91 ± 2% deuteration.

Reagent grade methanol, absolute ethanol, ethanol-*O*-*d* (Merck, Sharp, and Dohme) and *n*-propanol were distilled from magnesium and iodine according to the procedure described by Vogel (4). The higher alcohols, which were reagent grade or better, were refluxed over Linde Molecular Sieve 4 Å for several hours then distilled under nitrogen. Normally only the middle third of the distillate was retained. All solvents were stored under dry nitrogen prior to use.

Standardized stock solutions of sodium hydroxide (Fisher Scientific 0.10 and 1.0 *N*) were used as received. Stock solutions of the sodium alkoxides were prepared by adding freshly cut sodium metal, pre-washed in the solvent in question, to pure solvent maintained in an atmosphere of dry nitrogen. Solutions thus prepared were stored under nitrogen and standardized immediately before use by titration with 0.10 *N* HCl to the phenolphthalein-endpoint. Stock solutions of the sodium alkoxides were usually 0.05 to 0.10 *M* in concentration. Solutions of lower concentration were prepared by dilution.

Eastman 1-(*p*-hydroxyphenyl)-2,4,6-triphenylpyridin-

Can. J. Chem. Downloaded from www.nrcresearchpress.com by 210.87.254.5 on 09/05/12
For personal use only.

ium betaine was converted to the perchlorate salt as described by Dimroth *et al.* (5) and recrystallized from anhydrous methanol. After drying *in vacuo* over silica gel the pale yellow, needle-shaped crystals had m.p. 250 °C (uncorrected).

All other chemicals were reagent grade or better and were used without further purification.

Procedure

Kinetic measurements were carried out by means of a Durrum–Gibson stopped-flow spectrophotometer. Water from a constant temperature water bath was circulated through the cell compartment and drive syringe chamber to maintain the reacting solutions at a constant temperature.

All kinetic runs were carried out with base in large excess over TNB. Concentrations of TNB varied from 0.4×10^{-5} to 2.0×10^{-5} *M*. Concentrations of RO^- varied from 1.0×10^{-4} to 70×10^{-4} *M* except for the case R = H where HO^- varied from 2.5×10^{-2} to 25.0×10^{-2} *M*. The ionic strength of the reactant mixtures was not maintained constant except in reactions involving HO^- where μ was kept at 0.25 *M* using NaCl. At the low concentrations of base employed, even very low levels of absorbed CO_2 may well alter the actual base concentrations in an uncontrolled manner thereby rendering the experimental data inaccurate. To preclude CO_2 absorption all manipulations, such as preparation of the sodium alkoxide stock solutions, titration of these solutions with 0.10 *N* HCl, dilution of the stock solutions, and transfer of the base solutions to the "reservoir" syringes of the stopped-flow spectrophotometer, were performed under an atmosphere of dry nitrogen. Consistently reproducible kinetic results, the absence of any gentle rise in the infinity line as reported by Bernasconi (1), and linear absorbance *vs.* concentration of TNB plots passing through (0, 0), for solutions of constant base but variable TNB concentration suggest that errors due to CO_2 absorption have been largely eliminated.

Changes in concentration of the complex were normally followed by means of the absorbance at the long wavelength maximum. Pseudo-first-order rate constants (k_{obs}) were obtained from the slopes of the $\ln(A_\infty - A_t)$ *vs.* time plots where A_∞ and A_t refer to absorbances at times infinity and t respectively. Plots were normally linear to approximately 80% completion of the reaction. Individual k_{obs} values were reproducible to $\pm 3\%$ except for the reactions of TNB with isopropoxide at high temperature where the reproducibility was generally $\pm 5\%$.

Equilibrium constants for complex formation were determined by a spectrophotometric method using data obtained on a Cary 14 spectrophotometer. Since solutions used to determine equilibrium constants had approximately the same concentrations of base and TNB as those solutions used in the kinetic experiments, the precautions used to preclude CO_2 absorption in the kinetic experiments were also applied in all studies involving the determination of equilibrium constants.

In the E_t (5) measurements 3 to 5 mg of pure betaine perchlorate was weighed into a 25.0 ml volumetric flask, 0.10 ml of a 1% methanolic solution of sodium methoxide was added, and the flask filled to the mark with the solvent whose E_t was to be determined. Although the final solution always contained approximately 0.4% methanol and some sodium perchlorate, the presence of these species at the concentrations stated has little effect on the magnitude of the measured E_t (5). The absorption spectrum of the betaine was recorded on a Cary 14 spectrophotometer and the E_t of the solvent calculated from eq. 1, where $\bar{\nu}$ is the wavenumber (cm^{-1}) of the absorption maximum of betaine in the solvent (5).

$$[1] \qquad E_t \text{ (kcal mol}^{-1}) = 2.859 \times 10^{-3} \bar{\nu}$$

Results and Discussion

The reaction of TNB and RO^- under the conditions employed in our studies leads to the reversible formation of 1:1 σ-complexes **1** according to eq. 2. The 1:1 stoichiometry of the

[2] TNB + RO^- (in ROH) $\underset{k_{-1}}{\overset{k_1}{\rightleftharpoons}}$ 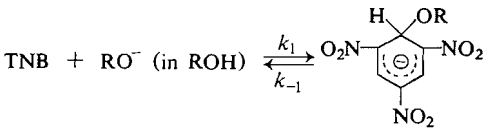

1

R = H, CH_3, C_2H_5, *n*-C_3H_7, *i*-C_3H_7, *n*-C_4H_9, *i*-C_4H_9, and *t*-C_4H_9

TNB–OR^- complexes where R = H, CH_3, and C_2H_5 has previously been established (1, 6–9). The 1:1 stoichiometry of each of the remaining complexes has been confirmed by the results obtained in the course of the kinetics and equilibrium studies of these systems and, in the case of the complex in which R = *n*-C_3H_7, through the use of the method of continuous variations (10) to establish the composition.

The spectral properties of the reaction products studied (Table 1) are fully in accord with the formulation of these species as σ-complexes (6, 11).

In all the systems studied k_{obs} was linearly related to the concentration of RO^- over the entire range of RO^- concentrations at all the temperatures studied. Typical data are shown in Fig. 1 for the reactions of TNB and *n*-propoxide ion at 4.0, 16.5, 25.0, 30.0, and 35.0 °C. The linearity of the k_{obs} *vs.* [RO^-] plots strongly suggests that ion-pairing effects are not a problem at the concentrations of base employed in these studies. Further support for this suggestion comes from the observation that, over the range of base concentrations studied, solutions of potassium *t*-butoxide yielded the same values of k_{obs} as did solutions of equal concentration of sodium *t*-butoxide. Of all the systems studied ion-pairing

TABLE 1. Absorption maxima and extinction coefficients of σ-complexes of some alkoxides with TNB in their respective alcohols at 25 °C

Base/solvent	λ_1 (nm)	λ_2 (nm)	$\varepsilon_1 \times 10^{-4}$ (1 mol^{-1} cm^{-1})	$\varepsilon_2 \times 10^{-4}$ (1 mol^{-1} cm^{-1})	$\varepsilon_1/\varepsilon_2$	Reference
CH_3O^-/CH_3OH	425	495	3.12	2.11	1.48	6
$C_2H_5O^-/C_2H_5OH$	424	497	3.39	2.28	1.49	6
n-$C_3H_7O^-/n$-C_3H_7OH	427	502	2.62 ± 0.02	1.74 ± 0.01	1.503 ± 0.008	This work
n-$C_4H_9O^-/n$-C_4H_9OH	428	504	2.61 ± 0.04	1.73 ± 0.01	1.508 ± 0.005	This work
i-$C_4H_9O^-/i$-C_4H_9OH	429	501	2.60 ± 0.01	1.73 ± 0.01	1.503 ± 0.005	This work
i-$C_3H_7O^-/i$-C_3H_7OH	427	501	2.59 ± 0.08	1.75 ± 0.03	1.480 ± 0.030	This work

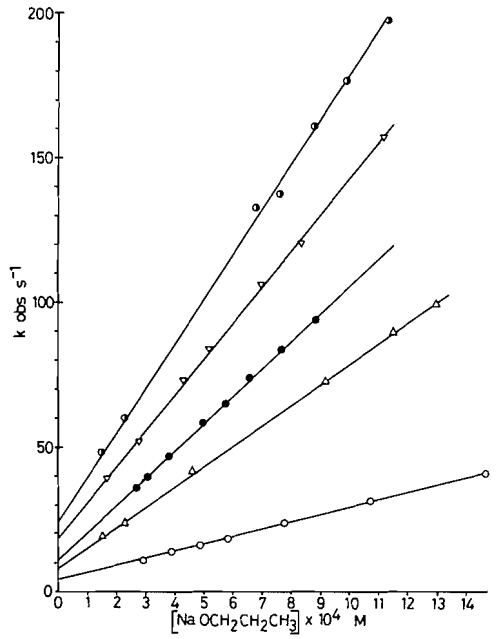

FIG. 1. Plot of k_{obs} *vs.* concentration of *n*-propoxide ion for the σ-complex formation reactions between 1,3,5-trinitrobenzene and *n*-propoxide in *n*-propanol at 4.0 (0), 16.5 (△), 25.0 (●), 30.0 (▽), and 35.0 °C (◑).

effects would be expected to be most pronounced in the *t*-butoxide – *t*-butanol system (12).

Since $[RO^-] \gg [TNB]$ in all runs

$$[3] \qquad k_{obs} = k_1[RO^-] + k_{-1}$$

Values of k_1 and k_{-1} were obtained in all cases from the "least squares" slopes and intercepts of plots of k_{obs} *vs.* $[RO^-]$. Because k_{-1} values are obtained from the intercepts of such plots the error associated with k_{-1} is always considerably larger than the error associated with k_1. When in addition the magnitude of k_{-1} is very small, as it is in the reactions of TNB with the lyate ions of the higher alcohols, the actual value of k_{-1} becomes very uncertain.

In Table 2 are listed specific rate constants (k_1 and k_{-1}), equilibrium constants determined spectrophotometrically (K), and kinetic and thermodynamic parameters associated with σ-complex formation between TNB and the various lyate ions according to eq. 1.

A substantial variation is found for the rate coefficients of complex formation with the various lyate ions. These are found to be in the ratio 1:304:1900:3660:3740:4960:3820:1500 for HO^-, CH_3O^-, $C_2H_5O^-$, n-$C_3H_7O^-$, n-$C_4H_9O^-$, i-$C_4H_9O^-$, i-$C_3H_7O^-$, and t-$C_4H_9O^-$.

Our value of k_1 (at 25.0 °C) for the TNB-CH_3O^- reaction agrees well with Bernasconi's (1) value for this reaction despite the fact that systems of different ionic strength were used in the studies and that we used the stopped-flow technique while Bernasconi used the temperature-jump technique to obtain rate constants. Agreement is much less satisfactory in the case of the TNB–HO^- and TNB–$C_2H_5O^-$ reactions. Exact comparisons in the case of the TNB–HO^- system are rendered difficult because reaction media of quite different ionic strengths (μ) were used in the two studies.[2]

In studies of the TNB–$C_2H_5O^-$ reaction we made no attempt to control μ ($\mu_{max} = 7.2 \times 10^{-3}$ *M*) and studied the reaction under conditions $[RO^-] \gg [TNB]$. Bernasconi (1) chose reaction conditions $[TNB] \gg [RO^-]$. In principle both modes of study should lead to the same values of k_1 and k_{-1}. While Bernasconi's and Ainscough and Caldin's values of k_1 for the TNB–$C_2H_5O^-$ at 25.0 °C apparently show reasonable agreement, it should be noted that

[2]Although results from other systems studied (13) suggest that ionic strength effects in the formation of 1:1 complexes should be negligible, no detailed information is available regarding ionic strength effects in the formation of 1:1 σ-complexes between nitroaromatics and uninegative bases.

Can. J. Chem. Downloaded from www.nrcresearchpress.com by 210.87.254.5 on 09/05/12
For personal use only.

Can. J. Chem. Downloaded from www.nrcresearchpress.com by 210.87.254.5 on 09/05/12
For personal use only.

TABLE 2. Kinetic and thermodynamic parameters of Meisenheimer complexes at 25 °C

	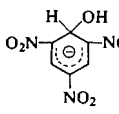 in H_2O	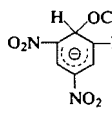 in CH_3OH	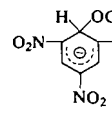 in C_2H_5OH	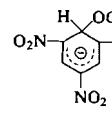 in n-C_3H_7OH	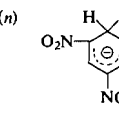 in n-C_4H_9OH	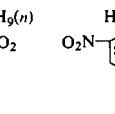 in i-C_4H_9OH	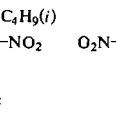 in i-C_3H_7OH	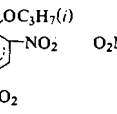 in t-C_4H_9OH
$k_1(M^{-1}\ s^{-1})$	25.3 (37.5)[a]	7700 (7050)[a]	49 500 (33 400)[a]	92 600 ± 1700[b]	94 700 ± 1000	125 800 ± 3600	96 700 ± 5000	38 000 ± 2000[c]
$k_{-1}(s^{-1})$	13.4 (9.8)[a]	357 (305)[a]	15.4 (27.5)[a]	11.9 ± 1.1	5.3 ± 0.3	1.7 ± 1.2	1.7 ± 2.2	<1
$k_1/k_{-1}(M^{-1})$	1.88 (3.73)[a]	21.6 (23.1)[a]	3100 (1210)[a]	7800	17 900	74 000	—	>38 000
$K(M^{-1})$	2.7[d,e]	16.6	2020	7080	14 360	53 130	204 000	—
ΔH_1^*(kcal mol^{-1})	15.6 ± 0.8[a]	10.2 ± 0.8[a]	8.7 ± 0.1[a] (11.7 ± 0.1)[f]	7.3 ± 0.6[g]	7.3 ± 0.6	8.0 ± 0.6	5.8 ± 0.4	6.5 ± 0.8
ΔS_1^*(cal deg^{-1} mol^{-1})	1.1 ± 2.7[a]	−6.7 ± 2.7[a]	−8.6 ± 3.4[a] (2.2 ± 0.6)[f]	−6.4 ± 2.3	−6.4 ± 2.3	−3.9 ± 2.3	−11.7 ± 1.4	−11.5 ± 2.7
ΔH_{-1}^*(kcal mol^{-1})	7.3 ± 0.8[a]	9.2 ± 0.8[a]	10.4 ± 1.2[a] (11.4 ± 0.2)[f]	10.3 ± 0.9[i] (11.7 ± 2.5)[h]	9.0 ± 0.7[i]	11.0 ± 1.8[i]	16.0 ± 1.0[i]	—
ΔS_{-1}^*(cal deg^{-1} mol^{-1})	−29.4 ± 2.7[a]	−16.3 ± 2.7[a]	−16.9 ± 4[a] (−14.3 ± 0.6)[f]	−14.0 ± 3.3	−19.7 ± 2.5	−16.9 ± 5.3	−2.0 ± 3.6	—
ΔH^0(kcal mol^{-1})	8.3 ± 1.6[a]	1.0 ± 1.6[a]	−1.4 ± 2.2[a] (0.3 ± 0.3)[f]	−3.0 ± 0.3	−1.7 ± 0.1	−3.0 ± 1.2	−10.2 ± 0.6	—
ΔG^0(kcal mol^{-1})				−5.25	−5.67	−6.45	−7.23	—
ΔS^0(cal deg^{-1} mol^{-1})	30.5 ± 5.4[a]	9.6 ± 5.4[a]	8.3 ± 7.4[a] (16.5 ± 1.5)[f]	7.6 ± 1.0	13.3 ± 0.2	13.0 ± 3.0	−9.7 ± 2.2	—
log $A_1(M^{-1}\ s^{-1})$				10.8 ± 0.5	10.8 ± 0.5	11.4 ± 0.5	9.7 ± 0.3	9.7 ± 0.6

[a]Reference 1.
[b]Error limits for k_1 and k_{-1} are based on the errors associated with the "least square" slopes and intercepts respectively of plots of k_{obs} *vs.* [RO$^-$].
[c]At 30 °C.
[d]Reference 7.
[e]Reference 8.
[f]Reference 9.
[g]Error limits for ΔH_1^* are based on the maximum and minimum slopes obtained in plots of log k_1 *vs.* $1/T$. Error limits for ΔS_1^* are based on the maximum and minimum intercepts obtained, at $1/T = 0$, in plots of log k_1 *vs.* $1/T$.
[h]Obtained from plots of log k_{-1} *vs.* $1/T$.
[i]$\Delta H_{-1}^* = \Delta H_1^* - \Delta H^0$.

Can. J. Chem. Downloaded from www.nrcresearchpress.com by 210.87.254.5 on 09/05/12
For personal use only.

Ainscough and Caldin (9) did not obtain k_1 at 25 °C directly but through the use of k_1 and E_a values determined at lower temperatures. As Bernasconi (1) points out the value of E_a reported by Ainscough and Caldin is probably in error (*vide infra*).

The trend in k_1 values is intelligible in terms of decreasing solvation of the lyate ion in passing from HO^- through to $i\text{-}C_4H_9O^-$. The lower values of k_1 recorded for $i\text{-}C_3H_7O^-$ and $t\text{-}C_4H_9O^-$ are seen to arise largely because low ΔH_1^+ values (in the range of ΔH_1^+ for R = $n\text{-}C_3H_7$ and $n\text{-}C_4H_9$) are offset by the significantly more negative values of ΔS_1^+ for these alkoxides as compared to the ΔS_1^+ values for R = $n\text{-}C_3H_7$ and $n\text{-}C_4H_9$. Both steric effects associated with formation of a carbon–oxygen bond in **1** and less efficient solvation of the $i\text{-}C_3H_7O^-$ and $t\text{-}C_4H_9O^-$ ions in their ground states would be expected to contribute to the more negative values of ΔS_1^+ in these systems. That steric effects are important in determining the magnitude of k_1 can be seen by comparing the ΔH_1^+ and ΔS_1^+ values for the systems R = $i\text{-}C_4H_9$ and $i\text{-}C_3H_7$.[3]

Our kinetic parameters ΔH_1^+ and ΔS_1^+ are in agreement with Bernasconi's results where R = H, CH_3, and C_2H_5. In the light of all the thermodynamic values reported it seems probable that Ainscough and Caldin's values of ΔH_1^+ and ΔS_1^+ for the TNB–$C_2H_5O^-$ reaction are in error.

Rate coefficients for reversion of complex to reactants (k_{-1}) show a less pronounced variation than do k_1 values in going from HO^- to $t\text{-}C_4H_9O^-$. Values of k_{-1} are in the ratio 1:26.6:1.15:0.89:0.39:0.12 < 0.12: ⩽ 0.07 for the same sequence of bases discussed above. Again, our value of k_{-1} for the TNB–CH_3O^- reaction agrees well with that reported by Bernasconi (1) while agreement in the TNB–HO^- and TNB–$C_2H_5O^-$ systems is less satisfactory. The surprisingly low value of k_{-1} for the TNB–HO^- system has been attributed by Bernasconi (1) to intramolecular hydrogen bonding to an ortho nitro group in complex **1**. Comparison of the ΔH_{-1}^+ and ΔS_{-1}^+ values for the TNB–HO^- system to the corresponding values in the remaining TNB–RO^- systems (where R = alkyl) indicates the major difference arises in the ΔS_{-1}^+ term since the ΔH_1^+ values do not change appreciably. The value of ΔH_{-1}^+ is unexpectedly high while the value of ΔS_{-1}^+ is unexpectedly low for the TNB – $i\text{-}C_3H_7O^-$ system. Both effects may be related to a much greater solvation of the σ-complex by $i\text{-}C_3H_7OH$. Detailed information regarding the heats of solution of TNB, sodium alkoxide and the sodium salt of the 1:1 σ-complex would be required to test this suggestion. Calorimetric studies of the type indicated have been reported by Larsen *et al.* (15) in connection with the reaction of sodium methoxide and 2,4,6-trinitroanisole in a wide range of methanol–dimethylsulfoxide mixtures. In this system, in passing from methanol to 95% dimethylsulfoxide–methanol, the heat of solution of sodium methoxide decreased by 10.6 kcal mol^{-1} while the heat of solution of the adduct increased by 7.0 kcal mol^{-1}.

In most cases in which equilibrium constants for complex formation (K) can be measured independently by a spectrophotometric technique the agreement between K and k_1/k_{-1} is reasonable. In general, because of uncertainties in k_{-1}, particularly at low values of k_{-1}, the ratios k_1/k_{-1} are best regarded as approximations only to the true values of K. For all the systems studied equilibrium constants determined spectrophotometrically are considered to be the more reliable except where K exceeds 5×10^5 l mol^{-1}.

Equilibrium constants for complex formation are in the ratio 1:9:1100:3900:7900:24,400:113,000 for HO^-, CH_3O^-, $C_2H_5O^-$, $n\text{-}C_3H_7O^-$, $n\text{-}C_4H_9O^-$, $i\text{-}C_4H_9O^-$, and $i\text{-}C_3H_7O^-$.

In the systems under study both solvent effects and base effects must necessarily play a role in determining the values of ΔH_1^+, ΔS_1^+, ΔH_{-1}^+, ΔS_{-1}^+, and ΔG^0. It is of interest to see what relationships, if any, exist between the observed thermodynamic and kinetic parameters and known solvent and base parameters.

For the cases R = CH_3, C_2H_5, $n\text{-}C_3H_7$, $i\text{-}C_3H_7$, $n\text{-}C_4H_9$, and $i\text{-}C_4H_9$ the log K *vs.* solvent parameter E_t (5, 16) is linear with a slope −0.57 (Fig. 2). The linear relationship between log K and the E_t of the solvents suggests that solvent effects play a major role in determining the equilibrium constants for reactions of the type under investigation

[3]A study of the replacement of halogens from 6-halogenobenzothiazoles by mercaptide ions in a common solvent (methanol) revealed that branching at the position α to the nucleophilic atom in the nucleophile resulted in a rate retardation whose magnitude was nearly independent of the size of the halogen displaced (14).

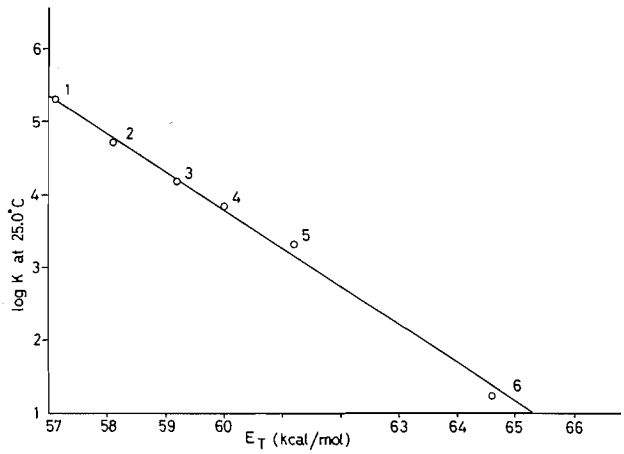

FIG. 2. Plot of log K at 25.0° for σ-complex formation according to eq. 2 *vs.* the solvent parameter E_t of the corresponding ROH. Points: 1, *i*-propanol; 2, *i*-butanol; 3, *n*-butanol; 4, *n*-propanol; 5, ethanol; 6, methanol.

(17). For σ-complex formation between cyanide ion and TNB in the alcohols a linear log K *vs.* E_t plot with slope −0.35 was found over the range R = CH_3, C_2H_5, *n*-C_3H_7, *i*-C_3H_7, *n*-C_4H_9, and *t*-C_4H_9 (17). The more negative slope observed in the reactions of TNB with RO^- undoubtedly reflects the combined effect of changing solvent and changing base strength as one proceeds from R = CH_3 to R = *n*-C_4H_9 in the RO^- series. For dilute alcoholic solutions (*e.g.*, 0.1 *M* alkali metal alkoxide in the corresponding alcohol) the order of basicity rises in passing from methanol (H_- = 12.66) to ethanol (H_- = 14.57) to *i*-propyl alcohol (H_- = 16.95) to *t*-butyl alcohol (H_- = 19.14) (18).

Log k_1 and log k_{-1} *vs.* E_t plots are also approximately linear for the cases R = CH_3, C_2H_5, *n*-C_3H_7, and *n*- and *i*-C_4H_9 with slopes −0.23 and 0.31 respectively. Employing the E_t values of *i*-C_3H_7OH and *t*-C_4H_9OH as bases, lower than expected values of log k_1 and higher than expected values of log k_{-1} are obtained for R = *i*-C_3H_7 and *t*-C_4H_9. When R = H both log k_1 and k_{-1} values are smaller than expected on the basis of the E_t for H_2O with log k_{-1} showing the most marked deviation from the expected value. This suggests that K for the case R = H is higher than expected on the basis of the E_t value for H_2O largely because of the abnormally small value of k_{-1}. A possible reason for the small value of k_{-1} in this system has already been advanced (1).

TABLE 3. Pseudo-first-order rate constants for σ-complex formation between 1,3,5-trinitrobenzene and 1,3,5-trinitrobenzene-d_3 with ethoxide ion in ethanol at 25.0 °C

$[NaOC_2H_5]$ ($M \times 10^{-4}$)	k_{obs}[a] (s^{-1})	
	TNB	TNB-d_3
3.6	13.4	13.3
6.7	21.8	21.6
12.2	34.7	34.6
21.6	51.6	51.5
25.4	59.4	59.6
29.0	70.0	70.5

[a] From plots of ln ($A_\infty - A_t$) *vs.* time; A measured at 426.5 nm; $[TNB]_0 = 0.82 \times 10^{-5} - 1.15 \times 10^{-5} M$.

As part of this study we also investigated the reaction of TNB-d_3 with ethoxide ion in ethanol. The data in Table 3 show that at the same concentration of ethoxide ion k_{obs} is, within experimental error, the same for the two substrates. We can discern no kinetic isotope effect associated with this σ-complex formation reaction. If a kinetic isotope effect $\{k_1(TNB)/k_1(TNB\text{-}d_3)\}$ exists, we estimate it is less than 1.03. Negligible kinetic isotope effects are to be expected for σ-complex formation reactions (19).

A solvent isotope effect is associated with σ-complex formation in the TNB–$C_2H_5O^-$ reaction as exemplified by the data in Table 4. At every base concentration k_{obs} for σ-complex formation is substantially larger in ethanol-*O*-*d*

Can. J. Chem. Downloaded from www.nrcresearchpress.com by 210.87.254.5 on 09/05/12
For personal use only.

TABLE 4. Pseudo-first-order rate constants for σ-complex formation between 1,3,5-trinitrobenzene and ethoxide ion in ethanol and ethanol-*O-d* at 25.0 °C

$[NaOC_2H_5]$ ($M \times 10^{-3}$)	k_{obs}[a] (s^{-1})	
	Ethanol	Ethanol-*O-d*
0.50	18.0	37.5
1.0	28.6	57.8
2.0	50.1	101.0
2.5	61.0	121.0
3.0	72.0	140.5
3.5	83.0	—
4.0	93.9	—

[a]From plots of ln $(A_\infty - A_t)$ *vs.* time; A measured at 426.5 nm; $[TNB]_0 = 1.13 \times 10^{-5}$ M.

than in ethanol. Analysis of the kinetic data yields solvent deuterium isotope effects $\{k_1(C_2H_5OD)/k_1(C_2H_5OH)\}$ and $\{k_{-1}(C_2H_5OD)/k_{-1}(C_2H_5OH)\}$ of 1.92 ± 0.05 and 2.4 ± 0.5 respectively. A solvent isotope effect $\{k_1(C_2H_5OD)/k_1(C_2H_5OH)\}$ of 1.84 has been reported by Bellobono *et al.* (20) for the reaction of ethoxide ion and 2,4-dinitrochlorobenzene while the reaction of ethoxide ion and 2,4,6-trinitrotoluene to form 2,4,6-trinitrobenzyl anion shows a solvent isotope effect of 1.82.[4] Solvent isotope effects $\{k_1(CH_3OD)/k_1(CH_3OH)\}$ of 1.96 and 1.62 have been reported for the σ-complex formation reactions between methoxide ion and 2,4-dinitroanisole (21) and methoxide ion and 2-cyano-4,6-dinitroanisole (22).

Financial support by the National Research Council of Canada is gratefully acknowledged.

[4]E. Buncel, A. R. Norris, K. E. Russell, and R. Tucker. To be published.

1. C. F. BERNASCONI. J. Am. Chem. Soc. **92**, 4682 (1970).
2. E. BUNCEL and E. A. SYMONS. Can. J. Chem. **44**, 771 (1966).
3. E. A. SYMONS. Ph.D. Thesis. Queen's University, Kingston, Ontario, 1969.
4. A. I. VOGEL. A Text-book of practical organic chemistry. 3rd Ed., Longmans, London.
5. K. DIMROTH, C. REICHHARDT, T. SIEPMANN, and F. BOHEMANN. Leibigs Ann. Chem. **661**, 1 (1963).
6. E. BUNCEL, A. R. NORRIS, and K. E. RUSSELL. Quart. Rev. London, **22**, 123 (1968).
7. T. ABE. Bull. Chem. Soc. Jap. **33**, 41 (1960).
8. V. GOLD and C. H. ROCHESTER. J. Chem. Soc. 1710 (1964).
9. J. B. AINSCOUGH and E. F. CALDIN. J. Chem. Soc. 2546 (1956).
10. P. JOB. Ann. de Chim. **9**, 113 (1928).
11. M. J. STRAUSS. Chem. Rev. **70**, 667 (1970).
12. W. H. SAUNDERS, JR., D. G. BUSHMAN, and A. F. COCKERILL. J. Am. Chem. Soc. **90**, 1775 (1968).
13. M. R. CRAMPTON. J. Chem. Soc. B, 1341 (1967).
14. G. BARTOLI, L. DINUNNO, and P. E. TODESCO. Tetrahedron Lett. 2369 (1968).
15. J. W. LARSEN, K. AMIN, and J. H. FENDLER. J. Am. Chem. Soc. In press
16. C. REICHHARDT. Angew. Chem. Int. Ed. Engl. **4**, 29 (1965).
17. E. BUNCEL, A. R. NORRIS, W. PROUDLOCK, and K. E. RUSSELL. Can. J. Chem. **47**, 4129 (1969).
18. J. F. COETZEE and C. D. RITCHIE. Solvent–solute interactions. Marcel Dekker Inc., New York, N.Y. 1969.
19. L. MELANDER. Isotope effects on reaction rates. Ronald Press, New York, N.Y., 1960.
20. I. R. BELLOBONO, P. BELTRAME, M. G. CATTANIA, and M. SIMONETTA. Tetrahedron Lett. 2673 (1968).
21. C. F. BERNASCONI. J. Am. Chem. Soc. **90**, 4982 (1968).
22. J. H. FENDLER, E. J. FENDLER, and C. E. GRIFFIN. J. Org. Chem. **34**, 689 (1969).

Can. J. Chem. Downloaded from www.nrcresearchpress.com by 210.87.254.5 on 09/05/12
For personal use only.

Can. J. Chem. Downloaded from www.nrcresearchpress.com by 210.87.254.40 on 09/05/12
For personal use only.

Crystal and Molecular Structure of 2-Bromo-11-ethyl-5,9-dimethoxytetracyclo[5.4.1.1^{4,12}.1^{8,11}]tetradecan-3-one, $C_{18}H_{27}BrO_3$

R. F. DUNPHY AND H. LYNTON

Department of Chemistry, University of New Brunswick, Fredericton, New Brunswick

Received March 11, 1971

The molecular structure of 2-bromo-11-ethyl-5,9-dimethoxytetracyclo[5.4.1.1^{4,12}.1^{8,11}]tetradecan-3-one, $C_{18}H_{27}BrO_3$, synthesized in an attempt to develop a method of conversion from an advanced relay compound to the alkaloid delphinine, has been determined by the heavy atom method. The compound crystallizes in the monoclinic system, space group $P2_1/c$, with unit cell dimensions $a = 9.684(9)$, $b = 13.481(15)$, $c = 12.988(14)$ Å, $\beta = 99.47(7)°$, and four molecules in the unit cell. The atomic parameters were refined by block-diagonal least squares using anisotropic thermal parameters. The hydrogen atom positions were established but the parameters were not refined. The final agreement residual for 816 observed reflections is $R = 0.044$.

The stereochemistry of the compound was found to be unsuitable for the delphinine synthesis.

La structure moléculaire du 2-bromo-11-ethyl-5,9-diméthoxytétracyclo[5.4.1.1^{4,12}.1^{8,11}]tétradecan-3-one, $C_{18}H_{27}O_3Br$, synthétisé dans l'espoir d'obtenir l'alcaloide delphinine à partir d'une étape intermédiaire avancée, a été déterminée par la méthode de l'atome lourd. Ce composé cristallise dans le système monoclinique, groupe d'espace $P2_1/c$. La maille élémentaire, contenant quatre molécules, a pour dimensions: $a = 9.684(9)$, $b = 13.481(15)$, $c = 12.988(14)$ Å, et $\beta = 99.47(7)°$. Les paramètres atomiques ont été affinés par moindres carrés (diagonalisation par blocs) en utilisant des facteurs thermiques anisotropes. Les positions des atomes d'hydrogène ont été établies mais n'ont pas été affinées. L'indice d'accord final est $R = 0.044$ pour 816 reflexions observées.

La stéréochimie de ce composé ne convient pas à la synthèse de la delphinine.

Canadian Journal of Chemistry, 49, 2497 (1971)

Introduction

In 1970, Wiesner *et al.* (1) reported the synthesis of an advanced relay compound and showed it to be indistinguishable from the product obtained by degradation of delphinine. A conversion of this relay compound to delphinine, if successful, will accomplish the total synthesis of this interesting alkaloid.

The model compound **1** (Fig. 1) has been synthesized by Wiesner and Tsai to develop the methods of conversion. Compound **2** (Fig. 1) has been prepared from the model compound and, if the new alicyclic *cisoid* ring system has the necessary *cis–exo* stereochemistry, ring contraction would yield the complete skeleton and stereochemistry of the delphinine C/D ring system (2). The method could then be applied to the relay compound to produce delphinine with some substituents missing, the addition of which would pose no fundamental problem. A sample of the compound **2** was submitted for X-ray investigation to determine whether the desired stereochemistry had been obtained.

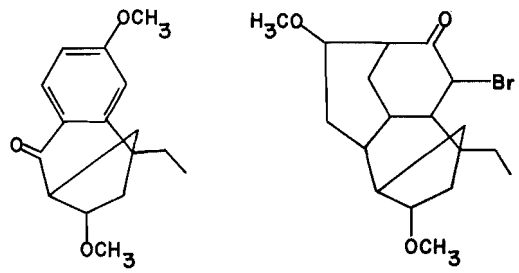

1 2

FIG. 1. Model compounds for the intermediates in the synthesis of delphinine.

Crystal Structure Analysis

Crystal data are as follows:

$C_{18}H_{27}BrO_3$ f.w. 371.4

Monoclinic, $a = 9.684(9)$, $b = 13.481(15)$, $c = 12.988(14)$ Å, $\beta = 99.47(7)°$, $v = 1672.5$ Å^3, $\rho_o = 1.45(3)$, $z = 4$, $\rho_c = 1.475$ (20 °C, Mo K$\bar{\alpha}$, $\lambda = 0.71069$ Å).

The unit cell dimensions and their estimated standard deviations were obtained from a least

TABLE 1. Final parameters (e.s.d.'s) ($x, y, z \times 10^4$; $U_{ij} \times 10^3$)
T.F. = $\exp[-2\pi^2(a^{*2}h^2U_{11} + \ldots + 2b^*c^*klU_{23} + \ldots)]$

	x	y	z	U_{11}	U_{22}	U_{33}	U_{23}	U_{13}	U_{12}
Br	2831(1)	4729(1)	2890(1)	143(1)	104(1)	118(1)	39(1)	21(1)	37(1)
O(1)	3404(7)	3730(5)	5353(5)	173(11)	80(9)	81(8)	−9(7)	43(7)	2(8)
O(2)	2873(7)	0645(4)	4530(5)	126(9)	54(8)	109(9)	11(6)	37(7)	2(7)
O(3)	9223(6)	2274(5)	5040(5)	77(8)	128(10)	70(8)	−19(7)	15(6)	15(7)
C(1)	4309(9)	3970(7)	3780(7)	71(12)	85(13)	66(12)	9(10)	12(9)	1(10)
C(2)	3471(10)	3387(7)	4483(7)	97(13)	75(13)	63(12)	−4(10)	15(10)	26(11)
C(3)	2788(10)	2421(6)	4112(7)	107(14)	35(11)	80(13)	7(13)	15(10)	0(10)
C(4)	3120(9)	2167(7)	3017(7)	57(13)	110(14)	58(12)	−18(11)	8(10)	−10(10)
C(5)	4683(10)	2228(7)	3058(7)	103(13)	59(12)	40(11)	−6(9)	19(10)	−3(10)
C(6)	5177(9)	3334(7)	3129(6)	60(12)	62(12)	60(11)	−13(10)	9(9)	6(9)
C(7)	3402(10)	1595(7)	4875(7)	98(13)	63(12)	76(12)	1(10)	31(10)	10(10)
C(8)	4971(10)	1571(7)	4952(7)	101(12)	61(13)	60(11)	15(9)	26(9)	15(11)
C(9)	5528(9)	1542(7)	3897(6)	88(12)	77(12)	39(11)	12(10)	24(9)	4(11)
C(10)	7125(9)	1735(6)	3993(6)	104(13)	55(12)	40(11)	−9(9)	19(9)	−4(10)
C(11)	7746(9)	2326(7)	4959(7)	75(13)	78(13)	58(12)	−8(10)	15(10)	−7(10)
C(12)	7201(9)	3399(7)	4700(7)	93(13)	71(13)	70(12)	−11(10)	10(10)	6(11)
C(13)	6767(9)	3422(7)	3487(6)	96(13)	59(12)	39(11)	−12(9)	14(9)	−2(10)
C(14)	7412(10)	2472(7)	3146(7)	101(14)	70(12)	49(12)	−21(10)	30(10)	−4(10)
C(15)	7291(9)	4384(7)	3006(7)	82(13)	77(14)	110(15)	11(10)	30(11)	−18(10)
C(16)	8819(11)	4590(9)	3279(9)	123(16)	139(17)	159(17)	22(14)	37(13)	−56(14)
C(17)	9964(11)	2656(9)	6002(8)	114(16)	184(19)	92(15)	−21(13)	−22(12)	−33(14)
C(18)	1436(9)	0526(7)	4577(8)	52(12)	120(17)	166(16)	5(13)	47(11)	−31(11)

squares evaluation of the positions of 12 independent reflections. The space group is $P2_1/c$ (C_{2h}^5) No. 14 in ref. 3.

Intensity data were collected on a Picker computer-controlled four-angle diffractometer using a $\theta/2\theta$ scan with β-filtered Mo Kα radiation and a scintillation detector. The two octants hkl and $\bar{h}kl$ were explored to a maximum of 2θ of 35°. There were 1142 accessible reflections in this region of which 816 were considered observed. The threshold was taken as 0.10 times the background count or 70 counts, whichever was greater. The specimen was an elongated crystal with dimensions 0.54 × 0.32 × 0.22 mm, the long direction being parallel to the b axis. The b axis of the crystal was mounted parallel to the ϕ direction of the diffractometer. The linear absorption coefficient for Mo Kα radiation is $\mu = 26.14$ cm^{-1}. No absorption or extinction corrections were applied.

The position of the bromine atom was established from a three-dimensional Patterson synthesis. All of the carbon and oxygen atoms were then located from a three-dimensional Fourier synthesis based on the phases determined by the bromine atom alone. All atoms were found to be in general positions. The method of refinement was by successive cycles of block-diagonal least squares, using 3 × 3 matrices for the positional parameters and 6 × 6 matrices for the anisotropic thermal parameters of each atom. The quantity minimized was

$$R_2 = \Sigma\omega(|F_o| - |F_c|)^2$$

for observed reflections only, using weighting function

$$\omega = \frac{1}{1 + [(|F_o| - P_2)/P_1]^4}$$

with $P_1 = 30$, $P_2 = 40$. Scattering factor curves used were those for Br, O, C, and H given in ref. 4. The bromine scattering curve was corrected for anomalous dispersion (5).

The final agreement residual

$$R = \Sigma(||F_o| - |F_c||)/\Sigma|F_o|$$

for all atoms except hydrogen was 0.069. A difference synthesis at this point showed the positions of all hydrogens as peaks with electron density between 0.4–0.5 eÅ^{-3} and no other electron density greater than 0.25 eÅ^{-3}. The hydrogens were assigned isotropic thermal parameters by the following scheme: for hydrogens on terminal methyl groups, $B = 5.00$; for those on the secondary side chain carbon, $B = 4.75$; for those on other secondary (bridging) carbons, $B = 4.50$; and for those attached to tertiary carbons, $B = 4.00$ Å^2. The positional and thermal parameters for the hydrogens were not refined during subsequent least squares

Can. J. Chem. Downloaded from www.nrcresearchpress.com by 210.87.254.40 on 09/05/12
For personal use only.

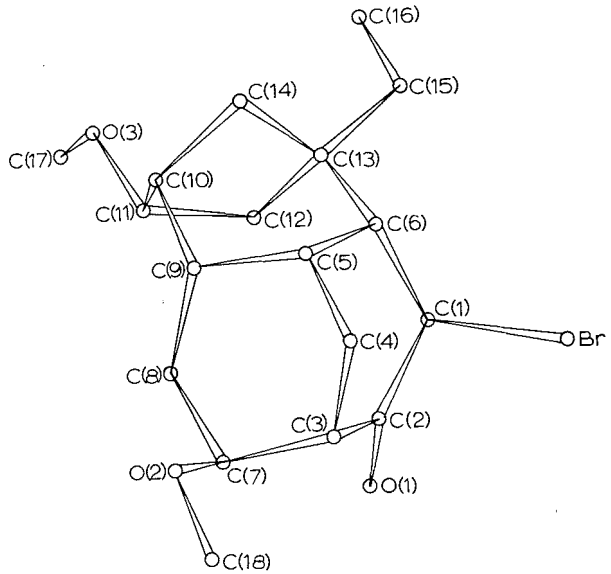

FIG. 2. General stereochemistry of the molecule.

TABLE 2. Parameters for the hydrogen atoms × 10^3
T.F. = $\exp[-8\pi^2 U(\sin\theta/\lambda)^2]$

Atoms		x	y	z	U(Å^2)
C(1)	H(1)	490	460	421	51
C(3)	H(2)	160	247	412	51
C(4)	H(3)	230	250	233	57
	H(4)	258	152	287	57
C(5)	H(5)	510	215	242	51
C(6)	H(6)	494	374	221	51
C(7)	H(7)	305	181	559	51
C(8)	H(8)	539	223	541	57
	H(9)	537	095	539	57
C(9)	H(10)	530	080	359	51
C(10)	H(11)	775	102	400	51
C(11)	H(12)	730	210	565	51
C(12)	H(13)	621	360	502	57
	H(14)	810	390	492	57
C(14)	H(15)	695	222	238	57
	H(16)	851	257	318	57
C(15)	H(17)	649	470	322	60
	H(18)	686	436	215	60
C(16)	H(19)	937	467	410	63
	H(20)	970	411	303	63
	H(21)	931	510	280	63
C(17)	H(22)	952	338	619	63
	H(23)	980	210	640	63
	H(24)	090	290	588	63
C(18)	H(25)	051	085	400	63
	H(26)	097	070	526	63
	H(27)	090	−022	425	63

cycles. In the last cycle no parameter shift exceeded 0.3 times the estimated standard deviation. The final agreement residual for the observed reflections, for all atoms, was $R = 0.044$. A set of structure factors for the final parameters given in Tables 1 and 2 has been placed in the depository of Unpublished Data.[1]

Discussion

The intramolecular bond distances and angles are given in Table 3. The general stereochemistry of the molecule and the numbering scheme used in this paper are shown in Fig. 2.

The general structure indicated in Fig. 1 is seen to be correct but the ring in question does not have the desired *exo* configuration. Hence, another method of conversion must be found for the formation of delphinine from the relay compound. The *endo* configuration of the ring gives the molecule a cage-like structure with the bromine, carboxyl, methoxy, and ethyl substituents pointing outward from the ring system. The new ring adopts the chair configuration while the other two six-membered rings are in the boat form, giving the molecule a fairly rigid structure.

Most of the bond lengths and angles shown in Table 3 are comparable with those for organic structures found in the literature, although there are several which are significantly different from the expected values. In particular, there is a very short bond C(15)—C(16) 1.490(14) Å. A "riding-

[1]Photocopies may be obtained, upon request, from the Depository of Unpublished Data, National Science Library, National Research Council of Canada, Ottawa, Canada K1A OR6.

Can. J. Chem. Downloaded from www.nrcresearchpress.com by 210.87.254.40 on 09/05/12
For personal use only.

TABLE 3. Intramolecular distances and angles (e.s.d.'s in parentheses)

Atoms	Distance (Å)	Atoms	Angle (degrees)
Br—C(1)	1.972(9)	C(7)—O(2)—C(18)	113.2(7)
		C(11)—O(3)—C(17)	113.7(7)
O(1)—C(2)	1.232(11)		
O(2)—C(7)	1.425(11)	Br—C(1)—C(2)	102.2(6)
O(2)—C(18)	1.412(11)	Br—C(1)—C(6)	112.0(6)
O(3)—C(11)	1.418(11)	C(2)—C(1)—C(6)	115.5(7)
O(3)—C(17)	1.431(12)	O(1)—C(2)—C(1)	117.9(8)
		O(1)—C(2)—C(3)	122.2(8)
C(1)—C(2)	1.535(13)	C(1)—C(2)—C(3)	120.0(8)
C(1)—C(6)	1.546(12)	C(2)—C(3)—C(4)	109.9(7)
C(2)—C(3)	1.504(13)	C(2)—C(3)—C(7)	108.4(7)
C(3)—C(4)	1.548(13)	C(4)—C(3)—C(7)	108.4(7)
C(3)—C(7)	1.543(13)	C(3)—C(4)—C(5)	108.3(7)
C(4)—C(5)	1.507(13)	C(4)—C(5)—C(6)	110.4(7)
C(5)—C(6)	1.565(13)	C(4)—C(5)—C(9)	113.7(7)
C(5)—C(9)	1.556(12)	C(6)—C(5)—C(9)	113.9(7)
C(6)—C(13)	1.539(12)	C(1)—C(6)—C(5)	111.8(7)
C(7)—C(8)	1.507(14)	C(1)—C(6)—C(13)	113.5(7)
C(8)—C(9)	1.554(13)	C(5)—C(6)—C(13)	111.9(7)
C(9)—C(10)	1.553(13)	O(2)—C(7)—C(3)	111.5(7)
C(10)—C(11)	1.524(12)	O(2)—C(7)—C(8)	107.9(7)
C(10)—C(14)	1.542(12)	C(3)—C(7)—C(8)	109.6(8)
C(11)—C(12)	1.557(13)	C(7)—C(8)—C(9)	115.8(8)
C(12)—C(13)	1.564(12)	C(5)—C(9)—C(8)	112.6(7)
C(13)—C(14)	1.523(13)	C(5)—C(9)—C(10)	111.0(7)
C(13)—C(15)	1.560(13)	C(8)—C(9)—C(10)	114.2(7)
C(15)—C(16)	1.490(14)	C(9)—C(10)—C(11)	114.0(7)
		C(9)—C(10)—C(14)	110.2(7)
		C(11)—C(10)—C(14)	99.2(7)
		O(3)—C(11)—C(10)	107.0(7)
		O(3)—C(11)—C(12)	111.3(7)
		C(10)—C(11)—C(12)	103.5(7)
		C(11)—C(12)—C(13)	105.2(7)
		C(6)—C(13)—C(12)	113.1(7)
		C(6)—C(13)—C(14)	106.6(7)
		C(6)—C(13)—C(15)	108.6(7)
		C(12)—C(13)—C(14)	102.8(7)
		C(12)—C(13)—C(15)	111.8(7)
		C(14)—C(13)—C(15)	114.0(7)
		C(10)—C(14)—C(13)	101.7(7)
		C(13)—C(15)—C(16)	115.8(8)

motion" correction to this bond length increases the distance to 1.508 Å. A more detailed analysis of the thermal motion may provide an explanation for the remaining differences.

The four molecules in the cell are oriented with the longest dimension of the molecule roughly parallel to the *a* axis. The closest approach distance between two molecules in this structure is 3.307(12) Å between O(3) of one molecule and C(18) of the molecule in the next cell along the *a* direction.

We wish to thank Dr. K. Wiesner for suggesting the problem, Mr. T. Y. R. Tsai for a sample of the compound, Dr. F. R. Ahmed of the Biochemistry Laboratory, National Research Council of Canada, for use of his computer programs, and the National Research Council of Canada for financial support.

1. K. WIESNER, E. W. K. JAY, C. DEMERSON. T. KANNO, J. KREPINSKÝ, LIZZIE POON, T. Y. R. TSAI, A. VILIM, and C. S. WU. Exper. **26**, 1030 (1970).
2. K. WIESNER, F. BICKELHAUPT, and D. R. BABIN. Exper. **15**, 93 (1959). K. WIESNER, F. BICKELHAUPT, D. R. BABIN, and M. GÖTZ. Tetrahedron Lett. **3**, 11 (1959); Tetrahedron, **9**, 254 (1960). K. WIESNER, O. L. SIMMONS, and R. H. WIGHTMAN. Tetrahedron Lett. **15**, 23 (1960).
3. International tables for X-ray crystallography. Vol. I. The Kynoch Press, Birmingham, England, 1965. Section 4.3.
4. International tables for X-ray crystallography. Vol. III. The Kynoch Press, Birmingham, England, 1962. Table 3.3.1.A.
5. International tables for X-ray crystallography. Vol. III. The Kynoch Press, Birmingham, England, 1962. Table 3.3.2.C.

Can. J. Chem. Downloaded from www.nrcresearchpress.com by 210.87.254.40 on 09/05/12
For personal use only.

Can. J. Chem. Downloaded from www.nrcresearchpress.com by 210.87.254.105 on 09/05/12
For personal use only.

Oxidative Degradation of a Podocarpic Acid Derivative

TSE-LOK HO[1]

Department of Chemistry, University of New Brunswick, Fredericton, New Brunswick

Received March 29, 1971

The dichromate oxidation of methyl-7-methyl-6,8,11,13-podocarpatetraen-19-oate, (**5**), is reported.

L'oxydation par le dichromate du méthyl-7 podocarpatétraène-6,8,11,13 oate-19 (**5**) de méthyle est rapportée.

Canadian Journal of Chemistry, 49, 2501 (1971)

During the study of ring B expansion of methyl *O*-methylpodocarpate (**1**) which served as a model in a projected synthesis of aconitine-type diterpene alkaloids (1), we discovered a novel oxidative degradation.

It was intended to prepare the exocyclic olefin **2**, a useful intermediate for our purpose (2), from the well-known 7-keto derivative **3** of **1**.

We first attempted the Reformatsky reaction on **3**, hoping that further transformations of the product **4** by dehydration, saponification and pyrolysis would yield the desired olefin. Surprisingly, direct acid treatment of the crude product gave only the styrene **5**, whose structure followed from spectroscopic data.

Wittig olefination (3), when applied to ketone **3**, also led to the isomerized product **5**. The definite structure of **5** was settled on a firm basis by its preparation by dehydration of the methyl Grignard product of **3**.

Dichromate oxidation of the styrene **5** gave, unexpectedly, methyl *O*-methyl-5,6-dehydro-7-ketopodocarpate (**6**). The physical properties of this substance are consistent with those reported by Wenkert *et al.* (4), who prepared it by a different route. Hydrogenation of **6** yielded methyl *O*-methylpodocarpate.

The mechanistic pathway of the oxidation may be envisaged as outlined in Scheme 1. It is noteworthy that a close analogy of the initial steps may be found in the cleavage of cycloalkenes to dialdehydes by chromyl trichloroacetate (5).

Experimental

Melting points were determined on a Kofler microscope hot-stage and are uncorrected. The i.r. spectra were

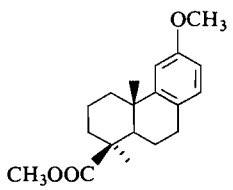

1

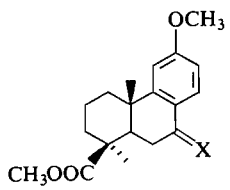

2 X = CH_2
3 X = O

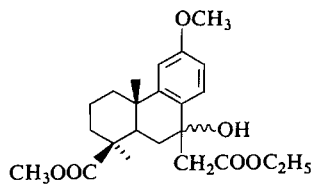

4

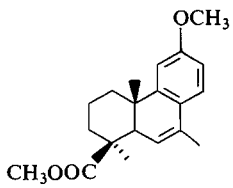

5

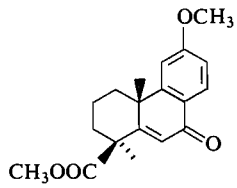

6

[1]Present address: Department of Chemistry, University of Sherbrooke, Sherbrooke, Quebec.

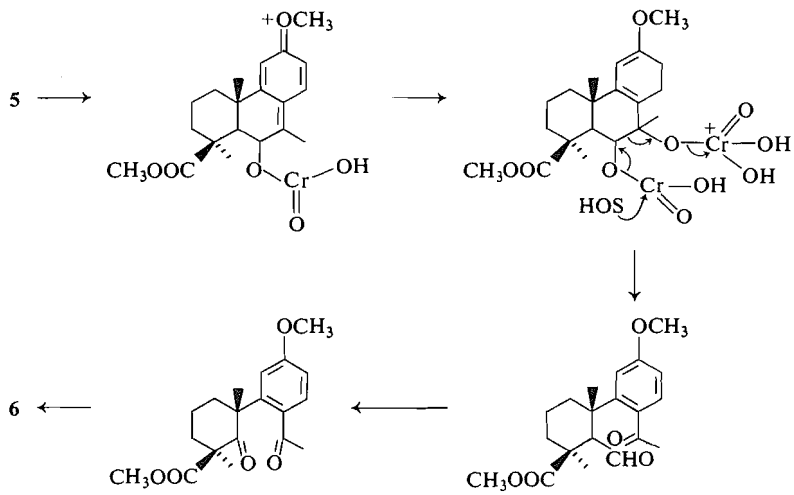

SCHEME I

recorded on a Perkin–Elmer model 21 spectrophotometer. The u.v. spectra were taken on a Beckman DK-2 spectrophotometer. The n.m.r. spectra were measured in $CDCl_3$ on a Varian HR-60 spectrometer operated at 56.4 MHz, with TMS as internal standard.

Reformatsky Reaction, Dehydration of 3

To a stirred, refluxing suspension of 0.65 g of activated zinc dust and a crystal of iodine in 10 ml of anhydrous benzene was introduced from a dropping funnel of a solution of 0.95 g of methyl *O*-methyl-7-ketopodocarpate (**3**) and 1.7 g of ethyl bromoacetate. An additional 0.20 g of zinc dust and 0.50 g of ethyl bromoacetate were added after 1 and 1.5 h, respectively. The reaction was allowed to proceed overnight, the mixture was cooled and poured into 10% aqueous sulfuric acid. The layers were separated and the aqueous phase was further extracted with chloroform. An orange brown oil was obtained from the dried organic extracts.

The crude product (2.71 g, combined from two identical runs) was dissolved in 50 ml of benzene containing 1.0 g of *p*-toluenesulfonic acid monohydrate, and was brought to reflux under a Dean–Stark water separator for 24 h. The contents were poured into ice-cold sodium bicarbonate solution, extracted with chloroform. The dried organic phase was evaporated to dryness and the residue (1.8 g) was chromatographed on 50 g of neutral alumina (Woelm, activity II) to furnish 1.099 g of pure styrene **5**, m.p. 84–86°, and 0.20 g of **3**. An analytical sample of **5** was prepared by sublimation under high vacuum. The i.r.: ν_{max} (CCl_4) 1732 (ester), 1615 cm^{-1}; u.v.: λ_{max} (log ε) 271.5 (4.10), 218.5 (4.21); n.m.r.: τ ($CDCl_3$) 9.16 (3H, s, CH_3), 8.73 (3H, s, CH_3), 7.94 (3H, br, s, CH_3), 6.32 (3H, s, $COOCH_3$), 6.19 (3H, s, $ArOCH_3$), 3.86 (1H, br, $=CH$), 3.42, 3.25, 2.91 (3H, ArH).

Anal. Calcd. for $C_{20}H_{26}O_3$: C, 76.50; H, 8.35; O, 15.29. Found: C, 76.57, 76.38; H, 8.30, 8.41; O, 14.81.

Wittig Reaction on 3

To a solution of phenyllithium prepared from 0.14 g of lithium and 1.57 g of bromobenzene in 100 ml of ether was added 4.35 g of methyl triphenylphosphonium bromide. After 2 h stirring at 25° under nitrogen, the ylid solution was cooled in an ice-bath, and a solution of 1.05 g of methyl *O*-methyl-7-ketopodocarpate in 30 ml of dry tetrahydrofuran was introduced. The reaction mixture was allowed to warm up to room temperature and left aside overnight, then finally heated under reflux for 5 h. After removal of the solvents, the residue was triturated several times with ether and filtered through an alumina column. Further chromatography of the product over 50 g of neutral alumina (Woelm, activity II) yielded 0.49 g of the styrene **5**, identical with the compound obtained from the Reformatsky-dehydration reactions (i.r., n.m.r., t.l.c., m.p., mixture m.p. 84–86°).

From later fractions of the chromatogram, 0.336 g of unreacted **3** was recovered.

Grignard Reaction, Dehydration of 3

To the Grignard reagent prepared from 0.38 g of magnesium turnings and 1 ml of methyl iodide, diluted to 100 ml with anhydrous ether, was added 1.0 g of finely pulverized ketone **3** with vigorous magnetic stirring. The reaction mixture was then refluxed overnight, cooled, and destroyed with aqueous ammonium chloride. The aqueous layer after separation was extracted with benzene. Evaporation of the dried organic solution gave 1.0 g of a crude product.

Direct dehydration with 1.0 g of *p*-toluenesulfonic acid monohydrate in 50 ml of benzene at reflux yielded 0.9 g of material. Pure styrene **5** (0.602 g) was isolated by chromatography on alumina. Some unreacted ketone (0.246 g) contaminated with a small amount of **5** was collected from later fractions.

Dichromate Oxidation of 5

Sodium dichromate dihydrate (80 mg) was added to a solution of 75 mg of styrene **5** in 5 ml of glacial acetic acid. After heating in a boiling water bath for 3 h, the reaction mixture was cooled, poured into crushed ice,

Can. J. Chem. Downloaded from www.nrcresearchpress.com by 210.87.254.105 on 09/05/12
For personal use only.

neutralized with sodium carbonate, and extracted with chloroform. Evaporation of the dried extracts *in vacuo* afforded 80 mg of material. Purification of the product by column chromatography (neutral alumina, Woelm, activity II) yielded 40 mg of the cross-conjugated ketone **6**, m.p. 175–178.5°, after crystallization from methanol (lit. (5) m.p. 173–175°). The i.r.: ν_{max} ($CHCl_3$) 1730 (ester), 1652 (ketone), 1602 (Ar) cm^{-1}; u.v.: λ_{max} (log ε) (C_2H_5OH) 302.5 (4.10), 242.5 nm (4.22); n.m.r.: τ ($CDCl_3$) 8.65 (3H, s, CH_3), 8.47 (3H, s, CH_3), 6.35 (3H, s, $COOCH_3$), 6.15 (3H, s, $ArOCH_3$), 3.43 (1H, s, H-6), 3.05 (2H, m, ArH), 1.87 (1H, d, $J \simeq 10$ Hz, ArH).

Hydrogenation of Ketone 6

The ketone **6** (0.109 g) was hydrogenated in 10 ml of ethanol with 12 mg of 10% Pd–C for 20 h. The catalyst was removed by filtration (Celite) and the filtrate was evaporated to dryness. The product (0.105 g) obtained crystallized on standing and was recrystallized from methanol, m.p. 126–129°. This specimen was found to be identical with methyl *O*-methylpodocarpate (i.r., n.m.r., t.l.c., mixture m.p. 128–129.5°).

The author is grateful to Prof. Z. Valenta for guidance and the Department of Chemistry, University of New Brunswick, for financial support.

1. K. Wiesner, M. Götz, D. L. Simmons, and L. R. Fowler. Coll. Czech. Chem. Commun. **28**, 2462 (1963).
2. E. J. Corey, M. Ohno, R. B. Mitra, and P. A. Vatakencherry. J. Am. Chem. Soc. **86**, 478 (1964).
3. A. Maercker. Org. React. **14**, 270 (1965).
4. E. Wenkert, P. Beak, R. W. J. Carney, J. W. Chamberlin, D. B. R. Johnston, C. D. Roth, and A. Tahara. Can. J. Chem. **41**, 1924 (1963).
5. H. Schildknecht and W. Föttinger. Ann. **659**, 20 (1962).

Can. J. Chem. Downloaded from www.nrcresearchpress.com by 210.87.254.105 on 09/05/12
For personal use only.

Can. J. Chem. Downloaded from www.nrcresearchpress.com by 210.87.254.6 on 09/05/12
For personal use only.

Lewis Acid – Base Interactions Between Bis-π-cyclopentadienyl Tungsten and Molybdenum Dihydrides, Cp_2MH_2, and some Main Group III Moieties

A. STORR AND B. S. THOMAS

Chemistry Department, University of British Columbia, Vancouver 8, British Columbia

Received January 14, 1971

Combination of the Lewis bases Cp_2MH_2 (where M = W or Mo) with the Group III Lewis acids AlR_3 (where R = Me, Et, or Ph) and $AlMe_2H$ has yielded a series of 1:1 complexes of the type $Cp_2MH_2.AlR_3$. A number of the complexes undergoes a slow elimination of hydrogen or alkane in benzene solution. Attempts to isolate mixed hydride adducts of the type, $Cp_2MH_2.M'H_3$ (where M' = Al or Ga), were unsuccessful.

La combinaison des bases de Lewis Cp_2MH_2 (M = W ou Mo) avec les acides de Lewis du groupe III, AlR_3 (R = Me, Et ou Ph) et $AlMe_2H$, conduit à une des séries de complexes 1:1 du type $Cp_2MH_2.AlR_3$. Un certain nombre de ces complexes perdent de l'hydrogène ou un alkane, en solution dans le benzène. Les tentatives en vue d'isoler des hydrures doubles du type, $Cp_2MH_2.M'H_3$ (M' = Al ou Ga) sont demeurées vaines.

Canadian Journal of Chemistry, **49**, 2504 (1971)

The transition metal hydrides, Cp_2MH_2 (where M = W or Mo), have been shown to act as Lewis bases (1, 2). In the present study we were interested in extending the range of transition metal – Group III derivative compounds by investigating reactions between these two hydrides and a number of potential Group III acceptor moieties. It was found that organo aluminum derivatives AlR_3 (where R = Me, Et, or Ph) and $AlMe_2H$ all form 1:1 complexes with the tungsten and molybdenum hydrides. The compounds are, in general, yellow crystalline solids which are monomeric in benzene solution. However, with dimethyl aluminum hydride as the acceptor moiety only the tungsten compound could be isolated from solution, the molybdenum adduct decomposing on removal of solvent.

The infrared spectra of the complexes in benzene solution in the region 4000–250 cm^{-1} show all the characteristic bands individually displayed by the separate components with no noteworthy changes due to complex formation. These observations effectively rule out bridge structures of the type

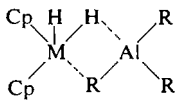

and indicate in all probability the presence of a direct metal–metal bond in the complexes. A similar conclusion was reached by Brunner *et al.* (3) for the complex $Cp_2WH_2.AlMe_3$ on the basis of their infrared (i.r.) data and low temperature nuclear magnetic resonance (n.m.r.) measurements.

Proton n.m.r. data collected on benzene solutions of the complexes are summarized in Table 1. The cyclopentadienyl-hydrogen signals show fine splittings due to coupling to the M—H protons but only at high field strengths and small sweep widths ($J_{Cp-W-H} \simeq 0.5$–0.7 c.p.s.). In general the M—H signals are fairly broad and couplings to cyclopentadienyl ring protons were not resolved. On standing the appearance of additional signals to those listed in Table 1 indicate the slow decomposition, with alkane elimination, of some of the complexes in benzene solution. Thus, $Cp_2MoH_2.AlMe_3$, $Cp_2MoH_2.AlEt_3$, and $Cp_2WH_2.AlEt_3$ all decompose slowly at room temperature with evolution of alkane, and on long standing, the deposition of solid material from the benzene solutions. In the typical case of $Cp_2WH_2.AlEt_3$, the proton n.m.r. spectrum of a freshly prepared sample is illustrated in Fig. 1(*a*). After several days the spectrum of the solution appears as shown in Fig. 1(*b*) with a sharp new signal (τ = 9.2 p.p.m.) appearing in addition to the signals observed initially. The new signal is assigned to the presence of ethane in the sample, an assignment initially suggested by the pressure build-up within the n.m.r. tube and confirmed by previous measurements on the chemical shift of ethane (4). Initially even with the presence of ethane indicated by the spectrum, the solution in the n.m.r. tube remained clear,

TABLE 1. ^{1}H n.m.r. data for complexes of bis-π-cyclopentadienyl molybdenum and tungsten dihydrides with some aluminum alkyls

Compound	τ_{Cp}	τ_{MH}	τ_{Al-R}	$\tau_{Al-R(uncomplexed)}$
Cp_2WH_2	5.76	22.28	—	—
$Cp_2WH_2.AlMe_3$	5.81	23.29	10.14	10.33
$Cp_2WH_2.AlMe_2H$	5.78	22.47	10.14	10.49
$Cp_2WH_2.AlEt_3$	5.78	22.43	8.50*, 9.62†	8.87*, 9.69†
$Cp_2WH_2.AlPh_3$	5.97	22.57	—	—
Cp_2MoH_2	5.62	18.77	—	—
$Cp_2MoH_2.AlMe_3$	5.66	18.77	10.15	10.33
$Cp_2MoH_2.AlEt_3$	5.69	18.84	8.54*, 9.71†	8.87*, 9.69†
$Cp_2MoH_2.AlPh_3$	5.84	18.50	—	—

*Triplet (CH_3 protons).
†Quartet (CH_2 protons).

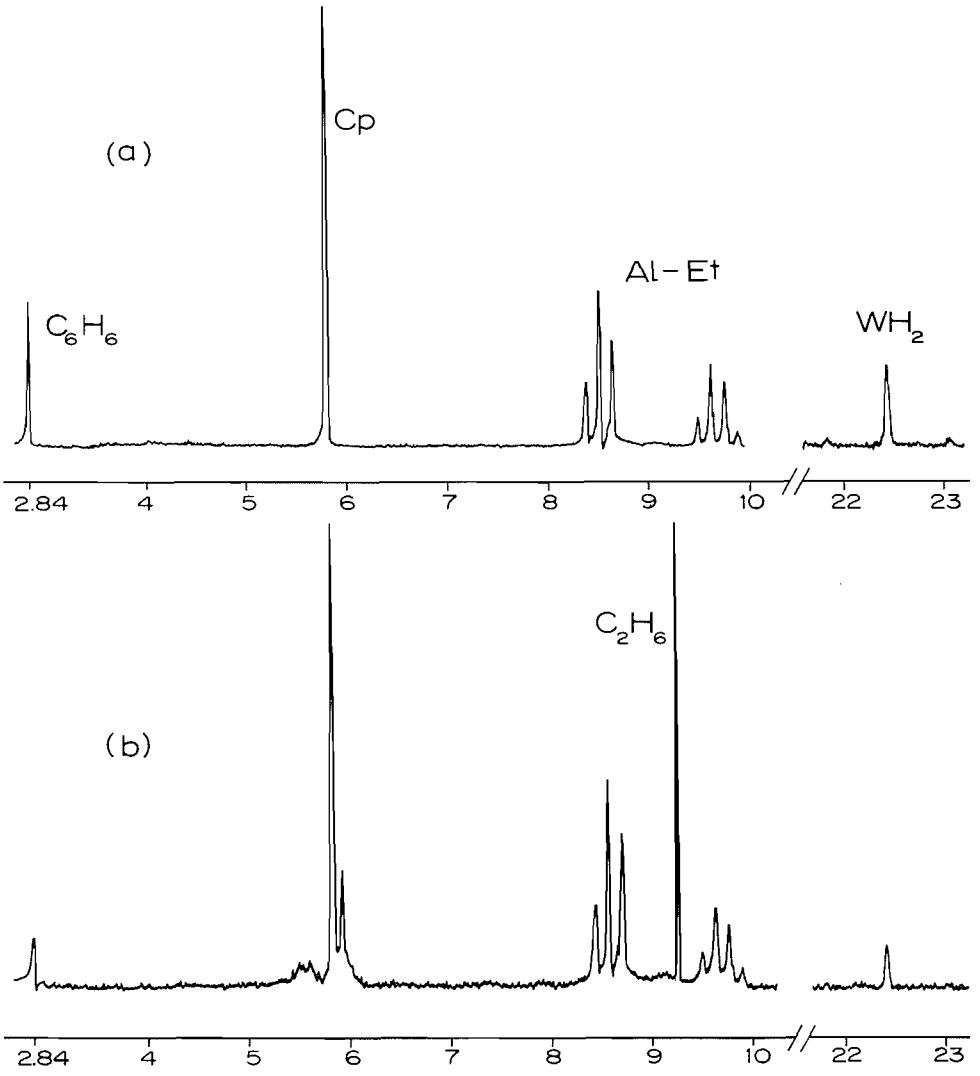

FIG. 1. ^{1}H n.m.r. spectrum of $Cp_2WH_2.AlEt_3$ in benzene solution at 60 Mc/s. (*a*) freshly prepared, (*b*) after several days.

Can. J. Chem. Downloaded from www.nrcresearchpress.com by 210.87.254.6 on 09/05/12
For personal use only.

Can. J. Chem. Downloaded from www.nrcresearchpress.com by 210.87.254.6 on 09/05/12
For personal use only.

but on long standing a dark brown solid of uncertain composition was deposited. The appearance of the ethane signal coincided with a more complicated signal for the cyclopentadienyl rings and a reduction in the relative intensity of the M—H signal. These observations suggest that although soluble low molecular weight species are initially formed following ethane elimination, these gradually polymerize to yield insoluble, cross-linked, materials containing a network of tungsten and aluminum atoms. In the case of dimethyl aluminum hydride adducts hydrogen is eliminated in preference to methane, possibly because of the greater polarity of the aluminum hydrogen bond. With the trimethyl aluminum complexes, methane was evolved only from the molybdenum compound at room temperature in benzene solution. (A signal due to methane appeared in the n.m.r. spectrum at $\tau = 9.9$ p.p.m.) Even after prolonged periods at room temperature, benzene solutions of $Cp_2WH_2.AlMe_3$ gave no evidence of methane elimination. This observation is in agreement with the generality (2) that transition metal basicity increases down a group of the *d* block elements in contrast to the trend usually observed for main group bases.

Our inability to prepare stable mixed hydride derivatives of the type $Cp_2MH_2AlH_3$ demonstrates the reduced Lewis acidity of the "AlH_3" unit over the AlR_3 moieties. The reaction of lithium aluminum hydride with the tungsten base and hydrogen chloride did indicate the formation of an unstable complex which deposited polymeric $(AlH_3)_x$ from benzene solution.

$$Cp_2WH_2AlH_3 \xrightarrow[\text{room temperature}]{C_6H_6} Cp_2WH_2 + \frac{1}{x}(AlH_3)_x$$

The i.r. spectrum of the initially clear solution displayed both W—H and Al—H absorptions. On standing, a white solid was deposited slowly from the solution and the intensity of the Al—H absorption decreased until finally the spectrum was that of pure Cp_2WH_2 in benzene solution. The white solid was characterized as $(AlH_3)_x$ which is known to be insoluble in benzene solution (5). The corresponding gallane reaction gave no indication of complex formation to yield $Cp_2WH_2.GaH_3$, and the "GaH_3" unit released by the action of hydrogen chloride on the lithium gallium hydride promptly decomposed to give hydrogen and gallium metal in characteristic fashion (6).

Experimental

Materials were handled in a conventional high vacuum line or in a glove box under an atmosphere of oxygen-free dry nitrogen. All solvents were thoroughly dried and redistilled before use.

Starting Materials

Bis-π-cyclopentadienyl molybdenum and tungsten dihydrides were prepared by the method of Green *et al.* (7). Trimethyl aluminum and triethyl aluminum (Alfa Inorganics) were purified by reduced pressure distillation. Triphenyl aluminum was prepared by the reaction of diphenyl mercury with a slight excess of aluminum foil in refluxing toluene. Lithium aluminum hydride was purified by extracting the crude material (Alfa Inorganics) with diethyl ether, and an ether solution of lithium gallium hydride was obtained by the standard procedure (8). Hydrogen chloride gas (Matheson Co., Inc.) was carefully dried by repeated passage over phosphorus pentoxide before use. Dimethyl aluminum hydride was prepared by the reaction of trimethyl boron (K and K Laboratories, Inc.) on lithium aluminum hydride in a sealed bulb, and purified by vacuum transfer (9).

Spectra

Definitive infrared spectra were recorded on a Perkin–Elmer Model 457 spectrometer (4000–250 cm^{-1}). The samples were run as benzene solutions, the cells being loaded in the glove box.

Proton n.m.r. spectra were obtained on Varian HA-100 and T-60 instruments. The benzene solutions were prepared in the glove box and the sample tubes sealed off to prevent oxidation and hydrolysis. All τ values are referred to benzene as $\tau_{C_6H_6} = 2.84$ p.p.m. Concentrations of all the solutions were kept roughly the same (~0.3 *M*) to minimize any possible concentration dependence of the signals.

Molecular Weights

Cryoscopic molecular weight determinations were conducted using benzene as solvent. The apparatus was designed to provide a nitrogen blanket over the solution to prevent atmospheric interference.

Analyses

The active hydrogen and alkyl group contents of the complexes were determined gas volumetrically after hydrolysis with a methanol–water mixture. All gas volumes are quoted at standard temperature and pressure. The aluminum content of the hydrolysate was determined gravimetrically as the 8-hydroxyquinolate (10).

Preparative Details

(a) Preparation of Aluminum Alkyl (Aryl) Derivatives

The complexes $Cp_2MH_2.AlR_3$ and $Cp_2MH_2.AlMe_2H$ were all prepared by the same general procedure which can be illustrated by the preparation of $Cp_2WH_2.AlEt_3$:

TABLE 2. Analytical data

Complex	Mol. wt. data		Analysis			
			Found		Calcd.	
	Found	Calcd.	Al	R(hydrolysable)	Al	R(hydrolysable)
$Cp_2WH_2.AlMe_3$	400	388	6.90	11.4	6.95	11.6
$Cp_2WH_2.AlEt_3$	405	430	6.25	20.0	6.30	20.2
$Cp_2WH_2.AlMe_2H$	404	374	7.24	—	7.22	—
$Cp_2WH_2.AlPh_3$	620	574	4.66	—	4.70	—
$Cp_2MoH_2.AlMe_3$	306	300	9.10	15.2	9.00	15.0
$Cp_2MoH_2.AlEt_3$	361	342	7.95	25.9	7.90	25.4
$Cp_2MoH_2.AlMe_2H$	290	286	—	—	—	—
$Cp_2MoH_2.AlPh_3$	477	486	5.60	—	5.55	—

Bis-π-cyclopentadienyl tungsten dihydride (0.4486 g, 1.42 mmol) was dissolved in benzene (20 ml) and triethyl aluminum (0.1620 g, 1.42 mmol) was added dropwise. The solvent was pumped away to leave the yellow, crystalline complex, $Cp_2WH_2.AlEt_3$. Analytical data for the complexes are listed in Table 2.

(b) Attempted Preparation of Mixed Hydride Species

Hydrogen chloride (21.6 ml, 0.96 mmol) was condensed onto a mixture of bis-π-cyclopentadienyl tungsten dihydride (0.2806 g, 0.96 mmol) and excess lithium

$$Cp_2WH_2 + HCl + LiAlH_4 \rightarrow Cp_2WH_2.AlH_3 + H_2 + LiCl$$

aluminum hydride (0.1 g, 2.6 mmol) in diethyl ether (20 ml). The mixture was warmed to room temperature with stirring and the volume of hydrogen evolved measured (23.0 ml, 1.02 mmol). The ether was removed at −80° and the product extracted with benzene. The solution displayed both W—H and Al—H stretching frequencies in its infrared spectrum but on standing deposited a white solid. Similar results were obtained using bis-π-cyclopentadienyl molybdenum dihydride as the Lewis base. However, in similar reactions employing lithium gallium hydride, no evidence of even transient complex formation was obtained.

We thank the National Research Council of Canada for financial support.

1. J. C. KOTZ and D. G. PEDROTTY. Organometal. Chem. Rev. A, **4**, 479 (1969).
2. D. F. SHRIVER. Acc. Res. **3**, 231 (1970).
3. H. BRUNNER, P. C. WAILES, and H. D. KAEZ. Inorg. Nucl. Chem. Lett. **1**, 125 (1965).
4. J. A. POPLE, W. G. SCHNEIDER, and H. J. BERNSTEIN. High-resolution nuclear magnetic resonance. McGraw-Hill, New York. 1959.
5. B. S. THOMAS. Ph.D. Thesis. University of Newcastle-upon-Tyne, Newcastle-upon-Tyne, England. 1969.
6. N. N. GREENWOOD and M. G. H. WALLBRIDGE. J. Chem. Soc. 3912 (1963).
7. M. L. H. GREEN, J. A. MCCLEVERTY, L. PRATT, and G. WILKINSON. J. Chem. Soc. 4854 (1961).
8. N. N. GREENWOOD, A. STORR, and M. G. H. WALLBRIDGE. Inorg. Chem. **2**, 1036 (1963).
9. T. WARTIK and H. I. SCHLESINGER. J. Am. Chem. Soc. **75**, 835 (1953).
10. I. M. KOLTHOFF and E. B. SANDELL. Textbook of quantitative inorganic analysis. 3rd. ed. Macmillan, New York. 1952. p. 321.

Can. J. Chem. Downloaded from www.nrcresearchpress.com by 210.87.254.6 on 09/05/12
For personal use only.

Can. J. Chem. Downloaded from www.nrcresearchpress.com by 210.87.254.5 on 09/05/12
For personal use only.

^{35}Cl Nuclear Quadrupole Resonance of Alkyl Chloroformates, Alkyl Acid Chlorides, and Carbamyl Chlorides

R. M. HART AND M. A. WHITEHEAD[1]

Radiofrequency Spectroscopy Laboratory, Chemistry Department, McGill University, The Royal Institution for the Advancement of Learning, Montreal 110, Quebec

Received February 22, 1971

The ^{35}Cl nuclear quadrupole resonance (n.q.r.) frequencies at 77 °K of twenty-two chloroformates, twenty-eight acid chlorides, two thiocarbonyl molecules, and five carbamyl chlorides are reported.

On rapporte les fréquences de résonance nucléaire quadrupolaire du ^{35}Cl à 77 °K de vingt-deux chloroformates, vingt-huit chlorures d'acides, deux molécules thiocarbonylées et cinq chlorures de carbamoyle.

Canadian Journal of Chemistry, 49, 2508 (1971)

Introduction

The planarity (1, 2) of the —X—COCl unit suggests π-bonding, and the difference in π-bonding when X is R, O, S, or N could be measured by comparing the ^{35}Cl n.q.r. in equivalent molecules. Unfortunately, no resonances were detected in —SCOCl molecules nor in —NCSCl molecules. Frequencies were obtained for thirteen pairs of molecules, RCOCl and ROCOCl, and the frequency variation within each series was small. The frequency variation is qualitatively discussed.

Experimental

Commercial samples were used and purified by distillation and sublimation.

A modified Dean type externally quenched superregenerative oscillator with phase-sensitive detection and strip chart recording was used to measure the ^{35}Cl n.q.r. frequencies, as previously described (3).

1. The Chloroformate Molecules (Table 1)

The frequencies of the *n*-alkyl chloroformates are approximately constant for R greater than *n*-C_3H_7, in agreement with the behavior of the frequencies in the RCl series (4) and with the normal σ-inductive effects of organic chemistry in such alkyl molecules (5–7).

A comparison of the frequencies from the RCl, RCH_2Cl, RCOCl, and ROCOCl series shows that the frequencies are roughly correlated when R is a saturated organic group such as CH_3 and XCH_2 (where X is halogen), or when an unsaturated group, such as Ph is separated from the chlorine by a saturated linkage. The frequency variation is most pronounced in the RCl system and least pronounced in the RCOCl series. When the group R is unsaturated and capable of conjugation, the RCl and RCOCl frequencies roughly correlate, and the ROCOCl and RCH_2Cl frequencies roughly correlate; since in RCl π-conjugation to the chlorine is possible while in RCH_2Cl it is impossible, these correlations suggest that ROCOCl shows no π-conjugation to the chlorine while RCOCl does show π-conjugation to the chlorine. There is, however, no linear correlation between the frequencies of the RCl and RCOCl or the RCH_2Cl and ROCOCl series. Table 2 gives the results for CNDO/2 calculations on four chloroformate molecules with R equal to CH_3, CH_2F, CHF_2, and CF_3. The calculations use Santry and Segal parameters (8) and the Townes and Dailey formula (9). They show that there is little or no π-bonding to the chlorine from the carbon (4) and that it does not change with increased fluorine substitution. The frequency changes are, consequently, σ-induced. Thus $C_6H_5CH_2$— has a frequency within the *n*-alkyl range, as do $CH_2{=}CHCH_2$ and $Cl(CH_2)_3$; the other fluorine or chlorine substituted *n*-alkyl groups fall in the normal σ-inductive order (10–12). The similarity of the frequencies for C_6H_5— and *p*-$CH_3OC_6H_4$— support such a σ-inductive view, but it must always be remembered that any large change in the σ-bond between the carbon and chlorine will always cause a change in the π-bond between the carbon and chlorine (13), however, the specific amount of π-character in each molecule must be calculated (16). The changes, although small,

[1]Author to whom correspondence to be addressed.

TABLE 1. ^{35}Cl n.q.r. frequencies of chloroformates at 77 °K[a]

Molecule	Frequency (MHz)	
	Acyl chlorine	Carbon chlorine
CH_3OCOCl	34.257	
C_2H_5OCOCl	34.270, 34.364 (33.858)[c]	
n-C_3H_7OCOCl	33.823	
n-C_4H_9OCOCl	33.746	
n-$C_5H_{11}OCOCl$	33.770	
n-$C_6H_{13}OCOCl$	33.749	
n-$C_7H_{15}OCOCl$	33.806	
n-$C_8H_{17}OCOCl$	33.873	
$(CH_3)_2CHOCOCl$	33.798, 33.701	
$(CH_3)_2CHCH_2OCOCl$	34.030, 34.082	
O-$(CH_2CH_2OCOCl)_2$	34.102, 34.848	
$CH_2{=}CHCH_2OCOCl$	34.282	
C_6H_5OCOCl	34.818	
p-$CH_3OC_6H_4OCOCl$	34.943	
$C_6H_5CH_2OCOCl$	33.772	
$(CF_3)_3COCOCl$	36.737	
C_2F_5OCOCl	36.563, 36.731	
i-C_3F_7OCOCl	36.258	
$F_5SOCOCl$	36.604	
Cl_3CCH_2OCOCl	35.691	38.746, 38.918, 39.141
$ClCH_2CH_2OCOCl$	34.436[b]	34.319[b]
$ClCH_2CH_2CH_2OCOCl$	34.194, 33.968	33.370, 33.069

[a]Attempts to crystallize samples of $(CH_2OCOCl)_2$ were unsuccessful. No frequencies were detected in CF_3OCOCl or $CH_3(CF_3)_2COCOCl$. All multiple interactions are of equal intensity.
[b]These assignments are arbitrary.
[c]Reference 24.

account for the lack of linearity in the correlation of RCl and ROCOCl frequencies. Furthermore Table 2 demonstrates that small changes in σ and π can cause large frequency differences. In the calculations the —OCOCl group was assumed to have the same geometry in all four molecules, and the rough correlation between the ROCOCl and RCH_2Cl frequencies supports such an assumption: some chloroformates have been postulated to have dioxan structures such as $ClCO_2CCl_3$ being 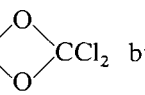 but this has been disproved by i.r. measurements on similar compounds in CCl_4, and there is no evidence for such structures in the solid state (14). Dipole moments have favored the R to be *cis* to Cl in RXCOCl (15) and electron diffraction (1) has shown *cis* for the methyl chloroformate only. The ^{35}Cl n.q.r. frequencies do not give any evidence on these points, except that the regularity of the frequency change with R suggests similar structures for all molecules.

The similarity of the frequencies of $F_5SOCOCl$ and C_2F_5OCOCl shows that the sulfur, although capable of d_π–p_π conjugation with the —OCOCl group, nevertheless affects the chlorine by σ induction.

2. The Acid Chloride Molecules (Table 3)

The frequencies for the *n*-alkyl acid chlorides are approximately constant for R greater than C_3H_7, with less variation than in the chloroformates, and in the expected σ-inductive sequence (4, 16, 17).

The low frequencies of the RCOCl molecules is due to large π-bonding to the chlorine (4); consequently the C_6H_5— and *p*-$CH_3OC_6H_4$— groups are conjugated to the Cl in RCOCl, but σ-inductive in ROCOCl. The $(CH_3)_3$— group of pivaloylchloride results in this molecule $(CH_3)_3$-CCOCl having the *lowest* ^{35}Cl—C n.q.r. frequency observed (17).

The chloro, fluoro, and bromo substituted molecules show acyl chlorine frequencies in agreement with inductive effects due to the high electronegativity of the halogen bonding orbitals (18). The F_3C— molecule has a lower frequency than the Cl_3F— molecule; similar trends occur in the chloroalkanes and α-chloro ethers (4), where they have been explained as hyperconjugation between the C—Cl bond and the fluorine lone

Can. J. Chem. Downloaded from www.nrcresearchpress.com by 210.87.254.5 on 09/05/12
For personal use only.

Can. J. Chem. Downloaded from www.nrcresearchpress.com by 210.87.254.5 on 09/05/12
For personal use only.

TABLE 2. CNDO/2 calculations on four chloroformate molecules using Santry and Segal parameters (8) and the Townes and Dailey equation (9)

Molecule	Atom populations							Chlorine orbital populations[a]				ν (MHz) ^{35}Cl	
	H	—O—	=O	—C<	>C=	Cl	F	p_x	p_y	p_z	q_{zz}	Calculated	Experimental
$ClOCOCH_3$	0.99	6.22	6.24	3.87	3.50	7.22	—	1.96	1.98	1.35	0.62	34.29	34.257
$ClOCOCH_2F$	1.00	6.23	6.23	3.65	3.50	7.21	7.18	1.96	1.98	1.34	0.63	34.61	—
$ClOCOCHF_2$	1.00	6.23	6.23	3.47	3.49	7.20	7.19	1.96	1.98	1.33	0.64	35.51	—
$ClOCOCF_3$	—	6.24	6.22	3.29	3.50	7.17	7.19	1.96	1.99	1.29	0.685	37.43	—

[a] The accuracy of these populations is governed by the accuracy of the geometry input for the molecules.

TABLE 3. ^{35}Cl n.q.r. frequencies of carboxylic acid chlorides at 77 °K[j]

Molecule	Frequency (MHz)	
	Acyl chlorine[a]	Non-acyl chlorines[a]
CH_3COCl	28.909, 29.079	
C_2H_5COCl	29.138	
n-C_3H_7COCl	29.004	
n-$C_5H_{11}COCl$	28.991	
n-$C_6H_{13}COCl$	29.084, 29.150	
n-$C_7H_{15}COCl$	29.067	
$(CH_3)_2CHCOCl$ (*iso*-butyrylchloride)	28.950	
$(CH_3)_2CHCH_2COCl$ (*iso*-valerylchloride)	28.807	
$(CH_3)_3CCOCl$ (pivaloylchloride)	28.355	
$CH_2{=}CHCOCl$ (acryloylchloride)	29.954, 30.124	
$CH_3CH{=}CHCOCl$ (crotonylchloride)	29.482	
$ClCH{=}C(Cl)COCl$[d]	32.482, 32.517	36.001[h], 36.092[h], 37.609[i], 37.872[i]
$CH_3OC(O)COCl$ (ethylchloro oxylate)	31.929	
N-$(C(COCl)CH_2CH_2)_2$ (pyridine-2 6-dicarboxylicacidchloride)	31.454, 31.892[d]	
$ClSO_2CH_2COCl$	31.973, 32.501	(34.951, 35.191)
C_6H_5COCl	29.914[g]	
p-$CH_3OC_6H_4COCl$	30.091[g]	
$ClCOCl$	(35.081, 36.225)[b]	
Cl_3CCOCl[c]	33.721	40.132, 40.473, 40.613
n-C_3F_7COCl	33.753	
C_2F_5COCl	33.412	
CF_3COCl	33.438[d]	
$CClF_2COCl$	33.444[d]	(—)[f]
CCl_2HCOCl[e]	32.147, 32.962	38.353, 38.521, 39.189, 39.386
$CClH_2COCl$[e]	30.437	37.517
$CBrH_2COCl$	30.452	
$ClCH_2CH_2COCl$	29.471	34.018
$ClCH_2CH_2CH_2COCl$	29.027	32.875

[a]All multiple interactions are of equal intensity.
[b]Reference 25.
[c]Reference 26.
[d]Very broad interactions.
[e]Reference 27.
[f]It is surprising that no expected resonance at 40 MHz was observed, perhaps due to random orientation of the $—CClF_2$ group.
[g]Reported at 29.93 MHz and 30.09, respectively (28).
[h]α-C—Cl bond.
[i]β-C—Cl bond.
[j]No quadrupolar interactions were detected in methylchloro-oxylate; valeryl, cinnamoyl, or itaconyl chloride.

pairs (19). In the present case hyperconjugation is between the fluorine lone pairs and the CO antibonding molecular orbital. Inductive effects cease beyond C_3 as in the *n*-alkyl series.

C_6H_5— raises the frequency of the RCOCl above that of the R equal to *n*-alkyl by 1 MHz (compared to 0.6 MHz in ROCOCl) while *p*-$CH_3OC_6H_4$ raises the frequency by 1.16 MHz (compared to 0.73 MHz in ROCOCl). Consequently the π-bonding to the chlorine enhances the σ-bond effect, shown by these groups in ROCOCl, by approximately 0.4 MHz.

The reported ^{35}Cl frequencies in $COCl_2$ seem too high in view of the other frequencies in Table 3. Substitution of a single chlorine in place of a perhalo group should not raise the frequency by 2.5 MHz; it may, however, be isomeric (20). The possible isomers are the *trans* and *staggered* forms.

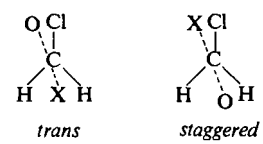

trans *staggered*

For the chloroacetyl chlorides these have been shown to exist in the liquid; however, in the solid

Can. J. Chem. Downloaded from www.nrcresearchpress.com by 210.87.254.5 on 09/05/12
For personal use only.

TABLE 4. ^{35}Cl n.q.r frequencies of two thiocarbonyl molecules at 77 °K[a]

Molecule		Frequency (MHz)
Name	Formula	
p-Chlorophenyldithiocarbonylchloride	$ClC_6H_4SC(S)Cl$	35.443 (34.284)[b]
Phenoxythiocarbonylchloride	$C_6H_5OC(S)Cl$	35.825
(Phenylchloroformate (for comparison)	$C_6H_5OC(O)Cl$	34.818)

[a]No resonances were detected in thiocarbonyl chloride $CSCl_2$ or any other sulfur analogues of Tables 1 and 3.
[b]Aromatic, Cl—C_6H_4—.

TABLE 5. ^{35}Cl n.q.r. frequencies of carbamyl chlorides at 77 °K

Molecule		Frequency (MHz)
Name	Formula	
Dimethylcarbamylchloride	$(CH_3)_2NCOCl$	31.909
Diethylcarbamylchloride	$(C_2H_5)_2NCOCl$	31.879[a]
Diphenylcarbamylchloride	$(C_6H_5)_2NCOCl$	33.202
Methylphenylcarbamylchloride	$(CH_3)(C_6H_5)NCOCl$	32.664
Ethylphenylcarbamylchloride	$(C_2H_5)(C_6H_5)NCOCl$	32.951

[a]2 kHz above frequency in ref. 19.

only the *trans* isomer exists for CH_3COF, $ClCH_2COF$, CH_3COCl, $ClCH_2COCl$, $ClCH_2COBr$, and CH_3COBr (20*a*). For $COCl_2$ the solid state has been shown to have an ordered structure but with unexplained residual entropy, which may be due to both isomers existing in the solid, but there is no evidence to establish this (20*b*).

3. The Thiocarbonyl Molecules (Table 4)

On σ-orbital electronegativity arguments the phenoxythiocarbonyl chloride frequency should be lower than that of phenylchloroformate. However, the π-orbital to chlorine could be affected by the stronger CS π bond (18).

4. The Carbamyl Molecules (Table 5)

The unsymmetrically substituted molecules both had intense resonances which exhibited normal temperature dependence, with no break in frequency dependence and no line width peculiarities (21) between 77 °K and room temperature. This suggests that CN bond reorientation (22, 23) does not occur in this range of temperature. The diphenylcarbamylchloride resonance is very weak.

The frequencies are in accord with σ-bond inductive effects from electronegativity considerations (10–13, 18) with the unsymmetrically substituted molecules between the symmetrical parent molecule frequencies. The high frequencies in the thiocarbamyl and carbamyl molecules suggest that like the chloroformates there is little π-bonding to the chlorine.

This research was supported by the National Research Council of Canada, to whom R.M.H. is grateful for a Bursary, 1969–1970. The McGill Committee on Research is thanked for finance of a frequency meter, and summer support for R.M.H., 1970. The McGill Computing Centre provided facilities on their IBM 360/75 computer. Mr. J. Grabenstetter did the CNDO calculations. Dr. D. E. Young of Allied Chemicals, Morristown, New Jersey, is thanked for providing samples of the fluorochloroformates prior to publication of their preparation.

1. J. M. O'GORMAN, W. SHAND, JR., and W. SCHOMAKER. J. Am. Chem. Soc. **72**, 4222 (1950).
2. K. M. SINNOT. J. Chem. Phys. **34**, 851 (1961).
3. R. CLIPSHAM, R. M. HART, and M. A. WHITEHEAD. J. Chem. Soc. A, 584 (1969). R. M. HART and M. A. WHITEHEAD. J. Chem. Soc. To be published.
4. E. A. C. LUCKEN. Nuclear quadrupole coupling constant. Academic Press, New York. 1969.
5. N. C. BAIRD and M. A. WHITEHEAD. Theor. chim. Acta, **6**, 167 (1966).
6. R. HOFFMANN. J. Chem. Phys. **39**, 1397 (1963).
7. C. SANDORFY. Can. J. Chem. **33**, 1337 (1955).
8. D. P. SANTRY and G. A. SEGAL. J. Chem. Phys. **47**, 158 (1967).
9. W. GORDY, W. V. SMITH, and R. F. TRAMBARULO. Microwave spectroscopy. John Wiley, New York. 1953. p. 269.
10. M. J. S. DEWAR. Molecular orbital theory of organic chemistry. McGraw-Hill, New York. 1970.
11. J. HINZE, M. A. WHITEHEAD, and H. H. JAFFE. J. Am. Chem. Soc. **85**, 148 (1963).
12. M. KAPLANSKY and M. A. WHITEHEAD. Mol. Phys. **16**, 481 (1969).

Can. J. Chem. Downloaded from www.nrcresearchpress.com by 210.87.254.5 on 09/05/12
For personal use only.

13. M. KAPLANSKY and M. A. WHITEHEAD. Mol. Phys. **15**, 149 (1968).
14. J. L. HALES, J. IDRIS JONES, and W. KYNASTRON. J. Chem. Soc. 615 (1957); J. Chem. Soc. 618 (1957).
15. (*a*) A. QUEEN, T. A. NOUR, M. N. PADDON-ROW, and K. PRESTON. Can. J. Chem. **48**, 522 (1970). (*b*) E. BOCK and D. I. WACHA. Can. J. Chem. **45**, 3177 (1967). (*c*) A. QUEEN, T. A. NOUR, and E. BOCK. Can. J. Chem. **43**, 556 (1965).
16. J. A. POPLE and D. L. BEVERIDGE. Approximate molecular orbital theory. McGraw-Hill, Toronto. 1970.
17. M. A. WHITEHEAD, N. C. BAIRD, and M. KAPLANSKY. Theor. chim. Acta, **3**. 135 (1965).
18. J. HINZE and H. H. JAFFE. J. Am. Chem. Soc. **84**, 540 (1962).
19. E. A. C. LUCKEN. J. Chem. Soc. 2954 (1959); Chem. Commun. 425 (1970).
20. (*a*) A. Y. KHAN and N. JONATHAN. J. Chem. Phys. **50**, 1801 (1969). (*b*) B. ZASLOW, M. ATOJI, and W. N. LIPSCOMB. Acta Cryst. **5**, 833 (1952).
21. R. M. HART and M. A. WHITEHEAD. Mol. Phys. **19**, 383 (1970).
22. R. C. NEUMANN, D. N. ROARK, and V. JONAS. J. Am. Chem. Soc. **89**, 3412 (1967).
23. A. E. LEMIRE and J. C. THOMPSON. Can. J. Chem. **48**, 824 (1969).
24. T. L. WEATHERLY and Q. WILLIAMS. J. Chem. Phys. **22**, 958 (1954).
25. R. LIVINGSTONE. J. Phys. Chem. **57**, 496 (1953).
26. H. C. ALLAN. J. Phys. Chem. **57**, 501 (1953).
27. P. J. BRAY. J. Chem. Phys. **23**, 703 (1955).
28. D. W. MCCALL and H. S. GUTOWSKY. J. Chem. Phys. **21**, 1300 (1953).

Can. J. Chem. Downloaded from www.nrcresearchpress.com by 210.87.254.5 on 09/05/12
For personal use only.

Electron Spin Resonance of γ-Irradiated Dicyandiamide

G. LIND AND R. KEWLEY
Department of Chemistry, Queen's University, Kingston, Ontario

Received February 9, 1971

The X-band e.s.r. spectra of single crystal and powder samples of γ-irradiated dicyandiamide, $(H_2N)_2CNCN$, have been observed. The results show that three radical species are formed on irradiation at room temperature. One of these radicals, which gives a single broad line spectrum of width 8.5 G and $g = 2.0040$, has not been identified. The other two species are considered both to have the same chemical formula $NH_2\dot{C}(NH)NCN$ but one is a π-electron radical whereas the other is a σ-electron radical with a very large proton hyperfine splitting in the range of 73–81 G. The production of two types of radicals by radiation damage to the same $—NH_2$ group of dicyandiamide is explained in terms of the ease of formation of π- and σ-electron radicals as influenced by geometrical considerations stemming from the hydrogen bonding in the dicyandiamide crystal.

On observe la bande X du spectre de e.s.r. d'un cristal unique et d'échantillons en poudre de dicyandiamide, $(H_2N)_2CNCN$, irradiés par des rayons γ. Les résultats indiquent que trois espèces radicalaires se forment sous irradiation à température de la pièce. L'un de ces radicaux, donnant un spectre constitué d'un signal large et unique de largeur 8.5 G et $g = 2.0040$, n'a pas été identifié. On suppose que les deux autres espèces ont la même formule chimique $NH_2\dot{C}(NH)NCN$ mais que l'un d'eux est un radical π-électronique et que l'autre est un radical σ-électronique donnant lieu à un important dédoublement hyperfin de proton dans la région de 73–81 G. La formation de deux espèces de radicaux, obtenus par suite des dommages causés par les radiations sur le même groupe $—NH_2$ du dicyandiamide, est expliquée en terme de facilité de formation des radicaux π- et σ-électroniques; ceci par suite de considérations géométriques provenant des liaisons hydrogène dans le cristal de dicyandiamide.

Canadian Journal of Chemistry, 49, 2514 (1971)

Introduction

In e.s.r. studies of radiation damage to carboxylic acids a frequent occurrence has been the observation of radicals containing the grouping $—\dot{C}HCOOH$, in which the unpaired electron occupies a π molecular orbital (1). On the other hand, an e.s.r. study of the formyl radical $H\dot{C}O$ (2) showed that this species has an unusually large proton hyperfine splitting of 137 G, which is inconsistent with the magnitude expected for a π-electron radical. Flow system experiments in which hydrogen was abstracted by OH radicals from acetamide and formamide yielded radicals identified as $\dot{C}H_2CONH_2$ and $HCO\dot{N}H$ (3). The former radical is a normal π-radical having closely equivalent methylene protons with $a_H = 21.28$ G. The latter radical has fairly large nitrogen hyperfine coupling, $a_N = 21.65$ G, and one proton with $a_H = 30.55$ G. Later, by means of deuteration, studies of temperature variation of hyperfine coupling constants and line width dependence on p*H*, this species was shown in fact to be not $HCO\dot{N}H$ but $O\dot{C}NH_2$ (4). It was described as a "non-π" radical analogous to the formyl radical, the small proton hyperfine coupling, relative to that in $H\dot{C}O$, being attributed to the substantial spin density at the nitrogen atom.

Recently e.s.r. studies following irradiation of malonamide (5, 6) and cyanoacetylurea (7) have shown that two types of radicals, designated π-electron and σ-electron, can be produced from a particular substance by radiation damage. The π-electron radicals are characterized primarily by CH proton hyperfine coupling constants in the range 7 to 33 G with $a_{iso} \sim 20$ G (in $H_2NCO\dot{C}HCONH_2$ (6) and $NC\dot{C}HCONH$-$CONH_2$ (7)). The latter value is similar to the hyperfine splitting constant a_H of the methyl radical and to values of Q_H found in aromatic radical ions (8). The σ-electron radicals, $H_2NCOCH_2CO\dot{N}H$ and $NCCH_2CONHCO\dot{N}H$, have much larger proton hyperfine coupling constants which are in the range 79 to 87 G, with $a_{iso} \sim 80$ G. In contrast to these results an e.s.r. investigation of γ-irradiated pentafluoropropionamide (9) showed the presence of the two species $CF_3\dot{C}FCONH_2$ and $CF_3CF_2CO\dot{N}H$, both of which are considered to be π-electron radicals, although it may be noted that a detailed study of the latter radical was not feasible under the conditions of the experiment. X-Irradiation

of hydroxyurea produces a radical first thought to be H_2NCONH but later identified as NH_2CONHO· which is a π-radical with the unpaired electron centered on oxygen (10, 11). The same radical can also be produced by oxidation in aqueous solution, see (12) for example, and has been shown to have $a_H^{NH} = 12.5$ G and $a_N^{NH} = 8.2$ G (10, 13).

The present work was undertaken in order to concentrate attention on the effects of radiation on the $-NH_2$ group. Dicyandiamide (1-cyanoguanidine), $(H_2N)_2C{=}N{-}C{\equiv}N$, offers the possibilities of formation of both π- and σ-electron radicals centered on nitrogen without complications in the e.s.r. signal due to a π-electron radical centered on carbon or oxygen. Another interesting feature of the substance is the extensive hydrogen bonding in the crystal, which causes inequivalence of the two protons of each of the two amino groups in the molecule, with the anticipated result that more than one radical may be produced by damage to an NH_2 group by high energy radiation.

Experimental

The powder and single crystal studies were carried out using reagent grade samples supplied by Eastman Organic Chemicals and the Aldrich Chemical Company, Inc. Both gave the same e.s.r. spectrum following 1.5 h of γ-irradiation of powder samples. The γ-ray dosage used throughout both the powder and single crystal investigations was 8×10^{17} eV/g/min, irradiation being carried out in a ^{60}Co Gamma cell (A.E.C.L.) at room temperature.

The crystal structure parameters and atom positions for dicyandiamide are well known from previous investigations (14–17). The space group is *C2/c*. The unit cell contains eight molecules of $C_2H_4N_4$ and has the parameters: $a = 15.00$, $b = 4.44$, $c = 13.12$ Å, and $\beta = 115°$ 20′ (15). The neutron diffraction study (17) proved that the correct structural formula of the molecule in the crystal is the diamino form. Of considerable importance to the present work is the fact that in the crystal the molecule is almost entirely planar and that hydrogen bonding joins the molecules together in "infinite" layers which are closely parallel to the (310) and (3$\bar{1}$0) planes.

The single crystal used in this work was of dimensions 1 mm × 1.5 mm × 4 mm and was grown by the hydrothermal process (18) at 30 °C. The faces of the crystal were identified and its initial orientation was found, using X-ray diffraction. A smaller crystal, having a similar but sharper diffraction pattern, was used with a precession camera to redetermine the unit cell parameters as $a = 15.0$, $b = 4.49$, $c = 13.2$ Å, and $\beta = 115°$ 5′, which are in good agreement with the results of Hughes (15) given above. The 1 mm × 1.5 mm × 4 mm crystal was found to be elongated along the *c*-axis with the (001), (310), and (3$\bar{1}$0) faces well developed. The (310) and (3$\bar{1}$0) faces are

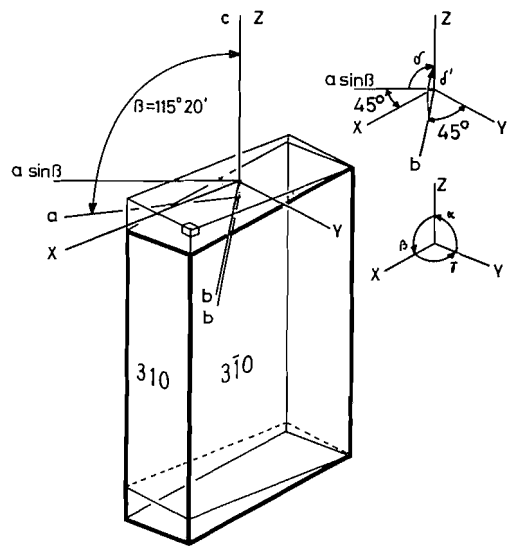

FIG. 1. The form of the single crystal showing the choice of the reference axes. The angles α, β, γ, δ, and δ′ are defined at the upper right.

very nearly at right angles (89° 36′). The orthogonal axes of rotation chosen initially for the single crystal study are designated *X*, *Y*, and *Z*. Rotations were also carried out about the axes $a \sin \beta$ and *b*. The *Z*-axis is the same as the crystal *c*-axis, the *X*-axis is at right angles to the (310) plane, and the *Y*-axis is at right angles to *X* and *Z* and lies very closely along the (3$\bar{1}$0) axis, see Fig. 1, and is indistinguishable from it within experimental error. After 24 h exposure to γ radiation the crystal was mounted by means of silicone grease on plexiglass plates which could be inserted into a holder, allowing rotation about the chosen directions. The silicone grease gave no e.s.r. signal. However, the holder and plate were found to have an e.s.r. spectrum consisting of a very broad line, width ~500 G, centered at a field of 2900 G and a second broad line of 250 G width at a field of 1300 G. Neither of these signals interfered with the study of the e.s.r. spectra from the crystal. The orientation of the mounted crystal could be read to ±0.5°. The error in mounting the crystal on the plate is, however, somewhat larger, approximately 3–5°. For the powder measurements irradiation was carried out for periods up to 24 h. After irradiation samples were transferred to 3 mm quartz tubes. The e.s.r. spectra were recorded with a Varian 4502 X-band spectrometer equipped with a 9 in. magnet and a V-4532 dual cavity. The standard used was an aqueous solution containing peroxylamine disulfonate which was taken to have a g value of 2.00550 and a hyperfine separation of 13.00 G between the low field and center line of the ^{14}N three line hyperfine pattern (19). Most of the e.s.r. spectra, including those of the single crystal, were taken at room temperature. For work at low and high temperatures the V-4557 variable temperature accessory together with a V-4540 temperature controller were used, temperature being measured with a resistance type temperature sensor to an accuracy of ±5 °C.

Results

(i) Powder

The powder, when subjected to γ radiation for periods up to about 7 h, gave an e.s.r. signal at room temperature which is the superposition of two overlapping spectra, which we call spectra A and B. For irradiation periods above 7 h an additional spectrum, C, could be observed so the complete e.s.r. signal is made up of the three overlapping spectra A, B, and C. Intensity comparisons for spectrum B at various times during the first 16 h of irradiation showed that the radical species concerned increases in amount in a linear manner with time. This observation furnishes good evidence that the radicals responsible for spectra B and C are produced simultaneously from dicyandiamide, not by consecutive processes. The lack of observation of spectrum C during the first 7 h can be attributed to its overlapping with the more intense spectrum B. For all irradiation periods up to 24 h spectrum B disappeared irreversibly when the irradiated powder was heated to 150 °C, the e.s.r. signal being observed after returing the sample to room temperature. Having available the experimental spectra A + B, A, A + B + C, and A + C it was possible by subtraction to separate out the individual spectra B and C, see Fig. 2. The species giving rise to spectra A, B, and C are all stable at room temperature over a period of several months.

Spectrum A is a single line with its center at $\mathbf{g} = 2.0040 \pm 0.0004$ and a line width of about 8.5 G. The radical giving this signal has not been identified. Spectrum C is due to an unpaired electron interacting with one proton and one nitrogen nucleus. From the powder spectrum one principal value of each of the nitrogen and proton hyperfine tensors could be determined and these values are consistent with a π-electron radical, see Table 1. Spectrum C is similar to an e.s.r. spectrum reported by Morton (20) which he obtained by γ-irradiation of a single crystal of $(NH_4)_2HPO_4$. This spectrum was explained as being that of a π-electron radical centered on nitrogen, a fragment of the form $H—\overset{+}{N}\diagdown\!\diagup$. Later, however, Symons and Atkins (21) doubted this and considered alternative explanations to be either (*i*) the species NH_3^+, with two protons not exhibiting interaction with the unpaired electron due to hydrogen bonding to a phosphate group or (*ii*) a species of the form X—N—H where X is a phosphate oxygen. The spectrum B, which disappears on heating, may be seen to consist of two well-separated three-line groups each having two shoulders, one on each side, as shown in Fig. 2. The pair of strong triplets show the presence of one proton and one nitrogen nucleus. The shoulders indicate that interaction of the unpaired electron with a second nitrogen could be taking place. Applying the theory of e.s.r. spectra of polycrystalline matrices (ref. 1, pp. 323–332), to the powder spectrum allows for this radical the determination of two of the **g**-tensor elements and also two of the elements of the proton hyperfine tensor, see Fig. 2. The nature of the spectrum does not allow a clear distinction to be drawn between an axially symmetric **g**-tensor with elements $g_\parallel$ and $g_\perp$ and a tensor with three unequal elements, in which case one of the **g**-values has not been determined. Also from the powder spectrum alone it is difficult to distinguish between the coupling of one nitrogen nucleus with two different tensor elements in its hyperfine tensor and two nitrogen nuclei interacting with the unpaired electron. However, the width of the shoulders does indicate that there are two nitrogen nuclei interacting. This indeed is proved by the single crystal results.

The values of the proton hyperfine coupling constants of spectrum B, see Table 1, are not consistent with the presence of a π-electron

TABLE 1. Observed values for elements of the g-tensors, the proton hyperfine coupling tensors and the nitrogen hyperfine coupling tensors for spectra B and C of γ-irradiated dicyandiamide powder*

Spectrum B	g_1	= 2.0028 (0.0004)
	g_2	= 2.0040 (0.0004)
	g_3	= ?
	A_1(H)	= 80.4 (4) G
	A_2(H)	= 73.2 (1.0) G
	A_3(H)	= ?
	$A_1(N_1)$	= 25.5 (3.0) G
	$A_2(N_1)$	= 0 (2.0) G
	$A_3(N_1)$	= ?
	$A_1(N_2)$	< 5 G
	$A_2(N_2)$	= 6.5 (1.0) G
	$A_3(N_2)$	= ?
Spectrum C†	g_2	= 2.0031 (0.0004)
	A_2(H)	= 29.4 (1.0) G
	A_2(N)	= 15.8 (1.0) G

*Tensor elements not given in the table could not be found either from the powder or single crystal measurements.

†Only one element of each of the g-tensor and the nitrogen and proton hyperfine coupling tensors is determined.

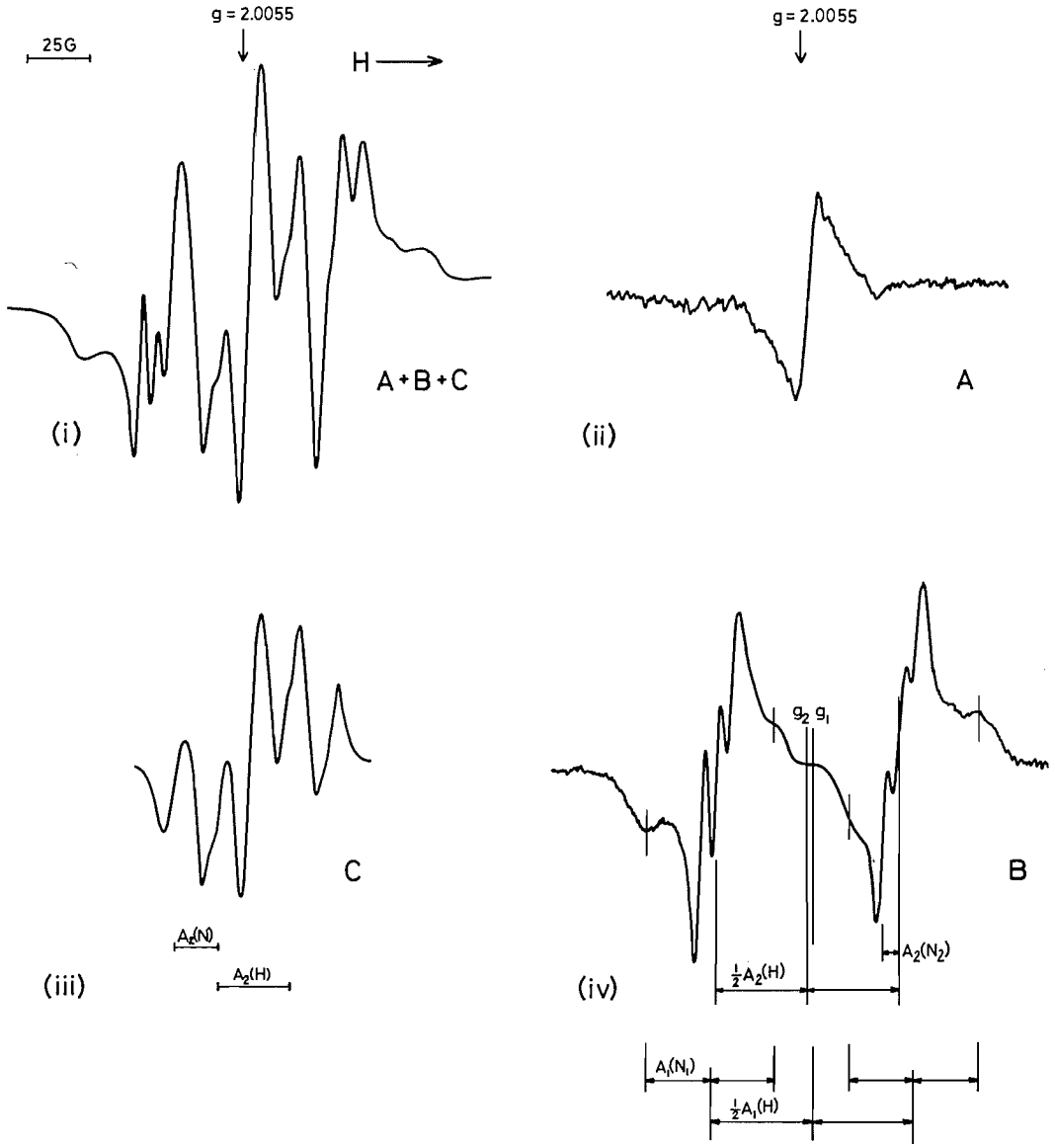

FIG. 2: Spectra from the powder experiments, taken at a klystron frequency of 9.5 GHz. (*i*) Trace of the X-band e.s.r. spectrum of dicyandiamide after 20 h of γ-irradiation at room temperature. (*ii*) Spectrum of unidentified species (A) observed following 3 h of irradiation followed by heating to 150 °C. (*iii*) Spectrum of the π-radical (C), obtained by subtracting the spectrum of the unidentified radical (A) from the residual spectrum (A + C), observed after γ-irradiating for 20 h and then heating to 150 °C to remove spectrum B. (*iv*) Spectrum of the σ-radical (B), also obtained by subtraction. The figure shows how the values of the derived g and hyperfine tensor elements were deduced.

radical but do allow the possibility of a σ-electron radical with $\rho_H^\sigma \approx 0.14$, Two of the principal values, $A_1(H)$ and $A_2(H)$, of the proton hyperfine splitting tensor were arrived at by measuring the positions of the weaker shoulders and stronger triplets, respectively. The same measurements also gave the values of g_1 and g_2 and also $A_1(N_1)$ and $A_2(N_2)$ in Table 1.

(ii) Single Crystal

The e.s.r. spectra of the dicyandiamide single crystal, irradiated and studied at room tempera-

ture, were recorded at 10° intervals for rotation about the *X*, *Y*, *Z*, *a* sin β, and *b* axes (angles α, β, γ, δ′, and δ, respectively) and in addition at 2° intervals for $0° \leqslant \gamma \leqslant 45°$ and 1° intervals for γ near 135°. These smaller intervals were chosen in an attempt to gain additional information concerning the nitrogen hyperfine splitting, particularly to study the movement of the outermost weak satellites described below. The spectra observed for the single crystal can again be understood as due to superposition of the three spectra A, B, and C, taking into account the possibility of magnetically non-equivalent sites, particularly for the spectrum B. Because of the overlapping of spectra it was not possible to carry out complete determinations of the magnitudes and direction cosines of principal values of g, $A(N_1)$, $A(N_2)$, and A(H) tensors. Even so, the results allow some interesting deductions to be made concerning the nature and orientation of the radicals responsible for spectrum B.

The e.s.r. spectra with the magnetic field in the *YZ* and *XZ* planes are not well resolved and show only a slight dependence on the angles α and β. At most angles α and β the spectrum consists of three broad lines similar to those shown in Fig. 3 but at a few orientations of the field in the *YZ* and *XZ* planes each of the outermost lines showed a further splitting into a strong 1:1:1 triplet with some weaker satellite peaks on both sides. There is a significant improvement in the resolution of the hyperfine structure when the magnetic field is in the *XY* plane, with the triplet structure and satellites becoming most obvious at $\gamma = 45°$, and also at $\gamma = 135°$, compare Figs. 3 and 4. In addition to the angular variation in the spectra required by the symmetry of the host crystal, the spectra also repeat exactly after 90°, *i.e.* e.s.r. (γ) = e.s.r. (90° + γ). The best resolution was found at $\gamma = 45$ and 135°, indicating probable equivalence of different magnetic sites at these orientations. For rotation about the *b* axis $\delta = 0$ corresponded to $\gamma = 135°$ and about the *a* sin β axis $\delta' = 0$ was the same as $\gamma = 45°$. The e.s.r. spectra with the magnetic field in the *bc* plane (angle δ′) showed the expected symmetry with respect to the *c*(*Z*) axis, *i.e.* e.s.r. (90° − δ′) ≡ e.s.r. (90° + δ′). The spectra with the magnetic field in the *ac* plane (angle δ) did not show this symmetry with respect to the *c* axis and differed from those in the *bc* plane in having very good resolution over a fairly wide range of values of δ, with two well-resolved nine-line groups being observed near $\delta = 30°$, see Fig. 5.

The observed behavior is interpreted as follows. The e.s.r. spectra for $\gamma = 45$ and 135° are due to overlapping of spectra from radicals in two inequivalent magnetic sites, see Fig. 4. The large doublet splitting is caused by interaction of the unpaired electron with one proton. A fairly large and anisotropic hyperfine interaction occurs with one nitrogen, hyperfine coupling tensor $A(N_1)$, and a smaller and more isotropic coupling takes place with a second nitrogen, hyperfine coupling tensor $A(N_2)$. At $\gamma = 45$ and 135° the two overlapping spectra give rise to two 1:1:1:4:4:4:1:1:1 groups. The unusually large proton splitting shows the presence of a σ-radical which is produced by loss of one of the hydrogens from either of the two $-NH_2$ groups. This is dealt with in greater detail in the discussion

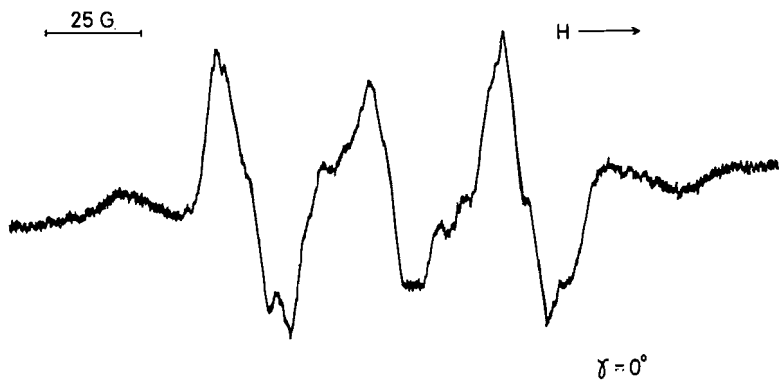

FIG. 3. The 9.5 GHz e.s.r. spectrum of the γ-irradiated dicyandiamide crystal with the magnetic field along the (310) or *X* direction.

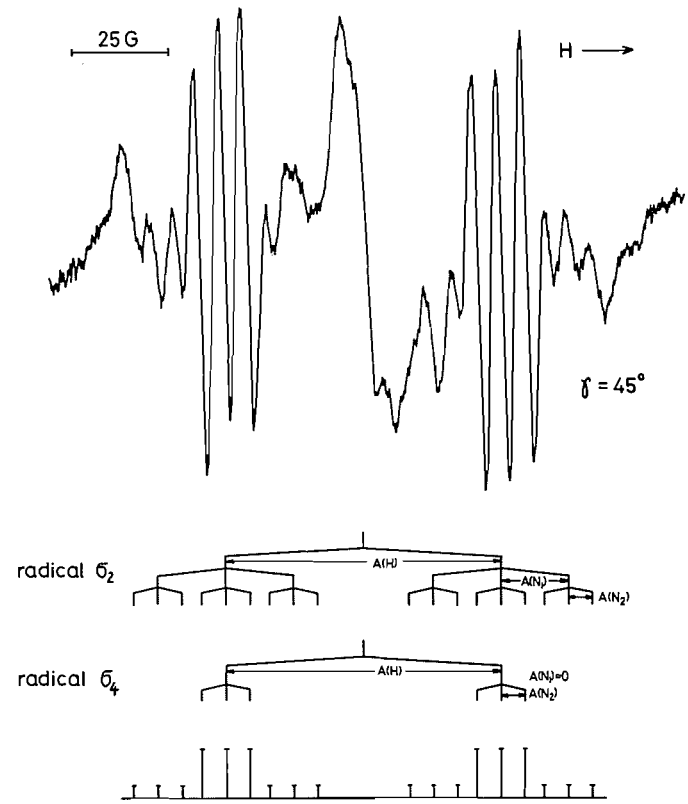

FIG. 4. The 9.5 GHz e.s.r. spectrum of the γ-irradiated single crystal with the magnetic field along the *b* axis. At this orientation the two lattice sites of radical formed by loss of H_2 are magnetically equivalent as are those for the radical formed by loss of H_4.

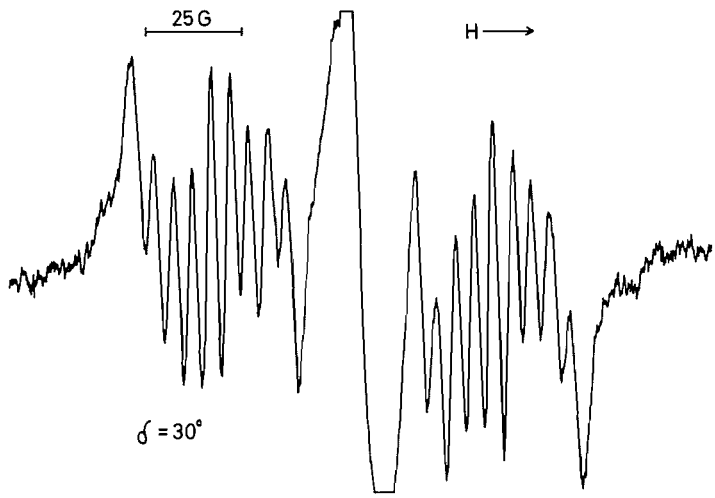

FIG. 5. The 9.5 GHz e.s.r. spectrum of the γ-irradiated dicyandiamide single crystal for the magnetic field orientation $\delta = 30°$ in the *ac* plane.

below. The large coupling, tensor A(H), can then be attributed to the remaining hydrogen in the —ṄH fragment and the tensor $A(N_1)$ to this nitrogen. The further and quite isotropic splitting may belong to the nitrogen of the undamaged $-\dot{N}H_2$ group or possibly to one of the two CN nitrogens. The results for rotation about the *b* and *a* sin β axes confirm that the *ac* plane is a mirror plane for the crystal, an important fact which is utilized below in the discussion section.

When the γ-irradiated single crystal was heated to 150 °C for 5 min and then cooled to room temperature the strong outer triplets and weaker satellites (spectrum B, $\gamma = 45°$) disappeared leaving behind a broad line of width approximately 13 G and having two shoulders. This residual spectrum is similar to the spectrum A + C obtained from the powder. However, the resolution for this spectrum was not sufficiently good to allow the determination of any further information beyond that already found from the powder study.

The single crystal spectra thus confirm the main conclusions of the powder work showing, in addition to the single line spectrum A, spectra B and C from two different types of radicals, one in which the unpaired electron interacts with one proton and two N nuclei (B) and one in which the unpaired electron appears to interact with one proton and only one N nucleus (C).

Discussion

In order to understand the nature of the radicals observed in this study it is necessary first to consider in some detail the dicyandiamide molecule and its crystal structure. Arguing from the observed internuclear distances Hughes (15) concluded that the cyanimino group, NCN, could be represented in terms of the resonance structures

$:N\equiv C-\ddot{N}\diagdown$ (25%) $\qquad :\bar{\ddot{N}}=C=\ddot{N}\diagdown$ (75%)

and that in the guanidine group, $NC(NH_2)_2$, the C—N distances indicate considerable delocalization of the carbon–nitrogen double bond. The heavy atoms in the guanidine group should thus be planar. The most recent studies of the crystal structure (16, 17) show that all the atoms of a particular molecule lie nearly in the same plane with the exception of H_3 and N_1, see Fig. 6. The molecular planes, held together by interplanar hydrogen bonding, are very close to the crystal $(3\bar{1}0)$ and (310) planes.

In the undamaged crystal the $-NH_2$ group angles are as shown in Fig. 6. They were calculated using the data of Rannev and Ozerov (17). The angle $C_2N_4H_4$ is 124° so that after the removal of H_3 formation of a π-electron radical could take place with very little disturbance in the position of the hydrogen bonded atom H_4, which lies in the plane of the molecule. The nitrogen N_4 would thus achieve an approximately sp^2 hybridization state. The same argument may be applied to the group $C_2N_3H_2$. The angle $C_2N_4H_3$ is 108° so that after the loss of H_4 formation of a so-called σ-electron radical (2, 5, 7, 22) can occur, again with only small readjustments of the atom positions. The nitrogen N_4 would now reach a state of approximately sp^3 hybridization. We consider that in this case π-electron radical formation does not occur because of the constraint placed upon H_3 by hydrogen bonding to N_1 of an adjacent molecule. Again we can apply the argument to the residual atoms $C_2N_3H_1$ after loss of H_2. This model thus leads to the four possibilities, shown in Chart 1, for radical formation after the loss of one of the four hydrogen atoms in the molecule, assuming that all four N—H bonds may be broken. The notation here is that for example π_3 means a π-electron radical formed by loss of H_3.

π-Radicals

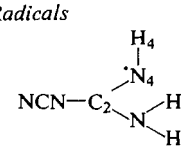

π_3

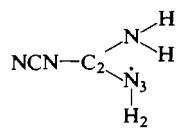

π_1

σ-Radicals

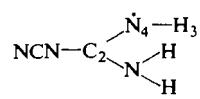

σ_4

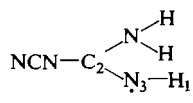

σ_2

Chart 1

The dicyandiamide crystal belongs to the space group *C2/c*. Although there are eight molecules per unit cell, their positions are related by inversion and translation in such a way that for a given

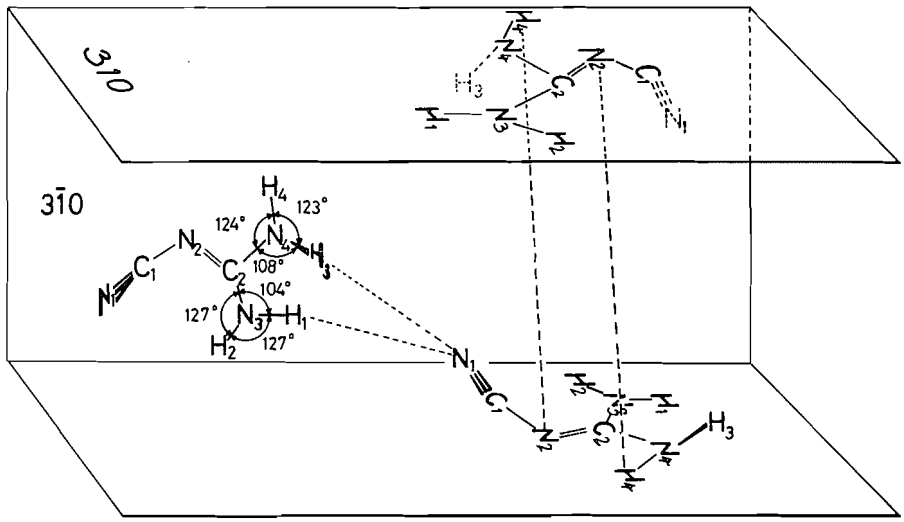

FIG. 6. Schematic diagram showing the arrangement of atoms in the dicyandiamide crystal structure. For each molecule all atoms are coplanar except H_3 and N_1. Hydrogen bonding to molecules in other planes is indicated by dashed lines. The bond lengths are not to scale.

radical there can be only two inequivalent magnetic sites. These must be related to each other by reflection in the *ac* plane. We refer to these two positions as I and II, respectively. It is then possible to have four π-radicals in magnetically non-equivalent positions: π_1(I), π_1(II), π_3(I), and π_3(II) and also four σ-radicals σ_2(I), σ_2(II), σ_4(I), and σ_4(II). The four π-radical positions could give rise to the e.s.r. spectrum C, observed in both powder and single crystal and found to be less well resolved in the latter case. The four σ-radical positions produce spectrum B. This assumes that when either the N_4H_4 or N_3H_2 bond is broken the orbital in which the now unpaired electron is located is able to take up a position consistent with sp^3 hybridization. This reorientation appears to be more likely than a change in the position of either H_3 or H_1, which are both constrained by hydrogen bonding. Assuming that the orbital containing the unpaired electron points along a direction which makes angles of 109° 28′ with the adjacent NH and CN bonds and from the two resulting solutions choosing the direction closest to the direction of the original unbroken N_4H_4 or N_3H_2 bond, then the directions shown in Fig. 7 were obtained. These directions should be the ones in which the largest value of the $A(N_1)$ tensor is found for the four σ-radical positions. It may be seen from Fig. 7 that the projections of these directions on the XY plane lie close to $a \sin \beta$ or $\gamma = 135°$ for σ_4(I) and σ_4(II) and close to b or $\gamma = 45°$ for σ_2(I) and σ_2(II). For the field in the XY plane we should therefore find maxima in $A(N_1)$ for these four directions. These four maxima may be taken in two sets of two, one pair near $\gamma = 45°$ and one near $\gamma = 135°$. At $\gamma = 45$ and 135°, crossing of each pair of $A(N_1)$ curves takes place giving only two distinguishable e.s.r. patterns, or two different values of $A(N_1)$. At most of the other values of γ four signals should be present. The condition that only two distinguishable patterns can be observed also holds for the field anywhere in the *ac* plane, the mirror plane. This is not generally true for the field in the *bc* plane. However, for the *bc* plane the condition e.s.r. $(90° + \delta') \equiv$ e.s.r. $(90° - \delta')$ must hold which is found experimentally to be the case. Although experimental points could only be obtained near $\gamma = 45$ and 135° for the field in the XY plane the measured values of $A(N_1)$ in these regions and the general features of the variation of the spectra for rotation of the crystal about the b, Z, and $a \sin \beta$ axes give strong support to the proposed model.

The following considerations can be made to give a better understanding of the reason for the large proton hyperfine coupling in the σ-electron radical. The interaction between the magnetic moments of an electron and a nucleus can be

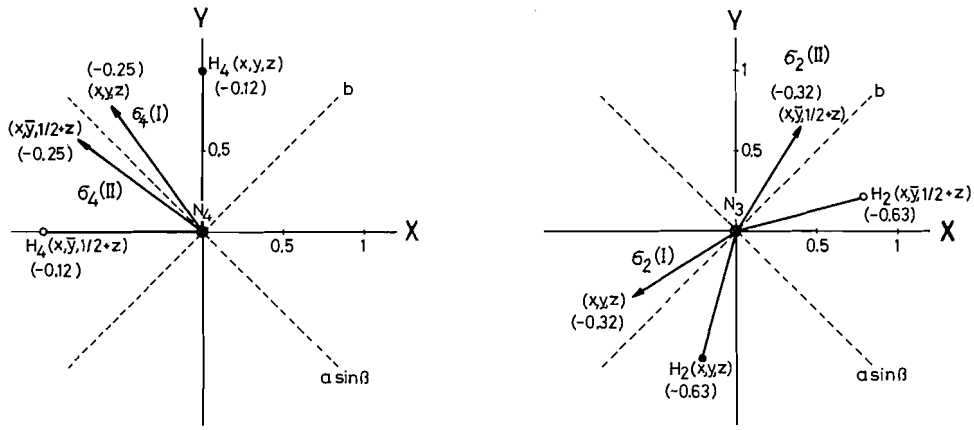

FIG. 7. Calculated directions of the orbital containing the unpaired electron for each of the four different magnetic sites of the σ-radical: σ_2(I), σ_2(II), σ_4(I), and σ_4(II). The Z coordinates are given in brackets. The orbital directions are taken to be unit vectors (1 Å). For each pair of sites the nitrogen atoms have been superimposed at the origin.

expressed in the usual way as the sum of the isotropic Fermi contact and anisotropic dipole–dipole terms: $H_{hf} = H_F + H_D$. If the unpaired electron is in a $p_z(\pi)$ orbital the probability density in the p-orbital nodal plane is zero. Even so protons in the planar methyl radical and in the rings of aromatic radicals do show some non-zero isotropic hyperfine coupling (8). This happens because of σπ spin polarization, brought about through exchange interaction coupling together the spins of the σ-electrons in the C—H bond with the $p_z(\pi)$ electron of the carbon. The isotropic term H_F in such a case can be written

$$[1] \quad H_F = \frac{8\pi}{3} g_e\beta_e g_N\beta_N\rho(r_N)(\hat{I}\cdot\hat{S}) = K\rho(r_N)(\hat{I}\cdot\hat{S}) = a(\hat{I}\cdot\hat{S})$$

where $\rho(r_N)$ is the unpaired electron density at the nucleus. Also

$$[2] \quad \rho(r_N) = \pi^2(r_N) - \frac{4}{\sqrt{6}}\lambda\sigma(r_N)\sigma^*(r_N) \quad (\lambda^2 \ll 1)$$

where λ is the coefficient which determines the magnitude of the configurational admixture of one of the two excited doublet states with the ground doublet (23, 24). $\pi^2(r_N)$ is the π-type spin density of the electron at the proton. σ and σ* refer to bonding and antibonding orbitals, respectively.

Without the admixture of the excited doublet term to the ground doublet term the unpaired electron density would be

$$[3] \quad \rho(r_N) = \pi^2(r_N)$$

In the case of an aromatic ring proton

$$[4] \quad \pi^2(r_N) = 0$$

Equations 1 and 2 then lead to

$$[5] \quad a_{H\mu} = Q_{CH}\rho_\mu^\pi \qquad Q_{CH} < 0$$

for the hyperfine coupling of the proton H_μ, which is the McConnell relation. ρ_μ^π is the π-electron density at the carbon atom, C_μ, to which the proton is bound. It should be noted that ρ_μ^π is the integrated spin density, obtained by integration of $\rho(r_N)$ over the π-orbital located at the carbon atom. It is easily seen that the McConnell relation [5] holds only for a nucleus which lies in the nodal plane of the π-orbital, in other words when the condition [4] is fulfilled. If [4] does not hold then

$$[6] \quad a_{H\mu} = K_H\pi^2(r_H) + Q_{CH}\rho_\mu^\pi$$

($K_H = 2.3626 \times 10^{-22}$ G cm^3) and the isotropic proton hyperfine splitting, $a_{H\mu}$, now depends very strongly on the position of the proton as defined by r_H.

In 1959 Karplus (25) carried out a valence bond calculation for the methyl radical of the dependence of the proton hyperfine splitting on the angle θ between the symmetry axis and each C—H bond. The calculation was made in terms of a seven electron – seven orbital model for CH_3 as well as for a three electron – three orbital model. These calculations show that a_H is

strongly dependent on the magnitude of θ. For example with θ = 90°, 109° 28′, and 144° 45′, corresponding to planar (sp^2), tetrahedral (sp^3), and pyramidal (p^3) hybridization, respectively, the following results were obtained: θ = 90° (sp^2), $23.4 < a_H < 34.6$ G; θ = 109° 28′ (sp^3), $34.5 < a_H < 44.1$ G; θ = 144° 45′ (p^3), $145.3 < a_H < 179.3$ G.

Although the corresponding angle between the N—H bond and the orbital containing the unpaired electron in the σ-electron radical of the present study is not known precisely it is probably near the tetrahedral angle which could lead to the large observed proton hyperfine coupling.

We should like to thank Mrs. J. D. Savage for growing single crystals of dicyandiamide and also Professor R. D. Heyding for identifying crystal faces and axes. We acknowledge the generous support given to this work by the National Research Council of Canada.

1. P. B. AYSCOUGH. Electron spin resonance in chemistry. Methuen. 1967. p. 228. Table 7.9.
2. F. J. ADRIAN, E. L. COCHRAN, and V. A. BOWERS. J. Chem. Phys. **36**, 1661 (1962).
3. P. SMITH and P. B. WOOD. Can. J. Chem. **44**, 3085 (1966).
4. R. LIVINGSTON and H. ZELDES. J. Chem. Phys. **47**, 4173 (1967).
5. N. CYR and W. C. LIN. J. Chem. Phys. **50**, 3701 (1969).
6. H. N. REXROAD, Y. H. HAHN, and W. J. TEMPLE. J. Chem. Phys. **42**, 324 (1965).
7. P. W. LAU and W. C. LIN. J. Chem. Phys. **51**, 5139 (1969).
8. A. CARRINGTON and A. D. MCLACHLAN. Introduction to magnetic resonance. Harper and Row. 1967. p. 83. Table 6.1.
9. R. J. LONTZ. J. Chem. Phys. **45**, 1339 (1966).
10. H. W. SHIELDS, P. J. HAMRICK, and W. REDWINE. J. Chem. Phys. **46**, 2510 (1967).
11. K. REISS and H. W. SHIELDS. J. Chem. Phys. **50**, 4368 (1969).
12. W. M. FOX and P. SMITH. J. Chem. Phys. **48**, 1868L (1968).
13. A. LUND and T. GILLBRO. J. Mag. Res. **2**, 164 (1970).
14. K. HEYDRICH. Z. Krist. **48**, 278 (1910–1911).
15. E. W. HUGHES. J. Am. Chem. Soc. **62**, 1258 (1940).
16. Z. V. ZVONKOVA, V. YA. KRIVNOV, and A. N. KHVATKINA. Doklady Phys. Chem. **155**, 261 (1964).
17. N. V. RANNEV and R. P. OZEROV. Doklady Phys. Chem. **155**, 426 (1964).
18. Scientific American. January 1968. p. 128.
19. Varian "EPR at Work" series. No. 28.
20. J. R. MORTON. J. Phys. Chem. Solids, **24**, 209 (1963).
21. P. W. ATKINS and M. C. R. SYMONS. The structure of inorganic radicals. Elsevier. 1967. pp. 107–108.
22. E. L. COCHRAN, F. J. ADRIAN, and V. A. BOWERS. J. Chem. Phys. **40**, 213 (1964).
23. S. I. WEISSMAN. J. Chem. Phys. **25**, 890 (1956).
24. F. GERSON. Hochauflösende ESR-Spektroskopie 1, Verlag Chemie, GmbH, Weinheim/Bergstr. 1967. pp. 74–84.
25. M. KARPLUS. J. Chem. Phys. **30**, 15 (1959).

Can. J. Chem. Downloaded from www.nrcresearchpress.com by 210.87.254.42 on 09/05/12
For personal use only.

Trimethylstannylarsines

J. W. ANDERSON AND J. E. DRAKE
Department of Chemistry, University of Windsor, Windsor, Ontario

Received February 15, 1971

Tin arsines which contain an As—H bond, namely trimethylstannylarsine, bis-trimethylstannylarsine, and phenyl(trimethylstannyl)arsine, have been prepared and characterized. Alternative preparations of other trimethylstannylarsines are also discussed.

Des arsines d'étain contenant une liaison As—H, la triméthylstannylarsine, la bis-triméthylstannylarsine, et la phényl (triméthylstannyl) arsine, ont été préparés et caractérisés. D'autres modes de préparation de triméthylstannylarsines sont discutés.

Canadian Journal of Chemistry, 49, 2524 (1971)

Introduction

Several routes have been established for the formation of silyl- and germyl-arsines in which there are no organo-substituents on arsenic. Lithium tetra-arsinoaluminate has been used in the preparation of mono- and bis-arsino substituted silanes and mono-arsino substituted germanes by reaction with the appropriate bromides (1). Trisilylarsine and mono-, di-, and tri-germylarsines were prepared from the reaction of arsino-potassium with bromosilane (2) or bromogermane (3). Under carefully controlled conditions followed by acidification with hydrogen sulfide, this route has been used for the synthesis of mono- and di-silylarsine (4). Exchange reactions between silylarsines and halogeno-germanes have also been used to produce germylarsines (1, 3, 5).

Methods for the preparation of tertiary arsines containing an Sn—As bond include amine cleavage (6) and removal of hydrogen chloride from arsine and a tin chloride using a tertiary amine (7).

We have attempted the preparation of primary and secondary (*i.e.*, As—H containing) tin arsines by related methods. Compounds of this type have not been prepared previously (8).

Experimental

Apparatus

The experiments were carried out in conventional Pyrex glass vacuum systems. The i.r. spectra were recorded on a Beckman IR 12 spectrometer in a gas cell (5 cm path length) or in an air-tight cell-holder between KBr plates for liquid samples; the values given are cm^{-1}. The ^1H n.m.r. spectra were recorded in sealed n.m.r. tubes (*ca.* 2 mm o.d.) on a JEOL C-60 HL spectrometer, and molecular weights were determined by freezing-point depression of benzene.

Starting Materials

Commercial trimethyl (chloro)- and trimethyl(bromo)-stannane (Alfa Inorganics) were used as supplied and their purity checked by their n.m.r. spectra (9). Arsine was prepared by the action of water on sodium arsenide; methylarsine from reduction of sodium methyl arsenate with zinc and hydrochloric acid; and phenylarsine by the lithium tetrahydroaluminate reduction of phenyl-(dichloro)arsine. Arsino-potassium was prepared from arsine and potassium in liquid ammonia and lithium tetra-arsinoaluminate from arsine and lithium tetrahydroaluminate (10). Silylarsine and the methyl(silyl)-arsines were prepared from bromosilane and the appropriate arsinoaluminates (1) and the phenyl(silyl)-arsines from bromosilane and the corresponding lithium phenylarsenides. Diethyl(trimethylstannyl)amine was prepared from lithium diethylamide and trimethyl(chloro)-stannane (11).

Reduction of Trimethylbromostannane with Lithium Tetra-arsinoaluminate

Typically, trimethylbromostannane (2.49 g; *ca.* 10 mmol) was condensed onto a monoglyme solution of lithium tetra-arsinoaluminate (12.5 mmol) and the mixture held at −45° for *ca.* 10 min. Separation of the products by trap-to-trap distillation gave trimethylstannylarsine (0.217 g; 0.9 mmol), in a trap at 0° while the solvent, arsine, and a mixture of methylstannanes passed through into a −196° trap.

Reaction of Trimethylbromostannane with Arsino-potassium

Typically, trimethylbromostannane (2.18 g; *ca.*9 mmol) and arsino-potassium (10.1 mmol) each in diethylether, were mixed together slowly and held at −78° for 3 h. After this time, arsine (identified by its i.r. spectrum) and solvent were distilled off as the vessel was warmed to room temperature. Tris-trimethylstannylarsine (1.53 g; *ca.* 2.7 mmol) was then distilled, by gentle warming, from the reaction vessel. In all cases where the least volatile fraction was the desired product, the latter was distilled from the reaction vessel to the storage trap, usually a tube suitable for n.m.r. analysis, by surrounding the trap with liquid nitrogen and then providing the minimum of heat from a mantle.

In a similar manner, trimethylbromostannane (2.5 g; *ca.* 10.5 mmol) was mixed with excess arsino-potassium

Can. J. Chem. Downloaded from www.nrcresearchpress.com by 210.87.254.42 on 09/05/12
For personal use only.

(39 mmol). Arsine was pumped away at −78° and the residue treated with excess hydrogen sulfide for 1 h. After removal of solvent, distillation using a Leroy Column (12) gave three distinct fractions, trimethylstannylarsine (0.55 g; 2.3 mmol), bis-trimethylstannylarsine (0.36 g; 0.9 mmol), and tris-trimethylstannylarsine (0.45 g; 0.8 mmol). A similar residue, when treated with methyl iodide gave dimethyl(trimethylstannyl)-arsine, methyl(bis-trimethylstannyl)arsine, and tris-trimethylstannylarsine.

Further Anion Reactions

(a) Tris-trimethylstannylarsine (1.36 g; 2.4 mmol) and monoglyme were trapped onto potassium (5.0 mmol) and the system allowed to warm to room temperature. The monoglyme solution changed color from blue to various shades of brown. Excess hydrogen sulfide was immediately added and after 10 min the volatile materials, which included arsine, tetramethylstannane, and trimethylstannane (identified by n.m.r. spectra), were pumped away. Bis-trimethylstannylarsine (0.32 g; 0.8 mmol) was then distilled, by gentle warming, from the reaction vessel.

(b) In a similar manner, phenyl(bis-trimethylstannyl)-arsine (1.44 g; 3.0 mmol) and potassium (5.9 mmol) in monoglyme gave, after treatment with H_2S and pumping off volatile products, phenyl(trimethylstannyl)arsine (0.32 g; 1.0 mmol).

(c) In a similar manner, methyl(bis-trimethylstannyl)-arsine (0.79 g; 2 mmol) and potassium (4 mmol) in monoglyme gave only a small amount of methyl(bis-trimethylstannyl)arsine in the less volatile fraction.

Reaction of Trimethylchlorostannane with Dimethyl(silyl)arsine

Typically, dimethyl(silyl)arsine (1.37 g; *ca.* 10.1 mmol) and a small quantity of diethylether were distilled onto trimethylchlorostannane (2.0 g; *ca.* 10 mmol) and allowed to warm from −196° to room temperature. Chlorosilane (identified by its i.r. spectrum) and the ether were pumped away leaving dimethyl(trimethylstannyl)arsine (2.72 g; *ca.* 10.1 mmol) which was poured into a ^1H n.m.r. tube attached as a side-arm to the reaction vessel.

Reaction of Trimethylchlorostannane with Methyl(disilyl)arsine, Diphenyl(silyl)arsine, and Phenyl(disilyl)arsine

As described above, the reaction of trimethylchlorostannane (4.04 g; *ca.* 20 mmol) with methyl(disilyl) arsine (1.49 g; *ca.* 10.5 mmol) gave methyl(bis-trimethylstannyl)arsine (4.12 g; *ca.* 9.9 mmol); trimethylchlorostannane (1.45 g; *ca.* 7.3 mmol) with diphenyl(silyl)-arsine (1.84 g; 7.1 mmol) gave diphenyl(trimethylstannyl)arsine (2.81 g; 7.1 mmol); and trimethylchlorostannane (2.97 g; 14.9 mmol) with phenyl(disilyl) arsine (1.58 g; 7.4 mmol) gave phenyl(bis-trimethylstannyl)arsine (3.65 g; 7.5 mmol).

Reaction of Trimethylchlorostannane with Silylarsine

(a) Silylarsine (*ca.* 1 mmol) and diethylether were distilled onto trimethylchlorostannane (0.2 g; *ca.* 1 mmol) and allowed to warm to —78° when arsine was evolved. On warming to room temperature, trisilylarsine (identified by its i.r. spectrum (13)) distilled off leaving mainly unreacted trimethylchlorostannane.

(b) An equimolar amount of silylarsine was distilled onto trimethylchlorostannane in an n.m.r. tube which was then sealed. The ^1H n.m.r. spectrum only showed peaks attributable to arsine (14), trisilylarsine (15), and trimethylchlorostannane (9).

An equimolar amount of silylarsine was distilled onto trimethylbromostannane in an n.m.r. tube which was then sealed. The ^1H n.m.r. spectrum, taken immediately the tube had warmed to room temperature, only showed peaks attributable to the starting materials. After 1 h the only peaks were those attributable to trisilylarsine and arsine (in a ratio of *ca.* 3:2) and unchanged trimethylbromostannane.

Reaction of Trimethyl(bromo)stannane with Trimethylstannylarsine

Equimolar amounts of trimethyl(bromo)stannane and trimethylstannylarsine were held at room temperature in a 10 ml reaction vessel. Arsine (identified by its i.r. spectrum) was evolved and after *ca.* 6 h the remaining mixture consisted only of tris-trimethylstannylarsine and trimethyl(bromo)stannane; the latter was pumped away leaving the former.

Reaction of Diethyl(trimethylstannyl)amine with Phenylarsine

Typically, phenylarsine (0.4 g; 2.5 mmol) in diethylether was slowly added to a stirred solution of diethyl (trimethylstannyl)amine (1.17 g; 5 mmol) at room temperature. Diethylamine (identified by its i.r. spectrum) was pumped off at room temperature along with the solvent. Phenyl(bis-trimethylstannyl)arsine (0.9 g; 1.9 mmol) was then distilled, by gentle warming, from the reaction vessel.

Reaction of Diethyl(trimethylstannyl)amine with Methylarsine

Typically, gaseous methylarsine (2.5 mmol) was slowly admitted over a stirred diethylether solution of diethyl(trimethylstannyl)amine (1.18 g; 5 mmol) at room temperature. Diethylamine and solvent were pumped away after 40 min at room temperature. Methyl(bis-trimethylstannyl)arsine (0.6 g; 1.4 mmol) was then distilled, by gentle warming, from the reaction vessel.

Characterizations

Tris-trimethylstannylarsine, methyl(bis-trimethylstannyl)arsine, dimethyl(trimethylstannyl)arsine, diphenyl-(trimethylstannyl)arsine, and phenyl(bis-trimethylstannyl)arsine were characterized by their molecular weights and i.r. and ^1H n.m.r. spectra (8), and their cleavage reactions with HBr.

Trimethylstannylarsine

Me_3SnAsH_2 (Mol. Wt. Calcd.: 240.6. Found: 238). Its ^1H n.m.r. parameters are displayed, along with related species, in Table 1. Its i.r. spectrum showed the following main features: 2975s and 2908m (CH_3 stretches); 2076s (AsH_2 stretch); 1415w, 1185m (CH_3 deformations); 950m (AsH_2 deformation); 766m, 715 (CH_3 rocks); 570 v.w.; 519s, 499m (Sn—C_3 stretches).

Bis-trimethylstannylarsine

$(Me_3Sn)_2$ AsH (Mol. Wt. Calcd.: 403.3. Found: 421). Its ^1H n.m.r. parameters are displayed in Table 1. Its i.r. spectrum showed the following main features: 2979s, 2902m (CH_3 stretches); 2089s (AsH stretch); 1420m,

TABLE 1. The n.m.r. parameters of tin arsines and other trimethylstannyl derivatives*

Compound	δ SnC*H*	$J\,117_{SnCH}$	$J\,119_{SnCH}$	Compound	$J\,117_{SnCH}$	$J\,119_{SnCH}$
Me_3SnAsH_2†	0.31	47.5	50	Me_3SnCl‖	56.1	58.5
$Me_3SnAsHPh$‡	0.34	48	50	Me_3SnBr‖	55.8	58.4
$Me_3SnAsMe_2$	0.22	47	49.5	Me_3SnI‖	55.6	58.0
$Me_3SnAsPh_2$	0.21	48	50.5	$(Me_3Sn)_2O$‖	53.6	56.0
$(Me_3Sn)_2AsH$‡	0.36	§	§	$(Me_3Sn)_2S$‖	53.9	56.3
$(Me_3Sn)_2AsMe$	0.39	47.5	50	$(Me_3Sn)_2Se$‖	53.5	56.0
$(Me_3Sn)_2AsPh$	0.35	48	50	Me_3SnSMe¶	54.5	59.9
$(Me_3Sn)_3As$	0.37	47.5	50	$Me_3SnSeMe$¶	53.4	55.9
				$(Me_3Sn)_3P$**	49.7	52.2

*All chemical shifts in p.p.m. downfield from TMS and coupling constants in Hz.
†δ As*H* 1.1.
‡δ As*H* not observed.
§Not observed.
‖See ref. 9.
¶See ref. 28.
**See ref. 18.

1186m (CH_3 deformations); 938w (AsH bend); 760m, 710w (CH_3 rocks); 522s, 502m (Sn—C_3 stretches).

Phenyl(trimethylstannyl)arsine

$(Me_3Sn)AsHPh$ (Mol. Wt. Calcd.: 317.6. Found: 335). Its ^1H n.m.r. parameters are displayed in Table 1. Its i.r. spectrum showed the following main features attributable to the phenyl-group itself: 3061s, 3098m, 1583s, 1484s, 1335w, 1320w, 1300w, 1155w, 1072m, 1023s, 998m, 842w, 736s, 693s, 665w, 616w, in addition to the following: 2979s, 2909s (CH_3 stretches); 2084s (AsH stretch); 1433s, 1184s (CH_3 deformations); 959m (AsH bend); 765s (CH_3 rock); 520s, 501s (Sn—C_3 stretches); 452s.

Reaction with Hydrogen Bromide

Trimethylstannylarsine (1.0 mmol) and hydrogen bromide (1.0 mmol) were held together at room temperature for 1/2 h giving trimethyl(bromo)stannane (0.9 mmol) and arsine (0.9 mmol). Similarly bis-trimethylstannylarsine (0.5 mmol) and hydrogen bromide (1.0 mmol) gave trimethyl(bromo)stannane (1.0 mmol) and arsine (0.5 mmol) and phenyl(trimethylstannyl)arsine 1.1 mmol) and hydrogen bromide (1.1 mmol) gave trimethyl(bromo)stannane (1.0 mmol) and phenylarsine (1.1 mmol), all identified by n.m.r. spectra.

Other Reactions

Trimethylstannylarsine (1.1 mmol) and hydrogen sulfide (0.7 mmol) were held together at room temperature for 1 h. The products volatile at −78° were removed and sealed up in a 2 mm n.m.r. tube. Integration of the spectrum showed that there was a 5:1 mixture of hydrogen sulfide and arsine. The tube was broken open and the contents returned to the reaction vessel and left at room temperature overnight. The products were then separated to give bis(trimethylstannyl)sulphide (0.5 mmol; identified by its n.m.r. spectrum) and arsine (1.2 mmol; containing a little hydrogen sulfide).

Trimethylstannylarsine (1.6 mmol) and water (0.9 mmol) were maintained at room temperature for 13 h. Arsine (0.9 mmol) was evolved and the water (0.9 mmol) was recovered.

Discussion

Trimethylstannylarsine, Me_3SnAsH_2, is prepared, albeit in low yield, by the reaction between lithium tetra-arsinoaluminate and less trimethylbromostannane than required by the stoichiometry of reaction, eq. 1. Increasing the proportion of bromide to that used in similar reactions involving silanes and germanes (1) gave even lower yields.

$$[1]\quad 4Me_3SnBr + LiAl(AsH_2)_4 = 4Me_3SnAsH_2 + LiBr + AlBr_3$$

Trimethylstannylarsine and bis-trimethylstannylarsine, $(Me_3Sn)_2AsH$, can both be prepared from the reaction of trimethylbromostannane and arsino-potassium under controlled conditions. With equimolar amounts of reactants, tris-trimethylstannylarsine, $(Me_3Sn)_3As$, is formed in good yield, as might be expected because a tertiary product is common in such anion reactions (2). However, with a large excess of arsino-potassium, subsequent acidification with hydrogen sulfide leads to the liberation of mono- and bis-trimethylstannylarsine, eq. 2. The mechanism of formation of related complex ions has been discussed for phosphine systems (2, 4). The rapid condensation of primary and secondary silyl- and germyl-arsines is a familiar feature of their chemistry (16), so condensation to produce

$$[2]\quad [AsH_2]^- \xrightarrow{Me_3SnBr} \begin{cases} [Me_3SnAsH]^- \xrightarrow[(H^+)]{H_2S} Me_3SnAsH_2 \\ [(Me_3Sn)_2As]^- \xrightarrow[(H^+)]{H_2S} (Me_3Sn)_2AsH \end{cases}$$

Can. J. Chem. Downloaded from www.nrcresearchpress.com by 210.87.254.42 on 09/05/12
For personal use only.

Can. J. Chem. Downloaded from www.nrcresearchpress.com by 210.87.254.42 on 09/05/12
For personal use only.

tris-trimethylstannylarsine is not unexpected. In addition, we find, both under sealed-tube and vacuum-line conditions, that trimethylstannylhalides catalyze such condensation processes, eq. 3.

$$[3]\quad \left.\begin{matrix}3SiH_3AsH_2\\ 3Me_3SnAsH_2\end{matrix}\right\} \xrightarrow[X = Cl, Br]{Me_3SnX} \left\{\begin{matrix}(SiH_3)_3As + 2AsH_3\\ (Me_3Sn)_3As + 2AsH_3\end{matrix}\right.$$

Bis-trimethylstannylarsine and phenyl(trimethylstannyl)arsine can also be prepared when the corresponding trimethylstannylarsine anions, formed by reaction of dry potassium in diglyme, eq. 4, are immediately acidified with hydrogen

$$[4]\quad (Me_3Sn)_2AsR \xrightarrow{2K} [Me_3SnAsR]^- + Me_3Sn^- + 2K^+$$
$$(R = Me_3Sn, Ph, Me)$$

sulfide. Trimethylstannane and tetramethylstannane are also liberated. Evidently, these systems involve complex processes and acidification must be rapid if As—H containing arsines are to be extracted. Hydrogen sulfide has been used successfully in similar systems (3) and in the time of the reaction, it does not attack Sn—As bonds. However, over a longer period, trimethylstannylarsine reacts with H_2S to give some trimethylstannylsulfide and arsine.

The solutions, eq. 4, presumed to contain the methyl(trimethylstannyl)arsine anion, $[Me_3SnAsMe]^-$, did not give $Me_3SnAsMeH$ on acidification. The latter presumably disproportionates to give only the starting material, $(Me_3Sn)_2AsMe$ in the less volatile fraction. Similarly, when the solutions containing trimethylstannylarsine anions, eq. 2, are treated with methyliodide, only methyl(bis-trimethylstannyl)arsine, eq. 5, is found although methyl(trimethylstannyl)arsine might also have been

$$[5]\quad [(Me_3Sn)_2As]^- + MeI \longrightarrow (Me_3Sn)_2AsMe + I^-$$

expected from the corresponding reaction with $[Me_3SnAsH]^-$. The formation of small amounts of dimethyl(trimethylstannyl)arsine in this experiment could result from interaction with excess $[AsH_2]^-$, eq. 6, followed by reaction with methyliodide.

$$[6]\quad \text{"}Me_3SnAsHMe\text{"} + [AsH_2]^- \longrightarrow AsH_3 + [Me_3SnAsMe]^-$$

The use of a lithium alkyl or lithium tetrahydroaluminate (17–19) to cleave an Sn—As bond followed by acidification did not lead to better yields of As—H containing tin arsines than the potassium method.

Tin arsines have previously been prepared by methods outlined in eqs. 7 and 8 (6, 7). Even with a large excess of arsine used as the solvent

$$[7]\quad 3Me_3SnCl + AsH_3 + 3Et_3N \longrightarrow 3Et_3NHCl + (Me_3Sn)_3As$$

$$[8]\quad Me_3SnNMe_2 + R_2AsH \longrightarrow Me_3SnAsR_2 + Me_2NH\ (R = Ph, Me)$$

we were unable to prepare any As—H containing tin arsines by either of these methods. Diethyl(trimethylstannyl)amine reacts smoothly with phenyl- and methyl-arsine, eq. 9, to give the tertiary arsines.

$$[9]\quad 2Me_3SnNEt_2 + RAsH_2 \longrightarrow (Me_3Sn)_2AsR + 2Et_2NH$$
$$(R = Ph, Me)$$

The exchange reactions between silylarsines and methyl(halogeno)germanes have resulted in the formation of mono- and bis-arsino-methylgermanes (1). However, extension to the methyl(halogeno)stannanes is not promising since trimethyl(halogeno)stannanes so effectively catalyze the condensation of silylarsine or trimethylstannylarsine (3). In this the tin halides parallel bromosilane which also assists condensation (20) rather than bromogermanes which exchange.

However, trimethyl(chloro)stannane does react in a similar manner to trimethyl(halogeno)- and halogeno-germanes with dimethyl(silyl)-, diphenyl(silyl)-, methyl(disilyl)-, and phenyl(disilyl)-arsines forming dimethyl(trimethylstannyl)-, diphenyl(trimethylstannyl)-, methyl(bis-trimethylstannyl)- and phenyl(bis-trimethylstannyl)-arsines respectively, eqs. 10 and 11, in excellent yields.

$$[10]\quad SiH_3AsR_2 + Me_3SnCl \longrightarrow Me_3SnAsR_2 + SiH_3Cl$$

$$[11]\quad (SiH_3)_2AsR + 2Me_3SnCl \longrightarrow (Me_3Sn)_2AsR + 2SiH_3Cl$$
$$(R = Me, Ph)$$

The new compounds were characterized by their molecular weights, i.r. and ^1H n.m.r. spectra, and by their reactions with hydrogen

Can. J. Chem. Downloaded from www.nrcresearchpress.com by 210.87.254.42 on 09/05/12
For personal use only.

bromide. Anhydrous hydrogen halides quantitatively cleave tin arsines giving well-known easily-identifiable products and thus present a useful method of on-line analysis which has been utilized for other group IV arsines (1, 3). The new arsines are thermally unstable and decompose into the parent arsine and the fully substituted tin arsine. As such, satisfactory mass spectral data are difficult to obtain although the parent peak (*m/e* 236–246) for trimethylstannyl arsine was clear.

The i.r. spectra of the new compounds are listed in the Experimental section together with assignments made by comparison with the spectra of phenylarsine (21), related silyl- (22, 23), germyl- (1, 24), and trimethylstannylarsines (7), and other trimethylstannyl (25) compounds.

The n.m.r. spectra are displayed in Table 1. The Sn*CH* chemical shifts and coupling constants confirm the characterization of the new compounds as tin arsines. In particular the Sn—C—H coupling constants remain in a very narrow range regardless of the differing substitution on arsenic. The coupling constants for other trimethylstannyl compounds fall into quite distinct and characteristic ranges depending on the group of the periodic table to which the element bound to tin belongs, rather than being electronegativity dependent. Although As—H resonances are usually broad due to quadrupole relaxation, we believe our failure to detect those in bis-trimethylstannylarsine and phenyl(trimethylstannyl)arsine was due to exchange processes taking place. We have observed similar phenomena in related trimethylgermyl species but are as yet unable to determine the cause. In view of this and the failure to detect the Sn—C—H satellites in bis-trimethylstannylarsine, the value for the chemical shift for this compound must be regarded as provisional.

Several reactions of trimethylstannylarsine were investigated. The Sn—As bond is cleaved rapidly by hydrogen bromide, slowly by hydrogen sulfide, and water only catalyzes its condensation. This order of reactivity is consistent with their acidity and in this respect the tin arsine parallels primary germyl arsines (1, 26), rather than silyl arsines, which are rapidly cleaved by water. The primary tin arsine parallels both the analogous silicon and germanium arsines in that there is no interaction or insertion with carbon dioxide or carbon disulfide (1). This is not unexpected as even dimethyl(trimethylstannyl)arsine only forms a weak adduct with carbon disulfide (27).

We thank the National Research Council of Canada for financial support.

1. J. W. Anderson and J. E. Drake. J. Chem. Soc. A, 3131 (1970).
2. E. Amberger and H. D. Boeters. Chem. Ber. **97**, 1999 (1964).
3. E. A. V. Ebsworth, D. W. H. Rankin, and G. M. Sheldrick. J. Chem. Soc. A, 2828 (1968).
4. C. Glidewell and G. M. Sheldrick. J. Chem. Soc. A, 350 (1969).
5. J. E. Drake, N. Goddard, and J. Simpson. Inorg. Nucl. Chem. Lett. **4**, 361 (1968).
6. K. Jones and M. F. Lappert. J. Organomet. Chem. **3**, 295 (1965).
7. H. Schumann and A. Roth. Chem. Ber. **102**, 3713 (1969).
8. E. W. Abel and S. M. Illingworth. Organomet. Chem. Rev. A, **5**, 143 (1970).
9. H. Schmidbauer and I. Ruidisch. Inorg. Chem. **3**, 599 (1964).
10. J. W. Anderson and J. E. Drake. Inorg. Nucl. Chem. Lett. **5**, 887 (1969).
11. K. Jones and M. F. Lappert. J. Chem. Soc. 1944 (1965).
12. D. J. LeRoy. Can. J. Res. **28**B, 492 (1950).
13. G. Davidson, L. A. Woodward, E. A. V. Ebsworth, and G. M. Sheldrick. Spectrochim. Acta, **23**, 2609 (1967).
14. E. A. V. Ebsworth and G. M. Sheldrick. Trans. Faraday Soc. **63**, 1071 (1967).
15. E. A. V. Ebsworth and G. M. Sheldrick. Trans. Faraday Soc. **62**, 3282 (1966).
16. J. E. Drake and C. Riddle. Quart. Rev. **24**, 263 (1970).
17. G. Fritz and G. Becker. Z. anorg. allg. Chem. **372**, 180 and 196 (1970).
18. H. Schumann, P. Schwabe, and O. Stelzer. Chem. Ber. **102**, 2900 (1969).
19. J. W. Anderson and J. E. Drake. J. Chem. Soc. In press.
20. J. Simpson. Ph. D. Thesis, Southampton University, Southampton, England, 1967.
21. H. Stenzenberger and H. Schindlbaur. Spectrochim. Acta, **26**A, 1713 (1970).
22. H. Burger, U. Goetze, and W. Sawodny. Spectrochim. Acta, **26**A, 671 (1970).
23. J. E. Drake and C. Riddle. Spectrochim. Acta, **26**A, 1697 (1970).
24. J. E. Drake, C. Riddle, K. M. Mackay, S. R. Stobart, and K. J. Sutton. Spectrochim. Acta, **25**A, 941 (1969).
25. H. Kriegsmann, H. Hoffmann, and H. Geissler. Z. anorg. allg. Chem. **341**, 24 (1965).
26. J. E. Drake and C. Riddle. J. Chem. Soc. A, 2709 (1968).
27. E. W. Abel, R. Honigschmidt-Grossich, and S. M. Illingworth. J. Chem. Soc. A, 2623 (1968).
28. E. W. Abel and D. B. Brady. J. Organomet. Chem. **11**, 145 (1968).

Can. J. Chem. Downloaded from www.nrcresearchpress.com by 210.87.254.6 on 09/05/12
For personal use only.

Organobismuth Compounds.[1] III. Preparation and Infrared Spectra of Triphenylbismuth(V) Derivatives of Dibasic Acids

R. G. GOEL AND H. S. PRASAD

Department of Chemistry, University of Guelph, Guelph, Ontario

Received February 8, 1971

Triphenylbismuth carbonate, oxalate, sulfate, selenate, and chromate have been prepared and their solid state infrared (i.r.) spectra have been studied in the frequency region 4000 to 200 cm^{-1}. The i.r. spectroscopic results indicate that, like the corresponding trimethyl- and triphenylantimony(V) derivatives, these compounds also have non-ionic polymeric structures containing bridging anion groups and five co-ordinate bismuth. The i.r. frequencies associated with the bismuth–anion stretching vibrations appear to occur at 300 cm^{-1} for the carbonate and below 300 cm^{-1} for the other compounds.

Le carbonate, l'oxalate, le sélénate et le chromate de triphénylbismuth ont été préparés et leur spectres i.r. étudiés en phase solide dans la région de 4000 à 200 cm^{-1} de fréquence. Les résultats de spectroscopie i.r. indiquent que comme dans les dérivés triméthyl et triphényl antimoine(V) correspondants, ces composés, dont les structures polymériques ne ressemblent pas à celle du fer, contiennent également des groupes anions servant de ponts et des atomes de bismuth pentacoordonnés. Les fréquences i.r. associées avec les vibrations d'élongation bismuth-anion apparaissent à 300 cm^{-1} pour le carbonate et au-dessous de 300 cm^{-1} pour les autres composés.

Canadian Journal of Chemistry, 49, 2529 (1971)

Introduction

Amongst the organic compounds of pentavalent bismuth only the triphenylbismuth(V) derivatives of monobasic acids have been well studied and the information about the constitution and structural features of these compounds has been obtained only recently. We have shown that triphenylbismuth(V) derivatives such as Ph_3BiX_2 (1), where X = halide, pseudohalide, nitrate or carboxylate, are molecular compounds containing five co-ordinate bismuth. The structure of triphenylbismuth dichloride (2) has been shown to be trigonal bipyramidal by X-ray crystallography.

With the exception of the reported preparation of triphenylbismuth carbonate and sulfate (3) no information had been obtained on organobismuth(V) derivatives of dibasic acids. In continuation of our studies on the structural aspects of organic derivatives of pentavalent antimony and bismuth we now report on the preparation and infrared spectroscopic studies of triphenylbismuth carbonate, oxalate, sulfate, selenate, and chromate.

Results and Discussion

Triphenylbismuth carbonate, oxalate, sulfate, and selenate are white solids; the chromate is a yellow solid. Freshly prepared samples of all the compounds are stable at room temperature for a few days, however, the chromate decomposes upon exposure to light. Upon prolonged storage at room temperature all the compounds decompose slowly. Samples stored in a refrigerator did not show any sign of decomposition over a period of several weeks. With the exception of the chromate, these compounds are insoluble in water and most of the common organic solvents such as CH_3CN, CH_3NO_2, DMF, and DMSO. The chromate is slightly soluble in DMF and DMSO. Triphenylbismuth selenate and chromate are also slightly soluble in formamide. The equivalent conductances of 2×10^{-3} *M* solutions of the selenate and the chromate in formamide are 0.31 and 5.92 $ohm^{-1}\,cm^2\,equiv^{-1}$, respectively. No suitable solvent could be found to determine the conductance of other compounds.

Infrared Spectra

The i.r. spectra of these compounds were studied in the solid state in the frequency range of 4000 to 200 cm^{-1}. In the region 4000 to 300 cm^{-1} the i.r. absorption bands due to the triphenylbismuth group for all the compounds studied are almost identical to those observed for triphenylbismuth dihalides (1). The absorption frequencies due to the anion group can therefore be identified

[1]For Part II, see ref. 12.

TABLE 1. Infrared absorption frequencies* due to X group in Ph_3BiX compounds

Ph_3BiCO_3	$Ph_3BiC_2O_4$	Ph_3BiSO_4	Ph_3BiSeO_4	Ph_3BiCrO_4
1552 vs	1642 vs	1250 vs	950 s	954 s
1295–1255 vs†	1610 s	1120 vs	892 s	925 s
1032 m	1425 m	960 s	796 m	828 m
835 w	1250–1232 vs§	920 vs	760 vs	770 s
750–680 m‡	830 w	630 m	460 m (sh)	404 sh
	770 s	600 m	410 sh	385 s
	365 s	475 w	396 s	364 sh
			370 s	314 w

*In cm^{-1}; m, medium; s, strong; sh, shoulder; vs, very strong; w, weak.
†The band shows several components.
‡Overlap with phenyl bands.
§Doublet.

for each compound and these frequencies are recorded in Table 1.

On comparing the data in Table 1 with the i.r. frequencies of the respective anions (4) it is evident that these compounds do not contain free anions. The non-ionic nature of these compounds is also demonstrated by the conductance data for the triphenylbismuth selenate and the chromate. Previous i.r. spectroscopic studies (5–7) on trimethyl- and triphenylantimony(V) derivatives of divalent oxy-anions indicate that in each of these compounds the anion group acts as a bridging ligand. The i.r. spectroscopic data shown in Table 1 also indicate a similar function for the anion group in the bismuth compounds included in this investigation. Although the i.r. spectral features of triphenylbismuth(V) derivatives are similar to those observed for the analogous antimony compounds (5–7), a comparison of the anion stretching frequencies in the analogous bismuth and antimony compounds indicates that the anion–metal co-ordinate bond is weaker in bismuth compounds.

Bismuth–Anion Stretching Frequencies and Other Low Frequency Bands

The i.r. spectrum of triphenylbismuth (8) in 400 to 200 cm^{-1} region shows two strong bands at 237 and 220 cm^{-1} and a shoulder at 207 cm^{-1}. The 237 and 220 cm^{-1} bands have been assigned to Whiffen's *t*-vibration (9) and the 207 cm^{-1} shoulder has been attributed to Whiffen's *x*-vibration (9). The bands due to the *t*- and *x*-vibrations in triphenylbismuth dihalides, dinitrate, diacetate, and diisocyanate (1) also occur below 250 cm^{-1}. The i.r. spectra of triphenylbismuth carbonate, oxalate, sulfate, selenate, and the chromate in the region 400 to 200 cm^{-1} are shown in Fig. 1. By comparing these spectra with the spectra of triphenylbismuth (8) and triphenylbismuth dihalides (1) the absorption frequencies below 250 cm^{-1} can be assigned to the *t*- and *x*-vibrations of the triphenylbismuth group. The spectrum of triphenylbismuth carbonate shows a strong band at 300 cm^{-1}. This band can be assigned to the stretching frequency of the bismuth–carbonate bond (O—Bi—O str.). The assignments for the bismuth–anion stretching frequencies for the other compounds cannot be made with certainty. The spectrum of the oxalate shows a strong band at 365 cm^{-1}. This band is more likely due to the oxalate group since the C—O—C bending and the CO_2 rocking modes of the oxalate group (10) have been reported to absorb in this region. Another strong band for the oxalate is observed in the region 252–244 cm^{-1}. This band is not very well resolved but it appears to have two components. It is likely that the two components of this band correspond to the bismuth–oxalate stretching vibration and one of the *t*-vibrations. The spectra of triphenylbismuth sulfate, selenate, and the chromate also show a strong band at *ca.* 250 cm^{-1} and this band may be due to the bismuth–anion stretching vibration. However, due to the presence of *t*-vibration in the 250–200 cm^{-1} region these assignments can only be considered as tentative. The bands at 396 and 370 cm^{-1} in the spectrum of the selenate are certainly due to selenate group. Similarly the bands at 385, 368, and 314 in the spectrum of the chromate arise due to the absorption by chromate group.

In conclusion, the triphenylbismuth(V) derivatives of the divalent oxy-anions appear to be structurally similar to the analogous antimony compounds. Their solid state i.r. spectra are indicative of a polymeric structure involving five co-ordinate bismuth and bridging anion. The

Can. J. Chem. Downloaded from www.nrcresearchpress.com by 210.87.254.6 on 09/05/12
For personal use only.

Can. J. Chem. Downloaded from www.nrcresearchpress.com by 210.87.254.6 on 09/05/12
For personal use only.

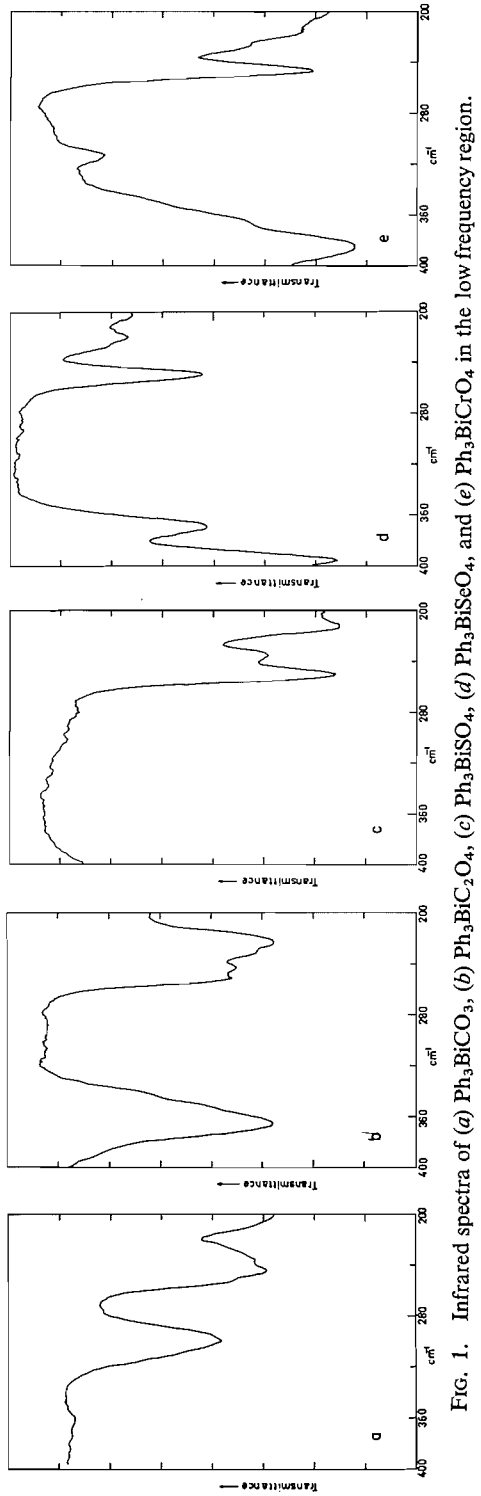

FIG. 1. Infrared spectra of (*a*) Ph_3BiCO_3, (*b*) $Ph_3BiC_2O_4$, (*c*) Ph_3BiSO_4, (*d*) Ph_3BiSeO_4, and (*e*) Ph_3BiCrO_4 in the low frequency region.

TABLE 2. Analytical data and melting points for Ph_3BiX compounds

	Analysis (%)				
	Found		Calculated		
Compound	C	H	C	H	Melting point (°C)
Ph_3BiSO_4*	39.78	2.68	40.54	2.81	200†
Ph_3BiSeO_4	36.37	2.49	37.06	2.59	180†
Ph_3BiCO_3	45.38	2.94	45.61	3.02	164–165§
$Ph_3BiC_2O_4$	45.28	2.71	45.46	2.86	177†
Ph_3BiCrO_4	38.74	2.61	38.86	2.71	111‡

*Sulfur, found: 6.25%, calculated: 6.01%.
†Decomposed without melting.
‡Melted with explosion.
§Melted with decomposition.

insolubility of these compounds in even very polar organic solvents also suggests the existence of a strong intermolecular bonding. The bismuth–anion stretching frequency in triphenylbismuth carbonate appears to occur at 300 cm^{-1}. For the other compounds this frequency is indicated to occur at *ca.* 250 cm^{-1} or lower.

Experimental

Microanalyses were performed in this department or by Schwarzkopf Microanalytical Laboratory, New York. The analytical data and melting points are recorded in Table 2.

Triphenylbismuth dichloride was prepared as described previously (1). Formamide was purified by the method of Mann (11). Other chemicals were reagent grade and were used without further purification.

Preparation of Compounds

(1) Triphenylbismuth Carbonate, Oxalate, and Chromate

A preparation (3) which involves bubbling carbon dioxide through a solution of triphenylbismuth dibromide containing excess of sodium hydroxide is reported to afford impure triphenylbismuth carbonate. Pure triphenylbismuth carbonate was obtained by the reaction of triphenylbismuth dichloride with an aqueous solution of potassium carbonate. Triphenylbismuth oxalate and chromate were also prepared by this method. In a typical preparation 0.0133 mol of the appropriate potassium salt was dissolved in about 25 ml of distilled water and to this solution was added 0.0033 mol of triphenylbismuth dichloride. The mixture was stirred for 8 h in the dark, and then filtered. The residue was washed several times with water till it was free from the potassium salt. It was further washed with acetone to free it from unreacted triphenylbismuth dichloride and then dried under vacuum at room temperature. The yield in each case (calculated according to the amount of triphenylbismuth dichloride taken) was approximately 40%. The low yields are due to incomplete reaction because in each case unreacted triphenylbismuth dichloride was recovered.

(2) Triphenylbismuth Sulfate

It was prepared by the reaction of concentrated sulfuric acid on triphenylbismuth dichloride as described in the literature (3). Yield, 70%.

(3) Triphenylbismuth selenate

A dilute solution of selenic acid was added dropwise with stirring to triphenylbismuth carbonate at about 10 °C until there was no effervescence. The triphenylbismuth selenate separated as fine white powder. It was filtered, washed with water to remove excess of acid, and finally washed with acetone. It was then dried under vacuum at room temperature. Yield, 100%.

Physical Measurements

Infrared spectra were recorded on a Beckman IR-12 double beam spectrophotometer using KRS-5 and polyethylene windows. The samples were prepared as mulls in Nujol or Halocarbon oil. The conductances were measured at 25° with a Beckman RC-18 conductivity bridge. The melting points were determined with a Gallenkamp melting point apparatus and are uncorrected.

We are grateful for the financial support of the National Research Council of Canada.

1. R. G. GOEL and H. S. PRASAD. Can. J. Chem. **48**, 2488 (1970).
2. D. M. HAWLEY and G. FERGUSON. J. Chem. Soc. A, 2539 (1968).
3. F. CHALLENGER and A. E. GODDARD. J. Chem. Soc. **CXVII**, 762 (1920).
4. K. NAKAMOTO. Infrared spectra of inorganic and co-ordination compounds. 2nd ed. John Wiley and Sons, Inc., New York. 1970.
5. H. C. CLARK and R. G. GOEL. Inorg. Chem. **5**, 998 (1966).
6. R. G. GOEL, P. N. JOSHI, D. R. RIDLEY, and R. E. BEAUMONT. Can. J. Chem. **47**, 1423 (1969).
7. G. O. DOAK, G. G. LONG, and L. D. FREEDMAN. J. Organometal. Chem. Amsterdam, **4**, 82 (1965).
8. K. SHOBATAKE, C. POSTMUS, J. R. FERRARO, and K. NAKAMOTO. Appl. Spectrosc. **23**, 12 (1969).
9. D. H. WHIFFEN. J. Chem. Soc. 1350 (1956).
10. J. K. WILMSHURST. J. Mol. Spectrosc. **21**, 49 (1966).
11. C. K. MANN. *In* Electroanalytical chemistry. Vol. 3. *Edited by* A. J. Bard. Marcel Dekker, Inc., New York. 1969. p. 57.
12. R. G. GOEL and H. S. PRASAD. J. Chem. Soc. A, 562 (1971).

Can. J. Chem. Downloaded from www.nrcresearchpress.com by 210.87.254.6 on 09/05/12
For personal use only.

Can. J. Chem. Downloaded from www.nrcresearchpress.com by 210.87.254.105 on 09/05/12
For personal use only.

Vibrational Spectra of 1,1-Dichlorocyclopropane

J. M. FREEMAN[1] AND P. J. ROBINSON

Chemistry Department, University of Manchester Institute of Science and Technology, Manchester M60 1QD, England

Received September 23, 1970[2]

Infrared and Raman spectra of 1,1-dichlorocyclopropane are reported. Force constants were determined by an iterative computer procedure for two possible sets of assignments of the normal mode frequencies. It is suggested that in the correct assignment the methylene rocking modes are at higher frequency than the twisting modes.

Les spectres infrarouge et Raman du dichloro-1,1-cyclopropane sont décrits. Les constantes de force ont été déterminées au calculateur par une méthode itérative pour les deux systèmes possibles d'attribution des modes normaux de fréquence. Il est suggéré que dans l'attribution correcte, les modes de rotation des groupes méthyléneques se trouvent à une fréquence plus élevée que les modes de torsion.

Canadian Journal of Chemistry, 49, 2533 (1971)

Introduction

The vibrational analysis for 1,1-dichlorocyclopropane was of interest in connection with unimolecular reaction rate calculations (1). The infrared and Raman spectra and the skeletal analysis had been reported by Kay (2), but the infrared (i.r.) spectra obtained during kinetic work (3) did not entirely agree with Kay's, and errors were found in his **F** and **G** matrices. It was therefore of interest to re-analyze the spectra and to carry out a complete vibrational analysis of the molecule. The vibrational spectra of a number of other three-membered ring systems have been analyzed (2, 4–6), and points of specific interest in the present work were the assignments of the ring deformation and methylene wagging frequencies in A_1 and of the methylene rocking and twisting modes in A_2 and B_1; it has been suggested (4) that the rocks rather than the twists should have the higher frequencies.

Spectra

1,1-Dichlorocyclopropane was prepared as described previously (3) and purified by preparative g.l.c.; it was chromatographically pure on several g.l.c. columns.

Infrared spectra were recorded for capillary films or 10% solutions in carbon tetrachloride or cyclohexane on Unicam SP 100 and Perkin–Elmer 457 or 621 spectrophotometers, and for the vapor on the PE621. The Raman spectrum of the pure liquid was recorded on a Spex instrument using Ar^+ 488 nm laser excitation.[3] For many lines our spectra differed from Kay's by only a few cm^{-1} and Kay's figures were used for consistency.

The molecule of 1,1-dichlorocyclopropane has C_{2v} symmetry and has 21 fundamental vibrations, 4 in the C—H stretching region. The vibrations comprise $7A_1$ (i.r. and Raman active; Raman polarized) $+ 4A_2$ (Raman only, depolarized) $+ 5B_1 + 5B_2$ (i.r. and Raman active; Raman depolarized). The assignments used in the calculations are given in Table 5, together with those of Kay, and are discussed below.

C—H Stretching Vibrations

Four bands are expected in this region, but only two resolvable absorptions were observed; 3022 (s,vs,p) and 3100 (m,m,d) cm^{-1} (here and below the i.r. and Raman strengths and the Raman polarization are quoted in parentheses after the reciprocal wavelength). Kay's band at 3048 cm^{-1} is spurious and his assignments in A_2 and B_2 were reversed (see Table 5).

Other Vibrations

Thirteen of the remaining seventeen fundamentals were reasonably strong and agreed with Kay's spectra, and Kay's assignments were used for these lines: 1454 (s,w,p), 1409 (vs,w,d), 1238 (vs,s,p), 1130 (vs,vw,?), 1037 (vs,vw,p), 952 (s,m,d), 874 (w,s,p), 772 (s,vw,?), 717 (vs,m,d),

[1]Present address: ICS/24, Shell Chemicals Limited, Carrington, Cheshire, England.

[2]Revision received March 15, 1971.

[3]We thank Dr. M. I. Ware (University of Manchester) and Dr. V. Fawcett (University of Bradford) for recording the Raman spectrum, and Professor D. A. Long (University of Bradford) for use of the spectrometer.

TABLE 1. Symmetry coordinates

A_1 coordinates	
$S_1 = (r_1 + r_2 + r')/\sqrt{3}$	(ring breath)
$S_2 = (r_1 + r_2 - 2r')/\sqrt{6}$	(ring def.)
$S_3 = (s_1 + s_2)/\sqrt{2}$	(CCl stretch)
$S_4 = (t_1 + t_2 + t_3 + t_4)/2$	(CH stretch)
$S_5 = (\alpha_1 + \alpha_2 + \alpha_3 + \alpha_4)/2$	(CCl_2 def.)
$S_6 = (\beta_1 + \beta_2 + \beta_3 + \beta_4 + \beta_5 + \beta_6 + \beta_7 + \beta_8)/\sqrt{8}$	(CH_2 def.)
$S_7 = (\beta_1 + \beta_2 - \beta_3 - \beta_4 - \beta_5 - \beta_6 + \beta_7 + \beta_8)/\sqrt{8}$	(CH_2 wag)
A_2 coordinates	
$S_8 = (t_1 - t_2 - t_3 + t_4)/2$	(CH stretch)
$S_9 = (\alpha_1 - \alpha_2 - \alpha_3 + \alpha_4)/2$	(CCl_2 twist)
$S_{10} = (\beta_1 - \beta_2 + \beta_3 - \beta_4 - \beta_5 + \beta_6 - \beta_7 + \beta_8)/\sqrt{8}$	(CH_2 rock)
$S_{11} = (\beta_1 - \beta_2 - \beta_3 + \beta_4 + \beta_5 - \beta_6 - \beta_7 + \beta_8)/\sqrt{8}$	(CH_2 twist)
B_1 coordinates	
$S_{12} = (s_1 - s_2)/\sqrt{2}$	(CCl stretch)
$S_{13} = (t_1 - t_2 + t_3 - t_4)/2$	(CH stretch)
$S_{14} = (\alpha_1 + \alpha_2 - \alpha_3 - \alpha_4)/2$	(CCl_2 rock)
$S_{15} = (\beta_1 - \beta_2 + \beta_3 - \beta_4 + \beta_5 - \beta_6 + \beta_7 - \beta_8)/\sqrt{8}$	(CH_2 rock)
$S_{16} = (\beta_1 - \beta_2 - \beta_3 + \beta_4 - \beta_5 + \beta_6 + \beta_7 - \beta_8)/\sqrt{8}$	(CH_2 twist)
B_2 coordinates	
$S_{17} = (r_1 - r_2)/\sqrt{2}$	(ring def.)
$S_{18} = (t_1 + t_2 - t_3 - t_4)/2$	(CH stretch)
$S_{19} = (\alpha_1 - \alpha_2 + \alpha_3 - \alpha_4)/2$	(CCl_2 wag)
$S_{20} = (\beta_1 + \beta_2 + \beta_3 + \beta_4 - \beta_5 - \beta_6 - \beta_7 - \beta_8)/\sqrt{8}$	(CH_2 def.)
$S_{21} = (\beta_1 + \beta_2 - \beta_3 - \beta_4 + \beta_5 + \beta_6 - \beta_7 - \beta_8)/\sqrt{8}$	(CH_2 wag)

500 (vs,vs,p), 404 (—,m,d), 300 (—,m,d), 272 (m,m,d) cm^{-1}. The five polarized Raman lines were clearly A_1 fundamentals, and to these was added the apparently depolarized line at 272 cm^{-1}. The bands at 404 and 300 cm^{-1} were both virtually absent from the i.r., but only one frequency as low as this can be assigned to A_2. Following Kay, 300 cm^{-1} was placed in A_2 and 404 cm^{-1} in B_2.

The four remaining vibrations are more problematical. The strong i.r. band at 1292 cm^{-1} in Kay's vapor spectrum was absent from our i.r. spectra,[4] and for the corresponding B_1 vibration we used instead a band at 1212 (m,vw,?) cm^{-1}. The 1292 cm^{-1} Raman line was used in one series of calculations to replace the 1164 cm^{-1} band placed by Kay in A_2, since the latter was also infrared active. Kay's A_2 band at 825 cm^{-1} was absent from our spectra and was replaced by 809 (—,w,?) cm^{-1}. Finally, the 443 cm^{-1} Raman line used by Kay as a B_1 fundamental was very weak in our spectra and must be considered of doubtful validity, although we used it for want of an adequate substitute.

Other Bands

These are listed for completeness, but not discussed further: 2914, 2848, 2826, 2683, 2650, 2556, 2476, 2361, 2326, 2274, 2210, 2166, 2110, 2088, 1983, 1933, 1903, 1871, 1834, 1809, 1748, 1636 (all w or vw,—), 1375 (—,vw,p), 1330 (vw,—), 1163 (m,w,d), 1061 (m,vw,?), 1012 (w,—), 900 (vw,—), 790 (w,—), 633 (vw,—) 596 (—,vw,?), 251 (w,—) cm^{-1}.

[4]In ref. 3 the spurious band was wrongly quoted as 1321 cm^{-1}.

Calculations

Coordinates and Geometry

The internal coordinates were labelled as shown in Fig. 1. The geometry deduced from microwave spectra by Flygare, Narath, and Gwinn (7) was used. In their work the ring was

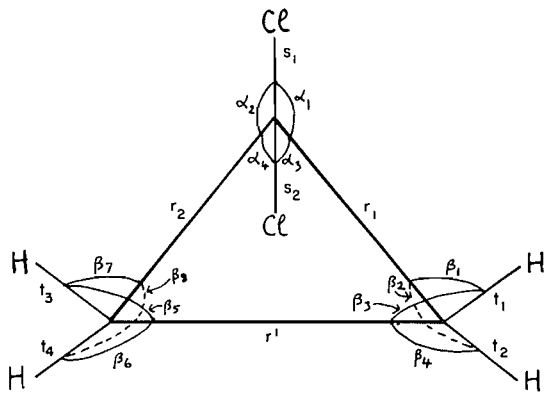

FIG. 1. Internal coordinates for 1,1-dichlorocyclopropane.

Can. J. Chem. Downloaded from www.nrcresearchpress.com by 210.87.254.105 on 09/05/12
For personal use only.

TABLE 2. G matrices for 1,1-dichlorocyclopropane (upper triangles quoted)

A_1 vibrations						
0.25000	0.00000	−0.06364	−0.08634	−0.06671	−0.15402	0.00000
	0.12500	−0.04500	0.03053	−0.01193	0.03081	−0.09807
		0.07720	0.00000	0.03826	0.00851	0.00851
			1.03679	0.00861	0.07401	−0.00578
				0.04968	0.01761	−0.01873
					1.28409	0.00825
						0.64879
A_2 vibrations						
1.11400	0.08861	−0.26871	0.06298			
	0.07047	−0.19526	0.04576			
		1.75004	−0.13876			
			0.56005			
B_1 vibrations						
.14666	0.00000	−0.17425	0.08764	0.08764		
	1.11400	0.08861	−0.14276	−0.06298		
		0.33449	−0.23307	−0.17510		
			1.39008	0.13878		
				0.62510		
B_2 vibrations						
0.12500	−0.05287	−0.05880	−0.05336	−0.05662		
	1.03679	0.00861	0.06246	0.00578		
		0.09568	−0.00391	−0.04914		
			1.25183	−0.00825		
				0.72598		

found to be virtually equilateral, with $r_i = r' =$ 0.1532 nm, $s_i = 0.1734$ nm, $t_i = 0.1085$ nm, $\angle$ HCH = 117.58°, and $\angle$ ClCCl = 114.63°; hence $\angle$ CCH = 116.65° and $\angle$ CCCl = 117.88°. Atomic weights were taken as 1.008, 12.000, and 34.97 for H, C, and ^{35}Cl, respectively. The symmetry coordinates (Table 1) were those of Kay (ref. 2, appendix II),[5] in which B_2 representations are symmetric with respect to the plane of the ring.

G Matrices

In preliminary work, algebraic expressions were used for the **G** elements relevant to the skeletal vibrations. These agreed with those in Kay's Appendix III except for

$$\mathbf{G}_{A_1}(3,5) = 2^{\frac{1}{2}}aC[d(2A^2 - G - 1) + eA(G - 1)]$$

$$\mathbf{G}_{A_1}(5,5) = [d^2(-7A^2 + 3G + 3) + 2deA(4A^2 - 2G - 1) + e^2(3 + 2A^2G - 6A^2)]aC^2 + \tfrac{1}{2}e^2(3 - 4A^2)bC^2$$

$$\mathbf{G}_{B_2}(3,3) = [d^2(G + 1 - A^2) - 2deA + e^2]aC^2 + \tfrac{1}{2}be^2C^2$$

where a, C etc. are as defined by Kay. Later, the **G** elements for the full analysis were obtained by an iterative numerical method (8). These are given in Table 2; the skeletal elements agree well with the values from the algebraic expressions.

[5]Note that on pp. 71 and 92 Kay reverses the representations B_1 and B_2.

F Matrices

The potential function used included the six direct force constants and initially 20 of the 26 interactions between adjacent coordinates. The force constants and simplifying assumptions used are listed in Table 4, together with the shorthand nomenclature used in Table 3, which was produced by computer (9) and gives the corresponding symmetry force constants in terms of valence force constants (*i.e.*, **F**). The skeletal elements agree with those of Kay apart from expected differences and a misprint and error in Kay's version of $\mathbf{F}_{A_1}(2,2)$ and $\mathbf{F}_{A_1}(2,3)$, respectively.

Determination of Force Constants

Force constants for a number of assignments were obtained by iterative fitting of calculated frequencies to the "observed" frequencies, using the computer program described previously (9). An important feature of this program is the attention paid to correct correlation between the calculated and observed frequencies by consideration of the potential energy distribution, without which serious errors can arise (9, 10). The number of indeterminate force constants was reduced to 19 by fixing $f(t)$ and $f(tt)$, assuming that $f(\beta_1\beta_2) = f(\beta_3\beta_4)$ and $f(r_1\beta_1) = f(r'\beta_1)$, and by fixing $f(ss)$, $f(rt)$, and $f(r't)$ at zero after initial itera-

Can. J. Chem. Downloaded from www.nrcresearchpress.com by 210.87.254.105 on 09/05/12
For personal use only.

TABLE 3. F matrices (upper triangles quoted; nomenclature amplified in Table 4)

A_1 vibrations

$(2r + r' + 2rr + 4rr')/3,\ \sqrt{2}(r - r' + rr - rr')/3,\ 4rs/\sqrt{6},\ 2(rt + r't)/\sqrt{3},\ 2(r\alpha + r\alpha')/\sqrt{3},\ 4rs/\sqrt{6},\ 0$
$(r + 2r' + rr - 4rr')/3,\ 2rs/\sqrt{3},\ 2(rt - r't)/\sqrt{6},\ 2(r\alpha + r\alpha')/\sqrt{6},\ -r\beta/\sqrt{3},\ \sqrt{3}r\beta$
$(s + ss),\ 0,\ \sqrt{2}(s\alpha + s\alpha'),\ 0,\ 0$
$(t + tt),\ 0,\ 0,\ 0$
$(\alpha + \alpha\alpha_1 + \alpha\alpha_2 + \alpha\alpha_3),\ 0,\ 0$
$(\beta + \beta\beta_1 + \beta\beta_2 + \beta\beta_3),\ 0$
$(\beta + \beta\beta_1 - \beta\beta_2 - \beta\beta_3)$

A_2 vibrations

$(t - tt),\ 0,\ 0,\ 0$
$(\alpha - \alpha\alpha_1 - \alpha\alpha_2 + \alpha\alpha_3),\ 0,\ 0$
$(\beta - \beta\beta_1 + \beta\beta_2 - \beta\beta_3),\ 0$
$(\beta - \beta\beta_1 - \beta\beta_2 + \beta\beta_3)$

B_1 vibrations

$(s - ss),\ 0,\ \sqrt{2}(s\alpha - s\alpha'),\ 0,\ 0$
$(t - tt),\ 0,\ 0,\ 0$
$(\alpha + \alpha\alpha_1 - \alpha\alpha_2 - \alpha\alpha_3),\ 0,\ 0$
$(\beta - \beta\beta_1 + \beta\beta_2 - \beta\beta_3),\ 0$
$(\beta - \beta\beta_1 - \beta\beta_2 + \beta\beta_3)$

B_2 vibrations

$(r - rr),\ \sqrt{2}rt,\ \sqrt{2}(r\alpha - r\alpha'),\ r\beta,\ r\beta$
$(t + tt),\ 0,\ 0,\ 0$
$(\alpha - \alpha\alpha_1 + \alpha\alpha_2 - \alpha\alpha_3),\ 0,\ 0$
$(\beta + \beta\beta_1 + \beta\beta_2 + \beta\beta_3),\ 0$
$(\beta + \beta\beta_1 - \beta\beta_2 - \beta\beta_3)$

TABLE 4. Optimized force constants[a]

Force constant	Symbol in Table 5	Value for assignment 1	Value for assignment 2
$f(r)$	r	4.596	4.583
$f(r')$	r'	4.463	4.465
$f(s)$	s	3.424	3.407
$f(t)$	t	5.115[b]	5.115[b]
$f(\alpha)$	α	1.453	1.460
$f(\beta)$	β	0.889	0.780
$f(\beta_1\beta_2)$, $f(\beta_3\beta_4)$ [c]	$\beta\beta_1$	0.049	0.184
$f(\beta_1\beta_3)$	$\beta\beta_2$	−0.299	−0.008
$f(\beta_1\beta_4)$	$\beta\beta_3$	0.305	0.016
$f(rr)$	rr	−0.374	−0.375
$f(rr')$	rr'	−0.186	−0.218
$f(rs)$	rs	0.321	0.331
$f(tt)$	tt	0.050[b]	0.050[b]
$f(\alpha_1\alpha_2)$	$\alpha\alpha_1$	−0.029	−0.028
$f(\alpha_1\alpha_3)$	$\alpha\alpha_2$	0.248	0.230
$f(\alpha_1\alpha_4)$	$\alpha\alpha_3$	0.105	0.103
$f(s_1\alpha_1)$	$s\alpha$	0.414	0.406
$f(s_1\alpha_3)$	$s\alpha'$	−0.407	−0.414
$f(r_1\alpha_1)$	$r\alpha$	0.363	0.388
$f(r_1\alpha_2)$	$r\alpha'$	−0.186	−0.188
$f(r_1\beta_1)$, $f(r'\beta_1)$ [c]	$r\beta$	0.159	0.211
$f(ss)$	ss	0[d]	0[d]
$f(rt)$	rt	0[d]	0[d]
$f(r't)$	$r't$	0[d]	0[d]
$f(t_1\beta_j)$, $f(r_1\beta_3)$, $f(r_3\beta_1)$	Assumed to be zero		

[a]Units are mdyn Å^{-1} = 10^2 N m^{-1}, mdyn Å rad^{-2} = 10^{-18} N m rad^{-2}, or mdyn rad^{-1} = 10^{-8} N rad^{-1} as appropriate.
[b]Fixed.
[c]Assumed equal.
[d]Iteration gave small values (*ca.* 0.01) which were imprecisely determined and therefore replaced by zero.

Can. J. Chem. Downloaded from www.nrcresearchpress.com by 210.87.254.105 on 09/05/12
For personal use only.

TABLE 5. Comparison of assigned and calculated reciprocal wavelengths/cm^{-1}

Vibration[a]		Kay's assignment	Assignment 1		Assignment 2	
			$\bar{\nu}$(Obsd.)	$\bar{\nu}$(Calcd.)	$\bar{\nu}$(Obsd.)	$\bar{\nu}$(Calcd.)
A_1 species						
Ring breathing	(S_1)	1238	1238	1225[b]	1238	1228
Ring def.	(S_2)	1037	874	886[c]	874	907[d]
CCl stretch	(S_3)	500	500	494[e]	500	494[e]
CH stretch	(S_4)	3022	3022	3025	3022	3025
CCl_2 def.	(S_5)	272	272	254	272	254
CH_2 def.	(S_6)	1454	1454	1444	1454	1434
CH_2 wag	(S_7)	874	1037	1085[f]	1037	1069[f]
A_2 species						
CH stretch	(S_8)	3048	3106	3111	3106	3111
CCl_2 twist	(S_9)	300	300	306	300	314
CH_2 rock	(S_{10})	825	809	831	1291	1296
CH_2 twist	(S_{11})	1164	1164	1181	809	757
B_1 species						
CCl stretch	(S_{12})	717	717	660	717	647
CH stretch	(S_{13})	3096	3096	3101	3096	3101
CCl_2 rock	(S_{14})	443	443	422	443	431
CH_2 rock	(S_{15})	772	772	768[g]	1212	1197
CH_2 twist	(S_{16})	1292	1212	1278	772	850[h]
B_2 species						
Ring def.	(S_{17})	952	952	936	952	938
CH stretch	(S_{18})	3106	3022	3019	3022	3019
CCl_2 wag	(S_{19})	404	404	397	404	396
CH_2 def.	(S_{20})	1409	1409	1410	1409	1428
CH_2 wag	(S_{21})	1130	1130	1098	1130	1101

[a]Symmetry coordinate contributing > 80% of potential energy of normal vibration, unless otherwise noted.
[b]$0.75S_1 + 0.17S_6$, *etc.*
[c]$0.45S_7 + 0.42S_2$, *etc.*
[d]$0.46S_2 + 0.42S_7$, *etc.*
[e]*ca.* $0.72S_3 + 0.13S_2$, *etc.*
[f]*ca.* $0.55S_7 + 0.42S_2$, *etc.*
[g]$0.67S_{15} + 0.16S_{12}$, *etc.*
[h]$0.63S_{16} + 0.21S_{12}$, *etc.*

tions showed that these constants were small and had little effect on the results of the calculation.

In no case was the fit as good as might be desired, and the results will be quoted only for two models, which differ essentially in the assignments of the methylene rocks and twists. The derived force constants for the two assignments are given in Table 4 and the assignments are compared with the calculated frequencies in Table 5. Vibrations are assigned to those normal modes having the largest potential energy contribution (9), although in a few cases (noted in Table 5) the mixing is too great for any single assignment to be really meaningful. For example, we attribute little significance to our reversal of Kay's assignments for the A_1 ring deformation and methylene wagging vibrations.

Discussion

It was clear from the progress of the convergence of the iterative method that a close fit between the observed and calculated frequencies could not be obtained using the adopted force field. Although it is possible that further refinement in the force field defined in Table 3 may have improved the agreement between the experiment and theory, it was thought that such action was not worthwhile in view of the substantial doubts concerning the assignments of the observed frequencies. Unavailable information, such as the vibrational frequencies of isotopically substituted dichlorocyclopropanes (*e.g.* $C_3D_4Cl_2$), would help to define the force field more closely, and hence to decide more rigorously on the present doubtful assignments in $C_3H_4Cl_2$.

On the basis of normal coordinate analyses of ethylene oxide, ethylene oxide-d_4, and ethylene sulfide, it has been suggested (4) that the CH_2 rocks should have a higher frequency than the CH_2 twists in three-membered ring systems. The factors involved were the physical acceptability of the force constants defining each assignment

Can. J. Chem. Downloaded from www.nrcresearchpress.com by 210.87.254.105 on 09/05/12
For personal use only.

TABLE 6. Group force constants for methylene modes (assignment 1, twists higher; assignment 2, rocks higher)

Mode	Force constant expression	1,1-Dichlorocyclopropane		Ethylene oxide		Ethylene sulfide	
		Asst. 1	Asst. 2	Asst. 1	Asst. 2	Asst. 1	Asst. 2
CH_2 def.	$\beta + \beta\beta_1 + \beta\beta_2 + \beta\beta_3$	0.944	0.972	[a]	[a]	[a]	[a]
CH_2 wag	$\beta + \beta\beta_1 - \beta\beta_2 - \beta\beta_3$	0.932	0.956	1.128	1.128	0.781	0.781
CH_2 rock	$\beta - \beta\beta_1 + \beta\beta_2 - \beta\beta_3$	0.236	0.572	0.259	0.554	0.333	0.421
CH_2 twist	$\beta - \beta\beta_1 - \beta\beta_2 + \beta\beta_3$	1.444	0.620	1.513	0.701	0.782	0.620

[a]Not calculated; group factorization procedure used.

and the difficulty in defining a valence force field capable of reproducing the symmetry force fields corresponding to the reverse assignment. Similar considerations apply here, the off-diagonal valence force constants being much larger for assignment 1 than for assignment 2. It is also useful to consider Table 6, where group force constants are quoted; the CH_2 def., wag, rock, and twist force constants have much closer values for assignment 2, as may be expected physically. Table 6 also includes the corresponding force constants for ethylene oxide and sulfide (4), and as might be expected the results are rather similar to those for dichlorocyclopropane.

1. K. A. HOLBROOK, J. S. PALMER, K. A. W. PARRY, and P. J. ROBINSON. Trans. Faraday Soc. **66**, 869 (1970).
2. M. I. KAY. Ph.D. Thesis. Rensselaer Polytechnic Institute, 1962. (Available from University Microfilms Inc., *cf.* Diss. Abs. **25**, 130 (1964–5).)
3. K. A. W. PARRY and P. J. ROBINSON. J. Chem. Soc. B, 49 (1969).
4. J. M. FREEMAN and T. HENSHALL. Can. J. Chem. **46**, 2129, 2136 (1968).
5. J. E. KATON, W. R. FEAIRHELLER, and J. T. MILLER. J. Chem. Phys. **49**, 823 (1968) and references cited therein.
6. J. R. DURIG, S. F. BUSH, and W. C. HARRIS. J. Chem. Phys. **50**, 2851 (1969) and references cited therein.
7. W. M. FLYGARE, A. NARATH, and W. D. GWINN. J. Chem. Phys. **36**, 200 (1962).
8. J. M. FREEMAN. J. Mol. Spectrom. **30**, 51 (1969).
9. J. M. FREEMAN and T. HENSHALL. J. Mol. Spectrom. **25**, 101 (1968).
10. C. D. NEEDHAM and J. OVEREND. Spectrochim. Acta, **22**, 1383 (1966).

Can. J. Chem. Downloaded from www.nrcresearchpress.com by 210.87.254.105 on 09/05/12
For personal use only.

Can. J. Chem. Downloaded from www.nrcresearchpress.com by 210.87.254.40 on 09/05/12
For personal use only.

Crystal and Molecular Structure of Difluorochlorine(III)-hexafluoroarsenate(V), ClF_2AsF_6

H. Lynton and J. Passmore

Department of Chemistry, University of New Brunswick, Fredericton, New Brunswick

Received March 22, 1971

Crystals of difluorochlorine(III)hexafluoroarsenate(V), ClF_2AsF_6, are monoclinic, space group $A2/a$, $a = 10.676(9)$, $b = 7.673(7)$, $c = 8.064(7)$ Å, $\beta = 113.40(5)°$. The structure was refined by three dimensional least squares methods to $R = 0.045$ for 185 independent observed reflections. The chlorine atom has two nearest fluorine neighbors at 1.541(14) Å, with a F—Cl—F angle of 103.17(0.70) °, and two longer fluorine bonds at 2.339(14) Å. All five atoms lie in a plane. The arsenic atom is octahedrally coordinated to six fluorine atoms and is connected to two ClF_2^+ groups via *trans* fluorine bridges.

Les cristaux de difluorochlorure(III)hexafluoroarsénate(V), ClF_2AsF_6, appartiennent au système monoclinique, groupe espace $A2/a$, $a = 10.676(9)$, $b = 7.673(7)$, $c = 8.064(7)$ Å, $\beta = 113.40(5)°$. La structure a été affinée par la méthode des moindres carrés, avec $R = 0.045$ pour 185 réflexions indépendantes observées. L'atome de chlore a deux atomes de fluor à proximité immédiate, situés à 1.541(14) Å et faisant un angle F—Cl—F de 103.17(0.70)°, et deux atomes de fluor plus éloignés situés à 2.339(14) Å. Les cinq atomes sont dans un même plan. L'atome d'arsenique est coordonné d'une façon octahédrique aux six atomes de fluor et est relié à deux groupes ClF_2^+ au moyen de ponts fluor en position *trans*.

Canadian Journal of Chemistry, 49, 2539 (1971)

Introduction

This work arose out of an attempt to determine the crystal structure of ClF_2IrF_6 (1, 2). The results indicated a greater F—Cl—F angle than that suggested by various spectroscopic investigations of related compounds (3–5) and the corresponding F—Br—F angle in BrF_2SbF_6 (6, 7). As the standard deviations for ClF_2IrF_6 were large, the structural determination of the crystallographically more favorable ClF_2AsF_6 was undertaken. While this work was in progress, the crystal structure of ClF_2SbF_6 was reported (8). ClF_2AsF_6 is of interest as a ClF_3 – Lewis acid adduct, and also as a ClF_2^+-containing compound. Halogen and interhalogen cations have recently been reviewed (9).

Experimental

Chlorine trifluoride and arsenic pentafluoride were supplied by Ozark–Mahoning Company and were used without further purification. Gaseous reagents were manipulated in a Monel vacuum line fitted with Whitey (IKS-316) stainless steel valves and Swagelok compression fittings. The solid was transferred in a "Dri-Lab" manufactured by Vacuum Atmospheres Corporation, Los Angeles, California.

Arsenic pentafluoride was distilled onto chlorine trifluoride in a Kel-F trap. An adduct formed which dissolved in excess chlorine trifluoride. The solid was vacuated at 0° to remove volatile material. The compound was identified as ClF_2AsF_6 from the infrared spectrum (3) of the powdered solid between silver chloride plates. Lumps of the solid were sealed under atmospheric pressure into thin walled quartz capillaries, o.d. 0.5 in. The capillaries were placed horizontally on the sides of a beaker at various distances from its base which was heated at 80°. Good single crystals grew overnight by sublimation.

Crystal Structure Analysis

Crystal data are as follows:

ClF_2AsF_6 f.w. = 262.4

Monoclinic, $a = 10.676(9)$, $b = 7.673(7)$, $c = 8.064(7)$ Å, $\beta = 113.40(5)°$, $v = 606.3$ Å^3, $z = 4$, $\rho_c = 2.874$ (20 °C, MoKα, $\lambda = 0.71069$ Å).

The unit cell dimensions and their estimated standard deviations were obtained from a least squares evaluation of the positions of 12 independent reflections. The volume is consistent with $z = 4$, since 32 fluorine atoms in the unit cell give a volume per fluorine atom of 19 Å^3, comparable with the usual value of 18 Å^3 for approximate close-packing. The space group is $A2/a$ (C_{2h}^6) No. 15 in *International Tables for X-Ray Crystallography*, Vol. 1 (10).

Intensity data were collected on a Picker computer-controlled four-angle diffractometer using a $\theta/2\theta$ scan with β filtered MoKα radiation and a scintillation detector. The region of reciprocal space explored was the two octants hkl and $\bar{h}kl$ to a maximum 2θ of 40°. In this region 292 reflections were accessible, of which 185 were considered to be observed. The threshold was taken as 0.07 × background count. The specimen was roughly rectangular in shape, 0.2 mm long and 0.04 mm in cross section, mounted in a quartz capillary tube. The linear absorption coefficient for MoKα radiation is $\mu = 64.7$ cm^{-1}. No corrections were made for either absorption or extinction.

The positions of all atoms were established from a three dimensional Patterson synthesis. Arsenic and chlorine atoms were found to occupy the special positions *4a* and

Can. J. Chem. Downloaded from www.nrcresearchpress.com by 210.87.254.40 on 09/05/12
For personal use only.

TABLE 1. Final parameters*

Atom	$x \times 10^4$	$y \times 10^4$	$z \times 10^4$	$u_{11} \times 10^3$	$u_{22} \times 10^3$	$u_{33} \times 10^3$	$u_{23} \times 10^3$	$u_{13} \times 10^3$	$u_{12} \times 10^3$
As	0	0	0	80(2)	93(3)	78(2)	27(5)	22(2)	1(5)
Cl	2500	3504(9)	0	88(7)	99(8)	95(8)	0	15(6)	0
F(*1*)	−0228(13)	−0167(15)	1957(15)	254(20)	321(26)	128(15)	1(24)	100(14)	−65(26)
F(*2*)	1365(11)	1418(19)	1006(16)	140(15)	229(20)	136(15)	1(16)	18(12)	−119(18)
F(*3*)	1030(15)	−1679(18)	0594(24)	204(22)	151(19)	373(34)	−8(21)	63(21)	59(19)
F(*4*)	1655(12)	4752(15)	0646(16)	202(17)	123(16)	193(17)	−8(15)	48(13)	36(16)

*Estimated standard deviations in parentheses; t.f. = $\exp[-2\pi^2(a^{*2}h^2u_{11} + \cdots + 2b^*c^*klu_{23} + \cdots)]$.

TABLE 2. Interatomic distances and angles in the AsF_6^- group*

Bond distance		Bond angle	
Bond	Distance (Å)	Bonds	Angle (deg)
As—F(*1*)	1.694(12)	F(*1*)—As—F(*2*)	90.93(0.66)
As—F(*2*)	1.740(13)	F(*1*)—As—F(*3*)	89.78(0.78)
As—F(*3*)	1.637(16)	F(*2*)—As—F(*3*)	90.85(0.73)
		F(*1*)—As—F′(*2*)	89.07(0.66)
F(*1*)—F(*2*)	2.448(20)	F(*1*)—As—F′(*3*)	90.22(0.78)
F(*1*)—F(*3*)	2.352(23)	F(*2*)—As—F′(*3*)	89.15(0.73)
F(*2*)—F(*3*)	2.407(20)		
F(*1*)—F′(*2*)	2.408(17)	As—F(*2*)—Cl	136.02(0.69)
F(*1*)—F′(*3*)	2.361(22)		
F(*2*)—F′(*3*)	2.371(22)		

*F′ atoms related to F atoms by center of symmetry at the arsenic atom; estimated standard deviations in parentheses.

4e, respectively. The structure was refined by successive cycles of block-diagonal least squares, using 3 × 3 matrices for the positional parameters and 6 × 6 for the anisotropic thermal parameters of each atom. The quantity minimized was $R_2 = \Sigma w(|F_o| - |F_c|)^2$ for observed reflections only, using weighting function $w = 1/\{1 + [(|F_o| - P_2)/P_1]^4\}$, with $P_1 = 45$ and $P_2 = 55$. Scattering factor curves used were those for As, Cl, and F given in *International Tables for X-Ray Crystallography*, Vol. III (11) corrected for anomalous dispersion (12).

After refinement was complete, a difference synthesis showed a small amount of remaining electron density nowhere greater than 0.4 e $Å^{-3}$. The final agreement residual $R = \Sigma(||F_o| - |F_c||)/\Sigma|F_o|$ was 0.045. A set of structure factors for the final parameters given in Table 1 has been placed in the Depository of Unpublished Data.[1]

Discussion

The atomic arrangement is shown in Fig. 1. The arsenic atoms lie on centers of symmetry at 000 and 0, ½, ½ and the chlorine atoms lie on the two-fold axes. Each arsenic is surrounded octahedrally by six fluorine atoms; all F—As—F angles (Table 2) are not significantly different from 90°. Two fluorine atoms from each AsF_6^- anion provide *trans* bridges to two ClF_2^+ cations. The arsenic to bridging fluorine F(*2*) distance 1.740(13) Å is probably significantly longer than As—F(*1*) 1.694(12) Å and significantly longer than the shortest terminal bond As—F(*3*) 1.637 (16) Å. The coordination around the chlorine atom is shown in Fig. 2, and the corresponding distances are given in Table 3. The ClF_2^+ and the bridging fluorines lie within 0.04 Å of the best mean plane through the five atoms (Table 4). The

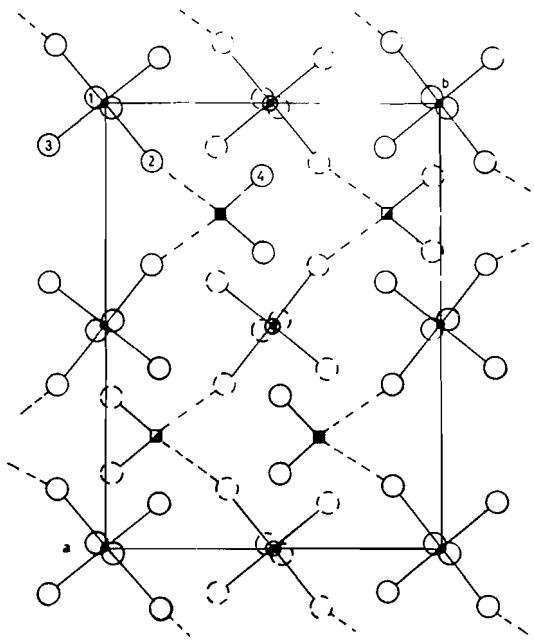

FIG. 1. Projection of the structure along the *c* axis. ○, ○, Fluorine atoms; ◉, arsenic atom at $z = ½$; ●, arsenic atom at $z = 0$; ■, chlorine atom at $z = 0$; ◩, chlorine atom at $z = ½$.

atoms F(*3*), F″(*3*), F(*1*), and F″(*1*) are situated towards the F(*4*), F″(*4*) side of the chlorine atom at about van der Waal's distance away.

Table 5 compares the structural information found for the ClF_2^+ ion in ClF_2AsF_6 and ClF_2SbF_6. The bridging fluorines are also essentially coplanar with the ClF_2^+ in ClF_2SbF_6 (8) (as is the BrF_2^+ in BrF_2SbF_6 (6, 7)). The most obvious difference is the F—Cl—F angle, 103.17(0.70)° in ClF_2AsF_6 compared with 95.9(3.1)° in ClF_2SbF_6,

[1]Copies may be obtained free of charge, upon request, from the Depository of Unpublished Data, National Science Library, National Research Council of Canada, Ottawa, Canada.

Can. J. Chem. Downloaded from www.nrcresearchpress.com by 210.87.254.40 on 09/05/12
For personal use only.

TABLE 3. A selected list of distances and angles showing the chlorine coordination*

Bond distance		Bond angle	
Bond	Distance (Å)	Bonds	Angle (deg)
Cl—F(*1*)	3.141(14)	F(*2*)—Cl—F(*4*)	81.64(0.59)
Cl—F(*2*)	2.339(14)	F(*2*)—Cl—F″(*2*)	93.62(0.47)
Cl—F(*3*)	3.267(18)	F(*4*)—Cl—F″(*4*)	103.17(0.70)
Cl—F(*4*)	1.541(14)		
		F(*1*)—Cl—F″(*1*)	142.11(0.41)
F(*1*)—F(*3*)	2.352(23)	F(*3*)—Cl—F″(*3*)	175.06(0.44)
F(*1*)—F(*4*)	2.853(17)		
F(*2*)—F(*4*)	2.607(18)		
F(*2*)—F″(*3*)	3.365(21)		
F(*2*)—F″(*2*)	3.411(18)		
F(*3*)—F″(*4*)	3.249(21)		
F(*4*)—F″(*4*)	2.416(19)		

*F″ atoms related to F atoms by twofold axis through chlorine atom; estimated standard deviations in parentheses.

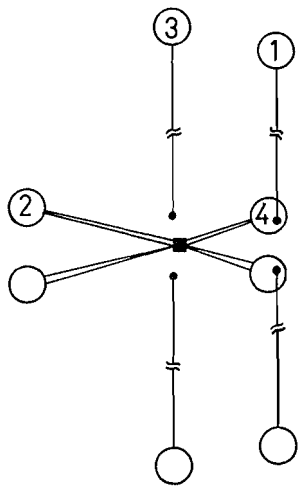

FIG. 2. Coordination around the chlorine atom. ○, Fluorine atoms; ■, chlorine atom; ●, position of the fluorine atoms projected onto the Cl, F(*2*), F″(*2*), F(*4*), F″(*4*) plane.

TABLE 4. Best mean plane through atoms Cl, F(*2*), F(*4*), F″(*2*), and F″(*4*)*

Atom	Distance from plane (Å)
Cl	0
F(2)	−0.03(1)
F(4)	0.04(1)
F″(2)	−0.04(1)
F″(4)	0.03(1)

*Equation of plane: $-0.423X - Y - 0.906Z + 1.129 = 0$, referred to an orthogonal set of axes, X along a, Y along b, and Z along c^*. Estimated standard deviations in parentheses.

TABLE 5. A comparison of the ClF_2^+ structure in ClF_2AsF_6 and ClF_2SbF_6 (8)*

Parameter	ClF_2AsF_6	ClF_2SbF_6
Cl—F [ClF_2^+] distance	1.541(14) Å	1.57(3) Å 1.58(3) Å
Cl — bridging fluorine distance	2.339(14) Å	2.43(3) Å 2.33(3) Å
F—Cl—F [ClF_2^+] angle	103.17(0.70)°	95.9(3.1)°
F—Cl—F [bridge] angle	93.62(0.47)°	89.9(1.9)°

*Estimated standard deviations in parentheses.

although the difference is only "possibly significant". The chlorine atom in ClF_2SbF_6 also has four fluorine atoms at about van der Waal's distance away 3.08(3), 2.96(3), 3.11(3), and 2.99 (3) Å (8), two above and two below the ClF_2^+ plane, but in a different orientation to that found for ClF_2AsF_6. In other respects the structures are similar.

Interest in the bonding of interhalogen compounds has centered around the question of whether or not d orbital participation is important (13). The F—Cl—F angle of 103.17 (0.70)° in ClF_2^+ suggests that a bonding model that uses exclusively p (14) or d^2sp^3 orbitals would not be appropriate. It is possible that the structure can be represented mainly in terms of valence bond structures **1** and **2**, structure **1** having the most importance.

Both valence structures favor a planar arrangement of the chlorine atom and its four nearest neighbors, structure **1** on steric grounds and structure **2** from electronic considerations. The arrangement of the four fluorine atoms at about van der Waal's distance from the chlorine atom

Can. J. Chem. Downloaded from www.nrcresearchpress.com by 210.87.254.40 on 09/05/12
For personal use only.

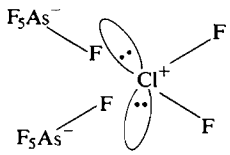

1

Ionic structure
chlorine sp^3 hybridized

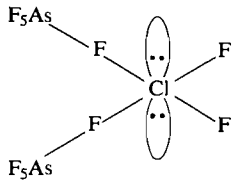

2

Bridging structure
chlorine d^2sp^3 hybridized

would favor lone pairs having the orientation of valence bond structure **1** (see Fig. 2). The F—Cl—F angle is larger than the corresponding angle in PF_3, 97.8 ± 0.2° (15) and SCl_2, 100.3° (error unspecified) (16). This could be due to greater p_π–d_π bonding in ClF_2^+. The ClF bond distance is 1.541(14) Å, significantly less than that in ClF gas, 1.6281 Å (17), and is the shortest chlorine–fluorine distance so far reported.

The F—Br—F angle in BrF_2SbF_6 is 93.5(2.1)° and the fluorine bridging is stronger than in ClF_2AsF_6 (see Table 6). It is possible that for the bromine compound, structure **2** has more importance. It has been pointed out that the physical properties of BrF_2SbF_6 suggest extensive fluorine bridging (18). The infrared and Raman spectra of both BrF_2AsF_6 and BrF_2SbF_6 (19, 20) are more complicated than their chlorine analogues (3–5); however, this could be due to the fact that the arsenic and antimony atoms in ClF_2AsF_6 and ClF_2SbF_6 lie on centers of symmetry reducing the number of bands by the operation of the mutual exclusion rule.

The fluorine bridging is probably stronger in ClF_2AsF_6 than in ClF_2SbF_6, and if the arguments concerning bridging and bond angle have any validity, then the F—Cl—F angle in the antimony adduct should be the largest. The evidence suggests that this is probably not the case; however, the large standard deviations for ClF_2SbF_6 make comparisons somewhat speculative.

TABLE 6. Structural data for BrF_2^+ in BrF_2SbF_6 (6, 7)

Parameter	Value
Br—F [BrF_2^+]	1.69(2) Å
Br — bridging fluorine	2.29(2) Å
F—Br—F [BrF_2^+] angle	93.5(2.1)°
F—Br—F [bridge] angle*	95.3(1.4)°
Ratio of bridging Br—F distance to Br — terminal fluorine distance	1.36
Corresponding ratio for ClF_2AsF_6	1.52

*Arsenic atoms linked to BrF_2 by *cis* fluorine bridges; estimated standard deviations in parentheses.

We wish to acknowledge the support of the National Research Council of Canada, the Defence Research Board, and the University of New Brunswick Research Fund. We also wish to thank Dr. F. R. Ahmed of the Biochemistry Laboratory, NRCC for use of his computer programs.

1. J. PASSMORE. Ph.D. Thesis. University of British Columbia, Vancouver, British Columbia, 1967.
2. J. PASSMORE. Unpublished results.
3. K. O. CHRISTE and W. SAWODNY. Inorg. Chem. **6**, 313 (1967).
4. R. J. GILLESPIE and M. J. MORTON. Inorg. Chem. **9**, 616 (1970).
5. J. SHAMIR and I. YAROSLAVSKI. Third European Symposium on Fluorine Chemistry. Aix-en-Provence. September 1970. Abstr. p. 73.
6. A. J. EDWARDS and G. R. JONES. Chem. Commun. 1304 (1967).
7. A. J. EDWARDS and G. R. JONES. J. Chem. Soc. A, 1467 (1969).
8. A. J. EDWARDS and R. J. C. SILLS. J. Chem. Soc. A, 2697 (1970).
9. R. J. GILLESPIE and M. J. MORTON. Quart. Rev. In press.
10. International Tables for X-Ray Crystallography. Vol. I. The Kynoch Press, Birmingham, England. 1965.
11. International Tables for X-Ray Crystallography. Vol. III. The Kynoch Press, Birmingham, England. 1962. Table 3.3.1.A.
12. International Tables for X-Ray Crystallography. Vol III. The Kynoch Press, Birmingham, England. 1962. Table 3.3.2.C.
13. F. A. COTTON and G. W. WILKINSON. Advanced inorganic chemistry. 2nd ed. Interscience Publ., N.Y. 1966. Chap. 15 and references therein.
14. E. H. WIEBANGA and D. KRACHT. Inorg. Chem. **8**, 738 (1969).
15. Y. MORINO, K. KUCHITSU, and T. MORITANI. Inorg. Chem. **8**, 867 (1969).
16. H. STAMMREICH, R. FORNERIS, and K. STONE. J. Chem. Phys. **23**, 972 (1955).
17. Tables of interatomic distances and configuration in molecules and ions. Chem. Soc. Special Publication No. 11. 1958.
18. H. C. CLARK. Halogen fluorides and other covalent fluorides. Chem. Rev. **58**, 883 (1958).
19. K. O. CHRISTE and C. J. SCHACK. Inorg. Chem. **9**, 2296 (1970).
20. T. SURLES, H. H. HYMAN, L. A. QUARTERMAN, and A. I. POPOV. Inorg. Chem. **9**, 2726 (1970).

Can. J. Chem. Downloaded from www.nrcresearchpress.com by 210.87.254.40 on 09/05/12
For personal use only.

Can. J. Chem. Downloaded from www.nrcresearchpress.com by 210.87.254.105 on 09/05/12
For personal use only.

Vibrational Spectra of Peroxydisulfuryl Difluoride $S_2O_6F_2$ and the Halogen Derivatives $FOSO_2F$ and $ClOSO_2F$

A. M. QURESHI, L. E. LEVCHUK, AND F. AUBKE[1]

Department of Chemistry, University of British Columbia, Vancouver 8, British Columbia

Received February 11, 1971

Vibrational spectra of the halogenfluorosulfates $FOSO_2F$ and $ClOSO_2F$ are recorded and C_s symmetry is suggested for the molecules. For peroxydisulfuryl difluoride a staggered non-planar configuration with C_2 symmetry is indicated by the polarized Raman spectra.

Les spectres de vibration d'halogénofluorosulfates, $FOSO_2F$ et $ClOSO_2F$, sont rapportés et une symétrie C_s est envisagée pour ces molécules. Pour le peroxyde de bis (fluorure de sulfuryle), le spectre Raman polarisé révèle une configuration décalée non planaire, avec une symétrie C_2.

Canadian Journal of Chemistry, 49, 2544 (1971)

Peroxydisulfuryl difluoride, $S_2O_6F_2$, has been known for some time (1, 2) and has proven to be an extremely versatile reagent in synthetic inorganic chemistry (3–5). Even though some relevant structural details, such as the infrared spectrum in the NaCl region (1), the ^{19}F nuclear magnetic resonance (n.m.r.) spectrum and the reversible dissociation into SO_3F radicals (6, 7) at elevated temperature, indicating the presence of a peroxy group, are reported, the molecular structure is not known in detail and the complete vibrational spectrum has not been investigated.

The same holds true for the two halogen derivatives fluorine fluorosulfate $FOSO_2F$ (8) and chlorine fluorosulfate $ClOSO_2F$ (9). Infrared spectra, mostly on the gaseous compounds, are reported (8, 10*a*, 10*b*, 11) but these are with one exception (10*b*) limited to the transparency range of AgCl. This has allowed only a limited assignment of the vibrational absorption bands.

Raman spectra, which should be extremely helpful in determining the molecular geometry, and low temperature infrared spectra except for $ClOSO_2F$, are not reported. Both should permit the assignment of the vibrational modes.

A number of related molecules, where vibrational studies are reported, can be used as examples in the attempted assignment. They include HSO_3F (12–14), $BrOSO_2F$ (15), and the polysulfurylfluorides $S_2O_5F_2$ and $S_3O_8F_2$ (16) and the peroxysulfate ion $S_2O_8^{2-}$ (17). It was found necessary to reinvestigate the Raman spectrum of HSO_3F (12), where not all expected vibrational modes had been found previously.

[1]To whom correspondence should be addressed.

Experimental

Peroxydisulfuryl difluoride was prepared according to Cady and Shreeve (18) in a catalytic flow reaction. The compound was distilled repeatedly in a greaseless vacuum line. The purity of $S_2O_6F_2$ and of the halogen fluorosulfates was checked by ^{19}F n.m.r. and vapor density measurements. Fluorine fluorosulfate is obtained in the same flow reaction as a by-product and purified by repeated vacuum distillation. Since handling this compound can be hazardous, only small quantities were prepared and safety precautions were taken. Chlorine fluorosulfate is obtained according to Gilbreath and Cady (9). The compound was distilled in a metal vacuum line. A monel reactor of about 100 ml contents with a Whitey valve was used. Fluorosulfuric acid was purified by double distillation as described previously (19).

Raman samples were contained either in an ordinary 7 mm o.d. Pyrex tube ($S_2O_6F_2$) or quartz tube ($ClOSO_2F$) or in a 12 mm o.d. thick wall Pyrex tube ($FOSO_2F$), all with a flattened bottom. The samples were flame sealed after filling. The starting materials were supplied from Allied Chemical Corporation (F_2, SO_3, HSO_3F) or from Matheson of Canada (Cl_2). The identity and purity of the compounds was checked by ^{19}F n.m.r.

Infrared spectra were obtained on Perkin Elmer grating spectrophotometers 457 (for routine work on gaseous samples) and 225 (for low temperature studies). The spectra on gaseous samples were obtained with a monel infrared cell of 80 mm pathlength fitted with silver chloride windows (Harshaw Chemicals) and Whitey valves. The low temperature spectra were obtained with CsI windows, using a metallic Dewar container (Andonain Associated Inc.).

Raman spectra were obtained on a Cary 81 spectrometer equipped with a Spectra Physics model 125 He–Ne laser.

Results

Well-resolved Raman and infrared spectra were obtained for all three compounds. The Raman spectra for $FOSO_2F$ and $ClOSO_2F$ are shown in Figs. 1 and 2, the Raman spectrum of

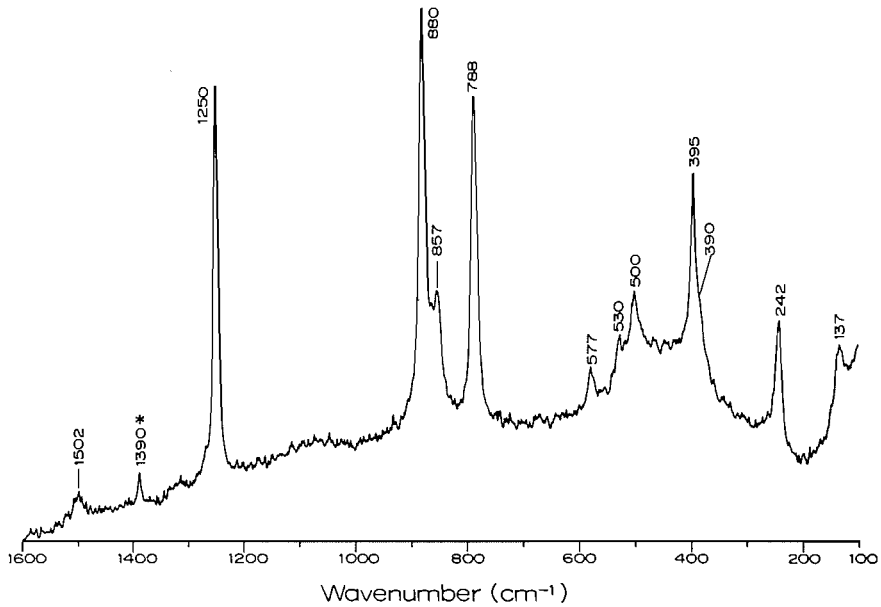

FIG. 1. Raman spectrum of $FOSO_2F$.

$S_2O_6F_2$ is reproduced in Fig. 3. The observed absorption bands are listed together with a proposed assignment in Table 1 for HSO_3F, $FOSO_2F$, and $ClOSO_2F$ and in Table 2 for $S_2O_6F_2$. Also listed are estimated intensities and calculated polarization ratios.

Discussion

From previous infrared and ^{19}F n.m.r. studies it can be concluded that the compounds $XOSO_2F$ with X = H, F, or Cl are true fluorosulfates, the observed chemical shifts fall into the range of other SO_3F compounds (20), with X linked over oxygen to sulfur. It can also be assumed that this X—O—S group is non-linear as postulated by the Gillespie–Nyholm valence shell electron pair repulsion model (21) and as found, for example, in compounds such as SF_5OF (22) or in the triatomic molecules X_2O (23). If in addition a hindrance of free rotation around the S—O bond in this X—O—S group is assumed, presumably caused by some weaker $p\pi \rightarrow d\pi$ bonding as postulated by Cruikshank (24), one would expect two different configurations, one belonging to the point group C_s with X and F co-planar and the other C_1 where both are not co-planar. For the C_S configuration *cis*- and *trans*-isomers are expected.

As can be seen from Table 1, the polarized Raman spectra show the presence of four (HSO_3F, $FOSO_2F$) and three ($ClOSO_2F$) depolarized modes, thus favoring point group C_s over C_1 in good agreement with previous work on HSO_3F (12).

The twelve expected vibrational modes are conveniently described as SO_2 stretching modes (symmetric (a') and asymmetric, S—F, S—OX, and O—X stretching (all a'), SO_2 and OX bonding (a'). S—OX and SF wagging, SO_2 rocking (a''), and SO_3F and SOX torsions (a'') all of which are observed for $FOSO_2F$. In case of $ClOSO_2F$, the SOCl torsion mode is not observed. This band is expected to occur below 100 cm^{-1} judging from the position of the corresponding band for $FOSO_2F$ at 137 cm^{-1}.

The O—H stretching mode for HSO_3F found at 3150 and 3050 cm^{-1} (13) is not observed in the Raman spectrum in agreement with previous work (12). Two new Raman bands are observed for this compound, both fairly weak, a depolarized band at 686 cm^{-1} and a presumably polarized band at 490 cm^{-1}. The former is assigned in agreement with Savoie and Giguère (13) as OH torsion mode, the latter which is not observed in the infrared spectrum is assigned as S—F wagging mode. The proposed assignment for HSO_3F departs only in this regard from previous proposals (13) where coincidence of

Can. J. Chem. Downloaded from www.nrcresearchpress.com by 210.87.254.105 on 09/05/12
For personal use only.

Can. J. Chem. Downloaded from www.nrcresearchpress.com by 210.87.254.105 on 09/05/12
For personal use only.

TABLE 1. Vibrational spectra of XSO_3F*

HSO_3F		$FOSO_2F$					$ClOSO_2F$				
		Raman liquid			Infrared		Raman (liquid)				
Raman (cm^{-1})	Infrared (13) (cm^{-1})	Frequency (cm^{-1})	Intensity	ρ	Gas (cm^{-1})	Solid (cm^{-1})	Frequency (cm^{-1})	Intensity	ρ	Infrared solid (10*b*) (cm^{-1})	Assignment
1443	1440	1502	0.4	1.0 dp	1501	1485 vs	1478	0.5	1.0 dp	1458	SO_2 asym. stretch (*a''*)
		1390	0.4			1465 m,sh					
1205	1230	1250	8.5	0.22 p	1248	1241 vs	1225	4.5	0.10 p	1238	SO_2 sym. stretch (*a'*)
961	960	788	7.0	0.28 p	789	776 s 783	856	1.5	0.40 p	876	S—OX stretch (*a'*)
851	837	857	3.0	0.53 p	852	846 s	830	1.5	0.60 p	837	S—F stretch (*a'*)
(2940)	3125	880	10.0	0.28 p	879	875 s	706	10.0	0.15 p	709	O—X stretch (*a*)
						606 602 vw					
560	556	577	0.8	p	575	569 s	573	0.7	p	573	SO_2 bend (*a'*)
1179	1170	242	3.0	0.50 p			212	2.5	0.50 p		S—O—X bend (*a'*)
						544					
						539 w				545	
						531					
552	554	530	0.5	1.0 dp	523	519 s	534	0.7	1.0 dp	532	SO_2 rock (*a''*)
490		500	1.5	0.27		495 ms	486	4.5	0.65 p	487	SF wag (*a'*)
686	667†	137	1.0	1.0 dp	—	—	—				S—OX torsion (*a''*)
393	396	390	1.0	dp	—	380 s	389	0.6	1.0 dp	390	SO twisting (*a''*)
405	429	395	4.0	0.60 p	—	395 m,sh	363	8.0	0.37 p	364	S—OX wag (*a'*)

*vs = very strong, s = strong, m = medium, w = weak, vw = very weak, b = broad, sh = shoulder, p = polarized, dp = depolarized, ρ = polarization ratio.
†Our interpretation.

Can. J. Chem. Downloaded from www.nrcresearchpress.com by 210.87.254.105 on 09/05/12
For personal use only.

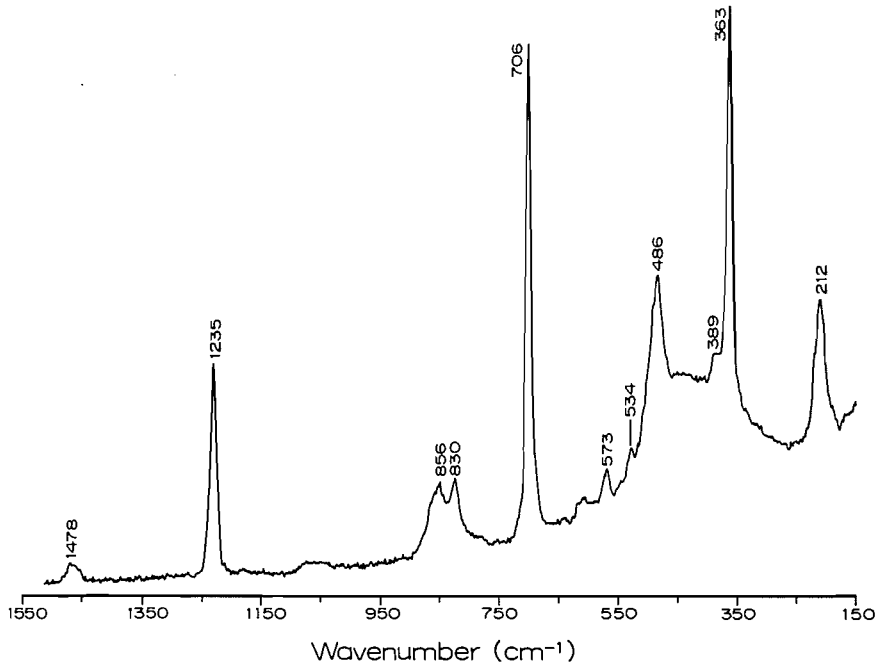

FIG. 2. Raman spectrum of $ClOSO_2F$.

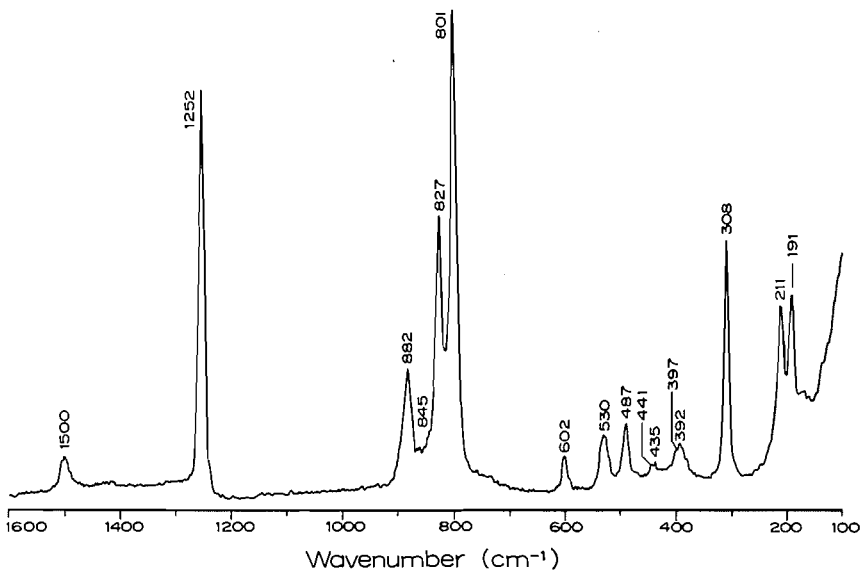

FIG. 3. Raman spectrum of $S_2O_6F_2$.

this band with the torsion mode at 390 cm^{-1} had been suggested.

Both $FOSO_2F$ and $ClOSO_2F$ are found to have absorption bands in the same region. The fact that hydrogen bridge-bonding in the liquid acid is mainly responsible for the low SO_2 stretching vibrations is obvious from the reported infrared studies on gaseous HSO_3F (13, 14). The corresponding bands are higher for $FOSO_2F$ and also for $ClOSO_2F$, even though some molecular

TABLE 2. Vibrational spectra of $S_2O_6F_2$*

Raman			Infrared frequency (cm^{-1})		Approximate assignment of fundamentals
Frequency (cm^{-1})	Intensity	Polarization ratio, ρ	80 °K	Gas	
				2740 vw	
			1908 vw		
			1680 vw	1690 vw	
				1645 vw	
			1485 vs		
1500	1.0	1.0 dp	1467 w,sh	1498	ν_{SO_2} asym.
				1350 w,b	P branch
1252	8.0	0.19 p	1247 m,sh	1248 vs	ν_{SO_2} sym.
			1239 vs	1162 m,b	R branch
			1080 vw		
			1020 vw	1030 vw	
882	2.5	0.33 p	880 m	878 m	ν_{SF}
845	w,sh	?	847 vs	847 vs	ν_{SO} asym.
827	4.0	0.88 dp	822 m		ν_{SO} sym.
801	10.0	0.08 p	794 m	795 m	ν_{O-O}
			748 s	752 s	
			656 vw		
602	0.5	0.90 dp	595 m	598 w,sh	SO_2 bend
			588 m		
			572 w	565 w	
530	0.5	1.0 dp	532 m,sh		SO_2 rock
			517 vs	524 s	
487	0.5	0.46 p	481 w		SF wag
441	0.2	?	437 m		SOO bend
435	0.3	1.0 dp			SOO bend
397	0.5	? dp	385 m,w		SO_2F torsion or SOO wag
392	0.7	0.57 p	378 m,w		SOO wag
308	5.0	0.60 p	302 w		S—OO bend
211	3.0	0.33 p			Deformation
191	3.5	0.33 p			

*v = very, s = strong, m = medium, w = weak, sh = shoulder, b = broad, p = polarized, dp = depolarized.

association, presumably via Cl...OS interaction, is evidenced by the wide liquid range and the observed Trouton constant (9).

No evidence of similar association is apparent for $FOSO_2F$. The vibrational bands are identical for the liquid and the gaseous sample within the error limits and only for the solid spectrum an expected shift to lower frequencies of about 10 cm^{-1} is noted. In addition some bands appear to be split in the low temperature spectrum, presumably due to factor group splitting. Poor resolution in the range lower than 300 cm^{-1} did not allow us to detect the bands at ~240 and 137 cm^{-1} in the infrared spectrum.

Whereas a straightforward assignment is possible in the high and in the low frequency range, some ambiguity is expected in the range of 700 to 900 cm^{-1} where three fundamentals ν_{S-F}, ν_{OF}, and ν_{S-OF} occur, all *a'* modes and thus polarized in the Raman spectrum. The previous assignment (8) based on a comparison of the $FOSO_2F$ and the CH_3OSO_2F bands in this reagent had suggested for ν_{OF} a frequency at 880 cm^{-1}, for ν_{SF} a value of 852 cm^{-1}, and for ν_{S-OF} 789 cm^{-1}. This appears quite reasonable even when compared to more recent assignment made on related molecules.

The O—F stretching frequency is normally found at slightly higher wavenumbers, *e.g.* at 945 cm^{-1} for CF_3OF (25) and at 937 cm^{-1} for $FONO_2$ (26*a*, *b*) but for SF_5OF (27) a lower value of 888 cm^{-1} is suggested. Where covalently bound SO_3F groups are found, the SF stretch is normally expected to be higher than 800 cm^{-1}, thus favoring the 852 cm^{-1} mode over the band at 788 cm^{-1}, which is best described as ν_{S-OF}. All other bands are easily assigned in good analogy to HSO_3F.

For $ClOSO_2F$ similar difficulties are encountered. The strong, polarized band at 706 cm^{-1} is best assigned as ν_{Cl-O} even though for $ClONO_2$ a higher value, 809 cm^{-1}, has been suggested for the identical vibration (28). For chloroxyperfluoroalkanes (29) the Cl—O stretch is found in

Can. J. Chem. Downloaded from www.nrcresearchpress.com by 210.87.254.105 on 09/05/12
For personal use only.

Can. J. Chem. Downloaded from www.nrcresearchpress.com by 210.87.254.105 on 09/05/12
For personal use only.

the range of 780–750 cm^{-1}, for SF_5OCl a frequency of 720 cm^{-1} is suggested (30). Our assignment is also in good agreement with the interpretation of the infrared spectrum (10*a*, *b*, 11).

Both bands at 856 and at 830 cm^{-1} are in the expected range of the S—F stretching mode. We assign the lower value to ν_{S-F} for the following reasons. In terminal monodentate SO_3F groups, where strong molecular associations as, for example, in HSO_3F is absent, such as $BrOSO_2F$ (15), $[Br(OSO_2F)_4]^-$ (31), $[I(OSO_2F)_4]^-$ (31), CF_3OSO_2F (32), and NF_2OSO_2F (32), ν_{SF} is found in the relatively narrow frequency range of 830–840 cm^{-1}. Furthermore it has been demonstrated by Gillespie and Robinson (33) on a number of examples, that in tetrahedrally coordinated sulfur compounds of the type XSO_2Y both the SO_2 stretching modes and ν_{S-Y} depend on the electronegativity of X as, for example, found for SO_2F_2 *vs.* $ClSO_2F$ (34).

If this argument applies also to $FOSO_2F$ and $ClOSO_2F$ both the SO_2 stretching modes and ν_{SF} should occur at lower wavenumbers for $ClOSO_2F$, as is in fact observed.

The band at 856 cm^{-1} is correspondingly assigned as ν_{S-OCl}. All remaining bands are assigned in close analogy to $HOSO_2F$ and $FOSO_2F$. The low temperature infrared spectrum is reported by Christie *et al.* (10*b*) and was therefore not recorded by us.

For $FOSO_2F$ a spurious, unassigned band at 1390 cm^{-1} was noted in some Raman samples but appeared to be absent in the infrared spectrum. The band is therefore ignored in the interpretation.

Peroxydisulfuryl difluoride can be regarded as a true peroxide, as discussed before, of the type R_2O_2 where $R = SO_2F$. Following an interpretation of the vibrational spectrum in terms of group frequencies, one would expect the SO_2F bands to occur in approximately the same region as previously established for the halogenfluorosulfates and HSO_3F. For the S_2O_2 skeleton in $S_2O_6F_2$, three reasonable structural possibilities can be discussed: (*a*) a planar *cis* configuration belonging to point group C_{2v}, (*b*) a planar *trans* configuration, point group C_{2h}, and (*c*) a non planar, staggered form with C_2 symmetry.

Previous structural studies on related compounds have confirmed model (*c*) for $(SF_5)_2O_2$ (35), H_2O_2 (23), and $(CH_3)_2O_2$ (36) where dihedral angles between the two X—O—O planes are found to be between 100 and 110°. For the ion $S_2O_8^{2-}$ isoelectronic to $S_2O_6F_2$, however, configuration (*b*) has been suggested as a result of a vibrational study (17) in analogy to the ion $P_2O_8^{4-}$ (37). This is confirmed by X-ray diffraction, for $(NH_4)_2S_2O_8$ (38, 39) and $Cs_2S_2O_8$ (38), but for $K_2S_2O_8$ (40) again the staggered configuration is suggested. No precedents could be found for configuration (*a*) among the peroxides. This structural type is only found, where strong multiple bonding between the bridging atoms exists as, for example, in *cis*-N_2F_2 (41, 42), *cis*-$(C_6H_5)_2N_2$ (43), and *cis*-$N_2O_2^{2-}$ (44). For all these compounds the corresponding *trans* isomers are found as well with grossly different vibrational absorption characteristics. This is clearly not the case for $S_2O_6F_2$, where the O—O bond is found to be very weak (6, 7).

Even though a clear distinction between configuration (*a*) and (*c*) by vibrational spectroscopy is feasible but rather difficult, only one torsion mode would be infrared (i.r.) active and Raman polarized for C_2 but i.r. inactive and Raman depolarized for C_{2v}, the transform (*b*) would have a center of symmetry with 3 modes only i.r. active and 3 modes only Raman active as postulated by the mutual exclusion rule and as found for *trans* difluorodiazine (45, 46). Inclusion of the SO_2F groups in the discussion will add a fourth likely structural possibility when both SO_2F groups are oriented in such a way that all symmetry is reduced to C_1. One would expect 24 polarized Raman and i.r. active modes. For point group C_2 all 24 modes would be Raman and i.r. active, but only 13 would be polarized. For C_{2h} 13 modes would be i.r. active and 12 Raman active with 8 polarized modes. And finally for C_{2v} one expects 19 i.r. active and 24 Raman active modes with 8 being polarized.

The vibrational spectra are listed in Table 2. Agreement with the previously reported gas phase infrared spectrum (1) is good. The following features are interesting. Strong vibrational coupling as observed for $S_2O_5F_2$ and other polysulfuryl halides appears to be absent here, because the SO_2F group bands are not split. The appearance of shoulders in the low temperature i.r. spectrum is not observable in the gas phase spectrum and may be considered as solid state splitting. The reason for the absence of coupling in $S_2O_6F_2$ can be seen in the rather weak oxygen–

Can. J. Chem. Downloaded from www.nrcresearchpress.com by 210.87.254.105 on 09/05/12
For personal use only.

oxygen bond (6, 7), linking both SO_2F. Since seven individual vibrational modes can be assigned to this group, ν_{SO_2} symmetric and antisymmetric, V_{S-F}, SO_2 bend, SO_2 rock, SF wag, and a torsion mode, coincidence of these modes for the two SO_2F groups would reduce the number of observable bands from 24 to 17.

Assignment of the seven SO_2F modes shows good agreement with the corresponding bands for $FOSO_2F$. We assign the bands at 1500 and 1252 cm^{-1} as SO_2 stretches, 882 cm^{-1} as SF stretch slightly higher than found for $S_2O_5F_2$ (16), 602 cm^{-1} as SO_2 bending mode, 530 cm^{-1} as SO_2 rock 487 cm^{-1} as SF wag, and 397 cm^{-1} as torsional mode. Of these 3 are clearly polarized and 3 depolarized, the band 397 cm^{-1} is uncertain.

The region between 800 and 900 cm^{-1} shows a certain complexity. In addition to the mentioned SF stretch at 882 cm^{-1} the S—O stretch and the O—O stretch should occur in this region. In fact a very intense, polarized band at 801 cm^{-1} is found in the Raman spectrum with a very low depolarized ratio, assignable as ν_{O-O}. The position is slightly lower than found for the $S_2O_8^{2-}$ ion, where bands in the region of 834 to 810 cm^{-1} are observed depending on the cation type (17). In addition two more absorption bands are observed in this region, a weak shoulder in the Raman spectra at 845 cm^{-1} with a corresponding intense infrared band at 847 cm^{-1} and a Raman band at 827 cm^{-1} observable also in the infrared spectrum at 80 °K. We assign both bands as asymmetric and symmetric SO stretches. The gaseous infrared spectrum does not show this band, probably obscured by the strong 847 cm^{-1} absorption, but a weak band at 795 cm^{-1} becomes visible. This and the band at 878 cm^{-1} had been interpreted previously as P and R branches of the 847 cm^{-1} band (1). Since the 847 mode is not totally symmetrical and both the 878 and the 795 cm^{-1} are observable in the spectrum at 80 °K where typical P and R branches as the ones at 1350 and 1162 cm^{-1} have vanished, the previous assignment is improbable.

The band 795 cm^{-1} is now assigned as ν_{O-O}. The occurrence of this band in the infrared spectrum is in disagreement with the findings for the ions $S_2O_8^{2-}$ (17) and $P_2O_8^{4-}$ (37) and not consistent with the C_{2h} model.

As found for the SO stretches, some splitting seems to occur also for the SOO bending modes at 392 and 397 cm^{-1} and the SO wag at 441 and 435 cm^{-1}. The 397 cm^{-1} bands seem to coincide with the previously assigned torsional mode. As shown in Fig. 3 the bands are indeed rather broad.

The remaining bands are tentatively assigned as SOOS bend at 308 cm^{-1} and two torsional modes at 211 and 191 cm^{-1}. All are clearly polarized. It appears that of the 17 observed bands 8 are clearly polarized and 5 are clearly depolarized. The situation in the remaining four low intensity modes is uncertain. This fact already is inconsistent with point group C_1, where all modes would be polarized. The results are, however, most consistent with a staggered configuration (*c*). Furthermore, all Raman active bands appear also in the infrared spectrum down to 300 cm^{-1}. Beyond this region the resolution in the i.r. spectrum has become too poor.

In addition to the discussed infrared bands and some weak intensity combination bands, two strong absorptions are found in both the low temperature and the gas phase infrared spectrum. Both bands at 1030 and 748 cm^{-1} are without Raman counterparts, whereas the first one is undoubtedly due to a small SiF_4 impurity, the band at 748 cm^{-1} is difficult to explain. In spite of the relatively high intensity it is felt that this absorption band may not be due to a fundamental vibration, because no corresponding Raman band is found. One could, however, argue that a possibly weak and depolarized band in this region might be obscured by the intense band at 801 cm^{-1}, which is somewhat unlikely, considering the sharpness of this band as is evident in the figure. Even then only two possible interpretations of the 748 cm^{-1} absorption could be discussed: as S—O asymmetric stretch or as SO_2 rocking mode. The first possibility would imply that the symmetric SO stretch occurs at higher frequencies than the asymmetric one, in disagreement with findings for $S_2O_8^{2-}$. The second alternative is not very likely because in the spectra of $FOSO_2F$ and $ClOSO_2F$ no evidence for a deformation mode as high up as 750 cm^{-1} is found. The proposed assignment, favoring C_2 symmetry would imply that in the molecular fragment O—OSO_2F the O—O—S—F grouping would be planar otherwise the symmetry would be reduced to C_1. This is in fact identical to the

situation for HSO_3F and the halogen fluorosulfates where the X—O—S—F group was found to be planar.

It follows that $S_2O_6F_2$ and the halogenfluorosulfates are structurally related. The preference for the proposed structures could be seen in lone electron pair repulsion between lone pairs on different oxygen and halogen atoms as suggested for H_2O_2 (47, 48). This reasoning would favor a *trans* arrangement for halogenfluorosulfate rather than a *cis* one. It is hoped that future structural studies will confirm the suggested configurations.

Financial support from the National Research Council of Canada is gratefully acknowledged. We wish to thank Dr. R. D. Spratley and Mr. P. Tchir for their help in obtaining the low temperature infrared spectra and Mr. E. Matter for his help in building the metal manifold and metal reactors used in the preparation.

1. F. B. DUDLEY and G. H. CADY. J. Am. Chem. Soc. **79**, 513 (1957).
2. U. WANNAGAT and G. MENNICKEN. Z. anorg. allg. chem. **278**, 310 (1955).
3. G. H. CADY. Adv. Inorg. Radiochem. **2**, 105 (1960).
4. S. M. WILLIAMSON. Prog. Inorg. Chem. 7, 39 (1966).
5. A. A. WOOLF. *In* New pathways in inorganic chemistry. *Edited by* E. A. V. Ebsworth, A. G. Maddock, and A. G. Sharpe. Cambridge Press. 1968. p. 327.
6. F. B. DUDLEY and G. H. CADY. J. Am. Chem. Soc. **85**, 3375 (1963).
7. E. CASTELLANO, R. GATTI, J. E. SICRE, and H. J. SCHUMACHER. Z. Phys. Chem. N.F. **42**, 174 (1964).
8. F. B. DUDLEY, G. H. CADY, and D. F. EGGERS. J. Am. Chem. Soc. **78**, 290 (1956).
9. W. P. GILBREATH and G. H. CADY. Inorg. Chem. **2**, 496 (1963).
10. (*a*) C. J. SCHACK and R. D. WILSON. Inorg. Chem. **9**, 311 (1970). (*b*) K. O. CHRISTE, C. J. SCHACK, and E. C. CURTIS. Spectrochim. Acta, **26A**, 2367 (1970).
11. C. V. HARDIN, C. T. RATCLIFFE, L. R. ANDERSON, and W. B. FOX. Inorg. Chem. **9**, 1938 (1970).
12. R. J. GILLESPIE and E. A. ROBINSON. Can. J. Chem. **40**, 644 (1962).
13. R. SAVOIE and P. A. GIGUÈRE. Can. J. Chem. **42**, 277 (1964).
14. S. M. CHACKALACKAL and F. E. STAFFORD. J. Am. Chem. Soc. **88**, 4815 (1966).
15. A. M. QURESHI and F. AUBKE. Inorg. Chem. **10**, 1116 (1971).
16. R. J. GILLESPIE and E. A. ROBINSON. Can. J. Chem. **39**, 2179 (1961).
17. A. SIMON and H. RICHTER. Z. anorg. allg. Chem. **315**, 196 (1962).
18. G. H. CADY and J. M. SHREEVE. Inorg. Syn. 7, 124 (1963).
19. J. BARR, R. J. GILLESPIE, and R. C. THOMPSON. Inorg. Chem. **3**, 1149 (1964).
20. F. A. HOHORST and J. M. SHREEVE. Inorg. Chem. **5**, 2069 (1966).
21. R. J. GILLESPIE and R. S. NYHOLM. Quart. Rev. Chem. Soc. **11**, 339 (1957).
22. R. A. CRAWFORD, F. B. DUDLEY, and K. HEDBERG. J. Am. Chem. Soc. **81**, 5287 (1959).
23. Tables of Interatomic Distances and Configuration in Molecules and Ions. Special Publication No. 11, The Chemical Society, London. 1958.
24. D. W. CRUIKSHANK. J. Chem. Soc. 5489 (1961).
25. R. T. LAGEMANN, E. A. JONES, and P. J. H. WOLTZ. J. Chem. Phys. **20**, 1768 (1952).
26. (*a*) W. E. SKIENS and G. H. CADY. J. Am. Chem. Soc. **80**, 5640 (1960). (*b*) A. J. ARVIA, L. F. R. CAFFERATA, and H. J. SCHUMACHER. Chem. Ber. **96**, 1187 (1963).
27. F. B. DUDLEY, G. H. CADY, and D. F. EGGERS. J. Am. Chem. Soc. **78**, 1553 (1956).
28. R. H. MILLER, D. L. BERNITT, and I. C. HISATSUNE. Spectrochim. Acta, **23A**, 223 (1967); see also ref. 26(*b*) and K. BRÄNDLE, M. SCHMEISSER, and W. LÜTTKE. Chem. Ber. **93**, 2300 (1960).
29. C. J. SCHACK and W. MAYA. J. Am. Chem. Soc. **91**, 2902 (1969).
30. C. J. SCHACK, R. D. WILSON, J. S. MUIRHEAD, and S. N. COHZ. J. Am. Chem. Soc. **91**, 2907 (1969).
31. H. A. CARTER, S. P. L. JONES, and F. AUBKE. Inorg. Chem. **9**, 2485 (1970).
32. A. M. QURESHI and F. AUBKE. Unpublished results.
33. R. J. GILLESPIE and E. A. ROBINSON. Can. J. Chem. **41**, 2074 (1963).
34. T. BIRCHALL and R. J. GILLESPIE. Spectrochim. Acta, **22**, 681 (1966).
35. R. B. HARVEY and S. H. BAUER. J. Am. Chem. Soc. **76**, 261 (1954).
36. W. SHAND as quoted in P. W. ALLEN and L. E. SUTTON. Acta Cryst. **3**, 46 (1950).
37. A. SIMON and H. RICHTER. Z. anorg. allg. Chem. **304**, 1 (1960).
38. W. H. ZACHARIASSEN and R. C. L. MOONEY. Z. Kristallogr. Mineral. Petrogr. Abstr. **88A**, 63 (1934).
39. B. K. SIVERTSEN and H. SORUM. Z. Kristallogr. **130**, 449 (1969).
40. R. C. KEEN. Z. Kristallogr. Mineral. Petrogr. Abstr. **91A**, 129 (1935).
41. R. K. BOHN and S. H. BAUER. Inorg. Chem. **6**, 309 (1967).
42. S. T. KING and J. OVEREND. Spectrochim. Acta, **23A**, 61 (1967).
43. G. C. HAMPSON and J. M. ROBERTSON. J. Chem. Soc. 409 (1941).
44. J. GOUBEAU and K. LAITENBERGER. Z. anorg. Chem. **320**, 78 (1963).
45. S. T. KING and J. OVEREND. Spectrochim. Acta, **22**, 689 (1966).
46. J. SHAMIR and H. H. HYMAN. Spectrochim. Acta, **23A**, 1191 (1967).
47. W. G. PENNY and G. B. B. M. SUTHERLAND. Trans. Faraday Soc. **30**, 898 (1934).
48. E. N. LASSETTRE and L. B. DEAN. J. Chem. Phys. **17**, 317 (1949).

Can. J. Chem. Downloaded from www.nrcresearchpress.com by 210.87.254.105 on 09/05/12
For personal use only.

Can. J. Chem. Downloaded from www.nrcresearchpress.com by 210.87.254.105 on 09/05/12
For personal use only.

The Kinetics and Mechanism of the Chloride–Chlorate Reaction in Moderately Concentrated Solutions of $HClO_4$ and H_2SO_4 at 25 °C

P. Crisci and F. Lenzi

Département de génie chimique, École Polytechnique, Université de Montréal, Montréal, Québec

Received December 4, 1970

The stoichiometry and kinetics of the reaction

[1] $$2H^+ + ClO_3^- + Cl^- \rightarrow ClO_2 + \tfrac{1}{2}Cl_2 + H_2O$$

have been determined at 25 °C in 3.0 – 5.8 *M* $HClO_4$ and compare well with the results obtained in aqueous H_2SO_4. A mechanism involving a semi-ideal treatment of the dehydration equilibrium

$$H^+.4H_2O \rightleftarrows H^+.H_2O + 3H_2O$$

is consistent with the kinetic data in both media.

La stoechiométrie et la cinétique de la réaction

[1] $$2H^+ + ClO_3^- + Cl^- \rightarrow ClO_2 + \tfrac{1}{2}Cl_2 + H_2O$$

ont été déterminées à 25 °C pour des solutions de $HClO_4$ de 3.0–5.8 *M*; les résultats se comparent bien avec ceux obtenus dans H_2SO_4 aqueux. Un mécanisme impliquant un traitement semiidéal de l'équilibre de déshydratation:

$$H^+.4H_2O \rightleftarrows H^+.H_2O + 3H_2O$$

est consistant avec les données cinétiques dans les deux milieux.

Canadian Journal of Chemistry, 49, 2552 (1971)

Introduction

Reaction 1 has been postulated (1, 2) to be fundamental to reactions involving the reduction of chlorate to chlorine dioxide in moderately concentrated acid solutions. The stoichiometry and kinetics of reaction 1 in 2–6 *M* H_2SO_4 have been investigated previously (2–4). The stoichiometry was shown to be consistent with [1] if the chlorate:chloride ratio was greater than one (2, 3, 7, 9, 10).

The kinetic data (3, 4) showed that the rate of formation of ClO_2 was: (*a*) first order in chlorate towards high ($\simeq 5$ *M* H_2SO_4) acidities, changing to second order towards low ($\simeq 2$ *M* H_2SO_4) acidities, (*b*) second order in chloride throughout the acidity range, (*c*) 11–13th order in stoichiometric H_2SO_4, with the lower order at lower acidities.

Chlorine was found to have an inhibiting effect on the reaction (as opposed to chlorine dioxide), the effect being greater at lower acidities (3, 4).

The chlorate order had been found to be variable at any given low acidity (2). It was also noted that lithium, sodium, and potassium nitrates had a rate-enhancing effect in the order $Li^+ > Na^+ > K^+$; this was interpreted in terms of increasing hydration causing an increase in effective acidity (4).

The order with respect to chlorate at a fixed sodium ion concentration (the sum of the sodium nitrate and sodium chlorate concentrations being maintained constant) was accordingly redetermined and found (3) to be indeed constant at any given acidity, with values given in (*a*) above. This implied that in the early work (2) the simultaneous change of sodium concentration with that of chlorate had influenced the results, and indicates that for reactions occurring in such an acidity range (2–6 *M* H_2SO_4), specific ionic strength may be more important than general ionic strength.

Mechanism [2], [3] below was proposed (3)

[2] $$3H^+ + 2Cl^- + ClO_3^- \underset{k_2'}{\overset{k_2}{\rightleftarrows}} HClO_2 + Cl_2 + H_2O$$

[3] $$HClO_2 + H^+ + ClO_3^- \xrightarrow{k_3} 2ClO_2 + H_2O$$

which led to the rate expression

[4] $$\frac{d[ClO_2]}{dt} = \frac{2k_2k_3[H^+]^4[ClO_3^-]^2[Cl^-]^2}{k_2'[Cl_2]a_w + k_3[H^+][ClO_3^-]}$$

for large chlorate:chloride ratios, and thus ac-

Can. J. Chem. Downloaded from www.nrcresearchpress.com by 210.87.254.105 on 09/05/12
For personal use only.

counted for the observed kinetics with respect to Cl^-, ClO_3^-, and chlorine.

It was suggested (4) that the equilibrium

$$[5] \qquad H^+.4H_2O \overset{K_5}{\rightleftarrows} H^+ + 4H_2O$$

would account for the very high (11–13) order with respect to stoichiometric H_2SO_4, as well as the rate enhancing effect of highly hydrated ions such as Li^+; substituting

$$[H^+] = K_5[H^+.4H_2O]/a_w^4$$

(see Appendix 1) in equation 4 gave

$$[6] \qquad \frac{d[ClO_2]}{dt} = \frac{2k_2k_3K_5^4[Cl^-]^2[ClO_3^-]^2[H^+.4H_2O]^4}{k_2'[Cl_2]a_w^{17} + k_3K_5[H^+.4H_2O][ClO_3^-]a_w^{12}}$$

which enabled the reaction order with respect to stoichiometric H_2SO_4 for the range 2.0–4.4 *M* to be calculated to be 11, in approximate agreement with experiment (4).

However, the existence of totally unhydrated protons even at relatively low concentration has been questioned.[1]

In order to confirm the above interpretation, which implies that the reaction rate is independent of the acid anion (except for its effect on the water activity term), it was decided to investigate the stoichiometry and kinetics of the chloride–chlorate reaction in aqueous perchloric acid, which is completely dissociated[2] to 6 *M* (6), and for which water activity values are available (12).

Experimental

Stoichiometry

The analytical methods used were those described previously (2, 7) except for the determination of Cl^- and ClO_3^-. Chloride was obtained gravimetrically as AgCl, and chlorate was reduced to chloride by Fe^{2+} which was again determined as AgCl according to the procedure given in Treadwell (8).

Kinetics

The experimental methods used were those described previously (3, 4) except that the "2-syringe method" of mixing the reactants was used exclusively.

Sodium ion concentration was maintained constant for the chlorate order runs at 2.50 and 3.83 *M* $HClO_4$ by adding varying amounts of sodium nitrate in such a way as to keep the sum of $NaNO_3$ and $NaClO_3$ equal to 1.400 *M* at 2.50 *M* $HClO_4$ and 0.625 *M* at 3.83 *M* $HClO_4$ for the reasons previously (3, 4) described.

[1]M. Lister. Private communication.

[2]Although H_2SO_4 is not completely dissociated it so happens that the ratio of H^+ to stoichiometric H_2SO_4 remains approximately constant at 1.3:1 over the range 2–6 *M* as shown by Young's Raman spectral results at 25 °C (5, 11). This enables the approximation [H^+ hydrated] $\simeq$ 1.3[stoichiometric H_2SO_4] to be made in section *Effect of Acidity* under Discussion.

Results

Stoichiometry

Chlorine balances were obtained to within 2% of total chlorine reacted. For 4.9 to 6.4 *M* $HClO_4$ and initial chlorate to chloride ratios of 4:1, the stoichiometry was consistent with

$$[1] \quad 2H^+ + ClO_3^- + Cl^- \rightarrow ClO_2 + \tfrac{1}{2}Cl_2 + H_2O$$

$$[7] \qquad 6H^+ + ClO_3^- + 5Cl^- \rightarrow 3Cl_2 + 3H_2O$$

the ratio of ClO_2:Cl_2 produced being 1.90 $\pm$ 0.06, implying that 99.4% of the chlorate reacted according to reaction 1. The ratio of ClO_2:Cl_2 diminished to 1.6 at acidities below 3 *M* $HClO_4$ for 4:1 initial ClO_3^-:Cl^- ratios, and also diminished to 1.7–1.8 (at 4.9 to 6.4 *M* $HClO_4$) for initial ClO_3^-:Cl^- ratios of 2.5:1 and 1:1.

These stoichiometric results are in accord with those obtained previously in H_2SO_4 and HCl (2, 3, 7, 9, 10): the ratio of ClO_2:Cl_2 obtained, and hence the relative amounts of chlorate reacting according to reactions 1 and 7, is determined by the ratio of ClO_3^- to Cl^- present in the reacting solution. The ratio of ClO_2:Cl_2 approaches 2 (*i.e.* 100% reaction 1) as the ratio of ClO_3^- to Cl^- increases to high values.

The results reported here for $HClO_4$ follow the same trend of increasing ClO_2:Cl_2 ratio as the ClO_3^-:Cl^- ratio increases; even at the lowest ClO_2:Cl_2 ratio of 1.6:1 obtained, 96% of the chlorate reacts according to reaction 1.

A ratio of ClO_3^-:Cl^- of 24:1 was accordingly used in this work for the main kinetic investigation of the effect of acidity (Fig. 6); in the previous work in H_2SO_4 (3, 4) reported in Fig. 8, the ratio used for the acidity effect experiments was 20:1.

The minimum chlorate:chloride ratio used was 1.7:1 at 4.47 and 2.42 *M* $HClO_4$ during the investigation of the order with respect to chloride

reported in Fig. 1. The second point in Fig. 1 is at a ClO_3^- to Cl^- ratio of 2.5:1 followed by a point at a 5:1 ratio. Figure 1 shows little change in kinetic regime with changing chlorate:chloride ratio, which was also the case for the experiments carried out in H_2SO_4 and reported in refs.

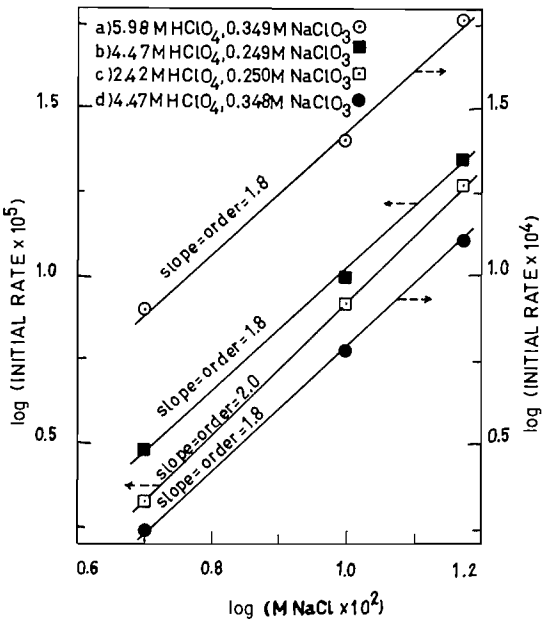

FIG. 1. Order w.r.t. chloride at different chlorate and acid concentrations.

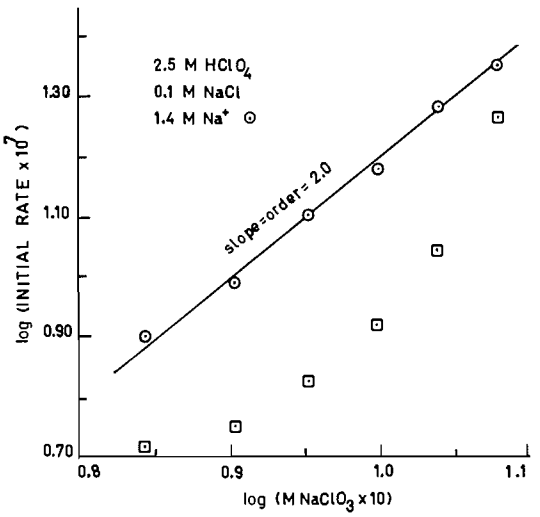

FIG. 2. Order w.r.t. chlorate at 2.5 *M* $HClO_4$, with Na^+ maintained at 1.4 *M* by the presence of varying amounts of $NaNO_3$. The squares represent rate values without the addition of $NaNO_3$.

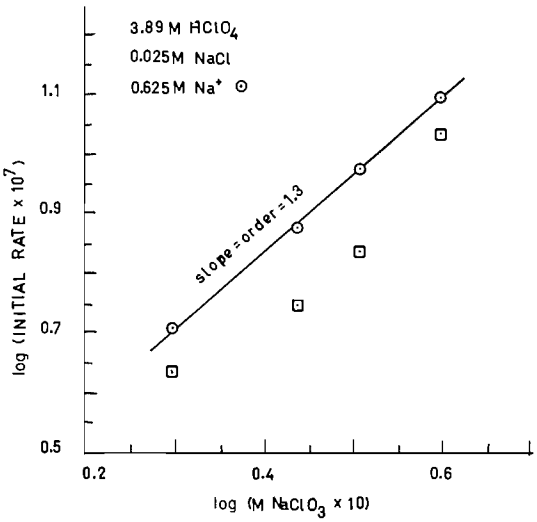

FIG. 3. Order w.r.t. chlorate at 3.89 *M* $HClO_4$, with Na^+ maintained at 0.625 *M* by the presence of varying amounts of $NaNO_3$. The squares represent rate values without the addition of $NaNO_3$.

2, 3, 7, and 9. Again Figs. 2, 3, and 4 show no discernible change in kinetic regimes with changing ClO_3^-:Cl^- ratios.

Kinetics

Initial rates of ClO_2 formation, which are a measure of reaction 1 only, are reported throughout in mol l^{-1} s^{-1}. Each point reported is the mean of the 3 or 4 initial rate measurements for a given set of experimental conditions; however, the results in Table 1 were calculated using individual points.

The deviations from the mean of each set of 3 or 4 initial rates were obtained. The maximum deviation from the mean for any such set was $\pm 10\%$ of the mean. The average maximum deviation from the mean over all the sets was $\pm 7\%$, the higher deviations occurring at the lower acidities, as was also the case for H_2SO_4 (3, 4).

The data are reported in Figs. 1–7.

(*a*) Results of the order with respect to chloride are shown in Fig. 1.

(*b*) Results of the order with respect to chlorate are shown in Figs. 2, 3, and 4.

(*c*) Results of the order with respect to $HClO_4$ are shown in Figs. 5 and 6. In Figs. 5, 6, and 8 the extremities of each vertical line representing a set of runs at each acidity correspond to the

Can. J. Chem. Downloaded from www.nrcresearchpress.com by 210.87.254.105 on 09/05/12
For personal use only.

TABLE 1. Analysis of the experimental Van't Hoff data for $HClO_4$ and H_2SO_4

Acid	Experimental range	No. of experimental points	Slope*	Standard deviation	Linear correlation coefficient	$\Sigma(x - \bar{x})^2$
Single straight line						
$HClO_4$ (Fig. 5)	2.66–5.66 *M*	36	12.25±0.31	0.09	0.997	0.3080
(Fig. 6)	3.00–5.80 *M*	18	12.57±0.37	0.07	0.998	0.0801
H_2SO_4 (Fig. 8)	3.00–6.07 *M*	45	12.33±0.42	0.08	0.994	0.2624
Best two straight lines						
Lower slope						
$HClO_4$ (Fig. 5)	2.66–4.10 *M*	24	10.83±0.31	0.04	0.998	
(Fig. 6)	3.00–3.89 *M*	9	11.42±1.55	0.07	0.989	
H_2SO_4 (Fig. 8)	3.00–4.52 *M*	15	10.67±0.44	0.04	0.998	
Higher slope						
$HClO_4$ (Fig. 5)	4.10–5.66 *M*	16	13.87±0.27	0.03	0.999	0.0514†
(Fig. 6)	3.89–5.80 *M*	12	12.91±0.28	0.05	0.999	0.0566
H_2SO_4 (Fig. 8)	4.52–6.07 *M*	36	13.44±0.82	0.12	0.987	0.1183

*The slope ranges are calculated for a 95% degree of confidence.
†The sums of the square deviations refer to the results for both straight lines taken together.

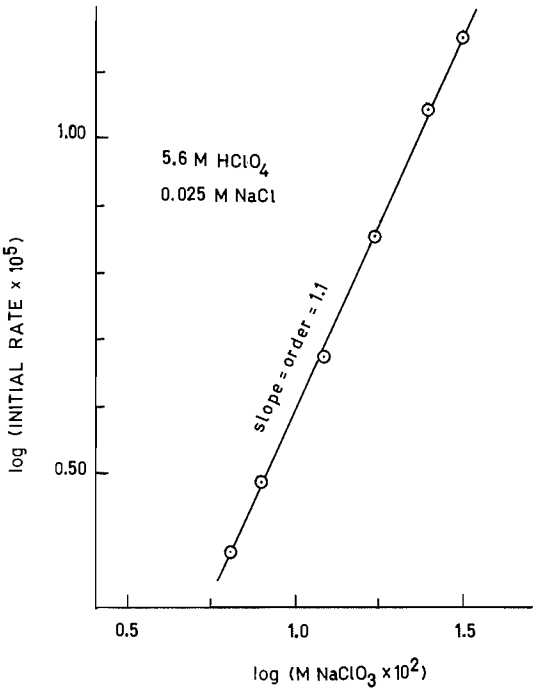

FIG. 4. Order w.r.t. chlorate at 5.6 *M* $HClO_4$. Na^+ was not maintained constant since even the maximum value (0.025 + 0.316 = 0.341 *M*) is small compared to 5.6 *M* in H^+.

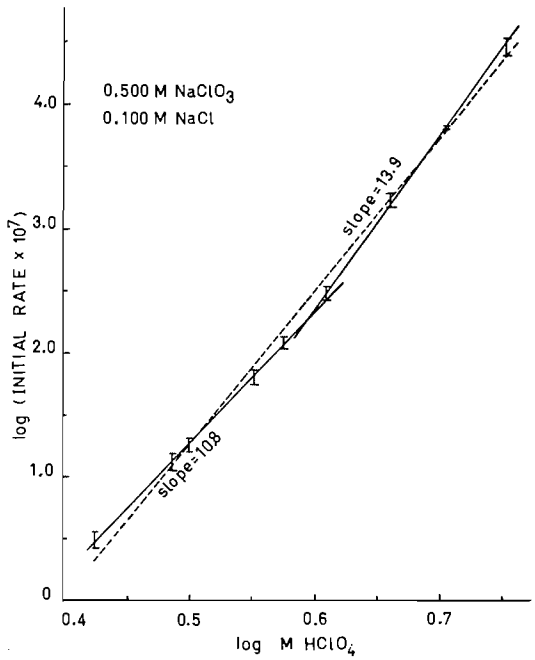

FIG. 5. The effect of stoichiometric $HClO_4$ for 0.500 *M* $NaClO_3$, 0.100 *M* NaCl. The straight lines are those calculated from the data by the 2 straight lines method (see Table 1).

maximum and minimum values of the initial rate of formation of ClO_2 obtained for the set.

(*d*) The effect of chlorine is shown indirectly in Fig. 7, where $1/(d[ClO_2]/dt)$ is plotted *vs.* $[ClO_2]$ at two different acidities. The diminishing slope of the actual experimental $[ClO_2]$ *vs.* time plots or the increase in reciprocal rates with $[ClO_2]$ shown in Fig. 7 cannot be ascribed to the time-diminishing concentration of the reactants, since only a small fraction of the initial chlorate and chloride will have reacted for the experimental conditions in question.

Can. J. Chem. Downloaded from www.nrcresearchpress.com by 210.87.254.105 on 09/05/12
For personal use only.

Can. J. Chem. Downloaded from www.nrcresearchpress.com by 210.87.254.105 on 09/05/12
For personal use only.

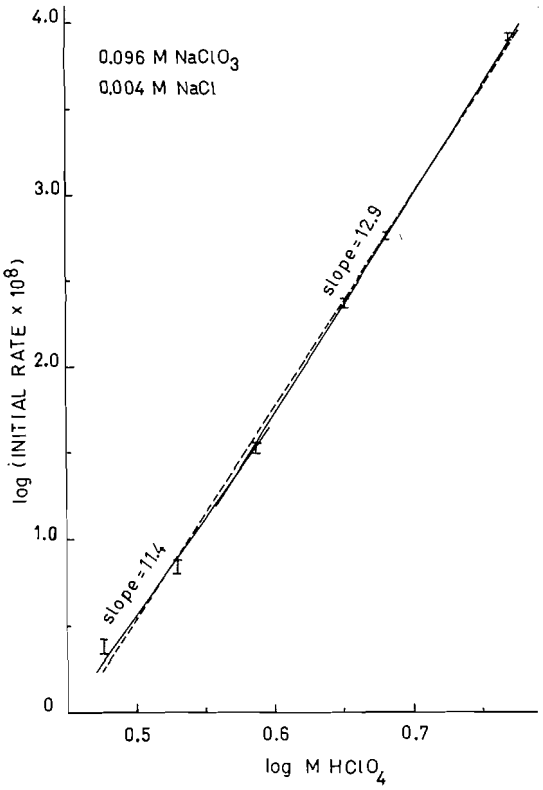

FIG. 6. The effect of stoichiometric $HClO_4$ for 0.096 *M* $NaClO_3$, 0.004 *M* NaCl. The straight lines are those calculated from the data by the 2 straight lines method (see Table 1).

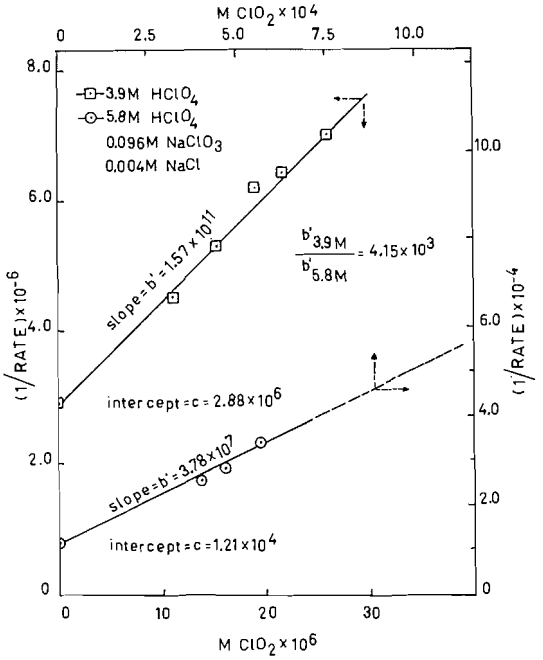

FIG. 7. The differential inhibiting effect of chlorine.

It has been shown (3) that in H_2SO_4 the ratio of ClO_2:Cl_2 is independent of time for the small chlorate conversion involved, and assuming this to be also true in $HClO_4$ (since both stoichiometric and kinetic results are similar in both media), the $[ClO_2]$ can be interpreted as being equivalent to $\alpha[Cl_2]$, where α is a constant over the conversion range, and $\simeq 2.0$ since the ratio of ClO_3^- to Cl^- used is 24:1.

Thus the linearity obtained in Fig. 7 shows that $1/(d[ClO_2]/dt)$ is of the form $b[Cl_2] + c$, there b and c are constants independent of Cl_2, which is consistent with rate equation 4 with respect to the effect of chlorine.

The ratio of the two slopes of Fig. 7 is 4.15×10^3 showing that the coefficient of the $[Cl_2]$ term in rate equation 4 (or rate equation 8 in Discussion section) is much higher at lower acidity. This supports the interpretation previously made for H_2SO_4 (4): that is, the differential inhibiting effect of chlorine with respect to

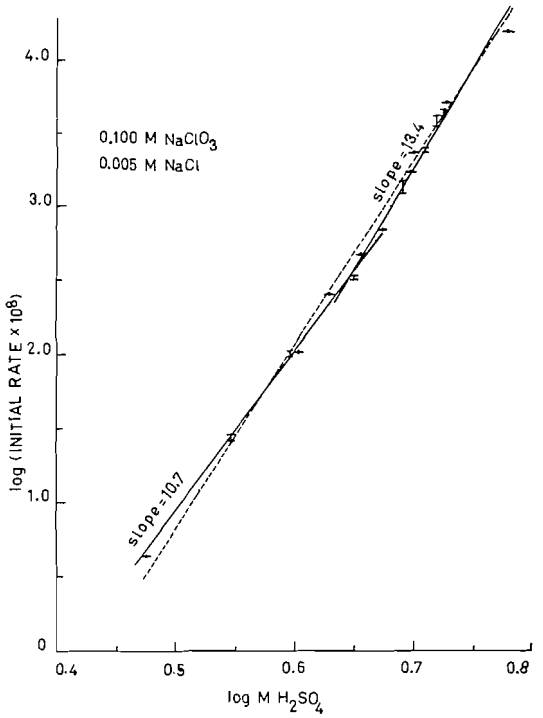

FIG. 8. The effect of stoichiometric H_2SO_4; experimental data from (3). The straight lines are those calculated from the data by the 2 straight lines method (see Table 1).

Can. J. Chem. Downloaded from www.nrcresearchpress.com by 210.87.254.105 on 09/05/12
For personal use only.

acidity is due to the presence of a higher power of water activity in the $[Cl_2]$ term of the denominator of the rate-equation than in the $[ClO_3^-]$ term.

Discussion

The orders with respect to Cl^-, ClO_3^-, and $HClO_4$ as well as the effect of chlorine are in good agreement with the data previously obtained for H_2SO_4 as reaction medium (see Introduction). This implies that the role of the acid anion is small, and substantiates mechanism [2], [3], and [4] as far as the effects of Cl^-, ClO_3^-, and Cl_2 are concerned.

The Effect of Acidity

Let

$$H^+.mH_2O \rightleftarrows H^+.(m-n)H_2O + nH_2O$$

be a general dehydration equilibrium with equilibrium constant (in mole fraction units)

$$K = \frac{[H^+.(m-n)H_2O]}{[H^+.mH_2O]} \times a_w^n$$

where $[H^+.(m-n)H_2O]$ and $[H^+.mH_2O]$ are concentrations in mol l^{-1} of solution.

This expression can be derived as in Appendix 1. The "minimum" or less radical assumption, that $f_{H^+(m-n)H_2O}/f_{H^+.mH_2O}$ is independent of concentration (as opposed to the more drastic assumption, $f_{H^+(m-n)H_2O}/f_{H^+.mH_2O} \simeq 1$) is difficult to prove or disprove except operationally, but it is no more radical than, for example, Bell and Bascombe's (13) assumption that $f_{BH^+} \simeq f_{H^+\text{ hydrated}}$.

On the assumption that K is small (that is, there is much more of the more hydrated than the less hydrated species in the experimental acidity range up to 5.8 M $HClO_4$), the stoichiometric acid molarity (or 1.3 × stoichiometric acid molarity in the case of H_2SO_4, see footnote 2) can be substituted for $[H^+.mH_2O]$, and supposing further that the less hydrated (and hence more reactive) species $H^+.(m-n)H_2O$ is the one that mainly participates in steps [2] and [3], rate equation 4 becomes

$$[8] \qquad \frac{d[ClO_2]}{dt} = \frac{2k_2k_3K^4[H^+.mH_2O]^4[Cl^-]^2[ClO_3^-]^2}{k_2'[Cl_2]a_w^{(3m+n+1)} + k_3K[H^+.mH_2O][ClO_3^-]a_w^{3n}}$$

Rate equation 8 is qualitatively consistent with the experimental order change with respect to chlorate from 2 at low acidity towards unity at high acidity, as well as the differential (with respect to acidity) inhibiting effect of chlorine.

At high acidity (where a_w is relatively small, $[H^+.mH_2O]$ is relatively large) the first term in the denominator of rate equation 8 may be small compared to the second term, as shown by the approximately first order in chlorate and reduced chlorine inhibiting effect. Thus at high acidity the reaction rate would depend on $[H^+.mH_2O]^3$ (*i.e.* the stoichiometric acid concentration to the 3rd power) as well as on a_w^{-3n}.

Similar considerations suggest that at low acidity (where a_w is relatively large, $[H^+.mH_2O]$ is relatively small) the second term in the denominator may be small compared to the first term, as shown by the approximately second order in chlorate and enhanced chlorine inhibiting effect. Thus at low acidity the reaction rate would depend on $[H^+.mH_2O]^4$ (*i.e.* the stoichiometric acid concentration to the 4th power) as well as on $a_w^{-(3m+n+1)}$.

A rigorously constant order with respect to stoichiometric concentration would not be expected from rate equation 8 for an extended experimental acid concentration range, since there would be an increasing contribution of the "ClO_3^-" or right hand side term in the denominator of [8] as the acidity increased. In fact, the points in Figs. 5, 6, and 8 appear to lie on curves showing slight slope increases with increasing acidity.

The rate data shown in Figs. 5, 6, and 8 can be correlated by single straight lines obtained by least squares. The sums of the squares of the deviations from these straight lines, together with the ranges of their slopes for a 95% degree of confidence, and linear correlation coefficients are given in Table 1. However, a consideration of the observation of increasing slope (or order) with increasing acidity suggests that a better fit might be obtained with a two straight line correlation.

This was achieved by calculating the sum of the squares of the deviations for all possible combinations of two straight lines and choosing as the best combination the one giving the least overall sum of the squares of the deviations.

These optimum combinations are also given in

$$[8a] \qquad \begin{pmatrix}\text{order}\\ \text{high acidity}\end{pmatrix} = \frac{\log \left[\frac{(M_{acid})_2}{(M_{acid})_1}\right]^3 \left[\frac{a_{w_1}}{a_{w_2}}\right]^{3n}}{\log \frac{(M_{acid})_2}{(M_{acid})_1}}$$

Table 1 (and plotted in Figs. 5, 6, and 8) and show appreciably smaller sums of squares of deviations than the corresponding single straight lines.

Although the direct verification of rate-expression [8] with respect to acidity changes is not feasible at this stage, it is possible to develop two approximate limiting forms, valid at high and low acidity, respectively, which can yield calculated values of the order with respect to stoichiometric H_2SO_4 or $HClO_4$.

At high acidity, when the right or "chlorate side" of the denominator of [8] predominates over the left or "chlorine side" (as indicated by the experimental order with respect to chlorate tending to unity and the reduced inhibiting effect of chlorine), a repeated application of [8] at two acidities, neglecting the Cl_2 side relative to the chlorate side of the denominator, will yield a calculated order with respect to stoichiometric acid between the two acidities.

Similarly at low acidities, neglecting the chlorate side relative to the chlorine side of the denominator of [8] (as indicated by the experimental order with respect to chlorate tending towards 2 and the enhanced inhibiting effect of chlorine), limiting order expression [8*b*] is obtained

$$[8b] \qquad \begin{pmatrix}\text{order}\\ \text{low acidity}\end{pmatrix} = \frac{\log \left[\frac{(M_{acid})_2}{(M_{acid})_1}\right]^4 \left[\frac{a_{w_1}}{a_{w_2}}\right]^{3m+n+1}}{\log \frac{(M_{acid})_2}{(M_{acid})_1}}$$

For eqs. 8*a* and 8*b* to be used to calculate orders (for different assumed values of n and n and m, respectively) for comparison with those experimentally determined, the latter have to be obtained from the rate data determined with $[ClO_3^-]$ and $[Cl^-]$ low enough relative to the acid concentration for the approximation $a_{w(\text{pure aqueous acid solution})} \simeq a_{w(\text{reacting solution})}$ to be valid.[3] This is probably so for the data of Fig. 6, where $M_{NaClO_3} = 0.096$ and $M_{NaCl} = 0.004\ M$ in $HClO_4$ of concentration 3.00 to 5.80 M, since by far the greatest contributor to the lowering of a_w from 1.00 to the actual value will be the 3.00 (or more) M acid compared to the 0.100 M total salt concentration. The cationic or Na^+ hydration is approximately half that of the proton (4), and this will probably lessen even further the dehydrating contribution of the salts relative to that of the acid, on the assumption that cationic hydration is relatively more important than anionic hydration.

[3]More accurately, it is the ratio of $(a_{w_1}/a_{w_2})_{(\text{pure aqueous acid solution})} \simeq (a_{w_1}/a_{w_2})_{(\text{reacting solution})}$ that is involved, and this for fairly close values of a_{w_1} and a_{w_2}, see Tables 2 and 3.

TABLE 2. Values of the order calculated from expression 8*a* at high acidity

Acid	n	Calculated order
$HClO_4$*	2	11.5
	3	15.7
	4	19.9
	5	24.1
H_2SO_4†	2	10.9
	3	14.8
	4	18.7
	5	22.7

*Figure 6; $M_1 = 4.81$, $M_2 = 5.80$; $a_{w1} = 0.630$, $a_{w2} = 0.484$; experimental order (two straight lines from Table 1) = 12.91 ± 0.28.
†Figure 8; $M_1 = 5.30$, $M_2 = 6.07$; $a_{w1} = 0.565$, $a_{w2} = 0.474$; experimental order (two straight lines from Table 1) = 13.44 ± 0.82.

Similar considerations apply to the data of Fig. 8, *i.e.* 0.100 M $NaClO_3$ and 0.005 M NaCl for a 3–6.1 M range of $[H_2SO_4]$, which is equivalent to a $3 \times 1.3 - 6.1 \times 1.3$ M range in H^+ (see footnote 2). Clearly the data of Fig. 5, where $NaClO_3$ was 0.500 M and NaCl was 0.100 M, are not suitable for comparisons of calculated and experimental orders, and are not included in Tables 2 and 3. However, the orders

Can. J. Chem. Downloaded from www.nrcresearchpress.com by 210.87.254.105 on 09/05/12
For personal use only.

TABLE 3. Values of the order calculated from expression 8*b* at low acidity

		Order		
		n =		
Acid	*m*	3	4	5
$HClO_4$*	3	9.3	—	—
	4	10.2	10.6	—
	5	11.7	12.1	12.5
H_2SO_4†	3	9.7	—	—
	4	11.0	11.4	—
	5	12.3	12.7	13.2

*Figure 6; $M_1 = 3.00$, $M_2 = 3.52$; $a_{w1} = 0.828$, $a_{w2} = 0.777$; experimental order (two straight lines) from Table 1 = 11.42 ± 1.55.
†Figure 8; $M_1 = 3.00$, $M_2 = 3.75$; $a_{w1} = 0.824$, $a_{w2} = 0.742$; experimental order (two straight lines) from Table 1 = 10.67 ± 0.44.

obtained in Table 1 for the data of Fig. 5 afford some back-handed justification for the

$$a_{w\ (\text{pure aqueous acid solution})} = a_{w\ (\text{reacting solution})}$$

assumption. The "2-slope analyses" for the data of Fig. 5 and Fig. 6 give results in fairly close agreement, even though the ratio of acid to salt is much lower for the data of Fig. 5. The difference between 0.600 *M* and 0.100 *M* total salt concentration is much greater than that between the 0.1 *M* total salt for Fig. 6 and the ideal zero total salt concentration which would ensure a_w equality.

Values of a_w (12, 13) for the pure acid–water solutions have accordingly been used for Tables 2 and 3 which give a comparison of experimental orders (from Table 1) and those calculated using order expressions 8*a* and 8*b*.

Table 2 compares the experimental order at higher acidity as obtained from Table 1 with that calculated by eq. 8*a* using different values of *n*. Too large an acidity interval cannot be taken for the order calculation, since order expression 8*a* would become less valid as the $[Cl_2]$ term in the denominator of [8] becomes increasingly important as the acidity decreases. On the other hand, too small an acidity range cannot be taken since a reasonably large difference in a_w is required for a meaningful order calculation. Accordingly ranges a_{w_1} to $a_{w_2} = 0.630$ to 0.484 and 0.565 to 0.492 were chosen, respectively, for the $HClO_4$- and H_2SO_4-order calculations, each a_w range corresponding to one half the experimental a_w range from Table 1. The higher a_w's of the ranges correspond to 4.81 *M* $HClO_4$ and 5.30 *M* H_2SO_4 where the order with respect to chlorate is close to 1.1–1.2 (see Figs. 3, 4 and refs. 2, 3), indicating only slight Cl_2-term interference.

Order values calculated via expression 8*a* can be shown (Appendix 2) to be larger than the experimental order. Thus the results in Table 2 indicate that $n > 2$; that values of $n \geqslant 3$ are consistent with experiment, and that values of *n* much larger than 3 would appear to be increasingly improbable.

The acceptance of Lister's comment[1] on the relative improbability of the existence of the bare proton (even as an intermediate) in moderately concentrated acid solutions suggests that the probable reacting intermediate is H_3O^+; thus $m - n = 1$ and hence $m = 4$.

Table 3 compares experimental and calculated orders for different values of *n* and *m* for the lower acidity ranges. Calculated orders were obtained via expression 8*b* and half the experimental a_w ranges of Table 1. The model discrimination is not comparable to that of Table 2 because of the smaller a_w ranges on the one hand (larger a_w ranges would cause more uncertainty in the application of [8*b*] due to the increasing ClO_3^- term contribution), and larger experimental uncertainties on the other. The experimental uncertainties at the lower acidity are due to the low $[ClO_3^-]$ and $[Cl^-]$ imposed by the $a_{w(\text{reacting solution})} \simeq a_{w(\text{pure aqueous acid})}$ restraint. The results of Fig. 5 show better precision but the water activity approximation is less valid.

Table 3 shows that the lower acidity results for both acids are at least not inconsistent with the model $m = 4$, $n = 3$ suggested by the calculations of Table 2, and also confirms the coarser approach previously used (4).

Both hydrated species in the postulated equilibrium

$$[9] \qquad H_9O_4^+ \rightleftarrows H_3O^+ + 3H_2O$$

have previously been proposed (15). Although it would appear over-optimistic to infer that the tetra and mono hydrated proton species are the only ones present, it seems reasonable to conclude that equilibrium [9] treated semi-ideally can be of use in correlating the behavior of systems in moderately concentrated acid solutions when the a_w are known or can be approximated.

Can. J. Chem. Downloaded from www.nrcresearchpress.com by 210.87.254.105 on 09/05/12
For personal use only.

Can. J. Chem. Downloaded from www.nrcresearchpress.com by 210.87.254.105 on 09/05/12
For personal use only.

Verification

Rate equation 8 can be inverted to give

$$\frac{1}{\frac{d[ClO_2]}{dt}} = \frac{1}{r} = \frac{k_2'}{2k_2k_3K^4}\,\frac{a_w^{3m+n+1}}{M^4[Cl^-]^2[ClO_3^-]^2}\,[Cl_2] + \frac{a_w^{3n}}{2k_2K^3M^3[Cl^-]^2[ClO_3^-]}$$

where M is the stoichiometric acid molarity (for $HClO_4$).

For the low conversion experimental conditions of Fig. 7, all terms other than $[Cl_2]$ (and $[ClO_2]$) can be considered constant and equal to their original values at the start of the reaction. Using the relation $[ClO_2] = \alpha[Cl_2]$ established for H_2SO_4 (3), and taking $\alpha = 1.9$,

$$[8c] \qquad \frac{1}{r} = \frac{k_2'}{2k_2k_3K_4}\,\frac{a_w^{3m+n+1}[ClO_2]}{M^4[Cl^-]^2[ClO_3^-]^2 1.9} + \frac{a_w^{3n}}{2k_2K^3M^3[Cl^-]^2[ClO_3^-]}$$

which is the linear form

$$\frac{1}{r} = b'[ClO_2] + c$$

obtained in Fig. 7.

Comparing the theoretical and experimental inverse rate expressions yields that $b'_{(5.8\,M\,HClO_4)}$, the experimental slope from Fig. 7 for the results at 5.8 M $HClO_4$,

$$b'_{(5.8\,M\,HClO_4)} = 3.78 \times 10^7 = \frac{k_2' a_w^{3m+n+1}}{2k_2k_3K_4M^4[Cl^-]^2[ClO_3^-]^2 \times 1.9}$$

and intercept c

$$c_{(5.8\,M\,HClO_4)} = 1.21 \times 10^4 = \frac{a_w^{3n}}{2k_2K^3M^3[Cl^-]^2[ClO_3^-]}$$

Substituting the numerical values of $a_w = 0.484$ (14) (the water activity at 5.8 M $HClO_4$), $M = 5.8$, $[Cl^-] = 0.004\,M$, and $[ClO_3^-] = 0.096\,M$, corresponding to the experimental conditions for the results at 5.8 M $HClO_4$ reported in Fig. 7, the expressions for $b'_{(5.8\,M\,HClO_4)}$ and $c_{(5.8\,M\,HClO_4)}$ can be solved for $k_2'/2k_2k_3K$ and $1/2k_2K^3$ for different ascribed values of n and m. The values calculated for these constants are given in Table 4 for different combinations of values of n and m.

TABLE 4. Calculations of the grouped constants from the rate data at 5.8 M $HClO_4$ in Fig. 7

	$\frac{k_2'}{2k_2k_3K^4} \times 10^{-9}$	$\frac{1}{2k_2K^3} \times 10^{-3}$
$m = 3, n = 3$	0.159	2.46
$m = 4, n = 3$	1.42	2.46
$m = 4, n = 4$	2.64	22.4
$m = 5, n = 3$	12.1	2.46
$m = 5, n = 4$	25.2	22.4

The values of $k_2'/2k_2k_3K^4$ and $1/2k_2K^3$ in Table 4 can now be used to calculate otherwise *ab initio* reciprocal rates from eq. 8*c* for different combinations of values of n and m.

Reciprocal rates at different values of ClO_2 are available at 3.9 M $HClO_4$ (Fig. 7). These are compared to different values of calculated reciprocal rates in Table 5.

The best integral combination of n and m is verified to be $m = 4$, $n = 3$, although slightly higher values of both parameters would improve the agreement.

Finally, the two terms in the denominator of [8] can be compared at different acidities for a given $[Cl_2] = 10^{-5}$ M/l using the values of $k_2'/2k_2k_3K$ and $1/2k_2K^3$ of Table 4 for model $m = 4$, $n = 3$. This is done in Table 6 where the value of $R = k_2'a_w^{16}[Cl_2]/k_3KM[ClO_3^-]a_w^9$ is compared at high (5.8 M $HClO_4$), intermediate (3.9 M $HClO_4$), and low (2.5 M $HClO_4$) acidities from the point of view of the differential inhibiting effect of chlorine. Table 6 verifies that the model $m = 4$, $n = 3$ conforms with the observation that the inhibiting effect of chlorine is high at low acidities, and conversely.

TABLE 5. Comparison of calculated and experimental values of $1/r$ at 3.9 M $HClO_4$

		$(1/r)_{calcd.} \times 10^{-6}$ (1 s/M)						
				% error for model*		% error for model*		
$[ClO_2] \times 10^6$ (M/l)	$(1/r)_{exp.} \times 10^{-6}$ (1 s/M)	$m = 3$ $n = 3$	$m = 4$ $n = 3$	$m = 4$ $n = 3$	$m = 4$ $n = 4$	$m = 4$ $n = 4$	$m = 5$ $n = 3$	$m = 5$ $n = 4$
0	2.88	1.43	1.43	50	5.42	88	1.43	5.42
11.1	4.45	2.05	2.99	33	7.68	72	7.41	14.2
15.4	5.25	2.29	3.60	31	8.65	65	9.70	17.6
19.2	6.13	2.50	4.10	33	9.32	52	11.7	20.6
21.6	6.36	2.64	4.47	30	9.82	54	13.0	22.6
26.0	6.93	2.88	5.08	27	10.7	54	15.3	26.0

*% error refers to $\{|(1/r)_{calcd.} - (1/r)_{exp.}|/(1/r)_{exp.}\} \times 100$.

TABLE 6. Comparison of the terms in the denominator of eq. 8 for $[Cl_2] = 10^{-5}$ M/l

$HClO_4$ (M)	R
5.8	6.46×10^{-2}
3.9	1.82
2.5	8.95

Appendix 1

On the Activity Coefficients of the more Hydrated and less Hydrated Species

$$H^+.4H_2O \overset{K_5}{\rightleftharpoons} H^+ + 4H_2O$$

K_5, the equilibrium constant in mole fraction units, is given by

$$K_5 = \frac{f_{H^+} x_{H^+} a_w^4}{f_{H^+.4H_2O} x_{H^+.4H_2O}}$$

$$= \frac{f_{H^+} \frac{n_{H^+}}{n_t} a_w^4}{f_{H^+.4H_2O} \frac{n_{H^+.4H_2O}}{n_t}}$$

$$= \frac{f_{H^+}}{f_{H^+.4H_2O}} \frac{n_{H^+}}{n_{H^+.4H_2O}} a_w^4$$

where the f's are the activity coefficients on the mole fraction scale, the x's are the mole fractions, a_w is the water activity of the solution, n_{H^+}, $n_{H^+.4H_2O}$, and n_t are the number of moles of H^+, $H^+.4H_2O$, and the total number of moles present, respectively.

The "maximum" assumption would be that $f_{H^+} \simeq f_{H^+.4H_2O}$; since non-idealities due to Debye–Hückel effects, overall hydration effects and change of water structure effects would already be accounted for in the a_w term, and individual ionic hydration effects would be accounted for by equilibrium [5] itself.

Alternatively, the less radical assumption that $f_{H^+}/f_{H^+.4H_2O} = p$, where p is independent of concentration, will give the expression

$$K_5' = \frac{K_5}{p} = \frac{n_{H^+}}{n_{H^+.4H_2O}} a_w^4$$

whence for 1 l of solution

$$K_5 \text{ or } K_5' = \frac{\text{moles (per litre) of } H^+}{\text{moles (per litre) of } H^+.4H_2O} \times a_w^4$$

and thus

$$[H^+] = K_5 \text{ (or } K_5') \frac{[H^+.4H_2O]}{a_w^4}$$

Appendix 2

On the Comparison Between Calculated and Experimental Orders in Table 2

Let the rate of reaction 1 (at an acid concentration sufficiently high for eq. 8 to hold with no appreciable Cl_2 term contribution) be represented by point *2* in Fig. 9 (a Van't Hoff plot). Let the experimental rate at some lower acidity M_1 be represented by point *1*. The experimental order will be given by the slope of the line *1–2* in Fig. 9.

The rate at acidity M_1 can be calculated using the "no-Cl_2" form of rate expression 8;

$$r_{calcd. \text{ at } M_1} = \frac{2k_2K^3[Cl^-]^2[ClO_3^-]M^3}{a_w^{3n}}$$

Now

$$r_{exp. \text{ at } M_1} = \frac{2k_2K^3[Cl^-]^2[ClO_3^-]M^{3+\delta}}{a_w^{3n+\varepsilon}}$$

Can. J. Chem. Downloaded from www.nrcresearchpress.com by 210.87.254.105 on 09/05/12
For personal use only.

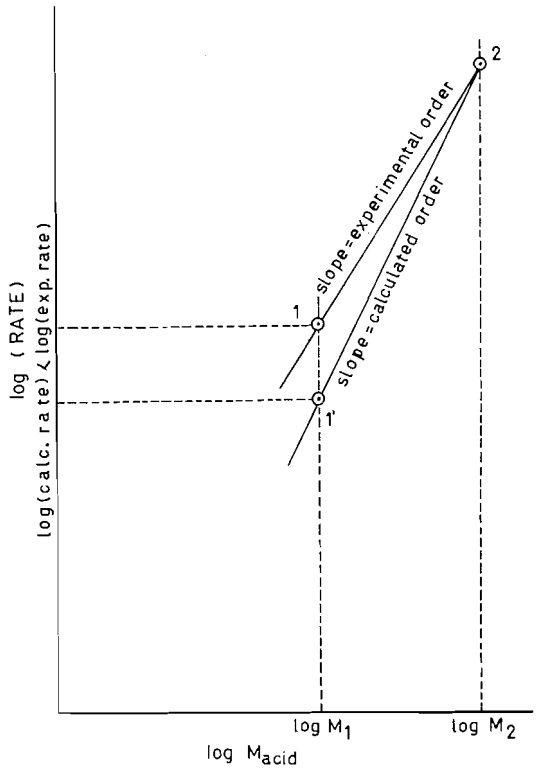

FIG. 9. Comparison of calculated and experimental orders at high acidity.

where δ and ε are positive numbers representing lumped corrections due to the contribution of the Cl_2 term in the denominator of [8]; since $M > 1$ and $a_w < 1$, the numerator in $r_{exp.} >$ numerator in $r_{calcd.}$ and the denominator in $r_{exp.} <$ denominator in $r_{calcd.}$, leading to the result that $r_{exp.} > r_{calcd.}$.

Thus the point *1'* in Fig. 9 representing the calculated rate at M_1 will be lower than the experimental rate represented by point *1*.

Hence the slope of *1'–2* will be greater than the slope of *1–2*, *i.e.* the calculated order will be higher than that determined experimentally.

The authors wish to thank Professor M. Lister for his comment on $H^+.H_2O$ and H^+, Mr. P. Krick for carrying out the experiments on the stoichiometry, and the National Research Council of Canada for operating grant A-4520.

1. W. H. RAPSON. Can. J. Chem. Eng. **36**, 262 (1958).
2. F. LENZI and W. H. RAPSON. Pulp Paper Mag. Can. **63**, 9T-442 (1962).
3. C. C. HONG, F. LENZI, and W. H. RAPSON. Can. J. Chem. Eng. **45**, 349 (1967).
4. F. LENZI and W. H. RAPSON. Can. J. Chem. **46**, 979, 3615 (1968).
5. T. F. YOUNG. Rec. Chem. Prog. **12**, 81 (1951).
6. J. W. AKITT, A. K. COVINGTON, J. G. FREEMAN, and T. H. LILLEY. Trans. Faraday Soc. **65**, 2701 (1969).
7. F. LENZI. Ph.D. Thesis. Department of Chemical Engineering and Applied Chemistry, University of Toronto, Toronto, Ontario. 1965.
8. F. P. TREADWELL. Chimie Analytique, Tome II, Dunod, Paris. 1925. p. 424.
9. F. LENZI. M.A.Sc. Thesis. University of Toronto, Toronto, Ontario. 1956.
10. K. LUTHER and F. MACDOUGALL. Z. phys. Chem. **62**, 199 (1908).
11. E. B. ROBERTSON and H. B. DUNFORD. Can. J. Chem. **86**, 5080 (1964).
12. R. A. ROBINSON and O. J. BAKER. Trans. Roy. Soc. New Zealand, **76**, 250 (1946).
13. K. H. BASCOMBE and R. P. BELL. Discuss. Faraday Soc. **24**, 158 (1957).
14. S. SHANKMAN and A. R. GORDON. J. Am. Chem. Soc. **61**, 2370 (1939).
15. H. L. CLEVER. J. Chem. Educ. **40**, 637 (1963).

Can. J. Chem. Downloaded from www.nrcresearchpress.com by 210.87.254.105 on 09/05/12
For personal use only.

Can. J. Chem. Downloaded from www.nrcresearchpress.com by 210.87.254.42 on 09/05/12
For personal use only.

The Influence of Heteroatom-substituted Methyl Groups and of Vinyl Groups (CR_2=CR—) Attached to C-2 of 1,3-Dioxolanes on the Ease and Direction of Hydrogenolysis of the 1,3-Dioxolanes by AlH_2Cl, AlH_3, or $LiAlH_4$[1]

H. A. Davis and R. K. Brown

Department of Chemistry, University of Alberta, Edmonton, Alberta

Received March 26, 1971

Heteroatom substituents on the methyl group of 2-methyl-1,3-dioxolane retard the rate of hydrogenolysis by AlH_2Cl of ether solutions of the 2-substituted 1,3-dioxolanes. The effectiveness of the heteroatoms in decreasing the ease of hydrogenolysis is H < S < O < Br < NR_2. This retardation is thought to be due to the destabilization of the transition state leading to the intermediate oxocarbonium ion, caused by the electronegativity of the heteroatom and/or coordination of some of the AlH_2Cl with the heteroatom.

AlH_2Cl or AlH_3 in diethyl ether at room temperature reduces 2-vinyl- or 2-[alkyl (or aryl) substituted vinyl]-1,3-dioxolanes to only the β,γ-unsaturated alkyl β-hydroxyethyl ether, the product expected from hydride ion addition to C-2 of the 1,3-dioxolane. The ease of hydrogenolysis increases with increasing alkyl (or aryl) substitution on the 2-vinyl group.

$LiAlH_4$ in diethyl ether at room temperature, or in di-*n*-propyl ether or 1,2-dimethoxyethane (DME) at room temperature or reflux temperature, reduces 2-vinyl-1,3-dioxolane only to α-propenyl β-hydroxyethyl ether. This product is the result of hydride addition to the β-carbon of the vinyl group accompanied by ring opening and double bond migration. Alkyl substituents attached to the vinyl group of 2-vinyl-1,3-dioxolane markedly retard the rate of hydrogenolysis by $LiAlH_4$ in the dialkyl ethers at room temperature, but at the reflux temperature (90°) of di-*n*-propyl ether the 2-alkylated vinyl-1,3-dioxolanes are hydrogenolyzed, but only to the β,γ-unsaturated alkyl β-hydroxyethyl ether. In refluxing DME (80°) the 2-alkylated vinyl-1,3-dioxolanes give primarily, if not exclusively, the α,β-unsaturated alkyl β-hydroxyethyl ether. A rationale is suggested to account for these results.

$LiAlH_4$ in diethyl ether reduces 2-styryl-1,3-dioxolane only to β-phenylethyl-1,3-dioxolane, by hydride addition to the olefinic carbon β to the phenyl group.

Les substituants hétéroatomiques situés sur le groupe méthyle du méthyl-2 dioxolane-1,3 ralentissent la vitesse d'hydrogénolyse par AlH_2Cl des solutions éthérées des dioxolanes-1,3 substitués en 2. L'efficacité des hétéroatomes dans la diminution de la facilité d'hydrogénolyse est H < S < O < Br < NR_2. On pense que ce ralentissement est du à la déstabilisation de l'état de transition qui conduit à l'ion oxocarbonium intermédiaire à cause de l'électronégativité de l'hétéroatome et/ou de la coordination d'une certaine quantité de AlH_2Cl avec l'hétéroatome.

AlH_2Cl ou AlH_3 dans l'éther diéthylique réduit quantitativement à la température ordinaire les vinyl-2 ou les vinyl-2 [substitués par un groupe alkyle (ou aryle)] dioxolanes-1,3 en alkyl β,γ-insaturé β-hydroxyéthyl éther qui est le produit attendu lors de l'addition d'un ion hydrure sur le C-2 d'un dioxolane-1,3. La facilité de l'hydrogénolyse croît avec l'augmentation de la substitution par un groupe alkyle (ou aryle) sur le groupe vinyle en position 2.

$LiAlH_4$ dans l'éther diéthylique à la température ordinaire, ou dans l'éther di-*n*-propylique ou dans le diméthoxy-1,2 éthane (DME) à la température ordinaire ou au reflux du solvant, réduit le vinyl-2 dioxolane-1,3 quantitativement en α-propenyl β-hydroxyéthyl éther, le produit se forme par suite de l'addition de l'hydrure sur le carbon en β du groupe vinyle suivie d'une ouverture de cycle et d'une migration de la double liaison. Les substituants alkylés sur le groupe vinyle des vinyl-2 dioxolanes-1,3 ralentissent de façon notable la vitesse d'hydrogénolyse par $LiAlH_4$ dans les dialkyl éthers à la température ordinaire mais, à la température de reflux (90°) de l'éther di-*n*-propylique, les vinyl-2 [substitués par un groupe alkyle] dioxolanes-1,3 subissent l'hydrogénolyse pour donner uniquement l'alkyl β,γ-insaturé β-hydroxyéthyl éther. Au reflux du DME (80°), les vinyl-2 [substitués par un groupe alkyle] dioxolanes-1,3 donnent d'abord, sinon exclusivement, l'alkyl α,β-insaturé β-hydroxyéthyl éther. On propose un raisonnement pour rendre compte de ces résultats.

$LiAlH_4$ dans l'éther diéthylique réduit le styryl-2 dioxolane-1,3 seulement en β-phényléthyl dioxolane-1,3 par addition de l'hydrure sur le carbone olifinique en β du groupe phényle.

Canadian Journal of Chemistry, 49, 2563 (1971)

---

[1]From the thesis of H. A. Davis submitted to the Faculty of Graduate Studies, University of Alberta, Edmonton, Alberta, as part of the requirements for the Ph.D. degree, 1970.

Can. J. Chem. Downloaded from www.nrcresearchpress.com by 210.87.254.42 on 09/05/12
For personal use only.

Introduction

It has been shown that substituents on C-2 of the 1,3-dioxolane ring have a much greater effect on the rate of reductive cleavage by "mixed hydride" reagents ($LiAlH_4$ + $AlCl_3$) than do the same substituents situated on any other ring carbon atom (1). Electron donor substituents (R = methyl or phenyl in Scheme 1) attached to C-2 accelerate the cleavage by stabilization of the transition state leading to the formation of the intermediate oxocarbonium ion, the step which is considered to be rate determining (1–4), whereas electron-withdrawing groups (chloromethyl, dichloromethyl) attached to C-2 retard the reductive cleavage.

This paper describes the effect of a number of C-2 substituents which could participate in the stabilization of the transition state leading to the formation of such an oxocarbonium ion intermediate, either by electromeric or anchimeric assistance and thus accelerate the rate of hydrogenolysis of the 1,3-dioxolane ring.

Results and Discussion

Hydrogenolysis with AlH_2Cl or AlH_3 was done by first preparing the reducing species in ether solution by mixture of the appropriate amounts of $AlCl_3$ and $LiAlH_4$ (5) followed by the addition of the 1,3-dioxolane. Competitive reductions were made by the addition of an equimolar mixture of the two 1,3-dioxolanes to an ether solution of AlH_2Cl or AlH_3 sufficient to reduce only half of the mixture of dioxolanes. Recoveries of starting material and products were generally 80–95%. Reduction products were stable under the conditions of the reaction as had been found previously (1). Analyses of the products were made by comparison of the g.l.c. retention times with those of known samples, or by isolation and characterization of the product(s) whenever there was any doubt as to identity. The relative peak areas in the g.l.c. were used directly as quantitative measures of the products since it had been found that these differed in detector response at the most by only 10%, and in the great majority of cases by less than 5%. This practice was considered reasonable since the differences in relative amounts of products obtained were generally much greater than 10%. For those few cases in which the differences in proportion of products were small and considered to be significant, the difference in detector response was taken into consideration.

Hydrogenolysis with AlH_2Cl or AlH_3

(i) 2-Methyl-1,3-dioxolanes Containing a Heteroatom Attached to the C-2 Methyl Group

It is known that certain atoms, suitably situated in a molecule, can enhance the rate of a reaction by anchimeric assistance in the rate controlling step (6, 7). In order to determine if this phenomenon could occur in the hydrogenolysis of acetals, several 2-methyl-1,3-dioxolanes were prepared, containing a heteroatom directly attached to the C-2 methyl group. The heteroatoms chosen were O, S, Br, and N, atoms considered to be capable of providing anchimeric assistance and also able to survive under the reaction conditions. These α-substituted 1,3-dioxolanes were hydrogenolized with AlH_2Cl in ether solution at room temperature. The results are shown in Table 1.

It is seen that the replacement of a hydrogen atom on the methyl group of 2-methyl-1,3-dioxolane by a heteroatom *retards* the hydrogenolysis, the order of decreasing rate of reaction

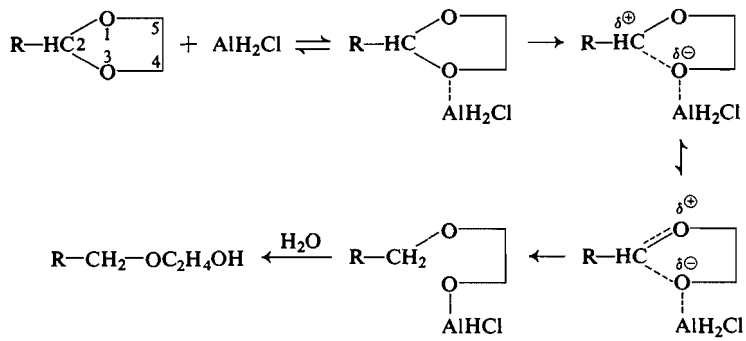

SCHEME 1

TABLE 1. Hydrogenolysis by AlH_2Cl in ether of some 2-methyl-1,3-dioxolanes containing a heteroatom attached to the C-2 methyl group

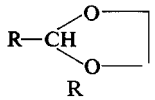

R	Time (h)	Extent of reduction (%)	Total recovery (%)	Reduction product(s)
CH_3—	0.5	100*	90	$C_2H_5OC_2H_4OH$
CH_3—SCH_2—	0.5	45	90	$CH_3SC_2H_4OC_2H_4OH$
CH_3—O—CH_2—	24	70	90	$CH_3OC_2H_4OC_2H_4OH$
—$BrCH_2$—	24	17	90	$BrC_2H_4OC_2H_4OH$
$(CH_3)_2NCH_2$—	24	0	30†	

*Complete reduction occurred well within 30 min.
†This recovery could not be improved.

being H > S > O > Br > NR_2. This rate reduction could be due to the following causes either separately or in combination. (*a*) The electronegativity of the heteroatom decreases the ability of the methyl group to stabilize the transition state leading to the intermediate oxocarbonium ion. (*b*) The association of some of the reducing agent (a Lewis acid) with the heteroatom, thus increasing the electron-withdrawing power of the heteroatom. (*c*) The association suggested in (*b*) would decrease the effective concentration of the AlH_2Cl. A similar effect due to O and S substituents on the rate of hydrolysis of diethylacetals of substituted acetaldehyde has been noted by Speck *et al.* (8). They found the rate of hydrolysis of the diethylacetals of the following aldehydes to be acetaldehyde ≫ methylthioacetaldehyde > methoxyacetaldehyde, and attributed this to the electronegativity of the substituent which caused destabilization of the intermediate carbonium ion. The greater retardation for the methoxy- compared to the methylthioacetaldehyde diethylacetal was considered to be due to the greater degree of protonation of the oxygen analogue. The apparently greater degree of association of protons or of Lewis acids with the heteroatom of oxygen ethers compared to sulfur ethers has been noted previously (9 and references therein). The results shown in Table 1 are corroborated by the competitive hydrogenolysis of these compounds with a limited amount of AlH_2Cl. These are shown in Table 2.

TABLE 2. Relative rates of room temperature hydrogenolysis by AlH_2Cl in ether of some 2-methyl-1,3-dioxolanes containing a heteroatom attached to the C-2 methyl group

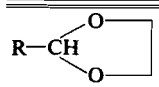

R	Relative rate
CH_3—	1.
CH_3SCH_2—	0.15
CH_3OCH_2—	0.02
$BrCH_2$—	<0.02

The data in Tables 1 and 2 indicate that anchimeric assistance by formation of the cyclic "onium" species (structure **A**) is insignificant and actually may not occur. If it does, it is well submerged by effects resulting in retardation of the reaction.

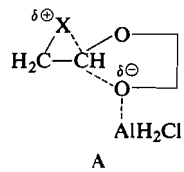

A

(ii) 1,3-Dioxolanes Containing a Vinyl or Phenyl Group Attached to C-2

Hydrogenolysis of 2-phenyl-1,3-dioxolane with a 1:1 molar ratio of $LiAlH_4$ and $AlCl_3$ has been reported to proceed more rapidly than does similar reduction of 2-methyl-1,3-dioxolane (1), presumably because of the greater degree of stabilization of the intermediate oxocarbonium ion by the phenyl substituent than by the methyl group at C-2. We were interested in determining whether similar stabilization would be offered by the double bond of α,β-unsaturated aldehyde ethyleneacetals (2-vinyl- or 2-substituted vinyl-1,3-dioxolanes). Accordingly a number of such acetals in ether were hydrogenolyzed at room temperature first separately with AlH_2Cl to determine the product(s) which could be obtained, and then competitively with a limited amount of AlH_3 to discover the relative ease of hydrogenoly-

Can. J. Chem. Downloaded from www.nrcresearchpress.com by 210.87.254.42 on 09/05/12
For personal use only.

TABLE 3. Hydrogenolysis of ether solutions of some 2-vinyl and 2-aryl-1,3-dioxolanes with AlH_2Cl*

R	Total recovery (%)	Reduction product(s)
CH_2=CH—	80	CH_2=$CHCH_2OC_2H_4OH$
CH_3CH=CH—	85	CH_3CH=CH—$CH_2OC_2H_4OH$
CH_2=$C(CH_3)$—	85	CH_2=$C(CH_3)CH_2OC_2H_4OH$
C_2H_5CH=CH—	90	C_2H_5CH=$CHCH_2OC_2H_4OH$
$(CH_3)_2C$=CH—	90	$(CH_3)_2C$=$CHCH_2OC_2H_4OH$
C_6H_5—	90	$C_6H_5CH_2OC_2H_4OH$
p-$CH_3OC_6H_4$—	90	*p*-$CH_3OC_6H_4CH_2OC_2H_4OH$
o-$CH_3OC_6H_4$—	90	*o*-$CH_3OC_6H_4CH_2OC_2H_4OH$
C_6H_5CH=CH—	90	C_6H_5CH=$CHCH_2OC_2H_4OH$

*All reactions were done at 25° for 30 min, and all were complete within this time.

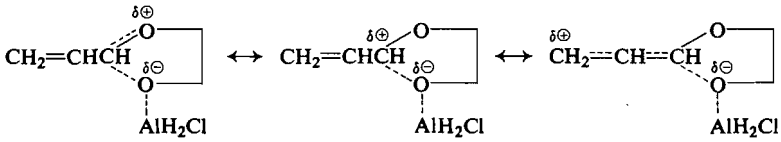

SCHEME 2

sis. The reason for using AlH_3 for the competitive reactions was that the rate of reduction is slower with AlH_3 than with AlH_2Cl (5) and this *might* permit selectivity in rates of reduction to be better perceived. Furthermore it had already been established both in the present work and in that reported previously (5), that the same products are obtained from hydrogenolysis of 1,3-dioxolanes by AlH_3 as by AlH_2Cl. The results are shown in Tables 3 and 4 respectively.

The results in Tables 3 and 4 show that in each case only one and the same product is obtained, in nearly quantitative yield, using either of the two reducing agents, and that this product is the one resulting from hydride addition to the methine carbon (C-2) of the 1,3-dioxolane ring to give the β,γ-unsaturated ether. No evidence was obtained for the formation, even in small amount, of the product resulting from addition of the hydride ion to the β carbon of the vinyl substituent attached to C-2, to give the α,β-unsaturated ether resulting from double bond migration and 1,3-dioxolane ring opening. The exclusive formation of the β,γ-unsaturated ether may be due to the overwhelming predominance of the more stable carbonium ion, that stabilized by both the adjacent oxygen atoms and the allylic system (Scheme 2). The complete absence of the α,β-unsaturated ether supports the view that not only is there the marked predominance of the more stable carbonium ion resulting from considerable C—O bond stretching due to the effect of the Lewis acid, but also that hydride addition to C-2 of the ring might well occur by a four-center transition state (structure **B**).

TABLE 4. Relative rates of hydrogenolysis of ether solutions of some 2-vinyl- and 2-aryl-1,3-dioxolanes with AlH_3 at 25°*,†

R	Relative rate
CH_3—	0.025
CH_2=CH—	1.0
CH_2=$C(CH_3)$—	1.6
C_6H_5—	1.7
CH_3CH=CH—	4.0
C_2H_5CH=CH—	7.0
$(CH_3)_2C$=CH—	15.
p-$CH_3OC_6H_4$—	20.
C_6H_5CH=CH—	Very great

*Products obtained and analyzed for by g.l.c. were those shown in Table 3. No other products were detected.

†Equimolar quantities of two acetals in ether solution were treated with AlH_3, sufficient to reduce only half of these two acetals. Each competitive reaction was done at least twice.

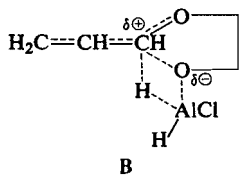

B

Can. J. Chem. Downloaded from www.nrcresearchpress.com by 210.87.254.42 on 09/05/12
For personal use only.

Can. J. Chem. Downloaded from www.nrcresearchpress.com by 210.87.254.42 on 09/05/12
For personal use only.

Hydrogenolysis with $LiAlH_4$

Acetals and ketals are reported to be stable to $LiAlH_4$ in ether solution, and this permits the protection of carbonyl groups of ketones and aldehydes during hydride reduction of other functional groups in the molecule (10). However, the addition of a Lewis acid such as $AlCl_3$ to the $LiAlH_4$ reduction system does permit the hydrogenolysis of dialkylacetals and ketals to simple ethers (11, 12) and of cyclic acetals and ketals (1,3-dioxolanes and 1,3-dioxanes) to β-hydroxyethers (1–4, 9, 13, 14). Since electron donor substituents at C-2 of the 1,3-dioxolane ring greatly increase the ease of hydrogenolysis of one of the C—O bonds (1) by "mixed hydride" ($AlCl_3$ + $LiAlH_4$) (5, 15) the possibility was explored as to whether a Lewis acid such as $AlCl_3$ was necessary for the hydrogenolysis of these more active acetals and whether $LiAlH_4$ alone in ether would be sufficient. Accordingly, several 1,3-dioxolanes containing a vinyl or aryl substituent at C-2 were hydrogenolyzed with $LiAlH_4$, first in diethyl ether at room temperature (Table 5), then in refluxing (80°) 1,2-dimethoxyethane (DME) (Table 6), and finally in refluxing (90°) di-*n*-propyl ether (Table 7).

It is seen that $LiAlH_4$ in diethyl ether at room temperature does hydrogenolyze acrolein ethyleneacetal (2-vinyl-1,3-dioxolane) slowly (32 and 76% in 24 and 48 h respectively) by ring opening and simultaneous double bond migration to form the α,β-unsaturated ether, β-hydroxyethyl α-propenyl ether (experiment 1, Table 5). In di-*n*-propyl ether, $LiAlH_4$ converted 2-vinyl-1,3-dioxolane to the same α,β-unsaturated ether to the extent of 70% in 24 h at 25°, and completely in 2 h at 90° (experiments 1*a* and *b*, Table 7). In DME, $LiAlH_4$ reduced 2-vinyl-1,3-dioxolane also to the α,β-unsaturated ether completely at 80° in 24 h, but barely at all at room temperature in 24 h. In none of these solvents was there any evidence for the formation of the alternate reduction product, the β,γ-unsaturated ether, allyl β-hydroxyethyl ether, the product from direct hydride addition to the methine carbon (C-2) of the 1,3-dioxolane ring.

The 2-vinyl-1,3-dioxolanes possessing one or more alkyl substituents attached to the vinyl moiety, failed to react at all with $LiAlH_4$ at room temperature (or at 25°) in diethyl ether (experiments 2*a–d*, Table 5) or in di-*n*-propyl ether (experiments 2*a–c*, Table 7). However at 90° in di-*n*-propyl ether they were reduced completely within 12 h but only to the β,γ-unsaturated ether, the product expected from ring cleavage and hydride ion addition to the methine carbon (experiments 3–5, Table 7). In DME at 80°, $LiAlH_4$ also hydrogenolyzed the 2-alkylvinyl-1,3-dioxolanes, though more slowly than in di-*n*-propyl ether, but the product in all but one case was primarily, if not totally, the α,β-unsaturated ether, accompanied by 0–6% of the β,γ-unsaturated ether (experiments 2–4, Table 6). The exception was β-methylcrotonaldehyde ethyleneacetal from which the proportion of the β,γ- to α,β-unsaturated ether obtained was ~2:1 (experiment 5, Table 6).

The remarkable difference in the type of product obtained from $LiAlH_4$ hydrogenolysis of these 2-alkylvinyl-1,3-dioxolanes in DME on the one hand and in the dialkyl ethers on the other, is interesting. Those obtained in the dialkyl ether (except for the product obtained from the parent compound 2-vinyl-1,3-dioxolane) are the β,γ-unsaturated ethers which must arise from C_2—O_1 bond breaking and hydride addition to C-2 (*cf.* Scheme 1) as has been observed for the hydrogenolysis of 1,3-dioxolanes by the Lewis acid species AlH_2Cl and AlH_3 (1, 5, and Table 3 of the present work). In DME, hydride ion addition occurs at the olefinic carbon atom remote from the methine carbon, with consequent, or simultaneous, cleavage of the C_2—O_1 bond of the ring and migration of the double bond to the α,β position. The similarity of the hydrogenolysis products obtained in di-*n*-propyl ether with $LiAlH_4$ to those obtained by AlH_2Cl in diethyl ether suggests the participation of a species which can associate with the oxygen atom of the 1,3-dioxolane ring and thus promote C_2—O_1 bond stretching to develop carbonium ion character at C-2 which then would lead to hydride addition at C-2.

The increase in reducing ability of $LiAlH_4$ in DME compared with that in diethyl ether has been ascribed to the greater cation solvating ability of the DME (16). The lower ability of di-*n*-propyl ether to solvate the Li cation, would thus allow $Li^{\oplus}$ to associate to a greater extent with an oxygen atom of the dioxolane. Not only would $Li^{\oplus}$ thus promote C_2—O_1 bond stretching, but the $AlH_4^{\ominus}$ ion would remain in the vicinity of the associated $Li^{\oplus}$ and thus be in a good position to transfer a hydride ion to C-2 (Scheme 3). In DME, the $Li^{\oplus}$ cation is highly solvated by the diether (structure **C**) thus decreasing the extent to which $Li^{\oplus}$ associates with the dioxolane.

Can. J. Chem. Downloaded from www.nrcresearchpress.com by 210.87.254.42 on 09/05/12
For personal use only.

TABLE 5. Hydrogenolysis of some C-2 vinyl or aryl substituted 1,3-dioxolanes with $LiAlH_4$ in diethyl ether at room temperature

Experiment no.	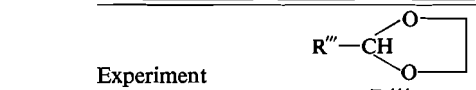	Time(h)	Extent of reduction (%)	Total recovery (%)	Reduction product(s)
1	*a* CH_2=CH—	24	32	80	CH_3CH=$CHOC_2H_4OH$
	b	48	76	80	
2	RR′C=CHR″— *a* R = CH_3, R′ = R″ = H *b* R = R′ = H, R″ = CH_3 *c* R = C_2H_5, R′ = R″ = H *d* R = R′ = CH_3, R″ = H	96	0	85	
3	*p*-$CH_3OC_6H_4$—	72	0	90	
4	*o*-$CH_3OC_6H_4$—	144	0	90	
5	C_6H_5CH=CH—	24	100	90	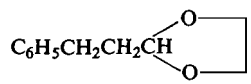
6	C_6H_5CH=CH—	24	100	90	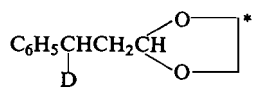 *
7	C_6H_5CH=CH—	24	100	90	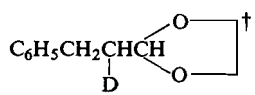 †

*Hydrogenolysis was carried out with $LiAlH_4$ as for experiment 5, but the solution was treated with a D_2O solution of sodium hydroxide to destroy the complex.
†Hydrogenolysis was carried out with $LiAlD_4$ and the solution then treated with a H_2O solution of sodium hydroxide to destroy the complex.

Can. J. Chem. Downloaded from www.nrcresearchpress.com by 210.87.254.42 on 09/05/12
For personal use only.

TABLE 6. Hydrogenolysis of some C-2 vinyl substituted 1,3-dioxolanes with $LiAlH_4$ in 1,2-dimethoxyethane at 80°

Experiment no.	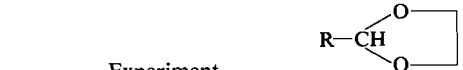 R	Time(h)	Extent of reduction (%)	Total recovery (%)	Reduction product(s)	Relative amount (%)
1	CH_2=CH—	24	100*	80	CH_2=$CHCH_2OC_2H_4OH$ CH_3CH=$CHOC_2H_4OH$	0 100
2	CH_3CH=CH—	70	70	80	CH_3CH=$CHCH_2OC_2H_4OH$ CH_3CH_2CH=$CHOC_2H_4OH$	5 95
3	CH_2=$C(CH_3)$—	70	45	80	CH_2=$C(CH_3)CH_2OC_2H_4OH$ $(CH_3)_2C$=$CHOC_2H_4OH$	0 100
4	C_2H_5CH=CH—	70	65	80	C_2H_5CH=$CHCH_2OC_2H_4OH$ $C_2H_5CH_2CH$=$CHOC_2H_4OH$	6 94
5	$(CH_3)_2C$=CH—	70	60	80	$(CH_3)_2C$=$CHCH_2OC_2H_4OH$ $(CH_3)_2CHCH$=$CHOC_2H_4OH$	65 35

*At room temperature, little reaction occurred in 24 h; only a trace of the α,β-unsaturated product was detected.

TABLE 7. Hydrogenolysis of some C-2 vinyl substituted 1,3-dioxolanes with $LiAlH_4$ in di-*n*-propyl ether at 90°*

Experiment no.	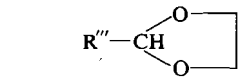 R‴	Time(h)	Extent of reduction (%)	Total recovery (%)	Reduction product(s)
1	*a* CH_2=CH—	24 (at 25°)	70	90	CH_3CH=$CHOC_2H_4OH$
	b	2	100	90	
2	RR′C=CR″—	24 (at 25°)	0	85	
	a R = CH_3, R′ = R″ = H *b* R = C_2H_5, R′ = R″ = H *c* R = R′ = CH_3, R″ = H				
3	CH_3CH=CH—	2	100	90	CH_3CH=$CHCH_2OC_2H_4OH$
4	*a* C_2H_5CH=CH—	2	50	90	C_2H_5CH=$CHCH_2OC_2H_4OH$
	b	12	100	90	
5	*a* $(CH_3)_2C$=CH—	2	80	90	$(CH_3)_2C$=$CHCH_2OC_2H_4OH$
	b	12	100	90	

*Some experiments (1*a*, 2*a*–*c*) were carried out at 25° in order to compare the results with those obtained at 90° (experiments 3–5).

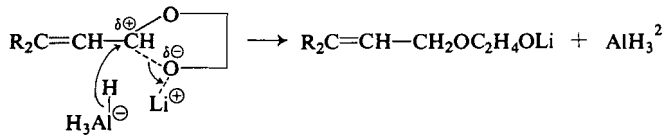

SCHEME 3

The $AlH_4^{\ominus}$ thus "liberated" cannot easily approach C-2 of the dioxolane ring because of the repulsion due to the partial negative charge on the oxygen atom(s) of the ring. The alternative position of attack by $AlH_4^{\ominus}$ is at the β carbon of

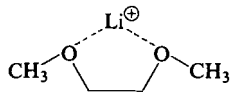

C

the vinyl group, since the latter will be polarized by the electronegative oxygen atoms of the dioxolane ring. This would lead to simultaneous double bond migration and ring cleavage to produce the α,β-unsaturated ether (Scheme 4). Alkyl groups (R) attached to the vinyl moiety would delocalize the partial positive charge developed on the vinyl group and hence attack by $AlH_4^{\ominus}$ on the vinyl moiety would be more difficult (*cf.* Table 6). *Two* alkyl groups on the β carbon of the vinyl substituent would favor electron-donation towards the ring to allow sufficient C_2—O_1 bond stretching to cause $AlH_4^{\ominus}$ to attack C-2 and produce the β,γ-unsaturated ether in greater proportion (Experiment 5, Table 6).

It is significant that in both solvents used, the dialkyl ether or DME, $LiAlH_4$ reduces the parent compound, 2-vinyl-1,3-dioxolane, only to the α,β-unsaturated ether (experiment 1 in Tables 5–7). This must mean that $LiAlH_4$ prefers attack at the β carbon of the vinyl group, and that alkyl substituents attached to the vinyl unit have a pronounced effect in changing the course of reaction. It is possible that a steric effect of these alkyl substituents plays a part by reducing the ease of approach by $AlH_4^{\ominus}$ or $LiAlH_4$ to the β carbon of the vinyl group. However, models show that there is ample room for such approach, and this is corroborated by the fact that the methyl group on the α carbon of the vinyl moiety completely inhibits hydride addition to the β carbon (experiment 3, Table 6) even though the β carbon is sterically as accessible as it is in 2-vinyl-1,3-dioxolane.[3]

A final point of interest is the reduction of only the double bond of cinnamaldehyde ethyleneacetal by $LiAlH_4$ in diethyl ether at room temperature (experiments 5–7, Table 5). Olefinic double bonds normally are not reduced by $LiAlH_4$, although a few cases of such reduction have been reported. For example the double bond of α,β-unsaturated carbonyl compounds has been reduced by $LiAlH_4$ (17, 18) and allyl alcohol has been reduced to *n*-propyl alcohol (19) while ω-nitro styrene is converted to β-phenylethylamine (20). It is clear from the deuteration experiments (experiments 6 and 7, Table 5) that $LiAlH_4$ attacks the olefinic carbon atom β to the phenyl ring, and this occurs very likely because the formation of a negative charge on the carbon α to the phenyl ring is more easily accomplished than it is on the carbon α to the dioxolane ring.

Experimental

Boiling points and melting points are uncorrected. The g.l.c. analyses were made with an F and M Model 700 instrument, equipped with 12′ × 1/8″ columns packed with either butanediol succinate, 20% on Gas-Chrom P (60–80 mesh) or silicone rubber SE30, 20% on Gas-Chrom P(60–80 mesh). Helium was the carrier gas at a flow rate of about 40 ml/min. For preparative g.l.c., an Aerograph Autoprep, Model A-700 (Wilkins Instrument and Research Co.) was employed, with a 12′ × 1/4″ column packed with butanediol succinate, 20% on Gas-Chrom P (60–80 mesh). Helium was the carrier gas. The column temperature and type of column used was dependent upon the boiling points of the compounds. For some analytical work on the F and M Model 700, the temperature was linearly programmed to achieve better resolution. The temperature was increased at the rate of 7.5°/min, starting from 80–100°, with the terminal temperature determined by the column stability. Quantitative analyses were made by measuring the areas of the peaks corresponding to the compounds obtained. In most cases, these areas were compared with those obtained from

[2]The AlH_3 so liberated could also reduce the 2-vinyl-1,3-dioxolane as shown in Tables 3 and 4.

[3]One of the referees has suggested that the reason why acrolein ethyleneacetal hydrogenolyzes only to the α,β-unsaturated ether is that it is less sterically encumbered than all the other α,β-unsaturated acetals employed. Only when the steric requirements increase does there occur a delicate balance between steric requirements and solvent effects.

Can. J. Chem. Downloaded from www.nrcresearchpress.com by 210.87.254.42 on 09/05/12
For personal use only.

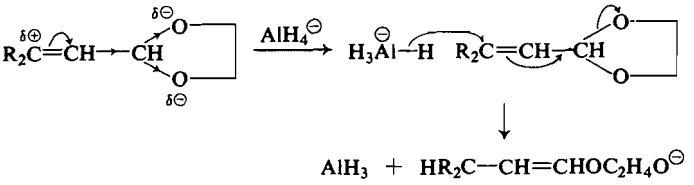

SCHEME 4

known and weighed artificial mixtures, and it was found that equimolar mixtures gave peaks whose areas differed by less than 5%. In a few cases the error was somewhat greater, but within 10%.

The i.r. spectra were recorded with a Perkin–Elmer Model 21 instrument.

The p.m.r. spectra were recorded on either a Varian Associates A-60 or A-55/60A instrument by Mr. R. Swindlehurst and assistants in this Department. All spectra were referred to tetramethylsilane.

The p.m.r. and i.r. spectra were obtained for all compounds and in all cases were consistent with the structure assigned.

Elemental analyses were made by Mrs. D. Mahlow of this Department.

The drying agent for solutions was anhydrous magnesium sulfate unless otherwise stated. Solvents were removed by rotary evaporator under reduced pressure unless otherwise stated.

Preparation of Substituted 1,3-Dioxolanes

2-Methyl-1,3-dioxolane was prepared by the method of Hibbert and Pimm (21). Yield 51%; b.p. 72° at 700 mm° η_D^{25} 1.3912; lit. b.p. 83–85° at 760 mm (21).

2-(Methoxymethyl)-1,3-dioxolane was prepared from methoxyacetaldehyde diethylacetal (Aldrich Chemical Co.) and ethylene glycol according to the alcohol exchange method of McElvain and Curry (22). Yield, 70%; b.p. 130° at 710 mm; η_D^{24} 1.4216; lit. b.p. 57–58° at 18 mm; η_D^{20} 1.4201 (23).

2-(Bromomethyl)-1,3-dioxolane was made from bromoacetaldehyde diethylacetal and ethylene glycol (22). Yield, 70%; b.p. 60° at 15 mm; η_D^{23} 1.4805; lit. b.p. 175° at 745 mm; η_D^{25} 1.4805 (22).

2-(Methylthiomethyl)-1,3-dioxolane. To a stirred solution of 11.5 g (0.24 mol) of methyl mercaptan in 300 ml of dry DME, cooled to −10° by means of an ice–salt bath, was added 5.8 g (0.24 mol) of sodium hydride in 1 g portions. When the hydride had been added, the cooling bath was removed and the reaction mixture stirred at room temperature for 2 h. 2-(Bromomethyl)-1,3-dioxolane (40 g, 0.24 mol) was added and the mixture then heated under reflux for 2 h and subsequently cooled to room temperature. The precipitated sodium bromide was removed by suction filtration, and the filtrate freed from solvent. The pale yellow residue was distilled under vacuum to give 15 g (47%) of colorless liquid, b.p. 64–65° at 15 mm; η_D^{24} 1.4820.

Anal. Calcd. for $C_5H_{10}O_2S$: C, 44.75; H, 7.46; S, 23.85. Found: C, 44.57; H, 7.28; S, 24.00.

The 60 MHz p.m.r. spectrum in CCl_4 showed a triplet at τ 5.09 (1H, $J \sim 4.5$ Hz), a multiplet between 6.05 and 6.32 (4H); a doublet at 7.47 (2H, $J \sim 4.5$ Hz), a singlet at 7.89 (3H).

2-(Dimethylaminomethyl)-1,3-dioxolane was prepared according to published directions (24). From 70 ml of 33% aqueous dimethylamine and 25 g of 2-(bromomethyl-1,3-dioxolane) was obtained 12 g (60%) of liquid boiling at 59–60° at 20 mm; η_D^{25} 1.4320; lit. b.p. 68° at 20 mm (24).

Anal. Calcd. for $C_6H_{13}NO_2$: C, 54.96; H, 9.92; N, 10.69. Found: C, 54.58; H, 9.86; N, 10.51.

The 60 MHz p.m.r. spectrum in CCl_4 showed a triplet at τ 5.21 (1H, $J \sim 4$ Hz); a multiplet centered at 6.22 (4H); a doublet at 7.62 (2H, $J \sim 4$ Hz); a singlet at 7.78 (6H).

2-Vinyl-1,3-dioxolane was made by a modification of a published procedure (25) as described by Davis and Brown (26).

2-(1-Propenyl)-1,3-dioxolane was prepared according to published directions (27). Yield, 56%; b.p. 69° at 50 mm; η_D^{26} 1.4405; lit. b.p. 71° at 50 mm; η_D^{30} 1.4380 (27).

The following five compounds were prepared by the same method used to make 2-(1-propenyl)-1,3-dioxolane above.

2-(α-Methylvinyl)-1,3-dioxolane, described previously (26).

2-Phenyl-1,3-dioxolane from benzaldehyde and ethylene glycol. Yield, 85%; b.p. 87° at 5 mm; η_D^{25} 1.5248; lit. b.p. 101° at 10 mm (28); η_D^{20} 1.5270 (29).

2-(o-Methoxyphenyl)-1,3-dioxolane from *o*-methoxybenzaldehyde and ethylene glycol. Yield, 80%; b.p. 117° at 2 mm; η_D^{24} 1.5325; lit. b.p. 119.5–120.5° at 3 mm; η_D^{20} 1.5343 (30).

2-(p-Methoxyphenyl)-1,3-dioxolane from *p*-anisaldehyde and ethylene glycol. Yield, 83%; b.p. 139° at 8 mm; η_D^{24} 1.5335; lit. b.p. 158–160° at 17 mm; $\eta_D^{19.5}$ 1.4306 (30).

2-Styryl-1,3-dioxolane from cinnamaldehyde and ethylene glycol. Yield, 65%; b.p. 84° at 0.1 mm; η_D^{24} 1.5625. This liquid crystallized on standing at room temperature for 1 h. Recrystallization from petroleum ether gave colorless needles, m.p. 29.5–31°.

Anal. Calcd. for $C_{11}H_{12}O_2$: C, 74.98; H, 6.86. Found: C, 75.03; H, 6.94.

The 60 MHz p.m.r. spectrum in CCl_4 showed a broad multiplet between τ 2.40 and 2.81 (5H); a doublet at 3.22 (1H, olefinic, $J \sim 16$ Hz); a doublet of doublets at 3.88 (1H, olefinic, $J \sim 16$, $J \sim 5$ Hz); a doublet at 4.62 (1H, $J \sim 5$ Hz); a multiplet centered at 6.08 (4 H).

2-(1-Butenyl)-1,3-dioxolane was obtained from the dehydrohalogenation of 2-(1-bromobutyl)-1,3-dioxolane (26).

2-(2-Methyl-1-propenyl)-1,3-dioxolane was obtained from the dehydrohalogenation of 2-(1-bromo-2-methyl-1-propyl)-1,3-dioxolane (26).

Can. J. Chem. Downloaded from www.nrcresearchpress.com by 210.87.254.42 on 09/05/12
For personal use only.

Can. J. Chem. Downloaded from www.nrcresearchpress.com by 210.87.254.42 on 09/05/12
For personal use only.

Preparation of some Authentic Products of Hydrogenolysis

2-Allyloxyethanol

This was prepared by the following modification of the published method (31).

To a solution of 62 g (1 mol) of dry ethylene glycol in 300 ml of dry DME was added 19.2 g (0.4 mol) of sodium hydride. The resulting mixture was stirred at room temperature for 2 h and then 48.4 g (0.4 mol) of allyl bromide was added. The mixture was heated under reflux for 2 h and was then cooled to room temperature. The solid material was removed by suction filtration and the filtrate was freed from solvent. The residual oil was distilled under reduced pressure, giving 27 g (67%) of colorless liquid, b.p. 46° at 5 mm; η_D^{25} 1.4333; lit. b.p. 63–64° at 18–19 mm; η_D^{20} 1.4356 (31).

2-Crotyloxyethanol

This compound was prepared from crotyl bromide and ethylene glycol by the same method used to synthesize 2-allyloxyethanol above. Yield, 65%; b.p. 81° at 18 mm; η_D^{27} 1.4383; lit. b.p. 85–87° at 21–22 mm; η_D^{20} 1.4428 (32).

The crotyl bromide was prepared by the method of Winstein and Young (33). The b.p. 46–48° at 94 mm; η_D^{23} 1.4787; lit. b.p. 49° at 93 mm; η_D^{25} 1.4795 (33).

2-(2-Methylthioethoxy)ethanol

The precursor, *2-methylthioethanol* was prepared as follows. To a solution of 39 g (0.5 mol) of 2-mercaptoethanol in 300 ml of dry DME was added 12 g (0.5 mol) of sodium hydride. The resulting mixture was stirred at room temperature for 2 h. Iodomethane (71 g, 0.5 mol) was then added and the mixture was stirred overnight at room temperature. The solids were removed by suction filtration and the filtrate was freed from solvent. The residue was taken up in 200 ml of dry ether and the solution filtered to remove the precipitate, and then freed from ether. The residue was distilled to give 25 g (54%) of colorless liquid, b.p. 78° at 30 mm; η_D^{24} 1.4869; lit. b.p. 61° at 10 mm; η_D^{20} 1.4930 (34).

To a solution of 4 g (0.044 mol) of 2-methylthioethanol in 200 ml of dry DME was added 1.05 g (0.044 mol) of sodium hydride. After the mixture had been stirred for 2 h, ethyl chloroacetate (5.4 g, 0.044 mol) was added and the resulting mixture was heated under reflux overnight. The cooled reaction mixture was freed from solids and then from solvent. The residue, in 50 ml of dry ether was filtered from additional precipitate and the filtrate freed from ether. The crude product was added to a solution of 1.7 g (0.044 mol) of $LiAlH_4$ in 100 ml of dry ether. The mixture was stirred for 0.5 h and then treated with 10 ml of a 15% aqueous solution of potassium hydroxide. This was then diluted with 50 ml of water and the resulting mixture extracted continuously with ether for 12 h. The dried ether extract was filtered free of solid, and solvent removed. The residue was distilled under reduced pressure to give 2.3 g (52%) of colorless liquid, b.p. 84° at 2.5 mm; η_D^{24} 1.4837.

Anal. Calcd. for $C_5H_{12}O_2S$: C, 44.10; H, 8.83; S, 23.52. Found: C, 44.01; H, 8.82; S, 23.40.

The 60 MHz p.m.r. spectrum in CCl_4 showed a multiplet between τ 6.20 and 6.81 (7H), a triplet at 7.35 (—S—CH_2—, $J \sim 7$ Hz), and a singlet at 7.88 (CH_3—S—).

The i.r. spectrum (neat) showed a broad band between 3640 and 3210 (OH stretching) and a broad band between 1150 and 1010 cm^{-1} (C—O— stretching).

2-(2-Dimethylaminoethoxy)ethanol

The precursor, *ethyl (2-dimethylaminoethoxy)acetate* was prepared by a modification of the general procedure of Leffler and Calkins (35). To a stirred solution of 30 g (0.337 mol) of 2-(dimethylamino)-ethanol and 41.2 g (0.337 mol) of ethyl chloroacetate in 400 ml of dry DME cooled to −10° by an ice–salt bath, was added sodium hydride (8.1 g, 0.337 mol) in 1 g portions. When the addition was complete, the reaction mixture was allowed to attain room temperature and then stirred for 24 h. The solids were removed by suction filtration and the filtrate was freed from solvent. The residue was dissolved in 100 ml of dry ether and the precipitated solid again removed by filtration. The ether was removed from the filtrate and the residue distilled under reduced pressure. Yield, 25 g (42%); b.p. 64° at 0.5 mm; η_D^{23} 1.4265.

Anal. Calcd. for $C_8H_{17}NO_3$: C, 54.86; H, 9.71; N, 8.00. Found: C, 54.92; H, 9.66; N, 7.81.

The 60 MHz p.m.r. spectrum in CCl_4 showed a quartet at τ 5.89 (2H, $J \sim 7$ Hz), a singlet at 6.08 (2H), a triplet at 6.48 (2H, $J \sim 6$ Hz), a triplet at 7.58 (2H, $J \approx 6$ Hz), a singlet at 7.83 (6H), and a triplet at 8.77 (3H, $J \approx 7$ Hz).

The i.r. spectrum (neat) showed a strong band at 1760 (C═O) and a broad band between 1220 and 1110 cm^{-1} (C—O— stretching).

Ethyl (2-dimethylaminoethoxy)acetate (10 g, 0.06 mol) was added dropwise to a stirred solution of 2.08 g (0.06 mol) of $LiAlH_4$ in 50 ml of dry ether. When the ester had been added, the reaction mixture was stirred for 1 h at room temperature and then 10 ml of a 15% aqueous solution of potassium hydroxide was added. This was diluted with 50 ml of water and the mixture extracted continuously for 12 h with ether. The ether extract was dried, then freed of drying agent and solvent. The residue was distilled under reduced pressure to give 6 g (60%) of colorless liquid, b.p. 60–61° at 4 mm; η_D^{25} 1.4390.

Anal. Calcd. for $C_6H_{15}NO_2$: C, 54.14; H, 11.28; N, 10.53. Found: C, 54.23; H, 11.34; N, 10.65.

The 60 MHz p.m.r. spectrum in CCl_4 showed a singlet at τ 5.31 (1H), a singlet at 6.54 (6H), a triplet at 7.59 (2H, $J \approx 5.5$ Hz), and a singlet at 7.80 (6H).

The i.r. spectrum in CCl_4 showed a broad band between 3600 and 3050 (OH) and a broad band between 1170 and 1030 cm^{-1} (C—O—).

2-Benzyloxyethanol was prepared according to published directions (1).

2-Ethoxyethanol, from Eastman Kodak Co.

Diethyleneglycol monomethyl ether, from Fisher Scientific Co.

2-(β-Bromoethoxy)ethanol was not prepared since hydrogenolysis of 2-bromomethyl-1,3-dioxolane gave only 2-ethoxyethanol as result of loss of Br.

Products Obtained from Hydrogenolysis Reactions

The majority of hydrogenolysis products were obtained by their isolation from the mixture obtained from the hydrogenolysis reactions. These were identified by elemental analysis, i.r. and p.m.r. spectra. These, along with their physical constants and spectral data, are shown in Tables 8 and 9.

Can. J. Chem. Downloaded from www.nrcresearchpress.com by 210.87.254.42 on 09/05/12
For personal use only.

TABLE 8. Physical constants of products isolated from the hydrogenolysis reactions

Product	Boiling point (°C (mm))	η_D(°C)	Analysis	
			Calculated	Found
cis-$CH_3CH{=}CHOC_2H_4OH$	66–72 (22) (1:1 mixture of *cis* and *trans*)	1.4408(25)	C 58.80 H 9.87	58.61 10.17
trans-$CH_3CH{=}CHOC_2H_4OH$		1.4391(25)	58.80 9.87	58.51 9.85
cis-$C_2H_5CH{=}CHOC_2H_4OH$	72–79(20) (1:1 mixture of *cis* and *trans*)	1.4417(25)	62.04 10.41	62.20 10.84
trans-$C_2H_5CH{=}CHOC_2H_4OH$		1.4413(25)	62.04 10.41	62.26 10.17
$CH_2{=}C(CH_3)CH_2OC_2H_4OH$	69–71(20)	1.4382(25)	62.04 10.41	62.15 10.67
$(CH_3)_2C{=}CHOC_2H_4OH$	74(18)	1.4449(25)	62.04 10.41	61.80 9.83
$C_2H_5CH{=}CHCH_2OC_2H_4OH$	64(4)	1.4434(22)	64.58 10.84	64.38 10.40
cis-$C_3H_7CH{=}CHOC_2H_4OH$	60–68(10) (1:1 mixture of *cis* and *trans*)	1.4414(26)	64.58 10.84	64.43 10.66
trans-$C_3H_7CH{=}CHOC_2H_4OH$		1.4446(25)	64.58 10.84	64.60 10.93
$(CH_3)_2C{=}CHCH_2OC_2H_4OH$	69(4.5)	1.4502(22)	64.58 10.84	64.52 10.73
$(CH_3)_2CHCH{=}CHOC_2H_4OH$	74–75(5)	1.4532(24)	64.58 10.84	64.29 10.71
$C_6H_5CH_2CH_2CH(OCH_2CH_2O)$	60(0.1)	1.5167(24)	74.13 7.92	73.94 7.72
$C_6H_5CHDCH_2CH(OCH_2CH_2O)$	60(0.1)	1.5170(24)	73.71 D+H 8.17	73.84 8.17
$C_6H_5CH_2CHDCH(OCH_2CH_2O)$	60(.01)	1.5165(24)	73.71 D+H 8.17	73.73 7.78
$C_6H_5CH{=}CHCH_2OC_2H_4OH$	92(0.05)	1.5553(27)	74.13 7.92	74.10 7.72
o-$CH_3OC_6H_4CH_2OC_2H_4OH$	102(0.5)	1.5300(21)	65.92 7.74	65.66 7.76
p-$CH_3OC_6H_4CH_2OC_2H_4OH$	109(0.5)	1.5285(23)	65.92 7.74	65.97 8.00

Can. J. Chem. Downloaded from www.nrcresearchpress.com by 210.87.254.42 on 09/05/12
For personal use only.

TABLE 9. Spectral data for the compounds shown in Table 8

Compound (R=C_2H_4OH)	Proton magnetic resonance				Infrared	
	H-	Multiplicity	Chemical shift (τ)	Coupling (Hz)*	Absorption (cm^{-1})	Assignment
cis-$CH_3CH{=}CHOR$	1	2 quartets	4.10	$J_{1,2}\sim7$; $J_{1,3}\sim1.5$	3650–3150(S)	O—H
	2	2 overlapping quartets	5.68	$J_{1,2}\sim J_{2,3}\sim7$	3040	vinyl C—H
	3	2 doublets	8.46	$J_{2,3}\sim7$; $J_{1,3}\sim1.5$	1670(S)	vinyl ether
trans-$CH_3CH{=}CHOR$	1	2 quartets	3.79	$J_{1,2}\sim13$; $J_{1,3}\sim1.5$	3650–3150(S)	O—H
	2	2 overlapping quartets	5.28	$J_{1,2}\sim13$; $J_{2,3}\sim7$	3060	vinyl C—H
	3	2 doublets	8.45	$J_{2,3}\sim7$; $J_{1,3}\sim1.5$	1650(S)	vinyl ether
cis-$CH_3CH_2CH{=}CHOR$	1	2 triplets	4.13	$J_{1,2}\sim6.0$; $J_{1,3}\sim1$	3650–3150(S)	O—H
	2	2 overlapping triplets	5.71	$J_{1,2}\sim6.0$; $J_{2,3}\sim7$	3030	vinyl C—H
	3	multiplet	7.6–8.3		1660(S)	vinyl ether
	4	triplet	9.06	$J_{3,4}\sim7$		
trans-$CH_3CH_2CH{=}CHOR$	1	2 triplets	3.78	$J_{1,2}\sim12.5$; $J_{1,3}\sim1.5$	3650–3150(S)	O—H
	2	2 overlapping triplets	5.24	$J_{1,2}\sim12.5$; $J_{2,3}\sim7$	3050	vinyl C—H
	3	multiplet	7.8–8.4		1650(S)	vinyl ether
	4	triplet	9.0	$J_{3,4}\sim7$		
$CH_2{=}C(CH_3)CH_2OR$	1	singlet	6.12	$w/2\sim3$	3650–3150	O—H
	2	singlet	8.28	$w/2\sim3$	1650(w)	C=C
	3	multiplet	5.0–5.2			
$(CH_3)_2C{=}CHOR$	1	multiplet	4.15–4.30		3600–3100(S)	O—H
	2	multiplet	8.46	$w/2\sim6$	1685(S)	vinyl ether
$CH_3CH_2CH{=}CHCH_2OR$	1	multiplet	5.95–6.2		3650–3250	O—H
	2, 3	multiplet	4.0–4.85		1675(w)	C=C
	4	multiplet	7.7–8.2			
	5	triplet	9.0	$J\sim7.0$		
cis-$CH_3CH_2CH_2CH{=}CHOR$	1	2 triplets	4.09	$J_{1,2}\sim6.5$; $J_{1,3}\sim1$	3650–3100(S)	O—H
	2	2 overlapping triplets	5.70	$J_{1,2}\sim6.5$; $J_{2,3}\sim6.5$	3050	vinyl C—H
					1680(S)	vinyl ether
trans-$CH_3CH_2CH_2CH{=}CHOR$	1	2 triplets	3.80	$J_{1,2}\sim12.5$; $J_{1,3}\sim1$	3650–3150(S)	O—H
	2	2 overlapping triplets	5.30	$J_{1,2}\sim12.5$; $J_{2,3}\sim7$	3070	vinyl C—H
					1655(S)	vinyl ether
$(CH_3)_2C{=}CHCH_2OR$	1	doublet	6.03	$J_{1,2}\sim7$	3650–3100(S)	O—H
	2	complicated triplet	4.70		1680(w)	C=C
	3	2 singlets	8.26, 8.33			
$(CH_3)_2CHCH{=}CHOR$	1	doublet	3.80	$J_{1,2}\sim12.5$; $J_{1,3}\sim1$	3650–3100(S)	O—H
	2	2 overlapping triplets	5.32	$J_{1,2}\sim12.5$; $J_{2,3}\sim7$	1650(S)	vinyl ether
	3, 4	multiplets	7.8–9.3			

Can. J. Chem. Downloaded from www.nrcresearchpress.com by 210.87.254.42 on 09/05/12
For personal use only.

TABLE 9.—*Concluded*

Compound (R=C_2H_4OH)	Proton magnetic resonance				Infrared	
	H-	Multiplicity	Chemical shift (τ)	Coupling (Hz)*	Absorption (cm^{-1})	Assignment
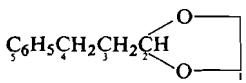	1	multiplet	6.04–6.34		1600 and 1680(w)	C=C
	2	triplet	5.24	$J_{2,3}$~4.5		
	3	multiplet	7.92–8.33			
	4	multiplet	7.14–7.46			
	5	singlet	2.87			
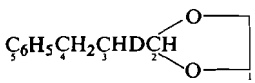	1	multiplet	6.04–6.34			
	2	doublet	5.23	$J_{2,3}$~4.5		
	3	multiplet	7.92–8.33			
	4	doublet	7.33			
	5	singlet	2.87			
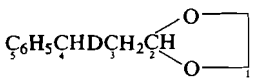	1	multiplet	6.04–6.34			
	2	triplet	5.24	$J_{2,3}$~4.5		
	3	multiplet	7.92–8.33			
	4	multiplet	7.14–7.46			
	5	singlet	2.87			
$C_6H_5CH=CHCH_2OR$	1	doublet	5.96	$J_{1,2}$~5	3650–3120(S)	O—H
	2, 3	multiplets	3.62–3.91			
	4	singlet	2.88			
o-$CH_3OC_6H_4CH_2OR$	1	singlet	5.50		3650–3150(S)	O—H
	2	multiplet	2.56–3.40			
	3	singlet	6.27			
p-$CH_3OC_6H_4CH_2OR$	1	singlet	5.70		3650–3150	O—H
	2	2 doublets	2.90, 3.34	J~8		
	3	singlet	6.35			

*Approximate values from observation.

Can. J. Chem. Downloaded from www.nrcresearchpress.com by 210.87.254.42 on 09/05/12
For personal use only.

Hydrogenolysis with AlH_2Cl

The procedure employed was based on that described by Diner (36). The following reduction of 2-vinyl-1,3-dioxolane is typical.

A solution of $LiAlH_4$ (0.5 g, 0.015 mol) in 15 ml of dry ether was cooled in ice to 5°. To this was added dropwise an ether solution of $AlCl_3$ (previously prepared by the addition of $AlCl_3$ (1.99 g, 0.015 mol) in small portions to 15 ml of dry ether kept at 5°). This mixed hydride solution was stirred at room temperature for 15 min and then 2-vinyl-1,3-dioxolane (3 g, 0.03 mol) was added. The resulting mixture was stirred for 30 min at room temperature and then a solution of 15% potassium hydroxide in water was added dropwise until no further reaction occurred. The colorless precipitate (lithium aluminate) was separated by suction filtration and the ether removed from the filtrate by fractional distillation. The residue (85% recovery) was analyzed by g.l.c. and found to be composed of only 2-allyloxyethanol, identical with an authentic sample.

This procedure was employed for the AlH_2Cl reductions of the compounds shown in Tables 1–3, for the reduction periods shown. Tables 8 and 9 give the physical and spectral properties of those compounds isolated from the hydrogenolysis reactions and then characterized.

Competitive Hydrogenolysis with AlH_2Cl

The following general procedure was used.

An ether solution of AlH_2Cl was obtained from $LiAlH_4$ (0.143 g, 0.0037 mol) and $AlCl_3$ (0.5 g, 0.0037 mol) in 20 ml of dry ether as described above. When this had been stirred for 15 min, a mixture of 2-methyl-1,3-dioxolane (0.66 g, 0.0075 mol) and 2-(methylthiomethyl)-1,3-dioxolane (1 g, 0.0075 mol) was added. The subsequent procedure was the same as that described above except that after the aqueous potassium hydroxide had been added, an additional quantity (50 ml) of water was added and the resulting mixture was extracted continuously with ether overnight. The ether extract was dried, filtered, and the filtrate freed from ether by fractional distillation at atmospheric pressure. The residue (90% recovery), when analyzed by g.l.c., was found to be composed only of a 7:1 ratio of 2-ethoxyethanol and 2-(2-methylthioethoxy)ethanol, identified by comparison of the retention times with those of authentic samples. Other pairs of compounds were reduced similarly and the results are shown in Table 2.

Reduction with $LiAlH_4$

The procedure was the same as that used above for the reduction with AlH_2Cl. By this method, acrolein ethyleneacetal (2-vinyl-1,3-dioxolane) (3 g, 0.03 mol), treated with $LiAlH_4$ (1.14 g, 0.03 mol) in 30 ml of dry ether for 48 h, gave after work-up (85% recovery) a 1:1 mixture of *cis*- and *trans*-2-(α-propenyloxy)ethanol, identified by their elemental analyses, p.m.r. and i.r. spectra after isolation and separation by preparative g.l.c. Tables 5–7 show details of the experiments and the results obtained for other 1,3-dioxolanes, while Tables 8 and 9 provide physical and spectral data for the compounds isolated.

Competitive Reductions with AlH_3

The procedure was the same as that used for the competitive reductions with AlH_2Cl. The AlH_3 was prepared according to published directions (5, 15). The results are shown in Table 4.

We thank the National Research Council of Canada for financial assistance throughout the course of this work. One of us (HAD) thanks the National Research Council of Canada for the award of a Bursary for the academic year 1969–1970.

1. B. E. Leggetter and R. K. Brown. Can. J. Chem. **42**, 990 (1964).
2. B. E. Leggetter and R. K. Brown. Can. J. Chem. **43**, 1030 (1965).
3. E. L. Eliel, B. E. Nowak, R. A. Daignault, and V. G. Badding. J. Org. Chem. **30**, 2441 (1965).
4. W. W. Zajac, Jr. and K. J. Byrne. J. Org. Chem. **35**, 3375 (1970).
5. U. E. Diner, H. A. Davis, and R. K. Brown. Can. J. Chem. **45**, 207 (1967).
6. S. Winstein. Bull. Soc. Chim. Fr. **18**, C55 (1951).
7. A. Streitwieser, Jr. Chem. Rev. **56**, 675 (1956).
8. J. C. Speck, Jr., D. J. Rynbrandt, and I. H. Kochevar. J. Am. Chem. Soc. **87**, 4979 (1965).
9. B. E. Leggetter and R. K. Brown. Can. J. Chem. **41**, 2671 (1963).
10. N. G. Gaylord. Reduction with complex metal hydrides. Interscience Publishers Inc., New York, N.Y., 1956. pp. 673–680.
11. E. L. Eliel and M. N. Rerick. J. Org. Chem. **23**, 1088 (1958).
12. E. L. Eliel. Record Chem. Progr. (Kresge–Hooker Sci. Lib.) **23**, 129 (1961).
13. E. L. Eliel, V. G. Badding, and M. N. Rerick. J. Am. Chem. Soc. **84**, 2371 (1962).
14. E. L. Eliel, L. A. Pilato, and V. G. Badding. J. Am. Chem. Soc. **84**, 2377 (1962).
15. E. C. Ashby and J. Prather. J. Am. Chem. Soc. **88**, 729 (1966).
16. M. J. Jorgenson and A. F. Thacher. Chem. Commun. 973 (1968).
17. R. E. Lutz and J. S. Gillespie, Jr. J. Am. Chem. Soc. **72**, 2002 (1950).
18. R. E. Lutz and D. F. Hinkley. J. Am. Chem. Soc. **72**, 4091 (1950).
19. F. A. Hochstein and W. G. Brown. J. Am. Chem. Soc. **70**, 3484 (1948).
20. R. F. Nystrom and W. G. Brown. J. Am. Chem. Soc. **70**, 3738 (1948).
21. H. Hibbert and J. A. Pimm. J. Am. Chem. Soc. **46**, 1286 (1924).
22. S. McElvain and M. J. Curry. J. Am. Chem. Soc. **70**, 3781 (1948).
23. M. F. Shotakovskii, N. V. Kusnetsov, Che-Min Yang, and G. G. Balezina. Izv. Akad. Nauk SSSR, Otd. Khim. Nauk. 2220 (1962). Chem. Abstr. **58**, 13783 (1963).
24. Brit. Pat. 595 963, December 23, 1947. Chem. Abstr. **42**, P3436 (1948).
25. R. F. Fischer and C. W. Smith. J. Org. Chem. **25**, 319 (1960).
26. H. A. Davis and R. K. Brown. Can. J. Chem. **49**, 2321 (1971).

27. D. L. HEYWOOD and B. PHILLIPS. J. Org. Chem. **25**, 1699 (1960).
28. M. SULZBACHER, E. BERGMANN, and E. PARISER. J. Am. Chem. Soc. **70**, 2827 (1948).
29. A. RIECHE, E. SCHMITZ, and E. BEYER. Chem. Ber. **91**, 1935 (1958).
30. E. J. SALMI and K. KYRKI. Suomen Kemistilehti. **19B**, 97 (1946); Chem. Abstr. **41**, 5480 (1947).
31. C. D. HURD and M. A. POLLACK. J. Am. Chem. Soc. **60**, 1905 (1938).
32. B. I. MIKHANT'EV and E. A. PYRAKHINA. Zhur. Obshchei. Khim. **30**, 958 (1960); Chem. Abstr. **55**, 370 (1961).
33. S. WINSTEIN and W. G. YOUNG. J. Am. Chem. Soc. **58**, 104 (1936).
34. M. SELIM–DORGANS, M. SELIM, and H. GAULT. C. R. **244**, 1047 (1957); Chem. Abstr. **51**, 1206 (1957).
35. M. T. LEFFLER and A. E. CALKINS. *In* Organic syntheses. Coll. Vol. III, John Wiley and Sons, Inc., New York, N.Y., 1955. p. 544.
36. U. E. DINER. Ph.D. Thesis. Department of Chemistry, University of Alberta, Edmonton, Alberta, 1967.

Can. J. Chem. Downloaded from www.nrcresearchpress.com by 210.87.254.42 on 09/05/12
For personal use only.

Can. J. Chem. Downloaded from www.nrcresearchpress.com by 210.87.254.5 on 09/05/12
For personal use only.

Fully Fluorinated Alkoxides. Part V. Derivatives of Tetrafluorocatechol

CELIA MACDONALD, A. J. TOMLINSON, AND C. J. WILLIS[1]
Department of Chemistry, University of Western Ontario, London 72, Ontario

Received March 16, 1971

Tetrafluorocatechol (tetrafluoro-1,2-dihydroxybenzene) has been found to form isolable complexes with transition metals (Ni^{2+}, Cu^{2+}, and Fe^{3+}), and with germanium, acting as a chelating, dinegative, ligand. These complexes are few in number and of limited stability, suggesting that tetrafluorocatechol has less applicability as a ligand than related highly halogenated organic molecules. Complexes of tetrabromocatechol with Ni^{2+} are also described.

Le tétrafluoropyrocathécol (tétrafluoro dihydroxy-1,2 benzène) forme des complexes isolables avec des métaux de transition (Ni^{2+}, Cu^{2+} et Fe^{3+}) et avec le germanium, et fonctionne comme un ligand chélatant porteur de deux charges négatives. Ces complexes sont peu nombreux et leur stabilité est limitée ce qui suggère que le tétrafluoropyrocathécol est moins utile en tant que ligand que des molécules organiques correspondantes fortement halogénées. Les complexes obtenus entre le tétrabromopyrocathécol et le Ni^{2+} sont également rapportés.

Canadian Journal of Chemistry, 49, 2578 (1971)

Introduction

We have previously shown (1) that stable complexes of various first-row transition elements, including Mn(II), Fe(III), Ni(II), Cu(II), and Zn(II), may be produced by reaction of the metal ion with perfluoropinacol in aqueous solution. The pinacol is effectively ionized to the dinegative ion $[OC(CF_3)_2C(CF_3)_2O]^{2-}$ (PFP), and complexes with metal ions have the composition $[M(PFP)_2]^{2-}$ and $[M(PFP)_3]^{3-}$ for M^{2+} and M^{3+} ions respectively.

The ready formation of stable chelated alkoxides by the fluorinated diol may be attributed to the increased proton acidity resulting from the inductive effect of the 12 fluorine atoms in the molecule, and it was of interest to attempt to extend this study to analogous fluorinated aromatic diols. Tetrafluoro-1,2-dihydroxybenzene (tetrafluorocatechol, TFC) is the simplest molecule of this type. Although this compound has been known for some years, no complexes of it have yet been reported, although in the initial account of its preparation (2) it was noted that it gave a blue color with aqueous ferric chloride.

Complexes of TFC would also be of interest because of their relation to the so-called "dithiolene" complexes (**1** and **2**; X = S, Y = H) which often undergo a series of electron transfer processes, resulting in values of Z from -2 to

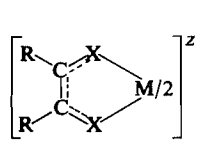

1

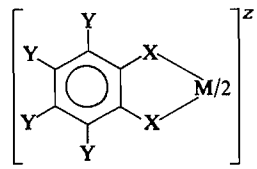

2

$+2$ (3–7). In many of these complexes, the groups R are electronegative (*e.g.* CN or CF_3) and the delocalization of the electron density between metal and ligand orbitals leads to greater stability of the "reduced" members of a series. Complexes of catechol (**2**, X = O, Y = H) have been reported over many years, but only recently has a series of well-characterized compounds containing catechol or tetrachlorocatechol (Y = Cl) been obtained and shown to undergo electron transfer reactions (8).

In a report of reactions of tetrafluorobenzene-1,2-dithiol (**2**, X = S, Y = F), it is suggested that this ligand gives complexes of metals in high oxidation states, such as Ni(III) and Cu(III) (9), but other workers have said that a meaningful oxidation state cannot be assigned to a metal atom in a system of this type (7).

Results and Discussion

Metal complexes of tetrafluorocatechol proved to be considerably less stable and more difficult to prepare than those of perfluoropinacol, and only a limited number could be characterized. Of the metals studied, copper(II) was the only

[1]To whom enquiries should be addressed. For part IV, see ref. 1.

Can. J. Chem. Downloaded from www.nrcresearchpress.com by 210.87.254.5 on 09/05/12
For personal use only.

one for which we were able to prepare a complex having tetrafluorocatechol as the sole ligand on the metal ion; namely $K_2[Cu(TFC)_2]$, a dark purple solid reversibly forming a green dihydrate. This compound was made by the addition of potassium hydroxide to methanolic Cu^{2+} in the presence of the ligand, oxygen being excluded.

With nickel(II), which readily forms the complex $[Ni(PFP)_2]^{2-}$ with perfluoropinacol, no analogous tetrafluorocatechol complex could be isolated. However, neutral mixed ligand complexes of nickel could be prepared with nitrogen or phosphorus donors and tetrafluorocatechol, *e.g.* (TMED)Ni(TFC), where TMED = tetramethylethylenediamine, $(PEt_3)_2Ni(TFC)$, and (diphos)Ni(TFC), where diphos = 1,2-bis(diphenylphosphino)ethane. These three compounds were brown and diamagnetic, with similar electronic spectra, and were assumed to have a square planar configuration, as do the corresponding perfluoropinacol complexes (10). The TMED complex formed a green, paramagnetic (μ_{eff} = 3.18 B.M.), air-sensitive dihydrate, having an electronic spectrum typical of octahedral nickel(II); this is presumably the product of the coordination of two molecules of water to the nickel atom in the complex.

When TMED was added to a copper(II) solution containing tetrafluorocatechol in an attempt to prepare (TMED)Cu(TFC), the amine acted as a base rather than a ligand, and the product was characterized as $[H_2TMED]^{2+}$-$[Cu(TFC)_2]^{2-}$.

No compound could be prepared in which three tetrafluorocatechol molecules were chelated around a metal ion, whereas perfluoropinacol readily forms such complexes with Fe^{3+} and Al^{3+} (1). Tetrafluorocatechol did, as previously reported, give a blue coloration with iron(III), this reaction providing a sensitive test for the presence of the compound, but it was not easy to isolate a stable solid adduct. However, addition of TMED gave a black complex, soluble in methanol to give a blue solution, which analyzed for $(TMED)Fe(TFC)_2$. It did not appear likely that this compound contained iron(IV), as its magnetic moment (6.1 B.M.) was very similar to that of the known perfluoropinacol complex of iron(III) (6.0 B.M.) and in the region usually found for high-spin iron(III) compounds. The Mossbauer spectrum of the complex was also consistent with the presence of iron(III).

To preserve charge balance, this molecule must therefore contain an additional proton. It does not appear that the amine is protonated, as complexes of this type, such as the compound $[H_2TMED]^{2+}[Cu(TFC)_2]^{2-}$ described above, together with analogous perfluoropinacol derivatives (10), have a strong characteristic absorption in the 2300–2700 cm^{-1} region of their i.r. spectra, which is absent in the iron complex. We suggest, therefore, that the proton is attached to the oxygen atom of a TFC molecule, and probably hydrogen-bonded to a second oxygen. The i.r. spectrum does not show any absorption assignable with certainty to such a grouping, but this is frequently the case with hydrogen-bonded hydroxyl groups, *e.g.* in nickel bis(dimethylglyoxime) (11).

The resulting structure, in which six-coordinate iron(III) is chelated by a neutral TMED molecule and two TFC molecules, one singly ionized and the other doubly ionized, is in agreement with the available evidence, but cannot be regarded as conclusively established. Attempts to remove the proton by treatment with base, to give an anionic iron complex, resulted only in decomposition.

A brief investigation was made of the ability of tetrafluorocatechol to form cyclic derivatives of main group elements, as does catechol (12). Of the group IV elements, no simple derivatives of the type $M(TFC)_2$ could be prepared, but, in the presence of base, germanium gave the adduct $Ge(TFC)_2 \cdot 2DMF$ (DMF = dimethylformamide), which was more stable to atmospheric oxidation and hydrolysis than the transition metal derivatives described above. However, no analogous stoichiometric compound of silicon or tin could be isolated using DMF or other donor molecules.

With many other metals, evidence was obtained for complex formation with tetrafluorocatechol, but no stable derivative could be isolated. With manganese(II), for example, pale green crystals of a complex separated when base was added to a solution containing TFC and Mn^{2+}, but the crystals decomposed in the course of a few hours, even when kept under vacuum in the dark.

From the rather meagre range of tetrafluorocatechol complexes isolated, it is difficult to obtain a detailed picture of the properties of the

Can. J. Chem. Downloaded from www.nrcresearchpress.com by 210.87.254.5 on 09/05/12
For personal use only.

ligand. It appears to produce a smaller ligand field splitting than similar ligands, as the first absorption maximum in the spectrum of the complex $[Cu(TFC)_2]^{2-}$ occurs at 13 500 cm^{-1}, compared with $[Cu(C_6H_4O_2)_2]^{2-}$, 15 000; $[Cu(C_6Cl_4O_2)_2]^{2-}$, 14 800 (8), and $[Cu(PFP)_2]^{2-}$, 15 100 cm^{-1} (10).

The very limited oxidative stability of the tetrafluorocatechol complexes was unexpected, as previous workers (8) have shown that complete replacement of hydrogen by chlorine in a catechol complex leads to much greater stability. In an effort to throw further light on this point, we have briefly investigated the properties of tetrabromocatechol (TBC) as a ligand, since no report of such complexes has yet appeared. Like other catechols studied, tetrabromocatechol is very readily oxidized in basic solution, but it proved a slightly better ligand than tetrafluorocatechol. With nickel(II), the complexes $[Me_4N^+]_2[Ni(TBC)_2]^{2-}$, (TMED)Ni(TBC), and $(PEt_3)_2Ni(TBC)$ were isolated as yellow or brown, diamagnetic, solids, considerably more stable than either the catechol or the tetrafluorocatechol nickel complexes.

The instability of complexes of fully halogenated catechols appears, therefore, to reach a maximum in the tetrafluorocatechol derivatives. We suggest that this may derive from the highly polar nature of the carbon–fluorine bond, which, in the presence of a system where electron transfer processes may readily occur, leads to ready elimination of a fluoride ion and consequent decomposition of the complex. Consistent with this, we have frequently found fluoride ion present in the decomposition products resulting from tetrafluorocatechol reactions. We conclude, therefore, that this ligand will be of restricted use in the preparation of metal complexes, and will lack the general applicability of perfluoropinacol.

Experimental

General

All reactions with tetrafluorocatechol and tetrabromocatechol were carried out under an atmosphere of nitrogen using outgassed solvents. The i.r. spectra were recorded as Nujol mulls on a Beckman model IR-10 instrument and visible spectra on a Beckman DK-1 instrument. Abbreviations used in describing spectra are: vs, very strong; s, strong; m, medium; w, weak; br, broad; sh, shoulder. ^{19}F n.m.r. spectra were recorded on a Varian model HA-100 spectrometer at 94.1 mHz. Magnetic moments were determined at 25° by the Gouy method using $Hg[Co(CNS)_4]$ as standard. Microanalyses were performed by Alfred Bernhardt Laboratories.

Tetrafluorocatechol

This compound was prepared by the procedure of Burdon *et al.* (2) up to the point where the benzodioxin and aluminum chloride were refluxed in benzene for 6 h and the mixture poured on ice. We then extracted the mixture repeatedly with approximately 1 *M* sodium hydroxide solution, the aqueous layer being run *immediately* into 2 *M* hydrochloric acid (the catechol oxidizes rapidly in basic solution). More acid was then added to p*H* about 1.0, and the solution extracted with diethyl ether until the extract no longer gave a coloration with aqueous ferric chloride. The ether was then dried ($MgSO_4$) and evaporated, and the semi-solid residue purified by repeated sublimation to give tetrafluorocatechol (m.p. 66–68°, lit. m.p. 67–69°). The ^{19}F n.m.r. spectrum showed a typical AA′XX′ spectrum (doublet of quartets) centered at 175.5 and 183.7 p.p.m. from $CFCl_3$. The i.r. spectrum showed absorptions at 3640(s), 3550(s), 3200(br), 2700(m), 2440(w), 2340(w), 2110(w), 1750(w), 1635(s), 1520(vs), 1480(s), 1320(s), 1225(s), 1160(w), 1150(w), 1135(w), 1000(s), and 795(m) cm^{-1}.

Use of the work-up procedure given by previous workers resulted in poorer yield and considerable contamination of the product with dibenzyl. Despite many attempts to improve the efficiency of this preparation by varying the reaction conditions, we were unable to obtain a yield over 10% based on hexafluorobenzene.

Reaction of TFC with Fe^{3+} and TMED

Excess TMED (2 ml) was added to TFC (0.8 g) in anhydrous methanol (10 ml) and iron(III) acetate (0.78 g) in methanol was added dropwise. After stirring for 4 h, the deep blue solution was filtered and evaporated to give the iron complex tetramethylethylenediaminebis(tetrafluorocatechol) iron(III) as a black powder.

Anal. Calcd. for $C_{18}H_{17}F_8O_4N_2Fe$: C, 40.6; H, 3.2; F, 28.5; N, 5.3; Fe, 10.5. Found: C, 40.7; H, 3.4; F, 28.9; N, 5.4; Fe, 10.3.

The electronic spectrum (MeOH solution) showed bands at 580 (ε = 3500) and 390 mμ (ε = 2200).

The i.r. spectrum showed absorptions at 2720(w), 1600(w), 1480(s), 1290(w), 1270(w), 1255(w), 1125(m), 1025(s), 1010(s), 980(s), 955(m), 805(m), 770(w), and 725(w) cm^{-1}.

The complex had a magnetic moment of 6.1 B.M. and gave a non-conducting solution in methanol. Its Mossbauer spectrum showed a center shift of 0.68 ± 0.07 mm/s, relative to sodium nitroprusside, a value typical of iron(III) compounds(13).

Reaction of TFC with Ni^{2+} and TMED

TFC (1.3 g) in ethanol (10 ml) was mixed with nickel nitrate hexahydrate (2.08 g) in water (15 ml). TMED was added dropwise with stirring until the p*H* of the solution reached 10, by which time a green precipitate had appeared. After stirring 10 min, the mixture was filtered and the precipitate recrystallized from methanol, washed with dichloromethane, and dried briefly *in vacuo* at 25°. Analysis showed it to be tetramethylethylenediamine nickel tetrafluorocatecholate dihydrate.

Anal. Calcd. for $C_{12}H_{20}F_4O_4N_2Ni$: C, 36.9; H, 5.2; F, 19.4; N, 7.2; Ni, 15.0. Found: C, 36.8; H, 5.3; F, 20.7; N, 7.5; Ni, 15.6.

Can. J. Chem. Downloaded from www.nrcresearchpress.com by 210.87.254.5 on 09/05/12
For personal use only.

The electronic spectrum (diffuse reflectance) showed peaks at 400(sh), 720(br), 855(sh), and 920(w) mμ; in solution (MeOH) the peaks were at 475(sh), 650, 1054, and 1452 mμ. The magnetic moment at 25° was 3.18 B.M.

On keeping at 65° *in vacuo* for 48 h, the green dihydrate was converted to the brown anhydrous tetramethylethylenediamine nickel tetrafluorocatecholate.

Anal. Calcd. for $C_{12}H_{16}F_4O_2N_2Ni$: C, 40.6; H, 4.5; F, 21.4; N, 7.9; Ni, 16.5. Found: C, 40.9; H, 4.5; F, 21.5; N, 8.0; Ni, 16.5.

The complex dissolved in anhydrous methanol to give a green solution absorbing at 475(sh), 651, 1055 and 1453 mμ. In dichloromethane, it gave a brown solution absorbing at 380(sh) and 475 mμ.

The i.r. spectrum showed peaks at 1760(m), 1470(br,s), 1290(s), 1243(w), 1200(w), 1132(s), 1100(w), 1077(w), 1047(w), 1000(br,s), 819(s), 772(m), 725(m), and 628(m) cm^{-1}.

This compound and the five succeeding nickel complexes were diamagnetic.

Reaction of TFC with Ni^{2+} and Triethylphosphine

TFC (0.9 g) and nickel nitrate hexahydrate (1.4 g) were dissolved in methanol (10 ml) and PEt_3 (0.6 g) added with stirring. Shiny brown crystals precipitated and were recrystallized from methanol to give bis(triethylphosphine nickel tetrafluorocatecholate.

Anal. Calcd. for $C_{18}H_{30}F_4O_2NiP_2$: C, 45.5; H, 6.4; F, 16.0; Ni, 12.4. Found: C, 45.3; H, 6.0; F, 16.2; Ni, 12.5.

Mol. Wt. Calcd.: 475. Found (osmometric in benzene): 520.

The electronic spectrum (CH_2Cl_2 solution) showed bands at 415 (ε = 530) and 575 mμ (ε = 170). A diffuse reflectance spectrum gave peaks at 412 and 562 mμ. The i.r. spectrum showed peaks at 1470(s), 1295(s), 1250(m), 1128(s), 1000(s,br), 776(s), 730(s), and 685(w) cm^{-1}.

Reaction of TFC with Ni^{2+} and 1,2-Bis(diphenylphosphino)ethane (diphos)

TFC (0.6 g) and nickel(II) sulfate hexahydrate (1.65 g) in methanol (10 ml) were mixed with diphos (1.5 g) in tetrahydrofuran (15 ml) and stirred for 1 h. A brown crystalline material separated which was identified as diphos nickel tetrafluorocatecholate.

Anal. Calcd. for $C_{32}H_{24}F_4O_2P_2Ni$: C, 60.3; H, 3.8; F, 11.9. Found: C, 60.4; H, 3.9; F, 12.2.

The electronic spectrum (CH_2Cl_2 solution) showed one band at 570 mμ (ε = 220). The i.r. spectrum showed peaks at 2405(w), 1915(w), 1815(w), 1760(w), 1700(w), 1465(s), 1280(s), 1180(w), 1155(w), 1115(m), 1095(m), 1000(s), 865(m), 805(m), 745(s), 710(s), 700(s), 685(s), and 645(m) cm^{-1}.

Reaction of Tetrabromocatechol with Ni^{2+} and PEt_3

This preparation was carried out in the same manner as that of the corresponding TFC complex. The compound bis(triethylphosphine) nickel tetrafluorocatecholate formed brown crystals.

Anal. Calcd. for $C_{18}H_{30}Br_4O_2NiP_2$: C, 30.1; H, 4.2; Br, 44.5; Ni, 8.2. Found: C, 29.9; H, 3.9; Br, 44.4; Ni, 8.3.

The electronic spectrum (CH_2Cl_2 solution) showed one band at 560 mμ (ε = 170). The i.r. spectrum showed peaks at 1450(s), 1350(m), 1275(s), 1240(s), 1220(m), 1035(s), 1010(w), 980(w), 945(s), 768(s), 750(s), 730(s), and 635(m) cm^{-1}.

Tetramethylammonium Bis(tetrabromocatechol)nickelate(II)

Stoichiometric amounts of tetrabromocatechol and nickel nitrate were dissolved in methanol and tetramethylammonium hydroxide (15% in methanol) added dropwise with stirring. The complex precipitated as brown plates.

Anal. Calcd. for $C_{20}H_{24}O_4Br_8N_2Ni$: C, 22.8; H, 2.3; N, 2.7; Br, 60.6; Ni, 5.6. Found: C, 22.6; H, 2.5; N, 2.5; Br, 60.5; Ni, 5.6.

The i.r. spectrum showed peaks at 1485(s), 1350(m), 1274(s), 1233(s), 1031(m), 950(s), 935(s), 785(s), 750(s), and 640(w) cm^{-1}.

Reaction of Tetrabromocatechol, Ni^{2+}, and TMED

Tetrabromocatechol (2.0 g) and nickel nitrate (1.4 g) were dissolved in methanol (30 ml) and TMED (6.0 g) added. The dark brown precipitate was recrystallized from methanol to give tetramethylethylenediamine nickel tetrabromocatecholate.

Anal. Calcd. for $C_{12}H_{16}Br_4O_2N_2Ni$: C, 24.1; H, 2.7; N, 4.7; Br, 53.4; Ni, 9.8. Found: C, 24.3; H, 2.8; N, 4.8; Br, 53.5; Ni, 10.0.

The electronic spectrum (acetone solution) showed a band at 485 mμ (ε = 105). The i.r. spectrum showed peaks at 1435(s), 1340(m), 1270(s), 1232(s), 1205(w), 1120(w), 1040(m), 1010(m), 985(w), 940(s), 815(s), 770(s), 745(s), and 645(w), cm^{-1}.

Reaction of TFC with Cu^{2+}

TFC and copper sulfate pentahydrate in a 2:1 molar ratio were dissolved in methanol and methanolic potassium hydroxide added to p*H* 7, at which point an olive-green solid precipitated. On drying *in vacuo* at 65° for 48 h, the solid became purple, in which state it was analyzed as potassium bis(tetrafluorocatechol) cuprate.

Anal. Calcd. for $C_{12}F_8O_4CuK_2$: C, 28.7; F, 30.3; Cu, 12.7. Found: C, 28.9; F, 30.2; Cu, 12.9.

The electronic spectrum (methanol solution) showed one band at 740 mμ (ε = 220). In the i.r. spectrum, peaks were at 1620(m), 1495(s), 1275(m), 1135(m), 1000(s), and 720(m) cm^{-1}.

The purple solid rapidly reverted to the green color on exposure to atmosphere.

Reaction of TFC with Cu^{2+} and TMED

TFC (0.4 g) and copper sulfate pentahydrate (0.55 g) in water (10 ml) were kept under vacuum and TMED (0.5 g) distilled into the flask. The resulting slurry was filtered to give a grey–green powder insoluble in common solvents. Analysis identified it as tetramethylethylenediammonium bis(tetrafluorocatechol) cuprate.

Anal. Calcd. for $C_{18}H_{18}F_8N_2O_4Cu$: C, 39.9; H, 2.6; F, 28.1; N, 5.2. Found: C, 40.3; H, 2.7; F, 28.5; N, 5.1.

The i.r. spectrum showed peaks at 2610(w), 2360(s,br), 1620(m), 1490(s), 1275(s), 1155(m), 1120(s), 1070(m), 1000(s), 790(w), and 725(m) cm^{-1}.

Reaction of TFC and $GeCl_4$ in DMF

To TFC (1.0 g) in DMF (25 ml) was added germanium tetrachloride (0.59 g). A white solid formed initially, then redissolved. After stirring 15 min, the volume of the solution was then reduced to 5 ml, and a white solid

separated. It was recrystallized from methanol to give bis(dimethylformamide) germanium bis(tetrafluorocatecholate).

Anal. Calcd. for $C_{18}H_{14}F_8O_4N_2Ge$: C, 37.4; H, 2.4; F, 26.3; N, 4.8. Found: C, 37.3; H, 2.6; F, 26.5; N, 4.9.

The i.r. spectrum showed peaks at 1760(w), 1650(s), 1510(s), 1490(s), 1350(s), 1270(m), 1250(m), 1170(w), 1150(s), 1130(w), 1080(w), 1000(s), 870(w), 760(w), 710(s), and 675(s) cm^{-1}.

Financial support of this work was provided by the National Research Council of Canada. We are indebted to Dr. G. M. Bancroft, of this department, for kindly determining the Mossbauer spectrum.

1. M. ALLAN and C. J. WILLIS. J. Am. Chem. Soc. **90**, 5343 (1968).
2. J. BURDON, V. A. DAMODARAN, and J. C. TATLOW. J. Chem. Soc. 763 (1964).
3. H. B. GRAY. *In* Transition metal chemistry. Vol. 1. *Edited by* R. L. Carlin. Marcel Dekker Inc., New York, N.Y., 1965. p. 239.
4. G. N. SCHRAUZER. *In* Transition metal chemistry. Vol. 4. *Edited by* R. L. Carlin. Marcel Dekker Inc., New York, N.Y., 1968. p. 299.
5. F. LALOR *et al.* J. Am. Chem. Soc. **89**, 2278 (1967).
6. R. H. HOLM, A. C. BALCH, A. DAVISON, A. H. MAKI, and T. E. BERRY. J. Am. Chem. Soc. **89**, 2866 (1967).
7. A. L. BALCH, I. G. DANCE, and R. H. HOLM. J. Am. Chem. Soc. **90**, 1139 (1968).
8. F. ROHRSCHEID, A. L. BALCH, and R. H. HOLM. Inorg. Chem. **5**, 1542 (1966).
9. A. CALLAGHAN, A. J. LAYTON, and R. S. NYHOLM. Chem. Commun. 399 (1969).
10. W. S. CRIPPS and C. J. WILLIS. Unpublished observations.
11. R. E. RUNDLE and M. PARASOL. J. Chem. Phys. **20**, 1487 (1952).
12. H. J. EMELÉUS and J. J. ZUCKERMAN. J. Organomet. Chem., **1**, 328 (1964).
13. G. M. BANCROFT, A. G. MADDOCK, W. K. ONG, and R. H. PRINCE. J. Chem. Soc. A, 723 (1966); 1966 (1967).

Can. J. Chem. Downloaded from www.nrcresearchpress.com by 210.87.254.5 on 09/05/12
For personal use only.

A Method for Gas–Liquid Chromatographic Identification of *O*-Methyl Ethers of 2-Deoxy-2-methylamino-D-glucose and 2-Deoxy-2-methylamino-D-galactose[1]

P. A. J. GORIN AND R. J. MAGUS

National Research Council of Canada, Prairie Regional Laboratory, Saskatoon, Saskatchewan

Received March 23, 1971

A method is described for the g.l.c. identification of *O*-methyl ethers that can be formed on methylation–fragmentation analysis of polymers containing 2-acetamido-2-deoxy-D-glucopyranose or 2-acetamido-2-deoxy-D-galactopyranose units. The possible 2-deoxy-*O*-methyl-2-methylamino-D-glucoses and -D-galactoses and their derived hexitols, were converted to their acetates and trimethylsilyl ethers. The g.l.c. was carried out using a number of liquid phases and the retention times of the derivatives were found to be sufficiently diverse to make positive identifications of unknowns feasible.

Une méthode est décrite pour identifier par c.l.g les éthers *O*-méthylés pouvant se former pendant les analyses par méthylation et fragmentation de polymères contenant soit l'unité acétamido-2 désoxy-2 D-glucopyranose soit l'unité acétamido-2 désoxy-2 D-galactopyranose. Les composés possibles, les désoxy-2 *O*-méthyl méthylamino-2 D-glucoses et D-galactoses ainsi que leurs dérivés hexitols, ont été transformés en acétates et éthers triméthylsililés correspondants. En utilisant un certain nombre de phases liquides, la c.l.g conduit, pour les dérivés, a des temps de retention suffisamment différents pour permettre une bonne identification des composés inconnus.

Canadian Journal of Chemistry, 49, 2583 (1971)

Partially *O*-methylated 2-deoxy-2-methylamino derivatives of D-glucose (1) and D-galactose (2) have been synthesized to serve as standards in structural investigations of polymers or oligomers containing 2-acetamido-2-deoxy-D-glucopyranose and 2-acetamido-2-deoxy-D-galactopyranose units, respectively. These fragments can be formed when methylation by the Kuhn (3) (methyl iodide-*N*,*N*-dimethylformamide – silver oxide) or Hakomori (4, 5) (methyl iodide–sodium hydride–dimethyl sulfoxide) procedures are carried out and the product hydrolyzed by acid. Two effective methods for identification of the *N*-methyl hexosamine derivatives are by means of an amino acid analyzer and by g.l.c. as trimethylsilyl (t.m.s.) ethers (1, 2). The former method can be used (6–8) when a 0.2–1.0 mg sample of *O*-methyl ether is available. Each derivative has a characteristic retention time and gives an absorption maximum of 570 mμ on reaction with ninhydrin. When only microgram quantities are available, however, the g.l.c. method must be used. To increase the effectiveness of the g.l.c. analysis of complex mixtures of *O*-methyl sugars a more detailed investigation of the g.l.c. properties of the above standards was made. The present work describes the preparation of a number of new derivatives and the determination of their retention times on a variety of liquid phases.

A previous g.l.c. examination of the t.m.s. ethers of 2-deoxy-*O*-methyl-2-methylamino-D-glucoses (1) and their D-galactose isomers (2) showed that most of the hexoses can be distinguished, even though each compound generally gives rise to two peaks, arising from the α- and the β-anomer. However, Perry and Webb (9) have obtained a superior separation by g.l.c. of the acetates of derived 2-amino-2-deoxy-*O*-methyl-D-glucitols using a column containing neopentyl glycol sebacate (NPGSb) at 245°, where only one peak is formed from each parent hexitol. Although the acetates of 2-deoxy-*O*-methyl-2-methylamino-D-hexitols could neither be eluted from the column under these conditions nor from a column containing diethylene glycol adipate – diethylene glycol (4:1), a separation was obtained using a UC W-98 (a methyl vinyl silicone) liquid phase at 210° (Table 1). Different emergence orders were observed using the t.m.s. ethers on UC W-98 liquid phase at 160° and NPGSb liquid phase at 140° (Table 1). The acetates were prepared using acetic anhydride – pyridine at 100°, a process which results in formation of *O*-acetyl, *N*-acetyl derivatives. Treatment of the hexitols with trimethylsilyl chloride – hexamethyldisilazanepyridine at 100° (10) should result in formation of *O*-, but

[1]NRCC No. 12001.

Can. J. Chem. Downloaded from www.nrcresearchpress.com by 210.87.254.6 on 09/05/12
For personal use only.

TABLE 1. Retention times, in minutes, of derivatives of 2-deoxy-*O*-methyl-2-methylamino derivatives of D-glucitol and D-galactitol

O-Methyl derivative of 2-deoxy-2-methyl-amino-D-hexitol	Retention time (min)		
	Trimethylsilyl derivatives on NPGSb at 140°*	Trimethylsilyl derivatives on UC W-98 at 160°†	Acetates on UC W-98 at 210°
Glucitol series			
Unsubstituted	9.4	8.40	3.85
3-	8.3	5.81	3.08
4-	7.8	5.63	3.60
6-	6.8	5.32	2.70
3,4-Di-	8.2	4.08	2.53
3,6-Di-	6.6	3.68	2.10
4,6-Di-	5.8	3.53	2.37
3,4,6-Tri-	6.8	2.62	1.65
Galactitol series			
Unsubstituted	8.8	7.99	4.00
3-	9.2	6.28	3.35
4-	7.6	5.55	3.80
6-	7.2	5.38	2.70
3,4-Di-	9.2	4.58	2.87
3,6-Di-	7.6	4.22	2.20
4,6-Di-	6.7	3.70	2.45
3,4,6-Tri-	9.6	3.05	1.88

*NPGSb, neopentylglycol sebacate.
†UC W-98, a methyl vinyl silicone.

not *N*-trimethylsilyl derivatives by analogy with the trimethylsilylation of galactosamine (11). The acetylation and etherification processes are effective since all of the resulting derivatives gave one peak on g.l.c.

Another series of retention times was obtained using the t.m.s. ethers of 2-deoxy-*O*-methyl-2-methylamino-D-hexoses on UC W-98 liquid phase at 160° and the corresponding acetates on UC W-98 at 210° (Table 2). The emergence orders differ from each other and from those obtained with the t.m.s. ethers on NPGSb at 140° (1, 2; Table 2).

It can be seen from Tables 1 and 2 that by use of the six different g.l.c. conditions a good resolution of the 2-deoxy-*O*-methyl-*N*-methyl-amino derivatives of D-glucose and D-galactose can be obtained together with a wide variance in their emergence orders. It should therefore be possible to methylate a polysaccharide known to contain 2-acetamido-2-deoxy-D-glucose or -D-galactose units, hydrolyze the product, and detect the resulting *O*-methyl-*N*-methyl derivative(s) in the presence of other *O*-methyl ethers. It appears that superimposition of the g.l.c. signals of these two types of compound under six analysis conditions is unlikely. An alternative method of identification of *N*-methyl sugars in a methylation product is possible in which they are concentrated by ion-exchange chromatography prior to g.l.c. A suggested procedure is reduction of the methylation mixture by sodium borohydride followed by preferential absorption of the *N*-methyl hexitol on a column of a cation-type ion exchange resin. It can then be eluted with aqueous ammonium hydroxide and examined by the g.l.c. procedure.

Experimental

Preparation of Derivatives for Gas–Liquid Chromatography

(1) Preparation of 2-Deoxy-O-methyl-2-methylamino-D-hexitols

N-Methyl-hexosamine hydrochlorides (10 mg) were dissolved in water (1 ml) containing sodium borohydride (5 mg). After 3 h excess reagent was destroyed with acetic acid and the solutions evaporated to dryness. Boric acid was removed as trimethyl borate by dissolving the residues in methanol and evaporating, a process that was repeated three times.

(2) Preparation of Acetates

Samples of *N*-methyl-hexosamine hydrochloride and *N*-methyl-hexosaminitol containing approximately 1 mg of material were treated with acetic anhydride – pyridine (0.2 ml:0.2 ml) at 100° for 2 h and the solutions then evaporated *in vacuo*. The residues were dissolved in chloroform (0.5 ml) and applied to the g.l.c. columns in 3 μl aliquots.

Can. J. Chem. Downloaded from www.nrcresearchpress.com by 210.87.254.6 on 09/05/12
For personal use only.

TABLE 2. Retention times, in minutes, of derivatives of 2-deoxy-*O*-methyl-2-methylamino derivatives of D-glucose and D-galactose on g.l.c.

O-Methyl derivative of 2-deoxy-2-methyl-amino-D-hexose	Retention times (min)		
	Trimethylsilyl derivatives on NPGSb at 140° (1, 2)	Trimethylsilyl derivatives on UC W-98 at 160°	Acetates on UC W-98 at 210°
Glucose series			
Unsubstituted	12.4(76%), 20.4(24%)	3.95(15%), 5.86(60%) 8.02(25%)	1.72(28%), 3.63(72%)
3-	9.4(81%), 12.8(19%)	3.54(90%), 4.56(10%)	1.39(15%), 3.35(85%)
4-	7.3(73%), 12.3(27%)	3.36(76%), 4.46(24%)	1.42(22%), 3.13(78%)
6-	13.8(78%), 16.6(22%)	4.45(73%), 5.10(27%)	1.17(25%), 2.39(75%)
3,4-Di-	6.5(84%), 9.4(16%)	2.30(99%), 2.70(1%)	1.07(8%), 2.49(92%)
3,6-Di-	10.4	2.59(83%), 2.88(17%)	0.88(8%), 2.17(92%)
4,6-Di-	8.1(80%), 10.6(20%)	2.35(78%), 2.80(22%)	0.90(13%), 1.95(87%)
3,4,6-Tri-	7.3	1.55	1.50
Galactose series			
Unsubstituted	9.2(67%), 12.9(23%)	4.90(71%), 5.40(29%)	1.92(21%), 3.57(39%) 3.73(39%)
3-	9.9 , 11.6	3.68	1.50(17%), 3.02(83%)
4-	9.5(78%), 14.5(22%)	3.60(76%), 4.44(24%)	1.50(35%), 3.29(65%)
6-	8.5(89%), 11.5(11%)	3.33(94%), 3.70(6%)	1.27(16%), 2.45(84%)
3,4-Di-	12.4(76%), 15.8(24%)	2.87(70%), 3.15(30%)	1.19(15%), 2.67(85%)
3,6-Di-	8.7 , 10.2	2.37(95%), 2.94(5%)	2.00(14%), 2.10(86%)
4,6-Di-	7.7(75%), 12.2(25%)	2.20(85%), 2.74(15%)	0.97(27%), 2.08(73%)
3,4,6-Tri-	10.2(76%), 12.8(24%)	1.69(89%), 1.88(11%)	0.74(20%), 1.67(80%)

(3) Trimethylsilyl Ethers

One milligram samples of sugar were converted to the t.m.s. ethers by the method of Sweeley *et al.* (10). Two-tenths of a milliliter of reagent was used and the solutions (3 μl) were applied directly to the g.l.c. column.

Gas–Liquid Chromatographic Procedure

The columns used are as follows: *(1)* a 3 ft × 1/8 in. (i.d.) glass column containing 10% of NPGSb (Applied Science Laboratories, State College, Pennsylvania) on silanized, acid-washed Chromosorb W (80–100 mesh), pretreated with Silyl 8 column conditioner (0.2 ml; Pierce Chemical Company). *(2)* A 4 ft × 1/8 in. (i.d.) glass column containing 3.8% of silicone gum UC W-98 (Chromatographic Specialties Ltd., Brockville, Ontario) on silanized, acid-washed Chromosorb W (80–100 mesh).

The g.l.c. unit was a Hewlett–Packard Model 402 incorporating a hydrogen flame detector operated under the following conditions: H_2 pressure: 12 p.s.i., rotameter reading 2.5; He pressure: 45 p.s.i., rotameter reading 3; air pressure: 30 p.s.i., rotameter reading 3.75.

1. P. A. J. GORIN and A. J. FINLAYSON. Carbohydr. Res. **18**, 269 (1971).
2. P. A. J. GORIN. Carbohydr. Res. **18**, 281 (1971).
3. R. KUHN, H. TRISCHMANN, and I. LÖW. Angew. Chem. **67**, 32 (1955).
4. S. HAKOMORI. J. Biochem. Tokyo, **55**, 205 (1964).
5. H. BJÖRNDAL, C. G. HELLERQVIST, B. LINDBERG, and S. SVENSSON. Angew. Chem. **9**, 610 (1970).
6. P. A. J. GORIN. Can. J. Chem. **49**, 527 (1971).
7. P. A. J. GORIN and D. E. EVELEIGH. Biochem. **9**, 5023 (1970).
8. P. A. J. GORIN, J. F. T. SPENCER, and A. J. FINLAYSON. Carbohydr. Res. **16**, 161 (1971).
9. M. B. PERRY and A. C. WEBB. Can. J. Chem. **47**, 4091 (1969).
10. C. C. SWEELEY, R. BENTLEY, M. MAKITA, and W. W. WELLS. J. Am. Chem. Soc. **85**, 2497 (1963).
11. C. C. SWEELEY, D. VANCE, and G. MARINETTI *editors*. Lipid chromatographic analysis, Marcel Dekker Co., New York, N.Y. 1967. pp. 465–495.

Can. J. Chem. Downloaded from www.nrcresearchpress.com by 210.87.254.6 on 09/05/12
For personal use only.

Can. J. Chem. Downloaded from www.nrcresearchpress.com by 210.87.254.40 on 09/05/12
For personal use only.

Oxydation des alcènes par l'ion thallique. I. Stéréochimie et mécanisme de l'oxydation des cyclohexènes

C. Freppel, R. Favier, J.-C. Richer, et M. Zador
Département de Chimie, Université de Montréal, Montréal, Québec

Reçu le 15 mars 1971

L'étude de la stéréochimie des diols formés dans l'oxydation du tert-butyl-3 cyclohexène par le sulfate thallique a permis de mettre en évidence la participation du groupe hydroxyle en α lors de la rupture de la liaison C—Tl de l'intermédiaire organothalleux. En effet, seuls les diols *trans* ont été obtenus ce qui exclut la substitution S_N2 par l'eau. Il est suggéré que l'oxydation thallique en milieu aqueux peut constituer une synthèse en une seule étape de diols *trans* dans le cas des systèmes rigides où l'organothalleux intermédiaire a une configuration diaxiale. La formation d'un seul diol diaxial lors de l'oxydation du tert-butyl-4 cyclohexène tend à confirmer cette hypothèse.

The stereochemistry of the diols obtained by oxidation of 3-*t*-butylcyclohexene by thallic sulfate indicates that the α hydroxyl group participates in the breaking of the C—Tl bond of the intermediate organothallous compound. The fact that only the *trans* diols are obtained indicates that an S_N2 substitution of the thallium can be excluded. We suggest that the thallic oxidation in aqueous media of olefin of rigid conformation is an excellent one-step method of preparing *trans* diols. The formation of the *trans* diaxial diol upon oxidation of 4-*t*-butylcyclohexene tends to confirm that hypothesis.

Canadian Journal of Chemistry, 49, 2586 (1971)

Introduction

Au cours des dernières années l'étude de l'oxydation thallique de nombreuses substances organiques a été effectuée (1). L'oxydation thallique des oléfines conduit à la formation de diols-1,2 ainsi qu'à la formation de produits carbonylés qui peuvent être prépondérants en milieu non-aqueux (2, 3).

Bien que le mécanisme réactionnel ait déjà été discuté par plusieurs auteurs (1–5), le mécanisme de rupture du lien C—Tl conduisant aux diols-1,2 n'a pas été élucidé quant à savoir s'il se fait par attaque S_N2 du solvant ou par participation du groupe hydroxyle en α. En vue d'élucider ce point nous avons étudié l'oxydation du tert-butyl-3 cyclohexène par le sulfate thallique en système hétérogène solution aqueuse de sulfate thallique – oléfine surnageant.

Le tert-butyl-3 cyclohexène a été choisi à cause de la rigidité de sa conformation, ce qui permet l'obtention de renseignements univoques sur le mécanisme réactionnel. De plus, l'identification des quatre diols isomères conformationnels est possible par comparaison avec les produits purs (6). La nature des diols obtenus permet de préciser la stéréochimie de la réaction, et ceci en comparaison avec les études d'addition électrophile effectuées sur ce système (7).

Pour compléter les résultats il nous semblait intéressant de les comparer avec ceux pour le cyclohexène, obtenus dans les mêmes conditions.

Le sulfate thallique en milieu aqueux a été choisi comme réactif pour plusieurs raisons: (*i*) il est très facile à préparer, (*ii*) sa réactivité n'est pas trop influencée par la présence d'ions sulfate (8), (*iii*) l'extraction des produits n'est pas affectée par la présence d'acide perchlorique qui est à éviter à cause de son instabilité en milieu anhydre, et (*iv*) il n'y a pas de réactions secondaires avec le solvant.

Résultats et discussions

L'oxydation du cyclohexène (**1**) par le sulfate thallique conduit avec un faible rendement à de nombreux produits d'oxydation (**2**, **3**, **4**, **5**, et **6**).

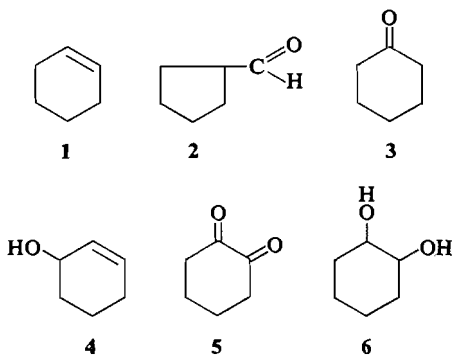

1 **2** **3** **4** **5** **6**

Can. J. Chem. Downloaded from www.nrcresearchpress.com by 210.87.254.40 on 09/05/12
For personal use only.

TABLEAU 1. Produits d'oxydation du cyclohexène

Produit	2	3	4	5	6
Temps de rétention (min), colonne *a**	10.5	15.0	25.5	46.5	144.0
Temps de rétention (min), colonne *b*†	3.0	4.7	10.4	22.0	67.6

*Colonne *a*: 12′ × ¼″, Carbowax 4000, 6% déposé sur Fluoropak 40 60–80 mesh; débit: 12 ml/s gaz porteur; N_2; T = 155 °C; Chromatographe Varian, Aerographe 90-P.
†Colonne *b*: 6′ × 1/8″, DEGS 15% déposé sur gaz chrom. R 80–100 mesh; débit: 1 ml/s; gaz porteur N_2; T = 120 °C; Chromatographe F.M. 700.

Le tableau 1 résume les résultats obtenus. L'identification des produits a été effectuée par c.p.g. par superposition des pics grâce à des produits de référence.

L'oxydation du tert-butyl-3 cyclohexène (**7**) conduit avec un bon rendement principalement à un mélange de diols *trans* (**8** et **9**) isomères (R = H).

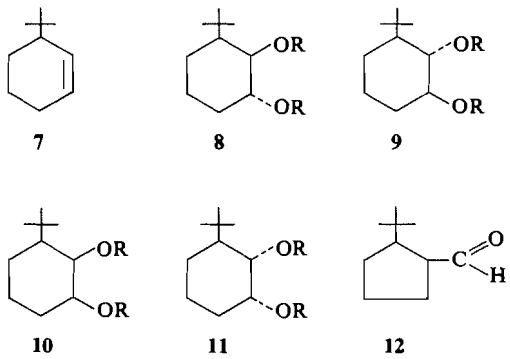

7 **8** **9**

10 **11** **12**

Le tableau 2 résume les quantités relatives des produits obtenus.

D'après les résultats obtenus pour les deux systèmes les constatations suivantes s'imposent: (*i*) l'oxydation qui est très peu sélective dans le cas du cyclohexène et qui donne des produits d'oxydation successive, apparaît au contraire très sélective dans le cas du tert-butyl-3 cyclohexène, (*ii*) alors que la réaction est pratiquement instantanée avec le cyclohexène, celle du tert-butyl-3 cyclohexène est très lente, (*iii*) l'oxydation du tert-butyl-3 cyclohexène conduit uniquement à des diols *trans* (**8** et **9**) à l'exclusion des diols *cis* (**10** et **11**), (*iv*) cette réaction permet donc la synthèse en une seule étape des diols *trans* (**8** et **9**).

TABLEAU 2. Produits d'oxydation du tert-butyl-3 cyclohexène

Produit R = $Si(CH_3)_3$	8	9	10	11	Inconnu†
Temps de rétention (min)*	5.2	8.1	7.2	6.5	
Pourcentage (%)	73	10	1<	1<	12

*Colonne 6′ × 1/8″, UCW98, 10% déposé sur Diatoport S 80–100 mesh; débit: 40 ml/min; gaz porteur: N_2; T = 170 °C; Chromatographe: F.M. 700.
†Selon toute probabilité d'après des indications spectroscopiques et par analogie au cas du cyclohexène il s'agit de l'aldéhyde **12**.

Le mécanisme du schéma 1 permet de rendre compte d'une manière cohérente des différences observées entre les deux systèmes et permet de préciser le mécanisme intime de formation des diols par oxydation thallique.

Dans toutes les réactions la première étape est celle de formation d'un complexe entre l'ion thallique et la double liaison, un ion ponté à trois centres, comme cela est généralement admis par analogie avec l'oxymercuration (3–5). Ce type d'intermédiaire, semblable à un ion bromonium cyclique, a été proposé récemment lors de l'étude de l'influence des substituants sur la vitesse d'oxydation par l'acétate thallique (10).

Dans le cas du tert-butyl-3 cyclohexène deux différents ions pontés, *cis* **13** et *trans* **14** peuvent exister. L'ouverture de l'ion ponté *cis* **13** donne exclusivement un seul organothalleux **15** alors que son isomère *trans* **14** en donne deux, **16** et **17**. Ceci est analogue à l'ouverture d'ions pontés de ce type observés dans l'addition électrophile sur le tert-butyl-3 cyclohexène (6) et (7).

Le fait que les seuls produits observés soient des diols *trans* (**8** et **9**) à l'exclusion de diols *cis* (**10** et **11**), d'une part indique la nécessité de faire appel à un ion ponté à trois centres et constitue donc une nouvelle preuve de son existence et, d'autre part, est en accord avec un mécanisme faisant intervenir la participation du groupe hydroxyle des intermédiaires organothalleux (**15**, **16**, et **17**). Les résultats prouvent sans ambiguité qu'il n'y a pas de substitution S_N2 du Tl par le solvant tel qu'invoqué par plusieurs auteurs (3–5). Il est évident que le mécanisme de participation ne peut être prépondérant que si l'organothalleux intermédiaire a la configuration *trans* diaxiale **15**. Dans le cas d'un organothalleux diéquatorial, le mécanisme de régression de cycle est sans doute favorisé. Il est à noter que les résultats seraient compatibles avec un mécanisme S_Ni avec rétention de configuration ou avec la formation d'un intermédiaire époxyde à partir de **15**, **16**, et **17**, mais aucune évidence expérimen-

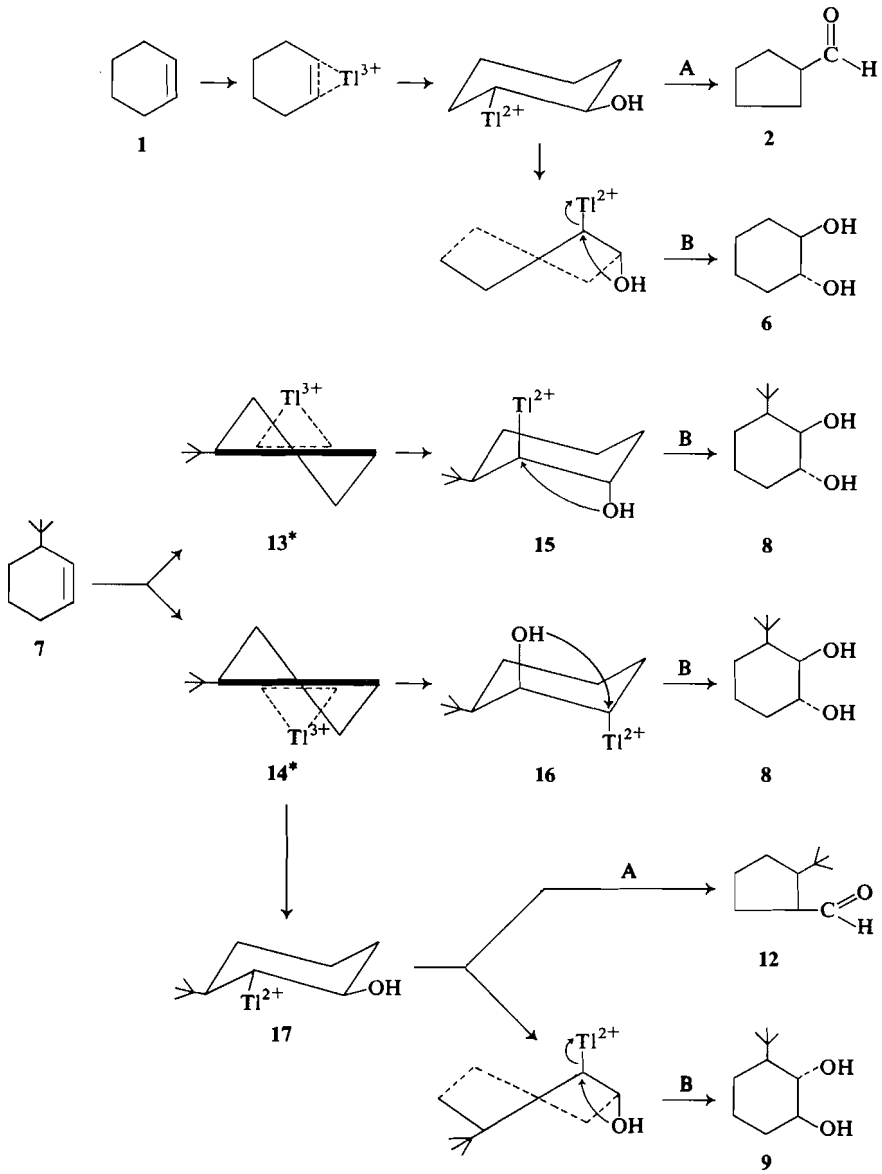

SCHÉMA 1. (A) Régression de cycle, (B) participation, où Tl^{3+} représente diverses espèces thallique en solution (8). *La représentation des conformations est identique à celle souvent utilisée pour les époxydes cyclohexaniques (9).

tale n'est disponible pour confirmer une ou l'autre de ces hypothèses.

Dans le cas du cyclohexène, l'ouverture de l'ion ponté conduit principalement à l'organothalleux diéquatorial, qui par un mécanisme de régression pouvant devenir prépondérant dans certaines conditions (3), conduit à l'aldéhyde **2** correspondant. Bien que l'intermédiaire chaise diaxiale conduirait aussi aux diols *trans*, on n'en a pas tenu compte étant donné qu'il est largement défavorisé par rapport à son isomère diéquatorial.

Pour conclure, le mécanisme, proposé pour la formation de diols-1,2 par oxydation thallique d'oléfines en solution aqueuse, peut être généralisé de la manière suivante: formation d'un ion ponté à trois centres, ouverture en un organothalleux et, participation du groupe hydroxyle lors de la rupture de la liaison C—Tl. L'applica-

Can. J. Chem. Downloaded from www.nrcresearchpress.com by 210.87.254.40 on 09/05/12
For personal use only.

Can. J. Chem. Downloaded from www.nrcresearchpress.com by 210.87.254.40 on 09/05/12
For personal use only.

tion de ce mécanisme très général à la synthèse de diols-1,2 nécessite cependant une condition: l'organothalleux intermédiaire doit être de nature *trans* diaxial. Cette condition est réalisée dans le cas du tert-butyl-4 cyclohexène et, comme prévu par le mécanisme proposé on obtient exclusivement un diol *trans* diaxial, le tert-butyl-4 *cis* cyclohexane-diol-1,2 *trans*. De plus, si l'on désire des rendements en diols élevés, l'oxydation en milieu aqueux est la plus avantageuse à cause de la prépondérance de la participation du groupe hydroxyle.

En conclusion, il est donc probable que dans d'autres systèmes rigides, tels les stéroides, la méthode d'oxydation thallique en milieu aqueux hétérogène puisse constituer une méthode intéressante de synthèse en une seule étape de diols *trans* et nous poursuivons nos travaux dans ce domaine.

Partie expérimentale

(1) Oxydation du tert-butyl-3 cyclohexène

Dans un ballon à fond rond de 2 l, 2.2 mmol de tert-butyl-3 cyclohexène est ajouté à 900 ml d'eau et à 4 mmol de sulfate thallique obtenu par dissolution de l'oxyde thallique dans 100 ml d'une solution d'acide sulfurique 2 *M*. Le mélange réactionnel est agité 6 jours à 35 °C puis la solution est saturée de sel et extraite trois fois avec 400 ml d'éther. La solution aqueuse est rendue basique et extraite à nouveau avec 400 ml d'éther. Les phases éthérées sont réunies et neutralisées jusqu'à p*H* neutre au moyen d'une solution aqueuse de soude. La solution organique est séchée sur du carbonate de sodium anhydre et concentrée sous vide pour donner 250 mg (ρ = 67%) d'un produit huileux dont la c.p.g. sur une petite partie sililée (11) indique la présence de 73% du diol *trans* diaxial **8**, 10% du diol *trans* diéquatorial **9**, et 18% d'un produit non identifié.

Une expérience similaire réalisée à température ordinaire pendant 4 jours conduit à un produit constitué par 57% de tert-butyl-3 cyclohexène (**1**) n'ayant pas réagit, 6.5% d'un produit non identifié, et 36.5% de diol constitué par 88% de diol diaxial **8** et 12% de diol diéquatorial **9**.

Les diols isomères **8**, **9**, **10**, et **11** ont été préparés par la méthode décrite auparavant (6).

(2) Oxydation du cyclohexène

L'oxydation du cyclohexène a été réalisé dans des conditions analogues mais la réaction a été terminée au bout d'une dizaine de minutes. Par suite de la grande solubilité de certains des composés dans l'eau ainsi que l'instabilité de l'aldéhyde **2**, le pourcentage des produits obtenu après extraction n'a pas de signification. Toutefois l'aldéhyde **2** est le produit majeur et la quantité de diol formé ne dépasse probablement pas 5%.

(3) Oxydation du tert-butyl-4 cyclohexène

L'oxydation du tert-butyl-4 cyclohexène a été réalisée de la même manière que **7**, mais la réaction étant beaucoup plus rapide, elle était terminée au bout de 4 h. En partant de 2 g de tert-butyl-4 cyclohexène, après trois extractions à l'acétate d'éthyle, on a obtenu 1.15 g de tert-butyl-4 *cis* cyclohexanediol-1,2 *trans* cristallin qui est le seul produit obtenu. L'identification du produit a été effectuée par comparaison des spectres r.m.n. et i.r. avec le produit de référence obtenu par l'ouverture des époxydes correspondants (12). Les points de fusions sont identiques, p.f. 143–144 °C (litt. (12) 141–142 °C).

Les auteurs remercient le Conseil National de Recherches du Canada et le Ministère de l'Education du Québec pour les octrois de recherches accordés.

1. R. R. GRINSTEAD. J. Org. Chem. **26**, 238 (1961); H. J. KABBE. Ann. **656**, 204 (1962); C. B. ANDERSON et S. WINSTEIN. J. Org. Chem. **28**, 605 (1963); S. UEMURA, R. KITO, et K. ICHIKAWA. Nippon Kagaku Zasshi (Jap.) **87**, 986 (1966); K. WIBERG et W. KOCH. Tetrahedron Lett. 1179 (1966); S. UEMURA, A. TABATA, M. OKANO, et K. ICHIKAWA. Chem. Commun. 1630 (1970); E. C. TAYLOR et A. MCKILLOP. Account. Chem. Res. **3**, 338 (1970).
2. P. M. HENRY. J. Am. Chem. Soc. **87**, 4423 (1965).
3. A. MCKILLOP, J. D. HUNT, E. C. TAYLOR, et F. KIENZLE. Tetrahedron Lett. No. **60**, 5275 (1970).
4. P. M. HENRY. Advan. Chem. Ser. No. 70, 126 (1968).
5. R. FAVIER et M. ZADOR. Can. J. Chem. **47**, 3539 (1969).
6. J.-C. RICHER et C. FREPPEL. Can. J. Chem. **48**, 145 (1970).
7. J.-C. RICHER et C. FREPPEL. Tetrahedron Lett. No. **51**, 4411 (1969); C. FREPPEL. Thèse de doctorat. Université de Montréal, Montréal, Québec, 1971.
8. R. FAVIER et M. ZADOR. Can. J. Chem. **48**, 2407 (1970).
9. M. HANACK. Conformation theory. Academic Press, 1965. p. 149.
10. R. J. OUELLETTE, G. KORDOSKY, C. LEVIN, et S. WILLIAMS. J. Org. Chem. **34**, 4104 (1969).
11. J. HEDGLEY et W. G. OVEREND. Chem. Ind. 378 (1968); C. SWEELEY, R. BENTLEY, M. MAKITA, et W. WELLS. J. Am. Chem. Soc. **85**, 2497 (1963); A. E. PIERCE. Silylation of organic compounds. Pierce Chemical Co., 1968; Handbook of silylation. Handbook GPA-3. Pierce Chemical Co., 1970.
12. C. W. DAVEY, E. L. MCGINNIS, J. M. MCKEOWN, G. D. MEAKINS, M. W. PEMBERTON, et R. N. YOUNG. J. Chem. Soc. 2674 (1968); N. A. LEBEL et R. F. CZAJA. J. Org. Chem. **26**, 4768 (1961).

Can. J. Chem. Downloaded from www.nrcresearchpress.com by 210.87.254.42 on 09/05/12
For personal use only.

Oxydation des alcènes par l'ion thallique. II. Méthode d'oxydation électrochimique catalysée par l'ion thallique

R. Favier, C. Freppel, J.-C. Richer, et M. Zador
Département de chimie, Université de Montréal, Montréal, Québec

Reçu le 2 avril 1971

L'oxydation électrochimique de substrats organique contenant des liaisons doubles a été réalisée. L'ion thallique joue un rôle d'intermédiaire ou de catalyseur dans l'oxydation:

$$Tl(I) \xrightarrow{\text{anode}} Tl(III)$$

$$Tl(III) + \text{alcène} \longrightarrow \text{produits} + Tl(I)$$

En effectuant l'oxydation à potentiel contrôlé et dans un système à compartiments anodique et cathodique séparés on a obtenu des rendements faradayiques intéressants, ce qui permet l'application de la méthode en synthèse dans les cas où l'oxydation thallique est sélective.

Electrochemical oxidation of organic substrates containing double bonds has been accomplished. Thallic ion is a catalyst in the oxidation:

$$Tl(I) \xrightarrow{\text{anode}} Tl(III)$$

$$Tl(III) + \text{alkene} \longrightarrow \text{products} + Tl(I)$$

Relatively high current efficiencies are obtained while performing the oxidation at controlled potential, and by separating the anodic and cathodic compartments; this fact allows the use of this method in synthesis in cases where the thallic oxidation is selective.

Canadian Journal of Chemistry, **49**, 2590 (1971)

Introduction

Comme le montre la littérature récente, le Tl(III) oxyde des substances contenant une liaison double sans dégrader ces dernières et, dans certains cas, peut conduire à la synthèse en une seule étape d'un produit d'oxydation (1).

Le but du présent travail est la mise au point d'une méthode électrochimique permettant l'oxydation électrochimique de diverses oléfines où le Tl(I) est réoxydé *in situ* et le Tl(III) ne joue donc qu'un rôle d'intermédiaire d'après le schéma:

[1] $$Tl(I) \xrightarrow{\text{anode}} Tl(III)$$

[2] $$Tl(III) + \text{alcène} \longrightarrow \text{produits} + Tl(I)$$

Dans la somme des éqs. 1 et 2, les deux états d'oxydation du thallium disparaissent; le thallium a donc un rôle de catalyseur de l'oxydation électrochimique de l'alcène. La transformation du Tl(I) en Tl(III) est connue (2), et dernièrement une méthode continue a pu être réalisée (3). Toutefois à cause du potentiel d'oxydo-réduction élevé du système Tl^+/Tl^{3+}, $E_0 = 1.25$ V (4), et à cause de la possibilité d'oxydation des substances organiques à des potentiels élevés, une étude approfondie est nécessaire: ceci est aussi important si l'on désire obtenir des rendements faradayiques élevés.

Résultats et discussions

Les considérations théoriques, confirmées par des essais préliminaires, montrent que pour empêcher la réduction du Tl(I) à la cathode, il est indispensable de travailler à l'aide d'un système à deux compartiments.

Pour trouver le domaine d'oxydation du Tl(I), on a étudié les diagrammes d'intensité–potentiel (5) du Tl(I) et du solvant avec l'électrolyte de support, dans les conditions expérimentales, choisies pour l'oxydation par la suite: aux mêmes concentrations, utilisant les mêmes électrodes fixes à grande surface, agitation magnétique etc.

Les résultats montrent qu'aux environs d'un potentiel, E, de 2 V par rapport au calomel saturé, l'oxydation du Tl(I) se fait de manière satisfaisante (courbe *a*, fig. 1). L'étude similaire de l'électrolyte support ($HClO_4$ dans l'eau) en

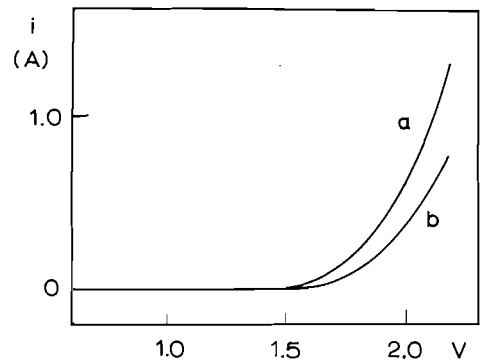

FIG. 1. Diagrammes intensité–potentiel. Solvant, H_2O; $T = 26 \pm 0.5$ °C; agitation magnétique; $[HClO_4] = 1.0\ M$; courbe *a*, $[TlClO_4] = 1.0 \times 10^{-2}\ M$; courbe *b*, $[TlClO_4] = 0$, avec ou sans cyclohexanedione-1,2 cyclohexène, tert-butyl-3 cyclohexène.

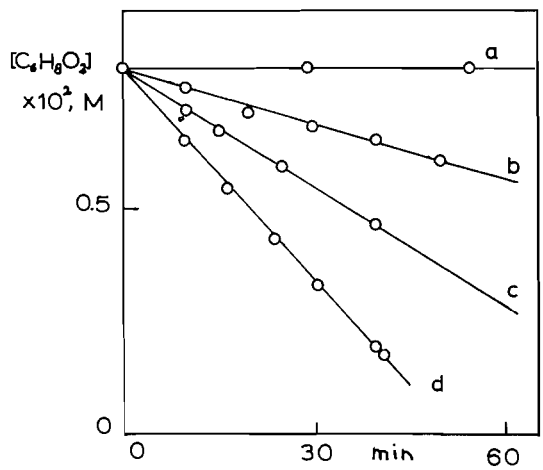

FIG. 2. Oxydation de la cyclohexanedione-1,2. Solvant, H_2O; $T = 26 \pm 0.5$ °C; agitation magnétique; $[HClO_4] = 0.9\ M$; courbe *a*, $[TlClO_4] = 0$, $E = 2.0$ V; courbe *b*, $[TlClO_4] = 1.0 \times 10^{-2}\ M$, $E = 1.9$ V; courbe *c*, $[TlClO_4] = 1.0 \times 10^{-2}\ M$, $E = 2.0$ V; courbe *d*, $[TlClO_4] = 1.0 \times 10^{-2}\ M$, $E = 2.15$ V.

absence de Tl(I) révèle qu'à ces potentiels l'oxydation de l'eau est loin d'être négligeable (courbe *b*, fig. 1) ce qui se manifeste par un dégagement d'oxygène à l'anode. Il en découle qu'il est nécessaire d'opérer à des potentiels aux environs de 2 V et que si on veut un rendement faradayique raisonnable, on ne peut pas augmenter ce potentiel au delà de 2 à 2.2 V; il est impossible donc d'opérer aux potentiels correspondants au courant limite du système Tl^+/Tl^{3+}.

Oxydation de la cyclohexanedione-1,2

Pour trouver les caractéristiques générales de l'oxydation électrochimique, la cyclohexanedione-1,2 a été étudiée comme exemple type étant donné que (*i*) la disparition de sa forme énol prépondérante peut être facilement suivie par spectrophotométrie u.v., (*ii*) sa grande solubilité dans l'eau permet une étude sur un système homogène, et (*iii*) la cinétique de son oxydation par le Tl(III) est connue dans diverses conditions (6, 7).

La fig. 2 montre quelques résultats types obtenus lors de l'oxydation à potentiel contrôlé (8). La courbe *a* représente une expérience en absence de $TlClO_4$; on constate que le réactif seul ne subit aucune oxydation. Les autres courbes représentent la disparition de la cyclohexanedione-1,2 en présence du Tl(I) d'après le schéma suivant:

$$[3] \qquad Tl^+ \xrightarrow{\text{anode}} Tl^{3+} + 2e^-$$

$$[4] \qquad Tl^{3+} + C_6H_8O_2 + H_2O \longrightarrow Tl^+ + C_6H_8O_3 + 2H^+$$

L'oxydation se fait à vitesse constante, qui est d'ailleurs celle de l'éq. 3; l'étape suivante, [4], est très rapide dans les conditions expérimentales (6) et la concentration du Tl(III) reste très petite tant qu'il reste du réactif en solution. Le temps de demi-vie du Tl(III) au début de la réaction est de l'ordre de 0.05 min (6) ce qui est très petit par rapport à l'échelle de temps de la fig. 2. Comme la concentration du Tl(I) reste pratiquement constante, la vitesse d'oxydation anodique reste stationnaire. Les résultats, tels que présentés à la fig. 2 permettent de calculer le rendement faradayique, *R*, dans diverses conditions. Il est défini par:

$$R = -\frac{d[C_6H_8O_2]}{dt} \times \frac{VnF}{i}$$

où *V* est le volume total du compartiment anodique; *n* est le nombre d'électrons impliqués, 2; *F* est le faraday; *i* est le courant moyen; et *t* le temps.

Les rendements faradayiques sont résumés au tableau 1; ils sont tous nettement inférieurs à un ce qui est normal à cause de l'oxydation de l'eau aux potentiels utilisés. La comparaison des expériences *1*, *2*, et *3* montre que bien que la vitesse de l'oxydation du réactif augmente par augmentation du potentiel imposé (fig. 2), le rendement faradayique diminue dans les mêmes conditions, parce que l'oxydation de l'eau

Can. J. Chem. Downloaded from www.nrcresearchpress.com by 210.87.254.42 on 09/05/12
For personal use only.

TABLEAU 1. Rendements faradayiques de l'oxydation de la cyclohexanedione-1,2*

Expérience	Compartiment anodique (*M*) $[TlClO_4]$	Compartiment anodique (*M*) $[C_6H_8O_2]$	Potentiel(V) (par rapport au calomel)	Courant moyen(A)	R
1	1.0×10^{-2}	7.8×10^{-3}	1.9	0.09	0.33 ± 0.05
2	1.0×10^{-2}	7.8×10^{-3}	2.0	0.25	0.24 ± 0.04
3	1.0×10^{-2}	7.8×10^{-3}	2.15	0.8	0.14 ± 0.02
4	5.0×10^{-3}	7.4×10^{-3}	1.9	0.09	0.24 ± 0.04
5†	1.0×10^{-2}	1.1×10^{-2}	2.0	0.13	0.13 ± 0.02
6‡	1.0×10^{-2}	0.95×10^{-2}	8.0‡	0.7	0.21 ± 0.03

*Solvant, H_2O; $[HClO_4] = 0.9\ M$; volume de solution dans chaque compartiment, 200 ml; $T = 26 \pm 0.5$ °C
†Solvant, acétonitrile–eau 60% v/v; $[HClO_4] = 0.72\ M$.
‡Système à deux électrodes, source D.C.

TABLEAU 2. Oxydation des cyclohexènes

Produit	Temps de rétention (min) Colonne *a*	Colonne *b*	Colonne *c*	%
A. Cyclohexène; $R = 0.2 \pm 0.03$				
Cyclopentane carboxaldehyde	10.5	3.0		16.6
Cyclohexanone	15.0	4.7		16.8
Cyclohexène-2-ol	25.5	14.		22.7
Cyclohexanedione-1,2	46.5	22.		26.7
Cyclohexanediol-1,2	144	67.6		15.4
B. tert-Butyl-3 cyclohexène; $R = 0.16 \pm 0.02$				
tert-Butyl-3 cyclohexanediol-1 *trans*, 2 *cis**			14.6	44.3
tert-Butyl-3 cyclohexanediol-1 *cis*, 2 *trans*			16.2	33.2
Inconnu†			12.0	22.5

*Les termes *cis* et *trans* précisent la configuration d'un substituant par rapport au groupe tert-butyl supposé équatorial dans tous les cas.
†D'après les évidences spectroscopiques il s'agit probablement du tert-butyl-2 cyclopentane carboxaldehyde.

devient de plus en plus importante. La diminution du rendement faradayique quand on diminue la concentration du Tl(I) peut être expliquée de la même manière (expériences *1* et *4*). Finalement, l'utilisation d'un mélange d'acétonitrile–eau comme solvant, fait également diminuer le rendement (expérience *5*). Nous avons observé une anomalie de la courbe intensité–potentiel de ce système commençant à ~1.4 V, due probablement à la réaction du solvant (9). L'oxydation dans ce solvant a été étudiée en vue de son utilisation dans le cas de certaines oléfines complètement insolubles dans l'eau.

Les résultats obtenus lors de l'étude à potentiel contrôlé, à l'aide de l'appareillage à trois électrodes, ont permis de trouver les conditions expérimentales, tel que la différence de potentiel entre l'électrode de travail et l'électrode auxiliaire, pour l'utilisation d'une source D.C. à potentiel variable. Ce dernier est beaucoup plus accessible et courant dans les laboratoires ou dans l'industrie et si son utilisation se fait dans de bonnes conditions, permet d'obtenir des résultats semblables aux précédents (expérience *6*).

Oxydation du cyclohexène et du tert-butyl-3 cyclohexène

L'oxydation des cyclohexènes a été effectuée dans un système hétérogène: solution aqueuse–alcène surnageant avec des rapports alcène/Tl(I) = 100–200. Les résultats sont groupés dans le tableau 2. Les rendements faradayiques sont du même ordre de grandeur que ceux obtenus auparavant. Les produits sont les mêmes que ceux obtenus lors de l'oxydation directe par le sulfate thallique (10) avec une augmentation de la proportion des produits d'oxydation successive. Dans le cas du tert-butyl-3 cyclohexène seules les diols *trans* sont obtenus comme lors de l'oxydation directe (10).

L'ensemble des résultats obtenus permet donc de conclure, qu'en choisissant avec soin le potentiel, l'oxydation électrochimique, catalysée par le Tl(III), de composés organiques à liaison double peut être effectuée avec des rendements faradayiques intéressants. Evidemment la sélectivité de cette méthode ne peut pas dépasser celle de l'oxydation directe par le Tl(III) mais elle offre comme avantage d'être relativement peu

Can. J. Chem. Downloaded from www.nrcresearchpress.com by 210.87.254.42 on 09/05/12
For personal use only.

couteuse, nécessitant d'une part une source D.C. à potentiel variable simple et d'autre part, de faibles quantités de sels thalleux pour la transformation de grandes quantités de substrats organiques.

Partie expérimentale

Appareillage

La cellule réactionnelle a deux compartiments cylindriques, d'un volume de 300 ml chacun, qui sont séparés par un verre frité, type M, de 27 mm de diamètre se trouvant au milieu du tube de verre reliant les deux compartiments; dans ce système la diffusion du Tl^+ est négligeable d'un compartiment à l'autre. La cellule a été placée dans un thermostat pour maintenir la température constante. Les courbes intensité–potentiel ont été réalisées à l'aide d'un appareil Tacussel Servovit-9A, un milliampèremètre Tacussel Bluxy 427 et un enregistreur X-Y Sefram TRVAC.

L'oxydation à potentiel contrôlé a été réalisée à l'aide d'un potentiostat Tacussel-PRT 20-2X en utilisant un système à trois électrodes dont deux sont placées dans le compartiment anodique, l'électrode de travail et l'électrode de référence au calomel saturé, la troisième, l'électrode auxiliaire se trouve au compartiment cathodique. L'électrode de travail et l'électrode auxiliaire sont en platine de 10 cm^2 et de 6 cm^2 respectivement.

Le générateur D.C. à potentiel variable est un Electro Product Laboratories Inc. Mode D-612T filtered D.C. Power supply.

Préparation du perchlorate thalleux

Le perchlorate thalleux a été obtenu par réduction du perchlorate thallique en solution par le peroxyde d'hydrogène; par abaissement de la température, le perchlorate thalleux précipite de la solution contenant environ 4 *M* d'ions perchlorate; la solution de perchlorate thallique a été obtenu par dissolution de l'oxyde thallique (Fairmount Chemical Co. Inc.) dans l'acide perchlorique.

Oxydation de la cyclohexanedione-1,2

Les solutions de cyclohexanedione-1,2 ont été fraîchement préparées pour chaque série d'expériences par dissolution du réactif solide (J. T. Baker) étant donné qu'en conservant les solutions pendant de longues périodes la forme énolique se transforme en cétone (6, 11).

L'oxydation a été effectuée à potentiel contrôlé ou en utilisant la source D.C. La disparition de la forme énolique dans le compartiment anodique a été suivie par l'analyse spectrophotométrique des échantillons prélevés à intervalles réguliers à la longueur d'onde $\lambda = 265$ mμ. Le volume des solutions est de 200 ml dans chacun des compartiment; le compartiment cathodique contient de l'acide perchlorique comme électrolyte à la même concentration que celle du compartiment anodique.

Oxydation du cyclohexène

La composition du compartiment anodique est la suivante: 200 ml de solution aqueuse 0.9 *M* en $HClO_4$ et 0.01 *M* en $TlClO_4$ + 20 ml de cyclohexène ($\sim$ 0.2 mol). L'oxydation est effectuée à potentiel contrôlé: 2.1 V (par rapport au calomel): $i = 0.3$ A. Après 96 h la totalité de l'alcène disparaît; l'extraction continue au chloroforme conduit à un mélange de produits correspondant à $\sim$60% de l'alcène de départ, ce qui correspond à un rendement faradayique d'au moins 0.2. L'identification des produits est effectuée par c.p.g. par superposition des pics avec des produits de référence. Le cyclopentane carboxaldéhyde a été obtenu par ozonolyse du cyclopentyl-3 acrylate d'éthyle. Colonne *a*: 12′ × 1/4″, Carbowax 4000, 6% Fluoropak 40 60–80 débit: 12 ml/s; gaz porteur N_2; T = 155 °C; Chromatographe Varian, Aerographe 90P. Colonne *b*: 6′ × 1/8″: DEGS 15% gaz chrom. R 80–100; débit 1 ml/s; gaz porteur N_2; T = 120 °C; Chromatographe F.M. 700.

Oxydation du tert-butyl-3 cyclohexène

Les méthodes et conditions expérimentales sont identiques à celles décrites ci-dessus. La quantité d'alcène étant de 15 ml ($\sim$0.095 mol), après 96 h la totalité a réagit ($R \sim 0.16$). La chromatographie a été effectuée sur les esters sililés. Les produits de référence ont été obtenus par ouverture des époxydes (12). Colonne *c*: 6′ × 1/4″; 10% Sil Gum Rub UC-98 diatoport 80–100; débit: 1 ml/s; T = 160 °C; Chromatographe F. M. 700.

Les auteurs remercient le Conseil National de Recherches du Canada et le Ministère de l'Education du Québec pour les octrois de recherches accordés ainsi que le professeur M. Abraham du Département de Chimie pour avoir bien voulu mettre à leur disposition divers appareils électrochimiques.

1. R. R. Grinstead. J. Org. Chem. **26**, 238 (1961); H. J. Kabbe. Ann. **656**, 204 (1962); C. B. Anderson et S. Winstein. J. Org. Chem. **28**, 605 (1963); P. M. Henry. J. Am. Chem. Soc. **87**, 4423 (1965); S. Nemura, R. Kito, et K. Ichikawa. Nippon Kagaku Zasshi (Jap.) **87**, 986 (1966); A. McKillop, J. D. Hunt, E. C. Taylor, et F. Kienzle. Tetrahedron Lett. **60**, 5275 (1970).
2. W. Frendlich. Nouveau traité de chimie minérale. Masson, 1961. p. 901.
3. A. H. Frye. Fr. 1556518; Chem. Abstr. **72**, 17996*d* (1970).
4. W. M. Latimer. Oxidation potentials. Prentice-Hall 1959. p. 165.
5. G. Milazzo. Electrochimie. Dunod, 1969. p. 284; R. W. Murray et C. N. Reilley. *Dans* Treatise on analytical chemistry. I. M. Kolthoff et P. J. Elving, éditeurs. Part. I. Vol. 4. Interscience, 1963. p. 2170.
6. R. Favier et M. Zador. Can. J. Chem. **47**, 3539 (1969).
7. R. Favier et M. Zador. Can. J. Chem. **48**, 2407 (1970).
8. G. Milazzo. Electrochimie. Dunod, 1969. p. 302; R. W. Murray et C. N. Reilley. *Dans* Treatise on analytical chemistry. I. M. Kolthoff et P. J. Elving, éditeurs. Part I, Vol. 4. Interscience, 1963. p. 2196.
9. R. Favier. Thèse de doctorat. Université de Montréal, Montréal, Québec, 1970.
10. C. Freppel. Thèse de doctorat. Université de Montréal, Montréal, Québec, 1971.
11. R. Bakule et F. A. Long. J. Am. Chem. Soc. **85**, 2309 (1963).
12. J.-C. Richer et C. Freppel. Can. J. Chem. **48**, 145 (1970).

Can. J. Chem. Downloaded from www.nrcresearchpress.com by 210.87.254.42 on 09/05/12
For personal use only.

Can. J. Chem. Downloaded from www.nrcresearchpress.com by 210.87.254.42 on 09/05/12
For personal use only.

Isomérisation des époxydes

KRZYSZTOF JANKOWSKI ET JEAN-YVES DAIGLE
Département de Chimie, Université de Moncton, Moncton, Nouveau-Brunswick

Reçu le 30 mars, 1971

L'isomérisation des époxydes sur les cycles à cinq et à six a été réalisée par l'action du cyanate de potassium en milieu éthanol–eau. Les spectres de r.m.n. des époxydes *trans* et *cis* ont été étudiés.

Isomerization of five and six-membered ring epoxides was realized through the action of potassium cyanate in ethanol–water medium. The n.m.r. spectra of *trans* and *cis* epoxides were studied.

Canadian Journal of Chemistry, 49, 2594 (1971)

En s'inspirant de la réaction d'obtention d'épithiocyclohexane (1), par l'action de thiocyanate de potassium sur l'époxycyclohexane, nous avons réalisé l'isomérisation des époxydes par le traitement avec le cyanate de potassium (schéma 1).

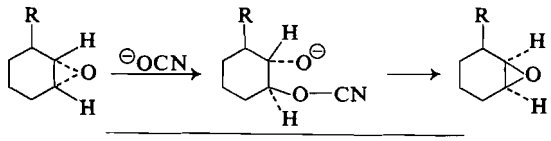

SCHÉMA 1

L'époxyde *trans* (du départ) s'isomèrise donc en époxyde *cis* et la réaction atteint probablement un équilibre. L'isomérisation des époxydes avec notre méthode peut être appliquée là où l'obtention d'un époxyde spécifique est difficile (p. ex. pour des époxydes stéroidaux (2)). Tout d'abord l'époxydation de méthyl-2 cyclopentene (1) avec l'acide *m*-chloroperbenzoïque donne un mélange d'époxydes *trans* **2***a* et *cis* **2***b* avec un rapport 60:40.

L'époxydation de l'hydroxy-2 cyclohexene (**3**) avec même peracide donne principalement l'époxyde *trans* **4***a* (3).

Les preuves de l'isomérisation ont été apportés par l'étude des spectres r.m.n. (tableaux 1 et 2).

Le mélange des époxydes **2***a* et *b* après l'isomérisation dans des conditions standards a révélé la présence de 44% d'isomère **2***a* et 56% d'isomère **2***b*. Nous avons observé que les protons oxiranniques d'époxyde *trans* se trouvent déplacés $\Delta\delta = +0.06$ p.p.m. par rapport aux mêmes protons d'un époxyde *cis*. Cette différence nous a servi pour l'identification des époxydes.

Nous avons observé que les époxycyclohexanes s'isomèrisent mieux que les époxycyclopentanes. Le signal du proton sur le noyau oxirannique d'époxyde *trans* est également déplacé ($\Delta\delta = +0.12$ p.p.m.) vers les champs plus bas par rapport au même proton d'époxyde *cis*. Cette relation a déjà été observée par nous mêmes (2) et par Tori *et al.* (4) et en général la différence est plus grande pour les époxydes sur les cycles à six que des époxydes sur les cycles à cinq.

L'action du cyanate de potassium sur l'époxyde acétylé **6***a* donne en plus de l'isomérisation (20%), le mélange des deux autres époxydes **4***a* et *b* dû à la déacétylation en milieu basique (les protons oxiranniques 3.31 et 3.18, les protons en α d'hydroxyle 4.1 p.p.m.).

Les preuves supplémentaires des structures des époxydes ont été obtenues par l'étude des spectres r.m.n. des dérivés hydroxylés (ouverture des époxydes en milieu basique).

Le mélange des époxydes **2***a* et *b* hydrolysé a donné principalement le méthyl-3 cyclopentanediol-1,2 (**7**) possédant la structure *trans* diéquatorial des deux groupements hydroxylés (déplacement chimiques des C*H*O 2.73 et 3.15). On voit également deux signaux du méthyle 0.37 et 0.44 p.p.m. attribuables aux méthyles axial et équatorial correspondants.

L'époxyde **4***b* hydroxylé (i.r. 3480 cm^{-1} pont hydrogène (5) absent pour la structure **4***a*) a donné le cyclohexane-triol-1,2,3-D,L-1,2/3 (**8**). Nous avons isolé également une petite quantité d'un cyclohexane-triol-1,2,3-*méso*-1,3/2 (**9**) obtenu par l'attaque nucléophile sur l'autre carbone d'époxyde.

Les structures **8** et **9** ont été prouvées par des spectres r.m.n. Le triol **8** donne un spectre identique à celui décrit par McCasland *et al.* (6), déplacements chimiques des protons en α d'hydroxyle 4.10, 3.45, et 3.78 p.p.m.

L'autre triol **9** a donné les signaux pour deux protons en α d'hydroxyle (symmétrie) à 3.40 p.p.m. et un proton à 3.10 p.p.m. Ces données

TABLEAU 1. Isomérisation des époxydes

Produits	% d'isomérisation*
trans-Méthyl-3 époxy-1,2 cyclopentane (**2***a*)	45
cis-Méthyl-3 époxy-1,2 cyclopentane (**2***b*)	28
cis-Hydroxy-3 époxy-1,2 cyclohexane (**4***b*)	65
trans-Hydroxy-3 époxy-1,2 cyclohexane (**4***a*)	35
trans-Acétoxy-3 époxy-1,2 cyclohexane (**6***a*)	20†
cis-Acétoxy-3 époxy-1,2 cyclohexane (**6***b*)	30†

*Par les spectres de r.m.n.
†Déacétylation des produits; ~50% du matériel isomère hydroxylé *trans* et *cis*.

TABLEAU 2. Données physiques des produits **1–9**

Produit	Point d'ébullition (°C/mm Hg)	Résonance magnétique nucléaire δ (p.p.m.) $CDCl_3$ —CH—CH—	Δδ OH *cis–trans*	Autres
1 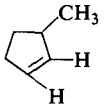	83	—	—	CH=CH 5.8, CH_3 0.94, CH_2—C=C 2.2 cycle 0.8–1.3
2*a** 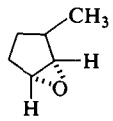	144–7	3.34	0.05	CH_3 0.73, cycle 0.8–1.4
2*b** 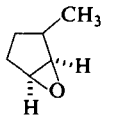	144–7	3.29	—	CH_3 0.82, cycle 0.8–1.3
7† 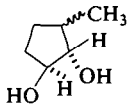	130–3/12	—	—	CH_3 0.44 et 0.37, OH 3.7 (échange) CH_3—C(OH)—CH(3.15)(OH)—CH(2.73)(OH), cycle 0.8–1.7
3 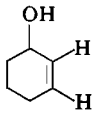	63–5/12	—	—	OH 3.75 (échange) *CH*—OH 4.12 CH=CH 5.73 cycle 1.6–2.1
4*b* 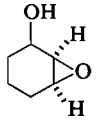	83–50/9	3.19	—	OH 3.38 (échange) *CH*—OH 3.94 cycle 1.2–2.1
4*a* 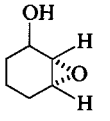	110/1.8	3.31	0.12	OH 3.2 (échange) *CH*—OH 3.96 cycle 1.3–2.0

Can. J. Chem. Downloaded from www.nrcresearchpress.com by 210.87.254.42 on 09/05/12
For personal use only.

TABLEAU 2. Données physiques des produits **1–9**

Produit	Point d'ébullition (°C/mm Hg)	Résonance magnétique nucléaire δ (p.p.m.) $CDCl_3$		
		—CH(O)—CH—	Δδ *OH cis–trans*	Autres
5 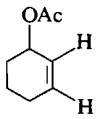	68–71/12	—	—	CH_3COO 1.95 CH—OCO 5.17 CH=CH 5.77 cycle 1.5–1.9
6*a* 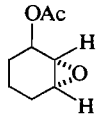	92/0.05	3.17	—	$OCOCH_3$ 2.07 CH—OCO 5.1 cycle 1.3–2.0
6*b* 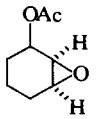	92–4/14	3.05	0.12	CH_3COO 2.03 CH—OCO 4.98 cycle 1.3–1.9
8‡ (6) 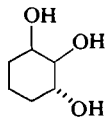	220/0.05	—	—	*CH*—O 4.10, 3.45 et 3.78
9‡ (6) 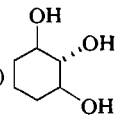	55/0.08	—	—	*CH*O 3.40 (2H), 3.10 (1H)

*Anal. calc. pour $C_6H_{10}O$ (98.1): C, 73.43; H, 10.27. Trouvé; C, 73.11; H, 9.95.
†Anal. calc. pour $C_6H_{12}O_2$ (116.2): C, 62.04; H, 10.41. Trouvé; C, 62.21; H, 10.45.
‡Spectre dans D_2O.

concordent bien avec la littérature (5). On a obtenu également une petite quantité du produit insaturé, l'élimination en milieu basique caractérisée par le proton oléfinique à ~5. 7 p.p.m. (p.é. 45°/25 mm). Finalement l'ouverture d'époxyde **6***a* dans la même condition donne le mélange des triols **8** et **9** à cause de la déacétylation du produit de départ suivi de l'hydrolyse.

Toutefois pour avoir plus de preuves de structures, des études avec l'oxygène marqué seront tentées.

Partie expérimentale

Les spectres de r.m.n. ont été enregistrés à l'aide de spectrophotomètre Varian A-60 et Varian HA-100 dans $CDCl_3$ ou D_2O (concentration ~5%).

Les spectres i.r. ont été enregistrés avec un appareil Perkin–Elmer, modèle 237-B ($CHCl_3$).

Les analyses élémentaires ont été faites par la Compagnie Midwest Microlab, Indianapolis, Indiana.

Les points d'ébullition n'ont pas été corrigés.

Les époxydes ont été purifiés par distillation; le rendement de la distillation est 70–90%.

Le produit **5** a été obtenu avec le rendement de 60% par l'acétylation du produit **3** (Aldrich Chemicals) selon une méthode habituelle (pyridine-anhydride acétique).

Epoxydation des oléfines

Une solution d'oléfine (0.12 mol) en benzène anhydre (200 ml) et une solution d'acide *m*-chloroperbenzoïque 0.48 mol (200 ml) ont été refroidies (0°) et ensuite mélangées. Le mélange a été agité pendant 48 h, puis lavé avec le carbonate de potassium à 10% et le solvant a été évaporé *in vacuo*. Le produit pur a été obtenu par distillation.

Isomérisation des époxydes

L'époxyde (0.01 mol) a été ajouté à une solution de cyanate de potassium (0.01 mol) en éthanol–eau (1:1, 10 ml). Cette solution a été agitée pendant 48 h (25°). Le produit brut a été extrait avec le chloroforme et seché avec le sulfate de sodium anhydre. Le solvant a été évaporé *in vacuo* et le produit a été distillé.

Can. J. Chem. Downloaded from www.nrcresearchpress.com by 210.87.254.42 on 09/05/12
For personal use only.

Ouverture des époxydes

L'époxyde (1 g) a été ajouté à une solution d'hydroxyde de sodium à 10% dans l'éthanol (10 ml). Le mélange a été agité pendant 50 h. Le produit a été extrait avec le chloroforme, l'extrait a été seché avec le sulfate de sodium anhydre, puis le solvant a été évaporé sous vide et le produit a été distillé.

Les auteurs remercient le Conseil National de Recherches du Canada, le Département de Chimie de l'Université de Montréal, et la Compagnie Bristol-Myers pour l'aide apportée à ce travail.

1. E. E. VAN TAMELEN. J. Am. Chem. Soc. **73**, 3444 (1951).
2. K. JANKOWSKI et J.-Y. DAIGLE. Synth. 32 (1971).
3. H. B. HENBEST et R. A. L. WILSON. J. Chem. Soc. 1958 (1957).
4. K. TORI, T. KOMENO, et T. NAKAGAWA. J. Org. Chem. **29**, 1136 (1964).
5. R. STEYN et H. Z. SABLE. Tetrahedron, 3579 (1969).
6. G. E. MCCASLAND, M. D. NAUMANN, et L. J. DURKAM. J. Org. Chem. **30**, 3079 (1966). H. Z. SABLE, W. M. RITCHEY, et J. E. NORDLANDER. J. Org. Chem. **30**, 3771 (1966). G. FARGES et A. KERGOMAND. Bull. Soc. Chim. Fr. 4476 (1969).

Can. J. Chem. Downloaded from www.nrcresearchpress.com by 210.87.254.42 on 09/05/12
For personal use only.

Can. J. Chem. Downloaded from www.nrcresearchpress.com by 210.87.254.105 on 09/05/12
For personal use only.

Composés de coordination de molécules soufrées. II. Complexes pseudo-tétraédriques et plan du nickel(II) avec quelques dithiole-1,2 thiones-3

FRANÇOIS YVES PETILLON ET JACQUES EMILE GUERCHAIS
Laboratoire de Chimie Minérale, U.E.R. des Sciences, Avenue Le Gorgeu, Université de Brest, 29N, France

Reçu le 10 mars 1971

L'étude dans l'infrarouge lointain permet de distinguer les complexes NiI_2L_2 pseudo-tétraédriques, originaux (L = $R_1R_2C_3S_3$ où $R_1 = CH_3$ et $R_2 = H$, $R_1 = R_2 = CH_3$, $R_1 = C_4H_3S$ et $R_2 = H$) du composé plan $NiI_2L'_2$ (L' = $R_1R_2C_3S_3$ où $R_1 = C_6H_5$ et $R_2 = H$). Les spectres électroniques enregistrés à l'état solide confirment cette distinction. Le déplacement de la bande $\nu_{C=S}$ de la molécule de dithiole-1,2 thione-3, qui rentre dans la sphère de coordination, est plus important dans les composés du cobalt(II) que dans ceux du nickel(II).

The study of the far infrared spectral region permits one to distinguish between the pseudo-tetrahedral complexes NiI_2L_2 (L = $R_1R_2C_3S_3$ where $R_1 = CH_3$ and $R_2 = H$, $R_1 = R_2 = CH_3$, $R_1 = C_4H_3S$ and $R_2 = H$) and the square planar complex $NiI_2L'_2$ (L' = $R_1R_2C_3S_3$ where $R_1 = C_6H_5$ and $R_2 = H$). The electronic spectra recorded in the solid state confirm the distinction. The displacement of the band $\nu_{C=S}$ of the molecule 1,2-dithiol-3-thione which enters the sphere of coordination is more marked in the complexes of cobalt(II) than in the corresponding nickel(II) complexes.

Canadian Journal of Chemistry, 49, 2598 (1971)

Introduction

Jusqu'à ce jour, ce sont essentiellement les complexes avec les sels de métaux lourds qui ont été isolés avec les dithiole-1,2 thiones-3 ($HgCl_2$, $HgBr_2$, $SbCl_3$, $SbCl_5$, CdI_2, $AgNO_3$, $AuCl_4$, $PdCl_4$, $PtCl_4$, $BiCl_3$, $SnCl_4$) (1 à 4), c'est-à-dire en majorité des composés avec les ions métalliques de la classe B définie par Ahrand, Chatt et Davies (5), ceci en raison de leur attrait pour l'atome de soufre polarisable. Parmi les éléments de la première série de transition, seuls les composés avec le cuivre et le fer, respectivement aux degrés d'oxydation deux et trois, ont été mentionnés (6).

Dans le cadre d'une étude sur les complexes métalliques des dithiole-1,2 thiones-3, nous avons dans un travail récent (7), préparé et étudié les composés du cobalt(II).

Dans ces derniers complexes l'entourage pseudo-tétraédrique du métal a été mis en évidence et sa coordination à la molécule organique par le soufre de la fonction thione a été suggérée. Il était intéressant d'étudier le comportement du nickel(II) vis-à-vis de ces coordinats cycliques soufrés. Aussi nous avons isolé les complexes iodés du nickel(II) avec différentes dithiole-1,2 thiones-3 substituées $R_1R_2C_3S_3$, où R_1 et R_2 sont des radicaux hydrogène, méthyle, phényle ou thiényle.

Pour les nouveaux composés obtenus nous proposons un entourage du métal en nous basant sur les spectres électroniques, les propriétés magnétiques et une étude dans l'infrarouge lointain. Nous verrons l'influence de la coordination sur les principales bandes d'absorption des molécules organiques. L'éventualité d'une coordination π sera discutée.

Partie expérimentale

Produits de départ

Les dithiole-1,2 thiones-3 ont été préparées selon des procédés décrits dans la littérature (8) par action du P_4S_{10} soit sur la R_1 dimercapto-propénone, soit sur le β,β'-diéthoxypropionate d'éthyle dans le xylène à reflux; elles ont été recristallisées dans l'acétone. L'iodure de nickel anhydre utilisé est un produit K & K Laboratories, Inc.

Etudes spectroscopiques

Les spectres infrarouges ont été enregistrés sur un appareil 225 Perkin–Elmer. La méthode de suspension dans le nujol a été utilisée dans toute la longueur du spectre.

Les spectres électroniques sont obtenus à l'aide d'un appareil Beckman DK 2A, en utilisant une sphère de réflectance.

Mesures des susceptibilités magnétiques

Les mesures ont été réalisées à la température ordinaire, selon la méthode de Gouy. Les corrections de diamagnétisme ont été calculées à partir des tables données dans la littérature (9).

Préparation des complexes

On dissout à chaud 0.005 mole de dithiole-1,2 thione-3 et 0.0025 mole d'iodure de nickel anhydre dans de

TABLEAU 1. Résultats analytiques

Complexes	C %		H %		S %		I %		Ni %	
	Calc.	Tr.	Calc.	Tr.	Calc.	Tr.	Calc.	Tr.	Calc.	Tr.
$NiI_2(C_3H_2S_3)_2$	12.40	12.4	0.69	0.83	33.11	33.3	43.68	43.4	10.10	9.97
$NiI_2(C_4H_4S_3)_2$	15.77	15.8	1.32	1.48	31.58	31.6	41.67	40.9	9.64	10.07
$NiI_2(C_5H_6S_3)_2$	18.85	18.8	1.89	2.08	30.19	30.2	39.84	39.6	9.21	9.01
$NiI_2(C_7H_4S_4)_2$	22.56	22.6	1.08	1.14	34.42	34.0	34.05	33.4	7.87	7.91
$NiI_2(C_9H_6S_3)_2$	29.48	29.4	1.65	1.66	26.24	26.2	34.62	34.2	8.00	8.05

l'acétone fraîchement distillée (~300 ml). On porte le mélange à reflux pendant 30 min sous agitation. On évapore une partie du solvant, un solide noir ou vert-sombre précipite. On recristallise le complexe dans de l'acétone. On obtient une poudre cristalline.

Analyses

Le carbone, l'hydrogène et le soufre ont été analysés par le service central de microanalyse du C.N.R.S. de Thiais. L'iodure est dosé par potentiométrie avec une solution de nitrate d'argent titrée. Le nickel(II) a été dosé par précipitation avec la diméthylglyoxime sous forme de $Ni(C_4H_7N_2O_2)_2$. Celui-ci a été séché vers 110 °C jusqu'à poids constant.

Résultats et discussion

Mesures magnétiques et conductimétriques

Les complexes obtenus sont peu solubles dans les solvants usuels (tétrachlorure de carbone, nitrométhane, nitrobenzène, chloroforme), et s'y décomposent très rapidement. De vert sombre les solutions deviennent jaunes ou brunes, au bout de quelques minutes. Même les solutions acétoniques ne sont pas très stables à faible concentration. Il a donc été impossible de mesurer leur conductivité.

Les résultats de l'analyse centésimale (tableau 1) sont en accord avec la formule NiI_2L_2, où L représente le coordinat organique. Plusieurs entourages du nickel sont possibles. D'autre part, bien qu'une structure ionique du type $[NiL_4]^{2+}[NiI_4]^{2-}$ ne soit pas à exclure a priori en l'absence de données conductimétriques, nous verrons que les spectres obtenus dans l'infrarouge lointain nous permettent d'écarter cette solution.

Les valeurs des moments magnétiques des produits (tableau 4) suggèrent un entourage plan du métal pour le di-iodobis (phényl-5 dithiole-1,2 thione-3) nickel(II) (composé *A*), et une symétrie pseudo-tétraédrique pour les quatre autres complexes (composés *B*). Pour ces derniers la contribution orbitale diminue avec l'encombrement stérique des substituants R_1 et R_2 des dithiole-1,2 thiones-3

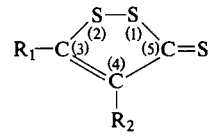

ce qui est logique, et le moment magnétique passe de 3.68 mB pour le di-iodobis (dithiole-1,2 thione-3) nickel(II), à 3.29 mB pour le di-iodobis (thiényl-5 dithiole-1,2 thione-3) nickel(II). Notons enfin que certains échantillons du complexe A présentent un léger paramagnétisme (<0.8 mB) qui serait probablement dû à la présence d'un isomère tétraédrique.

Spectres électroniques

Les spectres électroniques des complexes enregistrés à partir de solutions dans l'acétone sont identiques à ceux des coordinats organiques correspondants; cependant, ceux des composés $NiI_2(C_5H_6S_3)_2$ et $NiI_2(C_4H_4S_3)_2$ sont typiques d'une symétrie pseudo-tétraédrique, mais différent des spectres enregistrés à l'état solide. Aucune conclusion ne peut dont être tirée de cette étude en solution.

Composés B

Dans le domaine de fréquence 3000–15000 cm^{-1} les spectres par réflectance mettent en évidence trois à quatre bandes principales, caractéristiques d'un environnement pseudo-tétraédrique du nickel(II) (10) (voir tableau 2). Dans une symétrie T_d, trois transitions autorisées par spin sont attendues dans le visible. Par suite de l'abaissement de la symétrie à C_{2v} la transition ν_3, $^3T_1(F) \rightarrow {}^3T_1(P)$ apparaît en général sous forme de trois composantes ($^3T_1 \rightarrow {}^3A_2$, $^3T_1 \rightarrow {}^3B_1$, $^3T_1 \rightarrow {}^3B_2$), de même que la transition ν_1, $^3T_1(F) \rightarrow {}^3T_2(F)$, seule ν_2 n'est pas affectée. Sur les spectres une bande unique, assez intense, située vers 9000 cm^{-1} peut être assignée à la transition ν_2, $^3T_1(F) \rightarrow {}^3A_2(F)$. Un massif d'intensité notable, apparaissant entre 15000 et 11000 cm^{-1} serait l'enveloppe des pics corres-

Can. J. Chem. Downloaded from www.nrcresearchpress.com by 210.87.254.105 on 09/05/12
For personal use only.

Can. J. Chem. Downloaded from www.nrcresearchpress.com by 210.87.254.105 on 09/05/12
For personal use only.

TABLEAU 2. Attribution des bandes d'absorption des spectres électroniques des complexes (cm^{-1})

$NiI_2(R_1R_2C_3S_3)_2$	ν_1 $^3T_1(F) \rightarrow {}^3T_2(F)$	$^3T_1(F) \rightarrow {}^1D$†	ν_2 $^3T_1(F) \rightarrow {}^3A_2(F)$	ν_3 $^3T_1(F) \rightarrow {}^3T_1(P)$	$^3T_1(F) \rightarrow {}^1G$†		ν_1 $^1A_g \rightarrow {}^1B_{3g}$	Transfert de charge
$R_1 = R_2 = H$	~4160,6000		8980	13280				17480
$R_1 = CH_3, R_2 = H$	4470,5490		9025	11750	16080*			17640
$R_1 = R_2 = CH_3$	4480,5360		9115	11780				17860
$R_1 = C_4H_3S, R_2 = H$	4810	6780,7750	9410	12190				17920
$R_1 = C_6H_5, R_2 = H$						11490*†	18750* 16030	

*Epaulement.
†Transition interdite par spin.

TABLEAU 3. Moments magnétiques et valeurs des paramètres électroniques des complexes

Complexes	μ(mB)	$\nu_3(cm^{-1})$	$\nu_2(cm^{-1})$	$\nu_1(cm^{-1})$	$\Delta(cm^{-1})$	$B'(cm^{-1})$	$\beta = B'/B$
$NiI_2(C_3H_2S_3)_2$	3.68	13280	8980		4480	650	0.63
$NiI_2(C_4H_4S_3)_2$	3.61	11750	9025		4830	548	0.53
$NiI_2(C_5H_6S_3)_2$	3.59	11780	9115		4880	545	0.52
$NiI_2(C_7H_4S_4)_2$	3.29	12190	9410		5040	565	0.55
$NiI_2(C_9H_6S_3)_2$	dia.			16030			

TABLEAU 4. Comparaison des champs des coordinats entre les complexes pseudo-tétraédriques du cobalt(II) et du nickel(II) (cm^{-1})

			X = I	
Complexes	X = Cl, Co (7)	X = Br, Co (7)	Co (7)	Ni
$MeX_2(C_3H_2S_3)_2$	4040	3760	3660	4480
$MeX_2(C_4H_4S_3)_2$			3630	4830
$MeX_2(C_9H_6S_3)_2$	3720	3590	3360	
$MeX_2(C_7H_4S_4)_2$	3300	3290	3270	5040

pondants à la transition ν_3. L'attribution de ν_1 est plus délicate du fait de la présence dans le proche infrarouge de bandes de vibrations carbone–hydrogène des coordinats organiques. Cependant les absorptions notées entre 4000 et 6000 cm^{-1} peuvent être attribuées à la transition ν_1 qui dans nos composés présentent en général deux composantes. Sur les spectres des complexes $NiI_2(C_7H_4S_4)_2$ et $NiI_2(C_4H_4S_3)_2$ on observe respectivement deux bandes de très faibles intensités à 6780 cm^{-1} et 7750 cm^{-1} et une épaule à 16080 cm^{-1} qui correspondent très probablement aux transitions interdites par spin $^3T_1(F) \rightarrow {}^1D$ d'une part et $^3T_1(F) \rightarrow {}^1G$ d'autre part. Etant donné son intensité le pic noté vers 17000 cm^{-1} est dû à une transition du type $\pi \rightarrow \pi$. Cette bande de transfert de charges, signalée par Ouchi et coll. (11, 12) entre 24000 et 21000 cm^{-1}, se retrouve donc sur nos spectres à une fréquence anormalement basse et est responsable de la couleur noire des produits étudiés. Au-delà de 20000 cm^{-1} il est difficile d'attribuer les différentes absorptions présentes sur les spectres, en effet les bandes dues aux coordinats organiques interfèrent avec celles d'éventuelles transitions des complexes.

Les valeurs des champs des coordinats Δ et celles des intégrales de répulsion électronique de Racah B' (tableau 3) ont été calculées à partir des fréquences ν_2 et ν_3 par la résolution des équations établies par Underhill et Billing (13) dans le cadre d'une symétrie tétraédrique.

Comparons les valeurs du champ Δ dans la série des composés du nickel(II) d'une part, et dans celle correspondante du cobalt(II) d'autre part (tableaux 3 et 4). Alors que ce champ diminue avec un encombrement stérique plus important des substituants R_1 et R_2 des molécules R_1-5 R_2-4 dithiole-1,2 thiones-3, dans le cas des produits cobalteux il augmente, au contraire, dans celui des composés du nickel(II). Pour le cobalt cet abaissement du champ des coordinats dû à un encombrement a été interprété (7) comme résultant d'un allongement de la liaison Co—S. Pour les complexes du nickel(II) on aurait donc un accroîssement du caractère covalent de la liaison Ni—S. Ce phénomène pourrait s'expliquer par l'existence dans les coordinats organiques d'une part d'une conjugaison soit du groupement CH_3 soit d'une liaison π du thiényle avec une double liaison du cycle dithiolique, d'autre part dans le cas de substituants méthyle d'un effet supplémentaire inductif +I du CH_3; ces deux contributions créent un excès de charges négatives sur le soufre de la fonction thione.

Les valeurs de la constante de Racah B' pour tous ces complexes sont de l'ordre de 52 à 63% de celles de l'ion libre Ni^{2+} (1030 cm^{-1}). Ce faible pourcentage s'explique par un recouvrement orbital important résultant de l'entourage du métal par deux atomes de soufre et deux ions iodures volumineux et très polarisables.

Composé A

Le diamagnétisme et le spectre électronique (tableau 2) du complexe vert sombre NiI_2-$(C_9H_6S_3)_2$ militent en faveur d'un entourage plan du métal. Le passage d'une symétrie tétra-

Can. J. Chem. Downloaded from www.nrcresearchpress.com by 210.87.254.105 on 09/05/12
For personal use only.

TABLEAU 5. Attribution des principales bandes d'absorption des coordinats organiques et de leurs complexes avec le nickel(II) dans l'infrarouge lointain (cm^{-1})*

Compound	ν_{Ni-I}	ν_{Ni-S}	ν_{noyau}	$\delta_{C=S}$	$\gamma_{C=S}$	$\nu_{Ni-S} + \delta_{noyau}$
$C_3H_2S_3$ (20, 21)			380(TF)	354(M)	264(M)	
$NiI_2(C_3H_2S_3)_2$	230(tf)	363(Mf)†				
	211(MF)	320(tf)	387(M)	‡	338(tf)	
$C_4H_4S_3$ (20)			380(F)	316(Mf)	218(f)	
$NiI_2(C_4H_4S_3)_2$	230(ép)	‡				
	210(F)	300(f)	382(F)	355(Mf)	290(f)	458(f)
$C_5H_6S_3$ (20)			393(M)	275(Mf)		
$NiI_2(C_5H_6S_3)_2$	228(ép)	368(f)				
	210(M)	‡	397(Mf)	‡		
$C_7H_4S_4$			387(Mf)	347 } (tf) 343 }		
$NiI_2(C_7H_4S_4)_2$	229(ép)	‡				529(Mf)†
	214(M)	317(Mf)	390(MF)	‡		589(M)
$C_9H_6S_3$ (20, 21)			389(Mf)	344(Mf)	286(Mf)	
$NiI_2(C_9H_6S_3)_2$	292(MF)	380(Mf)				
	272(f)	‡	390(Mf)	‡	‡	

*(TF) = très intense; (F) = intense; (MF) = moyenne-forte; (M) = moyenne; (Mf) = moyenne-faible; (f) = faible; (tf) = très faible; (ép) = épaulement.
†Bandes dont l'attribution est incertaine.
‡Bandes n'apparaissant pas sur les spectres.

édrique (composés *B*) à une symétrie plane (composé *A*) résulterait d'un encombrement stérique plus important de la phényl-5 dithiole-1,2 thione-3. Dans l'hypothèse d'une symétrie D_{2h} quatre absorptions sont théoriquement attendues (14). Sur le spectre du complexe étudié on observe un seul pic intense à 16030 cm^{-1} qui serait l'enveloppe de trois bandes correspondant aux transitions $b_{2g} \rightarrow b_{1g}$, $e_g \rightarrow b_{1g}$, $a_{1g} \rightarrow b_{1g}$. L'épaulement situé vers 18750 cm^{-1} serait provoqué par la quatrième transition $e_g \rightarrow b_{2g}$. Dans l'ultraviolet il devient délicat d'effectuer une attribution par suite de l'existence de bandes dues aux transitions du coordinat organique.

La non isotypie de *A* et de $CoI_2(C_9H_6S_3)_2$ a été constatée sur les films de Debye–Scherrer, ceci est en accord avec l'existence d'un complexe plan *A* et de composés tétraédriques *B*.

Etude des complexes par spectroscopie infrarouge

La bande caractéristique de la vibration ν_{Ni-X} (où X est un halogène) est située selon Coates et Parkin (15) à des fréquences plus élevées dans les composés plans que dans les tétraédriques. Ils assignent la bande pointée à 280 cm^{-1} à la vibration de valence ν_{Ni-I} dans le composé plan $Ni(Me_3P)_2I_2$, tandis que Clark et Williams (16) l'attribuent à celle située vers 220 cm^{-1} dans les complexes tétraédriques. On observe (tableau 5) sur les spectres des produits (*B*) un pic de forte intensité à 210 cm^{-1} qui par comparaison avec les travaux de Clark peut être considéré comme typique de la liaison Ni–I. Aucune absorption n'existe dans cette région spectrale pour le complexe *A*, par contre deux bandes supplémentaires de forte et faible intensité apparaissent vers 290 cm^{-1}, domaine où sont normalement attendues les vibrations de valence nickel-iode pour un composé plan. Ceci confirme l'hypothèse d'un entourage plan du métal dans le diiodobis (phényl-5 dithiole-1,2 thione-3) nickel(II). D'après ces résultats on voit (tableau 5) qu'une formule ionique du type $[NiL_4][NiI_4]$ n'est pas possible par suite de la présence de l'absorption ν_{Ni-I} à des fréquences supérieures à celle observée par Sabatini et Sacconi (17) pour l'ion $[NiI_4]^{2-}$, soit 189 cm^{-1}.

Alors que dans l'infrarouge lointain les spectres des complexes de la dithiole-1,2 thione-3 avec le cobalt(II) présentent une absorption forte vers 310 cm^{-1} caractéristique d'une vibration ν_{Co-S}, aucune bande intense supplémentaire n'est à signaler, dans cette région, sur ceux des composés du nickel(II). Seul un pic de faible intensité est visible entre 210 et 400 cm^{-1} domaine où est décelée habituellement la bande de vibration ν_{Ni-S} (18). La liaison métal – molécule organique peut s'effectuer selon deux

Can. J. Chem. Downloaded from www.nrcresearchpress.com by 210.87.254.105 on 09/05/12
For personal use only.

Can. J. Chem. Downloaded from www.nrcresearchpress.com by 210.87.254.105 on 09/05/12
For personal use only.

modes différents: ou le nickel(II) est coordonné à la dithiole-1,2 thione-3 par un soufre, ou il est lié par une coordination π perpendiculaire à la liaison C=S. L'absence de bande intense supplémentaire entre 210 et 400 cm^{-1} serait en accord avec cette dernière solution, puisqu'une bande due à une coordination π est probablement située en dessous de 200 cm^{-1}. Dans le cas d'une telle liaison une structure peut être envisagée à laquelle correspond, dans l'hypothèse généralement admise d'une coordination bidentate (19) une formule brute NiI_2L, en désaccord avec les résultats de l'analyse centésimale. Ceci suggère d'attribuer les bandes de faible intensité, situées vers 310 et 370 cm^{-1} aux vibrations ν_{Ni-S}, symétrique et antisymétrique, et de proposer une coordination par le soufre. La faible perturbation de la vibration $\nu_{C=S}$ (tableau 6) confirme notre hypothèse, en effet une coordination π de la liaison C=S au métal se traduirait par un déplacement très important vers les basses fréquences de la bande caractéristique de cette vibration (18).

La détermination de l'identité du donneur est rendue délicate par la présence de trois atomes de soufre. Pour les composés du cobalt nous avons proposé une coordination du métal par le soufre de la fonction thione (7). Ce travail n'apporte, à ce sujet, aucun argument définitif confirmant ou infirmant cette hypothèse. On note cependant que les bandes attribuées aux vibrations $\delta_{C=S} + \delta_{noyau}$, $\delta_{C=S}$ et $\gamma_{C=S}$ (20) disparaissent ou sont fortement perturbées par la coordination (tableau 6); ce fait milite en faveur d'une liaison du métal par le soufre de la fonction thione. Alors que la fréquence de la vibration $\nu_{C=S}$ (20, 21) augmente systématiquement dans les complexes du cobalt, avec le nickel on constate que le déplacement de cette bande est très faible; dans le cas du composé avec le substituant thiényle elle ne subit aucune altération tandis que dans celui du substituant diméthyle elle est même déplacée vers les basses fréquences. On a interprété (7) le déplacement vers les grands nombres d'onde des composés du cobalt comme résultant d'un draînage des électrons du cycle aromatique de la dithiole-1,2 thione-3 vers le métal, draînage qui compense, au maximum, la diminution de l'ordre de la liaison C=S par suite de la coordination. Pour les complexes du nickel(II) avec les dithiole-1,2 thiones-3 substituées, l'effet mésomère dû au groupement méthyle ou thiényle diminue le caractère π de la liaison C=S; cet effet contrebalance l'influence du déplacement du courant du cycle, ce qui explique dans ce cas les déplacements négligeables ou nuls (tableau 6) vers les hautes fréquences de la bande de vibration $\nu_{C=S}$.

TABLEAU 6. Attribution de quelques bandes d'absorption des molécules organiques et de leurs complexes avec le nickel(II) entre 2000 et 500 cm^{-1}

Coordinates organique ou complexes	ν_{S-s} ou ν_{C-C}	$\nu_{C=S}$	$\delta_{C=S} + \delta_{noyau}$
$C_3H_2S_3$ (20, 21)	1463(TF) 562(MF)	1164(F)	562(F)
$NiI_2(C_3H_2S_3)_2$	1456(F) 554(MF)	1180(F)	554(F)
$C_4H_4S_3$ (20)	1547 1520 (F) 560(F)	1178(F)	655(F)
$NiI_2(C_4H_4S_3)_2$	1482(F) 557(F)	1188(F)	*
$C_5H_6S_3$ (20)	1515(MF)	1162(F)	515(F)
$NiI_2(C_4H_4S_3)_2$	1486(MF)	1156(F)	522(F)
$C_7H_4S_4$	1477(F) 552(M)	1184(F) 1179(ép)	660(F)
$NiI_2(C_7H_4S_4)_2$	1446(F) 550(M)	1184(F)	680(F)
$C_9H_6S_3$ (20, 21)	1480(F) 532(MF)	1180(F) 1173(ép)	583(MF)
$NiI_2(C_9H_6S_3)_2$	1462(F) 516(M)	1189(F) 1178(MF)	580(f)

*Bandes n'apparaissant pas sur les spectres.

Conclusion

Les différents résultats obtenus nous permettent de conclure à un environnement pseudo-tétraédrique du nickel dans les complexes $NiI_2(R_1R_2C_3S_3)_2$ dans le cas où $R_1 = CH_3$ et $R_2 = H$, $R_1 = R_2 = CH_3$, $R_1 = C_4H_3S$ et $R_2 = H$, et à un entourage plan dans le cas où $R_1 = C_6H_5$ et $R_2 = H$. L'examen des spectres infrarouges suggère une coordination du nickel à la molécule organique par le soufre de la fonction thione. Mais seule une étude radiocristallographique complète permettrait d'affirmer l'existence d'une telle liaison.

Nous remercions M. Daniel Gentric pour les discussions fructueuses que nous avons eues au sujet des spectres infrarouges des dithiole-1,2 thiones-3.

1. N. LOZAC'H et O. GAUDIN. C. R. Acad. Sci. Paris, Ser. C, **225**, 1162 (1947).
2. M. G. VORONKOV et F. P. TSIPER. Zh. Anal. Khim. **6**, 331 (1951).

3. P. S. LANDIS et L. A. HAMILTON. J. Org. Chem. **25**, 1742 (1960).
4. B. BÖTTCHER et A. LUTTRINGHAUS. Ann. **89**, 557 (1947).
5. S. AHRAND, J. CHATT, et N. R. DAVIES. Quart. Rev. **12**, 265 (1958).
6. M. G. VORONKOV, A. S. BROUN, et G. B. KARPENKO. J. Gen. Chem. U.R.S.S., **19**, 1927 (1949).
7. F. PETILLON et J. E. GUERCHAIS. Bull. Soc. Chim. France, sous presse.
8. A. THUILLIER et J. VIALLE. Bull. Soc. Chim. France, **9**, 1398 (1959).
9. J. LEWIS et R. G. WILKINS. Modern coordination chemistry, Interscience publishers Inc., New York. 1964.
10. D. M. L. GOODGAME, M. GOODGAME, et F. A. COTTON. J. Amer. Chem. Soc. **83**, 4161 (1961).
11. A. OUCHI, M. HYODO, et Y. TAKAHASHI. Bull. Chem. Soc. Jap. **40**, 2819 (1967).
12. A. OUCHI, M. NAKATANI, et Y. TAKAHASHI. Bull. Chem. Soc. Jap. **41**, 2044 (1968).
13. A. E. UNDERHILL et D. E. BILLING. Nature, **210**, 834 (1966).
14. Q. LOONEY et B. E. DOUGLAS. Inorg. Chem. **9**, 1955 (1970).
15. G. E. COATES et C. PARKIN. J. Chem. Soc. 421 (1963).
16. R. J. H. CLARK et C. S. WILLIAMS. Inorg. Chem. **4**, 350 (1965).
17. A. SABATINI et L. SACCONI. J. Amer. Chem. Soc. **86**, 17 (1964).
18. D. M. ADAMS. Metal-ligand and related vibrations. Edward Arnold publishers Ltd., London, 1967.
19. M. C. BAIRD et G. WILKINSON. J. Chem. Soc. (A), 865 (1967).
20. D. GENTRIC et P. SAUMAGNE, à paraître.
21. J. FABIAN et R. MAYER. Chem. Ind. 1962 (1966).

Can. J. Chem. Downloaded from www.nrcresearchpress.com by 210.87.254.105 on 09/05/12
For personal use only.

Can. J. Chem. Downloaded from www.nrcresearchpress.com by 210.87.254.5 on 09/05/12
For personal use only.

Viscosities, Densities, and Refractive Indices of Binary Liquid Mixtures

MIGUEL KATZ, PEDRO W. LOBO, A. SANCHO MIÑANO, AND HORACIO SÓLIMO

Cátedra de Físico-Química, Facultad de Ciencias Exactas y Tecnología, Universidad Nacional de Tucumán. Argentina

Received March 22, 1971

The viscosities, densities, and refractive indices at 25, 30, 35, and 40 °C were determined for the systems: aniline + toluene (A + T), *N*,*N*-dimethylaniline + toluene (DMA + T), and aniline + *n*-butanol (A + B). From the experimental results the excess volume, excess viscosity, and excess molar free energy of activation of flow were calculated. The deviations from ideality for the excess thermodynamic functions are more important for the systems (A + T) and (A + B) than for (DMA + T). This fact is explained by the existence of dispersion forces in the mixture and by the presence of hydrogen bonds in pure aniline and pure butanol.

Les valeurs de la viscosité, densité et indice de réfraction ont été déterminées à 25, 30, 35 et 40 °C pour les systèmes: aniline + toluène (A + T), *N*,*N*-diméthylaniline + toluène (DMA + T) et aniline + *n*-butanol (A + B). Les fonctions d'excès relatives au volume, viscosité et énergie libre molaire d'activation de l'écoulement ont été calculées. Les déviations de l'idéalité pour les fonctions thermodynamiques d'excès sont plus grandes pour les systèmes (A + T) et (A + B) que pour le système (DMA + T). Ce fait trouve son explication dans l'existence de forces de dispersion dans le mélange et par la présence de ponts hydrogène dans l'aniline pure et dans le butanol pur.

Canadian Journal of Chemistry, 49, 2605 (1971)

Introduction

Viscosities of binary liquid non-electrolyte mixtures have been studied to obtain information about the type and degree of interaction between molecules of the components of some binary systems. Positive deviations from ideal behavior means strong interaction between unlike molecules, but if negative deviations are present, dispersion forces are dominant (1).

The following systems: aniline + toluene (A + T), *N*,*N*-dimethylaniline + toluene (DMA + T), and aniline + *n*-butanol (A + B) were chosen because these four substances have polar characteristics and two of them (A and B) show hydrogen bonding.

Densities, viscosities, and refractive indices for the three systems at different mole fractions were measured at 25, 30, 35, and 40 °C. Some data about these three physical constants of the pure compounds and of the systems are tabulated in the literature (2, 3).

From the experimental results the following thermodynamic functions have been calculated: ΔV^E (excess molar volume), $\Delta\eta^E$ (excess of viscosity), and $\Delta^* G^E$ (excess molar free energy of activation of flow).

Experimental

Density

Densities were determined with a Robertson specific gravity bottle (4). The total pycnometer volume was about 20 ml and was calibrated with doubly distilled water at every temperature. All weighings were made on a digital Sartorius Selecta balance and corrected to vacuum.

A thermostatically controlled bath constant to ±0.01 °C was used. Temperatures were read from calibrated thermometers.

Viscosity

Viscosities of pure liquids and mixtures have been determined with a Cannon–Fenske viscosimeter calibrated with doubly distilled water, benzene, and sucrose solutions (5). Kinetic energy corrections were applied to viscosity data.

In making determinations, both pycnometer and viscosimeter were maintained in the bath until at least two consecutive measurements of the liquid height in the capillaries or the flow time indicated that the sample had reached the temperature of the bath.

Refractive Index

The refractive index for the sodium D line of the pure components and mixtures were measured with a Jena dipping refractometer with an accuracy of ±0.00002.

Materials and Solutions

Toluene, Merck p.a., was twice distilled over dried P_2O_5 at reduced pressure and only the middle half of each distillation was recovered. Aniline, Merck p.a., was distilled twice over zinc dust and over anhydrous Na_2SO_4

at reduced pressure. We recover too, only the middle half of each of two distillations. *N,N*-dimethylaniline, Erba RS electronic grade, and *n*-butanol, Merck chromatoquality grade, were used without further purification. Water was twice distilled from alkaline permanganate.

Mixtures were prepared by mixing weighed amounts of the pure liquids to prevent evaporation.

Results

The experimental molar fractions, densities, viscosities, and refractive indices at 25, 30, 35, and 40 °C for the three systems are listed in Tables 1, 2, and 3.

The excess thermodynamic functions (6) were calculated with the following equations

$$\Delta\eta^E = \eta - (x_1\eta_1 + x_2\eta_2)$$

$$\Delta V^E = V - (x_1V_1 + x_2V_2)$$

$$\Delta^*G^E = RT[\ln \eta V - (x_1 \ln \eta_1 V_1 + x_2 \ln \eta_2 V_2)]$$

where η, η_1, and η_2 = viscosity of the mixture and of the pure components; V, V_1, and V_2 = molar volume of the mixture and of the pure components; R = gas constant. The molar volume V of the mixture is defined by

$$V = \frac{x_1M_1 + x_2M_2}{\rho}$$

where M_1 and M_2 are the molecular weights of the components.

Excess thermodynamic functions at 25 °C are plotted against molar fraction of one component: $x_1 = x_A$ (for the system A + T and A + B) and $x_1 = x_{DMA}$ (for the systems DMA + T) in Figs. 1, 2, and 3.

Discussion

The experimental values of viscosities for the A + T system listed in Table 1 show a relatively high decrease on the initial addition of toluene. This behavior is characteristic of systems in which at least one of the components exhibits hydrogen bonding (7). It is possible that for aniline (8), the existence of hydrogen bonding exists between the amine group with another of the same kind (N—H···N) or with the benzene ring of another molecule of aniline. Figure 1 shows for the A + T system a minimum value of $\Delta\eta^E$ at x_1=0.65 in agreement with what has been said above and with the possibility of hydrogen bonding of the aniline group with the benzene ring of toluene.

For the system A + B (see Fig. 1), the minimum is at $x_1 = 0.55$, giving an almost symmetrical curve. This change in position of the minimum value with respect to the A + T system can be explained by hydrogen bonding of the type (O—H···O) between the *n*-butanol

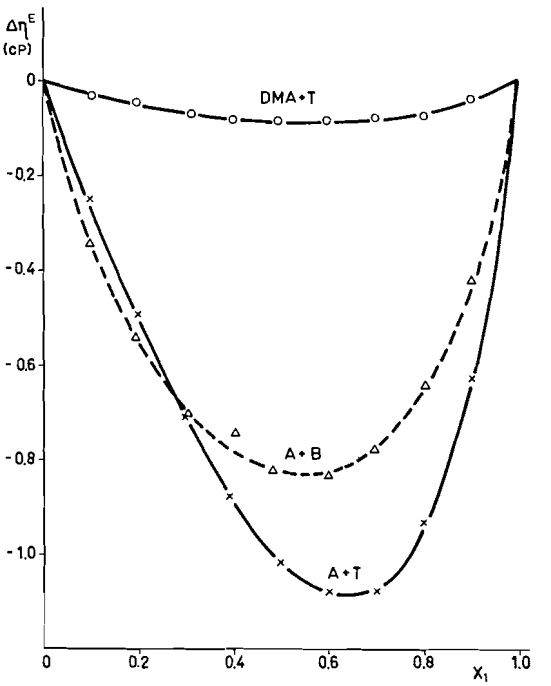

FIG. 1. $\Delta\eta^E$ *vs.* x_1.

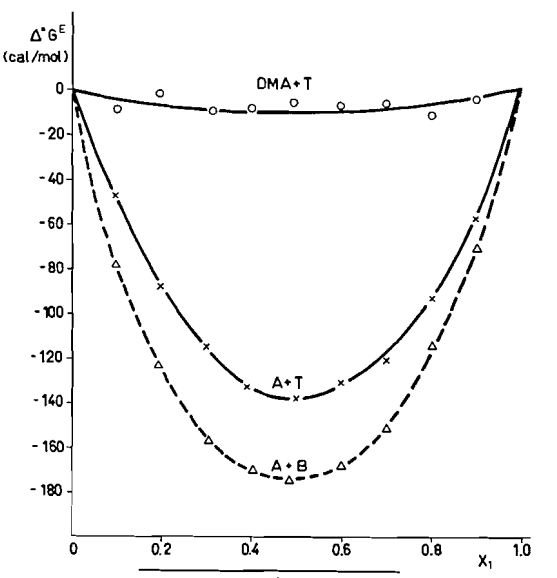

FIG. 2. Δ^*G^E *vs.* x_1.

Can. J. Chem. Downloaded from www.nrcresearchpress.com by 210.87.254.5 on 09/05/12
For personal use only.

Can. J. Chem. Downloaded from www.nrcresearchpress.com by 210.87.254.5 on 09/05/12
For personal use only.

TABLE 1. Experimental results for the aniline + toluene system

	ρ (g/cc)				η (cP)				n_D			
x_1*	25 °C	30 °C	35 °C	40 °C	25 °C	30 °C	35 °C	40 °C	25 °C	30 °C	35 °C	40 °C
1.00000	1.01745	1.01321	1.00928	1.00457	3.773	3.184	2.748	2.345	1.58392	1.58128	1.57852	1.57564
0.89980	1.00017	0.99568	0.99142	0.98725	2.822	2.423	2.122	1.863	1.57378	1.57103	1.56842	1.56587
0.80091	0.98263	0.97911	0.97511	0.97063	2.199	1.907	1.696	1.486	1.56366	1.56078	1.55879	1.55619
0.69777	0.96684	0.96232	0.95779	0.95339	1.723	1.522	1.367	1.216	1.55402	1.55137	1.54883	1.54617
0.60028	0.95095	0.94611	0.94214	0.93764	1.406	1.253	1.139	1.030	1.54482	1.54178	1.53932	1.53674
0.49932	0.93487	0.93039	0.92599	0.92161	1.146	1.074	0.954	0.872	1.53547	1.53256	1.52928	1.52786
0.39168	0.91815	0.91312	0.90910	0.90521	0.940	0.867	0.803	0.740	1.52625	1.52348	1.52121	1.51845
0.30038	0.90469	0.90005	0.89556	0.89105	0.814	0.752	0.720	0.650	1.51852	1.51571	1.51316	1.51052
0.19802	0.89022	0.88610	0.88208	0.87715	0.701	0.653	0.615	0.570	1.50975	1.50722	1.50461	1.50190
0.09770	0.87577	0.87105	0.86649	0.86179	0.620	0.576	0.545	0.495	1.50180	1.49908	1.49645	1.49363
0.00000	0.86213	0.85753	0.85305	0.84834	0.557	0.524	0.501	0.470	1.49430	1.49149	1.48867	1.48589

*x_1 = molar fraction of aniline.

TABLE 2. Experimental results for the *N,N*-dimethylaniline + toluene system

	ρ (g/cc)				η (cP)				n_D			
x_1*	25 °C	30 °C	35 °C	40 °C	25 °C	30 °C	35 °C	40 °C	25 °C	30 °C	35 °C	40 °C
1.00000	0.95232	0.94815	0.94393	0.93975	1.288	1.173	1.078	0.985	1.55661	1.55389	1.55157	1.54913
0.89832	0.94474	0.94056	0.93649	0.93230	1.173	1.070	0.999	0.914	1.55141	1.54880	1.54628	1.54403
0.80146	0.93693	0.93275	0.92869	0.92431	1.066	0.988	0.918	0.851	1.54632	1.54379	1.54124	1.53873
0.70104	0.92891	0.92465	0.92055	0.91621	0.989	0.911	0.854	0.780	1.53937	1.53822	1.53586	1.53346
0.59735	0.92081	0.91611	0.91206	0.90783	0.906	0.834	0.782	0.726	1.53491	1.53227	1.52921	1.52656
0.49296	0.91138	0.90705	0.90265	0.89824	0.831	0.770	0.726	0.664	1.52793	1.52527	1.52278	1.52025
0.40110	0.90284	0.89831	0.89380	0.88921	0.767	0.714	0.671	0.619	1.52213	1.51936	1.51692	1.51438
0.31251	0.89464	0.89011	0.88586	0.88123	0.711	0.668	0.625	0.586	1.51644	1.51372	1.51118	1.50855
0.19611	0.88325	0.87876	0.87418	0.86952	0.653	0.604	0.570	0.536	1.50856	1.50565	1.50317	1.50066
0.10112	0.87335	0.86871	0.86409	0.85947	0.597	0.561	0.532	0.499	1.50174	1.49883	1.49628	1.49365
0.00000	0.86213	0.85753	0.85305	0.84834	0.557	0.524	0.501	0.470	1.49430	1.49149	1.48867	1.48589

*x_1 = molar fraction of *N,N*-dimethylaniline.

Can. J. Chem. Downloaded from www.nrcresearchpress.com by 210.87.254.5 on 09/05/12
For personal use only.

TABLE 3. Experimental results for the aniline + *n*-butanol system

	ρ (g/cc)				η (cP)				n_D			
x_1*	25 °C	30 °C	35 °C	40 °C	25 °C	30 °C	35 °C	40 °C	25 °C	30 °C	35 °C	40 °C
1.00000	1.01745	1.01321	1.00928	1.00457	3.773	3.184	2.748	2.345	1.58392	1.58128	1.57852	1.57564
0.89956	0.99749	0.99313	0.98867	0.98418	3.231	2.745	2.375	2.048	1.56500	1.56211	1.55991	1.55716
0.80276	0.97788	0.97352	0.96926	0.96484	2.899	2.468	2.144	1.861	1.54700	1.54449	1.54197	1.53949
0.69459	0.95600	0.95161	0.94711	0.94272	2.637	2.248	1.971	1.709	1.52662	1.52422	1.52148	1.51925
0.60049	0.93641	0.93200	0.92778	0.92344	2.474	2.130	1.857	1.613	1.50903	1.50666	1.50424	1.50194
0.48372	0.91202	0.90776	0.90350	0.89900	2.343	2.010	1.770	1.529	1.48781	1.48534	1.48314	1.48062
0.40554	0.89534	0.89110	0.88689	0.88257	2.287	1.965	1.722	1.468	1.47276	1.47039	1.46831	1.46608
0.30514	0.87388	0.86970	0.86561	0.86128	2.249	1.941	1.703	1.440	1.45490	1.45278	1.45043	1.44825
0.19349	0.84957	0.84545	0.84136	0.83720	2.278	1.965	1.734	1.500	1.43427	1.43208	1.42994	1.42783
0.09983	0.82880	0.82472	0.82078	0.81672	2.368	2.049	1.800	1.568	1.41685	1.41477	1.41279	1.41072
0.00000	0.80590	0.80221	0.79822	0.79436	2.592	2.224	1.958	1.700	1.39744	1.39548	1.39358	1.39165

*x_1 = molar fraction of aniline.

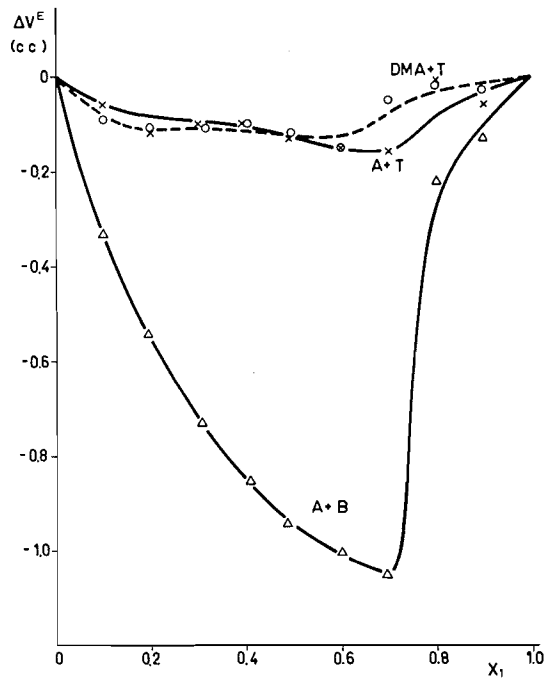

FIG. 3. ΔV^E *vs.* x_1.

molecules (9) and by other types of hydrogen bonding described for the aniline molecule. The DMA + T system (see Fig. 1) shows a $\Delta\eta^E$ value close to zero which would mean the absence of hydrogen bonding in the components.

It is considered that $\Delta\eta^E$ is negative for systems in which dispersion forces are dominant, becoming less negative and then increasingly positive as the strength of interaction increases (1).

From the analysis of Fig. 2 we may conclude that for the system A + B, where both components are associated in the pure state, more negative Δ^*G^E values are obtained than for the A + T system, where only A shows hydrogen bonding. This result is in agreement with the expected variation of the ΔH^* and $T\Delta S^*$ functions for non-ideal mixtures of the type previously described (10).

For the DMA + T system, the value of Δ^*G^E is close to that expected for ideal behavior.

The negative values of ΔV^E are explained by Prigogine (11) in terms of the different sizes of the molecules or the dipole–dipole interaction between them. This effect is observed in the A + B system in a stronger way than in the other two, mainly because of the different sizes of a cycle molecule and a linear one.

We have calculated the excess thermodynamic functions at 25, 30, 35, and 40 °C. The values obtained tend to become less negative and then increasingly positive as the temperature increases, which is in accord with the nature of these functions. Only $\Delta\eta^E$, ΔV^E, and Δ^*G^E at 25 °C are shown, since for the other temperatures the curves are similar.

The almost linear variation of the refractive indices for the three systems in terms of the composition (see Tables 1, 2, and 3) is in agreement with the conclusion of Loiseleur (12) for a large number of ideal and non-ideal systems. Neither the polar characteristics of the substances studied nor the existence of hydrogen bonding in the aniline and *n*-butanol seem to have any important effect on the linear dependence of this property with concentration.

1. R. J. FORT and W. R. MOORE. Trans. Faraday Soc. **62**, 1112 (1966).
2. J. TIMMERMANS. Physico-chemical constants of binary systems in concentrated solutions. Interscience Publ., New York. 1959. pp. 150, 552, 555, 560, and 561.
3. A. WEISSBERGER, E. S. PROSKAUER, J. A. RIDDICK, and E. E. TOOPS. Organic solvents. Vol. VII. 2nd. ed. Interscience Publ., New York. 1955. p. 94.
4. G. R. ROBERTSON. Ind. Eng. Chem. **11**, 464 (1939).
5. International Critical Tables. Vol. V. McGraw-Hill Book Co., Inc. 1925. p. 23.
6. P. K. KATTI and M. M. CHAUDHRI. J. Chem. Eng. Data, **9**, 442 (1964).
7. G. P. JOHARI. J. Chem. Eng. Data, **13**, 541 (1968).
8. R. J. W. LE FÈVRE, L. RADOM, and G. L. D. RITCHIE. J. Chem. Soc. B, 913 (1969).
9. B. YA LEVIN. Zh. Fiz. Khim. **28**, 1399 (1954).
10. G. M. BARROW. Química-física. Vol. II. Reverté Ed. 1968. p. 655.
11. I. PRIGOGINE. The molecular theory of solutions. North Holland Publishing Co., Amsterdam. 1957.
12. H. LOISELEUR. Thèse de Doctorat-ès-Sciences, Lyon. 1965. p. 80.

Can. J. Chem. Downloaded from www.nrcresearchpress.com by 210.87.254.5 on 09/05/12
For personal use only.

Can. J. Chem. Downloaded from www.nrcresearchpress.com by 210.87.254.105 on 09/05/12
For personal use only.

NOTES

A Novel Synthesis of β-Hydroxyvaline

CASIMIR BERSE AND PIERRE BESSETTE[1]

Department of Chemistry, Université de Montréal, Montréal, Québec

Received February 5, 1971

The synthesis of β-hydroxyvaline from ethyl β,β-dimethylacrylate through 1,2-di(ethoxycarbonyl)-3,3-dimethylaziridine as intermediate shows a new way of preparation of this amino acid.

La synthèse de la β-hydroxyvaline à partir du β,β-diméthylacrylate d'éthyle en passant par le diéthoxycarbonyl-1,2 diméthyl-3,3 aziridine comme intermédiaire, illustre une nouvelle méthode de synthèse de cet acide aminé.

Canadian Journal of Chemistry, 49, 2610 (1971)

Until now several methods have been used to synthesize β-hydroxyvaline (1–7). However in none of these methods was 1,2-di(ethoxycarbonyl)-3,3-dimethylaziridine (**3**) used as intermediate.

The objective of our work was the preparation of such an aziridine. The opening of this aziridine with different reagents could be a general method for the synthesis of different derivatives of valine. The hydrolysis of these derivatives will lead to the corresponding amino acids. This note shows that the synthesis of such an aziridine is possible and the opening of the aziridine ring leads to the β-hydroxyvaline. Thus by following the method similar to that described by Lwowski and Maricich (8) the reaction of ethyl β,β-dimethylacrylate with *N*-(*p*-nitrobenzenesulfonoxy)urethan in the presence of triethylamine permitted the formation of the aziridine **3**, b.p. 110–115/0.1 mm Hg (dec.), yield 14% (see Scheme 1). Opening of the aziridine **3** with acetic acid gave ethyl 3-acetoxy-2-(ethoxycarbonylamino)-3-methylbutanoate (**4**), b.p. 115 ± 5°/0.09 mm Hg, yield 25%, and ethyl 2-(ethoxycarbonylamino)-3-methyl-3-butenoate (**5**) b.p. 90–100°/0.09 mm Hg, yield 28%. Compounds **4** and **5** were separated by chromatography. Alkaline hydrolysis of **4** with aqueous potassium hydroxide followed by elution on Rexyn 101 H gave β-hydroxyvaline (**6**), m.p. 221–223° (lit. 226–227° (5)), yield 10%.

[1]Holder of an NRCC Studentship, 1968–1971.

The synthesis of penicillamine using the novel method described herein is presently under active investigation in our laboratory.

Experimental

Solutions were concentrated under reduced pressure using a rotary evaporator and a water bath at a temperature of 40° and less. Reaction mixtures and products were examined by t.l.c. using silica gel GF-254, hexane–ether (50:50 v/v), and spray of 50% sulfuric acid in ethanol followed by heating at 200 °C. Melting and boiling points were uncorrected.

The i.r. spectra were recorded on a Beckman model IR-8 double beam spectrometer. The n.m.r. spectra were recorded on a Varian A-60 spectrometer. Mass spectra were done on a Hitachi–Perkin–Elmer model RMU 6-D. Elemental analyses were performed by Midwest Microlab Inc., Indianapolis, Indiana.

Ethyl β,β-Dimethylacrylate (1)

Product **1** was obtained from β,β-dimethyl acrylic acid by the method described by Moureu and Chovin (9); b.p. 152–153 °C (lit. (9) 153 °C).

N-(p-Nitrobenzenesulfonoxy)urethan (2)

Product **2** was prepared from *N*-hydroxyurethan and *p*-nitrobenzenesulfonyl chloride as described by Lwowski and Maricich (8); m.p. 114 °C (lit. (8) 116.4–116.8 °C).

1,2-Di(ethoxycarbonyl)-3,3-dimethylaziridine (3)

To a solution of 4.28 g (0.030 mol) of **1** and of 8.705 g (0.030 mol) of **2** in dichloromethane (100 ml) was added with stirring over a period of 1 h a solution of 3.33 g (0.033 mol) of triethylamine in dichloromethane (20 ml). After the mixture was stirred for 3 h, it was poured into ether (1000 ml). Triethylammonium *p*-nitrobenzenesulfonate was eliminated by filtration and the solution concentrated under reduced pressure. The oily residue was chromatographed on silica gel with hexane–ether

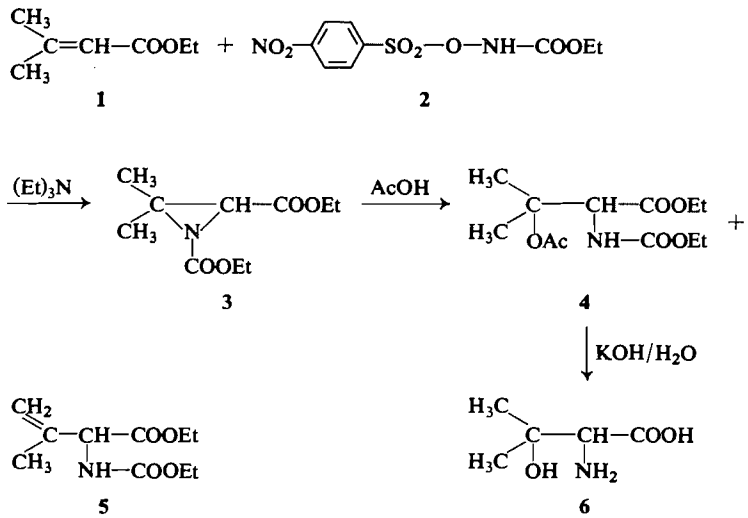

SCHEME 1

(90:10 v/v) as eluant to give the pure aziridine **3**; yield 0.89 g (14%), t.l.c. R_f 0.50; b.p. 110–115°/0.10 mm Hg (dec.); i.r. bands ($CHCl_3$) at 1720, 1382, and 1370 cm^{-1}; τ(CCl_4) 8.76 and 8.74 (6H, triplet), 8.71 and 8.69 (6H, singlet), 7.17 (1H, singlet), 5.91 and 5.96 (4H, quadruplet); mass spectra *m/e* 215.

Anal. Calcd. for $C_{10}H_{17}NO_4$: C, 55.79; H, 7.96. Found: C, 55.51; H, 7.84.

Ethyl 3-Acetoxy-2-(ethoxycarbonylamino)-3-methylbutanoate (4) and Ethyl 2-(Ethoxycarbonylamino)-3-methyl-3-butenoate (5)

Compound **3**, (4.80 g, 0.022 mol), was added slowly during 3 h to glacial acetic acid (35 ml) at reflux. Once the addition finished the acetic acid was removed *in vacuo*, ether (200 ml) was added, the solution was dried over K_2CO_3, filtered, and evaporated. The oily residue was chromatographed on silica gel and eluted with hexane–ether (90:10 v/v) to obtain products **4** and **5**.

Product **4**, 1.720 g (28%); t.l.c. R_f 0.40; b.p. 115 ± 5°/0.09 mm Hg; i.r. bands (CCl_4) at 3460, 1745, 1730, and 1510 cm^{-1}; τ (CCl_4) 8.71 and 8.77 (6H, triplet), 8.47 and 8.53 (6H, singlet), 8.09 (3H, singlet), 5.83 and 5.93 (4H, quadruplet), 5.51 (1H, doublet), and 4.23 (1H, doublet).

Anal. Calcd. for $C_{12}H_{21}O_6N$: C, 52.35; H, 7.68. Found: C, 52.76; H, 7.97.

Product **5**, 1.19 g (25%); t.l.c. R_f 0.50; b.p. 90–100°/0.09 mm Hg; i.r. bands (CCl_4) at 3460, 1730, 1650, and 1500 cm^{-1}; τ (CCl_4) 8.73 and 8.77 (6H, triplet), 8.23 (3H, singlet), 5.83 and 5.93 (4H, quadruplet), 5.35 (1H, doublet), 5.05 (2H, multiplet), 4.43 (1H, doublet); mass spectra *m/e* 215.

Anal. Calcd. for $C_{10}H_{17}NO_4$: C, 55.79; H, 7.96. Found: C, 55.62; H, 7.68.

β-*Hydroxyvaline (6)*

Compound **4**, (1.720 g, 0.0062 mol), was added to 25 ml of an aqueous solution of 1.00 *N* potassium hydroxide and heated at reflux for 18 h. The solution was concentrated *in vacuo* and passed on Rexyn 101H (10 g) and eluted with water. After evaporation of the water the yellow residue was crystallized in methanol to give β-hydroxyvaline 75 mg (10%), m.p. 221–223° (lit. (5) 226–227°); i.r. bands (Nujol) at 3200, 1670, 1600, and 1560 cm^{-1}; τ (D_2O) 8.53 and 8.73 (6H, singlet), 6.38 (1H, singlet) 6.15 (4.6H, DHO singlet).

Anal. Calcd. for $C_5H_{11}NO_3$: C, 45.03; H, 8.25. Found: C, 44.91; H, 7.94.

We thank the National Research Council of Canada for financial support.

1. EMIL ABDERHALDEN and KURT HEYNS. Ber. **67B**, 530 (1934).
2. M. A. PROKOF'EV and M. M. BOTVINNIK. Compt. rend. acad. sci. U.R.S.S. **25**, 488 (1939).
3. SUEO TATSUOKA, TAKENOBU UENO, and KEISABURO HIRATA. J. Pharm. Soc. Jap. **70**, 229 (1950).
4. K. RÜFENACHT. Helv. Chim. Acta, **35**, 762 (1952).
5. T. KANEKO and T. INUI. J. Chem. Soc. Jap. Pure Chem. Sect. (Nippon Kagaku Zasshi), **82**, 743 (1961).
6. A. SCHOEBERL and A. ERNSBERGER. Naturwiss. **53** (4), 107 (1966).
7. JUN-ICHI OH-HASHI and KAORU HARADA. Bull. Chem. Soc. Jap. **39**, 2287 (1966).
8. W. LWOWSKI and T. J. MARICICH. J. Am. Chem. Soc. **87**, 3630 (1965).
9. H. MOUREU and P. CHOVIN. Bull. Soc. Chim. Fr. 586 (1953).

Can. J. Chem. Downloaded from www.nrcresearchpress.com by 210.87.254.105 on 09/05/12
For personal use only.

Action du chloroformiate d'éthyle sur les lactames. Préparation sélective d'éthers lactimiques et de *N*-éthoxycarbonyl-lactames

R. GAUTHIER,[1] P. BLONDEAU,[2] C. BERSE, ET D. GRAVEL
Département de Chimie, Université de Montréal, B.P.6128, Montréal, Québec

Reçu le 3 mars 1971

La réactivité de quelques lactames carbocycliques et de quelques γ-thiolactames vis-à-vis du chloroformiate d'éthyle est étudiée. A 25°, lorsqu'il y a réaction, on observe la formation du chlorhydrate de l'éther lactimique correspondant, en accord avec la littérature. A 110°, la *N*-éthoxycarbonyl-lactame correspondante est formée avec de bons rendements. Des essais ont montré que l'éther lactimique libre est très probablement un intermédiaire dans cette réaction.

The reactivity of some carbocyclic lactams and some γ-thiolactams with ethyl chloroformate has been studied. At 25°, when reaction takes place, the corresponding lactim ether hydrochloride is formed in accord with the literature. At 110° however, the reaction yields the corresponding *N*-ethoxycarbonyl lactam in good yield. Investigation showed the free lactim ether to be a probable intermediate in this reaction.

Canadian Journal of Chemistry, 49, 2612 (1971)

La formation de chlorhydrates d'éthers lactimiques par l'action du chloroformiate d'éthyle sur des lactames ou des amides est déjà connue (1–3). Hechelhammer (1), en particulier, a obtenu l'éthoxy-7 tétrahydro-3,4,5,6 azépine-2*H* (**1**) en faisant réagir une quantité stoechiométrique de caprolactame (**2**) avec le chloroformiate d'éthyle dans le benzène à 25°, et en neutralisant le chlorhydrate du produit formé avec du carbonate de calcium.

Dans le cadre de nos travaux sur la réactivité des oxo-5 thiazépines-1,4, nous avons tenté la formation d'éthers lactimiques du type de l'éthoxy-5 méthoxycarbonyl-3 dihydro-2,3 thiazépine-1,4 (**3**).

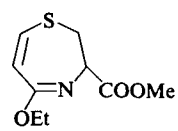

3

Pour ce faire, nous avons mis en réaction la méthoxycarbonyl-3 oxo-5 tétrahydro-2,3,4,5 thiazépine-1,4 (**4**) avec le chloroformiate d'éthyle dans le benzène à 25°. Cependant, dans ces conditions, la thiazépine **4** n'a donné aucune réaction. En répétant la réaction à différentes températures (25, 50, 75, 80, et 110°) avec le toluène comme solvant, aucune réaction n'a eu lieu jusqu'à la température de reflux; après 12 h de reflux cependant, une chromatographie sur couche mince de gel de silice a montré que le produit de départ s'était complètement transformé en un seul produit de réaction: non pas l'éther lactimique attendu **3**, mais bien l'éthoxycarbonyl-4 méthoxycarbonyl-3 oxo-5 tétrahydro-2,3,4,5 thiazépine-1,4 (**5**) avec un rendement quantitatif. La structure du produit **5** a été établie sans difficulté à l'aide des spectres u.v., i.r., de r.m.n., et de masse.

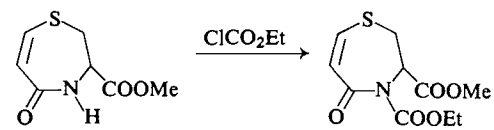

4 **5**

Devant le résultat surprenant de cette réaction, nous l'avons répétée sur une série de lactames, pour deux raisons principales: d'abord tenter d'en faire une préparation générale des *N*-éthoxycarbonyl-lactames et aussi pour essayer d'obtenir une ébauche du mécanisme de la réaction. On sait que si les *N*-alkoxycarbonyl-amides (*N*-acyl carbamates) sont facilement préparées par acylation des carbamates correspondants (4–6), les *N*-alkoxycarbonyl-lactames par contre sont très mal connues: une seule préparation est décrite dans la littérature. En effet, Falkenstein et Dörfel (7) rapportent la préparation d'une série de ces composés selon une méthode non-publiée de Kiefer; la séquence des réactions utilisées est représentée par l'éq. 1.

[1]Boursier pré-doctorat du CNRC, 1968–1971.
[2]Boursier pré-doctorat du CNRC, 1965–1969.

Can. J. Chem. Downloaded from www.nrcresearchpress.com by 210.87.254.42 on 09/05/12
For personal use only.

[1] 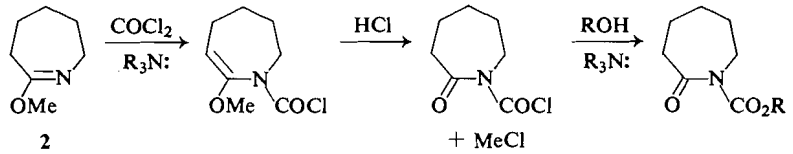

Quoique cette préparation fournisse d'excellents rendements, elle nécessite néanmoins une série de quatre étapes.

Etant donné la simplicité de la méthode au chloroformiate d'éthyle, la réaction a donc été reprise à 25° et à 110° sur les lactames suivantes: méthoxycarbonyl-3 oxo-5 perhydrothiazépine-1,4 (**6**), oxo-5 perhydrothiazépine-1,4 (**7**), caprolactame (**2**), et valérolactame (**8**). Un excès de 9 mol de chloroformiate d'éthyle a été utilisé dans

TABLEAU 1. Réaction des lactames avec le chloroformiate d'éthyle

	25 °C	110 °C
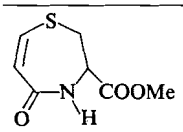 **4***	—	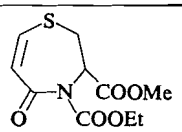 **5‡**
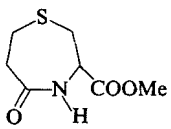 **6***	—	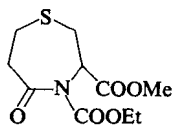 **13‡**
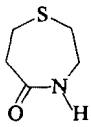 **7†**	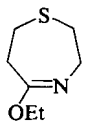 **10‡**	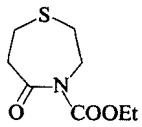 **14‡**
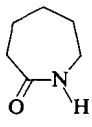 **2**	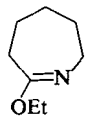 **1**	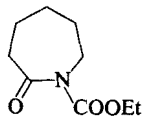 **15**
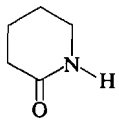 **8**	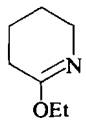 **11‡**	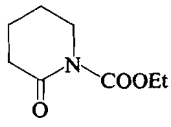 **16‡**
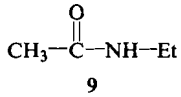 **9**	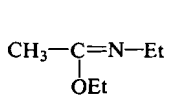 **12§**	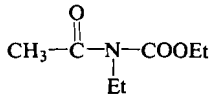 **17** (~2–3%)

*Préparation: P. Blondeau. Thèse de Doctorat. Faculté des Sciences, Université de Montréal, Montréal, Québec, juillet 1970.

†Préparation: voir réf. 9.

‡Ces produits nouveaux ont été identifiés par leurs données spectrales, ainsi que l'analyse élémentaire (sauf pour les produits **5**, **11**, et **13**).

§Isolé sous forme de chlorhydrate, tel que décrit par Suydam *et al.* (3).

Can. J. Chem. Downloaded from www.nrcresearchpress.com by 210.87.254.42 on 09/05/12
For personal use only.

TABLEAU 2. Rendements et constantes physiques des produits formés

Produit de départ	Rendement (%)	Point d'ébullition (°C/mm)	Analyse			
			Trouvé		Calculé	
			C	H	C	H
(A) Ethers lactimiques						
10	41	100/50	52.97	8.19	52.79	8.23
1	*	*				
11	50	50/20				
(B) N-Ethoxycarbonyl-lactames						
5	~100	†				
13	~100	†				
14	75	122/0.05	47.46	6.70	47.27	6.44
15	55	86/0.05	58.47	8.19	58.36	8.16
16	70	92/0.08	56.12	7.65	56.24	7.90

*Voir réf. 1.
†Les produits sont isolés par évaporation du solvant. D'après les spectres, ils ne contiennent pas d'impuretés décelables. Dû aux petites quantités disponibles, ils n'ont pu être distillés. De plus, ils se décomposent sur gel de silice.

Can. J. Chem. Downloaded from www.nrcresearchpress.com by 210.87.254.42 on 09/05/12
For personal use only.

,us les cas. Les produits majeurs obtenus sont décrits dans le tableau 1.

On remarque dans le tableau 1 que dans tous les cas, il a été possible d'isoler la *N*-éthoxycarbonyl-lactame. Dans le cas des produits **4** et **6**, il a été impossible d'obtenir l'éther lactimique correspondant, même en variant les conditions de température et de concentration; en élevant la température, on voit plutôt apparaître la *N*-éthoxycarbonyl-lactame. Il est à noter également que l'expérience a été tentée sur une amide, la *N*-éthylacétamide (**9**). Quelles que soient les conditions utilisées, il a été impossible d'obtenir la *N*-éthoxycarbonyl-amide[3] correspondante (**17**) avec un rendement supérieur à 2 ou 3%. Les rendements de réaction, ainsi que les constantes physiques des produits, sont rapportés dans le tableau 2. Les déplacements chimiques des groupements éthoxyles des différents produits dans le spectre de r.m.n. ainsi que certaines absorptions caractéristiques en i.r. sont rapportés dans le tableau 3.

Il est intéressant de noter que lors de la réaction de la valérolactame (**8**) avec le chloroformiate d'éthyle, un produit secondaire a pu être isolé par chromatographie sur gel de silice, avec un rendement de 18%. Ce produit donne un test de Beilstein positif ainsi qu'un précipité avec le nitrate d'argent à chaud; d'après les spectres i.r., de r.m.n., et de masse,[4] la structure **18** est attribuée au produit.

Il est très probable que des produits secondaires du même type se forment avec les autres lactames étudiées mais toutefois, ils n'ont pas été remarqués lors de la purification du produit de réaction.

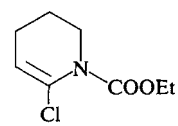

18

A la lumière des résultats obtenus, il semblait logique de supposer que l'éther lactimique ou son chlorhydrate pouvait être un intermédiaire dans la formation de la *N*-éthoxycarbonyl-lactame. Pour vérifier cette hypothèse, nous avons fait réagir l'éthoxy-7 tétrahydro-3,4,5,6 azépine-2*H* (**1**) ainsi que son chlorhydrate avec un excès de chloroformiate d'éthyle dans le toluène à 110°. Dans les deux cas, nous avons pu isoler la *N*-éthoxycarbonylcaprolactame (**15**) avec des rendements de même ordre qu'avec la caprolactame (**2**). Des résultats analogues ont aussi été observés avec l'éther lactimique **11**.

Il faut faire remarquer également qu'avec les lactames **6**, **7**, et **8**, on observe en cours de réaction à 110° la formation d'un précipité; si on filtre ce précipité, on constate qu'il s'agit du chlorhydrate

[3]Le produit **17** n'a pu être obtenu parfaitement pur; il a été identifié par comparaison des spectres i.r. et de r.m.n. avec ceux du produit authentique préparé par les méthodes connues (4, 8).

[4]Le produit est trop instable pour qu'on puisse en obtenir une analyse élémentaire.

TABLEAU 3. Données spectrales des produits formés

Produit	Résonance magnétique nucléaire (—O—C_2H_5)(δ) CH_3	CH_2	Infrarouge (cm^{-1}) C=N	
(A) Ethers lactimiques				
10	1.25	4.00	1675	
1	1.25	4.00	1670	
11	1.15	3.95	1675	
	CH_3	CH_2	C=O ester*	C=O lactame
(B) N-Ethoxycarbonyl-lactames				
5	1.40	4.35	masqué	1715
13	1.25	4.25	1770 (épaulement)	1715
14	1.40	4.35	1775	1715
15	1.40	4.35	1770	1715
16	1.40	4.30	1775	1715

*La bande carbonyle de la partie ester (—$COOC_2H_5$) est toujours de faible intensité, alors que la bande carbonyle de la partie lactame (—C(=O)—N) est toujours de forte intensité.

de l'éther lactimique correspondant;[5] si, d'autre part, on laisse la réaction suivre son cours, ce précipité disparaît graduellement.

Les résultats décrits ci-haut permettent donc de suggérer le mécanisme décrit au schéma 1.[6]

Dans le cas de réactions effectuées soit sur la caprolactame (**2**) soit sur l'éther lactimique correspondant **1**, nous avons isolé et caractérisé du chlorure d'éthyle par condensation des produits volatils émanant du mélange réactionnel à 110°. Toutefois, il est connu que les chlorhydrates des éthers lactimiques se décomposent à haute température pour redonner la lactame de départ ainsi que le chlorure d'alkyle correspondant (2). La présence du chlorure d'éthyle dans le cas présent n'est donc pas un argument définitif. Quant à la formation du chlorhydrate de l'éther lactimique, Suydam *et al.* (3) ont déjà suggéré un mécanisme plausible pour rendre compte de sa formation.

Le mécanisme suggéré, sans être totalement prouvé, rend toutefois compte des produits formés et pourrait éventuellement servir de base à une étude quantitative de la réaction.

Notons enfin que la méthode au chloroformiate permet de préparer en une seule étape les *N*-alkoxycarbonyl-lactames, agents d'activation utiles en polymérisation anionique des lactames (7).

Partie expérimentale

Les spectres i.r. ont été pris sur un spectrophotomètre "Beckmann" modèle IR-8 à double réseau.

Les spectres de masse ont été enregistrés sur un spectromètre de masse "Hitachi–Perkin–Elmer" modèle RMu 6-D.

Les spectres de r.m.n. ont été déterminés sur un spectromètre modèle JNM-4H-100 de la Compagnie Jeolco. Le tétraméthylsilane est utilisé comme référence interne et le $CDCl_3$ comme solvant.

Les points de fusion et d'ébullition ne sont pas corrigés.

Les analyses élémentaires ont été effectuées par Midwest Microlab Inc., Indianapolis, Indiana.

(1) Réaction à 25 °C (procédure-type)

La lactame[7] (~0.02 mol) est dissoute dans du toluène anhydre (200 ml) et le chloroformiate d'éthyle (20 ml, ~0.2 mol) est ajouté en une portion. Le mélange est agité à 25 °C pendant 12 h. Le précipité est ensuite filtré et lavé avec du toluène, puis agité quelques minutes avec du carbonate de potassium 50% (50 ml). Le mélange est extrait trois fois à l'éther, et la solution éthérée séchée sur carbonate de sodium. L'éther est évaporé *in vacuo*, et le résidu distillé sous vide.

(2) Réaction à 110 °C (procédure-type)

La lactame (~0.02 mol) est dissoute dans du toluène anhydre (200 ml) et le chloroformiate d'éthyle (20 ml,

[5]L'identification a été faite à l'aide du spectre i.r. du produit après neutralisation.

[6]Le mécanisme est illustré à l'aide de la valérolactame (**8**). La voie *a* semble générale pour toutes les lactames alors que la voie *b* n'a été mise en évidence que dans le cas particulier représenté.

[7]Avec les lactames **4** et **6**, aucune réaction n'a été observée, même en élevant la température. Si on élève trop la température, on voit plutôt apparaître la *N*-éthoxycarbonyl-lactame.

Can. J. Chem. Downloaded from www.nrcresearchpress.com by 210.87.254.42 on 09/05/12
For personal use only.

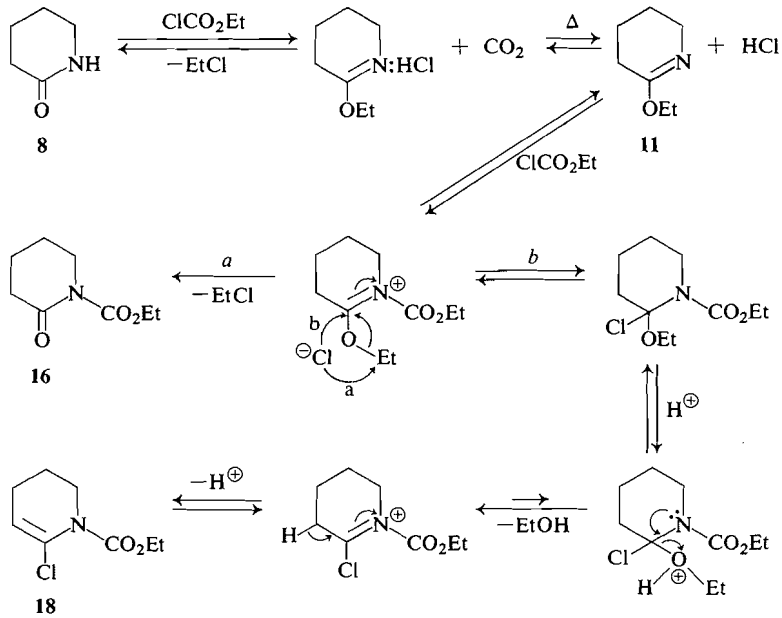

SCHÉMA 1

~0.2 mol) est ajouté en une portion. Le mélange est porté à reflux pendant 12 h. Le solvant et l'excès de chloroformiate d'éthyle sont ensuite évaporés *in vacuo*, et le résidu distillé sous vide poussé à l'aide d'une colonne Vigreux (15 po), ou chromatographié sur gel de silice.

Dans le cas de la pipéridone-2 (**8**), on peut isoler par chromatographie le produit secondaire **18**, qui est repurifié par distillation dans un appareil semi-micro, p.éb. ~70°/0.2 mm.

En i.r., ce produit montre des bandes caractéristiques à 1715 (C=O) et 1660 cm^{-1} (C=C(N)Cl). En r.m.n., on observe des absorptions à δ 1.38 (t, 3H), 1.8 (m, 2H), 2.2 (m, 2H), 3.67 (m, 2H), 4.20 (q, 2H), et 5.38 (t, 1H). Le spectre de masse montre un ion moléculaire à *m/e* 189 ainsi qu'un pic à *m/e* 191 dans le rapport de 3:1.

(3) Mise en évidence du chlorure d'éthyle

La caprolactame (**2**) (20 g, 0.177 mol) est dissoute dans du toluène anhydre (500 ml) et le chloroformiate d'éthyle (50 ml, 0.5 mol) est ajouté en une portion. Pendant que le mélange est chauffé à reflux, on recueille les gaz qui se dégagent au bout du réfrigérant à l'aide d'un piège à glace sèche. Après le traitement habituel, on peut isoler la *N*-éthoxycarbonylcaprolactame (**15**) (14.0 g, 0.076 mol) avec un rendement de 43%. Après distillation fractionnée des produits de condensation dans le piège froid, on peut caractériser une certaine quantité de chlorure d'éthyle (5 ml, 0.075 mol), p.éb. 13 °C. L'identification a été faite par comparaison du spectre de r.m.n. avec celui d'un échantillon authentique. L'expérience a été répétée à partir de l'éther lactimique **1**, et des résultats à peu près identiques ont été obtenus.

Les auteurs remercient le Conseil National de Recherches du Canada pour l'aide financière apportée sous forme de bourses d'études (R.G. et P.B.) et d'octrois de recherche (C.B. et D.G.).

1. W. HECHELHAMMER. Brev. allemand, 948, 973 (1956).
2. R. ROGER et D. G. NEILSON. Chem. Rev. **61**, 179 (1961).
3. F. H. SUYDAM, W. E GRETH, et N. R. LANGERMEN. J. Org. Chem. **34**, 292 (1969).
4. D. BEN-ISHAI et E. KATCHALSKI. J. Org. Chem. **16**, 1025 (1951).
5. R. K. RALPH et G. SHAW. J. Chem. Soc. 1877 (1956).
6. M. PIANKA et D. J. POLTON. J. Chem. Soc. 983 (1960).
7. G. FALKENSTEIN et H. DÖRFEL. Makromol. Chem. **127**, 34 (1969).
8. L. HUNTER et N. G. REYNOLDS. J. Chem. Soc. 2857 (1950).
9. C. BARKENBUS, J. F. DIEHL, et G. R. VOGEL. J. Org. Chem. **20**, 871 (1955).

Can. J. Chem. Downloaded from www.nrcresearchpress.com by 210.87.254.42 on 09/05/12
For personal use only.

The Master Equation for the Dissociation of a Dilute Diatomic Gas. IV. The Bottleneck Phenomenon

E. KAMARATOS AND H. O. PRITCHARD
Centre for Research in Experimental Space Science, York University, Downsview, Ontario

Received April 2, 1971

Once the initial transients have died out, the rate constant for the dissociation or recombination of a dilute diatomic gas bears the same kind of relationship to individual translation–vibration transition probabilities as does the conductance of a generalized resistance network to the individual resistance components. Thus, it is not possible to single out any one transition which "controls" the rate of dissociation or recombination.

Une fois que les phénomènes initiaux ont disparu, la constante de vitesse de la dissociation ou de la recombinaison d'un gaz diatomique dilué apporte le même genre de relation aux probabilités de transition individuelle translation-vibration que ne le fait la conductance d'un réseau généralisé de résistances aux résistances composantes individuelles. Ainsi, il n'est possible d'isoler aucune transition qui "contrôle" la vitesse de dissociation ou de recombinaison.

Canadian Journal of Chemistry, 49, 2617 (1971)

Can. J. Chem. Downloaded from www.nrcresearchpress.com by 210.87.254.105 on 09/05/12
For personal use only.

In Part III[1] of this series (1), it was shown empirically that the rate constant for the dissociation (or recombination) of a diatomic gas can be determined by finding the numerically smallest eigenvalue d_{n-1} of a submatrix $\mathbf{A}_{00}$ of the relaxation matrix. The off-diagonal elements of $\mathbf{A}_{00}$ are simply the specific transition rates W_{ij} $(= ZP_{ij})$ between all the bound states, and each diagonal element is the negative sum of the specific dissociation rate from that state and all the other elements in the row (eq. III (5)). The eigenvalue d_{n-1} is related to the desired rate constants through eqs. III (21) and III (22) *viz.*

$$k_{d,M} = -[M]^{-1}d_{n-1}$$

and

$$k_{r,M} = -K^{-1}[M]^{-1}d_{n-1}$$

where K is the equilibrium constant and [M] is the inert gas concentration. The minuteness of the inaccuracies of these two relationships is now well established (1–3).

Also in Part III, we found considerable circumstantial evidence for the existence of some kind of bottleneck in the dissociation process: the two most compelling points were that an increase of a factor of 1000 in the dominant bound-continuum rate coefficient caused only a 5% increase in the rate of dissociation; and that when sets of transition probabilities were chosen which did not have this property, the rate constant for recombination changed its behavior completely from a slow decline with increasing temperature to a very rapid increase with increasing temperature (Fig. III (3)). An attempt was made to define the bottleneck by determining which pair of transition probabilities P_{ij} and P_{ji} perturbed the eigenvalue d_{n-1} (*i.e.* the rate constant) the most; it was found that with the particular set of transition probabilities chosen, this criterion characterized the bottleneck as being somewhat diffuse, extending approximately over the levels $v = 9$ to $v = 13$ in H_2, with the $v = 10 \leftrightarrow 11$ and $v = 11 \leftrightarrow 12$ transitions the most important contributors.

In this Note we examine, by numerical experiment, the sensitivity of the rate constant for the recombination of H atoms by a third body M to variations in the assumed transition probabilities in the bottleneck region; the calculations were performed for two temperatures 2000 and 3000 °K to try to connect the temperature coefficient of $k_{r,M}$ to those of the bottleneck transition probabilities. The standard set of T–V transition probabilities were taken to be those given by the prescription eq. III (1), and Fig. 1(*a*) shows the variation of $k_{r,M}$ at 2000 °K for gross variations in the $10 \leftrightarrow 11$, $11 \leftrightarrow 12$, and $12 \leftrightarrow 13$ transition probabilities; similar data for 3000 °K are shown in Fig. 1(*b*). As already noted, $k_{r,M}$ is most sensitive to perturbations in the $10 \leftrightarrow 11$ and $11 \leftrightarrow 12$ transition probabilities. However, the most striking feature is the remark-

[1]Equations in this paper are designated by a prefix III; the reader is referred to refs. 1 and 2 for further clarification of the symbols used.

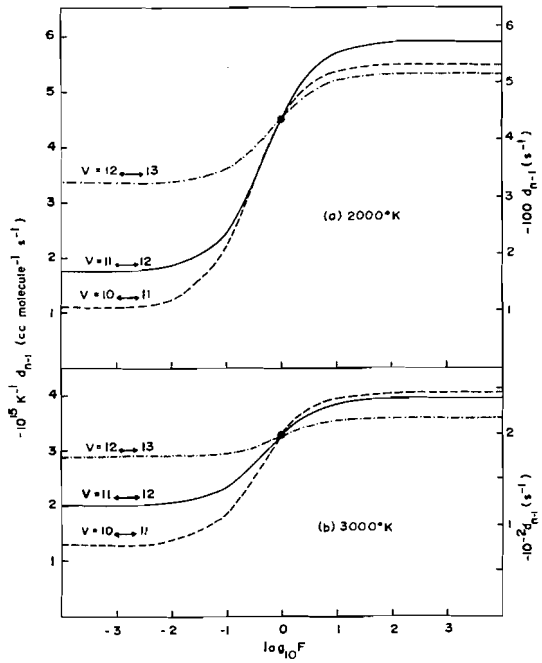

FIG. 1. Variation of the rate constants $k_{r,M}$ and $k_{d,M}$ for variations in the transition probabilities $P_{i,i+1}$ and $P_{i+1,i}$ when each pair of probabilities was multiplied in turn by the factor F. The left-hand ordinate is $-10^{15}K^{-1}d_{n-1}(= 10^{15}[M]k_{r,M}$ from eq. III (22)) and the right hand ordinate is proportional to $-d_{n-1}(= [M]k_{d,M}$ from eq. III (21)); [M] = 3.5×10^{19} molecules cc^{-1} in each case.

able insensitivity of the rate constant to large changes in the probabilities. For example, a decrease in the $11 \leftrightarrow 12$ transition probability by a factor of 100 reduces $k_{r,M}$ by a factor of about 2.5 at 2000 °K and 2.3 at 3000 °K: the rate constants are about a factor of two less sensitive to large increases in transition probability than to large decreases; and that beyond a factor of 100 change in $P_{i,i+1}$ and $P_{i+1,i}$ there is no further change in the rate constant. Small variations were also examined, and the rate constants were found to be roughly linear functions of the logarithm of the perturbed probability for variations of less than a factor of two, becoming rapidly non-linear beyond that. However, since the rate constant $k_{r,M}$ has different sensitivities to each individual transition probability at each temperature, and each transition probability has its own individual temperature coefficient, there is obviously no *simple* factor which determines the temperature coefficient of $k_{r,M}$; the temperature coefficient of the dissociation rate constant $k_{d,M}$ is of course *dominated* by the Boltzmann factor $\exp(-D_0/kT)$, this being to first order the temperature coefficient of the equilibrium constant K.

Some calculations were made to examine the actual differences that would occur in the reaction process, using dissociation as an example. It was found that if the transition probability for the $11 \leftrightarrow 12$ transition was reduced, all pseudo-steady populations $v = 0$ to 11 were higher, whilst those of $v = 12$, 13, and 14 were lower than in the unperturbed calculation at the same reaction time. As a result, all transition rates $R_{ij}(= W_{ij}n_j)$ between states $v = 0$ to 11 increased, both upwards and downwards: above $v = 12$, all rates decreased, again in both directions. Also, since the lower populations were inflated and the upper populations were depressed, upward multiple quantum jumps across the bottleneck increased in rate, whilst downward multiple quantum jumps across the bottleneck decreased in rate; nevertheless, since single quantum jumps are dominant during the pseudo-steady regime (2), the overall rate of dissociation *decreases*. On the other hand, if the $11 \leftrightarrow 12$ transition probability was increased, all these properties were reversed; also, the behavior in recombination processes is complementary.

Returning to the discussion of the behavior demonstrated in Fig. 1, the explanation in qualitative terms is very simple. If we increase the ease of the transition $v = 11 \leftrightarrow 12$, we increase the rate; but if we increase it so far that it no longer presents any impediment to the flow of molecules, other transitions (co-operatively) become rate determining, so the rate does not increase unboundedly. Alternatively, if we reduce the ease of this transition, we decrease the rate, but if we reduce it so far that it presents an infinite barrier to the flow of molecules, they can still get round the barrier by multiple quantum jumps (mainly in this case $v = 11 \leftrightarrow 13$ and $v = 10 \leftrightarrow 12$) so that the rate does not fall to zero. An analogy which is easy to visualize is that of an n-point resistance network, with resistances r_{ij} connecting each point in the network. If one of the elements $r_{i,i+i}$ is decreased to zero, there is a small increase in the conductance c of the network, whereas if $r_{i,i+i}$ becomes an open circuit there is a small decrease in the conductance of the network, since there are many other paths that the current can

Can. J. Chem. Downloaded from www.nrcresearchpress.com by 210.87.254.105 on 09/05/12
For personal use only.

take. In fact, there is a remarkable similarity between eq. III (5) and the network conductance equations, *viz.*

$$i = Cv$$

In this equation i is a column vector whose first element is $-i$ (the current), the last element is $+i$ and all other elements are zero (the precise analogue of the steady-state assumption for dn_i/dt in dissociation); v is a column vector of the voltages at each network point; and $\mathbf{C}$ is a symmetric matrix with off-diagonal elements c_{ij} (the individual conductances) and diagonal elements equal to the negative sum of all other elements in the row. We have performed some calculations on arbitrary 16-point resistance networks, and verified that the behavior of the network conductance[2] is similar to that observed in Fig. 1. Other network systems, *e.g.*, the flow of traffic through city streets, are equally useful in trying to achieve a *qualitative* understanding of these dissociation–recombination processes.

In summary, our calculations demonstrate the complexity of the factors determining the dissociation or recombination rate of a molecule; it is clear that what has been termed the bottleneck (4) is a diffuse and co-operative phenomenon, and that no single element in it has a significant causal relationship to the overall rate. In our view, it seems that future advances in our understanding of this aspect of the problem will more likely come from the establishment of eigenvalue theorems for the matrix $\mathbf{A}_{00}$ than by further numerical experiment. For example, the variation of every pair of single-step bound–bound transition probabilities in $\mathbf{A}_{00}$ gives rise to an effect on the rate constant similar to those shown in Fig. 1 except that the dispersion can vary from a factor of about 6 as seen in Fig. 1(*a*) to parts-per-million or even less. These tiny dispersions occur when the perturbation of a pair of transition probabilities simply perturbs one eigenvalue only as described in Part III; the larger dispersions discussed here arise almost like a residue in d_{n-1}, when the resultant perturbation happens to spread over several of the other eigenvalues.

We would like to acknowledge assistance from R. A. Koehler and D. L. S. McElwain in these calculations.

1. D. L. S. McElwain and H. O. Pritchard. Thirteenth Symposium (International) on Combustion. The Combustion Institute. 1971. p. 35.
2. D. L. S. McElwain and H. O. Pritchard. J. Am. Chem. Soc. **91**, 7693 (1969).
3. C. A. Brau. J. Chem. Phys. **47**, 1153 (1967).
4. D. G. Rush and H. O. Pritchard. Eleventh Symposium (International) on Combustion. The Combustion Institute. 1967. p. 13.

[2]If processes taking place during the transient period become experimentally accessible, the extension of this analogy to capacitative resistance networks might be instructive and useful.

Erratum: Kinetic Isotope Effects in the Radiation-induced Oxidation of Alcohols by Hydrogen Peroxide in Aqueous Solution

C. E. Burchill and G. F. Thompson
Department of Chemistry, University of Manitoba, Winnipeg 19, Manitoba

Received May 6, 1971

(Ref. Can. J. Chem. **49**, 1305 (1971))

Canadian Journal of Chemistry, 49, 2619 (1971)

On page 1306, eq. 8 should read as follows:

[8] $2\beta \rightarrow$ 2,5-Hexanediol or other products

Can. J. Chem. Downloaded from www.nrcresearchpress.com by 210.87.254.105 on 09/05/12
For personal use only.

Can. J. Chem. Downloaded from www.nrcresearchpress.com by 210.87.254.40 on 09/05/12
For personal use only.

Stereoselective Total Synthesis of (+)-Copaborneol, (+)-Copaisoborneol, and (+)-Copacamphor[1]

EDWARD PIERS,[2] RONALD W. BRITTON, ROBERT J. KEZIERE, AND R. DEAN SMILLIE
Department of Chemistry, University of British Columbia, Vancouver 8, British Columbia

Received May 11, 1971

A stereoselective total synthesis of the novel tricyclic sesquiterpenoids (+)-copaborneol (**1**), (+)-copacamphor (**2**), and (+)-copaisoborneol (**3**) is described. This work fully corroborates the structure and absolute stereochemistry assigned to the three sesquiterpenoids.

Une synthèse totale et stéréosélective de nouveaux sesquiterpènes tricycliques, le (+)-copabornéol (**1**), le (+)-copacamphre (**2**), et le (+)-copaisobornéol (**3**), est décrite. Ce travail confirme pleinement la structure et la stéréochimie absolue attribuée à ces trois sesquiterpènes.

Canadian Journal of Chemistry, 49, 2620 (1971)

The novel tricyclic sesquiterpenoid (+)-copaborneol is the major C_{15}-alcohol occurring in the wood of *Pinus silvestris* L. (1) and in Swedish sulfate turpentine (2) and has been assigned (3, 4) structure and absolute stereochemistry as depicted in **1**. Oxidation of this alcohol afforded (+)-copacamphor (**2**) (3, 4). Reduction of the latter with lithium aluminum hydride gave (+)-copaisoborneol (**3**), while reduction with sodium in ethanol yielded (+)-copaborneol (**1**) (3, 4). We report here a stereoselective total synthesis of these three sesquiterpenoids via a route which fully corroborates the structural and absolute stereochemical assignments.

Conversion of (+)-carvomenthone (**4**), with absolute configuration as shown (5), into the corresponding *n*-butylthiomethylene derivative **5** was accomplished by standard procedures (6). Alkylation (potassium *t*-butoxide in *t*-butyl alcohol) of the latter with methyl 2-iodopropionate was highly regioselective[3] and stereoselective and gave, after removal of the blocking group (6) and esterification of the resulting keto acid, the keto ester **6** in 62% yield.[4] Treatment of keto ester **6** with sodium bis(trimethylsilyl)amide (8) in refluxing dimethoxyethane, followed by quenching of the reaction mixture with acetic acid, afforded a 90% yield of the substituted bicyclo[3.2.1]octadione **7**, m.p. 76–77°, $[\alpha]_D^{20}$ −56°.

When the diketone **7** was reacted with 1 equiv of sodium bis(trimethylsilyl)amide (8) in benzene, and the resulting solution was treated with excess acetyl chloride, the enol acetate **8** was obtained in 90% yield. Hydrogenation (platinum oxide, ethanol) of the latter gave only one keto acetate and the p.m.r. spectrum of this material was in full accord with the assigned structure **9**. In particular, the proton on C-6 appeared as a pair of doublets (τ 4.65) with $J_{5,6} = 7.5$ and $J_{6,7} = 10.5$ Hz. Furthermore, the bridgehead proton at C-5 also produced a pair of doublets (τ 7.16), with $J_{4,5} = 3.5$ and $J_{5,6} = 7.5$ Hz. Molecular models clearly indicate that these spectral data are consistent only with the keto

[1]Financial support for this work by the National Research Council of Canada is gratefully acknowledged.

[2]Fellow of the Alfred P. Sloan Foundation, 1970–1972.

[3]Interestingly, alkylation of **5** with methyl 2-bromopropionate under a variety of conditions consistently gave mixtures of *O*- and *C*-alkylation products. For an excellent discussion regarding *O*- *vs.* *C*-alkylation of ambident anions, see ref. 7.

[4]The stereochemistry of **6** and of other synthetic intermediates was unambiguously established on the basis of chemical correlation with compounds of known stereochemistry, conformational analysis, and/or analysis of spectral data. New compounds gave satisfactory analytical data and showed spectral properties in complete accordance with the assigned structures.

Can. J. Chem. Downloaded from www.nrcresearchpress.com by 210.87.254.40 on 09/05/12
For personal use only.

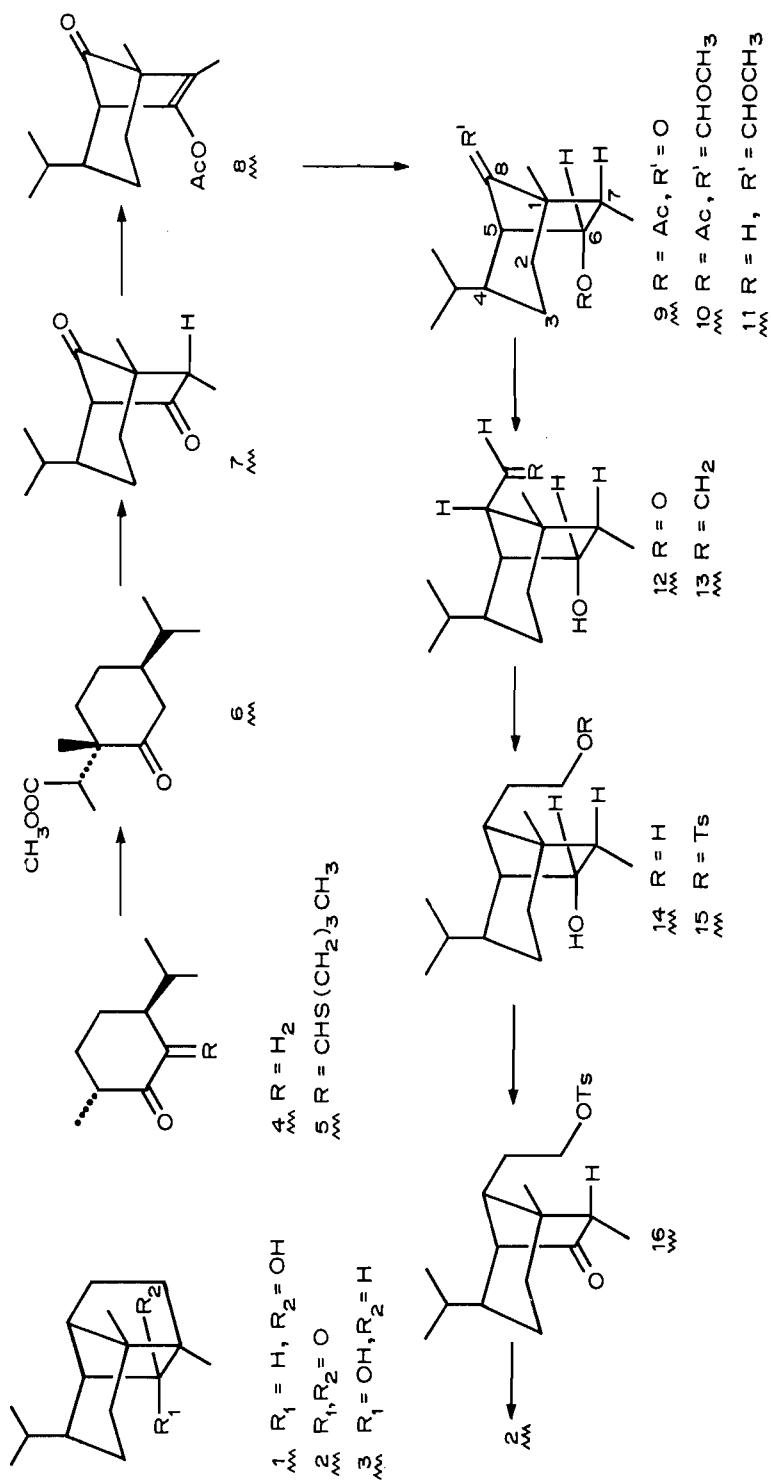

acetate possessing the stereochemistry depicted in **9**, assuming that the hydrogenation proceeded in a *cis* manner.[5]

Treatment of keto acetate **9** with methoxymethylenetriphenylphosphorane in ether gave an isomeric mixture of the enol ether acetates **10**, accompanied by some of the corresponding alcohols **11**. Successive subjection of this mixture to reduction (lithium aluminum hydride), hydrolysis (aqueous perchloric acid in ether), and equilibration (aqueous potassium carbonate in methanol) afforded, in 50% yield from **9**, the hydroxy aldehyde **12**. Reaction of the latter with methylenetriphenylphosphorane in dimethyl sulfoxide (9) gave, in 92% yield, the olefinic alcohol **13**, $[\alpha]_D^{20}$ +43°. Hydroboration–oxidation (10) of **13** led to the diol **14**, which upon treatment with *p*-toluenesulfonyl chloride in pyridine followed by Collins oxidation (11) of the resulting mono tosylate **15**, afforded the crystalline keto tosylate **16**, m.p. 114–114.5° (45% yield from **13**).

Treatment of **16** with 0.1 *M* methylsulfinyl carbanion (12) in dimethyl sulfoxide afforded in 82% yield, (+)-copacamphor (**2**), $[\alpha]_D^{23}$ +106°; i.r. (film) 5.75, 9.60, 9.87 μ; p.m.r. τ 9.06, 9.10 (singlets, tertiary methyls), 9.09, 9.11 (doublets, J = 6.4 Hz, isopropyl methyls). This material was shown to be identical (i.r., p.m.r., g.l.c. retention times, specific rotation) with authentic (+)-copacamphor.[6] Since the latter compound had previously (3, 4) been converted into both (+)-copaborneol (**1**) and (+)-copaisoborneol (**3**), the work described above also completes the total synthesis of these two sesquiterpenoids.

1. L. WESTFELT. Acta. Chem. Scand. **20**, 2829 (1966).
2. L. WESTFELT. Acta. Chem. Scand. **20**, 2841 (1966).
3. M. KOLBE and L. WESTFELT. Acta. Chem. Scand. **21**, 585 (1967).
4. M. KOLBE-HAUGWITZ and L. WESTFELT. Acta. Chem. Scand. **24**, 1623 (1970).
5. E. J. COREY and N. NOZOE. J. Am. Chem. Soc. **87**, 5728 (1965), and references therein.
6. R. E. IRELAND and J. A. MARSHALL. J. Org. Chem. **27**, 1615 (1962) and references therein.
7. W. J. LE NOBLE. Synth. 1 (1970).
8. M. TANABE and D. F. CROW. Chem. Commun. 1498 (1969), and references therein.
9. R. GREENWALD, M. CHAYKOVSKY, and E. J. COREY. J. Org. Chem. **28**, 1128 (1963).
10. G. ZWEIFEL and H. C. BROWN. Org. React. **13**, 1 (1963).
11. J. C. COLLINS, W. W. HESS, and F. J. FRANK. Tetrahedron Lett. 3363 (1968); R. RATCLIFFE and R. RODEHORST. J. Org. Chem. **35**, 4000 (1970).
12. E. J. COREY and M. CHAYKOVSKY. J. Am. Chem. Soc. **87**, 1345 (1965).

[5]It is pertinent to point out that the proton adjacent to the hydroxyl group in copaisoborneol appears as a doublet with J = 8 Hz, while that in copaborneol appears as a broad singlet (4).

[6]We are very grateful to Dr. L. Westfelt for a generous sample of (+)-copacamphor.

Can. J. Chem. Downloaded from www.nrcresearchpress.com by 210.87.254.40 on 09/05/12
For personal use only.

Stereoselective Total Synthesis of (−)-Copacamphene and (−)-Cyclocopacamphene[1]

EDWARD PIERS,[2] RONALD W. BRITTON, ROBERT J. KEZIERE, AND R. DEAN SMILLIE
Department of Chemistry, University of British Columbia, Vancouver 8, British Columbia

Received May 11, 1971

An efficient and highly stereoselective total synthesis of the novel sesquiterpenes (−)-copacamphene (**1**) and (−)-cyclocopacamphene (**3**) is described. This work fully corroborates the structure and absolute stereochemistry assigned to the two sesquiterpenes.

Une méthode de synthèse totale, efficace et hautement stéréosélective de nouveaux sesquiterpènes, le (−)-copacamphène (**1**) et le (−)-cyclocopacamphène (**3**), est décrite. Ce travail confirme pleinement la structure et la stéréochimie absolue attribuée à ces deux sesquiterpènes.

Canadian Journal of Chemistry, 49, 2623 (1971)

The structure (1) and absolute stereochemistry (2) of the novel tricyclic sesquiterpene (+)-copacamphene have been assigned as depicted in **1**. Although this material has apparently not as yet been isolated from a natural source, it has been obtained by rearrangement of a copaborneol derivative (1, 2). Very recently, racemic copacamphene has been obtained by total synthesis (3). A closely related compound, (+)-cyclocopacamphene (**2**) has been obtained from cyclocopacamphenic acid (4) and, apparently, occurs in vetiver oil (4). Although it has been suggested that (+)-cyclocopacamphene has absolute stereochemistry as depicted in **2** (4), this point has not yet received unambiguous verification. We report here the total synthesis of (−)-copacamphene (**1**)[3] and of (−)-cyclocopacamphene (**3**) via a highly stereoselective route which provides unambiguous evidence for the structure and absolute stereochemistry of these compounds.

Reaction of the diketone **4**, of known absolute stereochemistry (5), with 1 equiv of sodium borohydride in methanol gave the keto alcohol **5**.[4] Conversion of the latter into the corresponding tosylhydrazone **6**, followed by reaction of the latter with methyllithium in tetrahydrofuran (6) gave the olefinic alcohol **7**. Collins oxidation (7) of **7** afforded, in 67% overall yield from the diketone **4**, the keto olefin **8**, $[\alpha]_D^{23}$ −29°.

Reaction of **8** with methoxymethylenetriphenylphosphorane in dimethyl sulfoxide (8) (40°, 1.5 h) gave, in high yield, a mixture of isomeric enol ethers **9**. Successive subjection of the latter to hydrolysis (35% perchloric acid in ether), equilibration (potassium carbonate in methanol), Wittig reaction (methylenetriphenylphosphorane in dimethyl sulfoxide), and hydroboration–oxidation (disiamylborane in tetrahydrofuran; hydrogen peroxide – sodium hydroxide (9)) afforded (66% yield from **9**) the olefinic alcohol **10**, $[\alpha]_D^{20}$ +8.5°. Treatment of **10** with *p*-toluenesulfonyl chloride in pyridine at 25° gave the olefinic tosylate **11** which, presumably largely due to the proximity of the tosylate functionality and the olefinic double bond, exhibited a high propensity toward eliminative cyclization. Thus, merely allowing **11** to stand at room temperature gave, after filtration of the resultant material through a silica gel column, a 90% yield (from **10**) of a mixture consisting nearly entirely of (−)-copacamphene (**1**), accompanied by very small amounts of two as yet unidentified compounds. Pure synthetic (−)-copacamphene (**1**), readily obtained from this mixture by chromatography of the latter over silver nitrate impregnated silica gel, exhibited $[\alpha]_D^{21}$ −159°; i.r. (film) 3.26, 6.03, 6.83, 7.20, 7.30, 11.42 μ; p.m.r. τ 5.21, 5.49 (singlets, olefinic protons), 7.54 (broad signal, allylic proton), 9.00 (singlet, tertiary methyl), 9.10 (doublet, J = 6.0 Hz, isopropyl methyls). These spectral data are in excellent agreement with

[1]Financial support for this work from the National Research Council of Canada is gratefully acknowledged.

[2]Fellow of the Alfred P. Sloan Foundation, 1970–1972.

[3]Although Kolbe-Haugwitz and Westfelt (2) were correct in their assignments regarding absolute stereochemistry, we have found that copacamphene of absolute configuration as shown in **1** is levorotatory ($[\alpha]_D^{21}$ −159°, *vide infra*) and not dextrorotatory ($[\alpha]_D$ +28.9°) as reported (1, 2). Neither we nor Dr. Westfelt (private communication) have as yet been able to trace the reason for this discrepancy.

[4]New compounds gave satisfactory analytical data and showed spectral properties in complete accord with the assigned structures.

Can. J. Chem. Downloaded from www.nrcresearchpress.com by 210.87.254.5 on 09/05/12
For personal use only.

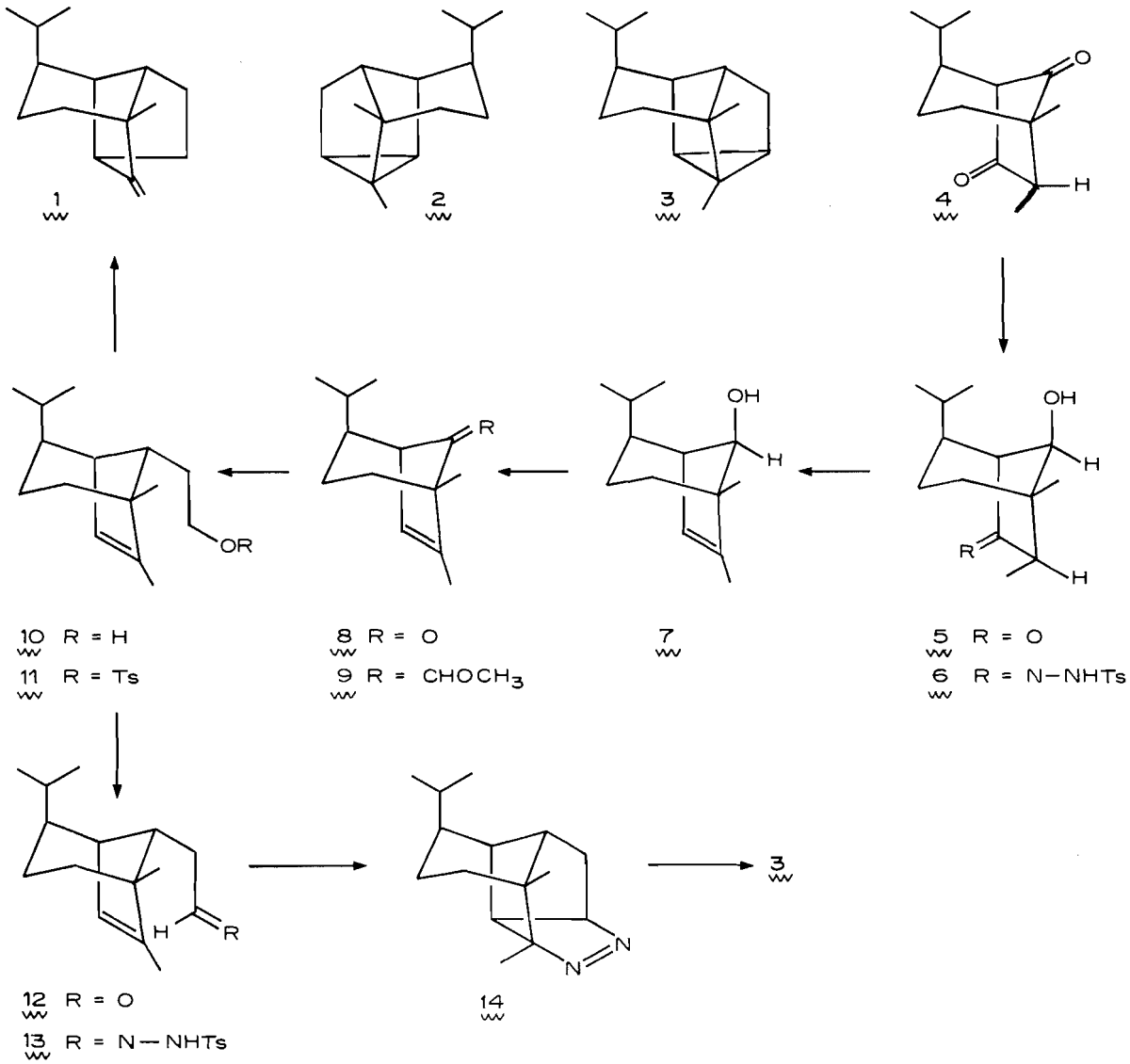

those published for copacamphene (2, 3) and, indeed, our synthetic (−)-copacamphene exhibited spectral data and g.l.c. retention times identical with those of (±)-copacamphene (3).[5]

Oxidation (7) of **10** gave, in 91% yield, the olefinic aldehyde **12**, $[\alpha]_D^{21}$ −39°, which was converted, by reaction with *p*-toluenesulfonylhydrazide in benzene, into the corresponding tosylhydrazone **13**. Pyrolysis (120–140°) of the lithium salt of the latter under reduced pressure (0.25 mm) with direct distillation of the product (10) afforded (81% yield from **12**) the pyrazoline **14**,[6] $[\alpha]_D^{22}$ +95°. The structure of the latter was clearly shown by the p.m.r. spectrum, which exhibited only one proton (τ 5.11) adjacent to the —N=N— moiety (12). Photolysis of **14** in ether gave a quantitative yield of (−)-cyclocopacamphene (**3**), $[\alpha]_D^{21}$ −42°; i.r. (film) 3.29, 6.85,

[5]We are very grateful to Professor J. E. McMurry for a sample of this compound.

[6]The facile intramolecular 1,3-dipolar cycloaddition of the intermediate olefinic diazoalkane to give **14** is presumably a function of the proximity of the two reacting functional groups and of the fairly strained nature of the olefinic double bond (see ref. 11).

Can. J. Chem. Downloaded from www.nrcresearchpress.com by 210.87.254.5 on 09/05/12
For personal use only.

7.21, 7.28, 11.60, 11.80, 12.10 μ; p.m.r. τ 8.99, 9.26 (singlets, tertiary methyls), 9.10, 9.13 (doublets, $J = 6.5$ Hz, isopropyl methyls), 9.32, 9.37 (broad signals, cyclopropyl protons). The i.r. and p.m.r. spectra of this material were identical with those of authentic (+)-cyclocopacamphene (**2**) (4).[7]

1. M. KOLBE and L. WESTFELT. Acta. Chem. Scand. **21**, 585 (1967).
2. M. KOLBE-HAUGWITZ and L. WESTFELT. Acta. Chem. Scand. **24**, 1623 (1970).
3. J. E. MCMURRY. Tetrahedron Lett. 3731 (1970).
4. F. KIDO, R. SAKUMA, H. UDA, and A. YOSHIKOSHI. Tetrahedron Lett. 3169 (1969).
5. E. PIERS, R. W. BRITTON, R. J. KEZIERE, and R. D. SMILLIE. This issue.
6. A. K. BOSE and N. G. STEINBERG. Synth. 595 (1970), and references therein.
7. J. C. COLLINS, W. W. HESS, and F. J. FRANK. Tetrahedron Lett. 3363 (1968); R. RATCLIFFE and R. RODEHORST. J. Org. Chem. **35**, 4000 (1970).
8. R. GREENWALD, M. CHAYKOVSKY, and E. J. COREY. J. Org. Chem. **28**, 1128 (1963).
9. G. ZWEIFEL and H. C. BROWN. Org. React. **13**, 1 (1963).
10. G. M. KAUFMAN, J. A. SMITH, G. G. VANDER STOUW, and H. SHECHTER. J. Am. Chem. Soc. **87**, 935 (1965).
11. G. W. COWELL and A. LEDWITH. Q. Rev. **24**, 119 (1970).
12. R. J. CRAWFORD, A. MISHRA, and R. J. DUMMEL. J. Am. Chem. Soc. **88**, 3959 (1966).

[7]F. Kido, Ph.D. Thesis, Tohoku University, Sendai, Japan, 1970. We are grateful to Dr. Kido for his help in carrying out this comparison.

Can. J. Chem. Downloaded from www.nrcresearchpress.com by 210.87.254.5 on 09/05/12
For personal use only.

Can. J. Chem. Downloaded from www.nrcresearchpress.com by 210.87.254.42 on 09/05/12
For personal use only.

Canadian Journal of Chemistry

Published by THE NATIONAL RESEARCH COUNCIL OF CANADA

VOLUME 49 AUGUST 15, 1971 NUMBER 16

The Kinetics of the Thermal Insertion Reaction of Tin(II) Halides with Cyclopentadienylnickel Carbonyl Dimer

P. F. BARRETT AND RONALD R. CLANCY

Department of Chemistry, Trent University, Peterborough, Ontario

Received March 23, 1971

The kinetics of the thermal insertion of $SnCl_2$ and $SnBr_2$ into the metal–metal bond of $[\pi\text{-}C_5H_5NiCO]_2$ have been studied. On the basis of the kinetic data a bimolecular mechanism, involving direct attack of the tin(II) halide on the nickel dimer, has been proposed. The thermal insertion with tin(II) bromide was found to proceed with an activation enthalpy of 19.4 ± 0.2 kcal/mol and an activation entropy of -8.8 ± 0.4 cal deg^{-1} mol^{-1}. For the thermal insertion with tin(II) chloride a $\Delta H^{\ddagger}$ and $\Delta S^{\ddagger}$ of 22.5 ± 0.2 kcal/mol and -4.0 ± 0.2 cal deg^{-1} mol^{-1}, respectively, were observed.

La cinétique de l'insertion thermique de $SnCl_2$ et $SnBr_2$ dans la liaison métal-métal de $[\pi\text{-}C_5H_5NiCO]_2$ a été étudiée. Sur la base des données cinétiques, on propose un mécanisme bimoléculaire, impliquant une attaque directe du halogénure d'étain(II) sur le dimère du nickel. L'insertion thermique avec le bromure d'étain(II) procède avec une enthalpie d'activation de 19.4 ± 0.2 kcal/mol et avec une entropie d'activation de -8.8 ± 0.4 cal deg^{-1} mol^{-1}. Pour l'insertion thermique avec le chlorure d'étain(II), on observe pour $\Delta H^{\ddagger}$ et $\Delta S^{\ddagger}$ respectivement les valeurs de 22.5 ± 0.2 kcal/mol et -4.0 ± 0.2 cal deg^{-1} mol^{-1}.

Canadian Journal of Chemistry, 49, 2627 (1971)

Introduction

Cyclopentadienylnickel carbonyl dimer exists as a doubly carbonyl bridged species (1, 2) containing a covalent Ni—Ni bond. The insertion of tin(II) chloride into this bond was first reported by Patmore and Graham (3) and we have found that tin(II) bromide forms a similar insertion product.

Previous studies (4, 5) have reported the kinetics of the insertion of tin(II) halides into the metal–metal bonds of hexacarbonylbis(tri-*n*-butyl-phosphine)dicobalt and cyclopentadienyl-iron dicarbonyl dimer. From these investigations information regarding the strength of metal–metal bonds has been obtained as well as details of the mechanisms of insertion reactions.

In this paper we report the kinetic investigation of the thermal insertion of $SnCl_2$ and $SnBr_2$ into the metal–metal bond of cyclopentadienylnickel carbonyl dimer.

Experimental and Results

Materials

Cyclopentadienylnickel carbonyl dimer, $[\pi\text{-}C_5H_5NiCO]_2$, was prepared from dicyclopentadienylnickel and nickel carbonyl (Alpha Inorganics Inc.) using methods previously described (1, 2). Anhydrous tin(II) chloride was prepared by dehydrating the dihydrate (Fisher Scientific Co.) with acetic anhydride (6). Anhydrous tin(II) bromide (K & K Laboratories Inc.) was prepared in a similar manner but under a nitrogen atmosphere. The anhydrous $SnCl_2$ and $SnBr_2$ were stored in light-tight containers in vacuo over P_2O_5. Tetrahydrofuran (Fisher Scientific Co.; Certified grade) was dried by refluxing over sodium wire and was freshly distilled immediately before use in the kinetic runs.

Preparation of Insertion Products

Dichlorobis(π-cyclopentadienylcarbonylnickel)tin(IV) was prepared using the method of Patmore and Graham (3). Dibromobis(π-cyclopentadienylcarbonylnickel)tin(IV) was prepared in a similar manner, all work being done in a nitrogen atmosphere. The product gave dark green, air stable, needlelike crystals, m.p. 116°.

Anal. Calcd. for $[\pi\text{-}C_5H_5NiCO]_2SnBr_2$: C, 24.75; H, 1.72; Br, 27.39. Found: C, 24.71; H, 1.98; Br, 27.31.[1]

Kinetics

The thermal insertion of tin(II) chloride into the metal–metal bond of cyclopentadienylnickel carbonyl dimer was studied by recording the appearance of the insertion product at 600 mμ using a Unicam SP800 spectrophotometer. The reaction mixture underwent a color change

[1]This analysis was carried out by Dr. Franz Pascher, Microanalytical Laboratory, Bonn, West Germany.

Can. J. Chem. Downloaded from www.nrcresearchpress.com by 210.87.254.42 on 09/05/12
For personal use only.

from red to green during the course of the reaction and gave an isosbestic point at 556 mμ indicating that there was a simple conversion from reactants to product. For each run 10 ml of a THF solution of known tin(II) chloride concentration was thermostated to the desired temperature and then used to completely fill a 1 cm stoppered silica cell containing an amount of $[\pi\text{-}C_5H_5NiCO]_2$ required to give an approximately 1.5×10^{-3} *M* solution. Pseudo first-order kinetics were observed in all cases. Plots of log $(A_\infty - A_t)$, where A_∞ and A_t are the absorbances at 600 mμ for times ∞ and t, respectively, were linear for over 50% reaction.

A_∞ was due solely to the absorbance of the product $[\pi\text{-}C_5H_5NiCO]_2SnCl_2$ but because of the uncertainty in the initial concentration of $[\pi\text{-}C_5H_5NiCO]_2$, a value for A_∞ could not be determined directly. The following outlines the method used to calculate A_∞ at 600 mμ from the absorbance at the isosbestic point (556 mμ). The molar absorptivity (ε) of $[\pi\text{-}C_5H_5NiCO]_2$ must be identical with that of $[\pi\text{-}C_5H_5NiCO]_2SnCl_2$ at 556 mμ and was calculated to be 1.37×10^3 from a Beer's law plot of $[\pi\text{-}C_5H_5NiCO]_2SnCl_2$ at this wavelength. In a given run, the final concentration of product could then be determined from the absorbance at the isosbestic point. Using this value for the final concentration of product, A_∞ could be calculated from a Beer's law plot of $[\pi\text{-}C_5H_5NiCO]_2SnCl_2$ at 600 mμ, the wavelength at which the kinetics were studied. The molar absorptivity at this wavelength was found to be 1.41×10^3. Data for the Beer's law plots of $[\pi\text{-}C_5H_5NiCO]_2SnCl_2$ were obtained from THF solutions which were 0.5 *M* in $SnCl_2$ under which conditions the insertion product was considerably more stable.

The thermal insertion reaction with tin(II) bromide could not be studied in the visible by following the appearance of the insertion product because of the instability of this product and the resulting uncertainties in interpreting the absorbance data. The reaction could however, be studied kinetically by following the disappearance of the bridging carbonyl band of $[\pi\text{-}C_5H_5NiCO]_2$ in the infrared (1844 cm^{-1}) since the subsequent decomposition of the insertion product did not affect this region of the spectrum. $[\pi\text{-}C_5H_5NiCO]_2$ was found to be stable under actual reaction conditions for times well in excess of those of the actual kinetic runs. For the runs themselves, 10 ml of a THF solution containing a known concentration of $SnBr_2$ was thermostated and quickly added to a three-necked flask containing the nickel dimer. A nitrogen atmosphere was maintained in the vessel throughout and the bridging carbonyl region in the infrared spectrum was scanned using a Perkin–Elmer 621 spectrophotometer immediately upon removal of an aliquot by means of a syringe. As samples were removed the nitrogen atmosphere was maintained by means of a small positive pressure. Time intervals were taken from the moment the samples were removed from the reaction vessel. From the transmittances, linear plots of log $(A_t - A_\infty)$ against time were obtained where A_t and A_∞ are the absorbances at time t and ∞, respectively. Plots were linear for well over two half-lives. A base line of the spectrum was obtained from the absorbance of a solution of $SnBr_2$ run against the reference solvent THF. A_∞ was found to be zero in all cases.

The observed pseudo first-order rate constants for the $SnBr_2$ and $SnCl_2$ insertions reactions, k_{obs}, are plotted in Figs. 1 and 2 as functions of tin(II) halide concentration. The lines were fitted by a least squares analysis (7) using the origin as an experimental point since there was no evidence for decomposition of the cyclopentadienylnickel carbonyl dimer.

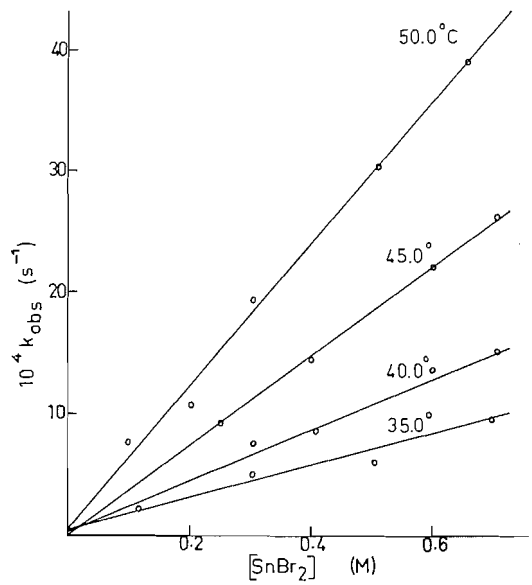

FIG. 1. Plot of the observed pseudo first-order rate constant *vs.* tin(II) bromide concentration for the thermal reaction $[\pi\text{-}C_5H_5NiCO]_2 + SnBr_2 \rightarrow [\pi\text{-}C_5H_5NiCO]_2SnBr_2$ in THF.

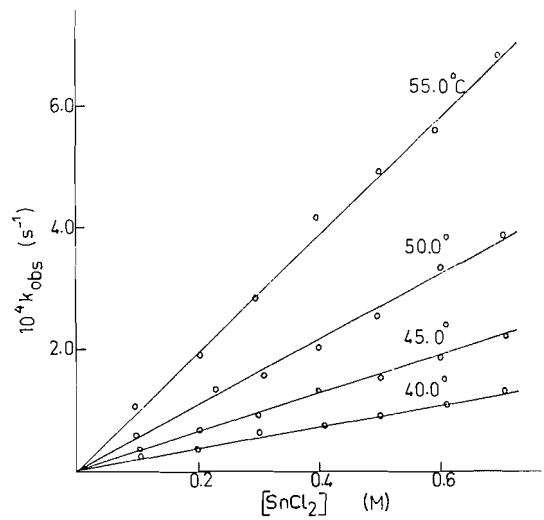

FIG. 2. Plot of the observed pseudo first-order rate constant *vs.* tin(II) chloride concentration for the thermal reaction $[\pi\text{-}C_5H_5NiCO]_2 + SnCl_2 \rightarrow [\pi\text{-}C_5H_5NiCO_2]SnCl_2$.

Can. J. Chem. Downloaded from www.nrcresearchpress.com by 210.87.254.42 on 09/05/12
For personal use only.

Discussion

Figures 1 and 2 show that the pseudo first-order rate constant, k_{obs}, for the insertion of tin(II) halides into the metal–metal bond of $[\pi\text{-}C_5H_5NiCO]_2$ varies directly with tin(II) halide concentration over the range of concentrations studied. The most obvious mechanism to account for this behavior would involve the direct bimolecular attack of the tin(II) halide on the $[\pi\text{-}C_5H_5NiCO]_2$ dimer. In the insertion of tin(II) halides into the metal–metal bonds of the similar complexes $[PBu_3Co(CO)_3]_2$ (4) and $[\pi\text{-}C_5H_5Fe(CO)_2]_2$ (5), however, the kinetic data could only be explained by invoking the following two stage mechanism

$$A_2 \underset{k_{-1}}{\overset{k_1}{\rightleftharpoons}} A_2^* \xrightarrow[B]{k_2} ABA$$

where A_2 represents the metal dimer, A_2^* is a reactive intermediate, B is the tin(II) halide, and ABA the insertion product. In the case of the $[\pi\text{-}C_5H_5Fe(CO)_2]_2$ reaction, this was the only mechanism proposed while in the case of the $[PBu_3Co(CO)_3]_2$ reaction, it was one of two mechanisms which were suggested to operate concurrently. In the light of these results one might have expected the $[\pi\text{-}C_5H_5NiCO]_2$ complex to react by a similar mechanism, and indeed when the concentration of A_2^* is small and $k_2[B] \ll k_{-1}$ the rate law for this two-step mechanism reduces to

$$[1] \qquad \frac{-d[A_2]}{dt} = \frac{k_1 k_2}{k_{-1}}[B][A_2]$$

which is consistent with our kinetic data since the k_{obs} then becomes directly proportional to the tin(II) halide concentration.

Although the kinetic data alone cannot distinguish between these two mechanisms, other indirect evidence suggests that it is unlikely that the $[\pi\text{-}C_5H_5NiCO]_2$ complex reacts in the same way as the $[\pi\text{-}C_5H_5Fe(CO)_2]_2$ and $[PBu_3Co(CO)_3]_2$ complexes via a two-step mechanism, but rather is subjected to direct bimolecular attack by the tin(II) halides. In the first place a two-step mechanism was proposed in the reactions of $[PBu_3Co(CO)_3]_2$ and $[\pi\text{-}C_5H_5Fe(CO)_2]_2$ in order to account for curvature of the plots of k_{obs} against tin(II) halide concentration, whereas no such curvature is observed in the insertion reactions of $[\pi\text{-}C_5H_5NiCO]_2$. Secondly, in the substitution reactions of $Mn_2(CO)_{10}$ and $Re_2(CO)_{10}$ (8), and in the insertion reactions of $[\pi\text{-}C_5H_5Fe(CO)_2]_2$ and $[PBu_3Co(CO)_3]_2$, which are all proposed to occur via the two-step mechanism, the reactive intermediates involved, A_2^* have all been suggested to be species in which the two halves of each of the dimers are held together solely by a single carbonyl bridge. Since the $[\pi\text{-}C_5H_5NiCO]_2$ complex shows no evidence of existing in a non carbonyl bridged form, (1, 2) the proposal of a singly carbonyl bridged reactive intermediate would seem less plausible in this case. Finally, Ellgen (9) has studied the reactions of $[\pi\text{-}C_5H_5NiCO]_2$ with carbon monoxide, triphenylarsine, triphenylphosphite, and other similar ligands and has found no evidence to suggest that the mechanism involved anything but the direct attack of the incoming ligand on the nickel dimer.

Values of k, the calculated second-order rate constant, and the thermodynamic parameters calculated from the observed rate data are listed in Tables 1 and 2. The negative $\Delta S^{\ddagger}$ is consistent with an associative type of mechanism. The $\Delta S^{\ddagger}$ for the insertion of $SnBr_2$ into the metal–metal bond of $[\pi\text{-}C_5H_5NiCO]_2$ is more negative than for the $SnCl_2$ insertion reaction. This is consistent with $SnBr_2$ being a better nucleophile than $SnCl_2$ for the soft (10) nickel dimer, thus forming a "tighter" or more ordered transition state in an associative reaction mechanism. The $\Delta H^{\ddagger}$ is also slightly lower for the $SnBr_2$ insertion reaction,

TABLE 1. Kinetic parameters for the $SnBr_2$ thermal reaction*

Temperature (°C)	10^4k (l mol^{-1} s^{-1})
50.0	49.3±3.7
45.0	37.2±0.5
40.0	21.5±1.3
35.0	13.1±0.8

*The uncertainties are standard deviations; $\Delta H^{\ddagger}$ = 19.4 ± 0.2 kcal mol^{-1}; $\Delta S^{\ddagger}$ = −8.8 ± 0.4 cal deg^{-1} mol^{-1}.

TABLE 2. Kinetic parameters for the $SnCl_2$ thermal reaction*

Temperature (°C)	10^4k (l mol^{-1} s^{-1})
55.0	9.75±0.27
50.0	5.93±0.18
45.0	3.09±0.05
40.0	1.76±0.06

*The uncertainties are standard deviations; $\Delta H^{\ddagger}$ = 22.5 ± 0.2 kcal mol^{-1}; $\Delta S^{\ddagger}$ = −4.0 ± 0.2 cal deg^{-1} mol^{-1}.

again consistent with $SnBr_2$ being better for direct nucleophilic attack than $SnCl_2$.

It is interesting that the insertion of tin(II) halides into the metal–metal bonds of $[\pi\text{-}C_5H_5NiCO]_2$ and $[\pi\text{-}C_5H_5Fe(CO)_2]_2$ involves two completely different mechanisms. In the insertion reaction with $[\pi\text{-}C_5H_5Fe(CO)_2]_2$ the only mechanism appears to be a two-stage one involving a reactive intermediate, while the insertion of tin(II) halides into $[\pi\text{-}C_5H_5NiCO]_2$ seems to proceed solely by a one-step, bimolecular type mechanism. Part of the explanation for this may lie in the fact that on going from Fe to Ni across the first transition series, the effective nuclear charge on the metal is increasing, making it more susceptible to direct nucleophilic attack by the incoming tin(II) halide. In addition, $[\pi\text{-}C_5H_5NiCO]_2$ contains two fewer carbonyl groups which would make this dimer sterically more susceptible to direct attack than the more hindered $[\pi\text{-}C_5H_5Fe(CO)_2]_2$.

The insertion reaction of tin(II) halides with $[PBu_3Co(CO)_3]_2$ has been found to proceed via both a two-step, dissociative type mechanism as well as by a one-step, bimolecular mechanism. Although this complex is not entirely analogous to the nickel and iron dimers, there does appear to be an increasing tendency for these insertion reactions to proceed via a single-step, bimolecular mechanism rather than by a two-stage type mechanism as the atomic number of the metal increases along the first transition series.

Since the insertion reaction involving the $[\pi\text{-}C_5H_5NiCO]_2$ dimer is postulated to proceed solely via a bimolecular mechanism, it has not been possible to interpret the data in a way which would give any information regarding the strength of the Ni—Ni bond.

The authors wish to thank the Department of University Affairs of the Province of Ontario and the National Research Council of Canada for financial support. One of us (R.R.C.) also wishes to thank the National Research Council of Canada for a Postgraduate Scholarship.

1. E. O. Fischer and C. Palm. Chem. Ber. **91**, 1725 (1958).
2. J. F. Tilney-Bassett. J. Chem. Soc. 577 (1961).
3. D. J. Patmore and W. A. G. Graham. Inorg. Chem. **5**, 1405 (1966).
4. P. F. Barrett and A. J. Poë. J. Chem. Soc. A, 429 (1968).
5. P. F. Barrett and K. K. W. Sun. Can. J. Chem. **48**, 3300 (1970).
6. G. Brauer. (*Editor*). Handbook of preparative inorganic chemistry. Vol. 1. Academic Press, New York. 1963. p. 728.
7. J. Mandel. The statistical analysis of experimental data. Interscience, New York. 1964. pp. 141–144 and pp. 272–278.
8. L. I. B. Haines and A. J. Poë. J. Chem. Soc. A, 2826 (1969).
9. P. C. Ellgen. Inorg. Chem. **10**, 232 (1971).
10. Ralph G. Pearson. J. Am. Chem. Soc. **85**, 3532 (1963).

Can. J. Chem. Downloaded from www.nrcresearchpress.com by 210.87.254.42 on 09/05/12
For personal use only.

Application of the Congruence Principle to Viscosities of 1-Chloroalkane Binary Mixtures

B. M. COURSEY[1] AND E. L. HERIC[2]

Department of Chemistry, University of Georgia, Athens, Georgia

Received April 13, 1971

Viscosities are reported at 25 °C in five 1-chloroalkane binary systems. Mixture data are presented both as kinematic viscosity and as excess Gibbs free energy of activation for flow. The latter quantity is correlated with the average chain length in the mixtures by graphical and analytical forms of Brønsted and Koefoed's principle of congruence. This correlation serves as a basis for prediction of mixture viscosities for 1-chloroalkane pairs having chain lengths within the observed extremes: 1-chlorobutane and 1-chlorooctadecane. Errors as kinematic viscosity by this method are less than 5.5% for the systems studied.

Les viscosités de cinq systèmes binaires de chloro-1 alcanes sont rapportées à 25 °C. Pour l'écoulement, les données d'un mélange sont présentées en termes de viscosité cinématique et d'excès d'énergie libre d'activation de Gibbs. Cette dernière quantité est reliée à la longueur moyenne de chaine dans les mélanges au moyen des formes graphiques et analytiques du principe de congruence de Brønsted et Koefoed. Cette corrélation est utilisée comme base de prédiction pour les viscotiés de mélanges formé de paires de chloro-1 alcanes ayant de longueurs de chaine comprises entre les extrêmes observés, à savoir le chloro-1 butane et le chloro-1 octadécane. Pour les systèmes étudiés, les erreurs de viscosité cinématique par cette méthode sont inférieures à 5.5%.

Canadian Journal of Chemistry, 49, 2631 (1971)

Introduction

The congruence principle of Brønsted and Koefoed (1) is often used for demonstrating internal consistency of *n*-alkane mixtures. Mixtures are said to be congruent which have the same average chain length, n, through the requirement that

$$[1] \qquad n = \sum_i x_i n_i$$

where x_i and n_i are mole fraction and chain length, respectively, of species i. Although the principle was originally used for free energies, it has since been applied to a number of equilibrium properties of *n*-alkane mixtures (2–5). In a previous paper (6), the authors have shown that the principle is also applicable to viscosities of *n*-alkane mixtures.

The present work demonstrates that the congruence principle may also be used for correlation and prediction of viscometric properties in mixtures of 1-chloroalkanes. For mixtures of homologs, the principle may be expressed as (7)

$$[2] \qquad \Delta_{pq:n} = f(n) - x_p f(n_p) - x_q f(n_q)$$

where $\Delta_{pq:n}$ is the molar excess thermodynamic mixing property for two species of chain length n_p and n_q, and $f(n)$ is some state function of the homologous series. The function, of course, is dependent on the property considered and intensive variables of the system. At various times the following functions have been used

$$f(n) = \sum_j A_j n^j \qquad \text{McGlashan (7)}$$

$$= \sum_j B_{-j}/n^j \qquad \text{Diaz-Peña and Martin (8)}$$

$$= \sum_j C_{-j}/(n-2)^j \qquad \text{Hijmans and Holleman (9)}$$

$$= \Delta_{mt:n} \qquad \text{Hijmans (3)}$$

The first three are analytical functions which are series expansions in various powers of the average chain length with constants A_j, B_{-j}, C_{-j}, respectively. The last is a graphical method based on the observed behavior in a mixture of the extreme components of chain lengths n_m and n_t. All of these functions are evaluated for some pair of extreme components and then used to predict the behavior of component pairs within the extremes through eq. 2. Both the series expansion in $(1/n)$ and the graphical method have been examined in the present study.

[1]Present address: U.S. Army Engineer Reactors Group, Fort Belvoir, Virginia.

[2]To whom correspondence should be addressed.

TABLE 1. Properties of purified components at 25 °C

Compound	Molecular weight (g/mol)	Kinematic viscosity (cS)		Experimental dynamic viscosity (cP)
		Experimental	Literature[a]	
1-Chlorobutane	92.569	0.4837	0.476–0.499	0.4261
1-Chlorohexane	120.624	0.7952	0.795–0.796	0.6945
1-Chlorooctane	148.678	1.298	1.305–1.32	1.128
1-Chlorodecane	176.732	2.046		1.772
1-Chlorododecane	204.786	3.089	3.07	2.668
1-Chlorotetradecane	232.840	4.496		3.875
1-Chlorohexadecane	260.894	6.299	6.40	5.421
1-Chlorooctadecane[b]	288.949	8.590		7.385

[a]From five sources identified in ref. 11.
[b]Supercooled liquid.

In order to apply the congruence principle to mixture viscosities (6), the transport property is first converted to a thermodynamic activation property. Kinematic viscosity, ν, may be related to the Gibbs free energy of activation for flow, Δ^*G, by the Eyring viscosity equation (10)

$$[3] \qquad \nu = (hN/M) \exp (\Delta^*G/RT)$$

where h = Planck's constant, N = Avogadro's number, M = molecular weight, R = molar gas constant, and T = temperature in °K. If free energy activation barriers are assumed additive for mixtures, then for an ideal mixture

$$[4] \qquad \Delta^*G^{ideal} = \sum_i x_i \Delta^*G_i$$

Molar excess Gibbs free energy of activation for flow

$$[5] \qquad \Delta^*G^E = \Delta^*G - \Delta^*G^{ideal}$$

which on rearrangement of eqs. 3–5 becomes

$$[6] \quad \Delta^*G^E = RT\left[\ln (\nu M) - \sum_i x_i \ln (\nu_i M_i)\right]$$

If $\Delta^*G^E > 0$, then the viscosity is greater than that of an ideal mixture. Equation 6 provides a property suitable for treatment with the congruence principle.

Equipment

The equipment and techniques used in this work have been described previously (11, 12). A water bath thermostatically controlled to ±0.01 °C was used. Bath temperature was monitored with a Beckman thermometer which had been set with a calibrated thermometer. The calibration of the latter was against an NBS certified standard. Times were measured with an electric stop clock which had been calibrated against an electronic time standard. All weighings were made with a Mettler 300-g-capacity precision balance with certified weights.

Viscosities were determined with Cannon–Fenske ASTM viscometers with different capillary diameters because of the 20-fold increase in viscosity in the 1-chloroalkane series. Three NBS oils of certified viscosity were employed as primary standards for the ASTM 50 and 100 viscometers. Kinetic energy corrections compared favorably with those predicted for the given capillary diameters (13).

The viscometers were maintained in the bath until constant flow time was obtained. As room temperature was only slightly lower than 25 °C, temperature equilibrium was established rapidly. Evaporation losses from the viscometers were negligible.

Liquids were mixed in a 50-ml modified glass syringe sealed by glass at the needle end. Again, evaporation rates were negligible. Transfer to viscometers was by overpressure through capillary tubing installed within the syringe plunger. The glass equipment was provided with ball and socket joints to minimize evaporation on transfer. Joints were treated with hexane to remove traces of non-volatile components.

Materials

Purification procedures for the materials used in this study have been described (11). The referenced study contains a comparison of experimental and literature values for densities and refractive indices as well as viscosities. Some properties of the pure components are given in Table 1. Experimental values represent the mean of at least three determinations.

Results

It is evident from Table 1 that there are some significant differences between experimental and literature values for kinematic viscosities. The comparison with literature values must be qualified, however, because no single work has reported viscosities for the range of compounds. The greatest disagreement is for 1-chlorobutane, although the present value is within the range of literature values. Moreover analytical chromatographs for all the compounds used in this work (11) indicated satisfactory purity.

Experimental kinematic viscosities for mixtures in the five binary systems are given in Table 2.

TABLE 2. Viscosities of 1-chloroalkane binary mixtures at 25 °C

Binary mixture	Mole fraction of first-named component	Kinematic viscosity (cS)	Δ^*G^E (cal/mol)
1-Chlorododecane + 1-chlorobutane	0.2298	0.8880	145.0
	0.2967	1.026	162.1
	0.4384	1.354	174.7
	0.5232	1.571	168.2
1-Chlorohexadecane + 1-chlorohexane	0.2988	1.857	176.1
	0.4443	2.548	188.8
	0.5461	3.104	179.0
	0.6874	3.975	144.3
1-Chlorotetradecane + 1-chlorooctane	0.3092	2.067	61.3
	0.4608	2.515	67.5
	0.4966	2.625	66.6
	0.5383	2.759	65.0
1-Chlorooctadecane + 1-chlorodecane	0.3008	3.528	83.1
	0.4486	4.398	89.9
	0.4943	4.691	89.3
	0.5496	5.052	85.6
1-Chlorooctadecane + 1-chlorohexadecane	0.4625	7.320	4.8
	0.4934	7.390	4.7
	0.5449	7.505	4.4

Also shown there are the excess molar Gibbs free energies of activation for flow calculated with eq. 6. Replication of measurements on the pure components indicate an estimated precision of $\pm 0.1\%$ in kinematic viscosity. This corresponds to experimental error of ± 0.7 cal/mol in Δ^*G^E.

Discussion

For the application of the congruence principle, results will also be considered from two systems reported previously (12): 1-chlorobutane + 1-chlorohexane and 1-chlorobutane + 1-chlorooctadecane. As stated previously, the graphical form of the congruence principle (3) is a special case of eq. 2. This method is demonstrated in Fig. 1 for Δ^*G^E in the 1-chloroalkane systems. The experimental values for the excess for the extreme components, in this case $\Delta_{418:n}$, are plotted *vs.* the average chain length. The excesses for the other component pairs, $\Delta_{pq:n}$, within the extremes, n_m, n_t, are superimposed as described previously (6). The agreement of the data in Fig. 1 parallels that found for other properties within homologous series (3, 8). The error by this method in predicting mixture viscosities is shown in Table 3. Errors have been expressed both as Δ^*G^E and as kinematic viscosity.

An analytical form of the congruence principle (8) utilizing a series expansion in reciprocal powers of n has also been examined. The function $f(n)$ has the following form

$$[7]\quad f(n) = B_1 n + B_0 + B_{-1}/n + B_{-2}/n^2 + B_{-3}/n^3 + \cdots$$

The first two terms do not contribute to the excess.

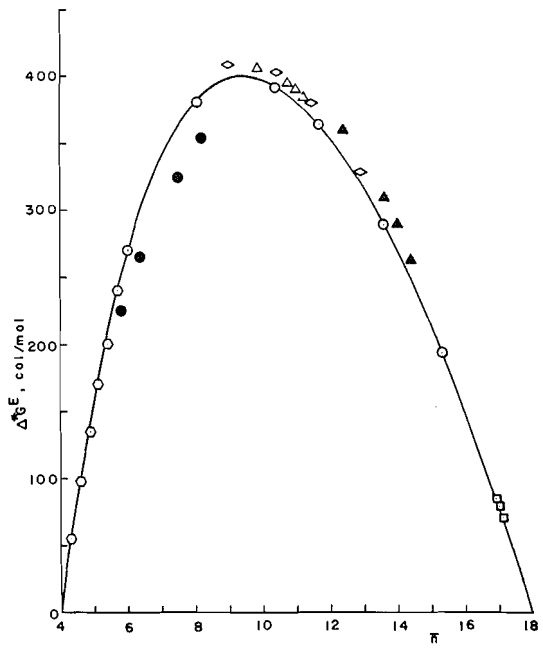

FIG. 1. Application of Hijmans' graphical form of the congruence principle (3) to Δ^*G^E in 1-chloroalkane binary mixtures. ○, $C_4Cl + C_{18}Cl$; ●, $C_4Cl + C_{12}Cl$; ⬡, $C_4Cl + C_6Cl$; ◇, $C_6Cl + C_{16}Cl$; △, $C_8Cl + C_{14}Cl$; ▲, $C_{10}Cl + C_{18}Cl$; □, $C_{16}Cl + C_{18}Cl$.

TABLE 3. Application of the congruence principle to Δ^*G^E in 1-chloroalkane mixtures

System[a]	Range of average chain length	Range of kinematic viscosity (cS)	Error by graphical method		Error by analytical method	
			As[b] Δ^*G^E (cal/mol)	As[c] %v	As[b] Δ^*G^E (cal/mol)	As[c] %v
$C_4Cl + C_{18}Cl$[d]	6.01–15.27	1.042 –6.272	—	—	—	—
$C_4Cl + C_{12}Cl$	5.84– 8.19	0.8880–1.571	28.9	5.3 (−)	29.9	5.4 (−)
$C_4Cl + C_6Cl$[d]	4.31– 5.72	0.5315–0.7511	3.2	0.6 (−)	10.7	1.8 (−)
$C_6Cl + C_{16}Cl$	8.99–12.87	1.857 –3.975	11.5	2.0 (+)	10.7	1.8 (+)
$C_8Cl + C_{14}Cl$	9.86–11.23	2.067 –2.759	8.5	1.4 (+)	6.4	1.1 (+)
$C_{10}Cl + C_{18}Cl$	12.41–14.40	3.528 –5.052	20.3	3.4 (+)	21.0	3.5 (+)
$C_{16}Cl + C_{18}Cl$	16.93–17.09	7.320 –7.505	3.1	0.5 (+)	2.0	0.3 (+)

[a]The number of hydrogens and the prefix *n*- have been deleted for the system components.
[b]Standard error for the system is defined as $[\Sigma(\text{experimental value} - \text{calculated value})^2/\text{number of observations}]^{1/2}$.
[c]Standard % error as kinematic viscosity, v, is defined as $[\Sigma\ 100[(\text{experimental value} - \text{calculated value})/\text{experimental value}]^2/\text{number of observations}]^{1/2}$. The predominant sign of the error is indicated in parentheses.
[d]Data for these systems are given in ref. 12.

Substitution of the above function into eq. 2 on rearrangement yields

$$[8]\quad \Delta_{pq:n} = B_{-1}\delta_{-1} + B_{-2}\delta_{-2} + B_{-3}\delta_{-3} + \cdots$$

where Δ is an abbreviation for Δ^*G^E, and δ is composition variable with δ_{-j} defined by

$$\delta_{-j} = (1/n^j) - (x_p/n_p{}^j) - (x_q/n_q{}^j)$$

The constants B_{-j} were found by a least-squares fit of the experimental data (12) for the reference system: 1-chlorobutane + 1-chlorooctadecane. The following three constants were sufficient to fit the data for this system within experimental error

$$B_{-1} = -24\,350 \text{ cal/mol}$$

$$B_{-2} = 76\,390 \text{ cal/mol}$$

$$B_{-3} = -104\,800 \text{ cal/mol}$$

The analytical method has a disadvantage noted previously (9). Contributions from individual terms exceed the value of the excess itself and this makes the predicted excess dependent on the physically irrelevant number of terms taken. Columns 6 and 7 of Table 3 show the error in predicted Δ^*G^E and kinematic viscosity by eq. 8 using the three coefficients.

A comparison of errors by the analytical and graphical techniques in Table 3 indicates little difference in the two methods. The greatest error by either method occurs in the 1-chlorobutane + 1-chlorododecane system where the predicted kinematic viscosities are ~5% greater than the experimental values.

Previous applications of the congruence principle have been limited to the approach given thus far: *i.e.*, calculated and experimental values are tabulated for several systems and a general discussion is given of the relative agreement. It must be noted, however, that there are 105 possible binary systems of the 1-chloroalkanes having carbon numbers between 4 and 18. It is possible with the congruence principle to predict the excess as a function of composition in all of these systems with roughly the same error as shown in Table 3. Using a digital computer we have examined Δ^*G^E in these 105 systems.

The principles of the method are straightforward. We have already established the functional dependence of the excess on the three variables n_p, n_q, and x_p by eqs. 2 and 8. It is possible to display the excess graphically as a function of n_p and n_q for two cases: (*1*) the composition is held constant, for instance at $x_p = 0.5$, or (*2*) the excess is maximized with respect to composition. The method is demonstrated here using the maximum value of the excess.

An iterative technique was used to calculate the excess for a large number of pairs, n_p, n_q, and a Newton–Raphson method was used to find the maximum excess for each pair. The resultant excess "surface" is shown in Fig. 2. Each of the 105 real systems is represented by a point in the x,y plane. Systems along the diagonal correspond to $n_p = n_q$, for which the excess must equal zero. Coordinates for each of the systems examined in this work are indicated on the figure. The error associated with the surface at each of these points is essentially the same as that given in column 6 of Table 3. Closer

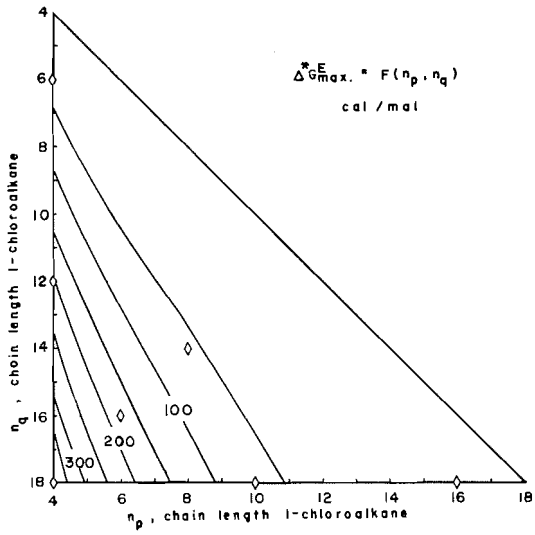

FIG. 2. $\Delta^*G_{max}{}^E$ as a function of chain length of the component species in 1-chloroalkane binary mixtures, eq. 8. The curves represent constant values of the excess function at 50 cal/mol increments. The x-y coordinates of systems studied are indicated by a ◇.

agreement between experimental and calculated values would not substantially affect the shape of the surface.

Examination of Fig. 2 yields some useful information about the general viscometric behavior of these systems. All of the systems exhibit positive deviations from ideal mixing (Δ^*G^E positive) and the magnitude of the excess increases with the difference in chain lengths when a single component is mixed with successive homologs. This parallels the behavior observed for n-alkane systems (6). It is also observed that a given difference in chain lengths for two short components has a more pronounced effect on the excess than the same difference for two long chain components.

An explanation of the observed viscometric behavior in 1-chloroalkane systems based on molecular arguments was given in a previous paper (12). Basically the positive deviations from ideal mixture viscosity are ascribed to the difference in flow mechanisms for the two components. The short chain molecules are assumed to flow by gross molecular rotation while the longer chain molecules flow by a combination of segmental jumping and rotation about carbon–carbon bonds. These assumptions are further substantiated by reference again to Fig. 2. The excess is slight for mixtures of long chains since they have a similar flow mechanism. However, the excess increases sharply for 1-chlorobutane mixed with longer chains which are assumed to have a different flow mechanism.

No attempt has been made in this work to resolve hydrocarbon (or chain) effects and dipole effects for 1-chloroalkane mixtures. In a previous paper, however, we have resolved these effects for n-hexadecane mixed with the same 1-chloroalkanes studied here (14).

This work was supported in part by the Petroleum Research Fund which is administered by the American Chemical Society.

1. J. N. BRØNSTED and J. KOEFOED. K. danske. Vidensk. Selsk. Skr., Mat. fys. Medd. **22**, 1 (1946).
2. J. H. VAN DER WAAL and J. J. HERMAN. Rec. Trav. Chim. Pays-Bas. **69**, 949 (1950); **69**, 971 (1950).
3. J. HIJMANS. Mol. Phys. **1**, 307 (1958).
4. TH. HOLLEMAN and J. HIJMANS. Physica, **28**, 604 (1962).
5. TH. HOLLEMAN. Physica, **31**, 49 (1965).
6. B. M. COURSEY and E. L. HERIC. Mol. Phys. **13**, 287 (1967).
7. M. L. MCGLASHAN. Mol. Phys. **4**, 87 (1961).
8. M. DIAZ-PEÑA and F. F. MARTIN. Anales Real. Soc. Espan. Fis-Quim. **60B**, 9 (1964).
9. J. HIJMANS and TH. HOLLEMAN. Mol. Phys. **4**, 91 (1961).
10. S. GLASSTONE, K. J. LAIDLER, and H. EYRING. The theory of rate processes. McGraw-Hill, New York. 1941. p. 484.
11. B. M. COURSEY and E. L. HERIC. J. Chem. Eng. Data, **14**, 426 (1969).
12. E. L. HERIC and B. M. COURSEY. J. Chem. Eng. Data, **15**, 536 (1970).
13. E. A. WILLIHNGANZ, W. B. MCCLURE, M. R. FENSKE, and R. V. MCGREW. Ind. Eng. Chem. Anal. Ed. **6**, 231 (1934).
14. E. L. HERIC and B. M. COURSEY. Can. J. Chem. Eng. **48**, 568 (1970).

Can. J. Chem. Downloaded from www.nrcresearchpress.com by 210.87.254.6 on 09/05/12
For personal use only.

The Thermal Pressure and Energy–Volume Coefficients of the Methyl Alcohol – Water and *t*-Butyl Alcohol – Water Systems

DIGBY D. MACDONALD[1] AND J. B. HYNE
Department of Chemistry, University of Calgary, Calgary, Alberta

Received April 30, 1971

Thermal pressure and energy–volume coefficients have been determined for various methyl alcohol – water and *t*-butyl alcohol – water mixtures at several temperatures in the range 19–55 °C. The energy–volume coefficient is found to pass through a maximum at 0.3–0.4 mole fraction methyl alcohol and 0.1 mole fraction *t*-butyl alcohol. This behavior is consistent with the average intermolecular distance passing through a minimum in both systems at the corresponding solvent compositions. The relationship between the energy–volume coefficient, the cohesive energy density, and the structure of aqueous binary systems is examined. The temperature dependence of the thermal pressure coefficient is discussed in terms of the effect of temperature on the susceptibility of the entropy of the two systems to isothermal expansion.

Le coefficient thermique de la pression et le coefficient d'énergie–volume ont été déterminés pour divers mélanges d'alcool méthylique-eau et alcool *t*-butylique-eau à plusieurs températures entre 19 et 55 °C. Le coefficient énergie–volume passe par un maximum pour une fraction molaire d'alcool méthylique comprise entre 0.3 et 0.4 et pour une fraction molaire d'alcool *t*-butylique de 0.1. Ce comportement concorde avec le fait que la distance intermoléculaire moyenne passe par un minimum pour les deux systèmes aux compositions correspondantes en solvant. La relation entre le coefficient d'énergie–volume, la densité d'énergie de cohésion et la structure des systèmes aqueux binaires est examinée. La variation du coefficient thermique de la pression avec la température est analysée en termes d'effet de température sur la sensibilité de l'entropie des deux systèmes à l'expansion isotherme.

Canadian Journal of Chemistry, 49, 2636 (1971)

Introduction

The thermodynamic and physical properties of alcohol–water mixtures have been studied extensively and are well reviewed by Franks and Ives (1). In spite of the great deal of work performed on these systems doubt still remains as to the detailed interactions and structure present in these liquid mixtures. In two recent publications (2, 3), however, we have demonstrated that additional information on the structure of binary liquid systems may be obtained from an examination of the behavior of the energy–volume coefficient and cohesive energy density. In this paper we report detailed studies of the energy–volume coefficient and the cohesive energy density behavior of methyl alcohol – water and *t*-butyl alcohol – water mixtures. These two systems were chosen since they exhibit positive deviations from Raoult's Law (1). This behavior is determined by large negative excess entropies, suggesting considerable changes in liquid structure on mixing the components.

[1]Present address: Research Chemistry Branch, Atomic Energy of Canada Ltd., Pinawa, Manitoba.

Experimental

Materials

Reagent grade methyl alcohol and *t*-butyl alcohol were dried over calcium oxide and distilled twice at atmospheric pressure in an efficient still. The refractive indices of both liquids agreed well with accepted values and no impurities could be detected by vapor phase chromatography (v.p.c.).

Aqueous mixtures were prepared by weight using doubly distilled water and were degassed by the freeze–pump–thaw technique.

Apparatus and Method

Thermal pressure coefficients were measured at four temperatures in the range 19–55 °C for various alcohol–water mixtures using the constant-volume thermometer described earlier (3). The same precautions described in this earlier study (3) were exercized here in order to eliminate errors due to the heat of compression of the oil (pressurizing medium) and sample liquid.

Results

Plots of applied pressure (P) *vs.* temperature (T) at constant volume over the range of temperature employed in each determination (0.8–2.0 °C) were linear, demonstrating that the data are adequately represented by eq. 1.

$$P = mT + C \qquad [1]$$

TABLE 1. Thermal pressure and energy – volume coefficients for methyl alcohol – water mixtures at various temperatures

T (°C)	γ_V (atm deg^{-1})	$\left(\frac{\partial U}{\partial V}\right)_T$ (atm)	T (°C)	γ_V (atm deg^{-1})	$\left(\frac{\partial U}{\partial V}\right)_T$ (atm)
	0.100 mole fraction MeOH			*0.200 mole fraction MeOH*	
19.0	7.75	2264.2	24.1	12.38	3680.1
30.8	9.70	2948.4	29.0	12.65	3822.3
40.1	10.97	3436.5	39.5	13.42	4195.9
51.4	12.53	4066.7	51.5	14.20	4610.2
	0.300 mole fraction MeOH			*0.400 mole fraction MeOH*	
19.5	13.71	4012.4	23.9	13.91	4132.1
30.8	14.37	4367.9	34.2	13.91	4275.4
40.1	14.36	4498.4	42.2	14.02	4421.4
54.4	14.73	4825.0	53.5	14.05	4589.6
	0.500 mole fraction MeOH			*0.700 mole fraction MeOH*	
21.7	13.72	4045.5	22.0	11.74	3465.2
31.2	13.60	4139.3	31.8	11.60	3537.5
41.1	13.46	4229.9	42.0	11.01	3469.9
50.4	12.94	4186.9	50.9	10.94	3545.2
	*1.000 mole fraction MeOH**				
23.0	9.80	2902.4			
30.5	9.27	2814.9			
40.3	8.94	2802.3			
51.3	8.44	2738.4			

*Reference 16, reports $\gamma_V = 9.7$ atm deg^{-1} at 20 °C.

The gradient m is equal to the observed thermal pressure coefficient $\gamma_V^{obs} = [(\partial P/\partial T)_V^{obs}]$. Each γ_V^{obs} value, however, requires correction for the finite expansion and compression of glass. This correction is made using eq. 2 (3),

$$[2] \qquad \gamma_V = \gamma_V^{obs}\left(\frac{\alpha_1}{\gamma_V^{obs}\beta_g + \alpha_1 - \alpha_g}\right)$$

where α_g and β_g are the coefficients of thermal expansion and compressibility of Pyrex glass (9.9×10^{-6} deg^{-1} and 3.06×10^{-6} atm^{-1}, respectively, (4)) and α_1 is the coefficient of expansion of the sample liquid. Numerical values for α_1 were calculated from temperature–density data (5, 6) taken from the literature.

Energy–volume coefficients, $(\partial U/\partial V)_T$, were calculated from the thermal pressure coefficients using the "thermodynamic equation of state".

$$[3] \qquad \left(\frac{\partial U}{\partial V}\right)_T = T\left(\frac{\partial P}{\partial T}\right)_V - P$$

For all the mixed and pure liquids investigated in this work $T\gamma_V$ is very much greater than the applied pressure P and eq. 3 reduces to eq. 4.

$$[4] \qquad \left(\frac{\partial U}{\partial V}\right)_T = T\gamma_{V,P=1\text{ atm}}$$

The thermal pressure and energy–volume coefficients computed at several temperatures using eqs. 2 and 4, respectively, are listed in Tables 1 and 2. Both parameters were reproducible to $\pm 1 - 2\%$ and where comparison is possible the values obtained in this work are in good agreement with data taken from the literature.

Numerical values for γ_V, $(\partial U/\partial V)_T$ and the temperature dependence of γ_V were calculated graphically at 25 °C and are listed in Table 2. The $(\partial\gamma_V/\partial T)$ values are considered accurate to ± 0.015 atm deg^{-2}.

The energy–volume coefficient is related (3) to the cohesive energy density $(\Delta U_V/V)_T$ by eq. 5.

$$[5] \qquad \left(\frac{\partial U}{\partial V}\right)_T = n\left(\frac{\Delta U_V}{V}\right)_T$$

where ΔU_V is the energy of vaporization of the liquid to the perfect gas state and V is the molar volume of the liquid at temperature T. The energy of vaporization per mole of mixture can be calculated (3) using eq. 6.

$$[6] \quad \Delta U_V = X_1\Delta H_{V,1} + X_2\Delta H_{V,2} - \Delta H_M - RT$$

The quantities $\Delta H_{V,1}$ and $\Delta H_{V,2}$ are enthalpies of vaporization of components 1 and 2, respec-

Can. J. Chem. Downloaded from www.nrcresearchpress.com by 210.87.254.6 on 09/05/12
For personal use only.

TABLE 2. Thermal pressure and energy–volume coefficients for *t*-butyl alcohol – water mixtures at various temperatures

T (°C)	γ_V (atm deg^{-1})	$\left(\frac{\partial U}{\partial V}\right)_T$ (atm)	T (°C)	γ_V (atm deg^{-1})	$\left(\frac{\partial U}{\partial V}\right)_T$ (atm)
	0.050 mole fraction t-BuOH			*0.100 mole fraction t-BuOH*	
25.7	13.12	3921	21.1	15.57	4581
36.4	14.33	4436	39.4	14.96	4676
44.3	14.79	4695	55.0	14.59	4788
52.5	15.05	4901			
	0.200 mole fraction t-BuOH			*0.300 mole fraction t-BuOH*	
24.0	13.97	4151	24.3	12.81	3811
33.9	13.85	4253	36.7	12.49	3870
44.3	13.29	4219	42.4	12.62	3982
53.3	13.16	4296	52.4	12.18	3965
	0.400 mole fraction t-BuOH			*0.600 mole fraction t-BuOH*	
24.4	11.94	3553	24.7	11.19	3333
35.5	11.94	3685	34.9	10.94	3370
43.7	11.56	3663	43.5	10.61	3360
53.0	11.37	3708	53.7	10.35	3383
	0.800 mole fraction t-BuOH			*1.000 mole fraction t-BuOH**	
23.9	10.63	3158	29.2	10.36	3133
35.4	10.30	3178	41.8	9.73	3066
43.9	9.91	3142	59.2	9.07	3015
54.5	9.65	3162			

*Reference 16 reports $\gamma_V = 11.2$ atm deg^{-1} at 20 °C.

TABLE 3. Thermal pressure, energy–volume, and cohesive energy density parameters for methyl alcohol – water mixtures at 25 °C

Mole fraction methyl alcohol	γ_V (atm deg^{-1})	$\left(\frac{\partial U}{\partial V}\right)_T$ (atm)	$\left(\frac{\Delta U_V}{V}\right)_T$ (atm)	n	$\left(\frac{\partial \gamma_V}{\partial \gamma_T}\right)$ (atm deg^{-2})
0.000*	5.68	1694	22 684	0.074	0.223
0.100	8.65	2579	20 456	0.126	0.152
0.200	12.45	3712	18 415	0.202	0.066
0.300	14.10	4204	16 570	0.254	0.023
0.400	13.95	4159	14 958	0.278	0.005
0.500	13.55	4040	13 604	0.297	−0.020
0.700	11.70	3489	11 188	0.312	−0.030
1.000	9.70	2892	8 488	0.341	−0.050

*Data for pure water taken from ref. 3.

TABLE 4. Thermal pressure, energy–volume, and cohesive energy density parameters for *t*-butyl alcohol – water mixtures at 25 °C

Mole fraction *t*-butyl alcohol	γ_V (atm deg^{-1})	$\left(\frac{\partial U}{\partial V}\right)_T$ (atm)	$\left(\frac{\Delta U_V}{V}\right)_T$ (atm)	n	$\left(\frac{\partial \gamma_V}{\partial T}\right)$ (atm deg^{-2})
0.050	12.95	3861	19 448	0.199	0.150
0.100	15.43	4601	16 704	0.275	−0.030
0.200	14.05	4189	12 881	0.325	−0.031
0.300	12.85	3831	10 461	0.366	−0.021
0.400	12.05	3593	8 798	0.408	−0.022
0.600	11.20	3339	6 667	0.501	−0.031
0.800	10.58	3155	5 392	0.585	−0.035
1.000	10.52	3137	4 591	0.693	−0.045

Can. J. Chem. Downloaded from www.nrcresearchpress.com by 210.87.254.6 on 09/05/12
For personal use only.

Can. J. Chem. Downloaded from www.nrcresearchpress.com by 210.87.254.6 on 09/05/12
For personal use only.

tively, to the perfect gas state and ΔH_M is the heat of mixing per mole of mixture. The enthalpies of vaporization of water, methyl alcohol, and *t*-butyl alcohol to the perfect gas state at 25 °C are 10.52 kcal mol^{-1} (7), 8.96 kcal mol^{-1} (7), and 11.15 kcal mol^{-1} (8, 9), respectively. Energies of vaporization for the various alcohol–water mixtures were calculated using these data and heats of mixing taken from the literature (6, 10). Division of the ΔU_V values by the corresponding molar volumes results in the cohesive energy densities. The cohesive energy densities are listed in Tables 3 and 4 together with energy–volume coefficients interpolated at 25 °C from data listed in Table 1. Numerical values for *n* are also listed and were calculated using eq. 5.

Discussion

Energy–Volume Coefficients

The variation of the energy–volume coefficient, $(\partial U/\partial V)_T$, with solvent composition for the methyl alcohol – water and *t*-butyl alcohol – water systems is illustrated in Figs. 1 and 2, respectively. Both systems exhibit a maximum in the variation of $(\partial U/\partial V)_T$ with composition. Many other properties (both intensive and extensive) of these aqueous organic binary systems exhibit extremum behavior in the same region of solvent composition (1).

In terms of classical mechanics the total energy of a fluid, *U*, may be regarded as the sum of three terms (3, 11–13).

$$[7] \qquad U = U(T) + U_A + U_R$$

The quantity $U(T)$ is the mean kinetic energy of the molecules at their equilibrium positions and U_A and U_R are the potential energies due to attractive and repulsive interactions, respectively. Since $U(T)$ depends only on temperature then differentiation of *U* with respect to volume at constant temperature yields eq. 8 for the energy–volume coefficient of the system.

$$[8] \qquad \left(\frac{\partial U}{\partial V}\right)_T = \left(\frac{\partial U_A}{\partial V}\right)_T + \left(\frac{\partial U_R}{\partial V}\right)_T$$

Equation 8 demonstrates that the behavior of the experimentally measured energy–volume coefficient is determined by the separate components for intermolecular attraction and repulsion. This treatment has been used previously to interpret the energy–volume coefficient behavior of pure liquids (11–13) and dimethyl sulfoxide – water mixtures (3).

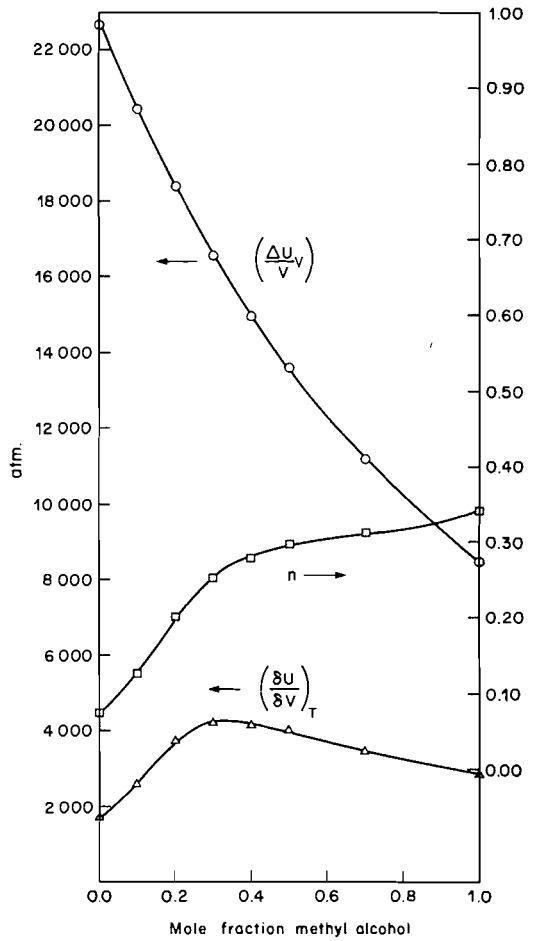

FIG. 1. Energy–volume coefficients and cohesive energy density parameters form ethyl alcohol – water mixtures at 25 °C.

U_A and U_R are known to vary with intermolecular distance (*r*), and therefore volume (*V*), as shown in Fig. 3. It is clear from this schematic representation that $(\partial U_A/\partial V)_T$ and $(\partial U_R/\partial V)_T$ are positive and negative, respectively, and vary with volume as has been recently elaborated by Barton (14). Since the sum of these two terms, $(\partial U/\partial V)_T$, is observed to be positive, the attractive term must be numerically larger than the repulsive term (see eq. 8). The behavior of $(\partial U/\partial V)_T$ as a function of solvent composition must therefore be determined principally by the corresponding behavior of the attractive interaction term $(\partial U_A/\partial V)_T$. Since this dominant

Can. J. Chem. Downloaded from www.nrcresearchpress.com by 210.87.254.6 on 09/05/12
For personal use only.

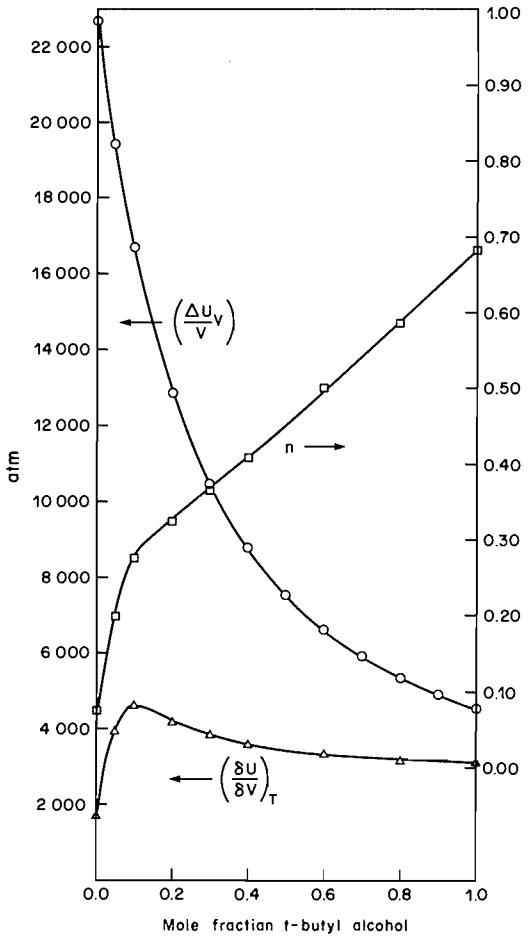

FIG. 2. Energy–volume coefficients and cohesive energy density parameters for *t*-butyl alcohol – water mixtures at 25 °C.

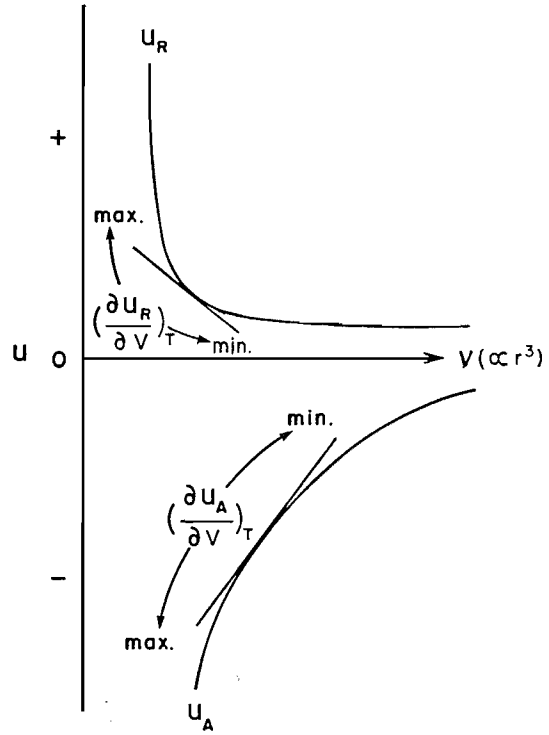

FIG. 3. Schematic representation of intermolecular interaction potential energy curves.

term is required to pass through a maximum to yield the observed behavior of the sum term, $(\partial U/\partial V)_T$, the free volume V or intermolecular distance r, as represented by the x-axis in Fig. 3, must pass through a minimum. Hence it can be concluded that the observed positive maximum in $(\partial U/\partial V)_T$ for both methyl and *t*-butyl alcohol mixtures with water is indicative of minimum free volume and intermolecular separation at these solvent compositions in both binaries.

This conclusion provides an interesting rationale for the recently reported behavior of the volume of activation for the solvolysis of benzyl chloride in aqueous alcohol solvent mixtures (15). It was found in these studies that the minimum in the activation volume as a function of solvent composition was largely if not exclusively the result of a corresponding *maximum* in the initial state partial molal volume. Benzyl chloride, in this initial state is non-ionic and only weakly polar and hence its partial molal volume should reflect predominantly "hole formation". Hence if the free volume (and intermolecular separation) of the solvent passes through a minimum, as has been concluded in this work, the expansion of the solvent required to form a hole of sufficient size to accommodate the solute and hence the solute's partial molal volume must pass through a maximum. Accordingly, the partial molal volume behavior of benzyl chloride in the two alcohol–water systems of interest is consistent with the free volume model proposed above to account for the variation of $(\partial U/\partial V)_T$ with solvent composition.

Cohesive Energy Densities

The relationship between the energy–volume coefficient and the cohesive energy density is expressed by eq. 5. This relationship has been examined for one component systems (16, 17)

Can. J. Chem. Downloaded from www.nrcresearchpress.com by 210.87.254.6 on 09/05/12
For personal use only.

and recently for dimethyl sulfoxide – water mixtures (3). Equivalent analyses for the alcohol–water systems investigated in the present study are presented in Figs. 1 and 2. These plots show that neither n nor $(\Delta U_V/V)_T$ exhibit extremum behavior as a function of solvent composition although their product, $(\partial U/\partial V)_T$, does. This extremum behavior of $(\partial U/\partial V)_T$ is clearly the result of the non-compensatory behavior of the component n and $(\Delta U_V/V)_T$ terms. It is interesting to note that these same non-compensatory trends in the behavior of n and $(\Delta U_V/V)_T$ found for the alcohol–water systems are also found in the dimethyl sulfoxide – water system (3) despite the fact that the alcohol–water mixtures exhibit positive deviations from Raoult's law as opposed to the dimethyl sulfoxide – water system which exhibits large negative deviations from ideality (18).

The physical significance of n is not clear (16) so that any relationship between this parameter and "liquid structure" remains tenuous. However, compilations of values of n by Allen, Gee, and Wilson (16) and Hildebrand (17) reveal that for non-polar liquids n is approximately equal to one. For strongly associated liquids, however, n is much less than unity and especially so for hydrogen bonded liquids. Thus, the overall increase in n from pure water to pure alcohol may reflect a general decrease in the overall hydrogen bonding in the system. Additionally, n is almost twice as large for the more hydrophobic pure *t*-butyl alcohol as for pure methyl alcohol suggesting a greater degree of hydrogen bonding in the latter system. This conclusion agrees with the results of infrared spectroscopy (1).

In as much as n may be a measure of the extent to which the solvent systems are hydrogen bonded, it is worth observing that the value of n at that mole fraction at which $(\partial U/\partial V)_T$ is a maximum is virtually the same in both systems, *viz.* 0.26. Since the maximum in $(\partial U/\partial V)_T$ was associated with a corresponding minimum in both free volume and intermolecular distance it is not unreasonable that the degree of hydrogen bonding in both systems would be similar under these conditions. In the case of dimethyl sulfoxide – water mixtures (3), however, the value of n at the $(\partial U/\partial V)_T$ maximum is 0.45. This considerable difference between the hydroxyl containing cosolvents and the sulfoxide is in keeping with the reasonable expectation that it is the polar groups within the cosolvents that determine the degree of hydrogen bonding and hence the value of n at minimum free volume.

Entropy–Volume–Temperature Relationship

The thermodynamic relationship between the thermal pressure coefficient and the volume derivative of the entropy of a system at equilibrium is given by eq. 9.

$$[9] \qquad \gamma_V = \left(\frac{\partial S}{\partial V}\right)_T$$

Data compiled in Tables 3 and 4 show that γ_V passes through a maximum in both systems at 0.3–0.4 mole fraction methyl alcohol and 0.1 mole fraction *t*-butyl alcohol. According to eq. 9 these are the compositions at which the entropy and hence the degree of ordering of both systems is most susceptible to isothermal expansion.

The temperature dependence of γ_V as a function of solvent composition for both alcohol–water systems is illustrated in Fig. 4. These plots exhibit the same general trends that were found for the dimethyl sulfoxide – water system (3), *i.e.* $(\partial\gamma_V/\partial T)$ changes sign from positive to negative in highly aqueous mixtures and is quite insensitive to changes in solvent composition at high organic mole fractions. The change in sign can be rationalized as follows.

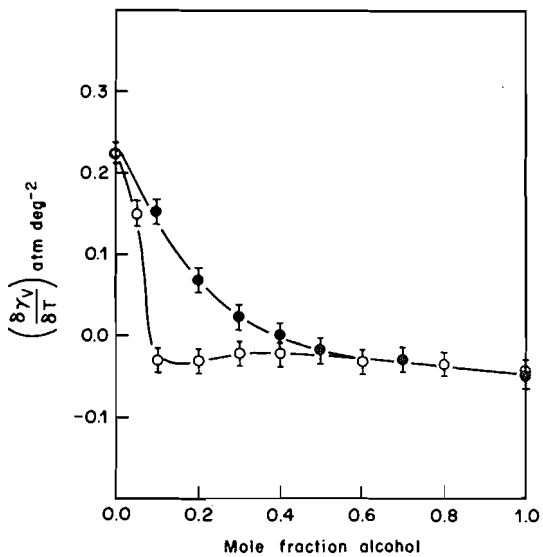

FIG. 4. Plot of $(\partial\gamma_V/\partial T)$ *vs.* solvent composition for methyl alcohol – water mixtures (●) and *t*-butyl alcohol – water mixtures (○) at 25 °C.

The open "flickering cluster" configurations in water are not favored energetically at smaller volumes, *i.e.* entropy increases as volume decreases and hence for *these configurations* $(\partial S/\partial V)_T$ is negative.[2] With increasing temperature, however, these "flickering cluster" configurations are broken down and their contribution to the total $(\partial S/\partial V)_T$ of the system is less negative. This may account for the positive value for $(\partial\gamma_V/\partial T) = (\partial^2 S/\partial T\partial V)$ in the highly aqueous system. The pure alcohols, however, do not possess the open structure characteristic of water, but rather the molecules tend to associate in chains of varying lengths (1). These structures should be less favored energetically at higher volumes and therefore make a positive contribution to $(\partial S/\partial V)_T$ for the system. As the temperature is increased the alcohol chains are broken down and their contribution to $(\partial S/\partial V)_T$ for the system is less positive, *i.e.* $(\partial\gamma_V/\partial T)$ is negative. The solvent composition at which $(\partial\gamma_V/\partial T)$ is zero represents the point at which the negative contributions to $(\partial\gamma_V/\partial T)$ exactly balance the positive ones. It is interesting to note that this point occurs at a much lower organic mole fraction in *t*-butyl alcohol – water mixtures than in methyl alcohol – water mixtures. This suggests that the positive contribution to $(\partial\gamma_V/\partial T)$ from the "flickering clusters" is more rapidly reduced by addition of *t*-butyl alcohol to water than by the addition of methyl alcohol to water. A molecular interpretation of this observation must, however, await more detailed investigation of the highly aqueous systems. It is possible that the rapid reduction in the positive contribution to $(\partial\gamma_V/\partial T)$ on the addition of *t*-butyl alcohol to water reflects the ability of this alcohol to "buttress" flickering clusters (1) and therefore stabilize the open structure of liquid water against disruption by compression.

[2]For water in the temperature range 0 to 3.98 °C $(\partial S/\partial V)_T = \gamma_V$ is negative (19). In this case few of the "flickering cluster" configurations have been disrupted by thermal agitation and the sign of $(\partial S/\partial V)_T$ for the system is determined by the influence of volume changes on the stability of the clusters.

Financial assistance for this work from the National Research Council of Canada is gratefully acknowledged. The authors also express their appreciation of valuable discussions with Dr. F. L. Swinton, University of Strathclyde.

1. F. Franks and D. J. G. Ives. Quart. Rev. Chem. Soc. **20**, 1 (1966).
2. D. D. Macdonald, J. B. Hyne, and F. L. Swinton. J. Am. Chem. Soc. **92**, 6355 (1970).
3. D. D. Macdonald and J. B. Hyne. Can. J. Chem. **49**, 611 (1971).
4. C. F. Lau, G. N. Malcolm, and D. V. Fenby. Aust. J. Chem. **22**, 855 (1969).
5. S. Z. Mikhail and W. R. Kimel. J. Chem. Eng. Data, **6**, 533 (1961).
6. J. Kenttamaa, E. Tommila, and M. Martti. Ann. Acad. Sci. Fenn. Ser AII (93) 1 (1959).
7. D. R. Stull, E. F. Westrum, and G. C. Sinke. The chemical thermodynamics of organic compounds. Wiley, N.Y. 1969.
8. E. T. Beynon, Jr. and J. J. McKetta. J. Phys. Chem. **67**, 2761 (1963).
9. H. A. Skinner and A. Snelson. Trans. Faraday Soc. **56**, 1776 (1960).
10. L. Benjamin and G. C. Benson. J. Phys. Chem. **67**, 858 (1963).
11. R. E. Gibson and O. H. Loeffler. J. Am. Chem. Soc. **61**, 2515 (1939).
12. R. E. Gibson and O. H. Loeffler. J. Am. Chem. Soc. **63**, 898 (1941).
13. W. A. Adams and K. J. Laidler. Can. J. Chem. **45**, 123 (1967).
14. A. F. M. Barton. J. Chem. Ed. **48**, 156 (1971).
15. H. S. Golinkin, I. Lee, and J. B. Hyne. J. Am. Chem. Soc. **89**, 1307 (1967).
16. G. Allen, G. Gee, and G. J. Wilson. Polymer, **1**, 456 (1960).
17. J. H. Hildebrand. Phys. Rev. **34**, 984 (1929).
18. J. Kenttamaa and J. J. Lindberg. Suomen Kem. B**33**, 104 (1960).
19. J. S. Rowlinson. Liquids and liquid mixtures Butterworths, London. 2nd Ed. 1969.

Can. J. Chem. Downloaded from www.nrcresearchpress.com by 210.87.254.6 on 09/05/12
For personal use only.

Can. J. Chem. Downloaded from www.nrcresearchpress.com by 210.87.254.40 on 09/05/12
For personal use only.

Kinetics of Charge Scavenging in γ-Irradiated Liquid Cyclohexane: A Comparison Between Different Ion–Electron Spacial Distribution Functions Used with Two Diffusion Approximations[1]

JEAN-POL DODELET AND GORDON R. FREEMAN
Chemistry Department, University of Alberta, Edmonton, Alberta

Received January 13, 1971

The form of the spacial distribution function of ions and electrons in an irradiated liquid is not accurately known and several types of function have been assumed by different workers. The various forms are compared and used in the calculation of electron–solute reaction yields in liquid cyclohexane. Our previously used semi-empirical distribution function (YSE) and a power function (YP) give satisfactory results, but a three dimensional, single parameter Gaussian (YG1) and a delta function (YD) do not. The prescribed diffusion approximation has also been inserted into the model for comparison with earlier work. No improvement was obtained. Whereas our previous approximations may lead to an underestimate of the geminate neutralization times, the prescribed diffusion approximation may lead to an overestimate of them.

La forme de la fonction de distribution spatiale des ions et électrons dans un liquide irradié n'est pas connue avec précision et plusieurs types de fonctions ont été proposés par différents chercheurs. Les différentes formes sont comparées et utilisées dans le calcul des rendements des réactions électrons–solutés dans le cyclohexane liquide. On obtient des résultats satisfaisants en utilisant une fonction de distribution semi-empirique (YSE), que nous avons déjà définie dans des travaux antérieurs, ainsi qu'une fonction faisant intervenir une puissance (YP); il n'en est pas de même si on utilise une fonction Gausienne tri-dimensionelle à paramètre unique ou une fonction delta (YD). A titre de comparaison, l'approximation de diffusion a également été introduite dans le modèle; elle n'apporte aucune amelioration. Alors que nos approximations précédentes sembleraient conduire à une sous-estimation des temps de neutralisation géminées, l'approximation de diffusion conduirait au contraire à une sur-estimation de ceux-ci.

Canadian Journal of Chemistry, 49, 2643 (1971)

I. Introduction

The kinetics of ion and electron reactions in γ-irradiated liquid hydrocarbons have been described by a stochastic model (1–3). For example, the yield of product from an electron–solute reaction is calculated from the probability that a radiation produced electron will meet and react with a solute molecule before it reacts with a radiolytic positive ion. The calculations involve the relative spacial distributions of the ions and electrons and the relative motions of the ions and electrons under the dual influence of their mutual coulombic field and thermal forces. In previous publications from this laboratory a semiempirical spacial distribution function has been used (3). The relative motions of the ions and electrons have been represented by a simple but approximate equation (2, 3).

To further our understanding of the reaction kinetics we have now tested several types of distribution function and a different motion-equation in the model. The results are reported in this article.

[1]Supported by the National Research Council of Canada.

II. Effect of the Form of the Initial Spacial Distribution of the Charges

The initial distance y between a thermalized electron and its parent ion is not the same for all ion–electron pairs. The form of the distribution function $N(y)$ is not precisely known and several types of function have been used by different workers (see Section II-2). One of the purposes of this article is to compare them.

The effect of the form of the $N(y)$ function on the calculated nitrogen yields from solutions of nitrous oxide in cyclohexane (4) is described in the following sections.

(1) The Model

Readers are referred to ref. 3 for a detailed description of the model. The required equations are summarized below.

The number of molecules of nitrogen formed

Can. J. Chem. Downloaded from www.nrcresearchpress.com by 210.87.254.40 on 09/05/12
For personal use only.

per 100 eV absorbed by the solvent, $g(N_2)$, is given by eq. 1.

$$[1] \quad g(N_2) = [\sum N(y)\Phi_-/\sum N(y)]g(N_2)_{max}$$

where $N(y)$ is the relative number of thermalized electron–ion pairs that have an initial separation distance y and Φ_- is the total probability that an electron with a given y value will be scavenged.

$$[2] \quad \Phi_- = \phi_{fi} + \phi_-(1 - \phi_{fi})$$

where ϕ_{fi} is the fraction of ion pairs with a given value of y that become free ions.

$$[3] \quad \phi_{fi} = \exp(-\xi^2/\varepsilon ykT)$$

where ξ is the charge on an electron, ε is the dielectric constant of the liquid, k is Boltzmann's constant, and T is the absolute temperature. The probability that a certain pair of charges will undergo geminate neutralization is $(1 - \phi_{fi})$ and the probability that the electron in such a pair will be scavenged by a solute molecule before the former meets its counter ion is ϕ_-.

$$[4] \quad \phi_- = 1 - (1 - f_-N_s)^{\beta-\nu}$$

where f_- is the encounter efficiency of the reaction between the electron and the solute, N_s is the mole fraction of solute in the solution, β_- is an adjustable parameter, and ν is given by

$$[5] \quad \nu = 1.39 \times 10^7\varepsilon(y^3 - r_0^3)\ \text{cm}^2/\text{V}$$

where r_0 is the distance of the last electron jump to undergo neutralization. The units of y and r_0 in eq. 5 are cm.

Attention is focussed on the reactions of the electrons that are undergoing geminate neutralization. When the solute concentration is great enough to scavenge a significant fraction of the electrons undergoing geminate neutralization, all the "free ion" electrons become scavenged; eq. 2 refers to this region.

Finally, the free ion yield is given by eq. 6.

$$[6] \quad g(N_2)_{fi} = [\sum N(y)\phi_{fi}/\sum N(y)]g(N_2)_{max}$$

(2) Calculations Using Different Forms of the Initial Distribution Function N(y)

Ion–electron distribution functions that have been used or discussed by different workers fall into six categories. In general, simpler distribution functions have been used in more complex kinetics models, and vice versa.

In probability calculations the shapes of the distribution functions, rather than their absolute magnitudes, are important. To facilitate a comparison of the functions used, each was normalized to $\int_0^\infty N(y)dy = N_0 = 5000$, where 5000 is a convenient arbitrary number.

(a) Semi-empirical Function (YSE)

This type of function is partially derived from secondary electron energy distributions and range–energy relations (3, 7–9). The YSE $N(>y)$ function used in the present work (Fig. 1) was constructed from data in ref. 3. The resulting calculated free ion yield is $g_{fi} = 0.13$, in agreement with the experimentally measured value 0.13 ± 0.02 (5, 6).

The experimental yields of nitrogen from solutions of nitrous oxide in cyclohexane (4) are plotted in Fig. 2. The value of $g(N_2)_{max}$ is taken as 5.0 (Fig. 2). To calculate "theoretical" nitrogen yields a value of β_- in the vicinity of 10^{15} V/cm^2 and $r_0 = 1 \times 10^{-7}$ cm were assumed. With a given value of β_-, a value of $g(N_2)$ was calculated for each of the nitrous oxide concentrations used experimentally. The calculated and

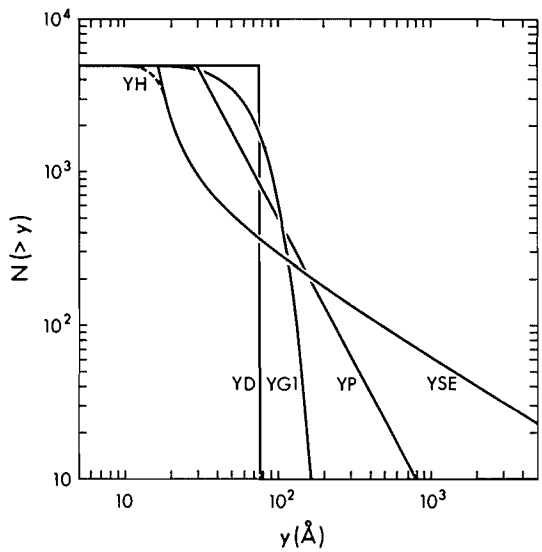

FIG. 1. Different $N(>y)$ functions that give "best" $g(N_2)$ curves for solutions of nitrous oxide. YD, $N(y) = 5000\ \delta(y - 76\ \text{Å})$; YG1, $b = 59$ Å, see eq. 12; YP, $N(>y) = 2.0 \times 10^{-9}\ y^{-1.9}$ for $y \geq 2.9 \times 10^{-7}$ cm, $N(>y) = 5000$ for $y \leq 2.9 \times 10^{-7}$ cm; YSE, semi-empirical, full curve; YH, $y_0 = 8$ Å, $j = 21$ Å (see eq. 15), dashed-curve upper portion and lower portion same as YSE.

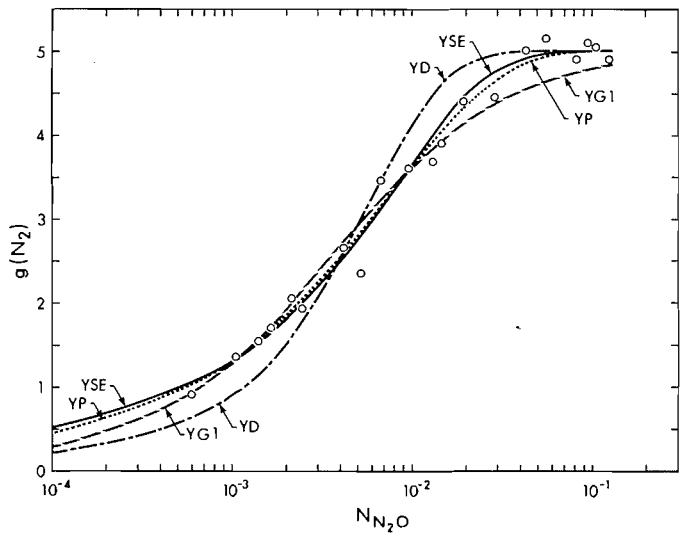

FIG. 2. $g(N_2)$ as a function of the mole fraction of nitrous oxide, N_{N_2O}. ○, experimental (4). The curves are the best calculable with the $N(y)$ functions indicated. The same curves are obtained whether r_0 is taken as 0 or 10 Å.

experimental yields were then compared. The magnitude of error in the calculated yields was estimated by averaging the absolute quantity $|g(N_2)_{exp} - g(N_2)_{calcd}|$ over all the points.

$$[7]\quad \text{Error} = \left(\sum_{i=1}^{n} |g(N_2)_{exp} - g(N_2)_{calcd}|_i\right) \Big/ n$$

The error was calculated for a series of β_- values, and a minimum error was sought. The minimum error was 0.13 g units per point obtained with $\beta_- = 6.9 \times 10^{14}$ V/cm^2. The corresponding calculated nitrogen yields are represented by the full curve in Fig. 2.

The above calculations were repeated with $r_0 = 0$. The minimum error in this case was 0.14 g units per point, only slightly greater than that obtained with $r_0 = 10$ Å.

(b) Power Function (YP)

This function is an arbitrary simplification of YSE and has the form (10, 11)

$$[8a]\quad N(>y) = Ky^{-x} \qquad y \geq y_{min}$$

$$[8b]\quad N(>y) = N_0 \qquad y \leq y_{min}$$

YP is adjusted to fit the free ion yield, $g_{fi} = 0.13$. Only two of the three parameters K, x, and y_{min} are independently adjustable because the behavior is limited by eq. 8*b*. Furthermore, reasonable values of the free ion yield can only be obtained with positive values of x.

The stages of the YP calculations were as follows.

A. (*1*) Choose an arbitrary value of x and calculate g_{fi} as a function of y_{min} (or K). (*2*) Repeat *A*(*1*) for a series of values of x.

B. Pick the value of y_{min} (or K) for each x that gives the value of $g_{fi} = 0.13$.

C. (*1*) With a pair of values of x and y_{min} from *B*, and $r_0 = 1 \times 10^{-7}$ cm, calculate $g(N_2)$ curves for a series of values of β_- and pick the β_- that gives the minimum error. (*2*) Repeat *C*(*1*) for each value of x and its corresponding y_{min}.

D. Pick the best value of x as the one that gives the smallest error.

E. Repeat *C* and *D* with $r_0 = 0$.

The results of the stage *A* calculations are shown in Fig. 3 for x values ranging from 0.5 to 4.5. The experimental value of g_{fi} is marked on each curve, indicating the appropriate value of y_{min} for each x (stage *B* of the calculations). The value of y_{min} that gives the correct g_{fi} increases with increasing x. A value of y_{min} less than 1 Å would have no physical significance, so x must be greater than 0.5.

From the calculations of stage *C* the best value of β_- for each value of x was determined. It was found that as x decreased the best value of β_- increased in a roughly hyperbolic fashion.

Stage *D*: a plot of the minimum error at each x against x contained a distinct minimum. The

Can. J. Chem. Downloaded from www.nrcresearchpress.com by 210.87.254.40 on 09/05/12
For personal use only.

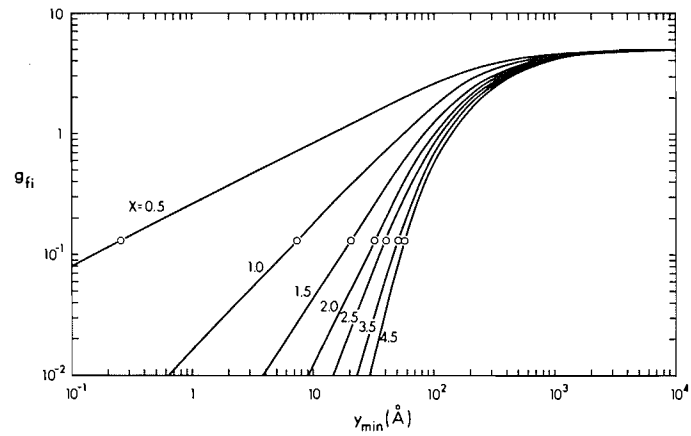

FIG. 3. Calculated values of g_{fi} as a function of y_{min} for several values of x in YP (eq. 8). ○, experimental $g_{fi} = 0.13$.

smallest error with $r_0 = 1 \times 10^{-7}$ cm was 0.12 g units per point, obtained with $x = 1.9$.

The above calculations were repeated with $r_0 = 0$ (stage E). The results were the same as those with $r_0 = 1 \times 10^{-7}$ cm.

The nitrogen yields calculated with the best YP function [9] are displayed by the curve labelled YP in Fig. 2.

$$[9a] \quad N(>y) = 2.0 \times 10^{-9} y^{-1.9} \qquad y \geqslant 2.9 \times 10^{-7} \text{ cm}$$

$$[9b] \quad N(>y) = 5000 \qquad y \leqslant 2.9 \times 10^{-7} \text{ cm}$$

(c) Delta Function (YD)

This function represents the gross approximation that all secondary electrons have the same range (12–15).

$$[10] \quad N(y) = N_0 \delta(y - y_d)$$

Equation 10 is the limiting case of eq. 8 with $x = \infty$ and $y_{min} = y_d$.

The free ion yield $g_{fi} = 0.13$ leads to the value $y_d = 7.6 \times 10^{-7}$ cm. Thus,

$$[11] \quad N(y) = 5000\delta(y - 7.6 \times 10^{-7} \text{ cm})$$

The nitrogen yields calculated from eq. 11 gave a minimum error of 0.30 g units per point, with r_0 equal to either zero or 10 Å. The best nitrogen yields calculable from the YD function are shown in Fig. 2.

(d) One-parameter Gaussian Function (YG1)

The Gaussian function most often used is a three dimensional function with one adjustable parameter (13, 14)

$$[12] \quad N(y) = N_0(4y^2/\pi^{1/2}b^3) \exp(-y^2/b^2)$$

where the parameter b indicates the width of the distribution and in the present instance is also the most probable value of y.

The free ion yield in cyclohexane requires $b = 59$ Å. Using this value of b and r_0 equal to either 0 or 10 Å, the calculated nitrogen yields give a minimum error of 0.18 g units per point. The calculated curve is shown in Fig. 2.

(e) Two-parameter Gaussian Function (YG2)

A more general Gaussian than eq. 12 is eq. 13, which is a three dimensional function with two adjustable parameters (y_0 and b, see Fig. 4).

$$[13] \quad N(\bar{y}) = N(y_b) = N_0(4y_b^2/\pi^{1/2}b^3) \exp(-y_b^2/b^2)$$

where $\bar{y}$ is the value of y averaged over all angles, for a given pair of values of y_0 and b.

$$[14] \quad \bar{y} = \int_0^\pi y \frac{\sin\theta}{2} d\theta = \int_0^\pi (y_0^2 + y_b^2 + 2y_0 y_b \cos\theta)^{1/2} \frac{\sin\theta}{2} d\theta$$

Equation 13 is equivalent to eq. 12 when $y_0 = 0$, and to eq. 10 when $b = 0$. Equations analogous to eq. 14 are also used to average y^2 and y^3 over all angles, when required.

The nitrogen yields calculated with eq. 13 give a minimum error of 0.15 g units per point, with $y_0 = 18$ Å, $b = 58$ Å. The calculated nitrogen yield curve is very similar to that for YG1 in Fig. 2, except that the lower end is shifted slightly

Can. J. Chem. Downloaded from www.nrcresearchpress.com by 210.87.254.40 on 09/05/12
For personal use only.

Can. J. Chem. Downloaded from www.nrcresearchpress.com by 210.87.254.40 on 09/05/12
For personal use only.

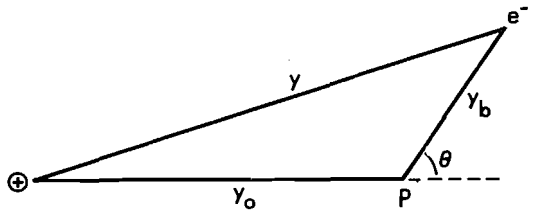

FIG. 4. Illustration of the symbols in the 3-dimensional Gaussian YG2. y_0 is a constant. y_b has a 3 dimensional Gaussian distribution about the point P, and the most probable value of y_b is the b in eq. 13. The value of y is $y = (y_0^2 + y_b^2 + 2y_0y_b \cos\theta)^{1/2}$. The distribution of y is symmetrical about the y_0 axis, and the probability of occurrence of a given value of θ is proportional to sin θ.

downwards and the upper end is shifted upwards by 0.07 g units.

The $N(>y)$ curve for YG2 is essentially the same as that for YG1 in Fig. 1, but the left-hand end is shifted to higher y values by 2–3 Å.

(f) YH

A hybrid between the semi-empirical function and a Gaussian (3, 16, 17) was made by cutting off the low-y end of the YSE function and fitting the amputated portion into a Gaussian form. The junction between the Gaussian and YSE portions is denoted by j (Fig. 5).

In YH, any arbitrary value of $y_0 < j$ can serve as the origin for the Gaussian. The values of y_0 and j automatically fix the value of the Gaussian dispersion parameter b. The YH function is

$$[15a] \qquad N(y) = 0 \quad y \leqslant y_0$$

$$[15b] \qquad N(y) = N_0[4(y - y_0)^2/\pi^{1/2}(b - y_0)^3] \exp[-(y - y_0)^2/(b - y_0)^2] \quad y_0 \leqslant y \leqslant j$$

$$[15c] \qquad N(y) = \text{YSE} \quad y \geqslant j$$

where $N_0 = 5000$.

The values of y and j were each varied in 1 Å jumps over a sufficiently wide range to locate the smallest minimum error. The smallest error was 0.13 g units per point, obtained for $j = 21$ Å and $y_0 = 8$ Å. The corresponding $g(N_2)$ curve was essentially the same as that for YSE in Fig. 2, except that it was shifted slightly towards the YP curve at high N_2O concentrations.

(g) YC

$N(y)$ = constant, *i.e.* all values of y are equally probable (14). This function corresponds to YP with $x = -1$. However, x must be >0.5 (Section II *2b*), so the YC function is impossible.

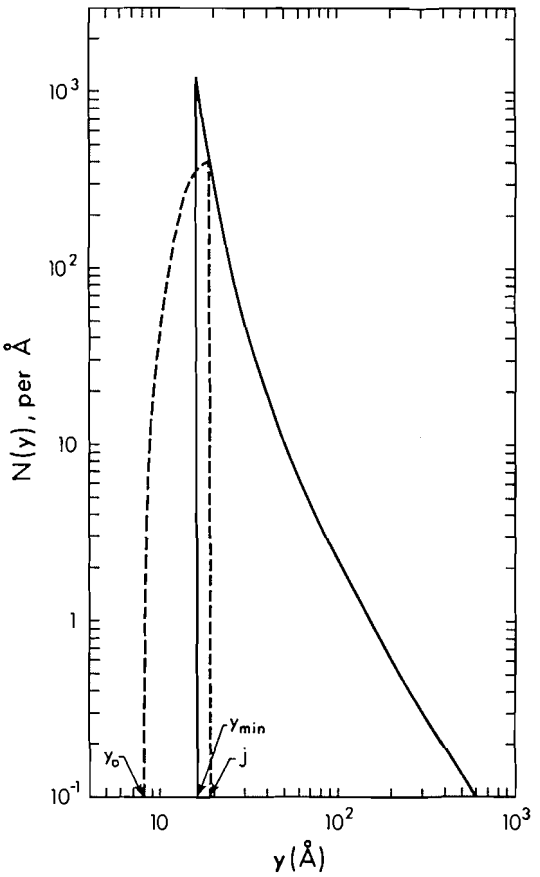

FIG. 5. YSE- and YH-$N(y)$ functions: full curve is the YSE-$N(y)$ function obtained by differentiating the YSE-$N(>y)$ curve in Fig. 1; dashed curve is the Gaussian portion of the YH function that gives the best fit to the experimental nitrogen yields; $y_0 = 8$ Å, $y_{min} = 16$ Å, $j = 19$ Å.

(3) Comparison of the Results from the Different N(y) Functions

(*a*) The functions YP, YG2, and YH each have two freely adjustable parameters, while YD and YG1 each have one. As expected the two-parameter functions gave better results than did those with one parameter (Table 1). However, it is interesting that YSE, in which no parameter was freely adjusted, gave results that were almost as good as those from the two-parameter functions. The YSE function was originally constructed during the interpretation of the variation of the free ion yields in a series of liquids (7) and

TABLE 1. Median values of y, minimum errors, and best values of β_- obtained for several $N(y)$ distributions in cyclohexane

Distribution	y_{med} (Å)*	$r_0 = 0$ Error (g/point)	$r_0 = 0$ β_- (10^{13} V/cm^2)	Distribution parameters
YSE	19	0.14	58.0	—
YP	42	0.12	6.3	$x = 1.9, K = 2.0 \times 10^{-9}$
YD	76	0.30	1.4	$y_d = 76$ Å
YG1	65	0.18	2.6	$b = 59$ Å
YG2	67	0.15	2.3	$b = 58$ Å, $y_0 = 18$ Å
YH	19	0.13	65.0	$j = 21$ Å, $y_0 = 8$ Å

*Median value of y.

has been applied without alteration to the scavenging model.

(*b*) The results are not sensitive to the choice of the value of r_0 from zero to 10 Å.

(*c*) Within the present framework, the broader forms of $N(y)$ function tend to give the smaller errors (Fig. 1 and Table 1).

(*d*) By way of comparison with other models (16–18), it should be mentioned that the scavenging yields $[g(N_2) - g_{fi}]$ calculated from the present model using the YSE function vary linearly with the square root of the scavenger concentration at low concentrations (Fig. 6). The yields calculated with the other $N(y)$ distribution functions deviate from linear square root plots; the amount of deviation from linearity obtained from the different functions increased in the order YSE < YP < YG1 < YD (Fig. 6). Experimental scavenging yields give linear "square root plots" at low concentrations (2, 9, 16, 18, 19), so from this point of view the YSE and YP functions are satisfactory while YG1 and YD are not.

It is also instructive to see the calculated yields plotted against the first power of the scavenger concentration at low concentrations (Fig. 7). The plots obtained using the YG1 and YD functions have linear regions in the vicinity of zero concentration. Thus the YD and YG1 function lead to G(scavenged) $\propto$ [S]$^{1.0}$ at low [S], which is

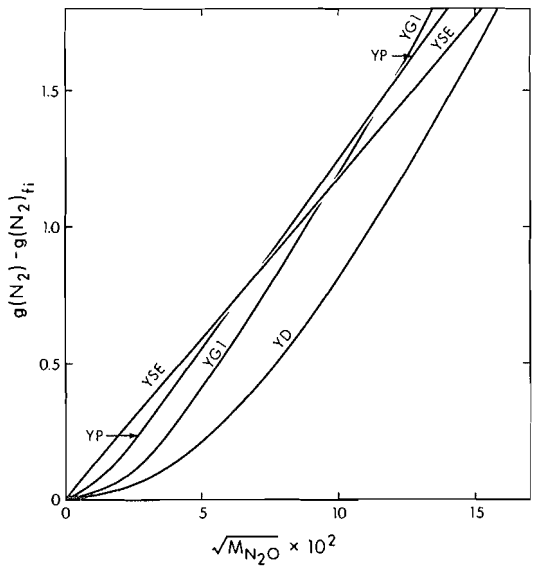

FIG. 6. Calculated values of $[g(N_2) - g_{fi}]$ for solutions of nitrous oxide in cyclohexane, plotted against the square root of the molarity of the nitrous oxide. The $N(y)$ distribution functions used in the calculations are indicated on the curves.

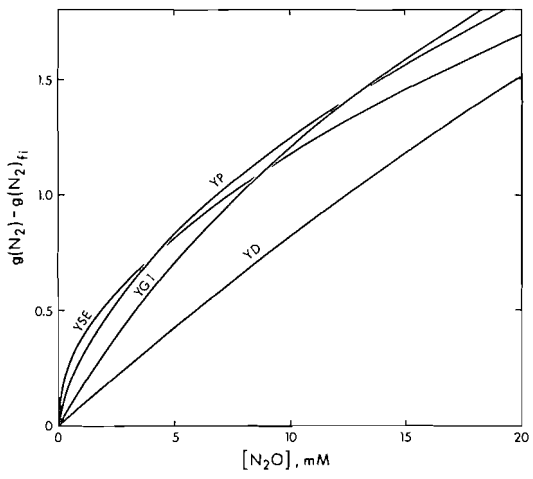

FIG. 7. Calculated values of $[g(N_2) - g_{fi}]$ for solutions of nitrous oxide in cyclohexane, plotted against the molarity of the nitrous oxide. The $N(y)$ distribution functions used in the calculations are indicated on the curves.

Can. J. Chem. Downloaded from www.nrcresearchpress.com by 210.87.254.40 on 09/05/12
For personal use only.

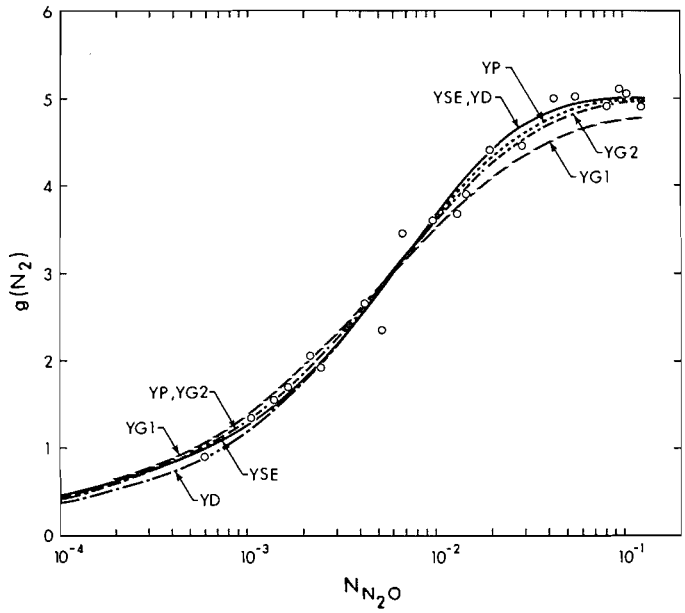

FIG. 8. $g(N_2)$ calculated by the prescribed diffusion method. ○, experimental (4). The $N(y)$ distributions used are indicated.

the wrong mathematical form. This is an alternative demonstration that the functions YD and YG1 are unsatisfactory in this model.

III. Effect of the Form of the Diffusive Motion of the Charge Pairs

In previous publications from this laboratory it has been assumed that the lifetime t_{gn} of an ion pair that undergoes geminate neutralization is simply governed by the ion mobilities $(u_+ + u_-)$, the mutual electric field between the two charges, and the drift distance $(y - r_0)$ (2, 3).

$$[16]\quad t_{gn} = \varepsilon(y^3 - r_0^3)/4.32 \times 10^{-7}(u_+ + u_-)\ \text{s}$$

However, eq. 16 tends to underestimate the neutralization time because it underemphasizes the effect of the random diffusion on the drift of the ions in their mutual electric field. A more complete description of the ion lifetimes is given by the prescribed diffusion approximation (13, 15). It is therefore desirable to insert the prescribed diffusion approximation into our kinetic equations to determine its effect on the calculated results.

The method in Section II used an average geminate neutralization time for a thermalized electron–ion pair that had a certain initial separation distance y. The prescribed diffusion method, on the other hand, considers the probability of neutralization as a function of time for each initial distance y. The probability F_y that an ion pair will remain unneutralized at time t, having started their Brownian motion from time zero at the initial separation y, is described by eq. 17 (15).

$$[17]\quad -\mathrm{d}F_y = \frac{e^2F_y}{\varepsilon kT(4\pi D)^{1/2}t^{3/2}}\exp(-y^2/4Dt)\,\mathrm{d}t$$

where $-\mathrm{d}F_y$ is the fraction of ion pairs that undergo neutralization during the interval between the times t and $t + \mathrm{d}t$, and D is the sum of the diffusion coefficients of the positive and negative species (taken approximately equal to that of the electron, 9×10^{-3} cm^2/s (20)).

In the prescribed diffusion method eqs. 1, 3, and 6 remain unchanged, but the total probability Φ_- that an electron with a given y value will be scavenged when the mole fraction of solute is N_s becomes

$$[18]\quad \Phi_- = 1 - \int_{t=0}^{\infty}(1 - f_-N_s)^{\alpha t}\,\mathrm{d}F_y$$

where $\alpha = b/t_1$, b is the number of new neighbors

Can. J. Chem. Downloaded from www.nrcresearchpress.com by 210.87.254.40 on 09/05/12
For personal use only.

TABLE 2. Summary of prescribed diffusion results

Distribution	y_{med} (Å)*	Error (g/point)	$\alpha(10^{12}\ s^{-1})$	Distribution parameters
YSE	19	0.14	218.0	—
YP	52	0.13	19.0	$x = 2.5, K = 4.8 \times 10^{-13}$
YD	76	0.14	7.7	$y_d = 76$ Å
YG1	65	0.20	15.0	$b = 59$ Å
YG2	77	0.13	10.0	$b = 55$ Å, $y_0 = 37$ Å

*Median value of y.

that an electron meets during the time t_1, and t_1 is the average time required for one diffusive jump of the electron.

The calculations have five general steps: (*a*) pick a form of $N(y)$ function from Section II; (*b*) pick a specific $N(y)$ function of that form that gives the correct free ion yield; (*c*) use the function and eqs. 1, 17, and 18 to calculate $g(N_2)$ at different nitrous oxide concentrations, adjusting the value of α to find the one that gives the smallest error (eq. 7); (*d*) pick another $N(y)$ function of the same form, if another exists, and repeat (*b*)–(*d*); (*e*) pick another form of $N(y)$ function and repeat (*b*)–(*e*).

The forms of $N(y)$ function used were YSE, YP, YD, YG1, and YG2. The function YSE is not freely adjustable and there is only one function of each of the forms YD and YG1 that gives the correct free ion yield. Thus the YSE, YD, and YG1 functions used here were exactly the same as those used in Section II. However, YP and YG2 each have two adjustable parameters, and the "best fit" functions of these forms are not the same in the prescribed diffusion method as they were in Section II.

The results of the calculations are summarized in Fig. 8 and Table 2. The YG1 distribution gave the largest error. The other functions gave satisfactory agreement.

IV. Comparison

The only striking contrast between the results of the y^3 method (Section II) and the prescribed diffusion method is that the narrowest $N(y)$ distribution function, YD, gave the largest error in the former and one of the smallest errors in the latter. The YD function is unrealistically narrow, and the preceding results might indicate that the prescribed diffusion method overestimates the spread of neutralization times in the liquid.

1. G. R. FREEMAN. J. Chem. Phys. **43**, 93 (1965).
2. J. W. BUCHANAN and F. WILLIAMS. J. Chem. Phys. **44**, 4377 (1966).
3. G. R. FREEMAN. J. Chem. Phys. **46**, 2822 (1967).
4. M. G. ROBINSON and G. R. FREEMAN. J. Chem. Phys. **48**, 983 (1968).
5. W. F. SCHMIDT and A. O. ALLEN. J. Phys. Chem. **72**, 3730 (1968).
6. P. H. TEWARI and G. R. FREEMAN. J. Chem. Phys. **49**, 4394 (1968).
7. G. R. FREEMAN and J. M. FAYADH. J. Chem. Phys. **43**, 86 (1965).
8. A. HUMMEL, A. O. ALLEN, and F. H. WATSON, JR. J. Chem. Phys. **44**, 3431 (1966).
9. G. R. FREEMAN. Radiat. Res. Rev. **1**, 1 (1968), Elsevier Publishing Co., Amsterdam.
10. L. G. WALKER. Ph.D. Thesis. University of Alberta, Edmonton, Alberta. 1967.
11. J. A. LEONE and W. A. HAMILL. J. Chem. Phys. **49**, 5304 (1968).
12. G. R. FREEMAN. J. Chem. Phys. **39**, 1580 (1963).
13. A. MOZUMDER. J. Chem. Phys. **48**, 1659 (1968).
14. P. LUDWIG. J. Chem. Phys. **50**, 1787 (1969).
15. A. MOZUMDER. J. Chem. Phys. **50**, 3153, 3162 (1969).
16. A. MOZUMDER and J. L. MAGEE. J. Chem. Phys. **47**, 939 (1967).
17. A. HUMMEL. J. Chem. Phys. **48**, 3268 (1968).
18. J. M. WARMAN, K.-D. ASMUS, and R. H. SCHULER. Adv. Chem. Ser. **82**, 25 (1968).
19. F. WILLIAMS. J. Am. Chem. Soc. **86**, 3954 (1964).
20. W. F. SCHMIDT and A. O. ALLEN. J. Chem. Phys. **52**, 4788 (1970).

Can. J. Chem. Downloaded from www.nrcresearchpress.com by 210.87.254.40 on 09/05/12
For personal use only.

Can. J. Chem. Downloaded from www.nrcresearchpress.com by 210.87.254.5 on 09/05/12
For personal use only.

Effect of Pressure on the Rates of Reaction of Radiolysis Intermediates in Liquid *n*-Hexane[1]

KAMAL N. JHA AND GORDON R. FREEMAN
Chemistry Department, University of Alberta, Edmonton 7, Alberta

Received April 20, 1971

The yield of hydrogen from pure hexane, $G(H_2) = 5.3 \pm 0.2$ was independent of pressure in the range 1 bar to 4.6 kbars. The G values of H_2, HD, and D_2 obtained from 11 mol% C_6D_{14} in C_6H_{14} were independent of pressure and were respectively, 4.85, 0.34, and 0.11. The electron and hydrogen atom scavenging efficiencies of carbon tetrachloride and hexadiene-1,3, and the hydrogen atom scavenging efficiency of hexene-1 were independent of pressure. The positive ion scavenging efficiencies of benzene and aniline increased with increasing pressure. The volume of activation for the hydrogen atom reaction with *n*-hexane is essentially the same as that for the reaction with hexene-1. The pressure dependence of the charge scavenging reactions has been interpreted in terms of the kinetics of spur processes. The treatment is consistent with the fact that the efficiency of the electron scavenging reactions is independent of pressure. The increased efficiency of positive ion reaction under pressure implies that the ratio of the diffusion coefficients of the radiolytic positive ion and electron, D_+/D_-, increases with increasing pressure.

Le rendement en hydrogène pour l'hexane pur, $G(H_2) = 5.3 \pm 0.2$, est indépendant de la pression dans le domaine de 1 bar à 4.6 kbar. Les valeurs G de H_2, HD et D_2 obtenues à partir de 11 mole% de C_6D_{14} dans C_6H_{14} sont indépendantes de la pression et sont respectivement de 4.85, 0.34 et 0.11. L'efficacité du tétrachlorure de carbone et de l'hexadiène-1,3 pour capturer les électrons et les atomes d'hydrogène ainsi que l'efficacité de l'hexène-1 pour capturer les atomes d'hydrogène est indépendante de la pression. L'efficacité du benzène et de l'aniline pour capturer les ions positifs augmente en même temps que la pression. Le volume d'activation pour la réaction d'atomes d'hydrogène avec le *n*-hexane est essentiellement le même que pour la réaction avec l'hexène-1. La dépendance de la pression sur les réactions de capture des charges est interprétée en termes de cinétique des reactions dans les grapées. L'augmentation de l'efficacité des réactions des ions positifs, sous l'effet de la pression, implique que le rapport des coefficients de diffusion des ions positifs crées sous irradiation et des électrons, D_+/D_-, augmente avec la pression.

Canadian Journal of Chemistry, 49, 2651 (1971)

Introduction

Information about the behavior of radiolysis intermediates in liquids can be obtained by studying the effect of pressure upon their relative rates of reaction (1–4). To this end, charge scavenging reactions have been studied in *n*-hexane at the pressures 1 bar and 4.6 kbars.

A similar investigation of charge scavenging in liquid cyclopentane has recently been reported (5). The charge scavengers N_2O, ND_3, and C_2H_5OD were used. The results obtained were similar to those reported here for liquid *n*-hexane.

Experimental

Phillips Research Grade *n*-hexane was used after the removal of traces of olefin by treatment with concentrated sulfuric acid (3). The treated hexane was then washed with water, dried, and distilled by standard techniques. Phillips Research Grade hexene-1 and benzene, Reagent Grade aniline from Shawinigan Chemicals and hexadiene-1,3 from Sapon Laboratories were distilled before use. Carbon tetrachloride from Fisher Scientific Co. was washed with sodium carbonate solution prior to use. Ethanol from United States Industrial Chemicals and perdeuterio *n*-hexane from Merck, Sharp and Dohme were used as received.

The high pressure system has been described elsewhere (1–3). The hydrostatic liquid used in the high pressure system was Esso Bayol 35 from Imperial Oil Limited. Specially ground 5 cm^3 glass syringes (East Rutherford Syringes, Inc.) sealed to 5/20 standard-taper inner joints (Fischer and Porter Ltd), capped with corresponding outer joints were used as reaction vessels for most of the experiments. The hydrogen yields obtained from the syringe technique were reproducible at 1 bar but at 4.6 kbars it was observed that the syringes began to jam after several (~5) runs and resulted in low hydrogen yields. For this reason no syringe was used more than three times under high pressure. The hydrogen yields under such conditions were reproducible and found to be independent of pressure. To check the reliability of the syringe technique a goosenecked cell was used, in which a mercury column separates the sample from the pressurizing oil and transmits the pressure (5). The hydrogen yields from such cells gave $G(H_2) = 5.3 \pm 0.2$ independent of pressure, equal to those obtained from the syringe technique.

[1]This work was presented in part at the C.I.C.–A.C.S joint meeting in Toronto, May 28, 1970.

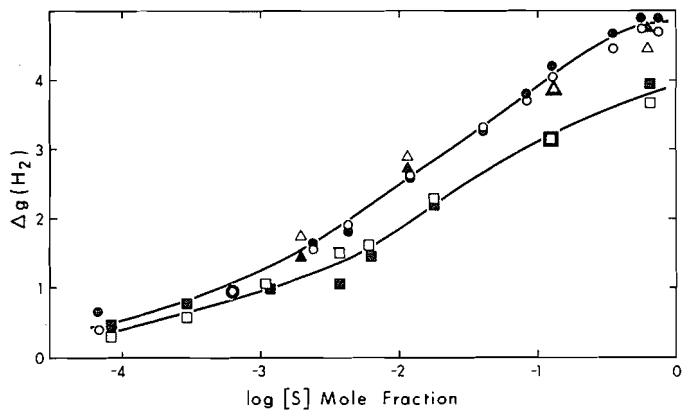

FIG. 1. $\Delta g(H_2)$ from *n*-hexane as a function of solute concentration. Carbon tetrachloride, ○; hexadiene-1,3, △; hexene-1, □. Open symbols, 1 bar; filled symbols, 4.6 kbars.

Several samples were irradiated in mercury-free Pyrex cells to compare the hydrogen yields in the presence and absence of mercury. The value obtained under this condition was $G(H_2) = 5.3$, which shows that mercury has no detectable effect on the hydrogen yield.

For the syringe samples, *n*-hexane and its solutions were deaerated by bubbling with argon for 10 min before irradiation. The change in concentrations of solutions after such treatment was negligible because the vapor pressures of the solutes are close to that of *n*-hexane, and secondly, evaporation of the solutions was less than 3%. Solutions of known concentrations of scavengers were prepared volumetrically or gravimetrically. Analysis of the irradiated samples was performed with a modified Van Slyke apparatus attached to a gas chromatograph with a thermal conductivity detector (6). For the separation of hydrogen, an 8 ft molecular sieve (Linde 5A from Union Carbide) column was used with argon carrier gas.

Samples were prepared in the goosenecked and Pyrex cells by standard vacuum techniques. Hydrogen from the irradiated samples was collected by a Toepler pump and injected into the gas chromatograph (11).

Irradiation was performed at 23° with a ^{60}Co γ-source. Special sample holders were used for the different types of cells to reproduce their position in the high pressure vessel. The amount of sample used was chosen such that the volume at the irradiation pressure equalled 3.2 cm^3. This required 2.10 g at 1 bar and 2.62 g at 4.6 kbars (*7a*). The same volume was used at each pressure to simplify the dosimetry inside the pressure bomb. The dose rate, determined by a Fricke dosimeter, was 8.1×10^{16} eV/g min in *n*-hexane (*7b*). The dose was 6.5×10^{17} eV/g.

The isotopic composition of hydrogen from the C_6D_{14}–C_6H_{14} solution was determined using a CEC 21-614 mass spectrometer.

Results

The yields of hydrogen obtained from the different cells agreed with each other within experimental error. Pure *n*-hexane gave $G(H_2) = 5.3 \pm 0.2$, independent of pressure over the range 1 bar to 4.6 kbars. This value is in agreement with previously published values at atmospheric pressure (8–10).

The yields from the solutions are expressed as *g* values, based on the energy initially absorbed in the solvent only. That is, $g = G/\varepsilon_s$, where ε_s is the electron fraction of solvent in the solution. A correction was made to the hydrogen yields for the direct radiolysis of ethanol, hexene-1, and hexadiene-1,3 in the solutions using $G(H_2) = 5.1$ for ethanol, 0.8 for hexene-1, and 0.2 for hexadiene-1,3 (assumed equal to that from cyclohexadiene-1,3 (11)). The hydrogen yield from benzene is so low (0.04) that no correction was necessary.

The *G* values of H_2, HD, and D_2 obtained from 11 mol% C_6D_{14} in C_6H_{14} were, respectively, 4.86, 0.33, 0.11 at 1 bar and 4.84, 0.35, 0.11 at 4.6 kbars. The yields are independent of pressure.

Figure 1 displays $\Delta g(H_2) = g(H_2)_0 - g(H_2)$ against the mole fractions of carbon tetrachloride, hexadiene-1,3, and hexene-1 at 1 bar and 4.6 kbars. $\Delta g(H_2)$ is independent of pressure for all three solutes. Carbon tetrachloride and hexadiene-1,3 are equally efficient as scavengers, while hexene-1 is about three-fold less efficient.

Figure 2 depicts $\Delta g(H_2)$ against mole fraction of aniline at 1 bar and at 4.6 kbars. The efficiency of scavenging hydrogen precursors by aniline increases with increasing pressure. Unfortunately, higher concentrations of aniline could not be used because of its limited solubility in *n*-hexane.

The effect of benzene is similar to that of aniline, but the pressure effect on the former is greater than that on the latter (*cf.* Figs 2 and 3).

Can. J. Chem. Downloaded from www.nrcresearchpress.com by 210.87.254.5 on 09/05/12
For personal use only.

TABLE 1. Relative efficiencies of scavengers in liquid *n*-hexane

Solute	$k_{1\ bar}$	$k_{4.6\ kbars}$	Probable species scavenged
Carbon tetrachloride	1.0	1.0	e^-, H
Hexadiene-1,3	1.0	1.0	e^-, H
Hexene-1	0.4	0.4	H, +
Aniline	0.2	0.4	+, H
Benzene	0.2	0.6	+, H
Benzene + 10% ethanol	0.1	0.5	H, +

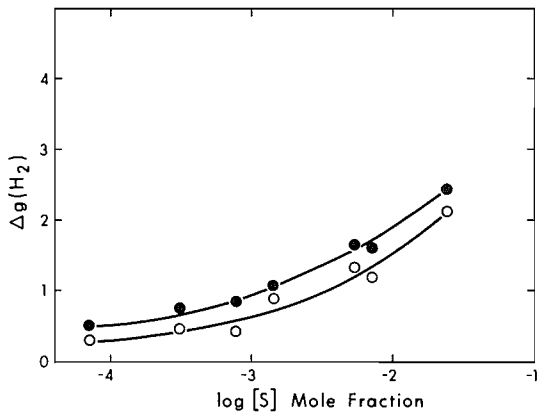

FIG. 2. $\Delta g(H_2)$ from *n*-hexane as a function of aniline concentration. ○, 1 bar; ●, 4.6 kbars.

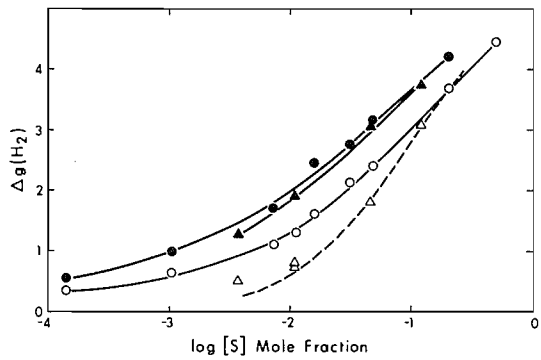

FIG. 3. $\Delta g(H_2)$ from *n*-hexane as a function of solute concentration. Benzene: ○, 1 bar; ●, 4.6 kbars. 10 mol% ethanol + benzene: △, 1 bar; ▲, 4.6 kbars (dashed line at 1 bar was calculated using $k_{17}/k_{16} = 13$).

Addition of 10 mol% ethanol to the *n*-hexane benzene solutions decreases the scavenging efficiency of benzene at 1 bar but at 4.6 kbars the effect of ethanol is greatly reduced (Fig. 3). At 4.6 kbars benzene solutions more concentrated than 0.2 mole fraction broke the cells, probably due to freezing of the solutions.

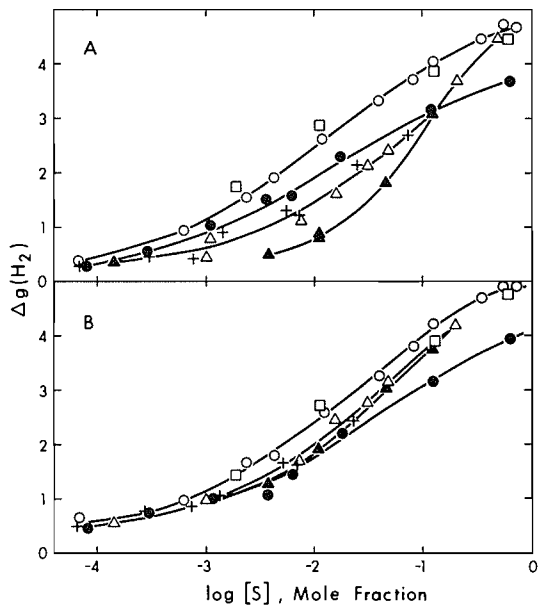

FIG. 4. $\Delta g(H_2)$ from *n*-hexane as a function of solute concentration. *A*: 1 bar; *B*: 4.6 kbars. ○, carbon tetrachloride; □, hexadiene-1,3; ●, hexene-1; +, aniline; △, benzene; ▲, benzene + 10 mol% ethanol.

The different effects of pressure on the different scavenger solutions are strikingly demonstrated in Fig. 4. The aniline and benzene curves at 1 bar are lower than the hexene-1 curve at low solute concentrations, but they are above the hexene-1 curve at 4.6 kbars.

The relative efficiencies of the different scavengers at 1 bar and 4.6 kbars are listed in Table 1.

Discussion

The mechanism for hydrogen formation in the γ radiolysis of liquid *n*-hexane can be represented as follows

[1] $C_6H_{14} \rightsquigarrow C_6H_{14}^+ + e^-$

[2] $C_6H_{14} \rightsquigarrow C_6H_{14}^*$

Can. J. Chem. Downloaded from www.nrcresearchpress.com by 210.87.254.5 on 09/05/12
For personal use only.

Can. J. Chem. Downloaded from www.nrcresearchpress.com by 210.87.254.5 on 09/05/12
For personal use only.

[3] $C_6H_{14}^+ + e^- \rightarrow C_6H_{14}^*$

[4] $C_6H_{14}^* \rightarrow H, H_2$, products

[5] $H + C_6H_{14} \rightarrow H_2 + C_6H_{13}$

The lack of a pressure effect on the yield of hydrogen from pure hexane or on the isotopic composition of the hydrogen from the C_6D_{14}–C_6H_{14} solution indicates that the yields of reactions 4 and 5 are unaffected by pressure. It also seems probable that there is no net effect of pressure on reactions 1–3 over the range used. No pressure effect on the yields of reactions 3 and 5 would be expected, since they have no competing reactions in the mechanism.

The hydrogen yield from liquid cyclopentane was also independent of pressure (5).

A. Carbon Tetrachloride, Hexadiene-1,3, and Hexene-1 Solutions

Carbon tetrachloride and conjugated diolefins have been shown to scavenge both electrons and hydrogen atoms in hydrocarbon and aqueous solutions (12, 13).

[6] $e^- + CCl_4 \rightarrow CCl_4^- (\rightarrow CCl_3 + Cl^-)$

[7] $e^- + C_6H_{10} \rightarrow C_6H_{10}^-$

[8] $C_6H_{14}^+ + (Cl^- \text{ or } C_6H_{10}^-) \rightarrow$ no H or H_2

[9] $H + CCl_4 \rightarrow HCl + CCl_3$

[10] $H + C_6H_{10} \rightarrow C_6H_{11}$

The absence of an appreciable pressure effect on the scavenging efficiencies of these solutes (Fig. 1) indicates that the net influences of pressure on reactions 3, 6, and 7 are equal to each other, and that the influences on reactions 5, 9, and 10 equal each other. This is in agreement with similar observations in other systems (5, 14, 15).

Mono-olefins such as hexene-1 scavenge hydrogen atoms at low concentrations (13, 16) and possibly also positive ions at high concentrations (17). The lack of a pressure effect on the scavenging efficiency of hexene-1 is consistent with the occurrence of reaction 11 in competition with reaction 5, since the two types of reaction have similar volumes of activation (14).

[11] $H + C_6H_{12} \rightarrow C_6H_{13}$

B. Benzene, Benzene + Ethanol, and Aniline Solutions

Benzene has been suggested to scavenge hydrogen atoms in the liquid phase (12, 13, 18). In solid phase solutions it has also been reported to scavenge electrons (19–22) and positive charge (19, 22–24).

The scavenging efficiency of benzene increased with increasing pressure (Fig. 3), whereas the efficiencies of the electron and hydrogen atom scavengers were unaffected by pressure (part *A*). This seemed to indicate that the pressure effect on the benzene solutions was due to positive ion reactions. To test this possibility, ethanol was added as a competitive scavenger for the positive ions.

[12] $C_6H_{14}^+ + C_6H_6 \rightarrow C_6H_{14} + C_6H_6^+$

[13] $C_6H_6^+ + e^- \rightarrow$ negligible H_2

[14] $C_6H_{14}^+ + C_2H_5OH \rightarrow C_6H_{13} + C_2H_5OH_2^+$

[15] $C_2H_5OH_2^+ + e^- \rightarrow C_2H_5OH + H$

Whereas benzene inhibits hydrogen formation and ethanol does not, so addition of ethanol should diminish the effectiveness of benzene as a hydrogen inhibitor. Such was found to be the case at atmospheric pressure, but the ethanol effect was much reduced at 4.6 kbars (Fig. 3). It therefore appears that $\Delta V_{14}^{\ddagger} > \Delta V_{12}^{\ddagger}$, where $\Delta V^{\ddagger}$ is the volume of activation.

To obtain further evidence about the effect of pressure on positive ion reaction efficiencies, aniline was used as a scavenger (25–28). Amines have been shown to react with radiolytic cations (17, 25–28). Increasing the pressure on the aniline solutions increased the scavenging efficiency (Fig. 3). The main effect of low concentrations of benzene and aniline on the radiolysis of *n*-hexane at 1 bar appears to be the scavenging of positive ions. However, in the presence of 10 mol% ethanol benzene acts mainly as a hydrogen atom scavenger. The dashed curve in Fig. 3 was calculated using homogeneous kinetics with $k_{17}/k_{16} = 13$ and $\Delta g(H_2)_{max} = 4.8$; RH in reaction 16 can be either hexane or ethanol.

[16] $H + RH \rightarrow H_2 + R$

[17] $H + C_6H_6 \rightarrow C_6H_7$

The value $\Delta g(H_2)_{max} = 4.8$ was estimated from the carbon tetrachloride experiments, in which both hydrogen atoms and the geminate neutralization reaction were being scavenged.

At 4.6 kbars reaction 12 is favored over reaction 14, and the ethanol interferes relatively little with the benzene reaction.

It has been suggested that benzene scavenges electrons prior to solvation in methanol–water

Can. J. Chem. Downloaded from www.nrcresearchpress.com by 210.87.254.5 on 09/05/12
For personal use only.

glassy solids at 77 °K (20) and that phenol, which is analogous to our aniline, scavenges unsolvated electrons in the above matrices as well as in water (20, 21). However, there is no evidence that these compounds scavenge electrons in liquid *n*-hexane.

Kinetics Considerations

The fact that the volume of activation for the hydrogen atom reaction with hexane (abstraction) is essentially the same as that for the reaction with hexene-1 (addition) can be rationalized by assuming that there is a tight activated complex in each reaction. It has been estimated that $\Delta V^{\ddagger}$ for $H + CH_4 \rightarrow H_2 + CH_3$ is about -9 cm^3/mol (14). In the same way one may estimate $\Delta V_5^{\ddagger} \approx -9$ cm^3/mol and $\Delta V_{11}^{\ddagger} \approx -10$ cm^3/mol.

The pressure dependence of the charge scavenging reactions must be interpreted in terms of the kinetics of spur processes. Several treatments of the kinetics of charge scavenging in the γ radiolysis of liquids have been made (29–32). In general, they indicate that the concentration of scavenger required to scavenge a given fraction of the geminate electrons or positive ions is related to a reaction efficiency parameter. To interpret the pressure results in terms of the stochastic model the complete exponent $v\beta$ of the concentration factor (29, 32) must be considered. For electron scavenging (29),

$$[18]\quad v\beta_- = \frac{1.39 \times 10^7 \varepsilon y^3}{(u_+ + u_-)} \left\{ \frac{b_- D_-}{\lambda_-^2} + \frac{b_s D_s}{\lambda_s^2} \right\}$$

The pressure sensitivities of the dielectric constant ε, the secondary electron range y, and the mean free path λ are approximately $\varepsilon \propto \rho$, $y \propto \rho^{-1}$, $\lambda \propto \rho^{-1}$, where ρ is the density. One may therefore write

$$[19]\quad v\beta_- \approx c'(D_- + D_s)/(u_+ + u_-) = c(D_- + D_s)/(D_+ + D_-)$$

where c' and c are factors that are essentially independent of pressure, D is a diffusion coefficient, u is a mobility, and the subscripts $+$, $-$, and s refer to the geminate positive ions and electrons and the scavenger, respectively. From the data presently available (29–31) values of D_+ and D_s are much smaller than D_- and therefore, eq. 19 reduces to eq. 20,

$$[20]\quad v\beta_- \approx c$$

which implies that the efficiency of electron scavenging should be independent of pressure. The results demonstrate that this is essentially true (Fig. 1).

For positive ion scavenging, the equation analogous to [19] is

$$[21]\quad v\beta_+ \approx c(D_+ + D_s)/(D_+ + D_-)$$

Results from benzene, benzene + ethanol, and aniline solutions in hexane indicate that $v\beta_+$ increases with an increase in pressure. The respective increases are ~3-fold, 4-fold, and 2-fold on going from 1 bar to 4.6 kbars (Figs. 2 and 3). The increase in $v\beta_+$ with increasing pressure is ascribed to an increase in the ratio $(D_+ + D_s)/(D_+ + D_-)$ because c is essentially independent of pressure. D_s will decrease with increasing pressure as a result of the increasing viscosity of the solution, so the value of the ratio $D_+/(D_+ + D_-)$ must increase more than does $v\beta_+$; the value of the ratio D_+/D_- must increase even more.

The increase in D_+/D_- has a spectrum of possible causes, ranging from both diffusion coefficients decreasing but with D_+ decreasing less rapidly than D_-, to both coefficients increasing, but with D_+ increasing more rapidly than D_-. A definite choice cannot yet be made among the various possibilities. However, considering that electrons can be trapped in disordered systems (33–39) and that the positive charges appear to migrate limited but significant distances by charge exchange during radiolysis of solid hydrocarbons (24, 40), we tend to favor the interpretation that D_+ increases or remains the same while D_- remains the same or decreases with increasing pressure. Hentz and Brazier (5) came to a similar conclusion regarding the cyclopentane system.

Preliminary experiments were done by W. Skrlac and G. B. Evans. We are grateful to the National Research Council of Canada for financial assistance.

1. D. L. Dugle and G. R. Freeman. J. Phys. Chem. **70**, 1256 (1966).
2. R. R. Hentz, Farhataziz, D. J. Milner, and M. Burton. J. Chem. Phys. **46**, 2995 (1967).
3. D. W. Brazier and G. R. Freeman. Can. J. Chem. **47**, 885 (1969).
4. R. R. Hentz and R. J. Knight. J. Chem. Phys. **52**, 2456 (1970).
5. R. R. Hentz and D. W. Brazier. J. Chem. Phys. **54**, 554 (1971).
6. Farhataziz. J. Phys. Chem. **71**, 598 (1967).

7. (*a*) D. W. BRAZIER and G. R. FREEMAN. Can. J. Chem. **47**, 893 (1969). (*b*) G. R. FREEMAN. Can. J. Chem. **38**, 1043 (1960).
8. T. J. HARDWICK. J. Phys. Chem. **66**, 2246 (1962).
9. M. G. ROBINSON and G. R. FREEMAN. J. Chem. Phys. **48**, 983 (1968).
10. T. KIMURA, K. FUEKI, and Z. KURI. Bull. Chem. Soc. Japan, **43**, 1657 (1970).
11. E. D. STOVER and G. R. FREEMAN. Can. J. Chem. **46**, 2109 (1968).
12. M. ANBAR and P. NETA. Int. J. Appl. Rad. Isot. **16**, 227 (1965).
13. B. D. MICHAEL and E. J. HART. J. Phys. Chem. **74**, 2878 (1970).
14. (*a*) S. D. HAMANN. *In* Physico-chemical effects of pressure. Butterworths Scientific Publ., London. 1957. pp. 166–172; (*b*) W. J. LE NOBLE. Prog. Phys. Org. Chem. **5**, 207 (1967), see pp. 241–298.
15. R. R. HENTZ, FARHATAZIZ, and D. J. MILNER. J. Chem. Phys. **49**, 2153 (1967).
16. F. BUSI and G. R. FREEMAN. J. Phys. Chem. In press.
17. T. SHIDA and W. H. HAMILL. J. Am. Chem. Soc. **88**, 5376 (1966).
18. M. C. SAUER, JR. and I. MANI. J. Phys. Chem. **72**, 3856 (1968).
19. T. SHIDA and W. H. HAMILL. J. Chem. Phys. **44**, 4372 (1966).
20. T. SAWAI and W. H. HAMILL. J. Phys. Chem. **73**, 2750 (1969).
21. T. SAWAI and W. H. HAMILL. J. Phys. Chem. **74**, 3914 (1970).
22. A. EKSTROM. J. Phys. Chem. **74**, 1705 (1970).
23. T. SHIDA and W. H. HAMILL. J. Chem. Phys. **44**, 2375 (1966).
24. P. W. F. LOUWRIER and W. H. HAMILL. J. Phys. Chem. **74**, 1418 (1970).
25. E. J. LAND and G. PORTER. Trans. Faraday Soc. **59**, 2027 (1963).
26. T. SHIDA and W. H. HAMILL. J. Chem. Phys. **44**, 2369 (1966).
27. M. ANBAR, D. MEYERSTEIN, and P. NETA. Nature, **209**, 1348 (1966).
28. R. COOPER and J. K. THOMAS. J. Chem. Phys. **48**, 5103 (1968).
29. G. R. FREEMAN. J. Chem. Phys. **46**, 2822 (1967).
30. A. HUMMEL. J. Chem. Phys. **48**, 3268 (1968).
31. J. M. WARMAN, K.-D. ASMUS, and R. H. SCHULER. Advan. Chem. Ser. **82**, 25 (1968).
32. J.-P. DODELET and G. R. FREEMAN. Can. J. Chem. This issue.
33. J. P. GUARINO and W. H. HAMILL. J. Am. Chem. Soc. **86**, 777 (1964).
34. G. R. FREEMAN and J. M. FAYADH. J. Chem. Phys. **43**, 86 (1965).
35. N. F. MOTT. Adv. Phys. **16**, 49 (1967).
36. M. SILVER, D. G. ONN, P. SMEJTEK, and K. MASUDA. Phys. Rev. Lett. **19**, 626 (1967).
37. J. LIN, K. TSUJI, and F. WILLIAMS. J. Am. Chem. Soc. **90**, 2766 (1968).
38. J. T. RICHARDS and J. K. THOMAS. J. Chem. Phys. **53**, 218 (1970).
39. A. EKSTROM, R. SUENRAM, and J. E. WILLIAMS. J. Phys. Chem. **74**, 1888 (1970).
40. A. EKSTROM and J. E. WILLARD. J. Phys. Chem. **74**, 1708 (1970).

Can. J. Chem. Downloaded from www.nrcresearchpress.com by 210.87.254.5 on 09/05/12
For personal use only.

Can. J. Chem. Downloaded from www.nrcresearchpress.com by 210.87.254.5 on 09/05/12
For personal use only.

The Electroreduction of Periodate Anion in Alkaline Media

W. R. FAWCETT AND Y. C. KUO LEE
Department of Chemistry, University of Guelph, Guelph, Ontario

Received February 1, 1971

The electroreduction of periodate anion was studied at a dropping mercury electrode in aqueous solutions in the pH range 11–13.3 where the process is markedly affected by the double layer. The electrode reaction was found to be complex, its mechanism depending on both pH and ionic strength. The effects of the double layer on the component reactions are discussed with respect to current theoretical developments.

L'électroréduction de l'anion périodate a été étudiée au moyen d'une électrode à gouttes de mercure, en solution aqueuse et dans une zone de pH comprise entre 11 et 13.3, où le processus est pronfondément influencé par la double couche. La réaction à l'électrode est compliquée et son mécanisme dépend à la fois du pH et de la force ionique. Les effets de la double couche sur les réactions des constituants sont discutés par rapport aux résultats théoriques actuels.

Canadian Journal of Chemistry, 49, 2657 (1971)

Introduction

As the result of several experimental investigations (1–4), it has been found that periodate anion in aqueous solution is reduced at a dropping mercury electrode in two steps, the first being a two electron reduction to iodate anion, and the second, a six electron reduction of iodate to iodide anion. The first polarographic wave was normal in acidic media (1, 2); however, in alkaline media, an anomalous current minimum, whose depth depended on pH, ionic strength, and the nature of the base electrolyte cation, appeared at potentials cathodic of the working electrode's electrocapillary maximum (e.c.m.) where the diffusion limited current was expected (1, 3, 4). Lamy (4) attributed the minimum to a double layer effect, namely, repulsion of the reacting anion from the similarly charged electrode (5), and thereby accounted for the dependence on ionic strength. On the basis of existing thermodynamic data for the solution equilibria of periodate (6), he assumed that the predominant species at high pH was $H_3IO_6^{2-}$ and concluded that the pH dependence resulted from the fact that the electroactive species was $H_4IO_6^-$ formed from the dinegative anion in a labile protonation reaction preceding electron transfer. However, more recent studies of periodate equilibria (7–9) have shown that the species $H_2IO_6^{3-}$ and $H_2I_2O_{10}^{4-}$ are present in the pH range 11–14 so that pH dependence also results from variations in the bulk concentrations of the various anions. On reexamining the double layer effect in this system, it was found that the charge on the predominant reacting species depended on both pH and ionic strength (10). Further details of the results of this reexamination are presented in the following paper.

Experimental and Method of Data Analysis

Current–voltage curves for the reduction of periodate anion were measured at a dropping mercury electrode with various combinations of alkali metal hydroxides and fluorides as base electrolytes. The base electrolytes were chosen so that kinetic data would be obtained with a given cation as a function of pH at constant ionic strength and vice versa. The apparatus, experimental procedure, and general methods of reagent purification have been described previously (10). CsOH was prepared from a solution of CsCl by electrolysis according to the method outlined by Vogel (11). AnalaR grade sodium and potassium periodate were used as depolarizers without further purification. The depolarizer concentration was always 5×10^{-4} M.

The rate of charge transfer at a given potential was calculated from the current measured at the end of the lifetime of a given mercury drop, the droptime, and the corresponding current which would flow if the process were diffusion controlled. The calculation was based on Koutecký's theory for irreversible electrode processes and included corrections for electrode sphericity (10). The necessary double layer data, namely values of electrode charge density, q, and outer Helmholtz plane (o.H.p.) potential, ϕ_2 as functions of electrode potential were calculated from the capacity data of Grahame and Payne as outlined previously (10). For convenience, the kinetic data are reported in terms of $(\ln k)/f$ where k is the rate constant (cm s^{-1}) and $f = F/RT$ (V).

Results and Discussion

A typical current–potential curve for periodate anion reduction at a mercury electrode is shown

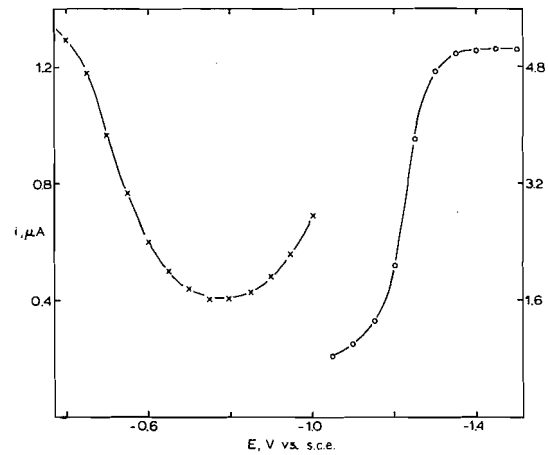

FIG. 1. Current–potential curve for the electroreduction of 5×10^{-4} *M* $NaIO_4$ at a dropping mercury electrode in 0.1 *M* NaOH at 25 °C. Capillary characteristics: flow rate = 0.296 mg s^{-1}, drop time = 8.75 s at −0.4 V, 6.86 s at −1.5 V. Points (×) correspond to the left hand ordinate scale and (○) to the right hand scale.

in Fig. 1. The kinetic data of interest in this investigation, namely that for reduction of periodate to iodate, were obtained in the region of the current minimum. The potential at which current due to the second process, reduction of iodate to iodide, became significant was determined by a simple extrapolation procedure. A plot of log $[i/(i_{d2} - i)]$ *vs.* electrode potential was made with data in the potential region of the second wave; i is the observed current and i_{d2}, the diffusion limited current for the second process. The resulting plot was linear over the rising portion of the second wave and had a slope of 12 V^{-1}. The potential at which a current of 6×10^{-3} μA would flow according to the above linear relationship was determined by extrapolation. This current was the smallest which could be detected for typical experimental conditions of current measurement in the region of the minimum. By this procedure it was found that current flowing due to the second process could be considered negligible at potentials anodic of −0.950 V with respect to the standard calomel electrode.

The diffusion coefficients required for calculation of the diffusion limited current over the potential range of the current minima were determined from the limiting current for the second wave. These constants could not be calculated from current densities measured at potentials anodic of the e.c.m. because of the presence of polarographic maxima of the second kind. The apparent diffusion coefficients obtained were found to decrease with increase in both ionic strength and p*H*. These changes are attributed respectively to the effects of ionic atmosphere on diffusion of the reacting ions, and to the participation of more than one ion in the mass transfer process. According to the equilibrium constants determined by Buist *et al.* (9), both $H_3IO_6^{2-}$ and $H_2IO_6^{3-}$ were present in the solutions to a significant extent under the given experimental conditions. For a stoichiometric periodate concentration of $5 \times 10^{-4}M$, the concentration of $H_2I_2O_{10}^{4-}$ was negligible except at lower p*H*. Since the largest amount present in any of the systems corresponded to approximately 2% of the total periodate concentration, its presence was neglected in the calculations described below. If both the dinegative and trinegative ions react at the electrode, then, according to the Ilkovič equation[1] one may write (12)

$$[1] \quad D_{app}^{1/2} = \frac{K_{b3}}{K_{b3} + C_{OH}} D_2^{1/2} + \frac{C_{OH}}{K_{b3} + C_{OH}} D_3^{1/2}$$

where D_{app} is the apparent value of the diffusion coefficient calculated from the diffusion limited current, D_2 and D_3, the diffusion coefficients for the two anions at a given ionic strength, K_{b3}, the basicity constant for $H_2IO_3^{3-}$ at the given ionic strength, and C_{OH}, the hydroxyl ion concentration. The parameters K_{b3}, $D_2^{1/2}$, and $D_3^{1/2}$ were determined from the values of $D_{app}^{1/2}$ as a function of C_{OH} at constant ionic strength using the generalized least squares procedure of Wentworth (14). The results are summarized in Table 1. Values of K_{b3} at zero ionic strength were calculated using single ion activity coefficients estimated according to Davies' equation (15). The weighted average for K_{b3} ($\mu = 0$) from the results in Table 1 is $(1.53 \pm 0.14) \times 10^{-2}$, a result which agrees well with that of Buist *et al.* (9). As expected,

[1]Strictly speaking this calculation should be based on Koutecký's equation (13) for the diffusion limited current which includes a correction for electrode sphericity. However, the precision with which the diffusion coefficients could be determined was too low to warrant this refinement.

Can. J. Chem. Downloaded from www.nrcresearchpress.com by 210.87.254.5 on 09/05/12
For personal use only.

TABLE 1. Parameters obtained by least squares fit of diffusion coefficient data to eq. 1

Ionic strength (μ, M)	Number of data points	$K_{b3} \times 10^3$	$D_2^{1/2} \times 10^3$ (cm $s^{-1/2}$)	$D_3^{1/2} \times 10^3$ (cm $s^{-1/2}$)
0.01*	11	10.2	2.73	2.60
0.02	18	6.65 ± 11.0	2.71 ± 0.05	2.52 ± 0.09
0.05	22	9.2 ± 6.4	2.71 ± 0.04	2.43 ± 0.05
0.1	23	5.1 ± 3.2	2.67 ± 0.05	2.39 ± 0.03
0.2	21	5.0 ± 2.7	2.66 ± 0.07	2.31 ± 0.02

*The non-linear least squares procedure was not convergent in this case. K_{b3} was calculated as described in the paper from values obtained at other ionic strengths; $D_2^{1/2}$ and $D_3^{1/2}$ were then determined from a linear least squares fit of the data to eq. 1.

the values of D_2 and D_3 decrease with increase in ionic strength, the decrease for the trinegative ion being greater than that for the dinegative. Finally, it was assumed that the diffusion limited current in the region of the current minimum was due to diffusion of $H_3IO_6^{2-}$ only, and accordingly, calculated using the tabulated values of $D_2^{1/2}$. This assumption is discussed below.

Kinetic data obtained at ionic strength 0.05 for varying pH with Na^+ as the base electrolyte cation are shown in Fig. 2. At constant electrode potential on the rational scale, ϕ_m, the structure of the double layer for the various base electrolytes involved was the same assuming that neither fluoride or hydroxyl anions are specifically absorbed at cathodic potentials (16). The variation of reaction rate with pH at constant ϕ_m is attributed to variation in the concentration of the electroreducible species, or of another species involved in a chemical reaction preceding the electron transfer step and producing the electroreducible species. It was also noted that the potential at which the current reached a minimum changed with pH, becoming slightly more anodic as the pH increased. This observation can be ascribed to a gradual change in mechanism with change in concentration of the electroreducible species. Kinetic data for varying ionic strength at pH 12 are shown in Fig. 3. These results are obviously attributable to a double layer effect. As the ionic strength is decreased, the potential drop across the diffuse layer, ϕ_2, increases at

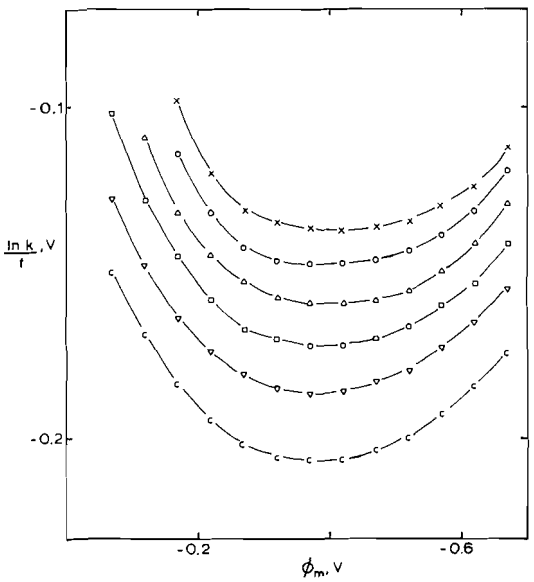

FIG. 2. Kinetic data for the electroreduction of periodate anion as a function of pH and potential at constant ionic strength (0.05). The hydroxyl ion concentrations are 0.001 (×), 0.002 (○), 0.005 (△), 0.01 (□), 0.02 (▽), and 0.05 (C).

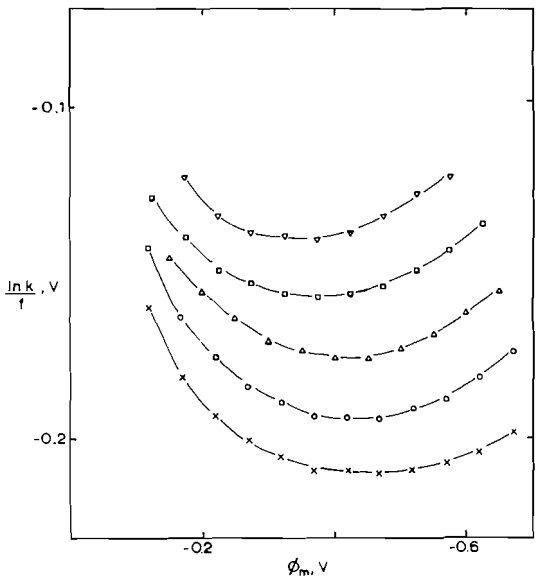

FIG. 3. Kinetic data for the electroreduction of periodate anion as a function of ionic strength and potential at constant pH (12). The ionic strengths are 0.01 (×), 0.02 (○), 0.05 (△), 0.1 (□), and 0.2 (▽).

Can. J. Chem. Downloaded from www.nrcresearchpress.com by 210.87.254.5 on 09/05/12
For personal use only.

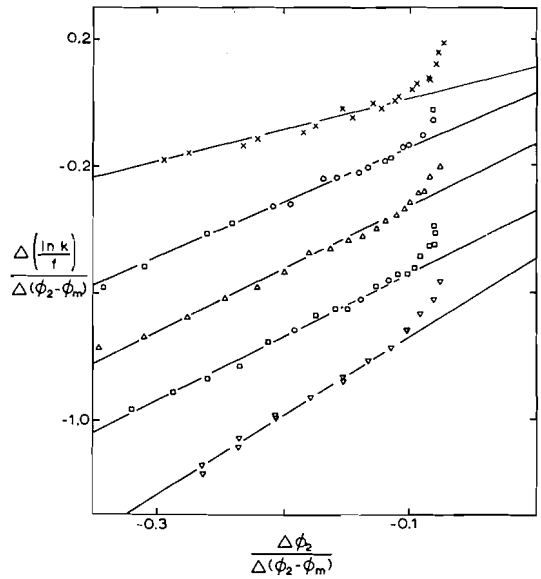

FIG. 4. Differential plots of kinetic data for the electroreduction of periodate anion in NaOH solutions of varying concentration: 0.01 (×), 0.02 (○), 0.05 (△), 0.1 (□), and 0.2 (▽). The ordinate scale is correct for the uppermost plot; for the sake of clarity the other plots have been shifted down by 0.2 units each.

constant ϕ_m so that the reacting anion is increasingly repelled from the electrode.

A simple differential technique described earlier (10) was used to determine the charge on the reacting species. Typical differential plots for data obtained in NaOH solutions of varying concentration with finite differences calculated at 50 mV increments in ϕ_m are shown in Fig. 4. The slope of the plots depended on both p*H* and ionic strength, increasing with increase in ionic strength, and in some cases, with p*H*. In summary, the slopes in the limit of low ϕ_m were approximately 1 for $\mu = 0.01$, between 1 and 2 for $\mu = 0.02$, 2 for $\mu = 0.05$ and 0.1, and between 2 and 3 for $\mu = 0.2$ *M*. In all cases the corresponding intercepts were greater than zero, indicating that the rate controlling step was electron transfer. Then, the slope is equal to the charge z on the ion transported through the double layer to the reaction site. In contrast to results for the peroxydisulfate system (17, 18), the differential plots did not always display a smooth increase in slope, and in some cases, had distinct points of inflection.

From the above results it was concluded that the mechanism of periodate reduction involves parallel reaction steps, the important step being direct reduction of the divalent species. At low ionic strength and p*H*, the reduction of a monovalent anion produced from the divalent species in a preceding protonation or ion-pairing reaction is predominant, whereas at high ionic strength and p*H* reduction of the trivalent ion is possible. The higher slope in differential plots at $\mu = 0.2$ is not conclusive evidence of participation of $H_2IO_6^{3-}$ in the electrode reaction in the potential region of the minimum. As the ionic strength increases the range of $\Delta\phi_2/\Delta(\phi_2 - \phi_m)$ decreases. All differential plots had higher slopes at the most negative values of $\Delta\phi_2/\Delta(\phi_2 - \phi_m)$ due to distortion of the current–potential curves in the region of the e.c.m. by polarographic maxima. For $\mu = 0.2$, this potential region corresponds to values of $\Delta\phi_2/\Delta(\phi_2 - \phi_m)$ between -0.28 and -0.18. In addition, an increase in the slope of the differential plots with increase in the abscissa variable similar to that found for peroxydisulfate (17, 18) is apparent in the differential plots. These two effects probably distort the differential plots at $\mu = 0.2$ sufficiently that they cannot be used to determine the charge. If reduction of the trivalent ion contributed significantly to the current in the region of the minimum, this current would not decrease with increase in p*H* since an increase in p*H* results in an increase in $H_2IO_3^{3-}$ concentration. From the intercepts obtained with integral slopes in the limit of low ϕ_m, transfer coefficients of 0.26 ± 0.01 for reduction of $H_3IO_3^{2-}$ and 0.11 ± 0.01 for reduction of the monovalent anion were determined.

The validity of the conclusions drawn from the differential plots was confirmed by analyzing the p*H* dependence of kinetic data at constant ionic strength. Neglecting any contribution of ion pairs to the total current, the rate of reaction at constant potential may be written

$$[2] \qquad v = k_1a_1 + k_2a_2 + k_3a_3$$

where a_z is the activity of the periodate species with charge $-z$ and k_z, the corresponding rate constant. When current–potential data are analyzed according to Koutecký's theory, a rate constant is calculated with the assumption that there is only one reactant at a concentration equal to the stoichiometric concentration of the depolarizer, C_s. Defining an apparent rate

Can. J. Chem. Downloaded from www.nrcresearchpress.com by 210.87.254.5 on 09/05/12
For personal use only.

Can. J. Chem. Downloaded from www.nrcresearchpress.com by 210.87.254.5 on 09/05/12
For personal use only.

constant k_{app} equal to v/C_s and assuming that the predominant species in solution are $H_3IO_6^{2-}$ and $H_2IO_6^{3-}$, eq. 2 may be rewritten

$$[3] \quad k_{app} = \frac{k_1\gamma_1 K_{b2} K_{b3}}{K_{b3}C_{OH} + C_{OH}^2} + \frac{k_2\gamma_2 K_{b3}}{K_{b3} + C_{OH}} + \frac{k_3\gamma_3 C_{OH}}{K_{b3} + C_{OH}}$$

where K_{b2} is the basicity constant for $H_3IO_6^{2-}$ and γ_z the single ion activity coefficient. The mechanism of periodate reduction was confirmed by determining the dependence of k_{app} $(K_{b3} + C_{OH})$ on C_{OH}. In order to minimize the effects of possible errors in correcting for concentration overpotential, values of k_{app} were calculated from data in the vicinity of the minimum current. For ionic strengths in the range 0.01–0.2 with K_{b3} calculated from $K_{b3}(\mu = 0) = 1.53 \times 10^{-2}$, $k_{app}(K_{b3} + C_{OH})$ decreased with increase in C_{OH}, indicating that reduction of $H_4IO_6^-$ and $H_3IO_6^{2-}$ contributed to the observed current. There was no indication of increase in $k_{app}(K_{b3} + C_{OH})$ with C_{OH}, that is, of a contribution from reduction of $H_2IO_6^{3-}$ even at the highest pH and ionic strength where this reaction would be favored. On this basis, it was concluded that k_3C_3 was negligible in the potential region of the current minimum. Furthermore, the major species diffusing to the electrode from the bulk was $H_3IO_6^{2-}$ so that the reversible current in this potential region would be the diffusion limited current for $H_3IO_6^{2-}$, its calculation being based on the diffusion coefficient D_2.

The rate constants k_1 and k_2 were determined at constant ionic strength and constant potential from a least squares fit of the equation

$$[4] \quad k_{app}(K_{b3} + C_{OH}) = \frac{k_1\gamma_1 K_{b2} K_{b3}}{C_{OH}} + k_2\gamma_2 K_{b3}$$

to the kinetic data. The equilibrium constants and activity coefficients were calculated as described above, $K_{b2}(\mu = 0)$ being set equal to 2.05×10^{-6} (9). Results at $\mu = 0.01$ and 0.02 are presented in the form of corrected Tafel plots in Fig. 5. The plots were linear in the potential range $\phi_m = -0.2$ to -0.5 V and yielded transfer coefficients of 0.26 for reduction of $H_3IO_6^{2-}$ and 0.11 for reduction of $H_4IO_6^-$. These results agree with those obtained from the differential plots and are excellent confirmation of the proposed mechanism. It was observed

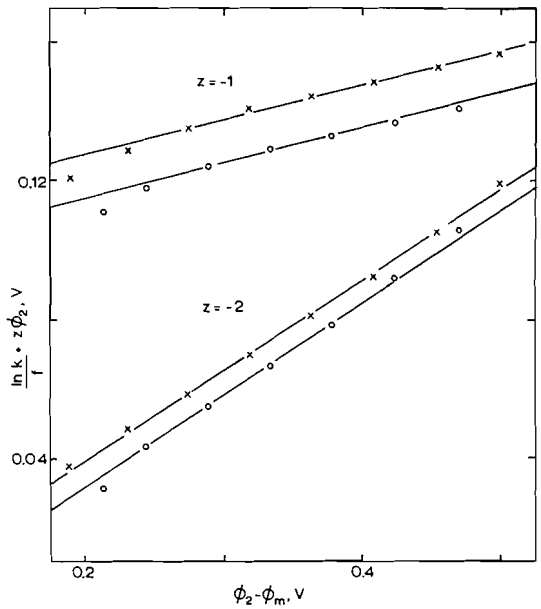

FIG. 5. Corrected Tafel plots of kinetic data for the electroreduction of $H_4IO_6^-$ (upper curves) and $H_3IO_6^{2-}$ (lower curves) at ionic strengths 0.01 (×) and 0.02 (○).

that the rate constant for reduction of the monovalent species was always greater than that for the divalent species at a given ionic strength. It is difficult to offer a qualitative explanation of this observation because the data were obtained at potentials far cathodic of the standard potentials,[2] and because the reactions are complex. However, if electron transfer is the rate controlling step in both reactions, current theories (19, 20) predict that the exchange current for the $H_3IO_6^{2-}$ would be less than that for the $H_4IO_6^-$ reaction since the work of solvent reorganization would increase with the charge on the reacting anion. It was also noted the rate constant for a given reaction decreased at constant potential with increase in ionic strength. A similar observation was made with data for the electroreduction of peroxydisulfate anion (18) where it was attributed to errors in the ϕ_2 potential as estimated by the Gouy–Chapman theory.

In the above analysis it was assumed that ion pairs such as $NaH_3IO_6^-$ and $NaH_2IO_6^{2-}$ do not participate in the reaction mechanism.

[2]The standard potentials are approximately 0.7 and 0.9 V with respect to standard hydrogen electrode for the $H_3IO_6^{2-}$ and $H_4IO_6^-$ reactions, respectively.

Can. J. Chem. Downloaded from www.nrcresearchpress.com by 210.87.254.5 on 09/05/12
For personal use only.

The concentration of $NaH_2IO_6^{2-}$ in the bulk of the solution will be proportional to the concentration of $H_2IO_6^{3-}$ and therefore will increase with pH at constant ionic strength. Thus, on the basis of the same arguments presented above for $H_2IO_6^{3-}$, it can be assumed that reduction of $NaH_2IO_6^{2-}$ does not contribute significantly to the observed current. If $NaH_3IO_6^-$ participates in the reaction scheme, then eq. 4 must be rewritten as follows

$$[5]\quad k_{app}(K_{b3} + C_{OH}) = \frac{k_1\gamma_1 K_{b2}K_{b3}}{C_{OH}} + k_2\gamma_2 K_{b3} + k_1'\gamma_2 K_{f2}K_{b3}C_M$$

where k_1' is the rate constant for reduction of $NaH_3IO_6^-$, C_M, the concentration of cations and K_{f2}, the formation constant for $NaH_3IO_6^-$. In deriving eq. 5 it is assumed that the concentration of $NaH_3IO_6^-$ is very much less than that of $H_3IO_6^{2-}$. At first sight, it would appear that, if $NaH_3IO_6^-$ contributed to the observed current, values of k_2 calculated by fitting the data to eq. 4 would increase with increase in ionic strength. However, this conclusion is invalid if the individual rate constants k_2 and k_1' are given by the Frumkin equation. From eq. 5 and Frumkin's theory, one may write

$$[6]\quad k_2 + k_1'K_{f2}C_M = k_{20}\exp(2f\phi_2) \times \exp[\beta_2 f(\phi_2 - \phi_m)] + k_{10}'K_{f2}C_M\exp(f\phi_2) \times \exp[\beta_1' f(\phi_2 - \phi_m)]$$

where k_{20} and k_{10}' are the corresponding rate constants at the e.c.m., and β_2 and β_1', the respective transfer coefficients. From the Gouy–Chapman theory, at potentials sufficiently cathodic of the e.c.m.

$$[7]\quad \exp(f\phi_2) = \frac{\theta C_M}{K_i^2(\phi_m - \phi_2)^2}$$

where K_i is the integral capacity of the inner layer and θ, a constant for a given solvent. Thus, eq. 6 may be written

$$[8]\quad k_2 + k_1'K_{f2}C_M = k_{20}\exp(2f\phi_2) \times \exp[\beta_2 f(\phi_2 - \phi_m)] + k_{10}'K_{f2}K_i^2(\phi_2 - \phi_m)^2 \times \exp(2f\phi_2)\exp[\beta_1' f(\phi_2 - \phi_m)]/\theta$$

Since K_i is independent of ionic strength in the absence of specific adsorption, corrected Tafel plots ($\ln(k_2 + k_1'K_{f2}C_M) - 2f\phi_2$ *vs.* $\phi_2 - \phi_m$) would be independent of ionic strength; however, they would not be linear if $k_1'K_{f2}C_M$ is comparable in magnitude to k_2. In the present case, since the corrected Tafel plots are linear over a wide potential range, it is concluded that $NaH_3IO_6^-$ does not participate significantly in the reaction scheme.

The reduction of periodate anion was also studied in base electrolyte solutions of KOH and CsOH. The cation effect observed was similar to that reported for other systems (5), the reaction rate increasing at constant overpotential with increase in the base electrolyte cation's atomic number. From differential plots, it was concluded that the charge on the reacting anion varied with ionic strength and pH in a manner which paralleled exactly changes in base electrolytes where the cation was Na^+. Furthermore, the slope of corrected Tafel plots in the limit that $\phi_2 - \phi_m$ approached zero depended on the nature of the cation, increasing in the order $Na^+ < K^+ < Cs^+$. Similar observations have been made with kinetic data for anion reduction in both water and formamide (21). Values of the limiting slopes for the two reactions with different base electrolyte cations are summarized in Table 2.

The observed variations in Tafel slope with nature of the double layer cation can be accounted for if the reacting species is in the inner part of the double layer in the transition state (17). In this case the limiting Tafel slope is given by

$$[9]\quad \beta_0 = \alpha - \lambda_0(\alpha - z)$$

where α is the overall transfer coefficient for a complex electrode reaction, and $(1 - \lambda_0) = x_r/x_{20}$, x_r being the distance of the charge center of the reacting particle in the transition state from the electrode and x_{20}, the thickness of the inner layer at the e.c.m. The variation with double layer cation is due to a change in inner layer thickness with the nature of the cation

TABLE 2. Limiting Tafel slope β_0 as a function of charge on the reacting anion and nature of the base electrolyte cation

	β_0 when charge on anion =	
Base electrolyte cation	−1	−2
Na^+	0.11	0.26
K^+	0.13	0.29
Cs^+	0.17	0.40

Can. J. Chem. Downloaded from www.nrcresearchpress.com by 210.87.254.5 on 09/05/12
For personal use only.

at the o.H.p., the thickness of the inner layer decreasing as the atomic number of the alkali metal cation increases. An increase in x_{20} results in a decrease in λ_0 and thus a decrease in β_0, as is observed. The validity of this explanation can be tested easily with the above results. For a given reaction it is reasonable to assume that α and x_r do not vary with variation in the double layer cation. Thus, the relative change in $\beta_0 - z = (\alpha - z)x_r/x_{20}$ will reflect the relative change in $1/x_{20}$. From the observed Tafel slopes it was found that $(\beta_0 - z)_{Na^+}$: $(\beta_0 - z)_{K^+}$: $(\beta_0 - z)_{Cs^+}$ was constant within experimental error for the two reactions and had an average value of 1:1.02:1.06. This result agrees favorably with that found with the same cations for the electroreduction of peroxydisulfate in water (1:1.03:1.06) (17).

Several explanations can be offered for the variation in Tafel slope with charge on the reaction anion. This could be attributed to a change in overall transfer coefficient α. On the other hand, if the transfer coefficients for the two reactions are the same, the variation in β_0 could be ascribed to an increase in x_r, that is, a decrease in λ_0, with increase in charge on the reacting anion. However, variation in β_0 with x_r would have to be sufficient to offset the explicit variation with z which is in the opposite direction.

Finally, there was some curvature in the corrected Tafel plots at potentials greater than $\phi_m = -0.2$ V, their slope increasing somewhat with increase in potential in the anodic direction. Although there are several theoretical explanations of curvature in corrected Tafel plots (17, 22) other than ion pairing, no conclusions can be drawn in the present case. The curvature was observed in a potential region where errors in the calculated reaction rate are liable to be large due to the difficulties involved in correcting for mass transfer.

The authors wish to thank Dr. R. K. Boyd and M. Anderson for suggesting the non-linear least squares technique used in the data analysis and for making available their computer program. The financial assistance of the National Research Council of Canada and the Department of University Affairs (Ontario) is gratefully acknowledged.

1. P. Souchay. Anal. Chim. Acta, **2**, 17 (1948).
2. R. H. Coe and L. B. Rogers. J. Am. Chem. Soc. **70**, 3276 (1948).
3. L. Jenšovský. Coll. Czech. Chem. Commun. **22**, 181 (1957).
4. F. Lamy. Mémoire de Licence, Université Libre de Bruxelles, 1961.
5. A. N. Frumkin. Z. Elektrochem. **59**, 807 (1955).
6. C. E. Crouthamel, H. V. Meek, D. S. Martin, and C. V. Banks. J. Am. Chem. Soc. **71**, 3031 (1949). C. E. Crouthamel, A. M. Hayes, and D. S. Martin. J. Am. Chem. Soc. **73**, 82 (1951).
7. J. Haladjian, R. Sabbah, and P. Bianco. J. Chim. Phys. **65**, 1751 (1968).
8. J. Aveston. J. Chem. Soc. Sec. A, 273 (1969).
9. G. J. Buist, W. C. P. Hipperson, and J. D. Lewis. J. Chem. Soc. Sec. A, 307 (1969).
10. W. R. Fawcett, J. E. Kent, and Y. C. Kuo Lee. J. Electroanal. Chem. **20**, 357 (1969).
11. A. I. Vogel. Textbook of quantitative inorganic analysis. Longmans, London. 1961. p. 239.
12. N. Tanaka, K. Ogino, and G. Sato. Bull. Chem. Soc. Japan, **39**, 366 (1966).
13. J. Koutecký. Czech. J. Phys. **2**, 50 (1953).
14. W. E. Wentworth. J. Chem. Educ. **42**, 96 (1965).
15. C. W. Davies. Ion association. Butterworths, London. 1962. p. 41.
16. R. Payne. J. Electroanal. Chem. **6**, 486 (1963).
17. W. R. Fawcett. J. Electroanal. Chem. **22**, 19 (1969).
18. W. R. Fawcett and M. D. Mackey. J. Electroanal. Chem. **27**, 219 (1970).
19. R. A. Marcus. Ann. Rev. Phys. Chem. **15**, 155 (1964).
20. V. G. Levich. Adv. Electrochem. Electrochem. Eng. **4**, 249 (1966).
21. W. R. Fawcett, D. J. Bieman, and M. D. Mackey. Coll. Czech. Chem. Commun. **36**, 503 (1971).
22. D. M. Mohilner. J. Phys. Chem. **73**, 2652 (1969).

Can. J. Chem. Downloaded from www.nrcresearchpress.com by 210.87.254.105 on 09/05/12
For personal use only.

Reactions of Tertiary Hypohalites[1]

V. BOIDO[2] AND O. E. EDWARDS
Biochemistry Laboratory, National Research Council of Canada, Ottawa, Canada

Received April 5, 1971

Metallic silver initiates short-chain homolytic decomposition of tertiary alkyl hypochlorites and hypobromites. Evidence is presented that the reaction of tertiary alcohols with silver oxide – mercuric oxide – bromine involves formation and homolytic decomposition of alkyl hypobromite followed by cyclization of γ-bromo alcohols. A convenient synthesis of tricyclo[4.3.1.0^{3,8}]decan-4-one (4-proto-adamantanone) is described.

L'argent métallique initie la décomposition homolytique en chaîne courte d'hypochlorites et d'hypobromites d'alkyles tertiaires. On présente une preuve d'après laquelle la réaction entre les alcools tertiaires et le réactif oxyde d'argent-oxyde de mercure-brome implique la formation et la décomposition homolytique d'hypobromite d'alkyle, suivie par la cyclisation des γ-bromo alcools. On décrit une voie d'accès facile à la tricyclo [4.3.1.0^{3,8}] décanone-4 (protoadamantanone-4).

Canadian Journal of Chemistry, **49**, 2664 (1971)

Recent work in these laboratories has shown that the action of metallic silver on chloramides (1) and chloramines (2) produces the corresponding nitrogen radicals. Since no hydrogen chloride or chloride ions are produced, the possibility of radical chains involving chlorine atoms (3) is precluded. In addition no metallic ions are present in solution to provide complications due to oxidation–reduction processes (4). Hence this method of generating the radicals has valuable potential for the study of the reactions of nitrogen radicals in the ground state in solution.

A comparable possibility existed for the preparation of alkoxy radicals from hypohalites (eq. 1). The formation of a number of tertiary alkoxy radicals by this method

[1] $$ROCl + Ag^0 \rightarrow RO\cdot + AgCl$$

and study of their reactions is reported in this paper.

The first cases studied were those of 2-methylpent-2-yl hypochlorite (**1**) and hypobromite. The monomeric products characterized when **1** reacted with metallic silver at room temperature in acetonitrile are shown in eq. 2.

The γ-chloro alcohol produced could be readily cyclized to 2,2-dimethyltetrahydrofuran (**2**). The ratio of hypochlorite decomposed to silver chloride formed was 4:1.

2-methylpent-2-yl hypobromite behaved similarly when treated with Tollens' silver, but the chain length was shorter.

In a reexamination of the work of Sneen and Matheny (5) we treated 2-methylpentan-2-ol with bromine, mercuric oxide, and silver oxide at 0–5 °C in pentane. The product was the corresponding hypobromite. This decomposed near room temperature into acetone, 2-pentanone, and 5-bromo-2-methylpentan-2-ol. The latter cyclized slowly at room temperature to 2,2-dimethyltetrahydrofuran (**2**). The cyclization was markedly accelerated by silver oxide.

When the bromine, oxides, and alcohol reagents were mixed rapidly at room temperature in an attempt to duplicate the conditions of Sneen and Matheny, the temperature rose and reaction was complete in 10 min. No hypobromite was left, and 2,2-dimethyltetrahydrofuran had been formed. In addition acetone was shown to be present, hence the overall reaction was the same as thermal decomposition of the hypobromite followed by silver oxide induced cyclization of the γ-bromo alcohol.

As an example of a monocyclic tertiary hypohalite, 1-methylcyclopent-1-yl hypochlorite (**3**) was chosen for study. Cairns and Englund had shown (6) that this decomposed thermally to give a high yield of 6-chloropentan-2-one (**4**). Metallic silver converted **3** into **4** rapidly at room temperature. The ratio of hypochlorite converted to silver chloride produced was 9.7:1.

[1]NRCC No. 12007.
Presented in part at the Annual Meeting of the Chemical Institute of Canada, Halifax, Nova Scotia, May 31–June 2, 1971.
[2]Postdoctoral Fellow of the Consiglio Nazionale delle Ricerche (Rome), 1969–1970.

Can. J. Chem. Downloaded from www.nrcresearchpress.com by 210.87.254.105 on 09/05/12
For personal use only.

[2] 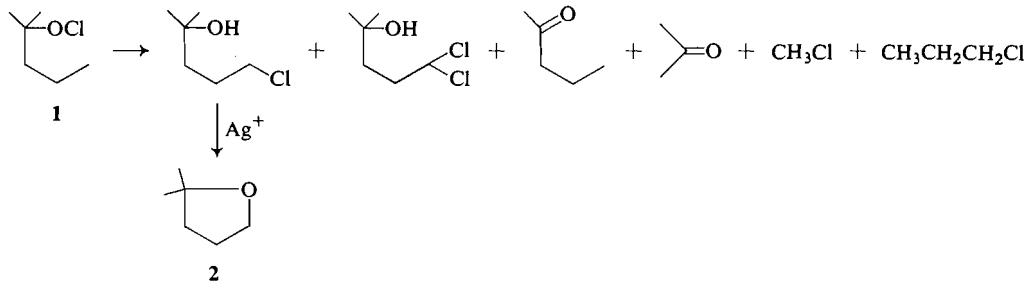

1 2

The next examples studied were 1-methyl-1-phenylethyl hypochlorite (**5**) and 1,1-diphenylethyl hypochlorite (**6**). Somewhat to our surprise

3 4

5 gave nearly exclusively fission to acetophenone (eq. 3). The ratio of ROCl/silver chloride produced was 2.4. In contrast 6 gave predominantly

[3] 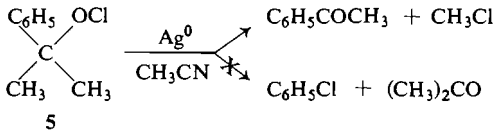

5

1,1-diphenylethanol, 22% of acetophenone, but no benzophenone (eq. 4). The ROCl/AgCl ratio was 1.7.

[4] 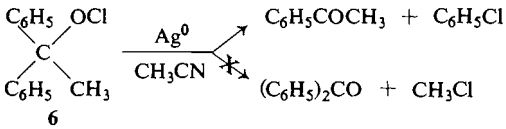

6

Our attention was attracted to recent syntheses (7) of tricyclo[4.3.1.$0^{3,8}$]decane (protoadamantane) and its derivatives. It occurred to us that 1-adamantyl hypohalites (**7**) might be converted under homolytic conditions into the corresponding 3-*endo*halobicyclo[3.3.1]nonan-7-ones (**8**), which could be cyclized to 4-protoadamantanone (**9**).

Treatment of 1-adamantyl hypochlorite in acetonitrile with Tollens' silver led to rapid reaction to give a mixture of 1-adamantanol, chlorinated adamantanols, the bicyclic ketone **8** (X = Cl), and dichloro ketones. Under the conditions chosen 4 mol of hypochlorite were decomposed for each mol of silver chloride produced. The yield of chloro ketones (calculated as **8**, X = Cl) was estimated to be 40.5%. In comparable experiments at 0° 1-adamantyl hypobromite gave an estimated 33% of bromo ketones (calculated as **8**, X = Br).

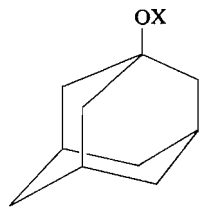

7

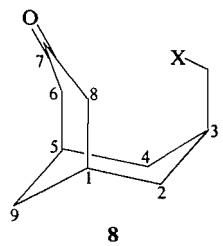

8

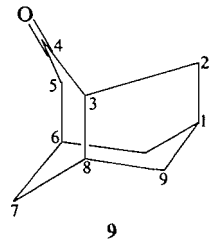

9

The thermal decomposition of 1-adamantyl hypochlorite was very slow in refluxing carbon tetrachloride or chlorobenzene at 110°. However it decomposed rapidly in refluxing acetonitrile. The estimated yield of chloro ketones produced was 64%. The hypobromite decomposed quite rapidly when heated in all three solvents giving approximately 63% of bromo ketones rich in **8** (X = Br).

Finally photolysis of 1-adamantyl hypochlorite in carbon tetrachloride gave a lower yield of **8** (X = Cl) than the silver initiated reaction hence was not studied in detail.

The chloro or bromo ketones **8** could be cyclized at room temperature using sodium hydride in tetrahydrofuran to give good yields (*ca.* 37% based on hypohalite used) of 4-protoadamantanone (**9**). While this work was in progress Black and Gill (8) reported the preparation of **8** (X = I) from "1-adamantyl hypoiodite",

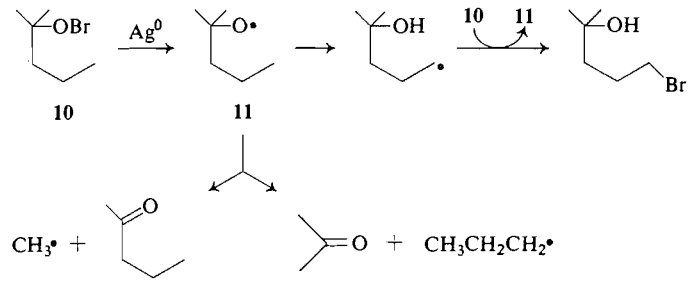

[5]

and its conversion into protoadamantanone in an overall yield of 34%. Lunn (9) has also prepared and characterized the bicyclic iodoketone (**8**, X = I), and described its cyclization into 4-protoadamantanone (overall yield 32%). A synthesis of **9** by deamination of 2-aminoadamantan-1-ol has recently been reported by Lenoir and Schleyer (10).

Discussion

The products from the silver initiated decomposition of 2-methylpent-2-yl hypochlorite and hypobromite are exactly what would be expected for a homolytic chain reaction (eq. 5). The fact that the Sneen and Matheny (5) conditions produce hypobromites which are thermolabile, and that the products from 2-methylpent-2-yl hypobromite fit the above homolytic pattern, suggest that their postulate of reaction involving cationic oxygen is in error. It appears that the unique role of the silver oxide is to cyclize the γ-bromo alcohol. This conclusion is in harmony with those of Akhtar and co-workers (11) and Smolinsky and Feuer (12).

The cyclization of primary and secondary alcohols using the bromine – silver oxide or iodine – mercuric oxide combination recently described by Mihailovic and co-workers (13) is not inconsistent with homolytic decomposition of intermediate hypohalites. Finally, the claim by Sommer and co-workers (14) that their observed solvent effects support a cationic oxygen mechanism for the silver oxide – bromine – secondary alcohol reactions is not convincing. The addition of tetrahydrofurans, or the use of ethers as solvents was shown to eliminate an induction period and increase the yield of cyclic ethers at the expense of ketonic products. We suggest that this effect is most simply explained as initiation of homolytic decomposition of the alkyl hypobromites by peroxide in the ethers (see ref. 1).

The direction of fission of 1-methyl-1-phenylethoxy radical suggests that the transition state for the decomposition resembles the products, and that the difference in energy of formation of phenyl or methyl radicals is more than offset by development of acetophenone resonance[3] (eq. 6).

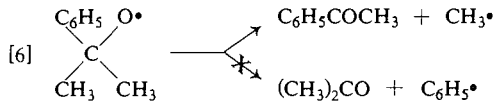

[6]

In the case of 1,1-diphenylethoxy radical however, the resonance energy gain in producing benzophenone is probably slightly more than that for formation of acetophenone.[4] Hence the nearly exclusive formation of the latter and phenyl radicals (eq. 7) suggests that these radicals are at least 5 kcal/mol more stable than methyl radicals.

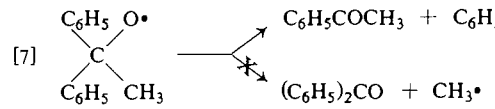

[7]

In view of the compactness of the adamantane skeleton, it was an open question whether or not the 1-adamantoxy radical would undergo fission to the keto alkyl radical (eq. 8). However, the

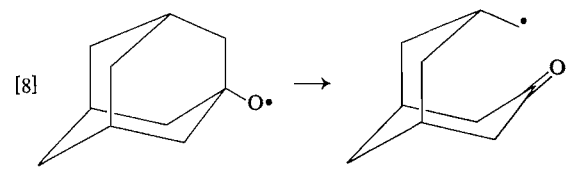

[8]

free energy of activation for the fission must be low since the reaction competes favorably with

[3]However there is no clear correlation with the accepted value for acetophenone resonance (only 1 kcal/mol more than benzene) (15).

[4]The resonance contribution of the benzophenone carbonyl is estimated to be zero (15) but this seems improbable.

Can. J. Chem. Downloaded from www.nrcresearchpress.com by 210.87.254.105 on 09/05/12
For personal use only.

Can. J. Chem. Downloaded from www.nrcresearchpress.com by 210.87.254.105 on 09/05/12
For personal use only.

the abstraction of hydrogen from solvent and other molecules.

Black and Gill (8) considered the thermal decomposition of 1-adamantyl hypoiodite[5] and the other hypohalites studied to be homolytic. Our results with metallic silver prove that the adamantoxy radical does give the bicyclic ketone. However, the solvent effect on the thermal decomposition of the hypochlorite is only consistent with charge development in the transition state, which probably resembles **12**. Even in

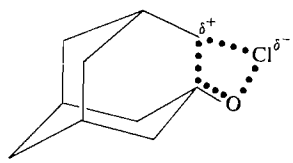

12

acetonitrile, however, considerable adamantanol and chlorinated adamantanol were produced, hence a simultaneous homolytic fission of the hypochlorite was taking place. In view of the apparent absence of a solvent effect, the thermal decomposition of the hypobromite appears to be more homolytic in character. However the yield of bromoketones (*ca.* 63%), in contrast to the 33% yield for the pure homolytic process (silver initiated), suggests that a bond reorganization process is the main reaction path rather than reaction via adamantoxy radicals.

Experimental

The acetonitrile used was spectroscopic quality. The metallic silver used was a light brown solid produced by the action of formaldehyde on silver ammonium ion solution (Tollens' reagent), then thorough washing with water. It was prepared fresh for each experiment.

The g.l.c. was done on a 1/4″ × 6′ column of silicone rubber (10% SE30 on acid-washed silanized chromosorb W). Alumina was Woelm neutral grade, with activities according to Brockmann and Schodder (16).

Silver chloride was estimated by extraction into aqueous ammonia, filtration, reprecipitation by acid, filtration, and drying at 100°. Silver bromide was estimated by dissolving unreacted silver in nitric acid, filtration, washing, and drying. Yields and ratios are corrected for aliquots removed for titration.

Action of Silver on 2-Methyl-pent-2-yl Hypochlorite

Glacial acetic acid (10 ml) was added with stirring to an ice-cold mixture of 2.38 g of 2-methylpentan-2-ol and 150 ml of strongly alkaline 8% sodium hypochlorite solution. After 2 h stirring at 5 °C, the mixture was extracted with pentane. The pentane solution was washed with sodium carbonate solution then dried over sodium sulfate. The solvent was removed below room temperature on a rotating evaporator leaving 2.48 g of yellow oil. Its i.r. spectrum in methylene chloride showed the presence of a small amount of parent alcohol and a ketone.

The oil was dissolved in 22.5 ml of acetonitrile and 2.5 ml of water (final volume near 27 ml). Titration of 1 ml showed the presence of 1.57 g of hypochlorite. The remaining solution was purged with a stream of nitrogen. Tollens' silver from 2.6 g of silver nitrate was then added in portions over 20 min while stirring under nitrogen. After a total reaction time of 30 min only 1% of the hypochlorite remained. This was destroyed by addition of more silver, then the suspension was filtered. The precipitate was washed with acetonitrile.

The combined filtrates were distilled through a short Vigreux column giving (*a*) 2 ml of fore-run and (*b*) 20 ml b.p. near 80° (bath up to 120°). A residue (*c*) of 1.3 g remained.

The fore-run (*a*) and a methanol solution of trimethylamine was heated in a sealed tube at 100° for 5 h. The solvent was then distilled leaving 87 mg of crystalline salt. Its n.m.r. spectrum in D_2O had signals near δ 1.0 (triplet, J = 7 Hz), 1.2–2.1 (broad multiplet), 3.1 (sharp singlet), and 3.3 (triplet, J = 7) in intensity ratios of 3:2:11:2. This corresponds to a mixture containing 85% of trimethyl propylammonium iodide and 15% of tetramethylammonium iodide.

The main distillate (*b*) was partially dried using sodium sulfate. To this was added 1 g of *p*-nitrophenylhydrazine and the mixture held near 75° for 1 h by which time no carbonyl absorption was left in its i.r. spectrum. The solvent was removed under reduced pressure and the residue taken up in methylene chloride. The solution was washed twice with 2 *N* sulfuric acid, then with sodium carbonate solution.

The distillate from quaternary salt formation of fore-run (*a*) was treated in the same way. The combined hydrazone weighed 824 mg. Its n.m.r. spectrum contained peaks at δ 1.18 (triplet, J = 7 Hz) and at 1.96 and 2.10 corresponding to the *p*-nitrophenylhydrazones of 2-pentanone (1.18, 1.96, and 2.10) and acetone (1.93 and 2.08).

The intensities corresponded to 55% acetone derivative and 45% 2-pentanone, with a total ketone yield of 47%.

The residue (*c*) was dissolved in acetonitrile and stirred at room temperature with silver oxide from 657 mg of silver nitrate for 3 h. The suspension was filtered, the filtrate diluted with an equal volume of water, and extracted with pentane. The dried pentane solution was concentrated to small volume using a Vigreux still head. The residue gave n.m.r. signals at δ 1.24 (sharp) and 3.88 (triplet, J = 7 Hz) corresponding to the signals from authentic 2,2-dimethyltetrahydrofuran. The i.r. spectrum of the residue had seven peaks in the fingerprint region identical with those of 2,2-dimethyltetrahydrofuran, and the mixture gave a g.l.c. peak at the same retention time as authentic ether.

In another run, the fraction corresponding to (*c*) was distilled over a short path under 10 mm pressure. Distillate collected at a bath temperature up to 70° was a bad mixture but that collected at 70–100° contained approximately 50% of 5-chloro-2-methylpentan-2-ol as indicated

[5]Lunn (9) points out that the hypoiodite may not be involved in the cleavage by lead tetraacetate – iodine reagent.

Can. J. Chem. Downloaded from www.nrcresearchpress.com by 210.87.254.105 on 09/05/12
For personal use only.

by n.m.r. signals at δ 0.74 (sharp) and 4.15 (triplet, J = 6.5 Hz).

Anal. Calcd. for $C_6H_{13}ClO$: Cl, 38.53. Found: 40.76.

This fraction and the residue gave an n.m.r. triplet at δ 5.85 (J = 6 Hz) corresponding to the presence of 5,5-dichloro-2-methylpentan-2-ol.

The silver chloride produced weighed 307 mg. Hence the ROCl/AgCl ratio was 4.

Action of Silver on 2-Methylpent-2-yl Hypobromite

Hypobromous acid was prepared from 3.99 g of bromine in 120 ml of water at 0° using 9.3 g of silver sulfate in the dark. The solution was decanted from silver bromide and added to a solution of 2.3 g (22.5 mmol) of 2-methylpentan-2-ol in 50 ml of trichlorofluoromethane. After 15 min vigorous mixing at 0° the organic layer was separated, washed with ice-water, and dried over sodium sulfate. The solvent was removed at 0° on a rotating evaporator and the residue dissolved in 30 ml of acetonitrile. Iodimetric titration showed the presence of 15.5 mmol of hypobromite.

Tollens' silver from 4.29 g of silver nitrate was added under nitrogen to a solution of the hypobromite (15.2 mmol) in 30 ml of acetonitrile. After 0.5 h stirring at 0° under nitrogen, all the hypobromite had reacted.

The solids were removed by filtration then the bulk of the acetonitrile removed by distillation (oil bath). The residue was dissolved in ether, the ether solution washed four times with water, dried, and distilled. The brown mobile oil had an n.m.r. spectrum corresponding to 5-bromo-2-methylpentan-2-ol (221 mg, 1.22 mmol). The characteristic signals were a singlet at δ 1.31 and a triplet (J = 6.5 Hz) at δ 3.63 in the ratio of 3:1.

To the distilled acetonitrile was added 1.5 g of *p*-nitrophenylhydrazine and a few drops of acetic acid. The mixture was refluxed for 1 h, then the solvent removed under reduced pressure. The residue was taken up in methylene chloride. The solution was washed three times with 2 *N* sulfuric acid, with sodium carbonate solution, then with water, dried, and distilled. A crystalline residue (1.1 g) remained. Examination of its n.m.r. spectrum showed it to consist of 63% *p*-nitrophenylhydrazone of 2-pentanone (3.14 mmol) (δ 1.18 (triplet J = 7 Hz), 1.96, and 2.1) and 37% acetone derivative (δ 1.93 and 2.08).

The amount of silver bromide produced was 1.79 g (9.5 mmol) *i.e.* ROBr/AgBr = 1.6.

Thermal Decomposition of 2-Methylpent-2-yl Hypobromite

(1) In an attempt to duplicate the conditions of Sneen and Matheny (5) a suspension was prepared of 1.6 g of 2-methyl-2-pentanol, 5.10 g of yellow mercuric oxide, and 2.37 g of silver oxide in 30 ml of dry pentane. To the stirred mixture in dim light, 1.0 g of bromine was added. The temperature of the mixture rose to 35° due to heat of reaction. After 10 mins stirring the mixture was filtered and the salts washed with pentane. The bulk of the solvent was removed by distillation. Both the distillate (*A*) and residue (*B*) contained carbonyl compounds (i.r.). The carbonyl compound in the distillate (*A*) was converted to its *p*-nitrophenylhydrazone by addition of 1.4 g of *p*-nitrophenylhydrazine, 20 ml of acetonitrile, 20 ml of ethanol, and 4 drops of acetic acid, then refluxing the solution for 1 h. The solvents were removed and the derivative purified as described in the silver catalyzed reaction. It proved to be 325 mg of quite pure acetone *p*-nitrophenylhydrazone (two 3H singlets at δ 1.98 and 2.13).

The residue (*B*) gave an i.r. band at 1050 cm^{-1} (C—O—C) and had n.m.r. signals characteristic of 2,2-dimethyltetrahydrofuran (δ 1.25 (singlet), 3.92 (triplet, J = 6.5 Hz)).

(2) The above reaction was repeated, except that the bromine was added slowly while the temperature was kept below 5 °C. After 10 min the solution was filtered. The filtrate did not show any —OH or C=O stretching bands in the i.r., nor the characteristic C—O—C band, hence the product was apparently 2-methylpent-2-yl hypobromite.

The solution was then refluxed in the dark until colorless (15 min), at which time no hypobromite remained (iodimetry). The i.r. spectrum now showed bands at *ca.* 3200 (OH), 1720, and a very weak band at 1056 cm^{-1}. The solution was divided into two equal parts.

From one part, the solvent was removed at 0° under 20 mm pressure. The residue contained 5-bromo-2-methylpentan-2-ol as indicated by n.m.r. signals at δ 3.53 (triplet, J = 6.5 Hz) and 1.28 (singlet) in the ratio 1:3 and a pair of peaks with equal intensity at *m/e* 162 and 164 (M^+-H_2O) in its mass spectrum. The presence of 5,5-dibromo-2-methylpentan-2-ol was indicated by an n.m.r. triplet at δ 5.90 (J = 6 Hz).

To the other part was added 1.2 g of silver oxide and the mixture stirred at room temperature for 10 min. The i.r. spectrum of the solution now had bands at *ca.* 3450 cm^{-1} (weaker) while one at 1050 cm^{-1} (C—O—C) had become very strong. Stirring for 4 h effected no further marked change in the spectrum.

After filtration, the solution was passed through a column of 14 g of alumina, activity IV. The substance eluted with pentane was very volatile, some passed with the pentane when this was distilled through a short Vigreux column. The residue (312 mg) which still contained a little pentane had spectra characteristic of 2,2-dimethyltetrahydrofuran (ν_{max}(pentane) 1050 cm^{-1}; n.m.r signals at δ 1.25 (singlet) and 3.9 (triplet, J = 7 Hz) in the ratio 3:1).

Action of Silver on 1-Methylcyclopentyl Hypochlorite

A solution of 2.5 g (25 mmol) of 1-methylcyclopentanol and 5.7 ml of acetic acid in 10 ml of acetonitrile was added slowly with stirring in the dark to 50 ml of ice-cold 11.6% aqueous sodium hypochlorite solution. After 45 min stirring at 0°, the mixture was diluted with cold water and extracted twice with pentane. The pentane solution was washed with 3 20 ml portions of 3% sodium bicarbonate solution then with water. The dried pentane solution contained 20.2 mmol of hypochlorite. Its i.r. spectrum showed the absence of alcohol, but a weak carbonyl band was present at 1720 cm^{-1}.

Moist Tollens' silver, freshly prepared from 3.98 g of silver nitrate, was added over 20 min under dry nitrogen in semi-darkness to a stirred solution of 14.2 mmol of the hypochlorite in 40 ml of acetonitrile. The hypochlorite was completely destroyed in less than 0.5 h (a blank run without silver showed no reaction under these conditions).

The solution was filtered. The filtrate was reduced to small volume under reduced pressure, then the residual liquid distilled over a short path under 15 mm pressure. The first fraction of 0.21 g (bath up to 70°) was a mixture of 1-methylcyclopentanol and 6-chlorohexan-2-one in the

Can. J. Chem. Downloaded from www.nrcresearchpress.com by 210.87.254.105 on 09/05/12
For personal use only.

ratio 1:5 as estimated by g.l.c. (105°; retention time 105 and 375 s, respectively). The second fraction of 1.518 g was nearly pure 6-chlorohexan-2-one (1% 1-methylcyclopentanol). The n.m.r. spectrum of the ketone had peaks at δ 1.78 (m, 4H), 2.18 (s, 3H), 2.53 (t, 2H, J = 6.5 Hz), 3.60 (t, 2H, J = 6.5 Hz). It was further characterized as its 2,4-dinitrophenylhydrazone, m.p. 80–81°, (lit. (17) m.p. 81.5°). The yield of the chloro ketone was estimated to be 1.77 g (13.2 mmol, 93%).

The silver chloride produced in the reaction weighed 0.21 g (1.47 mmol). Hence the ratio of ROCl/AgCl was approximately 9.7.

Action of Silver on 2-Phenylprop-2-yl Hypochlorite

A solution of 2.04 g of 2-phenylpropan-2-ol in 5 ml of acetonitrile was added to 50 ml of ice-cold sodium hypochlorite solution (chlorine bubbled into a solution of 9 g of sodium hydroxide in 50 ml of water until the pH reached 5). The mixture was stirred in an ice bath for 3 h then extracted with pentane. The dried pentane solution was concentrated under reduced pressure leaving a faintly yellow oil. This was dissolved in acetonitrile to make 25 ml of solution containing 13.4 mmol of hypochlorite and a trace of ketone (ν_{max} 1695 cm^{-1}).

Tollens' silver from 907 mg of silver nitrate was added to the stirred hypochlorite solution, maintained at 0–5° under nitrogen. After 0.25 h 32% of the hypochlorite had reacted; after 1 h, 53%; 2 h, 68%. The reaction was pushed to completion by addition of fresh silver. The remaining 21.5 ml of solution was filtered. To the filtrate was added 2.1 g of *p*-nitrophenylhydrazine. The mixture was maintained at *ca.* 80° for 1 h then the bulk of the solvent was removed under reduced pressure. The residue was taken up in methylene chloride and excess *p*-nitrophenylhydrazine removed by washing with dilute sulfuric acid, then with water. The methylene chloride was removed, and the residue boiled with hexane. The crystals were collected by filtration, giving 1.58 g, m.p. 165–175°. After two recrystallizations it had m.p. 181°. Its mixed m.p. with acetophenone *p*-nitrophenylhydrazone (184°) was 182° and their n.m.r. spectra were identical. There was no sign of acetone in the original reaction mixture (i.r.) or the *p*-nitrophenylhydrazone.

The hexane extract from the *p*-nitrophenylhydrazone contained 695 mg of oil whose n.m.r. and i.r. spectra showed it to be mainly 2-phenylpropan-2-ol.

The amount of silver chloride produced was 727 mg corresponding to an ROCl/AgCl ratio of approximately 2.4.

In a parallel run (1.2 g hypochlorite in 30 ml of acetonitrile) in which the weight ratio of hypochlorite to silver was 3.4 the reaction was very fast; 68% reacted in 0.5 h, 86% in 1 h. The chain length produced, as measured by silver chloride, was 4.5. Hence the reaction is sensitive, probably to traces of oxygen.

A blank run showed that the hypochlorite was only partially converted to ketone when left at 0° for 64 h.

Action of Silver on 1,1-Diphenylethyl Hypochlorite

A solution of 2.48 g of 1,1-diphenylethanol (12.5 mmol) in 10 ml of acetonitrile containing 2.4 ml of acetic acid was added dropwise to a stirred ice-cold 11% sodium hypochlorite solution (strongly basic) in diffuse light. The mixture was stirred at 0–5 °C for 45 min. It was then diluted with water and the product extracted into carbon tetrachloride. This was washed twice with 3% sodium bicarbonate solution. The dried solution ($MgSO_4$) had no OH stretching absorption and contained 12.5 mmol of hypochlorite (iodimetry). The solvent was removed under reduced pressure at 0–5 °C and the crystalline residue dissolved in 40 ml of acetonitrile.

Tollens' silver (acetonitrile washed) from 2.85 g of silver nitrate (16.8 mmol) was added in portions during 20 min to the stirred ice-cold solution of the hypochlorite under nitrogen in semi-darkness. The extent of reaction was: 0.5 h, 74%; 1 h, 78%; 2 h, 84%; 3.5 h, 86%. The reaction was pushed to completion by adding silver from 0.47 ml of silver nitrate, then the suspension was filtered. The g.l.c. examination of the filtrate showed the major products to be 1,1-diphenylethanol, acetophenone, and chlorobenzene. The solvent was removed under reduced pressure at 5 °C. The crystalline solid was recovered by filtration using pentane for washing. It proved to be 508 mg of 1,1-diphenylethanol. The pentane filtrate was passed through a column of 50 g of alumina, activity II. Forty-five milliliters of benzene eluate left an oil on evaporation at 0°. The g.l.c. showed the presence of chlorobenzene, acetophenone, and 1,1-diphenylethanol. Its n.m.r. spectrum had signals corresponding to the methyl groups of acetophenone (δ 2.5) and 1,1-diphenylethanol (δ 1.92) and to the presence of a trace of ω-chloroacetophenone (δ 4.6).

A second 45 ml of benzene eluted 0.417 g of 1,1-diphenylethanol, and 100 ml of benzene containing 5% of methanol eluted a further 0.55 of this carbinol.

The oil from the first benzene eluate was dissolved in 20 ml of ethanol containing 1 g of *p*-nitrophenylhydrazine. The solution was refluxed for 45 min then the solvent removed under reduced pressure. The residue was dissolved in methylene chloride. The solution was washed twice with 2 *N* sulfuric acid then four times with water. The dried solution was distilled, and the crystalline residue extracted repeatedly with boiling hexane. The insoluble material had m.p. 178–181° and mixed m.p. with acetophenone *p*-nitrophenylhydrazone 180–184°; yield 0.52 g (2.04 mmol). The hexane extracts yielded 0.138 g of 1,1-diphenylethanol.

The yield of once-recrystallized 1,1-diphenylethanol, m.p. 80–81°, was 1.29 g (6.5 mmol).

The amount of silver chloride produced in the reaction was 1.062 g (7.4 mmol). The ROCl/AgCl ratio was 1.7.

The yield of acetophenone, corrected for aliquots removed, was 22%. No benzophenone was detected among the products.

1-Adamantyl Hypobromite

Hypobromous acid was prepared from 1.05 g of bromine and 2.18 g of silver sulfate in 30 ml of water at 0–5 °C in semi-darkness. A solution of 765 mg of 1-adamantanol in 10 ml of methylene chloride was added and the mixture stirred in an ice bath. More solid silver sulfate was added at intervals during 1 h of stirring. The light brown organic layer was separated and the aqueous layer washed with more methylene chloride. Evaporation of the methylene chloride under reduced pressure left a pale brown crystalline residue. Iodimetry showed this to contain 4.2×10^{-3} mol of hypobromite (84%).

Action of Silver on 1-Adamantyl Hypobromite

A solution of 4.2×10^{-3} mol of hypobromite in 15 ml

Can. J. Chem. Downloaded from www.nrcresearchpress.com by 210.87.254.105 on 09/05/12
For personal use only.

of acetonitrile was prepared. Its i.r. spectrum showed that only a trace of carbonyl compounds were present.

The solution was purged with nitrogen, then Tollens' silver from 1.25 g of silver nitrate (washed with acetonitrile) was added. After 0.5 h stirring at 0° under nitrogen, 98.5% of the hypobromite had reacted. After a further half hour of stirring the mixture was filtered and the solid washed with acetonitrile. The filtrate was taken to near dryness below room temperature under reduced pressure. The residue was dissolved in methylene chloride, then the solution washed with water, dried, and the solvent evaporated. The residue was adsorbed from benzene onto 17.5 g of silica gel. Benzene – methylene chloride mixture and methylene chloride eluted ketonic material and finally mixtures of ketone and alcohol. The total yield of ketone produced was estimated to be 33% (monobromo ketone). This was cyclized using excess sodium hydride in tetrahydrofuran at room temperature during 18 h. The product was passed in pentane solution through a column of 1 g of alumina, activity II. The pentane eluate was sublimed at temperatures up to 190°, 1 atm giving 136 mg of fairly pure protoadamantanone (**9**). Its identity was confirmed by t.l.c. and i.r. spectrum in comparison with authentic material. The precipitate contained 100 mg of nearly pure 1-adamantanol which was removed by a chloroform wash.

The silver bromide produced weighed 413 mg. The ratio of hypobromite reacted to silver bromide was 1.9.

Thermal Decomposition of 1-Adamantyl Hypobromite

A solution of 3.0 mmol of the hypobromite in 25 ml of acetonitrile was refluxed in semi-darkness under nitrogen. Decomposition was complete in 0.5 h. The solvent was removed under reduced pressure, leaving a residue of 940 mg whose i.r. spectrum showed the presence of hydroxyl and carbonyl groups. It was extracted twice with hot pentane. The pentane insoluble fraction (180 mg) contained 20.4% bromine, and appeared to be a mixture of brominated adamantanols.

The pentane-soluble products were adsorbed from methylene chloride onto 14 g of silica gel. Eluates (15 ml each) 1 and 2 gave 127 mg whose n.m.r. and i.r. spectrum showed it to be 3-bromomethylbicyclo[3.3.1]nonan-7-one (**8**, X = Br) and a component with ν_{max} 1730 cm^{-1} and extra n.m.r. signals at δ 4.18 (doublet) and 4.9 (doublet). Eluates 3–10 (325 mg) were nearly pure **8** (X = Br). Eluates 11–15 (methylene chloride – ether) contained some ketone but were rich in alcohols. Their bromine content was only 6.6%. The total yield of ketonic product (calculated as **8** (X = Br)) was 63% based on original hypobromite.

After removal of an analytic sample, fractions 3–10 were cyclized using sodium hydride (see preparation of protoadamantanone), giving 180 mg of sublimed crystalline product. By g.l.c. this contained 90% of protoadamantanone. The total possible yield of protoadamantanone was estimated to be 40%.

The decomposition of 1-adamantyl hypobromite in refluxing carbon tetrachloride was fast (0.5 h). The ratio of carbonyl absorption to CH stretching absorption in the i.r. spectrum of the total product showed the yield of **8** to be comparable to that in the thermal decomposition in acetonitrile.

*3-Bromomethylbicyclo[3.3.1]nonan-7-one(**8**, X = Br)*

After recrystallization from pentane this formed plates, m.p. 62–63°. It had $\nu_{max}(CHCl_3)$ 1705 cm^{-1} and n.m.r. signals at δ 3.23 (2H, doublet, J = 6.5 Hz), 2.75 to 1.5 (11H, multiplet), and 0.98 (2H, broad signal).

Anal. Calcd. for $C_{10}H_{15}BrO$: C, 51.97; H, 6.54; Br, 34.57. Found: C, 51.87; H, 6.47; Br, 34.90.

Tricyclo[4.3.1.$0^{3,8}$]decan-4-one (4-Protoadamantanone)

To a solution of 88 mg of 3-bromomethylbicyclo[3.3.1]-nonan-7-one in 5 ml of anhydrous tetrahydrofuran was added 50 mg of a 50% dispersion of sodium hydride in oil. The mixture was stirred overnight while protected from moisture and carbon dioxide. The suspension was filtered through Celite, and the solid washed with pentane. The residue after removal of the pentane was sublimed at 35–40° under 10^{-2} mm. The 53 mg of crystalline sublimate had m.p. 205–208° (sealed capillary). After removal of two minor impurities by t.l.c., recrystallization from pentane, and resublimation, it had m.p. 208–210°. It gave a parent ion with *m/e* 150, $\nu_{max}(CHCl_3)$ 1705^{-1} and an n.m.r. signal at δ 2.72 (approximately 2H) probably arising from the proton on C-3 and the equatorial proton on C-5.

Anal. Calcd. for $C_{10}H_{14}O$: C, 79.95; H. 9.39. Found: C, 79.78; H, 9.22.

1-Adamantyl Hypochlorite

1-Adamantanol (810 mg, 5.33 mmol) was dissolved in 10 ml of acetonitrile and 4 ml of acetic acid. The solution was added dropwise to 40 ml of a stirred ice-cold 11% solution of sodium hypochlorite in water (strongly alkaline) over the course of 15 min. The mixture was stirred vigorously at 0° in diffuse light for 1 h. The product was extracted into pentane and the pentane solution washed with water then twice with 3% sodium bicarbonate solution. After drying the pentane was evaporated, leaving a white solid. This was dissolved in 20 ml of acetonitrile. Its i.r. spectrum showed the presence of only a trace of carbonyl compound, but the carbonyl peak grew steadily in intensity in the i.r. beam. Iodimetry showed the presence of 4.84×10^{-3} mol (91%) of hypochlorite.

Action of Silver on 1-Adamantyl Hypochlorite

A solution of 4.8 mmol of the hypochlorite in 20 ml of acetonitrile was purged with nitrogen. Tollens' silver from 1.5 g of silver nitrate (washed with acetonitrile) was added and the mixture stirred under nitrogen in an ice bath. After 0.5 h no hypochlorite was left. The solids were removed by filtration and the solvent removed nearly completely under reduced pressure below room temperature. The residue was taken up in methylene chloride then the solution washed with water, dried, and distilled. The products were adsorbed from benzene onto 25 g of silica gel. Benzene – methylene chloride (1:1) eluted 329 mg of colorless oil which was the chloroketone **8** (X = Cl) contaminated with dichloroketone.

Anal. Calcd. for $C_{10}H_{15}ClO$: Cl, 18.99. Found: Cl, 23.4.

Methylene chloride eluted 44 mg of the chloroketone containing some alcohols. The total yield of chloroketones (calculated as **8**) was estimated to be 1.86 mmol (40.5%). Methanol in chloroform eluted 521 mg of crystalline alcohols. The chlorine content (12.7%) cor-

Can. J. Chem. Downloaded from www.nrcresearchpress.com by 210.87.254.105 on 09/05/12
For personal use only.

responded to 67% of monochloroadamantanol in the mixture.

The yield of silver chloride (1.14 mmol) corresponded to a hypochlorite to silver chloride ratio of 4.

Thermal Decomposition of 1-Adamantyl Hypochlorite

(a) In Acetonitrile

A solution containing 3.36 mmol of the hypochlorite and 250 mg of adamantanol in 25 ml of acetonitrile was refluxed in dim light under nitrogen. After 0.5 h, 70% had reacted; 1.5 h, 83%; 2 h, 87%. The reaction was complete in 4 h. The solvent was removed under reduced pressure and the residue adsorbed from benzene onto 16 g of silica gel. The benzene eluates (50 ml) gave 66 mg of oil with $\nu_{max}(CH_2Cl_2)$ 1730 cm^{-1} and containing 37.3% chlorine. Methylene chloride eluted 381 mg of oil with ν_{max} 1705 cm^{-1} and an n.m.r. spectrum coincident with that of 3-chloromethylbicyclo[3.3.1]nonan-7-one. Further methylene chloride eluates (61 mg) were partly crystalline and contained considerable alcohol as well as the chloro ketone. The monochloroketone yield was estimated to be 64% based on starting hypochlorite. Methanol eluted 320 mg of crystalline alcohols containing 16.1% chlorine.

(b) In Carbon Tetrachloride

A solution of 3.9 mmol of the hypochlorite in 40 ml of carbon tetrachloride was refluxed under nitrogen. Decomposition was complete in 24 h.

(c) In Chlorobenzene

A solution of 2.94 mmol of the hypochlorite in 25 ml of chlorobenzene was heated at 110° under nitrogen. Decomposition was complete in 20 h. The products from both (*b*) and (*c*) after removal of solvents under reduced pressure gave i.r. spectra in methylene chloride with ν_{max}3600, 3420, and 1715 cm^{-1}. The relative intensity of the peaks was comparable to that for the crude product from the silver-initiated decomposition of the hypochlorite.

Photochemical Decomposition of 1-Adamantyl Hypochlorite

Nitrogen was bubbled for a few minutes through a solution of 2.3 mmol of the hypochlorite in 35 ml of carbon tetrachloride at 0 °C. The solution was then irradiated with light from a 100 W Hanovia high pressure mercury lamp filtered by a Corax sleeve. Decomposition was complete in less than 0.5 h. The solution now had i.r. absorption at 3600, 3370, and 1725 cm^{-1}. The intensity of the carbonyl absorption relative to the CH stretching absorption was less than that in the thermal or silver-initiated reactions in acetonitrile.

Comparable results were obtained when the hypochlorite was photolyzed at −10° in trichlorofluoromethane.

3-Chloromethylbicyclo[3.3.1]nonan-7-one

The colorless oil from thermal decomposition of 7 (X = Cl) was distilled over a short path under 10^{-2} mm at a bath temperature of 60°. It had $\nu_{max}(CH_2Cl_2)$ 1705 cm^{-1} and gave n.m.r. signals at δ 3.35 (2H doublet), 2.18–1.6 (11H mult.), and a broad 2H signal centered at δ 1.10.

Anal. Calcd. for $C_{10}H_{15}ClO$ (mol. ion *m/e* 186): C, 64.33, H, 8.10; Cl, 18.99. Found (186): C, 64.11; H, 7.92; Cl, 19.18.

The chloro ketone cyclized smoothly when treated with sodium hydride in tetrahydrofuran at room temperature (see cyclization of the bromo ketone). From 350 mg of the crude chloro ketone from the thermal reaction 186 mg of crude 4-protoadamantanone was obtained. The g.l.c. showed this to be over 90% pure. The contaminant was a chloro ketone as shown by analysis (1.4% chlorine).

We are grateful to the Consiglio Nazionale delle Ricerche (Rome) for fellowship support. We thank Mr. H. Seguin for analyses and Mr. M. Lesage for assistance with g.l.c.

1. O. E. Edwards, J. M. Paton, M. H. Benn, R. E. Mitchell, C. Watanatada, and K. N. Vohra. Can. J. Chem. **49**, 1648 (1971).
2. O. E. Edwards, D. Vocelle, and J. W. ApSimon. In pre aration. O. E. Edwards and D. P. Paskovich. Unpublished work.
3. C. Walling and J. A. McGuinness. J. Am. Chem. Soc. **91**, 2053 (1969).
4. F. Minisci, R. Galli, and G. Pollina. Chim. Ind. (Milan) **47**, 736 (1965).
5. R. A. Sneen and N. P. Matheny. J. Am. Chem. Soc. **86**, 5503 (1964).
6. T. L. Cairns and B. E. Englund. J. Org. Chem. **21**, 140 (1956).
7. B. R. Vogt. Tetrahedron Lett. 1575 (1968). M. L. Sinnott, H. J. Storesund, and M. C. Whiting. Chem. Commun. 1000 (1969). J. R. Alford and M. A. McKervey. Chem. Commun. 615 (1970). L. A. Spurlock and K. P. Clark. Abstr. of the 157th Natl. Am. Chem. Soc. Meeting, Minneapolis, Minnesota, April 13–18, 1969. Organic 134.
8. R. M. Black and G. B. Gill. Chem. Commun. 972 (1970).
9. W. H. W. Lunn. J. Chem. Soc. C, 2124 (1970).
10. D. Lenoir and P. v. R. Schleyer. Chem. Commun. 941 (1970).
11. M. Akhtar, P. Hunt, and P. B. Dewhurst. J. Am. Chem. Soc. **87**, 1807 (1965).
12. G. Smolinsky and B. I. Feuer. J. Org. Chem. **30**, 3216 (1965).
13. M. L. Mihailovic, Z. Cekovic, and J. Stankovic. Chem. Commun. 981 (1969).
14. A. Deluzarche, A. Maillard, P. Rimmelin, F. Schue, and J. M. Sommer. Chem. Commun. 976 (1970).
15. G. W. Wheland. Resonance in organic chemistry. J. Wiley and Sons, New York, N. Y., 1955. p. 99.
16. H. Brockmann and H. Schodder. Ber. **74**, 73 (1941).
17. J. W. Wilt and J. W. Hill. J. Org. Chem. **26**, 3523 (1961).

Can. J. Chem. Downloaded from www.nrcresearchpress.com by 210.87.254.40 on 09/05/12
For personal use only.

Eistert's Methyl Enol Ethers of Acetylacetone

DENNIS V. C. AWANG
Food and Drug Directorate, Department of National Health and Welfare, Ottawa, Canada

Received April 5, 1971

The configuration and conformation of the two isomeric methyl enol ethers of acetylacetone (**1**) have been unequivocally demonstrated. The n.m.r. solvent shift data and observation of nuclear Overhauser effects support an s-*cis* conformation for the more stable isomer **2** bearing acetyl *trans* to methoxyl while indicating an s-*trans* conformation for the less stable enol ether **3** having acetyl *cis* to methoxyl. The facile acid-catalyzed isomerization of **3** to **2** apparently proceeds by reversible protonation of carbonyl oxygen since no deuterium incorporation is observed when the isomerization is performed in acetic acid-d_4.

La configuration et la conformation des deux éthers méthyl énoliques de l'acétylacétone (**1**) ont été démontrées sans ambiguité possible. La r.m.n., les données relatives aux déplacements chimiques par les solvants ainsi que l'observation de l'effet nucléaire Overhauser confirment une conformation s-*cis* pour l'isomère le plus stable (**2**) ayant le groupe acétyle en position *trans* par rapport au groupement méthoxyle. Une conformation s-*trans* est attribuée à l'éther énolique le moins stable (**3**) ayant le groupe acétyle en position *cis* par rapport au groupe méthoxyle. L'isomérisation acido-catalysée très facile de **3** en **2** procède apparemment par une protonation réversible de l'oxygène du carbonyle puisqu'aucune incorporation de deutérium n'est observée lorsque l'isomérisation est effectuée dans l'acide acétique-d_4.

Canadian Journal of Chemistry, 49, 2672 (1971)

Eistert *et al.* (1) by careful manipulation, were able to isolate from the reaction of acetylacetone (**1**) and diazomethane in absolute ether, two compounds which they designated "*cis*"- and "*trans*"-methyl enol ethers. On the basis of qualitative rate data and the difference in chemical behavior of the two ethers towards ferric chloride and aqueous sodium hydroxide solutions it was concluded that the initially formed, higher-boiling enol ether was the "*cis*" isomer; the latter was transformed into the low-boiling "*trans*" isomer at a rate dependent upon conditions. The mechanism suggested by these workers for the reaction of **1** with diazomethane involves methylation of the s-*cis* enol **1***a*, but while this implies initial formation of an enol ether bearing acetyl *cis* to methoxyl and in the s-*cis* conformation, the question of conformation of the material isolated was not specifically addressed; no direct reference was made to the structure of their "*trans*" enol ether.

Recently (2) it has been noted that the less stable isomer, also referred to as "*cis*", can be converted to the more stable "*trans*" isomer by heating. It was reported also that the n.m.r. signal for the vinylic proton of the "*cis*" isomer appears at higher field than that of the "*trans*"; but neither the conditions under which the spectra were observed nor the chemical shifts of the other protons in the molecules were recorded.

Results and Discussion

The results here communicated firmly establish that the ethers of Eistert *et al.* are *cis–trans* configurational isomers and that the *configuration* of their "*cis*" isomer is as was then suggested. The conformation of the latter isomer as well as the configuration and conformation of their "*trans*" isomer have also been elucidated.

The stable isomer (**2**) was the only enol ether observed when **1** was methylated using dimethylsulfate or methanol – sulfuric acid. The unstable isomer (**3**) is the exclusive *primary* product of the diazomethane reaction. Attempted distillation of crude **3** at atmospheric pressure resulted in quantitative conversion to **2**, although **3** could be purified without isomerization by careful distillation under reduced pressure.

Relatively free rotation about the central bond of the α,β-unsaturated ketone system affords enol ethers **2** and **3** a choice of s-*cis* and s-*trans* conformations, as illustrated in Scheme 1. By analogy with mesityl oxide, whose conformation has been established by a variety of approaches (4), **2** may reasonably be expected to exist predominantly in the s-*cis* conformation **2***a*. However, a survey of the literature reveals no precedent which dictates the choice of conformation for **3**.

The conformation and configuration of the two enol ethers are dramatically portrayed by the solvent-induced chemical shifts (Table 1) ob-

TABLE 1. Chemical shifts induced in the n.m.r. signals of the methyl enol ethers of acetylacetone and dimedone by aromatic solvents

Compound	$\Delta_{aromatic}^{CCl_4}$ (p.p.m.)	=CH	=CCH	OCH	COCH
2*a*	C_6H_6	+0.17	−0.12	+0.43	+0.07
	C_5H_5N	−0.10	−0.15	+0.13	−0.08
3*b*	C_6H_6	−0.15	+0.43	+0.52	−0.10
	C_5H_5N	−0.27	+0.13	+0.17	−0.33
Methyl enol ether of dimedone*	C_6H_6†	−0.12	+0.25	+0.58	0.00
	C_5H_5N†	−0.25	0.00	+0.12	−0.13

*See ref. 9.
†The *gem*-dimethyl proton signal suffers shifts of +0.12 and +0.13 p.p.m. on passing to solution in benzene and pyridine, respectively.

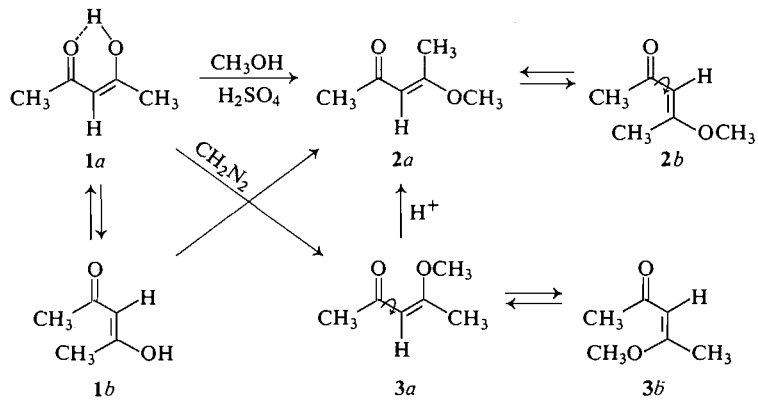

SCHEME 1

served in the n.m.r. spectrum on passing from dilute solution in carbon tetrachloride to dilute solution in benzene or pyridine ($\Delta = \delta_{CCl_4} - \delta_{aromatic}$ p.p.m.); the signs and magnitudes of the observed shifts are in accord with the generalization, well established for α,β-unsaturated ketones, that the signals of protons lying behind a reference plane[1] suffer positive shifts whereas those of protons in front of the plane undergo negative shifts and those of protons close to the plane exhibit very small and variable shifts (4, 5).

For ether **2**, the large and positive values of $\Delta_{C_6H_6}^{CCl_4}$ for the methoxy and vinylic proton resonance signals, concomitant with an appreciable negative value for the allylic methyl proton signal are compatible only with s-*cis* formulation **2***a*. By contrast, ether **3** exhibits positive values of $\Delta_{aromatic}^{CCl_4}$ for methoxyl and allylic methyl protons and negative values for its vinylic proton, consistent with its representation as the s-*trans* conformer **3***b*.[2]

The assignments of the signals for acetyl methyl and allylic protons made on the basis of line width[3] are reinforced by observation of the chemical shifts induced on passing from dilute solution in carbon tetrachloride to dilute solution

[1]Perpendicular to the αC—CO—α′C plane, through the carbonyl carbon atom for benzene-induced shifts and through the α-carbon atoms in the case of pyridine-induced shifts.

[2]Note that for **3** the benzene-induced shifts are appreciably greater on the positive side of the reference plane, whereas the emphasis is reversed in the case of pyridine hifts. Also, compared with ether **3**, the shifts induced by pyridine in the protons of **2** are neither as decidedly different nor as obviously rationalized; this is possibly a consequence of interference with solvent complexing at carbonyl by the ether grouping which is closer to the "collision plane" in **2**. These observations suggest that pyridine-induced shifts should be regarded with rather greater caution than benzene-induced shifts when used in the diagnosis of conformational attitudes.

[3]Although neither *cis* nor *trans* coupling constants for vinylic-allylic proton interaction, clearly observed in mesityl oxide (J = 1.2, 1.4 Hz) (3), could be ascertained for these enol ethers, appreciable broadening of the β-methyl signals, compared with those of the acetyl methyls, could be perceived.

Can. J. Chem. Downloaded from www.nrcresearchpress.com by 210.87.254.40 on 09/05/12
For personal use only.

TABLE 2. Chemical shifts induced in the n.m.r. signals of the methyl enol ethers of acetylacetone and dimedone by "proton-donating" solvents

Compound	$\Delta_{CDCl_3}^{CCl_4}$ or $\Delta_{CH_3OH}^{CCl_4}$ (p.p.m.)	=CH	=CCH	OCH	COCH
2*a*	$CDCl_3$	−0.10	−0.07	−0.03	−0.10
	CH_3OH	−0.23	−0.04	−0.05	−0.10
3*b*	$CDCl_3$	−0.15	−0.02	−0.20	−0.10
	CH_3OH	−0.19	−0.07	−0.25	−0.09
Methyl enol ether of dimedone	$CDCl_3$	−0.13	−0.08	0.00	−0.13
	CH_3OH	−0.18	−0.12	−0.05	−0.13

in "proton-donating" solvents (Table 2). These effects although not as dramatic as those observed on passing to aromatic solvents can be rationalized using the generalization that the magnitude of the chemical shift (resulting from association of solvent with carbonyl oxygen) is inversely proportional to the distance by which the proton is separated from the carbonyl oxygen atom.[4] The large anomalous effect observed for the methoxy protons of **3***b* is imputed to participation of a lone pair on methoxyl oxygen in neutralization of positive charge generated at the carbonyl carbon atom; this observation also argues against structure **2***b*.[5]

The configurations of ethers **2** and **3** are further confirmed by observation of nuclear Overhauser effects (n.O.e.'s) (7). Irradiation of the methoxyl and acetyl protons of **2** results in 30 and 12% increases, respectively, in the integrated intensity of the vinylic proton signal while no such enhancement occurs upon irradiation of the allylic methyl protons; in sharp contrast, irradiation of the methoxyl protons produced no appreciable change in the integrated intensity of the signal for the vinylic proton of ether **3**, but irradiation of its allylic and acetyl methyl protons effected increases of 20 and 13% respectively.

The formation of enol ether **3** is readily rationalized on the basis of a mechanism involving methylation of the s-*cis* enol of acetylacetone **1***a* (8). Loss of the enolic proton would expose the carbonyl and enolic oxygen atoms to the unshielded mutual repulsion of their respective lone pairs; rotation about the carbonyl to olefinic bond produces the more stable s-*trans* conformation **3***b*, a reversal of the order of stability of s-*cis* and s-*trans* isomers which obtains when methoxyl is replaced by methyl (in mesityl oxide).

It has not been possible to assess the importance of the intermediacy of either s-*trans* enol **1***b* or ether **3** in the formation of **2** by the other methods of methylation.

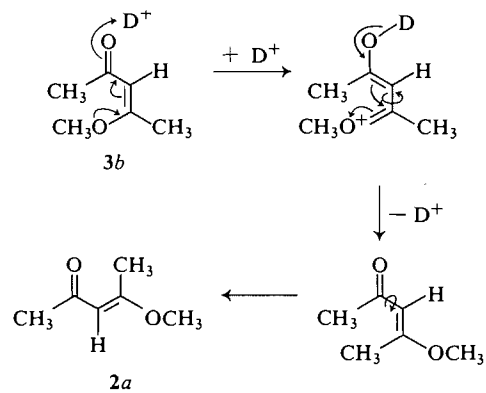

SCHEME 2

The isomerization of **3** and **2** is acid-catalyzed, quantitative conversion occurring within seconds at the probe temperature of the n.m.r. spectrometer (40 °C), when a few crystals of *p*-toluenesulfonic acid are added to a 10% chloroform-*d*

[4]Shifts induced by trifluoroacetic acid, usually helpful in making such assignments, could not be determined for these enol ethers since they were readily degraded by the acid at the probe temperature of the spectrometer.

[5]It should be noted that although appearance of the n.m.r. signal for the vinylic proton of **2** at lower field than that of **3** (Δ = 0.44 p.p.m.) is consistent with deshielding of the former proton due to the anisotropic effect of a *cis* enoxy group (6) an accurate assessment of the magnitude of this effect cannot be made. The major contribution to the difference in chemical shift is probably due to the change in the anisotropic effect of the carbonyl group brought about by purely conformational change: for example, in carbon tetrachloride, the signal for the vinylic proton of mesityl oxide appears at 0.33 and 0.30 p.p.m., respectively, downfield from that of isophorone and 3-methylcyclohex-2-enone.

Can. J. Chem. Downloaded from www.nrcresearchpress.com by 210.87.254.40 on 09/05/12
For personal use only.

solution of **3**. The mechanism of this acid-catalyzed isomerization is probably that illustrated in Scheme 2 since isomerization in acetic acid-d_4[6] does not lead to any detectable deuterium incorporation: mechanisms involving the intermediacy of enol or the protonation of the olefinic bond would result in reduction and enhancement, respectively, of the ratio of integrated intensities of methyl to vinylic proton signals in the n.m.r. spectrum.

Experimental

The n.m.r. spectra were recorded using a Varian A-60A spectrometer; spectral grade solvents containing tetramethylsilane (TMS) as internal reference were employed in all cases. The i.r. spectra were obtained with a Perkin–Elmer Model 621 spectrophotometer, and u.v. spectra on a Beckman DB spectrophotometer.

Enol Ether 3

An ice-cold ethereal-alcoholic solution (0.36 M, 100 ml) of diazomethane (Diazald) was added in one portion to 3 g (0.03 mol) of acetylacetone. The solution was magnetically stirred in the dark at room temperature overnight (approximately 16 h), dried over anhydrous potassium carbonate, and solvent removed under reduced pressure below 40 °C. The residue consisted of enol ether **3** better than 95% pure by n.m.r. The ether was purified by distillation under reduced pressure, b.p. 56–58°/3.5 mm; spectral characteristics for **3** are: n.m.r. (CCl_4, internal TMS) δ 4.96 (s, 1H), 3.80 (s, 3H, OCH_3), 2.13 (s, 3H, $—COCH_3$), 2.00 (s, 3H, $=CCH_3$) p.p.m.; i.r. (neat) ν 1650, 1615 (C=), 1075 (C—O—C) cm^{-1}; u.v. (95% EtOH) λ_{max} 260 nm (ε 10 910).

Enol Ether 2

Distillation at atmospheric pressure of the residue from methylation yielded pure **2**, b.p. 162–164°/758 mm. Spectral characteristics for **2** are: n.m.r. (CCl_4, internal TMS) δ 5.40 (s, 1H), 3.61 (s, 3H, OCH_3), 2.18 (s, 3H, $=CCH_3$), 2.03 (s, 3H, $—COCH_3$) p.p.m.; i.r. (neat) ν 1680, 1580 (C=), 1070 (C—O—C) cm^{-1}; u.v. (95% EtOH) λ_{max} 250 nm (ε 13 700).

[6]Isomerization takes place during minutes at 40 °C; a singlet due to ether **3** can be observed at δ 5.27 (**2** at δ 5.62) which disappears during the time taken for a second n.m.r. scan.

The author acknowledges the technical assistance of Mr. A. Vincent and is grateful to Mr. H. W. Avdovich for recording the 60 MHz n.m.r. spectra. Special thanks are due to Dr. R. A. Bell of McMaster University for examination of the n.O.e.'s. The counsel and assistance of Prof. J. W. ApSimon of Carleton University, as well as helpful discussions with my colleague Dr. W. L. Wilson, are also appreciated.

1. B. Eistert, F. Arndt, L. Loewe, and E. Ayca. Chem. Ber. **84**, 156 (1951).
2. S. T. Yoffe, E. I. Fedin, P. V. Petrovskii, and M. I. Kabachnik. Tetrahedron Lett. 2661 (1966).
3. J. V. Hatton and R. E. Richards. Mol. Phys. **5**, 153 (1962).
4. (*a*) J. E. Baldwin. J. Org. Chem. **30**, 2423 (1965). (*b*) J. Ronayne, M. V. Sargent, and D. H. Williams. J. Am. Chem. Soc. **88**, 5288 (1966), and references therein.
5. (*a*) N. S. Bhacca and D. H. Williams. Tetrahedron Lett. 3127 (1964). (*b*) C. J. Timmons. Chem. Commun. 576 (1965). (*c*) D. H. Williams and N. S. Bhacca. Tetrahedron, **21**, 1641, 2021 (1965). (*d*) J. Connelly and R. McCrindle. Chem. Ind. (Lond.). 379 (1965). (*e*) D. H. Williams. Tetrahedron Lett. 2305 (1965). (*f*) D. H. Williams, and D. A. Wilson. J. Chem. Soc. B, 144 (1966). (*g*) F. H. Cottee and C. J. Timmons. J. Chem. Soc. B, 326 (1968).
6. R. Noyori, H. Inoue, and M. Katô. J. Am. Chem. Soc. **92**, 6699 (1970).
7. F. A. L. Anet and A. J. R. Bourn. J. Am. Chem. Soc. **87**, 5250 (1965).
8. G. S. Hammond and R. M. Williams. J. Org. Chem. **27**, 3775 (1962).
9. K. Arakawa and M. Irie. Chem. Pharm. Bull. Tokyo, **5**, 524 (1957).

Can. J. Chem. Downloaded from www.nrcresearchpress.com by 210.87.254.40 on 09/05/12
For personal use only.

Can. J. Chem. Downloaded from www.nrcresearchpress.com by 210.87.254.6 on 09/05/12
For personal use only.

Synthetic Cardenolides and Related Products. II.[1] Lactams[2]

J. M. FERLAND, Y. LEFEBVRE, R. DINOI, AND R. DEGHENGHI
Ayerst Research Laboratories, Montreal, Quebec

Received March 25, 1971

On treatment of cardenolides with ammonia or methylamine two isomers are obtained, 21-amino-14β,21-oxidonorcholan-23-oic acid lactam and 21-amino-14β-hydroxy-16β,21-oxidonorcholan-23-oic acid lactam. The assignment of stereochemistry to each isomer is based on the n.m.r. spectra and the correlation with the structure of isodigitoxigenin or isogitoxigenin.

Les cardénolides réagissent avec l'ammoniaque ou la méthylamine pour conduire à deux isomères à savoir les lactames des acides amino-21 oxydo-14β,21 norcholanoïque-23 et amino-21 hydroxy-14β oxydo-16β,21 norcholanoïque-23. La stéréochimie de chaque isomère a été établie au moyen des spectres de r.m.n. et par corrélation avec la structure de l'isodigitoxigénine ou l'isogitoxigénine.

Canadian Journal of Chemistry, 49, 2676 (1971)

Naturally occurring cardenolides such as digitoxin and gitoxin or their aglycones were treated with ammonia or methylamine at room temperature to yield a lactol-amide (**5**). Two isomeric lactams (**A** and **B**), consistent with structure (**6**), were obtained when the lactol-amides were treated under acidic conditions or when cardenolides were heated in an autoclave at 110 °C. These isomers were separated only in the case of the aglycones (R = H or Ac).

As shown in Scheme 1 the same products were obtained by treating isodigitoxigenin (**4**) with ammonia or amines.

These results are not surprising in view of the acetal-type structure of isodigitoxigenin (3, 4) or in view of the great tendency of cardenolides to cyclize to the "iso-" form **4** in basic medium (5).

The stereochemistry of the predominant isodigitoxigenin (**4**) (R = R_2 = H) has been postulated on conformational grounds by Schindler and Reichstein (5) as having the 20(*S*), 21(*R*) fusion of the E/F rings (**7**).

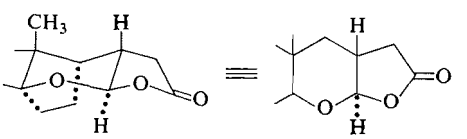

7 [20(*S*),21(*R*)]

Our n.m.r. data, however, do not support the *trans* configuration.[3] The coupling constant *J* for the 21-proton is 5 Hz and consistent with an axial–equatorial angle of *ca.* 40° indicating a *cis* junction, which we describe as 20(*S*),21(*S*) (**8**)[4] (6).

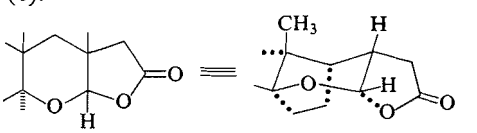

8 [20(*S*),21(*S*)]

In order to prove that the product described as **8** possesses the more stable equatorial side chain and not the opposite *cis* conformation, the following experiments were performed. Isodigitoxigenin (**4**) was converted into the known ester **11***b* according to the method described by Jacobs and Gustus (7) (Scheme 2).

Under acidic conditions one would expect to lose control of the stereochemistry at C-21 going through the carboxonium ion **10** but not at C-20. The lactol-ester (**11***b*), isolated in low yield, has now a half-width (*w*/2) of 14 Hz indicating a *trans*-diaxial configuration of the 20–21 protons. Moreover, its mutarotation in

[1]See ref. 1.

[2]The work described in this paper was presented in part at the 155th A.C.S. Meeting, San Francisco. California, April 5, 1968. Abstract Papers A.C.S. No. 155, 69N (1968), and at the 6th International Symposium on the Chemistry of Natural Products, Mexico, April 22, 1969 (2).

[3]The *trans* junction of the lactone ring in α-santonin, as a classical example, shows a coupling constant of *J* = 11 Hz for the C-1 proton.

[4]The same conclusion was drawn by Pettit *et al.* (6) using the coupling constant.

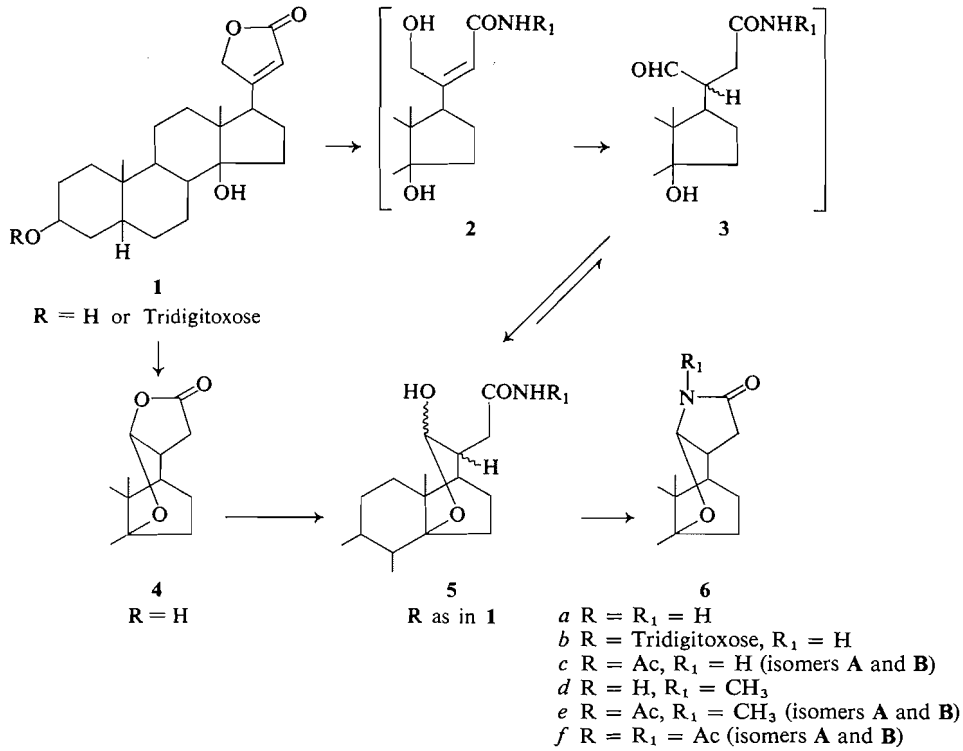

SCHEME 1

THF–water containing a trace of hydrochloric acid (α_D +5.7 increasing to 10.4°) is consistent with the epimerization of an equatorial alcohol to an axial one (8). Reacidification of the lactol-acid **11***a* regenerates isodigitoxigenin (**4**) in excellent yield. Carbon-20 must be equatorial, and it follows structure 20(*S*),21(*S*) for isodigitoxigenin accepting the physical data cited above.

The major lactam "**A**" isolated in 25% yield (**6***c*), has a coupling constant $J = 6$ Hz for the C-21 proton (axial–equatorial) and we assign the same *cis*-structure 20(*S*),21(*R*) (**13**) present in isodigitoxigenin.[5] The minor lactam "**B**" (**6***c*) (3% yield) has a half-width $w/2 = 6$ Hz for the C-21 proton and therefore must possess the alternative *cis* configuration 20(*R*),21(*S*) (**14**) as indicated in Scheme 3 (9).

The lactamization must occur from **5** through the carboxonium ion **12** to **13** and **14**. Additional evidence for the structure of the minor lactam **14** is provided by a deshielding of the C-18 protons (1.12 p.p.m.) while C-18 of **13** absorb at 1.0 p.p.m. due to proximity of the lactam function. Partial formation of the less stable axial side chain during the shift of the double bond from **2** to **3** or epimerization at C-20 of the intermediate amine-aldehyde **3** followed by lactamization are the probable mechanisms of the formation of this minor isomer.

An analogous reaction took place with gitoxigenin (**15**), which possesses a 16β-hydroxyl function, when similarly treated with methyl amine (Scheme 4).

A major and a minor isomer (**A** and **B**) were isolated in a 10/1 ratio. Similar lactamizations are reported by Barton *et al.* (3) in their paper on the diterpenoid bitter principle clerodin,

[5]Katzung *et al.* (9) have repeated our work and assigned *trans*-structure 20(*S*),21(*S*) to our *cis* product **13** and *cis*-structure 20(*S*),21(*R*) to the alternative *cis* (**14**) in agreement with our earlier communication in San Francisco (1*c*) but not consistent with our later (2) and present analysis.

Can. J. Chem. Downloaded from www.nrcresearchpress.com by 210.87.254.6 on 09/05/12
For personal use only.

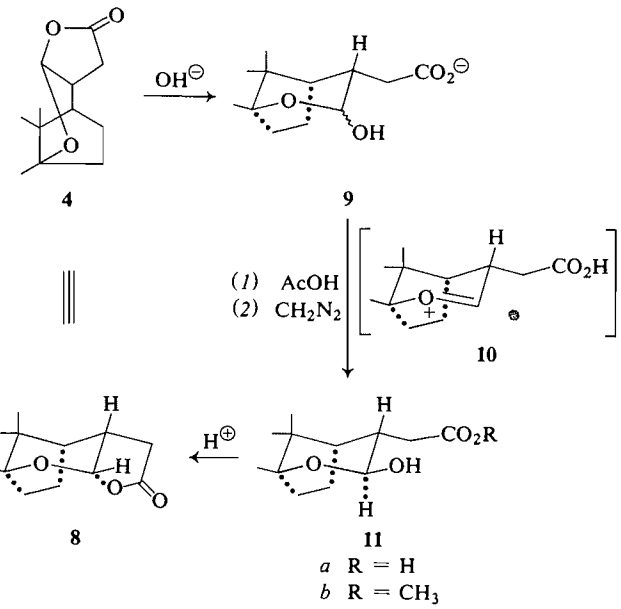

4 9 10 8 11

a R = H
b R = CH_3

SCHEME 2

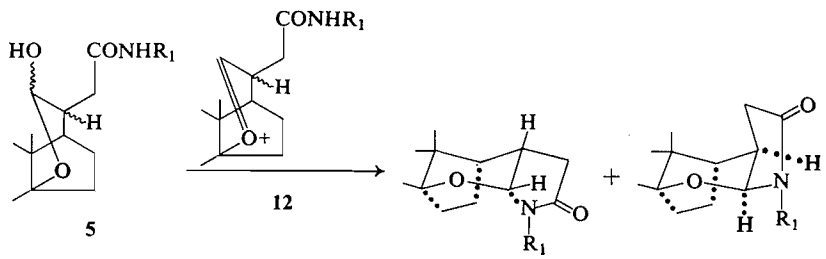

5 12 13 14

SCHEME 3

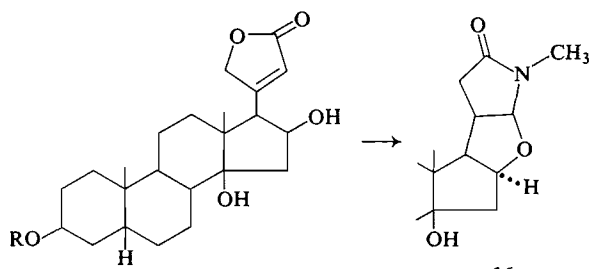

15
R = H

16
a R = H
b R = Ac

SCHEME 4

and more recently by German workers (4) who describe the bicyclic system hexahydrofuro-[2,3*b*]pyrrol-2-one. Clearly, only the two *cis* structures are possible (Scheme 5).

The major isomer is assigned the 20(*S*),21(*R*) structure **18** on steric grounds; a strong interaction is found in the minor isomer **19** between the 18-angular methyl group and the CH_2 at C-22. The 21-proton coupling constant is $J = 5$ and 6 Hz respectively as expected for a *cis*-junction.

Can. J. Chem. Downloaded from www.nrcresearchpress.com by 210.87.254.6 on 09/05/12
For personal use only.

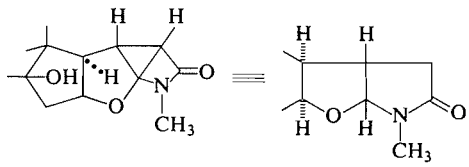

17 [20(*S*),21(*R*)]

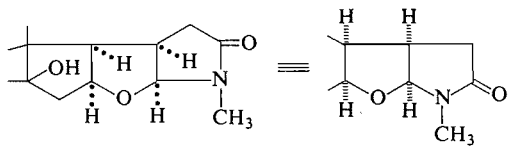

19 [20(*R*),21(*S*)]

SCHEME 5

In isogitoxigenin acetate $J = 5$ Hz for the C-21 proton centered at 6.02 p.p.m.

Experimental[6]

3β-Acetoxy-21-amino-14β,21-oxidonorcholan-23-oic Acid Lactams (6c)

Procedure A

Digitoxigenin (9.6 g) in methanol (500 ml) was saturated with dry ammonia at 0 °C. It was then heated at 110 °C in a Paar bomb apparatus for 24 h. After cooling, the solution was evaporated and the solid obtained, dissolved in ethanol (500 ml) and sulfuric acid 2% in water (50 ml) and refluxed for 2 h. The alcohol was evaporated to one quarter of its initial volume and poured into ice-cold water. The solid appearing was filtered, washed with water, and dried to give the crude 3β-hydroxy title compound, m.p. 254–256 °C (6.9 g).

The crude lactams (6.9 g) were acetylated in pyridine (70 ml) and acetic anhydride (35 ml) overnight. The solution was poured into ice-cold water and the solid obtained, filtered, washed with water, and dried. The crude acetates (6.9 g) were chromatographed on silica gel (300 ml fractions collected). Both isomers were eluted with a mixture of methylene chloride – ethyl acetate (45/55). The fractions containing mainly the more polar isomer (as shown by t.l.c.) were combined and crystallized from methylene chloride – ether to give 2.3 g of the analytical sample of isomer **13**, *3β-acetoxy-21-amino-14β,20(S),21(R)-oxidonorcholan-23-oic acid lactam*, m.p. 256–258 °C, $[\alpha]_D$ ($CHCl_3$) −35.8°.

Anal. Calcd. for $C_{25}H_{37}NO_4$: C, 72.26; H, 8.97; N, 3.37. Found: C, 72.07; H, 8.82; N, 3.35.

The i.r.: ν_{max}($CHCl_3$) 3400, 3200, 1710, and 1690 cm^{-1}; n.m.r. ($CDCl_3$): 5.47 (21H, $J = 5$ Hz doublet), 1.0 (C-18 and -19 CH_3), 6.56 p.p.m. (N—H).

[6]Melting points are uncorrected. The i.r. spectra were taken on a Perkin–Elmer 21 apparatus and n.m.r. were recorded on a Varian A-60-A spectrometer operating at 60 MHz/s; TMS was used as internal standard. Grace Davidson silica gel was used.

The richer fractions in the less polar isomer (as shown by t.l.c.) were combined and crystallized from methylene chloride – ether to give 0.210 g of the analytical sample of isomer **14**, *3β-acetoxy-21-amino-14β,20(R),21(S)-oxidonorcholan-23-oic acid lactam*, m.p. 227–229 °C, $[\alpha]_D$ ($CHCl_3$) −28.6°.

Anal. Calcd. for $C_{25}H_{37}NO_4$: C, 72.26; H, 8.97; N, 3.37. Found: C, 71.97; H, 8.87; N, 3.37.

The i.r.: ν_{max}($CHCl_3$) 3400, 3200, 1710, and 1690 cm^{-1}; n.m.r. ($CDCl_3$): 5.28 (C-21 H, $w/2 = 6$ Hz), 1.12 (C-18 CH_3), 1.0 (C-19 CH_3), and 6.56 p.p.m. (N–H).

Procedure B

A solution of digitoxigenin (3.0 g) in methanol (50 ml) and water (1 ml) was saturated with ammonia at 0 °C. The well-stoppered flask was left at room temperature for 8 days. The solid which had deposited (1.6 g) was filtered and dried to give the crude *3β-hydroxy-14β,21-oxido-21-hydroxy-norcholan-23-oic acid amide* (**5**), m.p. 259–262 °C.

The crude amide was refluxed in ethanol (160 ml) containing sulfuric acid 2% (16 ml) for 2 h. It was acetylated and chromatographed as in procedure A. Both products isolated were identical in all respects to the two isomers isolated in procedure A.

Procedure C

A suspension of isodigitoxigenin (1.0 g) in methanol (100 ml) was saturated with dry ammonia at 0 °C. It was treated as in procedure A and the isomers isolated were in all respects identical with products isolated in procedure A.

3β-Tridigitosyl-14β,21-oxido-21-amino-norcholan-23-oic Acid Lactam (6b)

A solution of digitoxin (2.0 g) in methanol (120 ml) was saturated with dry ammonia at 0 °C. It was then heated at 110 °C in a Paar bomb for 16 h. The solution was evaporated under vacuum to one half of its initial volume, acidified with 0.1 *N* sulfuric acid, and poured into water. The solid appearing was filtered, washed with water and taken into chloroform. The organic solution was dried and evaporated. The crude product was crystallized three times from methylene chloride – ether to give 400 mg. The analytical sample was obtained after one more recrystallization from the same solvents, m.p. 244–246 °C, $[\alpha]_D$ ($CHCl_3$) −6.7.

Anal. Calcd. for $C_{41}H_{65}NO_{12}$: C, 64.46; H, 8.57; N, 1.82. Found: C, 64.37; H, 8.59; N, 1.77.

The i.r.: ν_{max}($CHCl_3$) 3400 and 1690 cm^{-1}.

3β-Hydroxy-20(S),21(R)-(N-acetylamino)-14β,21-oxidonorcholan-23-oic Acid Lactam-3-acetate (6f) (Isomer 13)

A solution of lactam-3-acetate (isomer **13**) (0.300 g) in pyridine (3 ml) and acetic anhydride (3 ml) was heated for 16 h on the steam bath. After cooling, the solution was poured onto ice-cold water and the solid obtained filtered, washed with water, dried, and chromatographed on silica gel. The fractions eluted (0.260 g) with 25% ethyl acetate in methylene chloride were crystallized from ether, m.p. 221–223 °C, $[\alpha]_D$ ($CHCl_3$) −81.5°.

Anal. Calcd. for $C_{27}H_{39}NO_5$: C, 70.87; H, 8.50; N, 3.06. Found: C, 71.37; H, 8.13; N, 3.15.

Can. J. Chem. Downloaded from www.nrcresearchpress.com by 210.87.254.6 on 09/05/12
For personal use only.

Can. J. Chem. Downloaded from www.nrcresearchpress.com by 210.87.254.6 on 09/05/12
For personal use only.

The i.r.: $\nu_{max}(CHCl_3)$ 1720 and 1110 cm^{-1}; n.m.r. ($CDCl_3$): 5.85 (C-21 H, doublet J = 7 Hz), 1.07 (C-18 CH_3) 1.00 (C-19 CH_3), 2.47 p.p.m. (N—Ac).

3β-Hydroxy-20(R),21(S)-(N-acetylamino)-14β,21-oxidonorcholan-23-oic Acid Lactam-3-acetate (6f) (Isomer 14)

A solution of lactam-3-acetate (isomer **14**) (0.125 g) was acetylated as in the previous case and chromatographed. The fractions eluted with 6% ethyl acetate in methylene chloride (0.070) were crystallized from ether, m.p. 208–210 °C, $[\alpha]_D$ ($CHCl_3$) +33.9°.

Anal. Calcd. for $C_{27}H_{39}NO_5$: C, 70.87; H, 8.59; N, 3.06. Found: C, 70.91; H, 8.67; N, 3.22.

The i.r.: $\nu_{max}(CHCl_3)$ 1720 and 1110 cm^{-1}; n.m.r.: 5.85 (C-21 H, doublet J = 7 Hz), 1.12 (C-18 Me), 0.93 (C-19 CH_3), 2.47 p.p.m. (N—Ac).

3β-Acetoxy-21-(N-methylamino)-14β,21-oxidonorcholan-23-oic Acid Lactam (6e)

A solution of digitoxigenin (2.6 g) in methanol (70 ml) saturated at 0 °C with methylamine was left in a well-stoppered flask at room temperature for 40 h. The solvent was then evaporated and the solid obtained refluxed in ethanol (100 ml) and sulfuric acid 2% (10 ml) for 2 h. The alcohol was evaporated to one quarter of its initial volume and poured into ice-cold water. The solid appearing was filtered, washed with water to leave the crude *3β-hydroxy-21-(N-methylamino)-14β,21-oxidonorcholan-23-oic acid lactam* (**6d**) (2.6 g).

This crude alcohol (1.0 g) was acetylated and chromatographed as in procedure A. Two isomers were eluted in methylene chloride – ether 50/50. The richer fractions in the less polar isomer (as shown by t.l.c.) were combined and crystallized twice from methylene chloride – ether to give the pure *3β-acetoxy-20(R),21(S)-(N-methylamino)-14β,21-oxidonorcholan-23-oic acid lactam* (6*e*) (0.030 g) (isomer **13**), m.p. 242–244 °C, $[\alpha]_D$ ($CHCl_3$) −26.8°.

Anal. Calcd. for $C_{26}H_{39}NO_4$: C, 72.69; H, 9.15; N, 3.26. Found: C, 72.44; H, 8.99; N, 3.53.

The i.r.: $\nu_{max}(CHCl_3)$ 1720, 1675, 1255, 1088, and 1020 cm^{-1}; n.m.r. ($CDCl_3$): 5.1 (C-21 H, doublet J = 6 Hz), 1.05 (C-18 Me), 1.02 (C-19 Me), 2.80 p.p.m. (N—CH_3).

The richer fractions in the more polar isomer (as shown by t.l.c.) were combined and crystallized twice from methylene chloride – ether to give the pure *3β-acetoxy-20(S),21(R)-(N-methylamino)-14β,21-oxidonorcholan-23-oic acid lactam* (**6e**) (isomer **14**) (0.600 g), m.p. 212–214 °C, $[\alpha]_D$($CHCl_3$) −33.8°.

Anal. Calcd. for $C_{26}H_{39}NO_4$: C, 72.69; H, 9.15; N, 3.26. Found: C, 72.61; H, 8.95; N, 3.37.

The i.r.: $\nu_{max}(CHCl_3)$ 1720, 1675, 1255, 1082, and 1020 cm^{-1}; n.m.r. ($CDCl_3$): 5.1 (C-21 H, doublet J = 6 Hz), 1.05 (C-18 Me), 1.00 (C-19 Me), 2.88 p.p.m. (N—CH_3).

3β,14β-Dihydroxy-21-(N-methylamino)-16β,21-oxidonorcholan-23-oic Acid Lactam (16)

A solution of gitoxigenin (1.0 g) in methanol (100 ml) was saturated at 0 °C with dry methylamine and left in a well-stoppered flask at room temperature for 40 h. The solution was then evaporated and refluxed in methanol (60 ml) containing 0.1 *N* sulfuric acid (30 ml) for 15 min. After neutralization with pyridine, the solution was evaporated to one half of its initial volume, salt saturated and extracted with chloroform. The organic layer was washed with water, dried, and evaporated to leave the crude *3β,14β-dihydroxy-21-(N-methylamino)-16β,21-oxidonorcholan-23-oic acid lactam* (**16a**).

This alcohol was acetylated and chromatographed as in procedure A. The fractions eluted in methylene chloride – ethyl acetate (50/50) were combined and crystallized from methylene chloride – ether to give (0.250 g) the pure *3β,14β-dihydroxy-20(S),21(R)-(N-methylamino)-16β,21-oxidonorcholan-23-oic acid lactam acetate* (isomer **18**), m.p. 225–227 °C, $[\alpha]_D$ ($CHCl_3$) +23.9°.

Anal. Calcd. for $C_{26}H_{39}NO_5$: C, 70.08; H, 8.82; N, 3.14. Found: C, 69.76; H, 8.55; N, 3.15.

The i.r. $\nu_{max}(CHCl_3)$ 3600, 1720, and 1685 cm^{-1}; n.m.r. ($CDCl_3$): 5.0 (C-21 H, doublet J = 5 Hz), 1.05 (C-18 Me), 0.93 (C-19 Me), 2.42 (N—CH_3), 4.55 p.p.m. (C-16 H, triplet J = 7 Hz).

The fractions eluted with ethyl acetate were combined and crystallized several times from methylene chloride – ether to give (0.025 g) of the pure *3β,14β-dihydroxy-20(R),21(S)-(N-methylamino)-16β,21-oxidonorcholan-23-oic acid lactam acetate* (isomer **19**), m.p. 274–276 °C, $[\alpha]_D$ ($CHCl_3$) −28.5°.

Anal. Calcd. for $C_{26}H_{39}NO_5$: C, 70.08; H, 8.82; N, 3.14. Found C, 70.37; H, 9.03; N, 3.43.

The i.r.: $\nu_{max}(CHCl_3)$ 3600, 1720, and 1685 cm^{-1}; n.m.r. ($CDCl_3$): 5.38 (C-21 H, doublet J = 6), 1.08 (C-18 Me), 0.93 (C-19 Me), 2.81 (N—CH_3), 4.63 p.p.m. (C-16 H, triplet J = 7 Hz).

The authors wish to thank Dr. G. Schilling and his associates for analytical data and Mr. W. Turnbull for rotation measurements.

1.(*a*) J. M. Ferland and Y. Lefebvre. U.S. Patent 3 462 412; Chem. Abstr. **71**, 113, 228 (1969). (*b*) J. M. Ferland, Y. Lefebvre, R. Deghenghi, and K. Wiesner. Tetrahedron Lett. 3617 (1966). (*c*) 155th A.C.S. Meeting, San Francisco, California, April 5, 1968. Abstr. Papers A.C.S. No. 155, 69N (1968).
2. R. Deghenghi. Pure and Appl. Chem. **21**, 153 (1970).
3. D. H. R. Barton, H. T. Cheung, A. D. Cross, L. M. Jackman, and M. Martin-Smith. J. Chem. Soc. 5061 (1961).
4. C. Lange, H. Wamhoff, and F. Korte. Angew. Chem. Intern. Ed. 7, 303 (1968).
5. O. Schindler and T. Reichstein. Helv. Chim. Acta, **39**, 1876 (1956).
6. G. R. Pettit, T. R. Kasturi, J. C. Knight, and J. Occolowitz. J. Org. Chem. **35**, 1404 (1970).
7. W. A. Jacobs and L. Gustus. J. Biol. Chem. **78**, 573 (1928).
8. J. T. Edward, P. F. Morand, and I. Puskas. Can. J. Chem. **39**, 2069 (1961).
9. B. G. Katzung, J. A. Munoz, D. Y. Shirachi, A. J. Trevor, H. H. Chang, and M. E. Wolff. Exper. **26**, 1189 (1970).

Can. J. Chem. Downloaded from www.nrcresearchpress.com by 210.87.254.105 on 09/05/12
For personal use only.

Electrolysis of α-Chloro- and α-Fluorocarboxylic Acids

PARKASH C. ARORA AND R. G. WOOLFORD
Department of Chemistry, University of Waterloo, Waterloo, Ontario

Received March 8, 1971

The electrolysis of α-chlorovaleric, α-chlorocaproic, and α-chloroisobutyric acids in methanol gave none of the Kolbe dimer; the main products were chloroester and hydrogen ester with aldehydes and acetals formed in lesser amounts. In water, straight chain α-chloroacids gave dimeric esters as the major product. However, Kolbe dimer was formed in fairly good yields together with small amounts of fluoro-ester and acetal, when α-fluorocaproic and α-fluoroheptanoic acids were electrolyzed in methanol. No Kolbe dimer was produced from 2-fluoro-2-ethylbutanoic and α-fluorophenylacetic acids; the corresponding ketone or aldehyde was the major product.

Les électrolyses dans le méthanol des acides α-chlorovalérique, α-chlorocaproïque, et α-chloroisobutyrique ne conduisent pas aux dimères de Kolbe; les produits principaux sont les chloro-esters et les hydrogénoesters; en plus petite quantité se forment des aldéhydes et des acétals. Dans l'eau, les α-chloroacides en chaine droite conduisent aux esters dimériques en tant que produits majoritaires. Cependant, dans l'électrolyse dans le méthanol des acides α-fluorocaproïque et α-fluoroheptanoïque, des dimères de Kolbe se forment avec un assez bon rendement avec toutefois de petites quantités de fluoro-esters et d'acétals.

Canadian Journal of Chemistry, 49, 2681 (1971)

In a previous paper (1) from this laboratory, the electrolysis of α-bromocarboxylic acids in methanol produced hydrogen ester and bromoester as major products. The results were regarded as the result of attack of an initial carboxy radical on the solvent. Reduction of C—Br to C—H in both the ester and acid occurred at the cathode with migration of Br^- to the anode and oxidation there to Br_2. Electrolysis experiments with branched chain α-bromoacids in water indicated production of carbonium ions. In all the acids studied, no Kolbe dimer was detected, nor were other possible products such as alcohols, ethers, and paraffins obtained. Hoping to understand better the electrochemical processes involved with α-halo substituents, the behavior of α-chloro- and α-fluorocarboxylic acids during Kolbe electrolysis was examined. It was anticipated especially that the smaller, more stable fluoro-substituent might allow dimer formation to occur. Conway and Dzieciuch (2) previously found that normal Kolbe coupling took place with trifluoroacetic acid; this reaction was the only previous example of successful coupling with an α-fluoro substituent present.

The electrolyses of α-chlorocarboxylic acids were carried out in methanol and water. The results of various electrolysis reactions of α-chlorovaleric, α-chlorocaproic, and α-chloroisobutyric acids in methanol (Scheme 1) are summarized in Table 1 and show that chloroester is the major organic product. Hydrogen ester is formed in low yields with the ratio of hydrogen ester to chloro ester increasing as the time of electrolysis is increased. The straight-chain α-chloroacids also produced acetals in low yield but this behavior was not observed with the branched-chain acid. It is probable that the corresponding acetal was formed from the branched-chain chloroacid, but because of volatility was lost under the experimental conditions used.

The presence of 1-chloropentane in trace amounts in the electrolysis products of α-chlorocaproic acid shows that, at least in part, radical

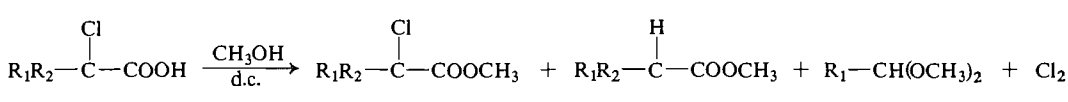

SCHEME 1

Can. J. Chem. Downloaded from www.nrcresearchpress.com by 210.87.254.105 on 09/05/12
For personal use only.

TABLE 1. Electrolysis of α-chlorocarboxylic acids in methanol

Acid used (10 g)	Solvent (ml)	Current (A)	Time (h)	Temperature (°C)	Weight of neutral fraction (g)	Weight of acidic fraction (g)	Yield % of		
							Chloro ester	Hydrogen ester	Acetal
α-Chlorovaleric acid	30	0.8	6	45	2.8	6.7	60	trace	2.4
	30	1.0	18	45	2.9	6.5	63	trace	trace
	50	0.6	24	30	2.9	6.0	24	6.2	5.0
	50	1.1	24	34	4.5	5.1	45	11	9.9
α-Chlorocaproic acid	30	0.6	8	35	2.3	6.5	41	nil	—
	30	1.0	12	6	2.0	6.9	41	5.1	6.9*
	30	1.2	24	38	4.2	1.8	24	7.3	7.2*
	35	0.7	24	37	6.3	2.3	23	19	14
α-Chloroisobutyric acid	30	0.8	6	35	0.7	8.6	30	5.5	—
	30	0.8	12	32	1.1	8.8	37	4.4	—
	60	1.0	6	30	1.2	8.3	24	8.1	—
	30	0.8	24	35	4.4	5.3	65	11	—

*Approximately 2% free aldehyde also isolated in these cases. Trace amounts of 1-chloropentane were also found.

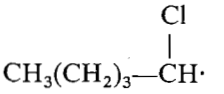

was converted to saturated chloroalkane. Such behavior was not observed in the case of α-chlorovaleric or α-chloroisobutyric acid. Divided cell and control experiments for the chloroacids similar to those conducted for the bromoacids showed essentially the same results. Reduction of C—Cl to C—H occurred at the cathode, with Cl^- migration to the anode and formation there of Cl_2. Esterification occurred at the anode only, whereas some of the side products such as aldehydes and acetals were found in the cathode compartment. Control experiments on esterification (with no electrolysis) showed that prolonged heating of α-chloroacids in methanol produced very little (*ca.* 5–8%) ester.

In water, α-chlorovaleric and α-chlorocaproic acid (straight-chain acids) behaved differently from the analogous α-bromoacids. With the straight-chain chloroacids the major electrolysis product was 1′-chloro-1′-butyl 2-chloropentanoate (40%) from α-chlorovaleric acid and 1′-chloro-1′-pentyl 2-chlorohexanoate (38%) from α-chlorocaproic acid. Such esters were not isolated from α-bromoacids. No Kolbe dimer was detected, nor were other possible esters found (*i.e.* those in which one or two C—Cl → C—H conversions occurred); some unidentified high molecular weight compounds were also produced. The formation of esters in electrolysis reactions in water can be explained by combination of carboxy and alkyl radicals absorbed on the electrode surface and is consistent with mechanisms proposed by Troeger and Ewars (3) and Kaufler and Herzog (4). Alternatively a further oxidation of the alkyl radical could occur yielding the corresponding carbonium ion, which would give the same ester by combination with the initial carboxylate anion (Scheme 2). Carbonium ions are usually produced only when secondary or tertiary species can form (a good general discussion of radical and carbonium ion intermediates during Kolbe electrolysis may be found in recent work by Skell and coworkers (ref. 5 and articles cited therein) and by Eberson (6)). Perhaps in this case some stabilization by the resonance form $CH_3(CH_2)_n—CH{=}Cl^+$ may be involved. Such ester formation from a carbonium ion intermediate avoids the involvement of a carboxy radical which is known to have a short lifetime (*ca.* 10^{-9} s) in chemical processes, although it is believed to be longer-lived when absorbed on a platinum electrode. Lack of Kolbe dimer from these α-chloroacids would also be consistent with a carbonium ion species. The present results also indicate that the C—Cl bond is more stable than C—Br in the α-bromoacids and there is negligible or very little reduction of this C—Cl bond during electrolysis.

Electrolysis in water of α-chloroisobutyric acid (a branched-chain acid) produced mainly ketones rather than esters. Products obtained were acetone (18.3%), 1,1-dichloroacetone (2.4%), and 1,3-dichloroacetone (0.8%). As discussed for the bromo analog, it is likely that acetone was the major reaction product at the electrode but, being miscible in water and very volatile, either reacted further with chlorine or was lost in the exit gas stream. Some high molecular weight substances were also formed which could not be obtained pure. The similarity of products from electrolysis of α-chloroisobutyric acid in water and the corresponding α-bromoacid reported earlier (1) indicates that product formation can be interpreted in terms of the production of a carbonium ion $(CH_3)_2\overset{+}{C}—Cl$ which picks up OH^- from water with the ketone resulting.

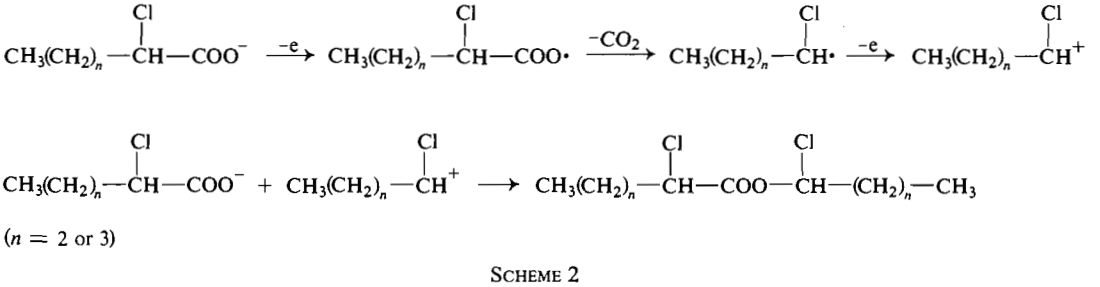

($n = 2$ or 3)

SCHEME 2

Can. J. Chem. Downloaded from www.nrcresearchpress.com by 210.87.254.105 on 09/05/12
For personal use only.

Can. J. Chem. Downloaded from www.nrcresearchpress.com by 210.87.254.105 on 09/05/12
For personal use only.

TABLE 2. Electrolysis of α-fluorocaproic acid in methanol

Acid used (10 g)	Solvent (ml)	Current (A)	Time (h)	Temperature (°C)	Weight of neutral fraction (g)	Weight of acidic fraction (g)	Yield % of				
							Fluoro ester **2**	Hydrogen ester **3**	Acetal **4**	Kolbe dimer **5***a*	Kolbe dimer **5***b*
α-Fluorocaproic acid	30	0.8	6	35	3.8	1.5	4.2	1.6	7.0	16	17
	30	0.8	12	32	5.4	1.8	6.4	nil	27	19	20
	30	0.8	24	30	4.8	2.3	12	trace	20	12	17
	30	0.8	12	43	5.0	1.0	4.4	nil	4.4	32	33
	30	1.0	12	6	4.3	2.5	7.7	—	19	20	20

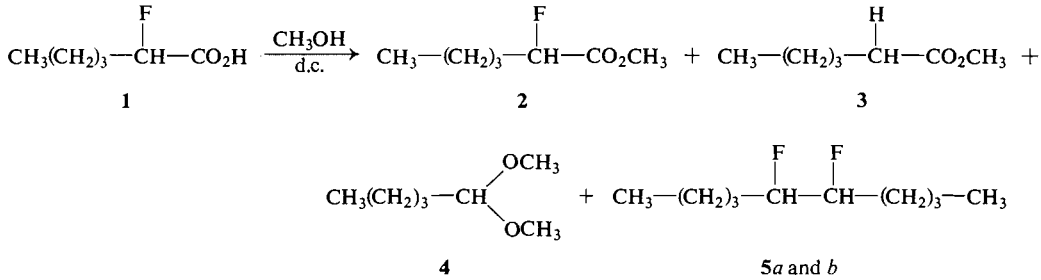

SCHEME 3

α-Bromo- and α-chloro-substituted acids did not produce normal Kolbe coupling reactions and while similar to some extent in their reactions, the chloro-substituent was not as easily lost by reduction to C—H. Therefore it seemed reasonable to ascertain if a halogen atom smaller in size would allow dimer formation (also a C—F bond would be expected to be even less easily converted to C—H). As a start, efforts were concentrated on α-fluorocaproic acid. The results of various electrolysis reactions of this fluoroacid in methanol are given in Table 2 and products are illustrated in Scheme 3.

Fluoroester **2** was produced in poor yield compared to the analogous chloroester and the acetal yield was variable. The major products were difluorides **5***a* and *b*. Both showed essentially identical n.m.r. absorption attributable to methyl at 9.03 τ, methylene at 8.4 and 8.2 τ and methine, four broad multiplets centered at 5.7 τ (*gem* $J_{HF} \sim 50$ and *vic* $J_{HF} \sim 20$ Hz); both showed similar i.r. absorption at 1060 (C—F) cm^{-1}. This evidence in conjunction with microanalytical data confirms structure **5** and indicates the two dimers are the anticipated diastereomers formed in essentially equal amounts. Both these compounds appeared as two separate peaks (g.l.c.) and could easily be isolated at temperature programming of 170–190°. Further efforts to distinguish between these diastereomers were not attempted. Monomeric 1-fluoropentane $CH_3(CH_2)_3CH_2F$ was anticipated as a possible product but no trace was found. In all the electrolyses of α-fluorocaproic acid, changes in concentration and time appeared to have little effect but at higher temperature the ratio of dimeric compounds to other products is increased. 1,1-Dimethoxypentane, **4**, formed in *ca.* 20% yield was identified by its n.m.r. and i.r. spectra and comparison of its g.l.c. retention time with an authentic sample. A small quantity of valeraldehyde was also detected by g.l.c.

To determine how typical dimer formation was during Kolbe electrolysis, we decided to extend our study to some other α-fluoroacids, *viz.* α-fluoroheptanoic acid, 2-fluoro-2-ethylbutanoic acid, and α-fluorophenylacetic acid. Electrolysis of α-fluoroheptanoic acid in methanol gave the Kolbe dimer 6,7-difluorododecane (both diastereomers),

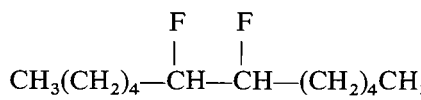

Structures were confirmed as in the previous case. On the other hand the branched-chain fluoroacid, 2-fluoro-2-ethylbutanoic acid, gave 3-pentanone (24–32%) as major electrolysis product as well as the expected fluoroester (6–9%). Several electrolyses of this acid in methanol revealed that changes in temperature, current density, temperature, concentration, or time did not result in dimer formation. Similar behavior was observed when α-fluorophenylacetic acid was electrolyzed where the only product formed was benzaldehyde (for comparison, the corresponding α-bromophenylacetic acid gave hydrogen ester as major product (80%) along with very little (2.5%) bromoester but essentially no benzaldehyde). The lack of dimer formation from these latter two acids is not surprising since carbonium ion formation leading to carbonyl products is much more likely.

The work described herein represents the first detailed study of the electrolysis of α-chloro and α-fluorocarboxylic acids. The results for α-chloroacids in methanol are essentially the same as for α-bromoacids, except that the reduction of C—Cl is less pronounced in the chloroacids. In water the straight-chain α-chloroacids produced

Can. J. Chem. Downloaded from www.nrcresearchpress.com by 210.87.254.105 on 09/05/12
For personal use only.

Can. J. Chem. Downloaded from www.nrcresearchpress.com by 210.87.254.105 on 09/05/12
For personal use only.

esters. With the α-fluoroacids the straight-chain α-fluoro-caproic and -heptanoic acids produced the Kolbe dimers possibly because the fluorine atom being smaller allows the

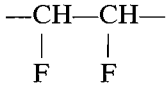

linkage to form more easily. Also C—F is less easily reduced to C—H. The difluoro dimer should also be more stable under electrolysis conditions, since Br_2 and Cl_2 can be lost[1] from the appropriate dihalide but not F_2 from the difluoride.

Experimental

General

α-Chlorovaleric acid (7, 8), α-chlorocaproic acid (7, 8), and α-chloroisobutyric acid (9) were prepared according to methods described in the literature. The fluoroacids were synthesized according to the method of Pattison *et al.* (10, 11) but yields on large scale preparations were poor especially for the branched-chain acid. Microanalyses were obtained from Schwarzkopf Microanalytical Laboratory, Woodside, New York. The g.l.c. analyses and separations were carried out on an Aerograph Autoprep model 700 with a 10′ × 3/8″ column with a 30% loading on Chromosorb W of either silicon gum rubber SE-30 or Carbowax 20M. Temperature programming was used in the range 170–250°. Detector temperature was kept *ca.* 25° above the column temperature when collection of the sample was desired. The i.r. spectra were taken with a Beckman IR-10 spectrophotometer either on thin liquid films or in CCl_4 solution. The n.m.r. spectra were obtained with a Varian T-60 spectrometer, absorptions being quoted in τ values against tetramethylsilane.

The conventional electrolysis cell, general method of electrolysis, isolation of products, and divided cell experimental details have been described before (1, 12).

Electrolysis of α-Chloro Acids in Methanol

The results of these electrolyses at various temperatures and concentrations are found in Table 1. The products were identified by comparison with authentic samples, especially in their g.l.c. behavior and i.r. spectra.

For comparison, certain control reactions were run. Refluxing of α-chloro acids under electrolysis conditions, but with no current resulted in some esterification (10–13%). Prolonged heating (40–50°) of α-chloro acids (no electrolysis) gave no conversion to hydrogen acid but did produce some (5–8%) esterification. However, when some methyl α-chloroesters were subjected to electrolysis (under similar condition to those shown in Table 1), they gave considerable amounts of the appropriate hydrogen esters (35–40%).

[1]We have observed the loss of Br_2 under our electrolysis conditions from *vic*-dibromoacids but have not done any detailed studies. Other than studies on α,β-dihaloacids, there are not many recorded examples in this area.

Electrolysis of α-Chlorovaleric and α-Chlorocaproic Acids in Water

Potassium hydroxide (4.2 g, 0.075 mol) was dissolved in water (60 ml) and α-chlorovaleric acid (25.5 g, 0.187 mol) was added. A current of 1.25 A was passed for 40 h and the temperature was kept at 10–15° with an ice bath. After isolation of neutral and acidic fractions in the usual manner, a light brown neutral oil (12.9 g) was collected. The neutral fraction showed (g.l.c.) a major fraction (40%); a small sample of this compound was isolated with the Autoprep-700 using an SE-30 column, temperature programming from 160–200°, and a detector temperature of 250°, and was identified as 1′-chloro-1′-butyl 2-chloropentanoate. The i.r. spectrum showed strong absorption at 1770 cm^{-1} (CCl_4). The n.m.r. spectrum showed peaks at τ 9.1, 8.8, 5.9, and 3.8 with integrated areas of 6:4:4:1:1. The triplet at τ 5.9 indicated

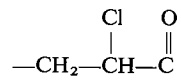

whereas the triplet at τ 3.8 indicated

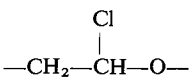

Anal. Calcd. for $C_9H_{16}O_2Cl_2$: C, 47.60; H, 7.51; Cl, 31.24. Found: C, 47.85; H, 7.15; Cl, 31.18.

Similarly α-chlorocaproic acid (31.0 g, 0.2 mol) was electrolyzed at 1.2 A for 36 h. A dark brown neutral oil (14.1 g) was collected which when subjected to fractional distillation under reduced pressure decomposed. From a fresh sample of neutral oil 1′-chloro-1′-pentyl 2-chlorohexanoate was isolated by g.l.c. This ester has the same spectral features as 1′-chloro-1′-butyl 2-chloropentanoate.

Anal. Calcd. for $C_{11}H_{20}O_2Cl_2$: C, 51.78; H, 7.84; Cl, 27.81; Found: C, 51.87; H, 7.74; Cl, 28.00.

Electrolysis of α-Chloroisobutyric Acid in Water

α-Chloroisobutyric acid (30.6 g, 0.25 mol) was added to a solution of potassium hydroxide (5.7 g) in water (65 ml). A current of 1.5 A was passed for 28 h and the temperature was kept at 20–25°. Work-up as usual gave 9.4 g of neutral product, which was mainly acetone (18.3%), 1-chloroacetone (6.1%), 1,1-dichloroacetone (2.4%), and 1,3-dichloroacetone (0.8%).

Electrolysis of α-Fluorocaproic and α-Fluoroheptanoic Acids in Methanol

The results of several electrolyses of α-fluorocaproic acid are shown in Table 2. The fluoroester was confirmed by use of an authentic sample. Hydrogen ester was absent. Three other components were isolated by g.l.c. using the SE-30 column, temperature programming of 170–190°, and a detector temperature of 220°. One component was identified as 1,1-dimethoxypentane $CH_3(CH_2)_3—CH(OCH_3)_2$. The i.r. spectrum in CCl_4 solution showed bands at 1050 and 1130 cm^{-1}; the n.m.r. spectrum showed four groups of peaks at τ 8.9, 8.7, 6.8, and 5.8 with relative intensities of 3:6:6:1. This compound had identical g.l.c. behavior when compared with an authentic sample prepared according to the method of Lorette and Howard (13). The other two components appeared from the elemental analysis to be diasterioisomers.

Anal. Calcd. for

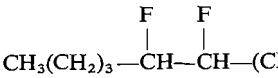

$CH_3(CH_2)_3—CH—CH—(CH_2)_3—CH_3$, $(C_{10}H_{20}F_2)$:

C, 67.41; H, 11.23; F, 21.34. Found for one diastereomer: C, 67.18; H, 11.00; F, 21.72. Found for the other diastereomer: C, 67.77; H, 11.61; F, 21.32.

The i.r. spectrum in each case showed a band at 1060 (C—F) cm^{-1}. The n.m.r. spectra of each isomer showed signals for methyl at 9.03 τ, methylene at 8.4 and 8.2 τ, and methine, four broad multiplets centered at 5.7 τ (*gem* J_{HF} 50 and *vic* J_{HF} 20 Hz). The refractive indices of these diastereomers were very similar (n_D^{24} 1.4018 and 1.4027 respectively); the first isomer remained a colorless oil on cooling in ice but the second isomer solidified.

Similar electrolysis of α-fluoroheptanoic acid was carried out in methanol under identical conditions with that of α-fluorocaproic acid. The neutral fractions from three runs were examined only for dimeric compounds which constituted *ca.* 40–60% of the neutral fraction. Two compounds were isolated with the Autoprep Model 700, in a similar fashion to the isolation of the two diasterioisomers obtained from the electrolysis of α-fluorocaproic acid (g.l.c., two separate peaks).

Anal. Calcd. for

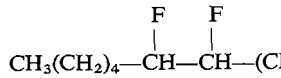

$CH_3(CH_2)_4—CH—CH—(CH_2)_4—CH_3$, $(C_{12}H_{24}F_2)$:

C, 69.90; H, 11.65; F, 18.90. Found for one diastereomer: C, 69.56; H, 11.65; F, 18.50. Found for the other diastereomer: C, 69.72; H, 11.82; F, 18.58.

We wish to thank the National Research Council of Canada for support of this work.

1. R. G. Woolford, Judy Soong, and W. S. Lin. Can. J. Chem. **45**, 1837 (1967).
2. B. E. Conway and M. Dzieciuch. Proc. Chem. Soc. 121 (1962).
3. J. Troeger and E. Ewars. J. Prakt. Chem. Ser. **2**, 58, 127 (1898).
4. F. Kaufler and C. Herzog. Ber. **42**, 2870 (1909).
5. P. H. Reichenbacher, M. D. Morris, and P. S. Skell. J. Am. Chem. Soc. **90**, 3432 (1968).
6. L. Eberson. J. Am. Chem. Soc. **91**, 2402 (1969).
7. R. Adams and R. M. Kamm. Org. Synth. Coll. Vol. 1, 250 (1956).
8. R. H. Horn, R. B. Miller, and S. N. Slater. J. Chem. Soc. 2900 (1950).
9. D. G. Kundinger, E. A. Ikenberry, E. B. W. Ovist, J. G. Peterson, and C. R. Dick. J. Am. Chem. Soc. **82**, 2953 (1960).
10. F. H. Dean, J. H. Amin, and F. L. M. Pattison. Org. Synth. **46**, 10, 37 (1966).
11. F. L. M. Pattison, R. L. Buchanan, and F. H. Dean. Can. J. Chem. **43**, 1700 (1965).
12. R. G. Woolford and W. S. Lin. Can. J. Chem. **44**, 2783 (1966).
13. N. B. Lorette and W. L. Howard. J. Org. Chem. **25**, 521 (1960).

Can. J. Chem. Downloaded from www.nrcresearchpress.com by 210.87.254.105 on 09/05/12
For personal use only.

Can. J. Chem. Downloaded from www.nrcresearchpress.com by 210.87.254.105 on 09/05/12
For personal use only.

The Dichloroiodine(III) and Dibromoiodine(III) Cations in Sulfuric Acid

J. B. SENIOR AND J. L. GROVER

Department of Chemistry, St. Paul's College, University of Manitoba, Winnipeg 19, Manitoba
and
Department of Chemistry and Chemical Engineering, University of Saskatchewan, Saskatoon, Saskatchewan[1]

Received February 8, 1971

The results of measurements of the conductivities and freezing points of solutions formed by adding chlorine or bromine to solutions of iodic acid and iodine (mole ratio $I_2/HIO_3 = 2.0$) in sulfuric acid are reported. The results provide evidence for the formation of the ions ICl_2^+ and IBr_2^+ in these solutions. Ultraviolet–visible spectra of the solutions are reported.

On rapporte les résultats des mesures de conductivité et de détermination des points de congélation de solutions obtenues en ajoutant du chlore ou du brome à des solutions d'acide iodique et d'iode (rapport molaire $I_2/HIO_2 = 2.0$) dans l'acide sulfurique. Les résultats apportent des preuves quant à la formation d'ions ICl_2^+ et IBr_2^+ dans ces solutions. On rapporte les spectres u.v.—visible des solutions.

Canadian Journal of Chemistry, 49, 2688 (1971)

Introduction

Garrett, Gillespie, and Senior (1) reported the formation of the polyhalogen cations I_3^+, I_5^+, I_2Cl^+, and I_2Br^+ in solutions prepared by adding iodine alone or iodine and iodine monochloride or monobromide, respectively, to solutions of iodic acid in sulfuric acid. These workers also reported conductance data which suggest that the dichloroiodine(III) cation, ICl_2^+, is formed, along with I_2Cl^+, when iodine monochloride alone is added to solutions of iodic acid in sulfuric acid. They pointed out that the hitherto unreported dibromoiodine(III) cation, IBr_2^+, would be isoelectronic with the known compound $TeBr_2$ and hence that its existence was very probable. The cation ICl_2^+ is known to exist in the compounds $ICl_3.AlCl_3$ and $ICl_3.SbCl_5$ whose crystal structures were determined by Vonk and Wiebenga (2). Aubke and Cady (3) prepared ICl_2SO_3F as a low-melting, apparently impure solid. They did not report on its behavior in solution, although they found that the related compound I_3SO_3F gave I_3^+ in solution in fluorosulfuric acid.

While our work was in progress, Gillespie and Malhotra (4) presented conductometric and cryoscopic evidence for the formation of ICl_2^+ in solutions of iodine trichloride in disulfuric acid.

In the present work, chlorine or bromine was added to solutions in 100% sulfuric acid, containing iodic acid and iodine in the mole ratio $I_2/HIO_3 = 2.0$, corresponding to the formal +1 oxidation state of iodine. The freezing points and electrical conductivities of the resulting solutions provide evidence for the formation of the cations ICl_2^+ and IBr_2^+, respectively.

[1]Present address of J. B. Senior, to whom correspondence should be addressed.

Results and Discussion

The Systems $(HIO_3 + 2I_2) - Cl_2$ and $(HIO_3 + 2I_2) - Br_2$

In each conductometric experiment the starting solution contained iodic acid and iodine in the mole ratio $I_2/HIO_3 = 2.00 \pm 0.03$. Successive additions of the halogen X_2 (X = Cl or Br) were made, and the conductance measured following each addition. Graphs of specific conductance *vs.* the mole ratio $X_2/(HIO_3 + 2I_2)$ were plotted. Conductance values at the mole ratio 5.0, obtained from these graphs by interpolation, are shown in Table 1.

In each cryoscopic experiment, the starting solution had a different value of the mole ratio $X_2/(HIO_3 + 2I_2)$. This solution was diluted by successive additions of 100% sulfuric acid to give a range of concentrations. A curve of freezing point *vs.* the stoichiometric concentration of iodic acid was plotted from the results of each experiment, and values of the freezing point at round molal concentrations of iodic acid were obtained by interpolation. The interpolated data were plotted to give a set of graphs of freezing point *vs.* the mole ratio $X_2/(HIO_3 + 2I_2)$, each for a fixed stoichiometric molality of iodic acid. Values of the freezing point at the mole ratio 5.0, obtained from these curves, are given in Table 2.

TABLE 1. Interpolated conductivities and values of γ

Mole ratio $Cl_2/(HIO_3 + 2I_2) = 5.0$			Mole ratio $Br_2/(HIO_3 + 2I_2) = 5.0$		
$10^2 wHIO_3$*	Conductivity $\times 10^2$ (ohm^{-1} cm^{-1})	γ	$10^2 wHIO_3$*	Conductivity $\times 10^2$ (ohm^{-1} cm^{-1})	γ
0.600	1.460	—	0.509	1.322	7.7
0.924	1.815	7.8	0.546	1.346	7.7
1.009	1.845	7.7	0.837	1.658	7.7
1.291	2.150	7.6	0.939	1.798	7.7
1.386	2.233	7.5	1.243	2.129	7.8
1.584	2.474	7.5	1.461	2.385	7.8
1.841	2.688	7.5	1.666	2.597	7.8
2.051	2.908	7.6	1.764	2.711	7.9
2.380	3.165	7.5	1.954	2.885	7.9
2.488	3.311	7.5	2.214	3.170	8.0

*w = molonity, *i.e.* moles solute (kg solution)$^{-1}$ (10).

TABLE 2. Interpolated freezing points and values of ν

	Mole ratio $Cl_2/(HIO_3 + 2I_2) = 5.0$		Mole ratio $Br_2/(HIO_3 + 2I_2) = 5.0$	
$10^2 mHIO_3$*	Freezing point (°C)	ν	Freezing point (°C)	ν
0.50	10.060	16.9	10.064	16.7
0.75	9.850	16.1	9.836	16.4
1.00	9.635	15.7	9.600	16.3
1.25	9.430	15.3	9.384	15.9
1.50	9.222	15.0	9.170	15.6
1.75	9.006	14.8	8.944	15.4
2.00	9.798	14.7	8.702	15.5
2.25	8.580	14.6	8.480	15.3
2.50	8.370	14.5	8.255	—

*Uncorrected for solvent used in reaction.

The curves of conductance and freezing point *vs.* the mole ratio $X_2/(HIO_3 + 2I_2)$ for X = Cl and the conductance curves for X = Br showed breaks close to the mole ratio 5.0. The conductance increased very little beyond this mole ratio, while the freezing point continued to be depressed but less steeply. Cryoscopic experiments were not done for high enough mole ratios to show clearly whether or not there was a break in the freezing point curves in the case X = Br. Before addition of X_2, the solutions were a dirty green color. As X_2 was added, the color gradually changed to a bright orange-red (X = Cl) or a deep red-brown (X = Br), the color change being complete at the mole ratio 5.0. At mole ratios less than 5.0, free halogen vapor was not visible over the solutions, but at mole ratios greater than 5.0 the solutions had an appreciable vapor pressure of X_2. Values of ν, the number of moles of particles produced in solution per mole of iodic acid, were calculated from the freezing point data for the 5.0 mole ratio (Table 2). These values have been corrected for the repression of solvent self-ionization (5) and for solvent used up in the reaction. Values of γ, the number of moles of hydrogensulfate ions produced per mole of iodic acid, were calculated by comparison of the curves of conductance *vs.* concentration at the 5.0 mole ratio, with that for the solute water (6) (Table 1).

Reaction to give ICl_2^+ or IBr_2^+ would take place according to the overall equation

$$[1]\quad HIO_3 + 2I_2 + 5X_2 + 8H_2SO_4 \rightleftharpoons 5IX_2^+ + 3H_3O^+ + 8HSO_4^-$$

$$\nu = 16,\ \gamma = 8\ (X = Cl \text{ or } Br)$$

The experimental values of ν and γ are in good agreement with the predicted values in both cases. The small decrease in ν with increasing concentration can probably be explained by incomplete ionization of the water formed (7). No other reasonable ionization scheme can be found, consistent with the observed ν and γ values.

It should be emphasized that eq. 1 is a net stoichiometric equation only, and there is no suggestion that it represents a mechanism for the formation of IX_2^+. It has been shown (1) that the

Can. J. Chem. Downloaded from www.nrcresearchpress.com by 210.87.254.105 on 09/05/12
For personal use only.

Can. J. Chem. Downloaded from www.nrcresearchpress.com by 210.87.254.105 on 09/05/12
For personal use only.

main iodine-containing species in a solution of $HIO_3 + 2I_2$ in 100% H_2SO_4 are IO^+, $IOSO_4H$, and I_3^+, and these species are no doubt involved in a possibly quite complicated sequence of reactions leading to the final products shown.

The fact that the conductance does not increase significantly after the mole ratio 5.0, while the freezing point continues to be depressed, suggests that the excess of chlorine dissolves in the molecular form rather than reacting to give an ICl_4^+ ion, analogous to I_5^+.

The u.v.–visible absorption spectrum of the ICl_2^+ ion in these solutions shows absorption maxima at 360 nm ($\varepsilon = 56.7 \pm 1.3$) and 452 nm ($\varepsilon = 44.9 \pm 1.2$) while IBr_2^+ gives a maximum at 358 nm ($\varepsilon = 544 \pm 20$) and a broad shoulder at about 540 nm.

In a single conductivity experiment, iodine trichloride was added to a solution of $HIO_3 + 0.33I_2$. The conductivity curve showed a break close to $ICl_3/(HIO_3 + 0.33I_2) = 3.33$, and the value of γ at this mole ratio was 7.7, in agreement with reaction according to the overall equation

$$[2] \quad 3HIO_3 + I_2 + 10ICl_3 + 24H_2SO_4 \rightleftharpoons 15ICl_2^+ + 9H_3O^+ + 24HSO_4^- \qquad \gamma = 8$$

It is of interest that iodine trichloride alone is only sparingly soluble in 100% sulfuric acid, and does not appear to give ICl_2^+ in this solvent, in contrast to its reported behavior in disulfuric acid (4).

Experimental

Iodic acid was recrystallized from dilute (1:4) nitric acid and air-dried at room temperature. *Iodine* (reagent grade) was used without further purification. *Bromine* (reagent grade) was dried over phosphorus pentoxide and distilled. *Chlorine* (Matheson of Canada Ltd.) was dried by passing it over Drierite, then over phosphorus pentoxide.

Freezing points were measured by the Beckman method (8), using a solid stem mercury-in-glass thermometer, graduated in 0.01 °C and read to 0.001 °C, which was calibrated against a platinum resistance thermometer. Freezing of the supercooled solutions was induced by dropping into the cryoscope a small piece of platinum which had been cooled in liquid nitrogen. This has been found to be more reliable than the method used by the earlier workers (8).

The conductivity cells used for the $(HIO_3 + 2I_2) - Br_2$ system have been described previously (9). In early conductance experiments on the $(HIO_3 + 2I_2) - Cl_2$ system, the same cells were used, and the mole ratio $Cl_2/(HIO_3 + 2I_2)$ was determined by removing aliquots of solution for analysis immediately following each conductance measurement. In later experiments, a cell was used which was small enough to be weighed to 1 mg before and after each addition of chlorine. Undissolved chlorine was swept from the cell by a stream of dry nitrogen before each weighing. The cell consisted of a small mixing flask and a side-arm containing the electrodes. The solution was withdrawn into the side-arm for measurements. The initial solution for each cryoscopic experiment on the $(HIO_3 + 2I_2) - Cl_2$ system was prepared in this cell, and a weighed amount transferred to the cryoscope. Conductance measurements were made with the cells immersed in an oil thermostat regulated at 25 ± 0.002 °C by means of a Bayley Instrument Co. Model 116 Precision Temperature Controller. The temperature of the bath was measured by a calibrated solid stem mercury-in-glass thermometer. Resistances of solutions were measured using a Beckman Model RC 18 conductivity bridge.

Full details of the conductometric and cryoscopic results are available elsewhere.[2]

Ultraviolet–visible spectra were recorded on a Cary 14 spectrophotometer, using 1 cm quartz cells.

We are grateful to the National Research Council of Canada for financial support of this work.

1. R. A. Garrett, R. J. Gillespie, and J. B. Senior. Inorg. Chem. **4**, 563 (1965).
2. C. G. Vonk and E H. Wiebenga. Acta Cryst. **12**, 859 (1959).
3. F. Aubke and G. H. Cady. Inorg. Chem. **4**, 269 (1965).
4. R. J. Gillespie and K. C. Malhotra. Inorg. Chem. **8**, 1751 (1969).
5. S. J. Bass, R. J. Gillespie, and E. A. Robinson. J. Chem. Soc. 821 (1960).
6. S. J. Bass, R. J. Gillespie, R. H. Flowers, E. A. Robinson, and C. Solomons. J. Chem. Soc. 4320 (1960).
7. S. J. Bass, R. J. Gillespie, and J. V. Oubridge. J. Chem. Soc. 837 (1960).
8. R. J. Gillespie, E. D. Hughes, and C. K. Ingold. J. Chem. Soc. 2473 (1950).
9. R. J. Gillespie and J. B. Senior. Inorg. Chem. **3**, 440 (1964).
10. R. J. Gillespie and C. Solomons. J. Chem. Educ. **37**. 202 (1960).

[2]Full details of the experimental results may be obtained free of charge, upon request, from the Depository of Unpublished Data, National Science Library, National Research Council of Canada, Ottawa, Canada.

Can. J. Chem. Downloaded from www.nrcresearchpress.com by 210.87.254.40 on 09/05/12
For personal use only.

Composition of Tetrahydrofuran Hydrate and the Effect of Pressure on the Decomposition[1]

S. R. GOUGH AND D. W. DAVIDSON
Division of Chemistry, National Research Council of Canada, Ottawa, Canada

Received March 12, 1971

The decomposition temperature of the structure II clathrate hydrate of tetrahydrofuran has been followed to pressures above 3 kbars, where the hydrate is found to decompose incongruently in the regions of stability of ices III and II, with no evidence of formation of a denser hydrate. From measurements of liquid solution densities and of volume changes at hydrate decomposition the density of the hydrate was obtained. Comparison with the X-ray lattice dimension indicates that at least 98% of the large cages are occupied, the principal uncertainty being in the lattice parameter. A similar treatment is made of Tammann and Krige's data (23) for chloroform hydrate. Analysis of the results of 18 composition determinations of structure II hydrates shows no statistical evidence of departure from the ideal composition of 17 mol of water per mol of hydrate former.

La température de décomposition du clathrate hydraté de structure II du tétrahydrofuranne a été suivie jusqu'à des pressions supérieures à 3 kbar; il a été trouvé que dans ces régions de stabilité des glaces III et II l'hydrate se décompose d'une façon aberrante sans preuve de formation d'un hydrate plus dense. A partir des mesures de densité des solutions liquides et des changements de volume à la décomposition de l'hydrate, il a été possible d'obtenir la densité de l'hydrate. La comparaison avec la dimension du réseau obtenu par rayons X indique qu'au moins 98% des grandes cages sont occupées, l'incertitude principale étant dans le paramètre rétuculaire. A partir des données de Tamman et Krige une analyse similaire est effectuée pour le chloroforme hydraté. Les analyses des résultats se rapportant à 18 déterminations de composition d'hydratés ayant la structure II ne montrent aucune preuve statistique d'écart par rapport à la composition idéale de 17 mol d'eau par mole de générateur d'hydrate.

Canadian Journal of Chemistry, 49, 2691 (1971)

Among the diverse molecules now known to form "gas hydrates" of von Stackelberg's structures I and II (1) are a number of ethers and ketones which are distinguished from the classical gas-hydrate formers by their solubility in water and by the possibility of hydrogen bonding with the host water molecules of the clathrate structures. Ethylene oxide (2, 3) and trimethylene oxide (4) form hydrates of type I. Structure II hydrates are formed by dimethyl ether (1), by trimethylene oxide, tetrahydrofuran, 2,5-dihydrofuran, propylene oxide, and 1,3-dioxolane (4, 5) and by acetone (6, 7) and cyclobutanone (5, 8). With the exception of the study by Glew and Rath (9) of the variable composition of ethylene oxide hydrate, there appears to be no accurate information about the degree of occupancy of the cages or the heat of formation of these hydrates.

Trimethylene oxide (4) and acetone (8) hydrates decompose incongruently. Of the other structure II hydrates only tetrahydrofuran hydrate melts appreciably above 0 °C. This hydrate is therefore most easily distinguished from ice and has been chosen for further study.

Tetrahydrofuran hydrate was first reported by Palmer (10) who found from melting point *vs.* concentration curves a composition of between 13 and 16 molecules of water per molecule of tetrahydrofuran (THF), with a probable formula of $THF \cdot 14H_2O$. Erva (11) obtained a congruent melting point of 4.38 °C at an approximate composition of $THF \cdot 16H_2O$. Several nugatory irregularities in the melting points of solutions of higher THF content were interpreted as peritectic points of lower hydrates (11) or in terms of discrete association complexes in liquid solution (12). They are more likely to be related to the incorporation of different amounts of air in different hydrate samples.

Among several indirect methods (13) of determining the composition of clathrate hydrates, one which is particularly applicable to the hydrates of water-soluble molecules depends on comparison of measured hydrate density with the composition-dependent density calculated from the X-ray unit cell dimensions. Glew and Rath (9) have used the results of flotation mea-

[1]NRCC No. 12002.

surements of the density of ethylene oxide hydrate in conjunction with the lattice parameter to obtain compositions of this hydrate. We have determined the density of THF hydrate from measurements of the volume change at hydrate decomposition and of the density of the liquid solution. Volume, capacitance, and thermal-analysis measurements were made to high pressures to determine the effect of pressure on the hydrate–solution equilibrium and to look for evidence of a transformation of the hydrate to a denser crystallographic form. Heats of formation of the hydrate were estimated from the results.

Experimental Methods

The initial measurements were made to define the region of stability of THF hydrate in the pressure–temperature plane. The decomposition of the hydrate was followed by the capacitance, conductance, and volume changes which accompanied increase of temperature or pressure through the decomposition region. Some experiments were also made with pressure decreasing. The cell used was that previously described (Fig. 1(*b*) of ref. 14), with essentially the same methods of control and measurement of temperature and pressure. The electrical measurements were normally made at 20 kHz. The driving piston was coupled to a slow-speed motor to effect rotational oscillation through $\pm 4°$ and thereby to reduce piston friction. Volume changes were measured in terms of displacement of this piston which was monitored to 10 μin. by a dial gauge.

Solutions were prepared from conductivity water and THF which had been distilled over calcium hydride. Analysis by vapor phase chromatography showed the THF to contain 0.1% of volatile impurity. Compositions ranged from $THF{\cdot}17.0H_2O$ to $THF{\cdot}16.8H_2O$. Hydrate was normally prepared by cooling to below 0 °C and conditioning at +2 °C and 1 atm for about 12 h, followed by over-night conditioning at a temperature and pressure near the starting point of the decomposition measurements.

Most hydrate samples showed relatively small capacitance and volume changes associated with the melting of ice: conductance was particularly sensitive to such eutectic melting. For these samples both ice and hydrate melting data were recorded. Since the measuring thermocouple was outside the pressure vessel (14) in these measurements, melting points were taken as the temperatures at the onset of melting, upon which there was usually agreement to within a few tenths of a degree among the parameters measured. Figure 1 illustrates such warming curves. Measurements with varying pressure refer to equilibrated temperatures, but the transitions tended to occur over a range of pressure and to show hysteresis when the pressure change was reversed (Fig. 2). Nevertheless, the hydrate and ice melting points appear to have been generally defined to better than 1° and 100 bars.

Considerably more accurate determination of the variation of hydrate decomposition temperature (and volume) with pressure to 1400 bars was realized by insertion of a calibrated Chromel–Alumel thermocouple into the center of the sample, the insulated leads, swaged in a stainless steel tube, being brought out through the lower electrode and piston. Since the presence of the thermocouple interfered with the electrical measurements, the decomposition temperature was determined from the dilatometric and thermal (temperature *vs.* time) measurements only, as the mid-points of the volume changes or of the thermal steps. An example is shown in Fig. 3. All such measurements were made with a sample of composition $THF{\cdot}16.69H_2O$ at a heating rate of about 0.2°/min.

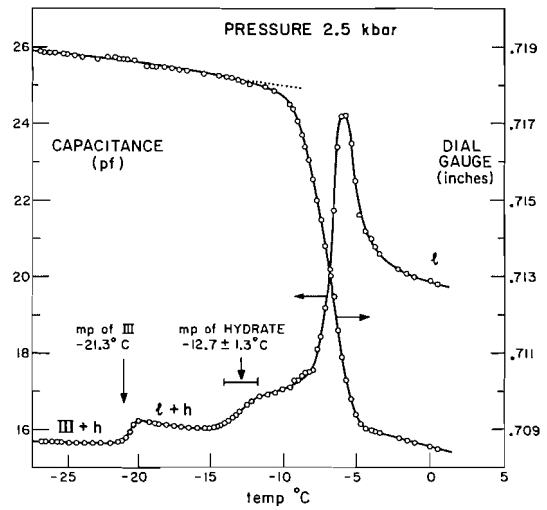

FIG. 1. Illustration of capacitance and volume changes at temperatures of phase changes in the THF–water system.

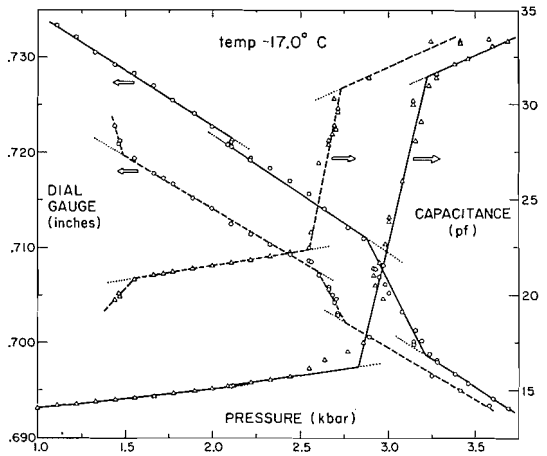

FIG. 2. Capacitance and volume changes at pressures of hydrate decomposition (pressure increasing, solid lines) and formation (pressure decreasing, broken lines).

Can. J. Chem. Downloaded from www.nrcresearchpress.com by 210.87.254.40 on 09/05/12
For personal use only.

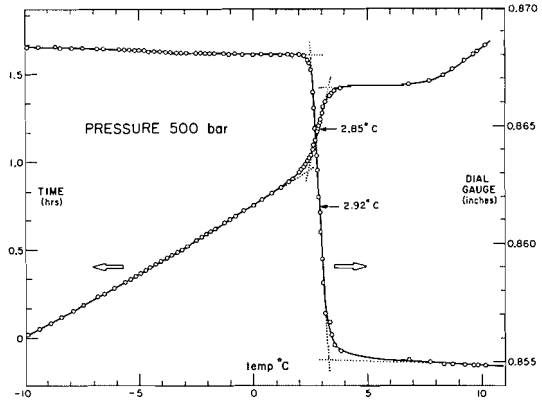

FIG. 3. Example of determination of temperature and volume change of decomposition of THF hydrate.

Densities of liquid solutions near 4 °C were measured with a quartz pycnometer of 11 ml capacity designed after Kirshenbaum (15) and calibrated with mercury and water at 4 °C. The bath temperature was regulated to ±0.01 °C and measured with a platinum resistance thermometer.

Results

Solution Densities

The densities of a solution of composition THF·16.98H_2O at four temperatures near the hydrate decomposition point at 1 atm are given in Table 1, along with a single measurement of a more dilute solution. The accuracy is considered to be ±0.00003 g/cm³, with a relative accuracy with respect to temperature change of the first solution of ±0.00001 g/cm³. These data are sufficient to define the dependence on composition and temperature necessary for determination of the density at the decomposition temperature and over the range of possible hydrate compositions considered below. The appreciable decrease of density with increase of temperature is not surprising, since Wada and Umeda (16) found that THF lowers the temperature of maximum density of water. Extrapolation of their results suggests this temperature to be about −15 °C for a composition of THF·17H_2O.

Phase Equilibria of THF Hydrate

Figure 4 (heavy line) shows the region of stability of THF hydrate. At pressures below 3.05 kbar the hydrate melts congruently to a liquid of greater density, the curvature of the temperature–pressure line being determined by the larger compressibility and thermal contraction of the liquid. This part of the hydrate decomposition curve intersects the freezing curve of ice III in the presence of liquid of hydrate composition at −19.8 °C and 3.05 kbar. At higher pressures the hydrate (h) "melts" incongruently to give ice III and a peritectic liquid (l), the dependence of decomposition temperature on pressure becoming increasingly great as ice III is formed in greater proportion. The decomposition curves in this region were not well enough defined to distinguish between the h → III + l and h → V + l curves, ice V (as shown by its melting behavior) having been obtained in most pressurizing runs within the region of stability of ice III. When the ice formed is V, the melting of the hydrate remains congruent to about −21.4 °C and 3.12 kbar. At lower temperatures the equilibrium decomposition is to ice II and THF-rich liquid. Dielectric studies (to be published elsewhere) show the hydrate to be stable to at least 3.5 kbar at −62 °C.

There was no evidence of formation of a denser hydrate.

TABLE 1. Densities of THF solutions

Composition	Temperature (°C)	Density (g/cm³)
THF·16.98H_2O	4.03_5	0.99730
	4.13_3	0.99726
	4.31_1	0.99719
	4.67_5	0.99706
THF·17.99H_2O	3.98_0	0.99768

Melting of Ice in the Presence of THF

Over its full range, the curve corresponding to eutectic melting of ice I in the presence of hydrate (Fig. 4) lies about 1° below the melting curve of ice I given by Bridgman (17). This suggests that the eutectic composition shows little variation over this pressure range from its value (0.9 mol% THF (11)) at 1 bar and that the partial molar volume of water (V_1) in the eutectic liquid is not much different from the molar volume of pure water (V_1^0) at the same pressure. The increasing depression of the freezing point of ice III with increase of pressure corresponds to increasing THF content of the eutectic solution, which reaches the hydrate composition at the intersection with the hydrate melting curve. On the other hand, the increasing depression of the freezing point of ice V, 5° at 6.2 kbar, is due to an increasing value of $V_1^0 - V_1$, where V_1 refers to the liquid of the same composition as the hydrate.

Can. J. Chem. Downloaded from www.nrcresearchpress.com by 210.87.254.40 on 09/05/12
For personal use only.

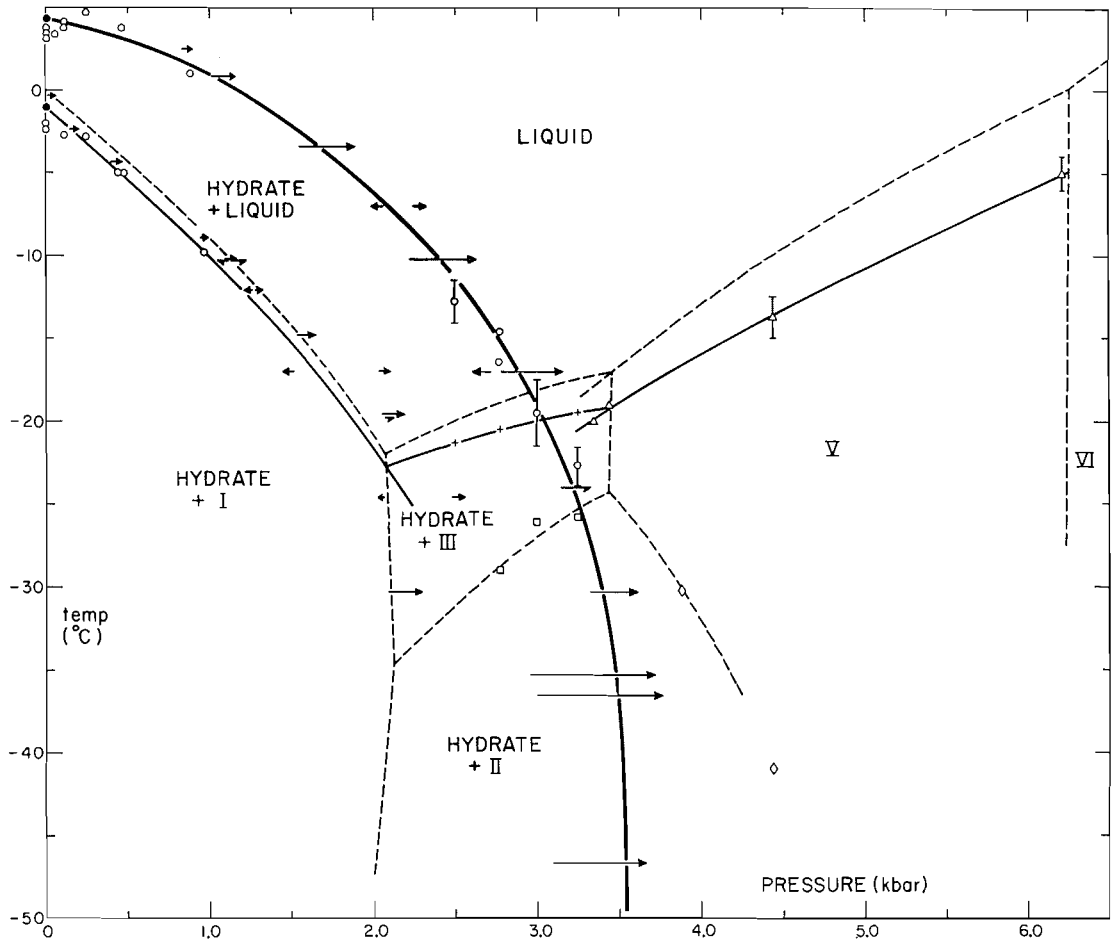

FIG. 4. Phase diagram of the THF–water system. The heavy line is the decomposition curve of THF hydrate, light lines are water-rich eutectic points (to left of heavy line) or melting points of ice in the THF·17H_2O system (to right), and broken lines are Bridgman's phase boundaries in the water system.

Dependence of Decomposition Temperature on Pressure

The decomposition temperature of THF·16.69-H_2O given by the mid-points of the thermal steps in the temperature *vs.* time curves were measured at 17 pressures between 1 and 1400 bars. The results (Fig. 5) are given, to a standard deviation (σ) of 0.080°, by

$$[1] \quad t(°C) = (4.126 \pm 0.035) - (2.280 \pm 0.139) \times 10^{-3} P - (1.150 \pm 0.112) \times 10^{-6} P^2$$

where P is the pressure in bars.

The temperatures at the mid-points of the corresponding volume changes were measured at 14 pressures (Fig. 5) and are given, with $\sigma = 0.093°$, by

$$[2] \quad t\,(°C) = (4.279 \pm 0.082) - (2.375 \pm 0.259) \times 10^{-3} P - (1.169 \pm 0.176) \times 10^{-6} P^2$$

No reduction of variance was achieved by the inclusion of terms in P^3 in the least squares analyses.

The mid-points of the decomposition curves were chosen for greatest accuracy of the pressure dependence of the melting points. Equations 1 and 2 are expected to underestimate the melting

Can. J. Chem. Downloaded from www.nrcresearchpress.com by 210.87.254.40 on 09/05/12
For personal use only.

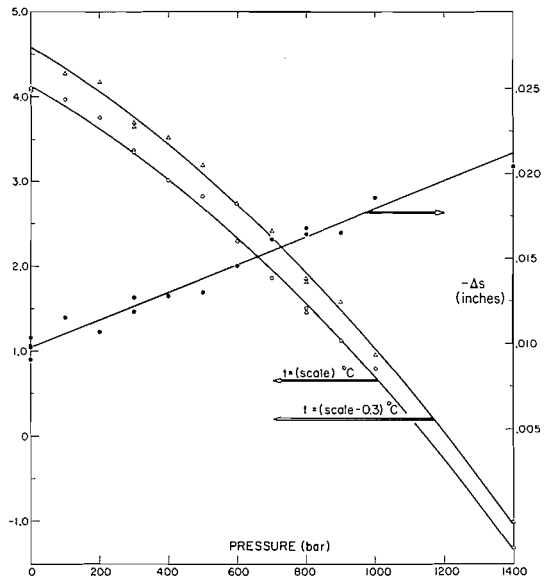

FIG. 5. Pressure dependence of decomposition temperature from thermal (○) and volume (△) measurements and of change of piston displacement (●) at decomposition. (The decomposition temperatures from volume measurements are displaced upward by 0.3 °C.)

point of the hydrate at 1 bar because of the central position in the sample of the measuring thermocouple. This appears to be less true of eq. 2, possibly because of some lag of the piston behind the change of volume.

The linear coefficients in eqs. 1 and 2 may be combined to yield

$$[3] \quad \left(\frac{dt}{dP}\right)_{P\to 0} = -(2.301 \pm 0.122) \times 10^{-3}$$

degrees per bar, the error quoted, like those of eqs. 1 and 2, being the standard error.

Volume Change of Hydrate Decomposition

Seventeen measurements of the change of dilatometer gauge reading for THF·16.69H_2O at pressures between 1 and 1400 bars (Fig. 5) gave

$$[4] \quad \Delta s \text{ (in.)} = -(0.00972 \pm 0.00021) - (8.22 \pm 0.35) \times 10^{-6} P$$

The value of σ (0.00057 in.) was scarcely improved, and the constant term hardly affected, by inclusion of a term in P^2.

Division of Δs for $P = 1$ bar, by the length of the column of liquid solution at 4.4 °C gave

$$[5] \quad \Delta v/v = \Delta s/s = -(0.01470 \pm 0.00034)$$

for the relative change of volume. From Table 1 the density of liquid THF·16.69H_2O at 4.4 °C may be taken as 0.99705 ± 0.00004 g cm^{-3}, whence the change of volume is -5.496 ± 0.129 cm^3 per mol of THF·16.69H_2O.

This volume change is not quite the desired volume change for congruent melting of 1 mol of hydrate of composition THF·nH_2O, since $n > 16.69$. Some melting of the hydrate occurs over the whole temperature between the THF-rich eutectic temperature and the final melting point. Examination of the volume *vs.* temperature curves shows that a contribution to the *measured* volume change is first detected about 1° below the temperature of final melting. Erva's data (11) show the liquid composition to be THF·7.5H_2O at this temperature. The measured volume change then corresponds to

$$[6] \quad x[\text{THF}\cdot n\text{H}_2\text{O(h)}] + (1 - x)[\text{THF}\cdot 7.5\text{H}_2\text{O(l)}] \rightarrow [\text{THF}\cdot 16.69\text{H}_2\text{O(l)}]$$

where $x = 9.19/(n - 7.5)$ is the fraction of THF present in the hydrate at the onset of melting.

Reaction 6 may be considered as the sum of the processes of melting x mol of hydrate and of mixing x mol of liquid THF·nH_2O with $(1 - x)$ mol of liquid THF·7.5H_2O. The volume change of mixing is zero for an ideal solution. The density measurements of THF–water solutions at 25 °C by Critchfield *et al.* (18) give zero for this volume change, with n near 17, to within the experimental accuracy of 0.02%. We ascribe the whole of the measured volume change to the melting of x mol of hydrate and put for the melting of 1 mol

$$[7] \quad \Delta V(\text{h} \rightarrow \text{l}) = \frac{-5.496}{x} \pm \frac{1}{x}\sqrt{30.25(1 - x)^2 + 0.0640}$$

The error estimate[2] has been conservatively written to include an uncertainty in the correction $(1/x)$ of the order of magnitude of the correction itself and the original standard error of the measured volume change has been expanded to the 95% confidence level.

[2]The error in x is assumed to be $x(1 - x)$ and in the measured volume change 1.96×0.129 cm^3.

Can. J. Chem. Downloaded from www.nrcresearchpress.com by 210.87.254.40 on 09/05/12
For personal use only.

Can. J. Chem. Downloaded from www.nrcresearchpress.com by 210.87.254.40 on 09/05/12
For personal use only.

Hydrate Composition

The molar volume of THF·nH$_2$O(l) at 4.4° may be written as

$$[8] \quad V(\mathrm{l}) = \frac{72.10 + 18.015n}{0.99716 + 0.000364(n - 16.98)} \text{ cm}^3$$

and that of the solid hydrate as

$$[9] \quad V(\mathrm{h}) = \frac{Nna^3}{136} \text{ cm}^3$$

where N is Avogadro's number and a is the dimension of the cubic unit cell which contains 136 water molecules. Unfortunately, a is not accurately known at the decomposition temperature of the hydrate. Von Stackelberg and Meuthen's value (2) of 17.18 Å at −10 °C appears to be uncertain by as much as 0.10 Å. The more accurate values of Sargent and Calvert (5), *viz.*, 17.13 ± 0.03 Å at −163 °C and two values of 17.170 ± 0.004 and 17.162 ± 0.007 Å at −137 °C (the errors are σ's), refer to much lower temperatures. The values (5) for the closely related hydrate of dihydrofuran, almost identical with those of THF hydrate at −137 °C, include 17.22 ± 0.01 Å at −40 °C. Extrapolation of the combined data for THF and dihydrofuran hydrates to 4 °C gives 17.24 Å, to which we assign a maximum uncertainty of ±0.03 Å.

In Fig. 6 volumes given by eq. 7 and by the difference between eqs. 8 and 9 are plotted against n for values of a between 17.21 and 17.27 Å.

The most probable value of n is 16.86. For the range of lattice parameters allowed, values between about 16.4 and 17.5 are formally permitted. It is unlikely, however, that THF (maximum diameter 5.9 Å (2)) can occupy the small cages of free diameter 4.9 Å and therefore that n is less than 17. It may also be noted that a = 17.21 Å, for which n is 17.34 ± 0.20, is much less likely than a = 17.23 Å, with n = 17.01 ± 0.16. We conclude, at about the 90% confidence level, that at least 98% of the large cages are occupied.

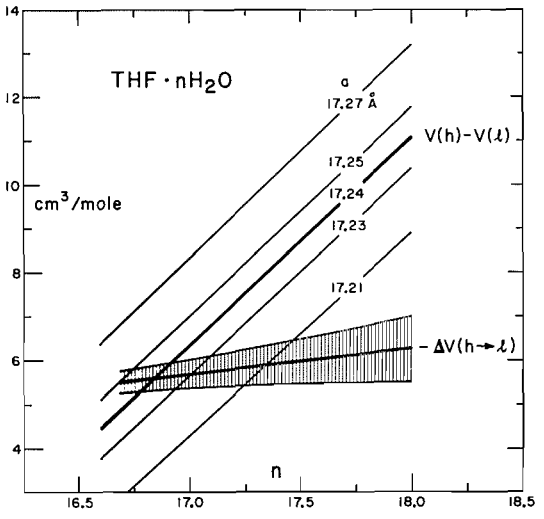

FIG. 6. Dependence of volume change at decomposition on composition of THF hydrate.

Effect of Air on Hydrate Properties

Under the conditions of our experiments, in which the only air present was that initially dissolved in the liquid, the effect of air on the volume changes discussed above may be shown to be negligible. Saturation with air at 1 atm affects the density of liquid water only in the sixth decimal place (19) and therefore may be assumed to have a negligible effect on the density of the THF solution. If the air present in the solution (assumed to be the amount soluble in water at 4 °C) is entirely taken into the small cages of the hydrate, the hydrate density is increased by 0.000034 g/cm^3 and the volume change of melting reduced by only 0.013 cm^3/mol.

It is well-known that some hydrates grown in the presence of air incorporate large quantities of air in their cages, with a consequent increase of stability (see refs. 13 and 20, for example). A simple experiment showed this to be true of THF hydrate. A sample of THF·16.79H$_2$O was slowly frozen and conditioned in an ice bath for several hours. The warming curve obtained in an air-jacketed glass vessel showed the great bulk of the sample to melt at 4.45 °C. With further warming the remaining crystals gradually melted with the evolution of air bubbles and only completely disappeared at 5.0 °C. It is likely that the presence of air accounts for Palmer's report (10) of two maximum melting points at 5.07 and 5.37 °C. The available data suggest that the melting point of THF hydrate containing little or no air lies at 4.4 ± 0.1 °C.

Heats of Decomposition

The enthalpy change of congruent melting at negligible pressure is given by

$$[10] \quad \Delta H(\mathrm{h} \rightarrow \mathrm{l}) = \frac{T\Delta V(\mathrm{h} \rightarrow \mathrm{l})}{\left(\frac{\mathrm{d}t}{\mathrm{d}P}\right)_{P \rightarrow 0}}$$

The pressure coefficient of the melting point is

Can. J. Chem. Downloaded from www.nrcresearchpress.com by 210.87.254.40 on 09/05/12
For personal use only.

TABLE 2. Enthalpies of decomposition of THF hydrate

Decomposition	Temperature (°C)	ΔH (kcal/mol)
$h \rightarrow l$	4.4	16.7±1.9
$h \rightarrow l_1 + l_2$	4.4	19.5±2.0
$h \rightarrow l_1 + g$	4.4	27.1±2.0
$h \rightarrow l_1 + g$	0	26.5±2.1
$h \rightarrow I + g$	0	2.1±2.1

given by eq. 3. With $\Delta V(h \rightarrow l) = -5.8 \pm 0.3$ cm^3, $\Delta H(h \rightarrow l) = 16.7 \pm 1.9$ kcal/mol, at about the 95% confidence level.

We have crudely measured the heat of mixing of 1 mol of THF and 17 mol of water at a mean temperature of 4 °C, and found $\Delta H(l_1 + l_2 \rightarrow l) = -2.8 \pm 0.2$ kcal. This value is consistent with values read from Erva's figure (21), *viz.*, −2.25 and −2.60 kcal for mixing at 25 and 15 °C, respectively. The heat of vaporization of liquid THF at 4.4 °C is found from the vapor pressure equation (22) to be $\Delta H(l_2 \rightarrow g) = 7.6 \pm 0.1$ kcal/mol. These quantities, together with estimates of specific heats between 4.4 and 0 °C, give the enthalpy changes shown in Table 2.

Discussion

Chloroform Hydrate

The only comparable study of the volume change of decomposition of a structure II hydrate appears to be that of Tammann and Krige (23), who measured the volume change and temperature of decomposition of chloroform hydrate to the sparingly miscible liquids at pressures to 2 kbar. Analysis of their data gives, with $\sigma = 0.00144$ cm^3/g,

$$[11] \quad \Delta v = (0.01956 \pm 0.00174) - (5.547 \pm 0.470) \times 10^{-5} P + (1.0353 \pm 0.2476) \times 10^{-8} P^2$$

for the change in volume per gram of hydrate. These volume changes were measured indirectly from the changes of pressure at decomposition and were corrected (23) for the considerable amounts of excess water present. From eq. 11, $\Delta V(h \rightarrow l_1 + l_2)$ per mol of hydrate at 1 bar (and about 2 °C) may be written as a function of n.

The solubility at 2 °C of chloroform in water is only 0.96 and of water in chloroform only 0.02 weight % (24). Little error is introduced by assuming additivity of molar volumes in these dilute solutions:

$$[8'] \quad V(l_1 + l_2) = \frac{119.39}{1.5222} + \frac{18.015n}{0.999947}$$

where the density of chloroform is from Timmermans (25). $V(h)$ is given by eq. 9 with $a = 17.33 \pm 0.10$ Å (26).

The volume differences for chloroform hydrate are shown in Fig. 7. The uncertainty shown for $\Delta V(h \rightarrow l_1 + l_2)$ is double the standard error of the constant term in eq. 11.

The most probable value of n is 17.25, but a value as high as 19.0 cannot be definitely excluded because of the large uncertainty of the lattice parameter. Conversely, if, as there is good reason to assume (see below), the large cages are at least 98% occupied, the value of a is defined between 17.30 and 17.37 Å.

The pressure-dependence of the decomposition temperature of chloroform hydrate was not measured (23) with sufficient accuracy to permit a useful estimation of $\Delta H(h \rightarrow l_1 + l_2)$ from eq. 10. This quantity was found to be 22.9 kcal/mol by a calorimetric study made in 1885 (27). Addition of the heat of vaporization of chloroform at 2 °C gives $\Delta H(h \rightarrow l_1 + g) \simeq 30.7$ kcal/mol.

Critical Decomposition Temperatures of Structure II Hydrates

For THF and chloroform hydrates the decomposition temperature is highest in the absence of externally-applied pressure. The melting tempera-

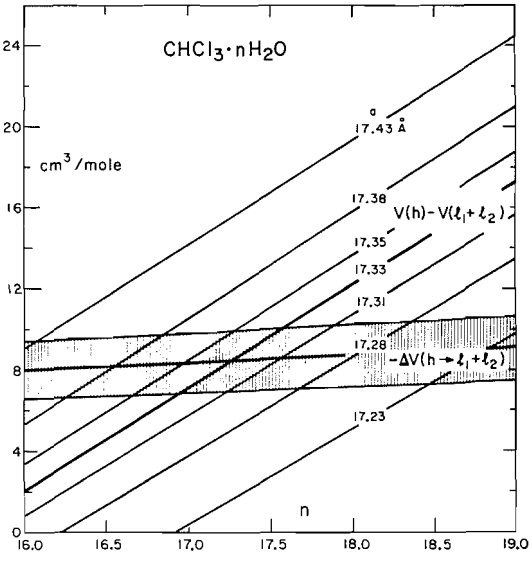

FIG. 7. Dependence of volume change at decomposition on composition of chloroform hydrate.

TABLE 3. Composition of structure II hydrates*

Hydrate	ΔH_1 (h → l_1 + g) (kcal/mol)	ΔH_2 (h → I + g) (kcal/mol)	From ΔH_1–ΔH_2		From effect of NaCl		Direct analysis
			n	*w*	*n*	*w*	*n*
SF_6	29.57	5.14	17.02(33)	3			
Cyclopropane	29.2	6.42	15.87(34)	1	17.05(34)	3	
(Deuterate)	32.37	6.44	17.18(35)†	3			
n-Propane	32.1	6.34	17.94(36)	1	17.9 (37)	1	19.7(38)
Isobutane	30.5	5.45	17.45(39)	2	17.50(39)	2	17.1(40)
CH_3I	31.4	7.3	16.79(13)	1			
$CHCl_3$	30.7‡		17.25§	1			18 (27) 17.7(31)
$CHCl_2F$	32.72	8.51	16.86(41)	2	16.80(42)	2	
CCl_3F	35.45	11.57	16.63(42)	0			
CCl_2F_2	30.14	7.79	15.57(42)	0			
$CBrClF_2$	32.567 31.86(43)	8.254	16.94(29)	4	16.57(43)	2	
$CBrF_3$	29.42	6.99	15.62(42)	0			
CH_3CH_2Cl	31.9	8.7	16.16(13)	1			
CH_3CClF_2	31.11	7.49	16.45(44)	1	17.18(44)	2	
C_4H_8O	27.1‡		16.86§	3			

*Reference numbers in parentheses.
†Based on heat of fusion of D_2O of 1515 cal/mol.
‡Indirect value (see text).
§Present result from the density measurement method.

ture measured under the saturated vapor pressure of the hydrate is therefore a true "critical decomposition temperature", a result probably generally true of all simple structure II hydrates which decompose to give liquids. On the other hand, acetone hydrate decomposes to ice (and relatively acetone-rich liquid) at its incongruent melting point (8), which may be expected to rise somewhat with the application of pressure.

Compositions of Structure II Hydrates

Table 3 gives the results of earlier composition studies of structure II hydrates. The second and third columns show, respectively, the molar heats of decomposition into liquid water and gaseous hydrate-former and into ice I and gaseous hydrate-former, as derived from the dependence of pressure on temperature along the respective three-phase equilibrium lines. The difference between these heats at 0 °C is $n\Delta H(\mathrm{I} \rightarrow l_1)$ (28). The value *n* so obtained, with the heat of fusion of ice taken as 1435.7 cal/mol, is given in column 4. These values of *n* vary greatly in accuracy, not only with the number and accuracy of the original data, but also with the adequacy of the corrections made for gas imperfection, the presence of water vapor in the gas, and the effect of finite solubility of hydrate-former in water. Only Glew (29) appears to have combined accurate measurements with a proper statistical study of the errors. We have attempted to represent the relative accuracy of individual values of *n* in terms of weights (*w*) assigned on a scale of 0 to 4.

Values of *n* in column 6 were derived from the shift of the h–l_1–g equilibrium produced by addition of NaCl, according to the method of Miller and Strong (30). The values in the final column are the results of various attempts at direct analysis and are generally of lower accuracy. An exception is the analysis of chloroform hydrate by Barrer and Ruzicka (31) who found the large cages to be 94 to 98% occupied by chloroform with measurements made in the presence of various "help gases".

Consideration of these results suggests that in no case has a statistically significant departure from the ideal composition of $n = 17$ been demonstrated. Certainly this is true of the results as a whole. With cases of $w = 0$ omitted, the unweighted mean of the values of *n* in columns 4 and 6 is 16.99 ± 0.54. More realistically, weighting according to w^2 gives 17.01 ± 0.31. Thus at about the 85% level of confidence, more than 98% of the large cages are occupied.

We conclude that the available composition data for structure II hydrates are of insufficient accuracy to test the extent of applicability of the relation between the μ-potential of water in equilibrium with the clathrate (μ_1) and that of

Can. J. Chem. Downloaded from www.nrcresearchpress.com by 210.87.254.40 on 09/05/12
For personal use only.

the empty lattice (μ_1^0),

$$[12] \qquad \mu_1 = \mu_1^0 + \frac{kT}{17}\ln\left(1 - \frac{17}{n}\right)$$

given by the ideal solid solution theory (32). Equation 12 predicts an invariable composition for these hydrates in equilibrium with ice at a fixed temperature and pressure and gives $(\mu_1^0 - \mu_1) > 125$ cal/mol for more than 98% occupancy of the cages at 0 °C.

We are greatly indebted to R. E. Hawkins for technical assistance.

1. M. von Stackelberg and H. R. Müller. Z. Elektrochem. **58**, 25 (1954).
2. M. von Stackelberg and B Meuthen. Z. Elektrochem. **62**, 130 (1958).
3. R. K. MacMullan and G. A. Jeffrey. J. Chem. Phys. **42**, 2725 (1965).
4. R. E. Hawkins and D. W. Davidson. J. Phys. Chem. **70**, 1889 (1966).
5. D. F. Sargent and L. D. Calvert. J. Phys. Chem. **70**, 2689 (1966).
6. A. S. Quist and H. S. Frank. J. Phys. Chem. **65**, 560 (1961).
7. G. J. Wilson and D. W. Davidson. Can. J. Chem. **41**, 264 (1963).
8. B. Morris and D. W. Davidson. Can. J. Chem. **49**, 1243 (1971).
9. D. N. Glew and N. S. Rath. J. Chem. Phys. **44**, 1710 (1966).
10. H. A. Palmer. Thesis. University of Oklahoma. 1950.
11. J. Erva. Suomen Kemistil. **29B**, 183 (1956).
12. K. L. Pinder. Can. J. Chem. Eng. **43**, 271, 274 (1965).
13. M. von Stackelberg. Naturwiss. **36**, 327, 359 (1949).
14. S. R. Gough and D. W. Davidson. J. Chem. Phys. **52**, 5442 (1970).
15. I. Kirshenbaum. Physical properties and analysis of heavy water. McGraw-Hill Book Co., Inc., New York. 1951. p. 6.
16. G. Wada and S. Umeda. Bull. Chem. Soc. Japan, **35**, 1797 (1962).
17. P. W. Bridgman. Proc. Am. Acad. Arts Sci. **47**, 441 (1912).
18. F. E. Critchfield, J. A. Gibson, Jr., and J. L. Hall. J. Am. Chem. Soc. **75**, 6044 (1953).
19. Landolt-Bornstein Zahlenwerte und Funktionen. Vol. IV. 6th ed. Springer-Verlag, Berlin. Part 1, p. 101.
20. M. von Stackelberg and W. Meinhold. Z. Elektrochem. **58**, 40 (1954).
21. J. Erva. Suomen Kemistil. **28B**, 131 (1955).
22. R. Cigna and E. Sebastiani. Annali di Chim. **54**, 1048 (1964).
23. G. Tammann and G. J. R. Krige. Z. anorg. allgem. Chem. **146**, 179 (1925).
24. Landolt-Bornstein Zahlenwerte und Funktionen. Vol. II. Part 2*b*, p. 3–400.
25. J. Timmermans. Proc. Roy. Soc. Dublin, **13**, 327 (1912).
26. M. von Stackelberg and W. Jahns. Z. Elektrochem. **58**, 162 (1954).
27. G. Chancel and F. Parmentier. Compt. rend. **100**, 27 (1885).
28. F. E. C. Scheffer and G. Meyer. Proc. Roy. Acad. Sci. Amsterdam, **21**, 1204 (1919); **21**, 1338 (1919).
29. D. N. Glew. Can. J. Chem. **38**, 208 (1960).
30. B. Miller and E. R. Strong, Jr. Am. Gas Assoc. Monthly, **28**, No. 2, 63 (1946).
31. R. M. Barrer and D. J. Ruzicka. Trans. Faraday Soc. **58**, 2239 (1962).
32. J. H. van der Waals and J. C. Platteeuw. Adv. Chem. Phys. **2**, 1 (1959).
33. L. D. Sortland and D. B. Robinson. Can. J. Chem. Eng. **42**, 38 (1964).
34. D. R. Hafemann and S. L. Miller. J. Phys. Chem. **73**, 1392 (1969).
35. D. R. Hafemann and S. L. Miller. J. Phys. Chem. **73**, 1398 (1969).
36. W. M. Deaton and E. M. Frost, Jr. Monograph No. 8, U.S. Bureau of Mines. 1946.
37. A. J. Barduhn, H. E. Towlson, and Y. C. Hu. Am. Inst. Chem. Eng. J. **8**, No. 2, 176 (1962).
38. P. J. Ceccotti. Ind. Eng. Chem. Fundam. **5**, No. 2, 106 (1966).
39. A. J. Barduhn, O. S. Rouher, and D. J. Fontagne. U.S. Office of Saline Water, Res. Dev. Prog. Report 366, 1968.
40. T. Uchida and I. Hayana. Govt. Chem. Ind. Res. Inst. Tokyo, **59**, 382 (1964).
41. W. P. Banks, B. O. Heston, and F. F. Blankenship. J. Phys. Chem. **58**, 962 (1954).
42. T. A. Wittsruck, W. S. Brey, Jr., and W. H. Rodebush. J. Chem. Eng. Data, **6**, 343 (1961).
43. Syracuse Univ. Res. Inst. U.S. Office of Saline Water Res. Dev. Prog. Report, 70, 1963.
44. F. A. Briggs, Y. C. Hu, and A. J. Barduhn. U.S. Office of Saline Water Res. Dev. Prog. Report 59, 1962.

Can. J. Chem. Downloaded from www.nrcresearchpress.com by 210.87.254.40 on 09/05/12
For personal use only.

Can. J. Chem. Downloaded from www.nrcresearchpress.com by 210.87.254.6 on 09/05/12
For personal use only.

Thermodynamic Constants of Tetracyanoethylene Complexes with Methylated Benzenes

S. C. LIAO[1] AND R. K. CHAN[2]

Department of Chemistry, University of Western Ontario, London, Ontario

Received October 8, 1970

Formation constants, and enthalpy, free energy, and entropy changes for the tetracyanoethylene complexes with a *complete* series of methyl-substituted benzenes have been evaluated from the charge-transfer spectra over a temperature range of 1–50 °C in carbon tetrachloride solutions. From the literature data, it is deduced that various competing side interactions may not be significant compared to 1:1 electron donor–acceptor complex formation under certain experimental conditions. Some correlations among thermodynamic properties and vertical ionization potentials of the donors are discussed.

Les constantes de formation et les changements d'enthalpie, d'énergie libre et d'entropie de complexes du tétracyanoéthylène avec une série complète de benzènes substitués par des groupes méthyles ont été évalués à partir des spectres de transfert de charges déterminés en solution de tétrachlorure de carbone à des températures entre 1 et 50 °C. D'après les données de la littérature, il est déduit que les diverses interactions compétitives ne seraient pas significatives, dans certaines conditions expérimentales, comparées avec la formation d'un complexe 1:1 entre les donneurs et accepteurs d'électrons. Quelques corrélations entre les propriétés thermodynamiques et le potentiel vertical d'ionisation des donneurs sont discutées.

Canadian Journal of Chemistry, 49, 2700 (1971)

Introduction

The formation constants of tetracyanoethylene (TCNE) complexes with methyl-substituted benzenes have been investigated in different solvents and in gas phase (1–14). Compared with many evaluations of the formation constants, relatively few values for the ΔH^0 and ΔF^0 have been reported for the TCNE complexes in carbon tetrachloride solutions (Table 1). In this work the thermodynamic properties of the TCNE complexes with a *complete* series of methyl-substituted benzene donors have been determined in carbon tetrachloride over the temperature range 1–50 °C from the visible charge-transfer spectra. Some correlations among thermodynamic properties and vertical ionization potential are discussed.

Experimental

Materials were purified as described previously (15).

The charge-transfer spectra were measured by determining the variations in the intensity of visible absorption by the TCNE complexes as a function of the concentrations of the complex components in carbon tetrachloride solutions. The standard TCNE stock solutions for benzene, dimethylbenzenes, and trimethylbenzenes were prepared at room temperature by dissolving TCNE in donor. Different concentrations of solutions for spectral determinations were then prepared by diluting a set of stock solutions with carbon tetrachloride in a 10 ml volumetric flask. The concentrations, in the order of $1\text{–}4 \times 10^{-4}$ M/l, were chosen so that the measured absorbances were in the region of 0.3–0.8 at room temperature. A slightly different method was used for preparing the stock solutions of tetramethylbenzenes, pentamethylbenzene, and hexamethylbenzene. Enough carbon tetrachloride was added to a 50 ml volumetric flask containing 6–8 mg of TCNE and 3–4 mg of donor. The stock solution was diluted again as before.

The samples of TCNE were weighed in a Cahn Electrobalance M-10 with an accuracy of 0.001 mg. The initial concentrations of all solutions were established through the mixing of known volumes of solutions or of pure components, the densities of which were known. It was assumed that the volumes were additive in all cases for evaluating the initial concentrations of TCNE and donor. The temperature corrections for concentrations of solutions between 1 and 50 °C were calculated to be $\pm 2\%$ with respect to 25 °C corresponding to ± 0.02 in $\ln K_N$ or ± 0.01 kcal mol^{-1} in ΔF^0_N which were within the estimated experimental errors of ± 0.02 kcal mol^{-1}. Therefore, the corrections were neglected.

All visible spectra were taken on a Cary 14 recording spectrophotometer with 1 cm cells from 1 to 50 °C at 5 to 10° intervals. The temperature was maintained to ± 0.5 °C by circulation of water from a thermostat to the sample cell block and was measured by means of a copper–constantan thermocouple with a Hewlett–Packard 7100B recorder. No variation in absorbance was found within ± 0.5 °C.

Formation constants, K_N, in terms of mole fraction were evaluated from Benesi–Hildebrand (B–H) equation (16)

$$[1] \qquad \frac{C_A l}{A_{max}} = \left(\frac{1}{K_N \varepsilon_{max}}\right)\frac{1}{N_D} + \frac{1}{\varepsilon_{max}}$$

[1]Present address: Department of Chemistry, University of Michigan, Ann Arbor, Mich. 48104.

[2]To whom all correspondence should be addressed.

TABLE 1. Formation constants and some thermodynamic properties of TCNE complexes with methylated benzenes

Donor	t (°C)	Solvent	K_N	K_c (l/mol)	$-\Delta H^0$ (kcal/mol)	$-\Delta F^0$ (kcal/mol)	$-\Delta S^0$ (cal/mol deg)	Reference
C_6H_6	25	CH_2Cl_2		0.153				13
	25	$CHCl_3$		0.28 ±0.05				8
	25	CCl_4		0.887±0.030				13
	20	CCl_4	10.7		3.34	1.38	6.7	2
$C_6H_5CH_3$	25	CH_2Cl_2		0.310				13
	25	CCl_4		1.76 ±0.061				13
1,3,5-$(CH_3)_3C_6H_3$	25	CH_2Cl_2		1.46				13
	25	CCl_4		8.54 ±0.34				13
1,2,4,5-$(CH_3)_4C_6H_2$	20	CCl_4	145		5.48	2.90	8.8	2
$C_6(CH_3)_6$	25	CH_2Cl_2		7.2 ±0.2				4
	27.5	1,2-$C_2H_4Cl_2$		15.9	5.49	1.69	12.6	9
	25	$CHCl_3$		19.6				8
	25	CCl_4		123 ±8.8				13
	20	CCl_4	1530		7.75	4.27	11.9	2

where C_A is the initial molar concentration of TCNE and N_D refer to the initial donor concentration in mole fraction units, l represents the thickness of the cell in cm, and A_{max} and ε_{max} are maximum absorbance and molar absorptivity of the complex, respectively.

The enthalpy changes at the standard state, ΔH^0_N, were calculated from the temperature dependence of the corresponding K_N. Values of ΔF^0_N and ΔS^0_N were obtained from

$$[2] \qquad \Delta F^0_N = -RT \ln K_N = \Delta H^0_N - T\Delta S^0_N$$

Results and Discussion

Because inconsistent results were found in the literatures for the formation constants of electron donor–acceptor complexes in the solution, many alternate equations, similar to B–H equation, for evaluating the formation constants have been introduced as summarized by Briegleb (17) and Foster (18). These equations give divergent results and some of them are in good agreement with the values obtained from B–H equation within the experimental errors (11). Therefore the simple B–H equation should be valid in the system of 1:1 complex under the conditions of large excess of donor compared to the acceptor and of negligible solvent competition with either donor or acceptor.

The results for formation constants are affected adversely by the misuse of B–H equation for some complex systems. Besides D + A $\rightleftharpoons$ DA in solution, the contact charge-transfer complex (19), carbon tetrachloride complexes with methylated benzenes (20–24), TCNE complex with dichloromethane (1, 13), and the possible presence of termolecular complexes (8, 14, 25) have been discussed in the literatures. Furthermore, there is a possibility that either of the components may self-associate in some systems (26) or that the free donor, acceptor, and complex occur in solution each with a solvation shell (27).

For the TCNE systems with methylated benzene in carbon tetrachloride, we may neglect the complications due to their insignificant effects in view of the experimental conditions and errors. The most serious interference is probably the formation of carbon tetrachloride complexes with methylated benzenes. However, as shown in Table 2, the values are small compared with the formation constants of the corresponding TCNE complexes. For instance, K_c of benzene complex with TCNE in cylcohexane at 22 °C is 2.00 l/mol (5) while the complex with carbon tetrachloride at 25 °C is 0.076 ± 0.057 l/mol (24).

The present experimental conditions of the TCNE complexes have met the requirements of the B–H equation presented by Person (28) that the donor concentration in the most concentrated solution must be greater than about one tenth of the formation constant. Foster (18) also has pointed out that if the initial concentration ratio of donor to acceptor is about 10:1, the changes in the apparent values of formation constant are less than the experimental error. Recently, Deranleau (29) has proposed that the most accurate values of formation constant or molar absorptivity are obtained when the saturation fraction of the most dilute component lies between 0.2 and 0.8; outside this region, the determined values become somewhat uncertain.

Can. J. Chem. Downloaded from www.nrcresearchpress.com by 210.87.254.6 on 09/05/12
For personal use only.

TABLE 2. Formation constants of some complexes with carbon tetrachloride and dichloromethane

Acceptor	Donor	t (°C)	Solvent	K_N	K_c (l/mol)	Reference
CCl_4	C_6H_6	25	n-C_6H_{14}		0.009±0.004	21
	C_6H_6	25	n-C_6H_{14}		0.001±0.02*	24
	C_6H_6	25	c-C_6H_{12}		0.076±0.057	24
	1,3-$(CH_3)_2C_6H_4$	25	c-C_6H_{12}		0.112±0.028	24
	1,4-$(CH_3)_2C_6H_4$	25	c-C_6H_{12}		0.136±0.018	24
	1,3,5-$(CH_3)_3C_6H_3$	25	n-C_6H_{14}		0.113±0.044	21
	1,3,5-$(CH_3)_3C_6H_3$	25	c-C_6H_{12}		0.252±0.036	24
	$C_6(CH_3)_6$	25	n-C_6H_{14}		0.64 ±0.12	23
	$C_6(CH_3)_6$	25	n-C_6H_{14}		0.648±0.092*	24
	$C_6(CH_3)_6$	25	c-C_6H_{12}		0.550±0.160	24
TCNE	CH_2Cl_2	22	$CHCl_3$	0.21		1
	CH_2Cl_2	25	CCl_4	2.64	0.29 ±0.020	13

*Recalculated value from the preceding entry.

TABLE 3. Formation constants of methyl-substituted benzene–TCNE complexes in carbon tetrachloride*

	Donor	K_N at T(°K) = 274	283	293	298	303	313	323	λ_{max} (mμ)
1	C_6H_6	9.8	8.3	7.1	6.4	6.2	5.1	4.6	384
2	$C_6H_5CH_3$	18.5	15.6	13.5	11.8	11.2	9.5	8.2	403
3	1,2-$(CH_3)_2C_6H_4$	28.0	26.7	19.7	18.6	16.7			426
4	1,3-$(CH_3)_2C_6H_4$	36.3		25.0	29.5		18.6		432
5	1,4-$(CH_3)_2C_6H_4$	36.4	29.0	22.9	21.0	18.7	15.9	14.7	398
		44.2	30.6	24.6	22.0	19.9	16.2	14.6	460
6	1,2,3-$(CH_3)_3C_6H_3$	67.6	65.3	47.1	47.1		34.2	26.7	455
7	1,2,4-$(CH_3)_3C_6H_3$		61.3	44.2	43.2		32.1	25.7	435
		71.3	59.5	44.3	43.5		30.2	23.5	472
8	1,3,5-$(CH_3)_3C_6H_3$	72.7	64.5	49.1	39.2		31.7	25.8	455
9	1,2,3,4-$(CH_3)_4C_6H_2$	350	230	199	174	154	117	78.5	481
10	1,2,3,5-$(CH_3)_4C_6H_2$		187	153	138	118	96.5	74.6	477
11	1,2,4,5-$(CH_3)_4C_6H_2$	378	291	233	180	170	126	114	462
		351	268	204	168	180	118	109	525
12	$C_6H(CH_3)_5$		722	492	425	390	284	217	511
13	$C_6(CH_3)_6$		1795	1337	1025	890	680	432	536

*For the complexes having doublet maximum intensities, the values on the first row are calculated from shorter wavelength and the second from longer wavelength.

The points which define the straight line in B–H equation or others are measured experimentally and, therefore, subject to errors. Hence, the straight line has some uncertainty in its slope and intercept leading to some uncertainty in formation constants (30). The accuracy of the absorbance is about 0.002–0.003, especially for the absorbance beyond the range of 0.3–0.8 leading to estimated errors of ± 0.02 kcal mol^{-1} in ΔF^0_N, ± 0.2 kcal mol^{-1} in ΔH^0_N, and ± 0.6 cal deg^{-1} mol^{-1} in ΔS^0_N. The values of formation constants, K_N, are tabulated in Table 3. For those complexes exhibiting doublets in the spectra, the values evaluated from two different maximum absorption bands agree within the experimental errors.

The formation constants evaluated from the charge-transfer spectra (Table 1) increase with increasing refractive index of the solvent, from dichloromethane ($n_D^{20} = 1.424$), 1,2-dichloroethane (1.445), chloroform (1.446), to carbon tetrachloride (1.460). The trend of increasing formation constant presumably arises through the decreasing competition of solvation with either donor or acceptor. Therefore, carbon tetrachloride may be regarded as the most "inert" solvent in this series. In addition, there is no evidence of deviation from linearity for the ln K_N against $1/T$ plot over a 50° temperature range for the systems studied. This indicates that only 1:1 complex exists (9) under the present experimental conditions. Thus, the formation of carbon tetrachloride complexes with methylbenzenes is comparatively insignif-

Can. J. Chem. Downloaded from www.nrcresearchpress.com by 210.87.254.6 on 09/05/12
For personal use only.

TABLE 4. Standard free energies and enthalpies of formation for the TCNE complexes with methylated benzenes in carbon tetrachloride* (unit: kcal/mol)

	Donor	$-\Delta F^0_N$ at T(°K) = 274	283	293	298	303	313	323	$-\Delta H^0_N$
1	C_6H_6	1.24	1.19	1.14	1.10	1.09	1.01	0.97	2.7
2	$C_6H_5CH_3$	1.59	1.54	1.51	1.46	1.45	1.40	1.35	3.0
3	1,2-$(CH_3)_2C_6H_4$	1.81	1.84	1.73	1.73	1.70			3.4
4	1,3-$(CH_3)_2C_6H_4$	1.96		1.87	2.00		1.82		3.3
5	1,4-$(CH_3)_2C_6H_4$	1.96	1.89	1.82	1.80	1.76	1.72	1.72	
		2.06	1.92	1.86	1.83	1.80	1.73	1.72	3.6
6	1,2,3-$(CH_3)_3C_6H_3$	2.29	2.21	2.24	2.35		2.21	2.13	4.2
7	1,2,4-$(CH_3)_3C_6H_3$		2.31	2.21	2.23		2.16	2.09	
		2.33	2.30	2.21	2.23		2.13	2.03	4.1
8	1,3,5-$(CH_3)_3C_6H_3$	2.34	2.34	2.27	2.17		2.15	2.09	4.1
9	1,2,3,4-$(CH_3)_4C_6H_2$	3.19	2.95	3.08	3.05	3.03	2.96	2.80	4.6
10	1,2,3,5-$(CH_3)_4C_6H_2$		2.94	2.93	2.92	2.87	2.84	2.77	4.5
11	1,2,4,5-$(CH_3)_4C_6H_2$	3.23	3.19	3.18	3.08	3.09	3.01	3.04	
		3.19	3.15	3.10	3.03	3.13	2.97	3.02	4.8
12	$C_6H(CH_3)_5$		3.70	3.61	3.58	3.59	3.51	3.45	5.5
13	$C_6(CH_3)_6$		4.21	4.19	4.11	4.09	4.06	3.90	6.4

*For the complexes having doublet maximum intensities ΔF^0_N in the first row are calculated from the shorter wavelength and the second from longer wavelength; the values of ΔH^0_N are average values.

TABLE 5. Standard entropy changes of formation for the TCNE complexes with methylated benzenes in carbon tetrachloride* ($-\Delta S^0_N$: cal/mol deg)

	Donor	$-\Delta S^0_N$ at T(°K) = 274	283	293	298	303	313	323
1	C_6H_6	5.33	5.34	5.32	5.37	5.31	5.40	5.36
2	$C_6H_5CH_3$	5.15	5.16	5.09	5.17	5.12	5.11	5.11
3	1,2-$(CH_3)_2C_6H_4$	5.80	5.51	5.70	5.60	5.61		
4	1,3-$(CH_3)_2C_6H_4$	4.89		4.88	4.36		4.73	
5	1,4-$(CH_3)_2C_6H_4$	5.99	6.04	6.08	6.04	6.07	6.00	5.82
		5.62	5.94	5.94	5.94	5.94	5.97	5.82
6	1,2,3-$(CH_3)_3C_6H_3$	6.97	7.03	6.69	6.21		6.36	6.41
7	1,2,4-$(CH_3)_3C_6H_3$		6.33	6.45	6.28		6.20	6.22
		6.46	6.36	6.45	6.28		6.29	6.41
8	1,3,5-$(CH_3)_3C_6H_3$	5.42	6.22	6.23	6.48		6.23	6.22
9	1,2,3,4-$(CH_3)_4C_6H_2$	5.15	5.83	5.19	5.20	5.18	5.24	5.17
10	1,2,3,5-$(CH_3)_4C_6H_2$		5.51	5.36	5.30	5.38	5.30	5.36
11	1,2,4,5-$(CH_3)_4C_6H_2$	5.73	5.69	5.53	5.77	5.64	5.37	5.36
		5.88	5.83	5.80	5.94	5.51	5.85	5.51
12	$C_6H(CH_3)_5$		6.36	6.45	6.44	6.30	6.36	6.35
13	$C_6(CH_3)_6$		7.74	7.54	7.68	7.62	7.48	7.74

*For the complexes having doublet maximum intensities the values in the first row are calculated from the shorter wavelength and the second from longer wavelength.

icant. Foster and Matheson (9) also have indicated that, under the conditions of approximately equal concentrations of donor and acceptor used, a single 1:1 hexamethylbenzene–TCNE complex in 1,2-dichloroethane is formed with no significant contributions from isomeric complexes or from contact charge transfer.

The thermodynamic constants, ΔF^0_N, ΔH^0_N, and ΔS^0_N based on K_N values are tabulated in Tables 4 and 5, respectively. The decreases (*i.e.*, more negative) in ΔH^0_N with increasing methylation on the benzene ring are accompanied by parallel decreases in ΔF^0_N and ΔS^0_N. There is little difference in the thermodynamic quantities for the isomers having the same number of methyl substituents, which implies that the evidence for the steric repression of complex formation by the methyl groups in these $b\pi$–$a\pi$ complexes is lacking. It is apparent that the entropy changes show a slight decrease with increasing number of methyl substituents. However, the entropies do not vary widely for the series of TCNE complexes, from 5 to 7 cal/mol deg only. Similar phenomena are also reported

Can. J. Chem. Downloaded from www.nrcresearchpress.com by 210.87.254.6 on 09/05/12
For personal use only.

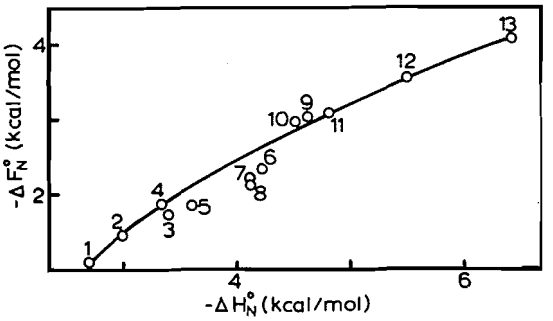

FIG. 1. Relation between free energy and enthalpy of formation for TCNE complexes with methylbenzenes in carbon tetrachloride at 25 °C. Numbers refer to the donors in Table 4.

for the entropies of formation for a number of iodine complexes with methylbenzenes, which are all of the order of 4 to 5 cal/mol deg (31).

The expected correlation between $\Delta F^0{}_N$ and $\Delta H^0{}_N$ (Fig. 1) implies that the decrease in free energy or entropy on forming the complex becomes greater due to the more restricted configuration of the atoms as the complex become more stable. It has been shown that the contribution to enthalpy of formation is mainly from the energy of electron donor–acceptor interaction with a small contribution from the changes in translational, rotational, and vibrational energy levels of the reactants on complex formation (32). Values of $-\Delta H^0{}_N$ are usually of the order of 3 to 7 kcal/mol which show that interaction between the components is weaker than the classical or ionic bonding. The correlations between the relative strength of the electron donor–acceptor interaction as estimated from $\Delta H^0{}_N$ or $\Delta F^0{}_N$ and the strength of the donor as measured by its vertical ionization potentials (15) for the TCNE complexes are shown in Fig. 2. In general, regular, though non-linear, relationships are observed between $\Delta H^0{}_N$ and I_D, and between $\Delta F^0{}_N$ and I_D for a series of complexes involving a common acceptor. It is deduced that the complex formation increases with the donor strength to release an electron from the bonding π orbital similar to parallel studies by infrared and proton resonance spectroscopy and by calorimetry (33).

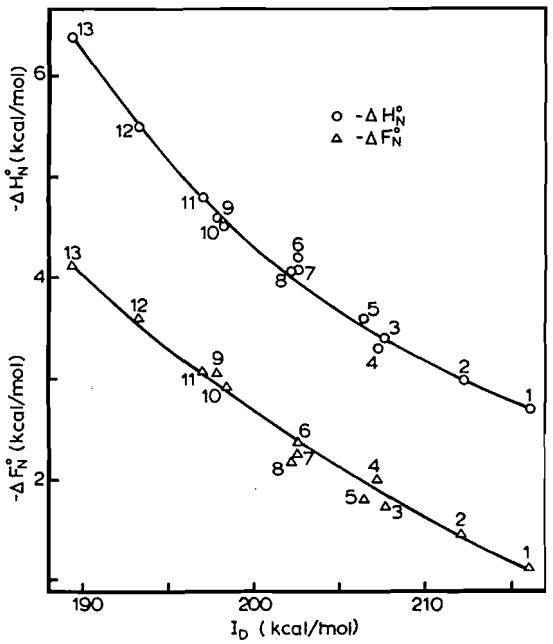

FIG. 2. Correlations of the free energies, and enthalpies of the TCNE complexes at 25 °C with the vertical ionization potentials of methylbenzenes. Numbers refer to the donors in Table 4.

The financial support from the National Research Council of Canada is gratefully acknowledged.

1. R. E. MERRIFIELD and W. D. PHILLIPS. J. Amer. Chem. Soc. **80**, 2778 (1958).
2. G. BRIEGLEB, J. CZEKALLA, and G. REUSS. Z. Phys. Chem. Frankfurt, **30**, 333 (1961).
3. J. ROBERT GOTT and WILLIAM G. MAISCH. J. Phys. Chem. **39**, 2229 (1963).
4. M. E. PEOVER. Trans. Faraday Soc. **60**, 417 (1964).
5. P. H. EMSLIE and R. FOSTER. Tetrahedron, **21**, 2851 (1965).
6. M. KROLL and M. L. GINTER. J. Phys. Chem. **69**, 3671 (1965).
7. A. R. COOPER, C. W. P. CROWNE, and P. G. FARRELL. Trans. Faraday Soc. **62**, 18 (1966).
8. M. J. S. DEWAR and C. C. THOMPSON, Jr. Tetrahedron supp. 7, 97 (1966).
9. R. FOSTER and I. B. C. MATHESON. Spectrochim Acta, **23A**, 2037 (1967).
10. A. H. EWARD. Trans. Faraday Soc. **64**, 733 (1968).
11. M. KROLL. J. Amer. Chem. Soc. **90**, 1097 (1968).
12. P. H. EMSLIE, R. FOSTER, I. HORMAN, J. W. MORRIS, and D. R. TWISELTON. J. Chem. Soc. B, 1161 (1969).
13. R. X. EWALL and A. J. SONNESSA. J. Amer. Chem. Soc. **92**, 2845 (1970).
14. P. J. TROTTER and D. A. YPHANTIS. J. Phys. Chem. **74**, 1399 (1970).
15. R. K. CHAN and S. C. LIAO. Can. J. Chem. **48**, 299 (1970).
16. H. A. BENESI and J. H. HILDEBRAND. J. Amer. Chem. Soc. **71**, 2703 (1949).
17. G. BRIEGLEB. Electronen-Donor-Acceptor-Komplexe. Springer Verlag, Berlin. 1961. Chap. 12.
18. R. FOSTER. Organic Charge-Transfer Complexes. Academic Press, London. 1969. Chap. 6 and p. 158.
19. L. F. ORGEL and R. S. MULLIKEN. J. Amer. Chem. Soc. **79**, 4839 (1957).
20. R. ANDERSON, R. CAMBIO, and J. M. PRAUSNITZ. Amer. Inst. Chem. Engineers J. **8**, 66 (1962).

Can. J. Chem. Downloaded from www.nrcresearchpress.com by 210.87.254.6 on 09/05/12
For personal use only.

21. R. ANDERSON and J. M. PRAUSNITZ. J. Chem. Phys. **39**, 1225 (1963); **40**, 3443 (1964).
22. F. DÖRR and G. BUTTGEREIT. Ber. Bunsenges. Phys. Chem. **67**, 867 (1963).
23. R. F. WEIMER and J. M. PRAUSNITZ. J. Chem. Phys. **42**, 3643 (1965).
24. D. R. ROSSEINSKY and H. KELLAWI. J. Chem. Soc. A, 1207 (1969).
25. S. CARTER. J. Chem. Soc. A, 404 (1968).
26. D. W. TANNER and T. C. BRUICE. J. Phys. Chem. **70**, 3816 (1966).
27. C. CARTER, J. N. MURRELL, and E. J. ROSCH. J. Chem. Soc. 2048 (1965).
28. W. B. PERSON. J. Amer. Chem. Soc. **87**, 167(1965).
29. D. A. DERANLEAU. J. Amer. Chem. Soc. **91**, 4044 (1969).
30. R. S. MULLIKEN and W. B. PERSON. Molecular Complexes. Wiley–Interscience, New York. 1969. p. 90.
31. C. VAN DE STOLPE. Thesis. Solvatie van Jodium in Organische Oplosmiddelen. University of Amsterdam. 1953.
32. W. B. PERSON. J. Amer. Chem. Soc. **84**, 536 (1962).
33. J. C. D. BRAND, G. EGLINTON, and J. TYRRELL. J. Chem. Soc. 5914 (1965).

Can. J. Chem. Downloaded from www.nrcresearchpress.com by 210.87.254.6 on 09/05/12
For personal use only.

Can. J. Chem. Downloaded from www.nrcresearchpress.com by 210.87.254.5 on 09/05/12
For personal use only.

Synthesis of Some New Phosphino Acetylenes

A. J. CARTY, N. K. HOTA, T. W. NG, H. A. PATEL,[1] AND T. J. O'CONNOR
Department of Chemistry, University of Waterloo, Waterloo, Ontario

Received November 30, 1970

The synthesis and characterization of the new phosphino acetylenes $(C_6H_5)_2PC{\equiv}CCF_3$, $(C_6H_5)_2PC{\equiv}CC(CH_3)_3$, $(C_6H_5)_2PC{\equiv}CP(C_6F_5)_2$, $(C_6F_5)_2PC{\equiv}CCH_3$, $(C_6F_5)_2PC{\equiv}CC_6H_5$, $(C_6H_5)_2PC{\equiv}CP[N(C_2H_5)_2]_2$, the mixed arsine–phosphine $(C_6H_5)_2PC{\equiv}CAs(C_6H_5)_2$, and the arsino acetylene $(C_6H_5)_2AsC{\equiv}CCF_3$ are reported.

On rapporte la synthèse et la caractérisation des nouveaux phosphino-acétylènes $(C_6H_5)_2PC{\equiv}CCF_3$, $(C_6H_5)_2PC{\equiv}CC(CH_3)_3$, $(C_6H_5)_2PC{\equiv}CP(C_6F_5)_2$, $(C_6F_5)_2PC{\equiv}CCH_3$, $(C_6F_5)_2PC{\equiv}CC_6H_5$, $(C_6H_5)_2PC{\equiv}CP[N(C_2H_5)_2]_2$, de l'arsine-phosphine mixte $(C_6H_5)_2PC{\equiv}CAs(C_6H_5)_2$, et de l'arsino-acétylène $(C_6H_5)_2AsC{\equiv}CCF_3$.

Canadian Journal of Chemistry, 49, 2706 (1971)

Introduction

During the past decade a number of tertiary phosphines containing α-acetylenic groups have been characterized (1). These include trialkynylphosphines $P(C{\equiv}CR)_3$ (2–4), dialkyl or diaryl alkynylphosphines $R_2'PC{\equiv}CR$ (5–10), aryldialkynylphosphines $R'P(C{\equiv}CR)_2$ (3), acetylenic diphosphines $R_2PC{\equiv}CPR_2$ (5, 11–13), and a variety of organometal phosphines with α-acetylenic substituents (14). Our interest in the coordinating properties of acetylenic phosphines and diphosphines (15) prompted us to attempt the synthesis of several ligands having substituents of varying electronegativity on the phosphorus atom or hydrocarbon residue. In this paper we report the preparation and characterization of $(C_6H_5)_2PC{\equiv}CCF_3$, $(C_6H_5)_2AsC{\equiv}CCF_3$, $(C_6H_5)_2PC{\equiv}CC(CH_3)_3$, $(C_6F_5)_2PC{\equiv}CCH_3$, $(C_6F_5)_2PC{\equiv}CC_6H_5$, $(C_6H_5)_2PC{\equiv}CP(C_6F_5)_2$, $(C_6H_5)_2PC{\equiv}CP[N(C_2H_5)_2]_2$, and $(C_6H_5)_2PC{\equiv}CAs(C_6H_5)_2$.

Experimental

The following compounds were obtained commercially: C_6F_5Br (Fluorochem Ltd.), $(C_6H_5)_2PCl$ (Orgmet Inc.), $(CH_3)_3CC{\equiv}CH$ (Farchan Research Laboratories), $CF_3C{\equiv}CH$ (Pierce Chemical Co.) $(C_6H_5)_2AsCl$ (Strem Chemicals), n-C_4H_9Li (Alfa Inorganics).

Phosphine and Arsine Syntheses

$(C_6H_5)_2PC{\equiv}CCF_3$

Two methods were used for the synthesis of this compound.

(*a*) Diethylaminodiphenylphosphine $(C_6H_5)_2PN(C_2H_5)_2$ was prepared from diethylamine and diphenylchlorophosphine by the method of Ewart and co-workers (16). Diethylaminodiphenylphosphine (5.0 g) was weighed into a Carius tube, pentane (5 ml) added, and a slight excess (3.0 g) of 3,3,3-trifluoropropyne condensed into the tube *in vacuo*. The tube was sealed and allowed to warm to room temperature. Reaction appeared to be complete after *ca.* 3 h. The tube was cooled, vented, and washed with pentane. Fractionation of the liquid remaining after pentane removal afforded the required product in 45% yield.

(*b*) 3,3,3-Trifluoropropyne (9.4 g) was condensed at −78° into a Carius tube, the tube cooled, opened, and the propyne added to ether (25 ml) at −78° in a two-necked flask equipped with magnetic stirrer, dropping funnel, and nitrogen inlet. The stoichiometric reaction quantity of *n*-butyllithium (3 *M* in hexane) with ether (20 ml) was then added dropwise via the funnel, the temperature being maintained at −78°. After 1 h diphenylchlorophosphine (22.1 g) in ether (25 ml) was added slowly while stirring. The reaction mixture was then allowed to warm to room temperature and stirred for 1 further h. Ether was removed on a rotary evaporator and benzene added to precipitate lithium chloride. After filtration, benzene was removed and the black filtrate was distilled under reduced pressure to yield colorless $(C_6H_5)_2PC{\equiv}CCF_3$ (65%).

$(C_6H_5)_2AsC{\equiv}CCF_3$

This compound was prepared as above using $(C_6H_5)_2AsCl$ for $(C_6H_5)_2PCl$. Method (*b*) again gave better yields.

$(C_6H_5)_2PC{\equiv}CC(CH_3)_3$[2]

The lithium salt of 3,3-dimethyl-1-butyne was made by the reaction of the acetylene (8.2 g) with *n*-butyllithium at −78°. After addition of $(C_6H_5)_2PCl$ (22.1 g) in ether (25 ml) the flask was warmed to room temperature. The white precipitate was dissolved in a minimum of chloroform and water (30 ml) added. The organic layer was dried over magnesium sulfate, evaporated to half volume, and cooled overnight at 0°. The product was obtained as white needles (68%).

$(C_6F_5)_2PC{\equiv}CCH_3$

Bis(pentafluorophenyl)chlorophosphine was synthe-

[1]Predoctoral Fellow supported by Arapahoe Chemicals, Division of Syntex Corporation, Palo Alto, California.

[2]We thank Mr. J. Slezak for help in the synthesis of this compound.

TABLE 1. Acetylenic phosphine syntheses

Compound	Yield	Melting point (°C)	Boiling point (°C)	ν (C≡C)† (cm^{-1})	%C Calcd.	%C Found	%H Calcd.	%H Found
$(C_6H_5)_2PC{\equiv}CCF_3$	45* 65		70–71 (0.1 mm)	2200	64.79	64.70	3.62	3.61
$(C_6H_5)_2AsC{\equiv}CCF_3$	65		79–80 (0.1 mm)	2200	55.95	55.86	3.13	3.01
$(C_6H_5)_2PC{\equiv}CC(CH_3)_3$	68	33–34		2171 2220	81.20	80.96	7.14	7.15
$(C_6F_5)_2PC{\equiv}CCH_3$	52		91–95 (0.4 mm)	2200	44.70	44.55	0.88	0.74
$(C_6F_5)_2PC{\equiv}CC_6H_5$	62	89		2170	51.52	51.46	1.07	0.96
$(C_6H_5)_2PC{\equiv}CP(C_6F_5)_2$	66	102		2103	54.39	54.12	1.76	1.81
$(C_6H_5)_2PC{\equiv}CP[N(C_2H_5)_2]_2$	44		145–148 (0.001 mm)	2119	68.80	68.70	7.80	7.90
$(C_6H_5)_2PC{\equiv}CAs(C_6H_5)_2$	50	86–87		2092‡	71.30	71.01	4.56	4.60
$(C_6H_5)_2PC{\equiv}CCH_3$	82	31	146 (0.6 mm)	2195				

*From $(C_6H_5)_2PN(C_2H_5)_2 + CF_3C{\equiv}CH$.
†Solutions in $CHCl_3$.
‡Raman measurement in CCl_4.

sized as described by Magnelli and co-workers (17). To lithium propynylide (0.1 mol) in ether/hexane 1:1 at −78° (from $CH_3C{\equiv}CH + n\text{-}C_4H_9Li$) was added an ether solution of bis(pentafluorophenyl)chlorophosphine (0.1 mol). The solution was allowed to reach room temperature then stirred for a further 2 h to give a reddish solution. Ether was removed *in vacuo*, petrol ether (40–60°) (50 ml) added, and the mixture filtered. The filtrate was distilled under reduced pressure yielding $(C_6F_5)_2PC{\equiv}CCH_3$ as a colorless liquid in 52% yield based on the chloride.

$(C_6F_5)_2PC{\equiv}CC_6H_5$

This compound was prepared in an identical fashion to the above using phenylacetylene for propyne. Colorless crystals (62%) were obtained.

$(C_6H_5)_2PC{\equiv}CP(C_6F_5)_2$

Diphenylethynylphosphine $(C_6H_5)_2PC{\equiv}CH$ was prepared according to the method of Charrier and co-workers (10). To an ether/hexane solution of $(C_6H_5)_2PC{\equiv}CLi$ (from $(C_6H_5)_2PC{\equiv}CH$ (4.0 g) and $n\text{-}C_4H_9Li$ (9.6 ml of 2/m) in hexane) was added with stirring 7.2 g of $(C_6F_5)_2PCl$ in ether (25 ml). Work-up was similar to that for $(C_6F_5)_2PC{\equiv}CCH_3$ and yielded colorless crystals (66%) which were recrystallized from ethanol.

$(C_6H_5)_2PC{\equiv}CAs(C_6H_5)_2$

This compound was prepared from $(C_6H_5)_2PC{\equiv}CLi$ and $(C_6H_5)_2AsCl$ in a similar manner to the above. Recrystallization of the product from chloroform/ethanol gave colorless needles (50%).

$(C_6H_5)_2PC{\equiv}CCH_3$ and $(C_6H_5)_2PC{\equiv}CC_6H_5$

These were prepared from the appropriate acetylene via the *n*-butyllithium method above. This gives superior yields to the Grignard preparation used earlier by Charrier and co-workers (10).

$(C_6H_5)_2PC{\equiv}CP[N(C_2H_5)_2]_2$

Bis(diethylamino)chlorophosphine $[(C_2H_5)_2N]_2PCl$ was obtained as a liquid b.p. 60–62° (0.6 mm) from phosphorus trichloride and diethylamine as previously described (18). The chlorophosphine (14.5 g) in ether (25 ml) was added dropwise to $(C_6H_5)_2PC{\equiv}CLi$ (from $(C_6H_5)_2PC{\equiv}CH$ (15.0 g) + $n\text{-}C_4H_9Li$ (36 ml of 2 *M*)) in ether/hexane at −78°. After warming to room temperature the reaction was completed by stirring for 1 h. The brown suspension remaining was filtered under nitrogen and the solvent removed *in vacuo*. Dry petrol-ether (40–60°) was added to precipitate lithium chloride, then the mixture filtered. After removal of solvent the residue was distilled at 10^{-3} mm. The fraction collected at 145–148° was the desired product. Considerable decomposition occurred on distillation, the yield being 44%.

Physical Measurements

The i.r. spectra were recorded on a Beckman IR 9 spectrometer as solutions in chloroform. Mass spectra were measured with a Perkin–Elmer RMU-6E instrument. The mass spectra of the phosphines are given in Table 2 and ν (C≡C) stretching frequencies of the ligands in Table 1.

Results and Discussion

The compounds prepared (Table 1) considerably extend the range of known phosphino acetylenes. The derivative $(C_6H_5)_2PC{\equiv}CAs(C_6H_5)_2$ is the first acetylenic mixed phosphine–arsine to be described. Compounds $(C_6H_5)_2PC{\equiv}CP(C_6F_5)_2$ and $(C_6H_5)_2PC{\equiv}CP[N(C_2H_5)_2]_2$ represent the first examples of unsymmetrical acetylenic diphosphines. Compounds of this type are expected to be of importance in the direct measurement of three-bond P–P coupling constants in n.m.r. spectroscopy (19).

We wish to draw attention to the synthetic utility of the compound $(C_6H_5)_2PC{\equiv}CH$ which is readily preparable (10) from $(C_6H_5)_2PCl$ and the mono-Grignard of acetylene. Reaction of $(C_6H_5)_2PC{\equiv}CH$ with *n*-butyllithium in ether or hexane gives high yields of lithium diphenylphosphinoethynylide $(C_6H_5)_2PC{\equiv}CLi$. This salt can then be used for the preparation of unsymmetrical species in good yield via reaction with R_2PCl or R_2AsCl.

Unlike the alkyldiphenylphosphines, the α-

Can. J. Chem. Downloaded from www.nrcresearchpress.com by 210.87.254.5 on 09/05/12
For personal use only.

TABLE 2. Mass spectral data for most abundant fragment ions of phosphinoacetylenes*

Compound	*m/e* (% Relative abundance)
$(C_6H_5)_2PC{\equiv}CCF_3$	279(20) 278(100) 277(11) 258(7) 246(5) 228(12) 227(7) 210(7) 209(35) 207(11) 201(9) 190(6) 189(20) 183(8) 178(7) 165(5) 154(16) 152(10) 151(31) 141(5) 132(8) 131(8) 127(9) 109(7) 108(66) 107(32) 78(6) 77(18) 76(5) 63(6) 51(21) 50(7) 39(7)
$(C_6H_5)_2AsC{\equiv}CCF_3$	322(65) 302(12) 282(44) 253(4) 245(8) 229(8) 228(21) 227(13) 209(67) 195(20) 190(4) 189(6) 178(10) 176(16) 154(79) 153(28) 152(100) 151(96) 127(25) 101(11) 78(10) 77(40) 75(11) 74(9) 63(6) 51(47) 50(19) 39(10)
$(C_6H_5)_2PC{\equiv}CCH_3$	224(100) 209(61) 147(39) 183(37) 165(27) 115(36) 108(28) 107(48) 78(13) 77(55) 63(17) 51(71) 50(21) 39(25)
$(C_6H_5)_2PC{\equiv}CC_6H_5$	286(42) 285(21) 209(28) 207(15) 183(15) 254(14) 178(100) 165(14) 154(7) 152(15) 143(16) 132(18) 177(12) 108(23) 107(30) 102(17) 78(31) 77(41) 76(16) 63(19) 51(41) 50(23) 39(32)
$(C_6H_5)_2PC{\equiv}CC(CH_3)_3$	266(8) 91(6) 77(15) 71(8) 70(6) 69(13) 65(19) 63(15) 57(100) 53(19) 52(7) 51(74) 50(21) 45(8) 41(27) 39(27)
$(C_6H_5)_2PC{\equiv}CP(C_6H_5)_2$	394(84) 210(15) 209(100) 207(13) 185(62) 184(8) 183(55) 178(8) 165(8) 152(6) 139(7) 108(6) 107(10) 77(10) 51(10) 39(6)
$(C_6H_5)_2PC{\equiv}CAs(C_6H_5)_2$	439(32) 438(100) 284(8) 282(3) 261(4) 259(11) 253(6) 252(25) 229(8) 227(10) 210(6) 209(32) 207(14) 186(6) 185(38) 184(6) 183(43) 178(20) 165(8) 152(10) 107(8) 77(5)
$(C_6H_5)_2PC{\equiv}CP[N(C_2H_5)_2]_2$	243(18) 242(86) 241(6) 213(14) 201(14) 200(87) 199(100) 198(7) 186(28) 185(30) 184(13) 183(65) 170(5) 152(12) 133(7) 124(13) 121(18) 115(5) 109(18) 108(59) 107(26) 91(35) 78(5) 77(9) 73(18) 72(11) 65(5) 58(54) 51(12) 44(22) 39(9)
$(C_6F_5)_2PC{\equiv}CCH_3$	404(29) 382(8) 366(6) 353(19) 276(50) 261(7) 255(8) 237(22) 215(13) 206(12) 205(10) 198(30) 192(17) 187(15) 186(8) 168(19) 167(5) 129(10) 117(10) 110(26) 109(15) 99(7) 93(10) 89(8) 83(12) 70(60) 69(100) 65(13) 57(11) 51(12) 39(17)
$(C_6F_5)_2PC{\equiv}CC_6H_5$	466(1) 397(3) 378(6) 347(7) 300(15) 299(100) 279(17) 274(6) 268(70) 233(13) 230(23) 217(5) 204(6) 198(23) 179(5) 151(70) 132(15) 131(20) 117(10) 110(20) 108(23) 107(10) 99(10) 93(7) 69(27)
$(C_6F_5)_2PC{\equiv}CP(C_6H_5)_2$	574(6) 389(4) 299(6) 210(17) 209(100) 207(9) 185(10) 183(16) 179(6) 178(7) 165(7) 132(5) 108(9) 107(14) 77(7) 69(6) 65(6) 63(9) 57(10) 51(7) 39(9)

*Spectra were measured at 70 eV.

acetylenic phosphines (Table 1) show little tendency to oxidize spontaneously in air although P=O stretching bands can be found in the i.r. spectra of samples recovered after long periods in non-degassed solvents. Other workers have likewise noted the stabilizing effect of α-acetylenic substituents on tertiary phosphines (4, 20). The presence of strongly electron-withdrawing substituents on either phosphorus or the hydrocarbon residue appears to have no marked effect on the ease of oxidation of the phosphorus atoms. Slow decomposition of $(C_6H_5)_2MC{\equiv}CCF_3$ (M = P, As) and $(C_6H_5)_2PC{\equiv}CP[N(C_2H_5)_2]_2$ occurs on prolonged standing at room temperature. We have, however, noted distinct differences in the behavior of $(C_6H_5)_2PC{\equiv}CCH_3$ and $(C_6H_5)_2PC{\equiv}CCF_3$ toward iron carbonyls with the C≡C bond of the latter being considerably more reactive (21).

The i.r. spectra of the compounds in the range 2000–650 cm^{-1} resemble those of trivalent phosphorus compounds with similar substituents (10, 16, 22) and are not reported here. The main feature of interest concerns the ν (C≡C) frequency of the acetylenes. For the compounds $(C_6H_5)_2PC{\equiv}CCF_3$, $(C_6H_5)_2AsC{\equiv}CCF_3$, $(C_6F_5)_2PC{\equiv}CCH_3$, $(C_6F_5)_2PC{\equiv}CC_6H_5$, and $(C_6H_5)_2PC{\equiv}CCH_3$, the C≡C stretching vibration appears at the lower end of the range (2300–2175 cm^{-1}) normally found for disubstituted acetylenes (23). The compound $(C_6H_5)_2PC{\equiv}CC(CH_3)_3$ exhibits two bands in the ν (C≡C) region, as observed for several derivatives of $HC{\equiv}CC(CH_3)_3$ (4). The two unsymmetrical diphosphines show a weak–medium intensity band due to ν (C≡C) in the i.r. at frequencies close to the value of 2097 cm^{-1} observed for ν (C≡C) of $(C_6H_5)_2PC{\equiv}CP(C_6H_5)_2$ in the Raman (12). The mixed phosphine–arsine ligand has no band in the i.r. attributable to ν (C≡C) but in the Raman a strong line appears at 2092 cm^{-1}. As we have previously pointed out (24) these low C≡C stretching frequencies may be indicative of a π type interaction between phos-

Can. J. Chem. Downloaded from www.nrcresearchpress.com by 210.87.254.5 on 09/05/12
For personal use only.

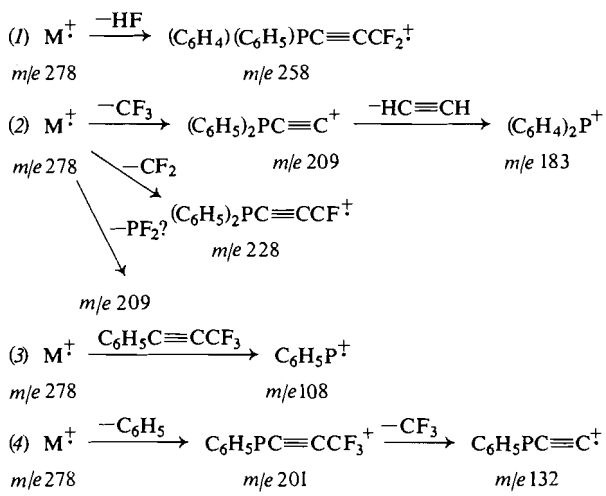

SCHEME 1. SOME possible fragmentation pathways for $(C_6H_5)_2PC{\equiv}CCF_3$.

phorus and the acetylenic carbon atom. A similar effect, but to a lesser extent, may be operative in the acetylenes having only one phosphorus or arsenic substituent. Similar conclusions have been reached from an X-ray study of $(C_6H_5)_2PC{\equiv}CP(C_6H_5)_2$ (25) and from i.r. studies of the analogous silicon species (26).

Mass Spectra

The abundances of major ions in the mass spectra of the phosphines prepared are given in Table 2. Spectra were recorded to obtain accurate molecular weights and to provide confirmation of the stoichiometries of the products. With the exception of $(C_6H_5)_2PC{\equiv}CP[N(C_2H_5)_2]_2$ all the phosphines exhibit parent ion peaks in the mass spectra. The absence of peaks at *m/e* higher than that of the parent ion testifies to the purity of the products. For $(C_6H_5)_2PC{\equiv}CCF_3$, $(C_6H_5)_2PC{\equiv}CCH_3$, and $(C_6H_5)_2PC{\equiv}CAs(C_6H_5)_2$ the $M^{+\cdot}$ ions are most abundant. The fragmentation patterns for $(C_6H_5)_2PC{\equiv}CCF_3$ and $(C_6H_5)_2AsC{\equiv}CCF_3$[3] are complex, apparently involving at least four mechanistic pathways as given for $(C_6H_5)_2PC{\equiv}CCF_3$ in Scheme 1. The initial fragmentation steps involving loss of HF, CF_3, and $C_6H_5C{\equiv}CCF_3$ are all supported by the appearance of appropriate metastable ions. It should be kept in mind however that $C_6H_5P^{+\cdot}$ could be the end product of several different fragmentation pathways in addition to *3*. From the ion abundances *2* and *3* appear to be dominant. In addition however rearrangement occurs during fragmentation since ions such as $C_6H_5C{\equiv}CC_6H_5^+$ (*m/e* 178) and $C_6H_5C_3F_4^+$ (*m/e* 189) are found in reasonable abundance. Similar behavior has been noted in the mass spectra of related fluorophosphines (27). For $(C_6H_5)_2AsC{\equiv}CCF_3$ biphenylene (or $C_6H_5As^{\cdot+}$) (*m/e* 152) is the base ion and mechanisms *1* and *3* are apparently more important than *2* or *4*. The relative abundances of $(C_6H_4)_2As^+$ (*m/e* 227) and $(C_6H_4)_2P^+$ (*m/e* 183) do not differ significantly. $(C_6H_5)As^{+\cdot}$ (*m/e* 152) is however more abundant than $(C_6H_5)P^{+\cdot}$ (*m/e* 108). A similar trend has been noted by Miller and Rake (28) in the mass spectra of pentafluorophenyl phosphorus and arsenic derivatives. An ion of *m/e* 209 carries a significant amount of ion current in $(C_6H_5)_2AsC{\equiv}CCF_3$. This may arise via loss of AsF_2 from $M^{+\cdot}$ followed by rearrangement. The appropriate metastable ion was found for this reaction. For both $(C_6H_5)_2PC{\equiv}CCF_3$ and $(C_6H_5)_2AsC{\equiv}CCF_3$ the presence of fragments $(C_6H_5)_2MC{\equiv}C^+$ (*m/e* 209, M = P; 253, M = As), $C_6H_5MC{\equiv}CCF_3^+$ (*m/e* 201, M = P; 245, M = As) and $C_6H_5MC{\equiv}C^{+\cdot}$ (*m/e* 132, M = P) provide confirmation of the expected structures.

The spectra of the unfluorinated species $(C_6H_5)_2PC{\equiv}CR$ (R = CH_3, C_6H_5, $C(CH_3)_3$) are simpler than their fluorinated analogues. The base ions are M^+ for R = CH_3, $C_6H_5C{\equiv}CC_6H_5^+$

[3]NOTE ADDED IN PROOF: Exact mass measurements on ions in the mass spectrum of $(C_6H_5)_2AsC{\equiv}CCF_3$ confirm the identity of fragments arising from loss of HF, AsF_2, C_6H_5, and $C_6H_5C{\equiv}CCF_3$ from $M^{+\cdot}$.

Can. J. Chem. Downloaded from www.nrcresearchpress.com by 210.87.254.5 on 09/05/12
For personal use only.

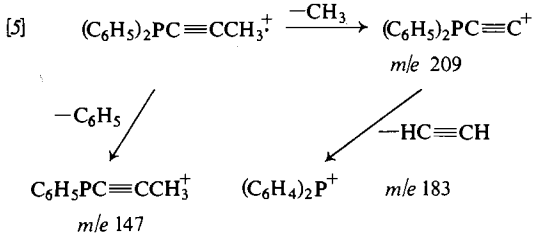

SCHEME 2

for R = C_6H_5, and $(CH_3)_3C^+$ for R = $(CH_3)_3C$. Two fragmentation patterns of importance are *5* shown in Scheme 2 for $(C_6H_5)_2PC{\equiv}CCH_3$. Metastables were found for both reactions. A similar mechanism is operative for $(C_6H_5)_2PC{\equiv}CC_6H_5$ and again supported by appropriate metastable peaks. The high abundance of $C_6H_5C{\equiv}CC_6H_5^+$ in the phenyl acetylene suggests either rearrangement of $(C_6H_5)_2PC{\equiv}C^+$ after elimination of P or direct elimination of C_6H_5P from $(C_6H_5)_2PC{\equiv}CC_6H_5^{\cdot+}$. The latter reaction gave a strong metastable at *m/e* 110.8. For $(C_6H_5)_2PC{\equiv}CR$ (R = CH_3, C_6H_5) the fragments $(C_6H_4)_2P^+$ (*m/e* 183), $(C_6H_4)_2CR^+$ (*m/e* 115, R = CH_3; 177 R = C_6H_5), $C_6H_5P^{\cdot+}$ (*m/e* 108), $C_6H_5^+$ (*m/e* 77), $C_5H_3^+$ (*m/e* 63), $C_4H_3^+$ (*m/e* 51), $C_4H_2^+$ (*m/e* 50), $C_3H_3^+$ (*m/e* 39) appear in reasonable abundance. For $(C_6H_5)_2PC{\equiv}CC(CH_3)_3$ the major ions apart from M^+ appear at low *m/e*.

The diphosphine $(C_6H_5)_2PC{\equiv}CP(C_6H_5)_2$ and the mixed P, As compound $(C_6H_5)_2PC{\equiv}CAs(C_6H_5)_2$ show similar fragmentation patterns with loss of $(C_6H_5)_2P$ and $(C_6H_5)_2As$ being the major reactions. Both decompositions were supported by metastable transitions. The ions $(C_6H_4)_2M^+$ (M = P), which appear in most spectra presumably result from loss of $HC{\equiv}CH$ from $(C_6H_5)_2PC{\equiv}C^+$ (*m/e* 209).

No parent ion was observed for $(C_6H_5)_2PC{\equiv}CP[N(C_2H_5)_2]_2$. However, the occurrence of fragments $(C_6H_5)_2PC_2PH_2^+$ (*m/e* 242), $[(C_2H_5)_2N]_2PC{\equiv}C^+$ (*m/e* 199), $(C_6H_5)_2P^+$ (*m/e* 185), and $(C_6H_4)_2P^+$ (*m/e* 183) leave little doubt that the compound is correctly formulated.

In $(C_6H_5)_2PC{\equiv}CAs(C_6H_5)_2$ and $(C_6H_5)_2PC{\equiv}CP[N(C_2H_5)_2]_2$ cleavage of *either* the $C{-}P(C_6H_5)_2$ or $C{-}MR_2$ (M = As, R = C_6H_5; M = P, R = $N(C_2H_5)_2$) bonds may occur as a first fragmentation step. In the unsymmetrical pentafluorophenyl derivative $(C_6F_5)_2PC{\equiv}CP(C_6H_5)_2$ the most abundant peak is $(C_6H_5)_2PC{\equiv}C^+$, suggesting preferential cleavage of the $C{-}P(C_6F_5)_2$ bond. A strong metastable ion supports this assignment. Loss of $HC{\equiv}CH$ from $(C_6H_5)_2PC{\equiv}C^+$ then leads to $(C_6H_4)_2P^+$ at *m/e* 183.

For the compounds $(C_6F_5)_2PC{\equiv}CR$ (R = C_6H_5, CH_3) the dominant reactions (both give metastable peaks) involve loss of C_6F_5 from M^+ and loss of C_6F_5P (or $C_6F_5C{\equiv}CR$) from $M^{\cdot+}$. Loss of R appears to be of minor importance in the fragmentation of these phosphines in contrast to the behavior of the unfluorinated analogues. Compound $(C_6F_5)PC{\equiv}CC_6H_5^+$ is the base ion for $(C_6F_5)_2PC{\equiv}CC_6H_5$ and CF_3^+ (or PF_2^+) for $(C_6F_5)_2PC{\equiv}CCH_3$. Rearrangement following fragmentation also appears to be essential in order to account for several ions in high abundance in the mass spectra of these derivatives.

We thank Arapahoe Chemicals, Division of Syntex Corporation, for financial support of this work. The continued support of the National Research Council of Canada is appreciated.

1. B. I. IONIN, G. M. BOGOLYUBOV, and A. A. PETROV. Russ. Chem. Rev. Engl. Trans. **36**, 249 (1967) and references therein.
2. W. VOSKUIL and J. F. ARENS. Rec. Trav. Chim. **83**, 1301 (1964).
3. H. HARTMANN and A. MEIXNER. Naturwiss. **50**, 403 (1963).
4. H. F. REIFF, and B. C. PANT. J. Organomet. Chem. **17**, 165 (1969).
5. W. VOSKUIL and J. F. ARENS. Rec, Trav. Chim. **81**, 993 (1962).
6. W. CHODKIEWICZ, P. CADIOT, and A. WILLEMART. Compt. Rend. **250**, 866 (1960).
7. J. C. BILLIOTTE, G. POURCELOT, LE QUAN MINH, J. SOULIE, W. CHODKIEWICZ, P. CADIOT, and A. WILLEMART. Bull. Soc. Chim. Fr. 1890 (1960).
8. I. A. MARETINA and A. A. PETROV. Zhur. Obshch. Khim. **34**, 1685 (1964).
9. K. ISSLEIB and G. HARZFELD. Chem. Ber. **95**, 268 (1962).
10. C. CHARRIER, W. CHODKIEWICZ, and P. CADIOT. Bull. Soc. Chim. Fr. 1002 (1966).
11. H. HARTMANN, C. BEERMANN, and H. CZEMPIK. Z. Anorg. Chem. **287**, 261 (1956).
12. A. J. CARTY and A. EFRATY. Inorg. Chem. **8**, 543 (1969).
13. F. A. HART and J. CHATT. J. Chem. Soc. 1385 (1960).
14. W. SIEBERT, W. E. DAVIDSOHN, and M. C. HENRY. J. Organomet. Chem. **17**, 65 (1969) and references therein.
15. A. J. CARTY, T. W. NG, A. EFRATY, and T. BIRCHALL. Inorg. Chem. **9**, 1263 (1970) and references therein.
16. G. EWART, D. S. PAYNE, A. L. PORTE, and A. P. LANE. J. Chem. Soc. 3984 (1962).

Can. J. Chem. Downloaded from www.nrcresearchpress.com by 210.87.254.5 on 09/05/12
For personal use only.

17. D. D. MAGNELLI, G. TESI, J. U. LOWE JR., and W. E. MCQUISTION. Inorg. Chem. **5**, 457 (1966).
18. K. ISSLEIB and W. SEIDEL. Chem. Ber. **92**, 2681 (1959).
19. F. B. OGILVIE, J. M. JENKINS, and J. G. VERKADE. J. Am. Chem. Soc. **92**, 1916 (1970).
20. B. C. PANT and H. F. REIFF. J. Organomet. Chem. **15**, 65 (1968).
21. A. J. CARTY and T. O'CONNOR. Unpublished results.
22. A. L. HENNE and M. NAGER. J. Am. Chem. Soc. **73**, 1042 (1951).
23. K. NAKANISHI. Infrared absorption spectroscopy. Holden-Day, San Francisco, California, 1962. p. 28.
24. A. J. CARTY and A. EFRATY. Chem. Commun. 1559 (1968).
25. J. C. J. BART. Acta Cryst B**25**, 489 (1969).
26. R. WEST and C. S. KRAIHANZEL. Inorg. Chem. **1**, 967 (1962).
27. R. G. CAVELL and R. C. DOBBIE. Inorg. Chem. **7**, 101 (1968).
28. J. M. MILLER and A. T. RAKE. J. Chem. Soc. A, 1881 (1970).

Can. J. Chem. Downloaded from www.nrcresearchpress.com by 210.87.254.5 on 09/05/12
For personal use only.

Can. J. Chem. Downloaded from www.nrcresearchpress.com by 210.87.254.5 on 09/05/12
For personal use only.

Synthetic Studies of Hydronaphthacenic Antibiotics. I. The Synthesis of 4-Demethoxy-7-*O*-methyl Daunomycinone

C. M. WONG, D. POPIEN, R. SCHWENK, AND J. TE RAA
Department of Chemistry, University of Manitoba, Winnipeg 19, Manitoba

Received March 23, 1971

Daunomycin is a new and very promising antitumor antibiotic. This communication reports the synthesis of (*dl*)-4-demethoxy-7-*O*-methyl daunomycinone as part of a scheme toward the total synthesis of daunomycin.

La daunomycine est un antibiotique nouveau et prometteur contre les tumeurs. Cette communication relate la synthèse du *dl* déméthoxy-4 *O*-méthyl-7 daunomycinone en tant qu'étape en vue de la synthèse totale de la daunomycine.

Canadian Journal of Chemistry, 49, 2712 (1971)

Introduction

In the last two decades numerous antibiotics with a linear tetracyclic skeleton have been isolated from different kinds of bacterial cultures (1). The tetracyclines attracted the attention of many organic chemists due to their very complicated structures and their potent antibacterial properties. Thus the syntheses of tetracyclines have been reported by many research groups since 1962 (2). Rhodomycins (3) are another group of antibiotics having a linear tetracyclic skeleton but which are not as potent against bacteria as the tetracyclines. However, two members recently isolated, daunomycin (rubidomycin) (**1**) and adriamycin (**2**) (5), have shown very high activity against tumors (4) and have been used successfully in treating acute lymphomas.

Daunomycin under mild acid hydrolysis gives an amino-sugar daunosamine (**3**) and a tetracyclic hydronaphthacenequinone aglycone daunomycinone (**4**). The synthesis of **3** and its derivatives was reported recently (6). A synthesis of the tetracyclic system **5** and the condensation of **5** with glucose was also reported (7). However, the synthesis of the tetracyclic aglycone **4** has not been reported and we are reporting our synthesis of 4-demethoxy-7-*O*-methyl daunomycinone (**6**) as a working model toward the total synthesis of daunomycin and adriamycin.

Results and Discussion

Condensing 2,5-dimethoxybenzaldehyde with 2,4-pentanedione in benzene solution in the presence of piperidine and acetic acid gave almost quantitatively the diketone **7**, which upon hydrogenation in ethanol using 5% Pd/C as catalyst, gave the diketone **8**. This compound, when freshly distilled, existed in an equilibrium between the keto and the enol form. This was evident from the n.m.r. spectrum which showed a small peak at $-6.50\ \tau$ corresponding to the enol proton with an area integrated to about one-third of a hydrogen; a singlet at $6.58\ \tau$ corresponding to the benzylic hydrogens of the enol-form and a doublet at $7.06\ \tau$ corresponding to the benzylic hydrogens of the keto-form. On standing, the diketone **8** crystallized entirely in the enol-form; this was shown by the n.m.r. spectrum which now had a singlet at $-6.63\ \tau$ for the enol proton integrating to exactly one hydrogen.

The diketone **8** was then alkylated with ethyl-bromoacetate and sodium hydride in anhydrous tetrahydrofuran to give the keto-ester **9** which on treatment with aqueous sodium hydroxide solution underwent a reversed Claisen followed by the hydrolysis of the ester to give the keto-acid **10**. Cyclization of **10** in the presence of hydrofluoric acid gave the tetralone **11** or the lactone **12** depending on the concentration and the reaction temperature. At 35 °C and low concentration of **10**, the tetralone **11** was isolated in 72% yield together with the lactone **12** in about 5% yield. At 0 °C and high concentration of **10**, the lactone **12** was isolated as the major product.

Hydrogenolysis of **11** in acidic ethanolic solution in the presence of 5% Pd/C gave the tetralin **13**, which upon oxidation in *t*-butyl alcohol with potassium *t*-butoxide and oxygen followed by reduction with zinc gave the hydroxyketone **14** in

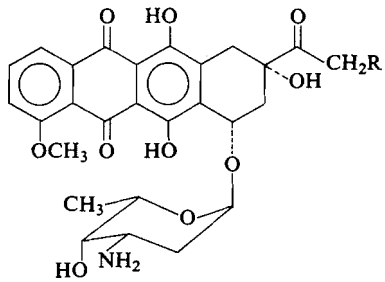

1 R = H
2 R = OH

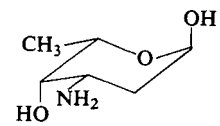

3

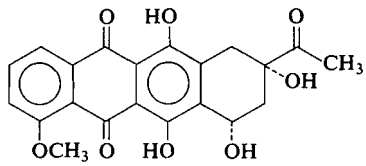

4

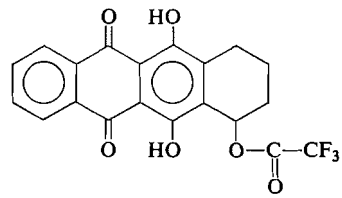

5

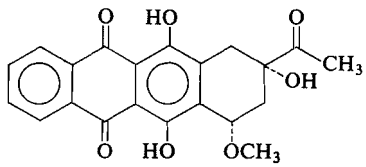

6

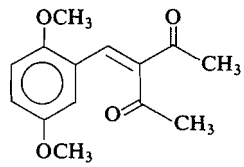

7

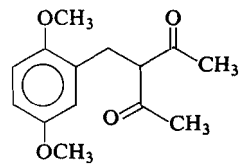

8

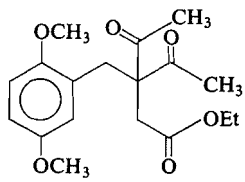

9

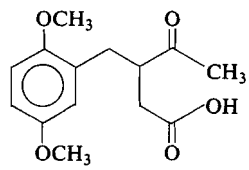

10

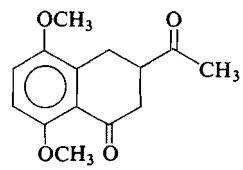

11

excellent yield. The use of sodium *t*-butoxide however, gave less than 5% yield, possibly due to the low solubility of the sodium salt at the reaction temperature.

In order to ascertain that the hydroxy group is in the tertiary position, the tetralin **13** was reduced with sodium borohydride to the corresponding alcohol and eventually converted to the olefinic mixture **15** by tosyl chloride and pyridine. Osmium tetroxide oxidation of **15** to the diol **16** followed by oxidation with dicyclohexylcarbodiimide and dimethylsulfoxide gave the identical hydroxyketone **14**.

Condensing **14** with phthalic acid monomethyl ester in trifluoroacetic anhydride solution followed by basic hydrolysis and then cyclization with hydrofluoric acid gave the tetracyclic hydroxyketone **17**. This was then converted to

Can. J. Chem. Downloaded from www.nrcresearchpress.com by 210.87.254.5 on 09/05/12
For personal use only.

Can. J. Chem. Downloaded from www.nrcresearchpress.com by 210.87.254.5 on 09/05/12
For personal use only.

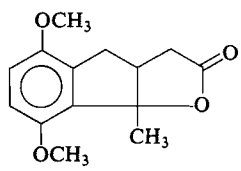

12

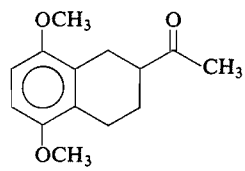

13

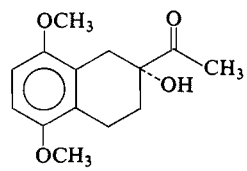

14

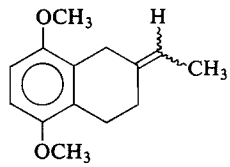

15

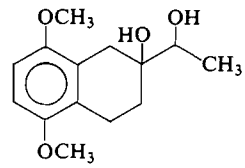

16

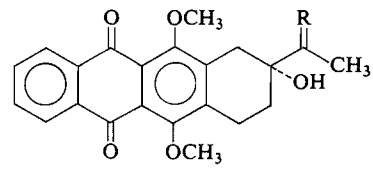

17 R = O
18 R = O—CH_2
O—CH_2

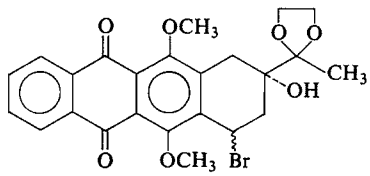

19

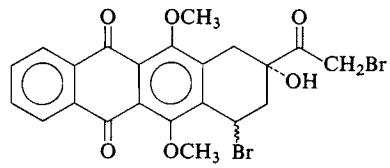

20

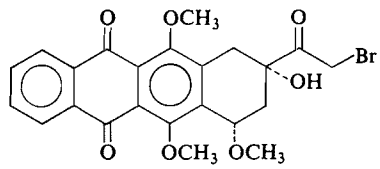

21

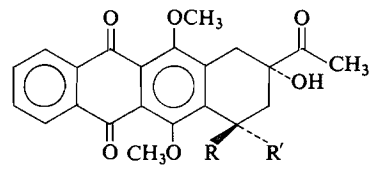

22 R = OCH_3; R′ = H
23 R = H; R′ = OCH_3

the ketal **18** making the two benzylic positions different enough to be selectively attacked by *N*-bromosuccinimide on the less hindered position. Thus refluxing the ketal **18** with *N*-bromosuccinimide in carbon tetrachloride in the presence of a trace of benzoyl peroxide gave the unstable bromoketal **19** and the dibromide **20**. This mixture, without purification, was then refluxed in anhydrous methanol to give **21**, **22**, and **23** which were separated from each other by t.l.c. on silica.

The stereochemistry of **21**, **22**, and **23** was assigned mainly on the basis of the n.m.r. spectra of **14**, **17**, **18**, **21**, **22**, and **23**. Under identical conditions, the hydroxy protons of **14**, **17**, **18**, and **22** had chemical shifts higher than 6 τ while those of **21** and **23** were lower than 5 τ. The chemical shift differences are interpreted as being a result of the existence of hydrogen bonding between the hydroxy proton and the C_7—OCH_3 groups in **21** and **23**.

The fact that the C_7-isomer of **21** was not observed and that there was twice as much of **23** produced as **22** would indicate that the conversion

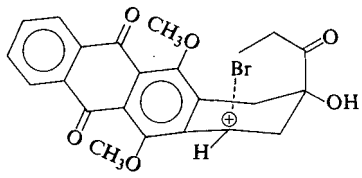

24
26 Br replaced by H

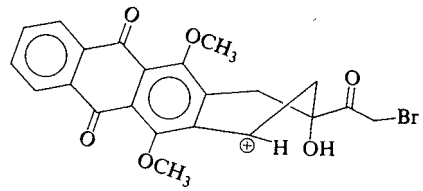

25
27 Br replaced by H

of **19** and **20** to **21**, **22**, and **23** went through a partially stereospecific S_N1 process.[1] The C_7-carbonium ion formed when **20** is refluxed in methanol exists mainly in the conformation **24** which is more stable than the other conformation **25** due to the presence of a bridging between the bromine atom and the carbonium ion.[2] Thus methanol can only come from the α-side giving the C_7-*O*-methyl group *cis* to the C_9-hydroxy group. On the other hand, the carbonium ions **26** and **27** are very similar energetically. In the former case methanol will come mainly from the α-side due to the steric effect of the axial C_9-acetyl group while in the latter case, approach of methanol from the β-side is slightly favored.

[1]In another series of investigations, the conversion of **i** to **ii** by aluminum chloride in refluxing benzene was accompanied by the formation of **iii**, also dissolving **ii** in chloroform in the presence of trifluoroacetic acid gave the corresponding trifluoroacetate **iv**. These results would indicate that the formation of a carbonium ion was very easy.

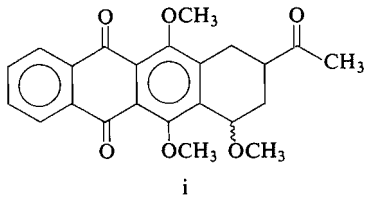

i

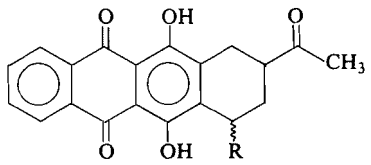

ii R = OCH_3
iii R = C_6H_5
iv R = $O-\overset{O}{\overset{\|}{C}}-CF_3$

[2]This will be proven further in the synthetic approach to adriamycin.

The hydroxyketone **23** was then hydrolyzed to the red crystalline 4-demethoxy-7-*O*-methyl daunomycinone (6) in benzene solution in the presence of aluminum chloride (5*b*).

Experimental

Melting points and boiling points are uncorrected. The i.r. spectra (cm^{-1}) were recorded on a Perkin–Elmer model 700 spectrophotometer using methylene chloride as solvent or as otherwise specified. The n.m.r. spectra (τ) were recorded on a Varian Model A56/60A MHz spectrometer using deuterated chloroform as solvent and tetramethylsilane as internal standard. Mass spectra were recorded on a Hitachi Perkin–Elmer Model RMU-6D or a Finnigan Model 1015 mass-spectrometer. High resolution mass spectra were recorded on the MS9 mass-spectrometer of the Chemistry Department, University of Alberta, Edmonton, Alberta. Microanalyses were performed by Dr. Daesslé of Montreal and Dr. Yates of Arizona.

Preparation of 3-Acetyl-4-(2′,5′-dimethoxyphenyl) 3-Buten-2-one (7)

A benzene solution (500 ml) containing 2,5-dimethoxybenzaldehyde (100 g), 2,4-pentanedione (80 g), piperidine (4 ml), and acetic acid (12 ml) was refluxed in a 1 l flask equipped with a condenser and a water separator, for 2 h. The benzene was then removed under reduced pressure and the residue which crystallized on standing (148 g) could be purified by recrystallization from methanol; m.p. 65–66 °C; i.r. 1710 and 1700 (ketones), 1665 (C=C), 1620 and 1595 (aromatic); n.m.r. 2.51 (s, 1H, olefinic), 3.33 (s, 3H, aromatic), 6.33 (s, 3H, OCH_3), 6.45 (s, 3H, OCH_3), 7.82 (s, 3H, $COCH_3$), 8.00 (s, 3H, $COCH_3$).

Preparation of 3-Acetyl-4-(2′,5′-dimethoxyphenyl) 2-Butanone (8)

The crude product **7** above was dissolved in 200 ml of distilled ethanol and filtered into a 3 l flask containing Pd/C (5%, 13 g) and distilled ethanol (1.3 l). The solution was then hydrogenated at atmospheric pressure until the uptake of hydrogen ceased. The catalyst was removed by filtration and the ethanol evaporated under reduced pressure. The residue was purified by distillation (b.p. 150–155 °C at 0.5 mm Hg) (133 g). The distillate crystallized on standing and was recrystallized from carbon tetrachloride and petroleum ether; m.p. 63–68 °C; i.r. 1600 (broad); n.m.r. −6.63 (s, 1H, enol), 3.17–3.58 (m, 3H, aromatic), 6.24 (s, 3H, OCH_3), 6.34 (s, 3H, OCH_3), 6.47 (s, 2H, benzylic), 8.00 (s, 6H, $C-CH_3$).

Can. J. Chem. Downloaded from www.nrcresearchpress.com by 210.87.254.5 on 09/05/12
For personal use only.

Can. J. Chem. Downloaded from www.nrcresearchpress.com by 210.87.254.5 on 09/05/12
For personal use only.

*Preparation of 3-Acetyl-4-(2',5'-dimethoxyphenyl) Butanoic Acid (**10**)*

To a 1 l flask equipped with a mechanical stirrer, a condenser, and a dropping funnel, freshly distilled dry tetrahydrofuran (600 ml), the diketone **8** (30 g), and sodium hydride (6 g 50% mineral oil suspension) in small portions were added. The tetrahydrofuran solution was heated to a gentle reflux and ethyl bromoacetate (21 g) in dry tetrahydrofuran (50 ml) was added through the dropping funnel over a period of 15 min. After refluxing for 1 h, most of the tetrahydrofuran was distilled off and water (100 ml) was added to the residue. The aqueous solution was extracted exhaustively with benzene. The benzene solution was dried over magnesium sulfate, and evaporated under reduced pressure to give the crude crystalline keto-ester **9** (40 g) which could be recrystallized from methanol; m.p. 66–67 °C; i.r. 1735 (ester), 1700 (ketone), 1600 (aromatic); n.m.r. 3.35 (m, 3H, aromatic), 5.86 (q, 2H, $COOCH_2$—CH_3), 6.30 (s, 3H, OCH_3), 6.37 (s, 3H, OCH_3), 6.58 (s, 2H, benzylic), 7.18 (s, 2H, CH_2—$COOC_2H_5$), 7.80 (s, 6H, $COCH_3$), 8.75 (t, 3H, $COOCH_2CH_3$).

Anal. Calcd. for $C_{18}H_{24}O_6$: C, 64.27; H, 7.19. Found: C, 64.11; H, 6.99.

The keto-ester **9** was then hydrolyzed by heating in a sodium hydroxide solution (8%, 250 ml) at 65 °C for 3 h. The basic solution was then washed with benzene and acidified with cold concentrated hydrochloric acid. The keto-acid precipitate **10** was filtered and dried in a desiccator to give 27 g of white solid which was further purified by recrystallization from methanol, m.p. 106–107 °C; i.r. 1740 (acid), 1700 (ketone); n.m.r. −2.10 (s, 1H, COOH), 2.70 (m, 3H, aromatic), 5.97 (s, 3H, $COCH_3$).

Anal. Calcd. for $C_{14}H_{18}O_5$: C, 63.13; H, 6.76. Found: C, 63.30; H, 6.58.

*Cyclization of Keto-acid **10***

The keto-acid **10** (10 g) was added with stirring into a polyethylene reaction flask containing hydrofluoric acid (100 ml). After stirring for 3 h in a water bath at 20 °C, the temperature was raised to 40 °C to evaporate the remaining hydrofluoric acid. The residue was diluted with water and extracted exhaustively with chloroform. The chloroform solution was washed with sodium bicarbonate solution, dried, and then evaporated to dryness under reduced pressure. Upon addition of methanol to the residue, the tetralone **11** crystallized and was then collected by filtration. The mother liquor was evaporated to dryness and the residue was dissolved in benzene. After stirring the benzene solution with sodium hydroxide solution (25 ml, 8%) for 2 h, the benzene layer was separated, washed with water, and dried over magnesium sulfate and evaporated to dryness. Upon addition of methanol and ether, another crop of tetralone **11** crystallized and was collected as before. The combined tetralone **11** (6.7 g) was further purified by recrystallization from methanol ether; m.p. 123–125 °C; i.r. 1710 (ketone), 1685 (conjugated ketone), 1590 (aromatic); n.m.r. 3.20 (q, 2H, aromatic), 6.20 (s, 3H, OCH_3), 6.23 (s, 3H, OCH_3), 7.97 (s, 3H, $COCH_3$); mass spectrum 248 (m^+/e), 205 (M-$COCH_3$).

The aqueous sodium hydroxide solution was acidified with concentrated hydrochloric acid and then extracted with chloroform. Evaporating the chloroform solution to dryness gave lactone **12** (450 mg) which was purified by recrystallization from methanol; m.p. 137–138 °C; i.r. 1765 (lactone), 1610 (aromatic); n.m.r. 3.38 (s, 3H, aromatic), 6.26 (s, 3H, OCH_3), 6.30 (s, 3H, OCH_3), 8.21 (s, 3H, t-CH_3); mass spectrum 248 (m^+/e), 233 (M-CH_3), 190 (2-methyl, 4,7-dimethoxyindene cation).

*Preparation of 1,4-Dimethoxy-6-hydroxy-6-acetyl Tetralin (**14**)*

A solution of the tetralone **11** (10 g), distilled ethanol (400 ml), concentrated hydrochloric acid (10 ml), water (40 ml), and 5% Pd/C (2 g) was hydrogenated at atmospheric pressure and room temperature for 6 h with mechanical shaking. After filtering the catalyst, the alcoholic solution was evaporated to dryness under reduced pressure. The residue was recrystallized from ethanol and petroleum ether to give the crystalline monoketone **13** (8.4 g); m.p. 81–82 °C; i.r. 1715 (ketone), 1610 (aromatic); n.m.r. 3.41 (s, 2H, aromatic), 6.26 (s, 6H, OCH_3), 7.80 (s, 3H, $COCH_3$).

The monoketone **13** (5.7 g) dissolved in dry t-butyl alcohol (50 ml) was added to an oxygen-saturated t-butyl alcohol solution (400 ml) in a 1 l flask containing potassium t-butoxide prepared by dissolving freshly cut potassium (8 g) in the t-butyl alcohol. Dry oxygen was bubbled through a gas dispersion tube into the solution for exactly 5 min keeping the reaction temperature at 35 °C. The solution was then cooled in an ice bath and glacial acetic acid was added until the solution became acidic. Zinc dust (20 g) was added immediately and the solution was then stirred at room temperature for 6 h. The zinc was then removed by filtration and the filtrate was evaporated to a syrupy residue at 50 °C under reduced pressure. The residue was diluted with water and extracted exhaustively with chloroform. The chloroform solution was dried over magnesium sulfate and evaporated to dryness to give the crude crystalline hydroxyketone **14** (5.5 g) which was purified by recrystallization from methanol and ether; m.p. 100–102 °C; i.r. 3525 (OH), 1705 (ketone), 1600 (aromatic); n.m.r. 3.40 (s, 2H, aromatic), 6.26 (s, 3H, OCH_3), 6.30 (s, 3H, OCH_3), 6.42 (s, 1H, OH), 7.75 (s, 3H, $COCH_3$).

Anal. Calcd. for $C_{14}H_{18}O_4$: C, 67.12; H, 7.20. Found: C, 67.18; H, 7.20.

*Preparation of the Tetracyclic Hydroxyketone **17***

Trifluoroacetic anhydride (10 ml) was added to a mixture of the hydroxyketone **14** (2 g) and the phthalic acid monomethyl ester (4 g). The solution was refluxed under dry nitrogen atmosphere overnight. After removing the trifluoroacetic anhydride under reduced pressure, the residue was hydrolyzed by 8% sodium hydroxide solution (30 ml) at 65 °C. The basic aqueous solution was washed with chloroform and then acidified by concentrated hydrochloric acid. The acidic solution was then extracted exhaustively with chloroform. Evaporating the chloroform solution to dryness as usual gave a dark brown residue which, without purification, was then dissolved in hydrofluoric acid (10 ml) in a polyethylene flask and then worked-up as described in the preparation of the tetralone **11**. The dark yellow residue was purified by preparative t.l.c. on alumina to give the yellow crystalline tetracyclic hydroxyketone **17** (700 mg) which could be recrystallized

Can. J. Chem. Downloaded from www.nrcresearchpress.com by 210.87.254.5 on 09/05/12
For personal use only.

from methanol; m.p. 184–186 °C; i.r. 3510 (OH), 1710 (ketone), 1670 (quinone), 1600 and 1560 (aromatic); n.m.r. 1.73–2.34 (m, 4H, aromatic), 6.10 (s, 3H, OCH_3), 6.15 (s, 3H, OCH_3), 6.20 (s, 1H, OH), 6.91 (broad s, 4H, benzylic); mass spectrum 380 (m^+/e), 362 (M-H_2O), 337 (M-$COCH_3$).

Anal. Calcd. for $C_{22}H_{20}O_6$: C, 69.49; H, 5.29. Found: C, 69.55; H, 5.13.

Preparation of 4-Demethoxy Daunomycinone Trimethyl Ether (23)

A benzene solution (60 ml) of the hydroxyketone **17** (600 mg), ethylene glycol (1 ml), and anhydrous *p*-toluenesulfonic acid (50 mg) was distilled at a very slow rate. After about 30 ml of benzene was collected, the residual benzene was washed with sodium carbonate solution and then evaporated to dryness under reduced pressure to give quantitatively the crystalline ketal **18** which could be recrystallized from benzene, m.p. 185–186 °C; i.r. showed the absence of 1710 peak. The ketal **18** was then refluxed in carbon tetrachloride solution (50 ml) containing *N*-bromosuccinimide (290 mg) and a trace of benzoylperoxide for 45 min under dry nitrogen atmosphere. The solution was then evaporated under reduced pressure at room temperature to about 10 ml and the succinimide was then removed by filtration. The orange solution, without further purification, was refluxed in anhydrous methanol (50 ml) overnight under dry nitrogen. After evaporating the methanolic solution to dryness under reduced pressure, concentrated hydrochloric acid (3 ml) and water (10 ml) in 30 ml of tetrahydrofuran were added and the solution was stirred at room temperature for 4 days. After most of the tetrahydrofuran was removed under reduced pressure, the residue was diluted with water and extracted by chloroform exhaustively. Washing the chloroform solution with dilute sodium bicarbonate solution and evaporating the chloroform solution to dryness gave a dark orange residue which was separated by t.l.c. on silica into three major fractions corresponding to compounds **21**, **22**, and **23**.

The bromoketone **21** (95 mg) was further purified by recrystallization from methanol; m.p. 176–178 °C; i.r. 3475 (OH), 1735 (ketone), 1670 (quinone), 1595 and 1560 (aromatic); n.m.r. 1.74–2.35 (m, 4H, aromatic), 4.81 (s, 1H, OH), 5.08 (t, 1H, C_7—H), 5.20 (s, 2H, $CO\mathit{CH}_2Br$), 6.04 (s, 3H, OCH_3), 6.13 (s, 3H, OCH_3), 6.43 (s, 3H, C_7—OCH_3); mass spectrum 490 (m^+/e Br-81), 488 (m^+/e Br-79), 367 (M-$COCH_2Br$), 359 (M-H_2O, CH_3OH, Br), 335 (M-CH_3OH, $COCH_2Br$). This bromoketone was converted to **23** via zinc and acetic acid.

The crude hydroxyketone **22** (110 mg) was further purified by t.l.c. on silica followed by recrystallization from methanol; m.p. 192–193 °C; i.r. 3525 (OH), 1715 (ketone), 1675 (quinone), 1600 and 1575 (aromatic); n.m.r. 1.70–2.33 (m, 4H, aromatic), 4.95 (q, 1H, $J = 2$, $J = 4.5$ Hz, C_7—H), 6.03 (s, 3H, OCH_3), 6.08 (s, 3H, OCH_3), 6.14 (s, 1H, OH), 6.50–7.12 (q, 2H, $J = 15$ Hz, C_{10}—H_2), 6.65 (s, 3H, C_7—OCH_3), 7.29 (d of d, 1H, $J = 2$, $J = 15$ Hz, C_8—H), 8.04 (d of d, 1H, $J = 4.5$, $J = 15$ Hz, C_8—H); mass spectrum 410 (m^+/e), 392 (M-H_2O), 335 (M-CH_3OH, $COCH_3$), 307 (M-$COCH_3$, CH_3OH, CO).

The hydroxyketone **23** (220 mg) was recrystallized from methanol; m.p. 194–195 °C; i.r. 3475 (OH), 1710 (ketone), 1670 (quinone), 1595 and 1560 (aromatic); n.m.r. 1.70–2.33 (m, 4H, aromatic), 4.96 (s, 1H, OH), 5.04 (d of d, 1H, $J = 2$, $J = 4$ Hz, C_7—H), 6.01 (s, 3H, OCH_3), 6.10 (s, 3H, OCH_3), 6.42 (s, 3H, C_7—OCH_3), 6.70–6.85 (m, 2H, C_{10}—H_2), 7.35–7.67 (m, 1H, C_8—H), 7.93–8.24 (d of d, 1H, $J = 4$, $J = 15$ Hz, C_8—H); mass spectrum 410 (m^+/e), 392 (M-H_2O), 360 (M-H_2O, CH_3OH), 335 (M-CH_3OH, $COCH_3$), and 307 (M-CH_3OH, $COCH_3$, CO).

Anal. Calcd. for $C_{23}H_{22}O_7$ (mol. ion 410.1365): C, 67.31; H, 5.36. Found (410.1360 (high resolution mass spectrum)): C, 67.30; H, 5.33.

Preparation of 4-Demethoxy-7-O-methyl Daunomycinone (6)

The hydroxyketone **23** (140 mg) and aluminum chloride (300 mg) in benzene solution (20 ml) were stirred together with sea sand at 50 °C overnight under dry nitrogen atmosphere. The benzene solution was then extracted twice with an aqueous oxalic acid solution (20 ml, 5%) and the combined oxalic acid solution was extracted with chloroform. The combined benzene and chloroform solutions were then dried over sodium sulfate and evaporated to dryness under reduced pressure giving a red solid residue. The residue was then purified by t.l.c. on silica to give the red crystalline 4-demethoxy-7-*O*-methyl daunomycinone (**6**) (96 mg) which was recrystallized from a large volume of chloroform; m.p. 250–254 °C; i.r. ($CHCl_3$) 3400 (OH), 3400–2700 (phenols), 1715 (ketone), 1625 (quinone), 1595 (aromatic); n.m.r.[3] −3.50 (s, 1H, phenol), −3.20 (s, 1H, phenol), 1.50–2.03 (m, 4H, aromatic), 4.80 (s, 1H, C_9—OH), 4.92 (d of d, 1H, C_7—H), 6.20 (s, 3H, OCH_3), 6.64 (q, 2H, C_{10}—H_2), 7.37 (s, 3H, $COCH_3$); mass spectrum 382 (m^+/e), 332 (M-H_2O, CH_3OH), 307 (M-$COCH_3$, CH_3OH), 289 (M-$COCH_3$, H_2O, CH_3OH).

Mol. Ion Calcd. for $C_{21}H_{18}O_7$: 382.1053. Found (high resolution mass spectrum): 382.1050.

The synthesis toward daunomycin and adriamycin is progressing and results will be reported later.

The authors would like to express their gratitude to the National Research Council of Canada for financial support and Drs. Camerino and Mondelli for a sample of daunomycinone for spectroscopic comparison.

1. (*a*) J. Cook and W. Carruthers. Progress in organic chemistry. Vol. 7. Butterworths and Co. Ltd., London, 1968. p. 1–34. (*b*) H. Brockmann and K. Pauer. Naturwissen. **37**, 492 (1952).
2. (*a*) R. B. Woodward. Pure and Appl. Chem. **6**, 561 (1963). (*b*) A. I. Gurevick, M. G. Karapetyan, M. N. Kolosov, V. G. Korobko, V. V. Onoprienko, S. A. Popravko, and M. M. Shemyakin. Tetrahedron Lett. 131 (1967). (*c*) H. Muxfeldt. J. Am. Chem. Soc. **90**, 6534 (1968). (*d*) D. H. R. Barton. Chem. in Brit. **6**, No. 7, 301 (1970).
3. H. Brockmann, T. Waehneldt, and Jurgen Niemeyer. Tetrahedron Lett. 415 (1969).

[3]Recorded on an A56/60A 60 MHz spectrometer with the help of a Varian Model C-1024 time averaging computer.

4. (*a*) A. DI MARCO, M. GAETANI, P. OREZZI, B. M. SCARPINATO, R. SILVESTRINI, M. SOLDATI, T. DASDIA, and L. VALENTINI. Nature, **706** (1964). (*b*) J. A. STOCK. Chem. in Brit. **6**, No. 1, 11 (1970).
5. (*a*) H. BROCKMANN, H. BROCKMANN JR., and JURGEN NIEMEYER. Tetrahedron Lett. No. 45, 4719 (1969). (*b*) F. ARCAMONE, G. FRANCESCHI, P. OREZZI, and S. PENCO. Tetrahedron Lett. No. 30, 3349 (1968). (*c*) R. H. IWAMOTO, P. LIM, and N. S. BHACCA. Tetrahedron Lett. No. 36, 3891 (1968). (*d*) F. ARCAMONE, G. FRANCESCHI, S. PENCO, and A. SELVA. Tetrahedron Lett. No. 13, 1007 (1969).
6. (*a*) J. P. MARSH JR., C. W. MOSHER, E. M. ACTON, L. GOODMAN. Chem. Commun. 973 (1967). (*b*) H. BAER, K. CAPEK, and M. C. COOK. Can. J. Chem. **48**, 89 (1969).
7. J. P. MARSH JR., R. H. IWAMOTO, and LEON GOODMAN. Chem. Commun. 589 (1968).

Can. J. Chem. Downloaded from www.nrcresearchpress.com by 210.87.254.5 on 09/05/12
For personal use only.

Can. J. Chem. Downloaded from www.nrcresearchpress.com by 210.87.254.42 on 09/05/12
For personal use only.

Mössbauer Spectra and Electric Dipole Moments of Organotin(IV) Complexes with Monodentate Donor Ligands

F. PATRICIA MULLINS

Department of Chemistry, Mount St. Vincent University, Halifax, Nova Scotia

Received March 8, 1971

Mössbauer spectra and electric dipole moment data are reported for R_2SnCl_2 and $RSnCl_3$ complexes with Y type ligands where R = C_4H_9, C_6H_5 and Y = Ph_3PO, Ph_3AsO, Bu_3PO, and Ph_3P. Quadrupole splittings and dipole moments are consistent with *trans* C—Sn—C bonds in the $R_2SnCl_2Y_2$ complexes. In the trigonal bipyramidal Ph_2SnCl_2Y complexes, the two phenyl groups are assumed to be in equatorial positions. Data for the $RSnCl_3Y_2$ complexes suggest that in $BuSnCl_3(Ph_3AsO)_2$ and $BuSnCl_3(Ph_3P)_2$ two Cl atoms are *trans* and that in $BuSnCl_3(Ph_3PO)_2$ and $PhSnCl_3(Ph_3PO)_2$ the three Cl atoms are *cis*.

On rapporte les données obtenues à partir des spectres de Mössbauer et des moments dipolaires électriques pour les complexes R_2SnCl_2 et $RSnCl_3$ avec des ligands du type Y, ou R = C_4H_9, C_6H_5 et Y = Ph_3PO, PhAsO, Bu_3PO et Ph_3P. Les dédoublements quadrupolaires et les moments dipolaires sont consistants avec des liaisons C—Sn—C *trans* dans les complexes $R_2SnCl_2Y_2$. On suppose que dans le complexe Ph_2SnCl_2Y trigonal bipyramidal, les deux groupes phényles occupent la position équatoriale. Les données obtenues pour les complexes $RSnCl_3Y_2$ suggèrent que dans $BuSnCl_3(Ph_3AsO)_2$ et $BuSnCl_3(Ph_3P)_2$, les atomes de chlore sont en position *trans* et que dans $BuSnCl_3(Ph_3PO)_2$ et $PhSnCl_3(Ph_3PO)_2$ les trois atomes de chlore sont en position *cis*.

Canadian Journal of Chemistry, 49, 2719 (1971)

Introduction

Within the past ten years there has been considerable interest in the interpretation of Mössbauer spectra of SnX_4, $RSnX_3$, R_2SnX_2, and R_3SnX complexes as a means of determining the structure of these compounds. Most of the work on organotin(IV) complexes has been done with bidentate and to a lesser extent monodentate ligands containing N, O, S, and P donor atoms. In some cases the study of the Mössbauer parameters of these tin complexes has been linked with other experimental methods of structural determination, for example, using X-ray (1), electron spin resonance (2), nuclear quadrupole resonance (3), nuclear magnetic resonance (4–6), infrared spectra (6–12), and electric dipole moments (13–16).

The purpose of the present study was to broaden the correlation between the Mössbauer and electric moment studies previously undertaken on R_2SnX_2 and $RSnX_3$ complexes (13–16) by using monodentate rather than bidentate ligands, as well as to compare the present results with those obtained in an investigation of SnX_4 complexes with similar O and P donor ligands (10, 11, 15). It was of interest to discover whether the R groups in the R_2SnCl_2 complexes would remain *trans* in $R_2SnCl_2Y_2$ complexes where the monodentate ligands are more bulky than R and whether these ligands would have a *trans* or *cis* arrangement in the complexes. It was also of interest to ascertain the effect of the monodentate *vs.* bidentate ligand on the position of the lone R in $RSnCl_3$ complexes. It is true, of course, that the configurations of molecules may differ from the solid state to solutions. However, previous studies (13, 14) have shown an *excellent* correlation between the configurations of octahedral tin(IV) complexes containing two carbon–tin bonds as revealed by Mössbauer measurements on solids and as indicated in solution by dielectric constant measurements. This observed correlation certainly makes it worthwhile to extend the comparison of Mössbauer and dielectric constant measurements to $R_2SnCl_2 \cdot L_2$ compounds. The previous correlations also suggest that in the absence of determining crystal packing factors the configurations of $RSnCl_3 \cdot L_2$ complexes may well be similar in the solid state and in solution. Two of the complexes were not sufficiently soluble in benzene to allow for dielectric constant measurements. Although 1:2 complexes have been reported for Ph_2SnCl_2 with Ph_3PO and Ph_3AsO (17), the various

TABLE 1. Analyses and melting points of R_2SnX_2 and $RSnX_3$ complexes

Complex	Analysis (%) Found C	Found H	Calcd. C	Calcd. H	Melting point
$(C_6H_5)_2SnCl_2(C_{12}H_{27}PO)_2$	55.33	8.21	55.40	8.27	115–17
$(C_4H_9)_2SnCl_2(C_{12}H_{27}PO)_2$	52.15	9.78	51.91	9.81	34–36
$(C_4H_9)_2SnCl_2(C_{18}H_{15}PO)_2$	61.70	5.85	61.42	5.62	83–85
$(C_4H_9)_2SnCl_2(C_{18}H_{15}AsO)_2$	54.78	5.05	55.73	5.10	110-d
$(C_6H_5)_2SnCl_2(C_{18}H_{15}AsO)$	53.98	4.04	54.09	3.78	190–92
$(C_6H_5)_2SnCl_2(C_{18}H_{15}PO)$	57.26	4.13	57.92	4.05	173–75
$C_6H_5SnCl_3(C_{18}H_{15}PO)_2$	57.42	4.48	58.74	4.11	143-d
$C_4H_9SnCl_3(C_{18}H_{15}PO)_2$	57.09	4.79	57.27	4.67	128–30
$C_4H_9SnCl_3(C_{18}H_{15}AsO)_2$	51.61	4.17	51.84	4.24	76-d
$C_4H_9SnCl_3(C_{18}H_{15}P)_2$	60.48	5.12	59.55	4.87	65-d

methods attempted yielded compounds whose analyses and Mössbauer parameters indicated the presence of 1:1 complexes.

Experimental

Preparation of Compounds

Phenyltin and *n*-butyltin trichloride, diphenyl and di-*n*-butyltin dichloride were obtained from Alfa Inorganics Inc. Triphenylphosphine was purchased from Matheson, Coleman and Bell. Triphenylphosphine oxide, triphenylarsine oxide, and tributylphosphine oxide were obtained from Eastman Organic Chemicals. All solvents were Baker Analyzed Reagents. Thiophene-free benzene was refluxed over phosphorus pentoxide for several hours before being distilled.

Complexes of $R_2SnCl_2Y_2$ were prepared by mixing the ligand and R_2SnCl_2 or $RSnCl_3$ in a 2:1 ratio in an appropriate solvent: hot absolute ethanol was used for R_2SnCl_2 and $BuSnCl_3$ complexes with Ph_3PO; absolute ether for $PhSnCl_3(Ph_3PO)_2$; ether–benzene for $BuSnCl_3$ with Ph_3P; ether-ethanol for the Ph_3AsO and Bu_3PO complexes. The Ph_3AsO complexes of PH_2SnCl_2 and Bu_2SnCl_2 and the Ph_2SnCl_2 complexes of Ph_3PO and Bu_3PO were obtained as white precipitates. The other complexes were obtained as white powders, except $BuSnCl_3(Ph_3P)_2$ which was cream colored, by evaporation of cooled solutions of benzene and absolute ether. All solids were washed with petroleum ether (b.p. 30–60°) and dried under vacuum at room temperature overnight. Attempts to isolate other complexes of these ligands and Ph_3As with the starting compounds were not successful.

Analytical data and melting points for the complexes are given in Table 1.

Mössbauer Spectra

These were obtained with an Austin Science Associates Mössbauer Spectrometer Drive Model S3, with Model K3 constant acceleration linear motor, pre-amplifier, a Reuter Stokes Model RSG-61 proportional counter tube filled with krypton–carbon dioxide, a Northern Scientific Inc. modified 512 channel analyzer with a single channel analyzer and time base generator, Model NS-600 and a Teletype readout. A 10 mC $Ba^{119m}SnO_3$ source obtained from New England Nuclear Corporation was used at room temperature. The finely divided solid absorbers were placed between beryllium windows and mounted in a copper sample holder attached to a metal Dewar automatically filled with liquid nitrogen. Data were accumulated until at least 2×10^5 counts per channel were collected to reduce statistical error. The data thus obtained were treated by computer analysis as described previously (16).

The spectrometer was calibrated periodically against chemically pure SnO_2 and natural iron foil obtained from New England Nuclear Corporation. The parameters were read from the plotted curves and the difference between replicate measurements was less than 0.05 mm s^{-1}. The spectrum of Bu_2SnCl_2 $(Bu_3PO)_2$ is illustrated in Fig. 1.

Dielectric Constants of Benzene Solutions

These were obtained at 25 °C as in previous investigations (18) using an oscillator similar to that described by Estok (19). The reproducibility of dielectric constants of benzene and solutions was ± 0.0005 and this was taken as the relative precision of measurements (Table 2). Electric moments were calculated by the method of Higasi (20), using a value of 0.8481 for β (21).

Infrared spectra of potassium bromide discs and benzene solutions were obtained with a Perkin–Elmer 521 and a Beckman IR-33 spectrometer.

Discussion of Results

The isomer shifts relative to SnO_2, quadrupole splittings and dipole moment data obtained for the compounds studied are listed in Table 3. Asymmetries in the doublet Mössbauer spectra are present in most of the compounds. The programmed data yielded intensity ratios (area of peak *1*/peak *2*); **1** (1.41), **2** (0.65), **3** (0.81), **6** (1.17), **7** (0.87), **11** (1.19). Previous comparisons of dipole moments obtained by calculations of Higasi with those from the LeFevre and Vine modification of the Hedestrand equation indicate that density and index of refraction measure-

Can. J. Chem. Downloaded from www.nrcresearchpress.com by 210.87.254.42 on 09/05/12
For personal use only.

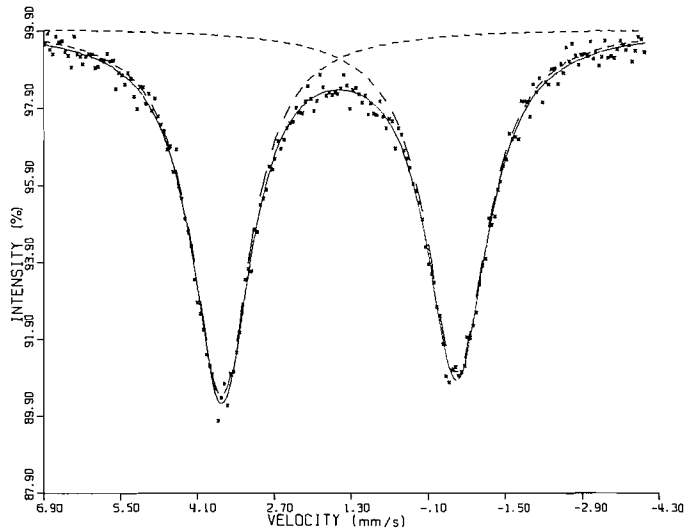

FIG. 1. ^{119m}Sn Mössbauer spectrum of $Bu_2SnCl_2(Bu_3PO)_2$ *vs.* a $Ba^{119m}SnO_3$ source.

TABLE 2. Dielectric constants of benzene solutions at 25 °C

$100wf_2$	ε	$100wf_2$	ε
$(C_6H_5)_2SnCl_2(Bu_3PO)_2$		$(C_4H_9)_2SnCl_2(Bu_3PO)_2$	
0.00	(2.2730)	0.00	(2.2730)
1.03	2.3733	1.11	2.4757
1.93	2.4427	1.96	2.6467
4.03	2.6021	3.67	3.0335
$(C_4H_9)_2SnCl_2(Ph_3PO)_2$		$(C_4H_9)_2SnCl_2(Ph_3AsO)_2$	
1.17	2.4432	0.93	2.4434
1.53	2.4985	1.18	2.4847
2.12	2.5948	1.34	2.5209
$(C_6H_5)_2SnCl_2(Ph_3PO)$		$(C_6H_5)_2SnCl_2(Ph_3AsO)$	
0.71	2.3796	0.21	2.3105
1.35	2.4854	0.41	2.3463
1.82	2.5644	0.70	2.3939
$C_4H_9SnCl_3(Ph_3PO)_2$		$C_4H_9SnCl_3(Ph_3AsO)_2$	
0.85	2.4182	0.14	2.2994
1.17	2.4738	0.24	2.3126
1.49	2.5263	0.35	2.3271
$C_4H_9SnCl_3(Ph_3P)_2$		$(C_4H_9)_3PO$	
0.57	2.2983	1.30	2.3974
0.83	2.3111	2.25	2.4910
0.97	2.3161	3.13	2.5773

ments are unnecessary (13, 14). The moments of R_2SnCl_2 and $RSnCl_3$ with Ph_3PO compare with values of 9.5 and 10.1 D reported for dioxane solutions of $SnCl_4$ and $SnBr_4$ respectively with Ph_3PO (15).

R_2SnCl_2 Compounds

The quadrupole splittings obtained indicate that these complexes have octahedral configurations with the R groups *trans* except for **6** and **7** which, in accord with the chemical analyses obtained, are indicative of five-coordinate tin.

For compounds **3**–**5** the splittings are similar to those of the corresponding α,α′-dipyridyl and *o*-phenanthroline complexes (13), indicating similar electron releases to tin by the oxygen and nitrogen donors. The splitting obtained for **2** larger than that previously obtained for *trans* diphenyl compounds (14) may be attributed to a differing degree of distortion from octahedral symmetry, as suggested by Poller *et al.* (8). The smaller isomer shifts obtained for the diphenyl *vs.* the dibutyl compounds are as expected from the difference in the electron releasing ability of the two R groups.

In a crystal structure of $[Me_2SnClterpy]^+$-$[Me_2SnCl_3]^-$ (22), the methyl groups were found to be *trans* with a C—Sn—C angle of 159° in the distorted octahedral cation and in the equatorial plane with a C—Sn—C angle of 140° in the trigonal bipyramidal anion; the more electronegative Cl ligands were bonded preferentially in the axial positions as observed in other examples of trigonal bipyramidal structures with different ligands coordinated to a main group element (23). Equatorial positions have also been assigned to R groups in series of trigonal bipyramidal compounds studied by Zuckermann and co-workers (24), Parish and Platt (25), and Brill and Long (26). The quadru-

Can. J. Chem. Downloaded from www.nrcresearchpress.com by 210.87.254.42 on 09/05/12
For personal use only.

TABLE 3. Mössbauer* and electric moment† data

Compound	δ	ΔE_Q	Γ_1	Γ_2	$100wf_2$	$\Delta\varepsilon/wf_2$	μ_H (D)	$\mu_{diss.}$‡ (D)
1. Bu_3PO					1.3–3.1	9.6	4.30	±0.03
2. $Ph_2SnCl_2(Bu_3PO)_2$	1.20	3.81	0.95	1.01	4.0	10.2	8.56	7.45
3. $Bu_2SnCl_2(Bu_3PO)_2$	1.49	4.13	0.85	0.93	3.7	20.7	>11.9	7.5
4. $Bu_2SnCl_2(Ph_3PO)_2$	1.62	4.11	0.97	1.03	2.1	15.2	>11.0	7.5
5. $Bu_2SnCl_2(Ph_3AsO)_2$	1.49	4.04	1.09	1.13	1.4	18.0	>12.5	8.95
6. $Ph_2SnCl_2(Ph_3AsO)$	1.21	2.83	0.99	0.92	0.7	17.3	>10.3	7.03
7. $Ph_2SnCl_2(Ph_3PO)$	1.25	2.98	0.97	1.00	1.8	16.0	> 9.6	6.1
8. $PhSnCl_3(Ph_3PO)_2$	0.80	2.01	1.19	1.38				
9. $BuSnCl_3(Ph_3PO)_2$§	1.05	2.36	0.97	0.96	1.5	17.1	>11.5	7.5
10. $BuSnCl_3(Ph_3AsO)_2$	0.90	1.81	0.99	1.03	0.35	17.5	12.2	8.95
11. $BuSnCl_3(Ph_3P)_2$	1.23	1.73	0.90	0.82				

*In mm s^{-1}; absorber temperatures 78 °K; δ is expressed relative to SnO_2; δ and ΔE_Q are 0.07 mm s^{-1} and Γ are 0.10 mm s^{-1}.
†wf_2 and $\Delta\varepsilon/wf_2$ are for the largest concentrations used, except for 2 and 10 which are extrapolated values; infrared spectra for benzene solutions of other complexes showed partial dissociation.
‡Values for complete dissociation.
§Reference 9 quotes δ = 1.10 mm s^{-1}; ΔE_Q 2.32 mm s^{-1}.

pole splitting (q.s.) values for **6** and **7** are in agreement with the values calculated by Parish and Platt for such a configuration (25). Zuckerman (24) also interpreted his observed increases in J ($^{119}Sn—C—^1H$) as arising from increasing concentration of s character in the Sn—C bond. Therefore, the values of 100 *vs.* 88 Hz obtained for J in dimethyltin dichloride complexes with Ph_3AsO and Ph_3PO, respectively (17), would lead one to expect greater i.s. and q.s. values for the triphenylarsine oxide complexes as obtained by Yeats *et al.* for the $SnCl_4$ complexes with these ligands (10). For the R_2SnCl_2 complexes with these two donor ligands, **4** and **5**, and **6** and **7**, the R_3PO complexes show the larger i.s. and q.s. values. The explanation for this reversal is not evident at this time. Steric effects resulting in distortions, particularly of the C—Sn—C angle, may be responsible for this anomaly (27, 28).

Stretching frequencies for Y ligands have been reported as follows: ν(P—O) 1190–1202 cm^{-1} (Ph_3PO), 1166 cm^{-1} (Me_3PO), ν(As—O) 880–881 cm^{-1} (Ph_3AsO) (9, 17, 29–33); ν(P—O) 1160 cm^{-1} (Bu_3PO, this work). Shifts to the following frequencies were noted on complex formation: ν(P—O) 1107 cm^{-1} (**2**), 1115 cm^{-1} (**3**), 1155 cm^{-1} (**4**), 1140 cm^{-1} (**7**), 1142 cm^{-1} (**8**), 1160 cm^{-1} (**9**); ν(As—O) 850 cm^{-1} (**5**), 860 cm^{-1} (**6**), and 855 cm^{-1} (**10**). These values agree well with values reported for these or similar compounds (9, 17, 30). Infrared spectra were taken of benzene solutions of the complexes, where solubility permitted, to determine whether or not dissociation was taking place in solution. Most of the complexes showed both shifted and unshifted peaks in solution, evidence of partial dissociation. The extent of dissociation varied from very slight for **2**, **7**, and **10** to considerable for **4** and **9**. In general, frequencies were shifted to slightly higher values in benzene solutions as compared to KBr disc values. Unfortunately, as stated by Jensen and Nielsèn (32), the frequencies of triphenylphosphine complexes do not differ much from those of the ligand; therefore, it was not possible to determine the degree of dissociation of **11** in solution from the infrared spectrum. From dielectric constant measurements of rather dilute solutions of $BuSnCl_3(Ph_3P)_2$ an electric moment of 5.77 D was calculated which compares with a moment of 4.75 D for complete dissociation.

In a crystal structure determination of $Me_2SnCl_2(C_5H_5NO)_2$ (34), all identical ligands were found to be *trans* with little distortion from octahedral symmetry, and the Sn—O—N bond angle 117°, which is quite close to the Sn—O—P angle assumed below. In their study of the electric moments of transition metal complexes, Schafer and Curran (35) obtained a good correlation between calculated and experimental values in $ZnCl_2(HMPA)_2$ (HMPA = hexamethylphosphoramide) by assuming the P—O—M angle to be 125°, with one ligand in the conformation of minimum moment and the other in conformation of maximum moment. As previous work has indicated similar polarizabilities for Sn(IV) and Zn(II) (14), this same value has been taken for the P—O—M angle in the octahedral tin phosphine oxide complexes, along with the

Can. J. Chem. Downloaded from www.nrcresearchpress.com by 210.87.254.42 on 09/05/12
For personal use only.

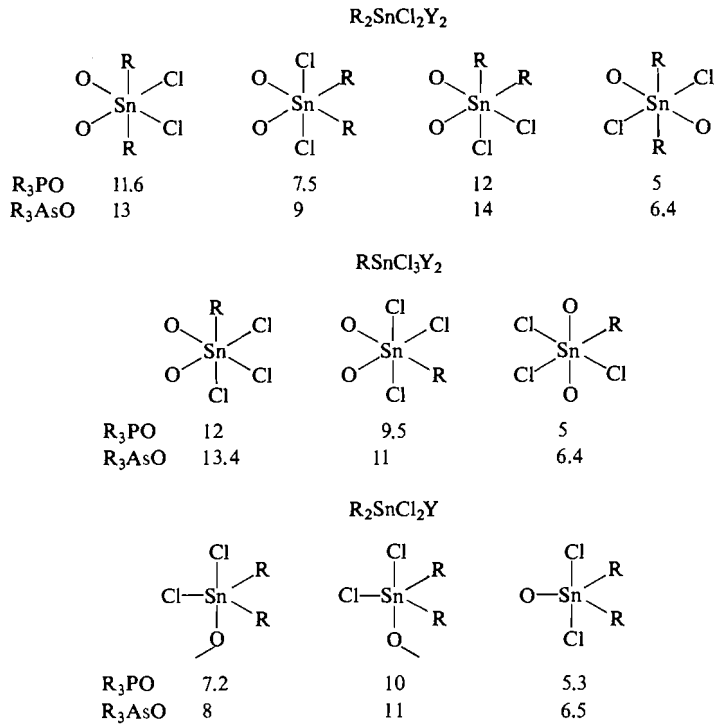

FIG. 2. Dipole moments calculated for various configurations of complexes.

assumption that the N→M—Cl moment in pyridine type complexes is 0.3 D greater than the O→M—Cl moment in HMPA type complexes (35). Using this assumption, the O→Sn—Cl resultant for two vectors at 90° has been obtained from the following calculations

$$N{\rightarrow}Sn{-}Cl_{resultant} = \mu_{Bu_2SnCl_2\cdot o\text{-phen}} - \mu_{o\text{-phen}} = 11.3 - 4.1 = 7.2 \text{ D (ref. 13)}$$

$$O{\rightarrow}Sn{-}Cl_{resultant} = N{\rightarrow}Sn{-}Cl_{resultant} - 1.16(0.3) = 7.2 - 0.4 = 6.8 \text{ D (ref. 35)}$$

The O→Sn—Cl vector can then be taken as 6.8/1.414 = 4.8 D, so that if the moment of Sn—Cl is from 3.2–3.4 D (13), a value of approximately 1.5 D is obtained for O→Sn. This is to be distinguished from the value of 2.8 D estimated for a normal covalent Sn—O bond moment (14). From the moment of 4.37 D for Bu_2SnCl_2 (13), the Bu—Sn—Cl vector can be taken as 3.77 D. The resultant of two R_3Y bond moments at 90° to each other is 6.09 D for Ph_3PO, 6.08 D for Bu_3PO, 7.83 D for Ph_3AsO(μ_{Ph_3PO} = 4.31 D, μ_{Ph_3AsO} = 5.54 D (36); μ_{Bu_3PO} = 4.30 D). The equal electric moments of Bu_3PO and Ph_3PO indicate a balance between the greater σ electron release by the alkyl group and the

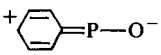

π-electron delocalization in the triphenyl compound.

In the calculation for possible configurations, the angle which these resultants make with the rest of the molecule must be taken into account. Varying degrees of distortion from the assumed Y—O—M angle must be considered as well as distortions from octahedral symmetry. The small Sn—C bond moment has been neglected in most cases; this would yield a difference of approximately ±0.4 D for butyl *vs.* phenyl compounds. The calculated moment for complete dissociation values were obtained from the square root of the sum of the squares for the moments of the components (μ_{BuSnCl_3} = 4.32 D, $\mu_{Ph_2SnCl_2}$ = 4.32 D (37)). The values calculated for *cis* Y groups assume maximum and minimum orientation for the two groups as stated previ-

Can. J. Chem. Downloaded from www.nrcresearchpress.com by 210.87.254.42 on 09/05/12
For personal use only.

Can. J. Chem. Downloaded from www.nrcresearchpress.com by 210.87.254.42 on 09/05/12
For personal use only.

ously. In calculating the moments of *trans* Y groups, one has to consider random orientation of these groups. The moment for the R_3PO random orientation about the O—Sn—O axis has been calculated from the equation $\mu = 1.41\ m \sin\theta$ (38), where m is the moment of R_3PO, θ is the angle that the moment makes with the O—Sn—O axis, 55° in the present case; this gives a value of 5.0 D for configurations with *trans* R_3PO groups, 6.4 D for *trans* R_3AsO groups, lower than the experimental values obtained.

As stated previously q.s. values for **3–5** indicate a *trans*-R configuration is present in the solid state and experimental dipole moments suggest a *trans*-R, *cis*-Cl, *cis*-O configuration is present in solution. In the case of Ph_2SnCl_2-$(Bu_3PO)_2$, dipole moment data indicate a possible mixture of *cis* and *trans* Bu_3PO groups in solution. A comparison of experimental and calculated moments for **6** and **7**, suggests equatorial diphenyl groups, axial–equatorial Cl atoms, and random orientation of the O group in axial position, as indicated previously for solid R_2SnX_3 compounds (22–25). Some possible configurations with calculated values are shown in Fig. 2.

$RSnX_3Y_2$ Complexes

The Mössbauer data for **10**, **11** are sufficiently close to the values obtained for complexes having bidentate nitrogen groups (16) to postulate similar configurations, with two Cl atoms *trans* in both cases. However, in accord with the observation of Parish and Platt (27), the relatively large quadrupole splitting for $BuSnCl_3$-$(Ph_3PO)_2$ suggests the possibility of a different configuration for this complex in the solid form and electric moment calculations indicate that in solution this complex has three *cis* Cl atoms and two *cis* PO groups. The dipole moment data for $BuSnCl_3(Ph_3AsO)_2$ does not clearly distinguish between this configuration and one in which two Cl atoms are *trans*. The smaller i.s. and q.s. values for $PhSnCl_3(Ph_3PO)_2$, **8**, than for $BuSnCl_3(Ph_3PO)_2$, **9**, reflect the greater tin share of the electrons of the C—Sn bond in the butyl compound. Again, the smaller isomer shift for $BuSnCl_3(Ph_3AsO)_2$ *vs.* $BuSnCl_3(Ph_3PO)_2$ appears as an interesting anomaly, which it is hoped may be resolved in the course of further research on another series of compounds.

The author is grateful to the National Research Council of Canada for financial support and to Dr. M. Falk of the Atlantic Regional Laboratory in Halifax for the use of research facilities. Special thanks are due to Dr. W. Lieper and his research assistants of the Physics Department of Dalhousie University for the use of a Mössbauer spectrometer and computer program. Gratitude is expressed to Br. C. Curran of the University of Notre Dame for helpful discussions.

1. A. G. Davies, H. J. Milledge, D. C. Puxley, and P. J. Smith. J. Chem. Soc. A, 2862 (1970).
2. M. Barber, P. Swift, D. Cunningham, and M. J. Frazer. J. Chem. Soc. D, 1338 (1970).
3. D. E. Williams and C. W. Kocher. J. Chem. Phys. **52**, 1480 (1970).
4. J. C. Hill, R. S. Drago, and R. H. Herber. J. Am. Chem. Soc. **91**, 1644 (1969).
5. T. Chivers and J. R. Sams. J. Chem. Soc. A, 928 (1970).
6. B. Gassenheimer and R. H. Herber. Inorg. Chem. **8**, 1120 (1969).
7. R. C. Poller and J. N. R. Ruddick. J. Chem. Soc. A, 2273 (1969).
8. R. C. Poller, J. N. R. Ruddick, M. Thevarasa, and W. R. McWhinnie. J. Chem. Soc. A, 2327 (1969).
9. A. G. Davies, L. Smith, and P. J. Smith. J. Organometal. Chem. Amsterdam, **23**, 135 (1970).
10. P. A. Yeats, J. R. Sams, and F. Aubke. Inorg. Chem. **9**, 740 (1970).
11. A. J. Carty, T. Hinsperger, L. Mihichuk, and H. D. Sharma. Inorg. Chem. **9**, 2573 (1970).
12. D. Petridis, F. P. Mullins, and C. Curran. Inorg. Chem. **9**, 1270 (1970).
13. M. A. Mullins and C. Curran. Inorg. Chem. **6**, 2017 (1967).
14. M. A. Mullins and C. Curran. Inorg. Chem. **7**, 2584 (1968).
15. J. Philip, M. A. Mullins, and C. Curran. Inorg. Chem. **7**, 1895 (1968).
16. F. P. Mullins. Can. J. Chem. **48**, 1677 (1970).
17. V. G. K. Das and W. Kitching. J. Organometal. Chem. Amsterdam, **13**, 523 (1968).
18. C. Curran, P. A. McCusker, and H. S. Makowski. J. Am. Chem. Soc. **79**, 5188 (1957).
19. G. K. Estok. J. Chem. Educ. **39**, 478 (1962).
20. K. Higasi. Bull. Inst. Phys. Chem. Res. Tokyo, **22**, 805 (1943).
21. E. Claeys, G. van der Kelen, and Z. Eeckhaut. Bull. Soc. Chim. Belges, **70**, 462 (1961).
22. F. W. B. Einstein and B. R. Penfold. J. Chem. Soc. A, 3019 (1968).
23. E. L. Muetterties, W. Mahler, K. J. Packer, and R. Schmultzer. Inorg. Chem. **3**, 1298 (1964).
24. N. W. G. Debye, E. Rosenberg, and J. J. Zuckerman. J. Am. Chem. Soc. **90**, 3234 (1968).
25. R. V. Parish and R. H. Platt. Inorg. Chim. Acta, **4**, 65 (1970).
26. T. B. Brill and G. G. Long. Inorg. Chem. **9**, 1980 (1970).
27. R. V. Parish and R. H. Platt. J. Chem. Soc. A, 2145 (1969).

28. R. V. PARISH and R. H. PLATT. Inorg. Chim. Acta, **4**, 589 (1970).
29. G. B. DEACON and J. H. S. GREEN. Spectrochim. Acta, **24**(A), 845 (1968).
30. J. P. CLARK, V. M. LANGFORD, and C. J. WILKINS. J. Chem. Soc. A, 792 (1967).
31. S. H. HUNTER, V. M. LANGFORD, G. A. RODLEY, and C. J. WILKINS. J. Chem. Soc. A, 305 (1968).
32. K. A. JENSEN and P. H. NIELSEN. Acta Chem. Scand. **17**, 1875 (1963).
33. G. A. RODLEY, D. M. L. GOODGAME, and F. A. COTTON. J. Chem. Soc. 1499 (1965).
34. E. A. BLOM, B. R. PENFOLD, and W. T. ROBINSON. J. Chem. Soc. A, 913 (1969).
35. M. SCHAFER and C. CURRAN. Inorg. Chem. **4**, 623 (1965).
36. A. L. MCCLELLAN. *In* Tables of experimental dipole moments. W. H. Freeman and Co. San Francisco and London. 1963. pp 511, 513.
37. H. H. HUANG, K. M. HUI, and K. K. CHIU. J. Organometal Chem. Amsterdam, **11**, 515 (1968).
38. J. W. WILLIAMS. Z. Phys. Chem. A, **138**, 75 (1928).

Can. J. Chem. Downloaded from www.nrcresearchpress.com by 210.87.254.42 on 09/05/12
For personal use only.

Can. J. Chem. Downloaded from www.nrcresearchpress.com by 210.87.254.105 on 09/05/12
For personal use only.

Reactions of Sodium *N,N*-Diethyldithiocarbamate and Potassium Ethyl Xanthate with some 3d Transition Metal Halides in the presence of 2,2′-Bipyridyl and 1,10-Phenanthroline

D. G. Holah and C. N. Murphy

Department of Chemistry, Lakehead University, Thunder Bay, Ontario

Received April 13, 1971

The synthesis and some properties of ethylxanthate (Xan^-) complexes, $MXan_2$ and $MXan_3^-$ (M = manganese(II) and iron(II)) are reported. Reactions between divalent metal halides (manganese, iron, cobalt, nickel, copper, and zinc) and Xan^- and between the metal halides and *N,N*-diethyldithiocarbamate (dtc^-) in the presence of nitrogen bases 1,10-phenanthroline (phen) and 2,2′-bipyridyl (bipy) are described. The major products of these reactions are complexes of the type $MXan_2$.Base and $Mdtc_2$.Base (with notable exceptions). In the former series with bipy, two different crystalline modifications of the manganese, iron, and cobalt complexes are formed, and copper(II) is reduced to copper(I) by Xan^- in the presence of both bases. In the nickel–dtc system with bipy, $Nidtc_2$ is produced, while with phen, the complex $[Niphen_3]dtc_2$ is formed. The latter reacts very rapidly with methylene chloride. $Cudtc_2$ is produced from the copper(II)/base/dtc reactions.

On rapporte la synthèse et quelques propriétés des complexes obtenus avec l'éthyl xanthate (Xan^-), $MXan_2$ et $MXan_3^-$ (M = manganèse(II) et fer(II)). On décrit les réactions entre les halogénures de métaux divalents (manganèse, fer, cobalt, nickel, cuivre et zinc) et Xan^- ainsi qu'entre les halogénures métalliques et le *N,N*-diéthyldithiocarbamate (dtc^-) en présence de composés azotés servant de base, à savoir la phénanthroline-1,10(phen) et la bipyridyle-2,2′(bipy). Les produits principaux de ces réactions sont des complexes du type $MXan_2$.Base et $Mdtc_2$.Base (avec certaines exceptions). Dans les premières séries, avec la bipy, deux modifications cristallines différentes se forment pour les complexes avec le manganèse, le fer et le cobalt; de plus, le cuivre(II) est réduit en cuivre(I) par le Xan^- en présence des deux bases. Dans le système nickel–dtc, avec la bipy, on forme $Nidtc_2$, alors qu'avec la phen, on forme le complexe $[Niphen_3]dtc_2$. Ce dernier réagit très rapidement avec le chlorure de méthylène. On forme le complexe $Cudtc_2$ par les réactions entre cuivre(II)/base/dtc.

Canadian Journal of Chemistry, 49, 2726 (1971)

Introduction

A study of the electronic and molecular structure of transition metal complexes of the type ML_2, where L are 1,1-dithiolate ligands such as

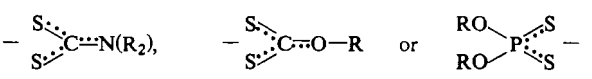

R = Et, L = dtc R = Et, L = Xan R = Et, L = dtp

are often made difficult by the instability of these species, particularly in the case of dithiocarbamates and xanthates. For example, the $Mdtc_2$ complexes (M = Cr, Mn, Fe) are exceedingly sensitive to air oxidation (1) while there seems to be no reliable documentation of $Codtc_2$ (1, 2). The $Mdtp_2$ and $MXan_2$ complexes (M = Cr, Mn, Fe, Co) are less studied although there is a brief mention (3) of $FeXan_2$. It is interesting that one tris(xanthate) complex, $(R_4N)NiXan_3$, has been characterized (4–6) while in the dithiocarbamate series the formulation (7) of a complex as $Na[Codtc_3]$ has been questioned (8), and there seems to be no authentic example of a $Mdtc_3$ species.

The stability of the MS_4 entity does appear (9, 10) to be affected by varying the size of the group R, but is clearly increased by incorporating a base adduct onto the MS_4 species (10). Adducts of the dtp complexes with various bases, such as 2,2′-bipyridyl (bipy) 1,10-phenanthroline (phen) and various substituted derivatives of the latter, have been studied and some structures which include both 5 and 6 coordinated metal ions determined (10). Much less information is available on adducts of dithiocarbamates and xanthates. With the latter, $NiXan_2$.bipy has been studied, one report (11) suggesting four coordinate nickel with another suggesting a *cis*-octahedral arrangement (12). Very recently (5), various adducts of $NiXan_2$ including $NiXan_2$.bipy and $NiXan_2$.phen have been studied particularly regarding the assignment of infrared vibrations. With dithiocarbamates, $Codtc_2$.phen has been synthesized (13) and contains high spin cobalt(II).

Can. J. Chem. Downloaded from www.nrcresearchpress.com by 210.87.254.105 on 09/05/12
For personal use only.

Considering the fact that no reliable report of the preparation of $Codtc_2$ exists, the base has clearly had a profound stabilizing influence on the cobalt(II)–dtc system.

This paper reports our studies aimed at (*i*) isolating new bis and tris(xanthate) and tris-(dithiocarbamate) metal complexes and (*ii*) examining the ability of nitrogen bases 2,2′-bipyridyl and 1,10-phenanthroline to stabilize the metal xanthates and dithiocarbamates.

Experimental

Reagent grade phen, bipy, KXan, and $Nadtc.3H_2O$ were used without further purification, as were the hydrated metal chlorides. Many of the complexes prepared in this work are air-sensitive and much of the experimental work was therefore carried out in a nitrogen-filled glove box (~100 p.p.m. oxygen).

Preparation of Complexes

$MXan_2$ (M=Mn,Fe)

The complexes were prepared in a nitrogen atmosphere by reacting a 1:2 mole ratio of the metal(II) halide and KXan in aqueous solution. The yellow manganese complex is appreciably water soluble and the solution was therefore evaporated to dryness. The insoluble iron(II) complex was dried under vacuum. Acetonitrile solutions of the complexes, which are extremely air-sensitive, were allowed to run down an alumina column (deactivated with ethylacetate) and the brightly colored liquors concentrated by removal of the solvent at room temperature under vacuum. Addition of ether or benzene produced solids which were dried under vacuum. $FeXan_2$ decomposes after several days even when stored under vacuum.

$(Et_4N)MXan_3$ (M=Mn, Fe)

Crude oily products were obtained by adding in a nitrogen atmosphere, an aqueous solution of KXan to one of the metal(II) halide and Et_4NCl until the mole ratio was 3:1:1, respectively. The oils, which solidified after scratching, were dried under vacuum and recrystallized from acetonitrile or methylene chloride on addition of ether.

$MXan_2.phen$ (M=Mn, Fe, Co, Ni, Zn)

These compounds were prepared by adding aqueous KXan to a solution of the metal(II) chloride and phen (mole ratio 2:1:1, respectively). The solids were dried under vacuum and recrystallized from methylene chloride on addition of ether (For M=Co, in a nitrogen atmosphere) in approximately 50% yields.

$MXan_2.bipy$ (M=Mn, Fe, Co, Ni, Zn)

Two different crystalline modifications, α and β, were obtained for M=Fe, Co, and Ni. In all cases low yields (between 25 and 40%) were observed, and the reactions, although usually reliable, occasionally gave unexpected and non-reproducible products (particularly the reaction involving the α-Fe complex).

In all cases, except for α-Co, an aqueous solution of KXan was added to a solution of the metal(II) chloride and bipy (2:1:1 or 2:1:2 mole ratios), the crude product washed several times with water, and dried under vacuum. (For the α and β cobalt complexes the reactions were carried out in a nitrogen atmosphere.)

Mn: The crude product was recrystallized several times from methylene chloride by addition of ether. The solid decomposes within hours in air and within several days when sealed under vacuum.

β-*Fe*: This is the red material remaining after the above crude product was washed with water. Most organic solvents resulted either in the oxidation of the iron or transformation of the complex to the α-phase.

α-*Fe*: The red β-phase becomes deep blue in methylene chloride and brown crystals of the α-phase were obtained by addition of ether. The solid becomes red and amorphous after several days.

α-*Co*: The $KXan/CoCl_2$/bipy reaction using 2:1:1 stoichiometries was carried out in acetone. Crystals of the α-phase were obtained by removal of the acetone under vacuum and recrystallizing the residue from a methylene chloride solution by addition of ether.

β-*Co*: The crude product from the aqueous reaction was recrystallized from benzene on addition of high boiling petroleum ether.

β-*Ni*: The aqueous reaction involving nickel(II) differed from the other reactions in that yields were considerably improved when the mixture was allowed to stand for several days. The β-phase was recrystallized several times from methylene chloride on addition of ether.

α-*Ni*: A methylene chloride solution of the β-phase was run down an alumina column (deactivated with ethylacetate). The α-phase was obtained from the green layer after concentration and addition of ether, although occasionally a brown layer was also observed, from which the β phase could be isolated as above.

Zn: This was obtained by recrystallizing the crude product from methylene chloride on addition of ether.

Reactions involving Copper(II)

Addition of an aqueous solution of KXan to one of copper(II) chloride and the base in 2:1:1 mole ratios resulted in the formation of red precipitates both for bipy and phen. The latter product contains dixanthogen and a compound identical (X-ray isomorphous) with a compound prepared from copper(I) chloride, KXan, and phen in a 1:1:1 mole ratio. The above red product could not be recrystallized from organic solvents, since the yellow CuXan was immediately produced on addition of the solvent, with dixanthogen being recovered from the solution.

$Mdtc_2.phen$ (M=Mn, Fe, Co, Zn)

These complexes were prepared by reacting metal(II) halides and phen (1:3 ratio) in water followed by the slow addition, with stirring, of the stoichiometric amount of Nadtc in water. The complexes were washed with water in which they are insoluble, and dried under vacuum. The complexes were recrystallized from methylene chloride (Mn, Fe, Co in a nitrogen atmosphere), washed with ether and dried under vacuum. The blue species, formed by reacting copper(I) chloride with phen in water reacted immediately with Nadtc to give a precipitate of $Cudtc_2$, while the $CrCl_2$/phen/dtc reaction resulted in oxidation of the metal.

$Niphen_3dtc_2$

A bright yellow solid is formed when an aqueous solu-

Can. J. Chem. Downloaded from www.nrcresearchpress.com by 210.87.254.105 on 09/05/12
For personal use only.

TABLE 1. Chemical analyses and electronic properties

Compound	Color	Analyses: Required M	C	H	N	Found M	C	H	N	μ_{eff}	Band	ε	Assignment
$MnXan_2$	Yellow	18.5	24.2	3.4		18.5	22.9	3.5		4.8	15 900 sh	—	
$(Et_4N)MnXan_3$	Yellow	10.0	37.2	6.4		10.4	37.4	6.4		6.0	14 700 sh	—	
$[MnXan_2 0.85Bipy]$	Yellow		40.3	4.1	5.5		39.4	3.8	5.4	5.6	14 700 sh	—	$^6A_{1g} \rightarrow {}^4T_{1g}$
$[MnXan_2phen]$	Yellow		45.3	3.8	5.9		45.3	3.8	6.0	6.0	15 400 sh	—	
$[Mndtc_2phen]$	Pink		49.7	5.3	10.5		50.2	5.3	10.6	6.0	14 300 sh,w	—	
$[Mndtc_2bipy]$	Pink		47.3	5.6	11.0		47.9	5.7	10.9	6.0	14 300 sh	—	
$FeXan_2$	Red		24.2	3.4			23.7	3.4		4.4	8 560	8.8	
$(Et_4N)FeXan_3$	Red	10.2				10.0				5.5	7 150 sh 8 500	11.7	
α-$[FeXan_2bipy]$	Brown		42.4	4.0	6.2		42.2	3.9	6.3	4.8	8 700 11 500	—	$^5T_{2g} \rightarrow {}^5E_g$
β-$[FeXan_2bipy]$	Red		42.4	4.0	6.2		42.0	3.8	6.4	*	8 600		
$[FeXan_2phen]$	Red-blue		45.2	3.8	5.9		46.0	3.9	6.2	5.1	8 600 11 500 sh	—	
$[Fedtc_2phen]$	Blue		49.6	5.3	10.5		49.6	5.1	10.4	*	9 500 sh	—	
$[Fedtc_2bipy]$	Blue		47.2	5.6	11.0		47.0	5.5	10.9	*	8 900 sh	—	
α-$[CoXan_2bipy]$	Olive		42.0	3.9	6.1		42.7	4.5	6.2	4.4	8 700	7.9	
β-$[CoXan_2bipy]$	Brown		42.0	3.9	6.1		41.0	3.7	5.4	4.6	8 700	4.8	
$[CoXan_2phen]$	Brown		44.9	3.8	5.8		45.3	3.6	6.0	4.8	8 600	5.6	$^4T_{1g} \rightarrow {}^4T_{2g}$
$[Codtc_2bipy]$	Brown		47.0	5.5	11.0		46.9	5.6	10.7	5.0	8 700	—	
$[Codtc_2phen]$	Brown	See ref. 13								5.1	8 750	—	
β-$[NiXan_2bipy]$	Brown		42.0	4.0	6.1		41.3	3.9	6.1	3.0	9 250 sh 10 400	21	$^3A_{2g} \rightarrow {}^3T_{2g}$
											16 700	24	$\rightarrow {}^3T_{1g}(F)$
$[Niphen_3]dtc_2$	Orange		61.7	5.0	12.5		61.5	5.2	12.8	2.99	11 100 sh 12 700	—	$\rightarrow {}^3T_{2g}$
$[Niphen_3]Cl_2.2CH_2Cl_2$	Tan		53.5	3.3	9.8		54.5	3.8	10.2	—	11 100 sh 12 700	—	$\rightarrow {}^3T_{2g}$
											19 100	—	$\rightarrow {}^3T_{1g}(F)$
$[Niphen_3]Cl_2.2EtOH$	Pink		63.1	4.7	11.0		62.3	5.1	11.0	—	11 100 sh 12 700	—	$\rightarrow {}^3T_{2g}$
$[ZnXan_2bipy]$	White		41.5	3.9	6.0		42.0	3.7	6.2	Dia	—		
$[ZnXan_2phen]$	White		44.4	3.7	5.7		44.6	3.5	5.8	Dia	—		
$[Zndtc_2bipy]$	Yellow		46.4	5.5	10.8		46.2	5.5	10.7	Dia	—		

*Insufficient pure material obtained for a Gouy measurement.

Can. J. Chem. Downloaded from www.nrcresearchpress.com by 210.87.254.105 on 09/05/12
For personal use only.

tion of a stoichiometric amount of Nadtc is added to the red aqueous solution of nickel(II) chloride and phen (1:3). After washing with water, the complex was dried under vacuum, when the color slowly changed from yellow to orange. The resultant red solid was recrystallized from acetonitrile–ether, washed with ether and dried under vacuum, yielding bright yellow-orange crystals of $Niphen_3dtc_2$. This compound is very soluble in methylene chloride giving initially a deep blood-red solution but within 2–5 s the color is largely discharged and yellow crystals appear. These were removed, washed with methylene chloride, dried under vacuum and identified as $Niphen_3Cl_2.2CH_2Cl_2$. The methylene chloride solution and washings were evaporated at room temperature and the residue extracted into benzene solution, which yielded crystals (14) of dtc_2CH_2 on addition of ether.

The yellow crystals of $Niphen_3Cl_2.2CH_2Cl_2$ dissolve in ethanol and on addition of ether pink crystals which analyzed close to $Niphen_3Cl_2.2EtOH$ are precipitated. This product is identical with the pink solid formed by reacting nickel(II) chloride with 3 mol of phen and recrystallizing from ethanol.

$Mdtc_2.bipy$ (M=Mn, Fe, Co, Zn)

These complexes were made in an analogous manner to the phen complexes, with the manganese, iron, and cobalt complexes being recrystallized in a nitrogen atmosphere. Reactions of the nickel and copper systems both resulted in the formation of $Nidtc_2$ and $Cudtc_2$, respectively.

Analyses and Physical Measurements

Element analyses were carried out under the supervision of W. J. Buis at the Micro-Analytical Department of the Institute for Organic Chemistry TNO, Utrecht, The Netherlands, and are recorded in Table 1. X-Ray powder photographs and mass spectral studies were carried out as previously described (14). Magnetic moments were measured in a double ended Gouy tube suspended from a semi-micro balance between the poles of a Varian electromagnet. The tube was calibrated with $HgCo(CNS)_4$, $Nien_3S_2O_3$, and $CuSO_4.5H_2O$, using standard diamagnetic corrections (15). The tube constant β, measured using $HgCo(CNS)_4$ was used to calculate the susceptibilities of the latter two complexes. Agreement was within 1% of the published values. Visible solution and reflectance spectra were recorded on a Cary 14 spectrophotometer.

Results and Discussion

All the complexes prepared in this work are listed in Table 1, together with chemical analyses and colors.

Like the corresponding bis(dithiocarbamate)-metal(II) complexes, the bis(xanthate) complexes of manganese and iron are air sensitive, and indeed the iron complex appears to decompose slowly when stored under vacuum. The complexes have identical X-ray powder photographs which are radically different from those (12) of the previously reported square planar $NiXan_2$ and tetrahedral $ZnXan_2$. Both appear to have magnetic moments (Table 1) somewhat lower than required for high spin d^5 and d^6 configurations, although reflectance spectra (Table 1) suggest the presence of essentially 6-coordinated metal ions. It is possible that this is achieved through polymerization, which may, through slight metal–metal interaction, account for the lowering of the magnetic moments. It is significant that the xanthate series form compounds of the type $MXan_3^-$ and these species can be obtained as solid, tetraethylammonium salts, as has been previously reported (4–6) for M = Ni. The analogous manganese(II) and iron(II) complexes have now been prepared and both show normal high spin magnetic properties and reflectance spectra again indicative of 6 coordination. The X-ray powder photographs of the iron and nickel(II) complexes are identical, with the manganese(II) pattern very similar. All attempts, in both aqueous and non aqueous solutions, at preparing $MXan_2$ and $MXan_3^-$ compounds for M = chromium(II), cobalt(II), and copper(II) resulted in oxidation of the first two species and reduction of the latter. However, there is a report (16) of the formation of cobalt(II) xanthate in acid solution (p*H* 2.5–3.5), although our attempts at the preparations of $CoXan_2$ and $(R_4N)CoXan_3$ in sulfuric acid solutions under oxygen free conditions resulted in the formation of $CoXan_3$. Also all attempts to make complexes of the type $Mdtc_3^-$ either by reactions of metal halide, tetraalkylammonium halide, and Nadtc (1:1:3) or by reactions of $Mdtc_2$ with excess Nadtc in the presence of R_4NCl in various solvents resulted in the isolation of starting materials or the $Mdtc_2$ species. This is likely due to the increased strength of the M—S bonds in dithiocarbamates compared to the xanthates and may also be a reflection of the considerable stabilities of the dimeric $Mdtc_2$ species and the square planar $Nidtc_2$ (12). The previous report (7) of the complex $NaCodtc_3$ appears to be in error (8) although recently (17) an octahedral complex of nickel with three dithiocarbamate ions has been studied.

There are significant differences in the way in which KXan and Nadtc react with the metal halides when the bases phen and bipy are present. Thus in the dithiocarbamate system, two moles of dithiolate react with a solution or suspension of $MBase_3^{2+}$. When less base is used, *e.g.*, a ratio

Can. J. Chem. Downloaded from www.nrcresearchpress.com by 210.87.254.105 on 09/05/12
For personal use only.

of metal:base:ligand of 1:2:2 or 1:1:2, extensive oxidation of the metal can occur, particularly with manganese(II). However, with reactions involving xanthate, ratios of 1:1:2 appear to be adequate for the isolation of the $MXan_2$.Base complexes. It is interesting that in this series when the base is bipyridyl, two crystalline forms of the same complex are obtained for M = Fe, Co, and Ni and are arbitrarily labeled α and β. The α phases are all X-ray isomorphous with the manganese complex. We have repeated the literature method (16) for the preparation of $NiXan_2$.bipy, namely the reaction between $NiXan_2$ and bipy in ether, and find the complex to be isomorphous with the α-phase. Furthermore, reported magnetic and electronic spectral properties of this material (and $NiXan_2$.phen) are identical with our data which are therefore omitted from Table 1. The β phases are all different crystalline forms. When the base is phen, then only complexes of cobalt and nickel show isomorphism. However, all the complexes including the nickel complex (16) show normal high spin behavior and reflectance and solution spectra consistent with octahedral metal ions. While both bases have clearly stabilized cobalt(II) in the presence of xanthate, many of the complexes, particularly with bipy, tend to decompose slowly both in air and when stored under nitrogen. Indeed no satisfactory chemical analysis was obtained for $MnXan_2$.bipy, rather the analysis always indicating the presence of approximately 0.9 molecule of base.

However, it was not possible to stabilize the copper(II) xanthate system in the presence of base. The red products isolated from the reactions of solutions of copper(II) and base with xanthate were washed with water and dried under vacuum. All attempts to recrystallize the diamagnetic red products from organic solvents resulted in the immediate appearance of the yellow CuXan. Chemical analyses (C 42.2, H 3.9, N 6.5%) of the red phen product while approximating to that required for $CuXan_2$.phen (C 44.4, H 3.7, N 5.8%), is also consistent with the presence of an intimate mixture of CuXan.phen and dixanthogen (the latter being insoluble in water and readily identified by bands in its infrared spectrum (18)). These results can be rationalized by considering the potential data of Table 2.

Thus, it is apparent that the reduction of either Cu^{2+} or $Cubipy_2^{2+}$ by Xan^- is thermodynamically favorable and that the presence or absence of base makes little difference to the stability of the copper(II) system.

TABLE 2. Potential data

Reaction	Potential (V)	Reference
$Xan^- \rightarrow \frac{1}{2} Xan_2 + e$	0.136	19
$Cu^{2+} \rightarrow Cu^+ - e$	0.15	20
$Cubipy_2^{2+} \rightarrow Cubipy_2^+ - e$	0.12	21

Reactions between the metal halides, base, and xanthate in 1:3:2 mole ratios give different products which will be described in a later publication (22).

There are significant differences in the way that Nadtc reacts with $Mphen_3^{2+}$ and $Mbipy_3^{2+}$ when M = Ni. With elements manganese, iron, and cobalt both bases give similar adducts, $Mdtc_2$.Base with members of each series being isomorphous and therefore probably isostructural, except for $Mndtc_2$.bipy. All these solid complexes appear to be air stable in marked contrast to the behavior of the $Mdtc_2$ complexes themselves. In both series the electronic properties are similar to those of the xanthate complexes.

It is interesting that reactions involving copper(II) result in the immediate formation of $Cudtc_2$, with no evidence of any formation of $Cudtc_2$.Base. A similar reaction occurs with nickel(II) when the base is bipy, although with phen, $Niphen_3dtc_2$ is the final product.

The formation and reactions of this compound are summarized in Fig. 1. The nature of the yellow solid is not clear and little can be done to establish its composition since as soon as it is dried it begins to turn to the orange product.

$[Niphen_3]dtc_2$ dissolves in methylene chloride to give a deep red solution, although within several seconds the color is largely discharged and tan colored crystals deposit. The reaction between dtc^- and CH_2Cl_2 is clearly extremely fast, much faster in fact than the reaction (14) between Nadtc and methylene chloride, which must be refluxed for several hours in order to obtain an appreciable yield of CH_2dtc_2. It may be that the latter reaction is relatively slow because of the insolubility of Nadtc in methylene chloride, while in the above reaction the dtc^- species is in solution and therefore probably able to react with the solvent much more rapidly.

Chemical analyses indicate the presence of close

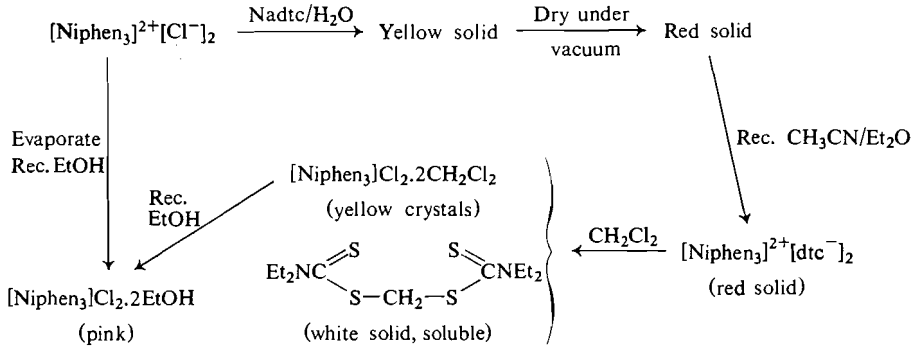

FIG. 1. Reactions of $[Niphen_3]Cl_2$.

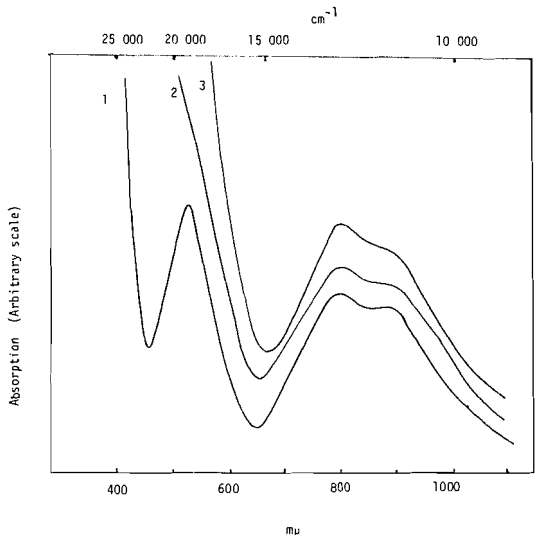

FIG. 2. Reflectance spectra of species containing the $[Niphen_3]^{2+}$ ion. (*1*) $[Niphen_3]Cl_2.2EtOH$, (*2*) $[Niphen_3]Cl_2.2CH_2Cl_2$, (*3*) $[Niphen_3]dtc_2$.

to two molecules of both methylene chloride and ethanol associated with the $[Niphen_3]Cl_2$ species. This was verified by mass spectral studies which clearly indicate the presence of both solvents. Thus, the mass spectrum (direct inlet, 80 eV, 160 °C) of the methylene chloride adduct shows very strong bands at *m/e* 86, 84, 51, and 49 while the ethanol adduct has a particularly strong peak at *m/e* 46. These molecules do not appear to be readily removed at 10^{-3} Torr at room temperature although they are removed at 10^{-6} Torr at slightly higher temperatures. The only indication of solvent in the infrared spectra of these compounds is the presence of a small band at 3220 cm^{-1} in the ethanol adduct. The reflectance spectra in Fig. 2 clearly indicates that the cation $[Niphen_3]^{2+}$ is present in all three compounds, although it is surprising that the presence of methylene chloride has resulted in the charge-transfer band moving to lower energies compared to its position in the ethanol adduct. The splitting of the $^3A_{2g} \rightarrow {}^3T_{2g}$ transition may arise from distortions of the $Niphen_3^{2+}$ ion, although the $^3A_{2g} \rightarrow {}^3T_{2g}$ band does not show similar splittings, at least at room temperature (23). Phenanthroline does not appear to react readily with $Nidtc_2$ once the latter has formed, probably an indication of the strength of the Ni—S bonds in the square planar molecule.

Several attempts have been made, by ebulliometry in methylene chloride solutions, to measure the molecular weight of a variety of the complexes reported here. In all cases the complexes either proved too insoluble or amorphous residues, indicative of decomposition of the complexes, appeared in the ebulliometer, making accurate measurements impossible (6).

The assignment of various bands in the infrared spectra of these complexes will be considered with the report of the products from the metal–base–Xan reactions in 1:3:2 mole ratios, as these products shed some light on the assignments.

We thank the Senate Research Committee of Lakehead University Thunder Bay, Ontario, the National Research Council of Canada, and the Ontario Department of University Affairs for generous financial support of this work.

1. J. P. FACKLER, JR. and D. G. HOLAH. Inorg. Nucl. Chem. Lett. **2**, 251 (1966).
2. I. M. BHATT and K. P. SONI. J. Indian Chem. Soc. **45**, 277 (1968). I. M. BHATT, K. P. SONI, and A. M. TRIVEDI. Indian J. Chem. **6**, 753 (1968). L. H.

Can. J. Chem. Downloaded from www.nrcresearchpress.com by 210.87.254.105 on 09/05/12
For personal use only.

PIGNOLET, R. A. LEWIS, and R. H. HOLM. J. Am. Chem. Soc. **93**, 360 (1971).
3. K. BURGER, E. PAPP-MOLNAR, H. VAGARHELYI-NAGY, and L. KORECZ. Magy. Kem. Foly. **76**, 138 (1970). Chem. Abstr. **73**, 19124*x* (1970).
4. D. COUCOUVANIS and J. P. FACKLER, JR. Inorg. Chem. **6**, 2047 (1967).
5. A. D'ADDARIO, D. G. HOLAH, and K. KNOX. Unpublished work. A. D'Addario. Ph.D. Thesis. 1970. Univ. Microfilms, Ann Arbor, Michigan.
6. M. R. HUNT, A. G. KRUGER, L. SMITH, and G. WINTER. Aust. J. Chem. **24**, 53 (1971). A. G. KRUGER and G. WINTER. Aust. J. Chem. **24**, 161 (1971).
7. G. D'ASCENZO and W. WENDLANDT. J. Therm. Anal. **1**, 423 (1969).
8. D. G. HOLAH and C. N. MURPHY. J. Therm. Anal. In press.
9. M. DELEPINE and L. COMPIN. Bull Soc. Chim. Fr. **27**, 474 (1920).
10. S. E. LIVINGSTONE and A. E. MIHKELSON. Inorg. Chem. **9**, 2545 (1970).
11. H. KREBS, E. F. WEBER, and H. FASSBENDER. Z. Anorg. Allg. Chem. **276**, 128 (1954).
12. D. COUCOUVANIS. Prog. Inorg. Chem. **11**, 233 (1970).
13. E. PAGLIA. Gazz. Chim. Ital. **87**, 1133 (1957); Chem. Abstr. **52**, 12644*d* (1958).
14. P. R. HECKLEY, D. G. HOLAH, A. N. HUGHES, and F. LEH. Can. J. Chem. **48**, 3827 (1970).
15. B. N. FIGGIS and J. LEWIS. Mod. Coord. Chem. 415 (1960).
16. A. L. ZAGYANSKII. Zh. Prikl. Khim. **38**, 942 (1965); Chem. Abstr. **63**, 2369*f* (1965).
17. A. AVDEEF, J. P. FACKLER, JR., and R. G. FISCHER, JR. J. Am. Chem. Soc. **92**, 6972 (1970).
18. L. H. LITTLE, G. W. POLING, and J. LEJA. Can. J. Chem. **39**, 745 (1961).
19. V. M. SHULMAN and S. V. LARIONOV. Izv. Sib. Otd. Akad. Nauk. SSSR Ser. Khim. Nauk. **5**, 35 (1967); Chem. Abstr. **69**, 24021*h* (1968).
20. A. I. VOGEL. Textbook of quantitative inorganic analysis. Longmans. 3rd ed. p. 89.
21. B. R. JAMES, M. PARRIS, and R. J. P. WILLIAMS. J. Chem. Soc. 4630 (1961).
22. D. G. HOLAH and C. N. MURPHY. To be published.
23. R. L. CHIANG and R. S. DRAGO. Inorg. Chem. **10**, 453 (1971).

Can. J. Chem. Downloaded from www.nrcresearchpress.com by 210.87.254.105 on 09/05/12
For personal use only.

Can. J. Chem. Downloaded from www.nrcresearchpress.com by 210.87.254.40 on 09/05/12
For personal use only.

Étude cinétique de quelques cellules électrochimiques de métaphosphate de sodium ($NaPO_3$) fondu[1,2]

E. J. Casey et A. R. Dubois

Centre de recherches pour la défense, Ottawa, Canada

Reçu le 31 août 1970[3]

Les métaphosphates fondus et déshydratés ne réagissent pas avec le platine et le quartz à 650 °C; il a donc été possible d'etudier en détail les processus chimiques et électrochimiques d'abord avec des électrodes de platine puis ensuite avec des électrodes de nickel. Des études ont aussi été faites avec les métaux suivants: Fe, Cu, Ca, Ag.

Le dégagement anodique d'oxygène sur le platine à partir du métaphosphate de sodium fondu laisse voir un hystérésis dans la courbe V/I et un comportement Tafel ($d\eta/d \log i = 2.3RT/\beta nF$) d'une exactitude surprenante impliquant que la décharge lente d'un électron détermine la vitesse de réaction sur un domaine étendu de vitesses. Le processus cathodique est complexe et le dépôt contient du sodium élémentaire dans le platine.

Le phosphure de nickel $Ni_{12}P_5$ prédomine comme produit d'autocorrosion sur le Ni. Ce produit est réduit activement s'il est couplé électrochimiquement avec le Ca, et de la même façon est activement oxydé par O_2. L'électrolyse poussée introduit du nickel supplémentaire à l'anode ou du phosphore à la cathode et modifie la structure cristalline du produit.

Les résultats de l'analyse thermique différentielle (ATD), de l'analyse par spectroscopie r.m.n.-phosphore et de la solubilité du sel résiduel dans l'eau démontrent que la structure trimérique du sel fondu est modifiée par l'électrolyse. L'anolyte diffère du catholyte. Le sel fondu électrolysé présente une conduction ionique et électronique à 650 °C mais les facteurs de transport électronique semblent être déterminés par un processus d'injection à la cathode.

Plusieurs réactions se produisent aux interfaces électrodes–électrolyte et dans l'électrolyte, dont la nature chimique et électrochimique et la cinétique sont envisagées. Les résultats expérimentaux obtenus conduisent à penser qu'un contrôle de la cellule électrochimique permet d'orienter sélectivement les produits de la réaction, phosphures métalliques, phosphore, phosphine, métaphosphates polymériques, le dépôt métallique et produits métal-phosphore semiconducteurs. On envisage également la possibilité d'une pile $Ca|NaPO_3|Ni$ et d'une pile à combustible sur $Ni|NaPO_3|O_2$.

Interest in the possible use of molten metaphosphates as electrolyte and as reactant in electrochemical cells has been examined from the points of view of both electrochemical synthesis and sources of electrical energy. Both are shown to be possible.

The anodic evolution of O_2 from carefully dried molten $NaPO_3$ on Pt shows hysteresis in the V/I curve, and also shows Tafel behavior ($d\eta/d \log i = 2.3RT/\beta nF$) with surprising exactness, which implicates one-electron slow discharge as rate-determining over a considerable range of rate of reaction. The cathodic process is complex, but includes deposition of Na into the Pt if the melt is dry.

On Ni the phosphide $Ni_{12}P_5$ predominates as the autocorrosion product. This material is actively reduced if electrochemically coupled with Ca, and can be electrochemically oxidized by O_2. Forced electrolysis inserts extra nickel into a phosphide anode, or phosphorus into a phosphide cathode, and modifies its crystal structure. The trimeric structure of the melt is modified by electrolysis, as shown by DTA tracings, by phosphorus-n.m.r. spectra, by changes of color and of solubility of the products in water. Anolyte product differs from catholyte product. The electrolyzed melt can leak charge both electronically and electrolytically at 650 °C, but electronic transport is tenuous and seems to be determined by an injection process at the cathode. Reactions and mechanisms are proposed for the various processes, including a phosphate shuttle to account for loss of charge.

Indications are that metal phosphides, phosphorus, phosphine, polymeric metaphosphates with various physical properties, metal cladding, and semiconducting metallo-phosphorus products could be selectively produced if sufficient controls were to be imposed on a suitably designed electrochemical reactor.

Canadian Journal of Chemistry, 49, 2733 (1971)

---

[1]Communication présentée partiellement aux Congrès de l'ACFAS, 1966–68, et à la Conférence sur l'Electrochimie à l'Université de Montréal les 1 et 2 juin 1970.

[2]Référence à rappeler au CRDO: Rapport No. 643.

[3]La révision reçue le 23 avril 1971.

Can. J. Chem. Downloaded from www.nrcresearchpress.com by 210.87.254.40 on 09/05/12
For personal use only.

Introduction

Cet exposé décrit une étude entreprise sur des cellules électrochimiques utilisant comme électrolyte du métaphosphate de sodium fondu à 650 °C. Le but initial de ce travail était de mieux comprendre les phénomènes chimiques et électrochimiques qui y prennent place.

La littérature concernant l'électrolyse ignée du métaphosphate de sodium est très disposée et fragmentaire. Ainsi Couch (1) mentionne la formation de couches de phosphures dures de nickel formées sur une électrode de nickel, lors d'une simple immersion ou d'une électrolyse. Grueber et aussi Frank et Inman (2) rapportent la préparation de phosphore très pur à la cathode par électrolyse. Bekturov (3) montre que le phosphore pouvait être obtenu par action d'un gaz reducteur sur le métaphosphate de sodium fondu. Le travail analytique le plus complet semblent cependant être encore celui de Chêne (4).

Bien qu'on ait observé que l'évolution anodique d'oxygène et le dépôt cathodique de sodium ainsi que la corrosion rapide de la plupart des métaux (même le platine sous les conditions réductrices) apparaissent dans les metaphosphates fondus, la démonstration est incomplète et peu convaincante, surtout en ce qui concerne le méchanisme des réactions. Dans son livre Van Wazer (5) passe en revue presque toute la littérature pertinente antérieure.

En 1960, Delimarskii *et al.* (6) présentèrent une communication expliquant en détail l'effet d'additifs solides sur le métaphosphate pur fondu. Frank et Inman (2) mentionnent de l'évidence pour la dépolymérisation de chaînes du métaphosphate avant de perdre leurs charges à la cathode. Certain auteurs prétendent également que le P^{5+} du métaphosphate peut subir une réduction de plusieurs électrons, jusqu'à P^{3-}. Une telle réaction de transfert présente un grand intérêt à la fois fondamental (compréhension du mécanisme des réactions) et pratique (synthèse électrochimique et piles énergétiques utilisant des sels fondus). Cette étude des métaphosphates fondus provient directement du travail de Senderoff (7) décelant le présence de phosphine du cours de la réduction de cet oxyanion dans les piles thermiques.

Nous avons étudié le comportement de plusieurs métaux dont le platine, le calcium, le nickel, le cuivre et le fer, en présence de sel fondu pur, soit par immersion simple, soit par traitement anodique et cathodique. La première partie décrit les caractéristiques chimiques de l'électrolyte et la cellule de mesures. La seconde partie est consacrée aux comportements électrochimiques.

Phénomènes chimiques

Le métaphosphate de sodium (B & A réagent) contenait 2% d'eau en plus des autres impuretés décrites (métaux lourds: Pb et Fe, 0.005%; As, 0.001%; sulfate, 0.01% et chlore, 0.003%). Les travaux préliminaires ont montré que ce produit attaquait un grand nombre de matériaux utilisés comme creusets à 650 °C et réagissait violemment avec le Ca métallique pour produire du phosphine; il attaque même le Pt dans des conditions réductrices. Toutefois la déshydratation a pu être réalisée efficacement par le procédé suivant: sous pression réduite ($\simeq$10 nm), la température du sel fondu était élevée à près de 900 °C dans un tube en quartz (Fig. 1) pour une période de trois heures; on le refroidissait ensuite à 800 °C sous vide pour 16 h. Après un

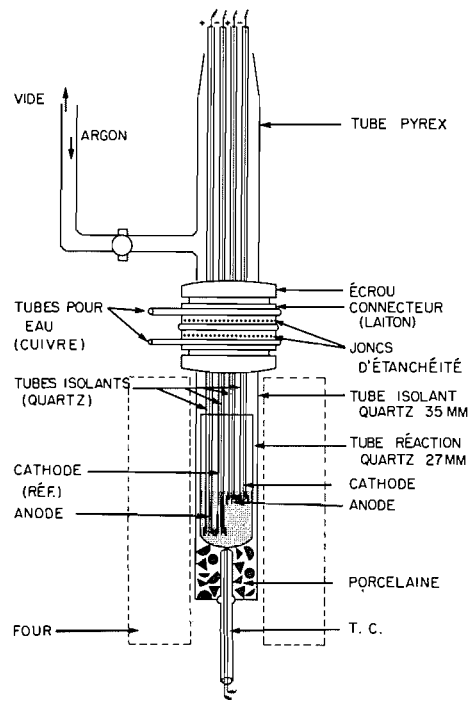

FIG. 1. Appareil. A noter que la chemise, les gaines des électrodes, les cloches d'échantillonage et le récipient de la cellule sont en quartz. Deux électrodes auxiliaires Pt/sel/Pt composent le potentiel de référence: à 10 μA/cm² le potentiel était 1.15 V sûr, et l'anode était utilisée comme référence.

Can. J. Chem. Downloaded from www.nrcresearchpress.com by 210.87.254.40 on 09/05/12
For personal use only.

tel traitement, le sel fondu n'attaquait plus le Pt dans des conditions réductrices et était inerte vis à vis calcium métallique, et l'analyse du sel fondu par la méthode Karl Fisher a montré une teneur en eau de moins de 0.02%, apparemment retenue dans la structure polymérique du sel fondu. Une analyse spectrographique d'un tel sel fondu déshydraté révéla de faibles traces de Cu, Al, Mg, Fe, un trace de Si mais ne put déceler du Pt ou du Ni. Hydraté ou non, le sel fondu est visqueux entre 600 et 750 °C et la viscosité de NaH_2PO_4 soigneusement déshydraté jusqu'à $NaPO_3$ a été étudiée (8*a*). Bien qu'on ait révélé l'existence d'une part d'une structure trimérique cyclique et d'autre part d'une structure polymérique à longue chaîne (5), la composition anionique précise du sel fondu dépend probablement de la teneur en eau du sel fondu considéré et de l'histoire thermique du sel fondu bien que ce dernier point n'ait pas encore été étudié expérimentalement d'une façon systématique. Le montant de Na_2O en excès est aussi très important: avec son excès la conductibilité ne change pas, mais la viscosité diminue beaucoup (8*b*).

Les diagrammes de diffraction de rayons-X de sels déshydratés ne diffèrent pas sensiblement de celui de $NaPO_3$, mais il apparaît parfois dans le thermogramme différentiel un grand pic exothermique à 320 °C indiquant une réaction (probablement la formation d'un polymère) qui ne peut être isolé des effets de l'histoire thermique antérieure de l'échantillon.

Le chauffage de mélanges équivalents de Na_2O et de P_2O_5 donne une vive réaction exothermique vers 300 °C. On en conclut que le sel fondu ne peut être considéré comme une simple solution de Na_2O et P_2O_5. Ce point a été soulevé et discuté par d'autres auteurs (9).

Produits d'électrolyse dans le sel fondu

Dans le sel fondu déshydraté, le Pt résiste aussi bien à l'attaque anodique que cathodique. (L'inertie du calcium dans le sel fondu après immersion indique que ce dernier est suffisamment déshydraté.) A des faibles densités de courant, l'anode de Pt atteint rapidement une tension stable tandis que celle de la cathode s'accroît lentement et au début de façon erratique; puis après quelques heures il s'établit une différence de potentiel d'environ 1.1–1.2 V entre l'anode et la cathode, potentiel stable à quelques mV près. A des densités de courant plus élevées, la cellule atteint le potentiel d'environ 1.2 V plus rapidement, et si l'électrolyse persiste, un dépôt noir apparaît à la cathode tandis qu'un produit jaune-orange soluble est produit à l'anode.

Le spectre de diffraction de rayons-X du sel fondu déshydraté solidifié et refroidi présente très peu d'intérêt car coloré ou non, le verre ainsi formé était généralement inerte aux rayons-X. L'analyse thermique différentielle était souvent aussi indéfinie; le thermogramme dépend plus du taux de refroidissement antérieur que de la présence de la substance colorée.

Ce chromophore jaune persiste parfois même quand le sel solidifié et refroidi est dissout dans l'eau; il présente une large bande d'absorption avec un maximum à 410 nm. Si l'on prolonge l'électrolyse du sel fondu déshydraté à 650 °C entre les deux électrodes de Pt, le composé formé à l'anode devient plus foncé (brun doré). Comme un complexe à transfert de charge, la couleur change avec la température, réversiblement: du brun doré à 650 °C au brun à 750 °C, au jaune à 610 °C. (On peut noter les couleurs Munsell (10) dans le tableau 1. Ce n'était pas possible d'obtenir des spectra d'absorption parce que le fondu électrolysé était un peu brumeux, un peu bourbeux.)

De plus, le $NaPO_3$ avant l'électrolyse montre dans l'eau une absorption r.m.n.-P à $+21 \pm 1$ p.p.m. en prenant de la H_3PO_4 à 85% comme le zéro de référence; mais l'anolyte jaune montre en plus une résonance à $+10 \pm 1$ p.p.m. indiquant qu'il existe un nouvel environnement du phosphore dans l'anolyte formé par le traitement anodique. La résonance se produit à un niveau d'énergie caractéristique d'un "polymétaphosphate" (11). Un modèle de ce qui se produit a été conçu à partir de (*a*) ces nouveaux faits, (*b*) les travaux de Griffith et Rutt (12) qui associent le groupe C_{3v} (trimère en forme de chaise) à $NaPO_3$ dans l'état solide (basé sur les spectres i.r. et Raman), (*c*) la supposition que le groupe C_{3v} persiste dans le sel fondu, (*d*) des idées basées sur des revues récentes des complexes chromophoriques inorganiques par Jørgensen (13). Le mécanisme que nous proposons pour l'oxydation anodique du sel fondu est illustré dans la Fig. 2. On peut donc voir que le nouveau modèle explique, du moins qualitativement, le dégagement d'oxygène, le nouvel environnement du phosphore ainsi que la présence du chromophore; de plus, il suggère

TABLEAU 1. Couleurs du sel fondu ($NaPO_3$) électrolysé à diverses températures (électrodes de nickel)

Température (°C)	Description Munsell*	Observations
697.7		Brun pâle
704.4	Nuance: R, Y, R 10.0 R, Valeur 5 Chroma 10	Brun pâle
655.3	10.0 R, Valeur 4 Chroma 10	Brun pâle
595.3	10.0 R, Valeur 5 Chroma 8	Brun pâle
510.9		Brun plus pâle, brun jaunâtre
412.1	Nuance: YR-Y, 10.0 YR Valeur 7, Chroma 8	Plus jaune
713.1	Nuance: YR, 2.5 YR Valeur 5, Chroma 10	Brun pâle
641.6	Nuance: YR, 2.5 YR Valeur 5, Chroma 6	Brun pâle
548.5	Nuance: YR, 5.0 YR Valeur 6, Chroma 8	Brun plus pâle
392.4	Nuance: Y, 2.5 Y Valeur 6, Chroma 6	Couleur brune est disparue tend vers jaune
214.7	Nuance: Y, 5.0 Y Valeur 8, Chroma 6	Solidifie, se fissure jaune
24	Nuance: Y-GY, 10.0 Y Valeur 7, Chroma 6	Solide, jaune-vert pâle

*R = red, Y = yellow.

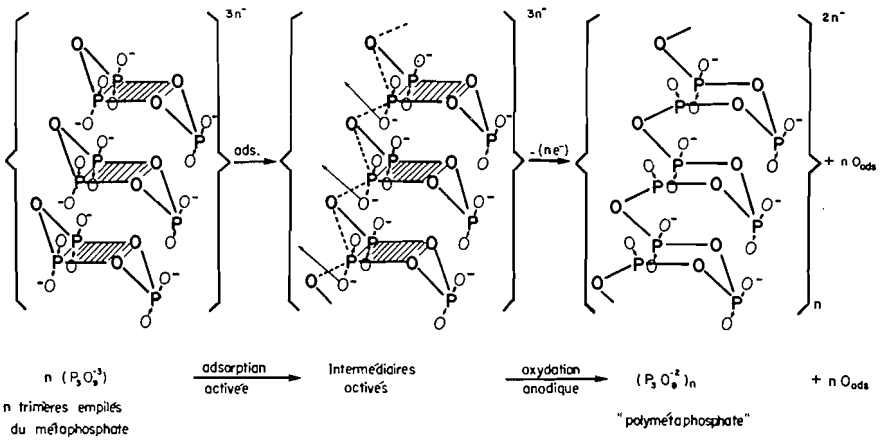

FIG. 2. Représentation schématique de l'oxydation anodique du sel fondu.

pourquoi la solubilité de l'anolyte est beaucoup plus faible que celle du $NaPO_3$ avant l'électrolyse. En effet, le modèle suggère que l'oxydation anodique produit une espèce polymérique inhabituelle en ouvrant les trimères et en créant de nouvelles liaisons P—O—P transversales. Hélices et serpentins désordonnées sont tous les deux possibles, mais il est très peu probable que les liaisons transversales se fassent tout à fait au hasard. La configuration pourrait avoir des modes capables de semiconductivité par liaison π. Toutefois, notre image de l'activité chromophorique n'est pas encore très claire, parce qu'on doit avoir égard au lieu spectral du maximum d'absorption d'O_3^- (14) ainsi que des quelques bandes fortes de PO (15), dont les maxima sont aussi près de 410 nm.

L'anolyte solidifié se dissout généralement plus rapidement dans l'eau à la température de la pièce que le catholyte, ce dernier laissant un

Can. J. Chem. Downloaded from www.nrcresearchpress.com by 210.87.254.40 on 09/05/12
For personal use only.

TABLEAU 2. Dix phosphures de nickel: Ni_xP_y

Phosphures	$x:y$	Ni/P Relat. Atom.	Evidences: Diagr. phase	Evidences: Tension de vapeur	Composition par analyse	Diffractions des rayons-X: Cristal unique	Diffractions des rayons-X: Poudre
Métaux durs							
1-	3:1	3.0	Réfs. 25, 27	Réf. 31	Réf. 4	Réf. 26	Réf. 32
2-	5:2	2.5	Réfs. 25, 27	Réf. 31	Réf. 4	Part.	Réf. 29
3-	12:5	2.4	Deux	Non	Probablement	Réf. 26	Réf. 32
et	7:3	2.33	Seul.	Non	Probablement	Non	ASTM 3-1101
4-	2:1	2.0	Réfs. 25, 27	Réf. 31	Réf. 4	Réf. 26	Réf. 32
5-	5:3	1.67	Réf. 25	Non	Peut-être	Non	Non
6-	5:4	1.25	Réf. 27	Non	Probablement	Réf. 28	Réf. 27
Métaux mous							
1-	6:5	1.2	Peut-être	Réfs. 30, 31	Réf. 4	Non	Non
2-	1:1	1.0	Réf. 27	Non		Réf. 26	Réf. 27
3-	1:2	0.5	Réf. 27	Réfs. 30, 31	Probablement	Réf. 26	ASTM 13-213
4-	1:3	0.33	Réf. 27	Réfs. 30, 31	Probablement	Non	Réfs. 27, 31

résidu fibreux amorphe aux rayons-X. Les structures de l'anolyte et du catholyte sont évidemment différentes.

Oxydation métallique

Le platine et l'or ne sont pas attaqués appréciablement après qu'on a soigneusement déshydraté le sel fondu. L'oxygène se dégage à l'anode de platine. Par contre, les métaux plus actifs tel Ca, Ni, Cu, Fe sont attaqués lentement. Nous décrivons tout d'abord les aspects phénomènologiques.

Le nickel, immergé pendant deux heures à 650 °C dans un électrolyte de $NaPO_3$ fondu déshydraté, se revêt d'une couche métallique grise très dure (Fig. 3*a*) dont le diagramme de diffraction des rayons-X était celui de $Ni_{12}P_5$ (Ni_7P_3 dans la littérature antérieure), tel que décrit par Rundqvist (16). Ce dépôt est fortement magnétique et insoluble dans l'eau. Il se solubilise lentement dans les acides forts. Les neuf autres phosphures connus du nickel, tableau 2, n'apparaissent pas. De plus, le $Ni_{12}P_5$ est produit en assez grande quantité sous forme apparemment de cristaux isolés. Ce sont des lamelles minces, brillantes, à fractures conchoïdales, d'une longueur d'environ 0.1 mm, ressortant de la surface du Ni dans le sel fondu (Fig. 3*a*).

L'oxydation anodique du nickel immédiatement après son immersion dans le sel fondu ne produit pas de lamelles. On a pu déterminer que le produit sous forme d'une mince couche grise était composé de $Ni_{12}P_5$ en plus d'un autre composant encore inconnu.

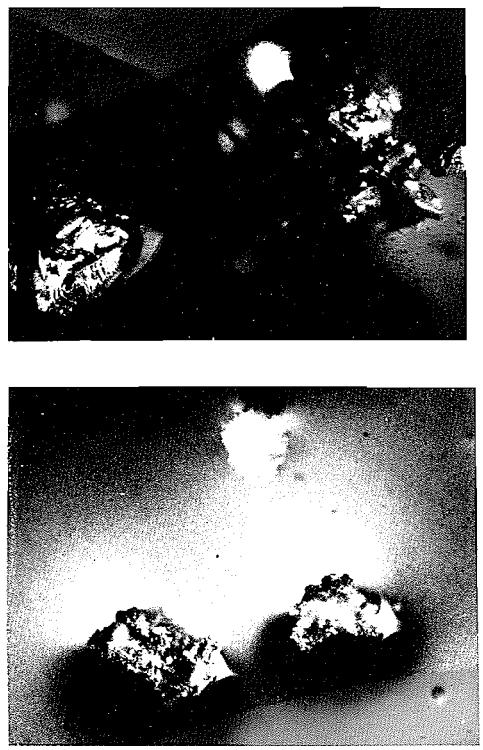

FIG. 3. Photographie des produits formés sur le Ni: (*a*) des cristaux de $Ni_{12}P_5$ (*b*) produit cathodique inconnu. Grandeur des photos: 125×.

Des spécimens de nickel coulé, corrodé à l'acide, ainsi que du nickel fritté en poudre (85% poreux), ont montré sensiblement les mêmes produits, bien que la substance frittée anodisée produisait des lignes supplémentaires

Can. J. Chem. Downloaded from www.nrcresearchpress.com by 210.87.254.40 on 09/05/12
For personal use only.

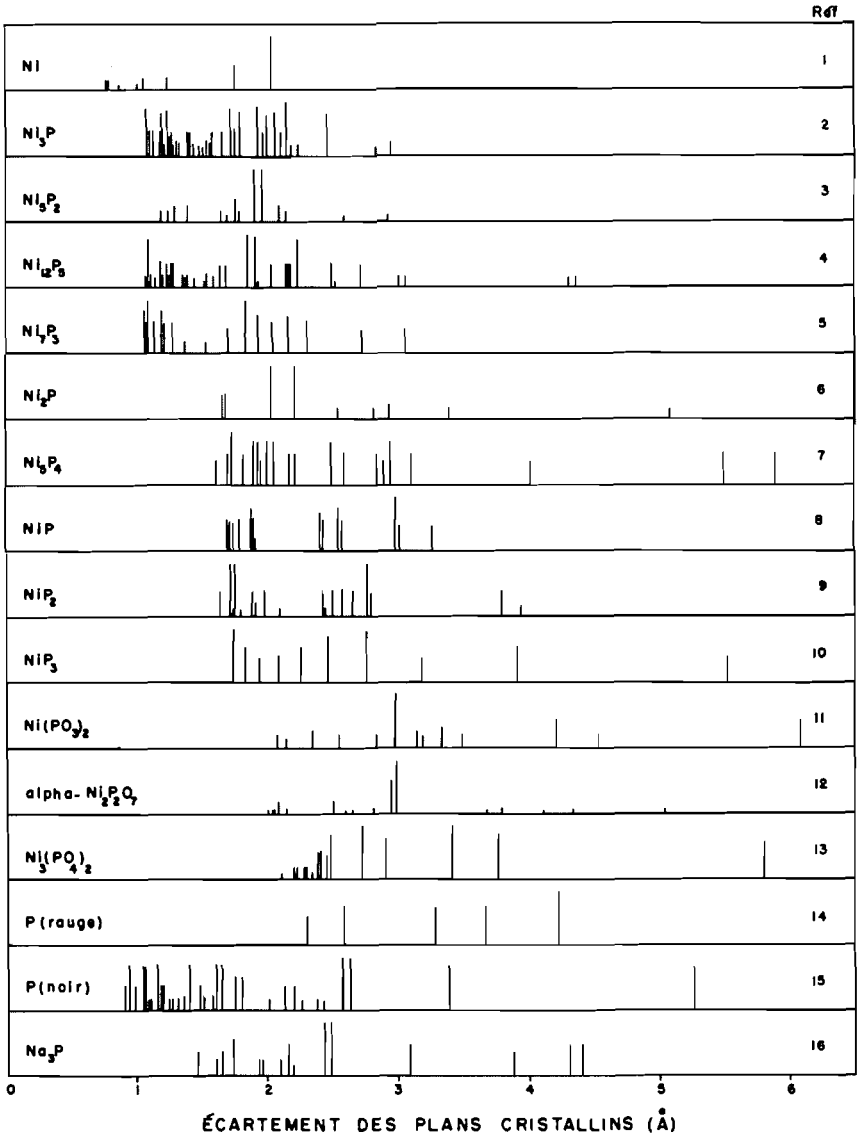

FIG. 4. Diagrammes de diffraction des rayons-X de phosphures connus et de quelques produits de réaction possibles: *1*, "X-ray Powder Data File" ASTM fiche numéro 4-0850; *2*, réf. 26; *3*, réf. 29; *4*, même que 2; *5*, ASTM fiche numéro 3-1101; *6*, ASTM fiche numéro 3-0953; *7*, réf. 27; *8*, même que 7; *9*, réf. 26; *10*, même que 2; *11*, réf. 33; *12*, même que 11; *13*, même que 11; *14*, ASTM fiche numéro 2-0266; *15*, ASTM fiche numéro 9-20; *16*, ASTM fiche numéro 4-0764.

dans le diagramme de diffraction, résultant probablement d'une couche d'oxyde sur le produit du départ. Un ensemble de diagrammes connus pour les phosphures de nickel ou d'autres produits de réactions probables est donné dans la Fig. 4. Ces diagrammes peuvent être comparés avec un produit de réaction anodique non identifié dont le diagramme apparait dans la Fig. 5*a*.

Les produits de réactions anodiques de cuivre, de fer et de calcium n'ont pas été étudiés avec autant de précision que ceux de nickel, mais les phosphures de cuivre et de fer ont été identifiés surtout.

Réduction cathodique

Dans le but de préciser un point expérimental qui veut que le Pt soit attaqué par le méta-

Can. J. Chem. Downloaded from www.nrcresearchpress.com by 210.87.254.40 on 09/05/12
For personal use only.

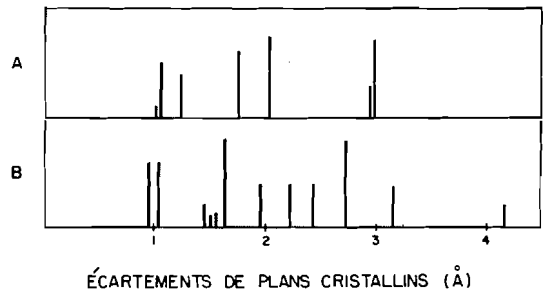

FIG. 5. Diagramme de diffraction des rayons-X du (*a*) produit anodique (*b*) produit cathodique, non identifiés.

phosphate fondu sous des conditions réductrices (17), nous soulignons que l'attaque ne se fait pas si le sel fondu est soigneusement déshydraté jusqu'au point d'être inerte au calcium.

Pendant la réduction cathodique à 650 °C du Pt dans le métaphosphate fondu déshydraté une couche mince du produit de réaction est deposée sur le Pt. L'identification de ce matériel suit.

Par l'analyse quantitative spectroscopique à flamme d'échantillons en surface, il a été démontré que la charge accumulée par le dépôt électrolytique pouvait être attribuée au dépôt de sodium sur et dans le Pt. Toutefois du phosphore (pas nécessairement élémentaire) apparaît toujours dans l'analyse. Etant donné le mince dépôt (estimé par les mesures coulombiennes à environ de 100 couches atomiques sur le Pt), le produit de réaction pourrait être un phosphure tel que PtP_2 ou Na_3P, ou même un phosphite. Toutefois on s'attendrait à ce que ces deux derniers, réagissent violemment quand le produit est introduit dans l'eau. Les connaissances actuelles nous portent à croire que le produit sur le Pt est du Na, tout probablement dans le Pt sous forme d'un alliage Pt–Na, avec aussi la possibilité de trouver du phosphore élémentaire. D'autres auteurs ont trouvé du phosphore élémentaire sur des cathodes de tungstène et de charbon (2), mais nous n'avons jamais pu obtenir d'indications certaines du phosphore sur la surface du platine; la couche était toujours trop mince.

Le nickel se comporte différemment. Tandis que le potentiel du Pt varie et devient graduellement plus négatif pendant une réaction cathodique, le nickel se charge et il prend immédiatement un potentiel qui est le même que le potentiel stable du platine comme cathode. La réduction du Ni se produit très bien à une légère surtension, et une mince pellicule (Fig. 3*b*) d'un gris pâle en résulte. Quand des échantillons lavés de ce produit (non-magnétique) sont isolés du sel solidifié vitreux, à la température ambiante, ils donnent une simple structure cubique, dont le diagramme de diffraction des rayons-X n'est pas connu (Fig. 5*b*). Le produit non lavé, qui contient probablement une portion du sel réduit ainsi que la substance grise fournit en plus deux autres diagrammes séparables mais non identifiables, révélant deux autres produits. Chacun d'eux présente deux larges distances (5–10 Å) réticulaires, distinctes et séparables, tel qu'on trouve dans une structure défectueuse (18).

Ainsi, nos connaissances indiquent la présence de 5 produits cathodiques différents: *A*, $NaPO_3$ amorphe, vitreux, fibreux, soluble lentement à l'eau chaude; *B*, Na en alliage avec le Pt, et possiblement avec le Ni ainsi qu'avec d'autres métaux étudiés; *C*, un "phosphure gris" avec une structure cubique (appelé ultérieurement "P(Na)", formé sur le Ni; *D–E*, deux autres substances cristallines avec des défectuosités dans le réseau cristallin, tout probablement des formes défectueuses du phosphure gris inconnu de *C*.

Une attention particulière a déjà été porté au "phosphure gris" (*C*). Chêne, dans un travail remarquable, a déclaré en 1941 que des phosphures massifs de plusieurs compositions différents peuvent être produits à la cathode, selon la température, la densité du courant et les solides ajoutés au sel fondu. D'autres chercheurs ont aussi déclaré la formation de phosphures cependant sans évidence. Grueber en 1956 prétendait que le phosphore très pur est en lui-même un constituant majeur. Cependant, dans toutes ces études anciennes, les analyses ont été faites sur des échantillons macroscopiques, qui, d'après nos expériences, devraient être hétérogènes.

Dans le présent travail, le dépôt gris *C* est cristalline mais n'est pas fortement magnétique. Les cristallites présentent un spectre de diffraction (cubique simple) à 7 lignes, qui n'a pas encore été identifié. La Fig. 5 montre les quatre plus fortes espaces à: 2.73, 1.64, 1.05 et 0.96 Å. L'analyse à la microsonde a révélé que les cristallites contiennent principalement du phosphore avec du nickel comme partie composante mineure et une quantité indéterminée de Na.

Ainsi *C* n'est peut-être pas simplement un des phosphures de nickel à haute teneur en phos-

Can. J. Chem. Downloaded from www.nrcresearchpress.com by 210.87.254.40 on 09/05/12
For personal use only.

Can. J. Chem. Downloaded from www.nrcresearchpress.com by 210.87.254.40 on 09/05/12
For personal use only.

phore. Ceci pourrait être un phosphure de sodium, ou bien un nouvel allotrope du phosphore élémentaire. Puisque le comportement électrochimique du dépôt Na-sur-Pt, Pt(Na), est semblable à celui du dépôt gris qui a été produit cathodiquement sur le Ni, il semble probable que le dépôt cathodique est une solution de sodium–phosphore qui peut être stabilisée, soit dans le nickel, soit dans le platine. Il semble donc y avoir deux possibilités pour le Ni, soit un composé tel que Na_3P rapporté, ou une substance semi-métallique, sodium-dans-phosphore, P(Na), retenue dans une matrice de Ni limité. En l'absence de preuves par diagrammes de diffraction des rayons-X pour Na_3P, nous devons supposer que ce dernier est plus probable.

La stabilité de la charge retenue par le phosphure gris est variable.

Phénomènes électrochimiques

Observations générales

Avec une telle variété dans les possibilités de réactions découvertes par les études des changements chimiques et rapportée dans la section précédente, on voit que l'interprétation des mesures électrochimiques sur ce système est capricieuse. Toutefois certaines mesures ont été faites qui non seulement décrivent le comportement du système mais conduisent à une meilleure compréhension des processus dont il est le siège.

Les méthodes utilisées sur des électrodes simples étaient toutes conventionnelles: (*a*) mesures de la quantité d'électricité, (*b*) comportement *V*/*I*, (*c*) décroissance de potentiel en circuit ouvert. Quelques caractéristiques électriques des cellules de conversion d'énergie ont aussi été déterminées. Les observations les plus générales peuvent être résumées de la façon suivante:

(*a*) Le potentiel pendant le dégagement de l'oxygène du Pt est assez stable pout être utilisé comme potentiel de référence. Son comportement *V*/*I* est remarquablement semblable à celui en solution aqueuse, par exemple d'une part l'hystérésis et d'autre part des valeurs semblables de la pente Tafel sont observées.

(*b*) Les potentiels en circuit ouvert du Ni, Cu, Fe sont tous semblables à celui du Pt une fois ce dernier réduit cathodiquement dans le sel fondu: environ 1.2 V cette électrode étant négative par rapport à l'électrode de référence Pt/O_2; mais celle du Ca est environ 2.6 V négative elle aussi par rapport à l'électrode de référence.

(*c*) Les surtensions sont de façon prédominante, non-ohmiques. Après l'interruption du courant, le potentiel décroît lentement sur une période de quelques secondes.

(*d*) Les densités de courant limites pour des oxydations de métaux actifs sont basses: généralement de l'ordre de 0.1 A/cm^2.

L'électrode à gaz O_2

Le sel déshydraté se décompose à l'anode pour libérer un gaz constitué principalement d'oxygène. La réaction anodique globale pourrait suivre

$$2PO_3^- \rightarrow P_2O_5 + \tfrac{1}{2}O_2 + 2e^-$$

Nous la discuterons en détail plus tard, après que nous examinerons les résultats électrochimiques.

Le comportement Tafel et la décroissance de potentiel ont été déterminés. Contrairement à la cathode, le potentiel de l'anode décroît très rapidement vers la valeur réversible deux ou trois secondes après l'interruption du courant; par la suite, la décroissance sur les derniers 100 mV est très lente. dη/d log t varie d'un essai à l'autre. La moyenne est d'environ 49 mV/décade de temps et correspond probablement à un processus de désorption lente contrôlé par la diffusion. Nous n'avons pas fait de mesures rapides de la décroissance du potentiel pour des temps inférieurs à 1.0 s.

Le comportement de Tafel sur 2½ ordres de grandeur (Fig. 6) a révélé l'existence probable de deux types différents de sous-couches à partir

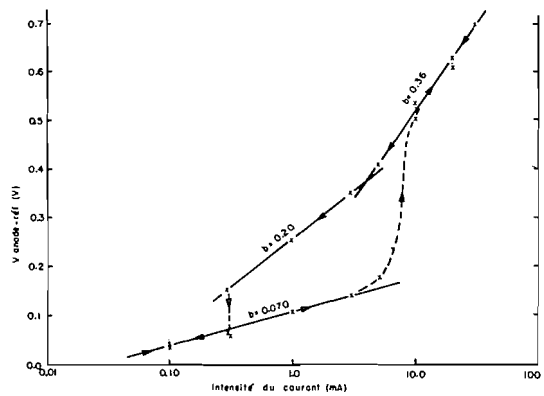

FIG. 6. Renseignement *V*/*I* de l'évolution d'oxygène sur le Pt dans le $NaPO_3$ à 650 °C. Si $\beta = 0.5$ et $n = 1$, alors $b = 2 \times 2.3RT/n\beta F = 0.36$, impliquant que la décharge lente à partir de PtO_x est l'étape déterminante de la vitesse. Ref: O_2 sur Pt à 10 μA/cm^2.

Can. J. Chem. Downloaded from www.nrcresearchpress.com by 210.87.254.40 on 09/05/12
For personal use only.

desquelles l'oxygène peut évoluer. Une des sous-couches est stable à une faible densité de courant avec une faible valeur de $b \equiv d\eta/d \log I$ (de l'ordre de 0.07 V/décade), et l'autre existe principalement à une forte densité de courant avec une valeur de b environ 0.36 V/décade. Cependant une fois formée, cette dernière peut continuer à exister si la densité de courant est réduite lentement et systématiquement à des valeurs où on ne trouve généralement que le premier type de sous-couche. Il a été suggéré que la sous-couche pourrait être du PtP_2 ou du PtO, existant aux faibles densités de courant, et PtO_x formé à des densités de courant élevées. Le comportement est tel que chacun d'eux semble pouvoir remplacer l'autre, l'oxyde supérieur remplaçant le phosphure ou l'oxyde inférieur à une densité de courant élevée et l'inverse à des densités de courant faibles.

Aux plus hautes densités de courant, la pente mesurée, 0.36, concorde remarquablement avec la valeur théorique prédite par $2 \times 2.3RT/F$ pour un processus dans lequel la décharge lente d'une espèce adsorbée de la solution est l'étape déterminante de la vitesse pourvu qu'un seul électron soit transféré et que le facteur de symétrie soit de 0.5. Ceci n'est apparemment pas un cas isolé car on a trouvé (19) que la réaction d'évolution gazeuse anodique de $NaNO_2$ fondu a aussi des valeurs de b données par $2 \times 2.3RT/F$ sur trois ordres de grandeur de densité de courant aussi bien à 244 qu'à 310 °C. Dans ce cas on croyait que la réaction primaire devait être $NO_2^- \rightarrow NO_2 + e^-$. De la même façon, la décharge du nitrate montre le même genre de comportement de Tafel, impliquant une décharge lente de NO_3^- du moins sur un domaine limité de densités de courant (20). Ainsi, par analogie, nous avons conclu dans le cas du $NaPO_3$ que l'étape lente est la décharge de PO_3^- du polymère absorbé sur la surface PtO_x saturé en oxygène.

Pour des densités de courant intermédiaires, b devient constant à 0.20 et non pas à 0.18 comme on s'y attendrait si l'étape déterminante était la combinaison lente d'atomes d'oxygène sur le PtO_x; cette valeur supérieure est peut-être due au fait que x est maintenant moindre ou bien encore due au remplacement partiel de l'oxygène par le phosphore de la sous-couche. Même aux densités de courant plus faibles, il est possible que la couche d'oxyde soit remplacée par une couche beaucoup plus catalytique de phosphure. (Dans un cas, du PtP_2 a été isolé du sel fondu et identifié par diffraction des rayons-X à la fin de l'expérience.) Aux densités de courant intermédiaires et faibles, la situation semble être aussi compliquée que dans les bisulfates, les sulfates et les carbonates (21).

La région de transition a été étudiée en détail en examinant les effets de l'interruption du courant. A 5 mA, par exemple, on note souvent le phénomène de surtension anodique. On observe surtout ce phénomène chez des métaux actifs qui peuvent donner lieu à deux oxydes (Ag en solution aqueuse de KOH; Pb en solution aqueuse de H_2SO_4, *e.g.*), cette surtension transitoire se produit lorsqu'on passe d'un oxyde inférieur à un oxyde supérieur. Dans le cas présent, la surtension se produit seulement si l'électrode a un repos d'au moins 2 min en circuit ouvert avant l'oxydation anodique et de façon générale la surtension est d'autant plus marquée que ce repos est prolongé. Décrit d'une autre façon: si le potentiel baisse de plus de 400 mV durant le repos, la surtension anodique peut se produire lors de la prochaine charge anodique. On peut expliquer cette surtension en l'attribuant au phosphore élémentaire qui, provenant du phosphure, pénètre dans la couche PtO_x lors que la réaction a lieu après une période de repos au cours de laquelle le phosphure a pu s'accumuler.

La tension à laquelle l'oxygène se dégage dans la région transitoire semble dépendre largement du degré de saturation de PtO_x en O ou de l'activité catalytique de PtO_x pour la libération d'oxygène. Ainsi la tension finale atteinte par l'électrode faiblement catalytique (i_0 faible) peut dépasser de 60 mV celle d'une électrode fortement catalytique (i_0 élevé).

Il existe donc trois types de sites sur lesquels PO_3^- peut se décharger et où l'oxygène peut se dégager du sel fondu trimérique: Pt pur, qui existe avant l'anodisation de la surface et possiblement après sur la surface de l'électrode; les sites PtP_2; et les sites PtO_x.

Considérons deux routes alternatives pour l'oxydation de PO_3^-. Supposons que la "simple décharge"

$$PO_3^- \rightarrow PO_{3\ ads.} + e^-$$

soit suivie de la décomposition non électrochimique pour produire O_2

$$PO_{3\ ads} \rightarrow P + 3/2\ O_2\uparrow$$

ou

$$PO_{3\ ads} \rightarrow PO + O_2\uparrow$$

ou

$$PO_{3\ ads} \rightarrow PO_2 + \tfrac{1}{2}O_2\uparrow$$

Alternativement, si le sel $NaPO_3$ fondu a été décomposé partiellement jusqu'à Na_2O dissout dans P_2O_5 (9), du "Na_2O" venant du sel fondu se décharge sur l'anode pour donner O_{ads} et la "décharge électrochimique" de PO_3^- procède comme

$$PO_3^- + O_{ads} \rightarrow O_2\uparrow + PO_{2\ ads} + e^-$$

suivie de la décomposition

$$PO_{2\ ads} \rightarrow P + O_2\uparrow$$

ou

$$PO_{2\ ads} \rightarrow PO + \tfrac{1}{2}O_2$$

Il est concevable que O_2 provienne directement de la décharge d'ions O_2^-. Dans ce cas, le transfert d'électron en une seule étape requise pour que $b = 0.36$ doit être le suivant:

$$O^-_{ads} \rightarrow O_{ads} + e^-$$

suivie d'une réaction de combinaison conduisant au dégagement d'oxygène. Toutefois, les produits phosphoreux doivent encore être expliqués de façon rationnelle.

Maintenant nous pouvons décrire la Fig. 6 comme suit: Aux faibles densités de courant l'oxygène se dégage à partir d'une sous-couche dont la composition PtO/PtP_2 varie en fonction de la densité de courant, et $b = 0.07$. Cependant, au-dessus d'une densité de courant critique, PtO_x se développe, et O_2 évolue à une vitesse limitée par la décharge lente de PO_3^-, et $b = 0.36$. En abaissant la densité de courant même d'un facteur de dix, le PtO_x demeure protégé, mais la vitesse devient limitée par la décharge électrochimique de PO_3^- avec O_{ads}, et $b = 0.2$. Enfin, si nous voulons réduire la densité de courant à des valeurs trop faibles, le PtO_x n'est plus protégé par l'oxygène évolué, et la sous-couche se reforme.

Les faits suivants s'accordent avec les deux mécanismes de décharge: (*a*) Le phosphore rouge élémentaire a été identifié une fois sublimé de l'anode; (*b*) Le composé noirâtre PtP_2 a été isolé et identifié par diffraction de rayons-X, (*c*) Il n'y a aucune preuve de l'échappement d'un PO_2 gazeux.

Réductions cathodiques

Le sel fondu fournit un produit de réaction de telle sorte que la cathode de Pt agit comme

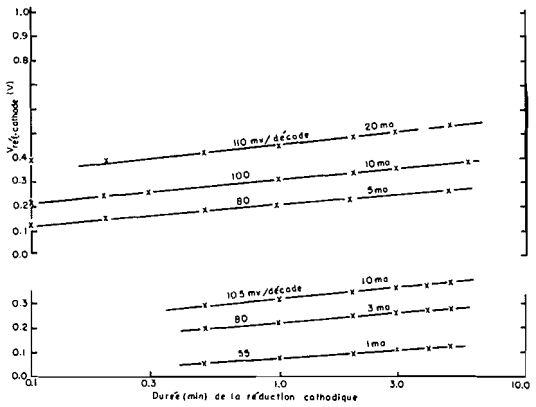

FIG. 7. Potentiel de la cathode à 650 °C durant le dépôt électrolytique de "P(Na)" sur le Pt à partir du $NaPO_3$ asséché. Deux expériences, équation de Nernst: $V \propto \log a_{Na(Pt)} = \log (it/nF)$.

une électrode métal-amalgame. Bien que Brester ait proposé un comportement semblable en 1866 dans réf. 24 nous pouvons maintenant présenter trois sortes de preuves. Ainsi dès le début de la réduction cathodique, la tension prend une valeur de 0.8 V cathodique à l'électrode d'oxygène et devient progressivement plus cathodique suivant l'équation de Nernst, $E\alpha \log q$, lors du passage de la charge q. La Fig. 7 illustre ce fait. De plus, en circuit ouvert, la tension décline lentement et tout se passe comme si le produit cathodique (Na ?) diffuse dans le Pt ou est corrodé par le sel fondu ou les deux. Le déclin est classique en ce que sur deux ordres de grandeur du temps, $d\eta/d \log (t + \theta)$ est constant et égal à 15 mV/décade de temps si le traitement cathodique préalable a été réalisé à de fortes densités de courant, sinon les valeurs sont quelque peu plus faibles. Ce fait est illustré dans la Fig. 8. Ceci est le comportement attendu si une espèce active électrochimiquement s'échappe par un mécanisme sous le contrôle de la diffusion soit dans l'électrode ou dans l'électrolyte sur une surface plane infinie (22).

Enfin, la phase formée par la réduction cathodique peut être oxydée anodiquement pour récupérer la charge. Ainsi, le produit de réaction tenant la charge coulombienne peut subir une oxydation anodique, et la quantité de la charge coulombienne associée, q_a, peut être mesurée. On trouve que le rendement, q_a/q_a^0, du dépôt électrolytique est de 100% aux fortes densités de courant, mais il diminue jusqu'à 20% aux faibles densités de courant (Fig. 9).

Can. J. Chem. Downloaded from www.nrcresearchpress.com by 210.87.254.40 on 09/05/12
For personal use only.

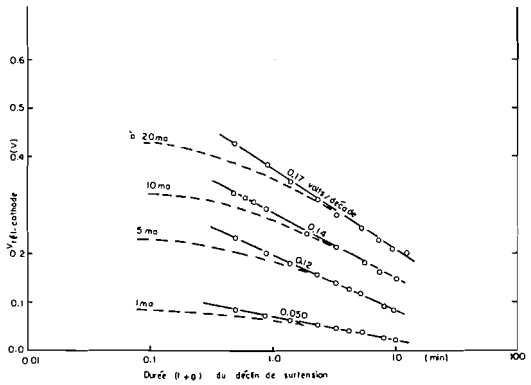

FIG. 8. Déclin de potentiel du dépôt électrolytique de la cathode en circuit ouvert sous contrôle de la diffusion du Na (?) des profondeurs du solide à la surface. Ligne pleine: $\theta = 0.4$ min.

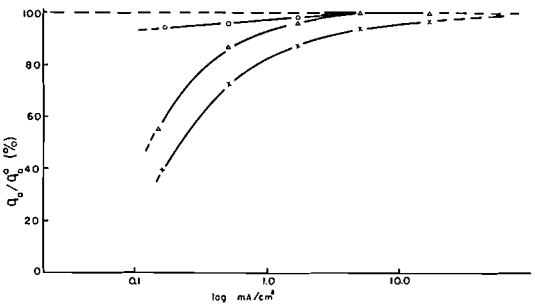

FIG. 9. Fraction de charge cathodique retrouvée à 650 °C par oxydation anodique immédiate sur le Pt dans le $NaPO_3$ asséché, en fonction de la densité de courant. ×, électrode fraîche; ○, électrode ayant complété plusieurs cycles. Dépôt électrolytique constant à 300 mC. $I_a = I_c$. Semiconductivité ou navette?

Parfois la quantité récupérée est moindre que celle qui a été déposée. Une partie de la charge perdue peut parfois être retrouvée par un second traitement anodique suivant un court intervalle en circuit ouvert; tout se passe comme si Na diffusait du sein de l'électrode de Pt vers la surface durant cet intervalle. Toutefois, surtout à de faibles densités de courant, une majeure fraction est perdue et ne peut être retrouvée.

Nous pouvons imaginer deux explications de ces phénomènes: (*1*) la conductivité électronique se produit; (*2*) il existe une "navette électrochimique" dans le sel fondu électrolysé. Nous avons déjà indiqué (Fig. 2) comment la conductivité électronique est possible dans cet électrolyte.

En détail nous supposons une "navette" dans laquelle des ions et des espèces neutres produiraient un court-circuit dans l'électrolyte entre les deux électrodes, quand le circuit extérieur est ouvert, par exemple

Réactions anodiques

[1a] $2PO_3^- \rightarrow 2PO_3 + 2e^-$

[2a] $PO_3 \rightarrow PO_2 + \frac{1}{2}O_2$

[3a] $PO_2 + PO_3 \rightarrow P_2O_5$

$$2PO_3^- \rightarrow P_2O_5 + \tfrac{1}{2}O_2 + 2e^-$$

Réactions cathodiques

[1c] $P_2O_5 + e^- \rightarrow PO_3^- + PO_2$

[2c] $PO_3 + e^- \rightarrow PO_3^-$

[3c] $\frac{1}{2}O_2 + PO_2 \rightarrow PO_3$

$$\tfrac{1}{2}O_2 + P_2O_5 + 2e^- \rightarrow 2PO_3^-$$

On connait bien que l'électrolyte doit être saturé avec de l'oxygène à l'anode. Nous suggérons qu'à la cathode il y aurait assez d'oxygène pour supporter la réaction 3c (l'entredeux n'est que 2 cm). Le P_2O_5 et l'oxygène pourraient diffuser à la cathode, et les ions PO_3^- à l'anode. Donc les deux réactions électrodiques contiennent un court-circuit électrolytique entre les deux électrodes. Ce procédé cyclique nous appelons "la navette électrochimique": c'est un système rédox PO_3^-/P_2O_5 qui conduit la charge entre les deux électrodes quand le circuit est ouvert. On voit qu'il pourrait y avoir un transfert de charge mais aucune réaction globale.

Ainsi, on voit dans la Fig. 9 que le rendement de charge est une fonction de la densité de courant ($I_{cath} = I_{anod}$). De ces renseignements, l'effet d'une "navette" de phosphate ou de la conduction électronique (laquelle réaction se passe) peut être estimée à 0.2 mA/cm^2, mais variable (3 expériences avec le même sel fondu et les mêmes électrodes: 3 courbes Fig. 9). Comme autres exemples, citons Al^+/Al^{3+} une navette dans les cryolytes fondus, et NO_2^-/NO_3^- une navette des solutions aqueuses de KOH.

La rétention de charge du dépôt cathodique dans le sel fondu peut être mesurée pendant des périodes prolongés de repos. Ceci est illustré dans la Fig. 10. Le courant aussi bien pour la charge que la décharge est de 10 mA/cm^2 et l'efficacité du courant (Fig. 9) est de 100%. Dans la Fig. 10 on peut noter que la stabilité varie, voir même améliorée, avec le vieillissement de l'électrode, et qu'une charge de 30% est retenue

Can. J. Chem. Downloaded from www.nrcresearchpress.com by 210.87.254.40 on 09/05/12
For personal use only.

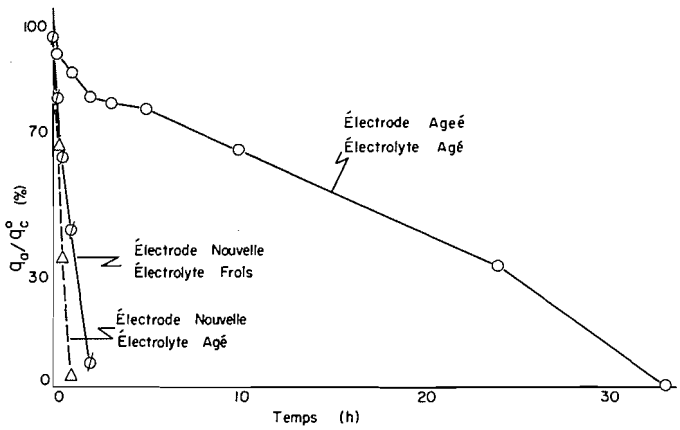

FIG. 10. Rétention de charge du "P(Na)" déposé cathodiquement et contrôlé par son état solide à la surface de l'électrode.

même après 24 h. Tandis que la variation dans le rendement du dépôt électrolytique peut être interprétée comme étant due à la semiconductivité ou à l'action de navette dans l'électrolyte; la rétention de charge est d'abord une propriété de l'électrode et non de l'électrolyte. Basée sur les travaux analytiques réalisés sur des dépôts cathodiques sur le Pt et le Ni, la variation de conductivité électronique et de stabilité peut être due au fait que la composition du dépôt cathodique varie avec la densité du courant et la charge totale traversée, étant donné que c'est probablement un composé hétérogène. D'une part, si le Pt et le Ni métallique sont à découvert et peuvent injecter des électrons dans le sel fondu, le P_2O_5 peut être réduit; donc l'opération de navette sera possible et la rétention de charge sera faible. D'autre part, si le semiconducteur P ou Na_3P sépare le métal de l'électrolyte, la navette peut être inopérante; donc le Pt(Na) ou le P(Na) ne sera pas facilement attaqué par le sel fondu. Il faut noter le fait que les fortes densités de courant favorisent des phosphures avec une forte teneur en phosphore et il en résulte une haute efficacité de courant. Il semble que la pellicule cathodique exercerait un grand nombre de contrôles subtils sur le procédé de ce système électrochimique. Il est intéressant que ce comportement est semblable à celui de l'électrode à oxyde de vanadium (23) dont la composition contrôle le processus d'injection anodique qui se produit sur sa surface catalytique. Il faut bien noter que le comportement cathodique des électrons de Pt dans le sel fondu seché est tout a fait différent de celui rapporté par les autres chercheurs (2) qui ont utilisés les électrodes de charbon et de tungstène. A 650 °C même un petit peu d'eau rendra les cathodes très actives.

Nous tenons à remercier sincèrement MM. L. G. Wilson (diffraction des rayons-X) et C. L Gardner (r.m.n.-P), de ces laboratoires, pour leur contribution scientifique. Nos remerciements aussi à MM. K. N. Campney et L. Ricard qui ont effectué quelques essais préliminaires d'électrolyse dans notre laboratoire; à M. J. F. Rowland et ses collègues du Ministère des Energie, Mines et Ressources qui ont fait les analyses spectroscopiques et au microsonde; à M. P. Lenfant et ses collègues de l'Institut de recherches de l'Hydro-Québec, qui nous ont envoyé beaucoup de commentaires utiles pendant la préparation du rapport; et enfin à Mlle Louise Nadon de l'Université de Montréal et adjointe aux recherches ici durant l'été 1970, et Mme F. Holmes de ce laboratoire, pour l'assistance technique et l'encouragement linguistique.

Les renseignements reçus de M. S. Rundqvist, Université d'Uppsala, nous ont facilité l'identification des produits de nickel.

1. D. E. COUCH. Hard phosphide coatings on nickel. U.S. Pat. 3,236,752, Fév. 26, 1966.
2. (*a*) B. A. GRÜBER. Préparation électrolytique de phosphore très pur. U.S. Pat. 2,965,552, Déc. 20, 1960. (*b*) E. FRANKS et D. INMAN. J. Electroanal. Chem. **26**, 13 (1970).
3. A. B. BEKTUROV. Tr. Inst. Khim. Nauk. Akad. Nauk. Kaz. SSR, **10**, 94 (1964).
4. M. CHÊNE. Ann. de Chim. **15**, 187 (1941).
5. J. R. VAN WAZER. Phosphorus and its compounds. Vol. 1, Interscience Publishers, New York. 1958.
6. YU. K. DELIMARSKII, V. N. ANDREEVA, and G. D. NAZARENKO. Propriétés thermodynamiques d'oxydes dissous dans du métaphosphate de sodium fondu

Can. J. Chem. Downloaded from www.nrcresearchpress.com by 210.87.254.40 on 09/05/12
For personal use only.

et du borax. Proc. All-Union Conf on Phys. Chem. of Molten Salts & Slags, Nov. 1960, p. 559.
7. S. SENDEROFF. Comm. privée.
8. (*a*) G. J. JANZ et G. R. LAKSHMINARAYANAN. Molten salts. Vol. 2. NSRDS-NBS 28, US Govt. Printing Office, Wash., D.C., 20402, 1969; aussi J. HLAKIK et G. MORAND. Electrochimie des sels fondus. Masson & Cie Eds, Paris. 1969. (*b*) B. R. HUBBLE et J. L. COPELAND. J. Chem. Eng. Data, **15**, 441 (1970).
9. V. N. ANDREEVA. Ukranian J. Chem. **21**, 569 (1955).
10. Munsell Book of Color, Munsell Color Corp., Baltimore, Md., 1942.
11. J. R. VAN WAZER. J. Am. Chem. Soc. **78**, 5709 (1956).
12. W. P. GRIFFITH and K. J. RUTT. J. Chem. Soc. A, 2332 (1968).
13. G. K. JØRGENSEN. *In* Werner Centennial. Amer. Chem. Soc., Washington, D.C. 1967 p. 169.
14. M. EBERT and A. HOWARD. Current topics in radiation research. Vol. III. North-Holland Publ. Co., Amsterdam. 1967. p. 67.
15. S. MROZOWSKI and C. SANTARAM. J. Opt. Soc. Am. **56**, 1174 (1966).
16. S. RUNDQVIST and E. LARSSON. Acta Chem. Scand. **13**, 551 (1959); S. RUNDQVIST. Diagramme poudre de $Ni_{12}P_5$ et d'autres phosphures. Comm. privée, 1968.
17. The use and maintenance of platinum laboratory apparatus, Platinum and platinum products. Johnson Matthey and Mallory Ltd. JAT 504, Feb., 1957.
18. L. MANDLECORN (*Editor*). Non-stoichiometric compounds. Academic Press, New York. 1964.
19. A. J. ARVÍA *et al.* Electrochim. Acta, **11**, 1173 (1966); **15**, 124 (1970).
20. W. E. TRIACA and A. J. ARVÍA. Electrochim. Acta, **10**, 419 (1965).
21. B. W. BURROWS and G. J. HILLS. Electrochim. Acta, **15**, 456 (1970); aussi H. FLOOD et T. FORLAND. Discuss. Faraday Soc. **1**, 302 (1947), par exemple.
22. W. JOST. Diffusion in solids, liquids, and gases. Academic Press, New York. 1952.
23. W. P. GOMES. Surface Sci. **19**, 181 (1970); T. FREUND. J. Phys. Chem. **73**, 468 (1969).
24. A. BRESTER. Arch. Neerl, **1**, 296 (1866).
25. N. KONSTANTINOW. Z. Anorg. Chem. **60**, 405 (1909).
26. S. RUNDQVIST *et al.* Acta Chem. Scand. **16**, 242 (1962); **16**, 922 (1962); **13**, 551 (1959).
27 E. LARSSON. Arkiv. Kemi, **23**, 335 (1965).
28. M. ELFSTROM. Acta Chem. Scand. **19**, 1694 (1965).
29. L. D. CALVERT *et al.* Can. J. Chem. **42**, 1511 (1964).
30. J. R. VAN WAZER. Phosphorus and its compounds. Interscience, London. 1958. p. 169.
31. W. BILTZ et M. HEIMBRECHT. Anorg. Chem. **237**, 132 (1938).
32. S. RUNDQVIST. Comm. privée.
33. S. E. SARVER. Trans. Brit. Cer. Soc. **65**, 198 (1966).

Can. J. Chem. Downloaded from www.nrcresearchpress.com by 210.87.254.40 on 09/05/12
For personal use only.

Can. J. Chem. Downloaded from www.nrcresearchpress.com by 210.87.254.40 on 09/05/12
For personal use only.

NOTES

Protonated Cyclopropanes. VI.[1] Solvolyses of 1-^{14}C-1-Propylmercuric Perchlorate

C. C. Lee and Joyce Law

Department of Chemistry and Chemical Engineering, University of Saskatchewan, Saskatoon, Saskatchewan

Received April 26, 1971

The solvolysis of 1-^{14}C-1-propylmercuric perchlorate in 10% dioxane – 90% H_2O, HOAc, or HCOOH gave, respectively, about 0.6, 2.5, or 3.5% isotopic scramblings, the rearranged ^{14}C-label being distributed approximately equally over C-2 and -3. The results are considered in relation to protonated cyclopropanes as possible intermediates.

La solvolyse du perchlorate de ^{14}C-1 propyl-1 mercure dans des mélanges 10% dioxane – 90% H_2O, ACOH, ou HCOOH a donné respectivement environ 0.6, 2.5, et 3.5% d'échanges isotopiques. Le ^{14}C-marqué se distribue à peu près également sur les carbones en position 2 et 3. Les résultats sont interprétés en fonction de cyclopropanes protonés comme intermédiaires possibles.

Canadian Journal of Chemistry, 49, 2746 (1971)

In recent years, there has been considerable interest in protonated cyclopropanes as reaction intermediates and isotopic scrambling studies have provided some of the definitive experimental data in support of such intermediates (1). As an extension of our recent work on isotopic scramblings in the 1-propyl system (2, 3), solvolytic studies on 1-^{14}C-1-propylmercuric perchlorate (**1**-$HgClO_4$-1-^{14}C) have been carried out. The acetolysis of 1-^{14}C-1-propyl tosylate (**1**-OTs-1-^{14}C) gave no isotopic scrambling (4), while the formolysis of **1**-OTs-1-^{14}C at reflux temperature was found to give a product with 0.83% of the label rearranged from C-1 to -2 and -3 (4). However, this latter small amount of isotope position rearrangement was not observed by Karabatsos and coworkers (5) in the formolysis at 75° of deuterium-labeled **1**-OTs-1,1-d_2 and **1**-OTs-2,2-d_2. Since the solvolytic demercuration of an alkylmercuric perchlorate generates an alkyl cation with neutral mercury as the leaving group (6, 7), the resulting cation may be destabilized, a so-called "hot" carbonium ion, as the leaving group is incapable of forming a stable ion-pair with the cation. It would, therefore, be of interest to study the solvolysis of **1**-$HgClO_4$-1-^{14}C and compare the isotopic scrambling data with previous results such as those from the solvolysis of **1**-OTs-1-^{14}C.

1-$HgClO_4$-1-^{14}C, derived from equimolar quantities of **1**-HgOAc-1-^{14}C and $HClO_4$, was solvolyzed in 10% dioxane – 90% H_2O (by volume), HOAc, or HCOOH. Both 1-propyl and 2-propyl alcohols, acetates, or formates were obtained. The yields and product distributions as determined in preliminary trials with ordinary **1**-$HgClO_4$ are given in Table 1.

In the experiments with **1**-$HgClO_4$-1-^{14}C, the acetate and formate products were hydrolyzed to the alcohols and these as well as the mixture of 1-propanol and 2-propanol from the solvolysis in aqueous dioxane were separated by preparative v.p.c. The samples of **1**-OH-x-^{14}C so obtained were degraded to give the isotopic distribution in the 1-propyl group by conversion to propionic acid, to acetic acid, and then to methylamine as previously described (8). The results are summarized in Table 2.

The formation of both 1-propyl and 2-propyl products (Table 1), the latter resulting from a 1,2-hydride shift in the 1-propyl cation, and the finding that the major part of the 1-propyl product is isotopically unrearranged with the ^{14}C-label remaining at C-1 (Table 2) suggest that in the solvolyses of **1**-$HgClO_4$ under the present conditions, the reaction pathways may be concurrent direct displacement and cationic processes. Such concurrent processes would be analogous to the recent conclusions of Schleyer and coworkers (9–11) that solvolyses of β-arylalkyl systems involve separate and discrete solvent-assisted and aryl-assisted pathways. The

[1]For paper V, see ref. 3.

TABLE 1. Yields and distributions of 1-propyl and 2-propyl products from solvolyses of 1-propylmercuric perchlorate

Solvent	Yield (%)	Product distribution (%)* 1-Propyl	2-Propyl
10% Dioxane–90% H_2O	30	92	8
10% Dioxane–90% H_2O containing 10% NaOH	14	100	Trace
HOAc	70	82	18
HCOOH	70	80	20

*Determined by v.p.c.

TABLE 2. Activity distributions in the x-^{14}C-1-propanol derived from solvolyses of 1-^{14}C-1-propylmercuric perchlorate (**1**-$HgClO_4$-1-^{14}C)

Solvent	Run	Specific activity (c.p.m./mmol)* $CH_3CH_2CH_2OH$†	CH_3COOH‡	CH_3NH_2§	^{14}C-Distribution (%) C-1	C-2	C-3
10% Dioxane – 90% H_2O‖	1	94 000	544	260	99.4	0.3	0.3
	2	107 000	600	290	99.4	0.3	0.3
	3	114 000	660	310	99.4	0.3	0.3
HOAc	1	114 000	2800	1300	97.5	1.4	1.1
	2	134 500	3100	1500	97.7	1.2	1.1
	3	113 000	2700	1250	97.6	1.3	1.1
HCOOH	1	98 000	3150	1500	96.8	1.6	1.6
	2	72 600	2700	1100	96.3	2.1	1.6
	3	126 600	4200	1960	96.7	1.8	1.5

*Measured by a liquid scintillation counter and corrected for quenching. Statistical errors were within ± 1% of the observed activities.
†Assayed as the α-naphthylurethane.
‡Assayed as the *p*-nitrobenzyl ester.
§Assayed as the *p*-toluenesulfonamide.
‖A similar solvolysis with the solvent containing 10% NaOH gave a product with essentially no scrambling (less than 0.1%) of the ^{14}C from C-1 to -2 and -3.

isotopic scrambling from C-1 to C-2 and -3 as summarized in Table 2 may be interpreted as resulting from some involvement of protonated cyclopropane as part of the ionic processes. The extent of such scrambling is lowest in the product from solvolysis in aqueous dioxane, and this may be attributed to a predominant direct displacement in this nucleophilic solvent system. It may also be of interest to note that the amounts of scrambling in the 1-propyl products from acetolysis and formolysis of **1**-$HgClO_4$-1-^{14}C are greater than the analogous data from acetolysis and formolysis of **1**-OTs-1-^{14}C (4), but are roughly of the same order of magnitude as observed in the deamination of **1**-NH_2-1-^{14}C (8, 12), the deamination being another reaction involving a "hot" carbonium ion.

Isotopic scramblings in the 1-propyl group have generally been discussed in terms of equilibrating corner-protonated (**2**) or edge-protonated (**3**) cyclopropanes. Collins (13) has predicted that in reactions with a 1-propyl

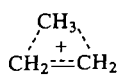

2

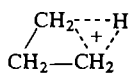

3

substrate labeled at C-1 with isotopic carbon, if products were formed before equilibrium has been established, for processes involving equilibrating corner-protonated cyclopropanes, isotope position rearrangement from C-1 to -3 can never be greater than from C-1 to -2, while for processes involving equilibrating edge-protonated cyclopropanes, rearrangement of the label from C-1 to -3 can be greater than from C-1 to -2. Recent attempts in this laboratory (2, 3) to obtain evidence for edge-protonation in accordance with this prediction have failed. The present finding of approximately equal amounts of rearrangement of the ^{14}C-label from C-1 to -2 and to -3 again failed to provide a differentiation between corner- and edge-protonation. Since the carbonium ion generated from solvolytic demercuration may be "hot" or of high energy,

Can. J. Chem. Downloaded from www.nrcresearchpress.com by 210.87.254.40 on 09/05/12
For personal use only.

Can. J. Chem. Downloaded from www.nrcresearchpress.com by 210.87.254.40 on 09/05/12
For personal use only.

that small portion of the reaction which may have proceeded via equilibrating protonated cyclopropanes likely would have been completely equilibrated before product formation, resulting in equal amounts of scrambling of the label from C-1 to -2 and to -3.

In connection with the representation of the structure of protonated cyclopropane as corner- or edge-protonated **2** or **3**, it may be of interest to point out that very recently, *ab initio* calculations on the structures and relative stabilities of $C_3H_7^+$ cations with complete geometry optimization have been carried out by Radom *et al.* (ref. 14 and private communications from L. Radom). The results suggested that besides the stable 2-propyl cation, a "methyl eclipsed 1-propyl cation" with distorted geometry, which could be regarded as a "distorted corner-protonated cyclopropane", may well correspond to the only other potential minimum in the complete $C_3H_7^+$ surface. These conclusions are in sharp contrast to earlier interpretations of experimental data in terms of corner- and edge-protonated cyclopropanes **2** and **3**, neither of which was found by Radom and coworkers to correspond to an energy minimum. However, these calculated energies apply only to ions in the gas phase and solvation may alter the picture. Professor Schleyer (P. v. R. Schleyer, private communications) has also used the term "partially-bridged" structure in describing the methyl eclipsed 1-propyl cation. These calculations do suggest the possibility that isotopic scramblings such as those observed in the present work could have resulted from equilibrating partially-bridged structures with **2** and **3** as transition states.

Experimental

1-^{14}C-1-Propylmercuric Acetate (1-HgOAc-1-^{14}C)

The preparation of **1**-HgOAc-1-^{14}C was carried out using the general method described by Ouellette (15), involving the conversion of 1-^{14}C-1-chloropropane (**1**-Cl-1-^{14}C) (3) to the Grignard reagent, treatment with $HgCl_2$ to give **1**-HgCl-1-^{14}C, m.p. 140–141° (lit. (16), m.p. 140°), and reaction of the latter with AgOAc to give **1**-HgOAc-1-^{14}C, m.p. 55–56° (lit. (15), m.p. 55.4–56.2°).

Solvolysis Reactions

The solvents employed were 10% dioxane – 90% H_2O (by volume), redistilled, reagent grade glacial acetic acid, and redistilled, reagent grade, 98–100% formic acid. A solution of 8.0 g (0.026 mol) of **1**-HgOAc-1-^{14}C and 2.5 ml (0.027 mol) of 70% $HClO_4$ in 50 ml of solvent was heated under reflux for 8 h. The resulting material was then cooled in an ice–salt bath and neutralized with 25% NaOH solution. In the case of acetolysis of formolysis, more NaOH was added to give a final concentration of about 10% and the alkaline mixture was refluxed for 2 h to hydrolyze the ester products. The 1-propanol and 2-propanol obtained were recovered by continuous ether extraction and purified by preparative v.p.c. using a Carbowax column as previously described by Lee and Kruger (8). The degradation of the 1-propanol to give the ^{14}C-distribution in the 1-propyl group was also effected as described by Lee and Kruger (8).

The financial support given by the National Research Council of Canada and the valuable discussions on the structure of the protonated cyclopropane given by Professor P. v. R. Schleyer are gratefully acknowledged.

1. C. C. Lee. Prog. Phys. Org. Chem. **7**, 129 (1970).
2. C. C. Lee and W. K.-Y. Chwang. Can. J. Chem. **48**, 1025 (1970).
3. C. C. Lee and D. J. Woodcock. J. Am. Chem. Soc. **92**, 5992 (1970).
4. C. C. Lee and J. E. Kruger. Can. J. Chem. **44**, 2343 (1966).
5. G. J. Karabatsos, J. L. Fry, and S. Meyerson. J. Am. Chem. Soc. **92**, 614 (1970).
6. F. R. Jensen and R. J. Ouellette. J. Am. Chem. Soc. **83**, 4477 (1961).
7. F. R. Jensen and R. J. Ouellette. J. Am. Chem. Soc. **83**, 4478 (1961).
8. C. C. Lee and J. E. Kruger. Tetrahedron, **23**, 2539 (1967).
9. P. v. R. Schleyer and C. J. Lancelot. J. Am. Chem. Soc. **91**, 4297 (1969).
10. J. M. Harris, F. L. Schadt, P. v. R. Schleyer, and C. J. Lancelot. J. Am. Chem. Soc. **91**, 7508 (1969).
11. H. C. Brown, C. J. Kim, C. J. Lancelot, and P. v. R. Schleyer. J. Am. Chem. Soc. **92**, 5244 (1970).
12. C. C. Lee and K.-M. Wan. J. Am. Chem. Soc. **91**, 6416 (1969).
13. C. J. Collins. Chem. Rev. **69**, 543 (1969).
14. L. Radom, J. A. Pople, V. Buss, and P. v. R. Schleyer. J. Am. Chem. Soc. **93**, 1813 (1971).
15. R. J. Ouellette. Ph.D. Thesis. University of California, Berkeley, California, 1962.
16. C. S. Marvel, C. G. Gauerke, and E. L. Hill. J. Am. Chem. Soc. **47**, 3009 (1925).

Reaction of Bis(trifluoromethyl)diazomethane with Bis(trimethylsilyl)acetylene

W. R. CULLEN AND F. L. HOU
Chemistry Department, University of British Columbia, Vancouver 8, British Columbia

Received April 29, 1971

The reaction of bis(trifluoromethyl)diazomethane with bis(trimethylsilyl)acetylene yields 1,2-bis-(trimethylsilyl)-3,3-bis(trifluoromethyl)cyclopropene in low yield. The cyclopropene has an unexpectedly high C=C stretching frequency.

La réaction du bis(trifluorométhyl) diazométhane avec le bis(triméthylsilyl) acétylène conduit au bis(triméthylsilyl)-1,2 bis(trifluorométhyl)-3,3 cyclopropène avec un faible rendement. Le cyclopropène a une fréquence d'élongation C=C anormalement élevée.

Canadian Journal of Chemistry, 49, 2749 (1971)

Although a number of cyclopropenes have been prepared containing a single sigma-bonded metal or metalloid substituent (1–3), no examples were known where two or more of the substituents on the cyclopropene were of this nature. We wish to report that the reaction of bis(trifluoromethyl)diazomethane with bis(trimethylsilyl)acetylene under the influence of u.v. irradiation produces 1,2-bis(trimethylsilyl)-3,3-bis(trifluoromethyl)cyclopropene in low (6%) yield.

[1] $(CF_3)_2CN_2 + (CH_3)_3SiC{\equiv}CSi(CH_3)_3 \xrightarrow{h\nu}$

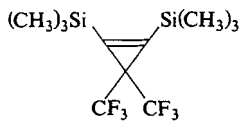

The same method has been used to prepare 3,3-bis(trifluoromethyl)cyclopropenes from the acetylenes $CF_3C{\equiv}CR$ (R = H, CF_3, $(CH_3)_3Sn$, $(CH_3)_3Ge$) (2). The "organic" acetylenes give mainly isopyrazoles by 1,3-dipolar addition together with some cyclopropenes. The former yield cyclopropenes by nitrogen elimination on heating. No evidence for an intermediate isopyrazole was obtained from the reaction of eq. 1 although we recognize that here also the isopyrazole could have been the source of the cyclopropene.

The structure of the product follows from its singlet ^1H and ^{19}F n.m.r. spectra, which have the expected chemical shift values, and the strong "double-bond" stretching frequency (4) in the i.r. spectrum at 1946 or 1928 cm^{-1}. This frequency is one of the highest recorded for a cyclopropene and is unexpected in view of the previously observed trend that electropositive groups in the vinylic position lower the frequency (2).

Experimental

All volatile reagents and products were manipulated in a standard vacuum system. The i.r. spectra were recorded on a Perkin–Elmer 457 spectrophotometer. The n.m.r. spectra were recorded using a Varian T60 instrument. Microanalyses were performed by Mr. Peter Borda of this Department.

Bis(trimethylsilyl)acetylene (0.85 g, 5.0 mmol) (5) and bis(trifluoromethyl)diazomethane (1.0 g, 5.6 mmol) (6) were sealed in a Pyrex tube and irradiated with a 200 W u.v. lamp at a distance of 10 cm for 6 days. The less volatile contents of the tube which condensed in a trap at −78°, were separated by v.p.c. (20% SF-96 at 140°) into 11 components. Only the seventh and eleventh fractions could be collected and identified. The former proved to be unreacted acetylene (0.40 g) and the latter the cyclopropene (0.091 g, 5.7% yield).

Anal. Calcd. for $C_{11}H_{18}Si_2F_6$: C, 41.2; H, 5.62; F, 35.6. Found: C, 41.3; H, 5.73; F, 35.3.

The ^1H n.m.r. spectrum (CCl_4 solution) consisted of a singlet at 0.29 p.p.m. downfield from internal TMS. The same solution gave a ^{19}F spectrum consisting of a singlet at 57.5 p.p.m. upfield from external $CFCl_3$. The i.r. spectrum showed the following absorptions (liquid film): 2975(m), 2905(w), 1946(s), 1928(s), 1396(s), 1332(s), 1300(m), 1258(s), 1160(s,br.), 1020(w), 970(s), 860(s,br.), 822(m,sh.), 768(m), 712(s), 700(m,sh.), 688(m,sh.), 650(w), 620(m) cm^{-1}.

We thank the National Research Council of Canada for financial support.

1. W. R. CULLEN. Fluorine Chem. Rev. **3**, 73 (1969).
2. W. R. CULLEN and M. C. WALDMAN. Can. J. Chem. **48**, 1885 (1970).
3. W. R. CULLEN and M. C. WALDMAN. J. Fluorine Chem. In press.
4. G. L. GLOSS. Adv. Alicyclic Chem. **1**, 53 (1963).
5. R. WEST and L. C. QUASS. J. Organomet. Chem. **18**, 55 (1969).
6. D. M. GALE, W. J. MIDDLETON, and C. G. KRESPAN. J. Am. Chem. Soc. **88**, 3617 (1966).

Can. J. Chem. Downloaded from www.nrcresearchpress.com by 210.87.254.42 on 09/05/12
For personal use only.

Preparation of 7-Ethyl-2-naphthoic Acid[1]

D. K. R. STEWART
Research Station, Canada Department of Agriculture, Kentville, Nova Scotia

Received January 28, 1971

7-Ethyl-2-naphthoic acid was synthesized by cyclization of the formylation product of ethyl-4-(4′-ethylphenyl)-butyrate and dehydrogenation of the resulting 7-ethyl-3,4-dihydronaphthoic acid.

L'acide éthyl-7 naphthoïque-2 a été synthétisé par cyclisation du produit de formylation de l'ester éthylique de l'acide (éthyl-4′ phényl)-4 butanoïque et par déshydrogénation de l'acide éthyl-7 dihydro-3,4 naphthoïque résultant.

Canadian Journal of Chemistry, **49**, 2750 (1971)

Can. J. Chem. Downloaded from www.nrcresearchpress.com by 210.87.254.6 on 09/05/12
For personal use only.

Some time ago while the author was engaged in the synthesis of 1-methyl-6-ethyl-3-azaphenanthrene, a key degradation product of atisine, Locke and Pelletier (1) published a preliminary account of their work. Their synthesis (2) proceeded from 7-ethyl-1-tetralone via a mixture of isomers of 2-(7′-ethyl-1′-oxo-1′,2′,3′,4′-tetrahydro-2′-naphthyl)-propionic acid to α-methyl-7-ethyl-2-naphthaleneacetic acid (**1**), Pictet–Spengler cyclization of the corresponding amine and dehydrogenation to the azaphenanthrene.

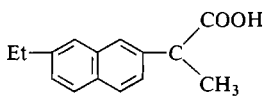

1

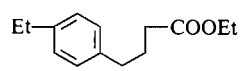

2

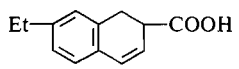

3

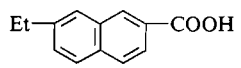

4

Our route proceeded from ethyl-4-(4′-ethylphenyl)-butyrate (**2**) via 7-ethyl-3,4-dihydronaphthoic acid (**3**) and 7-ethyl-2-naphthoic acid (**4**) to **1** and followed the same course thereafter. Since the acids **3** and **4** have not yet been described and may be of some value in the chemistry of natural products, their preparation is reported here.

In a series of reactions similar to that employed by Holmes and Trevoy (3) for the preparation of 7-methoxy-2-naphthoic acid, ethyl-4-(4′-ethylphenyl)-butyrate (**2**) was formylated with isoamyl formate/sodium ethoxide and the product cyclized with H_3PO_4/H_2SO_4 to yield a mixture of esters of **3**. Dehydrogenation of **3** with sulfur yielded **4** which was converted via Wolff rearrangement of the ethyldiazoketone to the known acid **1**. This route thus provides an alternate pathway to the azaphenanthrene.

[1]Contribution No. 1407.

Experimental

7-Ethyl-3,4-dihydro-2-naphthoic Acid (3)

Isoamyl formate (40.7 g) in ether (150 ml) was added to a cold ethereal suspension of alcohol-free sodium ethoxide prepared from sodium (6.8 g). A solution of ethyl-4-(4′-ethylphenyl)-butyrate (4) (65.5 g) in ether (100 ml) was then added with stirring and cooling. The reaction mixture was kept at 0 °C for 2 h and room temperature for 4 days. The deep red solution was then stirred into 500 g of ice and water. The unreacted starting material was recovered by separating the ether layer and extracting the aqueous layer twice with ether. The aqueous solution of the sodium enolate of ethyl-2-formyl-4-(4′-ethylphenyl)-butyrate was acidified and the oily formyl derivative was extracted with ether. The ether solution was washed with water and bicarbonate solution, then dried over sodium sulfate and the isoamyl formate removed under water aspirator vacuum. The heat sensitive formylation product (43.4 g) was added dropwise to a vigorously stirred mixture of orthophosphoric acid, sp. gr. 1.75 (170 ml), and sulfuric acid, sp. gr. 1.83 (36 ml), cooled to −10°. The mixture was stirred for 2 h, poured into ice water, and extracted with ether. The extract was washed with water and bicarbonate solution, then dried over sodium sulfate. A mixture of the ethyl and isoamyl esters of 7-ethyl-3,4-dihydro-2-naphthoic acid (29.5 g) was obtained. Saponification with NaOH in ethanol and crystallization from benzene yielded 15.0 g acid **3**, m.p. 133–134°; λ_{max} (EtOH) 234 (ε 23 300), 280 mμ (ε 17 200).

Anal. Calcd. for $C_{13}H_{14}O_2$: C, 77.20; H, 6.98. Found: C, 77.38; H, 7.12.

7-Ethyl-2-naphthoic Acid (4)

Acid **3** (4.00 g) was mixed with powdered sulfur (0.64 g) in a round-bottom flask and heated in a wax bath at 240°. H_2S was freely evolved for 15 min and heating was continued for an additional 30 min. The melt was cooled, dissolved in aqueous NaOH, and extracted with chloroform. The basic solution was then acidified and the acid **4** extracted with ether. The methyl ester was formed by

refluxing for 4 h with methanol (100 ml) and H_2SO_4 (4 ml). The crude ester was purified by vacuum distillation (120°/0.5 mm) yielding 3.02 g methyl ester which was crystallized from methanol, m.p. 46–47°. The free acid **4** was obtained by saponification and crystallized from acetone, m.p. 174–175°; λ_{max} (EtOH) 236 (ε 54 200), 280 (ε 6740), 338 mμ (ε 1380).

Anal. Calcd. for $C_{13}H_{12}O_2$: C, 77.98; H, 6.04. Found: C, 77.84; H, 5.95.

Acid **4** was converted, via Wolff rearrangement of the ethyldiazoketone prepared from the acid chloride and diazoethane, to the known α-methyl-7-ethyl-2-naphthaleneacetic acid (**1**), m.p. 109–110° (2).

Anal. Calcd. for $C_{15}H_{16}O_2$: C, 78.92; H, 7.06. Found: C, 79.11; H, 6.87.

Grateful acknowledgment is made to the National Research Council of Canada for a Postdoctorate Fellowship (1955–1956), to Dr. O. E. Edwards for his interest in this work, and to Mr. H. Seguin for the analyses.

1. D. M. Locke and S. W. Pelletier. J. Am. Chem. Soc. **80**, 2588 (1958).
2. D. M. Locke and S. W. Pelletier. J. Am. Chem. Soc. **81**, 2246 (1959).
3. H. L. Holmes and L. W. Trevoy. Can. J. Res. **22B**, 56 (1944).
4. F. G. Badder and F. L. Warren. J. Chem. Soc. 944 (1939).

Structure of the Second Coordination Sphere of Transition Metal Complexes. III. Ion Pairing involving Cobalt Complexes

D. R. Eaton and Linda Seville
Department of Chemistry, McMaster University, Hamilton, Ontario

AND

J. P. Jesson
Central Research Department, E. I. Du Pont de Nemours and Co., Wilmington, Delaware

Received March 16, 1971

The structure of the ion pair formed between Co(II) bistripyrazolylmethane ions and PF_6^- ions in acetonitrile solution has been investigated. Isotropic shifts observed in the ^{19}F nuclear magnetic resonance (n.m.r.) spectra of the anion have been used for this purpose. It is concluded that the preferred position of the anion lies close to the symmetry axis of the cobalt complex and that a contact ion pair is involved. This result is contrasted with previous studies of second sphere coordination involving neutral molecules.

On examine la structure de la paire d'ion formée dans une solution d'acétonitrile entre les ions Co(II) bistripyrazolylméthane et PF_6^-. On utilise à cet effet le déplacement isotrope observé dans le spectre r.m.n. de ^{19}F de l'anion. Il en a été déduit que la position préférentielle de l'anion est celle qui se trouve proche de l'axe de symétrie du complexe avec le cobalt; de plus une paire d'ion de contact est impliquée. Ce résultat est en désacord avec des études précédentes ou des molécules neutres étaient impliquées dans une deuxième sphère de coordination.

Canadian Journal of Chemistry, **49**, 2751 (1971)

In previous papers (1, 2) in this series we have discussed the role of neutral molecules in the second coordination sphere of Co(II) complexes. Evidence for a "double layer" structure in which the dipoles of the second sphere ligands were oriented in the opposite sense to those of the first sphere ligands was brought forward. The main thrust of our interest in this area is towards an understanding of the detailed mechanisms of the ligand exchange reactions involved in homogeneous catalysis. Most such reactions occur in non-aqueous solvents and in the absence of ionic species. Nevertheless it is of interest to ask how ionic second sphere ligands fit into this picture of second coordination sphere structure and the question may well be one of importance for enzymatically catalyzed reactions in aqueous media. Relatively little (3) is known about the detailed geometry of such ion pairs. In the present note we wish to report data on an ionic system closely related to the cobalt complexes previously studied.

The complexes in question are based on the Co(II) bis(tripyrazolylmethane) (4) ion $Co[HCpz_3]_2^{2+}$. The structure of this ion is shown in

Can. J. Chem. Downloaded from www.nrcresearchpress.com by 210.87.254.6 on 09/05/12
For personal use only.

refluxing for 4 h with methanol (100 ml) and H_2SO_4 (4 ml). The crude ester was purified by vacuum distillation (120°/0.5 mm) yielding 3.02 g methyl ester which was crystallized from methanol, m.p. 46–47°. The free acid **4** was obtained by saponification and crystallized from acetone, m.p. 174–175°; λ_{max} (EtOH) 236 (ε 54 200), 280 (ε 6740), 338 mμ (ε 1380).

Anal. Calcd. for $C_{13}H_{12}O_2$: C, 77.98; H, 6.04. Found: C, 77.84; H, 5.95.

Acid **4** was converted, via Wolff rearrangement of the ethyldiazoketone prepared from the acid chloride and diazoethane, to the known α-methyl-7-ethyl-2-naphthaleneacetic acid (**1**), m.p. 109–110° (2).

Anal. Calcd. for $C_{15}H_{16}O_2$: C, 78.92; H, 7.06. Found: C, 79.11; H, 6.87.

Grateful acknowledgment is made to the National Research Council of Canada for a Postdoctorate Fellowship (1955–1956), to Dr. O. E. Edwards for his interest in this work, and to Mr. H. Seguin for the analyses.

1. D. M. Locke and S. W. Pelletier. J. Am. Chem. Soc. **80**, 2588 (1958).
2. D. M. Locke and S. W. Pelletier. J. Am. Chem. Soc. **81**, 2246 (1959).
3. H. L. Holmes and L. W. Trevoy. Can. J. Res. **22B**, 56 (1944).
4. F. G. Badder and F. L. Warren. J. Chem. Soc. 944 (1939).

Structure of the Second Coordination Sphere of Transition Metal Complexes. III. Ion Pairing involving Cobalt Complexes

D. R. Eaton and Linda Seville
Department of Chemistry, McMaster University, Hamilton, Ontario

AND

J. P. Jesson
Central Research Department, E. I. Du Pont de Nemours and Co., Wilmington, Delaware

Received March 16, 1971

The structure of the ion pair formed between Co(II) bistripyrazolylmethane ions and PF_6^- ions in acetonitrile solution has been investigated. Isotropic shifts observed in the ^{19}F nuclear magnetic resonance (n.m.r.) spectra of the anion have been used for this purpose. It is concluded that the preferred position of the anion lies close to the symmetry axis of the cobalt complex and that a contact ion pair is involved. This result is contrasted with previous studies of second sphere coordination involving neutral molecules.

On examine la structure de la paire d'ion formée dans une solution d'acétonitrile entre les ions Co(II) bistripyrazolylméthane et PF_6^-. On utilise à cet effet le déplacement isotrope observé dans le spectre r.m.n. de ^{19}F de l'anion. Il en a été déduit que la position préférentielle de l'anion est celle qui se trouve proche de l'axe de symétrie du complexe avec le cobalt; de plus une paire d'ion de contact est impliquée. Ce résultat est en désacord avec des études précédentes ou des molécules neutres étaient impliquées dans une deuxième sphère de coordination.

Canadian Journal of Chemistry, **49**, 2751 (1971)

In previous papers (1, 2) in this series we have discussed the role of neutral molecules in the second coordination sphere of Co(II) complexes. Evidence for a "double layer" structure in which the dipoles of the second sphere ligands were oriented in the opposite sense to those of the first sphere ligands was brought forward. The main thrust of our interest in this area is towards an understanding of the detailed mechanisms of the ligand exchange reactions involved in homogeneous catalysis. Most such reactions occur in non-aqueous solvents and in the absence of ionic species. Nevertheless it is of interest to ask how ionic second sphere ligands fit into this picture of second coordination sphere structure and the question may well be one of importance for enzymatically catalyzed reactions in aqueous media. Relatively little (3) is known about the detailed geometry of such ion pairs. In the present note we wish to report data on an ionic system closely related to the cobalt complexes previously studied.

The complexes in question are based on the Co(II) bis(tripyrazolylmethane) (4) ion $Co[HCpz_3]_2^{2+}$. The structure of this ion is shown in

Can. J. Chem. Downloaded from www.nrcresearchpress.com by 210.87.254.105 on 09/05/12
For personal use only.

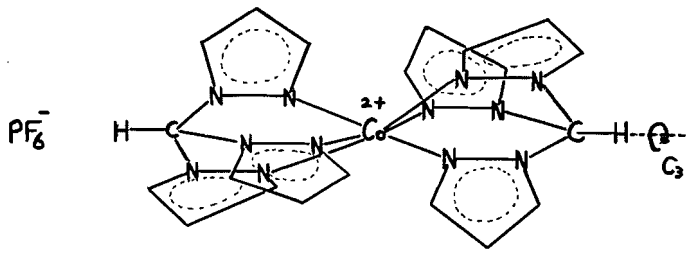

FIG. 1. Structure of the $Co[HCpz_3]_2^{2+}$ ion.

Fig. 1. They are derived from the Co(II) pyrazolyl borates studied previously by replacing the two boron atoms with carbon atoms. The two series of complexes are isoelectronic but the additional nuclear charge of carbon gives rise to a dipositive ion rather than a neutral molecule. Jesson (5) has studied the electron spin resonance (e.s.r.) spectra of these compounds and has shown that they have g values closely similar to the boron analogues. The large anisotropy of the g values makes them particularly suitable for ion pairing studies based on the dipolar interactions (6) between magnetic nuclei of the counter ion and the unpaired electrons located on the cobalt (7). There have been several previous studies of ion-pairing based on dipolar shifts but most have been hampered by a lack of information regarding the directions of the magnetic axes within the molecule and the sign and magnitude of the magnetic anisotropy (8–13).[1]

Dipolar interaction gives rise to shifts in the n.m.r. frequencies of the nuclei in question given by the formula[2]

$$\frac{\Delta\nu}{\nu} = -D\frac{(3\cos^2\theta - 1)}{r^3}(g_{\parallel} - g_{\perp})$$

In principle D and $(g_{\parallel} - g_{\perp})$ are known from Jesson's work and measurement of the dipolar shift $\Delta\nu/\nu$ leads to the geometric factor $(3\cos^2\theta - 1)/r^3$ where r is the distance of the interacting nucleus from the Co atom and θ is the angle between a line joining this nucleus to the Co and the threefold principal axis of the molecule (see Fig. 1). In practice, as will become apparent below, the lability of the ion pairs limits the amount of quantitative information which can be obtained from this type of measurement. Nevertheless it is possible to carry out a qualitative analysis of the data which provides an informative comparison of the role of ions and neutral molecules in the second coordination sphere.

An initial problem is presented by the choice of a counter ion. Six or seven complexes were tried but the solubility of the majority of them, particularly those involving doubly charged anions, was insufficient to allow n.m.r. studies. $Co[HCpz_3]_2(PF_6)_2$ has reasonable solubility in acetonitrile and the fluorine nuclei on the anion provide a suitable probe. One may therefore compare ^{19}F chemical shifts of $Co[HCpz_3]_2(PF_6)_2$ with those of $Zn[HCpz_3]_2(PF_6)_2$. The zinc complex is structurally very similar to the cobalt complex and differs from it significantly only in that it lacks unpaired electrons so that the possibility of dipolar shifts does not arise. In both cases the ^{19}F spectrum shows a doublet of spacing 708 Hz. The doublet splitting arises from coupling with the ^{31}P nucleus. The observation of this simple spectrum shows that the PF_6^- ion is changing its environment sufficiently rapidly to make all the fluorines appear equivalent. The chemical shifts for the zinc complex, relative to Freon 112 internal standard, vary only slightly with concentration (10–20 Hz). Those of the cobalt complex vary substantially. In Table 1 the chemical shifts of the Co complex relative to the Zn complex at different concentrations are given. Several points should be

[1]It has been suggested several times in the literature (14–16) that isotropic shifts in ion pairs may be contact rather than dipolar in nature. This implies that the forces holding together the ions are to some extent covalent. The present case does not seem at all favorable for such an interaction. There is no extensive delocalization of the spin and the closest possible approach of the PF_6^- to the Co ion is 5 or 6 Å at which distance orbital overlap would be negligible. In addition the known large magnetic anisotropy of these complexes forms the basis for a positive prediction of a dipolar shift mechanism. We therefore feel justified in disregarding the possibility that contact interactions may determine the observed shifts.

[2]This formula assumes a threefold or higher axis, which we have in the present case, and also neglects the second order Zeeman term. This latter limitation would be important for quantitative applications.

Can. J. Chem. Downloaded from www.nrcresearchpress.com by 210.87.254.105 on 09/05/12
For personal use only.

Can. J. Chem. Downloaded from www.nrcresearchpress.com by 210.87.254.105 on 09/05/12
For personal use only.

TABLE 1. Concentration and temperature dependence of ^{19}F resonance of $Co[HCpz_3]_2(PF_6)_2$ in acetonitrile

Concentration (M/lt)	Δν* (Hz)	Temperature (°C)	Δν* (Hz)
0.006	− 69	76	−199
0.011	−113	64	−212
0.023	−171	50	−227
0.046	−241	40	−237
0.093	−336	17	−259
0.185	−463	5	−274
		− 5	−285
		−15	−300
		−25	−310
		−35	−318

*Shifts at 56.4 MHz relative to Zn complex.

noted. The PF_6^- resonance in the cobalt compound always occurs to low field of that in the zinc compound with the difference increasing to 400–500 Hz at the highest obtainable concentration of cobalt complex. The difference approaches zero at low concentration of cobalt complex. The most plausible explanation is that in both cases there is ionic dissociation

$$M[HCpz_3]_2(PF_6)_2 \rightleftharpoons M[HCpz_3]_2(PF_6)^+ + PF_6^-$$

$$M[HCpz_3]_2(PF_6)^+ \rightleftharpoons M[HCpz_3]_2^{2+} + PF_6^-$$

At low concentrations the predominant species is PF_6^-. At higher concentrations ion pairing causes a significant dipolar shift for the Co compound.

Two further experiments provide additional evidence for the above equilibria. In the first, chemical shifts were measured for mixtures of the Co and Zn complexes of the same total concentration. In all cases only a single doublet is observed and its position varies linearly with the fraction of cobalt complex. Rapid exchange between the ion pairs is indicated with the fraction complexed to cobalt, which determines the extent of the shift, varying in the manner expected for dissociative equilibria. In Table 1 results showing the temperature dependence of the ^{19}F shifts for the cobalt compound are also given. The increasing shift at low temperatures arises predominantly from the temperature dependence of the magnetic susceptibility of the cobalt complex and confirms that the shifts arise from interaction with the unpaired electrons on the cobalt.

In order to obtain geometric parameters we require the chemical shift of the undissociated cobalt ion-pair. In view of the extensive dissociation demonstrated by the above results and of the existence of two dissociative equilibria this shift is not easy to obtain. Further, a previous discussion has shown (1) that even given such a shift there are inevitable ambiguities in translating the data into concrete geometric parameters when the complexes involved are labile on the n.m.r. time scale. This latter condition holds in the present case. We shall therefore be content with a very approximate treatment which will however serve to illustrate the structural point we wish to make. Zero dissociation of the complex is expected either at infinite concentration or at zero dielectric constant of the solvent. Extrapolation to the latter limit proves to be the more convenient. The cobalt shifts relative to zinc were therefore measured in mixtures of acetonitrile and carbon tetrachloride, to reduce the dielectric constant, and acetonitrile and water, to enhance the dielectric constant. As anticipated the shifts are larger in the low dielectric constant mixtures. Dielectric constants were obtained by measuring the proportions of the solvents by n.m.r. integration of their peaks and assuming proportionality on a volume basis. The dependence of the shift appears to be linear with dielectric constant as is shown in Fig. 2. Extrapolation gives $\Delta\nu_0$ -1375 ± 75 Hz. More realistically we should perhaps say $\Delta\nu_0$ lies between -1000 and -2000 Hz. It is, however, very clearly negative and of this order of magnitude. The former feature shows immediately that $(3\cos^2\theta - 1)$ is positive and hence that the preferred geometry of the ion pair involves approach of the PF_6^- in a direction more nearly parallel to the axis of the cobalt complex (see Fig. 1) than perpendicular to it. This result is exactly opposite to that obtained for neutral second sphere ligands (1, 2). If it is assumed that the preferred approach is along the symmetry axis and if the formula derived by LaMar (8) for the dipolar shift of a freely tumbling counter ion is used, the observed intercept corresponds to a Co–P separation of 8.1 ± 0.1 Å.[3] A model shows that this is very similar to the closest separation in this orientation allowed by the Van der Waals radii of the ions (~8 Å). Again, we do not wish to stress this numerical agreement, which is probab-

[3]A referee has pointed out that there is an error in LaMar's equation. However, the corrected equation changes the calculated separation by less than 1%. At this large separation the shift is insensitive to the exact model chosen for tumbling of the anion and other sources of error are far more important.

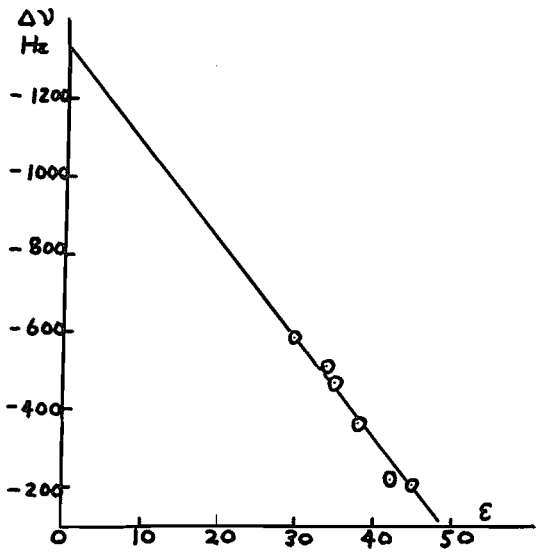

FIG. 2. ^{19}F isotropic shifts of $Co[HCpz_3]_2(PF_6)_2$ as a function of the dielectric constant of the solvent.

ly fortuitous, but do take the result as a clear indication that we are dealing with a contact ion pair, rather than a solvent separated ion pair, with a preferred geometry approximately that shown in Fig. 1.

The significant feature of this result is that the preferred geometry of the ionic second sphere complex is indeed different from that of a neutral second sphere complex. The favored positions, corresponding to closest approach to the central metal atom, may be taken up by dipolar solvent molecules interacting with the negatively charged primary ligands. The counter ion must then be fitted into the resulting structure by taking up the next best position. Bearing in mind that ion–ion interactions fall off less rapidly with distance than ion–dipole or ion-induced dipole interactions this is perhaps not unreasonable from an electrostatic point of view. It is also reminiscent of the much more familiar situation in which solution of a simple salt in water leads to an aquated cation with the anion relegated to the second coordination sphere. It is apparent that the detailed second coordination sphere structure could be changed dramatically by the presence of charge bearing substituents at positions comparatively remote from the central ligand bearing metal atom.

Experimental

^{19}F n.m.r. spectra were obtained at 56.4 Mc/s using a Varian DP instrument. Freon 112 was used as an internal calibrant. There is some dependence of the shifts on the concentration of Freon 112 so that calibrant concentrations were kept as low as possible. Integrated proton spectra of the solvents were obtained on a Varian A60 instrument.

We are indebted to the National Research Council of Canada for financial support of this research and to Dr. S. Trofimenko of the Central Research Dept., E. I. Du Pont Company for kindly donating the complexes.

1. D. R. EATON. Can. J. Chem. **47**, 2645 (1969).
2. D. R. EATON, H. O. OHORODNYK, and L. SEVILLE. Can. J. Chem. **49**, 1218 (1971).
3. P. BECK. Coord. Chem. Rev. **3**, 91 (1968). See also ref. 1 and references therein.
4. W. HÜCKEL and H. BRETSCHNEIDER. Chem. Ber. **70**, 2024 (1937).
5. J. P. JESSON. J. Chem. Phys. **45**, 1049 (1966).
6. H. E. MCCONNELL and R. E. ROBERTSON. J. Chem. Phys. **29**, 1361 (1958).
7. G. N. LAMAR. J. Chem. Phys. **41**, 2992 (1964).
8. G. N. LAMAR. J. Chem. Phys. **43**, 235 (1965).
9. W. D. HORROCKS, R. H. FISCHER, J. R. HUTCHISON, and G. N. LAMAR. J. Am. Chem. Soc. **88**, 2436 (1966).
10. G. N. LAMAR, R. H. FISCHER, and W. D. HORROCKS. Inorg. Chem. **6**, 1798 (1967).
11. R. H. FISCHER and W. D. HORROCKS. Inorg. Chem. **7**, 2659 (1968).
12. I. M. WALKER and R. S. DRAGO. J. Am. Chem. Soc. **90**, 6951 (1968).
13. J. C. FANNING and R. S. DRAGO. J. Am. Chem. Soc. **90**, 3987 (1968).
14. P. K. BURKART, H. P. FRITZ, W. GRETNER, H. J. KELLER, and K. E. SCHWARZHAUS. Inorg. Nucl. Chem. Lett. **4**, 237 (1968).
15. D. G. BROWN and R. S. DRAGO. J. Am. Chem. Soc. **92**, 1871 (1970).
16. H. P. FRITZ, W. C. GRETNER, H. J. KELLER, and K. E. SCHWARZHAUS. Z. Naturforsch. **25B**, 174 (1970).

Can. J. Chem. Downloaded from www.nrcresearchpress.com by 210.87.254.105 on 09/05/12
For personal use only.

Methyl 2,3-*O*-Isopropylidene-β-D-*ribo*-pentodialdofuranoside: a Useful Intermediate in Chain Extension Reactions[1]

ROGER F. BUTTERWORTH[2] AND STEPHEN HANESSIAN
Department of Chemistry, University of Montreal, Montreal, Quebec.

Received March 17, 1971

Oxidation of methyl 2,3-*O*-isopropylidene-β-D-ribofuranoside with the "Pfitzner–Moffatt" reagent (methyl sulfoxide – dicyclohexylcarbodiimide) provides an efficient route to the corresponding 5-aldehydo derivative. Oxidation with methyl sulfoxide – acetic anhydride mixtures affords low yields of the aldehyde, the 5-acetate and 5-*O*-methylthiomethyl ether derivatives being the principal products.

L'oxydation du méthyl 2,3-*O*-isopropylidene-β-D-ribofuranoside avec le réactif de Pftizner et Moffatt (diméthyl sulfoxide – dicyclohexylcarbodiimide) introduit une méthode efficace d'obtention du dérivé 5-aldehydo correspondant. D'autre part, l'oxydation avec le couple diméthyl sulfoxide – anhydride acétique fournit un rendement faible en aldéhyde, les dérivés secondaires 5-*O*-acétyl et l'éther 5-*O*-méthylthiomethyl étant les produits principaux.

Canadian Journal of Chemistry, 49, 2755 (1971)

The discovery and application of mild and efficient oxidants for the conversion in high yield of isolated hydroxyl groups to the corresponding aldehydes or ketones (1) in carbohydrate chemistry, has brought about a renewed interest in the chemistry of carbonyl sugars (2). Uloses and aldehydo sugars are now commonly used as reactive intermediates in the synthesis of deoxy, amino, and branched-chain sugars, frequently found in many antibiotics (3).

In view of the biological importance of derivatives of D-ribofuranose and the ready availability (4, 5) of methyl 2,3-*O*-isopropylidene-β-D-ribofuranoside (**1**), the synthesis of the aldehydo sugar **2** was undertaken. Application of recently developed chain-extension reactions would then offer a useful route to modified derivatives of D-ribofuranose.[3]

Methyl 2,3-*O*-isopropylidene-β-D-ribofuranoside (**1**) is now readily obtainable (4, 5) directly from D-ribose in yields of over 70%. In the present investigation, we note that n.m.r. studies of the product **1**, even prior to purification, reveal the absence of measurable quantities of either ribopyranosides or the α-furanoside.[4]

Treatment of the pure **1** with methyl sulfoxide – dicyclohexylcarbodiimide (6) afforded the crude aldehyde **2** in 76% yield (see Scheme 1). Attempts to purify the product by multiple distillation were unsuccessful, affording low yields of pure product. Chromatographic separation, followed by distillation, afforded the pure aldehyde **2** in 48% yield as a colorless syrup. The n.m.r. spectrum of **2** in CCl_4 (Fig. 1) was consistent with the assigned structure, showing an aldehydo proton singlet at τ 0.3. In D_2O, however, the n.m.r. spectrum showed the presence of the hydrate **3** in solution, the H-5 proton appearing as a doublet at τ 6.0 ($J_{4,5}$ = 7.7 Hz). A crystalline *p*-nitrophenylhydrazone **4** was prepared in the usual manner.

Treatment of **1** with methyl sulfoxide and acetic anhydride (7) gave only low yields of the aldehyde **2**, the two major products being methyl 5-*O*-acetyl-2,3-*O*-isopropylidene-β-D-ribofuranoside (**5**) and the methylthiomethyl ether derivative **6**. Removal of excess reagents by lyophilization (8), followed by de-esterification of the mixture and final chromatographic separation afforded methyl 2,3-*O*-isopropylidene-5-*O*-methylthiomethyl-β-D-ribofuranoside (**6**) as a syrup,

[1]Presented in part at the 161st Meeting of the American Chemical Society, April 1971, Los Angeles, California, CARB 15.

[2]Postdoctoral Fellow, 1969–1971.

[3]The reaction of **1** with various Wittig-type reagents affords the expected chain-extended and branched products in high yields. Results to be reported from this laboratory.

[4]The β anomeric configuration for **1** has previously been assigned on the basis of n.m.r. spectral studies (5).

Can. J. Chem. Downloaded from www.nrcresearchpress.com by 210.87.254.42 on 09/05/12
For personal use only.

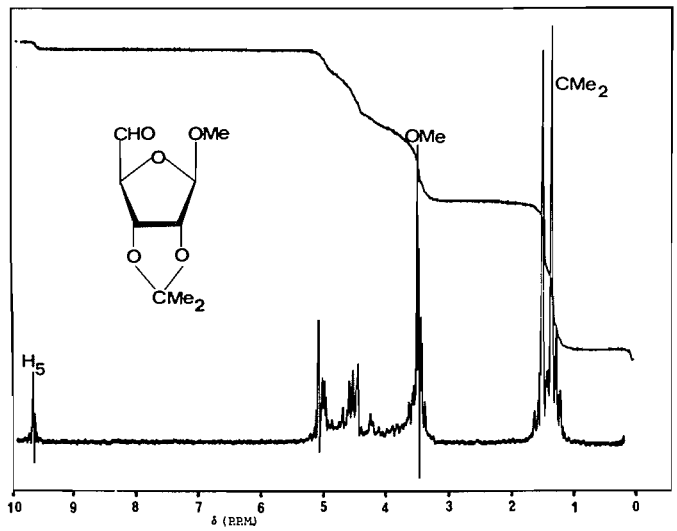

FIG. 1. The 100 MHz n.m.r. spectrum of methyl 2,3-*O*-isopropylidene-β-D-*ribo*-pentodialdofuranoside (**2**) (CCl_4 solution).

which was the major product present in the initial reaction mixture. The structure of **6** was established by n.m.r. spectroscopy and by desulfurization to the 5-*O*-methyl ether derivative **7**. The n.m.r. spectra of compounds **5** and **6** are shown in Fig. 2. Due to the proximity of peaks due to the acetyl and thiomethyl protons, caution should be exercized in assigning structures based on the appearances of such resonances in the n.m.r. spectra of the products of oxidation using DMSO/acetic anhydride.

The relative distribution of acetate and methylthiomethyl ether by-products obtained upon attempted oxidation of isolated hydroxyl groups of carbohydrates using DMSO and acetic anhydride is worthy of comment. From a consideration of published data (1), the extent of thioether formation appears to be dependent upon the nature of the hydroxyl group to be oxidized, as well as its steric and electronic environment. Thus, thioether formation appears to decrease in the order: OH(primary) > OH(secondary equatorial) > OH(secondary axial). In some cases (9), for example, when the secondary alcohol to be oxidized has an azido group on the adjacent carbon atom, the major product of oxidation using DMSO/acetic anhydride has been shown to be corresponding acetate. In the presence of a vicinal phenylthio substituent, the corresponding enol acetate can be formed (10) indicating the possible importance of electronic effects.

Attempts to prepare the aldehyde **2** by treatment of **1** with ruthenium tetroxide (11) met with little success, affording extensive decomposition and very low yields of oxidized product. This result is surprising in view of the report by Berkowitz and Rylander (12) that ruthenium tetroxide converts primary alcohols to the corresponding aldehydes or carboxylic acids. Similarly, attempts to effect a "Kornblum-type" oxidation (13) of the type recently reported (14) from this laboratory, by treatment of the 5-*O*-*p*-tolylsulfonyl ester of **1** with DMSO in the presence of sodium bicarbonate led to partial detosylation with no detectable quantity of aldehyde, even at elevated temperatures.

Experimental

General

Melting points are uncorrected. The i.r. spectra were recorded with a Beckmann IR-8 instrument. The t.l.c. was performed on plates coated with silica gel GF_{250} (Merck) and the spots were detected with a solution of 10% v/v sulfuric acid in ethanol, after the plates were heated at 110°. Sulfur-containing compounds were also detected using a 0.05 *M* sulfuric acid solution containing 1% of potassium permanganate. Column chromatography was performed using silica gel (Baker) 60–200 mesh. The developing system used both for column and t.l.c. was benzene – ethyl acetate, 3.5:1. The n.m.r. spectra were measured with a JEOL-4H-100 100 MHz

Can. J. Chem. Downloaded from www.nrcresearchpress.com by 210.87.254.42 on 09/05/12
For personal use only.

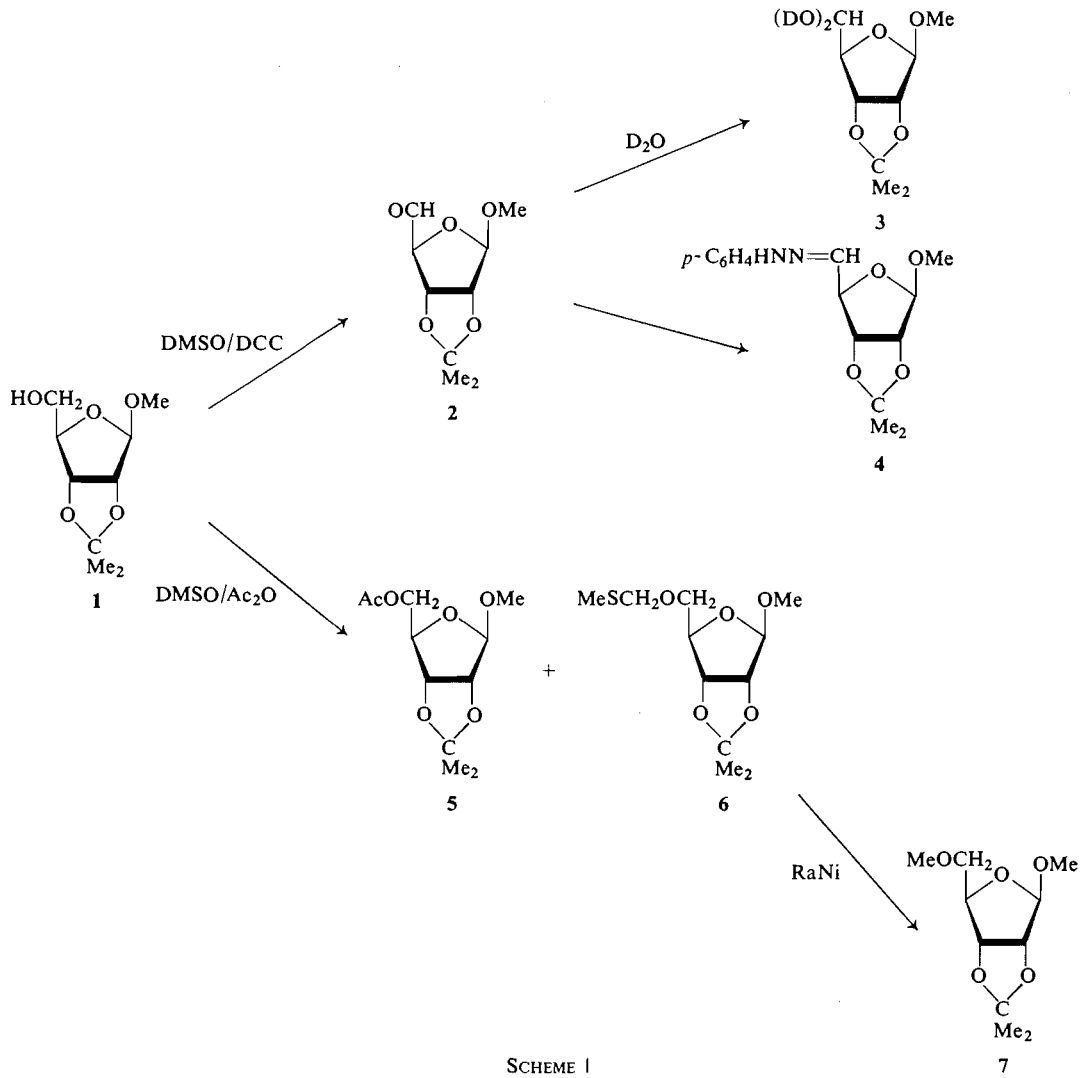

SCHEME I

instrument with an operating temperature of 30°; internal standards were, in the case of CCl_4 solutions, tetramethylsilane, and for D_2O solutions, sodium 4,4-dimethyl-4-silapentane-1-sulfonate. Optical rotations were measured with a Rudolph Model 80 photoelectric polarimeter (Caldwell, New Jersey).

Methyl 2,3-O-Isopropylidene-β-D-ribo-pentodialdofuranoside (2)

Freshly distilled methyl 2,3-*O*-isopropylidene-β-D-ribofuranoside (**1**, 8.0 g) in dry methyl sulfoxide (25 ml) was added to a mixture of methyl sulfoxide (40 ml), dry benzene (50 ml), and pyridine (3.2 ml) containing trifluoroacetic acid (1.6 ml). To the stirred solution was added dicyclohexylcarbodiimide (25 g) and the reaction mixture was stirred at 5 °C for 2 h, then at room temperature overnight. After this time, t.l.c. indicated that reaction had terminated. The mixture was filtered and a solution of oxalic acid (20 g) in methanol (50 ml) was added to the filtrate in small portions, with stirring. The resulting suspension was stirred 1 h at room temperature then filtered, the filtrate was washed with saturated sodium hydrogen carbonate solution (3 × 100 ml), the aqueous layer was extracted with ethyl acetate (150 ml) and the organic extracts were combined and dried (Na_2SO_4). Removal of solvent afforded a syrup which was dissolved in a little acetone and insoluble dicyclohexylurea was removed by filtration. Repetition of this treatment several times, followed by removal of solvent afforded a mobile syrup (6.14 g, 76%). Attempts to purify the product by repeated distillation were unsuccessful. A portion (2.5 g) was

Can. J. Chem. Downloaded from www.nrcresearchpress.com by 210.87.254.42 on 09/05/12
For personal use only.

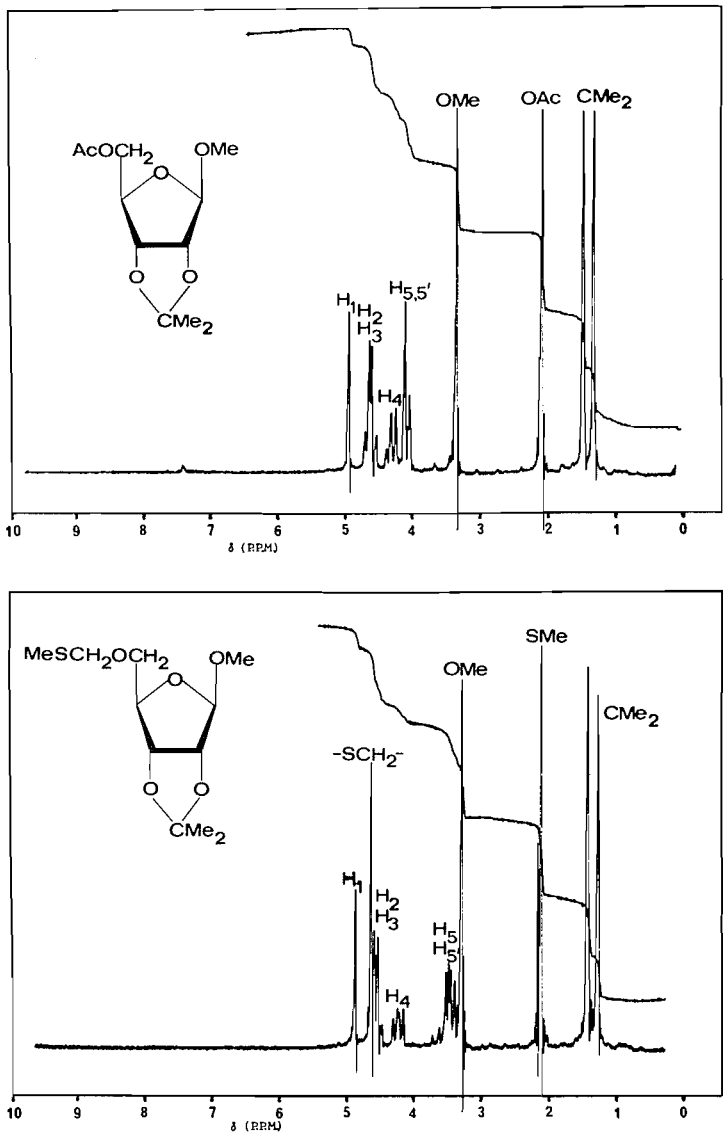

FIG. 2. The 100 MHz n.m.r. spectra of methyl 5-*O*-acetyl-2,3-*O*-isopropylidene-β-D-ribofuranoside (**5**) and methyl 2,3-*O*-isopropylidene-5-*O*-methylthiomethyl-β-D-ribofuranoside (**6**) (CCl_4 solution).

purified by chromatography on a column containing silica gel (300 g) using benzene – ethyl acetate, 3.5:1, as developer. Removal of solvent from combined fractions containing the product yielded a colorless syrup (1.2 g, 48%); b.p. 75°/0.2 Torr; $[\alpha]_D^{23}$ −91° (*c* 2, $CHCl_3$). The i.r. spectrum showed a strong carbonyl absorption at 1730 cm^{-1} but negligible absorption in the OH region. The n.m.r. data (see Fig. 1): τ 0.35 (1-proton singlet, $J_{4,5} \approx 0$ Hz, H_5), 4.9 (1-proton singlet, H-1), 5.0–6.0 (3-proton multiplet, H-2, -3, -4), 6.6 (3-proton singlet, OCH_3), 8.6, 8.8 3-proton singlets, $C(CH_3)_2$.

Methyl 2,3-O-Isopropylidene-β-D-ribo-pentodialdofuranoside p-Nitrophenylhydrazone (4)

To a solution of the aldehyde **2** (0.25 g) in methanol (5 ml) was added a solution of *p*-nitrophenylhydrazine hydrochloride (0.35 g) in a mixture of water (5 ml) and pyridine (1 ml) and the mixture was stored 40 h at room temperature. Removal of solvent afforded a syrup which

Can. J. Chem. Downloaded from www.nrcresearchpress.com by 210.87.254.42 on 09/05/12
For personal use only.

Can. J. Chem. Downloaded from www.nrcresearchpress.com by 210.87.254.42 on 09/05/12
For personal use only.

was dissolved in ether and washed successively with water, dilute H_2SO_4, and 5% sodium hydrogen carbonate solution. The solution was dried (Na_2SO_4) and evaporated to a syrup which crystallized from ether–hexane to give yellow needles of the hydrazone **4**, (0.31 g), m.p. 151–152°; $[\alpha]_D^{24}$ −49° (*c* 1, $CHCl_3$)

Anal. Calcd. for $C_{15}H_{19}N_3O_6$: C, 53.41; H, 5.68; N, 12.46. Found: C, 53.58; H, 5.75; N, 12.60.

Treatment of Methyl 2,3-O-Isopropylidene-β-D-ribofuranoside with Methyl Sulfoxide – Acetic Anhydride

Methyl 2,3-*O*-isopropylidene-β-D-ribofuranoside (4, 5), (**1**, 2.5 g) in dry methyl sulfoxide (35 ml) was treated with acetic anhydride (20 ml) and the reaction mixture was stored 36 h at room temperature. The t.l.c. showed the presence of three products, of which, the minor component having an R_f identical to that of the authentic aldehyde **2**. Removal of solvent and excess reagents by lyophilization afforded a pale yellow syrup (2.9 g) which was partitioned between water (75 ml) and petroleum ether (b.p. 30–60°), (50 ml). The organic layer was washed with a saturated solution of sodium hydrogen carbonate (2 × 15 ml), then with water (2 × 15 ml) and dried (Na_2SO_4). Removal of solvent yielded a colorless syrup (1.39 g), shown by t.l.c. to be a mixture of two products, the minor component having an R_f identical to that of an authentic sample of methyl 5-*O*-acetyl-2,3-*O*-isopropylidene-β-D-ribofuranoside (**5**); n.m.r. data (see Fig. 2): τ 5.0 (1-proton singlet, H-1), 5.4 (2-proton AB quartet, $J_{2,3}$ = 3.5 Hz, H-2,3), 5.6–6.0 (3-proton multiplet, H-4, -5, -5′), 6.6 (3-proton singlet OCH_3), 7.9 (3-proton singlet, —O—C(=O)—CH_3), 8.6, 8.8 (3-proton singlets $C(CH_3)_2$). Treatment of the mixture with 20 ml of a solution of methanol, saturated with ammonia at 0°, for 24 h, followed by removal of reagents by evaporation gave a syrupy product, shown by comparative t.l.c. studies to contain **1** and a major product of higher chromatographic mobility. Separation of the mixture (1.06 g) by chromatography on a column containing 125 g of silica gel afforded the major product (0.64 g) as a colorless syrup, $[\alpha]_D^{24}$ −60(*c* 2, $CHCl_3$). The n.m.r. spectrum of this product in CCl_4 (see Fig. 2) was consistent with the assignment of its structure as methyl 2,3-*O*-isopropylidene-5-*O*-methylthiomethyl-β-D-ribofuranoside (**6**); n.m.r. data (see Fig. 2); τ 5.1 (1-proton singlet, H-1), 5.3 (2-proton singlet —CH_2S—), 5.4 (2-proton AB quartet, $J_{2,3}$ = 3.5 Hz, H-2,3), 5.8, (1-proton multiplet, H-4), 6.6 (2-proton multiplet, H-5, -5′), 6.75 (3-proton singlet, OCH_3), 7.9 (3-proton singlet, —SCH_3), 8.6, 8.76 (3-proton singlets, $C(CH_3)_2$). Treatment of a solution of **6**, (0.25 g) in methanol (5 ml), with Raney nickel (1.25 g) at reflux for 8 h, gave, after filtration and removal of solvent a product (0.13 g), chromatographically and spectroscopically indistinguishable from an authentic sample of methyl 2,3-*O*-isopropylidene-5-*O*-methyl-β-D-ribofuranoside **7**, prepared by methylation (Ag_2O, MeI) of **1**.

1. R. F. Butterworth and S. Hanessian. Synth. **2**, 70 (1971).
2. O. Theander. Advan. Carbohydr. Chem. **17**, 223 (1962).
3. S. Hanessian and T. H. Haskell. *In* The carbohydrates. 3rd Ed. Vol. IIA. Academic Press Inc., New York, N.Y., 1970. p. 139.
4. P. A. Levene and A. T. Stiller. J. Biol. Chem. **104**, 299 (1934).
5. N. J. Leonard and K. L. Carraway. J. Heterocycl. Chem. **3**, 485 (1966).
6. K. E. Pfitzner and J. G. Moffatt. J. Am. Chem. Soc. **85**, 3027 (1963).
7. J. D. Albright and L. Goldman. J. Org. Chem. **30**, 1107 (1965).
8. D. Horton and J. S. Jewell. Carbohydr. Res. **2**, 251 (1966).
9. Y. Ali and A. C. Richardson. J. Chem. Soc. C, 320 (1969).
10. S. Hanessian and A. P. A. Staub. Chem. Ind. London, 1436 (1970).
11. P. J. Beynon, P. M. Collins, P. T. Doganges, and W. G. Overend. J. Chem. Soc. C, 1131 (1966).
12. L. M. Berkowitz and P. N. Rylander. J. Am. Chem. Soc. **80**, 6682 (1958).
13. N. Kornblum, J. W. Powers, G. J. Anderson, W. J. Jones, H. O. Lasson, O. Levand, and W. M. Wearer. J. Am. Chem. Soc. **79**, 6562 (1957).
14. S. Hanessian and A. P. A. Staub. Carbohydr. Res. **14**, 424 (1970).

Erratum: Collisional Deactivation Rates of $N_2^+(B^2\Sigma_u^+)$

G. I. Mackay and R. E. March
Department of Chemistry, Trent University, Peterborough, Ontario

Received May 27, 1971

(Ref.: Can. J. Chem. **49**, 1268 (1971))

Canadian Journal of Chemistry, **49**, 2759 (1971)

Drawings of Figs. 1 and 2 should be interchanged, captions are correct as printed.

Can. J. Chem. Downloaded from www.nrcresearchpress.com by 210.87.254.42 on 09/05/12
For personal use only.

Photochemistry of Metal Olefin Complexes. Isomerization and Stereospecific Cyclodimerization of Silver Cycloalkene Complexes

F. LEH, S. K. WONG, AND J. K. S. WAN
Department of Chemistry, Queen's University, Kingston, Ontario

Received May 17, 1971

Photolysis of $AgClO_4$ – 1-methylene cyclohexane complex in pure polycrystalline state or in methanol solution leads to isomerization of the complex to $AgClO_4$ – 1-methylcyclohexene. The isomerized complex undergoes further photochemical cyclodimerization giving the stereospecific *exo-trans-exo* dimer of the 1-methylcyclohexene and colloidal silver. Similar photoisomerization and a less stereospecific photodimerization were observed in the photolysis of the polycyclic $AgClO_4$ – β-pinene complex.

La photolyse du complexe méthylène-1 cyclohexane – $AgClO_4$ soit sous forme polycristalline soit en solution dans le méthanol conduit à une isomérisation du complexe en méthyl-1 cyclohexène – $AgClO_4$. Le complexe isomérisé subit une cyclodimérisation photochimique ultérieure pour donner d'une façon stéréospécifique le dimère *exo-trans-exo* du méthyl-1 cyclohexène et de l'argent colloïdal. De la même façon, une photoisomérisation et une photodimérisation moins stéréospécifique sont observées dans la photolyse du complexe polycyclique β-pinène – $AgClO_4$.

Canadian Journal of Chemistry, 49, 2760 (1971)

Although recent interests in the Ag^+-catalyzed rearrangements of strain polycyclic alkanes are developing rapidly (1–6), surprisingly little effort has been devoted to explore the photochemical reactivity of the well-known silver–olefin complexes. We report here the photoisomerization and the stereospecific photocyclodimerization of $AgClO_4$ complexes of 1-methylene cyclohexane and 1-methylcyclohexene. Similar photochemical reactions of the silver – β-pinene complex are also observed. These results indicate that the photochemical reactivity of these silver–olefin complexes are distinctly different from those of the free ligands and may be of general interest to synthetic and mechanistic organic photochemistry.

The complexes were prepared by addition of the corresponding olefins to an acetone solution of $AgClO_4$ at 0 °C. The white crystalline products were filtered, washed, and dried over P_2O_5. Silver analyses of these solid complexes indicated a 2:1 olefin to Ag ratio. Since the i.r. and n.m.r. data characterizing these complexes are not available in the literature, they are presented here in Table 1.

The $AgClO_4$ – 1-methylene cyclohexane complex was found to be stable in the dark at 0 °C for several weeks. Irradiation of a methanol solution of this complex (0.1 *M*) with u.v. (2537 Å) effects firstly an isomerization to silver – 1-methylcyclohexene. The photoisomerization can be readily followed by n.m.r. and/or i.r. analyses showing the conversion of a complexed exocyclic olefin to a complexed endocycloalkene. The rate of the photoisomerization process is apparently independent of temperature within the range 10–30 °C. However, photolysis of the complex in the pure solid state leads to a tenfold increase in the rate of conversion. Prolonged irradiation of the complex either in solution or in the solid state for several hours results in secondary photochemical reaction of the isomer product giving the sole *exo-trans-exo* cyclic dimer of the 1-methylcyclohexene and colloidal silver via a stereospecific photocyclodimerization. It was confirmed by further experiments involving separate photolyses of $AgClO_4$ – 1-methylene cyclohexane and $AgClO_4$ – 1-methylcyclohexene alone that the photoisomerization is a nonreversible process, in that the endocyclic olefin complex is photostable. However, it was also demonstrated that only the endocyclic olefin complex undergoes photodimerization by stereospecific cycloaddition with a yield up to 20%

TABLE 1. The i.r. and n.m.r. characterization of the silver olefin complexes

Compound	$\nu_{C=C}(cm^{-1})$	Proton chemical shifts* (c.p.s.)		
		CH_3	CH_2(olefinic)	CH(olefinic)
1-Methylene cyclohexane	1644	—	271.1	—
$AgClO_4$ – 1-methylene cyclohexane	1584	—	292.0	—
1-Methylcyclohexene	1671	92.8	—	319.5
$AgClO_4$ – 1-methylcyclohexene	1620	99.4	—	335.0
$AgClO_4$ – α-pinene	1616, 1581	103.0	—	317.5
$AgClO_4$ – β-pinene	1638, 1580	—	273.4	—

*Recorded with a Bruker HX60 spectrometer using TMS as reference.

after several hours irradiation. Dimerization was, in fact, the only photochemical reaction for silver – 1-methylcyclohexene. In all cases, no other products resulting from addition of solvent to the olefin complexes were observed.

There are at least six possible stereoisomers which can be formed via cyclodimerization of the 1-methylcyclohexene ligand. However, only one stereospecific photodimer was obtained which was separated by g.l.c. using an 8 ft column packed with nitrile silicon gum XE60 (10%) on Chromosorb P. The molecular weight of the dimer was confirmed by mass spectrometric analysis which shows that the base peak is in fact the dimer parent ion (*m/e* 192). The i.r. spectrum of the dimer shows absorption maxima at 1576, 1466, 1451, 1020, 926, and 841 cm^{-1} which are consistent with the spectra due to cyclohexane and cyclobutane derivatives. The p.m.r. spectrum of the photodimer recorded with a Bruker HX60 high resolution spectrometer, displays a complex absorption pattern centered at 2.15 p.p.m. which is probably due to the cyclobutane protons and the cyclohexane methylene protons having similar chemical shifts. The methyl protons on the cyclobutane ring are associated with the absorption centered at 1.68 p.p.m. Since the protons of the cyclobutane ring in the *trans* configuration are likely to have resonance at higher field (7), we tentatively assign the photodimer to the *exo-trans-exo* configuration **1**. Absolute assignment will have to await further study.

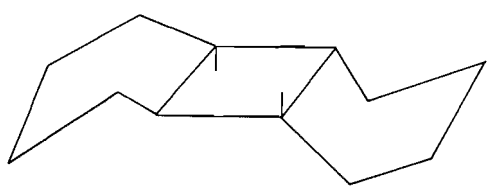

1

It is apparent that the photochemical behavior of the above silver–olefin complexes is in marked contrast to that of the free olefins. For example, Kropp and Krauss (8) have studied the xylene-photosensitized reaction of 1-methylcyclohexene in both methanol and hydrocarbon solvents. In protic media, photoisomerization to the exocyclic 1-methylene cyclohexane as well as conversion to ether by addition of a solvent molecule to the olefin, were the principal courses of reaction. These authors also found that the exocyclic isomer is photo-stable, thus the photoisomerization is non-reversible. This is exactly opposite to the photochemical behavior of the corresponding silver complexes. Furthermore, photosensitized reaction of 1-methylcyclohexene in hydrocarbon solvent also leads to dimerization yielding a mixture of at least six different dimers (8). This again is distinctly different from the stereospecific photocyclodimerization of the corresponding silver complex. On the other hand, Herling and co-workers (9) have found that thermal isomerization of 1-methylene cyclohexane to 1-methylcyclohexene can be effected by using sodium–alumina as the catalyst at 25 °C. However, thermal isomerization of silver–1-methylene cyclohexane at room temperature in the dark has not been observed.

The mechanistic implications of these results are being investigated by flash photolysis and by low temperature e.s.r. spectroscopy. Our preliminary e.s.r. results suggest that photochemical reactions may involve radical intermediates such as the Ag^+–cyclohexenyl radical and trapped H atoms. Silver – cycloalkenyl radicals have been observed in γ-radiolysis of solid silver cycloalkene complexes (10, 11).

Similar photochemical behavior was observed for the polycyclic silver – β-pinene and silver – α-pinene complexes. Only silver – β-pinene was found to photoisomerize to the more stable

Can. J. Chem. Downloaded from www.nrcresearchpress.com by 210.87.254.42 on 09/05/12
For personal use only.

silver – α-pinene complex. However, photodimerization via less stereospecific routes was found to occur in both α- and β-complexes.

Financial support by the National Research Council of Canada and the Public Health Department, is gratefully acknowledged.

1. P. G. GASSMAN and T. J. ATKINS. J. Am. Chem. Soc. **93**, 1042 (1971).
2. L. A. PAQUETTE, S. E. WILSON, and R. P. HENZEL. J. Am. Chem. Soc. **93**, 1288 (1971).
3. L. A. PAQUETTE and J. C. STOWELL. J. Am. Chem. Soc. **92**, 2584 (1970).
4. L. A. PAQUETTE. J. Am. Chem. Soc. **92**, 5765 (1970).
5. L. A. PAQUETTE, G. R. ALLEN, and R. P. HENZEL. J. Am. Chem. Soc. **92**, 7002 (1970).
6. L. CASSAR, P. E. EATON, and J. HALPERN. J. Am. Chem. Soc. **92**, 6366 (1970).
7. D. VALENTINE, N. J. TURRO, and G. S. HAMMOND. J. Am. Chem. Soc. **86**, 5202 (1964).
8. P. J. KROPP and H. J. KRAUSS. J. Am. Chem. Soc. **89**, 5199 (1967).
9. J. HERLING, J. SHABTAI, and E. GIL-AV. J. Am. Chem. Soc. **87**, 4107 (1965).
10. D. R. GEE and J. K. S. WAN. Can J. Chem. **49**, 160 (1971).
11. D. R. GEE, K. E. RUSSELL, and J. K. S. WAN. Can. J. Chem. **48**, 2740 (1970).

Can. J. Chem. Downloaded from www.nrcresearchpress.com by 210.87.254.42 on 09/05/12
For personal use only.

Can. J. Chem. Downloaded from www.nrcresearchpress.com by 210.87.254.42 on 09/05/12
For personal use only.

Canadian Journal of Chemistry

Published by THE NATIONAL RESEARCH COUNCIL OF CANADA

VOLUME 49 SEPTEMBER 1, 1971 NUMBER 17

Oxidation of Hydrocarbons. III. Kinetics and Mechanism of the Oxidation of Arenes by Aqueous Sodium Dichromate[1]

DONALD G. LEE AND UDO A. SPITZER[2]

Department of Chemistry, University of Saskatchewan, Regina Campus, Regina, Saskatchewan

Received April 26, 1971

The kinetics of the oxidation of several sodium *p*-alkylbenzenesulfonates by aqueous dichromate have been studied under slightly acidic conditions (pH = 7.0 to 5.4). The results indicate that the only active oxidant under these conditions is the acid chromate ion, $HCrO_4^-$, and that the reaction probably involves a free radical process.

Les cinétiques de l'oxydation de quelques *p*-alkylbenzènesulfonates de sodium par le dichromate aqueux ont été étudiées sous des conditions légèrement acide (pH = 7.0 à 5.4). Les résultats indiquent que dans ces conditions, la seule espèce oxydante active est l'ion chromate acide, $HCrO_4^-$, et que la réaction fait probablement intervenir un processus par radicaux libres.

Canadian Journal of Chemistry, 49, 2763 (1971)

Introduction

The oxidation of arenes by aqueous sodium dichromate is a reaction of considerable synthetic potential since it results in selective oxidation of side chains with little or no ring degradation (1, 2). For example, using this procedure, 2-methylnaphthalene can be converted to 2-naphthoic acid in almost quantitative yields whereas the use of most other oxidants, including acidic chromium(VI), results in the formation of a considerable amount of 2-methylnaphthoquinone (3). Other attractive features of this procedure include the ease with which products can be recovered, and the reaction has consequently found several synthetic applications (4–6).

Despite its apparent synthetic utility only one study dealing with the mechanism of the reaction has been reported (7). In this investigation, Bixel and Drayer found that the oxidation of *o*-toluic acid using a 30% aqueous solution of $Na_2Cr_2O_7$ followed the rate law expressed in eq. 1, and they suggested that the reaction was initiated by the abstraction of a hydrogen atom in the rate determining step. However, these authors noted that their data could also be successfully accommodated by other mechanisms as well.

$$[1] \quad v = k[Cr_2O_7^{2-}][o\text{-Toluic Acid}][H^+]$$

Other workers reported that oxidations of arenes with side chains two or more carbon atoms in length underwent reaction at the terminal carbon (8). However, this report was later shown to be erroneous; oxidation occurs only at the α-position (9).

In the present work we have attempted to increase our understanding of the mechanism of the reaction by studying the oxidation of arenes with different types of side chains. Because of the low solubility of hydrocarbons in aqueous media it was found that reproducible rate constants could be obtained only if the arenes contained an additional group which increased their solubility in water. The *p*-sulfonate group functions admirably in this respect since it increases the solubility of the arene, but is itself inert to oxidation. Furthermore, judging from its small σ-value (10), it should not have a large electronic effect on the rate of reaction.

[1]For parts I and II of this series, see refs. 9 and 20.

[2]Saskatchewan Research Council Scholarship holder 1968–1970.

Can. J. Chem. Downloaded from www.nrcresearchpress.com by 210.87.254.42 on 09/05/12
For personal use only.

Experimental

Apparatus

The reaction vessel was a Parr #4501 stirrer type Pressure Reaction Vessel with the following specifications: capacity, 2000 ml; bomb material, T-316 stainless steel; pressure gauge range, 0 to 2000 p.s.i.; heater, W1OM auto transformer 1500 W; circuitry, 60 cycles, 115 V a.c.; stirrer, mechanical, 520 r.p.m. The temperature was monitored by a custom dial thermometer with a range of 0–250°. This range was verified from 100–250° by a chromel–alumel thermocouple. The accuracy (±0.5°) was limited by the temperature control apparatus. Samples for kinetic analysis were withdrawn through the liquid sampling valve by means of a simple glass apparatus which prevented loss of water vapor.

Preparation of Sodium p-Sulfonates of Toluene, Toluene-α-d_3, Ethylbenzene, Isopropylbenzene, and t-Butylbenzene

These salts were prepared according to the general procedure described by Fieser (11) after the arenes had been purified by repeated treatments with cold concentrated H_2SO_4 to remove thiophene derivatives and then distilled. The following ratios were observed although the quantities of each arene varied. To 0.3 mol of arene at 100° were added 19 ml of 97% H_2SO_4 with stirring at such a rate that the temperature did not exceed 120°. The resulting solution was kept at 110° until the organic layer disappeared (usually 1 h). This mixture was allowed to cool to 50° and then poured into 100 ml of water. The organic layer was removed using a separatory funnel. The aqueous solution was partially neutralized by the careful addition of 15 g of sodium bicarbonate. Sodium chloride (40 g) was then added, the mixture was heated to boiling and just enough water was added to bring all the salt into solution. The mixture was cooled in ice and the crystals were collected. The recovered crystals were redissolved in hot water and treated with 40 g NaCl and the product was again recovered. The product was recrystallized once more in this manner and then once from water. The yield at this point was only 30% but the purity was 98% or better as determined from carbon–hydrogen analysis. The impurities were in all cases resistant to oxidation (as judged from the fact that compounds at different stages of purification gave the same rate constants). The analysis for these compounds are listed below.

Anal. Calcd. for sodium *p*-toluenesulfonate: C, 43.29; H, 3.63. Found: C, 43.10; H, 3.51.

Anal. Calcd. for sodium *p*-(α-d_3)-toluenesulfonate: C, 42.60. Found: C, 40.38.

Anal. Calcd. for sodium *p*-ethylbenzenesulfonate: C, 46.15; H, 4.36. Found: C, 45.98; H, 4.38.

Anal. Calcd. for sodium *p*-isopropylbenzenesulfonate: C, 48.64; H, 4.99. Found: C, 49.08; H, 4.91.

Anal. Calcd. for sodium *p*-*t*-butylbenzenesulfonate: C, 50.83; H, 5.55. Found: C, 46.61; H, 5.35.

Although the purity of sodium *p*-*t*-butylbenzenesulfonate was not high according to the analysis it was found that this compound was resistant to oxidation under our conditions, thus supporting the conclusion that the impurities which contaminated these compounds are not oxidizable. Similarly the deuterated compound, because of the excessive cost of starting material, was recrystallized only twice to give a yield of 50% and a purity of 95%. In the preparation of solutions for kinetic experiments the substrate concentration was always corrected for purity.

Kinetic Method

The rate of oxidation was followed by spectrophotometrically observing the decrease of [Cr^{VI}] with respect to time. Since the reaction temperatures were all too high for direct spectrophotometric observation samples were withdrawn at known time intervals. These samples were quenched by quickly cooling to room temperature using a Dry Ice – ethanol slurry. After centrifuging to remove suspended Cr_2O_3 the samples were analyzed at 364 nm for Cr^{VI} using a Unicam Model SP-500 Series 2 spectrophotometer. At this wavelength Cr^{VI} has an absorption peak in the phosphate buffer solutions that was found to obey Beer's Law (12).

The reactants were first mixed together in an aqueous phosphate buffer at room temperature. (The ionic strength of the buffers was maintained at 1.2.) The reactor was then sealed, purged with purified nitrogen, charged with 320 p.s.i. of nitrogen, and heated to and stabilized at the desired temperature. This usually required ½ to 1 h of heating, but since the reaction half lives were always long in comparison, this warm up time could be neglected.

Good pseudo first order rate plots, all with correlation coefficients of 0.993 or greater, were obtained for that portion of the reaction taking place after the warm up time. Two typical plots for the oxidation of *p*-ethylbenzenesulfonate are reproduced in Fig. 1. The data were processed by the method of least squares utilizing an IBM #360 computer.

Results

Initially, attempts were made to investigate the rate law for the oxidation of ethylbenzene by using unsubstituted arenes as substrates, but it soon became apparent that the investigation was severely hampered by poor reproducibility. This was attributed to the low solubility of arenes in aqueous media. However, it was observed that the arene oxidation proceeded at a rate that was approximately equal to that of the corresponding arene sulfonate, and in order to obtain precise rate constants, it was necessary to use these more soluble derivatives. The data obtained are summarized in Table 1.

Discussion

From the data presented in Table 1, it is possible to define the rate law for the oxidation of sodium *p*-ethylbenzenesulfonate.

The good straight line plots obtained in Fig. 1, where ln (absorbance) is plotted against time indicates that the reaction is first order in Cr^{VI}.

The order with respect to arene was then obtained by maintaining the acidity constant and

TABLE 1. Oxidation of sulfonated arenes (X—C$_6$H$_4$—SO$_3$Na)*

X	Initial reductant concentration (M)	Temperature (°C)	pH (25°)	$k_1 \times 10^5$(s^{-1})	$k_2 \times 10^3$(M^{-1}s^{-1})†
C_2H_5	0.0198	200.0	5.45	3.03	1.93
C_2H_5	0.0199	200.0	5.45	3.41	2.16
C_2H_5	0.0395	200.0	5.45	7.02	1.98
C_2H_5	0.0448	200.0	5.45	8.11	1.99
C_2H_5	0.0450	200.0	5.45	8.47	2.07
C_2H_5	0.0674	200.0	5.45	12.6	1.99
C_2H_5	0.0674	200.0	5.45	13.2	2.08
C_2H_5	0.1123	200.0	5.45	22.4	2.07
C_2H_5	0.1126	200.0	5.45	22.1	2.03
C_2H_5	0.0674	178.0	5.43	3.52	0.558
C_2H_5	0.0679	189.0	5.42	6.57	1.03
C_2H_5	0.0676	218.0	5.42	24.8	3.91
C_2H_5	0.0672	216.0	5.42	25.1	3.97
C_2H_5	0.0677	200.0	5.42	12.8	2.01
C_2H_5	0.0677	200.0	5.42	12.7	2.00
C_2H_5	0.0451	200.0	5.03	6.67	1.62
C_2H_5	0.0460	200.0	6.03	6.09	1.45
C_2H_5	0.0449	200.0	6.56	3.62	0.888
C_2H_5	0.0688	200.0	7.02	2.92	0.452
C_2H_5	0.0677	196.0	5.43	8.92	1.40
CH_3	0.0971	200.0	5.42	3.93	0.417
CH_3	0.0969	200.0	5.42	3.72	0.395
CD_3	0.0328	200.0	5.31	0.267	0.089
i-C_3H_7	0.0440	200.0	5.42	11.2	3.14
i-C_3H_7	0.0878	200.0	5.42	20.9	2.62
i-C_3H_7	0.0878	200.0	5.42	22.3	2.80
i-C_3H_7	0.0675	200±3	5.48	11.7	1.97
i-C_3H_7	0.0940	200.0	5.31	2.15	2.51
t-C_4H_9	0.0568	200.0	5.43	No reaction after 25 h	

*[Cr^{VI}] = 5.45 × 10^{-3} M in $H_2PO_4^-$/HPO_4^{2-} buffer, μ = 1.2.
†$k_2 = k_1$/[Arene]. The arene concentrations are those which would pertain at the half-time of the reactions, assuming that the methyl, ethyl, and isopropyl side chains are oxidized respectively to the corresponding carboxylic acids, ketones and alcohols (9, 12).

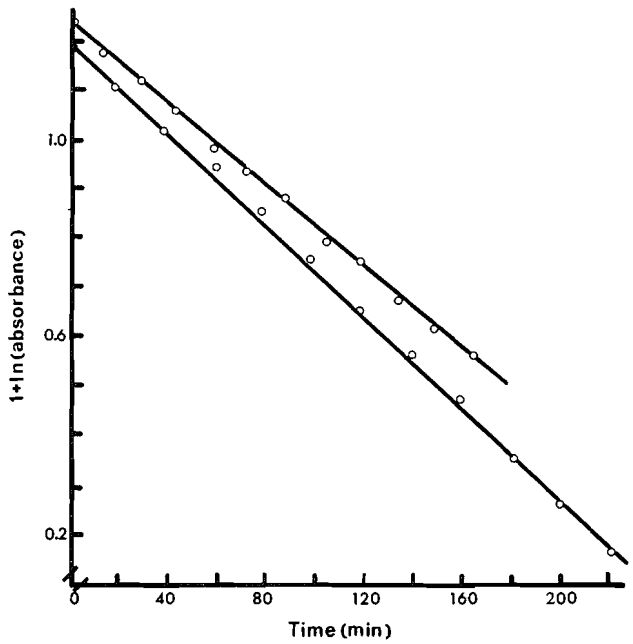

FIG. 1. Typical pseudo first order plots for the oxidation of sodium p-ethylbenzenesulfonate.

Can. J. Chem. Downloaded from www.nrcresearchpress.com by 210.87.254.42 on 09/05/12
For personal use only.

Can. J. Chem. Downloaded from www.nrcresearchpress.com by 210.87.254.42 on 09/05/12
For personal use only.

varying the arene concentration. The pseudo first order rate constants were found to be directly dependent on the concentration of arene when the oxidation of sodium *p*-ethylbenzenesulfonate was studied at a p*H* of 5.45 and 200 °C. This is indicated by the constancy of the k_2 values for the first nine experiments in Table 1.

When attempts were made to evaluate the order with respect to acidity in a similar manner by varying the p*H*, it was found that a plot of log k_2 *vs.* p*H* gave a curve rather than a straight line (see Fig. 2). However, this apparently complex dependence upon acidity is really a result of the analytical method used which measures the concentration of all chromium(VI) species present in solution. Under neutral conditions the primary chromium(VI) species present in dilute solutions are CrO_4^{2-} and $HCrO_4^-$ (1*a*). If it is assumed that $HCrO_4^-$ is the only active oxidant, it can be concluded from the derivation presented in the Appendix that the rate of reaction should be dependent on a complex function of acidity, $[H^+]/([H^+] + K)$, where K is the acid dissociation constant of $HCrO_4^-$. In accordance with this derivation, it was found that a plot of log k_2 against log $([H^+]/([H^+] + K))$ gave a straight line with slope of 1.05 ± 0.09 (see Fig. 3). Hence, the reaction apparently depends only upon p*H* in so far as it controls the equilibrium between $HCrO_4^-$ and CrO_4^{2-}.

From these considerations the rate law for the oxidation of arenes under neutral conditions is of the form,

$$v = k[\text{arene}][Cr^{VI}]([H^+]/[H^+] + 3.0 \times 10^{-7})$$

or

$$v = k[\text{arene}][HCrO_4^-]$$

At this point it is of value to consider the differences observed between acidic and neutral chromium(VI) oxidations. Wiberg and Evans (15) thoroughly studied the acidic chromium(VI) oxidation of diphenylmethane and found the rate law,

$$v = k[\text{Total } Cr^{VI}][\text{diphenylmethane}]h_0$$

where h_0 is the Hammett acidity function. But under these conditions, chromium(VI) exists primarily as H_2CrO_4 and $HCrO_4^-$ and it is noteworthy that ring degradation becomes extensive, particularly when polycyclic aromatic hydrocarbons are used as the substrates (13). However, neutral chromium(VI) oxidations, where $HCrO_4^-$ is the major oxidant, do not attack aromatic (9) or polyaromatic ring systems

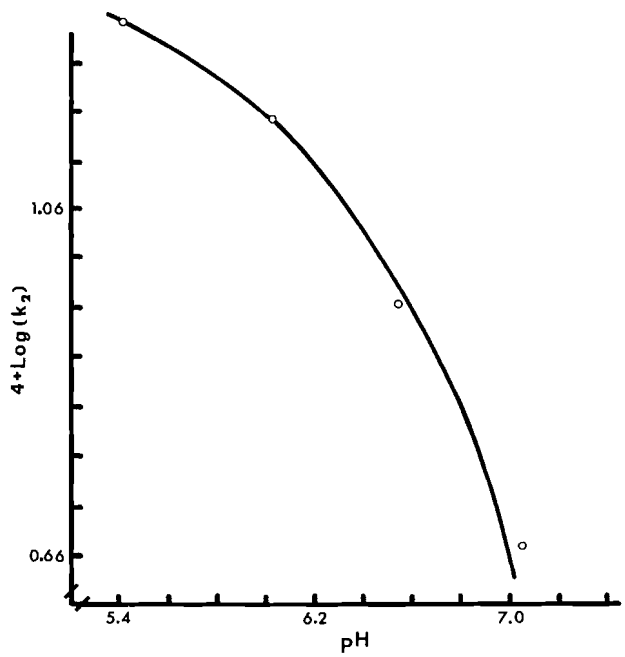

FIG. 2. Plot of log k_2 against p*H* for the oxidation of sodium *p*-ethylbenzenesulfonate.

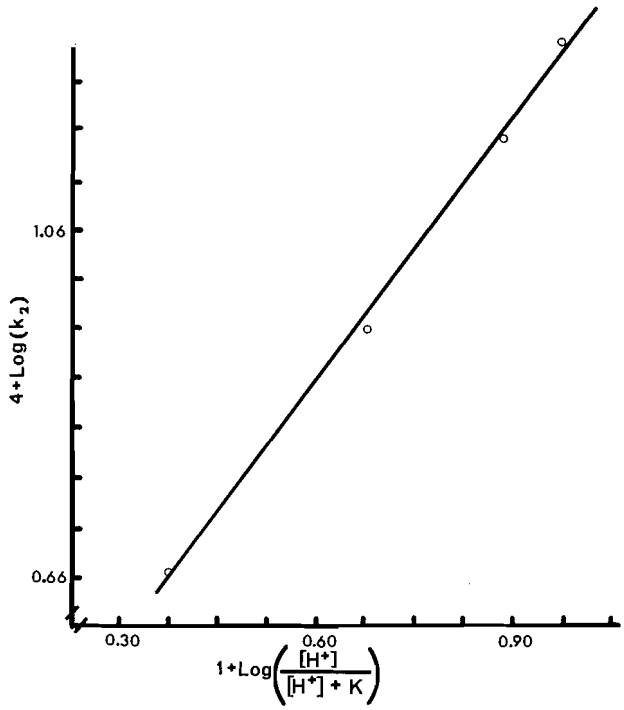

FIG. 3. Dependence of k_2 upon acidity for the oxidation of sodium *p*-ethylbenzenesulfonate. K is the acid dissociation constant of $HCrO_4^-$. Slope = 1.0, correlation coefficient = 0.975.

(3). It thus becomes attractive to propose that H_2CrO_4 (or $H_3CrO_4^+$) is responsible for the ring degradation. An alternative explanation could be that at higher acidities the ring systems become protonated and are thus rendered more susceptible to oxidation.

From the rate law, it can be concluded that the transition state for neutral chromium(VI) oxidations is composed of one molecule of arene and one of acid chromate anion. The observation of a primary deuterium isotope effect, k_H/k_D = 4.6, when the rates of reaction of sodium *p*-toluenesulfonate and its α,α,α-d_3 analogue are compared indicates that the cleavage of the carbon–hydrogen bond is the rate determining step.

The thermodynamic parameters (see Fig. 4) are close to those obtained for the acidic chromium(VI) oxidations of alcohols, $\Delta S^{\neq}$ (arene) = −22.8 e.u., $\Delta S^{\neq}$ (2-propanol) ≐ −35 e.u., $\Delta H^{\neq}$ (arene) = 21.0 kcal/mol, $\Delta H^{\neq}$ (2-propanol ≐ 12 kcal/mol, thus suggesting the possibility that a similar mechanism may be operating (14).

By comparing the relative rates of 1°:2°:3° carbon–hydrogen bond cleavage, it is also possible to distinguish between homolytic cleavage (radical abstraction) or heterolytic cleavage (hydride ion abstraction). Table 2 illustrates

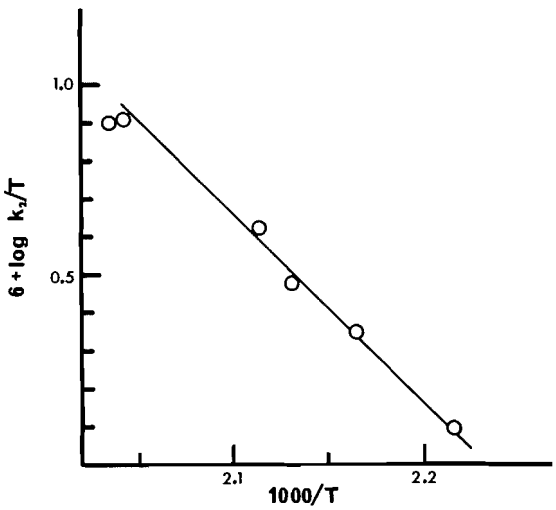

FIG. 4. Thermodynamic parameters for the oxidation of sodium *p*-ethylbenzenesulfonate. $\Delta H^{\neq}$ = 21.0 kcal/mol, $\Delta S^{\neq}$ = −22.8 e.u., slope = −4.59, correlation coefficient = 0.996.

Can. J. Chem. Downloaded from www.nrcresearchpress.com by 210.87.254.42 on 09/05/12
For personal use only.

TABLE 2. Comparative rates for different types of side chains*

Arene	$k_2 \times 10^4 (M^{-1}s^{-1})$†	Ratio	Free radical formation‡	Carbonium ion formation§
Sodium *p*-toluenesulfonate	4.06	1	1	1
Sodium *p*-ethylbenzenesulfonate	20.0	5	4	10^2
Sodium *p*-isopropylbenzenesulfonate	28.5	7	13	10^5

*pH = 5.42, temperature = 200°.
†The k_2 values are the averages of two or more experiments.
‡Hydrogen abstraction by methyl radicals from toluene, ethylbenzene, and isopropylbenzene (18).
§Solvolysis rates for the chlorides of toluene, ethylbenzene, and isopropylbenzene (19).

that the comparative rates are very similar to those observed for reactions known to proceed by a radical mechanism. Hydrogen abstraction has also been suggested for the acidic chromium-(VI) oxidation of toluene, ethylbenzene, and triphenylmethane where the ratio of 1°:2°:3° was found to be 1:3:8 (15). It is likely that this abstraction does not result in a completely free radical since the oxidation of styrene under similar conditions yielded no polymers (12). The radical can rather be visualized as being trapped in a solvent cage with Cr^V, a more powerful oxidant than Cr^{VI} (16). This would lead to further rapid oxidation.

Appendix

In the particular pH region where these experiments were performed two chromium species are present (CrO_4^{2-} and $HCrO_4^-$), both of which are detected spectrophotometrically (1*a*). Since the spectrophotometric analytical technique used at 364 nm does not distinguish between the two species the absorbance recorded is really due to $[Cr^{VI}]_{total} = [HCrO_4^-] + [CrO_4^{2-}]$. It is known that CrO_4^{2-} is oxidatively inactive since at p$H \geq 9$ no oxidation occurs, so it can be assumed that the only effective oxidant is the acid chromate anion, *i.e.* $v = k[\text{substrate}]\,[HCrO_4^-]$. However, as a result of the analytical technique, the rate is measured as $-d[Cr^{VI}]_{total}/dt$. These two parts of the rate equation can be equated using the equilibrium constant for the acid chromate anion–chromate dianion system which is known to be 3.0×10^{-7} at 25° (1*a*). After the following calculations are performed, the rate equation can be expressed in terms of $[Cr^{VI}]_{total}$.

$$\frac{[CrO_4^{2-}][H^+]}{[HCrO_4^-]} = 3.0 \times 10^{-7} = K = \frac{[CrO_4^{2-}][H^+]}{[Cr^{VI}]_T - [CrO_4^{2-}]}$$

$$K[Cr^{VI}]_T - K[CrO_4^{2-}] = [CrO_4^{2-}][H^+]$$

$$K[Cr^{VI}]_T = [CrO_4^{2-}]([H^+] + K)$$

$$[2] \qquad [CrO_4^{2-}] = [Cr^{VI}]_T\left(\frac{K}{[H^+] + K}\right)$$

$$-d[Cr^{VI}]/dt = k[\text{substrate}][HCrO_4^-]$$

$$[3] \qquad = k[\text{substrate}]([Cr^{VI}]_T - [CrO_4^{2-}])$$

substituting eq. 2 into eq. 3,

$$-d[Cr^{VI}]_T/dt = k[\text{substrate}]\left([Cr^{VI}]_T - [Cr^{VI}]_T\left(\frac{K}{[H^+] + K}\right)\right)$$

$$= k[\text{substrate}][Cr^{VI}]_T\left(1 - \frac{K}{[H^+] + K}\right)$$

$$= k[\text{substrate}][Cr^{VI}]_T\left(\frac{H^+}{[H^+] + K}\right)$$

Can. J. Chem. Downloaded from www.nrcresearchpress.com by 210.87.254.42 on 09/05/12
For personal use only.

The rates of oxidation were found to be linearly dependent on this somewhat unusual acidity function, thus indicating that the basic assumption was correct, *i.e.* $v = k[\text{substrate}]\ [HCrO_4^-]$. It should be noted that the equilibrium constant used was determined at 25° whereas the kinetic investigations were at about 200°. Similarly the p*H* measurements were all made at 25° and although it is not at present known how *K* responds to temperature changes it is known that the changes in p*H* are small in the phosphate buffer system used (17). The derivation thus rests on the assumption that changes in *K* as the temperature increases are either small or parallel to changes in the p*H* of the phosphate buffer system.

The authors are grateful to the National Research Council of Canada for the award of an operating grant (D.G.L.) and to the Saskatchewan Research Council for the award of a scholarship (U.A.S.).

1. K. B. WIBERG. *In* Oxidation in organic chemistry. Part A. K. B. Wiberg, *editor*. Academic Press, New York, N.Y., 1965. pp. 83–105 (*a*) p. 71.
2. D. G. LEE. *In* Oxidation; techniques and applications in organic synthesis. R. L. Augustine, *editor*. Marcel Dekker, New York, N.Y., 1969. pp. 31–36.
3. L. FRIEDMAN, D. L. FISHEL, and H. SHECHTER. J. Org. Chem. **30**, 1453 (1965).
4. L. F. FIESER and M. FIESER. Reagents for organic synthesis. John Wiley & Sons, Inc., New York, N.Y., 1967. p. 1061.
5. L. FRIEDMAN. Org. Synth. **43**, 80 (1963).
6. M. S. NEWMAN and H. BODEN. J. Org. Chem. **26**, 1759 (1961).
7. J. C. BIXEL and D. DRAYER. I. and E. C. Process Des. and Dev. **5**, 376 (1966).
8. R. H. REITSEMA and N. L. ALLPHIN. J. Org. Chem. **27**, 27 (1962).
9. D. G. LEE and U. A. SPITZER. J. Org. Chem. **34**, 1493 (1969).
10. D. H. MCDANIEL and H. C. BROWN. J. Org. Chem. **23**, 420 (1958).
11. L. F. FIESER. Experiments in organic chemistry. D. C. Heath and Company, Boston, Massachusetts. 1957, p. 144.
12. U. A. SPITZER. M.Sc. Thesis. University of Saskatchewan, Regina Campus, Regina, Saskatchewan, 1970.
13. L. F. FIESER, W. P. CAMPBELL, E. M. FREY, and M. D. GATES. J. Am. Chem. Soc. **61**, 3216 (1939).
14. R. STEWART. Oxidation mechanisms. W. A. Benjamins, New York, N.Y., 1964. p. 37–48.
15. K. B. WIBERG and R. J. EVANS. Tetrahedron, **8**, 313 (1960).
16. J. ROČEK. Tetrahedron Lett. 135 (1962).
17. Handbook of chemistry and physics. 49th Edition. R. C. Weast, *editor*. The Chemical Rubber Co., Cleveland, Ohio, 1969. p. D80.
18. W. A. PRYER. Introduction to free radical chemistry. Prentice-Hall Inc., Englewood Cliffs, N.J., 1966. p. 56.
19. A. STREITWIESER. Solvolytic displacement reactions. McGraw-Hill, New York, 1962. p. 44.
20. D. G. LEE and B. E. SINGER. Can. J. Chem. **48**, 2674 (1970).

Can. J. Chem. Downloaded from www.nrcresearchpress.com by 210.87.254.42 on 09/05/12
For personal use only.

Can. J. Chem. Downloaded from www.nrcresearchpress.com by 210.87.254.42 on 09/05/12
For personal use only.

Novel Chemical Shift Changes of Carbohydrates Induced by Lanthanide Shift Reagents: Some Experimental Optimizations[1]

IAN ARMITAGE AND L. D. HALL

Department of Chemistry, The University of British Columbia, Vancouver 8, British Columbia

Received March 15, 1971

The ^{1}H n.m.r. spectra of 1,2:5,6-di-*O*-isopropylidene-α-D-glucofuranose (**4**), of 1,2:5,6-di-*O*-isopropylidene-α-D-allofuranose (**5**), and of their 3-*O*-acetyl derivatives **6** and **7**, respectively have been separately measured in the presence of varying concentrations of the tris{dipivaloylmethane} derivatives of europium (**1**), thulium (**2**), and praseodymium (**3**). For these derivatives, both europium (**1**) and thulium (**2**) induce shifts to low field whereas praseodymium (**3**) produces high field shifts; for any individual proton the magnitude of the induced shift is shown to be linearly proportional to the amount of added reagent and is best followed by addition of volume aliquots of a dilute solution of the lanthanide. It is shown that simplistic rationales concerning the relationship between the magnitudes of induced shifts and the geometry of the substrate system can be entirely misleading; the D-*gluco*-derivative **4** is particularly noteworthy in this regard. Since the magnitudes of the induced shifts are temperature dependent it is important to report the temperature at which experiments are performed. For **1** the induced shifts are *ca.* 2.2 times larger for carbon tetrachloride solutions than for deuterochloroform solutions when operating under otherwise identical conditions.

Les spectres de r.m.n. de ^{1}H du 1,2:5,6-di-*O*-isopropylidène-α-D glucofuranose (**4**), du 1,2:5,6-di-*O*-isopropylidène-α-D-allofuranose (**5**) et de leurs dérivés respectifs 3-*O*-acétylés **6** et **7** ont été séparement mesurés en présence des dérivés tris (dipivaloylméthane), en concentrations variables, de l'europium (**1**), du thulium (**2**), et du praseodymium (**3**). Pour ces dérivés, à la fois ceux de l'europium (**1**) et du thulium (**2**) provoquent des déplacements à champ faible tandis que celui du praseodymium (**3**) donne des déplacements à champ fort; pour chaque proton, l'importance du déplacement induit est proportionnellement linéaire à la quantité de réactif ajouté. Cette variation est mieux appréciée par addition de volumes d'une solution diluée de lanthanide. On montre que des raisonnements trop simples concernant la relation qui lie l'importance des déplacements induits et la géométrie du substrat peuvent être entièrement erronés. L'exemple du dérivé D-glucosidique **4** est particulièrement significatif à cet égard. Puisque l'importance des déplacements induits dépend de la température, il est important de noter la température à laquelle les expériences sont faites. Pour le composé **1**, les déplacements induits sont 2.2 fois plus importants pour des solutions de tétrachlorure de carbone que pour des solutions de deutero chloroforme lorsqu'on opère dans des conditions par ailleurs identiques.

Canadian Journal of Chemistry, **49**, 2770 (1971)

Introduction

One of the principle shortcomings of ^{1}H n.m.r. spectroscopy as a method for studying the structures of complex organic substances is associated with the intrinsically low sensitivity of ^{1}H chemical shifts to changes in chemical and stereochemical environment. As a result, it often happens that a resonance of particular interest is obscured by the fortuitous overlap of other resonances. Although the spectra of monosaccharide derivatives are not commonly complicated by this hazard, it remains that direct spectral assignments are occasionally precluded by a small chemical shift between a pair of protons; for example, the resonances of C-6 methylene protons are often difficult to observe.

Over the years this laboratory has been concerned with the development and evaluation of methods for simplifying the proton spectra of carbohydrate derivatives and in this regard we have variously described the use of spin-decoupling (2), solvent shifts (3), high-magnetic fields (4), and ^{1}H–{^{1}H} INDOR spectroscopy (5). In the present paper we shall discuss several lanthanide, tris{dipivaloylmethane} derivatives which appear to have considerable potential as reagents for inducing large chemical shift changes in the ^{1}H n.m.r. spectra of carbohydrate substances dissolved in organic solvents.

The potential of lanthanide complexes as "chemical-shift" reagents was first recognised by Hinckley (6) in 1969 and since then we (1) and a large number of other workers have out-

[1]For a preliminary communication of some of these data, see ref. 1. The present paper is Part 1 of a series "Nuclear Magnetic Resonance Studies of Paramagnetic Systems".

Can. J. Chem. Downloaded from www.nrcresearchpress.com by 210.87.254.42 on 09/05/12
For personal use only.

lined a variety of europium (7) and other lanthanide (8) systems which respond favorably. Most of these studies have been concerned with organic systems having a single "chelating" substituent, usually a hydroxyl group, and our initial concern was to demonstrate that monosaccharide derivatives, which are potentially polyfunctional can also give useful results. We shall also be concerned here with details of what we regard to be the most useful way of using these lanthanide reagents, with particular emphasis on the tris{dipivaloylmethane} derivatives of europium (**1**), thulium (**2**) and praseodymium (**3**). For convenience, four derivatives of the 1,2:5,6-di-*O*-isopropylidene-α-D-hexofuranose system (**4**–**7**), which were available from other studies in our laboratory were chosen as the substrate molecules. Other merits of these derivatives are that they all have reasonably well

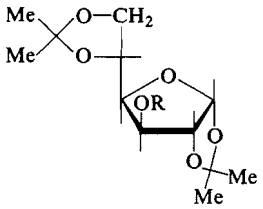

4 R = H
6 R = $\overset{\overset{O}{\|}}{C}CH_3$

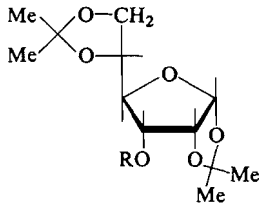

5 R = H
7 R = $\overset{\overset{O}{\|}}{C}CH_3$

defined geometries and each has one group, either an hydroxyl or acetoxyl group, likely to provide the major association site for the lanthanide reagent, together with many additional functionalities likely to provide weaker "donor-bonds."

Results and Discussion

The syntheses of tris{dipivaloylmethane} derivatives of europium (**1**), thulium (**2**), and of praseodymium (**3**) following the standard literature procedures (9), present no difficulties. During preliminary experiments no particular attempts were made to perform the measurements with rigorously dried reagents or solvents and the spectra which were obtained showed considerable line-broadening, even with **1**. The experiments described here used freshly sublimed lanthanide reagents (**1**, **2**, or **3**) and carefully dried solvents and substrates, and for **1** no significant line-broadening was observed up to 0.15 mol equiv added reagent. The effect of deliberately adding a small amount of water to a solution is shown in Fig. 1. A comparison between the spectra shown in Figs. 1A and B indicates the effect which the added europium reagent, **1**, has had on the ^1H spectrum of **4**. The outcome of adding water to this system is shown in Fig. 1C. Clearly the added water has almost entirely eliminated the induced shift; from Fig. 1A, $\tau_{H\text{-}1} = 4.080$, $\tau_{H\text{-}2} = 5.489$ and from Fig. 1C $\tau_{H\text{-}1} = 4.060$, and $\tau_{H\text{-}2} = 5.463$. This implies that the water associates more strongly with **1** than does the carbohydrate derivative **4**; a practical outcome of this phenomenon is given later in this paper.

Preliminary experiments also established that the rather small[2] quantities (<0.15 mol equiv; <25 mg; $<3.5 \times 10^{-5}$ mol) of lanthanide reagent needed to produce interesting chemical shift changes, were most conveniently obtained by the addition of volume aliquots of a freshly prepared stock solution of the reagent. This procedure also provided an automatic access to two important sets of data: (*i*), plots of the magnitude of induced shifts as a function of the amount of added reagent and (*ii*), the spectrum of the compound having the optimal dispersion of chemical shifts and hence the maximal number of measurable coupling constants. This latter aspect is clearly illustrated in Fig. 1, which shows spectra of 1,2:5,6-di-*O*-isopropylidene-α-D-glucofuranose (**4**). The spectrum in Fig. 1B shows the effect of 9.84×10^{-2} mol equiv of added europium (**1**); all seven ring-proton resonances are clearly resolved.

Following preliminary evaluations, a routine series of spectra were measured in which aliquots of each of the lanthanide reagents **1**, **2**, and **3** were added to each of the four sugars **4**, **5**, **6**, and **7**, using deuterochloroform solutions throughout. For brevity, we shall center our discussion on the behavior of the D-*gluco*-derivative, **4**.

The plots shown in Figs. 2, 3, and 4 are typical and indicate that there is a linear relationship between the magnitude of an induced shift and the amount of added lanthanide reagent, at

[2]It will be noted that throughout this work we have intentionally kept the amount of added lanthanide to a minimum. It is possible to add far larger quantities but for carbohydrate derivatives this is not generally necessary.

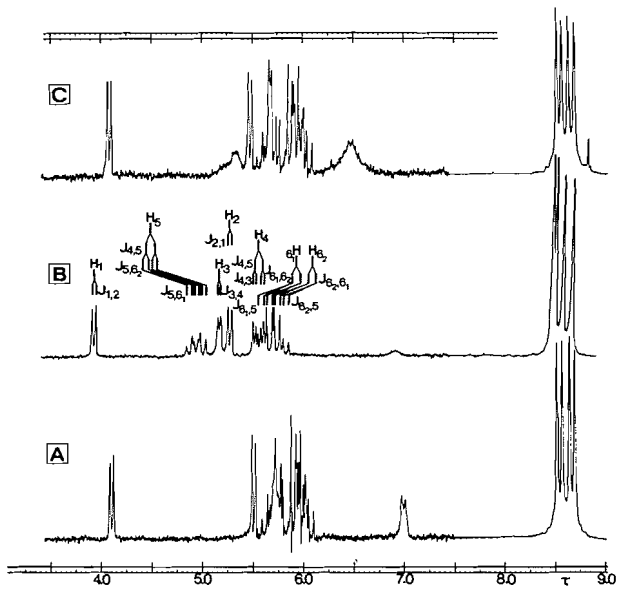

FIG. 1. The ^{1}H n.m.r. spectra (100 MHz) of 1,2:5,6-di-*O*-isopropylidene-α-D-glucofuranose (**4**, 0.0842 g) in deuterochloroform (0.5 ml). [A] The normal spectrum. [B] The spectrum after the addition of europium tris {dipivaloylmethane} (**4**, 9.84×10^{-2} mol equiv). [C] As for [B] but with the further addition of water (0.01 ml, 1.55 mol equiv per mol of **4**). A diagrammatic representation of the first-order assignment is given above the spectrum shown in [B].

least up to *ca.* 0.15 mol equiv. The linearity of these plots implies that on the n.m.r. time scale the exchange between the "free" and "complexed" lanthanide reagent must be in the fast exchange limit. Besides providing a convenient means for indicating the progress of an experiment and for obtaining the spectrum having the optimal dispersion of chemical shifts, this linear relationship provides for the recovery of the chemical shift data which would otherwise be lost; thus, extrapolation of a shift–concentration plot back to zero concentration of the added lanthanide gives the "normal" shift of that particular proton. However, it must be emphasized that this useful procedure can be subject to a sizeable experimental error. A notable illustration of this point is given in Fig. 3 for the thulium reagent (**2**). It can be seen that there is a "lag" during the addition of the first 0.01 mol equiv of **2**; furthermore, the lag is identical for all observable protons. These observations are consistent with the presence of a small amount of water in the carbohydrate sample, which complexes preferentially with the thulium reagent; in accord with this suggestion the lag was decreased by further drying of the carbohydrate **4**.

Similar results were obtained with the same sample of the D-*gluco*-derivative **4** in conjunction with the europium (**1**) and praseodymium (**3**) reagents; these data are summarized in Table 1. It is of interest to note that the final magnitude of the error induced by this effect is dependent on the slope of the shift–concentration plot for that particular resonance; the greater the slope the greater will be the error. Fortunately this potential hazard need not be troublesome since it is only necessary for the normal chemical shift of *one* proton to be directly measurable; this then provides a correction factor which can be applied to the other measurements.

The excellent results which can be obtained by extrapolations of shift–concentration plots

TABLE 1. Chemical shifts (τ-values) for 1,2:5,6-di-*O*-isopropylidene-α-D-glucofuranose (**4**) in "chloroform" solution obtained by direct measurement and by extrapolation of the plots shown in Figs. 2, 3, and 4 back to zero concentration of lanthanide reagent

Proton	Extrapolated chemical shift values			Values by direct observation
	τ_0(Eu)	τ_0(Tm)	τ_0(Pr)	
H-1	4.085	4.300	4.070	4.075
H-2	5.500	5.760	5.480	5.488
H-3	5.745	6.575	5.700*	*ca* 5.7
H-4	5.820	6.415	5.920	—†
H-5	5.710	*	5.700	5.677

*This value was not plotted in Fig.4.
†Indeterminate.

Can. J. Chem. Downloaded from www.nrcresearchpress.com by 210.87.254.42 on 09/05/12
For personal use only.

Can. J. Chem. Downloaded from www.nrcresearchpress.com by 210.87.254.42 on 09/05/12
For personal use only.

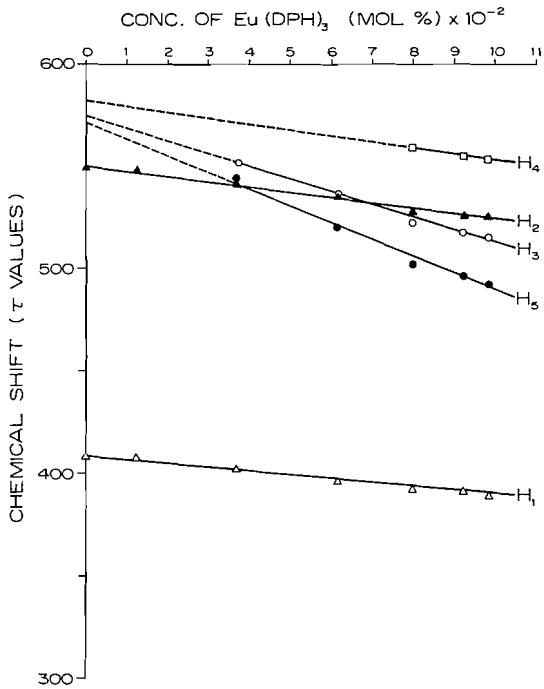

FIG. 2. Chemical shifts observed for a solution of 1,2:5,6-di-*O*-isopropylidene-α-D-glucofuranose (**4**, 0.0842 g) in deuterochloroform (0.6 ml) following the dropwise addition of a solution of europium tris{dipivaloylmethane} (**1**, 0.3115 g) in deuterochloroform (1 ml). The dotted sections of the plots shown for the H-4, -3, and -5 resonances apply over the region where assignments were considered to be insufficiently accurate to be included here.

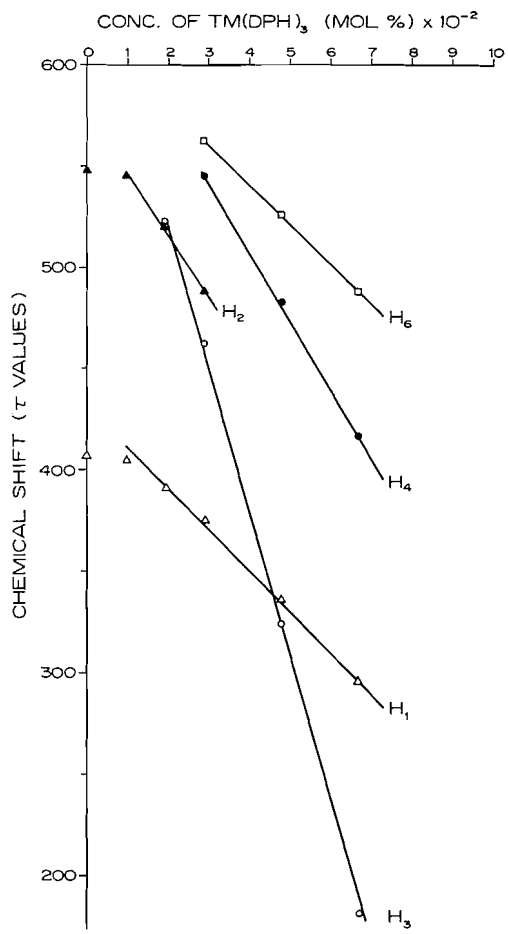

FIG. 3. Plot of the chemical shift changes observed for a solution of 1,2:5,6-di-*O*-isopropylidene-α-D-glucofuranose (**4**, 0.0897 g) in deuterochloroform (0.6 ml) induced by thulium tris{dipivaloylmethane} (**2**). The chemical shifts of the two H-6 resonances remained essentially the same throughout the experiment. The chemical shift of the H-5 resonance ran roughly parallel with that of H-4; it could not be measured with sufficient accuracy to justify its inclusion here.

when no water impurity is present are typified in the data listed in Table 2 for 3-*O*-acetyl-1,2:5,6-di-*O*-isopropylidene-α-D-glucofuranose (**6**); with care, even better agreement can be obtained.

It is interesting to note that for the compounds we have studied the thulium reagent **2** generally produces larger changes in chemical shifts than an equivalent amount of the europium reagent **1**. Insofar that the shifts induced by europium (**1**) are already very large, there seems to be at this time little advantage in using the thulium reagent **2** except possibly for conformationally mobile systems. Furthermore, the fact that for any particular amount of induced shift, **2** appears to cause significantly more line broadening[3] than **1**, also dictates in favor of **1**. Although there may

TABLE 2. Chemical shifts (τ-values) for 3-*O*-acetyl 1,2:5,6-di-*O*-isopropylidene-α-D-glucofuranose (**6**) in deuterochloroform solution, showing values obtained by direct measurements and by extrapolation to zero concentration of a shift–concentration plot for the addition of lanthanide reagents **1**, **2**, and **3**

	Chemical shifts			
	Extrapolated values			
Proton	τ_0(Eu)	τ_0(Tm)	τ_0(Pr)	Direct values
H-1	4.165	4.160	4.113	4.152
H-2	5.550	5.555	5.470	5.522
H-3	4.825	4.835	4.710	4.765

[3]This point is being further investigated.

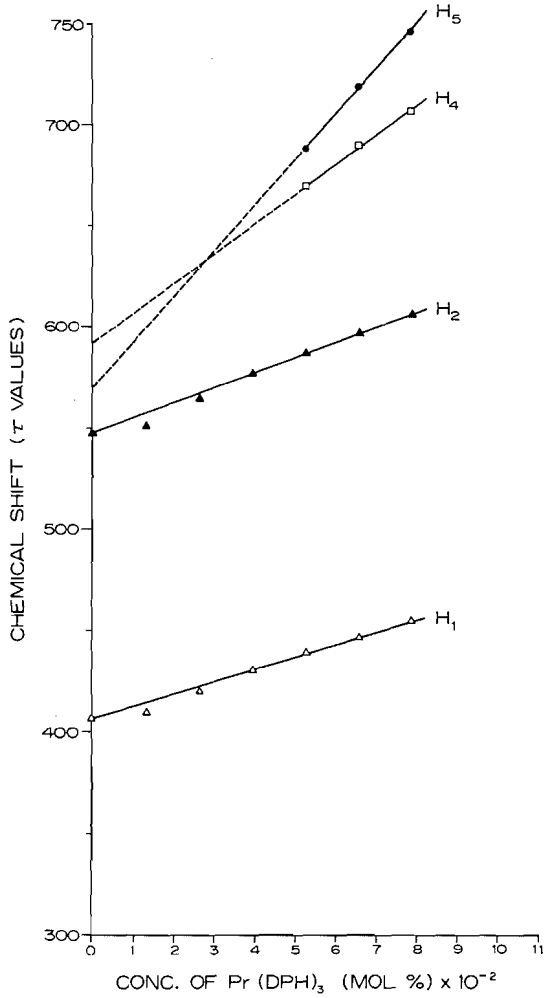

FIG. 4. Plot of the chemical shift changes induced by praseodymium tris{dipivaloylmethane} (**3**) in the proton spectra of 1,2:5,6-di-*O*-isopropylidene-α-D-glucofuranose (**4**, 0.0964 g) in chloroform (0.6 ml). The H-3 resonance moves at approximately the same rate as the H-4 resonance, that is at a rate less than that of H-5.

be occasions when it is advantageous to use the shifts to high field induced by the praseodymium reagent **3** this is certainly not the case for derivatives **4**–**7**; virtually no additional data could be obtained for these substances.

Several serendipitous observations made during the course of this study provide some interesting insights and may serve as cautions against some of the simplistic rationalizations which have been implied elsewhere, and which we consider to be either incorrect or misleading.

For simple aliphatic derivatives it is often found that the protons which are nearest in terms of bond separation to the functional group predominantly engaged in complexing with the lanthanide, are the ones which undergo the largest induced shifts. However, it would be totally naive to anticipate that this same situation should necessarily pertain to more complex molecules, particularly cyclic systems, although in principle it can. Instead, it must be emphasized that *if the shifts induced by lanthanide reagents arise via the pseudo-contact mechanism, as has generally been assumed (10), then an angular dependence must also be included in calculations of induced shift-changes.*

An indication of the complications which can arise for cyclic systems is afforded by the results for 1,2:5,6-di-*O*-isopropylidene-α-D-glucofuranose (**4**). According to results from aliphatic derivatives, one might have assumed that the C-3 hydroxyl group would be the principle donor group and hence that the H-3 resonance should undergo the largest shift. As can be seen from the Fig. 1 this is not so, and H-5 shifts 1.35 times as fast as the H-3 resonance. Interestingly, the other three compounds **5**, **6**, **7** do behave in a "normal" fashion with **1**, with H-3 undergoing the largest shift. The "anomalous" behavior of **4** is further compounded by the observation that with the thulium reagent **2**, H-3 does shift the most.

There are several possible reasons for the unusual behavior of **4** with europium (**1**). It could be that the geometry of this compound is uniquely suitable for forming a second donor bond with the europium reagent **1**, but not with the thulium reagent **2**. An alternative rationale is that the angle factor implicit in the $\cos^2 \phi$ term of the formulation of the pseudo-contact interaction is different for europium (**1**) than it is for thulium (**2**). We prefer to wait for additional mechanistic insight before commenting further. It is, however, interesting to note that the large value of $J_{4,5}$ 7.8 Hz for **4** implies that H-5 is *transoid* with respect to H-4 and is hence located quite near to the C-3 hydroxyl group. For the present it suffices to note that this behavior would certainly not have been expected on the basis of simplistic arguments.

A further chance observation, which we have not yet had the opportunity to pursue is that the

Can. J. Chem. Downloaded from www.nrcresearchpress.com by 210.87.254.42 on 09/05/12
For personal use only.

Can. J. Chem. Downloaded from www.nrcresearchpress.com by 210.87.254.42 on 09/05/12
For personal use only.

magnitudes of induced shifts appear to be significantly solvent dependent. For example we have measured the shift-changes of the D-*gluco* derivative **4**, induced by europium (**1**), for both chloroform (or deuterochloroform) and carbon tetrachloride solutions. For H-1, -3, and -5, the shift induced by a certain amount of europium (**1**) is 2.2 times larger in a carbon tetrachloride solution than it is for a chloroform solution. Should this observation have any generality it will provide the basis for some interesting chemical speculations.

To the best of our knowledge our preliminary communication (1) contains the only reference to date of the temperature dependence of lanthanide induced chemical shift changes; as the temperature is decreased so the magnitude of the shift increases. This has a number of important implications which we shall discuss elsewhere. Suffice for the present comment that it is possible to increase the "effectiveness" of a lanthanide reagent by decreasing the temperature at which the measurements are made. For example, as part of a separate series of experiments (11) we made the measurements summarized in Table 3. For H-5 the shift induced at *ca.* −47 °C by 9.4×10^{-2} mol equiv of **1** is 2.5 times that produced by the same amount of reagent at 33°C.

In a preliminary communication Crump and coworkers (8*b*) have suggested that the absolute concentration of a solution is important in determining the magnitude of an induced shift. We have repeated on several occasions the measurements discussed in this paper and do find discrepancies between individual determinations; however, we have detected no systematic regularity in these deviations and feel that it is quite likely that they represent the large experimental errors associated with this type of measurement. It is noteworthy, however, that in our experiments the *molar* concentrations of both lanthanide and substrate (*ca.* 0.6 *M*) are varied simultaneously. Other experiments which involve only changes in lanthanide do indeed show a substrate dependence (11). The same workers (8*b*) have also commented that "... the shift ratios of protons in any given substrate remain the same whichever lanthanide is used". That our chemical shift changes appear to be in very poor accord with this suggestion is demonstrated by the data summarized in Table 4.

In summary then, we have shown that lanthanide tris{dipivaloylmethane} derivatives do indeed produce useful chemical shift changes in the ^{1}H n.m.r. spectra of carbohydrates and that the reagents are used most effectively by dropwise addition of aliquots of a dilute solution. Even for potentially polyfunctional derivatives of the sort described in this paper, the induced chemical shift changes are proportional to the amount of reagent added; extrapolation of chemical shifts back to zero lanthanide concentration then affords the basic chemical shift data of the substrate system, providing that the substrate has been rigorously dried. Insofar as the induced shifts are very dependent on the temperature at which the measurements are made, it is obvious that it may prove difficult to intercompare data obtained in different laboratories, indeed it is often very difficult to obtain reproducible data. Finally, we have shown that assumptions as to which particular proton is likely to undergo the largest change in shift may lead to erroneous assignments.

Further studies on lanthanide shift reagents are clearly of interest; for example, the stoichiometry of the lanthanide-substrate equilibrium is not yet known. In particular it seems necessary to develop a fuller model for the relationship between the magnitudes of induced shifts and the conformations of both the free and associated substrates.

TABLE 3. Chemical shift data (τ-values) for 5-hydroxy-1,2,3,4,7,7-hexachloronorborn-2-ene* in deuterochloroform showing the effect of added† europium tris{dipivaloylmethane} (**1**) and of a temperature change

	Normal shifts	Shifts in presence of **1**	
Proton	At 33 °C	At 33 °C	At − 47.5 °C
H-6	8.028	7.615	7.17
H-6′	7.155	6.998	6.79
H-5	5.238	4.720	3.95

*0.0951 g in 0.6 ml.
†9.4×10^{-2} *M* equiv.

TABLE 4. Ratios of the chemical shift changes of selected pairs of protons of 1,2:5,6-di-*O*-isopropylidene-α-D-glucofuranose (**4**) in deuterochloroform solution after the addition of lanthanide tris{dipivaloylmethane}

	Numerical value of ratio		
Protons considered	Eu(**1**)	Tm(**2**)	Pr(**3**)
H-1/H-3	0.30	0.29	0.48
H-3/H-5	0.74	1.78	0.58

Can. J. Chem. Downloaded from www.nrcresearchpress.com by 210.87.254.42 on 09/05/12
For personal use only.

Experimental

Europium tris{dipivaloylmethane} (**1**) was prepared from europium oxide[4] following the method of Eisentraut and Sievers (9). The thulium reagent **2** and the praseodymium reagent **3** were prepared by the same route, but starting from the corresponding nitrate salt.[4] 2,2,6,6-Tetramethyl-3,5-heptanedione was purchased from Eastman Organic Chemicals, a division of Eastman Kodak Co.

The carbohydrate derivatives **4**–**7** were stock samples and had m.p. and n.m.r. parameters in entire accord with the assigned structures.

A sample of the lanthanide reagent and of the carbohydrate were vacuum sublimed immediately prior to an experiment. The lanthanide was dissolved in either deuterochloroform, chloroform, or carbon tetrachloride (*ca.* 0.4 g/ml). Aliquots of this standard solution were added via a 0.10 ml syringe to a solution of the carbohydrate (*ca.* 0.18 g/ml).

All n.m.r. measurements were made with a modified Varian HA-100 spectrometer, operating in the frequency-swept mode with a probe temperature of 35.0 °C. For experiments using the europium and thulium reagents (**1**, **2**) deuterochloroform solutions were used, with internal tetramethylsilane as the reference signal for the field-frequency lock. Experiments with the praseodymium reagent **3** were made with chloroform [5] solutions and the chloroform resonance was used to provide a lock signal; some tetramethylsilane was added to provide a chemical shift reference.

This work was supported by grants from the National Research Council of Canada. It is a pleasure to thank Dr. Peter Legzdins of this Department for many helpful discussions concerning the synthesis and handling of lanthanide derivatives.

1. I. Armitage and L. D. Hall. Chem. Ind. London, 1537 (1970).
2. R. J. Abraham, R. Freeman, L. D. Hall, and K. A. McLauchlan. J. Chem. Soc. 2080 (1962).
3. L. D. Hall. Adv. Carbohydr. Chem. **19**, 51 (1964).
4. L. D. Hall, J. F. Manville, and N. S. Bhacca. Can. J. Chem. **47**, 1 (1969).
5. R. Burton, L. D. Hall, and P. R. Steiner. Can. J. Chem. **48**, 2679 (1970).
6. C. C. Hinckley. J. Am. Chem. Soc. **91**, 5160 (1969).
7. (*a*) J. K. M. Sanders and D. H. Williams. J. Chem. Soc. D, 422 (1970). (*b*) P. V. Demarco, T. K. Elzey, R. B. Lewis, and E. Wenkert. J. Am. Chem. Soc. **92**, 5734 (1970). (*c*) P. V. Demarco, T. K. Elzey, R. B. Lewis, and E. Wenkert. J. Am. Chem. Soc. **92**, 5737 (1970). (*d*) G. H. Wahl, Jr., and M. R. Peterson, Jr. J. Chem. Soc. D, 1167 (1970). (*e*) R. R. Fraser and Y. Y. Wigfield. Chem. Commun. 1471 (1970). (*f*) G. M. Whitesides and D. W. Lewis. J. Am. Chem. Soc. **92**, 6979 (1970). (*g*) F. I. Carroll and J. T. Blackwell. Tetrahedron Lett. **48**, 4173 (1970). (*h*) K. J. Liska, A. F. Fentiman, Jr., and R. L. Foltz. Tetrahedron Lett. **53**, 4657 (1970). (*i*) A. F. Cockerill and D. M. Rackham. Tetrahedron Lett. **59**, 5149 (1970). (*j*) A. F. Cockerill and D. M. Rackham. Tetrahedron Lett. **59**, 5153 (1970). (*k*) C. C. Hinckley. J. Org. Chem. **35**, 2834 (1970). (*l*) G. H. Wahl and M. R. Peterson. Varian Instrum. Appl. **4**, 6 (1970). (*m*) L. H. Keith. Tetrahedron Lett. **1**, 3 (1971). (*n*) J. K. M. Sanders and D. H. Williams. J. Am. Chem. Soc. **93**, 641 (1971). (*o*) D. G. Buckley, G. H. Green, E. Ritchie, and W. C. Taylor. Chem. Ind. London, 298 (1971). (*p*) P. Belanger, C. Freppel, D. Tizane, and J. C. Richer. Chem. Commun. 266 (1971). (*q*) K. K. Andersen and J. J. Uebel. Tetrahedron Lett. **60**, 5253 (1970). (*r*) S. G. Levine and R. E. Hicks. Tetrahedron Lett. **4**, 311 (1971). (*s*) K. Tori, Y. Yoshimura, and R. Muneyuki. Tetrahedron Lett. **4**, 333 (1971). (*t*) R. A. Bauman. Tetrahedron Lett. **5**, 419 (1971). (*u*) Z. W. Wolkowski. Tetrahedron Lett. **12**, 825 (1971). (*v*) C. C. Hinckley, M. R. Klotz, and F. Patil. J. Amer. Chem. Soc. **93**, 2417 (1971). (*w*) O. Achmatowicz, Jr., A. Ejchart, J. Jurczak, L. Kozerski, and J. St. Pyrek. Chem. Commun. 98 (1971). (*x*) T. H. Siddall. Chem. Commun. 452 (1971).
8. (*a*) J. Briggs, G. J. Frost, F. A. Hart, G. P. Moss, and M. L. Staniforth. J. Chem. Soc. D, 749 (1970). (*b*) D. R. Crump, J. K. M. Sanders and D. H. Williams. Tetrahedron Lett. **50**, 4419 (1970). (*c*) P. Girard, H. Kagan, and S. David. Bull. Soc. Chim. Fr. **12**, 4515 (1970). (*d*) R. E. Rondeau and R. E. Sievers. J. Am. Chem. Soc. **93**, 1522 (1971). (*e*) J. Briggs, F. A. Hart, G. P. Moss, and E. W. Randall. Chem. Comm. 364 (1971). (*f*) R. F. Butterworth, A. G. Pernet, and S. Hanessian. Can. J. Chem. **49**, 981 (1971). (*g*) C. Beaute, Z. W. Wolkowski, and N. Thoai. Tetrahedron Lett. **12**, 817 (1971). (*h*) Z. W. Wolkowski. Tetrahedron Lett. **12**, 821 (1971). (*i*) H. Hart and G. M. Love. Tetrahedron Lett. **7**, 625 (1971). (*j*) P. Belanger, C. Freppel, D. Tizane, and J.-C. Richer. Can. J. Chem. **49**, 1985 (1971). (*k*) N. Ahmad, N. S. Bhacca, J. Selbin, and J. D. Wander. J. Am. Chem. Soc. **93**, 2564 (1971).
9. K. J. Eisentraut and R. E. Sievers. J. Am. Chem. Soc. **87**, 5254 (1965).
10. D. R. Eaton. J. Am. Chem. Soc. **87**, 3097 (1965).
11. I. Armitage and L. D. Hall. Unpublished results.

[4]Obtained from Alfa Inorganics, Inc.

[5]Ethanol-free chloroform was obtained by standing A.R. Grade chloroform over granular, self-indicating silica gel. The n.m.r. spectrum of this material shows no signs of ethanol resonances, even when the instrument was operating at the highest possible gain.

Can. J. Chem. Downloaded from www.nrcresearchpress.com by 210.87.254.42 on 09/05/12
For personal use only.

Kinetics and Mechanism of Hydrogen Exchange in the 2,4,6-Trihydroxybenzenonium Ion[1]

A. J. KRESGE,[2] Y. CHIANG,[2] AND S. A. SHAPIRO

Lash Miller Chemical Laboratories, Department of Chemistry, University of Toronto, Toronto 181, Ontario

Received May 17, 1971

The n.m.r. line-broadening method was used to measure rates of hydrogen exchange in the 2,4,6-trihydroxybenzenonium ion (carbon-protonated phloroglucinol) in a series of concentrated sulfuric and perchloric acid solutions. Comparison of separately determined rates of exchange of protons in the methylene and vinyl groups of this ion allows a concerted mechanism for the exchange reaction to be excluded and shows that exchange must occur through intermediate formation of completely deprotonated 1,3,5-trihydroxybenzene. This assignment of reaction mechanism allows transformation of the data into deprotonation rate constants, which, together with previously measured positions of equilibrium, permit estimation of specific rates of protonation of 1,3,5-trihydroxybenzene, k_+; the latter are in good agreement with the rate of aromatic hydrogen exchange of 1,3,5-trihydroxybenzene measured by an isotopic tracer method at lower acidities. The kinetic acidity dependence of k_+ is unusually shallow; this, coupled with the much steeper acidity dependences of other aromatic protonation reactions, serves to reinforce the growing realization that there is no unique relationship between kinetic acidity dependence and reaction mechanism.

La méthode d'élargissement de raies en r.m.n. a été utilisée pour mesurer les vitesses d'échange d'hydrogène dans l'ion trihydroxy-2,4,6 benzenonium (phloroglucinol protoné sur un carbone) dans une série de solutions d'acide sulfurique et d'acide perchlorique concentré. La comparaison des vitesses d'échange des protons des groupes méthylènes et vinyles de cet ion déterminées séparément, permet d'exclure un mécanisme concerté pour la réaction d'échange et montre que cet échange doit se faire par l'intermédiaire du trihydroxy-1,3,5 benzène entièrement déprotoné. L'attribution de ce mécanisme réactionnel permet de traduire ces résultats en constantes de vitesses de déprotonation, lesquelles, en liaison avec les positions d'équilibre, préalablement mesurées, permettent une estimation des vitesses spécifiques k_+, de protonation du trihydroxy-1,3,5 benzène. Ces dernières sont en bon accord avec la vitesse d'échange d'hydrogène aromatique du trihydroxy-1,3,5 benzène mesurée par une méthode de traceur isotopique à plus faible acidité. L'influence de l'acidité sur la constante cinétique k_+ est inhabituellement faible; ceci, relié à l'influence beaucoup plus forte de l'acidité sur d'autres réactions de protonation de composés aromatiques permet de renforcer l'idée qu'il n'y a pas de relation unique entre l'influence de l'acidité sur la cinétique et le mécanisme de la réaction.

Canadian Journal of Chemistry, 49, 2777 (1971)

Introduction

Comparison of the acidity dependence of the rate of aromatic hydrogen exchange (eq. 1) in concentrated acid solutions with the acidity dependence of the position of equilibrium between the aromatic substrate and its benzenonium ion conjugate acid (eq. 2) has, within recent years, afforded new insight into the nature of concentrated acid solutions (1–6). These conclusions rest upon the assumption that acid-catalyzed exchange occurs only through successive protonation and deprotonation of the aromatic substrate, and that the kinetic and equilibrium measurements therefore refer to the same chemical reaction. Should exchange take place by some other reaction path which circumvents proton addition or removal, such as, for example, a concerted mechanism which exchanges protons in the benzenonium ion while avoiding deprotonation (eq. 3), these conclusions would be upset.

[1] 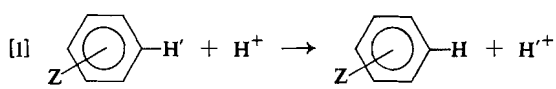

[2] 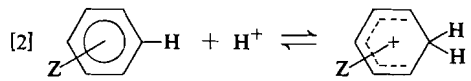

Fortunately, it is possible to test for the presence of such a concerted reaction, for that mechanism and the deprotonation–reprotonation reaction scheme lead to different ratios of rates of exchange at different sites in the benzenonium

[1]Aromatic Protonation X. For Part IX, see ref. 6.

[2]Permanent address: Department of Chemistry, Illinois Institute of Technology, Chicago, Illinois 60616.

[3] 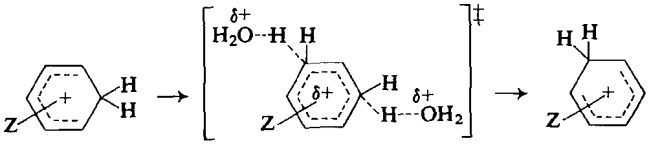

[4] 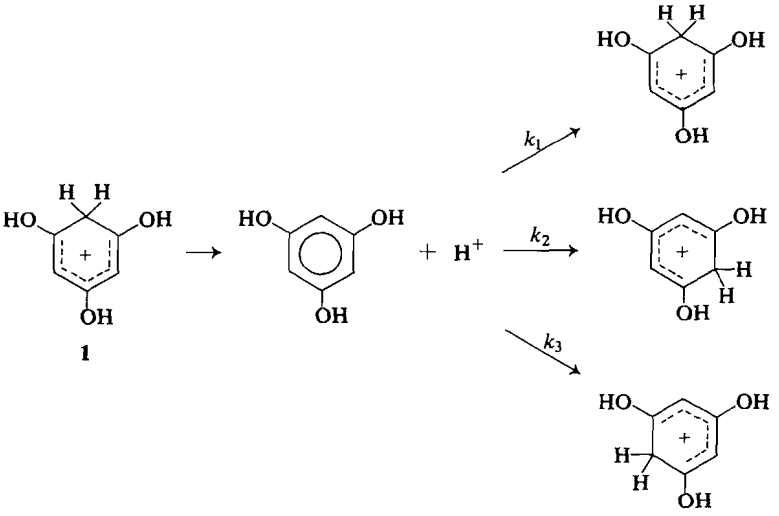

ion. Consider, for example, the case of phloroglucinol, the molecule used in the present study. When hydrogen exchange in the conjugate acid of this substance, the 2,4,6-trihydroxybenzenonium ion (**1**), occurs by the deprotonation–reprotonation mechanism, free 1,3,5-trihydroxybenzene is formed, and this then reaccepts a proton with equal probability at any one of its three equivalent basic sites (eq. 4). The specific rates of these three reprotonation reactions must be the same, but it is useful to distinguish them as k_1, k_2, and k_3 because the consequences of the three reactions on the lifetimes of the methylene group hydrogens and the vinyl group hydrogens of the 2,4,6-trihydroxybenzenonium ion, τ_m and τ_v respectively, are different. Reprotonation at the same site replaces one of the methylene group hydrogens but restores the other to its original state; the coefficient of k_1 in the rate law for methylene group exchange is therefore 0.5 (eq. 5).

$$[5] \quad -d[{=}CH_2]/dt = (0.5k_1 + k_2 + k_3)[THB] = 2.5k[THB]$$

Reprotonation at a different site, on the other hand, removes the original methylene group completely, and the coefficients of k_2 and k_3 in this rate law are therefore each unity. Exchange of vinyl group hydrogens is not effected at all by reprotonation at the same site, and only half of the original vinyl group is lost by reprotonation at either one of the other sites; this leads to the rate law for vinyl group exchange given as eq. 6.

$$[6] \quad -d[{=}CH{-}]/dt = (0.0k_1 + 0.5k_2 + 0.5k_3)[THB] = 1.0k[THB]$$

Comparison of eqs. 5 and 6 shows that exchange of methylene group hydrogens will occur 2.5 times as fast as exchange of vinyl group hydrogens ($\tau_v = 2.5\tau_m$) provided that the deprotonation–reprotonation mechanism is operating.

The concerted mechanism requires proton removal and proton addition to occur at different sites, and it therefore necessarily leads to formation of a new benzenonium ion at each act of exchange (eq. 7). This has the effect of blocking one of the reactions which occur in the deprotona-

[7] 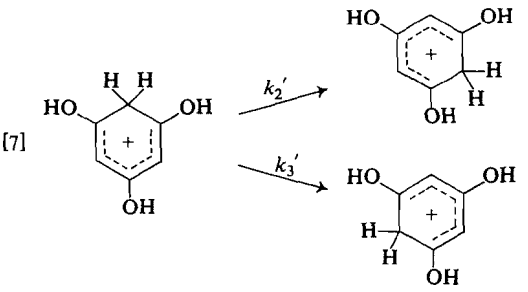

Can. J. Chem. Downloaded from www.nrcresearchpress.com by 210.87.254.42 on 09/05/12
For personal use only.

Can. J. Chem. Downloaded from www.nrcresearchpress.com by 210.87.254.42 on 09/05/12
For personal use only.

tion–reprotonation reaction scheme, and that leads to the rate laws shown in eqs. 8 and 9. The

$$[8] \quad -d[{=}CH_2]/dt = (k_2' + k_3')[THBH^+] = 2.0k'[THBH^+]$$

$$[9] \quad -d[{=}CH{-}]/dt = (0.5k_2' + 0.5k_3')[THBH^+] = 1.0k'[THBH^+]$$

concerted mechanism, therefore, gives a rate of exchange of methylene group hydrogens which is only twice that of the vinyl group hydrogens ($\tau_v = 2.0\tau_m$), a prediction different from that for the deprotonation–reprotonation mechanism.

It is difficult, if not impossible, to compare rates of methylene and vinyl group hydrogen exchange in benzenonium ions using the conventional tracer method of monitoring aromatic hydrogen exchange. Benzenonium ions, however, generally give well-separated methylene and vinyl group n.m.r. signals, which, under certain conditions, experience lifetime broadening and can therefore be used to determine rates of hydrogen exchange (7). The 2,4,6-trihydroxybenzenonium ion is particularly well suited for this purpose, for its spectrum contains only two lines at τ 3.7 (vinyl group) and 5.9 p.p.m. (methylene group) which broaden appreciably in moderately concentrated aqueous sulfuric and perchloric acids (8). This substance was therefore chosen for the present test of the concerted mechanism.

Experimental

Materials

The water of hydration was removed from phloroglucinol dihydrate (Fisher Scientific Co., Reagent Grade) by drying in an oven at 110° for 24 h. Acetone was Mallinckrodt ANALAR grade and was used without further treatment. Reagent grade 95% sulfuric acid and 70% perchloric acid were diluted with distilled water to approximately desired strengths, and exact concentrations were then determined by titration (by weight) with standard base.

Solutions for kinetic measurement were prepared by combining weighed amounts of anhydrous phloroglucinol and acid solution, adding a trace of acetone and shaking (and sometimes heating gently) to complete solution. Since the effect of added phloroglucinol on H_0 values and other measures of the acid strength of concentrated solutions is not known, phloroglucinol concentrations were kept as low as possible (2–4 weight % = 0.3–0.5 *M*) without impairing the quality of the n.m.r. signals, and acid strengths were evaluated on the basis of the acid concentration before phloroglucinol was added. Molarities and acidity function values were calculated from weight % using recently provided interpolation functions (9*a*, 10).

Kinetics

Spectra were taken with a Varian A-60 spectrometer operating at an r.f. field no greater than 0.05 mG and a sweep rate of 0.1–0.2 Hz/s; the fact that all lines were accurately Lorentzian in shape indicates that these conditions ensured slow passage and avoided saturation. The methylene and vinyl group portions of the spectra were recorded on ordinary chart paper using a convenient horizontal scale (0.5–2 Hz/cm) and a spectral amplitude sufficient to give a large vertical deflection; each line was scanned 3–4 times in order to average out noise. The sample (probe) temperature was determined by measuring the separation between hydroxyl and methyl group signals from a sample of methanol and using relationships between this parameter and temperature provided in the literature (11). During the course of a day's operations, temperature fluctuations never exceeded 0.2°, but variations from day to day sometimes were of the order of 1°. The experiments in H_2SO_4 were done at 33.1–33.8° and those in $HClO_4$ at 32.7–34.0°.

Full line widths at half-heights, $\delta\nu$, were determined from these traces by reading off intensities, I_l, at 15–25 frequencies, ν_l, spaced regularly throughout each line, and then fitting these data by the method of least squares to the Lorentzian line-shape function given as eq. 10.

$$[10] \quad \frac{I_l - I_0}{I_{max} - I_0} = \frac{1}{1 + [(2/\delta\nu)(\nu_l - \nu_0)]^2}$$

In this expression, I_0 is the base line and I_{max} is the maximum intensity, *i.e.* the peak height at the mid-point of the spectral line, ν_0. This function falls off only very gradually at distances far removed from ν_0, and it is significant, therefore, that base lines obtained by least squares fit were usually lower by appreciable amounts (as much as 50%) than base lines drawn by eye through the bottoms of the spectral lines; this indicates that the scans seldom covered a frequency range large enough for accurate visual analysis. Compliance to eq. 10 containing the least squares parameters was invariably well within the experimental uncertainty of the data; on the other hand, when visually-determined parameters were used in the equation, the fit was usually poor, especially in the spectral tails.

Average lifetimes, τ, of methylene or vinyl group hydrogens were calculated from line-widths using eq. 11.

$$[11] \quad \pi\delta\nu = \tau^{-1} + T_2^{-1}$$

The natural line-width in the absence of hydrogen exchange, T_2^{-1}, was approximated as the width at half-height of the signal from a trace of acetone dissolved in each kinetic sample. This signal proved to be wider for H_2SO_4 solutions than for $HClO_4$ solutions, but in each acid it was approximately independent of acid concentration; constant values of 0.6 Hz for H_2SO_4 and 0.4 Hz for $HClO_4$ were therefore adopted.

The data obtained in this way are summarized in Tables 1 and 2.

Results and Discussion

These kinetic experiments allow a particularly straightforward choice between the two mechanisms for hydrogen exchange in the 2,4,6-trihy-

TABLE 1. Line widths of n.m.r. signals from the 2,4,6-trihydroxybenzenonium ion in aqueous sulfuric acid*

Weight % H_2SO_4†	Weight % THB‡	C_{THB} (M)§	δν (Hz)‖ =CH_2	δν (Hz)‖ =CH—	τ_v/τ_m
72.3	2.09	0.28	—	24.0±1.1	—
75.5	2.28	0.31	44.5±3.5	15.5±0.5	2.94±0.25
75.5	2.40	0.33	44.6±1.6	15.8±0.8	2.90±0.17
77.9	2.06	0.29	20.6±0.8	9.40±0.26	2.28±0.11
77.9	2.47	0.34	20.0±0.6	9.00±0.40	2.31±0.12
77.9	2.52	0.35	22.4±0.6	9.30±0.13	2.50±0.06
80.3	2.49	0.35	14.1±0.5	6.22±0.08	2.41±0.09
80.3	2.54	0.35	13.5±0.6	5.80±0.06	2.49±0.10
80.3	2.89	0.41	13.3±0.2	5.95±0.18	2.37±0.07
83.3	2.26	0.32	9.02±0.20	3.85±0.07	2.60±0.07
83.3	3.08	0.44	9.72±0.25	4.05±0.08	2.64±0.08
83.3	3.78	0.55	9.87±0.39	3.96±0.08	2.77±0.12
				Average	2.56±0.07¶

*At 33.1–33.8°.
†Weight % H_2SO_4 before addition of phloroglucinol.
‡Weight % of phloroglucinol in the final solution.
§Molar concentration of phloroglucinol estimated using the volume of the acid solution only.
‖Error estimates are standard deviations obtained from the least squares analysis.
¶Standard deviation of the mean.

TABLE 2. Line widths of n.m.r. signals from the 2,4,6-trihydroxybenzenonium ion in aqueous perchloric acid*

Weight % $HClO_4$†	Weight % THB‡	C_{THB} (M)§	δν (Hz)‖ =CH_2	δν (Hz)‖ =CH—	τ_v/τ_m
64.0	3.06	0.32	58.0±4.0	21.1±1.3	2.78±0.26
64.8	2.32	0.30	44.8±2.1	15.5±0.5	2.95±0.17
65.6	2.42	0.32	32.8±1.7	14.0±0.6	2.38±0.16
65.6	2.93	0.38	34.1±0.3	13.4±0.5	2.60±0.10
66.4	2.23	0.29	28.0±0.5	11.3±0.4	2.54±0.47
66.4	2.63	0.35	25.4±0.1	11.7±0.3	2.21±0.13
67.7	2.87	0.38	21.4±0.9	8.77±0.12	2.51±0.11
68.4	2.52	0.34	16.5±0.6	6.87±0.21	2.48±0.10
68.4	2.52	0.34	16.8±0.4	6.87±0.17	2.53±0.10
69.4	2.39	0.32	12.9±0.3	5.68±0.11	2.37±0.08
70.4	2.34	0.32	10.3±0.3	4.45±0.20	2.42±0.12
70.4	2.74	0.37	9.9±0.2	4.54±0.10	2.27±0.07
				Average	2.50±0.06¶

*At 32.7–34.0°.
†Weight % $HClO_4$ before addition of phloroglucinol.
‡Weight % phloroglucinol in the final solution.
§Molar concentration of phloroglucinol estimated using the volume of the acid solution only.
‖Error estimates are standard deviations obtained from the least squares analysis.
¶Standard deviation of the mean.

droxybenzenonium ion, represented as eqs. 4 and 7. The data presented in Table 1 show that the average value of τ_v/τ_m measured in 11 separate experiments at four different sulfuric acid concentrations is 2.56 ± 0.07; this is within experimental error of the value 2.50 demanded by the kinetic analysis for a deprotonation–reprotonation scheme (eqs.4–6), but is clearly incompatible with $\tau_v/\tau_m = 2.00$ required for a concerted reaction mechanism (eqs. 7–9). The results for perchloric acid are in complete accord with this: $\tau_v/\tau_m = 2.50 \pm 0.06$ for 12 experiments at eight different acid concentrations.

These results show that the mechanism favored by hydrogen exchange in the 2,4,6-trihydroxybenzenonium ion is the deprotonation–reprotonation scheme shown as eq. 4, and that, at the very most, only a few per cent of the reaction can occur through the concerted mechanism of eq. 7. It would seem reasonably safe, therefore, to com-

Can. J. Chem. Downloaded from www.nrcresearchpress.com by 210.87.254.42 on 09/05/12
For personal use only.

[12] 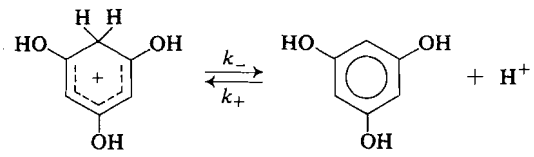

pare rates of aromatic hydrogen exchange with equilibria of benzenonium ion formation under the assumption that these are two different manifestations of the same chemical process.

With this mechanistic assignment in hand, it is possible to transform the data of Tables 1 and 2 into specific rates of deprotonation of the conjugate acid of phloroglucinol, k_- (eq. 12). The constant k_+ of eq. 12 is the specific rate of reprotonation at all basic sites, and it is therefore equal to the sum of the three individual rate constants k_1, k_2, and k_3 used in eq. 4. The rate law of eq. 5 can then be transformed into that shown as eq. 13, which, since the system is at equilibrium and

$$[13] \qquad \frac{-\mathrm{d}[{=}\mathrm{CH_2}]}{\mathrm{d}t} = \frac{2.5}{3.0}k_+[\mathrm{THB}]$$

$k_+[\mathrm{THB}] = k_-[\mathrm{THBH^+}]$ is equivalent to eq. 14. This shows that the specific rate of deprotona-

$$[14] \qquad \frac{-\mathrm{d}[{=}\mathrm{CH_2}]}{[\mathrm{THBH^+}]\,\mathrm{d}t} = \tau_m^{-1} = \frac{2.5}{3.0}k_-$$

tion, k_-, may be obtained by multiplying τ_m^{-1} by the factor 3.0/2.5. A similar treatment of the rate of exchange of vinyl group protons (eqs. 15 and 16) shows that k_- is also available from τ_v^{-1} but here the multiplicative constant is 3.0.

$$[15] \qquad \frac{-\mathrm{d}[{=}\mathrm{CH}{-}]}{\mathrm{d}t} = \tfrac{1}{3}k_+[\mathrm{THB}]$$

$$[16] \qquad \frac{-\mathrm{d}[{=}\mathrm{CH}{-}]}{[\mathrm{THBH^+}]\,\mathrm{d}t} = \tau_v^{-1} = \tfrac{1}{3}k_-$$

The results of this analysis are presented in Tables 3 and 4 together with some conventional measures of the acid strength of the concentrated acid solutions in which these experiments were performed. It may be seen, first of all, that k_- decreases with increasing acidity, as is appropriate for a deprotonation and therefore base-catalyzed reaction. This decrease, however, is considerably more precipitous than expected were the basic strength of these solutions just the inverse of acid concentration, and it would seem that here, as with many acid-catalyzed reactions in concentrated acid solutions, an indicator acidity function is a more appropriate measure of acid-base strength. Figure 1 shows that the H_0 function does in fact correlate the data reasonably well, giving slopes $\mathrm{d}(\log k)/\mathrm{d}(H_0)$ of 0.52 ± 0.02 in sulfuric acid and 0.42 ± 0.01 in perchloric acid.

The fact that this correlation shows essentially no difference in deprotonation rate between sulfuric and perchloric acid solutions of the same

TABLE 3. Rates of deprotonation of 2,4,6-trihydroxybenzenonium ion and reprotonation of 1,3,5-trihydroxybenzene in aqueous sulfuric acid*

Weight % H_2SO_4†	$C_{H_2SO_4}$ (M)†	H_0†,‡	k_- (s^{-1})§	$\frac{[THBH^+]}{[THB]}$‖	$10^4\,k_+$ (s^{-1})§
72.3	12.1	−6.22	—, 221	474	—, 10.5
75.5	12.9	−6.70	166, 141	1530	25.4, 21.6
75.5	12.9	−6.70	166, 143		25.4, 21.9
77.9	13.5	−7.07	75.6, 83.1	3780	28.6, 31.4
77.9	13.5	−7.07	73.2, 79.2	3780	27.7, 29.9
77.9	13.5	−7.07	82.2, 82.2	3780	31.1, 31.1
80.3	14.2	−7.44	51.0, 53.0	9350	47.7, 49.6
80.3	14.2	−7.44	48.7, 49.1	9350	45.5, 45.9
80.3	14.2	−7.44	47.8, 50.4	9350	44.7, 47.1
83.3	15.0	−7.92	31.8, 30.6	30300	96.4, 92.7
83.3	15.0	−7.92	35.0, 31.7	30300	106, 96.1
83.3	15.0	−7.92	34.4, 32.6	30300	104, 98.8

*At 33.1–33.8°.
†Measures of acid strength refer to H_2SO_4 before addition of phloroglucinol.
‡Reference 14.
§The first rate constant in each set is based on τ_m and the second, on τ_v.
‖Extrapolated from the data of ref. 10 using the relationship $\log([THBH^+]/[THB]) = -3.930 - 1.062(H_0)$.

Can. J. Chem. Downloaded from www.nrcresearchpress.com by 210.87.254.42 on 09/05/12
For personal use only.

TABLE 4. Rates of deprotonation of 2,4,6-trihydroxybenzenonium ion and reprotonation of 1,3,5-trihydroxybenzene in aqueous perchloric acid*

Weight % $HClO_4$†	C_{HClO_4} (M)†‡	H_0†,‡	k_- (s^{-1})§	$\frac{[THBH^+]}{[THB]}$‖	$10^4\,k_+$ (s^{-1})§
64.0	10.1	−6.12	217, 195	71.8	1.56, 1.40
64.8	10.3	−6.32	167, 143	102	1.70, 1.46
65.6	10.5	−6.52	122, 128	143	1.74, 1.83
65.6	10.5	−6.52	127, 122	143	1.82, 1.74
66.4	10.7	−6.75	104, 103	206	2.14, 2.12
66.4	10.7	−6.75	94.3, 107	206	1.94, 2.20
67.7	11.0	−7.07	79.2, 78.9	341	2.70, 2.69
68.4	11.2	−7.26	60.7, 61.1	467	2.83, 2.85
68.4	11.2	−7.26	61.9, 61.1	467	2.89, 2.85
69.4	11.4	−7.53	47.3, 49.8	744	3.52, 3.71
70.4	11.7	−7.82	35.4, 39.0	1230	4.35, 4.80
70.4	11.7	−7.82	37.2, 38.3	1230	4.58, 4.71

*At 32.7–34.0°.
†Measures of acid strength refer to $HClO_4$ before addition of phloroglucinol.
‡Reference 9.
§In each set, the first rate constant is based on τ_m and the second on τ_γ.
‖Extrapolated from the data of ref. 10 using the relationship $\log([THBH^+]/[THB]) = -3.588 - 0.546(H_c)$.

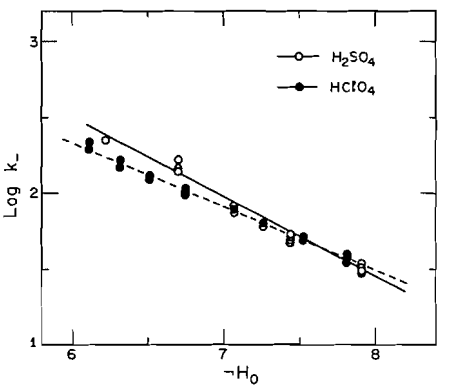

FIG. 1. Relationship between the specific rate of deprotonation of 2,4,6-trihydroxybenzenonium ion and the H_0 acidity function.

H_0 value, however, is disturbing. An indicator acidity function such as H_0 is based on equilibrium measurements, and it thus presumably reflects the equilibrium acidity of the medium. This may well be different from the kinetic acidity, and, in particular, a sulfuric acid solution, with its additional general acid-general base pair, HSO_4^-–SO_4^{2-}, available to protonate and/or deprotonate a substrate, might be expected to have a greater kinetic acidity than a perchloric acid solution of the same H_0. Such differences in kinetic and equilibrium acidity are in fact not uncommon; a particularly relevant case is the increase in the rate of detritiation of 1,3-dimethoxybenzene-4-*t* observed in going from perchloric acid solutions to sulfuric acid solutions at constant H_0 (5).

This work on 1,3-dimethoxybenzene suggests, moreover, that the H_0 scale, based as it is on primary aniline indicators, is not altogether appropriate for correlating rates of aromatic hydrogen exchange, and that an acidity function which uses indicator bases more similar in structure to the carbonium ions generated in aromatic hydrogen exchange, might be more suitable; this conclusion is reinforced by more recent investigations of equilibrium aromatic protonation (10). It is significant, therefore, that correlations of the present rate data with H_c, a recently constructed acidity function which uses only conjugate bases of carbonium ions as indicators (12), does show the present reaction to be more rapid in sulfuric acid than in perchloric acid. Perhaps even more appropriate for this purpose than the H_c function would be an acidity scale based upon phloroglucinol itself. The extent of protonation of phloroglucinol has recently been measured in sulfuric and in perchloric acids (10), and extrapolation of these data to the regions for which k_- is available gives the values of $[THBH^+]/[THB]$ listed in Tables 3 and 4. Figure 2 shows the correlation of the present rate data using this measure of acid strength; it may be seen that, at constant extent of protonation of 1,3,5-trihydroxybenzene, the 2,4,6-trihydroxybenzenonium ion loses protons to sulfuric acid *ca.* four times more rapidly than to perchloric acid.

The availability of these values of $[THBH^+]/[THB]$ makes it possible to estimate specific rates of protonation of phloroglucinol, k_+, by using the equilibrium relationship $k_+[THB] =$

Can. J. Chem. Downloaded from www.nrcresearchpress.com by 210.87.254.42 on 09/05/12
For personal use only.

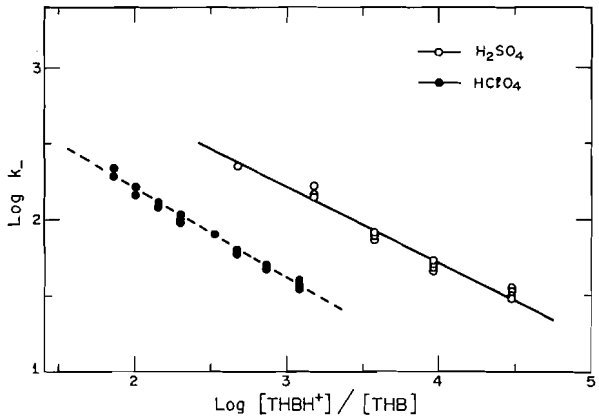

FIG. 2. Relationship between the specific rate of deprotonation of 2,4,6-trihydroxybenzenonium ion and an acidity function based upon the equilibrium protonation of 1,3,5-trihydroxybenzene.

$k_-[THBH^+]$; values of k_+ obtained in this way are listed in Tables 3 and 4. These rate constants are composed of $[THBH^+]/[THB]$ measured at 25° (10) and k_- determined at 33–34°, but the uncertainty in k_+ introduced by this difference in temperature is likely to be well under a factor of two, for extents of protonation of weak bases in concentrated acids usually do not change very rapidly with temperature (13–16). The effect of temperature, moreover, will be much the same on all of the values of $[THBH^+]/[THB]$ involved, and the uncertainty in relative values of k_+ should thus be an order of magnitude less than that in their absolute magnitude. Any conclusions drawn from the manner in which k_+ changes as a function of some other variable, *e.g.* acidity of the medium, should therefore be quite reliable.

The acidity dependence of k_+ is in fact unusually shallow; for example, in sulfuric acid $-d(\log k_+)/d(H_0) = 0.54 \pm 0.02$ and the Bunnett–Olsen parameter ϕ (17) has the value 0.49 ± 0.02, while in perchloric acid $-d(\log k_+)/d(H_0) = 0.30 \pm 0.01$ and $\phi = 0.73 \pm 0.01$. Though uncommon, this behavior is nevertheless readily understandable in terms of the two factors which control kinetic acidity dependence: (*1*) substrate structure and (*2*) transition state structure (6). The substrate here, phloroglucinol, shows a relatively shallow acidity dependence even in its equilibrium protonation, principally because its conjugate acid interacts strongly with solvent water by forming hydrogen bonds through its positively charged hydroxyl groups (10, 18). The rate of proton addition to phloroglucinol cannot show an acidity dependence any steeper than this, and, in fact, the kinetic acidity dependence should be somewhat more shallow than the equilibrium acidity dependence because this reaction, being quite rapid, will have an early transition state in which only a fraction of the equilibrium acidity dependence can be realized. In support of this is the fact that the data of Table 4 give an acidity exponent, α_A (4, 6), of 0.38 ± 0.01, which can be taken to mean that the protonation transition state lies about four-tenths of the way along the reaction coordinate between 1,3,5-trihydroxybenzene and the 2,4,6-trihydroxybenzenonium ion.

This unusually low kinetic acidity dependence, when coupled with the considerably steeper ones shown by some other aromatic protonation reactions proceeding by the same mechanism (3, 6, 16), adds to the growing realization that kinetic acidity dependence is not a sharply defined characteristic of reaction mechanism and points up the danger of drawing mechanistic conclusions from kinetic acidity dependence alone. In particular, the value of ϕ for the present reaction occurring in perchloric acid, 0.73, and that evaluated by Bunnett and Olsen (17) for the protonation of azulene using the data of ref. 16, −0.42, cover almost all of the range available to this parameter.

These relationships between k_+ and the acidity of the medium make it possible to compare the present results with the rate of aromatic hydrogen exchange in phloroglucinol measured by the tracer method at lower acidities (6). Perhaps the best function down which to make the necessary extrapolation is $\log([THBH^+]/[THB])$, and use of the relationship $\log k_+ = 3.366 + 0.415 \log([THBH^+]/[THB])$ gives a value of 2.7×10^2

Can. J. Chem. Downloaded from www.nrcresearchpress.com by 210.87.254.42 on 09/05/12
For personal use only.

s^{-1} for k_+ in 28.1 weight % $HClO_4$, the most concentrated acid in which the tracer measurements were done. These tracer experiments determined the rate of loss of tritium from one position of 1,3,5-trihydroxybenzene, and the rate constant measured, k_{-t}, therefore differs from k_+ of the present work by a statistical factor of three plus an isotope effect: $k_{-t} = (k_+/3)/(1 + k_H/k_T)$; in addition, the tracer work was done at 1.4° whereas the present measurements refer to 33–34°. Neither the temperature coefficient of k_{-t} nor the isotope effect k_H/k_T is known for 1,3,5-trihydroxybenzene, but these quantities are available for the same reaction of 1,3,5-trimethoxybenzene; since these two substrates are quite similar both in structure and in reactivity, it would seem not unreasonable to apply the trimethoxybenzene data to the present case. In the interval 1.4–33.5°, k_{-t} for 1,3,5-trimethoxybenzene increases by a factor of 22 (19) and k_H/k_T for this substrate is 20 (20); combination of these numbers with the measured value of k_{-t} for 1,3,5-trihydroxybenzene at 1.4° in 28.1 weight % $HClO_4$, 1.3×10^{-1} s^{-1} (6), gives $k_+(33.5°) = 1.8 \times 10^2$ s^{-1}. This is only 30% less than the value extrapolated from the present experiments, which, in view of the approximations made, must be considered to be very good agreement.

The authors are indebted to the National Research Council of Canada for a grant which made this research possible; to Professor W. F. Reynolds, Professor J. C. Thompson, and Mrs. A. E. Lemire for help with the nmr method of measuring reaction rates; and to Professor K. Yates, in whose laboratory this work was performed, for his most generous hospitality.

1. A. J. KRESGE and Y. CHIANG. Proc. Chem. Soc. 81 (1961).
2. F. A. LONG and J. SCHULZE. J. Am. Chem. Soc. **83**, 3340 (1961).
3. J. SCHULZE and F. A. LONG. J. Am. Chem. Soc. **86**, 331 (1964).
4. A. J. KRESGE, R. A. MORE O'FERRALL, L. E. HAKKA, and V. P. VITULLO. Chem. Commun. 46 (1965).
5. A. J. KRESGE, L. E. HAKKA, S. MYLONAKIS, and Y. SATO. Disc. Faraday Soc. **39**, 75 (1965).
6. A. J. KRESGE, S. G. MYLONAKIS, Y. SATO, and V. P. VITULLO. J. Am. Chem. Soc. In press.
7. D. M. BROUWER, E. L. MACKOR, and C. MACLEAN. *In* Carbonium ions. *Edited by* G. A. Olah and P. von R. Schleyer. Vol. II. John Wiley and Sons, New York, 1970. Chapt. 20.
8. A. J. KRESGE, Y. CHIANG, and L. E. HAKKA. J. Am. Chem. Soc. In press.
9. (*a*) A. J. KRESGE and H. J. CHEN. Unpublished work; (*b*) K. YATES and H. WAI. J. Am. Chem. Soc. **86**, 5408 (1964).
10. A. J. KRESGE, H. J. CHEN, L. E. HAKKA, and J. E. KOUBA. J. Am. Chem. Soc. In press.
11. A. L. VAN GEET. Anal. Chem. **42**, 679 (1970).
12. M. T. REAGAN. J. Am. Chem. Soc. **91**, 5506 (1969).
13. E. M. ARNETT and R. D. BUSHICK. J. Am. Chem. Soc. **86**, 1564 (1964).
14. C. D. JOHNSON, A. R. KATRITZKY, and S. A. SHAPIRO. J. Am. Chem. Soc. **91**, 6654 (1969).
15. P. TICKLE, A. G. BRIGGS, and J. M. WILSON. J. Chem. Soc. B, 65 (1970).
16. B. C. CHALLIS and F. A. LONG. J. Am. Chem. Soc. **87**, 1196 (1965).
17. J. F. BUNNETT and F. P. OLSEN. Can. J. Chem. **44**, 1917 (1966).
18. W. M. SCHUBERT and R. H. QUACCHIA. J. Am. Chem. Soc. **85**, 1278 (1963).
19. A. J. KRESGE, Y. CHIANG, and Y. SATO. J. Am. Chem. Soc. **89**, 4418 (1967).
20. A. J. KRESGE and Y. CHIANG. J. Am. Chem. Soc. **89**, 4411 (1967).

Can. J. Chem. Downloaded from www.nrcresearchpress.com by 210.87.254.42 on 09/05/12
For personal use only.

Can. J. Chem. Downloaded from www.nrcresearchpress.com by 210.87.254.6 on 09/05/12
For personal use only.

Isocarbostyrils. I. Electrophilic Substitution Reactions

D. E. HORNING, G. LACASSE, AND J. M. MUCHOWSKI[1]

Bristol Laboratories of Canada, Candiac, Quebec

Received April 19, 1971

The electrophilic substitution of *N*-alkylated isocarbostyrils was examined in considerable detail. Bromination, acylation, nitration, and acid-catalyzed condensation with formaldehyde occurred exclusively at C-4 under relatively mild conditions. The acylation of isocarbostyrils has heretofore not been reported.

The bromination of 2-methyl-5-nitroisocarbostyril in aqueous acetic acid gave 2-methyl-3,4-dihydro-3-hydroxy-4-bromo-5-nitroisocarbostyril (7) of unknown stereochemistry, as the sole product. When heated above its melting point, 7 lost the elements of water to give the "normal" product of bromination **8**.

In aqueous acetic acid, excess bromine was shown to convert isocarbostyrils to the corresponding 3,4-dihydro-3-hydroxy-4,4-dibromo derivatives whose structures were supported by spectral and degradative evidence.

La substitution électrophile d'isocarbostyriles *N*-alkylés a été examinée avec beaucoup de soin. Sous des conditions relativement douces, la bromation, l'acylation, la nitration, et la condensation acido-catalysée avec le formaldéhyde, se fait exclusivement sur C-4. L'acylation des isocarbostyriles n'a jusqu'a présent jamais été rapportée.

La bromation du méthyl-2 nitro-5 isocarbostyrile dans l'acide acétique aqueux conduit au seul méthyl-2 dihydro-3,4 hydroxy-3 bromo-4 nitro-5 isocarbostyrile (7) de stéréochimie inconnue. Lorsque le composé 7 est chauffé au-dessus de son point de fusion, il y a élimination d'eau et formation du produit "normal" de bromation **8**.

Dans l'acide acétique aqueux, un excès de brome transforme les isocarbostyriles en dérivés dihydro-3,4 hydroxy-3 dibromo-4,4 correspondants, dont les structures sont confirmées par des preuves spectrales et de dégradation.

Canadian Journal of Chemistry, **49**, 2785 (1971)

2-Pyridone (**1**; R = H) and its *N*-alkylated derivatives are electron-rich heterocyclic systems which are generally considered to possess a substantial degree of aromatic character (1–3). These compounds undergo electrophilic substitution with ease at the 3- and the 5-positions, with substitution often, but by no means always, occurring preferentially at C-3 (4–7; see also ref. 2, pp. 659–671). Quinolin-2-one (**2**, R = H; carbostyril), isoquinolin-1-one (**3**, R = H; isocarbostyril), and the *N*-alkylated derivatives thereof, are expected to have properties somewhat similar to 2-pyridones, but with the obvious difference that electrophilic attack of the hetero ring would be confined to one carbon atom (C-3 in **2** and C-4 in **3**).

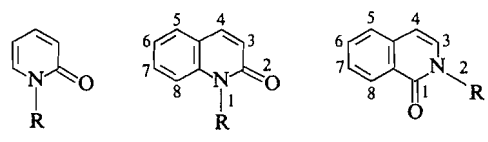

1 **2** **3**

[1]To whom enquiries concerning this paper should be addressed.

In connection with several synthetic objectives, it was necessary to examine the behavior of various electrophilic reagents toward selected members of the isocarbostyril family. When this investigation was initiated (1963), only a few examples of electrophilic substitution in the isocarbostyril[2] series had been described (8–12). These, and studies which have appeared since then, are described in the main body of this paper.

The great majority of this work was restricted to *N*-substituted isocarbostyrils because of the ease with which they were prepared from isoquinolines (see Experimental), and because an *N*-substituent was expected to ensure that the lactam form[3] was the species undergoing reaction.

Halogenation

The bromination of 2-methylisocarbostyril (**3**, R = CH_3) was first described by Bamberger and Frew in 1894 (9). A monobromo compound

[2]The carbostyril series will not be considered further in this paper. References 13 and 14 should be consulted for pertinent data in this area.

[3]Electrophilic substitution of isocarbostyril (**3**, R = H) could occur via the lactam form, the enol form, or a mixture of both forms. See section on nitration, below.

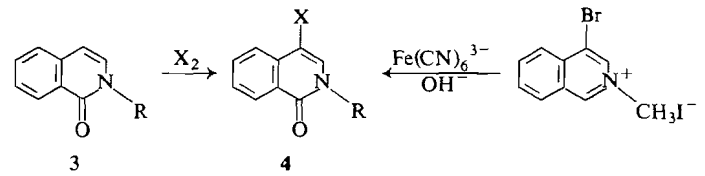

SCHEME 1

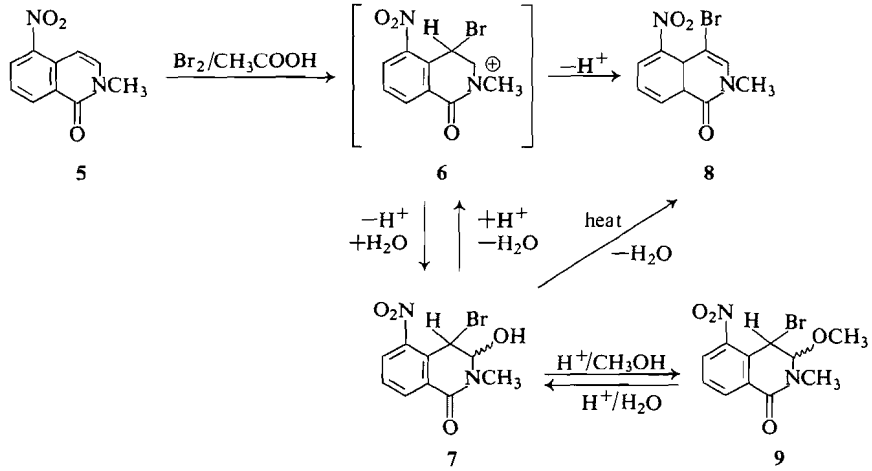

SCHEME 2

of unspecified structure was obtained in high yield. In 1958, Robison and Robison (10) reported that the oxidative chlorination or bromination ($HX + H_2O_2$) of isocarbostyril produced 4-chloro- or 4-bromoisocarbostyril (**4**, X = Cl, Br; R = H: see Scheme 1) respectively. Very shortly thereafter, Ochiai and Kawazoe (12) showed that the bromination of isocarbostyril in acetic acid gave 4-bromoisocarbostyril, the structure of which was confirmed by conversion to the known 1-chloro-4-bromoisoquinoline.

In this study the addition of a molecular equivalent of bromine in acetic acid to a solution of 2-methylisocarbostyril in the same solvent, gave a monobromo compound with properties in agreement with those previously reported (9). This compound was shown to be 2-methyl-4-bromoisocarbostyril (**4**, X = Br; R = CH_3) by direct comparison with a specimen synthesized by the alkaline ferricyanide oxidation of 4-bromoisoquinoline methiodide. The bromination of several other isocarbostyrils under the same conditions gave the corresponding 4-monobromo derivatives (see Table 1) in every case but one (see below). The structures of these compounds were assigned by analogy to the examples cited above, and were supported by their characteristic n.m.r. spectral properties (see Table 2).

The bromination of 2-methyl-5-nitroisocarbostyril (**5**, see Scheme 2) under the usual conditions (*i.e.* bromine in acetic acid followed by an aqueous work-up), gave a 1:1 mixture of two monobromo compounds. One of these, a lemon yellow solid, was clearly 2-methyl-4-bromo-5-nitroisocarbostyril (**8**) as deduced from its elemental analysis and spectral properties. The other, a pale yellow solid, analyzed for $C_{10}H_9BrN_2O_4$ (*i.e.* **8** + 1 H_2O), and had a broad i.r. absorption (Nujol mull) at 3262 cm^{-1}. The n.m.r. spectrum (see Table 2) confirmed the presence of an intact 1,2,3-trisubstituted benzene system (for typical ABC spectra see ref. 17*b*), the absence of other absorptions in the aromatic region, and in addition, showed three single proton absorptions at δ 5.32 (J = 2.3 Hz), 5.79 (J = 2.3 Hz) and 6.85 ($w/2$ = 13 Hz, exchanged with D_2O). These data when viewed together left little doubt that the light yellow compound possessed the bromohydrin structure **7**. Finally, it is of interest to note that the bromination of **5** in 10% aqueous acetic acid gave **7** as the sole product, and that **7** was converted to **8** when heated to its melting point.

Can. J. Chem. Downloaded from www.nrcresearchpress.com by 210.87.254.6 on 09/05/12
For personal use only.

Can. J. Chem. Downloaded from www.nrcresearchpress.com by 210.87.254.6 on 09/05/12
For personal use only.

TABLE 1. Yields and physical constants* of some brominated isocarbostyrils

Compound				Yield	Melting	Crystallization	% Calculated				% Found			
No.	X	R	R′	(%)	point (°C)	solvent	C	H	Br	N	C	H	Br	N
4	Br	H	—	95	247–248†	Acetonitrile	48.25	2.69	—	6.25	48.46	2.60	—	6.31
4	Br	CH_3	—	80	128–129‡	Cyclohexane:benzene(10:1)	50.43	3.39	33.57	—	50.63	3.38	33.31	—
4	Br	$C_6H_5CH_2$	—	58	85–86§	Cyclohexane:benzene(10:1)	61.16	3.85	—	4.46	61.23	3.82	—	4.61
12	—	CH_3	CH_3	76	133–135‖	Cyclohexane:benzene(trace)	52.40	4.00	—	—	52.27	4.02	—	—
7	—	—	—	79	137–139‖ 220–227¶	1,2-Dichloroethane	39.88	3.01	26.55	—	40.18	3.17	26.64	—
8	—	—	—	81**	231–233	1,2-Dichloroethane	42.41	2.49	28.25	—	42.30	2.45	28.26	—
9	—	—	—	86	146–148	Methanol	41.92	3.52	25.37	—	42.18	3.63	25.46	—
11	—	H	H	71	130–135	1,2-Dichloroethane	33.67	2.20	49.79	—	33.84	2.26	49.66	—
11	—	CH_3	H	79	121–122	Benzene	35.85	2.71	47.71	4.18	35.57	2.62	48.31	4.18
11	—	CH_3	CH_3	75	104–105¶ 184–186	Cyclohexane:benzene(1:1)	37.84	3.18	45.80	—	38.08	3.17	45.83	—
13	—	—	—	88	151–154††	Cyclohexane:benzene(2:1)	36.07	2.12	48.00	—	36.48	2.28	48.20	—

*Yields refer to once crystallized products, the melting points are those of the analytical specimens.
†Literature (10) m.p. 248–249°.
‡Literature (9) m.p. 132°.
§After sublimation at 80°/0.001 mm.
‖After sublimation at 85°/0.001 mm.
¶Double melting point observed only on fast heating (sample placed in apparatus 10° before lower m.p.). On slow heating only the higher melting point was observed.
**Yield obtained on thermolysis of 7.
††Literature (19) m.p. 140°.

Can. J. Chem. Downloaded from www.nrcresearchpress.com by 210.87.254.6 on 09/05/12
For personal use only.

TABLE 2. The i.r. and n.m.r. spectra of some brominated isocarbostyrils

Compound					Nuclear magnetic resonance spectra (δ)†								
						Aromatic							
No.	X	R	R′	Infrared spectra* (cm^{-1})	Solvent	8	7	6	5	3	NCH_3	OH	Other
4	Br	H	—	3165,1690,1662‡	A§	8.51(q)‖	----------7.97–7.53(m)¶----------				—	—	NH 11.50
4	Br	CH_3	—	1652	B	8.65(q)	-------7.89–7.33(m)----------7.36				3.53	—	—
4	Br	$C_6H_5CH_2$	—	1652	B	8.48(q)	----------7.87–7.27(m)----------				—	—	NCH_2 5.18 C_6H_5 7.32
12	—	CH_3	CH_3	1645	B	8.38(q)	----7.62(m)**----7.88(q)			—	3.47	—	C—CH_3 2.60
7	—	—	—	3262,1656,1537,1349‡	A	8.34(q)††	7.75(q)	8.28(q)††	—	—	3.20	6.85‡‡	H-4 5.79(d, J = 2.3) H-3 5.32(d, J = 2.3)
8	—	—	—	1648,1525,1354‡	A	8.33(q)††	7.71(t)	8.54(q)††	—	8.10	3.55	—	—
9	—	—	—	1656,1526,1343‡	A	8.39(m)	7.85(q)	8.39(m)	—	—	3.45††	—	H-4 6.02(d, J = 2.8) H-3 5.26(d, J = 2.8) OCH_3 3.30††
11	—	H	H	3327,3190,1663‡	A	----------7.85–7.35(m)----------				—	—	9.0(d)	H-3 5.23(d, J = 4.1) NH 5.8(width ~ 4δ)
11	—	CH_3	H	3190,1646‡	A	----------8.02–7.38(m)----------				—	3.15	5.67§§	H-3 5.43
11	—	CH_3	CH_3	3500,3312,1653	B	8.12(q)	----7.57(m)¶¶----8.12(q)			—	3.27	4.20	C—CH_3 1.70
13	—	—	—	1730,1683	B	8.14(q)	----7.64(m)¶¶----8.12(q)			—	3.48	—	—

*Recorded in chloroform (unless specified otherwise) with a Perkin–Elmer 237B grating spectrophotometer or a Unicam SP-200G i.r. spectrophotometer.
†Recorded with a Varian A-60A spectrometer.
‡Recorded as a Nujol mull.
§A = DMSO-d_6; B = $CDCl_3$.
‖d = Doublet, m = multiplet, q = quartet, t = triplet; all other absorptions had singlet multiplicity.
¶The dotted line indicates the protons which make up the multiplet; in this case H-3 to -7.
**Twelve-line multiplet.
††The assignment could be the reverse of that indicated.
‡‡$w/2$ = 13 Hz.
§§This absorption ($w/2$ = 12 Hz) observed after addition of HCl gas to the solution.
¶¶Ten-line multiplet.

Can. J. Chem. Downloaded from www.nrcresearchpress.com by 210.87.254.6 on 09/05/12
For personal use only.

The formation of **7** was interpreted as occurring via the relatively stable cationic species **6** which, when produced, did not readily lose a proton because of the severe non-bonded bromine–nitro group interaction expected in the product. Instead, the carbonium ion could revert to the starting material by the expulsion of Br^+, or be trapped by a suitable nucleophile.[4] The stability of **6** was shown to be appreciable, since acid-catalyzed methanolysis of **7** gave the methyl ether **9** as the major product. It would be of considerable mechanistic interest to undertake a kinetic investigation of the bromination of **3** and its 4-deuterio derivative, to determine if the formation of **4** also occurred with rate limiting proton loss from an intermediate analogous to **6**.

The question of the stereochemistry of the bromohydrin **7** and its methyl ether **9** must now be considered. The dihedral angles between the protons on C-3 and -4 for the most stable conformers[5] of the *cis*- and the *trans*-isomers of **7** and **9**, as measured from Dreiding models, were *ca.* 50 and 70° respectively. These values corresponded to coupling constants of 3.1 Hz for the *cis*- and 0.6 Hz for the *trans*-isomers as calculated from the Karplus equation (17*a*). The measured *J* values of 2.3 and 2.8 Hz respectively, for **7** and **9**, would therefore be indicative of a *cis* disposition of the substituents in these compounds. This conclusion must, however, be regarded with circumspection on at least two counts. Firstly, it is not known whether the so called less favored conformer of the *trans*-isomer can in reality be disregarded completely. As little as 20–25% of this conformer would make the calculated *J* values agree with those observed. Secondly, the known (18) effect of electronegative substituents on vicinal H–H coupling constants makes a stereochemical assignment especially hazardous when both isomers are not available.

In view of the likelihood that **9** (and probably **7** on the basis of the similar *J* value) was the product of thermodynamic control, an unambiguous assignment of its geometry would clearly be of interest.[6]

In connection with other synthetic studies, it was necessary to determine if the polybromination of isocarbostyrils could be effected. The addition of a molecular equivalent of bromine to 2-methyl-4-bromoisocarbostyril (**12**, R = CH_3; R′ = H; see Scheme 3) resulted in the relatively slow formation of a dibromo alcohol **11** (R = CH_3; R′ = H), which could also be obtained directly from 2-methylisocarbostyril (**10**, R = CH_3; R′ = H) and an excess of bromine.[7] The structure of this compound was established on the basis of analytical, spectral, and degradative evidence. For example, oxidation of the above dibromo carbinolamide with sodium dichromate in sulfuric acid gave the known (19) dibromo imide **13**, which was reduced with potassium iodide in aqueous acetic acid to *N*-methylhomophthalimide (**14**).

The bromination of isocarbostyril (**10**, R = R′ = H) and 2,3-dimethylisocarbostyril (**10**, R = R′ = CH_3) gave dibromo carbinolamides analogous to that derived from 2-methylisocarbostyril. In no case was there any evidence (i.r., n.m.r.) for the existence of the open chain tautomer **15** of **11**. Similar conclusions can be drawn from the published spectral data for cyclic carbinolamides in the 2-azaphenalone series (20).

Acylation

The acylation of isocarbostyrils does not appear to have heretofore been reported (see note added in revision at end of discussion).

Vilsmeier–Haack formylation of 2-methylisocarbostyril (Scheme 4) gave a mono aldehyde

[4]Examples of steric retardation of product formation in the bromination of certain aromatic systems are known; *e.g.* see refs. 15 and 16.

[5]There were two possible conformers for each isomer, but in both cases, one conformer was considered as less likely because of a large non-bonded repulsion between the 4-bromo and the 5-nitro groups. The dihedral angle for both conformers of the *cis*-isomer was the same (*ca.* 50°); for the less favored (?) conformer of the *trans*-isomer, the measured angle was *ca.* 175° (*J* = 9.2 Hz).

[6]A referee has suggested that some information concerning the stereochemistry of **7** and **9** might be derived from a study of the behavior of **7** towards base. This possibility had already been examined by us in a cursory way, but the results obtained were not interpretable in a clear cut manner. For example, **7** did react with sodium hydride in dimethylformamide, but a complex mixture of products (six by t.l.c.), at least some of the components of which still contained halogen (strong positive Beilstein test), was obtained.

[7]Normally these brominations were effected in 10% aqueous acetic acid, but the same products were obtained if the reaction was performed in glacial acetic acid. This would tend to indicate that in the absence of water, the product was either a tribromide, a dibromo acetate, or a mixture of both, and that the carbinolamide was produced during the aqueous work-up.

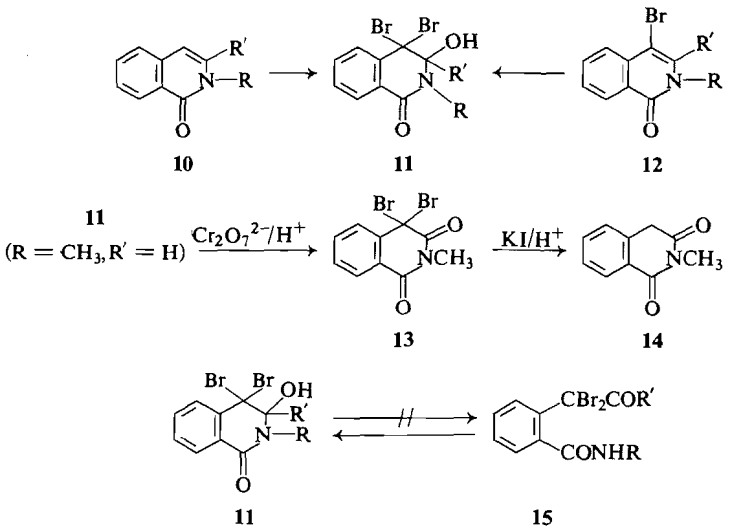

SCHEME 3

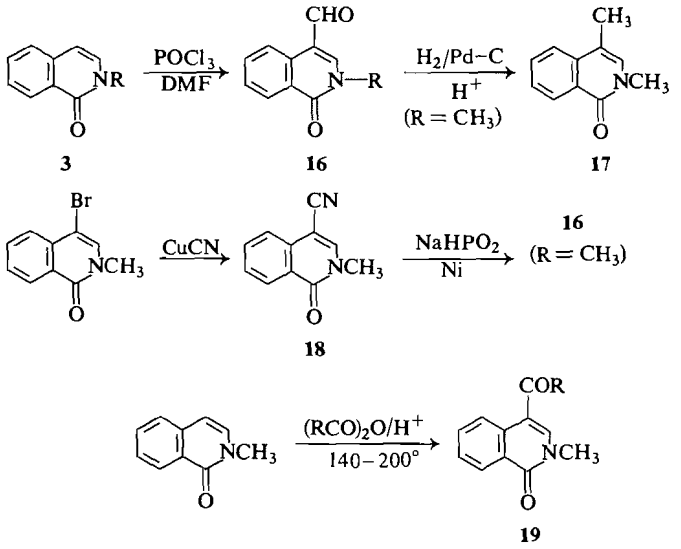

SCHEME 4

(**16**, R = CH_3; see Tables 3 and 4) which was catalytically reduced to a dimethylisocarbostyril **17** different from 2,3-dimethylisocarbostyril. That the formyl group had occupied the 4-position was proved unequivocally by the synthesis of **16** (R = CH_3) from 2-methyl-4-cyanoisocarbostyril (**18**).

2-Benzylisocarbostyril (**3**, R = $C_6H_5CH_2$) furnished a product analogous to **16** (R = CH_3), but isocarbostyril itself reacted very slowly under the same conditions to produce 1-chloroisoquinoline.

Other acyl groups could be incorporated into the isocarbostyril system by the sulfuric acid catalyzed acylation with carboxylic acid anhydrides. For example, a solution of 2-methylisocarbostyril in acetic anhydride containing the catalyst gave the 4-acetyl derivative **19** (R = CH_3) in 72% yield, after 1 h at reflux temperature. The 4-benzoyl analogue **19** (R = C_6H_5) was obtained under somewhat more vigorous conditions from benzoic anhydride (40% yield from isoquinoline methiodide). Sainsbury *et al.* (21) have prepared this compound in poor yield

Can. J. Chem. Downloaded from www.nrcresearchpress.com by 210.87.254.6 on 09/05/12
For personal use only.

Can. J. Chem. Downloaded from www.nrcresearchpress.com by 210.87.254.6 on 09/05/12
For personal use only.

TABLE 3. Yields and physical constants* of some 4-substituted isocarbostyrils

Compound			Yield	Melting	Crystallization	% Calculated			% Found		
No.	R	R′	(%)	point (°C)	solvent	C	H	N	C	H	N
16	CH_3	—	75	155–156	Cyclohexane:benzene(1:1)	70.58	4.85	—	70.54	4.77	—
16	$C_6H_5CH_2$	—	60	114–115†	Benzene	77.55	4.98	5.32	77.87	5.08	5.33
17	—	—	66	80–82‡	Cyclohexane	76.27	6.40	—	76.35	6.42	—
18	—	—	74§	197–199‖	Benzene	71.71	4.38	—	71.88	4.68	—
19	CH_3	—	72	142–144	Cyclohexane:benzene(1:1)	71.63	5.51	6.96	71.91	5.53	7.10
19	C_6H_5	—	64	131–133¶	Cyclohexane:benzene(3:1)	77.55	4.98	5.32	77.12	5.00	5.18
21	CH_3	H	36.5**	163–165††	Cyclohexane:benzene(1:1)	58.83	3.95	13.73	58.62	3.96	13.40
27	—	—	66‡‡	302–305§§	Acetonitrile	76.35	5.49	8.48	76.43	5.59	8.51

*Yields refer to once crystallized products, the melting points are those of the analytical specimens.
†After sublimation at 105°/0.001 mm.
‡After sublimation at 70°/0.001 mm.
§Yield obtained by the alkaline ferricyanide oxidation of the corresponding isoquinoline methiodide. The yield from 4 (R = CH_3, X = Br) and cuprous cyanide was 65%.
‖Literature (32) m.p. 198°.
¶Literature (21) m.p. 134–135°.
**Yield using acetyl nitrate. With nitrous acid the yield was 18%.
††After sublimation at 125°/0.005 mm.
‡‡Yield based on recovered starting material.
§§Literature (23) m.p. 302–304°.

TABLE 4. The i.r. and n.m.r. spectra of some 4-substituted isocarbostyrils*

Compound			Infrared spectra	Nuclear magnetic resonance spectra (δ)						
				Aromatic						
No.	R	R′	(cm^{-1})	8	7	6	5	3	NCH_3	Other
16	CH_3	—	2745,1693,1655	8.56(q)	--8.08–7.56(m)†	---	9.16(q)	7.87	3.79	CHO 9.99
16	$C_6H_5CH_2$	—	2740,1694,1662	8.47(q)	--7.88–7.42(m)	----	9.00(q)	7.73	—	CHO 9.72; C_6H_5 7.37; CH_2 5.28
19	CH_3	—	1644	8.38(q)	--7.83–7.33(m)‡	---	8.88(q)	7.90	3.62	C—CH_3 2.50
19	C_6H_5	—	1630,1655	8.42(q)§	--7.87–7.28(m)	----	8.47(q)§	------‖	3.57	—
21	CH_3	H	1677,1519,1322	8.44(q)§	--8.02–7.64(m)¶	------	8.57(q)§	8.90	3.73**	—
27	—	—	1658,1627	8.74(q)	-------8.16–7.80(m)	----------		7.34	3.97††	CH_2 4.70

*See footnotes * and † in Table 2.
†See footnotes ‖ and ¶ in Table 2.
‡Twelve-line multiplet.
§The assignment could be the reverse of that indicated.
‖H-3 and the five phenyl protons made up part of the multiplet at δ 7.87–7.28.
¶Ten-line multiplet.
**Recorded in $CDCl_3$ containing 10% by volume of DMSO-d_6.
††Recorded in $CDCl_3$ containing 10% by volume of trifluoroacetic acid.

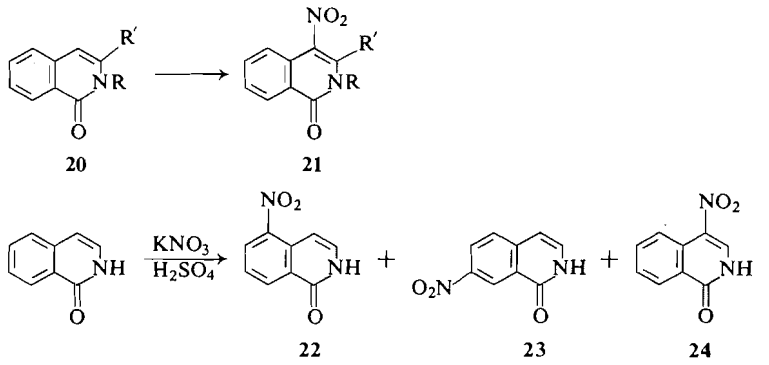

SCHEME 5

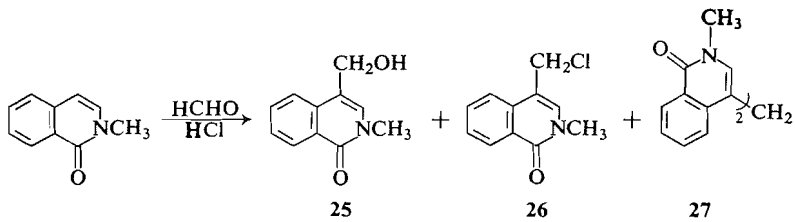

SCHEME 6

(12% from isoquinoline methiodide) by the aerial oxidation of the product of benzoylation of 2-methyl-1,2-dihydroisoquinoline.

Nitration

In 1886, Gabriel (8) reported that treatment of 3-phenylisocarbostyril (**20**, R = H; R′ = C_6H_5; see Scheme 5) with dinitrogen tetroxide in acetic acid gave the 4-nitro derivative **21** (R = H; R′ = C_6H_5), but no evidence was given in support of this structure. The nitration of isocarbostyril with potassium nitrate in sulfuric acid has been said (11) to produce 6- and 8-nitroisocarbostyril, but this disclosure was undoubtedly erroneous since Kawazoe and Yoshioka (13) have recently shown that the n.m.r. spectra of the two major products were fully consistent with 5- (**22**) and 7-nitroisocarbostyril (**23**) respectively. These authors also described the formation of a third mono nitro compound (trace amounts) to which they tentatively assigned the 4-nitro structure **24**.

We have studied the nitration of 2-methylisocarbostyril (**20**, R = CH_3; R′ = H) with nitrous acid in acetic acid (22) and with nitric acid in acetic anhydride (acetyl nitrate). The same mono nitro compound was obtained in both cases. The n.m.r. spectrum (Table 4) of this compound was fully compatible with that expected for 2-methyl-4-nitroisocarbostyril (**21**, R = CH_3; R′ = H). Since we have never observed electrophilic substitution at any position other than C-4, even when conditions were such that disubstitution could have taken place, it is tempting to suggest that the major nitration products observed by Kawazoe and Yoshioka were those derived from the *N*-protonated hydroxy tautomer of isocarbostyril.[8] This proposal is not consistent, however, with the results of the sulfuric acid promoted deuteration experiments[9] which showed that the proton at C-4 is most readily exchanged.

Condensation with Formaldehyde

Tomisawa *et al.* (23) recently reported that 2-methylisocarbostyril condensed with formaldehyde to give mixtures of products, the composition of which depended on the reaction conditions. For example, in the presence of hydrochloric acid, acetic anhydride, and sodium acetate (100°), a 1:1 mixture of the alcohol **25** (see Scheme 6) and the bis-isocarbostyrilmethane **27** was obtained. In the absence of sodium acetate and at room temperature, a 1:3 mixture of the chloro-

[8]Indeed, this proposal has been made by Kawazoe and Yoshioka (13) to account for the above results.

[9]In 61% D_2SO_4, H-4 of isocarbostyril was completely exchanged after 4 h at 140°; H-5 and -7 were totally exchanged after 4 h at 180° (13).

Can. J. Chem. Downloaded from www.nrcresearchpress.com by 210.87.254.6 on 09/05/12
For personal use only.

Can. J. Chem. Downloaded from www.nrcresearchpress.com by 210.87.254.6 on 09/05/12
For personal use only.

methyl compound **26** and the bis-isocarbostyrilmethane **27** was produced.

Our interest in the above condensation stemmed from an attempt to effect an acid-catalyzed (hydrochloric acid) Mannich reaction between 2-methylisocarbostyril, paraformaldehyde, and dimethylamine hydrochloride (refluxing ethanol). The only product, formed in low yield, was the bis-isocarbostyrilmethane (**27**). This compound was produced in significantly better yield when the reaction time was lengthened and when dimethylamine hydrochloride was omitted from the reaction mixture. The same compound was obtained as a by-product during the acid-catalyzed hydrogenolysis of 2-methylisocarbostyril-4-aldehyde (**16**, R = CH_3).

In summary, isocarbostyrils undergo electrophilic substitution with an ease approaching that observed for indoles, although the substitution pattern of the latter group of compounds bears only a superficial resemblance to that described for isocarbostyrils (24). The accessibility of 4-substituted isocarbostyrils opens up an area with a substantial synthetic potential. The following paper (25) describes one application of some of the data described herein.

Note Added in Revision

After this manuscript had been submitted to the referees, Professor H. Tomisawa (Tohoku College of Pharmacy, Sendai, Japan) informed us that he also had successfully acylated *N*-substituted isocarbostyrils, and that these results were presented at the annual meeting of the Japanese Pharmaceutical Society in the summer of 1970. We thank Professor Tomisawa for providing us with this information.

Experimental

The melting points were determined in a Gallenkamp m.p. apparatus and are not corrected.

Preparation of the 2-Alkylisoquinolinium Iodides

2-Methylisoquinolinium iodide was prepared according to the method of Freund and Bode (26). The other 2-alkylisoquinolinium salts were prepared as follows.

A solution of the isoquinoline in acetonitrile (30 ml/g of the base) containing a 10 mol % excess of the alkyl iodide (benzyl iodide was prepared *in situ* from equimolar amounts of benzyl chloride and anhydrous sodium iodide (15 min in boiling acetonitrile followed by filtration to remove sodium chloride)) was heated at reflux temperature for 1–17 h. If the salt did not crystallize on cooling, the acetonitrile was removed *in vacuo* and the residue was crystallized from a suitable solvent. The yields of the pure salts ranged from 70–90%. All of the salts but one (see below) were known compounds and had physical constants in agreement with those given in the literature.

2-Methyl-4-cyanoisoquinolinium iodide was obtained in 88% yield. After crystallization from alcohol it had m.p. 255–256°.

Anal. Calcd. for $C_{10}H_6N_2$:CH_3I: C, 44.62; H, 3.06. Found: C, 44.74; H, 3.34.

Preparation of the Isocarbostyrils

Isocarbostyril was prepared either by the method of Chichibabin and Kursanova (27) or by the method of Robison and Robison (28).

All of the *N*-substituted isocarbostyrils but two (see below) were prepared by the alkaline ferricyanide oxidation of the corresponding 2-alkylisoquinolinium iodides. The method was in essence that described by Haworth and Perkin (29). The general procedure is given below.

To a stirred solution of the isoquinolinium salt (0.05 mol) in water (250 ml) was added a solution of 85% potassium hydroxide (11.22 g) in water (110 ml). This was followed immediately by the addition of a solution of potassium ferricyanide (49.4 g) in water (300 ml). The mixture was stirred for 1 h at room temperature, the product was extracted into a suitable solvent, and then purified by distillation or by crystallization from an appropriate solvent. The yields ranged from 45–95%.

2,3-Dimethylisocarbostyril (**10**, R = R′ = CH_3) was obtained in very low yield by the above method. It was, however, preparable in satisfactory yield as follows:

2,3-Dimethylisoquinolinium iodide (37.0 g, 130 mmol) was added all at once to a solution of 85% potassium hydroxide (34.3 g) in water (650 ml). The mixture was stirred at room temperature under a slight positive pressure of oxygen for 2.5 h. The mixture was then stirred with dichloromethane (100 ml) and benzene (150 ml) until the solids were dissolved. The organic phase was separated and combined with a benzene extract of the aqueous phase. The aqueous phase was stirred under oxygen for an additional 24 h and then extracted as above. The combined extracts were washed with 10% hydrochloric acid (to remove the 1,2-dihydroisoquinoline), and then with water. The extract was dried over sodium sulfate, the solvent was removed *in vacuo*, and the solid residue was recrystallized from cyclohexane (charcoal) to give 8.7 g (39%) of a solid m.p. 100–102° (lit. (30) m.p. 101–102°).

Monobromination of the Isocarbostyrils

The following procedure was typical. To a stirred solution of the isocarbostyril in glacial acetic acid (10–20 ml/g) was added an equimolar amount of bromine in acetic acid (5–10 ml/g of bromine) at a rate such that the reaction temperature did not exceed 30°. After an additional 0.5 to 1.5 h at room temperature the reaction mixture was poured into a large volume of ice-water, the mixture was stirred for *ca.* 10 min, and the product was extracted into dichloromethane or collected by filtration. The physical constants and spectral data for these compounds are recorded in Tables 1 and 2.

When 2-methyl-5-nitroisocarbostyril (**5**) was brominated in the above manner a 1:1 mixture of compounds **7** and **8** was obtained. After crystallization of the mixture from benzene the two products were separated mechanically and crystallized to constant m.p. Compounds **7** and

Can. J. Chem. Downloaded from www.nrcresearchpress.com by 210.87.254.6 on 09/05/12
For personal use only.

8 were more conveniently prepared in the manner described below.

2-Methyl-3,4-dihydro-3-hydroxy-4-bromo-5-nitroisocarbostyril (7)

To a solution of 2-methyl-5-nitroisocarbostyril (4.09 g, 20.1 mmol) in 10% aqueous acetic acid (200 ml) was added a solution of bromine (6.42 g, 40.2 mmol) in the same solvent system (50 ml). After 5 h at room temperature the reaction was poured into a large volume of ice-water and the product was extracted into dichloromethane. The extract was washed with water, dried over sodium sulfate, and evaporated *in vacuo*. The residue was slurried with 1,2-dichloroethane and the insoluble material (4.54 g, 79%) was collected by filtration. It was identical to the bromohydrin obtained as one component of the mixture described above.

2-Methyl-4-bromo-5-nitroisocarbostyril (8)

The above bromohydrin (602 mg, 2 mmol) was heated at 150°/10 mm for 10 min. The residual solid was crystallized from 1,2-dichloroethane to give a lemon yellow solid (461 mg, 81%) m.p. 225–230° (dec). Three further crystallizations gave material m.p. 231–233° (dec.) identical to the sample obtained as part of the mixture described above.

2-Methyl-3,4-dihydro-3-methoxy-4-bromo-5-nitroisocarbostyril (9)

A solution of the bromohydrin **7** (2.00 g, 6.65 mmol) and *p*-toluenesulfonic acid monohydrate (20 mg) in methanol (35 ml) was heated under reflux for 3 h. When the solution was cooled in ice, a solid (1.81 g, 86%), m.p. 138–143°, crystallized from solution. Three further crystallizations of the methoxy compound raised its m.p. to 146–148°. Evaporation of the original mother liquor and crystallization of the residue from 1,2-dichloroethane gave a solid (108 mg, 6%), m.p. 226–228° identical to the bromoisocarbostyril (**8**) described above.

Dibromination of the Isocarbostyrils

A solution of the isocarbostyril in 10% aqueous acetic acid (20–30 ml/g) was treated in the usual manner with 3 mol equiv of bromine in the same solvent system (5 ml/g of bromine). When the addition was completed stirring was continued for 2–3 h at room temperature and then the mixture was poured with stirring into a large volume of ice-water. After *ca.* ½ h the product was collected by filtration or extracted into a suitable solvent. Further purification of these materials was effected by crystallization from a suitable solvent. See Tables 1 and 2.

N-Methyl-4,4-dibromohomophthalimide (13)

A stirred solution of the dibromocarbinolamide (**11**, R = CH_3 = R′= H; 3.35 g, 10 mmol) in acetic acid which was 2.5 *M* in sulfuric acid (200 ml) was treated with 0.694 *M* sodium dichromate solution in 2.5 *M* sulfuric acid (5.64 ml, 3.66 mmol) at a rate such that the reaction temperature did not exceed 35°. When the addition was completed, stirring at room temperature was continued for 1 h, the mixture was then poured into a large volume of ice-water and the product was extracted into dichloromethane. The extract was washed with water, dried over sodium sulfate, and evaporated *in vacuo*. Crystallization of the residue from benzene–cyclohexane (1:2) gave the product in two crops, m.p. 151–154 (2.943 g) and 145–150° (0.411 g) (lit. (19) m.p. 140°).

N-Methylhomophthalimide (14)

Pulverized potassium iodide (1.332 g, 8 mmol) was added to a solution of the dibromohomophthalimide (0.333 g, 1 mmol) in 30% aqueous acetic acid (20 ml). The liberated iodine was destroyed by the addition of solid sodium bisulfite. The clear solution was poured into a large volume of ice-water, the product was extracted into dichloromethane, the extract was washed with water, and then dried over sodium sulfate. The solvent was removed *in vacuo* and the residue was sublimed at 70°/0.001 mm to give *N*-methylhomophthalimide (0.161 g, 92%) m.p. 120–122°. A mixed melting point with an authentic specimen of *N*-methylhomophthalimide (34) was undepressed.

Vilsmeier–Haack Formylation of the Isocarbostyrils

The formylating agent was prepared in the usual manner at 0° from dry dimethyl formamide (39.2 g, 440 mmol) and phosphorous oxychloride (16.9 g, 110 mmol). A solution of the isocarbostyril (100 mmol) in dry dimethylformamide (13 g) was added dropwise at 0° with stirring over a 0.5 h period, and then the reaction was heated on a steam bath for 2.5–4 h. The hot solution was poured into ice-water and the product was isolated by filtration, or by extraction into a suitable solvent. Further purification was effected by crystallization from an appropriate solvent system (see Table 3).

Preparation of 2-Methyl-4-formylisocarbostyril (16, R = CH_3) from 2-Methyl-4-cyanoisocarbostyril (18)

The nitrile **18** was prepared from 2-methyl-4-bromoisocarbostyril and cuprous cyanide in *N*-methyl-2-pyrrolidone (31); *e.g.*, a mixture of the bromoisocarbostyril (0.900 g, 3.78 mmol) and cuprous cyanide (0.610 g, 6.82 mmol) in *N*-methyl-2-pyrrolidone (10 ml) was heated at reflux temperature for 2.5 h. The hot solution was poured into aqueous sodium cyanide solution (50 ml, 25% (weight)), the mixture was shaken vigorously and then filtered through Celite. The filter cake was washed with dichloromethane, the organic phase was separated and combined with a dichloromethane extract of the aqueous phase. The solvent was removed *in vacuo*, the residue was dissolved in toluene, and the resulting solution was washed with 10% (weight) sodium cyanide solution and then with water. The dried solution (sodium sulfate) was evaporated *in vacuo* and the residue was crystallized from benzene to give the nitrile (0.451 g, 65%) m.p. 195–197°. One recrystallization of this solid gave material with m.p. 197–199° identical in all respects to the nitrile obtained by the alkaline ferricyanide oxidation of 2-methyl-4-cyanoisoquinolinium iodide. Thuillier *et al.* (32) reported m.p. 198° for this compound.

A suspension of the nitrile (0.802 g) and sodium hypophosphite (1.6 g) in 1:1:2 water – acetic acid – pyridine (28 ml) containing Raney nickel (0.5 g) was stirred at 40–45° for 4 h (see ref. 33). The solution was poured into water and extracted with dichloromethane. The extract was washed with water, dried over sodium sulfate, and evaporated *in vacuo*. The residue was crystallized from 1:1 benzene:cyclohexane to give the aldehyde

Can. J. Chem. Downloaded from www.nrcresearchpress.com by 210.87.254.6 on 09/05/12
For personal use only.

(0.360 g) m.p. 151–153°. Several crystallizations gave material m.p. 155–156° identical in all respects with that prepared by the Vilsmeier–Haack method.

*2,4-Dimethylisocarbostyril (**17**)*

A solution of the above aldehyde (7.48 g, 40 mmol) in glacial acetic acid (200 ml) containing perchloric acid (8 ml, 60–62%) and 10% palladium-on-charcoal (750 mg) was hydrogenated at room temperature and an initial hydrogen pressure of 46 p.s.i.g. After 13 h the catalyst was removed by filtration through Celite. The filtrate was concentrated to a small volume *in vacuo*, the residue was diluted with water and extracted with dichloromethane. The extract was washed with sodium carbonate solution (50 g/l), then with water, and finally it was dried over sodium sulfate and evaporated *in vacuo*. The residue was separated into a benzene soluble oil and a benzene insoluble solid. The solid (1.10 g, 17%) had m.p. 290–298°. On crystallization from acetonitrile, material with m.p. 297–302°, with an i.r. spectrum indistinguishable from the bis-isocarbostyril methane **27**, was obtained.

The benzene solution from above was evaporated *in vacuo* and the residue was evaporatively distilled at 140°/0.01 mm to give an oil (4.57 g, 66%) which solidified spontaneously. After crystallization from cyclohexane and sublimation *in vacuo* at 70°/0.001 mm, a white solid m.p. 80–82° was obtained. Admixture of this material with 2,3-dimethylisocarbostyril caused a depression of the m.p. to 55–65°.

*2-Methyl-4-acetylisocarbostyril (**19**, $R = CH_3$)*

A solution of 2-methylisocarbostyril (4.78 g, 30 mmol) in acetic anhydride (10 ml) containing concentrated sulfuric acid (10 drops) was heated at reflux temperature for 1 h. The hot solution was poured into water (150 ml) and after 1 h the product was extracted into dichloromethane. The extract was washed with water, dried over sodium sulfate, and evaporated *in vacuo*. The solid residue was chromatographed on neutral alumina (Fluka, Activity II; 300 g) using 10% chloroform in benzene as the eluant. The first 200 ml of the eluate was discarded, the next 3.2 l contained the product which was crystallized from 1:1 benzene cyclohexane. The ketone (4.35 g, 72%) had m.p. 142–144°.

*2-Methyl-4-benzoylisocarbostyril (**19**, $R = C_6H_5$)*

A mixture of 2-methylisocarbostyril (15.9 g, 100 mmol), benzoic anhydride (67.9 g, 300 mmol) and concentrated sulfuric acid (30 drops) was heated in an oil bath at 200° under a slight positive pressure of nitrogen for 40 h. To the melt was cautiously added methanol (300 ml) and 2 *N* sodium hydroxide (300 ml) and the resultant was heated at reflux temperature for 1 h. The methanol was removed *in vacuo*, the residue was diluted with water and extracted with ethyl acetate. The extract was washed well with water, dried over sodium sulfate, and evaporated *in vacuo*. The solid residue was crystallized from benzene–cyclohexane (1:3) to give the product in two crops, m.p. 131–132 (15.1 g) and 128–131° (1.7 g).

*2-Methyl-4-nitroisocarbostyril (**21**, $R = CH_3$; $R' = H$)*

(a) Nitration with Acetyl Nitrate

To a stirred and cooled solution of 2-methylisocarbostyril (1.59 g, 10 mmol) in acetic anhydride (6.0 ml) was added a solution of concentrated nitric acid (0.71 ml) in acetic acid (3.0 ml) at a rate such that the reaction temperature did not exceed 5°. The cooling bath was removed, but the temperature was not allowed to exceed 25° (periodic cooling was necessary). After 0.5 h the reaction had ceased, the solution was poured into ice-water and the product was extracted into dichloromethane. The extract was washed with water, dried over sodium sulfate, and evaporated *in vacuo*. The residue was chromatographed on neutral alumina (Fluka, Activity II; 50 g) using benzene as the eluant (50 ml fractions). The product was present in fractions 3–7. Evaporation of the solvent and crystallization of the residue from 1:1 benzene cyclohexane gave a pale yellow crystalline solid (0.745 g, 36.5%) m.p. 163–165°.

(b) Nitration with Nitrous Acid

To a stirred, cooled solution of 2-methylisocarbostyril (7.96 g, 50 mmol) in glacial acetic acid, which was 2.5 *M* in sulfuric acid (100 ml), and water (10 ml), was added a solution of sodium nitrite (10.35 g, 150 mmol) in water (30 ml) at a rate such that the reaction temperature did not exceed 10°. After 4 h at 10–15°, the reaction was diluted with water and the product was extracted into benzene. The extract was washed with water, dried over sodium sulfate, and evaporated *in vacuo*. The residue was chromatographed on neutral alumina (Activity II, 320 g) as before (100 ml fractions). The product was contained in fractions 4–16. Crystallization of this material gave a product, m.p. 163–165° (1.59 g, 18%) identical in all respects to the nitration product obtained as described above.

Acid-catalyzed Condensation of 2-Methylisocarbostyril with Formaldehyde

2-Methylisocarbostyril (1.59 g, 10 mmol), paraformaldehyde (0.396 g, 4.4 mmol) in 95% ethanol (5 ml), containing concentrated hydrochloric acid (0.05 ml), was heated under reflux for 18.5 h. The reaction mixture was cooled to room temperature and the bis-isocarbostyrilmethane **27** (0.500 g, 66% based on recovered starting material), m.p. 297–300° was collected by filtration. The filtrate was diluted with water, and extracted with benzene. Evaporation of the dried extract *in vacuo* gave 0.862 g of starting material. Three crystallizations of crude **27** from acetonitrile gave a solid with m.p. 302–305°. (lit. (23), m.p. 302–304°).

1. A. R. KATRITZKY and J. M. LAGOWSKI. Heterocyclic chemistry. Methuen and Co. Ltd., London, 1960. pp. 51–52.
2. H. MEISLICH. Pyridine and its derivatives. Part III. *Edited by* E. Klingsberg. Interscience Publishers, New York, N.Y., 1962. pp. 627–628.
3. J. A. ELVIDGE and L. M. JACKMAN. J. Chem. Soc. 859 (1961).
4. R. A. ABRAMOVITCH and J. G. SAHA. Advances in heterocyclic chemistry. Vol. VI. *Edited by* A. R. Katritzky and A. J. Boulton. Academic Press, New York, N.Y., 1966. pp. 253–265.
5. A. R. KATRITZKY and J. M. LAGOWSKI. The principles of heterocyclic chemistry. Academic Press, New York, N.Y., 1968. pp. 38–40.
6. L. A. PAQUETTE. Principles of modern heterocyclic chemistry. W. A. Benjamin Inc., New York, N.Y., 1968. pp. 234–235.

7. L. A. PAQUETTE and W. C. FARLEY. J. Org. Chem. **32**, 2725 (1967).
8. S. GABRIEL. Chem. Ber. **19**, 830 (1886).
9. E. BAMBERGER and W. FREW. Chem. Ber. **27**, 198 (1894).
10. M. M. ROBISON and B. L. ROBISON. J. Org. Chem. **23**, 1071 (1958).
11. (*a*) M. IKEHARA and J. SHIMIZU. Proced. of the 9th Jap. Pharm. Conv. 118 (1956); see ref. 12, p. 25. (*b*) T. HASHIMOTO and S. NAGASE. Proced. of the 12th Jap. Pharm. Conv. 235 (1959); see ref. 12, p. 25.
12. E. OCHIAI and Y. KAWAZOE. Chem. Pharm. Bull. Tokyo, **8**, 24 (1960).
13. Y. KAWAZOE and Y. YOSHIOKA. Chem. Pharm. Bull. Tokyo, **16**, 715 (1968).
14. H. TOMISAWA, Y. KOBAYASHI, H. HONGO, and R. FUJITA. Chem. Pharm. Bull. Tokyo, **18**, 919 (1970).
15. R. O. C. NORMAN and R. TAYLOR. Electrophilic substitution in benzenoid compounds. Elsevier Publishing Co., Amsterdam, 1965. p. 123.
16. (*a*) E. BACIOCCHI and G. ILLUMINATI. Progress in physical organic chemistry. Vol. 5. *Edited by* A. Streitweiser, Jr. and R. W. Taft. Interscience Publishers, New York, N.Y., 1967. pp. 18 and 19. (*b*) E. BACIOCCHI, G. ILLUMINATI, G. SLEITER, and F. STEGEL. J. Am. Chem. Soc. **89**, 125 (1967).
17. (*a*) M. KARPLUS. J. Am. Chem. Soc. **85**, 2870 (1963). (*b*) J. EMSLEY, J. FEENEY, and L. H. SUTCLIFFE. High resolution nuclear magnetic resonance spectroscopy. Vol. I. Pergamon Press, London, 1965. p. 377.
18. H. BOOTH. Tetrahedron Lett. 411 (1965).
19. C. FOURNIER and J. DECOMBE. Bull. Soc. Chim. Fr. 3367 (1967).
20. A. WARSHAWSKY and D. BEN-ISHAI. J. Heterocycl. Chem. **6**, 681 (1969).
21. M. SAINSBURY, S. F. DYKE, and A. R. MARSHALL. Tetrahedron **22**, 2445 (1966).
22. C. A. BUNTON, E. D. HUGHES, C. K. INGOLD, D. I. H. JACOBS, M. H. JONES, G. J. MINKOFF, and R. I. REED. J. Chem. Soc. 2628 (1950).
23. H. TOMISAWA, K. SAITO, H. HONGO, and R. FUJITA. Chem. Pharm. Bull. Tokyo, **18**, 937 (1970).
24. P. L. JULIAN, E. W. MEYER and H. C. PRINTY. Heterocyclic compounds. Vol. III. *Edited by* R. C. Elderfield. John Wiley and Sons, Inc., New York, N.Y., 1952. pp. 1–73.
25. D. E. HORNING, G. LACASSE, and J. M. MUCHOWSKI. Can. J. Chem. This issue.
26. M. FREUND and G. BODE. Chem. Ber. **42**, 1746 (1909).
27. A. E. CHICHIBABIN and A. I. KURSANOVA. J. Russ. Phys. Chem. Soc. **62**, 1211 (1930); Chem. Abstr. **25**, 2727 (1931).
28. M. M. ROBISON and B. L. ROBISON. J. Org. Chem. **21**, 1337 (1956).
29. R. D. HAWORTH and W. H. PERKIN, JR. J. Chem. Soc. **127**, 1434 (1925).
30. L. G. S. BROOKER and F. L. WHITE. J. Am. Chem. Soc. **73**, 1094 (1951).
31. M. S. NEWMAN and H. BODEN. J. Org. Chem. **26**, 2525 (1961).
32. G. THUILLIER, B. MARCOT, J. ¢RUANES, and P. RUMPF. Bull. Soc. Chim. Fr. 4770 (1967).
33. O. G. BACKEBERG and B. STASKUN. J. Chem. Soc. 3691 (1962).
34. J. M. MUCHOWSKI. Can. J. Chem. **47**, 857 (1969).

Can. J. Chem. Downloaded from www.nrcresearchpress.com by 210.87.254.6 on 09/05/12
For personal use only.

Can. J. Chem. Downloaded from www.nrcresearchpress.com by 210.87.254.40 on 09/05/12
For personal use only.

Isocarbostyrils. II.[1] The Conversion of 2-Methyl-4-acyl-5-nitroisocarbostyrils to 2-Substituted Indole-4-carboxylic Acids

D. E. HORNING, G. LACASSE, AND J. M. MUCHOWSKI[2]
Bristol Laboratories of Canada, Candiac, Quebec

Received April 19, 1971

The sulfuric acid catalyzed acylation of 2-methyl-5-nitroisocarbostyril with carboxylic acid anhydrides gave the corresponding 4-acylated derivatives **3**, which underwent reductive cyclization to 2-substituted derivatives of 4-methyl-1,3,4,5-tetrahydropyrrolo[4.3.2.*de*]isoquinolin-5-one (**4**). Alkaline hydrolysis of the six-membered lactam in **4** was accompanied by a retro-Mannich reaction to produce 2-substituted indole-4-carboxylic acids in about 40% overall yield from **3**.

L'acylation catalysée par l'acide sulfurique du méthyl-2 nitro-5 isocarbostyrile par les anhydrides des acides carboxyliques conduit aux dérivés **3** acylés en-4 correspondants. Ces derniers subissent une cyclisation pour donner les dérivés substitués en-2 du méthyl-4 tétrahydro-1,3,4,5 pyrrolo[4.3.2.*de*]-isoquinolinone-5 (**4**). L'hydrolyse alcaline de la lactane à six chainons dans **4** est accompagnée d'une réaction rétro-Mannich pour donner les acides indole carboxyliques-4 substitués en position-2, et cela avec un rendement global d'environ 40% à partir de **3**.

Canadian Journal of Chemistry, 49, 2797 (1971)

The synthesis of indoles bearing a 4-carbonyl function (**1**, X = H, OR, NH_2, etc.), or a substituent at that position which could be readily transformed to a carbonyl group (*e.g.*, CH_2OH, CN, etc.) has been the subject of extensive investigation during the past three decades (1–8). An appreciable number of these studies stemmed from the need to prepare suitable precursors for the synthesis of lysergic acid and closely related compounds (see refs. 1–3, for example). In the preceding paper (9), it was reported that *N*-alkylisocarbostyrils were readily acylated at the 4-position. This was an important observation, since it was apparent to us that 2-methyl-5-nitroisocarbostyril (**2**) was a potential source of 4-carbonyl indoles if acylation could be effected at C-4. There would then remain only the problem of devising an appropriate ring closing – ring opening reaction sequence, which, when applied to **3**, would provide a 4-carbonyl indole. This paper describes a successful three-step transformation of 2-methyl-5-nitroisocarbostyril to some 2-substituted indole-4-carboxylic acids.

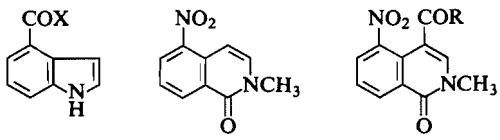

1 **2** **3**

When 2-methyl-5-nitroisocarbostyril and carboxylic acid anhydrides were heated together (95–150°) in the presence of a catalytic amount of sulfuric acid, the 4-acylated compounds **3** (R = CH_3, C_2H_5, C_6H_5) were formed in satisfactory yields. It is noteworthy that these conditions were milder than those required for the acylation of 2-methylisocarbostyril (9). For example, acetylation and benzoylation of 2-methylisocarbostyril required reaction temperatures of 140 and 200° respectively, whereas the corresponding reactions on 2-methyl-5-nitroisocarbostyril occurred readily at 95 and 150°. This observation is quite remarkable in view of the anticipated adverse steric effect of the *peri* nitro group in **2** on an entering acylium ion. Whereas the acylation of **2** was accomplished with surprising ease, it was equally unexpected that formylation could not be effected under conditions which were successful for 2-methylisocarbostyril, or under a large number of other variants of the Vilsmeier–Haack reaction.[3]

The structures of the 4-acylated-5-nitroiso-

[1]For Part 1, see ref. 9.

[2]To whom inquiries concerning this paper should be addressed.

[3]A referee has suggested that one explanation for this observation is that Vilsmeier–Haack complexes may have greater steric requirements than solvated acylium ions.

TABLE 1. Yields and melting points of some isocarbostyril and indole compounds

Compound No.	R	R′	Yield(%)	Melting point(°C)	Crystallization solvent	% Calculated C	H	N	% Found C	H	N
3	CH_3	—	70	200–202	Benzene	58.53	4.09	11.39	58.62	4.25	11.70
3	C_2H_5	—	42	177–178	Cyclohexane: benzene(1:1)	59.99	4.65	—	59.88	4.58	—
3	C_6H_5	—	50–65	167–169*	Benzene	66.23	3.92	9.09	66.37	4.02	8.89
4	CH_3	—	>40	311–312†	Acetonitrile	71.97	6.04	14.00	72.28	6.25	14.26
4	C_6H_5	—	55	276–278†	Ethanol	77.84	5.38	10.68	77.94	5.58	10.70
6	CH_3	H	39–46‡	230–232	Ethanol: water(3:2)	68.56	5.18	8.00	68.66	5.31	7.88
6	CH_3	CH_3	80	131–132§	Cyclohexane: benzene(4:1)	69.82	5.86	—	69.76	5.68	—
6	C_6H_5	H	77	266–268	Ethanol: water(3:2)	75.93	4.67	5.90	76.04	4.74	5.85
6	C_6H_5	CH_3	90	125–127	Cyclohexane: benzene(10:1)	76.47	5.22	—	76.65	5.34	—

*Occasionally a modification with m.p. 177–179° was obtained.
†Melting point taken in a sealed, evacuated capillary.
‡Yield based on 3 (R = CH_3) as the starting material.
§After sublimation at 100°/0.001 mm.

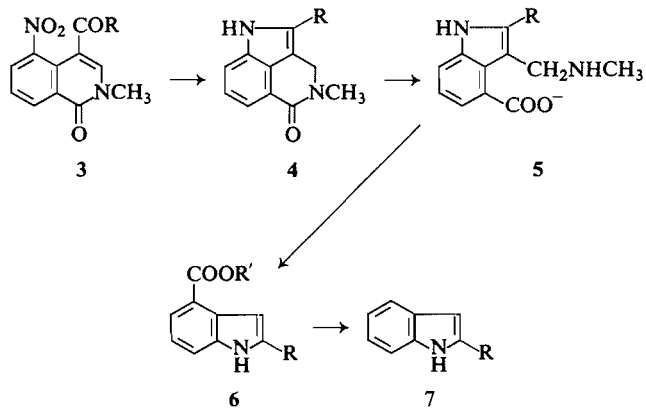

3 4 5 6 7

SCHEME 1

carbostyrils were supported by their elemental analyses (Table 1), characteristic n.m.r. spectra (Table 2), and by the chemical transformations described below. For instance, catalytic hydrogenation of the nitroacetyl derivative **3** (R = CH_3) resulted not only in the expected ring closure, but also was accompanied by migration of the isocarbostyril double bond into the newly formed five-membered ring. The tricyclic compound thus produced **4** (R = CH_3) is the first member of the hitherto unknown pyrrolo-[4.3.2-*de*]isoquinoline ring system.[4] Although this compound was indefinitely stable in the solid state, solutions of it were rapidly oxidized to tarry substances on exposure to air. The phenyl substituted analogue **4** (R = C_6H_5)[5] was, however, sufficiently air insensitive to be handled without special precautions. The tricyclic nature of these compounds was substantiated by their n.m.r. spectra, elemental analysis (see Tables 1 and 2), and the transformation described below and shown in Scheme 1.

On the basis of previous observations (11, 12), it was concluded that the cleavage of **4** to an indole-4-carboxylic acid would be most readily accomplished under alkaline conditions. At that time, it was not known whether the product would be an amino acid **5**, or if a retro-Mannich reaction would occur to give a desmethyl-

[4]Proposed numbering for this ring system. For the numbering of the related quinoline analogue see ref. 10.

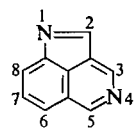

[5]The cyclization of **3** (R = C_2H_5) was not attempted.

Can. J. Chem. Downloaded from www.nrcresearchpress.com by 210.87.254.40 on 09/05/12
For personal use only.

Can. J. Chem. Downloaded from www.nrcresearchpress.com by 210.87.254.40 on 09/05/12
For personal use only.

TABLE 2. The n.m.r. spectra of some isocarbostyril and indole compounds*

Compound				Aromatic								
No.	R	R′	Solvent	8	7	6	5	3	NCH_3	NH	CCH_3	Other
3	CH_3	—	A†	8.39(q)‡	7.83(t)	8.66(q)	—	8.66	3.68	—	2.55	——
3	C_2H_5	—	B	8.16(q)	7.58(t)	8.62(q)	—	7.81	3.67	—	1.18(t) $J = 7.2$	CH_2 2.84(q) $J = 7.2$
3	C_6H_5	—	B	8.36(q)	7.84(t)	8.89(q)	—	7.77	3.70	—	—	C_6H_5 8.12(m, 2H) 7.74(m, 3H)
4	CH_3	—	A	- - - -	7.02–7.58(m)§	- - - -	—	—	3.15	11.11 ($w/2 = 9$)	2.55	CH_2 4.88
4	C_6H_5	—	A	- - - -	7.47(m)‖	- - - -	—	—	3.17	11.76 ($w/2 = 4$)	—	CH_2 5.17
6	CH_3	CH_3	B	—	7.42(m)¶	7.14(q)	7.87(q)	6.86(m)¶	—	8.14 ($w/2 = 12$)	2.38**	OCH_3 3.97
6	C_6H_5	CH_3	B	—	- - - - 7.42(m)‖	- - - -	7.88(q)	—	—	8.92 ($w/2 = 8$)	—	OCH_3 3.96

*The spectra were recorded with a Varian A-60A spectrometer and are expressed in p.p.m. (δ) from internal tetramethylsilane. J values expressed in Hz.
†A = DMSO-d_6; B = $CDCl_3$.
‡m = Multiplet, q = quartet, t = triplet; all other absorptions had singlet multiplicity.
§Seven lines of an AB_2 multiplet with A at δ 7.22 and B at δ 7.49 and $J_{AB} = 7.7$.
‖This multiplet also contained the five protons of the phenyl group at C-2.
¶These absorptions contained considerable fine structure.
**H-3 and the methyl group at C-2 were also mutually weakly coupled (< 1 Hz).

TABLE 3. The u.v. and i.r. spectra of some methyl-indole-4-carboxylates

Compound No.	R	R′	Ultraviolet spectra* λ_{max}(mμ) / log ε	Infrared spectra† (cm^{-1})
6	H	CH_3‡	214 (4.18) 230 (4.33) 314 (3.91)	3466, 3360, 1710
6	CH_3	CH_3	213 (4.20) 233 (4.37) 329 (3.89)	3460, 3355, 1710
6	C_6H_5	CH_3	218 (4.35) 243 (4.36) 250§ (4.26) 270 (4.19) 325§ (4.17) 349 (4.24)	3460, 3350, 1711

*Measured in 95% ethanol on a Unicam SP 800 u.v. spectrophotometer.
†Recorded in chloroform on a Unicam SP-200G i.r. spectrophotometer.
‡Prepared as described in ref. 1.
§Shoulder.

aminomethyl acid **6** (R′ = H). An indication that the latter reaction might occur was to be found in the observations of Powers (13), which showed that indoles bearing a 3-substituent at the aldehyde level of oxidation underwent loss of that substituent in strongly alkaline media.[6] In any event, heating an aqueous dimethyl sulfoxide solution of **4** (R = C_6H_5) containing an excess of potassium hydroxide, under reflux, effected its direct conversion to 2-phenylindole-4-carboxylic acid (**6**, R = C_6H_5, R′ = H) in 77% yield.[7] The same reaction could be accomplished on **4** (R = CH_3), but in this case, because of its sensitivity toward aerial oxidation, the tricyclic indole was used without purification. In this way, 2-methylindole-4-carboxylic acid (**6**, R = CH_3, R′ = H) was obtained in 39–46% overall yield from **3** (R = CH_3).

The gross structure of 2-phenylindole-4-carboxylic acid was corroborated by an elemental analysis, and by the u.v., i.r. (Table 3), and n.m.r. spectra of the methyl ester. Furthermore, cupric ion catalyzed decarboxylation of the carboxylic acid gave the known 2-phenylindole (**7**, R = C_6H_5). 2-Methylindole-4-carboxylic acid did not decarboxylate under the same conditions, but the spectral data (Tables 2 and 3) measured for the methyl ester strongly supported the assigned structure. The n.m.r. spectrum of the aromatic protons of **6** (R = R′ = CH_3) was especially definitive. The quartet at δ 7.87 was assigned to H-5 which was deshielded by the methoxycarbonyl group at C-4, while the broad absorption at δ 8.14 was due to the NH proton. The finely structured apparent doublet centered at δ 7.42 and the narrow multiplet at δ 6.86 were attributed, respectively, to H-7 and -3, which were weakly long range (< 1 Hz) coupled. The remaining, partially obscured quartet centered at δ 7.14, was ascribed to H-6. Acid-catalyzed deuterium exchange caused the disappearance of the signals due to H-1 and -3 with concurrent simplification of the H-6 resonance to a clean quartet. A small (0.6–1 Hz) long range coupling between H-3 and -7 in indoles has been observed previously (17, 18).

Experimental

The melting points were determined in a Gallenkamp m.p. apparatus and are not corrected.

2-Methyl-5-nitroisocarbostyril (m.p. 115–116°, lit. (19) m.p. 120°) was prepared in 85–95% yield by the alkaline ferricyanide oxidation of 2-methyl-5-nitroisoquinolinium iodide (see ref. 9).

Methyl indole-4-carboxylate (m.p. 67–69°, lit. (*1b*) m.p. 69.5–70.5°; after crystallization from cyclohexane and sublimation at 60°/0.001 mm) was obtained from the carboxylic acid (*1a*) and ethereal diazomethane.

[6]Certain 5-hydroxy-4-dialkylaminomethylindoles have recently been shown to undergo a base-catalyzed reverse Mannich reaction (14).

[7]When the hydrolysis was carried out in aqueous ethanol or aqueous ethylene glycol a mixture of two carboxylic acids was obtained. The major (60% yield), less soluble, product was shown to be **6** (R = C_6H_5) by direct comparison with the product obtained in the absence of alcoholic solvents. The minor (20% yield), more soluble, acid (m.p. 214–216°) was considered to be 2-phenyl-3-methylindole-4-carboxylic acid on the basis of its elemental analysis (Found: C, 76.36; H, 4.94; N, 5.75), spectral data (i.r. (Nujol), 3365, 2655, 2570, 1680 cm^{-1}; n.m.r. (DMSO-d_6), δ 2.57 (s, 3H), 7.14–8.14 (m, 8H), 11.72 (s, 1H), 12.08 (s, 1H)), and decarboxylation (see above) to 2-phenyl-3-methylindole (15). The minor product must have been formed via reduction of the intermediate **5** (R = C_6H_5) by the alcoholic solvent. Primary alcohols are known (16) to function as reducing agents in aqueous alkaline media, but the conditions (320–380°, sealed tube) are rather more vigorous than those described herein.

Can. J. Chem. Downloaded from www.nrcresearchpress.com by 210.87.254.40 on 09/05/12
For personal use only.

Can. J. Chem. Downloaded from www.nrcresearchpress.com by 210.87.254.40 on 09/05/12
For personal use only.

2-Methyl-4-acetyl-5-nitroisocarbostyril (3, R = CH_3)

2-Methyl-5-nitroisocarbostyril (8.16 g, 40 mmol), acetic anhydride (18 ml), and concentrated sulfuric acid (5 drops) were heated on a steam bath for 4 h. The dark colored solution was cooled to room temperature, water (25 ml) was added, and the mixture was heated on a steam bath until a single phase was produced (*ca.* 10 min). The solution was poured into a large volume of water, the product was extracted into dichloromethane, the extract was washed well with water, dried over sodium sulfate, and then evaporated *in vacuo*. The residue was crystallized from benzene to give the product in two crops, m.p. 197–200 (5.70 g) and 194–197° (1.17 g). Upon recrystallization from 2-propanol the m.p. was raised to 200–202°.

2-Methyl-4-propionyl-5-nitroisocarbostyril (3, R = C_2H_5)

This compound was prepared in the same manner as the above acetyl compound, with the exception that propionic anhydride was used and the reaction time was lengthened to 6 h. The product (m.p. 175–176°, 42% yield) was crystallized from benzene: cyclohexane (2:1).

2-Methyl-4-benzoyl-5-nitroisocarbostyril (3, R = C_6H_5)

Benzoic anhydride (13.6 g, 60 mmol), 2-methyl-5-nitroisocarbostyril (4.08 g, 20 mmol), and concentrated sulfuric acid (8 drops) were heated together at 150° (oil bath) under a slight positive pressure of nitrogen for 17 h. To the hot melt was added acetonitrile (20 ml), pyridine (10 ml), and water (10 ml) and the solution was heated at reflux temperature for 1 h. The solution was poured into ice-water, sodium carbonate solution (200 g/l) was added until alkalinity was achieved, the product was extracted into dichloromethane and the extract was dried over sodium sulfate, and evaporated *in vacuo*. The oily solid was taken up in chloroform and placed on a column of Florisil (100 g, 100–200 mesh, packed in benzene). The column was developed with chloroform; the first 350 ml of the eluate was discarded, the product was contained in the next 2.4 l. The product was crystallized from benzene:cyclohexane (4:1). The first crop had m.p. 165–167°, subsequent crops had a lower m.p. (153–157°) but on crystallization from 1:1 benzene cyclohexane material with m.p. 165–167° was obtained. The total yield of product with m.p. 165–167° ranged from 3.08–4.00 g (50–65%).

2,4-Dimethyl-1,3,4,5-tetrahydropyrrolo-[4,3,2-de]isoquinolin-5-one (4, R = CH_3)

2-Methyl-4-acetyl-5-nitroisocarbostyril (1.64 g, 6 mmol) and 10% palladium-on-charcoal (200 mg) in ethanol (100 ml) were hydrogenated at room temperature and an initial hydrogen pressure of 60 p.s.i.g. The theoretical amount of hydrogen was absorbed in 1 h. Some of the product had separated from solution; it was collected (680 mg of product and catalyst) by filtration in an atmosphere of nitrogen. It was sufficiently pure to be purified by crystallization in the manner described below. The filtrate was evaporated *in vacuo* at 30°; the residue was slurried with toluene, and the insoluble material (693 mg) was collected by filtration and sublimed at 190–195°/0.001 mm. A yellow solid (381 mg) m.p. 311–312° (evacuated capillary) was obtained. The sublimate was dissolved in boiling acetonitrile (through which a slow stream of nitrogen was bubbled) and on cooling in ice, the product crystallized. The m.p. remained unchanged.

2-Phenyl-4-methyl-1,3,4,5-tetrahydropyrrolo-[4,3,2-de]isoquinolin-5-one (4, R = C_6H_5)

2-Methyl-4-benzoyl-5-nitroisocarbostyril was catalytically reduced in the same manner as described above (1.5 h). The product was sufficiently stable in solution to be handled without special precautions. The catalyst was removed by filtration through Celite, the filtrate was evaporated *in vacuo* and the residue was crystallized from ethanol. The product, m.p. 270–274° (evacuated capillary), was obtained in 55% yield. Further crystallization raised the m.p. to 276–278°.

2-Methylindole-4-carboxylic Acid (6, R = CH_3, R′ = H)

2-Methyl-4-acetyl-5-nitroisocarbostyril (1.64 g, 6 mmol) and 10% palladium-on-charcoal (200 mg) in absolute ethanol (100 ml) was hydrogenated as before. The contents of the hydrogenation vessel were transferred in an atmosphere of nitrogen to a 500 ml round-bottomed flask. The solvent was removed *in vacuo* at 30° and a solution of 85% potassium hydroxide (8.4 g) in 50% aqueous dimethylsulfoxide (120 ml) was added to the residue. The mixture was stirred magnetically under reflux for 17 h while a gentle flow of nitrogen was maintained through the apparatus. Concentrated hydrochloric acid was carefully added to the cooled solution until the dissolved silica precipitated from solution (still weakly basic). The mixture was filtered, the filter cake was washed well with water, and the filtrate was made acidic with concentrated hydrochloric acid. The product was extracted into ethyl acetate, the extract was shaken with sodium carbonate (100 g/l), the basic solution thus obtained was acidified with concentrated hydrochloric acid, and the product was extracted into ethyl acetate. The extract was washed with water, dried over sodium sulfate, and evaporated *in vacuo*. The residue (1.06–1.24 g) was taken up in methanol, silica gel (5 g, Merck, activity II–III) was added, and the mixture was evaporated to dryness *in vacuo*. This mixture was placed on top of a dry packed column of silica gel (100 g) and the column was developed with ethyl acetate. The product was contained in the first 250 ml of the eluate. It was crystallized from aqueous ethanol (2:3) to give the carboxylic acid in two crops, m.p. 225–229 (356–368 mg) and 219–223° (49–96 mg). The yield of the combined crops ranged from 39–46% based on the starting nitro ketone.

The methyl ester was prepared by adding an excess of ethereal diazomethane to an ice cold methanolic solution of the carboxylic acid. The ester was crystallized from cyclohexane:benzene (4:1) to give material m.p. 130–131°.

2-Phenylindole-4-carboxylic Acid (6, R = C_6H_5, R′ = H)

The tricyclic indole (524 mg, 2 mmol) and 85% potassium hydroxide (2.5 g) in 50% aqueous dimethylsulfoxide (30 ml) was heated at reflux temperature for 20 h. The reaction was processed as before, the sodium carbonate soluble fraction being crystallized from 3:2 aqueous ethanol (chromatography was unnecessary). The product (385 mg, 77%) had m.p. 265–267°.

The methyl ester was prepared in the usual manner using ethereal diazomethane. It had m.p. 124.5–126°, after crystallization from cyclohexane:benzene (10:1).

Decarboxylation of 2-Phenylindole-4-carboxylic Acid

An intimate mixture of the carboxylic acid (40.2 mg) and basic cupric carbonate (1.8 mg), contained in a 10 ml flask equipped with a water cooled condenser, was heated under a slight vacuum at 270° until gas evolution had ceased. Full water pump vacuum (10 mm) was then applied and the bath temperature was increased to 320° during a ½ h period. The sublimate was taken up in dichloromethane and the solution was extracted with aqueous sodium carbonate (100 g/l). The aqueous phase was made acidic with concentrated hydrochloric acid and the mixture was extracted with ethyl acetate. The extract was washed with water, dried over sodium sulfate, and evaporated *in vacuo* to give recovered carboxylic acid (14.8 mg).

The dichloromethane phase from above was washed with water, dried over sodium sulfate, and evaporated *in vacuo*. The residue was sublimed at 140–145°/0.005 mm to give 2-phenyl indole (9.2 mg) m.p. 185–186°; mixed m.p. with authentic 2-phenyl indole, 186–188°. The solution i.r. spectrum ($CHCl_3$) was identical to that of an authentic specimen (20).

1. (*a*) F. C. Uhle. J. Am. Chem. Soc. **71**, 761 (1949). (*b*) F. C. Uhle, C. M. McEwen Jr., H. Schroter, C. Yuan, and B. W. Baker. J. Am. Chem. Soc. **82**, 1200 (1962).
2. (*a*) H. Plieninger, K. Suhr, G. Werst, and B. Kiefer. Chem. Ber. **89**, 270 (1956). (*b*) H. Plieninger and W. Lehnert. Chem. Ber. **100**, 2427 (1967).
3. H. Plieninger and W. Muller. Chem. Ber. **93**, 2024, 2029 (1960).
4. J. Szmuzkovicz. J. Org. Chem. **29**, 843 (1964).
5. M. von Strandtmann, M. P. Cohen, and J. Shavel Jr. J. Med. Chem. **8**, 200 (1965).
6. O. Yonemitsu, P. Cerutti, and B. Witkop. J. Am. Chem. Soc. **88**, 3941 (1966).
7. H. Plieninger and H. Klinga. Chem. Ber. **101**, 2605 (1968).
8. S. A. Monti and W. O. Johnson. Tetrahedron, **26**, 3685 (1970).
9. D. E. Horning, G. Lacasse, and J. M. Muchowski. Can. J. Chem. This issue.
10. A. M. Patterson, L. T. Capell, and D. F. Walker. The ring index. Second edition. McGregor and Werner Inc., 1960. p. 375.
11. R. A. Abramovitch and D. Shapiro. J. Chem. Soc. 4589 (1956).
12. R. A. Abramovitch and J. M. Muchowski. Can. J. Chem. **38**, 554 (1960).
13. J. C. Powers. Tetrahedron Lett. 655 (1965).
14. S. A. Monti and G. D. Castillo, Jr. J. Org. Chem. **35**, 3764 (1970).
15. H. M. Kissman, D. W. Farnsworth, and B. Witkop. J. Am. Chem. Soc. **74**, 3948 (1952).
16. E. E. Ried, H. Worthington, and A. W. Larcher. J. Am. Chem. Soc. **61**, 99 (1939).
17. J. A. Elvidge and K. G. Foster. J. Chem. Soc. 981 (1964).
18. J-Y. Lallemand and T. Bernath. Bull. Soc. Chim. Fr. 4091 (1970).
19. H. Decker. J. Prakt. Chem. **47**, 28 (1893).
20. R. L. Shriner, W. C. Ashley, and E. Welch. Organic syntheses. Coll. Vol. III. John Wiley and Sons Inc., New York, N.Y., 1960. p. 725.

Can. J. Chem. Downloaded from www.nrcresearchpress.com by 210.87.254.40 on 09/05/12
For personal use only.

Can. J. Chem. Downloaded from www.nrcresearchpress.com by 210.87.254.6 on 09/05/12
For personal use only.

Thermodynamic Analysis of the Hammett Equation, the Temperature Dependence of ρ, and the Isoequilibrium (Isokinetic) Relationship[1]

LOREN G. HEPLER

Department of Chemistry, The University of Lethbridge, Lethbridge, Alberta

Exact thermodynamic analysis of the Hammett equation has led to four differential equations relating $\delta\Delta H^0$, $\delta\Delta S^0$, $\delta\Delta C_p^0$, $d\rho/dT$, and $d^2\rho/dT^2$. Similar equations can be obtained in terms of activation parameters $\Delta H^{\ddagger}$, etc. For temperature independent $\delta\Delta H^0$ and $\delta\Delta S^0$ and therefore $\delta\Delta C_p^0 = 0$, two of these differential equations lead to $\rho = \rho_\infty[1 - (\beta_i/T)]$ and the familiar isoequilibrium (isokinetic) equation $\delta\Delta H^0 = \beta_i\delta\Delta S^0$. The "isoequilibrium (isokinetic) temperature" represented here by β_i is a temperature independent constant of integration. For constant non-zero $\delta\Delta C_p^0$ we similarly obtain more complicated expressions for ρ and the "isoequilibrium (isokinetic) temperature." These findings are considered in relation to a model in which environmental contributions (due to solute–solvent interactions) to $\delta\Delta H^0$ and $\delta\Delta S^0$ are related by a parameter β_e. The relationship between β_i and β_e is established, and it is shown that in general $\beta_i \neq \beta_e$.

L'analyse thermodynamique exacte de l'équation de Hammett a conduit à quatre équations différentielles se rapportant à $\delta\Delta H^0$, $\delta\Delta S^0$, $\delta\Delta C_p^0$, $d\rho/dT$ et $d^2\rho/dT^2$. Des équations semblables peuvent être obtenues en termes de paramètres d'activation $\Delta H^{\ddagger}$, etc. Lorsque $\delta\Delta H^0$ et $\delta\Delta S^0$ sont indépendants de la température et que, par conséquent, $\delta\Delta C_p^0 = 0$, deux de ces équations différentielles amènent à $\rho = \rho_\infty[1 - (\beta_i/T)]$ et à l'équation habituelle d'isoéquilibre (isocinétique) $\delta\Delta H^0 = \beta_i\delta\Delta S^0$. La "température d'isoéquilibre (isocinétique)" représentée ici par β_i est une constante d'intégration indépendante de la température. Pour une valeur $\delta\Delta C_p^0$ constante et non nulle, nous obtenons de la même manière des expressions plus compliquées pour ρ et la "température d'isoéquilibre (isocinétique)". Ces données sont envisagées en fonction d'un modèle dans lequel les contributions de l'environnement à $\delta\Delta H^0$ et $\delta\Delta S^0$ dues aux intéractions soluté-solvant) sont évaluées par un paramètre β_e. La relation entre β_i et β_e est établie et on montre que, en général $\beta_i \neq \beta_e$.

Canadian Journal of Chemistry, 49, 2803 (1971)

Introduction

The empirical successes of the Hammett equation in correlating a wide variety of equilibrium and rate data are well known. Considerable progress has been made (1–6) in gaining some understanding of why the Hammett equation works as well as it does, and also elucidating its thermodynamic consequences. Among problems that remain partly unresolved are those involving the temperature dependence of the Hammett ρ parameter and the relationships between the Hammett ρ and two different β parameters that have been widely used. This paper is devoted first to detailed thermodynamic analysis of the Hammett equation and then to the relationship of this analysis to an extrathermodynamic model for substituent and solvent effects.

Thermodynamic Consequences of the Hammett Equation

The Hammett equation can be applied to the effect of substituents on acid ionizations as represented by the equation

$$[1]\quad HA^z(S) + R^{z-1}(S) = A^{z-1}(S) + HR^z(S)$$

in which HA^z is a substituted acid, HR^z is a reference acid, and (S) is used to denote that the preceding substance is in solution. We denote the equilibrium constant for reaction 1 by K, which is equal to K_{HA}/K_{HR}, and write the Hammett equation as

$$[2]\quad \log K \simeq \rho\sigma$$

Thus we also have

$$[3]\quad \delta\Delta G^0 = -2.3RT\rho\sigma$$

in which $\delta\Delta G^0 = \Delta G_{HA}^0 - \Delta G_{HR}^0$. The Hammett equation has also been applied similarly to substituent effects on equilibrium constants and rate constants for a wide variety of other reactions.

All of the following derivations are carried out in terms of standard state thermodynamic functions indicated by the superscript zero, but could equally well be done in terms of a ratio of rate constants such as $k_{subst.}/k_{ref.}$ and

[1]Presented in part at the Nobel Workshop in Biochemical Thermochemistry at the Chemical Center University of Lund, Lund, Sweden, 1971.

Can. J. Chem. Downloaded from www.nrcresearchpress.com by 210.87.254.6 on 09/05/12
For personal use only.

the related activation parameters commonly represented by $\Delta G^{\ddagger}$, etc.

It is a general empirical observation that the Hammett equation "works" about as well at one temperature as another. We shall therefore begin our thermodynamic analysis on the basis that eq. 2 is exactly valid over the entire temperature range of interest. According to the original and still used definitions of the parameters in the Hammett eq. 2, the substituent parameter σ is independent of temperature ($d\sigma/dT = 0$), while the reaction–solvent parameter ρ may depend on temperature.

Differentiation of eq. 2 with respect to temperature and combination of the resulting equations with well known thermodynamic equations leads to a number of further equations, of which the following are of immediate interest

$$[4] \quad \delta\Delta H^0 = 2.3RT^2(d\rho/dT)\sigma$$

$$[5] \quad \delta\Delta S^0 = 2.3R[\rho + T(d\rho/dT)]\sigma$$

$$[6] \quad \delta\Delta H^0 = \left[\frac{T^2(d\rho/dT)}{\rho + T(d\rho/dT)}\right]\delta\Delta S^0$$

$$[7] \quad \delta\Delta C_p{}^0 = 2.3R\sigma[T^2(d^2\rho/dT^2) + 2T(d\rho/dT)]$$

In these equations $\delta\Delta H^0 = \Delta H_{HA}{}^0 - \Delta H_{HR}{}^0$, and similarly for both $\delta\Delta S^0$ and $\delta\Delta C_p{}^0$.

Accuracy of most experimental data is such that we are limited to consideration of both $\delta\Delta H^0$ and $\delta\Delta S^0$ (and maybe more especially $\delta\Delta H^{\ddagger}$ and $\delta\Delta S^{\ddagger}$) as temperature independent constants. It therefore follows from $d\delta\Delta H^0/dT = \delta\Delta C_p{}^0$ and $d\delta\Delta S^0/dT = \delta\Delta C_p{}^0/T$ that in these common cases we must take $\delta\Delta C_p{}^0 = 0$. From eq. 7 we therefore have

$$[8] \quad T^2(d^2\rho/dT^2) + 2T(d\rho/dT) = 0$$

The general solution of the differential eq. 8 is a two constant equation of the form

$$[9] \quad \rho = C_1 + C_2/T$$

It is more convenient for us to use symbols similar to those introduced by Leffler and Grunwald (2). Thus we write this general equation with its two constants of integration as

$$[10] \quad \rho = \rho_\infty(1 - \beta_i/T)$$

in which the subscript *i* on β is used to emphasize that we are here concerned with the quantity called the *i*sokinetic or *i*soequilibrium temperature by Leffler and Grunwald (2) and others. It is a necessary requirement of differential eq. 8 that this β_i be independent of temperature. To show that this β_i is indeed the same as the isokinetic or isoequilibrium temperature used by Leffler and Grunwald (2), we substitute ρ and $d\rho/dT = \rho_\infty\beta_i/T^2$ from eq. 10 into eq. 6 to obtain

$$[11] \quad \delta\Delta H^0 = \beta_i\delta\Delta S^0$$

It should now be emphasized that $\log K = \rho\sigma$ and $\delta\Delta C_p{}^0 = 0$, both valid over a range of temperature, necessarily lead by exact thermodynamics and the solution of differential eq. 8 to the temperature dependence of ρ given in eqs. 9 and 10 and to the isoequilibrium (isokinetic) relationship of eq. 11 in which β_i is independent of temperature.

For a reaction series with $\delta\Delta S^0 = 0$ at all temperatures, eq. 5 requires that

$$[12] \quad \rho + T(d\rho/dT) = 0$$

The solution of this differential equation is

$$[13] \quad \rho = C_2/T \quad (\text{for } \delta\Delta S^0 = 0)$$

in which we have a special case corresponding to $C_1 = 0$ in eq. 9. For a reaction series with $\delta\Delta H^0 = 0$ at all temperatures, eq. 4 requires that

$$[14] \quad d\rho/dT = 0$$

Thus in this special case we have a temperature independent ρ as in

$$[15] \quad \rho = C_1 \quad \text{or } \rho = \rho_\infty \quad (\text{for } \delta\Delta H^0 = 0)$$

Now we turn to consideration of reaction series for which both $\delta\Delta H^0$ and $\delta\Delta S^0$ vary with temperature and for which we therefore have $\delta\Delta C_p{}^0 \neq 0$. The simplest case is that in which non-zero $\delta\Delta C_p{}^0$ is independent of temperature, which now requires that we find the appropriate solution for the differential eq. 7. This solution may be written in the form

$$[16] \quad \rho = \rho^*\left[1 - \frac{\beta^*}{T} + \frac{\delta\Delta C_p{}^0}{2.3R\sigma\rho^*}\ln T\right]$$

First we note that for the special case of $\delta\Delta C_p{}^0 = 0$, eq. 16 reduces to eq. 10 with $\rho_\infty = \rho^*$ and $\beta_i = \beta^*$.

Substitution of ρ, $d\rho/dT$, and $d^2\rho/dT^2$ from eq. 16 into eq. 6 gives us

$$[17]\quad \delta\Delta H^0 = \left[\frac{\beta^* + \frac{T\delta\Delta C_p^0}{2.3R\rho^*\sigma}}{1 + \frac{\delta\Delta C_p^0}{2.3R\rho^*\sigma}(1 + \ln T)}\right]\delta\Delta S^0$$

Again we note that for $\delta\Delta C_p^0 = 0$ we obtain a simplification to $\delta\Delta H^0 = \beta^*\delta\Delta S^0$, which is the same as eq. 11 already obtained for this special case.

Leffler was apparently the first to observe and express the now common linear relationship between $\delta\Delta H^0$ and $\delta\Delta S^0$ (or $\delta\Delta H^{\ddagger}$ and $\delta\Delta S^{\ddagger}$) in terms of the isoequilibrium (isokinetic) eq. 11. Although some published examples of linear enthalpy–entropy relationships have been justly criticized as spurious because of experimental errors or large uncertainties, particularly when enthalpies and entropies are derived from $d \ln K/dT$ or $d \ln k/dT$, there is now considerable empirical support for the applicability of eq. 11 to a variety of reaction series. Leffler and Grunwald (2) and Hammett (1) have shown in different ways that the isoequilibrium (isokinetic) temperature here denoted by β_i is a temperature independent constant when $\delta\Delta C_p^0 = 0$ in agreement with the present identification of β_i as one of the constants of integration obtained from differential eq. 8. It is worth emphasizing that the isoequilibrium (isokinetic) relationship of eq. 11 with constant β_i is a rigorous thermodynamic consequence of the Hammett equation and $\delta\Delta C_p^0 = 0$.

Leffler and Grunwald (2) have cited a number of empirical β_i values and have noted that many of these values are close to the experimental temperature under consideration. They have presented some theoretical explanation for this observation and also the generalization that β_i is expected to be positive. The purely thermodynamic treatment given here, in which β_i appears as a constant of integration, requires no particular numerical value or even sign for β_i. As shown later in this paper, a reaction model that is consistent with the present thermodynamic analysis can give further information about the magnitude of β_i.

Since we have few data to justify consideration of temperature dependent $\delta\Delta H^0$ and $\delta\Delta S^0$ values with $\delta\Delta C_p^0 \neq 0$, the treatment given in eqs. 8–15 is all that is appropriate for most reaction series. But because there is a slow accumulation of more accurate data applicable over wider ranges of temperature to justify taking $\delta\Delta C_p^0 \neq 0$, and because it is of value to ascertain the limits of applicability of such useful empirical relationships as the Hammett equation, we now give careful consideration to eqs. 16 and 17.

In eq. 16 we have ρ expressed partly in terms of $\delta\Delta C_p^0/\sigma$. This is directly contrary to the definitions of ρ and σ, which require that these two parameters be independent of each other. It is therefore a thermodynamic requirement of the Hammett equation that $\delta\Delta C_p^0/\sigma$ be a constant so that the right hand side of eq. 16 becomes effectively independent of σ. Because of the $\ln T$ term in eq. 16 we expect to observe a slight curvature in graphs of ρ *vs.* $1/T$ when $\delta\Delta C_p^0 \neq 0$.

The term in brackets in eq. 17 also involves $\delta\Delta C_p^0/\sigma$, but it was shown above that the independence of ρ and σ in the Hammett equation requires that this ratio be constant in any reaction series. Thus it is still appropriate to describe eq. 17 as an isoequilibrium (isokinetic) relationship. The isoequilibrium (isokinetic) "temperature" previously denoted by β_i is now a function of temperature rather than a constant.

There are a number of reaction series that do exhibit the various proportionalities that have been derived by thermodynamic analysis of the Hammett equation. On the other hand, it is becoming well known that the Hammett equation often provides a good approximate correlation of both equilibrium and rate constants even when enthalpies and entropies vary in apparently erratic fashion and there is no good isoequilibrium (isokinetic) relationship. In the next section of this paper, in which a particular reaction model is described, it is shown that "compensation" of contributions of solute–solvent interactions to enthalpies and entropies can account for the approximate success of the Hammett equation even when its derivative thermodynamic consequences are far from being satisfied.

A Model for Thermodynamics of Substituent and Solvent Effects

It has been shown previously (3–7) that it is useful to express thermodynamic functions for reactions of type represented by eq. 1 in terms of "*int*ernal" and "*env*ironmental" contributions as in the following

Can. J. Chem. Downloaded from www.nrcresearchpress.com by 210.87.254.6 on 09/05/12
For personal use only.

Can. J. Chem. Downloaded from www.nrcresearchpress.com by 210.87.254.6 on 09/05/12
For personal use only.

[18] $$\delta\Delta H^0 = \delta\Delta H_{int} + \delta\Delta H_{env}$$

[19] $$\delta\Delta S^0 = \delta\Delta S_{int} + \delta\Delta S_{env}$$

King (8) has clearly described these contributions as follows: "*Internal effects* are those intrinsic to the molecules of the acid and base. *Environmental effects* are those which result from interaction of the molecules of the acid and base with the solvent." Similar definitions apply to other solute species in other reaction series.

A useful and reasonable expression of the proportional relationship between $\delta\Delta H_{env}$ and $\delta\Delta S_{env}$ is (5, 6)

[20] $$\delta\Delta H_{env} = \beta_e\delta\Delta S_{env} + \gamma\delta\Delta H_{int}$$

in which β_e is an "environmental" parameter (*not* the same as β_i) and γ is a parameter that depends on the solvent and the temperature. Because $\delta\Delta S_{int} \simeq 0$ (7) for many symmetrical reactions of type represented by eq. 1, we can write eq. 20 as

[21] $$\delta\Delta H_{env} = \beta_e\delta\Delta S^0 + \gamma\delta\Delta H_{int}$$

A wide variety of evidence (4–11) shows that the environmental parameter β_e is approximately equal to the temperature of the solution so that we henceforth take

[22] $$\beta_e = T$$

It has been shown (5, 6) that eqs. 18–22 lead to

[23] $$\delta\Delta G^0 = \delta\Delta H_{int}(1 + \gamma)$$

and thence

[24] $$\rho\sigma = [C(1 + \gamma)/2.3RT][-\delta\Delta H_{int}/C]$$

in which C is an arbitrary proportionality constant. We identify $C(1 + \gamma)/2.3RT$ with ρ and $-\delta\Delta H_{int}/C$ with σ. Thus this reaction model correctly leads to a linear free energy relationship with ρ that is dependent on solvent and temperature and to σ that is dependent only on the substituent. It is "compensation" of $\delta\Delta H_{env}$ and $\delta\Delta S_{env}$ that is responsible for the simple form of eqs. 23 and 24, which permit us to understand substituent effects largely in terms of "internal" enthalpy or energy. Furthermore, it is this partial compensation of $\delta\Delta H_{env}$ and $\delta\Delta S_{env}$ that accounts for the observation that the Hammett equation gives a good approximate correlation of equilibrium and rate constants even when enthalpies and entropies are not in accord with the thermodynamic requirements of the Hammett equation.

Differentiation of eq. 23 with respect to temperature (taking $\delta\Delta H_{int}$ to be independent of temperature as done previously for σ) leads to the following

[25] $$\delta\Delta H^0 = C[T(d\gamma/dT) - (1 + \gamma)]\sigma$$

[26] $$\delta\Delta S^0 = -\delta\Delta H_{int}(d\gamma/dT) = C(d\gamma/dT)\sigma$$

In eqs. 25 and 26 we have $\delta\Delta H^0$ and $\delta\Delta S^0$ both proportional to σ, as in eqs. 4 and 5 obtained directly from the Hammett equation.

Further combination of equations leads to the isoequilibrium (isokinetic) relationship

[27] $$\delta\Delta H^0 = \left[T - \frac{1 + \gamma}{d\gamma/dT}\right]\delta\Delta S^0 = \left[\beta_e - \frac{1 + \gamma}{d\gamma/dT}\right]\delta\Delta S^0$$

Since the terms in brackets in eq. 27 correspond to the isoequilibrium (isokinetic) temperature denoted in this paper by β_i, we have

[28] $$\beta_i = \beta_e - \frac{1 + \gamma}{d\gamma/dT} = T - \frac{1 + \gamma}{d\gamma/dT}$$

Although β parameters without subscripts have incorrectly been taken to be the same, eq. 28 clearly shows that β_i is not equal to β_e. When $(1 + \gamma)/(d\gamma/dT)$ is small compared to T, we find that $\beta_i \simeq T$ as commonly observed. On the other hand, there is no requirement that $(1 + \gamma)/(d\gamma/dT)$ be small, in which case β_i may be much larger than T or even negative. It should be noted, however, that negative β_i values are rare and that several of these are quite uncertain.

Differentiation of either eq. 25 or 26 with respect to temperature and combination with either $d\delta\Delta H^0/dT = \delta\Delta C_p^0$ or $d\delta\Delta S^0/dT = \delta\Delta C_p^0/T$ leads to

[29] $$\delta\Delta C_p^0 = CT(d^2\gamma/dT^2)\sigma$$

Thus this reaction model leads to $\delta\Delta C_p^0$ proportional to σ, as required by the Hammett equation.

When $\delta\Delta C_p^0 = 0$, eq. 29 leads to

[30] $$d^2\gamma/dT^2 = 0$$

A general solution of this differential equation is

[31] $$\gamma = a + bT \quad (\delta\Delta C_p^0 = 0)$$

and we therefore also have

Can. J. Chem. Downloaded from www.nrcresearchpress.com by 210.87.254.6 on 09/05/12
For personal use only.

[32] $\beta_i = -(1 + a)/b$

Again, β_i is independent of temperature because we take $\delta\Delta C_p^0 = 0$.

Conclusions and Summary

Because some of the thermodynamic consequences of the Hammett equation and the dichotomized enthalpy–entropy model for substituent and solvent effects may be obscured by mathematical details, a verbal summary may be useful. It should also be emphasized that some of the present conclusions concerning the temperature dependence of ρ and the isoequilibrium (isokinetic) relationship have been deduced previously (1, 2) in other ways.

The assumed validity of the Hammett equation over a range of temperature *requires* by thermodynamics that $\delta\Delta H^0$ and $\delta\Delta S^0$ be proportional to σ and therefore that $\delta\Delta H^0$ be proportional to $\delta\Delta S^0$. The exact validity of the Hammett equation with independent ρ and σ values also requires that $\delta\Delta C_p^0$ be proportional to σ or equal to zero. When $\delta\Delta C_p^0 = 0$ we find that $\rho = \rho_\infty[1 - (\beta_i/T)]$ and that $\delta\Delta H^0 = \beta_i\delta\Delta S^0$ with β_i independent of T. When $\delta\Delta C_p^0 \neq 0$, we have $\beta_i = f(T)$. If $\delta\Delta C_p^0$ is neither proportional to σ nor equal to zero, then ρ is a function of σ and we can no longer have an exactly linear relationship between $\delta\Delta H^0$ and $\delta\Delta S^0$. These statements are totally independent of all reaction models. Similar statements about $\delta\Delta H^{\ddagger}$, $\delta\Delta S^{\ddagger}$, and $\delta\Delta C_p^{\ddagger}$ are dependent on the applicability of thermodynamics to the transition state theory and the various activation parameters.

A useful model for substituent and solvent effects is one in which thermodynamic functions are taken to be sums of environmental and internal contributions. This model can account for the general form of the Hammett equation and the temperature dependence of ρ. It also leads to $\delta\Delta H^0$, $\delta\Delta S^0$, and $\delta\Delta C_p^0$ proportional to σ and thence to an isoequilibrium (isokinetic) relationship, all similar to the thermodynamic requirements of the Hammett equation. The environmental parameter β_e that occurs in this model is not the same as the isoequilibrium (isokinetic) temperature β_i, but is instead (approximately) equal to the experimental temperature. A relationship between β_i and β_e or T is derived in terms of the solvent parameter γ.

The solvent parameter γ is related to the solvent-reaction parameter ρ of the Hammett equation. It remains to be seen whether it is possible to obtain more useful information from γ values than from ρ values.

An important but inexact consequence which follows from $\beta_e \simeq T$ is that there is substantial "compensation" of $\delta\Delta H_{env}$ by $\delta\Delta S_{env}$ so that the Hammett equation is approximately satisfied even when $\delta\Delta H^0$ and $\delta\Delta S^0$ vary in erratic ways contrary to the exact thermodynamic requirements of proportionality to σ.

I am grateful to Douglas Dolman for many helpful discussions and to the authors of refs. 1 and 2, whose writings have provided the background and much of the impetus for the work reported here. I also thank the National Research Council of Canada and the Research Corporation for their support of experimental research that has led to some of this paper.

1. L. P. Hammett. Physical-organic chemistry. 2nd ed. McGraw-Hill, New York, N.Y. 1970.
2. J. E. Leffler and E. Grunwald. Rates and equilibria of organic reactions. Wiley, New York, N.Y. 1963.
3. P. D. Bolton and L. G. Hepler. Q. Rev. In press.
4. L. G. Hepler. J. Am. Chem. Soc. **85**, 3089 (1963).
5. J. W. Larson and L. G. Hepler. J. Org. Chem. **33**, 3961 (1968).
6. J. W. Larson and L. G. Hepler. *In* Solute–solvent interactions. *Edited by* J. F. Coetzee and C. D. Ritchie. Marcel Dekker, Inc., New York, N.Y. 1969.
7. L. G. Hepler and W. F. O'Hara. J. Phys. Chem. **65**, 811 (1961).
8. E. J. King. Acid–base equilibria. Pergamon Press, Inc., Oxford, England. 1965.
9. D. J. G. Ives and P. D. Marsden. J. Chem. Soc. 649 (1965).
10. C. D. Ritchie and W. F. Sager. Prog. Phys. Org. Chem. **2**, 323 (1964); C. D. Ritchie, Symposium on Linear Free Energy Correlations, Durham, North Carolina. 1964.
11. L. G. Hepler. J. Phys. Chem. **68**, 2645 (1964).

Can. J. Chem. Downloaded from www.nrcresearchpress.com by 210.87.254.6 on 09/05/12
For personal use only.

^{121}Sb Mössbauer: Antimony–Fluorine Systems

T. BIRCHALL AND B. DELLAVALLE
Department of Chemistry, McMaster University, Hamilton, Ontario

Received March 12, 1971

^{121}Sb Mössbauer data are presented for $NaSbF_4$, $KSbF_4$, KSb_2F_7, K_2SbF_5, $KSbF_6$, $CsSb_2F_{11}$, and $(NH_4)_2SbCl_5$. Attempts are made to rationalize the data in terms of known structural parameters.

Les données Mössbauer relatives à ^{121}Sb sont présentées pour $NaSbF_4$, $KSbF_4$, KSb_2F_7, K_2SbF_5, $KSbF_6$, $CsSb_2F_{11}$, et $(NH_4)_2SbCl_5$. On essaye de rationaliser les données en termes de paramètres structuraux connus.

Canadian Journal of Chemistry, 49, 2808 (1971)

Introduction

Mössbauer spectroscopy is being increasingly used in structural investigations of inorganic systems. We have become interested in applying the technique to a study of compounds of antimony, and although a number of papers have been published in this area (1–5), the interpretation of data has often been hampered by a lack of reliable structural information. A catalogue of Mössbauer parameters for compounds of known structure is necessary before the technique can be reliably used in obtaining structural imformation about compounds of unknown structure. To this end we decided to study the much quoted fluoro-anions of antimony(III) (6). These antimony–fluorine compounds were reported (7–10) to have structures in which the antimony was coordinated to 3 to 5 fluorines, and such a variation in environment would be expected to produce significant changes in Mössbauer parameters. Recently some of these compounds have been reinvestigated and shown to have structures which differed considerably from those previously reported. For example, SbF_3 has recently been shown to be polymeric (11), with six fluorine neighbors, rather than molecular (7), and KSb_2F_7 to consist of chains of SbF_4^- and SbF_3 units (12) rather than the simple $Sb_2F_7^-$ ion (8).

We here report the Mössbauer parameters for a number of these fluoro-antimony anions and attempt to rationalize the data in terms of the structural data available. In addition we also include our data on $KSbF_6$, and $CsSb_2F_{11}$.

Experimental

Preparation of Compounds

Attempts were made to prepare all of the compounds reported by Bystrom *et al.* according to their procedures (8–10). However, these were not always successful. For example all attempts to prepare KSb_4F_{13} resulted in KSb_2F_7 and it is extremely unlikely that the former compound exists. It is interesting to note that Bystrom and Wilhelmi (8) provide no analytical data for this compound.

KSb_2F_7

Several procedures yielded samples of this compound. Dissolution of Sb_2O_3 and K_2CO_3 in a 2:1 mole ratio in aqueous HF and allowing the solution to cool produced crystals of KSb_2F_7. KSb_2F_7 was also obtained from the attempted preparation of KSb_4F_{13}, and from Bystrom and Wilhelmi's (8) procedure for obtaining K_2SbF_5, except that the residue was recrystallized at room temperature from aqueous HF. Analysis: Sb found 59.0% theoretical 58.7%.

$NaSbF_4$

This was prepared by dissolving Sb_2O_3 and Na_2CO_3 in a 1:1 molar ratio in excess aqueous HF, evaporating to dryness and recrystallizing from water at room temperature. Clear colorless crystals were obtained. Analysis: Sb found 54.3% theoretical 55.1%.

$KSbF_4$

This was prepared in an analogous manner to the sodium salt, to yield a white powdery compound. Analysis: Sb found 52.1% theoretical 51.4%.

K_2SbF_5

This compound was obtained while attempting to prepare K_3SbF_6 by dissolving Sb_2O_3 and K_2CO_3 in a 1:3 mole ratio in excess aqueous HF. The solution was evaporated to dryness and the residue recrystallized twice from water at room temperature to give clear colorless crystals. Analysis: Sb found 41.0% theoretical 41.3%.

$KSbF_6$ was obtained from Ozark-Mahoning Co. and used without further purification. $CsSb_2F_{11}$ was kindly supplied by Dr. P. A. W. Dean formerly of this department.

Mössbauer Spectra

The Mössbauer spectra were recorded on apparatus previously described (13) except that a Xe–CO_2 proportional counter was used instead of a scintillation counter. The source was a 0.5 mCi $Ba^{121}Sn(Sb)O_3$ obtained from New England Nuclear and the single

Can. J. Chem. Downloaded from www.nrcresearchpress.com by 210.87.254.6 on 09/05/12
For personal use only.

channel analyzer was set on the escape peak of the 37.2 keV γ ray. The source was at room temperature while all samples were cooled to liquid nitrogen temperatures. The Sb(III) samples contained ~25 mg Sb/cm while those of Sb(V) contained ~40 mg Sb/cm. All of the spectra were obtained from finely powdered samples. The drive system was calibrated, before and after each spectrum, using Pd.^{57}Co and a standard iron foil. All spectra were computer fitted to an eight line quadrupole split pattern using a modification of Gabriel and Ruby's (14) program kindly supplied by G. J. Long, University of Missouri. All isomer shifts are with respect to InSb at liquid nitrogen temperature as zero isomer shift.

Results and Discussion

The Mössbauer isomer shift may be written simply as δ = constant $(\Delta R/R)\ \Delta|\psi s(0)|^2$ where $\Delta R/R$ is the change in nuclear radius on going from the ground to excited state and $\Delta|\psi s(0)|^2$ represents the difference in s electron density between the source and absorber. For ^{121}Sb, $\Delta R/R$ has been established as having a negative sign (15), hence the more negative the isomer shift the higher the s electron density at the nucleus. For ^{121}Sb, I = 7/2 and 5/2, the presence of an electric field gradient results in a splitting of the absorption into an eight line pattern which cannot be completely resolved due to the relatively large natural line width. The intensities of these lines are governed by the Clebsch–Gordan coefficients, and their relative positions by the magnitudes of the quadrupole moments for the ground and excited states, the size of the electric field gradient and upon the asymmetry parameter. The broad asymmetric resonance absorption which results when an electric field gradient is present must therefore be computer fitted in order to arrive at accurate Mössbauer parameters. In this work we have taken the ratio of quadrupole moments (Q 7/2/Q 5/2) to be 1.34 (15). Because of the unequal intensities of all transitions, the shape of the absorption envelope immediately yields the sign of the quadrupole splitting and hence the sign of the electric field gradient. Since Q for ^{121}Sb is negative, a positive quadrupole splitting means a negative electric field gradient and a concentration of charge along the symmetry axis. Such additional information is not normally obtained from ^{57}Fe or ^{119}Sn spectra.

The Mössbauer data obtained are summarized in Table 1 and representative spectra are shown in Fig. 1. The data has been arranged in order of increasing isomer shift or decreasing s electron density, with the Sb(III) compounds having much more negative shifts than those of Sb(V). This is to be expected since the higher oxidation state has no 5s electron pair. Also included in Table 1, for the purposes of comparison, are data for $(NH_4)_2SbCl_5$ and SbF_3. The data for SbF_3 are that of Ruby *et al.* (16) while that for $(NH_4)_2SbCl_5$ is the result of a more accurate analysis of a spectrum which we have already reported elsewhere (5).

Of the Sb(III) compounds examined the SbF_4^- and $Sb_2F_7^-$ ions have been reported as having novel structures: the $KSbF_4$ salt having a tetrameric anion $[Sb_4F_{16}]^{4-}$ with a square pyramidal arrangement about each antimony and a lone pair occupying the sixth coordination position (9), while $CsSb_2F_7$ contained discrete $Sb_2F_7^-$ ions with a trigonal bipyramidal arrangement about each antimony with one of the equatorial positions being occupied by the lone pair (8). These structures have been accepted and widely referred to for many years (6). The structure of SbF_3 had been reported as consisting of discrete molecules with a pyramidal arrangement of fluorines about antimony (7). There appeared, then, to be a considerable variation in coordination about Sb(III) in these Sb—F systems and large variation in Mössbauer parameters might have been expected. Careful reading of Bystrom *et al.* later papers (9, 10) reveals that he regarded the apparent changes in coordination number

TABLE 1. Mössbauer data for some antimony fluoride systems

Compound	Isomer shift	Quadrupole coupling constant (e^2qQ)	Line width	%Absorption
$(NH_4)_2\ SbCl_5$	−6.52±0.11	+11.2±1.8	2.9	8.6
SbF_3[16]	−6.0 ±0.2	+19.6±0.8		
$KSbF_4$	−5.02±0.15	+15.2±1.1	3.0	7.4
$NaSbF_4$	−4.96±0.09	+15.1±1.0	2.8	7.0
KSb_2F_7	−4.62±0.09	+17.0±0.9	2.8	8.7
K_2SbF_5	−4.11±0.09	+16.1±0.6	2.5	11.5
$CsSb_2F_{11}$	+10.95±0.06	+5.2±1.7	2.5	4.6
$KSbF_6$	+11.42±0.03	+3.1±1.5	2.9	10.4

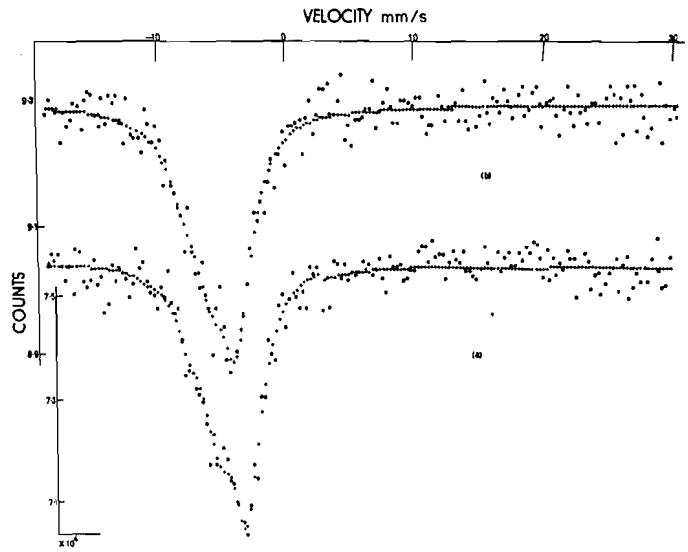

FIG. 1. ^{121}Mössbauer spectra of (*a*) K_2SbF_5; (*b*) $NaSbF_4$, at liquid nitrogen temperature. ○, experimental counts; +, computed counts.

with some suspicion, and suggested that the structures of SbF_3, KSb_4F_{13}, and $CsSb_2F_7$ should be reinvestigated.

Recently Edwards (11) has shown that SbF_3 is not molecular, but polymeric with bridging fluorines to give an arrangement in which there are six fluorines about each antimony in a distorted octahedral arrangement. The distortion being due to the stereochemically active 5s electron pair. We have been unable to obtain any compound with an analysis corresponding to KSb_4F_{13}: the data reported by Bystrom and Wilhelmi (8) for this stoichiometry may well have been that of a mixture of SbF_3 and KF. Further evidence on the $Sb_2F_7^-$ anion has very recently (12) shown the previously accepted structure (8) to be incorrect. Again there are no discrete ions and this structure should be regarded as made up of SbF_4^- and SbF_3 units with interaction between units via fluorine bridges so that the whole structure resembles a chain. This results in two antimony environments, one six coordinate (5 fluorines and a lone pair), and the other five coordinate (4 fluorines and a lone pair). Mastin (12) has also reexamined the data for $NaSbF_4$ and finds this to be essentially as reported (10), but he was unable to prepare suitable crystals of the corresponding potassium salt to verify its structure. The sodium salt has each SbF_4^- ion sharing two fluorines with two other SbF_4^- units, so that each Sb has five fluorines and a lone pair to give a distorted octahedral arrangement about the antimony. The ion should be written as $[SbF_4]_n^{n-}$. A similarly distorted octahedral geometry is observed in the SbF_5^{2-} ion (8) as well as in the analogous chloro salt $(NH_4)_2SbCl_5$ (17).

Thus, apart from SbF_3 and one site in KSb_2F_7, the environments about Sb(III) all appear to be distorted octahedra and the Mössbauer data in Table 1 can be explained on this basis. One can describe the bonding in terms of sp^3d^2 hybridization with an electron pair occupying one position of the octahedron. A comparison of the data for the $SbCl_5^{2-}$ and SbF_5^{2-} salts shows that the former has the higher s electron density at the Sb nucleus: the less electronegative chlorine being less efficient at removing electron density from the central antimony than is fluorine. There is also a more marked difference in quadrupole splitting between these two salts which can again be attributed to electronegativity differences in the halogens. Since the quadrupole coupling constants are all positive this means that there is a negative electric field gradient and an excess of electron density along the symmetry axis as compared to the equatorial plane. The four equatorial fluorines by virtue of their greater electron withdrawing power would therefore create more asymmetry than four chlorines and a greater quadrupole splitting results as is observed.

Can. J. Chem. Downloaded from www.nrcresearchpress.com by 210.87.254.6 on 09/05/12
For personal use only.

Can. J. Chem. Downloaded from www.nrcresearchpress.com by 210.87.254.6 on 09/05/12
For personal use only.

Since $NaSbF_4$ has been shown to have a chain structure *i.e.*, $(SbF_4)_n^{n-}$ by two independent groups (10, 12), as described above, it seems reasonable to suppose that the potassium salt with identical Mössbauer parameters will also have the same structure. Thus the tetrameric structure for $KSbF_4$, originally proposed by Bystrom *et al.* (9), may be incorrect. The lower isomer shift and smaller quadrupole splitting compared to K_2SbF_5 indicate that the bridging fluorines are less effective at removing electron density from the antimony than are terminal fluorines.

Examination of the crystallographic data for KSb_2F_7 indicates that there are two antimony sites, one with five near fluorine neighbors and the other with four near fluorines. Both sites are very distorted due to the stereochemically active lone pair. We have been unable to resolve the Mössbauer spectrum for this compound into components due to each site, and the data reported are the result of fitting one eight line pattern to the absorption envelope. The site having 5 fluorines might be expected to have an isomer shift close to that for SbF_5^{2-}, while that having only 4 fluorines would be expected to have a higher s electron density and a lower shift, since four fluorines will withdraw less electron density than five fluorines. We note that the "average" shift for KSb_2F_7 is indeed more negative than K_2SbF_5. The value for the quadrupole coupling constant for this compound cannot be interpreted though we feel that the positive value is realistic. If $Sb_2F_7^-$ had had a structure in which each antimony was surrounded by four fluorines and a lone pair of electrons in a distorted trigonal bipyramidal arrangement, then the lone pair in the equatorial plane would have resulted in a positive electric field gradient at the Sb and hence a negative value for the quadrupole coupling constant. This is not observed and is added support for the polymeric structure (12).

The Mössbauer data for SbF_3 also fall into place as a result of the recent structure redetermination (11). Because of the significant interactions between the SbF_3 units, all fluorines can be regarded as bridging, and since a bridging fluorine appears to be less efficient at removing electron density than a terminal fluorine, a relatively high s electron density remains on the antimony. Alternatively one might regard the antimony as seven coordinate (six fluorines and a lone pair) with the lone pair in a hybrid orbital having considerable s character, giving a relatively high s electron density at Sb and hence a lower isomer shift. In cases where the 5s pair is stereochemically inactive, as in $[Co(NH_3)_6][SbCl_6]$, isomer shifts as low as -11.2 mm/s are observed (5). The large quadrupole coupling is evidence that the 5s electron pair is not completely inactive and is clearly consistent with the distorted structure (11).

Two salts of Sb(V) have been examined and the relevant data are given in Table 1. Mössbauer data on SbF_6^- salts have been reported previously by Ruby *et al.* (16) and Bryukhanov *et al.* (18). The isomer shift of the sodium salt is 10.4 ± 0.2 mm/s (18) while that for the potassium salt is given as 12.3 ± 0.4 mm/s (16), both with respect to InSb. We find an isomer shift of $+11.42$ mm/s for $KSbF_6$, but a direct comparison between our data and that of Ruby *et al.* (16) may not be valid since they recorded their spectra at 4.2 °K. However, since our data and that of the Russian workers (18) both refer to InSb at liquid nitrogen temperature, a comparison is allowable. The sodium salt has a lower isomer shift than the potassium salt by 1 mm/s. Part of this difference may be experimental error but it is interesting to note that these salts do have different crystal structures. Sodium hexafluoroantimonate(V) (19) has the same structure as $LiSbF_6$ (20), with a perfect octahedron of fluorines about each antimony. However, in $KSbF_6$ this octahedron is distorted (21). It is also noted that the Sb—F bond length is 1.877 Å in $LiSbF_6$ but 1.77 Å in $KSbF_6$. Such differences are significant and if the sodium salt has a similar Sb—F bond length to that found in $LiSbF_6$ then the difference in isomer between $NaSbF_6$ and $KSbF_6$ are accounted for. However, only the data for $LiSbF_6$ can be considered accurate and the others should probably be reinvestigated.

Bryukhanov *et al.* (18) found no quadrupole splitting in the sodium hexafluoroantimonate(V) as would have been expected for the regular octahedral arrangement discussed above. A splitting was reported for the $KSbF_6$ (16) which we confirm, although our value is considerably less (+3.1 mm/s) than that previously reported (+8.0 mm/s) (16). Both results confirm that this salt indeed has a distorted anion. We feel that our lower value is the more realistic in view of the crystallographic evidence.

The data for the $Sb_2F_{11}^-$ salt can be rationalized on terms of the known structural information. Although the structure of the Cs^+ salt is

unknown, it seems reasonable that the anion will resemble that in $XeF.Sb_2F_{11}$ (22) where two SbF_5 units are linked by a fluorine bridge. Since a bridging fluorine will remove less electron density from the central atom than a terminal fluorine, one would expect the Sb in $Sb_2F_{11}^-$ to have a higher s electron density than in SbF_6^-, and hence a lower isomer shift. This is indeed observed. One also notes a larger quadrupole splitting in $Sb_2F_{11}^-$ than in SbF_6^-. In the Sb_2F_{11} fragment of $XeF.Sb_2F_{11}$ there are three Sb—F distances 1.78–1.80 Å and 1.90–1.93 Å for the two kinds of terminal fluorine, and a longer bond 2.05 Å to the bridging fluorine. The quadrupole splitting found for $CsSb_2F_{11}$ is clearly in accord with a similarly distorted antimony environment.

We hope to make use of the data presented here in a Mössbauer analysis of more complex antimony–fluorine systems.

We wish to thank the National Research Council of Canada for supporting this work and for a fellowship for B.D.V.

1. J. G. Stevens and L. H. Bowen. Mössbauer Eff. Methodol. **5**, 27 (1969) and refs therein.
2. T. Birchall and B. DellaValle. Chem. Commun. 675 (1970).
3. G. G. Long and L. H. Bowen. Inorg. Nucl. Chem. Lett. **6**, 837 (1970).
4. G. G. Long, J. G. Stevens, R. J. Tullbane, and L. H. Bowen. J. Am. Chem. Soc. **92**, 4230 (1970).
5. T. Birchall, B. DellaValle, E. Martineau, and J. B. Milne. J. Chem. Soc. A, 1855 (1971).
6. F. A. Cotton and G. Wilkinson. Advanced inorganic chemistry. 2nd ed. Interscience, New York. 1967. p. 493.
7. A. Bystrom and A. Westgren. Arkiv. Kemi Miner. **17**, 1 (1943).
8. A. Bystrom and K. A. Wilhelmi. Arkiv Kemi, **3**, 17, 373, 461 (1951).
9. A. Bystrom, S. Bückland, and K. A. Wilhelmi. Arkiv Kemi, **4**, 175 (1952).
10. A. Bystrom, S. Bückland, and K. A. Wilhelmi. Arkiv. Kemi, **6**, 77 (1953).
11. A. J. Edwards. J. Chem. Soc. A, 2751 (1970).
12. S. H. Mastin. Private communication. S. H. Mastin and R. R. Ryan. Inorg. Chem. In press.
13. T. Birchall. Can. J. Chem. **47**, 1351 (1969).
14. J. A. Gabriel and S. L. Ruby. Nucl. Instr. Methods, **36**, 23 (1965).
15. J. G. Stevens and S. L. Ruby. Phys. Lett. **32A**, 91 (1970).
16. S. L. Ruby, G. M. Kalvius, G. B. Beard, and R. L. Snyder. Phys. Rev. **159**, 239 (1967).
17. M. Edstrand, M. Inge, and N. Ingri. Acta Chem. Scand. **9**, 122 (1955).
18. V. A. Bryukhanov, B. Z. Iofa, V. Kotkhekar, S. I. Semenov, and V. S. Shpinel. Soviet Phys. JETP, **26**, 912 (1968).
19. H. Bode and H. Clausen. Z. anorg. Chem. **265**, 229 (1951).
20. J. H. Burns. Acta Cryst. **15**, 1098 (1962).
21. H. Bode and E. Voss. Z. anorg. Chem. **264**, 144 (1951).
22. V. M. McRae, R. D. Peacock, and D. R. Russell. Chem. Commun. 629 (1969).

Can. J. Chem. Downloaded from www.nrcresearchpress.com by 210.87.254.6 on 09/05/12
For personal use only.

Can. J. Chem. Downloaded from www.nrcresearchpress.com by 210.87.254.5 on 09/05/12
For personal use only.

Studies on Metal Hydroxy Compounds. XIII. Thermal Analyses and Decomposition Kinetics of Hydroxystannates of Bivalent Metals

P. RAMAMURTHY AND E. A. SECCO

Chemistry Department, St. Francis Xavier University, Antigonish, Nova Scotia

Received March 8, 1971

The thermal analyses of hexahydroxystannates of bivalent metals of the type $Me[Sn(OH)_6]$, where Me = Zn, Co, Cu, Ni, Mn, Ca, Mg, Cd, Sr, reveal that the primary mode of decomposition occurs by dehydroxylation and subsequent decomposition of the metastannate residue occurs in the Zn, Cu, Mn, Ca, and Mg compounds. Calorimetric measurements along with related enthalpic values for the decomposition reaction are given. The kinetics of thermal decomposition of all compounds studied, except the Cd and Mg analogues, follow first order reaction kinetics up to $\alpha \sim 0.9$.

Les analyses thermiques d'hexahydroxystannates de métaux divalents du type $Me[Sn(OH)_6]$, avec Me = Zn, Co, Cu, Ni, Mn, Ca, Mg, Cd, Sr, indiquent que le premier mode de décomposition se fait par déshydroxylation, et que la décomposition subséquente du métastannate résiduel se fait dans les composés du Zn, Cu, Mn, Ca et Mg. Des mesures calorimétriques, de pair avec les valeurs d'enthalpies, sont rapportées pour la décomposition.

Les cinétiques de la décomposition thermique de tous les composés étudiés, à l'exception des analogues du Cd et Mg, obéissent aux réactions cinétiques de premier ordre jusqu'à $\alpha \sim 0.9$.

Canadian Journal of Chemistry, 49, 2813 (1971)

Introduction

Hexahydroxystannates of the general formula $Me[Sn(OH)_6]$, where Me is a bivalent metal, have been known for some time (1, 2) but hitherto no detailed work has been reported on their mode of decomposition and decomposition kinetics.

The existence of $Me[Sn(OH)_6]$ type compounds was thought to provide an opportunity to probe the effect of the metal species Me on the $-Sn(OH)_6$ portion of the molecule. Any effect arising from the Me species might be expected to manifest itself indirectly on the thermal stability, mode of decomposition, and decomposition kinetics of the compound.

The purpose of this paper is to report on a physico-chemical study involving thermal analyses and decomposition kinetics of $Me[Sn(OH)_6]$ compounds where Me represents a bivalent transition metal or Group II*a* metal.

Experimental

All compounds used in this study were prepared in this laboratory by following procedure described in the literature (2, 3). In each preparation, the precipitate was filtered, washed thoroughly with distilled water, and dried at 110 °C overnight.

The identities of the reactant compounds were confirmed by the available X-ray diffraction patterns (3). Those compounds for which X-ray patterns were not available were confirmed in an indirect manner by correlating the thermogravimetric analysis with the X-ray patterns of the solid residues; furthermore, the unknown X-ray patterns had to resemble the known patterns in their essential features.

The heating curves, calorimetric measurements, and isothermal kinetic traces were obtained as previously described (4–6). The heating rate used was 20 °C/min and an ambient atmosphere of dry N_2 (Matheson Prepurified Grade with a stated impurity of 0.003% O_2) at a flow rate of 2SCFH was maintained during all experiments.

Results and Discussion

Thermogravimetry

The results of thermogravimetry are presented in Table 1; the proposed reaction for each compound is that which best fits the observed weight loss. The only step observed in the decomposition reaction is via dehydroxylation which is represented by the general equation

$$[1] \quad Me[Sn(OH)_6]_{(s)} \rightarrow MeSnO_{3(s)} + 3H_2O_{(g)}$$

The products of decomposition were identified by X-ray diffraction and correlated with DTA curves.

Differential Thermal Analysis

The DTA results are given in Table 2 with two thermal effects in evidence. The first effect is endothermic observed in all compounds and corresponds to dehydroxylation according to [1]. The second effect is an exotherm observed

Can. J. Chem. Downloaded from www.nrcresearchpress.com by 210.87.254.5 on 09/05/12
For personal use only.

TABLE 1. Thermogravimetric results

Compound	Temperature range (°C)	% of total weight lost	
		Observed	Calculated
$Zn[Sn(OH)_6]$	200–450	18.10	18.20
$Co[Sn(OH)_6]$	195–355	19.10	19.30
$Cu[Sn(OH)_6]$	185–350	18.91	19.00
$Ni[Sn(OH)_6]$	200–450	19.43	19.30
$Mn[Sn(OH)_6]$	200–400	19.70	19.62
$Ca[Sn(OH)_6]$	200–460	20.75	20.70
$Mg[Sn(OH)_6]$	230–460	21.79	22.00
$Cd[Sn(OH)_6]$	200–350	16.12	16.20
$Sr[Sn(OH)_6]$	225–450	17.00	17.10

TABLE 2. Differential thermal analysis

Compound	Peak number	Peak temperature (°C)	Reaction number
$Zn[Sn(OH)_6]$	1	300	1
	2*	750	2
$Co[Sn(OH)_6]$	1	320	1
$Cu[Sn(OH)_6]$	1	250	1
	2*	630	2*a*
$Ni[Sn(OH)_6]$	1	320	1
$Mn[Sn(OH)_6]$	1	280	1
	2*	560	2*a*
$Ca[Sn(OH)_6]$	1	370	1
	2*	760	2
$Mg[Sn(OH)_6]$	1	340	1
	2*	650	2
$Cd[Sn(OH)_6]$	1	270	1
$Sr[Sn(OH)_6]$	1	320	1

*Exotherms.

with Zn, Cu, Mn, Ca, and Mg and assigned to the decomposition of the metastannate according to the general equations (7),

[2] $$2MeSnO_3 \rightarrow Me_2SnO_4 + SnO_2$$

or

[2*a*] $$MeSnO_3 \rightarrow MeO + SnO_2$$

These latter modes of decomposition, [2] and [2*a*], do not involve any weight change and therefore are not observable in thermogravimetry; the reaction products were, however, identified by X-ray diffraction patterns.

Calorimetric Measurements

The calorimetric results along with the related enthalpic values for the decomposition of the compounds according to reaction 1 with the onset–terminal temperature limits are presented in Table 3; the literature value of decomposition of $Sn(OH)_4$ is included for comparison. The ΔH^0_f of the various hydroxystannates could not be calculated since the heats of formation of the products, $MeSnO_3$, are not reported in the literature.

Reaction Kinetics Data

The experimental α, t data for the decomposition reactions were processed through a large number of kinetic rate expressions. The best linear relations between the experimental data and the known rate expressions over the maximum reaction fraction ($\alpha \sim 0.9$) for all compounds, excepting $Cd[Sn(OH)_6]$, and over the temperature range studied are given in Table 4. All the compounds studied, except the Cd and Mg compounds, obey first order reaction kinetics up to $\alpha \sim 0.9$.

The rate data for $Cd[Sn(OH)_6]$ fit a power law relationship in the initial accelerating stage up to $\alpha = 0.4$, *i.e.*

$$\alpha = kt^n$$

where n is found to be in the range 1.5–1.8. The non-integral and temperature dependent nature of "n" have been interpreted by Thomas and Tompkins (8).

The $Mg[Sn(OH)_6]$ decomposition reaction follows a phase boundary control reaction mechanism as shown by the fitting of its kinetic data to the three-dimensional contracting sphere model equation, *viz*

$$1 - (1 - \alpha)^{1/3} = kt$$

The column of $\log_{10} A$ shows that all compounds, except $Cd[Sn(OH)_6]$, possess a value of $A < 10^{13}$. From the Arrhenius rate equation, in the form derived from activated complex theory (6)

$$k_r = \left[10^{13}\frac{Q^*}{Q}\right] e^{-E_a/RT} = A\, e^{-E_a/RT}$$

A values of 10^6–10^{12} are interpreted in terms of a complex restricted in its modes of rotation to varied degrees as discussed by Cordes (9). A linear relationship is evident for the activation energy E_a and heat of decomposition ΔH as displayed in Fig. 1. The intercept value of *ca.* 3 kcal/mol might represent the net activation energy E_n for decomposition. The relationship is expressed in equation form, $E_a = E_n + \Delta H$, where the dependence of E_a could be ascribed

TABLE 3

Compound	Temperature range (°C)	Heat of decomposition* ΔH/mol of H_2O formed (kcal)	Heat of decomposition* ΔH/mol of compound decomposed (kcal)
$Zn[Sn(OH)_6]$	200–340	5.07	15.21±0.21
$Co[Sn(OH)_6]$	250–370	5.48	16.46±0.05
$Cu[Sn(OH)_6]$	185–295	6.79	20.36±0.04
$Ni[Sn(OH)_6]$	200–360	8.51	25.55±0.28
$Mn[Sn(OH)_6]$	190–320	7.09	21.28±0.31
$Ca[Sn(OH)_6]$	250–400	10.90	32.60±0.51
$Mg[Sn(OH)_6]$	240–400	7.39	22.18±0.32
$Cd[Sn(OH)_6]$	210–350	11.80	35.40±0.50
$Sr[Sn(OH)_6]$	240–360	4.71	14.14±0.11
$Sn(OH)_4$†		8.05	16.10†

*All determinations were done in duplicate; ΔH values are given with their average deviations.
†Included for comparison purposes; ΔH value taken from N.B.S. Circular No. 500.

TABLE 4. Kinetic results for decomposition

Compound	Temperature range (°C)	Number of temperatures	Rate expression	Activation energy E_a (Kcal)	log A
$Zn[Sn(OH)_6]$	220–260	5	First order	16.3 ±0.5	6.60
$Co[Sn(OH)_6]$	260–300	4	First order	20.9 ±1.5	7.41
$Cu[Sn(OH)_6]$	180–240	5	First order	21.9 ±1.1	7.03
$Ni[Sn(OH)_6]$	260–300	4	First order	27.19±0.91	9.04
$Mn[Sn(OH)_6]$	200–250	4	First order	27.00±1.72	11.22
$Ca[Sn(OH)_6]$	300–350	4	First order	33.67±1.70	11.94
$Sr[Sn(OH)_6]$	270–320	5	First order	19.70±0.75	7.00
$Cd[Sn(OH)_6]$	210–250	4	$\alpha = kt^n (\alpha < 0.4)$ First order ($\alpha > 0.4$)	39.36±2.1 48.9 ±2.8	13.48 23.25
$Mg[Sn(OH)_6]$	250–310	4	$[1 - (1 - \alpha)^{1/3}] = kt$	27.17±1.25	9.16

directly to ΔH. A more meaningful relationship would be, therefore, between ΔH and a fundamental property, such as the ionization potential, of the Me species (Fig. 2). The plot approximates a linear dependence for the bivalent metals of the "first transition" series and Mg; Cd and Sr, apparent exceptions to the linear relationship, belong to the "second transition" series.

The structure of $Me[Sn(OH)_6]$ compounds is reported to consist of discrete $Sn(OH)_6^{2-}$ groups as determined from spectroscopic studies (2). Crystal structure studies of $Me[Sn(OH)_6]$, however, (*i*) report ReO_3 type structures (3*a*) with Me, and Sn species alternating on Re sites and (*ii*) show the metallic species bound to 6OH groups in a pseudo-octahedral coordination (3). Whatever the exact structure of $Me[Sn(OH)_6]$, two types of reactive bound OH groups may be assumed to be present, that is, Me—OH and Sn—OH bonded groups. It is expected the OH bound to Sn to be essentially of constant character in all compounds and also the character of OH bonded to Me is expected to be a function of the nature of Me. Furthermore, if first-order rate kinetics in dehydroxylation reactions of hydroxy compounds (10) is due to the high mobility of free H and bearing in mind the amphoteric nature of stannic hydroxide, then it is suggested that mobile H arises from the [—Sn—O...H] site. Any effect due to the nature of Me is expected therefore to reflect itself on the [—Me—OH] portion.

A simple interpretation for the inverse dependence of ΔH with ionization potential, assuming all other factors to remain constant, might be given in terms of —Me—OH character. As the ionization potential of Me increases, the contribution of negative charge by Me to the electronegative O is minimal so that the OH is covalently bonded to Me resulting in a relatively

Can. J. Chem. Downloaded from www.nrcresearchpress.com by 210.87.254.5 on 09/05/12
For personal use only.

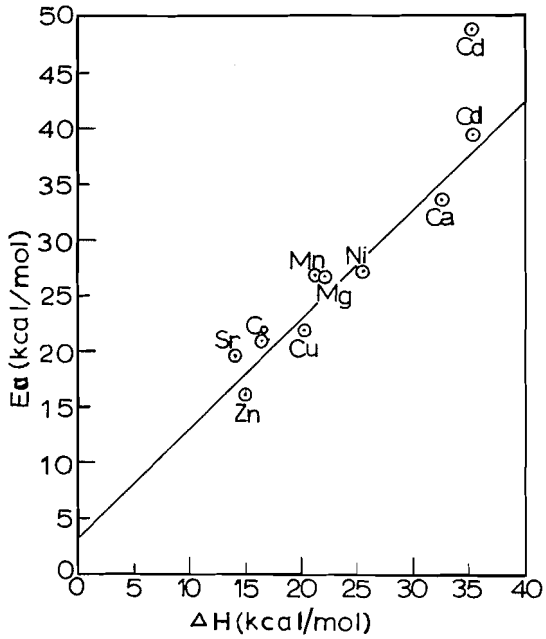

FIG. 1. Plot of activation energy E_a *vs.* heat of decomposition ΔH.

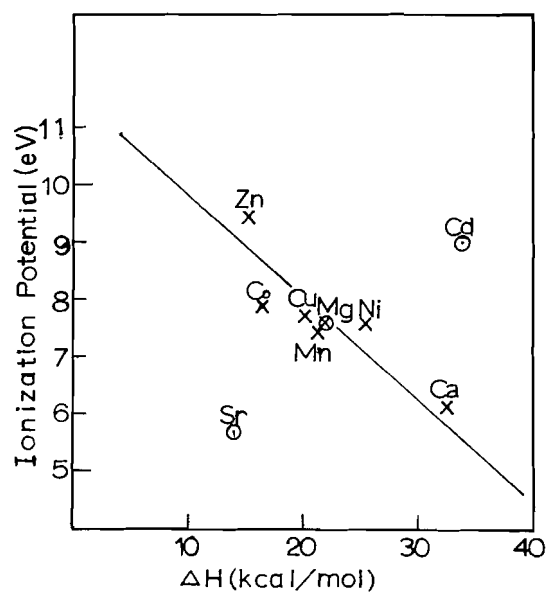

FIG. 2. Plot of ionization potential of the metal species *vs.* heat of decomposition ΔH.

weak [—Me...OH] bond. Conversely, for Me of low ionization potential the contribution of negative charge to O is much greater so OH becomes negatively charged with [—Me^+—OH^-] assuming an ionic character with increased strength. However, a more realistic interpretation must involve an interplay of the effect of the ionization potential of Me on OH groups bonded to both Me and Sn.

The authors are indebted to the National Research Council of Canada for financial support of this research program.

1. J. W. MELLOR. Comprehensive treatise on inorganic and theoretical chemistry. Vol. VII. Longmans, Green and Co., Ltd., New York. 1927. pp. 416–421.
2. T. DUPUIS, C. DUVAL, and J. LECOMTE. Compt. Rend. **257**, 3080 (1963).
3. H. STRUNZ and B. CONTAG. Acta Cryst. **13**, 601 (1960). I. MORGENSTERN-BADARAU, Y. BILLIET, P. POIX, and A. MICHEL. Comp. Rend. **260** (13), 3688 (1965).
4. O. K. SRIVASTAVA and E. A. SECCO. Can. J. Chem. **45**, 579 (1967).
5. P. RAMAMURTHY and E. A. SECCO. Can. J. Chem. **46**, 3605 (1968); **47**, 2185 (1969).
6. P. RAMAMURTHY and E. A. SECCO. Can. J. Chem. **47**, 2181 (1969).
7. T. DUPUIS. Chem. Anal. **50**, 302 (1968).
8. J. G. N. THOMAS and F. C. TOMPKINS. Proc. Roy. Soc. London, Ser. A. **209**, 550 (1951); **210**, 111 (1951).
9. H. F. CORDES. J. Phys. Chem. **72**, 2185 (1968).
10. P. RAMAMURTHY and E. A. SECCO. Can. J. Chem. **48**, 2617 (1970).

Can. J. Chem. Downloaded from www.nrcresearchpress.com by 210.87.254.5 on 09/05/12
For personal use only.

Can. J. Chem. Downloaded from www.nrcresearchpress.com by 210.87.254.5 on 09/05/12
For personal use only.

The Influence of Sulfoxides and Sulfones on the Temperature of Maximum Density of Water

DIGBY D. MACDONALD,[1] M. D. SMITH, AND J. B. HYNE
Department of Chemistry, University of Calgary, Calgary, Alberta

Received March 11, 1971

The influence of dimethyl sulfoxide (DMSO), diethyl sulfoxide (DESO), tetramethylene sulfoxide (TMSO), and tetramethylene sulfone ($TMSO_2$) on the temperature of maximum density of water has been investigated. It is concluded that in dilute solution DESO stabilizes the characteristic three-dimensional structure of water. The other solutes, however, destabilize the structure of water over the entire concentration range studied (0–1.3 $\times$ 10^{-2} mole fraction solute).

L'influence du diméthyl sulfoxyde (DMSO), diéthyl sulfoxyde (DESO), tétraméthylène sulfoxyde (TMSO) et tétraméthylène sulfone ($TMSO_2$) sur la température du maximum de densité de l'eau, a été étudiée. Il en a été déduit qu'en solution diluée, le DESO stabilise la structure caractéristique à trois dimensions de l'eau. Les autres solutés, par contre, déstabilisent la structure de l'eau sur toute l'échelle de concentration étudiée (0–1.3 $\times$ 10^{-2} fraction molaire de soluté).

Canadian Journal of Chemistry, **49**, 2817 (1971)

Introduction

The influence of various solutes on the temperature of maximum density (TMD) of water has been used in a number of investigations (1–5) to determine the effect of dissolved substances on the structural properties of water. This method is particularly useful since the observed effects are readily interpreted in terms of changes in concentration of the "structured" and "unstructured" components of liquid water (3). Previous studies by Wada and Umeda (1, 2) and by Franks and Watson (3) have demonstrated that certain organic solutes (*e.g.* alcohols, amines) shift the "structured–unstructured" equilibrium in liquid water in the direction of the "structured" component. Other solutes (*e.g.* acetonitrile, propionitrile, acetamide, and 1,4-dioxane) have the reverse effect (2). These two classes of solutes are commonly referred to as "water-structure makers" and "water-structure breakers", respectively.

In view of the growing importance of sulfoxides and sulfones as solutes in biochemical and physico-chemical investigations involving water as solvent, the present study was undertaken to determine their influence on the structure of liquid water. The compounds chosen for this study were dimethyl sulfoxide (DMSO), diethyl sulfoxide (DESO), tetramethylene sulfoxide (TMSO), and tetramethylene sulfone ($TMSO_2$). This series permitted us to examine various relationships between the structural properties of the solutes and their abilities to perturb the structure of liquid water.

[1]Present address: Research Chemistry Branch, Whiteshell Nuclear Research Establishment, Pinawa, Manitoba.

Experimental

Apparatus and Method

Temperatures of maximum density were determined by observing the temperature of minimum volume using a 100 ml dilatometer of conventional design (3). The dilatometer was filled with solution and cooled slowly to approximately 5 °C. Air bubbles were carefully excluded. The dilatometer was then thermostated in an oil bath controlled to better than $\pm$0.02 °C. The position of the meniscus was determined with a cathetometer at eight temperatures within $\pm$1.5 °C of the TMD of each solution. After each temperature setting thermal equilibration was indicated by time independence of the solvent meniscus in the capillary. This required about 15 min and a further 15 min were allowed to elapse before reading the meniscus position. All temperature measurements were made with a 6° Beckman thermometer which was calibrated against a platinum resistance thermometer.

Molar volumes of the various solutes were measured at several temperatures using a mercury displacement dilatometer (6). The measurements were made in a 30 °C range extending from about 5 °C above the melting point. The dilatometer was periodically calibrated using degassed conductivity grade water.

Materials

All four compounds were dried over freshly cut calcium hydride and distilled under reduced pressure (~0.1 mm Hg). The middle 70% cuts were collected and stored in tightly stoppered flasks. Chromatographic analysis showed no impurities greater than 0.5% by

Can. J. Chem. Downloaded from www.nrcresearchpress.com by 210.87.254.5 on 09/05/12
For personal use only.

weight. The melting points of the various compounds agreed well with published values (Table 1). We could find no reliable melting point for TMSO in the literature. In this case we have used density as a criterion of purity and find excellent agreement between the density measured in this study and that quoted by Jeffery, Parker, and Vogel (9).

All solutions were prepared by weight using doubly-distilled conductivity grade water. The water was degassed by boiling prior to preparation of the solutions.

Results

The TMDs were determined graphically from the parabolic meniscus position *vs.* temperature plots. It was found that the observed TMD of water in our apparatus occurred at 4.40 °C, 0.42 °C higher than the accepted value of 3.98 °C. This type of discrepancy has been noted previously (1, 4) and has been attributed to expansion of the dilatometer. Accordingly, all observed TMDs were corrected by subtracting 0.42 °C.

Numerical values for $\Delta\theta$, the shift in the TMD from 3.98 °C (*i.e.* TMD − 3.98), for various concentrations of the four compounds in water are listed in Table 2. In order to check the accuracy of the experimental method the TMDs of three potassium chloride solutions were measured and compared with data taken from the literature. The comparison is presented in Fig. 1. The $\Delta\theta$ values illustrated in Fig. 1 were reproducible to ± 0.1 °C and clearly lie on the same line as that generated by literature values to within this limit of error. All other $\Delta\theta$ values reported in this work have the same uncertainty limits.

The numerical values for $(\partial V^0/\partial T)_p$ listed in Table 1 were calculated directly from plots of V^0 *vs.* T. These plots were found to be linear, within experimental error, demonstrating that the $(\partial V^0/\partial T)_p$ values are not strongly dependent on temperature. Accordingly, these values are used in calculating ideal solute induced shifts in the TMD of water (see the following section). The $(\partial V^0/\partial T)_p$ values are considered accurate to better than $\pm 2\%$ as determined by inspection of the V^0 *vs.* T plots.

TABLE 1. Physical properties of the pure solute

Solute	Melting point (°C) This work	Melting point (°C) Literature	$(\partial V^0/\partial T)_p$ (ml mol^{-1} deg^{-1})
DMSO	19.5	18.55 (7) 19–20 (8)	0.0667 (20–50 °C)*
DESO	20.0	19–20 (8)	0.0923 (20–50 °C)
TMSO	(1.17249)†	(1.1725 (9))†	0.0683 (18–50 °C)
$TMSO_2$	25.0	24.8 (9)	0.0669 (30–50 °C)

*Temperature range over which $(\partial V^0/\partial T)_p$ was measured.
†Density at 20.00 °C in g ml^{-1}

TABLE 2. Solute-induced shifts in the temperature of maximum density of water

Compound	$\chi \times 10^2$*	$-\Delta\theta$ (°C)
DMSO	0	0
	0.3198	0.83
	0.6341	1.75
	0.9749	2.72
	1.2930	3.75
DESO	0	0
	0.2542	0.63
	0.5118	1.35
	0.9270	2.77
	1.2006	3.92
TMSO	0	0
	0.2489	0.80
	0.4319	1.40
	0.6887	2.35
	0.9650	3.38
$TMSO_2$	0	0
	0.2027	1.38
	0.3925	2.66
	0.6132	4.24

*Mole fraction.

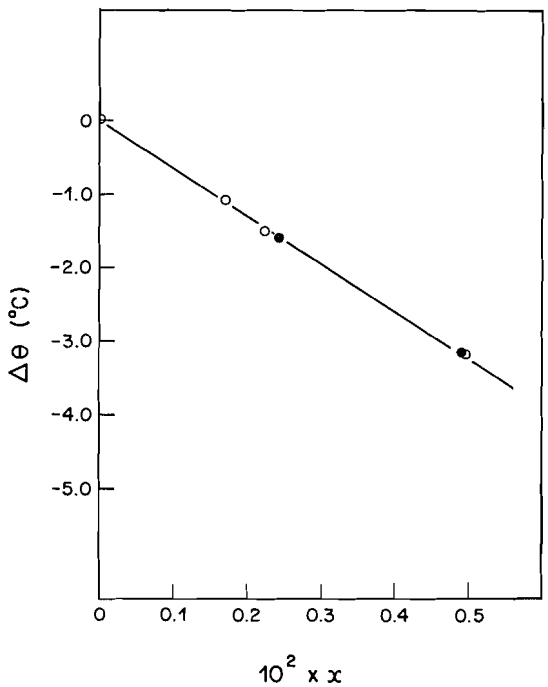

FIG. 1. The influence of potassium chloride mole fraction on the TMD of water. ○, this work; ●, ref. 16.

Can. J. Chem. Downloaded from www.nrcresearchpress.com by 210.87.254.5 on 09/05/12
For personal use only.

Discussion

The shifts in the TMD of water produced by the four compounds studied in this work are shown in Fig. 2. In all cases $\Delta\theta$ becomes more negative with increasing concentration of the solute species. This behavior is commonly found (1–5) and was recognized as early as 1839 by Despretz (10, 11).

Wada and Umeda (1, 2) and later Franks and Watson (3) have shown that the observed shift in the TMD can be divided into an ideal contribution ($\Delta\theta_i$) and a non-ideal contribution ($\Delta\theta_s$). Thermodynamic reasoning shows that this relationship may be written as eq. 1.

$$[1]\quad \Delta\theta = -\left(\frac{\chi}{1-\chi}\cdot\frac{(\partial V^0/\partial T)_p}{2\alpha_1 V_1^*}\right) - \left(\frac{(\partial \Delta V_x^M/\partial T)}{2(1-\chi)\alpha_1 V_1^*}\right) = \Delta\theta_i + \Delta\theta_s$$

where V^0 is the molar volume of the solute, V_1^* is the molar volume of water at 3.98 °C (*i.e.* 18.016 ml mol^{-1}), ΔV_x^M is the excess volume of mixing, χ is the mole fraction of solute, and α_1 is a constant which defines the parabolic variation of the molar volume of water with temperature about the TMD (1, 3). This constant has a numerical value of 7.80×10^{-6} deg^{-2} (1). For an ideal solution ΔV_x^M is zero at all temperatures so the shift in the TMD becomes numerically equal to the first term on the right hand side of eq. 1, $\Delta\theta_i$. For dilute real systems $\chi/(1-\chi) \rightarrow \chi$ and $(1-\chi) \rightarrow 1$ so eq. 1 can be reduced to eq. 2.

$$[2]\quad \Delta\theta = -\frac{(\partial V^0/\partial T)_p}{2\alpha_1 V_1^*}\cdot\chi - \frac{(\partial \Delta V_x^M/\partial T)}{2\alpha_1 V_1^*}$$

Equation 2 predicts that if $(\partial \Delta V_x^M/\partial T)$ is a linear function of χ then $\Delta\theta$ will vary linearly with composition thus obeying the Depretz rule (10, 11). The data plotted in Figs. 1 and 2 reveal that potassium chloride and $TMSO_2$ obey the Depretz rule whereas the other compounds examined do not. This observation shows that for potassium chloride and $TMSO_2$ $(\partial \Delta V_x^M/\partial T)$ is a linear function of χ. For the three less dipolar sulfoxides, however, $(\partial \Delta V_x^M/\partial T)$ must vary non-linearly with χ over the composition range considered resulting in the observed non-linear dependence of $\Delta\theta$ on χ. Unfortunately no direct measurements of $(\partial \Delta V_x^M/\partial T)$ as a function of χ have been made for these systems with sufficient accuracy to test the above predictions.

Numerical data contained in Table 1 permit calculation of $\Delta\theta_i$ for the various sulfoxide and sulfone solutions employed in this study. The results of these calculations are illustrated in Fig. 3. Two points should be noted. First, $\Delta\theta_i$ is always negative and varies linearly with χ (see eq. 2). Second, the relative abilities of the compounds to depress $\Delta\theta$ (Fig. 2) and $\Delta\theta_i$ (Fig. 3) are not the same. This clearly demonstrates that the non-ideal term ($\Delta\theta_s$) makes a significant contribution to the behavior of $\Delta\theta$ for the compounds studied.

The non-ideal contribution to the solute-induced shifts in the TMD of water have also been calculated (eq. 1) and are plotted in Fig. 4. Previous investigations (1–3) suggest that *non-electrolytes* which stabilize the characteristic three-dimensional structure of water against thermal destruction, *i.e.*, "water – structure makers", exhibit positive values for $\Delta\theta_s$.[2] Ac-

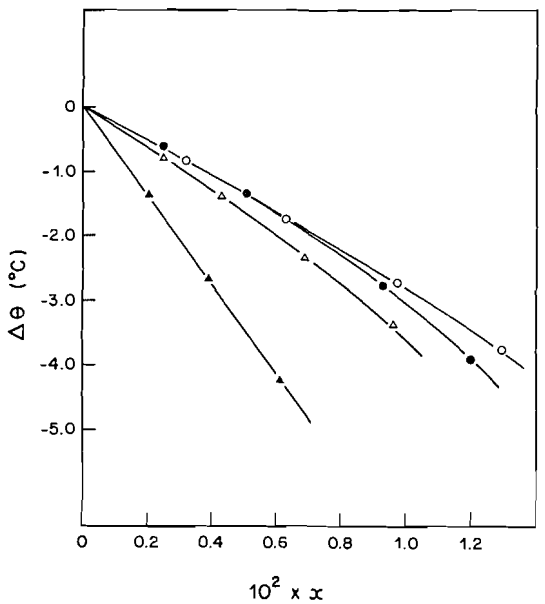

FIG. 2. The overall influence ($\Delta\theta$) of sulfoxides and sulfone mole fraction on the TMD of water. ○, DMSO; ●, DESO; △, TMSO; ▲, $TMSO_2$.

[2]Recent work by Wada and Miura (12) and Sarma and Ahluwalia (13) suggests that this generalization may not hold true for "structure-making" ionic solutes such as the tetra-alkyl ammonium halides. The reader is referred to these papers for a detailed discussion of this apparent anomaly.

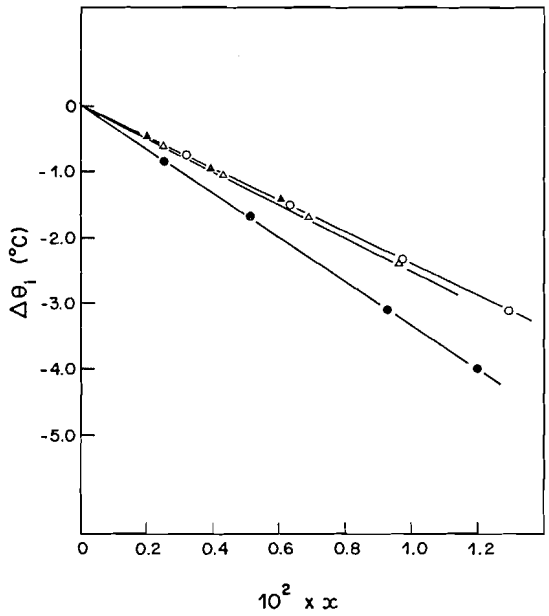

FIG. 3. Ideal component of the shift ($\Delta\theta_i$) in the TMD of water as a function of mole fraction. ○, DMSO; ●, DESO; △, TMSO; ▲, $TMSO_2$.

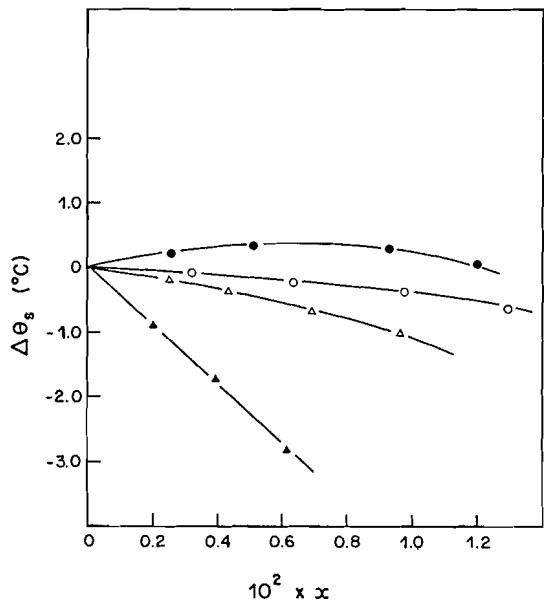

FIG. 4. Non-ideal component of the shift ($\Delta\theta_s$) in the TMD of water as a function of mole fraction. ○, DMSO; ●, DESO; △, TMSO; ▲, $TMSO_2$.

cording to the above interpretation of the four solutes investigated here only DESO can be considered as a "water-structure maker" and then only in dilute solution ($<1.2 \times 10^{-2}$ mol fraction). The other three solutes appear to destabilize or break-down the characteristic three-dimensional structure of liquid water apparently in the increasing order of effectiveness DMSO < TMSO < $TMSO_2$. A recent study by Safford *et al.* (14) showed that small additions of DMSO to water sharpen the peaks in the radial distribution function derived from X-ray diffraction and also the intermolecular frequency spectrum of water derived from neutron inelastic scattering. These data indicate that DMSO increases the molecular order in water. On the other hand, a more recent study by Brink and Falk (15) has shown that addition of a few mol% of DMSO to water does not change the average value or the width of distribution of hydrogen bond energies derived from infrared spectroscopy. These latter data indicate that small additions of DMSO have little effect on the structure of water. In the present study, however, we find that DMSO produces a small negative $\Delta\theta_s$ suggesting that this compound destabilizes or breaks down the characteristic three-dimensional structure of liquid water. This contrasts with the findings of both Safford *et al.* and Brink and Falk. It is possible, though not considered likely, that the different conclusions reflect different experimental temperatures, *i.e.* 4 °C for the present study but 25 °C for the other two. It is more likely, however, that the three experimental techniques respond to different phenomena.

If the ability of a solute to perturb the structure of water can be regarded as a sum of group effects, as proposed by Wada and Umeda (2), then the data plotted in Fig. 4 provide a means of determining the effect of varying the hydrophobic nature and the hydrophilic nature of the solute on its ability to "make" or "break" the structure of liquid water. In the sulfoxide series the structure making tendencies fall in the order DESO > DMSO > TMSO. Since the sulfoxide group is common to all three compounds then this order reflects the relative abilities of the diethyl, dimethyl, and tetramethylene groups to stabilize water structure. The observation that a diethyl configuration has a greater structure making ability than a dimethyl configuration is expected since previous investigations (1–3) have shown that hydrophobic structure making ability increases with carbon

Can. J. Chem. Downloaded from www.nrcresearchpress.com by 210.87.254.5 on 09/05/12
For personal use only.

Can. J. Chem. Downloaded from www.nrcresearchpress.com by 210.87.254.5 on 09/05/12
For personal use only.

chain length. On the other hand, comparison of the behavior of DESO and TMSO (Fig. 4) shows that the open chain configuration (DESO) has a much greater ability to stabilize water structure than the closed ring configuration (TMSO), even though both compounds possess four carbon atoms. This difference is too large to reflect merely the different number of hydrogen atoms. Instead, it is likely that the greater degree of conformational freedom possessed by DESO allows this compound to adopt a more efficient structure making configuration in the open three-dimensional structure which is characteristic of liquid water.

The effect of varying the hydrophilic nature of the solute may be examined by comparing the $\Delta\theta_s$ *vs.* χ curves for TMSO and $TMSO_2$ plotted in Fig. 4. These curves clearly show that a sulfone group ($>SO_2$) is much more efficient at destabilizing water structure than a sulfoxide group ($>SO$). Wada and Umeda (2) have demonstrated that the water-structure breaking ability of a hydrophilic group increases with its group dipole moment. Since sulfones have larger dipole moments than sulfoxides (16) the relationship found above is expected.

Finally, the $\Delta\theta_s$ *vs.* χ curve for DESO plotted in Fig. 4 passes through a maximum at about 0.7×10^{-2} mole fraction solute, indicating that the structure making ability of DESO is optimized at this composition. This observation suggests that at this concentration the structure making ability of DESO is counterbalanced by the structure breaking effect of its sulfoxide dipole, and further additions of DESO to the system result in the destruction of the stabilized water clusters by a bulk effect, *i.e.* the water molecules become too dilute to maintain co-operative hydrogen bonding. This explanation can also account for the curved $\Delta\theta_s$ *vs.* χ curves (Fig. 4) for DMSO and TMSO, both of which are water-structure destabilizers. At low concentrations solute–water dipole–dipole interaction or hydrogen bonding are the dominant mechanisms in destabilizing water clusters. At higher concentrations, however, the water-structure destabilizing bulk effect of the solute is superimposed on the above mechanism resulting in $(\partial\Delta\theta_s/\partial\chi)$ becoming more negative with increasing solute concentration.

Financial assistance for this work from the National Research Council of Canada is gratefully acknowledged.

1. G. WADA and S. UMEDA. Bull. Chem. Soc. Jap. **35**, 646 (1962).
2. G. WADA and S. UMEDA. Bull. Chem. Soc. Jap. **35**, 1797 (1962).
3. F. FRANKS and B. WATSON. Trans. Faraday Soc. **63**, 329 (1967).
4. A. J. DARNELL and J. GREYSON. J. Phys. Chem. **72**, 3021 (1968).
5. A. J. DARNELL and J. GREYSON. J. Phys. Chem. **72**, 3032 (1968).
6. R. E. GIBSON and O. H. LOEFFLER. J. Am. Chem. Soc. **61**, 2515 (1939).
7. D. MARTIN, A. WEISE, and H. J. NICLAS. Angew Chem. Int. Ed. **6**, 318 (1967).
8. C. C. ADDISON and J. C. SHELDON. J. Chem. Soc. 2705 (1956).
9. G. H. JEFFERY, R. PARKER, and A. I. VOGEL. J. Chem. Soc. 570 (1961).
10. M. C. DESPRETZ. Ann. Chim. Phys. **70**, 49 (1839).
11. M. C. DESPRETZ. Ann. Chim. Phys. **73**, 296 (1840).
12. G. WADA and M. MIURA. Bull. Chem. Soc. Jap. **42**, 2498 (1969).
13. T. S. SARMA and J. C. AHLUWALIA. J. Phys. Chem. **74**, 3457 (1970).
14. G. J. SAFFORD, P. C. SCHAFFER, P. S. LEUNG, G. F. DOEBBLER, G. W. BRADY, and E. F. X. LYDEN. J. Chem. Phys. **50**, 2140 (1969).
15. G. BRINK and M. FALK. J. Mol. Struct. **5**, 27 (1970).
16. J.W. SMITH. Electric dipole moments. Butterworths, London. 1955. p. 230.

Can. J. Chem. Downloaded from www.nrcresearchpress.com by 210.87.254.5 on 09/05/12
For personal use only.

The Decomposition of Aqueous Sodium Bromite

C. L. Lee and M. W. Lister
Department of Chemistry, University of Toronto, Toronto 181, Ontario

Received March 24, 1971

An investigation of the rate of decomposition of aqueous sodium bromite is described. The main reactions are: $2BrO_2^- \rightarrow BrO^- + BrO_3^-$ and $Br^- + BrO_2^- \rightarrow 2BrO^-$, followed by $BrO^- + BrO_2^- \rightarrow Br^- + BrO_3^-$. The rate constants and activation parameters of the decomposition reactions are reported. As the second reaction is the reverse of that previously studied in the decomposition of sodium hypobromite, its equilibrium constant (at various temperatures) can be obtained, and hence the thermodynamic properties of aqueous bromite ions. These are briefly compared with the properties of similar ions containing bromine or chlorine.

On décrit les recherches entreprises en vue de déterminer la vitesse de décomposition d'une solution aqueuse de bromite de sodium. Les réactions principales sont: $2BrO_2^- \rightarrow BrO^- + BrO_3^-$ et $Br^- + BrO_2^- \rightarrow 2BrO^-$ puis $BrO^- + BrO_2^- \rightarrow Br^- + BrO_3^-$. On rapporte les constantes de vitesse et les paramètres d'activation pour ces réactions de décomposition. Puisque la deuxième réaction est l'inverse de celle étudiée précédemment pour la décomposition de l'hypobromite de sodium, sa constante d'équilibre (à différente température) peut être obtenue et par conséquent les propriétés thermodynamique des ions bromites en solution aqueuse. Celles-ci sont brièvement comparées avec les propriétés d'ions similaires contenant du brome ou du chlore.

Canadian Journal of Chemistry, 49, 2822 (1971)

This paper is concerned with the kinetic and, to a lesser extent, thermodynamic stability of bromite ions in aqueous solution. The results permit some comparisons to be made amongst the series of bromine oxyions, and these in turn are briefly compared with the analogous chlorine compounds. Bromite ions have been relatively little investigated, but a study of their kinetic stability was made by Engel, Oplatka, and Perlmutter-Hayman (1) as part of their research on hypobromite ions. We have examined their decomposition under somewhat different conditions and over a range of temperature, and a comparison with their results will be made later in this paper. A fairly extensive investigation of the conditions of formation of bromite from hypobromite ions, and of the preparation of sodium bromite, has been made by Breiss (2). The present work was done at sufficiently high p*H*, so that protonated species (particularly HOBr) would be present only at very low concentrations. Acidified sodium bromite decomposes rapidly, so presumably other reactions, not investigated in the present work, are then important.

Experimental

Sodium Bromite

Several sources were used for the reagent. Firstly, it was prepared by the method of Breiss (2), which gave crystals of the trihydrate, $NaBrO_2.3H_2O$. Secondly, crystals of the same composition were made available by La Société d'Études Chimiques pour l'Industrie et l'Agriculture, of Argenteuil, France, to whom we are much indebted. Thirdly, a solution of the compound was obtained from the Olin Mathieson Chemical Corporation of New York, and this solution was evaporated and the sodium bromite recrystallized. Most of the experiments used material from the first two sources. Since the solid showed a tendency to decompose, the crystals were dissolved in dilute sodium hydroxide solution to give a stock solution that was reasonably stable, and which was diluted as required for the experiments.

Sodium hydroxide and bromine, used in the preparation of sodium bromite, were of analytical reagent grade, as were the sodium bromide and sodium perchlorate which were added to the solutions in the kinetic experiments.

Apparatus

In the kinetic runs, samples of the appropriate solution were sealed in Pyrex glass ampoules, and immersed in a thermostat for known lengths of time. The thermostat contained silicone oil, controlled to ± 0.02 °C. The solutions contained sodium bromite, sodium hydroxide, sodium bromide (not added in some runs), and sodium perchlorate to adjust the ionic strength to a value of 0.50. At suitable times the ampoules were removed, rapidly cooled, and the contents analyzed.

Analysis of Solutions

The solutions in general contained sodium bromide, hypobromite, bromite, and bromate, sodium hydroxide and possibly a little carbonate. The sodium perchlorate present was assumed not to react, so its concentration was known from the amount added initially. The sodium bromide concentration was also known from the amount put in initially, plus the amount formed in the reaction (see below).

The sodium bromite and hypobromite were estimated

Can. J. Chem. Downloaded from www.nrcresearchpress.com by 210.87.254.5 on 09/05/12
For personal use only.

spectrophotometrically with a Beckmann DU Spectrophotometer. Their extinction coefficients were measured from the absorbances of freshly prepared alkaline solutions; in the case of sodium hypobromite this was made in the usual way by adding bromine to cold sodium hydroxide solution. It was checked by polarography that these solutions did not contain appreciable amounts of the other ion (*e.g.* hypobromite in the bromite solution). The polarographic experiments would have detected 0.5% of the other ion as impurity. The extinction coefficients found were as follows:

	Extinction coefficient	
Wavelength (nm)	NaBrO	$NaBrO_2$
296	113.2	114.6
300	140.5	112.4
310	220.2	100.0
320	284.5	90.0
330	303.2	83.6
340	278.1	73.7
350	220.8	60.4
360	155.0	44.6
370	94.9	30.8
380	56.6	20.5

The solutions used to obtain these extinction coefficients were standardized by titration with arsenious oxide at a p*H* regulated by excess sodium bicarbonate (3). The arsenious oxide reacts with both sodium hypobromite and bromite. In the kinetic runs measurements were made at 296 and 380 mμ, and it was checked that the other species present did not contribute appreciably to the absorbances at these wavelengths.

It was found that the total oxidizing normality, measured by the iodine liberated on adding excess potassium iodide and sulfuric acid, did not change during a run, so presumably oxygen is not evolved. Consequently changes in bromide and bromate concentrations could be calculated from the mass balance of bromine and oxygen atoms. The absence of oxygen evolution was confirmed (within moderate limits) by the fact that the ampoules did not develop increased pressure during a run.

The concentration of sodium hydroxide was found by adding excess hydrogen peroxide to a sample, boiling to destroy the excess, followed by titration with standard acid. The hydrogen peroxide reacts with both sodium bromite and hypobromite.

Mechanism and Calculation of Rate Constants

Engel, Oplatka, and Perlmutter-Hayman (1) proposed a mechanism for the decomposition of sodium bromite. Our results fit their mechanism, though with some difference in the relative contributions of the various reactions. They found a dependence of the rate on p*H*,while under the conditions of the present experiments (0.06 to 0.18 *M* sodium hydroxide), no change in rate constant was found with varying $[OH^-]$. They interpreted their results as showing that at the lower p*H* of most of their experiments protonated species are reacting. Presumably these species are present in such low concentrations under the conditions of our experiments as to have no effect. However, it should be mentioned that in the somewhat analogous decomposition of hyperbromite ions, the rate increases with $[OH^-]$, and the rate in fact passes through a minimum at about the p*H* values we have used (3, 4). It is possible, therefore, that a similar minimum occurs for bromite ions, and that the apparent lack of p*H* dependence arises because our experiments fall in the region of this minimum.

We can therefore re-write their mechanism, and propose that the following reactions occur:

$$[1] \qquad 2BrO_2^- \xrightarrow{k_1} BrO_3^- + BrO^-$$

$$[2] \qquad BrO^- + BrO_2^- \xrightarrow{k_2} BrO_3^- + Br^-$$

$$[3] \qquad Br^- + BrO_2^- \xrightarrow{k_3} 2BrO^-$$

$$[4] \qquad 2BrO^- \xrightarrow{k_4} Br^- + BrO_2^-$$

Reaction 4 is the reverse of reaction 3, and is the initial step in the decomposition of hypobromite ions. Engel, Oplatka, and Perlmutter-Hayman found that, at 25 °C and at the concentrations they used, reaction 3 was more important than reaction 1. However, in our experiments, both reaction paths made appreciable contributions, with reaction 1 predominating.

The mechanism above gives rate equations which could not be integrated, but since k_2 is relatively high, the steady state approximation was made that $d[BrO^-]/dt = 0$. From this, putting $[Br^-] = x$, $[BrO^-] = y$, and $[BrO_2^-] = z$, we get

$$2k_4y^2 + k_2yz - k_1z^2 - 2k_3xz = 0$$

Values of k_4 are known (1, 4, 5), and also of k_2 (5), and these combined with the values of k_1 and k_3 obtained below show that the term $2k_4y^2$ is small enough to be neglected. Hence $y = (k_1z + 2k_3x)/k_2$. With this approximation, the rate equations can be integrated to give (with $\beta = x_0/z_0$)

$$\frac{1}{z} = \frac{k_3 - 3k_1 + 3(k_3\beta + k_1)\, e^{k_3(3\beta+1)z_0t}}{k_3(3\beta + 1)z_0}$$

Can. J. Chem. Downloaded from www.nrcresearchpress.com by 210.87.254.5 on 09/05/12
For personal use only.

A plot of $1/z$ against t should give an exponential curve of increasing slope, but it was found that our experimental results were such that the curvature was very slight during the decomposition of the first 20–25% of the sodium bromite. The slope $d(1/z)/dt$ is

$$3(k_3\beta + k_1)e^{k_3(3\beta + 1)z_0 t}$$

and the initial slope is $3(k_3\beta + k_1)$. In practice, we took an average slope, $(1/z - 1/z_0)/t$, over the first part of the reaction. This average slope can be shown to be $S_0\,(e^{ct} - 1)/ct$, where S_0 is the initial slope, and $c = k_3(3\beta + 1)z_0$. The average slope was therefore corrected to give the initial slope by this expression. This involves a knowledge of k_3, which was obtained as described below. The process of correction was repeated until the value of k_3 used to obtain S_0 was the same as the final value of k_3. Finally S_0 was plotted against β, which gave a linear plot, though with some scatter. The best line through the points was obtained by least mean squares, and k_1 and k_3 were obtained from this line, since $S_0 = 3(k_3\beta + k_1)$. The corrections from the average to the initial slopes were mostly under 5%, and in only one run above 10%.

After the rate constants had been obtained, the validity of the steady state approximation was checked as follows. Firstly, the concentrations of hypobromite ion, which are also obtainable from the measured absorbances, were compared with the steady state values given by $(k_1z + 2k_3x)/k_2$. However, $[BrO^-]$ was always so low, that the most that can be said is that the values were of the right order of magnitude. In a typical run $[BrO_2^-] = 0.05\ M$, and the calculated $[BrO^-] = 0.0004\ M$. As the extinction coefficients are not very different, it follows that a very small error in absorbance gives a large error in $[BrO^-]$. Secondly, the differential equations were integrated numerically, with the assumption that initially $[BrO^-] = 0$. It was found that the steady state concentration of hypobromite had developed rapidly compared with the rate of decomposition of the bromite. 95% of the steady state $[BrO^-]$ was reached during the first 1 to 2½% of the bromite decomposition, the exact amount depending chiefly on the concentration of bromide ions. At the same time the slope, which starts low if $[BrO^-]$ is initially zero, had risen to 97 to 98% of its steady state value. The first sample was taken after a time that was long enough to ensure firstly that temperature equilibrium had been reached and secondly that steady state conditions had been virtually established.

Results

Table 1 gives the results for the main series of runs at 76.6 °C. The slopes are corrected on the assumption that $k_3 = 3.925 \times 10^{-7}\ M^{-1}\ s^{-1}$, and the least mean squares line drawn through S_0 plotted against β gives $k_3 = 3.917 \times 10^{-7} M^{-1}\ s^{-1}$. The best value for k_3 is therefore $3.92 \times 10^{-7}\ M^{-1}\ s^{-1}$. The value derived for k_1 is $3.04 \times 10^{-6}\ M^{-1}\ s^{-1}$.

Similar data for 86.0 °C are given in Table 2. Here the slopes are corrected on the assumption that $k_3 = 6.90 \times 10^{-7}\ M^{-1}\ s^{-1}$, and the resulting plot of S_0 against β makes $k_3 = 6.896 \times 10^{-7}\ M^{-1}\ s^{-1}$. Hence the best value for k_3 is $6.90 \times 10^{-7}\ M^{-1}\ s^{-1}$, and the value for k_1 is found to be $8.10 \times 10^{-6}\ M^{-1}\ s^{-1}$. Table 2 also contains data for 96.7 °C. The slopes are corrected with $k_3 = 12.08 \times 10^{-7}\ M^{-1}\ s^{-1}$, and these in turn give $k_3 = 12.06 \times 10^{-7}\ M^{-1}\ s^{-1}$. The best value for k_3 is taken to be $12.07 \times 10^{-7}\ M^{-1}\ s^{-1}$, and the value of k_1 is found to be $24.79 \times 10^{-6}\ M^{-1}\ s^{-1}$.

A plot of $\log k_1$ or $\log k_3$ against $1/T$ is reasonably linear in both cases. For k_1, the activation energy is 26.8_5 kcal/mol. If we assume that $\Delta H^{\ddagger}$ is independent of temperature, then $\Delta H^{\ddagger} = 26.2_5$ kcal/mol (at 25 °C) and $\Delta S^{\ddagger} = -7.3$ cal/deg mol; $\log k_1$ extrapolated to 25 °C is −8.43. For k_3, the activation energy is 13.7 kcal/mol. From this, $\Delta H^{\ddagger} = 13.1$ kcal/mol (at 25 °C) and $\Delta S^{\ddagger}$ is −47 cal/deg mol; $\log k_3$ extrapolated to 25 °C is −7.96.

The slope, S_0, and hence the rate constants do not appear to depend on the concentration of hydroxide ions present. Neither k_1 nor k_3 gave any systematic trend with $[OH^-]$ over the range 0.06 to 0.18 M.

Discussion

The results of the present work differ somewhat from those of Engel, Oplatka, and Perlmutter-Hayman (1), but the differences can be attributed to different experimental conditions. Firstly, these workers find the rate decreases with increasing pH, by a factor of 3 for every pH unit. However, their results are only for pH values of 8.5, 9.7, and 13.0, and they did not investigate whether there is any change around pH 13. Our

TABLE 1. Decomposition of sodium bromite at 76.6 °C

Run	$[BrO_2^-]_0 \times 10^2$ (M)	$[Br^-]_0 \times 10^2$ (M)	$[OH^-]$ (M)	$S_0 \times 10^5$ (M^{-1} s^{-1})	β
1	7.72	1.11	0.1030	0.913	0.144
2	9.28	1.33	0.1040	0.913	0.143
3	8.43	3.45	0.1380	0.937	0.409
4	8.55	25.11	0.1400	1.188	2.935
5	8.28	17.02	0.1355	1.058	2.056
6	4.12	16.55	0.0725	1.483	4.023
7	7.32	0.76	0.1263	0.877	0.104
8	3.66	0.36	0.0632	0.951	0.098
9	4.89	0.51	0.1662	0.953	0.104
10	5.05	0.51	0.0842	0.940	0.101
11	5.04	0.51	0.0842	0.966	0.101
12	4.24	0.43	0.0716	0.908	0.101
13	3.85	16.66	0.0631	1.435	4.323
14	5.41	34.52	0.1442	1.641	6.376
15	5.39	22.91	0.1426	1.423	4.254
16	5.33	12.21	0.1410	1.193	2.292
17	5.97	15.03	0.1581	1.254	2.516
18	5.89	6.59	0.1562	1.028	1.118
19	5.27	6.69	0.1378	1.113	1.268
20	3.34	20.98	0.0897	1.625	6.284
21	6.65	18.74	0.1791	1.200	2.817
22	3.34	14.02	0.0897	1.489	4.192
23	5.79	30.98	0.1561	1.498	5.347

TABLE 2. Decomposition of sodium bromite at 86.0 °C

Run	Temperature (°C)	$[BrO_2^-]_0 \times 10^{-2}$ (M)	$[Br^-]_0 \times 10^{-2}$ (M)	$[OH^-]$ (M)	$S_0 \times 10^5$ (M^{-1} s^{-1})	β
24	86.0	3.91	35.86	0.0808	4.34	9.172
25	"	4.42	23.18	0.0912	3.53	5.429
26	"	5.18	12.13	0.1069	2.94	2.344
27	"	5.18	0.24	0.1069	2.59	0.046
28	"	5.21	6.53	0.1056	2.63	1.253
29	"	5.12	0.24	0.1076	2.33	0.047
30	96.7	3.89	19.04	0.0805	9.24	4.884
31	"	5.23	12.81	0.1081	8.41	2.448
32	"	5.14	0.24	0.1062	7.40	0.047
33	"	5.26	30.22	0.1086	9.44	5.748

results indicate that at high pH, the rate does not change with pH; this is presumably because protonated species (such as HOBr), which could offer alternative routes for the reaction, are effectively absent in 0.1 M sodium hydroxide. Hence we have written the reactions as occurring between ions.

Secondly, the earlier workers found that at 25 °C the reaction $Br^- + BrO_2^- \rightarrow 2BrO^-$ predominated under their experimental conditions. However, the rate constants they quote are not very different: in our nomenclature, they give $k_1 = 1.3 \times 10^{-4}$ M^{-1} s^{-1}, and $k_3 = 1.43 \times 10^{-4}$ M^{-1} s^{-1}. At high temperatures, we find k_1 greater than k_3, but the activation parameters are such that this order reverses at low temperatures, and the rate constants extrapolated to 25 °C are $k_1 = 3.7 \times 10^{-9}$, $k_3 = 1.1 \times 10^{-8}$ M^{-1} s^{-1}. This is a long extrapolation, but at least it agrees with Engel, Oplatka, and Perlmutter-Hayman's result that k_3 is more important at low temperatures. Their rate constants quoted above are for a pH of 8.5, which is presumably why they are much larger than ours. However, the discrepancy is larger than would be expected from their observations on the effect of pH, and cannot at present be explained.

The results allow some calculations to be made on the thermodynamic properties of bromite ions. Reactions 3 and 4 above lead to an equilibrium

$$Br^- + BrO_2^- \underset{k_4}{\overset{k_3}{\rightleftharpoons}} 2BrO^-$$

with the activation parameters: reaction 3 has $\Delta H^{\ddagger} = 13.1$ kcal/mol, $\Delta S^{\ddagger} = -47$ cal/deg mol;

Can. J. Chem. Downloaded from www.nrcresearchpress.com by 210.87.254.5 on 09/05/12
For personal use only.

TABLE 3. Conventional thermodynamic quantities for aqueous ions at 25 °C

Ion	ΔH^0_f	ΔG^0_f	S^0	Ion	ΔH^0_f	ΔG^0_f	S^0
Cl^-	−40.0	−31.35	13.2	Br^-	−28.9	−24.6	19.3
ClO^-	−25.4	−8.9	10.0	BrO^-	−21.9	−8.0	12.0
ClO_2^-	−16.6	2.7	24.1	BrO_2^-	−8.9	6.5	30.5
ClO_3^-	−25.15	−2.15	38.8	BrO_3^-	-16.2_5	4.3	38.6
ClO_4^-	−31.0	−2.1	43.5	BrO_4^-	2.9	28.9	44.7
$Cl_2O_2^{2-\ddagger}$	−26.3	10.1	8.7	$Br_2O_2^{2-\ddagger}$	−25.0	9.1	3.0

and reaction 4 has $\Delta H^{\ddagger} = 18.8$ kcal/mol, $\Delta S^{\ddagger} = -21$ cal/deg mol (5). Hence ΔH for the reaction in the k_3 direction is −5.7 kcal/mol, and ΔS is −26 cal/deg mol. Thermodynamic data on dilute aqueous solutions are for sodium bromide: $\Delta H^0_f = -86.2$, $\Delta G^0_f = -87.2$ kcal/mol, $S^0 = 33.7$ cal/deg mol; and for sodium hypobromite: $\Delta H^0_f = -79.1$, $\Delta G^0_f = -70.6$ kcal/mol, $S^0 = 26.4$ cal/deg mol (6, 7). Hence calculated values for sodium bromite (aq) are: $\Delta H_f^0 = -66.3$ kcal/mol, and $S^0 = 45$ cal/deg mol. These results, combined with data for the elements in sodium bromite, make the value for its $\Delta G^0_f = -56.1$ kcal/mol. Some confirmation of this is provided by the value for ΔH^0_f of −66.0 kcal/mol from calorimetric measurements on the reaction of aqueous sodium bromite and sodium sulfite (8). Table 3 summarizes values for chlorine and bromine oxyions, in order to show that the values deduced above for sodium bromite (aq) are reasonable. The data come from refs. 6, 7, and 9. Values are included for the activated species $X_2O_2^{2-\ddagger}$ (for $Cl_2O_2^{2-\ddagger}$, see ref. 10). The values in Table 3 are conventional values, relative to H^+ (aq) as zero.

The general trends of these quantities are similar, apart from the well-known low stability of perbromates. As regards bromite ions, their ΔH^0_f, relative to the other bromine ions, is somewhat more positive compared to the chlorine series. This is somewhat offset by their higher entropy, so that there is less contrast in ΔG^0_f. Thus the equilibrium constant for $X^- + XO_2^- \rightleftharpoons 2XO^-$ is calculated to be 1.4×10^{-3} for the bromine compounds, and 1.4×10^{-11} for chlorine. The activated species $X_2O_2^{2-\ddagger}$ are also not very different in the two series, although here the entropy of the bromine species is somewhat lower. At present, it does not seem to be possible to explain these differences in detail.

In a recent paper (11), Massagli, Indelli, and Pergola report results of the decomposition of bromite at pH of 8.5 and below. Their results follow a rate equation

$$\text{Rate} = [HBrO_2][Br^-]\{k_1 + k_2[H^+]\}$$

which is evidently a different mechanism from ours, the difference being presumably attributable to the much lower pH of their experiments.

1. P. ENGEL, A. OPLATKA, and B. PERLMUTTER-HAYMAN. J. Am. Chem. Soc. **76**, 2010 (1954).
2. J. BREISS. Ph.D. Thesis. L'université de Strasbourg, Strasbourg, France. 1959.
3. R. M. CHAPIN. J. Am. Chem. Soc. **56**, 2211 (1934).
4. B. PERLMUTTER-HAYMAN and G. STEIN. J. Phys. Chem. **63**, 734 (1959).
5. M. W. LISTER and P. E. MCLEOD. Can. J. Chem. In publication.
6. W. M. LATIMER. Oxidation potentials. 2nd ed. Prentice-Hall, Inc., New York. 1952.
7. National Bureau of Standards Circular 500, U.S. Government Printing Office, Washington.
8. M. B. KENNEDY and M. W. LISTER. Unpublished result.
9. G. K. JOHNSON, P. N. SMITH, E. H. APPELMAN, and W. N. HUBBARD. Inorg. Chem. **9**, 119 (1970).
10. M. W. LISTER. Can. J. Chem. **34**, 465 (1956).
11. A. MASSAGLI, A. INDELLI, and F. PERGOLA. Inorg. Chim. Acta, **4**, 593 (1970).

Can. J. Chem. Downloaded from www.nrcresearchpress.com by 210.87.254.5 on 09/05/12
For personal use only.

Can. J. Chem. Downloaded from www.nrcresearchpress.com by 210.87.254.105 on 09/05/12
For personal use only.

The Decomposition of Perchloric Acid on Metal Oxide Catalysts

R. GILBERT[1] AND P. W. M. JACOBS

Department of Chemistry, The University of Western Ontario, London 72, Ontario

Received February 9, 1971

The thermal decomposition of perchloric acid has been investigated on five Harshaw catalysts: copper chromite, alumina, iron(III) oxide, copper(II) oxide, and manganese(IV) oxide (the last three being supported on alumina). Manganese(IV) oxide gave complex kinetics which were not fully analyzed but on the other four catalysts the reaction was first order. Activation energies were: copper chromite, 54 kcal/mol; alumina, 28.8 kcal/mol; iron(III) oxide, 28.6 kcal/mol; copper(II) oxide, 39.0 kcal/mol. A mechanism is proposed for the decomposition which involves proton transfer to an acceptor (typically an O^{2-} ion) in the catalyst surface followed by decomposition of the ClO_4^- anion formed in this process. Some observations on the catalyzed thermal decomposition of ammonium perchlorate are presented.

L'étude de la décomposition thermique de l'acide perchlorique a été faite à partir de cinq catalyseurs de Harshaw: le chromite de cuivre, l'alumine, les oxydes de fer(III), de cuivre(II) et de manganèse(IV) (les trois derniers ayant comme support l'alumine). L'oxyde de manganèse(IV) donne des cinétiques complexes qui n'ont pas été complètement élucidées mais pour les quatre autres catalyseurs, la réaction est du premier ordre. Les énergies d'activation sont de 54 kcal/mol pour le chromite de cuivre, de 28.8 kcal/mol pour l'alumine, de 28.6 kcal/mol pour l'oxyde de fer(III) et de 39.0 kcal/mol pour l'oxyde de cuivre(II). Un mécanisme est proposé pour la décomposition: il y a transfert de proton sur un accepteur (un ion O^{2-} typique) à la surface du catalyseur puis décomposition de l'anion ClO_4^- formé dans ce processus. Quelques observations sur la décomposition thermique catalysée du perchlorate d'ammonium sont aussi présentées.

Canadian Journal of Chemistry, 49, 2827 (1971)

In the course of their study of the thermal decomposition and ignition of ammonium perchlorate, Jacobs and Russell-Jones (1) suggested that the catalytic activity of copper chromite might be due to its ability to catalyze the thermal decomposition of perchloric acid which is produced in the initial step of the decomposition of ammonium perchlorate by proton transfer (2, 3). At that time only the uncatalyzed thermal decomposition of perchloric acid had been studied (4). This reaction appears to be heterogeneous in Pyrex glass reaction vessels at low temperatures (4–6) but homogeneous at high temperatures (4, 6). Further studies of the perchloric acid decomposition and particularly the effect on this of metal oxide catalysts, which are the traditional catalysts for the ammonium perchlorate decomposition, clearly were required. While this work was in progress Solymosi *et al.* published a preliminary report (7) of the effect of a number of oxide catalysts on the decomposition of perchloric acid and later a detailed account (8) of the decomposition on chromium oxide catalysts. In this paper we describe the decomposition of perchloric acid on copper chromite, on alumina, and on iron(III) oxide, copper(II) oxide, and manganese(IV) oxide supported on alumina.

Experimental

The catalysts were supplied by the Harshaw Chemical Co. and are identified by their catalogue numbers. They were in the form of small pellets 1/8 in. long and 1/8 in. in diameter. The surface areas of the catalysts are given in Table 1. The decomposition was studied by a flow method using nitrogen as the carrier gas. The diameter of the catalyst bed was 22 mm. The effluent gases from the

TABLE 1. Description of catalysts

Harshaw number	Nominal composition (by weight)	Color	Surface area ($m^2\ g^{-1}$)
Cu-0203	78% CuO 20% Cr_2O_3	Dark brown	10–13
Fe-0301	20% Fe_2O_3 on Al_2O_3	Rust brown	41
Cu-0803	10% CuO on Al_2O_3	Black	137
Al-0104	99% Al_2O_3	White	80
Mn-0201	19% MnO_2 on Al_2O_3	Black	69

[1]Present address: Department of Chemistry, The University of West Indies, Mona, Kingston 7, Jamaica.

Can. J. Chem. Downloaded from www.nrcresearchpress.com by 210.87.254.105 on 09/05/12
For personal use only.

reactor were passed through a trap containing standard NaOH. Analysis of the contents of this trap, after time t, for Cl^-, OCl^-, and OH^- gave the amount of decomposition of $HClO_4$. The residence time, t_r, was calculated from the flow rate and the volume of the reactor. Further details of experimental technique have been given elsewhere (6).

Results

Kinetics

Iron(III) Oxide

A 30 g sample of the catalyst Fe-0301 with a surface area of 1.23×10^3 m^2 was studied at five temperatures in the range 177 to 238 °C. The initial perchloric acid concentration was varied from 2×10^{-4} to 1×10^{-3} mol/l and residence times t_r of 0.05 to 0.7 min were employed. After an initial conditioning period in which the activity increased, reproducible results were obtained. The reaction was of first order, as shown by the plots of $\log (a/a_0)$ *vs.* t_r, a_0 being the initial acid concentration and a the concentration of acid after a residence time t_r (Fig. 1). Points corresponding to different values of a_0 are not distinguished because the fractional decomposition in a given t_r is insensitive to a_0 in the range covered. The catalyst showed no visible signs of attack by the perchloric acid.

Alumina

A 30 g sample of Al-0104 having a surface area of 2.36×10^3 m^2 was studied at five temperatures in the range 176 to 251 °C. The initial acid concentration was in the range 3.2 to 4.0 $\times$ 10^{-4} mol/l and residence times from 0.06 to 1.0 min were employed. No conditioning period was required and the activity of the catalyst remained constant. The reaction was first order at all temperatures studied.

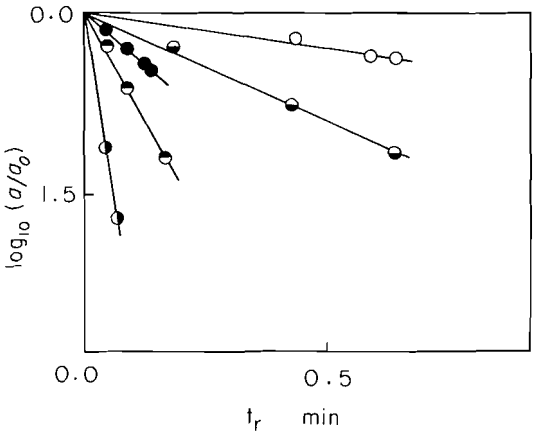

FIG. 1. First order plots for the decomposition of perchloric acid on iron(III) oxide. ○, 176.7 °C; ◒, 196.1 °C; ●, 206.5 °C; ◓, 216.7 °C; ◑, 238.5 °C.

Copper(II) Oxide

A 10 g sample of Cu-0803 having a surface area of 1.37×10^3 m^2 was studied at six temperatures in the range 196 to 250 °C. The initial acid concentration was varied from 2×10^{-4} to 1.5×10^{-3} mol/l and residence times of 0.05 to 0.2 min were used. The activity decreased initially until a relatively constant value was reached. The decomposition was then first order in the above temperature range. At the conclusion of the experiments it was noted that the cupric oxide had partly changed in color from black to green.

Copper Chromite

Two 30 g samples of Cu-0203, each having surface areas of 3.45×10^2 m^2 were used. Both samples were studied at 261 °C and the second sample was also studied at five other temperatures before non-reproducible results were obtained. The initial perchloric acid concentration was varied in the range 3.5 to 9.9 $\times$ 10^{-4} mol/l; residence times were between 0.05 and 0.26 min. Preliminary work showed that initially all the perchloric acid which was passed over the catalyst was consumed but that after a few runs, the catalytic decomposition could be observed. The activity of the catalyst then increased to more than ten times its original value. A second sample showed the same sequence. After this initial conditioning, results were fairly reproducible for about 15 runs but then they gradually became less reproducible and the activity generally decreased. In the reproducible region the decomposition obeyed first order kinetics. Both catalyst samples were visibly attacked by the perchloric acid producing a ginger colored product.

Manganese(IV) Oxide

A 30 g sample of Mn-0201 with a surface area of 2.06×10^3 m^2 was studied at five temperatures in the range 142 to 207 °C. Reproducibility was excellent but the kinetics were not first order. Plots of fractional decomposition α against residence time in Fig. 2 show an initial acceleratory period. Attempts were made to fit these data to a number of Langmuir–Hinshelwood type models but without success. At

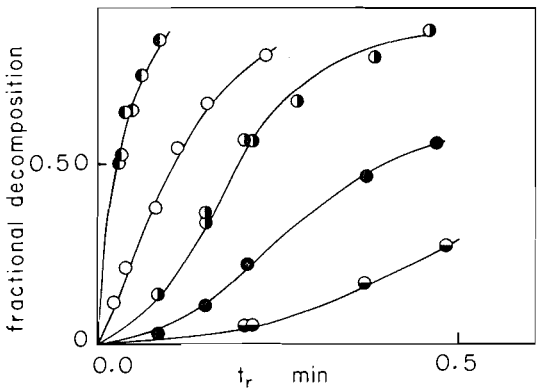

FIG. 2. Decomposition of perchloric acid on manganese(IV) oxide. The plots show the fraction decomposed in a residence time t_r. ◐, 207.2 °C; ○, 197.3 °C; ◑, 177.6 °C; ●, 159.0 °C; ◒, 142.2 °C.

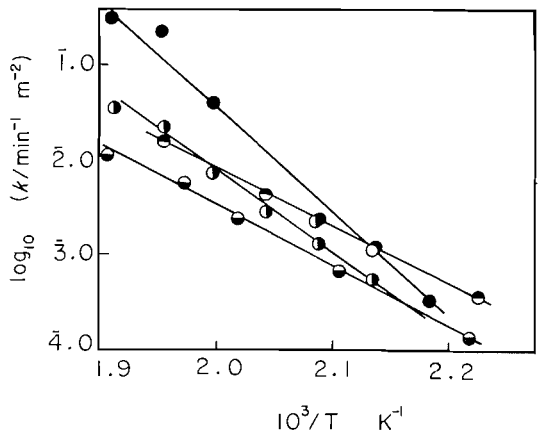

FIG. 3. Arrhenius plots showing the relative activity of four Harshaw catalysts for the decomposition of perchloric acid. ◒, Al-0104; ◑, Cu-0803; ◓, Fe-0301; ●, Cu-0203. Physical characteristics of the catalysts are given in Table 1.

177 °C the fractional decomposition was observed to decrease slightly with increasing acid concentration, suggesting an apparent order of less than unity. Manganese(IV) oxide is an excellent catalyst and highly reproducible results can be obtained with it, but the results were not analyzed in detail because it was felt that self-heating was probably the cause of the acceleratory reaction.

Arrhenius Parameters

The decomposition of perchloric acid is first order on all the catalysts tried apart from Mn-0201. A composite Arrhenius plot is shown in Fig. 3, and the Arrhenius parameters are summarized in Table 2.

TABLE 2. Arrhenius parameters

Catalyst	Apparent activation energy (kcal/mol)	Specific preexponential factor (min^{-1} m^{-2})
Cu-0203	54.0	2.5×10^{22}
Fe-0301	28.6	2.5×10^{10}
Al-0104	28.8	1.3×10^{10}
Cu-0803	39.0	8.0×10^{14}

Discussion

All five of the Harshaw catalysts used catalyzed the decomposition of perchloric acid. Cu-0203 is a pelleted form of Cu-0202 which is used extensively in solid propellant compositions. Its composition corresponds (9) to $CuCr_2O_4$.7CuO; no thermal changes in the catalyst are expected in the temperature range in which it was used. Pearson (9) has shown that alternate exposures of Harshaw Cu-0202 to fuels (ethylene, isobutene or ammonia) and to oxygen resulted in reduction and oxidation of the catalyst and that this was a bulk effect. With these reactants the weight of the catalyst never exceeded 100% of the initial weight, *i.e.* oxygen did not oxidize the Cr(III) present. Alternate exposures to isobutene and perchloric acid induced a similar redox cycle but in this instance the catalyst did show a net weight gain after exposure to perchloric acid. At the same time catalyst samples changed color from black to reddish brown and chromate ion was detected in an alkaline extract, confirming oxidation to Cr(VI). Similar changes were observed in our Cu-0203 catalyst. Initially, all the perchloric acid is consumed so that it must be reacting with the catalyst; then the activity gradually increases until a stable catalyst results. The initial conditioning must correspond to the formation of surface chromate which then functioned as the actual catalyst in this work. It should be noted that cupric chromate, with the empirical formula $CuCrO_4$.1.75Cu$(OH)_2$, is also used in propellant compositions and the same redox cycles as are observed on copper chromite can be induced in copper chromate (9).

Solymosi and Börcsök (8) found that the activity of chromium oxide catalysts lay in the order Cr(III) > Cr(IV) ≫ Cr(VI) and that the

Can. J. Chem. Downloaded from www.nrcresearchpress.com by 210.87.254.105 on 09/05/12
For personal use only.

activity of chromium(III) oxide declined due to surface oxidation. The activation energy for decomposition of perchloric acid on Cr(III) oxide (fresh) is 31 kcal/mol (8) and on copper chromite (pre-treated) is 54 kcal/mol while that on cupric oxide is 39 kcal/mol (Table 2). Furthermore the activities of the chromite and cupric oxide catalysts are different. The measured activity of the conditioned chromite must be due, therefore, to the Cr(VI) formed.

Perchloric acid was also observed to react with cupric oxide probably forming the chloride and the oxychloride (9). Since the decomposition kinetics were only studied in the reproducible region the activation parameters (Table 2) correspond to perchloric acid decomposition on the reacted surface containing Cl^- and OCl^- as well as O^{2-} and Cu^{2+} ions.

No visible changes were observed following decomposition on ferric oxide, alumina, or manganese(IV) oxide although there was a conditioning period on ferric oxide. This could have corresponded to oxidation of some iron(II) present but this was not tested for specifically.

Mechanism

Solymosi and Börcsök (8) have suggested that the activity of perchloric acid catalysts is connected with the stability of the corresponding metal perchlorate. We now propose a mechanism for the catalyzed decomposition of perchloric acid that is consistent with this proposal. The requirements for decomposition in this model are (*i*) adsorption of $HClO_4$ molecules on the catalyst, (*ii*) the presence of a proton acceptor in the surface, (*iii*) thermal instability of the metal perchlorate complex formed. The process is depicted in Fig. 4 for an alumina catalyst. The adsorbed perchloric acid (*i*) loses a proton to a surface oxide ion (*ii*). Repetition of this process gives two adjacent OH^- ions from which water can be eliminated. Metallic perchlorates decompose to yield either the chloride or the oxide (10) or, in the case of cupric perchlorate, the oxychloride. In Fig. 4 we presume the oxide is formed. The mechanism (10) in the case of barium and magnesium perchlorates is successive removal of O atoms from ClO_4^- until ClO^- is formed; the ClO^- ions can then either lose a further oxygen atom or decompose bimolecularly to $O^{2-} + Cl_2$. The key step determining the activity of the catalyst is clearly

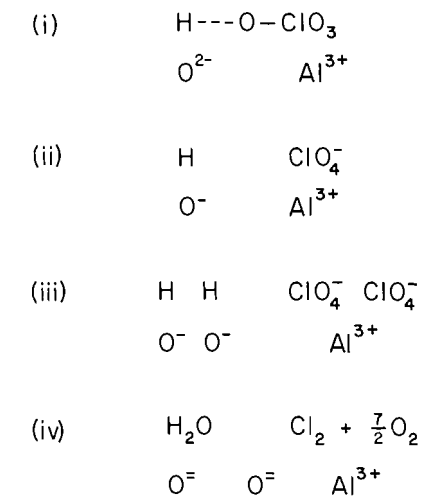

FIG. 4. Schematic representation of the proposed mechanism of decomposition of perchloric acid on metal oxide catalysts. Alumina is used as an example. The essential feature is proton transfer to an acceptor in the catalyst surface followed by decomposition of the resulting ClO_4^- anion.

the (unimolecular) decomposition of ClO_4^- and this will be influenced by the properties of the cation: presumably small cations of high charge will exert the greatest perturbing effect on the $O—ClO_3^-$ bond.

On chromium(III) oxide Solymosi and Börcsök (8) observed ClO_2 to be formed at low temperatures and this would imply a bimolecular decomposition of ClO_4^- ions rather than the unimolecular decomposition discussed above. If further work shows ClO_2 formation to occur quite generally, then the bimolecular decomposition of ClO_4^- will be established as the preferred route. In metallic perchlorates the ClO_4^- decomposes unimolecularly in barium and magnesium perchlorates (10, 11) but bimolecularly in the group I perchlorates (12).

Implications for Ammonium Perchlorate Decomposition

There have been no previously recorded investigations of the catalytic effect of Cu-0803, Fe-0301, and Mn-0201 on the decomposition of ammonium perchlorate although the metal oxides contained in these catalysts are known to be positive catalysts for the ammonium perchlorate decomposition. The catalytic activity of these Harshaw catalysts towards ammonium perchlorate was therefore confirmed in a number

Can. J. Chem. Downloaded from www.nrcresearchpress.com by 210.87.254.105 on 09/05/12
For personal use only.

Can. J. Chem. Downloaded from www.nrcresearchpress.com by 210.87.254.105 on 09/05/12
For personal use only.

of experiments using a Perkin–Elmer Differential Scanning Calorimeter. In a previous summary of the activity of catalysts for the high-temperature decomposition of ammonium perchlorate (*i.e.* at temperatures at which the ammonia and perchloric acid desorb into the gas phase) Jacobs and Whitehead (13) classified catalysts into two groups: (*A*) those like magnesium oxide which react with ammonium perchlorate to form the corresponding metallic perchlorate and then form a molten phase, and (*B*) those like copper(II) oxide which do not form a melt and in which any reaction is limited to the catalyst surface. The mechanism of decomposition for group *B* was believed to involve the catalyzed decomposition of perchloric acid (1) while that for group *A* to consist essentially (11, 14) of proton transfer from NH_4^+ to O^{2-} ions, with decomposition of ClO_4^- to regenerate oxide ions. If the views on the mechanism of decomposition of perchloric acid expressed above (Fig. 4) are basically correct, then we see how similar the two catalytic mechanisms really are. For group *A* proton transfer from NH_4^+ to O^{2-} occurs directly while for group *B* proton transfer from NH_4^+ to ClO_4^- is followed by proton transfer from $HClO_4$ to the O^{2-} (or Cl^- or other proton acceptor) in the catalyst. Evidence supporting this view comes from the work of Boldyreva, Bezrukov, and Boldyrev (15) who showed that copper(II) oxide (and several other oxides from group *B*) can catalyze the decomposition of ammonium perchlorate even when separated physically from it so that it is the perchloric acid diffusing to the catalyst through the vapor phase whose decomposition is being facilitated. The work of Solymosi and Börcsök (8) also supports these mechanisms: these authors observe that while ZnO, CdO, and MgO all form perchlorates only ZnO is an active catalyst for the perchloric acid decomposition at ~350 °C and they attribute this (quite correctly in our view) to the greater thermal stability of magnesium and cadmium perchlorates compared to that of zinc perchlorate. It follows that in catalyzing the thermal decomposition of ammonium perchlorate CdO and MgO (group *A*) are not acting by catalyzing the decomposition of perchloric acid.

The explanation of the generally close parallel between catalytic activity for perchloric acid decomposition and ammonium perchlorate decomposition (7, 16) would thus seem to have a sufficient basis in the mechanisms presented and discussed in this paper.

This research was supported by the Defence Research Board, the National Research Council of Canada, and the Province of Ontario (through a graduate fellowship to R.G.).

1. P. W. M. Jacobs and A. Russell-Jones. Eleventh Symposium (International) on Combustion (The Combustion Institute, Pittsburgh, *Pa.*, 1967) p. 457.
2. P. W. M. Jacobs and A. Russell-Jones. AIAA J. **5**, 829 (1967).
3. G. L. Pellett and A. R. Saunders. AIAA Sixth Aerospace Sciences Meeting, New York, January 1969 (AIAA Pre-print No. 68-140).
4. J. B. Levy. J. Phys. Chem. **66**, 1092 (1962).
5. D. J. Sibbett and J. M. Lobato. Aerojet-General Corp., Azusa, Calif., Rept. No. 1782, April 1960 (AD 240 274).
6. R. Gilbert and P. W. M. Jacobs. Comb. Flame. In press.
7. F. Solymosi, S. Börcsök, and M. E. Lázár. Comb. Flame, **12**, 398 (1968).
8. F. Solymosi and S. Börcsök. J. Chem. Soc. 601 (1970).
9. G. S. Pearson. Comb. Flame, **14**, 73 (1970).
10. R. Acheson and P. W. M. Jacobs. Can. J. Chem. **47**, 3031 (1969).
11. R. Acheson and P. W. M. Jacobs. J. Phys. Chem. **74**, 281 (1970).
12. H. F. Cordes and S. R. Smith. J. Phys. Chem. **72**, 2189 (1968).
13. P. W. M. Jacobs and H. M. Whitehead. Chem. Rev. **69**, 551 (1969).
14. R. Acheson and P. W. M. Jacobs. AIAA J. **8**, 1483 (1970).
15. A. A. Boldyreva, B. N. Bezrukov, and V. V. Boldyrev. Kinet. Catal. (U.S.S.R.) **8**, 258 (1967).
16. G. S. Pearson and D. Sutton. AIAA J. **5**, 344 (1967).

Can. J. Chem. Downloaded from www.nrcresearchpress.com by 210.87.254.42 on 09/05/12
For personal use only.

Low Surface Coverage Interactions of Sulfur Dioxide on Selected Transition Metal Catalysts from 273 to 423 °K

R. W. GLASS AND R. A. ROSS
Department of Chemistry, Lakehead University, Thunder Bay, Ontario

Received April 13, 1971

Calorimetric heats of adsorption for sulfur dioxide at low surface coverages from 0.004 to 0.600 μmol m^{-2} on a number of supported transition metal catalysts have been measured between 273 and 423 °K mainly by an adiabatic technique. The catalysts included Fe_2O_3, Mn_2O_3, V_2O_5, $MnSO_4$, and "NiS" all supported on silica gel.

Sulfur dioxide adsorption/desorption isotherms, nitrogen adsorption data, and chemical and infrared analyses were also determined to provide further ancillary information.

Heats of adsorption at 423 °K for adsorbed amounts of 0.004 μmol m^{-2} varied with the adsorbent from nearly 39.0 for Mn_2O_3 on silica gel to 23.0 kcal mol^{-1} for the silica gel support medium. With increase in surface coverage to 0.600 μmol m^{-2} the heat values begin to steady at 6 to 7, 7 to 8, and 8 to 9 kcal mol^{-1} at 423, 373, and 323 °K, respectively, and less discrimination is observed among the various materials. Preadsorption of small amounts of sulfur dioxide on the supported oxides followed by oxygen admission caused sharp initial falls of as much as 7 to 8 kcal mol^{-1} in the heat values whereas preadsorption of oxygen followed by sulfur dioxide gave only slight heat increases of around 1 kcal mol^{-1}.

It is proposed that sulfur dioxide is chemisorbed on all surfaces with the strongest interactions occurring at the lowest coverages. Sulfates are formed on the oxides as confirmed by chemical analysis, and it is postulated that multiple hydrogen bond formation occurs on silica gel through the interaction of sulfur dioxide oxygen atoms with surface hydroxy groups.

Les chaleurs calorimétriques d'adsorption du dioxyde de soufre (à faible surface couverte; de 0.004 à 0.600 μmol m^{-2}) sur un certain nombre de catalyseurs de métaux de transition fixés sur un support, ont été étudiées entre 273 et 423 °K au moyen d'une technique adiabatique. Sur un support commun en gel de silice, les catalyseurs incluent Fe_2O_3, Mn_2O_3, V_2O_5, $MnSO_4$ et "NiS".

Les isothermes adsorption/désorption pour le dioxyde de soufre, les données relatives à l'adsorption de l'azote ainsi que les analyses chimiques et infrarouges ont été déterminées dans le but d'informations secondaires ultérieures.

Les chaleurs d'adsorption à 423 °K pour des quantités adsorbées de 0.004 μmol m^{-2} varient avec l'adsorbant entre 39.0 pour Mn_2O_3 fixé sur du gel de silice, à 23.0 kcal mol^{-1} pour le support en gel de silice. Lorsque la surface couverte augmente jusqu'à 0.600 μmol m^{-2}, les valeurs des chaleurs d'adsorption s'étalent entre 6 et 7 à 423 °K, 7 et 8 à 373 °K, 8 et 9 à 323 °K. Dans ce cas, les différences observées entre les divers produits sont nettement plus faibles. Une préadsorption de dioxyde de soufre en petite quantité sur les oxydes fixés sur un support, suivie d'une admission d'oxygène provoque une chute initiale brutale de 7 à 8 kcal mol^{-1} des valeurs de chaleur d'adsorption; au contraire, une préadsorption d'oxygène suivie de dioxyde de soufre n'augmente que de 1 kcal mol^{-1} les chaleurs d'adsorption.

Il est suggéré que le dioxyde de soufre est chemisorbé sur toutes les surfaces mais que les interactions les plus fortes ont lieu sur des surfaces faiblement couvertes. La formation de sulfates sur les oxydes est confirmée par des analyses chimiques; il est postulé que la formation de liaisons hydrogène multiples se produit sur le gel de silice par suite de l'interaction des atomes d'oxygène du dioxyde de soufre avec les groupes hydroxyles de surface.

Canadian Journal of Chemistry, 49, 2832 (1971)

Introduction

This investigation contributes to a series of studies of the adsorption of sulfur-containing gases on various solids. The studies are largely motivated by the possibility of using adsorption or adsorption with catalysis as effective processes for the removal of deleterious sulfur compounds from industrial stack gases.

Although considerable work has been reported on the mechanism and kinetics of the heterogeneous oxidation of sulfur dioxide on catalytic solids (1, 2), comparatively little adsorption data have been determined for the gas. In particular, thermodynamic information is extremely sparse; most noticeably for systems where chemical adsorption is likely to occur.

Earlier, results were described (3) for the adsorption of sulfur dioxide on silica gels in the temperature range 263 to 323 °K when both adsorption–desorption isotherms and isosteric

Can. J. Chem. Downloaded from www.nrcresearchpress.com by 210.87.254.42 on 09/05/12
For personal use only.

heats for surface coverages above one-tenth of a monolayer were determined. These data showed that physisorption was the dominant process although some chemical interaction with surface hydroxy groups appeared to take place.

In the present work calorimetric heats of adsorption of sulfur dioxide have been determined between 273 and 423 °K for silica gel and a range of catalytic solids, namely Mn_2O_3, V_2O_5, Fe_2O_3, $MnSO_4$, and "NiS", supported on silica gels. Further, several experiments have been carried out at 423 °K in which small amounts of either oxygen or sulfur dioxide were preadsorbed by the catalysts and the heats of adsorption on stepwise addition of the other gas measured. Complete sulfur dioxide adsorption–desorption isotherms have been determined for each supported catalyst at several temperatures from 273 to 423 °K and chemical and infrared analyses used to identify the products of the adsorption reactions.

Experimental

Materials

Supported metal oxides were prepared by impregnating Davison '923' grade silica gel (surface area 630 m^2/g; particle size, 75–150 μ) with an approximately 1 *M* solution of the appropriate metal nitrate for 6 h. After filtering and washing, the material was heated in air at 550 °C for 12 h to decompose the nitrate. Supported manganese(II) sulfate adsorbent was prepared by impregnating the gel with a 1 *M* solution of manganese(II) sulfate for 6 h and then heat-treating in air at 550 °C for 12 h. Nickel sulfide on silica gel was prepared by impregnating the gel with a 1 *M* solution of nickel nitrate for 6 h and then adding directly a 0.05 *M* solution of ammonium sulfide. The material was then filtered and washed before heat-treatment in air at 550 °C for 12 h.

Particles of the various adsorbents were examined by optical microscopy before and after use in the adsorption experiments. Photomicrographs (×70) were taken for record purposes. Except for the supported nickel sulfide all adsorbents showed evidence of aggregation after heat treatment at 550 °C. The particle size range increased to 75–225 μ with a very small proportion, <1%, of fine particles <75 μ present which indicated a small amount of disintegration. The manganese(III), iron(III), and vanadium(V) oxides were uniformly dispersed into the individual gel particles as indicated by the uniformity of color throughout the samples examined. The dispersion of nickel(II) sulfide and manganese(II) sulfate was not as uniform, which might be anticipated. With the former, the gel particles had a fairly uniform grey color but fine black 'dots' of material, presumably "NiS", were observed sticking to practically all particles while with the latter a very small amount of fine crystals (~1–10 μ) of manganese(II) sulfate was present in addition to the impregnated gel particles. Observations in color changes which resulted from the adsorption experiments are referred to later.

The following properties were determined for the finished adsorbents: (*a*) silica gel (surface area 590 m^2/g), (*b*) 2.50% Mn (as Mn_2O_3 *w/w*; 475 m^2/g), (*c*) 9.50% V (as V_2O_5 *w/w*; 450 m^2/g), (*d*) 3.20% Mn (as $MnSO_4$ *w/w*; 460 m^2/g), (*e*) 9.20% Fe (as Fe_2O_3 *w/w*; 555 m^2/g), and (*f*) 2.80% Ni (as "NiS" *w/w*; 390 m^2/g).

The supported nickel sulfide adsorbent (*f*) was assumed to have a one-to-one nickel/sulfur ratio and because of the complex nature of the supported catalysts no attempt was made to measure possible nonstoichiometric compositions. Surface areas were determined by low-temperature nitrogen adsorption at 77 °K.

Immediately before making adsorption measurements all adsorbents were activated at 240 °C for 2 h in air, transferred to the appropriate apparatus and then outgassed at 100 °C for 30 min at $<10^{-5}$ mm.

Sulfur dioxide (Matheson Co.) was anhydrous quality and was drawn directly from the cylinder after line-flushing to a trap attached to the apparatus. It was then outgassed at 10^{-4} mm and vacuum distilled over trays of phosphorous pentoxide. Middle portions only were used and g.l.c. analysis showed these to be >99.99% pure. Helium (Canadian Liquid Air Ltd.) was 99.995% pure and oxygen (Canadian Liquid Air Ltd.) 99.6% minimum prior to drying in desiccant columns.

Apparatus

Adsorption–desorption isotherms were determined in an all-glass vacuum system using a quartz spring microbalance (4). The quartz spring had a sensitivity of 403 mm g^{-1} at room temperature. At 273 °K the adsorption chamber was placed in an ice-bath controlled to ±0.01°. For higher temperatures a noninductively wound metal furnace was used. The furnace was insulated with asbestos rope and placed in a vacuum jacket. Tests showed that the temperature could be held to better than ±0.1° at 423 °K.

Heats of adsorption were determined calorimetrically in a vessel similar to that described (5). At 273 °K the outer jacket was air filled and the adsorption heats determined isothermally. At temperatures above 273 °K it was not possible to obtain temperature control of the required accuracy for the minimum 45 min necessary for isothermal determinations. Hence, the calorimeter was then operated adiabatically with its outer jacket evacuated, giving control to ±0.01°. In all experiments helium at 6 to 7 mm pressure was introduced to maximize the thermal conductivity prior to admission of the other gases.

The heats quoted were measured for the conditions $(dT/dt) = 0$ which normally occurred about 1 min after admission of the gas to the calorimeter. A cooling correction was applied to the observed temperature rise by extrapolating the linear portion of the cooling curve immediately after the maximum to a point midway between 't_{max}' and 't_0'. Four to five electrical calibrations were carried out in each run, prior to, during, and after adsorption. These were accurate to ±1% with no significant trends while the shapes of the temperature/time calibration traces were identical to those for the gas additions. The measurement technique was adapted from that used by Smith and Ford (6).

At 20 to 30 cm, well above the experimental pressure range, the heat of compression was measured with helium and instantaneous and maximum temperature

rises of 0.005° were observed. These values were well within the limits of experimental error when compared with the temperature rises of about 1° observed in the normal adsorption experiments at much lower pressures.

Results

Heats of Adsorption

The values were determined for a range of sulfur dioxide surface coverages from 0.004 to 0.200 μmol m^{-2} on all six adsorbents and normally at three temperatures for each adsorbent between 273 and 423 °K. Table 1 summarizes the heat values obtained at 423 °K.

A useful approximate figure for the degree of surface coverage can be calculated assuming close-packing and a cross-sectional area (7) of 22.9 $Å^2$ for an adsorbed sulfur dioxide molecule at 423 °K. With these assumptions, 0.700 μmol m^{-2} can be shown to be approximately equivalent to one-tenth of a monolayer at that temperature.

Heats of adsorption on several of the catalysts were measured to higher values of surface coverage at 323, 373, and 423 °K. There was a marked tendency for the value to appear to level out at amounts adsorbed between 0.200 and 0.300 μmol m^{-2}, particularly at the higher temperatures when fairly steady values of the heats of adsorption seemed to be approached. These data are shown for silica gel in Fig. 1. The results obtained with supported manganese(II) sulfate showed different characteristics to those of silica gel and the other supported catalysts. The differences were most marked at 323 °K where a comparatively sluggish fall from *ca.* 30 kcal mol^{-1} at 0.004 μmol m^{-2} to a value of 9 to 10 kcal mol^{-1} at 0.400 μmol m^{-2} was observed, Fig. 2.

Additional experiments were carried out with silica gel to test the possibility of surface dehydration occurring during adsorption of sulfur dioxide at 423 °K. The heat curve was measured up to a coverage of 0.100 μmol m^{-2} and the gas then desorbed at the same temperature at 10^{-5} mm. Samples of the desorbed gas were analyzed with a Beckman IR-12 infrared spectrophotometer. No trace of water could be detected in the samples while sulfur dioxide was easily identified by the strong asymmetric stretching frequency at 1362 cm^{-1}. After desorption, sulfur dioxide was readmitted to the gel and the whole procedure repeated thrice. Each time the heat curves obtained were identical with that in Fig. 1 within the limits of experimental error. For example, at a coverage of 0.004 μmol m^{-2} the

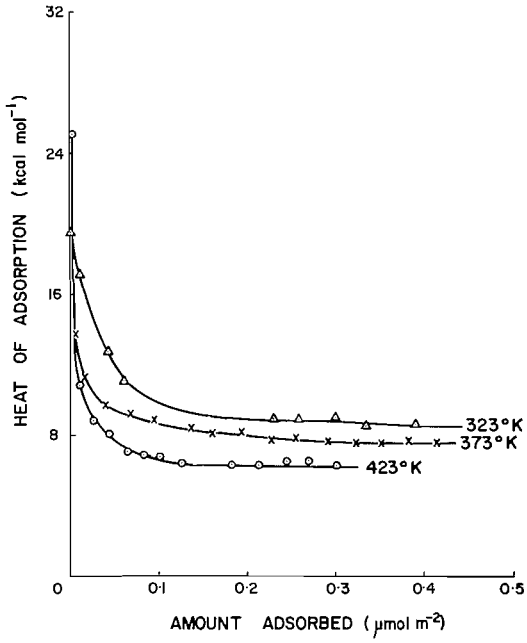

FIG. 1. Variation of heat of adsorption of sulfur dioxide with amount adsorbed on silica gel.

TABLE 1. Heats of adsorption (kcal mol^{-1}) at 423 °K for low surface coverages of sulfur dioxide on silica gel and catalysts supported on silica gel*

Surface coverage (μmol m^{-2})	Heat of adsorption (kcal mol^{-1})					
	Silica gel	Mn_2O_3	V_2O_5	Fe_2O_3	$MnSO_4$	"NiS"
0.004	23.0	38.8	24.0	32.0	28.0	28.0
0.010	11.1	17.4	17.6	18.0	17.5	18.0
0.020	9.6	13.0	13.8	12.2	15.2	14.8
0.040	8.2	9.7	10.7	9.6	13.0	12.8
0.120	6.4	6.6	8.6	7.4	9.7	10.9
0.200	6.3	6.0	7.8	6.7	9.0	10.3

*Tabulation of all data obtained in this study, not all of which are presented here, can be obtained free of charge, upon request, from the Depository of Unpublished Data, National Science Library, National Research Council of Canada, Ottawa, Canada.

Can. J. Chem. Downloaded from www.nrcresearchpress.com by 210.87.254.42 on 09/05/12
For personal use only.

Can. J. Chem. Downloaded from www.nrcresearchpress.com by 210.87.254.42 on 09/05/12
For personal use only.

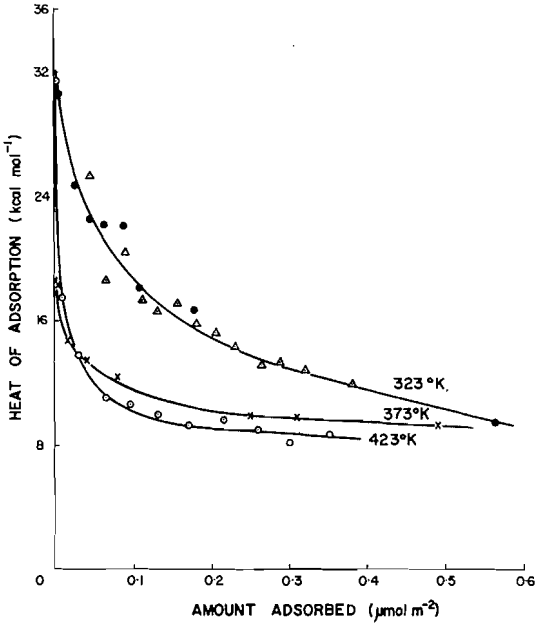

FIG. 2. Variation of heat of adsorption of sulfur dioxide with amount adsorbed on $MnSO_4$/silica gel.

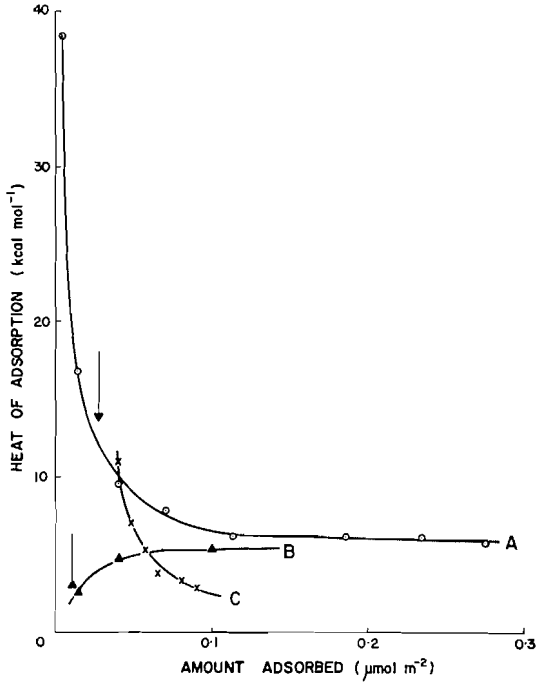

FIG. 3. Adsorptions on Mn_2O_3/silica gel at 423 °K.

heat of adsorption in each case was 24 ± 1 kcal mol^{-1}. Separate experiments in which 'massive' samples, *ca.* 5g, of silica gel were equilibrated with sulfur dioxide at 423 °K also failed to show the presence of water in the desorbed gas samples when examined in the spectrophotometer.

Sulfur Dioxide/Oxygen Interactions

Several experiments were carried out in which either oxygen or sulfur dioxide was preadsorbed by the catalytic solids prior to exposure to the other gas. Thus at 423 °K, 0.028 μmol m^{-2} of sulfur dioxide was preadsorbed in one dose on Mn_2O_3/silica gel. Oxygen was then admitted to the system in small quotas and heats of adsorption measured for amounts adsorbed up to 0.100 μmol m^{-2}. For the first three additions maximum increases of 1.58, 1.18, and 0.78 mm pressure were observed at system equilibrium which was achieved at each stage in about 45 min. With the fourth and subsequent oxygen additions no such pressure increases occurred. The measured heats, curve *C*, are shown in Fig. 3 along with the heat curves for sulfur dioxide on Mn_2O_3/silica gel, *A*, and sulfur dioxide on the same adsorbent after preadsorption of 0.011 μmol m^{-2} of oxygen, *B*.

Very similar results to those in Fig. 3 were obtained when the oxygen experiments with preadsorbed sulfur dioxide were repeated at the same temperature using silica gel and supported V_2O_5 and Fe_2O_3 as adsorbents.

When oxygen was preadsorbed in quantities from 0.011 to 0.015 μmol m^{-2} at pressures from 65 to 80 mm on the supported Mn_2O_3, V_2O_5, and Fe_2O_3 adsorbents, small heats of adsorption were recorded on subsequent admission of quotas of sulfur dioxide. For Mn_2O_3/silica gel the heat increased with each addition to the final measured value of 5.3 kcal mol^{-1} at 0.100 μmol m^{-2}, Fig. 3. The time taken to reach equilibrium in these experiments was from 3 to 4 h.

Analytical Examinations

Studies were made of both desorbed gas fractions and solid residues after adsorption of sulfur dioxide and the sulfur dioxide/oxygen compositions on the supported oxides to investigate the possibility of the formation of sulfur trioxide either in the gas phase or as an adsorbed complex or both. Further, particular experiments were designed in which oxygen was adsorbed at 423 °K on a 'massive' sample, *ca.* 7 g, of Fe_2O_3/silica gel containing preadsorbed sulfur dioxide using similar relative quantities of the gases as

Can. J. Chem. Downloaded from www.nrcresearchpress.com by 210.87.254.42 on 09/05/12
For personal use only.

those in the calorimeter experiments. After desorption, solid samples were examined by the potassium bromide disc technique. However, the SO_3 asymmetric stretching vibration (8) at 1391 cm^{-1} lay within a very broad and diffuse Si—O band which occurred from about 1150 to 1450 cm^{-1}. Hence no conclusion could be made.

The spectra of desorbed gas samples were carefully examined using the optimum working conditions of the spectrophotometer and a slight perturbation was detected at 1391 cm^{-1} in three out of five experiments with the 'massive' sample. Hence the presence of extremely small quantities of sulfur trioxide could not be ruled out.

More significantly, qualitative chemical analysis (see, for example, ref. 9) of the oxide sample residues after the sulfur dioxide calorimeter experiments gave clear evidence that sulfate formation had occurred. Careful comparative tests with the original adsorbents showed that very small amounts of sulfate were formed on both Mn_2O_3 and V_2O_5 while a larger quantity was evident in the Fe_2O_3 residue. Quantitative analysis was not attempted.

Adsorption–Desorption Isotherms

Sulfur dioxide isotherms were determined at 273, 323, 373, 423, and 473 °K. The isotherm shapes were very similar for each adsorbent at a given temperature.

Figure 4(*a*) shows the adsorption–desorption isotherms obtained with Mn_2O_3/silica gel. Adsorption equilibrium times varied with the temperature and pressure. At 273 °K the times increased with increase in pressure from not more than 30 min at pressures up to 250 mm to approximately 2 h at 700 mm.

Hysteresis was present at 273, 323, and 373 °K, negligibly so at 423 °K and not at all at 473 °K. The shape of the hysteresis loop at 273 °K was completely different from those obtained at the higher temperatures. Hysteresis was observed over a limited range from 450 to 700 mm while at 323 and 373 °K it extended over the complete pressure range. On pumping out, the sulfur dioxide was removed within 30 min for experiments at 273, 323, and 373 °K, but at 423 and 473 °K about 0.015 μmol m^{-1} remained.

Figures 4(*b*), (*c*), and (*d*) show similar characteristics at each temperature for supported V_2O_5, Fe_2O_3, and $MnSO_4$, respectively. Adsorption equilibrium times were of the same order of magnitude as for Mn_2O_3/silica gel and all the sulfur dioxide could be removed on pumping out, except at 423 and 473 °K when again approximately 0.015 μmol m^{-2}, as sulfur dioxide, was retained by the adsorbent.

Discussion

The high heats of adsorption shown in Table 1 for 0.004 μmol m^{-2} refer to an extremely small amount of adsorbed gas when compared with that required to complete a monolayer although in molecular terms the figure represents between 10^{14} and 10^{15} molecules adsorbed per m^2 of surface. When the surface concentration of adsorbed sulfur dioxide is increased fifty times to 0.200 μmol m^{-2} the measured heats fall by factors of three to six which indicates significantly that the strongest gas/solid interactions are located within a surface occupancy of less than one-hundredth of a monolayer. This conclusion is confirmed by the isotherm measurements where similar quantities of sulfur dioxide appeared to be irreversibly adsorbed at 423 and 473 °K.

At the lowest coverage measured the heat of adsorption of sulfur dioxide on Mn_2O_3/silica gel was 38.8 kcal mol^{-1} at 423 °K. At this temperature the heat of formation of manganese(II) sulfate as calculated from published tables (10) is −43.2 kcal mol^{-1} according to the reaction

$$Mn_2O_3(s)+SO_2(g) \rightarrow MnO(s)+MnSO_4(s)$$

Formation of manganese(II) sulfite and manganese(IV) oxide from the same reactants (10) has a $\Delta H_f = -19.0$ kcal mol^{-1} and hence sulfate formation seems likely. Chemical tests on the residues from both 423 and 473 °K confirmed the presence of small amounts of sulfate.

Similarly, sulfate was detected in used V_2O_5/silica gel samples after sulfur dioxide adsorptions at 423 °K and also a distinct color change in this material was observed from the original pale yellow to pale brown when it was removed from the reaction chamber. This observation is also indicative of sulfate formation (10). At this temperature the heat of formation calculated for $VOSO_4$ from the two reactants is −40.5 kcal mol^{-1}, almost twice the measured heat of adsorption at 0.004 μmol m^{-2}. However, it is stressed that the formation of these traces of

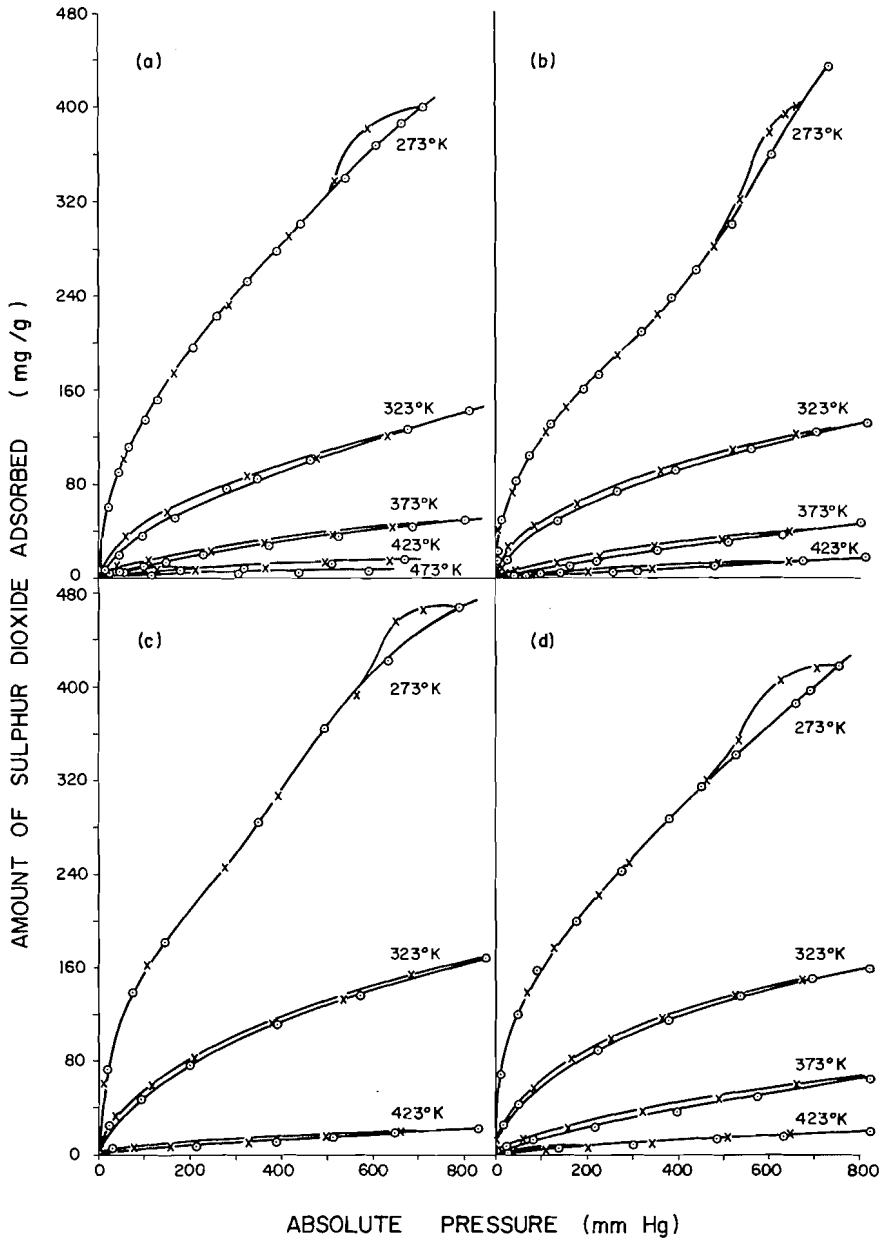

FIG. 4. Adsorption/desorption isotherms for sulfur dioxide on (*a*) Mn_2O_3/silica gel, (*b*) V_2O_5/silica gel, (*c*) Fe_2O_3/silica gel, and (*d*) $MnSO_4$/silica gel. To convert the ordinates (mg/g) to μmol/m^2, multiply the plotted values by (*a*) 0.0329, (*b*) 0.0347, (*c*) 0.0340, and (*d*) 0.0282, respectively.

sulfates on the oxide catalysts is not interpreted as excluding strong chemisorptive but reversible interactions from contributing to the measured heat values at 0.004 μmol m^{-2} since the sulfur dioxide molecules are adsorbed on an essentially heterogeneous surface matrix. Rather it is suggested that the largest contribution to the heat of adsorption arises at a few surface loci where the supported oxides are endowed with favorable geometric and chemical properties for sulfate formation. It is not possible to identify these loci with the present techniques.

Can. J. Chem. Downloaded from www.nrcresearchpress.com by 210.87.254.42 on 09/05/12
For personal use only.

Can. J. Chem. Downloaded from www.nrcresearchpress.com by 210.87.254.42 on 09/05/12
For personal use only.

Continued dosing of all of the supported oxide catalysts with sulfur dioxide up to 0.300 μmol m^{-2} at 423 °K results in a smooth decrease in the adsorption heat values which begin to steady at between 6.0 and 8.0 kcal mol^{-1}. Hence the gas/solid interactions become progressively weaker as the surface coverage increases. Probably little or no significant adsorbate/adsorbate interactions occur (see, for example, ref. 11) in agreement also with the very low degrees of surface coverage in these experiments.

Further information on the state of the adsorbed sulfur dioxide molecules can be deduced from the preadsorption experiments, Fig. 3. Thus preadsorption of sulfur dioxide on all of the adsorbents and subsequent addition of small oxygen quotas causes increases in the pressure of the system and the surface equilibrium is slow to settle on each addition. The adsorption heats fall fairly sharply from 11.3 to 3.5 kcal mol^{-1} over the first four oxygen additions indicating that oxygen is weakly adsorbed in comparison with sulfur dioxide.

The catalytic reaction between SO_2 and O_2 to give SO_3 does not proceed readily on any of these oxides until around 600 °K and while the reaction mechanism has been variously interpreted (12–14), there is general agreement that sulfur dioxide is chemisorbed and reacts with either gas phase oxygen species (12) or adsorbed oxygen atoms (13) or ions (14). Whichever way, the formation of sulfur trioxide requires dissociation of some oxygen which would cause a pressure increase in the system if occurring in the gas phase prior to either reaction or adsorption followed by reaction. Only small pressure rises were detected consistent with the very small amount of sulfur trioxide likely to be present. Electrical resistance measurements of the adsorption of (SO_2 + O_2) mixtures on evaporated carbon films (15) at 473 and 523 °K have been interpreted as indicating that oxygen is weakly adsorbed also on those surfaces and that an (SO_3) adsorbed complex may be present. Any sulfur trioxide formed on the adsorbents and subsequently desorbed should be perfectly stable in the gas phase at 423 °K since $\log_{10} K_p$ for $SO_3(g) \rightleftharpoons SO_2(g) + \frac{1}{2}O_2(g)$ is -7.94 and -5.33, respectively (16) at 400 and 500 °K.

Adsorption of sulfur dioxide on all solids with oxygen preadsorbed causes an increase in the heat to a value approaching that for the normal surfaces which is again compatible with a stronger surface interaction with sulfur dioxide. The abnormal length of time required to achieve system equilibrium in these experiments may be due simply to the slowness of diffusion of the sulfur dioxide molecules to the surface in the presence of the large quantities of gas-phase oxygen that were required to produce 0.011 to 0.015 μmol m^{-2} of the adsorbed gas.

The heats of adsorption on silica gels of sulfur dioxide at 263 °K, boiling point, approach the value of the heat of liquefaction as the monolayer coverage nears completion (3). At the higher temperatures studied here the heats of liquefaction (16) are 5.07 (8.44), 3.96 (27.40), and 1.73 kcal mol^{-1} (68.67 atm) at 323, 373, and 423 °K, respectively. At these three temperatures the heats of adsorption are 9.0, 8.0, and 6.3 kcal mol^{-1} for 0.200 μmol m^{-2} surface coverage at pressures very much less than 1 atm. Hence, even at the highest coverages studied the gas/solid interactions still seem likely to involve chemical adsorption.

After heat treatment at 550 °C there are about 3 to 4 μmol m^{-2} of hydroxy groups present on the silica gel surface (17). Some of these groups are still bonded to adjacent silicon atoms about 3 Å apart (18). Since the normal ⟨O—S—O in sulfur dioxide (10) is 119.54° the O—O distance will be about 2.5 Å, which allows the possibility of orbital interactions between sulfur dioxide oxygen atoms and hydroxy hydrogens on the gel surface. For adsorbed water on silica gel it is now accepted (19) that the molecules are linked via their oxygen atoms to two adjacent hydroxy groups by hydrogen bonds (20). Adsorption of sulfur dioxide presents a more complex situation since the geometry of the interaction as well as the bonding possibilities indicates that the sulfur atom could be linked to the surface by four, two, one or even three hydrogen bonds formed through its oxygen atoms interacting with suitably spaced hydroxy groups. High adsorption heats of 23.0 to 25.0 kcal mol^{-1} at 423 °K for 0.004 μmol m^{-2} adsorbed in the absence of surface dehydration reactions suggests that several bridge linkages of the O—H···O type may be formed since one such arrangement normally involves from 3 to 6 kcal mol^{-1} of energy (21). The fall in the heat values with surface coverage, Fig. 1, could then be due to a progressive increase in the contributions of single and dual modes of attachment to the surface.

The results obtained with supported man-

ganese(II) sulfate and 'nickel sulfide' at 423 °K are very similar. Again the values at the lowest coverages in particular indicate chemisorption which has already been postulated (22) to explain the sorption of sulfur dioxide on nickel(IV) sulfide at 393 °K.

Clear differences are apparent in the heat curves for silica gel and manganese(II) sulfate on silica gel, Figs. 1 and 2; noticeably so at 323 °K where the sulfate heats are from 2 to 10 kcal mol^{-1} higher than those for the gel with the greatest differences observed at low coverages. Contributions to the heat of adsorption on manganese(II) sulfate from complex interactions between surface sulfate species and the initially adsorbed sulfur dioxide molecules may account for these effects.

Differences in the adsorption/desorption isotherms for sulfur dioxide on the various supported catalysts are only obvious for those measured at 273 °K. At 323 °K and higher both the amounts adsorbed and the isotherm pattern are almost entirely independent of the chemical nature of the adsorbent. Equilibrium amounts adsorbed fall sharply with increase in temperature in each case and at 423 and 473 °K pressure increase has little effect on the incremental adsorbed amounts. At 473 °K adsorption is confined to a small area of the external surface and there is little or no pore contribution as is evident from the absence of hysteresis. The critical temperature for sulfur dioxide (16) is 430 °K and observations on other systems particularly for carbon dioxide on silica gel (23), have also shown that hysteresis disappears at temperatures above or close to the critical temperature of the adsorbate.

The shapes of the 273 °K hysteresis loops were analyzed as previously outlined (24). The only significant feature was with respect to the supported manganese(II) sulfate where the width of loop separation was nearly twice that of the oxides indicating a greater difference in the chemical potential of the adsorbed sulfur dioxide molecules on the sulfate surface between the two extreme adsorbed states (25).

1. P. MARS and J. G. H. MAESSON. J. Catal. **10**, 1 (1968).
2. A. REGNER, A. SIMECEK, and J. VOLSOLSOBE. Collect. Czech. Chem. Commun. **33**(7), 2162 (1968).
3. W. J. JONES and R. A. ROSS. J. Chem. Soc. A, 1021 (1967).
4. T. W. BOYLE, W. J. GAW, and R. A. ROSS. J. Chem. Soc. 240 (1965).
5. E. ROBINSON and R. A. ROSS. J. Chem. Soc. A, 2521 (1969).
6. W. R. SMITH and D. G. FORD. J. Phys. Chem. **69**(10), 3587 (1965).
7. P. H. EMMETT and S. BRUNAUER. J. Am. Chem. Soc. **59**, 1553 (1937).
8. R. J. LOVEJOY, J. H. COLWELL, D. F. EGGERS, and G. D. HALSEY. J. Chem. Phys. **36**, 612 (1962).
9. F. FEIGL. Spot tests in inorganic analysis. Elsevier, New York. 1958.
10. Handbook of chemistry and physics. Chemical Rubber Publishing Co., Cleveland. 1970.
11. A. CLARK. The theory of adsorption and catalysis. *Edited by* E. M. Loebl. Academic Press, New York. 1970.
12. M. THODOS. Chem. Eng. Sci. **21**(12), 1191 (1966).
13. Y. KANEKO and H. ODANAKA. J. Res. Inst. Catal. Hokkaido Univ. **14**(3), 213 (1966).
14. A. SIMECEK and A. REGNER. Collect. Czech. Chem. Commun. **33**(8), 2540 (1968).
15. I. S. MCLINTOCK and J. C. ORR. Nature, **225**, 629 (1970).
16. D. BIENSTOCK, L. W. BRUNN, E. M. MURPHY, and H. E. BENSON. Bureau of Mines Information Circular, 7836 (1958).
17. W. J. JONES and R. A. ROSS. J. Chem. Soc. A, 1787 (1968).
18. A. V. KISELEV and V. I. LYGIN. Russ. Chem. Rev. **31**(3), 175 (1962).
19. H. P. BOEHM. Adv. Catal. **16**, 226 (1966).
20. B. B. DARLOW and R. A. ROSS. Nature, **198**, 4884 (1963).
21. A. V. KISELEV and V. I. LYGIN. Infrared spectra of adsorbed species. *Edited by* L. H. Little. Academic Press, New York. 1966.
22. J. P. BUDELOT and D. DELAFOSSE. Compt. Rend. **259**(2), 385 (1964).
23. M. M. DUBININ, B. P. BERING, V. V. SERPINSKY, and B. N. VASILEV. Surface phenomena in chemistry and biology. Pergamon, New York. 1958.
24. E. ROBINSON and R. A. ROSS. Can. J. Chem. **48**, 13 (1970).
25. D. H. EVERETT. The solid–gas interface. Vol. 2 *Edited by* E. A. Flood. Marcel Dekker, Inc., New York. 1967.

Can. J. Chem. Downloaded from www.nrcresearchpress.com by 210.87.254.42 on 09/05/12
For personal use only.

Can. J. Chem. Downloaded from www.nrcresearchpress.com by 210.87.254.5 on 09/05/12
For personal use only.

Theoretical Studies of Nonbenzenoid Hydrocarbons: 16 π-Electron Systems

F. W. Birss and N. K. Das Gupta[1]

Department of Chemistry, University of Alberta, Edmonton, Alberta

Received May 29, 1970[2]

Hückel and self-consistent-field semi-empirical π-electron molecular orbital calculations on pentalenoheptalene are reported and the results compared to those of pyrene, acepleiadylene, napth[*cde*]azulene, and cyclohept[*bc*]acenaphthylene which contain the same number of π electrons. Resonance energies of all molecules calculated by the methods of Dewar and Whitehead are reported. It is suggested that pentalenoheptalene can be treated as two fused azulene nuclei.

Utilisant la méthode de Hückel et la méthode semi-empirique s.c.f., on a effectué des calculs d'orbitales moléculaires pour les électrons π du pentalénoheptaléne; on compare ces résultats avec ceux du pyrène, de l'acépléiadylène, du naphto[*cde*]azulène et du cyclohepta[*bc*]acénaphtylène qui contient le même nombre d'électrons π. On a calculé les énergies de résonance de toutes les molécules par les méthodes de Dewar et de Whitehead. Il apparaîtrait que le pentalénoheptalène peut être considéré comme deux noyaux d'azulène qui ont été attachés ensemble.

Canadian Journal of Chemistry, 49, 2840 (1971)

Introduction

Recently Hafner *et al.* (1) have reported the synthesis of 4-methyl-pentaleno[6,6*a*,1,2-*def*]-heptalene. This molecule belongs to a relatively small class of compounds with fused five- and seven-membered rings with planar structure. As such it is amenable to theoretical treatment within the π-electron approximation. Other molecules in this class, notably azulene, pentalene, heptalene, pentenoazulene, and pentenoheptalene have been studied by various authors (2–4) with particular interest in the aromatic nature of such molecules. In this paper we report calculations on pentalenoheptalene along with the π-isoelectronic molecules acepleiadylene, napth-[*cde*]azulene, and cyclohept[*bc*]acenaphthylene within the π-electron approximation using Hückel and self-consistent-field molecular orbital methods. Heilbronner and co-workers (5) have reported calculations on these molecules by a modified Pariser–Parr–Pople method which involves neglect of many of the two-electron repulsion integrals included in the present work.

Method and Parameters

The Hückel calculations were of the simplest type, assuming equal one-center and neighboring two-center coulomb integrals throughout the molecule. Self-consistent-field molecular orbitals were obtained by a linear combination of atomic orbitals-molecular orbitals (l.c.a.o.-m.o.) method similar to that introduced by Pariser and Parr (6) and Pople (7). The orbitals are expressed as eigenvectors of the matrix representation of the closed-shell Hartree–Fock operator (8).

$$F = H + \sum_{i=1}^{8} (2J_i - K_i)$$

within the zero-differential overlap approximation. Assuming one $2p_\pi$ atomic orbital, represented as χ, on each center, the matrix elements are

$$F_{kk} = \langle\chi_k|F|\chi_k\rangle = \alpha_k + \sum_{m=1}^{16} q_m\gamma_{km} - \tfrac{1}{2}q_k\gamma_{kk}$$

$$F_{kl} = \beta_{kl} - \tfrac{1}{2}p_{kl}\gamma_{kl}$$

for neighboring k and l. For non-neighboring centers β_{kl} is assumed to be zero. The one-center one-electron integrals, α_k, are given by

$$\alpha_k = \langle\chi_k|H_1|\chi_k\rangle = -I - \sum_{\substack{m\neq k\\=1}}^{16} \gamma_{km}$$

with I the ionization energy of the carbon atom in its sp^2 valence state (9), 11.16 eV. The two-electron integrals, γ_{kl}, were calculated by the method of Ohno (10)

$$\gamma_{kl} = \langle\chi_k(1)\chi_k(1)|1/r_{12}|\chi_l(2)\chi_l(2)\rangle$$
$$= e^2/(a^2 + R_{kl}^2)^{1/2}$$
$$= 14.397/(1.328^2 + R_{kl}^2)^{1/2}\ \text{eV}$$

[1]On leave of absence from Department of Chemistry, Visva-Bharati University, Santiniketan, West Bengal, India.

[2]Revision received February 12, 1971.

Can. J. Chem. Downloaded from www.nrcresearchpress.com by 210.87.254.5 on 09/05/12
For personal use only.

with R_{kl} the internuclear distance in Å. The parameter a is chosen such that the one-center two-electron integral has the value 11.134 eV, the difference between the ionization energy and electron affinity of carbon in its sp^2 valence state (9).

The one-electron integrals between neighboring centers, β_{kl}, were the source of two types of calculation reported below. In one a constant value, -1.7901 eV, was used. This was obtained by the method of Chung and Dewar (11) using the value of γ_{kk} given above, assuming an average neighboring internuclear distance of 1.40 Å. In the other type β_{kl}, dependent upon the internuclear distance, was obtained by the method of Lo and Whitehead (12).The designations s.c.f.(*a*) and s.c.f.(*b*) are used to denote the type of β integral used, the former indicating β dependent on internuclear distance, the latter indicating the constant value.

The charge density at a center

$$q_k = 2 \sum_{i=1}^{8} C_{ki}^2$$

and bond order

$$p_{kl} = 2 \sum_{i=1}^{8} C_{ki} C_{li}$$

are obtained from the eigenvector components C_{ki}. For the first s.c.f. iteration the eigenvectors produced by the Hückel calculation were used for calculation of the contributions of the J_i and K_i operators to the **F** matrix elements. Self-consistency was declared when all components for occupied orbitals agreed within five figures after the decimal in a comparison of vector components of successive iterations.

Molecular Geometry

The structures of 4-methyl-pentaleno[6,6*a*,1,2-*def*]heptalene (13) and acepleiadylene (14) are known; they are planar. The structures of the other molecules were not found in the literature. For naphth[*cde*]azulene, a planar structure assuming all bond lengths equal to 1.40 Å which gave reasonable bond angles was obtained. For cyclohept[*bc*]acenaphthylene a planar structure with reasonable bond angles could not be obtained with all bond lengths equal to 1.40 Å. Therefore a compromise structure was used, with bond lengths varying from 1.36 to 1.46 Å, similar to the range for the molecules of known structure. The geometries used in the present calculation are given in Fig. 1, with labels *I*: pentaleno[*def*]-heptalene, *II*: acepleiadylene, *III*: naphth[*cde*]-azulene, *IV*: cyclohept[*bc*]acenaphthylene. Henceforth these molecules will be referred to as pentalenoheptalene, acepleiadylene, napthazulene, and cycloheptacenaphthylene.

Bond Orders and Bond Lengths

The calculated bond orders and available experimental bond lengths are given in Tables 1 to 4 along with empirical bond lengths obtained from the relation of Dewar and Gleicher (15)

$$R_{kl} = 1.504 - 0.166 p_{kl}$$

The agreement of any set of theoretical bond lengths with the experimental is somewhat erratic as experience with similar compounds would lead one to anticipate. Nevertheless we suggest that the similarity of bond length and bond order for the 9–10 bond of azulene and the 11–15 and 13–16 bonds of pentalenoheptalene indicates that the latter may be treated as two fused azulene structures as against fused pentalene and heptalene.

Taking the highest bond orders together indicates that the Kekule structure *A*, shown with others in Fig. 2, is dominant in the description of pentalenoheptalene. Structures *B* and *C* are perhaps more strongly contributing than *D*. The situation is similar for the other molecules with structure *A* less dominant. The Kekule structures which contribute to each bond are given in Tables 1 to 4.

The relatively high bond orders of the 6–7 and 8–9 bonds of pentalenoheptalene, the 5–6 and 7–8 bonds of acepleiadylene, the 8–9 and 10–14 bonds of naphthazulene, and the 5–6 and 7–8 bonds of cycloheptacenaphthylene suggest that these molecules may exhibit dienophilic activity in these regions.

Charge Densities and Dipole Moments

The charge densities for the molecules are given in Table 5. As in azulene, the π-electron density of the five-membered rings is increased at the expense of the seven-membered rings, with a tendency to establish a local sextet in all rings. This is also reflected by the theoretical π dipole moments given in Table 6 with the angles shown in Fig. 1, labelling the s.c.f. result as *1* (the angles given by the two methods of β determination being indistinguishable) and the Hückel result as *2*.

The dipole moment of acepleiadylene has been

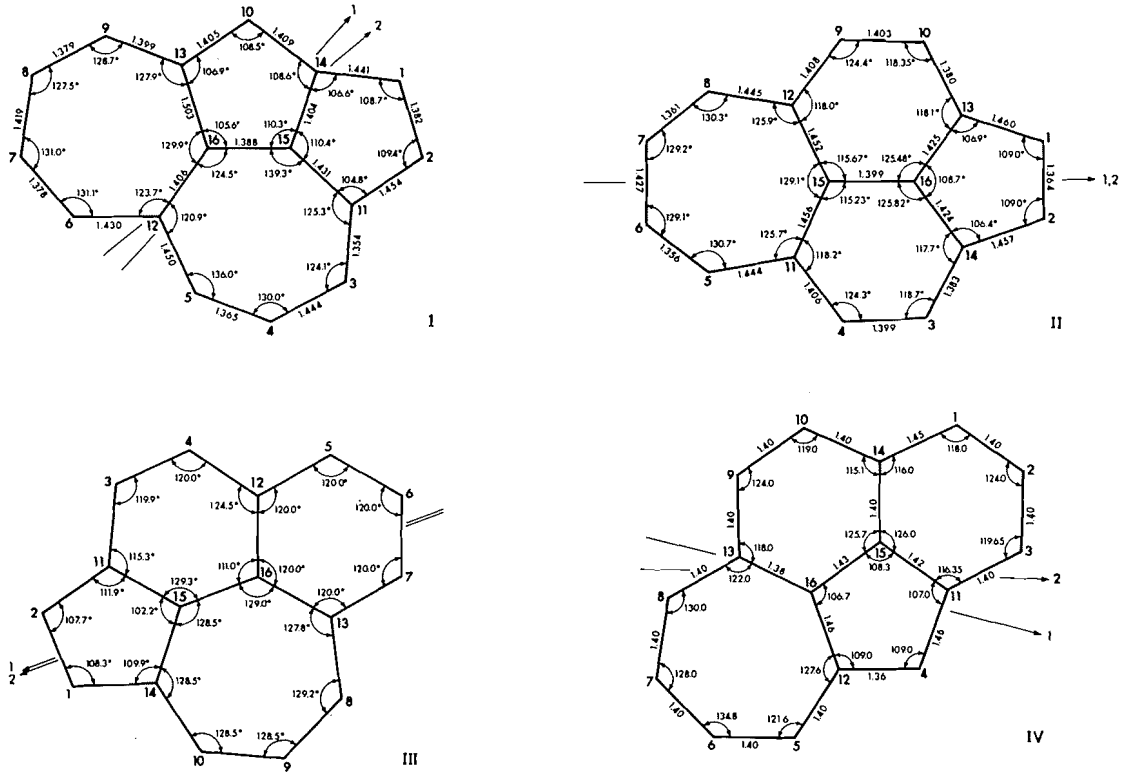

FIG. 1. Geometries and dipole moment vectors.

TABLE 1. Bond orders and bond lengths for pentalenoheptalene

	Bond order			Bond length (Å)			
				Calculated			
Bond	H.m.o.	s.c.f. (*a*)	s.c.f. (*b*)	s.c.f. (*a*)	s.c.f. (*b*)	Obsd.	Kekule structures
1– 2	0.7419	0.8849	0.8258	1.357	1.367	1.382	*A, C, D*
2–11	0.5196	0.3230	0.4206	1.450	1.434	1.454	*B*
3–11	0.6315	0.8255	0.7063	1.367	1.387	1.354	*A, C*
3– 4	0.6096	0.4069	0.5607	1.437	1.411	1.444	*B, D*
4– 5	0.6985	0.8545	0.7437	1.362	1.381	1.365	*A, C*
5–12	0.5356	0.3915	0.5170	1.439	1.418	1.450	*B, D*
12– 6	0.5226	0.4566	0.4493	1.428	1.429	1.430	*C*
6– 7	0.7198	0.8016	0.7922	1.371	1.373	1.378	*A, B, D*
7– 8	0.5742	0.4741	0.4848	1.425	1.424	1.419	*C*
8– 9	0.7167	0.7931	0.7879	1.372	1.373	1.379	*A, B, D*
9–13	0.5292	0.4692	0.4553	1.426	1.428	1.399	*C*
13–10	0.6402	0.7237	0.6869	1.384	1.390	1.405	*A, B*
10–14	0.5509	0.5490	0.5648	1.413	1.410	1.409	*C, D*
1–14	0.5058	0.3583	0.4178	1.445	1.435	1.441	*B*
14–15	0.5397	0.6491	0.6002	1.396	1.404	1.404	*A*
11–15	0.4250	0.3110	0.3760	1.452	1.442	1.431	*D*
12–16	0.5349	0.6708	0.5940	1.393	1.405	1.406	*A*
15–16	0.5586	0.5246	0.5231	1.417	1.417	1.388	*B, C*
13–16	0.4200	0.2747	0.3782	1.458	1.441	1.503	*D*

Can. J. Chem. Downloaded from www.nrcresearchpress.com by 210.87.254.5 on 09/05/12
For personal use only.

TABLE 2. Bond orders and bond lengths for acepleiadylene

Bond	Bond order		Bond length (Å)			Kekule structures
			Calculated			
	s.c.f. (*a*)	s.c.f. (*b*)	s.c.f. (*a*)	s.c.f. (*b*)	Obsd.	
1– 2	0.9114	0.8591	1.353	1.361	1.364	*A, C, B*
2–14	0.3049	0.3879	1.453	1.440	1.457	*D*
3–14	0.7303	0.6710	1.383	1.393	1.383	*A, B*
3– 4	0.5762	0.6280	1.408	1.400	1.399	*C, D*
4–11	0.7265	0.6693	1.383	1.393	1.406	*A, B*
5–11	0.3121	0.3833	1.452	1.440	1.444	*D*
6– 5	0.8986	0.8477	1.355	1.363	1.356	*A, C, B*
6– 7	0.3372	0.4206	1.448	1.434	1.427	*D*
7– 8	0.8982	0.8476	1.355	1.363	1.361	*A, C, B*
8–12	0.3131	0.3836	1.452	1.440	1.445	*D*
9–12	0.7320	0.6702	1.383	1.393	1.408	*A, C*
9–10	0.5686	0.6269	1.410	1.400	1.403	*B, D*
10–13	0.7365	0.6721	1.382	1.392	1.380	*A, C*
1–13	0.3019	0.3875	1.454	1.440	1.460	*D*
13–16	0.4714	0.4937	1.426	1.422	1.425	*B*
14–16	0.4771	0.4947	1.425	1.422	1.424	*C*
11–15	0.4772	0.4964	1.425	1.422	1.456	*C*
12–15	0.4700	0.4952	1.426	1.422	1.452	*B*
15–16	0.6280	0.5791	1.400	1.410	1.399	

TABLE 3. Bond orders and bond lengths for naphthazulene

Bond	Bond order		Calculated bond length (Å)		Kekule structures
	s.c.f. (*a*)	s.c.f. (*b*)	s.c.f. (*a*)	s.c.f. (*b*)	
1– 2	0.8352	0.8351	1.365	1.365	*A, B, C*
2–11	0.4260	0.4257	1.433	1.433	*D*
3–11	0.5092	0.5084	1.420	1.420	*B*
3– 4	0.7859	0.7867	1.374	1.373	*A, C, D*
4–12	0.4866	0.4856	1.423	1.423	*B*
5–12	0.5725	0.5722	1.409	1.409	*C, D*
5– 6	0.7069	0.7072	1.387	1.387	*A, B*
6– 7	0.6302	0.6300	1.399	1.399	*C, D*
7–13	0.6579	0.6583	1.395	1.395	*A, B*
8–13	0.4120	0.4109	1.436	1.436	*D*
8– 9	0.8155	0.8163	1.369	1.369	*A, B, C*
9–10	0.4739	0.4730	1.425	1.426	*D*
10–14	0.7631	0.7635	1.377	1.377	*A, B, C*
1–14	0.4127	0.4133	1.436	1.435	*D*
14–15	0.3309	0.3299	1.449	1.449	
15–16	0.5245	0.5235	1.417	1.417	*B, D*
13–16	0.5018	0.5021	1.421	1.421	*C*
12–16	0.5455	0.5465	1.414	1.413	*A*
11–15	0.6439	0.6450	1.397	1.397	*A, C*

determined experimentally at 0.49 D (16). Theoretical values for the π dipole moment have been obtained (17) by Pullman, 1.0 D, and by Julg, 0.9 D, compared with 1.2 and 2.0 D in the present work.

Spectra, Ionization Energies, Electron Affinities

The experimental spectra of the molecules studied here have a large number of peak maxima, many of which are not clearly resolved. Therefore, the best that one can expect in a comparison of the theoretical and observed transition energies is a general correlation over quite wide spectral regions. Tables 7 to 10 display this comparison. Except for pentalenoheptalene, the reported experimental values were measured from published curves (18), taking only clearly pronounced maxima. For pentalenoheptalene, the same criterion was used, based upon the peak maxima reported by Hafner *et al.* (1) and the spectra given by Heilbronner and co-workers (5).

In addition to the observed peak maxima in-

Can. J. Chem. Downloaded from www.nrcresearchpress.com by 210.87.254.5 on 09/05/12
For personal use only.

TABLE 4. Bond orders and bond lengths for cycloheptacenaphthylene

Bond	Bond order		Calculated bond length (Å)		Kekule structures
	s.c.f. (*a*)	s.c.f. (*b*)	s.c.f. (*a*)	s.c.f. (*b*)	
1– 2	0.7574	0.7139	1.378	1.386	*A, C*
2– 3	0.5781	0.6229	1.408	1.401	*B, D*
3–11	0.7160	0.6642	1.385	1.394	*A, C*
4–11	0.3395	0.4157	1.448	1.435	*D*
4–12	0.8424	0.7920	1.364	1.373	*A, B, C*
5–12	0.3711	0.3985	1.442	1.438	*D*
5– 6	0.8494	0.8313	1.363	1.366	*A, B, C*
6– 7	0.4198	0.4413	1.434	1.431	*D*
7– 8	0.8488	0.8314	1.363	1.366	*A, B, C*
8–13	0.3811	0.4079	1.441	1.436	*D*
9–13	0.5075	0.5119	1.420	1.419	*B*
9–10	0.7826	0.7821	1.374	1.374	*A, B, D*
10–14	0.5041	0.4931	1.420	1.422	*C*
1–14	0.5125	0.5639	1.419	1.410	*B, D*
14–15	0.5893	0.5491	1.406	1.413	*A*
11–15	0.4842	0.4981	1.424	1.421	*B*
15–16	0.5085	0.5268	1.420	1.417	*C, D*
13–16	0.6879	0.6505	1.390	1.396	*A, B*
12–16	0.2707	0.3242	1.459	1.450	

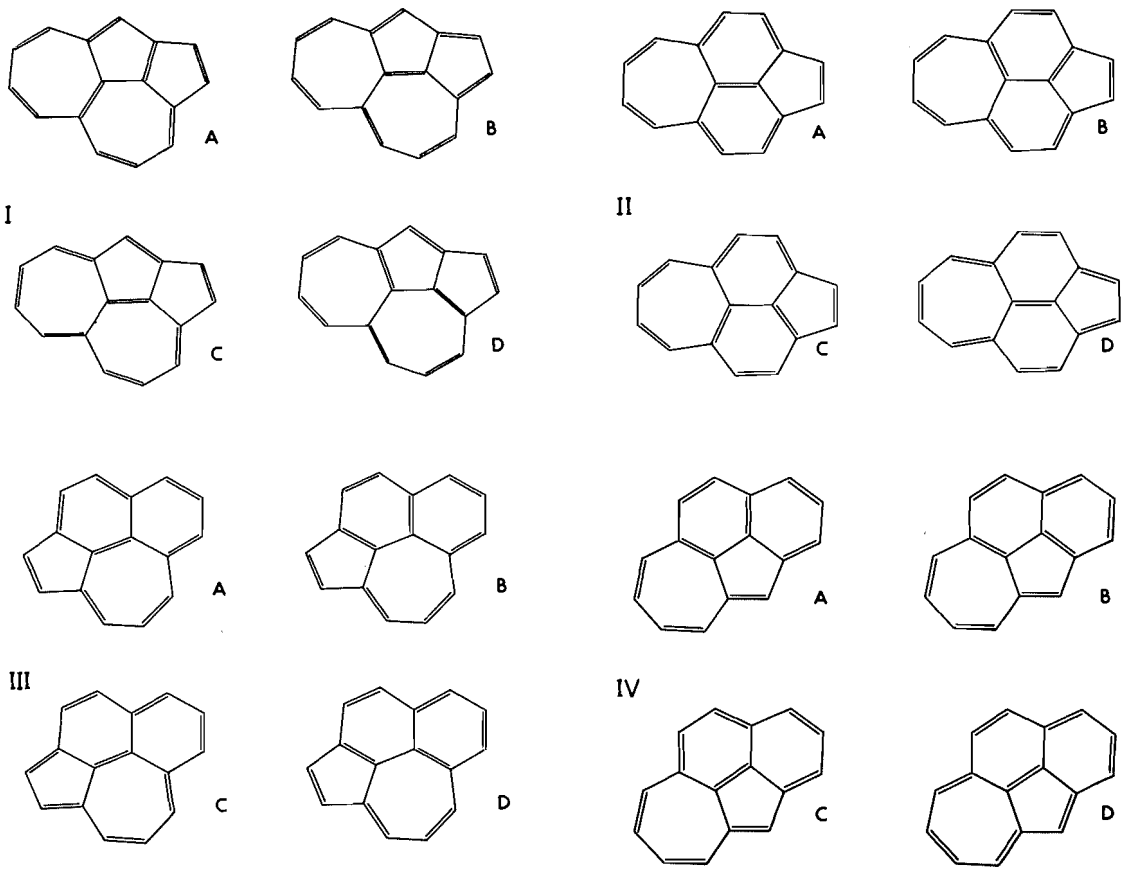

FIG. 2. Kekule structures.

Can. J. Chem. Downloaded from www.nrcresearchpress.com by 210.87.254.5 on 09/05/12
For personal use only.

Can. J. Chem. Downloaded from www.nrcresearchpress.com by 210.87.254.5 on 09/05/12
For personal use only.

TABLE 5. Charge densities

	Pentalenoheptalene			Acepleiadylene		Naphthazulene		Cycloheptace-naphthylene	
Center	H.m.o.	s.c.f. (*a*)	s.c.f. (*b*)	s.c.f. (*a*)	s.c.f. (*b*)	s.c.f. (*a*)	s.c.f. (*b*)	s.c.f. (*a*)	s.c.f. (*b*)
1	0.9867	0.9495	0.9052	1.0175	1.0298	1.0742	1.0741	0.9836	0.9782
2	1.1096	1.0842	1.1303	1.0173	1.0297	0.9920	0.9920	1.0151	1.0228
3	0.9210	1.0063	1.0203	0.9522	0.9227	0.9561	0.9561	0.9729	0.9624
4	0.9378	0.9438	0.9250	1.0427	1.0701	1.0531	1.0531	1.0631	1.0806
5	0.9396	1.0263	1.0424	0.9910	0.9816	0.9998	0.9996	0.9472	0.9213
6	1.0293	1.0870	1.1112	0.9925	0.9867	0.9975	0.9976	1.0261	1.0436
7	0.9265	0.9003	0.8779	0.9921	0.9866	1.0165	1.0162	0.9655	0.9440
8	1.0328	1.0929	1.1182	0.9913	0.9816	0.9077	0.9076	1.0179	1.0338
9	0.9104	0.8876	0.8559	1.0433	1.0702	1.0505	1.0509	1.0318	1.0474
10	1.0754	1.0006	0.9642	0.9513	0.9225	0.8867	0.8866	0.9650	0.9442
11	0.9669	0.9176	0.8728	0.9723	0.9587	1.0597	1.0595	0.9953	0.9966
12	0.9178	0.8882	0.8861	0.9719	0.9587	0.9907	0.9906	1.0142	1.0228
13	1.0713	1.1011	1.1412	1.0247	1.0396	1.0318	1.0321	0.9519	0.9224
14	1.1142	1.0675	1.1079	1.0247	1.0395	1.0086	1.0087	1.0144	1.0196
15	1.1639	1.0910	1.1318	0.9983	0.9862	1.0199	1.0200	1.0287	1.0457
16	0.8968	0.9562	0.9096	1.0170	1.0357	0.9553	0.9556	1.0073	1.0146

TABLE 6. π dipole moments

	Dipole moment (D)		
Molecule	H.m.o.	s.c.f. (*a*)	s.c.f. (*b*)
Pentalenoheptalene	5.62	1.68	1.51
Acepleiadylene	8.27	1.15	2.06
Naphthazulene	5.70	1.71	1.70
Cycloheptacenaphthylene	4.33	0.60	0.87

TABLE 7. Transition energies (eV) for pentalenoheptalene

s.c.f. (*a*)			s.c.f. (*b*)			Heilbronner and co-workers (5)
Orbitals	Theoretical	Observed	Orbitals	Theoretical	Observed	
8 → 9	2.5	2.3	8 → 9	2.2	2.3	2.4
8 → 10	3.2	2.8	7 → 9	2.9	2.8	3.1
7 → 10	3.4	2.9	8 → 10	3.0	2.9	3.3
8 → 11	3.5	3.4	8 → 11	3.4	3.4	
7 → 9	3.5		7 → 10	3.4		
7 → 11	4.2		6 → 9	3.8		3.7
6 → 9	4.3	4.3	6 → 10	4.1	4.3	4.1
6 → 10	4.3		7 → 11	4.3		4.3
5 → 9	4.9	4.9	5 → 9	5.0	4.9	4.4
6 → 11	5.5		6 → 11	5.0		

cluded in the tables there is in every case a number of observed maxima at low transition energies for which no theoretical counterpart was found. Dinghra and Poole (19) have discussed these transitions in the case of pentalenoheptalene. Aside from these bands the agreement between experiment and theory is good. It is encouraging to note that the orbital transitions occurring in each grouping shown in Tables 7 to 10 remain almost constant as the style of β integral evaluation is changed.

The last columns in Tables 7 to 10 show the results obtained by Heilbronner and co-workers (5) using a modified form of the Pariser–Parr–Pople method. The agreement of these results with experiment and with those obtained in this work is also good.

According to Koopmans' theorem (20), the ionization energy should be well approximated by the highest occupied orbital energy. It has commonly been observed (21) that values obtained by this method are 1 to 2 eV too high. Hoyland and

TABLE 8. Transition energies (eV) for acepleiadylene

s.c.f.(*a*)				s.c.f.(*b*)				Heilbronner and co-workers (5)	
Orbitals	Symmetry	Theoretical	Observed	Orbitals	Symmetry	Theoretical	Observed	Symmetry	Theoretical
			2.5				2.5	$^1A_1$	2.59
$8 \rightarrow 10$	$^1B_2$	3.3	3.0	$8 \rightarrow 10$	$^1B_2$	2.9		$^1B_2$	2.89
$8 \rightarrow 9$	$^1B_2$	3.6	3.8	$7 \rightarrow 9$	$^1A_1$	3.1	3.0	$^1B_2$	3.14
$7 \rightarrow 9$	$^1A_1$	3.6		$8 \rightarrow 9$	$^1B_2$	3.3			
$6 \rightarrow 9$	$^1A_1$	4.0	4.0	$6 \rightarrow 9$	$^1A_1$	3.9	3.8	$^1A_1$	3.45
$8 \rightarrow 11$	$^1B_2$	4.3		$8 \rightarrow 11$	$^1B_2$	4.2	4.0	$^1B_2$	4.34
$7 \rightarrow 10$	$^1A_1$	5.0		$7 \rightarrow 10$	$^1A_1$	4.4			
$6 \rightarrow 10$	$^1A_1$	5.0	4.9	$6 \rightarrow 10$	$^1A_1$	4.6		$^1A_1$	4.58
$7 \rightarrow 11$	$^1A_1$	5.0		$7 \rightarrow 11$	$^1A_1$	4.7	4.9		
$5 \rightarrow 9$	$^1A_1$	5.3		$5 \rightarrow 9$	$^1A_1$	5.0		$^1B_2$	4.76
$8 \rightarrow 12$	$^1B_2$	5.7	5.8	$8 \rightarrow 12$	$^1B_2$	5.4			
							5.8		

TABLE 9. Transition energies (eV) for napthazulene

	s.c.f.(*a*)		s.c.f.(*b*)		Heilbronner and co-workers (5)
Orbitals	Theoretical	Observed	Theoretical	Observed	
$8 \rightarrow 9$	2.6	2.3	2.6	2.3	2.10
		2.8		2.8	
$7 \rightarrow 9$	2.9	3.0	2.9	3.0	2.89
		3.4		3.4	
$8 \rightarrow 10$	3.7	3.6	3.7	3.6	
		3.7		3.7	3.61
$8 \rightarrow 11$	3.9		3.8		3.90
$7 \rightarrow 10$	4.2	4.0	4.1	4.0	
$6 \rightarrow 9$	4.3		4.2		
					4.31
$5 \rightarrow 9$	4.8	4.6	4.7	4.6	4.51
$7 \rightarrow 11$	4.8		4.8		

TABLE 10. Transition energies (eV) for cycloheptacenaphthylene

	s.c.f.(*a*)		s.c.f.(*b*)		Heilbronner and co-workers (5)
Orbitals	Theoretical	Observed	Theoretical	Observed	
					2.23
$8 \rightarrow 10$	2.9	2.9	2.8	2.9	2.90
		3.0		3.0	
$8 \rightarrow 9$	3.3	3.2	2.9	3.2	
		3.4			3.78
$6 \rightarrow 9$	3.8		3.5	3.4	
					3.83
$7 \rightarrow 9$	4.0		3.9		
$7 \rightarrow 10$	4.4	4.3	4.3		4.18
$8 \rightarrow 11$	4.5		4.4	4.3	4.37
$6 \rightarrow 10$	4.7		4.6		4.61
$5 \rightarrow 9$	5.1	4.9	5.0	4.9	
$7 \rightarrow 11$	5.1		5.2		

Can. J. Chem. Downloaded from www.nrcresearchpress.com by 210.87.254.5 on 09/05/12
For personal use only.

Can. J. Chem. Downloaded from www.nrcresearchpress.com by 210.87.254.5 on 09/05/12
For personal use only.

Goodman (22) have shown that the discrepancy can be accounted for by σ-core contraction and π-orbital deformation in the ionized molecule.

In the context of constant-β calculations, Bloor (2) has proposed a general corrected ionization energy for hydrocarbons as $-(\varepsilon_h + 1.33)$ eV, where ε_h is the highest occupied orbital energy. He also proposes that the half-wave reduction potential, measured in 95% aqueous dioxane, can be fitted by the form $-(\varepsilon_l + 4.77)$ eV, where ε_l is the lowest unoccupied orbital energy.

Values for the uncorrected ionization energy, based upon Koopmans' theorem, the ionization energy corrected by Bloor's method and for the lowest unoccupied orbital energy and the corresponding half wave potential, $\varepsilon_{1/2}$, obtained by Bloor's method are given in Table 11.

Also included in Table 11 are ionization energies and electron affinities calculated as the difference in total calculated energy of the neutral molecule and the total energy obtained in an open shell calculation on the positive or negative ion. Since identical basic integrals were used in all cases, these values should reflect the correction due to π-orbital deformation, neglecting σ-core contraction.

Resonance Stabilization

Delocalization energies (d.e.) per electron (d.e./e), based upon Hückel calculations, for the series naphthalene, phenanthrene, and pyrene are (23) 0.37, 0.39, and 0.41, respectively, indicating that this quantity increases with the size of the molecule. A similar increase occurs (23) in the series azulene, 1,2-benzazulene and cycloheptacenaphthylene (naptho(1,9,8,7-*aji*)azulene) with values 0.34, 0.36, and 0.39, respectively. Comparison between these series indicates a lowering in d.e./e with the replacement of a naphthalene by an azulene unit while maintaining the number of electrons and rings constant. This feature is also shown by the series pyrene, napthazulene, and pentalenoheptalene in which the naphthalene units of pyrene are successively replaced by azulene units. The d.e./e values are 0.41, 0.39, and 0.37, respectively, indicating that the molecules with successively greater numbers of azulene nuclei are successively somewhat less resonance stabilized.

Chung and Dewar (11) have proposed that the resonance stabilization may be expressed as

$$E_R^{(b)} = n(A_0 + a_1 A_1) + E_{\pi b}$$

where $A_0 = -1.0871$ eV, determined from the empirical resonance stabilization of benzene, $A_1 = -0.1627$ eV, the difference in the bond energies of "aromatic" and single carbon–carbon σ bonds,

$$a_1 = \frac{1}{n}(n' - n/2)$$

with n the number of π-electrons and n' the number of carbon–carbon single bonds in a reference valence bond structure. $E_{\pi b}$ is the π-bonding energy determined by

$$-E_{\pi b} = 2\beta \sum_{i<j} p_{ij} + \tfrac{1}{4}\sum_i q_i^2\gamma_{ii} + \sum_{i<j}[(q_i - 1)(q_j - 1) - \tfrac{1}{2}p_{ij}^2]\gamma_{ij}$$

Lo and Whitehead (12) give the resonance energy as

$$E_R^{(a)} = E_{\sigma b} + E_{\pi b} - (n' E_{C-C} + n'' E_{C=C})$$

with $E_{\pi b}$ and n' defined as above, n'' the number of double bonds in a reference valence bond structure, $E_{\sigma b}$ the σ-bonding energy determined by the method given by those authors, $E_{C-C} = 3.9115$ eV is the single bond energy at 1.505 Å C—C distance and $E_{C=C} = 5.6033$ eV is the double bond energy at 1.334 Å C—C distance. They also maintain that the stabilization energy per carbon–carbon bond, rather than the delocalization

TABLE 11. Measures of the ionization energy and electron affinity (eV)

	Ionization energy measures				Electron affinity measures			
	Orbital energy		I, Bloor	$E_{ion} - E_{molecule}$	Orbital energy		$\varepsilon_{1/2}$, Bloor	$E_{molecule} - E_{ion}$
Molecule	s.c.f.(*a*)	s.c.f.(*b*)	s.c.f.(*b*)	s.c.f.(*a*)	s.c.f.(*a*)	s.c.f.(*b*)	s.c.f.(*b*)	s.c.f.(*a*)
Pentalenoheptalene	−8.87	−8.69	7.36	8.72	−2.22	−2.32	−2.45	−2.30
Acepleiadylene	−9.14	−8.94	7.61	9.02	−2.10	−2.33	−2.44	−2.04
Napthazulene	−8.88	−8.87	7.54	8.72	−2.54	−2.54	−2.23	−2.91
Cycloheptacenaphthylene	−8.92	−8.75	7.42	8.73	−2.09	−2.29	−2.48	−2.29

TABLE 12. Energy quantities (eV)

Molecule	Calculation	$E_{\pi b}$	$E_{\sigma b}$	$E_R^{(a)}$	$E_R^{(b)}$	$E_R^{(a)}$ per bond
Naphthalene	Reference 12	14.600	40.576	3.690	3.566	0.3355
	s.c.f.(*b*)	14.508	40.608	3.630	3.474	0.330
	Reference 11	13.462			2.429	
Azulene	s.c.f.(*a*)	13.736	40.283	2.534	2.703	0.230
	s.c.f.(*b*)	13.408	40.386	2.309	2.374	0.210
	Reference 11	12.398			1.365	
Pyrene	Reference 12	23.886	70.456	6.489	6.004	0.3415
	s.c.f.(*b*)	24.013	70.141	6.301	6.131	0.3316
	Reference 11	22.335			4.453	
Pentalenoheptalene	s.c.f.(*a*)	22.520	70.231	4.898	4.638	0.258
	s.c.f. (*b*)	22.364	69.255	3.765	4.482	0.198
Acepleiadylene	s.c.f. (*a*)	23.360	70.308	5.815	5.479	0.306
	s.c.f.(*b*)	23.138	69.274	4.559	5.253	0.240
Napthazulene	s.c.f.(*a*)	23.512	69.633	5.292	5.631	0.279
	s.c.f.(*b*)	23.159	70.134	5.440	5.277	0.286
Cycloheptacenaphthylene	s.c.f.(*a*)	23.158	70.133	5.438	5.277	0.286
	s.c.f.(*b*)	23.111	69.639	4.896	5.229	0.258

energy per electron, is of prime significance in a comparison of π-bonding in conjugated systems.

Table 12 contains values of the quantities described above. For comparison we have included values for naphthalene, azulene, and pyrene as given by Chung and Dewar (11) and Lo and Whitehead (12). The two methods give good agreement for the molecules discussed in this paper but inconsistencies appear in the case of naphthalene and pyrene. We believe that this is due to the smaller value of γ_{11} chosen by Chung and Dewar in evaluating β, since recalculation of naphthalene with integral values consistent with the methods described in this paper leads to good agreement of the resonance energies calculated by the two methods.

The resonance stabilization per carbon–carbon bond can be used to arrange the ground states of the molecules in order of stability

pyrene > acepleiadylene > cycloheptacenaphthylene > napthazulene > pentalenoheptalene

although the three molecules in the middle of the sequence have so similar resonance energies that the order may be interchanged by minor variations in the choice of integral values.

The stabilization energy per carbon–carbon bond may also be used in a discussion of the aromaticity of the molecules. For that purpose, the aromatic molecules naphthalene and azulene, with stabilization energies per carbon–carbon bond of 0.34 and 0.23, respectively, serve as useful reference points. All the molecules fall in this range, pyrene with the value 0.34 and pentalenoheptalene with the value 0.26, suggesting that all are aromatic but that this character decreases with the number of benzenoid rings.

Like pentalene, heptalene, acenaphthylene, and pentenoazulene, pentalenoheptalene has $4n\pi$ electrons as well as being representable by more than one Kekule structure. Within Hückel's rule, such molecules should not exhibit aromatic character. Pentalene and heptalene are in fact typically olefinic, pentenoazulene is pseudoaromatic whereas acenaphthylene is aromatic. As for pentalenoheptalene, its stability, as expressed by the stabilization energy per carbon–carbon bond, resistance to electrophilic attack, and increase of electron density in the five-membered rings at the expense of that in the seven-membered rings, suggest that it may be effectively classified as an aromatic compound.

We are grateful to the National Research Council of Canada for financial support and to the Computing Center of The University of Alberta for making available facilities for the computations involved.

1. K. HAFNER, R. FLEISCHER, and K. FRITZ. Angew. Chem. Int. Ed. **4**, 69 (1965).
2. J. E. BLOOR. Can. J. Chem. **43**, 3026 (1965) and references therein.
3. T. NAKAJIMA, Y. YAGUCHI, R. KAERIYAMA, and Y. NEMOTO. Bull. Chem. Soc. Japan, **37**, 272 (1963) and references therein.

Can. J. Chem. Downloaded from www.nrcresearchpress.com by 210.87.254.5 on 09/05/12
For personal use only.

4. M. A. ALI and C. A. COULSON. Mol. Phys. **4**, 65 (1961). N. K. DAS GUPTA and M. A. ALI. Theor. Chim. Acta, **4**, 101 (1966).
5. P. BAUMGARTNER, E. WELTIN, G. WAGNIERE, and E. HEILBRONNER. Helv. Chim. Acta, **48**, 751 (1965).
6. R. PARISER and R. G. PARR. J. Chem. Phys. **21**, 466, 767 (1953).
7. J. A. POPLE. Trans. Faraday Soc. **49**, 1375 (1953).
8. C. C. J. ROOTHAN. Rev. Mod. Phys. **23**, 69 (1951).
9. J. HINZE and H. H. JAFFE. J. Am. Chem. Soc. **84**, 540 (1962).
10. K. OHNO. Theor. Chim. Acta, **2**, 219 (1964).
11. A. L. H. CHUNG and M. J. S. DEWAR. J. Chem. Phys. **42**, 756 (1965).
12. D. H. LO and M. A. WHITEHEAD. Can. J. Chem. **46**, 2027 (1968).
13. H. J. LINDNER. Chem. Ber. **102**, 2456 (1969).
14. A. W. HANSEN. Acta Cryst. **13**, 215 (1960); **21**, 97 (1966).
15. M. J. S. DEWAR and GLEICHER. J. Am. Chem. Soc. **87**, 685 (1965).
16. D. A. PITT, A. J. PETRO, and C. P. SMYTH. J. Am. Chem. Soc. **79**, 5633 (1957).
17. B. PULLMAN, A. PULLMAN, G. BERTHIER, and J. PONTIS. J. Chim. Phys. **49**, 20 (1952). P. FRANCOIS and A. JULG. J. Chim. Phys. **65**, 1180 (1968).
18. V. BOEKELHEIDE and G. K. VICK. J. Am. Chem. Soc. **78**, 653 (1956). P. D. GARDNER, C. E. WULFMAN, and C. L. OSBORN. J. Am. Chem. Soc. **80**, 143 (1958). D. H. REID, W. H. STAFFORD, and J. P. WARD. J. Chem. Soc. London, 1193 (1955).
19. R. C. DHINGRA and J. A. POOLE. J. Chem. Phys. **48**, 4829 (1968); J. Phys. Chem. **72**, 4577 (1968). K. C. Lim (*Editor*) Molecular luminescence. W. A. Benjamin, Inc. 1969. p. 813.
20. T. KOOPMANS. Physica, **1**, 104 (1934).
21. C. MOSER. J. Chim. Phys. **52**, 24 (1955).
22. J. R. HOYLAND and L. GOODMAN. J. Chem. Phys. **33**, 946 (1960).
23. A. STREITWIESER, JR. and J. I. BRAUMAN. Supplemental Tables of Molecular Orbital Calculations, with C. A. Coulson and A. Streitwieser, Jr., A Dictionary of π Electron Calculations, Pergamon Press, New York. 1965.

Can. J. Chem. Downloaded from www.nrcresearchpress.com by 210.87.254.5 on 09/05/12
For personal use only.

Can. J. Chem. Downloaded from www.nrcresearchpress.com by 210.87.254.42 on 09/05/12
For personal use only.

Base-induced Rearrangement of γ-Diketones. I. The Rearrangement of 1,2,2-Triphenyl-1,4-pentanedione to 1,3,3-Triphenyl-1,4-pentanedione[1]

PETER YATES, G. D. ABRAMS, MICHAEL J. BETTS, AND S. GOLDSTEIN
Lash Miller Chemical Laboratories, University of Toronto, Toronto 5, Ontario

Received March 18, 1971

Treatment of 4-hydroxy-2,2-diphenyl-3-pentenoic acid lactone (**3**) with phenyllithium gives 1,2,2-triphenyl-1,4-pentanedione (**2**), 1,3,3-triphenyl-1,4-pentanedione (**7**), and 3,3-diphenylpropiophenone (**16**). The γ-diketone **7** is shown to arise via rearrangement of an anion of the γ-diketone **2**. The formation of 1,2,3-triphenyl-1,4-pentanedione (**27**) is not observed, nor is **27** converted to **7** on treatment with base. It is concluded that the rearrangement proceeds via two homoenolate anion intermediates rather than via two 1,2 phenyl shifts.

Le traitement de la lactone de l'acide hydroxy-4 diphényl-2,2 pentène-3 oique (**3**) avec le phényllithium conduit aux triphényl-1,2,2 pentanedione-1,4 (**2**), triphényl-1,3,3 pentanedione-1,4 (**7**), et diphényl-3,3 propiophénone (**16**). Il est montré que la γ-dicétone **7** provient d'une transposition de l'anion de la γ-dicétone **2**. La formation de la triphényl-1,2,3 pentanedione-1,4 (**27**) n'est pas observée; par traitement basique **27** n'est pas non plus transformé en **7**. On en déduit que la transposition procède par l'intermédiaire de deux anions homoénolates plutôt que par deux migrations 1,2 de phényle.

Canadian Journal of Chemistry, 49, 2850 (1971)

In connection with studies of the i.r. spectra of cyclopentenones (2), the synthesis of 3,4,4-triphenyl-2-cyclopentenone (**1**) was undertaken. It was anticipated that this could be prepared from 1,2,2-triphenyl-1,4-pentanedione (**2**), which could be obtained by the reaction of the lactone **3** with phenyllithium. Previous work (3) suggested that **3** could be prepared by the reaction of diazoacetone (**4**) with diphenylketene (**5**).

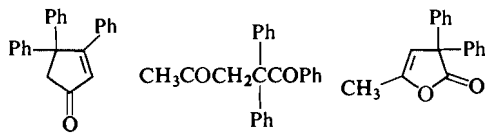

1 **2** **3**

In the event (Scheme 1), the reaction of **4** with **5** gave a mixture of products from which two compounds, $C_{17}H_{14}O_2$, were isolated. One of these, obtained in 11% yield, is identified as the desired lactone **3** by its i.r. and p.m.r. spectra.[2] The other, major product is assigned structure **6** (or the alternative enol) on the basis of its spectra[2] and the fact that it gives a positive test for a chelated enol on treatment with anhydrous methanolic ferric chloride; the formation of this type of product finds analogy in the reaction of diphenylketene with ethyl diazoacetate reported by Kende (4).

When the lactone **3** was treated with phenyllithium in ether for 20 min followed by work-up in aqueous acid, three products were obtained (Scheme 2). Two of these are isomers, $C_{23}H_{20}O_2$, and on the basis of their spectra (Table 1) are considered to be **2** and 1,3,3-triphenyl-1,4-pentanedione (**7**). The relationship of the u.v. spectra of the two isomers led to the assignment of structure **2** to the compound m.p. 154.5–155.5° (42%) and of structure **7** to the compound m.p. 152.5–154° (4%), in that the hypsochromic and hypochromic shifts of the high intensity maximum in the spectrum of the former relative to the latter can be attributed to a departure from coplanarity of the benzoyl phenyl and carbonyl groups of **2** due to the adjacent *gem*-diphenyl grouping. These assignments were corroborated by conversion of

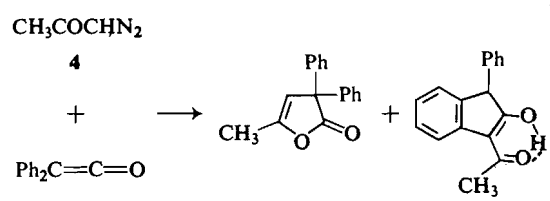

SCHEME 1

[1]Preliminary reports on part of this work have appeared (1).

[2]See Experimental.

TABLE 1. Spectra of 1,2,2- and 1,3,3-triphenyl-1,4-pentanediones

Compound	2	7
Melting point (°C)	154.5–155.5	152.5–154
λ_{max} (CCl_4) (μ)	5.79, 5.96, 7.36 (m)	5.85 (sh), 5.90, 7.40 (m)
λ_{max} (EtOH) [mμ(ε)]	239 (9800), 316 (sh, 310)	242.5 (13 800), 276.5 (sh, 1580)
δ ($CDCl_3$)	1.91 (s, 3H), 3.71 (s, 2H), 7.0–7.6 (m, 15H)	2.17 (s, 3H), 4.14 (s, 2H), 7.1–7.5 (m, 13H), 7.7–7.9 (m, 2H)

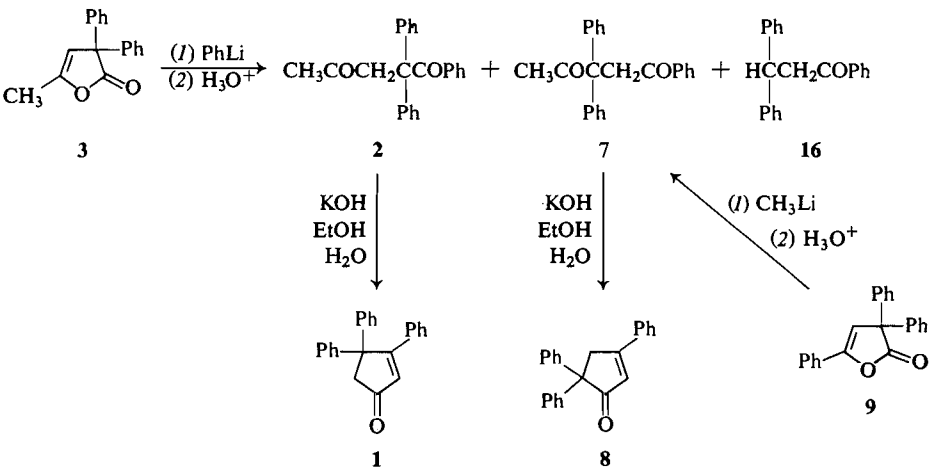

SCHEME 2

2 and **7** with aqueous ethanolic base to the cyclopentenones **1** and **8**, respectively. These products are readily distinguishable on the basis of their p.m.r. spectra;[2] as discussed elsewhere (2), the carbonyl-stretching band in the i.r. spectrum of **1** (unsubstituted at C-5) is split while that in the spectrum of **8** (substituted at C-5) is unsplit. Confirmation for the structural assignment for **7** was provided by its independent synthesis by treatment of the lactone **9** with methyllithium. In contrast to **3**, **9** was obtained in 77% yield by reaction of diphenylketene (**5**) with 2-diazoacetophenone (**10**) (3): two minor products, assigned structures **11** and **12**, were also isolated from the reaction mixture (Scheme 3). The i.r. and u.v. spectra of **11** closely resemble those of **13** (5); its formation again finds analogy in the reaction of diphenylketene with ethyl diazoacetate (4). The yellow compound **12** has a u.v. spectrum similar to that of **14** (6) and gives diphenylacetic acid on hydrolysis; its formation can readily be envisaged as proceeding via reaction of **15**, the analogue of **6**, with diphenylketene.

The third product formed on treatment of lactone **3** with phenyllithium was shown to be 3,3-diphenylpropiophenone (**16**) by direct comparison with an authentic sample.[3]

The most probable pathway for the formation of the diketone **7** from **3** appeared to be via rearrangement of the anion **17**, formed by reaction of **3** with phenyllithium, to the anion **18**. That this is the case was indicated by the observation that the yield of **7** relative to **2** increased with longer reaction times. Further, when **2** was treated with sodium methoxide in ether it was converted to a mixture of the cyclopentenones **1** and **8**; under these conditions **1** was not converted to **8**, and thus it may be concluded that **2** undergoes partial base-induced conversion to an anion of **7**, which then gives **8**.

Two general types of pathway may be envisaged as accounting for the rearrangement of the anion

[3]We thank Professor R. E. Lutz, University of Virginia, for his kindness in providing this sample (7).

Can. J. Chem. Downloaded from www.nrcresearchpress.com by 210.87.254.42 on 09/05/12
For personal use only.

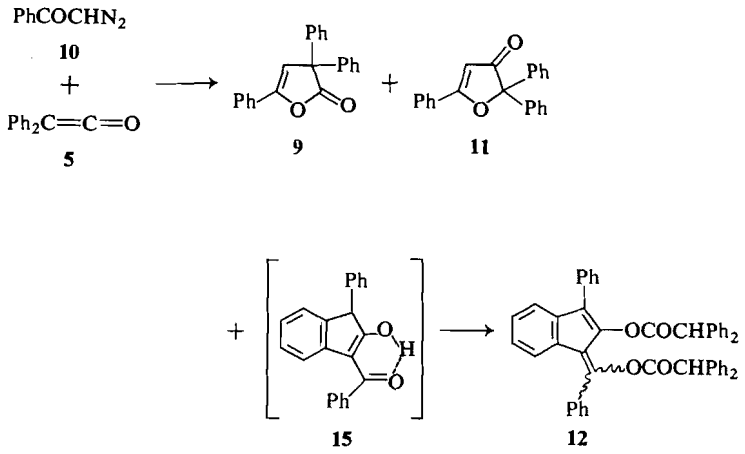

SCHEME 3

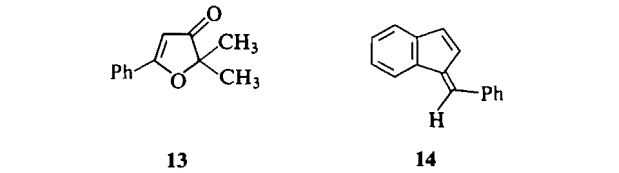

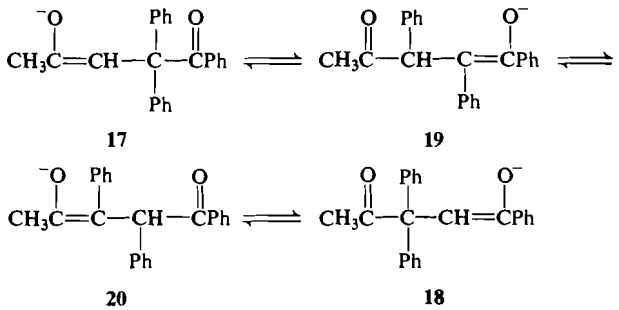

SCHEME 4

17 to the anion **18**.[4] In the first (Scheme 4), migration of a phenyl group could occur to give **19**, followed by hydrogen migration to give **20**, which would give **18** upon migration of the second phenyl group.

Such 1,2 migrations of phenyl groups to anionic centers find ample precedent in the work of Zimmerman, Grovenstein, and their coworkers (8). However, the postulate of a step involving hydrogen migration is less attractive. Consideration of a suprafacial [1,2] sigmatropic shift of hydrogen to an anionic center in terms of conservation of orbital symmetry (9, 10) shows that it is symmetry-forbidden, and no concerted intramolecular pathway is available for such a transformation. The same considerations apply to the more extended π-system of **19**. This restriction does not apply to phenyl migration, where a p-orbital at the migrating carbon atom can be utilized for simultaneous bonding to the atoms between which migration is occurring (9, 11). These considerations do not exclude the possibility that the conversion of **19** to **20** could occur by a non-concerted intramolecular process involving a radical anion – radical pair, as in the case of certain Stevens and Wittig rearrangements (11, 12), or by an intermolecular process involving

[4]Consideration of the reaction in terms of free anions is, of course, an approximation, since it neglects the presence of the cationoid species. Also neglected are any effects due to the presence of inorganic salts in the organolithium reagents.

Can. J. Chem. Downloaded from www.nrcresearchpress.com by 210.87.254.42 on 09/05/12
For personal use only.

Can. J. Chem. Downloaded from www.nrcresearchpress.com by 210.87.254.42 on 09/05/12
For personal use only.

protonation followed by deprotonation. However, the first process seems energetically most unfavorable (12*a*) in the case of hydrogen migration since a hydrogen atom would be one member of the radical pair, while the second process is likely to be unfavorable since it would require abstraction of a proton from an anionic species.[5]

In the second type of mechanism (Scheme 5), the anion **17** could give the homoenolate anion **21**, followed consecutively by formation of the anion **22** and a second homoenolate anion, **23**, which would give rise to the anion **18**. The intermediacy of homoenolate ions in several base-induced reactions of ketones has been demonstrated by Nickon and others (13), and Freeman and Plonka (14) have proposed the intermediacy of a homoenolate ion in a closely related case. A point of importance relating to Scheme 5 concerns the anion **22**; this is expected to be considerably less stable than the ion **22***a* that would be derived from it by 1,2 hydrogen migration. Indeed, should **22***a*, the enolate ion of the β-diketone **24**, be formed, it would be anticipated that the reaction would terminate at this stage. However, the suprafacial hydrogen migration required to effect the intramolecular conversion of **22** to **22***a* is symmetry-forbidden as discussed above, and thus formation of **22***a* would not be expected to occur readily.

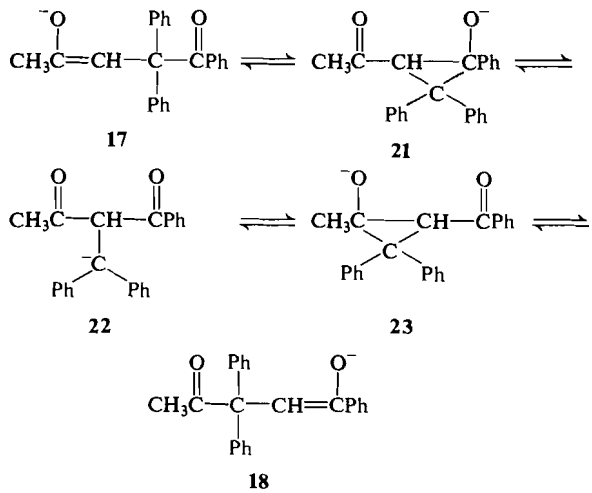

SCHEME 5

A more concerted version of Scheme 5 is possible and in this connection it is of interest to note its relationship to the mechanism proposed by Woodward and Kovach (15) many years ago for the acid-catalyzed rearrangement of santonic acid (**25**) to parasantonide (**26**). This was postulated to proceed via a concerted process involving (quasi) cyclopropanols analogous to the homoenolate ions **21** and **23**.

Scheme 5 is preferred to Scheme 4 because of the inclusion in the latter of a symmetry-forbidden step. Furthermore, experimental evidence confirms that the rearrangement does not proceed via Scheme 4. Were this scheme operative, it would be expected that significant amounts of the anions **19** and **20** would be present in the reaction mixture prior to quenching and that upon quenching the products would include the corresponding protonated species, 1,2,3-triphenyl-1,4-pentanedione (**27**). However, examination of the spectra of the total crude reaction product obtained from the treatment of **3** with phenyllithium failed to reveal the presence of any **27**.

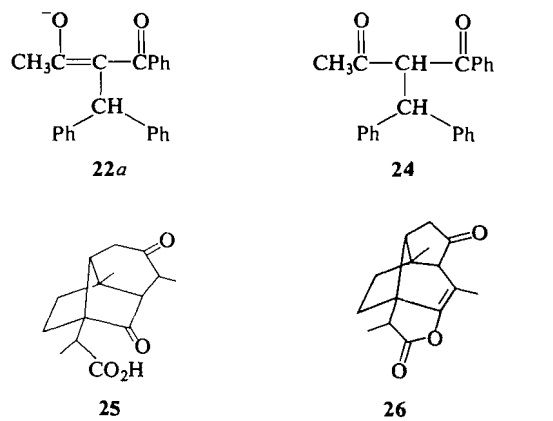

In order to test further the possibility of the intermediacy of **19** and **20** in the rearrangement, the synthesis of the diketone **27** was undertaken. Treatment of deoxybenzoin (**28**) in tetrahydrofuran with sodium hydride followed by 1-bromo-1-phenyl-2-propanone (**29**) gave a mixture of the diastereomers of **27** in low yield (Scheme 6). These were separated by fractional crystallization and identified on the basis of their elemental analyses and spectra (Table 2). Formed in addition were an isomeric compound, considered to

[5]The fact that increase in the reaction time beyond that required for the complete consumption of **3** leads to an increased yield of **7** shows that if an intermolecular proton transfer step is involved it must be able to proceed in the presence of anionic species alone.

TABLE 2. Spectra of the diastereomers of 1,2,3-triphenyl-1,4-pentanedione

Compound	*27a*	*27b*
Melting point (°C)	155–155.5	187–188
λ_{max} (CCl_4) (μ)	5.85, 5.96, 7.41 (m), 7.79 (w), 8.02 (w), 14.32	5.85, 5.96, 7.41 (m), 7.83, 14.35
λ_{max} (EtOH) [mμ(ε)]	247 (14 800)	248 (13 200)
δ ($CDCl_3$)	2.15 (s, 3H), 4.60 (d, J = 11 Hz, 1H), 5.20 (d, J = 11 Hz, 1H), 7.3 (m, 13H), 8.05 (m, 2H)	1.92 (s, 3H), 4.84 (d, J = 11 Hz, 1H), 5.60 (d, J = 11 Hz, 1H), 7.4 (m, 13 H), 7.9 (m, 2H)

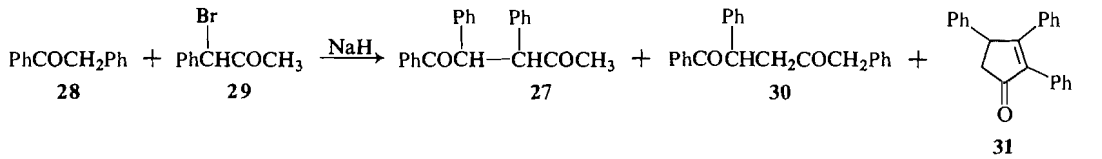

SCHEME 6

be 1,2,5-triphenyl-1,4-pentanedione (**30**) on spectroscopic grounds,[2] and 2,3,4-triphenyl-2-cyclopentenone (**31**), identified by comparison with an authentic sample (16) (Scheme 6). The relationship between **30** and **31** was confirmed by the observation that the former was converted to the latter by treatment with methanolic sodium methoxide. The pathway for the formation of **30** has not been established; possibilities include (*i*) isomerization of **29** to 1-bromo-3-phenyl-2-propanone followed by reaction with the anion of **28** and (*ii*) isomerization of the enol ether formed by *O*-alkylation of **28** by **29**.

When **27***a*, the lower-melting diastereomer of **27**, was treated with sodium methoxide in ether under conditions that led to the conversion of **2** to a mixture of the cyclopentenones **1** and **8**, neither of these products nor their precursors, **2** and **7**, could be detected in the reaction mixture. Much of compound **27***a* was recovered unchanged, together with several products formed in small amount; one of these was identified as the diastereomer **27***b* on the basis of its R_f value, and another is tentatively considered to be 3,4,5-triphenyl-2-cyclopentenone, the cyclization product from **27**, but was not fully characterized. The fact that **27** is not converted to either **2** or **7** nor to their cyclization products, **1** and **8**, under these conditions excludes it as an intermediate in the conversion of **2** to **7** and thus eliminates a mechanism of the type depicted in Scheme 4.

A mechanism of the type shown in Scheme 5 is therefore considered to be the best representation of the rearrangement pathway. The third product, 3,3-diphenylpropiophenone (**16**), from the reaction of phenyllithium with **3** is formed in variable yield and may result from the adventitious entry of water into the reaction mixture after consumption of the phenyllithium. It might also arise via attack of phenyllithium on **18**, **21**, or **22**. It is not formed by cleavage of **24** during the aqueous work-up, since **24** is stable under these conditions.

Each of the steps in Scheme 5 should be reversible as depicted. However, when the diketone **7** was treated with sodium methoxide in ether, only the cyclopentenone **8** was formed. This suggests that **7** does not undergo significant rearrangement to **2**, although it does not establish this unambiguously since it is possible that cyclization to **8** occurred more rapidly than rearrangement to **2**. Decisive evidence for the failure of the rearrangement to occur in the reverse direction to any significant extent was supplied by the observation that treatment of the lactone **9** with methyllithium gave only **7** and that no trace of **2** could be detected in the p.m.r. spectrum of the crude reaction product after several hours of reaction. It may be concluded that the equilibrium between the anions **17** and **18** very highly favors the latter.[6]

Full acceptance of the type of mechanism shown in Scheme 5 requires the demonstration that the geminal phenyl groups remain attached to the same carbon atom, since this represents a decisive distinction between mechanisms involv-

[6]In related cases, it has been established that the rearrangement is reversible; the position of equilibrium in the present case will be discussed in relation to these cases (17).

Can. J. Chem. Downloaded from www.nrcresearchpress.com by 210.87.254.42 on 09/05/12
For personal use only.

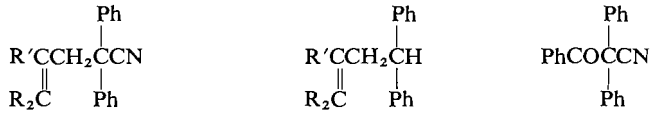

39 R = R′ = Ph
40 R = H; R′ = CH_3

41 R = R′ = Ph
42 R = H; R′ = CH_3

43

ing homoenolate ions and those involving 1,2 phenyl migrations. In order to test this, methods were sought for the preparation of **2** with an isotopic label at C-3. Its synthesis via **3** was unsatisfactory for this purpose because of the low yield obtained in the preparation of **3**. In spite of a variety of approaches, no success was achieved. Some of the observations made in the course of this search are not without intrinsic interest and they will be discussed here briefly.

Alkylation of diphenylacetonitrile with ethyl bromoacetate in the presence of aqueous sodium hydroxide and benzyltriethylammonium chloride gave the ester **32** in excellent yield.[7] The ester was hydrolyzed to the acid **33**, which was treated with 2 equiv of phenylmagnesium bromide in the expectation that it would be converted to the keto acid **34**. However, elimination of cyanide ion occurred to give the unsaturated acid **35**; a similar result was obtained when phenyllithium was used. When excess Grignard reagent was used the unsaturated alcohol **36** was obtained. The dinitrile

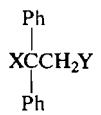

32 X = CN; Y = CO_2Et
33 X = CN; Y = CO_2H
34 X = COPh; Y = CO_2H
37 X = Y = CN

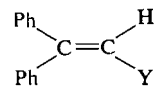

35 Y = CO_2H
36 Y = CPh_2OH
38 Y = CN

37, prepared by alkylation of diphenylacetonitrile with chloroacetonitrile (18), on treatment with methylmagnesium iodide or methyllithium gave the unsaturated nitrile **38** in similar fashion.

Alkylation of diphenylacetonitrile with 2,3,3-triphenylallyl bromide and with methallyl chloride in the presence of 50% aqueous sodium hydroxide and benzyltriethylammonium chloride gave the nitriles **39** and **40**, respectively. It was hoped that treatment of these with methyllithium would convert the nitrile groups to acetyl groups. However, cleavage of a carbon–carbon bond occurred in each case to give the hydrocarbons **41** and **42**, respectively. Such cleavage has been observed in related cases (19) and presumably involves elimination of acetonitrile from the lithium derivative of the imine formed as an intermediate in the attack of the methyllithium on the nitrile group. The preference for elimination in these cases and those referred to above presumably stems from the severe steric crowding at the carbon atom bearing the geminal phenyl groups. A similar cause must underlie the failure of another approach involving attempts to protect the carbonyl group of the keto nitrile **43**, prepared by benzoylation of diphenylacetonitrile.

Although these attempts to find an efficient route for the synthesis of labeled **2** failed, success attended the synthesis of a related labeled γ-diketone, and the study of its rearrangement has corroborated the mechanistic conclusions reached here (*1b*).

Experimental

Reaction of Diazoacetone and Diphenylketene. Formation of 4-Hydroxy-2,2-diphenyl-3-pentenoic Acid Lactone (3) and 3-Acetyl-2-hydroxy-1-phenylindene (6)

A solution of diazoacetone (**4**) was prepared by addition during 2.25 h of acetyl chloride (32.3 g, 412 mmol) in petroleum ether (80 ml) with stirring to 0.704 *M* ethereal diazomethane (1385 ml; 975 mmol) in an ice-water bath. The volume of the solution was reduced to *ca.* 100 ml by evaporation under reduced pressure at room temperature, and the remaining solution was diluted with benzene (800 ml).

This solution was added dropwise to a stirred solution of diphenylketene (**5**)[8] (47.1 g, 242 mmol) in benzene (1 l) at room temperature under nitrogen, and the mixture was stirred under these conditions overnight. The reaction mixture was concentrated to *ca.* 750 ml by distillation under reduced pressure under nitrogen. It was then washed three times with aqueous 5% sodium bicarbonate and once with saturated aqueous sodium chloride, and dried. Removal of the solvent gave a brown oil (57.6 g) from which some **6** (8.49 g) was separated by repeated solution in boiling ether, cooling, scratching, and filtering,

[7]This method of alkylation, that of Lange and Makosza (18), is preferable to methods involving alkoxides as the basic condensing agent because of its simplicity.

[8]Prepared by the method of Smith and Hoehn (20); to avoid severe bumping and frothing it was found necessary to distil the reaction mixture under nitrogen at water aspirator pressure to remove benzene prior to distillation of the diphenylketene at 3–4 mm.

Can. J. Chem. Downloaded from www.nrcresearchpress.com by 210.87.254.42 on 09/05/12
For personal use only.

Can. J. Chem. Downloaded from www.nrcresearchpress.com by 210.87.254.42 on 09/05/12
For personal use only.

followed by evaporation of the mother liquor. The residue was dissolved in petroleum ether – benzene (3:2) and chromatographed on silica gel (Davison; 800 g) with the same solvent mixture as eluent; 100-ml fractions were collected. Evaporation of fractions 42–76 gave crude **3** as a yellowish solid (6.05 g). A further quantity of crude **3** was obtained by evaporation of fractions 35–41 and heating of the combined residues at *ca.* 75° (0.025 mm) to volatilize the major contaminant, which was shown to be phenyl benzoate by spectral comparison with an authentic sample.

The total crude **3** (6.87 g) was rechromatographed on silica gel (100 g), packed and eluted with petroleum ether – benzene (3:2); 25-ml fractions were collected. Combination of fractions shown by their i.r. spectra to be rich in **3** and evaporation of the solvent yielded **3** as a colorless solid (6.33 g, 11% based on diphenylketene), m.p. 49–52°; λ_{max} (CCl_4) 5.54, 5.92 μ(m); δ (CCl_4) 2.10 (d, J = 1.5 Hz, 3H), 5.63 (q, J = 1.5 Hz, 1H), 7.26 (s, 10 H). Several sublimations at 70° (0.005 mm) failed to improve the m.p.

Anal. Calcd. for $C_{17}H_{14}O_2$: C, 81.58; H, 5.64. Found: C, 81.40; H, 5.59.

Further elution of the original chromatographic column with petroleum ether – benzene (3:2) gave **6** which was combined with the material obtained by treatment of the crude reaction product with ether. Eight recrystallizations from hexane gave **6** as colorless crystals, m.p. 125–126°; λ_{max} (CCl_4) 6.03, 6.22 μ(br); λ_{max} (MeOH) 254.5 (ε 9300), 278 (ε 7100), 287.5 (ε 7400), 340 mμ (ε 6000); δ ($CDCl_3$) 2.43 (s, 3H), 4.59 (s, 1H), 7.0–7.5 (m, 9H), *ca.* 14.1 (br s, 1H); blue-green coloration with anhydrous methanolic ferric chloride.

Anal. Calcd. for $C_{17}H_{14}O_2$: C, 81.58; H, 5.64. Found: C, 81.37; H, 5.69.

*Reaction of **3** with Phenyllithium. Formation of 1,2,2-Triphenyl-1,4-pentanedione (**2**), 1,3,3-Triphenyl-1,4-pentanedione (**7**), and 3,3-Diphenylpropiophenone (**16**)*

To a solution of **3** (294 mg, 1.18 mmol) in ether (25 ml) was added a 0.291 *M* ethereal solution of phenyllithium (8.0 ml; 2.33 mmol). The mixture was stirred under nitrogen at room temperature for 20 min and then acidified with 1.1 *N* hydrochloric acid. The ethereal phase was washed twice with aqueous 5% sodium bicarbonate and three times with water, and dried. Evaporation of the ether gave an oily solid (400 mg), which was triturated with hexane to give **2** (140 mg). Recrystallization from hexane gave **2** as colorless crystals, m.p. 154.5–155.5°.[9]

Anal. Calcd. for $C_{23}H_{20}O_2$: C, 84.12; H, 6.14. Found: C, 84.13; H, 6.34.

The mother liquors were stripped of solvent, and the residue was taken up in chloroform and separated into three major solid fractions by preparative t.l.c. on silica gel plates (with phosphor) with elution with 5% ethyl acetate – carbon tetrachloride. The solid fraction with the lowest R_f value consisted of **2** (55 mg; total yield of pure product: 163 mg, 42%). The next fraction (40 mg) had a closely similar R_f value and was recrystallized from isopropyl alcohol to give **7** (16 mg, 4%) m.p. 146–147°. Three recrystallizations from cyclohexane gave **7** as colorless crystals, m.p. 152.5–154°.[9]

[9]For spectra, see Table 1.

Anal. Calcd. for $C_{23}H_{20}O_2$: C, 84.12; H, 6.14. Found: C, 83.99; H, 6.15.

The third solid fraction (28 mg) was recrystallized from methanol to give **16** (19 mg, 6%), m.p. 94–95° (lit. (7) m.p. 94°), undepressed on admixture with an authentic sample;[3] λ_{max} ($CHCl_3$) 5.93 μ; λ_{max} (EtOH) 241.5 mμ (log ε 13 200); δ ($CDCl_3$) 3.68 (d, J = 7.3 Hz, 2H), 4.83 (t, J = 7.3 Hz, 1H), 7.0–7.5 (m, 13H), 7.8–8.0 (m, 2H).

Anal. Calcd. for $C_{21}H_{18}O$: C, 88.08; H, 6.34. Found: C, 88.13; H, 6.32.

When the reaction time was extended to 2.5 h and the product mixture was again resolved by preparative t.l.c. and crystallization, there was obtained **2** (18%) and **7** (27%) together with the corresponding cyclopentenones **1** (3%) and **8** (5%) (*vide infra*) (total yields of unrearranged and rearranged products: 21 and 32%, respectively).

*Reaction of **2** with Aqueous Ethanolic Potassium Hydroxide. Formation of 3,4,4-Triphenyl-2-cyclopentenone (**1**)*

A solution of **2** (248 mg, 0.756 mmol) in a 5% solution of potassium hydroxide in ethanol–water (4:1, 15 ml) was boiled under reflux for 30 min. The mixture was neutralized with 2 *N* hydrochloric acid and diluted with water, and solvent was distilled until the vapor temperature reached 98°. The residue was extracted four times with dichloromethane, and the extracts were washed twice with water and dried. Evaporation of the solvent gave a solid, which was crystallized from ethanol to yield **1** (117 mg, 50%), m.p. 173–179°. Further recrystallization from several solvents did not give a sharp-melting solid; the product consisted of two types of crystals, long needles and irregular globular forms, that were separated by hand picking and shown to have identical i.r. spectra in solution; λ_{max} (CCl_4) 5.80 (sh), 5.87 μ; λ_{max} (EtOH) 290 mμ (ε 17 000); δ ($CDCl_3$) 3.30 (s, 2H), 6.84 (s, 1H), 7.0–7.5 (m, 15H).

Anal. Calcd. for $C_{23}H_{18}O$: C, 89.00; H, 5.85. Found: C, 88.86; H, 5.83.

*Reaction of **7** with Aqueous Ethanolic Potassium Hydroxide. Formation of 3,5,5-Triphenyl-2-cyclopentenone (**8**)*

A solution of **7** (64 mg, 0.20 mmol) in a 5% solution of potassium hydroxide in ethanol–water (4:1) was boiled for 30 min. Work-up as in the case of **2** above gave a solid, which was crystallized from methanol to yield **8** (38 mg, 63%), m.p. 152–154°. This product was also obtained, together with **1**, when a mixture of **2** and **7** was chromatographed on neutral alumina; one recrystallization from hexane and two from methanol gave an analytical sample, m.p. 155–156.5°; λ_{max} (CCl_4) 5.87 μ; λ_{max} (EtOH) 288.5 mμ (ε 22 900); δ ($CDCl_3$) 3.83 (d, J= 1.5 Hz, 2H), 6.63 (t, J = 1.5 Hz, 1H), 7.0–7.9 (m, 15H).

Anal. Calcd. for $C_{23}H_{18}O$: C, 89.00; H, 5.85. Found: C, 88.77; H, 5.93.

*Reaction of 2-Diazoacetophenone and Diphenylketene. Formation of 4-Hydroxy-2,2,4-triphenyl-3-butenoic Acid Lactone (**9**), 2,2,5-Triphenyl-3(2H)-furanone (**11**), and **12**[10]*

To a solution of 2-diazoacetophenone (**10**) (21) (4.25 g, 29 mmol) in ether (30 ml) was added diphenylketene (**5**)

[10]*Cf.* ref. 3.

Can. J. Chem. Downloaded from www.nrcresearchpress.com by 210.87.254.42 on 09/05/12
For personal use only.

(22) (6.25 g, 32 mmol) in a nitrogen atmosphere. Brisk evolution of nitrogen occurred and the mixture was stirred under nitrogen at room temperature for 2 h, and then heated under nitrogen on the steam bath for a further 2 h after removal of most of the ether. The resulting oil (10.75 g) was dissolved in hot petroleum ether (b.p. 60–70°) and chromatographed on a silica gel column (Davison; 800 g) packed in the same solvent. The column was eluted with petroleum ether containing increasing amounts of ether (2% increments). Elution with 8% ether – petroleum ether gave **9** (7.00 g, 77% based on **10**), which was obtained after recrystallization from ethanol as colorless needles, m.p. 117.5–118.5° (lit. (3) m.p. 121–121.5°, 120°); λ_{max} 5.55, 6.03 μ(w); δ ($CDCl_3$) 6.33 (s, 1H); 7.2–7.5 (m, 13H), 7.6–7.8 (m, 2H).

The fractions eluted with 20% ether–petroleum gave **12** (2.17 g, 11%), which was obtained after recrystallization from ethanol as yellow needles, m.p. 183–184°; λ_{max} 5.71, 6.15 μ(m); λ_{max} (EtOH) 253 (ε 20 100), 259 (ε 19 400), 283.5 (ε 16 700), 333.5 mμ (ε 14 300); δ ($CDCl_3$) 3.90 (s, 1H), 5.34 (s, 1H), 6.8–7.6 (m, 34H).

Anal. Calcd. for $C_{50}H_{36}O_4$: C, 85.70; H, 5.18. Found: C, 85.21, 85.13; H, 5.09, 5.03.

Hydrolysis of **12** in 2-methoxyethanol with aqueous sodium hydroxide on the steam bath followed by recrystallization of the acid fraction from petroleum ether gave diphenylacetic acid, m.p. 146–147°, undepressed on admixture with an authentic sample; the i.r. spectra of the two samples were identical.

The fractions eluted with 26–28% ether – petroleum ether gave **11** (0.76 g, 8%), which was obtained after recrystallization from ethanol as colorless needles, m.p. 175–175.5°; λ_{max} (CCl_4) 5.89 μ; λ_{max} (EtOH) 247 (ε 6100), 309 mμ (ε 16 900); δ ($CDCl_3$) 6.11 (s, 1H), 7.35–7.6 (m, 13H), 8.0 (m, 2H); *m/e* (relative abundance) 312 (43), 283 (16), 207 (98), 179 (100), 105 (47).

Anal. Calcd. for $C_{22}H_{16}O_2$: C, 84.59; H, 5.16. Found: C, 84.36; H, 5.25.

Reaction of ***9*** *with Methyllithium. Formation of* ***7***

To a solution of **9** (500 mg, 1.60 mmol) in ether (40 ml) under nitrogen was added 1.75 *M* ethereal methyllithium (1.5 ml, 2.6 mmol). The mixture was stirred at room temperature for 25 min and then treated with 2 *N* sulfuric acid (15 ml). The ethereal layer was separated, washed with aqueous sodium bicarbonate and saturated aqueous sodium chloride, and dried. Evaporation of the ether gave a white solid that was crystallized from methanol to give **7** (470 mg, 89%), m.p. 148–148.5°. The p.m.r. spectrum of the crude product gave no evidence for the presence of **2**. When the reaction was allowed to proceed for 5 h, the yield of **7** was reduced to 77%, but again the p.m.r. spectrum of the crude product failed to show the presence of **2**.

Reaction of ***2*** *with Sodium Methoxide in Ether*

Sodium hydride (22 mg of a 54% dispersion in mineral oil; 0.49 mmol) was washed twice with petroleum ether and once with ether to remove mineral oil, and suspended in ether (25 ml) with stirring under nitrogen. To the stirred suspension was added a solution of **2** (127 mg, 0.39 mmol) in ether (35 ml) followed by two drops of methanol. After 3 days the mixture was treated with 1.2 *N* hydrochloric acid (25 ml). The ethereal layer was separated, and the aqueous layer was extracted twice with ether. The combined ethereal solutions were washed with aqueous 5% sodium bicarbonate and dried. The solvent was evaporated to give a solid residue (110 mg), which was resolved into two major components by preparative t.l.c. on silica gel (with phosphor) with elution with 5% ethyl acetate – carbon tetrachloride. The faster-moving major component (32 mg) was recrystallized from hexane–methanol to give **8** as colorless needles (25 mg, 21%), m.p. 150.5–152.5°. The slower-moving major component (43 mg) was crystallized from cyclohexane to give **1** as colorless crystals (35 mg, 29%), m.p. 168–173°.

When a solution of **1** in ether was treated with sodium hydride and methanol for 3 days and the mixture was worked-up as above, **1** was recovered quantitatively.

When a solution of **7** (61 mg) in ether was treated similarly, it was converted to **8** (43 mg, 75%), m.p. 148–150°; the p.m.r. spectrum of the total crude reaction product failed to show the presence of **1**.

*Reaction of the Sodium Derivative of Deoxybenzoin with 1-Bromo-1-phenylacetone. Formation of the Diastereomers of 1,2,3-Triphenyl-1,4-pentanedione (****27****), 1,2,5-Triphenyl-1,4-pentanedione (****30****), and 2,3,4-Triphenyl-2-cyclopentenone (****31****)*

Sodium hydride (460 mg of 54% dispersion in mineral oil; 10.3 mmol) was suspended in tetrahydrofuran (15 ml) in a nitrogen atmosphere. Deoxybenzoin (1.96, 10.0 mmol) dissolved in a little tetrahydrofuran was added. The mixture was warmed for 15 min, after which time hydrogen evolution had ceased. 1-Bromo-1-phenylacetone (23) (2.13 g, 10 mmol) was added and the mixture was boiled under reflux for 5 h. It was then poured into water and extracted with benzene. The extract was dried and stripped of solvent to give an orange gum, which was chromatographed on silica gel (150 g) packed in benzene–petroleum ether (2:3). Elution was commenced with mixtures of these solvents, the proportion of benzene being progressively increased. With benzene as eluent, deoxybenzoin (1.42 g, 72% recovery) was eluted. Elution was continued with benzene containing increasing amounts of ether. With 10% ether an oil (1.37 g) was eluted that was fractionated by preparative t.l.c. on silica with multiple gradient elution with 2–6% ether in petroleum ether to give a mixture of the diastereomers **27** (259 mg, 8%), together with **30** (409 mg, 12.5%) and **31** (233 mg, 7.5%) as the major components in order of decreasing R_f values.

Crystallization of the mixture of diastereomers **27** from methanol (20 ml) gave **27***b* as colorless needles (55 mg), m.p. 187–188° after recrystallization from methanol.[11]

Anal. Calcd. for $C_{23}H_{20}O_2$: C, 84.12; H, 6.14. Found: C, 83.94; H, 6.11.

On slow evaporation of the mother liquors a mixture of fine needles (**27***b*) and large prisms (**27***a*) crystallized. On dilution with methanol and heating, the needles dissolved more rapidly than the prisms, which were separated by filtration of the hot solution. Recrystallization from methanol gave **27***a*, m.p. 155–155.5°.[11]

Anal. Calcd. for $C_{23}H_{20}O_2$: C, 84.12; H, 6.14. Found: C, 83.87, 84.58; H, 6.54, 6.18.

Concentration of the mother liquors followed by

[11]For spectra, see Table 2.

Can. J. Chem. Downloaded from www.nrcresearchpress.com by 210.87.254.42 on 09/05/12
For personal use only.

repetition of the above separation processes together with hand-picking of crystals gave further **27***b* (total yield: 80 mg), m.p. 187–188°, and **27***a* (total yield; 137 mg), m.p. 154–155°.

Several recrystallizations of **30** from methanol gave crystals, m.p. 112.5–113°; λ_{max} (CCl_4) 5.86, 5.97 μ; λ_{max} (EtOH) 246 mμ (ε 13 600); δ ($CDCl_3$) 2.76 (dd, J = 4, 18 Hz, 1H), 3.62 (dd, J = 10, 18 Hz, 1H), 3.74 (s, 2H), 5.13 (dd, J = 4, 10 Hz, 1H), 7.26 (m, 13H), 8.0 (m, 2H); *m/e* (relative abundance) 328 (0.8), 237 (47), 105 (100).

Anal. Calcd. for $C_{23}H_{20}O_2$: C, 84.12; H, 6.14. Found: C, 84.24; H, 6.09.

Compound **31** was purified by preparative t.l.c. on silica with multiple elution with 5% ether – petroleum ether followed by recrystallization from methanol with treatment with Norit. It was obtained as pale yellow prisms, m.p. 139.5–140.5°, undepressed on admixture with an authentic sample prepared by the method of Koelsch and Geissman (16*a*); the i.r. spectra of the two samples were identical.

Reaction of 30 with Aqueous Ethanolic Sodium Hydroxide

A solution of **30** (59 mg) in ethanol (2 ml) was treated with 1 *N* aqueous sodium hydroxide (0.4 ml), and the resulting yellow solution was warmed briefly on the steam bath, acidified by the addition of 1 *N* hydrochloric acid (0.45 ml), and evaporated to dryness. The organic material was extracted from the residue with methanol, and the extract was concentrated to small volume. On standing, the concentrate deposited yellow crystals, which were recrystallized from methanol to give **31** (35 mg, 63%) as very pale yellow prisms, m.p. 140–140.5°, undepressed on admixture with an authentic sample (16*a*).

Reaction of 27a with Sodium Methoxide in Ether

Compound **27***a* (27 mg, 0.082 mmol) in ether (15 ml) was treated with sodium hydride (7.4 mg of a 54% dispersion in mineral oil; 0.17 mmol) and methanol (one drop) as in the case of **2**. Preparative t.l.c. on silica gel (with phosphor) with multiple elution with 50 and 80% benzene – petroleum ether gave **27***a* (18 mg, 67%) and several minor fractions, which did not include **1**, **2**, **7**, or **8**. One of these fractions (2.5 mg) had an R_f value identical with that of **27***b*. A second (4 mg) was tentatively identified as 3,4,5-triphenyl-2-cyclopentenone: λ_{max} (CCl_4) 5.85 μ; λ_{max} (EtOH) 286.5 mμ (ε ~ 14 000); δ ($CDCl_3$) 3.53, 4.60, 6.85, 7.3.

2-Benzhydryl-1-phenyl-1,3-butanedione (24)

The β-diketone **24** was prepared from benzhydrol and benzoylacetone by the method of Fosse (24) in 95% yield; m.p. 149.5–150.5° (lit. (24) m.p. 148–150°); λ_{max} 5.78, 5.96 μ; λ_{max} (EtOH) 252 (ε 16 100), 274 mμ (sh, ε 3000); λ_{max} (EtOH–NaOH) 315 mμ (ε 9500); δ ($CDCl_3$) 2.02 (s, 3H), 5.12 (d, J = 12 Hz, 1H), 5.63 (d, J = 12 Hz, 1H), 7.0–7.5 (m, 13H), 7.9–8.1 (m, 2H).

Anal. Calcd. for $C_{23}H_{20}O_2$: C, 84.12; H, 6.14. Found: C, 83.90; H, 6.22.

Compound **24** gave a negative test with anhydrous methanolic ferric chloride and was recovered unchanged after its ethereal solution was stirred for 1 h with either 5% aqueous sodium bicarbonate or 1.2 *N* hydrochloric acid.

Ethyl 3-Cyano-3,3-diphenylpropionate (32)

A mixture of diphenylacetonitrile (1.93 g, 10.0 mmol), 50% aqueous sodium hydroxide (5 ml), and benzene (5 ml) was vigorously stirred to give an emulsion. Benzyltriethylammonium chloride (20 mg) was added, producing an intense red coloration, and the reaction flask was flushed with nitrogen. Ethyl bromoacetate (1.67 g, 10.0 mmol) was added from a dropping funnel. The mixture became warm, and the red color was discharged within 10 min. After 1 h the mixture was poured into water, and extracted with benzene. The extract was washed with dilute hydrochloric acid and saturated aqueous sodium chloride, and dried. Evaporation of the solvent gave a colorless crystalline residue (2.68 g) that was twice recrystallized from ethanol to give **32** (2.10 g, 75%) as colorless prisms, m.p. 103.5–105° (lit. (25) m.p. 103–105°); λ_{max} (CCl_4) 4.49 (w), 5.71, 5.75 μ; δ ($CDCl_3$) 1.10 (t, J = 7 Hz, 3H), 3.42 (s, 2H), 4.07 (q, J = 7 Hz, 2H), 7.37 (s, 10H).

3-Cyano-3,3-diphenylpropionic Acid (33)

The ester **32** (2.01 g, 7.20 mmol) was dissolved in 70% aqueous ethanol (20 ml) containing potassium hydroxide (4 g), and the solution was heated on the steam bath for 30 min. Acidification with dilute hydrochloric acid gave a copious precipitate, which was filtered and crystallized from aqueous ethanol to give **33** (1.71 g, 95%) as colorless prisms, m.p. 182–183° (lit. (25) m.p. 183–184°); λ_{max} ($CHCl_3$) 3–4, 4.50 (w), 5.79 μ; δ ($CDCl_3$–Me_2CO) 3.48 (s), 7.37 (m), 8.33 (br s).

Reaction of 33 with Phenylmagnesium Bromide or Phenyllithium. Formation of 3,3-Diphenylacrylic Acid (35) and 1,1,3,3-Tetraphenyl-2-propen-1-ol (36)

(*A*) A solution of phenylmagnesium bromide was prepared from magnesium (26 mg, 1.1 mg-at.) and bromobenzene (173 mg, 1.1 mmol) in boiling, dry tetrahydrofuran (5 ml) under nitrogen. The solution was cooled to room temperature, and to it was added a solution of **33** (126 mg, 0.50 mmol) in dry tetrahydrofuran (5 ml). The mixture was stirred overnight, and then treated with 2 *N* sulfuric acid (10 ml). The resulting mixture was boiled under reflux for 45 min, cooled, and extracted with chloroform. The chloroform extract was extracted twice with aqueous 10% sodium carbonate. The combined basic extracts were acidified, and the mixture was extracted with chloroform. This chloroform extract was dried and stripped of solvent to give **35** (95 mg, 85%), which was obtained as long needles, m.p. 160–161° (lit. (26) m.p. 162°) after several crystallizations from aqueous methanol; λ_{max} (CCl_4) 3–4, 5.95 μ; λ_{max} (EtOH) 275 mμ (ε 12 900); *m/e* (relative abundance) 224 (100), 207 (18), 179 (42), 178 (37), 123 (13).

(*B*) Compound **33** (500 mg, 1.99 mmol) was treated with phenylmagnesium bromide (23 mmol) in tetrahydrofuran (40 ml) as in section *A*. The mixture was boiled under reflux for 2 h, cooled, and treated with 2 *N* sulfuric acid (25 ml). The resulting mixture was boiled under reflux for 1 h, cooled and extracted with ether. The extract was dried and stripped of solvent to give an orange gum (1.48 g), which was dissolved in 20% benzene – petroleum ether and chromatographed on silica (50 g). Elution was conducted with petroleum ether containing increasing amounts of benzene, followed by benzene. The latter eluted crude **36** (470 mg, 65%), which was crystallized several times from heptane to give prisms, m.p. 137–137.5° (lit. (27) m.p. 138–139°); λ_{max} (CCl_4) 2.80 (m),

Can. J. Chem. Downloaded from www.nrcresearchpress.com by 210.87.254.42 on 09/05/12
For personal use only.

6.15 μ (w); δ ($CDCl_3$) 2.44 (s, 1H, absent after D_2O treatment), 6.88 (s, 1H), 7.1–7.6 (m, 20H); *m/e* (relative abundance) 362 (1), 168 (16), 167 (100), 105 (20).

(*C*) A solution of **33** (126 mg, 0.50 mmol) in tetrahydrofuran (6 ml) was treated with a solution of phenyllithium (1.54 mmol) in ether (2 ml). The mixture was boiled under reflux for 5 h and worked-up as in section *A* to give **35** (69 mg, 62%), m.p. 159–160°.

2,2-Diphenylsuccinonitrile (37) (18)

A mixture of diphenylacetonitrile (2.50 g, 13.0 mmol), 50% aqueous sodium hydroxide (10 ml), and benzyltriethylammonium chloride (50 mg) was stirred to give an emulsion. A solution of chloroacetonitrile (0.755 g, 10.0 mmol) in benzene (5 ml) was added at such a rate that the temperature of the mixture was maintained at 30–35° (20 min). After 30 min of stirring, more chloroacetonitrile (0.378 g, 5.0 mmol) was added in benzene. After a further 30 min of stirring, the mixture was poured into water. The benzene layer was separated, washed once with water, twice with 2 *N* sulfuric acid, and once with saturated aqueous sodium chloride, dried, and stripped of solvent. The residual solid was twice crystallized from methanol (once with Norit treatment) to give **37** (2.26 g, 75%), m.p. 110–111° (lit. (18) m.p. 111°); λ_{max} ($CHCl_3$) 4.50 μ (m); δ ($CDCl_3$) 3.40 (s, 2H), 7.40 (s, 10H).

Reaction of 37 with Methylmagnesium Iodide or Methyllithium. Formation of 3,3-Diphenylacrylonitrile (38)

A solution of methylmagnesium iodide was prepared from magnesium (27 mg, 1.1 mg-at.) and methyl iodide (156 mg, 1.1 mmol) in ether (3 ml) under nitrogen. To it was added a solution of **37** (116 mg, 0.50 mmol) in ether (15 ml). The mixture was boiled under reflux for 2 h, cooled, and treated with 2 *N* sulfuric acid (5 ml). The resulting mixture was boiled under reflux for 2 h, cooled, and extracted with ether. The extract was washed twice with aqueous 10% sodium carbonate and once with saturated aqueous sodium chloride, dried, and stripped of solvent. The residue was subjected to preparative t.l.c. on silica with five elutions with 25% benzene – petroleum ether. The major fraction was a yellow gum, which on treatment with chloroform gave a small amount of solid residue. Filtration of the chloroform solution and removal of the solvent gave **38** as an oil (54 mg, 53%); λ_{max} (CCl_4) 4.51 μ; δ ($CDCl_3$) 5.73 (s, 1H); 7.3–7.5 (m, 10H).

Similar treatment of **37** (464 mg, 2.00 mmol) in tetrahydrofuran with methyllithium (2.3 mmol) in ether gave **38** as the major product together with unconsumed **37**.

2,2,4,5,5-Pentaphenyl-4-pentenonitrile (39)

A mixture of diphenylacetonitrile (276 mg, 1.43 mmol), 50% aqueous sodium hydroxide (9 ml), and benzene (10 ml) was stirred vigorously under nitrogen to give an emulsion. Benzyltriethylammonium chloride (40 mg) was added to give a deep red coloration, followed by a solution of 2,3,3-triphenylallyl bromide (28) (500 mg, 1.43 mmol) in benzene (20 ml). The red coloration was rapidly lost,[12] and stirring was continued at room temperature for 22 h. The mixture was diluted with an equal volume of water, the benzene layer was separated, and the aqueous layer was extracted twice with benzene. The combined benzene solutions were washed with water and saturated aqueous sodium chloride, dried, and stripped of solvent. The residue was recrystallized from 2-methoxyethanol to give **39** (496 mg, 75%), m.p. 215–217°. Two recrystallizations from this solvent raised the m.p. to 218.5–219°; λ_{max} (CCl_4) 4.49 μ (w); δ ($CDCl_3$) 3.73 (s, 2H), 6.9–7.3 (m, 25H); *m/e* (relative abundance) 461 (1), 270 (28), 269 (100), 193 (19), 192 (14), 191 (43), 178 (8), 165 (15).

Anal. Calcd. for $C_{35}H_{27}N$: C, 91.07; H, 5.90; N, 3.03. Found: C, 91.40; H, 5.82; N, 3.08.

Reaction of 39 with Methyllithium. Formation of 1,1,2,4,4-Pentaphenyl-1-butene (41)

A solution of **39** (335 mg, 0.73 mmol) in dry tetrahydrofuran (25 ml) under nitrogen was treated with 1.75 *M* methyllithium (1.5 ml, 2.6 mmol) in ether. The mixture was stirred at room temperature for 24 h, cooled in ice, and treated with 2 *N* sulfuric acid (6 ml). The organic layer was separated, and the aqueous layer was extracted twice with ether. The combined organic solutions were washed with aqueous 5% sodium bicarbonate and saturated aqueous sodium chloride, dried, and stripped of solvent to give crystalline **41** (307 mg, 100%), m.p. 152–152.5° after two recrystallizations from heptane; δ 3.22 (d, J = 7.5 Hz, 2H), 3.93 (t, J = 7.5 Hz, 1H), 6.6–7.4 (m, 25H); *m/e* (relative abundance) 436 (5), 269 (100), 191 (32).

Anal. Calcd. for $C_{34}H_{28}$: C, 93.53; H, 6.47. Found: C, 93.64; H, 6.47.

4-Methyl-2,2-diphenyl-4-pentenonitrile (40)

Diphenylacetonitrile (7.00 g, 36.3 mmol) in benzene (50 ml) was alkylated with methallyl chloride (3.5 g, 39 mmol), 50% aqueous sodium hydroxide (25 ml), and benzyltriethylammonium chloride (200 mg) by the procedure described for the preparation of **39** to give **40** (8.5 g, 95%) as a colorless oil, b.p. 126–127° (0.03 mm); λ_{max} (CCl_4) 4.49 (w), 6.05 μ (m); δ (CCl_4) 1.51 (m, 3H), 3.03 (br s, 2H), 4.69 (m, 1H), 4.86 (m, 1H), 7.3 (m, 10H); *m/e* (relative abundance) 247 (18), 193 (22), 192 (100), 165 (46).

Anal. Calcd. for $C_{18}H_{17}N$: C, 87.41; H, 6.93; N, 5.66. Found: C, 87.46; H, 6.93; N, 5.50.

Reaction of 40 with Methyllithium. Formation of 2-Methyl-4,4-diphenyl-1-butene (42)

A solution of **40** (192 mg, 0.78 mmol) in ether (8 ml) under nitrogen was treated with 1.75 *M* methyllithium (1 ml) in ether. The mixture was stirred for 19 h at −8 to −10°, and then treated with 2 *N* sulfuric acid (5 ml). The resulting mixture was worked-up as in the case of the corresponding reaction of **39** to give **42** as an oil (160 mg, 93%), b.p. 78–80° (0.01 mm); λ_{max} (CCl_4) 6.06 μ (m); δ (CCl_4) 1.63 (m, 3H), 2.71 (d, J = 8 Hz, 2H) 4.11 (t, J = 8 Hz, 1H), 4.55 (m, 1H), 4.64 (m, 1H), 7.2 (m, 10H).

Anal. Calcd. for $C_{17}H_{18}$: C, 91.84; H, 8.16. Found: C, 92.07; H, 8.10.

3-Oxo-2,2,3-triphenylpropionitrile (43)

Diphenylacetonitrile (965 mg, 5.00 mmol) in benzene (50 ml) was acylated with benzoyl chloride (1.405 g, 10.00 mmol), 50% aqueous sodium hydroxide (25 ml), and benzyltriethylammonium chloride (125 mg) as above, except that the reaction time was reduced to 10 min.

[12]A run that was terminated at this point showed that the loss of the red color did not signal the completion of the reaction.

Crystallization of the crude product, **43**, from methanol gave colorless prisms (955 mg, 64%), m.p. 125–127°. Recrystallization from methanol raised the m.p. to 128–129°; λ_{max} (CCl_4) 4.48 (w), 5.90 μ; λ_{max} (EtOH) 254.5 mμ (ε 12 500); δ ($CDCl_3$) 7.35 (br s, 13H), 7.8–8.0 (m, 2H); *m/e* (relative abundance) 297 (0.1), 190 (2.5), 165 (13), 106 (8), 105 (100).

Anal. Calcd. for $C_{21}H_{15}NO$: C, 84.82; H, 5.09; N, 4.71. Found: C, 85.03; H, 4.99; N, 4.79.

Attempts to ketalize and thioketalize **43** with ethylene glycol and 1,2-ethanedithiol, respectively, were unsuccessful.

We thank the National Research Council of Canada for generous support of this work. G.D.A. thanks the Province of Ontario for a Graduate Fellowship. Preliminary experiments by Dr. L. L. Williams (29) are gratefully acknowledged.

1. (*a*) P. Yates, G. D. Abrams, and S. Goldstein. J. Am. Chem. Soc. **91**, 6868 (1969). (*b*) M. J. Betts and P. Yates. J. Am. Chem. Soc. **92**, 6982 (1970).
2. P. Yates and L. L. Williams. J. Am. Chem. Soc. **80**, 5896 (1958); P. Yates, G. D. Abrams, and L. L. Williams. Tetrahedron Lett. 4341 (1969).
3. (*a*) P. Yates and T. J. Clark. Tetrahedron Lett. 435 (1961). (*b*) W. Reid and H. Mengler. Ann. **651**, 54 (1962).
4. A. S. Kende. Chem. Ind. (Lond.), 1053 (1956).
5. R. E. Rosenkranz, K. Allner, R. Good, W. von Philipsborn, and C. H. Eugster. Helv. Chim. Acta, **46**, 1259 (1963); A. Hofmann, W. von Philipsborn, and C. H. Eugster. Helv. Chim. Acta, **48**, 1322 (1965); G. Casnati, A. Quilico, A. Ricca, and P. Vita Finzi. Gazz. Chim. Ital. **96**, 1073 (1966).
6. E. D. Bergmann and Y. Hirshberg. Bull. Soc. Chim. Fr. [5] **17**, 1091 (1950).
7. R. E. Lutz and J. O. Weiss. J. Am. Chem. Soc. **77**, 1814 (1955).
8. E. Grovenstein, Jr., and L. C. Rogers. J. Am. Chem. Soc. **86**, 854 (1964), and earlier references quoted therein; H. E. Zimmerman and A. Zweig. J. Am. Chem. Soc. **83**, 1196 (1961); H. E. Zimmerman and F. J. Smentowski. J. Am. Chem. Soc. **79**, 5455 (1957).
9. R. B. Woodward and R. Hoffmann. The conservation of orbital symmetry. Academic Press, Inc., New York, N.Y., 1970.
10. N. F. Phelan, H. H. Jaffé, and M. Orchin. J. Chem. Educ. **44**, 626 (1967).
11. U. Schöllkopf, U. Ludwig, G. Ostermann, and M. Patsch. Tetrahedron Lett. 3415 (1969).
12. (*a*) P. T. Lansbury, V. A. Pattison, J. D. Sidler, and J. B. Bieber. J. Am. Chem. Soc. **88**, 78 (1966). (*b*) H. Schäfer, U. Schöllkopf, and D. Walter. Tetrahedron Lett. 2809 (1968); J. E. Baldwin, J. Debernardis, and J. E. Patrick. Tetrahedron Lett. 353 (1970).
13. A. Nickon and J. L. Lambert. J. Am. Chem. Soc. **84**, 4604 (1962); A. Nickon, H. Kwasnik, T. Swartz, R. O. Williams, and J. B. Digorgio. J. Am. Chem. Soc. **87**, 1615 (1965); R. Howe and S. Winstein. J. Am. Chem. Soc. **87**, 915 (1965); T. Fukunaga. J. Am. Chem. Soc. **87**, 916 (1965).
14. J. P. Freeman and J. H. Plonka. J. Am. Chem. Soc. **88**, 3662 (1966).
15. R. B. Woodward and E. G. Kovach. J. Am. Chem. Soc. **72**, 1009 (1950).
16. (*a*) C. F. Koelsch and T. A. Geissman. J. Org. Chem. **3**, 480 (1938). (*b*) J. M. Dunston. Ph.D. Thesis. University of Toronto, Toronto, Ontario, 1965; P. Bladon, S. McVey, P. L. Pauson, G. H. Broadhead, and W. M. Horspool. J. Chem. Soc. C, 306 (1966).
17. P. Yates and M. J. Betts. To be submitted for publication.
18. J. Lange and M. Makosza. Roczniki Chem. **41**, 1303 (1967); Chem. Abstr. **68**, 29374 (1968).
19. Ramart-Lucas and F. Salmon-Legagneur. Bull. Soc. Chim. Fr. [4] **43**, 321 (1928); F. F. Blicke and E.-P. Tsao. J. Am. Chem. Soc. **75**, 5587 (1953).
20. L. I. Smith and H. H. Hoehn. Org. Synth. Coll. Vol. 3, 356 (1955).
21. P. Yates and B. L. Shapiro. J. Am. Chem. Soc. **81**, 212 (1959).
22. R. Huisgen and L. A. Feiler. Chem. Ber. **102**, 3391 (1969).
23. P. E. Verkade and E. F. J. Janetzky. Rec. trav. chim. **62**, 775 (1943).
24. R. Fosse. Compt. Rend. **145**, 1290 (1908).
25. F. Salmon-Legagneur. Bull. Soc. Chim. Fr. [5] **19**, 580 (1952).
26. H. Rupe and E. Busolt. Ber. **40**, 4537 (1907).
27. D. Vorländer and C. Siebert. Ber. **39**, 1024 (1906).
28. R. O. C. Norman and C. B. Thomas. J. Chem. Soc. B, 598 (1967).
29. L. L. Williams. Ph.D. Thesis. Harvard University, Cambridge, Mass., 1961.

Can. J. Chem. Downloaded from www.nrcresearchpress.com by 210.87.254.42 on 09/05/12
For personal use only.

Can. J. Chem. Downloaded from www.nrcresearchpress.com by 210.87.254.42 on 09/05/12
For personal use only.

Temperature Dependence of Disproportionation–Combination Ratios for Alkyl Radicals in Liquid Methane[1,2]

HUGH A. GILLIS

Division of Physics, National Research Council of Canada, Ottawa, Canada[3]

and

Radiation Research Laboratories, Mellon Institute, Carnegie-Mellon University, Pittsburgh, Pa. 15213

Received February 16, 1971

The ratios of rate constants for disproportionation to combination have been measured for ethyl radicals and for *i*-propyl radicals in liquid methane between −181 and −94 °C. The radicals were generated by γ-radiolysis of dilute methane solutions of ethylene-d_4 or propylene-d_6. The activation energy for combination was found to exceed that for disproportionation by 290 ± 30 cal mol^{-1} for ethyl radicals and by 255 ± 25 cal mol^{-1} for *i*-propyl radicals. In both cases the disproportionation–combination ratio in the liquid, extrapolated to room temperature, is greater than that in the gas phase by a factor of about 2.5. These results are interpreted as indicating that disproportionation and combination reactions proceed by way of different transition states.

Les rapports des constantes de vitesse dismutation sur combinaison ont été mesurés pour les radicaux éthyles et *i*-propyles dans le méthane liquide entre −181 et −94 °C. Ces radicaux ont été engendrés par radiolyse-γ de solutions d'éthylène-d_4 ou de propylène-d_6 dans le méthane. L'énergie d'activation pour la combinaison s'est averée dépasser celle de dismutation par 290 ± 30 cal mol^{-1} pour les radicaux éthyles et par 255 ± 25 cal mol^{-1} pour les radicaux *i*-propyles. Dans les deux cas, le rapport dismutation sur combinaison dans le liquide, extrapolé à la température de la pièce, dépasse par un facteur d'environ 2.5 celui obtenu en phase gazeuse. L'interprétation de ces résultats indiquent que les réactions de dismutation et de combinaison se font par passage par des états de transition différents.

Canadian Journal of Chemistry, 49, 2861 (1971)

Introduction

Measurements of ratios of rate constants for disproportionation to combination (k_d/k_c) of alkyl radicals in a liquid at various temperatures are of interest for two principal reasons: (*a*) They are important in photochemical and radiation chemical studies on liquid hydrocarbons at low temperatures in deducing radical yields from final product yields; (*b*) They should give some information about the nature of the transition state(s) involved in these reactions. One of the main reasons for proposals that the same transition state is involved in the two reactions is that several authors concluded that these ratios remain constant within experimental error over a wide temperature range in the gas phase.[4]

In an earlier study (3) liquid methane was γ-irradiated in the pure state and with small amounts of added ethylene or propylene at a single temperature, −161 °C. The effects of these olefins on the major products were interpreted by a simple hydrogen atom scavenging mechanism. The k_d/k_c ratios for both the reaction of two ethyl radicals and the reaction of two isopropyl radicals were found to be much higher than gas phase values. In the present study k_d/k_c ratios for these radical pairs were determined from product yields over almost the whole temperature range at which methane is a liquid with the object of measuring any difference in activation energies. Deuterated olefins were used with the expectation that isotopic analysis would reveal whether there are contributions to the yields of the disproportionation and combination products from other reactions. Also it was hoped that the isotope effect in the disproportionation reaction could be measured.

Experimental

Materials

Matheson research grade methane (minimum purity 99.99 mol %) was treated in an effort to remove traces of water, ethane, and higher hydrocarbons. It was first passed through a trap containing thoroughly degassed silica gel at −120 °C. The last 20% was discarded. It was then passed through a spiral trap at −159 °C

[1]Supported in part by the U.S. Atomic Energy Commission.

[2]NRCC No. 12117.

[3]Present address

[4]See the tabulation of estimates of k_d/k_c for ethyl radicals at various temperatures in ref. 1; see also ref. 2.

Can. J. Chem. Downloaded from www.nrcresearchpress.com by 210.87.254.42 on 09/05/12
For personal use only.

packed with glass wool. Analysis of this purified methane by gas chromatography and mass spectrometry gave the following upper limits: O_2, 7; C_2H_4, 0.02; C_2H_6, 0.02; C_3H_8, 0.01 p.p.m.

Ethylene-d_4 and propylene-d_6 were obtained from Merck, Sharpe and Dohme and used as received except that they were pumped on at −196 °C.

Irradiation Conditions

A sample of 0.29 g in a glass cell was positioned in a Dewar flask in the irradiation chamber of a Co^{60} source. At the highest temperature about 2%, and at lower temperatures somewhat less, of the sample was in the gas phase. Sample temperatures of −94, −129, −161, and −181 °C were achieved by the use of a frozen toluene slush, a frozen *n*-pentane slush, boiling methane, and boiling oxygen (at a pressure about 15 cm above atmospheric), respectively, in the Dewar flask. The temperature was monitored during an irradiation with a thermocouple.

Two different Gammacell Co^{60} sources used provided dose rates of approximately 1.5×10^{18} and 1.0×10^{18} eV g^{-1} min^{-1}. Dose rates were determined by Fricke dosimetry with water in the Dewar flask, and dose rates for the samples were calculated by applying corrections for the electron density of the methane and the refrigerant. Only ratios of yields are of significance in this work so that exact doses are unimportant. Samples were given doses in the range $1.5–3.1 \times 10^{20}$ eV g^{-1}.

Product Analyses

Hydrocarbons were analyzed by gas chromatography in the same manner as in the previous study (3) with an F and M 5750 instrument equipped with a splitter, dual thermal conductivity and dual hydrogen flame detectors. Separated products were often trapped for mass spectrometric analysis at the exit of the thermal conductivity detector.

Isotopic analyses of various deuterated products were made mass spectrometrically. Analyses of products from solutions of C_3D_6 in CH_4 were performed at Mellon Institute on a Consolidated Model 21-101 instrument. Cracking patterns and sensitivities for detection of C_3D_8 and C_3H_8 were obtained by the use of authentic samples. The patterns obtained by Scala *et al.* (4) were used for C_3HD_7 (assumed to be $CD_3CD_2CHD_2$) and $C_3H_2D_6$ (assumed to be $CD_3CHDCHD_2$). Sensitivities for C_3HD_7 and $C_3H_2D_6$ were obtained by interpolation between those for C_3D_8 and C_3H_8.

Isotopic analyses of product ethanes from solutions of C_2D_4 in CH_4 were performed at the National Research Council of Canada, Ottawa, on an Atlas CH_4 mass spectrometer at an ionizing voltage of 14 eV with the use of calibrations obtained by Amenomiya and Pottie (5). The spectra of the propane and *n*-butane products from these solutions were also determined by this method. The percentages of $C_3H_3D_5$ in the propane and *n*-C_4HD_9 in the *n*-butane were calculated from the parent peaks, and the qualitative conclusions about relative contributions of other isotopic species given below in Results and Discussion were deduced.

Results and Discussion

Propylene-d_6 Solutions

The main radical reactions in this system are expected to be:

[1] $CH_4 \rightsquigarrow H, CH_3$

[2] $H + C_3D_6 \rightarrow CHD_2CDCD_3$

[3] $CH_3 + CHD_2CDCD_3 \rightarrow CHD_2CD(CH_3)CD_3$

[4] $\rightarrow CH_3D + C_3HD_5$

[5] $\rightarrow CH_4 + C_3D_6$

[6] $2CHD_2CDCD_3 \rightarrow$ Diisopropyl-d_{12}

[7] $\rightarrow CHD_2CD_2CD_3 + C_3HD_5$

[8] $\rightarrow CHD_2CHDCD_3 + C_3D_6$

The results in Table 1 show that the main isotopic propane species are C_3HD_7 and $C_3H_2D_6$ as expected from the above reactions. The effect of oxygen, added at a concentration such that it should scavenge most free radicals but not react otherwise to a significant extent (6), is to reduce the isobutane, diisopropyl, and propane yields to practically zero.[5] The small residual yields of C_3H_8 and C_3D_8 indicate approximately 30% non-radical contribution to these products. The remainder of the C_3H_8 must come from the reaction of C_2H_5 with CH_3. Independent evidence that there is a small yield of C_2H_5 radicals, in the absence of O_2, came from mass spectrometric analysis of the *i*-pentane from one of the runs at −129.5 °C, which showed that it is at least mainly $CH_3CH_2CD(CHD_2)CD_3$, and presumably results from a combination reaction of C_2H_5 with CHD_2CDCD_3. In the earlier work (3) it was suggested that *i*-pentane could result from the addition of methyl radicals to propylene followed by the reaction of the resulting sec-butyl radicals with methyl radicals. However that would produce $CH_3CD_2CD(CH_3)CD_3$, rather than the species found, and hence cannot be important.[6]

[5]It has been shown (3) that some of the ethane produced in a solution containing oxygen comes from the insertion reactions of methylene radicals into methane, and the rest probably is produced by the combination of methyl radicals in spurs. The possibility that methylene radicals could be complicating the system by preferentially reacting with the added olefin was considered, and rejected because in the experiments with ethylene solutions, the most likely products of such reactions, cyclopropane and propylene, were found to be insignificant.

[6]The API spectrum for undeuterated *i*-pentane gives the peak at mass 43 as the largest, and the peak at mass 57 is the largest in the C_4 region with an intensity of 54.5% of the 43. Therefore $CH_3CD_2CD(CH_3)CD_3$ would be expected to give peaks at masses 60 and 63 of

TABLE 1. Product yields from solutions of C_3D_6 in CH_4

T °C	−94.4	−94.4	−129.5	−129.5	−161	−161	−181	−181
Average mol % C_3D_6	0.056	0.062	0.037	0.071	0.058	0.069*	0.109	0.070
$G(C_2H_4)$	0.18	0.22	0.22	0.24	0.25	0.14	0.26	0.26
$G(C_2H_6)$	1.97	1.87	1.89	1.81	1.86	0.71	1.86	1.87
$G(-C_3D_6)$	8.4	8.6	5.1	5.9	4.3	7.5	4.3	4.0
$G(C_3HD_5)$	0.57	0.61	0.59	0.59	0.70	0.03	0.78	0.79
$G(C_3D_8)$	0.113	0.116	0.053	0.056	0.033	0.010	0.030	0.026
$G(C_3HD_7)$	0.596	0.628	0.416	0.441	0.426	0.005	0.377	0.407
$G(C_3H_2D_6)$	0.233	0.232	0.178	0.159	0.155	0.003	0.119	0.137
$G(C_3H_8)$	0.059	0.054	0.065	0.046	0.057	0.016	0.107	0.051
G(*i*-Butane)	1.15	1.31	0.95	0.94	0.72	0.003	0.56	0.57
G(*n*-Butane)	0.039	0.045	0.024	0.022	0.014	0.002	0.012	0.011
G(*i*-Pentane)	0.046	0.042	0.043	0.033	—	0.001	0.016	—
G(Diisopropyl)	0.425	0.427	0.241	0.250	0.174	0.001	0.130	0.131
k_d/k_c	2.14	2.20	2.62	2.55	3.47	—	3.98	4.29
%D	10.2	9.7	6.4	7.5	4.2	—	4.8	3.6
k_H/k_D	1.46	1.38	1.41	1.25	1.04	—	1.01	1.04

*Also contained 0.50 mol % O_2.

For the reaction of two *i*-propyl radicals, k_d/k_c should be given by $[0.7\,G(C_3D_8) + G(C_3HD_7) + G(C_3H_2D_6)]/G$(diisopropyl).These ratios are given in Table 1, and the points are shown on an Arrhenius plot in Fig. 1. The slope of the line corresponds to a difference in activation energies, $E_c - E_d = 255 \pm 25$ cal mol^{-1}. The extrapolated k_d/k_c at room temperature is 1.63 ± 0.12, as compared to the gas phase value of 0.69 (7).

The results in Table 1 show that consumption of C_3D_6 is somewhat greater than can be accounted for by the propane, *i*-butane and diisopropyl products, despite the fact that the fraction of energy absorbed directly by the solute must be negligible. Also mass spectrometric analysis of the *i*-butane product showed that although most of it is the expected *i*-butane-d_6, a significant fraction of it is *i*-butane-d_7, which must result from the addition to C_3D_6 of D atoms from decomposition of C_3D_6, followed by reaction of the *i*-C_3D_7 with CH_3. For each experiment the %D (yield of D atoms divided by the total yield of H plus D atoms) was calculated from this *i*-butane data, and these are given in Table 1. Some of the C_3D_8 must come from the disproportionation of *i*-C_3D_7 radicals.

about equal intensity as the largest C_4 peaks, and a large peak at mass 47 and no significant peak at 49. On the other hand $CH_3CH_2CD(CHD_2)CH_3$ should give peaks at 60 and 61 of approximately equal intensity as the largest peaks in the C_4 region and a very large 49 peak. The mass spectrum of the product *i*-pentane shows that the peak at mass 49 is the largest in the spectrum, and peaks at masses 60, 61, and 63 are 31, 28, and 4%, respectively, of the 49 peak. Therefore this *i*-pentane is at least mainly $CH_3CH_2CD(CHD_2)CD_3$.

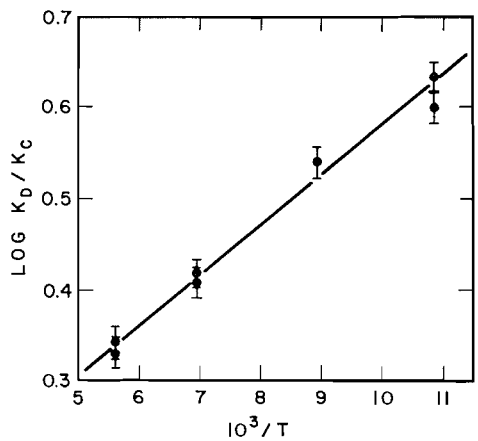

FIG. 1. Arrhenius plot of k_d/k_c ratios for the mutual reaction of *i*-propyl-d_6 radicals in liquid methane.

In the radiolysis of solutions of ethylene-d_4 in liquid ethane it was found that decomposition of the solute to give D_2 and D became increasingly important as the concentration of solute was raised, and this effect was ascribed to a charge transfer reaction (6). In a solution of C_3D_6 in methane a transfer of charge to C_3D_6, followed by neutralization of $C_3D_6^+$ and decomposition of the highly excited C_3D_6, would similarly account for the extra consumption of C_3D_6 and the production of D atoms. The occurrence of such reactions would not change the interpretation that the deuterated propanes and diisopropyl originate only in the disproportionation and combination of *i*-propyl radicals.

Originally it was hoped that both the isotope effect (k_H/k_D) in the disproportionation of two

Can. J. Chem. Downloaded from www.nrcresearchpress.com by 210.87.254.42 on 09/05/12
For personal use only.

Can. J. Chem. Downloaded from www.nrcresearchpress.com by 210.87.254.42 on 09/05/12
For personal use only.

i-C_3HD_6 radicals, and k_d/k_c for the reaction of CH_3 and i-C_3HD_6 could be measured in these experiments. The former can be calculated to a first approximation from the relationship

$$\frac{k_H}{k_D} = 5\frac{G(C_3H_2D_6)}{G(C_3HD_7)}$$

which is based on the assumption that H or D atoms are transferred only from the methyl groups. The k_d/k_c ratio for the reaction of CH_3 and i-C_3HD_6 would be inferred from the yield of propylene-d_5 after subtracting the amount produced in reaction 7, and the yield of i-butane. However for both calculations corrections have to be made for the following: (*a*) the appreciable yield of D atoms which give i-C_3D_7 radicals; (*b*) the considerable consumption of C_3D_6, and production and consumption of C_3HD_5; (*c*) the isotopic impurity in the C_3D_6. It turns out that these corrections make it impossible to estimate k_d/k_c for the reaction of CH_3 with i-C_3HD_6 radicals. Estimates of k_H/k_D for the disproportionation of two i-C_3HD_6 radicals after the above corrections were made are given in Table 1. Because of the magnitude of the corrections these estimates are possibly quite inaccurate, and in particular the change with temperature may not be significant.

Ethylene-d_4 Solutions

The results obtained by irradiating ethylene-d_4 solutions at various temperatures are shown in Table 2. The main radical reactions in this system are expected to be [1] and

[9] $H + C_2D_4 \rightarrow CHD_2CD_2$

[10] $CH_3 + CHD_2CD_2 \rightarrow CH_3CD_2CHD_2$

[11] $\rightarrow CH_3D + C_2HD_3$

[12] $\rightarrow CH_4 + C_2D_4$

[13] $2CHD_2CD_2 \rightarrow n$-$CHD_2CD_2CD_2CHD_2$

[14] $\rightarrow CHD_2CD_3 + C_2HD_3$

[15] $\rightarrow CHD_2CHD_2 + C_2D_4$

The low-voltage mass spectrum of the n-butane product indicates that the largest component is n-$C_4H_2D_8$, the product of reaction 13, with smaller amounts of n-C_4HD_9 and n-$C_4H_3D_7$ and a maximum of 2% n-C_4H_{10}. Small amounts of other deuterated species would not have been seen. The low-voltage mass spectrum of propane shows that the main component is $C_3H_4D_4$, the product of reaction 10, with smaller amounts of $C_3H_3D_5$ and $C_3H_5D_3$. The maximum C_3H_8 content ranges from 5.0% at −94.4 °C to 8.5% at −181 °C. The n-C_4HD_9 and $C_3H_3D_5$ must result from the sequence of D atoms adding to C_2D_4, and the resulting C_2D_5 radicals combining with either C_2HD_4 or CH_3 radicals. The percentage of D atoms in the total of H + D atoms was calculated for both the propane and n-butane products, and at all temperatures agreement is within 10%. The average values are given in Table 2. As with the CH_4–C_3D_6 solutions, the production of D atoms is accompanied by a greater consumption of C_2D_4 than can be accounted for by reaction 9, and the yield of D atoms is higher at higher temperatures and concentrations. The product $C_3H_5D_3$ and n-$C_4H_3D_7$ must result from addition of H atoms to C_2HD_3, present as an isotopic impurity in the C_2D_4 and also produced by reactions 11 and 14, followed by combination of the $C_2H_2D_3$ radicals with CH_3 and C_2HD_4 radicals. The percent C_2HD_3 calculated on this basis from the product n-$C_4H_3D_7$ agreed well with direct analyses of C_2HD_3 in the C_2D_4 that were done for three of the experiments in Table 2.

Isotope effects in the disproportionation reaction of two ethyl radicals were calculated at different temperatures in an analogous fashion as for two i-C_3HD_6 radicals, from the measured ratios of C_2HD_5 to $C_2H_2D_4$, and the percentages of H and D atoms, and C_2D_4 and C_2HD_3. Values found for k_H/k_D are given in Table 2. Again these are expected to be rather imprecise ($\pm$0.25). These calculations also indicate that about half of the product C_2D_6 can be accounted for by disproportionation of C_2D_5 radicals; the origin of the rest is unknown.

For the reaction of two ethyl radicals, k_d/k_c should be given by $[0.5\,G(C_2D_6) + G(C_2HD_5) + G(C_2H_2D_4) + G(C_2H_3D_3)]/G(n\text{-butanes})$. These ratios are given in Table 2, and the points are shown on an Arrhenius plot in Fig. 2. The slope of the line corresponds to a difference in activation energies, $E_c - E_d = 290 \pm 30$ cal mol^{-1}. The extrapolated k_d/k_c at room temperature is 0.34 ± 0.05, as compared to the gas phase value of 0.13 (7). It is noteworthy that this ($E_c - E_d$) is very similar to that obtained for i-propyl radicals, and also that the extrapolated k_d/k_c for the liquid at room temperature is 2.6 and 2.4 times the gas phase value for i-propyl and ethyl radicals, respectively.

TABLE 2. Product yields from solutions of C_2D_4 in CH_4

T °C	−94.4	−129.5	−129.5	−161	−181
Average mol % C_2D_4	0.085	0.092	0.036	0.089	0.093
$G(-C_2D_4)$	11.5	7.5	6.2	5.8	5.2
$G(C_2D_6)$	0.058	0.029	0.022	0.013	0.016
$G(C_2HD_5)$	0.282	0.247	0.216	0.193	0.229
$G(C_2H_2D_4)$	0.156	0.168	0.172	0.146	0.147
$G(C_2H_3D_3)$	0.016	0.011	0.017	0.012	0.008
$G(C_2H_6)$	1.90	2.06	1.98	2.03	2.05
G(Propanes)	2.08	1.65	1.52	1.30	1.12
G(*n*-Butanes)	1.09	0.69	0.64	0.49	0.39
k_d/k_c	0.44	0.64	0.65	0.73	1.01
%D	9.7	7.0	5.1	2.8	2.9
k_H/k_D	1.38	1.47	1.75	1.55	1.24

Comparison with Other Work

The conclusion that can be drawn from this work is that k_d/k_c ratios for alkyl radicals depend both on temperature and phase; $E_c - E_d \simeq 270$ cal mol^{-1}, and the extrapolated ratios at room temperature are higher in the liquid than those reported for the gas phase. Similar conclusions have been reached by some of the authors who have reported on these problems. Thus Dixon *et al.* (8) found that k_d/k_c for ethyl radicals reacting in a cage in liquid isooctane is proportional to $T^{-0.86}$, which corresponds to $E_c - E_d \simeq 400$ cal mol^{-1}. For ethyl radicals in liquid methane at −184° they found $k_d/k_c = 0.35$, which is much lower than the value of 1.01 found in this work. For ethyl radicals in liquid isooctane at 65° they reported $k_d/k_c = 0.14$, which is the same as the gas phase value. Sheldon and Kochi (9) found k_d/k_c for ethyl radicals of 0.15 and 0.12 in *n*-pentane and decalin at 30°, which is essentially the same as the gas phase value.[7] For *i*-propyl radicals in decalin at 30° they obtained 1.2, which is almost twice what is probably the best gas phase value (7). Bakale and Gillis (6) found $k_d/k_c = 0.41 \pm 0.06$ for C_2HD_4 radicals in liquid ethane at −78 °C; this point would fit well on Fig. 2. Klein *et al.* (10) measured disproportionation and combination products from the reaction of isopropyl radicals produced in the photolysis of solid and gaseous azoisopropane over the temperature range 77–380 °K. The points for both the gas and solid phase experiments fitted reasonably on the same Arrhenius plot, the slope of which gave $E_c - E_d = 260 \pm 25$ cal mol^{-1}. However the interpretation of these experiments is clouded by the fact that at 77 °K k_d/k_c was 2, in contrast to the value of 9 measured at this temperature by the same authors for an experiment involving hydrogen atom addition to solid propylene (11).

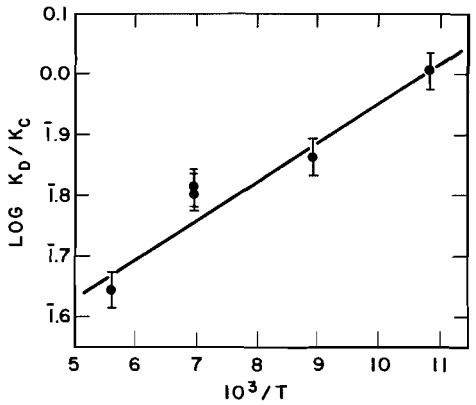

FIG. 2. Arrhenius plot of k_d/k_c ratios for the mutual reaction of ethyl-d_4 radicals in liquid methane.

It has been pointed out by one of the referees that the isotope effect in disproportionation found in this work indicates that k_d/k_c ratios might be quite sensitive to isotopic substitution, and therefore direct comparisons of k_d/k_c ratios for CHD_2CDCD_3 and C_2HD_4 radicals with those found for the corresponding undeuterated species in other laboratories might not be meaningful. Unfortunately the origin of the isotope effect is not known. If the transition states for disproportionation and combination are different, then the isotope effect seen here

[7]It might be expected that the reason for the higher values of k_d/k_c in this study as compared to that of Dixon *et al.* (8) is that reaction took place in a solvent cage in the latter, whereas in the present work the ethyl and *i*-propyl radicals are free in solution. However from their observation that the values of k_d/k_c for a number of alkyl radicals were the same in various solvents in which the percentages of radicals reacting in a cage were different, Sheldon and Kochi (9) concluded that k_d/k_c ratios for alkyl radicals in a cage are essentially the same as for those free in solution.

Can. J. Chem. Downloaded from www.nrcresearchpress.com by 210.87.254.42 on 09/05/12
For personal use only.

Can. J. Chem. Downloaded from www.nrcresearchpress.com by 210.87.254.42 on 09/05/12
For personal use only.

must be in the disproportionation reaction. If k_H/k_D is taken as 1.3, from Table 1, then k_d/k_c should be at most 24% larger for CH_3CHCH_3 than for CHD_2CDCD_3. However if only one transition state is involved, then the isotope effect could really be an inverse secondary effect on the combination reaction, and k_d/k_c might be larger for CH_3CHCH_3 than for CHD_2CDCD_3 by somewhat more than 24%. The results of the earlier study (3) on the radiolysis of liquid methane have a direct bearing on this question. In that investigation k_d/k_c was measured at -161 °C for CH_3CHCH_2D radicals, produced from solutions of C_3H_6 in CD_4. The average k_d/k_c from three experiments, recalculated on the same basis as used here, was 3.3 as compared to 3.5 in the present study. This strongly indicates that in fact k_d/k_c ratios are not influenced by isotopic substitution to an extent greater than the combined error limits of approximately 25%.

One might expect that there should also be an effect of temperature on k_d/k_c in the gas phase. A recent study by Reid and LeRoy (12) concluded tentatively that $E_c - E_d = -900$ cal mol^{-1} for ethyl radicals in the gas phase, and a paper by James and Suart (13) reported that $E_c - E_d = 250$ cal mol^{-1} for the mutual interaction of tert-butyl radicals. Konar (14) treated literature data by the thermodynamic formulation of reaction rates, and concluded that E_c is probably not equal to E_d for all alkyl radicals. But many experimental studies have concluded that k_d/k_c is independent of temperature within experimental error (1, 2). However the ranges of $\Delta(1/T)$ covered in the gas phase studies were much smaller than in this work, so the small $E_c - E_d$ found here would not have been seen easily. Thus the range 25–225 °C covered in a study by James and Steacie (15) corresponds to $\Delta(1/T) = 1.35 \times 10^{-3}$, as compared to $\Delta(1/T) = 5.26 \times 10^{-3}$ in this study.

Significance of Nonzero $E_c - E_d$

The most straightforward interpretation of a finite $(E_c - E_d)$ and a phase effect on k_d/k_c is simply that disproportionation and combination proceed by way of different transition states and although both activation energies are small, that for combination is about 270 cal mol^{-1} larger. These results are compatible with the proposal by Benson (16) that both reactions involve transition states with considerable ionic character, but the transition states are different, and there could be more contribution from ionic states to the transition state for disproportionation. Solvation in the liquid phase, even in a nonpolar liquid like methane, would therefore be expected to favor disproportionation.

Stefani (17) measured k_d/k_c ratios for ethyl radicals at 65 °C in ten different solvents covering a range of polarities, from isooctane to ethylene glycol. He found that the log of k_d/k_c is a linear function of the square root of the internal pressure of the solvent. He applied equations developed by Hildebrand and Scott (18*a*) to describe thermodynamic properties of regular solutions, and concluded that the solvent polarity effect is due to a larger internal pressure of the transition state for combination as compared to the internal pressure of the transition state for disproportionation. Also he concluded that the dependence of k_d/k_c on temperature in condensed phases is due to the effect of temperature on the internal pressure of the solvent, and not due to a real difference in activation energies. As indicated above, k_d/k_c for ethyl radicals in isooctane at 65 °C is much lower than any of the values reported here, although the internal pressures are comparable. Nevertheless the log of k_d/k_c taken from Fig. 2 was plotted against the square root of internal pressure of methane over the temperature range -168 to -126 °C for which the internal pressures of methane are available (19). The slope obtained, with internal pressure in atmospheres, was 20×10^{-3}, as compared to a slope of 4.76×10^{-3} obtained by Stefani. It must be concluded that the results of this work are not explicable by Stefani's treatment. A more general criticism of Stefani's treatment is that, as Hildebrand and Scott (18*b*) point out, the use of solubility parameters (the solubility parameter, δ, is the square root of the internal pressure) for polar molecules is somewhat questionable, unless the dipole is reasonably well buried within the molecule. Further, they indicate that temperature corrections for δ are of little value because the solubility parameter equations are rather crude approximations. Hence it must be considered that Stefani's explanation of the temperature and phase effects on k_d/k_c is rather dubious.

The author is very grateful to Dr. R. F. Pottie and Mr. R. L. Sander of the National Research Council of Canada for doing mass spectrometric analyses.

1. D. P. DINGLEDY and J. G. CALVERT. J. Am. Chem. Soc. **85**, 856 (1963).
2. J. A. KERR and A. F. TROTMAN-DICKENSON. *In* Progress in reaction kinetics. Vol. 1. *Edited by* G. Porter. Pergamon Press, London, 1961. p. 105.
3. H. A. GILLIS. J. Phys. Chem. **71**, 1089 (1967).
4. A. A. SCALA, S. G. LIAS, and P. AUSLOOS. J. Am. Chem. Soc. **88**, 5701 (1966).
5. Y. AMENOMIYA and R. F. POTTIE. Can. J. Chem. **46**, 1735 (1968).
6. G. BAKALE and H. A. GILLIS. J. Phys. Chem. **73**, 2178 (1969).
7. J. O. TERRY and J. H. FUTRELL. Can. J. Chem. **45**, 2327 (1967).
8. P. S. DIXON, A. P. STEFANI, and M. SZWARC. J. Am. Chem. Soc. **85**, 2551 (1963).
9. R. A. SHELDON and J. K. KOCHI. J. Am. Chem. Soc. **92**, 4395 (1970).
10. R. KLEIN, M. D. SCHEER, and R. KELLEY. J. Phys. Chem. **68**, 598 (1964).
11. R. KLEIN, M. D. SCHEER, and J. G. WALLER. J. Phys. Chem. **64**, 1249 (1960).
12. L. E. REID and D. J. LEROY. Can. J. Chem. **46**, 3275 (1968).
13. D. G. L. JAMES and R. D. SUART. Trans. Faraday Soc. **65**, 175 (1969).
14. R. S. KONAR. Int. J. Chem. Kinet. **2**, 419 (1970).
15. D. G. L. JAMES and E. W. R. STEACIE. Proc. Roy. Soc. (Lond.), A**244**, 289 (1958).
16. S. W. BENSON. *In* Advances in photochemistry. Vol. 2. *Edited by* W. A. Noyes, Jr., G. S. Hammond, and J. N. Pitts, Jr. Interscience Publishers, New York, N.Y. 1964. p. 1.
17. A. P. STEFANI. J. Am. Chem. Soc. **90**, 1694 (1968).
18. (*a*) J. H. HILDEBRAND and R. L. SCOTT. Regular solutions. Prentice-Hall, Inc., Englewood Cliffs, N.J., 1962. (*b*) pp. 169-170.
19. D. S. CHOI and M. S. JHON. Chem. Phys. Lett. **5**, 57 (1970).

Can. J. Chem. Downloaded from www.nrcresearchpress.com by 210.87.254.42 on 09/05/12
For personal use only.

Can. J. Chem. Downloaded from www.nrcresearchpress.com by 210.87.254.5 on 09/05/12
For personal use only.

Spectroscopic Evidence for the Formation of the Mercurous Ion in Irradiated Acetates

R. S. Eachus and F. G. Herring
Chemistry Department, University of British Columbia, Vancouver 8, British Columbia

Received February 25, 1971

The Hg(I) center has been produced by γ-irradiation both in Hg(II) doped cadmium acetate trihydrate and pure mercuric acetate. Both electron paramagnetic resonance and optical spectroscopy have been used to identify this species. The results indicate that the Hg(I) ion is produced in a covalent environment.

La formation de Hg(I) est produite par l'irradiation-γ à la fois de Hg(II) additionné d'acétate de cadmium trihydraté et d'acétate mercurique pur. Cette espèce a été identifiée à la fois par résonance paramagnétique électronique et par spectroscopie optique. Les résultats indiquent que l'ion Hg(I) est produit dans un environnement covalent.

Canadian Journal of Chemistry, 49, 2868 (1971)

Introduction

The effect of crystal structure on the production of radicals in irradiated acetates has been the subject of a recent publication (1). At 77 °K, the hydrated metal acetates gave methyl radicals as the primary product, whereas the anhydrous salts gave other species, usually the $CH_2CO_2^-$ radical. The products of C—C bond rupture are stabilized by the hydrogen bond network present in hydrated salts. In this study the effect of the metal ion was ignored. However, recent results (2–4) have indicated that the metal ions can play an important role in the radiolysis of their salts. For example, it was necessary to invoke cation-involvement to account for the unusual electron paramagnetic resonance (e.p.r.) spectra exhibited by polycrystalline Group IB and IIB metal carbonates and nitrates exposed to γ-rays (2). The species $(CdCO_3)^-$, $(Ag_2CO_3)^-$, $(CdNO_3)$, and $(AgNO_3)^-$, essentially covalent entities, were identified. Also, we recently reported that the exposure of the double salt $CaCd(CH_3.CO_2)_4 6H_2O$ to γ-rays at 77 °K resulted in the formation of Cd(I) and the methyl radical; on warming these centers decayed to produce the acetate fragment, $CH_2CO_2^-$ (3, 4). It would appear that the formation of low oxidation states of the metal ion, on irradiation, will occur when the cation present in the undamaged crystal has a high inelastic scattering cross section for electrons. The present investigation forms part of a comprehensive examination of the role of metal ions, which have high electron-capture cross-sections in radiation damage processes.

We wish to report the formation of the Hg(I) ion in single crystals of cadmium acetate dihydrate containing mercuric acetate as a substitutional impurity. Rogers and Kispert (1) reported that the exposure of pure mercuric acetate to high energy radiation gave paramagnetic species which were responsible for a very asymmetric e.p.r. pattern. These radicals were not identified. We have reexamined this e.p.r. spectrum and, in the light of the data obtained from Hg(II) doped in $Cd(CH_3CO_2)_2.2H_2O$, identify the principle products as $CH_2CO_2^-$ and the mercurous ion, no methyl radicals are formed in the anhydrous mercuric acetate.

The mercurous ion was first thought to have been isolated in a γ-irradiated aqueous glass containing a mercuric salt (5). Identification was based upon the observation of a single asymmetric line in the e.p.r. spectrum of the glass. The tail of a weak optical absorption (λ_{max} below 240 nm) has also been observed in a sulfuric acid glass which was tentatively assigned to the Laporte forbidden $^2D_{3/2} \leftarrow {}^2S_{1/2}$ transition in Hg(I). More convincing evidence for the existence of Hg(I) from radiation studies of acidic glasses containing Hg(II) has recently been presented (7). The detection of weak hyperfine features associated with the magnetic ^{199}Hg and ^{201}Hg isotopes established the identity of the species.

We have endeavored to relate optical studies to

Can. J. Chem. Downloaded from www.nrcresearchpress.com by 210.87.254.5 on 09/05/12
For personal use only.

the e.p.r. results to make this first report of the stabilization of the Hg(I) ion as a molecular complex in a crystalline environment. The data derived is used to probe both the electronic structure and the environment of the radical.

Experimental

Single crystals of pure cadmium acetate and cadmium acetate containing the mercuric ion as a substitutional impurity (0.5 wt% of $Hg(CH_3CO_2)_2$) were grown from aqueous solution. Large, colorless, monoclinic crystals were readily obtained. Samples were exposed to ^{60}Co γ-rays at both 77 °K and ambient temperatures, the doses varying from 0.3 to 3.0 Mrads. Electron paramagnetic resonance measurements were made at 77 and 295 °K on a conventional X-band spectrometer. Optical absorption spectra were recorded on a Cary-14 recording spectrophotometer incorporating a single crystal holder and an adjustable reference-beam attenuator. On exposure to γ-rays at room temperature, single crystals of cadmium acetate dihydrate were reduced to powder within 2 h. To reduce this efflorescence selected crystals were irradiated at 77 °K and subsequently annealed to 300 °K for investigation.

In addition to the experiments on doped cadmium acetate dihydrate the radiation damage in mercuric acetate was investigated. In this case however, the experiments were carried out on the polycrystalline material due to the difficulty in growing adequate single crystals.

Results

(a) Radiation Damage in Hg(II) doped Cadmium Acetate Dihydrate

The irradiation of pure $Cd(CH_3CO_2)_2.2H_2O$ at 77 °K with the subsequent annealing to 300 °K led to the well characterized $CH_2CO_2^-$ radical (8), a colorless stable fragment being formed. In contrast, a single-crystal of cadmium acetate dihydrate containing the mercuric ion as a substitutional impurity was rendered deep yellow on exposure to γ-rays. This yellow coloration is associated with a paramagnetic species (A) which also gives rise to the distinctive e.p.r. spectrum displayed in Fig. 1. The weaker triplet of features in the spectrum, centered around 3300 G, arise from $CH_2CO_2^-$. It may be noted here that when the irradiated crystal of Hg(II) doped cadmium acetate was annealed at room temperature for several days, this acetate fragment decayed with the concomitant formation of a second center (labelled B in Fig. 1). Intensive e.p.r. and e.n.do.r. investigations are now in progress in order to identify this species and it will be discussed in detail in a subsequent publication. During this annealing period the concentration of the original center A decreased slowly.

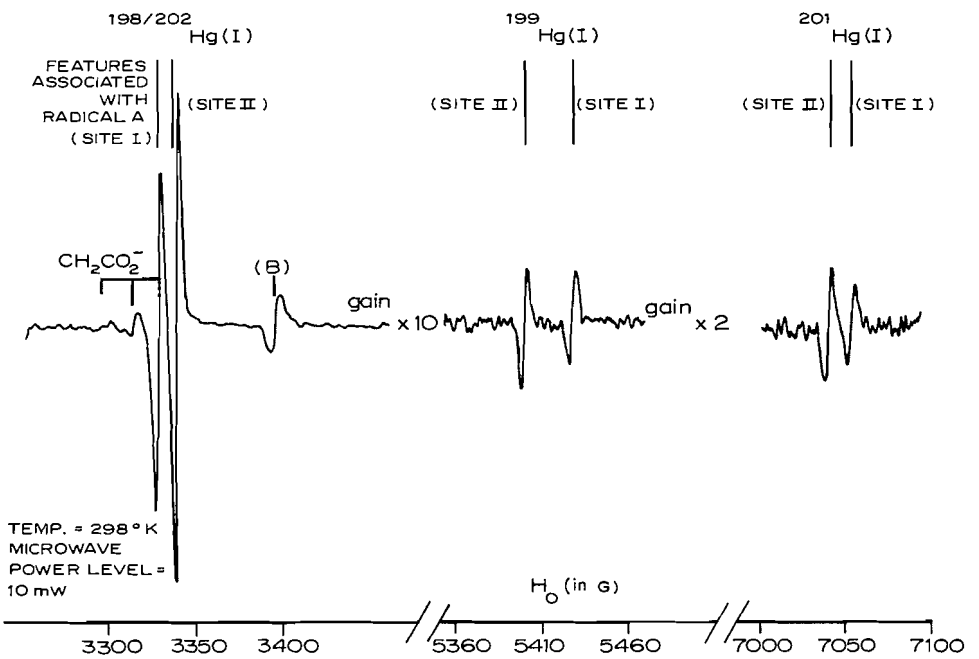

FIG. 1. Electron paramagnetic resonance spectrum of the Hg(I) impurity center in single-crystal $Cd(CH_3CO_2)_2.2H_2O$. $\theta = 40°$ in the bc'-plane.

Cadmium acetate dihydrate grows as large, monoclinic, prismatic crystals from aqueous solution and has the following unit cell parameters $a:b:c = 2.6076:1:2.1473$ and $\beta = 101° 25.5'$ (9). For the present e.p.r. investigation rotations were performed about the *a*- and *b*-axes, and a third orthogonal direction, *c'*, which makes an angle of 11°25.5′ to *c* (Fig. 2*a*). Figure 3 is a plot of the angular dependence of the spectrum of radical (A) with the applied magnetic field (H_0) in the *bc'*-plane; it will be noticed that there are two non-equivalent sites for this radical.

An examination of the e.p.r. spectrum of radical A measured at high incident microwave powers showed that each hyperfine line was accompanied by a weak pair of satellite lines. The intensity of these weaker resonances increased, with respect to the main lines, as the microwave power increased. Their separation was also field dependent, being 10.6 G at $H_0 = 3300$ G and 9.4 G at $H_0 = 5300$ G. This behavior is characteristic of features arising from the sympathetic spin-inversion of neighboring protons (10).

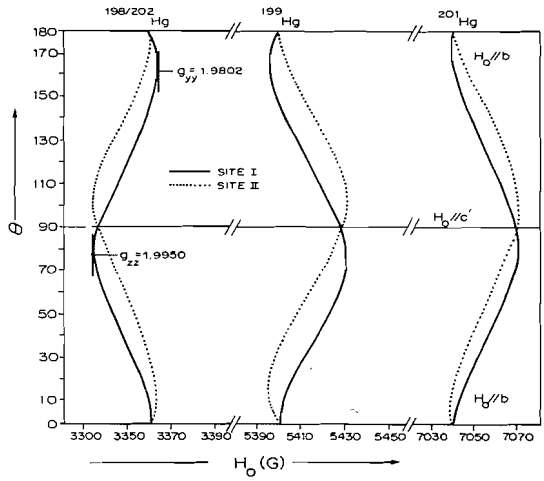

FIG. 3. Angular variation of the Hg(I) hyperfine features in the *bc'*-plane for the two distinguishable sites.

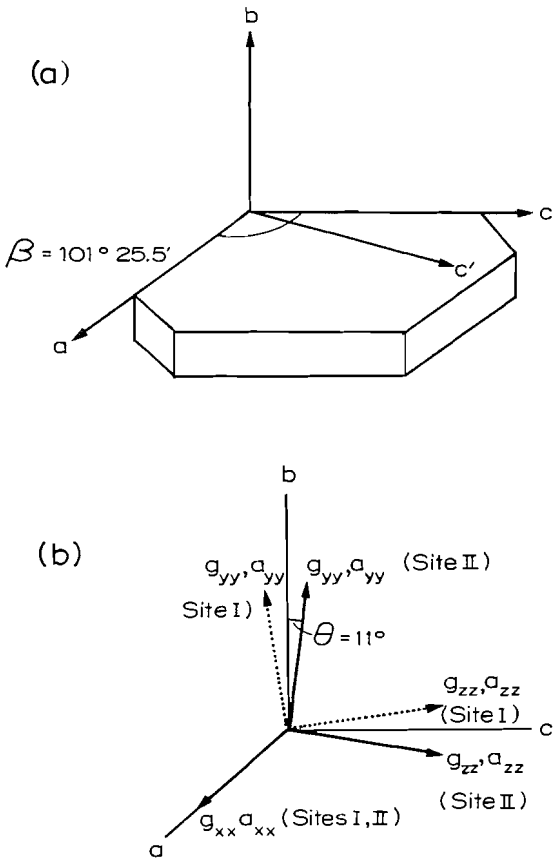

FIG. 2. (*a*) Crystal morphology and chosen axis system for $Cd(CH_3CO_2)_2.2H_2O$; (*b*) orientations of the principle values of the **g**- and hyperfine tensors relative to the chosen axis system.

The optical absorption spectrum of the irradiated crystal was characterized by a broad absorption having a maximum intensity at 305 nm.

(b) Radiation Damage in pure Mercuric Acetate

Irradiation of mercuric acetate at 77 °K resulted in the formation of a species whose electron spin resonance (e.s.r.) spectrum was identical to that of radical (A) in Hg(II) doped cadmium acetate. Although this species was stable indefinitely at this lower temperature, it decayed on warming to room temperature after approximately 2 h. The product of this decay was the $\dot{C}H_2CO_2^-$ radical.

Discussion

The magnetic and optical properties of radical (A) are those expected for the trapped mercurous ion. There are two magnetic isotopes of mercury in natural abundance (^{199}Hg, $I = \frac{1}{2}$, $\mu_N = 0.4979$ nuclear magnetons, 16.86%; ^{201}Hg, $I = \frac{3}{2}$, $\mu_N = -0.5513$ nuclear magnetons, 13.24%). The electronic energy levels expected for the ground state of Hg(I) are shown in Fig. 4. For this ion the isotropic hyperfine coupling constants are very large [$A_{iso}(^{199}Hg) \approx 28.0$ GHz and $A_{iso}(^{201}Hg) \approx 10.0$ GHz] so that the "normal" e.p.r. transitions which occur at lowest field, are not in-

Can. J. Chem. Downloaded from www.nrcresearchpress.com by 210.87.254.5 on 09/05/12
For personal use only.

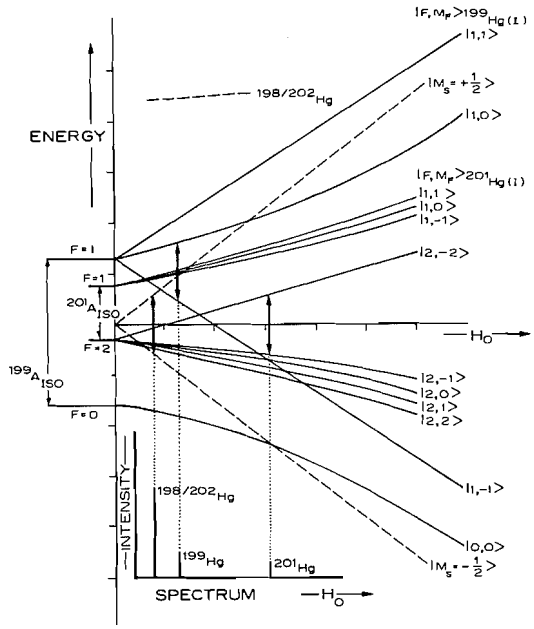

FIG. 4. Energy level diagram for the two magnetic isotopes of Hg(I). Note: $\mu_N(^{199}Hg)$ is positive whereas $\mu_N(^{201}Hg)$ is negative. The observed transitions are indicated on the constructed spectrum.

duced at the X-band operating frequency of 9.3 GHz. Consequently, we only detect the transitions

$$|F = 1, m_F = 0\rangle \leftrightarrow |F = 1, m_F = -1\rangle$$
at 5300 G for ^{199}Hg

$$|F = 2, m_F = -2\rangle \leftrightarrow |F = 2, m_F = -1\rangle$$
at 7000 G for ^{201}Hg

$$|S = \tfrac{1}{2}, m_S = \tfrac{1}{2}\rangle \leftrightarrow |S = \tfrac{1}{2}, m_S = -\tfrac{1}{2}\rangle$$
at 3300 G for $^{198/202}Hg$

where $\boldsymbol{F} = \boldsymbol{I} + \boldsymbol{S}$

The phenomenological spin Hamiltonian parameters given in Table 1 were computed from spectra measured in the *ab*-, *ac'*-, and *bc'*-crystal planes using a program written by Dr. J. A. Hebden based on the general method of Byfleet *et al.* (11). The experimental data were fitted to the general Hamiltonian

$$\beta\, \boldsymbol{H}\cdot\mathbf{g}\cdot\boldsymbol{S} + \boldsymbol{S}\cdot\mathbf{A}\cdot\boldsymbol{I} + Q'[I_z^2 - \tfrac{1}{3}I(I+1)] - \gamma\beta_N\, \boldsymbol{H}\cdot\boldsymbol{I}$$

in the usual notation.

Q', a redundant parameter for the 198/202 and 199-isotopes was calculated to be close to zero for the $^{201}Hg(I)$ ion. g_{xx} and a_{xx} are parallel to the crystallographic *a*-axis whilst g_{yy}, a_{yy}, and g_{zz}, a_{zz} lie in the *bc'*-plane and approximately 11° from *b* and *c'*, respectively (Fig. 2*b*). Included in Table 1 are the e.p.r. parameters, estimated using the Breit–Rabi approximation, for the Hg(I) ion trapped in a rigid, aqueous perchloric acid matrix. Eachus *et al.* (7) attributed the significant discrepancy between the experimental value of A_{iso}^{i} (^{201}Hg) and that calculated from the observed A_{iso}^{i} (^{199}Hg) value, to the effect of a large quadrupole term in the spin Hamiltonian. No such discrepancy has been found in the present work and in fact it appears that Q for $^{201}Hg(I)$ is very small; we feel that the errors incurred in the use of the Breit–Rabi expression led to the apparent discrepancy.

The optical absorption with a maximum at 305 nm is assigned to the Laporte-allowed $^2P_{\frac{1}{2},\frac{1}{2}} \leftarrow {}^2S_{\frac{1}{2}}$ transition of the mercurous ion. The analogous transition occurs at 300 nm for the pseudo-isoelectronic Cd(I) ion in both aqueous solutions (12) and rigid glasses (6). Brown and Dainton (6) observed that there is a significant blue shift of the P ← S transitions for the isoelectronic systems Ag^0, Cd^+, and In^{2+} as the atomic number increases. Consequently, we would expect a similar shift to lower energy on going from Tl^{2+} to Hg^+ in the analogous third row series (optical absorption data for trapped Au^0 are not available for comparison). If our assignment is correct, this is observed (λ_{max} Tl^{2+} = 267 nm (6)). It is surprising that Dainton and co-workers were unable to detect an optical absorption for Hg(I) in a rigid acid matrix. However, they did report that the tail of a band having a λ_{max} below 240 nm was apparent and Treinin (13) has assigned this high-energy absorption to the Laporte-forbidden $^2D_{\frac{1}{2},\frac{1}{2}} \leftarrow {}^2S_{\frac{1}{2}}$ transitions which occur at 198 nm in the gas phase. This band is expected to be intense for mercury in view of the pronounced *jj*-coupling. We feel that the absence of a P ← S transition for Hg(I) in rigid H_2SO_4 reflects the "free-ion" nature of the radical in this matrix. Conversely, the detection of an absorption at 305 nm in cadmium acetate dihydrate would suggest that the mercurous ion is stabilized as a molecular complex in this environment. This conclusion is further substantiated both by the reduction of the Fermi contact term relative to other studies and by the orthorhombic character of the mercury hyperfine tensor in the crystalline environment.

Can. J. Chem. Downloaded from www.nrcresearchpress.com by 210.87.254.5 on 09/05/12
For personal use only.

Can. J. Chem. Downloaded from www.nrcresearchpress.com by 210.87.254.5 on 09/05/12
For personal use only.

TABLE 1. Magnetic data for a number of mercury-containing paramagnetic species

Radical	Matrix	g-tensor				^{199}Hg-hyperfine tensor (G)				Reference
		g_{xx}	g_{yy}	g_{zz}	g_{iso}	B_{xx}	B_{yy}	B_{zz}	A_{iso}	
Hg(I)	$Cd(CH_3CO_2)_2.2H_2O$	1.979_3	1.980_2	1.995_0	1.984_8	−62	−17	+79	$9\,100 \pm 20$	This work
$(HgCO_3)^-$	$CdCO_3$								$13\,000 \pm 200$	2
Hg(I)	7 *m* $HClO_4$				1.99_7				$12\,500 \pm 100$[a]	7
Hg(I)	CH_3CH_2OH				1.98_7				$11\,500 \pm 100$	7
Hg(I)	$Hg(CH_3CO_2)_2$	2.002	2.002_2	1.995_0	1.999_8	−53	−93	+146	$9\,007 \pm 20$	This work

Can. J. Chem. Downloaded from www.nrcresearchpress.com by 210.87.254.5 on 09/05/12
For personal use only.

The factors which control the magnitude of the Fermi contact term have been discussed previously (4) in connection with the Cd(I) ion produced by radiation damage in calcium tetraacetate cadmium(II) hexahydrate. The fact that the Fermi contact interaction of the present center is substantially reduced relative to the Hg(I) produced in $CdCO_3$ (2) reflects the increased covalent interaction of the acetate ligands with the Hg(I) relative to the carbonate anion.

The crystal structure of cadmium acetate is, as yet, undetermined, however, the symmetry of the experimental **g**-tensor and the unusual form of the anisotropic hyperfine interaction tensor (-62, -17, $+79$ G for ^{199}Hg(I)) can be understood if the coordinated mercurous ion is assumed to occupy a site of C_2 or lower symmetry. It should be noted here that the values of the anisotropic part of the hyperfine coupling tensor may be in error to some degree since they are obtained by the subtraction of two large numbers.

Similarly the center observed in γ-irradiated mercuric acetate shows a large isotropic hyperfine coupling and a highly anisotropic term, consequently it would appear that the Hg(I) produced has a very low site symmetry similar to that in cadmium acetate. The differences in the magnitude of these parameters to those observed in the cadmium reflect the differences in crystal structure between cadmium and mercuric acetates.

The ground state of a mercurous ion in C_2 symmetry would be a linear combination of those mercury orbitals that transform as the irreducible representation A of C_2 point group. A consideration of these orbitals readily shows that such an orbital could produce the anisotropic hyperfine coupling observed. In addition the transformation properties of L_z, L_x, and L_y indicate that in C_2 symmetry g_{zz} will be close to the free spin value and the Δg_{yy} may be significant. However, without a more complete knowledge of the likely environment of the metal ion in cadmium acetate dihydrate or mercury acetate it is not possible to make a more quantitative interpretation of the data. Crystal structure studies on the Group IIB acetates are at present being undertaken (14) and it is hoped that these investigations and the further radiation damage studies we are undertaking will lead to a better understanding of the processes involved.

The authors wish to thank Professor C. A. McDowell for his interest in this work and the National Research Council of Canada for financial support.

1. M. T. Rogers and L. D. Kispert. Radiat. Chem. (Adv. Chem. Ser.) **2**, 327 (1968).
2. M. C. R. Symons and R. S. Eachus. Chem. Commun. 70 (1970).
3. R. S. Eachus and F. G. Herring. Chem. Phys. Lett. **5**, 405 (1970).
4. R. S. Eachus and F. G. Herring. Can. J. Chem. **49**, 562 (1971).
5. P. N. Moorthy and J. J. Weiss. Adv. Chem. Ser. **50**, 180 (1965).
6. D. M. Brown and F. S. Dainton. Trans. Faraday Soc. **62**, 1139 (1966).
7. R. S. Eachus, M. C. R. Symons, and J. K. Yandell. Chem. Commun. 979 (1969).
8. A Horsfield, J. R. Marton, and D. H. Whiffen. Mol. Phys. **4**, 327 (1961).
9. P. Groth. Chem. Kristallogr. (1908, Leipzig: W. Englemann).
10. G. I. Trammell, H. Zeldes, and R. Livingston. Phys. Rev. **110**, 630 (1958).
11. C. R. Byfleet, D. P. Chong, J. A. Hebden, and C. A. McDowell. J. Mag. Res. **2**, 69 (1970).
12. G. E. Adams, J. H. Baxendale, and J. W. Boag. Proc. Chem. Soc. 241 (1963).
13. A. Treinin. *In* Radical ions. *Edited by* E. T. Kaiser and L. Keran. Interscience, 1968. p. 525.
14. J. Trotter and W. Harrison. Unpublished work.

Can. J. Chem. Downloaded from www.nrcresearchpress.com by 210.87.254.42 on 09/05/12
For personal use only.

Couplings into Methylene Groups: a New Nuclear Magnetic Resonance Approach to Stereochemistry

K. N. SLESSOR AND A. S. TRACEY
Department of Chemistry, Simon Fraser University, Burnaby 2, British Columbia

Received December 17, 1970

A method of assigning dihedral angles to hydrogens adjacent to a methylene function by using computer analyzed n.m.r. coupling constants in a modified Karplus equation is presented. The "Dihedral Angle Estimation by the Ratio Method" (DAERM) is based on the assumption that, although the magnitudes of the Karplus constants, k_1 and k_2, vary, the ratio of k_1 to k_2 is a constant. Dihedral angles computed in this way seem not to be influenced by the effects of ring strain and substituent electronegativity. The conformational preferences of several four- to six-membered ring systems, some containing oxygen and sulfur atoms, have been investigated by this method. Molecular features such as ring puckering and flattening are indicated by DAERM as are some subtle electrostatic influences.

Une méthode qui consiste à assigner des angles dièdres aux hydrogènes adjacents à un groupe méthylène est présentée. A cet effet, on utilise les constantes r.m.n. de couplage, que l'on analyse par ordinateur suivant une équation de Karplus modifiée. "L'Estimation d'Angle Dièdre par la Méthode du Rapport" (EADMR) est fondée sur l'hypothèse que si la grandeur des constantes de Karplus (k_1 et k_2) varient, par contre, le rapport k_1 sur k_2 demeure constant. Les angles dièdres calculés de cette manière ne semblent pas influencés par les effets de tension de cycle et par l'électronégativité des substituants. Par cette méthode il a été possible de déterminer les conformations préférentielles de quelques systèmes cycliques de quatre à six chaînons, certains contenant des atomes d'oxygène et de soufre. Certaines particularités moléculaires comme le gauchissement et l'applatissement du noyau apparaissent dans la EADMR; il en est de même de quelques subtiles influences électrostatiques.

Canadian Journal of Chemistry, 49, 2874 (1971)

Introduction

The eq. 1 relating dihedral angle and coupling constant, reported by Karplus in 1959 (1), has maintained its essential features after several years of experimental and theoretical investigations. The limitations of the equation have been stressed by a number of workers (2, 3), including Karplus himself (4). The variation of the theoretically derived constants k_1 and k_2 with molecular and substituent properties, such as ring size and electronegativity have been noted and these have been attributed (3) to changes in magnitude of the electron exchange term, which is the major contributor to the Karplus constants, k_1 and k_2.

This report presents conformational results based on calculation of dihedral angles from a modified Karplus equation. Variations in Karplus constants are accommodated in this method through the assumption that the ratio of the Karplus constants k_1/k_2 is a constant. From the theoretical parameters calculated by Karplus (1), the ratio k_1/k_2 is very nearly equal to 0.9. Using accurate coupling constants, dihedral angles can be calculated for a hydrogen vicinal to a methylene function without prior assignment of Karplus constants and without consideration of the electronic perturbations affecting the system.[1] This process is termed the "Dihedral Angle Estimation by the Ratio Method" (DAERM).

The original form of eq. 1 is used, in which J is the vicinal coupling constant; k, the Karplus constant; Φ, the dihedral angle subtended by the coupled nuclei; and c, a constant.

$$[1a] \quad J_1 = k_1 \cos^2 \Phi_1 - c \qquad 0 \leq \Phi_1 \leq 90°$$

$$[1b] \quad J_2 = k_2 \cos^2 \Phi_2 - c \qquad 90 \leq \Phi_2 \leq 180°$$

The four possible arrangements of a hydrogen adjacent to a methylene group in a saturated system are shown in Fig. 1. Only cases A, B, and C will be discussed as case D is seldom, if ever, found in ring systems. From case A, the two equations describing the system are 1*a* and *b*, where $k_1 = k_1'$ since both Φ_1 and Φ_2 are less than 90°, and therefore [2] is obtained.

$$[2] \quad \frac{J_1 + c}{J_2 + c} = \frac{\cos^2 \Phi_1}{\cos^2 (\omega - \Phi_1)}$$

Assuming a regular tetrahedral system (ω =

[1] An attempt to separate electronic effects from stereochemical influences has been reported (5).

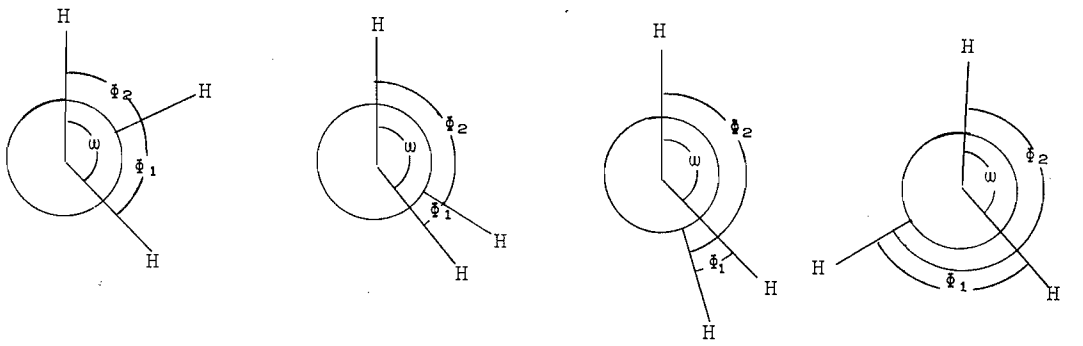

FIG. 1. Four arrangements of the —C—C—H system.
H H

120°) and using the theoretical value (1) of 0.28 for c, a complete solution for the angles Φ_1 and Φ_2 is possible from the coupling constants, J_1 and J_2, without knowledge of the Karplus constant, k_1, for that system. Cases B and C can be resolved in a similar manner, as shown in eqs. 3 (case B) and 4 (case C).

$$[3] \qquad \frac{J_1 + c}{J_2 + c} = \frac{k_1}{k_2} \frac{\cos^2 \Phi_1}{\cos^2 (\omega - \Phi_1)}$$

$$[4] \qquad \frac{J_1 + c}{J_2 + c} = \frac{k_1}{k_2} \frac{\cos^2 \Phi_1}{\cos^2 (\omega + \Phi_1)}$$

Having assumed a value of 0.9 for k_1/k_2, complete solutions for cases B and C are possible. If electronegativity and other substituent effects are reflected solely in the magnitude of the Karplus constants, DAERM should result in a sensitive probe into the angular relationship between vicinally coupled nuclei, as well as the electronic situation prevailing in the system being investigated. Testing of DAERM was undertaken through application of the method to ring systems having four to six atoms for which n.m.r. parameters were available.

Method

In order to easily evaluate the utility of DAERM, a short Fortran program[2] was written for the IBM 360/50 computer which calculated the possible angle sets for a given set of coupling constants from eqs. 2–4. DAERM provides two solutions for each set of coupling constants, one with both dihedral angles less than 90° (*i.e.* case A), the other with one angle less than, the other greater than 90° (*i.e.* either case B or C).

An example of the application of DAERM is provided by consideration of the computer analyzed low temperature proton n.m.r. parameters of octadeuterocyclohexane obtained by Garbisch and Griffith (6). One signal indicated two couplings of 3.65 and 13.12 Hz and, without prior assignment of their origin, DAERM allows four possible solutions as seen in Table 1.

Sets *ii* and *iv* are equivalent and can be rejected as the required Karplus constants are much too large. Unacceptably large calculated Karplus constants can often be used to rule out possible angular solutions and thus simplify the analysis. The second signal from octadeuterocyclohexane was analyzed as two couplings, 2.96 and 3.65 Hz. Again, without prior assignment, four solutions are seen in Table 2.

It is obvious that sets *vi* and *viii* are equivalent and that one set (*viii*) can be discarded. From Table 1 the coupling of 3.65 Hz is associated with two possible angles (sets *i* and *iii*).

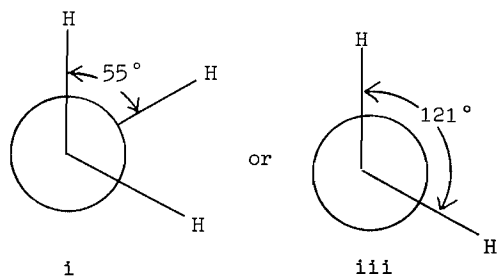

From Table 2 the three solutions for the coupling of 3.65 Hz are *v*, 152; *vi*(*viii*), 58; and *vii*, 23°. Thus, the only compatible set of solutions is *i* and *vi*.

[2]Available upon request.

Can. J. Chem. Downloaded from www.nrcresearchpress.com by 210.87.254.42 on 09/05/12
For personal use only.

TABLE 1.* DAERM calculations† on 3.65 and 13.12 Hz couplings

	Observed coupling constants		Calculated dihedral angles		Calculated Karplus constants	
Set	J_1	J_2	Φ_1	Φ_2	k_1	k_2
i	3.65	13.12	55	175	12.14	13.49
ii	3.65	13.12	70	50	32.78	36.43
iii	13.12	3.65	1	121	13.40	14.89
iv	13.12	3.65	50	70	32.78	36.43

*In all Tables and discussion, Φ_1 is the *cis* angle; Φ_2 the *trans* angle; k_1 the calculated Karplus constant for less than 90°; k_2 for greater than 90°.
†$k_1/k_2 = 0.9$, $\omega = 120°$.

TABLE 2. DAERM calculations* on 2.96 and 3.65 Hz couplings

	Observed coupling constants		Calculated dihedral angles		Calculated Karplus constants	
Set	J_1	J_2	Φ_1	Φ_2	k_1	k_2
v	2.96	3.65	32	152	4.52	5.02
vi	2.96	3.65	62	58	14.32	15.91
vii	3.65	2.96	23	143	4.61	5.13
viii	3.65	2.96	58	62	14.32	15.91

*$k_1/k_2 = 0.9$, $\omega = 120°$.

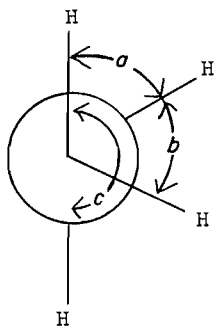

Angle *a*, 55 → 58°, gives rise to the J_{ae} coupling of 3.65 Hz; *b*, 62 → 65°, gives rise to the J_{ee} coupling of 2.96 Hz, and *c*, 175 → 178°, gives rise to the J_{aa} coupling of 13.12 Hz. It is important to note that the assignments were made without prior knowledge of the proton identities and without assigning numerical values of the Karplus constants. DAERM predicts a flattened chair conformation with proton assignments identical to Garbisch and Griffith (6).

Prior to further application of DAERM, an investigation of two main features of this method was carried out. These were: (*1*) distortion of the system from regular tetrahedral geometry ($\omega \neq 120°$), and (*2*) variation of the parameter, k_1/k_2. Using the octadeuterocyclohexane data with a k_1/k_2 constant at 0.9, the effect of distortion from tetrahedral geometry can be evaluated by plotting the calculated angle Φ_2 against values of ω. The value of ω was varied over the range 110 to 130°, which is beyond the range of distortions expected for normal tetrahedral systems. Figure 2 shows the results in which the angles obtained from the two sets of octadeuterocyclohexane couplings, J_{ae}, J_{ee}, and J_{ae}, J_{aa}, give two curves intersecting at a ω value of 115°. Karplus constants calculated for $\omega = 115°$ reassuringly provide identical results, $k_1 = 12.4$ and $k_2 = 13.8$, from the two sets of couplings.

The Φ_2 solutions should be the same from either set of couplings and as this value is influenced by the ratio k_1/k_2, the variation of k_1/k_2 with ω was investigated and the results presented in Fig. 3.

From theory, a ratio of unity or greater for k_1/k_2 cannot be accepted and, thus, Fig. 3 indicates that ω for cyclohexane is less than 120°. This in turn suggests that if constant p character is assumed for the bonding about carbon, the angle subtended by H—C—H at each methylene grouping in cyclohexane is smaller than the expected tetrahedral angle. Eliel *et al.* (7) has calculated an H—C—H angle of 107.3° from the cyclohexane electron diffraction data of Davis and Hassel (8). This value corresponds with an ω value of approximately 116° (9) and is in keeping with a ratio of very nearly 0.9. Figures 2 and 3 emphasize the inter-relationship between ω and the ratio k_1/k_2, and also provide an appreciation of the range permitted in the magnitude of the values.

From computer analyzed n.m.r. parameters, the conformation of a cyclohexane derivative has been determined to a degree where ring flattening and distortion from tetrahedral geometry are apparent. This method is considered to be of significance in assigning conformational properties to cyclic molecules in particular, as we shall describe in the succeeding section.

Discussion

An essential prerequisite of DAERM is the availability of n.m.r. coupling parameters of hydrogen nuclei vicinal to a methylene function. Four cyclohexyl systems for which such data

Can. J. Chem. Downloaded from www.nrcresearchpress.com by 210.87.254.42 on 09/05/12
For personal use only.

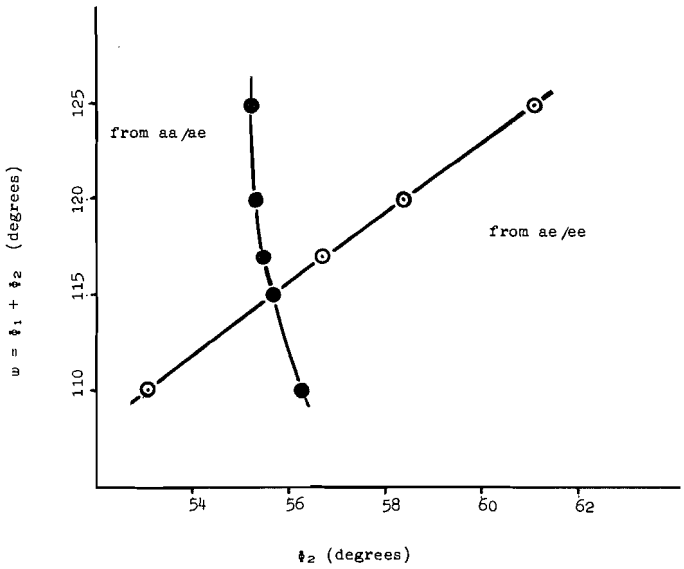

FIG. 2. Variation of ω with Φ_2.

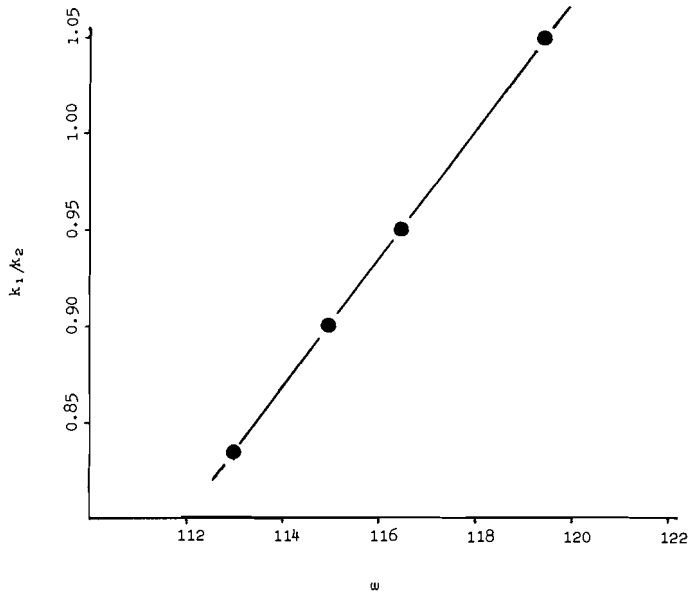

FIG. 3. Variation of k_1/k_2 with ω.

were available are now considered. A ratio of 0.9 and an ω value of 115° are assigned from which not only Φ_1 and Φ_2 but the Karplus constants, k_1 and k_2, which correspond to these acceptable solutions, are calculated.

Table 3 illustrates an essential point of DAERM. Although large variations exist in the reported coupling constants, all the Φ_1 angles are reasonably constant in the range 46–57°, and the Karplus constants are rather variable. Possibly more striking is the series of six-membered heterocycles shown in Table 4. Angles and constants were calculated using a ratio of 0.9 and tetrahedral geometry, ω = 120°, for the carbon atoms involved in the coupling. As seen in the cyclohexyl derivatives, rather large changes in

Can. J. Chem. Downloaded from www.nrcresearchpress.com by 210.87.254.42 on 09/05/12
For personal use only.

Can. J. Chem. Downloaded from www.nrcresearchpress.com by 210.87.254.42 on 09/05/12
For personal use only.

TABLE 3. The n.m.r. and DAERM data for cyclohexane derivatives

Reference	Compound	No.	R	Solvent	Observed coupling constants			Calculated angles*		Calculated Karplus constants	
					J_{aa}	J_{ea}	J_{ee}	Φ_1	Φ_2	k_1	k_2
10	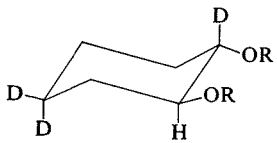	**1***a*	Ac	CCl_4	11.0	3.5	—	53	168	10.6	11.8
		b	H	$CHCl_3$	11.0	4.5	—	50	165	11.0	12.2
		b	D	D_2O	10.5	4.1	—	49	164	10.4	11.6
		c	Ditosyl	$CHCl_3$	7.9	3.6	—	46	161	8.2	9.1
		d	Isopropylidene	CCl_4	11.0	3.5	—	53	168	10.6	11.8
11	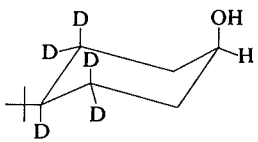	**2**		CCl_4	—	3.0	2.7	57	58	10.9	12.1
11	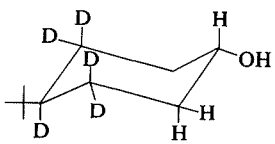	**3**		CCl_4	11.1	4.3	—	52	167	12.0	13.4
11	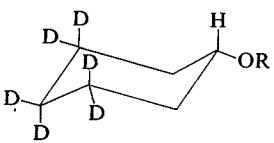	**4***a*	H	CCl_4	9.8	3.9	—	49	164	9.8	10.9
		a	D	D_2O	10.2	4.1	—	49	164	10.2	11.3
		b	Ac	CS_2(room temperature)	9.3	3.9	—	48	163	9.4	10.4
		b	Ac	$CS_2(-110°)$	11.4	4.2	—	51	166	11.2	12.5

*The calculated angles presented in Tables 3 and 4 must be treated with caution, since these are derived from first order couplings which may vary considerably from the actual values. In addition, some of these examples may exhibit errors due to the configurational dependence of electronegative substituents. These errors, combined with possible conformation mobility in these systems, limit the use of the calculated parameters to qualitative comparisons.

Can. J. Chem. Downloaded from www.nrcresearchpress.com by 210.87.254.42 on 09/05/12
For personal use only.

TABLE 4. Nuclear magnetic resonance DAERM data for heterocycles

Reference	Compound	No.	Solvent	Coupling constants		Calculated angles*		Calculated Karplus constants	
				J_{cis}	J_{trans}	Φ_1	Φ_2	k_1	k_2
12	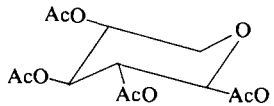	**5**	$CHCl_3$	4.2	8.1	43	163	8.1	9.0
13	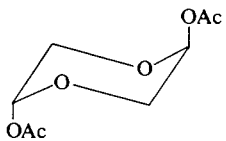	**6**		1.5	1.0	57	63	5.9	6.6
14	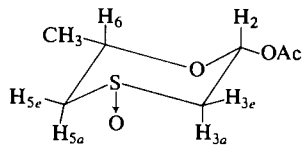	**7**	$CDCl_3$	$J_{2,3e}$ 1.6 $J_{5e,6}$ 1.8	$J_{2,3a}$ 10.1 $J_{5a,6}$ 11.5	63 64	183 184	9.4 10.7	10.4 11.8
14	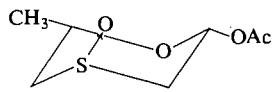	**8**	$CDCl_3$	$J_{2,3e}$ 1.9 $J_{5e,6}$ 1.9	$J_{2,3a}$ 9.8 $J_{5a,6}$ 10.8	61 62	181 182	9.1 10.0	10.1 11.1

*See footnote *, Table 3.

Can. J. Chem. Downloaded from www.nrcresearchpress.com by 210.87.254.42 on 09/05/12
For personal use only.

the calculated Karplus constants are evident for these heterocyclic derivatives, but these seem to bear little relation to the conformation of the molecule. The overall conformation of these molecules is of interest as the oxygen heterocycles show the expected flattening and the sulfoxides the expected puckering due to the bonding angles of the hetero atoms (15). The conformational mobility of these compounds at room temperature will result in time averaged dihedral angles and a general lowering of the calculated Karplus constants as can be seen in **4***b*, Table 3.

DAERM calculations on four-membered rings were made possible by the recent report of computer analyzed spectra of several thietanes. The results are presented in Table 5 using the proton assignments of the original workers (16, 17).

Four of the five compounds (**9–13**) gave DAERM angles in very good agreement with the reported angles, but the fifth, *trans*-2,4-diphenylthietane-1-oxide (**13**) gave quite different solutions. In contrast to the severely distorted molecule originally proposed (17), DAERM indicates a molecule flattened slightly in a manner which allows the phenyl groups to approach pseudo-equatorial positions. The possibility of incorrect proton assignments was excluded since DAERM predicted an impossibly distorted molecule for the alternate assignment.

Five-membered rings have posed a more complex problem in conformational analysis because of their very low barrier to pseudo-rotation. The bicyclo[2.2.1]heptane system is free from such complexities as the bridge locks the molecule in a single conformer. Table 6 represents the first-order coupling constants obtained by Williamson (18) on the hexachlorobicyclo[2.2.1]-heptenes and the DAERM calculated angles and Karplus constants. Not unexpectedly, the magnitude of the Karplus constants appears to be inversely proportional to the electronegativity of the substituent. This inverse relationship has been predicted on a theoretical basis (4) and a number of examples of the inverse dependence of J with electronegative substituents have been reported (see for example Williamson (18) and Cohen and Schaefer (19)).

As the $C_1—C_2—C_3$ bond angle in these systems is found to be significantly smaller than the tetrahedral angle (100° *vs.* 109.5°) (20), the angle between hydrogens on the methylene group at position 2 can be expected to be greater than the

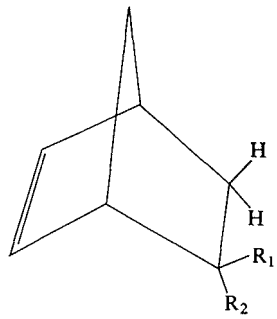

15

a $R_1 = —\overset{\overset{O}{\|}}{C}—OCH_3$; $R_2 = H$

b $R_1 = —H$; $R_2 = —\overset{\overset{O}{\|}}{C}—OCH_3$

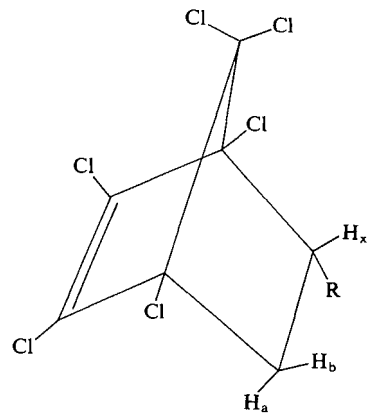

14

tetrahedral angle (21). Assuming a distortion of a few degrees ($\omega = 125°$), both the amount of twist about the $C_2—C_3$ bond and the Karplus constants decrease by a small amount (Table 7). These latter results are in better agreement with the magnitude of twists found by X-ray studies (22).

Our studies with DAERM suggest that in certain systems having couplings varying with solvent, the major reason for this may be a change in the Karplus constants rather than the conformation of the molecule (*e.g.* Table 3, compounds **1***b* and **4***a*). It would thus be very unwise to interpret variations in coupling constants on varying the solvent as changes in conformer populations until this point has been clarified.

Two general points are worth mentioning. The

Can. J. Chem. Downloaded from www.nrcresearchpress.com by 210.87.254.42 on 09/05/12
For personal use only.

TABLE 5. Conformational analysis of some thietanes

Reference	Compound	No.	Reported coupling (Hz)	Reported angle	DAERM* angle	Calculated Karplus constants
16	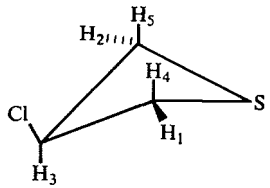	**9**	$J_{1,3}$ 7.670 $J_{3,4}$ 9.343	27.6 152.9	29 156	10.3, 11.5
17	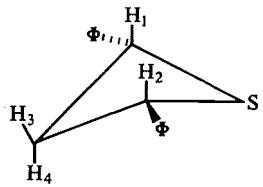	**10**	$J_{1,3}$ 7.35 $J_{1,4}$ 9.95	30.0 —	32 159	10.5, 11.7
17	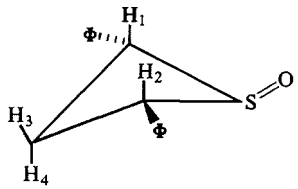	**11**	$J_{1,3}$ 9.53 $J_{1,4}$ 12.62	31.6 159.1	31 159	13.4, 14.9
17	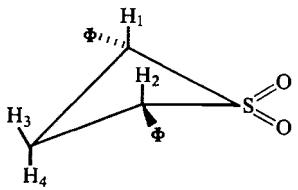	**12**	$J_{1,3}$ 9.17 $J_{1,4}$ 11.12	27.7 —	29 156	12.3, 13.6
17	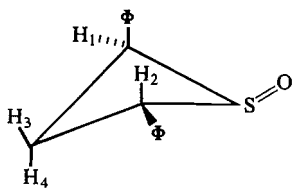	**13**	$J_{1,3}$ 3.16 $J_{1,4}$ 8.79 $J_{2,3}$ 10.24 $J_{2,4}$ 11.90	91.0 36.5 26.5 154.0	126 2 27 155	9.1, 10.1 13.3, 14.8

*ω = 127.6 as assigned by Dodson *et al.* (17).

Can. J. Chem. Downloaded from www.nrcresearchpress.com by 210.87.254.42 on 09/05/12
For personal use only.

TABLE 6. The n.m.r. and DAERM data* for hexachlorobicyclo[2.2.1]hept-5-ene derivatives

Compound 14	R	J_{ax}	J_{bx}	Calculated angles		Calculated Karplus constants		Substituent electronegativities from ref. 18
				Φ_{ax}	Φ_{bx}	k_1	k_2	
a	—CN	4.6	9.3	132	12	10.0	11.1	2.49
b	—C(=O)—OH	4.4	8.5	133	13	9.2	10.2	2.60
c	—C_6H_5	4.2	8.9	131	11	9.5	10.6	2.75
d	—Cl	3.2	8.0	128	8	8.4	9.4	3.25
e	—OH	2.4	7.4	124	4	7.7	8.6	3.43
f	—OAc	2.5	7.6	124	4	7.9	8.8	3.80

*$\omega = 120°$.

TABLE 7. Variation in ω for C-2 and -3 of bicyclo[2.2.1] hept-5-enes

Reference	Compound	R	ω	*cis* angle	*trans* angle	k_1	k_2
18	**14***b*	—C(=O)—OH	120	13	133	9.2	10.2
		—C(=O)—OH	125	8	133	9.0	10.2
18	**14***e*	—OH	120	4	124	7.7	8.6
		—OH	125	1	124	7.7	8.6
23	**15***a*	—C(=O)—OCH_3	120	10	130	10.0	11.1
			125	5	130	9.8	10.8
23	**15***b*	—C(=O)—OCH_3	120	11	131	9.6	10.7
			125	7	132	9.4	10.5

ratio, $k_1/k_2 = 0.9$, has been established only for cyclohexane and although variations in this value only affect the calculated angles by a few degrees, molecular orbital calculations indicate this value decreases with electronegative substituents (24). As far as we are aware, no information for systems expected to show this effect is available. The configurational dependence of electronegative substituents on couplings is only partially compensated for in DAERM through an internal averaging process. Thus, the applicability of DAERM is limited when electronegative substituents are bonded directly to the molecular segment under consideration. The error introduced will be maximal when the electronegative substituent is anti-periplanar to any of the hydrogen nuclei under consideration and minimal in the case of hydrocarbons and rings in which electronegative groups are not aligned in a *trans*-diaxial orientation with the hydrogen atoms. A formal correction could be introduced if such parameters were available, but only at the expense of computational simplicity.

Conclusions

Dihedral Angle Estimation by The Ratio Method (DAERM) is a means of establishing conformational preference without prior assignment of Karplus constants and in some systems without prior assignment of proton identities. The basic requirement of DAERM is a methylene group coupled vicinally to one or more hydrogens for which the n.m.r. parameters have been accurately determined. Using this data, the required angular solutions may be obtained from simple calculations. Such solutions not only allow assignment of conformational properties to the molecule but also allow calculation of the Karplus constants for the system. An advantage of DAERM is the determination of the dihedral angle from two vicinal couplings which improves the reliability of the solutions obtained. In the examples given, DAERM easily provided solutions agreeing well with the known conformational properties of the molecules studied.

We wish to thank Drs. K. Bowden, E. J. Wells, and especially L. D. Hall for very valuable discussions. We are pleased to acknowledge the financial support of the National Research Council of Canada.

1. M. KARPLUS. J. Chem. Phys. **30**, 11 (1959).
2. J. W. EMSLEY, J. FEENY, and L. H. SUTCLIFFE. High resolution nuclear magnetic resonance. Vol. 2. Pergamon Press Ltd., New York, N.Y., 1966.
3. M. BARFIELD and D. M. GRANT. Advances in magnetic resonance. Vol. 1. *Edited by* J. S. Waugh, Academic Press Inc., New York, N.Y., 1965.
4. M. KARPLUS. J. Am. Chem. Soc. **85**, 2870 (1963).
5. J. B. LAMBERT. J. Am. Chem. Soc. **89**, 1836 (1967); H. R. BUYS. Rec. Trav. Chim. **88**, 1003 (1969); J. B. LAMBERT. Accts. Chem. Res. **4**, 87 (1971).
6. E. W. GARBISCH and M. G. GRIFFITH. J. Am. Chem. Soc. **90**, 6543 (1968).
7. E. L. ELIEL, N. L. ALLINGER, S. J. ANGYAL, and G. A. MORRISON. Conformational analysis. Interscience Publishers Inc., New York, N.Y., 1965. p. 455.
8. M. DAVIS and O. HASSEL. Acta Chem. Scand. **17** 1181 (1963).
9. J. B. HENDRICKSON. J. Am. Chem. Soc. **83**, 4537 (1961).
10. R. U. LEMIEUX and J. W. LOWN. Tetrahedron Lett. 1229 (1963).

Can. J. Chem. Downloaded from www.nrcresearchpress.com by 210.87.254.42 on 09/05/12
For personal use only.

11. F. A. L. ANET. J. Am. Chem. Soc. **84**, 1053 (1962).
12. R. U. LEMIEUX and J. HOWARD. Can. J. Chem. **41**, 308 (1963).
13. L. D. HALL. Carbohydr. Res. **4**, 429 (1967).
14. A. B. FOSTER, T. D. INCH, M. H. QADIR, and J. M. WEBBER. Chem. Commun. 1086 (1968).
15. Reference 7. p. 249.
16. W. D. KELLER, T. R. LUSEBRINK, and C. H. SEDERHOLM. J. Chem. Phys. **44**, 782 (1966).
17. R. M. DODSON, E. H. JANCIS, and G. CLOSE. J. Org. Chem. **35**, 2520 (1970).
18. K. L. WILLIAMSON. J. Am. Chem. Soc. **85**, 516 (1963).
19. A. D. COHEN and I. SCHAEFER. Molec. Phys. **10**, 209 (1966).
20. D. A. BRUECKNER, T. A. HAMOR, J. M. ROBERTSON, and G. A. SIM. J. Chem. Soc. 799 (1962).
21. Reference 7. p. 448.
22. C. ALTONA and M. SUNDARALINGAM. J. Am. Chem. Soc. **92**, 1995 (1970).
23. F. A. L. ANET, H. H. LEE, and J. L. SUDMEIER. J. Am. Chem. Soc. **89**, 4431 (1967).
24. G. E. MACIEL, J. W. MCIVER, Jr., N. S. OSTLUND, and J. A. POPLE. J. Am. Chem. Soc. **92**, 4497 (1970).

Can. J. Chem. Downloaded from www.nrcresearchpress.com by 210.87.254.42 on 09/05/12
For personal use only.

Can. J. Chem. Downloaded from www.nrcresearchpress.com by 210.87.254.5 on 09/05/12
For personal use only.

Pressure Effect on the Kinetics of Reaction Between Solid NaCl and $ZrCl_4$ or $HfCl_4$ Vapors

P. PINT AND S. N. FLENGAS

Department of Metallurgy and Materials Science, University of Toronto, Toronto 181, Ontario

Received April 30, 1971

The kinetics of reaction between single crystals of sodium chloride and zirconium tetrachloride and hafnium tetrachloride vapors, to form sodium hexachlorozirconate and sodium hexachlorohafnate, respectively, have been investigated as a function of the tetrachloride pressures at a constant temperature of 485 °C. The rate of formation of Na_2ZrCl_6 is kinetically more favorable. The heterogeneous reaction is diffusion controlled, with the rate of diffusion depending on the availability of Cl^- vacancies.

Les cinétiques à température constante (485 °C) des réactions entre des cristaux uniques de chlorure de sodium avec des vapeurs de tétrachlorure de zirconium et d'hafnium, ont été étudiées en fonctions des pressions en tétrachlorure. Ces réactions conduisent respectivement à l'hexachlorozirconate de sodium et à l'hexachlorohafnate de sodium. La vitesse de formation de Na_2ZrCl_6 est cinétiquement plus favorable. Ces réactions hétérogènes sont contrôlées par diffusion et la vitesse de diffusion dépend de la disponibilité des espèces Cl^-.

Canadian Journal of Chemistry, **49**, 2885 (1971)

Introduction

Compounds of the general formula M_2XCl_6 (where M is an alkali metal cation, and X is Zr, Hf, or Ti) have been prepared by the reaction between solid MCl and gaseous XCl_4 (1–5). These compounds are of interest because of their possible uses for the recovery of the metals Zr, Hf, and Ti by fused salt electrolysis (6, 7) and for the purification of $ZrCl_4$ for applications requiring a low Hf content (8).

In a previous investigation (9) the rate of formation of Na_2ZrCl_6 was measured as a function of temperature. In the present work the effect of applied pressure of $ZrCl_4$ and of $HfCl_4$, on the rate of formation of the compounds Na_2ZrCl_6 and Na_2HfCl_6, respectively, was investigated at a constant reaction temperature of 485 °C.

Experimental

The apparatus for measuring the kinetics of the reaction is shown in Fig. 1.

The method involved the measurement of the weight increase of a single crystal of NaCl suspended from a quartz spring balance. The increase in weight was due to the reaction

$$[1] \qquad 2NaCl_{(s)} + XCl_{4\,(v)} \rightarrow Na_2XCl_{6\,(s)}$$

where X is Hf or Zr.

The crystals of sodium chloride were smooth and hexahedral, of approximate size 0.6 × 0.6 × 1.0 cm, and were cleaved from larger crystals. For every pressure run a new sodium chloride crystal was used.

To control the temperature of the $ZrCl_4$ or $HfCl_4$ to within ±1 °C, the ampoule containing the $ZrCl_4$ or $HfCl_4$ was placed into a brass block, into which two controlling chromel–alumel thermocouples had been inserted. This temperature fluctuation corresponds to a change in the $ZrCl_4$ or $HfCl_4$ vapor pressures of only ±15 Torr, at a total applied pressure of 700 Torr (10).

To ensure that the ampoule containing the $ZrCl_4$ or $HfCl_4$ was at the lowest temperature of the total system, a temperature profile of the system was taken prior to each experiment.

The vapor pressures were measured directly using the liquid tin isoteniscope incorporated in the system as shown in Fig. 1.

At the beginning of a run the furnace was heated to the desired temperature, and then wheeled into position over the cell containing the tetrachlorides. This procedure reduced the time-lag required by the system to reach its equilibrium.

The quartz spring balance was calibrated at the reaction temperature of 485 ± 2 °C. The spring constant was about 4.5% higher than that at room temperature.

To establish the pressure dependence of the rate of formation of Na_2ZrCl_2, six applied pressures were investigated, ranging from approximately 70 Torr to 1 atm. In the case of Na_2HfCl_6 formation, four different pressures between 100 Torr and 1 atm were applied.

The decomposition pressures of the compounds at the reaction temperature are of the order of 10 Torr (11, 12). Accordingly, the thermodynamic "drive" for the reaction is the difference between the applied and the decomposition pressures.

The microscopic examination of polished, partially reacted samples indicated the existence of two distinct layers. The definite separation of the two layers is shown in Fig. 2(*a*). It may be seen that the advancing interface is planar and symmetrical with the original shape retained, as expected for an isotropic material such as NaCl. Some rounding of the corners can also be seen (Fig. 2(*b*)). The outer layer represents the compound

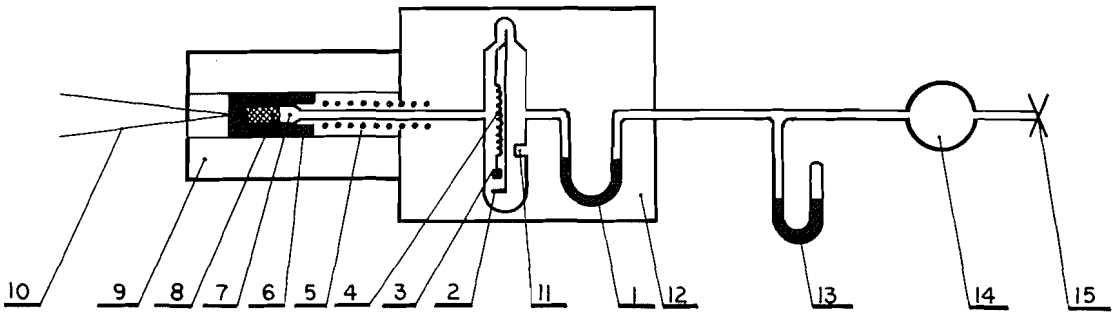

FIG. 1. Apparatus for kinetic studies. *1*, Sn manometer; *2*, reference point; *3*, salt crystal; *4*, quartz spring; *5*, auxilliary windings; *6*, brass block; *7*, quartz ampoule; *8*, solid XCl_4; *9*, sliding furnace; *10*, measuring thermocouple; *11*, thermocouple well; *12*, reaction furnace; *13*, Hg manometer; *14*, expansion bulb; *15*, 3-way stopcock.

Na_2XCl_6 and the inner, the unreacted core of NaCl. The compositions of the outer layers were verified to be the stoichiometric compounds by considering the initial weight and the final weight of the NaCl crystals, as well as the increase in weight of the sample due to the reaction with the vapors.

The dimensions of the NaCl crystals were measured with a micrometer. The final dimensions and weights of the unreacted NaCl were obtained by mechanically removing the outer layers.

Data Treatment

For any diffusion controlled heterogeneous reaction Fick's first law of diffusion may be written as

$$[2] \qquad \frac{dn}{dt} = -DA\left(\frac{\delta c}{\delta x}\right)_x$$

where D is the diffusion coefficient and the number of moles dn of substance diffusing across a sectional plane of surface area A cm^2 in the time dt is proportional to the concentration gradient $\delta c/\delta x$.

If it is assumed that the concentration gradient of the diffusing species depends only on the pressure of the tetrachloride vapor, it is evident that throughout a reaction the boundary conditions of the diffusing species should remain constant at a constant applied pressure.

Assuming the establishment of a steady state, at any given time, the change in the number of gram moles of reacted substance, dN, (where N is proportional to n), occupying a volume dV, is given by

$$dN = (\rho/M)dV = (\rho/M)\,A\,d(\Delta X)$$

where ρ is the density of the reaction product, M is the molecular weight, A the surface area, and ΔX the thickness of the reacted layer. Accordingly eq. 2 may be written as

$$[3] \qquad \frac{dN}{dt} = \frac{\rho A}{M}\frac{d(\Delta X)}{dt} = -DA\frac{k}{\Delta X}$$

By integrating eq. 3; one has

$$[4] \qquad \Delta X^2 = k^1 t$$

where k^1 and k are constant. This equation defines a parabola and relates ΔX to the time of reaction.

Since the thickness ΔX of the Na_2ZrCl_6 and Na_2HfCl_6 layers cannot be precisely estimated from weight gain measurements due to lack of density data for the compounds at the working temperature, a more suitable parameter for correlating the kinetic data is the decrease in the thickness ΔL of the reacting NaCl crystal. This parameter also corrects for the change in the surface area of the NaCl as the reaction takes place. The quantity ΔL may be calculated from the weight gain measurements by the following method.

For an isotropic crystal such as NaCl, of dimensions X, Y, and Z the decrease ΔL is expected to be equal in all three directions. During reaction the volume of the NaCl crystal decreases according to

$$d(\Delta V)_{NaCl} = (XY + YZ + XZ)\,d(\Delta L)$$

If X_0, Y_0, and Z_0 are the initial dimensions of the crystal, the instantaneous dimensions may be expressed as

$$X = X_0 - \Delta L$$
$$Y = Y_0 - \Delta L$$
$$Z = Z_0 - \Delta L$$

Substituting these relationships and integration from $\Delta L = 0$ at $\Delta V = 0$ to $\Delta L = \Delta L$ at $\Delta V = \Delta V$,

Can. J. Chem. Downloaded from www.nrcresearchpress.com by 210.87.254.5 on 09/05/12
For personal use only.

Can. J. Chem. Downloaded from www.nrcresearchpress.com by 210.87.254.5 on 09/05/12
For personal use only.

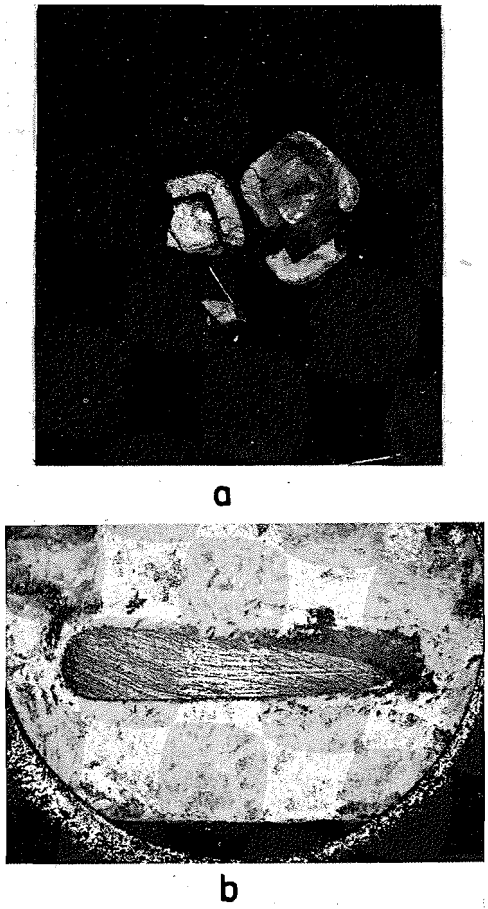

FIG. 2. Macrographs of reacted crystals. (*a*): Approximately 1.5×. Na_2ZrCl_6 and NaCl core. (*b*): Approximately 5×. Na_2ZrCl_6 and NaCl core.

$$[5]\quad (\Delta V)_{NaCl} = (X_0Y_0 + X_0Z_0 + Y_0Z_0)\Delta L - (X_0 + Y_0 + Z_0)\Delta L^2 + \Delta L^3$$

From the stoichiometry of reaction 1,

$$(W)_{NaCl} = \frac{2(W)_{XCl_4}(M)_{NaCl}}{(M)_{XCl_4}}$$

and since $(V)_{NaCl} = (W/\rho)_{NaCl}$ it is readily seen that

$$[6]\quad (\Delta W)_{XCl_4} = \frac{(\Delta V)_{NaCl}(M)_{XCl_4}(\rho)_{NaCl}}{(M)_{NaCl}}$$

where, V, W, M, and ρ represent the volume, weight, molecular weight, and density, respectively. From eqs. 5 and 6 the penetration ΔL can be calculated from the increase in weight due to the reaction with XCl_4 vapor. If a graphical method is used, the change in weight of the various crystals may be plotted as a function of arbitrarily chosen values of ΔL. From these graphs values of ΔL are obtained for the experimentally measured weight changes at the noted times of measurement.

For this calculation the density of the NaCl at 485 °C was obtained from the volumetric coefficient of expansion of NaCl at 20 °C ($\alpha_V = 1.21 \times 10^{-4}$/deg). To correct for the increase in dimensions of the NaCl at the working temperature, the linear coefficient of expansion was estimated from the volumetric coefficient. This correction was insignificant.

Results

Plots of ΔL^2 *vs.* time are shown in Figs. 3 and 4, for various pressures of $ZrCl_4$ and $HfCl_4$. The curves are linear and indicate a diffusion controlled mechanism. The data are summarized in Table 1.

ΔL values were also measured directly from partially reacted crystals from which the reacted layers had been removed. In all cases the measured ΔL agreed to within 5% of the calculated values.

The effect of pressure on the reaction rate is shown in Fig. 5, where the apparent reaction

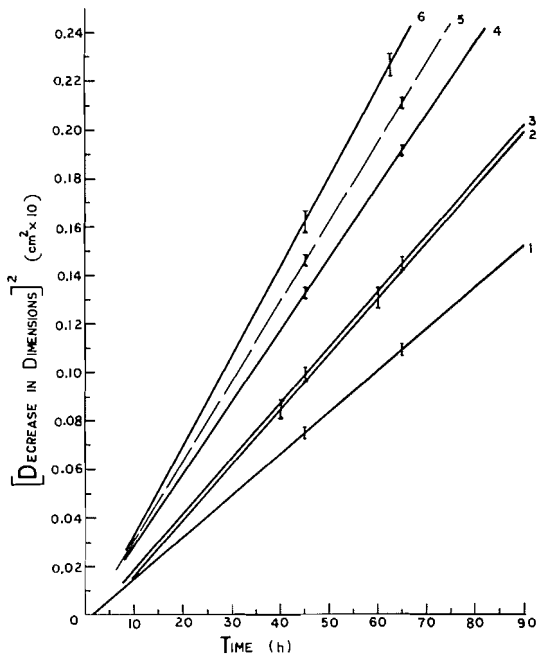

FIG. 3. (Decrease in dimensions of NaCl)² *vs.* time for Na_2ZrCl_6 formation. P_{ZrCl_4} in Torr for run *1*, 68; *2*, 165; *3*, 155; *4*, 308; *5*, 490 (extrapolated); and *6*, 670.

TABLE 1. Summary of data

Run number	Pressure (Torr)	Equation of line	Standard deviation	No. of points measured
		$ZrCl_4$–NaCl system		
1	68	$\Delta L^2 = 0.1709\times10^{-3}t - 0.2151\times10^{-3}$	0.2565×10^{-3}	17
2	165	$\Delta L^2 = 0.2319\times10^{-3}t - 0.9201\times10^{-3}$	0.4129×10^{-3}	19
3	155	$\Delta L^2 = 0.2293\times10^{-3}t - 0.4377\times10^{-3}$	0.2784×10^{-3}	42
4	308	$\Delta L^2 = 0.2989\times10^{-3}t - 0.1191\times10^{-3}$	0.2358×10^{-3}	38
5	490	$\Delta L^2 = 0.3310\times10^{-3}t - 0.2971\times10^{-3}$	0.1994×10^{-3}	6
6	670	$\Delta L^2 = 0.3767\times10^{-3}t - 0.6728\times10^{-3}$	0.4709×10^{-3}	20
		$HfCl_4$–NaCl system		
1	174	$\Delta L^2 = 0.1415\times10^{-3}t - 0.2161\times10^{-3}$	0.2015×10^{-3}	35
2	322	$\Delta L^2 = 0.1727\times10^{-3}t - 0.3094\times10^{-3}$	0.2081×10^{-3}	30
3	526	$\Delta L^2 = 0.1850\times10^{-3}t - 0.3187\times10^{-3}$	0.2729×10^{-3}	26
4	667	$\Delta L^2 = 0.1981\times10^{-3}t - 0.5376\times10^{-3}$	0.3956×10^{-3}	25

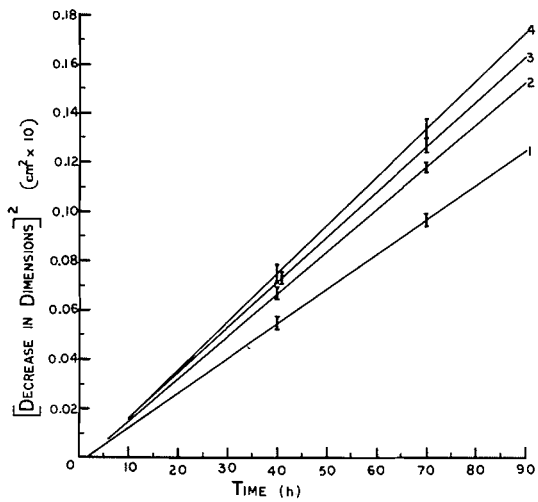

FIG. 4. (Decrease in dimensions of NaCl)² *vs.* time for Na_2HfCl_6 formation. P_{HfCl_4} in Torr for run *1*, 174; *2*, 322; *3*, 526; and *4*, 667.

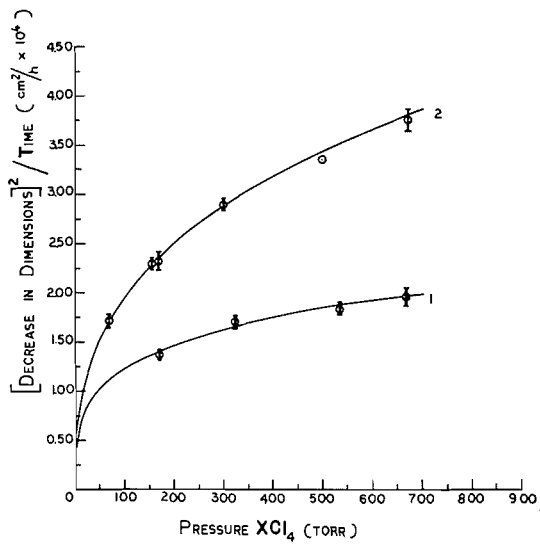

FIG. 5. Apparent reaction rate constant *vs.* pressure of $HfCl_4$ and $ZrCl_4$. *1*, $HfCl_4$ systems. *2*, $ZrCl_4$ systems.

rate constants are plotted *vs.* pressure. The curves in Fig. 5 are represented by the equations

$$[7] \qquad K^1_{Na_2ZrCl_6} = AP_{ZrCl_4}{}^{1/2.8}$$

and

$$[8] \qquad K^1_{Na_2HfCl_6} = BP_{HfCl_4}{}^{1/4.1}$$

which were determined from the least squares plots of log P_{XCl_4} *vs.* log K^1. It is seen that the reaction between NaCl and $ZrCl_4$ is kinetically favored as compared with that of NaCl and $HfCl_4$. Thus, the removal of Hf from Zr by preferential reaction of the $HfCl_4$ vapor with solid NaCl is favored thermodynamically (8) but not kinetically. However, since the proposed method of separation (8) uses powdered NaCl of large surface-to-volume ratio, the kinetic disadvantage is not significant.

Discussion

Generally, parabolic reaction rates indicate that a diffusion process is rate determining. As was seen the effect of pressure on the apparent reaction rate constant differs for the two compounds. Thus, it is probable that the mechanisms of diffusion differ.

Since the $ZrCl_4$ and $HfCl_4$ are relatively large molecules, and as no appreciable porosity was observed at the working temperature, it is unlikely that the molecular vapors are the diffusing species.

Can. J. Chem. Downloaded from www.nrcresearchpress.com by 210.87.254.5 on 09/05/12
For personal use only.

Can. J. Chem. Downloaded from www.nrcresearchpress.com by 210.87.254.5 on 09/05/12
For personal use only.

Although it is known (13) that alkali halides contain Schottky type defects, there is no information regarding the defect structure of the alkali chlorozirconates or hafnates.

The form of the equation describing the pressure dependence of the rate of reaction for the Na_2HfCl_6 and Na_2ZrCl_6 systems may be explained if the presence of an intermediate compound $NaXCl_5$ is postulated. The existence of $NaZrCl_5$ has been implied in phase diagram studies (14–16), where, depending upon the author, it appears as congruently (16) or incongruently melting (14, 15). No previous indication for the presence of $NaHfCl_5$ can be found in the literature. A complex ion of the type Na_2XCl_6 in an ionic solid can be understood by a configuration characterized by a finite co-ordination number. The strength of the bonds between the central cation X and the Cl^- anions, and also the bond distances should be different from those defining a hypothetical noncomplexed state. The condition of local electrical neutrality makes it necessary for the Na^+ cations to be bonded to the central X cations through bridging Cl^- anions.

Accordingly, the XCl_4 vapor is expected to react with the rigid Na_2XCl_6 lattice by direct bonding with surface Cl^- anions.

The following reaction mechanisms may be postulated depending whether one or two bridging chloride anions are reacting with the XCl_4 vapor to form the intermediate $[XCl_5^-]^*$ species.

[9] $$XCl_6^{2-} + XCl_{4\,(v)} \rightarrow 2[XCl_5^-]^* + [Cl_v^-]$$

where $[Cl_v^-] = \frac{1}{2}[XCl_5^-]^*$ or

[10] $$XCl_6^{2-} + XCl_{4\,(v)} \rightarrow 2[XCl_5^-]^* + 2[Cl_v^-]$$

where $[Cl_v^-] = [XCl_5^-]^*$ and $[Cl_v^-]$ indicates the concentration of chloride anion vacancies.

If the rate of diffusion is proportional to the concentration of vacancies the rate of reaction shall depend on the availability of Cl^- vacancies. The Cl^- ions are expected to diffuse from the NaCl inner layer, through the structure containing the Cl^- vacancies, to the gas–solid interface where the formation of the complex species is completed according to

$$[XCl_5^-]^* + Cl^- \rightarrow XCl_6^{2-}$$

The sodium cations are more mobile than the much larger Cl^- anions and therefore should not contribute to the kinetics of the reaction. The Na^+ cations follow the Cl^- anions through the largely open structure of the ionic lattice because of the electrostatic attractions.

The pressure effect on the kinetics is understood in terms of the concentration of XCl_5^- species at the gas–solid interface in accordance with either reactions 9 or 10.

From reactions 9 and 10, the corresponding forms for the equilibrium constants are written as

[11] $$K_9 = \frac{[XCl_5^-]^{*2}[Cl_v^-]}{P_{XCl_4}}$$

or

[12] $$[Cl_v^-] = K_9{}^1 P_{XCl_4}{}^{1/3}$$

and

[13] $$K_{10} = \frac{[XCl_5^-]^{*2}[Cl_v^-]^2}{P_{XCl_4}}$$

or

[14] $$[Cl_v^-] = K_{10}{}^1 P_{XCl_4}{}^{1/4}$$

For this calculation, the $a_{XCl_6^{2-}}$ in pure Na_2XCl_6 is taken to be unity.

From the experimental results the rates of reaction for the $ZrCl_4$–NaCl system appeár to follow reaction 9, as the pressure dependence approximates the 1/3 law, while the system NaCl–$HfCl_4$ appears to follow reaction 10 as the pressure dependence of the rate of reaction approximates the 1/4 law.

The effect of temperature on the kinetics of the reaction between NaCl and $ZrCl_4$ vapor, at the constant pressure of 600 Torr, has been previously investigated in this laboratory (9) and the apparent activation energy was found to have the low value of 12.3 ± 3 kcal/mol. In agreement with the proposed vacancy model, the increase in temperature is expected to decrease the concentration of Cl^- vacancies, because the effective thermodynamic drive for reaction 9 decreases as the decomposition pressure of the complex Na_2ZrCl_6 increases. This effect, however, is counteracted by the increasing rate of diffusion at higher temperatures.

Hence the overall temperature dependence should represent the combination of those two effects and should yield an apparent activation energy which is less than the activation energy usually observed in diffusion controlled processes.

The authors are indebted to the Defence Research Board for its financial aid.

1. S. N. FLENGAS and T. R. INGRAHAM. Can. J. Chem. **38**, 813 (1960).
2. R. L. LISTER and S. N. FLENGAS. Can. J. Chem. **41**, 1548 (1963).
3. J. E. DUTRIZAC and S. N. FLENGAS. Advances in Extractive Metallurgy Symposium. April 17–20, 1967. Institute of Mining and Metallurgy, London, England.
4. R. L. LISTER and S. N. FLENGAS. Can. J. Chem. **42**, 1102 (1964).
5. P. PINT. Kinetic and thermodynamic properties of some alkali chlorozirconate and chlorohafinate compounds. M.A.Sc. Thesis. University of Toronto, Toronto 181, Ontario. 1968.
6. P. PINT and S. N. FLENGAS. Paper presented at Conference of Metallurgists. Aug. 25–27, 1969. Windsor, Ontario.
7. S. N. FLENGAS and P. PINT. Can. Metal. Q. **8**, No. 2, 151 (1969).
8. J. E. DUTRIZAC and S. N. FLENGAS. Canadian Patent 863258. Feb. 9, 1971.
9. J. E. DUTRIZAC and S. N. FLENGAS. Can. J. Chem. **45**, 2317 (1967).
10. A. A. PALKO, A. D. RYON, and D. W. KUHN. J. Phys. Chem. **63**, 319 (1958).
11. S. N. FLENGAS, J. E. DUTRIZAC, and R. L. LISTER. Can. J. Chem. **46**, 495 (1968).
12. I. S. MOROZOV and SUN IN-CHZHU. Russ. J. Inorg. Chem. Vol. 4. No. 11, 1959.
13. W. JOST. Diffusion in solids, liquids, gases. Academic Press Inc., New York. 1960.
14. I. S. MOROZOV and B. G. KORSHUNOV. Russ. J. Inorg. Chem. **1**, 145 (1956).
15. L. J. HOWELL, R. C. SOMMER, and H. H. KELLOGG. Trans. A.I.M.E. Jan. 1957. p. 193.
16. R. V. HORRIGAN. Trans. A.I.M.E. Oct. 1955. p. 1118.

Can. J. Chem. Downloaded from www.nrcresearchpress.com by 210.87.254.5 on 09/05/12
For personal use only.

Can. J. Chem. Downloaded from www.nrcresearchpress.com by 210.87.254.6 on 09/05/12
For personal use only.

Photochemistry of Oximes III.[1] The Photochemical Beckmann Rearrangement

M. CUNNINGHAM, L. S. NG LIM, AND G. JUST
Department of Chemistry, McGill University, Montreal 110, Quebec

Received May 13, 1971

Cycloalkanone oximes of ring-size four to fifteen are shown to yield lactams upon irradiation in methanol solution. Acyclic ketoximes similarly yield Beckmann-type products in methanol solution. Unlike the Beckmann rearrangement, unsymmetrically α-substituted cyclohexanone oximes give mixtures of approximately equal parts of both possible lactam isomers. The photolysis of oximes epimeric at the α-carbon gives products in which the α-center has retained its configuration. The results are interpreted in terms of a concerted breakdown of an oxazirane intermediate.

Par irradiation en solution méthanolique, les oximes de cyclohexanones, dont le cycle comprend entre six et quinze chaînons, conduisent à des lactames. De la même façon, les cétoximes acycliques conduisent en solution méthanolique, à des produits de type Beckmann. Par contre, les oximes de cyclohexanones substituées en α d'une manière dissymétrique conduisent, d'une façon différente à la transposition de Beckmann, aux deux lactames isomères possibles avec environ une égale probabilité. La photolyse d'oximes épimères au carbone α, conduit à des produits où le centre α conserve sa configuration. Les résultats sont interprétés en terme d'une rupture concertée d'une oxazirane intermédiaire.

Canadian Journal of Chemistry, **49**, 2891 (1971)

Introduction

It has been reported (1, 2) that oximes are photosensitive compounds and that the products formed by the photolysis of cyclohexanone oxime (**1**) were solvent dependent, caprolactam (**3**) being formed from the photodecomposition of **1** in methanol and caproamide (**4**) being formed in iso-propanol. The results of further studies (2*d*) of the photoreaction in iso-propanol have been interpreted in terms of an oxazirane (**2**) as the

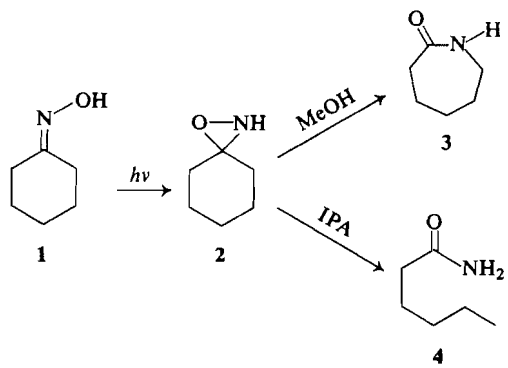

intermediate. We wish now to report in detail on the photoreaction of cyclic and acyclic ketoximes in methanol which results in the formation of Beckmann-type products.

[1]For part II in this series, see ref. 2*d*.

Results

(a) The Effect of α-Substitution on the Photolysis of Cyclohexanone Oximes

The photolysis of α-methyl cyclohexanone oximes is similar to that of cyclohexanone oxime (**1**). The photo-products were isolated in a pure state by t.l.c. in most cases and shown, where possible, to be identical with authentic samples. New compounds were adequately characterized by spectral and analytical data. The yields of the various photoreactions are summarized in Table 1.

(b) Lactam Ratios Formed in the Photolysis of Unsymmetrically α-Substituted Cyclohexanone Oximes

In a previous paper, (2*d*) we reported that the photolysis of unsymmetrically α-substituted cyclohexanone oximes in iso-propanol solution gave preferential cleavage of the bond to the more highly substituted carbon atom, presumably because the more stable free radical was formed. Photolysis in methanol solution gave no such preference for α-cleavage; approximately equal amounts of both possible lactam isomers were formed. The results of the photolysis of three

TABLE 1. Photolysis yields of α-substituted cyclohexanone oximes in methanol solution*

Starting oxime	% Yield			
	Ketone	Oxime	Amide	Lactam
Cyclohexanone oxime	5	27	4	37
2,2,6,6-Tetradeuterocyclohexanone oxime	5	27	7	35
2-Methylcyclohexanone oxime	6	25	4†	38†
2,2-Dimethylcyclohexanone oxime	7	30	3†	36†
2,6-Dimethylcyclohexanone oxime‡	4	15	3	43
2,2,6-Trimethylcyclohexanone oxime	6	23	1†	42†
2,2,6,6-Tetramethylcyclohexanone oxime	13	11	6	44
3,3,5,5-Tetramethylcyclohexanone oxime	9	23	4	41

*All photolyses reported were carried out in a standard manner.
†These are combined yields of both possible isomers.
‡A mixture of *cis* (90%) and *trans* (10%) isomers.

TABLE 2. Lactam ratios formed during the photolysis of unsymmetrically substituted cyclohexanone oximes*

Oxime	Lactam isomers	Ratio
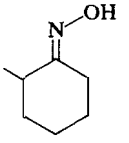	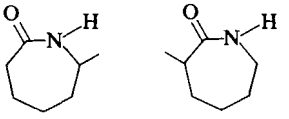	50/50±0.5
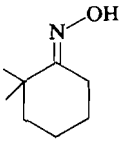	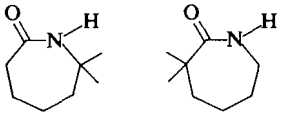	50/50
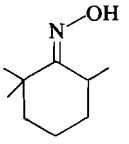	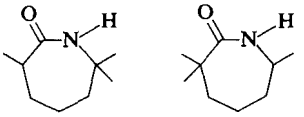	44/56

*All photolyses reported were carried out in a standard manner.

unsymmetrically α-substituted cyclohexanone oximes are summarized in Table 2.

(c) The Photolysis of Medium Sized Ring Ketoximes

The data of Table 2 indicate that free radical intermediates are probably not involved in the photoreaction in methanol solution. To test this hypothesis, the photolysis of a large ring ketoxime, cyclopentadecanone oxime, and of medium ring oximes was studied. If free radical intermediates were involved in the photoreaction a large ring ketoxime would be expected to give little lactam since, once opened, it would close again only to a limited extent. The medium rings should be even more sensitive to radical-type intermediates since ring strain, particularly for nine- and ten-membered rings, would prevent radical recombination. In fact, the lactam yield was little affected by ring size. The results are summarized in Table 3.[2] All compounds described therein were isolated in a pure state by t.l.c. and shown to be identical with authentic

[2]Other cyclic oximes have been included for comparison.

Can. J. Chem. Downloaded from www.nrcresearchpress.com by 210.87.254.6 on 09/05/12
For personal use only.

TABLE 3. The effect of ring size on the photoreaction*

Starting oxime	% Yield				
	Ketone	Oxime remaining	Amide	Lactam	Lactam corrected†
Cyclobutanone oxime	2	65	4	4	11
Cyclopentanone oxime	2	55	7	13	29
Cyclohexanone oxime	5	29	4	37	52
Cycloheptanone oxime	10	16	10	32	38
Cyclooctanone oxime	11	6	15	38	40
Cyclononanone oxime	12	4	13	42	44
Cyclodecanone oxime	17	8	13	34	37
Cycloundecanone oxime	13	11	9	40	45
Cyclododecanone oxime	9	16	6	42	50
Cyclopentadecanone oxime	10	42	6	44	76

*All photolyses reported were carried out in a standard manner.
†Corrected for unreacted oxime.

TABLE 4. Photolysis yields of some α-epimeric oximes*

Oxime	% Yield				
	Ketone	Oxime	Amide	Beckmann product	Epimeric Beckmann product†
Menthone oxime	7	29	3	45	>2
Isomenthone oxime	6	16	3	53	>2
cis-2,6-Dimethylcyclohexanone oxime	6	14	3	44	>1
trans-2,6-Dimethylcyclohexanone oxime	5	47	1	26	>1

*All photolyses reported were carried out in a standard manner.
†The limit of detection was of the order of 1–2%.

samples with the exception of the small and common ring ketones which were too volatile to be isolated.

(d) The Photolysis of Menthone and Isomenthone Oxime and of cis-2,6- and trans-2,6-Dimethylcyclohexanone Oxime

The photolysis of menthone oxime (**5**) and isomenthone oxime (**6**) could, in principle, each give four isomeric lactams, **7**–**10**. Only lactams **7** and **8** were found among the photoproducts of **5**. The lactams isolated were identical to those obtained by the Beckmann rearrangement of menthone oxime. Similarly, photolysis and a Beckmann rearrangement of isomenthone oxime (**6**) gave the same lactams, **9** and **10**.

In like manner, photolysis and a Beckmann rearrangement of *cis*-2,6-dimethylcyclohexanone oxime (**11**) and *trans*-2,6-dimethylcyclohexanone oxime (**12**) gave only lactams **8** and **14** respectively. The results are summarized in Table 4.

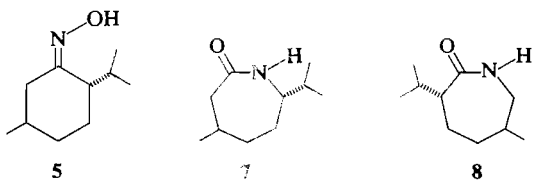

5 **7** **8**

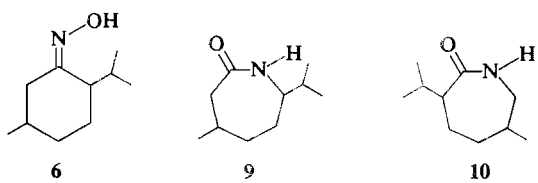

6 **9** **10**

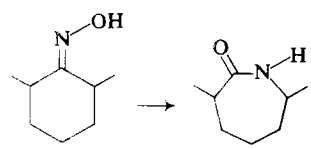

11 **13**

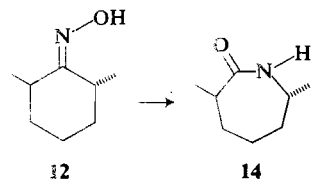

12 **14**

Can. J. Chem. Downloaded from www.nrcresearchpress.com by 210.87.254.6 on 09/05/12
For personal use only.

TABLE 5. Photolysis yields of various acyclic oximes*

Starting oxime	% Yield			
	Ketone	Oxime	Reductive α-cleavage	Beckmann-type products
Acetone oxime	†	44	11	2
Methyl ethyl ketone oxime	†	41	10	12
Diethyl ketone oxime	<1	31	10	21
Methyl *t*-butyl ketone oxime	<1	54	2	10
Di-isopropyl ketone oxime	4	28	4	34
Di-*t*-butyl ketone oxime	5	28	5	24

*All photolyses reported were carried out in a standard manner.
†Not determined

It was noted that recovered isomenthone oxime contained small amounts of menthone oxime and that recovered *cis*-2,6-dimethylcyclohexanone oxime contained some *trans*-2,6-dimethylcyclohexanone oxime.

(e) Photolysis of the Acyclic Ketoximes

The photolysis of the acyclic ketoximes was similar to that of cyclohexanone oxime (**1**), giving mainly Beckmann-type products in methanol. The results of the photolysis of a number of acyclic ketoximes are given in Table 5.

Discussion

(a) The Beckmann Rearrangement

The photolysis of the α-substituted cyclohexanone oximes has been shown to yield the corresponding lactams in good yield. This proves interesting since it suggests a method of extending the usefulness of the Beckmann rearrangement, for which the yield decreases sharply as the degree of α-substitution increases (3). In particular, a Beckmann rearrangement on 2,2,6,6-tetramethylcyclohexanone oxime gives only nitrile and no lactam, while the photoreaction gives a 60% lactam yield.

Furthermore, in the case of unsymmetrically substituted cyclohexanone ketoximes, both possible lactam isomers are formed in good yield in a 1:1 ratio by photolysis. A preponderance of one isomer is formed by the normal Beckmann rearrangement.

(b) The Mechanism of the Photoreaction

Although a free radical intermediate is almost certainly involved in the photolysis of oximes in iso-propanol solution (2), the evidence rules against such intermediates in the photoreaction in methanol. Taylor *et al.* (1) have shown the reaction to be only partly quenched by oxygen. In iso-propanol solution, the reaction is strongly quenched. Also, the ratio of lactam isomers formed in the photolysis of unsymmetrically α-substituted cyclohexanone oximes is almost unity. It is of the order of 6–10:1 for the amide isomers resulting from the photolysis in iso-propanol. Should a radical mechanism be involved, a ratio of lactam isomers similar to the amide isomer ratio would be expected. A large ring (cyclopentadecanone) ketoxime photolyzed normally giving a good yield of lactam as do the ketoximes of the medium rings. If these rings opened to form free radical intermediates, they should close again to the lactams only to a limited extent. Finally, menthone oxime and isomenthone oxime rearranged to the same lactams as those resulting from the Beckmann rearrangement, demonstrating that retention of configuration of the migrating group has occurred during the photo-rearrangement.[3] These results are not compatible with a free radical intermediate and are best explained by a mechanism in which the migrating group never becomes kinetically free of the migration terminus. In a subsequent paper, it will be shown that the photolysis of oxazirane **2** does indeed give caprolactam.

Experimental

All melting points were determined in open capillaries on a Gallenkamp melting point apparatus and are uncorrected. The i.r. spectra were recorded on a Perkin–Elmer 337 grating-type spectrometer as dilute carbon tetrachloride solutions. The n.m.r. spectra were recorded on a Varian A-60 spectrometer operating at 60 MHz (TMS, 0.00 p.p.m.). Merck silica gel HF was used for t.l.c. The photolysis yields were determined by v.p.c. on a Hewlitt–Packard 5751B instrument equipped with dual flame ionization detectors and a disc integrator. Except where noted, the yields were determined on 6 ft × 1/8 in.

[3]A similar finding has recently been reported (11).

Can. J. Chem. Downloaded from www.nrcresearchpress.com by 210.87.254.6 on 09/05/12
For personal use only.

Can. J. Chem. Downloaded from www.nrcresearchpress.com by 210.87.254.6 on 09/05/12
For personal use only.

stainless steel columns packed with 10% Carbowax 20M on high performance chromosorb W (100/120 mesh). All photolyses were carried out in quartz cells in a Rayonet Photochemical Reactor, model 1061, available from the Southern New England Ultraviolet Company, Middletown, Connecticut. The total energy output of the reactor was 32 W of which about 90% was emitted at the 253.7 nm mercury line. All photolyses were carried out in spectroquality methanol available from Matheson, Coleman and Bell.

General Procedure for the Photolysis of Oximes

A solution of the oxime (1 mmol) in methanol (100 ml) was placed in a quartz cell and nitrogen was bubbled through the solution for 20 min (the nitrogen atmosphere was maintained by a mercury seal). All solutions were photolyzed for 2 h, then concentrated to 10 ml for v.p.c. analysis, and/or to 1 ml for separation by t.l.c.

The required *ketones* were either commercially available or prepared by known methods (4–9).

The required *oximes* were prepared by standard methods (10) and sublimed to literature melting points.

cis- and trans-Dimethylcyclohexanone Oxime

cis-2,6-Dimethylcyclohexanone oxime (**11**) was prepared from commercially available 2,6-dimethylcyclohexanone[4] (90% *cis*). Several recrystallizations from hexane gave the pure *cis* oxime, m.p. 77.0–78.0°.

The *trans* isomer (**12**) was obtained by heating to reflux overnight 2,6-dimethylcyclohexanone[4] with 2 equiv of hydroxylamine hydrochloride and 3 equiv of potassium hydroxide in methanol solution. The oxime was shown by v.p.c. to be a mixture (68% *trans* – 32% *cis*). Several recrystallizations from methanol gave the pure *trans* isomer, m.p. 120.5–121.0°.

2,2,4,4-Tetramethyl-3-pentanone Oxime

2,2,4,4-Tetramethyl-3-pentanone oxime was prepared by heating the ketone to reflux with a concentrated solution of hydroxylamine acetate (0.64 g/cc) in methanol for 2 weeks. The oxime was isolated as a crystalline compound in 22% yield and melted, after sublimation and recrystallization, at 159–161°. The i.r. spectrum showed an absorption (O—H) at 3600 cm^{-1}. The n.m.r. spectrum showed signals at δ 1.25 (9H), 1.40 (9H), and 9.50 p.p.m. (1H).

Anal. Calcd. for $C_9H_{19}NO$: C, 68.74; H, 12.18; N, 8.91. Found: C, 69.08; H, 12.08; N, 8.90.

All *amides* and *lactams* were prepared by known procedures.

Attempts to prepare 2,2,6,6-tetramethylcaprolactam by a Beckmann rearrangement were without success. The crude product remaining after extraction showed no carbonyl band in the i.r. spectrum, but always a strong nitrile band.

trans- and cis-2,6-Dimethylcaprolactam

trans-2,6-Dimethylcaprolactam (**14**) was prepared by treating *trans*-2,6-dimethylcyclohexanone oxime (1 g) with thionyl chloride (1 ml) in methylene chloride solution (25 ml) at 0° for 30 min. The product was shown to be a mixture of *cis* and *trans* isomers by v.p.c. The mixture was enriched to 15% *cis* and 85% *trans* by chromatography on alumina (activity I). Fractional sublimation (40°/1 mm) gave the pure *trans* lactam, m.p. 77.0–78.0°.

cis-2,6-Dimethylcaprolactam (**13**) was prepared in an analogous manner. The crude product obtained in 64% yield was purified by recrystallization (hexane) to m.p. 71.0–72.0°.

All lactams and amides obtained in the photolyses of oximes were compared with authentic samples except for the one reported below, which has not yet been described, and which will serve as a typical example of the photolysis mixture work-up.

The Photolysis of 2,2,6,6-Tetramethylcyclohexanone Oxime

Photolysis of 2,2,6,6-tetramethylcyclohexanone oxime yielded, upon work-up by preparative t.l.c. using a benzene–ether eluant (1:1), unreacted oxime, R_f 0.93 and 2,2,6,6-tetramethylcaprolactam, R_f 0.46. Recrystallization of the lactam from pentane gave platelets, m.p. 113.5–114.5°. The i.r. spectrum showed a strong carbonyl absorption at 1640 and an N—H absorption band at 3380 cm^{-1}. The n.m.r. spectrum (CCl_4 solution) showed two methyl singlets at 1.17 (6H) and 1.30 (6H), the ring protons at 1.70 (6H), and a D_2O exchangeable proton at 7.17 p.p.m. (1H).

Anal. Calcd. for $C_{10}H_{19}NO$: C, 70.96; H, 11.32; N, 8.28. Found: C, 70.82; H, 11.12; N, 8.19.

The Photolysis of Unsymmetrically Substituted Cyclohexanone Oximes

Photolysis of these oximes gave lactam mixtures which could be separated by t.l.c. The relative amounts of isomers were determined by g.l.c. and n.m.r. spectroscopy.

The Photolysis of α-Epimeric Oximes

Photolysis of menthone oxime gave a mixture of lactams. Although it gave a single peak in the gas chromatograph on a polar column (10% Carbowax 20M), it separated into two peaks on a 5% OV-210 column. These peaks had the same retention times as the two lactam isomers resulting from a Beckmann rearrangement on menthone oxime and were different from the retention times of the two lactam isomers resulting from a Beckmann rearrangement on isomenthone oxime.

Photolysis of isomenthone oxime similarly gave a mixture of lactams, which separated into two peaks in the gas chromatograph on a 5% OV-210 column. The two peaks had the same retention times as the two lactam isomers resulting from a Beckmann rearrangement on isomenthone oxime and different retention times from the lactam isomers resulting from a Beckmann rearrangement on menthone oxime.

We would like to thank the National Research Council of Canada for financial support.

1. R. T. TAYLOR, M. DOUEK, and G. JUST. Tetrahedron Lett. 4143 (1966).
2. (*a*) J. H. AMIN and P. DE MAYO. Tetrahedron Lett. 1585 (1963). (*b*) M. DOUEK. Ph.D. Thesis. McGill University, Montreal, Quebec, 1966. (*c*) L. S. NG. Ph.D. Thesis. McGill University, Montreal, Quebec, 1968. (*d*) G. JUST and L. S. NG. Can. J. Chem. **46**, 3381 (1968). (*e*) T. OINE and T. MUKAI. Tetrahedron

[4]Aldrich Chemical Company.

Lett. 157 (1969). (*f*) H. IZAWA, P. DE MAYO, and T. TABATA. Can. J. Chem. **47**, 51 (1969). (*g*) B. Fox and H. ROSENBERG. Chem. Commun. 1115 (1969).
3. L. DONARUMA and W. HELDT. The Beckmann rearrangement. *In* Organic reactions. Vol. 11. *Edited by* R. Adams. John Wiley and Sons, New York, N.Y., 1960. p. 1.
4. P. BEST, J. LETTLER, and W. WATERS. J. Chem. Soc. Part 1, 822 (1962).
5. W. S. JOHNSON and H. POSVIC. J. Am. Chem. Soc. **69**, 1361 (1947).
6. K. DAHL. Ph.D. Thesis. McGill University, Montreal, Quebec, 1966.
7. H. C. BROWN and C. P. GARG. J. Am. Chem. Soc. **83**, 2952 (1961).
8. I. C. NIGAIN and L. LEVI. Anal. Chem. **35**, 1087 (1963).
9. J. E. DUBOIS, B. LEHEUP, S. MOLNARFI, F. HENNEGUIN, and P. BAUER. Bull. Soc. Chim. 2024 (1964).
10. R. SHRINER, R. FUSON, and D. CURTIN. The systematic identification of organic compounds, 5th Ed. John Wiley and Sons, New York, N.Y., 1964. p. 290.
11. H. SUGINOME and H. TAKAHASHI. Tetrahedron Lett. 5119 (1970).

Can. J. Chem. Downloaded from www.nrcresearchpress.com by 210.87.254.6 on 09/05/12
For personal use only.

Can. J. Chem. Downloaded from www.nrcresearchpress.com by 210.87.254.42 on 09/05/12
For personal use only.

Dehydration of Amides to Nitriles Initiated by Hexamethylphosphoric Triamide

RICHARD S. MONSON AND DEGGARY N. PRIEST
Department of Chemistry, California State College, Hayward, California 94542

Received May 4, 1971

Aliphatic and aromatic carboxamides are found to undergo ready dehydration in hexamethylphosphoric triamide at 220–240° affording the corresponding nitriles in good yield.

Les carboxamides aliphatiques et aromatiques subissent une déshydratation facile dans le HMPT à 220–240° et conduisent aux nitriles correspondants avec un bon rendement.

Canadian Journal of Chemistry, 49, 2897 (1971)

Hexamethylphosphoric triamide (HMPT) has found wide use as a reaction medium (1, 2), but has only recently been observed (3) to act as a dehydrating agent in the conversion of alcohols to olefins at elevated temperatures. In the course of our investigations into the chemistry of HMPT (3, 4), we have observed another dehydration reaction initiated by HMPT which is the subject of this report.

When primary aliphatic or aromatic carboxamides were heated to reflux in approximately a three-fold molar excess of HMPT (pot temperatures of 220–240°), a copious evolution of dimethylamine was observed. If the corresponding nitrile is volatile (b.p. <170°), it was then observed to distill from the reaction flask in a good state of purity but for the presence of dimethylamine. A simple work-up affords the pure nitrile. For high boiling products, a 2 h reflux is sufficient to allow conversion of amides to nitriles. The yields of nitriles obtained by these procedures are given in Table 1.

TABLE 1. Nitriles by HMPT dehydration of amides

Amide	Yield of corresponding nitrile (%)	Method
Propionamide	94	Distillation
n-Butyramide	75	Distillation
Hexanoamide	78	Distillation
Benzamide	67	Reflux
Phenylacetamide	75	Reflux
Adipamide	49	Reflux

The rapid evolution of dimethylamine, when considered in the light of the known propensity of HMPT to exchange with hydroxylic compounds (1, 3) suggests that the initial step of the reaction is the formation of a phosphorodiamidate derivative of the enol form of the amide (eq. 1). The basic solvent may then initiate the elimination of this leaving group affording the nitrile (eq. 2).

Conventional reagents for carrying out the dehydration of amides to nitriles are usually extremely reactive towards many functional groups, and the reaction by-products may also be reactive.

[1] $$R{-}CONH_2 \rightleftharpoons R{-}C(=NH){-}OH \xrightarrow{HMPT} R{-}C(=NH){-}O{-}P(=O)(NMe_2)_2 + Me_2NH \uparrow$$

[2] $$R{-}C(=N\text{H})\text{-}O{-}P(=O)(NMe_2)_2 \longrightarrow R{-}C{\equiv}N + {}^{\ominus}O{-}P(=O)(NMe_2)_2$$

$$\ddot{O}{=}P(NMe_2)_3 \qquad HO^{\oplus}{=}P(NMe_2)_3$$

Thionyl chloride, for example, effectively dehydrates amides but generates hydrogen chloride in the process making it an unsuitable reagent for acid-sensitive compounds. On the other hand, neither HMPT or its reaction products are highly reactive offering a possible advantage in the preparation of sensitive nitriles.

Experimental

All amides employed were the commercially available materials. HMPT, technical grade, was used without purification. Products were identified by comparison of their retention times in g.l.p.c. with authentic samples. Analysis by g.l.p.c. was carried out on an Aerograph Model 600 HyFi with flame ionization detector, column 15% SE-30 on acid washed Chromosorb, 1/8 in. × 2 m.

Dehydration of Amides

(a) Distillation Method

The amide (0.1 mol) is added to 65 ml of HMPT in a set-up arranged for distillation. The mixture is brought to reflux (pot, 220–240°) and dimethylamine and the nitrile distill from the reaction vessel over a period of about 2 h. The distillate is taken up in ether, the ethereal solution is washed three times with brine, and the dried (sodium sulfate) solution concentrated under reduced pressure. Distillation of the residue affords the desired nitrile.

(b) Reflux Method

The same proportions of amide and HMPT are refluxed together for 2 h. The cooled reaction mixture is diluted with 100 ml of brine and extracted with ether. (Disubstituted nitriles may require extraction into chloroform due to their limited solubility in ether.) The organic phase is washed, dried, concentrated, and distilled as above.

1. H. NORMANT. Angew Chem. Intern. Ed. **6**, 1046 (1967).
2. H. NORMANT. Colloq. Int. Centre Nat. Rech. Sci. No. 182, 207 (1970).
3. R. S. MONSON. Tetrahedron Lett. 567 (1971).
4. R. S. MONSON. Chem. Commun. 113 (1971).

An Attempted Synthesis of 4,5-Bis(dimethylamino)-1,2,3-thiadiazole

JAMES E. OLIVER AND JERRY B. STOKES

Entomology Research Division, Agricultural Research Center, USDA, Beltsville, Maryland 20705

Received April 26, 1971

Oxidation of 2-hydrazono-*N,N,N',N'*-tetramethylthiooxamide (**8**) by various reagents did not provide the expected thiadiazole **4**, but rather gave azines **11** and **12**. It is postulated that the hydrazone derived from **8** lost nitrogen to give carbene **14** which in turn produced **11** and **12**.

L'oxydation du l'hydrazono-2 tétraméthyl-*N,N,N',N'* thiooxamide (**8**) par différents réactifs ne conduit pas au thiadiazole **4** attendu, mais plutôt aux azines **11** et **12**. Il est suggéré que l'hydrazone qui dérive de **8**, perd l'azote et conduit au carbène **14** qui à son tour produit **11** et **12**.

Canadian Journal of Chemistry, 49, 2898 (1971)

3,5 - Bis(dimethylamino) - 1,2,4 - dithiazolium chloride (**1**) (1), hexamethylphosphoric triamide (**2**) (2), and hexamethylmelamine (**3**) (3) are all chemosterilants (4) against house flies (*Musca domestica* L.) and certain other insects. In at least the latter two cases, replacement of dimethylamino substituents by other groups tends to result in reduction of male-sterilizing activity (2, 3). In the hope of discovering new insect sterilants and defining requirements for activity in dimethylamino-substituted compounds, we decided to synthesize a series of bis(dimethylamino) heterocyclic compounds including 4,5-bis-(dimethylamino)-1,2,3-thiadiazole (**4**).

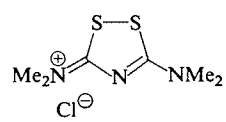

1

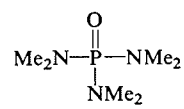

2

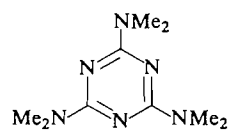

3

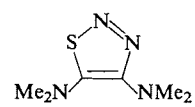

4

Can. J. Chem. Downloaded from www.nrcresearchpress.com by 210.87.254.42 on 09/05/12
For personal use only.

Thionyl chloride, for example, effectively dehydrates amides but generates hydrogen chloride in the process making it an unsuitable reagent for acid-sensitive compounds. On the other hand, neither HMPT or its reaction products are highly reactive offering a possible advantage in the preparation of sensitive nitriles.

Experimental

All amides employed were the commercially available materials. HMPT, technical grade, was used without purification. Products were identified by comparison of their retention times in g.l.p.c. with authentic samples. Analysis by g.l.p.c. was carried out on an Aerograph Model 600 HyFi with flame ionization detector, column 15% SE-30 on acid washed Chromosorb, 1/8 in. × 2 m.

Dehydration of Amides

(a) Distillation Method

The amide (0.1 mol) is added to 65 ml of HMPT in a set-up arranged for distillation. The mixture is brought to reflux (pot, 220–240°) and dimethylamine and the nitrile distill from the reaction vessel over a period of about 2 h. The distillate is taken up in ether, the ethereal solution is washed three times with brine, and the dried (sodium sulfate) solution concentrated under reduced pressure. Distillation of the residue affords the desired nitrile.

(b) Reflux Method

The same proportions of amide and HMPT are refluxed together for 2 h. The cooled reaction mixture is diluted with 100 ml of brine and extracted with ether. (Disubstituted nitriles may require extraction into chloroform due to their limited solubility in ether.) The organic phase is washed, dried, concentrated, and distilled as above.

1. H. NORMANT. Angew Chem. Intern. Ed. **6**, 1046 (1967).
2. H. NORMANT. Colloq. Int. Centre Nat. Rech. Sci. No. 182, 207 (1970).
3. R. S. MONSON. Tetrahedron Lett. 567 (1971).
4. R. S. MONSON. Chem. Commun. 113 (1971).

Can. J. Chem. Downloaded from www.nrcresearchpress.com by 210.87.254.5 on 09/05/12
For personal use only.

An Attempted Synthesis of 4,5-Bis(dimethylamino)-1,2,3-thiadiazole

JAMES E. OLIVER AND JERRY B. STOKES
Entomology Research Division, Agricultural Research Center, USDA, Beltsville, Maryland 20705

Received April 26, 1971

Oxidation of 2-hydrazono-*N,N,N',N'*-tetramethylthiooxamide (**8**) by various reagents did not provide the expected thiadiazole **4**, but rather gave azines **11** and **12**. It is postulated that the hydrazone derived from **8** lost nitrogen to give carbene **14** which in turn produced **11** and **12**.

L'oxydation du l'hydrazono-2 tétraméthyl-*N,N,N',N'* thiooxamide (**8**) par différents réactifs ne conduit pas au thiadiazole **4** attendu, mais plutôt aux azines **11** et **12**. Il est suggéré que l'hydrazone qui dérive de **8**, perd l'azote et conduit au carbène **14** qui à son tour produit **11** et **12**.

Canadian Journal of Chemistry, 49, 2898 (1971)

3,5 - Bis(dimethylamino) - 1,2,4 - dithiazolium chloride (**1**) (1), hexamethylphosphoric triamide (**2**) (2), and hexamethylmelamine (**3**) (3) are all chemosterilants (4) against house flies (*Musca domestica* L.) and certain other insects. In at least the latter two cases, replacement of dimethylamino substituents by other groups tends to result in reduction of male-sterilizing activity (2, 3). In the hope of discovering new insect sterilants and defining requirements for activity in dimethylamino-substituted compounds, we decided to synthesize a series of bis(dimethylamino) heterocyclic compounds including 4,5-bis-(dimethylamino)-1,2,3-thiadiazole (**4**).

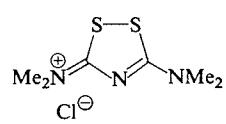

1

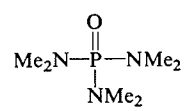

2

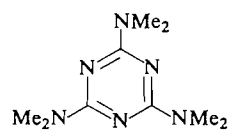

3

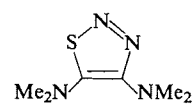

4

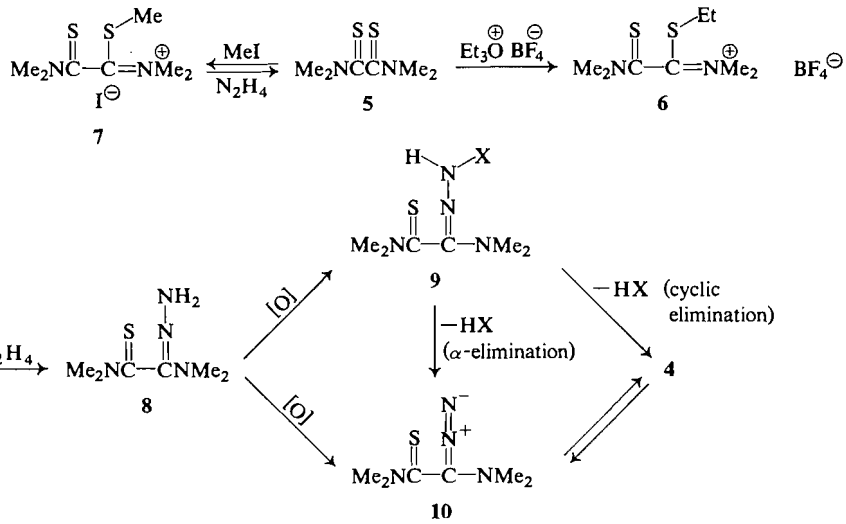

SCHEME 1

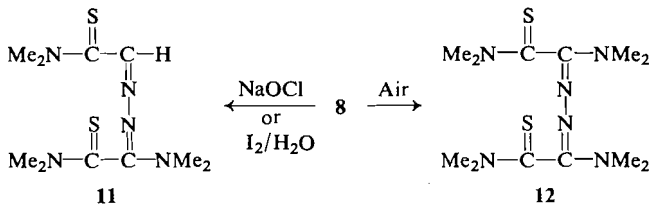

SCHEME 2

A few amino-substituted 1,2,3-thiadiazoles have been reported (5–7), but none of the synthetic methods seemed readily adaptable to synthesis of bis(dialkylamino)-1,2,3-thiadiazoles. For example, the reactions of diazoalkanes with isothiocyanates (7) necessarily provide monosubstituted amines, and the most general synthesis of the ring system involves the direct introduction of a diazo function into an activated methylene position and thus invariably produces carboxyl or acyl substituted thiadiazoles.

We therefore undertook a new synthesis of the ring system wherein the diazo function or its equivalent would be created by oxidation of the corresponding hydrazone. The required hydrazonothiooxamide **8** was synthesized as shown in Scheme 1. *N,N,N′,N′*-Tetramethyldithiooxamide (**5**)(8) was alkylated with triethyloxonium tetrafluoroborate to provide the *S*-ethyl salt **6** which reacted smoothly with hydrazine to give **8**. Methyl iodide also alkylated **5** to give the *S*-methyl salt **7**; however **7** reacted with hydrazine to regenerate **5**, presumably because of attack by hydrazine on the *S*-methyl.

Pross and Sternhell (9) and Barton, *et al* (10) have reported that hydrazones are oxidized to diazo compounds by iodine in the presence of base and have postulated that an *N*-iodohydrazone is formed that loses HI to give the diazo compound. We reasoned that hydrazone **8** should react analogously with iodine, and that loss of HI from the *N*-iodohydrazone **9** should occur by one of two pathways, either of which would provide the thiadiazole **4**; α-elimination would give the diazothioamide **10** which could spontaneously cyclize to **4** (5, 11) whereas cyclic elimination involving displacement of iodide by the thiocarbonyl would provide **4** directly.

When **8** was reacted with iodine in aqueous sodium carbonate at 0–5°, the only product isolated (75%) was a yellow solid identified as the azine **11** (see Scheme 2). The same azine was obtained in about 50% yield from the oxidation of **8** with aqueous sodium hypochlorite.

Can. J. Chem. Downloaded from www.nrcresearchpress.com by 210.87.254.5 on 09/05/12
For personal use only.

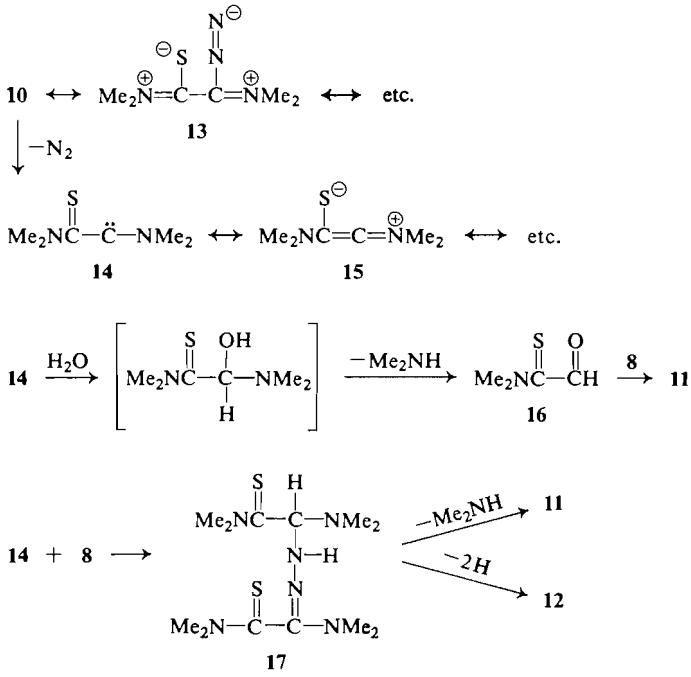

SCHEME 3

Hydrazone **8** was also slowly oxidized by air; a neat sample that had remained at room temperature for two weeks was found to contain a yellow solid different from that isolated from the iodine and hypochlorite oxidations. The material has been identified as the symmetrical azine **12**.

Mercuric oxide and silver oxide have also been reported (12) to oxidize hydrazones to diazo compounds; however **8** was recovered unchanged after attempted reaction with each of these reagents. 1-Chlorobenzotriazole (13) in methylene chloride oxidized **8** to a mixture of **11** and **12** plus a small amount of unidentified material. We were unable to separate the mixture but its n.m.r. and i.r. spectra indicated a ratio of **11** to **12** of about 2:3.

Thus we have oxidized **8** under conditions reported to convert hydrazones to diazo compounds, but in spite of the proximity of the thioamide function, the expected cyclization (11) did not occur. Although there are a variety of mechanisms by which azines can be formed from hydrazones (9, 10) and diazo compounds (12,14, 15), we feel that the formation of **11** and **12** is best explained by loss of N_2 from **10** to give carbene **14**, and subsequent conversion (depending on the reaction medium) of **14** to **11** and **12** as indicated in Scheme 3. Resonance form **13** of the diazothioamide **10** indicates that both the terminal nitrogen and sulfur atoms, between which bond formation must occur for ring-closure, bear partial negative charges. Thus electron donation into the diazo function by the dimethylamino group[1] may promote carbene formation instead of ring formation.

Experimental[2]

Melting points were obtained on a Thomas Hoover Capillary Melting Point Apparatus and are uncorrected. The n.m.r. spectra were recorded on a Varian Model T-60 spectrophotometer and i.r. spectra were obtained on a Perkin–Elmer Model 137 sodium chloride prism spectrophotometer. Magnesium sulfate was employed as a drying agent. Microanalyses were performed by Galbraith Laboratories, Inc., Knoxville, Tennessee.

[(Dimethylthiocarbamoyl)(ethylthio)methylene]-dimethylammonium Tetrafluoroborate (6)

A solution of triethyloxonium tetrafluoroborate (30.3 g, 0.161 mol) in methylene chloride (160 ml) was

[1]A closely related phenomenon has recently been reported (16*a*, *b*) in the equilibration of dialkylamino substituted 1,2,3-triazoles with diazoamidines.

[2]Mention of a proprietary product or company does not necessarily imply endorsement of the product or company by the U.S. Department of Agriculture.

Can. J. Chem. Downloaded from www.nrcresearchpress.com by 210.87.254.5 on 09/05/12
For personal use only.

Can. J. Chem. Downloaded from www.nrcresearchpress.com by 210.87.254.5 on 09/05/12
For personal use only.

added dropwise to a stirred solution of *N,N,N',N'*-tetramethyldithiooxamide (**5**, (8), 28.4 g, 0.161 mol) in methylene chloride (160 ml) under nitrogen. The solution was allowed to stand overnight at room temperature, then the solvent was removed *in vacuo* to yield an oil that crystallized on standing. Recrystallization from tetrahydrofuran–acetonitrile afforded 43.2 g (92%) of **6**, m.p. 92–93.5°; i.r. ν ($CHCl_3$) 1607, 1545, 1405, 1060 cm^{-1}; n.m.r. δ ($CDCl_3$) 1.47 (t, 3), 3.22 (q, 2), 3.46 (s, 3), 3.57 (s, 3), 3.60 (s, 3), 3.63 (s, 3).

Anal. Calcd. for $C_8H_{17}BF_4N_2S_2$: C, 32.89; H, 5.86; N, 9.59; S, 21.95. Found: C, 32.69; H, 5.89; N, 9.54; S, 21.97.

[(Dimethylthiocarbamoyl)(methylthio)methylene]-dimethylammonium Iodide (7)

Methyl iodide (11.0 g, 0.077 mol) in methylene chloride (50 ml) was slowly added to a solution of **5** (13.2 g, 0.075 mol) in methylene chloride (200 ml). After addition, the solution was refluxed 4 h. Evaporation of the solvent and recrystallization of the residue from absolute ethanol gave 19.9 g (84%) of **7** m.p. 142–143°; i.r. ν, ($CHCl_3$) 1603, 1525, 1395, 1210, 1150, 1125 cm^{-1}; n.m.r. δ ($CDCl_3$) 2.87 (s, 3), 3.68 (s, 3), 3.78 (s, 3), 3.87 (s, 3), 3.90 (s, 3).

Anal. Calcd. for $C_7H_{15}IN_2S_2$: C, 26.42; H, 4.75; I, 39.88. Found: C, 26.37; H, 4.59; I, 39.68.

N,N,N',N'-Tetramethyl-1-thiooxamide 2-Hydrazone (8)

A solution of anhydrous hydrazine (4.8 g, 0.15 mol) in methylene chloride (100 ml) was added dropwise to a stirred solution of **6** (21.9 g, 0.075 mol) in methylene chloride (400 ml) under nitrogen at room temperature. The mixture was stirred overnight, filtered, and the filtrate was evaporated. The resulting orange oil was extracted with ether (150 ml) and the ether solution was dried, filtered and evaporated. Distillation of the residue yielded 11.1 g (85%) of **8**, b.p. 92–93° (0.08 mm), i.r. ν ($CHCl_3$) 1615, 1512, 1385, 1144, 934, 867 cm^{-1}; n.m.r. δ ($CDCl_3$) 2.83 (s, 6), 3.28 (s, 3), 3.50 (s, 3), 4.30 (s, 2).

Anal. Calcd. for $C_6H_{14}N_4S$: C, 41.35; H, 8.10; N, 32.15. Found: C, 41.17; H, 8.24; N, 32.23.

Recrystallization (benzene–hexane) of the pot residue from the distillation gave a small amount of **12** identical to that isolated from the air oxidation of **8** (*vide infra*).

Reaction of 7 with Hydrazine

Anhydrous hydrazine (0.150 g, 4.7 mmol) in absolute ethanol (5 ml) was added dropwise to a stirred solution of **7** (0.636 g, 2.0 mmol) in absolute ethanol (20 ml) at room temperature under nitrogen. The mixture was stirred overnight then the solvent was evaporated *in vacuo*. Extraction of the residue with benzene followed by recrystallization from benzene–hexane gave 0.290 g (83%) of **5**, m.p. 136–138°, whose i.r. spectrum was identical to that of the authentic material.

Oxidation of 8 with Iodine. N,N,N',N'-Tetramethyl-1-thiooxamide 2-Azine with N,N-Dimethyl-1-thioglyoxaldehyde (11)

A solution of iodine (0.254 g, 1.0 mmol) and potassium iodide (0.498 g, 3.0 mmol) in water (20 ml) was added dropwise to a cold (0–5°), stirred solution of **8** (0.174 g, 1.0 mmol) and sodium carbonate (0.106 g, 1.0 mmol) in water (10 ml). The mixture was stirred for 2 h during which time a yellow solid separated (0.103 g, 75%, m.p. 170–176°). Recrystallization from benzene gave pure **11**, m.p. 179.5–180°, i.r. ν ($CHCl_3$) 1590, 1530, 1398, 914, 873 cm^{-1}; n.m.r. δ ($CDCl_3$) 3.10 (s, 6), 3.19 (s, 3), 3.46 (s, 3), 3.48 (s, 3), 3.53 (s, 3), 8.23 (s, 1).[3]

Anal. Calcd. for $C_{10}H_{19}N_2S$: C, 43.93; H, 7.00; N, 25.61; S, 23.45. Found: C, 43.82; H, 6.95; N, 25.45; S, 23.31.

Oxidation of 8 with Sodium Hypochlorite

Aqueous sodium hypochlorite (3.45 ml, 5.25%) was added dropwise to a cold (0–5°) solution of **8** (0.523 g, 3.0 mmol) in water (10 ml). A yellow–orange solid gradually precipitated that was collected and recrystallized from benzene to give pure **11**, m.p. 179.5–180°, identical to that obtained from the iodine oxidation.

Air Oxidation of 8. N,N,N',N'-Tetramethyl-1-thiooxamide 2-Azine (12)

A sample of pure **8** was exposed to air at room temperature for 2 weeks. A yellow solid (**12**) slowly separated (*ca.* 5% conversion in this time); it was purified by recrystallization from benzene–hexane, m.p. 186.5–187.5°, i.r. ν ($CHCl_3$) 1567, 1520, 1372, 1148, 1050, 941, 868 cm^{-1}; n.m.r. δ ($CDCl_3$) 2.88 (s, 12), 3.23 (s, 6), 3.47 (s, 6) (17).

Anal. Calcd. for $C_{12}H_{24}N_6S_2$: C, 45.54; H, 7.64; N, 26.55; S, 20.26. Found: C, 45.47; H, 7.56; N, 26.26; S, 20.12.

Oxidation of 8 with 1-Chlorobenzotriazole (13)

A solution of 1-chlorobenzotriazole (0.766 g, 5.0 mmol) in methylene chloride (50 ml) was added dropwise to a cold (0–5°), stirred solution of **8** (0.87 g, 5.0 mmol) in methylene chloride (25 ml) under nitrogen. After stirring at room temperature overnight the solution was washed with 1 *N* sodium hydroxide (2 × 10 ml), then with water (10 ml), and finally with brine (10 ml). The organic layer was dried, filtered, and evaporated to yield 0.705 g of brown residue that was chromatographed on silica gel. Elution with 1:1 benzene–chloroform gave 0.439 g of a yellow semi-solid. The n.m.r. spectrum indicated a 60:40 ratio of **12** to **11** plus a small amount of unidentified material (n.m.r. δ ($CDCl_3$) 3.00 and 3.30). Further attempts at purification were unsuccessful.

1. R. L. Fye, G. C. LaBrecque, A. B. Borkovec, and J. Morgan, Jr. J. Econ. Entomol. **62**, 522 (1969).
2. P. H. Terry and A. B. Borkovec. J. Med. Chem. **10**, 118 (1967).
3. A. B. Borkovec and A. B. DeMilo. J. Med. Chem. **10**, 457 (1967).
4. A. B. Borkovec. Insect chemosterilants. Interscience, New York, N.Y., 1966.
5. D. L. Pain and R. Slack. J. Chem. Soc. 5166 (1965).
6. J. Goerdeler and G. Gnad. Tetrahedron Lett. 795 (1964).
7. J. Goerdeler and G. Gnad. Chem. Ber. **99**, 1618 (1966).

[3]Slow rotation around N—C bonds in thioamide is known to produce splitting in the n.m.r. signals of alkyl hydrogens (17).

8. H. L. KLOPPING and G. J. M. VAN DER KERK. Rec. Trav. Chim. Pays-Bas, **70**, 936 (1951).
9. A. PROSS and S. STERNHELL. Aust. J. Chem. **23**, 989 (1970).
10. D. H. R. BARTON, R. E. O'BRIEN, and S. J. STERNHELL. J. Chem. Soc. 470 (1962).
11. P. A. S. SMITH. The chemistry of open-chain organic nitrogen compounds. Vol. 2. W. A. Benjamin, Inc., New York, N.Y., 1966. p. 249.
12. P. A. S. SMITH. The chemistry of open-chain organic nitrogen compounds. Vol. 2. W. A. Benjamin, Inc., New York, N.Y., 1966. p. 165.
13. C. W. REES and R. C. STORR. Chem. Commun. 1305 (1968).
14. P. YATES, D. G. FARNUM, and D. W. WILEY. Tetrahedron, **18**, 891 (1962).
15. H. REIMLINGER. Chem. Ber. **97**, 339 (1964).
16. (*a*) R. E. HARMON, F. STANLEY, JR., S. K. GUPTA, and J. JOHNSON. J. Org. Chem. **35**, 3444 (1970). (*b*) M. REGITZ and G. HIMBERT. Tetrahedron Lett. 2823 (1970).
17. W. E. STEWART and T. H. SIDDALL, III. Chem. Rev. **70**, 517 (1970).

Optically Active Amines. Part XIII.[1] Circular Dichroism of the *N*-Salicylidene Derivatives of Alkylamines

HOWARD E. SMITH AND HARRY E. ENSLEY[2]
Department of Chemistry, Vanderbilt University, Nashville, Tennessee 37203

Received April 6, 1971

Comparison of the c.d. spectra of (*S*)-(+)-*N*-salicylidene-α-phenylethylamine with those of (*S*)-(+)-*N*-salicylidene-sec-butylamine and (*R*)-(−)-*N*-salicylidene-2,2-dimethyl-3-aminobutane confirms the conclusion that the strong rotational strength shown by *N*-salicylidene-α- and β-phenylalkylamines is due to an interaction of the π-electron system of the phenyl group and the salicylidenimino chromophore. The sign of the Cotton effects near 255 and 315 nm shown by the *N*-salicylidenes of alkylamines and cycloalkylamines, when these are conformationally defined, can be correlated with their absolute configurations using a planar sector rule, similar to that used for the interpretation of the c.d. and o.r.d. spectra of *N*-salicylidene-α- and β-phenylalkylamines.

La comparaison des spectres de d.c. du *S*-(+)-*N*-salicylidène α-phényléthylamine avec ceux du *S*-(+)-*N*-salicylidène sec-butylamine et R-(−)-*N*-salicylidène diméthyl-2,2 amino-3 butane confirme le fait que l'importance de la force de rotation qui se manifeste dans les *N*-salicylidène α et β-phénylalkylamines, est due à une interaction des électrons π du groupe phényle avec le chromophore salicylidenimino. Les signes des effets Cotton entre 255 et 315 nm dans les *N*-salicylidènes d'alkylamines, dans une conformation définie, peuvent être reliés aux configurations absolues en utilisant le même genre de règle que celle utilisée dans l'interprétation des spectres de d.c. et d.o.r. des *N*-salicylidène α et β-phénylalkylamines.

Canadian Journal of Chemistry, 49, 2902 (1971)

In an earlier paper (2), the optical rotatory dispersion (o.r.d.) curves of the *N*-salicylidenes [(*S*)-**1***b* and (*S*)-**2***b*] of (*S*)-(−)-α-phenylethylamine[3] [(*S*)-**1***a*] and (*S*)-(+)-α-benzylethylamine [(*S*)-**2***a*] were compared with that of the *N*-salicylidene [(*S*)-**3***b*] of (*S*)-(+)-sec-butylamine [(*S*)-**3***a*]. Both (*S*)-**1***b* and (*S*)-**2***b* in ethanol show

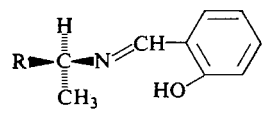

(*S*)-**1***b* R = C_6H_5
(*S*)-**2***b* R = $C_6H_5CH_2$
(*S*)-**3***b* R = C_2H_5

positive Cotton effects near 315 and 410 nm. In contrast, (*S*)-**3***b* is much weaker in rotatory power, and in ethanol only one weak peak at 437 nm could be observed. It was concluded that the strong rotational strength shown by *N*-salicylidene-α- and β-phenylalkylamines is due to an interaction of the π-electron system of the

[1]Part XII. H. E. Smith and A. A. Hicks (1).
[2]National Science Foundation Undergraduate Summer Fellow, 1969.
[3]Signs in parentheses refer to rotatory powers observed with sodium D-light for the amines as the neat liquid and for the *N*-salicylidenes as solutions in methanol.

Can. J. Chem. Downloaded from www.nrcresearchpress.com by 210.87.254.5 on 09/05/12
For personal use only.

8. H. L. KLOPPING and G. J. M. VAN DER KERK. Rec. Trav. Chim. Pays-Bas, **70**, 936 (1951).
9. A. PROSS and S. STERNHELL. Aust. J. Chem. **23**, 989 (1970).
10. D. H. R. BARTON, R. E. O'BRIEN, and S. J. STERNHELL. J. Chem. Soc. 470 (1962).
11. P. A. S. SMITH. The chemistry of open-chain organic nitrogen compounds. Vol. 2. W. A. Benjamin, Inc., New York, N.Y., 1966. p. 249.
12. P. A. S. SMITH. The chemistry of open-chain organic nitrogen compounds. Vol. 2. W. A. Benjamin, Inc., New York, N.Y., 1966. p. 165.
13. C. W. REES and R. C. STORR. Chem. Commun. 1305 (1968).
14. P. YATES, D. G. FARNUM, and D. W. WILEY. Tetrahedron, **18**, 891 (1962).
15. H. REIMLINGER. Chem. Ber. **97**, 339 (1964).
16. (*a*) R. E. HARMON, F. STANLEY, JR., S. K. GUPTA, and J. JOHNSON. J. Org. Chem. **35**, 3444 (1970). (*b*) M. REGITZ and G. HIMBERT. Tetrahedron Lett. 2823 (1970).
17. W. E. STEWART and T. H. SIDDALL, III. Chem. Rev. **70**, 517 (1970).

Optically Active Amines. Part XIII.[1] Circular Dichroism of the *N*-Salicylidene Derivatives of Alkylamines

HOWARD E. SMITH AND HARRY E. ENSLEY[2]
Department of Chemistry, Vanderbilt University, Nashville, Tennessee 37203

Received April 6, 1971

Comparison of the c.d. spectra of (*S*)-(+)-*N*-salicylidene-α-phenylethylamine with those of (*S*)-(+)-*N*-salicylidene-sec-butylamine and (*R*)-(−)-*N*-salicylidene-2,2-dimethyl-3-aminobutane confirms the conclusion that the strong rotational strength shown by *N*-salicylidene-α- and β-phenylalkylamines is due to an interaction of the π-electron system of the phenyl group and the salicylidenimino chromophore. The sign of the Cotton effects near 255 and 315 nm shown by the *N*-salicylidenes of alkylamines and cycloalkylamines, when these are conformationally defined, can be correlated with their absolute configurations using a planar sector rule, similar to that used for the interpretation of the c.d. and o.r.d. spectra of *N*-salicylidene-α- and β-phenylalkylamines.

La comparaison des spectres de d.c. du *S*-(+)-*N*-salicylidène α-phényléthylamine avec ceux du *S*-(+)-*N*-salicylidène sec-butylamine et R-(−)-*N*-salicylidène diméthyl-2,2 amino-3 butane confirme le fait que l'importance de la force de rotation qui se manifeste dans les *N*-salicylidène α et β-phénylalkylamines, est due à une interaction des électrons π du groupe phényle avec le chromophore salicylidenimino. Les signes des effets Cotton entre 255 et 315 nm dans les *N*-salicylidènes d'alkylamines, dans une conformation définie, peuvent être reliés aux configurations absolues en utilisant le même genre de règle que celle utilisée dans l'interprétation des spectres de d.c. et d.o.r. des *N*-salicylidène α et β-phénylalkylamines.

Canadian Journal of Chemistry, 49, 2902 (1971)

In an earlier paper (2), the optical rotatory dispersion (o.r.d.) curves of the *N*-salicylidenes [(*S*)-**1***b* and (*S*)-**2***b*] of (*S*)-(−)-α-phenylethylamine[3] [(*S*)-**1***a*] and (*S*)-(+)-α-benzylethylamine [(*S*)-**2***a*] were compared with that of the *N*-salicylidene [(*S*)-**3***b*] of (*S*)-(+)-sec-butylamine [(*S*)-**3***a*]. Both (*S*)-**1***b* and (*S*)-**2***b* in ethanol show

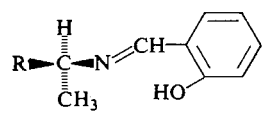

(*S*)-**1***b* R = C_6H_5
(*S*)-**2***b* R = $C_6H_5CH_2$
(*S*)-**3***b* R = C_2H_5

positive Cotton effects near 315 and 410 nm. In contrast, (*S*)-**3***b* is much weaker in rotatory power, and in ethanol only one weak peak at 437 nm could be observed. It was concluded that the strong rotational strength shown by *N*-salicylidene-α- and β-phenylalkylamines is due to an interaction of the π-electron system of the

[1]Part XII. H. E. Smith and A. A. Hicks (1).
[2]National Science Foundation Undergraduate Summer Fellow, 1969.
[3]Signs in parentheses refer to rotatory powers observed with sodium D-light for the amines as the neat liquid and for the *N*-salicylidenes as solutions in methanol.

Can. J. Chem. Downloaded from www.nrcresearchpress.com by 210.87.254.40 on 09/05/12
For personal use only.

TABLE 1. Spectral data for the *N*-salicylidene derivatives of some open-chain amines

Compound	Methanol		*n*-Hexane	
	The e.a. maxima* λ, nm (log ε)	The c.d. maxima† λ, nm ([θ])‡	The e.a. maxima* λ, nm (log ε)	The c.d. maxima† λ, nm ([θ])‡
(*S*)-**1***b*	404 (2.78)§‖	405 (+1100)§¶		
	315 (3.61)	315 (+18000)	320 (3.70)§	319 (+40000)§**
	283 (3.35)††			
		274 (−3000)		274 (−4000)
			262 (4.13)††	
	256 (4.14)	253 (+34000)	255 (4.18)	253 (+58000)
(*S*)-**3***b*	400 (3.22)	395 (+630)		
	314 (3.52)	313 (+1600)	318 (3.68)	315 (+2200)
	277 (3.60)			
	258 (4.00)††	253 (+4900)	260 (4.06)	255 (+3000)
	252 (4.04)		254 (4.09)	
(*R*)-**4***b*	399 (3.26)	400 (−1100)		
	314 (3.53)	315 (−2500)	317 (3.70)	314 (−2600)
	276 (3.64)			
	258 (4.02)††	261 (−6200)	261 (4.09)	261 (−6700)
	253 (4.05)		254 (4.14)	
(*S*)-**5***b*	400 (3.10)	396 (+710)	400 (1.25)†††‡‡	420 (−21)§§
	314 (3.56)	312 (+2700)	317 (3.66)	315 (+1800)
	275 (3.51)††			
		269 (−1900)		267 (−3800)
	257 (4.02)††		259 (4.06)††	
	254 (4.05)	248 (+6300)	255 (4.11)	251 (+8300)
(*R*)-**6***b*	400 (3.10)	388 (−160)	404 (1.47)‖‖	415 (+120)¶¶
	314 (3.58)	315 (−450)	319 (3.67)	316 (+1100)
	277 (3.54)††			
		267 (+6000)		267 (+6500)
	258 (4.04)††		260 (3.06)††	
	254 (4.08)	248 (−2300)	256 (4.11)	248 (−2900)

*For data not previously reported, 4.0 × 10^{-5} to 9.9 × 10^{-4} mol/l except for those maxima noted otherwise.
†For data not previously reported, temperature 25–28°; *c* 1.6 × 10^{-5} to 4.3 × 10^{-2} g/100 ml except for those maxima noted otherwise.
‡Molecular ellipticity.
§Data from ref. 4.
‖95% Ethanol as the solvent for this spectrum.
¶Absolute ethanol as the solvent for this spectrum.
**Isooctane as the solvent for this spectrum.
††Shoulder.
‡‡1.15 × 10^{-2} mol/l.
§§*c* 0.206 g/100 ml.
‖‖1.69 × 10^{-2} mol/l.
¶¶*c* 0.655 g/100 ml.

phenyl group and the salicylidenimino chromophore, the chirality of which gives the sign to the observed Cotton effects. This conclusion has been confirmed by subsequent o.r.d. and circular dichroism (c.d.) measurements with a substantial number of *N*-salicylidenes of α- and β-phenylalkylamines (3–5) and comparison of these measurements with similar ones made with the *N*-salicylidenes of steroidal amines (6–8) and of amino sugars (9). However, direct comparison of c.d. measurements with open-chain α- and β-phenylalkylamine derivatives with those of open-chain alkylamine derivatives has been lacking.

We now report the comparison of the electronic absorption (e.a.) and c.d. spectra of (*S*)-**1***b* with those of (*S*)-**3***b* as well as the *N*-salicylidene [(*R*)-**4***b*] of (*R*)-(−)-2,2-dimethyl-3-aminobutane (10) [(*R*)-(−)-pinacolylamine] [(*R*)-**4***a*]. (*S*)-**4***a* has been prepared earlier with a low rotatory power from (*R*)-tert-leucine (10). The complete resolution of (±)-**4***a* is now reported. In addition, the e.a. and c.d. spectra for the *N*-salicylidene [(*S*)-**5***b* and (*R*)-**6***b*] of (*S*)-(+)-2-amino-1-propanol (11) [(*S*)-**5***a*] and (*R*)-(−)-2-amino-1-butanol (12) [(*R*)-**6***a*] are also reported. The c.d. measurements with these latter two *N*-salicylidenes are pertinent to the interpretation of the c.d. spectra of salicylidenimino sugars (9).

Can. J. Chem. Downloaded from www.nrcresearchpress.com by 210.87.254.40 on 09/05/12
For personal use only.

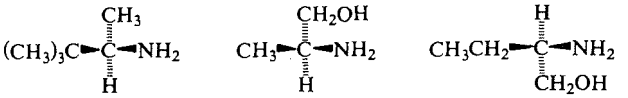

(*R*)-**4***a* (*S*)-**5***a* (*R*)-**6***a*

Results and Discussion

As seen in Table 1, the e.a. spectra of (*S*)-(+)-*N*-salicylidene-α-phenylethylamine [(*S*)-**1***b*], (*S*)-(+)-*N*-salicylidene-sec-butylamine [(*S*)-**3***b*], and (*R*)-(−)-*N*-salicylidene-2,2-dimethyl-3-aminobutane [(*R*)-**4***b*] in a particular solvent are the same. The absorption bands near 255 and 315 nm are assigned to electronic transitions of the intramolecularly hydrogen-bonded salicylidenimino group. The absorption band near 400 nm has been assigned, for the alkylamine *N*-salicylidenes in ethanol, to hydrogen-bonded complexes with the solvent (13) or to a tautomeric form (14). At high concentration, however, an absorption band near 400 nm is observed in the spectrum of *N*-salicylideneisopropylamine in carbon tetrachloride (13). This band disappears on dilution, and it is attributed to a small concentration of a dimeric species (13).

In the c.d. spectrum of (*S*)-**1***b*, the sign of the Cotton effects near 255 and 315 nm is correlated with the absolute configuration of (*S*)-**1***b* using a planar sector rule (5). Thus, in the preferred conformation of (*S*)-**1***b* (**7***a*), the phenyl group is behind the plane of the salicylidenimino chromophore, and in the spectrum, the two Cotton effects are positive. The c.d. maximum at 274 nm, not seen in the spectra of *N*-salicylidene-β-phenylalkylamines (3–5), has been assigned to a $\pi \rightarrow \pi^*$ transition of the phenyl ring of the amine moiety (4).

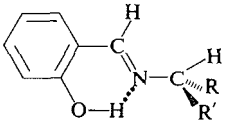

7

a R = C_6H_5; R′ = CH_3
b R = C_2H_5; R′ = CH_3
c R = CH_3; R′ = $C(CH_3)_3$
d R = CH_2OH; R′ = CH_3

For (*S*)-(+)-*N*-salicylidene-sec-butylamine [(*S*)-**3***b*] and (*R*)-(−)-*N*-salicylidene-2,2-dimethyl-3-aminobutane [(*R*)-**4***b*] corresponding c.d. maxima near 255 and 315 nm are observed. The intensities of these maxima are reduced since the interaction of a phenyl group with the salicylidenimino chromophore is no longer present. Both (*S*)-**3***b* and (*R*)-**4***b* have a preferred conformation (**7***b* and *c*) similar to that of (*S*)-**1***b*. As has been shown for alkyl-substituted cyclohexanones, the rotatory perturbation of the carbonyl chromophore by a tert-butyl group is larger than that by a methyl group (15). The rotatory perturbation of the salicylidenimino chromophore by an ethyl group may also be taken as larger than that by a methyl group. Using the same sector rule, (*S*)-**3***b* and (*R*)-**4***b* are predicted to show Cotton effects near 255 and 315 nm with signs as shown in Table 1.

Assuming a similar preferred conformation for the salicylidenimino group about its attachment bond and this sector rule, the sign of the Cotton effect near 315 nm shown by the *N*-salicylidenes of a number of 20-aminopregnanes can be predicted (6, 7). Much the same is true for the *N*-salicylidenes of cyclic amines, especially 17α-, 17β-, and 3α-amino steroids (8). For other cyclic amines, including other amino steroids, contributions from other salicylidenimino conformations may be important and perturbations by several remote groups may be significant (8). In these latter cases, predictions are sometimes unreliable.

The e.a. spectra of (*S*)-(+)-*N*-salicylidene-2-amino-1-propanol [(*S*)-**5***b*] and (*R*)-(+)-*N*-salicylidene-2-amino-1-butanol [(*R*)-**6***b*] in methanol are essentially the same as those of the others. In hexane, however, a weak absorption band near 400 nm is detected in each spectrum. The molecular absorptivity of the band decreases on dilution. The band may be due to a small concentration of the intermolecularly hydrogen-bonded dimer (13) in *n*-hexane.

The c.d. spectra of (*S*)-**5***b* and (*R*)-**6***b* also show an additional maximum near 268 nm. A maximum near this same wavelength is frequently present in the c.d. spectra of the *N*-salicylidene derivatives of α-hydroxy steroidal amines (8).

The rotatory perturbation of the salicylidenimino chromophore by a hydroxymethylene group is taken as greater than that by a methyl group. Application of the sector rule to a conformation of (*S*)-**5***b* (**7***d*) similar to the preferred conformation of (*R*)-**4***b* (**7***c*), predicts, as are observed, positive maxima near 255 and 315 nm

Can. J. Chem. Downloaded from www.nrcresearchpress.com by 210.87.254.40 on 09/05/12
For personal use only.

in the c.d. spectrum of (*S*)-**5***b*. The rotatory perturbation by a hydroxymethylene group is taken to be about the same as that by an ethyl group, and unusually low molecular ellipticities are found for the maxima near 255 and 315 nm in the c.d. spectrum of (*R*)-**6***b*. Also the sign of the maximum near 315 nm is different in the two solvents used.

Experimental

General

Boiling points are not corrected. The *N*-salicylidenes were prepared as previously reported (2). They had n.m.r. spectra compatible with their assigned structures. Optical rotations at the sodium D-line were obtained using a 1-dm sample tube. Elemental analyses were done by Galbraith Laboratories, Inc., Knoxville, Tennessee. The e.a. spectra were measured with a Cary Model 14 spectrophotometer using 1-cm sample cells. The c.d. spectra were measured at 25–28° with a Cary Model 60 spectropolarimeter with a Model 6001 accessory. The slit was programmed for a spectral band width of 1.5 nm, and a path length of 1 cm was used. Cut-off was indicated when the dynode voltage reached 400 V.

(S)-(+)-N-Salicylidene-sec-butylamine [(S)-3b][4]

This compound had $[\alpha]_D^{25}$ +73° (*c* 1.15, MeOH).

Resolution of (±)-2,2-Dimethyl-3-aminobutane [(±)-4a]

To 113.0 g (0.753 mol) of (+)-tartaric acid in 1000 ml of boiling 95% EtOH was added 75.0 g (0.741 mol) of (±)-**4***a*. On cooling the mixture to room temperature, there was deposited 141.2 g (152%) of solid, $[\alpha]_D^{23}$ +16° (*c* 2.78, H_2O). Four recrystallizations of this solid from 95% EtOH gave 59.1 g (63%) of the acid tartrate salt of (*R*)-**4***a*, $[\alpha]_D^{26}$ +16° (*c* 2.64, H_2O). Fifty grams of this salt was decomposed with 25% KOH, and the amine extracted into ether. The ethereal solution was dried (KOH), and the ether evaporated. Distillation of the residue gave 15.5 g (49%) of (*R*)-**4***a*, b.p. 100–103°, d_4^{20} 0.758, $[\alpha]_D^{23}$ −5.6° (neat), $[\alpha]_D^{25}$ −2.6° (*c* 5.10, MeOH) (lit. (10) $[\alpha]_D^{24}$ +0.70° (neat, *l* = 0.2 dm) for (*S*)-**4***a*).

The mother liquors from the above resolution were combined, and the solvent was removed. Decomposition of the residual salt gave 36.6 g (0.362 mol) of the partially racemic amine, $[\alpha]_D^{23}$ +2.02° (neat), which was combined with 54.4 g (0.362 mol) of (−)-tartaric acid in 500 ml of boiling 95% EtOH. On cooling this solution to room temperature, there was deposited 54.4 g (58%) of solid, $[\alpha]_D^{26}$ −16° (*c* 5.70, H_2O). After three recrystallizations of this solid from 95% EtOH, there was obtained 10.5 g (11%) of the acid tartrate salt of (*S*)-**4***a*, $[\alpha]_D^{25}$ −16° (*c* 4.69, H_2O).

The salt was decomposed and the amine purified as before. There was thus obtained 2.40 g (6.4%) of (*S*)-**4***a*, b.p. 100–103°, d_4^{20} 0.760, $[\alpha]_D^{24}$ +5.4° (neat), $[\alpha]_D^{24}$ +2.5° (*c* 5.10, MeOH).

[4]The preparation and characterization of this sample were reported earlier (2).

(±)-N-Salicylidene-2,2-dimethyl-3-aminobutane [(±)-4b]

From 5.06 g (50.0 mmol) of (±)-2,2-dimethyl-3-aminobutane [(±)-**4***a*] and 5.50 g (45.0 mmol) of salicylaldehyde in 15 ml of MeOH there was obtained 3.03 g (33%) of (±)-**4***b*, yellow oil, b.p. 82–84° (0.1 mm), n_D^{25} 1.5323, d_4^{20} 0.965.

Anal. Calcd. for $C_{13}H_{19}NO$: C, 76.05; H, 9.33; N, 6.82. Found: C, 76.21; H, 9.39; N, 7.05.

(R)-(−)-N-Salicylidene-2,2-dimethyl-3-aminobutane [(R)-4b]

From 4.10 g (40.5 mmol) of (*R*)-(−)-2,2-dimethyl-3-aminobutane [(*R*)-**4***a*] and 4.45 g (36.4 mmol) of salicylaldehyde in 50 ml of benzene there was obtained 3.54 g (47%) of (*R*)-**4***b*, yellow oil, b.p. 89–90° (0.2 mm), which on standing crystallized as yellow needles, m.p. *ca.* 30°, $[\alpha]_D^{24}$ −133° (*c* 2.04, MeOH).

Anal. Calcd. for $C_{13}H_{19}NO$: C, 76.05; H, 9.33; N, 6.82. Found: C, 76.21; H, 9.30; N, 7.04.

(S)-(+)-N-Salicylidene-2-amino-1-propanol [(S)-5b]

From 1.90 g (25.3 mmol) of (*S*)-(+)-2-amino-1-propanol [(*S*)-**5***a*], d_4^{20} 0.955, $[\alpha]_D^{24}$ +15.1° (neat), $[\alpha]_D^{24}$ +16° (*c* 4.99, MeOH) (lit. (16) $[\alpha]_D^{20}$ +15.8° (neat)), and 3.20 g (26.2 mmol) of salicylaldehyde in 10 ml of MeOH, there was obtained 3.67 g (81%) of (*S*)-**5***b*, yellow oil, b.p. 114–115° (0.3 mm), n_D^{25} 1.5815, $[\alpha]_D^{24}$ +76.2° (*c* 2.23, MeOH).

Anal. Calcd. for $C_{10}H_{13}NO_2$: C, 67.02; H, 7.31; N, 7.82. Found: C, 66.86; H, 7.15; N, 7.80.

(R)-(+)-N-Salicylidene-2-amino-1-butanol [(R)-6b]

From 4.68 g (52.5 mmol) of (*R*)-(−)-2-amino-1-butanol [(*R*)-**6***a*], d_4^{20} 0.936, $[\alpha]_D^{25}$ −10.2° (neat), $[\alpha]_D^{24}$ −10° (*c* 5.00, MeOH) (lit. (17, 18) $[\alpha]_D^{26}$ −9.92° (neat), $[\alpha]_D^{22}$ −10.00° (*c* 2, EtOH)), and 6.70 g (54.9 mmol) of salicylaldehyde in 20 ml of MeOH, there was obtained 7.15 g (70%) of (*R*)-**6***b*, recrystallized from *n*-hexane, yellow needles, m.p. 55–56° (corrected), $[\alpha]_D^{24}$ +8.1° (*c* 3.50, MeOH).

Anal. Calcd. for $C_{11}H_{15}NO_2$: C, 68.37; H, 7.82; N, 7.25. Found: C, 68.53; H, 7.67; N, 7.25.

1. H. E. Smith and A. A. Hicks. J. Org. Chem. In press.
2. H. E. Smith, S. L. Cook, and M. E. Warren, Jr. J. Org. Chem. **29**, 2265 (1964).
3. M. E. Warren, Jr. and H. E. Smith. J. Am. Chem. Soc. **87**, 1757 (1965).
4. H. E. Smith and R. Records. Tetrahedron, **22**, 813 (1966).
5. H. E. Smith and T. C. Willis. Tetrahedron, **26**, 107 (1970).
6. D. Bertin and M. Legrand. C.R. **256**, 960 (1963).
7. L. Velluz, M. Legrand, and M. Grosjean. Optical circular dichroism. Academic Press, New York, N.Y., 1965. pp. 156 and 240.
8. H. Ripperger, K. Schreiber, G. Snatzke, and K. Ponsold. Tetrahedron, **25**, 827 (1969).
9. S. Inouye. Chem. Phar. Bull. Tokyo, **15**, 1557 (1967).
10. H. Pracejus and S. Winter. Chem. Ber. **97**, 3173 (1964).

Can. J. Chem. Downloaded from www.nrcresearchpress.com by 210.87.254.40 on 09/05/12
For personal use only.

11. P. KARRER, P. PORTMANN, and M. SUTER. Helv. Chim. Acta, **31**, 1617 (1948).
12. A. M. KRITSYN, A. M. LIKHOSHERSTOV, T. V. PROTOPOPOVA, and A. P. SKOLDINOV. Dolk. Akad. Nauk SSSR, **145**, 332 (1962); Proc. Acad. Sci. U.S.S.R. **145**, 597 (1962).
13. J. CHARETTE, G. FALTLHANSL, and PH. TEYSSIE. Spectrochimica Acta, **20**, 597 (1964).
14. D. HEINERT and A. E. MARTELL. J. Am. Chem. Soc. **85**, 183, 188 (1963).
15. C. DJERASSI and W. KLYNE. J. Chem. Soc. 2390 (1963).
16. A. STOLL, J. PEYER, and A. HOFMANN. Helv. Chim. Acta, **26**, 929 (1943).
17. F. H. RADKE, R. B. FEARING, and S. W. FOX. J. Am. Chem. Soc. **76**, 2801 (1954).
18. S. TSUBOYAMA, K. TSUBOYAMA, and M. YANAGITA. Rika Gaku Kenkyusho Hokoku, **41**, 194 (1965); Chem. Abstr. **64**, 14079*g* (1966).

A Differential Scanning Calorimeter Study of Phase Transitions in Alkali Metal Stearates

J. A. RIPMEESTER[1] AND B. A. DUNELL
Chemistry Department, The University of British Columbia, Vancouver 8, British Columbia

Received September 22, 1970[2]

Differential scanning calorimeter thermograms have been obtained for the alkali metal stearates from 25 to 200 °C. Four different samples of different thermal history were studied for each soap, and differences in temperature and relative enthalpy of transitions were found to depend on the various sample histories. For lithium stearate good correlation is found between DSC and nuclear magnetic resonance (n.m.r.) results. Rubidium and caesium stearates seem to be less sensitive to thermal history than the sodium and potassium salts.

Des thermogrammes par calorimétrie différentielle de précision ont été obtenus pour des stéarates de métaux alcalins de 25 à 200 °C. Quatre échantillons différents avec une histoire thermique différente ont été étudiés pour chaque savon et les différences trouvées dans la température et l'enthalpie relative de transitions dépendent des différentes histoires. Pour le stéarate de lithium, il existe une bonne corrélation entre les résultats en DSC et en r.m.n. Les stéarates de rubidium et de caesium paraissent moins sensibles à l'histoire thermique que les sels de sodium et potassium.

Canadian Journal of Chemistry, **49**, 2906 (1971)

In the course of a broad line nuclear magnetic resonance study of alkali metal oleates and stearates (1), we examined a number of these soaps by the differential scanning calorimeter technique, using a Perkin–Elmer DSC 1-B instrument. In particular, DSC curves were run on different samples of the same substance of which the various samples had different thermal histories. As might be expected from previous work (2, 3), the thermal history had significant influence on the thermogram obtained for the sample. The temperatures of the various phase transitions as observed from the thermograms are also compared with transition temperatures observed by other techniques.

It may be worth noting at this point that in differential thermal analysis (DTA) the difference in temperature between the sample and a standard reference substance is measured, whereas in the differential scanning calorimeter (DSC) the difference in the energy required to keep sample and reference at the same temperature under constant rate of heating is recorded. In the DTA method, peaks are normally observed for both first and second order transitions, but in the DSC method peaks should accompany only first order transitions; the second order transitions should cause only a shift in the baseline of the thermogram. In this report only distinct peaks in the DSC thermograms are considered, so that all transitions listed for the DSC method should be first order.

Samples of alkali metal stearates were prepared from Eastman Kodak white label grade stearic acid and reagent grade alkali metal hydroxide by precipitation from hot ethanol and aqueous

[1]National Research Council of Canada Scholarship holder 1967–1970. Present address: Department of Chemistry and Chemical Engineering, University of Illinois, Urbana, Illinois 61801.

[2]Revision received June 7, 1971.

Can. J. Chem. Downloaded from www.nrcresearchpress.com by 210.87.254.40 on 09/05/12
For personal use only.

11. P. KARRER, P. PORTMANN, and M. SUTER. Helv. Chim. Acta, **31**, 1617 (1948).
12. A. M. KRITSYN, A. M. LIKHOSHERSTOV, T. V. PROTOPOPOVA, and A. P. SKOLDINOV. Dolk. Akad. Nauk SSSR, **145**, 332 (1962); Proc. Acad. Sci. U.S.S.R. **145**, 597 (1962).
13. J. CHARETTE, G. FALTLHANSL, and PH. TEYSSIE. Spectrochimica Acta, **20**, 597 (1964).
14. D. HEINERT and A. E. MARTELL. J. Am. Chem. Soc. **85**, 183, 188 (1963).
15. C. DJERASSI and W. KLYNE. J. Chem. Soc. 2390 (1963).
16. A. STOLL, J. PEYER, and A. HOFMANN. Helv. Chim. Acta, **26**, 929 (1943).
17. F. H. RADKE, R. B. FEARING, and S. W. FOX. J. Am. Chem. Soc. **76**, 2801 (1954).
18. S. TSUBOYAMA, K. TSUBOYAMA, and M. YANAGITA. Rika Gaku Kenkyusho Hokoku, **41**, 194 (1965); Chem. Abstr. **64**, 14079*g* (1966).

Can. J. Chem. Downloaded from www.nrcresearchpress.com by 210.87.254.6 on 09/05/12
For personal use only.

A Differential Scanning Calorimeter Study of Phase Transitions in Alkali Metal Stearates

J. A. RIPMEESTER[1] AND B. A. DUNELL
Chemistry Department, The University of British Columbia, Vancouver 8, British Columbia

Received September 22, 1970[2]

Differential scanning calorimeter thermograms have been obtained for the alkali metal stearates from 25 to 200 °C. Four different samples of different thermal history were studied for each soap, and differences in temperature and relative enthalpy of transitions were found to depend on the various sample histories. For lithium stearate good correlation is found between DSC and nuclear magnetic resonance (n.m.r.) results. Rubidium and caesium stearates seem to be less sensitive to thermal history than the sodium and potassium salts.

Des thermogrammes par calorimétrie différentielle de précision ont été obtenus pour des stéarates de métaux alcalins de 25 à 200 °C. Quatre échantillons différents avec une histoire thermique différente ont été étudiés pour chaque savon et les différences trouvées dans la température et l'enthalpie relative de transitions dépendent des différentes histoires. Pour le stéarate de lithium, il existe une bonne corrélation entre les résultats en DSC et en r.m.n. Les stéarates de rubidium et de caesium paraissent moins sensibles à l'histoire thermique que les sels de sodium et potassium.

Canadian Journal of Chemistry, **49**, 2906 (1971)

In the course of a broad line nuclear magnetic resonance study of alkali metal oleates and stearates (1), we examined a number of these soaps by the differential scanning calorimeter technique, using a Perkin–Elmer DSC 1-B instrument. In particular, DSC curves were run on different samples of the same substance of which the various samples had different thermal histories. As might be expected from previous work (2, 3), the thermal history had significant influence on the thermogram obtained for the sample. The temperatures of the various phase transitions as observed from the thermograms are also compared with transition temperatures observed by other techniques.

It may be worth noting at this point that in differential thermal analysis (DTA) the difference in temperature between the sample and a standard reference substance is measured, whereas in the differential scanning calorimeter (DSC) the difference in the energy required to keep sample and reference at the same temperature under constant rate of heating is recorded. In the DTA method, peaks are normally observed for both first and second order transitions, but in the DSC method peaks should accompany only first order transitions; the second order transitions should cause only a shift in the baseline of the thermogram. In this report only distinct peaks in the DSC thermograms are considered, so that all transitions listed for the DSC method should be first order.

Samples of alkali metal stearates were prepared from Eastman Kodak white label grade stearic acid and reagent grade alkali metal hydroxide by precipitation from hot ethanol and aqueous

[1]National Research Council of Canada Scholarship holder 1967–1970. Present address: Department of Chemistry and Chemical Engineering, University of Illinois, Urbana, Illinois 61801.

[2]Revision received June 7, 1971.

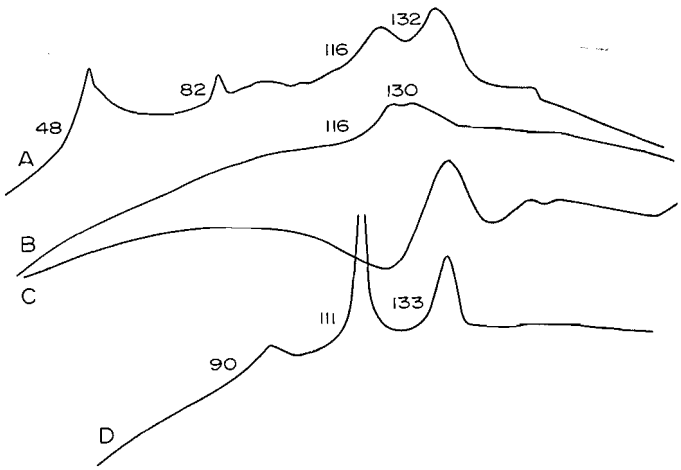

FIG. 1. Differential scanning calorimeter thermograms for four samples of sodium stearate of different thermal history. See text for details.

ethanol solutions (1). After the precipitated soap had been dried and recrystallized once from ethanol, four samples of each soap were prepared by the following treatment: samples *A* were kept under vacuum for one day at room temperature, samples *B* were kept under vacuum for 14 h at 110–120 °C and were run 24 h later, samples *C* were kept under vacuum for 28 h at 110–120 °C and were run 24 h later, and samples *D* were fused under vacuum and run about a week later. The samples were covered after preparation, but no special precautions were taken to keep them out of contact with the atmosphere when they were transferred to the DSC. Tank nitrogen passed around the sample during the DSC run. The thermogram was always run at a heating rate of 10 °C/min from room temperature to 200 °C.

The question has arisen as to whether this rate of heating is too rapid for substances in which some of the transitions occur sluggishly. In running DSC thermograms one must compromise between using a fast heating rate, thereby obtaining very well defined peaks, and using a slow heating rate in order to work at conditions closer to equilibrium, but thereby obtaining relatively small, poorly defined peaks. Pacor and Spier (4) report that with a DTA instrument they observed only little dependence of transition temperature upon heating rate for sodium salts of fatty acids containing from 10 to 19 carbon atoms for heating rates in the range of 1 to 16° per min. Using a sodium stearate sample and our DSC instrument, we find that there is a tendency for transition temperatures to be displaced to higher values as the rate of heating is increased. Differences of 1 to 3° in the temperatures of the major transitions up to 150 °C were observed between the thermograms for sodium stearate, one run at a rate of 2.5 °C/min and the other at 10 °C/min. It is felt that such differences are about equal to the experimental uncertainty of the method. Transition temperatures for heating rates of 2.5 °C/min and 40 °C/min were observed to differ by at most 10°, at least 2°, and on the average 5°, in the range up to 150 °C, the higher transition temperatures being obtained with the fast heating rate. A heating rate of 10 °C/min appears to be a satisfactory compromise in which systematic errors in transition temperatures are comparable with random errors and peaks in the thermogram are still well defined.

The thermograms for the four samples of sodium stearate are reproduced in Fig. 1 as examples of the type of behavior observed. The dependence of behavior on thermal history is clear, and the difficulty of determining transition temperatures is greater here than in any of the other soaps because of the long leading edges and general breadth of the peaks. The thermogram for sample *C* is especially difficult. In all cases the assignment of transition temperatures should be considered approximate. The transition temperature is taken to be that of the point at which the peak starts to break away from the base line. Transition temperatures are listed in Table 1 along with values obtained by X-ray methods (5,

Can. J. Chem. Downloaded from www.nrcresearchpress.com by 210.87.254.6 on 09/05/12
For personal use only.

TABLE 1. Transitions observed for the alkali metal stearates using the DSC method and other techniques

Alkali metal	DSC samples				X-Rays*	DTA†	n.m.r.‡	Dilatometry§
	A	*B*	*C*	*D*				
Li	112	112	112	110	122	118	114	115
	191	195	195	173	190	194	187–191	176
Na	48							
	82			90		93	85	90 (ref. 8)
	116	116		111		118	113	117 (ref. 8)
	132	130		133	133	136		132
						166		165
						196		193
K								51 (ref. 8)
	72	67, 75	67, 74	63	69	68, 77	60	65–70
	96	95		96				90
	104	104		102		106		
	132	132	132	130		134		
				138	139			
				149		148		
	149	152	152	153		163		162
					170		170	
						185		
Rb	59			58				
	82	80	81	78	84		75	75
	128	129						130
	137	135	137	136				
	141	141	142	140			143	
	186	172	191	189	177			160
Cs	60	62	63	59				
	72	72	71	71	70		70	70
	101	100	102	101	104		100	100
	114	115	114	114				
	129	132	129	128				
	184		182	184				170

*References 5 and 6.
†Reference 3.
‡References 2, 9, and 10.
§Reference 7, except where marked otherwise.

6), DTA (3), dilatometry (7, 8), and n.m.r. (2, 9, 10). The list of values obtained from other studies is intended to be representative rather than complete. Other results and a more extensive range of temperature than approximately 50 to 200 °C may be found in the references cited for Table 1 as well as in papers by Vold (11, 12), Ravich and Nechitaylo (13), Pace and Spier (4), and Puddington and co-workers (14).

In lithium stearate the higher temperature transition is shifted to lower temperature after the sample has been fused. The same behavior was observed (2) in an n.m.r. study of lithium stearate, and one may now conclude that the motional process which is manifested in this phase change involves a rate of reorientation of hydrocarbon chains which is great enough to be thermodynamically significant, and therefore much greater than the mere 10^4 or 10^5 s^{-1} which would be necessary to narrow the n.m.r. line.

In potassium stearate it is remarkable that no DSC transition was observed near 170 °C, where a transition is found by other techniques. We have no explanation for this. One may also note that in the rubidium and caesium stearates the effect of thermal history of the sample is less marked than in the other salts, and appears more in the variation in size of corresponding peaks than in significant shifts in the temperature at which peaks appear.

For sodium stearate Trzebowski (3) has reported three different DTA thermograms corresponding to an α form obtained by air drying at room temperature the precipitate from an aqueous alcohol solution, a β form obtained by heating to 55–60 °C and drying at this temperature, and a σ form obtained by heating above 110–135 °C. Trzebowski reports that DTA peaks occur for these three modifications, of which the α- and σ-forms should correspond to our samples *A* and

Can. J. Chem. Downloaded from www.nrcresearchpress.com by 210.87.254.6 on 09/05/12
For personal use only.

D, at the following temperatures: α-form 53, *ca.* 95, 99, 105, 122, and 136 °C; β-form, 97.5, 102, 122, and 136 °C; σ-form, 93, 118, and 136 °C. It appears that our sample *D* does correspond quite well in behavior with Trzebowski's σ-form, but other correspondences are doubtful.

The authors thank the National Research Council of Canada for financial support of this work and for the award of a Scholarship to J.A.R. We are also indebted to Dr. R. E. Pincock and Mr. K. R. Wilson for their helpfulness when we were using the DSC.

1. J. A. RIPMEESTER and B. A. DUNELL. Can. J. Chem. **49**, 731 (1971).
2. T. J. R. CYR, W. R. JANZEN, and B. A. DUNELL. Ordered fluids and liquid crystals. Adv. Chem. Ser. No. 63, Am. Chem. Soc. Washington, D.C. 1967. p. 13.
3. N. TRZEBOWSKI. Wiss. Z. der Friedrich-Schiller-Universität Jena, Math-Naturwiss. Reihe, **14**, 207 (1965).
4. P. PACOR and H. L. SPIER. J. Am. Oil Chem. Soc. **45**, 338 (1968).
5. B. GALLOT and A. SKOULIOS. Kolloid Z. u. Z. Polym. **209**, 164 (1966); **210**, 143 (1966); **213**, 143 (1967).
6. A. SKOULIOS and V. LUZZATTI. Acta Cryst. **14**, 278 (1961).
7. D. P. BENTON, P. G. HOWE, R. FARNAND, and I. E. PUDDINGTON. Can. J. Chem. **33**, 1798 (1955).
8. M. J. VOLD, M. MACOMBER, and R. D. VOLD. J. Am. Chem. Soc. **63**, 168 (1941).
9. R. F. GRANT and B. A. DUNELL. Can. J. Chem. **38**, 1951 (1960); **38**, 2395 (1960).
10. D. J. SHAW and B. A. DUNELL. Trans. Faraday Soc. **58**, 132 (1962).
11. R. D. VOLD. J. Am. Chem. Soc. **63**, 2915 (1941).
12. R. D. VOLD. J. Phys. Chem. **49**, 315 (1945).
13. G. B. RAVICH and N. A. NECHITAYLO. Doklady Akad. Nauk S.S.S.R. **83**, 117 (1952).
14. D. P. BENTON, P. G. HOWE, and I. E. PUDDINGTON. Can. J. Chem. **33**, 1384 (1955).

The Vapor Phase Radiolysis of Isopropanol and Water–Isopropanol Mixtures. II. Nitrous Oxide as Electron Scavenger[1,2]

M. G. BAILEY AND R. S. DIXON

Research Chemistry Branch, Atomic Energy of Canada Limited, Whiteshell Nuclear Research Establishment, Pinawa, Manitoba

Received March 25, 1971

Nitrous oxide reduces the hydrogen yield from water–isopropanol vapor mixtures by complete scavenging of electrons. Nitrogen is produced over the whole concentration range but the yield at higher isopropanol concentrations is much greater than the electron yield. The results indicate a competition between water and isopropanol for a secondary species resulting from electron attachment to N_2O. Reaction of this species with isopropanol leads to further N_2 whereas reaction with water does not. The reactive intermediate is most probably N_2O^- or $N_2O_2^-$.

Le protoxyde d'azote réduit le rendement en hydrogène de mélanges vapeurs eau–isopropanol en piégeant complètement les électrons. L'azote est produit pendant tout l'intervalle de concentration mais le rendement à concentration plus élevée en isopropanol est beaucoup plus grand que le rendement électronique. Les résultats indiquent qu'il y a compétition entre l'eau et l'isopropanol envers une deuxième espèce provenant de la fixation d'un électron sur N_2O. La réaction de cette espèce avec l'isopropanol fournit encore de l'azote alors que la réaction avec l'eau n'en fournit pas. L'intermédiaire réactif est probablement N_2O^- ou $N_2O_2^-$.

Canadian Journal of Chemistry, 49, 2909 (1971)

Previously we have studied the effects of some electron scavengers on the hydrogen yields from irradiated water–isopropanol mixtures in the vapor phase (1). In general the reduction in $G(H_2)$[3] was the same for each electron scavenger but we did not measure products from the

[1]AECL No. 3897.
[2]For part I, see ref. 1.
[3]Measured yields are written $G(X)$ and primary yields $g(x)$ molecules per 100 eV.

Can. J. Chem. Downloaded from www.nrcresearchpress.com by 210.87.254.6 on 09/05/12
For personal use only.

D, at the following temperatures: α-form 53, *ca.* 95, 99, 105, 122, and 136 °C; β-form, 97.5, 102, 122, and 136 °C; σ-form, 93, 118, and 136 °C. It appears that our sample *D* does correspond quite well in behavior with Trzebowski's σ-form, but other correspondences are doubtful.

The authors thank the National Research Council of Canada for financial support of this work and for the award of a Scholarship to J.A.R. We are also indebted to Dr. R. E. Pincock and Mr. K. R. Wilson for their helpfulness when we were using the DSC.

1. J. A. RIPMEESTER and B. A. DUNELL. Can. J. Chem. **49**, 731 (1971).
2. T. J. R. CYR, W. R. JANZEN, and B. A. DUNELL. Ordered fluids and liquid crystals. Adv. Chem. Ser. No. 63, Am. Chem. Soc. Washington, D.C. 1967. p. 13.
3. N. TRZEBOWSKI. Wiss. Z. der Friedrich-Schiller-Universität Jena, Math-Naturwiss. Reihe, **14**, 207 (1965).
4. P. PACOR and H. L. SPIER. J. Am. Oil Chem. Soc. **45**, 338 (1968).
5. B. GALLOT and A. SKOULIOS. Kolloid Z. u. Z. Polym. **209**, 164 (1966); **210**, 143 (1966); **213**, 143 (1967).
6. A. SKOULIOS and V. LUZZATTI. Acta Cryst. **14**, 278 (1961).
7. D. P. BENTON, P. G. HOWE, R. FARNAND, and I. E. PUDDINGTON. Can. J. Chem. **33**, 1798 (1955).
8. M. J. VOLD, M. MACOMBER, and R. D. VOLD. J. Am. Chem. Soc. **63**, 168 (1941).
9. R. F. GRANT and B. A. DUNELL. Can. J. Chem. **38**, 1951 (1960); **38**, 2395 (1960).
10. D. J. SHAW and B. A. DUNELL. Trans. Faraday Soc. **58**, 132 (1962).
11. R. D. VOLD. J. Am. Chem. Soc. **63**, 2915 (1941).
12. R. D. VOLD. J. Phys. Chem. **49**, 315 (1945).
13. G. B. RAVICH and N. A. NECHITAYLO. Doklady Akad. Nauk S.S.S.R. **83**, 117 (1952).
14. D. P. BENTON, P. G. HOWE, and I. E. PUDDINGTON. Can. J. Chem. **33**, 1384 (1955).

The Vapor Phase Radiolysis of Isopropanol and Water–Isopropanol Mixtures. II. Nitrous Oxide as Electron Scavenger[1,2]

M. G. BAILEY AND R. S. DIXON

Research Chemistry Branch, Atomic Energy of Canada Limited, Whiteshell Nuclear Research Establishment, Pinawa, Manitoba

Received March 25, 1971

Nitrous oxide reduces the hydrogen yield from water–isopropanol vapor mixtures by complete scavenging of electrons. Nitrogen is produced over the whole concentration range but the yield at higher isopropanol concentrations is much greater than the electron yield. The results indicate a competition between water and isopropanol for a secondary species resulting from electron attachment to N_2O. Reaction of this species with isopropanol leads to further N_2 whereas reaction with water does not. The reactive intermediate is most probably N_2O^- or $N_2O_2^-$.

Le protoxyde d'azote réduit le rendement en hydrogène de mélanges vapeurs eau–isopropanol en piégeant complètement les électrons. L'azote est produit pendant tout l'intervalle de concentration mais le rendement à concentration plus élevée en isopropanol est beaucoup plus grand que le rendement électronique. Les résultats indiquent qu'il y a compétition entre l'eau et l'isopropanol envers une deuxième espèce provenant de la fixation d'un électron sur N_2O. La réaction de cette espèce avec l'isopropanol fournit encore de l'azote alors que la réaction avec l'eau n'en fournit pas. L'intermédiaire réactif est probablement N_2O^- ou $N_2O_2^-$.

Canadian Journal of Chemistry, 49, 2909 (1971)

Previously we have studied the effects of some electron scavengers on the hydrogen yields from irradiated water–isopropanol mixtures in the vapor phase (1). In general the reduction in $G(H_2)$[3] was the same for each electron scavenger but we did not measure products from the

[1]AECL No. 3897.
[2]For part I, see ref. 1.
[3]Measured yields are written $G(X)$ and primary yields $g(x)$ molecules per 100 eV.

Can. J. Chem. Downloaded from www.nrcresearchpress.com by 210.87.254.42 on 09/05/12
For personal use only.

Can. J. Chem. Downloaded from www.nrcresearchpress.com by 210.87.254.42 on 09/05/12
For personal use only.

scavenging reaction. Nitrous oxide has been used extensively as an electron scavenger in gas phase radiolysis, and correlations made between the decrease in hydrogen yield and the production of nitrogen. Here we have extended our study of water–isopropanol mixtures by measuring yields of hydrogen and the production of nitrogen from mixtures containing nitrous oxide, and have found that the yield of N_2 is much higher than the yield of electrons in the system. Possible mechanisms are discussed.

The experimental details have been described previously (1). Irradiations were carried out at ~700 Torr pressure and 125 °C. The dose rate was $\sim 1.9 \times 10^{18}$ eV g^{-1} min^{-1} (estimated by the ethylene dosimeter (2) using $G(H_2) = 1.31$) and total doses were in the range 10^{19}–10^{20} eV g^{-1}. G-values were based on the total energy absorbed by both water and isopropanol. The energy absorbed by each component in the mixture was calculated, assuming it to be proportional to the electron density.

The hydrogen yields from water–isopropanol mixtures over the complete concentration range, with and without 2 mol% N_2O, are shown in Fig. 1. $G(H_2)$ shows a linear dependence on the fraction of energy absorbed by each component, in the presence and absence of N_2O. The effect of N_2O is due to electron capture by N_2O completely suppressing the neutralization reaction

$$[1] \quad e^- + H^+(H_2O)_x(C_3H_7OH)_y \rightarrow H + xH_2O + yC_3H_7OH$$

By extrapolating the straight lines in Fig. 1 to zero isopropanol and zero water concentrations, we obtain the yields of H atoms which arise from electrons in pure water and pure isopropanol. The values are $g(H)_w^e = 2.5 \pm 0.5$ and $g(H)_p^e = 3.5 \pm 0.5$, respectively. The hydrogen which remains in the presence of nitrous oxide represents the sum of the "residual" H atom yield plus the molecular hydrogen yield, designated $g(H)$ and $g(H_2)$, respectively. Figure 1 shows $g(H)_w + g(H_2)_w = 5.5 \pm 0.3$ and $g(H)_p + g(H_2)_p = 5.6 \pm 0.3$. These values in the presence of N_2O are in good agreement with our earlier results using other electron scavengers (1). Concentrations of N_2O higher than 2 mol% did not reduce $G(H_2)$ further showing that this quantity is sufficient to capture all the electrons. The effect of N_2O concentrations on $G(H_2)$ from pure isopropanol is shown in Fig. 2.

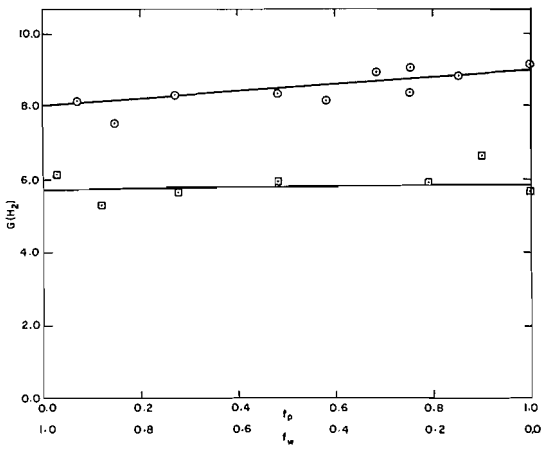

FIG. 1. Hydrogen yields from γ-irradiated water–isopropanol vapor mixtures at 125 °C and ~700 Torr. f_w and f_p are the fractions of energy absorbed by water and isopropanol, respectively. ○, No additive; □, with 2 mol% N_2O.

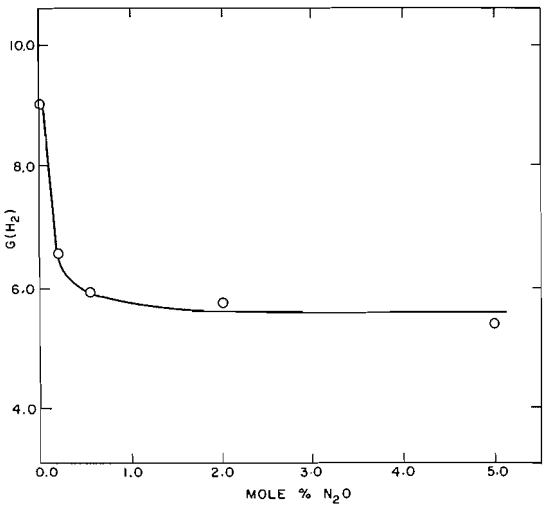

FIG. 2. Effect of N_2O concentration on $G(H_2)$ from isopropanol vapor at 125 °C and ~700 Torr.

The nitrogen yields from water–isopropanol mixtures containing various concentrations of N_2O are shown in Fig. 3. In all mixtures $G(N_2)$ increased rapidly up to a plateau value at ~2 mol% N_2O. However, the plateau values of $G(N_2)$ also increased with increasing fraction of isopropanol in the mixture, from 2.8 ± 0.3 at 0.2 mol% isopropanol to 12.5 ± 1.0 in pure isopropanol.

Figure 4 shows a plot of these plateau values

Can. J. Chem. Downloaded from www.nrcresearchpress.com by 210.87.254.42 on 09/05/12
For personal use only.

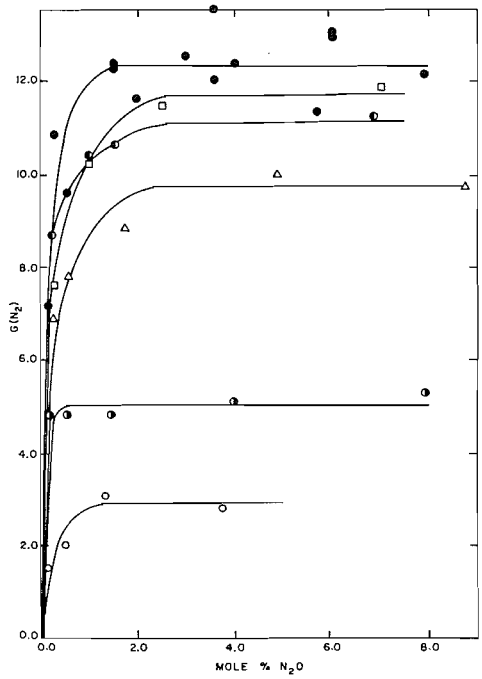

FIG. 3. Effect of N_2O concentration on $G(N_2)$ from water–isopropanol vapor mixtures at 125 °C and ~700 Torr. Isopropanol concentrations: ○, 0.2 mol%; ◑, 2.3 mol%; △, 10 mol%; ◐, 28 mol%; □, 51 mol%; ●, pure isopropanol.

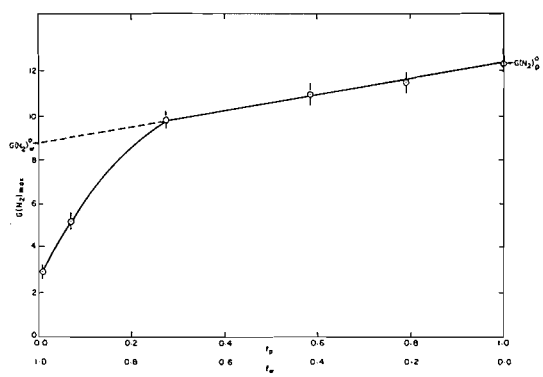

FIG. 4. Plot of $G(N_2)_{max}$ values from Fig. 3 against fraction of energy absorbed by water (f_w) and isopropanol (f_p).

$G(N_2)_{max}$ against the fraction of energy absorbed by the two components. $G(N_2)_{max}$ is seen to rise sharply up to $f_p \simeq 0.3$ and then increase more slowly and linearly up to $f_p = 1$. Extrapolation of the linear portion of the curve to $f_p = 0$ and $f_p = 1$ gives $G(N_2)_w^0 = 8.7 \pm 0.5$ and $G(N_2)_p^0 = 12.5 \pm 1.0$, respectively, as shown in Fig. 4.

Assuming electron capture to be a three-body process at the pressures used (3, 4)

[2] $$e^- + N_2O + M \rightarrow N_2O^- + M$$

the ion N_2O^- may react in several ways to produce N_2. If each N_2O^- yields one molecule of N_2 only, and no secondary reactions produce N_2, then $G(N_2)$ should equal $g(e)$. However, the N_2 yields are clearly much higher than the value of $g(e)$ and depend markedly on the fraction of isopropanol in the mixture. Despite this, the effect of SF_6, which suppresses virtually all the N_2 yield in both isopropanol and water–isopropanol mixtures, shows that most (possibly all) of the N_2 has the electron as precursor.

It is evident from Fig. 4 that a competition is occurring between water and isopropanol for some species X. Reaction of X with water leads to an overall yield of N_2 which equals $g(e)$, whereas reaction with isopropanol leads to a yield of N_2 which is greater than $g(e)$, the latter presumably by some short chain mechanism. The maximum yield of N_2 will therefore be obtained when all X reacts with isopropanol and Fig. 4 shows that this occurs at concentrations above ~10 mol% isopropanol ($f_p \sim 0.3$). The chain length may thus be calculated from the values of $G(N_2)_w^0$ and $G(N_2)_p^0$. Assuming that our values of $g(H)_w^e$ and $g(H)_p^e$ are equal to the respective electron yields, then $G(N_2)_w^0 \simeq 3.5\ g(e)_w$ and $G(N_2)_p^0 \simeq 3.6\ g(e)_p$, showing good agreement between the two estimates. These values would be slightly high if a small fraction of the electrons did not form H atoms on neutralization via reaction 1, since $g(H)^e$ would be slightly less than $g(e)$. The latter has been suggested in hydrocarbons (5, 6) but the evidence for it in water vapor (7) or alcohols (8) is sparse and inconclusive.

In hydrocarbon gases containing N_2O (6, 9–12), high nitrogen yields were explained mainly by a mechanism involving reaction of O^- with N_2O, the substrate or an additive. However, mass spectrometric (13), drift tube (14) and ion cyclotron resonance (15) experiments now show that O^- does not form N_2 on reaction with N_2O, at least at low kinetic energies (16). Recent results in the propane–HCl system (17) also indicate that O^- is not a precursor of N_2. Although the probability of forming O^- will be higher at 125 °C than at room temperature (18), we conclude that O^- is not responsible for the high N_2 yield in the present

system. The most probable identity of X is therefore N_2O^- or $N_2O_2^-$, the latter being formed by the reaction

[3] $$N_2O^- + N_2O \rightarrow N_2 + N_2O_2^-$$

Complete reaction of either N_2O^- or $N_2O_2^-$ with water

[4] $$N_2O^- + H_2O \rightarrow N_2 + OH + OH^-$$

[5] $$N_2O_2^- + H_2O \rightarrow N_2O + OH + OH^-$$

would lead to an overall yield of $G(N_2) = g(e)$, which corresponds to our experimental $G(N_2)$ at very low isopropanol concentrations.

The mode of attack of N_2O^- or $N_2O_2^-$ on the alcohol and the intermediates in the chain reaction are difficult to define specifically. Results in alkanes (10) indicate that the α-hydrogen of the alcohol is involved and, in our system, H-atom or proton abstraction at the α-H would result in the formation of $(CH_3)_2\dot{C}OH$ or $(CH_3)_2\bar{C}OH$. $(CH_3)_2\dot{C}OH$ is also formed in large yield, even at < 1 mol% isopropanol, by the reactions

[6] $$H + (CH_3)_2CHOH \rightarrow H_2 + (CH_3)_2\dot{C}OH$$

[7] $$OH + (CH_3)_2CHOH \rightarrow H_2O + (CH_3)_2\dot{C}OH$$

which appears to rule out H atom abstraction by N_2O^- or $N_2O_2^-$ as a major step in the chain reaction, unless some other product is important. The latter cannot be OH^-, as suggested in methylcyclohexane vapor (11), since in our system OH^- is also produced by reactions 4 and 5. Further, we see no reason why proton abstraction should occur at the α-H rather than from the —OH group or why the anion should not be protonated by H_2O. The latter also appears to rule out the radical ion $(CH_3)_2\dot{C}O^-$ which was proposed as chain carrier in aqueous alkaline isopropanol solutions (19) and alkaline liquid isopropanol (20).

It is clear that the intermediates in these chain reactions are not well identified in any gas phase system, but the necessity of an α-H in the alcohol does indicate a product resulting from attack at this α-H as one intermediate in the mechanism. However, despite the limited modes of attack, none of the possible products suggests itself immediately as the reaction intermediate.

The authors would like to thank Drs. P. J. Dyne, N. H. Sagert, K. W. Chambers, and F. P. Sargent for stimulating discussions and comments on the manuscript.

1. R. S. Dixon and M. G. Bailey. Adv. Chem. **82**, 247 (1968). Taken as Part I.
2. G. G. Meisels. J. Chem. Phys. **41**, 51 (1964).
3. A. V. Phelps and R. E. Voshall. J. Chem. Phys. **49**, 3246 (1968).
4. R. W. Fessenden and J. M. Warman. J. Chem. Phys. **49**, 4718 (1968).
5. P. J. Dyné. Can. J. Chem. **43**, 1080 (1965).
6. G. R. A. Johnson and J. M. Warman. Trans. Faraday Soc. **61**, 1709 (1965).
7. R. S. Dixon and M. G. Bailey. Can. J. Chem. **46**, 1957 (1968).
8. A. R. Anderson and J. A. Winter. *In* The chemistry of ionization and excitation. *Edited by* G. R. A. Johnson and G. Scholes. Taylor & Francis, London. 1967. p. 197.
9. J. M. Warman. J. Phys. Chem. **71**, 4066 (1967).
10. J. M. Warman. J. Phys. Chem. **72**, 52 (1968).
11. W. J. Holtslander and G. R. Freeman. Can. J. Chem. **45**, 1661 (1967).
12. N. H. Sagert, R. W. Robinson, and A. S. Blair. Can. J. Chem. **46**, 3511 (1968).
13. J. F. Paulson. Adv. Chem. **58**, 28 (1966).
14. J. L. Moruzzi and J. T. Dakin. J. Chem. Phys. **49**, 5000 (1968).
15. J. Schaefer and J. M. S. Henis. J. Chem. Phys. **49**, 5377 (1968).
16. J. F. Paulson. J. Chem. Phys. **52**, 959 (1970).
17. G. R. A. Johnson and J. L. Redpath. Trans. Faraday Soc. **66**, 861 (1970).
18. P. J. Chantry. J. Chem. Phys. **51**, 3369 (1969).
19. G. Scholes, M. Simic, and J. J. Weiss. Discuss. Faraday Soc. **36**, 214 (1963).
20. W. V. Sherman. J. Phys. Chem. **71**, 1695 (1967).

Can. J. Chem. Downloaded from www.nrcresearchpress.com by 210.87.254.42 on 09/05/12
For personal use only.

The Effect of Counter Ion and Crosslinking on the Bulk Volume Magnetic Susceptibility of Dowex 50W

PAUL H. WEINER

Department of Chemistry and Chemical Engineering, Stevens Institute of Technology, Hoboken, N.J. 07030

AND

DARRYL G. HOWERY[1]

Department of Chemistry, Brooklyn College of the City University of New York, Brooklyn, N.Y. 11210

Received February 15, 1971

The bulk volume magnetic susceptibility $\chi_{v,p}$ of packed beds of ten ionic forms of Dowex 50W having a crosslinking of 4, 8, and 12% divinylbenzene are measured using a spinning coaxial cell technique. Proton chemical shifts are referenced relative to external hexamethyldisiloxane (HMD). The measured values of $\chi_{v,p}$ range from -0.730 to -0.795 c.g.s. units. The absolute value of $\chi_{v,p}$ generally increases with an increase in atomic mass of the counter ion. For a given counter ion $|\chi_{v,p}|$ increases as the crosslinking increases. Chemical shifts for water external to and internal to the ion-exchange bead phase are corrected for bulk susceptibility differences between the reference and the packed bed. The widths at half height of the external water peak increase with an increase in $|\chi_{v,p}|$.

La susceptibilité magnétique volumique $\chi_{v,p}$ de couches tassées de dix formes ioniques de Dowex 50W ayant des liaisons transversales avec le divinylbenzène de 4, 8 et 12% est mesurée en utilisant la technique de la cellule coaxiale rotative.

Les déplacements chimiques des protons sont donnés par rapport à l'hexaméthyl disiloxane (HMD) pris comme référence externe. Les valeurs mesurées de $\chi_{v,p}$ vont de -0.730 à -0.795 unités c.g.s. La valeur absolue de $\chi_{v,p}$ croit généralement lorsque la masse atomique de l'ion opposé augmente.

Pour un ion opposé donné, $|\chi_{v,p}|$ augmente de la méme façon que le nombre de liaisons transversales. Les déplacements chimiques de l'eau extérieure et intérieure à la phase échangeuse d'ions en perles, sont corrigés à cause des différences de susceptibilité volumique qui existent entre la référence et la couche tassée. Les largeurs à mi-hauteur du pic de l'eau extérieure augmentent avec un accroissement de $|\chi_{v,p}|$.

Canadian Journal of Chemistry, 49, 2913 (1971)

Introduction

High resolution proton magnetic resonance (p.m.r.) studies of ion-exchange resins (1–7) are furnishing valuable information concerning the structure of water internal to the ion-exchange resin. For spherical ion-exchange beads suspended in water, the chemical shift of the resin-phase internal water is usually reported relative to the interstitial external water in the packed bed. Gordon (1) pointed out that changes in the bulk volume magnetic susceptibility of the packed bed alter line positions relative to an external standard but that the measured difference between the chemical shift of external water and that of internal water requires no correction for differences in bulk susceptibility of water and bead. We report here the application of a method for determining the bulk susceptibility of packed beds containing spherical ion-exchange resin beads. A knowledge of bulk susceptibilities then allows the calculation of corrected chemical shifts using external standards to measure chemical shifts.

The equation which must be used to obtain corrected chemical shift values when a coaxial sample cell is utilized is

$$[1]\quad \delta_{cor}^{HMD} = \delta_{obs}^{HMD} - (2\pi/3)(\chi_{v,s} - \chi_{v,p})$$

Here δ_{cor}^{HMD} is the corrected chemical shift in p.p.m. relative to the external reference standard (hexamethyldisiloxane in this study); δ_{obs}^{HMD} is the observed chemical shift; and $\chi_{v,s}$ and $\chi_{v,p}$ are the bulk volume magnetic susceptibilities of the reference solution and the packed bed, respectively. Resonance shifts which occur to the low-field side of the reference are positive.

The bulk susceptibility of an aqueous suspension of ion-exchange beads, needed for eq. 1, is determined by using the method of Malinowski and Weiner (8). It was shown that the bulk volume susceptibility of material contained in the central region of a spinning coaxial sample cell

[1]To whom all correspondence should be addressed.

Can. J. Chem. Downloaded from www.nrcresearchpress.com by 210.87.254.40 on 09/05/12
For personal use only.

Can. J. Chem. Downloaded from www.nrcresearchpress.com by 210.87.254.40 on 09/05/12
For personal use only.

could be determined from

$$[2]\quad \chi_{v,center} = \frac{[\nu_s^{(1)} - \nu_s^{(3)}]kr^2}{(a^2 + b^2)\pi\nu_0} = \frac{\nu_s^{(1)} - \nu_s^{(3)}}{72.65}$$

Here $\nu_s^{(1)}$ is the spinning frequency in Hz necessary to make the intensity of the first spinning sideband of the material in the annular region of the coaxial cell equal in intensity to the main band of that region (under the experimental conditions of reference annular and packed bed central); $\nu_s^{(3)}$ is the spinning frequency which produces equal intensities when the reference is annular and nitrogen gas at 1 atm pressure is central; k is the argument of a Bessel function; r is the mean radius of the annular region of the coaxial cell; a and b are the inner and outer radii of the central tube; and ν_0 is the spectrometer frequency in MHz. The spinning frequencies, $\nu_s^{(1)}$ and $\nu_s^{(3)}$, are determined by plotting relative peak height differences between main band and first sideband *vs.* the splitting between the two bands, and interpolating to find the spinning frequency when the relative peak height difference is zero. Because of the geometry of the coaxial cell, the first sideband appears at twice the sample spinning frequency. The right hand side of eq. 2 results when the constants are evaluated for the coaxial cell used in this work. Under the condition of equal peak height of main band and first sideband, the argument of the Bessel function takes the value of 1.4347.

The absolute signs of all $\nu_s^{(i)}$ (where $i = 1$ and 3) are determined by the field-gradient method proposed by Malinowski and Pierpaoli (9). In their method, if a change in the z-gradient produces asymmetric intermediate sidebands to the right (left) hand side of the main peak of the material in the annular region, then $\nu_s^{(i)}$ is positive (negative). Similarly, changing the x-gradient when $\nu_s^{(i)}$ is positive (negative) will produce asymmetric sidebands to the left (right) of the main peak of the annular region. The magnitude of $\nu_s^{(i)}$ should be determined only after all intermediate sidebands have been eliminated.

Since the packed bed – reference interface is cylindrical in a coaxial cell, corrections for differences in bulk susceptibility between reference and packed beds have to be made as indicated in eq. 1. Bernstein and Frei (10) pointed out that no additional susceptibility corrections need be made if the interface between two sample regions is spherical. For packed beds of spherical resin beads suspended in water, the interface between the external and internal water phases is spherical. Therefore, both regions of the packed beds experience the same magnetic field strength and no corrections have to be made for differences in bulk susceptibilities of the external and internal water phases.

Experimental

The ion exchange resins employed were Dowex AG 50W, 20–50 mesh, purchased from BioRad Laboratories. Details of resin pretreatment and of sample preparation have been reported (4). The exchange capacities of the sodium-form resin were found to be 4.62, 4.51, and 4.33 meq/g dry resin for crosslinkings of × 4, × 8, and × 12, respectively; the water contents determined by the centrifugation method for the three sodium-form resins were 0.62, 0.45, and 0.36 g/g wet resin, respectively. Spectra were taken at a probe temperature of 39 ± 1 °C on a Varian A-60A p.m.r. spectrometer utilizing a Hewlett–Packard Model 200AB wide range oscillator and a Hewlett–Packard Model 523DR frequency counter. The coaxial cell was a Wilmad Glass model number 516 of 5 mm outer diameter. The precision of the bulk susceptibilities is better than ±0.01 p.p.m.; the precision of uncorrected chemical shifts is better than ±1 Hz.

Results and Discussion

Results of studies on 10 ionic forms of Dowex 50W of crosslinkings × 4, × 8, and × 12 are summarized in Table 1.

The values of $\chi_{v,p}$ are all fairly similar to $\chi_{v,polystyrene}$ (= −0.690) (1) and to χ_{v,H_2O} (= −0.720). For ions in a given group the absolute value of $\chi_{v,p}$ increases with an increase in counter ion mass, as expected (11). For a given counter ion $|\chi_{v,p}|$ increases slightly with a decrease in water content of the ion-exchanger phase. The bulk susceptibility of the ion-exchanger bead, $\chi_{v,b}$, can be estimated by assuming additivity of the volumetric susceptibilities (12) of the two phases in the packed bed. For resin beads suspended in water, $\chi_{v,b}$ can be calculated from

$$[3]\quad \chi_{v,p} = 0.40\chi_{v,H_2O} + 0.60\chi_{v,b}$$

where the coefficients represent the approximate volume fractions of the two phases.

The constancy of the corrected chemical shifts for the external water calculated from eqs. 1 and 2 substantiates the method since the uncorrected chemical shifts for the external water (see Table 1) varied over the range 5.02–5.15 p.p.m. Chemical shifts for internal resin water referred to external tetramethylsilane–chloroform which were not corrected for susceptibility differences

TABLE 1. Bulk volume magnetic susceptibilities and corrected chemical shifts for packed beds of Dowex 50W

Form	X[a]	$-\chi_{v,p}$[b]	$-\chi_{v,b}$[c]	$\delta_{u,e}^{HMD}$[d]	$\delta_{c,e}^{HMD}$[e]		$\delta_{c,i}^{HMD}$[f]	w_e[g]
H^+	4	0.730	0.735	5.03	4.67		5.32	5
	8	0.735	0.745	5.04	4.67		6.00	9
	12	0.735	0.745	5.02	4.65		6.55	11
Na^+	4	0.740	0.755	5.03	4.65		4.53	12
	8	0.755	0.780	5.08	4.67		4.42	13
	12	0.765	0.795	5.08	4.65		4.32	15
NH_4^+	4	0.735	0.745	5.02	4.65		4.60	8
	8	0.745	0.760	5.04	4.65		4.55	11
	12	0.750	0.770	5.05	4.65		4.47	11
NMe_4^+	4	0.730	0.735	[h]		4.67[h]		8[i]
	8	0.745	0.760	[h]		4.63[h]		11[i]
	12	0.745	0.760	[h]		4.65[h]		13[i]
Rb^+	4	0.750	0.770	5.05	4.65		4.55	11
	8	0.775	0.810	5.08	4.63		4.40	17
	12	0.780	0.820	5.09	4.63		4.27	17
Mg^{2+}	4	0.750	0.770	5.05	4.65		4.82	8
	8	0.760	0.785	5.07	4.65		4.90	12
	12	0.770	0.805	5.09	4.65		5.02[j]	17
Ba^{2+}	4	0.780	0.820	[h]		4.58[h]		17[i]
	8	0.785	0.830	[h]		4.55[h]		21[i]
	12	0.795	0.845	[h]		4.57[h]		22[i]
Zn^{2+}	4	0.755	0.780	5.06	4.65		4.87	9
	8	0.770	0.805	5.07	4.63		5.02	15
	12	0.775	0.810	5.10	4.65		5.13	18
Cd^{2+}	4	0.760	0.785	5.09	4.67		4.82	10
	8	0.775	0.810	5.10	4.65		4.98	15
	12	0.795	0.845	5.15	4.65		5.02	18
La^{3+}	4	0.750	0.770	5.07	4.67		4.93	13
	8	0.765	0.795	5.08	4.65		5.02	14
	12	0.780	0.820	5.09	4.63		5.00	22

[a]Crosslinking.
[b]Bulk magnetic susceptibility of packed bed, p.p.m.
[c]Calculated volumetric susceptibility of ion-exchanger bead, p.p.m.
[d]Observed proton chemical shift for external (interstitial) water, p.p.m.
[e]Corrected proton chemical shift for external water, p.p.m.
[f]Corrected proton chemical shift for internal (resin phase) water, p.p.m.
[g]Width at half height for external water, Hz.
[h]Only one peak observed.
[i]Sum of external and internal water.
[j]Broad shoulder.

are generally in good agreement with the corrected chemical shifts since in chloroform, $\chi_{v,TMS}$ ($= -0.727$) differs in most cases so slightly from $\chi_{v,p}$ that the susceptibility correction in eq. 1 is insignificant.

Since the dependence of $\chi_{v,p}$ upon counter ion mass and crosslinking is established fairly completely in Table 1, values of $\chi_{v,p}$ for other resin forms of various crosslinkings can be estimated and the corresponding corrected chemical shifts can be calculated using eq. 1. Bulk susceptibility corrections become extremely important in studies of ion exchanger – mixed solvent systems (6, 7) where for many solvent pairs $\chi_{v,p}$ varies considerably with solvent composition. The method utilized in this work is applicable to any system containing spherical particles suspended in a fluid phase.

The widths at half height of the external water peak, w_e, increase with an increase in the absolute value of $\chi_{v,b}$, as predicted by Gordon (1). The correspondence between $\chi_{v,b}$ and w_e shown in Table 1 indicates that values of $\chi_{v,b}$ can be estimated to better than ± 0.02 from a determination of the width at half height of the external water peak.

1. J. E. GORDON. J. Phys. Chem. **66**, 1150 (1962).
2. L. S. FRANKEL. Anal. Chem. **42**, 1638 (1970) and references therein.
3. H. D. SHARMA and N. SUBRAMANIAN. Can. J. Chem. **49**, 457 (1971).

Can. J. Chem. Downloaded from www.nrcresearchpress.com by 210.87.254.40 on 09/05/12
For personal use only.

4. D. G. HOWERY and M. J. KITTAY. J. Macromolec. Sci. A4, 1003 (1970).
5. D. G. HOWERY and B. H. KOHN. Anal. Lett. **3**, 89 (1970).
6. L. S. FRANKEL. Can. J. Chem. **48**, 2432 (1970).
7. D. G. HOWERY, G. SENUM, and L. MADOFF. Anal. Lett. **3**, 483 (1970).
8. E. R. MALINOWSKI and P. H. WEINER. J. Am. Chem. Soc. **92**, 4193 (1970).
9. E. R. MALINOWSKI and A. R. PIERPAOLI. J. Mag. Resonance, **1**, 509 (1969).
10. H. J. BERNSTEIN and K. FREI. J. Chem. Phys. **37**, 1891 (1962).
11. L. N. MULAY. *In* Treatise on analytical chemistry. Vol. 4. Part 1. *Edited by* I. M. Kolthoff and P. J. Elving. John Wiley and Sons, Inc., New York. 1963. p. 1782.
12. J. A. POPLE, W. G. SCHNEIDER, and H. J. BERNSTEIN. High resolution nuclear magnetic resonance spectroscopy. McGraw-Hill Book Co., Inc., New York. 1959. p. 18.

Can. J. Chem. Downloaded from www.nrcresearchpress.com by 210.87.254.40 on 09/05/12
For personal use only.

The Norrish Type II Photodecomposition of Di-*n*-Butyl Terephthalate[1]

M. DAY AND D. M. WILES
Division of Chemistry, National Research Council of Canada, Ottawa, Canada

Received May 11, 1971

The liquid phase photolysis of undiluted di-*n*-butyl terephthalate yields 1-butene and carboxylic acid end groups as a result of a Norrish Type II photochemical rearrangement reaction. Quantum yields for the production of these two products have been determined and found to be $\phi_{1-\text{butene}} = 0.017$ and $\phi_{\text{COOH}} = 0.022$ in vacuum and $\phi_{1-\text{butene}} = 0.0050$ and $\phi_{\text{COOH}} = 0.0056$ in air.

La photolyse en phase liquide du téréphtalate de di-*n*-butyl non dilué conduit au butène-1 et à des terminaisons carboxyliques. Ceci est le résultat de la transposition photochimique du type "Norrish II". Les rendements quantiques de la formation de ces deux produits ont été déterminés et sont de $\phi_{\text{Butène-1}} = 0.017$ et $\phi_{\text{COOH}} = 0.022$ dans le vide et $\phi_{\text{Butène-1}} = 0.0050$ et $\phi_{\text{COOH}} = 0.0056$ dans l'air.

Canadian Journal of Chemistry, 49, 2916 (1971)

The photolyses of aliphatic and aromatic esters in which a β hydrogen atom occurs in the alcohol portion of the ester are known to yield an olefin and an acid as a result of an intramolecular process analogous to the Norrish Type II split of aldehydes and ketones (1–7). As a part of our studies of the photochemical decomposition of poly(ethylene terephthalate) (PET) in vacuum and air, we have examined the liquid phase photolysis of di-*n*-butyl terephthalate (DBT). Our objective was to determine the extent of Norrish Type II cleavage occurring in the photolysis of an aromatic di-ester similar in structure to the polymer, PET.

Degassed or air saturated undiluted DBT (4.5 ml) was sealed off after filling in a quartz cell (1 cm path). The ester was irradiated with the light from an Osram super pressure mercury lamp (HBO 200 W), filtered through a Corning filter CS 7-54 (range 225–420 nm) with 140 nm half band width and a 10 cm path water filter. After irradiation, volatile products were removed via a break seal and analyzed on a gas chromatograph equipped with a flame ionization detector. Quantitative analysis of the photolysis products indicated 1-butene was the main product. The concentrations of carboxylic acid end groups formed in the irradiated liquid as a result of photolysis were determined either by titrimetric analysis, or more conveniently by differential i.r. spectroscopy of the irradiated ester in comparison with the original liquid. The optical

[1]NRCC No. 12050.

4. D. G. HOWERY and M. J. KITTAY. J. Macromolec. Sci. A4, 1003 (1970).
5. D. G. HOWERY and B. H. KOHN. Anal. Lett. **3**, 89 (1970).
6. L. S. FRANKEL. Can. J. Chem. **48**, 2432 (1970).
7. D. G. HOWERY, G. SENUM, and L. MADOFF. Anal. Lett. **3**, 483 (1970).
8. E. R. MALINOWSKI and P. H. WEINER. J. Am. Chem. Soc. **92**, 4193 (1970).
9. E. R. MALINOWSKI and A. R. PIERPAOLI. J. Mag. Resonance, **1**, 509 (1969).
10. H. J. BERNSTEIN and K. FREI. J. Chem. Phys. **37**, 1891 (1962).
11. L. N. MULAY. *In* Treatise on analytical chemistry. Vol. 4. Part 1. *Edited by* I. M. Kolthoff and P. J. Elving. John Wiley and Sons, Inc., New York. 1963. p. 1782.
12. J. A. POPLE, W. G. SCHNEIDER, and H. J. BERNSTEIN. High resolution nuclear magnetic resonance spectroscopy. McGraw-Hill Book Co., Inc., New York. 1959. p. 18.

Can. J. Chem. Downloaded from www.nrcresearchpress.com by 210.87.254.40 on 09/05/12
For personal use only.

The Norrish Type II Photodecomposition of Di-*n*-Butyl Terephthalate[1]

M. DAY AND D. M. WILES
Division of Chemistry, National Research Council of Canada, Ottawa, Canada

Received May 11, 1971

The liquid phase photolysis of undiluted di-*n*-butyl terephthalate yields 1-butene and carboxylic acid end groups as a result of a Norrish Type II photochemical rearrangement reaction. Quantum yields for the production of these two products have been determined and found to be $\phi_{1-\text{butene}} = 0.017$ and $\phi_{\text{COOH}} = 0.022$ in vacuum and $\phi_{1-\text{butene}} = 0.0050$ and $\phi_{\text{COOH}} = 0.0056$ in air.

La photolyse en phase liquide du téréphtalate de di-*n*-butyl non dilué conduit au butène-1 et à des terminaisons carboxyliques. Ceci est le résultat de la transposition photochimique du type "Norrish II". Les rendements quantiques de la formation de ces deux produits ont été déterminés et sont de $\phi_{\text{Butène-1}} = 0.017$ et $\phi_{\text{COOH}} = 0.022$ dans le vide et $\phi_{\text{Butène-1}} = 0.0050$ et $\phi_{\text{COOH}} = 0.0056$ dans l'air.

Canadian Journal of Chemistry, 49, 2916 (1971)

The photolyses of aliphatic and aromatic esters in which a β hydrogen atom occurs in the alcohol portion of the ester are known to yield an olefin and an acid as a result of an intramolecular process analogous to the Norrish Type II split of aldehydes and ketones (1–7). As a part of our studies of the photochemical decomposition of poly(ethylene terephthalate) (PET) in vacuum and air, we have examined the liquid phase photolysis of di-*n*-butyl terephthalate (DBT). Our objective was to determine the extent of Norrish Type II cleavage occurring in the photolysis of an aromatic di-ester similar in structure to the polymer, PET.

Degassed or air saturated undiluted DBT (4.5 ml) was sealed off after filling in a quartz cell (1 cm path). The ester was irradiated with the light from an Osram super pressure mercury lamp (HBO 200 W), filtered through a Corning filter CS 7-54 (range 225–420 nm) with 140 nm half band width and a 10 cm path water filter. After irradiation, volatile products were removed via a break seal and analyzed on a gas chromatograph equipped with a flame ionization detector. Quantitative analysis of the photolysis products indicated 1-butene was the main product. The concentrations of carboxylic acid end groups formed in the irradiated liquid as a result of photolysis were determined either by titrimetric analysis, or more conveniently by differential i.r. spectroscopy of the irradiated ester in comparison with the original liquid. The optical

[1]NRCC No. 12050.

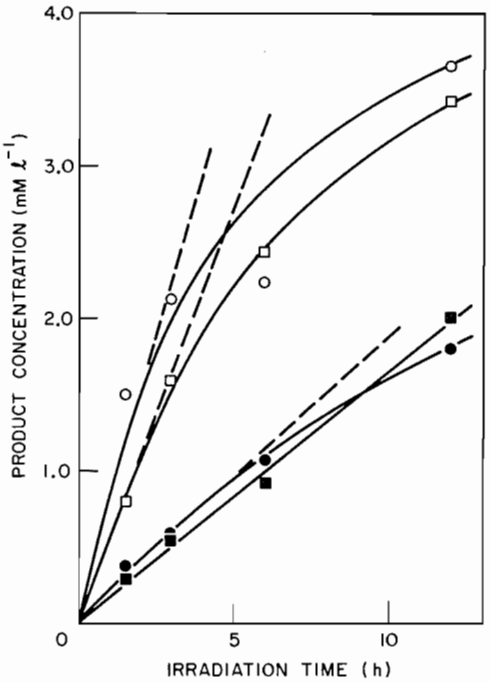

FIG. 1. Rate of formation of 1-butene in vacuum (□) and air (■) and —COOH in vacuum (○) and air (●) as a function of irradiation time.

density changes of the band centered at 3290 cm^{-1} was used to calculate the —COOH concentration. A molar extinction coefficient of $\varepsilon = 450 \pm 30$ was obtained from a comparison of the $o.d._{3290}$ and acid equivalence of several samples by non-aqueous potentiometric titrations.

The rates of formation of 1-butene and —COOH end groups as a function of irradiation time in air and vacuum are illustrated in Fig. 1. From these results, together with the light intensities on the cells (calibrated with an Eppley thermopile), the known spectral distribution of the lamp and the extinction coefficient for the undiluted DBT as a function of wavelength, calculations were made of the initial quantum yields for these two products. The photolysis of DBT under vacuum conditions gave acid end groups and 1-butene with initial quantum efficiencies of $\phi_{COOH} = 0.022$ and $\phi_{1-butene} = 0.017$. When the photolysis was carried out in air the initial quantum yields were reduced, ($\phi_{COOH} = 0.0056$; $\phi_{1-butene} = 0.0050$).

These results indicate that the following Norrish Type II intramolecular processes occur on photolysis

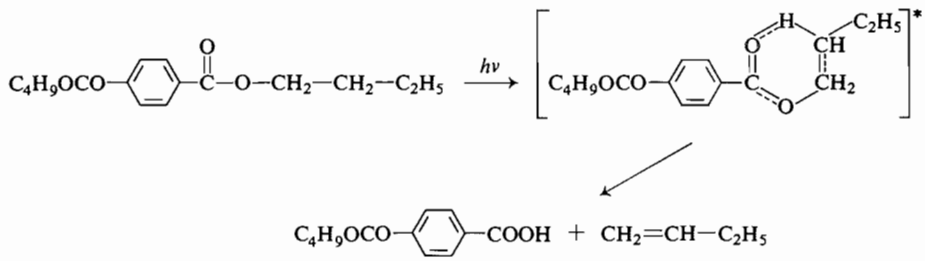

This process is consistent with the observations that 1-butene and carboxylic acid are the main products, and that the rates of formation of 1-butene and carboxylic acid end groups are comparable. The quantum yields obtained are also comparable to those reported for other esters of aromatic carboxylic acids photolyzed in solution (6, 7). The lower quantum yields obtained in air may be due to the influence of oxygen, in reducing the efficiency of reaction of the triplet-derived intermediate as suggested by Ausloos (5).

Thus the importance of the Norrish Type II cleavage in the photolysis of an aromatic diester has been established under our experimental conditions. This concludes our model compound investigation by establishing a possible mechanism which PET (the polymeric counterpart of DBT) may be expected to undergo. The actual photolysis of the polymer PET will be reported in a future publication.

1. P. AUSLOOS. Can. J. Chem. **36**, 383 (1958).
2. P. AUSLOOS. J. Am. Chem. Soc. **80**, 1310 (1958).
3. M. H. J. WIJNEN. J. Am. Chem. Soc. **82**, 3034 (1960).
4. R. BORKOWSKI and P. AUSLOOS. J. Am. Chem. Soc. **83**, 1053 (1961).
5. P. AUSLOOS and R. E. REBBERT. J. Phys. Chem. **67**, 163 (1963).
6. H. MORRISON, R. BRAINARD, and D. RICHARDSON. Chem. Commun. 1653 (1968).
7. J. A. BARLTROP and J. D. COYLE. J. Chem. Soc. B, 251 (1971).

Can. J. Chem. Downloaded from www.nrcresearchpress.com by 210.87.254.40 on 09/05/12
For personal use only.

Can. J. Chem. Downloaded from www.nrcresearchpress.com by 210.87.254.6 on 09/05/12
For personal use only.

COMMUNICATIONS

Electron Affinities from Thermal Proton-Transfer Reactions: C_6H_5 and $C_6H_5CH_2$

D. K. BOHME
Department of Chemistry, York University, Toronto, Ontario
AND
L. BREWSTER YOUNG
Mobil Chemical Company, Edison, New Jersey 08817

Received June 4, 1971

The observation of the preferred direction of proton transfer reactions in the gas phase at 300 °K has been employed to bracket the electron affinity, e.a., of the radicals C_6H_5 and $C_6H_5CH_2$ using well-established values for electron affinities and bond energies. The results indicate that 1.2 eV ≤ e.a.(C_6H_5) ≤ 1.6 eV and that 0.4 eV ≤ e.a.($C_6H_5CH_2$) ≤ 0.9 eV.

Les observations relatives à la direction préférentielle dans les réactions de transfert de proton en phase gazeuse et à 300 °K, ont été utilisées pour encadrer la valeur e.a. d'électron affinité pour les radicaux C_6H_5 et $C_6H_5CH_2$; à cet effet, des valeurs d'électron affinité et d'énergie de liaison bien établies, ont été utilisées. Les résultats indiquent que 1.2 eV ≤ e.a.(C_6H_5) ≤ 1.6 eV et que 0.4 eV ≤ e.a.($C_6H_5CH_2$) ≤ 0.9 eV.

Canadian Journal of Chemistry, 49, 2918 (1971)

Chemically useful values for the electron affinity of small molecules have recently become accessible through gas-phase investigations of the kinetics of negative ion – molecule reactions. For example, exothermic and endothermic negative-ion charge-transfer reactions have been employed to bracket unknown electron affinities between well-established electron affinities (1, 2). Electron affinities of molecules have also been determined from the translational energy thresholds for endothermic charge transfer reactions involving atomic halogen anions (3).

We report here the determination of electron affinities of selected radicals from bracketing experiments involving proton transfer reactions of the type

$$[1] \qquad X^- + YH \leftrightarrows Y^- + XH$$

proceeding in the gas phase at 300 °K. Although bracketing experiments can surpass the precision of other earlier techniques, they lack the precision of photodetachment (4) and electron impact (5) methods which, however, are often limited to the study of the electron affinity of atoms and small molecules.

The determination of the preferred direction of proton transfer in reaction 1 identifies the sign of the standard free energy change which, in turn, identifies the sign of the standard enthalpy change if the change in standard entropy can be neglected. The standard enthalpy change, $\Delta H°$, for reaction 1, is related to bond dissociation energy, D, and electron affinity, e.a., parameters in the following manner

$$[2] \quad \Delta H° = D(YH) - D(XH) + \text{e.a.}(X) - \text{e.a.}(Y)$$

Thus a knowledge of the sign of $\Delta H°$ and three of the four energy parameters allows the determination of a limiting value for the fourth parameter. The parameter of interest in these studies was the electron affinity of either X or Y.

The experiments were performed in a flowing afterglow system at the National Oceanic and Atmospheric Administration, Environmental Research Laboratories, in Boulder, Colorado. Details of the method of operation and data analysis have been thoroughly described elsewhere (6, 7). Helium was used as the buffer gas at a pressure *ca.* 0.4 Torr. H^- ions were generated by 25 eV electron impact on NH_3. The production of OH^- and $C_3H_5^-$ has been described previously (7) as has the generation of $C_6H_5^-$ and $C_6H_5CH_2^-$ (8). The concen-

TABLE 1. Summary of the kinetics of proton-transfer reactions investigated in the gas phase at 300 °K

Proton-transfer reaction	k_f*	k_r*	K
$C_6H_5^- + H_2O \rightleftarrows OH^- + C_6H_6$	$\gtrsim 5(-11)$	$< 5(-12)$	> 10
$H^- + C_6H_6 \rightleftarrows C_6H_5^- + H_2$	$\gtrsim 5(-11)$	$< 5(-12)$	> 10
$C_6H_5CH_2^- + C_2H_5OH \rightleftarrows C_2H_5O^- + C_6H_5CH_3$	$\gtrsim 5(-11)$	$< 5(-11)$	> 1
$C_3H_5^- + C_6H_5CH_3 \rightleftarrows C_6H_5CH_2^- + C_3H_6$	$\sim 1(-11)$	$< 1(-12)$	> 10
$OH^- + C_3H_6 \rightleftarrows C_3H_5^- + H_2O$	$2.7(-10)$		

*Units in cm^3 molecule^{-1} s^{-1}, (-11) denotes 10^{-11}.

trations of water, benzene, ethanol, and toluene in the reaction region were measured by monitoring the increase in total pressure in the reaction region as the vapors were introduced. As a result of the insensitivity of the capacitance manometer (with a 10 Torr sensing head) used in these experiments, the rate determinations for fast reactions using this technique led only to limiting values for rate constants.

A summary of the rate constant data obtained is given in Table 1. The last reaction listed has been reported previously (7). The ratio of the forward to the reverse rate constant was taken to be equal to the thermodynamic equilibrium constant since the energy distribution of both the ions, which undergo many thousand collisions with helium atoms before entering the reaction region, and the neutral reactants, which are added in thermal equilibrium at the operating temperature, is expected to be Boltzmann in all the forward and reverse reactions investigated. For each of the reactions listed in Table 1, the thermodynamic equilibrium constant was found to be greater than 1. Hence the standard free energy change is negative for all these reactions as written. We now make the assumption that the transfer of a proton is not accompanied by a significant change in entropy, *i.e.*, $T\Delta S^\circ \ll \Delta H^\circ$. Consequently, the five reactions listed in Table 1 are taken to be exothermic or thermoneutral at 300 °K. Relation 2 then leads to the limiting values 1.2 eV $\leq$ e.a.(C_6H_5) $\leq$ 1.6 eV and 0.4 eV $\leq$ e.a.($C_6H_5CH_2$) $\leq$ 0.9 eV. The electron affinities of H, OH, and C_2H_5O are taken to be well established at 0.754 eV (9), 1.83 eV (10), and 1.68 eV (11), respectively. The bond energies for H—H, HO—H, C_2H_5O—H, C_6H_5—H, and $C_6H_5CH_2$—H were taken to be 4.477 (12), 5.11 (12), 4.43 (13), 4.86 (14), and 3.69 (13), respectively.

The authors are aware of only one previous experimental determination of the electron affinity of these radicals. Page and Goode, who employ the magnetron technique they developed (15), report values ranging from 2.15 to 2.46 eV for e.a.(C_6H_5) and values ranging from 0.76 to 0.84 eV (with one value of 2.5 eV) for e.a. ($C_6H_5CH_2$). An early molecular orbital theory calculation by Hush and Pople (16) yielded e.a.($C_6H_5CH_2$) = 0.69 eV. The limiting values for e.a.($C_6H_5CH_2$) determined in these studies are in good agreement with the values (0.76 to 0.84 eV) determined by the magnetron technique and the value obtained from theoretical calculations. However, the limiting values determined in this study suggest a value for e.a.(C_6H_5) considerably lower than that obtained from the magnetron technique. An electron affinity e.a.-(C_6H_5) > 2.0 eV would make the first reaction in Table 1 endothermic (and $\Delta G^\circ > 0$) for ground-state reactants at 300 °K by more than 0.3 eV. We expect that our kinetic measurements deal with ground-state $C_6H_5^-$ ions and not $C_6H_5^-$ excited. Hence our result should represent a more accurate value for the electron affinity of C_6H_5.

1. K. KRAUS, W. MÜLLER-DUYSING, and H. NEUERT. Z. NATURFORSCH. **16**a, 1385 (1961).
2. C. LIFSHITZ and R. GRAJOWER. Int. J. Mass Spectry. Ion Phys. **3**, 5 (1969).
3. C. LIFSHITZ, B. M. HUGHES, and T. O. TIERNAN. Chem. Phys. Lett. **7**, 469 (1970).
4. L. M. BRANSCOMB. Atomic and molecular processes. *Edited by* D. R. Bates. Academic Press Inc., New York. 1962. Chap. 4.
5. P. J. CHANTRY and G. J. SCHULZ. Phys. Rev. **156**, 134 (1967).
6. E. E. FERGUSON, F. C. FEHSENFELD, and A. L. SCHMELTEKOPF. Advances in atomic and molecular physics. Vol. 5. Academic Press, Inc. New York. 1969.
7. D. K. BOHME and L. B. YOUNG. J. Am. Chem. Soc. **92**, 3301 (1970).
8. D. K. BOHME and L. B. YOUNG. J. Am. Chem. Soc. **92**, 7354 (1970).
9. C. L. PEKERIS. Phys. Rev. **126**, 1470 (1962).

Can. J. Chem. Downloaded from www.nrcresearchpress.com by 210.87.254.6 on 09/05/12
For personal use only.

10. L. M. BRANSCOMB. Phys. Rev. **148**, 11 (1966).
11. J. M. WILLIAMS and W. H. HAMILL. J. Chem. Phys. **49**, 4467 (1968).
12. G. HERZBERG. Molecular spectra and molecular structure. Vol. I. D. Van Nostrand Co. Inc., New York. Spectra of diatomic molecules. Vol. III. 2nd ed. 1953. Electronic spectra and electronic structure of polyatomic molecules. 1966.
13. J. A. KERR. Chem. Rev. **66**, 465 (1966).
14. D. M. GOLDEN and S. W. BENSON. Chem. Rev. **69**, 125 (1969).
15. F. M. PAGE and G. C. GOODE. Negative ions and the magnetron. Wiley-Interscience, New York. 1969.
16. N. S. HUSH and J. A. POPLE. Trans. Faraday Soc. **51**, 600 (1955).

Can. J. Chem. Downloaded from www.nrcresearchpress.com by 210.87.254.6 on 09/05/12
For personal use only.

Can. J. Chem. Downloaded from www.nrcresearchpress.com by 210.87.254.6 on 09/05/12
For personal use only.

Canadian Journal of Chemistry

Published by THE NATIONAL RESEARCH COUNCIL OF CANADA

VOLUME 49 SEPTEMBER 15, 1971 NUMBER 18

Infrared Spectra of Some Alkyl Platinum Compounds. Part II. Assignment of the CH Stretching Modes of a Methyl Group

B. A. MORROW[1] AND Y. BEAUCHAMP

Department of Chemistry, University of Ottawa, Ottawa, Canada

Received May 5, 1971

Several isotopically substituted triphenylphosphine stabilized dimethyl platinum compounds of the type $(Ph_3P)_2PtMe_2$ where Me = CH_3, CH_2D, CD_2H, and CD_3 have been prepared and their infrared spectra in the CH and CD stretching regions have been examined. The assignments of the stretching vibrations of the methyl group have been confirmed by means of an application of the Average Rule for isotopically substituted species. The possible application of the Average Rule as a general method for assigning CH stretching modes is discussed and it is suggested that the method could be used to confirm some recently proposed reassignments of the traditional Fox and Martin assignments. The method may also be used by surface chemists as a means of determining the number of hydrogen atoms in an adsorbed XH_n species.

Les composés diméthylés du platine du type $(Ph_3P)_2PtMe$, dans lesquels Me = CH_3, CH_2D, CD_2H et CD_3 ont été préparés et leurs spectres infrarouges dans les régions de vibrations d'élongation de CH et CD ont été examinés. Les attributions des vibrations d'élongation du groupe méthyle ont été confirmées grâce à l'application de la Règle de la Moyenne pour des espèces substituées par des isotopes. L'application possible de la Règle de la Moyenne comme une méthode générale pour l'attribution des modes de vibration CH est discutée et on suggère que la méthode pourrait être utilisée pour confirmer quelques réattributions récemment proposées des attributions traditionnelles de Fox et Martin. La méthode pourrait être aussi utilisée dans la chimie des surfaces comme un moyen de déterminer le nombre d'atomes d'hydrogène dans une espèce adsorbée XH_n.

Canadian Journal of Chemistry, **49**, 2921 (1971)

Introduction

The surface chemist who wishes to use infrared spectroscopy in order to study the nature of a surface–adsorbate species is severely hampered in making a complete vibrational analysis because the adsorbent is usually totally absorbing in-part of the infrared region (1). This problem is particularly critical in studying the spectra of hydrocarbons adsorbed on silica or alumina supported metal catalysts since the spectral regions below about 1200 cm^{-1} will be totally masked by the strong infrared absorptions of silica. Further, since it is usually only possible to utilize metal loadings of the order of 10–15% by weight, the deformation bands in 1400 cm^{-1} spectral region are often so weak so as to be undetectable (2). As a result, surface chemists often have to base any interpretation on a limited spectral region, which for hydrocarbons is usually the CH stretching region. In Part 1 of this series (3), the infrared spectra of some alkyl platinum compounds were discussed in relation to the spectra of chemisorbed hydrocarbons. In the present paper, the spectra of some partially deuterated methyl–platinum compounds are discussed. Because of the limited spectral region, the surface chemist often has to resort to isotopic substitution in order to confirm a spectral assignment, and it is important that the effects of such substitutions be well understood with reference to the spectra of model compounds.

A second point of interest is a current concern over the exact assignments of the CH stretching modes of a methyl group. Organic chemists have for years used the Fox and Martin assignments as an aid to identify this functional group (4, 5) and several interesting papers have recently

[1]To whom correspondence should be addressed.

TABLE 1. Observed methyl stretching frequencies of $(Ph_3P)_2PtMe_2$

Me	Wavenumber (cm^{-1})	Optical density	Assignment*	Average value of ν_s and ν_a (cm^{-1})†
CH_3	2934	0.11	ν_a	2908
	2878 (2856)‡	0.13	ν_s	(2915)
	2806	0.05	o.v.	
CH_2D	2923	0.045	ν_a	
	2881	0.073	ν_s	2907
	2154	0.03	ν(CD)	
CHD_2	2908	0.055	ν(CH)	
	2189	0.040	ν_a	2152
	2115	0.115	ν_s	
CD_3	2195	0.040	ν_a	
	2099 (2077)	0.045	ν_s	2156
	2050	0.035	o.v.	(2163)

*ν_a = asymmetric, ν_s = symmetric, o.v. = overtone.
†Using the Average Rule after correcting for Fermi resonance interaction. Values in parentheses are the average values without the Fermi resonance correction.
‡Corrected for Fermi resonance interaction with o.v. See text.

appeared in the literature in which these assignments are questioned (6, 7). This aspect will be discussed further later, but suffice it to say that it was anticipated in Part I (3) that the spectra of the partially deuterated methyl compounds should throw some light on the assignment problem. In this paper, the compounds $(Ph_3P)_2PtMe_3$ have been synthesized (Ph = phenyl, and Me = CH_3, CH_2D, CHD_2 or CD_3) and their infrared spectra in the CH and CD stretching regions have been analyzed.

Experimental

The *cis*-bis(triphenylphosphine)dimethylplatinum derivatives were prepared as in Part I (3). The CD_3Br, CH_2DBr, and CHD_2Br were obtained from Merck, Sharp and Dohme Ltd. of Montreal and were claimed to be of 98% isotopic purity (99.5% for CD_3Br). All spectra were run as saturated solutions in CCl_4 (about 10 mg/ml) on a Perkin–Elmer model 13G infrared spectrometer using a spectral slit width of about 3 cm^{-1}. The cell path length was 0.992 mm.

Results

Spectra in the CH and CD stretching regions are shown in Fig. 1, and the wavenumbers of the observed band of the methyl group ($< 3000\ cm^{-1}$ in the CH stretching region) are listed in Table 1.

Assignments

A methyl group is expected to give rise to three valence stretching modes in the infrared near 2800–3000 cm^{-1} for a CH_3 group, or near 2200–2000 cm^{-1} for a CD_3 group (5). When the 3-fold axis of symmetry is preserved, as for example in the methyl halides, one vibration is classified as being symmetric (ν_s) and two are asymmetric (ν_a) with respect to this axis, and the two asymmetric modes are degenerate. However, in most molecules which possess a methyl group, the 3-fold axis of symmetry is destroyed; but the

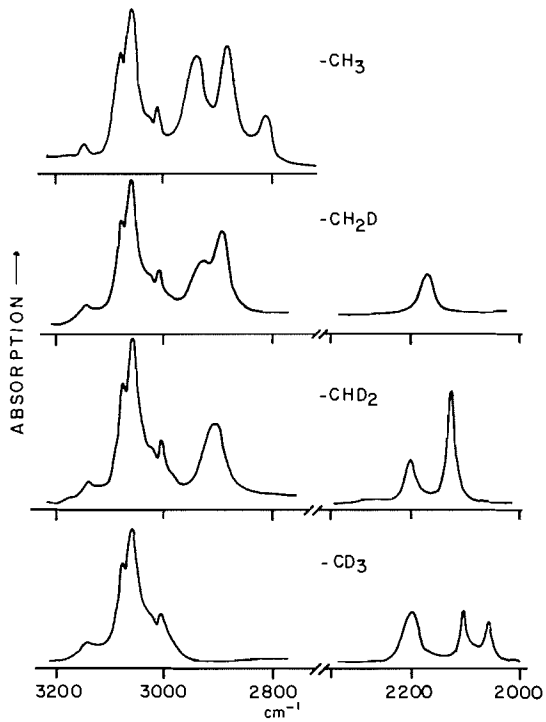

FIG. 1. Infrared spectra in the ν_{CH} and ν_{CD} region of $(Ph_3P)_2PtMe_2$ where Me = CH_3, CH_2D, CHD_2, and CD_3. All spectra were run as approximately 10^{-2} *M* solutions in CCl_4.

Can. J. Chem. Downloaded from www.nrcresearchpress.com by 210.87.254.6 on 09/05/12
For personal use only.

Can. J. Chem. Downloaded from www.nrcresearchpress.com by 210.87.254.6 on 09/05/12
For personal use only.

CH stretching vibrations are still commonly classified as being symmetric or asymmetric with respect to the localized 3-fold axis of the methyl group. In this case, the degeneracy of the two ν_a modes should be removed, but in practice, the vibrations of a methyl group are rather insensitive to its surroundings and the degeneracy is often preserved.

In a partially deuterated methyl group, CH_2D or CHD_2, the 3-fold symmetry is always destroyed and three distinct bands are to be expected. Therefore, a CH_2D group will give rise to one CD stretching mode and two CH_2 stretching modes, classified as ν_s and ν_a depending on whether the two CH bonds are vibrating in phase (symmetric) or out of phase (asymmetric).

In the present work, the infrared bands of the partially deuterated methyl derivatives, CH_2D and CHD_2 clearly show the predicted number of bands (Table 1) and where two bands are observed, the higher frequency mode can be assigned to ν_a for that species. These assignments can be further checked since the Average Rule (8) predicts that the XH and XD stretching frequencies of an XHD species should be the average of ν_a and ν_s of the corresponding XH_2 and XD_2 species, respectively. In the present case this rule is closely obeyed for CH_2D and CD_2H (Table 1), as it always is in other cases (8–10) although to be strictly correct this rule is an approximation which when valid should apply only to the root-mean-square values of the harmonic frequencies.

The spectrum of the CH_3 and CD_3 derivatives both exhibit three bands in the respective CH or CD stretching regions. This 3-band spectrum is commonly observed for the methyl group in a variety of environments although the band positions may be shifted to slightly higher or lower wavenumber depending on the nature of the atom to which the methyl carbon is attached (9, 11–15). The traditional Fox and Martin assignments (4) for a methyl group in a hydrocarbon place the "degenerate" ν_a modes near 2962 ± 10 cm^{-1}, and ν_s near 2872 ± 10 cm^{-1}, and accompanying these, a weaker band is often observed near 2810 cm^{-1} which is assigned to an overtone of a CH_3 deformation mode near 1450 cm^{-1}. Using this type of assignment scheme for the methyl platinum derivative, ν_a would occur at 2934 cm^{-1}, ν_s at 2878, and the band 2806 would be an overtone enhanced in intensity by Fermi resonance interaction with ν_s. It is also possible that the three bands could be assigned to the three anticipated CH stretching fundamentals since the 3-fold axis of symmetry is strictly speaking non-existent, or it is possible that the order of assignments suggested above are incorrect. The latter might particularly be the case for the CD_3 derivative where all three bands are of comparable intensity. There is no reason to assume that a Fermi resonance enhanced overtone should not be more intense than a fundamental; this situation has been invoked in a recent reassignment of the CH stretching bands of the Group IV tetramethyl derivatives (7).

There are numerous examples in the literature where assignments other than the Fox and Martin assignments are made (9); it is particularly common to ascribe the weaker low wavenumber band near 2810 cm^{-1} to ν_a. Indeed Adams (12) has examined the spectrum of $[(CH_3)_3P]_2Pt(CH_3)_2$ and $[(CH_3)_3P]_2Pt(CD_3)_2$ and although the spectrum of the $Pt–CH_3$ portion in the CH stretching region is partly obscured by the strong absorptions of the methyl phosphines, the CH stretching bands of $Pt–CH_3$ appear to be close to ours. On the basis of isotope shifts, Adams assigned a low wavenumber band at 2815 to ν_s, and was unable to decide which of the two "shoulders" near 2930 and 2885 was due to ν_a. Other examples are discussed below.

The correct assignments in the present case can be deduced from the wavenumbers of the bands of the partially deuterated species. Thus, using the Average Rule (8) again, the mean value of the three stretching modes of a methyl group should be very nearly equal to the single CH stretching mode of CHD_2, or to the average of two CH stretching modes of CH_2D. For the CH_3 derivative, if we assign the band at highest wavenumber to the doubly degenerate ν_a, and that at intermediate wavenumber to ν_s of CH_3, the calculated mean shown in Table 1 is somewhat higher than the mean of the two CH stretching vibrations of CH_2D, or of the single ν(CH) of CHD_2. A similar result is found for the CD_3 vibrations (Table 1). However, if, as assumed, ν_s is perturbed by Fermi resonance interaction with the band at 2806 (2050), then using the method of Hansen and Dennison (16, 17) to correct ν_s for this interaction, the predicted mean of the CH_3 and CD_3 vibrations is almost exactly equal to the "experimental" mean from CH_2D and CD_2H. This agreement is in fact far better than to be expected considering the approxima-

TABLE 2. Application of the Average Rule to the XH stretching vibrations of some pyramidal XH_3 species

Molecule	Wavenumbers (cm^{-1})	Average of ν_a and ν_s (cm^{-1})	Reference number
NH_3 [CCl_4 solution]	3416 (ν_a) 3312 (ν_s)	3381	18
NH_2D	3409 (ν_a) 3347 (ν_s)	3378	
NHD_2	3377		
NH_3 (gas)	3443 (ν_a) 3337 (ν_s)	3407	18
NH_2D	3411 (ν_a) 3366 (ν_s)	3388	
NHD_2	3402		
CH_3Cl (gas)	3042 (ν_a) 2966 (ν_s)	3017	9
CH_2DCl	3055 (ν_a) 2990 (ν_s)	3012	17
CHD_2Cl	3012		17
CH_3Br (gas)	3057 (ν_a) 2972 (ν_s)	3029	9
CH_2DBr	3052 (ν_a) 3001 (ν_s)	3027	17
CHD_2Br	3027		
CH_3I (gas)	3060 (ν_a) 2970 (ν_s)	3030	9
CH_2DI	3057 (ν_a) 3002 (ν_s)	3030	17
CHD_2I	3030		17

tions of the Average Rule, and of the Fermi resonance correction. However, it should be pointed out that using literature data, similar excellent agreement between predicted and "experimental" wavenumbers of the NH stretching modes of the partially deuterated ammonias (18) and for the partially deuterated methyl halides (9, 17) is also obtained (Table 2). Therefore, this technique clearly demonstrates the correctness of this assignment for the methyl stretching vibrations in both the CH and CD stretching regions, since no other assignment is compatible with the experimental results.

Further, since the wavenumbers of the bands observed by Adams for the Pt methyl group in $[(CH_3)_3P]_2Pt(CH_3)_2$ are very close to those observed in this work (12), it is clear that Adams' original assignments must be incorrect.

Discussion

The main conclusion to be reached from the present investigation is that caution must be exercised in assigning the CH stretching modes of a methyl group. As stated above, there are many examples in the literature where three bands have been observed from a methyl group in the CH stretching region and where the two higher wavenumber bands have been assigned to the two ν_a modes for which the degeneracy is assumed to be removed, and the low wavenumber band is assigned to ν_s. Some cases are listed in Table 3 and this work throws some doubt on the correctness of these assignments. Winther and Hummel (6) have recently re-examined the spectra of some ethyl containing compounds and have challenged the Fox and Martin assignments for the CH stretching modes in hydrocarbons, suggesting instead that ν_a is to be expected near 2962 cm^{-1}, but that ν_s should lie between 2940–2910 cm^{-1} and that the band near 2872 cm^{-1} which has formerly been assigned to ν_s is in fact an overtone of the methyl deformation mode. Apart from a shift in the absolute wavenumber, the difference in wavenumber between each of the three bands in this and other work is more compatible with Winther and Hummel's re-assignment. Therefore, the three bands listed in Table 3 for the stretching vibrations of a methyl

Can. J. Chem. Downloaded from www.nrcresearchpress.com by 210.87.254.6 on 09/05/12
For personal use only.

TABLE 3. Literature assignments of CH stretching modes of some CH_3 containing compounds

Compound	Wavenumbers	Assignments	Reference number
CH_3OH (liquid)	2978	ν_a	9, 19
	2951	ν_a	
	2838	ν_s	
CH_3OH (gas)	3005	ν_a	9, 19
	2965	ν_a	
	2843	ν_s	
CH_3NH_2	2961	ν_a	9
	2985	ν_a	
	2820	ν_s	
CH_3OCD_3	2992	ν_a	9
	2932	ν_a	
	2819	ν_s	
CD_3—$COOCH_3$	2957	ν_a	20
	2905	Combination band	
	2846	ν_s	
CD_3—$COOCD_2CH_3$	2982	ν_a	21
	2939	Combination band	
	2873	ν_s	

group should possibly be re-assigned in order of decreasing wavenumber to ν_a, ν_s, and a Fermi resonance enhanced overtone of a methyl deformation mode. Graham (7) has independently proposed this type of re-assignment for the Group IV tetramethyl compounds, and has suggested that a study of the temperature dependence of the half widths of these bands would confirm the correctness of these assignments. We would suggest that a study of the partially deuterated species, which is intrinsically simpler, could also be used as a check.

Conclusions

The essential correctness of the Average Rule has been demonstrated for the CH stretching modes of a methyl group of $(Ph_3P)_2Pt(CH_3)_2$ and its validity was also verified using literature data for some of the methyl halides, and for the NH stretching modes of ammonia. Surface chemists may reasonably safely use this rule as a means of determining the number of hydrogen atoms in an adsorbed terminal X—H_n group when studying the appropriate infrared spectra of the partially deuterated species. The method of partial deuteration also offers a method of checking the assignments of the CH stretching modes of compounds which contain methyl groups.

The financial support of the National Research Council of Canada is gratefully acknowledged.

1. L. H. LITTLE. Infrared spectra of adsorbed molecules. Academic Press Inc., New York. 1966.
2. N. SHEPPARD and J. W. WARD. J. Catal. **15**, 50 (1969).
3. B. A. MORROW. Can. J. Chem. **48**, 2192 (1970).
4. J. J. FOX and A. E. MARTIN. Proc. Roy. Soc. London. Ser. A. **167**, 257 (1938); **175**, 208 (1940).
5. L. J. BELLAMY. Infrared spectra of complex molecules. 2nd Ed. Methuen, London. 1958.
6. F. WINTHER and D. O. HUMMEL. Spectrochim. Acta, **25**A, 425 (1969).
7. S. C. GRAHAM. Spectrochim. Acta, **26**A, 345 (1970).
8. W. J. LEHMANN. J. Mol. Spectrosc. **7**, 261 (1961); **7**, 1 (1961).
9. T. SHIMANOUCHI. Tables of molecular vibrational frequencies. Parts 1, 2, and 3. U.S. Dept. of Commerce, NSRDS-NBS 6, -NBS 17, -NBS 11.
10. R. S. DENNEN, E. A. PIOTROWSKI, and F. F. CLEVELAND. J. Chem. Phys. **49**, 4385 (1968).
11. D. B. POWELL and N. SHEPPARD. Spectrochim. Acta, **21**, 559 (1965).
12. D. M. ADAMS. J. Chem. Soc. 1220 (1962).
13. B. NOLAN and R. N. JONES. J. Am. Chem. Soc. **75**, 5626 (1953).
14. D. E. CLEGG and J. R. HALL. Spectrochim. Acta, **21**, 357 (1965).
15. J. H. S. GREEN. Spectrochim. Acta, **24**A, 863 (1968).
16. G. E. HANSEN and D. M. DENNISON. J. Chem. Phys. **20**, 313 (1952).
17. J. R. RITER and D. F. EGGERS. J. Chem. Phys. **44**, 745 (1966).
18. J. CORSET, J. GUILLERMET, and J. LASCOMBE. Bull. Soc. Chim. Fr. 1231 (1966).
19. M. FALK and E. WHALLEY. J. Chem. Phys. **34**, 1554 (1961).
20. B. NOLIN and R. N. JONES. Can. J. Chem. **34**, 1382 (1956).
21. B. NOLIN and R. N. JONES. Can. J. Chem. **34**, 1392 (1956).

Can. J. Chem. Downloaded from www.nrcresearchpress.com by 210.87.254.6 on 09/05/12
For personal use only.

Can. J. Chem. Downloaded from www.nrcresearchpress.com by 210.87.254.42 on 09/05/12
For personal use only.

Complexes of Tungsten Halides with Group VI Donors: Adducts with Triphenylphosphine Chalcogenides

P. M. BOORMAN AND K. J. REIMER

Department of Chemistry, The University of Calgary, Calgary 44, Alberta

Received February 15, 1971

The preparation of complexes with the empirical formula WCl_5L (L = Ph_3PS, Ph_3PSe) and $WBr_4.Ph_3PS$ is reported. The tungsten chloride adducts have been formulated as $[W_2Cl_8L_2]2Cl$ on the basis of infrared spectra, molecular weight, and conductance measurements. The complex WBr_4Ph_3PS is probably a non-ionic dimer, but solubility problems make this suggestion tentative. No corresponding complex with Ph_3PSe could be isolated.

The shifts in ν(P—X) (X = S, Se) upon coordination are amongst the largest ever reported, and are indicative of bridging behavior by these ligands.

La préparation de complexes ayant pour formule empirique WCl_5L (L = Ph_3PS, Ph_3PSe) et $WBr_4.Ph_3PS$ est rapportée. Les produits d'addition avec le chlorure de tungstène ont pour formule $[W_2Cl_8L_2]2Cl$; ceci d'après les spectres infrarouges et les mesures de masse moléculaire et de conductance. Le complexe WBr_4Ph_3PS est probablement un dimère non ionique; des problèmes de solubilité rendent cependant cette suggestion hypothétique. Aucun complexe correspondant avec Ph_3PSe n'a été isolé.

Les déplacements de ν(P—X)(X = S, Se) d'après la coordination sont parmi les plus grands jamais rapportés et sont significatifs du phénomène de formation de ponts par ces ligands.

Canadian Journal of Chemistry, 49, 2926 (1971)

Introduction

Our interest in the chemistry of tungsten halides (1, 2) has led us to investigate their reactions with a wide variety of ligands with group VI donor atoms. We report here the reactions of triphenylphosphine chalcogenides with tungsten(VI) chloride and tungsten(V) chloride and bromide.

Although phosphine oxides in general, and Ph_3PO in particular, are known to form a wide variety of complexes with transition metal halides (3–7) and carbonyls (8) much less is known of comparable reactions with phosphine sulfides, selenides, and tellurides. Since reactions of tungsten halides with phosphine oxides had been reported previously (9) as yielding materials such as $WO_2Cl_2.2Ph_3PO$, which contained W=O bonds, we have confined our attention in the first instance to reactions with Ph_3PS and Ph_3PSe.[1]

Experimental

All preparative and handling procedures were carried out in a dry, nitrogen-filled glove-box.

[1]Extension to the telluride analogue was not possible since the latter compound is not stable (10).

Materials

Ph_3PS was obtained from Aldrich Chemicals and used after drying *in vacuo*. Ph_3PSe was prepared by the published methods (11, 12). Tungsten hexachloride and pentabromide were obtained from Alfa Inorganics, Beverley, Mass., and were carefully resublimed in sealed, evacuated tubes several times before use. WCl_5 was prepared by disproportionation of WCl_4 (13). Solvents were purified as before (1) and were thoroughly degassed before use.

Microanalyses were carried out by Alfred Bernhardt Microanalytical Laboratories. Halide determinations were also carried out independently in our laboratories by a standard potentiometric method.

Preparations

Two general synthetic methods were employed. Method II is preferable for reactions involving the more insoluble tungsten(V) halides.

Method I

Approximately 6 g of WCl_6 was dissolved in 500 ml of dry CCl_4 by magnetic stirring *in vacuo* and then the solution was filtered to remove any insoluble material. To the filtrate a 1.5:1 molar excess of the ligand was added via a filter stick. Precipitation of the product was immediate; it was filtered off on the stick and thoroughly washed with CCl_4 then dried *in vacuo*.

Method II

To a reaction flask containing a magnetic stirring bar and a suspension of the halide (*ca.* 1.5 g) in 150 ml of CCl_4 a slight molar excess of the ligand in 200 ml of CCl_4 was added. The reaction flask was evacuated and the mixture stirred for a period of 4 days to ensure com-

TABLE 1. Analytical data for complexes (analysis (%))

	C		H		Halogen		W		P		Chalcogenide	
Compound	Found	Calcd.	Found	Calcd.	Found	Calcd.	Found	Calcd.	Found	Calcd.	Found	Calcd.
WCl_5Ph_3PS	32.9	33.0	2.4	2.3	27.4	27.0	27.8	28.0	4.6	4.7	4.8	4.9
WCl_5Ph_3PSe	30.6	30.8	2.2	2.1	25.0	25.2	25.9	26.2	4.2	4.4	10.9	11.2
WBr_4Ph_3PS	26.8	27.1	2.1	1.9	40.0	40.1	22.7	23.0	3.7	3.9	4.2	4.0

plete reaction. The product was then filtered off, washed with CCl_4 then dried *in vacuo*.

WCl_5Ph_3Ps and WCl_5Ph_3PSe

These compounds were prepared in almost quantitative yield from WCl_6 and the ligands by Method I. WCl_5Ph_3PS was also prepared from WCl_5 by Method II. Its properties were identical when prepared by either route. Analytical data for the new compounds are presented in Table 1.

WBr_4Ph_3PS

This compound was prepared from WBr_5 by Method II. Reaction of WBr_5 and Ph_3PS using Method I yielded insignificant quantities of a green powder. It was impracticable to investigate these further although the identity of this product could well be WBr_5Ph_3PS.

$WBr_5 + Ph_3PSe$

This reaction was attempted by Method II but the product proved to be non-stoichiometric regardless of slight variations in the synthetic procedure.

Attempted Preparations of W(IV) Complexes

A standard technique for synthesis of compounds of the general formula WX_4L_2 is to displace RCN from the complexes $WX_4.2RCN$ with the appropriate ligand (14). In spite of numerous attempts using a variety of conditions we were unsuccessful in preparing W(IV) complexes with Ph_3PS or Ph_3PSe by this technique. Products obtained invariably contained some alkyl cyanide and free phosphine chalcogenide.

Physical Measurements

Conductance measurements were performed on *ca.* 10^{-3} *M* solutions in nitrobenzene at 25 °C, using an Industrial Instruments Model RC-18 Conductance Bridge.

Infrared spectra were recorded with a Perkin–Elmer Model 621 spectrophotometer, using Nujol mulls between CsI plates. Attempts to measure spectra in solution in the ν(PS) stretching frequency region were not successful, due either to instability of solutions or strong absorption of the solvent.

Electronic spectra (200–750 mμ) of dilute solutions of the complexes in acetonitrile were obtained using a Perkin–Elmer Model 202 spectrophotometer. Diffuse reflectance spectra were recorded over the range 270–700 mμ using a Cary 15 spectrophotometer with a standard attachment.

Magnetic susceptibility measurements were made at 22 °C by the Gouy Method. The susceptibilities were corrected for diamagnetism using Pascal's constants (15).

Molecular weight measurements were made cryoscopically in nitrobenzene. Temperatures were measured using an iron–constantan thermocouple connected to a Leeds and Northrup 7554 Model K4 potentiometer.

Results

The complexes with empirical formula WCl_5Ph_3PS (**1**) and WCl_5Ph_3PSe (**2**) were isolated as air sensitive yellow-green powders. All attempts at isolating crystalline samples using a wide variety of solvents and techniques were unsuccessful. The compounds decompose below their melting points. They were insoluble in non-polar solvents but moderately soluble in $PhNO_2$, $MeNO_2$, and MeCN.[2]

Addition of both complexes to benzene resulted in the formation of dark brown oil, and attempted preparation of **1** in benzene as solvent also gave rise to an oil of indefinite composition.

The compound of empirical formula WBr_4Ph_3PS (**3**) was isolated as an exceptionally air-sensitive brown solid. The analogous compound WBr_4Ph_3PSe could not be isolated in a pure form, although there was evidence from infrared spectral data of complex formation between WBr_5 and Ph_3PSe. **3** exhibited only slight solubility in $PhNO_2$ and $MeNO_2$ and was also insoluble in non-polar organic solvents.

Solution Measurements

Data are presented in Table 2. For compounds **1** and **2** the apparent molecular weights correspond best with values expected for dimers yielding 3 ions, *i.e.* $[W_2Cl_8L_2]^{2+}2Cl^-$. It will be noted that even allowing for the errors of such measurements the other likely formulations would have to be excluded. Furthermore when the conductance data are evaluated on this basis they show excellent agreement with molar conductance values expected for 2:1 electrolytes

[2]After standing for a few minutes solutions of **2** in $MeNO_2$ and MeCN deposited selenium, however.

Can. J. Chem. Downloaded from www.nrcresearchpress.com by 210.87.254.42 on 09/05/12
For personal use only.

TABLE 2. Molar conductance and molecular weight measurements for nitrobenzene solutions

Compound	Λ_m ohm^{-1} cm^2 (10^{-3} M)	Apparent molecular weight			
		Found*	Calculated		
			$[W_2Cl_8L_2]2Cl$	$[WCl_5L]$	$[WCl_4L_2][WCl_6]$
WCl_5Ph_3PS	40.2	465 ± 15	437	655	655
WCl_5Ph_3PSe	42.2	475 ± 15	468	702	702

*Molecular weight measurements were made at concentrations ranging from 10^{-3}–10^{-2} M.

(16). Allowing for some slight association of $[W_2Cl_8L_2]2Cl$ at the concentrations used for the molecular weight measurements, these data are very strong evidence for a binuclear structure.

The compound $WBr_4.Ph_3PS$ was insufficiently soluble to enable us to make molecular weight measurements, but the molar conductance of a 10^{-3} M solution in $PhNO_2$ was well below the value expected for a 1:1 electrolyte, when the solution was initially prepared. On standing the conductance increased and a white precipitate appeared.

Infrared Spectra

The spectra were recorded over the range 1400–200 cm^{-1} and pertinent frequencies are presented in Table 3. Assignments were made for ligand vibrations on the basis of those suggested by Jensen and Nielsen (17). The ligand spectra change remarkably little upon coordination, so that the most interesting feature is the change in the P—X stretching frequency. King and McQuillan (18) reported decreases in ν(P—S) as 40–50 cm^{-1} and in ν(P—Se) as 18–20 cm^{-1} for metal halide complexes of these ligands. Different authors have attributed this shift to lower frequencies to two possible reasons. Firstly (18) the pπ → dπ bond (X → P) could be weakened upon forming a M ← X bond as is observed for phosphine oxide (8, 19) and arsine oxide (20) complexes. Alternatively the decrease in frequency could be attributed to a mass effect, considering the M—X unit as a point mass (21).

TABLE 3. Infrared frequencies for triphenyl phosphine sulfide and triphenyl phosphine selenide complexes

Complex	Frequencies* (cm^{-1})	
	P—X	W—Cl
Ph_3PS	632 vs	
WCl_5Ph_3PS	536 s	329 sh, 324 sh, 319 vs
WBr_4Ph_3PS	536 s	
Ph_3PSe	555 vs	
WCl_5Ph_3PSe	532 sh	331 sh, 329 sh, 320 vs

*v = very, s = strong, sh = shoulder.

For the tungsten halide complexes we observe ν(P—S) and ν(P—Se) to decrease by 96 and 23 cm^{-1}, respectively. This could therefore be attributed to one of three factors.

Firstly the large value we observe might possibly be ascribed to a mass effect. However, since complexes of Au(I), Au(III), and Hg(II) halides with Ph_3PS exhibit much smaller shifts, in spite of the higher mass of the metals concerned, this argument is discounted.

Secondly the importance of electronic effects and their possible influence on the P—S π-bond might be considered. Since in the tungsten compounds only one (W(V)) or two (W(IV)) d electrons would be available for back donation to the sulfur it might be argued that this could result in localization of charge from the pπ–dπ P—S bond on to the sulfur. Even if this were possible the argument is no longer plausible when the (P—S) stretching frequencies for complexes of Nb(V) and Ta(V) chlorides are observed to be "normal" (22).

Thus the only logical explanation lies in assuming that the ligands are in fact bridging between two tungsten atoms, thus supporting the binuclear structure discussed above.

The argument is supported by three further observations. Firstly the possibility of structures involving W=S and W—P bonds (for the Ph_3PS products) is excluded, since on allowing a sample of WCl_5Ph_3PS to stand in moist air for a few minutes the free ligand Ph_3PS is regenerated (as evidenced by the introduction of a strong band attributable to ν(PS) for uncoordinated Ph_3PS). Secondly some impure samples exhibited bands which could be attributed to free ligand, bridging ligand, and to normally bonded ligand.

Can. J. Chem. Downloaded from www.nrcresearchpress.com by 210.87.254.42 on 09/05/12
For personal use only.

Can. J. Chem. Downloaded from www.nrcresearchpress.com by 210.87.254.42 on 09/05/12
For personal use only.

One such sample was obtained by dissolving WCl_5Ph_3PS in dichloromethane, and then removing the solvent.

Thirdly if the complex is binuclear there would be a strong possibility of chloride ions acting as the bridging groups. This situation is invariably accompanied by the observation of strong bands in the infrared spectrum at about 250 cm^{-1} (2, 23). Such bands are entirely absent.

While the above arguments have been directed specifically towards the compound $WCl_5.Ph_3PS$, all of our evidence supports the assignment of an identical structure for $WCl_5.Ph_3PSe$. In the latter case shifts in ν(P—Se) are much smaller. This has been attributed (18) to the less extensive P—Se π-character, and to the decreased sensitivity of ν(P—Se) owing to the larger mass of Se with respect to S.

We have not attempted to assign the bands in the region 300–340 cm^{-1} to individual ν(W—Cl) modes. However, assuming the local symmetry to be C_{2v} for the tungsten atoms, four W—Cl stretching modes would be predicted, whereas three are observed. Vibrational spectroscopy is frequently unreliable, however, for deducing the stereochemistry of complexes containing a heavy central atom (24).

For the compound $WBr_4.Ph_3PS$ ν(PS) is at the same frequency as for WCl_5Ph_3PS, hence again we suggest that the ligand is bridging. Little else can be derived from the spectrum of this compound, however.

Magnetic Moments and Electronic Spectra

The room temperature magnetic moments of the tungsten(V) complexes (Table 4) are within the range of values previously reported for tungsten in this oxidation state (25). We were unable to study the temperature dependence of the susceptibilities due to lack of facilities. The value of μ_{eff} for compound **3** is slightly lower than those often observed for W(IV). A variable temperature study of this compound would probably indicate antiferromagnetic behavior.

The electronic spectra (Table 5) suffer from the usual problems (1, 2) of interpretation in that the d–d bands are hidden by intense charge transfer bands with tails in the visible. However, it is notable that the reflectance spectra of **1** and **2** are extremely similar, again indicating that their structures are the same.

TABLE 4. Magnetic moment measurements

Compound	$\chi_m(\times 10^6)$	$\chi_m'(\times 10^6)$*	μ_{eff}(B.M.)
WCl_5Ph_3PS	55.7	361.9	0.925
WCl_5Ph_3PSe	26.2	340.4	0.897
WBr_4Ph_3PS	212.9	524.5	1.11

*Molar susceptibility (χ_m) corrected for diamagnetism of ligands using Pascal's constants.

TABLE 5. Electronic spectra of the tungsten chloride complexes

Compound	Conditions	λ_{max} (mμ)*
WCl_5Ph_3PS	MeCN	235(39.4), 272(26.2), 297(32.8), 345(22.2), 370(6.96)
	Reflectance	305sh, 335sh, 370, 445sh
WCl_5Ph_3PSe†	Reflectance	285, 335sh, 370, 445sh

*$\varepsilon_{max} \times 10^{-3}$ l mol^{-1} cm^{-1} in parentheses.
†Solution measurement not possible due to decomposition of complex.

We were unable to obtain solution spectra of compound **3** due to its insolubility, and attempts to obtain reflectance spectra were also unsuccessful even when the sample was diluted with $MgCO_3$.

Conclusion

The first complexes of tungsten halides with Group V chalcogenides have been prepared. The solution properties of the WCl_5 adducts indicate that they should be formulated as $[W_2Cl_8L_2]2Cl$ (L = Ph_3PS, Ph_3PSe).

The decrease in (P—X) (X = S, Se) upon coordination suggests bridging behavior by the chalcogen, giving the structural formulation

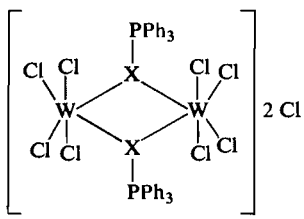

Such behavior has not previously been reported for these ligands although it is known in the case of Ph_3AsO (26).

The compound $WBr_4.Ph_3PS$ also appears to contain bridging Ph_3PS ligands, although in this

case solubility problems precluded some solution measurements necessary for a more complete characterization. Since the compound is probably a non-electrolyte, and polymeric structures would require tungsten to have a coordination number greater than 6, the most likely structure is

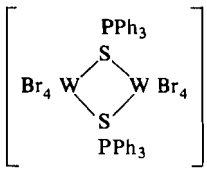

This structure is consistent with all of our data, but must remain speculative in the absence of molecular weight, and X-ray data.

Extensive attempts to isolate crystals suitable for X-ray structural studies have proved unsuccessful. However, both of the chloride complexes exhibit weak powder diffraction patterns.

We thank the National Research Council of Canada for financial support and for a Scholarship (to K.J.R.). The experimental assistance of Mrs. Monica Reimer and Mr. N. D. Cowie is gratefully acknowledged. We also thank Dr. K. A. Kerr and Mr. Brian Smith for help in acquiring X-ray powder diffraction measurements.

1. P. M. Boorman, N. N. Greenwood, M. A. Hildon, and R. V. Parish. J. Chem. Soc. A, 2002 (1968).
2. P. M. Boorman, N. N. Greenwood, and M. A. Hildon. J. Chem. Soc. A, 2466 (1968).
3. F. A. Cotton, D. M. L. Goodgame, and R. H. Soderburg. Inorg. Chem. **2**, 1162 (1963).
4. H. Gehrke, Jr. Diss. Abstr. **25**, 4952 (1965).
5. J. Lewis and R. Whyman. J. Chem. Soc. 6027 (1965).
6. K. W. Bagnall, D. Brown, and J. G. H. duPreez. J. Chem. Soc. 5217 (1965).
7. C. J. Wilkins and H. M. Haendler. J. Chem. Soc. 3174 (1965).
8. L. Chandrasegaran and G. A. Rodley. Inorg. Chem. **4**, 1360 (1965).
9. S. E. Feil. Diss. Abstr. **26**, 1338 (1965).
10. R. A. Zingaro, B. H. Steeves, and K. Irgolic. J. Organomet. Chem. **4**, 320 (1965).
11. R. A. Zingaro and E. A. Meyers. Inorg. Chem. **1**, 771 (1962).
12. P. Nicpon and D. W. Meek. Inorg. Syn. **10**, 157 (1967).
13. R. E. McCarley and T. M. Brown. Inorg. Chem. **3**, 1232 (1964).
14. E. A. Allen, B. J. Brisdon, and G. W. A. Fowles. J. Chem. Soc. 4531 (1964).
15. J. Lewis and R. G. Wilkins (*Editors*). Modern coordination chemistry. Interscience, New York. 1960.
16. C. M. Harris and R. S. Nyholm. J. Chem. Soc. 4375 (1956).
17. K. A. Jensen and P. H. Neilsen. Acta Chem. Scand. **17**, 1875 (1963).
18. M. G. King and G. P. McQuillan. J. Chem. Soc. A, 898 (1967).
19. J. Sheldon and S. Y. Tyree. J. Chem. Soc. **80**, 4775 (1958).
20. D. Phillips and S. Y. Tyree. J. Am. Chem. Soc. **83**, 1806 (1961).
21. J. A. W. Dalziel, A. F. le C. Holding, and B. E. Watts. J. Chem. Soc. A, 358 (1967).
22. P. M. Boorman and K. J. Reimer. To be published.
23. P. M. Boorman, N. N. Greenwood, M. A. Hildon, and H. J. Whitfield. J. Chem. Soc. A, 2017 (1967).
24. D. M. Adams. Metal ligand and related vibrations. Arnold, London. 1967.
25. R. V. Parish. Adv. Inorg. Chem. Radiochem. **9**, 315 (1966).
26. C-I. Brauden. Arkiv. Kemi, **22**, 485 (1964).

Can. J. Chem. Downloaded from www.nrcresearchpress.com by 210.87.254.42 on 09/05/12
For personal use only.

Can. J. Chem. Downloaded from www.nrcresearchpress.com by 210.87.254.40 on 09/05/12
For personal use only.

The Vibrational Spectra of Silane and Germane Derivatives. Part IV. The Infrared and Raman Spectra of the Iodo(methyl)germanes

J. W. ANDERSON, G. K. BARKER, J. E. DRAKE,[1] AND R. T. HEMMINGS
Department of Chemistry, University of Windsor, Windsor, Ontario

Received April 19, 1971

The infrared and Raman spectra of the series of iodo(methyl)germanes, CH_3GeI_3, $(CH_3)_2GeI_2$, and $(CH_3)_3GeI$ have been recorded. A normal coordinate analysis based on a modified valence force field confirms the *a priori* assignments for all of the fundamental frequencies except the torsional modes.

Les spectres infrarouges et Raman des séries de iodo (méthyl) germanes, CH_3GeI_3, $(CH_3)_2GeI_2$ et $(CH_3)_3GeI$ ont été enregistrés. Une analyse normale de coordination, fondée sur un champ de force valentiel modifié, confirme les attributions *a priori* de toutes les fréquences fondamentales à l'exception des modes de torsion.

Canadian Journal of Chemistry, 49, 2931 (1971)

Introduction

The vibrational spectra of the chloro- and bromo(methyl)germanes, $(CH_3)_nGeX_{4-n}$ (X = Cl, Br; n = 1, 2, and 3) have been studied by several workers (1–7). The work reported here is part of a continuing program on the vibrational analyses of various methylated and halogenated derivatives of germane. We investigated the vibrational spectra of the three iodo(methyl)-germanes, $(CH_3)_nGeI_{4-n}$ (n = 1, 2, and 3) to assist the interpretation of the spectra of other halogeno(methyl)germanes with lower symmetry elements and to confirm the assignments of previous authors. A full normal coordinate analysis was carried out to yield the best set of harmonic force constants, the eigenvectors, and the potential energy distributions for the molecules. Near the completion of this work, a vibrational analysis of tri-iodo(methyl)germane and its deuterated analogue was reported (8) which is in excellent agreement with our studies.

Experimental

The iodo(methyl)germanes were all prepared in high yield by the reaction of hydrogen iodide on the appropriate chloro(methyl)germanes, a method which has been used successfully for almost quantitative iodination in germane chemistry (9, 10). The compounds were purified by trap-to-trap distillation or fractional sublimation on a conventional Pyrex-glass, greaseless vacuum line. All samples for spectral analysis were estimated to be > 98% pure from their ^1H nuclear magnetic resonance (n.m.r.) spectra recorded on a Jeol C-60 HL high resolution spectrometer. Thus, tri-iodo(methyl)germane, CH_3GeI_3, was prepared by condensing trichloro(methyl)germane (*ca.* 1.1 mmol) (commercial sample, Alfa Inorganics) and excess of hydrogen iodide (*ca.* 4 mmol into a 50 ml reaction vessel at −196° and allowing the mixture to warm to room temperature. Reaction was complete after 1 h when infrared analysis showed the only volatiles to be hydrogen chloride (*ca.* 3.3 mmol), in a trap at −196°, and hydrogen iodide (*ca.* 0.7 mmol) in a trap at −78°. A pale yellow solid remained in the reaction vessel which was purified by sublimation and subsequently shown from its m.p. (45°) and ^1H n.m.r. spectrum to be CH_3GeI_3. Similarly, di-iodo(dimethyl)germane, $(CH_3)_2GeI_2$, and iodo(trimethyl)germane, $(CH_3)_3GeI$, were prepared by the reaction of excess hydrogen iodide on dichloro-(dimethyl)germane and chloro(trimethyl)germane, respectively (both available commercially, Alfa Inorganics).

The Raman spectra were recorded at room temperature on a Spectra-Physics 700 laser–Raman spectrometer using a helium–neon source. The sealed Pyrex glass tubes (*ca.* 1 mm o.d.) contained *ca.* 3 cm column length of neat liquid (for the volatile $(CH_3)_2GeI_2$ and $(CH_3)_3GeI$) or solid (for the involatile CH_3GeI_3). To permit Raman polarization data the tri-iodide was also run in CS_2 solution.

Infrared spectra were recorded at room temperature in the range 4000–200 cm^{-1} on a Beckman IR-12 infrared spectrometer using CsI plates for the liquid-film spectra of $(CH_3)_2GeI_2$ and $(CH_3)_3GeI$, or the CS_2 "smear" spectrum of CH_3GeI_3. A gas cell (10 cm path length) fitted with KBr windows was used for the gas phase spectrum of $(CH_3)_3GeI$. Scale expansion facilities on both instruments enabled strong sharp bands to be estimated to ± 1 cm^{-1} in the infrared spectrum and ± 2 cm^{-1} in the Raman effect.

An IBM s/360-50 computer was used for the normal coordinate calculations with the program SOTONVIB, a modified version of that described by Schachtschneider as GMAT and FPERT (11). A SVFF calculation was first attempted followed by modification of the inter-

[1]To whom correspondence should be addressed.

TABLE 1. Force constant listings*

Number	Motion	Force constant $(CH_3)_3GeI$	Force constant $(CH_3)_2GeI_2$	Force constant CH_3GeI_3
1	f_{CH}	4.8111	4.7903	4.8222
2	f_{GeC}	2.8696	2.8966	2.7863
3	f_{GeI}	1.1288	1.3422	1.2100
4	f_{HCH}	0.5011	0.4959	0.4858
5	$f_{HCGe^{\perp}}$	0.3619	0.3870	0.4214
6	$f_{HCGe^{\parallel}}$	0.5057	0.4795	
7	f_{CGeI}	0.4768	0.5180	0.5886
8	f_{CGeC}	0.4194	0.6916	—
9	f_{IGeI}	—	0.6616	0.6043
10	$f_{CH/CH}$	0.0409	0.0371	0.0278
11	$f_{GeC/GeC}$	0.0187	−0.0720	—
12	$f_{GeI/GeI}$	—	0.2103	0.2246
13	$f_{GeC/HCGe}$	0.0293	−0.0	0.0
14	$f_{HCGe^{\perp}/HCGe^{\parallel}}$	−0.0061	−0.0201	−0.0295
15	$f_{HCGe^{\perp}/HCGe^{\perp}}$	−0.0358	−0.0312	
16	$f_{HCH/HCH}$	−0.0059	−0.0105	−0.0110
17	$f_{CGeI/CGeI'}$	—	0.023021	—
18	$f_{CGeI/C'GeI}$	—	−0.1791	—
19	$f_{CGeI/C'GeI'}$	—	0.0135	—

*mdyn Å^{-1} for stretching, mdyn Å rad^{-2} for bending or bend–bend, and mdyn rad^{-1} for stretch–bend force constants.

TABLE 2. The vibrational spectrum of CH_3GeI_3*

Frequency (cm^{-1}) Infrared (CS_2 smear)	Raman (solid)†	Calculated	Assignment
3140 vw	—	—	$\nu_7 + \nu_{11} = 3151$
3002 m	2997 dp	3002.0	ν_7
2910 m	2908 p	2910.0	ν_1
2845 vw	—	—	$\nu_7 - \nu_{11} = 2853$
2440 w	—	—	$2\nu_2 = 2456$
2039 w	—	—	$\nu_2 + \nu_9 = 2040$
1831 m	—	—	$\nu_2 + \nu_3 = 1831$
1394 s	1396 dp	1394.0	ν_8
1228 m	1230 p	1228.5	ν_2
1195 vw	—	—	$2\nu_3 = 1202$
875 b sh	—	—	$\nu_9 + \nu_{12} = 877$
810 s	n.o.	809.9	ν_9
630 w sh	—	—	$\nu_2 - \nu_3 = 629$
601 s	607 p	600.9	ν_3
450 w	—	—	$\nu_{10} + \nu_4 = 447$
260 s			$\nu_4 + \nu_{12} = 263$
251 s	242 dp	241.5	ν_{10}
200 s	196 p	191.5	ν_4
	149 dp	148.5	ν_{11}
	91 p	90.2	ν_5
	67 dp	67.3	ν_{12}

*m = medium, s = strong, w = weak, v = very, sh = shoulder, p = polarized, dp = depolarized.
†Polarization data obtained from a CS_2 solution. Spectra recorded at room temperature.

action terms to give the best fit of calculated to observed absorption frequencies. The molecules were assumed to have "all tetrahedral" angles and the initial force constants were estimated from those previously calculated for $(CH_3)_3GeCl$ (4) and GeH_2I_2 (12). The reported literature values of the bond lengths of related compounds were used in the calculations *viz.* C—H, 1.093 Å; Ge—C, 1.954 Å; Ge—I, 2.5 Å. The observed and calculated frequencies are listed for each molecule (Tables 2, 4, and 6) with their assignments. The potential energy distributions (p.e.d.'s) amongst the force constants (Table 1) are listed (Tables 3, 5, 7).

Results and Discussion

Tri-iodo(methyl)germane, CH_3GeI_3

The molecule is assumed to have C_{3v} symmetry. The twelve fundamental modes are divided into

Can. J. Chem. Downloaded from www.nrcresearchpress.com by 210.87.254.40 on 09/05/12
For personal use only.

TABLE 3. Description of the fundamentals for CH_3GeI_3

Mode		Conventional description	Potential energy distributions
ν_1	a_1	CH_3 stretch (sym)	99(1) + 1(10)
ν_2	a_1	CH_3 def (sym)	7(2) + 54(4) + 47(5) − 6(14)
ν_3	a_1	GeC stretch	91(2) + 4(4) + 4(5)
ν_4	a_1	GeI_3 stretch (sym)	1(2) + 62(3) + 7(7) + 7(9) + 23(14)
ν_5	a_1	GeI_3 def (sym)	10(3) + 42(7) + 43(9) + 4(12)
ν_6	a_2	CH_3 torsion	Not observed or calculated
ν_7	e	CH_3 stretch (asym)	100(1)
ν_8	e	CH_3 def (asym)	94(4) + 3(5) + 2(16)
ν_9	e	CH_3 rock	3(4) + 89(5) + 6(14)
ν_{10}	e	GeI_3 stretch (asym)	79(3) + 27(7) + 8(9) − 15(12)
ν_{11}	e	GeI_3 rock	32(3) + 71(7) + 2(9) − 6(12)
ν_{12}	e	GeI_3 def (asym)	12(3) + 90(9) − 2(9)

TABLE 4. Vibrational spectrum of $(CH_3)_2GeI_2$*

Frequency (cm^{-1})			
Infrared (liquid)	Raman (liquid)	Calculated	Assignment
2990 w	2990 dp	2989.5	ν_1
		2989.3	ν_{10}
		2988.9	ν_{15}
		2988.9	ν_{21}
2907 w	2907 p	2906.1	ν_2
		2906.3	ν_{22}
2780 vw			$2\nu_3 = 2810$?
1405 m	1404 dp	1408.8	ν_3
		1404.3	ν_{11}
		1404.0	ν_{16}
		1408.5	ν_{23}
1235 m	1235 p	1236.3	ν_4
		1241.6	ν_{24}
848 s		837.0	ν_5
819 s		834.6	ν_{17}
770 m		773.9	ν_{25}
		756.3	ν_{12}
628 m	627 dp	633.5	ν_{26}
584 m	585 p	587.7	ν_6
245 s	242 dp	251.0	ν_{18}
222 m	220 p	232.8	ν_7
	195 p	175.5	ν_8
	175 dp	191.7	ν_{13}
		170.7	ν_{19}
	140 dp	135.0	ν_{27}
	73 p	77.0	ν_9

*Spectra recorded at room temperature.

five non-degenerate a_1 vibrations; six doubly degenerate e vibrations; and a single a_2 vibration. The a_1 and e modes should all be infrared active with the former polarized and the latter depolarized in the Raman effect. The a_2 mode is inactive. All eleven active fundamentals are observed and their description is given in Table 3 along with the potential energy distribution amongst the force constants. We make no further comment in view of the recent work by Durig *et al.* (8).

Di-iodo(dimethyl)germane, $(CH_3)_2GeI_2$

As with the corresponding chloride (3) the molecule $(CH_3)_2GeI_2$ is conveniently considered as having C_{2v} symmetry. The twenty-seven fundamental modes can be divided into nine, infrared active, a_1 modes which should appear as polarized bands in the Raman effect; five, infrared inactive, a_2 modes which, however, are Raman active leading to depolarized bands; and six b_1 and seven b_2 modes, all of which are infrared active and should give depolarized

Can. J. Chem. Downloaded from www.nrcresearchpress.com by 210.87.254.40 on 09/05/12
For personal use only.

TABLE 5. Description of the fundamentals for $(CH_3)_2GeI_2$

Mode		Conventional description	Potential energy distributions
ν_1		CH_3 stretch (asym)	100(1)
ν_2		CH_3 stretch (sym)	98(1) + 2(10)
ν_3		CH_3 def (asym)	94(4) + 3(6) + 2(16)
ν_4		CH_3 def (sym)	9(2) + 54(4) + 26(5) + 19(6)
ν_5	a_1	CH_3 rock (sym)	4(4) + 55(5) + 32(6) + 9(14)
ν_6		GeC_2 stretch (sym)	93(2) + 4(4) + 2(5) + 2(6) − 2(11)
ν_7		GeI_2 stretch (sym)	46(3) + 20(7) + 5(8) + 5(9) + 7(12)
ν_8		GeC_2 bending	32(2) + 20(7) + 44(8)
ν_9		GeI_2 bending (sciss)	7(3) + 15(7) + 78(9)
ν_{10}		CH_3 stretch (asym)	100(1)
ν_{11}		CH_3 def (asym)	95(4) + 3(6) + 2(16)
ν_{12}	a_2	CH_3 rock	3(4) + 91(6) + 5(13)
ν_{13}		GeI_2 bending (twist)	79(7) + 21(8)
ν_{14}		CH_3 torsion	Not observed or calculated
ν_{15}		CH stretch	100(1)
ν_{16}		CH_3 def (asym)	95(4) + 3(6) + 2(16)
ν_{17}		CH_3 rock	1(2) + 4(4) + 58(5) + 29(6) + 8(14)
ν_{18}	b_1	GeI_2 stretch (asym)	83(3) + 42(7) − 13(12) − 11(18)
ν_{19}		GeI_2 bending (rock)	77(7) + 3(17) + 20(18)
ν_{20}		CH_3 torsion	Not observed or calculated
ν_{21}		CH_3 stretch (asym)	100(1)
ν_{22}		CH_3 stretch (sym)	98(1) + 2(10)
ν_{23}		CH_3 def (asym)	93(4) + 3(5) + 2(16)
ν_{24}	b_2	CH_3 def (sym)	8(2) + 54(4) + 19(5) + 26(6) − 4(14)
ν_{25}		CH_3 rock	3(4) + 91(6) + 1(7) + 4(13)
ν_{26}		GeC_2 stretch (asym)	87(2) + 5(4) + 5(6) + 2(11)
ν_{27}		GeI_2 bending	35(3) + 101(7) − 6(11) − 3(17) − 26(18)

TABLE 6. Vibrational spectrum of $(CH_3)_3GeI$

Frequency (cm^{-1})				
Infrared		Raman		
Gas	Liquid	(liquid)	Calculated	Assignment
	3820, 3760			$\nu_2 + \nu_{19} = 3753$
	3690, vw			$\nu_{20} + \nu_{15} = 3678$
			2994.3	ν_1
			2995.4	ν_9
2990 w	2995 s	2995 dp	2996.1	ν_{13}
			2994.1	ν_{14}
			2912.9	ν_2
2910 w	2913 s	2913 p	2913.0	ν_{15}
	2795, 2480			$2\nu_{16} = 2830$, $2\nu_4 = 2490$
	2090, 1870 w			$\nu_2 - \nu_{19} = 2073$
	1815			$\nu_4 + \nu_{21} = 1870$, $\nu_4 + \nu_6 = 1825$
			1418.7	ν_3
			1410.2	ν_{10}
1410 vw	1415 s	1410 dp	1418.3	ν_{16}
			1411.0	ν_{17}
			1243.8	ν_4
1245 w	1245 s	1250 p	1245.1	ν_{18}
			836.3	ν_5
830 m	840 br s	832 dp	825.1	ν_{19}
730 m	765 s	n.o.	732.8	ν_{20}
			723.0	ν_{11}
617 w	625 s	623 dp	625.0	ν_{21}
570 w	580 s	578 p	579.8	ν_6
	228 s	224 p	231.9	ν_7
		179	143.2	ν_8
			180.6	ν_{22}
		132	133.2	ν_{23}

Can. J. Chem. Downloaded from www.nrcresearchpress.com by 210.87.254.40 on 09/05/12
For personal use only.

TABLE 7. Description of the fundamentals of $(CH_3)_3GeI$

Mode		Conventional description	Potential energy distribution
ν_1	a_1	CH_3 stretch (asym)	100(1)
ν_2		CH_3 stretch (sym)	98(1) + 2(10)
ν_3		CH_3 def (asym)	94(4) + 4(6)
ν_4		CH_3 def (sym)	7(2) + 54(4) + 25(5) − 5(15)
ν_5		CH_3 rock (sym)	1(2) + 4(4) + 27(5) + 62(6) + 10(15)
ν_6		GeC_3 stretch (sym)	90(2) + 3(4) + 3(5)
ν_7		GeI stretch	55(3) + 23(7) + 20(8)
ν_8		GeC_3 def (sym)	44(3) + 29(7) + 25(8)
ν_9	a_2	C—H stretch (asym)	100(1)
ν_{10}		CH_3 def (asym)	96(4) + 2(5) + 1(16)
ν_{11}		CH_3 rock (asym)	2(4) + 96(5) + 2(14)
ν_{12}		CH_3 torsion	Not observed or calculated
ν_{13}	e	CH_3 stretch (asym)	100(1)
ν_{14}		CH_3 stretch (asym)	100(1)
ν_{15}		CH_3 stretch (sym)	98(1) + 2(10)
ν_{16}		CH_3 def (asym)	94(4) + 4(6)
ν_{17}		CH_3 def (asym)	96(4) + 2(5)
ν_{18}		CH_3 def (sym)	8(2) + 54(4) + 24(5) + 20(6) − 5(14)
ν_{19}		CH_3 rock (sym)	4(4) + 29(5) + 62(6) + 10(14)
ν_{20}		CH_3 rock (asym)	2(2) + 2(4) + 92(5) + 1(8) + 2(13)
ν_{21}		GeC_3 stretch (asym)	90(2) + 4(4) + 5(5)
ν_{22}		GeC_3 def (asym)	1(7) + 97(8)
ν_{23}		GeC_3 rocking	98(7) + 1(8)
ν_{24}		CH_3 torsion	Not observed or calculated

Raman bands. A full description of these is presented in Table 5 along with the potential energy distributions amongst the force constants. There is no evidence in the spectra that permits reasonable assignments for the methyl torsional modes, ν_{14} and ν_{20}, but all of the remaining fundamentals are assigned (Table 4).

Iodo(trimethyl)germane, $(CH_3)_3GeI$

The molecule is assumed to have C_{3v} symmetry where the CH_3 groups are in their most symmetric positions. Twenty-four fundamental vibrations can be expected of which eight are a_1-type, four are a_2-type, and twelve are e-type. A description of these is presented in Table 7 along with the potential energy distributions amongst the force constants. The symmetric and asymmetric GeC_3 stretches ν_6 and ν_{21}, are assigned to polarized and depolarized bands at 580 and 625 cm^{-1}, respectively. The splitting of these asymmetric and symmetric modes is comparable to that in $(CH_3)_2GeI_2$. The GeI stretching mode, ν_7, appears as a polarized band at 224 cm^{-1} in the Raman spectrum.

The GeC_3 symmetric and asymmetric deformations ν_8 and ν_{22} are not resolved and are apparently contained in the broad band centered at 179 cm^{-1} in the Raman effect. This accidental degeneracy has been observed in other systems (4, 5) but it is interesting to note that the polarization data give no indication of the near coincidence of the symmetric and asymmetric deformations.

The two symmetric CH_3 rocking modes, ν_5 and ν_{19}, are assigned to a broad band at 840 cm^{-1} in the infrared. The results of the normal coordinate analysis confirm the assignment of the other CH_3 rocking mode, ν_{20} to a band at 730 cm^{-1} in the infrared. The a_2 mode, ν_{11}, is inactive in the infrared and too weak to be seen in the Raman spectrum but calculations give a frequency of 723 cm^{-1} for this vibration. These results are consistent with those currently accepted for the analysis of other methyl–germanium compounds (3, 4). A depolarized band at 132 cm^{-1} is attributable to the remaining GeC_3 rock, ν_{23}. Again, no indication appeared in any spectra for the CH_3 torsional modes, ν_{12} and ν_{24}, so no information could be obtained on the barrier hindering rotation around the carbon–germanium bond.

Force Constant Listings

The force constants listed in Table 1 are those calculated for the individual molecules. A very reasonable "fit" is found when average values of the stretching force constants are used although the bending modes do not exhibit such a high

Can. J. Chem. Downloaded from www.nrcresearchpress.com by 210.87.254.40 on 09/05/12
For personal use only.

Can. J. Chem. Downloaded from www.nrcresearchpress.com by 210.87.254.40 on 09/05/12
For personal use only.

degree of transferability, possibly due to the complex mixing we have observed amongst these modes.

Potential Energy Distributions

The potential energy distributions amongst the force constants are presented in Tables 3, 5, and 7. The symmetric and asymmetric CH_3 and GeC stretching modes in all three systems show almost total dependence on force constants one and two, respectively, consistent with their being essentially "pure stretches". By contrast, the GeI stretching modes are much less solely dependent on force constant three. The symmetric GeI stretches exhibit strong dependence on GeI/GeI stretch–stretch interactions and the CGeI and CGeC bending force constants as well as that of GeI stretching.

The asymmetric CH_3 deformation shows almost total dependence on force constant four but the symmetric CH_3 deformations show strong interaction with HCGe bending, and GeC stretching. The appearance of the GeC stretching force constant in the p.e.d. of the symmetrical deformations is noted in other methyl-germane derivatives that we are studying at this time. It is interesting to speculate that Fermi resonance between the first overtone of the symmetrical GeC stretch and the symmetrical CH_3 deformations might well be expected. However, complete splitting of bands is not observed although a shoulder is apparent on the low frequency side in each case.

The asymmetric GeC_3 deformation and GeC_3 rocking mode in $(CH_3)_3GeI$, the asymmetric GeI_3 deformation in CH_3GeI_3, and the CH_3 rocking vibrations in all molecules are essentially pure modes with little contribution from other force constants. The remaining modes are only approximately described by the conventional terminology. Thus, the GeC_2 (scissors) deformation in $(CH_3)_2GeI_2$ and symmetric GeC_3 deformation in $(CH_3)_3GeI$ have *ca.* 32 and 44% contribution from GeC stretching and GeI stretching, respectively, as well as significant contributions from CGeI bending. By contrast the symmetric GeI_2 (scissors) deformation in $(CH_3)_2GeI_2$ only has a small contribution from CGeI bending, but the remaining bending modes, the GeI_3 rock in CH_3GeI_3 and the GeI_2 wag and rock in $(CH_3)_2GeI_2$ all contain appreciable mixing among the force constants.

We wish to thank the National Research Council of Canada for financial support and express our great debt to Dr. D. E. Rogers of the University of Southampton for all his help on the programs SOTONVIB and FPERT.

1. D. F. Van De Vondel and G. P. Van Der Kelen. Bull. Soc. Chim. Belg. **74**, 453 (1965).
2. J. R. Aronson and J. R. Durig. Spectrochim. Acta, **20**, 219 (1964).
3. J. E. Griffiths. Spectrochim. Acta, **20**, 1335 (1964).
4. J. R. Durig, K. K. Lau, J. B. Turner, and J. Bragin. J. Mol. Spectrosc. **31**, 419 (1969).
5. D. F. Van De Vondel, G. P. Van Der Kelen, and G. Van Hooydonk. J. Organometal. Chem. **23**, 431 (1970).
6. M. I. Batuev, V. A. Ponomarenko, A. D. Matvecva, and G. Vzenhovo. Isv. Akad. Nauk SSSR. 2120 (1959).
7. V. E. Mironov and A. L Kravchenko Isv. Akad. Nauk SSSR. 988 (1965).
8. J. R. Durig, C. F. Jumper, and J. N. Willis, Jr. J. Mol. Spectrosc. **37**, 260 (1971).
9. S. Cradock and E. A. V. Ebsworth. J. Chem. Soc. A, 12 (1967).
10. J. E. Drake, R. T. Hemmings, and C. Riddle. J. Chem. Soc. A, 3359 (1970).
11. J. H. Schachtschneider. Vibrational analysis of polyatomic molecules VI: Shell Development Co. Emeryville, California. Project No. 31 450. December 1964. Tech. Report No. 57-65.
12. J. E. Drake and C. Riddle. J. Chem. Soc. A, 2114 (1969).

Can. J. Chem. Downloaded from www.nrcresearchpress.com by 210.87.254.40 on 09/05/12
For personal use only.

The Trifluoroacetic Acid Solvent System. Part II. Acids

M. G. HARRISS AND J. B. MILNE[1]

Department of Chemistry, University of Ottawa, Ottawa 2, Canada

Received April 21, 1971

^{19}F nuclear magnetic resonance (n.m.r.) studies show that SbF_5 forms $HSbF_5(OOCCF_3)$ in trifluoroacetic acid. This complex acid does not react with $(CF_3CO)_2O$ which must be added to carry out conductimetric studies in anhydrous $HOOCCF_3$. However, $HClO_4$, HSO_3F, and HNO_3 all react with $(CF_3CO)_2O$ to yield mixed anhydrides CF_3COClO_4, CF_3COSO_3F, and NO_2OOCCF_3. HBF_4 reacts with the anhydride to give CF_3COF while H_2SO_4 appears to be simply dehydrated to polysulfuric acids.

Les études de résonance magnétique nucléaire du fluor-19 indiquent que SbF_5 dans l'acide trifluoroacétique conduit à $HSbF_5(OOCCF_3)$. Ce complexe acide ne réagit pas avec $(CF_3CO)_2O$ qui doit être ajouté à $HOOCCF_3$ anhydre pour mener à bien des études conductimétriques. Cependant, $HClO_4$, HSO_3F et HNO_3 réagissent avec $(CF_3CO)_2O$ pour donner des anhydrides mixtes CF_3COClO_4, CF_3COSO_3F et NO_2OOCF_3. HBF_4 réagit avec l'anhydride pour donner CF_3COF alors que H_2SO_4 semble être déshydraté en acides polysulfuriques.

Canadian Journal of Chemistry, **49**, 2937 (1971)

Introduction

Trifluoroacetic acid is a very weak base (1) and, considering its good solvent properties (2), is of interest as a solvent for the titration of weakly basic substances. Some studies have already been carried out using perchloric acid as a titrant (3, 4). However, very few studies of acids in this solvent have been reported. According to electrical conductivity measurements, sulfuric acid is a non-electrolyte in trifluoroacetic acid (5). However, other authors, using indicator methods, report that sulfuric acid has a pK_a of 6.3 in the solvent (6). Pyrosulfuric (5), methanesulfonic and perchloric acids (6) are reported to behave as acids in trifluoroacetic acid. In view of the assumptions implicit in the indicator method for determining acid dissociation constants (6, 7) and the discrepancy in the behavior reported for sulfuric acid, it was considered of interest to study some strong acids in trifluoroacetic acid. The work reported here relies principally on nuclear magnetic resonance studies; the results of conductivity measurements are reported elsewhere (8).

Experimental

Materials

The trifluoroacetic acid was purified by distillation as described elsewhere (9).

Trifluoroacetic acid anhydride was prepared by refluxing the acid over P_2O_5 and then, distilling the product (b.p. 40.0 °C). Analar grade 71% perchloric acid, 98% sulfuric acid, 69% nitric acid, and 40% hydrofluoric acid were standardized by titration against sodium carbonate. Tetrafluoroboric acid was prepared from analytical grade boric acid and 40% hydrofluoric acid. Fluorosulfuric acid from Allied Chemical was doubly distilled before use (b.p. 160 °C). Antimony pentafluoride from Ozark-Mahoning was purified by distillation (b.p. 142 °C). Samples for n.m.r. spectra were made up by weight in precision n.m.r. tubes. All transfers were made in a dry box. Reaction was prevented by cooling the sample in liquid air until the tube was drawn off. Inserts made from Kel-F tubing supplied by Chemplast Co. Inc., Wayne, N.J. were used for the HBF_4 solutions initially, but no attack on glass was apparent in the n.m.r. spectra of solutions containing excess trifluoroacetic acid anhydride.

Fluorine n.m.r. spectra were taken on a Varian Associates HA-100 spectrometer. Except for the SbF_5 solutions all spectra were recorded at 25 °C.

Results and Discussion

The low dielectric constant of trifluoroacetic acid ($\varepsilon = 8.4$) requires that conductivity measurements be made at concentrations below $1.9 \times 10^{-4}\ M$ to observe ion-pairing without interference from higher ion aggregates (10). For this reason difficulties, arising from impurities in the solvent, water in particular, are greatly magnified. Acid containing as little as 0.00023% water has a water concentration equal to that of the limiting concentration at which simple ion-pair equilibria for an ionophore may be studied. For a very deliquescent solvent like trifluoroacetic acid sufficiently accurate removal of water to avoid interference with solute equilibria,

[1]To whom all correspondence should be addressed.

TABLE 1. Chemical shifts and peak areas for perchloric acid in trifluoroacetic acid anhydride*

Product	Chemical shift (p.p.m.)	Observed peak area	Calculated peak area (reaction 2)
$HOOCCF_3$	0.00	1.00	1.00
$(CF_3CO)_2O$	−0.54	0.483	0.485
CF_3COClO_4	−2.95	0.184	0.184

*Mole fractions $H_2O/(CF_3CO)_2O/HClO_4$; 0.286/0.585/0.129.

especially for acid solutes, is virtually impossible. For this reason a small amount of trifluoroacetic acid anhydride (0.5% by weight), which is a non-electrolyte in trifluoroacetic acid, was added for conductivity experiments (9). Nuclear magnetic resonance studies were made to establish whether the anhydride was inert towards acid solutes.

Perchloric Acid

Bessiere found perchloric acid to be an electrolyte in trifluoroacetic acid (6). Since the solvent used contained up to 36 p.p.m. water (0.002 *M*), the conductivity observed could be due to $H_3O^+ClO_4^-$ rather than $H_2OOCCF_3^+$-ClO_4^-. We have found that perchloric acid is a non-electrolyte in the presence of trifluoroacetic acid anhydride. This might suggest that perchloric acid exists in molecular form in the solvent, since any ion-pair that was formed would be expected to be dissociated to some degree. However, there is also the possibility of the dehydration reactions

[1] $2HClO_4 + (CF_3CO)_2O \rightarrow Cl_2O_7 + 2HOOCCF_3$

[2] $HClO_4 + (CF_3CO)_2O \rightarrow CF_3COClO_4 + HOOCCF_3$

The anhydrides formed in reactions 1 and 2 are expected to be non-electrolytes. Ionization of the mixed anhydride to give a trifluoroacetylium cation would be unlikely in view of the instability of this cation (11). Moreover, the isoelectronic CF_3COSO_3F behaves like a covalent compound (12). Fluorine n.m.r. was used to study the possibility of these reactions. The spectrum of a solution containing insufficient anhydride for complete removal of water consists of only one signal, indicating stoichiometric removal of water by anhydride. However, the addition of excess anhydride results in a spectrum with three peaks. This is consistent with reaction 2. The chemical shifts and peak areas for a solution with the composition in mole fraction units; $H_2O/(CF_3CO)_2O/HClO_4$; 0.286/0.585/0.129, are given in Table 1.

The observed peak areas are in good agreement with those required for reaction 2. A more extensive study of this reaction was not made because the solutions were of variable stability, turning yellow after a period of time varying from a few hours to a few days. When the solutions were frozen they turned a red color. The colors suggest the presence of chlorine dioxide or chlorine hexoxide.

Since perchloric acid reacts with trifluoroacetic acid anhydride and almost certainly reacts with water, further conductivity studies were considered unprofitable.

Fluorosulfuric Acid

The nuclear magnetic resonance spectrum of fluorosulfuric acid (0.38 mole fraction) in trifluoroacetic acid consists of two absorptions only, one in the F on S region, 116.3 p.p.m. to low field of the F on C peak. The areas correspond to the stoichiometry of the mixture and this shows that dehydration of trifluoroacetic acid does not take place. The spectra of solutions of fluorosulfuric acid in trifluoroacetic acid anhydride consist of 5 absorptions, 3 in the F on C region and 2 in the F on S region. No changes in the spectra were observed when the tubes were left standing for several weeks or heated to 100 °C for several days. The chemical shifts and peak areas are given in Table 2.

The spectra are consistent with the equilibrium

[3] $HSO_3F + (CF_3CO)_2O \rightleftarrows CF_3COSO_3F + HOOCCF_3$

The peaks *A*, *B*, and *C* are assigned to $HOOCCF_3$, $(CF_3CO)_2O$, and F on C in CF_3COSO_3F, respectively. The peaks *D* and *E* arise from F on S in HSO_3F and CF_3COSO_3F, respectively. The ratio of the area of peak *C* to peak *E* is 3:1

Can. J. Chem. Downloaded from www.nrcresearchpress.com by 210.87.254.40 on 09/05/12
For personal use only.

TABLE 2. Chemical shifts (p.p.m.) and peak areas (in parentheses) for solutions of fluorosulfuric acid in trifluoroacetic acid anhydride

Solution number	Mole fraction $HSO_3F/(CF_3CO)_2O$	Peak					
		A	*B*	*C*	*D*	*E*	*K*
1	0.370/0.630	0(4.79)	−0.21(30.1)	−1.68(3.08)	−116.6(2.68)	−122.7(1.00)	0.12
2	0.595/0.405	0(4.36)	−0.13(13.7)	−1.60(3.17)	−116.4(4.06)	−122.6(1.00)	0.16
3	0.796/0.204	0(3.32)	−0.08(5.76)	−1.56(3.10)	−116.3(6.83)	−122.3(1.00)	0.17

TABLE 3. Chemical shifts and peak area ratios* for solutions of H_2SO_4 in $(CF_3CO)_2O$

Solution number	Mole fractions $H_2O/(CF_3CO)_2O/H_2SO_4$	Observed peak area ratio	Calculated ratio for dehydration to H_2SO_4	Calculated ratio for dehydration to SO_3	Peak separation (c.p.s.)
1	0.139/0.422/0.439	6.5	0.49	∞	5.5
2	0.105/0.565/0.330	2.1	0.23	3.4	8.7
3	0.090/0.627/0.283	1.3	0.17	1.5	10.1
4	0.078/0.677/0.245	0.87	0.13	0.91	9.1

*$HOOCCF_3/(CF_3CO)_2O$.

within the error of the measurement for peaks so far apart. The chemical shifts of *C* and *E* and their separation are in good agreement with literature values for CF_3COSO_3F (12, 13), considering changes in solvent. The absence of coupling is consistent with the spectrum for CF_3COSO_3F (13); also it eliminates other possible products such as CF_3SO_3F (14) and CF_3SO_2F with fewer bonds between different fluorines which would show coupling. A small amount of water present causes peak *A* to be greater than peak *C* (although equilibrium 3 requires them to be equal). From the peak areas the equilibrium constant, *K*, for reaction 3 may be calculated and this is also given in Table 2. Considering the changing nature of the mixture, *K* is reasonably constant.

Because of the complication of mixed anhydride formation the conductivity of HSO_3F in $HOOCCF_3$ was not measured but the n.m.r. spectra suggest that the solvent is protonated by HSO_3F. In solutions of $(CF_3CO)_2O$ in $HOOCCF_3$, the acid peak lies 0.5 p.p.m. above the anhydride peak, varying slightly with changing concentration. In solutions containing HSO_3F the $HOOCCF_3$ peak shifts to lower field relative to $(CF_3CO)_2O$ with increasing HSO_3F mole fraction as would be expected if $H_2OOCCF_3^+$ were formed.

Sulfuric Acid

Solutions of concentrated H_2SO_4 in $(CF_3CO)_2O$ in the concentration range studied gave only 2 fluorine n.m.r. signals, one for anhydride and the other, displaced slightly to low field, for $HOOCCF_3$. The peak area ratios, chemical shifts and compositions are given in Table 3. The hypothetical area ratios for water removal to give H_2SO_4 and for complete dehydration to SO_3 are also given.

The high field peak increases in intensity relative to the other with increasing $(CF_3CO)_2O$ mole fraction and is assigned to anhydride. The low field peak is assigned to $HOOCCF_3$. The ratios of the areas of acid to anhydride show that anhydride removes the water and dehydrates H_2SO_4 as well. Three reactions may be considered

[4] $$nH_2SO_4 + (n-1)(CF_3CO)_2O \rightarrow H_2S_nO_{2n+1} + 2(n-1)HOOCCF_3$$

and

[5] $$H_2SO_4 + (CF_3CO)_2O \rightleftarrows (CF_3CO)HSO_4 + HOOCCF_3$$

[6] $$H_2SO_4 + 2(CF_3CO)_2O \rightleftarrows (CF_3CO)_2SO_4 + 2HOOCCF_3$$

However, for the equilibria 5 and 6 a third absorption for the mixed anhydride would be expected in the spectrum as for solutions of HSO_3F. Exchange with $HOOCCF_3$ or $(CF_3CO)_2O$, which would result in two peaks being observed, is unlikely. The compound $(CF_3CO)HSO_4$ has been prepared (15) by distillation of an equimolar mixture of SO_3 and $HOOCCF_3$ but it is said to undergo reaction with $HOOCCF_3$

Can. J. Chem. Downloaded from www.nrcresearchpress.com by 210.87.254.40 on 09/05/12
For personal use only.

TABLE 4. Chemical shifts and peak areas for the solution, $H_2O/(CF_3CO)_2O/HBF_4$; 0.380/0.560/0.060

Peak	Chemical shift (p.p.m.)	Observed area	Calculated area	Product
A	−90.6 (quartet)	~0.02	0.024	$CF_3CO\mathit{F}$
B	−1.25 (doublet)	0.069	0.073	$C\mathit{F}_3COF$
C	−0.50	0.304	0.293	$(CF_3CO)_2O$
D	0.00	1.00	1.00	$HOOCCF_3$
E	+53.1	~0.07	0.073	BF_3

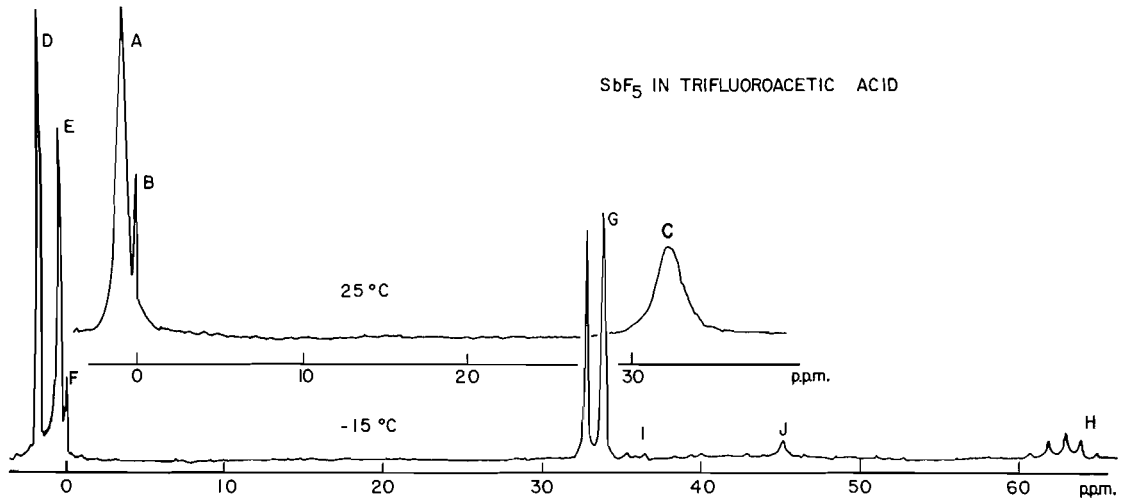

FIG. 1. ^{19}F nuclear magnetic resonance spectrum of a solution of composition $HOOCCF_3/(CF_3CO)_2O/SbF_5$ mole fraction, 0.639/0.023/0.338.

to give $(CF_3CO)_2O$. In the solutions studied here excess $HOOCCF_3$ is always present. The appearance of the $HOOCCF_3$ resonance to low field of $(CF_3CO)_2O$ suggests that the polysulfuric acids protonate $HOOCCF_3$.

Trifluoroacetic acid anhydride is a very strong dehydrating agent and, in terms of reaction 4, solution 1 corresponds to $n > 2$ (for $n = 2$, acid/anhydride area ratio is 5.7) and in solutions 3 and 4 the dehydration proceeds almost completely to SO_3.

Tetrafluoroboric Acid

The n.m.r. spectrum of a solution of $H_2O/(CF_3CO)_2O/HBF_4$, 0.474/0.450/0.076 mole fractions, consists of two resonances, that for $HOOCCF_3$ (area 1.000) and that for BF_4^- (area 0.116), shifted 70 p.p.m. to high field. Both the position and area of the high field peak are consistent with the presence of BF_4^-, which, from the stoichiometry of the mixture, should have an area of 0.113. Details of the spectrum of a solution, containing $(CF_3CO)_2O$ in excess of the sum of the moles of H_2O and HBF_4 together are given in Table 4. The spectrum is consistent with the reaction

[7] $(CF_3CO)_2O + HBF_4 \rightarrow$

$$CF_3COF + BF_3 + HOOCCF_3$$

The calculated areas in Table 4 are based upon the known stoichiometry of the solution assuming reaction 7 takes place. The chemical shift for BF_3 is comparable with the known value (14) and the shifts assigned to CF_3COF compare favorably with those of CF_3— and —COF groups (14). The coupling constant for CF_3COF was found to be 6.2 c.p.s. in the doublet and 5.6 c.p.s. in the quartet. Apparently CF_3CO^+-BF_4^- is not stable at room temperature similar to the corresponding hexafluorophosphate and arsenate (11).

Can. J. Chem. Downloaded from www.nrcresearchpress.com by 210.87.254.40 on 09/05/12
For personal use only.

Can. J. Chem. Downloaded from www.nrcresearchpress.com by 210.87.254.40 on 09/05/12
For personal use only.

Nitric Acid

The ^{19}F n.m.r. spectrum of a solution with the composition, $H_2O/(CF_3CO)_2O/HNO_3$; 0.337/0.446/0.217 mole fraction showed only one signal. Apparently H_2O is removed and the anhydride remaining reacts further with the HNO_3 according to one of two reactions

[8] $2HNO_3 + (CF_3CO)_2O \rightarrow 2HOOCCF_3 + N_2O_5$

[9] $HNO_3 + (CF_3CO)_2O \rightarrow NO_2OOCCF_3 + HOOCCF_3$

The spectrum of a solution containing anhydride in excess of that required for completion of reaction 9 ($H_2O/(CF_3CO)_2O/HNO_3$; 0.264/0.566/0.170) consists of two signals, with the weaker of the two 10.4 c.p.s. to low field of the other. This weaker peak is assigned to the excess anhydride. If reaction 8 is occurring, the peak area ratio ($HOOCCF_3/(CF_3CO)_2O$) would be 1.61. If reaction 9 takes place and the mixed anhydride exchanges with $HOOCCF_3$ the peak area ratio should be 3.31. The observed ratio is 3.42, indicating the formation of mixed anhydride. Exchange of NO_2OOCCF_3 with $HOOCCF_3$ is not unlikely in view of the feasibility of ionization to $NO_2^+OOCCF_3^-$.

Decomposition to form NO_2 was apparent in these solutions after several days.

Antimony Pentafluoride

The fluorine-n.m.r. spectra at 25 and -15 °C of a solution of SbF_5 in $HOOCCF_3$ with a small amount of $(CF_3CO)_2O$ added to ensure anhydrous conditions ($HOOCCF_3/(CF_3CO)_2O/SbF_5$, 0.639/0.023/0.338 mole fraction) are given in Fig. 1. The spectra of a more dilute solution (0.885/0.038/0.077 mole fractions) were similar except that the doublet *I* and the peak *J* were missing. The spectra bear close resemblance to those reported for SbF_5 dissolved in other solvents (16, 17) and are consistent with the reaction

[10] $HOOCCF_3 + SbF_5 \rightarrow HSbF_5(OOCCF_3)$

In the spectrum at 25 °C the peak *A* is assigned to $HOOCCF_3$ exchanging with $HSbF_5(OOCCF_3)$, the peak *B*, $(CF_3CO)_2O$, and the peak *C*, F on Sb in $HSbF_5(OOCCF_3)$. The peaks *A* and *C* are broadened by exchange processes. At -15 °C these processes have been slowed sufficiently and the spectrum of the F on Sb region consists of an AX_4 spectrum (peaks *G* and *H*) and the small peaks *I* and *J*. In addition, the peak *A* has split into two sharp peaks, *D* and *E*. The chemical shifts and areas of *D*, *G*, and *H* are those expected for the complex anion

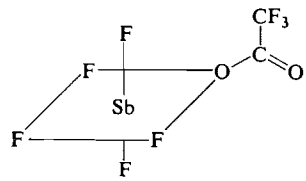

or its parent acid. The coupling constant for the fluorines *cis* and *trans* to the trifluoroacetate group is 98.0 c.p.s. which is comparable to that in other species (16, 17). The doublet *I* may arise from the dimer ion

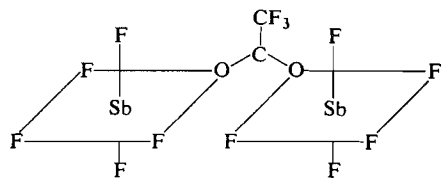

which also gives an AX_4 spectrum (16).

The other components of the spectra for these ions would be too weak to be observed. The single broad resonance *J* is assigned to SbF_6^- which has a chemical shift similar to that observed here (17, 18). The peak is broadened by quadrapole relaxation processes associated with the ^{121}Sb and ^{123}Sb species. The SbF_6^- could arise from a ligand redistribution reaction

$$2SbF_5(OOCCF_3)^- \rightleftarrows SbF_6^- + SbF_4(OOCCF_3)_2^-$$

which has been observed in other solutions with SbF_5 (17). The second species is expected to have a *cis* structure by analogy with other known $SbF_4X_2^-$ species (16, 17) and the intensity of the two triplets expected for this ion would be too weak for observation.

The addition of $KOOCCF_3$ to solutions of SbF_5 in $HOOCCF_3$ results in the precipitation of $KSbF_6$ which was identified by its X-ray powder diffraction pattern. The potassium analysis of the precipitate was slightly low for $KSbF_6$ (%K observed, 13.20; calculated for $KSbF_6$, 14.2; calculated for $KSbF_5(OOCCF_3)$, 10.6). The fluorine n.m.r. spectrum of the supernatant liquid from this reaction had no absorption in the F on Sb region but several peaks were observed in the F on C region. Further work is being carried out on this system.

Conclusion

To study acid behavior in $HOOCCF_3$, to which $(CF_3CO)_2O$ is added to ensure anhydrous conditions, an acid which does not react with anhydride is needed. The strong acids, $HClO_4$, HSO_3F, H_2SO_4, HNO_3, and HBF_4 all react with the anhydride. Antimony pentafluoride can be used for conductivity studies (8), although slight interference arises from side reactions. It is interesting that perchloric acid reacts completely to form the mixed anhydride while fluorosulfuric acid does not. It is known that fluorosulfuric acid is a considerably stronger acid than perchloric acid (19) and the protonation of $HOOCCF_3$ by HSO_3F could prevent complete reaction to the mixed anhydride. The preferential formation of the mixed anhydride to that of the symmetric anhydride has been previously reported (20) and may be a result of increased ionic contribution to the bonding in the mixed anhydride.

We thank the National Research Council of Canada for generous support and a bursary (M.G.H.).

1. J. Barr, R. J. Gillespie, and E. A. Robinson. Can. J. Chem. **39**, 1266 (1961).
2. R. Hara and G. H. Cady. J. Am. Chem. Soc. **76**, 4285 (1954).
3. J. E. DeVries, S. Schiff, and E. S. Gantz. Anal. Chem. **27**, 1814 (1955).
4. G. Kresze and V. Schmidt. Chem. Ber. **90**, 1687 (1957).
5. Y. Y. Fialkov and Y. Y. Borovikov. Vestn. Kievski. Politekhn. Inst., Ser. Khim. Mashinostroit i Tekhnol. **6**, 66 (1965).
6. Jacques Bessiere. Bull Soc. Chem. Fr. 3353 (1969).
7. I. M. Kolthoff and S. Bruckenstein. J. Am. Chem. Soc. **78**, 1 (1956).
8. M. G. Harriss and J. B. Milne. To be published.
9. M. G. Harriss and J. B. Milne. Can. J. Chem. **49**, 1888 (1971).
10. R. M. Fuoss and F. Accascina. Electrolytic conductance. Interscience, New York. 1959. p. 253.
11. E. Lindner and H. Kranz. Chem. Ber. **99**, 3800 (1966).
12. D. D. DesMarteau and G. H. Cady. Inorg. Chem. **5**, 169 (1966).
13. J. J. Delfino and J. M. Shreeve. Inorg. Chem. **5**, 308 (1966).
14. J. W. Emsley, J. Feeney, and L. H. Sutcliffe. High resolution nuclear magnetic resonance spectroscopy. Vol. 2. Pergamon Press, New York. 1966. p. 871.
15. John F. Dowdal. Chem. Abstr. **48**, P1425i (1954).
16. R. C. Thompson, J. Barr, R. J. Gillespie, J. B. Milne, and R. A. Rothenbury. Inorg. Chem. **4**, 1641 (1965).
17. P. A. Dean and R. J. Gillespie. J. Am. Chem. Soc. **91**, 7264 (1969).
18. R. J. Gillespie and K. C. Moss. J. Chem. Soc. 1170 (1966).
19. J. Barr, R. J. Gillespie, and E. A. Robinson. Can. J. Chem. **39**, 1266 (1961).
20. J. E. B. Randles, J. C. Tatlow, and J. M. Tedder. J. Chem. Soc. 436 (1954).

Can. J. Chem. Downloaded from www.nrcresearchpress.com by 210.87.254.40 on 09/05/12
For personal use only.

Can. J. Chem. Downloaded from www.nrcresearchpress.com by 210.87.254.5 on 09/05/12
For personal use only.

Ion Pairing and the Reaction of Alkali Metal Ferrocyanides and Persulfates

R. W. Chlebek and M. W. Lister

Received April 29, 1971

Osmometric measurements have been made on the alkali metal persulfates, and these are interpreted in terms of formation of ion pairs, $MS_2O_8^-$, by means of the method of Masterton and Berka (5). Equilibrium constants, and the derived thermodynamic quantities are deduced for the reactions $M^+ + S_2O_8^{2-} \rightleftharpoons MS_2O_8^-$. These results are applied to the interpretation of the kinetics of the reactions

$$2M_4Fe(CN)_6 + M_2S_2O_8 \rightarrow 2M_3Fe(CN)_6 + 2M_2SO_4$$

With M = K^+, Rb^+, and Cs^+, the reacting species are $MFe(CN)_6^{3-} + MS_2O_8^-$, with very similar rate constants; with M = Li^+, Na^+ the species are $MFe(CN)_6^{3-} + S_2O_8^{2-}$; and for lithium the reaction of $Fe(CN)_6^{4-} + S_2O_8^{2-}$ is also important. Rate constants and activation parameters are deduced.

Les mesures osmométriques ont été effectuées sur les persulfates d'un métal alcalin; les résultats sont interprétés en fonction de la formation d'une paire d'ions, $MS_2O_8^-$, suivant la méthode de Masterton et Berka (5). Les constantes d'équilibre et les quantités thermodynamiques qui en dérivent sont déduites des réactions $M^+ + S_2O_8^{2-} \rightleftharpoons MS_2O_8^-$. Ces résultats sont utilisés en vue de l'interprétation des cinétiques des réactions

$$2M_4Fe(CN)_6 + M_2S_2O_8 \rightarrow 2M_3Fe(CN)_6 + 2M_2SO_4$$

avec M = K^+, Rb^+ et Cs^+, les espèces réactionnelles sont $MFe(CN)_6^{3-} + MS_2O_8^-$, avec des constantes de vitesse très semblables; avec M = Li^+ et Na^+ les espèces réactionnelles sont $MFe(CN)_6^{3-} + S_2O_8^{2-}$; pour le lithium la réaction $Fe(CN)_6^{4-} + S_2O_8^{2-}$ est également importante. Les constantes de vitesse ainsi que les paramètres d'activation sont déduits.

Canadian Journal of Chemistry, 49, 2943 (1971)

In two earlier papers (1, 2), we reported measurements on the rates of the reactions

$$2M_4Fe(CN)_6 + M_2S_2O_8 \rightarrow 2M_3Fe(CN)_6 + 2M_2SO_4$$

where M is an alkali metal. These were interpreted in terms of ion pairs, such as $KFe(CN)_6^{3-}$, as the actual reacting species, and the criterion used was to discover which reaction path best followed the predictions of Brönsted's equation (3). This required a knowledge of the equilibrium constants of the reactions

$$M^+ + Fe(CN)_6^{4-} \rightleftharpoons MFe(CN)_6^{3-}$$

$$M^+ + S_2O_8^{2-} \rightleftharpoons MS_2O_8^-$$

Values of these constants are available in the literature for ferrocyanides (4), and we had made measurements (1) with a glass electrode on $KFe(CN)_6^{3-}$ and $KS_2O_8^-$, and also on the product ion pairs $KFe(CN)_6^{2-}$ and KSO_4^-. Values were not available for other persulfates, but since Masterton and Berka (5) had found fairly similar values for all alkali metal sulfates, it was assumed that the values of the equilibrium constants for all alkali metal persulfates were the same as the known value for $KS_2O_8^-$. The present paper reports values for these constants obtained by the method of Masterton and Berka (5), who used osmometric measurements and these values are in turn used to interpret the kinetic data. Water was the solvent throughout.

Experimental

Alkali Metal Persulfates

These were obtained by the methods already described (1, 2). Freshly prepared solutions were always used, and the concentrations were known, firstly from the weights of salt used, and secondly by titration. Two titrations were used: (*i*) excess ferrous ammonium sulfate solution was added and the excess was titrated with ceric ammonium sulfate, and (*ii*) potassium iodide was added and the resulting iodine was titrated with sodium thiosulfate.

Osmometric Measurements

These were done with a Mechrolab 301 A Vapor Pressure Osmometer. Potassium chloride solutions were used as the comparison solutions, and their osmotic coefficients were taken to be as given by Robinson and Stokes (6). The British Drug House AnalaR reagent grade of potassium chloride was used, the solution being made up by weight from the salt dried at 110 °C. Osmometric measurements were made at 25 and 37 °C.

Results

Table 1 gives the results of the osmometric measurements. The table gives the osmotic coefficient, ϕ_{12}, for various salt molalities *m*.

TABLE 1. Osmotic coefficients and equilibrium constants for ion pairing of alkali metal persulfates

Run	Salt	T	m	ϕ_{12}	α	K^c	I	K^0
1	$Na_2S_2O_8$	25.0 °C	0.0493	0.848	0.898	1.22	0.138	3.3
2	"	"	0.0950	0.826	0.826	1.21	0.252	3.7
3	"	"	0.0953	0.826	0.826	1.21	0.253	3.7
4	"	"	0.0980	0.818	0.795	1.46	0.254	4.5
5	$Rb_2S_2O_8$	"	0.0508	0.800	0.698	5.01	0.122	13.3
6	"	"	0.0526	0.784	0.635	6.65	0.120	17.5
7	"	"	0.0527	0.794	0.676	5.43	0.124	14.5
8	"	"	0.0722	0.780	0.635	4.87	0.164	13.8
9	"	"	0.0749	0.776	0.619	5.05	0.168	14.4
10	$Cs_2S_2O_8$	"	0.0507	0.762	0.540	10.87	0.106	27.8
11	"	"	0.0545	0.766	0.562	9.16	0.116	24.0
12	"	"	0.1073	0.729	0.437	8.40	0.201	24.7
13	"	"	0.1073	0.724	0.416	9.24	0.197	27.1
14	"	"	0.1091	0.725	0.419	8.91	0.201	26.3
15	$Na_2S_2O_8$	37.0	0.0496	0.836	0.850	1.95	0.134	5.4
16	"	"	0.0951	0.817	0.791	1.56	0.245	4.9
17	"	"	0.0952	0.818	0.795	1.52	0.246	4.8
18	$Rb_2S_2O_8$	"	0.0528	0.788	0.652	6.11	0.122	16.6
19	"	"	0.0529	0.794	0.677	5.40	0.124	14.8
20	"	"	0.0721	0.772	0.600	5.72	0.159	16.5
21	"	"	0.0722	0.773	0.603	5.61	0.160	16.2
22	$Cs_2S_2O_8$	"	0.0547	0.769	0.577	8.56	0.118	23.1
23	"	"	0.0551	0.770	0.579	8.33	0.119	22.5
24	"	"	0.1074	0.726	0.425	8.90	0.198	26.9
25	"	"	0.1074	0.730	0.442	8.24	0.202	25.0

From these are calculated the fractions of the ion pair dissociated, α, the ionic strength, I, and the equilibrium constant, defined as

$$K^c = \frac{[MS_2O_8^-]}{[M^+][S_2O_8^{2-}]}$$

at the particular ionic strength. The calculations followed Masterton and Berka's method (5). It was assumed that their osmotic coefficients for completely dissociated electrolytes held at both 25 and 37 °C. Table 1 also gives values of the equilibrium constant extrapolated to zero ionic strength. This extrapolation was made by the usual equation for single ion activity coefficients, f,

$$[1] \quad -\log f = Az^2\left(\frac{\sqrt{I}}{1 + Ba\sqrt{I}} - CI\right)$$

for an ion of charge z. Kielland found a value of $a = 4$ Å for persulfate ions (7), and an average value of 0.25 was used for C, (8), so that the equation used was

$$[2] \quad -\log f = Az^2\left(\frac{\sqrt{I}}{1 + 1.33\sqrt{I}} - 0.25I\right)$$

It may be noted that Masterton and Berka quote mean values of activity coefficients which approximately fit an equation

$$[3] \quad -\log f = Az^2\left(\frac{\sqrt{I}}{1 + 1.5\sqrt{I}} - 0.1I\right)$$

and use of this would increase K° to about 8% above the values given in Table 1.

In addition to the results given in Table 1, measurements were also made on lithium persulfate. The values of the osmotic coefficients were close to those given by Masterton and Berka for completely dissociated salts, so that we obtained no evidence of ion pairing in this case. As will be seen later, the kinetic measurements of lithium ferrocyanide and persulfate can be interpreted without invoking the participation of $LiS_2O_8^-$. Measurements were also made on potassium persulfate which gave equilibrium constants somewhat higher (about 20%) than those obtained by use of a glass electrode (1). Attempts to obtain constants by use of a glass electrode for the other alkali metals were unsuccessful, as the glass electrode readings were not steady enough, and a small change in cell voltage can give a large change in equilibrium constant.

Table 2 summarizes the results in the form of the average equilibrium constants, including those obtained earlier (1) for potassium persulfate. The derived thermodynamic quantities, ΔG^0, ΔH^0, and ΔS^0 are included. It may be

Can. J. Chem. Downloaded from www.nrcresearchpress.com by 210.87.254.5 on 09/05/12
For personal use only.

TABLE 2. Values of thermodynamic functions for $M^+ + S_2O_8^{2-} \rightleftharpoons MS_2O_8$

M^+	K^0 (M) 25 °C	K^0 (M) 37 °C	ΔG^0 (25 °C) (kcal/mol)	ΔH^0 (kcal/mol)	ΔS^0 (cal/deg mol)
Na^+	3.8	5.0	−0.79	4.3	17.0
K^+	8.2	9.4	−1.25	1.6	9.6
Rb^+	14.7	16.0	−1.59	1.3	9.8
Cs^+	26.0	24.4	−1.93	−1.0	3.2

noted that ΔG^0 changes much less than ΔH^0, since ΔH^0 and ΔS^0 in effect oppose each other.

Discussion

The original object of this research was to investigate the effect of ion pairing on the reaction of persulfate and ferrocyanide ions. Kinetic measurements on this reaction have already been reported (1, 2). In the case of the lithium, sodium, rubidium, and cesium salts, the conclusions reached were tentative, because equilibrium constants for the formation of alkali metal – persulfate ion pairs were not known. It is now possible to make a more quantitative comparison of the reactions.

The general method of treating the kinetic data, which appeared in Tables I to IV in ref. 2, was as follows. The concentrations of all the species present in a reacting mixture were calculated from the gross concentrations of the solutions, and from the equilibrium constants for ion pairing. These constants were those appropriate to the actual ionic strengths of the solutions, and were adjusted by means of activity coefficients calculated by eq. 2 above. Since the true ionic strength could only be found when the appropriate equilibrium constants were known, an iterative procedure was used, until the finally calculated ionic strength differed by less than 0.1% from that used in finding the equilibrium constants. Since the kinetic data were for 25 and 40 °C, the equilibrium constants for $MS_2O_8^-$ formation (obtained at 25 and 37 °C) were extrapolated to 40 °C, with the usual assumption that $\log K$ was linear in T^{-1}. A more serious assumption was necessitated by the fact that Shvedov and Nichugovskii's data on ferrocyanides (4) only applied to 25 °C, and data are not available for the other alkali metals. It was assumed that the temperature coefficients of all these equilibrium constants were the same as for the potassium ion pair, which was known from glass electrode measurements. As ΔH^0 for formation of the ion pair $KFe(CN)_6^{3-}$ is only 3.86 kcal, and as fairly small values are also found for the other potassium ion pairs involved (1), it was felt that this assumption would not introduce much error. Small corrections were made for ion pairing of rubidium and cesium with chloride, from data of Davies (ref. 8, p. 169), and also for alkali metal ferricyanide ion pair formation. The only known appropriate equilibrium constant is that for $KFe(CN)_6^{2-}$; this is close to one tenth of the value for $KFe(CN)_6^{3-}$, and it was assumed that this value of one tenth held for other alkali metals.

When all the concentrations were known, it was assumed that some particular pair of ions were the main reacting species, as follows:

Reacting species	Rate constant	Path
$Fe(CN)_6^{4-} + S_2O_8^{2-}$	k_1	4/2
$MFe(CN)_6^{3-} + S_2O_8^{2-}$	k_2	3/2
$Fe(CN)_6^{4-} + MS_2O_8^-$	k_3	4/1
$MFe(CN)_6^{3-} + MS_2O_8^-$	k_4	3/1

Values of k_1, etc., were calculated, and it was then seen which rate constant most closely followed the Brönsted equation. This rate constant was then supposed to belong to the correct mechanism of the reaction.

Some comments should be made on this procedure. Firstly, Brönsted's equation is

$$\log k = \log k^0 + 2Az_az_bF(I)$$

for reaction of ions of charge z_a, z_b, and $F(I)$ is the function of the ionic strength appearing in the extended Debye–Hückel equation, [1] above. $F(I)$ contains two constants Ba and C which vary somewhat from ion to ion, and it is not obvious which values should be used. Indeed, as we are dealing with various reacting species, and also a transition state species, it is not certain that the

Can. J. Chem. Downloaded from www.nrcresearchpress.com by 210.87.254.5 on 09/05/12
For personal use only.

TABLE 3. Values of d log k/d$F(I)$ obtained from various values of *Ba* and *C*; results for rubidium salts at 25 °C

Ba	*C*	d log k_1/d$F(I)$	d log k_2/d$F(I)$	d log k_3/d$F(I)$
1.0	0.2	12.0	8.25	2.67
1.0	0.25	12.8	8.75	2.83
1.0	0.3	13.6	9.35	3.02
0.9	0.3	12.8	8.8	2.84
0.93	0.3	13.0	8.95	2.89
1.3	0.3	16.3	11.2	3.62
Calculated value		8.14	6.11	3.05

TABLE 4. Best values of *Ba* and *C* from kinetic data

M^+	Path	T (°C)	*Ba*	*C*	Slope	log k^0 (M^{-1} s^{-1})
Li^+	4/2	25	1.0	0.3	8.14	−4.29
		40	1.0	0.3	8.38	−3.74
	3/2	25	1.0	0.3	6.11	−3.63
		40	1.0	0.3	6.29	−3.12
Na^+	3/2	25	1.0	0.2	6.12	−3.25
		40	1.0	0.2	6.10	−2.745
Rb^+	3/1	25	1.0	0.3	3.02	−1.437
		40	1.0	0.3	3.07	−1.087
Cs^+	3/1	25	1.0	0.1	3.02	−1.423
		40	1.0	0.1	3.05	−1.038

same constants apply throughout. The values in eq. 2 were used in adjusting the equilibrium constants, and various combinations of *Ba* and *C* were investigated in obtaining a fit with Brönsted's equation. The range of *Ba* investigated was 1.0 to 1.65, and the range of *C* was 0.1 to 0.3, in accordance with the values found to fit observed activity coefficients. Except with lithium, it was found that these ranges never allowed any ambiguity about the mechanism; for lithium (as will be seen) it is probable that two paths are important. Table 3, which contains results for the rubidium salts, shows the extent of the variation. This table gives the slopes of plots of log k against $F(I)$, which at 25 °C should have the value 1.018 $z_a z_b$. It can be seen that only k_4 gives agreement of observed and calculated slopes, which happens when $Ba = 1.0$, $C = 0.3$ approximately. Hence the reacting species are $RbFe(CN)_6^{3-}$ and $RbS_2O_8^-$. Similar calculations were made with Li^+, Na^+, and Cs^+.

Secondly, the equilibrium constants were taken to be those applying to the ionic strength at the start of the run. This ionic strength falls gradually, and calculations were made for the potassium salts at the mid point of the run, as well as at the beginning. The change in slope was always less than 1%, so that calculations at the initial ionic strength were taken to be sufficient.

Thirdly, with lithium a fit of the calculated and observed shapes was possible for both k_1 and k_2. The method cannot distinguish between k_2 and k_3, for both of which mechanisms the composition of the transition state species is $MFe(CN)_6$-$S_2O_8^{5-}$, so that the k_2 path only was arbitrarily chosen. It was therefore assumed that for lithium, both the k_1 and k_2 paths simultaneously contributed to the rate, and values were thus obtained for both constants. There was no evidence of this sort of behavior for sodium.

Table 4 gives the results of these calculations. The reaction path is indicated by the charges on the reacting species; *i.e.* $Fe(CN)_6^{4-} + S_2O_8^{2-}$ is 4/2. The values of *Ba* and *C* are those that give observed slopes most closely fitting Brönsted's equation (within the ranges of *Ba* and *C* quoted above). k^0 is the value of the rate constant extrapolated to zero ionic strength; k^0 is in units of M^{-1} s^{-1}. The usual activation parameters, $\Delta H^{\ddagger}$ and $\Delta S^{\ddagger}$, can be calculated from these results, and these are given in Table 5. Since the extrapolation to zero ionic strength follows slightly different equations for different M^+, Table 5 also contains values at $I = 0.1$. In the actual kinetic runs, the ionic strengths were varied from about 0.02 to 0.3 so $I = 0.1$ may be considered a typical value. Results reported earlier (1) on the 3/1 path for the potassium salts made $\Delta H^{\ddagger} = 9.0$ kcal/mol, and $\Delta S^{\ddagger} =$

Can. J. Chem. Downloaded from www.nrcresearchpress.com by 210.87.254.5 on 09/05/12
For personal use only.

TABLE 5. Calculated values of $\Delta H^{\ddagger}$ and $\Delta S^{\ddagger}$*

		$I = 0$		$I = 0.1$	
M^+	Path	$\Delta H^{\ddagger}$	$\Delta S^{\ddagger}$	$\Delta H^{\ddagger}$	$\Delta S^{\ddagger}$
Li^+	4/2	15.1	−27.5	16.5	−15
	3/2	13.9	−28.5	15.0	−19
Na^+	3/2	13.7	−25	14.6	−18.5
Rb^+	3/1	9.4	−32	9.65	−30
Cs^+	3/1	10.4	−28.5	10.55	−26.5

*$\Delta H^{\ddagger}$ in kcal/mol; $\Delta S^{\ddagger}$ in cal/deg mol.

−34.7 cal/deg mol at zero ionic strength; at $I = 0.1$, $\Delta H^{\ddagger} = 9.5$, and $\Delta S^{\ddagger} = -31$.

A few comments may be made on the quantities in Tables 4 and 5. It is found that the 3/1 paths for cesium, rubidium, and potassium (for which $\log k^0 = -1.402$ at 25 °C, and -1.085 at 40 °C) have fairly similar rate constants. Thus the ions do not seem to play a very specific role, and their behavior is perhaps merely a reflection of identical charge and not very different size (especially if hydrated). $\Delta H^{\ddagger}$ rises slightly from potassium to cesium, but this is offset by a rise in $\Delta S^{\ddagger}$. Possibly the somewhat smaller potassium ion permits a closer approach of the reacting ions in the activated complex leading to a smaller $\Delta H^{\ddagger}$ for electron transfer in the reaction, and also to a somewhat more tightly bound complex with a more negative $\Delta S^{\ddagger}$. Sodium salts behave differently, and this is not just a reflection of a lower degree of ion pairing. In fact if the 3/1 path for the sodium system had the same rate constant as for the potassium system, it would be the main route of the reaction, in spite of the lower concentrations of ion pairs. The reason for this change of behavior, which is evidently carried further in the lithium system, is not clear. $\Delta H^{\ddagger}$ and $\Delta S^{\ddagger}$ for all the reactions show some signs of a linear relation at $I = 0.1$, but this is almost totally obscured at $I = 0$. It may be noted that $\Delta H^{\ddagger}$ is on the average larger for reactions of ions with larger charges, though only by a small amount, as is to be expected for aqueous solutions.

Finally it may be noted that the 4/2 reaction will presumably be occurring in all reaction mixtures. However, it can be calculated from the rate constants and concentrations of various species, that in all the runs using an alkali metal other than lithium, it contributes only a small fraction to the total rate, and consequently went undetected.

1. R. W. CHLEBEK and M. W. LISTER. Can. J. Chem. **44**, 437 (1966).
2. R. W. CHLEBEK and M. W. LISTER. Can. J. Chem. **45**, 2411 (1967).
3. N. J. BRÖNSTED. Z. Phys. Chem. Leipzig, **102**, 169 (1922); **115**, 337 (1925).
4. V. P. SHVEDOV and G. F. NICHUGOVSKII. Radiokhimiya, **8**, 63 (1966).
5. W. L. MASTERTON and L. H. BERKA. J. Phys. Chem. **70**, 1924 (1966).
6. R. A. ROBINSON and R. H. STOKES. Electrolyte solutions. Butterworths Scientific Publications, London. 1959. 2nd edition.
7. J. KIELLAND. J. Am. Chem. Soc. **59**, 1675 (1937).
8. C. W. DAVIES. Ion association. Butterworths, London. 1962. pp. 39, 41.

Can. J. Chem. Downloaded from www.nrcresearchpress.com by 210.87.254.5 on 09/05/12
For personal use only.

Can. J. Chem. Downloaded from www.nrcresearchpress.com by 210.87.254.105 on 09/05/12
For personal use only.

The Structure of Derivatives of $[SCH_3Fe(CO)_3]_2$

J. P. Crow and W. R. Cullen
Chemistry Department, The University of British Columbia, Vancouver 8, British Columbia

Received May 12, 1971

$[SCH_3Fe(CO)_3]_2$ when separated into its two known isomers reacts with tertiary phosphines with retention of the sulfur-methyl group configuration. The reaction of the mixture of isomers of $[SCH_3Fe(CO)_3]_2$ with ditertiary phosphines and arsines has been studied. Some ligands give bridged complexes, and others chelates: one ligand gives both. The p.m.r. and Mössbauer spectra of these complexes are discussed.

Le composé $[SCH_3Fe(CO)_3]_2$, lorsqu'il est séparé en ses deux isomères connus, réagit avec les phosphines tertiaires avec rétention de la configuration du groupe méthyle-soufre. La réaction du mélange d'isomères de $[SCH_3Fe(CO)_3]_2$ avec les phosphines di-tertiaires et les arsines a été étudiée. Certains ligands donnent des complexes pontés et d'autres des chélates: un ligand donne les deux. Les spectres r.m.p. et Mössbauer de ces complexes sont discutés.

Canadian Journal of Chemistry, 2948 (1971)

Introduction

King has shown that $[SCH_3Fe(CO)_3]_2$ exists as two isomers **A** and **B** which can be separated chromatographically (1). The p.m.r. spectra of these compounds showed that isomer **A** contained inequivalent or *anti* sulfur-methyl groups and isomer **B** contained equivalent or *syn* sulfur-methyl groups. Later an X-ray crystallographic study of the *anti* isomer of $[SC_2H_5Fe(CO)_3]_2$ provided more details of the structure of these compounds (2). We have investigated the reactions of $[SCH_3Fe(CO)_3]_2$ with tertiary and ditertiary phosphines and assigned structures to the products on the basis of their infrared, proton magnetic resonance (p.m.r.), and Mössbauer spectra. Of particular interest are the reactions of fluorocarbon-bridged ditertiary phosphines and arsines such as **1** which are known to give bridged complexes with dicobalt octacarbonyl (3, 4), and triiron dodecacarbonyl (5, 6).

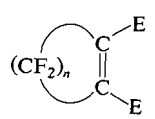

1*a* E = $As(CH_3)_2$, $n = 2$; $f_4$fars
1*b* E = $P(C_6H_5)_2$, $n = 2$; $f_4$fos
1*c* E = $P(C_6H_5)_2$, $n = 4$; $f_8$fos

Some related complexes have been previously prepared by other investigators (7) but little was said about their possible structures. A recent communication (8) describes the spectroscopic properties of a number of complexes of the sort $[SRFe(CO)_2P(C_6H_5)_3]_2$ and $[SRFe(CO)_2]_2$diphos (diphos = $(C_6H_5)_2PCH_2CH_2P(C_6H_5)_2$) and comments on some interesting structural features. Some of these have been found in the present investigation and in addition this paper describes, for the first time, separate reactions of the *syn* and *anti* isomers of the parent compound.

Experimental

Nuclear magnetic resonance (n.m.r.) spectra were run on a Varian T.60 spectrometer. Chemical shifts are reported in p.p.m. downfield from internal T.M.S. Mössbauer spectra were recorded at 80 °K and were processed as described in ref. 9. Infrared spectra were recorded on a Perkin–Elmer model 457 instrument. Microanalyses were done by Mr. P. Borda of this department. Ligands were prepared by literature methods (5, 9, 10) or were commercial samples.

Bis(methylthioirontricarbonyl) was prepared as in ref. 11 and separated into isomers by chromatography on alumina in pentane. $[C_6H_5SFe(CO)_3]_2$ and $S_2Fe_3(CO)_9$ and derivatives of these were made by the methods described in the literature (7, 12), purity was checked by melting points and infrared spectra. All other reactions were done under nitrogen by stirring equimolar amounts (2:1 for $[SCH_3Fe(CO)_2P(CH_3)_2C_6H_5]_2$) of the ligand and metal carbonyl in an aromatic solvent. Purification was effected by filtration of the solution followed by recrystallization from benzene/hexane to yield about 75% of the product. Reaction conditions and analyses for new compounds are shown in Table 1. Spectroscopic data are listed in Tables 2 and 3.

Results and Discussion

The **A** and **B** isomers of $[SCH_3Fe(CO)_3]_2$, henceforth called *anti-* and *syn-*, were separated by chromatography and were found to react

TABLE 1. Preparative and analytical data for thioironcarbonyl complexes

Complex	Reaction conditions			Analyses for new Complexes			
				Calcd.		Found	
	Solvent	Temperature (°C)	Time (h)	C	H	C	H
syn-$(SCH_3)_2Fe_2(CO)_5(CH_3)_2PC_6H_5$	Benzene	20	¼	37.2	3.3	37.3	3.3
anti-$(SCH_3)_2Fe_2(CO)_5(CH_3)_2PC_6H_5$	Benzene	20	½	37.2	3.3	37.2	3.5
syn-$(SCH_3)_2Fe_2(CO)_5P(C_6H_5)_3$	Benzene	20	¼	49.3	3.5	49.1	3.3
anti-$(SCH_3)_2Fe_2(CO)_5P(C_6H_5)_3$	Benzene	20	½	49.3	3.5	49.3	3.4
$[SCH_3Fe(CO)_2]_2f_4fos$ (chelate)*	Benzene	78	1	50.3	3.2	50.0	3.2
$[SCH_3Fe(CO)_2]_2f_8fos$ (chelate)	Benzene	78	1	47.4	2.8	47.4	2.7
$[SCH_3Fe(CO)_2(CH_3)_2PC_6H_5]_2$	Benzene	78	1	44.6	4.6	44.3	4.6
$[SCH_3Fe(CO)_2]_2f_4fos$ (bridged)	Xylene	140	3	50.3	3.2	50.9	3.3
$[SCH_3Fe(CO)_2]_2f_4fars$ (bridged)	Xylene	140	1	25.8	2.8	25.9	2.8
$S_2Fe_3(CO)_8P(C_6H_5)_3$	Hexane	60	4	43.5	2.1	43.6	2.1

*Converts to bridged form on refluxing in xylene for 3 h.

TABLE 2. Proton magnetic resonance spectra of the $(SCH_3Fe)_2(CO)_xL$ complexes*

Complex	S-methyl	P- or As-methyl
anti-$[SCH_3Fe(CO)_3]_2$	1.61, 2.12	—
syn-$[SCH_3Fe(CO)_3]_2$	2.08	—
anti-$[SCH_3Fe]_2(CO)_5P(CH_3)_2C_6H_5$	1.12, 1.80	1.83, 1.85. (J_{P-C-H} = 8 Hz) (7.8 → 7.2, C_6H_5)
syn-$[SCH_3Fe]_2(CO)_5P(CH_3)_2C_6H_5$	1.70	1.83. (J_{P-C-H} = 8 Hz) (7.8 → 7.2, C_6H_5)
anti-$[SCH_3Fe]_2(CO)_5P(C_6H_5)_3$	0.83, 1.55	(7.7 → 7.2, C_6H_5)
syn-$[SCH_3Fe]_2(CO)_5P(C_6H_5)_3$	1.60	(7.7 → 7.2, C_6H_5)
syn-$[SCH_3Fe(CO)_2P(CH_3)_2C_6H_5]_2$	1.50	1.74. (J_{P-C-H} = 8 Hz) (7.6 → 7.1, C_6H_5)
anti-$[SCH_3Fe(CO)_2]_2f_4fos$ (chelated)†	0.85, 1.80	(7.8 → 7.2, C_6H_5)
$[SCH_3Fe(CO)_2]_2f_4fars$ (bridged)	1.57, 1.71	1.57, 1.89

*Unless otherwise indicated all spectra were run in CS_2 solution.
†$CDCl_3$ solution.

with equimolar amounts of triphenyl- and dimethylphenylphosphine at room temperature, in benzene, to give complexes $(SCH_3)_2Fe_2(CO)_5$(ligand). The p.m.r. spectra of these complexes (Table 2) show that substitution occurs with retention of the sulfur-methyl configuration. Thus the tertiary phosphine complexes obtained from *syn*-$[SCH_3Fe(CO)_3]_2$ show one sulfur-methyl resonance in their p.m.r. spectra, whereas the complexes obtained from *anti*-$[SCH_3Fe(CO)_3]_2$ show two sulfur-methyl p.m.r. resonances separated by 0.70 p.p.m. The only significant change in the p.m.r. spectrum of $[SCH_3Fe(CO)_3]_2$ on substitution is a shift of the methyl resonances to higher field, and an increase of about 50% in the chemical shift between inequivalent methyl groups of the *anti* isomer. In these complexes, and in the other phosphorus complexes described later, a coupling P—Fe—S—C—H of about 1 Hz was also observed irrespective of the orientation of the S-methyl group.

Only one phosphorus-methyl resonance was observed in the p.m.r. spectrum of *syn*-$(SCH_3)_2Fe_2(CO)_5(CH_3)_2PC_6H_5$. This probably indicates that substitution by dimethylphenylphosphine occurs in the axial position (*cis* to both sulfur atoms), for only by substitution in this position is the molecule symmetrical enough to allow magnetic equivalence of the phosphorus-methyl groups.

The suggested structure of this molecule is shown in Fig. 1*a*. The isomer of this compound *anti*-$(SCH_3)_2Fe(CO)_5P(CH_3)_2C_6H_5$ which almost certainly is also substituted in the axial position does not have sufficient symmetry for equivalence of its P-methyl groups and hence shows two resonances attributable to these groups separated by 2 Hz (J_{P-C-H} = 8 Hz). Infrared and Mössbauer parameters (Table 3) of the complexes $(SCH_3)_2Fe_2(CO)_5L$ also show differences between the isomers. In the carbonyl stretching region of the infrared spectrum the *anti* isomers have five bands whereas the *syn* isomers show four bands. In addition the dimethylphenylphosphine com-

Can. J. Chem. Downloaded from www.nrcresearchpress.com by 210.87.254.105 on 09/05/12
For personal use only.

TABLE 3. Infrared (CO region) and Mössbauer parameters for $[SCH_3Fe(CO)_3]_2$ derivatives

Derivative	Infrared bands in region 2100–1800 cm^{-1}*	δ†	Δ†
syn-$(SCH_3)_2Fe_2(CO)_6$	2072(2) 2040(10) 1996(1) 1989(8)	0.29	1.00
anti-$(SCH_3)_2Fe_2(CO)_6$	2076(2) 2040(10) 2002(10) 1991(10)	0.29	0.88
syn-$(SCH_3)_2Fe_2(CO)_5P(CH_3)_2C_6H_5$	2046(9) 2040(2) 1986(10) 1970(9) 1930(4)	0.29	1.29
		0.30	0.78
anti-$(SCH_3)_2Fe_2(CO)_5P(CH_3)_2C_6H_5$	2050(9) 1987(10) 1976(7) 1966(6) 1934(3)	0.28	1.15
		0.29	0.70
syn-$(SCH_3)_2Fe_2(CO)_5P(C_6H_5)_3$	2050(10) 1985(10) 1972(9) 1928(3)	0.30	1.13
		0.32	0.73
anti-$(SCH_3)_2Fe_2(CO)_5P(C_6H_5)_3$	2048(10) 1988(10) 1979(8) 1968(5) 1936(3)	0.30 (Broad)	0.88
$(SCH_3)_2Fe_2(CO)_4f_4fos$ (chelated)	2028(10) 1966(9) 1958(8) (1934(1)) 1920(4)	0.28	1.14
		0.40	0.47
$(SCH_3)_2Fe_2(CO)_4f_8fos$ (chelated)	2032(10) 1968(10) 1960(8) 1916(3)	0.27	1.06
		0.42	0.76
$(SCH_3)_2Fe_2(CO)_4[(CH_3)_2PC_6H_5]_2$	1990(10) 1946(8) 1927(10)	0.28	1.00
$(SCH_3)_2Fe_2(CO)_4f_4fars$ (bridged)	1996(5) 1970(10) 1935(10)	0.36	1.08
$(SCH_3)_2Fe_2(CO)_4f_4fos$ (bridged)	2002(4) 1977(10) 1948(5) 1940(5)	0.33	1.01
$(SC_6H_5)_2Fe_2(CO)_6$	2084(5) 2046(10) 2006(10) 1996(10) 1986(2)	0.29	1.00
$(SC_6H_5)_2Fe_2(CO)_5P(C_6H_5)_3$	2056(8) 1990(10) 1976(3) 1944(2)	0.31	0.97
$S_2Fe_3(CO)_9$	2065(8) 2046(10) 2022(8) 2010(2)	0.29	0.57
$S_2Fe_3(CO)_8P(C_6H_5)_3$	2075(8) 2036(10) 2016(9) 2010(9) 1988(3) ~1976(3)	0.29	0.57
$S_2Fe_3(CO)_8P(C_4H_9\text{-}n)_3$	2072(4) 2045(1) 2031(9) 2014(10) 1974(4) 1961(4)	0.32	0.53

*In C_6H_{12} solution, relative intensities in parentheses.
†Isomer shift and quadrupole splitting values (at 80 °K) are in mm $s.^{-1}$ Shifts are quoted relative to sodium nitropruside.

plexes also show slight splitting of some of the carbonyl infrared bands which may be due to the presence of rotamers in solution. A related phenomenon has been noted by Jetz and Graham (13).

The Mössbauer spectra of $(SCH_3)_2Fe_2(CO)_5L$ complexes show quite large differences in the quadrupole splitting of the iron atoms in the *syn* and *anti* isomers (Table 3). In accordance with previous results (5, 9 and references therein), the isomer shift and quadrupole splitting parameter with the higher isomer shift value is assigned to the phosphine substituted iron atom. Thus complex formation decreases the quadrupole splitting of the substituted iron atom and increases the quadrupole splitting of the other iron atom. This effect is slightly more pronounced in the *syn* than in the *anti* isomers. $[SCH_3Fe(CO)_3]_2$ also shows quadrupole splitting differences between *anti* and *syn* isomers, perhaps an indication that in these complexes a change in the basic skeleton of the molecule accompanies *syn–anti* isomerism.

Attempts were also made to separate possible isomers of $[C_6H_5SFe(CO)_3]_2$ without success. The mono-triphenylphosphine derivative is certainly axially substituted as judged by its infrared spectrum.

With 2 mol of dimethylphenylphosphine and 1 mol of the bidentate ligands f_4fars, f_4fos, and f_8fos, (**1**), $[SCH_3Fe(CO)_3]_2$ (not separated into isomers) forms complexes which have carbonyl infrared spectra characteristic of disubstituted compounds. The complex $[SCH_3Fe(CO)_2P(CH_3)_2C_6H_5]_2$ has two equivalent iron atoms in its Mössbauer spectrum, and equivalent S-methyl groups in its p.m.r. spectrum, so the molecule has a *syn* configuration with both axial carbonyl groups displaced by the ligands. The p.m.r. spectrum also indicates that weak virtual coupling between the two phosphines is taking place in spite of the spatial separation between them. The number of bands in the CO stretching region of the infrared spectrum and their position is similar to that reported for $[SCH_3Fe(CO)_2P(C_6H_5)_3]$ (8) (the S-methyl orientation is not stated) which has also been assigned a structure in which the axial carbonyl groups are replaced.

With the cyclic phosphine ligand **1***b* and **1***c* complexes $(SCH_3)_2Fe_2(CO)_4(L—L)$ are formed under mild conditions. These have two Mössbauer environments, and two well separated S-methyl proton magnetic resonances. A structure with the ligand chelating and the S-methyl groups in the *anti* position (Fig. 1*b*) explains

Can. J. Chem. Downloaded from www.nrcresearchpress.com by 210.87.254.105 on 09/05/12
For personal use only.

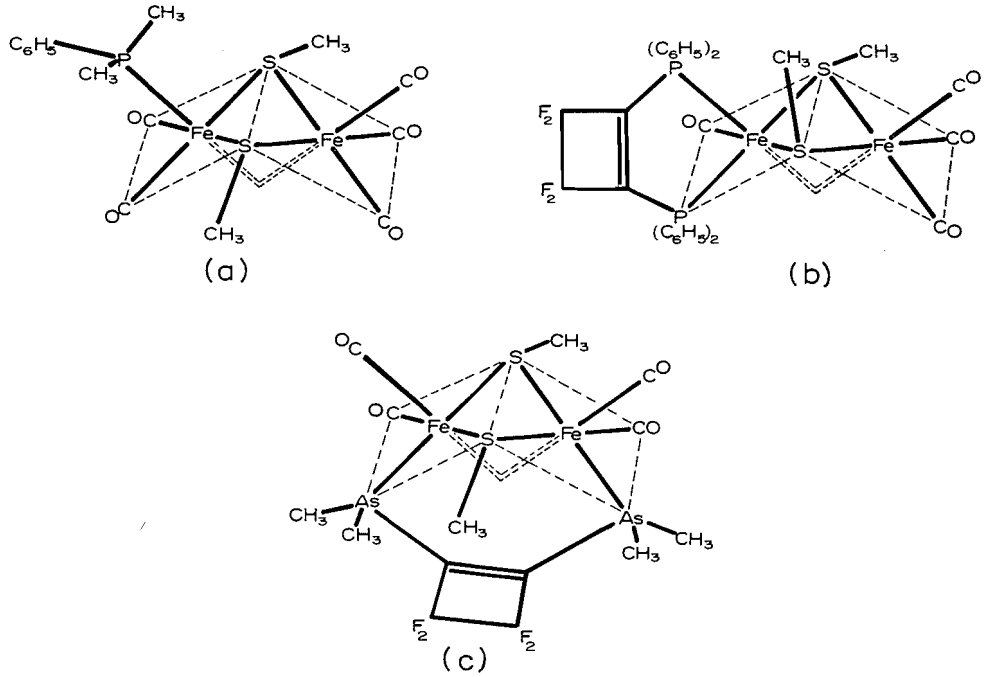

FIG. 1. Proposed structures of (*a*) *syn*-$(SCH_3Fe)_2(CO)_5P(CH_3)_2C_6H_5$, (*b*) $(SCH_3Fe)_2(CO)_4f_4fos$, (*c*) $(SCH_3Fe)_2(CO)_4f_4fars$.

these observations. Thus the chelated iron atom is the one with the greater isomer shift. The shifts are consistent with replacement of two carbonyl groups on one iron atom and none on the other. The infrared spectrum is similar to that of the diphos complex $(SCH_3)_2Fe(CO)_3Fe(CO)$diphos which is also believed to be chelated (7, 8). In Fig. 1*b* the ligand is shown occupying an axial and equatorial position. We believe that this is more likely than the equatorial–equatorial isomer because, as seen above, the axial carbonyl groups seem to be the more easily displaced.

The complexes $[SCH_3Fe(CO)_2]_2$(L—L) formed at higher temperatures with $f_4$fars and $f_4$fos have infrared and Mössbauer spectra which would result from the ligand bridging the two iron atoms. The Mössbauer spectra show that the iron atoms are equivalent and are mono-substituted. The p.m.r. spectrum of the $f_4$fars complex shows that while the As- and S-methyl groups are non-equivalent, the chemical shift values of the S-methyl groups are characteristic of the *syn* isomers. This spectrum would result when the ligand has displaced an equatorial carbonyl group (*i.e.* in the plane of Fe, S, S) from each iron atom (Fig. 1*c*). The infrared spectra of both $f_4$fars and $f_4$fos complexes are similar to that reported for the complex $[SCH_3Fe(CO)_2]_2(C_6H_5)_2PCH_2P(C_6H_5)_2$ which is also believed to be bridged (8).

The ability of fluorocarbon-bridged ligands such as **1** to yield bridged metal carbonyl complexes is well known (*e.g.* 3–6, 14). Indeed the proposed structure in Fig. 1*c* is very similar to that known for $f_4farsCo_2(CO)_6$ which contains the "folded book" skeleton with the ligand bridging two corners (3). These ligands, especially the phosphines, are also known to form chelate complexes with iron and Group VI carbonyls (9, 15), however, the isomers of $(SCH_3)_2Fe_2(CO)_4f_4fos$ are unusual because the ligand is either bridged or chelated.

The cluster compound $S_2Fe_3(CO)_9$ has a structure (16) which can be described in terms of two 6-coordinate iron atoms and one 7-coordinate one, and thus would be expected to have a Mössbauer spectrum of two quadrupole doublets. In fact the spectrum consists of one doublet. The derivatives $S_2Fe_3(CO)_8PR_3$ (R = C_6H_5, *n*-C_4H_9) also have a very similar Mössbauer spectrum

Can. J. Chem. Downloaded from www.nrcresearchpress.com by 210.87.254.105 on 09/05/12
For personal use only.

which seems to suggest that phosphine substitution at one iron atom alters its Mössbauer environment very little.

We thank the National Research Council of Canada for financial assistance and Dr. J. R. Sams for help in obtaining the Mössbauer spectra.

1. R. B. KING. J. Am. Chem. Soc. **84**, 2460 (1962).
2. L. F. DAHL and C. H. WEI. Inorg. Chem. **2**, 328 (1963).
3. J. P. CROW, W. R. CULLEN, W. HARRISON, and J. TROTTER. J. Am. Chem. Soc. **92**, 6339 (1970).
4. J. P. CROW and W. R. CULLEN. Inorg. Chem. In press.
5. W. R. CULLEN, D. A. HARBOURNE, B. V. LIENGME, and J. R. SAMS. Inorg. Chem. **9**, 702 (1970).
6. P. J. ROBERTS, B. R. PENFOLD, and J. TROTTER. Inorg. Chem. **9**, 2137 (1970).
7. W. HIEBER and A. ZEIDLER. Z. Anorg. Allgem. Chem. **329**, 92 (1964).
8. J. A. DE BEER, R. J. HAINES, R. GREATREX, and N. N. GREENWOOD. J. Organometal. Chem. **27**, C33 (1971).
9. W. R. CULLEN, D. A. HARBOURNE, B. V. LIENGME, and J. R. SAMS. Inorg. Chem. **8**, 95 (1969).
10. W. R. CULLEN, P. S. DHALIWAL, and C. J. STEWART. Inorg. Chem. **6**, 2256 (1967).
11. R. B. KING. Organometallic syntheses. Academic Press, New York, N.Y. 1965.
12. W. HIEBER and J. GRUBER. Z. Anorg. Allgem. Chem. **296**, 91 (1958).
13. W. JETZ and W. A. G. GRAHAM. J. Am. Chem. Soc. **89**, 2773 (1967).
14. P. J. ROBERTS and J. TROTTER. J. Chem. Soc. A, 3246 (1970).
15. W. R. CULLEN, D. F. DONG, and J. A. J. THOMPSON. Can. J. Chem. **47**, 4671 (1969).
16. C. H. WEI and L. F. DAHL. Inorg. Chem. **4**, 493 (1965).

Can. J. Chem. Downloaded from www.nrcresearchpress.com by 210.87.254.105 on 09/05/12
For personal use only.

Can. J. Chem. Downloaded from www.nrcresearchpress.com by 210.87.254.40 on 09/05/12
For personal use only.

Mouvements moléculaires et transitions de phases dans le perfluorométhylcyclohexane solide

BUU BAN
Laboratoire de Photophysique Moléculaire, Faculté des Sciences 91, Orsay, France

C. CHACHATY
Service de Chimie Physique, C.E.N. de Saclay, B.P. N°2, 91, Gif-sur-Yvette, France

ET

M. RENAUD ET R. FOURME
Laboratoire de Chimie Physique de l'Université Paris VI, Faculté des Sciences 91, Orsay, France

Reçu le 22 avril 1971

Le perfluorométhylcyclohexane a été étudié par diffraction de rayons X, r.m.n. et r.p.e. Les deux premières méthodes confirment l'existence de plusieurs phases thermodynamiquement stables entre 77 °K et le point de fusion (234 °K): phase I ($227 < T < 234$ °K), phase II ($173 < T < 227$ °K), phase III ($T < 173$ °K), ainsi que celle d'une phase métastable (II′) au-dessous de 130 °K. Lorsqu'on élève la température, la r.m.n. indique successivement la rotation de CF_3 (phases II′ et III), la réorientation de toute la molécule autour de l'axe pseudoternaire du cycle (phase II) puis sa réorientation isotrope (phase I). La r.p.e. fournit des renseignements analogues sur les mouvements des radicaux 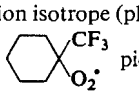 piégés dans le PFMCH. La comparaison entre l'anisotropie de g mesurée d'après la position des bandes des spectres r.p.e. et celle déduite de leur second moment suggère une large distribution des temps de corrélation de réorientation des radicaux dans la phase métastable.

Solid perfluoromethylcyclohexane has been studied by X-ray diffraction, n.m.r., and e.s.r. The two former methods confirm the existence of several thermodynamically stable crystalline phases between 77 °K and the melting point (234 °K): phase I ($227 < T < 234$ °K), phase II ($173 < T < 227$ °K), phase III ($T < 173$ °K) and that of a metastable phase (II′) below 130 °K. When the temperature is raised, the n.m.r. indicates successively the rotation of CF_3 (phases II′ and III), the reorientation of the molecule about the pseudothreefold axis of the ring (phase II), then its isotropic reorientation (phase I). Similar information is obtained from e.s.r. concerning the motions of 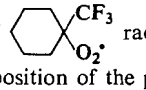 radicals trapped in PFMCH. The comparison between g anisotropy, measured from the position of the peaks of e.s.r. spectra and that deduced from their second moments suggests a wide distribution of reorientation correlation times for radicals in the metastable phase.

Canadian Journal of Chemistry, **49**, 2953 (1971)

I. Introduction

Les spectres de résonance paramagnétique électronique (r.p.e.) des radicaux piégés dans le perfluorométhylcyclohexane (PFMCH) irradié présentent d'importantes variations entre 77 °K et le point de fusion de ce composé (234 °K) (1). Ces variations ont été attribuées à des mouvements moleculaires associés aux transitions de phase qui ont été mises en évidence par des mesures de chaleur spécifique (2). Ces mesures ont permis de détecter deux points de transition entre 77 °K et le point de fusion (234 °K), l'un à 173 °K, l'autre à 226.6 °K. Nous désignerons respectivement par I, II et III les phases comprises dans les domaines de température $226\ °K < T < 234\ °K$, $173\ °K < T < 226\ °K$, $T < 173\ °K$. Dworkin (2) a également mentionné l'existence d'une phase métastable, que nous appellerons provisoirement phase IV, qui se transforme vers 120–140 °K en la phase III, avec dégagement de chaleur.

Nous nous sommes proposés de déterminer par r.p.e. les mouvements de réorientation des radicaux piégés dans le PFMCH en relation avec les mouvements des molécules de la matrice, que l'on étudie par résonance magnétique nucléaire

large bande (r.m.n.). Pour compléter et confirmer les résultats des expériences de résonance magnétique, les différentes phases du PFMCH solide ont été identifiées par diffraction de rayons X.

II. Techniques Expérimentales

Le PFMCH était un produit "Imperial Smelting" que nous avons utilisé tel quel après vérification de sa pureté par spectrométrie de masse (> 99.5%).[1]

(1) Diffraction de rayons X

L'étude des différentes phases cristallographiques du perfluorométhylcyclohexane (PFMCH) a été réalisée par la méthode des poudres, à l'aide d'une chambre de Weissenberg Stoe équipée d'un dispositif réfrigérant à jet d'azote gazeux (3). Un système de régulation stabilise la température du gaz à ± 0.5 degré autour du point choisi. Un étalonnage préalable à partir de substances connues permet de corriger les indications du thermocouple situé au voisinage de la sortie du Dewar dirigeant le jet gazeux et d'obtenir ainsi la température réelle de l'échantillon enformé dans un capillaire (ϕ 0.2 mm) en verre de Lindemann.

L'utilisation d'une chambre photographique (ϕ 57.8 mm) constituée de deux demi-cylindres rend aisé le chargement et le déchargement du film, sans perturber pour autant la température de la substance. En écartant les écrans de la chambre de Weissenberg de 2.5 mm de part et d'autre de son plan équatorial, le rayonnement diffracté par l'échantillon impressionne ce film sur une bande de 6 mm de largeur. Par translation manuelle de 10 mm du support de la chambre photographique entre chaque pose, il est ainsi possible d'enregistrer consécutivement, sur le même film, dix diagrammes Debye–Scherrer.

Tous les clichés ont été obtenus dans les mêmes conditions (Cu Kα, 26 kV, 20mA, 2 h d'exposition). Pour préciser les conditions nécessaires à l'obtention d'enregistrements de bonne qualité, nous avons refroidi l'échantillon de deux manières différentes: (*a*) un refroidissement lent a été effectué jusqu'à 230 °K. Après un premier diagramme, la température a été abaissée de 20° en 30 min, puis un nouveau diagramme a été recueilli, et le processus répété jusqu'à 90 °K; (*b*) le PFMCH a été trempé à 77 °K par un jet d'azote liquide, puis sa température a été ramenée de 90 à 230 °K à raison de 20° en 30 min, des clichés étant enregistrés à intervalles réguliers au cours du réchauffement.

L'examen des deux séries d'enregistrements montre que: (*a*) le refroidissement lent à partir de la phase liquide conduit à des diagrammes caractéristiques d'un solide constitué de quelques cristallites. En effet, le PFMCH dans sa forme I est pratiquement monocristallin; à 210 °K, les cristaux observés après la transition I–II sont encore assez gros et leur état de division ne se modifie guère par abaissement de la température; (*b*) la trempe à 77 °K, suivie d'un réchauffement lent, permet d'obtenir des diagrammes d'excellente qualité en raison de l'extrême division de la poudre cristalline. Pourtant, vers 230 °K, l'échantillon redevient spontanément quasiment monocristallin.

[1]Ces mesures ont été faites au C.E.A., dans le laboratoire de M. Botter que nous tenons à remercier ici.

Après avoir vérifié que la trempe par jet gazeux ou par projection d'azote liquide conduit aux mêmes résultats, nous avons décidé de commencer tout traitement thermique par une trempe gazeuse, la température de la substance pouvant ensuite être variée entre 90 et 210 °K.

(2) Résonance magnétique

Les expériences de résonance magnétique ont été effectuées à l'aide d'un spectromètre r.p.e. Varian V 4501 A convertible en spectromètre r.m.n. large bande par adjonction d'une unité radiofréquence V 4210 A. Les spectres étaient enregistrés en plaçant les échantillons dans un cryostat à circulation d'azote gazeux refroidi, situé dans la cavité r.p.e. ou la sonde r.m.n. La plupart des mesures ont été réalisées à des fréquences de l'ordre de 9250 MHz pour la r.p.e. et de 15 MHz pour la r.m.n. Au voisinage de 100 °K, le temps de relaxation spin-réseau T_1 des fluors, que nous n'avons pas mesuré, est suffisamment long pour provoquer une distorsion des spectres r.m.n. par passage rapide, même pour des vitesses de balayage aussi faibles que 0.5 G/min. Cette difficulté a été évitée en utilisant des échantillons non dégazés ou préalablement irradiés à 77 °K pour créer des centres paramagnétiques de façon à réduire T_1 (4). Nous avons vérifié que ces deux méthodes n'influaient pas sur la largeur et le second moment des spectres.

Le facteur g des radicaux du PFMCH a été mesuré en enregistrant simultanément les spectres r.p.e. des échantillons à étudier et celui d'un échantillon de goudron dispersé dans KCl dont la résonance se situe à $g = 2.0028$. Nous avons utilisé pour cela une cavité double V 4532 en tenant compte du gradient de champ magnétique entre les deux échantillons. Le champ était mesuré à l'aide d'un magnétomètre à résonance protonique Varian F8 relié à un fréquencemètre.

III. Résultats

(1) Diffraction de rayons X

(*a*) Après la trempe, nous avons enregistré des diagrammes Debye–Scherrer de 90 à 170 °K, puis de 170 à 90 °K et enfin de 90 à 170 °K, en faisant varier la température de 20° en 30 min entre deux clichés consécutifs: (*i*) au cours du premier réchauffement, les diagrammes obtenus à 90 et 110 °K sont caractéristiques d'une forme cristalline que nous avons appelée provisoirement "forme IV"; (*ii*) à 130 °K, on observe une autre variété que l'on conserve ensuite durant tout le traitement thermique. Cette forme est stable dans le domaine de température 90–170 °K et s'identifie avec la forme III observée par calorimétrie (2).

(*b*) Partant d'un échantillon trempé puis recuit à 170 °K afin d'obtenir la variété III, nous procédons à des enregistrements à 170 et 190 °K, puis de 190 à 90 °K et enfin de 90 à 170 °K, la température variant entre chaque exposition comme précédemment: (*i*) comme prévu, à 170 °K, nous avons la phase III; (*ii*) à 190 °K, nous

Can. J. Chem. Downloaded from www.nrcresearchpress.com by 210.87.254.40 on 09/05/12
For personal use only.

Can. J. Chem. Downloaded from www.nrcresearchpress.com by 210.87.254.40 on 09/05/12
For personal use only.

observons la forme II thermodynamiquement stable entre 173 et 226 °K; (*iii*), par refroidissement de 190 à 130 °K, la phase II se conserve, bien qu'en dessous de 173 °K on soit dans le domaine de la variété III; elle est alors thermodynamiquement instable. Il y a donc un retard à la transformation II–III; (*iv*), à 110 °K, une nouvelle forme II′ apparaît et est également observée aux températures successives de 90 et 110 °K; (*v*) enfin, entre 130 et 170 °K réapparaît la variété III.

On serait donc tenté de conclure que, selon le traitement thermique, le PFMCH présente trois formes cristallines stables (I, II et III) et deux formes métastables (II′ et IV). La superposition des clichés II et II′ montre qu'en fait la variété IV est un mélange de la forme II et de la forme II′, la première étant prédominante aux basses températures.

Une succession de clichés effectués à des intervalles de température plus petits a ensuite permis de préciser les domaines d'existence de ces différentes variétés. Entre 226 et 234 °K existe la forme I; de 226 à 173 °K, on trouve la phase II; au-dessous de 173 °K, la forme III est stable. La variété IV (mélange par trempe de la phase piégée II et de la phase II′) se transforme irréversiblement par réchauffement en III aux environs de 115 °K.

Quant à la phase II′, son domaine d'existence est essentiellement lié au traitement thermique que subit l'échantillon. Un refroidissement progressif rend II métastable et II′ apparaît vers 123–124 °K. Si l'abaissement de la température est poursuivi dans les mêmes conditions, II′ se conserve au-dessous de 123 °K, et ce n'est qu'au réchauffement que cette variété redonne III à 120–121 °K. Par contre, si l'on stabilise la température du PFMCH à 123–124 °K durant plusieurs heures, II′ se transforme spontanément en III.

Il résulte de toutes ces expériences que, quel que soit le mode de refroidissement appliqué à un échantillon polycristallin, la forme stable III ne peut être obtenue à partir de II qu'après passage, durant une période plus ou moins longue par la variété métastable II′. On peut rapprocher ces résultats de ceux établis par la r.m.n. (Fig. 1) et la calorimétrie.

Un abaissement lent de la température à partir de la phase liquide conduit spontanément, comme signalé plus haut, à un monocristal I; il nous a également été possible d'obtenir une tel monocristal par fusion de zone directement réalisée sur la tête goniométrique (5). La même technique permet aussi la fabrication d'un monocristal II. Ces échantillons ont été étudiés par la méthode du cristal tournant et les résultats obtenus sont mentionnés plus loin dans l'interprétation des données recueillies par la r.m.n.

(2) Résonance magnétique nucléaire

Les échantillons de PFMCH ont été solidifiés soit par trempe dans l'azote liquide ou par un courant d'azote gazeux (méthode A), soit par refroidissement par paliers de quinze à vingt minutes tous les cinq ou dix degrés (méthode B). Dans cette seconde méthode, les spectres sont enregistrés au cours du refroidissement progressif.

La Fig. 1 représente les largeurs ΔH et les seconds moments $\langle \Delta H^2 \rangle$ des spectres r.m.n. du PFMCH, en fonction de la température. Les courbes *a* et *a′*, *b* et *b′* correspondent respectivement aux méthodes A et B.

Quelle que soit la méthode de refroidissement initial des échantillons, lorsqu'on les réchauffe à partir de 100 °K, le second moment décroît tout d'abord de 9.5 G^2 à 7.2 G^2 puis augmente rapidement et d'une manière irréversible à 8–8.5 G^2 vers 130 °K. $\langle \Delta H^2 \rangle$ varie ensuite réversiblement entre 9.8 G^2 à 100 °K et 7.5 G^2 à 170 °K. Au-delà de 170–175 °K le second moment tombe à 1.1 ± 0.1 G^2 et demeure sensiblement constant jusqu'à 220 °K. Il décroît de nouveau au-delà de cette température et devient égal à 0.1 G^2 entre 225 et 234 °K. L'évolution de la largeur des spectres est tout à fait parallèle à celle du second moment (Fig. 1*a* et *b*).

Compte-tenu des résultats de calorimétrie (2) et de diffraction de rayons X, on peut admettre qu'une phase métastable est piégée par refroidissement direct des échantillons à 77 ou 90 °K. Il est probable qu'il s'agit de la phase II′, car l'inertie thermique des échantillons de r.m.n. ($\approx$ 1 ml) est très supérieure à celle des échantillons examinés aux rayons X ($\approx$ 1 mm^3) de sorte que la transformation II $\rightarrow$ II′ a le temps de s'effectuer au cours du refroidissement.

L'augmentation de ΔH et de $\langle \Delta H^2 \rangle$ au voisinage de 130 °K nous semble attribuable à la transformation de la phase II′ en phase III, stable au-dessous de 173 °K. Notons que cette transformation est irréversible, que nous ne l'avons

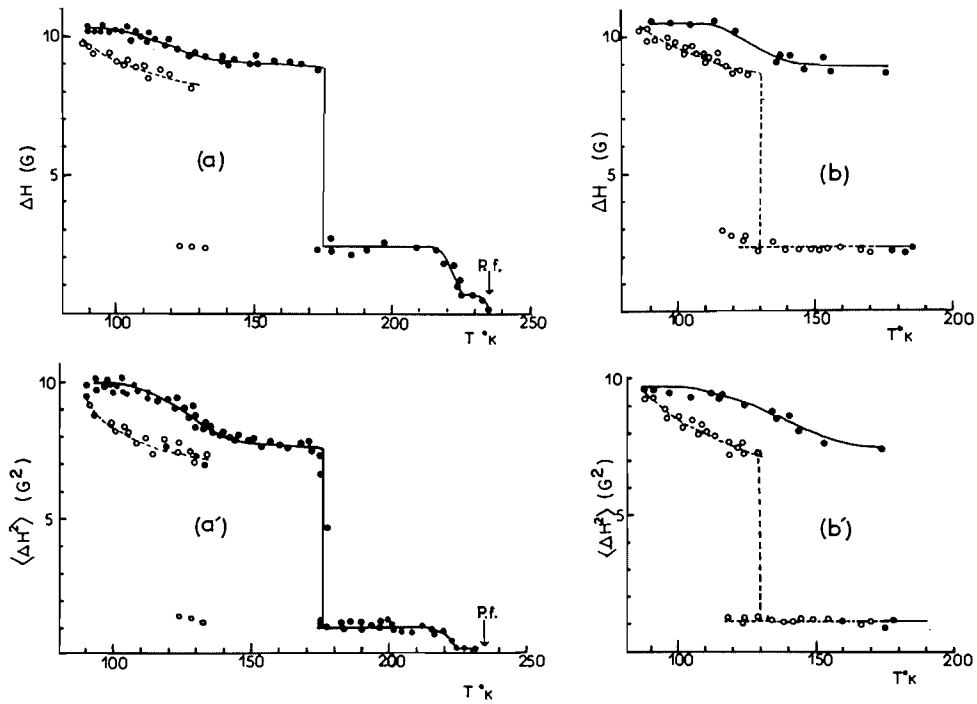

FIG. 1. Largeurs et seconds moments des spectres r.m.n. du PFMCH solide. Les figures *a* et *a'*, *b* et *b'* correspondent respectivement aux traitements thermiques A et B (voir paragraphe III, 2). En pointillés: courbes relatives aux phases métastables.

observée en r.m.n. que par réchauffement et que l'on enregistre transitoirement des spectres mixtes dont la composante étroite est semblable aux spectres obtenus entre 175 et 200 °K (Fig. 2*b* et *c*). Il nous paraît de même tout à fait probable que les paliers de 1.1 G^2 et de 0.1 G^2 correspondent aux phases II et I mentionnées précédemment.

Si l'on refroidit progressivement l'échantillon en partant de la phase II (méthode B) on constate que le palier de 1.1 G^2 caractéristique de cette phase persiste au-dessous de 173 °K, $\langle \Delta H^2 \rangle$ augmentant dans un intervalle de quelques degrés au voisinage de 130 °K pour rejoindre la courbe attribuée à la phase II' (Fig. 1*b'*).

Pour interpréter cet ensemble de résultats nous avons comparé les seconds moments des spectres de r.m.n. à des valeurs théoriques calculées à partir de différentes hypothèses sur la nature des mouvements moléculaires.

Pour un échantillon polycristallin en phase rigide l'expression du second moment d'un spectre de r.m.n. est (6, 7):

$$[1] \quad \langle \Delta H^2 \rangle = \tfrac{6}{5} I(I+1) g_N^2 \beta_N^2 N^{-1} \sum_{i>j} r_{ij}^{-6}$$

où I est le spin des noyaux dont on observe la résonance g_N le facteur de décomposition spectroscopique nucléaire, β_N le magnéton nucléaire, N est le nombre de noyaux en résonance dont on considère les interactions dipolaires et r_{ij} la distance qui sépare deux noyaux i et j. Dans le cas de fluors, l'expression [1] nous donne:

$$[2] \quad \langle \Delta H^2 \rangle (G^2) = 633.6 N^{-1} \times \sum_{i>j} r_{ij}^{-6}$$

La contribution intramoléculaire S_1 au second moment a été calculée pour différentes configurations du PFMCH en prenant r(C—C) = 1.54 Å, r(C—F) = 1.38 Å, $\angle$FCF = 109°28', valeurs indiquées dans la réf. 8. En supposant que CF_3 est bloqué en l'un des deux positions symétriques par rapport au cycle, qui sont sensiblement équivalentes, on trouve pour S_1: configuration chaise du cycle avec CF_3 équatorial: S_1 = 6.61 G^2; chaise avec CF_3 axial: S_1 = 9.89 G^2; bateau

Can. J. Chem. Downloaded from www.nrcresearchpress.com by 210.87.254.40 on 09/05/12
For personal use only.

Can. J. Chem. Downloaded from www.nrcresearchpress.com by 210.87.254.40 on 09/05/12
For personal use only.

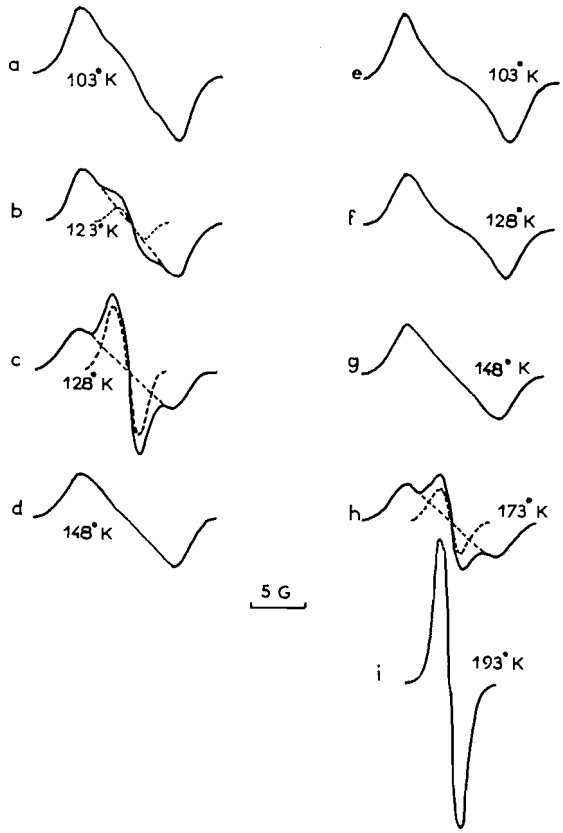

FIG. 2. Spectres r.m.n. du PFMCH solide. Les spectres *a* à *d* sont obtenus par trempe des échantillons (méthode A) et réchauffement continu. Les spectres *e*, *f*, *g* sont relatifs à la phase III, le spectre *h* à la transition III → II et le spectre *i* à la phase II.

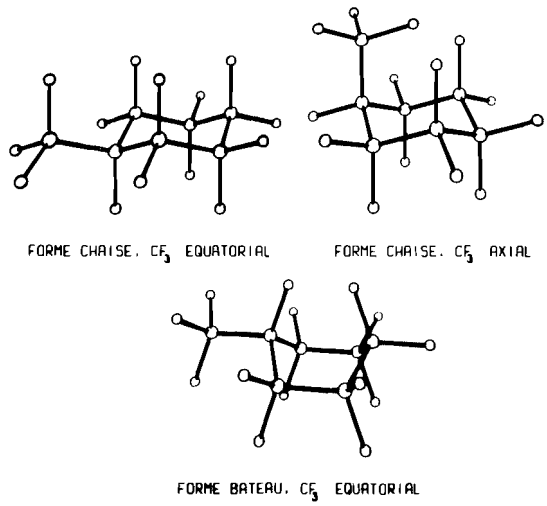

FIG. 3. Représentations moléculaires du PFMCH dessinées à l'aide du programme ORTEP (20) employé sur ordinateur UNIVAC 1108 et traceur de courbes Benson.

avec CF_3 équatorial: $S_1 = 9.87$ G^2. Ces trois configurations sont représentées sur la Fig. 3.

La configuration bateau avec CF_3 axial n'a pas été envisagée car elle amène presque en contact un fluor de CF_3 et un fluor du cycle. Il en est de même pour les formes bateaux asymétriques qui sont energétiquement défavorables (9). La valeur expérimentale maximum du second moment étant de 9.8 G^2, dont une fraction notable provient certainement de la contribution intermoléculaire S_2, nous ne retiendrons que la valeur $S_I = 6.6$ G^2 correspondant à la forme chaise avec CF_3 équatorial. Cette configuration est d'ailleurs celle du PFMCH en phase liquide (10).

Le calcul rigoureux du terme intermoléculaire S_2 n'a pu être effectué pour une phase rigide, faute de connaître la structure cristalline des phases III et II'. Nous avons cependant essayé d'évaluer S_2 à partir de deux approximations qui ont été utilisées dans le cas des molécules globulaires. L'approximation de Fratiello et Douglass (8) utilisée dans le cas du perfluorocyclohexane consiste à assimiler les molécules à des sphères à la surface desquelles les moments magnétiques sont uniformément répartis. Pour le PFMCH nous avons pris un rayon de sphère de 2.76 Å, déterminé d'après un modèle de Dreiding (11). La distance entre les centres de deux sphères voisines est alors: $R_i = 2 \times 2.76$ Å $+ 2 \times 1.35$ Å (rayon V. der Waals de F) $= 8.22$ Å. Cela nous donne une contribution à S_2 de 0.07 G^2 pour l'interaction entre les fluors de deux molécules voisines. Si l'on admet qu'une molécule est au maximum en contact avec douze voisines, on obtient $S_2 = 0.84$ G^2 au lieu de 9 8 G^2 − 6.6 G^2 = 3.2 G^2 (valeur expérimentale pour la phase III à 100 °K).

Dans l'autre approximation, proposée par Smith (12) on suppose une distribution des moments magnétiques continue au-delà d'une distance R du centre d'une molécule ce qui nous donne:

$$[3] \qquad S_2 \approx \tfrac{3}{5} I(I+1) g_N^2 \beta_N^2 \frac{4\pi}{3} \cdot \frac{N}{V} R^{-3}$$

où N est le nombre de fluors par maille de volume

Can. J. Chem. Downloaded from www.nrcresearchpress.com by 210.87.254.40 on 09/05/12
For personal use only.

V. La diffraction de rayons X indique pour la phase I un réseau cubique à 8 molécules par maille de volume $(13.2\ \text{Å})^3 = 2.3 \times 10^3\ \text{Å}^3$ et pour la phase II, un réseau quadratique à 24 molécules par maille de volume $13.2 \times (22.5)^2\ \text{Å}^3 = 6.67 \times 10^3\ \text{Å}^3$. Cela nous donne $N/V = 0.0487$ en phase I et $N/V = 0.0504$ en phase II. On peut admettre que pour les phases II′ et III le rapport N/V n'est pas très différent de celui des phases I et II, donc voisin de 0.05. En utilisant cette valeur dans la relation 3 avec $R = 2.76$ Å (rayon de la molécule), on obtient $S_2 = 3.15\ \text{G}^2$ en bon accord avec les valeurs expérimentales de $3.2 \pm 0.2\ \text{G}^2$ et de $3.0 \pm 0.2\ \text{G}^2$ déterminées pour les phases III et II′ au voisinage de 100 °K.

Nous allons maintenant calculer l'influence sur le second moment, de différents mouvements moléculaires. Quand un groupement ou une molécule dans son ensemble est en rotation autour d'un axe, l'expression du second moment devient (13):

$$[4]\quad \langle \Delta H^2 \rangle = \tfrac{6}{5} I(I+1) g_N^2 \beta_N^2 N^{-1} \times \sum_{i>j} \tfrac{1}{4}(3\cos^2 \gamma_{ij} - 1)^2 r_{ij}^{-6}$$

γ_{ij} étant l'angle entre un vecteur internucléaire r_{ij} et l'axe de rotation.

La contribution intramoléculaire de la forme chaise avec CF_3 équatorial ($S_1 = 6.61\ \text{G}^2$) comporte trois termes: interactions mutuelles des fluors de CF_3 bloqué $A_1 = 1.04\ \text{G}^2$, interaction CF_3—cycle $A_2 = 1.14\ \text{G}^2$, interactions mutuelles des fluors du cycle $A_3 = 4.43\ \text{G}^2$. La relation 4 permet de calculer que la rotation rapide de CF_3 autour de son axe ternaire réduit les deux premiers termes à $A_1' = 0.26\ \text{G}^2$ et $A_2' = 0.90\ \text{G}^2$, ce qui nous donne $S_1' = 5.59\ \text{G}^2$, A_3 demeurant inchangé. Le terme intermoléculaire S_2' a été calculé en admettant qu'il devient approximativement égal à

$$S_2 \times A_2'/A_2 = 3.2 \times 0.79\ \text{G}^2 = 2.53\ \text{G}^2$$

Le second moment théorique correspondant à la rotation de CF_3 est donc $\langle \Delta H^2 \rangle_{\text{calc}} = S_1' + S_2' = 8.12\ \text{G}^2$. Cette rotation rend compte en grande partie de la réduction du second moment expérimental qui décroît de $9.6 \pm 0.2\ \text{G}^2$ (100 °K) à $7.2 \pm 0.2\ \text{G}^2$ au voisinage des transitions II′ → III et III → II. La différence de $0.9 \pm 0.2\ \text{G}^2$ entre $\langle \Delta H^2 \rangle_{\text{calc}}$ et les valeurs expérimentales minima obtenues pour les phases III et II′ pourrait provenir de mouvements limités de rotation des molécules ou de la réorientation d'une partie d'entre elles, comme le laisse supposer l'existence de spectres mixtes au voisinage des points de transition (Fig. 2*b*, *c*, *h*).

Pour expliquer la diminution de 7 5 G^2 à 1.1 G^2 à la transition III → II (173 °K) nous avons envisagé la réorientation du PFMCH autour de l'axe pseudoternaire du cycle. Le terme intramoléculaire calculé est alors $S_1 = 0.92\ \text{G}^2$. Le terme intermoléculaire est évalué en supposant qu'il provient essentiellement de l'interaction entre molécules distantes de 8.22 Å de leurs deux plus proches voisines, suivant le même axe de rotation, les fluors étant "projetés" sur cet axe. Cette approximation nous donne $S_2 = 0.63\ \text{G}^2$ et donc $\langle \Delta H^2 \rangle_{\text{calc}} = 1.55\ \text{G}^2$. Pour une rotation du PFMCH selon son plus grand axe, on calcule $S_1 = 1.25\ \text{G}^2$ qui à elle seule dépasse la valeur expérimentale de $1.1\ \text{G}^2$ obtenue pour la phase II. La première de ces hypothèses paraît donc la plus vraisemblable.

Enfin dans le cas de la réorientation quasi-isotrope d'une molécule, le terme intramoléculaire s'annule, la contribution intermoléculaire pouvant être calculée en supposant les fluors groupés au centre de la molécule assimilée à une sphère (8):

$$[5]\quad \langle \Delta H^2 \rangle = S_2 = \tfrac{3}{5} I(I+1) g_N^2 \beta_N^2 N_0 \sum_i N_i R_i^{-6}$$

Nous avons vu qu'en phase I la maille est cubique ($a = 13.2$ Å) et contient huit molécules. En tenant compte par conséquent de l'interaction d'une molécule avec huit voisines et en prenant $R_i = 8.22$ Å comme précédemment on obtient $S_2 = 0.106\ \text{G}^2$ en accord avec la valeur expérimentale de $0.1 \pm 0.02\ \text{G}^2$ trouvée pour le second moment de la phase I. L'ensemble de nos valeurs expérimentales de $\langle \Delta H^2 \rangle$, comparées aux valeurs calculées (Tableau I) nous a donc permis de mettre en évidence trois mouvements moléculaires du PFMCH: la rotation de CF_3 en phases III et II′, la réorientation de l'ensemble de la molécule autour de l'axe pseudoternaire en phase II et la réorientation quasi isotrope en phase I.

La décroissance progressive de la largeur des spectres en phase III et II′ nous permet par ailleurs d'évaluer les fréquences de corrélation des mouvements moléculaires à partir de la relation (14, 15):

TABLEAU 1. Seconds moments des spectres r.m.n. du PFMCH

	Valeurs théoriques (G^2)			Valeurs expérimentales		
	S_1	S_2	$\langle \Delta H^2 \rangle$	T °K	Phase	$\langle \Delta H^2 \rangle$
Réseau rigide	6.61	3.18	9.79	100	III	9.8±0.2
				100	II′	9.6±0.2
Rotation CF_3	5.60	2.60	8.20	130	II′	7.2±0.2
				170	III	7.5±0.2
Réorientation autour de l'axe pseudoternaire du cycle	0.92	0.63	1.55	175–220	II	1.1±0.1
Réorientation quasi isotrope	0	0.10	0.10	225–232	I	0.1±0.02

$$[6] \quad \nu_c = \frac{\gamma}{16 \log_e 2} \Delta H \left[\tan \frac{\Delta H^2 - B^2}{C^2 - B^2} \cdot \frac{\pi}{2} \right]^{-1}$$

où ΔH est la largeur du spectre mesurée entre la maximum et le minimum de la dérivée d'absorption, B et C étant les valeurs limites de ΔH ($C > B$). Pour la phase II′ nous avons pris C = 9.8 G, B = 8.9 G et pour la phase III, C = 10.2 G, B = 9 G (*cf.* Fig. 1*a* et *b*). Le diagramme d'Arrhenius de ν_c donne respectivement pour les phases III et II′ les énergies d'activation E_1 = 5.5 kcal/mol et E_2 = 3.4 kcal/mol. Des mesures par écho de spin du temps de relaxation T_1, effectuées dans des conditions assez proches des nôtres (16) ont donné les énergies d'activation E_1' = 3.2 kcal/mol (phase III) et E_2' = 2.75 kcal/mol (phase métastable), de sorte que la valeur que nous avons trouvée pour E_1 paraît sujette à cautions.

(3) Résonance paramagnétique électronique

La structure hyperfine du spectre de 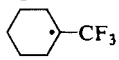 formé par irradiation γ du PFMCH est trop complexe pour permettre une étude détaillée des mouvements moléculaires de ce radical. Il a donc semblé préférable d'étudier le radical 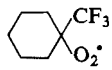 formé par irradiation du PFMCH en présence d'oxygène et dont le spectre ne dépend que de l'anisotropie de g. La peroxydation complète des radicaux 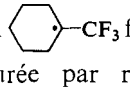 formés initialement à 77 °K est assurée par réchauffement progressif à 175–180 °K (phase II) et refroidissement rapide à 100 °K, dans le cryostat du spectromètre. On augmente ensuite la température de cinq en cinq degrés par paliers d'environ dix minutes en enregistrant les spectres. La recombinaison des radicaux devient rapide à partir de 160 °K ce qui exclut des mesures prolongées au-delà de cette température et donc l'usage de la méthode B utilisée pour les mesures de r.m.n.

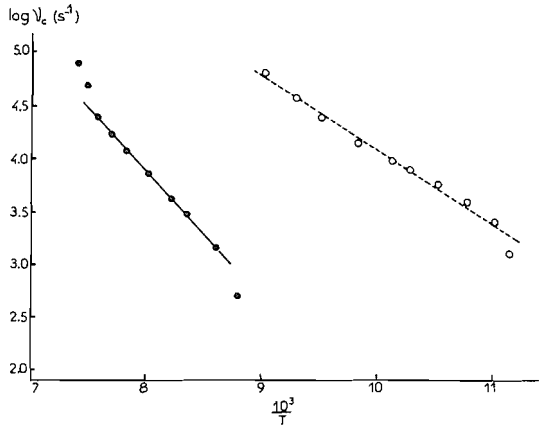

FIG. 4. Diagramme d'Arrhenius de la fréquence de corrélation de réorientation du PFMCH. En pointillés: phase II′, en traits pleins: phase III.

En phase II le spectre du radical peroxyle est une raie symétrique, centrée à g_{iso} = 2.0164 ± 0.0001 (Fig. 5*i*). Cette raie correspond soit à la réorientation isotrope du radical, soit comme on le verra plus loin, à la rotation simultanée du groupe C—O autour de la liaison C—O en position équatoriale, et du radical tout entier autour de l'axe pseudoternaire du cycle. A 77 °K par contre, en phase II′ ou III, le spectre de 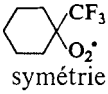 est caractéristique d'un tenseur g à symétrie axiale (17) avec $g_{\parallel}$ = 2.0395 ± 0.0001 (maximum du pic à champ faible) et $g_{\perp}$ = 2.00485 ± 0.0001 (minimum de la dérivée d'absorption du côté des champs élevés).

Au cours du réchauffement, le maximum du pic correspondant à $g_{\parallel}$ se déplace dans la direction

Can. J. Chem. Downloaded from www.nrcresearchpress.com by 210.87.254.40 on 09/05/12
For personal use only.

Can. J. Chem. Downloaded from www.nrcresearchpress.com by 210.87.254.40 on 09/05/12
For personal use only.

des champs élevés. La théorie de Kneubühl (17) permet d'attribuer ce déplacement aux mouvements de réorientation du radical. La valeur principale *apparente* $g_{\parallel}'$ est donnée en fonction du temps de corrélation de réorientation τ_c par la relation 7 que l'on peut déduire des relations 2 et 19 de la réf. 17:

$$[7] \quad g_{\parallel}'^2 = s + (g_{\parallel}^2 - s)\frac{2}{\pi}\arctan\left(\frac{\tau_c}{T_2}\right)$$

avec $s = (1/3)\,(g_{\parallel}^2 + 2g_{\perp}^2)$; s, a été calculé en prenant les valeurs principales du tenseur g déterminées d'après le spectre obtenu à 77 °K, en admettant que le radical soit bloqué à cette température. Le temps de relaxation dipolaire T_2 a été évalué à 10^{-8} s,[2] d'après la largeur de 13 G des gaussiennes élémentaires, qui donne le meilleur accord entre les spectres expérimentaux et les spectres reconstitués par calcul électronique en utilisant le programme de Lefebvre et Maruani (18) (Fig. 5*a* et *d*). $g_{\perp}'$ est donné en fonction de τ_c par une relation analogue à [7] mais sa variation est moins aisée à mesurer que celle de $g_{\parallel}'$.

$g_{\parallel}'$ et $g_{\perp}'$ convergent vers g_{iso} si le mouvement de réorientation du radical est isotrope. Si le mouvement se limite à la rotation de O—O autour de C—O, $g_{\parallel}'$ et $g_{\perp}'$ tendent respectivement vers

$$[8] \quad \begin{aligned} g_{\parallel}^{rot} &= g_{\parallel} - (g_{\parallel} - g_{\perp})\sin^2\alpha \\ g_{\perp}^{rot} &= \tfrac{1}{2}(3g_{iso} - g_{\parallel}^{rot}) \end{aligned}$$

α étant l'angle C—O—O. Pour $\alpha = 120°$ on obtient ainsi $g_{\parallel}^{rot} = 2.0135$ et $g_{\perp}^{rot} = 2.0178$.

Si enfin la rotation de O—O autour de C—O et la réorientation de tout le radical autour de l'axe pseudoternaire du cycle se produisent simultanément, $g_{\parallel}^{rot}$ et $g_{\perp}^{rot}$ demeurent inchangés pour une liaison C—O en position axiale ou deviennent respectivement égaux à 2.0167 et à 2.0162 si C—O est équatorial. Dans ce second cas, le spectre se confond pratiquement, étant donné la largeur de raie, avec le spectre de 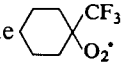

[2]Cette valeur de T_2 n'est donnée qu'à titre indicatif, la valeur exacte aurait pu être déterminée par des mesures de saturation progressive qu'il n'a pas été possible d'effectuer étant donné que le signal des radicaux peroxyles ne se sature pas à 77 °K, même à la puissance hyperfréquence maximum que nous pouvons utiliser (250 mW à la cavité).

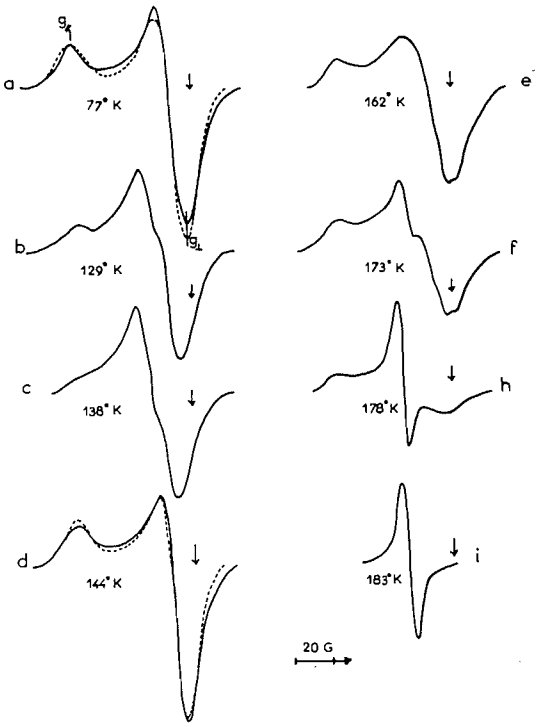

FIG. 5. Spectres r.p.e. des radicaux 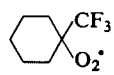

piégés dans le PFMCH. Les spectres *a* à *d* sont obtenus par trempe des échantillons après recuit en phase II et réchauffement continu. Les spectres *a* et *d* sont superposés aux spectres calculés (en pointillés) en prenant respectivement $g_{\parallel} = 2.03950$, $g_{\perp} = 2.00485$, $\lambda = 13.5$ G et $g_{\parallel} = 2.0380$, $g_{\perp} = 2.0056$, $\lambda = 13$ G. Les flèches verticales correspondent à $g_0 = 2.0028$, $H_0 = 3300$ G.

en réorientation isotrope. Il n'est pas exclu que cela se produise en phase II.

On peut constater sur la Fig. 6 que pour des échantillons trempés á 100 °K après recuit en phase II, $g_{\parallel}'$ décroît continuellement entre 100 et 130 °K et augmente dans un intervalle de quelques degrés au voisinage de 130 °K (courbe en pointillés). La relation 7 indique que cette augmentation est liée à un ralentissement des mouvements moléculaires. Si l'on refroidit de nouveau l'échantillon à 100 °K et qu'on le réchauffe ensuite à 160–170 °K, la décroissance de $g_{\parallel}'$ est continue et réversible (Fig. 6, courbe en trait plein). La comparaison des résultats de r.p.e. avec ceux de r.m.n. permet d'attribuer la première de ces courbes à la phase métastable II′, l'augmentation abrupte de $g_{\parallel}'$ à la transition II′ → III et la courbe en trait plein à la phase stable III.

Can. J. Chem. Downloaded from www.nrcresearchpress.com by 210.87.254.40 on 09/05/12
For personal use only.

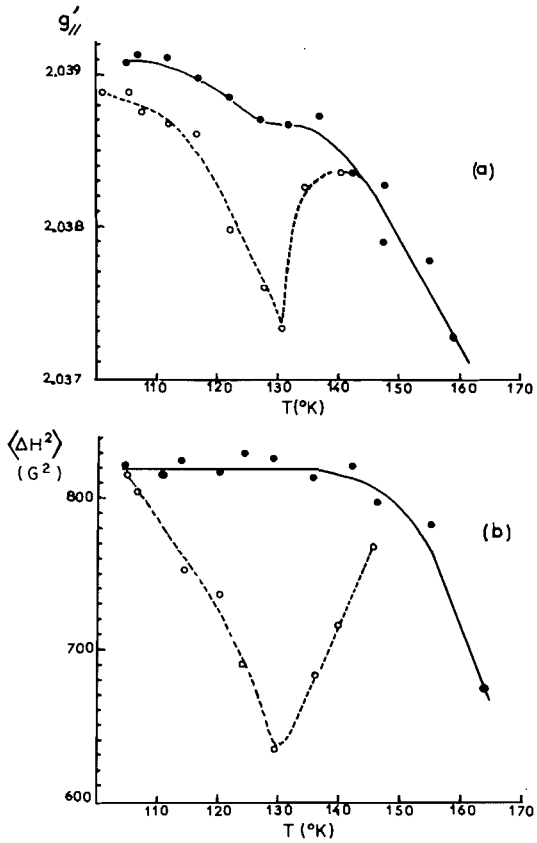

FIG. 6. Variation avec la température de $g_{\parallel}'$ (diagramme *a*) et du second moment des spectres r.p.e. de 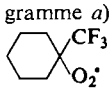 (diagramme *b*). En pointillés: phase II′ et transition II′ → III.

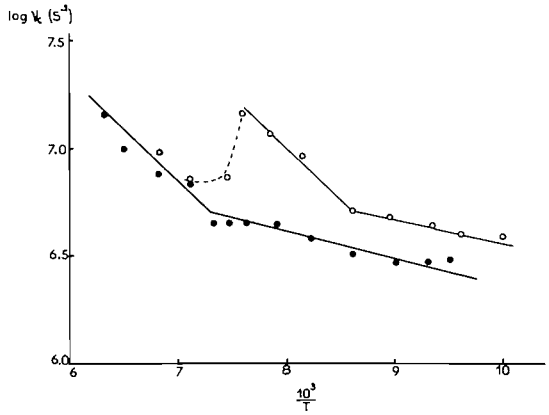

FIG. 7. Diagramme d'Arrhenius de la fréquence de corrélation de réorientation des radicaux peroxyles. ○ réchauffement continu après trempe à 77 °K des échantillons recuits en phase II. ●, phase III. En pointillés: transition II′ → III.

La relation 7 permet par ailleurs d'évaluer les temps de corrélation de réorientation et les énergies d'activation correspondantes pour les phases III et II′. Le diagramme d'Arrhenius de ν_c donne pour chacune de ces phases deux énergies d'activation $E_1 = 0.5 \pm 0.1$ kcal/mol et $E_2 = 2.5 \pm 0.2$ kcal/mol.

Dans le domaine de température étudié, la variation de $g_{\parallel}'$ est trop restreinte pour permettre de caractériser les mouvements moléculaires auxquels correspondent ces énergies d'activation. On peut noter cependant que E_1 est du même ordre de grandeur que celle trouvée par Sohma (19) pour la rotation de O—O autour de C—O dans le cas du radical ~~CF_2—$\underset{\displaystyle O_2^{\cdot}}{\overset{|}{CF}}$—$CF_2$~~ du téflon. L'énergie d'activation E_2 nous semble attribuable à la réorientation globale du radical 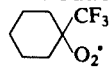 puisqu'elle se manifeste au voisinage des transitions II′ → III et III → II qui sont accompagnées d'une réorganisation du réseau. Le spectre "isotrope" de ce radical est effectivement observable en phase III à partir de 165 °K (Fig. 5) et parfois vers 130 °K à la transition II′ → III.

Nous avons également étudié la variation du deuxième moment $\langle \Delta H^2 \rangle$ des spectres de 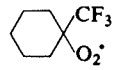 en fonction de la température. Pour un radical peroxyle, le second moment dépend essentiellement de l'anisotropie de g et a pour expression (18):

$$[9] \quad \langle \Delta H^2 \rangle \approx \frac{H_0^2}{5}(\varepsilon_{\parallel}^2 + \tfrac{8}{3}\varepsilon_{\perp}^2 + \tfrac{4}{3}\varepsilon_{\parallel}\varepsilon_{\perp}) + \frac{\lambda^2}{4}$$

où H_0 est la valeur du champ magnétique par rapport à laquelle on mesure $\langle \Delta H^2 \rangle$ soit dans le cas présent 3320 G pour $g_0 = 2.0028$. $\varepsilon_{\parallel}$ et $\varepsilon_{\perp}$ sont respectivement égaux à $g_{\parallel}'/g_0 - 1$ et à $g_{\perp}'/g_0 - 1$. Le terme $\lambda^2/4$ représente la contribution de la largeur de raie soit 42 G^2 pour $\lambda = 13$ G. Le premier terme de la relation 9 est largement prédominant puisqu'il peut varier de 800 G^2 pour un radical bloqué à 508 G^2 ou 511 G^2 pour la réorientation isotrope du radical et la seule rotation du groupe peroxyle.

Comme on peut le prévoir la variation de $\langle \Delta H^2 \rangle$ avec la température présente quelque

TABLEAU 2. Seconds moments des spectres r.p.e. de 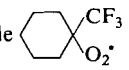

	Phase II′		Transition II′ → III		Phase III	
T (°K)	$\langle\Delta H^2\rangle$ (G²)	$\langle g_{\parallel}'\rangle$*	$\langle\Delta H^2\rangle$	$\langle g_{\parallel}'\rangle$	$\langle\Delta H^2\rangle$	$\langle g_{\parallel}'\rangle$
105	817	2.0387				
106					806	2.0382
109	748	2.0356				
111					817	2.0387
114	753	2.0358			826	2.0390
120	737	2.0350			819	2.0387
124	689	2.0325			830	2.0392
129	633	2.0290			827	2.0390
133			704	2.0340		
136			684	2.0322		
140			718	2.0342		
142			769	2.0366	822	2.0388
146					799	2.0380
155					784	2.0373
164					673	2.0316

*Valeurs calculées par la relation 9 avec $\lambda^2/4 = 42$ G².

analogie avec celle de $g_{\parallel}'$ (Fig. 6) en particulier pour la transition entre les phases II′ et III qui se traduit par un accroissement de $\langle\Delta H^2\rangle$. Le Tableau 2 donne quelques valeurs des seconds moments des spectres r.p.e. et les valeurs moyennes $\langle g_{\parallel}'\rangle$ que l'on peut en déduire par la relation 9.

Bien que les mesures de $\langle\Delta H^2\rangle$ ne soient pas très précises (reproductibilité de 3 à 5%), on peut noter dans la Fig. 6 et le Tableau 1 que pour la phase III les valeurs de $\langle g_{\parallel}'\rangle$ sont proches de celles de $g_{\parallel}'$ déduites directement des spectres. Pour la phase II′ et au voisinage de la transition III → II par contre, les valeurs de $\langle g_{\parallel}'\rangle$ sont systématiquement inférieures à celles de $g_{\parallel}'$. Nous attribuons cette différence à une large distribution des temps de corrélation dont le maximum correspond vraisemblablement à $g_{\parallel}'$. Il n'est effectivement pas possible, en prenant une seule valeur pour $g_{\parallel}'$ et pour $g_{\perp}'$ de reproduire par calcul électronique les spectres de la phase II′, entre 115 et 130 °K.

La dispersion des temps de corrélation est vraisemblablement liée à l'existence d'un spectre d'énergies d'activation de réorientation. En supposant que ce spectre soit une gaussienne de demi largeur σ:

$$[10]\quad N(E) = \frac{1}{\sigma\sqrt{2\pi}} \exp\left[-\frac{(E-E_0)^2}{2\sigma^2}\right]$$

On obtient pour $\tau = \tau_1 \exp(E/RT)$, la fonction de distribution:

$$[11]\quad N(\tau) = \frac{RT}{\sigma\sqrt{2\pi}} \exp\left[-\frac{R^2T^2}{2\sigma^2}\left(\log_e \frac{\tau}{\tau_0}\right)^2\right]$$

Soit $M_2(\tau)$ le second moment du spectre r.p.e. correspondant à une valeur unique de $g_{\parallel}'$ et de $g_{\perp}'$ donc de τ, la valeur du second moment correspondant à la distribution $N(\tau)$ est:

$$[12]\quad \langle\Delta H^2\rangle = \int_0^{\infty} M_2(\tau)N(\tau)\,d\tau$$

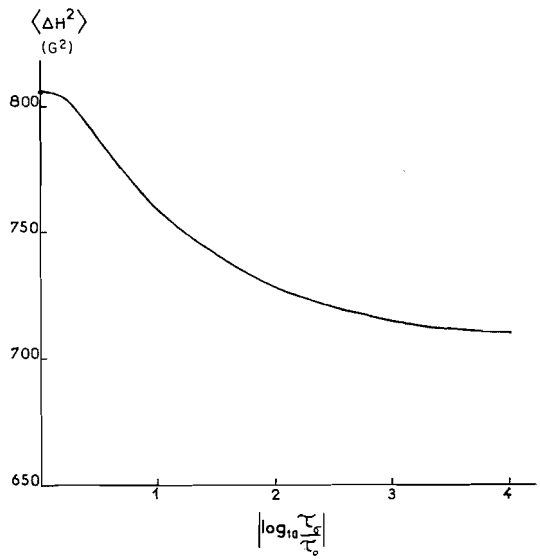

FIG. 8. $\langle\Delta H^2\rangle$ en fonction de la largeur de distribution des temps de corrélation $|\log_{10}\tau/\tau_0| = 0.43\,\sigma/RT$, pour $g_{\parallel}' = 2.0380$ ($\tau_0 = 10^{-7}$ s).

Can. J. Chem. Downloaded from www.nrcresearchpress.com by 210.87.254.40 on 09/05/12
For personal use only.

Can. J. Chem. Downloaded from www.nrcresearchpress.com by 210.87.254.40 on 09/05/12
For personal use only.

$M_2(\tau)$ pouvant être calculé à partir des relations 7 et 9 (Fig. 8).

A titre d'exemple, nous avons trouvé pour la phase II′ à 122 °K: $g_{\parallel}' = 2.0380$, $\tau_0 = 10^{-7}$ s ($M_2(\tau_0) = 806$ G^2). Le second moment expérimental est $\langle \Delta H^2 \rangle = 715$ G^2, ce qui nous donne $\sigma = 1.7$ kcal/mol ($E_0 = 2.5$ kcal/mol) et $\sigma/RT = 7$. Cette dernière valeur correspond à des temps de corrélation répartis entre 10^{-10} et 10^{-4} s.

IV. Conclusions

Les expériences de r.m.n. et de diffraction de rayons X confirment l'existence de trois phases thermodynamiquement stables entre 77 °K et le point de fusion, ainsi que celle d'une phase métastable que l'on peut piéger au dessous de 130 °K.

La comparaison des résultats de r.m.n. et de r.p.e. indique l'existence d'une corrélation entre les mouvements des radicaux et ceux des molécules de la matrice. Nous avons ainsi montré qu'en phase I les molécules de PFMCH sont en réorientation quasi-isotrope et il en est de même pour les radicaux 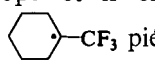 piégés dans cette phase (1). En phase II les molécules sont en rotation autour de l'axe pseudo-ternaire du cycle et l'on a vu que le spectre r.p.e. des radicaux peroxyles est interprétable par la composition de ce mouvement avec la rotation du groupe en position equatoriale. Enfin dans les phases II′ (métastable) et III on peut admettre que l'on observe en cours de réchauffement, d'abord les rotations intramoléculaires (de CF_3 ou de COO), puis la réorientation, probablement limitée, des molécules ou des radicaux, au voisinage des transitions II′ → III et III → II.

On peut noter sur les Figs. 4 et 7 que pour une même phase et une même température, les temps de corrélation de réorientation sont très différents pour les molécules de la matrice et pour les radicaux qui y sont piégés. Il est possible que les radicaux soient formés préférentiellement dans les défauts du réseau et possèdent de ce fait une plus grande liberté de réorientation que les molécules de la matrice. Plus vraisemblablement, cette différence apparente entre les temps de corrélation est inhérente aux méthodes de mesures, la r.m.n. étant utilisable dans le domaine $10^{-6} < \tau_c < 10^{-4}$ s et la r.p.e. dans le domaine $10^{-9} < \tau_c < 10^{-6}$ s. La possibilité de mesurer τ_c par ces deux méthodes, dans des conditions expérimentales indentiques, nous paraît la conséquence d'une très large distribution des temps de corrélation de réorientation, dans la phase métastable ainsi qu'au voisinage des points de transition.

L'un des auteurs (C.C.) remercie M. Sohma Professeur à l'Université d'Hokkaido pour lui avoir communiqué le prétirage d'un article (19) ainsi que M. Rigny, ingénieur au C.E.A., qui lui a fait connaître les résultats de mesures de relaxation effectuées dans son laboratoire (16).

1. C. Chachaty, A. Forchioni et M. Shiotani. Can. J. Chem. **48**, 435 (1970).
2. A. Dworkin. C.R. Acad. Sci. Paris, C **269**, 473 (1969).
3. M. Renaud et R. Fourme. Acta Cryst. **22**, 695 (1967).
4. C. Brot. Comptes Rendus du Xè Colloque Ampère, Leipzig, 1961. North Holland Publ., Amsterdam, 1962. p. 318.
5. M. Renaud et R. Fourme. Bull. Soc. Fr. Minér. Crist. **89**, 243 (1966).
6. J. H. Van Vleck. Phys. Rev. **74**, 1168 (1948).
7. H. S. Gutowsky, G. B. Kistiakowsky, G. E. Pake et E. M. Purcell. J. Chem. Phys. **17**, 972 (1949).
8. A. Fratiello et D. C. Douglass. J. Chem. Phys. **41**, 974 (1964).
9. J. Neel. J. Chim. Phys. **61**, 1381 (1964).
10. K. W. Jolley, L. H. Sutcliffe et S. M. Walker. Trans. Faraday Soc. **64**, 269 (1968).
11. A. S. Dreiding. Helv. Chim. Acta, **42**, 1399 (1959).
12. G. W. Smith. J. Chem. Phys. **42**, 4229 (1965).
13. H. S. Gutowsky et G. E. Pake. J. Chem. Phys. **18**, 162 (1950).
14. N. Bloembergen, E. M. Purcell et R. V. Pound. Phys. Rev. **73**, 679 (1948).
15. R. Kubo et K. Tomita. J. Phys. Soc. Jap. **9**, 888 (1954).
16. J. Garcin. Thèse de 3è Cycle, Université de Montpellier, 1970.
17. F. K. Kneubühl. J. Chem. Phys. **33**, 1074 (1960).
18. R. Lefebvre et J. Maruani. J. Chem. Phys. **42**, 1480 (1965).
19. S. Moriuchi, N. Nakamura, S. Shimada, H. Kashiwabara et J. Sohma. Polymer, **11**, 630 (1970).
20. C. K. Johnson. ORTEP, ORNL 3794 (1965).

Can. J. Chem. Downloaded from www.nrcresearchpress.com by 210.87.254.42 on 09/05/12
For personal use only.

Synthesis and Novel Rearrangement of 1,1,1-Trichloro-2-alken-4-ones

EBERHARD KIEHLMANN, PUI-WAH LOO, B. C. MENON, AND NORA MCGILLIVRAY
Department of Chemistry, Simon Fraser University, Burnaby 2, British Columbia

Received March 31, 1971

Strong mineral acids convert 1,1,1-trichloro-2-hydroxy-4-alkanones to 1,1,1-trichloro-2-alken-4-ones and 1,1,5-trichloro-1-alken-4-ones via an intramolecular chlorine shift from C-1 to -5 of an enol allylic system. Alternatively, 1,1,1-trichloro-2-alken-4-ones may be synthesized from 1,1,1-trichloro-2-hydroxy-4-alkanones by acetylation and elimination of acetic acid or by nucleophilic substitution with thionyl chloride followed by dehydrohalogenation. The two diastereomeric 1,1,1-trichloro-2-hydroxy-3-methyl-4-hexanones do not epimerize during acetylation, and the *erythro*-acetate resists elimination of acetic acid. Pyrolysis of 2-(1-hydroxy-2,2,2-trichloroethyl-)cyclohexanone yields 2-(2,2-dichlorovinyl)-2-cyclohexenone while treatment of 1,1,1,7,7,7-hexachloro-2,6-dihydroxy-4-heptanone with strong acid leads to the formation of 1,1,1,7,7,7-hexachloro-2,5-heptadien-4-one.

Des acides minéraux forts transforment les trichloro-1,1,1 hydroxy-2 alcanones-4 en trichloro-1,1,1 alcène-2 ones-4 et en trichloro-1,1,5 alcène-1 ones-4 par déplacement intramoléculaire du chlore du carbone en position 1 sur le carbone en position 5 d'un système énol allylique. Alternativement, les trichloro-1,1,1 alcène-2 ones-4 peuvent être synthétisés à partir des trichloro-1,1,1 hydroxy-2 alcanones-4 soit par acétylation et élimination de l'acide acétique soit par substitution nucléophile avec le chlorure de thionyle suivie d'une déshydrohalogénation. Il n'y a pas épimérisation au cours de l'acétylation des deux trichloro-1,1,1 hydroxy-2 méthyl-3 hexanones-4 diastéréoisomères et l'acétate érythro résiste à l'élimination de l'acide acétique. Le pyrolyse de la (hydroxy-1 trichloroéthyl-2,2,2)-2 cyclohexanone conduit à la (dichloro-2,2 vinyl)-2 cyclohexène-2 one tandis que le traitement de la hexachloro-1,1,1,-7,7,7 dihydroxy-2,6 heptanone-4 avec un acide fort n'amène pas la formation d'hexachloro-1,1,1,7,7,7 heptadiène-2,5 one-4.

Canadian Journal of Chemistry, 49, 2964 (1971)

In the course of our studies of the acetate-catalyzed crossed aldol condensation of chloral with aliphatic ketones in acetic anhydride (1) or glacial acetic acid (2) we observed that this reaction is not accompanied by dehydration of the resulting 1,1,1-trichloro-2-hydroxy-4-alkanones. The low tendency of trichloromethyl-substituted β-ketols to eliminate water (3) parallels the inertness of trichloromethylcarbinols in substitution reactions (4, 5) which has been attributed to the strengthening of the O-alkyl bond by the inductive electron-withdrawing effect of the three chlorine atoms attached to the adjacent carbon (6, 7). Since our attempts to effect the desired elimination reaction under mild neutral conditions using the recently recommended dicyclohexylcarbodiimide (8) in ether solution were not successful and since trichloromethylcarbinols are sensitive to strong base (9), we investigated the synthesis of the title compounds in neutral or acidic solution by three methods involving the conversion of the hydroxy group of the corresponding β-ketols to a better leaving group: protonation, acetylation, and replacement by chlorine.

Results and Discussion

1,1,1-Trichloro-2-penten-4-one has been prepared as early as 1893 (10) by heating acetone and chloral in a sealed tube, and a few years later (11) by treatment of 1,1,1-trichloro-2-hydroxy-4-pentanone with cold concentrated sulfuric acid. However, attempts by Auwers and Schmid (3) to prepare trichlorocrotonic acid from 4,4,4-trichloro-2-hydroxybutanoic acid under similar reaction conditions were unsuccessful. Baluja and coworkers (12, 13) have reported the synthesis of four 1,1,1-trichloro-2-alken-4-ones by pyrolysis of the corresponding β-ketols in molten potassium bisulfate and pointed out that prolonged thermal treatment leads to isomerization and fragmentation reactions.

Adopting a procedure previously described (14) for the dehydration of 1,1,1-trichloro-2-hydroxy-6-phenyl-5-hexen-4-one, we selected initially benzene (or toluene) and *p*-toluenesulfonic acid (TsOH) as solvent and catalyst, respectively. Although the expected 1,1,1-trichloro-4-phenyl-2-buten-4-one was formed in high yield from the corresponding phenyl-substituted ketol, application of this procedure to

[1] $\underset{a}{RCH_2COCHR'—CHOH—CCl_3} \xrightarrow{H^{\oplus}} \underset{b}{RCH_2COCR'=CH—CCl_3} + \underset{c}{RCHCl—CO—CHR'—CH=CCl_2}$

1 R = Et; R′ = H; **2** R = *i*-Pr; R′ = H; **3** R = R′ = Me

[2] $\underset{b}{R—CO—CH=CH—CCl_3} \xrightarrow[SiO_2]{\Delta} \underset{d}{R—CO—CHCl—CH=CCl_2}$

4 R = *t*-Bu; **5** R = CH_3; **6** R = C_6H_5

purely aliphatic 1,1,1-trichloro-2-hydroxy-4-alkanones of the general structure RCH_2COCHR'-$CHOHCCl_3$ (*a*) yielded discolored reaction mixtures containing in each case two isomeric olefins and a substantial quantity of unreacted starting material. Separation and spectroscopic analysis showed these two products to be the desired 1,1,1-trichloro-2-alken-4-one (*b*) and the corresponding isomeric 1,1,5-trichloro-1-alken-4-one (*c*, eq. 1). Treatment of *a* with molten potassium bisulfate (13) or with refluxing acetic acid containing a trace of sulfuric acid as catalyst gave similar results (Table 1). In the latter case, *c* was found to be the major product after prolonged reflux of the reaction mixture while flash pyrolysis over $KHSO_4$ yielded predominantly *b*. Starting from pure 1,1,1-trichloro-6-methyl-2-hepten-4-one (**2***b*), glacial acetic acid and sulfuric acid, isomerization to 1,1,5-trichloro-6-methyl-1-hepten-4-one (**2***c*) was observed after 6 h at 100°. These observations indicate that *c* is formed by a stepwise dehydration–rearrangement sequence. Close examination of the n.m.r. spectra of several crude product mixtures obtained from the crossed aldol condensation of chloral with dialkyl ketones in glacial acetic acid without added base catalyst (2) revealed that 1,1,5-trichloro-1-alken-4-ones (*c*) constitute the main by-product (<10%) formed under these conditions. All attempts to prepare 1,1,5-trichloro-1-penten-4-one by acid-catalyzed dehydration of 1,1,1-trichloro-2-hydroxy-4-pentanone or rearrangement of 1,1,1-trichloro-2-penten-4-one failed.

The structure assignments for the rearrangement products are based on their n.m.r. spectroscopic analysis. The olefinic protons of **1***c*, **2***c*, and **3***c* appeared at τ 3.93 (triplet), 3.89 (triplet), and 4.17 (two overlapping doublets, due to the existence of two diastereomeric structures), respectively, and were coupled to the protons of the adjacent carbon (**1***c*: τ 6.45, doublet, 2H; **2***c*: 6.43, doublet 2H; **3***c*: 6.01, multiplet, 1H). The protons attached to the chloro-substituted carbon atoms absorbed at τ 5.83 (triplet, **1***c*), 5.93 (doublet, **2***c*) and 5.60 (quartet, **3***c*) and were coupled to their respective vicinal protons (**1***c*: τ 8.10, multiplet, 2H; **2***c*: 7.62, multiplet, 1H; **3***c*: 8.40, doublet, 3H) with a coupling constant of 6.5 Hz. Although the fine-splitting of several peaks due to the non-equivalence of methylene protons near the asymmetric centers of **1***c* and **2***c* has not been taken into account in this simple first-order analysis, these chemical shifts and peak multiplicities are clearly inconsistent with the spectral parameters observed for **1***b*, **2***b*, and **3***b* (see Table 3) or with the pattern expected for the products of an allylic shift of chlorine (15) from C-1 of *b* to C-3 (see below).

To verify our structure assignments, we subjected several 1,1,1-trichloro-2-alken-4-ones (*b*) to those reaction conditions which have recently been reported (15) to lead to allylic rearrangements. These experiments confirmed the results obtained by Takeda for the silica-catalyzed rearrangment of methyl and phenyl 3,3,3-trichloro-1-propenyl ketone and showed that the corresponding tert-butyl alkenone **4***b* undergoes an analogous reaction (eq. 2). The co-product of acid-catalyzed dehydration of **4***a* described by Baluja (13) as the *cis*-isomer on the basis of i.r. absorption at 670 to 690 cm^{-1} (no n.m.r. or u.v. data reported) was actually found to be identical with the allylic isomer **4***d*. On the other hand, pyrolysis of **2***b* and **7***b* on silica did not lead to an analogous allylic shift but gave the 1,5-rearrangement products **2***c* and **7***c* shown in eq. 3 (see also eq. 1). The spectroscopic data observed for the previously described (16) 1,1-dichloro-6-methyl-1-hepten-4-one (n.m.r. τ 3.82 triplet for $—CH=CCl_2$ and 6.60 doublet for $—COCH_2$-$CH=CCl_2$; i.r. bands at 1625 and 1720 cm^{-1}; u.v. absorption maxima at 206 (ε 4700) and 273 nm (ε 150)) are very similar to those found for **2***c* thus providing further support for our structure assignment.

Although thermal allylic rearrangements of

Can. J. Chem. Downloaded from www.nrcresearchpress.com by 210.87.254.42 on 09/05/12
For personal use only.

Can. J. Chem. Downloaded from www.nrcresearchpress.com by 210.87.254.42 on 09/05/12
For personal use only.

TABLE 1. Reaction of 1,1,1-trichloro-2-hydroxy-4-alkanones with strong acids

Ketol structure (Q = —CHOH—CCl_3)	Solvent	Acid	Reaction temperature (°C)	Reaction time (h)	Product composition* (%)			
					Dehydration product *b*	Rearrangement product *c*	Starting material *a*	Other
C_6H_5—$COCH_2Q$	$C_6H_5CH_3$	TsOH	110	9.5	90	—	10	—
CH_3COCH_2Q	HOAc	H_2SO_4	100	44	42	—	50	8
$CH_3CH_2CH_2COCH_2Q$	C_6H_6	TsOH	80	24	33	46	21	—
do.	HOAc	H_2SO_4	100	24	6	58	30	6
CH_2CH_2COCHQ—CH_3†	HOAc	H_2SO_4	100	52	2	25	71	2
$(CH_3)_2CHCH_2COCH_2Q$	C_6H_6	TsOH	80	24	39	31	30	—
do.	HOAc	H_2SO_4	100	24	5	55	30	10
do.	—	$KHSO_4$	230	0.1	70	23	7	—
do.	—	$KHSO_4$	130	2	30	52	—	18
QCH_2COCH_2Q‡	C_6H_6	TsOH	110	17	90§	—	10	—

*Determined by v.p.c. of the crude product mixture on a 5 ft × 1/8 in. OV-17 column (110°).
†The *erythro*-compound initially used was found to epimerize under these conditions.
‡The m.p. 157–158°.
§Cl_3C—CH=CH—CO—CH=CH—CCl_3.

[3] $$R{-}CH_2{-}CO{-}CH = CH{-}CCl_3 \rightarrow R{-}CHCl{-}CO{-}CH_2{-}CH = CCl_2$$
(b, c)
$$R{-}CH_2{-}CO{-}CHCl{-}CH = CCl_2$$

2 R = *i*-Pr; 7 R = *t*-Bu

[4] $RCH_2COCH_2{-}CHOH{-}CCl_3$ (a)

$\downarrow H^{\oplus}$

$RCH_2COCH{=}CH{-}CCl_3$ (b) $\qquad$ $RCHCl{-}CO{-}CH_2{-}CH{=}CCl_2$ (c)

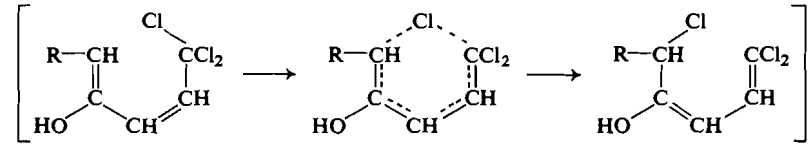

[5] 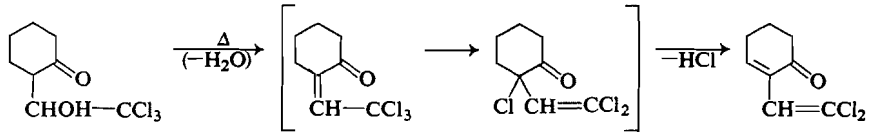

8*a*

1,1,1-trichloro-2-alkenes in the presence or absence of metal or metal oxide catalysts have been described by other authors (17–19), the shift of a chlorine atom from the γ- to the α′-position of an α,β-unsaturated ketone has to our knowledge not been reported before. Ohse *et al.* (20) observed thermal isomerization of trichlorocrotonic acid to 2,4,4-trichloro-3-butenoic acid in 90% yield while LeCoq (21) did not detect any 2,4,4-trichloro-3-butenal after prolonged heating of trichlorocrotonaldehyde in the presence of Lewis acids. We believe that acid-catalyzed enolization of *b* to form an enol allylic chloride (22) and the close proximity of the bulky trichloromethyl group to the α′-methylene carbon in certain conformations of this molecule are the major driving forces for a [1,5] sigmatropic transfer of chlorine which is presumed to be a thermally allowed suprafacial process (23) if orbital symmetry is to be conserved during the reaction (eq. 4).

The formation of 2-(2,2-dichlorovinyl)-2-cyclohexenone (eq. 5) by thermal decomposition of 2-(1-hydroxy-2,2,2-trichloroethyl)-cyclohexanone (**8***a*) during distillation appears to confirm this view. Since in this case the trichloromethyl group of the originally formed dehydration product cannot adopt a position favorable for a chlorine shift to the α′-carbon via a six-membered ring transition state, normal allylic rearrangement and elimination of hydrogen chloride lead to the observed product.

The acid-catalyzed dehydration of 1,1,1,7,7,7-hexachloro-2,6-dihydroxy-4-heptanone (**9***a*) in refluxing toluene was found to proceed without allylic rearrangement giving the highly conjugated, yellow 1,1,1,7,7,7-hexachloro-2,5-heptadien-4-one (**9***b*) in good yield (eq. 6).

Confirming and supplementing recently published data by Bowman and Williamson (24) we wish to report that **9***a* exists in two diastereomeric forms, and that both diastereomers (m.p. 119–121°, crystallized from chloroform; m.p. 157–158°, crystallized from ethanol) rather than the previously claimed (25) tetrahydro-2,5-bis(trichloromethyl)-4*H*-pyran-4-one are formed in the

Can. J. Chem. Downloaded from www.nrcresearchpress.com by 210.87.254.42 on 09/05/12
For personal use only.

[6]

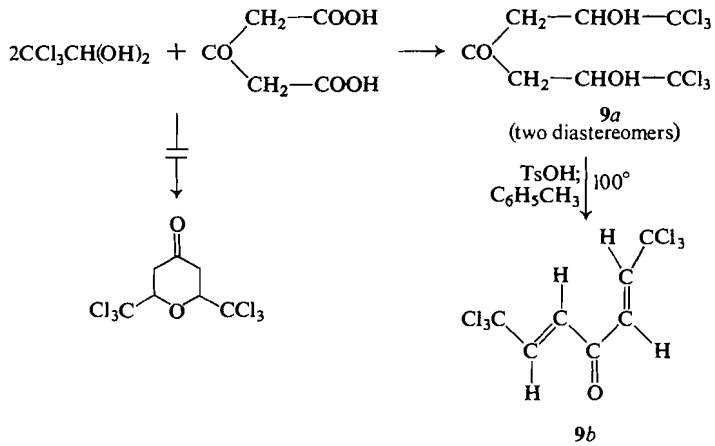

[7]

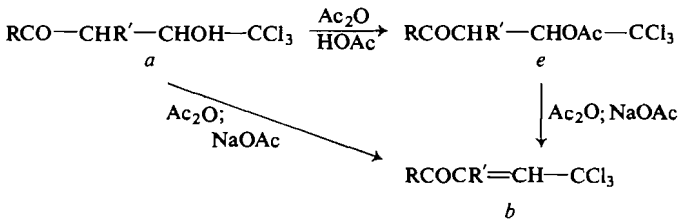

1 R = *n*-Pr; R′ = H
2 R = *i*-Bu; R′ = H
3 R = Et; R′ = Me
4 R = *t*-Bu; R′ = H
5 R = Me; R′ = H
7 R = *t*-BuCH$_2$; R′ = H
8 R = R′ = —(CH$_2$)$_4$—

condensation of chloral hydrate with acetonedicarboxylic acid.

A more satisfactory method for the preparation of 1,1,1-trichloro-2-alken-4-ones consists of the acetylation-elimination sequence shown in eq. 7. Auwers (3) used this procedure for the preparation of trichlorocrotonic acid from 4,4,4-trichloro-3-hydroxybutanoic acid. Our results of several acetylation experiments are summarized in Table 2. Although acetylation proceeds smoothly in refluxing acetic anhydride, only traces of ketol acetates *e* were detected in the crude product mixtures obtained from the acetate-catalyzed condensation of chloral hydrate with aliphatic ketones in acetic anhydride as solvent (1). In the absence of a catalyst or in the presence of catalytic amounts of glacial acetic acid, 1,1,1-trichloro-2-acetoxy-4-alkanones (*e*) were formed in high yields (Table 2) together with small quantities of the corresponding elimination products (*b*). When the reaction of **2***a* with acetic anhydride was monitored by v.p.c., the concentration of **2***e* was found to increase rapidly during the first 2 h (50% conversion after 2.5 h) and to reach a maximum at 70% conversion (10 h). After 24 h, the starting material had disappeared, and the product mixture contained ketol acetate (**2***e*), elimination product (**2***b*), and unidentified by-products in the approximate ratio 3.7:1:1. It is noteworthy that the two diastereomeric 1,1,1-trichloro-2-hydroxy-3-methyl-4-hexanones (*erythro-* and *threo-***3***a*) were converted to the corresponding acetates without detectable epimerization of starting material or product.[1] The *erythro*-isomer of 2-(1-hydroxy-2,2,2-trichloroethyl)-cyclohexanone (**8***a*), on the other hand, gave the corresponding acetate (*erythro-***8***e*) as major product together with small amounts of epimerized starting material and product (after 22 h at 100°).

By comparison of the carbonyl stretching

[1]For a discussion of configurational assignments for **3***a*, see ref. 1.

Can. J. Chem. Downloaded from www.nrcresearchpress.com by 210.87.254.42 on 09/05/12
For personal use only.

TABLE 2. Reaction of 1,1,1-trichloro-2-hydroxy-4-alkanones with acetic anhydride*

Ketol structure (Q = —CHOH—CCl_3)	Catalyst	Reaction time (h)	Yield† (g)	Product composition‡ (%)			
				Acetate *e*	Olefin *b*	Ketol *a*	Other
CH_3COCH_2Q	HOAc	14.5	12.1	79	20	1	trace
do.	—	15	12.0	80	11	9	—
do.	NaOAc	1.5	8.4	—	100	—	—
$CH_3CH_2CH_2COCH_2Q$	NaOAc	1.5	9.2	10	64	11	15
$(CH_3)_2CHCH_2COCH_2Q$	—	10	§	70	8	15	7
do.	—	24	12.7	65	18	—	17
do.	NaOAc	4	10.7	7	57	9	27
do.	NaOAc‖	15	11.0	5	80	5	10
$CH_3CH_2COCHQ—CH_3$¶	—	56	11.5	95	2	—	3
$CH_3CH_2COCHQ—CH_3$**	—	72	13.6	99	—	1	—
$(CH_3)_3CCOCH_2Q$	NaOAc	2	10.1	—	99	—	trace
$(CH_3)_3CCH_2COCH_2Q$	NaOAc	2	10.6	7	86	—	7

*Temperature 100°; initial reagent quantities; 0.05 mol ketol, 0.2 mol Ac_2O.
†Crude product after removal of Ac_2O and catalyst.
‡Analysis by v.p.c. of crude product mixture on a 5 ft × 1/8 in. OV-17, SE-52 or SE-30 column (120–140°).
§Reaction continued for an additional 14 h.
‖Catalyst (0.5 g) added after 14 h at 115°.
¶*Threo*, m.p. 37–38°.
**_Erythro_, m.p. 57–58°.

frequencies of the two diastereomeric 1,1,1-trichloro-2-hydroxy-3-methyl-4-hexanones (**3***a*) and their acetates (**3***e*) we were able to verify the presence of strong intramolecular hydrogen bonding in the *threo*-isomer of **3***a* (1). The carbonyl absorption bands of *threo*-**3***a* and *threo*-**3***e* were observed at 1700 and 1720 cm^{-1}, respectively. This blue-shift of 20 cm^{-1} on acetylation of the hydroxy group is of the same order of magnitude (13–24 cm^{-1}) reported by Stiles *et al.* (26) for a series of aromatic β-hydroxy ketones and can be attributed to the breaking of the hydrogen bond. The carbonyl peaks of both the *erythro*-ketol **3***a* and the *erythro*-acetate **3***e* appeared at 1720 cm^{-1}.

In the presence of sodium acetate, the reaction of 1,1,1-trichloro-2-hydroxy-4-alkanones (*a*) with acetic anhydride gives predominantly 1,1,1-trichloro-2-alken-4-ones (*b*) (Table 2). When a mixture of equimolar amounts of *threo*-ketol **3***a* and *threo*-acetate **3***e* was subjected to these reaction conditions and the progress of the reaction was monitored by v.p.c., the acetate was found to react more rapidly than the ketol. This result, in conjunction with the observed rapid and quantitative conversion of pure *threo*-acetate **3***e* to the corresponding alkenone **3***b* after only 45 min at 100° indicates that acetic acid is eliminated more readily from *threo*-**3***e* than water from *threo*-**3***a*, and that the dehydration reactions may proceed via acetylated intermediates.

It is interesting to note that even in the presence of sodium acetate the epimerization rate of diastereomeric acetates **3***e* is very slow relative to the rate of elimination, and that only traces of **3***b* were formed from *erythro*-**3***e*. Examination of space-filling molecular models indicates that this marked reactivity difference is probably due to destabilization of the transition state for *trans*-elimination of acetic acid from *erythro*-**3***e* caused by unfavorable non-bonding interactions between the bulky trichloromethyl group on the β-carbon and the methyl group on the α-carbon. In the most favorable conformation for *trans*-elimination of acetic acid from *threo*-**3***e*, on the other hand, the trichloromethyl and the methyl group reside in *anti*-position, and steric interactions between the trichloromethyl group and the alkyl-substituted carbonyl group can be minimized by free rotation about the R—CO—R′ single bonds (eq. 8). On this basis we have assigned structure **3***b* to the olefinic product.[2] This interpretation presumes that the most favored pathway for elimination involves a *trans*-concerted process.[3]

Since both the acid-catalyzed dehydration of

[2]Experiments to synthesize the other geometric isomer of **3***b* for a comparison of spectral and chemical properties are presently in progress.

[3]Cristol (32) and Truce (33) have used similar arguments and explained the low tendency of certain *threo*-β-chloro- and β-hydroxysulfones to undergo elimination reactions by repulsive steric interactions between the α-substituent (alkyl or phenyl) and the large sulfonyl group. In our case, the *erythro*-compound is less reactive because of the considerably larger steric requirements of the trichloromethyl group (compared to a methyl or phenyl group) and the smaller size of the carbonyl group (compared to a sulfonyl group).

Can. J. Chem. Downloaded from www.nrcresearchpress.com by 210.87.254.42 on 09/05/12
For personal use only.

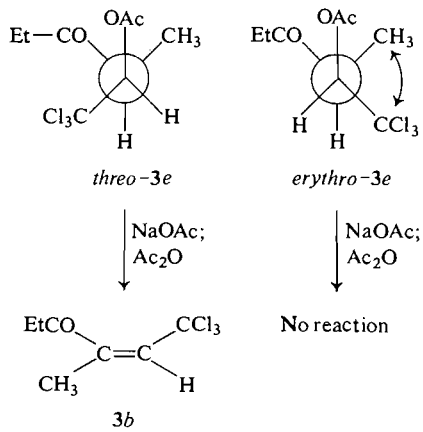

1,1,1-trichloro-2-hydroxy-4-alkanones (eq. 1) and the preparation of 1,1,1-trichloro-2-alken-4-ones via ketol acetates (see eq. 7 and last column of Table 2) are accompanied by undesirable side reactions and the separation of isomeric products proved to be difficult, we investigated the synthesis and dehydrohalogenation of 1,1,1,2-tetrachloro-4-alkanones (*f*) as an alternative route. Although Lucas reagent (5), aluminum chloride (27), and phosphorus pentachloride (19, 28) have been successfully used to replace the hydroxy group of trichloromethylcarbinols by chlorine, these substitution reactions are generally slow due to the electron-withdrawing effect and the steric bulk of the trichloromethyl group (4, 6, 7) and may lead to undesirable rearrangements or product decomposition (19, 29) under the drastic reaction conditions required. Thionyl chloride, on the other hand, has been reported (30) to react smoothly with aryl-substituted 1,1,1-trichloro-2-hydroxy-4-alkanones in the presence of pyridine to yield 1,1,1,2-tetrachloro-4-alkanones at low temperature and the corresponding dehydrohalogenation products at reflux temperature in chloroform.

Following this procedure, we obtained in high yield mixtures of 1,1,1,2-tetrachloro-4-alkanones (*f*) and 1,1,1-trichloro-2-alken-4-ones (*b*) with the substitution product generally predominating (eq. 9). Even at $-10°$ some *b* was formed, while in the absence of pyridine the starting material was quantitatively recovered. However, the *f*/*b* ratio was always found to be considerably higher when the reaction was carried out at lower temperatures (25 or 0° instead of reflux). This result together with the observation that **2***f* and **6***f* are readily dehydrohalogenated by pyridine in refluxing chloroform indicates that tetrachloro-

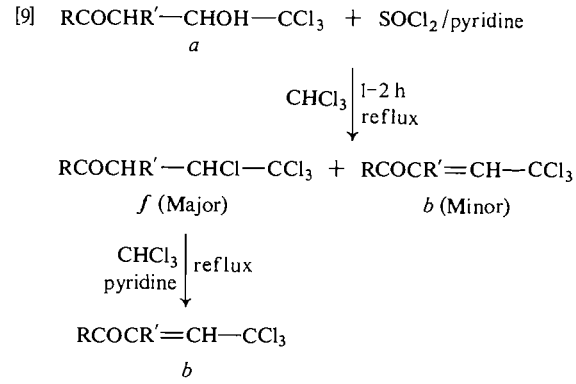

1 R = *n*-Pr; R′ = H
2 R = *i*-Bu; R′ = H
3 R = Et; R′ = Me
4 R = *t*-Bu; R′ = H
5 R = Me; R′ = H
6 R = C_6H_5; R′ = H
7 R = *t*-$BuCH_2$; R′ = H
10 R = Et; R′ = H
11 R = C_6H_5CH:CH, R′ = H

alkanones (*f*) may be involved as intermediates in the formation of the corresponding 1,1,1-trichloro-2-alken-4-ones (*b*). The conversion of the starting ketols *a* to the products shown in eq. 9 was generally 80–90% complete after 90 min reflux, and further extension of the reaction time led to extensive product decomposition (except for **6***a* and **11***a*). Similar results were obtained on treatment of **2***f* with sodium acetate in glacial acetic acid as dehydrohalogenating agent.

The two diastereomeric ketols *erythro*-**3***a* and *threo*-**3***a* were found to equilibrate rapidly under these reaction conditions to give a mixture of epimers which underwent normal substitution and dehydration. However, they reacted at a much slower rate (40–60% recovery of starting material after 90 min reflux time) than the other ketols which appears to be a consequence of the lower acidity of the hydrogen atom at the methyl-substituted α-carbon adjacent to the —CHOH— group. The two aryl-substituted 1,1,1-trichloro-2-hydroxy-4-alkanones **6***a* and **11***a* exhibited the highest reactivity of the 10 ketols studied and were quantitatively converted to their respective substitution (*f*, major) and dehydration (*b*, minor) products after 1 h at 60°. This result is in agreement with the observation by Roedig and Klappert (30) that **11***a* but not the corresponding diol C_6H_5CH=CH—CHOH—CH_2—CHOH—CCl_3 undergoes chlorine substitution at the trichloromethyl-substituted car-

Can. J. Chem. Downloaded from www.nrcresearchpress.com by 210.87.254.42 on 09/05/12
For personal use only.

[10] 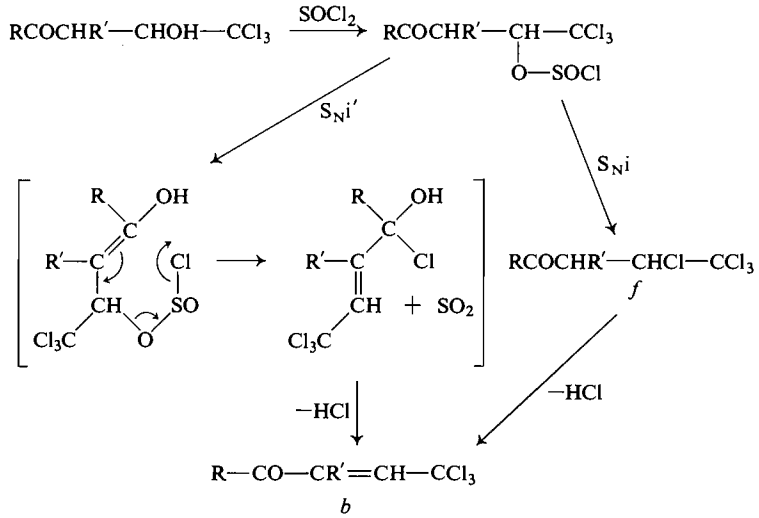

bon when treated with thionyl chloride and pyridine. Enolization to form a highly conjugated enol allylic system (22) appears to facilitate substitution, and the reaction of both aryl- and alkyl-substituted 1,1,1-trichloro-2-hydroxy-4-alkanones with thionyl chloride may well proceed by the S_Ni' mechanism which has been postulated by Pilgram and Ohse (31) and Steckel (19) for the analogous rearrangement of certain alkenyltrichloromethylcarbinols (eq. 10). However, the enol-stabilizing resonance effect involving the phenyl substituent of **11***a* does not render the trichloromethyl-substituted carbon so reactive as to permit solvolytic displacement of its hydroxy group. Thus, n.m.r. spectral analysis has shown that **11***a* can be recrystallized from methanol without structural change, and the reported (30) formation of 1,1,1-trichloro-2-methoxy-6-phenyl-5-hexen-4-one (or any other methoxy-substituted compound) under these conditions has been found to be in error.

Experimental

Elemental analyses were performed by A. Bernhardt Microanalytical Laboratory, Elbach, Germany. The u.v. spectra were run in 95% ethanol using a Unicam SP-200 spectrometer. The n.m.r. spectra were recorded on a Varian A 56/60 spectrometer using TMS as internal standard and $CDCl_3$ as solvent, and i.r. spectra on a Beckman IR-12 or a Perkin–Elmer 457 spectrometer using a dilute CCl_4 solution or a thin film of neat liquid (or melt) between sodium chloride plates.

The v.p.c. analyses were carried out on a Varian Aerograph Model 1200-1 HY-FI III gas chromatograph using a 5 ft × 1/8 in. column packed with 5% SE-30, 5% SE-52, or 2% OV-17 on Aeropak 30 (column temperature 110–140°) and nitrogen as carrier gas.

All 1,1,1-trichloro-2-hydroxy-4-alkanones were prepared from chloral and the respective ketones as previously described (1, 2). Thionyl chloride was distilled before use, while other chemicals were used without further purification (commercially available reagent grade quality).

Acid-catalyzed Dehydration of 1 1,1-Trichloro-2-hydroxy-4-alkanones

Method 1

Using a modified version of the procedure described before (14) for the preparation of **12***b*, a solution of 24.8 g (0.10 mol) of 1,1,1-trichloro-2-hydroxy-6-methyl-4-heptanone (**2***a*) and 6.0 g (0.03 mol) of *p*-toluenesulfonic acid in 160 ml benzene was vigorously refluxed for 24 h. Washing with water, drying over magnesium sulfate, and evaporation of the solvent under reduced pressure gave 20 g of a black oil which was found by v.p.c. analysis to contain 1,1,1-trichloro-6-methyl-2-hepten-4-one (**2***b*), 1,1,5-trichloro-6-methyl-1-hepten-4-one (**2***c*), and starting material in the ratio 39:31:30. Recrystallization from petroleum ether (60–100°) yielded 6 g of the starting ketol (**2***a*). Evaporation of the solvent from the mother liquor and vacuum distillation of the residue gave 8 g of a mixture of **2***b* and **2***c* boiling at 57–64°/0.01 mm. Small samples of pure **2***b* and **2***c* were obtained by repeated liquid partition chromatography of the distillate on silica using 20% (by volume) petroleum ether (60–100°) in benzene as eluent.

Compound **2***b*: m p. 17.5–18°, b.p. 57–60°/0.01 mm; i.r. (neat) 962 (H—C=), 1628 (C=C), 1678 and 1703 cm^{-1} (C=O); u.v. (95% EtOH) λ_{max} 223 (ε 12 000) and 336 nm (ε 38).

Anal. Calcd. for $C_8H_{11}OCl_3$: C, 41.86; H, 4.83; Cl, 46.37. Found: C, 41.69; H, 5.02; Cl, 46.41.

Compound **2***c*: b.p. 60–64°/0.01 mm.

Anal. Calcd. for $C_8H_{11}OCl_3$: C, 41.86; H, 4.83; Cl, 46.37. Found: C, 41.98; H, 4.72; Cl, 46.26.

The i.r. (neat) 1720 (C=C) and 1620 (C=C) cm^{-1}; u.v. (95% EtOH) λ_{max} 206 (ε 3500) and 270 nm (ε 1200).

Application of the same procedure to 1,1,1-trichloro-2-hydroxy-4-heptanone (**1***a*) yielded 1,1,1-trichloro-2-hepten-4-one (**1***b*), b.p. 48–49°/0.01 mm, and 1,1,5-tri-

Can. J. Chem. Downloaded from www.nrcresearchpress.com by 210.87.254.42 on 09/05/12
For personal use only.

Can. J. Chem. Downloaded from www.nrcresearchpress.com by 210.87.254.42 on 09/05/12
For personal use only.

TABLE 3. The n.m.r. chemical shifts (τ units) of 1,1,1-trichloro-2-acetoxy-4-alkanones, 1,1,1,2-tetrachloro-4-alkanones, and 1,1,1-trichloro-2-alken-4-ones

Compound	$-CH_2-CO-$	$-CO-CHR-CHX-$*	$-CHX-$*†	$-CO-CH=C<$*‡	$>C=CH-CCl_3$*‡
1*b*	7.35	—		3.39	2.95
e	7.57	6.91	4.03	—	—
f	7.50	6.75	5.00	—	—
2*b*	7.47	—	—	3.43	2.99
e	7.70	6.95	4.05	—	—
f	7.66	6.76	5.00	—	—
3*b*	7.28	—	—	—	2.87
e(*erythro*)	7.37	6.70	3.97	—	—
e(*threo*)	7.40	6.60	4.42	—	—
f	7.27	6.62	4.75	—	—
4*b*	—	—	—	3.13	2.97
f	—	6.63	4.93	—	—
5*b*	7.63	—	—	3.41	2.97
e	7.80	6.93	4.20	—	—
f	7.73	6.70	5.00	—	—
6*b*	—	—	—	2.53	2.65
f	—	6.15	4.73	—	—
7*b*	7 47	—	—	3.43	3.03
f	7.63	6.75	5.00	—	—
8*e*(*erythro*)	7.53	6.95	3.57	—	—
9*b*	—	—	—	3.11	2.78
10*b*	7.30	—	—	3.39	2.95
f	7.49	6.75	5.00	—	—
11*b*	—	—	—	3.05	2.80
f	—	6.49	4.81	—	—

*R = H or CH_3, X = OAc or Cl.
†Quartet (1:1:1:1) for $-CH_2-CHX-$, with J_{gtc} = 3.6–4.3 Hz and 7.1–7.8 Hz, respectively (except for **4***f* and **11***f*).
‡Doublet for each olefinic proton of —CH=CH—, with J = 14–16 Hz.

Can. J. Chem. Downloaded from www.nrcresearchpress.com by 210.87.254.42 on 09/05/12
For personal use only.

chloro-1-hepten-4-one (**1***c*), b.p. 55–60°/0.01 mm (see Tables 1 and 3).

Anal. Calcd. for $C_7H_9OCl_3$ (**1***c*): C, 39.01; H, 4.20; Cl, 49.35. Found: C, 38.88; H, 4.35; Cl, 49.30.

Reflux of a solution of 26.8 g (0.10 mol) of 1,1,1-trichloro-2-hydroxy-4-phenyl-4-butanone (**6***a*) and 2.0 g (0.01 mol) of *p*-toluenesulfonic acid in 160 ml toluene for 9.5 h and the usual work-up gave 24 g of a yellow, crude product from which 20 g (80% yield) of 1,1,1-trichloro-4-phenyl-2-buten-4-one (**6***b*), m.p. 99–100° (lit. (15) 98–99°) was obtained by recrystallization from petroleum ether (65–110°). The carbonyl and olefinic stretching vibrations of **6***b* were observed at 1680 and 1625 cm^{-1}, respectively, and u.v. absorption maxima (EtOH) at 233 (ε 7400) and 350 nm (ε 95).

Method 2

A solution of 12.4 g (0.05 mol) of **2***a* in 30 g of glacial acetic acid containing five drops of 10% sulfuric acid was heated at 100° for 24 h. After evaporation of the solvent the black reaction mixture was dissolved in ether, washed with water and 10% sodium bicarbonate solution, and dried over magnesium sulfate. Removal of the solvent left a dark oil (9.6 g) containing **2***c* (major product), unreacted starting material and a small amount of **2***b* (ratio of v.p.c. peak areas 11:6:1). Vacuum distillation furnished 5.5 g of distillate (b.p. 66–70°/0.025 mm) from which a pure sample of **2***c* was isolated by liquid partition chromatography as described before.

1,1,5-Trichloro-1-hepten-4-one (**1***c*) and 1,1,5-trichloro-1-hexen-3-methyl-4-one (**3***c*) were prepared by the same procedure from 1,1,1-trichloro-2-hydroxy-4-heptanone (**1***a*) and 1,1,1-trichloro-2-hydroxy-3-methyl-4-hexanone (**3***a*), respectively (see Table 1).

Method 3

According to the procedure described by Baluja and coworkers (12, 13) for the preparation of several 1,1,1-trichloro-2-alken-4-ones, 27 g (0.2 mol) of potassium bisulfate was dried at 100° and placed in a 100-ml three-necked flask equipped with thermometer and distillation assembly. After preheating the potassium bisulfate to 230°, 24.8 g (0.10 mol) of **2***a* was rapidly added over a 5-min period and the mixture was immediately distilled at aspirator vacuum (b.p. 115°/15 mm). Addition of ether to the distillate, washing with water, drying, and solvent evaporation gave 8.78 g (38% yield) of a yellow liquid which was found by v.p.c. and n.m.r. analysis to contain **2***b*, **2***c*, and **2***a* in the approximate ratio 70:23:7. When the original mixture of **2***a* and potassium bisulfate was refluxed for 2 h at 130° before distillation, n.m.r. and v.p.c. analysis of the crude distillate (18.6 g = 81% yield) revealed the formation of small amounts of several unidentified byproducts and an increase in the **2***c*/**2***b* ratio from 23/70 to 52/30 (Table 1).

Catalytic Rearrangement of 1,1,1-Trichloro-2-alken-4-ones

Adopting the procedure described in the literature (15) for the rearrangement of **5***b* and **6***b*, 6.38 g of silica gel (0.106 mol) was added to 6.38 g (0.028 mol) of 1,1,1-trichloro-5,5-dimethyl-2-hexen-4-one (**4***b*), and the mixture was heated for 17 h at 130° in a round-bottom flask equipped with reflux condenser. Vacuum distillation of the black semi-solid product mixture yielded 3.10 g (49% yield) of a clear yellow liquid, b.p. 36–38°/10 mm, which was found by n.m.r. and v.p.c. analysis to be pure 1,1,3-trichloro-5,5-dimethyl-1-hexen-4-one (**4***d*).

Spectroscopic Identification

Compound **4***d*: n.m.r. ($CDCl_3$) τ 3.69 (doublet, 1H, $—CH_A=CCl_2$), 4.50 (doublet, 1H, $—CH_BCl—$), and 8.76 (singlet, 9H, $(CH_3)_3C—$), J_{AB} = 10.0 Hz; i.r. (neat) 1625 (C=C) and 1725 cm^{-1} (C=O); u.v. (EtOH) λ_{max} 222 (ε 7700) and 297 nm (ε 130).

Subjecting 1,1,1-trichloro-2-penten-4-one (**5***b*) and 1,1,1-trichloro-4-phenyl-2-buten-4-one (**6***b*), respectively, to the same reaction conditions (15) gave the corresponding allylic rearrangement products **5***d* (27% yield of crude distillate b.p. 40–42°/0.2 mm, containing 8% unidentified byproduct) and **6***d* (20% yield of crude distillate, b.p. 120–125°/3.5 mm, containing 17% unidentified byproduct) with the following spectroscopic characteristics.

Compound **5***d*: n.m.r. ($CDCl_3$) τ 3.89 (doublet, 1H, $—CH_A=CCl_2$), 5.04 (doublet, 1H, $—CH_BCl—$), and 7.70 (singlet, 3H, CH_3), J_{AB} = 10 Hz (lit. (15) τ 3.96, 5.08, and 7.68, J_{AB} = 9 Hz); i.r. (neat) 1733 (C=O, lit. (15) 1730) and 1623 cm^{-1} (C=C); u.v. (EtOH) λ_{max} 221 (ε 8900) and 270 nm (ε 340).

Compound **6***d*: n.m.r. ($CDCl_3$) τ 1.95 and 2.50 (aromatic multiplet, 5H), 3.48 (doublet, 1H, $—CH_A=CCl_2$), and 4.06 (doublet, 1H, $—CH_BCl—$), J_{AB} = 9.5 Hz; i.r. (neat) 1620 (C=C) and 1700 cm^{-1} (C=O) (lit. (15) 1618 and 1690 cm^{-1}); u.v. (EtOH) λ_{max} 254 nm (ε 10 700).

Treatment of 1,1,1-trichloro-6-methyl-2-hepten-4-one (**2***b*) with silica at 130° resulted in the formation of 1,1,5-trichloro-6-methyl-1-hepten-4-one (**2***c*) (low yield), as identified by comparison of the n.m.r. spectrum of the distillate with that of an authentic sample of **2***c*, and one unidentified by-product. No absorption peaks were observed in the τ 4.0–5.1 range characteristic of the —CHCl— proton of 1,1,3-trichloro-1-alken-4-ones (see **4***d* and **5***d*).

Similarly, 1,1,1-trichloro-6,6-dimethyl-2-hepten-4-one (**7***b*) was found to rearrange on silica to 1,1,5-trichloro-6,6-dimethyl-1-hepten-4-one (**7***c*) rather than to 1,1,3-trichloro-6,6-dimethyl-1-hepten-4-one. In this experiment, 7.0 g (0.030 mol) of **7***b* yielded 1.16 g (20% yield) of **7***c* after 17 h heating at 130° on 7.0 g of silica and vacuum distillation (b.p. 109–114°/1.8 mm).

Compound **7***c*: n.m.r. ($CDCl_3$) τ 3.90 (triplet, 1H, $—CH=CCl_2$), 5.94 (singlet, 1H, —CHCl—), 6.45 (doublet, 2H, $—CH_2—$) and 8.91 (singlet, 9H, *t*-Bu); i.r. (neat) 1730 (C=O) and 1625 cm^{-1} (C=C).

Pyrolysis of 2-(1-Hydroxy-2,2,2-trichloroethyl)-cyclohexanone (8a)

It has been reported previously (2) that the condensation of chloral with cyclohexanone in glacial acetic acid results in complete product decomposition when carried out in the absence of a base catalyst; excessively high reaction temperatures and/or long reaction times had the same effect even in the presence of sodium acetate. Since decomposition, once it had started, proceeded rapidly and with evolution of hydrochloric acid, the following experiment was carried out with the sole intent to isolate and identify the major organic decomposition product.

Using the standard condensation procedure (2), a mixture of 30.7 g (0.31 mol) of cyclohexanone, 36.9 g (0.25 mol) of chloral, 5.1 g (0.063 mol) of anhydrous

Can. J. Chem. Downloaded from www.nrcresearchpress.com by 210.87.254.42 on 09/05/12
For personal use only.

sodium acetate, and 0.50 mol of glacial acetic acid was heated at 100° for 58 h at which time the evolution of hydrochloric acid fumes and black coloration of the reaction mixture indicated decomposition of the original condensation product (**8***a*). After another 6 h of reaction time, solvent and unreacted starting materials were evaporated, the residue was taken up in ether, washed with water and sodium bicarbonate solution, and dried over magnesium sulfate. Evaporation of the ether gave 48 g of a black viscous oil which was found by v.p.c. analysis to contain **8***a* and two more volatile products in the approximate ratio 8:35:7. The latter two compounds were separated from **8***a* by two high-vacuum distillations (b.p. 85–95°/0.025 mm), and the major component, 2-(2,2-dichlorovinyl)-2-cyclohexanone, was obtained in pure form by preparative gas chromatography on a 20 ft × 3/8 in. 30% SE-52 column at 250°. The originally colorless condensate in the collection tube turned blue-green on standing, the same color which was observed during distillation. The identity of the collected sample (> 96% pure) with the major component of the original crude product mixture was confirmed by re-injection into two analytical v.p.c. columns (OV-17 at 115° and SE-30 at 160°) and comparison of retention times. The structure assignment rests on the analytical and spectroscopic evidence listed below.

Anal. Calcd. for $C_8H_8Cl_2O$: C, 50.29; H, 4.22. Found: C, 50.00; H, 4.00.

Mass spectrometry (80 eV): peaks at *m/e* 190 (P), 192 (P + 2), and 194 (P + 4) in the relative intensity ratio 100:67:16 expected for a compound containing two chlorine atoms (theoretical ratio = 100:65:11), isotopic fragment peaks at *m/e* 162 (100%), 164 (61%), and 166 (13%) due to loss of CO, and base peak (P-chlorine) at *m/e* 155 (100%) with isotopic satellite at *m/e* 157 (34%, expected P/(P + 2) intensity ratio 100:33). The n.m.r. ($CDCl_3$): τ 2.55 (triplet, 1H, $=CH—CH_2—$), 3.28 (singlet, 1H, $—CH=CCl_2$), 7.52 (multiplet, 4H, $—CO—CH_2—$ and $=CH—CH_2—$), and 7.93 (multiplet, 2H, $—CH_2—CH_2—CH_2—$). The i.r. (neat): absorption maxima at 1676 ($>C=C—CO—$) and 1602 cm^{-1} (C=C, *s-cis*). The u.v./visible (95% EtOH): 215 (ε 33 000), 260 (ε 16 000), and 374 nm (ε 180); weak absorption at 642 nm due to colored impurity.

*Preparation of 1,1,1,7,7,7-Hexachloro-2,5-heptadien-4-one (**9b**)*

1,1,1,7,7,7 - Hexachloro - 2,6 - dihydroxy - 4 - heptanone (**9***a*), the precursor of **9***b*, was prepared according to the procedure described by Caujolle and coworkers (25). The crude product (light brown solid) obtained in 65% yield from chloral hydrate and acetonedicarboxylic acid in aqueous solution was recrystallized several times from chloroform to give **a white solid** (**9***a*-1) melting at 119–121°. Evaporation of the solvent from the mother liquors and several successive recrystallizations from ethanol yielded an isomeric white solid (**9***a*-2) melting at 157–158°. Spectroscopic characterization of these two compounds proved to be difficult due to their low solubility in water and most organic solvents (except dioxane, DMSO and trifluoroacetic acid).

Anal. Calcd. for $C_7H_8Cl_6O_3$ (**9***a*-1): C, 23.83; H, 2.29; Cl, 60.28. Found: C, 23.72; H, 2.44; Cl, 60.39.

Compound **9***a*-1: n.m.r. ($CDCl_3$, 57°) τ 5.33 (broad multiplet, 2H, $>CH—CCl_3$), 6.52 (broad singlet, 2H, —OH), and 6.90 (unsymmetrical triplet, 4H, $—CH_2—$); i.r. (KBr pellet, Beckman IR-12) 3450 (strong and broad, OH) and 1721 cm^{-1} (strong, with shoulder at 1708 cm^{-1}, C=O); i.r. (0.5 *M* solution in $CHCl_3$, Beckman IR-12) 3594 (sharp, with shoulder near 3500) and 1726 cm^{-1} (C=O).

Anal. Calcd. for $C_7H_8Cl_6O_3$ (**9***a*-2): C, 23.83; H, 2.29; Cl, 60.28. Found: C, 23.70; H, 2.43; Cl, 60.17.

Compound **9***a*-2: n.m.r. ($CDCl_3$, 57°) τ 5.32 (sharp 1:1:1:1 quartet, 2H, $>CH—CCl_3$), 6.63 (broad singlet, 2H, OH), and 6.90 (unsymmetrical triplet, 4H, $—CH_2—$); i.r. (KBr pellet) 3490 (strong and broad, OH) and 1725 cm^{-1} (C=O); i.r. (0.5 *M* solution in $CHCl_3$) 3594 (sharp, with shoulder near 3500) and 1726 cm^{-1} (C=O); lit. (23): i.r. (Nujol) of **9***a* (m.p. 124–126°) 3448 (OH) and 1710 cm^{-1} (C=O).

Dehydration was accomplished by refluxing (17 h) a solution of 5 g of **9***a*-2 in 40 ml of benzene in the presence of 0.4 g of *p*-toluenesulfonic acid using a Dean-Stark trap for removal of the water from the azeotrope. The resulting black solution was washed with water and aqueous sodium bicarbonate, and dried to give 1.5 g of *trans,trans*-1,1,1,7,7,7-hexachloro-2,5-dien-4-one (**9***b*), m.p. 70–72° (yellow), after several recrystallizations from cyclohexane and chloroform. The i.r. (KBr pellet, Beckman IR-12) 1628, 1640 (C=C), 1680 and 1698 cm^{-1} (C=O). The appearance of two absorption maxima for the carbonyl and the olefinic stretching vibrations, respectively, and the low C=O/C=C intensity ratio (approximately 1.0) of these peaks indicate the presence of both *s-cis* (1698 and 1628 cm^{-1}) and *s-trans* (1680 and 1640 cm^{-1}) conformers with the former predominating. The u.v. (EtOH) of **9***b*: λ_{max} 232 (ε 7300) and 325 nm (ε 63).

Acetylation of 1,1,1-Trichloro-2-hydroxy-4-alkanones

A solution of 11.7 g (0.05 mol) of 1,1,1-trichloro-2-hydroxy-3-methyl-4-hexanone (*erythro*-**3***a*) in 20.4 g (0.20 mol) of acetic anhydride was heated at 100° for 72 h. The pale yellow oil (13.6 g = 99% yield) obtained after removal of the solvent was distilled under high vacuum to give 11.85 g (86% yield) of 1,1,1-trichloro-2-acetoxy-3-methyl-4-hexanone (*erythro*-**3***e*), b.p. 76°/0.01 mm. The i.r. (solution in CCl_4) 1720 (ketone C=O) and 1760 cm^{-1} (ester C=O).

Anal. Calcd. for $C_9H_{13}O_3Cl_3$: C, 39.23; H, 4.76; Cl, 38.60. Found: C, 39.40; H, 4.90; Cl, 38.67.

The ketol acetates listed below were prepared by a similar procedure (data on reaction time, crude product yield, and product composition are summarized in Table 2, n.m.r. chemical shifts in Table 3).

1,1,1-Trichloro-2-acetoxy-3-methyl-4-hexanone (*threo*-**3***e*): b.p. 69–70°/0.01 mm; i.r. (solution in CCl_4) 1720 (ketone C=O) and 1761 cm^{-1} (ester C=O).

Anal. Calcd. for $C_9H_{13}O_3Cl_3$: C, 39.23; H, 4.76; Cl, 38.60. Found: C, 39.13; H, 4.19; Cl, 38.72.

1,1,1-Trichloro-2-acetoxy-6-methyl-4-heptanone (**2***e*): b.p. 88–89°/0.01 mm; i.r. (neat) 1720 (ketone C=O) and 1767 cm^{-1} (ester C=O).

Anal. Calcd. for $C_{10}H_{15}O_3Cl_3$: C, 41.47; H, 5.22; Cl, 36.73. Found: C, 41.33; H, 5.40; Cl, 36.89.

1,1,1-Trichloro-2-acetoxy-4-pentanone (**5***e*): b.p. 76–

Can. J. Chem. Downloaded from www.nrcresearchpress.com by 210.87.254.42 on 09/05/12
For personal use only.

77°/0.01 mm; i.r. (neat) 1725 (ketone C=O) and 1765 cm^{-1} (ester C=O). 2-(1-Acetoxy-2,2,2-trichloroethyl)-cyclohexanone (**8***e*): m.p. 110–111.5°; i.r. (Nujol) 1708 (ketone C=O) and 1754 cm^{-1} (ester C=O).

Preparation of 1,1,1-Trichloro-2-alken-4-ones from 1,1,1-Trichloro-2-acetoxy-4-alkanones

A solution of 82.5 g (0.33 mol) of 1,1,1-trichloro-2-hydroxy-6-methyl-4-heptanone (**2***a*) in 170 g (1.67 mol) of acetic anhydride was heated at 115° for 14 h to give a crude product mixture which was found by v.p.c. analysis to contain 1,1,1-trichloro-2-acetoxy-6-methyl-4-heptanone (**2***e*, 70%), 1,1,1-trichloro-6-methyl-2-hepten-4-one (**2***b*, 20%), unreacted starting material (6%), and one unidentified by-product (3%). Addition of 3 g of anhydrous sodium acetate at this point and continuation of the reaction for another hour changed the **2***b*/**2***e* product ratio from 20/70 to 80/5 and also resulted in an appreciable increase of the relative amount of undesirable by-products (from 3 to 10% of the total product mixture) which are believed to be isomers of **2***b*. The usual work-up procedure gave 73 g of crude product (brown liquid) from which 52.5 g (68% yield) of 95% pure **2***b* was obtained by vacuum distillation (b.p. 61–67°/0.1 mm).

When solutions of pure 1,1,1-trichloro-2-acetoxy-4-pentanone (**5***e*) and *threo*-1,1,1-trichloro-2-acetoxy-3-methyl-4-hexanone (*threo*-**3***e*), respectively, in acetic anhydride were heated at 100° for 45 min in the presence of anhydrous sodium acetate, the corresponding α,β-unsaturated ketones **5***b* and **3***b* could be isolated in nearly quantitative yield. The *erythro*-isomer of **3***e*, on the other hand, did not react under these conditions (85% recovery).

Characterization of 1,1,1-trichloro-2-penten-4-one (**5***b*): m.p. 20–20.5° (lit. (15) 25–26°).

Anal. Calcd. for $C_5H_5OCl_3$: C, 32.03; H, 2.68; Cl, 56.74. Found: C, 32.16; H, 2.82; Cl, 56.60.

The i.r. (neat) 1623 (C=C), 1678 and 1704 cm^{-1} (C=O, *transoid* and *cisoid*) (lit. (15) 1630, 1676, and 1700 cm^{-1}).

Acetate-catalyzed Dehydration of 1,1,1-Trichloro-2-hydroxy-4-alkanones

To a solution of 10.3 g (0.05 mol) of 1,1,1-trichloro-2-hydroxy-4-pentanone (**5***a*) in 20.5 g (0.20 mol) of acetic anhydride was added 1 g of anhydrous sodium acetate. The mixture was heated at 100° for 90 min. After evaporation of the solvent under vacuum, the residue was dissolved in 100 ml of ether and washed with water. The organic layer was dried with magnesium sulfate and the ether was evaporated to give 8.4 g of a yellow liquid from which 7.1 g (75% yield) of pure 1,1,1-trichloro-2-penten-4-one (**5***b*), was obtained by high-vacuum distillation (b.p. 41–42°/0.01 mm). 1,1,1-Trichloro-2-hepten-4-one (**1***b*), 1,1,1-trichloro-6-methyl-2-hepten-4-one (**2***b*), 1,1,1-trichloro-5,5-dimethyl-2-hexen-4-one (**4***b*), and 1,1,1-trichloro-6,6-dimethyl-2-hepten-4-one (**7***b*) were prepared from their respective ketols by the same procedure (see Table 2).

Reaction of Aliphatic 1,1,1-Trichloro-2-hydroxy-4-alkanones with Thionyl Chloride

Adopting the procedure described in the literature (30) for the preparation of aryl-substituted 1,1,1-trichloro-2-alken-4-ones, 0.022 mol of thionyl chloride and 100 ml of pyridine were added to a solution of 0.02 mol of 1,1,1-trichloro-2-hydroxy-4-alkanone (*a*) in 12 ml of chloroform, and the mixture was refluxed (60°) for 90 min. After washing with water and drying over magnesium sulfate, the solvent was removed by vacuum distillation and the crude product mixture was analyzed by n.m.r. spectroscopy for 1,1,1-trichloro-2-alken-4-one (*b*), 1,1,1,4-tetrachloro-4-alkanone (*f*), and starting material (*a*); v.p.c. analysis confirmed that no other compounds were present. Pure samples of *b* and *c* were obtained by fractional crystallization from petroleum ether (60–100°) or by partition chromatography on silicic acid using 80% (v/v) benzene/petroleum ether (30–60°) as eluent. When this procedure was applied to the 1,1,1-trichloro-2-hydroxy-4-alkanones listed below, the results specified in parentheses (weight of crude product mixture, product composition, product separation by vacuum distillation (v.d.), fractional crystallization (f.c.), or partition chromatography (p.c.)) were obtained.

1,1,1-Trichloro-2-hydroxy-4-heptanone (**1***a*) (4.8 g, 30% **1***b*/59% **1***f*, p.c.); i.r. of **1***f* (neat) 1719 cm^{-1} (C=O). 1,1,1-Trichloro-2-hydroxy-6-methyl-4-heptanone (**2***a*) (5.1 g, 45% **2***b*/49% **2***f*, f.c. and p.c.)

Anal. Calcd. for $C_8H_{12}OCl_4$ (**2***f*, m.p. 43–43.5°): C, 36.12; H, 4.55; Cl, 53.32; Found: C, 35.97; H, 4.65; Cl, 53.29. The i.r. (neat) 1720 cm^{-1} (C=O).

1,1,1-Trichloro-2-hydroxy-3-methyl-4-hexanone (*erythro*-**3***a*) (4.8 g, 18% **3***b*/24% **3***f*, p.c.); i.r. of **3***b* (neat) 1621 (C=C) and 1687 cm^{-1} (C=O). 1,1,1-Trichloro-2-hydroxy-5,5-dimethyl-4-hexanone (**4***a*) (5.4 g, 35% **4***b*/43% **4***f*, f.c.). Characterization of **4***b*: m.p. 45–47° (lit. (13) 51°); i.r. (neat) 1689 (C=O), 1617 (C=C), and 964 cm^{-1} (HC=, *trans*) (lit. (13) 970 cm^{-1}); u.v. (EtOH) λ_{max} 220 (ε 8100) and 335 nm (ε 47). Characterization of **4***f*: m.p. 118–120° (lit. (13) 122–123°).

Anal. Calcd. for $C_8H_{12}OCl_4$: C, 36.12; H, 4.55; Cl, 53.32; Found: C, 36.30; H, 4.75; Cl, 53.31.

1,1,1-Trichloro-2-hydroxy-4-pentanone (**5***a*) [4.4 g, 27% **5***b*/52% **5***f*, v.d. for **5***b*, p.c. for **5***f*]. 1,1,1-Trichloro-2-hydroxy-6,6-dimethyl-4-heptanone (**7***a*) (5.2 g, 53% **7***b*/42% **7***f*, f.c.). Characterization of **7***b*: b.p. 103°/1 mm; i.r. (Nujol) 1700, 1670 (C=O, *cisoid* and *transoid*), 1630 (C=C) and 960 cm^{-1} (*trans*, HC=); u.v. (EtOH) λ_{max} 222 (ε 13 500) and 340 nm (ε 49). Characterization of **7***f*: m.p. 49–50°; i.r. (neat) 1722 cm^{-1} (C=O).

Anal. Calcd. for $C_9H_{14}OCl_4$: C, 38.60; H, 5.03; Cl, 50.64. Found: C, 38.75; H, 5 14; Cl, 50.52.

1,1,1-Trichloro-2-hydroxy-4-hexanone (**10***a*) (4.5 g, 27% **10***b*/57% **10***f*, p.c.); i.r. of **10***f* (neat) 1724 cm^{-1} (C=O).

Reaction of Aryl-substituted 1,1,1-Trichloro-2-hydroxy-4-alkanones with Thionyl Chloride

Following the procedure described in the literature (30) for the preparation of aryl-substituted 1,1,1,2-tetrachloro-4-alkanones, a solution of 0.11 mol of thionyl chloride in 8 ml of chloroform was added drop-wise at 0–5° to a magnetically stirred solution of 26.8 g (0.10 mol) of 1,1,1-trichloro-2-hydroxy-4-phenyl-4-butanone (**6***a*) and 1.0 ml pyridine in 36 ml chloroform. After the addition was complete (approximately 1 h), stirring was continued for another hour at 0–5°, and then for 20 h at room temperature. Washing with water, drying and solvent evaporation gave 28 g of a yellow solid containing 1,1,1-trichloro-4-phenyl-2-buten-4-one (**6***b*) and 1,1,1,2-tetrachloro-4-phenyl-4-butanone (**6***f*) in the approximate ratio 1:2. The n.m.r. spectrum of the crude product mixture did not reveal the presence of any starting material.

Can. J. Chem. Downloaded from www.nrcresearchpress.com by 210.87.254.42 on 09/05/12
For personal use only.

Fractional crystallization from petroleum ether (60–100°) afforded pure **6***f* (less soluble), m.p. 62.5–63.5° (lit. (30) 63°) and **6***b* (from the mother liquor), m.p. 99–100° (lit. (15) 98–99°). The same two products were obtained in the approximate ratio **6***b*/**6***f* 2:3 when the reaction was carried out at reflux temperature (see preceding experiment).

Application of the reflux procedure (90 min at 60°, see before) to the pyridine-catalyzed reaction of 1,1,1-trichloro-2-hydroxy-6-phenyl-5-hexen-4-one (**11***a*) with thionyl chloride resulted in the quantitative conversion of starting material to a mixture containing 45% 1,1,1-trichloro-6-phenyl-2,5-hexadien-4-one (**11***b*) and 55% 1,1,1,2-tetrachloro-6-phenyl-5-hexen-4-one (**11***f*). Fractional crystallization from petroleum ether (60–100°) yielded samples of pure **11***b*, m.p. 93.5–95° (lit. (14, 30) 94–95°), and **11***f*, m.p. 79–80° (lit. (30) 83°). The starting ketol (**11***a*) did not undergo any chemical change when recrystallized from methanol, as evidenced by the complete identity of the two n.m.r. spectra taken before and after recrystallization, respectively, and by the absence in the latter spectrum of a singlet peak at the chemical shift expected for a methoxy group.

Dehydrohalogenation of 1,1,1,2-Tetrachloro-4-alkanones

To a 4:1 mixture (5.12 g) of 1,1,1,2-tetrachloro-6-methyl-4-heptanone (**2***f*) and 1,1,1-trichloro-6-methyl-2-hepten-4-one (**2***b*) obtained from 1,1,1-trichloro-2-hydroxy-6-methyl-4-heptanone (**2***a*) and thionyl chloride as described before was added 3 ml of chloroform and excess pyridine (1.7 ml, 0.021 mol), and the solution was refluxed at 60° for 8 h. The v.p.c. monitoring of the reaction progress revealed a gradual increase in the relative concentration of **2***b* at the expense of **2***f*. After 4 h the mixture was found to contain 50% **2***b*, 36% **2***f*, and small percentages of three unidentified by-products. The relative proportion of these by-products increased rapidly during the second half of the reaction until the product mixture contained only 10% **2***b* and 10% **2***f* after 8 h reflux time.

Similarly, stirring of a solution of a 67:26 (relative v.p.c. peak areas) mixture of **2***f* and **2***b* in glacial acetic acid in the presence of sodium acetate changed the percentage ratio to 40:50 after 12 h at room temperature, 34:63 after 200 min at 50°, and 33:42 after 22.5 h at 50° with a large percentage of by-products (25%) present in the final product mixture.

When a solution of 0.5 g of pure 1,1,1,2-tetrachloro-5,5-dimethyl-4-hexanone (**4***f*) in 3.5 g chloroform was heated at 100° for 24 h in the presence of two drops of pyridine, a reaction mixture was formed which was estimated by v.p.c. to contain starting material (**4***f*) and 1,1,1-trichloro-5,5-dimethyl-2-hexen-4-one (**4***b*) in the approximate ratio 3:7 and small quantities of unidentified by-products.

The authors wish to thank the National Research Council of Canada for the financial support of these investigations. The technical assistance of Miss Rosemary Wald is gratefully acknowledged.

1. E. Kiehlmann and P. W. Loo. Can. J. Chem. **47**, 2029 (1969).
2. E. Kiehlmann and P. W. Loo. Can. J. Chem. **49**, 1588 (1971).
3. K. von Auwers and M. Schmid. Chem. Ber. **46**, 487 (1913).
4. W. Gerrard and B. K. Howe. J. Chem. Soc. 505 (1955).
5. S. Mamedov, S. N. Ryzhova, and F. S. Gadzhizade. Zh. Org. Khim. **4**, 81 (1968).
6. F. I. Luknitskii and B. A. Vovsi. Zh. Org. Khim. **3**, 2142 (1967).
7. F. I. Luknitskii and B. A. Vovsi. Zh. Org. Khim. **3**, 794 (1967).
8. C. Alexandre and F. Rouessac. Tetrahedron Lett. 1011 (1970).
9. W. Reeve and C. W. Woods. J. Am. Chem. Soc. **82**, 4062 (1960).
10. J. Wislicenus and T. Kircheisen. Chem. Ber. **26**, 908 (1893).
11. J. Salkind. J. Russ. Phys. Chem. Ges. **30**, 906 (1899).
12. G. M. Baluja, A. M. Municio, and S. Vega. Anales Real Soc. Espan. Fis. Quim. (Madrid), Ser. B, **60**, 639 (1964).
13. G. M. Baluja. Anales Real Soc. Espan. Fis. Quim. (Madrid), Ser. B, **62**, 1009 (1966).
14. W. Reeve and E. Kiehlmann. J. Org. Chem. **31**, 2164 (1966).
15. A. Takeda and S. Tsuboi. J. Org. Chem. **35**, 2690 (1970).
16. E. Kiehlmann, R. J. Bianchi, and W. Reeve. Can. J. Chem. **47**, 1521 (1969).
17. D. G. Kundiger and H. N. Haney. J. Am. Chem. Soc. **76**, 615 (1954).
18. L. Fine. Ph.D. Thesis. University of Maryland, College Park, Maryland, 1962.
19. T. F. Steckel. Ph.D. Thesis. University of Maryland, College Park, Maryland, 1970.
20. H. Ohse, R. Palm, and H. Cherdron. Monatsh. Chem. **98**, 2138 (1967).
21. A. LeCoq. Ann. Chim. (Paris), **3**, 517 (1968).
22. F. G. Bordwell and M. W. Carlson. J. Am. Chem. Soc. **91**, 3951 (1969).
23. R. B. Woodward and R. Hoffmann. Angew. Chem. **81**, 845 (1969).
24. R. E. Bowman and R. N. Williamson. J. Chem. Soc. C, 101 (1970).
25. F. Caujolle, P. Couturier, and M. Doumerc. Bull. Soc. Chim. Fr. **17**, 22 (1950).
26. M. Stiles, R. R. Winkler, Y. Chang, and L. Traynor. J. Am. Chem. Soc. **86**, 3337 (1964).
27. W. Reeve, J. P. Mutchler, and C. L. Liotta. Can. J. Chem. **44**, 575 (1966).
28. H. L. Haller, P. D. Barlett, N. L. Drake, M. S. Newman, S. J. Cristol, C. M. Eaker, R. A. Hayes, G. W. Kilmer, B. Magerlein, G. P. Mueller, A. Schneider, and W. Wheatley. J. Am. Chem. Soc. **67**, 1591 (1945).
29. J. Colonge and G. Lartigau. Justus Liebigs Ann. Chem. **684**, 10 (1965).
30. A. Roedig and E. Klappert. Justus Liebigs Ann. Chem. **605**, 126 (1957).
31. K. Pilgram and H. Ohse. J. Org. Chem. **34**, 1586 (1969).
32. S. J. Cristol. J. Org. Chem. **28**, 2066 (1963).
33. W. E. Truce. J. Org. Chem. **35**, 1834 (1970).

Can. J. Chem. Downloaded from www.nrcresearchpress.com by 210.87.254.5 on 09/05/12
For personal use only.

Szilard–Chalmers Reactions in Dicyclopentadienyldiirontetracarbonyl

W. KANELLAKOPULOS-DROSSOPULOS AND D. R. WILES[1]
Institut fur Heisse Chemie, Kernforschungszentrum Karlsruhe, Germany

Received March 2, 1971

In neutron-irradiated solid $[CpFe(CO)_2]_2$ radioactive $FeCp_2$ and $Fe(CO)_5$ are formed, in addition to the radioactive parent compound. The radiochemical yields before annealing are 1.4, 3.2, and 16.0%, respectively. The predominance of $Fe(CO)_5$ over $FeCp_2$ is in keeping with previous observations. The yield of radioferrocene is not affected by subsequent thermal treatment at up to 75°, while the yields of the two carbonyl-containing compounds are increased up to 5.4 and 20.1%. The ferrocene yield is insensitive to irradiation time and temperature. From this insensitivity it is concluded that the Fe—Cp bonds are reformed by epithermal processes. Similarly the Fe—CO bonds are reformed by thermal as well as epithermal reactions.

Dans l'irradiation de $[CpFe(CO)_2]_2$ par les neutrons, il se forme du $FeCp_2$ et $Fe(CO)_5$ radioactif, en plus du composé radioactif parent. Les rendements radiochimiques avant le recuit sont respectivement de 1.4, 3.2 et 16.0%. La prédominance de $Fe(CO)_5$ sur $FeCp_2$ est en accord avec des observations précédentes. Le rendement en radioferrocène n'est pas affecté par un traitement thermique ultérieur jusqu'à 75°, alors que les rendements en composés contenant du carbonyle sont augmentés jusqu'à 5.4 et 20.1%. Le rendement en ferrocène est indépendant du temps et de la température d'irradiation. De cette non dépendance, il en a été conclu que les liaisons Fe-Cp se sont reformées par un processus épithermique. D'une façon analogue, les liaisons Fe-CO sont régénérées par des réactions aussi bien thermiques qu'épithermiques.

Canadian Journal of Chemistry, 49, 2977 (1971)

The chemical effects of neutron capture in π-bonded metalorganic compounds have been studied in a number of cases. Particularly interesting are the cyclopentadienylmetal carbonyls and the analogous benzenemetal carbonyls, where radical competition reactions can lead to the incorporation of the radioactive atoms into a small variety of distinct and different compounds without, apparently, having noticeable effect on the bulk material. Unfortunately, to date only two such systems have been studied. In neutron-irradiated benzenechromium tricarbonyl, Baumgärtner and Zahn (1) found a retention[2] of 10.0% of the radioactive atoms in their original chemical form, but also a radiochemical yield[2] of $^{51}Cr(\phi H)_2$ of 0.2% and of $Cr(CO)_6$, 13.5%. This surprisingly high yield of ^{51}Cr as the hexacarbonyl was matched in the $CpMn(CO)_3$ and $CH_3CpMn(CO)_3$ system (2) in that derivatives of the radical $—Mn(CO)_5$ were found to total some 9–10%, mostly present as $HMn(CO)_5$ and $CH_3Mn(CO)_5$. The yield of $^{56}MnCp_2$ could not be measured reliably, since a rapid exchange occurs between the carrier $MnCp_2$ and the radioactive atoms of the "inorganic" fraction.

It thus seems (2) that the newly radioactive metal atom is better able to accumulate carbonyl ligands than can be accounted for by the average composition of the target substance or by the metal–ring and metal–carbonyl bond strengths. To extend this study to another system, we have studied the binuclear $[CpFe(CO)_2]_2$ (3). Since iron has an even atomic number it does not form a monomeric Cp—Fe—CO compound, and the true structure involves two bridging carbonyls, with a *trans* configuration in the solid (4, 5).

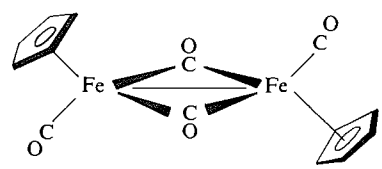

On chemical grounds one expects thermal decomposition to give ferrocene as the major molecular product (3). Likewise, radiolysis

[1]Permanent address: Chemistry Department, Carleton University, Ottawa, Canada.

[2]The retention and yield values given here and throughout this paper refer only to the radioactive atoms. These will be present in concentrations which may be some 10^{-10} to 10^{-12} mol%, and are detectable only because of their radioactivity. Macro quantities of these compounds are added to act as "carriers" during subsequent chemical operations.

Can. J. Chem. Downloaded from www.nrcresearchpress.com by 210.87.254.5 on 09/05/12
For personal use only.

usually causes primarily rupture of the metal–carbonyl bonds. This is contrary to the predictions of the generalization mentioned above which suggests that carbonyl formation ought to be favored. Thus the present system seems to be an unusually interesting one to study.

A further reason for choosing this compound lies in its binuclear structure. One should expect (6, 7) that greater retention or yield values would be found with the simpler molecules. While this is in part true, a number of contradictory results have appeared (7, 8). These seem to be explainable on the basis of rapid formation of simple "building blocks" which then combine or exchange to form the complex product molecule. Thus the high retentions in $Ru_3(CO)_{12}$ and $Fe_3(CO)_{12}$ were explained (7) by postulating $*Ru(CO)_4$ and $*Fe(CO)_4$ fragments, respectively, and the high retention in fulvalenehexacarbonylmanganese (8) is explainable by postulating the existence of highly reactive $C_5H_4*Mn(CO)_3$ fragments. Similarly, one might imagine the involvement of $Cp*Fe(CO)_2$ fragments as building blocks in the present system.[3]

Experimental

Dicyclopentadienyldiirontetracarbonyl was obtained from Atomergic Chemicals Co. and was purified by extraction and crystallization from boiling pentane.[4] The compound is somewhat sensitive to light, especially when in solution. Therefore the compound was stored in total darkness and handled in subdued light. In particular, fluorescent light was replaced by weak incandescent light, and the chromatograph columns were wrapped in aluminum foil. The compound was nicely crystalline, showing no visible signs of impurity. Mass spectrometric and infrared analyses[5] revealed no trace of impurity.

Irradiations were done in vacuo, at −78 °C in the Rohrpost position of the FR-2 Reactor, where the thermal flux was reportedly 9×10^{13} cm^{-2} s^{-1}. Irradiated samples were stored under liquid nitrogen until they were raised to room temperature for immediate processing. The samples were not analyzed for bulk decomposition at this stage. However, the appearance of the crystals was unchanged by the irradiation. Chromatographic tests failed to show the presence of any impurity such as $FeCp_2$ or $Fe(CO)_5$.

Samples to be processed were dissolved in 1 ml of $CHCl_3$, along with $FeCp_2$ and $Fe(CO)_5$ carriers, and 0.5 ml petroleum ether was then added. After being well mixed, the solution was put on the top of a silica gel column prepared under petroleum ether. Following elution of $Fe(CO)_5$ and $FeCp_2$, the eluant was replaced by $CHCl_3$ to effect elution of the target compound. Since $Fe(CO)_5$ is somewhat volatile, this fraction was collected in a tube containing concentrated HNO_3, to convert the iron to a non-volatile form. The ferrocene was further purified by sublimation under a gentle stream of nitrogen. Attempts to influence the distribution of the activity by scavenging with iodine (to produce $CpFe(CO)_2I$) met with failure, because of the bulk reaction of I_2 with the starting compound.

Radioactivity measurements were made using a well-type NaI scintillation counter. All samples were done in duplicate, comparing the activities with that of a reference sample composed of untreated crystals of the irradiated compound. Iron analyses were performed using Titriplex III solution with thiosalicylic acid as indicator (9), following total destruction of the compounds with H_2O_2 and HNO_3. Agreement between the duplicate samples was good, better than between different irradiations, for reasons which are not yet clear.

Results

The data obtained were somewhat scattered, despite all efforts to work carefully and reproducibly. The results are shown in Figs. 1, 2, and 3, in which are shown the values obtained for the yields[6] of the parent compounds, $Fe(CO)_5$ and $FeCp_2$, as functions of irradiation time, annealing time and annealing temperatures. It is seen immediately that the yield of $FeCp_2$ is evidently insensitive to any of these variables, and remains at about 1.4% regardless of the conditions. The two carbonyl-containing compounds seem to be more sensitive to external variables, and in approximately the same way, although the $Fe(CO)_5$ relatively more so than the target compound. It is noteworthy that the yield of $*Fe(CO)_5$ is higher than that of $*FeCp_2$, even without subsequent thermal treatment.

From Fig. 1 it is seen that the radiochemical yields of the two carbonyls increase somewhat as the irradiation time is increased from 3 to 10 min. This may be a result of the accompanying γ radiation, but we have no opportunity to check this hypothesis. Rather, we used a standard 10-min irradiation for all further experiments.

[3]An asterisk will be used in this paper to indicate that the metal atom following it is radioactive, and does not imply chemical excitation.

[4]We are grateful to Mr. E. Dornberger for performing this purification.

[5]We are grateful to Drs. W. Stieglitz and B. Kanellakopulos for these analyses.

[6]We shall use the term "yield" to refer to the fraction (or percent) of the total radioactivity of a specified type in the specified chemical form, including that of the parent compound. Corrections for chemical yield are, of course, included as are decay corrections when necessary. Any attempted distinction between retention and yield seems to be awkward, and occasionally misleading.

Can. J. Chem. Downloaded from www.nrcresearchpress.com by 210.87.254.5 on 09/05/12
For personal use only.

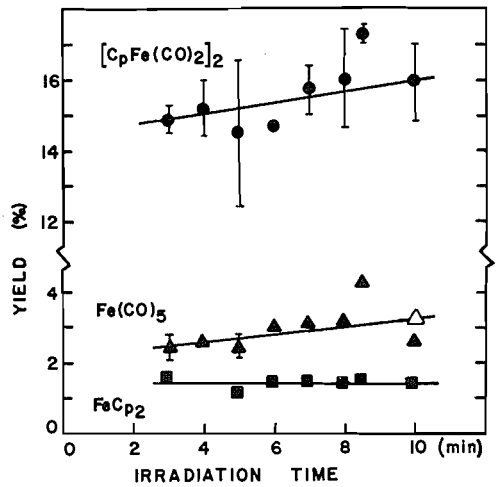

FIG. 1. Yields as a function of irradiation time at −78 °C, without annealing. The open point is taken for subsequent discussion as best representing the true value of the yield of $*Fe(CO)_5$ for a 10-min irradiation.

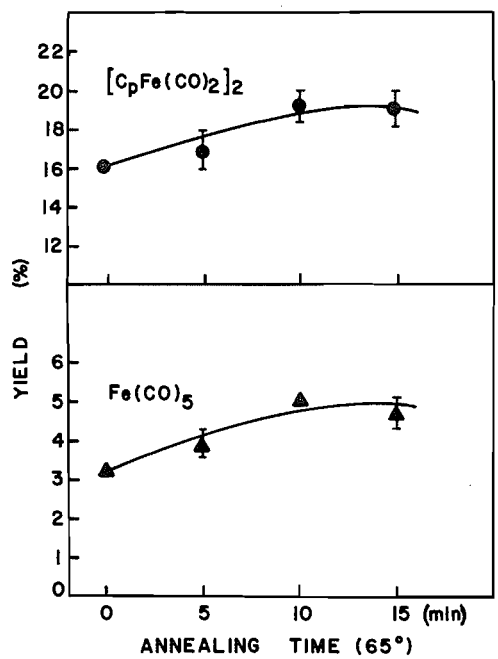

FIG. 2. Yields of $[Cp*Fe(CO)_2]_2$ and $*Fe(CO)_5$ as a function of annealing time at 65 °C, following 10 min irradiation at −78 °C.

The dependence on annealing time, Fig. 2, shows a gentle but distinct increase in the yields of the parent compound and $Fe(CO)_5$. The shapes of the curves cannot be given with certainty but the increase appears to occur mostly

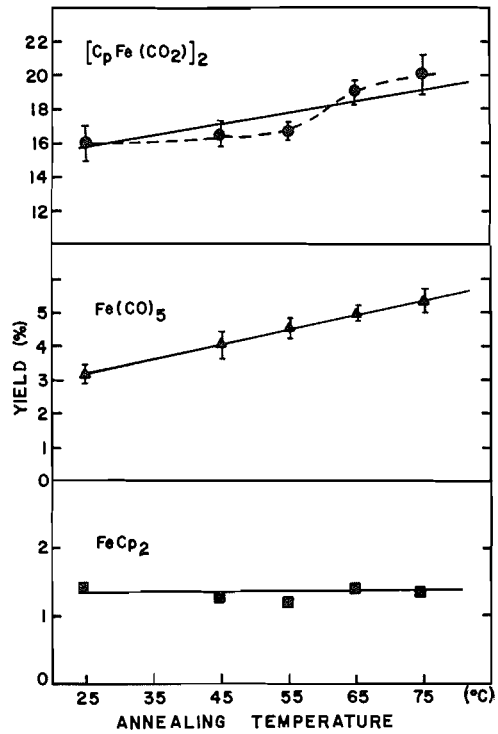

FIG. 3. Yields of $[Cp*Fe(CO)_2]_2$ and $*Fe(CO)_5$ after isochronal (15 min) annealing at various temperatures. The parameters for the straight lines drawn are given in Table 2.

in the first 10 min. Likewise the effect of increasing the annealing temperature, as given in Fig. 3, is to increase $Y_{[CpFe(CO)_2]_2}$ and $Y_{Fe(CO)_5}$, the latter relatively more. These data are given in Table 1.

The scatter in the data is too great to allow us to fix the shape of the curve of Y *vs.* temperature with great accuracy, although both can be represented to a first approximation as linear functions over the interval 25–75 °C

$$[1] \qquad Y_T^{15} = Y_{25} + \alpha\tau$$

where Y_T^{15} is the yield after 15 min of annealing at $T = 25 + \tau$ °C, and α is the slope of the line drawn in Fig. 3. It may be that the curve for $[CpFe(CO)_2]_2$ should better be taken as sigmoid in shape. Through all these changes, the yield of ferrocene-^{59}Fe remained essentially unchanged. The parameters for eq. 1 are given in Table 2.

In several irradiations carried out at reactor temperature, the ferrocene yield remained essentially unchanged at 1.4%. The other two yields were erratic but higher: up to 23 and 8%. Since

Can. J. Chem. Downloaded from www.nrcresearchpress.com by 210.87.254.5 on 09/05/12
For personal use only.

TABLE 1. Values obtained for the yields of ^{59}Fe in the chemical forms listed, following thermal treatment for 15 min at the indicated temperature*

	^{59}Fe yield		
T (°C)	$[CpFe(CO)_2]_2$	$Fe(CO)_5$	$FeCp_2$
25	16.0±1.1	2.53±0.23	1.40±0.04
45	16.5±0.8	4.13±0.37	1.31±0.05
55	16.7±0.4	4.71±0.57	1.22±0.07
65	19.1±0.7	4.70±0.22	1.35±0.05
75	20.1±1.2	5.37±0.35	1.36±0.08

*The uncertainty limits are the standard deviations of the means.

TABLE 2. Effect of isochronal annealing (15 min) at various temperatures, giving the parameters for eq. 1: $Y_T^{15} = Y_{25} + \alpha\tau$, where $T\,°C = 25 + \tau$, describing the straight lines in Fig. 3

Compound	Y_{25} (%)	α (% deg^{-1})	α/Y_{25}
$[CpFe(CO)_2]_2$	15.9	0.050	0.0031
$Fe(CO)_5$	3.2	0.044	0.013
$FeCp_2$	1.4	0.000	0.0000

the reactor temperature could be neither controlled nor measured, these data are of only qualitative significance.

Discussion

Assuming that the target molecule is initially destroyed,[7] there are these general stages during which reactions might occur between the radioactive atoms and various fragments and molecules to give the observed products:

(*i*) Hot (or epithermal) reactions can occur with recoil atoms either in flight (11, 12) or just at the end of their trajectory, while the surrounding region is still thermally or electronically excited (13, 14). This latter would also include the case of little recoil but extensive ionization by the Auger effect. It is not possible at present to make a reliable estimate of the time interval between the nuclear event and the time of attainment of a quasi-stable local state. Mössbauer experiments indicate that this time is shorter than about 10^{-9} s, for several ionic cobalt compounds (15). It is generally considered that these hot and epithermal reactions are insensitive to any experimental conditions which can be applied to solids.

(*ii*) Reactions can also occur in the untreated target after initial thermal excitation has been dissipated. These reactions, if fast, may be indistinguishable from epithermal and hot reactions. If they are slow enough, however, they will be susceptible to thermal, radiation, and other influences. An extensive literature on this subject deals largely with ionic salts, but some work has been reported on thermal and radiation annealing effects in π-organometallic compounds (2, 16, 17, 23).

(*iii*) Reactions may also occur during the chemical workup of the sample. While it is often possible to minimize these effects, and even to utilize them to capture unstable species (18, 2), there is seldom any real certainty that such reactions have *not* occurred. The greatest difficulty in this respect is assessing the probable chemical behavior of the unidentified carrier-free species, which may often include some 70–80% of the radioactive atoms. While it has been common to call this the "inorganic" fraction, its initial chemical nature is entirely unknown. It is thus possible that some unknown species could exchange or react with added carriers. The clearest example of this is the reaction (19) which leads to the accumulation of some 30% of the ^{56}Mn in the form of $MnCp_2$, from neutron-irradiated $Mn_2(CO)_{10}$! This might support a contention that at least some of the unknown species are ionic in nature, since $MnCp_2$ is known to be electrostatically bonded (20). The corresponding reaction of $FeCp_2$ with ^{59}Fe atoms is found to be very much less prominent, and an upper limit of 0.02% is indicated (21) for comparable conditions.

The insensitivity of the yield of $*FeCp_2$ to external influences, either during or after irradiation, suggests that the fate of the Fe—Cp bonds is determined by epithermal (or hot) processes, or that the $*FeCp_2$ is formed on dissolution by reaction between the carrier and some radioactive species which, though reactive, was trapped in a stable position in the solid. It seems unlikely that the latter would give rise to such highly reproducible results and, considering also the upper limit for exchange referred to above, we favor the former interpretation: that the Fe—Cp bonds are reformed by epithermal reactions.

The sensitivity of both of the carbonyl-containing compounds to external influences applied shows that an important fraction of the Fe- - -CO bonds are formed by thermal processes. The relative tendencies of thermal and other (epither-

[7]The few studies in which this has been investigated suggest that true failure of bond rupture occurs in only a very small fraction of the events (10).

Can. J. Chem. Downloaded from www.nrcresearchpress.com by 210.87.254.5 on 09/05/12
For personal use only.

mal and spurious) reactions can be derived from the values of α/Y_{25}. These values, given in Table 2, show the relative thermal tendency to be much the greater for $Fe(CO)_5$, and progressively less as the number of bonded Cp groups increases.

The fact that none of the observed product compounds decreases during annealing, but all either increase or remain constant, suggests that the three are produced independently by competitive reactions, and not by consecutive thermal reactions leading from one product to another. These latter are known in triphenylarsine (22) and suspected in $CpMn(CO)_3$ (23).

Reformation of the parent compound is most easily visualized as exchange of a $Cp^*Fe(CO)_2$ "monomer" with a molecule of the dimer. The $CpFe(CO)_2$ group is known as a constituent of a number of compounds (24). Its separate existence has been postulated by Haines and du Preez (25) as a reaction intermediate in the halogenation of $[CpFe(CO)_2]_2$. It seems possible that when trapped in a crystal lattice, the $CpFe(CO)_2$ monomer could have an independent existence, in the same way as $\cdot Mn(CO)_5$ is apparently stable in $Mn_2(CO)_{10}$ crystals, and thus be an available building block for reconstitution of the parent molecule. Although the usual form in the solid is the *trans* isomer both *cis* and *trans* are found in solution. A non-bridged structure, as is postulated (26) to account for the isomerization in solution, would be required for the most convenient exchange mechanism. Barrett and Sun (27) have estimated the energy required to break the two carbonyl bridges as 13 ± 2 kcal/mol, although the activation energy for isomerization will involve a rotational barrier as well. In an attempt to detect the presence of *cis*-$[CpFe(CO)_2]_2$ in the solid at higher temperatures, from which the presence of this nonbridged species could also be inferred, infrared (i.r.) spectra were run in KBr pellets at temperatures up to 80 °C. An increase in the intensity of a band at about 2000 cm^{-1}, assigned by Manning (26) to the *cis* compound, would indicate the formation of this species at higher temperatures. No variation in the relative band intensities was found between 20 and 80 °C.[8] It must thus be said that no evidence is at present available to support (or refute) the foregoing speculation on parent reformation.

[8]These spectra were kindly run by Dr. B. Kanellakopulos.

It is clear that a good deal of information on possible exchange reactions will be required before detailed statements can be made about the mechanisms of the radiochemical reactions described here. These data will be needed not only for CO groups, on which there are already extensive data, but also for Cp groups, which have not been studied, and for larger groups such as $CpFe(CO)_2$. Labelling of these large groups may perhaps most easily be accomplished by means of reactions such as are described in this paper (28). Preliminary studies have been made in this way on exchanges of the $—Mn(CO)_5$ group (29).

We express our sincere gratitude to Professor F. Baumgärtner for his constant interest and support, and for extending the hospitality of his Institute to D.R.W. We thank Mrs. E. Rauch for invaluable experimental assistance.

1. F. Baumgärtner and U. Zahn. Radiochim. Acta, **1**, 51 (1963).
2. I. G. de Jong, S. C. Srinivasan, and D. R. Wiles. Can. J. Chem. **47**, 1327 (1969).
3. T. S. Piper, F. A. Cotton, and G. Wilkinson. J. Inorg. Nucl. Chem. **1**, 165 (1955); B. F. Hallam, O. S. Mills, and P. L. Pauson. J. Inorg. Nucl. Chem. **1**, 313 (1955).
4. O. S. Mills. Acta Cryst. **11**, 62 (1958).
5. R. D. Fischer, A. Vogler, and K. Noack. J. Organomet. Chem. **7**, 135 (1967).
6. G. Harbottle. *In* Advances in inorganic chemistry and radiochemistry. Vol. I. *Edited by* H. J. Emeleus and A. G. Sharpe. 1959. p. 267.
7. S. R. Narayan and D. R. Wiles. Can. J. Chem. **47**, 1019 (1969).
8. I. G. de Jong and D. R. Wiles. Can. J. Chem. **48**, 1614 (1970).
9. E. Merck A.G. Komplexometrische Bestimmungs methoden mit Titriplex. Darmstadt.
10. U. Zahn. Radiochim. Acta, **7**, 170 (1967).
11. W. F. Libby. J. Am. Chem. Soc. **69**, 2523 (1947).
12. W. H. Wong and D. R. Wiles. Can. J. Chem. **46**, 3201 (1968).
13. J. E. Willard. Ann. Rev. Nucl. Sci. **3**, 193 (1953).
14. G. Harbottle and N. Sutin. J. Phys. Chem. **62**, 1344 (1958).
15. (*a*) W. Triftshäuser and P. P. Craig. Phys. Rev. **162**, 274 (1967). (*b*) P. Glentworth, A. L. Nichols, N. R. Large, and R. J. Bullock. Chem. Commun. 206 (1971).
16. U. Zahn, K. E. Collins, and C. H. Collins. Radiochim. Acta, **11**, 33 (1969).
17. H. R. Groening and G. Harbottle. Radiochim. Acta, **14**, 109 (1970).
18. I. G. de Jong and D. R. Wiles. Chem. Commun. 519 (1968).
19. S. C. Srinivasan. Ph.D. Thesis. Carleton University, Ottawa, Canada. 1970.

20. G. WILKINSON, F. A. COTTON, and J. M. BIRMINGHAM. J. Inorg. Nucl. Chem. **2**, 95 (1956).
21. W. KANELLAKOPULOS-DROSSOPULOS and D. R. WILES. In preparation.
22. G. GROSSMANN. Radiochim. Acta, **13**, 31 (1970).
23. T. COSTEA, I. NEGOESCU, P. VASUDEV, and D. R. WILES. Can. J. Chem. **44**, 885 (1966).
24. G. A. MELSON, P. F. STOKELY, and R. F. BRYAN. J. Chem. Soc. A, 2247 (1970).
25. R. J. HAINES and A. L. DU PREEZ. J. Chem. Soc. A, 2341 (1970).
26. A. R. MANNING. J. Chem. Soc. A, 1319 (1968).
27. P. F. BARRETT and K. K. W. SUN. Can. J. Chem. **48**, 3300 (1970).
28. S. C. SRINIVASAN and D. R. WILES. In preparation.
29. H. JAKUBINEK, S. C. SRINIVASAN, and D. R. WILES. Can. J. Chem. **49**, 2175 (1971).

Can. J. Chem. Downloaded from www.nrcresearchpress.com by 210.87.254.5 on 09/05/12
For personal use only.

Can. J. Chem. Downloaded from www.nrcresearchpress.com by 210.87.254.105 on 09/05/12
For personal use only.

Reactions of Alkylthio Derivatives of Aluminum with Aldehydes, Ketones, and Olefins

J. M. LALANCETTE, Y. BEAUREGARD, AND M. BHÉREUR
Département de Chimie, Faculté des Sciences, Université de Sherbrooke, Sherbrooke, Québec

Received March 22, 1971

The preparation of $((CH_3)_2CHS)_2AlCH_3$ and $(t\text{-}C_4H_9S)_2AlCH_3$ is reported. The reactions of $(RS)_2AlCH_3$ (R = CH_3, $(CH_3)_2CH$, $t\text{-}C_4H_9$) with ketones give aldol condensations leading to the corresponding conjugated ketones, with the acetyl group R—CO—CH_3; with other ketones, a mixture of thioacetal and enolthioether is obtained. With aldehydes, a mixture of thioacetal and enolthioether is observed. With olefins there is an addition of two RS groups on the site of the double bond, with a small percentage of allylic substitution. With conjugated ketone, the saturated ketone is obtained with the alkylthio group in β position. All those reactions proceed with good yields and appear quite general.

La préparation de $((CH_3)_2CHS)_2AlCH_3$ et de $(t\text{-}C_4H_9S)_2AlCH_3$ est rapportée. Les réactions de $(RS)_2AlCH_3$ (R = CH_3, $(CH_3)_2CH$, $t\text{-}C_4H_9$) avec les cétones donnent des condensations aldoliques conduisant à des cétones conjuguées, si le groupe acétyle R—CO—CH_3 est présent. Avec les autres cétones, un mélange de thioacétal et d'éther thioénolique est obtenu. Avec les aldéhydes un mélange du thioacétal et de l'éther thioénolique est observé. Avec les alcènes, on remarque l'addition de deux groupes RS sur le site de la liaison double ainsi qu'une certaine substitution en α du lien double. Avec les cétones conjuguées, des cétones saturées portant un groupe RS en position β sont obtenues. Ces réactions donnent de bons rendements.

Canadian Journal of Chemistry, **49**, 2983 (1971)

We have reported the preparation of thiomethyl derivatives of aluminum such as $(CH_3S)_2AlCH_3$ and $(CH_3S)_3Al$ and the reactions of those compounds with some inorganic and organic substrates (1). This paper will describe the reaction of organic derivatives of aluminum of general formula $(RS)_2AlCH_3$, where R = methyl, isopropyl, and *t*-butyl, with various aldehydes, ketones, and olefins.

The reactions of aluminum alkoxides with aldehydes and ketones are well known and widely used in organic chemistry. Depending on the experimental conditions those alkoxides can be used in oxydation or reduction reactions. The initial approach to the present work was to compare the effect of the substitution of RS groups with the RO groups on aluminum. With RS groups, the aluminum derivative was expected to give non-reversible reactions with oxygen bearing functional groups, contrary to Oppenauer oxidation, for example, when the reactions are essentially reversible. Such behavior was to be expected because of the important difference between the heat of formation of the Al—O and Al—S bonds: Al_2O_3 : $\Delta H°$: −399 kcal/mol; Al_2S_3 : $\Delta H°$: −121 kcal/mol (2). Such a large difference in heat of formation would render the system Al—S → Al—O irreversible towards Al—O.

We have noted however that the substitution of sulfur for oxygen on aluminum changes completely the reactivity of this reagent and entails very few similarities between those two families of aluminum derivatives.

Results and Discussions

Preparative Reactions

The general procedure for the preparation of alkylthio derivatives of aluminum has been reported (1). We have extended the scope of this method by using homologs of methanethiol as starting material such as isopropyl and *t*-butyl mercaptans. The pattern of the reaction was the same except that reflux temperatures were used instead of the low temperature conditions employed with methanethiol. In both cases, the product obtained was of the general formula $(RS)_2AlCH_3$, as shown by the various analyses. With R = methyl or isopropyl, the derivatives exist as a highly polymerized entity, insoluble in all non-destructive solvents. But with *t*-butyl, probably because of the steric hindrance created by the two bulky groups, and preventing its polymerization, the alkylthio aluminum derivative was then soluble in benzene and other nonpolar solvents. It has been possible, with this soluble material, to obtain i.r. and n.m.r. measurements. The elemental analyses was con-

[1] 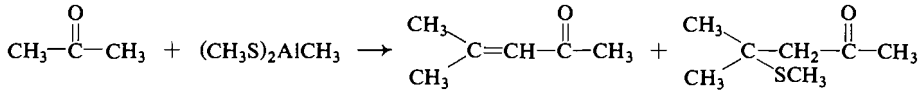

[2] 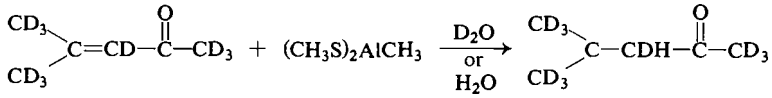

[3] 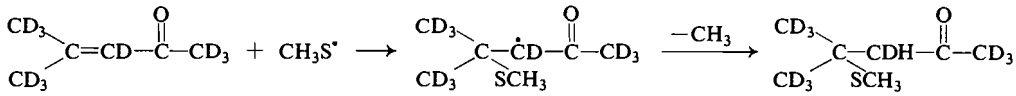

firmed with the n.m.r. of $(t\text{-}C_4H_9)_2AlCH_3$ where the two expected peaks were found at 1.48 (singlet, 3 protons) and 1.54 (singlet, 18 protons). It has been possible to obtain confirmation of the structure of $(CH_3S)_2AlCH_3$ by Raman spectroscopy.

Reactions with Ketones

Under mild experimental conditions, we have found that acetyl groups gave condensation reactions in presence of dithioalkyl derivatives of aluminum ($(RS)_2AlCH_3$ where R = methyl, isopropyl, or *t*-butyl). The condensation reaction appeared to be very specific for the acetyl groups, no such reaction being observed with other types of ketones. With ketones not having the acetyl groups, we obtained the corresponding thioketal and enol thioether with yields of the order of 60%. Such a specific reaction is of real synthetic interest. Acetone, for example, gave mesityl oxide and a similar reaction was noted with butanone, pinacolone, 4-methylpentanone-2, 3-methylbutanone. With the methylthio derivative of aluminum, the product of condensation was accompanied by a substance corresponding to the addition of one methylthio group on the double bond formed by the condensation (eq. 1). Besides those products, methyl sulfide and methyl disulfide were formed. The ratio of conjugated ketone to β-methylthio ketone was 2/1.

We have been able to show that the formation of the β-methylthio ketone was a secondary reaction occurring subsequent to the condensation of the starting ketone. By treating mesityloxide with $(CH_3S)_2AlCH_3$, the corresponding β-methylthio ketone was obtained with a good yield. The position of the methylthio group was clearly shown by n.m.r. In the case of mesityl oxide, for example, the β-methylthio derivative was showing three different CH_3 groups (ratio of protons: 6/3/3) and one CH_2 group (2 protons).

In order to ascertain the source of the protons of the CH_2 group in α to the carbonyl after addition of the CH_3S substituent, the reaction was repeated with deuterated mesityl oxide, the hydrolysis being done with D_2O and H_2O. Under both experimental conditions, the CHD group was found in the position α to the carbonyl (eq. 2). The presence of protons or deuterium in the position α to the carbonyl was clearly shown by n.m.r. From this result and from the presence of methyl sulfide and methyl disulfide among the reaction products, we believe that the reaction must be a radical process, the proton in the position being abstracted from one of the methyl groups on the aluminum derivative, after the addition of a CH_3S radical to the double bond (eq. 3). Experimental, and economical, difficulties prevented the verification of eq. 3 with $(CD_3S)_2$ $AlCD_3$ and protonated mesityl oxide.

When the aluminum derivative was prepared with a bulky substituent, such as the propyl or *t*-butyl groups, the secondary reaction leading to the β-alkylthio ketone was not observed, the sole reaction being condensation. This behavior was noted with acetone, 3-methylbutanone, and pinacolone. With acetophenone, α-isopropylthio styrene was obtained and with 1,1-diphenyl acetone, there was no condensation, the starting material being recovered by hydrolysis.

The condensation of two molecules of methyl ketone is quite general and stops after the reaction of two $COCH_3$ units. With a very hindered ketone like *t*-butyl methyl ketone, however, we found that by increasing the amount of methylthio aluminum derivative, polycondensation could be obtained. With a ratio of two carbonyl

Can. J. Chem. Downloaded from www.nrcresearchpress.com by 210.87.254.105 on 09/05/12
For personal use only.

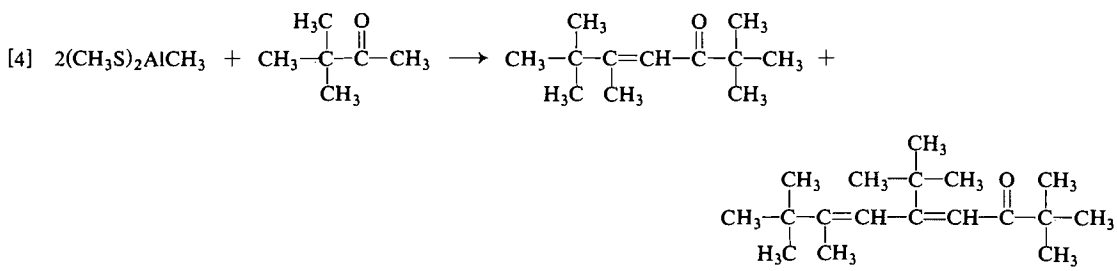

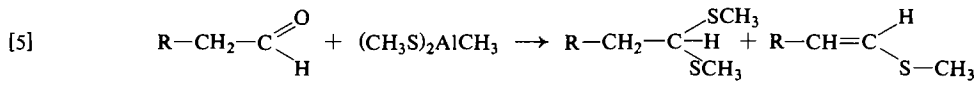

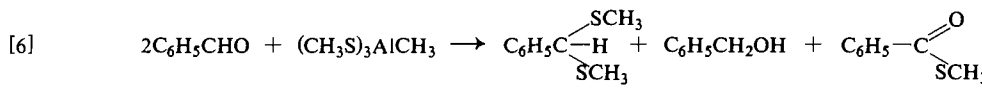

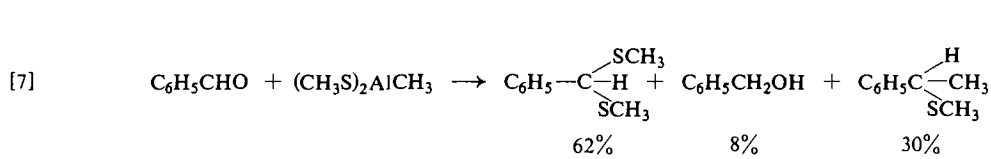

groups per aluminum, the normal product was obtained; but if the ratio reached one carbonyl group for two aluminum, then condensation was observed to proceed as shown in eq. 4: two or three molecules could then be involved in the condensation to give the constituents of the reaction mixture. Such a condensation of three molecules was observed solely with the above ketone; no similar reaction could be obtained with acetone, for example, even with a very large excess of the methylthio aluminum reagent.

Reactions with Aldehydes

With aliphatic aldehydes (phenylacetaldehyde, heptaldehyde, propionaldehyde, and butyraldehyde), the main reaction products were the corresponding thioacetals and thioenol ether (eq. 5). The ratio of thioacetal to methylthio olefin was of the order of 1/3.

With benzaldehyde the products of the reaction were the thioacetal, the thiolester, and smaller amounts of benzyl alcohol, when the ratio of aldehyde to reagent was of 2/1 (eq. 6). With a 1/1 molar ratio, then the thioacetal was the major product with lesser amounts of benzyl alcohol and methylthio ether (eq. 7). With cinnamaldehyde, the reaction products were the corresponding thioacetal and methylthioether, as observed with the 1/1 ratio reaction, eq. 6. The cinnamyl alcohol was not present in the reaction mixture but otherwise, the pattern of the reaction was quite similar to benzaldehyde.

The great variety of products, specially the presence of the methyl group on the carbonyl-bearing carbon cannot be explained easily. Clearly, a completely ionic mechanism cannot justify the formation of the thiol ester and the methylthioether. Consequently, as was the case with β-methylthio ketones and as it will be indicated with olefins, a free radical mechanism must be postulated to account for those products.

Reaction with Olefins and Conjugated Ketones

The reaction of $(CH_3S)_2AlCH_3$ has been examined with styrene, indene, and cyclohexene. In those experiments we have observed that there was an addition of two CH_3S groups to the double bond. With cyclohexene, beside the product of addition to the double bond, we found considerable allylic substitution (eq. 8). With conjugated ketones such as mesityl oxide, methyl vinyl ketone, cyclohexenone, isophorone, and *trans*-phenylbutanone, we observed the addition of the CH_3S group to the β position of the carbonyl to

Can. J. Chem. Downloaded from www.nrcresearchpress.com by 210.87.254.105 on 09/05/12
For personal use only.

[8] 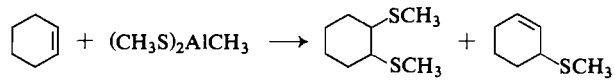

[9] 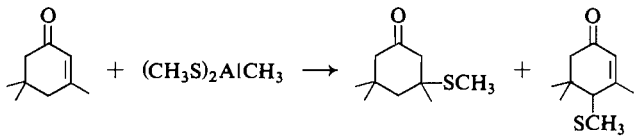

give the corresponding β-methylthio ketone. With isophorone some of the thiomethyl group was also found in the γ position (eq. 9).

Those results with olefins and conjugated ketones can only be explained by a radical attack either on the double bond or the conjugated double bond. The fact that the allylic groups could be involved in the reaction is another good indication in favor of a radical mechanism.

Mechanism of Reaction of $(RS)_2AlCH_3$

From those results obtained with aldehydes, ketones, and olefins, it is not easy to establish the precise mechanism of those reactions. In many instances, it is clear that the reaction must follow a radical path. The allylic substitution with olefins, the addition of the methylthio group with conjugated olefins such as mesityl oxide and the formation of methyl disulfide are strong indications of radical reactions. It has not been possible to use scavengers in order to corroborate those indications because of the reactivity of $(RS)_2AlCH_3$ with carbonyls, active methylene, or labile protons normally found on such substances.

Some of the reaction products, thioacetals and condensation products for example, can be explained by the acid character of substances like $(RS)_2AlCH_3$. But in every reaction where an ionic mechanism could prevail, there is also a product that cannot be easily accounted for without postulating a radical: methyl disulfide in the case of condensation reactions for example.

Consequently, although ionic mechanism cannot be ruled out entirely, the pattern of action of $(RS)_2AlCH_3$ must be strongly influenced by the capacity of this family of reagents to generate radicals.

Experimental

The i.r. measurements were made on a Perkin–Elmer spectrometer, model 257, in carbon tetrachloride solutions. The n.m.r. measurements were performed with a Varian A-60 instrument, using tetramethylsilane as internal reference. Mass spectrometric determinations were made with a Hitachi Perkin–Elmer machine, model RMV-6D. Melting points are not corrected. Elemental analyses are from Schwarzkopf Microanalytical Laboratory, New York. The v.p.c. measurements were made with a Microteck G-2000-R instrument. The u.v. spectra were recorded with a Cary 14 instrument. Raman measurements were made with a double monochromator Jarrell-Ash 25-100, using an argon laser at 4880 Å, the resolution being of the order of 1 cm^{-1}.

1. Preparation of Dithioalkyl Derivatives of Aluminum

The preparation of methyl bis(methylthio)aluminum has been reported (1).

The preparation of methyl bis(isopropylthio)aluminum was done according to the same procedure, except that after the addition of the mercaptan (1100 g) to the solution trimethyl aluminum (250 g), the solution was heated under reflux for 36 h. The expected derivative precipitated slowly and was isolated in a similar way as methyl bis(methylthio)aluminum.

With methyl bis(*t*-butylthio)aluminum, the procedure was the same as with the isopropyl derivative (1100 g of *t*-butyl mercaptan reacting with 250 g of trimethyl aluminum) except that benzene instead of pentane was used as solvent. The duration of the reflux was 3 days and the solvent was evaporated, in order to obtain the reaction product which then crystallized slowly. Yield: 90% based on $(CH_3)_3Al$: n.m.r. (benzene): singlet at 1.48 (3 protons) and singlet at 1.54 (18 protons).

The analyses were performed according to the methods described earlier (1).

Anal. Calc. for $(C_3H_7S)_2AlCH_3$: Al, 14.1. Found: Al, 15.2.

Anal. Calc. for $(C_4H_9S)_2AlCH_3$: Al, 12.2. Found: Al, 11.8%.

The Raman spectrum of methyl bis(methylthio)aluminum was determined in a sealed tube, with a sample of the solid material. Bands were observed at 2935 (strong), 2900 (medium), 2897 (medium), 2891 (medium), 1433 (weak), 1200 (weak), 700 (very strong), 576 (strong), 335 (very strong), 283 (very strong) cm^{-1}. The adsorption in the region of 700 cm^{-1} can be attributed to the C—S vibration, at 576 cm^{-1} to the Al—C vibration and 335 and 283 cm^{-1} to the Al—S vibration.

2. Reactions of Methyl Bis(alkylthio)aluminum with Ketones

2.1 Reaction with Acetone

In a conical flask, at room temperature, a suspension of 15 g (0.11 mol) of $(CH_3S)_3AlCH_3$ in 150 ml of dry pentane was treated with 12 g (0.20 mol) of acetone during 2 h. The reaction mixture turned rapidly to a yellowish

Can. J. Chem. Downloaded from www.nrcresearchpress.com by 210.87.254.105 on 09/05/12
For personal use only.

Can. J. Chem. Downloaded from www.nrcresearchpress.com by 210.87.254.105 on 09/05/12
For personal use only.

color. After this contact, the mixture was hydrolyzed by a slow addition of 10 ml of water and the aluminum hydroxide was filtered out. After drying over $MgSO_4$, the solvent was evaporated under vacuum leaving a yellow oil which was fractionated by distillation after analyses by v.p.c. Four components were found in this mixture. Methyl sulfide CH_3SCH_3 and methyl disulfide CH_3SSCH_3 were the first two products to appear upon v.p.c. chromatography. They were identified by comparison of their i.r. and n.m.r. spectra with those of authentic samples. The precise yield of those compounds has not been evaluated because of loss incurred by the evaporation of the solvent. They were present in more than trace amount, probably 20–30% of the total weight recovered at the end of the reaction. The third fraction, b.p. 129° was mesityl oxide, as shown by its n.m.r., i.r. and mass spectra which were identical with similar measurements made on an authentic sample. The last fraction, b.p. 78°/15 mm gave the following measurements. The n.m.r. δ: singlet (6 protons), 1.38; singlet (3 protons), 2.05; singlet (3 protons), 2.13; singlet (2 protons), 2.68. The i.r.: bands at 2980 (strong); 1710 (strong); 1180 (medium) cm^{-1}. Mass spectrum *m/e*: 41, 43, 47, 55, 83, 89, 98, 99, 146 (M^+). From those results, this last fraction must be 4-methyl-4-methylthiopentanone-2.

Anal. Calcd. for $C_7H_{14}OS$: C, 57.53; H, 9.58; S, 21.91. Found: C, 57.47; H, 9.62; S, 22.17.

The ratio of fraction 3 and 4 was 2/1 and the yield of those two fractions 65%.

The reactions with other ketones are reported in Table 1.

2.2 Reaction with Deuterated Mesityl Oxide

The reaction was performed with 5.4 g of perdeuterated mesityl oxide (Merck Sharp and Dohme), using experimental condition as in section 2.1 except that the hydrolysis was done with D_2O. The product gave an n.m.r. with a singlet (3 protons) at 2.03 and a triplet (1 proton) at 2.58 δ, $J = 2.2$ Hz, in accordance with the formulation $CD_3—CO—CHD—C(CD_3)_2SCH_3$.

The experiment was repeated under identical conditions except that the hydrolysis was done with H_2O. The same product was obtained, as indicated by similar n.m.r. and i.r spectra.

When the reaction was done with protonated mesityl oxide but the hydrolysis with D_2O, there was no incorporation of deuterium on the molecule: the ratio of the area of the peaks on n.m.r. of the reaction product were not affected and the i.r. did not indicate the presence of deuterium.

2.3 Reactions of Acetone with Methyl Bis(isopropylthio)aluminum

Using an experimental procedure as in section 2.1, acetone (11.6 g, 0.2 mol) was treated with methyl bis(isopropylthio)aluminum (19.2 g, 0.1 mol) in pentane at 0°, for 30 min. The usual procedures gave mesityl oxide (95% yield), identified by its n.m.r. and i.r. spectra.

2.4 Reactions of Acetone with Methyl Bis(t-butylthio)-aluminum

This reaction, on the same scale as in section 2.9 gave a high yield of the expected mesityl oxide. A similar behavior was noted with 3-methylbutanone and pinacolone, giving 2,5,6-trimethyl-4-heptene-3-one and 2,2,5,-6,6-pentamethyl-4-heptene-3-one with yields of 86 and 65% respectively. Those compounds were identified by comparison of their n.m.r. and i.r. spectra with authentic samples.

2.5 Reaction of Acetophenone

Using a similar experimental procedure as in section 2.1, acetophenone (12.0 g, 0.1 mol) and methyl bis(isopropylthio)aluminum (19.2 g, 0.1 mol) were reacted for 3 h at reflux temperature in pentane. The usual procedure gave 45% of α-isopropylthiostyrene. The n.m.r. δ: two doublets in the 1.15–1.40 region (6 protons); multiplet in the 2.50–3.30 region (1 proton); two doublets in the 5.1–5.5 region (2 protons); multiplet in the 7.3 region (5 protons). The i.r.: no band in the carbonyl region, band at 1665 cm^{-1} (weak). Mass spectrometry *m/e*: 120, 105, 77.

3. Reaction of Methyl Bis(alkylthio)aluminum with Aldehydes

3.1 Reaction with Benzaldehyde

In a 250 ml flask, a suspension of 6.8 g (0.05 mol) of methyl bis(thiomethyl)aluminum in 75 ml of anhydrous benzene was treated by 10.6 g (0.10 mol) of benzaldehyde. After a reflux of 1 h, the reaction mixture was cooled to 0°, hydrolyzed by water, and filtered. The organic phase, after drying over $MgSO_4$ was evaporated. The reaction mixture was formed of unreacted benzaldehyde (15%), thioacetal of benzaldehyde (15%), benzyl alcohol (29%), and methyl thiolbenzoate (41%). Those ratios were determined by v.p.c. on column 5 ft long, SE-30, 5%, at 150°. The benzaldehyde, its thioacetal, and benzyl alcohol were identified by comparison of their mass spectrum, v.p.c., and n.m.r. with those observed for samples. Methyl thiolbenzoate: the n.m.r. δ: singlet at 2.36 (3 protons); multiplet 7.35–7.83 (5 protons). The i.r. bands at 3090 (medium); 2980 (medium); 1665 (very strong); 1470 (strong) cm^{-1}. Mass spectrometry *m/e*: 152 (molecular ion), 105, 77, 51, 47.

Depending on the duration of the reaction, the temperature or the solvent (benzene or pentane) there was a slight variation of the yield of those compounds, up to 10%. However, those three products were always present.

When the reaction was repeated as above except that the molar ratio of aluminum derivative and benzaldehyde was 1/1, instead of 2/1, then the yield of thioacetal was increased, there was no longer methyl thiolbenzoate and a new compound, 1-phenyl-1-thiomethylethane appeared. In a typical experiment, no unreacted benzaldehyde was detected, there was 8% of benzyl alcohol, 62% of thioacetal, and 30% of $C_6H_5—CH(SCH_3)CH_3$, as shown by v.p.c. analysis.

1-Phenyl-1-thiomethylethane. The n.m.r. δ : doublet (3 protons) at 1.50; singlet (3 protons) at 1.78; quadruplet (1 proton) at 3.73; singlet (5 protons) at 7.15. The i.r.: bands at 3080 (medium); 3060 (medium); 3000 (strong); 2950 (strong); 1510 (strong); 1470 (very strong); 1455 (medium); 1240 (medium) cm^{-1}. Mass spectrometry *m/e*: 152 (molecular ion), 137, 121, 106, 105, 104, 103, 102, 77.

The reactions with other aldehydes are reported in Table 2.

4. Reaction of Olefins and Conjugated Ketones with Methyl Bis(methylthio)aluminum

4.1 Reaction with Cyclohexene

Using 8.0 g (0.59 mol) of methyl bis(methylthio)aluminum, the reaction with cyclohexene in excess was

Can. J. Chem. Downloaded from www.nrcresearchpress.com by 210.87.254.105 on 09/05/12
For personal use only.

TABLE 1. Reactions of $(CH_3S)_2AlCH_3$ with ketones

Ketone	Reaction products	Analysis (%) Calculated C	Calculated H	Calculated S	Found C	Found H	Found S	Nuclear magnetic resonance (δ)	Other
Butanone*	5-Methyl-4-heptene-3-one	76.19	11.11	—	75.97	11.19	—	5.45 (1H), 2.45 (4H), 1.30 (3H), 0.98 (6H)	b.p. 114°/15 mm
	5-Methyl-5-methylthio-3-heptanone	62.06	10.34	18.39	62.60	10.35	17.75	2.61 (2H), 2.45 (2H), 1.95 (3H), 1.70 (2H), 1.31 (3H), 1.0 (6H)	
Pinacolone*	2,2,5,6,6-Pentamethyl-4-heptene-3-one	79.12	12.08	—	79.22	12.22	—	6.31 (1H), 2.01 (3H), 1.11 (18H)	
4-Methylpentanone-2*	2,6,8-Trimethyl-5-nonene-4-one	79.12	12 08	—	79.13	12.20	—	6.05 (1H), 1.90–2.40 (9H), 0.85–1.10 (12H)	b.p. 139°/15 mm
3-Methylbutanone*	2,5,6-Trimethyl-4-heptene-3-one	77.87	11.77	—	77.87	11.74	—	5.38 (1H), 2.05–2.34 (2H), 1.87 (3H), 1.08–1.20 (12H)	b.p. 143°/12 mm
	2,5,6-Trimethyl-5-methylthio-heptanone-3							2.1–2.7 (4H), 2.00 (3H), 1.08–1.20 (12H)	b.p. 187–190°/12 mm
Methylvinylketone	4-Thiomethylbutanone†							2.06 (3H), 2.13 (3H), 2.65 (4H)	*m/e*: 118, 75, 71, 43
Cyclohexenone	3-Methylthiocyclohexanone‡	58.33	8.33	22.22	58.30	8.31	22 09	Multiplet 1.45–3.20, singlet at 2.10	*m/e*: 144, 97, 96, 69, 55, 44
Isophorone	4-Methylthio-3,5,5-trimethyl-2-cyclohexenone§							4.70–5.80 (2H), 1.70–2.32 (8H), 0.95–1.05 (6H)	*m/e*: 184, 168, 153, 105
	3-Methylthio-3,5,5-trimethylcyclo-hexanone‖							1.75–2.50, 2.01, 1.39, 1.16, 1.05	*m/e*: 186, 139, 83, 55
4-Phenyl-3-butenone	4-Phenyl-4-methylthiobutanone¶							7.66 (5H), 4.20 (1H), 2.88 (2H), 1.85–2.01 (6H)	*m/e*: 194, 147, 91, 43

*The dimerization of ketones gave yields of 80–90%.
†Yield: 85%.
‡Yield: 76%.
§Yield: 60%.
‖Yield: 16%.
¶Yield: 70%. The position of the CH_3S group was confirmed by reduction of the carbonyl by $NaBH_4$ and n.m.r. of the corresponding alcohol: multiplet at 2.88 δ.

TABLE 2. Reactions of $(CH_3S)_2AlCH_3$ with aldehydes and olefins

Reagent	Reaction products	Yield (%)	Nuclear magnetic resonance (δ)	Mass spectrometry (*m/e*)
Phenylacetaldehyde	2-Thiomethyl-1-phenylethene	26	2.33–2.35 (3H), 6.80–6.25 (2H), 7.32 (5H)	150, 135, 91, 45
	Thioacetal	68	1.98 (6H), 2.99 (2H), 3.73 (1H), 7.21 (5H)	198, 152, 107, 91, 47
Heptaldehyde	Thioacetal	70	3.58 (1H), 2.05 (6H), 0.78–2.28 (13H)	192, 145, 97, 87, 61
	1-Methylthio-1-heptene	21	2.16–2.21 (14H), 5.10–6.12 (2H)	144, 87, 81, 55
Cinnamaldehyde	Thioacetal	73	2.11 (6H), 4.29 (1H), 6.13 (1H), 6.50 (1H), 7.3 (5H)	163, 149, 115, 91, 47
	3-Methylthio-1-phenyl-1-butene	—	1.40 (3H), 1.94 (3H), 3.31 (1H), 6.01 (1H), 6.31 (1H), 7.28 (1H)	178, 131, 115, 91
Indene	2,3-Dimethylthioindene	55	2.00–2.19 (6H), 2.60–3.05 (1H), 3.16–3.70 (2H), 4.15 (1H), 7.15 (4H)	210, 163, 116, 115
Styrene	1,2-Dimethylthiophenylethane	75	1.80–1.88 (6H), 2.85 (2H), 3.80 (1H), 7.25 (5H)	198, 151, 137, 104, 91, 77

performed during 4 days at 110° in a pressure vessel. After hydrolysis and extraction with ethyl ether, two compounds were obtained weighing 3.2 g. This mixture was fractionated by preparative chromatography. The first fraction (1.8 g) was 3-methylthio-1-cyclohexene. The n.m.r. δ: multiplet between 1.45 and 2.25, including a singlet at 2.01 (9 protons); multiplet between 3.03 and 3.36 (1 proton); multiplet at 5.71 (2 protons). The i.r.: band at 1650 cm^{-1} (weak).

Anal. Calcd. for $C_7H_{12}S$: C, 65.62; H, 9.37; S, 25.00. Found: C, 65.59; H, 9.25; S, 25.16.

The second fraction weighing 0.9 g, was 1,2-dimethylthiocyclohexane. The n.m.r. δ: multiplet between 1.01 and 2.50, including a singlet at 2.13 (14 proton); multiplet between 2.58 and 2.90 (2 protons). Mass spectrometry *m/e*: 176 (molecular ion), 129, 81.

The reactions with other olefins are reported in Table 2.

The authors wish to thank the National Research Council of Canada for financial assistance and Professor A. Cabana for Raman measurements.

1. J. M. LALANCETTE, Y. BEAUREGARD, and M. BHEREUR. Can. J. Chem. **48**, 1093 (1970).
2. W. M. LATIMER. Oxidation potentials. Prentice-Hall, New York, N.Y., 1952. p. 282.

Can. J. Chem. Downloaded from www.nrcresearchpress.com by 210.87.254.105 on 09/05/12
For personal use only.

Can. J. Chem. Downloaded from www.nrcresearchpress.com by 210.87.254.105 on 09/05/12
For personal use only.

Reductions with Sulfurated Borohydrides. VI. The Reduction of Nitro, Nitrile, Amide, and Nitroso Groups

J. M. LALANCETTE AND J. R. BRINDLE

Département de Chimie, Faculté des Sciences, Université de Sherbrooke, Sherbrooke, Québec

Received March 22, 1971

Aromatic nitro compounds can be reduced with sulfurated sodium borohydride to the corresponding amine in high yields (≈80%) without affecting ester, nitrile, ether, halide or olefinic groups also present. With ortho-substituted nitro compounds the yields are around 60%.

Primary aliphatic nitro compounds are reduced to the corresponding nitrile in high yields. Secondary aliphatic nitro compounds are reduced to mixtures of ketones and the corresponding oxime. Tertiary aliphatic nitro compounds are not reduced.

Aromatic nitriles can be reduced to the corresponding amines with an excess of the reducing agent or converted to the corresponding thioamides with an excess of the nitrile.

Amides and nitroso can be reduced to the corresponding amines in moderate yields.

Les dérivés nitrés aromatiques peuvent être réduits en amines avec de bons rendements (≈80%) par l'hydrure de bore sulfuré, cette réduction pouvant être effectuée sans affecter les fonctions ester, nitrile, éther, halogène ou alcène présentes. Avec les dérivés ortho, les rendements sont de l'ordre de 60%.

Les dérivés nitrés aliphatiques primaires sont réduits en nitriles avec de bons rendements. Les dérivés nitrés aliphatiques secondaires sont réduits en un mélange de cétones et d'oximes correspondantes. Les dérivés nitrés aliphatiques tertiaires ne donnent pas de réaction.

Les nitriles aromatiques peuvent être réduits en amines, avec un excès de réducteur, ou en thioamides, avec un excès de nitrile.

Les amides et les nitroso peuvent être réduits en amines avec des rendements modérés.

Canadian Journal of Chemistry, 49, 2990 (1971)

We have reported the formation of sulfurated borohydrides (1, 2) according to eq. 1.

$$[1] \qquad NaBH_4 + 3S \xrightarrow[25°]{THF} NaBH_2S_3 + H_2$$

This sulfurated hydride has shown very distinctive properties in its reactions with aldehydes (3), ketones (4), and oximes (5).

We now wish to report the reduction of nitro, nitrile, amide, and nitroso groups with this new reducing agent.

Reduction of Nitro Derivatives with $NaBH_2S_3$

In order to appreciate the selectivity of $NaBH_2S_3$ a short survey of the reduction of nitro groups is indicated.

Catalytic hydrogenation, in presence of platinum or nickel (6) or chemical reduction by tin or iron, in presence of hydrochloric acid (7), can reduce simple nitro derivatives to the corresponding amines. Those procedures, however, are not very selective in presence of sensitive organic functions. With $LiAlH_4$ or mixtures of $LiAlH_4$.-$AlCl_3$, the reduction of aliphatic nitro groups generally proceeds to the level of the amino group (8). Because of the overwhelming reducing capacity of $LiAlH_4$, many other functional groups are also reduced under those conditions, such as esters, amides, nitriles, or halides. With aromatic nitro derivatives, reduction with $LiAlH_4$ leads mainly to azo derivatives and again, many other functional groups are reduced at the same time, when present (9).

With $NaBH_4$, aromatic or aliphatic nitro groups are not reduced, the only instance of reduction being observed in presence of palladium on carbon catalyst (10). With $LiBH_4$ low yields of amine (of the order of 20%) have been reported (11).

(a) Reduction of Aromatic Nitro Derivatives

We have found that sulfurated sodium borohydride can reduce aromatic nitro derivatives to the corresponding amines in very high yields. The experimental conditions of the reduction allow the transformation of the nitro group into the amino group without interference from halogen (F, Cl, Br, I), ester, nitrile, ether, or olefin groups. The results of those reductions, all performed under identical experimental conditions (24 h reflux in tetrahydrofuran (THF)) are reported in Table 1.

Can. J. Chem. Downloaded from www.nrcresearchpress.com by 210.87.254.105 on 09/05/12
For personal use only.

TABLE 1. Reduction of aromatic nitro compounds

Reagent	Product	Yield (%)	Reagent	Product	Yield (%)
Nitrobenzene	Aniline	84	*m*-Chloronitrobenzene	*m*-Chloroaniline	81
m-Nitrotoluene	*m*-Aminotoluene	80	*p*-Chloronitrobenzene	*p*-Chloroaniline	79
p-Nitrotoluene	*p*-Aminotoluene	65	*o*-Chloronitrobenzene	*o*-Chloroaniline	58
o-Nitrotoluene	*o*-Aminotoluene	63	*m*-Nitroanisole	*m*-Aminoanisole	81
o-Nitroethylbenzene	*o*-Aminoethylbenzene	62	*p*-Nitroanisole	*p*-Aminoanisole	65
Nitromesitylene	Aminomesitylene	50	*o*-Nitroanisole	*o*-Aminoanisole	73
o-Nitrobiphenyl	*o*-Aminobiphenyl	47	*m*-Nitroethylbenzoate	*m*-Aminoethylbenzoate	88
1-Nitronaphthalene	1-Aminonaphthalene	49	*p*-Nitroethylbenzoate	*p*-Aminoethylbenzoate	63
2-Nitronaphthalene	2-Aminonaphthalene	58	*o*-Nitroethylbenzoate	*o*-Aminoethylbenzoate	57
m-Nitrostyrene	*m*-Aminostyrene	85	*m*-Bromonitrobenzene	*m*-Bromoaniline	80
m-Fluoronitrobenzene	*m*-Fluoroaniline	77	*p*-Bromonitrobenzene	*p*-Bromoaniline	75
p-Fluoronitrobenzene	*p*-Fluoroaniline	90	*o*-Bromonitrobenzene	*o*-Bromoaniline	54
o-Fluoronitrobenzene	*o*-Fluoroaniline	50	*m*-Iodonitrobenzene	*m*-Iodoaniline	77
o-Nitroacetophenone	*o*-Nitro-1-hydroxyethylbenzene*	78	*p*-Iodonitrobenzene	*p*-Iodoaniline	67
m-Nitroacetophenone	*m*-Nitro-1-hydroxyethylbenzene*	83	*o*-Iodonitrobenzene	*o*-Iodoaniline	48
p-Nitroacetophenone	*p*-Nitro-1-hydroxyethylbenzene*	72	*p*-Nitrobenzophenone	Phenyl *p*-nitrophenyl carbinol*	88
			m-Dinitrobenzene	*m*-Nitroaniline†	44
			m-Dinitrobenzene	*m*-Diaminobenzene‡	82
			p-Nitrocyanobenzene	*p*-Aminocyanobenzene	60
			m-Nitrocyanobenzene	*m*-Aminocyanobenzene	74
			p-Dinitrobenzene§	*p*-Aminonitrobenzene	70

*Three hour contact at 0°.
†$NaBH_2S_3/NO_2$ ratio 1/1.
‡$NaBH_2S_3/NO_2$ ratio 4/1.
§Five hour contact at 25°.

Can. J. Chem. Downloaded from www.nrcresearchpress.com by 210.87.254.105 on 09/05/12
For personal use only.

Our results indicate that except with sterically hindered nitro groups, yields are generally in the range of 80%. With ortho derivatives, the lower yields are related to extraction problems caused by the solubility of ortho-substituted derivatives of aromatic bases. As indicated, nitroacetophenones can be reduced to the corresponding alcohols without affecting the nitro groups.

The stoichiometry of the reaction calls for a 1/1 molar ratio of reagent and reducing agent as shown by the variation of the yield of the reduction of nitrobenzene with $NaBH_2S_3$. With a 1/1 ratio ($NaBH_2S_3/NO_2$) and a long reaction time (85 h) a yield of aniline of 92% is obtained. If the ratio is decreased to 0.5/1, then the yield, after a reflux of 24 h, is decreased to 43%; a 0.25/1 ratio lowers the yield still further to 24%. From these variations of yield in relation to the ratio of reducing agent:nitro compound, we have concluded that the 1/1 ratio is the required stoichiometry for complete reduction. It is to be noted, however, that the second hydrogen on $NaBH_2S_3$ must be somewhat more difficult to involve in the reaction, since a yield of 95% of amine was obtained with a 2/1 ratio after only 24 h, three times more rapidly than with the 1/1 ratio.

We have been able to differentiate the action of the two hydrogen atoms of the reducing agent in the following way. One mole of nitrobenzene was treated by 2 mol of sulfurated sodium borohydride. The processing of an aliquot of this reaction mixture, after 24 h, proved that reduction was complete. Then 2 mol of nitro compounds were added in the form of an equimolar mixture of *o*-nitrotoluene and *p*-nitrotoluene. The flux was then continued for another 24 h. Upon extraction, it was found that only 31% of the second portion of nitro derivatives had been reduced and that the ratio of reduction was in favor of the less hindered derivative (*o*-aminotoluene, 25%; *p*-aminotoluene, 85%). A similar behavior was noted with a mixture of *o*- and *m*-nitrotoluene and was interpreted as an indication that the first hydrogen atom of the reducing agent is more easily available than the second, and that when it has been consumed, the resulting intermediate boric ester creates steric hindrance around the second hydrogen and renders it less reactive.

(b) Reduction of Aliphatic Nitro Derivatives

In the case of aliphatic nitro compounds, the structure of the substrate has a definite role on the orientation of the reaction. With primary nitro derivatives, such as phenylnitromethane, the main reaction product, obtained in a yield of 80%, is the corresponding nitrile. Small quantities of the corresponding oxime (10%) and amine (9%) are also observed along with a trace of the hydroxylamine. A similar behavior is noted with 1-nitropropane. In the case of the secondary nitro compound such as nitrocyclohexane, 45% of cyclohexanone, 30% of cyclohexanone oxime, 19% of *N*-cyclohexylhydroxylamine and traces of cyclohexylamine are observed. Similar results were obtained with 2-nitropropane, but the yields were lower, because of solubility and volatility of reaction products. With the tertiary nitro compound, using $(CH_3)_2C(NO_2)CH_2OAC$, no reaction was observed.

(c) Discussion

The use of sulfurated sodium borohydride offers very interesting possibilities for the reduction of nitro groups mainly because of its selectivity. It has advantages over present reagents, particularly when ester, halide, nitrile, amide or olefinic groups are also present in the molecule. With aliphatic nitro derivatives, the formation of nitriles, from primary nitro compounds, of ketones and oximes from secondary nitro compounds represents new reactions of real synthetic interest.

The mechanism of this reaction must be complex and at the present time is not fully understood. With an equimolecular ratio of reducing agent to nitro compounds, a near quantitative yield of amine is observed. This result indicates that besides the two hydrogen atoms, the sulfur atoms of $NaBH_2S_3$ must play a role in the reduction. It is to be noted that besides its reducing role, $NaBH_2S_3$ behaves as a dehydrogenating agent in the reduction of primary nitro groups for example. Such a behavior had been noted previously, with ketones (4).

In order to appreciate the relative importance of electronic and steric effects in the course of the reduction, various pairs of nitro derivatives have been reduced together. These results are reported in Table 2. It can be seen from these measurements that the relative ease of reduction of the

Can. J. Chem. Downloaded from www.nrcresearchpress.com by 210.87.254.105 on 09/05/12
For personal use only.

TABLE 2. Comparison of steric and electronic effects in the reduction of various nitro groups

Reagents	Total bases yield (%)*	Relative amine yield (%)†
o-$NO_2C_6H_4CH_3$ } p-$ClC_6H_4NO_2$	79	1 99
o-$NO_2C_6H_4CH_3$ } m-$ClC_6H_4NO_2$	96	15 85
o-$NO_2C_6H_4CH_3$ } o-$ClC_6H_4NO_2$	(39)‡	6 94
o-$NO_2C_6H_4CH_3$ } p-$NO_2C_6H_4OMe$	74	48 52
o-$NO_2C_6H_4CH_3$ } m-$NO_2C_6H_4OMe$	93	10 90
o-$NO_2C_6H_4CH_3$ } o-$NO_2C_6H_4OMe$	84	27 73
$C_6H_5NO_2$ } o-$NO_2C_6H_4CH_3$	90	86 14
o-$NO_2C_6H_4CH_3$ } m-$NO_2C_6H_4CH_3$	84	22 78
o-$NO_2C_6H_4CH_3$ } p-$NO_2C_6H_4CH_3$	82	29 71
o-$NO_2C_6H_4CH_3$ } o-$NO_2C_6H_4C_2H_5$	70	60 40
o-$NO_2C_6H_4CH_3$ } NO_2-Mesitylene	55	98 2
o-$NO_2C_6H_4CH_3$ } o-NO_2-Biphenyl	60	63 37
$C_6H_5NO_2$ } 1-NO_2-Naphthalene	85	56 44
$C_6H_5NO_2$ } 2-NO_2-Naphthalene	85	44 56

*Yields based on possible total NO_2 reduction *i.e.* 1 mol of reducer can reduce 1 mol of NO_2.
†Yields of each product for a given mixture.
‡Not representative because of difficulties of extraction.

nitro group is greatly influenced by substitution in the ortho position and by the electronic effects of substituents on the aromatic structure.

Reactions of Nitriles

We have indicated above that it is possible to reduce the nitro group in presence of nitrile, without interference by the C≡N function. However, under suitable conditions it is possible to convert aromatic nitriles into either amines or thioamides. With an excess of reducing agent (2/1 ratio of $NaBH_2S_3$ to C≡N), the amine is obtained. If this ratio is inverted (1/2 ratio of $NaBH_2S_3$ to C≡N), then the major product is the corresponding thioamide.

With aliphatic nitriles, the reaction led to complex mixtures containing products of the reaction of the α methylene group. Thus β-phenylacetonitrile gave the disulfide (**1**). The various reactions of nitriles are reported in Table 3.

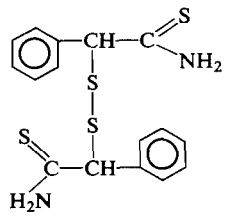

1

The reduction of nitriles to the corresponding amines is a well known reaction, but the formation, with good yields of aromatic thioamides from nitriles is a new method of preparation for those thioamides. The formation of thioamides from nitrile, by the action of H_2S in basic media, is known (12). With $NaBH_2S_3$, since the reaction takes place under anhydrous conditions and since $NaBH_2S_3$ alone does not give H_2S under the experimental conditions used, a mechanism calling for $NaBH_2S_3$ rather than H_2S must prevail.

Reduction of Amides and Nitroso Groups

The reduction of amides is difficult, and gives only moderate yields of the corresponding amines. Thus, benzamide gave a moderate yield of benzylamine, along with smaller amounts of dibenzylamine, thiobenzamide, and traces of benzonitrile. A similar behavior was observed with β-phenylacetamide.

Aliphatic nitroso compounds gave very complex mixtures. With nitrosobenzene, a yield of 80% of aniline was obtained with an equimolecular ratio of nitroso compound and reducing agent. When the ratio was increased to 2/1 the yield was about the same. Therefore it appears that half a mole of $NaBH_2S_3$ is required to reduce the nitroso group.

Experimental

The n.m.r. measurements were made with a Varian A-60 apparatus. The i.r. measurements were made with a Perkin–Elmer apparatus, model 257. The v.p.c. measurements were made with a Varian model 90P apparatus using a 5 ft Se30 column.

(1a) Optimal Conditions for Reduction of Nitrobenzene

To a suspension of 0.10 mol (13.2 g) of $NaBH_2S_3$ prepared as described before (3, 4), in 100 ml of tetra-

TABLE 3. Reductions of nitriles

Reagent	Ratio $NaBH_2S_3$/CN	Contact (h)	Temperature	Yield (%) Amine	Thioamide	Unreacted	Other
$C_6H_5C{\equiv}N$	1/1	24	Reflux	30	60	Traces	—
$C_6H_5C{\equiv}N$	1/2	24*	Reflux	15	80	Traces	—
$C_6H_5C{\equiv}N$	2/1	3	Reflux	63	30	Traces	—
$C_6H_5C{\equiv}N$	1/2	4	25°	18	78	Traces	—
$C_6H_5C{\equiv}N$	1/4	3	25°	6	31	50	—
$C_6H_5CH_2C{\equiv}N$	2/1	3	Reflux	38	—	—	Complex mixture
$C_6H_5CH_2C{\equiv}N$	1/2	3	Reflux	11	41	Traces	18% of **1**
$CH_3C(C_6H_5)_2{-}C{\equiv}N$	2/1	3	Reflux	24	Traces	Traces	—
$CH_3C(C_6H_5)_2{-}C{\equiv}N$	1/2	3	Reflux	10	Traces	Some	—
$CH(C_6H_5)_2{-}C{\equiv}N$	2/1	3	Reflux	39	≈25	10	15% CHO†
$CH(C_6H_5)_2{-}C{\equiv}N$	1/2	3	Reflux	11	38	47	4% CHO†
αNaphthylnitrile	2/1	3	Reflux	40	20	40	—
αNaphthylnitrile	1/2	3	Reflux	12	38	50	—
$CH_3C{\equiv}N$	1/2	24	Reflux	—	62	—	—
$CH_3(CH_2)_5C{\equiv}N$	2/1	3	Reflux	17	Traces	Traces	Disulfides present

*Three hour contact gave similar results.
†From n.m.r.

hydrofuran (THF), 0.10 mol (12.3 g) of nitrobenzene in 150 ml of THF was added dropwise. The reaction mixture was stirred and refluxed for 24 h, and was then evaporated to dryness, under reduced pressure, at room temperature. The residual solid was hydrolyzed with a 10% hydrochloric solution until p*H* 1 in presence of 250 ml of ethyl ether. The precipitated sulfur was filtered off and the filtrate washed repeatedly with ethyl ether. The aqueous fraction was neutralized to p*H* 11 with a 20% solution of NaOH, in presence of 200 ml of ethyl ether. The aqueous layer was extracted again with ether and the combined ether extracts were evaporated, giving an 84% yield of aniline. The i.r., v.p.c., and n.m.r. of the crude base confirmed its structure.

(1b) Other Reductions of Nitro Groups

The reduction of other nitro groups or mixtures of nitro derivatives has been done as described in section *1a*, the molar ratio of reagents and reducing agent, the duration and temperature of contact being indicated in Table 1. The compositions of the various mixtures has been determined by n.m.r. and v.p.c. The identification of the components of those mixtures was performed by preparative v.p.c. followed by analytical v.p.c., i.r., n.m.r., and mass spectrometry. In most cases, those measurements were compared with the results observed with authentic samples of pure bases. In Table 2, reflux for 24 h, of 0.2 mol of $NaBH_4$ and 0.1 mol of each of the nitro compounds were used in each case, the extraction procedure being the same as above.

(2) Reduction of Nitriles

The reduction of nitrile was done as described in section *1a* for nitro groups, the ratio of reagents and yields being reported in Table 3. The separation of amines from thioamide was done by extraction of the bases with 10% hydrochloric acid. The thioamides were recrystallized in CCl_4. The identification of the products thus obtained was done by comparison of n.m.r., v.p.c., and i.r. measurements obtained with authentic samples.

The structure of the disulfide **1** was established by the usual measurements. The n.m.r.: broad singlet at 2.60 (5 protons); singlet at 5.00 (1 proton); doublet at 0.5 τ (2 protons). Mass spectrometry: *m/e* 266, 232, 151, 117, 116, 91, 90, 98, 77, 64, 63, 62, 61, 60.

Anal. Calcd. for $C_{16}H_{16}N_2S_4$: C, 52.65; H, 4.38; N, 7.68; S, 53.17. Found: C, 50.84; H, 4.49; N, 7.27; S, 36.83; O, 0.0.

The differences in the calculated and found values of the elementary analysis are attributed to the difficulty of recrystallization (ethanol–water) of the disulfide. Yield: 5%.

(3) Reduction of Amides

The experimental procedure used is described in section *1a*, 0.2 mol of benzamide being treated by 0.4 mol of $NaBH_2S_3$. Using this stoichiometry with a reflux time of 120 h gave 46% of $C_6H_5CH_2NH_2$, 6% of $(C_6H_5CH_2)_2NH$ 16% of $C_6H_5CSNH_2$, and traces of C_6H_5CN and C_6H_5-CHO, while 31% of $C_6H_5CONH_2$ was recovered. For a reflux time of 24 h, the reaction gave 48% of primary amine, traces of secondary amine, 18% of thiobenzamide, and traces of benzaldehyde and benzonitrile, and about 30% of $C_6H_5CONH_2$ recovery. Approximately the same results were obtained for a contact time of 3 h. If equimolar quantities of reducing agent and amide were used for a contact time of 24 h reflux, the products were 22.4% of benzylamine, 2.5% of dibenzylamine, 25% of thiobenzamide and traces of benzonitrile and benzaldehyde with a recovery of about 50% of the starting benzamide. With a ratio of 4/1 of reducer to reagent for a 24 h reflux we obtained 45% of $C_6H_5CH_2NH_2$, 10% of $(C_6H_5CH_2)_2$-NH, 10% of $C_6H_5CSNH_2$, and traces of C_6H_5CN with about 35% of non-reacted benzamide. The dibenzylamine $(C_6H_5CH_2)_2NH$ was obtained by separation of the basic fraction on a silica gel column and identified by n.m.r., i.r., and mass spectroscopy.

Anal. Calcd. for $C_{14}H_{15}N$: C, 85.28; H, 7.62; N, 7.10. Found: C, 85.00; H, 7.50; N, 7.17.

The primary amine $C_6H_5CH_2NH_2$, the amide and

Can. J. Chem. Downloaded from www.nrcresearchpress.com by 210.87.254.105 on 09/05/12
For personal use only.

thioamide, and the aldehyde and nitrile were identified by n.m.r. and i.r. spectroscopy for all the mentioned experiments.

A molar ratio of 2/1 of reducing agent to 2-phenylacetamide for a reflux time of 24 h gave about 41% of 2-phenylethylamine. Some corresponding thioamide is believed to be formed and a large quantity of the initial amide was recovered.

(4) Reduction of Nitroso Compounds

The experimental procedure is the same as the one used in section *1a*. For an equimolar ratio of reducing agent/nitrosobenzene, we obtained an 82% yield of aniline, which was identified by n.m.r. and i.r. analysis. With a molar ratio of 1/2, a 75% yield of aniline was obtained.

The authors thank the National Research Council of Canada and the Defence Research Board of Canada (grant 9530-30) for financial assistance.

1. J. M. LALANCETTE, A. FRECHE, and R. MONTEUX. Can. J. Chem. **46** 2754 (1968).
2. J. M. LALANCETTE and M. ARNAC. Can. J. Chem. **47**, 3695 (1969).
3. J. M. LALANCETTE and A. FRECHE. Can. J Chem. **47**, 739 (1969).
4. J. M. LALANCETTE and A. FRECHE. Can. J. Chem. **48** 2366 (1970).
5. J. M. LALANCETTE and J. R. BRINDLE. Can. J. Chem. **48**, 735 (1970).
6. P. SABATIER and J. B. SENDERENS. C. R. **135**, 225 (1902).
7. V. MEYER. Ann. **171**, 1 (1874).
8. R. F. NYSTROM and W. G. BROWN. J. Am. Chem. Soc. **70**, 3738 (1948).
9. W. REID and F. MULLER. Chem. Ber. **85**, 470 (1952).
10. R. T. COUTTS and D. G. WIBBERLEY. J. Chem. Soc. 4610 (1963).
11. R. F. NYSTROM, S. W. CHAIKIN, and W. G. BROWN. J. Am. Chem. Soc. **71**, 3245 (1949).
12. A. E. S. FAIRFULLET, J. L. LOWE, and D. A. PEAK. J. Chem. Soc. 742 (1952).

Can. J. Chem. Downloaded from www.nrcresearchpress.com by 210.87.254.105 on 09/05/12
For personal use only.

Can. J. Chem. Downloaded from www.nrcresearchpress.com by 210.87.254.42 on 09/05/12
For personal use only.

The Reaction of Thallium with Hydrocarbons

J. M. LALANCETTE AND A. LACHANCE
Département de Chimie, Faculté des Sciences, Université de Sherbrooke, Sherbrooke, Québec

Received March 22, 1971

The exchange of the cyclopentadienyl anion between indium and thallium is reported along with exchange reactions between cyclopentadienylindiums, substituted with H, D, and CH_3. The pyrolysis of numerous hydrocarbons in presence of thallium to give the corresponding cyclopentadienylthallium derivative is described and related to the structure of the starting material.

L'échange de l'anion cyclopentadiényle entre l'indium et le thallium est rapporté, ainsi que des réactions d'échange entre certains cyclopentadiènеindiums substitués par H, D et CH_3. La pyrolyse d'hydrocarbures variés en présence de thallium pour donner le dérivé cyclopentadiénylthallium est décrite et reliée à la structure de l'hydrocarbure de départ.

Canadian Journal of Chemistry, **49**, 2996 (1971)

The lower elements of Group IIIA, namely indium and thallium, are known to give derivatives with cyclopentadiene involving the π electronic system of this molecule (1). Such compounds are obtained, in the case of indium (2), by the action of the cyclopentadienyl anion on a In^+ substrate. With thallium, a similar compound is formed either by the direct reaction of cyclopentadiene with the metal (3) or with a thallous salt (4), the reaction of the hydrocarbon with the metal being accompanied by an evolution of hydrogen. From the actual knowledge of the structure of those cyclopentadienyl derivatives of indium and thallium, and in analogy with ferrocene, the π system of the hydrocarbon is involved in a "half sandwich" structure as indicated in eqs. 1 and 2.

[1] $In^+ +$ 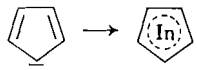 $\longrightarrow$

[2] $Tl^0 +$ $\longrightarrow \frac{1}{2}H_2 +$

The chemistry of cyclopentadienylindium is not easy because of the great sensitivity of this material towards light and oxygen. It can sublime as gold leaflets in darkness, under a vacuum better than 10^{-5} mm. The derivative of thallium is more stable. It can also sublime as pale yellow crystals and its resistance towards light and oxygen is somewhat better.

(1) Exchange of the Cyclopentadienyl Anion between Indium and Thallium

Because of the great difference in the stability and reactivity of those two compounds, we have postulated that an exchange of the ligand between the two metals was possible. The postulated reaction, as illustrated by eq. 3, was found to proceed quite easily.

[3] 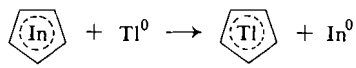

The reaction was performed simply by mixing freshly sublimed cyclopentadienylindium with finely divided thallium. By heating the mixture under high vacuum, the cyclopentadienylthallium sublimed. The displacement of equilibrium towards cyclopentadienylthallium in eq. 3 might be explained solely by the greater stability of the thallous derivative and the very high reactivity of the indium compounds. It has been possible to show, however, that such exchange reactions were very easily done, even when the thermodynamic properties of the metal derivatives were not much modified by the reaction. Such exchanges are described by eqs. 4 and 5. In the first case, deuterated cyclopentadienyl anion was shown to exchange easily with protonated cyclopentadienylindium. A similar behavior was noted with methyl cyclopentadienyl anion and cyclopentadienylindium. In both cases, the sublimate obtained from the mixture of the reagents indicated very clearly that both forms of cyclopentadiene (with and without deuterium or with and without methyl substituent) were bonded to the metal.

(2) Reactions with other Hydrocarbons

Such an exchange was interesting in itself and we tried to repeat the reaction with other dienes

[4] 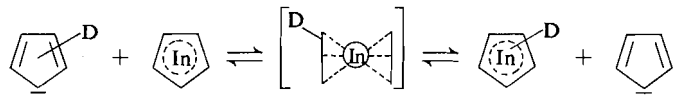

[5] 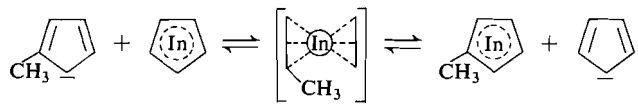

in order to broaden the scope of the reaction. Thallium was selected because it appeared more adequate than indium in its reactions with cyclopentadiene hydrocarbon. We found that at moderate temperature, conjugated dienes, such as cycloheptadiene would not react with thallium. At more elevated temperature, however, we were much surprised to find that several hydrocarbons gave the corresponding cyclopentadienethallium. We found that bicyclo[2,2,1]hepta-2,5-diene, 1,3-cyclohexadiene, 1,3-cycloheptadiene, 1,5-cyclooctadiene, 1,3-cyclooctadiene, 1,4-cyclohexadiene, cycloheptatriene, cycloheptene, cyclohexene, 2-pentene, 1-octene, cyclohexane, octane, and pentane, gave the corresponding cyclopentadienylthallium. However, benzene, cyclooctatraene, isoprene or isobutylene did not give the thallium derivative under similar experimental conditions. The cyclopentadienylthallium was sublimed and identified by its mass spectrum and by formation of ferrocene in ether, with $FeCl_3$ (5). The yield of the thallium derivative was of the order of 3% and about 60% of the starting hydrocarbon was recovered unreacted. Beside the thallium derivative, ethylene, acetylene, hydrogen, carbon, traces of benzene and polymeric material were also formed in the course of the reaction.

From those results, it can be concluded that the course of the thermal decomposition of an hydrocarbon of appropriate structure, a cyclopentadienyl anion or cyclopentadiene must be one of the intermediates. From the list of hydrocarbons cited above giving a positive reaction, it can be noted that with those substances, the partial structure **1** was always present, the unspecified bonds in **1** being involved in double bonds, C—C bonds or C—H bonds, depending on the cases.

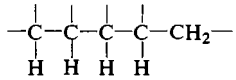

1

When such an arrangement was not present, the cyclopentadienylthallium was not formed. One explanation of this observation is that the partial structure **1** can act as a precursor of either cyclopentadiene or cyclopentadienyl anion, at the high temperature of the reaction, when the starting molecule is broken down. Either the hydrocarbon or its anion can then react with thallium metal to give the cyclopentadienyl derivative that sublimes before further decomposition. It is known (6) that the pyrolysis of mixtures of hydrocarbons can produce cyclopentadiene; the present work indicates the favorable structures for the formation of this substance.

The role of the thallium in this experiment must be twofold. First, it catalyzed the decomposition of the hydrocarbon as all metals do at high temperature. Secondly, its reactivity with the cyclopentadienyl structure and the volatility of the corresponding derivative render possible the observed trapping.

Experimental

Infrared measurements were made on a Perkin–Elmer spectrometer, model 257, in Nujol. The nuclear magnetic resonance (n.m.r.) measurements were performed with a Varian A-60 instrument, using tetramethylsilane as internal reference. Melting points were made with a "Buchi" melting point apparatus and are not corrected. Mass spectrometric determinations were made with a Hitachi Perkin–Elmer apparatus model RMV-6D.

(1) Preparation of Cyclopentadienylindium

Metallic sodium (0.6 g), finely cut, was introduced under nitrogen into a solution of 2.5 ml of cyclopentadiene freshly distilled, in 100 ml of absolute dry ether. The resulting mixture was refluxed with stirring for 12–14 h to form cyclopentadienylsodium. Indium tribromide (2.8 g) was then added, and the mixture was heated for another 12–14 h in the absence of air. After removal of the solvent by distillation at atmospheric pressure, the dry residue was sublimed under high vacuum (10^{-5} mm) by gradually raising the temperature to a maximum of 150°. This procedure gave pale yellow crystals of cyclopentadienylindium.

The mass spectrum of the product was taken under

Can. J. Chem. Downloaded from www.nrcresearchpress.com by 210.87.254.42 on 09/05/12
For personal use only.

Can. J. Chem. Downloaded from www.nrcresearchpress.com by 210.87.254.42 on 09/05/12
For personal use only.

very careful experimental conditions. All the time the product had to be kept under an inert gas such as helium and away from light, otherwise it would undergo to rapid decomposition by air or light. All manipulations were done inside a "Glove Bag" flushed with helium, the operation being performed in semi-darkness. The product was put in a small vial which was introduced into the mass spectrometer inlet. This procedure gave the expected peaks at *m/e* 180 and 178 for $C_5H_5{}^{115}In$ and $C_5H_5{}^{113}In$ with a ratio 95:5; at 115 and 113 for the two isotopes of indium; and at 65 and 66 for the cyclopentadienyl anion and cyclopentadiene. The isotopic ratio observed was correct for the natural mixture, at 180 and at 115.

(2) Preparation of Cyclopentadienylthallium

A mixture of 25 g of recrystallized Tl_2SO_4 and 10 g of KOH in 200 ml of water was treated at room temperature with 5 g of freshly distilled cyclopentadiene in a small amount of methanol. After stirring to completion of precipitation, the mixture was filtered and the precipitate was washed with ice-cold methanol and dried over KOH. The product was then purified by sublimation at 10^{-5} mm, gradually raising the temperature to 145°. This procedure gave pale white yellow crystals of cyclopentadienylthallium.

The product was submitted to a mass spectrometry determination with the same strict conditions that were used for the determination of cyclopentadienylindium. The expected peaks appeared at *m/e* 270 and 268 for $C_5H_5{}^{205}Tl$ and $C_5H_5{}^{203}Tl$, with a ratio 70:30; at 205 and 203 for thallium metal and at 66 and 65 for cyclopentadiene and cyclopentadienyl anion. The isotopic ratio was identical with the natural ratio of isotopes of Tl.

(3) Exchange between Cyclopentadienylindium and Thallium Metal

Cyclopentadienylindium (1.6 g) was prepared as above, starting from cyclopentadiene (16.4 g), sodium metal (4.8 g) and indium tribromide (21.9 g). Thin flakes of metallic thallium were prepared under nitrogen and mixed with the cyclopentadienylindium. The mixture was then heated at 50° for 30 min and sublimed at 10^{-5} mm, gradually raising the temperature to 90°. After 2 h, the product, pale white yellow crystals, was collected and submitted to mass spectrometry. The expected peaks were observed at *m/e* 270 and 268 for $C_5H_5{}^{205}Tl$ and $C_5H_5{}^{203}Tl$ with a ratio 70:30; at 205 and 203 for thallium metal; at 180 and 178 for $C_5H_5{}^{115}In$ and $C_5H_5{}^{113}In$; at 66 and 65 for cyclopentadiene and cyclopentadienyl anion.

(4) Exchange between Deuterated Cyclopentadienyl Anion and Cyclopentadienylindium

Metallic sodium (2.4 g) finely cut, was introduced under nitrogen into a solution of 8.2 g of cyclopentadiene freshly distilled in 300 ml of absolute dry ether. The resulting mixture was refluxed for 24 h to form cyclopentadienylsodium. After removal of the solvent under vacuum, 200 ml of dry *cis*-decalin were added and, keeping the system under nitrogen, the cyclopentadienylsodium was slowly hydrolyzed by adding D_2O. After hydrolysis, the NaOD was removed by decantation and the organic fraction dried over $MgSO_4$ and filtered. The deuterated cyclopentadiene was then distilled and the infrared spectra was showing a band of medium intensity at 2300 cm^{-1}.

Metallic sodium (2.7 g) was introduced under nitrogen into a solution of 9.3 g of deuterated cyclopentadiene in 200 ml of anhydrous ether. After refluxing for six days, the solvent was evaporated under vacuum and the solid residue was mixed with cyclopentadienylindium freshly sublimed.

The mixture was then heated at 50° for 10 min, then sublimed at 10^{-5} mm gradually raising the temperature to 140°. This procedure gave pale yellow crystals which were submitted to mass spectrometry analysis.

Peaks were obtained at *m/e* 183, 182, 181 for deuterated cyclopentadienylindium, at 180 and 178 for $C_5H_5{}^{115}In$ and $C_5H_5{}^{113}In$, at 115 and 113 for indium metal and at 68, 67, 66, and 65 for deuterated and non-deuterated cyclopentadiene and cyclopentadienyl anion.

(5) Exchange between Methylcyclopentadienyl Anion and Cyclopentadienylindium

Metallic sodium (5.6 g), finely cut, was introduced under helium into a solution of 17.4 g of freshly distilled methylcyclopentadiene in 200 ml of absolute dry ether. After refluxing for one week, the solvent was evaporated under vacuum and the methylcyclopentadienylsodium was then mixed with cyclopentadienylindium freshly sublimed.

After heating to 50° for 10 min, the mixture was sublimed at 10^{-5} mm gradually raising the temperature to 140°. The product (pale yellow crystals) was then submitted to a mass spectrometry analysis using the usual procedure.

The expected peaks were observed at *m/e* 194 for $CH_3C_5H_4{}^{115}In$, at 180 for $C_5H_5{}^{115}In$, at 80, 79 for methylcyclopentadiene and methylcyclopentadienyl anion and at 66, 65 for cyclopentadiene and cyclopentadienyl anion.

(6) Pyrolysis of various Hydrocarbons in presence of Thallium Metal

The reaction of cycloheptene with thallium metal to give cyclopentadienylthallium is described as a typical experiment. The experimental conditions were carefully controlled and with the apparatus used (Fig. 1), it was possible to reproduce the experiments without difficulties.

The thallium metal was washed several times with hexane to remove the high molecular weight hydrocarbon coating the pellets and after high vacuum drying introduced into a 100 ml flask. The apparatus was installed and a flow rate of approximately 19 c.c. of helium gas per minute was set on. A heating element covered by asbestos was wrapped around the thallium flask to give a temperature of 500° inside the vessel. It was important to wrap the heating elements around the whole flask. Cycloheptene was heated to its boiling point in a separate flask and a second heating element was used to keep the transfer line warm.

An acetone – Dry Ice trap was installed at the exit of the apparatus followed by a liquid air trap to condense all gases as volatile hydrocarbon vapors. Cycloheptene (5.57 g) was passed over thallium (17.9 g) at 500° for 24 h. After 1 h, pale yellow crystals began to appear at the top of the condenser. After this period, the product was

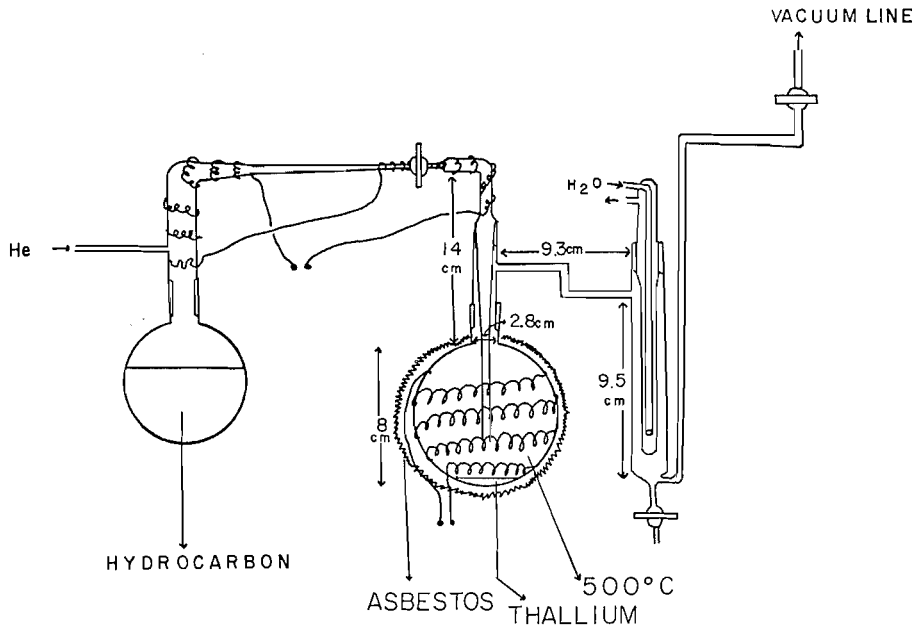

FIG. 1. Reaction apparatus.

sublimed at 10^{-5} mm, gradually raising the temperature to 145°. The unreacted liquid in the Dry Ice trap was mostly cycloheptene and traces of benzene (3.28 g). The gases trapped with liquid air were analyzed by infrared and shown to be ethylene and acetylene. The sublimation yielded white yellow crystals of cyclopentadienylthallium (0.167 g, 3% of reacted cycloheptene). A mass spectrometry analysis showed the expected peaks at *m/e* 270 and 268 for $C_5H_5{}^{205}Tl$ and $C_5H_5{}^{203}Tl$; at 205 and 203 for thallium metal with a ratio 70:30; and at 66 and 65 for cyclopentadiene and cyclopentadienyl anion.

A similar experiment was repeated with bicyclo(2,2,1)-hepta-2,5 diene, 1,3-cyclohexadiene, 1,3-cycloheptadiene, 1,5-cyclooctadiene, 1,3-cyclooctadiene, 1,4-cyclohexadiene, cycloheptatriene, cyclohexene, 2-pentene, 1-octene, cyclohexane, octane, and pentane, and cyclopentadienylthallium was obtained. With benzene, cyclooctatetraene, isoprene or isobutylene, no thallium derivative was observed.

Formation of Ferrocene

The thallium derivative obtained above was added to $FeCl_3.4H_2O$ (2 g) in a minimum quantity of ether and stirred for 1 h at 25°. After filtration over $MgSO_4$ and evaporation of the solvent, a sublimation at 25° yielded orange-yellow colored crystals of ferrocene. The product melted at 174.5 to 175.2° and an n.m.r. and infrared spectra were identical with the n.m.r. and infrared spectra of authentic ferrocene (5).

The ferrocene derivative was obtained in the course experiments with cyclohexane, 1-octene, octane, and cycloheptene.

The authors thank the National Research Council of Canada and the Defence Research Board of Canada (grant 9530-30) for financial assistance.

1. (*a*) F. A. COTTON and L. T. REYNOLDS. J. Am. Chem. Soc. **80**, 269 (1958). (*b*) A. G. LEE and G. M. SHELDRICK. Chem. Commun. 441 (1969).
2. E. O. FISCHER and H. P. HOFMANN. Angew. Chem. **69**, 639 (1957).
3. E. O. FISCHER and H. P. HOFMANN. Ber. **92**, 482 (1959).
4. E. O. FISCHER. Angew. Chem. **69**, 207 (1957).
5. A. N. NESMEYANOV and R. A. SOKOLIK. Methods of elemento-organic chemistry. Vol. 1. The World Publishing Co., Cleveland. 1967. p. 575.
6. F. SCHUTZ, W. BUSCHMANN, and W. WIESSBACH. Ber. **56**, 869 (1923).

Can. J. Chem. Downloaded from www.nrcresearchpress.com by 210.87.254.42 on 09/05/12
For personal use only.

Can. J. Chem. Downloaded from www.nrcresearchpress.com by 210.87.254.105 on 09/05/12
For personal use only.

Base-catalyzed Degradations of Carbohydrates. I. Synthesis and Alkaline Degradation of 2-*O*-β-D-Glucopyranosyl-3-*O*-methyl-D-glucose

G. O. Aspinall,[1] R. Khan, and Zofia Pawlak[2]

Department of Chemistry, Trent University, Peterborough, Ontario

Received May 19, 1971

2-*O*-β-D-Glucopyranosyl-3-*O*-methyl-D-glucose has been synthesized by two routes. Alkaline degradation of the disaccharide, followed by reduction, hydrolysis under extremely mild conditions, and further reduction, affords D-glucitol, and 3,4-dideoxy-*trans-erythro*- and -D-*threo*-hex-3-enitol.

Le 2-*O*-β-D-glucopyranosyl-3-*O*-méthyl-D-glucose a été synthétisé de deux façons. La dégradation alcaline du disaccharide suivie d'une réduction et hydrolyse sous des conditions extrêmement douces conduit, après réduction ultérieure, au D-glucitol et 3,4-didéoxy-*trans-erythro*- et -D-*threo*-hex-3-enitol.

Canadian Journal of Chemistry, 49, 3000 (1971)

2-*O*-β-D-Glucopyranosyl-3-*O*-methyl-D-glucose (**1**) was required as a model compound in connection with studies on the alkaline degradation of branched oligo- and polysaccharides. Methyl 4,6-*O*-benzylidene-2-*O*-(2,3,4,6-tetra-*O*-acetyl-β-D-glucopyranosyl)-3-*O*-methyl-α-D-glucopyranoside (**2**) was prepared by two routes: (*i*) by condensation of 2,3,4,6-tetra-*O*-acetyl-α-D-glucopyranosyl bromide and methyl 4,6-*O*-benzylidene-3-*O*-methyl-α-D-glucopyranoside (1), and (*ii*) by methylation of methyl 4,6-*O*-benzylidene-2-*O*-(2,3,4,6-tetra-*O*-acetyl-β-D-glucopyranosyl)-α-D-glucopyranoside (2, 3) with (*a*) methyl iodide and silver oxide in *N*,*N*-dimethylformamide or (*b*) diazomethane in the presence of boron trifluoride (4). Acetolysis of the glycoside (**2**) furnished a semi-crystalline disaccharide heptaacetate from which the disaccharide, 2-*O*-β-D-glucopyranosyl-3-*O*-methyl-D-glucose (**1**), was obtained on de-*O*-acetylation. The derived disaccharide alditol was characterized by the formation of a crystalline octaacetate and a crystalline octabenzoate.

Treatment of the disaccharide (**1**) with saturated lime-water gave a syrupy product whose u.v., i.r., and n.m.r. spectra indicated that elimination of methanol had occurred with the formation of 3-deoxy-2-*O*-β-D-glucopyranosyl-D-*erythro*-hex-2-enopyranose (**3**). The unsaturated disaccharide (**3**) was reduced with sodium borohydride, and mild treatment with cation-exchange resin during the work-up to destroy excess of hydride and remove sodium ions gave a syrupy mixture of products whose u.v. (λ_{max} 230 nm) and i.r. (ν_{max} 1690, 1640, and 975 cm^{-1}) spectra were consistent with the presence therein of the unsaturated ketose, 3,4-dideoxy-*trans*-D-*glycero*-hex-3-enos-2-ulose (5). The presence in the mixture of D-glucose and the unsaturated ketose was established by reduction with sodium borohydride to give D-glucitol, 3,4-dideoxy-*trans-erythro*-hex-3-enitol (**4**), and 3,4-dideoxy-*trans*-D-*threo*-hex-3-enitol (**5**), each of which was characterized by the formation of crystalline derivatives.

These results parallel those of Anet (5) on the

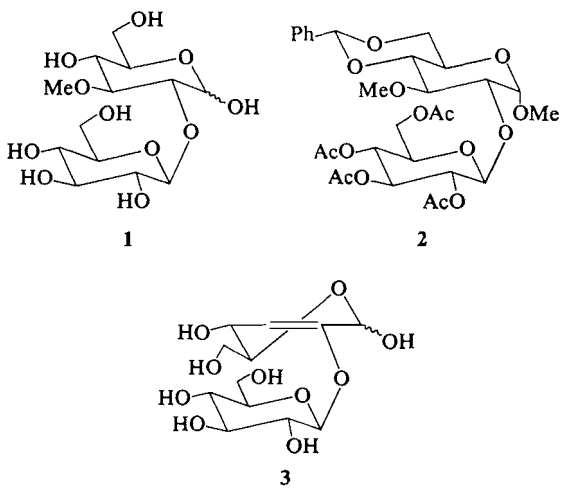

[1]To whom enquiries should be addressed.

[2]On leave (1969–1970) from the Department of Organic Chemistry, University of Warsaw, Poland.

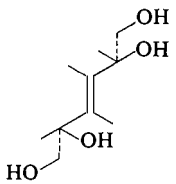

4

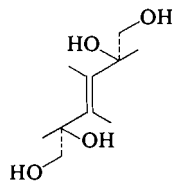

5

alkaline degradation of 2,3-di-*O*-methyl-D-glucose. It is noteworthy that the enol glycoside formed on reduction of the unsaturated disaccharide (**3**), like the enol ether, 3-deoxy-2-*O*-methyl-D-*erythro*-hex-2-enitol (5), is extremely labile to acid. The observed sequence of reactions may find application in the determination of the structure of branched oligosaccharides containing a 2,3-di-*O*-substituted reducing group in that (*i*) the 3-*O*-glycosyl substituent would be eliminated on alkaline degradation, (*ii*) the 2-*O*-glycosyl substituent would be subsequently liberated on very mild acid hydrolysis, and (*iii*) the formation of the epimeric hex-3-enitols would indicate the substitution pattern of the reducing sugar residue.

Experimental

Melting points are uncorrected. Optical rotations were measured with a Perkin–Elmer model 141 polarimeter at 20 ± 2°. The i.r. and u.v. spectra were measured on Unicam SP 200 and SP 800A spectrophotometers. The n.m.r. spectra were recorded on a JEOL C-60HL spectrometer with tetramethylsilane or sodium 4,4-dimethyl-4-silapentanesulfonate as internal standards. The t.l.c. was performed with Kieselgel G (Merck) as the adsorbent, and the dried plates were sprayed with ethanolic 5% sulfuric acid and heated at about 150°. Unless otherwise stated, column chromatography was carried out on silica gel (Davison grade 950, 60–200 mesh). Paper ionophoresis was in 0.05 *M* borate buffer at p*H* 10. Unless otherwise stated light petroleum refers to the fraction of b.p. 30–60°. Solutions were concentrated below 50° under reduced pressure.

Methyl 4,6-O-Benzylidene-3-O-methyl-α-D-glucopyranoside

Methyl 4,6-*O*-benzylidene-3-*O*-methyl-2-*O*-tosyl-α-D-glucopyranoside (1) (15 g) in refluxing methanol (400 ml) and benzene (500 ml) was treated with sodium (25 g) (6) for 6 h. The t.l.c. (chloroform–acetone, 4:0.3) showed a single product. Water (200 ml) was added to the cooled reaction mixture, organic solvents were removed, and the suspension was extracted with chloroform. The dried extract was concentrated and crystallization of the residue from methanol containing a little light petroleum gave methyl 4,6-*O*-benzylidene-3-*O*-methyl-α-D-glucopyranoside (9.5 g, 96%), m.p. 137–139° (unchanged on recrystallization), (lit. (1) m.p. 150–151°); n.m.r. data ($CDCl_3$): τ 2.4–2.8 (5-proton multiplet, aromatic H's), 4.40 (1-proton singlet, benzylidene–methine), 5.20 (1-proton doublet, splitting 4 Hz), 6.36, 6.54 (3-proton singlets, C-1 OMe and C-3 OMe), 7.2–7.45 (1-proton, OH).

Methyl 4,6-O-Benzylidene-2-O-(2,3,4,6-tetra-O-acetyl-β-D-glucopyranosyl)-3-O-methyl-α-D-glucopyranoside (2)

(*a*) Methyl 4,6-*O*-benzylidene-3-*O*-methyl-α-D-glucopyranoside (4 g) was dissolved by stirring for 2 h in dichloromethane (38 ml) in the presence of silver carbonate (4 g) and drierite (4 g). Iodine (1 g) and 2,3,4,6-tetra-*O*-acetyl-α-D-glucopyranosyl bromide (5.5 g) were added and the mixture was stirred for 42 h at room temperature. The mixture was filtered and concentration of the filtrate afforded a crystalline residue which, on trituration with methanol, gave a chromatographically pure product (5 g, 59%), m.p. 245–246°. Recrystallization from methanol gave compound **2**, m.p. 245–246°; $[\alpha]_D$ +33.7° (*c*, 1.15 in dichloromethane); n.m.r. data: τ 2.4–2.8 (5-proton multiplet, aromatic H's), 4.42 (1-proton singlet, benzylidene–methine H), 6.47, 6.57 (3-proton singlets, C-1 OMe and C-3 OMe), 7.9–8.05 (12 protons, OAc's).

Anal. Calcd. for $C_{29}H_{38}O_{15}$: C, 55.59; H, 6.07. Found: C, 55.33; H, 6.14.

(*b*) Methyl 4,6-*O*-benzylidene-2-*O*-(2,3,4,6-tetra-*O*-acetyl-β-D-glucopyranosyl)-α-D-glucopyranoside (1 g) and methyl iodide (2 ml) were stirred in *N*,*N*-dimethylformamide (15 ml) with silver oxide (1 g) for 30 h. The mixture was filtered, the filtrate was concentrated, and the residue was crystallized from ethoxyethanol to give compound **2**, m.p. 245–246°, $[\alpha]_D$ +33° (*c*, 1.0 in chloroform), whose n.m.r. spectrum was identical to that of the previously prepared sample.

(*c*) Methyl 4,6-*O*-benzylidene-2-*O*-(2,3,4,6-tetra-*O*-acetyl-β-D-glucopyranosyl)-α-D-glucopyranoside (0.5 g) was dissolved in dichloromethane (15 ml) at 0°, boron trifluoride etherate (0.05 ml) was added, and while the temperature was maintained at 0°, a white solid (polymethylene) was removed by filtration, and the filtrate was concentrated to a syrup which was crystallized from ethoxyethanol to give compound **2**, m.p. 243–245°, $[\alpha]_D$ +31° (*c*, 1.0 in chloroform), whose n.m.r. spectrum was identical with those of previously prepared samples.

2-O-β-D-Glucopyranosyl-3-O-methyl-D-glucose (1)

The foregoing glycoside (**2**) (4 g) in acetic anhydride (10 ml) was stirred with concentrated sulfuric acid 2% in acetic anhydride (20 ml) for 4 h. The mixture was poured into ice-water containing sodium hydrogen carbonate, the product was extracted with chloroform, and the chloroform extract was washed with water, dried, and concentrated to a syrup. The t.l.c. (chloroform–acetone, 4:0.3) showed a major component with fast-moving minor components with the mobilities of the peracetates of glucose and 3-*O*-methylglucose. The mixture was chromatographed on silica gel, elution with ether – light petroleum (3:1) and ether removing benzaldehyde and monosaccharide peracetates, and elution with ether–acetone (7.5:1) giving syrupy 1,4,6-tri-*O*-acetyl-2-*O*-(2,3,4,6-tetra-*O*-acetyl-β-D-glucopyranosyl)-3-*O*-methyl-

Can. J. Chem. Downloaded from www.nrcresearchpress.com by 210.87.254.105 on 09/05/12
For personal use only.

Can. J. Chem. Downloaded from www.nrcresearchpress.com by 210.87.254.105 on 09/05/12
For personal use only.

α-D-glucopyranose (2.8 g, 71%), $[\alpha]_D$ +35.3° (*c*, 1.34 in dichloromethane); n.m.r. data ($CDCl_3$): τ 3.77 (1-proton doublet, $J_{1,2}$ = 3 Hz, H-1), 6.57 (3-proton singlet, C-3 OMe), 7.85–8.05 (21 protons, OAc's).

Anal. Calcd. for $C_{27}H_{38}O_{18}$: C, 49.87; H, 5.89. Found: C, 49.91; H, 5.96.

This compound was later obtained in semi-crystalline form from ether–light petroleum.

Anal. Calcd. for $C_{27}H_{38}O_{18}$: C, 49.87; H, 5.89; OMe, 4.76. Found: C, 49.97; H, 5.86; OMe, 4.51.

Methanolic barium methoxide (1.5 *N*, 3 ml) was added to the above heptaacetate (3 g) in methanol (50 ml) and the mixture was kept at room temperature for 4 h. The solution was diluted with methanol and passed through columns of Amberlite resins IR-120(H) and IR-45(OH), the resins were washed with methanol–water (1:1), and the combined eluate and washings were concentrated to a syrup. The syrup was chromatographed on a column (90 × 1.5 cm) of Dowex resin 50 WX2 (Li^+; 200–400 mesh) with water as eluant to give chromatographically and ionophoretically pure syrupy 2-*O*-β-D-glucopyranosyl-3-*O*-methyl-D-glucose (**1**), $[\alpha]_D$ +19° → +13° (*c*, 1.0 in water); n.m.r. data (D_2O): τ 4.63 (1-proton doublet, $J_{1,2}$ = 3 Hz, H-1), 6.57 (3-proton singlet, C-3 OMe).

Anal. Calcd. for $C_{13}H_{24}O_{11}$: C, 43.71; H, 6.74; OMe, 8.70. Found (after drying over P_2O_5 at 60°): C, 43.40; H, 7.02; OMe, 8.41.

In subsequent preparations chromatographically pure disaccharide (**1**) was obtained by chromatography on a cellulose column using acetone–water (7:1) as eluant.

The disaccharide (**1**) (750 mg) was treated with sodium borohydride (125 mg) in water (25 ml) for 24 h. Excess of hydride was destroyed and sodium ions were removed by treatment with cation-exchanger, and the solution was concentrated several times with methanol to remove boric acid as methyl borate to give syrupy disaccharide alditol (500 mg). The syrup (200 mg) was treated with acetic anhydride and pyridine, and the product was recrystallized from ether–light petroleum (b.p. 30–60°) to give 1,4,5,6-tetra-*O*-acetyl-2-*O*-(2,3,4,6-tetra-*O*-acetyl-β-D-glucopyranosyl)-3-*O*-methyl-D-glucitol (300 mg), m.p. 88–90°, $[\alpha]_D$ −13.6° (*c*, 1.04 in dichloromethane); n.m.r. data ($CDCl_3$): τ 6.46 (3-proton singlet, C-3 OMe), 7.72–7.88 (24 protons, OAc's).

Anal. Calcd. for $C_{29}H_{42}O_{19}$: C, 50.21; H, 6.10. Found: C, 50.33; H, 6.16.

A further portion (100 mg) of the syrupy disaccharide alditol was treated with benzoyl chloride and pyridine, and the product was recrystallized from ethanol to give 1,4,5,6-tetra-*O*-benzoyl-2-*O*-(2,3,4,6-tetra-*O*-benzoyl-β-D-glucopyranosyl)-3-*O*-methyl-D-glucitol (75 mg), m.p. 80–83°, $[\alpha]_D$ +25.5° (*c*, 1.35 in dichloromethane).

Anal. Calcd. for $C_{69}H_{58}O_{19}$: C, 69.58; H, 4.91. Found: C, 69.49; H, 4.67.

Alkaline Degradation of Disaccharide (1)

The disaccharide (**1**) (1 g) was kept in oxygen-free saturated lime-water (100 ml) for 40 h at 50°. The cooled solution was neutralized with carbon dioxide and concentrated, the residue was extracted with acetone, and the extract was concentrated to a syrup, $[\alpha]_D$ +3° → −4° (*c*, 1.0 in water); λ_{max} (H_2O) 198 nm (ε 5500); ν_{max} (film) 1645 cm^{-1} (C=C); n.m.r. data (D_2O): OMe protons absent.

Anal. Calcd. for $C_{12}H_{20}O_{10}\cdot H_2O$: C, 42.10; H, 6.43. Found (after drying for 1 day at 40°): C, 41.99; H, 6.57.

Anal. Calcd. for $C_{12}H_{20}O_{10}$: C, 44.44; H, 6.17. Found (after extended drying at 40°): C, 43.40; H, 7.02.

Sodium borohydride (0.3 g) was added to the syrupy alkaline degradation product (0.2 g) in water (10 ml), and the solution was warmed to 40° and then kept at room temperature overnight. Excess of hydride was destroyed by the addition of acetone, sodium ions were removed by treatment with cation-exchange resin, and the solution was repeatedly concentrated with methanol to remove boric acid as methyl borate to give a syrup (0.2 g); λ_{max} (H_2O) 230 nm; ν_{max} (film) 1690 (C=O), 1640 (C=C), 975 cm^{-1} (*trans* H—C=C—H).

The syrup (0.2 g) containing the unsaturated ketose was treated with sodium borohydride (0.3 g) in water (10 ml) overnight and the reaction product was worked-up as described above. The t.l.c. of the resulting syrup (ethanol–chloroform, 3:1) showed components with the mobilities of glucitol and 3,4-dideoxy-*trans*-D-*threo*-hex-3-enitol. A further quantity (4 g) of syrup, similarly prepared, was separated by chromatography on a column of silica gel to give two fractions. The slower-moving component (1.6 g) was characterized as D-glucitol by conversion into the hexaacetate, m.p. and mixed m.p. 99°, $[\alpha]_D$ +9° (*c*, 1.0 in chloroform).

Anal. Calcd. for $C_{18}H_{26}O_{12}$: C, 49.76; H, 5.99. Found: C, 49.74; H, 5.88.

The faster-moving fraction (2 g) was triturated with warm acetone (4 ml) and separated into acetone-soluble and acetone-insoluble fractions. The acetone-soluble fraction (0.5 g) was stirred for 24 h with anhydrous cupric sulfate (2 g) in acetone (50 ml) containing concentrated sulfuric acid (0.15 ml). The filtered solution was neutralized with sodium carbonate, filtered, and concentrated to a syrup which was extracted with warm pentane. Removal of solvent from the extract and crystallization from methanol furnished 3,4-dideoxy-1,2:5,6-di-*O*-isopropylidene-*trans*-D-*threo*-hex-3-enitol (0.25 g), m.p. and mixed m.p. (with sample prepared by the method of Tipson and Cohen (7)) 80–81°, $[\alpha]_D$ +57.1° (*c*, 1.0 in chloroform).

Anal. Calcd. for $C_{12}H_{20}O_6$: C, 63.15; H, 8.78. Found: C, 62.98; H, 8.81.

The di-*O*-isopropylidene derivative (0.2 g) was heated at 50° for 1 h in 0.05 *N* hydrochloric acid in 50% aqueous methanol (3 ml). The cooled solution was diluted with water, neutralized with anion-exchanger, and concentrated. The residue was crystallized from ethanol to give 3,4-dideoxy-*trans*-D-*threo*-hex-3-enitol (**5**) (70 mg), m.p. and mixed m.p. 63–64°, $[\alpha]_D$ −14° (*c*, 1.0 in chloroform).

Anal. Calcd. for $C_6H_{12}O_4$: C, 48.64; H, 8.10. Found: C, 48.52; H, 8.38.

In a similar manner the acetone-insoluble fraction (0.5 g) was converted into 3,4-dideoxy-1,2:5,6-di-*O*-isopropylidene-*trans-erythro*-hex-3-enitol (0.3 g), m.p. and mixed m.p. (with sample prepared from 1,2:5,6-di-*O*-isopropylidene-D-glucitol 3,4-thionocarbonate (8)) 69–70°, $[\alpha]_D$ +0.5° (*c*, 1.0 in chloroform).

Anal. Calcd. for $C_{12}H_{20}O_4$: C, 63.15; H, 8.78. Found: C, 63.11; H, 9.09.

Hydrolysis of the di-*O*-isopropylidene derivative

furnished 3,4-dideoxy-*trans-erythro*-hex-3-enitol (**4**) (80 mg), m.p. and mixed m.p. 63–64°, $[\alpha]_D$ 0° (*c*, 5.0 in chloroform).

Anal. Calcd. for $C_6H_{12}O_4$: C, 48.64; H, 8.10. Found: C, 48.62; H, 8.40.

The authors wish to acknowledge financial support from the National Research Council of Canada.

1. H. R. BOLLIGER and D. A. PRINS. Helv. Chim. Acta, **28**, 465 (1945).
2. K. FREUDENBERG, H. TOEPFFER, and C. C. ANDERSEN. Ber. **61**, 1750 (1928); K. FREUDENBERG and K. SOFF. Ber. **69**, 1245 (1936).
3. B. COXON and H. G. FLETCHER, JR. J. Org. Chem. **26**, 2892 (1961).
4. I. O. MASTRONARDI, S. M. FLEMATTI, J. O. DEFERRARI, and E. G. GROS. Carbohydr. Res. **3**, 177 (1966).
5. E. F. L. J. ANET. Aust. J. Chem. **19**, 1677 (1966).
6. J. W. H. OLDHAM and G. J. ROBERTSON. J. Chem. Soc. 685 (1935).
7. R. S. TIPSON and A. COHEN. Carbohydr. Res. **1**, 338 (1965).
8. G. O. ASPINALL, N. W. H. CHEETHAM, and J. FURDOVA. Unpublished results.

Can. J. Chem. Downloaded from www.nrcresearchpress.com by 210.87.254.105 on 09/05/12
For personal use only.

Can. J. Chem. Downloaded from www.nrcresearchpress.com by 210.87.254.40 on 09/05/12
For personal use only.

Oligoribonucleotide Synthesis III.[1,2] Synthesis of Trinucleotides Using a Stepwise Phosphotriester Method

THOMAS NEILSON AND EVA S. WERSTIUK
Department of Biochemistry, McMaster University, Hamilton, Ontario

Received November 18, 1970[3]

A convenient general synthesis for protected di- and triribonucleotides of predetermined sequence is described. Starting with a 5′-*p*-methoxytrityl-2′-*O*-tetrahydropyranyl-ribonucleoside, the nucleoside unit destined to become the 5′-terminal of the oligomer, 2′-*O*-tetrahydropyranyl-nucleosides are coupled together by β,β,β-trichloroethyl 3′–5′-phosphotriester linkages. A two-step process is used for each coupling, (*a*) the terminal 3′-hydroxyl group is phosphorylated using β,β,β-trichloroethylphosphate activated by triisopropylbenzenesulfonyl chloride (TPS) and (*b*) re-activation of the newly inserted diphosphate grouping by TPS is followed by condensation with the 5′-hydroxyl of the incoming nucleoside derivative. These phosphotriester derivatives can be isolated and purified in good yield by silica gel column chromatography in methanol – methylene chloride. The fidelity of 3′–5′ linkage is checked. The p.m.r. spectra can indicate the nature and ratio of the bases in these protected oligomers. Deblocking conditions to give free trinucleoside diphosphates are described.

Une synthèse générale et pratique des di- et triribonucléotides protégés et de séquence prédéterminée est décrite. En partant du 5′-*p*-méthoxytrityl-2′-*O*-tétrahydropyranyl-ribonucléoside qui est le nucléoside unité destiné à devenir le groupe terminal en 5′ de l'oligomère, les 2′-*O*-tétrahydropyranyl-nucléosides sont couplés ensemble par des liens dus au β,β,β-trichloroéthyl 3′–5′-phosphotriester. Un processus en deux étapes est utilisé pour chaque couplage: (*a*) le groupe hydroxyl en 3′ terminal est phosphorylé en utilisant le β,β,β-trichloroéthylphosphate activé par le chlorure de triisopropylbenzènesulfonyl (TPS) et (*b*) la réactivation du groupement diphosphate, nouvellement inséré grâce au TPS est suivie d'une condensation avec le groupement hydroxylé en 5′ du dérivé nucléoside d'attaque. Ces dérivés phosphotriester peuvent être isolés et purifiés, avec un bon rendement, par chromatographie sur colonne de silica gel avec un mélange méthanol – chlorure de méthylène. La fidélité du couplage 3′–5′ a été vérifiée. Des spectres r.m.p. peuvent indiquer la nature et le pourcentage des composants dans ces oligomères protégés. Des conditions de débloçage pour obtenir des diphosphates trinucléoside libres sont décrites.

Canadian Journal of Chemistry, 49, 3004 (1971)

Oligoribonucleotide fragments corresponding to the anti-codon loop and neck region of transfer RNA_F^{Met} (*E. coli*) (3) and to the double stranded stem region (two complementary oligoribonucleotides) of transfer RNA_2^{Ala} (yeast) (4) have been isolated from partial Ribonuclease T1 digestions on the native molecules. Similar but reduced activities relative to their parents have been found in codon triplet and in aminoacyl-tRNA synthetase recognition respectively, indicating the elements for binding must be wholly or partially contained within the base sequence of those fragments. Specific points for transfer RNA interaction should become apparent on measuring the activities of a series of oligoribonucleotides with single base changes.

Only a limited number of oligonucleotides of known length and sequence are currently available, as fragments from enzymic digests are controlled by specific cleavage points in a polyribonucleotide. Chemical synthesis on the other hand is theoretically capable of providing all possible oligoribonucleotides. Should a particular sequence within a transfer RNA molecule be considered a possible function site, a 'tailor-made' oligoribonucleotide could be prepared and checked for activity. Thus sequences corresponding to (*a*) the anticodon loop and neck region of a transfer RNA_F^{Met} molecule may provide further information on the nature of anticodon–codon binding as well as clarify the function of the adjacent minor base and (*b*) the doubly stranded stem region (two complementary oligoribonucleotides) may establish the elements of aminoacyl-$tRNA_2^{Ala}$ synthetase recognition sites.

The current status of oligoribonucleotide synthesis leaves much to be desired. The general methods available (5, 6) provide no material longer than a trinucleotide. Because low capacity DEAE–cellulose chromatography in aqueous salt solutions was used as the purification pro-

[1]For part II, see ref. 1.
[2]A preliminary account has been published, see ref. 2.
[3]Revision received June 15, 1971.

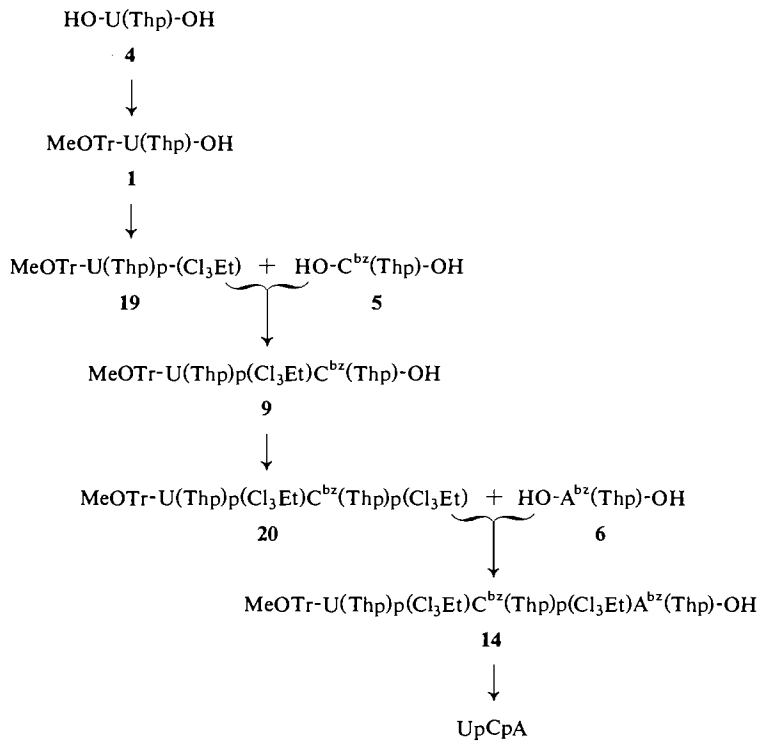

SCHEME 1

cedure, only small amounts of material were isolated. Interest in this area has been rekindled following two recent developments. (*a*) Ready solubility of tertiary phosphates of oligodeoxyribonucleotides in non-polar solvents allowed relatively large quantities of intermediates to be handled by silica gel chromatography (7–10). Consequently, the slower aqueous chromatographic procedures can be by-passed, at least until after the various protecting groups have been removed late in overall synthesis. (*b*) Mild mineral acid (p*H* 2) (11) accomplished smooth removal of the *O*-tetrahydropyranyl grouping with negligible isomerization of the 3′–5′-diphosphate internucleotidic linkage. Certain acid-labile protecting groups could now be used to block hydroxyl groups of ribofuranoside rings.

In this communication we report a new convenient stepwise synthesis for oligoribonucleotides, one which promises to be generally applicable to the preparation of mixed oligonucleotides. 2′-*O*-Tetrahydropyranyl-*N*-acylnucleosides (1, 11) are joined together in a stepwise manner using 3′–5′-phosphotriester linkages to give protected di- and triribonucleotides. The initial nucleoside in the phosphate coupling is a corresponding 5′-*O*-*p*-methoxytrityl derivative and is destined to become the 5′-terminal nucleoside in the proposed di- and triribonucleotide. Hence the synthesis starts from the 5′-terminal while most syntheses proceeded in the opposite direction. It is anticipated that coupling of these trinucleotides and subsequent deblocking of the product, will provide a block synthesis for much longer oligoribonucleotides of predetermined length and sequence.

Choice of the 'third group' of the phosphotriester internucleotidic linkage was the β,β,β-trichloroethyl grouping (Cl_3Et) which has been successfully employed in deoxyoligonucleotide synthesis by Eckstein (6, 12). Insertion followed a two stage procedure: (*a*) phosphorylation of 3′-hydroxyl group of a nucleoside with β,β,β-trichloroethylphosphoryl dichloride and (*b*) coupling of the new phosphate center with the 5′-hydroxyl group of the next nucleoside using triisopropylbenzenesulfonyl chloride (TPS). Conversion of the phosphotriester linkage to the native 3′–5′-diphosphate was effected by treatment with a Cu–Zn couple in *N*,*N*-dimethylformamide at 60°. A simplification of step *a* was employed in the present instance. β,β,β-Tri-

Can. J. Chem. Downloaded from www.nrcresearchpress.com by 210.87.254.40 on 09/05/12
For personal use only.

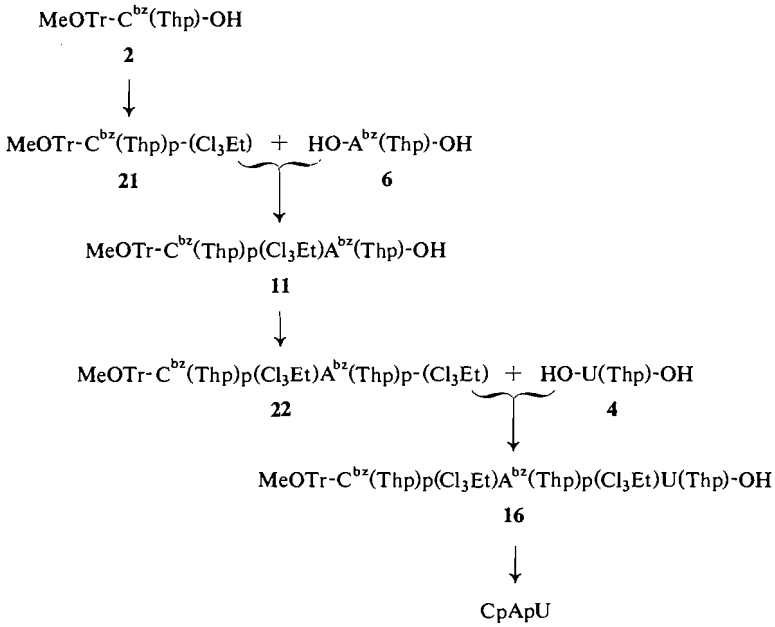

SCHEME 2

chloroethyl phosphate was activated in pyridine using TPS and this complex smoothly phosphorylated the 3′-secondary hydroxyl group of the nucleoside, thus by-passing the need of its more reactive and acidic phosphoryl dichloride derivative. Protected dinucleoside phosphates were prepared either using method A or B illustrated by the synthesis of blocked UpC (Scheme 1) and blocked CpA (Scheme 2) respectively. All protected trinucleoside diphosphates were prepared by the same method illustrated by the synthesis of blocked UpCpA (Scheme 1) and blocked CpApU (Scheme 2). Figure 1[4] shows the amounts of reactants and yields of products for the other protected di- and triribonucleotides prepared, as well as the method employed.

5′-*O*-*p*-Monomethoxytrityl-2′-*O*-tetrahydropyranyluridine (**1**) was prepared in 86% yield from the lower R_F diastereoisomer of 2′-*O*-tetrahydropyranyluridine (**4**) (11) by a high dilution procedure using 1.1 equiv of *p*-anisylchlorodiphenyl methane in pyridine – methylene chloride.

Preparation of Protected Dinucleoside Phosphates

Method A

The bis-cyclohexylamine salt of β,β,β-trichloroethylphosphate (12) was converted to its corresponding pyridinium salt and activated in pyridine using 2 equiv of TPS. Phosphorylation of **1** was carried out in pyridine, progress being monitored by t.l.c., to give 5′-*O*-*p*-methoxytrityl-2′-*O*-tetrahydropyranyluridine-3′-β,β,β-trichloroethylphosphate (**19**) as its pyridinium salt. Immediate activation of (**19**) with 1 equiv of TPS and coupling with the 5′-hydroxyl of N^4-benzoyl-2′-*O*-tetrahydropyranylcytidine (**5**) (1) (the higher R_F diastereoisomer was used as the low R_F diastereoisomer is only slightly soluble in pyridine) gave the blocked UpC, 5′-*O*-*p*-methoxytrityl-2′-*O*-tetrahydropyranyluridylyl(3′-β,β,β-trichloroethyl-5′)N^4-benzoyl-2′-*O*-tetrahydropyranylcytidine (**9**) in 63% yield over the two coupling steps. All phosphorylations were carried out in the dark under anhydrous conditions and preferably sealed under nitrogen. All blocked dinucleotides were eluted from silica gel columns by 2% methanol – methylene chloride. Although

[4]To condense the huge structural formulae necessary to describe a protected oligoribonucleotide, a shorthand method suggested by the IUPAC–IUB commission on Biochemical Nomenclature is adopted (Biochem. **9**, 4022 (1970)).

For example, 5′-*O*-*p*-methoxytrityl-2′-*O*-tetrahydropyranyluridylyl(3′-β,β,β-trichloroethyl-5′)N^4-benzoyl-2′-*O*-tetrahydropyranylcytidylyl(3′-β,β,β-trichloroethyl-5′)-N^6-benzoyl-2′-*O*-tetrahydropyranyladenosine can be written as MeOTr-U(Thp)p(Cl_3Et)C^{bz}(Thp)p(Cl_3Et)A^{bz}-(Thp)–OH.

Can. J. Chem. Downloaded from www.nrcresearchpress.com by 210.87.254.40 on 09/05/12
For personal use only.

Data of Protected Nucleosides

MeOTr-U(Thp)-OH(**1**); R_F 0.60 in 5% $CH_3OH—CH_2Cl_2$
MeOTr-C^{bz}(Thp)-OH(**2**); R_F 0.73 in 10% $CH_3OH—CH_2Cl_2$(1)
MeOTr-A^{bz}(Thp)-OH(**3**); R_F 0.90 in 5% $CH_3OH—CH_2Cl_2$(1)
HO-U(Thp)-OH(**4**); m.p. 185–187 °C; R_F 0.25 in 5% $CH_3OH—CH_2Cl_2$(11)
HO-C^{bz}(Thp)-OH(**5**); m.p. 162–164 °C; R_F 0.61 in 10% $CH_3OH—CH_2Cl_2$(1)
HO-A^{bz}(Thp)-OH(**6**); R_F 0.30 in 5% $CH_3OH—CH_2Cl_2$(1)
HO-G^{bz}(OH)-OH(**7**); m.p. 246–248 °C; R_F 0.14 in 15% $CH_3OH—CH_2Cl_2$(13)

Protected Dinucleoside Phosphates

Method A

1 (601 mg, 1 equiv) + **4** (656 mg, 2 equiv) → MeOTr-U(Thp)p(Cl_3Et)U(Thp)-OH(**8**) (700 mg, 62%)
1 (500 mg, 1 equiv) + **5** (720 mg, 2 equiv) → MeOTr-U(Thp)p(Cl_3Et)C^{bz}(Thp)-OH(**9**)(640 mg, 63%)
3 (350 mg, 1 equiv) + **6** (440 mg, 2 equiv) → MeOTr-A^{bz}(Thp)p(Cl_3Et)A^{bz}(Thp)-OH(**10**)(510 mg, 76%)

Method B

2 (480 mg, 1 equiv) + **6** (620 mg, 2 equiv) → MeOTr-C^{bz}(Thp)p(Cl_3Et)A^{bz}(Thp)-OH(**11**)(570 mg, 62%)
1 (250 mg, 1 equiv) + **6** (380 mg, 2 equiv) → MeOTr-U(Thp)p(Cl_3Et)A^{bz}(Thp)-OH(**12**)(250 mg, 48%)

Protected Trinucleoside Diphosphates

8 (224 mg, 1 equiv) + **4** (131 mg, 2 equiv) → MeOTr-U(Thp)p(Cl_3Et)U(Thp)p(Cl_3Et)U(Thp)-OH(**13**)(225 mg, 67%)
9 (250 mg, 1 equiv) + **6** (190 mg, 2 equiv) → MeOTr-U(Thp)p(Cl_3Et)C^{bz}(Thp)p(Cl_3Et)A^{bz}(Thp)-OH(**14**)(195 mg, 61%)
10 (215 mg, 1 equiv) + **7** (130 mg, 2 equiv) → MeOTr-U(Thp)p(Cl_3Et)A^{bz}(Thp)p(Cl_3Et)G^{bz}(OH)OH(**15**)(155 mg, 49%)
11 (399 mg, 1 equiv) + **4** (147 mg, 1.5 equiv) → MeOTr-C^{bz}(Thp)p(Cl_3Et)A^{bz}(Thp)p(Cl_3Et)U(Thp)OH(**16**)(278 mg, 48%)
12 (420 mg, 1 equiv) + **4** (152 mg, 1.5 equiv) → MeOTr-A^{bz}(Thp)p(Cl_3Et)A^{bz}(Thp)p(Cl_3Et)U(Thp)OH(**17**)(298 mg, 51%)
12 (348 mg, 1 equiv) + **7** (390 mg, 4 equiv) → MeOTr-A^{bz}(Thp)p(Cl_3Et)A^{bz}(Thp)p(Cl_3Et)G^{bz}(OH)OH(**18**)(126 mg, 25%)

FIG. 1. Summary of preparation of protected oligoribonucleotides.

19 is a salt, its large lipophilic trityl group allowed facile solution in methylene chloride, thus a simple extraction procedure could be used for its isolation.

Method B

The first stage of the formation of diphosphate linkage of blocked CpA, N^4-benzoyl-5′-*O*-*p*-methoxytrityl-2′-*O*-tetrahydropyranylcytidylyl-(3′-β,β,β-trichloroethyl-5′)N^6-benzoyl-2′-*O*-tetrahydropyranyladenosine (**11**), was described in method A. However, after the second coupling step, column chromatography was unable to separate cleanly **11** from excess N^6-benzoyl-2′-*O*-tetrahydropyranyladenosine (**6**) (1). Separation was accomplished by careful tritylation of the mixture in high dilution which ensured only 5′-*O*-tritylation. Excess **6** was converted to its corresponding 5′-trityl derivative **3** and silica gel column chromatographic separation of **3** and **11** was routine.

This 'back-tritylation' suggested a convenient method for checking the fidelity of the 3′–5′ linkages. Blocked dinucleotide material containing 3′–3′ linkages, arising from possible condensation with the 3′-hydroxyl of the incoming nucleoside, would obtain a second 5′-trityl group under mild tritylation conditions. Any such ditrityl material would be easily detected by t.l.c. Routine mild tritylation on all blocked dinucleotides showed no further reaction indicating the non-existence of 3′–3′-triphosphate formation. Steric interference between the neighboring 2′-*O*-tetrahydropyranyl group of the incoming nucleoside and the bulky arylsulfonic – phosphoric anhydride, together with the secondary nature of the 3′-hydroxyl group, apparently forbids reaction. Consequently no specific 3′-hydroxyl protection was necessary for the incoming nucleosides.

Preparation of Protected Triribonucleoside Diphosphates

Compound **9** was treated with the activated complex of bis-pyridinium β,β,β-trichloroethylphosphate and TPS to give blocked UpCp **20**, an intermediate in the formation of the phosphotriester bond. Immediate activation of **20** with TPS and condensation with N^6-benzoyl-2′-*O*-tetrahydropyranyladenosine (**6**) (1) gave the blocked triribonucleotide, UpCpA **14** in 61% yield over two steps. Elution of the protected trinucleotides occurred with 2.5–3.0% methanol – methylene chloride, those containing N^2-benzoylguanosine residues being more sluggish.

The p.m.r. data in Table 1 show the resonance bonds for the aromatic protons of the heterocyclic bases and for the anomeric protons of the protected di- and trinucleotides. Signals attributed to H-2 and -8 singlets of adenine, H-8 singlets of guanine, H-5 doublets of uracil, and 1′-anomeric doublets of the ribofuranoside moieties were

Can. J. Chem. Downloaded from www.nrcresearchpress.com by 210.87.254.40 on 09/05/12
For personal use only.

TABLE 1. The p.m.r. data of protected oligoribonucleotides

Protected compound	δ (p.p.m.) Aromatic protons	δ (p.p.m.) 1′-Anomeric protons
8 (UpU)	5.43 (2H, 2d, superimposed) H-5 of Us; 7.5 and 7.68 (2H, d, $J \sim 8$ Hz) H-6 of Us	5.95 (2H, 2d, superimposed) H-1′ of Us
9 (UpC)	5.42 (1H, d, $J \sim 8$ Hz) H-5 of U; 8.6 (1H, d, $J \sim 8$ Hz) H-6 of C; H-6 of U is under *o*-PhCO protons 8.1; H-5 of C is under trityl protons 7.3	5.8 (1H, d, $J \sim 8$ Hz) H-1′ of C; 6.05 (1H, d, $J \sim 6$ Hz) H-1′ of U
12 (UpA)	5.42 (1H, d, $J \sim 8$ Hz) H-5 of U; 8.60 and 8.65 (2H, s) H-2 and -8 of A; H-6 of U is under *o*-PhCO protons 8.1	6.05 (1H, d, $J \sim 6$ Hz) H-1′ of U; 6.3 (1H, d, $J \sim 4$ Hz) H-1′ of A
10 (ApA)	8.55 and 8.60 (2H, s) H-2 and -8 of A; 8.70 and 8.75 (2H, s) H-2 and -8 of A	6.30 (2H, 2d, $J \sim 6$ Hz superimposed) H-1′ of A
11 (CpA)	8.05 and 8.10 (2H, s) H-2 and -8 of A; H-6 of C is under *o*-PhCO protons 8.1; H-5 of C is under trityl protons 7.2	6.2 (2H, 2d, $J \sim 6$ Hz superimposed) H-1′ of C and A
14 (UpCpA)	5.42 (1H, 1 broad d) H-5 of U; 8.66 and 8.75 (2H, 2s) H-2 and -8 of A; H-6 of U and H-6 of C is under *o*-PhCO protons 8.05; H-5 of C is under trityl protons 7.3	5.98 (2H, 2d, superimposed) H-1′ of C and H-1′ of U; 6.26 (1H, d, $J \sim 5$ Hz) H-1′ of A
16 (CpApU)	5.65 (1H, d, $J \sim 10$ Hz) H-5 of U; 8.65 and 8.70 (2H, 2s) H-2 and -8 of A; H-6 of U and H-6 of C is under *o*-PhCO protons 8.05; H-5 of C is under trityl protons 7.3	5.98 (1H, d, $J \sim 4$ Hz) H-1′ of U; 6.3 (1H, d, $J \sim 6$ Hz) H-1′ of C; 6.6 (1H, d, $J \sim 6$ Hz) H-1′ of A
17 (ApApU)	8.53, 8.65, and 8.75 (4H, 4s, two are superimposed) H-2 and -8 of As; H-6 of U is under *o*-PhCO protons 8.1	5.98 (2H, 2d, superimposed) H-1′ of U and H-5 of U; 6.29 (2H, 2d, superimposed) H-1′ of As
18 (ApApG)	8.73, 8.65, 8.53, and 8.45 (4H, s) H-2 and -8 of As; 8.00 (1H, s) H-2 of G surrounded by *o*-PhCO protons 7.9–8.2	6.25 (2H, 2d, $J \sim 4$ Hz superimposed) H-1′ of As; 5.42 (1H, broadened) H-1′ of G

TABLE 2. Characterization of trinucleoside diphosphates

Deblocked triplets	R_F*	Literature R_F*	% Yield	Enzymic analysis
UpUpU	1.02	1.03	93	Up:U, 2:1 (PR)
UpCpA	0.56	0.57	90	Up:Cp:A, 1:1:1 (PR)
CpApU	0.59	0.57	87	C:pA:pU, 1:1:1 (SVD)
ApApU	0.45	0.46	91	A:pA:pU, 1:1:1(SVD)
ApApG	0.32	0.32	70	A:pA:pG, 1:1:1 (SVD)

*R_F's relative to Up as 1.00.

easily identified. The H-6 doublets of uracil and H-6 doublets of cytosine always lay under the ortho-protons of any *N*-benzoyl protecting groups, however, these multiplets always integrated for the correct number of protons. The H-5 doublets of cytidine were always obscured by the large phenyl resonance of the trityl group. Despite the existence of these overlapping resonances, the nature and ratio of the bases within a protected oligomer could be determined.

Deblocking of Trinucleoside Diphosphates

A three-step deblocking procedure was carried out in the following order. (*a*) β,β,β-Trichloroethyl groups were removed from the phosphate residue using a Cu–Zn couple (6, 12) in *N*,*N*-dimethylformamide for 1 day at 50 °C. (*b*) Ammonolysis of the amide groups on the heterocyclic bases was accomplished in half-saturated methanolic ammonia (1) for 2 days at room temperature. (*c*) Hydrolytic removal of the trityl and tetrahydropyranyl groups was achieved by maintaining the solution p*H* at 2 (11) for 1 day at ambient temperatures.

It is essential that the 2′-hydroxyl remains blocked during the alkaline conditions of ammo-

Can. J. Chem. Downloaded from www.nrcresearchpress.com by 210.87.254.40 on 09/05/12
For personal use only.

Can. J. Chem. Downloaded from www.nrcresearchpress.com by 210.87.254.40 on 09/05/12
For personal use only.

nolysis because of possible isomerization of the 3′–5′ phosphodiester bonds to a mixture of 2′–5′ and 3′–5′ phosphodiester linkages, thus destroying the whole purpose of specific 2′-blocking.

Characterization of the trinucleoside diphosphates, all one spot materials on p.c. and t.l.c. systems, was carried out by comparison with known R_F literature values (5). Base composition and the fidelity of the 3′–5′-phosphodiester linkages were checked using pancreatic ribonuclease (PR) or snake venom diesterase (SVD) digestions. Yields for the trinucleotides were calculated from spectrophotometric data assuming a 90% hypochromicity factor, all were *ca.* 80% (Table 2).

Experimental

The p.m.r. spectra were recorded on a Varian T60 or Varian HA-100 spectrometer in 10–15% (w/v) DMSO-d_6 – D_2O solutions, and line positions are reported in p.p.m. from the reference (TMS).

Silica gel (Baker Analyzed Reagent) was used for column chromatography; and Analtech prescored silica gel plates were employed for t.l.c. The plates were developed in 5 or 10% methanol in methylene chloride mixtures.

The t.l.c. detection was carried out using a ceric sulfate spray (1 g $H_4Ce(SO_4)_4$ in 10% aqueous sulfuric acid solution) and followed by heating the plates at 300–400 °C. Compounds containing a trityl group develop as yellow spots, while others appear as brown spots.

It was essential that moisture be excluded from all coupling reactions. After evaporation *in vacuo* of the pyridine solution, normal pressure was restored with dry nitrogen and *not* atmospheric air. All such evaporations were carried out in the temperature range 30–40 °C.

Emulsion, frequently obtained during methylene chloride extractions of aqueous pyridine solutions, was broken by the addition of a few milliliters of saturated sodium chloride solution.

*5′-O-Methoxytrityl-2′-O-tetrahydropyranyluridine (**1**)*

The lower R_F diastereoisomer of 2′-*O*-tetrahydropyranyluridine (**4**) (11) (1.6 g; m.p. 185–187°) was dissolved in anhydrous pyridine (8 ml) and methylene chloride (40 ml). *p*-Anisylchlorodiphenylmethane (1.65 g, 1.1 equiv) was added portionwise to the solution and the reaction mixture was sealed and left at room temperature overnight in the dark. The t.l.c. indicated the disappearance of starting material (R_F 0.1 → 0.6–0.9 in 5% CH_3OH–CH_2Cl_2). After quenching with ethanol (20 ml), the mixture was added to ice-water (100 ml) and extracted with methylene chloride (3 × 50 ml). The combined organic extracts were washed with distilled water (3 × 50 ml) and evaporated *in vacuo* to an oil, the last traces of pyridine being removed by co-distillation with toluene (2 × 25 ml). Column chromatography on silica gel was applied. Elution with 1% CH_3OH–CH_2Cl_2 gave the desired 5′-*O*-monotrityl material as an off-white solid foam (2.52 g, 86%) which was sufficiently pure for further conversions. The p.m.r. spectrum showed signals (δ TMS) at 7.85 (1H doublet, $J \sim 8$ Hz; 6-proton of uracil); 7.5 (14H multiplet; trityl aromatic protons); 6.10 (1H doublet; 1′-anomeric proton); 5.45 (1H doublet; $J \sim 8$ Hz; 5-proton of uracil); 4.95 (1H singlet; Thp acetal proton); 4.41 and 4.15 (3H multiplets, sugar protons); 3.85 (3H singlet; MeO of *p*-methoxytrityl); 1.65 (6H broad multiplet; *C*-methylenes of Thp).

Method A

*5′-O-p-Methoxytrityl-2′-O-tetrahydropyranyluridine-3′-β,β,β-trichloroethylphosphate (**19**)*

The bis-cyclohexylamine salt (720 mg, 2 equiv) of mono-β,β,β-trichloroethylphosphate (12) was dissolved in anhydrous pyridine (50 ml) (warming was necessary) and converted to the corresponding pyridinium salt by repetitive evaporation *in vacuo* and solution in pyridine (4 × 40 ml).

Triisopropylbenzenesulfonyl chloride (1 g, 4 equiv) was added to the pyridinium salt in pyridine (40 ml) whereupon a yellow coloration developed. Thirty minutes later, 5′-*O*-*p*-methoxytrityl-2′-*O*-tetrahydropyranyluridine (**1**) (500 mg, 1 equiv; R_F 0.6 in 5% CH_3OH–CH_2Cl_2) was added as a pyridine solution (5 ml). The reaction mixture was sealed under nitrogen and left at room temperature for 1–2 days in the dark. The t.l.c. indicated the phosphate coupling was complete (R_F 0.6 → 0.1 in 5% CH_3OH–CH_2Cl_2). Ice (5 g) was added and the quenched reaction left for 30 min, poured into ice-water (100 ml) and then extracted with methylene chloride (4 × 50 ml). The combined organic extracts were washed with distilled water (4 × 50 ml). Methylene chloride was removed by evaporation *in vacuo* and replaced by anhydrous pyridine (50 ml). This pyridine solution containing the pyridinium salt **19** of desired nucleotide derivative was used immediately to form blocked dinucleoside phosphate derivatives.

*5′-O-p-Methoxytrityl-2′-O-tetrahydropyranyluridylyl-(3′-β,β,β-trichloroethyl-5′)N⁴-benzoyl-2′-O-tetrahydropyranylcytidine (**9**)*

Triisopropylbenzenesulfonyl chloride (TPS) (500 mg, 2 equiv) was added to the pyridine solution of blocked uridylate derivative **19** prepared in the previous experiment and the activation was allowed to proceed for 30 min at room temperature in the dark. The high R_F diastereoisomer of N^4-benzoyl-2′-*O*-tetrahydropyranylcytidine (**5**) (1) (720 mg, 2 equiv; m.p. 162–164°; R_F 0.61 in 10% in CH_3OH–CH_2Cl_2) dissolved in anhydrous pyridine (10 ml) was added and the reaction mixture was left at room temperature for 1–2 days in the dark. After 1 day, a further portion of TPS (100 mg) was added to ensure complete reaction by the second day as indicated by t.l.c. (R_F 0.1 → 0.55 in 5% CH_3OH–CH_2Cl_2). Ice (5 g) was added and after 30 min the aqueous pyridine solution was poured into ice-water (50 ml) and extracted by methylene chloride (4 × 50 ml). The combined organic extracts were washed with water (4 × 50 ml) and evaporated *in vacuo* to an oily residue, the last traces of pyridine being removed by co-distillation with toluene (2 × 25 ml). The residue was dissolved in methylene chloride (50 ml) whereupon some triisopropylbenzenesulfonic acid separated and was removed. Column chromatography on silica gel was applied to the filtrate. Elution with 1.5% CH_3OH–CH_2Cl_2 gave a trace of 5′-*O*-*p*-methoxytrityl-2′-*O*-tetrahydropyranyluridine (**1**) and

Can. J. Chem. Downloaded from www.nrcresearchpress.com by 210.87.254.40 on 09/05/12
For personal use only.

the excess N^4-benzoyl-2′-*O*-tetrahydropyranylcytidine (**5**) (306 mg). The t.l.c. indicated that the expected order of elution should have been **1**, **19**, and **5**. Elution with 2% CH_3OH–CH_2Cl_2 gave the blocked dinucleotide (UpC) (640 mg, 63%) as a pale yellow solid foam.

*5′-O-p-Methoxytrityl-2′-O-tetrahydropyranyluridylyl-(3′-β,β,β-trichloroethyl-5′)N⁴-benzoyl-2′-O-tetrahydropyranylcytidine-3′-β,β,β-trichloroethyl-phosphate (**20**)*

The bis-cyclohexylamine salt (180 mg, 2 equiv) (12) of β,β,β-trichloroethylphosphate was converted to its corresponding pyridinium salt as described previously. Triisopropylbenzenesulfonyl chloride (250 mg, 4 equiv) was added to the pyridinium salt in anhydrous pyridine (5 ml). After 30 min, blocked UpC **9** (250 mg, 1 equiv) dissolved in pyridine (5 ml) was added to the yellow solution which was sealed under nitrogen and allowed to stand at room temperature for 1–2 days in the dark. The t.l.c. indicated almost complete reaction (R_F 0.55 → 0.1 in 5% CH_3OH–CH_2Cl_2). Ice (2 g) was added, followed 30 min later by a similar methylene chloride extraction process as used for **19**. Blocked UpCp **20** was obtained as its pyridinium salt in pyridine and was used immediately in the next step.

*5′-O-p-Methoxytrityl-2′-O-tetrahydropyranyluridylyl-(3′-β,β,β-trichloroethyl-5′)N⁴-benzoyl-2′-O-tetrahydropyranylcytidylyl(3′-β,β,β-trichloroethyl-5′)N⁶-benzoyl-2′-O-tetrahydropyranyladenosine (**14**)*

Triisopropylbenzenesulfonyl chloride (TPS) (125 mg, 2 equiv) was added to the pyridine solution of blocked UpCp **20** pyridinium salt (described above). After 30 min, N^6-benzoyl-2′-*O*-tetrahydropyranyladenosine (**6**) (1) (190 mg, 2 equiv; R_F: 0.30 in 5% CH_3OH–CH_2Cl_2) was added and the reaction mixture sealed under nitrogen and allowed to stand at room temperature for 1–2 days in the dark. A further portion of TPS (50 mg) was added after 1 day to ensure complete coupling by the second day, as indicated by t.l.c. in 5% CH_3OH–CH_2Cl_2 (R_F 0.1 → 0.50). A similar work-up to that used for **9** was employed and column chromatography on silica gel utilized for purification. Elution with 2% CH_3OH—CH_2Cl_2 (500 ml) gave some unreacted blocked UpC **9** (40 mg). Elution with 2.5% CH_3OH–CH_2Cl_2 (500 ml) gave excess blocked nucleoside **6** (80 mg). Elution with 3% CH_3OH–CH_2Cl_2 (750 ml) gave the blocked UpCpA **14** (195 mg, 61%) as a pale yellow solid foam. Again the column elution differed from that indicated by t.l.c. (**9**, **14**, and **6**).

Method B

*N⁴-Benzoyl-5′-O-p-methoxytrityl-2′-O-tetrahydropyranylcytidine-3′-β,β,β-trichloroethylphosphate (**21**)*

The bis-cyclohexylamine salt (0.608 g, 13.6 mmol; 2 equivs) of mono-β,β,β-trichloroethylphosphate was converted into its pyridinium salt as described previously. Triisopropylbenzenesulfonyl chloride (TPS) (0.840 g, 27.2 mmol; 4 equiv) was then added to the pyridinium salt. After 1 h, a pyridine solution of N^4-benzoyl-5′-*O*-*p*-methoxytrityl-2′-*O*-tetrahydropyranylcytidine (**2**) (1) (0.480 g, 6.8 mmol; 1 equiv; R_F: 0.63 in 5% CH_3OH–CH_2Cl_2) was added to the yellow solution and the reaction mixture sealed under nitrogen and set aside at room temperature in the dark. After 1–2 days t.l.c. indicated complete conversion into a product of R_F: 0.0–0.18 in 5% CH_3OH–CH_2Cl_2. Ice (5 g) was then added followed 30 min later by a similar methylene chloride extraction as described for **9**. Blocked Cp **21** was obtained as its pyridinium salt in pyridine and was used immediately to form blocked dinucleotide phosphate derivatives.

*N⁴-Benzoyl-5′-O-p-methoxytrityl-2′-O-tetrahydropyranylcytidylyl(3′-β,β,β-trichloroethyl-5′)N⁶-benzoyl-2′-O-tetrahydropyranyladenosine (**11**)*

Triisopropylbenzenesulfonyl chloride (TPS) (0.230 g, 7.5 mmol; 1.1 equiv) was added to the blocked cytidylate derivative **21** and the activation allowed to proceed for 30 min at room temperature in the dark. The low R_F diastereoisomer of N^6-benzoyl-2′-*O*-tetrahydropyranyladenosine (**6**) (1) (0.620 g, 13.6 mmol; 2 equivs; R_F: 0.19 in 5% CH_3OH–CH_2Cl_2) was then added, and the reaction mixture set aside at room temperature in the dark for 1–3 days. On the second day a further portion of TPS (0.115 g, 0.55 equiv) was added to speed coupling. The t.l.c. indicated *ca.* 90% conversion into a product of R_F: 0.49 in 5% CH_3OH–CH_2Cl_2. Ice (5 g) was then added to the mixture, and stirring continued for further 30 min. The reaction mixture was then poured into ice-water (60 ml) and repeatedly extracted with methylene chloride (5 × 30 ml). The combined organic extracts were washed with water (5 × 30 ml) and evaporated *in vacuo* to give an oily residue. The last traces of pyridine were removed by co-distillation with toluene (2 × 25 ml). Methylene chloride (30 ml) was then added to the residue, and the precipitated triisopropylbenzenesulfonic acid was filtered off. The filtrate was purified by chromatography on silica gel (40 g) in methylene chloride. Elution with 2.0% methanol – methylene chloride mixture (600 ml) yielded a *ca.* 1:1 mixture of **6** and **11** (0.813 g, R_F: 0.31 and 0.22 in 5% CH_3OH–CH_2Cl_2). Continued elution with 2.5% methanol – methylene chloride mixture (600 ml) gave an enriched sample **11** (0.436 g, R_F: 0.23 in 5% CH_3OH–CH_2Cl_2), which was purified further by chromatography on silica gel (40 g) as before. Pure CpA **11** was isolated (0.300 g, R_F: 0.22 in 5% CH_3OH–CH_2Cl_2) on elution with 2.5% methanol – methylene chloride mixture (400 ml). The mixture of **6** and **11** (obtained above) (0.813 g, R_F: 0.31 and 0.22 in 5% CH_3OH–CH_2Cl_2) was treated with an excess of *p*-anisylchlorodiphenylmethane (0.43 g, 1.4 mmol; *ca.* 1.5 equiv, based on a 1:1 mixture of **6** and **11**) in anhydrous pyridine (10 ml). The reaction mixture was set aside at room temperature in the dark. After 2 days t.l.c. indicated *complete* conversion of **6** into N^6-benzoyl-5′-*O*-*p*-methoxytrityl-2′-*O*-tetrahydropyranyladenosine (**3**) (1) (R_F: 0.78 in 5% CH_3OH–CH_2Cl_2). Ice (5 g) was then added, and stirring continued for further 30 min. The reaction mixture was then poured into ice-water (100 ml), and repeatedly extracted (5 × 30 ml) with methylene chloride. The combined organic extracts were washed with water (5 × 30 ml), and evaporated *in vacuo* to give a pale yellow glass. This material was purified by chromatography on silica gel (20 g) in methylene chloride. Elution with 1–2% methanol – methylene chloride mixtures (400 ml and 400 ml) yielded pure **3** (0.687 g, R_F: 0.80 in 5% CH_3OH–CH_2Cl_2). Continued elution with 2.5% methanol – methylene chloride mixtures yielded pure **11** (0.277 g; R_F: 0.33 in 5% CH_3OH–CH_2Cl_2) (total yield of **11** 0.577 g, 62%).

Can. J. Chem. Downloaded from www.nrcresearchpress.com by 210.87.254.40 on 09/05/12
For personal use only.

N^4-Benzoyl-5′-O-p-methoxytrityl-2′-O-tetrahydropyranylcytidylyl(3′-β,β,β-trichloroethyl-5′)N^6-benzoyl-2′-O-tetrahydropyranyladenosine-3′-β,β,β-trichloroethylphosphate (22)

The bis-cyclohexylamine salt (0.270 g, 6.0 mmol; 2 equivs) of mono-β,β,β-trichloroethylphosphate was converted into its pyridinium salt as described previously. Triisopropylbenzenesulfonyl chloride (TPS) (0.365 g, 12 mmol; 4 equivs) was then added to the pyridinium salt. After 1 h, a pyridine solution (5 ml) of blocked CpA **11** (0.399 g, 3 mmol; 1 equiv; R_F: 0.33 in 5% CH_3OH–CH_2Cl_2) was added to the yellow solution, and the reaction mixture sealed under nitrogen and set aside at room temperature in the dark. After 1–2 days t.l.c. indicated complete conversion into a product of R_F: 0.0–0.14 in 5% CH_3OH–CH_2Cl_2. Ice (5 g) was then added followed 30 min later by a similar methylene chloride extraction as described for **11**. Blocked CpAp **22** was obtained as its pyridinium salt in pyridine and was used immediately in the next step.

N^4-Benzoyl-5′-O-p-methoxytrityl-2′-O-tetrahydropyranylcytidylyl(3′-β,β,β-trichloroethyl-5′)N^6-benzoyl-2′-O-tetrahydropyranyladenylyl(3′-β,β,β-trichloroethyl-5′)2′-O-tetrahydropyranyluridine (16)

Triisopropylbenzenesulfonyl chloride (TPS) (0.97 mg, 3.3 mmol; 1.1 equiv) was added to the pyridine solution of blocked CpAp **22** pyridinium salt (described above). After 30 min the low R_F diastereoisomer of 2′-O-tetrahydropyranyluridine (**4**) (11) (0.147 g, 4.5 mmol; 1.5 equiv; R_F: 0.14 in 5% CH_3OH–CH_2Cl_2) was added, and the reaction mixture sealed under nitrogen, and set aside at room temperature for 1–3 days in the dark. A further portion of TPS (0.97 mg, 1.1 equiv) was added after 2 days to speed coupling. The t.l.c. indicated *ca.* 90% conversion into a product of R_F: 0.30 in 5% CH_3OH–CH_2Cl_2. After a similar work-up described for **9**, the product was purified by chromatography on silica gel (15 g) in methylene chloride. Elution with 2% methanol – methylene chloride mixture (400 ml) yielded an impure sample of **16** (0.205 g, R_F: 0.30 and 0.46 and 0.58 in 5% CH_3OH–CH_2Cl_2). Continued elution with 2.5–3.0% methanol – methylene chloride mixtures (600 ml + 600 ml) yielded a pure sample of CpApU **16**, (0.278 g, 48%; R_F: 0.30 in 5% CH_3OH–CH_2Cl_2) as a pale yellow solid foam.

Uridylyl(3′–5′)cytidylyl(3′–5′)adenosine (UpCpA)

5′-O-p-Methoxytrityl-2′-O-tetrahydropyranyluridylyl-(3′-β,β,β-trichloroethyl-5′)N^4-benzoyl-2′-O-tetrahydropyranylcytidylyl(3′-β,β,β-trichloroethyl-5′)N^6-benzoyl-2′-O-tetrahydropyranyladenosine (**14**) (10 mg) was dissolved in *N*,*N*-dimethylformamide (0.5 ml) and magnetically stirred with Cu–Zn couple (*ca.* 10 mg) for 1 day at 50 °C. The deblocking was followed by t.l.c. in 10% CH_3OH–CH_2Cl_2 (R_F: 0.8 → 0.0). An intermediate (R_F: 0.5) resulting from removal of only one of the β,β,β-trichloroethyl groups could be observed. Incomplete reaction could be corrected by an additional amount of Cu–Zn couple.

Half-saturated (at 0°) methanolic ammonia (1 ml) was added and the ammonolysis stirred for 2 days at room temperature. *N*-Ammonia solution (1 ml) was added and the Cu–Zn couple filtered off and washed with further dilute ammonia. Careful evaporation of the filtrate and washings *in vacuo* removed ammonia and methanol and brought the solution p*H* to 8–10. Dowex 50W (NH_4^+ form) (*ca.* 200 mg) was added and the mixture magnetically stirred for 15 min. The resin was filtered off and washed thoroughly in form of a short column with water. The filtrate and washings were pooled and the solution volume adjusted to *ca.* 10 ml by evaporation *in vacuo*. The o.d. loss for this treatment was 5%.

Hydrochloric acid solution (0.1 *N*) was added until solution p*H* was 2. Hydrolysis proceeded at room temperature for 1–2 days and was monitored by t.l.c.[5] on cellulose plates (R_F: 0.9 → 0.2). UpCpA (110 $O.D._{260}$, 90%) was isolated and purified using preparative paper chromatography.[5] Enzymic analysis using pancreatic ribonuclease (PR) showed complete digestion into equal amounts of Up,Cp, and A.

Cytidylyl(3′–5′)adenylyl(3′–5′)uridine (CpApU)

N^4-Benzoyl-5′-O-p-methoxytrityl-2′-O-tetrahydropyranyl cytidylyl(3′-β,β,β-trichloroethyl-5′)N^6-benzoyl-2′-O-tetrahydropyranyl adenylyl(3′-β,β,β-trichloroethyl-5′)-2′-O-tetrahydropyranyl uridine (**16**) (10 mg) was deblocked using the same procedure as for protected UpCpA **14**. CpApU (116 $O.D._{260}$, 87%) was isolated and purified using preparative paper chromatography.[5] Enzymic analysis using snake venom diesterase (SVD) showed complete digestion into equal amounts of C, pA, and pU.

Financial assistance from the Medical Research Council of Canada is gratefully acknowledged.

1. Part II, T. Neilson, and E. S. Werstiuk. Can. J. Chem. **49**, 493 (1971).
2. T. Neilson. Chem. Commun. 1139 (1969).
3. B. F. C. Clark, S. K. Dube, and K. A. Marcker. Nature, **219**, 484 (1968).
4. N. Imura, G. B. Weiss, R. W. Chambers. Nature, **222**, 1147 (1969).
5. R. Lohrman, D. Söll, H. Hayatsu, E. Ohtsuka, and H. G. Khorana. J. Am. Chem. Soc. **88**, 819 (1966).
6. A. Holy and J. Smrt. Coll. Czech. Chem. Commun. **31**, 3800 (1966).
7. F. Eckstein and I. Rizk. Angew. Chem. **79**, 684 and 939 (1967).
8. K. H. Sheit. Tetrahedron Lett. 3243 (1967).
9. R. L. Letsinger and K. K. Ogilvie. J. Am. Chem. Soc. **89**, 4801 (1967) and **91**, 3350 (1969).
10. C. B. Reese and R. Saffhill. Chem. Commun. 767 (1968).
11. B. E. Griffin, M. Jarman, and C. B. Reese, Tetrahedron, **24**, 639 (1968).
12. F. Eckstein. Chem. Ber. **100**, 2228 (1967).
13. S. Chladek and J. Smrt. Coll. Czech. Chem. Commun. **29**, 214 (1964).

[5]Paper chromatography was performed using the descending technique on Whatman No. 1 or 3 MM paper. The solvent system used for p.c. and t.l.c. on cellulose was ethanol – 1 *M* ammonium acetate, p*H* 7.5 (7:3, v/v). A short wave u.v. lamp was used for detection.

Can. J. Chem. Downloaded from www.nrcresearchpress.com by 210.87.254.6 on 09/05/12
For personal use only.

Alkylations of the Side-chain Nucleophiles of Cysteine, Methionine, Histidine, and Lysine Derivatives with Allyl Bromide, 1-Bromo-2-butyne, and 2-Bromoacetophenone

J. Bryan Jones and David W. Hysert

Lash Miller Chemical Laboratories, Department of Chemistry, University of Toronto, Toronto 181, Ontario

Received April 26, 1971

Comparative studies on the reactions of cysteine, methionine, histidine, and lysine derivatives with allyl bromide, 1-bromo-2-butyne, and 2-bromoacetophenone have been carried out in connection with an evaluation of the potential of reagents incorporating ethylenic and acetylenic functions for protein modification.

Des études comparatives sur les réactions de dérivés de la cystéine, histidine, et lysine avec le bromure d'allyle, le bromo-1 butyne-2 et la bromo-2 acétophénone, ont été menées à bien. Ces études sont reliées à une évaluation du potentiel des réactifs à l'incorporation de fonctions éthyléniques et acétyléniques pour une modification de protéines.

Canadian Journal of Chemistry, **49**, 3012 (1971)

Introduction

Our studies on alkylating agents containing ethylenic and/or acetylenic bonds were prompted by our interest in the design of bifunctional reagents of rigorously defined stereochemistry as structural probes (1) for proteins and nucleic acids and of *endo* or *exo* active site directed irreversible inhibitors (2) for which precise orientation of the alkylating function towards the selected target nucleophile could be achieved. Appropriate combinations of ethylenic and acetylenic bonds, with their unique *cis*/*trans* and linear geometries, appeared to provide an attractive possibility for achieving the degree of stereochemical control desired. However, in view of the potential instability of molecules containing poly-en/yne chains it was decided to carry out the exploratory surveys on relatively simple olefinic and acetylenic derivatives in order to determine the practicability of the concept. Since synthetic difficulties were anticipated with respect to the incorporation of many of the protein and nucleic acid alkylating functions of proven value (2–8) into polyunsaturated carrier molecules the more easily introducible allylic and propargylic halide functions were selected for the initial evaluations.[1]

Preliminary studies (16) had indicated allylic and propargylic bromides to be of potential value for modifying nucleophiles representative of those present in cysteine, methionine, histidine, and lysine residues and side-chain alkylations of selected derivatives of the latter amino acids themselves with allyl bromide (**1**) and 1-bromo-2-butyne (**2**) have now been carried out. For comparative purposes, all of the amino-acid derivatives studied were again reacted with 2-bromoacetophenone (**3**), which was taken as representative of the widely used α-halomethylcarbonyl series of protein alkylating agents (2–8).

The reactions of a spectrum of cysteine, methionine, histidine, and lysine derivatives with the alkylating agents **1**–**3** were surveyed initially and for each amino acid, compounds in which the α-amino groups were protected by acylation were used routinely. In contrast carboxyl groups were converted to appropriate esters only when alkylation of this function was found to constitute a significant competitive reaction. The most satisfactory experimental results were obtained with the derivatives **4**–**7** and the reactions observed for these compounds are summarized in Scheme 1. Each of the latter experiments was carried out in 30–50% aqueous ethanol solutions with the apparent p*H* being maintained within the range encountered *in vivo* either with a p*H*-stat or by the addition of the requisite amount of suitable bases, such as sodium hydroxide, sodium bicarbonate, sodium carbon-

[1]Somewhat surprisingly, in spite of their well documented susceptibility to nucleophilic attack (9) such functions have had very limited applications as biological or amino acid alkylating agents (10–15).

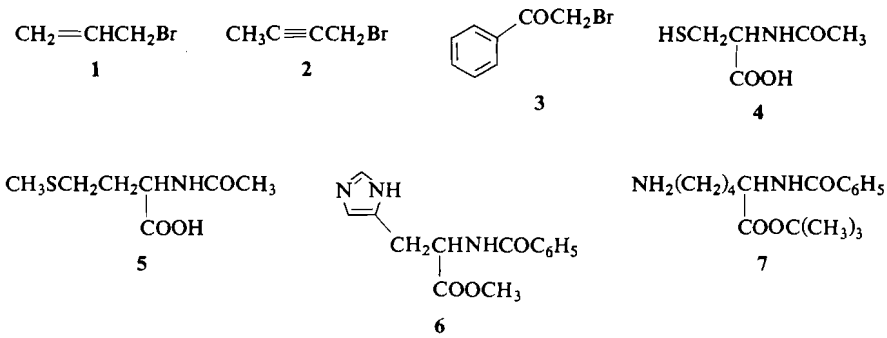

ate, and triethylamine. Although it was found convenient to repeat some reactions in non-aqueous solvents, such as methanol, ether or dimethylacetamide, in order to facilitate isolation and separation of the products, in no case was the product distribution found to be significantly different within the limited range of conditions surveyed.

Alkylation of *N*-acetyl-L-cysteine (**4**), with each of **1–3** in 30% aqueous ethanol at 25° at p*H* 8 proved to be facile and the expected products **8***a–c* were obtained in 85–95% yields. No further reactions to the corresponding sulfonium bromides nor alkylations of the carboxyl group were observed under the mild reaction conditions surveyed.

Reactions of **1–3** with *N*-acetyl-DL-methionine (**5**) in 30% aqueous ethanol at 25° also proceeded smoothly within the p*H* range 3–8 to give the expected sulfonium bromides **9***a–c* in excellent (95–100%) yields. Since **9***a–c* were obtained as non-crystallizable gums, elemental analyses were performed on the reineckate salt derivatives. Again no alkylations of the carboxyl group occurred nor did the often unstable (16, 17) sulfonium salts exhibit any tendencies to undergo decomposition.

Histidine studies were first attempted on the commercially available α-*N*-acetyl derivative **16**. When **16** was treated in refluxing 50% aqueous ethanol with stoichiometric amounts of **1–3**, mixtures were formed which contained carboxyl modified products in addition to the expected imidazole ring alkylation possibilities. Use of a large excess of the alkylating agents in dimethylacetamide as solvent converted compound **16** exclusively into the deliquescent, non-crystalline tris-alkylated salts **17** (Scheme 2). The complications arising from competitive alkylation of the carboxyl group and the product isolation difficulties encountered with α-*N*-acetyl histidine derivatives were finally overcome by using α-*N*-benzoyl-L-histidine methyl ester (**6**) as the substrate. Treatment of **6** either in 50% aqueous ethanol or in methanol at 25° with a moderate excess of allyl bromide (**1**) or 1-bromo-2-butyne (**2**), or with 1 equiv of 2-bromoacetophenone (**3**), afforded mixtures containing up to 90% of alkylated products in which the N-3 mono alkylated and N-1, N-3 bis-alkylated compounds, **10***a–c*, and **12***a–c* respectively, predominated. In addition, lesser (5–10%) amounts of the products of N-1 alkylation, **11***a–c*, were present. When a two-fold excess of 2-bromoacetophenone was used, the N-1, N-3 diphenacyl bromide **12***c* was formed exclusively in 98% yield. In the normal aqueous ethanol reaction solutions, and at elevated temperatures in methanol, hydrolyses of **12***a*, *b* to the corresponding zwitterions **13***a*, *b* proved to be serious competitive processes.

The structural assignments of the mono-alkylated histidine compounds were made on the basis of analyses of the spectral data and from steric considerations. Each of the mono-alkylated isomeric pairs **10** and **11** showed characteristic differences in their p.m.r. spectra. For the allyl and but-2-ynyl products, the positions of the C-4 proton peaks of the compounds assigned the N-3 structures exhibit upfield shifts of ≃0.5 p.p.m. relative to the same hydrogen resonances in the corresponding N-1 isomers. These differences can be accounted for by the anisotropic shielding of the C-4 proton to be expected for compounds such as **10***a*, *b* possessing an unsaturated substituent at N-3.[2] In addition,

[2]For the phenacyl derivatives **10***c* and **11***c*, the corresponding p.m.r. data were equivocal.

Can. J. Chem. Downloaded from www.nrcresearchpress.com by 210.87.254.6 on 09/05/12
For personal use only.

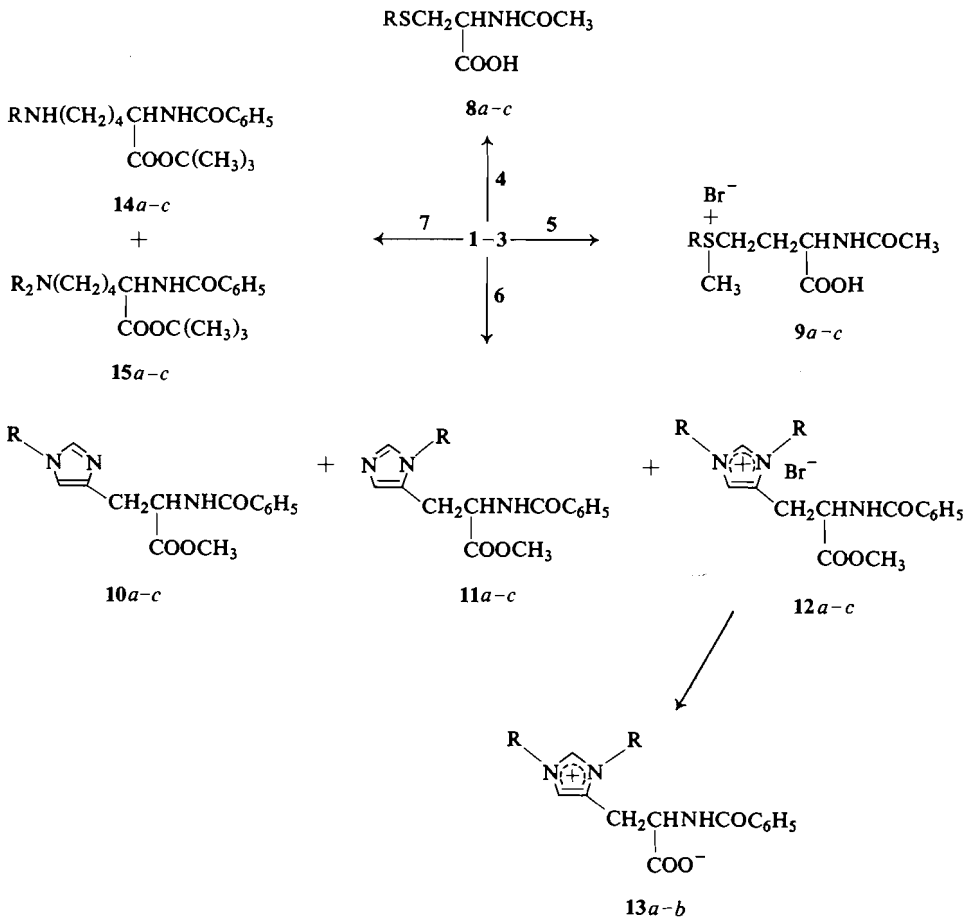

a R = $CH_2CH{=}CH_2$
b R = $CH_2C{\equiv}CCH_3$
c R = $CH_2COC_6H_5$

SCHEME 1

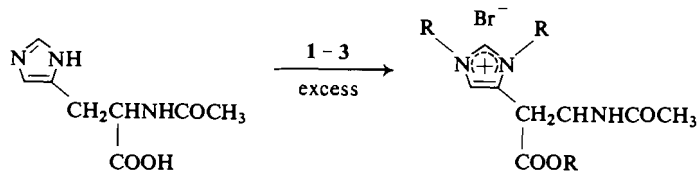

a R = $CH_2CH{=}CH_2$
b R = $CH_2C{\equiv}CCH_3$
c R = $CH_2COC_6H_5$

SCHEME 2

Can. J. Chem. Downloaded from www.nrcresearchpress.com by 210.87.254.6 on 09/05/12
For personal use only.

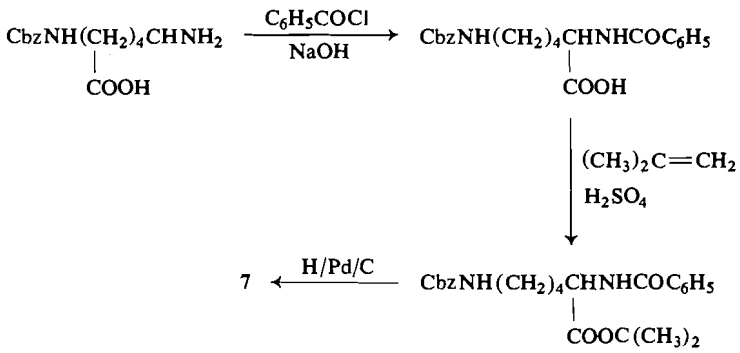

SCHEME 3

the α-amino hydrogen resonances of the N-3 compounds **10** exhibit downfield shifts of ≃0.5 p.p.m. relative to those of the same peaks in compounds **11**. Such chemical shift divergences can be rationalized in terms of intramolecular hydrogen bonding of the α-amino proton with N-1 for structures **10**;[3] the geometries of the isomeric N-1 substituted derivatives **11** do not allow such possibilities.

Examinations of molecular models of **6**, **10**, and **11** and considerations of the steric factors involved (*cf.* ref. 19) indicate that for both the mono- and bis-alkylation processes reactions at the N-3 positions should proceed much more readily than at the more hindered N-1 sites.[4]

In contrast to the amino acid residues discussed above, modifications of lysine ε-amino groups in proteins have been effected largely by reagents other than alkylating agents (5–8). However, a number of examples of their modification by halomethyl carbonyl reagents have been reported (5–8, 21).

Several lysine derivatives were evaluated in the search for a suitably protected compound. α-*N*-Acetyl-L-lysine (22) was rejected since its treatment with **1–3** gave complex mixtures of alkylation products which included significant proportions of carboxyl-modified compounds. Owing to the susceptibility to hydrolysis at p*H* 9 of the lysine methyl esters surveyed, protection of the carboxyl group as the less easily hydrolyzed *t*-butyl ester became necessary and the lysine derivative finally adopted was the α-*N*-benzoylated *t*-butyl ester **7**. This was prepared in 72% overall yield from ε-*N*-carbobenzyloxy-L-lysine as outlined in Scheme 3. Its alkylation by allyl bromide (**1**) and 1-bromo-2-butyne (**2**) proceeded smoothly in 50% aqueous ethanol at 25° within the p*H* range 9–11 to give the corresponding mono- and bis-alkylated derivatives **14***a*, *b* and **15***a*, *b* in solvent and p*H* dependent yields within the range 10 to 40%. In contrast the reaction of **7** with 2-bromoacetophenone (**3**) turned out to be exceedingly complex in both aqueous and non-aqueous solvents under a variety of reaction and work-up conditions. Disappointingly, none of **14***c* or **15***c*, nor any other identifiable products, could be isolated from the multiple component reaction mixture.[5] However, in view of the success already achieved with halomethylcarbonyl modification of other lysine ε-amino groups (5–8, 21) the inconclusive results of this last model reaction cannot be regarded as being representative of the types of reactions to be expected with suitable proteins.

The alkylation patterns observed above (Scheme 1) with allyl bromide (**1**), 1-bromo-2-butyne (**2**), and with the reference halomethylcarbonyl reagent **3**, largely parallel those of biological alkylating agents of proven value (2-8) and the results obtained confirm that the potential of appropriate compounds incorporat-

[3]The i.r. studies (18) have demonstrated the existence of such hydrogen bonding in various histidine derivatives. Although studies in the 900–750 cm^{-1} i.r. region were helpful in a similar structural assignment problem for *N*-carboxymethyl-L-histidines (19) the corresponding portions of the spectra of the isomeric pairs **10** and **11** were not sufficiently distinctive to be of value in this regard.

[4]Consideration of these factors was important with respect to the kinetic studies carried out subsequently (20).

[5]The complexity of the reaction mixture probably reflects the instability of the expected products **14***a* and **15***a*, and of 2-bromoacetophenone itself, to the moderately basic conditions surveyed (16, 23).

Can. J. Chem. Downloaded from www.nrcresearchpress.com by 210.87.254.6 on 09/05/12
For personal use only.

Can. J. Chem. Downloaded from www.nrcresearchpress.com by 210.87.254.6 on 09/05/12
For personal use only.

ing allylic and propargylic bromide functions for protein modification warrants further consideration. However, before their applicability with respect to the types of selective and/or sequential alkylations outlined in the Introduction can be realistically evaluated, further information on the relative rates and p*H* profiles to be expected for the various alkylation reactions is desirable. Kinetic studies which will provide some of these data are now in progress.

Experimental

All starting materials and products were purified until no impurities could be detected by g.l.c., t.l.c., and spectroscopic analyses. The p.l.c. separations were effected on silica gel G containing G.E. phosphor 118-2-7 using chloroform – methanol – ammonium hydroxide (90:15:1; v/v/v) as the developing solvent and the compounds were visualized with a Blak-Ray u.v. lamp (Ultra-Violet Products Inc.). All other general details of the methods, equipment, etc. used were as described previously (16). Since within each series of amino acid derivatives the alkylation procedures were generally identical, only the allyl bromide conditions have been fully described. The experimental procedures reported are those giving optimum yields of the desired products. Although in some cases this required the reaction to be carried out in non-aqueous solvents in order to facilitate the work-up procedure the analogous reactions in aqueous ethanol within the range of physiological p*H* always gave very similar product distributions.[4]

Materials

Allyl bromide (**1**), 1-bromo-2-butyne (**2**), and 2-bromoacetophenone (**3**) were obtained and purified as before (16). *N*-Acetyl-L-cysteine (**4**) and *N*-acetyl-DL-methionine (B.D.H.), L-histidine (Eastman), α-*N*-acetyl-L-histidine and α-*N*-acetyl-L-lysine (Calbiochem.), and ε-*N*-carbobenzoxy-L-lysine (Mann) were used as purchased. α-*N*-Benzoyl-L-histidine methyl ester (**6**), prisms from water, m.p. 158–159° (lit. (24) m.p. 160°) $[\alpha]_D^{22}$ −26.4° (*c*, 2.3 in CH_3OH) was prepared in 80% yield from L-histidine according to the procedure of Gerngross (24).

α-N-Benzoyl-L-lysine t-Butyl Ester (7)

ε-*N*-Carbobenzoxy-L-lysine was converted in 98% yield into its α-*N*-benzoyl derivative, microcrystals from benzene – petroleum ether b.p. 40–60° (1:1), m.p. 131–133° (lit. (25) m.p. 132–133°) as described by Irving and Gutman (25). The α-*N*-benzoyl-ε-*N*-carbobenzoxy-L-lysine obtained (20.1 g, 52 mmol) was dissolved at 0° in methylene chloride (200 ml) containing concentrated sulfuric acid (1 ml). Liquid isobutylene (35 g, 624 mmol) was then added and the mixture was shaken in a stoppered flask for 2 days. Following rotary evaporation of the reaction mixture, the residual solid was extracted with ether (3 × 150 ml) and the combined ether solution was washed successively with 5% aqueous hydrochloric acid (200 ml), 5% aqueous sodium hydroxide (200 ml), and saturated aqueous sodium chloride (200 ml). Evaporation of the dried ($MgSO_4$) ether solution gave a colorless solid (20.25 g) which after two recrystallizations from isopropyl ether yielded α-*N*-benzoyl-ε-*N*-carbobenzoxy-L-lysine *t*-butyl ester as fine needles (17.3 g), m.p. 86.5–87.5°, $[\alpha]_D^{25}$ −14.5° (*c*, 3.5 in CH_3OH); i.r. ($CHCl_3$) 3425, 3344, 1718, 1712, and 1653 cm^{-1}; p.m.r. ($CDCl_3$) δ 1.1–2.0 (6H, m, $NHCH_2(CH_2)_3$), 1.48 (9H, s, $OC(CH_3)_3$), 3.17 (2H, q, J = 5 Hz, $NHCH_2CH_2$), 4.69 (1H, q, J = 6 Hz, $CH_2CH(NH)CO$), 5.03 (2H, s, $C_6H_5CH_2O$), 5.20 (1H, m, J = 5 Hz, $CONHCH_2$), 6.93 (1H, d, J = 6 Hz, $CHNHCO$), 7.2–7.5 (8H, m, *m*- and *p*-aromatic, C_6H_5CO and $C_6H_5CH_2O$) and 7.7–8.0 p.p.m. (2H, m, *o*-aromatic, C_6H_5CO).

Anal. Calcd. for $C_{25}H_{32}N_2O_5$: C, 68.16; H, 7.32; N, 6.36. Found: C, 68.15; H, 7.52; N, 6.24.

A solution of α-*N*-benzoyl-ε-*N*-carbobenzoxy-L-lysine *t*-butyl ester (17.06 g, 38.7 mmol) in absolute ethanol (350 ml) containing concentrated hydrochloric acid (4 ml) and 10% palladium-on-charcoal (600 mg) was shaken in an atmosphere of hydrogen at 25° for 1 h. The filtered reaction solution was evaporated and the residual solid dissolved in 10% aqueous hydrochloric acid (200 ml). The acid extract was washed with ether (2 × 100 ml) and then brought to p*H* 12 with sodium hydroxide. Extraction of the basified mixture with ether (4 × 100 ml) followed by evaporation of the dried ($MgSO_4$) ether solution yielded an oil (9.95 g). Fractional distillation gave α-*N*-benzoyl-L-lysine *t*-butyl ester (7) b.p. 185–186°/0.1 Torr; $[\alpha]_D^{25}$ −19.3° (*c*, 2.3 in CH_3OH); i.r. ($CHCl_3$) 3448, 1721, and 1661 cm^{-1}; p.m.r. ($CDCl_3$) δ 1.0–2.6 (10H, m, $NH_2(CH_2)_4$), 1.50 (9H, s, $C(CH_3)_3$), 4.51 (1H, q, J = 5 Hz, $CH_2CH(NH)CO$), 7.5–7.6 (4H, m, *m*- and *p*-aromatic and $NHCO$), and 7.7–7.9 p.p.m. (2H, m, *o*-aromatic).

Anal. Calcd. for $C_{17}H_{26}N_2O_3$: C, 66.64; H, 8.55; N, 9.14. Found: C, 66.48; H, 8.73; N, 9.01.

Alkylation of N-Acetyl-L-cysteine (4)

(a) With Allyl Bromide (1)

Allyl bromide (2.42 g, 20 mmol) in methanol (20 ml) (or less conveniently, aqueous ethanol) was added with stirring at 25° to a solution of *N*-acetyl-L-cysteine (1.63 g, 10 mmol) in methanol (20 ml) containing 10 *N* aqueous sodium hydroxide (2.0 ml, 20 mmol). After stirring for a further 15 min, the reaction mixture was poured into water (400 ml) and the resulting solution was washed with ether (4 × 40 ml) and then acidified to p*H* 1 with concentrated hydrochloric acid. Sodium chloride (to saturation) was added and the mixture then extracted with chloroform (6 × 100 ml). Evaporation of the dried ($MgSO_4$) chloroform extracts afforded a solid residue (1.71 g) which was recrystallized from ethyl acetate to give *N*-acetyl-*S*-allyl-L-cysteine (**8***a*) as rhombs, m.p. 123–124° (lit. (14) m.p. 120–122°); $[\alpha]_D^{25}$ −31.0° (*c*, 2.2 in CH_3OH) (lit. (14) $[\alpha]_D^{21}$ −34°); i.r. (KBr) 3378, 1745, and 1727 cm^{-1}; p.m.r. (CF_3COOH) δ 2.28 (3H, s, $NHCOCH_3$), 3.20 (2H, d, J = 6 Hz, SCH_2CH), 3.24 (2H, d, J = 6 Hz, $CH_2{=}CHCH_2S$), 5.05 (1H, q, J = 6 Hz, $CH_2CH(NH)CO$), 5.26 (2H, d, J = 2 Hz, $CH_2{=}CHCH_2$), 5.6–6.0 (1H, m, $CH_2{=}CHCH_2$),[6] and 7.70 p.p.m. (1H, broad d, J = 6 Hz, $CHNHCO$).

(b) With 1-Bromo-2-butyne (2)

Reaction of *N*-acetyl-L-cysteine (1.63 g, 10 mmol) with 1-bromo-2-butyne (2.66 g, 20 mmol) for 25 min under the

[6]The shape of this proton resonance peak is characteristic of the allyl group.

Can. J. Chem. Downloaded from www.nrcresearchpress.com by 210.87.254.6 on 09/05/12
For personal use only.

above conditions yielded *N*-acetyl-*S*-(1-but-2-ynyl)-L-cysteine (**8***b*) as cubes (1.8 g) from 2-propanol-petroleum ether b.p. 40–60°, m.p. 101.5–102.5°; $[\alpha]_D^{25}$ −73.1° (*c*, 2.3 in CH_3OH); i.r (KBr) 3344, 1718, 1600, and 1548 cm^{-1}; p.m.r. (CF_3COOH) δ 1.77 (3H, t, J = 2 Hz, $CH_3C{\equiv}$), 2.28 (3H, s, $COCH_3$), 3.2–3.4 (4H, m, $\equiv CCH_2S$ and SCH_2CH), 5.05 (1H, q, J = 6 Hz, $SCH_2CH(NH)CO$), and 7.74 p.p.m. (1H, broad d, J = 6 Hz, $CHNHCO$).

Anal. Calcd. for $C_9H_{13}NO_3S$: C, 50.21; H, 6.09; N, 6.51; S, 14.89. Found: C, 50.24; H, 6.22; N, 6.39; S, 14.88.

(c) With 2-Bromoacetophenone (3)

Treatment of *N*-acetyl-L-cysteine (1.63 g, 10 mmol) with 2-bromoacetophenone (3.98 g, 20 mmol) and triethylamine (2.02 g, 20 mmol) under the conditions described for the allyl bromide reaction gave *N*-acetyl-*S*-phenacyl-L-cysteine (**8***c*), needles (2.4 g) from acetonitrile, m.p. 148–149°; $[\alpha]_D^{25}$ −43.0° (*c*, 1.1 in CH_3OH); i.r. (KBr) 3279, 1698, 1681, 1595, and 1550 cm^{-1}; p.m.r. (CF_3COOH) δ 2.32 (3H, s, $COCH_3$), 3.25 (2H, d, J = 5 Hz, SCH_2CH), 4.14 (2H, s, $COCH_2S$), 5.05 (1H, q, J = 5 Hz, $CH_2CH(NH)CO$), 7.46–7.90 (3H, m, *m*- and *p*-aromatic), 8.08 (2H, d of d, J = 1.6 Hz, *o*-aromatic), and 8.25 p.p.m. (1H, broad d, J = 7 Hz, $CHNHCO$).

Anal. Calcd. for $C_{13}H_{15}NO_4S$: C, 55.50; H, 5.38, N, 4.98; S, 11.40. Found: C, 55.41; H, 5.49; N, 5.16; S, 11.25.

Alkylation of N-Acetyl-DL-methionine (5)

(a) With Allyl Bromide (1)

Allyl bromide (1.21 g, 10 mmol) and *N*-acetyl-DL-methionine (0.96 g, 5 mmol) in 50% aqueous ethanol (50 ml) was stirred at 25° for 24 h. Water (40 ml) was added and the aqueous mixture was washed with chloroform (4 × 50 ml). The aqueous solution was then evaporated at 40°. The residual gum was dried *in vacuo* over P_2O_5 to give *N*-acetyl-*S*-allyl-DL-methionine sulfonium bromide (**9***a*) as a non-crystallizable, deliquescent glass (1.62 g), i.r. (KBr) 3226, 1730, 1661, and 1541 cm^{-1}; p.m.r, (CF_3COOH) δ 2.44 (3H, s, $COCH_3$), 2.69 (2H, broad m, CH_2CH_2CH), 2.98 (3H, s, $CH_3\overset{+}{S}$), 3.67 (2H, broad t, J = 7 Hz, $CH_2CH_2\overset{+}{S}$), 4.18 (2H, m, $CH_2{=}CHCH_2\overset{+}{S}$), 5.05 (1H, broad q, J = 7 Hz, $CH_2CH(NH)CO$), 5.63–6.16 (3H, m, $CH_2{=}CHCH_2$),[6] and 8.66 p.p.m. (1H, broad d, J = 7 Hz, $CHNHCO$). Elemental analysis was carried out on the reineckate (26) salt, m.p. 120°.

Anal. Calcd. for $C_{14}H_{24}N_7O_3S_5Cr$: C, 30.53; H, 4.39; N, 17.81; S, 29.11. Found: C, 30.34; H, 4.79; N, 17.99; S, 30.30.

(b) With 1-Bromo-2-butyne (2)

From *N*-acetyl-DL-methionine (0.96 g, 5 mmol) and 1-bromo-2-butyne (1.33 g, 10 mmol) under the above conditions was obtained *N*-acetyl-*S*-(1-but-2-ynyl)-DL-methionine sulfonium bromide (**9***b*) as a deliquescent, non-crystallizable glass (1.64 g), i.r. (KBr) 3257, 2247, 1730, 1661, and 1538 cm^{-1}; p.m.r. (CF_3COOH) δ 1.95 (3H, t, J = 2.5 Hz, $CH_3C{\equiv}$), 2.37 (3H, s, $COCH_3$), 2.60 (2H, broad m, CH_2CH_2CH), 3.0 (3H, s, $CH_3\overset{+}{S}$), 3.66 (2H broad t, J = 7 Hz, $\overset{+}{S}CH_2CH_2$), 4.32 (2H, broad m, $\equiv CCH_2\overset{+}{S}$), 5.0 (1H, broad q, J = 7 Hz, $CH_2CH(NH)CO$), and 8.40 p.p.m. (1H, broad d, J = 7 Hz, $CHNHCO$). Elemental analysis was performed on the reineckate (26) salt, m.p. 107–110° (dec.).

Anal. Calcd. for $C_{15}H_{24}N_7O_3S_5Cr$: C, 32.01; H, 4.30; N, 17.44; S, 28.50. Found: C, 31.70; H, 4.19; N, 16.69; S, 27.90.

(c) With 2-Bromoacetophenone (3)

Application of the above allyl bromide conditions to *N*-acetyl-DL-methionine (0.96 g, 5 mmol) and 2-bromoacetophenone (1.99 g, 10 mmol) afforded *N*-acetyl-*S*-phenacyl-DL-methionine sulfonium bromide (**9***c*) again as a deliquescent glass (1.86 g), i.r. (KBr) 3236, 1727, 1672, and 1538 cm^{-1}; p.m.r. (CF_3COOH) δ 2.38 (3H, s, $COCH_3$), 2.74 (2H, broad m, CH_2CH_2CH), 3.20 (3H, s, $CH_3\overset{+}{S}$), 3.88 (2H, broad m, $\overset{+}{S}CH_2CH_2$), 5.06 (1H, broad q, J = 7 Hz, $CH_2CH(NH)CO$), 5.45 and 5.59 (2H, ABq, J = 17 Hz, $COCH_2\overset{+}{S}$), 7.50–8.06 (5H, m, aromatic), and 8.40 p.p.m. (1H, broad d, J = 7 Hz, $CHNHCO$). The reineckate (26) salt derivative m.p. 116–117° (dec.) was used for elemental analytical characterization.

Anal. Calcd. for $C_{19}H_{26}N_7O_4S_5Cr$: C, 36.29; H, 4.17; N, 15.62; S, 25.50. Found: C, 36.34; H, 3.99; N, 14.96; S, 24.58.

Alkylation of α-N-Benzoyl-L-histidine Methyl Ester (6)

(a) With Allyl Bromide (1)

Allyl bromide (605 mg, 5 mmol), α-*N*-benzoyl-L-histidine methyl ester (273 mg, 1 mmol) and sodium bicarbonate (84 mg, 1 mmol) in methanol (10 ml) (or less conveniently, 50% aqueous ethanol) was stirred at 25° for 18 days. The reaction mixture was then evaporated and the residue extracted with boiling chloroform (or acetonitrile). Evaporation of the chloroform solution yielded a mixture from which the following compounds were isolated by p.l.c.

(i) α-*N*-Benzoyl-*N*-3-allyl-L-histidine methyl ester (**10***a*, R_f 0.92), as a glass (66 mg), i.r. ($CHCl_3$) 3425, 3322, 1739, and 1650 cm^{-1}; p.m.r. ($CDCl_3$) δ 3.16 (2H, d, J = 4 Hz, $=CCH_2CH$), 3.66 (3H, s, OCH_3), 4.46 (2H, d of t, J = 0.5 and 5Hz, $NCH_2CH{=}CH_2$), 4.9–5.4 (3H, m, CH_2-$CH{=}CH_2$ and $CH_2CH(NH)CO$), 5.7–6.2 (1H, m, $CH_2CH{=}CH_2$),[6] 6.76 (1H, broad s, $NCH{=}C$), 7.3–7.6 (4H, m, *m*- and *p*-aromatic and $NCHN$), 7.9–8.1 (2H, m, *o*-aromatic), and 8.50 p.p.m. (1H, broad d, J = 8 Hz, $CHNHCO$).

Mol. Wt. Calcd. for $C_{17}H_{19}N_3O_3$: 313.1426. Found (mass spectrum): 313.1425.

(ii) α-*N*-Benzoyl-*N*-1-allyl-L-histidine methyl ester (**11***a*, R_f 0.84), also as a glass (11 mg), i.r. ($CHCl_3$) 3448, 1742, and 1661 cm^{-1}; p.m.r. ($CDCl_3$) δ 3.28 (2H, broad d, J = 4 Hz, $=CCH_2CH$), 3.84 (3H, s, OCH_3), 4.4-4.7 (2H, m, $NCH_2CH{=}CH_2$), 4.8–5.4 (3H, m, $CH_2CH{=}CH_2$ and CH_2CHCO), 5.5–6.2 (1H, m, $CH_2CH{=}CH_2$),[6] and 7.2–8.0 p.p.m. (8H, m, aromatic, $NCH{=}C$, $NCHN$ and $CHNHCO$).

Mol. Wt. Calcd. for $C_{17}H_{19}N_3O_3$: 313.1426. Found (mass spectrum): 313.1428.

(iii) α-*N*-Benzoyl-*N*-1,*N*-3-diallyl-L-histidine methyl ester imidazolium bromide (**12***a*, R_f 0.37), a hygroscopic glass (88 mg) with i.r. ($CHCl_3$) 1742 and 1650 cm^{-1}; p.m.r. (CD_3CN) δ 3.42 (2H, m, $=CCH_2CH$), 3.74 (3H, s, OCH_3), 4.4–6.3 (11H, m, $\overset{+}{N}CH_2CH{=}CH_2$ and $CH(NH)CO$), 7.4–7.6 (4H, m, *m*- and *p*-aromatic and $\overset{+}{N}CH{=}C$), 7.9–8.1 (2H, m, *o*-aromatic), 8.68 (1H, d, J = 8 Hz, $CHNHCO$), and 8.85 p.p.m. (1H, s, $\overset{+}{N}CH\overset{+}{N}$).

Approximately 25% of the starting material **6**, R_f 0.65, was recovered from every reaction and in the aqueous

Can. J. Chem. Downloaded from www.nrcresearchpress.com by 210.87.254.6 on 09/05/12
For personal use only.

solvent reactions partial hydrolysis of **12***a* always occurred to give α-*N*-benzoyl-*N*-1,*N*-3-diallyl-L-histidine imidazolium carboxylate zwitterion (**13***a*, R_f 0.11) as a solid, m.p. 218–219.5°; i.r. (KBr) 1653, 1631, and 1418 cm^{-1}; p.m.r. (DMSO-d_6) δ 3.0–3.4 (2H, broad d, J = 6 Hz, $=CCH_2$-CH), 4.4–6.4 (11H, m, $\overset{+}{N}CH_2CH{=}CH_2$ and CH_2CH-(NH)CO), 7.3–8.0 (6H, m, aromatic and $\overset{+}{N}CH{=}$), 8.1–8.4 (1H, broad d, J = 7 Hz, CHN*H*CO), and 9.17 p.p.m. (1H, s, $\overset{+}{N}CH\overset{+}{N}$).

(b) With 1-Bromo-2-butyne (2)

From 1-bromo-2-butyne (665 mg, 5 mmol) and α-*N*-benzoyl-L-histidine methyl ester (273 mg, 1 mmol) under the above conditions were obtained:

(*i*) α-*N*-Benzoyl-*N*-3-(1-but-2-ynyl)-L-histidine methyl ester (**10***b*, R_f 0.90), as a gum (79 mg); i.r. ($CHCl_3$) 3436, 3333, 2247, 1736, 1653, and 1484 cm^{-1}; p.m.r. ($CDCl_3$) δ 1.81 (3H, t, J = 2 Hz, $CH_3C{\equiv}CCH_2$), 3.17 (2H, d, J = 5 Hz, $=CCH_2CH$), 3.69 (3H, s, OCH_3), 4.62 (2H, q, J = 2 Hz, $CH_3C{\equiv}CCH_2N$), 4.98 (1H, d of t, J = 5 and 7 Hz, CH_2CH(NH)CO), 6.88 (1H, s, $NCH{=}C$), 7.3-7.6 (3H, m, *m*- and *p*-aromatic), 7.62 (1H, s, NC*H*N), 7.85–8.05 (2H, m, *o*-aromatic), and 8.35 p.p.m. (1H, d, J = 7 Hz, CHN*H*CO).

Mol. Wt. Calcd. for $C_{18}H_{19}N_3O_3$: 325.1426. Found (mass spectrum): 325.1426.

(*ii*) α-*N*-Benzoyl-*N*-1-(1-but-2-ynyl)-L-histidine methyl ester (**11***b*, R_f 0.80) as a gum (65 mg); i.r. ($CHCl_3$) 3448, 3279, 2242, 1739, 1661, and 1481 cm^{-1}; p.m.r. ($CDCl_3$) δ 1.77 (3H, t, J = 1 Hz, $CH_3C{\equiv}CCH_2$), 3.33 (2H, d, J = 6 Hz, $=CCH_2CH$), 3.77 (3H, s, OCH_3), 4.62 (2H, q, J = 1 Hz, $CH_3C{\equiv}CCH_2N$), 5.03 (1H, q, J = 6 Hz, CH_2CH(NH)CO), 7.24 (1H, broad s, $NCH{=}C$), 7.3–7.6 (4H, m, *m*- and *p*-aromatic and NC*H*N) and 7.7–7.9 p.p.m. (3H, m, *o*-aromatic and CHN*H*CO).

Mol. Wt. Calcd. for $C_{18}H_{19}N_3O_3$: 325.1426. Found (mass spectrum): 325.1425.

(*iii*) α-*N*-Benzoyl-*N*-1,*N*-3-di(1-but-2-ynyl)-L-histidine methyl ester imidazolium bromide (**12***b*, R_f 0.53) as a hygroscopic glass (125 mg); i.r. ($CHCl_3$) 3268, 2252, 1736, 1650, and 1522 cm^{-1}; p.m.r. ($CDCl_3$) δ 1.73 and 1.83 (6H, two t, J = 1 Hz, $CH_3C{\equiv}CCH_2\overset{+}{N}$), 3.5–3.8 (2H, broad m, $=CCH_2CH$), 3.71 (3H, s, OCH_3), 5.02 and 5.21 (5H, two broad q and m, J = 1 Hz, $CH_3C{\equiv}CCH_2\overset{+}{N}$ and CH_2CH(NH)CO), 7.2–7.5 (3H, m, *m*- and *p*-aromatic), 7.74 (1H, s, $\overset{+}{N}CH{=}C$), 8.0–8.2 (2H, m, *o*-aromatic), 9.02 (1H, d, J = 8 Hz, CHN*H*CO), and 9.91 p.p.m. (1H, s, $\overset{+}{N}CH\overset{+}{N}$).

Anal. Calcd. for $C_{22}H_{24}BrN_3O_3$: C, 57.65; H, 5.28; N, 9.17; Br, 17.44. Found: C, 57.17; H, 5.24; N, 9.27; Br, 17.71.

Unchanged starting material **6**, R_f 0.61 (≃20%) was always recovered together with varying amounts of the product of hydrolysis of **12***b*, α-*N*-benzoyl-*N*-1,*N*-3-di(1-but-2-ynyl)-L-histidine imidazolium carboxylate zwitterion (**13***b*, R_f 0.18) which was isolated as a glassy solid i.r. (KBr) 2252, 1639, 1610, and 1385 cm^{-1}; p.m.r. (DMSO-d_6) δ 1.6–2.1 (6H, m, $CH_3C{\equiv}CCH_2$), 3.2–3.4 (2H, broad m, $=CCH_2CH$), 4.1–4.5 (1H, m, CH_2CH-(NH)CO), 5.0-5.3 (4H, m, $CH_3C{\equiv}CCH_2\overset{+}{N}$), 7.3–7.9 (6H, m, aromatic and $\overset{+}{N}CH{=}C$), 8.10 (1H, d, J = 6 Hz, CHN*H*CO), and 9.32 (1H, s, $\overset{+}{N}CH\overset{+}{N}$).

(c) With 2-Bromoacetophenone (3)

Under the conditions outlined above for allyl bromide, 2-bromoacetophenone (200 mg, 1 mmol), α-*N*-benzoyl-L-histidine methyl ester (273 mg, 1 mmol) and sodium bicarbonate (84 mg, 1 mmol) gave after a 2 day reaction period:

(*i*) α-*N*-Benzoyl-*N*-3-phenacyl-L-histidine methyl ester (**10***c*, R_f 0.84) as a glass (159 mg); i.r. ($CHCl_3$) 3436, 3333, 1736, 1698, and 1650 cm^{-1}; p.m.r. ($CDCl_3$) δ 3.12 (2H, d, J = 5 Hz, $=CCH_2CH$), 3.62 (3H, s, OCH_3), 4.96 (1H, m, CH_2CH(NH)CO), 5.35 (2H, s, $COCH_2N$), 6.78 (1H, s, $NCH{=}C$), 7.3–8.1 (11H, m, aromatic and NC*H*N), and 8.48 p.p.m. (1H, d, J = 8 Hz, CHN*H*CO).

Anal. Calcd. for $C_{22}H_{21}N_3O_4$: C, 67.50; H, 5.41; N, 10.74. Found: C, 67.00; H, 5.59; N, 10.04.

(*ii*) α-*N*-Benzoyl-*N*-1-phenacyl-L-histidine methyl ester (**11***c*, R_f 0.72) as a glass (11 mg); i.r. ($CHCl_3$) 3448, 1742, 1706, 1658, and 1486 cm^{-1}; p.m.r. ($CDCl_3$) δ 3.0–3.3 (2H, broad m, $=CCH_2CH$), 3.70 (3H, s, OCH_3), 4.7–5.1 (1H, broad m, CH_2CH(NH)CO), 5.46 (2H, broad s, $COCH_2N$), 6.54 (1H, broad s, $NCH{=}C$), 6.80 (1H, broad s, NC*H*N), 7.0–8.1 (10H, broad m, aromatic), and 8.70 p.p.m. (1H, broad d, J = 8 Hz, CHN*H*CO).

Anal. Calcd. for $C_{22}H_{21}N_3O_4$: C, 67.50; H, 5.41; N, 10.74. Found: C, 67.87; H, 5.81; N, 10.59.

(*iii*) α-*N*-Benzoyl-*N*-1,*N*-3-diphenacyl-L-histidine methyl ester imidazolium bromide (**12***c*, R_f 0.56) as a pale yellow solid (190 mg) m.p. 130–131.5°; i.r. (KBr) 3247, 1736, 1698, and 1650 cm^{-1}; p.m.r. ($CDCl_3$) δ 3.1–3.5 (2H, broad m, $=CCH_2CH$), 3.52 (3H, s, OCH_3), 4.7-5.1 (1H, broad m, CH_2CH(NH)CO), 5.95 and 6.18 (4H, two s, $COCH_2\overset{+}{N}$), 7.0–8.1 (16H, m, aromatic and $\overset{+}{N}CH{=}C$), 8.70 (1H, broad d, J = 7 Hz, CHN*H*CO), and 9.57 p.p.m. (1H, s, $\overset{+}{N}CH\overset{+}{N}$).

Anal. Calcd. for $C_{30}H_{28}BrN_3O_5$: C, 61.02; H, 4.78; N, 7.12. Found: C, 60.58; H, 5.07; N, 6.95.

Some (≃10%) starting material **6** (R_f 0.61) was always recovered but none of the zwitterion **13***c* was detected presumably owing to the decreased reaction period required for the 2-bromoacetophenone reactions.

When 2-bromoacetophenone was used in 5 *M* excess, a 98% yield of **12***c* was isolated.

Alkylation of α-N-Benzoyl-L-lysine t-Butyl Ester (7)

(a) With Allyl Bromide (1)

Allyl bromide (121 mg, 1 mmol), α-*N*-benzoyl-L-lysine *t*-butyl ester (306 mg, 1 mmol) and sodium carbonate (106 mg, 1 mmol) in ether (10 ml) (use of methanol or 50% aqueous ethanol also gives similar results) was stirred at 25° for 5 days. The mixture was then filtered and the filtrate evaporated. The p.l.c. of the residue gave:

(*i*) α-*N*-Benzoyl-ε-*N*-allyl-L-lysine *t*-butyl ester (**14***a*, R_f 0.73) as a gum (40 mg); i.r. ($CHCl_3$) 3436, 1733, and 1664 cm^{-1}; p.m.r. ($CDCl_3$) δ 1.49 (9H, s, $C(CH_3)_3$), 1.2–2.2 (6H, broad m, $NHCH_2(CH_2)_3CH$), 2.72 (2H, broad m, $NHCH_2CH_2$), 3.45 (2H, broad m, $CH_2{=}CHCH_2N$), 4.64 (1H, broad q, J = 6 Hz, CH_2CH(NH)CO), 5.1–5.4 (2H, m, $CH_2{=}CHCH_2$), 5.8–6.2 (1H, broad m, $CH_2{=}CHCH_2$),[6] 6.5–6.9 (1H, broad m, CHN*H*CO), 7.3–7.6 (3H, m, *m*- and *p*-aromatic) and 7.8–8.1 p.p.m. (2H, m, *o*-aromatic).

Mol. Wt. Calcd. for $C_{20}H_{30}N_2O_3$: 346.2256. Found (mass spectrum): 346.2253.

(*ii*) α-*N*-Benzoyl-ε-*N*,*N*-diallyl-L-lysine *t*-butyl ester (**15***a*, R_f 0.96) as a gum (205 mg); i.r. ($CHCl_3$) 3425, 1727, and 1664 cm^{-1}; p.m.r. ($CDCl_3$) δ 1.49 (9H, s, $C(CH_3)_3$), 1.2–2.1 (6H, m, $NCH_2(CH_2)_3$), 2.44 (2H, t, J = 6 Hz, NCH_2CH_2), 3.08 (4H, d, J = 6 Hz, $CH_2{=}CHCH_2N$), 4.72 (1H, q, J = 7 Hz, $CH_2CH(NH)CO$), 5.0–5.3 (4H, m, $CH_2{=}CHCH_2$), 5.6–6.1 (2H, m, $CH_2{=}CHCH_2$),[6] 7.10 (1H, d, J = 7 Hz, $CONHCH$), 7.3–7.5 (3H, m, *m*- and *p*-aromatic) and 7.75–7.95 p.p.m. (2H, m, *o*-aromatic).

Mol. Wt. Calcd. for $C_{23}H_{34}N_2O_3$: 386.2569. Found (mass spectrum): 386.2566.

Starting material **7** (5–10%) was recovered in each experiment from the p.l.c. band of R_f 0.4.

(b) With 1-Bromo-2-butyne (2)

From the reaction of 1-bromo-2-butyne (133 mg, 1 mmol), α-*N*-benzoyl-L-lysine *t*-butyl ester (306 mg, 1 mmol), and sodium carbonate (106 mg, 1 mmol) under the conditions above were obtained:

(*i*) α-*N*-Benzoyl-ε-*N*-(1-but-2-ynyl)-L-lysine *t*-butyl ester (**14***b*, R_f 0.80) as a viscous oil (38 mg); i.r. ($CHCl_3$) 3448, 1727, and 1661 cm^{-1}; p.m.r. ($CDCl_3$) δ 1.49 (9H, s, $C(CH_3)_3$), 1.78 (3H, m, $CH_3C{\equiv}CCH_2$), 1.3–2.1 (6H, broad m, $NHCH_2(CH_2)_3$), 2.77 (2H, broad m, $NHCH_2CH_2$), 3.45 (2H, m, $CH_3C{\equiv}CCH_2N$), 3.8–4.2 (1H, broad s, CH_2NHCH_2), 4.72 (1H, q, J = 6 Hz, $CH_2CH(NH)CO$), 7.04 (1H, d, J = 6 Hz, $CHNHCO$), 7.4–7.6 (3H, m, *m*- and *p*-aromatic), 7.8–8.0 p.p.m. (2H, m, *o*-aromatic).

Anal. Calcd. for $C_{21}H_{30}N_2O_3$: C, 70.36; H, 8.44; N, 7.82. Found: C, 70.08; H, 8.50; N, 7.64.

(*ii*) α-*N*-Benzoyl-ε-*N*,*N*-di(1-but-2-ynyl)-L-lysine *t*-butyl ester (**15***b*, R_f 0.98) as a gum (108 mg); i.r. ($CHCl_3$) 3448, 1727, and 1661 cm^{-1}; p.m.r. ($CDCl_3$) δ 1.49 (9H, s, $C(CH_3)_3$), 1.78 (6H, t, J = 2 Hz, $CH_3C{\equiv}CCH_2$), 1.4–2.2 (6H, broad m, $NCH_2(CH_2)_3$), 2.50 (2H, t, J = 6 Hz, NCH_2CH_2), 3.32 (4H, q, J = 2 Hz, $CH_3C{\equiv}CCH_2N$), 4.72 (1H, q, J = 6 Hz, $CH_2CH(NH)CO$), 6.92 (1H, d, J = 6 Hz, $CHNHCO$), 7.4–7.6 (3H, m, *m*- and *p*-aromatic), and 7.83–7.95 p.p.m. (2H, m, *o*-aromatic).

Anal. Calcd. for $C_{25}H_{34}N_2O_3$: C, 73.14; H, 8.35; N, 6.83. Found: C, 72.99; H, 8.17; N, 6.64.

Unchanged starting material **7** (≃10%) was contained in the p.l.c. band of R_f 0.37.

Grateful acknowledgment is made to the National Cancer Institute of Canada and the National Research Council of Canada for their support of this work and for the award (to D.W.H.) of an NRCC Science Scholarship.

1. F. WOLD. *In* Methods in enzymology. Vol. II. *Edited by* C. H. W. Hirs, Academic Press Inc., New York, N.Y., 1967, p. 617.
2. B. R. BAKER. Design of active site directed irreversible enzyme inhibitors. John Wiley and Sons Inc., New York, N.Y., 1967.
3. W. C. J. ROSS. Biological alkylating agents, Butterworth's, London, 1962.
4. S. J. SINGER. Adv. Prot. Chem. **22**, 1 (1967).
5. E. HABER. Ann. Rev. Biochem. **37**, 497 (1968).
6. L. A. COHEN. Ann. Rev. Biochem. **37**, 695 (1968).
7. B. L. VALEE and J. F. RIORDAN. Ann. Rev. Biochem. **38**, 733 (1969).
8. A. N. GLAZER. Ann. Rev. Biochem. **39**, 101 (1970).
9. R. H. DEWOLFE and W. G. YOUNG. Chem. Rev. **56**, 753 (1956).
10. G. TOENNIES and J. J. KOLB. J. Am. Chem. Soc. **67**, 849 (1945).
11. R. A. BRADSHAW, G. W. ROBINSON, G. M. HASS, and R. L. HILL. J. Biol. Chem. **244**, 1755 (1969).
12. C. BOLLACK and J. P. EBEL. Bull. Soc. Chim. Biol. **50**, 2351 (1968); C. BOLLACK, E. KLEIN, and J. P. EBEL. Bull. Soc. Chim. Biol. **50**, 2363 (1968).
13. J. F. CARSON and L. E. BOGGS. J. Org. Chem. **36**, 611 (1971) and previous papers.
14. A. STOLL and E. SEEBECK. Helv. Chim. Acta, **31**, 189 (1948).
15. A. L. MÜLLER and A. I. VIRTANIN. Acta Chem. Scand. **20**, 1163 (1966).
16. J. B. JONES and D. W. HYSERT. Can. J. Chem. **49**, 325 (1971) and references therein.
17. H. G. GUNDLACH, S. MOORE, and W. H. STEIN. J. Biol. Chem. **234**, 1761 (1959).
18. L. SCHUTTE, P. P. KLUIT, and E. HAVINGA. Tetrahedron Suppl. **7**, 295 (1966).
19. A. M. CRESTFIELD, W. H. STEIN, and S. MOORE. J. Biol. Chem. **238**, 2413 (1963).
20. J. B. JONES and D. W. HYSERT. Unpublished results.
21. P. CUATRECASAS, M. WILCHEK, and C. B. ANFINSEN. J. Biol. Chem. **244**, 4316 (1969).
22. A. NEUBERGER and F. SANGER. Biochem J. **37**, 515 (1943).
23. R. J. DEPASQUALE and M. VOGEL. J. Org. Chem. **35**, 1057 (1970).
24. O. GERNGROSS. Z. Physiol. Chem. **108**, 50 (1919).
25. C. C. IRVING and H. R. GUTMAN. J. Org. Chem. **24**, 1979 (1959).
26. B. F. AYCOCK, E. J. EISENBRAUN, and R. W. SCHRADER. J. Am. Chem. Soc. **73**, 1351 (1951).

Can. J. Chem. Downloaded from www.nrcresearchpress.com by 210.87.254.6 on 09/05/12
For personal use only.

Can. J. Chem. Downloaded from www.nrcresearchpress.com by 210.87.254.6 on 09/05/12
For personal use only.

The Structure of Fumarofine

C. K. Yu, J. K. Saunders, and D. B. MacLean
Department of Chemistry, McMaster University, Hamilton, Ontario

AND

R. H. F. Manske
Department of Chemistry, University of Waterloo, Waterloo, Ontario

Received April 14, 1971

A structure is proposed for fumarofine (F-38), an alkaloid of *Fumaria officinalis*. It is shown by spectroscopic methods to be another representative of the spirobenzylisoquinoline group of alkaloids.

Une structure est proposée pour la fumarofine (F-38), un alcaloïde du *Fumaria officinalis*. Par des méthodes spectroscopiques il est montré que celle-ci est apparentée au groupe spirobenzylisoquinoléine des alcaloïdes.

Canadian Journal of Chemistry, 49, 3020 (1971)

In 1938 Manske (1) isolated and identified several isoquinoline alkaloids from the plant *Fumaria officinalis* L. Among these were protopine, cryptopine, (±)-stylopine, (+)- and (±)-scoulerine, and sinactine. Besides these alkaloids of established structure, he reported the presence of two new alkaloids, F-37 ($C_{21}H_{23}NO_5$) and F-38 ($C_{20}H_{19}NO_6$). Two minor alkaloids were found later (2) in the same plant corresponding in composition to $C_{20}H_{21}NO_5$ and to $C_{20}H_{17}NO_5$, which were named fumaritine and fumariline, respectively. These alkaloids and F-37, fumaricine, have been shown to have a spirobenzylisoquinoline system (3). Here the structure of F-38, to which we assign the name fumarofine, will be reported.

Fumarofine (**1**) has absorption ascribed to a hydroxyl (3450 cm^{-1}) and a carbonyl (1700 cm^{-1}) group in its i.r. spectrum. An examination of its 100 MHz p.m.r. spectrum in DMSO-d_6 shows one singlet of area 1 at 8.65 δ which is assigned to a phenolic hydroxyl proton. A total area of seven protons is observed in the region 6.0–7.5 δ. One AB quartet centered at 7.18 and 7.36 δ (J_{AB} = 8 Hz) is assigned to ortho aromatic protons and a signal at 6.26 δ with an area of 2 to methylenedioxy protons. The three remaining singlets, two of which are probably due to para aromatic protons and one to an alcoholic OH, are at 7.24, 6.68, and 6.29 δ. A methoxyl signal at 3.80 δ is apparent in the spectrum. A signal at 4.33 δ (area 1) is probably due to a benzylic hydrogen geminal to a hydroxyl group. A disadvantage of the p.m.r. spectrum in DMSO-d_6 is the intense signal arising from undeuterated DMSO which obscures the signals in the high field region. Unfortunately, a spectrum in $CDCl_3$ could not be obtained because of insolubility. The data are recorded in Table 1.

When fumarofine was treated with diazomethane, its methyl ether, **2**, was obtained. The p.m.r. spectral data of **2** in DMSO-d_6 and in $CDCl_3$ are given in Table 1. In DMSO-d_6 the appearance of one additional methoxyl signal at 3.87 δ and the disappearance of the signal at 8.65 δ confirms that one phenolic hydroxyl group is present in fumarofine. In the region 6.0–7.5 δ, one AB quartet, one methylenedioxy signal, and three singlets are still observable. The signal corresponding to the benzylic hydrogen geminal to a hydroxyl group stays at 4.33 δ. When deuterium oxide was added to the solution of *O*-methylfumarofine in DMSO-d_6, the signal at 6.44 δ disappeared. This observation provides convincing evidence for the presence of an active hydrogen in the molecule, presumably a hydroxyl hydrogen.

When the p.m.r. spectrum of the methyl ether was run in $CDCl_3$, a signal appeared at 2.53 (area 3), which was obscured in the spectrum in DMSO-d_6, and is assigned to an *N*-methyl group.

In order to confirm the presence of one hydroxyl group in the molecule, the ether **2** was acetylated with acetic anhydride and pyridine to give **3**. The p.m.r. spectrum of **3** in $CDCl_3$ shows a signal assigned to an acetyl group at 2.22. The signal of the hydrogen geminal to the hydroxyl group in fumarofine methyl ether shifts

TABLE 1. The p.m.r. signals of **1**, **2**, and **3** in p.p.m. (δ)

	1 (in DMSO-d_6)	**2** (in DMSO-d_6)	**2** (in $CDCl_3$)	**3** (in $CDCl_3$)
H-1	7.24	7.41	7.29	7.30
2-OR_1	8.65	3.87	3.93	3.92
3-OCH_3	3.80	3.81	3.87	3.84
H-4	6.68	6.75	6.61	6.53
7-N—CH_3	—	—	2.53	2.63
12,13 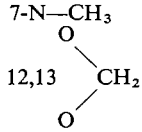	6.26	6.28	6.18	6.12
H-10	7.18	7.21	7.13	7.09
H-11	7.36	7.38	7.13	7.09
H-9	4.33	4.33	4.45	4.98
9-OR_2	6.29	6.44	6.18	2.22

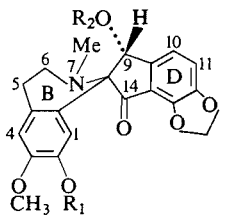

1 $R_1 = R_2 = H$

2 $R_1 = CH_3; R_2 = H$

3 $R_1 = CH_3; R_2 = CH_3—CO$

from 4.45 to 4.98 δ in the acetylated compound. In the region 6.0–7.5 δ, a signal at 7.09 δ (area 2) is assigned to two ortho protons, a signal at 6.12 δ (area 2) to the methylenedioxy group, and signals at 7.30 (area 1) and 6.53 δ (area 1) to two para aromatic protons. The data are given in Table 1.

Although i.r. and p.m.r. data reveal much about the functional groups and the structural units, the skeleton is still unknown. Since fumarofine occurs in the same plant as fumaricine, fumariline, and fumaritine, it may be structurally related to these alkaloids. Its properties preclude it belonging to the protoberberine, phthalide isoquinoline, or the protopine groups. When the mass spectrum of fumarofine is compared with those of the spirobenzylisoquinoline group found in the same plant (4) definite conclusions cannot be drawn about its structure. When, however, the spectra of sibiricine (4) and fumarofine are compared, there appears a remarkable similarity. Both compounds have the molecular ion peak as their base peak and most of the intense ions occur in the high mass end and in the region between *m/e* 140–200. Moreover, many peaks characteristic of a spirobenzylisoquinoline with a ketone and a hydroxyl group in the five-membered ring are present in fumarofine. It is, therefore, reasonable to assume that both compounds have the same carbon skeleton. The substitution pattern in fumarofine can be deduced from the presence of the dihydroisoquinolinium ion at *m/e* 192, which shows that the phenolic hydroxyl and methoxyl group must be present in ring A; therefore, the methylenedioxy group must be in ring D.

The spectral data suggest structure **1** but further p.m.r. data are required for a definitive assignment of the stereochemistry and the substitution pattern. In fumarofine the chemical shift difference of the aromatic AB quartet (δ_{HA} = 7.18, δ_{HB} = 7.36) indicates that the carbonyl is ortho to the methylenedioxy group. In those spirobenzylisoquinoline alkaloids of known structure in which the carbonyl group is ortho to the aromatic protons the chemical shift difference between two adjacent protons is much larger. For example, a difference of 0.4 p.p.m. is observed in sibiricine (5) because of the strong deshielding effect of the carbonyl function on the ortho proton. The substitution in ring D has been confirmed by a nuclear Overhauser effect (n.O.e.) experiment (6) in which an n.O.e. of 9% is observed at H-10 when H-9 in fumarofine is saturated.

Confirmation of the substitution pattern in ring A rests on the following n.O.e. experiment. Saturation of H-9 causes a 4% increase in area of the absorption at 7.24 δ which must be assigned to H-1, while saturation of the *O*-CH_3 results in an increase in area of 25% at 6.68 δ, presumably H-4. These data suggest that the

Can. J. Chem. Downloaded from www.nrcresearchpress.com by 210.87.254.6 on 09/05/12
For personal use only.

Can. J. Chem. Downloaded from www.nrcresearchpress.com by 210.87.254.6 on 09/05/12
For personal use only.

hydroxyl and methoxyl groups in ring A are at C-2 and -3, respectively. The structure of fumarofine is shown in structure **1**. Further evidence for the configuration at C-9 in structure **1** comes from the fact that H-9 is unaffected when the N—CH_3 is irradiated. If H-9 and N—CH_3 were on the same side of the plane of the five-membered ring a large n.O.e. would be expected. The n.O.e. data are recorded in Table 2.

The p.m.r. results on fumarofine differ from other members of this series in that there is an unusually large n.O.e. between H-9 and -5 and the chemical shift of H-1 is further downfield than in the related alkaloids, sibiricine (5) and fumariline (3). These facts can be explained by the conformation shown in **4** in which ring B is in a twist form and the OH is hydrogen bonded to the nitrogen causing the five-membered ring to be twisted so that the carbonyl group is closer to ring A with H-1 in the deshielding zone. H-9 is also forced to be closer to H-5. No such effect, however, is observed in sibiricine where the stereochemistry at C-9 is different. Thus, structure **4** is fully compatible with the mass spectral, i.r. and p.m.r. data.

One other piece of evidence supporting the proposed structure of fumarofine comes from its u.v. spectrum. The reported u.v. spectrum of **5** (7), λ_{max} (EtOH) 237 (4.52),[1] 292 (4.13), and 310 (4.01), is similar to that of sibiricine **8**, λ_{max} (EtOH) 205 (4.80), 240 (3.94), 291 (3.91) and 313 (3.99) but differs greatly from that of *O*-methylfumarofine, λ_{max} (EtOH) 208 (4.45), 235 (4.35), 259 (3.96), 286 (3.37), and 350 (3.40). On the other hand, the u.v. spectrum of **6**, λ_{max} (EtOH) 234 (4.47), 260 (4.08), 283 (3.60), and 354 (3.52), is similar to that of the methyl ether of fumarofine. The spectra of **5** and **6** are a composite of two chromophoric systems, the tetrahydroisoquinoline system and the 1-indanone system. The absorptions corresponding to the latter chromophore are different for different substitution patterns. The resemblance of the u.v. spectrum of **2** to that of **6** indicates that they have the same chromophoric system.

TABLE 2. The n.O.e.'s in **1**

Irradiated protons	Observed protons	% Area increase	Internuclear distance (A)*
H-9	H-1	4	3.35
H-9	H-10	9	2.88
H-5	H-9	16	2.65
N-CH_3	H-9	0	
O-CH_3	H-4	25	

*As measured from a Dreiding molecular model.

[1]Values of λ are in mμ and values of log ε are shown in parentheses.

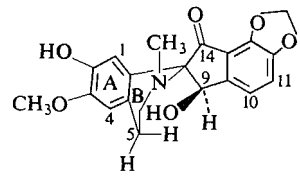

4

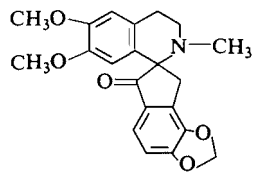

5

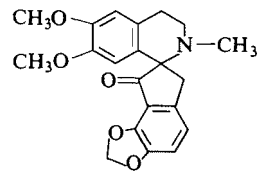

6

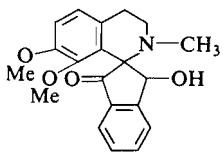

7

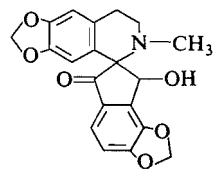

8

The characteristic ions in the mass spectra of the synthetic compound, **7** and sibiricine, **8** (4), are also found in the spectrum of fumarofine as expected. The spectrum (Fig. 1) is dominated by the molecular ion and the M-CH_3 ion. The molecular ion can undergo cleavage alpha to the >CHOH or alpha to the >C=O group in the five-membered ring to give ions **9** and **10**, respectively (Scheme 1). The former fragments by a mechanism already discussed (4) to the dihydroisoquinolinium ion **11** and the isoquinolinium ion at *m/e* 192 and 190, respectively, while the latter by processes already described (4) can lead to ion **12** at *m/e* 324 and to ion **13** at *m/e* 206.

When the spectrum is examined more closely, however, it seems to be more complicated than that of **8**. Many additional peaks appear in the high mass range, such as M-CO and its subsequent decomposition product ions. Multiplicity in the middle of the spectrum (*m/e* 150–220) appears, as shown in Fig. 1. One possible

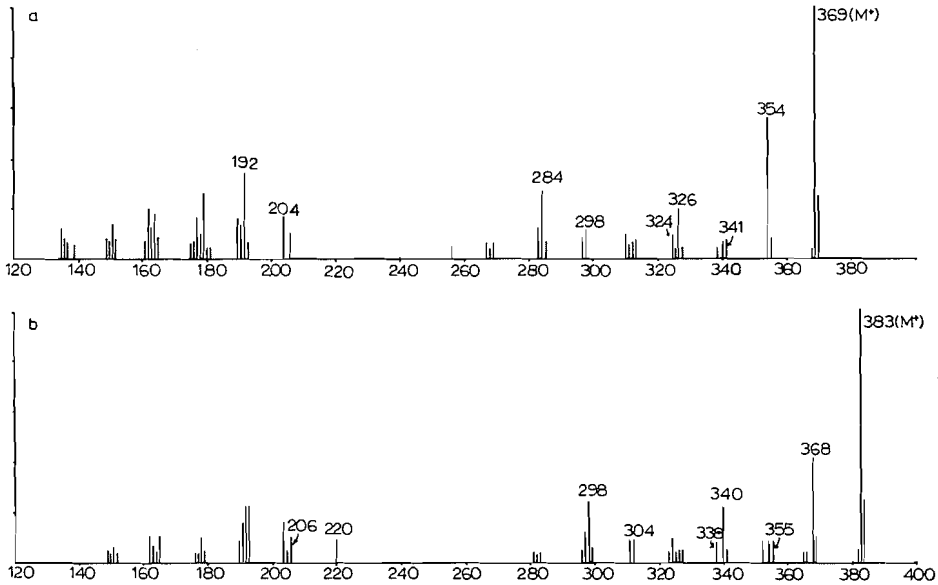

FIG. 1. The mass spectra of (*a*) fumarofine and (*b*) *O*-methylfumarofine.

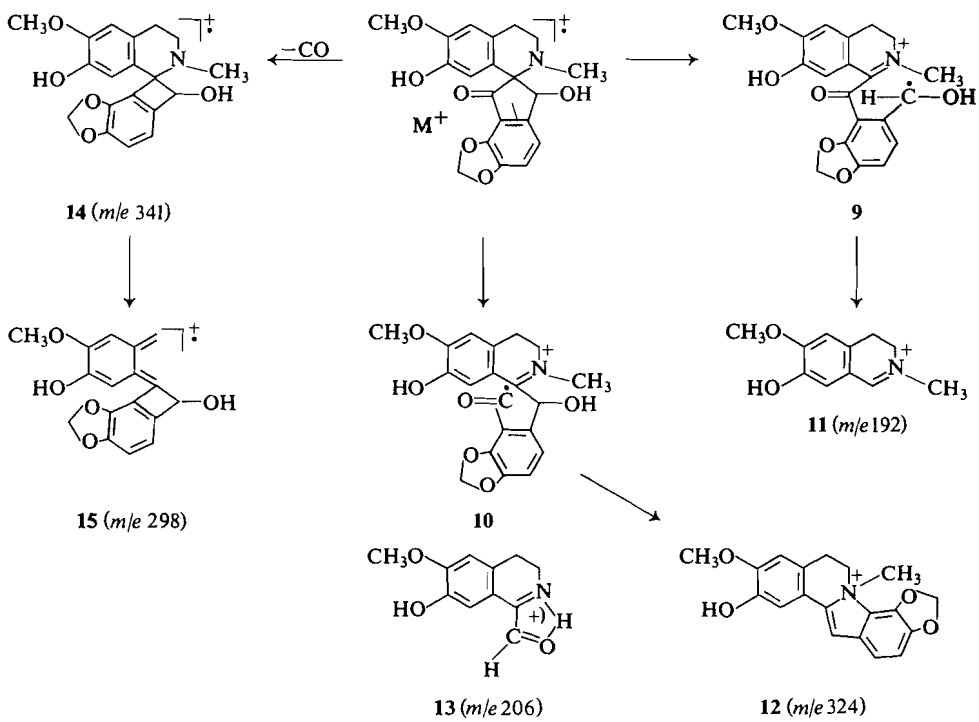

SCHEME 1

Can. J. Chem. Downloaded from www.nrcresearchpress.com by 210.87.254.6 on 09/05/12
For personal use only.

Can. J. Chem. Downloaded from www.nrcresearchpress.com by 210.87.254.6 on 09/05/12
For personal use only.

explanation for these differences is that the substitution of methoxyl and hydroxyl in ring A increases the possibility of the decomposition of the molecular ion as well as the fragment ions. Expulsion of CO from the molecular ion forms ion **14**, which by a retro-Diels–Alder decomposition can produce ion **15** at *m/e* 298. If the fragment C_3H_7N is lost from **14**, ion *m/e* 284 will be formed.

In the high mass range, there is a peak of composition $C_{18}H_{16}NO_5$, corresponding to the loss of CH_3CO which may arise by fragmentation of the aromatic ring. It is well documented that aromatic methyl ethers (8) can lose CH_3 and CO successively to give an ion, M-CH_3CO. Other possibilities are by loss of CH_3 from **14** or loss of CO from M-CH_3.

In the region *m/e* 150–200, most peaks are doublets and most of them contain a nitrogen atom. The source of these ions must be the isoquinoline moiety. The only useful and characteristic ion in this region, however, is the dihydroisoquinolinium ion, *m/e* 192, which is the most intense peak in this area.

The spectrum of *O*-methylfumarofine is also recorded in Fig. 1. In the high mass range (above *m/e* 250), all the peaks are 14 mass units higher than the corresponding peaks in fumarofine, and the peak intensities vary little. In the range between *m/e* 150 and 200 multiplicity of the peaks is much reduced in comparison to that of fumarofine. The peaks at *m/e* 192 and 206 in fumarofine are shifted to *m/e* 206 and 220 in **2**. These ions correspond to the isoquinolinium ion and the ion containing one nitrogen and three oxygens.

Experimental

Apparatus, Methods, and Materials

Mass spectra were determined on a C.E.C. 21-110B double-focusing mass spectrometer. Samples were introduced through a direct inlet system. Spectra are plotted in terms of relative abundance, with the most intense peak (base peak) taken as 100%. Only those peaks with an intensity equal to or greater than 3% of the most intense peak have been recorded.

The high resolution mass spectra were recorded on Ilford Q-2 photographic plates, which were developed in the usual manner. The spectra were then recorded on magnetic tape, using a Gaertner comparator-densitometer linked to a Datex system. They were processed on a CDC-6400 computer using a modified version of the HIRES program of Tunnicliff and Wadsworth (9).

The 100 MHz p.m.r. spectra were recorded using the frequency sweep mode of a Varian HA-100 spectrometer. Samples were dissolved in $CDCl_3$ or DMSO-d_6 using added TMS as the internal locking signal. Chemical shifts were measured relative to TMS using a V4315 frequency counter incorporated in the instrument. Double irradiation was achieved by employing a Hewlett-Packard 201C audiogenerator at the desired frequency.

A Perkin–Elmer 337 grating i.r. spectrometer was used to record i.r. spectra and a Cary 14 spectrometer was used for the u.v. spectrum.

Melting points were determined on a Kofler hot stage and are uncorrected.

Methylation of Fumarofine

Fumarofine (25 mg) was dissolved in methanol (5 ml) and excess diazomethane in ether added to the solution which was then allowed to stand for 3 h. The solvents were allowed to evaporate and the residue recrystallized from methanol–ether, m.p. 245–246 °C.

The u.v. spectrum: λ_{max} (EtOH) 208, 235, 259, 286, and 250 mμ; log ε 4.45, 3.96, 3.37, and 3.40.

The i.r. spectrum: ν_{OH} (KBr) 3450 cm^{-1}; $\nu_{C=O}$ (KBr) 1700 cm^{-1}.

Accurate mass measurement of the molecular ion gave the following result: calcd. for $C_{21}H_{21}NO_6$, 383.137; found, 383.138.

Acetylation of O-Methylfumarofine

O-Methylfumarofine (17 mg) was dissolved in acetic anhydride (4 ml) and pyridine (2 ml). The mixture was stirred at room temperature under a nitrogen atmosphere for 60 h. The excess acetic anhydride and pyridine were evaporated under reduced pressure, the residue triturated in aqueous sodium carbonate, and the suspension extracted several times with chloroform. The chloroform extract was dried over sodium sulfate, and evaporated to a residue which could not be induced to crystallize but on an analytical thin layer plate it showed only a single spot. The mass spectrum showed a molecular ion at *m/e* 425. Insufficient material was available for a combustion analysis.

We thank the National Research Council of Canada for financial support of this work.

1. R. H. F. Manske. Can. J. Res. B**16**, 438 (1938).
2. R. H. F. Manske. Can. J. Chem. **47**, 1103 (1969).
3. D. B. MacLean, R. A. Bell, J. K. Saunders, C.-Y. Chen, and R. H. F. Manske. Can. J. Chem. **47**, 3593 (1969).
4. C.-K. Yu and D. B. MacLean. This issue.
5. R. H. F. Manske, R. Rodrigo, D. B. MacLean, D. E. F. Gracey, and J. K. Saunders. Can. J. Chem. **47**, 3585 (1969).
6. J. K. Saunders, R. A. Bell, C.-Y. Chen, D. B. MacLean, and R. H. F. Manske. Can. J. Chem. **46**, 2876 (1968), and references therein.
7. F. Santavy, L. Hruban, V. Simanek, and D. Walterova. Collect. Czech. Chem. Commun. **35**, 2418 (1970).
8. H. Budzikiewicz, C. Djerassi, and D. H. Williams. Mass spectrometry of organic compounds. Holden-Day, Inc., San Francisco, California, 1967.
9. D. D. Tunnicliff and P. A. Wadsworth. Anal. Chem. **40**, 1826 (1968).

Can. J. Chem. Downloaded from www.nrcresearchpress.com by 210.87.254.105 on 09/05/12
For personal use only.

Mass Spectra of Spirobenzylisoquinoline Alkaloids

C. K. Yu and D. B. MacLean
Department of Chemistry, McMaster University, Hamilton, Ontario

Received April 14, 1971

The mass spectra of a number of spirobenzylisoquinoline alkaloids, several of their derivatives, and some model compounds are recorded and discussed. Fragmentation mechanisms are proposed for the formation of the major ions in the spectra of compounds containing one and two oxygen functions in the five-membered ring. The spectra of compounds containing a carbonyl group differ markedly from those having a hydroxyl group in the five-membered ring. Several model compounds were synthesized and characterized and their spectra compared with those of the alkaloids.

Les spectres de masse d'un certain nombre d'alcoloïdes du type spirobenzylisoquinoléine, de quelques uns de leurs dérivés, ainsi que de quelques composés types, sont rapportés et discutés. Des mécanismes de fragmentation sont proposés pour la formation des ions principaux dans les spectres des composé qui renferment une et deux fonctions oxygène dans le cycle à cinq atomes. Les spectres des composés qui renferment un groupement carbonyle différent considerablement de ceux ayant un groupe hydroxyle dans le noyau à cinq atomes. Plusieurs composés types ont été synthétisés et caractérisés dans le but de comparer leurs spectres avec ceux des alcaloïdes.

Canadian Journal of Chemistry, **49**, 3025 (1971)

The mass spectra of many classes of isoquinoline alkaloids have been investigated (1, 2) but a systematic study of the mass spectra of spirobenzylisoquinoline alkaloids has not been reported. Most of the known spirobenzylisoquinoline alkaloids were isolated several decades ago but it is only recently that their structures have been elucidated. The structures of known alkaloids are shown below along with two derivatives **4** and **8**. The mass spectra of ochotensine and ochotensimine have been reported (3) but their fragmentation does not show a characteristic pattern that can be used for diagnostic purposes. On the other hand the spirobenzylisoquinoline compounds with oxygenated substituents in the five-membered ring show distinct fragmentation patterns. The spectra of several alkaloids of this type have been reported (4–7) but none has been analyzed in detail. The present work will deal with the fragmentation pattern of known alkaloids of the spiro series oxygenated in the five-membered ring and with several model compounds.

The model compounds were synthesized by methods already described (8, 9). Since the compounds are new and the orientation of substituents found in one product differed from that reported (8) a description of the syntheses will precede a discussion of the mass spectra.

In 1968 the condensation of 3-hydroxy-4-methoxyphenylethyl amine with ninhydrin to a compound named 3-hydroxy-2-methoxyochotensinan-8,13-dione was reported (8). When we used the amine hydrochloride in the condensation with ninhydrin a different product was obtained to which we assign structure **11**. The phenol **11** was characterized as its *O*-methyl ether, **12**, as the former proved difficult to purify. The i.r. spectrum of **12** did not show hydroxyl absorption but had two absorptions in the carbonyl region at 1700 and 1745 cm^{-1}. The 60 MHz p.m.r. spectrum (Fig. 1) shows two methoxyl signals at 3.28 and 3.73 δ, one singlet of area 2 at 6.86 δ corresponding to two aromatic protons in ring A, a multiplet of area 4 in the region 7.7–8.1 δ arising from the protons in ring D, and signals from the remaining protons in the range 2.5–3.5 δ. When the spectrum was run on the 220 MHz instrument, the aromatic signal at 6.86 δ was split into a well-defined AB quartet with a coupling constant of 8 Hz (see inset Fig. 1). Thus, in the condensation of ninhydrin and 3-hydroxy-4-methoxyphenylethylamine under our conditions cyclization took place at the carbon ortho rather than para to the hydroxyl group to form **11** (Scheme 1).

Manske and Ahmed (9) have reported the synthesis of an analogue of ochrobirine in high yield. They treated 3,4-methylenedioxyphenylethylamine with ninhydrin in absolute ethanol at low temperature and were able to isolate pure para cyclized product **13**, which was later transferred into **14**, the analogue of ochrobirine,

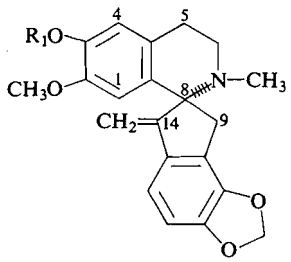

1 Ochotensimine $R_1 = CH_3$
2 Ochotensine $R_1 = H$

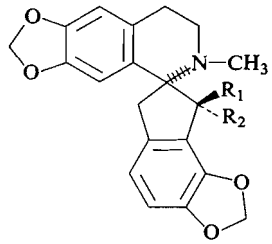

3 Fumariline $R_1 + R_2 = O$
4 Dihydrofumariline $R_1 = OH$; $R_2 = H$

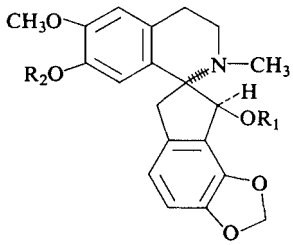

5 Fumaricine $R_1 = H$; $R_2 = CH_3$
6 Fumaritine $R_1 = H$; $R_2 = H$
7 Fumarophycine $R_1 = COCH_3$; $R_2 = H$
8 Diacetylfumaritine $R_1 = R_2 = COCH_3$

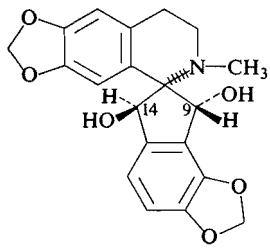

9 Ochrobirine

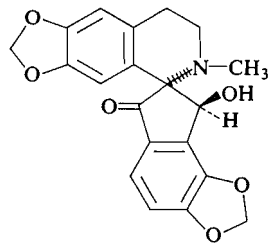

10 Sibiricine

by successive methylation and sodium borohydride reduction. We used their procedure with 3,4-dimethoxyphenylethylamine and ninhydrin at ice-water temperature. The product **15**, bright yellow crystals, melted at a temperature different from **12**. The p.m.r. spectrum of **15** had two singlets at 5.91 and 6.65 δ in the aromatic region replacing the AB quartet of **12**. Apparently, cyclization occurs at the para position in this instance as shown in Scheme 1. The signal at 6.65 δ is broader than the other singlet presumably because of benzylic coupling to H-5. The same situation has also been observed in the spectrum of sibiricine (5) in which two singlets, one at 6.54, the broader signal, and one at 6.04 δ, were assigned to H-4 and -1, respectively.

When compound **12** was methylated with formic acid and formaldehyde and reduced with sodium borohydride two major products were detected on t.l.c. They were separated by thick layer chromatography and subjected to spectroscopic investigation. Both products, **17** and **18**, were dihydro compounds as shown by their mass spectra and both show hydroxyl and carbonyl absorption in their i.r. spectra. When one carbonyl group is reduced, the interaction between R_1 and OCH_3 at C-1 (see

Can. J. Chem. Downloaded from www.nrcresearchpress.com by 210.87.254.105 on 09/05/12
For personal use only.

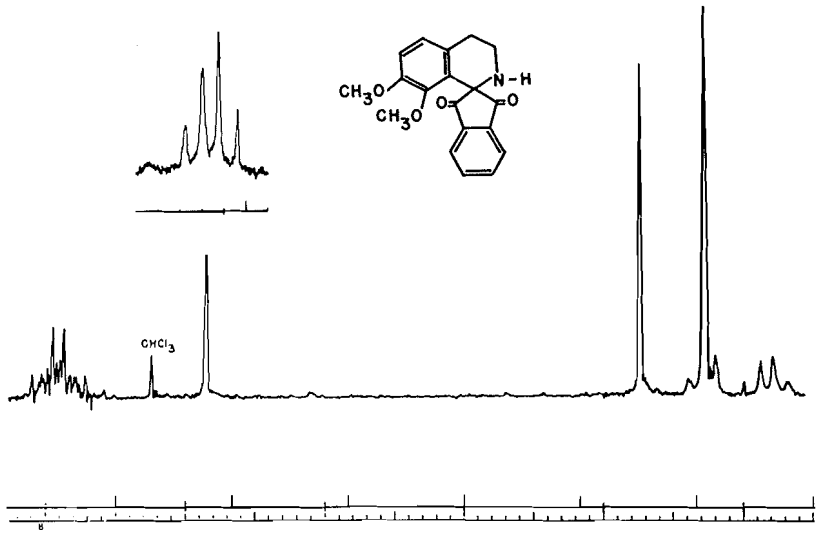

FIG. 1. The 60 MHz p.m.r. spectrum of **12**.

17 or **18**) is such that this OCH_3 group is forced to sit behind the remaining carbonyl group. The interaction between R_2 and N-CH_3 forces the *N*-methyl group to stay in front of the carbonyl group. As a result, the second carbonyl group is not readily accessible to hydride attack under mild reaction conditions and only dihydro compounds are obtained.

The assignment of stereochemistry to **17** and **18** is based on two facts. Firstly, on t.l.c. plates compound **17** has a higher R_f value than that of **18**, indicating that the latter is adsorbed more firmly on the surface of the silica gel. Since internal hydrogen bonding in **17** may reduce the interaction between adsorbent and compound (10) it moves faster on t.l.c. Secondly, when the 100 MHz p.m.r. spectra of the compounds are compared a sharp singlet is observed at 5.08 δ in **17** and a very broad signal centered at 5.26 δ in **18**. These signals are assigned to the C-9 protons in each case. Analogous signals have been observed in ochrobirine (6) in which the broad signal at 5.42 δ was assigned to the proton at H-14 on the same side of the plane as the N—CH_3 group while the sharp singlet at 4.88 δ was assigned to H-9 which is on the opposite side of the plane. Thus, the stereochemistry of **17** and **18** is established.

When **15** was reduced with sodium borohydride one major compound **16** was detected on t.l.c. The molecular ion peak in the mass spectrum appears four mass units higher than in **15**, indicating that both carbonyl groups are reduced in this instance. Since there is less steric hindrance present in this molecule, both carbonyl groups are accessible to hydride attack.

Before considering the mass spectra of the model compounds and the alkaloids with two oxygens in the five-membered ring it is appropriate to begin with compounds with one oxygen in the five-membered ring. Several compounds with one hydroxyl group are available, one with a single carbonyl group, and two with acetyl groups. The composition of all ions referred to in the subsequent discussion has been determined by high resolution mass spectrometry. Labelling studies on the natural compounds were precluded because of their paucity or because of lack of suitable chemical methods for introduction of label.

The mass spectra of dihydrofumariline (**4**), fumaricine (**5**), and fumaritine (**6**) have been published before (4) but are repeated here for convenience in Fig. 2. In Scheme 2 ions labelled *a*, *b*, and *c* are derived from fumaricine, fumaritine, and dihydrofumariline, respectively. The base peak, ion **20**, in the spectra of these compounds is assumed to arise as shown in Scheme 2. This mechanism has been supported by a deuterium labelling experiment, in which the hydroxyl hydrogen was replaced by deuterium causing a shift of one mass unit in the base peak.

Can. J. Chem. Downloaded from www.nrcresearchpress.com by 210.87.254.105 on 09/05/12
For personal use only.

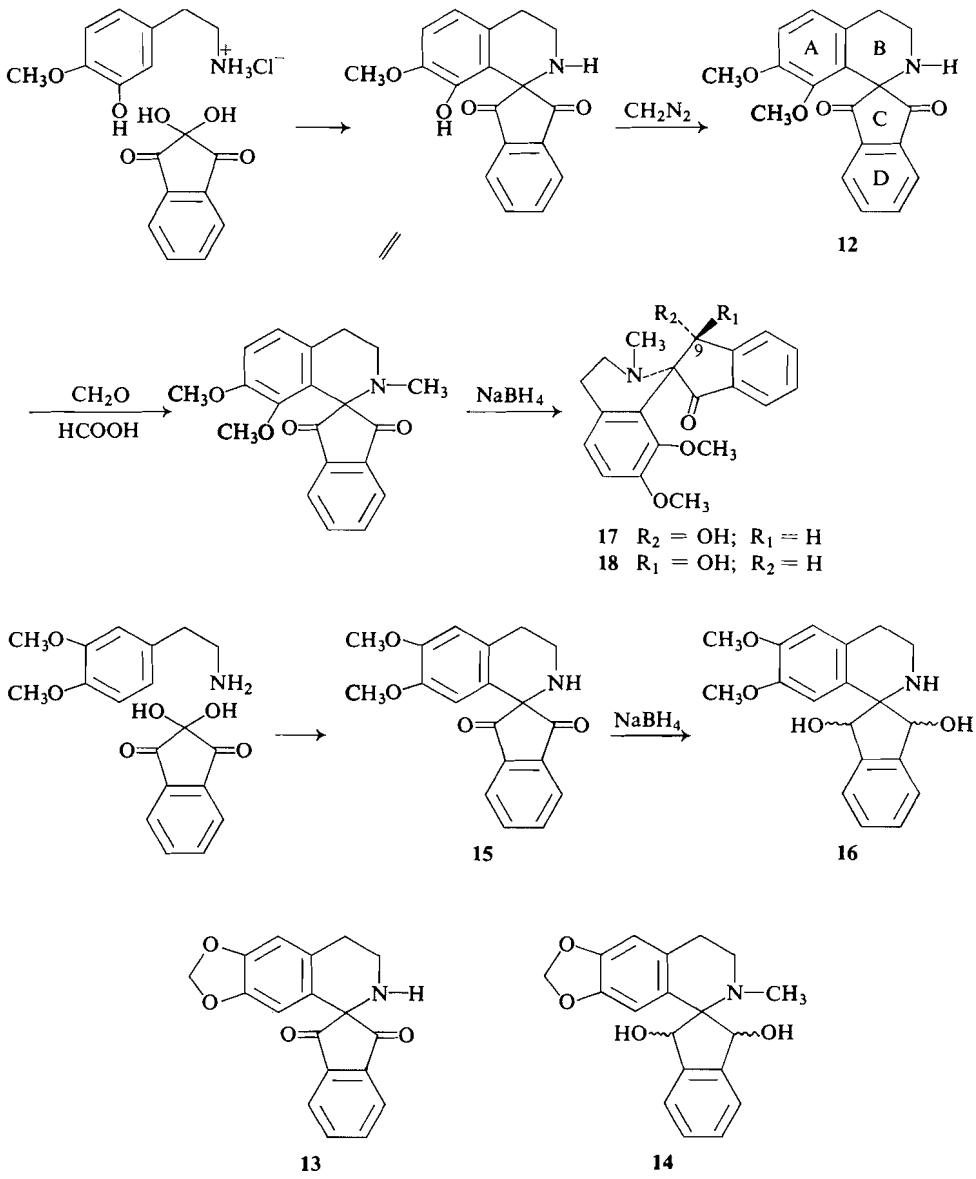

SCHEME 1

A small peak two mass units lower than the base peak is assigned to the isoquinolinium ion **21**, formed from **19** by C—C bond cleavage followed by the loss of one hydrogen from the isoquinoline moiety and rearrangement of another, or by loss of two hydrogens from **20**. Both ions, **20** and **21**, are characteristic of many isoquinoline alkaloids (1, 2). The same bond rupture with charge retention by the other portion of the molecule leads to ion **22**, *m/e* 163, which upon losing CO yields ion **23** at *m/e* 135 but both are of low intensity.

In the high mass end of the spectrum the M-CH_3 ion shows a constant intensity relative to the molecular ion ((intensity of M-CH_3)/(intensity of M^+) is about 1.4–1.7), which indicates that the source of the methyl radical must be a common structural unit, presumably the N—CH_3 group. In dihydrofumariline (**4**), the only source of the M-CH_3 ion is the methyl

Can. J. Chem. Downloaded from www.nrcresearchpress.com by 210.87.254.105 on 09/05/12
For personal use only.

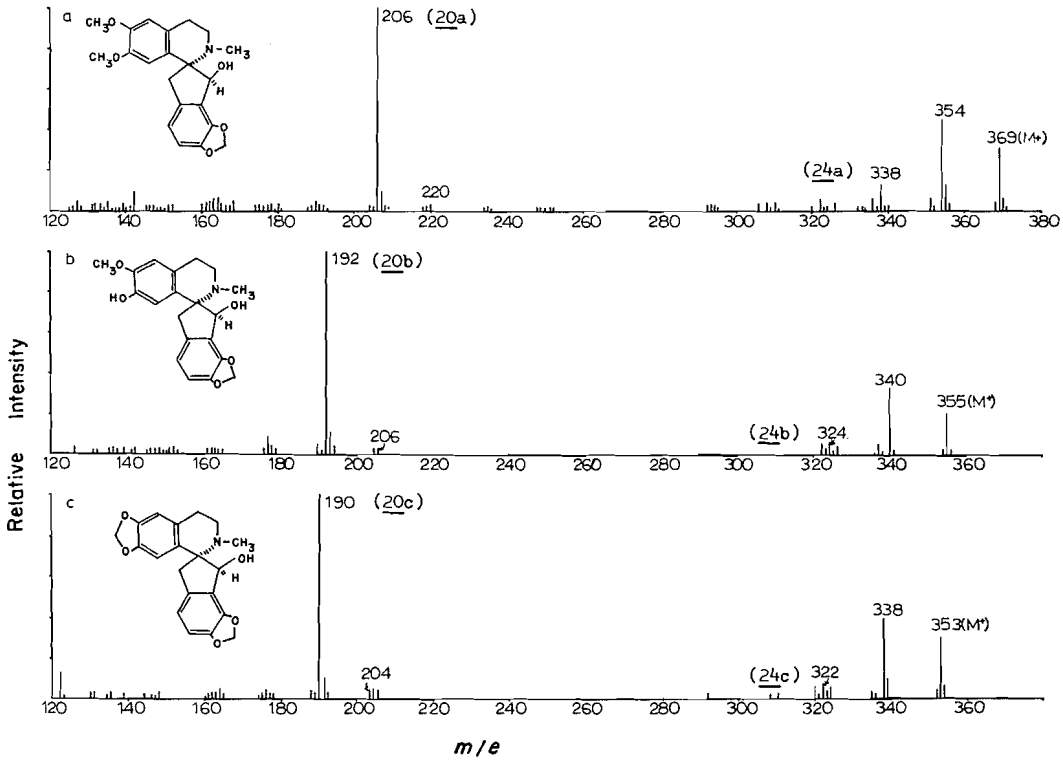

FIG. 2. The mass spectra of (*a*) fumaricine (**5**), (*b*) fumaritine (**6**), and (*c*) dihydrofumariline (**4**).

group attached to the nitrogen atom, and it is assumed that in these systems it is lost upon electron impact.

An M-31 peak is observed in all three cases corresponding in composition to M-OCH_3. In **5** and **6** this ion may be attributed to the loss of OCH_3 from the substituent in ring A. In **4**, however, the ion at M-31 can come only from another source. We propose that ion **19** expels a neutral fragment CH_2O and a radical H· to form an ion of type **24** which occurs in all of the spirobenzylisoquinoline compounds with oxygenated substituents in the five-membered ring. It is likely therefore that ions **24***a* and *b* contribute significantly to the M-31 peak in **5** and **6**, respectively.

An ion of low intensity 14 mass units higher than the base peak has been found to contain one nitrogen and three oxygen atoms; its structure will be discussed later.

The spectra of fumarophycine (**7**) and its *O*-acetate (**8**) are recorded in Fig. 3 (7, 11). They bear little resemblance to the unacetylated precursor **6** but are dominated by peaks arising from the acetyl groups. Both compounds lose CH_3CO and CH_3CO_2H forming ions at *m/e* 354 and 337, respectively, in **7** and at *m/e* 396 and 379, respectively, in **8**. Examination of the spectra under high resolution, however, shows the presence of ions common to **6**, **7**, and **8**, at *m/e* 355, 324, 206, 192, and 190. These ions are all relatively weak and the relationship among the compounds is apparent only when it is possible to determine the compositions by high resolution studies.

The spectrum of fumariline (**3**) (Fig. 4) is distinctly different from that of **4**, **5**, and **6**. It does not show an intense peak corresponding to **20***c*, since there is not a readily available hydrogen to facilitate the process for its formation. The isoquinolinium ion at *m/e* 188 (**21***c*), however, is still discernible in the spectrum since a process in which hydrogen is lost and undergoes rearrangement in the isoquinoline moiety is still feasible. The base peak at *m/e* 322 is a singlet and corresponds in composition to $C_{19}H_{16}NO_4$. It is apparently formed by ring opening to **25** with loss of CO followed or preceded by loss of H.

Can. J. Chem. Downloaded from www.nrcresearchpress.com by 210.87.254.105 on 09/05/12
For personal use only.

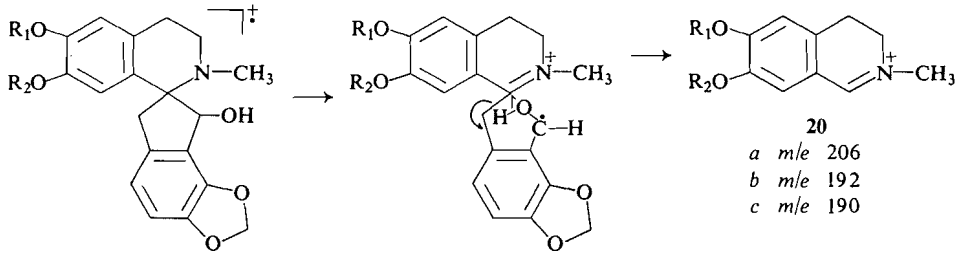

Fumaricine	*a* $R_1 = R_2 = CH_3$	*m/e* 369
Fumaritine	*b* $R_1 = CH_3$; $R_2 = H$	*m/e* 355
Dihydrofumariline	*c* $R_1 + R_2 = CH_2$	*m/e* 353

19

20
a *m/e* 206
b *m/e* 192
c *m/e* 190

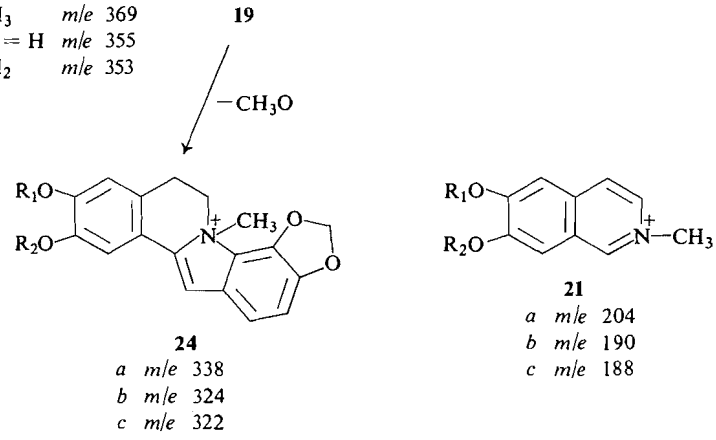

24
a *m/e* 338
b *m/e* 324
c *m/e* 322

21
a *m/e* 204
b *m/e* 190
c *m/e* 188

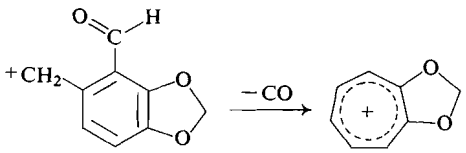

22 *m/e* 163 **23** *m/e* 135

SCHEME 2

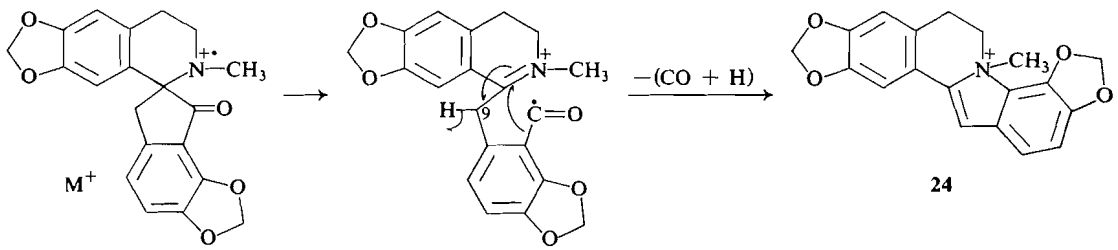

25 **24**

SCHEME 3

In the absence of a labelling experiment, the hydrogen is assumed to come from H-9 (Scheme 3). Upon loss of a molecule of formaldehyde from the methylenedioxy group ion **24***c* yields an ion at *m/e* 292 which decomposes further to give an ion at *m/e* 264, both of low intensity. A peak corresponding to M-CH_3 at *m/e* 336 is small but observable in the spectrum. The source of this methyl radical is probably the methyl group attached to the nitrogen atom.

Can. J. Chem. Downloaded from www.nrcresearchpress.com by 210.87.254.105 on 09/05/12
For personal use only.

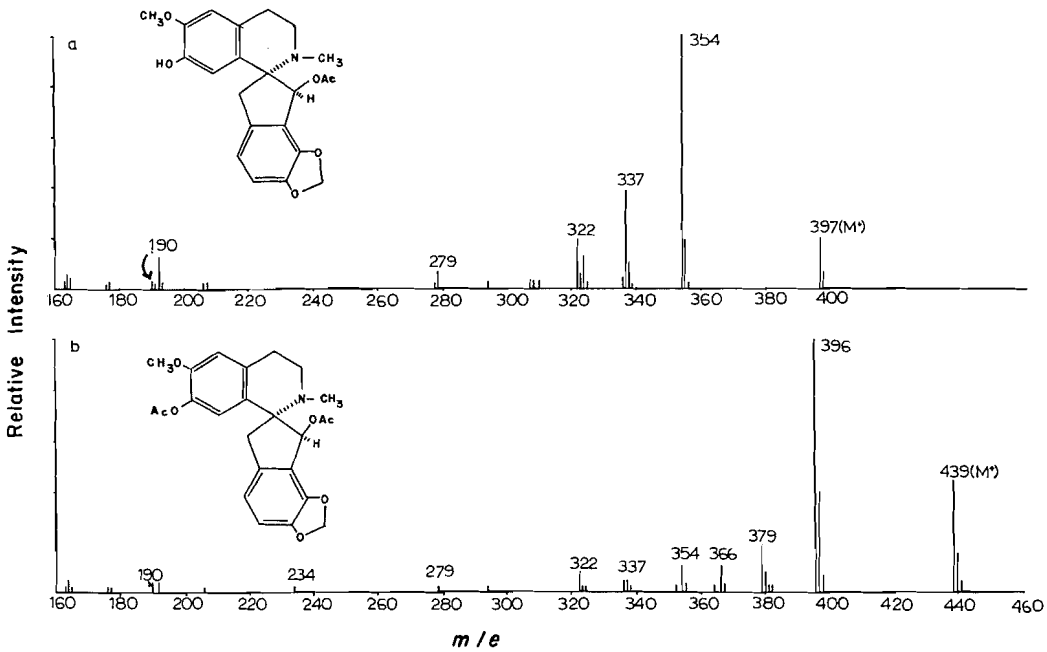

FIG. 3. The mass spectra of (*a*) fumarophycine (**7**) and (*b*) *o*-acetylfumarophycine (**8**).

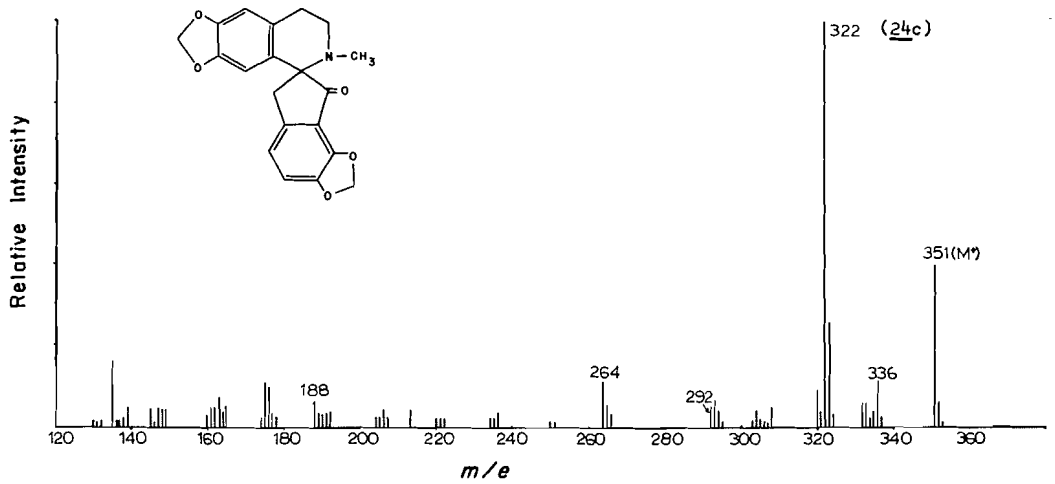

FIG. 4. The mass spectrum of fumariline (**3**).

The model compound **17** and sibiricine (**10**), both of which have a carbonyl and a hydroxyl group in the five-membered ring, are now examined. (The spectra of **17** and **18** are nearly identical and only one is discussed.) The spectrum of **17** is recorded in Fig. 5 and a scheme for its fragmentation in Scheme 4. The molecular ion is the most intense ion in the spectrum and fragmentation seems to be initiated by cleavage of the bonds β to nitrogen and adjacent to oxygen. Thus ion **26** is formed by cleavage adjacent to the OH group; its decomposition is analogous to that of **19** in the fumaricine series yielding **27** and **28** at *m/e* 206 and 204, respectively. Their intensity is nearly alike in contrast with fumaricine in which the ion of higher mass is

Can. J. Chem. Downloaded from www.nrcresearchpress.com by 210.87.254.105 on 09/05/12
For personal use only.

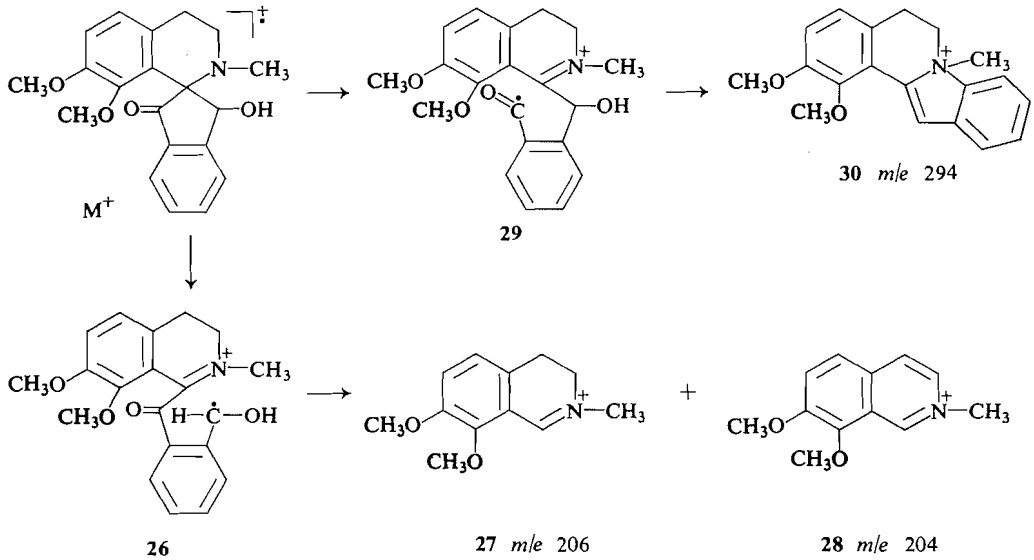

SCHEME 4

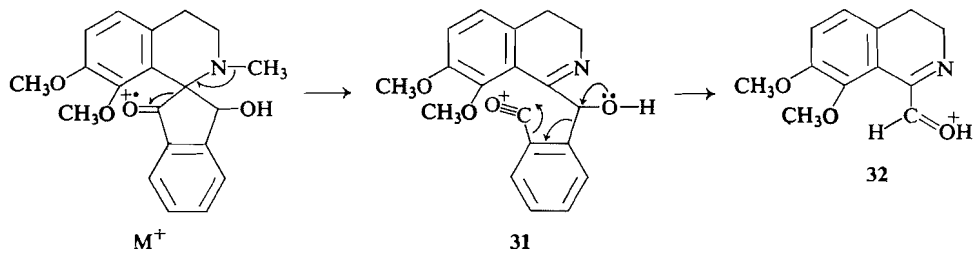

SCHEME 5

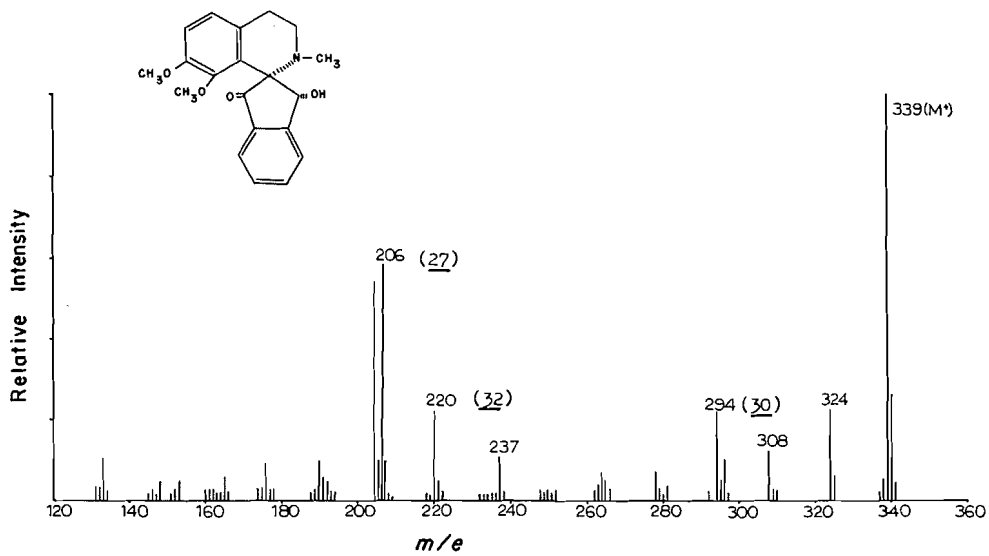

FIG. 5. The mass spectrum of compound **17**.

Can. J. Chem. Downloaded from www.nrcresearchpress.com by 210.87.254.105 on 09/05/12
For personal use only.

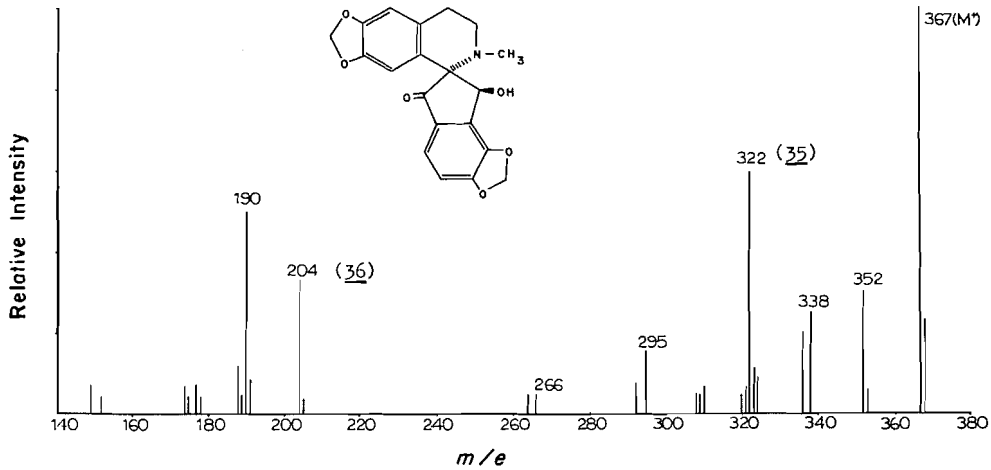

FIG. 6. The mass spectrum of sibiricine (**10**).

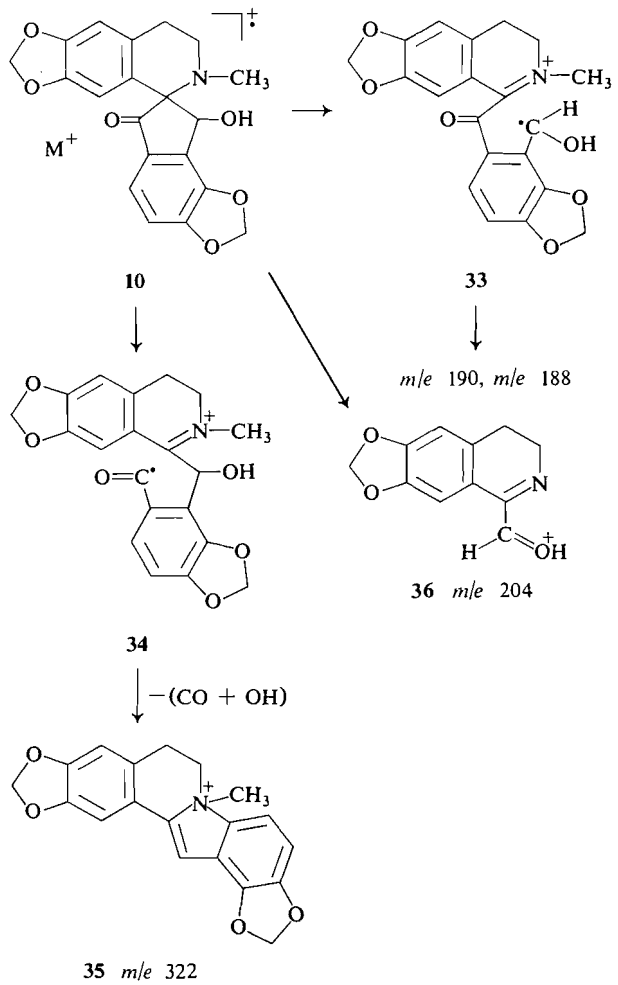

SCHEME 6

Can. J. Chem. Downloaded from www.nrcresearchpress.com by 210.87.254.105 on 09/05/12
For personal use only.

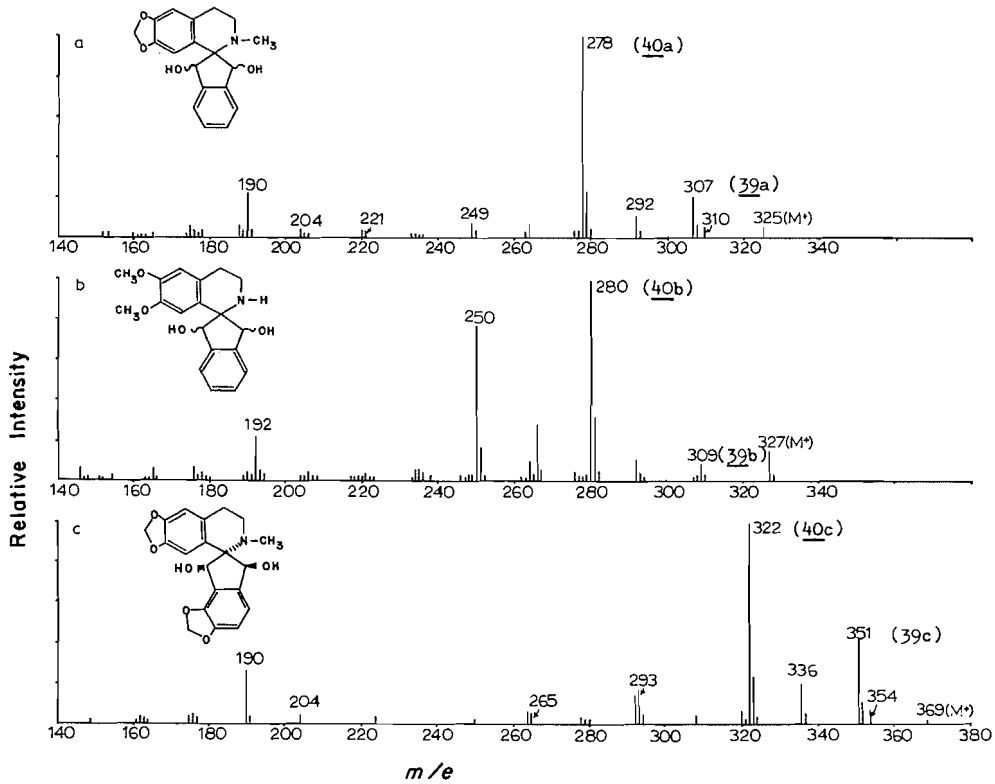

FIG. 7. The mass spectra of (*a*) compound **14**, (*b*) compound **16**, (*c*) ochrobirine (**9**).

much more intense. Fission of the bond adjacent to the carbonyl group leads to **29** which loses CO and OH to form **30**. (Compare Scheme 3 in which fumariline loses CO + H).

A moderately intense peak at *m/e* 220 has the composition $C_{12}H_{14}NO_3$ and must come from the isoquinoline moiety. It is postulated (Scheme 5) that the molecular ion expels a methyl radical from the nitrogen atom to form an intermediate ion **31** which decomposes to the daughter ion **32**. The process involves the loss of a methyl radical from the nitrogen atom, a fragmentation observed earlier in the spectrum of dihydrofumariline. Ions of type **32** occur in the spectra of all the spirobenzylisoquinoline compounds with hydroxyl groups in the five-membered ring but their intensity is very low in the spectra of fumaritine, fumaricine and dihydrofumariline.

The spectrum of sibiricine (**10**) (Fig. 6) and its fragmentation (Scheme 6) are very similar to that of **17**. The benzylic cleavage of the molecular ion may give either **33** or **34**, both of which may decompose further to give a series of peaks similar to those from **17**. Ion **34** can decompose by loss of CO and OH to give ion **35**, while ion **33** can give rise to the dihydroisoquinolinium ion, *m/e* 190, and the smaller isoquinolinium ion, *m/e* 188. The peak at *m/e* 204 (**36**) has one nitrogen and three oxygen atoms and must form in the manner shown in Scheme 5.

The loss of CH_3 is again a prominent peak (*m/e* 352) and must result through loss of the *N*-methyl group. The peak at *m/e* 338 corresponds to loss of CO and H and may form in the same way as ion **35** or by loss of CHO in one step from a methylenedioxy group. The spectra of **10** and **17** are alike and combine features found in the spectra of compounds with a carbonyl group in the five-membered ring, *e.g.* fumariline, and those with a hydroxyl group in the five-membered ring, *e.g.* dihydrofumariline.

The mass spectra of **14**, **16**, and ochrobirine (**9**) all of which have two hydroxyl groups in the spiro ring are recorded in Fig. 7. The spectra show a pattern distinct from that of sibiricine

Can. J. Chem. Downloaded from www.nrcresearchpress.com by 210.87.254.105 on 09/05/12
For personal use only.

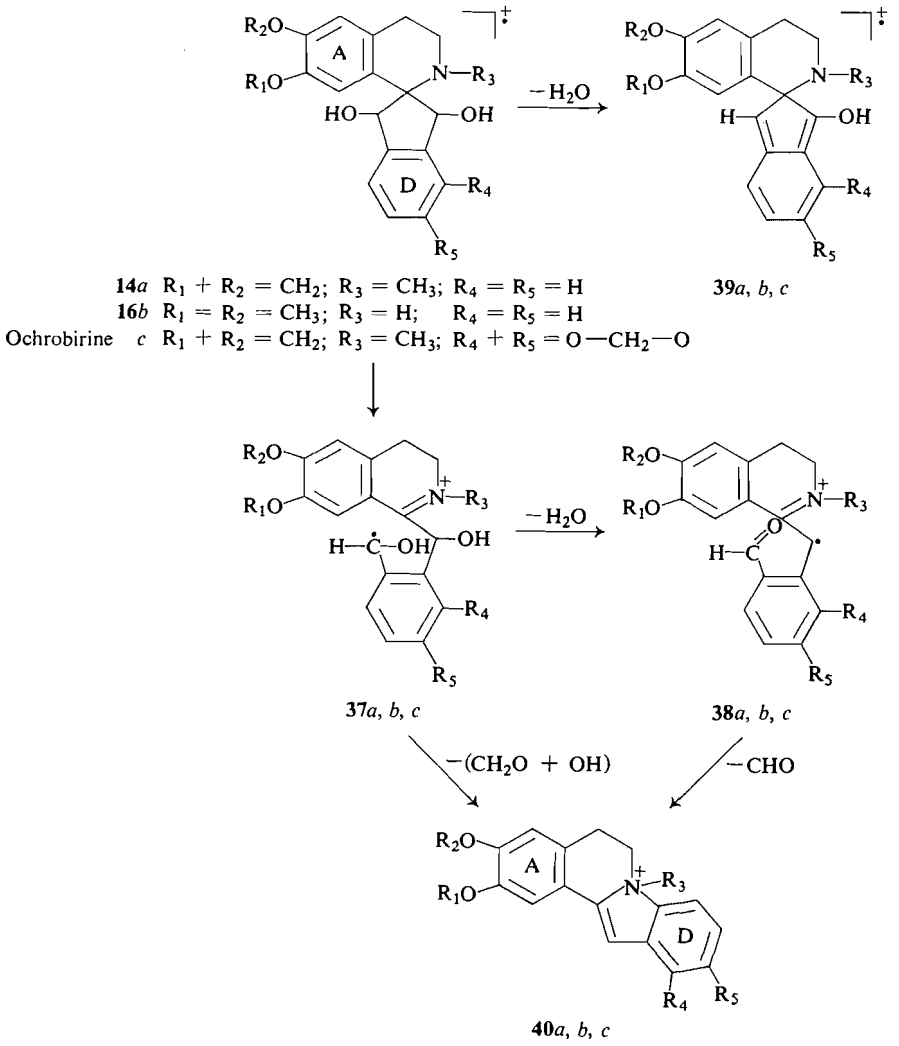

SCHEME 7

and of **17**. The parent peak is only 10% of the base peak or less, while in sibiricine (**10**) and **17** it is the base peak, and the dihydroisoquinolinium ion is reduced in intensity.

The M-H_2O and the base peak (M-CH_3O_2) may be formed by the processes shown in Scheme 7. The loss of H_2O from **37** leads to the more stable radical **38** in which the radical center is benzylic and also conjugated to the immonium ion. The M-H_2O peak may also come from the molecular ion directly to form ion **39**. The base peak, ion **40**, can be derived either from **38** by losing a CHO radical or from **37** by concerted elimination of the neutral fragments, CH_2O and OH. The latter process is analogous to the elimination of (CO + OH) from sibiricine, in which an M-OH ion peak cannot be detected. The course of further decomposition of **40***a*, *b*, and *c* is different, each depending on the substituents either in ring A or in ring D. Ion **40***a* loses a CHO radical followed by expulsion of CO to give small peaks at *m/e* 249 and 221, while ion **40***c* can lose either CHO or CH_2O, presumably from different rings, to yield ions at *m/e* 293 and 292, each of which is capable of losing a molecule of CO to produce the respective ions at *m/e* 265 and 264. The situation is quite different in **40***b* where two methoxyl groups are in ring A. The ejection of the stable neutral fragment, CH_2O, to give an even electron ion

Can. J. Chem. Downloaded from www.nrcresearchpress.com by 210.87.254.105 on 09/05/12
For personal use only.

Can. J. Chem. Downloaded from www.nrcresearchpress.com by 210.87.254.105 on 09/05/12
For personal use only.

seems to be a favorable process since the daughter ion peak at *m/e* 250 is quite intense. In the high mass range, when $R_3 = CH_3$, there is a small peak corresponding to M-CH_3. There is also a peak corresponding to M-($CH_3 + H_2O$), which can be derived either from ion M-CH_3 by losing H_2O or from M-H_2O by losing a CH_3 radical.

In the spectra of **14** and **9**, there is a small peak 14 mass units higher than the dihydroisoquinolinium ion and its composition has been determined to be $C_{11}H_{10}NO_3$. This ion will form in a manner similar to the corresponding ion in sibiricine and, therefore, can be assigned the structure **36** (Scheme 6).

Experimental

Apparatus, Methods, and Materials

Mass spectra were determined on a C.E.C. 21-110B double-focusing mass spectrometer. Samples were introduced through a direct inlet system. Spectra are plotted in terms of relative abundance, with the most intense peak (base peak) taken as 100%. Only those peaks with an intensity equal to or greater than 3% of the most intense peak have been recorded.

The high resolution mass spectra were recorded on Ilford Q-2 photographic plates, which were developed in the usual manner. The spectra were then recorded on magnetic tape, using a Gaertner comparator-densitometer linked to a Datex system. They were processed on a CDC-6400 computer using a modified version of the HIRES program of Tunnicliff and Wadsworth (12).

The p.m.r. spectra were routinely run on a Varian A-60 or Varian T-60 instrument in $CDCl_3$ using tetramethylsilane as internal standard. The 100 MHz spectra were recorded using the frequency sweep mode of a Varian HA-100 spectrometer. Samples were dissolved in $CDCl_3$ using added TMS as the internal locking signal. Chemical shifts were measured relative to TMS using a V4315 frequency counter incorporated in the instrument. Double irradiation was achieved by employing a Hewlett–Packard 201C audiogenerator at the desired frequency.

A Perkin–Elmer 337 grating i.r. spectrometer was used to record i.r. spectra.

Melting points were determined on a Kofler hot stage and are uncorrected.

The alkaloids, fumariline, fumaricine, fumaritine, sibiricine, ochrobirine, and compounds **13** and **14**, were obtained from Dr. R. H. F. Manske of the University of Waterloo, Waterloo, Ontario. Fumarophycine was obtained from Dr. N. M. Mollov of the Bulgarian Academy of Science, Sofia, Bulgaria.

*7-Methoxy-8-hydroxy-1,2,3,4-tetrahydroisoquinoline-1-spiro-2′-(1′,3′-indandione) (**11**)*

3-Hydroxy-4-methoxyphenylethylamine hydrochloride (940 mg), prepared according to the method of Ramirez and Burger (13), was added to a solution of ninhydrin (950 mg) in absolute alcohol (20 ml). The mixture was left at room temperature for 5 days. The solvent was evaporated, the residue dissolved in hot water, basified with saturated sodium bicarbonate solution, and extracted with chloroform. The chloroform extract was dried over sodium sulfate and evaporated to dryness. The red semi-crystalline solid obtained from chloroform–hexane melted at 92–95 °C. The mass spectrum showed a molecular ion at *m/e* 309.

*7,8-Dimethoxy-1,2,3,4-tetrahydroisoquinoline-1-spiro-2′-(1′,3′-indandione) (**12**)*

Compound **11** (70 mg) was dissolved in methanol (10 ml) and excess diazomethane in ether was added to the solution which was then allowed to stand for 3 h. The solvents were allowed to evaporate and the residue recrystallized from methanol. The yellow crystalline prisms melted at 158 °C. The i.r. spectrum: $\nu_{C=O}$ ($CHCl_3$) 1700, 1745 cm^{-1}.

Anal. Calcd. for $C_{19}H_{17}NO_4$: C, 70.6; H, 5.3. Found: C, 70.6; H, 5.4.

7,8-Dimethoxy-2-methyl-1,2,3,4-tetrahydroisoquinoline-1-spiro-2′-(1′,3′-indandione)

Compound **12** (50 mg) was mixed with formic acid (2 ml) and formaldehyde (2 ml), and heated on a steam bath for 12 h. Water was added to the mixture which was basified with saturated sodium bicarbonate solution and extracted with chloroform. The chloroform extract was washed with water, dried over sodium sulfate, and evaporated to dryness. The yellow residue was crystallized from methanol–ether, m.p. 158–159 °C. The i.r. spectrum: $\nu_{C=O}$ ($CHCl_3$) 1700, 1745 cm^{-1}.

Anal. Calcd. for $C_{20}H_{19}NO_4$: C, 71.2; H, 5.6; N, 4.2. Found: C, 71.2; H, 5.8; N, 4.3.

*6,7-Dimethoxy-1,2,3,4-tetrahydroisoquinoline-1-spiro-2′-(1′,3′-indandione) (**15**)*

The procedure for preparing **15** was similar to that for the preparation of **13** (9), but 3,4-dimethoxyphenylethylamine was used instead of 3,4-methylenedioxyphenylethylamine. The product **15** was recrystallized from chloroform–hexane, m.p. 175–179 °C. The i.r. spectrum: $\nu_{C=O}$ ($CHCl_3$) 1710, 1750 cm^{-1}.

Anal. Calcd. for $C_{19}H_{17}NO_4$: C, 70.6; H, 5.3; N, 4.6. Found: C, 70.5; H, 5.3; N, 4.6.

*6,7-Dimethoxy-1,2,3,4-tetrahydroisoquinoline-1-spiro-2′-(1′,3′-indandiol) (**16**)*

Compound **15** (100 mg) was dissolved in ethanol and sodium borohydride (100 mg) was added. The mixture was allowed to stand at room temperature for 2 h. The solvent was evaporated, water was added, and the mixture was extracted with ether. The ether extract was dried over potassium carbonate and evaporated to dryness. Compound **15** was purified on basic silica gel by thick layer chromatography and, after elution, recrystallized from ethanol, m.p. 176–180 °C. The i.r. spectrum: ν_{OH} ($CHCl_3$) 3560 cm^{-1}.

Anal. Calcd. for $C_{19}H_{21}NO_4$: C, 69.7; H, 6.4; N, 4.2. Found: C, 69.5; H, 6.3; N, 4.3.

*Preparation of **17** and **18***

Sodium borohydride (200 mg) was added slowly to a solution of 7,8-dimethoxy-2-methyl-1,2,3,4-tetrahydro-

isoquinoline-1-spiro-2′(1′,3′-indandione) (200 mg) in methanol (10 ml) and the mixture stirred at room temperature for 10 h. The solvent was evaporated, water (5 ml) was added, and the aqueous suspension was extracted with ether. The ether extract was dried over potassium carbonate and evaporated to dryness. The mixture was separated by thick layer chromatography on basic silica gel (developed in methanol–chloroform 1:20). The faster moving fraction after elution was crystallized from ethanol to give **17** (65 mg), m.p. 171–173 °C. The i.r. spectrum: $\nu_{C=O}$ ($CHCl_3$) 1705 cm^{-1}.

Anal. Calcd. for $C_{20}H_{21}NO_4$: C, 70.8; H, 6.2; N, 4.1. Found: C, 70.8; H, 6.2; N, 4.3.

The slower moving fraction after elution was crystallized from ethanol to give **18** (67 mg), m.p. 183–186 °C. The i.r. spectrum: $\nu_{C=O}$ ($CHCl_3$) 1710 cm^{-1}.

Anal. Calcd. for $C_{20}H_{21}NO_4$: C, 70.8; H, 6.2; N, 4.1. Found: C, 70.7; H, 6.2; N, 4.2.

We thank the National Research Council of Canada for financial support and Dr. R. H. F. Manske and Dr. N. M. Mollov for samples of the alkaloids used in this study.

1. H. Budzikiewicz, C. Djerassi, and D. H. Williams. Structure elucidation of natural products by mass spectrometry. Vol. 1. Holden-Day Inc., San Francisco, California, 1964.
2. K. Biemann. Fortschr. Chem. Org. Naturstoff, **24**, 1 (1966).
3. S. McLean, M.-S. Lin, and R. H. F. Manske. Can. J. Chem. **44**, 2449 (1966).
4. D. B. MacLean, R. A. Bell, J. K. Saunders, C.-Y. Chen, and R. H. F. Manske. Can. J. Chem. **47**, 3593 (1969).
5. R. H. F. Manske, R. Rodrigo, D. B. MacLean, D. E. F. Gracey, and J. K. Saunders. Can. J. Chem. **47**, 3585 (1969).
6. R. H. F. Manske, R. G. A. Rodrigo, D. B. MacLean, D. E. F. Gracey, and J. K. Saunders. Can. J. Chem. **47**, 3589 (1969).
7. M. Castillo, J. K. Saunders, D. B. MacLean, N. M. Mollov, and G. I. Yakimov. Can. J. Chem. **49**, 139 (1971).
8. T. Kametani, S. Takano, and S. Hibino. Yakugaku Zasshi, **88**, 1123 (1968).
9. R. H. F. Manske and Q. A. Ahmed. Can. J. Chem. **48**, 1280 (1970).
10. L. R. Snyder. Principles of adsorption chromatography. Marcel Dekker, Inc., New York, N.Y., 1968. p. 317.
11. N. M. Mollov, G. I. Yakimov, and P. O. Panov. C. R. Acad. Bulg. Sci. **20**, 557 (1967).
12. D. D. Tunnicliff and P. A. Wadsworth. Anal. Chem. **40**, 1826 (1968).
13. F. A. Ramirez and A. Burger. J. Am. Chem. Soc. **72**, 2781 (1950).

Can. J. Chem. Downloaded from www.nrcresearchpress.com by 210.87.254.105 on 09/05/12
For personal use only.

Can. J. Chem. Downloaded from www.nrcresearchpress.com by 210.87.254.105 on 09/05/12
For personal use only.

NOTES

An Apparent Stereochemical Effect in MnO_2 Oxidation of Some Allylic Alcohols

BERT FRASER-REID, BERNARD J. CARTHY, N. L. HOLDER, AND MARK YUNKER[1]
Department of Chemistry, University of Waterloo, Waterloo, Ontario

Received May 19, 1970[2]

3,4-Di-*O*-acetyl-D-xylal undergoes acid-catalyzed reaction with ethanol to give the anomeric mixture of ethyl 2,3-dideoxy-4-*O*-acetyl-D-*glycero*-pent-2-enopyranosides which can be separated after deacetylation. The α-D anomer **1** is readily oxidized by manganese dioxide to the α,β-unsaturated ketone but the β-D anomer **2** is inert. Thorough investigation of the 100 and 220 MHz n.m.r. spectra of **1** and **2**, their acetates, and dinitrobenzoates indicates that each exists conformationally pure in the half-chair form having the benefit of the anomeric effect. Hence in the oxidizable anomer **1** the C-4 allylic hydroxyl group is pseudo-equatorial; in the unoxidizable one it is pseudoaxial. Hydrogen bonding does not appear to be the reason for failure of **2** to oxidize.

The ethoxy groups of **1** and **2** are found to be ABX_3 system with unusually large separation for the AB protons.

Le di-*O*-acétyl-3,4-D-xylal soumis à une réaction acido-catalysée dans l'éthanol, donne un mélange anomérique de didéoxy-2,3-*O*-acétyl-4-D *glycéro*-pentene-2-pyranosides d'éthyle. L'isomère-α-D- **1** est rapidement oxydé par le bioxyde de manganèse en cétone α,β insaturée, par contre l'isomère β **2** est inerte. L'examen des composés **1** et **2** ainsi que de leurs dérivés acétates et dinitrobenzoates, en r.m.n. 100 et 220 MHz a montré que chacun des isomères est exclusivement sous forme d'une demie chaise grâce à "l'effet anomérique". Ainsi, l'isomère oxydé **1** possède une hydroxyle allylique en C-4 pseudo équatorial. Tandis que dans **2**, le même groupe est pseudo axial.

Les groupes éthoxy dans **1** et **2** forment des systèmes ABX_3 avec une séparation inhabituellement grande des protons AB.

Canadian Journal of Chemistry, **49**, 3038 (1971)

In a recent publication from this laboratory (1) it was reported that when ethanol reacted with 3,4-di-*O*-acetyl-D-xylal under boron trifluoride catalysis (2) a mixture was produced which, after deacetylation, could be separated chromatographically into what appeared to be α- and β-anomers of ethyl 2,3-dideoxy-D-*glycero*-pent-2-enopyranoside. The faster running component **1***a* behaved normally on manganese dioxide oxidation, being converted to an α,β-unsaturated ketone within 8 h. The slower running substance **2***a*, however, gave no evidence for ketone formation after 14 days of exposure to manganese dioxide.

It seemed strange that **1***a* and **2***a* would display such a difference in oxidizability if the only difference between both compounds was the orientation of the ethoxy group at the remote anomeric center. Both compounds characterized as their dinitrobenzoate esters **1***b* and **2***b* respectively gave satisfactory microanalyses (3). As expected for an anomeric pair, both **1***a* and **2***a* lost the aglycon readily (4) to give the same strong ion, **3**, corresponding to M^+-OCH_2CH_3 at

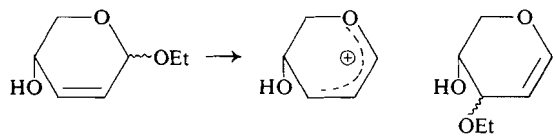

1*a* or **2***a* **3** **4**

m/e 99. Structure **4** which could also lead to ion **3** is excluded since **1** and **2** from their n.m.r. and i.r. spectra are not vinyl ethers.

The specific rotations for **1***a* and **2***a* were +22.2 and +44.3° respectively, but it was considered unwise to use these values for assigning configuration according to the original

[1]Undergraduate research participant, summer 1970. Department of Chemistry, University of Waterloo, Waterloo, Ontario.

[2]Revision received June 10, 1971.

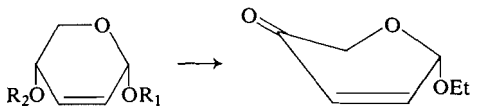

1 5

a R_1 = Et; R_2 = H
b R_1 = Et; R_2 = *o*-dinitrobenzoyl
c R_1 = Et; R_2 = Ac
12 R_1 = Me; R_2 = H

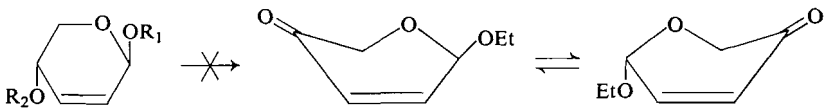

2*a* R_1 = Et ; R_2 = H
b R_1 = Et ; R_2 = *o*-dinitrobenzoyl
c R_1 = Et ; R_2 = Ac
13 R_1 = Me; R_2 = H

6

basis (5), since it is now clear that specific rotation and conformation are inextricably related (6).[3] Furthermore, no direct correlation could be established between the ketone and its alcohol progenitor since the ketones (**5** and **6**) obtainable from the anomers, form a DL pair and are therefore indistinguishable by n.m.r. spectroscopy.

The two substances were therefore subjected to detailed n.m.r. examination in the hope of finding an explanation for the difference in their oxidizability. The spectrum of the slower-running substance **2***a* will be discussed first since it is simpler.

Compound 2

The signal for H-1 in the 100 MHz spectrum of **2***a* (Fig. 1*b*) was a doublet (J_{12} = 3.0 Hz) completely devoid of any long-range coupling; *i.e.* J_{13} = 0. Recent studies on vinyl–allylic couplings indicate that a combination of three- and four-bond parameters such as this requires pseudoequatorial orientation for the allylic proton H-1 (7–9). These same criteria can also be applied at the other "end" of the molecule to H-4. Although the signal for H-4 itself is obscured, the three-bond coupling, J_{34}, can readily be deduced from the signal for H-3. Thus J_{34} = 4.0 Hz, and since the quartet for H-2 possesses no additional fine structure (Fig. 1*b*), $J_{24} \simeq$ 0 Hz. Hence the implication is that H-4 (like H-1) is pseudoequatorial, and compound **2** must either have the β-D-arrangement **7** or the α-D-arrangement **8**. Proof that these alternatives were correct, was supplied by the quartet at τ 5.88 whose geminal coupling of 13.0 Hz assigned it to one of the C-5 protons (shown below to be the axial, H′-5) the coupling of 3.0 Hz indicated gauche relationship to H-4.

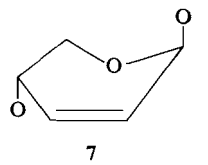

7

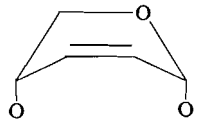

8

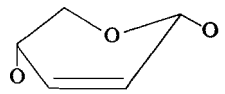

9

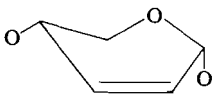

10

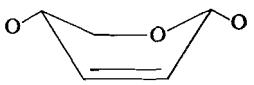

11

In order to confirm this reasoning, the dinitrobenzoate **2***b* was examined since H-4 had been made observable by the esterification (Fig. 2).

[3]Indeed, as will be seen, the more dextrorotatory substance is the β-D anomer, **2***a*, in contravention of the isorotation rules (5).

Can. J. Chem. Downloaded from www.nrcresearchpress.com by 210.87.254.105 on 09/05/12
For personal use only.

Can. J. Chem. Downloaded from www.nrcresearchpress.com by 210.87.254.105 on 09/05/12
For personal use only.

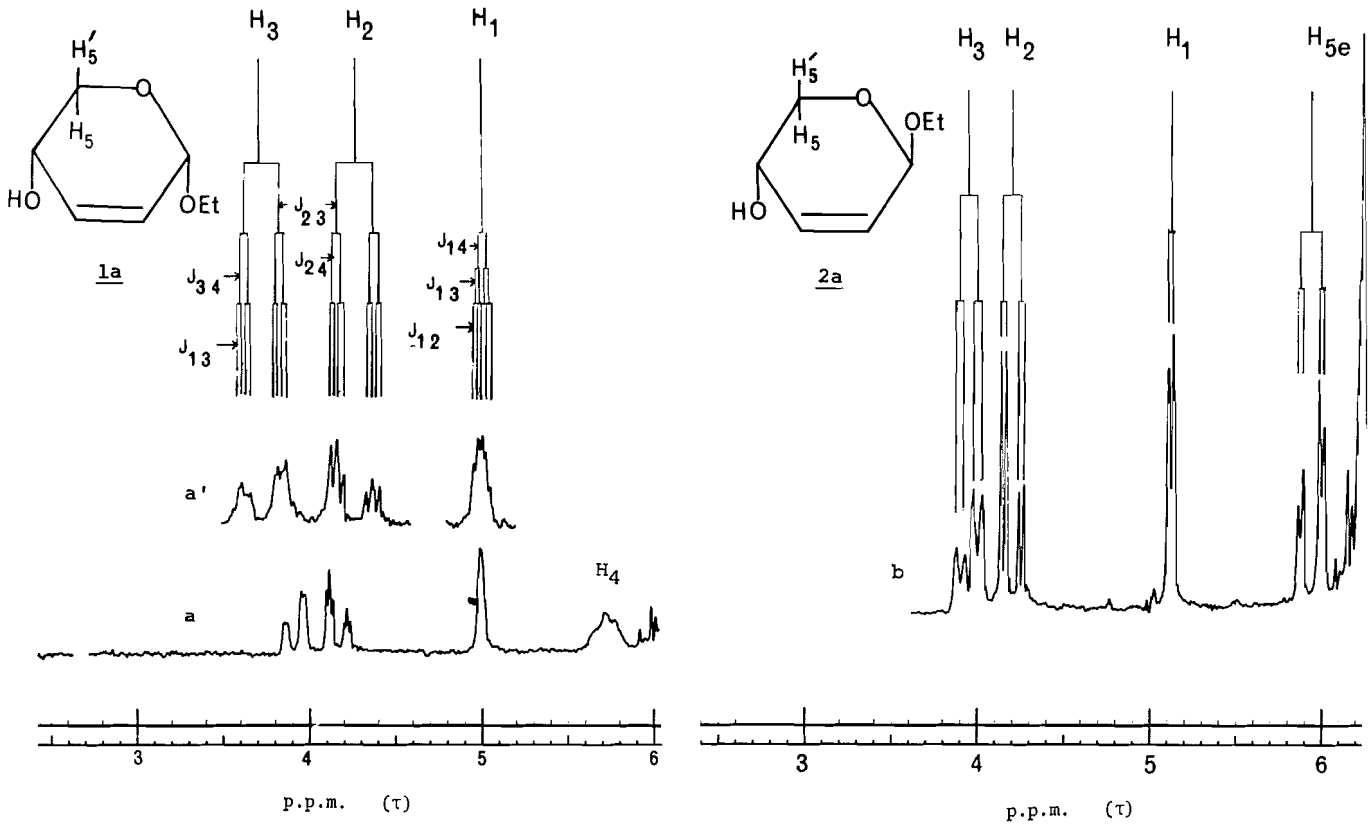

FIG. 1. The 100 MHz n.m.r. spectra of **1***a* (*a*) and **2***a* (*b*) in $CDCl_3$ (TMS). Sweep width in (*a*) and (*b*) is 1000 Hz; in (*a'*), 500 Hz.

Can. J. Chem. Downloaded from www.nrcresearchpress.com by 210.87.254.105 on 09/05/12
For personal use only.

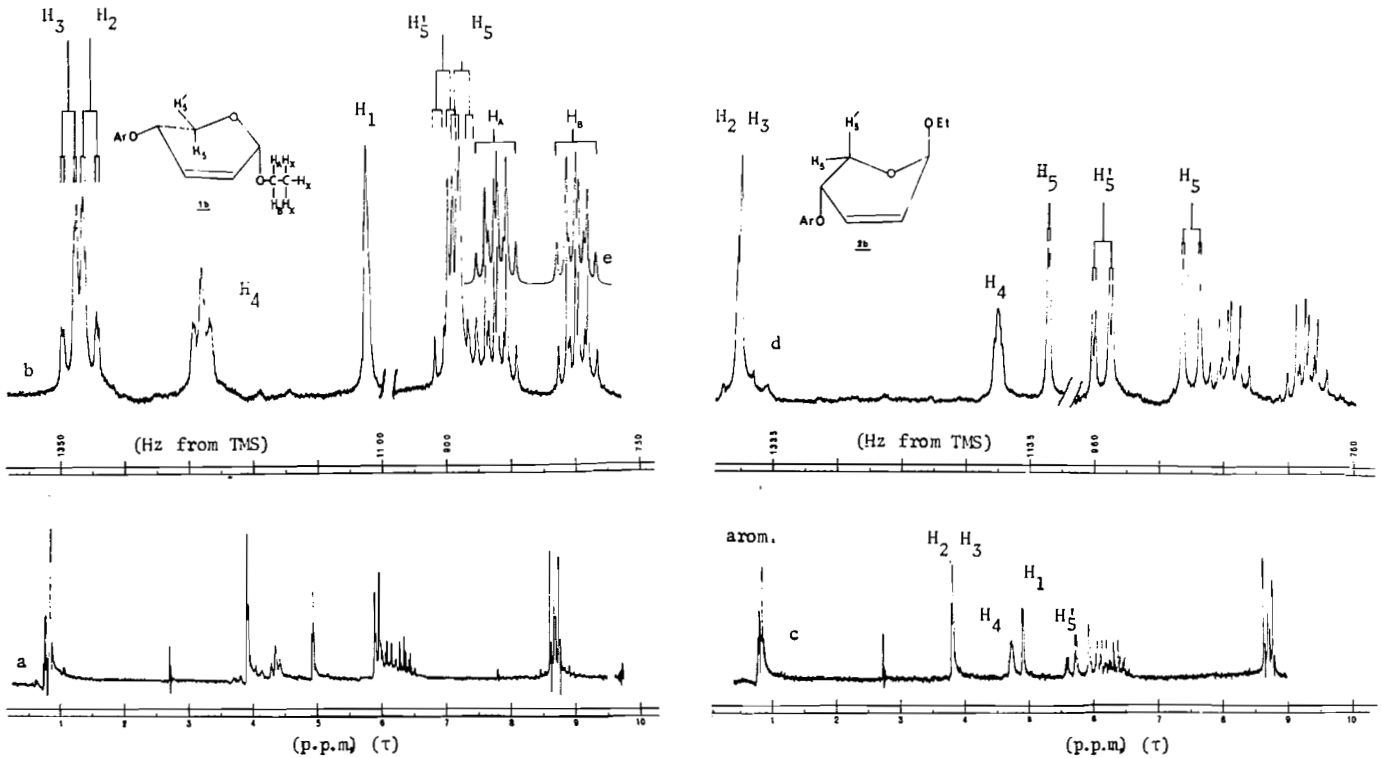

FIG. 2. (*a*) The 100 MHz and (*b*) 220 MHz n.m.r. spectra of **1***a* in $CDCl_3$ (TMS); (*c*) 100 MHz and (*d*) 220 MHz n.m.r. spectra of **2***b* in $CDCl_3$ (TMS); (*e*) computer simulated spectrum of the AB portion of an ABX_3 system. The 100 MHz spectra are at 1000 Hz sweep width, and the 220 MHz spectra are at 500 Hz sweep width. (Ar = 3 5-dinitrobenzoyl.)

TABLE 1. The n.m.r. parameters for ethyl α- and β-D-*glycero*-pent-2-enopyranosides in $CDCl_3$

	Chemical shifts from TMS (τ)						Coupling constants* (Hz)								
Compound	H-1	H-2	H-3	H-4	H′-5	H-5	J_{12}	J_{13}	J_{14}	J_{23}	J_{24}	J_{34}	J_{45}	$J_{45'}$	$J_{55'}$
1*a*†§	4.99	4.26	3.70	5.71	n.d.**	n.d.	2.5	1.1	1.5	10.0	1.3	2.5	n.d.	n.d.	n.d.
1*b*†¶	4.95	3.90–3.97		4.36	5.46	5.52	2.0	1.4	2.0	10.0	n.d.	1.6	7.5	6.0	11.5
1*c*†	5.05	Unresolved 4.10–4.15		4.68	Unresolved 6.18		~1.0	n.d.	n.d.	~0	n.d.	n.d.	7.0	7.0	0
2*a*‡§	5.13	4.20	3.95	n.d.	5.88	n.d.	3.0	0	0	10.0	0	4.0	n.d.	3.0	13.0
2*b*‡¶	4.99	Unresolved 3.73–3.83		4.73	5.67	6.03	1.5	0	0	n.d.	0	n.d.	1.7	2.5	13.5
2*c*‡‖	4.98	Unresolved 3.90–3.97		4.98	5.46	5.52	1.5	n.d.	0	0	n.d.	n.d.	~1.0	2.5	13.0

*|J| ± 0.2 read directly from spacings in the spectra interpreted on a first order basis.
†The α-D-isomers **1** or its esters in conformation **10**.
‡The β-D-isomers **2** or its esters in conformation **7**.
§100 MHz.
‖60 MHz.
¶220 MHz.
**n.d. Not determinable from spectrum.

It was necessary to ensure that esterification had affected only the chemical shift and not the orientation of H-4 or any other proton. One very dramatic effect of esterification was in the decreased chemical shift for the olefinic protons which now gave overlapping signals even at 220 MHz (Fig. 2*d*). Because of this, H-3, -2, and -1 which comprised an ABX system in **2***a* are transformed into an AA′X system in **2***b*. The spacings displayed by H-1 in the ester, J', are therefore expected to be the average of J_{12} and J_{13} (11). Using J_{12} and J_{13} (3.0 and 0 Hz respectively) obtained from the parent alcohol **2***a*, the calculated value for J' was found to be 1.5 Hz in agreement with the observed value, (recorded in Table 1 as J_{12}). However the doublet (for H-1) remained "pure" suggesting that esterification had not altered the orientation around C-1; *i.e.* H-1 was still pseudoequatorial in **2***b*. Nor had the arrangement around H-4 been altered since the low field quartet for the equatorial H′-5 showed no dramatic changes in either its chemical shift or its spacings as compared with the alcohol, **2***a* (see Table 1). The other C-5 proton (H-5) not readily discernable in **2***a* (Fig. 1*b*) but now obvious at τ 6.03 in the 220 MHz spectrum of **2***b* (Fig. 2*d*) had a vicinal coupling of 1.7 Hz. The two vicinal couplings indicate gauche relationships between *both* C-5 protons and H-4.

The information from H-1 and -4 taken in conjunction therefore confirms the above speculation that compound **2** exists in one of the conformations **7** and **8**. Arrangement **7** is clearly preferred on stereochemical grounds and accordingly, the values for J_{45} and J_{45}' observed in **2***b* (1.7 and 2.5 Hz respectively), are very close to those observed by Lemieux and Stevens (1.6 and 2.3) for 2-deoxy-β-D-ribopyranose triacetate, of known *1C* conformation (10). This observation implies incidentally that **2** must exist predominantly in the conformation **7**. Thus on this basis the axial C-5 proton deshielded by the C-1 oxygen is ascribed the low field quartet (Table 1).

Compound 1

Having assigned **2** as the β-D anomer in (conformation **7**) compound **1** must be the α-D alcohol, and it remained only to assign a suitable conformation from among the four possibilities **8**–**11**. The n.m.r. spectrum for **1***a* (Fig. 1*a*) was more complex than that for **2***a*, particularly for the H-1 signal. However by double irradiation experiments the couplings J_{12} and J_{24} were determined to be 2.5, and 1.3 Hz respectively. In view of the criteria outlined above (7–9) the large value for J_{12} indicates pseudoequatorial orientation for H-1, thereby eliminating **9** and **11**. The large values for the three- and four-bond vinyl–allylic couplings (J_{34} = 2.5 and J_{24} = 1.3 Hz) indicates pseudoaxial orientation for H-4, which therefore now eliminates **8** leaving only **10**.

The dinitrobenzoate ester **1***b* was also examined, and as with the β-D anomer **2***b*, esterifi-

Can. J. Chem. Downloaded from www.nrcresearchpress.com by 210.87.254.105 on 09/05/12
For personal use only.

Can. J. Chem. Downloaded from www.nrcresearchpress.com by 210.87.254.105 on 09/05/12
For personal use only.

cation had reduced the chemical shift for the olefinic protons making an AA'X system for H-2, -3, and -4 in the 100 MHz spectrum (Fig. 2*a*). As an added complication here, the C-5 protons were also unresolved (*vide infra*) thereby making H-4 the X-proton of *another* AA'X system. H-2, -3, -4, -5, and H'-5 of **1***b* therefore constituted an AA'MXX' system and the signal at τ 4.36 for H-4 (the M-proton) was understandably complex. To further compound the matter, double irradiation revealed a long-range coupling constant, J_{14}, of 2.0 Hz. In spite of these complications the major spacings (J') in H-4 should be derived from the largest couplings contributed to it, which are J_{45} and $J_{45'}$. Using typical values[4] of 8.9 and 4.7 Hz for these couplings, H-4 should appear as a broadened triplet with a calculated value for J' being the average of these, 6.8 Hz. The measured value in the 100 MHz spectrum (Fig. 1*a*) is 7.0 Hz.

The foregoing information would appear to imply that **1** must exist predominantly in conformation **10**. However it was impossible to obtain affirmation of this by studying the signals for the C-5 protons of the dinitrobenzoate **1***b* or acetate **1***c* since they were unresolved at 60 and 100 MHz. They therefore appeared as a doublet with J = 7.0 Hz (*e.g.* Fig. 2*a*). The 220 MHz spectrometer resolved these protons into two distinct AB quartets (Fig. 2*b*). The spacings observed (7.5 and 6.0 Hz) are in the acceptable range for *trans*-diaxial and equatorial–axial parameters for the system represented by **10** (12).

The presence of a homoallylic coupling (J_{14}) in the esters **1***b* and *c* but not in **2***b* and *c* is now readily explained since couplings of this type, which are thought to be transmitted through the intervening π-bond, follow the order 1,4-diaxial > 1,4-axial–equatorial > 1,4-equatorial-equatorial (13).

While this manuscript was being prepared a pertinent publication by Lemieux *et al.* appeared in which conformations of the methyl 2,3-dideoxy α-L and β-L-*glycero*-pent-2-enopyranosides were discussed (14). We prepared the methyl α-D (**12**) and β-D (**13**) enantiomers from D-xylal (or D-arabinal) diacetate and methanol as previously described for ethanol (1, 2). The n.m.r. spectra of these substances in DMSO-d_6 were identical in all respects with those kindly supplied by Professor Lemieux (14). Furthermore the spectra agreed in the expected manner with those of the ethyl analogues. Here again, difference in oxidizability of the anomers was observed *i.e.* **12** was smoothly oxidized while **13** was not.

These olefins (**1**, **2**, **12**, **13**) are expected to prefer the half-chair conformations (15) and since there are no serious non-bonded interactions to affect the outcome, the anomeric effect should have over-riding control and it is therefore not surprising that the half-chair forms chosen by these four substances, are those having the benefit of the anomeric effect (16, 17*a*). The result is that these substances appear to exist in much greater conformational purity than do most pentopyranose derivatives (10, 17).

The foregoing indicates that the hydroxyl groups in **1**, **2**, **12**, **13** are in different orientations, equatorial in the oxidizable substances (**1**, **12**) and axial in the unoxidizable, (**2**, **13**). However, this difference is not sufficient to account for the anomaly since steroidal allylic alcohols of either orientation are known to be oxidized (18). Another possible explanation is that hydrogen bonding of the hydroxyl group to the ring oxygen, possible only in the β-D anomers **2** and **13**, might prevent these alcohols from being oxidized. However, the allylic hydroxyl groups in epimers **14** and **15** are both oxidized to ketone **16** (19), although **14** should be as capable of hydrogen bonding to the ring oxygen as **2** or **13**.[5] In any event there is evidently a question as to the possible effects of stereochemistry on the oxidation of allylic alcohols. Experiments designed to clarify this issue are currently underway.

ABX_3 Spectra for some Ethoxy Groups

Magnetic non-equivalence for diastereotopic methylene protons of an ethoxy residue have been reported in several instances (20–22). Therefore the ABX 220 MHz spectra for the ethoxy aglycon of these substances (Fig. 2) would go unmentioned were it not for the unusually large magnitude of $|\nu_A - \nu_B|$. The value observed here, 0.28 p.p.m, is twice as large as that reported for ethoxy attached to carbon

[4]These values are the average of those reported by Lemieux and Stevens (10) in their Table II.

[5]A referee has suggested the possibility of a complex between the *cis* groupings of the α-D isomers (**1** and **12**) and manganese dioxide.

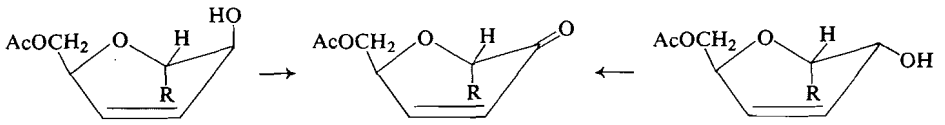

14
R = OEt

16

15

(21) although still much smaller than that for ethoxy attached to a hetero-atom (22). Thus in the 60 MHz spectrum, the ethoxy methylene protons appeared as a jumble of lines which could be reduced to two singlets at τ 6.09 and 6.37 by double irradiation of the τ 8.50 triplet.

The 16-line simulated spectrum for the AB portion (Fig. 2*e*) is shown along with the observed spectrum (Fig. 2*b*).

The phenomenon also occurs in the hexopyranoside analogues of **1** and **2**, and the large value $|\nu_A - \nu_B|$ is not associated with the double bond in these molecules, since their saturated derivatives also show the same effect.

The readiness with which these substances can be prepared allow for much easier access to these five-spin systems than the substituted propenes used elsewhere (23).

Experimental

The α- and β-anomers of ethyl 2,3-dideoxy-D-*glycero*-pent-2-enopyranoside (**1***a* and **2***a* respectively) were prepared from D-xylal diacetate as previously described (3) and separated by silica column chromatography using petroleum ether (35–60) – ethyl acetate (1:1) mixture as eluent. The acetates (**1***c*, **2***c*) and 3,5-dinitrobenzoates (**1***b*, **2***b*) were prepared by standard acylation methods.

The methyl analogues of **1** and **2** (**12** and **13** respectively) were also prepared in a similar way (3) from methanol and D-xylal diacetate or D-arabinal diacetate, the latter being obtained commercially from Raylo Chemicals Ltd., Edmonton, Alberta.

The alcohols **1**, **2**, **12**, and **13** were oxidized with manganese dioxide as previously described (1).

The n.m.r. spectra were determined on a Varian T60, a Varian HA 100 and/or a Varian 220 MHz spectrometer.

The simulated spectra were prepared using a modified version of LACOON III run on the IBM 360-75 belonging to the Faculty of Mathematics, University of Waterloo. The following data for the computations were derived from the 220 MHz spectra: $J_{AX} = J_{BX} = 7.0$, $J_{AB} = 9.5$ Hz; $\delta_A = 797.1$, $\delta_B = 860.5$, $\delta_X = 300.0$ Hz from TMS.

Financial support from the National Research Council of Canada is gratefully acknowledged. We express our gratitude to the staff of the Canadian 220 MHz NMR Centre for their help and to Professor L. W. Reeves for making available to us (1) his 100 MHz n.m.r. spectrometer and to Mr. R. Shaddick for operating it, and (2) a modified LACOON III program and to Dr. K. Shaw for assistance with the computation. We are grateful to Professor R. U. Lemieux and Dr. T. L. Nagabhushan for providing us with n.m.r. spectra of the α- and β-anomers of methyl 2,3-dideoxy-L-*glycero*-pent-2-enopyranoside.

1. B. Fraser-Reid, A. McLean, and E. W. Usherwood. J. Am. Chem. Soc. **91**, 5392 (1969).
2. R. J. Ferrier and N. Prasad. J. Chem. Soc. C, 570, 575 (1970).
3. B. Fraser-Reid, A. McLean, E. W. Usherwood, and M. Yunker. Can. J. Chem. **48**, 2877 (1970).
4. D. C. Jongh, T. Radford, J. D. Hribar, S. Hanessian, M. Bieber, G. Dawson, and C. C. Sweeley. J. Am. Chem. Soc. **91**, 1728 (1969); N. K. Kotchetkov and O. S. Chishov. Advan. Carbohydr. Chem. **21**, 39 (1966).
5. C. S. Hudson. Advan. Carbohydr. Chem. **3**, 1 (1948).
6. R. U. Lemieux and M. Hoffer. Can. J. Chem. **39**, 110 (1961); R. U. Lemieux and A. A. Pavia. Can. J. Chem. **46**, 1453 (1968).
7. (*a*) E. W. Garbisch. J. Am. Chem. Soc. **86**, 5562 (1962); (*b*) M. Sharma and R. K. Brown. Can. J. Chem. **44**, 2825 (1966).
8. R. U. Lemieux, E. Fraga, and K. A. Watanabe. Can. J. Chem. **46**, 61 (1968).
9. R. J. Ferrier and N. Prasad. J. Chem. Soc. C, 581 (1969).
10. R. U. Lemieux and J. D. Stevens. Can. J. Chem. **43**, 2059 (1965).
11. R. J. Abraham and H. J. Bernstein. Can. J. Chem. **39**, 216 (1961).
12. L. D. Hall and J. F. Manville. *In* Deoxy sugars. *Edited by* S. Hanessian. Advances in Chemistry Series, American Chemical Society, 1968, p. 236.
13. L. M. Jackman and S. Sternhell. Applications of n.m.r. spectroscopy in organic chemistry. Pergamon Press, New York, N.Y., 1969. p. 325.
14. R. U. Lemieux, K. A. Watanabe, and A. A. Pavia. Can. J. Chem. **47**, 4413 (1969).
15. E. L. Eliel. Stereochemistry of carbon compounds. McGraw Hill Book Company Inc., New York, N.Y., 1962. p. 239.
16. R. U. Lemieux. *In* Molecular rearrangements. Vol. 2, *Edited by* P. de Mayo. John Wiley and Sons, Inc., New York, N.Y., 1963.
17. (*a*) P. L. Durette and D. Horton. Chem. Commun. 1608 (1970); (*b*) P. L. Durette, D. Horton, and N. S. Bhacca. Carbohydr. Res. **10**, 565 (1969).

Can. J. Chem. Downloaded from www.nrcresearchpress.com by 210.87.254.105 on 09/05/12
For personal use only.

18. F. SONDHEIMER, C. AMENDOLLA, and G. ROSENKRANZ. J. Am. Chem. Soc. **75**, 5930 (1953).
19. N. L. HOLDER. Unpublished results.
20. E. O. BISHOP. Ann. Reports, **58**, 67 (1961).
21. G. M. WHITESIDES, D. HOLTZ, and J. D. ROBERTS. J. Am. Chem. Soc. **86**, 2628 (1964).
22. J. P. PRITCHARD and F. G. A. STONE. J. Am. Chem. Soc. **83**, 4138 (1961). P. R. SHAFER, D. R. DAVIS, M. VOGEL, K. MAGARAJAN, and J. D. ROBERTS. Proc. Nat. Acad. Sci. U.S.A. **47**, 49 (1961). J. S. WAUGH and F. A. COTTON. J. Phys. Chem. 65, 562 (1961).
23. R. W. FESSENDER and J. S. WAUGH. J. Chem. Phys. **30**, 944 (1959); J. D. SWALEN and C. A. REILLY. J. Chem. Phys. **34**, 2122 (1961).

Reaction of Iodine Azide with Cyclopentenone and Cyclohexenone

JOHN M. MCINTOSH
Department of Chemistry, University of Windsor, Windsor, Ontario

Received April 21, 1971

The addition of iodine azide to 2-cyclopentenone led to the formation of 2-iodo-2-cyclopentenone. A similar reaction with 2-cyclohexenone afforded the expected addition products in addition to 2-iodo-2-cyclohexenone.

L'addition d'azoture d'iode sur la cyclopentène-2 one conduit à l'iodo-2 cyclopentène-2 one. Une réaction similaire avec la cyclohexène-2 one conduit au produit d'addition attendu et à l'iodo-2 cyclohexène-2 one.

Canadian Journal of Chemistry, **49**, 3045 (1971)

In connection with other work, a sample of 3-aminocyclopentanone was required. From among many possible syntheses, the addition of iodine azide (1) to 2-cyclopentenone was selected. While this reaction was not expected to be regiospecific (2), separation of the reduction products 2-amino- and 3-aminocyclopentanone was not envisaged to be a problem of major proportions.

When 2-cyclopentenone (**1**) was treated with a solution of iodine azide in acetonitrile containing excess sodium azide according to the published procedure (1), the n.m.r. spectrum of the crude reaction mixture showed none of the expected absorptions for the addition products **3** (Scheme 1), but showed the product to be of the 2-substituted-2-cyclopentenone type. The i.r. spectrum showed strong azide and conjugated carbonyl absorptions (2120 and 1712 cm^{-1} respectively). Chromatography afforded 2-iodo-2-cyclopentenone (**4**) and a compound **A** whose stability precluded identification. When a solution of **4** was treated under the reaction conditions with iodine azide, t.l.c. of the product indicated a partial conversion into **A** had occurred. When the reaction was carried out in an n.m.r. tube, a very weak and broad absorption appeared at *ca.* 5 p.p.m. which remained constant throughout the reaction. Whether this absorption is due to the addition products **3** which are subsequently converted into **4**, or whether it is due to some small impurity is unclear. However, if the former is the case, the concentration of **3** cannot be more than 2% of the mixture at any time.

When the same reaction was applied to 2-cyclohexenone (**5**) (Scheme 2), the crude reaction mixture showed n.m.r. absorptions characteristic (2) of both of the two expected addition products **7***a* and *b* as well as of a 2-substituted-2-cyclohexenone in the ratio of 7:7:9 respectively. Chromatography afforded a mixture of **7***a* and *b* in the ratio of 1:1 (n.m.r.), and pure 2-iodo-2-cyclohexenone (**8***a*). Treatment of the crude mixture with triethyl amine in ether resulted in the disappearance of the n.m.r. signals between δ 4 and 7. The i.r. spectrum showed conjugated carbonyl and azide absorptions indicating the presence of **8***b*, but chromatography afforded only **8***a* in slightly increased yield.

Comparison of the base-catalyzed rate of exchange of cyclopentanone and cyclohexanone (7:1) (4) provides a rationale for the relative amounts of **3** and **7** in the two reaction mixtures. If these relative acidities also apply to **2** and **6** or

Can. J. Chem. Downloaded from www.nrcresearchpress.com by 210.87.254.105 on 09/05/12
For personal use only.

18. F. SONDHEIMER, C. AMENDOLLA, and G. ROSENKRANZ. J. Am. Chem. Soc. **75**, 5930 (1953).
19. N. L. HOLDER. Unpublished results.
20. E. O. BISHOP. Ann. Reports, **58**, 67 (1961).
21. G. M. WHITESIDES, D. HOLTZ, and J. D. ROBERTS. J. Am. Chem. Soc. **86**, 2628 (1964).
22. J. P. PRITCHARD and F. G. A. STONE. J. Am. Chem. Soc. **83**, 4138 (1961). P. R. SHAFER, D. R. DAVIS, M. VOGEL, K. MAGARAJAN, and J. D. ROBERTS. Proc. Nat. Acad. Sci. U.S.A. **47**, 49 (1961). J. S. WAUGH and F. A. COTTON. J. Phys. Chem. 65, 562 (1961).
23. R. W. FESSENDER and J. S. WAUGH. J. Chem. Phys. **30**, 944 (1959); J. D. SWALEN and C. A. REILLY. J. Chem. Phys. **34**, 2122 (1961).

Reaction of Iodine Azide with Cyclopentenone and Cyclohexenone

JOHN M. MCINTOSH
Department of Chemistry, University of Windsor, Windsor, Ontario

Received April 21, 1971

The addition of iodine azide to 2-cyclopentenone led to the formation of 2-iodo-2-cyclopentenone. A similar reaction with 2-cyclohexenone afforded the expected addition products in addition to 2-iodo-2-cyclohexenone.

L'addition d'azoture d'iode sur la cyclopentène-2 one conduit à l'iodo-2 cyclopentène-2 one. Une réaction similaire avec la cyclohexène-2 one conduit au produit d'addition attendu et à l'iodo-2 cyclohexène-2 one.

Canadian Journal of Chemistry, **49**, 3045 (1971)

In connection with other work, a sample of 3-aminocyclopentanone was required. From among many possible syntheses, the addition of iodine azide (1) to 2-cyclopentenone was selected. While this reaction was not expected to be regiospecific (2), separation of the reduction products 2-amino- and 3-aminocyclopentanone was not envisaged to be a problem of major proportions.

When 2-cyclopentenone (**1**) was treated with a solution of iodine azide in acetonitrile containing excess sodium azide according to the published procedure (1), the n.m.r. spectrum of the crude reaction mixture showed none of the expected absorptions for the addition products **3** (Scheme 1), but showed the product to be of the 2-substituted-2-cyclopentenone type. The i.r. spectrum showed strong azide and conjugated carbonyl absorptions (2120 and 1712 cm^{-1} respectively). Chromatography afforded 2-iodo-2-cyclopentenone (**4**) and a compound **A** whose stability precluded identification. When a solution of **4** was treated under the reaction conditions with iodine azide, t.l.c. of the product indicated a partial conversion into **A** had occurred. When the reaction was carried out in an n.m.r. tube, a very weak and broad absorption appeared at *ca.* 5 p.p.m. which remained constant throughout the reaction. Whether this absorption is due to the addition products **3** which are subsequently converted into **4**, or whether it is due to some small impurity is unclear. However, if the former is the case, the concentration of **3** cannot be more than 2% of the mixture at any time.

When the same reaction was applied to 2-cyclohexenone (**5**) (Scheme 2), the crude reaction mixture showed n.m.r. absorptions characteristic (2) of both of the two expected addition products **7***a* and *b* as well as of a 2-substituted-2-cyclohexenone in the ratio of 7:7:9 respectively. Chromatography afforded a mixture of **7***a* and *b* in the ratio of 1:1 (n.m.r.), and pure 2-iodo-2-cyclohexenone (**8***a*). Treatment of the crude mixture with triethyl amine in ether resulted in the disappearance of the n.m.r. signals between δ 4 and 7. The i.r. spectrum showed conjugated carbonyl and azide absorptions indicating the presence of **8***b*, but chromatography afforded only **8***a* in slightly increased yield.

Comparison of the base-catalyzed rate of exchange of cyclopentanone and cyclohexanone (7:1) (4) provides a rationale for the relative amounts of **3** and **7** in the two reaction mixtures. If these relative acidities also apply to **2** and **6** or

Can. J. Chem. Downloaded from www.nrcresearchpress.com by 210.87.254.42 on 09/05/12
For personal use only.

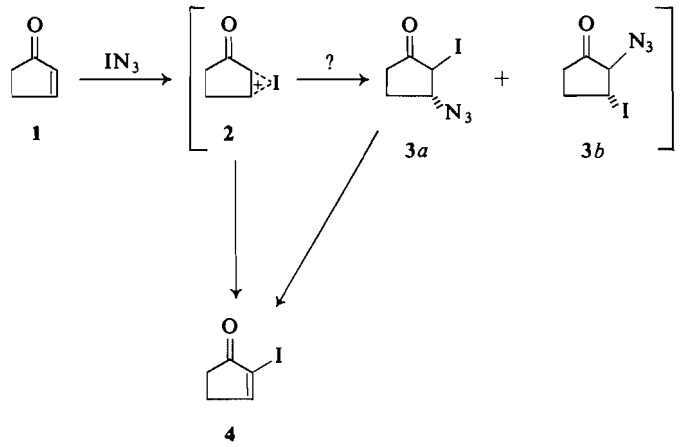

SCHEME 1

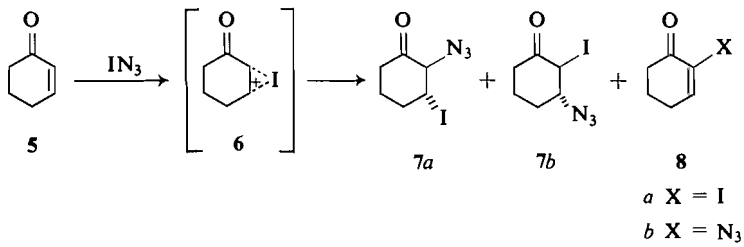

SCHEME 2

to **3** and **7**, it is clear that loss of a proton from **2** or **3** will be more favorable than a similar deprotonation of **6** or **7**.

The formation of 2-iodovinyl ketones from this reaction has not been reported previously. While Hassner *et al.* has reported (2, 3) the preparation of 2-azidovinyl ketones, either from the iodine azide adducts of conjugated ketones with sodium azide or from 2-bromovinyl ketones with sodium azide and hydrazoic acid in DMF, no mention of the presence of 2-iodovinyl ketones has been made. The reaction reported here, while not a general synthetic route, does provide a source of two members of this unusual class of compounds.

Experimental

The i.r. spectra were recorded on a Beckman IR 12 spectrometer in chloroform solution; n.m.r. spectra were obtained on a JEOLCO C6OHL spectrometer in deuteriochloroform and are reported in p.p.m. from an internal standard (TMS 0). Melting points are corrected. Microanalyses were performed by A. B. Gygli, Microanalysis Laboratory, Toronto, Ontario.

2-Iodo-2-cyclopentenone

To a slurry of 12.0 g (0.185 mol) of sodium azide in 45 ml of acetonitrile which had been cooled to −20°, was added 4.5 g (0.027 mol) of iodine monochloride in 10 ml of the same solvent over a period of 30 min. 2-Cyclopentenone (2.0 g, 0.026 mol) was added all at once and the reaction mixture was stirred for 24 h and allowed to rise to ambient temperature. The dark brown mixture was poured into 100 ml of water and the aqueous solution was extracted with three 60 ml portions of ether. The combined ethereal extracts were washed with two 50 ml portions of 10% sodium thiosulfate solution and two 50 ml portions of water and were dried over sodium sulfate. Evaporation gave 3.4 g of a brown oil which showed no n.m.r. absorptions between 4 and 8 p.p.m., but did show a triplet at δ 8.15. The i.r. spectrum showed a very weak shoulder at 1745 cm^{-1} and strong absorptions at 1720 and 2110 cm^{-1}. The t.l.c. (alumina, 50% petroleum ether, 48% benzene, 2% ethanol) showed the presence of two components with R_f values of 0.73 and 0.64.

Chromatography on silica gel using benzene – petroleum ether as eluent gave 1.53 g (30%) of **4**, m.p. 70.5–71.0° from petroleum ether: i.r. 3030, 2925, 1718, 1685 cm^{-1}; n.m.r. δ 8.15 (1H, t, J = 3 Hz), 3.00–2.37 (4H, mult); R_f 0.73.

Anal. Calcd. for C_5H_5IO: C, 28.86; H, 2.24; I, 61.03. Found: C, 28.87; H, 2.46; I, 61.23.

Further elution gave 0.7 g of a very unstable yellow

Can. J. Chem. Downloaded from www.nrcresearchpress.com by 210.87.254.42 on 09/05/12
For personal use only.

oil (A) which exhibited strong azide and conjugated carbonyl absorptions in the i.r. spectrum (2100, 1719, 1590 cm^{-1}) but no signals below δ 3.00 in the n.m.r. spectrum. This material decomposed to a black tar within minutes when solvent was removed. The t.l.c. indicated the presence of only the material with R_f 0.64.

2-Iodo-2-cyclohexenone

The reaction was run in exactly the same manner using the same molar quantities of reactants. Evaporation of the dried solution gave 5.6 g of a dark brown oil; n.m.r. δ 7.90 (t, J = 6 Hz), 4.83 (br), 4.60 (br d), 4.24 (mult), 3.7–1.5 (mult); i.r. 3030, 2960, 2880, 2110, 1715, 1690, 1590, 1575 cm^{-1}.

Assignment of the first three n.m.r. absorptions to **8***a*, 7*b*, and 7*a* (2) respectively gives a product distribution by n.m.r. integration of 9:7:7

Chromatography of the mixture on silica gel using benzene – petroleum ether as eluent gave a mixture of 7*a* and 7*b* in 20% yield

Anal. Calcd. for $C_6H_8N_3IO$: C, 27.17; H, 3.02. Found: C, 27.31; H, 2.93.

Further elution of the column with benzene and benzene–ethanol afforded **8***a* (2.53 g, 44%) as white crystals from petroleum ether, m.p. 46.0–47.0°: i.r. 3030, 2960, 2940, 2890, 2870, 1690, 1593 cm^{-1}; n.m.r. δ 7.90 (1H, t) 2.87–1.82 (6H, mult).

Anal. Calcd. for C_6H_7IO: C, 32.46; H, 3.18; I, 57.16. Found: C, 32.76; H, 3.46; I, 56.76.

Crude adduct (3.0 g) was dissolved in 100 ml ether and 5 ml of triethyl amine was added. The mixture was stirred at room temperature for 18 h, filtered, washed with two 50 ml portions of water, dried, and evaporated to give a dark oil; n.m.r. blank between δ 4.0 and 7.5; i.r. 2110, 1695 cm^{-1}. Purification as previously outlined afforded 1.65 g (55%) of **8***a*. A dark immobile band on the column may have been **8***b* or its decomposition products.

The financial assistance of the National Research Council of Canada and the technical assistance of Mr. D. Hill are gratefully acknowledged.

1. (*a*) A. HASSNER. Accts. Chem. Res. **4**, 9 (1971). (*b*) F. W. FOWLER, A. HASSNER, and L. A. LEVY. J. Am. Chem. Soc. **89**, 2077 (1967).
2. G. L'ABBÉ and A. HASSNER. J. Org. Chem. **36**, 258 (1971).
3. A. HASSNER, G. L'ABBÉ, and M. J. MILLER. J. Am. Chem. Soc. **93**, 981 (1971).
4. H. SCHECHTER, M. J. CULLIS, R. E. DESSEY, Y. OKUZUMI, and A. CHEN. J. Am. Chem. Soc. **84**, 2905 (1962).

Ozonation of Naphthalene with Water as Participating Solvent. Preparation of *o*-Phthalaldehyde

MURRAY G. STURROCK, BETTY J. CRAVY, AND VIRGINIA ALLEN WING
Department of Chemistry, Texas Woman's University, T.W.U. Station, Denton, Texas 76204

Received April 14, 1971

The water in aqueous acetone solutions acts as a participating solvent in the reaction of naphthalene with ozone forming hydroperoxy intermediates which are reduced to *o*-phthalaldehyde by conventional agents. The results are markedly different from those obtained in anhydrous solvents. Yields of product requiring no purification are 63%.

Dans des solutions aqueuses d'acétone, l'eau agit comme solvant de participation dans la réaction de l'ozone avec le naphtalène. Il se forme des hydropéroxy intermédiaires que sont réduits en *o*-phthaladéhyde par les agents conventionnels. Les résultats sont très différents de ceux obtenus dans des solvants anhydres. Les rendements en produit (ne demandant aucune purification) sont de 63%.

Canadian Journal of Chemistry, 49, 3047 (1971)

The profound effect that the presence of water in the solvent can have on the course of the reaction of a polycyclic aromatic hydrocarbon with ozone was first demonstrated some ten years ago (1) when yields of anthraquinone obtained directly from anthracene without the aid of reducing agents were improved from 28% in glacial acetic acid (2) to 73% in aqueous *t*-butanol (1). The anthracene reaction gave no useful isolable intermediate products and the mechanism of the ozonation reaction in aqueous media was studied first with phenanthrene (3) and later with pyrene (4). This is therefore the third in a series of reports devoted to the subject of ozonation in aqueous solvents.

The results of the work with anthracene,

Can. J. Chem. Downloaded from www.nrcresearchpress.com by 210.87.254.42 on 09/05/12
For personal use only.

oil (A) which exhibited strong azide and conjugated carbonyl absorptions in the i.r. spectrum (2100, 1719, 1590 cm^{-1}) but no signals below δ 3.00 in the n.m.r. spectrum. This material decomposed to a black tar within minutes when solvent was removed. The t.l.c. indicated the presence of only the material with R_f 0.64.

2-Iodo-2-cyclohexenone

The reaction was run in exactly the same manner using the same molar quantities of reactants. Evaporation of the dried solution gave 5.6 g of a dark brown oil; n.m.r. δ 7.90 (t, J = 6 Hz), 4.83 (br), 4.60 (br d), 4.24 (mult), 3.7–1.5 (mult); i.r. 3030, 2960, 2880, 2110, 1715, 1690, 1590, 1575 cm^{-1}.

Assignment of the first three n.m.r. absorptions to **8***a*, 7*b*, and 7*a* (2) respectively gives a product distribution by n.m.r. integration of 9:7:7

Chromatography of the mixture on silica gel using benzene – petroleum ether as eluent gave a mixture of 7*a* and 7*b* in 20% yield

Anal. Calcd. for $C_6H_8N_3IO$: C, 27.17; H, 3.02. Found: C, 27.31; H, 2.93.

Further elution of the column with benzene and benzene–ethanol afforded **8***a* (2.53 g, 44%) as white crystals from petroleum ether, m.p. 46.0–47.0°: i.r. 3030, 2960, 2940, 2890, 2870, 1690, 1593 cm^{-1}; n.m.r. δ 7.90 (1H, t) 2.87–1.82 (6H, mult).

Anal. Calcd. for C_6H_7IO: C, 32.46; H, 3.18; I, 57.16. Found: C, 32.76; H, 3.46; I, 56.76.

Crude adduct (3.0 g) was dissolved in 100 ml ether and 5 ml of triethyl amine was added. The mixture was stirred at room temperature for 18 h, filtered, washed with two 50 ml portions of water, dried, and evaporated to give a dark oil; n.m.r. blank between δ 4.0 and 7.5; i.r. 2110, 1695 cm^{-1}. Purification as previously outlined afforded 1.65 g (55%) of **8***a*. A dark immobile band on the column may have been **8***b* or its decomposition products.

The financial assistance of the National Research Council of Canada and the technical assistance of Mr. D. Hill are gratefully acknowledged.

1. (*a*) A. HASSNER. Accts. Chem. Res. **4**, 9 (1971). (*b*) F. W. FOWLER, A. HASSNER, and L. A. LEVY. J. Am. Chem. Soc. **89**, 2077 (1967).
2. G. L'ABBÉ and A. HASSNER. J. Org. Chem. **36**, 258 (1971).
3. A. HASSNER, G. L'ABBÉ, and M. J. MILLER. J. Am. Chem. Soc. **93**, 981 (1971).
4. H. SCHECHTER, M. J. CULLIS, R. E. DESSEY, Y. OKUZUMI, and A. CHEN. J. Am. Chem. Soc. **84**, 2905 (1962).

Ozonation of Naphthalene with Water as Participating Solvent. Preparation of *o*-Phthalaldehyde

MURRAY G. STURROCK, BETTY J. CRAVY, AND VIRGINIA ALLEN WING
Department of Chemistry, Texas Woman's University, T.W.U. Station, Denton, Texas 76204

Received April 14, 1971

The water in aqueous acetone solutions acts as a participating solvent in the reaction of naphthalene with ozone forming hydroperoxy intermediates which are reduced to *o*-phthalaldehyde by conventional agents. The results are markedly different from those obtained in anhydrous solvents. Yields of product requiring no purification are 63%.

Dans des solutions aqueuses d'acétone, l'eau agit comme solvant de participation dans la réaction de l'ozone avec le naphtalène. Il se forme des hydropéroxy intermédiaires que sont réduits en *o*-phthaladéhyde par les agents conventionnels. Les résultats sont très différents de ceux obtenus dans des solvants anhydres. Les rendements en produit (ne demandant aucune purification) sont de 63%.

Canadian Journal of Chemistry, 49, 3047 (1971)

The profound effect that the presence of water in the solvent can have on the course of the reaction of a polycyclic aromatic hydrocarbon with ozone was first demonstrated some ten years ago (1) when yields of anthraquinone obtained directly from anthracene without the aid of reducing agents were improved from 28% in glacial acetic acid (2) to 73% in aqueous *t*-butanol (1). The anthracene reaction gave no useful isolable intermediate products and the mechanism of the ozonation reaction in aqueous media was studied first with phenanthrene (3) and later with pyrene (4). This is therefore the third in a series of reports devoted to the subject of ozonation in aqueous solvents.

The results of the work with anthracene,

Can. J. Chem. Downloaded from www.nrcresearchpress.com by 210.87.254.40 on 09/05/12
For personal use only.

Can. J. Chem. Downloaded from www.nrcresearchpress.com by 210.87.254.40 on 09/05/12
For personal use only.

phenanthrene, and pyrene suggested that the effect of the presence of water during the ozonation of naphthalene would be to promote the formation of *o*-phthalaldehyde. This interesting but expensive dialdehyde has not been prepared heretofore in reasonable yield by the ozonation of naphthalene followed by conventional sodium iodide in acetic acid reduction of the ozonation products.

The reaction of ozone with naphthalene has been investigated by a number of workers (5–9). After some uncertainty (9), Bailey and co-workers concluded (10) that the explosive ozonation product isolated from the inert solvents used in all these studies was indeed the diozonide of naphthalene as originally reported by Harries (5). This group also made an extensive study of the reaction in anhydrous aliphatic alcohols, particularly anhydrous methanol, and isolated intermediate cyclic alkoxyhydroxyperoxides. They found, however, that the intermediates were completely resistant to reduction by sodium iodide in acetic acid (10). Only *o*-phthalaldehydic acid, or derivatives of it depending on the nature of the alcohol used as solvent and the type of work-up procedure, was recovered. Pappas and co-workers (11, 12) confirmed the surprising resistance of the cyclic hydroxymethoxyperoxide intermediate to reduction by sodium iodide. He was successful in obtaining a 40–50% yield of *o*-phthalaldehyde (as the bis[(2,4-dinitrophenyl)-hydrazone] derivative) by treating the cold methanolic ozonation product with dimethyl sulfide (11) and a 57% yield using triphenylphosphine (12).

The work with phenanthrene in aqueous *t*-butanol (3) had shown that water, like the aliphatic alcohols, acts as a participating solvent in the ozonation reaction and that the analogous cyclic dihydroxyperoxide decomposes quantitatively to biphenaldehyde on heating in aqueous solution. On the other hand, the cyclic methoxyhydroxyperoxide from phenanthrene yielded biphenaldehydic acid (13). The dihydroxyperoxide intermediate had not been isolated from the ozonation of phenanthrene in this earlier work (3) but had been prepared from biphenaldehyde and 30% hydrogen peroxide. Later it was prepared by the ozonation of phenanthrene in aqueous acetone (M. G. Sturrock, unpublished results). A series of equilibria including the open chain hydroxyhydroperoxide had been postulated to explain the results (3).

Considered in the light of the difference in the course of the reactions of ozone with phenanthrene and with anthracene in anhydrous and in aqueous solvents, it seemed probable that *o*-phthalaldehyde would result if the ozonation conditions were such that the formation of the intermediate hydroxyhydroperoxide would be favored, or better, that the formation of the cyclic alkoxyhydroxyperoxide would be precluded. Further support for the belief that *o*-phthalaldehyde could be prepared in this way was to be found in the process which had been patented for the removal of thionaphthene from crude coal tar naphthalene by the selective reaction of the thionaphthene using a deficiency of ozone and aqueous *t*-butanol as solvent (14). *o*-Phthalaldehyde had been detected qualitatively in these ozonation products (15).[1]

Accordingly, naphthalene was treated with two molar equivalents of ozone using aqueous acetone solutions as solvents. After conventional reduction with potassium iodide in acetic acid, removal of the acetone by evaporation, reduction of the liberated iodine with sodium thiosulfate solution, extracted with chloroform, and sublimation of the chloroform residue, pure *o*-phthalaldehyde was recovered. Yields of 63% were obtained consistently by this procedure. The principal product recovered when aqueous methanol was used as solvent was methyl-*o*-phthalaldehydate although *o*-phthalaldehyde could be detected qualitatively (15).[1] Yields of *o*-phthalaldehyde from ozonations made in aqueous *t*-butanol were slightly less than those in aqueous acetone, averaging 58% in a series of several experiments.

The conditions outlined in the Experimental evidently represent the optimum for this reaction in acetone–water solutions. Changes made in the ratio of acetone to water, in the quantity of naphthalene charged and, rather surprisingly, in the temperature of the ozonation step, had no significant effect on the yield. The results of typical experiments are given in Table 1.

It was evident at an early point in this work that the critical operation was the extraction of the *o*-phthalaldehyde from the aqueous solution after the reduction and evaporation of the acetone. Substitution of ethyl acetate or ethyl ether for chloroform made little difference in the

[1] *o*-Phthalaldehyde gives an intense blue–black coloration when treated with ammonia followed by acetic acid. The same color is developed when *o*-phthalaldehyde comes into contact with the skin.

TABLE 1. Ozonation of naphthalene in acetone–water mixtures

Naphthalene (g charged)	Ozone (*M* equiv)	Solvent (ml)		Temperature (°C) ozonation	*o*-Phthalaldehyde (% Yield)
		Acetone	Water		
5.0	2.1	105	45	27	61.6
5.0	2.1	105	45	27	63.9
5.0	2.1	105	45	26	60.1
5.0	2.1	75	75	27	57.5
2.5	2.1	62	22	26	61.5
5.0	2.1	105	45	−20	62.0
2.5	2.1	62	22	−20	59.0

yields obtained on sublimation. Steam distillation of the reduced product prior to extraction markedly reduced the efficiency of extraction probably as the result of increased hydration of the *o*-phthalaldehyde. The possibility of multipoint attack by ozone on the naphthalene molecule was discounted because unreacted naphthalene was not recovered when the amount of ozone absorbed was in the 2.1–2.2 *M* equiv range. A reddish gummy substance always remained at the end of the sublimation. This is believed to be a polymer of *o*-phthalaldehyde. A positive "Thiele test" (15) was obtained with it by treatment with ammonium hydroxide followed by acidification with acetic acid but the product could not be decomposed to any identifiable material. *o*-Phthalaldehydic acid formation was not a problem since the purity of the sublimed product remained high (m.p. 54–56°; lit. (16) 55.5–56°) regardless of the yield and of the final temperature used in sublimation. Undoubtedly some product was lost in the atmospheric temperature and pressure evaporation of the acetone after the reduction step. When the acetone was removed with a Rinco evaporator, the distillate gave positive "Thiele" tests. In a single experiment performed in acetone–water followed by a non-reductive work-up procedure, *o*-phthalaldehydic acid (m.p. 96–99°) was recovered in 62.5% yield. The literature (10) reports 88% yield of *o*-phthalaldehydic acid (m.p. 99°) from the low temperature ozonation of naphthalene in anhydrous methanol. Although the difference is believed to lie in incomplete extraction, the matter was not further investigated.

Aqueous methanol and aqueous ethanol proved to be unsuitable solvents for the preparation of *o*-phthalaldehyde. After treatment of the ozonation product with potassium iodide and acetic acid, the materials extracted with chloroform were esters of *o*-phthalaldehydic acid. This observation serves to illustrate the tendency of ethyl and methyl alcohols to form cyclic alkoxyhydroxyperoxides. In the case of phenanthrene these alkoxyhydroxyperoxides were found to decompose in a manner which retained the three atoms of oxygen of the original ozone molecule forming acidic products. The analogous hydroxyperoxides yield carbonyl derivatives (1, 3).

The results of this work have again demonstrated that water can act as a participating solvent in the ozonation of aromatic compounds and that its use is advantageous, particularly when aldehydic rather than acidic products are desired. *o*-Phthalaldehyde requiring no further purification is obtained by the ozonation of naphthalene in aqueous acetone solutions in yields which compare favorably with or exceed those reported by any procedure.

Experimental

The equipment and procedures used were those previously described (4). The naphthalene was reagent grade, m.p. 79–80°.[2] It was established that purification to m.p. 80.2° (14) had no discernable effect on the yields of *o*-phthalaldehyde. All other chemicals employed were also of reagent grade.

o-Phthalaldehyde by the Ozonation of Naphthalene

(A) Ozonation in Acetone–Water with Potassium Iodide Reduction

A stream of ozonized oxygen containing 1.73 g/ft³ of ozone was passed into a solution 5.0 g (0.039 mol) of naphthalene in 105 ml of acetone and 45 ml of water at a rate of 0.010 ft³/min. Under these conditions 98–99% of the ozone being introduced was absorbed. After 4 h the ozone absorption decreased to about 95% of that being introduced. A total of 4.1 g of ozone was passed into the reaction mixture of which 4.0 g (0.0834 mol) was absorbed. Immediately after completion of the ozonation, the product was treated with excess potassium iodide (13 g) and 5 ml of glacial acetic acid. The iodine released was reduced with 10% aqueous sodium thiosulfate solution and the acetone removed under reduced pressure at room temperature using a Rinco evaporator. The aqueous solution was extracted several times with

[2]Melting points were determined with an Electrothermal Melting Point Apparatus, standardized thermometer.

Can. J. Chem. Downloaded from www.nrcresearchpress.com by 210.87.254.40 on 09/05/12
For personal use only.

Can. J. Chem. Downloaded from www.nrcresearchpress.com by 210.87.254.40 on 09/05/12
For personal use only.

25 ml portions of chloroform. It was then saturated with sodium bicarbonate and again extracted several times with chloroform until the extract gave a negative test for *o*-phthalaldehyde (15). The chloroform was allowed to evaporate by overnight standing in an open beaker under mild magnetic stirrer agitation. The residue remaining, a light red or pinkish solid, was sublimed at a temperature of 45–60° under reduced pressure using ice-water in the cold finger of the sublimation apparatus. The sublimed product (3.33 g) light yellowish well formed crystals of *o*-phthalaldehyde, melted at 55–56°; lit. (16) 55.5–56°. The yield, 63.6% of theory, was typical of runs made in this manner.

Anal.[3] Calcd. for $C_8H_6O_2$: C, 71.65; H, 4.53. Found: C, 71.58; H, 4.50.

The n.m.r. spectrum obtained in $CDCl_3$ showed a singlet at -0.7 τ equivalent to two hydrogens and a multiplet from 1.8–2.2 τ equivalent to four hydrogens.[4]

After the sublimations were completed, that is to say when no further material was condensed on raising the temperature of the bath to 80–90°, a small quantity of red glass-like substance remained. The n.m.r. spectra, run on several different samples of the glass dissolved in acetone, invariably showed a singlet at -0.7 τ indicative of the aldehyde protons on *o*-phthalaldehyde and peaks at 1.7 τ to 2.7 τ corresponding to aromatic ring hydrogens. It is believed to be a polymeric phthalaldehyde.

(B) Ozonation in t-Butanol–Water with Potassium Iodide Reduction

A solution of 5.0 g of naphthalene in 105 ml of *t*-butanol and 45 ml of water was treated with a stream of ozonized oxygen containing 1.56 g/ft^3 of ozone at a rate of 0.0125 ft^3/min. Under these conditions 99% of the ozone introduced was absorbed. A total of 4.1 g of ozone was passed through the reaction mixture. Upon completion of the ozonation the product was treated in the manner described under section *A*. The yield of *o*-phthalaldehyde (m.p. 54–56°) was 3.05 g (58.3%).

(C) Ozonation in Acetone–Water with Dimethyl Sulfide Reduction

The ozonation was carried out using 5.0 g of naphthalene in a mixture of acetone and water as described under section *A*. Dimethyl sulfide (4 ml) was immediately added and the acetone allowed to evaporate at room temperature under gentle agitation. An additional 6 ml of reducing agent was added over the course of the next 3 h. Tests for active oxygen (potassium iodide) were made periodically until, after 4 h, a negative test was obtained. The solution was allowed to stand overnight to assure complete evaporation of the acetone. It was then extracted several times with chloroform and the extract allowed to evaporate. The yellow oil remaining was sublimed as previously described. The sublimed product gave a heavy "Thiele Test" (15) but was pasty and smelled strongly of dimethyl sulfoxide. An unsuccessful attempt was made to avoid the dimethyl sulfoxide difficulty by steam distillation prior to extraction. It is possible that this problem using dimethyl sulfide in the preparation of *o*-phthalaldehyde was encountered by Pappas *et al.* (12) since yields of this particular aldehyde were reported as the bis[(2,4-dinitrophenyl)hydrazone] derivative.

(D) Ozonation in Aqueous Methanol

A solution of 5.0 g of naphthalene in 105 ml of methanol and 45 ml of water was treated with 4.1 g of ozone as described in section *A*. After removal of the alcohol (Rinco, reduced pressure, bath temperature 34°), a brown oil separated. The aqueous solution was decanted and extracted with chloroform. The oil and the chloroform extract, were combined and the solvent removed by evaporation. The product remaining was crude methyl-*o*-phthalaldehydate. An n.m.r. spectrum of the oil in acetone showed a singlet at -0.7, a multiplet from 1.8 to 2.5, a broad singlet at 2.9, a broad singlet at 4.9, a singlet at 6.0, and several small peaks from 6.3 to 6.8 τ as well as a very small peak at about 9 τ. The peaks can be given the following assignments according to their chemical shifts: -0.7, aromatic aldehyde; 1.8 to 2.5, phenyl hydrogens; 4.9, hydroxyl proton; and 6.0 τ $C_6H_5COOCH_3$. On hydrolysis with sodium hydroxide solution followed by acidification, the oil yielded crude *o*-phthalaldehydic acid.

(E) Ozonation in Aqueous Ethanol

In a similar experiment using aqueous ethanol as solvent, the orange oil recovered was crude ethyl-*o*-phthalaldehydate. An n.m.r. spectrum of the oil in acetone showed a singlet at -0.7, a multiplet from 1.7 to 2.5, a quartet from 5.3 to 5.7 (centered at 5.5), a triplet from 8.5 to 8.7 τ (centered at 8.6), and a small impurity peak due to ethanol. The peaks can be given the following assignments according to their chemical shifts: -0.7, aromatic aldehyde; 1.7 to 2.5, phenyl hydrogens; quartet from 5.3 to 5.7, $C_6H_5COOCH_2CH_3$; and the triplet from 8.5 to 8.7 τ, $C_6H_5COOCH_2CH_3$.

3,6-Dihydroxy-4,5-benzo-1,2-dioxane (the Cyclic Dihydroxyperoxide)

(A) From o-Phthalaldehyde

o-Phthalaldehyde (1 g) was covered with 30% hydrogen peroxide and allowed to stand overnight in a refrigerator. White crystals, 0.39 g, (31 2%) m.p. 108–111° crude product separated. Recrystallization from ethyl acetate and petroleum ether gave 0.20 g of product m.p. 127–128°; lit. (18) 127–128°.

Anal. Calcd. for $C_8H_8O_4$: C, 57.15; H, 4.76. Found: C, 57.06; H, 4.72.

Three attempts were made to determine the active oxygen content of the product using the room temperature procedure (17) which had been used successfully in previous work (3, 4). The results were 26.7, 25.9, and 21.8% respectively, of the theoretical. The procedure of Rieche and Schmitz (18) which involves the use of higher temperatures during the reduction gave only 66.6% of theory.

(B) From the Ozonation of Naphthalene in Acetone–Water

A solution of 5.0 g of naphthalene in 105 ml of acetone and 45 ml of water was treated with 4.1 g of ozone in the manner described for the preparation of *o*-phthalaldehyde, section *A*. Removal of the acetone formed a cloudy solution which could not be induced to yield a crystalline product after standing several hours in an ice bath. The solution was extracted twice with 25 ml portions of ethyl

[3]Microanalyses were carried out using a Perkin–Elmer 240 Elemental Analyser.

[4]All n.m.r. spectra were obtained using a Varian A-60A Analytical Nuclear Magnetic Resonance Spectrometer.

acetate. The white crystals which formed as the ethyl acetate evaporated melted 99–150°. Recrystallization from ethyl acetate – petroleum ether (3:2), gave a product m.p. 129.5–131°, not depressed by an authentic sample of the cyclic dihydroxyperoxide m.p. 127–128°. The yield was low, 0.39 g, 6.0%. A quantity of crystals, 1.4 g, meanwhile had separated from the solution which had been extracted. The m.p. 107–115° was narrowed to 99–100° on recrystallization from water. Identification as *o*-phthalaldehydic acid was confirmed by elemental analysis.

Anal. Calcd. for $C_8H_6O_3$: C, 64.0; H, 4.0. Found: C, 64.12; H, 3.89.

o-Phthalaldehydic Acid by Ozonation in Aqueous Acetone, Alkaline Work-up

A solution of 2.5 g of naphthalene in 105 ml of acetone and 45 ml of water was treated with 2.05 g of ozone in the manner previously described. The product was refluxed with 25 ml of 15% sodium hydroxide solution for 30 min, cooled, acidified with hydrochloric acid and extracted five times with 25-ml portions of ethyl ether. The combined extracts were allowed to evaporate by overnight standing. The oil which remained was treated with a few drops of water and placed in the ice-bath. After several hours 1.83 g (62.4%) of *o*-phthalaldehydic acid, m.p. 96–99° separated, no depression with an authentic sample.

The authors are grateful to The Robert A. Welch Foundation, Houston, Texas, for the financial support of this work.

1. M. G. STURROCK, E. L. CLINE, and K. R. ROBINSON. U.S. Pat. 2 898 350. August 4, 1959.
2. P. S. BAILEY and J. B. ASHTON. J. Org. Chem. **22**, 98 (1957). See also P. S. BAILEY, P. KOLSAKER, B. SINHA, J. B. ASHTON, F. DOBINSON, and J. E. BATTERBEE. J. Org. Chem. **29**, 1400 (1964).
3. M. G. STURROCK, E. L. CLINE, and K. R. ROBINSON. J. Org. Chem. **28**, 2340 (1963).
4. M. G. STURROCK and R. A. DUNCAN. J. Org. Chem. **33**, 2149 (1968).
5. C. HARRIES. Ann. **343**, 336, 372 (1905).
6. L. SEEKLES. Rec. trav. chim. **42**, 706 (1923).
7. J. P. WIBAUT, L. W. F. KAMPSCHMIDT. Koninkl. Ned. Akad. Wet. Proc. 53, 1109 (1950).
8. L. W. F. KAMPSCHMIDT and J. P. WIBAUT. Rec. trav. chim. **73**, 431 (1954).
9. P. S. BAILEY and F. J. GARCIA-SHARP. J. Org. Chem. **22**, 1008 (1957).
10. P. S. BAILEY, S. S. BATH, F. DOBINSON, F. J. GARCIA-SHARP, and C. D. JOHNSON. J. Org. Chem. **29**, 697 (1964).
11. J. J. PAPPAS, W. P. KEAVENEY, E. GAUCHER, and M. BERGER. Tetrahedron Lett. No. 26, 4273 (1966).
12. J. J. PAPPAS, W. P. KEAVENEY, M. BERGER, and R. V. RUSH. J. Org. Chem. **33**, 787 (1968).
13. P. S. BAILEY. J. Am. Chem. Soc. **77**, 3811 (1956).
14. M. G. STURROCK, E. L. CLINE, K. R. ROBINSON, and R. J. LOVIN. U.S. Pat. 3 016 401. January 9, 1962.
15. J. THIELE and E. WINTER. Ann. **311**, 260 (1900).
16. J. C. BILL and D. S. TARBELL. Org. Synth. **14**, 82 (1954).
17. G. LOHAUS. Ann. **583**, 6 (1953) and endorsed by S. FLISZAR, D. GRAVEL, and E. CAVALLIERI. Can. J. Chem. **44**, 67 (1966).
18. A. RIECHE and E. SCHMITZ. Chem. Ber. **90**, 1082 (1957).

Ouverture normale d'époxydes aromatiques para-substitués par des α-mercapto esters

CASIMIR BERSE ET RONALD COULOMBE[1]

Département de chimie, Université de Montréal, Montréal, Québec

Reçu le 19 février 1971

Les α-mercaptoesters peuvent ouvrir le cycle oxirannique des époxydes aromatiques. Les produits formés résultent en grande majorité d'une ouverture normale du cycle et l'influence du substituant sur le noyau aromatique est de peu d'importance.

The three-membered ring of aromatic epoxides can be opened by α-mercaptoesters. The reaction products arise to a great extent by a normal opening of the ring and the substituent effect of the aromatic epoxide is of little importance.

Canadian Journal of Chemistry, 49, 3051 (1971)

Beaucoup de travaux (1–4) ont été effectués sur l'ouverture des époxydes par des acides aminés et nous avons été amenés à étudier cette réaction d'ouverture par des α-mercaptoesters aliphatiques. Même si le comportement des époxydes a déjà été étudié (5) en présence de thiols légers, aucun travail n'a été effectué avec des mercaptoesters.

Le schéma 1 résume les réactions effectuées dans la pyridine à reflux.

[1]Boursier pré-doctoral du CNRC 1969–1971.

Can. J. Chem. Downloaded from www.nrcresearchpress.com by 210.87.254.40 on 09/05/12
For personal use only.

acetate. The white crystals which formed as the ethyl acetate evaporated melted 99–150°. Recrystallization from ethyl acetate – petroleum ether (3:2), gave a product m.p. 129.5–131°, not depressed by an authentic sample of the cyclic dihydroxyperoxide m.p. 127–128°. The yield was low, 0.39 g, 6.0%. A quantity of crystals, 1.4 g, meanwhile had separated from the solution which had been extracted. The m.p. 107–115° was narrowed to 99–100° on recrystallization from water. Identification as *o*-phthalaldehydic acid was confirmed by elemental analysis.

Anal. Calcd. for $C_8H_6O_3$: C, 64.0; H, 4.0. Found: C, 64.12; H, 3.89.

o-Phthalaldehydic Acid by Ozonation in Aqueous Acetone, Alkaline Work-up

A solution of 2.5 g of naphthalene in 105 ml of acetone and 45 ml of water was treated with 2.05 g of ozone in the manner previously described. The product was refluxed with 25 ml of 15% sodium hydroxide solution for 30 min, cooled, acidified with hydrochloric acid and extracted five times with 25-ml portions of ethyl ether. The combined extracts were allowed to evaporate by overnight standing. The oil which remained was treated with a few drops of water and placed in the ice-bath. After several hours 1.83 g (62.4%) of *o*-phthalaldehydic acid, m.p. 96–99° separated, no depression with an authentic sample.

The authors are grateful to The Robert A. Welch Foundation, Houston, Texas, for the financial support of this work.

1. M. G. STURROCK, E. L. CLINE, and K. R. ROBINSON. U.S. Pat. 2 898 350. August 4, 1959.
2. P. S. BAILEY and J. B. ASHTON. J. Org. Chem. **22**, 98 (1957). See also P. S. BAILEY, P. KOLSAKER, B. SINHA, J. B. ASHTON, F. DOBINSON, and J. E. BATTERBEE. J. Org. Chem. **29**, 1400 (1964).
3. M. G. STURROCK, E. L. CLINE, and K. R. ROBINSON. J. Org. Chem. **28**, 2340 (1963).
4. M. G. STURROCK and R. A. DUNCAN. J. Org. Chem. **33**, 2149 (1968).
5. C. HARRIES. Ann. **343**, 336, 372 (1905).
6. L. SEEKLES. Rec. trav. chim. **42**, 706 (1923).
7. J. P. WIBAUT, L. W. F. KAMPSCHMIDT. Koninkl. Ned. Akad. Wet. Proc. 53, 1109 (1950).
8. L. W. F. KAMPSCHMIDT and J. P. WIBAUT. Rec. trav. chim. **73**, 431 (1954).
9. P. S. BAILEY and F. J. GARCIA-SHARP. J. Org. Chem. **22**, 1008 (1957).
10. P. S. BAILEY, S. S. BATH, F. DOBINSON, F. J. GARCIA-SHARP, and C. D. JOHNSON. J. Org. Chem. **29**, 697 (1964).
11. J. J. PAPPAS, W. P. KEAVENEY, E. GAUCHER, and M. BERGER. Tetrahedron Lett. No. 26, 4273 (1966).
12. J. J. PAPPAS, W. P. KEAVENEY, M. BERGER, and R. V. RUSH. J. Org. Chem. **33**, 787 (1968).
13. P. S. BAILEY. J. Am. Chem. Soc. **77**, 3811 (1956).
14. M. G. STURROCK, E. L. CLINE, K. R. ROBINSON, and R. J. LOVIN. U.S. Pat. 3 016 401. January 9, 1962.
15. J. THIELE and E. WINTER. Ann. **311**, 260 (1900).
16. J. C. BILL and D. S. TARBELL. Org. Synth. **14**, 82 (1954).
17. G. LOHAUS. Ann. **583**, 6 (1953) and endorsed by S. FLISZAR, D. GRAVEL, and E. CAVALLIERI. Can. J. Chem. **44**, 67 (1966).
18. A. RIECHE and E. SCHMITZ. Chem. Ber. **90**, 1082 (1957).

Ouverture normale d'époxydes aromatiques para-substitués par des α-mercapto esters

CASIMIR BERSE ET RONALD COULOMBE[1]

Département de chimie, Université de Montréal, Montréal, Québec

Reçu le 19 février 1971

Les α-mercaptoesters peuvent ouvrir le cycle oxirannique des époxydes aromatiques. Les produits formés résultent en grande majorité d'une ouverture normale du cycle et l'influence du substituant sur le noyau aromatique est de peu d'importance.

The three-membered ring of aromatic epoxides can be opened by α-mercaptoesters. The reaction products arise to a great extent by a normal opening of the ring and the substituent effect of the aromatic epoxide is of little importance.

Canadian Journal of Chemistry, 49, 3051 (1971)

Beaucoup de travaux (1–4) ont été effectués sur l'ouverture des époxydes par des acides aminés et nous avons été amenés à étudier cette réaction d'ouverture par des α-mercaptoesters aliphatiques. Même si le comportement des époxydes a déjà été étudié (5) en présence de thiols légers, aucun travail n'a été effectué avec des mercaptoesters.

Le schéma 1 résume les réactions effectuées dans la pyridine à reflux.

[1]Boursier pré-doctoral du CNRC 1969–1971.

Can. J. Chem. Downloaded from www.nrcresearchpress.com by 210.87.254.5 on 09/05/12
For personal use only.

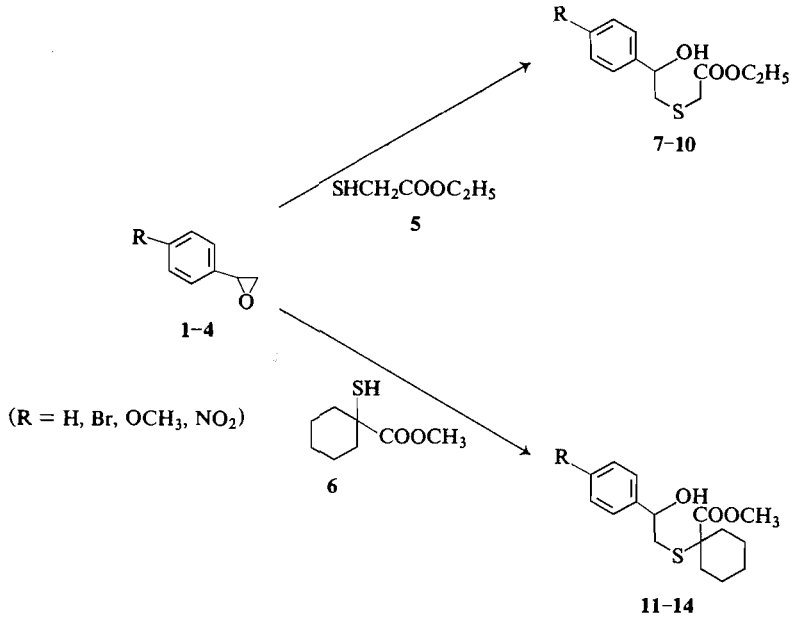

SCHÉMA 1[2]

TABLEAU 1. Résultats

Produit	Rendement* (%)	Spectre r.m.n. (δ) CCl_4 H_X†	CCl_4 H_{AB}‡	DMSO-d_6 *OH*
7 (R = H)	40	4.48	2.66	m
8 (R = Br)	44	4.64	2.74	—
9 (R = OCH_3)	16	4.59	2.70	—
10 (R = NO_2)	54	5.13	3.02	d
11 (R = H)	37	4.52	2.74	d(J = 4 Hz)
12 (R = Br)	50	4.50	2.73	d
13 (R = OCH_3)	55	4.48	~2.7	—
14 (R = NO_2)	45	4.70	2.82	—

*Rendement = $\frac{\text{Poids du produit final}}{\text{Poids du thiol + Poids de l'époxyde}}$

†Le centre des quatre raies du proton H_x est donné.
‡Le centre des deux sous-spectres AB est donné. Aucun J n'est calculé.

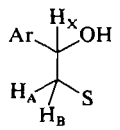

Les produits **7–14** furent généralement les produits majeurs et les produits secondaires n'eurent pas d'attention particulière. Il a été remarqué que dans ces conditions utilisées, la grande prédominance de l'ouverture fut normale et que l'influence du substituant sur le noyau aromatique fut de peu d'importance. Les produits résultant d'une ouverture anormale n'ont pu être séparés et caractérisés parce qu'ils étaient en trop faible quantité.

Tous les produits ont été identifiés grâce à des méthodes spectroscopiques et par des microanalyses. Nous reproduisons ici le tableau

[2]Les composés **1** et **5** sont disponibles commercialement.

Can. J. Chem. Downloaded from www.nrcresearchpress.com by 210.87.254.5 on 09/05/12
For personal use only.

TABLEAU 2. Analyses

Produit	Formule	Calculé (%) C	Calculé (%) H	Trouvé (%) C	Trouvé (%) H
7	$C_{12}H_{16}O_3S$	59.97	6.71	59.69	6.80
8	$C_{12}H_{15}BrO_3S$	45.21	4.73	44.87	4.68
9	$C_{13}H_{18}O_4S$	56.62	6.23	56.17	6.21
10	$C_{12}H_{15}NO_5S$	50.51	5.29	50.77	5.42
11	$C_{16}H_{22}O_3S$	65.29	7.53	65.07	7.35
12	$C_{16}H_{21}BrO_3S$	51.48	5.67	51.42	5.85
13	$C_{17}H_{24}O_4S$	62.90	7.45	63.17	7.36
14	$C_{16}H_{21}NO_5S$	57.75	6.71	57.52	6.93

des résultats (tableau 1). Chacun des produits **7–14** présente en r.m.n. un système ABX, la partie X représentant le proton benzylique. Tous les spectres sont pris dans le CCl_4 sauf pour le produit **10** où on ajoute une trace de $CDCl_3$ pour des raisons de solubilité. Certains spectres ont également été pris dans le DMSO-d_6 (6).

Les spectres i.r. des produits **7–14** montrèrent en solution dans CCl_4 les caractéristiques attendues pour ces produits, soit OH de type alcoolique et carbonyle à 1720 (± 5) cm^{-1}.

Il ne fait donc aucun doute quant à la structure de ces dérivés et à l'orientation de la réaction. Aucun mécanisme n'est proposé ici pour expliquer tant la sélectivité de l'ouverture que l'influence pratiquement indécelable du groupement attaché au noyau aromatique, contrairement à ce qui fut observé dans d'autres conditions expérimentales (7–9).

L'étude de la réactivité de ces composés **7–14** est en cours et fera l'objet d'une communication indépendante.

Partie expérimentale

Les spectres i.r. ont été pris sur un spectrophotomètre Beckman IR-8. Les spectres r.m.n. ont été pris sur un appareil JNM-4H-100 de Jeol et un appareil Varian T-60 avec le TMS comme référence interne.

Les analyses élémentaires ont été effectuées par Midwest Microlab Inc., à Indianapolis, Indiana.

Les points de fusion et d'ébullition ne sont pas corrigés.

Le mercaptocyclohexane carboxylate de méthyle (p.é. 60°/1.5 mm) a été préparé par la méthode de Jones *et al.* (10) à partir de l'acide α-bromocyclohexane carboxylique suivi d'estérification dans le méthanol. Les époxydes ont été préparés par la méthode de Shevchuk et Dombrovskii (11) et Fuchs et Vanderwerf (7) à partir des acétophénones correspondantes.

Toutes les ouvertures furent effectuées de la même façon. Le mercaptan et l'époxyde (mole à mole) furent dissous dans la pyridine (solution environ 10%) et portés à reflux environ trois heures. On constata la disparition du mercaptan par chromatographie sur couche mince. Le solvant fut retiré *in vacuo* et le résidu fut d'abord filtré sur une colonne de gel de silice pour éliminer les fractions polymériques avant d'être chromatographié dans l'hexane enrichi graduellement en éther. Les produits **7–14** n'ont en aucun cas été distillés car toute tentative entraîna la décomposition des produits. Ce sont tous des liquides jaunâtres à l'exception du composé **11** (p.f. sublimé: 54°).

Les produits ont été repurifiés par chromatographie sur colonne de gel de silice pour les microanalyses (voir tableau 2).

Nous remercions le Conseil National de Recherches du Canada de l'aide financière qui a rendu ce travail possible.

1. C. BERSE et K. JANKOWSKI. Can. J. Chem. **44**, 1513 (1966).
2. C. BERSE et K. JANKOWSKI. Can. J. Chem. **45**, 2865 (1967).
3. C. BERSE et K. JANKOWSKI. Can. J. Chem. **46**, 1835 (1968).
4. C. BERSE et K. JANKOWSKI. Can. J. Chem. **46**, 1939 (1968).
5. H. GILMAN et L. FULLHART. J. Am. Chem. Soc. **86**, 1478 (1949).
6. O. L. CHAPMAN et R. W. KING. J. Am. Chem. Soc. **86**, 1256 (1964).
7. R. FUCHS et C. A. VANDERWERF. J. Am. Chem. Soc. **76**, 1631 (1954).
8. C. O. GUSS. J. Am. Chem. Soc. **74**, 2561 (1952).
9. C. O GUSS et H. G. MAUTNER. J. Org. Chem. **16**, 887 (1951).
10. E. R. JONES, F. A. ROBINSON, et M. N. STRACHAN. J. Chem. Soc. 91 (1946).
11. M. I. SHEVCHUK et A. V. DOMBROVSKII. Chem. Abstr. **59**, 9921 g (1963).

Can. J. Chem. Downloaded from www.nrcresearchpress.com by 210.87.254.5 on 09/05/12
For personal use only.

Thermodynamics of Ionization of Fluoroalcohols in Aqueous Solution: Hexafluoropropan-2-ol and Hexafluoropropan-2,2-diol

EARL M. WOOLLEY[1] AND LOREN G. HEPLER
Department of Chemistry, The University of Lethbridge, Lethbridge, Alberta

AND

RODNEY S. ROCHE
Department of Chemistry, The University of Calgary, Calgary, Alberta

Received May 13, 1971

Calorimetric measurements have led to $\Delta H^0 = 6.37$ kcal mol^{-1} for ionization of aqueous hexafluoropropan-2-ol (HFIP) and to $\Delta H^0 = 6.00$ kcal mol^{-1} for ionization of aqueous hexafluoropropan-2,2-diol (HFPD). We have combined these values with our ΔG^0 values from p$K = 9.42$ for HFIP and p$K = 6.65$ for HFPD to obtain $\Delta S^0 = -21.7$ cal deg^{-1} mol^{-1} for ionization of aqueous HFIP and $\Delta S^0 = -10.3$ cal deg^{-1} mol^{-1} for ionization of aqueous HFPD. These results (all for 298 °K) show that most of the difference in pK values is due to the large difference in entropy of ionization. The ΔS^0 values can be explained largely in terms of solute–solvent interactions.

Les mesures calorimétriques conduisent à $\Delta H° = 6.37$ kcal mol^{-1} pour l'ionisation d'hexafluoropropanol-2 aqueux (HFIP) et à $\Delta H° = 6.00$ kcal mol^{-1} pour l'ionisation d'hexafluoropropanediol-2,2 aqueux (HFPD). En associant ces valeurs avec les valeurs de $\Delta G°$ obtenues à partir de p$K = 9.42$ pour HFIP et p$K = 6.65$ pour HFPD, on obtient $\Delta S° = -21.7$ cal deg^{-1} mol^{-1} pour l'ionisation de HFIP aqueux et $\Delta S° = -10.3$ cal deg^{-1} mol^{-1} pour l'ionisation de HFPD aqueux. Ces résultats (pour 298 °K) indiquent que la différence dans les valeurs de pK est principalement due aux différences importantes dans l'entropie d'ionisation. Les valeurs de $\Delta S°$ peuvent être rationalisées, en grande partie en invoquant des interactions soluté–solvant.

Canadian Journal of Chemistry, 49, 3054 (1971)

Introduction

Middleton and Lindsey (1) have reported p$K_a = 9.30$ for hexafluoropropan-2-ol (hexafluoroisopropanol, HFIP) and p$K_a = 6.58$ for hexafluoropropan-2,2-diol (hexafluoropropanediol, HFPD), presumably at about 25 °C, and have commented on the "abnormal acidity" of HFPD in terms of hydrogen bonding. Since earlier investigations (2) of thermodynamics of ionization of aqueous acids have shown that solute–solvent interactions and entropy effects can be as important as "internal energies" in relation to acid strengths and intramolecular hydrogen bonding, we have undertaken the calorimetric and e.m.f. measurements reported here. Also, it should be noted that there are no enthalpy and entropy data for ionization of other highly fluorinated acids or for any gem-diols.

Experimental

HFPD was prepared by stoichiometric addition of hexafluoroacetone (Mathieson) to water as described previously (3). The resulting HFPD was a stable gem-diol with melting point 44–46 °C. A solution of HFPD in CCl_4 (0.01 M) showed strong absorption at 3580 cm^{-1}, but no absorption in the 1800 cm^{-1} region (gaseous hexafluoroacetone has a carbonyl band at 1810 cm^{-1}) in this solution or in 1.0 M aqueous solution. No n–π^* or π–π^* transitions were observed in the u.v. spectrum.

HFIP was prepared by catalytic hydrogenation of hexafluoroacetone (PtO_2, 120 °C, maximum pressure 6000 p.s.i.) and purified by column fractionation at a reflux ratio of 10:1. The resulting HFIP was a colorless liquid, $n_D^{25\,°C} = 1.2748$, b.p. (760 mm Hg) = 59 °C.

Standard solutions were prepared by weighing HFIP and HFPD in a N_2 blanketed dry box, followed by addition of water to give known volumes of solutions of known concentrations, which were confirmed by titration with standard NaOH solution.

Calorimetric measurements were made with an LKB Precision Calorimetry System, used as a titration calorimeter. The titrant was supplied to the calorimeter by a Metrohm automatic titrator. Results refer to 25.0 °C and are reported in terms of the defined calorie (1 cal = 4.184 J).

Calorimetric titrations were carried out by adding known amounts of 0.2925 M NaOH to 95.5$_4$ ml of 0.01995 M HFIP or 0.01994 M HFPD. Heat effects associated with addition of three portions of NaOH solution were measured. Each of the first two portions neutralized about 45% of the acid originally present. The third portion contained enough NaOH to neutralize about 30% of the original acid. Molar heats of neutralization calculated from the heats associated with the first two additions of NaOH agreed with each other and also

[1]Present address: Department of Chemistry, Brigham Young University, Provo, Utah.

Can. J. Chem. Downloaded from www.nrcresearchpress.com by 210.87.254.42 on 09/05/12
For personal use only.

TABLE 1. Thermodynamics of ionization of HFIP (aq) and HFPD (aq) at 298 °K

Compound	pK	K	ΔG^0 (kcal mol^{-1})	ΔH^0 (kcal mol^{-1})	ΔS^0 (cal deg^{-1} mol^{-1})
HFIP	9.42 ± 0.04	$3.8(\pm 0.3) \times 10^{-10}$	12.85 ± 0.05	6.37 ± 0.06	-21.7 ± 0.03
HFPD	6.65 ± 0.02	$2.2(\pm 0.1) \times 10^{-7}$	9.07 ± 0.03	6.00 ± 0.04	-10.3 ± 0.2

with the heat of ionization calculated from the total heat associated with all three additions, thus demonstrating the absence of impurities with pK much different from the pK of the acid under investigation. Results of duplicate runs were in good agreement. In each case there were small corrections for heats of dilution, which were evaluated from results of separate measurements.

Ionization constants were determined by potentiometric titration at 25.0 °C with an Orion 801 pH meter with Beckman electrode pH 0–14. Initial concentrations of acid were 0.09974 M for HFIP and 0.08969 M for HFPD. Calculations, including activity coefficients, were carried out as described by King (4).

Results and Discussion

Results of our measurements are given in Table 1. Although our pH titrations were carried out with concentrations expressed as molarities, we report our results in terms of K, pK, ΔG^0, and ΔS^0 values based on the usual hypothetical one molal standard state (4). The reported ΔH^0 values are derived by combination of our heats of neutralization with $\Delta H^0 = 13.34$ kcal mol^{-1} for ionization of water (2, 5). The $\pm$ values given are our estimates of *total* uncertainties.

The results in Table 1 show that ~10% of the difference in ΔG^0 values is due to the difference in enthalpies of ionization, with the remaining ~90% of the ΔG^0 difference due to the difference in ΔS^0 of ionization. Since the ΔH^0 values can be regarded (2, 4, 6) as a sum of contributions from "internal" and "environmental" effects, we shall not try to interpret the small difference between the enthalpies of ionization of these compounds. On the other hand, the difference between the entropies of ionization can be interpreted (2, 4, 6, 7) largely in terms of solute–solvent interaction.

We begin by emphasizing that all available evidence shows that the equilibrium between hexafluoroacetone and water is such that it is appropriate to represent HFPD as a gem-diol rather than as a hydrated ketone. Next we note that the statistical effect of having two —OH groups on HFPD amounts to only 1.4 cal deg^{-1} mol^{-1} in ΔS^0, which is small compared to the observed 11.4 cal deg^{-1} mol^{-1} difference between ΔS^0 values for ionization of aqueous HFPD and HFIP.

Since our $\Delta S^0 = -21.7$ cal deg^{-1} mol^{-1} for ionization of aqueous HFIP is typical of many uncharged acids (2), we turn to consideration of either un-ionized HFPD or its anion as having an unusual partial molal entropy. In order for the ΔS^0 for ionization of aqueous HFPD to be less negative than usual, it is necessary that the partial molal entropy of un-ionized HFPD be unusually small or that the partial molal entropy of the HFPD anion be unusually large. We tentatively assume that the difference in entropies of ionization of aqueous HFPD and HFIP is due to an unusually large partial molal entropy for the anion of HFPD. This unusually large partial molal entropy for the anion of HFPD could result from an unusually small amount of "ordering" of water molecules around this ion.

The ordering of polar solvent molecules near anions of the type we are concerned with can be expressed in terms of the effective electrostatic field about the —O^- group. In the case of the HFPD anion the effective field near the —O^- group is diminished (compared to the field near the anion of HFIP) by the presence of the geminal —OH group that is oriented by intramolecular charge–dipole interaction. In molecules with appropriate geometry, this interaction leads to intramolecular hydrogen bonds.

In the absence of appropriate thermodynamic data for other acids of the gem-diol type, we turn to consideration of data in Table 2 for ionization of acids in which there may be intramolecular hydrogen bonding.

The ΔS^0 of ionization of *o*-hydroxybenzoic

TABLE 2. Entropies of ionization of aqueous acids at 298 °K (all ΔS^0 values from ref. 2)

Acid	ΔS^0 (cal deg^{-1} mol^{-1})
o-Hydroxybenzoic	−11.2
m-Hydroxybenzoic	−18.1
p-Hydroxybenzoic	−19.6
Maleic	−8.5
Fumaric	−13.8
Malic	−13.4
Succinic	−16.7

Can. J. Chem. Downloaded from www.nrcresearchpress.com by 210.87.254.42 on 09/05/12
For personal use only.

acid is larger (less negative) than ΔS^0 values for the *meta* or the *para* isomer. Similarly, ΔS^0 values for maleic acid and malic acid are greater than for fumaric and succinic acids. Thus we see that entropies of ionization for those acids in which we expect to find intramolecular hydrogen bonding in the anion are larger (less negative) than for "similar" acids in which the anion can have no intramolecular hydrogen bonding. It is reasonable to infer in these cases that the electrostatic field about the $-O^-$ group is diminished by hydrogen bonding, thus reducing "ordering" of solvent (as compared to similar anions without such intramolecular hydrogen bonding) in much the same way as the intramolecular charge–dipole interaction postulated above for the anion of HFPD.

We are grateful to the National Research Council of Canada for support of this research and to Douglas Dolman for his advice.

1. W. J. MIDDLETON and R. V. LINDSEY. J. Am. Chem. Soc. **86**, 4948 (1964).
2. J. W. LARSON and L. G. HEPLER. *In* Solute–solvent interactions. *Edited by* J. F. Coetzee and C. D. Ritchie. Marcel Dekker, Inc., New York, N.Y. 1969.
3. N. GRASSIE and R. S. ROCHE. J. Polymer Sci. **16** C, 4207 (1968).
4. E. J. KING. Acid–base equilibria. Pergamon Press, Inc., Oxford, England. 1965
5 R. N. GOLDBERG and L. G. HEPLER. J. Phys. Chem. **72**, 4654 (1968).
6. L. G. HEPLER. J. Am. Chem. Soc. **85**, 3089 (1963); L. G. HEPLER and W. F. O'HARA. J. Phys. Chem. **65**, 811 (1961).
7. L. P. FERNANDEZ and L. G. HEPLER. J. Am. Chem. Soc. **81**, 1783 (1959).

Crystal Structure of α-$Zn_3(VO_4)_2$

R. GOPAL AND C. CALVO
Institute for Materials Research, McMaster University, Hamilton, Ontario

Received January 25, 1971

α-$Zn_3(VO_4)_2$, the low temperature form of this compound, crystallizes in the orthorhombic space group *Cmca* with $a = 6.088(3)$, $b = 11.489(3)$, and $c = 8.280(3)$ Å and $Z = 4$. A total of 726 unique reflections were recorded from integrated precession photographs or with a manually set scintillation counter and used in a full matrix least squares refinement to a final R value of 0.089. The Zn ions lie in two types of octahedral sites while the V ions lie in sites showing tetrahedral coordination to oxygen atoms. The mean V—O bond length is 1.71 Å but one of the V—O bond lengths, involving an oxygen atom bonded to three Zn^{2+}, is 1.78(1) Å long. The average Zn—O bond lengths are 2.13 and 2.10 Å for the Zn ion with site symmetry $2/m$ and m site symmetry, respectively. α-$Zn_3(VO_4)_2$ is isostructural with $Mg_3(VO_4)_2$ and thus has a structure based upon a closest packing of oxygen atoms much like that found in spinel.

A basse température, le composé α-$Zn_3(VO_4)_2$, cristallise dans le système orthorhombique, groupe d'espace *Cmca* avec $a = 6.088(3)$, $b = 11.489(3)$ et $c = 8.280(3)$ Å et $Z = 4.726$ réflexions uniques ont été enregistrées soit à partir de photographies de précession intégrées soit au moyen d'un compteur de scintillement manuel et les résultats ont été affinés par moindre carrés jusqu'à une valeur finale $R = 0.089$. Les ions Zn se trouvent dans deux types de sites octahédriques alors que les ions V se trouvent dans des sites qui montrent une coordination tétrahédrique avec des atomes d'oxygène. La moyenne de la longueur de la liaison V—O est de 1.71 Å mais l'une des liaisons V—O, impliquant un atome d'oxygène lié à trois Zn^{2+}, a une longueur de 1.78(1) Å. Les moyennes des longueurs des liaisons Zn—O sont de 2.13 et 2.10 Å respectivement pour l'ion Zn ayant un site de symétrie $2/m$ et celui ayant un site de symétrie m. α-$Zn_3(VO_4)_2$ a la même structure que $Mg_3(VO_4)_2$ et de ce fait possède une structure fondée sur le tassement maximum des atomes d'oxygène un peu comme celle de la spinelle.

Canadian Journal of Chemistry, **49**, 3056 (1971)

The structures of $Mg_3(VO_4)_2$ (1), $Ni_3(VO_4)_2$ and the high temperature form of $Co_3(VO_4)_2$ (2) and the low temperature form of $Zn_3(VO_4)_2$, called α, are basically the same. The crystal structure of the first of these compounds has been refined by least squares methods using data obtained from a single crystal and the results indicate that three of the four V—O bond lengths about the VO_4 group are normal while the fourth is unusually long. The oxygen atom involved in this latter bond is shared with three Mg^{2+} ions, in addition to the vanadium, while the remaining

Can. J. Chem. Downloaded from www.nrcresearchpress.com by 210.87.254.42 on 09/05/12
For personal use only.

acid is larger (less negative) than ΔS^0 values for the *meta* or the *para* isomer. Similarly, ΔS^0 values for maleic acid and malic acid are greater than for fumaric and succinic acids. Thus we see that entropies of ionization for those acids in which we expect to find intramolecular hydrogen bonding in the anion are larger (less negative) than for "similar" acids in which the anion can have no intramolecular hydrogen bonding. It is reasonable to infer in these cases that the electrostatic field about the $-O^-$ group is diminished by hydrogen bonding, thus reducing "ordering" of solvent (as compared to similar anions without such intramolecular hydrogen bonding) in much the same way as the intramolecular charge–dipole interaction postulated above for the anion of HFPD.

We are grateful to the National Research Council of Canada for support of this research and to Douglas Dolman for his advice.

1. W. J. MIDDLETON and R. V. LINDSEY. J. Am. Chem. Soc. **86**, 4948 (1964).
2. J. W. LARSON and L. G. HEPLER. *In* Solute–solvent interactions. *Edited by* J. F. Coetzee and C. D. Ritchie. Marcel Dekker, Inc., New York, N.Y. 1969.
3. N. GRASSIE and R. S. ROCHE. J. Polymer Sci. **16** C, 4207 (1968).
4. E. J. KING. Acid–base equilibria. Pergamon Press, Inc., Oxford, England. 1965
5 R. N. GOLDBERG and L. G. HEPLER. J. Phys. Chem. **72**, 4654 (1968).
6. L. G. HEPLER. J. Am. Chem. Soc. **85**, 3089 (1963); L. G. HEPLER and W. F. O'HARA. J. Phys. Chem. **65**, 811 (1961).
7. L. P. FERNANDEZ and L. G. HEPLER. J. Am. Chem. Soc. **81**, 1783 (1959).

Crystal Structure of α-$Zn_3(VO_4)_2$

R. GOPAL AND C. CALVO
Institute for Materials Research, McMaster University, Hamilton, Ontario

Received January 25, 1971

α-$Zn_3(VO_4)_2$, the low temperature form of this compound, crystallizes in the orthorhombic space group *Cmca* with $a = 6.088(3)$, $b = 11.489(3)$, and $c = 8.280(3)$ Å and $Z = 4$. A total of 726 unique reflections were recorded from integrated precession photographs or with a manually set scintillation counter and used in a full matrix least squares refinement to a final R value of 0.089. The Zn ions lie in two types of octahedral sites while the V ions lie in sites showing tetrahedral coordination to oxygen atoms. The mean V—O bond length is 1.71 Å but one of the V—O bond lengths, involving an oxygen atom bonded to three Zn^{2+}, is 1.78(1) Å long. The average Zn—O bond lengths are 2.13 and 2.10 Å for the Zn ion with site symmetry $2/m$ and m site symmetry, respectively. α-$Zn_3(VO_4)_2$ is isostructural with $Mg_3(VO_4)_2$ and thus has a structure based upon a closest packing of oxygen atoms much like that found in spinel.

A basse température, le composé α-$Zn_3(VO_4)_2$, cristallise dans le système orthorhombique, groupe d'espace *Cmca* avec $a = 6.088(3)$, $b = 11.489(3)$ et $c = 8.280(3)$ Å et $Z = 4.726$ réflexions uniques ont été enregistrées soit à partir de photographies de précession intégrées soit au moyen d'un compteur de scintillement manuel et les résultats ont été affinés par moindre carrés jusqu'à une valeur finale $R = 0.089$. Les ions Zn se trouvent dans deux types de sites octahédriques alors que les ions V se trouvent dans des sites qui montrent une coordination tétrahédrique avec des atomes d'oxygène. La moyenne de la longueur de la liaison V—O est de 1.71 Å mais l'une des liaisons V—O, impliquant un atome d'oxygène lié à trois Zn^{2+}, a une longueur de 1.78(1) Å. Les moyennes des longueurs des liaisons Zn—O sont de 2.13 et 2.10 Å respectivement pour l'ion Zn ayant un site de symétrie $2/m$ et celui ayant un site de symétrie m. α-$Zn_3(VO_4)_2$ a la même structure que $Mg_3(VO_4)_2$ et de ce fait possède une structure fondée sur le tassement maximum des atomes d'oxygène un peu comme celle de la spinelle.

Canadian Journal of Chemistry, **49**, 3056 (1971)

The structures of $Mg_3(VO_4)_2$ (1), $Ni_3(VO_4)_2$ and the high temperature form of $Co_3(VO_4)_2$ (2) and the low temperature form of $Zn_3(VO_4)_2$, called α, are basically the same. The crystal structure of the first of these compounds has been refined by least squares methods using data obtained from a single crystal and the results indicate that three of the four V—O bond lengths about the VO_4 group are normal while the fourth is unusually long. The oxygen atom involved in this latter bond is shared with three Mg^{2+} ions, in addition to the vanadium, while the remaining

Can. J. Chem. Downloaded from www.nrcresearchpress.com by 210.87.254.40 on 09/05/12
For personal use only.

Can. J. Chem. Downloaded from www.nrcresearchpress.com by 210.87.254.40 on 09/05/12
For personal use only.

oxygen atoms are shared by only two magnesium atoms and the vanadium atom. The results of a recent refinement of X-ray and neutron powder data from $Co_3(VO_4)_2$ and $Ni_3(VO_4)_2$ are dissimilar in this detail (2). An environmental effect has been noted in α-$Mg_2P_2O_7$ (3), α-$Zn_2P_2O_7$ (4), and α-$Co_2P_2O_7$ (5) where bond length changes of the order of 0.05 Å in the diphosphate group have been noted as compared to 0.1 Å in $Mg_3(VO_4)_2$ (1). The structure of α-$Zn_3(VO_4)_2$ has been refined, in part, to determine whether a similar effect occurs in this material since there is a substantial difference in the electronegativity of the two cations, $Mg^{2+} = 1.2$ and $Zn^{2+} = 1.6$, as compared to 1.9 for V^{5+} (6).

α-$Zn_3(VO_4)_2$ undergoes two phase transformations upon increasing the temperature. The transition at 795 °C is sluggish but reversible while the one at 815 °C is rapid and reversible (7). An understanding of the driving forces for these transformations will require a detailed knowledge of the structure of each of the phases.

Crystals of α-$Zn_3(VO_4)_2$ were prepared from a slowly cooled melt containing stoichiometric amounts of ZnO and V_2O_5 in a platinum crucible. Unit cell parameters were determined by least squares refinement of single crystal photographs calibrated with the single crystal pattern of TiO_2 whose lattice parameters were taken to be $a = 4.5929$, $c = 2.9591$ Å (8). The values obtained are $a = 6.088(3)$, $b = 11.489(3)$, and $c = 8.280(3)$ Å using MoKα radiation ($\lambda_\alpha = 0.71069$ Å). A density of 5.0 g/cm^3 was measured with a pycnometer while the calculated density for $Z = 4$ is 4.88 g/cm^3. The assigned space group, *Cmca*, is the same as that of $Mg_3(VO_4)_2$ since the extinctions are $h + k$ odd for all reflections, l odd for $h0l$ and h and/or k odd for $hk0$. Intensities were measured from integrated precession photographs or with a manually set scintillation counter attached to a Supper Weissenberg camera using an ω scan. MoKα radiation was diffracted from a crystal whose size was 0.14 × 0.14 × 0.07 mm. The data set, consisting of nkl, $n = 0$ to 5; hkm, $m = 0$ and 1; and hpl, $p = 0$ to 4 were corrected for Lorentz and polarization effects and absorption.

The structure was refined by full matrix least squares procedures using 726 unique reflections. The final parameters of $Mg_3(VO_4)_2$ were used as trial coordinates and weights determined from the function $\omega = (30 + 0.2F_o + 0.012F_o^2)^{-1}$. The coefficients were chosen so that $\omega||F_o| - |F_c||^2$, the square of the difference between the observed and calculated structure factors would be independent of the local average of $|F_o|$. The weight was set to zero if the calculated intensity was less than the local minimum intensity. Common reflections were used to place all the data on a common scale. The atomic scattering curves were taken from the International Tables for X-Ray Diffraction and those for zinc and vanadium were corrected for dispersion (9). Refinement terminated when the calculated shifts in the varied parameters were all less than 1/3 of the calculated standard deviations. A full matrix least squares program written by J. S. Stephens for the CDC 6400 was used. The final R value was 0.089 while the weighted value is 0.116. The final atomic coordinates can be found in Table 1 while the observed and calculated structure factors are compared in Table 2.[1]

The bond lengths and angles are tabulated in Table 3 and, as with $Mg_3(VO_4)_2$, the three V—O bond lengths differ significantly. The V—O(2) bond length, involving that oxygen atom shared with three Zn^{2+}, is 1.79(1) Å long compared with 1.809(1) Å in $Mg_3(VO_4)_2$. In both structures the V—O(1) bond lengths are longer than the V—O(3) lengths. These values are 1.73(1) and 1.67(1) Å in the present case and 1.716(1) and 1.695(1) Å in $Mg_3(VO_4)_2$. The mean V—O bond length of 1.71 Å compares with the mean values of 1.70 and 1.71 Å found in $Ba_3(VO_4)_2$ (10). As a result of the larger errors in $\alpha Zn_3(VO_4)_2$ it cannot be concluded whether the individual V—O bond lengths between Mg and Zn orthovanadate differ significantly. On the other hand these results are completely reversed from those reported by Fuess *et al.* (2) on $Co_3(VO_4)_2$ and $Ni_3(VO_4)_2$ where the long V—O bond length corresponds to the V—O(1) bond. The O—V—O angles in the VO_4 tetrahedron do not deviate significantly from regularity and therefore the major distortion involves a radial displacement of O(2) from its ideal position, as is the case in $Mg_3(VO_4)_2$. The average ZnO bond lengths about Zn(1), lying in a site of $2/m$ symmetry, is 2.13 Å while the average Zn(2)—O bond length is 2.10 Å. This latter cation lies on the mirror plane. Both cations show substantially irregular octahedral coordination.

[1]Photocopies of Table 2 may be obtained free of charge, upon request, from the Depository of Unpublished Data, National Science Library, National Research Council of Canada, Ottawa, Canada.

Can. J. Chem. Downloaded from www.nrcresearchpress.com by 210.87.254.40 on 09/05/12
For personal use only.

TABLE 1. Positional and thermal parameters of $Zn_3(VO_4)_2$*

Atom	Position type	x	y	z	U_{11}†	U_{22}	U_{33}	U_{12}	U_{13}	U_{23}
Zn(1)	4(a)	0	0	0	0.010(1)	0.025(1)	0.012(1)	—	—	0.002(1)
Zn(2)	8(e)	1/4	0.1359(2)	1/4	0.010(1)	0.0236(8)	0.0158(7)	—	—	—
V	8(f)	0	0.3780(2)	0.1228(3)	0.004(1)	0.0116(9)	0.0099(8)	—	—	0.0016(8)
O(1)	8(f)	0	0.249(1)	0.232(1)	0.009(5)	0.023(5)	0.017(5)	—	—	0.007(4)
O(2)	8(f)	0	0.002(1)	0.245(1)	0.012(5)	0.020(4)	0.012(4)	—	—	0.004(4)
O(3)	16(g)	0.1186(8)	0.1186(8)	−0.005(1)	0.006(5)	0.024(4)	0.020(3)	−0.006(4)	0.002(3)	0.006(3)

*Estimated standard deviation in parentheses.
†U_{ij}'s in Å^2 are computed from $\beta_{ij} = 2\pi^2 b_i b_j U_{ij}$ where $T = \exp[-\beta_{11}h^2 + 2\beta_{12}hk + \ldots]$ appears in the structure factor expression and b_j are reciprocal lattice vectors.

TABLE 3. Bonding geometry in α-$Zn_3(VO_4)_2$ with estimated standard deviations in parentheses

Bond	Length (Å)	Bonds	Angle (deg)	Bonds	Angle (deg)
V—O(1)	1.73(1)	O(1)—V—O(2)	110.0(6)	O(2)—V—O(3)	109.7(4)
—O(2)	1.79(1)	—V—O(3)	2×109.0(4)	O(3)—V—O(3)′	108.4(5)
—O(3) 2×	1.67(1)				
Zn(1)—O(2)	2×2.04(1)	O(2)—Zn(1)—O(2)	180.0	O(3)—Zn(1)—O(3)	180
—O(3)	4×2.17(1)	—O(3)	4×89.2(3)	—O(3)	2×77.8(4)
Zn(2)—O(1)	2×2.01(1)	O(1)—Zn(2)—O(1)	99.1(4)	O(2)—Zn(2)—O(2)	89.2(3)
—O(2)	2×2.17(1)	—O(2)	85.9(4)	—O(3)	88.4(4)
—O(3)	2×2.13(1)	—O(2)	174.1(4)	—O(3)	84.0(4)
		—O(3)	92.6(4)	O(3)—Zn(2)—O(3)′	169.3(4)
		—O(3)	94.3(4)		

The crystal packing and the relationship between this structure and that of spinel have been discussed previously (1). One new feature concerns the phase transformations in this compound. A single crystal was heated and photographed *in situ*. The phase transformation is indeed sluggish and all attempts to convert a single crystal to the high temperature phase resulted in diffraction rings. It is thus curious that single crystals of the low temperature form survived the cooling process.

1. N. KRISHNAMACHARI and C. CALVO. Can. J. Chem. **49**, 1629 (1971).
2. H. FUESS, E. F. BERTAUT, R. PAUTHENET, and A. DURIF. Acta Cryst. **26B**, 2036 (1970).
3. C. CALVO. Acta Cryst. **23**, 298 (1969).
4. B. E. ROBERTSON and C. CALVO. J. Solid State Chem. **1**, 120 (1970).
5. N. KRISHNAMACHARI and C. CALVO. To be published.
6. S. S. BASTONOV. Russ. Chem. Rev. **37**, 332 (1968).
7. J. J. BROWN and F. A. HUMMEL. Trans. Br. Ceramic Soc. **64**, 387 (1965).
8. D. T. CROMER and K. HERRINGTON. J. Am. Chem. Soc. **77**, 4708 (1955).
9. International Tables for X-Ray Crystallography. Vol. III. Kynoch Press. 1962.
10. P. SÜSSE and M. J. BUERGER. Z. Krist. **131**, 161 (1970).

Studies on Horseradish Peroxidase. VII. A Kinetic Study of the Oxidation of Iodide by Horseradish Peroxidase Compound II

R. ROMAN, H. B. DUNFORD, AND M. EVETT
Department of Chemistry, University of Alberta, Edmonton, Alberta

Received April 1, 1971

The kinetics of the oxidation of iodide ion by horseradish peroxidase compound II have been studied as a function of p*H* at 25° and ionic strength of 0.11. The logarithm of the second-order rate constant decreases linearly from 2.3×10^5 to 0.1 M^{-1} s^{-1} with increasing p*H* over the p*H* range 2.7 to 9.0. The p*H* dependence of the reaction is explained in terms of an acid dissociation outside the p*H* range of the study.

Les cinétiques de l'oxydation d'ions iodure par le composé II (raifort peroxydase) ont été étudiées en fonction du p*H*, à 25 °C et avec une force ionique de 0.11. Le logarithm de la constante de vitesse du second ordre décroît linéairement de 2.3×10^5 jusqu'à 0.1 M^{-1} s^{-1} lorsque le p*H* augmente de 2.7 à 9.0. La dépendence du p*H* de la réaction est expliquée en fonction d'une dissociation acide, extérieure à la zone de p*H* étudiée.

Canadian Journal of Chemistry, **49**, 3059 (1971)

This work is part of a continuing series of studies the object of which is to elucidate the mechanism of the reactions of horseradish peroxidase (HRP). Previous studies have dealt with the effect of p*H* on the structure and kinetics of native HRP (1–4). More recently, we studied the kinetics of the reactions of two oxidized forms of HRP with ferrocyanide as a function of p*H*

Can. J. Chem. Downloaded from www.nrcresearchpress.com by 210.87.254.40 on 09/05/12
For personal use only.

TABLE 3. Bonding geometry in α-$Zn_3(VO_4)_2$ with estimated standard deviations in parentheses

Bond	Length (Å)	Bonds	Angle (deg)	Bonds	Angle (deg)
V—O(1)	1.73(1)	O(1)—V—O(2)	110.0(6)	O(2)—V—O(3)	109.7(4)
—O(2)	1.79(1)	—V—O(3)	2×109.0(4)	O(3)—V—O(3)′	108.4(5)
—O(3) 2×	1.67(1)				
Zn(1)—O(2)	2×2.04(1)	O(2)—Zn(1)—O(2)	180.0	O(3)—Zn(1)—O(3)	180
—O(3)	4×2.17(1)	—O(3)	4×89.2(3)	—O(3)	2×77.8(4)
Zn(2)—O(1)	2×2.01(1)	O(1)—Zn(2)—O(1)	99.1(4)	O(2)—Zn(2)—O(2)	89.2(3)
—O(2)	2×2.17(1)	—O(2)	85.9(4)	—O(3)	88.4(4)
—O(3)	2×2.13(1)	—O(2)	174.1(4)	—O(3)	84.0(4)
		—O(3)	92.6(4)	O(3)—Zn(2)—O(3)′	169.3(4)
		—O(3)	94.3(4)		

The crystal packing and the relationship between this structure and that of spinel have been discussed previously (1). One new feature concerns the phase transformations in this compound. A single crystal was heated and photographed *in situ*. The phase transformation is indeed sluggish and all attempts to convert a single crystal to the high temperature phase resulted in diffraction rings. It is thus curious that single crystals of the low temperature form survived the cooling process.

1. N. KRISHNAMACHARI and C. CALVO. Can. J. Chem. **49**, 1629 (1971).
2. H. FUESS, E. F. BERTAUT, R. PAUTHENET, and A. DURIF. Acta Cryst. **26B**, 2036 (1970).
3. C. CALVO. Acta Cryst. **23**, 298 (1969).
4. B. E. ROBERTSON and C. CALVO. J. Solid State Chem. **1**, 120 (1970).
5. N. KRISHNAMACHARI and C. CALVO. To be published.
6. S. S. BASTONOV. Russ. Chem. Rev. **37**, 332 (1968).
7. J. J. BROWN and F. A. HUMMEL. Trans. Br. Ceramic Soc. **64**, 387 (1965).
8. D. T. CROMER and K. HERRINGTON. J. Am. Chem. Soc. **77**, 4708 (1955).
9. International Tables for X-Ray Crystallography. Vol. III. Kynoch Press. 1962.
10. P. SÜSSE and M. J. BUERGER. Z. Krist. **131**, 161 (1970).

Studies on Horseradish Peroxidase. VII. A Kinetic Study of the Oxidation of Iodide by Horseradish Peroxidase Compound II

R. ROMAN, H. B. DUNFORD, AND M. EVETT
Department of Chemistry, University of Alberta, Edmonton, Alberta

Received April 1, 1971

The kinetics of the oxidation of iodide ion by horseradish peroxidase compound II have been studied as a function of p*H* at 25° and ionic strength of 0.11. The logarithm of the second-order rate constant decreases linearly from 2.3×10^5 to 0.1 M^{-1} s^{-1} with increasing p*H* over the p*H* range 2.7 to 9.0. The p*H* dependence of the reaction is explained in terms of an acid dissociation outside the p*H* range of the study.

Les cinétiques de l'oxydation d'ions iodure par le composé II (raifort peroxydase) ont été étudiées en fonction du p*H*, à 25 °C et avec une force ionique de 0.11. Le logarithm de la constante de vitesse du second ordre décroît linéairement de 2.3×10^5 jusqu'à 0.1 M^{-1} s^{-1} lorsque le p*H* augmente de 2.7 à 9.0. La dépendence du p*H* de la réaction est expliquée en fonction d'une dissociation acide, extérieure à la zone de p*H* étudiée.

Canadian Journal of Chemistry, **49**, 3059 (1971)

This work is part of a continuing series of studies the object of which is to elucidate the mechanism of the reactions of horseradish peroxidase (HRP). Previous studies have dealt with the effect of p*H* on the structure and kinetics of native HRP (1–4). More recently, we studied the kinetics of the reactions of two oxidized forms of HRP with ferrocyanide as a function of p*H*

Can. J. Chem. Downloaded from www.nrcresearchpress.com by 210.87.254.6 on 09/05/12
For personal use only.

Can. J. Chem. Downloaded from www.nrcresearchpress.com by 210.87.254.6 on 09/05/12
For personal use only.

(5, 6). The present work describes a p*H* study of the reaction of compound II of HRP with iodide. It is generally accepted that compound II (HRP-II) is an intermediate in the peroxidase-catalyzed reactions between hydrogen peroxide and a variety of reducing agents (7). It is possible to prepare HRP-II, which has one more oxidizing equivalent than native HRP, and to study its reactions in isolation from the other steps in the HRP cyclic reaction sequence. By studying one of its reactions over a p*H* range, it is possible to gain information concerning the ionizations which affect the active site of HRP-II for this reaction. Iodide was chosen as a substrate partly because its single ionization is outside the measurable p*H* range for the enzyme, thus simplifying the interpretation of the kinetic p*H* dependence.

The biological functions of most peroxidases are uncertain. However, it has been proposed that thyroid peroxidase functions in mammalian thyroid glands by oxidizing iodide in the synthesis of thyroxine (8). We thought that the readily available HRP might serve as a model for thyroid peroxidase, which at present can only be isolated in small quantities (9).

Experimental

Horseradish peroxidase was obtained from Boehringer-Mannheim either as a purified, lyophilized powder or as a highly purified ammonium sulfate suspension. The suspension, which had a p.n.[1] of 3.0 was dialyzed and passed through a millipore filter prior to use. The lyophilized powder (p.n. about 0.6) was purified by the method of Shannon *et al.* (10). From 0.1 to 0.5 g of the powder was dissolved in a sodium acetate buffer (p*H* 4.4 and ionic strength 0.005) and transferred to a Sephadex C50-(CM) column. The eluent was that of Shannon *et al.* The major peak was collected in 5 ml fractions and those of p.n. 2.8 or greater were combined and precipitated with ammonium sulfate (53 g/100 ml of solution) at −10 °C. The precipitate was dissolved, dialyzed, and passed through a millipore filter prior to use. Both enzyme preparations exhibited the same kinetic behavior and were sufficiently free from reducing impurities to give HRP-II a half-life of about 20 min. The fact that the observed reactions were first-order in HRP-II indicates that if more than one isozyme was present in detectable concentrations, these isozymes must react with similar rates. The concentration of HRP was determined spectrophotometrically at 403 nm using a molar absorptivity of $9.1 \times 10^4\ M^{-1}\ cm^{-1}$ (11).

All solutions were prepared from water that had been distilled from alkaline permanganate and then redistilled. Reagent grade inorganic chemicals were used without further purification. The ionic strength of all reaction mixtures was kept constant at 0.11 with 0.01 contributed by the buffer and the remainder by potassium nitrate and potassium iodide. Fresh solutions of potassium iodide were prepared weekly and were protected from light during storage. The concentrations of these iodide solutions were checked by titration with silver nitrate or with an Orion specific ion iodide electrode (84-53A); no change was detected during the storage period (12). The concentrations of the hydrogen peroxide solutions were determined spectrophotometrically by the molybdate-catalyzed oxidation of iodide (13, 14).

An Orion model 801 digital p*H* meter in conjunction with a Fisher combination electrode was used for p*H* measurements. A Beckman DU spectrophotometer was used for routine absorption measurements and a Cary 14 spectrophotometer was employed for recording spectra.

Kinetic measurements on solutions with p*H* lower than 6.5 were performed on a stopped flow apparatus; measurements on solutions with higher p*H* were performed on the Cary 14. The reaction was monitored by following the decrease in absorbance at 425 nm. All measurements were made with the solutions thermostatted at 25.0 °C. The stopped flow data were obtained as voltage *vs.* time measurements from oscilloscope traces. The observed first-order rate constants were determined by a nonlinear least squares fit to the equation

$$V_t = (V_0 - V_\infty)e^{-k_{obs}t} + V_\infty$$

where V_t, V_0, and V_∞ are the voltages observed at time t, at t equal to 0, and at t equal to ∞, respectively, and k_{obs} is the first-order rate constant. At the low absorbance changes used (0.04), voltage changes were taken to be proportional to changes in absorbance. For the analysis 20–30 points were taken per trace, and 4–8 traces were analyzed to give an average rate constant. The absorbance *vs.* time data from the Cary 14 experiments were analyzed in the same manner as the stopped flow data.

The preparation of HRP-II was similar to that described previously (5). It was found that the addition of an equimolar amount of hydrogen peroxide to HRP produced compound I, which could be converted to compound II by the addition of one-half of a molar equivalent of *p*-cresol. The absence of any compound I in the resulting mixture of HRP and HRP-II was verified spectrophotometrically (5). Care was taken in the preparation of HRP-II to avoid adding an excess of hydrogen peroxide, which would recycle part of the enzyme, resulting in anomalous kinetic results. For the same reason a small amount of HRP (*ca.* $10^{-9}\ M$) was added to solutions containing a mixture of buffer, iodide, and nitrate to remove any oxidizing impurity in these solutions. The buffer and the HRP-II solutions were not mixed prior to the reaction in the stopped flow apparatus to minimize decomposition of HRP-II at low p*H*. On the Cary 14 the reaction was performed by pipetting a solution of buffer, iodide, and nitrate into the HRP-II solution.

Results and Discussion

The kinetic behavior of the HRP-II-iodide reaction is consistent with the equation

[1]An acronym for purity number, the ratio of absorbance at 403 and 280 nm.

Can. J. Chem. Downloaded from www.nrcresearchpress.com by 210.87.254.6 on 09/05/12
For personal use only.

$$[1] \qquad \text{HRP-II} + I^- \xrightarrow{k_1} \text{HRP} + \tfrac{1}{2}I_2$$

All experiments were carried out with $[I^-]$ at least twenty times greater than the [HRP-II]; under these pseudo-first-order conditions the differential rate expression is

$$[2] \qquad -\mathrm{d}\frac{[\text{HRP-II}]}{\mathrm{d}t} = k_{obs}[\text{HRP-II}]$$

Values of k_1 are obtained from the equation

$$[3] \qquad k_{obs} = k_1[I^-]$$

This relation was verified by measuring k_{obs} over a range of iodide concentrations at a given p*H*. Plots of k_{obs} *vs.* $[I^-]$ are linear as shown in Fig. 1 for p*H* 3.41. Similar studies were carried out at p*H*'s 2.71, 2.99, 6.00, 8.66, and 9.05. At p*H* values below 3.4 and above 8.5 the k_{obs} *vs.* $[I^-]$ plots have a positive intercept indicating an appreciable spontaneous rate of reaction. The values of these intercepts are found never to be greater than 15% of the largest measured value of k_{obs}.

The values of k_1 as a function of p*H* are listed in Table 1 and $\log k_1$ is plotted *vs.* p*H* in Fig. 2. Where it was possible to overlap buffers, similar kinetic behavior was observed, indicating that there is no detectable effect due to buffers. We believe the values of k_1, the errors in which are mainly dependent on the errors in k_{obs} and in p*H*, are accurate to within $\pm 10\%$.

In a recent publication, Björkstén reported a value for the second-order rate constant, for the reaction of HRP-II and iodide, of $1.8 \times 10^2\ M^{-1}\ s^{-1}$ at p*H* 6.19 (15). Considering the different techniques employed in the two studies the agreement is reasonable with our value for the rate constant, $7.1 \times 10^1\ M^{-1}\ s^{-1}$, at the same p*H*. We feel that our value for the rate constant is more accurate, since it does not depend on the concentration of HRP-II or knowledge of the molar absorptivity differences between HRP-II and HRP.

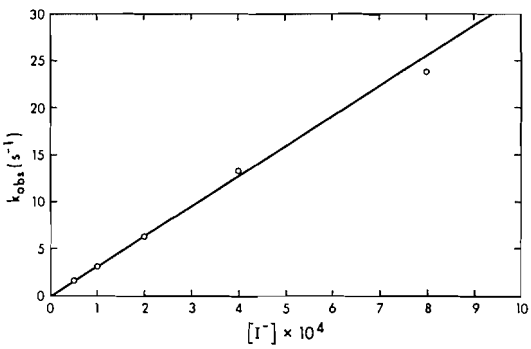

FIG. 1. Plot of k_{obs} *vs.* $[I^-]$ at p*H* 3.41 for the reaction between HRP-II and iodide. The straight line is the weighted linear least squares line. The slope, k_1, with its standard error is $(3.2 \pm 0.1) \times 10^4\ M^{-1}\ s^{-1}$. The intercept with its standard error is $-0.01 \pm 0.07\ s^{-1}$.

TABLE 1. Second-order rate constants for the HRP-II–iodide reaction at 25 °C

p*H*	k_1 ($M^{-1}\,s^{-1}$)	$[I^-]$ (M)	Buffer*
2.71	2.3×10^5	$0.5\text{–}2\times10^{-4}$	GH
2.99	8.8×10^4	$0.5\text{–}3\times10^{-4}$	GH
3.41	3.2×10^4	$0.5\text{–}8\times10^{-4}$	GH
4.03	9.1×10^3	1.0×10^{-3}	A
4.38	4.6×10^3	1.0×10^{-3}	A
4.68	2.1×10^3	2.5×10^{-3}	A
4.98	1.1×10^3	1.0×10^{-2}	A
5.01	9.7×10^2	5.0×10^{-3}	A
5.31	5.8×10^2	1.0×10^{-2}	CA
5.44	4.5×10^2	2.5×10^{-3}	A
5.58	3.1×10^2	1.0×10^{-2}	CA
6.00	1.2×10^2	$0.1\text{–}1.0\times10^{-2}$	P
6.53	3.4×10	3.3×10^{-4}	P
6.99	1.2×10	1.6×10^{-3}	T
7.46	4.3	9.1×10^{-3}	T
8.51	0.37	3.3×10^{-2}	B
8.66	0.29	$1.0\text{–}5.0\times10^{-2}$	T
9.05	0.10	$0.3\text{–}1.0\times10^{-1}$	C

*A, acetic acid – NaOH; B, borax–HNO_3; C, $NaHCO_3$–NaOH; CA, cacodylic acid – NaOH; GH, glycine–HNO_3; P, KH_2PO_4–NaOH; and T, tris–HNO_3.

The plot of $\log k_1$ *vs.* p*H* is a straight line with a slope of -1 within experimental error. This behavior can be explained most simply by assuming that there is a kinetically important ionization on either the enzyme or substrate which is outside the p*H* range covered in the study. The pK_A of hydriodic acid has been reported to be approximately -9 (16, 17). Using this ionization constant it can be shown that iodide and not hydriodic acid must be the reacting species since, over the range of p*H* and iodide concentration covered in our study, the reaction of hydriodic acid would require a rate constant that exceeded the diffusion controlled limit by a factor of 10^7. Thus the kinetic results can be explained if HRP-II exists in two forms with the protonated form reacting much more rapidly than the unprotonated form with iodide. This reaction mechanism can be written in general terms as

$$[4] \qquad \begin{array}{ccc} & & \text{HP-II} + I^- \xrightarrow{k_2} \\ & K_p \downarrow\uparrow & \\ & & \text{P-II} + I^- \xrightarrow{k_3} \end{array}$$

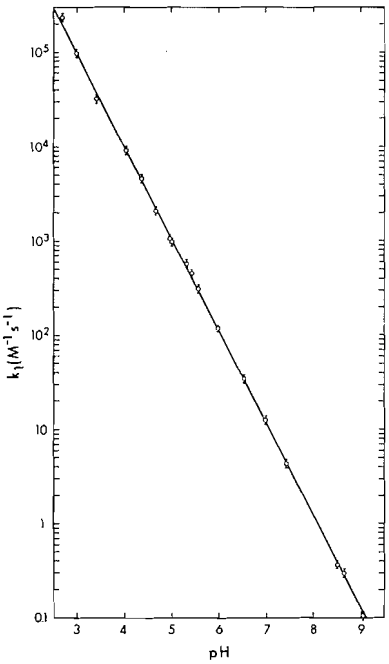

FIG. 2. Plot of log k_1 *vs.* p*H* for the reaction between HRP-II and iodide. The error limits drawn on the data points are based on an estimated standard deviation of ±10%. The solid line is the weighted linear least squares best fit line with a slope of −0.99 ± 0.006.

thus

$$[5] \qquad k_1 = \frac{k_2}{1 + \frac{K_p}{[H^+]}} + \frac{k_3}{1 + \frac{[H^+]}{K_p}}$$

Since the log k_1 *vs.* p*H* plot has a slope of −1 over the p*H* range of the study, we can conclude that (*1*) the term involving k_3 is negligible and (*2*) $K_p/[H^+] \gg 1$. The latter condition provides an estimate of the lower limit for K_p; the lowest p*H* of the study is 2.7 which means that K_p must be greater than 10^{-2} *M*. The maximum value of K_p must be such that k_2 does not exceed the diffusion-controlled limit ($10^{10}\ M^{-1}\ s^{-1}$). The combined effect of the above two conditions is to reduce eq. 5 to

$$[6] \qquad k_1 = \frac{k_2[H^+]}{K_p}$$

from which any point on the log k_1 *vs.* p*H* plot can be used to calculate that $k_2 = 10^8\ K_p$. Thus the maximum possible value of K_p would be 10^2 *M*. The minimum difference between k_2 and k_3 can be estimated at the highest p*H* on the log k_1 *vs.* p*H* plot. Assuming the minimum value for K_p of 10^{-2}, the relative concentrations of P-II and HP-II at p*H* 9.0 indicate that k_2 must be at least 10^7 times greater than k_3.

The log k_1 *vs.* p*H* plot for the iodide oxidation shows no indication of the kinetically important ionization with a pK_a value of 8.6, which exhibits a pronounced effect on the oxidation of ferrocyanide by Compound II (5).[2] If the rate determining steps for the reactions of the two substrates are the same, the influence of the ionization observed in the ferrocyanide reaction must result from interactions between HRP-II and substrate. The similarity in the overall acid catalysis for the two reactions suggests that the ionization characterized by K_p could exert its kinetic effect for all substrates of HRP-II. Further work involving different substrates is required to clarify the nature of these ionizations.

The authors are grateful to the National Research Council of Canada for financial support and to Dr. J. Critchlow for valuable discussion. R.R. acknowledges an NRCC Scholarship and a Government of Alberta Graduate Fellowship and M.E. an NRCC Postdoctoral Fellowship.

1. H. B. DUNFORD and R. A. ALBERTY. Biochem. **6**, 447 (1967).
2. W. D. ELLIS and H. B. DUNFORD. Biochem. **7**, 2054 (1968).
3. W. D. ELLIS and H. B. DUNFORD. Can. J. Biochem. **46**, 1231 (1968).
4. W. D. ELLIS and H. B. DUNFORD. Arch. Biochem. Biophys. **133**, 313 (1969).
5. B. B. HASINOFF and H. B. DUNFORD. Biochem. **9**, 4930 (1970).
6. H. B. DUNFORD and B. B. HASINOFF. *In* Advances in chemistry series 100, bioinorganic chemistry. *Edited by* R. F. Gould. American Chemical Society Publications, Washington, D.C. 1971. pp. 413–426.
7. A. S. BRILL. Compr. Biochem. **14**, 447 (1966).
8. T. HOSOYA. Gunma Symp. Endocrinol. **5**, 219 (1968).
9. A. TAUROG, M. L. LOTHROP, and R. W. ESTABROOK. Arch. Biochem. Biophys. **139**, 221 (1970).
10. L. M. SHANNON, E. KAY, and J. LEW. J. Biol. Chem. **241**, 2166 (1966).
11. D. KEILIN and E. F. HARTREE. Biochem. J. **49**, 88 (1951).
12. I. M. KOLTHOFF and E. B. SANDELL. Textbook of quantitative inorganic analysis. 3rd ed. MacMillan Co., New York, N.Y. 1963. p. 544.

[2]The apparently small effects attributed to two other ionizations on HRP-II in the oxidation of ferrocyanide have been shown to be within the experimental error limits by Mr. Meredith Cotton in our laboratory.

Can. J. Chem. Downloaded from www.nrcresearchpress.com by 210.87.254.6 on 09/05/12
For personal use only.

13. T. C. J. OVENSTON and W. T. REES. Anal. (London) **75**, 204 (1950).
14. R. W. RAMETTE and R. W. SANDFORD. J. Am. Chem. Soc. **87**, 5001 (1965).
15. F. BJÖRKSTÉN. Biochim. Biophys. Acta, **212**, 396 (1970).
16. F. A. COTTON and G. WILKINSON. Advanced inorganic chemistry. 2nd ed. John Wiley and Sons Inc., New York, N.Y. 1966. p. 223.
17. R. P. BELL. The proton in chemistry. Cornell University Press, Ithaca, N.Y. 1959. p. 89.

Can. J. Chem. Downloaded from www.nrcresearchpress.com by 210.87.254.6 on 09/05/12
For personal use only.

Molecular Beam Chemiluminescence. I. Kinetic Energy Dependence of the $NO + O_3 \rightarrow NO_2^* + O_2$ Reaction

ANTHONY E. REDPATH AND MICHAEL MENZINGER
Lash Miller Chemical Laboratories, University of Toronto, Toronto 181, Ontario

Received April 23, 1971

The visible chemiluminescence of the $NO + O_3 \rightarrow NO_2^* + O_2$ reaction has been studied as a function of collision energy using a supersonic molecular beam of NO. The reaction threshold $E_0 = 3.00 \pm 0.45$ kcal/mol is found to lie significantly below the Arrhenius activation energy of $E_a = 4.18 \pm 0.3$ kcal/mol. This clearly demonstrates the basic difference between the two quantities.

La chimioluminescence visible de la réaction $NO + O_3 \rightarrow NO_2^* + O_2$, a été étudiée en fonction de l'énergie de collision en utilisant un rayon moléculaire supersonique de NO. Le seuil réactionnel, $E_0 = 3.00 \pm 0.45$ kcal/mol se trouve donc être relativement plus bas que l'énergie d'activation d'Arrhenius qui est de $E_a = 4.18 \pm 0.3$ kcal/mol. Ceci démontre clairement la différence fondamentale entre les deux quantités.

Canadian Journal of Chemistry, **49**, 3063 (1971)

Despite the importance which the total reaction crossection $\sigma(E)$ as a function of collision energy plays in theories of elementary gas phase kinetics (1, 2), there is only a small number of neutral–neutral processes (3) for which this function has been determined either by photochemical (4) or by beam (5, 6) methods.

Variable energy molecular beams (chemical accelerators (7)) appear to offer the most obvious means for measuring $\sigma(E)$, but the problem of detecting the total flux of neutral products is serious and has so far precluded a broad application of this approach (3). However, light emitted during a chemiluminescent reaction is relatively easy to detect and its intensity bears a close relationship to the excitation function $\sigma(E)$. The combination of molecular beam with photon detection techniques has been termed molecular beam chemiluminescence (8). Compared to the infrared chemiluminescence studies pioneered by Polanyi and co-workers (9), electronic chemiluminescence in molecular beams has the advantage that the initial energy distribution is not as easily degraded by subsequent collisions during the short radiative lifetime of the emitters (10^{-6} s or less). This is the case even at pressures considerably higher than those employed in the present work.

We wish to report here beam studies of the visible emission from the reaction (10)[1]

$$[1] \qquad NO + O_3 \rightarrow NO_2^* + O_2 \quad (\downarrow h\nu)$$

as a function of collision energy (11).[2] Reaction 1 has been studied in some detail thermally in a flow system (12) and the following Arrhenius

[1]The first beam study of this process and related ones was carried out by Harrison and Scattergood (10) using crossed thermal beams. Due to the low collision energy, no signal attributable to reaction 1 could be detected.

[2]Govers (11) studied the same reaction, which also occurs via a reaction channel leading to NO_2 in its electronic ground state, using a supersonic molecular beam, at collision energies up to 10 kcal/mol. NO_2 was detected by a mass spectrometric technique involving a scatter box but wall reaction seemed to seriously interfere with the beam reaction, and no definite conclusions were reached.

13. T. C. J. OVENSTON and W. T. REES. Anal. (London) **75**, 204 (1950).
14. R. W. RAMETTE and R. W. SANDFORD. J. Am. Chem. Soc. **87**, 5001 (1965).
15. F. BJÖRKSTÉN. Biochim. Biophys. Acta, **212**, 396 (1970).
16. F. A. COTTON and G. WILKINSON. Advanced inorganic chemistry. 2nd ed. John Wiley and Sons Inc., New York, N.Y. 1966. p. 223.
17. R. P. BELL. The proton in chemistry. Cornell University Press, Ithaca, N.Y. 1959. p. 89.

Can. J. Chem. Downloaded from www.nrcresearchpress.com by 210.87.254.6 on 09/05/12
For personal use only.

Molecular Beam Chemiluminescence. I. Kinetic Energy Dependence of the $NO + O_3 \rightarrow NO_2^* + O_2$ Reaction

ANTHONY E. REDPATH AND MICHAEL MENZINGER
Lash Miller Chemical Laboratories, University of Toronto, Toronto 181, Ontario

Received April 23, 1971

The visible chemiluminescence of the $NO + O_3 \rightarrow NO_2^* + O_2$ reaction has been studied as a function of collision energy using a supersonic molecular beam of NO. The reaction threshold $E_0 = 3.00 \pm 0.45$ kcal/mol is found to lie significantly below the Arrhenius activation energy of $E_a = 4.18 \pm 0.3$ kcal/mol. This clearly demonstrates the basic difference between the two quantities.

La chimioluminescence visible de la réaction $NO + O_3 \rightarrow NO_2^* + O_2$, a été étudiée en fonction de l'énergie de collision en utilisant un rayon moléculaire supersonique de NO. Le seuil réactionnel, $E_0 = 3.00 \pm 0.45$ kcal/mol se trouve donc être relativement plus bas que l'énergie d'activation d'Arrhenius qui est de $E_a = 4.18 \pm 0.3$ kcal/mol. Ceci démontre clairement la différence fondamentale entre les deux quantités.

Canadian Journal of Chemistry, **49**, 3063 (1971)

Despite the importance which the total reaction crossection $\sigma(E)$ as a function of collision energy plays in theories of elementary gas phase kinetics (1, 2), there is only a small number of neutral–neutral processes (3) for which this function has been determined either by photochemical (4) or by beam (5, 6) methods.

Variable energy molecular beams (chemical accelerators (7)) appear to offer the most obvious means for measuring $\sigma(E)$, but the problem of detecting the total flux of neutral products is serious and has so far precluded a broad application of this approach (3). However, light emitted during a chemiluminescent reaction is relatively easy to detect and its intensity bears a close relationship to the excitation function $\sigma(E)$. The combination of molecular beam with photon detection techniques has been termed molecular beam chemiluminescence (8). Compared to the infrared chemiluminescence studies pioneered by Polanyi and co-workers (9), electronic chemiluminescence in molecular beams has the advantage that the initial energy distribution is not as easily degraded by subsequent collisions during the short radiative lifetime of the emitters (10^{-6} s or less). This is the case even at pressures considerably higher than those employed in the present work.

We wish to report here beam studies of the visible emission from the reaction (10)[1]

$$[1] \qquad NO + O_3 \rightarrow NO_2^* + O_2 \quad (\downarrow h\nu)$$

as a function of collision energy (11).[2] Reaction 1 has been studied in some detail thermally in a flow system (12) and the following Arrhenius

[1]The first beam study of this process and related ones was carried out by Harrison and Scattergood (10) using crossed thermal beams. Due to the low collision energy, no signal attributable to reaction 1 could be detected.

[2]Govers (11) studied the same reaction, which also occurs via a reaction channel leading to NO_2 in its electronic ground state, using a supersonic molecular beam, at collision energies up to 10 kcal/mol. NO_2 was detected by a mass spectrometric technique involving a scatter box but wall reaction seemed to seriously interfere with the beam reaction, and no definite conclusions were reached.

Can. J. Chem. Downloaded from www.nrcresearchpress.com by 210.87.254.6 on 09/05/12
For personal use only.

parameters are known: $A = (7.6 \pm 1.5) \times 10^{11}$ cm^3/mol s and $E_a = 4.18 \pm 0.3$ kcal/mol.

Experimental

A supersonic molecular beam (13) of NO (commercial grade (Matheson), purified by passage over Dry Ice cooled silica gel) seeded with varying amounts of hydrogen (Matheson, purity > 99.9%) for acceleration (14) of the heavy component was chopped, shot through a liquid nitrogen cooled, gold plated, scattering chamber, and monitored by an ionization gauge (15). Ozone was produced in a commercial ozonizer, selectively absorbed on Dry Ice cooled silica gel (11), and admitted to the scattering chamber through a Teflon needle valve. The scattering chamber pressure was measured by a conventional ionization gauge. The beam path within the scattering chamber was viewed by an RCA 6217 Photomultiplier. After lock-in amplification, the signal was measured as a function of the NO/H_2 mixing ratio, while the total nozzle pressure ($P_0 = 480$ Torr) and the scattering chamber pressure (typically $P_s = 3 \times 10^{-4}$ Torr) were kept constant. The kinetic energy of NO was computed from the formula (14)

$$[2] \quad E_{LAB} = \tfrac{1}{2} m_H V^2 = \frac{m_H}{m_M} \int_0^{T_0} C_{pM}\, dT$$

under the assumption of complete velocity equilibration of the two beam components during their isentropic expansion.

The formula expresses the final laboratory energy of the heavy component in terms of m_H, the molecular mass of the heavy component, m_M, the average mass of the gas mixture and C_M, the specific heat at constant pressure of the gas mixture. T_0 is the nozzle temperature. Considering the target molecules as stationary, the conversion to center of mass energies is straightforward. For an unambiguous analysis, a velocity selected beam should be used. Such work is now in progress and will be reported elsewhere.

Results and Discussion

Figure 1 gives the signal $S(E)$ as a function of collision energy. Since it was impractical to monitor the beam intensity with the ionization gauge, theoretical beam fluxes were obtained from the Valleau–Deckers theory (16). The normalized signal $S^n(E)$ is shown in Fig. 2.

As it turns out, the functional forms of $S(E)$ and $S^n(E)$ are similar, particularly up to a few kcal above threshold. As can be seen from $S^n(E)$, the levelling off of $S(E)$ above 8 kcal/mol is due to the intensity drop of the seeded beam at low NO/H_2 mixing ratios, and must not be mistaken for a similar trend in the reaction crossection. Care has to be taken in determining the threshold energy, in particular since the signal appears to approach zero asymptotically, and the measured

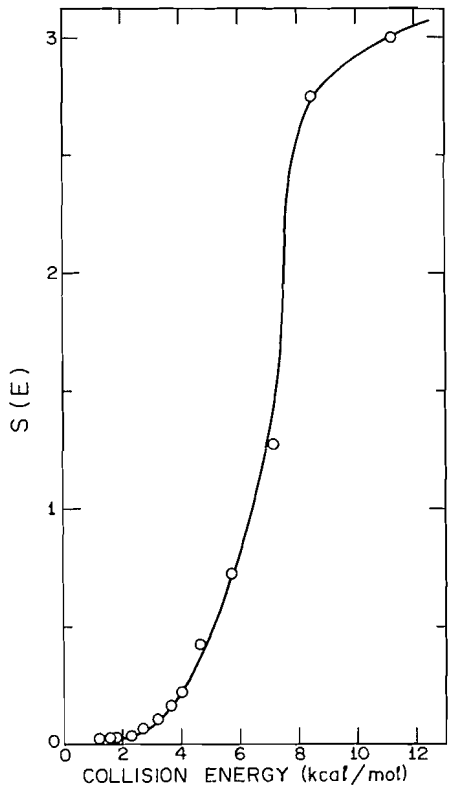

FIG. 1. Chemiluminescence signal (in arbitrary units) as function of the collision energy.

threshold depends sensitively on detection sensitivity and on the spread of collision energies. Our signal-to-noise ratio is $S/N \sim 75$ at 6 kcal/mol, and it decreases with decreasing energy (see insert to Fig. 2.). Subject to the finite detection sensitivity and to an assumed threshold law of the form

$$[3] \quad \sigma(E) = 0 \qquad \text{for } E < E_0$$
$$= C(E - E_0)^n \text{ for } E \geqslant E_0$$

where E_0 is the threshold and C and n are parameters, a least square fit of eq. 3 to $S^n(E)$ yields $E_0' = 2.20 \pm 0.25$ kcal/mol and $n = 2.00 \pm 0.15$. The true threshold E_0 is to be distinguished from the primed quantity E_0', which has not been corrected for the energy distribution in the beam. It has been observed (17) that contrary to theoretical expectations (18), the heavy component in a seeded beam can possess an energy spread of the order of RT_0, where T_0 is the nozzle temperature (300 °K in our case). Assuming this to be the case and taking the motion of the target

Can. J. Chem. Downloaded from www.nrcresearchpress.com by 210.87.254.6 on 09/05/12
For personal use only.

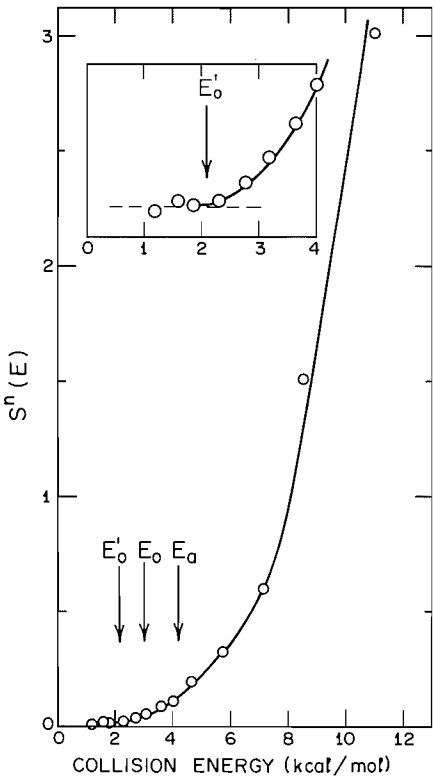

FIG. 2. Normalized signal (arbitrary units) as a function of the collision energy. The threshold region is shown enlarged in the insert. The constant background below 2 kcal is an apparative effect. E_0' is the onset of $S^n(E)$, E_0 is the true threshold energy, corrected for the energy distributions in beam and target, and E_a is the Arrhenius activation energy.

into account, the actual threshold E_0 will lie 0.8 ± 0.2 kcal/mol above the experimental value E_0'. A rigorous unfolding of the data has not been attempted due to our incomplete knowledge of the beam energy distribution. Subject to this restriction reaction 1 possesses a threshold at $E_0 = 3.00 \pm 0.45$ kcal/mol and the signal $S^n(E)$ rises above threshold according to the square ($n = 2.0 \pm 0.15$) of the excess energy.

While the meaning of the threshold energy E_0 is obvious, the Arrhenius activation energy E_a is not as simple a measure of microscopic collision energetics. It has been shown recently (19) that the activation energy is given by $E_a = \langle E^* \rangle - \langle E \rangle$ where $\langle E \rangle$ is the mean thermal energy of the reacting mixture ($\langle E \rangle = 3/2\ RT$ if internal degrees of freedom are neglected), and $\langle E^* \rangle$ represents the average energy of those collisions which lead to reaction. This latter quantity clearly depends on the threshold energy and on temperature as well as on the functional form of the reaction crossection $\sigma(E)$: if $\sigma(E)$ rises relatively quickly from threshold then $\langle E^* \rangle$ will lie close to E_0. On the other hand, if the reaction onset is very slow, as in the family of functions given by eq. 3 with $n > 2$, most of the reactive events occur at energies considerably in excess of E_0, and consequently the activation energy may greatly exceed the threshold. The considerable difference $E_a - E_0 = 1.18 \pm 0.75$ kcal is due primarily to the slow onset of the excitation function (19) and it clearly demonstrates the basic distinction between E_0 and E_a. For an excitation function $\sigma(E)$ of the form [3], an analytical expression for the activation energy E_a has been derived (20)

$$[4]\quad E_a = E_0 + RT\left\{(n + 1/2) - \frac{E_0}{E_0 + RT(n+1)}\right\}$$

The activation energies calculated from our E_0 and n values at the temperature limits and at the mean temperature of Clyne, Thrush, and Wayne's experiments (12*b*) are given in Table 1. The agreement between our computed activation energies and the experimental value of Clyne, Thrush, and Wayne is gratifying.

Furthermore, Table 1 shows that the computed activation energy carries a marked temperature dependence. A careful determination of the rate constant of reaction 1 over an extended temperature range should make this dependence suitable for direct experimental verification. In the above analysis we have tacitly substituted $S^n(E)$ for $\sigma(E)$. This seems justified since the thermal experiments (12) and the present study used the same detection technique.[3] $S^n(E)$ is to be regarded as

TABLE 1. Activation energy and temperature relationship

	E_a	
T (°K)	This work (kcal/mol)	Clyne–Wayne–Thrush (kcal/mol)
216	3.78 ± 0.46	
269	3.99 ± 0.48	4.18 ± 0.3
322	4.22 ± 0.50	

[3]Disregarding the somewhat different wavelength response of the photomultiplier used in (12*b*).

the partial crossection for formation of a detectable product.

To the best of the authors' knowledge this seems to be the first example of a reaction for which the threshold energy has been found to differ significantly from the activation energy.

Thanks are due to Professor J. M. Deckers who designed the vacuum chamber used in this work, and to Mr. K. Schaedlich, who helped during various stages of the experiment. Financial support by the National Research Council of Canada is gratefully acknowledged.

1. H. S. JOHNSTON. Gas phase reaction rate theory. The Ronald Press Co., N.Y. 1966.
2. K. J. LAIDLER. Theories of chemical reaction rates. McGraw Hill. 1969.
3. J. I. STEINFELD, and J. L. KINSEY. The determination of chemical reaction crossections. *In* Prog. React. Kinet. Vol. V. *Edited by* G. Poster. 1970. p. 1.
4. (*a*) A. KUPPERMANN and J. N. WHITE. J. Chem. Phys. **44**, 4352 (1966). (*b*) R. G. GANN, W. N. OLLISON, and J. DUBRIN. To be published.
5. (*a*) J. R. AIREY, E. F. GREENE, K. KODERA, G. P. RECK, and J. ROSS. J. Chem. Phys. **46**, 3287 (1967). (*b*) R. B. BERNSTEIN. Private communication.
6. M. MENZINGER and R. L. WOLFGANG. J. Chem. Phys. **50**, 2991 (1969).
7. R. L. WOLFGANG. Sci. Am. **219**, 44 (1968).
8. (*a*) M. C. MOULTON and D. R HERSHBACH. J. Chem. Phys. **44**, 3010 (1966). (*b*) CH. OTTINGER and R. N. ZARE. Chem. Phys. Lett. **5**, 243 (1970).
9. K. G. ANLAUF, P. J. KUNTZ, D. H. MAYLOTTE, P. D. PACEY, and J. C. POLANYI. Discuss. Faraday Soc. **44**, 183 (1967).
10. H. HARRISON and D. M. SCATTERGOOD. Bull. Am. Phys. Soc. **10**, 1211 (1961). Boeing Scientific Research Laboratories, Document D1-82-0480 (1966).
11. T. R. GOVERS. Ph.D. Thesis. University of Toronto. Toronto, Ontario. 1969.
12. (*a*) J. C. GREAVES and D. GARVIN. J. Chem. Phys. **30**, 348 (1959). (*b*) M. A. A. CLYNE, B. A. THRUSH, and R. P. WAYNE. Trans. Faraday Soc. **60**, 359 (1964). (*c*) P. N. CLOUGH and B. A. THRUSH. Trans. Faraday Soc. **63**, 915 (1967).
13. J. B. ANDERSON, R. P. ANDRES, and J. B. FENN. Adv. Chem. Phys. **X**, 275 (1966). (Interscience Publishers 1966).
14. N. ABUAF, J. B. ANDERSON, R. P. ANDRES, J. B. FENN, and D. G. H. MARSDEN. Sci. **155**, 997 (1967).
15. R. M. YEALLAND, R. L. LEROY, and J. M. DECKERS. Can. J. Chem. **45**, 2651 (1967).
16. J. P. VALLEAU and J. M. DECKERS. Can. J. Chem. **42**, 225 (1964); Can. J. Chem. **43**, 6 (1965).
17. J. B. ANDERSON. Entropie, **18**, 33 (1967).
18. N. ABUAF, J. B. ANDERSON, R. P. ANDRES, J. B. FENN, and D. R. MILLER. *In* Rarefied gas dynamics. *Edited by* C. L. Brundin. Fifth Symposium, Oxford, 1966) Vol. II. Academic Press. 1967. p. 1317.
19. M. MENZINGER and R. L. WOLFGANG. Angew Chem. (Int. Ed.) **8**, 438 (1969).
20. R. L. LEROY. J. Phys. Chem. **73**, 4338 (1969).

Can. J. Chem. Downloaded from www.nrcresearchpress.com by 210.87.254.6 on 09/05/12
For personal use only.

Can. J. Chem. Downloaded from www.nrcresearchpress.com by 210.87.254.42 on 09/05/12
For personal use only.

A Novel Nucleophilic Displacement of Benzoate by Sulfur During Thiation of 3-Deazauridine Tribenzoate[1,2]

MORRIS J. ROBINS
Department of Chemistry, The University of Alberta, Edmonton 7, Alberta

AND

BRUCE L. CURRIE, ROLAND K. ROBINS, AND ARTHUR D. BROOM
Departments of Chemistry and Biopharmaceutical Sciences, University of Utah, Salt Lake City, Utah

Received June 10, 1971

Thiation of 3-deazauridine tribenzoate [4-hydroxy-1-(2,3,5-tri-*O*-benzoyl-β-D-ribofuranosyl)-2-pyridone] (**1***a*) with phosphorus pentasulfide in moist β-picoline followed by debenzoylation gave 2-mercapto-1-(2-deoxy-β-D-arabinofuranosyl)pyridine-4-thione-$S_2 \rightarrow 2'$-cyclonucleoside (**2***b*). Thus, replacement of the heterocyclic oxygens by sulfur followed by a novel nucleophilic displacement of benzoate by mercaptide in the hot basic solution must have occurred.

L'action du pentasulfure de phosphore dans la β-picoline humide sur la déaza-3 uridine tribenzoate [hydroxy-4 (tri-2,3,5, *O*-benzoyl β-D-ribofuranosyl)-1 pyridone-2] (**1***a*) donne après débenzoylation le mercapto-2 (déoxy-2 β-D-arabinofuranosyl)-1 pyridine thione-4 cyclonucléoside-$S_2 \rightarrow 2'$ (**2***b*). Il en résulte qu'il s'est produit un remplacement des oxygènes hétérocycliques par du soufre, suivi d'un déplacement nucléophile du benzoate par un mercaptan, et ceci en solution basique chaude.

Canadian Journal of Chemistry, **49**, 3067 (1971)

Although several thio cyclonucleosides (heterocyclic $S \rightarrow$ sugar anhydronucleosides) have been synthesized by intramolecular nucleophilic displacement (1), sulfonyloxy or halogen leaving groups on the sugar have been employed (1, 2). For example, Wempen and Fox (1*c*) treated 3′-*O*-methanesulfonyl-2′-deoxy-2-thiothymidine with ethanolic triethylamine and obtained the corresponding $S_2 \rightarrow 3'$-cyclonucleoside.

Fox and coworkers (3) have reported the thiation of a number of benzoylated 4-ketopyrimidine nucleosides to give the corresponding 4-thione product using phosphorus pentasulfide in moist refluxing pyridine; and others (4) have used phosphorus pentasulfide in the higher boiling tetralin as solvent to introduce a 2-thione function into benzoylated 2-ketopyrimidine nucleosides. Indeed, benzoate is such a poor $B_{AL}2$ leaving group (5) it is not usually considered in nucleophilic displacement reactions except as a rather strong nucleophile in certain aprotic solvents (6) and the $B_{AL}1$ mechanism is highly unlikely unless stabilized carbonium ions result.

However, reaction of 1-(2,3,5-tri-*O*-benzoyl-β-D-ribofuranosyl)-4-hydroxy-2-pyridone (2′,3′,5′-tri-*O*-benzoyl-3-deazauridine) (**1***a*) with phosphorus pentasulfide in refluxing moist β-picoline gave a 92% yield of crystalline product which gave analytical results compatible with replacement of two oxygens by sulfur and concomitant loss of

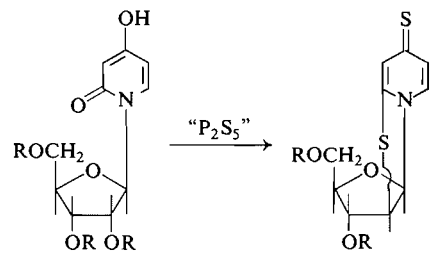

1
a R = —COPh
b R = —H

2
a R = —COPh
b R = —H

[1]This work was supported by Grant Number A5890 from The National Research Council of Canada and Grant Numbers CA-08109 and CA-05209 from the National Institutes of Health, USPHS.

[2]Abstracted in part from the Ph.D. dissertation of B. L. C., University of Utah, Salt Lake City, Utah, September, 1969.

Can. J. Chem. Downloaded from www.nrcresearchpress.com by 210.87.254.42 on 09/05/12
For personal use only.

the elements of benzoic acid. Treatment of this product, **2***a*, with hot alcoholic ammonia gave a debenzoylated product in 38% yield in which no displacement of sulfur had occurred. Reaction of **2***a* with an aqueous alcohol solution of triethylamine at room temperature gave the same compound, **2***b*, in 70% yield. Analytical data for this free nucleoside, **2***b*, suggested replacement of two oxygens by sulfur and loss of water from the parent 3-deazauridine, **1***b*. In view of the formation of the $O_2 \rightarrow 2'$-arabinosyl cyclonucleoside of 3-deazauridine (7) by the phenyl carbonate procedure, the corresponding dithio structure, **2***b*, was considered. This 1-(2-deoxy-β-D-arabinofuranosyl)-2-mercaptopyridine-4-thione-$S_2 \rightarrow$ 2′-cyclonucleoside, **2***b*, had m.p. 241.5–242.5° (dec.); $[\alpha]_D^{27}$ −200° (*c* 1, 50% DMF:H_2O); u.v.$_{max}$ (p*H* 1) 339, 275, 240 nm (ε 19 800, 8610, 13 400); (p*H* 11) 340, 263, 238 nm (ε 29 100, 5520, 13 500).

Anal. Calcd. for $C_{10}H_{11}NO_3S_2$: C, 46.68; H, 4.31; N, 5.45; S, 24.92. Found: C, 46.80; H, 4.29; N, 5.49; S, 24.68.

The absence of ionizable groups on the pyridine base is consistent with the small p*H* variation of the u.v. spectra.

The n.m.r. spectrum of **2***b* was determined in DMSO-d_6 on a Varian HA100 spectrometer. Resonance positions and first order coupling constants are as follows: δ 3.46 (m, 2, $H_{5',5''}$), 4.09 (m, 1, $H_{4'}$), 4.34 (d of d, 1, $J_{3'-4'} = 3.8$, $J_{3'-2'} = 2.8$ Hz, $H_{3'}$), overlapped with 4.41 (d of d, 1, $J_{2'-3'} = 2.8$, $J_{2'-1'} = 6$ Hz, $H_{2'}$), 4.95 (t, 1, $J_{5'\text{-OH-}5',5''} = 5.3$ Hz, 5′-*OH*), 5.90 (d, 1, $J_{3'\text{-OH-}3'} = 4.3$ Hz, 3′-*OH*), 6.52 (d, 1, $J_{1'-2'} = 6$ Hz, $H_{1'}$), 6.97 (d of d, 1, $J_{5-3} = 1.8$, $J_{5-6} = 7$ Hz, H_5), 7.18 (d, 1, $J_{3-5} = 1.8$ Hz, H_3), 7.66 (d, 1, $J_{6-5} = 7$ Hz, H_6). This spectral pattern was very similar to that of 1-(β-D-arabinofuranosyl)-2-hydroxy-4-pyridone-$O_2 \rightarrow$ 2′-cyclonucleoside (7) (the oxygen analog of **2***b*) taking into account the downfield shift induced by a thione sulfur (8) and the upfield shift of alkyl thio *vs.* alkyl oxygen protons (2′-H).[3]

Confirmation of the above assignments was provided by double irradiation experiments. Irradiation of the doublet at δ 6.52 (1′-H) collapsed the low field region of the δ 4.41 (2′-H) multiplet and intense irradiation at δ 4.37 collapsed the δ 6.52 doublet (1′-H) to a sharp singlet and the δ 5.90 doublet (3′-OH) to a singlet. Irradiation of the δ 5.90 doublet (3′-OH) simplified the pattern in the high field region of the δ 4.34 (3′-H) multiplet and allowed first order analysis of the 2′ and 3′ couplings.

A further proof of the cyclonucleoside structure of **2***b* is the fact that addition of D_2O removed only the δ 4.95 triplet and the δ 5.90 doublet (hydroxyl hydrogens) and simplified the 5′,5″-protons absorption to a doublet of doublets centered at δ 3.49 ($J_{5'-4'}$ and $J_{5''-4'} = 5.8$ and 2.8 Hz) but did not reduce the δ 7.18 doublet (3-H) even after prolonged heating. This behavior is also observed in the oxygen cyclonucleoside analog which has a fixed bond structure and is in contrast to the complete loss of the 3-H signal from structures such as 3-deazauridine (**1***b*) which can undergo keto–enol tautomerism in the 3,4-(—CH=COH—) system of the heterocycle (7).

Thus, thiation of the 2- and 4-keto functions of the pyridine base followed by nucleophilic displacement of the 2′-benzoyloxy group by 2-thio anion in the hot picoline solution must have occurred. This novel displacement is of potential use in the preparation of deoxynucleosides (1*b*) in the pyridine series. It would be of interest to investigate the generality of this one-step procedure in other heterocyclic nucleoside systems.

[3]For example, see spectra numbers 396 *vs.* 44 and 490 *vs.* 162 in ref. 9.

1. (*a*) G. SHAW and R. N. WARRENER. J. Chem. Soc. 50 (1959). (*b*) M. IKEHARA. Acc. Chem. Res. **2**, 47 (1969) and references therein. (*c*) I. Wempen and J. J. FOX. J. Org. Chem. **34**, 1020 (1969).
2. For a review see J. J. Fox. Pure and Appl. Chem. **18**, 223 (1969).
3. J. J. FOX, D. VAN PRAAG, I. WEMPEN, I. L. DOERR, L. CHEONG, J. E. KNOLL, M. E. EIDINOFF, A. BENDICH, and G. B. BROWN. J. Am. Chem. Soc. **81**, 178 (1959); and subsequent papers in this series.
4. T. UEDA, Y. IIDA, K. IKEDA, and Y. MIZUNO. Chem. Pharm. Bull. (Tokyo), **16**, 1788 (1968); P. Faerber and K.-H. SCHEIT. Chem. Ber. **103**, 1307 (1970).
5. A. G. DAVIES and J. KENYON. Quart. Rev. **9**, 203 (1955); E. S. GOULD. Mechanism and structure in organic chemistry. Holt, Rinehart and Winston, New York, N.Y., 1959. pp. 342–345.
6. E. J. REIST, L. GOODMAN, and B. R. BAKER. J. Am. Chem. Soc. **80**, 5775 (1958); E. J. REIST, R. R. SPENCER, and B. R. BAKER. J. Org. Chem. **24**, 1618 (1959).
7. M. J. ROBINS and B. L. CURRIE. Chem. Commun. 1547 (1968); B. L. CURRIE, R. K. ROBINS, and M. J. ROBINS. J. Heterocycl. Chem. **7**, 323 (1970).
8. W. E. STEWART and T. H. SIDALL, III. J. Phys. Chem. **74**, 2027 (1970); A. J. JONES, D. M. GRANT, M. W. WINKLEY, and R. K. ROBINS. J. Am. Chem. Soc. **92**, 4079 (1970); R. GREENHALGH and M. A. WEINBERGER. Can. J. Chem. **43**, 3340 (1965).
9. Varian high resolution NMR spectra catalogs. Varian Associates, 1963.

Photoreactions of Nitroso Compounds in Solution.[1] XIX Stereochemistry of Nitrosamine Photoaddition to Olefin

Y. L. CHOW, S. C. CHEN, AND D. W. L. CHANG
Department of Chemistry, Simon Fraser University, Burnaby 2, British Columbia

Received May 25, 1971

The stereochemical course of the photoaddition of nitrosamines to a carbon–carbon double bond was shown to follow a free radical mechanism initiated by aminium radicals. The photoaddition to cyclohexene was highly stereoselective in which the addendum approached in *anti*-diaxial mode. Similar photoadditions to *cis*- and *trans*-2-butenes were less stereoselective, giving mixtures of the *erythro*- and *threo*-adducts, owing to the rotation of the carbon–carbon single bond in the intermediate stage.

Le processus stéréochimique de la photoaddition des nitrosamines sur une double liaison carbone–carbone a été établi comme obéissant à un mécanisme par radical libre initié par des radicaux aminium. La photoaddition sur le cyclohexène est hautement stéréosélective lorsqu'il y a approche *anti*-diaxiale du réactif. Des photoadditions semblables sur les butanes-2 *cis* et *trans* étaient moins stéréosélectives, et donnent des mélanges de produits d'addition *érythro* et *thréo*. Ceci est dû à la rotation de la liaison simple carbone-carbone dans l'étape intermédiaire.

Canadian Journal of Chemistry, **49**, 3069 (1971)

Although photoaddition of nitrosamine to olefin requires the presence of an acid (1–3), the reaction lacks characteristics of a carbonium ion or a radical chain mechanism. The studies by flash excitation (1) have now shown that the aminium radical derived from the singlet excited state of a nitrosamine is initiating the addition to olefinic bond. The attack of an aminium radical, though electrophilic in nature, has to occur via free radical process; a purely electrophilic addition leads to an intermediate which violates the octet rule at the nitrogen center. The stereochemical studies of nitrosamine photoaddition concur with the above conclusion and afford interesting comparisons with the addition reactions of other nitrosyl derivatives (4–7).

We have established that the primary product from the nitrosamine photoaddition is a *C*-nitroso compound (3). In order to preserve the stereochemistry of the primary adduct **1**, it was necessary to prevent tautomerization of **1** to oxime **2** and to divert the secondary reactions (3) to dimer **3** and *N*-nitrosohydroxylamine (**4**). Ideally the final product should be **4** since **3** can reversibly dissociate to **2** via **1** under the conditions of isolation. Photolysis conditions have been established whereby reasonable yields of **3** and/or **4** can be obtained (3).

When the photoaddition of *N*-nitrosodimethylamine to cyclohexene (>350 nm at −40°) was interrupted after half reaction, the *anti*-dimer of *trans*-1-nitroso-2-dimethylamino-cyclohexane (**3***a*, m.p. 115–116°) was isolated in 16% yield.[2] As it is well established that the dimerization process is spontaneous and extremely rapid (8), it is apparent that *trans*-**1***a* is formed predominantly, if not exclusively. Photoaddition with 3–4 *M* excess of the nitrosamine in a Pyrex apparatus at −40° gave *trans*-1-(*N*-nitrosohydroxylamino)-2-dimethylaminocyclohexane (**4***a*, m.p. 108–111°) in 35% yield.[3] Reduction with $LiAlH_4$, followed by acetylation, of either crude **3***a* or crude **4***a* gave the same single product, *trans*-1-acetamido-2-dimethylaminocyclohexane (**5***a*), m.p. 82–84°. The *trans*-configuration of **3***a*, **4***a*, and **5***a* was deduced from the magnitude of the coupling constant (J = 8–10 Hz) between the methine protons. Thus the stereochemistry of **1** was not disturbed during the transformation to **4**.

The photoaddition of *N*-nitrosopiperidine to *trans*-2-butene yielded *erythro*-**4***b* (m.p. 34–36°)

[1]For Part XVIII of this series, see ref. 1.

[2]The yield of **3***a* was *ca.* 35% based on the nitrosamine consumed. The n.m.r. of the crude reaction mixture showed major signals due to **3***a* and minor signals due to **2***a*: the estimated yield of **3***a* on the bases of the n.m.r. signals is *ca.* 75%. Signals expected for the corresponding *cis*-isomer of **3***a* were not present.

[3]Since nitrosohydroxylamines **4***a* and *b* are readily soluble in water, quantitative isolation has not been achieved. A comparison of the n.m.r. spectrum of crude **4** with that of pure **4** showed that the former was slightly contaminated with oxime **2**.

Can. J. Chem. Downloaded from www.nrcresearchpress.com by 210.87.254.6 on 09/05/12
For personal use only.

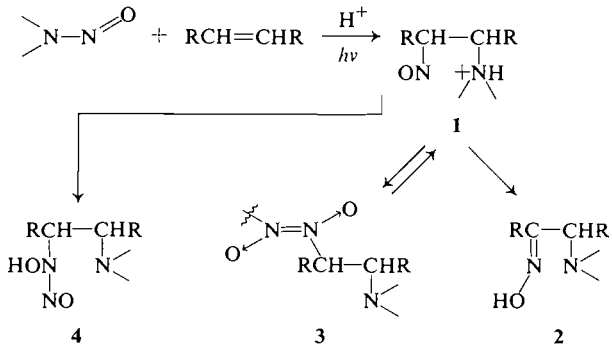

a R = $-(CH_2)_4-$
b R = $-CH_3$

and *threo*-**4***b* (m.p. 54–55°) in 4:1 ratio. Similar photoaddition to *cis*-2-butene yielded the *erythro*- and *threo*-**4***b* in 4:6 ratio. The *erythro* and *threo* ratio of **4***b* was 4:6 from both *cis*- and *trans*-2-butenes if the photoreaction was performed using a Corex filter. Although the stereochemistry of the adducts could not be deduced from the coupling constants of their methine protons (J = 10.5 and 10 Hz, respectively), a decision on the stereochemistry was, however, possible by comparison of their chemical behavior. The coupling constants of the methine protons indicate that both *threo*-**4***b* and *erythro*-**4***b* are overwhelmingly populated with the conformers indicated in which intramolecular hydrogen bonding is favored only in *threo*-**4***b* but not in *erythro*-**4***b*. This physical difference is revealed in the following observations: (*i*) The chemical shift of the n.m.r. signal for OH in *threo*-**4***b* (τ −1.4) is independent of variation in concentration while that of *erythro*-**4***b* (τ 0.38) is not. (*ii*) *Erythro*-**4***b* forms a green Cu^{2+} complex instantaneously while *threo*-**4***b* does not. Dimer **3***b* obtained from these photoadditions was shown to be a mixture of all the possible combinations from *threo*- and *erythro*-**1***b*. Although the % yields of **3***b* and **4***b* are only fair a low stereoselectivity during the course of photoaddition is established. Further it has been ascertained that butenes are not isomerized during the photolysis by v.p.c. analyses.[4]

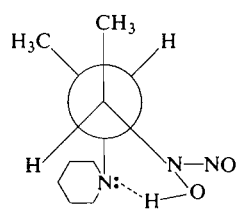

threo-**4***b*

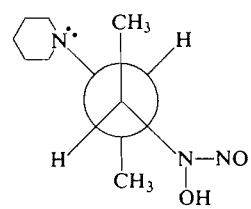

erythro-**4***b*

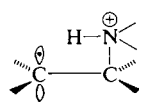

6

Since the photoaddition of *N*-nitrosodimethylamine to 4-*t*-butylcyclohexene gives predominantly those oximes (corresponding to **2***a*) having axial dimethylamino group (10), the aminium radical approaches the olefinic bond preferentially from axial direction to give the radical cation intermediate **6** and the mode of the addition is *anti*-parallel in a stepwise process. The predominance of the *trans*-adduct to cyclohexene suggests that combination of radical cation **6** with NO (or the equivalent) is very rapid;[5] the process requires less activation energy than the inversion barrier of the cyclohexyl radical. The observed mixtures of *erythro*- and *threo*-isomers in the photoaddition to the butenes may result from comparable activation energies required for the radical combination step and the rotation about the C—C bond in **6**.

The authors wish to thank the National Research Council of Canada and the President's Research Fund of Simon Fraser University for financial support.

[4]It is pertinent to point out that a nitrosamine photolytically adds to dienes efficiently instead of isomerizing dienes by sensitization (9).

[5]The photoaddition of *N*-nitrosopiperidine to β-pinene gives the addition product without cleaving the four-member ring. This requires that the corresponding intermediate **6** has very short lifetime (unpublished result; H. H. Quon of this laboratory).

Can. J. Chem. Downloaded from www.nrcresearchpress.com by 210.87.254.6 on 09/05/12
For personal use only.

1. M. P. LAU, A. CESSNA, Y. L. CHOW, and R. W. YIP. J. Am. Chem. Soc. In press.
2. Y. L. CHOW, S. C. CHEN, and C. J. COLÓN. J. Org. Chem. **32**, 2109 (1967).
3. Y. L. CHOW, S. C. CHEN, and D. W. L. CHANG. Can. J. Chem. **48**, 157 (1969).
4. M. OHNO, M. OKAMOTO, and K. NUKADA. Tetrahedron Lett. 4047 (1965).
5. J. MEINWALD, Y. C. MEINWALD, and T. N. BAKER, III. J. Am. Chem. Soc. **86**, 4074 (1964).
6. T. BEIER, H. G. HAWTHAL, and W. PRITZKOW. J. Prakt. Chem. **26**, 304 (1964).
7. H. C. HAMMAN and D. SWERN. Tetrahedron Lett. 3303 (1966); J. Am. Chem. Soc. **90**, 6481 (1968).
8. A. MACKOR, TH. A. J. W. WAJER, and TH. J. DEBOER. Tetrahedron Lett. 2757 (1967).
9. Y. L. CHOW, C. J. COLÓN, and D. W. L. CHANG. Can. J. Chem. **48** 1664 (1970): Y. L. CHOW, C. J. COLÓN, H. H. QUON, and T. MOJELSKY. Can. J. Chem. Submitted.
10. S. C. CHEN. Ph.D. Thesis. Simon Fraser University, Burnaby, British Columbia, 1970.

High Resolution Nuclear Magnetic Resonance Spectra of Bifluoride Ion and its Homologues

JOHN S. MARTIN AND FRED Y. FUJIWARA
Department of Chemistry, The University of Alberta, Edmonton 7, Alberta

Received June 1, 1971

The high resolution ^1H and ^{19}F nuclear magnetic resonance (n.m.r.) spectra of the four bihalide ions have been observed in aprotic solvents. The ^1H shielding is, in every case, 14 p.p.m. less than that in the related molecule. The spin–spin coupling in FHF^- is 120.5 ± 0.3 Hz.

Les spectres r.m.n. de ^1H et ^{19}F, à haute résolution, des quatre ions bihalogénures ont été pris dans des solvants aprotiques. Le blindage de ^1H est, dans tous les cas, inférieur de 14 p.p.m. à celui dans des molécules apparentées. Le couplage spin–spin dans FHF^- est de 120.5 ± 0.3 Hz.

Canadian Journal of Chemistry, **49**, 3071 (1971)

The bihalide anions, XHX^- (X = F, Cl, Br, I), which are stable in crystals and in solution, are chemical entities of unique structure. The hydrogen atom is located between the halogens. It is at the center of symmetry in FHF^- (1); in $ClHCl^-$ and $BrHBr^-$, its exact location appears to depend on its environment (2). The energies of formation from corresponding hydrogen halides and halide ions are in the range −15 to −40 kcal mol^{-1}. The three-center, hydrogen-bridged structure in these ions thus represents an extreme form of hydrogen bonding; its occurrence in such simple, symmetric systems makes their electronic structure one of fundamental interest.

The nuclear shieldings and couplings are sensitive probes of electronic structure. We have observed high resolution ^1H and ^{19}F spectra of the four bihalide ions, as tetraalkylammonium salts dissolved in aprotic solvents.

Tetrabutylammonium bifluoride was prepared from the bromide salt by exchange *in aquo* on a Dowex 21K fluoride column, then freeze dried, and pumped at 50°. On cooling, it gave waxy crystals of m.p. *ca.* 30°. In solution, this gave the ^1H spectrum shown in Fig. 1, at temperatures below +50° in CH_3CN and below −25° in CH_3NO_2. At higher temperatures, the multiplet structure broadened and collapsed, presumably because of interionic exchange.

The ^{19}F spectrum at low temperatures was a doublet, whose spacing, 120.5 ± 0.3 Hz, was equal to that in the ^1H spectrum. The spectra indicate that the two fluorines in FHF^- are symmetric with respect to the hydrogen, on the n.m.r. time scale.

The other bihalides were prepared in solution as follows. To a dilute solution of HCl, HBr, or HI was added the corresponding tetraalkylammonium halide salt. The single ^1H signal was observed to move to much lower shielding, as shown in Fig. 2. It remained sharp, thus indicating that, since it is exchanging rapidly between environments differing in shielding by *ca.* 14 p.p.m., the maximum residence times are of the order of a microsecond.

Can. J. Chem. Downloaded from www.nrcresearchpress.com by 210.87.254.6 on 09/05/12
For personal use only.

1. M. P. LAU, A. CESSNA, Y. L. CHOW, and R. W. YIP. J. Am. Chem. Soc. In press.
2. Y. L. CHOW, S. C. CHEN, and C. J. COLÓN. J. Org. Chem. **32**, 2109 (1967).
3. Y. L. CHOW, S. C. CHEN, and D. W. L. CHANG. Can. J. Chem. **48**, 157 (1969).
4. M. OHNO, M. OKAMOTO, and K. NUKADA. Tetrahedron Lett. 4047 (1965).
5. J. MEINWALD, Y. C. MEINWALD, and T. N. BAKER, III. J. Am. Chem. Soc. **86**, 4074 (1964).
6. T. BEIER, H. G. HAWTHAL, and W. PRITZKOW. J. Prakt. Chem. **26**, 304 (1964).
7. H. C. HAMMAN and D. SWERN. Tetrahedron Lett. 3303 (1966); J. Am. Chem. Soc. **90**, 6481 (1968).
8. A. MACKOR, TH. A. J. W. WAJER, and TH. J. DEBOER. Tetrahedron Lett. 2757 (1967).
9. Y. L. CHOW, C. J. COLÓN, and D. W. L. CHANG. Can. J. Chem. **48** 1664 (1970): Y. L. CHOW, C. J. COLÓN, H. H. QUON, and T. MOJELSKY. Can. J. Chem. Submitted.
10. S. C. CHEN. Ph.D. Thesis. Simon Fraser University, Burnaby, British Columbia, 1970.

High Resolution Nuclear Magnetic Resonance Spectra of Bifluoride Ion and its Homologues

JOHN S. MARTIN AND FRED Y. FUJIWARA
Department of Chemistry, The University of Alberta, Edmonton 7, Alberta

Received June 1, 1971

The high resolution ^1H and ^{19}F nuclear magnetic resonance (n.m.r.) spectra of the four bihalide ions have been observed in aprotic solvents. The ^1H shielding is, in every case, 14 p.p.m. less than that in the related molecule. The spin–spin coupling in FHF^- is 120.5 ± 0.3 Hz.

Les spectres r.m.n. de ^1H et ^{19}F, à haute résolution, des quatre ions bihalogénures ont été pris dans des solvants aprotiques. Le blindage de ^1H est, dans tous les cas, inférieur de 14 p.p.m. à celui dans des molécules apparentées. Le couplage spin–spin dans FHF^- est de 120.5 ± 0.3 Hz.

Canadian Journal of Chemistry, **49**, 3071 (1971)

The bihalide anions, XHX^- (X = F, Cl, Br, I), which are stable in crystals and in solution, are chemical entities of unique structure. The hydrogen atom is located between the halogens. It is at the center of symmetry in FHF^- (1); in $ClHCl^-$ and $BrHBr^-$, its exact location appears to depend on its environment (2). The energies of formation from corresponding hydrogen halides and halide ions are in the range −15 to −40 kcal mol^{-1}. The three-center, hydrogen-bridged structure in these ions thus represents an extreme form of hydrogen bonding; its occurrence in such simple, symmetric systems makes their electronic structure one of fundamental interest.

The nuclear shieldings and couplings are sensitive probes of electronic structure. We have observed high resolution ^1H and ^{19}F spectra of the four bihalide ions, as tetraalkylammonium salts dissolved in aprotic solvents.

Tetrabutylammonium bifluoride was prepared from the bromide salt by exchange *in aquo* on a Dowex 21K fluoride column, then freeze dried, and pumped at 50°. On cooling, it gave waxy crystals of m.p. *ca.* 30°. In solution, this gave the ^1H spectrum shown in Fig. 1, at temperatures below +50° in CH_3CN and below −25° in CH_3NO_2. At higher temperatures, the multiplet structure broadened and collapsed, presumably because of interionic exchange.

The ^{19}F spectrum at low temperatures was a doublet, whose spacing, 120.5 ± 0.3 Hz, was equal to that in the ^1H spectrum. The spectra indicate that the two fluorines in FHF^- are symmetric with respect to the hydrogen, on the n.m.r. time scale.

The other bihalides were prepared in solution as follows. To a dilute solution of HCl, HBr, or HI was added the corresponding tetraalkylammonium halide salt. The single ^1H signal was observed to move to much lower shielding, as shown in Fig. 2. It remained sharp, thus indicating that, since it is exchanging rapidly between environments differing in shielding by *ca.* 14 p.p.m., the maximum residence times are of the order of a microsecond.

Can. J. Chem. Downloaded from www.nrcresearchpress.com by 210.87.254.6 on 09/05/12
For personal use only.

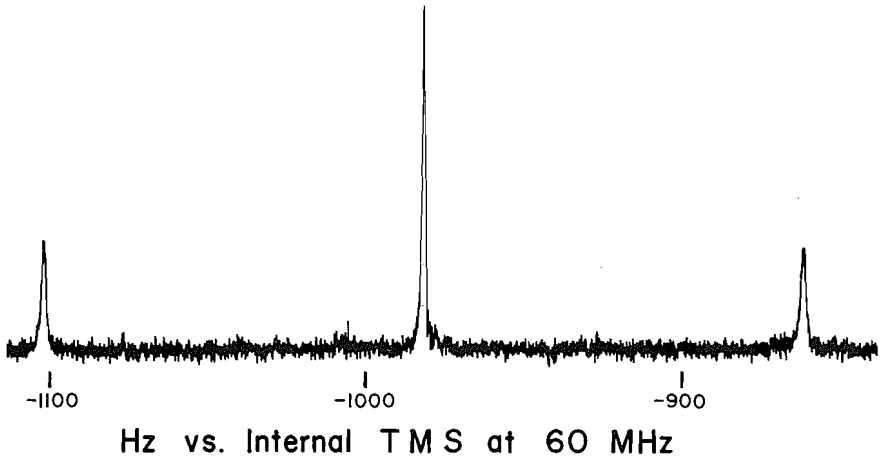

FIG. 1. The ^1H spectrum of bifluoride ion, as a 0.6 *M* solution of the tetrabutylammonium salt in acetonitrile at −30°. The intensities of the three lines were determined, by integration, to be in the proportion 1:2:1.

TABLE 1. ^1H shieldings of bihalide ions and the corresponding hydrogen halides, in p.p.m.

Shielding	F	Cl	Br	I
of XHX^-, *vs.* TMS	−16.3	−13.9	−10.2	−0.9
of HX gas, *vs.* CH_4	−2.1*	+0.45†	+4.35†	+13.25†
of XHX^-, absolute	14.8	17.2	20.9	30.2
of HX, absolute	28.8	31.4	35.3	44.2

*Reference 5.
†Reference 6.

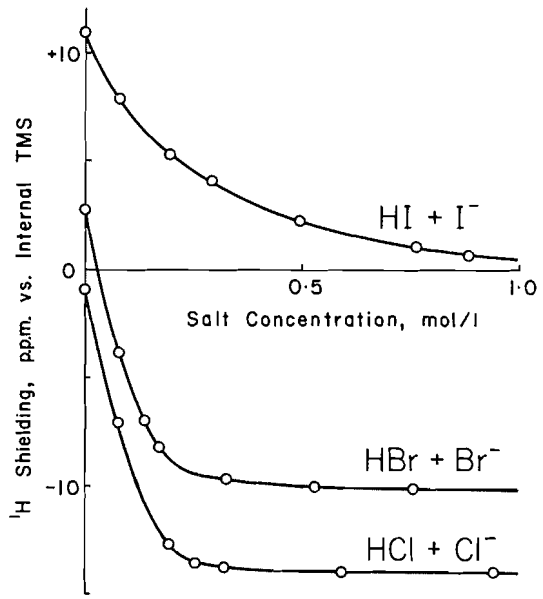

FIG. 2. Effect, on the ^1H shielding of 0.2 *M* hydrogen halide in symmetric tetrachloroethane, of added tetra-*n*-butylammonium halide.

It is evident from Fig. 2 that strong 1:1 complexes are formed between HCl and Cl^-, and between HBr and Br^-. The limiting shieldings, in excess salt, are taken as those of the bihalide ions, $ClHCl^-$ and $BrHBr^-$. It is evident that the iodide–HI complex is much weaker. The shielding of IHI^- was deduced by Benesi–Hildebrand–Scott analysis (3).

The observed ^1H shieldings are summarized in Table 1. To *ca.* 0.3 p.p.m., they are insensitive to the nature of the cation or the solvent, to concentration, and to temperature in the range studied (−80 to +70°). The absolute shieldings were determined using that of CH_4 (4).

It is remarkable that the decrease in ^1H shielding when a bihalide ion is formed happens to be nearly the same in all cases: about 14 p.p.m. This is an exceptionally large hydrogen bond shift, and represents a significant fraction of the total absolute shielding.

The ^1H shieldings may be accounted for by a simple "atom in a molecule" model, which provides a good description of the shieldings in

Can. J. Chem. Downloaded from www.nrcresearchpress.com by 210.87.254.6 on 09/05/12
For personal use only.

the hydrogen halides (7). In these cylindrically symmetric systems, it can be shown (8) that all significant contributions to the ^1H shielding increase with increasing 1s orbital population. The smaller shielding in the bihalide ion thus indicates that it has greater charge separation, in the sense $X^-H^+X^-$, than the molecule. This is in accord with recent s.c.f.-m.o. calculations (9), and with the nuclear quadrupole resonance (n.q.r.) spectra of $ClHCl^-$ and HCl (10).

The independent-electron m.o. model (11) predicts the opposite charge shift: greater 1s population in the ion than in the molecule. This presumably is a consequence of neglect of electron–electron repulsions, which *are* evaluated in the s.c.f. model. A very simple electrostatic picture of bihalide formation accounts for the charge shifts in an entirely natural way. As the halide ion, X^-, approaches the positive (H) region of the HX molecule, electronic charge is repelled out of the hydrogen orbital.

The ^{19}F shielding in bifluoride ion is somewhat temperature dependent, increasing from +67 to +71 p.p.m. *vs.* external neat CF_3COOH as the temperature increases from −20 to +70°. It agrees well with previous indirect determinations (12). Since the bifluoride ^{19}F shielding is intermediate between those of F^- and HF, it is also consistent with an electrostatic model of the FHF^- structure.

The H—F coupling in bifluoride, 120.5 ± 0.3 Hz, is about one fourth of that in the HF molecule, 521 Hz (13). This is also consistent with a smaller 1s population in the ion. A s.c.f.-m.o. calculation has already been published (14). While it failed by about 30% to fit the observed values of the couplings in HF and FHF^-, it nevertheless predicted with remarkable accuracy that they would be in the ratio 4:1.

1. J. A. Ibers. J. Chem. Phys. **41**, 25 (1964).
2. G. S. Stirling, C. J. Ludman, and T. C. Waddington. J. Chem. Phys. **52**, 2730 (1970); J. C. Evans and G. Y.-S. Lo. J. Phys. Chem. **71**, 3942 (1967); L. W. Schroeder. J. Chem. Phys. **52**, 1972 (1970).
3. R. L. Scott. Rec. Trav. Chim. Pays-Bas. **75**, 787 (1956).
4. D. K. Hindermann and C. D. Cornwell. J. Chem. Phys. **48**, 4148 (1968).
5. D. K. Hindermann and C. D. Cornwell. J. Chem. Phys. **48**, 2017 (1968).
6. W. G. Schneider, H. J. Bernstein, and J. A. Pople. J. Chem. Phys. **28**, 601 (1958).
7. C. Deverell. Mol. Phys. **18**, 319 (1970).
8. J. S. Martin and F. Y. Fujiwara. To be published.
9. P. A. Kollman and L. C. Allen. J. Am. Chem. Soc. **92**, 6101 (1970).
10. J. C. Evans and G. Y-S. Lo. J. Phys. Chem. **71**, 3697 (1967).
11. G. C. Pimentel. J. Chem. Phys. **19**, 446 (1951).
12. R. Haque and L. W. Reeves. J. Am. Chem. Soc. **89**, 250 (1967); K. Schaumburg and C. Deverell. J. Am. Chem. Soc. **90**, 2495 (1968).
13. E. L. Mackor, C. MacLean, and C. W. Hilbers. Rec. Trav. Chim. Pays-Bas. **87**, 655 (1968).
14. A. Azman, B. Borstnik, and J. Koller. Theoret. Chim. Acta, **13**, 262 (1969).

Can. J. Chem. Downloaded from www.nrcresearchpress.com by 210.87.254.6 on 09/05/12
For personal use only.

49
P-3075-4196
1971.

Canadian Journal of Chemistry

Published by THE NATIONAL RESEARCH COUNCIL OF CANADA

VOLUME 49 OCTOBER 1, 1971 NUMBER 19

Sur l'aptitude à l'extension du noyau pipéridique en fonction de la substitution de l'atome d'azote: réaction du diazométhane avec quelques pipéridones-4 et désamination nitreuse des aminométhyl-alcools correspondants[1]

H. FAVRE, Z. HAMLET,[2] R. LANTHIER,[3] ET M. MÉNARD[4]

Département de chimie, Université de Montréal, Montréal, Québec

Recu le 20 mai 1970[5]

L'aptitude à l'extension, mesurée par le rapport cétone agrandie/époxyde, varie considérablement en série pipéridique en fonction du substituant porté par l'atome d'azote. Elle est sensiblement la même lors de l'action du diazométhane sur les pipéridones-4 et de la désamination nitreuse des amino-alcools correspondants. Les valeurs sont de 0.01–0.1 pour un groupe phénylsulfonyle, de l'ordre de 0.3–0.6 pour un groupe benzoyle, et légèrement supérieures à 1 pour un groupe benzyle. Des effets électroniques (effets d'induction et de champ) sont à l'origine de ces différences. Le parallélisme entre les deux réactions indique que l'attaque nucléophile du diazométhane sur le groupe carbonyle peut fort bien engendrer la cétone agrandie et l'époxyde.

Aptitude to ring expansion in the piperidine series, measured by the ratio of ring expanded ketone to epoxide, varies considerably according to the nitrogen atom substituent. This ratio is essentially the same in the case of the reaction of diazomethane on 4-piperidones and the nitrous acid deamination of the corresponding aminoalcohols. The values of the ratio are 0.01–0.1 for a phenylsulfonyl group, of the order 0.3–0.6 for a benzoyl group and slightly greater than 1 for a benzyl group. Electronic effects (inductive and field effects) are the cause of these differences. Parallels between the two reactions indicate that nucleophilic attack of diazomethane on the carbonyl group can lead to the ring expanded ketone and the epoxide.

Canadian Journal of Chemistry, 49, 3075 (1971)

D'une manière générale, l'action des diazoalkanes sur les cyclanones **1** conduit à une extension de cycle (1, 2); il en va de même de la désamination nitreuse des aminométhyl-1 cyclanols **3** (1, 3). Dans les deux cas un époxyde spiranique **5** se forme, en quantité variable. Divers facteurs affectent le rapport cétone agrandie/époxyde; parmi ceux-ci, la présence d'un groupe électronégatif, tel que —OH, —Cl en α du groupe carbonyle, augmente la proportion d'époxyde. On peut ainsi s'attendre à ce que les hétérocycles saturés du type **1** (qui ont un groupe électronégatif en β du carbonyle) donnent à leur tour des proportions plus grandes d'époxyde que la tert-butyl-4 cyclohexanone: c'est en effet le cas (tableau 1) de la *p*-toluènesulfonyl-1 pipéridone-4 (**1***f*) (4), de la benzyl-1 pipéridone-4 (**1***b*) (5, 6), de la thiacyclohexanone-4 (**1***h*) (7); du côté des amino-alcools, la formation d'époxyde est nettement prédominante dans le cas de **3***g* (7); elle n'est pas connue pour l'aminoalcool **6** qui conduit à 45% de cétone agrandie (8). Ce mémoire traite d'une étude comparée de l'aptitude à l'extension des pipéridones-4 **1***b–e* et des amino-alcools correspondants **3***b*, *c*, et *e*.

[1]Tiré en partie des thèses de doctorat de R. Lanthier (1956) et M. Ménard (1959), Université de Montréal, Montréal, Québec.

[2]Boursier post-doctoral du Conseil National de Recherches du Canada (1962–1964); attaché de recherches (1964–1966). Adresse actuelle: Université Sir George Williams, Montréal, Québec.

[3]Boursier de l'Office Provincial de Recherches Scientifiques et boursier Canadian Industries Ltd. Adresse actuelle: Shawinigan Chemicals Ltd., Centre de recherches, Ste-Anne de Bellevue, Québec.

[4]Boursier du Conseil National de Recherches du Canada. Adresse actuelle: Bristol Laboratories of Canada, Candiac, Québec.

[5]Révision reçue le 6 mai 1971.

Can. J. Chem. Downloaded from www.nrcresearchpress.com by 210.87.254.5 on 09/05/12
For personal use only.

TABLEAU 1. Pourcentages de cétone agrandie et d'époxyde

X		Diazométhane					Désamination nitreuse				
		Cétone agrandie	Epoxyde	Aptitude	Référence		Cétone agrandie	Epoxyde	Aptitude	Référence	
$(CH_3)_3CCH=$	**1***a*	—	—	1.9–6.5	39	**3***a*	80*	20*	4.0	15	
$C_6H_5CH_2N=$	**1***b*	60†	—	—		**3***b*	60†	—	—		
		44‡	32‡	1.38	5, 6						
$C_6H_5CON=$	**1***c*	26§	40‡	0.65		**3***c*	20§	60‡	0.33		
p-$NO_2C_6H_4CON=$	**1***d*	32‡	53‡	0.60							
$C_6H_5SO_2N=$	**1***e*	9‡	82‖	0.11		**3***e*	<1¶	91‡	0.01		
p-$CH_3C_6H_4SO_2N=$	**1***f*	25‡	19‡	**	4						
$SO_2=$						**3***g*	14	67‡	0.21	7	
S=	**1***h*	42‡	40‡	1.0	7						
						6	57‡	—	—	8	

*Dosage par chromatographie en phase gazeuse.
†Semicarbazone.
‡Isolé comme tel.
§Phénylhydrazone.
‖Diéthylamino-alcool $C\begin{matrix}OH\\ \diagdown\\ CH_2—N(C_2H_5)_2\end{matrix}$.
¶Dinitro-2,4 phénylhydrazone.
**Séparation incomplète des composés de réaction.

Nous avons obtenu les phénylsulfonyl-1 et *p*-nitrobenzoyl-1 pipéridones-4 (**1***e* et *c*) en traitant le chlorhydrate de pipéridone-4 par les chlorures d'acides correspondants. Les benzoyl-1 et benzyl-1 pipéridones-4 sont connues (5, 9); la synthèse de la cétone **3***c* décrite par Morosawa peut être améliorée pour porter le rendement global de 30 à 69.5%.

Les amino-alcools **3***a–c* et *e* furent préparés par la voie classique: 1 → 2 → 3. La condensation de la cyclohexanone avec le nitrométhane s'effectue avec un rendement de 75% en présence d'une quantité équimoléculaire d'éthylate de sodium (10), tandis que le rendement baisse à 45% en présence d'une quantité catalytique du même composé (11). En présence d'une quantité équimoléculaire de méthylate de sodium, les cétones **1***c* et *e* conduisent aux nitro-alcools correspondants, avec des rendements respectifs de 66 et 85%. Seule une quantité catalytique de méthylate de sodium permet d'obtenir le nitro-alcool **1***b*: le rendement est alors de 85%.

Pour la réduction des nitro-alcools en amino-alcools nous avons mis en œuvre une méthode fort peu utilisée (12): les agents de réduction sont le sulfate ferreux et le fer en poudre, en milieu aqueux, neutre. Cette méthode permet de réduire quantitativement le nitrométhyl-1 cyclohexanol-1 (**2***a*) en amino-alcool **3***a*. Cette méthode permet d'obtenir, avec des rendements de 91 et 97% les amino-alcools **3***c* et *e*; elle ne s'applique pas au nitro-alcool benzylé **3***b*: dans ce cas, une réduction par le zinc dans l'acide acétique donne l'amino-alcool attendu. Les trois amino-alcools pipéridiques ont été oxydés en cétone par l'acide périodique, ce qui établit bien leur structure. Les amino-alcools **3***b* et *c* sont huileux et n'ont pas donné de sels cristallisés; ils ont été caractérisés par leurs spectres de r.m.n. et i.r.

Nous avons, pour fin de comparaison de l'action du diazométhane et de la désamination nitreuse, choisi les modes opératoires utilisés respectivement par Barbier (13), diazométhane engendré *in situ*, par décomposition de la nitrosométhylurée dans du méthanol en présence d'hydroxyde de potassium et par Tchoubar (14), acide acétique aqueux 25%. Au début de nos travaux, nous pensions que ces deux modes de réaction présentaient des analogies réelles, en ce que des essais préliminaires sur la cyclohexanone et sur l'amino-alcool correspondant indiquaient que la cétone agrandie représentait de 60 à 70% du mélange réactionnel, tandis que l'époxyde se formait à raison de 10–15%. Nous savons aujourd'hui, après des analyses poussées par chromatographie en phase gazeuse,[6] que ces deux modes opératoires ne présentent plus le parallélisme étroit du début (tableau 1). Ce qui était important, de toute façon, c'était de comparer le comportement des cétones et des amino-alcools dans des conditions identiques. Il s'est avéré que les méthodes choisies

[6]Le dosage de composés issus de la désamination a été publié (15); nous décrivons en détail les résultats de notre étude sur la formation des époxydes en série cyclohexanique à partir des cétones par l'action du diazométhane (39).

Can. J. Chem. Downloaded from www.nrcresearchpress.com by 210.87.254.5 on 09/05/12
For personal use only.

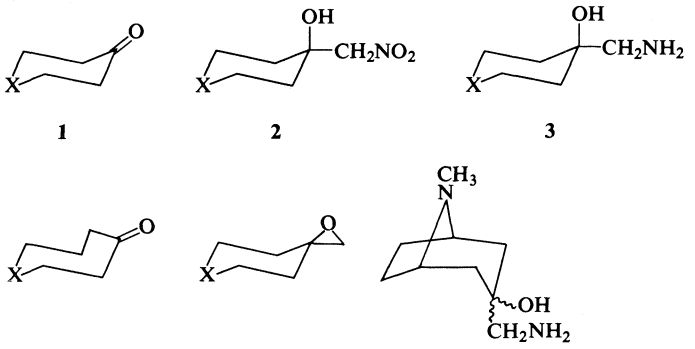

1 **2** **3**

4 **5** **6**

a X = $(CH_3)_3CCH$
b X = $C_6H_5CH_2N$
c X = C_6H_5CON
d X = *p*-$NO_2C_6H_4CON$
e X = $C_6H_5SO_2N$
f X = *p*-$CH_3C_8H_4SO_2N$
g X = SO_2
h X = S

permettaient de telles comparaisons, puisque les cétones et les amino-alcools ont tous réagi dans les conditions imposées, et ceci avec des rendements du même ordre de grandeur. Les résultats sont rapportés au tableau 1.

Tous les pourcentages du tableau 1, à l'exception de ceux correspondant à la série cyclohexanique, correspondent à des composés isolés, soit à l'état pur, soit sous forme de dérivés. Les époxydes présentent, dans les spectres de r.m.n., le singulet caractéristique du groupe 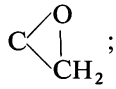 ; les cétones agrandies montrent l'abaissement de la fréquence C=O en i.r. caractéristique de l'agrandissement de cycle; de plus, les époxydes ont été synthétisés par la méthode de Corey et Chaykowsky (16) qui conduit avec des rendements supérieurs à 90% aux époxydes pipéridiques **5***b–e*. A la suite des sérieuses difficultés rencontrées dans le dosage du mélange issu de l'action du diazométhane avec la benzoyl-1 pipéridone-4, nous avons étudié cette réaction sur la *p*-nitrobenzoyl-1 pipéridone-4; tous les composés de réaction étant cristallins, le dosage fut plus facile et corrobore celui obtenu dans la série benzoylée. Nous n'avons jamais pu mettre en évidence la présence de l'époxyde **5***e* dans la série benzylée, tant à partir de la cétone[7] que de l'amino-alcool; dans des conditions expérimentales différentes, Morosowa (6) a réussi à l'isoler; ses résultats et les nôtres concordent de façon satisfaisante en ce qui concerne la cétone agrandie. Nous avons cherché également à mettre en évidence la formation d'azacyclo-octanones par une réaction ultérieure du diazométhane avec la première cétone agrandie mais sans succès; en série cyclohexanique, il ne se forme que très peu d'ailleurs de cétones supérieures à la cycloheptanone (2–3%), dans les conditions choisies pour la réaction. Trois points ressortent nettement de cette étude: (*1*) la formation d'époxyde peut être prépondérante, même exclusive dans la réaction de Tiffeneau–Demjanov et dans l'action du diazométhane appliquées à la série hétérocyclique; les observations d'Overberger et Katchman (7) en série thiannique peuvent ainsi être généralisées; (*2*) le parallélisme étroit entre l'aptitude à l'extension dans les deux réactions; (*3*) la bonne réactivité des cétones hétérocycliques dans les conditions expérimentales choisies et la dépendance de l'aptitude à l'extension de ces conditions expérimentales (les cétones **1***e* et *f* ont été soumises à des conditions expérimentales très différentes, tableau 1).

Le mécanisme de la désamination nitreuse a été établi à la suite de nombreux travaux (17–21). L'étape déterminante est le passage de l'ion diazonium au carbocation; les groupes antipériplanaires par rapport à l'ion diazonium ne participent pas à la formation du carbocation; les composés formés dépendent des vitesses relatives de réaction et de rotation du carbocation (**7**

[7]L'époxyde peut réagir avec l'hydroxyde de potassium pour donner un hydroxy-éther (39); une faible concentration en base et une courte durée de réaction tendent à supprimer cette réaction secondaire. Casy et Birnbaum (41) ne rapportent également que la cétone agrandie.

Can. J. Chem. Downloaded from www.nrcresearchpress.com by 210.87.254.5 on 09/05/12
For personal use only.

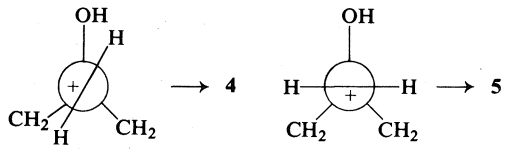

7 8

et **8** qui donnent **4** et **5**). Un groupe électronégatif, dans le cas des molécules **3***c*, *e*, et *f*, défavorisera la formation de la cétone agrandie en ralentissant la migration de la liaison C—C, celle-ci devant être fortement polarisée dans le sens du groupement électronégatif.

Une autre façon de considérer l'interaction entre le groupe électronégatif et le centre positif de réaction est de tenir compte de la distance qui sépare les points positifs (ou les dipôles) (22) au cours de l'extension de cycle et de la formation de l'époxyde; les charges positives sont plus rapprochées dans l'extension (**9***b*) que dans la formation de l'époxyde (**9***a*), défavorisant ainsi l'extension.[8]

9*a*

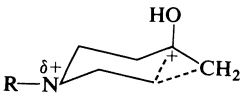

9*b*

Cette interaction entre charges positives se manifeste dans les amino-alcools, dont la basicité diminue en allant de la série cyclohexanique, à la série pipéridique et finalement à la série thiannique (tableau 2). Cette diminution de basicité, attribuable à un effet de champ, se retrouve en série pipérazinique (23). On connait d'autres exemples d'intervention d'un groupe sulfonyle. Le bioxyde d'amino-4 thianne (**10***a*) est nettement moins basique que l'amino-1 cyclohexane (24). Une interaction transannulaire se manifeste par un effet hypsochrome dans la série **11**, lorsque X passe de CH_2 à SO_2 (25, 26): il s'agit d'une opposition de deux charges positives, l'atome de soufre d'un côté, la structure de résonance $+C—C{=}C—O^-$ de l'autre. Le groupe sulfonyle empêche l'estérification de l'amino-alcool **10***b* (24). Finalement, le groupe sulfonyle retarde la solvolyse du système $C_6H_5SO_2(CH_2)_n C(CH_3)_2Cl$ par rapport à $H—CH_2—C(CH_3)_2Cl$: l'effet du groupe électronégatif s'atténue lorsque *n* passe de 1 à 2 à 3 (27). Cette dernière étude est intéressante par le fait qu'elle montre clairement, par une comparaison des groupes $=SO_2$ et $=SO$, que le groupe $=SO_2$ ne participe pas du tout à la réaction par ses oxygènes, comme le fait le groupe $=SO$ qui, en ce faisant, accélère la réaction (voir aussi (28)).

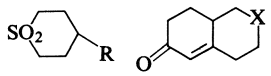

10 **11**

a R = NH_2
b R = $NHCH_2CH_2OH$

Le cas des amino-alcools comportant un deuxième groupe aminé basique soit **3***b* et **6** est intéressant. On se serait attendu, en raison de la charge positive sur l'azote tertiaire, en milieu acide, à une forte proportion d'époxyde dans ces désaminations, puisque la basicité d'une pipérazine est très faible lorsqu'un premier groupe NH est protoné (23) (tableau 2). Comme l'extension est prédominante, il faut admettre que la nature des interactions entre charges positives s'est profondément modifiée: l'apparition du carbocation pourrait modifier l'équilibre sel/base tertiaire; il se pourrait aussi que des interactions par ponts hydrogènes entre le sel d'ammonium de l'amine tertiaire et le groupe hydroxyle (par l'intermédiaire du solvant HOH (29, 30)) influent sensiblement sur l'aptitude du groupe hydroxyle à former un époxyde.

Nous n'avons jusqu'ici considéré que le seul effet électronégatif de l'hétéro-atome dans l'interprétation de l'aptitude à l'extension. On sait qu'il existe aussi des effets conformationnels (15, 31). D'une manière générale (32) on admet que la

TABLEAU 2. pK_a des amino-alcools **5** et d'amines apparentées

X	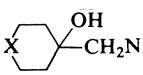	
$—CH_2—$	8.90	11.13
$C_6H_5—CON=$	8.30	7.78
$CH—SO_2N=$	8.29	
$p\text{-}CH_3—C_6H_4SO_2N=$		7.44
$—NH_2—$		5.52
$—SO_2—$	7.91	

[8]Seules les formules spatiales à groupes $—CH_2N_2^+$ et $—CH_2^+$ équatoriaux sont représentées (voir texte plus loin).

Can. J. Chem. Downloaded from www.nrcresearchpress.com by 210.87.254.5 on 09/05/12
For personal use only.

TABLEAU 3. Constantes de dissociation des cyanhydrines

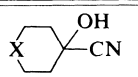

X	Déterminations	$K_d \times 10^{-3}$	K_d relative	Référence
—CH_2—	4	3.3	1	
C_6H_5—CH_2N=	3	4.6	1.4	
C_6H_5—CON=	3	5.9	1.8	
C_6H_5—SO_2N=	3	5.6	1.7	
—$CH(CH_3)$—			0.6	33, 34
—$C(CH_3)_2$—			2.5	34

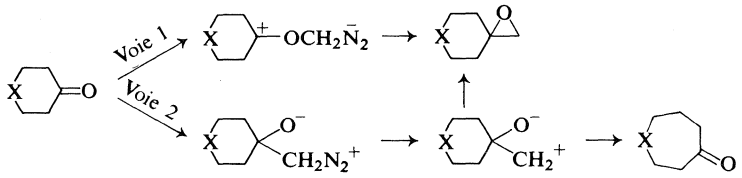

SCHÉMA 1

conformation d'une cétone hétérocyclique est semblable à celle de la cyclanone correspondante. Dans le but d'obtenir des renseignements sur des déformations possibles des cétones hétérocycliques **1***b*, *c*, et *e*, nous avons examiné les constantes de dissociation de leurs cyanhydrines (tableau 3). Elles sont voisines les unes des autres et légèrement supérieures à celle de la cyclohexanone. La différence est toutefois trop petite pour expliquer la formation prépondérante d'époxyde: des substituants en position 4 de la cyclohexanone et de l'amino-alcool correspondant n'affectent pas le rapport cétone agrandie/époxyde (2, 3). Par ailleurs, nous avons, en série cyclohexanique, détecté un effet conformationnel dans la réaction de Tiffeneau–Demjanov (15); cet effet a été observé également en série décalinique (31). Il se produit plus d'époxyde lorsque le groupe —CH_2NH_2 est équatorial que lorsqu'il est axial. La conformation équatoriale ou axiale du groupe —CH_2—NH_2 dans les amino-alcools hétérocycliques est difficile à préciser. D'une part, la valeur d'énergie conformationnelle du groupe =$C(OH)CH_3$ n'est pas égale à la somme des énergies conformationnelles des substituants OH et CH_3 pris séparément (35, 36). D'autre part, un substituant fonctionnel électronégatif, tel que carbonyle, augmente la proportion d'isomère ayant un groupe OH axial lorsqu'il est situé en position 4 dans un cyclohexanol (37). Il faut relever cependant que l'aminométhyl-1 cyclohexanol-1 réagit entièrement comme amino-alcool à groupe —CH_2NH_2 équatorial (15) dans des conditions identiques de réaction. Avec aussi un groupe —CH_2NH_2 équatorial[9] (formule spatiale **3**), nous nous trouverions dans les conditions les plus favorables à la formation de l'époxyde.

En ce qui regarde l'action du diazométhane sur les cétones hétérocycliques, l'explication électronique donnée pour la réaction de Tiffeneau–Demjanov s'applique dans l'hypothèse d'une attaque nucléophile du diazométhane sur la cétone selon la voie 2 du schéma 1.

La question du mécanisme de réaction n'est toutefois pas tranchée. Pour Bradley *et al.* (38) les voies 1 et 2 sont possibles, la voie 2 étant favorisée en présence de grandes quantités d'alcool. Nous montrons dans un autre article (39) que la *tert*-butyl-4 cyclohexanone réagit bien dans ce sens. Pour Gutsche et Bowers (40), la voie 2 ne conduirait qu'à la cétone agrandie, l'époxyde résultant entièrement de la voie 1. Le fait que la désamination nitreuse conduise aux époxydes, allié à celui que la réaction se fait dans du méthanol pur, milite en faveur de la voie 2. De plus, les travaux de Henbest (22) indiquent que la formation d'une charge positive en γ de l'hétéroatome dans la voie 1 est défavorisée par rapport à la formation de l'ion diazonium ou du carbocation, lorsque X est égal à C_6H_5—SO_2—N= et

[9]Dans la formule spatiale **3**, les groupements C_6H_5-CO= et $C_6H_5SO_2$— adopteraient une conformation comprise entre une conformation plane (due à la résonance (33)) et une conformation équatoriale (dans la méthyl-4 benzoyl-1 pipéridine (34), le groupe benzamide se trouve de préférence en conformation non plane).

Can. J. Chem. Downloaded from www.nrcresearchpress.com by 210.87.254.5 on 09/05/12
For personal use only.

C_6H_5—CO—N=; l'inverse sera vrai, par contre lorsque X est égal à C_6H_5—CH_2—N=; il est raisonnable, dès lors, d'envisager dans ce dernier cas que les deux voies 1 et 2 sont possibles.

Conclusion

Ce travail établit clairement que l'aptitude à l'extension des cétones hétérocycliques à six chaînons est limitée et fortement dépendante de la nature du substituant porté par l'atome d'azote dans les pipéridones-4.

Partie expérimentale[10]

1 Synthèse des cétones

*1.1 Benzyl-1 pipéridone-4 (**1b**)*

La synthèse de Morosawa (5) est améliorée par adjonction d'éthanol à la condensation de la benzylamine avec l'acrylate d'éthyle et l'utilisation d'une plus grande quantité d'acrylate d'éthyle (50 g d'amine, 100 ml d'éthanol anhydre et 200 g d'ester); le rendement est ainsi de 92%. L'utilisation d'hydrure de sodium, comme agent de cyclisation, augmente le rendement à 69.5%.[11]

*1.2 Benzoyl-1 pipéridone-4 (**1c**)*

Préparée selon (9), p. de f. 50–52°. Spectre i.r.: (CCl_4) 1723 (C=O), 1648 cm^{-1} (NC=O).

*1.3 p-Nitrobenzoyl-1 pipéridone-4 (**1d**)*

Benzoyle-1 carbéthoxy-3 pipéridone-4 (100 g) (9) sont chauffés à reflux pendant 2 h avec 400 ml d'acide chlorhydrique 6 *N*. L'acide benzoïque libéré est extrait à froid par de l'éther et la solution aqueuse est évaporée sous vide à une température inférieure à 60°. Le résidu est dissous dans 30 ml d'eau et transvasé dans un ballon à trois tubulures de 2 l surmonté d'un réfrigérant, d'un agitateur et d'une ampoule à addition. A cette solution, on ajoute 250 ml de chloroforme et, en agitant, 40 g de carbonate de sodium anhydre. Par l'ampoule, on laisse tomber lentement 67 g de chlorure de *p*-nitrobenzoyle dissous dans 300 ml de chloroforme. En agitant, on chauffe à reflux pendant 4 h.

Après ce temps, l'excès de chlorure de *p*-nitrobenzoyle est estérifié en refluant la solution avec 20 ml d'éthanol pendant 30 min. Le sel précipité est dissous dans le minimum d'eau glacée et décanté de la couche chloroformique; celle-ci est lavée successivement par Na_2CO_3 5% glacé, H_2O et HCl 5% et séchée sur Na_2SO_4. Par évaporation du solvant, on obtient un résidu huileux qui cristallise par addition d'éther. La recristallisation du résidu dans le butanol normal donne 63 g (70%) de **1***d* sous forme d'aiguilles incolores fondant à 118.5–119°. Spectre i.r.: (CCl_4) 1723 cm^{-1} (C=O).

Anal. calc. pour $C_{12}H_{12}O_4N_2$: C, 58.06; H, 4.87; N, 11.28. Trouvé: C, 57.76; H, 4.68; N, 11.31.

La 2,4-dinitrophénylhydrazone recristallisée dans le solvant mixte nitrométhane–éthanol, présente un p. de f. de 123–125°.

Anal. calc. pour $C_{18}H_{16}O_7N_6$: N, 19.22. Trouvé: N, 19.13.

L'oxime cristallise du mélange éthanol–eau sous forme d'aiguilles incolores fondant à 203.5–204°.

Anal. calc. pour $C_{12}H_{13}O_4N_3$: N, 15.96. Trouvé: N, 15.91.

*1.4 Phénylsulfonyl-1 pipéridone-4 (**1e**)*

La benzoyl-1 carbéthoxy-3 pipéridone-4 (100 g), obtenue selon McElvain et McMahon (9) est chauffée à l'ébullition à reflux avec 400 ml de HCl 6 *N* pendant 6 h. Après extraction de l'acide benzoïque par de l'éther, la solution est évaporée jusqu'à sec. Le résidu est dissous dans 40 ml d'eau on ajoute 400 ml de $CHCl_3$, 70 g de Na_2CO_3 finement pulvérisé et finalement sous bonne agitation et par petites portions 80 g de chlorure de benzènesulfonyle. Le mélange est agité durant 2 h à 25°, puis chauffé à l'ébullition pendant 2 h. Après filtration, la couche chloroformique est décantée, lavée avec HCl 5%, NaOH 5% puis avec une solution saturée de NaCl. Par distillation du solvant, on obtient un résidu rouge brun qui est repris par du tétrachlorure de carbone. Après traitement par du noir animal, on obtient la *phénylsulfonyl-1 pipéridone-4* (**1e**) sous forme de paillettes incolores, p. de f. 121–122° (rendement 74%). Spectre i.r.: (CCl_4) 1721 cm^{-1} (C=O).

Anal. calc. pour $C_{11}H_{13}O_3NS$: C, 55.21; H, 5.47; N, 5.85. Trouvé: C, 55.32; H, 5.48; N, 5.83.

L'oxime, cristallisée deux fois dans un mélange de méthanol et d'eau, fond à 172–173°.

Anal. calc. pour $C_{11}H_{14}O_3N_2S$: C, 51.95; H, 5.55; N, 11.02. Trouvé: C, 52.11; H, 5.92; N, 10.90.

La dinitro-2,4 phénylhydrazone, cristallisée dans l'éthanol, fond à 197°.

Anal. calc. pour $C_{17}H_{17}O_6N_5S$: C, 48.45; H, 4.54; N, 16.62. Trouvé: C, 48.74; H, 4.22; N, 16.78.

2 Nitro-alcools

*2.1 Benzyl-1 nitrométhyl-4 pipéridol-4 (**2b**)*

On dissout 40 g de benzyl-1 pipéridone-4 dans 75 ml de méthanol. On ajoute à cette solution 17.6 g de nitrométhane et 25 ml de méthanol dans lequel on a dissous auparavant 0.5 g de sodium. La solution résultante est refroidie pour quelques minutes puis laissée à la température ordinaire pendant 28 h. On verse le mélange réactionnel dans 400 ml d'eau glacée; il se dépose une huile que l'on extrait par du chloroforme. La solution est acidifiée par de l'acide acétique, puis rendue alcaline par addition d'une solution de $NaHCO_3$. La solution aqueuse est de nouveau extraite par du chloroforme. Les couches organiques sont réunies, lavées par une solution de $NaHCO_3$ et à l'eau et séchée sur Na_2SO_4 anhydre. Par

[10]Les points de fusion (p. de f.) ont été déterminés en tubes capillaires avec un thermomètre étalonné avec des substances pures de p. de f. connu. Les spectres i.r. ont été déterminés, en solution, au moyen d'un appareil Beckman IR 8, optique NaCl; en émulsion dans le Nujol, au moyen d'un appareil Perkin–Elmer modèle 112, double passage et simple faisceau, optique de chlorure de calcium. Les spectres de r.m.n. ont été enregistrés au moyen d'un appareil JEOL, 60 MHz, en solution dans le tétrachlorure de carbone, avec référence au tétraméthylsilane. Les analyses centésimales ont été effectuées par Geller Laboratories, Hackensack, New Jersey et M. Manser, Herrliberg.

[11]Une synthèse récente (42) conduit au chlorhydrate de benzyl-1 éthoxycarbonyl-3 pipéridone-4 avec un rendement de 52% à partir de l'amine.

Can. J. Chem. Downloaded from www.nrcresearchpress.com by 210.87.254.5 on 09/05/12
For personal use only.

Can. J. Chem. Downloaded from www.nrcresearchpress.com by 210.87.254.5 on 09/05/12
For personal use only.

évaporation du solvant, on obtient un résidu huileux qui cristallise par addition d'éther de pétrole (p.éb. 20–40°), 44.0 g (85%). La cristallisation dans l'éther de pétrole (p.éb. 65–110°) donne de très longues aiguilles incolores du nitro-alcool **2***b*, p. de f. 79°.

Spectre i.r. (CCl_4) 3590 et 3340 (—OH), 1540 et 1380 cm^{-1} (—NO_2). Spectre de r.m.n. (CCl_4) δ 7.3 (s, 5H, C_6H_5—), 4.16 (s, 2H, —CH_2—NO_2), 3.5 (s, 2H, —CH_2—N), 2.86 (s, 1H, —OH), 2.5 (m, 4H, —CH_2— adjacents à N du cycle), 1.7 (m, 4H, autres —CH_2— du cycle).

Anal. calc. pour $C_{13}H_{18}O_3N_2$: C, 62.38; H, 7.25; N, 11.19. Trouvé: C, 62.58; H, 7.42; N, 11.01.

2.2 Benzoyl-1 nitrométhyl-4 pipéridol-4 (2c)

Dans un ballon de 2 l à trois tubulures, muni d'une ampoule à décantation, d'un réfrigérant surmonté d'un tube à $CaCl_2$, d'un thermomètre plongeant jusqu'au fond du ballon et d'un agitateur mécanique à joint de mercure, on introduit 500 ml d'éthanol absolu et 11.4 g de sodium fraîchement coupé.

Quand tout le sodium est dissous, on ajoute, goutte à goutte, à la solution agitée maintenue à une température de 40°, une solution de 100 g de benzoyl-1 pipéridone-4 et 40 ml de nitrométhane dans 200 ml d'éthanol absolu. On continue l'agitation à la même température pendant 3 h puis on laisse le mélange au repos pour la nuit.

On ajoute 500 ml d'éther afin de précipiter complètement le sel sodé du nitro-alcool **2***c* formé puis on filtre. Le précipité est lavé plusieurs fois à l'éther.

Le sel est ensuite décomposé par la dissolution dans l'eau froide et addition lente d'acide acétique (35 ml) glacial; il se dépose une huile qui se solidifie facilement. Le mélange est extrait au chloroforme puis la solution organique est décantée lavée par $NaHCO_3$ et à l'eau, et séchée sur Na_2SO_4. Par évaporation du solvant, on obtient un résidu solide qui est, par la suite, cristallisé dans un mélange égal d'éthanol absolu et d'éther de pétrole (65–110°); il se sépare de la solution des aiguilles incolores, p. de f. 131–132° (rendement 85%).

Spectre i.r. (Nujol) 3260 (—OH) 1600 (—CON<), 1580 cm^{-1} (—NO_2). Spectre de r.m.n. (DMSO-d_6) δ 7.32 (s, 5H, C_6H_5—), 4.52 (s, 2H, —CH_2—NO_2), vers 3.2 et 1.6 (2 massifs, 8H, protons cycliques), 5.3 (s, 1H, —O*H*, échangeable en présence de D_2O).

Anal. calc. pour $C_{13}H_{16}O_4N_2$: C, 59.08; H, 6.10; N, 10.60. Trouvé: C, 59.30; H, 6.25; N, 10.68.

2.3 Nitrométhyl-4 phénylsulfonyl-1 pipéridol-4 (2e)

Selon le mode opératoire 2.2, 33.2 g de phénylsulfonyl-1 pipéridone-4 donnent après cristallisation dans le butanol normal 27.5 g d'aiguilles incolores de nitro-alcool **2***e* p. de f. 148.5–149.5° (rendement 66%).

Anal. calc. pour $C_{12}H_{16}O_5N_2S$: C, 47.99; H, 5.37; N, 9.33. Trouvé: C, 48.32; H, 5.29; N, 9.24.

3 Amino-alcools

3.1 Aminométhyl-1 cyclohexanol-1 (3a)

Dans un ballon à trois tubulures muni d'un agitateur à joint de mercure et d'un réfrigérant, on introduit 2.8 g de $FeSO_4 \cdot 7H_2O$, 150 ml d'eau, 25 g de fer en poudre, et 3 g de nitrométhyl-1 cyclohexanol-1 (p.éb. 130–132° sous 18 mm). Tout en maintenant une bonne agitation, le mélange est chauffé à l'ébullition à reflux durant 3 h. On extrait soigneusement par du chloroforme, puis on rend la solution aqueuse fortement alcaline par addition de NaOH 40%. Après filtration ou mieux centrifugation de l'hydroxyde ferreux formé, la solution alcaline est extraite par le chloroforme. On obtient après évaporation du solvant un résidu huileux incolore correspondant à un rendement de 100% en *aminométhyl-1 cyclohexanol-1*. Cet amino-alcool fut caractérisé par son chlorhydrate p. de f. 212–213° (Dauben *et al.* (43) donnent 215–216°).

3.2 Aminométhyl-4 benzyl-1 pipéridol-4 (3b)

Dans un ballon à trois tubulures de 500 ml, muni d'un agitateur mécanique et d'un thermomètre plongeant jusqu'au fond du ballon, on introduit 125 ml d'acide acétique et 34 g de zinc en poudre. Tout en maintenant une forte agitation et une température inférieure à 30°, on ajoute, par petites portions 12 g de nitro-alcool. On poursuit l'agitation pendant 6 h à 25°. On filtre les produits de réaction et on lave avec un peu d'acide acétique le zinc non transformé. Les filtrats d'acide acétique sont réunis puis distillés sous 10 mm à une température de 40° pour conduire à un résidu liquide; ce dernier est repris par l'eau et la solution aqueuse rendue alcaline par addition d'une solution de NaOH à 40%. L'extraction par trois portions d'éther de 100 ml chacune donne après évaporation du solvant 9.5 g d'huile jaune pâle correspondant à l'amino-alcool brut. Rendement 91%. Le chlorhydrate, l'acétate et le picrate sont des produits trop hygroscopiques pour être purifiés et analysés.

Spectre i.r. (CCl_4) vers 3400 cm^{-1}, bande très forte correspondant à —OH et —NH_2. Spectre de r.m.n. (CCl_4) δ 7.4 (s, 5H, C_6H_5—), 3.55 (s, CH_2 benzylique), 2.6 (m, 6H, 2 CH_2 du cycle et —CH_2— adjacent à —NH_2), 1.6 (m, autres —CH_2— du cycle), l'intégration montre de plus qu'il y a trois protons sous les pics décrits à 3.55 et 2.6, —NH_2 et OH. L'adjonction d'acides (CH_3COOH et HCl) élargit les pics à 3.55 et 2.6, confirmant la présence de deux atomes d'azote basiques dans la molécule. Le spectre de r.m.n. montre de plus qu'il ne reste dans cette amine aucune trace du composé de départ **2***b*.

Oxydation periodique

On dissout 1.0 g d'huile obtenue dans l'expérience précédente dans 10 ml de méthanol, puis on ajoute à la solution 1.0 g de HIO_4 dissous dans 50 ml d'eau, on laisse au repos pendant 24 h. La solution est concentrée jusqu'à 10 ml sous pression de 10 mm à une température de 40°, rendue alcaline par addition de soude à 10% et finalement extraite à l'éther par deux portions de 20 ml chacune. La solution éthérée est séchée puis évaporée au bain-marie; le résidu obtenu est ensuite dissous dans 10 ml de méthanol et traité par 1.0 g de chlorhydrate de semicarbazone, 1.5 g d'acétate de sodium, et 10 ml d'eau. Après contact de 24 h, on filtre le solide formé et cristallise ce dernier dans le butanol secondaire, on obtient des lamelles incolores p. de f. 195°. Cette semicarbazone ne donne pas de dépression, à l'essai de mélange avec une préparation authentique de semicarbazone de benzyl-1 pipéridone-4.

3.3 Aminométhyl-4 benzoyl-1 pipéridol-4 (3c)

Selon le mode opératoire 3.1, 3 g de nitro-alcool **2***c* donnent 2.6 g d'un résidu huileux, rendement 97%, qui constitue l'amino-alcool **3***c* brut. La formation d'un dérivé cristallisé (chlorhydrate, oxalate, acétate et picrate) a échoué.

Spectre i.r. (Nujol) 3450 (bande large, —OH et —NH_2),

Can. J. Chem. Downloaded from www.nrcresearchpress.com by 210.87.254.5 on 09/05/12
For personal use only.

1600 cm^{-1} (—CON<). Spectre de r.m.n. ($CDCl_3$) 6.98 (s, 5H, C_6H_5—), vers 3.2 et 1.4 (2 massifs, 4H chacun, protons cycliques), 2.4 (s large, 2H, —CH_2—NH_2), 2.2 (s large, 3H environ, —NH_2 et —OH, échangeables en présence de D_2O).

Oxydation periodique

On dissout 1 g d'amino-alcool **2***c* dans 10 ml de méthanol puis on ajoute à la solution 1 g de HIO_4 dissous dans 50 ml d'eau. On agite pendant quelques minutes et on laisse au repos pendant 24 h. On extrait alors la solution aqueuse par deux portions de 50 ml de $CHCl_3$. Le résidu huileux obtenu par évaporation de la solution de chloroforme est dissous dans 10 ml de méthanol. On ajoute à cette solution 1.0 g de phénylhydrazine et quelques gouttes d'acide acétique; on chauffe jusqu'à ébullition et on laisse refroidir pour obtenir des aiguilles jaunes pâles p. de f. 133°. Le p. de f. mixte avec un échantillon authentique de phénylhydrazone de benzoyl-1 pipéridone-4 ne donne aucune dépression.

3.4 Aminométhyl-4 phénylsulfonyl-1 pipéridol-4 (3e)

Selon le mode opératoire 3.1, 20 g de nitro-alcool **2***e* donnent 16.4 g (91%) d'amino-alcool brut **3***e*, p. de f. 124–125° après cristallisations répétées dans l'acétate d'éthyle et l'éther de pétrole, puis dans l'eau.

Anal. calc. pour $C_{12}H_{18}O_3N_2S$: C, 53.31; H, 6.71; N, 10.36. Trouvé: C, 53.80; H, 6.99; N, 10.18.

Le chlorhydrate, préparé dans l'éther par adjonction d'acide chlorhydrique gazeux, fond à 221–222°, après cristallisation dans un mélange d'isopropanol et d'éther.

Anal. calc. pour $C_{12}H_{19}O_3N_2SCl$: C, 46.97; H, 6.24; N, 9.13. Trouvé: C, 47.05; H, 6.25; N, 9.07.

Oxydation periodique

On dissout 1.0 g d'amino-alcool **3***e* dans 10 ml de méthanol et ajoute 1.0 g de HIO_4 en solution dans 5 ml d'eau. On agite pendant quelques minutes et abandonne pendant 5 h à 25°. Le volume de la solution est alors porté à 50 ml par adjonction d'eau. Après 24 h de contact, on recueille sur un filtre le précipité formé et on le cristallise dans le tétrachlorure de carbone. La phénylsulfonyl-1 pipéridone-4 (**1***e*) ainsi obtenue fond à 121–122°, seule ou en mélange avec un échantillon authentique.

4 Désamination nitreuse

4.1 Désamination nitreuse de l'amino-alcool (3b)

L'amino-alcool **3***b* (10 g) est dissous dans 100 ml d'acide acétique à 25%. En agitant et à température de 0°, on y ajoute, en 45 min, une solution de nitrite de sodium (4 g dans 20 ml d'eau). Après 2 h d'agitation à 0°, on ajoute au mélange réactionnel 6 g de chlorohydrate de semicarbazide et 9 g de $CH_3CO_2Na \cdot 3H_2O$. On agite jusqu'à dissolution complète, puis on laisse au repos toute la nuit. La solution est évaporée à sec; le résidu repris par de l'eau et la solution rendue alcaline par l'addition de soude à 40%; il se produit une précipitation d'un solide brun, lequel, cristallisé plusieurs fois dans le butanol secondaire (prismes) fond à 182–184°. Rendement 60% (en semicarbazone).

Anal. calc. pour $C_{14}H_{20}ON_4$: C, 64.58; H, 7.74; N, 21.53. Trouvé: C, 64.77; H, 7.71; N, 21.44.

Spectre de r.m.n. (DMSO-d_6) δ 8.93 (s, 1H, =N—NH —CO—), 7.4 (s, 5H, C_6H_5—), 6.3 (s, 2H, —CO—NH_2), 3.6 (s, 2H, —CH_2—N), 2.55 (bande unique, 8H, CH_2— adjacents à —N et C=N—), 1.8 (m, 2H, CH_2 restant du cycle).

4.2 Désamination nitreuse de l'amino-alcool (3c)

L'amino-alcool **3***c* (1.7 g) est dissous dans 25 ml d'acide acétique à 25%. Après refroidissement de la solution à 0°, on y ajoute, goutte à goutte, tout en maintenant une bonne agitation, 10 ml d'une solution de $NaNO_2$ (0.6 g dans 10 ml d'eau). L'agitation est continuée à 0° pendant 2 h. Le mélange réactionnel est extrait au chloroforme; la couche organique est ensuite lavée avec une solution de $NaHCO_3$ à 5%, à l'eau et séchée sur Na_2SO_4. On obtient par évaporation du solvant, une huile rouge très visqueuse; la distillation de cette huile sous vide poussé conduit à 1.4 g d'un produit visqueux incolore p.éb. 168–172°/0.6 mm. Le produit est traité par le réactif P de Girard et Sandulesco; 1.4 g de distillat sont chauffés à reflux pendant 1½ h avec 1.5 g de réactif, 15 ml de méthanol, et 1.5 ml d'acide acétique glacial. La solution est refroidie puis versée sur de la glace (50 g). Le mélange est extrait par cinq portions d'éther de 50 ml chacune; on obtient une solution éthérée (solution *A*) et une solution aqueuse (solution *B*).

Solution A

La solution est séchée puis concentrée jusqu'à 10 ml; il se forme par refroidissement une cristallisation de 0.95 g de *benzoyl-1 oxa-1 aza-5 spiro[5.2]octane* (**5***c*) (aiguilles incolores), p. de f. 83.5°. Rendement 60%. Le spectre i.r. ne montre aucune bande carbonyle. Le spectre r.m.n. est le suivant, dans CCl_4, en valeurs δ: quatre massifs de 2H, 1.25–1.6, 1.7–2.05, 3.3–3.7, et 3.7–4.1; singulet à 2.61 (2H correspondant à 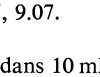); pic fin centré à 7.45 (5H, phényle).

Anal. calc. pour $C_{13}H_{15}O_2N$: C, 71.86; H, 6.96; N, 6.44. Trouvé: C, 71.60; H, 7.36; N, 6.44.

Solution B

On ajoute dans la solution aqueuse 20 ml de HCl 6 *N* et on laisse en contact pour la nuit. L'extraction par deux portions de 50 ml chacune de benzène et évaporation du solvant organique donne 0.32 g d'une huile jaune pâle correspondant à la benzoyl-1 aza-1 cycloheptanone-4 (**4***c*). Cette cétone que l'on n'a pas pu purifier par distillation donne facilement une phénylhydrazone p. de f. 201° (éthanol). Rendement brut 20%.

Anal. calc. pour $C_{19}H_{21}ON_3$: C, 74.23; H, 6.88; N, 13.67. Trouvé: C, 74.17; H, 7.01; N, 13.70.

Cette mise au point pour la séparation des produits de réaction est le résultat de plusieurs essais; il fut impossible de séparer le mélange par distillation fractionnée (p.éb. 168–172°/0.6 mm) ou par chromatographie sur une colonne d'alumine ou encore par cristallisation fractionnée. Seul le réactif P de Girard et Sandulesco a permis une séparation satisfaisante des substances cétoniques des autres composants du mélange.

4.3 Désamination nitreuse de l'amino-alcool (3e)

L'acétate de l'amino-alcool **3***e* (17.1 g) est dissous dans 100 ml d'acide acétique à 25%. Cette solution est agitée et maintenue à 0° à l'aide d'un bain de glace et de sel. On y ajoute graduellement durant 45 min une solution de nitrite de sodium (4.3 g dans 20 ml d'eau); il se forme un

Can. J. Chem. Downloaded from www.nrcresearchpress.com by 210.87.254.5 on 09/05/12
For personal use only.

volumineux précipité blanc; l'agitation est continuée durant 2 h à 0°. On extrait par le chloroforme et isole à la manière habituelle 11.9 g d'un solide blanc p. de f. 102–105°. Par cristallisation du produit brut dans le butanol secondaire, on obtient le *phénylsulfonyl-5 oxa-1 aza-5 spiro[5.2]octane* (**5***e*) p. de f. 106–107°, aiguilles incolores. Le spectre i.r. ne montre aucune bande carbonyle. Le spectre r.m.n. est le suivant, dans CCl_4, en valeur δ quatre massifs de 2H, 1.1–1.6, 1.6–2.4, 2.4–3.1, et 3.3–3.8; singulet 2.51 (2H, correspondant à); massif de 7.3 à 7.9 (5H, phényle).

Anal. calc. pour $C_{12}H_{15}O_3NS$: C, 56.89; H, 5.97; N, 5.53. Trouvé: C, 56.96; H, 5.95; N, 5.49.

On chauffe à l'ébullition un mélange de 1.0 g du produit brut, 1.0 g de dinitro-2,4 phénylhydrazine, et 35 ml de méthanol; après refroidissement, on ajoute 5 ml d'acide acétique glacial et porte à l'ébullition pendant quelques minutes. On isole après repos à la glacière, 2 mg de dinitro-2,4 phénylhydrazone p. de f. 167°, correspondant à la cétone agrandie **4***e* identique à celle décrite à la section 5.4 (plus loin).

5 Action du diazométhane sur les cétones

*5.1 Action du diazométhane sur la benzyl-1 pipéridone-4 (**1***b*)*

On dissout dans un ballon de 50 ml à trois tubulures, muni d'un agitateur mécanique et d'un thermomètre plongeant jusqu'au fond du ballon, 3 g de KOH à 80% et 5 g de benzyl-1 pipéridone-4 (**1***b*) dans 15 ml de méthanol.

On ajoute dans la solution fortement agitée, maintenue à 0°, en 30 min, 2.8 g de nitrosométhylurée. A la fin de l'addition, le mélange réactionnel est abandonné à 0° pendant 1 h, puis filtré et acidifié par 6 ml d'acide acétique glacial.

La solution acide est traitée par 6 g de chlorhydrate de semicarbazide et 8 g de $CH_3CO_2Na \cdot 3H_2O$; on chauffe au bain-marie pendant quelques minutes puis on laisse au repos pour la nuit.

En rendant la solution alcaline, il se produit un précipité blanc que l'on isole par filtration (5.5 g).

Après cinq cristallisations dans le butanol secondaire, on isole 3.9 g d'un produit pur (prismes) p. de f. 182–184°. Rendement 60% (en semicarbazone).

Le p. de f. de cette semicarbazone ne donne pas de dépression à l'essai de mélange avec celle obtenue par désamination nitreuse (section 4.1 plus haut).

*5.2 Action du diazométhane sur la benzoyl-1 pipéridone-4 (**1***c*)*

Dans un ballon de 300 ml à trois tubulures, muni d'un agitateur mécanique et d'un thermomètre plongeant jusqu'au fond du ballon, on introduit 125 ml de méthanol et 30 g de KOH aqueux 50%. La solution est refroidie jusqu'à 0° puis on y ajoute 50 g de benzoyl-1 pipéridone-4.

Tout en agitant fortement la solution maintenue à 0°, on ajoute, par petites portions 26.4 g de nitrosométhylurée. Le mélange est ensuite laissé en contact pendant 5 h à 0°, puis filtré et la solution claire neutralisée par de l'acide acétique glacial. La solution est concentrée jusqu'à un volume de 50 ml sous vide partiel et le résidu est repris par $CHCl_3$. La solution de chloroforme est lavée à l'eau, séchée et évaporée; on obtient 48 g d'un résidu huileux.

Le résidu (10 g) est traité par le réactif P de Girard et Sandulesco. On isole:

(*a*) Le produit cétonique (3 g) (test positif au réactif du *m*-dinitro-benzène) qui distille sous 0.2 mm à 165–170°. Ce produit (1 g) est traité par 1 g de phénylhydrazine dans le méthanol. Par cristallisation fractionnée, on obtient 0.76 g de phénylhydrazone, p. de f. 201°, peu soluble, caractérisée comme la phénylhydrazone de l'homopipéridone-4 *N*-benzoylée **4***c* par le p. de f. d'un mélange avec un échantillon décrit à la section 4.2 plus haut et 0.20 g de phénylhydrazone très soluble dans le méthanol dont le p. de f. de 133° ne donne pas de dépression avec un mélange de la phénylhydrazone de la benzoyl-1 pipéridone-4.

(*b*) La fraction non-cétonique (5.5 g) (huile très visqueuse) qui après cristallisation dans l'éther donne 4.3 g, p. de f. 83.5°, de l'époxyde **5***c*, caractérisé par p. de f. de mélange avec un échantillon préparé plus haut à la section 4.2 et 1.2 g d'un résidu huileux.

Il n'est possible dans ce cas d'établir qu'approximativement le bilan de la réaction qui s'établirait comme suit: cétone non-réagie: 9%, époxyde **5***c*: 40%, extension de cycle **4***c*: 26%. Le reste consiste en des mélanges non-résolvables.

*5.3 Réaction du diazométhane sur la p-nitrobenzoyle-1 pipéridone-4 (**1***d*)*

A un mélange de 250 ml de méthanol et 11.2 g d'une solution aqueuse de KOH 50% maintenue à 0° sont ajoutés 24.8 g de *p*-nitrobenzoyle-1 pipéridone-4 et, en agitant fortement et par petites portions, 10 g de nitrosométhylurée; après chaque addition, il faut attendre que la solution devienne incolore avant d'ajouter la portion suivante: après la fin de l'addition, le mélange réactionnel est laissé à la température ambiante pour la nuit, puis neutralisée par l'acide acétique; le solvant est évaporé et le résidu repris par 100 ml d'eau et 100 ml de chloroforme; la fraction aqueuse est de nouveau extraite au chloroforme; les fractions organiques réunies sont lavées par Na_2CO_3 5%, séchées et évaporées sous vide.

Le résidu (25 g) après trois cristallisations dans le méthanol, donne 14.0 g (53%) de l'époxyde **5***d*, sous forme de prismes incolores fondant à 145–146°. Spectre r.m.n. ($CDCl_3$) valeurs δ massif de 1.17 à 2.30 (4H), s à 2.77 (1H,); deux massifs de 3.20 à 4.70 (4H); d, 7.63 (2H, J = 9 Hz); d, 8.33 (2H, J = 9 Hz).

Anal. calc. pour $C_{13}H_{14}O_4N_2$: C, 59.53; H, 5.38; N, 10.68. Trouvé: C, 59.63; H, 5.34; N, 10.60.

Les filtrats de cristallisation de l'époxyde sont évaporés et recristallisés trois fois dans le butanol normal pour donner 6.3 g (26%) de la *p*-nitrobenzoyle-1 aza-1 cycloheptanone (**4***d*) fondant à 134°. Spectre i.r. (CCl_4) 1710 (C=O), 1650 cm^{-1} (N—C=O).

Anal. calc. pour $C_{13}H_{14}O_4N_2$: C, 59.53; H, 5.38; N, 10.68. Trouvé: C, 59.42; H, 5.43; N, 10.71.

La 2,4-dinitrophénylhydrazone de **4***d*, recristallisée dans le solvant mixte nitrométhane–éthanol, présente un p. de f. de 233°.

Anal. calc. pour $C_{19}H_{18}O_7N_6$: N, 18.99. Trouvé: N, 18.78.

Can. J. Chem. Downloaded from www.nrcresearchpress.com by 210.87.254.5 on 09/05/12
For personal use only.

Dosage de l'époxyde **5***d et de la cétone par la diéthylamine*

Le produit brut de l'action du diazométhane sur la cétone, 11 g, est chauffé 2 h à l'ébullition à reflux en présence de 5 g de diéthylamine dans 50 ml de méthanol. On abandonne pour la nuit à 25°. Les substances volatiles sont évaporées sous vide et le résidu repris par du chloroforme; on extrait par de l'acide acétique 10%. La solution chloroformique est lavée avec une solution aqueuse de carbonate de sodium 5%, séchée et évaporée. Le résidu, après deux cristallisations dans le butanol, donne 3.4 g (32%) de la cétone **4***d*.

La fraction "acide acétique" obtenue plus haut est saturée de carbonate de sodium et extraite par du chloroforme; on sèche cette solution et l'évapore; le résidu huileux est purifié par du charbon actif dans du butanol-2 et cristallisé dans ce solvant. On obtient 5.2 g de *diéthylaminométhyl-4 p-nitrobenzoyl-1 pipéridol-4* plaques incolores, p. de f. 113–114°. On obtient aussi ce composé à partir de l'époxyde **5***d* pur.

Anal. calc. pour $C_{17}H_{25}O_4N_3$: C, 60.88; H, 7.51; N, 12.52. Trouvé: C, 60.99; H, 7.42; N, 12.47.

*5.4 Réaction du diazométhane avec la benzènesulfonyl-1 pipéridone-4 (***1***e)*

On introduit dans un ballon à trois tubulures muni d'un agitateur mécanique et d'un thermomètre plongeant jusqu'au fond du ballon, 125 ml de méthanol, et 26 g de KOH aqueux 50%. La solution est refroidie jusqu'à 0°, puis on y ajoute 50 g de benzènesulfonyl-1 pipéridone-4; on agite jusqu'à dissolution complète, tout en maintenant la température à 0°. L'addition de 23.6 g de nitrosométhylurée pendant une période de 4 h provoque une évolution d'azote. Le mélange est abandonné durant 5 h à 0°; on filtre; la solution claire est neutralisée par de l'acide acétique glacial. On concentre jusqu'à un volume de 50 ml et on reprend par le chloroforme. On isole à la manière habituelle un résidu dont on retire par cristallisation dans l'alcool amylique tertiaire 4 g *de phénylsulfonyl-1 aza-1 cycloheptanone* (**5***e*), p. de f. 136–137°. Spectre i.r. (CCl_4) 1710 cm^{-1} (C=O).

Anal. calc. pour $C_{12}H_{15}O_3NS$: C, 56.89; H, 5.97; N, 5.53. Trouvé: C, 57.02; H, 6.12; N, 5.62.

Dinitro-3,4 phénylhydrazone: poudre orange, p. de f. 167°.

Anal. calc. pour $C_{18}H_{19}O_6N_5S$: N, 16.18. Trouvé: N, 16.02.

Par évaporation des eaux-mères de la cristallisation de la cétone **5***e*, on obtient un résidu (48.5 g); on traite ce dernier par 50 g de diéthylamine et 75 ml de méthanol à l'ébullition à reflux durant 6 h. Le mélange issu de la réaction est évaporé à sec et repris par le chloroforme. On sépare en partie neutre et partie basique par extraction par HCl 5%:

Partie neutre: 7.5 g de phénylsulfonyl-1 pipéridone-4 qui n'a pas réagi, p. de f. 121–122°.

Partie basique: 47.6 g de *diéthylaminométhyl-4 phénylsulfonyl-1 pipéridol-4*, p. de f. 87–88°. Cet amino-alcool est obtenu, avec un rendement de 84%, en mélangeant 2.0 g d'époxyde **5***e* pur, p. de f. 106–107°, obtenu à la section 4.3 plus haut, avec 15 g de diéthylamine et 50 ml de méthanol. Après repos de 1 h à température de 25°, on chauffe à reflux pendant 3 h. On évapore les substances volatiles et recristallise l'amino-alcool dans du cyclohexane pour obtenir des aiguilles incolores, p. de f. 87–88°.

Anal. calc. pour $C_{16}H_{26}O_3N_2S$: C, 58.86; H, 8.03; N, 8.58. Trouvé: C, 58.49; H, 8.23; N, 8.51.

Le bilan de la réaction s'établit comme suit: 50 g de cétone mise en réaction; 7.5 g retrouvée; 4 g de cétone agrandie et 47.6 g d'amino-alcool correspondant à 37 g d'époxyde **5***e*; l'époxyde et la cétone agrandie représentent respectivement 82 et 8.9% de rendement.

6 Synthèse des époxydes **5** *par la méthode de Corey et Chaykowsky (16)*

A une suspension agitée d'hydrure de sodium (10–12% d'excès par rapport aux 10 mmol requises) dans 30 ml de diméthylsulfoxyde anhydre, fraîchement distillé, on ajoute l'iodure de triméthylsulfoxonium (10–12% d'excès par rapport aux 10 mmol requises) sous forme de fine poudre, en maintenant le tout dans une atmosphère d'azote. Au bout de 20–30 min, on ajoute rapidement, toujours en atmosphère d'hydrogène, une solution de 10 mmol de la cétone dans 30 ml de diméthylsulfoxyde, anhydre et fraîchement distillé. Après agitation de 1 h, la température est portée à 50–60° pendant 1 h. Après refroidissement à 25°, le mélange est versé dans 500 ml d'eau glacée et le tout extrait par quatre portions de 100 ml de chloroforme. Après les lavages habituels à l'eau, séchage et évaporation, le résidu est cristallisé ou distillé. On prépare ainsi les époxydes: **5***b*, p.éb. 119–121° sous 0.45 mm, 96%,[12] caractérisé par son dérivé anilino de p. de f. 80–81°, décrit par Morosawa (6); **5***c*, p. de f. 84–85° (butanol-2), 93%; **5***d*, p. de f. 143–144° (butanol-2), 96%; au moment de l'introduction de la cétone dans la solution d'ylure à température de la pièce, une intense coloration bleue apparaît, qui devient bleu-vert foncé après 1 h à 50–60°; **5***e* p. de f. 107–108° (éther de pétrole), 86%. Les époxydes ainsi préparés et ceux obtenus par désamination nitreuse ou par l'action du diazométhane sur les cétones correspondantes sont identiques (c'est le cas de **5***c–e*).

7 Détermination des pK_a *des amino-alcools*

Les pK_a des amino-alcools étudiés furent déterminés suivant la méthode originale de Roberts *et al.* (48). L'aminométhyl-1 cyclohexanol fut préparé suivant la méthode décrite par Dauben *et al.* (43). Il fut fraîchement redistillé sous atmosphère d'azote avant les mesures. La valeur donnée pour le pK_a de l'amino-alcool **3***c* n'est qu'une valeur approchée puisqu'il fut impossible de purifier cet amino-alcool, soit par distillation, soit par cristallisation, soit par cristallisation d'un dérivé. La mesure fut donc effectuée sur le produit brut de la réaction, après élimination des impuretés non alcalines. La méthode décrite par Overberger et Katchman (7) fut employée pour l'obtention du bioxyde d'aminométhyl-4 hydroxy-4 thianne qui fut fraîchement sublimé avant les mesures.

Les échantillons (environ 0.5 mmol) furent titrés dans 100 ml d'éthanol 50% (v/v) fraîchement bouilli. Chacun des titrages fut effectué sous atmosphère d'azote avec une solution d'acide chlorhydrique fraîchement préparée dans l'éthanol à 50%. Les changements d'acidité au cours des titrages ont été suivis à l'aide d'un p*H*-mètre de marque

[12]On donne (44) un rendement de 33% pour cette réaction.

Can. J. Chem. Downloaded from www.nrcresearchpress.com by 210.87.254.5 on 09/05/12
For personal use only.

Beckman Modèle H2 monté d'une électrode de verre et d'une électrode de référence au calomel. Les pK_a donnés dans le tableau 2 correspondent à l'acidité au demi-titrage déterminé graphiquement en supposant une activité des ions égale à l'unité et en supposant l'échelle de l'appareil égale au logarithme de l'inverse de la concentration en ions hydrogène. Le pK_a de la cyclohexamine a été effectué comme mesure de vérification avec la valeur donnée dans la littérature. La valeur trouvée est identique, 9.83 (46).

8 Constantes de dissociation des cyanohydrines de la cyclohexanone et des pipéridones-4

Les constantes de dissociation des cyanohydrines des cétones rapportées dans le tableau 2 furent déterminées suivant la méthode décrite par Prelog et Kobelt (47). La cyclohexanone fut purifiée par l'intermédiaire de son dérivé bisulfitique et distillée sous atmosphère d'azote. L'éthanol à 95% employé comme solvant est reflué pendant quatre heures avec de la poussière de zinc et de l'hydroxyde de potassium de façon à éliminer toute trace d'aldéhydes. La solution d'acide cyanhydrique est préparée par dissolution de 55 g d'acide cyanhydrique liquide dans 2 l d'éthanol à 95%.

Nous remercions ceux qui ont subventionné ce travail: Ayerst Laboratories de Montréal et le Conseil National de Recherches du Canada (subvention T-14) et ceux qui ont accordé les bourses à R. Lanthier et M. Ménard, l'Office Provincial de Recherches Scientifiques, la Compagnie Canadian Industries Limited de Montréal et le Conseil National de Recherches du Canada.

1. C. D. Gutsche et D. Redmore. Advan. Alicyclic Chem. Suppl. **1**, 61 (1968).
2. C. D. Gutsche. Org. React. **8**, 364 (1954).
3. P. A. S. Smith et D. R. Baer. Org. React. **11**, 157 (1960).
4. R. A. Johnson, M. E. Herr, H. C. Murray, et G. S. Fonken. J. Org. Chem. **33**, 3187 (1968).
5. S. Morosawa. Bull. Chem. Soc. Jap. **31**, 418, (1958).
6. S. Morosawa. Bull. Chem. Soc. Jap. **33**, 575 (1960).
7. C. G. Overberger et A. Katchman. J. Am. Chem. Soc. **78**, 1965 (1956).
8. A. C. Cope, H. R. Nace, et L. L. Estes, Jr. J. Am. Chem. Soc. **72**, 1123 (1950).
9. S. M. McElvain et R. E. McMahon. J. Am. Chem. Soc. **71**, 901 (1949).
10. C. A. Grob et W. von Tcharner. Helv. Chim. Acta, **33**, 1070 (1950).
11. H. B. Fraser et G. A. R. Kon. J. Chem. Soc. 604 (1934).
12. H. H. Hodgson et D. P. Dodgson. J. Chem. Soc. 1004 (1948).
13. H. Barbier. Helv. Chim. Acta, **23**, 519 (1940).
14. B. Tchoubar. Bull. Soc. Chim. Fr. 164 (1949).
15. H. Favre et D. Gravel. Can. J. Chem. **41**, 1452 (1963).
16. E. J. Corey et M. Chaykowsky. J. Am. Chem. Soc. **87**, 1353 (1965).
17. D. Y. Curtin et M. C. Crew. J. Am. Chem. Soc. **77**, 354 (1955).
18. A. Streitweiser, Jr. J. Org. Chem. **22**, 861 (1957).
19. B. M. Benjamin, H. J. Schaeffer, et C. J. Collins. J. Am. Chem. Soc. **79**, 6160 (1957).
20. J. C. Martin et W. G. Bentrude. J. Org. Chem. **24**, 1902 (1959).
21. B. M. Benjamin, P. Wilder, Jr., et C. J. Collins. J. Am. Chem. Soc. **83**, 3654 (1961).
22. H. B. Henbest. Organic reaction mechanisms. The Chemical Society, London, 1965. p. 83.
23. H. K. Hall, Jr. J. Am. Chem. Soc. **78**, 2570 (1956).
24. C. Barkenbus et J. A. Wuellner. J. Am. Chem. Soc. **77**, 3866 (1955)
25. V. Georgian. Chem. Ind. London, 1480 (1957).
26. E. M. Kosower et D. C. Remy. Tetrahedron, **5**, 281 (1959).
27. F. Montanari, R. Danieli, H. Hogeveen, et C. Maccagnani. Tetrahedron Lett. 2685 (1964).
28. J. C. Martin et J. J. Uebel. J. Am. Chem. Soc. **86**, 2936 (1964).
29. V. Prelog et O. Häfliger. Helv. Chim. Acta, **33**, 2021 (1950).
30. J. Sicher, M. Tichy, F. Sipos, M. Svoboda, et J. Jonas. Collec. Czech. Commun. **29**, 1561 (1964).
31. R. G. Carlson et N. S. Behn. J. Org. Chem. **33**, 2069 (1968).
32. F. G. Riddell. Q. Rev. **21**, 364 (1967).
33. O. H. Wheeler et J. Z. Zabicky. Chem. Ind. London, 1388 (1956).
34. R. A. Benkeser et E. W. Bennett. J. Am. Chem. Soc. **80**, 5414 (1958).
35. J. J. Uebel et H. W. Goodwin. J. Org. Chem. **33**, 3317 (1968).
36. N. L. Allinger et C. D. Liang. J. Org. Chem. **33**, 3319 (1968).
37. R. D. Stolow et T. Groom. Tetrahedron Lett. 5781 (1968).
38. J. N. Bradley, G. W. Cowell, et A. Ledwith. J. Chem. Soc. 4334 (1964).
39. H. Favre, D. Gravel, M. Ménard, et J. Temler. Can. J. Chem. Ce numéro.
40. C. D. Gutsche et J. E. Bowers. J. Org. Chem. **32**, 1203 (1967).
41. A. F. Casy et H. Birnbaum. J. Chem. Soc. 5130 (1964).
42. N. E. Hoffman et A. Erinjeri. J. Heterocycl. Chem. **2**, 326 (1965).
43. H. J. Dauben, Jr., H. J. Ringold, R. H. Wade, et A. G. Anderson, Jr. J. Am. Chem. Soc. **73**, 2359 (1951).
44. M. Fishman et P. A. Cruickshank. J. Heterocycl. Chem. **5**, 467 (1968).
45. J. D. Roberts, E. A. McElhill, et R. Armstrong. J. Am. Chem. Soc. **71**, 2923 (1949).
46. J. D. Roberts et V. C. Chambers. J. Am. Chem. Soc. **73**, 5030 (1951).
47. V. Prelog et M. Kobelt. Helv. Chim. Acta, **32**, 1187 (1949).

Can. J. Chem. Downloaded from www.nrcresearchpress.com by 210.87.254.6 on 09/05/12
For personal use only.

La désamination nitreuse des aminométhyl-1 phénylsulfonyl-4 cyclohexanols-1 *cis* et *trans*[1]

H. Favre, Z. Hamlet,[2] M. Ménard,[3] G. Roblot,[4] et J. Temler
Département de Chimie, Université de Montréal, Montréal, Québec

Reçu le 20 mai 1970[5]

La désamination nitreuse de l'aminométhyl-1 phénylsulfonyl-4 cyclohexanol-1 *cis* donne 60% d'époxyde et 23% de cétone agrandie, tandis que son isomère *trans* donne 28% d'époxyde et 60% de cétone agrandie. La forte proportion d'époxyde s'explique par un effet inductif et de champ du groupe phénylsulfonyle; un effet conformationnel, qui fait qu'un groupe —CH_2NH_2 donne plus d'époxyde en conformation équatoriale qu'axiale, se retrouve également dans cette réaction. Cette étude a nécessité la préparation des phénylthio-4 et phénylsulfonyl-4 cyclohexanols et méthyl-1 cyclohexanols *cis* et *trans*.

Nitrous acid deamination of *cis*-1-aminomethyl-4-phenylsulfonyl-1-cyclohexanol gives 60% of epoxide and 23% of ring-expanded ketone whereas the *trans* isomer gives 28% of epoxide and 60% of ring-expanded ketone. The large proportion of epoxide is accounted for by the inductive effect and the field effect of the phenylsulfonyl group; a conformational effect wherein the CH_2NH_2 group leads to more epoxide when in an equatorial conformation than in an axial is also observed in this reaction. This study required the preparation of 4-phenylthio and 4-phenylsulfonyl cyclohexanols and *cis*- and *trans*-1-methyl cyclohexanols.

Canadian Journal of Chemistry, 49, 3086 (1971)

Dans le but de connaître la résultante des effets stéréoélectroniques et des effets de champ et d'induction sur la formation des époxydes et des cétones agrandies dans la désamination nitreuse, nous avons étudié les aminométhyl-1 phénylsulfonyl-4 cyclohexanols-1 *cis* et *trans* (**1** et **2**).[6] Du côté des effets stéréoélectroniques, nous avons montré (1) qu'en série cyclohexanique la conformation équatoriale ou axiale du groupe aminométhyle influençait le cours de la réaction, l'amino-alcool **3** donnant 20% d'époxyde, son isomère **4** 5% seulement. Cette observation était confirmée plus tard, en série décalinique (2). Du côté des effets de champ et d'induction, la présence d'un groupe électronégatif augmente sensiblement la formation d'époxyde, aux dépens de la cétone agrandie. Le groupe sulfonyle influence particulièrement la réaction: c'est ainsi qu'en série thiannique l'amino-alcool **5** conduit à 67% d'époxyde pour 14% de cétone agrandie (3), tandis qu'en série pipéridique (**6**) la cétone agrandie ne représente que des traces, l'époxyde se formant à plus de 99% (4) (tableau 1).

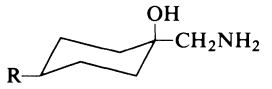

1 R = $C_6H_5SO_2$—
3 R = *tert*-butyle

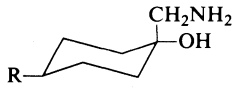

2 R = $C_6H_5SO_2$—
4 R = *tert*-butyle

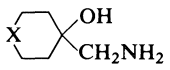

5 X = $-SO_2-$
6 X = $C_6H_5SO_2-N$

(A) Synthèse des amino-alcools 1 et 2 et désamination nitreuse

Nous avons choisi la voie classique (schéma 1) (5), cétone → nitro-alcool → amino-alcool, pour la préparation des amino-alcools **1** et **2**. L'ester-

[1]Tiré en partie de la thèse de doctorat de M. Ménard (1959) et du mémoire de maîtrise de G. Roblot (1967).

[2]Boursier post-doctoral du Conseil National de Recherches du Canada, 1962–1964; attaché de recherches, 1964–1966. Adresse actuelle: Université Sir George Williams, Montréal, Québec.

[3]Boursier du Conseil National de Recherches du Canada. Adresse actuelle: Bristol Laboratories of Canada, Candiac, Québec.

[4]Adresse actuelle: Institut des substances naturelles, Gif-sur-Yvette, France.

[5]Révision reçue le 6 mai 1971.

[6]Les configurations *cis* et *trans* correspondent aux groupes OH et $C_6H_5SO_2$ dans les composés **1**, **2**, **11**, **12**, **16**, et **17**, et OH et C_6H_5S dans **20** et **21**. Les époxydes seront *cis* et *trans* selon la configuration des alcools tertiaires d'ouverture.

La conformation des amino-alcools **1** et **2** doit comporter le groupe $C_6H_5—SO_2—$ équatorial dans les deux cas, vu la valeur *A* de 2.5 kcal/mol du groupe phénylsulfonyle (voir discussion plus loin).

TABLEAU 1. Pourcentages de formation d'époxyde et de cétone agrandie dans la désamination nitreuse

Amino-alcool de départ	Epoxyde (%)	Cétone agrandie (%)
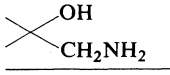	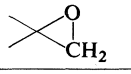	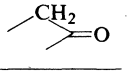
1	60*	23†
2	28‡	60*
3	20§	80§
4	5§	90§
5	67*	14
6	91*	Traces†

*Isolé comme tel.
†Isolé sous forme de dinitro-2,4 phénylhydrazone.
‡Isolé sous forme de pipéridino-alcool.
§Dosage par c.p.g.

lactone **7***a* sert de produit de départ (6, 7). Traitée par le thiophénolate de sodium (8), **7***a* donne l'acide ester **7***b*, qui conduit facilement au diester **7***c* et au diacide **7***d*. Une cyclisation de Dieckman du diester donne la cétone **8**, qu'il faut toutefois purifier par sa semicarbazone pour obtenir un produit très pur. Une oxydation par le peroxyde d'hydrogène dans l'acide acétique, selon (3), permet de convertir la cétone **8** en cétone **9**.

En présence d'une quantité équimoléculaire de méthylate de sodium (5, 9) (ou légèrement plus grande), la cétone **8** traitée par le nitrométhane conduit à un mélange de deux nitro-alcools isomères duquel nous avons retiré par cristallisation fractionnée 62% de l'isomère *trans* **10**, qui conduit par oxydation au nitro-alcool sulfonylé **11**. La cétone **9** ne conduit qu'à un nitro-alcool, qui est l'isomère *cis* **12**.

La réduction des nitro-alcools soit chimique par le fer en poudre et le sulfate ferreux, soit catalytique sur nickel de Raney (4), donne les deux amino-alcools isomères **1** et **2**. Les deux amino-alcools ont un pK_a identique et égal à 8.48; l'un **1**, fond à 130–131°, l'autre (**2**) à 171°.

La désamination nitreuse, effectuée dans les conditions déjà décrites (1, 4), solution aqueuse d'acide acétique à 25%, donne au départ de l'amino-alcool **1** un mélange de la cétone agrandie **14** et de l'époxyde **15**; par cristallisation, nous avons retiré du mélange 60% d'époxyde **15** pur, la cétone agrandie (23%) étant caractérisée par sa dinitro-2,4 phénylhydrazone. L'amino-alcool **2** engendre un mélange de la cétone agrandie **14** et de l'époxyde **13**; après traitement du mélange brut par de la pipéridine, nous avons obtenu par cristallisation, 60% de cétone **14** pure et 28% de pipéridino-alcool (**11***a*), correspondant à autant d'époxyde de **13**. Les pourcentages de cétones agrandies et d'époxyde sont rapportés au tableau 1.

(B) Configuration des amino-alcools 1 et 2

Le schéma 2 montre la corrélation de configuration qui permet d'attribuer la configuration *cis* à l'amino-alcool de p. de f. 130–131°. D'un côté, l'amino-alcool de p. de f. 130–131° (**1**) conduit par désamination nitreuse à l'époxyde de p. de f. 95–96° (**15**) et par hydrogénation de ce dernier, à l'alcool tertiaire de p. de f. 183–185° (**16**). D'un autre côté, l'action du méthylure de diméthyloxosulfonium (10) sur la phénylthio-4 cyclohexanone (**8**) conduit à un mélange des deux époxydes **18** et **19** dans le rapport 81:19, que nous avons transformé, par réduction par l'hydrure de lithium et d'aluminium, en un mélange des alcools tertiaires **20** et **21**; par cristallisation nous avons obtenu l'alcool **20** pur, de p. de f. 64.5–65°, qui donne par oxydation l'alcool sulfonylé **16**, de p. de f. 183–185°.

Du mélange résultant de l'action de l'iodure de méthylmagnésium sur la cétone **8**, nous avons tiré par chromatographie sur gel de silice, l'alcool **20** et son isomère **21**, de p. de f. 52–53° qui par oxydation conduit à l'alcool sulfonylé **17**, de p. de f. 55–56°. L'alcool **16** s'obtient également par cristallisation du mélange des alcools issus de l'action de l'iodure de méthylmagnésium sur la cétone **9**.

Nous avons choisi de déterminer les configurations des alcools **20** et **21**, pour connaître celle de l'amino-alcool **1** à l'aide de la corrélation établie plus haut, et nous avons mis en oeuvre la technique de r.m.n. Eliel et Gianni (11) ont montré que le signal de résonance du proton cyclohexanique adjacent au groupe C_6H_5—S— se situe à δ 2.85 pour le proton axial et à δ 3.52 pour le proton équatorial. Les spectres de r.m.n. des alcools **20** et **21** montrent un signal à, respectivement, δ 3.00 et 3.30; ces valeurs intermédiaires reflètent l'existence des équilibres **20***A* ⇄ **20***B* et **21***A* ⇄ **21***B*. Pour des valeurs de 0.35 kcal/mol pour $=C(OH)CH_3$ (12, 13) et 0.8 kcal/mol pour —S—C_6H_5 (11), les équilibres sont de l'ordre de 88:12 pour **20***A*:**20***B*, et 68:32 pour **21***A*:**21***B*. Pour fin d'attribution de configuration, il est clair que la valeur de δ 2.92 correspond à l'isomère qui contient le plus du

Can. J. Chem. Downloaded from www.nrcresearchpress.com by 210.87.254.6 on 09/05/12
For personal use only.

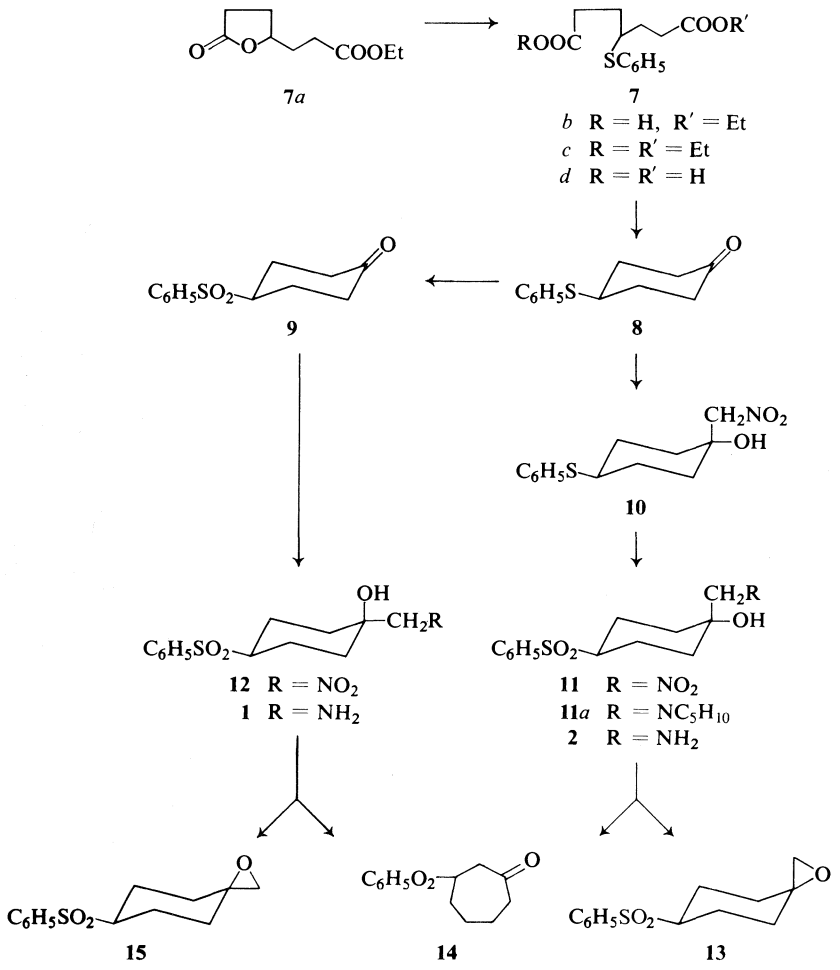

SCHÉMA 1

groupe C_6H_5—S— équatorial, soit l'isomère *cis* **20** (C_6H_5—S est *cis* par rapport à —OH).

De cette attribution de configuration, nous concluons que l'alcool sulfonylé **16**, qui résulte de l'oxydation de l'alcool **20**, doit avoir la configuration *cis* de même que les composés **1** et **15**.

Cette attribution de configuration n'est valable que si la règle de l'additivité des énergies conformationnelles des substituants —OH et C_6H_5—S s'applique à un cyclohexane porteur de ces groupes en position 1,4. Nous démontrons que cette condition est remplie par l'étude des phénylthio-4 cyclohexanols-1 *cis* et *trans* **24** et **25**; en déterminant sans ambiguité leur configuration, nous sommes en mesure de vérifier que les spectres de r.m.n. sont conformes aux équilibres conformationnels attendus. Il est bien entendu que nous utilisons la technique des déplacements chimiques dans un but strictement qualitatif et non quantitatif (14).

Nous avons synthétisé (schéma 3) les phénylthio-4 cyclohexanols-1 *cis* et *trans* par une méthode qui établit du même coup leur configuration, soit par la réaction du thiophénolate de sodium avec un tosylate. C'est une réaction S_N2 qui se fait avec l'inversion de configuration classique (15). Les monotosylates de cyclohexanediols 1,4 *cis* et *trans*, **23** et **22** sont connus (16); ils conduisent respectivement aux phénylthio-4 cyclohexanols-1 *trans* et *cis*, **25** et **24**. La valeur de l'énergie conformationnelle du substituant —OH varie entre 0.6 et 1.07 kcal/mol (11, 17–19) dans le tétrachlorure de carbone; celle du groupe —S—C_6H_5 dans ce solvant est fixée à 0.8 kcal/mol (11). En première approximation, ces valeurs permettent de retenir une

Can. J. Chem. Downloaded from www.nrcresearchpress.com by 210.87.254.6 on 09/05/12
For personal use only.

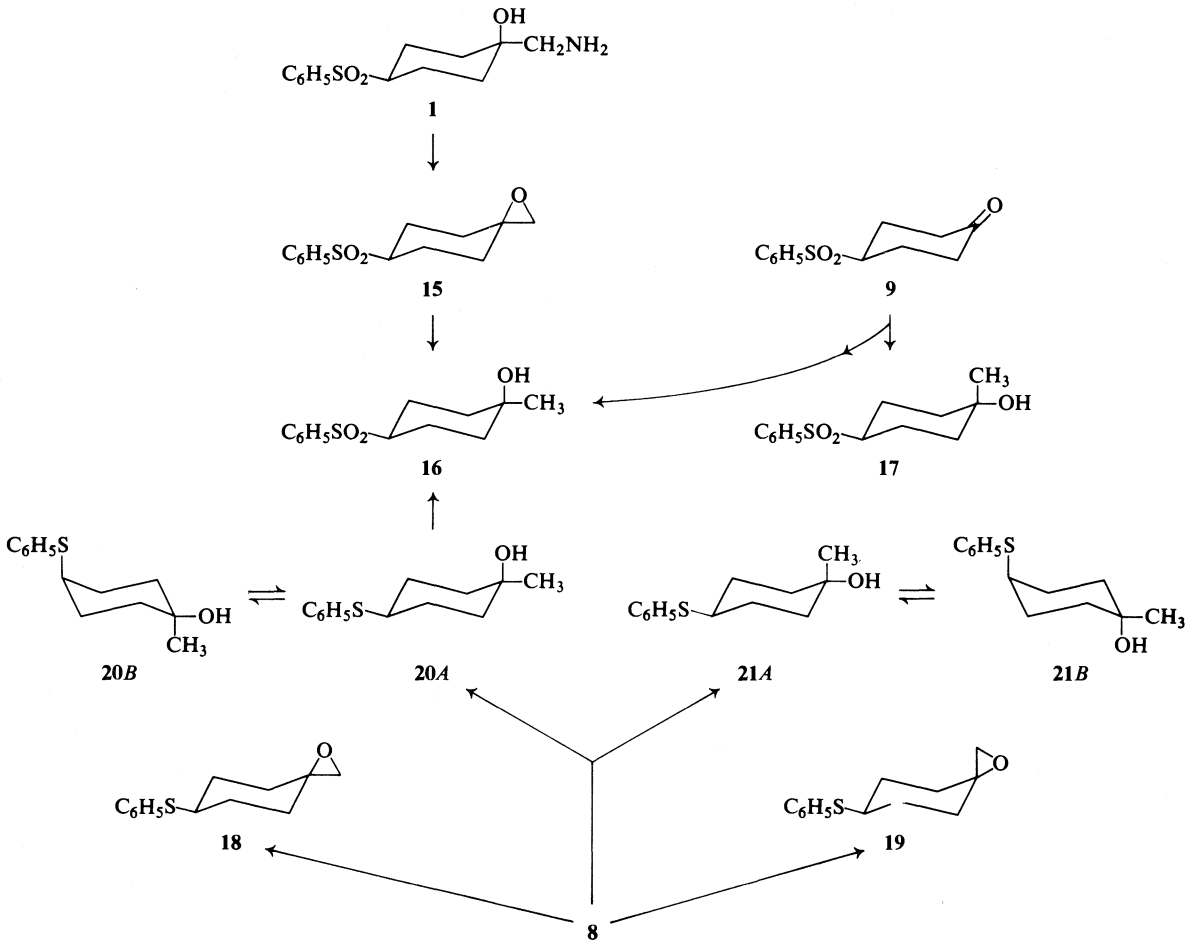

SCHÉMA 2

conformation diéquatoriale pour l'isomère *trans* et annoncent un équilibre voisin de 50:50 pour l'isomère **24***A*:**24***B cis*. Pour assurer la meilleure comparaison possible, nous choisissons le travail d'Eliel et Gianni (11) comme système de référence parce que les groupes C*H*—OH et C*H*—S—C_6H_5 y ont été étudiés dans des conditions identiques. Le tableau 2 rapporte les signaux observés dans les spectres de r.m.n. Il ressort clairement que l'isomère *trans*, comme attendu, a des valeurs inférieures à celles de l'isomère *cis*, tant pour le groupe C*H*—OH que pour le groupe C*H*—S—C_6H_5. Nous avons aussi mesuré les spectres r.m.n. dans le chloroforme deutérié; ils montrent des déplacements chimiques analogues. La règle de l'additivité jouant dans cette série, il est raisonnable de l'appliquer également aux cas des alcools tertiaires **20** et **21**.

Une confirmation des configurations *cis* et *trans* des alcools **24** et **25** vient de l'étude des phénylsulfonyl-4 cyclohexanols-4 *cis* et *trans* **26** et **27**. Par réduction catalytique sur nickel de Raney, la phénylsulfonyl-4 cyclohexanone (**9**) conduit à un alcool dont le spectre r.m.n., dans le chloroforme deutérié, présente une bande à δ 2.88 et une autre à 4.00 de largeur à demi hauteur de 9 Hz. Par réduction par l'hydrure de lithium et d'aluminium la cétone **9** conduit à un alcool dont le spectre r.m.n. montre une bande à δ 2.88 et une autre à 3.50 de largeur à demi hauteur de 23 Hz. On s'attend par l'examen des valeurs des énergies conformationnelles des groupes, SO_2—C_6H_5, 2.5 kcal/mol (20) et —OH, 0.6–1.07 (11, 17, 21) à ce que les deux alcools épimères aient un groupe phénylsulfonyle équatorial et se distinguent par l'orientation axiale et équatoriale du groupe hydroxyle. Il est manifeste dès lors que l'alcool de réduction catalytique est

Can. J. Chem. Downloaded from www.nrcresearchpress.com by 210.87.254.6 on 09/05/12
For personal use only.

TABLEAU 2. Spectres r.m.n. des alcools en valeurs δ*

	Solvant	C_6H_5—S—C*H*= Axial	C_6H_5—S—C*H*= Equatorial	HO—C*H*= Axial	HO—C*H*= Equatorial
tert-Butyl-4 cyclohexanol					
cis	CCl_4				3.93
trans	CCl_4			3.37	
tert-Butyl-4 phénylthio-1 cyclohexane					
cis	CCl_4		3.52		
trans	CCl_4	2.85			
Phénylthio-4 cyclohexanol-1					
cis	CCl_4	3.20 (16)		3.60 (15)	
trans	CCl_4	2.92 (29)		3.48 (27)	
cis	$CDCl_3$	3.25 (16)		3.90 (14)	
trans	$CDCl_3$	3.03 (22)		3.64 (22)	
Méthyl-1 phénylthio-4 cyclohexanol-1					
cis	CCl_4	2.92 (26)			
trans	CCl_4	3.30 (14)			
Phénylsulfonyl-4 cyclohexanol-1					
cis	$CDCl_3$	†			4.00 (9)
trans	$CDCl_3$	†		3.50 (23)	

*Entre parenthèses, on trouve la largeur à mi-hauteur, exprimée en Hz.
†Valeur de 2.88 pour $C_6H_5SO_2$—CH=, *cis* et *trans*.

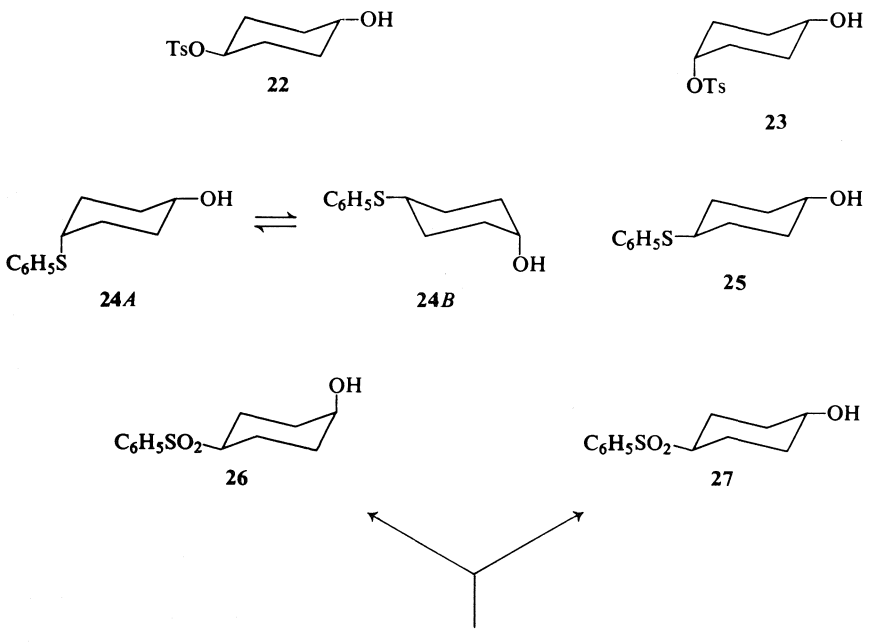

SCHÉMA 3

l'alcool *cis* (**26**) et l'alcool de réduction chimique, l'alcool *trans* (**27**). La corrélation de configuration entre les alcools sulfurés et les alcools sulfonylés se fait par oxydation du groupe sulfure de l'isomère *cis* **24**, selon la méthode de Paquette (22): nous avons bien obtenu l'alcool **26**, comme attendu.

(C) Conclusions

La désamination nitreuse des aminométhyl-1 phénylsulfonyl-4 cyclohexanols-1 *cis* et *trans* est régie par des facteurs de deux ordres. Un facteur électronique, dû à l'effet électronégatif du groupe sulfonyle augmente, par rapport à un groupe *tert*-butyle, la formation des époxydes. Un facteur

Can. J. Chem. Downloaded from www.nrcresearchpress.com by 210.87.254.6 on 09/05/12
For personal use only.

Can. J. Chem. Downloaded from www.nrcresearchpress.com by 210.87.254.6 on 09/05/12
For personal use only.

conformationnel, soit l'orientation axiale ou équatoriale du groupe $—CH_2—NH_2$, fait que la formation de l'époxyde est plus grande pour une orientation équatoriale que pour une orientation axiale.

Partie expérimentale

Les points de fusion (p. de f.) ont été déterminés en tubes capillaires, avec un thermomètre étalonné avec des substances pures de p. de f. connu en provenance du Bureau des Standards de Washington. Les spectres i.r. ont été déterminés au moyen d'un appareil Beckman IR-8, dans du chloroforme. Les spectres de r.m.n. ont été enregistrés au moyen d'un appareil Jeolco H60, en solution de tétrachlorure de carbone ou de chloroforme deutérié, avec référence au tétraméthylsilane. Les chromatographies sur plaque en couche mince ont été faites selon la technique décrite par Stahl (17). Les analyses centésimales sont de Midwest-Microlab Co. Indianapolis.

1 Cétones

1.1 Phénylthio-4 pimélate d'éthyle (7c)

A une solution de 12.5 g (0.55 at g) de sodium dans 250 ml de méthanol anhydre on ajoute assez rapidement 60 g (0.55 mol) de thiophénol. On évapore la solution résultante de moitié, on y ajoute 500 ml de toluène anhydre et l'on évapore de nouveau jusqu'au point d'ébullition du toluène. On obtient ainsi une suspension de thiophénolate de sodium dans le toluène ne contenant plus de méthanol. A cette suspension on ajoute 101 g (0.55 mol) de la lactone de l'hydroxy-4 pimélate d'éthyle **7***a* préparée selon (7) et l'on enlève complètement le solvant au bain-marie maintenu à 165°. Après la fin de l'évaporation le résidu est chauffé encore ½ h à 165°, refroidi, repris par 150 ml d'eau et lavé à l'éther. La solution aqueuse est acidifiée par de l'acide chlorhydrique concentré et extraite par de l'éther. Celui-ci est séché et évaporé pour donner 130 g d'une huile jaune très visqueuse. Ce résidu brut de réaction, p.éb. 198–210°/0.4 mm, équivalent de neutralisation 235, correspond au *phénylthio-4 monopimélate d'éthyle* (**7***b*) contenant un peu de diacide correspondant. Il est ajouté lentement à une solution de 65 g de chlorure de thionyle dans 500 ml d'éthanol absolu maintenu à 0° dans un bain de sel et de glace. Après la fin de l'addition on laisse le mélange réactionnel revenir lentement à la température de la pièce, puis on chauffe à reflux pendant ½ h. L'éthanol est alors évaporé sous vide et le résidu repris par de l'éther; celui-ci est lavé par du carbonate de sodium à 10%, séché et évaporé. Par distillation du résidu on obtient 132.4 g (75%) de *phénylthio-4 pimélate d'éthyle* (**7***c*) p.éb. 162°/0.7 mm; $n_D^{25} = 1.5145$. Le résidu brut de la réaction du thiophénolate de sodium avec la lactone de l'hydroxy-4 pimélate d'éthyle (2.4 g), sont laissés pendant 24 h à la température de la pièce, dans une solution de 0.6 g d'hydroxyde de sodium dans 20 ml d'eau. Après ce temps la solution est acidifiée par l'acide chlorhydrique concentré et refroidie à 0°. Le précipité est filtré et recristallisé dans un mélange éther – éther de pétrole pour donner 2.1 g d'*acide phénylthio-4 pimélique* (**7***d*) p. de f. 80–82°. Equivalent de neutralisation calculé, 134.2; trouvé, 133.9.

Anal. calc. pour $C_{13}H_{16}O_4S$: C, 58.18; H, 6.01. Trouvé: C, 57.90; H, 5.93.

1.2 Phénylthio-4 cyclohexanone (8)

En opérant sous atmosphère d'azote et en prenant les précautions usuelles, 109.4 g (0.34 mol) de phénylthio-4 pimélate d'éthyle sont ajoutés à une suspension vivement agitée de 16.3 g (0.68 mol) d'hydrure de sodium dans 600 ml de benzène anhydre. L'addition de 2 ml d'éthanol absolu amorce la réaction et amène une évolution immédiate d'hydrogène. Après 3 h de reflux, l'évolution d'hydrogène a complètement cessé, indiquant la fin de la réaction. Le mélange réactionnel est alors refroidi à 0° et traité consécutivement par 0.68 mol d'acide acétique glacial et 2.04 mol d'eau. L'acétate de sodium trihydraté formé est filtré et lavé plusieurs fois par le benzène. Le résidu obtenu de l'évaporation des filtrats benzéniques est ensuite chauffé à l'ébullition à reflux pendant 4 h avec une solution composée de 150 ml d'acide acétique glacial, 75 ml d'eau et 25 ml d'acide chlorhydrique 18%. La solution refroidie est extraite par l'éther; l'extrait éthéré est lavé avec une solution aqueuse de carbonate de sodium (10%), puis à l'eau; après séchage et évaporation de l'éther, la distillation du résidu fournit 52.4 g (75%) de *phénylthio-4 cyclohexanone* (**8**) p.éb. 130–135°/0.5 mm; $n_D^{24} = 1.5789$. Spectre i.r. (CCl_4) 1719 cm^{-1} (C=O).

Anal. calc. pour $C_{12}H_{14}OS$: C, 69.86; H, 6.84. Trouvé: C, 69.76; H, 6.72.

Dinitro-2,4 phénylhydrazone, p. de f. 149–150° (acétate d'éthyle).

Anal. calc. pour $C_{18}H_{18}O_4N_4S$: C, 55.94; H, 4.69; N, 14.50. Trouvé: C, 55.83; H, 4.70; N, 14.38.

Semicarbazone: p. de f. 137–138° (éthanol–eau).

Anal. calc. pour $C_{13}H_{17}ON_3S$: C, 59.28; H, 6.52; N, 15.97. Trouvé: C, 59.15; H, 6.55; N, 15.96.

1.3 Phénylsulfonyl-4 cyclohexanone (9)

On ajoute lentement 43.5 g de peroxyde d'hydrogène à 30% (10 ml par ½ h) à une solution de 38.7 g de phénylthio-4 cyclohexanone dans 300 ml d'acide acétique glacial maintenu à 5°. Après la fin de la réaction exothermique, le mélange réactionnel est agité à la température de la pièce pendant une nuit et chauffé au bain-marie pendant 2 h. Les solvants sont évaporés sous vide et le résidu est recristallisé dans l'isopropanol. On obtient ainsi 41.2 g (92%) de **9**, fondant à 125–125.5°. Spectre i.r. (CCl_4) 1725 cm^{-1} (C=O).

Anal. calc. pour $C_{12}H_{14}O_3S$: C, 60.47; H, 5.92. Trouvé: C, 60.32; H, 5.89.

Dinitro-2,4 phénylhydrazone: p. de f. 183–184° (chloroforme–éthanol).

Anal. calc. pour $C_{18}H_{18}O_6N_4S$: C, 51.67; H, 4.34; N, 13.39. Trouvé: C, 51.70; H, 4.31; N, 13.23.

Semicarbazone: p. de f. 191–194° (éthanol–eau).

Anal. calc. pour $C_{13}H_{17}O_3N_3S$: C, 52.86; H, 5.82; N, 14.23. Trouvé: C, 52.93; H, 5.76; N, 14.16.

2 Amino-alcool **1**

2.1 Nitrométhyl-1 phénylsulfonyl-4 cyclohexanol cis (12)

A une solution de 0.21 g (9×10^{-3} at g) de sodium dans 8 ml d'éthanol absolu on ajoute goutte à goutte une solution composée de 2 g (8.4×10^{-3} mol) de phénylsulfonyl-4 cyclohexanone, 0.8 g (13×10^{-3} mol) de nitrométhane et 15 ml de benzène anhydre. Le sel sodé du nitro-alcool précipite au fur-et-à-mesure de l'addition. Quand elle est terminée, le mélange est agité pendant 18 h à la température ambiante. On ajoute alors 20 ml d'éther

Can. J. Chem. Downloaded from www.nrcresearchpress.com by 210.87.254.6 on 09/05/12
For personal use only.

anhydre pour précipiter quantitativement le sel sodé du nitro-alcool; on le filtre, le dissout dans l'eau glacée et le neutralise avec 1 ml d'acide acétique glacial. Par filtration on obtient 2.33 g du nitro-alcool **12** brut fondant à 170–172°. Celui-ci recristallisé dans l'éthanol à 95%, donne 1.90 g (76%) de **12** fondant à 175–176°. Spectre r.m.n. (DMSO): δ 4.45, s, 2, $-CH_2NO_2$.[7]

Anal. calc. pour $C_{13}H_{17}O_5NS$: C, 52.16; H, 5.74; N, 4.69. Trouvé: C, 52.19; H, 5.75; N, 4.61.

2.2 Aminométhyl-1 phénylsulfonyl-4 cyclohexanol-1 cis (1)

(*a*) On hydrogène 6.0 g de nitro-alcool **12** dans 50 ml d'acide acétique glacial en présence de 2 g de nickel de Raney. La quantité théorique d'hydrogène est absorbée en 18 h. Le catalyseur est filtré et les filtrats sont évaporés sous vide. Le résidu est repris par l'eau, rendu fortement alcalin par de la soude à 20% et extrait par le chloroforme. Celui-ci est séché et évaporé pour donner 4.8 g (90%) de l'amino-alcool **1** fondant à 130–131° et ne présentant pas de dépression de p. de f. avec un échantillon préparé suivant *b*.

Anal. calc. pour $C_{13}H_{19}O_3NS$: C, 57.96; H, 7.11; N, 5.20. Trouvé: C, 57.92; H, 7.17; N, 5.28.

(*b*) Selon le mode opératoire 3.1 de notre travail antérieur (4), 1.6 g de nitro-alcool **12** donnent après cristallisation dans l'eau 1.2 g (83%) d'amino-alcool **1** sous formes de fines aiguilles fondant à 130.5–131°. Le pK_a, déterminé selon (4), est de 8.48.

3 Amino-alcool 2

3.1 Nitrométhyl-1 phénylthio-4 cyclohexanol trans (10)

En procédant comme décrit en 2.1, 60 g de phénylthio-4 cyclohexanone donnent 64 g d'une huile jaune pâle qui cristallise après quelques heures. Le p. de f. du produit brut est de 61–64°. Par crystallisation répétées dans un mélange éther – éther de pétrole on obtient 47.4 g (62%) de nitro-alcool **10** fondant à 69–70°. Les filtrats donnent une huile qu'il fut impossible de cristalliser.

Anal. calc. pour $C_{13}H_{17}O_3NS$: C, 58.44; H, 6.42; N, 5.24. Trouvé: C, 58.45; H, 6.49; N, 5.33.

3.2 Nitrométhyl-1 phénylsulfonyl-4 cyclohexanol-1 trans (11)

On dissout 25 g de nitro-alcool **10** dans un mélange de 30 ml d'anhydride acétique et de 30 ml d'acide acétique maintenu à 0–5° dans un bain de glace. A cette solution on ajoute lentement 30 ml de peroxyde d'hydrogène à 30%. Après la fin de la réaction exothermique, on laisse le mélange au repos pour la nuit. L'addition de 300 ml d'eau provoque une cristallisation abondante de fines aiguilles de nitro-alcool **11**, fondant à 126°. Par recristallisation dans un mélange éthanol–eau on obtient 21 g (75%) du nitro-alcool fondant à 132–134°. Spectre r.m.n. (DMSO) δ 4.55, s, 2, CH_2NO_2; $(CDCl)_3$, 4.53, s, 2, CH_2NO_2.[7]

Anal. calc. pour $C_{13}H_{17}O_5NS$: C, 52.16; H, 5.74; N, 4.69. Trouvé: C, 52.21; H, 5.92; N, 4.73.

3.3 Aminométhyl-1 phénylsulfonyl-4 cyclohexanol-1 trans (2)

(*a*) Selon le mode opératoire 2.2*a*, 18.2 g de nitro-alcool **11** sont hydrogénés et donnent 90% de l'amino-alcool **2** fondant à 171° et ne présentant pas de dépression de p. de f. avec un échantillon préparé suivant *b*.

Anal. calc. pour $C_{13}H_{19}O_3NS$: C, 57.96; H, 7.11; N, 5.20. Trouvé: C, 57.89; H, 7.14; N, 5.21.

(*b*) Selon le mode opératoire 3.1, de notre travail antérieur (4), 10 g de nitro-alcool **11** donnent après cristallisation dans l'eau 8.1 g (90%) d'amino-alcool **2** fondant à 171°. Le p. de f. de mélange avec son isomère *cis* est de 123–126°. Le pK_a, déterminé selon (4), est de 8.48.

4 Désamination nitreuse

4.1 Désamination nitreuse de l'aminométhyl-1 phénylsulfonyl-4 cyclohexanol cis (1)

A une solution de 1.1 g de l'amino-alcool **1** dans 10 ml d'acide acétique à 25% maintenue à 0° dans un bain de glace et de sel, on ajoute, goutte à goutte, une solution de 0.4 g de nitrite de sodium dans 2 ml d'eau. L'addition provoque la formation d'un volumineux précipité blanc. Le mélange est agité 2 h à 0° et extrait par du chloroforme. La couche organique est lavée par une solution aqueuse de bicarbonate de sodium à 10%, séchée et évaporée. On obtient ainsi 1.0 g d'une huile incolore qui cristallise lentement à froid. Par extraction du résidu avec trois portions de 150 ml d'éther, on isole une solution éthérée *B* et un résidu *C*. L'évaporation de la solution éthérée *B* donne 0.8 g d'un solide blanc fondant à 90–96°; celui-ci est recristallisé dans le butanol secondaire pour donner 0.6 g (60%) d'*époxyde de phénylsulfonyl-4 méthylène-1 cyclohexène cis* (**15**), p. de f. 95–96° après recristallisation dans le butanol-2.

Anal. calc. pour $C_{13}H_{16}O_3S$: C, 61.84; H, 6.39. Trouvé: C, 61.81; H, 6.48.

Le résidu *C* et les filtrats de cristallisation de l'époxyde **15** sont combinés, évaporés sous vide et traités par 10 ml d'une solution de dinitro-2,4 phénylhydrazine préparée suivant (23). On isole ainsi 0.4 g (correspondant à 0.23 g de cétone, soit 23%) de la dinitro-2,4 phénylhydrazone de la phénylsulfonyl-4 cycloheptanone (**14**) fondant à 196° et ne présentant pas de dépression de p. de f. avec un échantillon préparé suivant 4.2 plus loin.

4.2 Désamination nitreuse de l'aminométhyl-1 phénylsulfonyl-4 cyclohexanol trans (2)

L'amino-alcool **2** (14 g) est dissous dans 100 ml d'acide acétique à 25%. La solution résultante est maintenue à 0° dans un bain de glace et de sel. On y ajoute goutte à goutte, une solution de 4.2 g de nitrite de sodium dans 30 ml d'eau et l'on continue l'agitation pendant 2 h encore à la même température. Le mélange est extrait par le chloroforme; celui-ci est lavé par une solution aqueuse de bicarbonate de sodium à 5%, séché et évaporé. On isole ainsi 12.1 g d'une huile jaune pâle très visqueuse (*A*).

(*a*) L'huile *A* (3.0 g) fournit, après quatre cristallisations dans le solvant acétate d'éthyle – éther de pétrole 0.9 g (30%) de la *phénylsulfonyl-4 cycloheptanone* (**14**) fondant à 87–88°.

Anal. calc. pour $C_{13}H_{16}O_3S$: C, 61.87; H, 6.39. Trouvé: C, 61.81; H, 6.46.

Spectre i.r.: bande à 1709 cm^{-1} (C=O). Dinitro-2,4 phénylhydrazone: p. de f. 196–197° (chloroforme–éthanol).

Anal. calc. pour $C_{19}H_{20}O_6N_4S$: C, 52.77; H, 4.66; N, 12.95. Trouvé: C, 52.67; H, 4.68; N, 12.92.

[7]Pour fins de comparaison, les signaux de r.m.n. des *tert*-butyl-4 nitrométhyl-1 cyclohexanols-1 (1), apparaissent (CCl_4) comme singulets à δ 4.48 lorsque le groupe $-CH_2NO_2$ est axial, et à δ 4.30 lorsqu'il est équatorial.

Can. J. Chem. Downloaded from www.nrcresearchpress.com by 210.87.254.6 on 09/05/12
For personal use only.

(*b*) L'huile *A* (5.6 g) est chauffée à l'ébullition pendant 2 h avec 6 ml de pipéridine et 20 ml de méthanol. Le méthanol est évaporé sous vide et le résidu est repris par 100 ml de chloroforme et 50 ml d'acide chlorhydrique à 10%. La couche organique est séchée et évaporée pour donner 3.3 g (60%) de phénylsulfonyl-4 cycloheptanone fondant à 87–88° après recristallisation dans l'isopropanol. Le point de fusion mixte avec un échantillon obtenu suivant *a* est de 87°. La couche acide est neutralisée par de la soude à 20% et extraite par du chloroforme. Après séchage et évaporation du solvant on isole 2.7 g (correspondant à 1.6 g de l'époxyde **13**, soit 28%) de *pipéridinométhyl-1 phénylsulfonyl-4 cyclohexanol-1 trans* (**11***a*) fondant à 98–104°. Après cristallisation dans un mélange éther–alcool le p. de f. est porté à 103–104°.

Anal. calc. pour $C_{18}H_{27}O_3NS$: C, 64.06; H, 8.06; N, 4.15. Trouvé: C, 64.00; H, 8.08; N, 4.12.

Chlorhydrate préparé dans l'éther et recristallisé dans l'isopropanol: p. de f. 232–233°.

Anal. calc. pour $C_{18}H_{28}O_3NSCl$: C, 57.81; H, 7.55; N, 3.75. Trouvé: C, 57.80; H, 7.56; N, 3.84.

*5 Méthyl-1 phénylthio-4 cyclohexanols-1 cis et trans (**20** et **21**)*

A une solution d'iodure de méthylmagnésium préparée à partir de 6.2 g de magnésium et 2.40 g d'iodométhane dans 100 ml d'éther anhydre, on ajoute 6.2 g de phénylthio-4 cyclohexanone (**8**) en solution dans 50 ml d'éther anhydre. Après ébullition de 1.5 h et repos à 25° de 11 h, on ajoute à la solution éthérée 100 ml d'une solution aqueuse saturée de chlorure d'ammonium et on isole à la manière habituelle 7.0 g d'une huile incolore. Le spectre i.r. montre l'absence complète de cétone de départ. La c.p.g. montre deux pics dans le rapport 45–55 correspondant aux alcools **21** et **20**. Les alcools ont été séparés par chromatographie sur colonne de gel de silice (1.2 m), en utilisant comme éluant des fractions de 20 ml de benzène–acétone 9:1. On obtient ainsi, à partir de 3.7 g de mélange, 2.0 g (54%), fractions (10–22), de l'alcool *cis* **20** et 1.3 g (35%), fractions 28–45 de l'alcool *trans* **21**. Alcool *cis* **20**, p. de f. 64.5–65°, identique à celui décrit en 5*a*. Spectre i.r. (CCl_4) 3615 (bande fine, —OH non associé); 3580–3250 cm^{-1} (—OH associé). Spectre de r.m.n. (CCl_4) (valeurs δ) 1.17 (s, 3, $—CH_3$); de 1.20 à 2.20 (massif, 9); 2.92 (bande large, 1, largeur à demi hauteur 26 Hz, —S—CH=); de 7.10 à 1.50 (massif, 5, C_6H_5—).

Anal. calc. pour $C_{13}H_{18}OS$: C, 70.24; H, 8.11; S, 14.42. Trouvé: C, 70.41; H, 8.09; S, 14.60.

Alcool *trans* **21**, p. de f. 52–53°. Spectre i.r. (CCl_4) 3615 (bande fine, —OH non associé); 3580–3250 cm^{-1} (—OH associé). Spectre de r.m.n. (CCl_4) (valeurs δ) 1.20 (s, 3, $—CH_3$); de 1.25 à 2.20 (massif, 9); 3.3 (bande large, 1, largeur à demi hauteur 14 Hz, —S—CH=); de 7.10 à 7.50 (massif, 5, C_6H_5—S).

Anal. calc. pour $C_{13}H_{18}OS$: C, 70.24; H, 8.11; S, 14.42. Trouvé: C, 70.59; H, 8.26; S, 14.71.

*5a Méthyl-1 phénylthio-4 cyclohexanol-1 cis (**20**)*

(*a*) En suivant le mode opératoire de Corey et Chaykovsky (10): 20.6 g de phénylthio-4 cyclohexanone conduisent à 18.9 g du mélange des époxydes **18** et **19**, p.éb. 136–140°/0.4 mm. Le spectre i.r. ne montre ni cétone, ni alcool.

Anal. calc. pour $C_{13}H_{16}OS$: C, 70.87; H, 7.33; S, 14.55. Trouvé: C, 71.18; H, 7.61; S, 14.29.

En c.p.g. les deux époxydes sortent dans l'ordre **19** et **18**, (4% de FS 1265 sur Anachrom ABS: colonne de verre de 5.40 m, température de la colonne 200°).

(*b*) Le mélange des époxydes préparés en (*a*), 2.1 g est réduit par une suspension de 2.0 g d'hydrure de lithium et d'aluminium, dans 75 ml d'éther anhydre. Après 2.5 h d'ébullition, on isole à la manière habituelle 2.3 g d'alcool brut, constitué des deux alcools **21** et **20** dans le rapport 18–82 comme le montre la c.p.g. dans des conditions identiques à celles décrites en 5*a*. Par cristallisation de l'alcool brut dans le pentane, on obtient l'alcool **20** pur p. de f. 64.5–65°, homogène en c.p.g., identique à celui plus haut en 5.

*6 Méthyl-1 phénylsulfonyl-4 cyclohexanol-1 cis (**16**)*

*6.1 Par hydrogénation de l'époxyde **15***

On hydrogène 147 mg d'époxyde **15** p. de f. 95–96°, dans 25 ml d'éthanol anhydre en présence de palladium à 1% sur carbonate de calcium. On obtient 146 mg d'alcool **16** p. de f. 183.5–185° après cristallisation dans le butanol-2. Le spectre r.m.n. ($CDCl_3$) (valeurs δ) montre une bande fine à 1.22 ($—CH_3$), un massif de neuf protons de 1.00 à 2.10, une bande étalée $—SO_2—CH=$ à 2.90 et les protons aromatiques 5H, de 7.20 à 8.00. Spectre i.r., 3615 (bande fine, —OH non associé); 3590–3300 cm^{-1} (—OH associé).

Anal. calc. pour $C_{13}H_{18}O_3S$: C, 61.38; H, 7.13. Trouvé: C, 61.33; H, 7.12.

6.2 Par réaction de Grignard

A une solution de 24 g de phénylsulfonyl-4 cyclohexanone préparée plus haut selon 1.3 dans 200 ml de benzène anhydre, on ajoute lentement une solution de 18 g d'iodure de méthylmagnésium fraîchement préparée dans 100 ml d'éther anhydre. Après la fin de l'addition le mélange réactionnel est chauffé à reflux pendant 2 h, puis traité par 100 ml d'une solution saturée de chlorure d'ammonium. La couche organique est décantée, séchée, et évaporée. On obtient ainsi 25.1 g d'une huile très visqueuse qui cristallise lentement. Le produit est dissous dans 500 ml de benzène, absorbé sur 500 g d'alumine (activité I) et élué par fraction de 125 ml, par 500 ml de benzène, 500 ml d'éther (5%) – benzène, 1000 ml d'éther (10%) – benzène, 1000 ml d'éther (30%) – benzène, 500 ml d'éther (50%) – benzène, 500 ml d'éther (75%) – benzène, 500 ml de chloroforme (5%) – éther, 500 ml de chloroforme (10%) – éther, 500 ml de chloroforme (50%) – éther, 2500 ml de chloroforme, et 500 ml de méthanol (5%) – chloroforme. Des fractions de 1 à 30 (3.48 g) on tire par cristallisation dans le butanol secondaire 2.8 g de phénylsulfonyl-4 cyclohexanone. Les fractions 55 à 65 (8.29 g de p. de f. 160–168°) donnent, après recristallisation dans le butanol secondaire, 5.3 g de *méthyl-1 phénylsulfonyl-4 cyclohexanol-1* (**16**) p. de f. 183–184.5°, identique (p. de f. de mélange) à celui obtenu en 6.1. Les fractions 31 à 54 (6.07 g de p. de f. 107–127°) ne purent être cristallisées de même que les fractions 66 à 75 (7.16 g d'huile brune très visqueuse).

*6.3 Par oxydation de l'alcool **20***

On dissout 170 mg (3.15 mol) d'alcool **20** dans un mélange de 0.5 ml d'anhydride acétique et 0.5 ml d'acide acétique glacial. On refroidit le tout dans un bain de glace, puis ajoute 0.5 ml de péroxyde d'hydrogène à 30%. On abandonne à 0° durant 2½ h, puis à 25° pendant 12 h; on chauffe ensuite sur bain-marie pendant 30 min. On

Can. J. Chem. Downloaded from www.nrcresearchpress.com by 210.87.254.6 on 09/05/12
For personal use only.

ajoute goutte à goutte, à la solution chaude, de l'eau jusqu'à formation d'un léger trouble (10 gouttes environ). Par refroidissement dans l'armoire frigorifique, il se forme des aiguilles blanches, qui sont essorées, lavées avec de l'eau froide et séchées. Il s'agit de l'alcool qui fond à 183–185° et ne donne pas de dépression de point de fusion avec les échantillons préparés selon 6.1 et 6.2.

*7 Méthyl-1 phénylsulfonyl-4 cyclohexanol-trans (**17**)*

On oxyde l'alcool **21** (170 mg) comme décrit en 6.3 plus haut. L'alcool ne précipite pas sous forme cristalline, mais comme une huile. On évapore les solvants sous vide à 45° pendant 2 h et on ajoute au résidu 15 ml d'eau, chauffe à l'ébullition à reflux, concentre sous vide de 11 mm. Des cristaux précipitent à la température ambiante dans l'espace d'1/2 h. On essore les cristaux (90 mg), on les sèche à température ambiante. Il s'agit de l'alcool *trans*, qui se présente sous forme monohydratée, p. de f. 55–56°, avec décomposition. Spectre i.r. ($CHCl_3$) 3615 (bande fine, —OH non associé); 3590–3300 (—OH associé); 1310, 1150 cm^{-1} (—SO_2—). Spectre de r.m.n. ($CDCl_3$) (valeurs δ) 1.2 (s, 3, —CH_3); de 1.3 à 2.2 (massif, 9); 2.8 (bande large, 1, —SO_2—CH═); de 7.6 à 8.2 (massif, 5, C_6H_5—SO_2—). Spectre r.m.n. (DMSO-d_6) 1.1 (s, 3, —CH_3); 1.5 à 2.1 (massif, 8); 3.3 (bande large, 1, SO_2—CH═); 4.55 (s, 1, —OH); de 7.6 à 8.1 (massif, 5, C_6H_5—SO_2—). La bande due à la présence d'eau apparait à 3.47.

Anal. calc. pour $C_{13}H_{20}O_4S$: C, 57.32; H, 7.40; S, 11.77. Trouvé: C, 57.44; H, 7.25; S, 11.52.

*8 Phénylthio-4 cyclohexanol-1 cis (**24**)*

Une solution résultant de l'action de 0.137 g (6.0×10^{-3} at g) de sodium sur 10 ml d'éthanol anhydre additionnée de 0.73 g (6.64×10^{-3} mol) de thiophénol, est versée dans 80 ml d'une solution éthanolique de 1.5 g (5.6×10^{-3} mol) du monotosylate de cyclohexanediol-1,4 (**22**) p. de f. 108–111° (benzène – éther de pétrole) préparé selon Owen et Robins (16) p. de f. donné 112°. Après trois semaines à 25°, le précipité formé est filtré, et les eaux-mères, mises à sec, donnent 967 mg d'une huile dont la cristallisation dans l'éther de pétrole fournit 267 mg (23%) de *phénylthio-4 cyclohexanol-1 cis* (**24**) p. de f. 73–75°. La chromatographie sur couche mince ne montre qu'une seule tache (R_f 0.9; éluant: acétate d'éthyle, éther de pétrole, acétone, 3:1:1). Un échantillon analytique fond à 73.5–75° (éther de pétrole). Le spectre i.r. montre les bandes: OH libre 3610, OH lié 3430, C═C (aromatique) 1590 cm^{-1}; les suivantes apparaissent dans le composé *cis* mais sont absentes dans l'isomère *trans* 987 et 954 cm^{-1}. Le spectre r.m.n. montre ($CDCl_3$) (valeurs δ) entre 7.17 et 7.67 un massif correspondant à cinq protons (phényle); à 3.90 un pic correspondant à un proton (C*H*OH) (largeur à demi-hauteur 14 Hz); à 3.25 un pic correspondant à un proton (C*H*S) (largeur à demi-hauteur 16 Hz) entre 1.33 et 2.00, un massif correspondant à neuf protons. Le spectre, dans CCl_4, montre des bandes à 3.20, —SCH═ largeur à demi-hauteur 16 Hz et à 3.60 HOCH═ largeur à demi-hauteur 15 Hz.

Anal. calc. pour $C_{12}H_{16}OS$: C, 69.19; H, 7.74; S, 15.39. Trouvé: C, 69.53; H, 7.69; S, 15.19.

*9 Phénylthio-4 cyclohexanol trans (**25**)*

Une solution résultant de l'action de 0.529 g (2.3×10^{-3} at g) de sodium sur 10 ml d'éthanol–eau (4:1), additionnée de 2.57 g (23.4×10^{-3} mol) de thiophénol, est versée dans 70 ml d'une solution éthanol–eau (4:1) de 5.56 g (0.0205 mol) du monotosylate du cyclohexanediol-1, 4 *cis* **23**, p. de f. 93–93.5° (éther de pétrole – benzène) préparé selon Owens et Robins (16) p. de f. donné 94–95° (éther de pétrole – benzène). Après 7 jours à 0°, le solvant est évaporé sous vide et le résidu dissous dans du chloroforme. La solution, lavée successivement avec une solution de soude à 5% et à l'eau, puis séchée et évaporée fournit 2.94 g d'une huile jaune. Deux cristallisations dans l'éther de pétrole fournissent 0.736 g (17%) de *phénylthio-4 cyclohexanol trans* (**25**) p. de f. 73.5–74°. Cet alcool ne montre qu'une tache à la chromatographie sur couche mince (R_f 0.80, éluant: acétate d'éthyle, éther de pétrole, acétone, 3:1:1); deux taches apparaissent (R_f 0.8 et 0.9) quand il est mélangé avec le phénylthio-4 cyclohexanol *cis*. Le p. de f. mixte avec le phénylthio-4 cyclohexanol *cis* (**24**) est de 20° plus bas que ce dernier. Un échantillon analytique fond à 74.5–76° (éther de pétrole). Le spectre i.r. montre: OH libre 3610, OH lié 3430, C═C (aromatique) 1575 cm^{-1}; les pics suivants apparaissent dans le composé *trans* mais sont absents dans l'isomère *cis* 1447 (très fin), 1043, 750 cm^{-1} (très large). Le spectre r.m.n. montre ($CDCl_3$) valeurs δ entre 7.17 et 7.67, un massif de cinq protons (phényle); à 3.64, un pic correspondant à un proton (C*H*OH) (largeur à demi-hauteur 22 Hz); à 3.03, un pic correspondant à un proton (C*H*S) (largeur à demi-hauteur 22 Hz); entre 0.67 et 2.25, un massif correspondant à neuf protons. Le spectre r.m.n. dans CCl_4, montre le proton C*H*S à 2.92 (largeur à demi-hauteur 29 Hz) et le proton (C*H*OH—) à 3.48 (largeur à demi-hauteur 27 Hz).

Anal. calc. pour $C_{12}H_{16}OS$: C, 69.19; H, 7.74; S, 15.39. Trouvé: C, 68.87; H, 7.64; S, 14.94.

*10 Phénylsulfonyl-4 cyclohexanol-1 cis (**26**)*

10.1 Par réduction catalytique de la phénylsulfonyl-4 cyclohexanone

Le nickel de Raney (17 ml), préparé selon la méthode de Favre–Richer (24), est mélangé avec 10 g de phénylsulfonyl-4 cyclohexanone (9) et 1.5 l d'éthanol à 99%, dans une ampoule à hydrogénation. Quand l'hydrogénation est terminée, le mélange est filtré sous vide, sur de la terre de diatomée. Le solide est essoré avec 2 l d'acétone bouillante. L'évaporation fournit, après deux cristallisations dans le benzène, 5.73 g (57%) de *phénylsulfonyl-4 cyclohexanol-1 cis* (**26**) p. de f. 85–87° homogène à la chromatographie sur couche mince (R_f 0.7; éluant: acétate d'éthyle, éther de pétrole, acétone, 3:1:1). Les eaux-mères, incristallisables, présentent une bande carbonyle en i.r. Un échantillon analytique fond à 85–87° (benzène). Le spectre i.r. montre: OH libre 3610, OH lié 3510, C═C (aromatique) 1580, SO_2 1300, 1140 cm^{-1}; les pics suivants apparaissent dans le composé *cis*, mais sont absents dans l'isomère *trans* 950 (très fort), 925, 850, 750 (très large) cm^{-1}. Le spectre r.m.n. ($CDCl_3$) (valeurs δ) montre entre 7.33 et 8.08 un massif correspondant à cinq protons (phényle); à 4.00 un pic correspondant à un proton (C*H*OH) (largeur à demi-hauteur 9 Hz); à 2.88 un pic correspondant à un proton (C*H*SO_2—) (largeur à demi-hauteur 22 Hz); entre 1.00 et 2.17, un massif correspondant à neuf protons.

Can. J. Chem. Downloaded from www.nrcresearchpress.com by 210.87.254.6 on 09/05/12
For personal use only.

Anal. calc. pour $C_{12}H_{16}O_3S$: C, 59.97; H, 6.71; S, 13.34. Trouvé: C, 59.92; H, 6.60; S, 13.24.

p-Nitrobenzoate

Le *p*-nitrobenzoate est obtenu à partir de l'alcool *cis* selon la technique de Hennion et de Barrett (25) avec un rendement de 99%. Après six cristallisations dans l'éthanol anhydre, le p. de f. est constant, 168.5–170.5° (rendement 56%). Le p. de f. mixte avec le *p*-nitrobenzoate *trans* baisse de 25°. La chromatographie sur couche mince montre une seule tache, dès la première cristallisation (R_f 0.3; éluant: éther de pétrole, chloroforme, acétate d'éthyle, 3:1:1) tandis qu'un mélange de deux *p*-nitrobenzoates *cis* et *trans* donne deux taches (R_f 0.3 et 0.4) dans les mêmes conditions. Un échantillon analytique fond à 168.5–170.5° (éthanol anhydre). Le spectre i.r. montre: 1715 (C=O), 1300, 1140 (SO_2), 1520 (NO_2 sym.), 1340 cm^{-1} (NO_2 sym.); les pics suivants apparaissent dans le composé *cis* mais sont absents dans l'isomère *trans*: 1300, 990, 880, 850 cm^{-1}.

Le spectre r.m.n. présente ($CDCl_3$) (valeurs δ) de 7.41 et à 8.50, un massif correspondant à neuf protons (phényle); à 5.53, un pic correspondant à un proton (—C*H*—$OCOC_6H_5$) largeur à demi-hauteur 8 Hz; à 3.07, un pic correspondant à un proton (C*H*SO_2—) (largeur à demi-hauteur 22 Hz); entre 1.50 et 2.42, un massif correspondant à huit protons.

Anal. calc. pour $C_{19}H_{19}O_6NS$: C, 58.60; H, 4.92; S, 8.23. Trouvé: C, 58.41; H, 5.02; S, 8.33.

10.2 Par oxydation du phénylthio-4 cyclohexanol cis

On oxyde selon la technique de Paquette (22), 74 mg (0.356×10^{-3} mol) de phénylthio-4 cyclohexanol *cis*. On obtient, par extraction au chloroforme, 76.2 mg (89%) de phénylsulfonyl-4 cyclohexanol *cis* (**26**) qui recristallisé six fois dans le benzène, donne un p. de f. constant de 85–87° et ne montre pas de diminution de p. de f. quand il est mélangé avec le composé obtenu par réduction catalytique (0.1). De plus, il montre les mêmes spectres i.r. et r.m.n. que ce dernier.

*11 Phénylsulfonyl-4 cyclohexanol-1 trans (**27**)*

La phénylsulfonyl-4 cyclohexanone (**9**) (6.0 g, 0.025 mol) en solution dans 150 ml de tétrahydrofuranne (THF) anhydre, est ajouté goutte à goutte, à une suspension vivement agitée de 3.83 g d'hydrure de lithium aluminium (0.1 mol) dans 100 ml de THF anhydre. Le mélange devenu vert est chauffé jusqu'à reflux pendant 1½ h, puis, agité 10 h à 25°. L'excès d'hydrure est détruit avec 100 ml d'acide chlorhydrique à 10%. La solution est extraite au chloroforme. Les phases organiques réunies, lavées à l'eau, séchées, et évaporées sous vide à 20°, fournissent 6.0 g (100%) de *phénylsulfonyl-4 cyclohexanol trans* (**27**) brut.

Cet alcool brut est analysé en chromatographie sur couche mince, par un mélange de solvants: acétate d'éthyle, éther de pétrole, acétone 3:1:1; l'alcool brut de la réduction ci-dessus donne cinq taches: R_f 0.4 (très faible) non identifié; R_f 0.5, non identifié; R_f 0.6 phénylsulfonyl-4 cyclohexanol-1 *trans* (**27**), identifié par cochromatographie avec l'alcool *trans* pur; R_f 0.7 phénylsulfonyl-4 cyclohexanol *cis* (**26**) identifié en cochromatographie avec l'alcool *cis* pur obtenu en 6.1; R_f 0.9 non identifié.

L'alcool **27** brut fournit après plusieurs cristallisations dans l'eau le *phénylsulfonyl-4 cyclohexanol-1 trans* **27**, de p. de f. 40–50° (déc.). Un échantillon est cristallisé pour analyse dans le benzène: p. de f. 44–45° (déc.). Le spectre i.r. montre: OH libre 3610, OH lié 3510, C=C (aromatique) 1580 cm^{-1}; les pics suivants apparaissent dans le composé *trans* mais sont absents dans l'isomère *cis* 1148, 1050, (très forte intensité), 960, 720, 600 (forte intensité) cm^{-1}.

Le spectre r.m.n. ($CDCl_3$) (valeurs δ) montre de 7.33 à 8.00 un massif correspondant à cinq protons (phényle); à 3.50, un pic correspondant à un proton (C*H*OH) (largeur à demi-hauteur 23 Hz), à 2.88, un pic correspondant à un proton (C*H*SO_2—) (largeur à demi-hauteur 20 Hz) entre 0.83 et 2.58, un massif correspondant à neuf protons.

Anal. calc. pour $C_{12}H_{16}O_3S$: C, 59.97; H, 6.71; S, 13.34. Trouvé: C, 56.14; H, 7.02; S, 12.03.

Anal. calc. pour $C_{12}H_{16}O_3S{\cdot}H_2O$: C, 55.80; H, 7.02; S, 12.14.

p-Nitrobenzoate

On solubilise à chaud 0.835 g (5×10^{-3} mol) d'acide *p*-nitrobenzoïque et 1.20 g (5×10^{-3} mol) de phénylsulfonyl-4 cyclohexanol *trans* brut dans 65 ml de pyridine. La solution est additionnée de 1.24 g (6.5×10^{-3} mol) de chlorure de benzoyle, puis chauffée 2 h à 100° (préparation selon la technique de Hennion et de Barrett (25)). La solution refroidie, précipitée dans 200 ml d'un mélange glace-eau, filtrée, fournit 1.56 g (80%) de *p*-nitrobenzoate *trans*. Quatre cristallisations dans l'éthanol absolu donne le *p*-nitrobenzoate avec un p. de f. constant de 167–168.5° et un rendement de 27%. La chromatographie sur couche mince du *p*-nitrobenzoate brut avec un mélange: éther de pétrole, chloroforme, acétate d'éthyle, 3:1:1 donne deux taches à la première cristallisation (R_f 0.3 et 0.4): l'une (trace) correspond au *p*-nitrobenzoate *cis*, identifié par chromatographie avec le *p*-nitrobenzoate *cis* pur et l'autre, au *p*-nitrobenzoate *trans*, identifié par cochromatographie avec le *p*-nitrobenzoate *trans* pur p. de f. 167–168.5°. Un échantillon analytique fond à 167–168.5° (éthanol-anhydre). Le spectre i.r. montre les pics 1715 (C=O), 1520 (NO_2 asym.), 1340 (NO_2 sym.), 1300, 1140 cm^{-1} (SO_2); les pics suivants apparaissent dans le composé *trans* mais sont absents dans l'isomère *cis*: 1320, 940, 810, 610 cm^{-1}.

Le spectre r.m.n. ($CDCl_3$) (valeurs δ), montre entre 7.33 et 8.58, un massif correspondant à neuf protons (phényle); à 5.02, un pic correspondant à un proton ($CHOCOC_6H_5$) (largeur à demi-hauteur 23 Hz); à 3.05, un pic correspondant à un proton (C*H*SO_2—) (largeur à demi-hauteur 22 Hz) de 1.33 à 1.67, un massif correspondant à huit protons.

Anal. calc. pour $C_{19}H_{19}O_6NS$: C, 58.60; H, 4.92; S, 8.23. Trouvé: C, 58.46; H, 4.74; S, 8.30.

On mélange 2.66 g de *p*-nitrobenzoate *trans* (p. de f. 167–168.5°) avec une solution de 3.5 g de soude dans 30 ml d'eau et 45 ml de méthanol. Après 2 h de reflux, le méthanol est évaporé. Après 12 h au réfrigérateur, la suspension obtenue est filtrée. Un lavage à l'eau provoque une cristallisation instantanée dans le filtrat. La filtration fournit 0.38 g (23%) de phénylsulfonyl-4 cyclohexanol-*trans* (**27**) p. de f. 40–50° (déc.).

Nous remercions les Laboratoires Ayerst de Montréal et le Conseil National de Recherches du Canada de leur

aide financière (subventions T-14, A 0014 et A 5526, et bourse d'études à M.M.).

1. H. FAVRE et D. GRAVEL. Can. J. Chem. **41**, 1452 (1963).
2. R. G. CARLSON et N. S. BEHN. J. Org. Chem. **33**, 2069 (1968).
3. C. G. OVERBERGER et A. KATCHMAN. J. Am. Chem. Soc. **78**, 1965 (1956).
4. H. FAVRE, Z. HAMLET, R. LANTHIER, et M. MÉNARD. Can. J. Chem. Ce numéro.
5. H. H. DAUBEN, JR., H. J. RINGOLD, R. H. WADE, et A. G. ANDERSON, JR. J. Am. Chem. Soc. **73**, 2356 (1951).
6. W. S. EMERSON et R. I. LONGLEY, JR. Org. Synth. **33**, 25 (1953).
7. A. E. TCHITCHIBABINE. Bull. Soc. Chim. Fr. 670 (1941).
8. H. PLIENINGER. Chem. Ber. **83**, 265 (1950).
9. C. A. GROB et W. VON TCHARNER. Helv. Chim. Acta, **33**, 1070 (1950).
10. E. J. COREY et M. CHAYKOVSKY. J. Am. Chem. Soc. **87**, 1353 (1965).
11. E. L. ELIEL et M. H. GIANNI. Tetrahedron Lett. 97 (1962).
12. J. J. UEBEL et H. W. GOODWIN. J. Org. Chem. **33**, 3317 (1968).
13. N. L. ALLINGER et C. D. LIANG. J. Org. Chem. **33**, 3319 (1968).
14. F. R. JENSEN et B. H. BECK. J. Am. Chem. Soc. **90**, 3251 (1968).
15. E. L. ELIEL et R. S. RO. J. Am. Chem. Soc. **79**, 5995 (1957).
16. L. N. OWEN et P. A. ROBINS. J. Chem. Soc. 320 (1949).
17. A. H. LEWIN et S. WINSTEIN. J. Am. Chem. Soc. **84**, 2464 (1962).
18. J. REISSE, J. C. CELOTTI, D. ZIMMERMANN, et G. CHIURDOGLU. Tetrahedron Lett. 2145 (1964).
19. F. A. L. ANET. J. Am. Chem. Soc. **84**, 1053 (1962).
20. E. L. ELIEL, N. L. ALLINGER, S. J. ANGYAL, et G. A. MORRISON. Conformational analysis. Interscience Publishers, New York, N.Y., 1965. p. 439.
21. E. L. ELIEL, M. H. GIANNI, TH.H. WILLIAMS, et J. B. STOTHERS. Tetrahedron Lett. 741 (1962).
22. L. A. PAQUETTE. J. Am. Chem. Soc. **86**, 4383 (1964).
23. R. L. SHRINER, R. C. FUSON, et D. Y. CURTIN. The systematic identification of organic compounds. 5ème édition. John Wiley and Sons, Inc., New York, N.Y., 1964. p. 253.
24. H. FAVRE et J. C. RICHER. Can. J. Chem. **37**, 417 (1959).
25. G. F. HENNION et S. O. BARRETT. J. Am. Chem. Soc. **79**, 2146 (1957).
26. E. STAHL. Chemiker Ztg. **82**, 323 (1958).

Can. J. Chem. Downloaded from www.nrcresearchpress.com by 210.87.254.6 on 09/05/12
For personal use only.

Can. J. Chem. Downloaded from www.nrcresearchpress.com by 84.22.46.98 on 09/08/12
For personal use only.

La réaction du diazométhane avec les phénylsulfonyl-4, tert-butyl-4, et phénylthio-4 cyclohexanones[1]

H. Favre, D. Gravel, Z. Hamlet,[2] M. Ménard,[3] et J. Temler[4]

Département de chimie, Université de Montréal, Montréal, Québec

Reçu le 6 mai 1971

Ce mémoire traite de l'action du diazométhane *in situ* dans le méthanol en présence d'hydroxyde de potassium sur les phénylsulfonyl-4, tert-butyl-4, et phénylthio-4 cyclohexanones. Dans les deux derniers cas, les réactions conduisent à des mélanges contenant surtout les cétones agrandies accompagnées d'un peu des époxydes correspondants. Dans le premier cas, la cétone agrandie et les époxydes correspondants se forment en quantités égales. Cette formation élevée d'époxydes témoigne d'interactions électroniques transannulaires entre le groupe sulfonyle et la bétaine intermédiaire. Dans les réactions *ex situ* dans le méthanol, mais en l'absence d'hydroxyde de potassium, la cétone sulfonylée conduit essentiellement à l'acétal diméthylique, alors que les réactions des cétones tert-butylée et phénylthio suivent le même cours que lors des réactions *in situ*. L'hydroxyde de potassium exerce de plus une action particulière, en ouvrant les époxydes spiranniques et en conduisant à des éthers-alcools du type $\diagdown C(OH)—CH_2—O—CH_3$. Cette ouverture d'époxyde est avantageusement mise à profit pour obtenir des époxydes purs à partir de mélanges d'époxydes épimères. Les époxydes formés dans la réaction des trois cétones étudiées sont des mélanges d'isomères *cis–trans*, riches en isomères *cis*.

This paper describes the reaction of diazomethane generated *in situ*, methanolic potassium hydroxide solution, on 4-phenylsulfonyl, 4-tert-butyl, and 4-phenylthio-cyclohexanones. In the latter two cases, the reaction leads to mixtures containing mostly the enlarged ketones along with minor quantities of the corresponding epoxides. In the first case, the enlarged ketone and the corresponding epoxides are formed in equal amounts. This marked increase in the production of epoxides is indicative of transannular interactions between the sulfonyl group and the intermediate betaine. In the *ex situ* reactions, methanolic solutions without potassium hydroxide, phenylsulfonylcyclohexanone yields the corresponding dimethyl acetal almost exclusively whereas the tert-butyl and phenylthioketones follow the same course as in the *in situ* reactions. Furthermore, it has been observed in all cases that, under the conditions used, the potassium hydroxide leads to opening of the epoxide rings to yield hydroxy-ethers of the type $\diagdown C(OH)—CH_2—O—CH_3$. This epoxide-ring-opening was advantageously used in the preparation of pure epoxides from epimeric mixtures. The epoxides generated from the three ketones studied are mixtures of *cis–trans* isomers, rich in *cis* epimer.

Canadian Journal of Chemistry, 49, 3097 (1971)

Poursuivant notre étude de l'influence du groupe sulfonyle sur l'aptitude à l'extension des cétones à six chaînons (1) et des amino-alcools correspondants (1, 2), nous avons examiné la réaction de la phénylsulfonyl-4 cyclohexanone (**1***a*) avec le diazométhane. Nous avons examiné également le comportement, vis-à-vis de ce réactif, de la tert-butyl-4 cyclohexanone (**1***b*), que nous prenons comme système de référence. Finalement, nous avons étudié la phénylthio-4 cyclohexanone (**1***c*), dans le but de mettre en évidence les effets conformationnels et électroniques découlant de la présence du groupe phénylthio.

Nous avons effectué les réactions de deux manières: (*A*) *in situ*, selon le mode opératoire de Barbier (3), mis en oeuvre précédemment en série hétérocyclique (1), et (*B*) *ex situ*, dans le méthanol comme solvant ou selon la méthode de Bradley *et al.* (4), c'est-à-dire dans l'éther contenant des quantités catalytiques de méthanol. Les résultats sont rapportés aux tableaux 1 et 2.

Les produits de réaction sont en règle générale

[1]Tiré en partie des thèses de doctorat de D. Gravel et M. Ménard, Université de Montréal, Montréal, Québec.

[2]Boursier post-doctoral du Conseil National de Recherches du Canada (1962–64); attaché de recherches (1964–1966). Adresse actuelle: Université Sir George Williams, Montréal, Québec.

[3]Boursier du Conseil National de Recherches du Canada. Adresse actuelle: Bristol Laboratories of Canada, Candiac, Québec.

[4]Adresse actuelle: Domtar Limited, Central Research Laboratories, Senneville, Québec.

TABLEAU 1. Réactions *in situ* des cétones **1***a*, *b*, et *c* avec le diazométhane

Expérience*	Cétones **1**	Base	Température (°C)	Composés 1	2	5	6	7	Autres†	CA/E	Epoxyde *cis* (%)
1	*a*	KOH–eau	0–24	13	34	34	4	15	—	0.9	89
2	*a*	KOH–eau	0	30	30	31	3	6	—	0.9	91
3	*b*	KOH–eau	0–24	2	82	9 2‡	1 1‡	—	3	6.5	85
4	*b*	KOH–eau	0	15	52	12 12‡	0 5‡	—	4	1.9	83
5	*b*	K_2CO_3	0–24	32	45	18‡	5‡	—	0	2.0	78
6	*c*	KOH–eau	0–24	3	61	24	8	—	4	2.0	75
7	*c*	KOH–eau	0	2	65	23	7	—	3	2.3	77
8	*c*	K_2CO_3	0–24	10	57	22	9	—	2	1.9	71

*Dans toutes les expériences le diazométhane provient de la nitrosométhylurée, sauf dans l'expérience *7*, dans laquelle le *N*-méthyl *N*-nitroso toluènesulfonamide est mis en œuvre. Si dans les expériences *3* et *6* la nitrosométhylurée est remplacée par le *N*-méthyl *N*-nitroso toluènesulfonamide, les résultats sont reproductibles à 2% près.
†Les cétones agrandies plus lourdes que les cycloheptanones substituées figurent dans cette colonne.
‡Ces valeurs représentent les quantités d'époxydes que l'on retrouve à côté des éthers-alcools dans les expériences *3* et *4*; dans l'expérience *5* seuls les époxydes sont présents dans le mélange réactionnel.

TABLEAU 2. Réactions *ex situ* des cétones **1***a*, *b*, et *c* avec le diazométhane

Expérience	Cétones **1**	Solvents	Catalyseur* MeOH (mmol)	Température (°C)	Composés 1	2	3	4	Autres	CA/E	Epoxyde *cis* (%)
9	*a*	MeOH	—	24	25	18.5		(3.5)	53†		
10	*a*	MeOH	—	0	53				47†		
11	*b*	Ether	1	24	90	2.5	3.6	0.1	3.8‡		
12	*b*	Ether	5	24	87	6.0	4.0	0.1	2.9‡		
13	*b*	Ether	50	24	4	69	22	1	4§	3.1	96
14	*b*	MeOH	—	0–24	4	34	20	2	0	1.6	91
15	*c*	Ether	1	24	95	2.3	2.2	0.5	0	0.85	81
16	*c*	Ether	50	24	0	67	21	9	3§	2.4	70
17	*c*	MeOH	—	24	0	82	11.5	4.5	2§	5.3	72
18	*c*	MeOH	—	0–24	4	62	23	10	1§	1.9	70

*La quantité de MeOH, exprimée en mmol, correspond à 1 mmol de cétone.
†Correspond à l'acétal **7**.
‡Composé de nature inconnue.
§Cétones agrandies plus lourdes que les cétones **2**.

les cétones agrandies **2***a–c*, et les époxydes *cis* et *trans* **3***a–c* et **4***a–c*. Dans les réactions *in situ*, faites en présence d'hydroxyde de potassium, nous retrouvons également les éthers-alcools *cis* **5***a–c* et *trans* **6***a–c* (X = —OCH_3); la cétone **1***a* engendre de plus l'acétal **7**. Nous examinerons d'abord la préparation et la caractérisation de ces divers composés et ensuite leurs dosages dans les mélanges réactionnels.

Les cétones agrandies

Deux d'entre elles sont connues, **2***a* (2) et *b* (5). La cétone **2***c* s'obtient aisément par extension de cycle préparative de la cétone **1***c*. D'une manière générale, dans les conditions d'opération décrites, l'agrandissement de cycle s'arrête à toutes fins pratiques à la cycloheptanone. Dans le cas de la cétone **1***b*, la réaction conduit à quelques pourcents de cétones plus lourdes que **2***b*, qui sont certainement les tert-butyl-4 et -5 cyclo-octanones. En effet, en répétant le travail d'Anet *et al.* (6) c'est-à-dire la préparation d'anneaux à huit chaînons par extension de la cétone **1***b* par le diazométhane en présence d'éthérate de trifluorure de bore, nous avons obtenu un mélange des cétones à 7 et 8 membres dont les pics sont superposables, en c.p.g. à ceux de l'extension de cycle faite dans nos conditions.

Les époxydes

Les époxydes **3***a*, *b*, *c* et **4***a*, *b*, *c* se préparent avec de bons rendements par les méthodes de Corey et Chaykovsky (7). Les pourcentages d'isomère *cis* **3** sont rapportés au tableau 4. Les époxydes purs **3***a* et *b* sont connus de travaux antérieurs, respectivement réfs. 2 et 7. Le mélange 80–20 des époxydes **3***c* et **4***c* est également connu, à la suite de notre travail (2); une simple chromatographie

Can. J. Chem. Downloaded from www.nrcresearchpress.com by 84.22.46.98 on 09/08/12
For personal use only.

a R = $C_6H_5-SO_2-$; *b* R = tert-butyle; *c* R = C_6H_5-S-

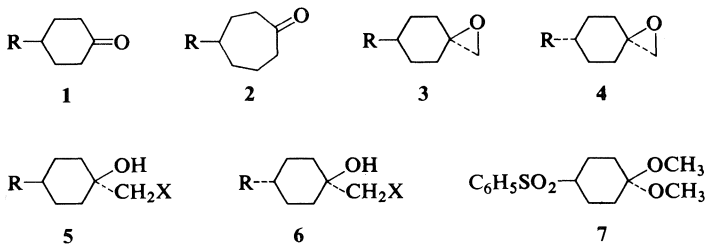

1 2 3 4

5 6 7

de ce mélange sur gel de silice permet d'obtenir l'isomère **3***c* pur. L'obtention des isomères **4***a*, *b*, et *c* résulte d'une méthode inédite. En traitant par de l'hydroxyde de potassium dans le méthanol un mélange des époxydes **3***a*–**4***a* riche en isomère **4***a*, les époxydes se transforment en éthers-alcools **5***a* et **6***a* (X = —OCH_3). Il est possible cependant d'arrêter la réaction au moment où tout l'époxyde **3***a* a réagi, alors qu'il reste encore de l'époxyde **4***a* dans le milieu. Une chromatographie sur gel de silice permet l'isolement de l'époxyde **4***a* pur. De la même manière, les époxydes **4***b* et *c* s'obtiennent à l'état pur.

Les éthers-alcools 5 et 6 (X = —OCH_3)

Ils résultent de l'action de l'hydroxyde de potassium sur les époxydes **3** et **4** dans du méthanol. Les composés **5***a* et *b* s'obtiennent purs au départ des époxydes purs **3***a* et *b*, ce qui établit leur configuration. Les isomères **6***a* et *b* s'obtiennent par ouverture et séparation chromatographique des mélanges riches en époxydes **4***a* et *b*. Le mélange 80–20 des époxydes **3***c*–**4***c*, réduit par l'hydrure de lithium et d'aluminium, donne un mélange 81–19 des alcools connus **5***c* et **6***c* (X = —H) (2) et par traitement par l'hydroxyde de potassium à un mélange 80–20 des éthers-alcools **5***c*–**6***c* (X = —OCH_3), ce qui établit leur configuration. Les six éthers-alcools purs décrits sont des alcools tertiaires, comme le montrent les spectres de r.m.n. mesurés dans le diméthylsulfoxyde deutérié (8).

L'acétal 7

Il s'obtient pur par l'action du méthanol sur la cétone **1***a*, en présence d'éthérate de trifluorure de bore.

Réactions et dosages des mélanges réactionnels

Les expériences ont été menées soit à l'échelle analytique soit à l'échelle préparative. A l'échelle analytique, les dosages ont demandé une longue mise au point. Le cas le plus simple est celui de l'analyse du mélange réactionnel issu de la réaction de la tert-butyl-4 cyclohexanone (**1***b*). En effet, la c.p.g. permet de doser simultanément les cétones **1***b* et **2***b*, les époxydes **3***b* et **4***b*, les éthers-alcools **5***b* et **6***b* et même les cétones agrandies plus lourdes que **2***b*. L'analyse par c.p.g. des époxydes **3***a* et **4***a* est impossible, en raison de leur décomposition. Il est par contre facile de doser par c.p.g., simultanément, les cétones **1***a* et **2***a*, les éthers-alcools **5***a* et **6***a* et l'acétal **7**. Nous avons donc converti totalement les époxydes en éthers-alcools avant le dosage par c.p.g. Nous avons procédé de la même manière dans le cas du mélange réactionnel issu de la cétone **1***c*.

La r.m.n. montre que les mélanges issus des réactions *in situ* en présence d'hydroxyde de potassium contiennent et les époxydes et les éthers-alcools. Les pics des protons méthyléniques (O—CH_2—) des éthers-alcools sont nettement différenciés de ceux des époxydes.

A côté de ces expériences, nous avons travaillé à l'échelle préparative, au départ des cétones **1***a* et *c*. La cétone **1***a* conduit à l'époxyde **3***a*, isolé sous forme de bromhydrine (50%) ou de pipéridino-alcool (39%), et à la cétone agrandie **2***a* isolée sous forme de dinitro-2,4 phénylhydrazone (25%). La cétone **1***c* permet d'obtenir la cétone agrandie **2***c* (64%) et l'époxyde **3***c* isolé comme pipéridino-alcool (**5**, X = $C_5H_{10}N$—). Du point de vue préparatif, l'extension de cycle de la phénylthio-4 cyclohexanone se fait bien, tandis que celle de la phénylsulfonyl-4 cyclohexanone en cétone agrandie **2***a*, est peu intéressante du fait de la grande quantité de cétone de départ qui reste inchangée. Par contre la cétone **2***a* se prépare avantageusement par la méthode de Tiffeneau–Demjanof décrite précédemment (2).

Can. J. Chem. Downloaded from www.nrcresearchpress.com by 84.22.46.98 on 09/08/12
For personal use only.

Can. J. Chem. Downloaded from www.nrcresearchpress.com by 84.22.46.98 on 09/08/12
For personal use only.

Discussion

La discussion porte sur trois points. (*1*) L'influence de l'hydroxyde de potassium. (*2*) Le rapport cétone agrandie/époxyde. (*3*) Le rapport *cis*/*trans* des époxydes.

(1) Influence de l'hydroxyde de potassium

Dans les trois cas étudiés, l'hydroxyde de potassium dans le méthanol convertit les époxydes **3** et **4** en éthers-alcools **5** et **6** (X = —OCH_3). Dans la réaction des cétones avec le diazométhane, cette conversion est partielle. Une faible quantité de base, un court temps de réaction et une température voisine de 0° sont les conditions qui préservent le mieux les époxydes. A titre d'exemple, nous pouvons citer les extensions préparatives des cétones **1***a* et *c*, qui donnent respectivement 39 et 29% d'époxydes, isolés sous forme de pipéridino-alcools. Les expériences *3* et *4* du tableau 1 donnent une idée de l'influence de la température. En série hétérocyclique, il est aussi possible d'obtenir les époxydes avec de bons rendements (1).

L'hydroxyde de potassium exerce d'autre part une action prépondérante sur le cours de la réaction de la cétone sulfonylée **1***a*. Dans les réactions *ex situ* (expériences *9* et *10*, tableau 2), le composé de réaction prépondérant est l'acétal **7**, tandis que les réactions *in situ* conduisent à la cétone agrandie et aux époxydes (expériences *1* et *2*, tableau 1). La présence ou l'absence de l'hydroxyde de potassium ne joue aucun rôle, quant à la nature des produits formés, dans le cas des cétones tert-butylée **1***b* et phénylthio **1***c*. Hassan et Casy (9), ont montré que les sels d'ammonium quaternaire des pipéridones-4 (**8**) existaient en solution alcoolique sous forme d'hémi-acétal **9**. Nous en déduisons que la cétone sulfonylée **1***a*, porteuse d'un groupe attracteur d'électrons, se comportera de la même façon et que le diazométhane agira comme agent d'acétalisation, comme il le fait avec d'autres hémi-acétals (10) et alcools (11). L'action de l'hydroxyde de potassium serait alors de réduire la formation de l'hémi-acétal et de permettre ainsi l'attaque nucléophile du diazométhane sur le groupe carbonyle.

Dans les réactions *in situ*, le remplacement de l'hydroxyde de potassium par le carbonate de potassium diminue le taux de réaction des cétones **1***b* et *c*, mais ne change pas la nature des produits formés (expériences *3* et *5*, et *6* et *8*, tableau 1). Dans le cas de la cétone sulfonylée **1***a*, le changement de base entraîne un changement total dans les produits de réaction; cette réaction est encore à l'étude.

8 X = $(CH_3)_2N^+$= **9** X = $(CH_3)_2N^+$=

10 X = $C_6H_5SO_2N$=

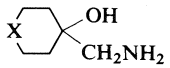

11 X = SO_2=

12 X = $C_6H_5SO_2N$=

(2) Rapport cétone agrandie/époxyde

Nous définissons l'aptitude à l'extension comme le rapport cétone agrandie/époxydes (CA/E), y compris les composés qui dérivent soit de la cétone agrandie soit des époxydes.

Les résultats des tableaux 1 et 2 indiquent que dépendant des conditions employées, les rapports CA/E varient pour une cétone donnée. Nous estimons cependant que dans des conditions expérimentales rigoureusement identiques une comparaison se justifie. Au tableau 3 figurent les rapports CA/E des cétones **1***a–c* obtenus *in situ* (expériences *1*, *3* et *6* du tableau 1) et celui obtenu dans le cas de la phénylsulfonyl-1 pipéridone-4 (**10**), dans des conditions expérimentales identiques (1). La cétone sulfonylée **1***a* occupe une position intermédiaire entre les deux extrêmes que représentent d'une part la tert-butyl-4 cyclohexanone (grande aptitude à l'extension) et la phénylsulfonyl-1 pipéridone-4 (**10**) (aptitude presque nulle à l'extension). Nous reviendrons plus loin au cas de la cétone **1***c*. Figurent aussi au tableau 3 les rapports CA/E pour les désaminations nitreuses des amino-alcools **5***a*, **6***a*, **5***b*, **6***b* (X = —NH_2) et **12** correspondant aux cétones **1***a*, **1***b* et **10** et celui de l'amino-alcool **11** étudié par Overberger et Katchman (12). Le parallélisme est remarquable entre l'action du diazométhane et les désaminations nitreuses: les amino-alcools **5***a* et **6***a* (X = —NH_2) occupent une position intermédiaire entre ceux dérivés de la tert-butyl-4 cyclohexanone (**5***b* et **6***b*) et ceux de la série hétérocyclique (**11** et **12**). Cette variation dans l'aptitude à l'extension témoigne d'interactions entre les groupes électronégatifs et les intermédiaires résultant de l'attaque nucléophile du diazométhane

TABLEAU 3. Aptitudes à l'extension (CA/E) de cétones cycliques et de leurs amino-alcools

Cétones de départ	Cétones agrandies (%)	Epoxydes (%)	CA/E	Référence	Amino-alcools	Cétones agrandies (%)	Epoxydes (%)	CA/E	Référence
1*b*	85*	13	6.5†		**5***b*	80	20	4	5
					6*b*	90	5	18	5
1*c*	65*	32	2†						
1*a*	34	38	0.9†		**5***a*	23	60	0.4	2
					6*a*	60	28	2	2
10	9	82	0.1	1	**12**	traces	91	0.01	1
					11	14	67	0.2	12

*Le chiffre indiqué comprend la cétone agrandie à 7 chaînons et tous les composés qui en dérivent (colonne "autres" du tableau 1).
†Tiré des expériences *1*, *3*, et *6* du tableau 1.

TABLEAU 4. Pourcentage de formation d'époxydes *cis* **3***a*, *b*, et *c*

Cétones **1**	CH_2N_2	$(CH_3)_2SO{=}CH_2$	$(CH_3)_2S{=}CH_2$
a	91–93	100	34
b	78–96	100*	32†
c	71–77	80	44

*Littérature (7) 100%.
†Littérature (7) 17%; la valeur de 32% que nous donnons ici résulte d'un dosage direct par c.p.g.

sur le groupe carbonyle et, d'un effet de distance, comme nous l'avons montré dans nos travaux antérieurs (1, 2).

Nos résultats nous amènent aussi à la conclusion que le groupe phénylthio de la cétone **1***c* n'exerce aucune influence sur le cours de la réaction, voir expériences *4* et *7*, *5*, et *8* du tableau 1, et *14* et *18* du tableau 2, car il se comporte d'une manière fort semblable au groupe tert-butyle, nécessairement inerte, de la cétone **1***b*. Les expériences *3* et *6* constituent cependant une exception.

Il est intéressant de relever que l'observation de Bradley *et al.* (4) au sujet de l'acétone - le rapport CA/E diminue avec la diminution de la quantité d'alcool utilisé comme catalyseur - s'applique aux cétones **1***b* et *c* (expériences *11–13*, *15*, *16* tableau 2). Cette augmentation, qui se fait toutefois au détriment du rendement en cétone agrandie et en époxydes, engendre des composés nouveaux dans le cas de la cétone **1***b*.

(3) Rapport cis/trans des époxydes

Il ressort clairement du tableau 4 que les époxydes *cis* prédominent largement dans les mélanges *cis*/*trans* dans la réaction du diazométhane avec des cyclohexanones substituées en position 4. Deux travaux ont récemment fait état de la prédominance de l'attaque équatoriale du diazométhane sur une décalone-2 (13) et un céto-3 stéroide (14). Notre étude confirme cette observation (tableau 4). Au départ de la tert-butyl-4 cyclohexanone (**1***b*), qui existe en conformation **13***b*, la formation prépondérante de l'époxyde *cis* **3***b*, ou en formule tridimentionnelle **14***b*, correspond à une attaque équatoriale du diazométhane. Il en sera de même pour la cétone **1***a*, en conformation **13***a*, qui engendre surtout l'époxyde *cis* **3***a*, donc **14***a*. Les résultats de la cétone **1***c* sont compatibles avec le fait que cette cétone existe sous les deux conformations **15**, qui par attaque équatoriale donneront un mélange des époxydes *cis* et *trans* **3***c*, **4***c* un peu plus pauvre en isomère *cis* que lorsque la cétone est rigide.

Nous comparons au tableau 4 les résultats de la formation des époxydes *trans* **3***a*, *b*, et *c* par l'action de trois réactifs: diazométhane, méthylures de diméthyloxosulfonium, et de diméthylsulfonium. On y retrouve un parallélisme certain entre l'action du diazométhane et celle du méthylure de diméthyloxosulfonium, cette dernière étant cependant beaucoup plus spécifique dans la formation des époxydes *cis*.

En conclusion, ce travail montre que, par rapport à un groupe tert-butyle en position 4 d'une cyclohexanone: un groupe phénylsulfonyle diminue considérablement l'aptitude à l'extension, mais ne touche pas à la formation prédominante d'époxyde équatorial; en revanche, un groupe phénylthio n'altère que peu l'aptitude à l'exten-

Can. J. Chem. Downloaded from www.nrcresearchpress.com by 84.22.46.98 on 09/08/12
For personal use only.

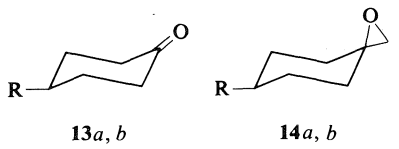

13*a*, *b* **14***a*, *b*

a R = $C_6H_5—SO_2—$

b R = tert-butyle

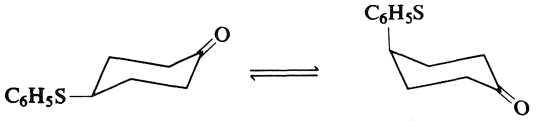

sion, mais donne par contre une moins grande stéréospécificité dans la formation des époxydes.

Partie expérimentale

Les spectres i.r. ont été déterminés à l'aide d'un spectrophotomètre Beckman IR8, avec un prisme à chlorure de sodium. Les spectres de r.m.n. ont été déterminés avec un appareil Jeolco C 60 H. Les valeurs sont exprimées en δ et données par rapport au tétraméthylsilane. Les liquides ont été distillés dans un tube à boules avant d'être analysés. Les analyses sont de C. Daesslé, Organic Microanalyses, Montréal.

1 Analyses par c.p.g.

Nous avons utilisé un appareil F & M 100, avec détection par ionisation à flamme.

Pour la cétone **1***a*, l'acétal **7**, la cétone **2***a*, et les éthers-alcools **5***a* et **6***a*, les temps de rétention sont les suivants, respectivement: 9, 10, 13, 15, et 19 min, dans les conditions suivantes: colonne de 3.8% de SE30 sur Anachrom ABS, 2.70 m de longueur, 8 mm de diamètre, température de 220° et débit de 70 ml/min; gaz porteur, He.

Pour les époxydes **3***b*, **4***b*, les éthers-alcools **5***b*, **6***b* et les cétones **1***b*, **2***b*, les temps de rétention sont les suivants, respectivement: 10, 12, 12.8, 16, 16.8, et 22 min; pour les cétones plus lourdes, probablement tert-butyl-4 et -5 cyclo-octanones, 25 et 27 min; dans les conditions suivantes: colonne de 4% QF1 sur Anachrom ABS, 6 m de longueur, 6 mm de diamètre, à température de 165° et débit de 45 ml/min, He. Les dosages des époxydes sont particulièrement délicats; il ne faut utiliser que des tubes de verre et surtout placer un tube de verre dans la chambre d'injection, pour éviter tout contact avec les parties métalliques de l'appareil.

Pour la cétone **3***c*, les éthers-alcools **6***c* et **5***c*, la cétone **2***c*, et les cétones plus lourdes que **2***c*, les temps de rétention sont respectivement: 15, 16, 18, 22.3, 26, et 28 min dans les conditions suivantes: colonne de 3.0% de QF1 sur Chromosorb G, 4.50 m de longueur et 3 mm de diamètre, à température de 195° et débit de 30 ml/min, He.

2 Epoxydes

2.1 Méthode au méthylure de diméthyloxosulfonium

Mode opératoire selon (7). La cétone **1***a* donne, avec 60% de rendement, l'époxyde **3***a*, p. de f. brut 70–80°, montant à 93–95° après une cristallisation dans l'éther, seul ou en mélange avec l'époxyde décrit en (2). La cétone **1***b* donne l'époxyde **3***b* pur, homogène en c.p.g. La cétone **1***c* donne, avec un rendement de 86%, un mélange 80–20 des époxydes **3***c* et **4***c* (dosage, section 3.33).

2.2 Méthode au méthylure de diméthylsulfonium

Mode opératoire selon (7). Les résultats sont donnés au tableau 4. Les époxydes **3***b*–**4***b* sont dosés par c.p.g. Les époxydes **3***a*–**4***a* sont dosés à la section 3.1.3 et les époxydes **3***c*–**4***c* à la section 3.3.3.

*3 Synthèse des éthers-alcools **5** et **6** (X = —OCH_3) et préparation des époxydes **3** et **4** purs*

3.1 Série de la phénylsulfonyl-4 cyclohexanone

*3.1.1 Préparation de l'époxyde **4***a* et des éthers-alcools **5***a* et **6***a* (X = —OCH_3)*

On dissout 1.1 g du mélange 34–66 des époxydes **3***a* et **4***a* dans 20 ml d'une solution préparée en dissolvant 3.7 g d'hydroxyde de potassium et 3.7 g d'eau dans 80 ml de méthanol. On agite 6 h à 24°. On neutralise par de l'acide acétique glacial, évapore sous vide à 40°. On reprend par du chloroforme; on lave cette solution par une solution aqueuse de bicarbonate de sodium, puis avec de l'eau jusqu'à neutralité. On sèche sur sulfate de magnésium et évapore le solvant. Le résidu, 1.0 g, est chromatographié sur 100 g de gel de silice; l'éluant est un mélange 58.0–38.2–3.8 d'acétate d'éthyle – cyclohexane – méthanol; on élue par des fractions de 15 ml. Les fractions 23 et 24 contiennent l'époxyde **4***a* (180 mg), les fractions 28–30 l'éther-alcool **6***a* (110 mg) et les fractions 33–37 l'éther-alcool **5***a* (250 mg).

*Epoxyde de méthylène-1 phénylsulfonyl-4 cyclohexane trans (**4***a*)*

Le p. de f. 79–80°. Spectre i.r. ($CHCl_3$): 3040 (époxyde), 1310 et 1150 cm^{-1} (—SO_2—). Spectre de r.m.n.:

($CDCl_3$): 1.4 à 2.5 (massif, 8H); 2.60 (s, 2H, 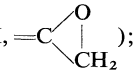); 3.00 (1H, —SO_2—); de 7.5 à 8.1 (massif, 5H, C_6H_5—).

Anal. calc. pour $C_{13}H_{16}O_3S$: C, 61.84; H, 6.39; S, 12.69. Trouvé: C, 61.90; H, 6.59; S, 12.89.

*Méthoxyméthyl-1 phénylsulfonyl-4 cyclohexanol cis (**5***a*)*

Le p. de f. 112–113.5° (éther). Spectre i.r. ($CHCl_3$): 3580 (OH non associé), 1310 et 1140 cm^{-1} (—SO_2—). Spectre de r.m.n. ($CDCl_3$): de 1.0 à 3.06 (9H): de 3.1 à 3.7 (bande étalée, 1H); 3.2 (s, 2H, C—CH_2—O) 3.39 (s, 3H, —OCH_3); de 7.4 à 8.1 (5H, C_6H_5). Dans DMSO-d_6, singulet (alcool tertiaire) à 4.35.

Anal. calc. pour $C_{14}H_{20}O_4S$: C, 59.13; H, 7.09; S, 11.26. Trouvé: C, 58.84; H, 6.85; S, 11.41.

*Méthoxyméthyl-1 phénylsulfonyl-4 cyclohexanol trans (**6***a*)*

Le p. de f. 73–74°. Spectre i.r. ($CHCl_3$): 3580 cm^{-1} (OH non associé). Spectre de r.m.n. ($CDCl_3$): de 1.1 à 3.1 (massif, 10H); 3.36 (s, 2H, C—CH_2—O); 3.41 (s, 3H, —OCH_3); de 7.5 à 8.1 (5H, C_6H_5). Dans DMSO-d_6, singulet (alcool tertiaire) à 4.52.

Can. J. Chem. Downloaded from www.nrcresearchpress.com by 84.22.46.98 on 09/08/12
For personal use only.

Can. J. Chem. Downloaded from www.nrcresearchpress.com by 84.22.46.98 on 09/08/12
For personal use only.

Anal. calc. pour $C_{14}H_{20}O_4S$: C, 59.13; H, 7.09; S, 11.26. Trouvé: C, 59.10; H, 7.21; S, 11.21.

3.1.2 Ouverture de l'époxyde 3a

L'époxyde **3***a* est traité par le mélange MeOH–KOH–eau pendant 24 h comme à la section précédente 3.1.1. Il en résulte après isolement et une cristallisation dans l'éther le composé **5***a*, de p. de f. 112–113, 5°. Une analyse par c.p.g. (selon la section 1) du produit brut ne montre qu'un pic, établissant ainsi la pureté stérique de l'époxyde **3***a* préparé à la section 2.1.

3.1.3 Ouverture du mélange des époxydes 3a et 4a

Le mélange des époxydes **3***a* et **4***a* conduit, par traitement par le mélange MeOH–KOH–eau comme à la section 3.1.2, à un mélange des éthers-alcools **5***a* et **6***a*. Un dosage par c.p.g., comme à la section 1, établit que les deux éthers-alcools **5***a* et **6***a* se trouvent dans les proportions 34–66.

3.2 Série de la tert-butyl-4 cyclohexanone

3.2.1 Préparation de l'époxyde 4b et des éthers-alcools 5b et 6b (X = —OCH₃)

On dissout 3.8 g du mélange (rapport 32–68) des époxydes **3***b* et **4***b* dans 68 ml d'une solution préparée en dissolvant 3.7 g d'hydroxyde de potassium et 3.7 g d'eau dans 100 ml de méthanol. On agite à 24°. Après 20 h, le pic correspondant à l'époxyde **3***b* a complètement disparu en c.p.g.; la réaction est interrompue. On neutralise par de l'acide acétique glacial, évapore sous vide à 40°. On reprend par de l'éther et isole, comme en 3.1.1, 3.5 g de produit que l'on chromatographie sur colonne de gel de silice, en utilisant un mélange 94–6 d'éther de pétrole et d'acétone, et en éluant par des fractions de 20 ml. Les fractions 6 à 12 contiennent l'époxyde **4***b* pur, 1.4 g (37%), les fractions 14 à 24 le composé **5***b*, 1.3 g (28.7%), et les fractions 25 à 28 le composé **6***b*, 0.3 g (6.6%).

Epoxyde de tert-butyl-4 méthylène-1 cyclohexane trans (4b)

Liquide, $n_D^{28} = 1.4598$. Spectre i.r. (CCl_4): 3040 cm^{-1} (oxiranne). Spectre de r.m.n. (CCl_4): 0.9 (s, 9H, tert-butyle); massif de 1.00 à 2.2 (9H): 2.43 (s, 2H,).

Anal. calc. pour $C_{11}H_{20}O$: C, 78.51; H, 11.98. Trouvé: C, 78.25; H, 11.80.

tert-Butyl-4 méthoxyméthyl-1 cyclohexanol cis (5b)

Liquide, $n_D^{28} = 1.4580$. Spectre i.r. (CCl_4): 3600 cm^{-1}, —OH non associé. Spectre de r.m.n. (CCl_4): 0.86 (s, 9H, tert-butyle); massif de 1 à 1.8 (9H); 1.97 (s, 1H, —OH); 3.10 (s, 2H, O—CH_2—O); 3.37 (s, 3H, —O—CH_3). Dans DMSO-d_6: singulet (alcool tertiaire à 4.02.

Anal. calc. pour $C_{12}H_{24}O_2$: C, 71.95; H, 12.08. Trouvé: C, 71.98; H, 12.13.

tert-Butyl-4 méthoxyméthyl-1 cyclohexanol trans (6b)

Liquide, $n_D^{28} = 1.4612$. Spectre i.r. (CCl_4): 3600 cm^{-1}, —OH non associé. Spectre de r.m.n. (CCl_4): 0.86 (s, 9H, tert-butyle); massif de 1 à 2.1 (9H); 2.33 (s, 1H, —OH); 3.30 (s, 2H, C—CH_2—O); 3.40 (s, 3H, —O—CH_3). Dans DMSO-d_6: singulet (alcool tertiaire) à 4.02.

Anal. calc. pour $C_{12}H_{24}O_2$: C, 71.95; H, 12.08. Trouvé: C, 71.59; H, 11.81.

3.2.2 Ouverture de l'époxyde 3b

On traite, comme plus haut à la section 3.1.2, l'époxyde **3***b* pur par le mélange MeOH–KOH–eau. On obtient l'éther-alcool **5***b*, caractérisé par son spectre de r.m.n., contenant 3% d'époxyde de départ, comme le montre l'analyse par c.p.g. faite selon la section 1.

3.3 Série de la phénylthio-4 cyclohexanone

3.3.1 Préparation de l'époxyde 4c et des éthers-alcools 5c et 6c

On traite 2.5 g d'un mélange 80–20% des époxydes **3***c* et **4***c* par 35 ml d'une solution préparée en dissolvant 3.7 g d'hydroxyde de potassium et 3.7 g d'eau dans 100 ml de méthanol. Après agitation de 10 h à 24°, on isole comme en 3.2.1 2.4 g de produit que l'on chromatographie sur 108 g de gel de silice, en utilisant comme éluant un mélange 92–8 d'éther de pétrole – acétone, et en éluant par des fractions de 20 ml. Les fractions 21–26 contiennent l'époxyde **3***c* pur (1.1 g), les fractions 31–36 contiennent l'éther-alcool **6***c* et les fractions 50–53 contiennent l'éther-alcool **5***c*.

Epoxyde de méthylène-1 phénylthio-4 cyclohexane trans (4c)

Liquide. Spectre i.r. (CCl_4): 3045 (époxyde). Spectre de r.m.n. (CCl_4): de 1.2 à 2.3 (massif, 8H); 2.47 (s, 2H,); 3.30 (bande, largeur à demi-hauteur 15 Hz 1H, —S—CH=); 7.2 (m, 5H, C_6H_5—).

Anal. calc. pour $C_{13}H_{16}OS$: C, 70.87; H, 7.32; S, 14.55. Trouvé: C, 70.55; H, 7.31; S, 14.28.

Méthoxyméthyl-1 phénylthio-4 cyclohexanol cis (5c)

Liquide. Spectre i.r. (CCl_4): 3600 cm^{-1} (OH non associé). Spectre de r.m.n. (CCl_4): de 0.98 à 2.51 (massif, 9H); 3.09 (s, 2H, C—CH_2—O—); et 3.33 (s, 3H, —OCH_3); sous ces deux singulets se trouve une bande large, 1H, —S—CH=; 7.2 (m, 5H, C_6H_5—). Dans DMSO-d_6: singulet (alcool tertiaire) à 4.17.

Anal. calc. pour $C_{14}H_{20}O_2S$: C, 66.63; H, 7.99; S, 12.69. Trouvé: C, 66.94; H, 8.23; S, 13.02.

Méthoxyméthyl-1 phénylthio-4 cyclohexanol trans (6c)

Liquide. Spectre i.r. (CCl_4): 3600 cm^{-1} (OH non associé). Spectre de r.m.n. (CCl_4): de 1.11 à 2.30 (massif, 9H); 3.2 (s, 2H, C—CH_2—O—) et 3.34 (s, 3H, —OCH_3); sous ces deux singulets se trouve une bande large, 1H, —S—CH=; 7.21 (m, 5H, C_6H_5—). Dans DMSO-d_6: singulet (alcool tertiaire) à 4.32.

Anal. calc. pour $C_{14}H_{20}O_2S$: C, 66.63; H, 7.99; S, 12.69. Trouvé: C, 66.42; H, 7.76; S, 12.61.

3.3.2 Epoxyde de méthylène-1 phénylthio-4 cyclohexane cis (3c)

On chromatographie sur colonne de gel de silice (125 g) 2.5 g du mélange 80–20% des époxydes **3***c* et **4***c* préparé à la section 2.1. Comme éluant, on utilise des portions de 20 ml du mélange 58–38 d'acétate d'éthyle – cyclohexane. Les fractions 24–27 contiennent l'époxyde **3***c* pur (0.6 g). Liquide. Spectre i.r. (CCl_4): 3045 cm^{-1} (époxyde). Spectre de r.m.n. (CCl_4): de 1.1 à 2.38 (massif, 8H); 2.48 (s, 2H, 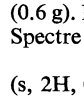); 3.13 (bande de largeur à demi-hauteur de 22 Hz) (1H, —S—CH=); 7.4 (m, 5H, C_6H_5).

Can. J. Chem. Downloaded from www.nrcresearchpress.com by 84.22.46.98 on 09/08/12
For personal use only.

Anal. calc. pour $C_{13}H_{16}OS$: C, 70.87; H, 7.32; S, 14.55. Trouvé: C, 70.96; H, 7.21; S, 14.36.

3.3.3 Dosage des époxydes 3c–4c en mélanges

La réduction des époxydes **3***c* et **4***c* par l'hydrure de lithium et d'aluminium conduit aux alcools **5***c* et **6***c* (X = H) déjà décrits (2). La réduction du mélange préparé en 2.1 plus haut conduit à un mélange contenant 81% d'alcool **5***c* et 19% d'alcool **6***c*, par analyse par c.p.g. dans les conditions décrites (2). Le même mélange d'époxydes conduit par traitement par le mélange MeOH–KOH–eau, comme en 3.3.1 plus haut, à un mélange des deux éthers-alcools **5***c* et **6***c* (X = —OCH_3) dans les proportions 80–20.

Le traitement par MeOH–KOH–eau, du mélange des époxydes **3***c*–**4***c* préparé en 2.2 conduit à un mélange des éthers-alcools **5***c* et **6***c* (X = —OCH_3) dans le rapport 44–56. La réduction du mélange des époxydes par l'hydrure de lithium et d'aluminium donne un mélange 50–50 des alcools **5***c* et **6***c* par analyse par c.p.g., selon (2).

4 Diméthoxy-1,1 phénylsulfonyl-4 cyclohexane (7)

On dissout 50 mg de la cétone **1***a* dans 3 ml de méthanol; on ajoute 0.05 ml d'éthérate de trifluorure de bore, et abandonne, avec agitation, pendant 12 h à 24°. On ajoute 7 gouttes d'une solution aqueuse saturée de bicarbonate de sodium. On évapore les solvants sous vide et reprend par du chloroforme. La solution chloroformique est lavée avec de l'eau, puis séchée sur sulfate de magnésium. On recueille 50 mg de cristaux blancs, qui après cristallisation dans l'éther, fondent à 92–93°. Spectre i.r. ($CHCl_3$): 2840 (OCH_3), 1310 et 1140 cm^{-1} (SO_2). Spectre de r.m.n. ($CDCl_3$): de 1.08 à 2.95 (massif, 9H); 3.09 (s, 3H, —OCH_3); 3.14 (s, 3H, —OCH_3); de 7.46 à 8.1 (massif, 5H, C_6H_5—).

Anal. calc. pour $C_{14}H_{20}O_4S$: C, 59.13; H, 7.09; S, 11.26. Trouvé: C, 59.21; H, 7.17; S, 11.37.

5 Réaction du diazométhane avec les cétones 1a, b, et c

5.1 Réactions in situ

Nous décrivons ici les réactions; les dosages par c.p.g., selon la section 1, figurent au tableau 1. La nitrosométhylurée se prépare selon (15).

5.1.1 Série de la phénylsulfonyl-4 cyclohexanone (1a)

Expérience 1

On dissout 238 mg (1 mmol) de cétone **1***a* dans 8 ml de méthanol refroidi à 0°; on ajoute à cette solution une solution de 112 mg d'hydroxyde de potassium dans 112 mg d'eau, puis par portions, pendant 90 min, 120 mg (1.15 mmol) de nitrosométhylurée. On agite à 0° 1 h de plus, puis à 24° pendant 18 h. On refroidi à 0°, neutralise par de l'acide acétique glacial, évapore le solvant, reprend le résidu par du chloroforme, lave une fois à l'eau, sèche sur sulfate de magnésium et évapore le chloroforme. On analyse par c.p.g.

Expérience 2

On manipule comme dans l'expérience *1*, sauf que l'agitation de 18 h à 24° est remplacée par une agitation de 5 h à 0°.

5.1.2 Série de la tert-butyl-4 cyclohexanone (1b)

Expérience 3

On prépare une solution de 37 ml de méthanol, 0.55 g d'hydroxyde de potassium et 0.55 g d'eau; on y dissout 771 mg de cétone **1** (5 mmol), refroidie à 0° et ajoute avec agitation, en 1.5 h 618.6 mg de nitrosométhylurée (6 mmol). On agite 1 h de plus à 0°, puis 18 h à 24°. On neutralise par de l'acide acétique, évapore le méthanol, reprend par de l'éther, lave à neutralité par de l'eau, sèche sur sulfate de magnésium et évapore l'éther. On dose par c.p.g.

Expérience 4

On opère comme au cours de l'expérience *3*, sauf que l'agitation de 18 h à 24° est remplacée par une agitation de 5 h à 0°.

Expérience 5

On opère comme à l'expérience *3*, sauf que l'hydroxyde de potassium et l'eau sont remplacés par 1.1 g de carbonate de potassium (pas d'eau).

5.1.3 Série de la phénylthio-4 cyclohexanone (1c)

Expérience 6 (tableau 1)

On dissout 206 mg (1 mmol) de cétone **1***c* dans 8 ml d'une solution préparée en dissolvant 0.55 g d'hydroxyde de potassium et 0.55 g d'eau dans 37 ml de méthanol. On y refroidi à 0°, et ajoute, avec agitation, en 90 min, 120 mg de nitrosométhylurée (1.15 mmol). On agite à 0° 1 h de plus, puis 18 h à 24°. On ajoute alors à la solution 8 ml d'une solution préparée en dissolvant 3.7 g d'hydroxyde de potassium et 3.7 g d'eau dans 100 ml de méthanol. On laisse agiter pendant 48 h. On neutralise par de l'acide acétique glacial, évapore le méthanol, reprend le résidu par de l'éther. On lave la solution éthérée à neutralité avec de l'eau, sèche sur sulfate de magnésium et évapore l'éther. On analyse par c.p.g.

Si l'on isole les composés de réaction après l'agitation de 18 h à 24°, on décèle un mélange d'époxydes et d'éthers-alcools, impossible à analyser par c.p.g.

Expérience 7

On manipule comme dans l'expérience *6*, sauf que l'agitation de 18 h à 24° est remplacée par une agitation de 5 h à 0°.

Expérience 8

On manipule comme dans l'expérience *6*, sauf que la solution initiale est faite de 8 ml de méthanol et 240 mg de carbonate de potassium.

5.2 Réactions ex situ

5.2.1 Préparation de la solution de diazométhane dans l'éther

En suivant les indications données en (15), on introduit par petites portions 20.6 g de nitrosométhylurée dans un ballon contenant 60 ml d'une solution aqueuse de KOH 50% et 200 ml d'éther pur maintenus à 5°. Une fois l'addition terminée, on adapte une colonne à distillation sur le ballon et distille lentement; la solution éthérée de diazométhane a un titre de 0.31 *M* (dosage par l'acide benzoïque).

5.2.2 Expérience 9–16 (tableau 2)

Expérience 9

A une solution de 238 mg (1 mmol) de cétone **1***a* dans 4 ml de méthanol maintenu à 24°, on ajoute d'un coup 3.6 ml (1.1 mmol) de la solution de diazométhane 0.31 *M* préparée en 5.2.1. On agite à température de 24° pendant 48 h, évapore les solvants et analyse par c.p.g. A cause de la très grande quantité d'acétal **7**, l'analyse des éthers-alcools est très approximative.

Can. J. Chem. Downloaded from www.nrcresearchpress.com by 84.22.46.98 on 09/08/12
For personal use only.

Expérience 10

On travaille comme dans l'expérience *9*, sauf que la température est maintenue à 0°.

Expérience 11

A une solution de 771 mg de cétone **1** (5 mmol), dans 20 ml d'éther, contenant 160 mg de méthanol (5 mmol), maintenue à 24 °C, on ajoute d'un coup 18 ml (6 mmol) d'une solution 0.31 *M* de diazométhane dans l'éther préparée de façon habituelle (22). On agite à température de 24° pendant 48 h et analyse par c.p.g.

Expérience 12

On opère comme au cours de l'essai *11*, sauf que la solution éthérée contient 320 mg de méthanol (10 mmol).

Expérience 13

On opère comme au cours de l'essai *11*, sauf que la solution est composée de 10 ml d'éther et 10 ml de méthanol (250 mmol).

Expérience 14

A une solution de 771 mg de cétone **1** (5 mmol), dans 20 ml de méthanol, à 0°, on ajoute pendant 1.5 h 18 ml d'une solution 0.31 *M* de diazométhane dans l'éther, gardée à 0°. On agite 1 h de plus à 0°, puis 18 h à 24°. On analyse par c.p.g.

Expérience 15

On prépare une solution de 206 mg (1 mmol) de cétone **1***c* dans 4 ml d'éther contenant 32 mg (1 mmol) de méthanol. A cette solution, maintenue à 24°, on ajoute d'un coup 3.6 ml (1.1 mmol) d'une solution 0.31 *M* de diazométhane dans l'éther préparée en 5.2.1 et maintenue à 24°. On laisse agiter 48 h à 24°, évapore le solvant. On ajoute au résidu 8 ml d'une solution formée en dissolvant 3.7 g d'hydroxyde de potassium et 3.7 g d'eau dans 80 ml de méthanol. Après agitation de 48 h, on neutralise par de l'acide acétique, évapore les solvants, reprend par de l'éther, lave une fois avec une solution aqueuse de bicarbonate de sodium puis à l'eau, sèche sur sulfate de magnésium anhydre et évapore l'éther. On dose le résidu par c.p.g.

Expérience 16

On opère comme dans l'expérience *15*, sauf que les 206 mg de cétone **1***c* étaient en solution dans 2 ml de méthanol (50 mmol) et 2 ml d'éther au début de la réaction.

Expérience 17

On opère comme dans l'expérience *15*, sauf que les 206 mg de cétone **1***c* étaient en solution dans 4 ml de méthanol au début de la réaction.

Expérience 18

On procède comme dans l'expérience *17*, sauf que la température était de 0° au lieu de 24° pour le début de la réaction.

*6 Réaction de la cétone **1***a *avec le diazométhane, à l'échelle préparative*

(*A*) On refroidit à 0° une solution de 11.0 de la cétone **1***a* dans 200 ml de méthanol. On y ajoute 5.6 g d'une solution d'hydroxyde de potassium 50% dans l'eau, puis par petites portions 5.0 g de nitrosométhylurée. On agite pendant 3 h à 0°, puis laisse revenir à 24° en 6 h. On neutralise par de l'acide acétique glacial, à 0°. On évapore les solvants sous vide, reprend le résidu par du chloroforme. On lave avec une solution aqueuse 10% de bicarbonate de sodium, on sèche sur sulfate de sodium et évapore le chloroforme. Le résidu est une huile jaune pâle (12.6 g).

(*B*) On agite pendant 1 h à 0°, 2.8 g du résidu obtenu en section *A* avec une solution de 3 ml d'acide bromhydrique à 40% dans 6 ml d'acétone. Une cristallisation abondante se produit. Par filtration, on recueille 1.8 g de *bromométhyl-1 phénylsulfonyl-4 cyclohexanol* (**5***a*, X = —Br), correspondant à 50% d'époxyde **3***a*, de p. de f. 160–162°, montant à 161–162° après une cristallisation dans l'acétone–eau.

Anal. calc. pour $C_{13}H_{17}O_3SBr$: C, 46.85; H, 5.14. Trouvé: C, 46.88; H, 5.21.

On agite 1.0 g de la bromhydrine **5***a*, 2 ml d'eau, 40 ml de méthanol, et 1.4 g d'oxyde d'argent fraîchement préparé pendant 2 h à 20°. On filtre l'oxyde d'argent, et on le lave avec du chloroforme. On évapore les solvants et recueille 0.7 g de l'époxyde **3***a*, p. de f. 95–96°, seul ou en mélange avec l'époxyde préparé antérieurement (2). Spectre de r.m.n. ($CDCl_3$): de 1.0 à 2.4 (massif, 8H); 2.67 (s, 2H,); 3.02 (bande de largeur à demi hauteur, 18 Hz, 1H, $—SO_2—CH=$); de 7.5 à 8.1 (massif, 5H, $C_6H_5—$).

(*C*) Les filtrats de formation et de cristallisation de la bromhydrine obtenus en section *B* sont évaporés sous vide de 11 mm, au bain-marie. Le résidu de 1.1 g est traité par 20 ml d'une solution de dinitro-2,4 phénylhydrazine préparée selon (19). On isole 2.7 g de dérivé fondant à 105–110°. Par cristallisation dans le chloroforme et l'éthanol on tire d'une part 0.7 g de dinitro-2,4 phénylhydrazone de la cétone **1***a* et 0.6 g de dinitro-2,4 phénylhydrazone de la cétone **2***a*, identiques à celles décrites (2).

(*D*) On chauffe à l'ébullition à reflux 6.2 g du résidu obtenu en section *A* avec 6 ml de pipéridine et 20 ml de méthanol. On évapore sous vide de 11 mm, au bain-marie et dissout le résidu dans 100 ml de chloroforme. On extrait la solution chloroformique par 50 ml d'acide chlorhydrique 10%. On décante la couche aqueuse, la neutralise par une solution d'hydroxyde de sodium 20% et extrait par du chloroforme. On sèche sur sulfate de sodium et évapore le chloroforme. On recueille 3.2 g (correspondant à 39% d'époxyde) d'amino-alcool fondant à 98–100°. Par cristallisation dans un mélange benzène-éther de pétrole on obtient le *phénylsulfonyl-4 pipéridinométhyl-1 cyclohexanol* (**5***a*, X = $—NC_5H_{10}$), p. de f. 115–116°. En mélange avec son isomère **5***b* de p. de f. 103–104°, déjà décrit (2) le p. de f. est de 74–77°.

Anal. calc. pour $C_{18}H_{27}O_3NS$: C, 64.06; H, 8.06; N, 4.15. Trouvé: C, 64.04; H, 8.07; N, 4.15.

Le *chlorhydrate* fond à 225–227°, après cristallisation dans l'isopropanol.

Anal. calc. pour $C_{18}H_{28}O_3NSCl$: C, 57.81; H, 7.55; N, 3.75. Trouvé: C, 57.81; H, 7.63; N, 3.74.

*7 Réaction de la cétone **1***c *avec le diazométhane, à l'échelle préparative*

(*A*) On prépare une solution à partir de 150 ml de méthanol, 2.75 g d'hydroxyde de potassium et 2.75 g d'eau; on le refroidit à 0°, y ajoute 10 g de la cétone **1***c*,

puis, par petites portions, 5 g de nitrosométhylurée. On attend que la solution soit redevenue incolore avant d'ajouter la portion suivante. On agite 3 h à 0°, laisse revenir à 20° en l'espace de 6 h, puis neutralise par de l'acide acétique glacial. On évapore sous vide de 11 mm, au bain-marie. On reprend le résidu par de l'éther, qu'on lave avec une solution 10% de bicarbonate de sodium, puis avec de l'eau; on sèche sur sulfate de sodium et évapore le solvant. Le résidu est une huile jaune pâle (10.8 g).

(*B*) On traite 1.06 g du résidu obtenu en section *A* par 1.0 g de chlorhydrate de semicarbazide et 1.0 g d'acétate de sodium dans 10 ml d'éthanol aqueux. On isole ainsi 0.69 g de *semicarbazone* de la cétone **2***c*, qui précipite (correspondant à 52% de cétone **2***c*), de p. de f. 168–169° après cristallisation dans l'éthanol étendu d'eau.

Anal. calc. pour $C_{14}H_{19}ON_3S$: C, 60.62; H, 6.91; N, 15.15. Trouvé: C, 60.55; H, 6.90; N, 15.15.

(*C*) On traite 0.50 g du résidu obtenu en section *A* par la dinitro-2,4 phénylhydrazine, selon (19). On obtient 0.51 g (correspondant à 56.5% de cétone **2***c*) de *dinitro-2,4 phénylhydrazone* de la cétone **2***c*, p. de f. 170–171° après cristallisation dans l'acétate d'éthyle – éthanol.

Anal. calc. pour $C_{19}H_{20}O_4N_4S$: C, 56.98; H, 5.03; N, 14.00. Trouvé: C, 56.88; H, 4.99; N, 14.04.

(*D*) On traite 9.0 g du résidu obtenu en section *A*, par 9 ml de pipéridine et 20 ml de méthanol à l'ébullition à reflux pendant 3 h. On évapore le méthanol sous vide, reprend le résidu par 150 ml d'éther et extrait par 50 ml d'acide chlorhydrique à 10%. La solution éthérée est séchée sur sulfate de sodium; on évapore l'éther. La distillation du résidu donne 5.75 g (64%) de *phénylthio-4 cyclohexanone* (**2***c*), p.éb. 128–130° sous 0.4 mm, n_D^{25} = 1.5755, homogène en c.p.g. selon les conditions données à la section 1. Spectre i.r. (CCl_4): 1707 cm^{-1} (C=O).

Anal. calc. pour $C_{13}H_{16}OS$: C, 70.86; H, 7.32. Trouvé: C, 70.97; H, 7.45.

La couche acide est neutralisée par de la soude à 20% et extraite par de l'éther. Après séchage et évaporation, du solvant on obtient 4.04 g (correspondant à 2.9 g d'époxyde **3***c*, soit 32% de rendement) de *phénylthio-4 pipéridinométhyl-1 cyclohexanol-1 cis* (**5***c*, X = —$C_5H_{10}N$—) sous forme d'une huile brune. Le *chlorhydrate*, préparé dans l'éther, fond à 157.5—159° après deux cristallisations dans le mélange isopropanol–éther.

Anal. calc. pour $C_{18}H_{28}ONSCl$: C, 63.22; H, 8.25; N, 4.10. Trouvé: C, 62.95; H, 8.14; N, 4.14.

On dissout 1.0 g de ce chlorhydrate dans 50 ml d'acide acétique à 50% refroidi à 0° et ajoute lentement une solution de 0.5 g de permanganate de potassium dans 10 ml d'acide acétique à 50%. Après décoloration par l'anhydride sulfureux et évaporation des solvants, le résidu est dissous dans de l'eau et lavé avec du chloroforme. La solution aqueuse est rendue alcaline par de la soude caustique à 20% et extraite par du chloroforme. On sèche et évapore le solvant. On obtient 1.0 g de phénylsulfonyl-4 pipéridinométhyl-1 cyclohexanol-1 *cis* (**5***a*, X = $C_5H_{10}N$—), p. de f. 98–100°, ne donnant pas de dépression en mélange avec un échantillon préparé plus haut à la section 6. Le p. de f. mixte avec l'isomère *trans*, obtenu antérieurement (2), est de 80–86°.

8 Réaction de la tert-butyl-4 cyclohexanone avec le diazométhane en présence d'éthérate de trifluorure de bore

A une solution de 771 mg de cétone **1***b* (5 mmol) dans 20 ml d'éther, à 0°, on ajoute 0.45 ml d'éthérate de trifluorure de bore fraîchement distillé, puis 20 ml d'une solution, refroidie à 0°, de diazométhane dans l'éther, préparée de la manière suivante: On ajoute 9.0 g de nitrosométhylurée à une solution refroidie à 0° de 20 ml d'hydroxyde de potassium à 50% et 40 ml d'éther, en 35 min, avec agitation. La couche éthérée est décantée et séchée sur de l'hydroxyde de potassium en pastilles, à 0°. L'addition se fait en 2 min, à raison de 4 portions de 5 ml chacune. L'analyse par c.p.g. donne les résultats suivants: (les pourcentages correspondent aux surfaces mesurées) **1***b*, 10%; **2***b*, 40%; cétones à 8 chaînons, 23 et 17%; cétones plus lourdes 10%. En ajoutant 40 ml de la solution de diazométhane dans l'éther, on obtient les résultats suivants: (les pourcentages correspondent aux surfaces mesurées) **1***b*, 0%, **2***b*, 10%; cétones à 8 chaînons, 37 et 26%; cétones plus lourdes à 31 et 33 min, 15%; à 39 min, 12%.

Nous remercions les Etablissements Dow Chemical of Canada Ltd, Montréal, de la tert-butyl-4 cyclohexanone mise à notre disposition. Nous remercions également les Laboratoires Ayerst, Montréal, le fonds de recherche non subventionnée de l'Université de Montréal et le Conseil National de Recherches du Canada de leur aide financière (subventions T-14, A-0014, et A-5526 et bourse d'études à D.G., Z.H. et M.M.).

1. H. Favre, Z. Hamlet, R. Lanthier, et M. Ménard. Can. J. Chem. Ce numéro.
2. H. Favre, M. Ménard, Z. Hamlet, G. Roblot, et J. Temler. Can. J. Chem. Ce numéro.
3. H. Barbier. Helv. Chim. Acta, **23**, 519 (1940).
4. J. N. Bradley, G. W. Cowell, et A. Ledwith. J. Chem. Soc. 4334 (1964).
5. H. Favre et D. Gravel. Can. J. Chem. **41**, 1452 (1963).
6. F. A. L. Anet, M. St-Jacques, et G. N. Chmurny. J. Am. Chem. Soc. **90**, 5243 (1968).
7. E. J. Corey et M. Chaykovsky. J. Am. Chem. Soc. **87**, 1353 (1965).
8. O. L. Chapman et R. W. King. J. Am. Chem. Soc. **86**, 1256 (1964).
9. M. M. A. Hassan et A. F. Casy. Org. Mag. Res. **1**, 389 (1969).
10. R. Kuhn et H. H. Baer. Ber. **86**, 724 (1953).
11. H. Zollinger. Azo and diazo chemistry, aliphatic and aromatic compounds. Interscience Publishers Inc., New York, N.Y., 1961. p. 69.
12. C. G. Overberger et A. Katchman. J. Am. Chem. Soc. **78**, 1965 (1956).
13. R. G. Carlson et N. S. Behn. J. Org. Chem. **33**, 2069 (1968).
14. J. B. Jones et P. Price. Chem. Commun. 1478 (1969).
15. A. I. Vogel. A text-book of practical organic chemistry. 3ème éd. John Wiley and Sons Inc., New York, N.Y., 1966. p. 969.

Can. J. Chem. Downloaded from www.nrcresearchpress.com by 84.22.46.98 on 09/08/12
For personal use only.

Ion Pair Formation in Solutions of Alkali Halides in Dimethyl Sulfoxide: Ultrasonic Absorption Studies[1]

D. R. DICKSON AND P. KRUUS
Department of Chemistry, Carleton University, Ottawa, Canada

Received February 4, 1971

The ultrasonic absorption of dimethyl sulfoxide solutions of several alkali halides has been studied in the frequency range 1.5 to 52 MHz. An excess absorption, relaxing between 3 and 8 MHz, was observed. The relaxation was assigned to the final step in the stepwise formation of a contact ion pair, with the relaxation frequency controlled by the rate of movement of a solvent molecule rather than an ion. Data on the system water – dimethyl sulfoxide are also presented and the effect of water on the relaxation discussed.

L'absorption ultra-sonique de plusieurs halogénures alcalins dans le diméthyl sulfoxyde a été étudiée dans l'intervalle de fréquence allant de 1.5 à 52 MHz. Un excès d'absorption, dont la relaxation se fait entre 3 et 8 MHz a été observée. La relaxation est attribuée à l'étape finale dans la formation graduelle d'une paire d'ion de contact. La fréquence de relaxation est contrôlée par la vitesse de déplacement d'une molécule de solvant plutôt que par celle d'un ion. Les données relatives au système eau-diméthyl sulfoxyde sont également présentées et l'effet de l'eau sur la relaxation est discutée.

Canadian Journal of Chemistry, **49**, 3107 (1971)

Can. J. Chem. Downloaded from www.nrcresearchpress.com by 210.87.254.6 on 09/05/12
For personal use only.

Introduction

Ion pairing was first studied by ultrasonics (1) following the observation of an anomalously large absorption coefficient for sea water. Detailed studies (2–6) have since shown that the stepwise ion association in aqueous solutions of 2–2 electrolytes could account for the absorption in excess of that expected from viscous losses. The assignment of mechanism was aided by a study of mixed solvent solutions of these salts (7); there are, however, still some discrepancies in both the data and its interpretation (4–6). The low concentration of ion pairs in aqueous solutions of 1–1 electrolytes excludes their showing an excess absorption except at salt concentrations much higher than that found in sea water (8). From extensive ultrasonic absorption measurements of aqueous solutions of the lanthanide salts it was concluded that the observed relaxation was a result of the formation of ion pairs (9). Absorption measurements of some aqueous electrolytes at hypersonic frequencies have recently been carried out by the method of Brillouin scattering. An excess absorption was only observed for multivalent electrolytes and very concentrated solutions of univalent salts (10).

Only a few ultrasonic studies of electrolytes dissolved in non-aqueous solvents have been attempted. Alkyl ammonium halides dissolved in nitrobenzene exhibit a relaxation in the region of 27 MHz; it was observed that addition of a small amount of methanol suppressed this relaxation (11). The excess absorption was attributed to the ion association equilibrium. It was suggested that the addition of methanol may have reduced the degree of ion pairing by solvating the anions, but the evidence was inconclusive. An investigation of the ultrasonic absorption properties of lithium chloride dissolved in a wide range of alcohols indicates that possibly two relaxations are present in these systems, one of which may be the ion association, ion pair dissociation equilibrium (12). A large single relaxation ascribed to this same equilibrium has been observed in solutions of hydrogen chloride in N,N-dimethyl formamide (13).

It was anticipated that an investigation by ultrasonics of dimethyl sulfoxide (DMSO) solutions of alkali halides might provide some information concerning ion pairing equilibria. This possibility was suggested by the results of previous studies of the physical chemistry of these solutions. Substantial ion pairing should be present, as discrepancies between experimentally determined activity coefficients and those predicted by the extended Debye–Hückel theory for lithium chloride and cesium iodide dissolved in DMSO have been accounted for by assuming ion pairing with an association constant of about 0.2 (14, 15).

Conductivity measurements suggest that only

[1]Taken in part from the thesis submitted by D. R. Dickson in partial fulfilment of the requirements for the M.Sc. degree.

TABLE 1. Systems studied with both the pulse and the streaming apparatus (20 °C)

System	Concentration (M l^{-1})	% by volume water	A (10^{-17} cm^{-1} s^2)	B (10^{-17} cm^{-1} s^2)	f_c (MHz)	$\bar{\mu}_m$
(1) NaCl	0.11	<0.1→1.0	19.0	45.0	7.9	10.0
(2) NaBr	0.16	<0.2→1.5	27.0	40.0	3.3	4.2
(3) NaBr	0.29	<0.2→1.5	85.0	45.0	3.3	7.3
(4) NaBr	0.42	<0.2→1.5	190.0	50.0	3.3	11.0
(5) NaBr	0.42	3.0→ —	119.0	49.0	3.3	6.4
(6) NaBr	0.42	6.0→ —	58.0	49.0	3.0	3.1
(7) NaI	0.26	<0.2→1.6	18.0	40.0	2.9	1.5
(8) NaI	0.55	<0.2→1.6	82.0	50.0	3.7	4.2
(9) NaI*	0.55		41.0	48.0	7.3	4.1
(10) NaI	1.00	<0.2→1.6	174.0	74.0	4.1	5.4
(11) NaI*	1.00		178.0	73.0	4.5	6.0
(12) LiBr*	0.40	<0.1→1.0	39.0	46.0	7.2	5.3
(13) LiBr*	0.60	<0.1→1.0	66.0	55.0	7.9	6.5
(14) KBr	0.53	<0.1→0.8	27.0	60.0	7.5	2.9
(15) $CaCl_2$	0.15	<0.2→ —	586.0	37.0	3.8	112.0
(16) $CaCl_2$	0.30	<0.2→ —	875.0	55.0	3.5	77.0
(17) $CaCl_2$	0.44	<0.2→ —	948.0	60.0	3.9	63.0

*Using only data from 10.6 to 52.8 MHz to fit the single relaxation equation.

the cations are solvated significantly (16). This is reasonable as the positive end of the DMSO dipole, which corresponds to the position of the sulfur atom, is shielded by the two methyl groups. The radii in angstroms of several ions dissolved in DMSO were estimated from the conductance data (17); the crystallographic radii (18) are enclosed in brackets: Na^+, 3.2 (0.95); K^+, 3.0 (1.33); Br^- 1.7 (1.95); I^-, 1.7 (2.16). Solutions of alkali halides in DMSO can possibly be described by more simple but realistic models because the anions are essentially unsolvated.

Ultrasonic absorption measurements in the frequency range 1.5 to 52 MHz were carried out on some such systems. The results are reported in Table 1 and discussed in terms of the stepwise formation of ion pairs. Measurements were also made on several other related systems in a more limited frequency range (10.5 to 52 MHz).

Experimental

The ultrasonic absorption coefficients were measured in the frequency range from 0.5 to 3.5 MHz with the streaming apparatus described below, and from 10.5 to 52 MHz with the pulse apparatus previously described in detail (19). The temperature of the absorption cells was controlled by a thermostatted water bath. The viscosity of each solution was determined with a Cannon–Fenske viscometer immersed in this bath.

The design of the streaming apparatus was based on the observation that the energy absorbed by a liquid from a sound beam results in a flow or streaming of the liquid in the direction of the beam (20). The absorption coefficient is determined from the streaming velocity and the sound radiation intensity. Figure 1 is a schematic diagram

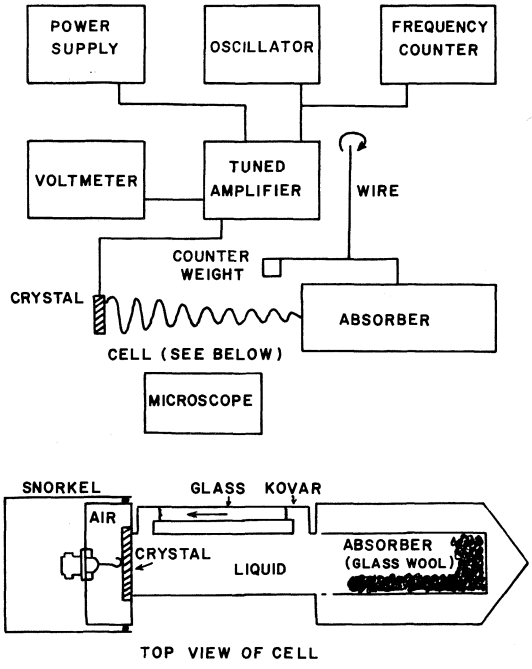

FIG. 1. Schematic diagram of the streaming apparatus.

of the cell and the electronics required to measure these quantities.

The stainless steel cell was constructed with a Pyrex side arm connected by means of Kovar glass-to-metal seals. The transducer was an X-cut quartz crystal of 2.8 cm diameter with a fundamental resonant frequency of 0.5 MHz. To ensure good electrical contact, the faces of the crystal were plated with a thin layer of gold or silver. The sound intensity was measured by the horizontal torque exerted by a stainless steel cylinder, 9.6 cm long

Can. J. Chem. Downloaded from www.nrcresearchpress.com by 210.87.254.6 on 09/05/12
For personal use only.

Can. J. Chem. Downloaded from www.nrcresearchpress.com by 210.87.254.6 on 09/05/12
For personal use only.

and 2.6 cm in diameter, packed with glass wool, and suspended from a torsion balance incorporating a 0.18 mm rolled phosphor bronze wire so as to be completely submerged in the liquid being studied and in the path of the sound beam.

The transducer was driven at 0.5, 1.5, 2.5, and 3.5 MHz by the output of the tuned amplifier, which amplified up to 800 V r.m.s. a continuous signal of the appropriate frequency from the Marconi TF 1370 oscillator. The frequency of the signal was determined with a Hewlett–Packard 5245 L frequency counter, and the voltage output of the amplifier was measured with a Marconi TF 2604 electronic voltmeter coupled by a 100× attenuating probe to the output of the amplifier. The power leads to the transducer were protected from water contact with snorkel arrangement.

To operate, the streaming apparatus was filled with the solution to be studied, ensuring that no air bubbles were trapped in the absorber. To enable measurement of the rate of streaming through the side arm, aluminum dust was suspended in the solution prior to filling. With the aid of reflected light, the particles were then observed under 15× magnification with a Bausch and Lomb stereomicroscope, and their rate of flow past a graticule contained in one of the eyepieces was measured.

To determine the absorption coefficient, α, eq. 1 had to be evaluated (20).

$$[1]\quad (\exp[20.4\alpha] - 1)(\exp 3.6\alpha) = K\eta \frac{u}{V^2}\frac{\Delta(V^2)}{\Delta R}$$

η is the viscosity in poise, u is the streaming velocity at the applied voltage V, $\Delta(V^2)$ is the change in the square of the applied voltage required to cause a constant change in the sound intensity ΔR, as determined with the torsion balance. K is a constant of the apparatus, calculated from the streaming velocity and radiation pressure observed when the cell was filled with carbon tetrachloride or chlorobenzene, for which the absorption coefficients were measured with the pulse apparatus. Only at 0.5 MHz was any difficulty experienced in obtaining reproducible results, due to the low absorption coefficient and the consequent low streaming velocity.

Solutions for both streaming and pulse measurements were prepared in a dry box from reagent grade salts (from Fisher, Anachemia or Baker) which had been dried to constant weight at 95 °C and from Fisher or British Drug Houses dimethyl sulfoxide which had been stored over grade 4 molecular sieve. DMSO refluxed over BaO and vacuum distilled below 65 °C gave essentially the same results, so this procedure for removing water was not employed. Solutions of HCl and HBr were made by passing dried gas into a burette inverted in a cooled flask of DMSO.

In spite of these precautions, the solutions were found to contain a significant amount of water after the streaming measurements. This water, which was absorbed from the atmosphere during the course of the measurements, was estimated from the intensity of its infrared absorption spectrum at 3500 cm^{-1}.

Attempts to measure the water content by the Karl Fischer titration (21) (Fisher So-K-3) were not successful, although this is a common method for such determinations. When the titrations were done by titrating excess Karl Fischer reagent with standard water in methanol solution (Fisher So-W-2) the method gave negative values for the water content, suggesting the possibility that DMSO interferes with the reagent.

Results

The relaxation parameters of the systems that were studied over the complete frequency range, that is by both the streaming and pulse techniques, are listed in Table 1. In addition, the water content of the solutions before and after the streaming measurements is listed. The relaxation parameters were determined by fitting an equation for a single relaxation to the experimental points by an unweighted least squares program. This equation (22) is of the form

$$[2]\qquad \frac{\alpha}{f^2} = A\left(1 + \frac{f^2}{f_c^2}\right)^{-1} + B$$

where α is the absorption coefficient, f is the frequency, f_c is the relaxation frequency, and B is the absorption due to viscosity and higher frequency relaxation processes. A is related to the molar maximum excess absorption per wavelength, $\bar{\mu}_m$, the concentration, c, and the velocity of sound, v, by the equation

$$[3]\qquad A = 2c\bar{\mu}_m/f_c v$$

The term, B, includes absorptions contributed by two processes. One is viscous absorption, α_η, calculated from the viscosity, η, by the equation (22)

$$[4]\qquad \frac{\alpha_\eta}{f^2} = \frac{8}{3}\pi^2\frac{\eta}{v^3}$$

The other is a result of equilibria which relax at frequencies above the range of observation. These processes could include an equilibrium between various solvent structures and an equilibrium resulting from the addition of an electrolyte. The structural absorption was assumed to be constant and equal to the difference between the observed absorption coefficient of pure DMSO and that calculated from the viscosity. The absorption estimated for the viscosity and structural relaxation for each solution was in nearly all cases insufficient to account for the magnitude of B.

Table 2 shows the absorption data for pure DMSO, containing less than 0.1% by volume of water. The addition of water to pure DMSO gives rise to a maximum in the absorption coefficient at a DMSO volume fraction of 0.75, that is, a mole

TABLE 2. Ultrasonic absorption and velocity data for pure dimethylsulfoxide

Temperature (°C)	α/f^2	α_η/f^2	α_s/f^2	v
	$(10^{-17}\ cm^{-1}\ s^2)$			$(m\ s^{-1})$
19	36.6	15.6	21.0	1513
25	34.2	14.5	20.7	1489
30	34.0	13.7	20.3	1473

fraction of about 0.4. This maximum corresponds to a maximum in the viscous absorption, Fig. 2. The difference between the two gives a curve more characteristic of mixtures of unassociated liquids (22); any association process giving rise to the viscosity maximum does not directly contribute to the ultrasonic absorption at these frequencies. Low frequency data, Fig. 3, suggest the possible presence of an absorption relaxing at about 0.6 MHz in a mixture with 0.75 volume fraction DMSO.

The effect of addition of water to salt solutions is illustrated for 0.44 M sodium bromide in DMSO in Fig. 4. The magnitude of A decreases with increasing water content but B and f_c remain constant. A rough extrapolation to zero water content suggests that for most of the results which depend on streaming measurements, the values of A could be as much as 40% higher in a water free system. Consequently, the relaxation parameters, f_c and $\bar{\mu}_m$, are possibly in error, and much of the detail concerning their variation with conditions

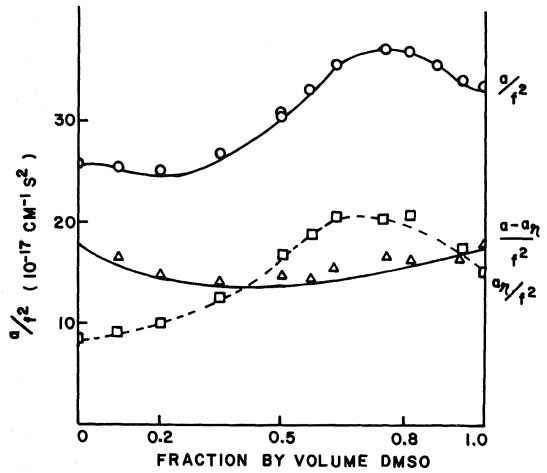

FIG. 2. Ultrasonic absorption in the system water–DMSO. Frequency 31 MHz: –○– experimental α/f^2; --□-- calculated viscous α_η/f^2; –△– difference $(\alpha - \alpha_\eta)/f^2$.

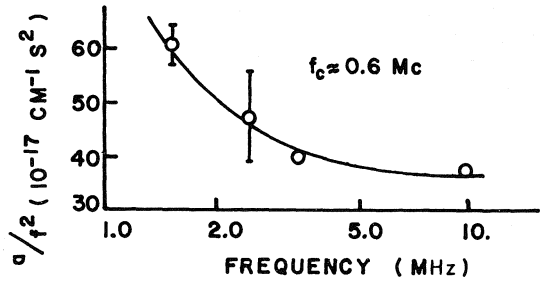

FIG. 3. Frequency dependence of ultrasonic absorption in a water–DMSO mixture; 0.75 volume fraction DMSO.

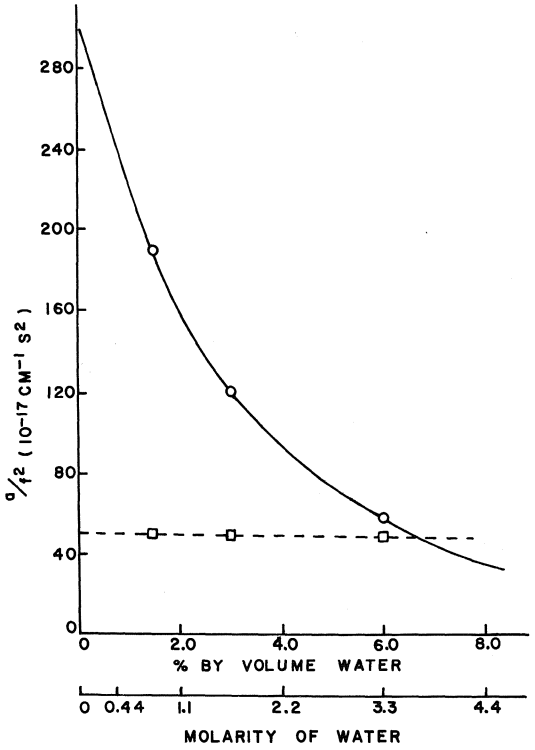

FIG. 4. The effect of water on absorption in a system 0.44 M in NaBr (systems 4, 5, 6, Table 2); –○– values of A; --□-- values of B.

may be obscured. Figure 5 shows a comparison of some curves generated from the relaxation parameters obtained from both pulse and streaming data with those obtained from pulse data alone. It was concluded that the low frequency data should be included when available, in spite of the error introduced by the absorption of water.

Only in the solutions of lithium bromide (systems 12, 13) does the shape of the relaxation

Can. J. Chem. Downloaded from www.nrcresearchpress.com by 210.87.254.6 on 09/05/12
For personal use only.

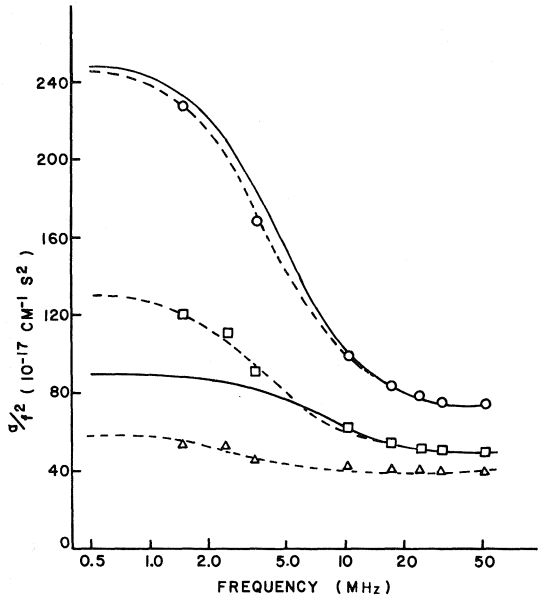

FIG. 5. Absorption in NaI solutions (systems 7 to 11, Table 1). ○ Experimental points, 1.00 *M*; □ experimental points, 0.55 *M*; △ experimental points, 0.26 *M*; — curve fitted using pulse data only; --- curve fitted using streaming and pulse data.

curves differ from those in Fig. 5. There appear to be two relaxations, one at about 7.5 MHz and the other at about 3 MHz. However, the data do not warrant fitting to an equation with more parameters than eq. 2. Because of this anomalous, but reproducible, nature of the LiBr relaxation curves, these two systems were not considered in searching for trends.

Some solutions were studied by the pulse apparatus in a limited frequency range; these were CsCl, CsI, HBr, $CaBr_2$, $MgBr_2$, HCl, KI, and LiCl. In the case of Cs salts, no excess absorption was found. The solutions of HBr had a large excess absorption but had strong odors of mercaptans. The $CaBr_2$ and $MgBr_2$ solutions also had large excess absorptions but could not be prepared without having considerable amounts of water present. Solutions of HCl (0.3 to 1.3 *M*) showed a strong absorption with $\bar{\mu}_m$ of the order of 60 and f_c at about 6 MHz. The KI (0.99 *M*) and LiCl (0.10 *M*) had, respectively, f_c equal to 2.3 and 4.1 MHz, and $\bar{\mu}_m$ 4.1 and 27.

The temperature dependence of f_c and $\bar{\mu}_m$ for solutions of NaI and NaBr was also investigated in this limited frequency range. A 10° rise in temperature did not affect the f_c or $\bar{\mu}_m$ significantly. In these systems the water content was <0.2%. However, there is considerable inaccuracy introduced in obtaining relaxation parameters in cases where the frequency range of the data does not extend below f_c.

The data in Table 1 show the relaxation frequency to be relatively independent of the salt concentration, the nature of the anion or cation, and the charge of the cation. This invariance may be real or it may be a result of the large experimental uncertainty of the low frequency data.

The molar excess absorption per wavelength on the other hand shows some variation with conditions. Three sets of systems, 2 to 4, 7 to 11, and 12 to 13, show increases in $\bar{\mu}_m$ with concentration while one, 15 to 17 shows a decrease. From a comparison of systems 1 with 2, and 3 with 7, it appears that $\bar{\mu}_m$ decreases with increasing anion size. Comparison of systems suggests that $\bar{\mu}_m$ also decreases with increasing cation size. The absence of an excess absorption for cesium salts and the data on KI and LiCl confirm these observations. Doubling the charge of the cation by substituting Ca^{2+} for Na^+ causes an approximately ten-fold increase in $\bar{\mu}_m$.

Discussion

Model for Ion Pairing Equilibria

The mechanism responsible for the excess absorption is assumed to be the stepwise association of free ions to form contact ion pairs. Proton exchange may be eliminated because of the low dissociation constant of the C—H bond of DMSO, and the relaxation of the ion atmosphere would contribute negligibly to the observed absorption coefficient. The ion association equilibria may be written as

$$[5]\quad M_s^+ + X^- \underset{k_{21}}{\overset{k_{12}}{\rightleftharpoons}} (M^+\text{–DMSO–}X^-)_s \underset{k_{32}}{\overset{k_{23}}{\rightleftharpoons}} (M^+\text{–}X^-)_s$$

1	2	3
Free ions	Solvent separated ion pair	Contact ion pair

where the subscript, s, denotes a solvated species.

The Bjerrum distance, that distance at which the electrostatic interaction energy between two ions becomes less than the mean thermal energy, is about 6 Å for an alkali halide in DMSO and about 12 Å for a 2–2 electrolyte in water. At separations exceeding these, the ions are considered to be free. Since two solvent molecules

Can. J. Chem. Downloaded from www.nrcresearchpress.com by 210.87.254.6 on 09/05/12
For personal use only.

Can. J. Chem. Downloaded from www.nrcresearchpress.com by 210.87.254.6 on 09/05/12
For personal use only.

are thought to separate the ions of the first ion pair formed by the association of 2–2 electrolytes in water (2), and since the DMSO molecule is larger than the water molecule, it is expected that steps intermediate to structures **1** and **2** need not be included in a description of the association of 1–1 electrolytes in DMSO.

Two relaxations should be observed for these coupled processes. The relaxation frequency, f_c, and the maximum excess absorption per wave length, $\bar{\mu}_m$, for each are given by equations available in references such as (23) and (24). They will not be given in detail here, as the lack of accuracy of the data as well as of necessary supporting thermodynamic data for the systems makes it impossible to apply these equations to the data.

Equilibrium 1 ⇌ 2

The rate coefficients for the diffusion controlled formation and dissociation of the solvent separated ion pair can be calculated by equations developed by Debye (26) and Eigen and DeMaeyer (27), respectively. For sodium bromide in DMSO, k_{12} is equal to 1.0×10^{10} l mol^{-1} s^{-1}, and k_{21} is equal to 3.0×10^9 s^{-1}. The relaxation frequency of this equilibrium should be about 10^9 Hz, much too high to account for the observed relaxation. The difference between B and the viscous absorption is probably partially due to this equilibrium.

Since the absorption coefficient of pure DMSO is much greater than the viscous absorption, losses due to a structural relaxation of the solvent are probably occurring. The addition of ions should tend to decrease the absorption resulting from this process, similar to the effect of dissolving alkali halides in water (24). The magnitude of the absorption due to the formation of the solvent separated ion pair is hence larger than the difference between the value of B obtained from the data and that estimated from viscous and structural absorption. The rate coefficients and thus the relaxation frequency of the association–dissociation equilibrium should not be very dependent on the nature of the cation due to shielding by the primary solvation sphere. However, if, as concluded from the conductance work, the anions are relatively unsolvated, the relaxation parameters should be anion dependent.

Equilibrium 2 ⇌ 3

The relaxation frequency of this equilibrium is governed by the magnitude of the rate constants k_{23} and k_{32}. It is, however, also dependent upon the magnitudes of k_{12}, k_{21}, the concentration of unpaired ions, and the activity coefficients of the system. The lack of a large variation of f_c with change of cation or anion suggests that the rate limiting step is governed more by the movement of a DMSO molecule into or out of the solvation sphere rather than the movement of any ion. The small change of f_c upon increasing the cation charge is somewhat puzzling. It may be that since the Bjerrum distance of the calcium ion is twice that of the alkali ions, the stepwise association mechanism should have two intermediate structures between the free ions and the contact ion pair, and therefore the relaxation observed at 3 to 4 MHz should be related to an equilibrium between two solvent separated ion pairs.

The magnitude of $\bar{\mu}_m$ is dependent among other things upon the degree of advancement of the equilibria, the rate constants, thermodynamic properties of the solution such as compressibility, thermal expansion, density, heat capacity, and activity coefficients. It is also dependent on the ΔV and ΔH of the equilibria. In view of the experimental uncertainties and the lack of knowledge of the equilibrium constant, K_{23}, an evaluation of any term such as ΔV or ΔH is impossible. $\bar{\mu}_m$ should be dependent on the concentration through the activity product, but the observed magnitude of the variation is surprising; this may be explained by a greater influence on the relaxation parameters due to water at lower concentrations. Increasing the size of the anion or cation causes a decrease in the excess absorption per wavelength, possibly as a result of a decrease in ΔV or ΔH, but most probably due to a change in the degree of association. The large decrease in A, and hence $\bar{\mu}_m$, upon addition of water to the solutions is presumably due to the hydration, and consequent stabilization with respect to association, of the free anions.

Conclusions

The relaxation observed in dimethyl sulfoxide solutions of alkali halides in the frequency range 3 to 8 MHz has been assigned to the second, final step of a stepwise association of the ions. Evidence of the presence of an absorption due to the first step was also obtained.

A limited experimental frequency range and difficulties in preventing atmospheric water from entering the solutions during measurement made

exact analysis of the phenomena impossible. The following qualitative trends were observed: (*1*) The relaxation frequency is relatively insensitive to changes in the cation, the anion, concentration, and temperature. (*2*) The molar excess absorption per wavelength decreases with increasing size of both the cation and the anion.

For a more quantitative, reliable analysis of the phenomena, it is necessary to acquire low frequency data on apparatus that would exclude atmospheric water from the solutions. It is expected that calculations of the energies of some simple but hopefully realistic models of the proposed structures, **2** and **3**, will also aid the analysis. Such work has been initiated with some preliminary successes (28).

The authors wish to thank Dr. J. E. Piercy and Mr. A. Raffler for assistance in planning and constructing the apparatus, Mr. D. G. Fecchio for Technical assistance, and Dr. C. H. Langford for helpful discussions. The project was supported financially by the National Research Council of Canada.

1. G. KURTZE and K. TAMM. Acustica, **3**, 33 (1953).
2. G. ATKINSON. Velocity and absorption of sound in equilibrium chemical systems. ARO Project No. 3417-C. CFSTI AD 642615. 1966.
3. L. GOLDFARB and E. YEAGER. Ultrasonic studies of diffusion controlled ionic association–dissociation. ONR Project No. NR 384-305. CFSTI AD 672359. 1968.
4. A. BECHTLER, K. G. BREITSCHWERDT, and K. TAMM. J. Chem. Phys. **52**, 2975 (1970).
5. P. HEMMES and S. PETRUCCI. J. Phys. Chem. **74**, 467 (1970).
6. L. G. JACKOPIN and E. YEAGER. J. Phys. Chem. **74**, 3766 (1970).
7. G. ATKINSON and S. K. KOR. J. Phys. Chem. **69**, 128 (1965).
8. H. KISTENMACHER, H. NISSEN, and H. WOLZ. Theses. Heidelberg Univ. 1968. *Cited by* K. Tamm. Reprint from the 6th International Congress on Acoustics. Vol. 1. Japan. August, 1968.
9. D. P. FAY and N. PURDIE. J. Phys. Chem. **74**, 1160 (1970).
10. C. J. MONTROSE and K. FRITSCH. J. Acoust. Soc. Am. **47**, 786 (1970).
11. S. PETRUCCI and M. BATTISTINI. J. Phys. Chem. **71**, 1181 (1967).
12. M. J. BLANDAMER, D. C. CLARKE, N. J. HIDDEN, and M. C. R. SYMONS. Trans. Faraday Soc. **64**, 2683 (1968).
13. S. C. CHAN and J. P. VALLEAU. Can. J. Chem. **46**, 853 (1968).
14. J. S. DUNNETT and R. P. H. GASSER. Trans. Faraday. Soc. **61**, 922 (1965).
15. M. D. ARCHER and R. P. H. GASSER. Trans. Faraday Soc. **62**, 3451 (1966).
16. P. G. SEARS, G. R. LESTER, and L. R. DAWSON. J. Phys. Chem. **60**, 1433 (1956).
17. J. E. PRUE and P. J. SHERRINGTON. Trans. Faraday Soc. **57**, 1795 (1961).
18. L. PAULING. The nature of the chemical bond. Cornell Univ., Ithaca. 1960.
19. R. J. FANNING and P. KRUUS. Can. J. Chem. **48**, 2052 (1970).
20. J. E. PIERCEY. J. de Phys. **17**, 405 (1956); J. E. PIERCEY and J. LAMB. Proc. Roy. Soc. London. Ser. A, **226**, 43 (1954); J. E. PIERCEY. Ultrasonic streaming and absorption in liquids. Ph.D. Thesis. Univ. of London. 1955.
21. J. MITCHELL, JR. Anal. Chem. **23**, 1069 (1951); Fisher Sc. Co. Technical Data Bulletin TD-119.
22. K. F. HERZFELD and T. A. LITOVITZ. Absorption and dispersion of ultrasonic waves. Academic Press. New York. 1959.
23. J. STUEHR and E. YEAGER. Physical acoustics. Vol. II. Part A. *Edited by* W. P. Mason. Academic Press, New York. 1965. p. 351.
24. K. TAMM. Handbuch der Physik. Vol. 11/1. *Edited by* S. Flügge. Springer, Berlin. 1961. p. 202.
25. D. MARTIN, A. WEISE, and H. J. NICLAS. Angew. Chem. **79**, 340 (1967).
26. P. DEBYE. Trans. Electrochem. Soc. **83**, 265 (1942).
27. M. EIGEN and L. DEMAEYER. Techniques of organic chemistry. Vol. 8. Part 2. *Edited by* A. Weissenberger. John Wiley and Sons, New York. 1963.
28. M. S. GOLDENBERG. B.Sc. Thesis. Carleton University, Ottawa. 1969.

Can. J. Chem. Downloaded from www.nrcresearchpress.com by 210.87.254.6 on 09/05/12
For personal use only.

Can. J. Chem. Downloaded from www.nrcresearchpress.com by 210.87.254.6 on 09/05/12
For personal use only.

Aqueous Nonelectrolyte Solutions. Part X. Mercury Solubility in Water[1]

D. N. GLEW AND D. A. HAMES
Research Department, Dow Chemical of Canada, Limited, Sarnia, Ontario

Received April 22, 1971

The solubility of mercury in water has been determined between 4 and 72 °C. Standard thermodynamic functions have been evaluated for mercury transfer from the liquid metal to aqueous solution and from aqueous solution to the gas phase. Mercury in water exhibits large positive deviations from Raoult's Law and shows a high relative volatility of 15 400 at 25 °C.

La solubilité du mercure dans l'eau a été déterminée entre 4 et 72 °C. Les fonctions thermodynamiques standards ont été évaluées pour le pasage du mercure du métal liquide à la solution aqueuse et de la solution aqueuse à la phase gazeuse. Dans l'eau, le mercure montre une déviation positive importante par rapport à la Loi de Raoult et une volatilité relative importante de 15 400 à 25 °C.

Canadian Journal of Chemistry, 49, 3114 (1971)

Introduction

Mercury dissolved in air-free water is monatomic and un-ionized with the zero-valent mercury atom in the spherically symmetric $^1S_0$ ground state (1).

The solubility equilibrium of liquid mercury with water has been measured previously (1–5) but these measurements are in serious disagreement at 25 °C. The early measurements at 25 °C, which are in good agreement with each other (2, 3), are considerably lower than more recent determinations using radioactive mercury (4) and neutron activation analysis (5). In contrast measurements at 85 °C are in good agreement (2, 5).

The temperature profile of the mercury solubility by Choi and Tuck (5) is suspect since it implies a constant enthalpy of mercury transfer into water which is inconsistent with the behavior of other aqueous nonelectrolytes (6–8).

In this work we have determined the solubility of mercury in water between 4 and 72 °C using atomic absorption for analysis.

Experimental

Material

Technical electrolytic grade mercury was purified by washing with 10% NaOH with agitation by a stream of air, washed with 5% HNO_3 with air agitation, filtered through a gold foil, rewashed with fresh 5% HNO_3, and distilled three times. A.C.S. grade sodium sulfite was supplied by Fisher Scientific Company, technical grade hydrazine hydrate by Matheson, Coleman and Bell, and reagent grade sodium borohydride by The British Drug Houses Limited. Grade A helium and Hi-Pure nitrogen were supplied by Liquid Carbonic Canadian Corporation Limited. Water was laboratory distilled.

Apparatus

The solubility cell previously described (9) was modified to include a 1 cm diameter fine glass frit at the lower end of the sampling tube 4 cm above the cell bottom. Cell temperatures, constant to ±0.01 °C, were maintained by the circulation of thermostated glycol–water through the outer jacket. The cell temperature was measured differentially with respect to a stainless steel block within the thermostat using a five-junction copper–constantan thermocouple. The temperature of the stainless steel block was measured using a standardized platinum resistance thermometer and Mueller bridge.

Method

The distilled water, continuously and vigorously stirred, was degassed for 2 h using a rotary oil pump. The pressure was restored to atmospheric several times by purging with nitrogen. Approximately 300 cm^3 water was then distilled under vacuum into the solubility vessel at 4 °C via an adaptor in the upper standard taper joint. Atmospheric pressure was restored by helium flow through the cell side-arm stopcock. After re-evacuation approximately 30 g mercury was then distilled into the cell. The helium flow was resumed, the adapter removed, approximately 0.001 *m* reducing agent (sodium sulfite, or hydrazine hydrate, or sodium borohydride) was added, and the cell stopper containing the upper Teflon bearing was replaced. The helium flow minimized air diffusion into the cell. The cell was evacuated again and restored to a slight positive pressure with helium. The cell contents were stirred continuously and the temperature adjusted to the preselected operating level.

The stirrer was stopped 2 h before sampling. A small helium pressure of 15 Torr above atmospheric was used to express a 5–10 g presample to clear the frit and tubing of non-equilibrated solution. A 10–20 g equilibrium sample was then immediately expressed into a weighed flask containing 1 ml 4% $KMnO_4$ and 1 ml 20% H_2SO_4. The flask was reweighed and the solution immediately

[1]Contribution No. 191.

Can. J. Chem. Downloaded from www.nrcresearchpress.com by 210.87.254.6 on 09/05/12
For personal use only.

analyzed for mercury by an atomic absorption method (10). Solubilities were approached from both above and below saturation.

As first shown by Stock *et al.* (2), mercury was readily oxidized by even very small traces of air and it was necessary to add small quantities of reducing agent to ensure that no mercury oxidation took place. If reducing agent was not added a noticeable oxidation took place within two days despite all efforts to prevent air leakage. Solubility was found to be unaffected by reducing agents concentrations between 0.001 and 0.02 *m*, in agreement with results using hypophosphorous acid (4).

In order to avoid sampling suspended mercury, which would give high apparent solubilities, the stirrer was stopped and the solution was withdrawn through the glass frit after 2 h. Equilibrium was reached in less than one day under our continuously stirred conditions, compared with ten days without stirring estimated by Pariaud and Archinard (3). To eliminate losses of the highly volatile mercury solute from the saturated solution (see Discussion section) the sample was immediately run into an excess of acid-permanganate.

All equilibrium constants were derived by the method of least-squares assuming that the logarithms of the equilibrium constants were normally distributed: this was consistent with the experimental determination of x_2^0 which was known with a constant percentage error. The standard thermodynamic function change values and their estimated standard errors, σ, were determined by the Clarke–Glew method (12).

TABLE 1. Solubility of mercury in water

Temperature (°C)	Solubility $x_2^0 \times 10^9$ Measured	Calculated	Reducing agent*
4.30	4.19	3.85	*d*
4.30	3.99	3.85	*d*
11.41	4.28	4.21	*b*
11.41	4.17	4.21	*b*
11.41	4.01	4.21	*b*
14.97	3.86	4.44	*a*
19.80	4.31	4.80	*a*
19.80	4.49	4.80	*a*
25.02	5.39	5.28	*d*
30.02	6.47	5.83	*c*
30.09	6.20	5.83	*a*
30.09	6.29	5.83	*a*
39.16	7.90	7.12	*a*
45.07	8.33	8.19	*b*
45.07	8.01	8.19	*b*
49.80	9.88	9.23	*a*
50.24	8.22	9.34	*a*
50.24	9.70	9.34	*a*
50.24	8.85	9.34	*a*
53.71	9.70	10.2	*b*
59.98	12.4	12.1	*a*
59.98	11.1	12.1	*a*
62.28	13.3	12.9	*b*
68.19	16.1	15.3	*a*
68.19	15.3	15.3	*a*
72.44	17.5	17.4	*b*

*a, sodium sulfite; *b*, hydrazine hydrate; *c*, sodium borohydride; and *d*, none.

Results

The temperature dependance of our measurements for the solubility of mercury in water between 4 and 72 °C is given by

$$[1] \quad \log_{10} x_2^0 = -122.811 + 4475.3/T + 40.2205 \log_{10} T$$

where x_2^0 is the mercury mole fraction and T is absolute temperature (0 °C = 273.15 K (11)). Table 1 compares our measured solubilities with those calculated from eq. 1. The estimated standard error on a single measurement is 7.5%. The final column of the table shows the reducing agent added, *a*, sodium sulfite; *b*, hydrazine hydrate; *c*, sodium borohydride; and *d*, no reducing agent. No significant difference was found between measurements taken with any of the three reducing agents over periods up to 14 days and with measurements after 1 day with no reducing agent.

A comparison of our solubilities with previous work (1–5) is shown in Fig. 1, where the logarithm of the mercury solubility in parts per million by weight is plotted against temperature. We find very good agreement between our measurements and the recent solubilities at 25 °C by Moser and Voigt (4) and by Choi and Tuck (5). Our extrapolated curve shows good agreement with the solubilities of Choi and Tuck at 80 and 90 °C (5), Stock *et al.* at 85 °C (2), and Bonhoeffer and Reichart at 120 °C (1). The earlier measurements at 25 °C by Stock *et al.* (2) and Pariaud and Archinard (3) are definitely too low and may have resulted from mercury losses caused by its very high relative volatility at this temperature. The measurements by Choi and Tuck at 35, 50, and 65 °C (5) are apparently too high. The measurement at 100 °C by Stock *et al.* (2) is also too high.

We derive the best equation for the mercury solubility x_2^0 in water between 0 and 120 °C.

$$[2] \quad \log_{10} x_2^0 = -128.089 + 4715.2/T + 42.0288 \log_{10} T$$

by the method of least squares combining the earlier measurements at 120 (1), 85 (2), 25 (4), and 25, 80, and 90 °C (5) with our measurements between 4 and 72 °C. The measurement by Stock *et al.* (2) at 100 °C was not included in determining eq. 2 because it was 28% above the value calculated from eq. 1.

The solubility of mercury in water together

TABLE 2. Solubility of mercury and standard thermodynamic function changes for mercury transfer into water*

Temperature (°C)	$x_2^0 \times 10^9$		$\Delta G_2^0(l_2 \rightarrow l_1)$ (cal/mol)		$\Delta H_2^0(l_2 \rightarrow l_1)$ (cal/mol)		$\Delta S_2^0(l_2 \rightarrow l_1)$ (cal/deg mol)	
	Value	σ	Value	σ	Value	σ	Value	σ
0.0	3.73	0.14	10 530	20	1 240	280	−34.0	0.94
5.0	3.91	0.11	10 700	16	1 660	250	−32.5	0.85
10.0	4.15	0.10	10 860	13	2 070	220	−31.0	0.76
15.0	4.46	0.08	11 010	11	2 490	200	−29.6	0.67
20.0	4.83	0.08	11 150	9	2 910	170	−28.1	0.58
25.0	5.28	0.08	11 290	9	3 330	150	−26.7	0.50
30.0	5.83	0.08	11 420	9	3 740	130	−25.3	0.43
35.0	6.48	0.10	11 550	9	4 160	110	−24.0	0.36
40.0	7.27	0.11	11 660	9	4 580	100	−22.6	0.32
45.0	8.20	0.13	11 770	10	5 000	90	−21.3	0.29
50.0	9.31	0.15	11 870	10	5 410	90	−20.0	0.29
55.0	10.6	0.17	11 970	11	5 830	100	−18.7	0.31
60.0	12.2	0.20	12 060	11	6 250	120	−17.4	0.35
65.0	14.1	0.23	12 150	11	6 670	130	−16.2	0.40
70.0	16.4	0.28	12 220	12	7 080	160	−15.0	0.46
75.0	19.1	0.35	12 300	12	7 500	180	−13.8	0.53
80.0	22.4	0.44	12 360	14	7 920	200	−12.6	0.60
85.0	26.3	0.58	12 420	16	8 340	230	−11.4	0.67
90.0	31.0	0.78	12 480	18	8 750	260	−10.2	0.74
100.0	43.6	1.5	12 570	24	9 590	310	−8.0	0.88
110.0	62.1	2.7	12 640	33	10 420	360	−5.8	1.0
120.0	89.1	5.0	12 680	43	11 260	420	−3.6	1.2

*$\Delta Cp_2^0(l_2 \rightarrow l_1) = 83.5 \pm 5.6$ cal/deg mol.

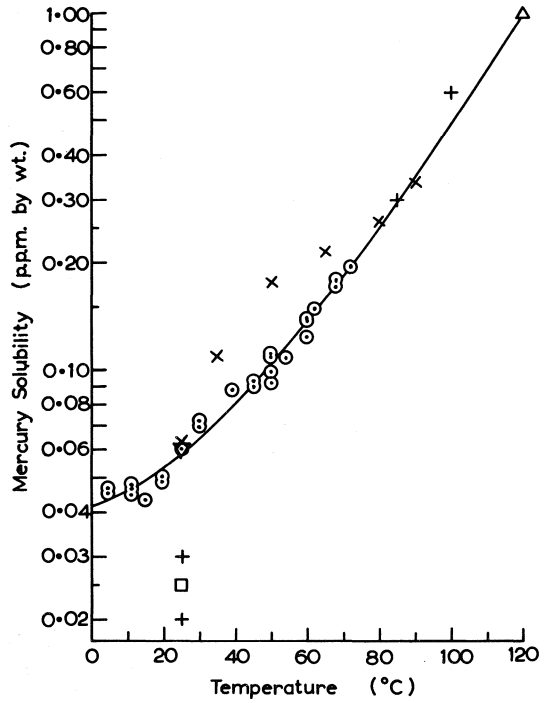

FIG. 1. The temperature dependence of the solubility of mercury △, Bonhoeffer and Reichart (1); +, Stock *et al.* (2); □, Pariaud and Archinard (3); ▽, Moser and Voigt (4); ×, Choi and Tuck (5); ⊙, this work. Solid curve calculated from eq. 2.

with its standard error, evaluated from eq. 2 between 0 and 120 °C, are presented in Table 2 and are shown by the solid line in Fig. 1. The table contains values with their errors, derived from eq. 2, for the standard thermodynamic function changes, $\Delta X_2^0(l_2 \rightarrow l_1)$, for the transfer at unit pressure of 1 mol mercury from the pure liquid metallic phase l_2 into an aqueous phase l_1 having unit mercury mole fraction.

Henry Law constants, $H_2 = p_2/x_2$ atm, were calculated as p_2^0/x_2^0 from the known mercury vapor pressure p_2^0 (13) with the experimental x_2^0 values used in calculating eq. 2. The least squares fit of this data, giving the best equation for the temperature dependence of H_2 between 0 and 120 °C, is

$$[3] \quad \log_{10} H_2 \text{ (atm)} = 135.636 - 8031.1/T - 42.8448 \log_{10} T$$

The Henry Law constant for mercury in water together with its standard error are evaluated from eq. 3 between 0 and 120 °C and presented in Table 3. The table contains values, derived from eq. 3, for the standard thermodynamic function changes, $\Delta X_2^0(l_1 \rightarrow g)$, for the transfer of 1 mol of mercury from the aqueous phase l_1 with unit mercury mole fraction and at 1 atm total pressure into the gas phase g containing an ideal mercury

Can. J. Chem. Downloaded from www.nrcresearchpress.com by 210.87.254.6 on 09/05/12
For personal use only.

TABLE 3. Henry law constants and standard thermodynamic functions for mercury evolution from water*

Temperature (°C)	$H_2 = p_2^0/x_2^0$ (atm)		$\Delta G_2^0(l_1 \rightarrow g)$ (cal/mol)		$\Delta H_2^0(l_1 \rightarrow g)$ (cal/mol)		$\Delta S_2^0(l_1 \rightarrow g)$ (cal/deg mol)	
	Value	σ	Value	σ	Value	σ	Value	σ
0.0	70	3	−2 310	20	13 490	280	57.8	0.95
5.0	109	3	−2 590	16	13 070	250	56.3	0.85
10.0	165	4	−2 870	13	12 640	220	54.8	0.76
15.0	242	5	−3 140	11	12 210	200	53.3	0.67
20.0	346	6	−3 400	9	11 790	170	51.8	0.58
25.0	482	7	−3 660	9	11 360	150	50.4	0.50
30.0	658	10	−3 910	9	10 940	130	49.0	0.43
35.0	878	13	−4 150	9	10 510	110	47.6	0.37
40.0	1 150	18	−4 380	10	10 090	100	46.2	0.32
45.0	1 470	23	−4 610	10	9 660	90	44.9	0.29
50.0	1 860	30	−4 830	10	9 230	90	43.5	0.29
55.0	2 300	38	−5 050	11	8 810	100	42.2	0.31
60.0	2 800	46	−5 260	11	8 380	120	40.9	0.35
65.0	3 370	56	−5 460	11	7 960	140	39.7	0.40
70.0	3 980	69	−5 650	12	7 530	160	38.4	0.47
75.0	4 640	85	−5 840	12	7 110	180	37.2	0.53
80.0	5 350	110	−6 020	14	6 680	210	36.0	0.60
85.0	6 080	140	−6 200	16	6 250	230	34.8	0.67
90.0	6 840	170	−6 370	18	5 830	260	33.6	0.74
100.0	8 360	280	−6 700	24	4 980	310	31.3	0.88
110.0	9 810	430	−7 000	33	4 130	360	29.0	1.0
120.0	11100	630	−7 280	43	3 270	420	26.8	1.2

*$\Delta C_{p_2}^0(l_1 \rightarrow g) = -85.1 \pm 5.6$ cal/deg mol.

vapor at 1 atm pressure. The standard errors on the thermodynamic functions in Tables 2 and 3 are nearly equal because the errors on the vapor pressures are very small compared with those on the solubility measurements.

Discussion

Mercury dissolved in water shows large positive deviations from Raoult's Law with activity coefficients $\gamma_2(\gamma_2 = 1/x_2^0)$ varying between 268 000 000 at 0 °C and 11 200 000 at 120 °C. The corresponding large positive values for $\Delta G_2^0(l_2 \rightarrow l_1)$ are predominantly due to the large negative entropy term at 0 °C, but to the large positive enthalpy term at 120 °C.

The Henry Law constants H_2, in Table 3, are very much greater than the known mercury saturation vapor pressure (13). The enthalpy change $\Delta H_2^0(l_1 \rightarrow g)$ of 13 490 ± 280 cal/mol at 0 °C is the largest yet determined for solute evolution from an aqueous solution, and directly reflects the strong attractive dispersion forces between the very polarizable mercury atom and its water neighbors. The very large $\Delta S_2^0(l_1 \rightarrow g)$ of 57.8 cal/deg mol at 0 °C is 37 cal/deg mol larger than Trouton's constant: this difference arises predominantly from orientation of water adjacent to the mercury solute. From the value of $\Delta C_{p_2}^0(l_1 \rightarrow g)$ and the heat capacity of mercury vapor (13) we obtain a partial molar heat capacity for aqueous mercury of 90.1 ± 5.6 cal/deg mol. This value is larger than expected for a small spherically symmetric monatomic solute (8) and indicates rapid thermal breakdown of the low temperature water orientations as the temperature is increased. H_2 attains a maximum value of 13 500 atm at 158 °C and then decreases with temperature.

The relative volatility of mercury solute with respect to water (H_2/p_1^0, where p_1^0 is the water vapor pressure in atm) is 15 400 at 25 °C and 8 360 at 100 °C, and shows the greater relative preference for mercury volatilization into the binary vapor phase at 25 than at 100 °C. The un-ionized monatomic mercury solute is readily lost by volatilization from its water solutions at normal temperatures.

1. K. F. BONHOEFFER and H. REICHART. Z. Phys. **67**, 780 (1931).
2. A. STOCK, F. CUCUEL, F. GERSTNER, H. KÖHLE, and H. LUX. Z. anorg. Chem. **217**, 241 (1934).
3. J. C. PARIAUD and P. ARCHINARD. Bull. Chim. Soc. Fr. 454 (1952).
4. H. C. MOSER and A. F. VOIGT. J. Am. Chem. Soc. **79**, 1837 (1957).
5. S. S. CHOI and D. G. TUCK. J. Chem. Soc. 4080 (1962).
6. D. D. ELEY. Trans. Faraday Soc. **35**, 1281 (1939).

Can. J. Chem. Downloaded from www.nrcresearchpress.com by 210.87.254.6 on 09/05/12
For personal use only.

7. D. N. GLEW and E. A. MOELWYN-HUGHES. Discuss. Faraday Soc. **15**, 150 (1953).
8. T. J. MORRISON and N. B. JOHNSTONE. J. Chem. Soc. 3441 (1954).
9. D. N. GLEW and D. A. HAMES. Can. J. Chem. **47**, 4651 (1969).
10. J. M. COLEMAN. Dow Chemical of Canada, Limited. Method for determination of mercury in effluents and process streams from a mercury-cell chlorine plant (Atomic absorption flameless method). This report is available, on request, from the Company.
11. Nat. Bur. Std. Tech. News Bull. **47**, 175 (1963).
12. E. C. W. CLARKE and D. N. GLEW. Trans. Faraday Soc. **62**, 539 (1966).
13. T. B. DOUGLAS, A. F. BALL, and D. C. GINNINGS. J. Res. Nat. Bur. Std. **46**, 334 (1951).

Can. J. Chem. Downloaded from www.nrcresearchpress.com by 210.87.254.6 on 09/05/12
For personal use only.

Can. J. Chem. Downloaded from www.nrcresearchpress.com by 210.87.254.105 on 09/05/12
For personal use only.

Reaction of Diphenylcyclopropenethione with Heteroaromatic Nitrogen Compounds

J. W. LOWN AND K. MATSUMOTO[1]

Department of Chemistry, University of Alberta, Edmonton, Alberta

Received May 19, 1971

Diphenylcyclopropenethione reacts with a variety of heteroaromatic nitrogen compounds to give in excellent yields four types of products (*a*) 6,7-diphenyl-8-thionpyrazolo[1,2-*a*]pyridazine and -cinnolines, (*b*) azaindolizinthiols, (*c*) azaindolizine disulfides, and (*d*) 1-methoxy-1,2-diphenyl-3-thionpyrrolidino-[1,2-*a*]isoquinoline and similar structures. Proof of structure of products of type *a* rests on their independent synthesis by the action of phosphorus pentasulfide on the known oxo-analogs. Products of type *b* are converted readily into type *c* by air oxidation. In products of type *d* a molecule of solvent methanol is incorporated in the structures.

La diphénylcyclopropènethione réagit avec un grand nombre de composés, ayant l'azote comme hétéroatome, pour donner avec un excellent rendement quatre types de composés (*a*) diphényl-6,7 thion-1,8 pyrazolo [1,2-*a*] pyridazine et -cinnolines, (*b*) azaindolizinthiols, (*c*) disulfure d'azaindolizine, et (*d*) méthoxy-1 diphényl-1,2 thion-3 pyrrolidino [1,2-*a*] isoquinoléine et des produits de structure semblable. Les preuves de structure des produits du type *a* reposent sur leurs synthèses indépendantes par l'action du pentasulfure de phosphore sur les analogues oxo connus. Les produits du type *b* sont transformés facilement en ceux du type *c* par oxydation par l'air. Dans les produits du type *d* une molécule du solvant (méthanol) est incorporée dans la structure.

Canadian Journal of Chemistry, 49, 3119 (1971)

We recently confirmed (1) and provided structure proof of an earlier tentative report by Breslow *et al.* (2) that diphenylcyclopropenone reacts with pyridine in refluxing methanol to give 1,2-diphenyl-3-indolizinyl *cis*-1,2-diphenylacrylate. We extended the reaction to include a variety of heteroaromatic nitrogen compounds and obtained in good yield either (*a*) 1,2-diphenyl-3-indolizinyl *cis*-1,2-diphenylacrylates and aza analogs, or (*b*) 5,6-diphenyl-7-hydroxypyrrolo-[1,2-*b*]pyridazines and similar structures, or (*c*) adducts in which cycloaddition takes place to the nitrogen–nitrogen bond of 1,2-diazines. Cycloheptenocyclopropenone in the examples studied forms heterocycles of type *b*.

The chemistry of diphenylcyclopropenethione (**1**) (3–5) has not received as much attention as its oxygen analog, diphenylcyclopropenone (**2**), probably because of its relative thermal instability.

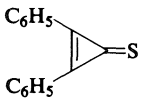

1

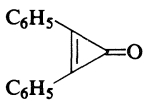

2

We report reactions of **1** with heteroaromatic nitrogen compounds which proceed smoothly at room temperature to give in excellent yield a variety of derivatives of aza analogs of indolizines.

The reactions of heteroaromatic nitrogen compounds with the thione **1** proved to be quite different from those with **2** reported earlier. The thione shows a marked propensity for addition to nitrogen–nitrogen double bonds whereas **2** undergoes such additions principally when addition to a carbon–nitrogen bond is precluded structurally (*e.g.* benzo[*c*]cinnoline (1)). In addition, the inability of the thione **1** to form sulfur analogs of indolizinyl *cis*-1,2-diphenylacrylates led to different behavior towards *e.g.* pyridine, pyrazine, and isoquinoline as was observed previously with **2**. Four principal product types were encountered.

Thionpyrazolo Structures

Pyridazine reacted smoothly with **1** in chloroform at room temperature to give a 1:1 addition product in 93% yield formulated as the 6,7-diphenyl-8-thionpyrazolo[1,2-*a*]pyridazine (**3**). This type of product is in contrast to the 5,6-diphenyl-7-hydroxypyrrolo[1,2-*b*]pyridazine (**4**) which was obtained from **2**.

Compound **3** showed a thioamide band in the

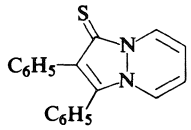

3

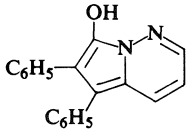

4

[1]NRCC Postdoctorate Fellow, 1969 to present.

Can. J. Chem. Downloaded from www.nrcresearchpress.com by 210.87.254.105 on 09/05/12
For personal use only.

i.r. spectrum and no evidence of the free thiol (negative tests with sodium nitroprusside and with 3,3′-dithiobis-(6-nitrobenzoic acid) (6)). In contrast **4** gave a positive ferric chloride test and exhibited a strong i.r. absorption at 3570 cm^{-1} for hydroxyl.

The thione also reacted readily with 3-methylpyridazine to give 4-methyl-6,7-diphenyl-8-thionpyrrolo[1,2-*a*]pyridazine **5**. The position of the methyl group in **5** is assigned on the basis of the known tendency of pyridazine to quaternize at the less hindered nitrogen (7) and since nucleophiles attack the carbon–sulfur bond of **1** (8) (*vide infra*).

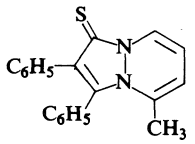

5

Adducts of types **3** and **5** proved to be the predominant type for **1** with 1,2-diazines while they are the exception in the reactions of **2**.

The thione **1** reacted quantitatively with benzo[*c*]cinnoline (where there is no vacant carbon alpha to nitrogen) to give 2,3-diphenyl-1-thionpyrazolo[1,2-*a*]benzo[*c*]cinnoline **6** with properties very similar to those of **3** and **5**. The structure of **6** was proven by its preparation in

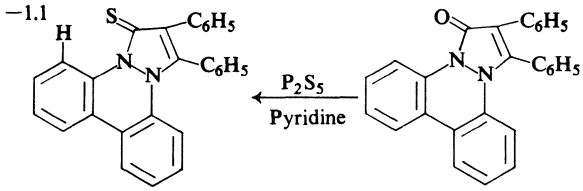

6 **7**

excellent yield from the known oxygen analog **7** (1) by heating with phosphorus pentasulfide in pyridine. Cinnoline also reacts with **1** in chloroform to give **8**, 2,3-diphenyl-1-thionpyrazolo-[1,2-*a*]cinnoline, in quantitative yield. 4-Methylcinnoline and cinnoline-4-carboxylic acid similarly reacted with the thione **1** to give 6-methyl-2,3-diphenyl-1-thionpyrazolo[1,2-*a*]-cinnoline (**9**), and 2,3-diphenyl-1-thionpyrazolo-[1,2-*a*]cinnoline-6-carboxylic acid (**10**), respectively in excellent yields.

Neither compound **3**, **5**, **6**, **8**, **9**, nor **10** showed any evidence of a thiol grouping and n.m.r. integrations in **9** and **10** showed all aromatic

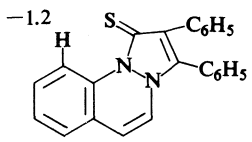

8

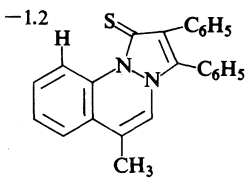

9

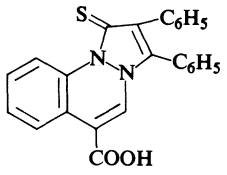

10

protons to be intact. Both **8** and **9** were prepared unambiguously by treatment of their respective oxygen analogs (prepared with diphenylcyclopropenone) with phosphorus pentasulfide in pyridine in excellent yields. The physical properties of these compounds were identical in every respect with those prepared directly from the thione, proving that the orientation of addition is the same for the thione **1** as for diphenylcyclopropenone and therefore that the initial attack by the heterocycles takes place at the C=S carbon. In agreement with this finding it has been shown recently that the thione undergoes nucleophilic attack at the C=S carbon by 1-(*N*-pyrrolidino)prop-1-ene (8). Structures containing pyrazolothione rings are well documented (9).

Substituents like the carbonyl group have generally very pronounced effects on the chemical shifts of *peri* protons (10). Such was found to be the case with the ketopyrazolo[1,2-*a*]cinnolines prepared previously with diphenylcyclopropenone, and the magnitude of the *peri*-effect for the adduct obtained with cinnoline was used to support the orientation of the addition (1). While no data are available in the literature on the magnitude of the *peri*-effect induced by an adjacent thione grouping, the magnitude of the paramagnetic shift on proton-12 in **6** (−1.10 p.p.m.), proton-10 in **9** (−1.20 p.p.m.), and proton-10 in **8** (−1.20 p.p.m.) indicate that the effect in these structurally unambiguous compounds is very similar to that of the carbonyl group. This property proved useful in assigning the structures of some 3-thionpyrrolidino compounds described below.

The analytical and spectral data for these new compounds are summarized in Tables 1 and 2.

Can. J. Chem. Downloaded from www.nrcresearchpress.com by 210.87.254.105 on 09/05/12
For personal use only.

TABLE 1. Reaction products of diphenylcyclopropenethione with heteroaromatic nitrogen compounds

Product	Reactant	Product type*	Melting point (°C)	Yield (%)	Found					Calculated				
					C	H	N	S	Molecular ion	C	H	N	S	Molecular ion
8	Cinnoline	A	267	96	78.46	4.96	7.69	9.06	352.1314	78.40	4.58	7.95	9.10	352.1314
9	4-Methylcinnoline	A	238	99†	—	—	5.97	6.88	366.1188	—	—	5.77	6.60	366.1191
6	Benzo[*c*]cinnoline	A	283	100	80.36	4.64	7.22	8.13	402.1184	80.57	4.51	6.96	7.97	402.1191
10	Cinnoline-4-carboxylic acid	A	289	100	72.93	4.15	6.88	8.05	396.0928	72.72	4.07	7.07	8.09	396.0933
5	3-Methylpyridazine	A	234	80	75.83	5.03	8.79	10.02	316.1030	75.99	5.10	8.86	10.14	316.1035
3	Pyridazine	A	219	93	75.46	4.64	8.97	10.69	302.0872	75.46	4.67	9.23	10.60	302.0878
12*c*	2,6-Dimethylpyrazine	B	144	68	76.46	5.60	8.22	9.40	330.1185	76.35	5.49	8.48	9.71	330.1191
12*b*	2-Methylpyrazine	B	130	75	76.16	5.33	8.78	10.18	316.1030	75.99	5.10	8.86	10.14	316.1035
11*b*	2-Aminopyrazine	C	288	70	—	—	13.02	10.09	632.1800	72.13	4.46	13.28	10.14	632.1817
14	Quinoxaline	B	255	56	78.30	4.33	7.87	9.05	352.1314	78.38	4.58	7.95	9.10	352.1314
12*a*	Pyrazine	(B + C)	B148	25	75.78	4.71	9.48	10.83	302.0870	75.46	4.67	9.27	10.60	302.0878
11*a*			C230	28	75.51	4.53	9.21	10.76	602.1599	75.70	4.35	9.30	10.65	602.1612
15	Isoquinoline	D	204	78	78.51	5.58	3.66	8.29	383.1336	78.29	5.52	3.65	8.37	383.1344
20	Quinazoline	D	185	31	74.72	5.49	7.06	8.50	384.1290	74.97	5.24	7.29	8.34	384.1296
21	Phthalazine	D	189	45	75.17	5.19	7.66	8.70	384.1290	74.97	5.24	7.29	8.34	384.1296

*A, 1:1 adduct exemplified by cinnoline adduct **7**; B, 1:1 adduct exemplified by pyrazine **11**; C, disulfide bridged product exemplified by pyrazine **10**; D, 1:1:1 adduct incorporating methanol exemplified by isoquinoline **15**.

†Incorporates 1 mol of $CHCl_3$ of solvation.

Can. J. Chem. Downloaded from www.nrcresearchpress.com by 210.87.254.105 on 09/05/12
For personal use only.

TABLE 2. Spectroscopic data on new heterocycles

Compound	Infrared spectrum (cm^{-1}) (KBr disc)	Nuclear magnetic resonance spectrum (δ)*			
		Solvent†	Indolizine ring and aryl protons	Methyl protons	Methine protons
8	1243 1356 1410	TFA	7.18, 7.90 (2H) ABq, J = 8 Hz (5,6 protons) 7.35–7.9 (13H) m; 8.65–8.95 (1H) m, (proton 10)	—	—
9	1035 1210 1394	TFA	7.1–8.2 (14H) m; 8.70–9.00 (1H) m, (proton 10)	2.51 (3H) d, J = 1 Hz	—
6	1071 1201 1439 1480	TFA	7.1–8.5 (17H) m, 8.5–8.75 (1H) m, (proton 10)	—	—
10	1241 1320 1700 (C=O)	$(CH_3)_2SO$	7.0–7.7 (12H) m; 7.83 (1H) s (proton 5); 8.4–8.65 (1H) m, (proton 10); 11.0 (1H) m, CO_2H	—	—
5	1235 1300 1404	$CDCl_3$ TFA	5.55–6.1 (2H) m; 6.9–7.7 (11H) m 6.4–7.02 (2H) m; 7.1–7.8 (10H); 7.8–8.2 (1H) m	3.40 (3H) s 3.20 (3H) s	—
12*c*	1065 1166 1315 1384 1455	TFA $CDCl_3$	6.6–8.0 (12H) m 6.65–7.6 (12H) m	3.28 (3H) s 2.52 (3H) s 2.66 (3H) s 2.32 (3H) s	
15	1067 1288 1560	$CDCl_3$	5.52, 5.85 (2H) ABq, J = 8 Hz (5,6 protons) 6.7–7.7 (14H) m	3.30 (3H) s	5.25 (1H) s 6.31 (1H) s
20	1070 1288 1567	$CDCl_3$	6.8–7.6 (15H) m	3.32 (3H) s	5.24 (1H) s 6.25 (1H) s
21	1070	$CDCl_3$	6.8–7.8 (15H) m	3.32 (3H) s	5.30 (1H) s 6.37 (1H) s

*All other new compounds gave normal n.m.r. and i.r. spectra with no unusual features.
†TFA = Trifluoroacetic acid.

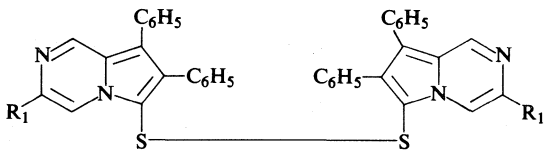

11

a $R_1 = H$
b $R_1 = NH_2$

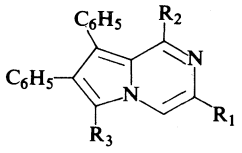

12

a $R_1 = H$; $R_2 = H$; $R_3 = SH$
b $R_1 = CH_3$; $R_2 = H$; $R_3 = SH$
c $R_1 = CH_3$; $R_2 = CH_3$; $R_3 = SH$
d $R_1 = CH_3$; $R_2 = CH_3$; $R_3 = OH$

Azaindolizinthiol and Azaindolizine Disulfide Structures

Pyrazine reacted readily with the thione **1** in methanol–chloroform in the presence of air to form a different type of product, the di-(7,8-diphenylpyrrolo[1,2-*a*]pyrazinyl)-6-sulfide **11***a* corresponding to a dimeric structure containing a disulfide bridge. Repetition of this reaction under nitrogen with the careful exclusion of oxygen afforded a mixture of the monomer 7,8-diphenylpyrrolo[1,2-*a*]pyrazine-6-thiol **12***a* and **11***a*. The thiol **12***a* was very sensitive to oxidation and could be converted quantitatively into the disulfide **11***a* by refluxing an aerated solution in chloroform.

Similarly 2-aminopyrazine reacts smoothly with the thione in methanol–chloroform at room temperature in the presence of air to give di-(3-amino-7,8-diphenylpyrrolo[1,2-*a*]pyrazinyl)-6-sulfide (**11***b*), in 70% yield.

2-Methylpyrazine reacted with **1** to give 3-methyl-7,8-diphenylpyrrolo[1,2-*a*]pyrazine thiol **12***b*, in 75% yield. In this reaction only one structural isomer was obtained which is tentatively assigned with the methyl group in the 3-position on the plausible grounds that cyclization to the pyrazine ring will take place preferentially on the less hindered side. Little is known about the tautomeric behavior of potential 2-thiolpyrrole derivatives except that they are thought to parallel the oxygen analogs which prefer the oxo form (11). Since spectroscopic examination did not lead to a clear-cut distinction between the two possible tautomeric forms of **12***a–c* no bias in favor of the thiol forms should be construed from the nomenclature used except that **12***a* evidently reacts through the thiol tautomer to form **11***a*.

2,6-Dimethylpyrazine reacts with **1** to form 1,3-dimethyl-7,8-diphenylpyrrolo[1,2-*a*]pyrazine-6-thiol (**12***c*) in good yield. Compounds **12***a–c* and the monomers corresponding to **11***a* and *b* are the sulfur counterparts of the 1,3-dimethyl-7,8-diphenyl-6-hydroxypyrrolo[1,2-*a*]-pyrazine (**12***d*) obtained by reaction of 2,6-dimethylpyrazine with **2**. Compounds **12***a–c* cannot form sulfur analogs of **13** (which is produced from pyrazine and **2**). This fact together with their facile oxidation to the disulfides presumably account for the observed lack of reactivity of the thione **1** towards pyridine and picolines. In contrast, as has been shown by Breslow and by the present authors, **2** reacts very vigorously under such conditions to form 1,2-diphenyl-3-indolizinyl-*cis*-1,2-diphenylacrylates like **13** (1, 2).

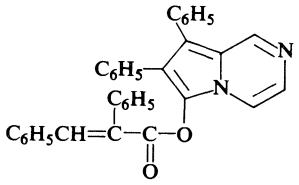

13

Quinoxaline reacted smoothly with **1** to form 2,3-diphenylpyrrolo[1,2-*a*]quinoxaline-1-thiol (**14**). In this respect quinoxaline reacts as a substituted pyrazine and differs radically from the behavior of the isomeric quinazoline and phthalazine.

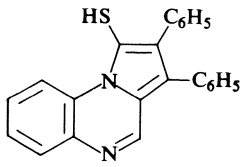

14

3-Thionpyrrolidino Structures

Isoquinoline and two nitrogen heterocycles quinazoline and phthalazine which share the same essential structural features with isoquinoline form a separate group in their reactions with **1**. Isoquinoline reacts very slowly with **1** in chloro-

Can. J. Chem. Downloaded from www.nrcresearchpress.com by 210.87.254.105 on 09/05/12
For personal use only.

Can. J. Chem. Downloaded from www.nrcresearchpress.com by 210.87.254.105 on 09/05/12
For personal use only.

form but in a methanol–chloroform mixture a rapid reaction ensues leading to a 1:1:1 adduct of the heterocycle:thione:methanol which is formulated as the 1-methoxy-1,2-di-phenyl-3-thionpyrrolidino[1,2-*a*]isoquinoline (**15**) on the basis of analytical and spectral evidence.

The n.m.r. spectrum shows the methine protons as two singlets at δ 5.25 and 6.31, the 5,6 protons as an AB quartet centered at δ 5.52 and 5.85 (J = 8 Hz) and the methoxy singlet at δ 3.30. This evidence disposes of the alternative structures, **16** (which would be expected to exhibit an AB quartet for the methine protons) and the Reissert-type structure **17** (which would show only one methine proton).

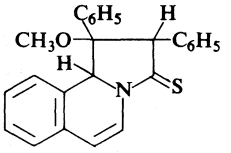

15

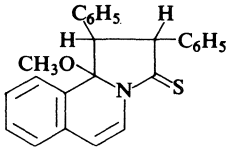

16

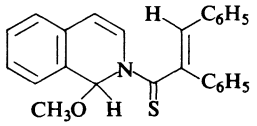

17

The absence of a low-field aromatic proton shifted by the *peri*-effect as observed in **5**–**8** discussed above argues against the alternative orientation of addition in **18**. Additionally, the compound **15** gives negative reactions with sodium nitroprusside and 3,3′-dithiobis-(6-nitrobenzoic acid), reagents which are specific for thiol groups, indicating the compound exists in the thione form shown.

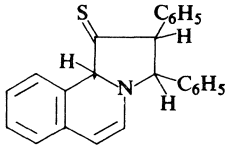

18

As remarked above there are few data available in the literature on the tautomeric behavior of thione-substituted five-membered ring heterocycles, except that existing evidence points to a parallel behavior with that of the oxygen analog (11). Since potential 2-hydroxypyrroles exist almost exclusively in the oxo form (12) and since certain pyrrolones have been shown to undergo conjugate addition of water to the carbon–carbon double bond (13) then **15** is plausibly formed by initial addition of **1** across the 1-2 positions of isoquinoline to give **19** followed by addition of methanol to the latter.

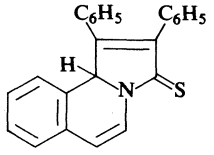

19

The corresponding product of the reaction of isoquinoline with **2** is 1,2-diphenyl-3-pyrrolo[1,2-*a*]isoquinolinyl *cis*-1,2-diphenylacrylate, in which addition has also taken place across the 1,2 carbon–nitrogen bond.

Controlled hydrolysis of **15** with 15 *N* sulfuric acid followed by neutralization afforded isoquinoline indicating that the isoquinoline moiety is retained in **15**.

Quinazoline similarly reacted with **1** in methanol–chloroform to give 1-methoxy-1,2-diphenyl-3-thionpyrrolidino[1,2-*c*]quinazoline **20**. As in the case of the analogous product formed with diphenylcyclopropenone, the structure is assigned on the basis of the known susceptibility of the 3-nitrogen of quinazoline to quaternize preferentially and the general reactivity of the 3,4 bond towards addition (14).

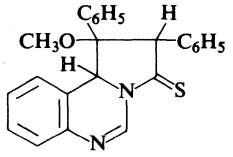

20

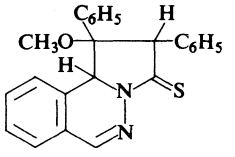

21

Phthalazine reacts with **1** to form the 1-methoxy-1,2-diphenyl-3-thionpyrrolidino[2,1-*a*]phthalazine (**21**). Evidently the 2,3 nitrogen–nitrogen bond in phthalazine has not a sufficiently high double bond character to dictate cycloaddition analogous to those of cinnoline, benzocinnoline, and pyridazine described earlier. Neither **20** nor **21** exhibit a *peri*-shifted aromatic proton suggesting a common orientation of addition of **1** to isoquinoline, quinazoline, and quinoxaline.

Can. J. Chem. Downloaded from www.nrcresearchpress.com by 210.87.254.105 on 09/05/12
For personal use only.

Experimental

Melting points were determined on a Fisher–Johns apparatus and are uncorrected. The i.r. spectra were recorded on a Perkin–Elmer model 421 spectrophotometer, and only the principal, sharply defined peaks are reported. The n.m.r. spectra were recorded on Varian A-60 and A-100 analytical spectrometers. The spectra were measured on approximately 10–15% (w/v) solutions in $CDCl_3$, with tetramethylsilane as a standard. Line positions are reported in p.p.m. from the reference. Absorption spectra were recorded in 'spectro'-grade solvents on a Beckman DB recording spectrophotometer. Mass spectra were determined on an Associated Electrical Industries MS-9 double focusing high resolution mass spectrometer. The ionization energy, in general, was 70 eV. Peak measurements were made by comparison with perfluorotributylamine at a resolving power of 15 000. Kieselgel DF-5 (Camag, Switzerland) and Eastman Kodak precoated sheets were used for t.l.c. Microanalyses were carried out by Dr. C. Daesslé, Organic Microanalysis Ltd., Montreal, Quebec and by Mrs. D. Mahlow of this department.

Diphenylcyclopropenethione

This compound was prepared according to the method of Eicher and Frenzel (4), see also (15).

Reaction of Diphenylcyclopropenethione with Heteroaromatic Nitrogen Compounds

The reaction conditions and purification procedures are illustrated by the following examples of each of the principal product types. The analytical and spectroscopic properties of other compounds similarly prepared are summarized in Tables 1 and 2.

(a) Reaction of Diphenylcyclopropenethione with Cinnoline

To a stirred, cooled (10°) solution of 1.71 g (7.7 mmol) of diphenylcyclopropenethione in 15 ml of chloroform was added dropwise a solution of 1.00 g (7.7 mmol) of cinnoline. Stirring was continued after completed addition for a further 12 h at room temperature during which time the solution adopted a red color. A yellow crystalline solid which had separated was collected and recrystallized from chloroform–ethanol to give 2.63 g (96% yield) of 2,3-diphenyl-1-thionpyrazolo[1,2-*a*]cinnoline (**8**) m.p. 267° (dec.).

Anal. Calcd. for $C_{23}H_{16}N_2S$ (mol. wt. 352.1314): C, 78.40; H, 5.03; N, 7.95; S, 9.10. Found (352.1314 (mass spectrum)): C, 78.46; H, 4.96; N, 7.69; S, 9.06.

The i.r. spectrum ν_{max} (KBr disc) 1410, 1356, 1243 cm^{-1} (C=S). The n.m.r. spectrum δ_{TMS} (CF_3COOH): 7.18, 7.90 (2H, ABq J = 8 Hz, 5,6 protons); 7.35–7.9 (13H, m, aromatic protons), 8.65–8.95 (1H, m, proton-10).

(b) Reaction of Diphenylcyclopropenethione with Pyrazine

(i) In the Presence of Oxygen

To a solution of 1.11 g (3 mmol) of diphenylcyclopropenethione in 15 ml of chloroform was added with stirring a solution of 0.40 g (5 mmol) of pyrazine in 10 ml of methanol. Stirring was continued for 3 days at room temperature. Evaporation of the solvent gave a dark brown solid, trituration of which with methanol afforded 0.68 g (45% yield) of di-(7,8-diphenylpyrrolo[1,2-*a*]pyrazinyl)-6-sulfide (**11***a*) as a yellow solid, m.p. 230° (dec.) (from chloroform–ethanol).

Anal. Calcd. for $C_{39}H_{26}N_4S_2$ (mol. wt. 602.1612): C, 75.90; H, 4.35; N, 9.30; S, 10.65. Found (602.1599 (mass spectrum)): C, 75.51; H, 4.53; N, 9.21; S, 10.76.

The n.m.r. spectrum δ_{TMS} ($CDCl_3$): 6.5–8.0 (m, aromatic protons).

(ii) In the Absence of Oxygen

A deoxygenated solution of 0.4 g (5 mmol) of pyrazine in 15 ml of methanol was added dropwise with stirring under nitrogen to a solution of 1.11 g (5 mmol) of diphenylcyclopropenethione in 15 ml of chloroform. The mixture was stirred for 2 days under nitrogen. After removal of the solvent *in vacuo*, methanol was added and the resulting yellow solid **11***a* identical with that obtained above was collected 0.42 g (28% yield) m.p. 230° (dec.). The filtrate was set aside at 0° for 1 day when a yellow crystalline solid separated which was collected, affording 0.38 g (25% yield) of 7,8-diphenylpyrrolo[1,2-*a*]pyrazine-6-thiol (**12***a*), m.p. 148° (from cold methanol under nitrogen).

Anal. Calcd. for $C_{19}H_{14}N_2S$: C, 75.46; H, 4.67; N, 9.27; S, 10.60. Found: C, 75.78; H, 4.71; N, 9.48; S, 10.83.

The n.m.r. spectrum δ_{TMS} ($CDCl_3$): 6.5–8.0 (m, aromatic protons). The latter compound **12***a* could be converted in the disulfide **11***a* by recrystallization from hot aerated chloroform.

(c) Reaction of Diphenylcyclopropenethione with Isoquinoline

A mixture of 1.11 g (5 mmol) of diphenylcyclopropenethione and 0.65 g (5 mmol) of isoquinoline in 15 ml of chloroform and 10 ml of methanol was stirred at room temperature for 24 h. The resulting pale yellow solid which separated was collected (0.19 g). Upon setting aside the filtrate for 7 days a further 0.52 g of product was obtained, representing 1.43 g (78% yield) of 1-methoxy-1,2-diphenyl-3-thionpyrrolidino[1,2-*a*]isoquinoline **15**, m.p. 204° (chloroform–methanol) as colorless crystals.

Anal. Calcd. for $C_{25}H_{21}NSO$: (mol. wt. 383.1344): C, 78.29; H, 6.95; N, 3.65; S, 8.37. Found (383.1336 (mass spectrum)): C, 78.51; H, 5.58; N, 3.66; S, 8.29.

The i.r. spectrum ν_{max} (Nujol mull) 1067, 1288, 1560 cm^{-1}. The n.m.r. spectrum δ_{TMS} ($CDCl_3$): 3.30 (3H, s, OCH_3); 5.25 and 6.31 (1H each, s, methine protons); 5.52, 5.85 (2H, ABq, J = 8 Hz, 5,6 protons), 6.7–7.7 (14H, m, aromatic protons).

Products of the three types exemplified above were obtained by similar procedures from other heteroaromatic nitrogen compounds. The analytical and spectral data are summarized in Tables 1 and 2.

Reaction of 2,3-Diphenyl-1-ketopyrazolo[1,2-a]cinnoline with Phosphorus Pentasulfide

A mixture of 0.34 g (1 mmol) of 2,3-diphenyl-1-ketopyrazolo[1,2-*a*]cinnoline and 0.44 g (2 mmol) of phosphorus pentasulfide in 20 ml of dry pyridine was heated under reflux for *ca.* 70 h with stirring. The solvent was removed *in vacuo* and the residual solid extracted with hot benzene. Evaporation of the benzene gave a yellow solid which was purified by recrystallization twice from chloroform–methanol to yield 0.30 g (88% yield) of 2,3-diphenyl-1-thionpyrazolo[1,2-*a*]cinnoline, m.p. 267°.

The physical and spectral characteristics of this com-

pound were identical with those of compound **8** prepared directly from the reaction of diphenylcyclopropenethione with cinnoline.

Reaction of Diphenylcyclopropenone with 4-Methylcinnoline

To a solution of 0.21 g (1 mmol) of diphenylcyclopropenone (15) in 15 ml of chloroform there was added with stirring at $-10°$ a solution of 0.14 g (1 mmol) of 4-methylcinnoline in 15 ml of methanol and stirring was continued for 2 h at $-10°$ and then 8 h at room temperature. The light green solid which separated was collected affording 0.32 g (91% yield) of 6-methyl-2,3-diphenyl-1-ketopyrazolo[1,2-*a*]cinnoline, m.p. 189° (chloroform–ethanol).

Anal. Calcd. for $C_{24}H_{18}N_2O$ (mol. wt. 350.1418): C, 82.26; H, 5.18; N, 7.99. Found (350.1419 (mass spectrum)): C, 82.14; H, 5.19; N, 8.00.

The i.r. spectrum ν_{max} (Nujol) 1641 cm^{-1} (C=O). The n.m.r. spectrum δ_{TMS}(CF_3COOH): 2.43 (3H, d, $J = 1$ Hz CH_3); 7.7–8.1 (13H, m, aromatic protons).

This material was converted into the thione in 84% yield identical in every respect to **9** by refluxing with phosphorus pentasulfide in pyridine. By a similar procedure compound **7** (1) was converted into **6**.

Acid-catalyzed Hydrolysis of 1-Methoxy-1,2-diphenyl-3-thionpyrrolidino[1,2-a]isoquinoline

A slurry of 0.766 g (2 mmol) of 1-methoxy-1,2-diphenyl-3-thionpyrrolidino[1,2-*a*]isoquinoline in 30 ml of 15 *N* sulfuric acid was heated to 80–100° for 2 h. A brown residue was collected and the filtrate neutralized with dilute aqueous potassium hydroxide and extracted with ether. Evaporation of the dried ($MgSO_4$) ether extract gave a yellow oil (0.33 g), the i.r. and n.m.r. spectra of which were superimposable with those of isoquinoline.

This research was supported by a grant from the National Research Council of Canada (to J.W.L.) and by the University of Alberta. We thank Mr. R. Swindlehurst and Dr. A. Hogg for the n.m.r. and mass spectra.

1. J. W. Lown and K. Matsumoto. Can. J. Chem. **49**, 1165 (1971).
2. R. Breslow, T. Eicher, A. Krebs, R. A. Peterson, and J. Posner. J. Am. Chem. Soc. **87**, 1320 (1965).
3. A. W. Krebs. Angew Chem. Int. Ed. **4**, 10 (1965).
4. T. Eicher and G. Frenzel. Z. Naturforsch, **20***b*, 2741 (1965).
5. T. Eicher and A. Hansen. Tetrahedron Lett. 1169 (1967).
6. G. L. Ellman. Arch. Biochem. Biophys. **82**, 70 (1959).
7. G. F. Duffin. Adv. Heterocycl. Chem. **3**, 19 (1964).
8. J. W. Lown and T. W. Maloney. Chem. and Ind. (Lond.) 870 (1970).
9. (*a*) R. H. Wiley and P. Wiley. Heterocyclic compounds. *Edited by* A. Weissberger. Interscience, New York, N.Y., 1964. p. 58. (*b*) T. L. Jacobs. *In* Heterocyclic compounds. *Edited by* R. C. Elderfield. Vol. 5. J. Wiley, New York, N.Y., 1957. p. 135. (*c*) A. Michaelis. Ann. **320**, 1 (1902).
10. L. M. Jackman and S. Sternhell. Applications of nuclear magnetic resonance spectroscopy in organic chemistry. 2nd ed. Pergamon Press, 1969. p. 204.
11. A. R. Katritzky and J. M. Lagowski. Adv. Heterocycl. Chem. **2**, 20, 60 (1963).
12. (*a*) Reference 10 p. 11, (*b*) H. Fischer and H. Orth. Die Chemie des Pyrrols. Vol. 1. Akademische Verlag, Liepzig, 1934. p. 124.
13. K. E. Schulte and J. Reisch. Arch. Pharm. **292**, 51 (1959).
14. (*a*) S. Gabriel and J. Colman. Chem. Ber. **37**, 3643 (1904). (*b*) A. Albert, W. L. F. Armarego, and E. Spinner. J. Chem. Soc. 5267 (1961). (*c*) A. Albert, W. L. F. Armarego, and E. Spinner. J. Chem. Soc. 2689 (1961). (*d*) T. Higashino. Yakugaku Zasshi **80**, 245 (1960); Chem. Abst. **54**, 13125e (1960).
15. J. W. Lown and T. W. Maloney. J. Org. Chem. **35**, 1716 (1970).

Can. J. Chem. Downloaded from www.nrcresearchpress.com by 210.87.254.105 on 09/05/12
For personal use only.

Can. J. Chem. Downloaded from www.nrcresearchpress.com by 210.87.254.5 on 09/05/12
For personal use only.

Etude polarographique des ozonides

J. GRIGNON ET S. FLISZÁR
Département de Chimie, Université de Montréal, Montréal, Québec

Reçu le 30 avril 1971

La réduction polarographique des ozonides du stilbène et d'une série de styrènes substitués dans le noyau a été étudiée. Une relation linéaire est observée entre les potentiels de demi-vague et les constantes σ de Hammett pour les ozonides des styrènes substitués. La constante ρ est positive, ce qui indique que l'étape déterminante est une réaction nucléophile. Un mécanisme est proposé pour la réaction d'électrode conduisant à la formation de 2 mol d'aldéhyde par mole d'ozonide.

The polarographic reduction of the ozonides of stilbene and of selected ring-substituted styrenes, yielding 2 mol of aldehyde per mole of ozonide, has been studied. With the substituted styrenes a Hammett relationship is observed for the half-wave potentials. The positive ρ constant (0.20) indicates that the determining step is a nucleophilic process. Possible mechanisms are discussed.

Canadian Journal of Chemistry, **49**, 3127 (1971)

Dans le cadre de l'étude des produits d'oxydation des corps gras, des caoutchoucs, des polymères, et des essences, de nombreuses publications et revues (1–3) ont traité du comportement polarographique des produits peroxydiques. Kůta et Quackenbush (4) ont, notamment, signalé les possibilités d'application des techniques polarographiques à l'étude des produits d'ozonation. Ainsi les méthoxyhydroperoxydes, engendrés lors de l'ozonation d'oléfines en présence de méthanol, ont fait l'objet d'un récent travail (5) et l'application analytique de la polarographie pour l'étude du mécanisme d'ozonolyse a été exposée (5–7). Il a également été montré (7) que les hydroxyperoxydes $R_2CH(OOR_1)OH$, examinés en polarographie, peuvent être facilement reconnus à côté de leurs alcoxyhydroperoxydes $R_2CH(OOH)$—OR_1 isomères.

Quelques conclusions générales se dégagent de l'ensemble de ces travaux: (*i*) Les composés peroxydiques d'une même classe sont réduits dans un domaine de potentiel restreint. Ainsi, par exemple, les potentiels de demi-vague observés pour les α-méthoxyhydroperoxydes R—$CH(OCH_3)$—OOH dans le tampon McIlvaine à p*H* 7, en présence de méthanol, sont compris entre −0.838 (R = H) et −0.200 V (R = *t*-C_4H_9) (5). Les divers types de composés peroxydiques peuvent être classés comme suit, par ordre de potentiel négatif croissant: peracides < hydroperoxydes < peroxydes. (*ii*) La réduction, irréversible, procède par la rupture de la liaison oxygène–oxygène, avec la participation de deux électrons, en une seule étape.

Dans le présent travail, les techniques polarographiques ont été appliquées à l'étude des ozonides du stilbène et des styrènes substitués dans le noyau (**1–6**).

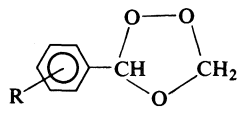

1 R = *p*-CH_3O
2 *p*-CH_3
3 H
4 *p*-Cl
5 *p*-Br
6 *m*-NO_2

Résultats et discussion

Les polarogrammes ont été obtenus, à moins d'indications contraires, par polarographie avec une tension alternative surimposée. Le solvant utilisé était un mélange 1:1 de benzène–méthanol et l'électrolyte de support du chlorure de lithium 0.5 *M*. Les polarogrammes des ozonides enregistrés dans ces conditions montrent deux pics. Le courant de réduction enregistré à un potentiel de 0 V est dû au méthanol contenu dans le solvant. Des deux pics polarographiques observés, le premier, c'est-à-dire celui qui apparaît au potentiel le moins négatif, est dû à la réduction de l'ozonide, tandis que le deuxième est causé par la réduction de l'aldéhyde aromatique engendré lors de l'électrolyse de l'ozonide. Ce point sera démontré par l'étude des potentiels de demi-vague et des temps de rétention en c.p.g. des produits obtenus par électrolyse préparative.

Can. J. Chem. Downloaded from www.nrcresearchpress.com by 210.87.254.5 on 09/05/12
For personal use only.

Le benzène–méthanol a été choisi comme solvant en raison de la faible solubilité des ozonides dans l'eau et dans le méthanol froid. Dans le benzène–méthanol, les ozonides subissent une décomposition lente: environ 15% de décomposition après 1 h à la température de 20 °C. Le méthanol semble être le principal agent affectant la stabilité des ozonides dans le solvant utilisé. Il est, en effet, généralement possible de conserver les ozonides pendant quelques semaines au réfrigérateur, purs ou en solution dans le benzène ou le tétrachlorure de carbone, tandis qu'en solution méthanolique ces mêmes ozonides sont presqu'entièrement décomposés en quelques jours. En raison de cette décomposition, les procédures expérimentales doivent être maintenues rigoureusement constantes.

Potentiels de demi-vague $E_{1/2}$

L'électrode de référence était constituée d'un fil d'argent plongé dans une solution d'électrolyte saturée en AgCl et séparée de la solution à analyser par un verre fritté fin.

Lors de l'utilisation d'un solvant non-aqueux la résistance de la solution n'est pas négligeable; il faut en tenir compte dans la mesure des potentiels de demi-vague. Il a été observé que la chute de tension due à la résistance de la solution est faible et indépendante de la concentration en dépolariseur dans le domaine de 1 à 32×10^{-4} *M* qui a été étudié. Elle est de 30 mV à un potentiel de -1.00 V et de 50 mV à -2.00 V. Dans ces conditions, l'aldéhyde benzoïque a un potentiel de demi-vague $E_{1/2}$ expérimental de -1.59 V, ce qui selon l'équation

$$E_{1/2} \text{ expérimental} = E_{1/2} \text{ corrigé} + iR$$

conduit à la valeur $E_{1/2}$ corrigé $= -1.55$ V, valeur voisine de celle de -1.58 V (par rapport à l'électrode de calomel saturée) observée par Willits *et al.* (8) dans une solution 0.3 *M* en LiCl dans le benzène–méthanol (1:1). Cette valeur du potentiel de demi-vague de l'aldéhyde benzoïque a été utilisée comme valeur étalon pour s'assurer de la reproductibilité de l'électrode de référence.

Les valeurs des potentiels de demi-vagues observées pour les ozonides étudiés sont rapportées au tableau 1. Il doit être noté que ces potentiels ont une légère tendance à être déplacés vers des valeurs plus négatives aux concentrations plus élevées. Les valeurs rapportées au tableau 1 ont été toutes mesurées à la concentration de 8×10^{-4} *M* en ozonide.

TABLEAU 1. Potentiels de demi-vague des ozonides $R_1C_6H_4—CH(O_3)CH—R_2$

R_1	R_2	$E_{1/2}$ expérimental (V)	$E_{1/2}$ corrigé (V)
p-CH_3O	H	−1.11	−1.08
p-CH_3		−1.05	−1.02
H		−1.01	−0.98
p-Cl		−0.98	−0.95
p-Br		−0.95	−0.92
m-NO_2		−0.87	−0.84
H	C_6H_5	−0.87	−0.84

Il ressort des résultats exposés au tableau 1 que les potentiels de demi-vague des ozonides des styrènes substitués dans le noyau varient régulièrement en fonction des substituants. La fig. 1 montre qu'une relation linéaire est obtenue en fonction des constantes de substituants σ de Hammett. La constante ρ est positive (+0.20), ce qui est en accord avec la majorité des processus de réduction électrochimique (9). Ceci indique que l'étape déterminant le potentiel est une réaction nucléophile, l'agent nucléophile étant probablement l'électron (ou l'électrode). Ceci exclut, donc, la possibilité d'une importance prédominante d'une attaque électrophile de la part, par exemple, d'un proton précédent le transfert d'électron.

Irréversibilité du processus d'électrode

Les oscillo-polarogrammes $i = f(E)$ ont montré, dans un grand domaine de vitesses de balayage, une irréversibilité complète du processus d'électrode pour tous les ozonides étudiés. En effet, aucun courant n'est observé sur la branche anodique des oscillo-polarogrammes pour des vitesses de balayage comprises entre 0.5 et 25 V/s. Pour des vitesses de balayage très grandes, par contre, supérieures à 200 V/s, un léger courant apparaît sur la branche anodique.

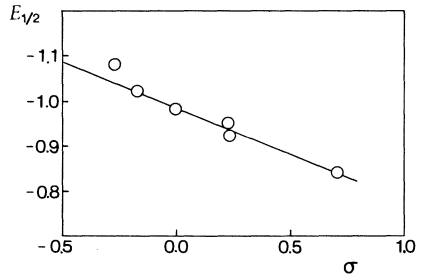

FIG. 1. Relation de Hammett entre $E_{1/2}$ et σ pour les ozonides des styrènes substitués.

Can. J. Chem. Downloaded from www.nrcresearchpress.com by 210.87.254.5 on 09/05/12
For personal use only.

Les pics cathodique et anodique sont alors décalés de 0.20 V.

L'irréversibilité du processus d'électrode, observée aux vitesses de balayage pas trop élevées, est confirmée par l'analyse logarithmique des courbes intensité-potentiel, d'après l'éq.:

$$E = E_{1/2} - (RT/\alpha nF) \ln[I/(I_1 - I)]$$

Le coefficient de transfert α calculé à partir des droites obtenues en portant $\ln[I/(I_1 - I)]$ en fonction de E est, pour tous les ozonides étudiés, de 0.10–0.13, compte tenu des deux électrons mis en jeu.

Nombre d'électrons mis en jeu dans le processus d'électrode

L'électrolyse à potentiel contrôlé a été effectuée sur des échantillons de 100 ml de solution environ 10^{-3} M en ozonide, en utilisant une nappe de mercure comme électrode. La température a été maintenue à 0 °C, afin de réduire la décomposition de l'ozonide: dans ces conditions le pic polarographique de l'ozonide demeure pratiquement inchangé après 1 h, ce qui est le temps généralement requis pour l'électrolyse. Le nombre d'électrons mis en jeu, n, a été déterminé d'après la quantité de courant requise pour réduire une quantité connue d'ozonide, ainsi que par l'étude des courbes $i = i(t)$ obtenues lors de l'électrolyse, d'après l'éq. (10):

$$\log \bar{i}_0 - \log \bar{i}_1 = \bar{i}_0 t/2.3nFC_{t=0}V$$

Les résultats des électrolyses rapportées au tableau 2 indiquent que la valeur expérimentale de n est voisine de 1.9 électron par molécule d'ozonide. Ce résultat, qui tend à montrer que $n = 2$, est en accord avec les valeurs de n observées lors de la réduction de divers composés peroxydiques (5, 7, 11).

Au cœur de la solution, la concentration en ozonide n'est pas identique à celle qui est mesurée à la surface de l'électrode. Ceci cause une erreur systématique qui pourrait expliquer, du moins en partie, le résultat approximatif obtenu.

TABLEAU 2. Détermination du nombre n d'électrons mis en jeu lors de la réduction des ozonides du stilbène et du styrène

Ozonide	Consommé (mmol)	Quantité d'électricité (C)	n*	n†
Stilbène	0.25	45	1.87	1.95
	0.20	34	1.76	1.63
Styrène	0.136	25.5	1.94	2.10
	0.133	24.8	1.93	1.73

*Calculé d'après la quantité d'électricité utilisée.
†Calculé d'après l'analyse logarithmique, par voie graphique.

Identification des produits d'électrolyse

L'électrolyse de 75 ml de solutions d'ozonide du stilbène, de concentrations comprises entre 5×10^{-3} et 1×10^{-2} M, a été effectuée à 0 °C avec une tension appliquée de −1.2 V par rapport à l'électrode Ag/AgCl. L'électrolyse a été conduite, dans chaque cas, jusqu'à la consommation complète de l'ozonide, attestée par l'absence du pic ozonide dans le polarogramme de la solution électrolysée. L'analyse de cette solution par c.p.g. a permis l'identification de l'aldéhyde benzoïque, par une comparaison des temps de rétention, au moyen d'un échantillon authentique de cet aldéhyde. Cette analyse a, de plus, permis de vérifier l'absence d'acide benzoïque dans la solution électrolysée. Les résultats sont rapportés dans le tableau 3.

Des expériences effectuées avec l'ozonide du stilbène, il ressort clairement que l'électrolyse d'une mole d'ozonide conduit à la formation de 2 mol d'aldéhyde benzoïque.

Des expériences similaires ont été faites avec l'ozonide du styrène. L'électrolyse de 100 ml de solution, environ 5×10^{-3} M en ozonide, a été effectuée à 0 °C sous une tension appliquée de −1.18 V par rapport à l'électrode Ag/AgCl. Après l'électrolyse, le polarogramme de la solution ne montre qu'un seul pic à −1.59 V, ce qui atteste la consommation complète de l'ozonide et confirme la présence de l'aldéhyde benzoïque. Comme pour l'ozonide du stilbène, le dosage de l'aldéhyde benzoïque a été effectué au moyen de son pic polarographique. Le deuxième produit attendu lors de l'électrolyse de l'ozonide du styrène, l'aldéhyde formique, ne se manifeste pas en polarographie. Dans le solvant utilisé, contenant 50% de méthanol, l'aldéhyde formique se retrouve, en effet, entièrement sous forme de son hémiacétal. Ce dernier n'étant pas réductible à l'électrode à goutte de mercure (9), il ne peut donc être décelé dans le polarogramme de la solution électrolysée. L'hémiacétal du formaldéhyde a été mis en évidence par c.p.g., par comparaison des temps de rétention avec une solution de styrène ozonée dans le méthanol. Son dosage a été effectué par une comparaison de la surface du pic chromatographique de l'hémiacétal dans

TABLEAU 3. Bilan matériel des électrolyses des ozonides du stilbène et du styrène

Ozonide	mmol consommé	PhCHO formé (mmol)	HCHO formé (mmol)	PhCHO / Ozonide	HCHO / Ozonide
Stilbène	0.75	1.42	—	1.89	—
	0.75	1.48	—	1.97	—
	0.395	0.773	—	1.96	—
Styrène	0.450	0.445	0.442	0.99	0.98
	0.448	0.433	0.399	0.97	0.92

la solution électrolysée avec la surface correspondante, déterminée à partir d'une solution de référence d'hémiacétal. La solution de référence a été obtenue par l'ozonolyse, à −20 °C, d'une quantité connue de styrène dans le méthanol pur, en tenant compte que l'ozonolyse d'une mole de styrène, dans ces conditions, conduit à la formation de 0.59 mol de formaldéhyde (12, 13), sous forme de son hémiacétal.

Les résultats exposés au tableau 3 indiquent clairement que l'électrolyse d'une mole d'ozonide de styrène aboutit à la formation d'une mole d'aldéhyde benzoïque et d'une mole d'aldéhyde formique.

Influence de la hauteur de la colonne de mercure

La proportionalité, observée au moyen d'un courant continu d'analyse, entre le courant limite et la hauteur (H) de la colonne de Hg, corrigée pour la tension interfaciale à la surface des gouttes de Hg (14), montre que ce courant est contrôlé par diffusion. Il s'est avéré nécessaire d'utiliser du bleu de méthylène pour supprimer les légers maxima qui apparaissent en polarographie lente. Il est à noter, cependant, que ces maxima disparaissent dès que la polarographie rapide ou à courant alternatif est utilisée.

Influence de la vitesse de balayage

Les courants maximum des oscillo-polarogrammes $i = f(E)$ ont été mesurés pour des vitesses de balayage comprises entre 0.5 et 25 V/s. Ainsi que le montre la fig. 2, les courants i_{max} sont linéairement reliés à la racine carrée de la vitesse de balayage, ce qui est caractéristique pour un courant contrôlé par diffusion, dans le cas d'un processus irréversible (15, 16). Le courant obéit alors à la relation:

$$i_{max} = k_2 qn(\alpha n_a)^{1/2} C D^{1/2} v^{1/2} \quad \text{(Ampère)}$$

Pour tous les ozonides étudiés, une légère influence de la vitesse de balayage sur les potentiels de demi-vague est également observé. Ces

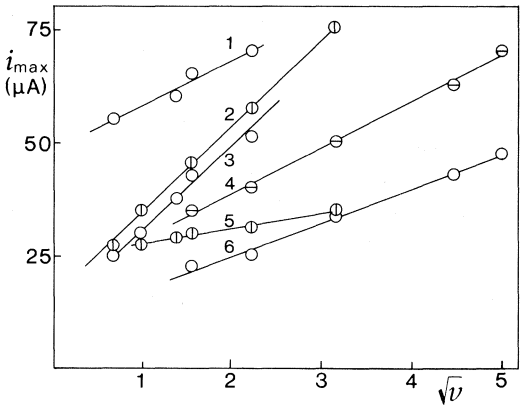

FIG. 2. Dépendance de i_{max} en fonction de la racine carrée de la vitesse (V/s) de balayage pour les ozonides du *p*-méthylstyrène (*1*), du *p*-méthoxystyrène (*2*), du *p*-bromostyrène (*3*), du styrène (*4*), du *p*-chlorostyrène (*5*), et du stilbène (*6*).

potentiels sont, en effet, d'autant plus déplacés vers les valeurs plus négatives que la vitesse de balayage est augmentée. En général, les potentiels sont plus négatifs d'environ 0.10 à 0.15 V pour $v = 25$ V/s qu'avec $v = 0.5$ V/s.

Influence de la température

L'influence de la température sur les pics polarographiques a été étudiée dans le domaine allant de 10 à 40 °C. Aucun effet notable n'a été relevé en ce qui a trait aux potentiels de demi-vague. Quant aux intensités de courants, leur dépendance de la température est illustrée par la fig. 3.

Les coefficients de température moyens, c'est-à-dire l'accroissement du courant par °C d'élévation de la température, rapportés à l'intensité de courant observée à 25 °C, dépendent de la nature de l'ozonide étudié (tableau 4).

Le sens de variation observé est l'inverse de ce à quoi on aurait pu s'attendre d'après les potentiels de demi-vague. La plus grande valeur observée,

Can. J. Chem. Downloaded from www.nrcresearchpress.com by 210.87.254.5 on 09/05/12
For personal use only.

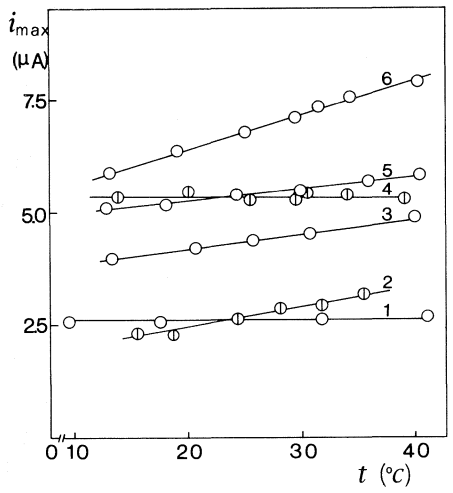

FIG. 3. Effet de température pour les ozonides du stilbène (*1*), du *p*-méthoxystyrène (*2*), du styrène (*3*), du *p*-bromostyrène (*4*), du *p*-chlorostyrène (*5*), et du *p*-méthylstyrène (*6*).

TABLEAU 4. Coefficients de température moyens pour la réduction des ozonides $R_1—C_6H_4—CH(O_3)CH—R_2$

R_2	R_1	Coefficients de température (%/°C)
H	*p*-CH_3O	1.8
	p-CH_3	1.1
	H	0.80
	p-Cl	0.50
	p-Br	0
C_6H_5	H	0

soit 1.8% par °C, correspond à celle indiquée par Zuman (17) pour le coefficient de température d'un courant contrôlé par diffusion.

Mécanisme proposé

L'ensemble des résultats expérimentaux suggère le mécanisme de réaction exposé ci-après (éq. 1);

[1] 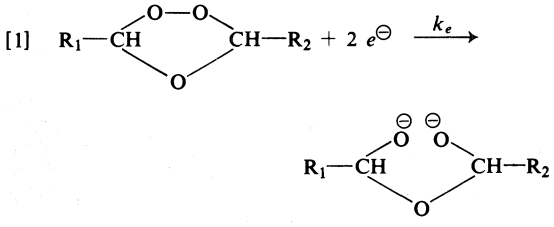

avec, pour les ozonides des styrènes substitués, $R_1 = RC_6H_4$ ou H, $R_2 =$ H ou RC_6H_4, et, pour l'ozonide du stilbène, $R_1 = R_2 = C_6H_5$.

L'étape 1 est bien confirmée par la corrélation des potentiels de demi-vague avec les constantes σ de Hammett (fig. 1) avec une pente ρ positive, ce qui montre que l'étape déterminante est une réaction nucléophile et exclut toute attaque électrophile précédent le transfert d'électrons en tant que processus déterminant la réaction.

L'étape suivante n'a, cependant, pas pu être précisée. Il est possible, en effet, d'expliquer la formation des produits observés par les réactions 2 et 3 ou, plus vraisemblablement, par une monoprotonation du dianion, selon la réaction 4.

[2] 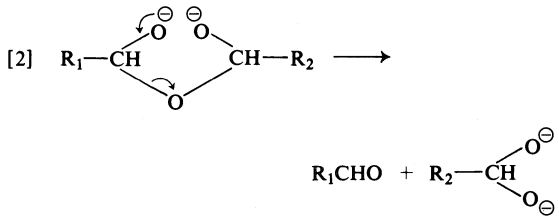

[3] 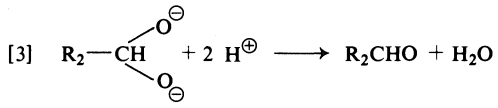

[4] 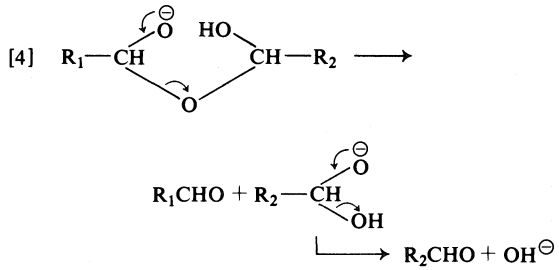

Il eut été intéressant d'étudier le comportement du potentiel de demi-vague et du courant limite en fonction du p*H*, en vue de mieux établir ces mécanismes. Cependant, en raison de la fragilité des ozonides et du milieu devant être employé, cette étude n'a pas pu être accomplie. Un essai a été effectué en utilisant un tampon constitué d'acide acétique et d'éthanolamine. Il s'est avéré que l'ozonide est rapidement décomposé dans ce milieu: environ 35% par heure, ce qui est attesté par la rapide décroissance du pic polarographique de l'ozonide. De plus, dans ce milieu, l'aldéhyde aromatique est réduit en deux étapes dans le domaine de p*H* compris entre p*H* 5 et 10 et l'un des deux pics de l'aldéhyde est très proche de

Can. J. Chem. Downloaded from www.nrcresearchpress.com by 210.87.254.5 on 09/05/12
For personal use only.

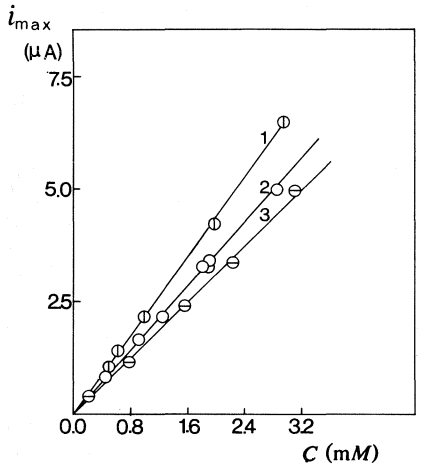

FIG. 4. Dépendance de i_{max} (μA) en fonction de la concentration C (mM) en ozonide du *p*-méthylstyrène (*1*), du *p*-bromostyrène (*2*), et du stilbène (*3*).

celui de l'ozonide, gênant ainsi considérablement les mesures.

Influence de la concentration en dépolariseur

L'intensité des courants limites a été étudiée en fonction de la concentration en ozonide, dans le benzène–méthanol (1:1) en présence de LiCl 0.5 *M*. Ainsi que l'indique la fig. 4, les intensités de courant enregistrés en polarographie à courant alternatif sont linéairement reliées aux concentrations en ozonide. Un contrôle soigneux des conditions expérimentales, en ce qui a trait, notamment, à la température, la pureté des solvants et le temps de dégazage, permet d'atteindre une reproductibilité satisfaisante ($\Delta i_{max} \leqslant 2\%$), ce qui permet des applications analytiques. Ainsi, dans le cas des ozonides des styrènes substitués où il n'y a pas de possibilité d'isomérie *cis–trans* et, par ailleurs, dans tous les cas où les proportions relatives des ozonides isomères *cis–trans* ne sont pas requises, la polarographie se révèle une méthode de dosage des ozonides, précise et très rapide.

Partie expérimentale

Les spectres de r.m.n. des ozonides préparés ont été enregistrés au moyen d'un spectromètre Jeolco C-60-H, en solution dans le tétrachlorure de carbone, en utilisant le tétraméthylsilane comme référence interne. Les spectres d'absorption i.r. ont été enregistrés au moyen d'un spectromètre Perkin–Elmer 621, en utilisant des solutions d'ozonide dans le tétrachlorure de carbone. Les analyses élémentaires ont été effectuées par le Dr. C. Daesslé (Organic Microanalyses, Montréal).

Produits utilisés

L'ozonide du stilbène (p.f. 74 °C) a été préparé selon Criegee *et al.* (18). Les ozonides **1–4** ont été préparés et purifiés selon (19) et les ozonides **5** et **6** ont été obtenus de manière similaire. L'ozonide du *p*-bromostyrène fond vers 15 °C.

Anal. calc. pour $C_8H_7O_3Br$: C, 41.58; H, 3.06; Br, 34.59. Trouvé: C, 41.42; H, 2.99; Br, 34.63.

Spectre r.m.n. (δ) dans le CCl_4: H_2, H_6, 7.58; H_3, H_5, 7.33; H_β, 5.95; H_α, 5.29; $H_{\alpha'}$, 5.24; J_{ortho} 8.0 Hz.

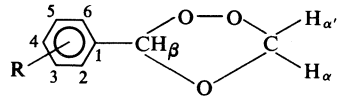

L'ozonide du *m*-nitrostyrène, liquide à la température ambiante, a donné l'analyse suivante.

Anal. calc. pour $C_8H_7O_3N$: C, 48.73; H, 3.58; N, 7.10. Trouvé: C, 48.80; H, 3.60; N, 6.90.

Spectre r.m.n. (δ) dans le CCl_4: H_2, H_4, 8.30; H_5, H_6, 7.75; H_β, 6.20; H_α, 5.43; $H_{\alpha'}$, 5.34. Les spectres r.m.n. d'une série d'ozonides de styrènes substitués dans le noyau ont fait l'objet d'une discussion antérieure (19). La position (*cis* ou *trans*) de H_α (ou de $H_{\alpha'}$) par rapport au cycle aromatique n'a pas pu être précisée à partir des présentes données expérimentales.

Polarographie

Les courbes intensité-potentiel ont été enregistrées à l'aide d'un polarographie Metrohm E-261-R. Cet appareil offre la double possibilité d'une analyse au moyen d'un voltage continu croissant linéairement ou d'une analyse à l'aide d'une tension alternative de faible amplitude surimposée au voltage continu d'analyse. Cette dernière technique, développée par Breyer *et al.* (20), a été utilisée dans la majeure partie du présent travail. La fréquence de la tension alternative utilisée a été de 60 Hz, et son amplitude de 50 mV. L'électrode à goutte de mercure était constituée d'un capillaire dont le mouvement de translation verticale, commandé par un électroaimant, assure un temps de goutte de 1/6 s pour un flux de mercure de 8.7 mg/s. L'électrode de référence était constituée d'un fil d'argent plongeant dans une solution d'électrolyte saturée en AgCl, séparée de la solution à analyser par un verre fritté fin. L'électrode auxiliaire était une électrode de tungstène commerciale.

La cellule de polarographie, d'une capacité utile de 25 ml, était munie d'une enceinte extérieure permettant une circulation d'eau à température constante. Le dégazage a été effectué à l'aide d'un courant d'azote saturé en solvant. La procédure polarographique consistait à placer 25 ml de solvant (benzène–méthanol, 1:1, LiCl 0.5 *M*) dans la cellule. Après un dégazage par un courant de N_2 (5 min), 1 ml de solution d'ozonide est ajouté. Après un deuxième dégazage le polarogramme est enregistré. Le benzène avait été purifié par un chauffage au reflux pendant 4 h, en présence de sodium, suivi d'une distillation. Le méthanol a été purifié par un chauffage au reflux en présence de copeaux de magnésium, pendant 4 h, suivi d'une distillation.

Oscillo-polarographie

Les oscillo-polarogrammes ont été obtenus à l'aide d'un appareillage comprenant: un générateur de tension

Can. J. Chem. Downloaded from www.nrcresearchpress.com by 210.87.254.5 on 09/05/12
For personal use only.

Can. J. Chem. Downloaded from www.nrcresearchpress.com by 210.87.254.5 on 09/05/12
For personal use only.

triangulaire Tacussel, un potentiostat Wenking-121, un oscilloscope Tektronix "Dual-Beam 502-A" muni d'une entrée différentielle X-Y et d'une boîte de résistance. Cet appareillage permet un balayage simple ou répétitif par une tension triangulaire. La gamme de vitesses de balayage va de quelques centièmes à quelques milliers de V/s. Pour l'étude du courant maximum en fonction de la racine carrée de la vitesse de balayage, un domaine restreint de vitesses intermédiaires allant de 0.5 à 25 V/s a été utilisé. L'utilisation de vitesses supérieures à 200 V/s a permis de noter l'apparition d'un léger pic anodique. Les électrodes utilisées sont les mêmes que celles décrites précédemment. Le temps de goutte a été ramené à 4 s.

Electrolyse à potentiel contrôlé

Les électrolyses ont été effectuées dans une cellule à trois compartiments, séparés par des verres frittés. La cellule était plongée dans un bain de glace afin de réduire la décomposition des ozonides. L'électrode de travail était constituée d'une nappe de mercure agitée au moyen d'un agitateur magnétique. L'électrode de contrôle était constituée d'un fil d'argent. L'électrode auxiliaire était une électrode de platine, immergée dans le compartiment central contenant du benzène–méthanol 1:1, 0.5 *M* en LiCl. La solution à électrolyser avait un volume de 75 à 100 ml.

Le solvant est dégazé par du N_2 et électrolysé au potentiel devant être utilisé par la suite pour l'ozonide, pendant 1 h ou jusqu'à la stabilisation du courant résiduel (0.1–0.3 mA). L'ozonide est ensuite ajouté et la solution est à nouveau dégazée pendant 10 min. Le courant d'azote est maintenu au-dessus de la solution durant toute la durée de l'électrolyse.

La tension était appliquée à l'aide d'un potentiostat Tacussel PRT-20, 2X. Le courant d'électrolyse a été noté au moyen d'un milliampèremètre, alors que son logarithme a été enregistré au moyen d'un enregistreur galvanométrique Graphispot GR VAC 2594, par l'intermédiaire d'un amplificateur à réponse logarithmique Logalex 0.1 A 8540 de Tacussel.

L'électrolyse de l'ozonide du stilbène a été effectuée sur des volumes d'environ 75–100 ml de solutions 5×10^{-3} à 10^{-2} *M* en ozonide. Le potentiel appliqué était de -1.2 V et la durée de l'électrolyse était de 1 à 2 h. A la fin de l'électrolyse, indiquée par un courant d'électrolyse proche de la valeur du courant résiduel et par un polarogramme ne présentant plus de pic à 0.87 V, un échantillon de 5 µl de la solution électrolysée a été analysé en chromatographie en phase gazeuse, au moyen d'un chromatographe F & M 5750 muni d'une colonne "Silicone-Rubber UCW-98" de 6 pd, à 100 °C. Les analyses ont bien confirmé que le temps de rétention du pic obtenu est identique à celui d'un échantillon authentique d'aldéhyde benzoïque. Le dosage de l'aldéhyde benzoïque au moyen de son pic polarographique révèle un rendement supérieur à 190% par rapport à l'ozonide consommé, ce que indique bien la formation de 2 mol d'aldéhyde par mole d'ozonide électrolysée.

L'électrolyse de l'ozonide du styrène a été effectuée dans les mêmes conditions que celles décrites pour l'ozonide du stilbène. L'analyse en c.p.g. a encore permi d'identifier et de doser l'aldéhyde benzoïque. Un autre échantillon de 5 µl de solution électrolysée, injectée sur une colonne "Carbowax 20M" de 6 pd à 30 °C permet l'identification de l'hémiacétal du méthanal, par comparaison du temps de rétention du pic obtenu avec celui d'une solution de styrène ozonée dans le méthanol. Le dosage de l'hémiacétal du méthanal a été effectué par comparaison des aires du pic de la solution électrolysée avec celui d'une solution de référence. La solution de référence a été préparée en ozonant 0.0171 g de styrène dans 25 ml de méthanol à -20 °C. Compte tenu du sens de clivage du styrène (13) qui est de 59% en faveur du méthanal, il se forme ainsi 3.88×10^{-3} *M* en hémiacétal de méthanal. Ces dosages ont révélé la formation d'une mole de chacune des aldéhydes par mole d'ozonide électrolysée.

Influence de la température et de la hauteur de la colonne de mercure

Ces deux études doivent être effectuées à l'aide d'un même échantillon d'ozonide dans tout le domaine de température ou de hauteur de colonne. Pour obtenir des mesures valables et reproductibles, il faut, avant chaque mesure, stabiliser soit la température, soit la hauteur de la colonne de mercure. La décomposition lente de l'ozonide exclut la possibilité de mettre un échantillon dans la cellule et d'effectuer toutes les mesures à l'aide de cet échantillon.

La méthode qui a donné les meilleurs résultats consiste à préparer une solution de base de 25 ml d'ozonide en utilisant comme solvant du benzène additionné d'un peu de méthanol (~1 ml). Cette solution est conservée dans la glace, à l'abri de la lumière. Pour chaque mesure, les conditions sont bien équilibrées avec 25 ml de solvant de polarographie. Ensuite 1 ml de la solution de base est ajouté. Après un dégazage, la mesure est enregistrée. Il a été vérifié que la solution de base reste inchangée durant une journée et que les premières mesures, reprises en fin de journée, redonnent les mêmes valeurs, aux erreurs expérimentales près. Il a également été vérifié que des polarogrammes pratiquement identiques, aux erreurs expérimentales près, sont enregistrés immédiatement après le dégazage de la solution et après un délai d'environ 3–5 min. Cette vérification permet de conclure que les coefficients de température observés (tableau 4) ne sauraient être imputés à une erreur due à la lente décomposition des ozonides.

Nous tenons à remercier M. le Dr. J. Carles de son aide précieuse lors de la préparation de quelques ozonides, ainsi que le Conseil National de Recherches du Canada pour une subvention qui a permis cette recherche.

1. L. S. SILBERT. J. Am. Oil Chem. Soc. **39**, 480 (1962).
2. A. H. M. COSIJN. Chem. Weekbl. **60**, 585 (1964).
3. M. BERNARD. Parfums, Cosmet., Savons, **1**, 467 (1958).
4. E. J. KŮTA et F. W. QUACKENBUSH. Anal. Chem. **32**, 1069 (1960).
5. J. RENARD et S. FLISZÁR. Can. J. Chem. **47**, 3333 (1969).
6. S. FLISZÁR et J. RENARD. Can. J. Chem. **48**, 3002 (1970).
7. G. KLUTSCH, J. GRIGNON, J. RENARD, et S. FLISZÁR. Can. J. Chem. **48**, 1598 (1970).
8. C. O. WILLITS, C. RICCIUTI, H. B. KNIGHT, et D. SWERN. Anal. Chem. **24**, 785 (1952).

9. P. ZUMAN. Substituent effects in organic polarography. Plenum Press, New York, N.Y., 1967. p. 97–98.
10. J. HEYROVSKÝ et J. KŮTA. Principles of polarography. Academic Press Inc., New York, N.Y., 1966, p. 277; G. A. GILBERT et E. K. RIDEAL. Trans. Faraday Soc. **47**, 396 (1951).
11. D. A. SKOOG et A. B. H. LAUWZECHA. Anal. Chem. **28**, 825 (1956).
12. P. ZUMAN. Organic polarographic analysis. Pergamon Press Ltd., New York, N.Y., 1964. p. 12–13.
13. S. FLISZÁR. Can. J. Chem. **44**, 2351 (1966); S. FLISZÁR et M. GRANGER. J. Am. Chem. Soc. **91**, 3330 (1969).
14. P. ZUMAN. Organic polarographic analysis. Pergamon Press Ltd., New York, N.Y., 1964. p. 23.
15. P. DELAHAY. J. Am. Chem. Soc. **75**, 1190 (1953).
16. H. MATSUDA et Y. AYABE. Z. Elektrochem. **59**, 494 (1955); J. HEYROVSKÝ et J. KŮTA. Principles of polarography. Academic Press, New York, N.Y., 1966. p. 505.
17. P. ZUMAN. Progress in physical organic chemistry. Vol. 5. Interscience Publishers Inc., New York, N.Y., 1967, p. 134.
18. R. CRIEGEE, A. KERCHOV, et H. ZINKE. Chem. Ber. **88**, 1878 (1955).
19. J. CARLES et S. FLISZÁR. Can. J. Chem. **48**, 1309 (1970).
20. B. BREYER, F. GUTMAN, et H. H. BAUER. Oesterr. Chem. Ztg. **57**, 67 (1956); B. BREYER, F. GUTMAN, et S. HACOBIAN. Aust. J. Sci. Res. Ser. **3**, 558 (1950).

Can. J. Chem. Downloaded from www.nrcresearchpress.com by 210.87.254.5 on 09/05/12
For personal use only.

Can. J. Chem. Downloaded from www.nrcresearchpress.com by 210.87.254.42 on 09/05/12
For personal use only.

Transannular Cyclizations of 6-Substituted Cyclodecynes[1]

R. J. Balf, Balaji Rao, and Larry Weiler[2]

Department of Chemistry, University of British Columbia, Vancouver 8, British Columbia

Received June 3, 1971

A series of 6-substituted cyclodecynes has been synthesized and the transannular cyclizations of these compounds were studied. The observed transannular cyclizations were highly stereoselective and give products containing the bicyclo[4.4.0]decane skeleton.

Une série de cyclodécynes substitués en position 6 a été synthétisée et les cyclisations *trans*-annulaires de ces composés ont été étudiées. Les cyclisations *trans*-annulaires observées sont très stéréosélectives et conduisent à des produits contenant le squelette du bicyclo[4.4.0] décane.

Canadian Journal of Chemistry, **49**, 3135 (1971)

Transannular reactions in medium-sized rings have been an area of extensive study for the past 15 years (1). We were interested in the transannular cyclizations of suitably substituted ten-membered rings as a new synthetic route to bicyclo[4.4.0]decanes and/or bicyclo[5.3.0]decanes. In particular we hoped to take advantage of the known susceptibility of the acetylenic bond to both electrophilic and nucleophilic attack (2). This is summarized in eq. 1. Most transannular

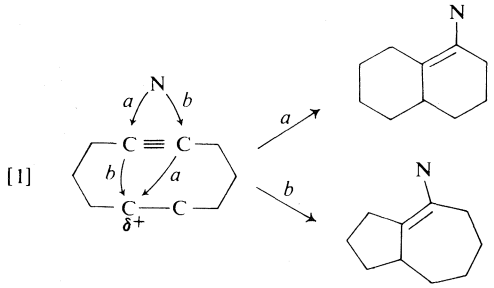

[1]

reactions in ten-membered rings appear to favor transition states involving six-membered rings (1, 3). However, the decomposition of cyclodecyl tosylhydrazone in an aprotic solvent yielded bicyclo[5.3.0]decane as the major product (4) and the peracid oxidation of cyclodecyne yielded *cis*-bicyclo[5.3.0]decan-2-one (5). Pyrolysis of epoxide **1** gave the aldehyde **2** (6). A transannular

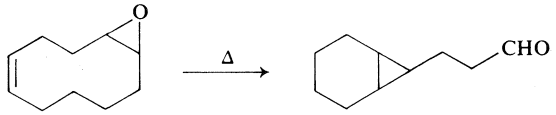

1 **2**

cyclization to a bicyclo[5.3.0]decane has been proposed for this and other related rearrangements of sesquiterpene epoxides (6, 7). On the other hand the solvolysis of *cis*- and *trans*-cyclodec-5-en-1-yl tosylates gave products containing the bicyclo[4.4.0]decane skeleton only (1, 8), indicating that these transannular reactions occur via six-membered ring transition states. The report that the solvolysis of 6-octyn-2-yl tosylate in trifluoroacetic acid proceeded preferentially to products containing a cyclopentane ring (9) suggested that the related 6-substituted cyclodecynes may undergo transannular cyclizations to bicyclo[5.3.0]decanes. However, solvolysis of cyclodec-5-yn-1-yl tosylate has recently been found to yield predominantly *cis*- and *trans*-decalone-1 together with small amounts of bicyclo[5.3.0]decanone-2 (10).

Our initial studies were concerned with cyclodecyn-6-one **3** (11).[3] Ketone **3** was stable to

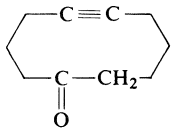

3

treatment with aqueous base. However, on treatment with aqueous acid the acetylenic ketone **3** gave an isomeric α,β-unsaturated ketone in high yield. It was quickly ascertained that this product was the octalone **4** by comparison of the spectroscopic properties and the v.p.c.

[1]A preliminary communication of a portion of this work has appeared. See ref. 27.

[2]Address correspondence to this author.

[3]We are grateful to Dr. Tanabe for a reference sample of **3** and spectral data as well as the details for the preparation of **3**.

retention times of the two materials. A sample of ketone **5** was prepared (12) and compared to the product from **3** and an authentic sample of **4**.

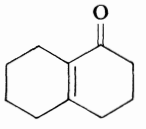

4

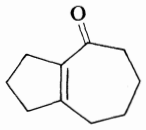

5

The ketones **4** and **5** could be clearly separated by v.p.c. and they had several differences in their i.r. spectra. When we carefully scrutinized the crude reaction mixture from the acid treatment of **3**, we could not find any trace of **5**. Several proton acids were found to be efficient catalysts in the isomerization of **3** to **4**. Lewis acids in aprotic solvents were also effective, for example, treatment of **3** with $BF_3 \cdot Et_2O$ in methylene chloride gave **4** in *ca.* 60% yield. We also studied the effect of solvent polarity on this isomerization. Although the isomerization was slower in nonpolar solvents, the yields of product **4** isolated were good (60–95%). One of the better procedures involves treating **3** with HCl in aqueous methanol to yield 95% **4**. In all of the above experiments we examined the crude reaction product for ketone **5** and in no case could any trace of **5** be detected in the reaction mixture. Furthermore, it was easy to show that ketone **5** is stable under these reaction conditions. All attempts to ketalize **3** gave only **4** and further reaction products of **4**.

The Birch reduction of open-chain γ-ethinyl ketones has been found to give only five-membered ring products (13). Hence we were interested in the course of this reduction of cyclodecyn-6-one **3**, since it is a cyclic γ-ethinyl ketone. On treatment with lithium in ammonia–tetrahydrofuran (13) **3** gave a mixture of the allylic alcohols **6** and **7** in the ratio of *ca.* 25:1 (*vide infra*) in excellent yield. These alcohols

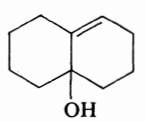

6

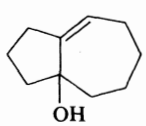

7

were rather prone to decompose and hence they were difficult to separate and fully characterize. For this reason these alcohols were oxidized in ethyl ether with aqueous chromic acid (14) to yield a mixture of **4** and **5** which could be readily separated and identified. This oxidative transformation and the spectral data of the alcohol **6** fully confirmed the structure of the major reduction product from **3**. A slight ambiguity existed in the case of the minor reduction product since structure **8** could be consistent with the spectral properties of this product.

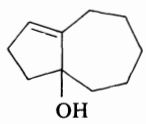

8

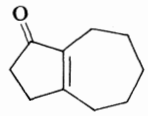

9

However, we rejected structure **8** by the fact that formation of **8** from **3** was unlikely on mechanistic grounds (13 and *vide infra*) and that the oxidative rearrangement of **8** to **5** was also unlikely. Alcohol **8** would be expected to give ketone **9** on oxidation. As the ketones **4** and **5** were separable by v.p.c. we used the ratio of **4**:**5** to estimate the ratio of alcohols in the reduction product from **3** since the alcohols themselves were not separable by the usual chromatographic techniques. Again the transannular cyclization of a cyclodecyne had occurred predominantly through a six-membered ring transition state; although in this case we did obtain a detectable amount of product arising from a five- (or seven-) membered transition state. This was consistent with the other transannular reactions of **3** but markedly different from the analogous reduction of open-chain compounds (13).

Reduction of cyclodecyn-6-one (**3**) with lithium aluminum hydride or sodium borohydride gave cyclodecyn-6-ol (**10**) in high yield.

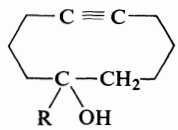

10 R = H
11 R = Me

Treatment of **3** with methyllithium or methylmagnesium bromide gave the alcohol **11**. No transannular products could be detected either spectroscopically or chromatographically. Therefore the carbonyl group in **3** is more nucleophilic in hydride reduction than the acetylenic

Can. J. Chem. Downloaded from www.nrcresearchpress.com by 210.87.254.42 on 09/05/12
For personal use only.

Can. J. Chem. Downloaded from www.nrcresearchpress.com by 210.87.254.42 on 09/05/12
For personal use only.

group. In fact we have not found a nucleophilic H, C, N, or O which will add to the triple bond in **3** before it attacks the carbonyl group. On treatment with excess dimethyllithium cuprate ketone **3** was recovered unchanged.

Treatment of cyclodecyn-6-ol (**10**) with refluxing methanolic HCl gave a good yield of *cis*- and *trans*-decalone-1 (**12** and **13**). We could not detect any of the isomeric bicyclo[5.3.0]decanone-2 (**14**) by v.p.c. The results differ slightly from the

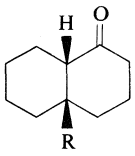

12 R = H
18 R = Me

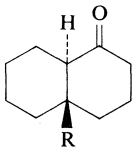

13 R = H
19 R = Me

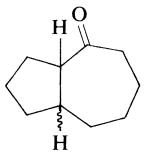

14

solvolysis and acetolysis of the tosylate from **10** which gave **12** and **13** as well as small amounts of *cis* and *trans*-**14** or either enol acetates (10). Since variation in solvent polarity did not effect the formation of **14** in the solvolysis experiments we cannot ascribe the difference between the solvolysis experiment (10) and the acid treatment of **10** to solvent effects.

When alcohol **10** was treated with $BF_3 \cdot Et_2O$ in methylene chloride a single very volatile product was obtained in good yield. The material was homogenous by t.l.c. and v.p.c., and no other product could be detected chromatographically or spectroscopically. Initially the spectroscopic data was confusing because of the presence of a band at 1705 cm^{-1} in the i.r. spectrum of the product. The molecular formula of this compound was established as $C_{10}H_{15}F$ by high resolution mass spectroscopy. The ^1H n.m.r. spectrum has a broad absorption between δ 1–3 and no other signals. The ^{19}F n.m.r. of the product has a relatively sharp singlet at 111 p.p.m. upfield from CCl_3F. These n.m.r. data are consistent with an olefinic fluorine (15) and the i.r. band at 1705 cm^{-1} is assigned to the double bond stretch of the fluoro olefin (15*b*, 16). The spectral data favor structure **15** for the fluoro olefin but they do not totally eliminate structure **16**. The ^{19}F n.m.r. data for a series of 1-fluorocycloalkenes are given in Table 1 (15*b*). Comparing the ^{19}F chemical shift and the J_{CH_2-CF} in the fluoro olefin from **10** with the data for the simple systems leads to the conclusion that these

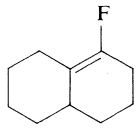

15

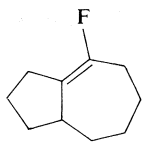

16

n.m.r. parameters favor the structure with the double bond in the smaller ring (15) for the fluoro olefin. This is further evidence of the homogeneity of the fluoro olefin, since **15** and **16** would be expected to show markedly shifted ^{19}F resonances.

To prove which structure was correct, **15** or **16**, we degraded the fluoro olefin in the following manner. The olefin was ozonized and the ozonide was worked-up oxidatively to give a keto acid with i.r. bands at 1705 and 1725 cm^{-1}. This is not consistent with a substituted cyclopentanone. In addition the acid was esterified to yield an ester with i.r. bands at 1705 and 1735 cm^{-1}. This ester was compared with an authentic sample of methyl 2-oxocyclohexylbutyrate **17** (17) which was prepared by the alkylation of the enamine from cyclohexanone

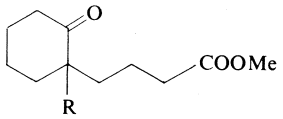

17 R = H
24 R = Me

with methyl γ-iodobutyrate. The two compounds were identical by spectroscopic data, v.p.c. retention times, and m.p. and mixed m.p. of their 2,4-DNP derivatives. Thus the fluoro olefin must have structure **15**. The chromatographic properties of **17** from the degradation of **15** again indicated that the fluoro olefin was a single compound.

The tertiary alcohol **11** was also treated with refluxing methanolic HCl and a mixture of ketones was isolated in reasonable yield. This

TABLE 1. The ^{19}F n.m.r. data for 1-fluorocycloalkenes (15*b*)

Compound	F(p.p.m.)*	$J_{CH_2-CF=C}$ (Hz)
1-Fluorocyclopentene	122.7	Small
1-Fluorocyclohexene	101.7	?
1-Fluorocycloheptene	91.1	11.5

*The ^{19}F chemical shifts are p.p.m. from CCl_3F.

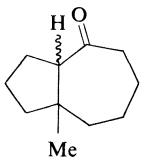

20 *cis*
21 *trans*

mixture consisted of **18**, **19**, **20**, and **21**. All four compounds could not be separated by v.p.c.; but by using a combination of v.p.c. and n.m.r. we were able to measure the relative amount of each isomer in the mixture. This transannular cyclization again was quite clean and free from side reactions. The ratios of **18**:**19** and **20**:**21** may be equilibrium values since they did not appear to change on prolonged acid treatment. We have not, as yet, investigated the reaction mixture at short reaction times to determine if the cyclization leads to a preference of either *cis* or *trans* isomer.

An authentic sample of the *cis* and *trans* isomers, **18** and **19**, was prepared by the conjugate addition of lithium dimethylcopper to the octalone **4** (18).[4] The conjugate addition yielded a predominance of the *cis* isomer **18**. These isomers could be equilibrated by acid or base and the *cis–trans* mixture was separable by v.p.c. The *cis* isomer **18** has an n.m.r. singlet at δ 1.02 and the *trans* isomer **19** has an n.m.r. singlet at δ 0.77 due to the angular methyl group. These assignments are in accord with n.m.r. signals for the C-19 methyl group in 5β-androstanone-4 (δ 1.12) and 5α-androstanone-4 (δ 0.74) (19). A sample of the *cis* and *trans* isomers, **20** and **21**, was prepared by the conjugate addition of lithium dimethylcopper to $\Delta^{1,7}$-bicyclo[5.3.0]-decanone-2 (**5**). These two isomers could also be separated by v.p.c. The *cis* isomer **20** has an n.m.r. singlet at δ 1.18 and the *trans* isomer **21** has an n.m.r. singlet at δ 0.72 due to the angular methyl group. All four isomers **18**–**21** could not be separated by v.p.c., however, by using a combination of v.p.c. and the intensity of the n.m.r. signals assigned to the angular methyl group in **18**–**21** we have found that the ratio of **18**:**19**:**20**:**21** from the acid-catalyzed cyclization of **11** was 1.0:1.4:0.1:0.25. This is the only example of transannular reactions of cyclodecynes in which we have found a significant amount of product resulting from cyclization through a five-membered ring transition state.

When alcohol **11** was treated with $BF_3 \cdot Et_2O$ in methylene chloride we again isolated a fluoro olefin in high yield. The product was homogeneous by a variety of chromatographic and spectroscopic techniques. The ^1H n.m.r. of this product has no vinyl protons but it does have a singlet at δ 1.05 due to the angular methyl group. The ^{19}F n.m.r. shows a relatively sharp singlet 110 p.p.m. upfield from CCl_3F. There is an i.r. absorption at 1700 cm^{-1} which is assigned to a monofluoro tetrasubstituted double bond stretching (*vide supra*). Again in this case there are two possible structures for the fluoro olefin, either **22** or **23**. The spectral data and our

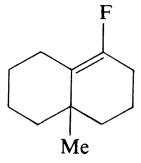

22

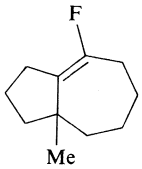

23

previous results led us to favor structure **22**. That is in fact the correct structure as proven by an oxidative sequence similar to that for compound **15**. Thus ozonolysis of the fluoro olefin from **11** and oxidative work-up gave a keto acid with a broad i.r. band at 1705 cm^{-1}. Esterification yielded methyl 1-methyl-2-oxocyclohexylbutyrate **24** which has i.r. bands at 1700 and 1730 cm^{-1}. No trace of the isomeric cyclopentanone which would arise from **23** could be found from the i.r. spectra of the keto acid and ester or from the v.p.c. of the ester.

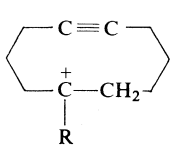

25

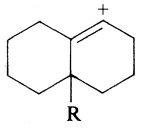

26

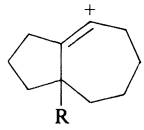

27

[4]We are grateful to Professor E. Piers and Miss W. M. Phillips for samples of **18** and **19**, and for their detailed experimental procedures.

Can. J. Chem. Downloaded from www.nrcresearchpress.com by 210.87.254.42 on 09/05/12
For personal use only.

Can. J. Chem. Downloaded from www.nrcresearchpress.com by 210.87.254.42 on 09/05/12
For personal use only.

If these cyclizations were to proceed via a free carbonium ion, **25**, then we would expect a preference for formation of **27** since the intermediary linear vinyl cation (9) should be more readily accommodated in a seven-membered ring (**27**) than a six-membered ring (**26**). It could be argued that **27** may be formed initially, and subsequently it rearranges entirely to **26**. However, recent evidence indicates that in fact **26** (R = H) rearranges to **27** (R = H) (20). Those reactions most likely to yield carbonium ions, for example, the solvolysis of the tosylate from **10** and acid treatment of **11** did lead to products which can be considered to arise from **27**. An examination of a molecular model of **3** or **10** suggests that C-1 and -2 are very nearly equidistant from C-6 and hence we might expect mixture of bicyclo[4.4.0]decanes and bicyclo-[5.3.0]decanes. However, we have found that there is a very strong preference for transannular cyclizations which proceed via a six-membered ring transition state. We feel that these cyclizations are essentially concerted, that is, the acetylene is simultaneously attacked by the electrophilic C-6 and an external nucleophile. Assuming that carbon atoms 1 and 2 approach sp^2 hybridization in the transition state for cyclization, then it appears, from models, that the transition state leading to the bicyclo[4.4.0]-decane skeleton has less steric interference and less torsional strain (21) than the transition state leading to the bicyclo[5.3.0]decane skeleton. Structure **28** is a Newman projection along

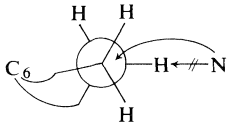

28

C-10, -1, -2, and -3. For *trans* coplanar addition of C-6 and a nucleophile to the triple bond it can be seen that one of the hydrogens on C-10 will sterically hinder the addition of the nucleophile to C-1; however, the nucleophile can add to C-2 with the two hydrogens on C-3 staggering it. This would explain the almost exclusive formation of products with a bicyclo[4.4.0]decane skeleton. Of course this does not explain the preponderance of **6** in the Birch reduction of **3**. Stork *et al.* (13*a*) have suggested that the Birch reduction of γ-ethinyl ketones involves a non-

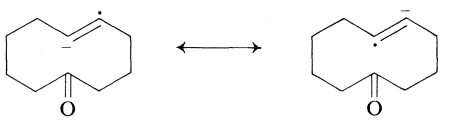

29

linear vinyl radical anion as an intermediate. Assuming that the analogous reduction of **3** involves a similar intermediate **29** then inspection of models of **29** shows a clear preference for formation of the six-membered ring product **6**. A related radical cyclization may be involved in the photochemical closure shown in eq. 2 (22).

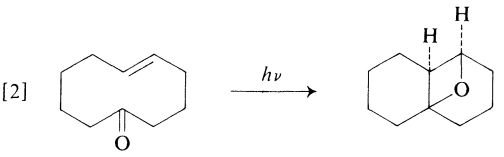

Experimental

Melting points were determined on a Kofler hot stage and are uncorrected. The i.r. spectra were recorded on a Perkin–Elmer model 700 and were calibrated using the 1601 cm^{-1} band of polystyrene. The ^1H n.m.r. spectra were recorded on either a Varian T-60 or Varian HA-100 and the ^{19}F n.m.r. spectra were recorded on a Varian T-60 equipped with a T-6-18 wide sweep module using CCl_3F as an internal standard. The mass spectra were obtained using an AEI MS-9 operating at 70 eV. Microanalyses were performed by Mr. Peter Borda, University of British Columbia. The v.p.c. analyses were performed with a Varian Aerograph 90-P-3 using column A, 5 ft × ¼ in. column of 3% SE 30 on Chromosorb W, and column B, 5 ft × ¼ in. column of 10% FFAP on Chromosorb W, or with a Perkin–Elmer Model 900 using column C, 5 ft × ⅛ in. column of 10% FFAP on Chromosorb W.

$\Delta^{1,7}$-Bicyclo[5.3.0]decenone-2 (5)

Compound **5** was prepared from $\Delta^{9,10}$-octalin by the method of Anderson and Nelson (12) to yield a product b.p. 114°/10 mm (lit. b.p. 126–128°/15 mm (12)).

Cyclodecyn-6-one (3)

A solution of 1.0 g (0.07 mol) of enone **5** in 20 ml of methanol was cooled in a water bath at 10° and treated with 10 ml of 30% hydrogen peroxide with stirring. A solution of 2 ml of 6 *N* sodium hydroxide in 5 ml of methanol was added dropwise over a period of ½ h and the resulting solution was stirred for an additional 15 h. The methanolic solution was diluted with 50 ml of water and extracted three times with methylene chloride. The extracts were combined, washed with brine solution until neutral, dried over anhydrous sodium sulfate, filtered, and the solvents were removed under reduced pressure. The residue was distilled at bath temperature 100°/0.6 mm to yield 0.82 g (74%) of 1,7-oxido-bicyclo[5.3.0]decanone-2.

A 1.61 g (0.097 mol) sample of the above epoxide was treated with tosylhydrazone under the conditions of

Can. J. Chem. Downloaded from www.nrcresearchpress.com by 210.87.254.42 on 09/05/12
For personal use only.

Schreiber *et al.* (11*b*) to yield cyclodecyn-6-one (**3**) which was distilled at a bath temperature of 55°/0.02 mm.

Acid Isomerization of Cyclodecyn-6-one (3)

(i) Methanolic Hydrochloric Acid

A 79 mg (0.53 mmol) sample of cyclodecyn-6-one (**3**) was dissolved in 1.5 ml of methanol containing one drop of concentrated hydrochloric acid and the solution was allowed to stand at room temperature for 12 h. Methanol was removed under reduced pressure, then the residue was dissolved in ether and washed with sodium bicarbonate solution. The organic extracts were dried over anhydrous sodium sulfate, filtered, and the solvents removed under reduced pressure. The residue was distilled at bath temperature of 70–80°/0.2 mm to yield 75 mg (95%) of octalone **4** which was compared by i.r. and v.p.c., column B, to an authentic sample of **4** prepared by the method of House and Thompson (23).

Compounds **4** and **5** were separated by v.p.c., column B, and no trace of **5** could be detected in crude reaction product above or in the sample of distilled **4**.

(ii) Boron Trifluoride Etherate in Methylene Chloride

A solution of 225 mg (1.5 mmol) of **3** in 10 ml of methylene chloride was treated with *ca.* 0.5 ml of boron trifluoride etherate. The solution was stirred and it turned dark green. After 10 min, the reaction mixture was washed with saturated aqueous sodium bicarbonate until the organic layer was colorless. The organic extracts were dried over anhydrous sodium sulfate, filtered, and the solvent removed under reduced pressure. The v.p.c. analysis, column B, showed only **4** to be present in the crude residue. This residue was distilled at bath temperature of 70–80°/0.2 mm to yield 133 mg (59%) of pure **4**.

(iii) Additional Conditions for Isomerization

The following conditions were also found to be effective in the isomerization of **3** to **4**: hydrochloric, hydrobromic, or perchloric acid in methanol, dioxane, or hexane at room temperature; refluxing acetic acid and zinc; *p*-toluenesulfonic acid in refluxing benzene; and mercuric chloride in refluxing methanol.

Attempted Ketalization of 3

A solution of 80 mg of **3**, 0.5 ml of ethylene glycol and a few crystals of *p*-toluenesulfonic acid in 50 ml of benzene was refluxed for 16 h. The benzene solution was washed with aqueous brine, dried over anhydrous sodium sulfate, filtered, and the solvent was removed under reduced pressure. A v.p.c., column B, and t.l.c. analysis indicated that the major component of the mixture was **4** and a small amount of unreacted **3**.

Birch Reduction of Cyclodecyn-6-one (3)

A solution of 165 mg (1.1 mmol) of **3** in 1 ml of dry tetrahydrofuran was added to 100 ml of liquid ammonia. The solution was stirred and very small pieces of lithium wire were added until a blue color persisted. Ammonium chloride was quickly added to render the solution colorless and the ammonia was allowed to evaporate. Water was added to the residue and the mixture was extracted with ethyl ether. The extracts were combined, washed with aqueous sodium chloride solution until neutral, dried over anhydrous sodium sulfate, filtered, and the solvents removed under reduced pressure to yield 168 mg of crude product. This semisolid showed no carbonyl absorption in the i.r. and it was sublimed at 25°/0.005 mm to give quantitative yield of product m.p. 61–69°; ν_{max} (CH_2Cl_2) 3580, 1605 cm^{-1}; δ (CCl_4) 5.4 (m, 1H), 1.2–2.6 (m, 15H); *m/e* calcd. for $C_{10}H_{16}O$: 152.1201; found: 152.1198; 152 (15%), 134 (58%), 119 (40%), 105 (52%), 91 (100%).

Oxidation of Alcohols from Birch Reduction of 3

The solution of the above alcohols from **3** (10 mg) in ethyl ether was added to an ice cold solution of 100 mg of chromium trioxide in 5 ml of water and 0.5 ml of concentrated sulfuric acid. The mixture was stirred for 2.5 h at 0° and then the ether layer was washed with water until neutral. The ether solution was dried over anhydrous sodium sulfate, filtered, and the solvent removed under reduced pressure to give an oily residue, ν_{max} ($CHCl_3$) 1650, 1630 cm^{-1}. This was analyzed by v.p.c., column C, and was found to contain **4** and **5** in the ratio of 25:1.

Cyclodecyn-6-ol (10)

Following the procedure of Hanack and Heumann (10) 15.2 mg (1.01 mmol) of **3** was reduced with lithium aluminum hydride (15 mg) in 10 ml of refluxing ethyl ether for 1½ h. The reaction mixture was cooled, treated with 5 ml of a saturated aqueous solution of potassium sodium tartrate, and the resulting mixture was stirred for 5 min. The aqueous layer was extracted with 2 × 20 ml of ethyl ether. The extracts were combined, dried over anhydrous sodium sulfate, filtered, and the solvents removed under reduced pressure. The residue was distilled at bath temperature of 85–90°/0.5 mm to yield 145 mg (94%) of **10**, ν_{max} (CH_2Cl_2) 3360 cm^{-1}; δ (CCl_4) 1.2–1.9 (m, 10H), 1.94 (b.s, 1H, exchangeable in D_2O), 2–2.4 (m, 4H), 4.2 (m, 1H).

6-Methylcyclodecyn-6-ol (11)

A solution of 1.7 g (0.011 mol) of **3** in dry tetrahydrofuran was treated dropwise with 7 ml of 2.3 *M* solution of methyllithium under nitrogen. After addition of methyllithium the solution was stirred for an additional 3½ h at room temperature. Excess methyllithium was decomposed with water. The aqueous layer was saturated with sodium chloride and extracted with ethyl ether. The extracts were combined, dried over anhydrous sodium sulfate, filtered, and the solvents removed under reduced pressure to yield an oily residue. This was purified by silica gel column chromatography using benzene – ethyl acetate (95:5 to 50:50) as eluant to give 500 mg (27%) of **11**. Due to its lability **11** could not be purified for combustion analysis; ν_{max} (film) 3390 cm^{-1}; δ ($CDCl_3$) 1.04 (s, 3H), 1.27 (s, 1H, exchangeable with D_2O), 1.2–1.8 (m, 10H), 1.9–2.4 (m, 4H); *m/e* 166 (8%), 151 (30%), 148 (26%), 133 (50%), 105 (52%), 91 (100%).

Acid Treatment of 10

A solution of 56 mg (3.71 mmol) of cyclodecyn-6-ol (**10**) and 2 drops of concentrated hydrochloric acid in 2 ml of methanol was refluxed for 3.5 h. The reaction mixture was poured into 30 ml of water and extracted with 30 ml of benzene – ethyl ether (1:1). The extracts were washed with 20 ml of saturated sodium bicarbonate solution and 20 ml of saturated sodium chloride, then dried over anhydrous sodium sulfate, filtered, and the solvents removed under reduced pressure. The residual oil was purified by preparative t.l.c. (silica gel – benzene – ethyl acetate, 9:1) to yield 8 mg of **10** and 42 mg (87%

Can. J. Chem. Downloaded from www.nrcresearchpress.com by 210.87.254.42 on 09/05/12
For personal use only.

based on unrecovered starting material) of decalones **12** and **13**. These were shown to be identical to authentic **12** and **13** by v.p.c., column C.

*cis- and trans-Decalone-1 (**12** and **13**)*

A mixture of **12** and **13** (24) was prepared by Birch reduction (Li, NH_3, NH_4Cl) of $\Delta^{9,10}$-octalone-1 (**4**) followed by Jones oxidation (25) of the 1-decol to **12** and **13**. The mixture so obtained was equilibrated as follows. A solution of 15 mg of **12** and **13** from above in 2 ml of methanol and 2 drops of 1 *N* sodium hydroxide was heated on a steam bath for 5 min and then diluted with 20 ml of water. The organic material was extracted with 20 ml of ethyl ether and the extracts were washed with saturated aqueous sodium chloride solution until the washings were neutral to litmus. These ketones were cleanly separable by v.p.c. on column B or C.

*cis- and trans-Bicyclo[5.3.0]decanone-2 (**14**)*

Birch reduction followed by Jones oxidation (25) of $\Delta^{1,7}$-bicyclo[5.3.0]decenone-2 (**5**) gave a mixture of isomers **14** which are equilibrated as above for **12** and **13**. Again the isomers **14** were separable by v.p.c. on column B or C.

*Treatment of **10** with Boron Trifluoride Etherate*

A solution of 190 mg (1.26 mmol) of cyclodecyn-6-ol (**10**) in 20 ml of dry methylene chloride was treated with 0.5 ml of boron trifluoride etherate and stirred at room temperature for 15 min. The brown reaction mixture was washed with saturated aqueous sodium bicarbonate until the organic layer became colorless. The methylene chloride solution then was dried over anhydrous sodium sulfate, filtered, and the solvents removed under reduced pressure. The very volatile residue was purified by preparative t.l.c. (silica gel – benzene) to yield 163 mg (85%) of fluoroalkene **15** which was homogeneous by v.p.c., columns B and C; ν_{max} (film) 1705 cm^{-1}; ^1H n.m.r. δ ($CDCl_3$) 1–3 (m); ^{19}F n.m.r. δ_{CCl_3F} (CCl_4) 111; *m/e* calcd. for $C_{10}H_{15}F$: 154.1158; found: 154.1102; 154 (10%), 135 (100%).

*Ozonolysis of **15***

A solution of 100 mg of **15** dissolved in 2 ml of methanol was cooled in a Dry Ice – acetone bath and ozone was passed through the solution until a light blue color appeared. The excess ozone was removed under reduced pressure. The ozonide solution was treated with 0.5 ml of 30% hydrogen peroxide and refluxed on a steam bath for 15 min. The reaction mixture was poured into 25 ml of water and extracted with 3 × 20 ml of ethyl ether. The extracts were combined, dried over anhydrous sodium sulfate, and the solvents removed under reduced pressure to yield crude 2-oxocyclohexylbutyric acid; ν_{max} ($CHCl_3$) 1705, 1725 cm^{-1}.

The crude acid was esterified with diazomethane and the resulting keto ester **17** was purified by t.l.c. (silica gel – chloroform) to give pure **17**; ν_{max} ($CHCl_3$) 1705, 1735 cm^{-1}. This was converted to its 2,4-DNP derivative m.p. 109–111°, mixed m.p. with 2,4-DNP of authentic **17** 108–111° (lit. m.p. 112° (17)).

*Methyl 2-Oxocyclohexylbutyrate (**17**)*

A 10.6 g (70 mmol) sample of the pyrrolidine enamine of cyclohexanone (26) was dissolved in 100 ml of dry ethanol and treated with 7.6 g (33.6 mmol) of methyl γ-iodobutyrate. This mixture was refluxed under nitrogen for 20 h. Then the solvent was removed under reduced pressure. The residue was stirred (5 min) with 20 ml of water and extracted with 50 ml of ethyl ether. The ethereal solution was washed with 3 × 10 ml of saturated sodium chloride solution (neutral to litmus), dried over anhydrous sodium sulfate, filtered, and the solvents removed under reduced pressure. The residue was distilled to yield 4 gm (60%) of **17** b.p. 60°/0.2 mm; ν_{max} ($CHCl_3$) 1710, 1730 cm^{-1}. A small portion was converted to its 2,4-DNP derivative, m.p. 110–113° (lit. m.p. 112° (17)).

*Acid Treatment of **11***

6-Methylcyclodecyn-6-ol (**11**) (20 mg) was dissolved in 2 ml of methanol containing one drop of concentrated hydrochloric acid and refluxed for 3.5 h. The mixture was diluted with 20 ml of water and extracted with 3 × 10 ml of ethyl ether. The extracts were combined, washed with 20 ml of saturated sodium bicarbonate solution, and 20 ml of saturated sodium chloride solution, dried over anhydrous sodium sulfate, filtered, and the solvents removed under reduced pressure. The residue was distilled, bath temperature of 85°/0.2 mm, to yield 13 mg (65%) of a mixture of ketones **18**, **19**, **20**, and **21** (v.p.c., columns B and C); ν_{max} ($CHCl_3$) 1705 cm^{-1}, no —OH stretch; δ (CCl_4) 0.72 (s), 0.77 (s), 1.03 (s), 1.20 (s).

*cis- and trans-7-Methylbicyclo[5.3.0]decanone-2 (**20** and **21**)*

Dimethyllithium cuprate was prepared from 571 mg (3.0 mmol) of dry cuprous iodide and *ca.* 4 ml of 2.3 *M* methyllithium in 100 ml of ethyl ether at 0°. A solution of 450 mg (3.0 mmol) of $\Delta^{1,7}$-bicyclo[5.3.0]decanone-2 (**5**) in 2 ml of dry ether was added dropwise under nitrogen to the cooled solution of dimethyllithium cuprate. After the addition was complete, the solution was stirred at 0° for an additional 2 h. The copper complex was decomposed with a saturated ammonium chloride solution and this mixture was stirred at room temperature for 1 h. The ether layer was separated, washed with saturated aqueous sodium chloride solution, dried over anhydrous sodium sulfate, filtered, and the solvents removed under reduced pressure. The residue was purified by preparative t.l.c. (silica gel – benzene) to yield 350 mg (70%) of **20** and **21**. This mixture of isomers was separated by v.p.c., column B; to give *cis*-7-methylbicyclo[5.3.0]decanone-2 (**20**) which distilled at bath temperature of 80°/0.2 mm; ν_{max} ($CHCl_3$) 1695 cm^{-1}; δ (CCl_4) 1.18 (s, 3H).

Anal. Calcd. for $C_{11}H_{18}O$: C, 79.47; H, 10.91. Found: C, 79.48; H, 10.83.

trans-7-Methylbicyclo[5.3.0]decanone-2 (**21**) was also obtained pure by v.p.c. This compound distilled at bath temperature of 82°/0.2 mm; ν_{max} ($CHCl_3$) 1695 cm^{-1}; δ (CCl_4) 0.72 (s, 3H).

Anal. Calcd. for $C_{11}H_{18}O$: C, 79.47; H, 10.91. Found: C, 79.43; H, 10.80.

*Treatment of **11** with Boron Trifluoride Etherate*

A solution of 222 mg (1.34 mmol) of 6-methylcyclodecyn-6-ol (**11**) and 0.5 ml of boron trifluoride etherate in 20 ml of dry methylene chloride was stirred at room temperature for 15 min. The resulting brown solution was washed with saturated aqueous sodium bicarbonate until the organic layer became colorless. Then the organic layer was dried over anhydrous sodium sulfate, filtered

and the solvents removed under reduced pressure. The volatile residue was purified by preparative t.l.c. (silica gel – benzene) to yield 191 mg (86%) of fluoroalkene **22**; ν_{max} (film) 1700 cm^{-1}; ^1H n.m.r. δ (CCl_4) 1.05 (s, 3H), 1.2–2 (m, 12H), 2.05 (d, $J \simeq 6$ Hz, 1H), 2.7 (d, $J \simeq 12$ Hz, 1H); ^{19}F n.m.r. δ_{CCl_3F} (CCl_4) 110; *m/e* calcd. for $C_{11}H_{17}F$: 168.1314; found: 168.1314; 168 (35%), 153 (100%), 149 (40%).

Ozonolysis of ***22***

A solution of 100 mg of **22** was ozonized under the same conditions as **15** above to yield crude 1-methyl-2-oxocyclohexylbutyric acid ν_{max} ($CHCl_3$) 1705 cm^{-1} (br).

The crude acid was esterified with diazomethane and purified by t.l.c. (silica gel – chloroform) to yield pure **24**; ν_{max} ($CHCl_3$) 1700, 1730 cm^{-1}; δ ($CDCl_3$) 1.0 (s, 3H), 1.1–1.9 (m, 10H), 2.3 (m, 4H), 3.6 (s, 3H); *m/e* 212 (5%), 181 (5%), 152 (5%), 112 (90%), 55 (100%).

A small portion of **24** was converted to its 2,4-DNP derivative, m.p. 99–100°.

Anal. Calcd. for $C_{18}H_{24}N_4O_6$: C, 55.10; H, 6.16; N, 14.28. Found: C, 54.93; H, 6.11; N, 14.56.

This research was supported by the Research Corporation, National Research Council of Canada, and the University of British Columbia.

1. A. C. Cope, M. M. Martin, and M. A. McKervey. Q. Rev. **20**, 119 (1966).
2. (*a*) E. Winterfeldt. *In* Chemistry of acetylenes. *Edited by* H. G. Viehe. M. Dekker, New York, N.Y., 1969. Chapt. 4. (*b*) T. F. Rutledge. Acetylenes and allenes. Van Nostrand – Reinhold, New York, N.Y., 1969. Chapt. 5. (*c*) S. I. Miller and R. Tanaka. *In* Selective organic transformations. Vol. 1. *Edited by* B. S. Thyagarajan. Wiley-Interscience, New York, N.Y., 1970. p. 143.
3. V. Prelog and J. G. Traynham. *In* Molecular rearrangements. Vol. 1. *Edited by* P. de Mayo. Wiley-Interscience, New York, N.Y., 1963. Chapt. 9.
4. (*a*) L. Friedman and H. Shechter. J. Am. Chem. Soc. **83**, 3159 (1961). (*b*) A. C. Cope, M. Brown, and G. L. Woo. J. Am. Chem. Soc. **87**, 3107 (1965).
5. J. Ciabattoni, R. A. Campbell, C. A. Renner, and P. W. Concannon. J. Am. Chem. Soc. **92**, 3826 (1970).
6. E. D. Brown, T. W. Sam, and J. K. Sutherland. Tetrahedron Lett. 5025 (1969).
7. K. Wada, Y. Enomoto, and K. Munakata. Tetrahedron Lett. 3357 (1969).
8. H. L. Goering, A. C. Olson, and H. H. Espy. J. Am. Chem. Soc. **78**, 5371 (1956).
9. P. E. Peterson and R. J. Kamat. J. Am. Chem. Soc. **91**, 4521 (1969).
10. M. Hanack and A. Heumann. Tetrahedron Lett. 5117 (1969).
11. (*a*) M. Tanabe, D. F. Crowe, and R. L. Dehn. Tetrahedron Lett. 3943 (1967). (*b*) J. Schreiber *et al.* Helv. Chim. Acta, **50**, 2101 (1967).
12. A. G. Anderson, Jr., and J. A. Nelson. J. Am. Chem. Soc. **73**, 232 (1951).
13. (*a*) G. Stork, S. Malhotra, H. Thompson, and M. Uchibayashi. J. Am. Chem. Soc. **87**, 1148 (1965). (*b*) P. Borrevang, J. Hjort, R. T. Rapala, and R. Edie. Tetrahedron Lett. 4905 (1968).
14. H. C. Brown, C. P. Garg, and K.-T. Liu. J. Org. Chem. **36**, 387 (1971).
15. (*a*) S. F. Campbell, A. G. Hudson, E. F. Mooney, A. E. Pedler, R. Stephens, and K. N. Wood. Spectrochim. Acta, **23A**, 2119 (1967). (*b*) D. R. Strobach and G. A. Boswell, Jr. J. Org. Chem. **36**, 818 (1971).
16. L. J. Bellamy. Advances in infrared group frequencies. Methuen and Co., London, 1968. p. 26.
17. A. Chatterjee. Tetrahedron Lett. 959 (1965).
18. J. W. Hoffman and M. L. Mole. Tetrahedron Lett. 501 (1971).
19. E. Glotter and D. Lavie. J. Chem. Soc. C, 2298 (1967).
20. W. D. Pfeifer, C. A. Bahn, P. v. R. Schleyer, S. Bocher, C. E. Harding, K. Hummel, M. Hanack, and P. J. Stang. J. Am. Chem. Soc. **93**, 1513 (1971).
21. P. v. R. Schleyer. J. Am. Chem. Soc. **89**, 699, 701 (1967).
22. G. L. Lange and M. Bosch. Tetrahedron Lett. 315 (1971).
23. H. O. House and H. W. Thompson. J. Org. Chem. **26**, 3729 (1961).
24. H. E. Zimmerman and A. Mais. J. Am. Chem. Soc. **81**, 3644 (1959).
25. A. Bowers, T. G. Halsall, E. R. H. Jones, and A. J. Lemin. J. Chem. Soc. 2555 (1953).
26. G. Stock, A. Brizzolara, H. Landesman, J. Szmuszkovicz, and R. Turrell. J. Am. Chem. Soc. **85**, 207 (1963).
27. B. Rao and L. Weiler. Tetrahedron Lett. 927 (1971).

Can. J. Chem. Downloaded from www.nrcresearchpress.com by 210.87.254.42 on 09/05/12
For personal use only.

Can. J. Chem. Downloaded from www.nrcresearchpress.com by 210.87.254.40 on 09/05/12
For personal use only.

Proton Magnetic Resonance Spectra of Some Amphetamines and Related Compounds and Observations on Rotamer Populations

K. Bailey, A. W. By, K. C. Graham, and D. Verner
Research Laboratories, Food and Drug Directorate, Ottawa, Canada

Received March 12, 1971

Data from the p.m.r. spectra of β-amino-, β-aminohydrochloride-, β-hydroxy-, and β-nitro-α-phenylpropanes having methyl or methoxy substituents on the phenyl ring (37 compounds in all) are presented. The α and β protons of the side-chain give a pattern usually analyzable as ABX. The data are discussed in terms of correlations of coupling constants and chemical shifts with electronegativity of the substituent groups, steric and electronic effects, and apparent changes in rotamer populations. Hydrogen-bonding between the amino group of amphetamines and a methoxyl function at the ortho position in the phenyl ring is indicated for the salts but not the free bases.

On présente les données relatives aux spectres r.m.p. de β-amine, chlorhydrate de β-amino, β-hydroxy, et β-nitro α-phénylpropanes, ayant des substituants méthyles ou méthoxy sur le noyau phényle (37 composés en tout). Les protons α et β sur la chaîne latérale donnent un spectre analysable habituellement selon un ABX. Les données sont discutées en fonction des relations des constantes de couplage et des déplacements chimiques avec l'électronégativité des groupes substituants, les effets stériques et électroniques et les modifications apparentes dans les populations des rotamères. La liaison hydrogène entre le groupe amine des amphétamines et le groupe méthoxy en position ortho sur le noyau phényle est établie dans les sels mais non dans les bases libres.

Canadian Journal of Chemistry, **49**, 3143 (1971)

The analysis of the p.m.r. spectra of organic molecules is an established technique in conformational analysis (1). 1,2-Disubstituted ethanes have received considerable attention (2) and the conformations of acetylcholine (3) and its seleno (4) and thio (4, 5) isologues and very recently its α- and β-methyl derivatives (6) have been investigated by these methods.

Some predictions have been made about the conformation of amphetamines (7). A model accounting for the psychotomimetic activity of methoxyamphetamines and phenethylamines was proposed (8) in which the conformational behavior of these compounds was suggested to be modified by intramolecular hydrogen bonding. Such models have been strongly criticized (7, 9). We were therefore interested in the possibility of analyzing the p.m.r. spectra of amphetamines having methoxy or methyl groups on the phenyl ring, and their salts (since amphetamines are virtually completely ionized at physiological p*H*), for rotamer populations. The methylene (benzylic, α) and methine (β) protons of the side-chain give rise to a spectral pattern ($\alpha_1\alpha_2\beta$) approximating the ABX type for fast rotation with unequal populations (1). To the end of investigating factors affecting the stability of the various rotameric forms, we also prepared and examined corresponding compounds **I** in which the amino function is replaced by hydroxyl and by nitro groups. Preliminary work on dimethoxyamphetamines has been presented (10).

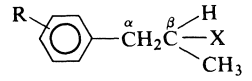

I

Discussion

We will assume at first that compounds $ArCH_2CH(CH_3)X$ exist in a dynamic equilibrium between the three classically staggered rotamers A, B, and C shown in Fig. 1 having mole fractions *a*, *b*, and *c* respectively.[1] The correspondence of protons α_1 and α_2 *as depicted* with the upfield (α′) or downfield (α) observed benzylic signals is discussed later in terms of the compound type. Vicinal coupling between protons is indicated in the figure, superscripts A, B, or C denoting the rotamer and subscripts *t* or *g* the coupling type (*trans* or *gauche*).

If $J\alpha_1\beta$ and $J\alpha_2\beta$ are the two observed (mean) vicinal couplings, then

[1]An approximate analysis of such a three-spin system for determining conformational equilibria has been presented by Snyder (11).

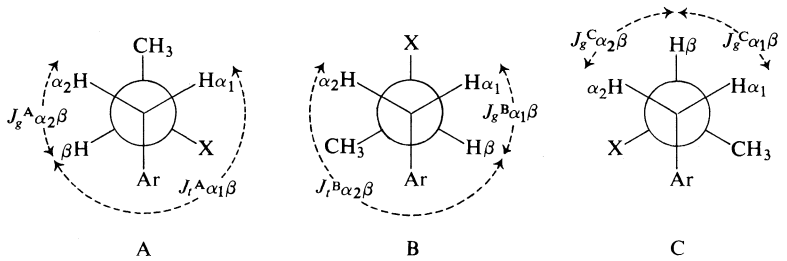

FIG. 1. Staggered rotamers of $ArCH_2CH(CH_3)X$; coupling constants indicated.

[1] $$J\alpha_1\beta = aJ_t^{A}\alpha_1\beta + bJ_g^{B}\alpha_1\beta + cJ_g^{C}\alpha_1\beta$$

[2] $$J\alpha_2\beta = aJ_g^{A}\alpha_2\beta + bJ_t^{B}\alpha_2\beta + cJ_g^{C}\alpha_2\beta$$

To simplify the present analysis for any one compound or series (X constant) the following approximations are made:

$$(i)\ J_t^{A}\alpha_1\beta = J_t^{B}\alpha_2\beta = J_t$$

$$(ii)\ J_g^{C}\alpha_1\beta \simeq J_g^{A}\alpha_2\beta = J_g$$

$$(iii)\ J_g^{C}\alpha_2\beta \simeq J_g^{B}\alpha_1\beta = J_{g'}$$

Equations 1 and 2 then reduce to the approximate form

[3] $$J\alpha_1\beta = aJ_t + bJ_{g'} + cJ_g$$

[4] $$J\alpha_2\beta = aJ_g + bJ_t + cJ_{g'}$$

also

[5] $$1 = a + b + c$$

The chief factors affecting these couplings in our series for constant dihedral angles depend on the electronegativities of the α and β substituents indicating that when X is more electronegative than CH_3, $J_{g'} > J_g$ (2, 12, 13). If the signals from the diastereotopic protons observed as α and α′ can be unambiguously assigned to the protons depicted as α_1 and α_2 in Fig. 1, and values of J_t, J_g, and $J_{g'}$, are available, then a, b, and c are easily obtained. If $J_g = J_{g'}$, simple algebra gives

$$a = \frac{J\alpha_1\beta - J_g}{J_t - J_g}$$

$$b = \frac{J\alpha_2\beta - J_g}{J_t - J_g}$$

and $$c = \frac{J_t + J_g - (J\alpha_1\beta + J\alpha_2\beta)}{J_t - J_g}$$

which are useful for preliminary estimates of rotamer stability.

The selection of suitable values for J_t, J_g, and $J_{g'}$ is hampered by the paucity of information on model compounds.

Other workers (14) have used $J_t = 12.0$ Hz as a starting point. This figure with the J_g and $J_{g'}$ values chosen below gives reasonable, greater than zero results for a, b, and c using our observed coupling constants. We therefore adopted $J_t = 12.0$ Hz as a suitable round number for the amphetamines. Abraham and Gatti (2) have recently devized precise equations for estimating vicinal coupling constants in 1,2-disubstituted ethanes, and it is reasonable that *changes* of the same order would be followed by our compounds. Averaging their coefficients and using Huggins' electronegativities (15) suggests that J_t decreases by about 0.7 Hz when X is changed from NH_2 to OH. The unchanged J_{vic} in triethylamine and tetraethylammonium salts (16) and work on *cis*-3-methyl-2-phenylmorpholine (17) indicates that J_t will be scarcely changed on protonation of the amphetamine amino group. 4-Nitro groups exert a negative increment on the (negative) geminal coupling of benzylic protons compared with NH_2 (18) and comparing compounds **1–6** with **19–24** (Table 1) shows a similar trend, the NO_2 seeming therefore to be less electronegative than NH_2 (10). Accordingly, J_t may increase (more positive) slightly when NO_2 is substituted for NH_2 in **I**.

The most important difference affecting the relative magnitudes of J_g and $J_{g'}$ seems to be the changing disposition of the CH_3 and X groups. Extrapolation of the coefficients for 1,2-disubstituted propanes (2) suggests the maximum difference (when X = N) to be about 1 Hz, and in the absence of definitive data $J_{g'} = 3.0$, $J_g = 2.0$, or $J_{g'} = J_g = 2.0$ are chosen as reasonable values for our compounds (19).

Table 2 shows how a, b, and c change with choice of J_t, J_g, and $J_{g'}$, for typical observed couplings. The calculated ratio of the two minor contributors is most affected by this choice, but

Can. J. Chem. Downloaded from www.nrcresearchpress.com by 210.87.254.40 on 09/05/12
For personal use only.

Can. J. Chem. Downloaded from www.nrcresearchpress.com by 210.87.254.40 on 09/05/12
For personal use only.

TABLE 1. Data from the p.m.r. spectra* of amphetamines and derivatives of structure I

Compound	Substitut on	X	ArR	β-H†	β-CH_3‡	$\overline{\alpha_1\alpha_2}$	$-J\alpha_1\alpha_2$ (Hz)	$\alpha_1 - \alpha_2$ (p.p.m.)	α′	(Jα′β)	α	(Jαβ)
1	2-CH_3	NH_2	7.69	6.87	8.86	7.36	13.1	9.05	7.43	(8.75)	7.28	(4.35)
2	3-		7.67	6.90	8.88	7.41	13.0	11.3	7.50	(8.5)	7.32	(4.3)
3	4-		7.70	6.90	8.90	7.45	13.2	11.2	7.54	(8.75)	7.36	(4.4)
4	2-CH_3O		6.20	6.80	8.88	7.37	12.9	10.8	7.45	(8.4)	7.28	(4.4)
5	3-		6.21	6.83	8.88	7.41	12.8	11.0	7.51	(8.3)	7.32	(4.5)
6	4-		6.23	6.88	8.92	7.45	13.0	9.5	7.55	(8.4)	7.39	(4.4)
7	2,3-$(CH_3)_2$		7.74, 7.80	6.88	8.89	7.37	13.2	11.1	7.46	(8.6)	7.28	(4.4)
8	2,4-		7.73, 7.73	6.87	8.90	7.42	13.3	9.7	7.50	(8.8)	7.34	(4.4)
9	2,5		7.73, 7.73	6.83	8.88	7.42	13.2	10.5	7.51	(8.8)	7.34	(4.4)
10	2,3-$(CH_3O)_2$		6.15, 6.18	6.81	8.88	7.37	12.7	8.1	7.44	(8.7)	7.30	(4.1)
11	2,4-		6.22, 6.22	6.84	8.92	7.45	13.0	10.9	7.54	(8.2)	7.36	(4.2)
12	2,5-		6.28, 6.28	6.83	8.91	7.43	12.5	10.3	7.51	(8.4)	7.35	(4.4)
13	3,4-		6.14, 6.14	6.85	8.88	7.44	13.0	10.1	7.53	(8.4)	7.35	(4.5)
14	3,5-		6.25, 6.25	6.83	8.89	7.47	13.0	12.0	7.57	(8.5)	7.37	(4.3)
15	2,3,4-$(CH_3O)_3$		6.07, 6.08, 6.18	6.82	8.90	7.44	13.0	10.8	7.53	(8.4)	7.35	(4.4)
16	2,4,5-		6.12, 6.17, 6.20	6.88	8.88	7.42	12.8	10.4	7.51	(8.4)	7.34	(4.5)
17	2,4,6-		6.20, 6.22, 6.22	6.90	8.91	7.40						
18	3,4,5-		6.10, 6.10, 6.12	6.83	8.81	7.42	13.0	13.9	7.55	(8.5)	7.32	(4.4)
19	2-CH_3	NO_2	7.70	5.25	8.48	6.84	14.0	21.95	7.01	(7.3)	6.67	(6.9)
20	3-		7.70	5.25	8.49	6.90	14.0	19.5	7.07	(7.05)	6.73	(6.95)
21	4-		7.70	5.26	8.50	6.90	14.0	18.5	7.05	(6.85)	6.75	(7.15)
22	2-CH_3O		6.20	5.10	8.51	6.86	13.6	13.1	6.97	(6.8)	6.75	(7.35)
23	3-		6.24	5.25	8.48	6.88	13.8	19.5	7.05	(6.9)	6.72	(7.1)
24	4-		6.25	5.29	8.50	6.90	14.0	17.0	7.04	(7.1)	6.76	(7.2)
25	2,5-$(CH_3O)_2$		6.24, 6.29	5.11	8.50	6.89	13.6	12.95	6.99	(6.5)	6.78	(7.1)
26	2-CH_3O	OH	6.22	5.95	8.81	7.24						
27	3-		6.23	6.00	8.80	7.32						
28	4-		6.23	6.05	8.81	7.35						
29	2,3-$(CH_3O)_2$	$NH_3^+Cl^-$	6.11, 6.16	6.35	8.61	6.95	13.0	15.9	7.09	(8.8)	6.82	(5.2)
30	2,4-		6.19, 6.23	6.40	8.64	7.01	13.1	16.0	7.14	(8.65)	6.87	(5.35)
31	2,5-		6.20, 6.27	6.40	8.61	6.99	13.1	13.6	7.10	(8.5)	6.88	(5.5)
32	3,4-(H_2O)		6.17, 6.19	?	8.64	7.00	13.0	27.7	7.23	(9.6)	6.77	(4.3)
33	3,5-		6.23, 6.23	6.45	8.60	7.00	13.1	25.2	7.20	(9.5)	6.79	(4.5)
34	2,3,4-$(CH_3O)_3$		6.06, 6.13, 6.18	?	8.61	7.00	13.2	17.1	7.15	(8.5)	6.86	(5.5)
35§	2,4,5-		6.13, 6.16, 6.16	?	8.61	7.01	13.0	14.0	7.13	(8.1)	6.90	(4.4)
36	2,4,6-		6.17, 6.17, 6.17	?	8.59	7.02						
37	3,4,5-		6.14, 6.14, 6.18	?	8.59	7.02	13.0	21.7	7.20	(9.2)	6.83	(4.8)

*τ-Values, measured with a Varian A-60A spectrometer using solutions at 40°, 10–15% in $CDCl_3$ containing TMS as internal standard. Signals (two recordings) were reproducible ± 0.01 p.p.m. Signals from the α and β protons were recorded at 100 Hz sweep width. Data from **10–14** have been presented before (10). Appropriate aromatic proton signals and integration ratios were observed.

†These signals were multiplets. Those from **34–37** were obscure: these salts are only moderately soluble in $CDCl_3$. Compound **32** crystallizes as a monohydrate, and the H_2O obscures the signal

‡Doublets: *J ca.* 6.5 Hz.

§Spectrum poor, lines 4 and 5 of ABX system not resolved, could lead to errors in $J_{\alpha_1\beta}$ and $J_{\alpha_2\beta}$.

TABLE 2. The effect of choice of J_t, $J_{g'}$, and J_g on apparent rotamer populations*

			Observed $J\alpha_1\beta = 5$, $J\alpha_2\beta = 8$			Observed $J\alpha_2\beta = 5$, $J\alpha_1\beta = 8$ Hz		
J_t	$J_{g'}$	J_g	*a*	*b*	*c*	*a*	*b*	*c*
11	2	2	33	67	0	67	33	0
13	2	2	27	55	18	55	27	18
12	2	2	30	60	10	60	30	10
12	3	2	24	58	18	57	29	14
12	2	1	31	63	6	60	36	4
12	3	1	25	61	14	57	35	8
12	4	1	21	58	21	55	33	12
			Observed $J\alpha_1\beta = 4$, $J\alpha_2\beta = 9$			Observed $J\alpha_2\beta = 4$, $J\alpha_1\beta = 9$ Hz		
			a	*b*	*c*	*a*	*b*	*c*
11	2	2	22	78	0	78	22	0
13	2	2	18	64	18	64	18	18
12	2	2	20	70	10	70	20	10
12	3	2	13	68	19	68	19	13
12	2	1	21	72	7	70	27	3
12	3	1	15	70	15	68	26	6
12	1	3	26	68	6	70	15	15

*a, b, and c expressed as mole fractions % to the nearest integer.

whatever the chosen constants, it is seen that the *direction* in which a and b change for various observed couplings is determined by the *observed* coupling constants. It is obviously unwise to make dogmatic statements from our results about the stability of the sterically disfavored rotamer C relative to that of the other minor rotamer, and small (*i.e.*, less than 10%) differences in apparent rotamer populations comparing *series* (X changing) should be viewed cautiously.

Results

Table 1 presents p.m.r. data for solutions of our compounds in deuterochloroform at 40 °C. The benzylic protons and the β proton give signals $\alpha_1\alpha_2\beta$ which were analyzed in the second order as ABX, assuming that $J\alpha_1\alpha_2$ is negative and $J\alpha_1\beta$ and $J\alpha_2\beta$ are positive. At first it is not possible to say which of α_1 and α_2 (Fig. 1) is at higher field, and Table 1 merely describes them as α and α′. Because the β-H is coupled to the α-CH_3, only the AB part was used to find $J\alpha_2\beta$ (1). In general these eight lines (numbered 1–8 from high to low field) were plainly visible, but for compounds **1–3** and **7–9** line 1 was obscured by the aromatic methyl signal and was calculated from $J\alpha_1\alpha_2$ revealed by lines 2–4, 5–7, and 6–8. Further, it happened that the broad NH_2 signal of compounds **1–3** came in the $\alpha_1\alpha_2$ region, although the AB lines projected from the envelope. Changing the concentration somewhat shifted the NH_2 signal and addition of D_2O caused its disappearance, but did not cause any detectable shift in any of the other lines, and the values recorded for **1–3** are for $CDCl_3$ solutions with D_2O added. We also noted that the presence of impurities, even to the extent of some 50–60% of crude reaction mixture in some cases, had no effect on the spectral analysis on comparison with purified material. These observations lend confidence in the spectra.

Table 1 shows that at 60 MHz, the coupling between α_1 and α_2 is about the same as their chemical shift difference. Indeed for compounds **17** and **36** (2,4,6-trimethoxy-substitution pattern) the signals are degenerate, resemble the A_2B case, and were not calculable as ABX. The methoxyphenyl propanols **26** and **28** also present an A_2B-like pattern at 60 MHz: lines 4 and 6 are superimposed, 3 and 5 partially overlap, and 1, 2, 7, and 8 are extremely weak.

Chemical Shifts

There is a trend for the band center of the α-protons ($\overline{\alpha_1\alpha_2}$) to shift slightly upfield in the monosubstituted series **1–3**, **4–6**, **19–21**, **22–24**, and **26–28** as the substituent shifts further from the benzylic carbon. The coupling constant data discussed below show that this is not due to consistent changes in the relative rotamer populations. The center $\overline{\alpha_1\alpha_2}$ of the other compounds remains approximately constant except that for

Can. J. Chem. Downloaded from www.nrcresearchpress.com by 210.87.254.40 on 09/05/12
For personal use only.

Can. J. Chem. Downloaded from www.nrcresearchpress.com by 210.87.254.40 on 09/05/12
For personal use only.

2,3-disubstituted compounds it appears at rather lower field. Steric hindrance to rotation of the phenyl ring and through-space effects from substituents seem unlikely explanations for this and we suggest that the effect results from the changing magnitude of inductive effects on the benzylic carbon (20). These influences should change $J\alpha_1\alpha_2$ very slightly (18) but no consistent pattern emerges from our results for these series.

The chemical shifts of the β-H and the β-CH_3 in the series **1–3**, **4–6**, **19–21**, and **26–28** are generally shifted to slightly higher fields as the substituent changes from the ortho to meta to the para position. Decreasing the population of rotamer C with this change (increasing the shielding of the β-H by the *gauche* aryl group) is unlikely on steric grounds and not supported by rotamer population changes derived from coupling constant data. For the nitro compounds **22–25** the effect on β-H is very marked and is discussed further below.

The downfield shifts observed in the β-CH_3, the β-H (and the $\overline{\alpha_1\alpha_2}$ signals), when the NH_2 group is protonated are considerably smaller than when the NH_2 is replaced by NO_2. Accordingly the J_t and J_g changes are probably greater on conversion of the NH_2 into NO_2 than on hydrochloride formation, which is in line with our earlier discussion and the calculations presented below.

Coupling Constants and Rotamer Populations

These are best discussed in terms of the compound type.

Amphetamines

Rotamer populations calculated from the appropriate expressions using $J_t = 12.0$, $J_{g'} = 3.0$ and $J_g = 2.0$ and using $J_t = 12.0$, $J_{g'} = J_g = 2.0$ (10) are in the Depository of Unpublished Data. The range of values found shows that there is almost no change in the conformational equilibria of the amphetamines as a result of changing the aromatic substitution pattern for methyl and methoxy substituents (*a* or $b \simeq 65$, *b* or $a \simeq 20$, $c \simeq 15\%$). This is readily seen in the coupling constants of Table 2. Reasons for supposing that α_1 will be at lower field than α_2 have been given (10) and if this is so, then rotamer B is predominant, in agreement with calculations (7). The amino group exerts greater steric demands than a nitro group (21). Our results for nitro compounds (below) show that A and B are roughly equally populated, hence an increase in *b* and a decrease in *a* on going from the nitro, series to the amino series appears reasonable. We conclude that for aryl-substituted amphetamines, the rotamer in which the amino and aryl functions are *trans* is the most stable and that at 40 °C it is present as some 55–70% of the equilibrium mixture in $CDCl_3$ solution.

The proposition (8) that hydrogen-bonding between the amino group and an oxygen atom at the ortho position to the side chain could seriously affect the conformational equilibria is not confirmed by our work on these free bases. An investigation of intra-molecular NH....O bonding in compound **4** by the i.r. sequential dilution technique showed only free NH absorption at 3635 and 3605 cm^{-1} at a concentration below 0.4% in carbon tetrachloride.[2]

Amphetamine Hydrochlorides

For the reasons given above, we consider that J_t, $J_{g'}$, and J_g, will be little changed from their values in the free bases. Table 3 presents results for methoxylated compounds in $CDCl_3$. There is obviously a significant difference between salts with an ortho oxygen and those without. The population of rotamer C is very low and considered to be zero in the following discussion of the four possibilities (average % given).

Case 1. Compounds with *o*-CH_3O have 65% A, others have 25% A.

Case 2. Compounds with *o*-CH_3O have 65% A, others have 75% A.

Case 3. Compounds with *o*-CH_3O have 35% A, others have 75% A.

Case 4. Compounds with *o*-CH_3O have 35% A, others have 25% A.

The shielding effects of a *gauche* or *trans* $NH_3^{(+)}Cl^{(-)}$ moiety have not been defined, although what follows confirms an earlier inference (22) that a *gauche* $NH_3^+....Cl^-$ has a shielding effect. Therefore the definition of which observed α signal corresponds with α_1 or α_2 and hence which of the calculated rotamer percentages applies to A and which to B is not at first possible. The following points are pertinent:

(i) Chemical Shifts of the Benzylic Protons

Assuming that the chemical shift changes between α_1 and α_2 of the salts are primarily due to effects from the β groups, then a linear rela-

[2]We thank Mr. J. C. Ethier for this result.

TABLE 3. Calculated rotamer populations of amphetamine hydrochlorides*

Compound	$J\alpha_1\beta > J\alpha_2\beta$			$J\alpha_1\beta < J\alpha_2\beta$		
	a	*b*	*c*	*a*	*b*	*c*
29	68	32	0	32	68	0
30	66.5	33.5	0	33.5	66.5	0
31	65	35	0	35	65	0
32	76	23	1	23	76	1
33	75	25	0	25	75	0
34	65	35	0	35	65	0
35†	61	24	15	24	61	15
37	72	28	0	28	72	0

*a, b, and c expressed as mole fractions %, using $J_t = 12, J_{g'} = J_g = 2$ Hz. For conditions of measurement see Table 1.
†Possible errors in $J\alpha\beta$ and $J\alpha'\beta$ (footnote §, Table 1) may be responsible for this apparently anomalous result.

tionship is expected between the chemical shift of α_1 with a rotamer percentage in one form A or B (C ≃ O) and similarly for α_2. There are fair fits with linearity when appropriate graphs are plotted for any of cases 1–4, and no conclusion can be drawn.

Case 1. For *o*-methoxylated salts, the H with larger coupling is α_1 which is observed upfield. Proton α_2 is shielded by a *gauche* CH_3 in both A and B, but when A dominates, α_1 has the greater *gauche* NH_3^+ effect which is therefore shielding. When A drops from 65 to 25%, α_2 shifts upfield (6.85 to 7.21 τ) because there is more *gauche* NH_3^+ influence. However, a deshielding effect of about 0.33 p.p.m. on α_1 (7.11 to 6.78 τ) for only a 40% decrease in *gauche* CH_3 influence (see A) seems to be somewhat excessive; *cis* and *trans* 3-methyl-2-phenylmorpholine hydrochlorides exist some 98% in the forms having *anti* and *gauche* 2-H/3-CH_3 conformations respectively in $CDCl_3$ solution and the 2-H signals are at 4.56 and 5.19 respectively (17).

Case 2. Similarly, shielding by *gauche* NH_3^+ is indicated, and as A increases, α_2 would shift downfield (6.85 to 6.78 τ) because (see rotamer B) there is a 10% decrease in the *gauche* NH_3^+ interaction. An upfield shift of about 0.1 p.p.m. (7.11 to 7.21 τ) for α_1 seems excessive for a 10% increase in the *gauche* CH_3 shielding.

Case 3. The relative magnitudes of the *gauche* CH_3 and NH_3^+ shielding or deshielding are important here and in case 4. The downfield shift for α_2 from 7.11 to 6.78 τ with decrease in B indicates that the *gauche* NH_3^+ has a shielding effect. Proton α_1 shifts from 6.85 to 7.21 τ which seems large for a 40% increase in the *gauche* CH_3 interaction.

Case 4. As in case 3, α_1 is at lower field because there is less shielding by the *gauche* CH_3 or because of *gauche* NH_3^+ effects. The shifts of α_2 (7.11 to 7.21 τ with increase in B) demonstrate that the *gauche* NH_3^+ has a shielding effect. The downfield shift in α_1 of about 0.07 p.p.m. (6.85 to 6.78 τ) for a 10% decrease in *gauche* CH_3 interaction is in fair agreement with the morpholine salts cited above.

Our initial assumptions and the small changes observed in the mean position of the benzylic signal with different substitution pattern do not allow a decision, although case 4 seems the most supportable. An important conclusion is that the NH_3^+ moiety *shields gauche* protons.

(ii) Chemical Shifts of the β-CH_3

If *a* is larger in the meta OCH_3 series, the β-CH_3 would be less shielded by the aryl group. Inspection of Tables 1 and 4 shows differences of β-CH_3 no greater than in the case of the free bases, where there is little change in rotamer populations, strongly suggesting that there is no major change in rotamer populations in the salts, *i.e.*, the "cross over" cases 1 and 3 are improbable. Table 4 shows that the downfield shifts of the β-CH_3 signal on going from the free amphetamines to their salts ($\Delta\tau$ CH_3) are generally greater for compounds with an *o*-CH_3O than for those without, *i.e.*, the increase of A in the ortho series on salt formation appears to be greater than for the meta series. The correlation is not good, but the results are best compatible with case 4.

From points *i* and *ii*, case 4 appears the most likely. Rotamer B is dominant, as for the free bases, but H-bonding or electrostatic interaction of some kind allows extra A in the ortho methoxyl series. Intramolecular hydrogen bonding between

Can. J. Chem. Downloaded from www.nrcresearchpress.com by 210.87.254.40 on 09/05/12
For personal use only.

TABLE 4. Changes in the chemical shift of the β-CH_3 group on protonation of amphetamines*

CH_3O-Substitution type	2,3-Di	2,4-Di	2,5-Di	2,3,4-Tri	2,4,5-Tri	3,4-Di	3,5-Di	3,4,5-Tri
τ β-CH_3 base (*i*)	8.88	8.92	8.91	8.90	8.88	8.88	8.89	8.81
τ β-CH_3 salt (*ii*)	8.61	8.64	8.61	8.61	8.61	8.64	8.60	8.59
Δτ CH_3 (= *i* − *ii*)	0.27	0.28	0.30	0.29	0.27	0.24	0.29	0.22
% A increase in salts†								
Case 1	47	40.5	41	41	36‡	−2	2	4
Case 2	47	40.5	41	41	36‡	51	52	48
Case 3	11	7.5	11	11	−1‡	51	52	48
Case 4	11	7.5	11	11	−1‡	−2	2	4

*For di- and trimethoxyamphetamines of Table 1 under the conditions described there, see footnote *.
†From difference in *a* values using $J_t = 12, J_{g'}$ (Table 3) $= J_g = 2$ Hz (*a* of bases ≃25%).
‡This value probably in error, see footnote †.

Can. J. Chem. Downloaded from www.nrcresearchpress.com by 210.87.254.40 on 09/05/12
For personal use only.

the protonated amino group and an ortho methoxyl is suggested by Snyder's model (7), and a similar interaction was inferred (22) for 1-(4-methoxyphenyl)-1-methoxy-2-aminopropane hydrochloride. An interaction with the aromatic bonds has been suggested as stabilizing the corresponding conformation for β-phenylethanols (21). Even if our estimate of *c* is somewhat inaccurate, it certainly seems that C is a small contributor. Rotamers A and C both have *gauche* aryl and NH_3^+ groups, so this agrees with the sterically favored B being dominant. Other amphetamine hydrochlorides were insufficiently soluble in $CDCl_3$ for spectral measurement. Amphetamines are protonated at physiological p*H*. Unfortunately, investigation of conformational behavior in water (using D_2O) was frustrated by the resultant chemical shift and/or coupling constant (rotamer population) changes: lines 4 and 6 were superimposed and 3 and 5 barely resolved. Results for other systems (23) suggest that the gross conformational features of the salts would be the same in different solvents. Our results (Table 5) provide evidence that amphetamine salts indeed exhibit conformational behavior of the type postulated by Snyder (8) but this does not correlate well with the degree of psychotomimetic activity.

1-Aryl-2-nitropropanes

The rotamer populations in Table 6 were calculated using $J_t = 13, J_{g'} = 3$, and $J_g = 2$ Hz. The increase in the chosen coupling constant values from that in amphetamines is in accord with the earlier discussion, and receives some experimental justification in that within this *J* *gauche* range, J_t must be increased if $a + b \not> 1$. Table 6 shows that for any one compound, *c* is little affected by the choice of which of α_1 and α_2 is at higher field. Because steric effects probably determine populations trends, it might be supposed that the greatest difference in *a* and *b* should be observed for the compounds with the substituent CH_3 or OCH_3 ortho to the side-chain. This seems to be the case if α_1 is at low field for the methyl compounds, but at high field for the methoxy compounds. However, the chemical shifts of the benzylic protons are about the same in both series and rotamer populations are little changed, so it seems more reasonable to expect that the same proton depicted as α_1 or α_2 (Fig. 1) appears at higher field in *both* series (and for the 2,5-dimethoxy compound **25**). Preliminary evidence suggested that the NO_2 group strongly shields *gauche* protons of a similar type (22), but a *gauche* CH_3 also shields and population changes (Table 6) are too small to allow an estimate of the relative magnitude of the shielding by these two groups, critical in deciding which of α_1 and α_2 is which. Rotamer A places the β-CH_3 *trans* to the aryl ring, and on steric grounds ($CH_3 > NO_2$) A would be the more stable. Our data for meta and para substituted compounds suggest that B is slightly more stable whether α_1 or α_2 is at high field, but the calculated *a*, *b*, and *c* depend on the chosen coupling constants and small errors in their values could reverse the order of apparent stability, since *a* and *b* are nearly equal.

TABLE 5. Data from the p.m.r. spectra* of dimethoxyamphetamine hydrochlorides

Compound†	$(CH_3O)_2Ar$	β-H‡	β-CH_3§	$\overline{\alpha_1\alpha_2}$
29	6.17, 6.26	6.40	8.77	7.10
30	6.25, 6.25	6.44	8.80	7.23
31	6.25, 6.28	6.4	8.78	7.18
32	6.23, 6.25	6.4	8.77	7.20
33	6.28, 6.28	6.4	8.77	7.20

*τ-Values, measured in D_2O solution (external TMS); otherwise see Table 1.
†See Table 1 for substitution pattern.
‡Multiplets, band-center not well defined.
§Doublets, *J ca.* 6.5 Hz.

TABLE 6. Calculated rotamer populations of 1-aryl-2-nitropropanes*

Compound	Substitution	% if α_1 at low field			% if α_1 at high field		
		a	*b*	*c*	*a*	*b*	*c*
19	2-CH_3	40.3	47.0	12.7	44.2	43.4	12.4
20	3-CH_3	40.9	44.6	14.5	41.9	43.7	14.4
21	4-CH_3	42.9	42.8	14.3	40.0	45.5	14.5
22	2-CH_3O	44.4	42.5	13.1	39.3	47.4	13.3
23	3-CH_3O	42.4	43.2	14.4	40.4	45.0	14.6
24	4-CH_3O	43.1	45.3	11.6	42.2	46.2	11.6
25	2,5-$(CH_3O)_2$	42.8	39.3	17.9	36.8	44.7	18.5

*a, b, and c expressed as mole fractions %, using $J_t = 13$, $J_{g'} = 3$, and $J_g = 2$ Hz. For conditions of measurement see Table 1.

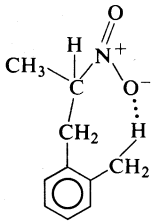

II

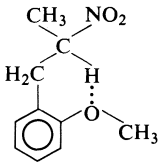

III

Extrapolation to the ortho compounds could be complicated by interactions of the type **II** and **III**. Although **II** is in our opinion unlikely, **III** is worth consideration: the β-H is rendered quite acidic by the nitro group. Type **III** may occur for rotamers A or B, probably with some distortion and lower symmetry imparted to the rotating phenyl ring. Evidence that this interaction occurs is found in the unusually low field resonance of the β-H in the ortho-methoxy compounds **22** and **25**. An increase in *c* might have such an affect (aryl group and β-H *trans*) but this does not seem to be the case for **22**. Further, the *o*-OCH_3 signal is at about 0.04 p.p.m. to lower field for **22** compared with **23** and **24**, whereas in the alcohols **26**–**28** and amphetamines **4**–**6** the differences are about 0.00 and 0.02 p.p.m. respectively. We conclude that for simple 1-aryl-2-nitropropanes the populations of rotamers A and B are roughly equal.

1-Aryl-2-propanols

A hydroxyl group is considerably less bulky than an amino group, and hence the ratio *b*:*a* is predicted to be less than in the case of amphetamines described earlier. In $CDCl_3$ solution at 40 °C the spectra of 1-aryl-2-propanols resemble the A_2B case. Since positive increments in J_{gem} result from the presence of more electronegative substituents (18) (*e.g.* O *cf.* N) the observation suggests that the chemical shift difference between the benzylic protons is now quite small. The same type of chemical shift *changes* occur as in the amino and nitro series. The low field position of $\overline{\alpha_1\alpha_2}$ in ortho methoxylated compounds is more marked; both it and the β-CH_3 signal are shifted by about 0.1 p.p.m. to lower field on changing the β substituent from NH_2 to OH, and the β-H is deshielded by about 0.8 p.p.m. Nibbering *et al.* (24) found that the corresponding vicinal couplings for solutions of 3,3,3-trideutero-1-phenylpropan-2-ol were not affected by concentration changes within the range 0.2–0.5 mol fraction in CCl_4. The benzylic protons were separated by about 6 Hz at 60 MHz. Their observed couplings (average 5.6 and 7.1 Hz) suggest populations of A (or B) about 36, B (or A) about 51, and C about 13%. Whatever assignment of signal to α_1 or α_2 is correct, the ratio *b*:*a* is lower than for the amphetamines, as predicted above.

Experimental

The compounds described here were prepared by standard methods, all were obtained as racemates.

Amphetamines

The appropriately substituted β-methyl-β-nitrostyrene was reduced using lithium aluminum hydride in ether or tetrahydrofuran. When a very impure amphetamine was obtained, it was generally isolated by regeneration from its hydrochloride. The common by-products of reaction seemed (p.m.r., i.r.) to be the corresponding oximes; their presence had no detectable effect on the p.m.r. spectrum of the amphetamine on the evidence from pure and impure materials. All 18 compounds were characterized as their hydrochlorides.

Amphetamine Hydrochlorides

These compounds were precipitated from ethereal solutions of the amphetamines on addition of a solution of hydrogen chloride in dry ether. All were recrystallized from isopropanol/hexane and gave satisfactory analyses (C, H, and N ±0.3%) except that 2,3- and 2,5-dimethylamphetamine hydrochloride were very hygroscopic:

Can. J. Chem. Downloaded from www.nrcresearchpress.com by 210.87.254.40 on 09/05/12
For personal use only.

Anal. Calcd. for $C_{11}H_{18}ClN$: C, 66.16; H, 9.09; N, 7.02; and Calcd. for $C_{11}H_{18}ClN \cdot \frac{1}{2}H_2O$: C, 63.28; H, 9.17; N, 6.71. Found: C, 63.18; H, 8.75; N, 6.76; and C, 63.94; H, 8.76; N, 6.70 respectively.

2,3,4-, 2,4,5-, and 2,4,6-Trimethoxyamphetamine appeared to be similarly hygroscopic.

Anal. Calcd. for $C_{12}H_{20}ClNO_3$: C, 55.09; H, 7.70; N, 5.35; and Calcd. for $C_{12}H_{20}ClNO_3 \cdot \frac{1}{2}H_2O$: C, 53.29; H, 7.82; N, 5.17. Found: C, 53.93; H, 7.41; N, 5.26; C, 53.87; H, 7.57; N, 5.27; and C, 53.71; H, 7.55; N, 5.37 respectively.

Satisfactory analyses were obtained after rigorous drying immediately before analysis. 3,4-Dimethoxyamphetamine hydrochloride was obtained as a stable monohydrate; 2,5-dimethoxyamphetamine hydrochloride deliquesces in moist air. We noted that literature values for the melting points of many amphetamine hydrochlorides differed considerably, and that our findings too were at variance; melting points seem to be affected by the presence of moisture absorbed from air.

1-Aryl-2-nitropropanes

The appropriately substituted β-methyl-β-nitrostyrene was reduced using sodium borohydride in methanol or ethanol at 30° (25). A large excess of reducing reagent was required before the yellow color of the nitrostyrene was completely discharged. Oximes appear to be the usual by-product, since on aqueous acid work-up, the corresponding phenylacetone (26) could be obtained. The nitropropane and phenylacetone were easily separated by silica gel column chromatography. The compounds were liquids, satisfactory analyses (C, H, and N) were obtained.

1-Aryl-2-propanols

The appropriately substituted phenylacetone was reduced using sodium borohydride in methanol. The alcohols were purified by column chromatography on silica gel.

We are grateful to Mr. H. W. Avdovich for his care in determining the p.m.r. spectra.

1. F. A. Bovey. Nuclear magnetic resonance spectroscopy. Academic Press, New York, N. Y., 1969.
2. R. J. Abraham and G. Gatti. J. Chem. Soc. B, 961 (1969).
3. C. C. J. Culvenor and N. S. Ham. J. Chem. Soc. D, 537 (1966).
4. R. J. Cushley and H. G. Mautner. Tetrahedron, 2151 (1970).
5. C. C. J. Culvenor and N. S. Ham. J. Chem. Soc. D, 1242 (1970).
6. (*a*) T. D. Inch, R. A. Chittenden, C. Dean. J. Pharm. Pharmac. **22**, 954 (1970). (*b*) A. F. Casy, M. M. A. Hassan, and E. C. Wu. J. Pharm. Sci. **60**, 67 (1971).
7. C. Chothia and P. Pauling. Proc. Natl. Acad. Sci. **63**, 1063 (1969).
8. S. H. Snyder and E. Richelson. Proc. Natl. Acad. Sci. **60**, 206 (1968).
9. S. Kang and J. P. Green. Proc. Natl. Acad. Sci. **67**, 62 (1970).
10. K. Bailey. J. Pharm. Sci. **60**, 1232 (1971).
11. E. I. Snyder. J. Am. Chem. Soc. **88**, 1165 (1966).
12. R. J. Abraham, L. Cavalli, and K. G. R. Pachler. Mol. Phys. **11**, 471 (1966).
13. H. Booth. Tetrahedron Lett. 411 (1965).
14. C. A. Kingsbury and D. C. Best. J. Org. Chem. **32**, 6 (1967).
15. M. L. Huggins. J. Am. Chem. Soc. **75**, 4123 (1953).
16. A. A. Bothner-By. Adv. Mag. Res. **1**, 203 (1965).
17. P. S. Portoghese. J. Med. Chem., **10**, 1057 (1967).
18. S. Sternhell. Q. Rev. 236 (1969).
19. Compare refs. 15 and 17; C. A. Kingsbury. J. Org. Chem. **35**, 1319 (1970); J. E. Forrest, R. A. Heacock, and T. P. Forrest. J. Pharm. Pharmac. **22**, 512 (1970).
20. *cf.* M. D. Bentley and M. J. S. Dewar. J. Org. Chem. **35** (1970).
21. J. McKenna. Conformational analysis of organic compounds. Royal Institute of Chemistry Lecture Series No. 1 (1966).
22. K. Bailey. Can. J. Chem. **48**, 3597 (1970).
23. E. I. Snyder. J. Am. Chem. Soc. **88**, 1155 (1966) and refs. 6*b* and 11.
24. N. M. M. Nibbering, K. Spaargaren, and P. J. van der Haak. Tetrahedron Lett. 4663 (1968).
25. A. Hassner and C. Heathcock. J. Org. Chem. **29**, 1350 (1964).
26. *cf.* R. V. Heinzelman. Org. Synth. Collect. Vol. 4, 573 (1963).

Can. J. Chem. Downloaded from www.nrcresearchpress.com by 210.87.254.40 on 09/05/12
For personal use only.

Can. J. Chem. Downloaded from www.nrcresearchpress.com by 210.87.254.5 on 09/05/12
For personal use only.

Influence of Lewis Acids on the Diels–Alder Reaction. IV. Reaction of 2-Methyl- and 2-Phenylfuran with Ethyl Propiolate[1]

A. W. McCulloch and A. G. McInnes

Atlantic Regional Laboratory, National Research Council of Canada, Halifax, Nova Scotia

Received April 29, 1971

The $AlCl_3$-promoted reactions of 2-methyl- and of 2-phenylfuran with ethyl propiolate afford as major products ethyl 5-hydroxy-2-methyl- and 2-phenylbenzoates (**6***a*, **6***b*). Also isolated as minor by-products of these reactions are ethyl 3-(2-furyl-5-methyl)acrylate (**5***a*), ethyl 3-(2-furyl-5-phenyl)acrylate (**5***b*), ethyl 3,3-di(2-furyl-5-methyl)propionate (**10***a*), ethyl 3,3-di(2-furyl-5-phenyl)propionate (**10***b*), and ethyl 2-hydroxy-5-methylbenzoate (**8***a*).

Les réactions amorcées par $AlCl_3$ entre le méthyl-2 et le phényl-2 furanne et le propiolate d'éthyle donnent comme produits majoritaires les hydroxy-5 méthyl-2 et phényl-2 benzoates d'éthyle (**6***a*, **6***b*). Ont été également isolés comme produits secondaires de ces réactions, le (furyl-2 méthyl-5)-3 acrylate d'éthyle (**5***a*), le (furyl-2 phényl-5)-3 acrylate d'éthyle (**5***b*), le di(furyl-2 méthyl-5)-3,3 propionate d'éthyle (**10***a*), le di(furyl-2 phényl-5)-3,3 propionate d'éthyle (**10***b*) et l'hydroxy-2 méthyl-5 benzoate d'éthyle (**8***a*).

Canadian Journal of Chemistry, 49, 3152 (1971)

We have recently reported the acid-catalyzed rearrangement of 1- and 1,4-substituted diethyl 7-oxabicyclo[2.2.1]2,5-heptadiene-2,3-dicarboxylate adducts **1** to 6- and 4,6-substituted diethyl 3-hydroxyphthalates **2** (1). Since formation of the adducts **1** is also accelerated by $AlCl_3$ this procedure has led to a one-step synthesis of polysubstituted aromatics.

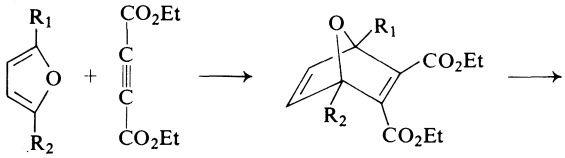

1

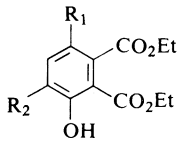

2

In an attempt to investigate the generality of this one-step synthesis from furans and acetylenes we have studied the use of ethyl propiolate as a dienophile: a brief preliminary account of some of this work has appeared (2). The present paper details the results of our studies of the reactions of 2-methyl- and 2-phenylfuran with ethyl propiolate.

In principle, reaction of a 2-substituted furan with ethyl propiolate can lead to the formation of two stereoisomeric 1:1 adducts, **3** and **4**, subsequent rearrangement of which would afford the phenolic esters, **6** and **8** respectively. However, results of various studies on the reactions of 2-substituted butadienes, such as isoprene, with methyl vinyl ketone (3), acrolein (3), methyl acrylate (4, 5), and acrylonitrile (4), or of a 1-substituted butadiene such as *trans*-piperylene with methyl acrylate (6) have indicated that the presence of $AlCl_3$ leads to enhanced stereoselectivity. In all cases involving a 1-substituted butadiene derivative the major product of the accelerated Diels–Alder addition is the 1,2-disubstituted adduct (7). By analogy therefore we would expect the product ratio **3**:**4**, and consequently **6**:**8**, to be high.

In practice we have found that the reactions of 2-methyl and 2-phenylfuran with ethyl propiolate in the presence of $AlCl_3$ at room temperature or below do in fact yield the phenolic compounds **6***a* and *b* as the major products. At these temperatures the intermediate adducts, **3** or **4**, were not detected, and all attempts to isolate them were unsuccessful.

Reaction of 2-Methylfuran with Ethyl Propiolate

Analysis of the crude product from a typical experiment indicated (*i*) that **6***a* was the major reaction product, (*ii*) that a considerable amount of polymerized 2-methylfuran was present (p.m.r. signals for this material could be readily identified by comparison with those observed in the spec-

[1]NRCC No. 12097.

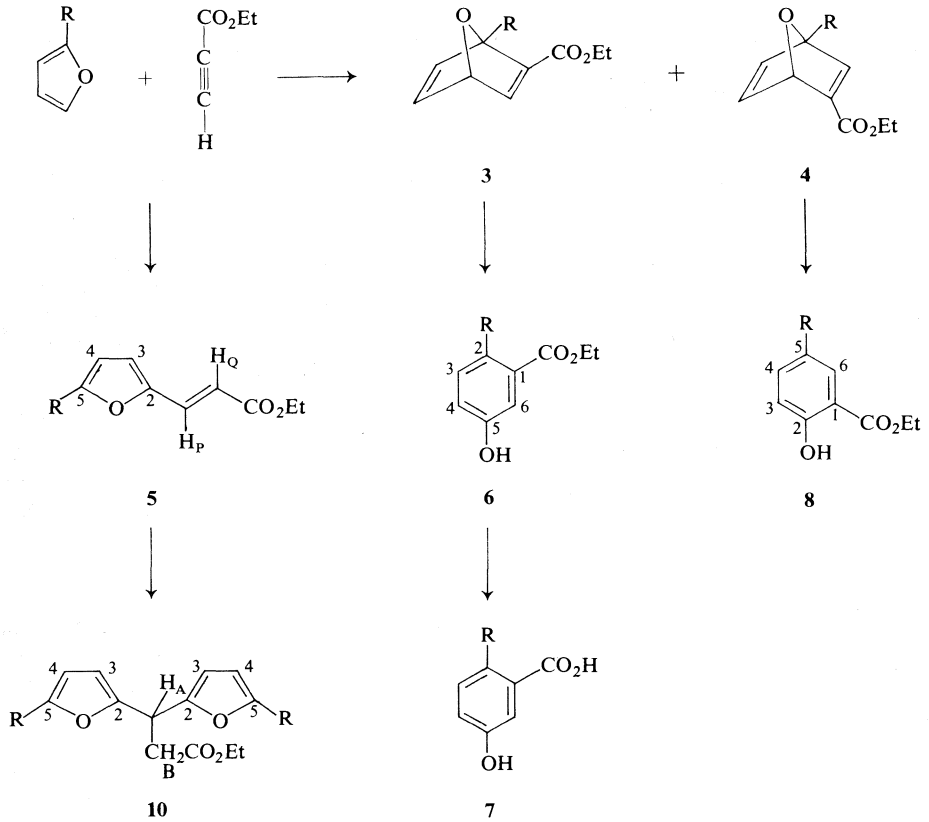

a R = CH_3;
b R = C_6H_5

trum of the orange gum obtained from a separate reaction involving only the diene and $AlCl_3$), and (*iii*) that **5***a*, **8***a*, and **10***a* were minor by-products (all <2%).

Compounds analogous to **5** are well known as reaction products from pyrroles and acetylenes (8) and are presumed to arise through a Michael-type addition process. Some speculation may be made regarding the mechanism. The reaction is presumably initiated by coordination of the carbonyl oxygen of the propiolate with $AlCl_3$. Nucleophilic attack by the furan on the β-carbon of the complexed ester would then lead (as shown in Scheme 1) to an allene-type intermediate, similar to that postulated by Huisgen *et al.* for the addition of amines to acetylenic esters (9). Abstraction of the ring proton then gives **5**: thus a process of *cis* addition yields a product having *trans* substituents. Formation of **10** may occur by a second analogous addition of the diene to **5**, again initiated by complexing between $AlCl_3$ and the ester carbonyl oxygen of **5**. We have isolated similar products from the $AlCl_3$-promoted reaction of *N*-methylpyrrole with methyl propiolate (10).

The meta-carbethoxyphenol **6***a* was readily soluble in base, whereas the strongly hydrogen-bonded ortho-carbethoxyphenol **8***a*, and the neutral components of the crude product, were insoluble. This facilitated isolation of **6***a*, which was obtained in *ca.* 30% yield after 30 min reaction at room temperature. The ester function of this compound underwent very facile hydrolysis. For example, if 5% NaOH was employed in the extraction procedure during work-up the product isolated after reacidification was predominantly **7***a*.

The by-products **5***a*, **8***a*, and **10***a* were separated from the resinified diene by column chromatography on silicic acid. Separation of the individual components required further purification by preparative t.l.c. and preparative g.l.p.c. The

Can. J. Chem. Downloaded from www.nrcresearchpress.com by 210.87.254.5 on 09/05/12
For personal use only.

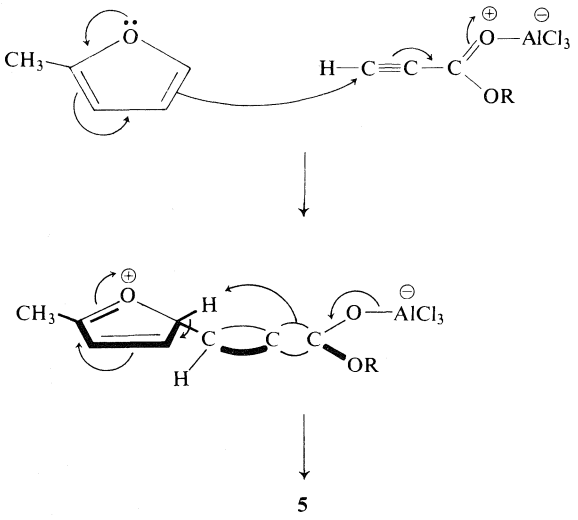

SCHEME 1

isolated yields of **5***a*, **8***a*, and **10***a* were 1.3, 0.2, and 0.7% respectively.

Reaction of 2-Phenylfuran with Ethyl Propiolate

The reaction with 2-phenylfuran followed an analogous pathway to that described above for 2-methylfuran, to give corresponding products. The reaction conditions, work-up procedures, and techniques of separation and purification were similar, but there were three important points of difference. (*i*) There was much less diene polymerization and consequently better product yields were obtained, (*ii*) although **5***b* (8%) and **10***b* (7%) could be isolated, no **8***b* was detected, indicating that steric control was greater in this reaction, and (*iii*) compound **6***b* was not readily hydrolyzed and so was the only compound obtained by base extraction of the crude reaction product.

Structures

The structures of the products were elucidated on the basis of p.m.r. (Tables 1–3), i.r., and mass spectral data (see Experimental).

Compounds 6a, 6b, and 8a

The acid-catalyzed rearrangement of 7-oxabicyclo[2.2.1]hepta-2,5-diene 2,3-dicarboxylates to 3-hydroxyphthalates is now well known (1). Analogous rearrangement of adducts **3** and **4** can lead *only* to structures **6** and **8** respectively. The major reaction products were unambiguously identified as **6***a* and *b* as follows:

(*a*) Non-bonded phenolic hydroxyl groups were evidenced by base solubility and by the chemical shift of the hydroxyl proton (3.00 in **6***a*, 3.49 τ in **6***b*). In the 3-hydroxyphthalates **2** (1), where the OH group is strongly hydrogen-bonded to an ortho carbethoxyl substituent, the chemical shift of the hydroxyl proton is at characteristically low field (*ca.* −1.0 τ).

(*b*) Both compounds showed i.r. absorptions for non-bonded ester carbonyl (1716 for **6***a*, 1713 cm^{-1} for **6***b*) and non-bonded phenolic hydroxyl (3610 for **6***a*, 3606 cm^{-1} for **6***b*) under conditions of high dilution (0.001 *M* in CCl_4). At higher concentrations absorptions for both free and intermolecularly hydrogen-bonded ester and hydroxyl were observed (see Experimental).

(*c*) Hydrolysis of **6***a* afforded the known hydroxy-acid **7***a*. The m.p. of the product (182–184°) was consistent with that reported in the literature (185°) (11).

(*d*) The chemical shifts of the carbethoxyl methylene (5.94 τ) and methyl (9.07 τ) hydrogens of **6***b* were diagnostic of an ortho phenyl substituent. Analogous shielding of carbethoxyl protons was observed (1) in diethyl 3-hydroxy-6-phenylphthalates (**2**, $R_1 = C_6H_5$).

The structure of **8***a* followed conversely from its insolubility in base, the relatively low-field position of the hydroxyl proton signal (−0.63 τ), and i.r. absorptions (0.002 *M* in CCl_4) for intramolecular hydrogen-bonded ester carbonyl (1666 cm^{-1}) and hydroxyl (broad band centered at 3200 cm^{-1}) groups.

Compounds 5a and b

The structures of the furylacrylate derivatives **5***a* and *b* were established on the basis of the following observations:

(*a*) The p.m.r. spectra (Table 2) of both compounds showed two very characteristic AB type systems for two olefinic and for two furan ring protons. The coupling ($J \approx 16$ Hz) between the olefinic protons suggests that these have a *trans* orientation (12), while that ($J \approx 3.4$ Hz) between the two ring protons indicates that they occupy positions 3 and 4 on the ring (13). Signals for carbethoxyl and ring methyl or phenyl hydrogens were also observed.

(*b*) Both **5***a* and *b* showed strong i.r. absorptions for conjugated ester carbonyl (1705 and 1700 cm^{-1} respectively) and for a conjugated double bond (1634 and 1620 cm^{-1} respectively). The *trans* stereochemistry of the double bond in **5***a*

Can. J. Chem. Downloaded from www.nrcresearchpress.com by 210.87.254.5 on 09/05/12
For personal use only.

Can. J. Chem. Downloaded from www.nrcresearchpress.com by 210.87.254.5 on 09/05/12
For personal use only.

TABLE 1. The p.m.r. parameters for **6***a*, **6***b*, **7***a*, and **8***a*

Compound	τ-Values			Aromatic hydrogens						
	—$CO_2CH_2CH_3$	−OH (−CO_2H)	R (CH_3 or C_6H_5)	H_3H_4* average τ	H_6 average τ	$\Delta\nu_{34}$ (Hz)	J_{34} (Hz)	J_{36} (Hz)	J_{46} (Hz)	Long-range coupling with ring CH_3 (Hz)
6*a*	8.66(3H, t), 5.65(2H, q)	3.00(1H, bs)	7.51(3H, bs)	2.99	2.55	7.9	8.6	0	2.5	H_3(0.3)
6*b*	9.07(3H, t), 5.94(2H, q)	3.49(1H, bs)	2.70(5H, s)	2.90	2.63	13.4	8.6	0	2.5	—
7*a*†		0.95(2H, bs)	7.49(3H, bs)	2.95	2.49	9.6	8.6	0	2.6	H_3(0.5), H_6(0.3)
8*a*	8.60(3H, t), 5.61(2H, q)	−0.63(1H, s)	7.72(3H, bs)	2.94	2.37	24.1	8.6	0	2.4	H_4(0.3), H_6(0.4)

*H_4 is at higher field than H_3 in **6***a*, **6***b*, and **7***a*: H_3 is at higher field than H_4 in **8***a*.
†Measured in acetone-d_6.

TABLE 2. The p.m.r. parameters for **5***a* and *b**

Compound	τ-Values		Olefinic and ring hydrogens										
									Long-range couplings (Hz)				
	$-CO_2CH_2CH_3$	R (CH_3 or C_6H_5)	H_PH_Q average τ	$\Delta\nu_{PQ}$ (Hz)	J_{PQ} (Hz)	H_3H_4 average τ	$\Delta\nu_{34}$ (Hz)	J_{34} (Hz)	H_3H_P	H_3H_Q	H_4H_P	H_4H_Q	$H_{3(CH_3)}$	$H_{4(CH_3)}$
5*a*	8.96(3H, t), 5.90(2H, q)	8.14(3H, bs)	2.97†	61.9	15.9	4.15‡	25.2	3.3	—	0.2	—	—	0.3	1.0
5*b*	8.93(3H, t), 5.87(2H, q)	2.3–3.1(5H, m)	2.93†	57.1	16.0	3.80‡	8.3	3.5	0.2	0.5	—	—	—	—

*Measured in benzene-d_6.
†H_Q is at higher field than H_P.
‡H_4 is at higher field than H_3 in **5***a*: H_3 is at higher field than H_4 in **5***b*.

TABLE 3. The p.m.r. parameters for **10***a* and *b*

Compound	τ-Values		H_A average τ	CH_2(B) average τ	J_{AB} (Hz)	H_3H_4 average τ	$\Delta\nu_{34}$ (Hz)	J_{34} (Hz)	Long-range couplings (Hz)					
	$-CO_2CH_2CH_3$	R (CH_3 or C_6H_5)							H_3H_A	H_4H_A	H_3H_B	H_4H_B	$H_{3(CH_3)}$	$H_{4(CH_3)}$
10*a*	8.80(3H, t), 5.88(2H, q)	7.75(3H, bs)	5.45	7.06	7.7	4.10*	5.6	3.1	—	—	—	—	0.3	0.9
10*b*	8.85(3H, t), 5.88(2H, q)	2.3–2.9(10H, m)	5.18	6.92	7.6	3.64*	19.4	3.3	0.8	0.2	0.2	—	—	—

*H_4 is at higher field than H_3 in **10***a*; H_3 is at higher field than H_4 in **10***b*.

Can. J. Chem. Downloaded from www.nrcresearchpress.com by 210.87.254.5 on 09/05/12
For personal use only.

was indicated by an absorption at 970 cm^{-1}; a similar assignment could not be made in the case of **5***b* since several bands occurred in this region of its i.r. spectrum.

(*c*) The mass spectra of **5***a* and *b* were characterized by ions of high abundance at *m/e* 135 and 197 respectively, corresponding to loss of 45 mass units ($-OC_2H_5$). The spectra also showed ions at *m/e* 43 and 105 (corresponding to CH_3CO and C_6H_5CO fragments), not present in those of **6***a* and *b*.

Compounds 10a and b

Elucidation of the structures of the difuryl propionate derivatives **10***a* and *b* was based on the following:

(*a*) The most characteristic feature of the p.m.r. spectra (Table 3) of **10***a* and *b* was the AB_2 type system (one-proton "triplet" and two-proton "doublet") observed in each case for the adjacent methine and methylene hydrogens. The four furan ring protons of each compound gave an AB type spectrum (J = 3.1–3.4 Hz), similar to those observed for the ring protons of **5***a* and *b*.

(*b*) Both **10***a* and *b* showed strong i.r. absorption for a saturated ester carbonyl group (1732 and 1731 cm^{-1} respectively).

(*c*) The mass spectra had base peaks at *m/e* 175 (**10***a*) and 299 (**10***b*), corresponding to a very characteristic loss of 87 mass units (by cleavage of the $-CH_2CO_2C_2H_5$ fragment). The spectra were also characterized by strong ions at *m/e* 43 (**10***a*) and 105 (**10***b*), for the fragments CH_3CO and C_6H_5CO.

Conclusions

The $AlCl_3$-promoted reactions of 2-monosubstituted furans with ethyl propiolate provides a convenient one-step route to 2-substituted-5-hydroxybenzoates, and extends the usefulness of this procedure in the preparation of aromatic compounds. Yields of course are limited in some cases by competitive diene polymerization. The reaction appears to be further limited to furans carrying an electron-releasing substituent: under the same experimental conditions, furfural and ethyl propiolate do not react.

Furan itself reacts with ethyl propiolate under the same conditions to give a mixture of 2:1 diadducts (9). Similar reactions of 2,5-disubstituted furans give mixtures of isomeric polysubstituted phenols, the isomer distribution being dependent on reaction conditions and substituent type (2). The full results of these investigations will be published shortly.

Experimental

The p.m.r. spectra were recorded with a Varian A-60A spectrometer equipped with a V-6058A spin-decoupler, using $CDCl_3$ as solvent (unless otherwise stated) and tetramethylsilane as internal standard. The chemical shifts and coupling constants reported are judged to have an accuracy of ±0.02 p.p.m. and ±0.3 Hz respectively. Values of small long-range couplings were estimated by comparison of the half-band widths of the appropriate coupled and decoupled signals. The i.r. spectra were obtained on a Perkin–Elmer model 521 spectrometer, and the mass spectra with a Dupont-C.E.C. model 21-491 spectrometer.

Reaction of 2-Methylfuran with Ethyl Propiolate

A solution of 2-methylfuran (6.56 g) in CH_2Cl_2 (120 ml) was added, at about 20°, to a mixture of ethyl propiolate (7.84 g) and anhydrous $AlCl_3$ (10.64 g) in CH_2Cl_2 (300 ml), to give a mixture 0.2 *M* in all three reagents. This was allowed to stand, with occasional shaking, for 30 min at room temperature, and was then shaken vigorously with cold water. The organic layer was separated, dried (Na_2SO_4), and evaporated to dryness.

(i) Isolation of 6a and 7a

The residue was dissolved in ether and the solution extracted thoroughly with 5% NaOH solution. After re-acidification (HCl) of the base extract to p*H* 1, extraction with ether afforded a semi-crystalline material (4.07 g). This was fractionated on the basis of solubility in $NaHCO_3$ solution. The bicarbonate-soluble fraction, after reacidification and extraction with ether, gave a colorless solid. Crystallization from water gave **7***a* as needles (2.63 g, 22%), subliming >165°, m.p. 182–184° (lit. 185° (11)); characteristic i.r. absorption (KBr) at 1680 cm^{-1}.

The bicarbonate-insoluble fraction gave a brown oil. Distillation at 120°/0.5 mm gave **6***a* as a cream-colored solid (640 mg, 4%), m.p. 53–55.5°. Ion of highest mass at *m/e* 180 ($C_{10}H_{12}O_3$ requires 180); characteristic i.r. absorptions (KBr) at 3400, 1672, and 1604 cm^{-1}; (0.005 *M* in CCl_4) at 3610, 3445 (broad), 1716 and 1685 cm^{-1} (shoulder); (0.001 *M* in CCl_4) at 3610 and 1716 cm^{-1}.

(ii) Isolation of 5a, 8a, and 10a

The NaOH-insoluble portion (5.69 g) of the crude product was recovered and washed thoroughly with petroleum-ether (b.p. 60–80°). This gave an insoluble pale brown amorphous solid (3.6 g), p.m.r. of which showed no ester or olefinic signals. The petrol-soluble fraction afforded an orange oil (2.0 g). This was chromatographed on a silicic acid column, with $CHCl_3$ as eluant. Fractions were collected in the following order:

(*a*) A pale yellow oil (95 mg), which on preparative t.l.c. (silica gel G, benzene : petroleum ether (1:1) as eluant) gave impure **8***a* (52 mg) of R_f 0.4. Final purification by preparative g.l.p.c. (5% carbowax on chromosorb G 8′ × 5/8″ column, operating at 170°) afforded **8***a* as a colorless oil (30 mg, 0.2%). Ion of highest mass at *m/e* 180 ($C_{10}H_{12}O_3$ requires 180). Characteristic i.r.

absorptions (0.002 *M* in CCl_4) at 3200 (broad) and 1666 cm^{-1}.

(*b*) The next fractions gave **10***a* as a pale yellow oil (135 mg, 0.7%), $n_D^{26} = 1.6551$. Ion of highest mass at *m/e* 262 ($C_{15}H_{18}O_4$ requires 262); characteristic i.r. absorption (liquid film) at 1732 cm^{-1}.

(*c*) The later fractions gave a pale yellow oil which was purified by preparative g.l.p.c. (20% carbowax on chromosorb W 8′ × 5/8″ column, operating at 150°) to give **5***a* as a colorless oil (190 mg, 1.3%), $n_D^{23} = 1.6551$, which crystallized on cooling to 0°. Ion of highest mass at *m/e* 180 ($C_{10}H_{12}O_3$ requires 180); characteristic i.r. absorptions (liquid film) at 1705, 1634, 1580, 1525, and 970 cm^{-1}.

Reaction of 2-Phenylfuran with Ethyl Propiolate

A solution of 2-phenylfuran (576 mg) in CH_2Cl_2 (6 ml) was added, at about 20°, to a mixture of ethyl propiolate (392 mg) and $AlCl_3$ (532 mg) in CH_2Cl_2 (14 ml), to give a mixture 0.2 *M* in all three reagents. After standing for 30 min at room temperature, with occasional shaking, the dark red reaction mixture was hydrolyzed as above.

(i) Isolation of ***6b***

The crude product was dissolved in ether and the solution extracted with 5% NaOH solution. Reacidification (HCl) and ether extraction gave **6***b* as a pale yellow gum (465 mg, 48%) which crystallized from petroleum ether as needles, m.p. 63–64°. Ion of highest mass at *m/e* 242 ($C_{15}H_{14}O_3$ requires 242); characteristic i.r. absorptions (KBr) at 3380, 3290, 1701, 1685, and 1600 cm^{-1}; (0.005 *M* in CCl_4) at 3605, 3440, 1713, and 1690 cm^{-1}; (0.001 *M* in CCl_4) at 3606 and 1713 cm^{-1}.

(ii) Isolation of ***5b*** *and* ***10b***

The NaOH-insoluble portion (385 mg) of the product was recovered to give a yellow oil which partially crystallized at 0°. This was submitted to preparative t.l.c. (silica gel G, $CHCl_3$ as eluant), fractions being collected as follows:

(*a*) A band of R_f 0.6 yielded **10***b* as a pale yellow oil (113 mg, 7%), $n_D^{26} = 1.6030$. Ion of highest mass at *m/e* 386 ($C_{25}H_{22}O_4$ requires 386); characteristic i.r. absorption (liquid film) at 1731 cm^{-1}.

(*b*) A band of R_f 0.4 yielded **5***b* as a pale yellow solid (78 mg, 8%) which was crystallized from petroleum ether (b.p. 60–80°) as colorless prisms, m.p. 79.5–81°. Ion of highest mass at *m/e* 242 ($C_{15}H_{14}O_3$ requires 242); characteristic i.r. absorptions (KBr) at 1700 and 1620 cm^{-1}.

We wish to thank Mrs. M. G. Flack and Mr. J. Van Ingen for their excellent technical assistance. Thanks are also due to Mr P. F. Seto for the i.r. spectra.

1. A. W. McCULLOCH, B. STANOVNIK, D. G. SMITH, and A. G. McINNES. Can. J. Chem. **47**, 4319 (1969). *cf.* P. VOGEL, B. WILLHALM, and H. PRINZBACH. Helv. Chim. Acta, **52**, 584 (1969); L. MAVOUNGOU GOMES. Compt. Rend. 270, *C*, 347 (1970); R. C. BANSAL, A. W. McCULLOCH, and A. G. McINNES. Can. J. Chem. **48**, 1472 (1970).
2. A. W. McCULLOCH and A. G. McINNES. Chem. Can. September, 1967. p. 51.
3. E. F. LUTZ and G. M. BAILEY. J. Am. Chem. Soc. **86**, 3899 (1964).
4. J-C. SOULA, D. LUMBROSO, M. HELLIN, and F. COUSSEMANT. Bull. Soc. Chim. Fr. 2065 (1966).
5. T. INUKAI and T. KOJIMA. J. Org. Chem. **31**, 1121 (1966).
6. T. INUKAI and T. KOJIMA. J. Org. Chem. **32**, 869 (1967).
7. J. SAUER. Angew. Chem. Inter. Ed. 6, 16 (1967).
8. R. M. ACHESON. *In* Advances in heterocyclic chemistry. Vol. 1. Academic Press, New York, N.Y., London, 1963. p. 125; K. SCHOFIELD. *In* Hetero-aromatic nitrogen compounds. Pyrroles and pyridines. Butterworths, London, 1967. p. 69–70. *cf.* R. C. BANSAL, A. W. McCULLOCH, and A. G. McINNES. Can. J. Chem. **47**, 2391 (1969).
9. R. HUISGEN, B. GIESE, and H. HUBER. Tetrahedron Lett. 1883 (1967).
10. R. K. BANSAL, A. W. McCULLOCH, D. G. SMITH, and A. G. McINNES. Unpublished work.
11. D. PELTIER. Compt. Rend. 236, 1972 (1953).
12. L. M. JACKMAN and S. STERNHELL. Applications of nuclear magnetic resonance spectroscopy in organic chemistry. 2nd ed. Pergamon Press, 1969. p. 301–302.
13. Reference 12, p. 306.

Can. J. Chem. Downloaded from www.nrcresearchpress.com by 210.87.254.5 on 09/05/12
For personal use only.

Can. J. Chem. Downloaded from www.nrcresearchpress.com by 210.87.254.105 on 09/05/12
For personal use only.

Solvent and Temperature Effects on Nitrogen Nuclear Spin Relaxation in Methyl Nitrate

CHRISTINE M. SHEPPERD, T. SCHAEFER, AND (IN PART) B. W. GOODWIN AND J. T'RAA
Chemistry Department, University of Manitoba, Winnipeg, Manitoba

Received February 22, 1971

Analysis of the proton resonance line shape yields quadrupolar relaxation times for the nitrogen nucleus in methyl nitrate, both neat and in solution with 14 different solvents. Variable temperature studies lead to activation parameters for molecular reorientation in dimethylformamide and in cyclohexane. Factors influencing the rotational rate of the solute molecule are elucidated; the results are analyzed in terms of various models for the correlation time characteristic of rotation in the liquid. None are successful in predicting the observed differences between reorientational rates in polar and nonpolar solvents. The Debye–Stokes model is evidently applicable to the solution in the polar dimethylformamide but not to the solution in the nonpolar saturated hydrocarbons. In the latter the inertial model of Steele is more satisfactory. Other solvents fall between these two extremes.

L'analyse de l'allure des bandes de résonance protonique donne les temps de relaxation quadripolaires pour l'atome d'azote du nitrate de méthyle à la fois pur et en solution dans quatorze différents solvants. Des études de variation de température permettent d'obtenir des paramètres d'activation pour la réorientation moléculaire dans la diméthylformamide et le cyclohexane. Les facteurs que influencent la vitesse de rotation de la molécule de soluté ont été élucidés; les résultats sont analysés en termes de modèles variables pour le temps de corrélation caractéristique d'une rotation dans le liquide. Aucun n'a permis de prédire avec succès les différences observées entre les vitesses de réorientation dans des solvants polaires et non polaires. Le modèle de Debye-Stokes est évidemment applicable à la solution dans la diméthylformamide polaire et non pas à la solution dans les hydrocarbures saturés non polaires. Dans ce dernier cas, le modèle rigide de Steele est plus satisfaisant. Pour les autres solvants, on se place entre ces deux extrêmes.

Canadian Journal of Chemistry, **49**, 3158 (1971)

Introduction

The existence of a quadrupole moment in the ^{14}N nucleus, and the presence of a non-spherically symmetric electric field at the nucleus due to the surrounding electron distribution, affect the magnetic resonance of the nitrogen nucleus and of other nuclei spin-coupled to it. Depending on the rate of the quadrupolar relaxation, the resonance of a spin-1/2 nucleus spin-coupled to a single nitrogen nucleus varies between the two extremes of a sharp triplet in the absence of relaxation and a sharp singlet when relaxation is very fast. It is possible to determine the quadrupolar relaxation time, T_q, of the nitrogen nucleus from an analysis of the proton resonance line shape (1).

T_q values provide a useful tool for the study of molecular reorientation in the liquid (2). The primary advantage of this approach rests on the premise that the electric field gradient is dominantly intramolecular and that the quadrupolar spin–lattice relaxation mechanism overwhelmingly predominates over the dipolar and spin-rotational relaxation of the ^{14}N nucleus. Accounting for relative translation in an expression for the relaxation time and the complication of including several mechanisms for relaxation can thus be neatly avoided by the use of quadrupolar nuclei. For a nucleus of spin 1 under conditions of extreme narrowing, the quadrupolar relaxation rate is given by (3)

$$[1] \qquad T_q^{-1} = 3/8(e^2qQ/\hbar)^2\tau_q$$

where $e^2qQ/\hbar$ is the nitrogen quadrupolar coupling constant and τ_q, the correlation time for molecular reorientation, is intimately coupled to molecular interactions. Hence the observed temperature, pressure, and solvent variations of T_q reflect the dependence of τ_q on these properties (the quadrupolar coupling constant, being an intramolecular parameter, is to a first approximation invariant to changes in temperature, etc.). In this paper we describe the procedure used to determine T_q and report the influence of temperature and solvent on the spin relaxation of ^{14}N in methyl nitrate. Our results will be discussed in terms of the various models proposed for molecular motion.

Can. J. Chem. Downloaded from www.nrcresearchpress.com by 210.87.254.105 on 09/05/12
For personal use only.

Experimental

1. Materials

Methyl nitrate was prepared by the esterification of methanol with nitric acid and purified by vacuum distillation. All solvents were of spectral grade and used without further purification. For temperature and solvent studies 15 mol% solutions of methyl nitrate plus a small amount of tetramethylsilane (TMS) were enclosed in glass tubes and carefully degassed by repeated freeze–pump–thaw cycles. Methyl nitrate is unstable to extremes of temperature and this fact was considered during the variable temperature work.

2. Nuclear Magnetic Resonance Measurements

All proton magnetic resonance (p.m.r.) spectra were measured on a Varian HA-100D spectrometer operated in the frequency sweep mode and locked to internal TMS. The spectrum of each sample was measured and calibrated (by a period averaging technique) at least six times, employing radiofrequency intensities well below saturation level and sweep rates of 0.02 Hz/s or less. The sample temperature was determined from a previously prepared calibration graph of dial-setting against actual temperature, as recorded by a thermocouple. Temperatures are accurate to ±1 °C.

3. Viscosity and Density Measurements

The viscosities and densities of 15 mol% methyl nitrate dimethylformamide (DMF) and methyl nitrate cyclohexane (C_6H_{12}) solutions were determined at different temperatures by standard techniques (Ostwald viscometer and pycnometer). The estimated error of the viscosity measurements is 2–3%.

Results and Discussion

1. Derivation of Relaxation Times T_q

The proton spectrum of methyl nitrate is shown in Fig. 1 at various temperatures in different solvents. The transition between singlet and triplet structures is clearly exhibited.

The theory underlying the shape of the absorption band was developed by Pople (1) and later modified to include the natural linewidth $(\pi T_2)^{-1}$ by Kintzinger *et al.* (4). The line shape expression $I(\nu)$ is given by

$$[2]\quad I(\nu) = \frac{C_1 + \Delta\nu^2(C_2 + \Delta\nu^2 C_3)}{C_4 + \Delta\nu^2[C_5 + \Delta\nu^2(C_6 + \Delta\nu^2)]}$$

where C_1 to C_6 are terms involving T_q, J (the ^{14}N—H coupling constant) and T_2 (the natural linewidth of the proton resonance in the absence of quadrupolar relaxation); $\Delta\nu$ is the shift in Hz from the center of the multiplet.

A program in Fortran IV was written for an IBM 360/65 computer equipped with a Calcomp plotter and used to construct theoretical absorption bands, $I(\nu)$, on the basis of eq. 2 for a variety of T_q values. Input parameters were J, T_2,[1] and a "reasonable" T_q value. A search was made around this central figure employing variable step sizes until iteration was almost complete. Spectra were then calculated at 0.0025 s

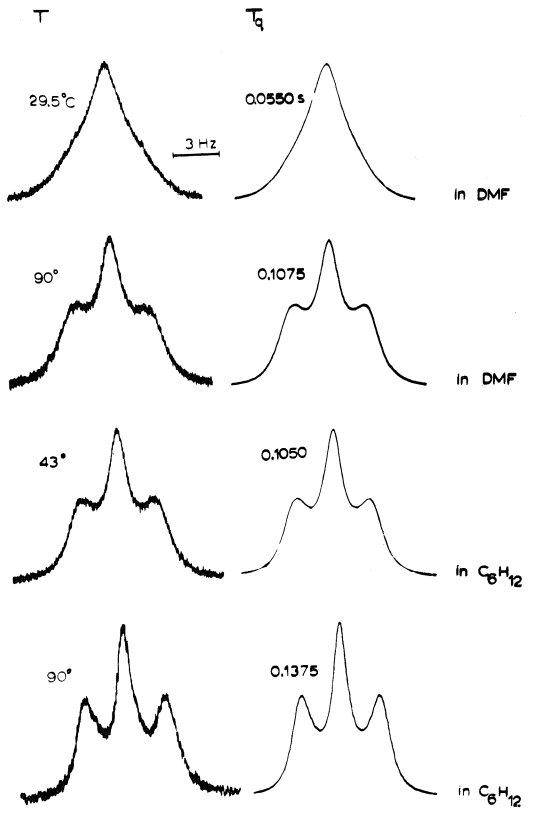

FIG. 1. Experimental and calculated resonance spectra of methyl nitrate in C_6H_{12} and DMF solutions at various representative temperatures and relaxation times.

[1]In none of the recorded spectra is the proton triplet sufficiently resolved to permit direct measurement of J and T_2. An effective T_2 was therefore determined from the solvent resonance since the linewidths of both solute and solvent (in the absence of exchange or relaxation effects) are determined by magnetic field inhomogeneities. $J(^{14}N—H)$ was obtained indirectly by recording the p.m.r. spectrum at high power and measuring the separation of the satellites caused ^{15}N—H coupling (0.36% abundance of ^{15}N). A neat sample and 50 mol% solutions in toluene and in chloroform all had $|J(^{15}N—H)| = 3.90 \pm 0.05$ Hz so that $|J(^{14}N—H)| = 2.78 \pm 0.04$ Hz because $\gamma^{15}N/\gamma^{14}N = -1.403$. This approach has been used previously (5) for ^{15}N–^{19}F coupling constants, but not, to our knowledge, for ^{15}N–^{1}H. It is interesting to note that Kintzinger (4) obtained a value of 2.75 Hz for $J(^{14}N—H)$ in methyl nitrate by complete line shape analysis involving iteration to a "best" set of J, T_2, and T_q values.

Can. J. Chem. Downloaded from www.nrcresearchpress.com by 210.87.254.105 on 09/05/12
For personal use only.

intervals, five on either side of the most probable T_q value, to enable a realistic error estimate to be made. Experimental and calculated spectra were compared visually by superimposing one on the other for different values of T_q until optimum agreement was found. For each temperature and solvent all experimentally recorded spectra were matched with the Calcomp plots; invariably this led to a "best" T_q value, with upper and lower limits estimated from the extreme T_q's which gave reasonable agreement. This is a rapid method for obtaining relaxation rates and also a reliable one since the entire line shape is fitted at the same time. However, at relaxation rates greater than the coupling constant $J(^{14}N—H)$, where the resonance is a broadened singlet, the fit is less sensitive to changes in T_q and the error limits are correspondingly larger.

In an attempt to overcome this problem an additional method of fitting the spectra was used in conjunction with visual matching. Application of a subroutine (developed previously for other rate studies) to the numerical output $I(\nu)$ of the main program generated certain characteristics of the resonance line shape which are sensitive to the rate of relaxation (*e.g.* positions of maxima and minima and their half-height linewidths). Comparison of these with the corresponding experimental parameters (as measured from the recorded spectra) permitted T_q values to be determined. Again, however, where the line shape is a broadened singlet fitting is less precise (T_q values are ± 0.005 s) than for a resolved triplet (where an error of ± 0.0025 s is associated with T_q). This represents an error of 2–5% in T_q which is somewhat less than that of conventional (spin-echo) methods for measuring ^{14}N spin–lattice relaxation times (6). Unfortunately this advantage is largely offset by the low sensitivity of the proton line shape to temperature. T_q changes by only 0.05 s in the entire 60 °C interval so that fitting of individual spectra to within at least 0.0025 s is necessary for an accurate determination of activation parameters. Examples of experimental and computer simulated spectra are given in Fig. 1. Tables 1 and 2 list the quadrupolar relaxation times for ^{14}N as a function of temperature (in the two solvents DMF and C_6H_{12}) and in 12 other solvents at ambient temperature.

TABLE 1. Quadrupole relaxation times, T_q, from fitted spectra for methyl nitrate

Dimethylformamide		Cyclohexane	
Temperature (°C)	T_q* (s)	Temperature (°C)	T_q* (s)
29.5	0.0550	28.5	0.0925
38.5	0.0625	38	0.1000 0.0975
49	0.0725	43	0.1050 0.1025
59	0.0800	48	0.1075 0.1050
69.5	0.0875	53	0.1100 0.1075
80	0.0975	58	0.1150 0.1125
90	0.1075	63	0.1175 0.1150
		68	0.1200 0.1175
		80	0.1300 0.1275
		90	0.1375

*Estimated error ± 0.0025 s. Where two values are given at one temperature they are the error limits.

2. *Activation Parameters*

The quadrupolar correlation time τ_q is determined only by reorientational motions so that its temperature dependence leads to activation parameters which can be unambiguously assigned to molecular rotation. If the temperature dependence follows the Arrhenius rate equation (2) then

$$[3] \qquad \tau_q = \tau_q^0 \exp(E_a/RT)$$

where τ_q^0 is an inverse frequency factor (and approximately constant) and E_a is an effective activation energy. From eq. 1 one then has

$$[4] \quad \log T_q = \log\left[\tau_q^0 \frac{3}{8}\left(\frac{e^2qQ}{\hbar}\right)^2\right]^{-1} - \frac{E_a}{2.303RT}$$

In Fig. 2 an Arrhenius plot of $\log T_q$ *vs.* $1/T$ is

TABLE 2. ^{14}N relaxation rates for methyl nitrate in various solvents at ambient temperature together with some physical properties of the solvent

Solvent	T_q (s)	Viscosity* (cP at 20 °C)	Dielectric constant* (20 °C)
1. CH_3CN	0.0950	0.325	38.8
2. CH_3COCH_3	0.0800	0.326	21.4
3. CS_2	0.0850	0.367	2.6
4. $CDCl_3$†	0.0650	0.563	5.1
5. C_7H_8	0.0800	0.590	2.4
6. C_6D_6†	0.0750	0.647	2.3
7. DMF	0.0550	0.924	37.6
8. CCl_4	0.0700	0.952	2.2
9. C_6H_{12}	0.0925	0.960	2.1
10. CH_3SOCH_3	0.0325	2.47	48.9
11. C_8H_{16}	0.0850	2.23	—
12. n-$C_{12}H_{26}$	0.0900	1.35(25°)	~2
13. n-$C_{16}H_{34}$	0.0800	3.63	~2
14. *cis*-Decalin	0.0775	3.38	~2
15. Neat	0.0625	—	23.9

*Data taken from International Tables (McGraw-Hill Book Company, Inc., New York, 1933).
†Physical properties taken to be those of the protonic species.

TABLE 3. Activation parameters for the reorientation of methyl nitrate*

Compound	E_a (kcal/mol)	$\tau_q^0 \times 10^4$ (s)	$\Delta G^{\ddagger}$ (at 353 °K) (kcal/mol)	$\Delta H^{\ddagger}$ (kcal/mol)	$\Delta S^{\ddagger}$ (kcal/deg mol)
C_6H_{12}	1.36±0.05	15.5±1	1.4±0.1	0.70±0.06	−2.1±0.2
DMF	2.38±0.06	4.7±0.4	1.6±0.1	1.73±0.7	0.3±0.2

*Quoted values are standard errors derived from the least squares analysis. They do not include uncertainties in T_2 and are probably therefore overly optimistic, since the line shape (and thus T_q) is known to be sensitive to changes in T_2 (5, 8).

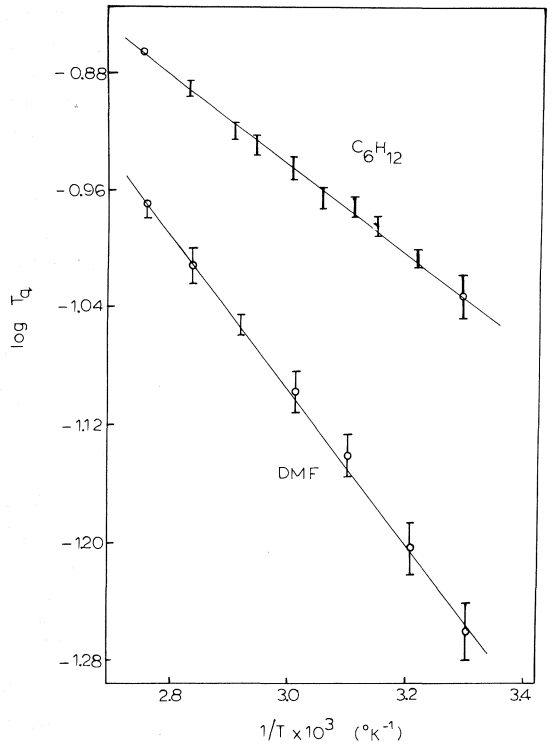

FIG. 2. A plot of log T_q *vs.* the reciprocal absolute temperature for the DMF and C_6H_{12} solution of methyl nitrate. The error bars were obtained as discussed in the text.

shown for the DMF and C_6H_{12} solutions. The points lie on a straight line within the limits of experimental accuracy but see refs. 2, 7. The activation energies and inverse frequency factors[2] are given in Table 3. Also listed are activation enthalpies and entropies[2] derived from plots of log T_q/T *vs.* $1/T$ as indicated by eq. 5 which follows from eq. 1 and the Eyring rate equation

$$[5] \quad \log \frac{T_q}{T} = \log\left(\frac{kf}{h}\right) - \log\left\{\frac{3}{8}\left(\frac{e^2qQ}{h}\right)^2\right\} + \frac{\Delta S^{\ddagger}}{4.577} - \frac{\Delta H^{\ddagger}}{4.577T}$$

k is the Boltzman constant and f the transmission coefficient (set equal to unity).

Comparison of the results of Table 3 with other work (see, for example 2, 4, 9–11) shows that the activation energies measured for methyl nitrate by the high-resolution p.m.r. method lie in the expected region; differences are generally compatible with the relative molecular shapes and sizes. A previously reported E_a value of 1.8 kcal/mol for the reorientation of methyl nitrate in tetrachloroethylene solution (4) lies between that found for DMF solution (2.38 kcal/mol) and C_6H_{12} solution (1.36 kcal/mol), demonstrating the effect of solvent on the activation parameters. While other workers have stressed the importance of viscosity in this respect (6, 12) the present results, involving two solvents of very similar viscosity (Table 2), show clearly that the dielectric constant is also significant; a larger barrier to molecular reorientation is presented by media of high dielectric constant than by less polar ones. This point is discussed further in the following sections.

3. *Solvent Dependence of Relaxation Rates*

It is apparent from the data in Tables 1 and 2 that T_q depends upon the nature of the solute–solvent system *i.e.* the rotational correlation time τ_q is sensitive to the solvent (6, 14–18). Bloembergen, Purcell, and Pound (19) applied Stokes' formula to Debye's theory of dielectric relaxation and proposed that for a sphere of radius a imbedded in a continuous medium of viscosity η

$$[6] \quad \tau_q = (4/3)\pi a^3 \eta / T$$

where T is the absolute temperature. Incorporating eq. 6 into eq. 1 shows that

[2]A knowledge of the ^{14}N quadrupole coupling constant in methyl nitrate is required in order to estimate the frequency factors and entropies from the intercept. Since e^2qQ/h has not been measured for this molecule an approximate value was estimated as in ref. 2; consequently the error in these activation parameters is doubtless larger than indicated in Table 3.

Can. J. Chem. Downloaded from www.nrcresearchpress.com by 210.87.254.105 on 09/05/12
For personal use only.

Can. J. Chem. Downloaded from www.nrcresearchpress.com by 210.87.254.105 on 09/05/12
For personal use only.

[7] $$T_q^{-1} = \frac{\pi a^3}{2}\left(\frac{e^2qQ}{\hbar}\right)^2 \frac{\eta}{T}$$

which predicts the temperature dependence of T_q^{-1} to parallel that of the ratio of viscosity to absolute temperature, provided the Debye–Stokes model is valid. Figure 3 shows these plots for C_6H_{12} and DMF solutions of methyl nitrate. With DMF solution the close agreement between activation energies computed from the relaxation rate curve of ^{14}N and the η/T curve indicates that the temperature dependence of the rotational motion is accurately described by the temperature dependence of η/T. These results support the Debye–Stokes model, eq. 6, where frictional forces alone are assumed to determine molecular motion. For the case of a strongly interacting solute–solvent system such as methyl nitrate/DMF (both highly polar) this approach appears to be a good approximation. Interestingly, Woessner *et al.* found a similar agreement for *n*-dodecane both neat and in carbon tetrachloride solution (17).

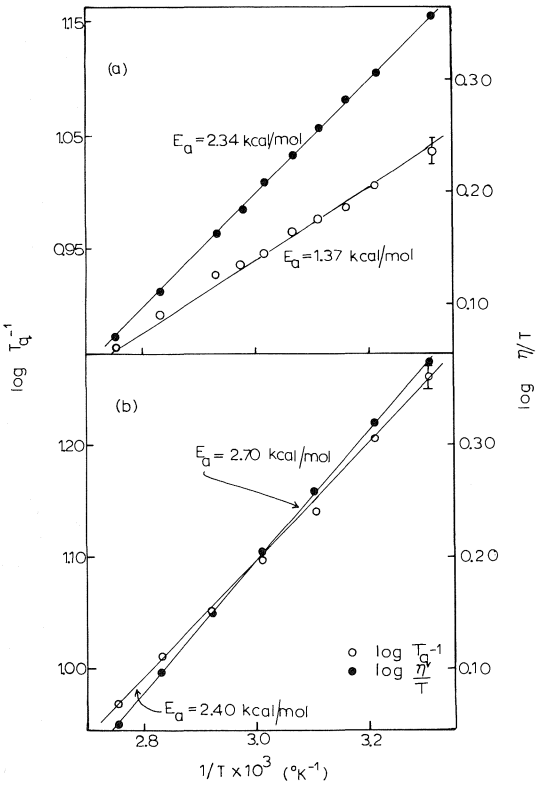

FIG. 3. The temperature dependences of the nitrogen relaxation rate and of viscosity for methyl nitrate in (*a*) C_6H_{12} solution and (*b*) DMF solution. Estimated error (shown only for one point) was obtained as discussed in the text.

However, for the methyl nitrate/C_6H_{12} system (and certain others (11, 20)) E_a for spin relaxation is found to be considerably less than that for η/T, yet large enough to rule out a dominance of molecular rotation by inertial effects, as has been suggested by Moniz *et al.* (21). This does not mean, however, that the rotation is independent of the moment of inertia. For a polar solute in a nonpolar solvent it is reasonable to assume that solute–solvent interactions will be less than for a polar solute/polar solvent pair *i.e.* that solute rotation in the former case involves less disturbance of neighboring molecules than in the latter system where simultaneous translation and rotation is probable. Now viscosity can be regarded as a measure of the momentum transfer between liquid layers moving with different velocities (a translational phenomenon) so that no relation between viscosity and rotational motion is expected unless simultaneous translation of other molecules is involved in rotation. Only in that case would the viscosity be a reasonable measure of the drag actually encountered by the rotating molecule. Thus the Debye–Stokes prediction of an equal temperature dependence for intramolecular relaxation and η (based on the assumption of a viscosity dependent rotational rate) depends critically on the nature of the molecular interactions in solution. It appears to be satisfactory for the rotation of methyl nitrate in DMF, but not in C_6H_{12} solution.

4. Solvent Dependence at Constant Temperature

It is also possible to test the dependence of correlation time on viscosity by changing the composition of the sample at constant temperature. The Debye–Stokes model predicts that the correlation time is directly proportional to the viscosity at a given temperature. Figure 4, using the data in Table 3, shows a scatter of points (greater than that found by Herbison-Evans and Richards (15) in similar studies) although a general trend of increasing relaxation rate with increasing viscosity and dielectric constant is apparent. It has been suggested (22) that the Debye–Stokes model could be improved by taking account of the discontinuous nature of the liquid medium through a microviscosity factor. This approach gives

Can. J. Chem. Downloaded from www.nrcresearchpress.com by 210.87.254.105 on 09/05/12
For personal use only.

[8] $$\tau_q = \frac{4\pi a^3 \eta}{3kT}\frac{a}{6b}$$

where b is the radius of the solvent molecule. Hence T_q^{-1} should depend linearly on η/b at constant temperature. However, this modification gave only marginal improvement to the plot in Fig. 4. An alternative approach, based on considerations of momentum transfer, has been given by Hill (23) and modified by Mitchell and Eisher (14). They obtain

[9] $$\tau_q = 2Ia\eta/\mu kT$$

where I is the average of the principal moments of inertia of the solute molecule and μ is the reduced mass of the solute–solvent system. A plot of T_q^{-1} *vs.* η/μ again gave a scatter of points similar to that in Fig. 4.

Closer examination of Fig. 4 and similar plots reveals that the data can be divided into two groups (ignoring for the moment points for the saturated hydrocarbons (9, 11–14). One 'straight' line can be drawn through the data for nonpolar but polarizable solvents (CS_2, $C_6H_5CH_3$, C_6D_6, CCl_4, (3, 5, 6, 8)) and another through the data for polar solvents as suggested by the broken lines in Fig. 4. Apparently an increase in dielectric constant enhances the relaxation rate over and above that brought about by an increase in viscosity. An empirical formula due to Murty (24),

[10] $$\tau_q = 6\pi\alpha\eta/(\varepsilon + 2)kT$$

(where α is the polarizability of the solute and ε the dielectric constant of the solvent) is successful for a number of liquids (25), although the methyl nitrate data certainly do not conform to eq. 10. In fact a plot of the data using eq. 10 shows that differences between polar and nonpolar solvents are accentuated.

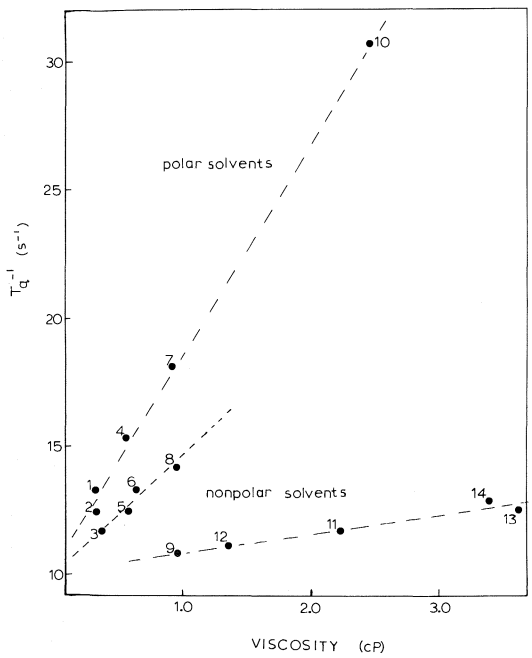

FIG. 4. ^{14}N relaxation rate as a function of viscosity for solutions of methyl nitrate, at ambient temperature. Solvents used were *1* = CH_3CN; *2* = acetone; *3* = CS_2; *4* = $CDCl_3$; *5* = $C_6H_5CH_3$; *6* = C_6D_6; *7* = DMF; *8* = CCl_4; *9* = C_6H_{12}; *10* = DMSO; *11* = C_8H_{16}; *12* = *n*-$C_{12}H_{26}$; *13* = *n*-$C_{16}H_{34}$; *14* = *cis*-decalin. The numbering is the same as in Table 2.

Figure 4 and plots based on eqs. 8 and 9 were designed to test the predictions of the Debye–Stokes, microviscosity, and modified Hill models, respectively. All appear to be inadequate as a description of the reorientation of methyl nitrate. In these plots a change in viscosity is accompanied by a change in numerous other physical properties associated with the new solvent; evidently the theories themselves are at fault or factors other than macroscopic viscosity are important in determining rates of molecular reorientation; or both may be true. That the data can be divided into two "straight" lines is probably significant and suggests that both the microviscosity and Hill theories are valid for a range of solvents where the molecular interactions do not vary appreciably. Indeed good agreement between experimental and calculated values of molecular correlation times has been variously reported for both theories (17, 18, 14, 26). The polarity of the solvent is clearly an important parameter, yet the relaxation rate does not depend on dielectric constant in the simple way suggested by Murty. Unfortunately our results do not suggest any alternative means of accounting explicitly for polar interactions in an expression for rotational correlation times.

5. *Relaxation in Saturated Hydrocarbon Solvents*

In Fig. 4 the points for ^{14}N relaxation in the saturated hydrocarbon solvents lie far below the rest and in fact show a relative independence of viscosity incompatible with any of the above theories. Moniz *et al.*'s model (21) of an inertial dominance of rotation is probably the most

satisfactory here, although the solute molecule is naturally not spherical or nonpolar!

Qualitatively, one might summarize as follows. The relatively large saturated hydrocarbon molecules each present a small segment of low polarizability to the polar methyl nitrate molecule and thus hinder the reorientation of the latter by almost the same amount, independently of the macroviscosity of the hydrocarbon liquid.[3] At the other extreme, the polar molecular DMF (and probably DMSO) interacts strongly with the solute molecule, dragging it along through the solvent and hence the macroviscosity of the solvent is a relatively acceptable measure of the hindrance to reorientation of the methyl nitrate molecule. The nonpolar but relatively polarizable solvents like CS_2 and CCl_4 (which also possess a large quadrupole moment relative to the saturated hydrocarbons) are then expected to and do fall between the two extremes represented by DMSO (point 10 in Fig. 4) and n-$C_{16}H_{34}$ (point 13 in Fig. 4).

Quantitatively it is difficult to see how a general model for these variations in relaxation time can be found.

6. *Internal Motion Effects of the Electric Field Gradient*

We assumed above that internal motions were not affecting T_q. Two internal motions able to reorient the field gradients at the nitrogen nucleus are rotation about the O—N bond and rotation of the methyl group about the C—N bond. If the nitrogen relaxation is to be affected the internal motion must reorient the field gradients relative to the molecular coordinate system at a rate comparable to the reorientation rate of the whole molecule.

The barrier to rotation about the O—N bond is 9.1 kcal/mol (27) and rotation about this bond is therefore much too slow to promote nitrogen relaxation in the temperatures under consideration. The barrier to internal rotation of the methyl group is 2.3 kcal/mol (27) and is therefore comparable to the barriers restricting the overall rotation. However, as pointed out by Wallach and Huntress (28) for the somewhat similar case of dimethylformamide, the orientations of the methyl group will likely have a very small effect on the orientation of the field gradient at the nitrogen (a large effect might be expected for deuterons placed in the methyl group).

[3]The chemical shift of the proton resonance of methyl nitrate in C_6H_{12} is independent of temperature, suggesting little dimerization of the solute molecules in these solvents.

We are grateful to the National Research Council of Canada for financial support.

1. J. A. Pople. Mol. Phys. **1**, 168 (1958).
2. W. B. Moniz and H. S. Gutowsky. J. Chem. Phys. **38**, 1155 (1963).
3. A. Abragam. The principles of nuclear magnetism. Oxford University Press, London. 1961.
4. J. P. Kintzinger, J. M. Lehn, and R. L. Williams. Mol. Phys. **17**, 135 (1969).
5. A. V. Cunliffe and R. K. Harris. Mol. Phys. **15**, 413 (1968).
6. T. D. Alger and H. S. Gutowsky. J. Chem. Phys. **48**, 4625 (1968).
7. J. G. Powles. Molecular relaxation processes. Chemical Society Special Publication Number 20, London. 1966. p. 127.
8. M. Broze and Z. Luz. J. Phys. Chem. **73**, 1600 (1969).
9. D. L. Hogenboom, D. E. O'Reilly, and E. M. Peterson. J. Chem. Phys. **52**, 2793 (1970).
10. T. T. Bopp. J. Chem. Phys. **47**, 3621 (1967).
11. D. E. O'Reilly and G. E. Schacher. J. Chem. Phys. **39**, 1768 (1963).
12. E. Rahkamaa. J. Chem. Phys. **48**, 531 (1968).
13. R. J. Abraham, L. Cavalli, and K. G. Pachler. Mol. Phys. **11**, 471 (1966).
14. R. W. Mitchell and M. Eisner. J. Chem. Phys. **33**, 86 (1960).
15. D. Herbison-Evans and R. E. Richards. Mol. Phys. **7**, 515 (1964).
16. E. Bock and E. Tomchuk. Can. J. Chem. **47**, 4635 (1969).
17. D. E. Woessner, B. S. Snowden, Jr., R. A. McKay, and E. T. Strom. J. Mag. Res. **1**, 105 (1969).
18. T. E. Burke and S. Chan. J. Mag. Res. **3**, 55 (1970).
19. N. Bloembergen, E. M. Purcell, and R. V. Pound. Phys. Rev. **73**, 679 (1948).
20. D. E. Woessner. J. Chem. Phys. **40**, 2341 (1964).
21. W. B. Moniz, W. A. Steele, and J. A. Dixon. J. Chem. Phys. **38**, 2418 (1963).
22. A. Gierer and K. Wirtz. Z. Naturforsch, **48**, 532 (1953).
23. N. E. Hill. Proc. Phys. Soc. London, B **67**, 149 (1954).
24. C. R. K. Murty. Indian J. Phys. **32**, 580 (1958).
25. R. C. Gupta, V. O. Agrawal, and S. S. Gupta. Ann. Der Phys. **20**, 209 (1967).
26. A. M. Pritchard and R. E. Richards. Trans. Faraday Soc. **62**, 1388 (1966).
27. W. B. Dixon and E. B. Wilson, Jr. J. Chem. Phys. **35**, 191 (1961).
28. D. Wallach and W. T. Huntress, Jr. J. Chem. Phys. **50**, 1219 (1969).

Can. J. Chem. Downloaded from www.nrcresearchpress.com by 210.87.254.105 on 09/05/12
For personal use only.

Can. J. Chem. Downloaded from www.nrcresearchpress.com by 210.87.254.40 on 09/05/12
For personal use only.

Successive Nucleophilic Substitution at Four-Coordinate Boron. Some Novel Chelated and Polynuclear Boron($n+$) Salts

SUE A. GENCHUR,[1] GARY L. SMITH,[2] AND HENRY C. KELLY[3]
Department of Chemistry, Texas Christian University, Fort Worth, Texas 76129

Received March 22, 1971

Reactions of various polyamines with the mono- and diiodoborane adducts of trimethylamine yield chelated and polynuclear boron($n+$) ions. Treatment of excess trimethylamine-monoiodoborane with *N,N′*-dimethylpiperazine, triethylenediamine, and *N,N,N′,N″,N″*-pentamethyldiethylenetriamine give the corresponding di- and trinuclear salts. At about 30°, the diiodoborane combines with triethylenediamine to give a dinuclear ion, but in refluxing benzene, the product is a polynuclear salt. Trimethylamine-diiodoborane reacts with pentamethyldiethylenetriamine (in excess) to produce a bicyclic chelate. The reaction between *N,N,N′,N′*-tetramethylethylenediamine (TMED) and the diiodoborane gives two chelated products, $[TMED(CH_3)_3NBH]^{2+}.2I^-$ and $(TMEDBHI)^+.I^-$. The latter salt, unlike its *B*-bromo and *B*-hydrido analogs, exhibits acidic behavior. This is tentatively explained by assuming a relatively high lability of the boron-bonded iodine.

Les réactions entre un certain nombre de polyamines et les produits mono- et diiodoborane de la triméthylamine conduisent à des ions bore($n+$), chélatés et polynucléaires. Le traitement d'un excès de monoiodoborane de triméthylamine avec la *N,N′*-diméthylpipérazine, la triéthylénediamine et la *N,N,N′,N′,N″,N″*-pentaneméthyldiéthylènetriamine conduit aux sels correspondants di- et trinucléaire. A 30 °C environ, le diiodoborane se combine avec la triéthylènediamine pour conduire à un ion dinucléaire, alors que dans le benzène au reflux, le produit obtenu est un sel polynucléaire. Le diiodoborane de la triméthylamine réagit avec la pentaméthyldiéthylènetriamine (en excès) pour donner un chélate bicyclique. La réaction entre la *N,N,N′,N′*-tétraméthylènediamine (TMED) et le diiodoborane conduit à deux composés chélatés, $[TMED(CH_3)_3NBH]^{2+}.2I^-$ et $(TMEDBHI)^+.I^-$. Ce dernier sel présente un caractère acide, à l'inverse de ses analogues portant un brome ou un hydrure en position *B*. Une tentative d'explication est donnée d'après laquelle la liaison bore-iode serait très labile.

Canadian Journal of Chemistry, **49**, 3165 (1971)

Introduction

Displacement reactions on amine-haloboranes have been shown by Nöth, Beyer, and Vetter (1) to be useful for the preparation of four-coordinate boron cations. This type of reaction has been considered a possible mechanistic step in a modified synthesis of such ions by Douglass (2) and has been applied widely for the preparation of a variety of bis(ligand) boronium ion salts (3–5). In one variation of this reaction, amine-haloboranes have been treated with selected diamines to produce chelated boronium ions and dinuclear boron(2+) salts (4–6). In this paper further extensions of such consecutive nucleophilic displacement at four-coordinate boron are examined through reactions of polyfunctional amines with the mono- and diiodoborane adducts of trimethylamine. Interesting chelated and polynuclear boron($n+$) ions, resulting from competing intra- and intermolecular reactions, are described.

[1]OSW Research Fellow, 1970–1971.
[2]OSW Research Fellow, 1969–1970
[3]To whom correspondence should be addressed.

Experimental

Materials

Trimethylamine-borane was obtained from Matheson, Coleman and Bell and was used without further purification. The mo o- and diiodoborane adducts were synthesized by methods similar to those of Nöth and Beyer (7, 8) involving the reaction of trimethylamine-borane with the appropriate stoichiometric quantities of iodine in refluxing benzene. These products were recovered by flash evaporation of the solvent and purified by vacuum sublimation (at 50° for the monoiodoborane and at 75° for the diiodoborane). Benzene was boiled under reflux over sodium and distilled immediately before use. The *N,N,N′,N′*-tetramethylethylenediamine (TMED) was obtained from Matheson, Coleman and Bell and was purified by distillation, b.p. 120–122°. Pentamethyldiethylenetriamine (PMDT) from K & K Laboratories was distilled before use, b.p. 200–202°. The 1,4-diazabicyclo(2.2.2)-octane (triethylenediamine) and dimethylpiperazine (DMP) also were obtained from K & K and were used without further purification. Boronium ion salts were prepared as water-soluble iodides as described below. The relatively insoluble PF_6^- salts of these ions were obtained by addition of crystalline NH_4PF_6 to 2–3% aqueous solutions of the iodides.

Apparatus

Infrared spectra were obtained with KBr wafers using a Perkin–Elmer Model 237 infrared spectrophotometer. Each of the salts synthesized from trimethylamine-

Can. J. Chem. Downloaded from www.nrcresearchpress.com by 210.87.254.40 on 09/05/12
For personal use only.

TABLE 1. Proton n.m.r. spectra

Salt	Signal	Relative intensity	Chemical shift (δ) p.p.m. in solvent		
			DMSO-d_6	CD_3CN	D_2O
$TED[(CH_3)_3NBH_2]_2^{2+}.2PF_6^-$*	Singlet, $(CH_3)_3N$	3.0	−3.0		
	Singlet, CH_2	2.0	−3.7		
$TED[(CH_3)_3NBHI]_2^{2+}.2PF_6^-$*	Singlet, $(CH_3)_3N$	3.2		−2.8	
	Singlet, CH_2	2.0		−3.4	
$DMP[(CH_3)_3NBH_2]_2^{2+}.2PF_6^-$†	Unsym doublet, $(CH_3)N$	3.0	−2.8		
	Broad singlet, CH_2	1.0	−3.4		
$PMDT[(CH_3)_3NBH_2]_3^{3+}.3PF_6^-$‡	Unsym triplet, $(CH_3)N$	21.0		−2.8	
	Multiplet, CH_2	4.1		−3.4 to −3.6	
$PMDTBH^{2+}.2PF_6^-$‡	Singlet, $(CH_3)N$	3.0		−2.2	
	Triplet, CH_2	15.4		−2.8	
	Singlet, $(CH_3)_2N$				
	Triplet CH_2	4.1		−3.3	
$TMED(CH_3)_3NBH^{2+}.2PF_6^-$	Unsym doublet, $(CH_3)N$	21.0	−3.2		
	Singlet, CH_2	4.0	−3.7		
$TMEDBHI^+.I^-$§	Singlet, $(CH_3)_2N$	13.0			−3.5
	Singlet, CH_2	4.0			−4.2
poly-$TED[(CH_3)_3NBH]^{2+}.2(C_6H_5)_4B^-$*	Singlet, $(CH_3)_3N$	2.6		−3.0	
	Multiplet, CH_2	3.0		−3.1 to −3.5	
	Multiplet, C_6H_5	6.2		−6.8 to −7.4	

*TED = triethylenediamine.
†DMP = dimethylpiperazine.
‡PMDT = pentamethyldiethylenetriamine.
§TMED = tetramethylethylenediamine.

TABLE 2. Conductance data

Salt	Solvent	Molar conductance (ohm^{-1})*	Charge type indicated
$TED[(CH_3)_3NBH_2]_2^{2+}.2PF_6^-$	CH_3CN	380	2:1
$TED[(CH_3)_3NBHI]_2^{2+}.2PF_6^-$	CH_3CN	387	2:1
$DMP[(CH_3)_3NBH_2]_2^{2+}.2PF_6^-$	CH_3CN	386	2:1
$PMDT[(CH_3)_3NBH_2]_3^{3+}.3PF_6^-$	CH_3CN	581	3:1
$PMDTBH^{2+}.2PF_6^-$	CH_3CN	394	2:1
$TMED(CH_3)_3NBH^{2+}.2I^-$	H_2O	273	2:1
$TMEDBHI^+.I^-$	H_2O	241	2:1
poly-$TED[(CH_3)_3NBH]^{2+}.2I^-$†	H_2O	140	

*Conductance values are for 0.001 *M* solutions.

†Concentration based on 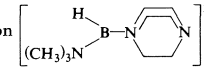 .$2I^-$ as the molecular unit.

monoiodoborane exhibited a doublet near 2500 cm^{-1}, indicative of the presence of the $—BH_2$ grouping, whereas spectra of salts prepared from the diiodoborane exhibited a singlet in this region characteristic of a single —B—H bond.

Proton nuclear magnetic resonance (n.m.r.) spectra (Table 1) were taken using a Varian A60-A n.m.r. spectrometer. Tetramethylsilane was used as an internal standard in acetonitrile-d_3 and dimethyl sulfoxide-d_6 and as an external standard with D_2O.

Conductivity measurements were made in acetonitrile and water employing a Fluke impedance bridge. The molar conductivities reported (Table 2) are for 0.001 *M* solutions of the salts.

Iodide and Hexafluorophosphate Salts of the N,N,N′,N′-Tetramethylethylenediaminetrimethylaminehydroboron(2+) Ion

A solution of 6.00 g (18.5 mmol) of trimethylaminediiodoborane in 10 ml of benzene was treated with 10 ml (65 mmol) of TMED and the mixture was stirred for 18 h at 75°. A solid product was recovered by vacuum filtration and a total of 2.05 g of unreacted diiodoborane was recovered from the filtrate by re-precipitation with petroleum ether. A portion of the solid reaction product was found to dissolve on the addition of methanol and the insoluble portion was separated by filtration. When the methanol filtrate was cooled in ice-water, some beige crystals identical to the original insoluble residue were obtained. This material was the iodide salt of the $(TMED)(CH_3)_3NBH^{2+}$ ion, which was identified as the PF_6^- salt (see below). Yield of iodide = 2.52 g (46.9% theory based on reacted diiodoborane). The iodide was recrystallized from methanol, m.p. 216–218° (decomp.). The hexafluorophosphate salt, obtained from an aqueous solution of the iodide and NH_4PF_6, was recrystallized from hot water, m.p. 272–273° (decomp.).

Anal. Calcd. for $C_9H_{26}BN_3^{2+}.2PF_6^-$ (477.06): C, 22.66; H, 5.49; N, 8.81. Found: C, 22.45; H, 5.50; N, 8.68.

N,N,N′,N′-Tetramethylethylenediamineiodohydroboron(1+) Iodide

This second product of the reaction of TMED with the diiodoborane was precipitated by the addition of benzene and petroleum ether to the methanol solution described above. Yield, 0.287 g (6.2% theory); m.p. 247–248° (decomp.).

Anal. Calcd. for $C_6H_{17}BIN_2^+.I^-$ (381.84): C, 18.87; H, 4.49; N, 7.34; I, 66.5. Found: C, 18.91; H, 4.63; N, 7.25; I, 65.0.

The iodide analysis was determined by a Volhard titration.

N,N,N′,N″,N″-Pentamethyldiethylenetriaminehydroboron(2+) Hexafluorophosphate

A total of 3.05 g (9.39 mmol) of trimethylaminediiodoborane was treated with 5 ml of pentamethyldiethylenetriamine (21 mmol) in 5 ml of benzene and the mixture was stirred for 18 h at 45°. The solid product was collected by filtration and dried *in vacuo*. Yield of the iodide, 0.301 g (7.9% theory). The hexafluorophosphate salt was precipitated and was purified by recrystallization from a mixture of acetonitrile and water, m.p. 211–213° (decomp.).

Anal. Calcd. for $C_9H_{24}BN_3^{2+}.2PF_6^-$ (475.05): C, 22.75; H, 5.09; N, 8.84. Found: C, 22.73; H, 5.32; N, 8.81.

Tris(trimethylaminedihydro)-μ3-N,N′,N″-(N,N,N′-N″,N″-pentamethyldiethylenetriamine)triboron(3+) Hexafluorophosphate

A 5.00 g (25.2 mmol) sample of trimethylamine-monoiodoborane was dissolved in about 50 ml benzene, and the solution treated with 20 ml of a benzene solution containing 0.726 g (4.19 mmol) of pentamethyldiethylenetriamine. After the mixture was stirred for 14 h at room temperature, the product was collected by filtration and dried *in vacuo*. Yield of the iodide, 2.35 g (73% theory). The PF_6^- salt was prepared and purified by recrystallization from hot water, m.p. (sealed capillary) 170–171° (decomp.).

Anal. Calcd. for $C_{18}H_{56}B_3N_6^{3+}.3PF_6^-$ (824.01): C, 26.24; H, 6.85; N, 10.20; P, 11.28. Found: C, 26.12; H, 6.71; N, 9.95; P, 11.07.

When the reaction was carried out using an excess of the triamine, the same product was formed in lower yield.

Bis(trimethylaminedihydro)-μ-N,N′-(N,N′-dimethylpiperazine)diboron(2+) Hexafluorophosphate

A 4.00 g (20.1 mmol) sample of trimethylaminemonoiodoborane was dissolved in 25 ml of dry benzene

Can. J. Chem. Downloaded from www.nrcresearchpress.com by 210.87.254.40 on 09/05/12
For personal use only.

Can. J. Chem. Downloaded from www.nrcresearchpress.com by 210.87.254.40 on 09/05/12
For personal use only.

under dry nitrogen and treated with 15 ml of a benzene solution containing 0.575 g (5.03 mmol) of dimethylpiperazine. The mixture was stirred at room temperature overnight. The product was collected by filtration and converted to the hexafluorophosphate salt which was purified by precipitation from dichloromethane solution *via* the addition of petroleum ether. Yield, 0.91 g (33% theory); m.p. (sealed capillary) 191.5–192.5° (decomp.).

Anal. Calcd. for $C_{12}H_{36}B_2N_4^{2+}.2PF_6^-$ (547.99): C, 26.30; H, 6.62; N, 10.22; P, 11.30. Found: C, 26.14; H, 6.66; N, 10.12; P, 11.07.

Bis(trimethylaminedihydro)-μ-N,N'-(1,4-diazabicyclo-(2.2.2)octane)diboron(2+) Hexafluorophosphate

A total of 5.00 g (25.2 mmol) of trimethylamine-monoiodoborane was dissolved in 30 ml benzene, and the flask was purged with dry nitrogen. A solution of 0.705 g (6.29 mmol) triethylenediamine in 30 ml benzene was added by means of an addition funnel. The solution was boiled under reflux for 2 h and then was allowed to stand at room temperature overnight. Yield of the iodide, 1.79 g (55.8% theory). The hexafluorophosphate salt was prepared, recrystallized from hot water, and dried *in vacuo*, m.p. 179.5–180.0° (decomp.).

Anal. Calcd. for $C_{12}H_{34}B_2N_4^{2+}.2PF_6^-$ (545.98): C, 26.40; H, 6.28; N, 10.26; P, 11.35. Found: C, 26.17; H, 6.42; N, 10.10; P, 11.07.

The experiment was repeated using an excess of triethylenediamine and the same product was obtained in lower yield.

Bis(trimethylamineiodohydro)-μ-N,N'-(1,4-diazabicyclo-(2.2.2)octane)diboron(2+) Hexafluorophosphate

A total of 1.49 g (13.3 mmol) of triethylenediamine was added to 7.14 g (22.0 mmol) of trimethylamine-diiodoborane in 30 ml benzene. The mixture was stirred at 30° for 12 h. The product was recovered by filtration and dried *in vacuo*. Yield, 2.05 g of the iodide salt (24.5% theory); m.p. 179–181° (decomp.). A hexafluorophosphate salt was obtained and was purified by recrystallization from hot water, m.p. 278–279° (decomp.).

Anal. Calcd. for $C_{12}H_{32}B_2I_2N_4^{2+}.2PF_6^-$ (797.77): C, 18.06; H, 4.04; N, 7.02. Found: C, 18.26; H, 3.97; N, 6.84.

Polymeric diazabicyclo(2.2.2)octanetrimethylamine-hydroboron(2+) Iodide

An 11.08 g (34.1 mmol) sample of trimethylamine-diiodoborane was dissolved in 100 ml benzene. A total of 5.67 g (51 mmol) of triethylenediamine was added slowly and the mixture was boiled under reflux for 40 h. Yield of the iodide, 13.62 g (93.8% theory); m.p. 164–171°, 171–180° (decomp.).

Anal. Calcd. for $C_{84}H_{208}B_{10}I_2N_{28}{}^{18+}.18I^-$: C, 23.70; H, 4.93; N, 9.21. Found: C, 23.81; H, 4.90; N, 9.21.

The theoretical analytical data are calculated assuming a chain length corresponding to ten boron atoms. The tetraphenylborate salt was formed by the addition of sodium tetraphenylborate to an aqueous solution of the iodide salt, m.p. 187–189° (decomp.).

Anal. Calcd. for $C_{84}H_{208}B_{10}I_2N_{28}{}^{18+}.18(C_{24}H_{20}B^-)$: C, 80.29; H, 7.42; N, 5.08; I, 3.29. Found: C, 63.87; H, 6.47; N, 6.46; I, 18.00.

Results and Discussion

Nucleophilic displacement by polyfunctional amines at four-coordinate boron in haloborane-amines may proceed by inter- and intramolecular pathways, and as expected, the dominant path is dependent on the nature of the substrate and on reaction conditions. Where chelation is possible, this route is generally favored when excess amine is employed. Thus, displacement in $(CH_3)_3NBHI_2$ with TMED in stoichiometric excess gives rise to chelation products **1** and **2**, essentially to the exclusion of a dinuclear complex.

[1] $(CH_3)_3NBHI_2 \xrightarrow[\text{(excess)}]{\text{TMED}}$

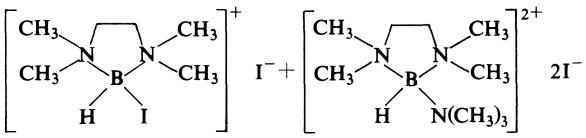

1 **2**

In a limited study of those reaction conditions favoring individual chelation products, it was found that the dipositive ion, **2**, was the only isolable product when the diiodoborane was employed in excess or when the reaction was carried out in refluxing benzene or refluxing neat TMED. Yields of **1** were improved when a large excess of TMED was employed and when a reaction temperature $< 60°$ was maintained (Table 3). It should be noted, however, that since the combined yields of **1** plus **2** were low in nearly all cases, a highly definitive statement on conditions affecting relative yields is not possible.

With $(CH_3)_3NBH_2I$ as a substrate, the hydride counterpart of **1**, namely, $TMEDBH_2{}^+I^-$ is obtained, and the *B*-bromo analog is formed from the reaction of TMED with $(CH_3)_3NBHBr_2$ (5). The fact that the bromide salt of the dipositive ion, **2**, was not observed in the reaction of the dibromoborane adduct with TMED is presumably due to bromide ion being a poorer leaving group than iodide. Moreover, **2** would not be expected to form via displacement in $(CH_3)_3NBH_2I$ since this would require the departure of the even poorer leaving group, H^-.

Unlike its *B*-bromo analog, complex **1** behaves as a moderately strong acid. A 0.011 *M* aqueous solution of this iodide salt exhibits a p*H* = 4.2. One equivalent of base is consumed on titration

TABLE 3. Product distribution for reaction of TMED with $(CH_3)_3NBHI_2$

Condition	Time (h)	Temperature (°C)	Recover yield, %* 1	2
20 ml TMED added to 6.00 g trimethylamine-diiodoborane in 10 ml benzene	24	51	20.1	—
3.57 g trimethylamine-diiodoborane dissolved in 35 ml neat TMED	24	55	4.3	—
10 ml TMED added to 6.00 g trimethylamine-diiodoborane dissolved in 10 ml benzene	24	56	12.2	11.0
	18	75	6.2	46.9
	3	80	—	31.8
	5	80	—	32.3
0.46 g TMED added to 3.48 g trimethylamine-diiodoborane dissolved in 10 ml benzene	44	65	—	3.4

*Products were separated and unreacted diiodoborane was recovered. Yields are based upon amounts of reacted diiodoborane.

[2] 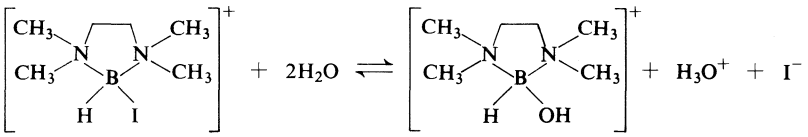

1 3

to the first (sharp) equivalence point (Fig. 1) and on further titration, a second equivalent is taken up with the development of a more gradual endpoint analogous to that obtained on neutralization of boric acid in the absence of a complexing agent such as mannitol or glycerol. Further, treatment of the iodide salt of **1** with $AgNO_3$ results in precipitation of all contained halogen (including boron-bonded iodine) as opposed to precipitation of only ionic bromide in the corresponding bromide salt of the *B*-bromo chelate. As a tentative explanation, it is suggested that the boron bonded iodine, unlike bromine, is relatively labile and that the acidity of complex **1** is due to hydrolytic dissociation.

There is no direct evidence for the *B*-hydroxo cation **3**, although it might be speculated that such a species is responsible for the consumption of a second equivalent of base (through the B—OH function). Addition of mannitol after the first equivalence point does not lower the p*H* of the solution, indicating that boric acid itself has not been formed. From Fig. 1, the pK_a of the more weakly acidic species is estimated to be 9.2. Conductivity measurements on aqueous solutions of **1** give a value for the molar conductance of 241 ohm^{-1}. This is in excess of the range of values expected for a 1:1 electrolyte, further suggesting that cation **1** may be partially dissociated in solution.

The reaction of excess pentamethyldiethylenetriamine (PMDT) with $(CH_3)_3NBHI_2$ resulted in successive intramolecular substitution to give (in low yield) the iodide salt of the chelated ion, **4**. This may reflect a somewhat greater tendency

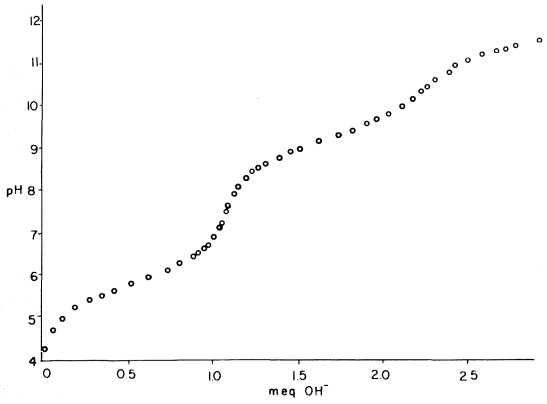

FIG. 1. Titration of 0.426 g (1.12 mmol) of (TMED)-$BHI^+.I^-$ with 0.120 *N* NaOH.

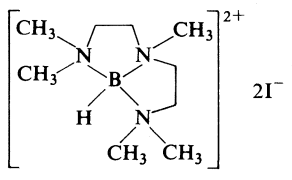

4

Can. J. Chem. Downloaded from www.nrcresearchpress.com by 210.87.254.40 on 09/05/12
For personal use only.

for chelation to occur with the diiodo adduct relative to the monoiodoborane, since the only isolable product obtained from the reaction of this triamine with $(CH_3)_3NBH_2I$ was one arising from intermolecular displacement, namely the trinuclear complex **5**.

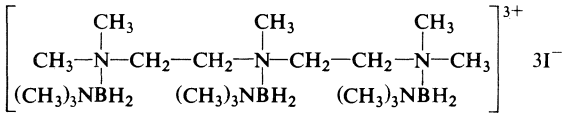

5

When dimethylpiperazine was reacted with a stoichiometric excess of the monoiodoborane, the dinuclear complex **6** was formed.

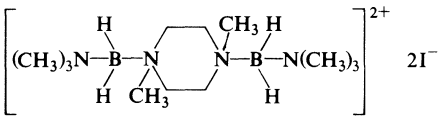

6

A bicyclic chelated boron(1+) ion containing dimethylpiperazine has been recently reported elsewhere (7).

With nitrogen at bridgehead positions as in diazabicyclo(2.2.2)octane (triethylenediamine), intramolecular substitution with chelation is precluded. The reaction of this difunctional nucleophile with $(CH_3)_3NBH_2I$ gave the dinuclear complex **7**.

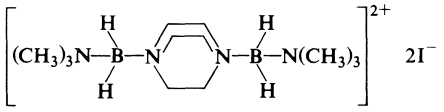

7

With the diiodoborane at 30°, the corresponding *B*-iodo derivative **8** was obtained.

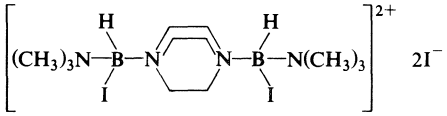

8

When the latter reaction is carried out with excess diamine in refluxing benzene, the formation of what is believed to be a polynuclear complex **9** occurs.

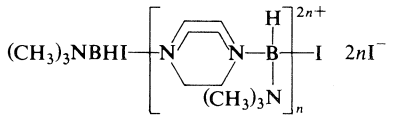

9

The theoretical analytical data for the polyion have been calculated assuming an average chain length corresponding to ten boron atoms, since at about this length, the analytical data change very slightly with change in size of the polymer. The ^1H n.m.r. spectrum of **8** shows a 3:2 ratio of methyl to methylene protons, while in the polymer, this ratio is about 5:6. This integration also is consistent with a polymer containing about ten boron atoms. The ratio would be expected to approach 3:4 as the length of the polymer chain becomes large. The tetraphenylborate salt of **9** was difficult to obtain in high purity as evidenced by the high iodine content and other discrepancies in the analytical data for this salt, as well as by the low intensity of the signal attributed to the phenyl protons of the $(C_6H_5)_4B^-$ ion in the ^1H n.m.r. spectrum. This is probably a result of the co-precipitation of I^- on formation of the insoluble tetraphenylborate salt. Such co-precipitation also has been observed during the isolation of other boron–nitrogen polyions prepared by vinyl polymerization reactions (9).

This research was supported by the Office of Saline Water, Grant No. 14-01-0001-2175 and by the Robert A. Welch Foundation and the Texas Christian University Research Foundation. Mr. Dennis L. Deavenport assisted in obtaining the n.m.r. spectra.

1. H. Nöth, H. Beyer, and H-J. Vetter. Ber. **97**, 110 (1964).
2. J. E. Douglass. J. Am. Chem. Soc. **86**, 5431 (1964).
3. K. C. Nainan and G. E. Ryschkewitsch. Inorg. Chem. **7**, 1316 (1968).
4. N. E. Miller, D. L. Reznicek, R. J. Rowatt, and K. R. Lundberg. Inorg. Chem. **8**, 862 (1969).
5. G. L. Smith and H. C. Kelly. Inorg. Chem. **8**, 2000 (1969).
6. G. E. Ryschkewitsch and T. E. Sullivan. Inorg. Chem. **9**, 899 (1970).
7. H. Nöth and H. Beyer. Ber. **93**, 2251 (1960).
8. J. R. Lowe, S. S. Uppal, C. Weidig, and H. C. Kelly. Inorg. Chem. **9**, 1423 (1970).
9. G. L. Smith, L. R. Johnson, and H. C. Kelly. Chem. Commun. 922 (1970).

Can. J. Chem. Downloaded from www.nrcresearchpress.com by 210.87.254.40 on 09/05/12
For personal use only.

Borane Adducts of Hydrazines and (Trifluoromethylphosphino) Hydrazines: a Nuclear Magnetic Resonance Study

L. K. PETERSON AND G. L. WILSON

Department of Chemistry, Simon Fraser University, Burnaby 2, British Columbia

Received May 17, 1971

Direct reactions between BX_3 (X = Me, F, Cl) and the methylhydrazines $MeNHNH_2$, Me_2NNH_2, Me_2NNHMe, and Me_2NNMe_2 yield 1:1 adducts in all cases except (*a*) BMe_3 and Me_2NNMe_2, which do not react; (*b*) BCl_3 and $MeNHNH_2$, Me_2NNH_2 or Me_2NNHMe, which result in hydrazinolysis of the B—Cl bond; and (*c*) BCl_3 with Me_2NNMe_2, which yields a dark brown, viscous liquid. However, the unstable 1:1 adducts $Me_2NNH_2BCl_3$ and $Me_2NNHMeBCl_3$ were prepared in solution, but were not isolated. On the basis of n.m.r. studies, it is concluded that adduct formation occurs at the more highly methylated nitrogen atom of Me_2NNH_2 and Me_2NNHMe; for $MeNHNH_2$, two isomeric adducts are formed with BF_3, in a 5:1 molar ratio, corresponding to complexation at the methylated nitrogen, and at the unsubstituted nitrogen atoms, respectively. A similar study of adduct formation between BX_3 and the trifluoromethylphosphinohydrazines $(CF_3)_2PNMeNMe_2$, $(CF_3)_2PNHNMe_2$, $(CF_3)_2PNMeNH_2$, and $(CF_3)_2PNHNHMe$ indicates that 1:1 adducts are formed in all cases except (*d*) BMe_3 with $(CF_3)_2PNMeNMe_2$, for which no reaction was observed; and (*e*) BCl_3 with $(CF_3)_2PNMeNH_2$ and $(CF_3)_2PNHNHMe$, for which elimination of $(CF_3)_2PCl$ was observed. The adducts are volatile white solids, except $(CF_3)_2PNMeNH_2BMe_3$, which is a colorless liquid at room temperature, and $(CF_3)_2PNMeNMe_2BCl_3$, which is a non-volatile solid. In only one case was it possible to deduce an unambiguous stereochemistry for the adduct from n.m.r. data, *viz.* $(CF_3)_2PNMeNH_2BX_3$, (X = Me, F) where complexation occurs at the terminal, least substituted nitrogen atom. In $(CF_3)_2PNMeNMe_2BF_3$ and in $(CF_3)_2PNHNHMeBF_3$, the NMe and the NMe_2 groups, and the PNH and NNH protons, respectively, are deshielded by the same, or very similar extents, so that an exclusive choice of structure cannot be made.

Les réactions directes entre BX_3 (X = Me, F, Cl) et les méthylhydrazines $MeNHNH_2$, Me_2NNH_2, Me_2NNHMe et Me_2NNMe_2 donnent dans tous les cas des produits d'addition 1:1 excepté: (*a*) BMe_3 et Me_2NNMe_2 qui ne réagissent pas; (*b*) BCl_3 et $MeNHNH_2$, Me_2NNH_2 et Me_2NNHMe ou il y a hydrazinolyse de la liaison B—Cl; et (*c*) BCl_3 avec Me_2NNMe_2 qui donne un liquide visqueux marron foncé. Toutefois, les produits d'addition 1:1 instables $Me_2NNH_2BCl_3$ et $Me_2NNHMeBCl_3$ ont été préparés en solution mais n'ont pas été isolés. Des études r.m.n. ont permis de conclure que la formation du produit d'addition se fait sur l'atome d'azote le plus complètement méthylé de Me_2NNH_2 et Me_2NNHMe. Pour $MeNHNH_2$, deux produits d'addition isomères se forment avec BF_3 dans le rapport molaire 5:1 ce qui correspond respectivement à la complexation sur l'azote méthylé et aux atomes d'azote non substitués. Une étude semblable de formation de produit d'addition entre BX_3 et les trifluorométhylphosphinohydrazines $(CF_3)_2PNMeNMe_2$, $(CF_3)_2PNHNMe_2$, $(CF_3)_2PNMeNH_2$, et $(CF_3)_2PNHNHMe$ indique que les produits d'addition 1:1 se forment dans tous les cas excepté pour (*d*) BMe_3 avec $(CF_3)_2PNMeNMe_2$ où aucune réaction n'est observée et; (*e*) BCl_3 avec $(CF_3)_2PNMeNH_2$ et $(CF_3)_2PNHNHMe$ pour lesquels on observe l'élimination de $(CF_3)_2PCl$. Les produits d'addition sont des solides volatiles blancs, sauf $(CF_3)_2PNMeNH_2BMe_3$ qui est un liquide incolore à la température ordinaire et $(CF_3)_2PNMeNMe_2BCl_3$ qui est un solide non volatile. Seulement dans un cas, il a été possible de déduire à partir des données r.m.n. une stéréochimie non ambiguë pour le produit d'addition, $(CF_3)_2PNMeNH_2BX_3$ (X = Me, F). Dans ce cas, la complexation se fait sur l'atome d'azote terminal, le moins substitué. Dans le cas de $(CF_3)_2PNMeNMe_2BF_3$ et de $(CF_3)_2PNHNHMeBF_3$, les groupes NMe et NMe_2 et les protons des groupements PNH et NNH, respectivement, sont déplacés avec des valeurs semblables ou très proches ce qui ne permet pas un choix exclusif de structure.

Canadian Journal of Chemistry, 49, 3171 (1971)

Can. J. Chem. Downloaded from www.nrcresearchpress.com by 210.87.254.5 on 09/05/12
For personal use only.

Discussion

The phosphinohydrazine skeleton, P—N—N, is potentially tribasic, with the two nitrogen atoms able to function as σ donors, while both σ and π acceptor capacity are possible for the phosphorus atom (1). In the case of (phenylphosphino) hydrazines $R_nP(NR'NMe_2)_{3-n}$ (n = 1, 2; R = C_6H_5; R′ = H, Me), studies of alkylation and chloramination reactions have shown that the phosphorus atom is more basic than either of the nitrogen atoms; the corresponding hydrazinophosphineoxides $R_nP(O)(NR'NMe_2)_{3-n}$ do not undergo alkylation or chloramination, indicating that both nitrogens are unreactive toward electron acceptor species (2). Similarly, adduct formation with boranes (3) and with carbonium species (2, 3) takes place at the phosphorus atom; surprisingly, even the terminal

Can. J. Chem. Downloaded from www.nrcresearchpress.com by 210.87.254.5 on 09/05/12
For personal use only.

nitrogen atom is unreactive toward electron acceptor molecules. Likewise, as in the case of aminophosphines, it is the phosphorus, rather than the nitrogen atom, that functions as the donor site toward acceptors based on boron (4), aluminum (5), phosphorus (6), carbonium (7), and transition metal species (8). Such findings are in keeping with the fact that trimethylphosphine is the most basic, toward BF_3, of the trimethyl derivatives of Group V elements (9). In the case of the P—N—N skeleton of $(CF_3)_2PNR'NMe_2$, one might expect diminished basicity of P due to the electronegative CF_3 substituents, and diminished basicity of the central N atom, due to π-bonding with phosphorus, thus leaving the terminal N atom as the most basic site in the molecule. This situation might be expected to preserve the P—N bond against cleavage reactions (10, 11) commonly found with aminophosphines and acidic species such as HCl (10), BF_3, and BCl_3 (12). However, if the lone pairs of electrons on the hydrazine moiety reside in essentially delocalized molecular orbitals, then the deactivating effect of the $(CF_3)_2P$ group may be transmitted to the terminal N atom as well. In order to resolve these speculations, the formation and stereochemistry of the adducts of a series of methylhydrazines, and of trifluoromethylphosphinohydrazines were studied, using mainly n.m.r. techniques.

The chemical shift for a given nucleus depends on several factors: (*a*) diamagnetic shielding caused by the electron cloud about the nucleus, (*b*) bulk diamagnetic susceptibility effects, (*c*) neighboring group anisotropic shielding, (*d*) intramolecular electric field effects, and (*e*) intermolecular interactions (13). By using internal reference standards, the need to correct for (*b*) was avoided. The effects (*c*) and (*d*) were assumed to be constant within each series of adducts studied. The solvent–solute and solute–solute interactions (*d*) may influence the chemical shift in terms of solvent, concentration, and temperature effects; variations among such effects were minimized by standardizing the experimental conditions for each series of adducts.

The possibility of exchange, for pure 1:1 adduct in solution, and for adduct in the presence of excess base, was checked using variable temperature n.m.r. studies.

Adducts of Amines and Hydrazines

A study of n.m.r. data pertaining to the adducts of ammonia and methylamines with BMe_3 and BF_3 shows that the latter acid is always more deshielding than the former; for the adjacent proton H—N→BX_3, the difference between the effects of BF_3 and BMe_3 is ~1.0 τ, whereas, for protons remote by two bonds, *e.g.* in H_3C—N→BX_3, the difference is ~0.2 τ (14).

The experimental n.m.r. data for hydrazines and their BX_3 adducts is collected in Table 1. A study of exchange processes indicated that, for the system $Me_2NNHMeBX_3 + Me_2NNHMe$ (X = Me, F, Cl), exchange was slowed by cooling to 10°; both intra- and intermolecular exchange of BX_3 among the basic centers is possible. For $Me_2NNH_2BMe_3 + Me_2NNH_2$, two separate signals for the NMe_2 groups of complexed and uncomplexed species were observed at −45°, the coalescence temperature being −25°. Thus an exchange rate $>25\ s^{-1}$ at room temperature is indicated (15). For $Me_2NNH_2BX_3 + Me_2NNH_2$ (X = F, Cl), separate signals for complexed and uncomplexed species were observed at +35°; for comparison within the set, measurements were made at −45°.

As for the methylamines, deshielding effects within the adducts of hydrazines, >N—N(R)-
| |
BX_3 and R—N—N→BX_3, are likewise trans-
|
mitted throughout the molecule, presumably with diminishing intensity as the number of intervening bonds increases. The NH chemical shifts, however, appear to be extremely sensitive to traces of moisture, and are therefore less reliable for stereochemical interpretations than data obtained for MeN protons. In $Me_2NNHMeBX_3$, the major deshielding effect occurs at the Me_2N group, indicating complexation at the more substituted N atom, *viz.*, $X_3B{\cdot}Me_2NNHMe$. In $Me_2NNH_2BX_3$, however, both the NH_2 and Me_2N protons experience substantial deshielding; the results for the NH_2 group were variable, depending upon the efficacy of drying. The data for the Me_2N group was comparable to that for the corresponding group in the BX_3 adducts of Me_2NNHMe, suggesting similar structures for the two complexes *viz.*, $X_3B{\cdot}Me_2NNHMe$.

The room temperature ^1H n.m.r. spectrum of $MeNHNH_2$ consists of two sharp peaks, of equal intensity, at 6.77 and 7.41 τ, corresponding to exchanging NH and NH_2 protons and to the Me group, respectively. At +39°, a 1:1 molar mixture of $MeNHNH_2$ and BMe_3 shows the same band at 7.41 τ for the MeN group, while a broad band

TABLE 1. The n.m.r. data for hydrazines and their BX_3 adducts*

Compound	Solvent	T °C	$-NH_2$	$\diagdown NH \diagup$	$-NMe_2$	$\diagdown NMe \diagup$	BMe_3	$BF_3(^{19}F)$
$MeNHNH_2$*[a]	$CDCl_3$	39	6.77	—	—	7.41	—	—
$MeNHNH_2BMe_3$†	$CDCl_3$	39	(6.03)	(6.03)	—	7.41	10.32	
$MeNHNH_2BF_3$*[a,c]	DMSO-d_6	39	6.70‡	—	—	7.33§	—	159.2‖
			2.62			7.23		151.6
			1.85					149.3
Me_2NNH_2*[a]	CH_2Cl_2	−45	6.76	—	7.58	—	—	—
$Me_2NNH_2BMe_3$*[a]	CH_2Cl_2	−45	6.19	—	7.39	—	10.33	—
$Me_2NNH_2BF_3$*[a,c]	CH_2Cl_2	−45	5.89		7.18	—	—	166.9¶
$Me_2NNH_2BCl_3$*[a]	DMSO-d_6	+35	5.05	—	6.97	—	—	—
Me_2NNHMe*[a]	CH_2Cl_2	+10	—	—	7.58	7.45	—	—
$Me_2NNHMeBMe_3$*	CH_2Cl_2	+10	—	6.22	7.50	7.50	10.30	—
$Me_2NNHMeBF_3$*[b,c]	CH_2Cl_2	+10	—	5.97	7.30	7.42	—	162.7¶
$Me_2NNHMeBCl_3$	CH_2Cl_2	+10	—	—	6.99	7.16	—	—
Me_2NNMe_2*[a]	$CDCl_3$	39	—	—	7.79	—	—	—
$Me_2NNMe_2BF_3$*[b,c]	DMSO-d_6	39	—	—	7.62	—	—	151.1
								149.2
								147.3
$Me_2NNMe_2BCl_3$*[b]	DMSO-d_6	39	—	—	7.18	—	—	—

*Chemical shifts were measured, using ~10% solutions, relative to (*a*) internal TMS; (*b*) external TMS, for ^1H nuclei (τ for TMS = 10.00); and (*c*) relative to external $CFCl_3$, for ^{19}F nuclei.
†Temperature dependent ^1H spectrum; see Discussion.
‡The NH peaks assigned thus: for $F_3BNH(Me)NH_2$, τ(NH), 1.85; (NH_2), 6.70; for $MeNHNH_2BF_3$, τ (exchanging NH and NH_2), 2.62; see Discussion.
§The MeN peaks assigned thus: $F_3BNH(Me)NH_2$, 7.33; $MeNHNH_2BF_3$, 7.23 τ; see Discussion.
‖The ^{19}F peaks assigned thus: $F_3BNH(Me)NH_2$, 159.2 p.p.m. J_{BF}, 1515 Hz; $MeNHNH_2BF_3$, 151.6 p.p.m., J_{BF}, 17.0 Hz; BF_4^- 149.3 p.p.m., J_{BF}, 1.0 Hz; see Discussion.
¶The B–F coupling constants were: for $Me_2NNH_2BF_3$, J_{BF}, 13.5 Hz; for $Me_2NNHMeBF_3$, J_{BF}, 14.2 Hz.

appears at 6.03 τ for the exchanging NH and NH_2 protons; at −40°, the spectrum consists of two doublets (mid points, 6.27 and 7.35 τ), in the intensity ratio 2:3. At the low temperature, it appears that exchange between NH and NH_2 has ceased, thus permitting coupling between the NH proton and (*a*) the MeN group (J_{NNCN} 5.8 Hz), and (*b*) the NH_2 group (J_{HNNH} 4.5 Hz). The theoretical 12-line spectrum of the NH proton was not observed. Similarly, at 39°, the spectrum for a mixture of $MeNHNH_2BMe_3$ and $MeNHNH_2$ (1:2 molar ratio) consisted of two peaks, indicative of equivalent NMe protons and equivalent NH and NH_2 protons. Thus the adduct is either fully dissociated at 39°, or rapid intermolecular exchange of BMe_3 amongst the hydrazine molecules is present. At −40°, however, the bands for complexed and uncomplexed species are distinguished. The bands were assigned on the basis of their relative intensities and the known composition of the mixture. Surprisingly, the signal for MeN (complexed) appears upfield relative to MeN (uncomplexed); an enhancement of hydrogen bonding interactions between complexed and free hydrazine may account for the deshielding of the free base, and may compensate for the deshielding, due to the BMe_3 moiety, within the complexed molecule.

The reaction of BF_3 with $MeNHNH_2$ gives a white crystalline adduct which is insoluble in $CDCl_3$, in CH_2Cl_2, and CH_2Cl_2, but dissolves in DMSO. The latter solvent, unfortunately, is unsuitable for low temperature n.m.r. studies. Both the ^1H and ^{19}F n.m.r. spectra are consistent with the presence of two isomers, (*a*) $F_3B{\cdot}MeNHNH_2$ and (*b*) $MeNHNH_2{\cdot}BF_3$, in a 5:1 molar ratio.

The ^1H n.m.r. spectrum consisted of bands which were assigned to MeN and to NH protons: two signals at 7.33 and 7.23 τ, in a 5:1 intensity ratio, corresponded to the MeN protons of isomers (*a*) and (*b*), respectively. The former signal is a poorly resolved 1:1:1:1 quartet, indicating coupling to the spin 3/2 ^{11}B nucleus (J_{BNCH} ~1.50; *cf.* J_{BNCH} for Me_3NBF_3, 1.54; for Me_2NHBF_3, 1.79; for $MeNH_2BF_3$, 2.05 Hz (14)). The three broad NH signals were assigned on the basis of their integrated intensities. Two bands for isomer (*a*) (at 6.70 (NH_2 group), and 1.85 τ (NH)) indicated the absence of exchange among the NH protons, whereas only one band (at 2.62 τ) indicated rapid intramolecular exchange among the corresponding protons of isomer (*b*); the intensity ratio was 2:1:3 for the three bands. The addition of excess $MeNHNH_2$ to a solution of the adduct gave rise to singlet MeN (at 7.43 τ) and NH (4.88 τ) signals, indicating rapid intermolecular exchange at +39°. The ^{19}F spectrum consisted of two major bands and an impurity band, the latter

Can. J. Chem. Downloaded from www.nrcresearchpress.com by 210.87.254.5 on 09/05/12
For personal use only.

TABLE 2. A study of adduct formation between BX_3 and trifluoromethylphosphinohydrazines*†

Compound	mmol	BMe_3	BF_3	BCl_3
$(CF_3)_2PNMeNMe_2$ **1**	Taken	0.587 (**1**) : 0.453*[a], ‡[a]	0.403 (**1**) : 1.501‡[b]	0.470 (**1**) : 0.679*[d], ‡[a], §
	Recovered		1.031	
	Used		0.470	
$(CF_3)_2PNHNMe_2$ **2**	Taken	0.725 (**2**) : 1.421‡[c]	2.019 (**2**) : 7.043‡[c]	0.623 (**2**) : 1.220‡[d], ‖
	Recovered	0.717	5.021	0.593
	Used	0.704	2.022	0.627
$(CF_3)_2PNMeNH_2$ **3**	Taken	0.485 (**3**) : 0.494*[b]	0.573 (**3**) : 0.571	*[c]
$(CF_3)_2PNHNHMe$ **4**	Taken	0.535 (**4**) : 0.529	1.276 (**4**) : 1.270	*[c]

*In all cases, volatile white solid 1:1 adducts were formed, except (*a*) $(CF_3)_2PNMeNMe_2 + BMe_3$, no evidence for adduct formation; (*b*) $(CF_3)_2PNMeNH_2 + BMe_3$, a colorless liquid 1:1 adduct; (*c*) in reactions between BCl_3 and $(CF_3)_2PNMeNH_2$ or $(CF_3)_2PNHNHMe$, the B—Cl bond was solvolyzed in preference to adduct formation; (*d*) $(CF_3)_2PNMeNMe_2 + BCl_3$, white, non-volatile 1:1 adduct.

†The adducts, or the component mixtures, were soluble in $CDCl_3$ and in $CFCl_3$.

‡Reactions were carried out: (*a*) in the absence of solvent; (*b*) in toluene; (*c*) in cyclohexane; (*d*) in chlorobenzene.

§For n.m.r. studies, the adduct was prepared in situ in an n.m.r. tube; a solution of the adduct in $CFCl_3$ slowly yielded a dark brown liquid, immiscible with $CFCl_3$.

‖A solution of the adduct in $CFCl_3$ slowly turned brown, and precipitated a white solid.

indicating the presence of a small amount of BF_4^- (a 1:1:1:1 quartet, δ at 149.3 p.p.m.; J_{BF} 1.0 Hz; spectrum for authentic BF_4^-, 149.8 p.p.m. and 1.0 Hz (16)). The main bands, in a 5:1 intensity ratio, were assigned to isomers (*a*) (δ, 150.2 p.p.m.; J_{BF} 15.5 Hz) and (*b*) (δ, 149.3 p.p.m.; J_{BF} 17.0 Hz), respectively; the higher field ^{19}F shift for isomer (*b*) is in accord with the expected greater basicity of the MeN center. The J_{BF} coupling constant is sensitive to the steric environment of the four coordinate nitrogen atom (*cf.* $Me_3N{\cdot}BF_3$, J_{BF} 13.8; $NH_3{\cdot}BF_3$, 13.8; $Me_2NH{\cdot}BF_3$, 15.5; $MeNH_2{\cdot}BF_3$, 15.7 Hz; (14)).

Adducts of Phosphinohydrazines

The (trifluoromethyl)phosphinohydrazine borane adducts were prepared by the reaction of BX_3 (X = Me, F, Cl) with the appropriate phosphinohydrazine dissolved in an inert solvent. Experimental details are summarized in Table 2.

The adducts of $(CF_3)_2PNMeNMe_2$ (**1**), $(CF_3)_2PNHNMe_2$ (**2**), $(CF_3)_2PNMeNH_2$ (**3**), and $(CF_3)_2PNHNHMe$ (**4**) with BX_3 (X = Me, F, Cl) vary in stability, both with respect to dissociation and with respect to chemical reaction. Thus $(CF_3)_2PNRNR'R''{\cdot}BCl_3$ adducts[1] undergo cleavage reactions, slowly for compounds **1** and **2**, but rapidly for **3** and **4**. In spite of the potential polybasic nature of the donor molecule, only 1:1 adducts were observed. The stoichiometry and stereochemistry of adduct formation were deduced from the n.m.r. spectra, and from determinations of the reaction ratios. In all cases the deshielding of the P atom, as measured by changes in the ^{19}F chemical shifts of the $(CF_3)_2P$ group upon complexation of the phosphinohydrazines, was relatively small (Table 3). Considerable deshielding effects were observed for protons attached directly, or indirectly via carbon, to the N atoms. The weak basicity of the P atom must be due to the electronegative CF_3 groups, which effectively reduce basicity in molecules such as $(CF_3)_2PMe$ and $(CF_3)_3P$. Of the two nitrogen atoms, one may be designated as "central", and the other as "terminal", within the P—N—N skeleton. The possible structures of complexes are illustrated in Fig. 1. These structures may be distinguished by the fact that BX_3 may be adjacent to, or one atom removed from, the (P)NR or (N)NR′R″ (R, R′, and R″ = H or Me) groupings. In theory, the actual location of the BX_3 group may be revealed by the observable deshielding effects on R or R′, on the basis that the order of deshielding will be: adjacent protons > protons remote by one bond > protons remote by two bonds.

As in the case of amines and hydrazines, more effective deshielding of N—H and N—CH_3 protons in the phosphinohydrazines is brought about by adduct formation with BF_3 than with BMe_3.

FIG. 1. Structures of phosphinohydrazine borane adducts.

[1]R, R′, R″ = H and/or Me.

Can. J. Chem. Downloaded from www.nrcresearchpress.com by 210.87.254.5 on 09/05/12
For personal use only.

TABLE 3. The n.m.r. data for trifluoromethylphosphinohydrazines and their BX_3 adducts*†

Compound	—NH_2	$\diagdown$NH$\diagup$	—NMe_2	$\diagdown$NMe$\diagup$	—BMe_3	—CF_3(^{19}F)	—BF_3(^{19}F)
$(CF_3)_2PNMeNMe_2$	—	—	7.50	7.13 $J_{P\sim H}$ 3.0 $J_{H\sim F}$ 0.7	—	63.4 $J_{P\sim F}$ 82.0	—
$(CF_3)_2PNMeNMe_2BMe_3$*[b]	—	—	7.50	7.14 $J_{P\sim H}$ 2.8 J_{FCPNCH} 0.7	9.32	61.5 $J_{P\sim F}$ 85.5	—
$(CF_3)_2PNMeNMe_2BF_3$*[b]	—	—	7.15	6.80 $J_{P\sim H}$ 2.0 J_{FCPNCH} 0.7		59.6 $J_{P\sim F}$ 88.5	153.4
$(CF_3)_2PNMeNMe_2BCl_3$*[b]	—	—	6.49‡	6.40 $J_{H\sim F}$ 0.7		58.1 $J_{P\sim F}$ 93.3	—
$(CF_3)_2PNHNMe_2$	—	5.95	7.50	—		63.5 $J_{P\sim F}$ 84.0	—
$(CF_3)_2PNHNMe_2BMe_3$*[a]	—	5.64	7.43	—	9.45	65.0 $J_{P\sim F}$ 83.0	—
$(CF_3)_2PNHNMe_2BF_3$*[a]	—	4.12 $J_{P\sim H}$ 11.0	7.07	—	9.45 $J_{P\sim F}$ 88.5	63.7	163.4
$(CF_3)_2PNHNMe_2BCl_3$	—	2.85	6.67	—	—	62.7 $J_{P\sim F}$ 89.0	—
$(CF_3)_2PNMeNH_2$	6.15	—	—	6.93 $J_{P\sim H}$ 8.5		60.6 $J_{P\sim F}$ 84.3	—
$(CF_3)_2PNMeNH_2BMe_3$*[a]	6.00	—	—	6.89 $J_{P\sim H}$ 8.5	9.45	60.6 $J_{P\sim F}$ 83.7	—
$(CF_3)_2PNMeNH_2BF_3$*[a]	3.80	—	—	6.72 $J_{P\sim H}$ 6.8		59.8 $J_{P\sim F}$ 89.5	148.5
$(CF_3)_2PNHNHMe$	—	5.70 (PNH) 6.39 (NNH)		7.37		63.8 $J_{P\sim F}$ 80.0	—
$(CF_3)_2PNHNHMeBMe_3$*[a]	—	5.03 (PNH) 5.47 (NNH)	—	7.27	10.02	63.5 $J_{P\sim F}$ 82.7	—
$(CF_3)_2PNHNHMeBF_3$*[a]	—	3.92 (PNH) 4.52 (NNH)	—	7.08§		62.9‖ $J_{P\sim F}$ 86.5	159.0

*Measurements were made using ~10% solutions in (*a*) $CDCl_3$, (*b*) $CFCl_3$.
†The ^{1}H chemical shifts are given relative to internal TMS, $\tau = 10.00$; ^{19}F shifts are given in p.p.m. relative to internal $CFCl_3$; coupling constants are reported in Hz.
‡A doublet, coupling not assigned.
§Temperature dependent signals; a doublet at +39°, with $J = 5.0$ Hz; coalescence temperature, 49°.
‖Temperature dependent signals: at +39°, a doublet of quartets, J_{F-F}, 8.0; first quartet, J_{PCF}, 86.0; second quartet, J_{PCF}, 87.0 Hz; coalescence temperature, 72°.

In many cases, however, the deshielding effect is transmitted to both of the N atoms of the hydrazine moiety, to essentially the same extent, so that a choice of structure cannot be made; for example, the NMe and NMe_2 groups in $(CF_3)_2PNMeNMe_2BF_3$, and the PNH and NNH protons in $(CF_3)_2PNHNHMeBF_3$, are deshielded to the same, or very similar, extents.

The band for the NMe protons in $(CF_3)_2PNMeNMe_2$, and in its adduct with BF_3, consists of two overlapping septets, indicative of coupling with the ^{31}P and ^{19}F nuclei. The NMe_2 group appears as a single absorption, devoid of fine structure. In $(CF_3)_2PNMeNMe_2BCl_3$, however, only one septet is present for the NMe protons, suggesting through-space coupling as the mechanism of the proton-fluorine interaction, while the band for the NMe_2 protons consists of a doublet (J(?)[2] 1.4 Hz). With $(CF_3)_2PNHNMe_2$ and its adducts, coupling between the ^{31}P nucleus and the NH proton is observed only for $(CF_3)_2PNHNMe_2BF_3$, suggesting coordination at the NH site. The possibility of a π-complex type of structure (Fig. 2), as has been suggested for hydrazine alane-complexes (17), cannot be excluded. In only one case, *viz.* $(CF_3)_2PNMeNH_2$-

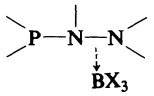

FIG. 2. Possible π-complex type of structure for phosphinohydrazine borane adducts.

[2]Not assigned.

Can. J. Chem. Downloaded from www.nrcresearchpress.com by 210.87.254.5 on 09/05/12
For personal use only.

TABLE 4. A study of adduct formation between BX_3 and methylhydrazines*†

Compound	mmol	BMe_3		BF_3	
$MeNHNH_2$	Taken	2.40§	2.43	2.29§	2.31
		White solid, 1:1 adduct, m.p. ~20°; soluble in $CDCl_3$, CH_2Cl_2		White solid, 1:1 adduct, m.p. ~50°; insoluble in $CDCl_3$, CH_2Cl_2; soluble in DMSO	
Me_2NNH_2	Taken	1.47	1.49	1.63	1.62
		White solid, 1:1 adduct, soluble in $CDCl_3$, $CDCl_3$, CH_2Cl_2		White solid, 1:1 adduct; soluble in $CDCl_3$, CH_2Cl_2	
Me_2NNHMe	Taken	1.72	1.84	1.38	1.41
	Recovered		0.14		
	Used		1.70		
		Colorless liquid, 1:1 adduct; soluble in CH_2Cl_2		Colorless liquid, 1:1 adduct; soluble in $CDCl_3$, CH_2Cl_2	
Me_2NNMe_2	Taken	1.25	1.24	1.25	1.26
	Recovered		1.24		
		No evidence for adduct formation		Colorless, non-volatile liquid adduct; insoluble in DCl_3, CH_2Cl_2; soluble in DMSO‡	

*Details are given for reactions performed in the absence of solvent; similar results were obtained for reactions carried out in solution.
†Reactions between (*a*) BCl_3 and $MeNHNH_2$ resulted in hydrazinolysis of the B—Cl bond; (*b*) BCl_3 and Me_2NNH_2 or Me_2NNHMe gave unstable 1:1 adducts only from reactions carried out in solution in cyclohexane; the adducts were insoluble in $CDCl_3$ and in CH_2Cl_2, but dissolved in DMSO; (*c*) BCl_3 and Me_2NNMe_2 proceeded vigorously at −33°, giving a dark brown viscous liquid, insoluble in $CDCl_3$ and CH_2Cl_2 but soluble in DMSO.
‡On standing, the solution became dark brown.
§This quantity, and those directly below, indicate mmoles of methylhydrazine taken.

BX_3 (X = Me, F) was it possible to deduce the stereochemistry of the adduct. The dominant deshielding effect occurs at the NH_2 protons, and of all adducts of phosphinohydrazines studied, the deshielding (by BF_3) of NH protons is greatest in this case. Thus the preferred structure involves complexation at the terminal, least substituted nitrogen atom (Fig. 3). With isomeric $(CF_3)_2$-PNHNHMe, where the central N atom is less sterically constrained, deshielding in the BX_3 adducts is experienced by both N atom centers. With $(CF_3)_2PNMeNMe_2$ and BMe_3, the absence of interactions associated with adduct formation was noted; indeed, a study with models showed severe steric crowding in the possible 1:1 adducts with BMe_3, but not with BF_3. A study of the shielding of the BX_3 moiety upon complexation reveals differing requirements for BMe_3 and BF_3: thus the largest shielding effect on BMe_3 occurs with $(CF_3)_2PNHNHMe$, whereas, in the case of BF_3, it is with $(CF_3)_2PNHNMe_2$. The greater steric requirements of the NMe_2 group, relative to NHMe, may be compensated by the possibility for hydrogen bonding in the BF_3, but not in the BMe_3, adduct (Fig. 3).

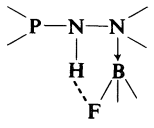

FIG. 3. Phosphinohydrazine–BF_3 structure showing hydrogen bonding.

Experimental

All materials were handled using a high vacuum system or a dry, inert atmosphere system. Hydrazine, methylhydrazine, and 1,1-dimethylhydrazine (K & K Chemicals) were dried over anhydrous barium hydroxide and further purified by low temperature column distillation and by vacuum fractionation. Trimethylhydrazine and tetramethylhydrazine were prepared and purified by the method of Class *et al.* (18). Trimethylboron, prepared by the method of Brown (19), boron trifluoride (Allied Chemicals), and boron trichloride (K & K), tetramethylsilane (Stohler Isotope Chemicals), and trichlorofluoromethane (Matheson, Coleman, and Bell) were purified by vacuum fractionation. Phosphinohydrazines were made according to published methods (20). Solvents were rigorously dried by standard methods, and purified by distillation or by vacuum fractionation.

The n.m.r. spectral measurements were made using a Varian A56/60 n.m.r. spectrometer, fitted with a Varian V-6057 variable temperature system which allowed spectral measurements from −60 to +200 °C. Temperature calibration was achieved using methanol or ethylene glycol.

Preparation of Adducts

Adducts were prepared in cold finger attachments on the vacuum system or *in situ* in n.m.r. tubes. In general, the borane was added to the pure hydrazine or phosphinohydrazine, or to a solution of the hydrazine, in the reaction tube; mixtures were allowed to equilibrate at −33° and at room temperature, and products were separated by vacuum fractionation. Volatile adducts were distilled under vacuum into n.m.r. tubes; non-volatile

Can. J. Chem. Downloaded from www.nrcresearchpress.com by 210.87.254.5 on 09/05/12
For personal use only.

derivatives were either prepared *in situ*, or were transferred in solution by means of a syringe, to n.m.r. tubes fitted with syringe caps. Details of experiments are summarized in Table 4. For consistency, n.m.r. measurements were made on solutions of the same concentration (see Table 2).

The financial assistance of the National Research Council of Canada is gratefully acknowledged.

1. E. W. AINSCOUGH, L. K. PETERSON, K. I. THÉ, and G. L. WILSON. Can. J. Chem. **47**, 3405 (1969) and references therein.
2. R. P. NIELSEN, J. F. VINCENT, and H. H. SISLER. Inorg. Chem. **2**, 760 (1963).
3. D. S. PAYNE. Chem. Commun. 327 (1965).
4. (*a*) E. FLUCK. *In* Topics in phosphorus chemistry. M. Grayson and E. J. Griffith, *editors*. Interscience, New York, N.Y. 1967. (*b*) M. D. LAPRADE and C. E. NORDMAN. Inorg. Chem. **8**, 1669 (1969). (*c*) G. TERHAAR, M. A. FLEMING, and R. W. PARRY. J. Am. Chem. Soc. **84**, 1767 (1962).
5. S. F. SPANGENBERG and H. H. SISLER. Inorg. Chem. **8**, 1004 (1969).
6. D. H. BROWN, K. D. CROSBIE. G. W. FRASER, and W. A. SHARP. J. Chem. Soc. (A) 551 (1969).
7. (*a*) A. B. BURG and P. J. SLOTA. J. Am. Chem. Soc. **80**, 1107 (1958). (*b*) R. M. KREN and H. H. SISLER. Inorg. Chem. **9**, 836 (1970).
8. (*a*) M. A. BEG and H. C. CLARK. Can. J. Chem. **38**, 119 (1960). (*b*) R. SCHMUTZLER. Inorg. Chem. **3**, 465 (1964). (*c*) C. G. BARLOW, J. F. NIXON, and M. WEBSTER. J. Chem. Soc. (A), 2216 and 2692 (1968). (*d*) K. COHN and R. W. PARRY. Inorg. Chem. **7**, 46 (1968). (*e*) C. G. BARLOW, J. F. NIXON, and J. R. SWAIN. J. Chem. Soc. A, 1082 (1969).
9. F. G. A. STONE. Q. Rev. **88**, 101 (1958).
10. A. B. BURG and J. HENERS. J. Am. Chem. Soc. **87**, 3092 (1965).
11. A. B. BURG. Accounts of Chem. Res. **2**, 353 (1969).
12. R. R. HOLMES and R. P. WAGNER. J. Am. Chem. Soc. **84**, 357 (1962).
13. J. W. EMSLEY, J. FENNEY, and L. H. SUTCLIFFE. High resolution nuclear magnetic resonance spectroscopy. Pergamon Press, 1966.
14. C. W. HEITSCH. Inorg. Chem. **4**, 1019 (1965).
15. H. KESSLER. Angew. Chem. Intern. Ed. **9**, 219 (1970).
16. E. J. WELLS. Private communication.
17. (*a*) N. R. FETTER and B. BARTOCHA. Can. J. Chem. **39**, 2001 (1961). (*b*) M. S. BAINS and D. C. BRADLEY. Can. J. Chem. **40**, 1351 (1962). (*c*) N. R. FETTER, B. BARTOCHA, F. E. BRINCKMAN, and D. W. MOORE. Can. J. Chem. **41**, 1353 (1963). (*d*) D. F. CLEMENS, W. R. BREY, and H. H. SISLER. Inorg. Chem. **2**, 1251 (1963).
18. J. B. CLASS, J. G. ASTON, and T. S. OAKWOOD. J. Am. Chem. Soc. **75**, 2937 (1953).
19. H. C. BROWN. J. Am. Chem. Soc. **67**, 374 (1945).
20. (*a*) L. K. PETERSON and G. L. WILSON. Can. J. Chem. **46**, 685 (1968). (*b*) L. K. PETERSON, G. L. WILSON, and K. I. THÉ. Can. J. Chem. **47**, 1025 (1969). (*c*) L. K. PETERSON and G. L. WILSON. Can. J. Chem. **47**, 4281 (1969).

Downloaded from www.nrcresearchpress.com by 210.87.254.5 on 09/05/12
For personal use only.

Can. J. Chem. Downloaded from www.nrcresearchpress.com by 210.87.254.40 on 09/05/12
For personal use only.

The Preparation of Some Heterocyclic Analogues of Triptycene

D. M. McKinnon and J. Y. Wong
Chemistry Department, University of Manitoba, Winnipeg, Manitoba

Received May 10, 1971

A variety of anthracenes react with dibenzoylethylene and diacetylethylene to give substituted bicyclooctadienes as Diels–Alder adducts. Treatment of these with phosphorus pentasulfide gives derivatives of benzenonaphtho[*c*]thiophenes, which are thiophene analogues of triptycene. Reaction of the anthracenes with dibenzoylacetylene gave substituted bicyclooctatrienes, which on treatment with phosphorus pentasulfide gave inseparable mixtures of the benzenonaphtho[*c*]thiophenes and benzenonaphtho[*c*]-furans. Attempted retro Diels–Alder reactions of the thiophenes were unsuccessful.

Quelques anthracènes réagissent avec le dibenzoyléthylène et le diacétyléthylène pour donner des bicyclooctadiènes substitués, qui sont des produits de la réaction de Diels–Alder. Le traitement de ces composés par le pentasulfure de phosphore conduit à des benzénonaphto[*c*]thiophènes, qui sont des composés du thiophène analogues au triptycène. La réaction entre les anthracènes et le dibenzoylacétylène conduit à des bicyclooctatriènes, qui par traitement au pentasulfure de phosphore donnent des mélanges non séparables de benzénonaphto[*c*]thiophènes et benzénonaphto[*c*]furannes. Les réactions retro Diels–Alder avec les thiophènes ne donnent aucun résultat.

Canadian Journal of Chemistry, 49, 3178 (1971)

Although the synthesis and properties of the interesting rigid symmetrical hydrocarbon triptycene (**1**) are well known (1), only a few examples are described of heterocyclic analogues, in which one or more of the ortho linked benzene rings are replaced by heterocyclic systems, particularly those with aromatic character. Recently some thiophene analogues have been made (2) by Diels–Alder type additions to naphtho[2,3-*b*]thiophene (**2**), and some 3,4-furo- and 4,5-pyridazo-analogues have been prepared (3*a*, *b*) from anthracene (**3***a*) via its adduct **4***a* with *cis*-dibenzoylethylene. Also, some heterotriptycenes, in which hetero atoms replace one or more bridgehead methine groups have been synthesized (4*a*, *b*).

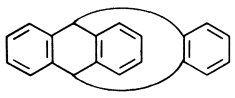

1

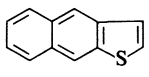

2

As part of our research on benzo[*c*]thiophene derivatives, we became interested in the preparation of these compounds, especially the hitherto unreported thiophene derivatives **5**, since in certain cases these contain the benzo[*c*]thiophene skeleton as an element of structure. The method of Wynberg used for the isomeric benzo[*b*]thiophenes is unsuitable for this type, particularly where monocyclic substituting rings are required. In addition the thiophenes **5** have higher symmetry and are more suitable for some spectroscopic investigations. Also, such compounds are of potential interest in investigations on interannular phenomena, such as have been suggested for triptycene (5, 6) in investigations on the reactivity of bridgehead substituents (6, 7), and as possible precursors of dehydrothiophene. These compounds are conveniently prepared by the following scheme.

trans-Dibenzoylethylene reacted with a variety of substituted anthracenes to give the corresponding dibenzodibenzoylbicyclooctadienes, **4***a–h*. In some cases Lewis acid catalysis by aluminum chloride was used. Treatment of these adducts with phosphorus pentasulfide in pyridine gave the desired thiophenes **5***a–h*, although in rather low yield, probably because of competing Diels–Alder reactions. Indeed when the reaction was attempted in other media only retro Diels–Alder products were obtained. Likewise dibenzoylacetylene reacted with anthracenes to give dibenzoyldibenzobicyclooctatrienes, **6***a–d*. Generally yields of these were better, in accord with its enhanced dienophilic properties compared to dibenzoylethylene. Surprisingly, although related compounds give thiophenes satisfactorily on treatment with phosphorus pentasulfide (8, 9) these adducts gave mixtures whose analyses and spectroscopic properties were consistent with mixtures of the desired thiophenes **5** and the corresponding furans. These could not be separated satisfactorily. Although the conversion

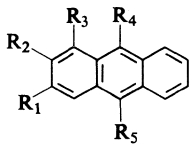

3

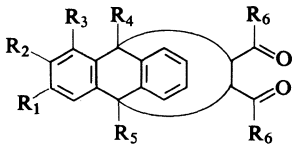

4

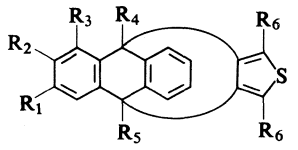

5

a $R_1 = R_2 = R_3 = R_4 = R_5 = H$; $R_6 = Ph$

b $R_1 = R_2 = R_3 = R_4 = H$; $R_5 = Me$; $R_6 = Ph$

c $R_1 = R_2 = R_3 = H$; $R_4 = R_5 = Me$; $R_6 = Ph$

d $R_1 = H$; $R_2 = Me$; $R_3 = R_4 = R_5 = H$; $R_6 = Ph$

e $R_1 = R_2 = R_3 = R_4 = H$; $R_5 = OMe$; $R_6 = Ph$

f $R_1 = R_2 = R_3 = R_4 = H$; $R_5 = Br$; $R_6 = Ph$

g $R_1 = H$; $R_2, R_3 = (—CH=CH—)_2$; $R_4 = R_5 = H$; $R_6 = Ph$

h $R_1, R_2 = (—CH=CH—)_2$, $R_3 = R_4 = R_5 = H$; $R_6 = Ph$

i $R_1 = R_2 = R_3 = R_4 = R_5 = H$; $R_6 = Me$

j $R_1 = R_2 = R_3 = R_4 = H$; $R_5 = R_6 = Me$

of the adducts **4** to the thiophenes **5** corresponds to a simple well-known thiophene synthesis (10), successful conversion of the adducts **6** must involve a reduction stage, perhaps by loss of sulfur or oxygen. A possible mechanism would proceed via a Cope-type rearrangement of a sulfurized (partially or complete) adduct **6** to a 1,2-thioxin or 1,2-dithiin respectively, which could extrude sulfur, similarly to known reactions (11), to form the furan or thiophene respectively.

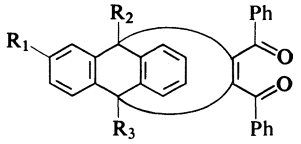

6

a $R_1 = R_2 = R_3 = H$

b $R_1 = R_2 = H$; $R_3 = Me$

c $R_1 = H$; $R_2 = R_3 = Me$

d $R_1 = Me$; $R_2 = R_3 = H$

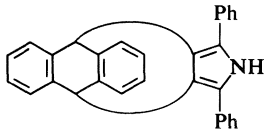

7

The preparations of the dibenzoylethylene and dibenzoylacetylene adducts of a variety of substituted anthracenes are summarized in Tables 1 and 2 respectively. The thiophenes **5***a–h* were colorless or pale yellow. Their structures follow from their analyses and mass spectral data. Partly to confirm the structures of the initial dibenzoylethylene adduct, a pyrrole derivative **7** was made by reaction of the adduct **4***a* with ammonium acetate, corresponding to a Paal–Knorr pyrrole synthesis (12, 13).

Acridine was also treated with dibenzoylethylene in an attempt to make a precursor of an azatriptycene analogue, but no adduct could be isolated.

We also attempted to obtain some other heteroanalogues starting from naphtho[2,3-*b*]thiophene (**2**) (14, 15). Unsuccessful attempts had been made to form a triptycene analogue from this by reaction with dehydrobenzene, but this compound is the basis of the successful preparation of Wynberg *et al.* (2). However, reaction with dibenzoylethylene in xylene was unsuccessful.

Attempts were also made to produce compounds without the bulky phenyl substituents on the thiophene ring. Thus anthracene (**3***a*) and 9-methylanthracene (**3***b*) reacted with diacetylethylene to form adducts, **4***i* and *j* respectively. One of these, **4***i*, has been previously reported (16) but with a different melting point. This is possibly due to the existence of optical isomers. Treatment of these with phosphorus pentasulfide in toluene gave the thiophenes, **5***l* and *j* respectively. Sulfurization in pyridine was unsuccessful, possibly due to the formation of base-catalyzed condensation products (16). With 2,5-dimethoxy-2,5-dihydrofuran, which would have permitted synthesis of compounds without substituents in the thiophene ring, anthracene did not form an adduct under any of the conditions tried.

These compounds are probably best named as derivatives of thiophene, although similar compounds have been named as substituted bicyclooctatrienes (3) or as derivatives of the correspon-

Can. J. Chem. Downloaded from www.nrcresearchpress.com by 210.87.254.40 on 09/05/12
For personal use only.

Can. J. Chem. Downloaded from www.nrcresearchpress.com by 210.87.254.40 on 09/05/12
For personal use only.

TABLE 1. Reaction of anthracenes with dibenzoylacetylene

Compound **3**	Solvent	Reaction time (h)	Product **6**	The m.p. (°C)	Yield (%)	Formula	Analysis (%) Calculated C	Calculated H	Found C	Found H
a	Xylene	16	*a*	207–208	87	$C_{30}H_{20}O_2$	87.38	4.85	87.27	5.01
b	Benzene	16	*b*	179	91	$C_{31}H_{22}O_2$	87.33	5.17	87.18	5.26
c	Benzene	16	*c*	261–263	96	$C_{32}H_{24}O_2$	87.27	5.45	87.14	5.41
d	Toluene	16	*d*	223	88	$C_{31}H_{22}O_2$	87.33	5.17	87.13	5.28

TABLE 2. Reaction of anthracenes with *trans*-dibenzoylethylene (DBE) or diacetylethylene (DAE)

Compound **3**	Reagent	Solvent	Reaction time (h)	Product **4**	The m.p. (°C)	Yield (%)	Formula	Analysis (%) Calculated C	Calculated H	Calculated Br	Found C	Found H	Found Br
a	DBE	Xylene	24	*a*	148–151	56	$C_{30}H_{22}O_2$	86.96	5.31	—	86.87	5.24	—
b	DBE	Ethanol	24	*b*	92	88	$C_{31}H_{24}O_2$	86.92	5.61	—	86.81	5.77	—
c	DBE	Ethanol	8	*c*	195	98	$C_{32}H_{26}O_2$	86.88	5.88	—	86.71	6.00	—
d	DBE	Toluene	12	*d*	112	70	$C_{33}H_{24}O_2$	86.92	5.61	—	86.77	5.46	—
e	DBE	Methanol	48	*e*	161	43	$C_{31}H_{24}O_3$	83.78	5.41	—	83.43	5.53	—
f	DBE	Toluene	48	*f*	93	12	$C_{30}H_{21}O_2Br$	73.02	4.26	16.23	72.97	4.44	16.05
g	DBE	Methylene chloride	120	*g*	116	19	$C_{34}H_{24}O_2$	87.93	5.17	—	87.61	5.26	—
h	DBE	Toluene	48	*h*	133	67	$C_{34}H_{24}O_2$	87.93	5.17	—	87.82	5.34	—
i	DAE	Toluene	48	*i*	182*	41	$C_{20}H_{18}O_2$	82.75	6.20	—	82.67	6.22	—
j	DAE	Toluene	48	*j*	188	55	$C_{21}H_{10}O_2$	82.89	6.58	—	82.70	6.63	—

*Literature (16), 211–213°.

Can. J. Chem. Downloaded from www.nrcresearchpress.com by 210.87.254.40 on 09/05/12
For personal use only.

ding polynuclear hydrocarbon (2). Thus the compound **5***a* would be named 1,3-diphenyl-4,9-dihydro-4,9-*o*-benzenonaphtho[2,3-*c*]thiophene. Where the three rings attached to the central methine carbon atoms are different, the compounds will be a mixture of enantiomers.

The n.m.r. spectra of these compounds are consistent with their analyses and properties. The methine protons give sharp singlets in a similar range to those found for triptycene (17, 18) and for a thiophene analogue (2). Values, however, for the compounds with phenyl substituents on the thiophene ring, lie at slightly lower field, probably due to the deshielding effects of the phenyl groups. In the phenanthro-compound **5***g* the shifts of the two methine protons are quite different from each other. In part this may be due to the difference in deshielding by the angularly fused aromatic ring, but it is more probably a steric effect, caused by interference of the 4 and 5 protons. Similar effects have been used to explain low field absorption of the 4,5-protons in phenanthrene (19, 20). The positions of the methine protons in the methyl compounds **5***i* and *j* are slightly higher than for triptycene. This once more probably represents a deshielding due to different effects of the dimethylthiophene compared to a benzene ring. In general the aromatic peaks in these thiophenes **5***a–h* are rather complex, but in the anthra-compound **5***h* a sharp singlet for the 5,10-protons was obtained. These are uncoupled to the other aromatic protons. Similar effects have been observed for the corresponding protons in anthracene and naphthacene (19, 21).

These thiophenes **5** are also of interest in that retro Diels–Alder reactions might provide interesting products. Two possible reactions might be envisaged for the compounds **5**.

Scheme 1*a* might provide a route to 3,4-dehydrothiophenes. Although the formation of some

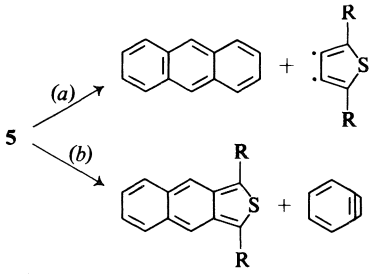

SCHEME 1

2,3-dehydrothiophenes has been demonstrated (22*a*, *b*) attempted preparation of the former led to products derived from the latter by rearrangement of the dehydrothiophene intermediate. Such rearrangements would be less likely with a 2,5-disubstituted intermediate such as in Scheme 1*a*, and the dehydrothiophene might be detectable, although decomposition to an acyclic diyne, as has been found in a related investigation (23), is also a possibility. Scheme 1*b* is interesting in that it could provide naphtho[2,3-*c*]thiophenes and dehydrobenzene. A similar reaction was proposed by Wynberg *et al.* (2). The dehydrobenzene could be trapped by a suitable diene, or in its absence, might react with the thiophene ring of the naphtho-[2,3-*c*]thiophene with eventual formation of a naphthacene derivative. Cava and VanMeter (24) have shown that in naphtho[2,3-*c*]thiophene Diels–Alder reactions occur in the heterocyclic ring. However, heating a mixture of the thiophene **5***a* and 9-methylanthracene gave substantially unchanged starting materials, along with only traces of other material.

Examination of the mass spectra of these compounds **5***a–d* indicated no significant peaks corresponding to decomposition by Scheme 1*a* or *b*. Apart from the parent peak, there were large peaks corresponding to mass 121, probably Ph·CS. Loss of this may occur by a similar process which leads to loss of HCS from Wynberg's compound (2), and from other thiophenes (25, 26). However, the mass spectra of the 1,3-dimethylcompounds **5***i* and *j* gave large ions for the parent anthracenes and for a mass of 110, which may correspond to decomposition by Scheme 1*a*. A chemical proof of this was sought by heating the thiophene **5***i* with 9-methylanthracene. However, only starting material was isolated, and no anthracene and thiophene **5***j* were obtained. We are forced to conclude that these proposed retro Diels–Alder reactions are not important.

Experimental

The n.m.r. spectra were obtained on a Varian model 56/60A spectrometer in deuterochloroform solution using tetramethylsilane as an internal standard. Mass spectra were obtained on a Finnegan 1015 quadrupole Mass spectrometer. Chromatography was performed on a "Camag" silica gel type D.S.F.5 supplied by Mondray Ltd. as 1 mm layers on glass plates. Development of plates, unless otherwise stated, was carried out using benzene with increasing proportions of chloroform. Melting points (m.p.) were obtained as a Fisher–Johns apparatus.

Can. J. Chem. Downloaded from www.nrcresearchpress.com by 210.87.254.40 on 09/05/12
For personal use only.

TABLE 3. Preparation of 4,9-dihydro-4,9-*o*-benzenonaphtho[2,3-*c*]thiophenes from diacyldibenzobicyclooctadienes

Compound 5	Reaction time (h)	The m.p. (°C)	Yield (%)	Formula	Analysis (%) Calculated C	H	S	Br	Found C	H	S	Br
*a**	96	235	59	$C_{30}H_{20}S$	87.38	4.85	7.77		87.20	4.98	7.87	
b†	48	147	27	$C_{31}H_{22}S$	87.32	5.17	7.50		87.14	5.36	7.30	
c‡	48	246–248	48	$C_{32}H_{24}S$	87.27	5.45	7.28		87.11	5.60	7.15	
d§	72	209	67	$C_{31}H_{22}S$	87.32	5.17	7.50		87.22	5.31	7.34	
*e***	72	137	47	$C_{31}H_{22}S$	84.16	4.98	7.24		84.01	4.79	7.17	
f††	48	132	77	$C_{30}H_{19}SBr$	73.32	3.87	6.52	16.29	73.24	3.90	6.62	16.31
g‡‡	48	161	71	$C_{34}H_{24}S$	88.31	4.76	6.93		88.06	4.66	7.09	
h§§	72	177	58	$C_{34}H_{24}S$	88.31	4.76	6.93		88.17	4.89	6.81	
i‖	48	282	22	$C_{20}H_{16}S$	83.33	5.56	11.11		83.31	5.70	11.04	
j¶	48	267	38	$C_{21}H_{18}S$	83.44	5.96	10.60		83.67	5.70	10.14	

*Mass spectrum, *m/e* 412 (parent peak), 291 (M-PhCS), 121 $PhCS^+$.
†Mass spectrum, *m/e* 426 (parent peak), 305 (M-PhCS), 121 $PhCS^+$.
‡Mass spectrum, *m/e* 440 (parent peak), 319 (M-PhCS), 121 $PhCS^+$.
§Mass spectrum, *m/e* 426 (parent peak), 305 (M-PhCS), 121 $PhCS^+$.
‖Mass spectrum, *m/e* 288 (parent peak), 178 (M-110), 110 (tentatively $C_4S(CH_3)_2$).
¶Mass spectrum, *m/e* 302 (parent peak), 192 (M-110), 110 (tentatively $C_4S(CH_3)_2$).
**Mass spectrum *m/e* 432 (parent peak).
††Mass spectrum *m/e* 491 (parent peak).
‡‡Mass spectrum *m/e* 464 (parent peak).
§§Mass spectrum *m/e* 464 (parent peak).

TABLE 4. The n.m.r. data of 4,9-dihydro-4,9-*o*-benzenonaphtho[2,3-*c*]thiophenes

Compound 5	τ-Values (Positions of groups or protons in parentheses)		
	Methine protons	Aromatic rings	Others
a	4.52 (4,9) 4.67 (4,9) in CS_2	3.26–2.51	
b	4.45 (9)	3.12–2.47	8.08 (4) methyl
c	—	3.05–2.43	8.10 (4,9) methyls
d	4.47 (4,9)	3.29–2.38	7.75 (6) methyls
e	4.45 (9)	3.15–2.17	6.16 (4) methoxy
f	4.54 (9)	3.09–2.22	—
g	4.35 (11), 3.74 (4)	3.21–1.80	—
h	4.40 (4,11)	3.19–2.40	2.40 (5,10), uncoupled to other aromatic protons
i	4.94 (4,9)	3.22–2.71	7.72 (1,3) methyls
j	4.96 (9)	3.21–2.18	7.72 (4) methyl, 7.67 (1,3) methyls

Reaction of Anthracenes with Dibenzoylacetylene to Form Substituted Dibenzodibenzoylbicyclooctatrienes, 6a–d

Equimolar amounts of the anthracenes and dibenzoylacetylene (27) were refluxed together in suitable solvents for suitable times. The solvents were removed by evaporation and the crude products were purified by chromatography. The results are summarized in Table 1.

Reaction of Anthracenes with trans-Dibenzoylethylene or trans-Diacetylethylene to Form Substituted Dibenzobicyclooctadienes 4a–i

Equimolar quantities of the anthracene and diacetylethylene (28) or dibenzoylethylene were refluxed together in a suitable solvent. In one case, **3***g*, the reaction was performed at room temperature under catalysis by a trace of aluminum chloride. The mixtures were worked up and the products purified by chromatography. The results are summarized in Table 3.

Conversion of Dibenzodibenzoylbicyclooctadienes to the Thiophenes, 5a–h

The diketones were refluxed with a small excess of phosphorus pentasulfide in pyridine for varying times. The mixtures were poured into water, and benzene extraction gave crude products which were purified by chromatography using benzene/petroleum ether as a developing solvent. Under u.v. light, two purple fluorescent bands were evident. The first was the parent anthracene, and the second was the required thiophene. The results are summarized in Table 3. Reaction in other solvents tried gave either retro Diels–Alder reactions or did not give satisfactory results. The n.m.r. spectra are summarized in Table 4.

Sulfurization of Diacetyldibenzobicyclooctadiene (4i, j) to form 1,3-Dimethyl-4,9-dihydro-4,9-o-benzenonaphtho[2,3-c]thiophene (5i, j)

These were prepared as for the previous compounds except toluene was used as a solvent. The products were crystallized from petroleum ether. Results are summarized in Table 3 and n.m.r. data in Table 4.

Sulfurization of Dibenzodibenzoylbicyclooctatriene (6a)

The diketone (0.5 g) and phosphorus pentasulfide (1 g) in pyridine (10 ml) were refluxed for 6 days. The mixture was poured into water and extracted with benzene. The dried extract was examined by chromatography and a colorless band separated. Evaporation gave a colorless amorphous material whose properties were consistent with a mixture of **5***a* and the corresponding furan prepared according to ref. 3.

Similar results were obtained for the compounds **6***b–d*.

Preparation of 1,3-Diphenyl-4,9-dihydro-4,9-o-benzenonaphtho[2,3-c]pyrrole (7)

Dibenzodibenzoylbicyclooctadiene (**4***a*) (0.5 g) and excess ammonium acetate in acetic acid (10 ml) were refluxed for 2½ h. Addition of water precipitated the pyrrole and thorough washing gave analytically pure material m.p. 269–271° (74%).

Anal. Calcd. for $C_{30}H_{21}N$: C, 91.14; H, 5.32; N, 3.54. Found: C, 90.98; H, 5.25; N, 3.49.

The n.m.r. spectrum of **7**, 4.52 (2H singlet, methine protons), 3.33 to 2.60 τ (19H bands, protons on the aromatic ring and proton on nitrogen).

Attempted Reaction of Acridine with trans-Dibenzoylethylene

Acridine (179 mg, 1 mmol) and dibenzoylethylene (236 mg, 1 mmol) in toluene (20 ml) were refluxed for 2 days. Examination of the mixture afforded only unreacted starting material. Different solvents likewise gave unsuccessful results.

Reaction of Naphtho[2,3-b]thiophene with trans-Dibenzoylethylene to Form 8

Naphtho[2,3-*b*]thiophene (276 mg, 1.5 mmol) and dibenzoylethylene (3.56 mg, 1.5 mmol) were heated together in xylene (10 ml) for 48 h. No adduct was obtained.

Attempted Reaction of Anthracene with 2,5-Dimethoxy-2,5-dihydrofuran

Anthracene (330 mg, 2 mmol) and 2,5-dimethoxy-2,5-dihydrofuran (520 mg, 4 mmol) were heated together in a variety of solvents for varying times. Under none of the conditions tried could adducts be isolated.

Attempted Reaction of 9-Methylanthracene and 1,3-Dimethyl-4,9-dihydro-4,9-o-benzenonaphtho-[2,3-c]thiophene

9-Methylanthracene (384 mg, 2 mmol) and the thiophene (288 mg, 1 mmol) were fused together at 240° for 2 h. The t.l.c. examination of the product indicated only unreacted starting material along with traces of other material.

Can. J. Chem. Downloaded from www.nrcresearchpress.com by 210.87.254.40 on 09/05/12
For personal use only.

The authors wish to thank the National Research Council of Canada for financial support, Dr. T. Schaefer and Dr. J. B. Westmore for valuable advice, and Mr. R. Dickinson and Mr. M. Arneson for the preparation of n.m.r. and mass spectra respectively.

1. P. D. BARTLETT and S. G. COHEN. J. Am. Chem. Soc. **64**, 2649 (1942).
2. H. WYNBERG, J. DEWIT, and H. J. M. SINNIGE. J. Org. Chem. **33**, 711 (1970).
3. P. BAUMGARTNER and G. HUGEL. Bull. Soc. Chim. Fr. 1005 (1954).
4. (*a*) G. WITTIG and G. STEINHOFF. Angew. Chem. **75**, 453 (1963). (*b*) C. F. WILCOX and M. P. STEVENS. J. Am. Chem. Soc. **84**, 1258 (1962).
5. (*a*) M. S. DEGROOT and J. H. VAN DER WAALS. Mol. Phys. **6**, 545 (1963). (*b*) D. HELLWINKEL and W. SCHENK. Angew. Chem. Int. Edn. **8**, 987 (1969).
6. P. D. BARTLETT and E. S. LEWIS. J. Am. Chem. Soc. **72**, 1005 (1950).
7. P. D. BARTLETT, M. J. RYAN, and S. G. COHEN. J. Am. Chem. Soc. **64**, 2649 (1942).
8. M. E. MANN and J. D. WHITE. Chem. Commun. 420 (1968).
9. M. AHMED, J. M. BUCHSHRIBER, and D. M. MCKINNON. Can. J. Chem. **68**, 1991 (1971).
10. W. STEINKOPFF. Die Chemie des Thiophenes. Theodore Steinkopff, Dresden, 1941.
11. W. SCHROTH, F. BILLIG, and G. REINHOLD. Angew Chem. Int. Edn. **6**, 698 (1967).
12. L. LEDERER and C. PAAL. Ber. **18**, 2594 (1885).
13. L. KNORR and K. HESS. Ber. **44**, 2762 (1911).
14. W. CARRUTHERS. J. Chem. Soc. 704 (1962).
15. W. CARRUTHERS. J. Chem. Soc. 4477 (1963).
16. T. PAVOLINI, F. GAMBARIN, and L. VERZA. Ann Chim. (Rome), **42**, 149 (1952).
17. K. G. KIDD, G. KOTOWYCZ, and T. SCHAEFER. Can. J. Chem. **45**, 2155 (1967).
18. W. B. SMITH and B. A. SHOULDERS. J. Phys. Chem. **69**, 2022 (1965).
19. N. JONATHON, S. GORDON, and B. P. DAILEY. J. Chem. Phys. **36**, 2443 (1962).
20. C. REID. J. Mol. Spectrosc. **1**, 18 (1957).
21. R. H. MARTIN, N. DEFAY, G. GEERTS-EVRARD, and S. DELAVARENNE. Tetrahedron, **20**, 1073 (1964).
22. (*a*) G. WITTIG and V. WAHL. Angew. Chem. **73**, 492 (1961). (*b*) G. WITTIG and M. RINGS. Ann. **719**, 127 (1969).
23. R. W. HOFFMAN. Dehydrobenzene and cycloalkynes. Academic Press, New York, N.Y., 1967. p. 290.
24. M. P. CAVA and J. P. VANMETER. J. Org. Chem. **34**, 538 (1969).
25. V. HANUS and V. CERMAK. Coll. Czech. Chem. Commun. **24**, 1602 (1959).
26. I. W. KINNEY and G. L. COOK. Anal. Chem. **24**, 1391 (1952); **25**, 1729 (1953).
27. R. E. LUTZ and W. R. SMITHEY. J. Org. Chem. **16**, 51 (1951).
28. K. F. ARMSTRONG and R. ROBINSON. J. Chem. Soc. 1650 (1934).

Can. J. Chem. Downloaded from www.nrcresearchpress.com by 210.87.254.40 on 09/05/12
For personal use only.

Can. J. Chem. Downloaded from www.nrcresearchpress.com by 210.87.254.40 on 09/05/12
For personal use only.

19-Hydroxy Steroids. II. The Synthesis of 3β,5,19-Trihydroxy-5β-cholestane[1]

PETER MORAND AND MORRIS KAUFMAN
Department of Chemistry, University of Ottawa, Ottawa, Canada

Received June 3, 1971

Chemical evidence is presented in support of the structures assigned to the isomeric epoxides **4***a* and **5***a* obtained by peracid oxidation of the double bond in 3β-acetoxycholest-5-en-19-ol (**2***a*). Reduction of 3β-acetoxy-5,6α-oxido-5α-cholestan-19-ol (**4***a*) with lithium aluminum hydride leads exclusively to the C-5 alcohol while reduction of 3β-acetoxy-5,6β-oxido-5β-cholestan-19-ol (**5***a*) with the same hydride results in the isolation of the C-5 and -6 alcohols in a ratio of 1:5. When an attempt was made to reduce the 5β,6β-epoxide **5***a* with lithium trimethoxyaluminohydride a rearrangement occurred. A structure is postulated for the compound isolated and a mechanism for its formation is discussed.

Des preuves chimiques sont présentées pour prouver les structures attribuées aux époxydes isomères **4***a* et **5***a*, obtenus par oxydation au péracide de la double liaison de l'acétoxy-3β cholestène-5 ol-19 (**2***a*). La réduction de l'acétoxy-3β oxydo-5,6α cholestan-5α ol-19 (**4***a*) par l'hydrure de lithium et d'aluminium conduit exclusivement à l'alcool en C-5 alors que la réduction de l'acétoxy-3β oxydo-5,6β cholestan-5β ol-19 (**5***a*) avec le même hydrure donne les alcools en C-5 et -6 dans un rapport 1:5. Une transposition se produit lorsqu'on tente de réduire l'époxyde-5β,6β, **5***a*, par l'hydrure de lithium triméthoxyaluminium. Une structure est proposée pour le composé isolé et on discute du mécanisme de sa formation.

Canadian Journal of Chemistry, **49**, 3185 (1971)

During the course of our investigation of approaches to the synthesis of cardiac-active steroids containing an oxygen atom at C-19 and hydroxyl groups in the 3β- and 5β-positions (1, 2) we were concerned with preparation of the model compound 3β,5,19-trihydroxy-5β-cholestane (**6***a*). The synthesis of this compound is described in this paper as well as the reactions and stereochemistry of some of the intermediates involved.

Epoxidation of 3β-Acetoxycholest-5-en-19-ol (2a) and of 3β,19-Diacetoxycholest-5-ene (2b)

Henbest and Wilson (3) have shown that hydroxyl groups play an important role in the stereoselective epoxidation of allylic double bonds in six-membered rings. More recently, non-allylic double bonds have been shown (4) to be similarly influenced by neighboring hydroxyl groups. For example, it has been reported that epoxidation of the ethylene ketal of 19-hydroxyandrost-5-ene-3,17-dione with monoperphthalic acid yields the 5β,6β-epoxide exclusively. These results were rationalized by assuming that in the transition state the peracid will be located on the β-side of the molecule because of interaction between the peracid, the hydroxyl group, and the double bond.

We found that, on treatment of 3β-acetoxycholest-5-en-19-ol (**2***a*) with excess monoperphthalic acid in ether, it is possible to obtain both 3β-acetoxy-5,6β-oxido-5β-cholestan-19-ol (**5***a*) and 3β-acetoxy-5,6α-oxido-5α-cholestan-19-ol (**4***a*). These compounds were isolated in yields of 72 and 14%, respectively. As expected, epoxidation of 3β,19-diacetoxycholest-5-ene (**2***b*) gave predominantly the 5α,6α-epoxide **4***b* along with a significant amount of the 5β,6β-epoxide **5***b*. The structures of these isomeric epoxides were first assigned on the basis of elemental analysis and i.r. and n.m.r. spectra which have been reported elsewhere (1). The chemical reactions described below confirm these configurational assignments.

Treatment of 3β-acetoxy-5,6α-oxido-5α-cholestan-19-ol (**4***a*) with a methanolic solution of hydrogen chloride afforded a compound which was identified as 6β,19-oxido-5α-cholestane-3β,5-diol (**1**). Mass spectral and elemental analyses for this compound indicated an empirical formula of $C_{27}H_{46}O_3$ and the i.r. spectrum showed the characteristic C-19 methylene band (5) of 6β,19-oxides at 1498 cm^{-1}. When 3β-acetoxy-5,6β-oxido-5β-cholestan-19-ol (**5***a*) was similarly treated with a methanolic solution of hydrogen chloride the product isolated gave a mass spectral analysis consistent with the empirical formula $C_{27}H_{45}ClO_2$ and the i.r. spectrum indicated a 6β,19-oxide (band at 1498

[1]For Part I, see ref. 1

Can. J. Chem. Downloaded from www.nrcresearchpress.com by 210.87.254.40 on 09/05/12
For personal use only.

cm^{-1}). This compound must therefore be 5-chloro-6β,19-oxido-5α-cholestan-3β-ol (**3**) (6) as would be expected from a 5β,6β-epoxide.

Reduction of Diastereomeric Epoxides

In acyclic compounds the reductive opening of epoxides with lithium aluminum hydride generally occurs at the least substituted carbon atom (7) to produce the more highly substituted alcohol. The addition of aluminum chloride has been found (8) to alter the course of such reductions yielding the least substituted alcohol as a product. However, in the case of epoxides in six-membered rings, hydride reduction is complicated by factors implicit in the Fürst–Plattner rule (9). For example, although the lithium aluminum hydride reduction of 5,6α-oxido-5α-cholestane leads exclusively to the C-5 alcohol (10), Hallsworth and Henbest (11) have reported that 5,6β-oxido-5β-cholestane yields both 5β-cholestan-5-ol (60%) and 5α-cholestan-6β-ol (31%) under these conditions. It is apparent that both the Fürst–Plattner rule and steric factors play a role in determining the course of the reduction for such epoxides. More recently Sweet and Brown (12) have shown that polar effects can be considered to influence the course of the lithium aluminum hydride reduction in *cis*- and *trans*-3,4-oxido-2-alkoxytetrahydropyrans.

Treatment of the 5α,6α-epoxide **4***b* with lithium aluminum hydride and acetylation of the product resulted in the isolation of 3β,19-diacetoxy-5α-cholestan-5-ol (**7**) whose empirical formula, $C_{31}H_{52}O_5$, was confirmed by elemental and mass spectral analyses. An examination of the half-band width (28 Hz) of the signal for the C-3 proton in the n.m.r. spectrum of this compound indicated an axial orientation (13). This is consistent with a 5α-hydroxyl group, arising from the reductive opening of the 5α,6α-epoxide in the normal manner (10).

Reduction of 3β-acetoxy-5,6β-oxido-5β-cholestan-19-ol (**5***a*) with lithium aluminum hydride and subsequent acetylation of the crude product led to the isolation of two substances in a ratio of about 1:5. The major product, after hydrolysis, treatment with a methanolic solution of hydrogen chloride, and reacetylation of the product, gave a substance which was identified as 3β-acetoxy-6β,19-oxido-5α-cholestane (**8***b*). The i.r. spectrum of the latter showed the characteristic absorption band (5) due to the C-19 methylene group of 6β,19-oxides indicating the presence of a 6β-hydroxyl group in the reduction product. In the n.m.r. spectrum, the observed value of 17 Hz for the half-band width of the signal for the C-3 proton was taken as evidence (13) for a *trans* A/B-ring junction. The structure of the major product in the lithium aluminum hydride reduction of the 5β,6β-epoxide must therefore be the one shown (**9***a*) in Scheme 1.

The second product isolated was identified, on the basis of its n.m.r. spectrum, as 3β,19-diacetoxy-5β-cholestan-5-ol (**6***b*). A half-band width of 9 Hz was observed for the signal for the 3α-proton indicating (13) that the A/B-ring junction must be *cis*. Hydrolysis of this substance led to the isolation of 3β,5,19-trihydroxy-5β-cholestane **6***a* whose empirical formula, $C_{27}H_{48}O_3$, was confirmed by elemental and mass spectral analyses.

The sharp decrease in the amount of the 5β-alcohol **6***a* formed compared to the proportion of this alcohol obtained in the case of the lithium aluminum hydride reduction of 5,6β-oxido-5β-cholestane (11) remains unexplained. However, since we were interested in finding means of improving the yield of 5β-alcohol by reduction of the 5β,6β-epoxide we turned our attention to other reducing agents. Brown and Weissman (14) have reported that in the reduction of unsymmetrical epoxides with lithium trimethoxyaluminohydride, hydride transfer occurs almost exclusively at the least substituted carbon. In view of this observation it might be predicted that the use of this reagent would lead to a higher yield of the 5β-alcohol **6***a*. Reduction of 3β-acetoxy-5,6β-oxido-5β-cholestan-19-ol (**5***a*) led to the formation of two products, neither of which resembled (t.l.c.) the compounds obtained on reduction with lithium aluminum hydride.

The separation of these materials was effected by column chromatography of the acetylated mixture. On the basis of the chemical and physical data presented below the structure of the first substance (50%) eluted from the column is formulated as (5*S*)-3β,6β,19-triacetoxy-1(10 → 5)*abeo*-cholest-9(10)-ene (**10***b*). The second substance (34%) could not be identified.

The n.m.r. spectrum of **10***b* was observed to be similar to that of 3β,6β,19-triacetoxy-5α-cholestane (**6***b*) in that two secondary and one primary acetoxy groups are indicated. Hydrolysis of this compound gave the corresponding triol **10***a*. Evidence that reduction had not occurred was obtained by examination of the mass spectrum

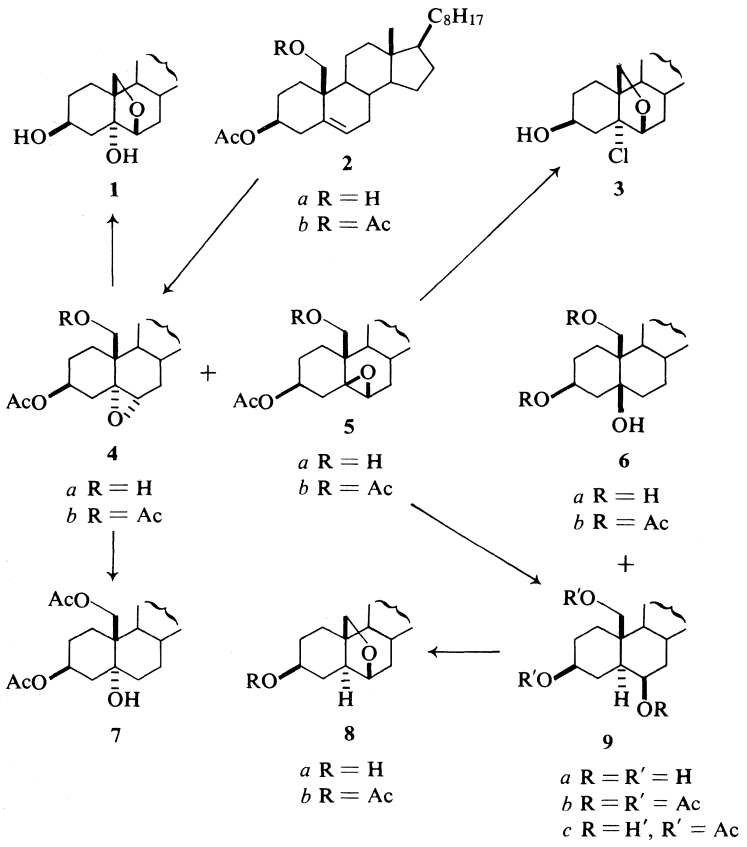

SCHEME 1

which showed an apparent molecular ion peak at 418 and not at 420 as would have been expected on reduction of the epoxide.

Treatment of this triol **10***a* with a dry methanolic solution of hydrogen chloride led to the isolation of a product which was identified as 5-chloro-6β,19-oxido-5α-cholestan-3β-ol (**3**), a compound prepared earlier from 3β-acetoxy-5,6β-oxido-5β-cholestan-19-ol (**5***a*). The two compounds were found to be identical by comparison of their mass spectra and melting points.

Several attempts were made to oxidize the triol **10***a* in order to examine the i.r. spectrum of the product for carbonyl absorption but we were unable to find the right conditions for the reaction to proceed cleanly enough to allow for separation of the products obtained.

Discussion

In order to rationalize the non-reductive rearrangement of the 5β,6β-epoxide **5***a*, a few observations should be made regarding the conformation of the A/B-rings of **5***a* and the nature of lithium trimethoxyaluminohydride as a reducing agent.

It can be seen from Dreiding models that the preferred conformation of the A-ring in 3β-acetoxy-5,6β-oxido-5β-cholestan-19-ol (**5***a*) is the "non-steroid" one (15, 16). As shown below, this conformation places the bond (C_1—C_{10}) which must migrate to form the 5,5′-spiro compound in a *trans* coplanar position (17) to the C—O bond at C-5.

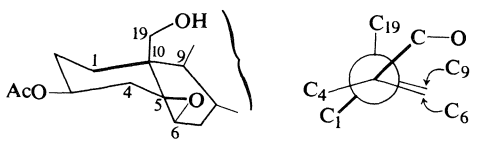

It is known (18) that in the formation of alkoxyaluminohydrides (Scheme 2) each successive step proceeds more slowly than the preceding one (*i.e.* A-1 > A-2 > A-3 > A-4). Resonance interaction of the type below which would assist the

Can. J. Chem. Downloaded from www.nrcresearchpress.com by 210.87.254.40 on 09/05/12
For personal use only.

$$AlH_4^- \xrightarrow[CH_3OH]{A\text{-}1} H_3Al{-}OCH_3^- \xrightarrow[CH_3OH]{A\text{-}2} H_2Al{-}(OCH_3)_2^- \xrightarrow[CH_3OH]{A\text{-}3} HAl{-}(OCH_3)_3^- \xrightarrow[CH_3OH]{A\text{-}4} Al{-}(OCH_3)_4^-$$

SCHEME 2

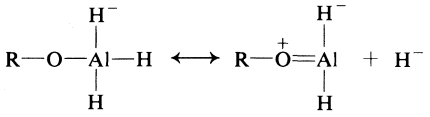

transfer of a hydride ion and accelerate the reaction, is not very effective because such overlap is between the 2p orbital electrons on oxygen and the vacant 3p orbitals of aluminum. This may result in the electron-withdrawing effect of the alkoxy group being dominant, thus retarding the reaction involving loss of a hydride ion.

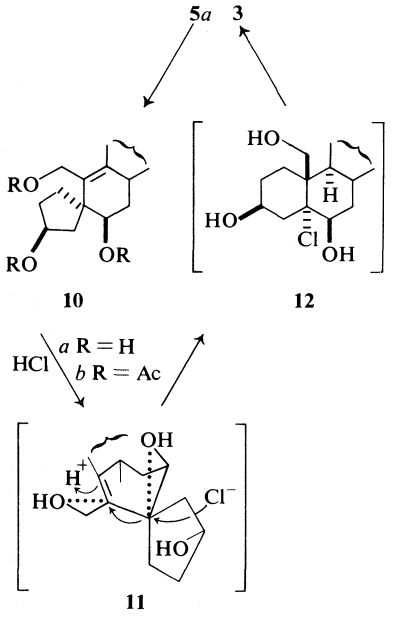

SCHEME 3

On treatment of 3β-acetoxy-5,6β-oxido-5β-cholestan-19-ol (**5***a*) with lithium trimethoxyaluminohydride the C-19 hydroxyl group, which lies directly above the 5β,6β-epoxide, may participate in the reaction by the formation of an intermediate with lithium trimethoxyaluminohydride similar to those postulated by others (19–21). The presence of such a complex could lead to the weakening of the C—O bond at C-5 with concomitant migration of the C_1—C_{10} bond and collapse of the proton at C-9 to give a C_9—C_{10} double bond (see Scheme 3).

The fact that only one major product is obtained on treatment of the 5,5′-spiro compound **10***a* with a solution of methanolic hydrogen chloride implies that the rearrangement involved in forming the 5α-chloro-6,19-oxide **3** is stereospecific. Here again, a participating role may be invoked for the C-19 hydroxyl group. If protonation of the C_9—C_{10} double bond is assumed to occur from the α-side of the molecule, the developing carbonium ion at C-10 would be protected from attack on the β-side by interaction with the C-19 hydroxyl group as shown in the postulated intermediate **11**. Migration of the bond of the five-membered ring attached to C-5 would then proceed from the α-side. Similarly the chloride ion would be directed to the α-side of the carbonium ion forming at C-5 due to interaction with the C-6 hydroxyl group situated on the β-side.

Experimental

Melting points were determined on a Hoover Uni-Melt apparatus and are uncorrected. The i.r. and n.m.r. spectra were recorded on a Beckman IR-8 infrared spectrophotometer and on a Varian V-4302 60 Mc spectrometer, respectively. Microanalyses were performed in the Microanalytical Laboratory of Dr. A. Bernhardt, Max Planck Institute, West Germany. SilicaR (200–300 mesh) was used as adsorbant for column chromatography and silica gel G (according to Stahl) was used as adsorbant for t.l.c. with sulfuric acid as spraying agent. In working up the products of reactions, the organic extracts were washed with dilute hydrochloric acid and/or sodium bicarbonate solution, dried over anhydrous magnesium sulfate, and evaporated to dryness under reduced pressure. In the hydride reduction experiments, excess reagent was destroyed with methanol and water and insoluble inorganic material was dissolved with 20% hydrochloric acid.

Epoxidation of 3β-Acetoxycholest-5-en-19-ol (2a)

Treatment of an ether solution of 3β-acetoxycholest-5-en-19-ol (**2***a*) (22) with an excess of monoperphthalic acid led to the isolation (1) of both *3β-acetoxy-5,6β-oxido-5β-cholestan-19-ol* (**5***a*) (72%, m.p. 129–130.5°) and *3β-acetoxy-5,6α-oxido-5α-cholestan-19-ol* (**4***a*) (14%, m.p. 184–186°).

Can. J. Chem. Downloaded from www.nrcresearchpress.com by 210.87.254.40 on 09/05/12
For personal use only.

Can. J. Chem. Downloaded from www.nrcresearchpress.com by 210.87.254.40 on 09/05/12
For personal use only.

Epoxidation of 3β,19-Diacetoxycholest-5-ene (2b)

3β,19-Diacetoxycholest-5-ene (**2***b*, 1.8 g, 2.5 mmol), prepared by acetylation of 3β-acetoxycholest-5-en-19-ol (**2***a*), was treated in ether solution with monoperphthalic acid (0.8 g, 5.0 mmol) at room temperature for 2 h. The solution was washed with a 20% aqueous solution of sodium sulfite and dried ($MgSO_4$). The phthalic acid was removed by elution on a silica gel (300 g) column with ether. Separation of the three main components of the crude product (0.73 g) was achieved by column chromatography using silica gel (300 g) as adsorbant and benzene as eluant.

The first substance (29 mg) collected from the column had the same R_f value as the starting material **2***b* by t.l.c. and was not characterized further. The second fraction (308 mg), which could not be crystallized, was identified as *3β,19-diacetoxy-5,6α-oxido-5α-cholestane* (**4***b*). A sample which appeared to be pure on t.l.c. exhibited n.m.r. ($CDCl_3$): τ 5.0 (multiplet, 3α-H, $w/2$ = 25 Hz), 6.0 (singlet, —CH_2O—), 7.02 (doublet, 6β-H, J = 3.0 Hz), 7.90, 8.0 (singlets, 19- and 3β-OAc, respectively); mass spectrum (70 eV) *m/e*: 442 and 382 (mol. wt. 502). The last component (210 mg) eluted from the column was identified as *3β,19-diacetoxy-5,6β-oxido-5β-cholestane* (**5***b*). The substance isolated exhibited n.m.r. ($CDCl_3$): τ 5.08 (multiplet, 3α-H, $w/2$ = 24 Hz), 5.65 (quartet, —CH_2O—, J_{AB} = 11 Hz), 7.0 (singlet, 6α-H), 7.86, 7.94 (singlets, 19- and 3β-OAc, respectively); mass spectrum (70 eV) *m/e*: 502 (molecular ion), 442, 382. 3β-Acetoxy-5,6β-oxido-5β-cholestan-19-ol (**5***a*, 50 mg, 1.08 mmol) obtained in the epoxidation of 3β-acetoxycholest-5-en-19-ol (**2***a*) was treated with acetic anhydride (1.0 ml) and pyridine (4.0 ml) for 12 h at 10°. Working-up in the usual manner gave a colorless oil (50 mg) which had identical n.m.r. and mass spectra as the product obtained in the epoxidation of 3β,19-diacetoxycholest-5-ene (**2***b*).

6β,19-Oxido-5α-cholestane-3β,5-diol (1)

3β-Acetoxy-5,6α-oxido-5α-cholestan-19-ol (**4***a*, 0.40 g, 0.87 mmol) was dissolved in methanol (50 ml) saturated with hydrogen chloride, and stirred at room temperature for 18 h. The volume of this solution was decreased under reduced pressure and then diluted with ether. The residue (0.39 g), obtained after working-up in the usual way, consisted mainly of two substances (t.l.c.) and was chromatographed on silica gel using benzene as eluant. In this manner 6β,19-oxido-5α-cholestane-3β,5-diol (**1**, 176 mg) was isolated, an analytical sample of which was obtained by crystallization from methanol; m.p. 222°; i.r. ($CHCl_3$): 3610 (OH groups), 1498 (—CH_2O—) cm^{-1}; mass spectrum (70 eV) *m/e*: 418 (molecular ion), 400, 382, 351.

Anal. Calcd. for $C_{27}H_{46}O_3$: C, 77.46; H, 11.08. Found: C, 77.35; H, 11.01.

Reduction of 3β,19-Diacetoxy-5,6α-oxido-5α-cholestane (4b) with $LiAlH_4$

Lithium aluminum hydride (0.10 g, 2.1 mmol) was added to a solution of 3β,19-diacetoxy-5,6α-oxido-5α-cholestane (**4***b*, 0.14 g, 0.32 mmol) in dry tetrahydrofuran (50 ml) and the mixture refluxed for 2 h. Working-up in the usual manner yielded a white solid (0.11 g) which was acetylated in a solution of acetic anhydride (1.0 ml) and pyridine (4.0 ml) at room temperature for 12 h. A crude product (130 mg) was isolated which yielded, upon crystallization from methanol, an analytical sample of *3β,19-diacetoxy-5α-cholestan-5-ol* (**7**) exhibiting m.p. 53–54°; n.m.r. ($CDCl_3$): τ 4.65 (multiplet, 3α-H, $w/2$ = 28 Hz), 5.65 (quartet, —CH_2O—, J_{AB} = 12 Hz), 7.90, 7.98 (singlets, 19- and 3β-OAc respectively); mass spectrum (70 eV) *m/e*: 444, 426, 384, 366 and 353 (mol. wt. 504).

Anal. Calcd. for $C_{31}H_{52}O_5$: C, 73.76; H, 10.38. Found: C, 73.77; H, 10.24.

Reduction of 3β-Acetoxy-5,6β-oxido-5β-cholestan-19-ol (5a) with $LiAlH_4$

3β-Acetoxy-5,6β-oxido-5β-cholestan-19-ol (**5***a*, 0.50 g, 1.08 mmol) was dissolved in dry tetrahydrofuran (300 ml). To this solution $LiAlH_4$ (1.5 g, 24.5 mmol) was added and the reaction mixture was refluxed with stirring for 24 h. Working-up in the usual way yielded a crude product (475 mg) which was found to consist of two substances (t.l.c.). This material was then acetylated with acetic anhydride (2.0 ml) and pyridine (8.0 ml) at room temperature for 12 h. A crude product (490 mg) was obtained from which three substances were isolated after chromatographic separation on silica gel (250 g) using benzene as eluant.

The first compound (140 mg, oil) was identified as *3β,6β,19-triacetoxy-5α-cholestane* (**9***b*) by its n.m.r. spectrum ($CDCl_3$) which exhibited signals at τ 5.15 (singlet, 6α-H, $w/2$ = 8 Hz), 5.25 (multiplet, 3α-H, $w/2$ = 26 Hz), 5.65 (singlet, —CH_2O—), 7.94, 7.98, 8.01 (singlets, 3 acetoxyl groups).

The second substance (65 mg, oil) eluted from the column was identified as *3β,19-diacetoxy-5β-cholestan-5-ol* (**6***b*) on the basis the n.m.r. spectrum ($CDCl_3$) which exhibited peaks at τ 4.80 (singlet, 3α-H, $w/2$ = 9 Hz), 5.64 (singlet, —CH_2O—), 7.95, 7.97 (singlets, 2 acetoxyl groups).

A third compound (161 mg, oil) eluted from the column was identified as *3β,19-diacetoxy-5α-cholestan-6β-ol* (**9***c*) by its n.m.r. spectrum ($CDCl_3$) which exhibited peaks at τ 5.30 (multiplet, 3α-H), 5.57 (singlet, —CH_2O—), 6.26 (singlet, 6α-H, $w/2$ = 7 Hz), 7.95, 8.0 (singlets, 2 acetoxyl groups).

A mixture (241 mg) containing 3β,6β,19-triacetoxy-5α-cholestane (**9***b*) and 3β,19-diacetoxy-5α-cholestan-6β-ol (**9***c*) was hydrolyzed in a 30% aqueous methanol – 30% sodium hydroxide solution at room temperature for 24 h. Working-up in the usual manner gave *3β,6β,19-trihydroxy-5α-cholestane* (**9***a*) and an analytical sample was obtained by crystallization from methanol–tetrahydrofuran; m.p. 230–231°; mass spectrum (70 eV) *m/e*: 402, 384, 372, 354 (mol. wt. 420).

Anal. Calcd. for $C_{27}H_{48}O_3$: C, 77.09; H, 11.50. Found: C, 77.15; H, 11.32.

3β,19-Diacetoxy-5β-cholestan-5-ol (**6***b*) was hydrolyzed in the same manner described above. An analytical sample of *3β,5,19-trihydroxy-5β-cholestane* (**6***a*), obtained by crystallization from methanol exhibited m.p. 145–146°; mass spectrum (70 eV) *m/e*: 402, 384, 372, 354 (mol. wt. 420).

Anal. Calcd. for $C_{27}H_{48}O_3$: C, 77.09; H, 11.50. Found: C, 76.66; H, 11.23.

6β,19-Oxido-5α-cholestan-3β-ol (8a)

3β,6β,19-Trihydroxy-5α-cholestane (**9***a*, 40 mg, 0.09

Can. J. Chem. Downloaded from www.nrcresearchpress.com by 210.87.254.40 on 09/05/12
For personal use only.

mmol) was treated with a dry methanolic solution of hydrogen chloride for 3 h at 50°. Working-up in the usual manner gave a crude product (35 mg) which, upon crystallization from acetone, provided an analytical sample of 6β,19-oxido-5α-cholestan-3β-ol (**8***a*); m.p. 131–134°; n.m.r. ($CDCl_3$): τ 6.02 (doublet, 6α-H, J_{ee} = 3 Hz), 6.29 (singlet, —CH_2O—), 6.29 (multiplet, 3α-H); mass spectrum (70 eV) *m/e*: 402 (molecular ion), 384, 371, 353; i.r. ($CHCl_3$): 3600 (—OH), 1495 (—CH_2O—) cm^{-1}.

The alcohol **8***a* was acetylated with acetic anhydride in pyridine and crystallization from methanol of the product isolated gave an analytical sample of *3β-acetoxy-6β,19-oxido-5α-cholestane* (**8***b*); m.p. 98–100°; n.m.r. ($CDCl_3$): τ 5.37 (multiplet, 3α-H, *w*/2 = 17 Hz), 6.04 (doublet, 6α-H, J_{ee} = 3 Hz), 6.46 (singlet, —CH_2O—), 7.98 (singlet, 3β-OAc).

Anal. Calcd. for $C_{29}H_{48}O_3$: C, 78.32; H, 10.88. Found: C, 78.21; H, 10.84.

*Reduction of 3β-Acetoxy-5,6β-oxido-5β-cholestan-19-ol (**5***a*) with Lithium Trimethoxyaluminohydride*

Lithium aluminum hydride (0.78 g, 20.8 mmol) was added to dry tetrahydrofuran (100 ml) in a three-necked flask, equipped with a stirrer and condenser. The system was purged with a steady stream of nitrogen. To this solution was added dry methanol (2.5 ml, 62.5 mmol) over a period of 10 min. 3β-Acetoxy-5,6β-oxido-5β-cholestan-19-ol (**5***a*) (0.50 g, 1.08 mmol) was added and the solution refluxed for 20 h. Working-up in the usual manner yielded a crude product (500 mg) which was acetylated in acetic anhydride (4.0 ml) and pyridine (10 ml) at room temperature for 12 h. The oil which was isolated was chromatographed on silica gel (300 g) using benzene as eluant. In this manner two substances were isolated, the first of which was identified as *(5S)-3β,6β,19-triacetoxy-1(10 → 5)abeo-cholest-9(10)-ene* (**10***b*) (240 mg). The n.m.r. spectrum of this compound showed peaks at τ 4.65 (multiplet, 3α-H, *w*/2 = 27 Hz), 4.85 (singlet, 6α-H, *w*/2 = 7 Hz), 5.45 (singlet, —CH_2O—), 7.86, 7.92, 7.99 (singlets, 3 acetoxyl groups). The second substance (170 mg) could not be identified.

Hydrolysis of the triacetate **10***b* isolated above with an aqueous (10%) methanolic solution of NaOH (10%) at room temperature provided, after crystallization from methanol, an analytical sample of *(5S)-3β,6β,19-trihydroxy-1(10 → 5)abeo-cholest-9(10)-ene* (**10***a*); m.p. 179–181°; mass spectrum (70 eV) *m/e*: 418 (molecular ion), 400, 388, 382, 370, 352.

Anal. Calcd. for $C_{27}H_{46}O_3$: C, 77.46; H, 11.08. Found: C, 76.84; H, 11.35.

*5-Chloro-6β,19-oxido-5α-cholestan-3β-ol (**3**)*

*(a) From 3β-Acetoxy-5,6β-oxido-5β-cholestan-19-ol (**5***a*)*

Treatment of 3β-acetoxy-5,6β-oxido-5β-cholestan-19-ol (**5***a*, 100 mg, 0.27 mmol) with a dry methanolic solution of hydrogen chloride at room temperature for 12 h yielded, after working-up in the usual manner, a white solid (94 mg). Crystallization of this material from aqueous acetone gave an analytical sample of 5-chloro-6β,19-oxido-5α-cholestan-3β-ol (**3**); m.p. 126–127.5° (lit. (6) m.p. 139–140°); i.r. ($CHCl_3$): 3610 (OH), 1498 (—CH_2O—) cm^{-1}; mass spectrum (70 eV) *m/e*: 436 (molecular ion), 418, 400, 382, 351.

*(b) From (5S)-3β,6β,19-Trihydroxy-1(10 → 5)abeo-cholest-9(10)-ene (**10***a*)*

(5*S*)-3β,6β,19-Trihydroxy-1(10 → 5)*abeo*-cholest-9(10)-ene (**10***a*, 30 mg, 0.09 mmol) was treated with a dry methanolic solution of hydrogen chloride at room temperature for 12 h. Working-up in the usual manner gave a crude product which was purified by chromatography on silica gel (10 g). Crystallization from aqueous acetone of the substance eluted gave a compound with m.p. 126–127.5°. A mixed m.p. with the 5-chloro-6β,19-oxido-5α-cholestan-3β-ol (**3**) prepared from **5***a* was undepressed. The i.r. and mass spectra of this compound were identical to that of the 5α-chloro-6β,19-oxide (**3**) obtained from **5***a*.

The authors are grateful to Dr. T. Durst for helpful discussions and acknowledge the financial support of the National Research Council of Canada.

1. R. R. Fraser, M. Kaufman, P. Morand, and G. Govil. Can. J. Chem. **47**, 403 (1969).
2. For comprehensive reviews of such compounds see E. Heftmann and E. Mosettig. Biochemistry of steroids. Reinhold Publishing Corp., New York, 1960. pp. 61–78; L. F. Fieser and M. Fieser. Steroids. Reinhold Publishing Corporation, New York, 1959. pp. 527–799; F. Sondheimer. Chem. Br. **1**, 454 (1969); Elsevier's encyclopedia of organic chemistry. Ser. III. Carboisocyclic condensed compounds. Steroids: Cardanolides, bufanolides, homosteroids. R. Radt (*Editor*). Springer-Verlag, Berlin, 1969. pp. 4506S–5002S.
3. H. B. Henbest and R. A. L. Wilson. J. Chem. Soc. 1958 (1957).
4. M. Mousseron, M. Mousseron-Canet, and J.-C. Guilleux. Compt. Rend. **258**, 3861 (1964); M. Mousseron-Canet and B. Lebeeuw. Compt. Rend. **260**, 4225 (1965); M. Mousseron-Canet, B. Lebeeuw, and J.-C. Lanet. Compt. Rend. **262**, 1438 (1966); M. Mousseron-Canet, and J.-C. Guilleux. Bull. Soc. Chim. Fr. 3853, 3858 (1966).
5. J. F. Bagli, P. Morand, and R. Gaudry. J. Org. Chem. **28**, 1207 (1963).
6. J. Kalvoda, K. Heusler, H. Ueberwasser, G. Anner, and A. Wettstein. Helv. Chim. Acta, **46**, 1361 (1963).
7. N. G. Gaylord. Reduction with complex metal hydrides. Interscience Publishers, Inc. New York. 1956. pp. 646–673.
8. E. L. Eliel and D. W. Delmonte. J. Am. Chem. Soc. **80**, 1744 (1958); E. L. Eliel and M. N. Rerick. J. Am. Chem. Soc. **82**, 1362 (1960).
9. A. Fürst and P. A. Plattner. Abstr. Papers, 12th Intern. Congr. Pure Appl. Chem. New York, 1951. p. 405; Helv. Chim. Acta, **32**, 275 (1949).
10. P. A. Plattner, H. Heusser, and M. Feurer. Helv. Chim. Acta, **32**, 587 (1949).
11. A. S. Hallsworth and H. B. Henbest. J. Chem. Soc. 4604 (1957).
12. F. Sweet and R. K. Brown. Can. J. Chem. **46**, 708 (1968).
13. N. S. Bhacca and D. H. Williams. Applications of NMR spectroscopy in organic chemistry. Holden-Day Inc., San Francisco, 1966. pp. 100–103.

14. H. C. BROWN and P. M. WEISSMAN. J. Am. Chem. Soc. **87**, 5614 (1965).
15. J. CASTELLS, G. A. FLETCHER, E. R. H. JONES, G. D. MEAKINS, and R. SWINDELLS. J. Chem. Soc. 2785 (1960).
16. *Cf.* A. T. DE B. ANDREWS, A. D. BOUL, G. D. MEAKINS, and M. J. SLEDGE. J. Chem. Soc. C, 1052 (1970).
17. *Cf.* J. W. BLUNT, M. P. HARTSHORN, and D. N. KIRK. J. Chem. Soc. C, 635 (1968); I. G. GUEST and B. A. MARPLES. J. Chem. Soc. C, 576 (1971).
18. H. O. HOUSE. Modern synthetic reactions. W. A. Benjamin, Inc., New York, 1965. pp. 24, 30.
19. E. L. ELIEL. J. Org. Chem. **28**, 1923 (1963).
20. H. B. HENBEST. J. Chem. Soc. 4478 (1961); Proc. Chem. Soc. London, 159 (1963).
21. E. GLOTTER, S. GREENFIELD, and D. LAVIE. Tetrahedron Lett. 5261 (1967).
22. R. M. MORIARITY and T. D. J. D'SILVA. Tetrahedron, **21**, 547 (1965).

Can. J. Chem. Downloaded from www.nrcresearchpress.com by 210.87.254.40 on 09/05/12
For personal use only.

Can. J. Chem. Downloaded from www.nrcresearchpress.com by 210.87.254.5 on 09/05/12
For personal use only.

Alkaline Epoxidation of Carbohydrate Nitroolefins[1,2]

HANS H. BAER AND WERNER RANK
Department of Chemistry, University of Ottawa, Ottawa 2, Canada

Received April 21, 1971

Action of hydrogen peroxide in a weakly alkaline medium upon nitroolefinic sugar derivatives led to α-nitroepoxides in excellent yields. Thus, methyl 4,6-*O*-benzylidene-2,3-dideoxy-3-nitro-α-D-*erythro*-hex-2-enopyranoside (**1**), its β-anomer **2**, and its α-D-*threo* epimer **3** stereospecifically gave methyl 2,3-anhydro-4,6-*O*-benzylidene-3-*C*-nitro-α-D-mannopyranoside (**6**), the β-D-*allo* isomer **7**, and the α-D-*talo* isomer **8**, respectively. The corresponding β-D-*threo* olefin **4** produced a mixture of the β-D-*gulo* (**9**) and β-D-*talo* (**10**) epoxides, with **9** strongly preponderating. The β-L-*gulo* (**11**) and β-L-*talo* (**12**) derivatives were made from the enantiomer **5** of **4**. Another route to α-nitroepoxides, originating from 3-bromo-3-deoxy-3-nitro sugars, furnished the β-D-*manno* isomer **13**.

L'action du peroxyde d'hydrogène en milieu faiblement basique sur des dérivés nitrooléfiniques des sucres, conduit à des α-nitroépoxydes avec un excellent rendement. Ainsi, le méthyl *O*-benzylidène-4,6 didéoxy-2,3 nitro-3 α-D-*érythro* hexène-2 pyranoside (**1**), son anomère β (**2**), et son épimère α-D-*thréo* (**3**) conduisent stéréospécifiquement et respectivement à l'anhydro-2,3 *O*-benzylidène-4,6 *C*-nitro-3-α-D-mannopyranoside (**6**), à l'isomère β-D-*allo* **7**, et à l'isomère α-D-*talo* **8**. L'oléfine β-D-*thréo* **4** correspondante, conduit à un mélange des époxydes β-D-*gulo* (**9**) et β-D-*talo* (**10**), le composé **9** étant en très grande prépondérance. Les dérivés β-L-*gulo* (**11**) et β-L-*talo* (**12**) ont été préparés à partir de l'énantiomère **5** de **4**. Une autre voie d'accès aux α-nitroépoxydes, ayant pour origine les dérivés bromo-3 déoxy-3 nitro-3 des sucres, conduit à l'isomère β-D-*manno* **13**.

Canadian Journal of Chemistry, **49**, 3192 (1971)

Recently, Newman and Angier (3) recorded the preparation and some chemical properties of compounds containing a hitherto unknown structural feature, namely, a nitro-substituted oxirane ring. They obtained such epoxides by the action of alkaline hydrogen peroxide upon phenyl and cyclohexyl derivatives of nitroethylene. We wish to report the synthesis of carbohydrate α-nitroepoxides which are believed to hold much promise for a considerable range of synthetic purposes.

The methyl 4,6-*O*-benzylidene-2,3-dideoxy-3-nitro-hex-2-enopyranosides **1–5** all reacted smoothly, in ethanolic solution at room temperature, with aqueous, 30% hydrogen peroxide at p*H* 8–9. Crystalline methyl 2,3-anhydro-3-*C*-nitrohexopyranosides were produced in yields of 75–90%. Epoxidation of the α- and β-D-*erythro* glycosides, **1** and **2**, and of the α-D-*threo* isomer, **3**, furnished single epoxides having the α-D-*manno* (**6**), β-D-*allo* (**7**), and α-D-*talo* (**8**) configurations, respectively.[3] As no evidence for formation of the alternative diastereoisomers was uncovered, these reactions appeared to be highly stereoselective. A lesser degree of stereoselectivity was observed with the β-D-*threo* isomer **4** which gave a mixture from which the β-D-*gulo* (**9**) and β-D-*talo* (**10**) products were isolated in a ratio of 5:1. In order to verify the differential behavior of **4**, the same reaction was performed with its enantiomer **5**, and the β-L-*gulo* (**11**) and β-L-*talo* (**12**) glycosides were obtained in a similar ratio of 6:1. Hence, in all cases epoxidation occurred preferentially from the side of the ring opposite to the glycosidic methoxyl group.

A different route to α-nitroepoxides was found in connection with a study on α-halonitro sugars which will be described in detail in a forthcoming article (5). Thus, the compounds **6** and **8** were also obtained by the action of base upon the 3-bromo-3-deoxy-3-nitro glycosides **14** and **15**, respectively. An additional α-nitroepoxide,

[1]Part XX in a series on the reactions of nitro sugars. For Part XIX see ref. 1.

[2]Reported on May 25, 1970, before the Chemical Institute of Canada and the American Chemical Society (2).

[3]After our preliminary report (2) appeared, a short communication (4) describing the preparation of **7** from **2** by the action of sodium hypochlorite was published.

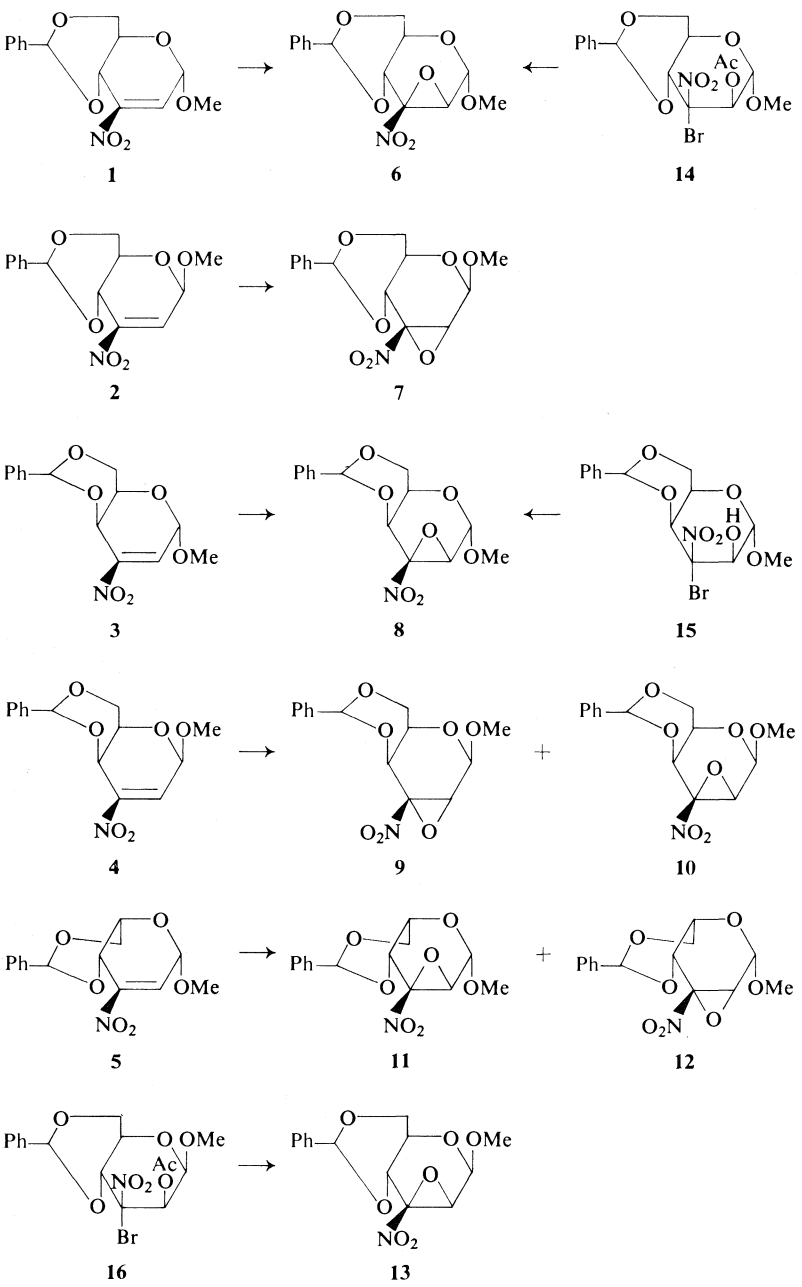

namely that with the β-D-*manno* configuration **13**, arose from the bromodeoxynitro glycoside **16**.

The structure of the stereoisomeric epoxides **6**–**13** was confirmed by elemental analysis and spectroscopy. Strong i.r. bands at about 1560 cm^{-1} indicated the nitro group, and n.m.r. spectra in $CDCl_3$ showed, except for the β-*talo* compounds **10** and **12**,[4] the presence of the benzy-

[4]Because of poor solubility no useful n.m.r. spectra were obtained from **10** and **12**.

Can. J. Chem. Downloaded from www.nrcresearchpress.com by 210.87.254.5 on 09/05/12
For personal use only.

TABLE 1. Chemical shifts (τ) of methyl 2,3-anhydro-4,6-*O*-benzylidene-3-nitrohexopyranosides

Compound	Configuration	$PhCHO_2$	H-1	H-2	H-4	H-5	H-6	H-6′	OCH_3
6	α-D-*manno*	4.44	5.15	6.29	~6.0	6.23	5.71	~6.0	6.55
7	β-D-*allo*	4.28	5.18	6.23	4.95	6.39	5.65	6.12	6.45
8	α-D-*talo*	4.33	4.91	6.29	4.37	6.24	5.63	5.76	6.56
9	β-D-*gulo*	4.37	5.21	5.74	5.10	6.59	5.67	5.94	6.46
13	β-D-*manno*	4.40	4.94	6.14	5.88	6.41	5.64	6.13	6.42

lidene acetal group (aromatic 5-proton multiplet near τ 2.6 and methine singlet near τ 4.3–4.4) and of the glycosidic methoxyl group (3-proton singlet at τ 6.42–6.46 in β-anomers, at 6.55–6.56 in α-anomers). Integration of the remaining signals revealed the presence of six skeletal protons in each case, as required by the structure. The chemical shifts measured in $CDCl_3$ solution are given in Table 1.

The configurations were assigned by means of n.m.r. data and circular dichroism (c.d.) curves (Fig. 1). Since the configurations at C-1, -4, and -5 of each compound were defined by the starting materials, it was necessary only to determine the steric dispositions of the epoxide oxygen atoms. Thus compounds **7** and **13**, which have identical stereochemistry with respect to C-1, -4, and -5, evidently differ only in the orientation of the epoxide ring. The stereochemical environment of the nitro chromophore is thereby made different, and as a result the compounds exhibit Cotton effects with opposite signs, even though they have the same anomeric configuration. Compound **6** (which on the basis of its origin could be the α-anomer of either **7** or **13**) shows the same Cotton effect as **13** and consequently is assigned the same epoxide configuration. Further evidence was provided by the n.m.r. spectra. It has been pointed out (6, 7) that in 2,3-anhydrohexopyranosides (including 4,6-*O* benzylidene derivatives) the anomeric proton shows no coupling with H-2 when these protons are *trans*-related, and that a small coupling is observed when they are *cis*-related. In **6** and **7** the H-1 signals were sharp singlets (100 MHz spectra at 250 Hz sweep width), whereas **13** gave an anomeric doublet with 0.8 Hz splitting. This is in agreement with the α-D-*manno* and β-D-*allo* configurations for **6** and **7**, respectively, and with the β-D-*manno* configuration for **13**.[5]

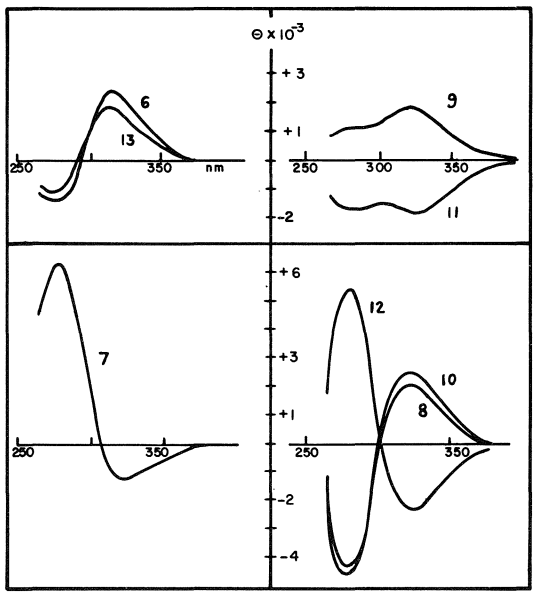

FIG. 1. Circular dichroism of carbohydrate α-nitroepoxides at 25° in dioxane. The authors are indebted to Dr. J. Kovář for these spectra.

Among the epoxides with *cis*-fused benzylidene rings, **8** and **10** give virtually identical c.d. curves. For this reason **10**, rather than **9**, is thought to be the anomer of **8**. The sign of the Cotton effect of **8** and **10** is the same as that of the anomeric pair **6** and **13**, and the two pairs are therefore allocated identical configuration with respect to the

[5]Methyl 2,3-anhydro-4,6-*O*-benzylidene-α-D-mannopyranoside exhibits $J_{1,2} = 0$ Hz whereas the α-D-*allo* isomer shows $J_{1,2} = 2.5$ Hz (6); the corresponding α-D-*allo* 4,6-diacetate shows $J_{1,2} = 1.5$ Hz, and the α-D-*manno* and β-D-*allo* 4,6-diacetates display $J_{1,2} = 0$ Hz (7). If **6**, **7**, and **13** would possess the α-D-*allo*, β-D-*manno*, and β-D-*allo* configurations, respectively, one would expect to find small $J_{1,2}$ couplings in the first two and no coupling in the last one, *i.e.* the reverse of what has been found. The value of **13** is somewhat smaller than had been anticipated, but it is to be noted that, in the half-chairs which these compounds are assumed to occupy, the dihedral angle between 1,2-*cis* protons varies slightly, depending on whether the protons are situated on the upper side of the ring (as in the α-D-*allo* case) or on the lower side (as in the β-D-*manno* case). Moreover, the nitro group may well exert some influence on the magnitude of this coupling.

Can. J. Chem. Downloaded from www.nrcresearchpress.com by 210.87.254.5 on 09/05/12
For personal use only.

TABLE 2. α-Nitroepoxides

Compound	Reaction time (min)	Yield (%)	Melting point (°C)	$[\alpha]_D^{25}$ in $CHCl_3$ (*c*, 0.5–0.8) (degrees)	Anal. Found for $C_{14}H_{15}NO_7$ (309.3)* C	H	N
Methyl 2,3-anhydro-4,6-*O*-benzylidene-3-*C*-nitro-							
-α-D-mannopyranoside (**6**)	90	77	173–174	+51.2	54.52	4.75	4.35
-β-D-allopyranoside (**7**)	30	89	204–205	−98.8	54.69	5.03	4.36
-α-D-talopyranoside (**8**)	40	84	215–216	+91.8	54.64	4.83	4.73
-β-D-gulopyranoside (**9**)	50	67.5	154–155	−62.1	54.56	5.05	4.34
-β-D-talopyranoside (**10**)	50	13	241–243 (dec.)	−31.2†	54.42	4.87	
-β-L-gulopyranoside (**11**)	45	64	154–156	+62.7			
-β-L-talopyranoside (**12**)	45	11	239–241 (dec.)				
-β-D-mannopyranoside (**13**)			182–183	−68.4	54.63	5.08	4.32

*Anal. Calcd. for $C_{14}H_{15}NO_7$: C, 54.45; H, 4.89; N, 4.53.
†In dimethylformamide.

epoxide ring. From the assignment of the α- and β-D-*talo* configurations to **8** and **10**, it follows that **9** must possess the β-D-*gulo* configuration. Although **9** shows an abnormal c.d. curve which is as yet unexplained (Fig. 1), both **9** and **8** exhibit zero coupling of H-1 and -2, conforming with *trans* arrangements of these protons.

The enantiomerism of **9** and **11**, and of **10** and **12**, was borne out by physical constants (Table 2), identical i.r. spectra, mirror image c.d. curves, and (for **9** and **11**)[4] identical n.m.r. spectra.

Inspection of Table 1 reveals a number of noteworthy regularities in chemical shifts. Thus, in the compounds having a *trans*-fused benzylidene ring, the methine proton resonates at higher field when the epoxide ring is *cis* to it than when it is *trans* (τ 4.44 and 4.40 *vs.* 4.28), and the same holds to a much stronger degree for H-4 (τ 6.0 and 5.88 *vs.* 4.95). In the compounds having a *cis*-fused benzylidene ring the chemical shifts of the H-4 protons (5.10 *vs.* 4.37) and of the methine protons (4.37 *vs.* 4.33) follow the same trend (although the last-mentioned difference is small and may not be significant). Ferrier and Prasad (7) have observed dependencies of H-4 shifts on the orientation of the 2,3-epoxy ring, but the effects they noted were much smaller than those in our compounds, and one has therefore to conclude that here the nitro group makes an important contribution. On the other hand, the chemical shifts of the protons H-2 differ little, and the same applies to the protons H-5. An exception is provided by **9** which gives an H-2 signal appreciably downfield, and an H-5 signal noticeably upfield, from the corresponding signals of the isomers. It is tempting to speculate

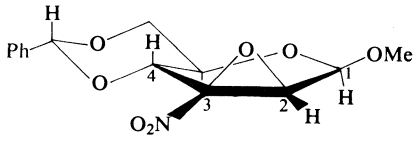

13

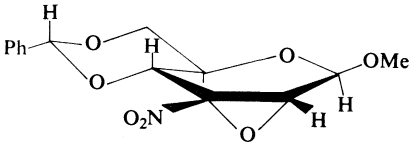

7

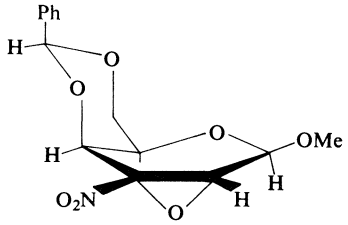

9

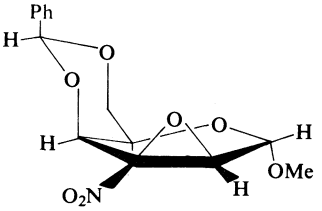

8

that this is caused by the same stereochemical feature that gives rise to the anomalous c.d. curve. No doubt the preferred torsional angle of the nitro group, which presumably is governed

Can. J. Chem. Downloaded from www.nrcresearchpress.com by 210.87.254.5 on 09/05/12
For personal use only.

by steric or dipolar effects originating chiefly from O-4 and O-2,3, is a determinant factor in both c.d. and p.m.r.[6]

Experimental

Melting points were taken using capillaries in an electrically heated aluminum block apparatus. The t.l.c. was performed on silica gel G (E. Merck AG, Darmstadt) with 3:2 (v/v) ethyl acetate – petroleum ether (b.p. 30–60°), and spots were made visible by ceric sulfate and heating. Optical rotations were measured in a Perkin–Elmer 141 automatic polarimeter, and c.d. curves were recorded with a Jasco ORD/UV-5 instrument. The n.m.r. spectra (100 MHz) were obtained, at sweep widths of 1000 and 250 Hz, from solutions in $CDCl_3$ containing tetramethylsilane.

General Procedure for Epoxidation

The starting compounds, namely the methyl 4,6-*O*-benzylidene-2,3-dideoxy-3-nitrohex-2-enopyranosides with α-D-*erythro* (**1**) (8), β-D-*erythro* (**2**) (9), α-D-*threo* (**3**) (8), and β-D-*threo* (**4**) (10) configuration were prepared according to the references cited, or by improved modifications (11, 12) of the original procedures. The β-L-*threo* isomer **5** (m.p. 159–161°, $[\alpha]_D$ +47.1° in dimethylformamide) was obtained from methyl 4,6-*O*-benzylidene-3-deoxy-3-nitro-β-L-galactopyranoside (13) by the method elaborated (10, 12) for its enantiomer **4** for which has been recorded m.p. 162°, $[\alpha]_D$ −47.8°.

To a solution of a given nitroolefinic sugar (200 mg) in ethanol (20 ml) was added 1 ml of aqueous, 30% hydrogen peroxide (reagent grade), and the p*H* of the mixture was adjusted to 8–9 by adding a few drops of *N* sodium hydroxide solution. The reaction mixture was stirred at room temperature for a specified time (Table 2) during which the epoxide began to crystallize, usually at an early stage. The reactions were monitored by t.l.c. which enabled a clear distinction between starting material and product in all cases. Complete consumption of the starting material was observed. The white, crystalline precipitate was removed by filtration, washed with a small amount of cold water (for **6** and **7**) or cold ethanol (for **8**, **10**, and **12**), and dried in a desiccator. By adding some water to the mother liquor and concentrating the solution under diminished pressure, second crops were obtained of **6** and **8**, whereas the mother liquors of sparingly soluble **10** and **12** furnished the more soluble **9** and **11**, respectively, which constituted the major reaction products. The products so obtained gave single spots on t.l.c. and had reasonably sharp melting points which were raised a few degrees only by recrystallization from 95% ethanol. Yields, physical constants, and microanalytical data for the epoxides **6**–**12** are given in Table 2. Also included in Table 2 are data for the β-D-*manno* isomer **13** although this compound was obtained in a different way (5).

[6]A substantially different over-all conformation as cause of the anomalous characteristics of **9** seems unlikely. Although **9** (and **8**) may exist with an inverted pyranose half-chair ($HC^5{}_O$) instead of the depicted half-chair ($HC^O{}_5$), the n.m.r. spectra militate against such inversion. Both compounds display only small vicinal couplings (2–2.5 Hz) in their H-5 and -6 signals, whereas the $HC^5{}_O$ form with a *cis*-fused 1,3-dioxane chair would have a 180° dihedral angle between H-5 and one of the H-6 protons, calling for a large *J* value. Compounds **7** and **13** indeed show the corresponding, large splitting (10 Hz) as required by the conformation depicted.

We thank the National Research Council of Canada for support of this work.

1. H. H. Baer and J. Kovář. Can. J. Chem. **49**, 1940 (1971).
2. H. H. Baer and W. Rank. Abstract of papers (CARBO, No. 12), Joint conference of the Chemical Institute of Canada and the American Chemical Society, Toronto, Ontario, May, 1970.
3. H. Newman and R. B. Angier. Tetrahedron, **26**, 825 (1970); Chem. Commun. 369 (1969).
4. T. Sakakibara, S. Kumazawa, and T. Nakagawa. Bull. Soc. Chem. Jap. **43**, 2655 (1970).
5. H. H. Baer and W. Rank. In preparation.
6. D. H. Buss, L. Hough, L. D. Hall, and J. F. Manville. Tetrahedron, **21**, 69 (1965).
7. R. J. Ferrier and N. Prasad. J. Chem. Soc. C. 575 (1969).
8. H. H. Baer and F. Kienzle. Can. J. Chem. **45**, 983 (1967).
9. H. H. Baer and T. Neilson. Can. J. Chem. **43**, 840 (1965).
10. H. H. Baer, F. Kienzle, and T. Neilson. Can. J. Chem. **43**, 1829 (1965).
11. H. H. Baer and W. Rank. To be published. Part XXVI of this series.
12. H. H. Baer. *In* Methods in carbohydrate chemistry, Vol. VI. [53]. Academic Press, New York, N.Y., 1971.
13. H. H. Baer and F. Kienzle. Can. J. Chem. **43**, 3074 (1965).

Can. J. Chem. Downloaded from www.nrcresearchpress.com by 210.87.254.5 on 09/05/12
For personal use only.

A Study of Steric Effects on Nitromethylene Acidity and the Mechanism of Epimerization in Partially Blocked Nitro Hexoses[1]

HANS H. BAER AND WERNER RANK
Department of Chemistry, University of Ottawa, Ottawa 2, Canada

Received April 21, 1971

The extent of nitronate formation in seven methyl 4,6-*O*-benzylidene-3-deoxy-3-nitrohexopyranosides and four methyl 4,6-*O*-benzylidene-2,3-dideoxy-3-nitrohexopyranosides in dilute potassium hydroxide solution was compared by means of u.v. spectroscopy. Considerable differences were found to exist in the nitromethylene acidities, and these were correlated with stereochemical features of the molecules. A facile *manno* → *gluco* epimerization occurring in this series was investigated. It was shown that, in alkaline alcoholic solution, the epimerization proceeds by an elimination–addition via an intermediate nitroalkene if the hydroxyl group at C-2 is acetylated. However, if the hydroxyl is free, the nitroalkene is not an intermediate and, in accord with the low nitromethylene acidity in this particular case, the mechanism is suggested to involve a reverse Henry reaction.

Le degré de formation de nitronate à partir de sept méthyl *O*-benzylidène-4,6 déoxy-3 nitro-3 hexopyranosides et de quatre méthyl *O*-benzylidène-4,6 didéoxy-2,3 nitro-3 hexopyranosides, en solution dans de l'hydroxyde de potassium dilué, a été comparé par spectroscopie u.v. Des différences considérables ont été trouvées en ce qui concerne les acidités des groupes nitrométhylènes; celles-ci ont été reliées aux caractères stéréochimiques des molécules. L'épimérisation facile *manno* → *gluco* qui se fait dans cette série a été étudiée. Il a été montré que, en solution alcoolique et alcaline, l'épimérisation se fait par une élimination–addition via un nitroalcène intermédiaire, si le groupe hydroxyle en C-2 est acétylé. Cependant, si l'hydroxyle est libre, le nitroalcène n'est pas un intermédiaire et, en accord avec la faible acidité du nitrométhylène dans ce cas particulier, le mécanisme implique probablement une réaction d'Henry inverse.

Canadian Journal of Chemistry, **49**, 3197 (1971)

Can. J. Chem. Downloaded from www.nrcresearchpress.com by 210.87.254.42 on 09/05/12
For personal use only.

In a preceding part of this series the influence of configuration on the thermodynamic stability of pentopyranoside nitronates was discussed (1). It was shown that conformational preferences and equilibria of epimerization in the sodium salts of methyl 3-deoxy-3-nitropentopyranosides can be rationalized on the basis of the nonbonded interaction between the nitronate group and an adjacent, equatorial hydroxyl group ($A^{(1,3)}$ effect). Concurrent studies with hexose derivatives provided further insights regarding the influence of steric factors on reactivity in nitro sugars. The present article reports observations concerning the behavior of 4,6-*O*-benzylidene derivatives of methyl 3-deoxy-3-nitrohexopyranosides in alkaline medium. Such acetals are useful derivatives that can serve for the separation of stereoisomers and as starting points for many syntheses (2, 3). However it has been recognized for some time (4) that the benzylidene group is prone to cleavage by way of base-promoted β-elimination, which may detract from its usefulness as a blocking group. The degree of sensitivity appears to be dependent on configuration, for it has been observed (5) that methyl 2-*O*-acetyl-4,6-*O*-benzylidene-3-deoxy-3-nitro-β-D-galactopyranoside undergoes reactions which entail the loss of the benzylidene group rather more readily than its *gluco* isomer. The first step in this type of reaction and in various other base-catalyzed reactions of primary and secondary nitro compounds is generally assumed to be proton abstraction to give a nitronate ion, and it was therefore decided to undertake a comparative study of nitronate formation in this series.

The extent of nitronate formation in the available methyl 4,6-*O*-benzylidene-3-deoxy-3-nitro- and 2,3-dideoxy-3-nitrohexopyranosides in 0.01–0.001 *N* ethanolic potassium hydroxide solution was examined by u.v. spectroscopy, making use of the high-intensity absorption in the 250 nm region which is due to the nitronate chromophore (4, 6, 7).[2] Table 1 lists molar absorbances (A_M) of

[1]Part XXI in a series on the reactions of nitro sugars. For Part XX see ref. 15.

[2]The absorption maximum of sodium methanenitronate in water is at 232 nm (8), and the maxima of the sodium salts of other primary and secondary nitroalkanes and nitrocycloalkanes fall in the region 226–244 nm (9).

TABLE 1. The u.v. absorptions produced by nitro glycosides in ethanolic potassium hydroxide solution

Compound	Configuration	Normality in KOH	λ_{max} (nm)	A_M*
1	α-D-*talo*	0.001	251	21700
2	α-D-*galacto*	0.01	254	10900
3	β-D-*galacto*	0.001	258	12100
		0.01	258	13500
4	α-D-*gluco*	0.001	250–260	500
5	β-D-*gluco*	0.001	250–260	500
6	α-D-*manno*	0.001	250–260	500
7	β-D-*manno*	0.001	250–260	500
8	α-D-*lyxo*	0.01	251	14100
9	β-D-*lyxo*	0.001	253	13800
		0.01	253	14500
10	α-D-*arabino*	0.001	252	1050
11	β-D-*arabino*	0.001	252	1050

*Molar absorbance = absorbance of a solution 10^{-4} *M* in nitro compound, multiplied by 10 000. The value would represent the molar extinction coefficient of the nitronate anion only in case of complete ionization.

the nitro compounds, which may be taken as a measure for the amount of nitronate present under the given conditions of alkalinity. The values recorded are maximum values, attained about 8 min after the addition of alkali to the nitro compounds. It is to be noted that establishment of the nitro–nitronate equilibrium, though rapid, is not instantaneous, and in systems developing a reasonably strong absorption the growth of the nitronate peak can be readily monitored in an automatic spectrometer. For example, **1** showed A_M 13 600, 15 400, 20 400, and 21 700 after 0.6, 1.5, 4, and 8 min (in 0.001 *N* KOH in ethanol). Then the peak decreased again (A_M 21 000 and 19 300 after 16 and 64 min), with concomitant appearance of a new peak near 300 nm. The latter phenomenon is due to a slow elimination reaction leading to an unsaturated nitronate (4).

It is seen that methyl 4,6-*O*-benzylidene-3-deoxy-3-nitro-α-D-talopyranoside (**1**) forms nitronate most easily. The α- and β-D-*galacto* isomers, **2** and **3**, do so less readily but still extensively, whereas the α- and β-D-*gluco* isomers, **4** and **5**, produce hardly any nitronate absorption and the amount of salt formed must be very small.[3] The α- and β-D-*manno* isomers, **6** and **7**, give rise to the same, insignificant absorptions and thus appear to behave like the *gluco* isomers. This seemed surprising at first sight but became understandable when their chemical fate was examined, as will be disclosed in a subsequent paragraph. The methyl 4,6-*O*-benzylidene-2,3-dideoxy-3-nitro-α- and β-D-*lyxo*-hexopyranosides (**8** and **9**) appear to form nitronate somewhat more readily than the D-*galacto* derivatives, and their α- and β-*arabino* isomers, **10** and **11**, behave similarly to the D-*gluco* derivatives but give rise to slightly greater absorptions. In summary, high-intensity absorption is observed when the oxygen atom O-4 is linked axially, and low absorption, when it is linked equatorially. In both cases, replacement of an equatorial hydroxyl group at C-2 by hydrogen moderately enhances the absorption. An axial hydroxyl at C-2 causes a strong increase when O-4 is axial also, but is without visible effect when O-4 is equatorial. We offer the following explanation for these observations.

In the nitronates expected to arise from the compounds that bear a *trans*-fused acetal ring (**4–7**, **10**, and **11**), one of the nitronate oxygens faces nonbonded interaction from the equatorial O-4. This condition [$A^{(1,3)}$ effect (10)], which is associated with an interaction energy of about 2 kcal/mol (1) and which cannot, in these rigid bicyclic systems, be relieved by a conformational change, constitutes a severe impediment to nitronate formation. In the compounds having a *cis*-fused acetal ring (**1–3**, **8**, and **9**), the (axial) O-4 does not so interfere. An equatorial hydroxyl group at C-2 could likewise be expected to hinder nitronate formation, and the lower extinctions given by the D-*galacto* and D-*gluco* compounds

[3]At higher concentration of alkali (0.1 *N* aqueous NaOH), **5** does produce a peak at 253 nm (4).

Can. J. Chem. Downloaded from www.nrcresearchpress.com by 210.87.254.42 on 09/05/12
For personal use only.

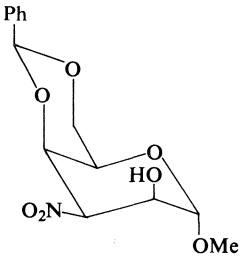

1

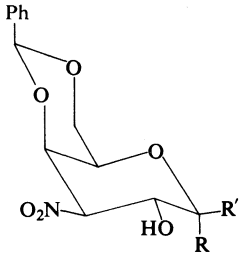

2 R = OMe; R′ = H
3 R = H; R′ = OMe

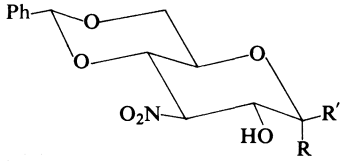

4 R = OMe; R′ = H
5 R = H; R′ = OMe

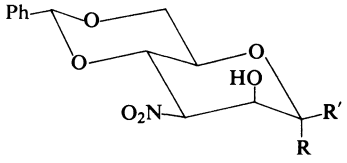

6 R = OMe; R′ = H
7 R = H; R′ = OMe

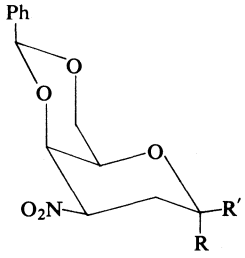

8 R = OMe; R′ = H
9 R = H; R′ = OMe

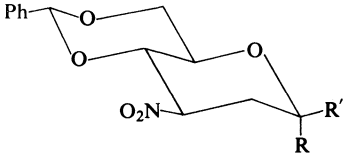

10 R = OMe; R′ = H
11 R = H; R′ = OMe

in comparison with their respective 2-deoxy analogs might be taken to bear this out. However the differences are small, and they may in fact be due entirely to a change in the inductive effect of C-2. At any rate it is clear that an equatorial hydroxyl at this position does not seriously interfere with nitronate formation, and one may therefore assume that its $A^{(1,3)}$ interaction is diminished substantially by a distortion of the pyranoside chair. A molecular model shows that flattening which the chair tends to incur by sp^2 hybridization of C-3 will mainly affect the position of C-2 (in the more flexible part of the ring), allowing an equatorially-attached hydroxyl to move downward and thus to recede from the nitronate oxygen atom. This movement should be opposed by an axial anomeric methoxyl group and indeed, the α-D-galactoside **2** seems to produce slightly less nitronate than its β-anomer **3** while the corresponding anomers **8** and **9** of the 2-deoxy series expectedly exhibit no significant difference. The ring distortion just mentioned also implies a lessening of steric interaction between an axially attached oxygen at C-4 and an opposing axial atom or group at C-2. Undoubtedly this is conducive to nitronate formation in the *galacto* and *lyxo* compounds, and it provides an especially pronounced driving force in the *talo* isomer **1**.

We have also estimated the pK_a values of some of the compounds by half-titration with sodium hydroxide in aqueous dioxane (Table 2). The

Can. J. Chem. Downloaded from www.nrcresearchpress.com by 210.87.254.42 on 09/05/12
For personal use only.

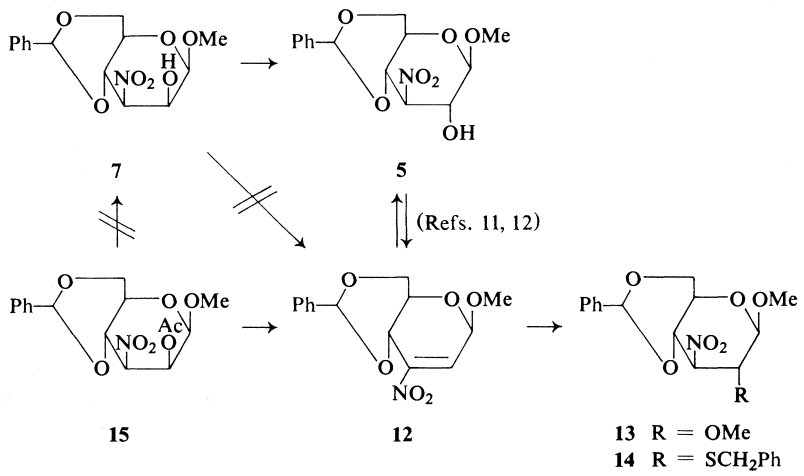

SCHEME 1

nitromethylene acidities so found qualitatively parallel the spectroscopically determined tendencies of salt formation, bearing out the influence of configuration.[4]

Although an equatorial disposition of O-4 obviously is the chief obstacle to facile nitronate formation in these benzylidenated glycosides, it nevertheless seemed remarkable that the mannosides **6** and **7**, with their axial 2-hydroxyl, did not perceptibly differ spectroscopically from the glucosides. However, it is recalled that the mannoside **7** was *epimerized* to **5** by refluxing in toluene or benzene in the presence of basic alumina or solid potassium hydroxide catalyst (11, 12). We have now found that it epimerizes more rapidly yet in alcoholic, alkaline solution at room temperature, and the observed u.v. spectrum therefore may well represent largely **5** rather than **7**. This epimerization, the facile occurrence of which was ascertained by isolation of **5** in preparative experiments using ethanolic potassium hydroxide or methanolic sodium methoxide solutions (and which was also performed with the α-anomer **6**), was of considerable interest with regard to its mechanism.

TABLE 2. Nitromethylene acidities

Compound	Configuration	pK_a*
1	α-D-*talo*	8.1
2	α-D-*galacto*	9.6
4	α-D-*gluco*	10.8
5	β-D-*gluco*	10.8
6	α-D-*manno*	11.0
8	α-D-*lyxo*	8.8
9	β-D-*lyxo*	8.3
10	α-D-*arabino*	10.7
11	β-D-*arabino*	10.5

*The p*H*-values observed potentiometrically in approximately 0.01 *M* solutions in dioxane upon half-titration with 0.002 *N* sodium hydroxide in water. We thank Dr. Jan Kovář for kindly performing these measurements.

It had been demonstrated that the glucoside **5** is dehydrated by heating in toluene (or benzene) in the presence of a solid base to give the nitroolefin **12**, and that **12** in turn can be easily hydrated back to **5**, so that it was reasonable to assume that the epimerization of **7** took the same course, via **12** (11, 12) (see Scheme 1). There is still no evidence to discount that pathway for the reaction under the conditions then employed. However, a mechanism that does not involve **12** has now been established to operate under the present conditions. If **12** were produced from **7**, then, in a methanolic medium containing sodium methoxide, **12** should add methanol to produce the 2-*O*-methyl ether (**13**) of **5**, rather than **5** itself. It has been shown previously (13) that **12** does indeed give **13** with great ease and we have now convinced ourselves that it does so even in the presence of a stoichiometric amount of water.[5] Furthermore, when **7** was treated with the strong nucleophile, sodium benzylmercaptide in meth-

[4]Compare also the similar dependence of acidity on the stereochemistry of the methyl 3-deoxy-3-nitropentopyranosides (1). Note that the spectroscopic and potentiometric data apply to different solvents; quantitative conclusions are not intended.

[5]By providing 1 mol of water per mol of **12** in excess methanol we simulated the conditions that would obtain upon dehydration of **7**.

Can. J. Chem. Downloaded from www.nrcresearchpress.com by 210.87.254.42 on 09/05/12
For personal use only.

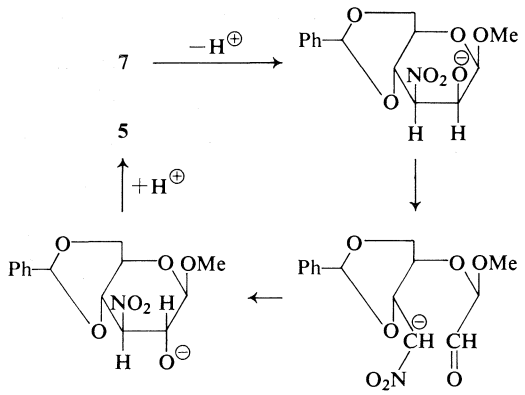

SCHEME 2

anol, the product was **5** and not the known benzylthio derivative **14**. An intermediacy of **12** can therefore be ruled out for these reactions. On the other hand, the *O*-acetyl derivative (**15**) of **7** furnished the methyl ether **13** in 88% yield upon reaction with methanolic potassium hydroxide, the reaction being complete within a few minutes at room temperature. This can only be explained by β-elimination of the acetoxy group to give intermediate **12**, and subsequent nucleophilic addition of methanol. For if **15** had suffered methanolysis of its acetyl rather than β-elimination of its acetoxy group, then **7** and hence **5** would have resulted. Numerous elimination–additions of this kind had previously been performed with the 2-acetates of the glucosides **4** and **5**. The conclusion can be drawn that abstraction of H-3 by base, however small its extent, is sufficient in the 2-acetates to permit elimination of the good leaving group, acetate ion, whereas in **7** it is not effective enough to induce departure of the poor leaving group, hydroxyl ion. Because of the difficulty in forming its nitronate, **7** incurs competitive deprotonation of the 2-hydroxyl group, and this leads to ring opening by reversal of a nitroalkane cyclization. Subsequent recyclization produces the thermodynamically more stable β-D-*gluco* epimer[6] (Scheme 2). Although the intermediate aldehydonitronate should have a high extinction coefficient, its concentration is not expected to reach a spectroscopically observable level. This mechanism was originally proposed by Grosheintz and Fischer (14) for the easy, epimeric equilibration of deoxynitroinositols, but it lacked experimental support and was not adopted in our subsequent work on nitro sugars, mainly because of theoretical considerations (2) and because of accumulating evidence for the role of nitroolefin intermediates in various base-catalyzed transformations (2, 4–7, 11–13). However, our recent studies on the epimerization of nitro pentosides (1) and of the above mannosides have demonstrated that the nitronate ⇄ nitroolefin pathway does not apply when the nitromethylene acidity is strongly reduced for steric reasons. In these cases, the secondary nitro group might be termed pseudo-tertiary, and it is suggested that a reverse Henry reaction (reverse nitroalkane-aldehyde addition), known to be facile only in β-hydroxy-*tert*-nitro compounds, must then account for epimerization.

[6]In contrast to the situation in the nitronates, there is no special hindrance between a nitro group on a tetrahedral carbon and an adjacent, equatorial hydroxyl.

Experimental

For general procedures and instrumental techniques, see preceding parts of this series (1, 15).

Materials

The following nitro glycosides were obtained according to the references given in parentheses: **1**, **8**, **10** (16); **3**, **4**, **7**, **15** (17); **5**, **11**, **12** (18); **9** (19). Preparation of the new α-D-*galacto* compound **2** (m.p. 166–167°; $[\alpha]_D$ +205°, *c* 0.5 in chloroform) and α-D-*manno* compound **6** (m.p. 138–139°); $[\alpha]_D$ +27.7°, *c* 0.8 in chloroform) will be disclosed elsewhere (3).

Ultraviolet Spectra

Accurately weighed samples (about 3.6 mg) of the nitro glycosides were dissolved in 10.00 ml of 99% ethanol. Aliquots containing 0.31 mg of **1**–**7** (mol. wt. 311) or 0.295 mg of **8**–**11** (mol. wt. 295) were withdrawn and their volumes (*e.g.* 0.85 ml) were made up to 10.00 ml with 0.01 or 0.001 *N* ethanolic potassium hydroxide solution as specified (Table 1), to give solutions that were 10^{-4} *M* in nitro compound. The spectra were measured in a Perkin–Elmer 202 spectrophotometer using 1-cm cells, with the reference cell containing ethanolic KOH of the same normality.

Reactions Concerning the manno → gluco Epimerization

(*a*) The β-D-mannoside **7** (62 mg) was dissolved in 0.1 *N* ethanolic potassium hydroxide (20 ml). After standing for 10 min at 25° the solution was deionized by cation exchange, filtered, and evaporated to give a solid that was recrystallized from methanol–water. The product (55 mg, 89%) melted at 180–181° and gave an i.r. spectrum identical with that of an authentic sample of the β-D-glucoside **5**; lit. (18), m.p. 181–182°. In a parallel run employing methanolic potassium hydroxide and ice cooling, t.l.c. revealed that the conversion of **7** was complete within a few minutes.

(*b*) A similar preparative experiment using the α-D-mannoside **6** furnished 81% of the α-D-glucoside **4**, m.p. 165–166°, $[\alpha]_D$ +82.1° (*c* 0.63 in ethanol), with an i.r.

Can. J. Chem. Downloaded from www.nrcresearchpress.com by 210.87.254.42 on 09/05/12
For personal use only.

spectrum identical to that of an authentic sample; lit. (17), m.p. 167°, $[\alpha]_D$ +82°.

(*c*) Compound **7** (62 mg) was dissolved in 20 ml of 0.1 *N* methanolic sodium methoxide solution. After standing at 25° for 2.5 h the solution was deionized and evaporated to give 57 mg (92%) of crystals which on recrystallization from methanol–water amounted to 53 mg (85%), m.p. 180–181°. They were identical with **5** according to t.l.c. and i.r. spectrum.

(*d*) Thiobenzyl alcohol (0.2 ml) was mixed with 0.1 *N* sodium methoxide solution (33 ml). After 15 min the mannoside **7** (103 mg) was added, and the reaction mixture was stirred at room temperature. According to t.l.c. **7** was completely converted into **5** after 30 min, and work-up after 60 min yielded 89 mg (86%) of recrystallized **5**, m.p. 179–181°. There was no evidence for formation of the known (13) benzylthio derivative **14**.

(*e*) To an ice cold solution of the 2-acetate **15** (70.5 mg) in methanol (5 ml) was added a 0.2 *N* methanolic potassium hydroxide solution (20 ml). It was revealed by t.l.c. that the reaction was complete after 2 min. Work-up by deionization and evaporation after 25 min furnished 57 mg (88%) of **13**, m.p. 184–185°, which was identified with an authentic sample by i.r. spectroscopy and an undepressed mixture melting point.

We thank the National Research Council of Canada for support of this work.

1. H. H. Baer and J. Kovář. Can. J. Chem. **49**, 1940 (1971).
2 H. H. Baer. Adv. Carbohydr. Chem. Biochem. **24**, 69 (1969).
3. H. H. Baer and W. Rank. To be submitted. Part XXVI of this series.
4. H. H. Baer and F. Kienzle. Ann. **695**, 192 (1966).
5. H. H. Baer and K. S. Ong. Can. J. Chem. **46**, 2511 (1968); J. Org. Chem. **34**, 560 (1969).
6. H. O. L. Fischer and H. H. Baer. Ann. **619**, 53 (1958).
7. H. H. Baer and W. Rank. Can. J. Chem. **43**, 3330 (1965).
8. G. Kortüm. Z. physik. Chem. **43B**, 279 (1939).
9. F. T. Williams, Jr., P. W. K. Flanagan, W. T. Taylor, and H. Schechter. J. Org. Chem. **30**, 2674 (1965).
10. F. Johnson and S. K. Malhotra. J. Am. Chem. Soc. **87**, 5492 (1965).
11. H. H. Baer and W. Rank. Can. J. Chem. **47**, 2811 (1969).
12. H. H. Baer and F. Kienzle. Can. J. Chem. **47**, 2819 (1969).
13. H. H. Baer, T. Neilson, and W. Rank. Can. J. Chem. **45**, 991 (1967).
14. J. M. Grosheintz and H. O. L. Fischer. J. Am. Chem. Soc. **70**, 1479 (1948).
15. H. H. Baer and W. Rank. Can. J. Chem. This issue.
16. H. H. Baer and F. Kienzle. Can. J. Chem. **45**, 983 (1967).
17. H. H. Baer, F. Kienzle, and T. Neilson. Can. J. Chem. **43**, 1829 (1965).
18. H. H. Baer and T. Neilson. Can. J. Chem. **43**, 840 (1965).
19. H. H. Baer and F. Kienzle. Can. J. Chem. **43**, 3074 (1965).

Can. J. Chem. Downloaded from www.nrcresearchpress.com by 210.87.254.42 on 09/05/12
For personal use only.

Can. J. Chem. Downloaded from www.nrcresearchpress.com by 210.87.254.105 on 09/05/12
For personal use only.

Acetonation of 3-Deoxy-3-nitro-D-glucose and Formation of a Derivative of 3-Deoxy-3-nitro-D-allose[1]

JAN KOVÁŘ AND HANS H. BAER
Department of Chemistry, University of Ottawa, Ottawa, Canada

Received May 28, 1971

Reaction of 3-deoxy-3-nitro-D-glucose (**1**) with acetone and triethyl orthoformate in the presence of hydrogen chloride gave crystalline 3-deoxy-1,2-*O*-isopropylidene-3-nitro-α-D-glucopyranose (**2**), 3-deoxy-1,2:4,6-di-*O*-isopropylidene-3-nitro-α-D-glucopyranose (**3**), and 3-deoxy-1,2:5,6-di-*O*-isopropylidene-3-nitro-α-D-glucofuranose (**5**) in proportions varying with the acid concentration. The furanose derivative **5** is thermodynamically favored. Partial acid hydrolysis of **5** gave 3-deoxy-1,2-*O*-isopropylidene-3-nitro-α-D-glucofuranose (**4**), whereas action of mild base caused epimerization to 3-deoxy-1,2:5,6-di-*O*-isopropylidene-3-nitro-α-D-allofuranose (**6**).

La réaction du déoxy-3 nitro-3 D-glucose (**1**) avec l'acétone et le triéthyl orthoformate en présence d'HCl conduit au déoxy-3 *O*-isopropylidène-1,2 nitro-3 α-D glucopyranose (**2**), au déoxy-3 di-*O* isopropylidène-1,2;4,6 nitro-3 α-D-glucopyranose (**3**), et au déoxy-3 di-*O*-isopropylidène-1,2;5,6 nitro-3 α-D-glucofuranose (**5**) en proportions variables selon la concentration en acide. Le dérivé furanosique **5** est thermodynamiquement favorisé. L'hydrolyse acide partielle de **5** donne le déoxy-3 *O*-isopropylidène-1,2 nitro-3 α-D-glucofuranose (**4**), alors que l'action d'une base faible provoque l'épimérisation en déoxy-3 di-*O*-isopropylidène-1,2;5,6 nitro-3 α-D-allofuranose (**6**).

Canadian Journal of Chemistry, **49**, 3203 (1971)

The familiar derivatization of carbohydrates with acetone has been applied to nitro sugars and nitro inositols in a few instances only (1–3). Thus, it has served as a means of separating a mixture of 6-deoxy-6-nitro-D-glucose and -L-idose, a pair of sugars that give furanoid di-*O*-isopropylidene derivatives even though one of the ketal moieties possesses the unfavorable, six-membered ring structure bridging C-3 and -5 (1). With a view to preparing a partially blocked compound for some synthetic project we decided to investigate the acetonation of 3-deoxy-3-nitro-D-glucose (**1**). This was undertaken in the expectation that the 1,2-mono- and 1,2:5,6-di-*O*-isopropylidene derivatives of the furanose form of **1** would be obtained, and no particular problems were anticipated. Although the goal was reached, a number of noteworthy complications occurred in its pursuit.

To begin with, the reaction of acetone with **1** appeared to be considerably less facile than that of D-glucose and most simple aldoses (4). A variety of conditions that included catalysis with boron trifluoride or cupric sulfate and sulfuric acid gave unsatisfactory results. High degrees of acetonation were eventually achieved when mixtures of acetone and triethyl orthoformate were employed and anhydrous hydrogen chloride in dioxane was provided as a catalyst (5). However, several products were formed in varying proportions, and the results of individual experiments seemed difficult to reproduce. The reaction remained vexing until influences of acid concentration and work-up operations had been studied in detail. Altogether five new products were encountered (see Scheme 1): 3-deoxy-1,2-*O*-isopropylidene-3-nitro-α-D-glucopyranose (**2**), 3-deoxy-1,2:4,6-di-*O*-isopropylidene-3-nitro-α-D-glucopyranose (**3**), 3-deoxy-1,2-*O*-isopropylidene-3-nitro-α-D-glucofuranose (**4**), 3-deoxy-1,2:5,6-di-*O*-isopropylidene-3-nitro-α-D-glucofuranose (**5**), and 3-deoxy-1,2:5,6-di-*O*-isopropylidene-3-nitro-α-D-allofuranose (**6**). Structural proof will be described in a later paragraph.

When acetonation of **1** was allowed to take place for 3 days at 4°, the predominant product at low hydrogen chloride concentration was the monoacetone pyranose **2**, and this was accompanied by the diacetone pyranose **3** and the diacetone furanose **5**. Among these minor products, **3** preponderated over **5** at lowest acidity of the medium. As the acidity was increased the proportion of **2** decreased relative to the combined amount of the diacetone derivatives, and in the latter, the proportion of **5** rose while that of **3**

[1]Part XXIII in a series on reactions of nitro sugars. For part XXII see ref. 27.

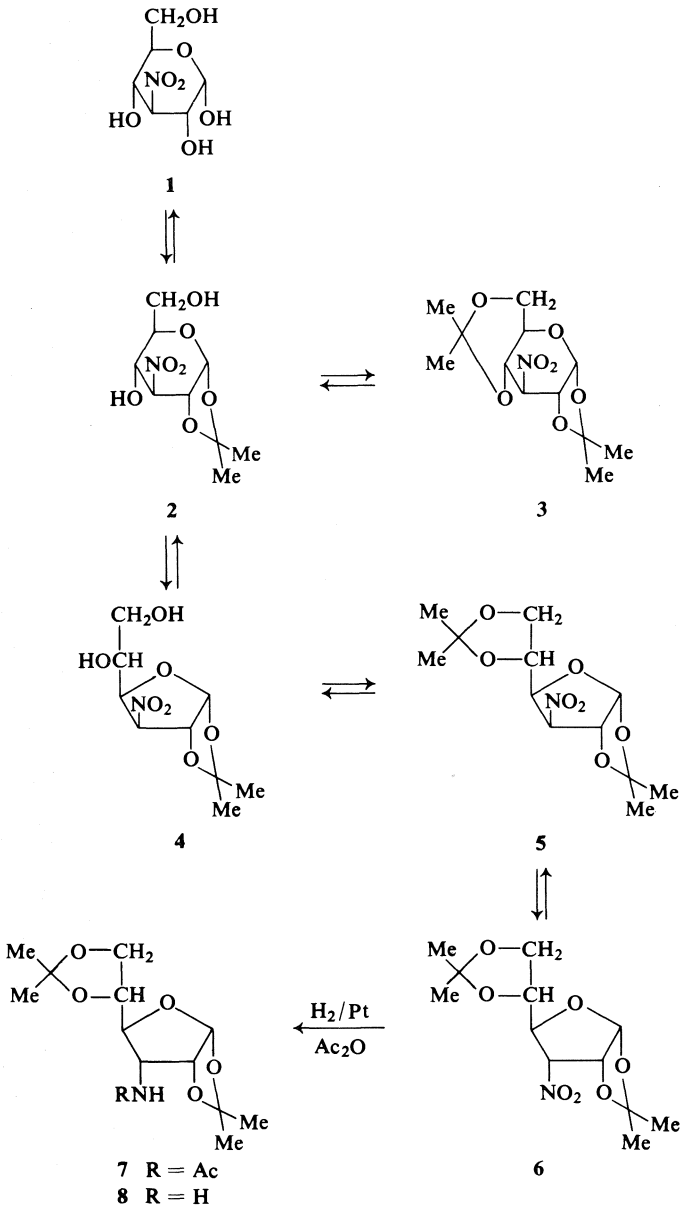

SCHEME 1

diminished. At sufficiently high acidity **5** thus became the predominant product. This is illustrated in Fig. 1 by data obtained in a set of preparative experiments performed under standardized conditions. It was possible to fractionate a given product mixture, by virtue of differential solubilities in chloroform and ethyl acetate, into unreacted **1**, monoacetone derivative **2**, and a fraction comprising the diacetone derivatives **3** and **5**. The ratios **3**:**5** were derived from n.m.r. spectra of the mixtures which displayed well-separated H-1 signals suitable for intensity comparison by integration. It is evident from the results that the nitro glucose reacts fastest in its pyranose form to give **2** and even **3** although these molecules, especially **3**, are sterically disfavored. The diacetone furanose **5** is formed comparatively slowly, but it is seen to be the thermodynamically most favored component since it begins to predominate when establishment of equilibrium is

Can. J. Chem. Downloaded from www.nrcresearchpress.com by 210.87.254.105 on 09/05/12
For personal use only.

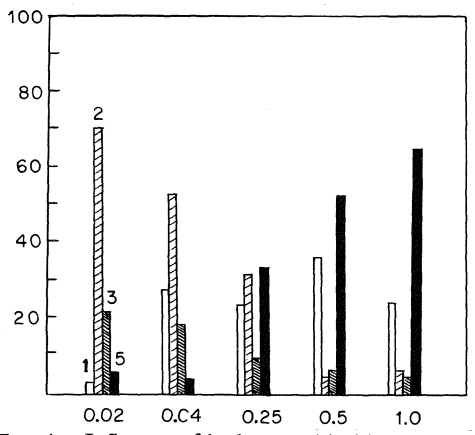

FIG. 1. Influence of hydrogen chloride concentration on the acetonation of **1**. Ordinate: Percentage composition of the reaction mixture. Abscissa: Normality of medium in hydrogen chloride.

promoted by growing amounts of catalyst.[2] In acetonations of D-glucose itself, ketals of the furanose form are produced invariably, and ketals of the pyranose form have not to our knowledge been encountered, presumably because kinetic control does not normally prevail. In the case of **1** apparently the slower over-all acetonation process permits isolation of kinetic products. As far as conversion of the compounds into **5** is concerned one must assume that the route passes through a monoacetone furanose. However, no such intermediate was detected under the reaction conditions discussed so far, and one has therefore to conclude that it rapidly accepts a second isopropylidene group.

The monoisopropylidene furanose **4** was, however, obtained from **5** by partial hydrolysis with 0.01 *N* sulfuric acid. Quite unexpectedly it was also produced when **5** was chromatographed on a column of silica gel.[3] Equally unexpected was the finding that similar chromatography of **5** on a different brand of silica gel[4] yielded yet another diisopropylidene sugar, namely the allofuranose derivative **6**. The phenomena thus associated with chromatographic work-up operations were not conducive to an easy unravelling of the acetonation reaction. We have now realized that the first-mentioned adsorbent[3] reacts sufficiently acidic to cause partial deacetonation whereas the second adsorbent[4] shows a weak base reactivity that catalyzes epimerization at the nitromethylene asymmetric center. Indeed, the two adsorbents are stained red and green, respectively, by a yellow chloroform extract of p*H* universal indicator paper. The same epimerization (**5** → **6**) was also brought about by the action of solid sodium bicarbonate in acetone, under which conditions an equilibrium containing the D-*gluco* and D-*allo* compounds in a ratio 4:5 was reached (Table 1). Although this epimerization is not very fast it may well lead to contamination of **5** by **6** during work-up of acetonations if, for removal of the acid catalyst, excessive amounts of bicarbonate are used for prolonged periods of time and without cooling of the mixture.

Attention has been drawn on many occasions (1, 2, 7–16) to the extraordinary ease with which certain structural and configurational changes are effected in nitro sugars by the action of base. However, the present instance is the first *gluco* → *allo* epimerization to be observed in this area. 3-Deoxy-3-nitro hexose derivatives with the *gluco*, *manno*, *galacto*, and *talo* configurations have been subjected to column chromatography (17, 18) or exposed to more strongly basic media (8, 10, 15, 16), and no inversions at C-3 were observed although other changes did occur. But the compounds referred to had the pyranose structure, with an equatorial nitro group having no tendency to become axial.[5] In the furanoses **5** and **6**,

TABLE 1. Epimeric equilibration of a mixture of **5** and **6**

Time (h)	Composition (%)		
	5	**6**	(3)*
0	74	21	5
0.75	70	25	5
2.5	66	30	4
20	47	49	4
44	44	52	4
116	43	52	5
150	41	53	6

*The starting mixture used for this particular experiment contained 5% of isomer 3. The amount of this component remained unchanged within the limits of experimental error, and its presence is considered irrelevant.

[2]The reaction is considered to be a reversible transacetalation involving 2,2-diethoxypropane (6) that originates from acetone and triethyl orthoformate.

[3]The silica gel used was designated as "desiccant, mesh 100–200, specification MIL D3716" and was supplied by Davison Chemical, Baltimore, Maryland.

[4]Silica gel designated "for column chromatography, mesh 70–325", supplied by E. Merck A.G., Darmstadt, Germany.

[5]Compare also our recent discussion of the preference for an equatorial nitro group in the methyl 3-deoxy-3-nitropentopyranosides (14).

Can. J. Chem. Downloaded from www.nrcresearchpress.com by 210.87.254.105 on 09/05/12
For personal use only.

a 3,4-*cis* arrangement obviously implies more strain than a 3,4-*trans* arrangement, and this factor seems to override the opposing strain difference in the 2,3-*cis* and -*trans* arrangements, thus favoring epimerization. This situation parallels that existing in recently reported syntheses (13, 19) of 3-deoxy-3-nitropentofuranosides by nitroalkane cyclization, where the main products had the *ribo* (3,4-*trans*) rather than the *xylo* (3,4-*cis*) configuration.

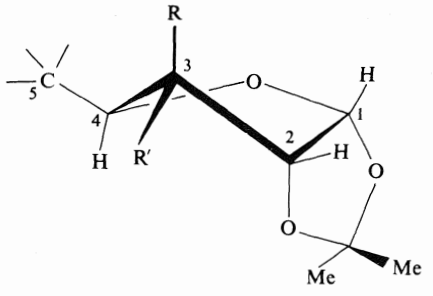

FIG. 2. The T_2^3 conformation of the furanose ring in **4** and **5** (R = NO_2; R′ = H) and **6** (R = H; R′ = NO_2).

Assignment of Structure

The monoisopropylidene sugar **4** consumed 1 *M* equiv of periodate, thereby being degraded to an aldehyde which was transformed, by reduction and subsequent deacetonation (20), into 3-deoxy-3-nitro-D-xylose. This established the constitution and configuration of **4** and its preparative precursor, the diacetone derivative **5**. The isomeric monoacetone derivative **2** was resistant against periodate, in keeping with the pyranoid structure assigned to it. It must also possess the D-*gluco* configuration since it yielded **5** on further acetonation, a fact which rules out the remote possibility that a configurational change had occurred in its formation or isolation. The diacetone compound **6** was elucidated by catalytic hydrogenation in the presence of acetic anhydride. This afforded a crystalline acetamido compound which was identified with the known (21) 3-acetamido-3-deoxy-1,2:5,6-di-*O*-isopropylidene-α-D-allofuranose (**7**) obtained by *N*-acetylation of an authentic sample of the parent amine **8** (21–23) (kindly provided by Dr. D. H. Ball, Natick, Massachusetts). Finally, the structural assignment for **3** was based on the nonidentity of this compound with the isomers **5** and **6** and appears reasonable in view of its formation from **1**, along with **2**, under mild conditions of acetonation.

In deuterochloroform solution the diacetone compounds **3**, **5**, and **6** are readily distinguished by the positions of their n.m.r. signals for H-1 (doublets with $J_{1,2}$ = 3.5–4.5 Hz), which occur at τ 4.40, 3.92, and 4.11, respectively. Whereas the monoacetone furanose **4** cannot be differentiated from **5** through the H-1 signal (τ 3.91), its H-5 and -6 signals (τ 6.2–6.4) occur farther upfield than those of **5** (τ 5.9–6.1) and may thus serve for distinction. In derivatives of 1,2-*O*-isopropylidene-α-D-glucofuranose the furanose ring has been deduced from n.m.r. spectra to exist in the T_2^3 twist conformation (24, 25). Our data for **4** and **5** tend to bear out this conformation as we found zero coupling between H-2 and -3, indicating a dihedral angle of the order of 90° between these protons. Although the spectrum of the *allo* compound **6** did not provide a similar indication for the conformation since the H-2, -3, and -4 signals were difficult to analyze, it appears reasonable to assume the same T_2^3 form. In the latter, **6** has an approximately 90° dihedral angle between the C_3—NO_2 and C_4—C_5 bonds, and this condition would explain the somewhat greater stability of **6** as compared to **5** where that angle is only about 30° (Fig. 2). In the inverted, T_3^2 form of **6**, the nitro group would interfere severely with one of the isopropylidene methyl groups, and the compound would be expected to be less stable than **5**.[6]

Experimental

For general preparative and instrumental techniques see preceding articles of this series (13–17, 26). 3-Deoxy-3-nitro-α-D-glucopyranose (**1**) was prepared as described (26); m.p. 182–184°, $[\alpha]_D$ +119 (2 min) → +112 (6 min) → +83° (2 h, in water). Reported, m.p. 176–177° (dec.), $[\alpha]_D$ +99.6 (6 min) → +73.9° (130 min). The t.l.c. was performed on 7-cm plates of silica gel G (E. Merck A.G., Darmstadt, Germany) and proved useful for distinguishing the nitro glucose **1** from the two monoisopropylidene derivatives **2** and **4** and the three diisopropylidene derivatives **3**, **5**, and **6**, as follows (R_f values in parentheses): *a*, with ethyl acetate, **1** (0.4), **2** and **4** (0.9), **3**, **5**, and **6** (1.0); *b*, with 1:1 ethyl acetate – chloroform, **1** (0.05), **2** and **4** (0.4), **3**, **5**, and **6** (0.9); *c*, with 1:5 ethyl acetate – chloroform, **1** (0.0), **2** and **4** (0.1), **5** (0.6), **6** (0.7), and **3** (0.85). The n.m.r. data (100 MHz) were obtained from $CDCl_3$ solutions unless other-

[6]NOTE ADDED IN PROOF: Nakagawa and coworkers have briefly reported (28) the synthesis of **6** by another route, and they have also obtained (29) a pyranoid diketal of **1**, namely, the cyclohexylidene analog of **3**.

Can. J. Chem. Downloaded from www.nrcresearchpress.com by 210.87.254.105 on 09/05/12
For personal use only.

Can. J. Chem. Downloaded from www.nrcresearchpress.com by 210.87.254.105 on 09/05/12
For personal use only.

wise indicated, and are expressed on the τ-scale with reference to internal tetramethylsilane.

3-Deoxy-1,2-O-isopropylidene-3-nitro-α-D-glucopyranose (2) and 3-Deoxy-1,2:4,6-di-O-isopropylidene-3-nitro-α-D-glucopyranose (3)

A solution of the nitro glucose **1** (335 mg, 1.6 mmol) in acetone (3.3 ml, dried over $CaCl_2$) and triethyl orthoformate (1.6 ml) was acidified with 0.03 ml of 4.9 *N* hydrogen chloride in dioxane. The reaction mixture was allowed to stand at about 25° for 3 days and was then neutralized by shaking with dry sodium bicarbonate for 1 min and filtered with some activated charcoal through layers of Dowex-1X2 ($CH_3CO_2^-$) and Amberlite IR-120 (H^+) (1 ml each, prewashed with acetone). The filtrate was evaporated to give a resinous material that was co-evaporated thrice with benzene, dried *in vacuo*, and then extracted with a total of 5–6 ml of boiling benzene, in three portions. A brown residue (62 mg) was discarded, and the extract was chromatographed on a column containing silica gel Merck[4] (15 g, containing 10% of added water). Elution with benzene (165 ml) furnished colorless crystals (116 mg) which upon recrystallization from ligroin gave pure **3** (49 mg), m.p. 128–129°, $[\alpha]_D$ + 134° (*c* 0.23, in methanol). The i.r. spectrum in chloroform showed NO_2 bands at 1555 and 1370 cm^{-1}, and bands at 1365, 1320, 1200, 1045, and 1010 cm^{-1} which were not present in the spectra of **5** and **6**. The n.m.r. data: τ 4.40 (doublet, J = 4.5 Hz, H-1), 5.2–5.6 (2-proton multiplet, H-2, -3), 5.8–6.3 (4-proton multiplet, H-4, -5, -6, -6′), 8.43, 8.57, 8.65, 8.65 (3-proton singlets, CH_3).

Anal. Calcd. for $C_{12}H_{19}NO_7$ (289.3): C, 49.81; H, 6.62; N, 4.85. Found: C, 49.77; H, 6.55; N, 5.03.

The ligroin mother liquor of the above recrystallization furnished a small amount of crystals melting at 110–111°. These were identical with compound **6** described further below.

After the elution of **3**, the chromatographic column was eluted with benzene containing increasing amounts of ethanol. With benzene–ethanol (20:1), compound **2** (115 mg) was obtained. It was recrystallized from ethyl acetate – ligroin; m.p. 180–181°, $[\alpha]_D$ +37° (*c*, 0.26, in methanol). The compound was almost insoluble in chloroform. The n.m.r. data (in acetone-d_6): τ 4.78 (doublet, J = 3 Hz, H-1), 5.2–5.5 (2-proton multiplet, H-2, -3), 5.9–6.4 (4-proton multiplet, H-4, -5, -6, -6′), 8.56, 8.70 (3-proton singlets, CH_3).

Anal. Calcd. for $C_9H_{15}NO_7$ (249.2): C, 43.39; H, 6.07; N, 5.62. Found: C, 43.53; H, 6.09; N, 5.77.

3-Deoxy-1,2:5,6,di-O-isopropylidene-3-nitro-α-D-glucofuranose (5)

A solution of **1** (414 mg) in dry acetone (5 ml) and triethyl orthoformate (1 ml) was acidified with 0.2 ml of 2.8 *N* hydrogen chloride in dioxane and kept at 25° for 4 days. The mixture was neutralized by stirring for 3 min with solid sodium bicarbonate, filtered, and evaporated to give a residue which was extracted three times with hot benzene. An amount of 148 mg of what was mainly unreacted **1** remained undissolved. The benzene extract was evaporated to give an oil which was transferred by means of chloroform onto a column containing 10 g of silica gel.[3] Elution with chloroform produced an oil (356 mg) that crystallized in part by trituration with petroleum ether (b.p. 30–60°). Recrystallization from petroleum ether gave **5** (122 mg), m.p. 60–62°, $[\alpha]_D$ +28° (*c*, 0.3, in benzene), and +4.5° (*c*, 0.3, in methanol). The i.r. spectrum in chloroform exhibited NO_2 bands at 1550 and 1370 cm^{-1} and, in the fingerprint region, was similar in general to, but different in some details from, the spectra of **3** and **6**. Especially a peak at 1085 cm^{-1} distinguished **5** from the isomers.

The n.m.r. data: τ 3.92 (doublet, $J_{1,2}$ = 3.5 Hz, H-1); 4.90 (doublet, $J_{3,4}$ = 4.0 Hz, H-3), 5.01 (doublet, $J_{1,2}$ = 3.5 Hz, H-2); 5.66 (quartet, $J_{3,4}$ = 4.0 and $J_{4,5}$ = 8 Hz, H-4); 5.9–6.1 (3-proton multiplet, H-5, -6, -6′); 8.50, 8.59, 8.69, 8.72 (3-proton singlets, CH_3).

Anal. Calcd. for $C_{12}H_{19}NO_7$ (289.3): C, 49.81; H, 6.62; N, 4.85. Found: C, 50.01; H, 6.60; N, 4.72.

A similar experiment was performed using 620 mg of **1** in 9 ml of a 5:1 acetone – triethyl orthoformate mixture acidified with 2 ml of 4.9 *N* hydrogen chloride in dioxane. The reaction was allowed to proceed at +4° for 3 days. The mixture was neutralized under ice cooling with sodium bicarbonate (2 g). The residue obtained on filtration and evaporation was extracted with cold chloroform (3 × 5 ml). The part that remained undissolved (250 mg) was mainly **1** (t.l.c.). The chloroform extract was concentrated to a small volume, cooled, and placed for 1 day in a refrigerator where it deposited crystals (58 mg) consisting mainly of **2** (t.l.c.). The filtrate from these crystals on evaporation gave an oil (720 mg) which according to n.m.r. spectroscopy contained **5** as the only carbohydrate besides dioxane (τ 6.32), acetone (τ 7.91), and acetone self-condensation products. These non-carbohydrate materials were removed by passing a chloroform solution of the oil through a column of silica gel Merck[4] (15 g) which was eluted with the same solvent (75 ml). Although the recovered carbohydrate (523 mg) was mainly **5** it now contained about 15% of **6**, according to n.m.r. spectroscopy. Two parts (109 and 155 mg) of this material were rechromatographed in the same manner, on 3 and 5 g of silica gel,[4] respectively. The materials recovered (94 and 139 mg, approximately 90%) contained **5** and **6** in the ratios of 75:25 and 67:33. See also the description of the formation **6** given further below.

Another experiment was performed similar to that just described, except that the monoacetone pyranose **2** served as the starting material, and passage of the product through silica gel was omitted. The experiment yielded **5** (70%) and a mixture of **1** and **2** (15–20%).

Influence of Hydrogen Chloride Concentration on the Acetonation

The results shown in Fig. 1 were obtained as follows. Samples of nitro glucose **1** (approximately 209 mg, 1 mmol) were suspended in 3 ml of a 5:1 (*v*/*v*) mixture of acetone and triethyl orthoformate. The suspensions were cooled with dry ice while hydrogen chloride in dioxane was added in amounts providing the acid normalities specified in Fig. 1. The reaction mixtures were stored at +4° for 3 days and then neutralized by stirring with solid sodium bicarbonate under ice cooling, filtered through cotton wool, and evaporated to dryness.

In each run the mixture of products so obtained was extracted three times with chloroform. The combined

Can. J. Chem. Downloaded from www.nrcresearchpress.com by 210.87.254.105 on 09/05/12
For personal use only.

extract (10 ml) was dried over $MgSO_4$ and evaporated to give an oil that was dissolved[7] in 0.5 ml of $CDCl_3$ for n.m.r. spectroscopic determination of the ratio of diisopropylidene derivatives. After evaporation, the dry weight was determined and taken to be the combined yield of **3** and **5**, as no monoisopropylidene derivative was present (t.l.c.) and the amount of **6** was negligible.

The chloroform-insoluble part of the reaction product was triturated with cold ethyl acetate (1 ml). After storage for 12 h at 4° the supernatant solution was removed from the undissolved residue. The latter was washed, dried, and weighed; it was mainly unreacted **1** as confirmed by t.l.c. and optical rotation (with mutarotation). The ethyl acetate solution was evaporated and the residue was weighed; it consisted mainly of the monoisopropylidene compound **2** (m.p. 180–181°; t.l.c.). There was some cross-contamination in the fractions of **1** and **2** but, in determining the weights, this was considered to cancel. Compound **4**, which in contrast to **2** is readily soluble in chloroform, was not encountered in these experiments.

3-Deoxy-1,2-O-isopropylidene-3-nitro-α-D-glucofuranose (4)

Compound **5** (126 mg) in acetone (1.2 ml) and 0.01 *N* sulfuric acid (12.5 ml) were boiled for 10 min. The cooled solution was treated with 0.7 ml of Dowex-1X2 (acetate form, prewashed with *N* acetic acid) for removal of the sulfuric acid. The solution was then evaporated and the residue (109 mg), after drying *in vacuo*, was triturated with cold benzene to give crystalline **4** (50 mg), m.p. 82–83°, $[\alpha]_D$ +64° (in benzene), +25° (in methanol), +41° (in water) (*c*, about 0.3). Infrared bands in chloroform were at 3580 and 3460 (broad, OH), 1545 and 1370 cm^{-1} (NO_2). The fingerprint pattern differed from those of **3**, **5**, and **6** by a band at 1055 cm^{-1}. The n.m.r. data: τ 3.91 (doublet, J = 3.5 Hz, H-1), 4.82 (doublet, J = 4.0 Hz, H-3), 4.98 (doublet, J = 3.5, H-2), 5.52 (quartet, $J_{3,4}$ = 4.0 and $J_{4,5}$ = 8 Hz, H-4), 6.2–6.4 (3-proton multiplet, H-5, -6, -6′), 8.50, 8.69 (3-proton singlets, CH_3).

Anal. Calcd. for $C_9H_{15}NO_7$ (249.2): C, 43.39; H, 6.07; N, 5.62. Found: C, 43.49; H, 6.19; N, 5.81.

Spectroscopically pure **5** (55 mg) dissolved in chloroform was chromatographed on silica gel Davison[3] (1.2 g). The column was successively eluted with chloroform (15 ml) and chloroform containing 2% of ethanol (12 ml). The latter eluant produced crystalline **4** (37 mg, 80%), m.p. 82–84°, in spectroscopically pure form. Similarly, **4** was several times obtained in 40% yield (based on **1**) when **1** was acetonated as described above for the preparation of **5** and the crude reaction mixture was chromatographed in this manner. However, attempted conversion of **5** into **4** by the action of silica gel failed in some experiments, **5** being recovered unchanged.

3-Deoxy-1,2:5,6-di-O-isopropylidene-3-nitro-α-D-allofuranose (6)

Compound **6** was first obtained in an attempt to prepare **5** as described above, with the use of an excess of sodium bicarbonate for neutralization (at room temperature for 20 min), and with the use of silica gel Merck[4] for chromatography. From mixtures of diisopropylidene derivatives so produced, **6** separated by crystallization from ligroin. It melted at 111.5–112° and had $[\alpha]_D$ +101° (*c*, 0.24, in methanol). Infrared bands (in chloroform) were at 1550 and 1370 cm^{-1} (NO_2), and in the fingerprint region the spectrum differed from that of **5** by the presence of bands at 1305 and 1100 cm^{-1} and absence of bands at 1335 and 1085 cm^{-1}.

The n.m.r. data: τ 4.11 (doublet, J = 3.5 Hz, H-1); 4.9–5.2 (3-proton multiplet, H-2, -3, -4); 5.8–6.2 (3-proton multiplet, H-5, -6, -6′); 8.48, 8.63, 8.70, 8.70 (3-proton singlets, CH_3).

Anal. Calcd. for $C_{12}H_{19}NO_7$ (289.3): C, 49.81; H, 6.62; N, 4.85. Found: C, 49.88; H, 6.65; N, 4.96.

A mixture[8] of diisopropylidene derivatives (180 mg) containing **5**, **6**, and **3** in the ratio 74:21:5 as determined by n.m.r. spectroscopy was dissolved in acetone (0.5 ml), sodium bicarbonate (50 mg) was added, and the mixture was allowed to stand at room temperature, with occasional swirling. At intervals, the change in composition (Table 1) was determined by recording the n.m.r. spectrum of the solution. It is noted that the amount of **3** remained unchanged during the epimeric equilibration of **5** and **6**. See also the formation of **6** mentioned above in the section dealing with **5**.

3-Acetamido-3-deoxy-1,2:5,6-di-O-isopropylidene-α-D-allofuranose (7)

A solution of **6** (25 mg) in methanol (2.5 ml) and acetic anhydride (0.15 ml) was hydrogenated over platinum dioxide at ordinary temperature and pressure. The reduction of the nitro group was monitored by u.v. spectroscopy (disappearance of nitronate absorption at 251 nm in alkaline medium) and required about 26 h. The filtered solution was evaporated to give a crystalline residue which upon recrystallization from ethyl acetate – ligroin afforded **7** (11 mg), m.p. 131.5–132°, $[\alpha]_D$ +76° (in chloroform), in good agreement with recorded values (21). The i.r. and n.m.r. spectra were superimposable with those of a sample that had been obtained by *N*-acetylation of authentic amine **8** (21–23).

We thank the National Research Council of Canada for financial support and Mrs. Siegrid Hancock and Mrs. Lisa Siemsen for technical assistance.

1. J. M. Grosheintz and H. O. L. Fischer. J. Am. Chem. Soc. **70**, 1476 (1948).
2. J. M. Grosheintz and H. O. L. Fischer. J. Am. Chem. Soc. **70**, 1479 (1948).
3. F. W. Lichtenthaler and H. O. L. Fischer. J. Am. Chem. Soc. **83**, 2005 (1961).
4. A. N. de Belder. Advan. Carbohydr. Chem. **20**, 219 (1965).
5. S. Chládek and J. Smrt. Coll. Czech. Chem. Commun. **28**, 1301 (1963).
6. S. J. Angyal and R. M. Hoskinson. J. Chem. Soc. 2985 (1962).
7. H. O. L. Fischer and H. H. Baer. Ann. **619**, 53 (1958).

[7]Usually a small amount of material crystallized and remained undissolved at this stage; it was combined with the main, chloroform-insoluble residue.

[8]Obtained by acetonation of **1**, as described previously, using a reaction medium 0.5 *N* in hydrogen chloride, and chromatography on silica gel[4].

8. H. H. BAER. J. Am. Chem. Soc. **84**, 83 (1962).
9. H. H. BAER and W. RANK. Can. J. Chem. **43**, 3330, 3462 (1965); **47**, 2811 (1969).
10. H. H. BAER and F. KIENZLE. Ann. **695**, 192 (1966).
11. H. H. BAER and F. KIENZLE. J. Org. Chem. **33**, 1823 (1968); Can. J. Chem. **47**, 2819 (1969).
12. H. H. BAER. Advan. Carbohydr. Chem. Biochem. **24**, 67 (1969).
13. H. H. BAER and M. BAYER. Can. J. Chem. **49**, 568 (1971).
14. H. H. BAER and J. KOVÁŘ. Can. J. Chem. **49**, 1940 (1971).
15. H. H. BAER and W. RANK. This issue.
16. J. KOVÁŘ, R. ČAPEK, and H. H. BAER. In press.
17. H. H. BAER and K. ČAPEK. Can. J. Chem. **47**, 99 (1969).
18. H. H. BAER and W. RANK. To be published as part XXVI of this series.
19. H. H. BAER and I. FURIĆ. J. Org. Chem. **33**, 3731 (1968).
20. J. KOVÁŘ and H. H. BAER. Can. J. Chem. This issue.
21. R. U. LEMIEUX and P. CHIU. J. Am. Chem. Soc. **80**, 4745 (1958); B. COXON and L. HOUGH. J. Chem. Soc. 1643 (1961).
22. K. FREUDENBERG, O. BURKHART, and E. BRAUN. Ber. **59**, 714 (1926).
23. M. L. WOLFROM, F. SHAFIZADEH, and R. K. ARMSTRONG. J. Am. Chem. Soc. **80**, 4585 (1958).
24. R. J. ABRAHAM, L. D. HALL, L. HOUGH, and W. A. MCLAUCHLAN. J. Chem. Soc. 3699 (1962).
25. L. HOUGH and A. C. RICHARDSON. *In* Rodd's chemistry of carbon compounds. Vol. I, Part F. *Edited by* S. Coffey. Elsevier Publishing Co., Amsterdam, 1967. p. 115.
26. H. H. BAER, W. RANK, and F. KIENZLE. Can. J. Chem. **48**, 1302 (1970).
27. W. RANK and H. H. BAER. This issue.
28. T. TAKAMOTO, R. SUDOH, and T. NAKAGAWA. Tetrahedron Lett. 2053 (1971).
29. T. SAKAKIBARA, T. TAKAMOTO, and T. NAKAGAWA. Bull. Chem. Soc. Japan, **44**, 865 (1971).

Can. J. Chem. Downloaded from www.nrcresearchpress.com by 210.87.254.105 on 09/05/12
For personal use only.

Can. J. Chem. Downloaded from www.nrcresearchpress.com by 210.87.254.5 on 09/05/12
For personal use only.

Chemistry of 2-Substituted Adamantanes. III.[1] Mass Spectra of 1- and 2-Adamantanethiol, 2-Adamantanol, and 2-Adamantanamine

J. W. GREIDANUS[2]

Department of Chemistry, The University of Calgary, Calgary 44, Alberta

Received November 16, 1970

The mass spectra of 1- and 2-adamantanethiol (**1** and **2***a*), 2-adamantanol (**2***c*), and 2-adamantanamine (**2***d*) have been studied. The isomeric thiols give almost identical spectra and loss of the sulfhydryl radical produces the most abundant ion, while the molecular ion peaks have 9 and 21% relative intensity for **1** and **2***a*, respectively. Elimination of H_2S is an insignificant process. In the fragmentation of **2***c* and *d*, loss of H_2O and NH_3 as a single group occurs (metastable peaks), giving M-H_2O and M-NH_3 ions, both at *m/e* 134; this produces the base peak for **2***c* and the second most intense (93%) peak for **2***d*. Further fragmentation of these ions results in very similar peak patterns for **2***c* and *d*. The amine shows a very intense molecular ion peak (79%) and an M-1 base peak ion. The mass spectra of **2***c* and *d* are very different from those of 1-adamantanol and 1-adamantanamine.

Les spectres de masse des adamantanethiols-1 et -2 (**1** et **2***a*), de l'adamantanol-2 (**2***c*), et de l'adamentanamine-2 ont été étudiés. Les thiols isomères donnent des spectres pratiquement identiques et la perte du radical sulfhydrile conduit à l'ion le plus abondant alors que l'intensité relative des pics dues aux ions moléculaires de **1** et **2***a* est respectivement de 9 et 21%. L'élimination de H_2S est un processus insignifiant. Dans la fragmentation de **2***c* et *d*, la perte des seuls groupes H_2O et NH_3 se produit (pics métastables), pour donner les ions M-H_2O et M-NH_3, tout deux situés à *m/e* = 134; ceci conduit au pic de base pour **2***c* et au deuxième pic le plus important (93%) pour **2***d*. La fragmentation ultérieure de ces ions conduit à des systèmes très semblables pour **2***c* et *d*. L'amine présente un ion moléculaire très intense (79%) et un pic de base à M-1. Les spectres de masse de **2***c* et *d* sont très différents de ceux de l'adamantanol-1 et de l'adamantamine-1.

Canadian Journal of Chemistry, 49, 3210 (1971)

Introduction

Some time ago Dolejšek *et al.* (1) reported the mass spectra of a variety of 1-substituted adamantane compounds, and suggested a number of fragmentation reactions to account for the observed data. Although there has been very much interest in the chemistry of adamantanes in the last few years, no mass spectral study has been reported to our knowledge for 2-substituted adamantanes. Such a study was started by us because of its intrinsic interest, as well as for the purpose of identification and, if possible, of analysis of isomer mixtures by low-resolution mass spectroscopy.

As will be seen from the results, such an analysis would be well feasible in some cases, but would be much harder in another instance.

Experimental

The compounds investigated were obtained from commercial sources (1-adamantanamine, 2-adamantanamine) or prepared by published procedures (1-adamantanol (2), 2-adamantanol (3), 1-adamantanethiol (4), 2-adamantanethiol (5), and 2-methylthioadamantane (5)), and carefully purified.

The mass spectra, some of which are shown in Figs. 1 and 2, were recorded with a Varian Atlas CH-5 spectrometer, with a nominal ionizing energy of 70 or 12 eV, a source temperature of 250°, and by use of a direct probe (20–25°). The relative intensities of the peaks are given as percentages of the most intense peak (base peak) in a spectrum. Peaks with a relative intensity lower than 2% were not reproduced, unless they had a special significance.

Results and Discussion

1- and 2-Adamantanethiol

The molecular ion peaks (*m/e* 168) in the mass spectra (70 eV) of the thiols **1** (Fig. 1*a*) and **2***a* (Fig. 1*b*) are of medium to high relative intensity (8.5 and 21%, respectively) and the base peak in both spectra is found at *m/e* 135. A metastable peak for the transformation M → (M-SH) is present at *m/e* 108.5 (calcd. 108.5) in the spectra (at 70 and 12 eV).

Elimination of hydrogen sulfide is a process of very minor significance, especially in the tertiary thiol **1** where peak *m/e* 134 has a relative intensity of only 0.5% (70 eV). Although it has been

[1]For Part II of this series, see ref. 5.

[2]Present address: School of Natural Sciences, University of Zambia, P.O. Box 2379, Lusaka, Zambia.

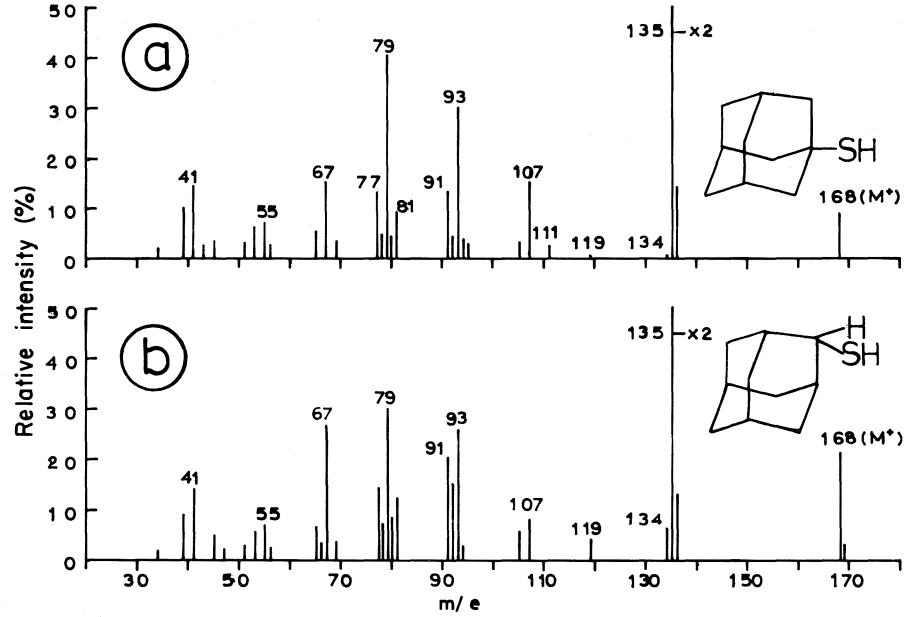

FIG. 1. Mass spectra (70 eV) of (*a*) 1-adamantanethiol and (*b*) 2-adamantanethiol.

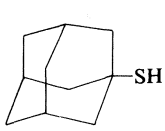

1

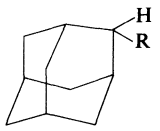

2

a R = SH
b R = SCH_3
c R = OH
d R = NH_2

established (6) that loss of H_2S is an important fragmentation of the molecular ion of secondary thiols (especially at low electron energies), we observed on lowering the ionizing energy to 12 eV only negligible changes in the relative intensities of the *m/e* 134 peaks in either of the thiols. At this low ionizing energy the molecular ion gave rise to the base peak (*m/e* 168) and peak M-33 had a relative intensity of 89%. No metastable peak corresponding to the loss of hydrogen sulfide from the molecular ion could be found in the spectrum of **2***a*. The finding that loss of H_2S from the molecular ion of **1** does not play any role in the fragmentation is not surprising as a favorable spatial relationship for a 1,3- or 1,4-elimination is not present in the molecule.

The M-H_2S ion (*m/e* 134) is a likely precursor (eq. 1) for the formation of fragment $C_9H_{11}^+$ as

[1] $C_{10}H_{14}^+$ (*m/e* 134) $\xrightarrow[*]{-CH_3^\cdot}$ $C_9H_{11}^+$ (*m/e* 119)

the metastable peak for this transformation (*m/e* 105.7) is present in the spectrum of **2***a*.

Loss of the neutral fragment $C_4H_9^\cdot$ from the molecular ion of various 1-substituted adamantanes gives rise to the most abundant ion in the spectra of 1-adamantanol (**3***a*) and 1-adamantanamine (**3***b*). These fragmentations have been formulated by Dolejšek *et al.* (1) as the formation of protonated phenol (**5***a*) and aniline (**5***b*), respectively (eq. 2).

In the spectrum of 1-adamantanethiol (**1**) only a weak peak is present at *m/e* 111 (2.4% relative intensity) and the fragmentation M → M-57 plays therefore no significant role in this compound. This behavior was unexpected as sulfur is known (7) to participate readily in the type of new bond formation that would lead to **4** (X = SH).

The approximately ten times higher intensity of the peaks at *m/e* 134 and 119, and the double intensity of the molecular ion peak in the spectrum of **2***a* are the main differences between the spectra of **1** and **2***a*. Except for some minor variations in relative intensities the rest of the spectra are virtually the same even when the many metastable peaks are compared.

It is clear that 1-adamantanethiol (**1**) belongs in

Can. J. Chem. Downloaded from www.nrcresearchpress.com by 210.87.254.5 on 09/05/12
For personal use only.

Can. J. Chem. Downloaded from www.nrcresearchpress.com by 210.87.254.5 on 09/05/12
For personal use only.

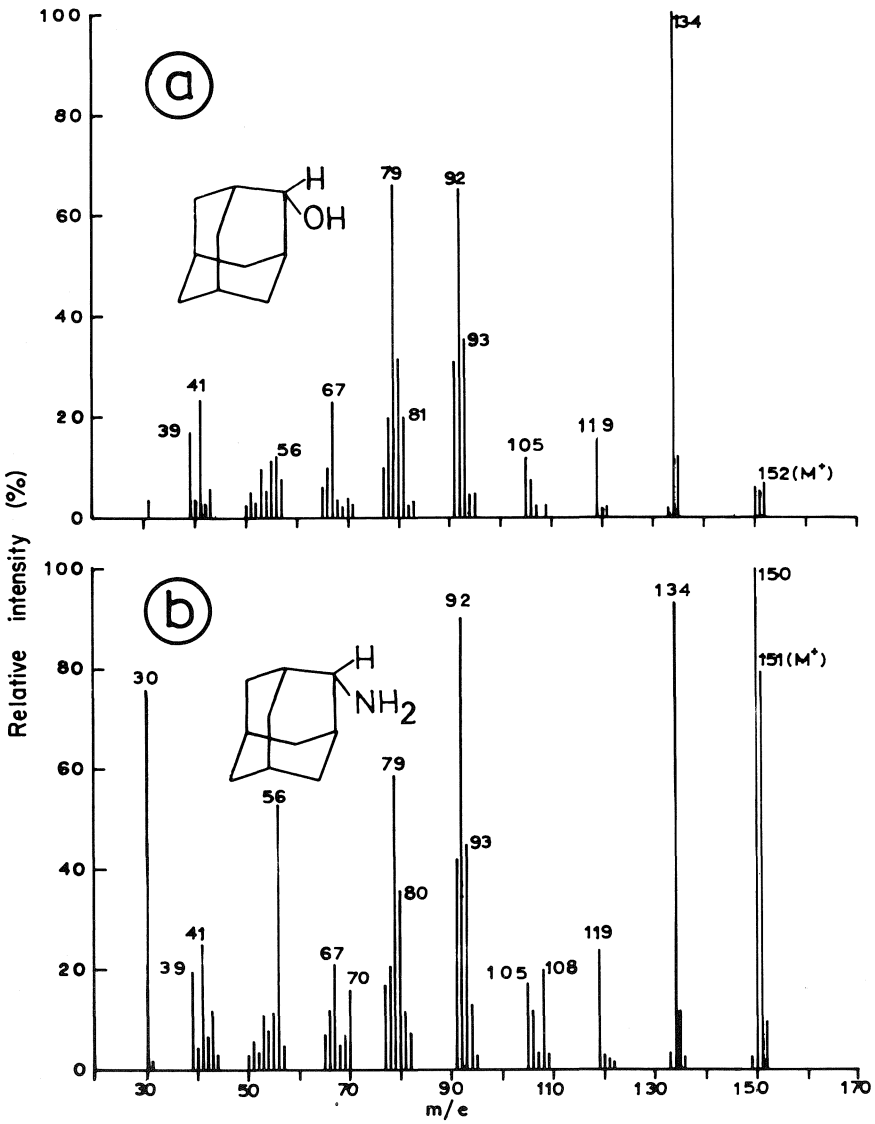

FIG. 2. Mass spectra (70 eV) of (*a*) 2-adamantanol and (*b*) 2-adamantanamine.

[2]

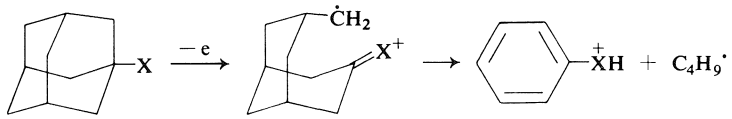

1 X = SH
3*a* X = OH
b X = NH_2

4*a* X = OH (*m/e* 152)
b X = NH_2 (*m/e* 151)

5*a* X = OH (*m/e* 95)
b X = NH_2 (*m/e* 94)

the same group as 1-nitro, 1-bromo-, and 1-alkyladamantane (1). All lose their substituent readily, forming $C_{10}H_{15}^+$ which upon further fragmentation produces many even-electron ions. Metastable peaks for the transformations involving $C_{10}H_{15}^+$ and its derived ions are listed in Table 1. Those for the transformations numbered 6 and 10 were not reported by Dolejšek *et al.* (1) for any of their 1-substituted adamantanes which showed the same fragmentation behavior. These

TABLE 1. Metastable ion peaks (*m/e*) for transformations $A^+ \rightarrow B^+ + C$ involving $C_{10}H_{15}^+$ and smaller fragments in the spectra of **1** and **2***a*

Transformation no.	A(*m/e*)	B(*m/e*)	C	*m/e**
1	$C_{10}H_{15}$(135)	C_8H_{11}(107)	C_2H_4	84.8
2	$C_{10}H_{15}$(135)	C_7H_9(93)	C_3H_6	64.1
3	$C_{10}H_{15}$(135)	C_6H_9(81)	C_4H_6	48.6
4	$C_{10}H_{15}$(135)	C_6H_7(79)	C_4H_8	46.2
5	$C_{10}H_{15}$(135)	C_5H_7(67)	C_5H_8	33.3
6	C_8H_{11}(107)	C_7H_7(91)	CH_4	77.4
7	C_8H_{11}(107)	C_6H_7(79)	C_2H_4	58.3
8	C_7H_9(93)	C_7H_7(91)	H_2	89.0
9	C_6H_7(79)	C_6H_5(77)	H_2	75.0
10	C_5H_7(67)	C_3H_5(41)	C_2H_2	25.1

*Calculated values; observed values differed at the most 0.2 *m/e* units from these.

authors suggested that a metastable peak at *m/e* 37.1 probably arose from fragmentation of an ion *m/e* 121 (eq. 3). However in their spectra, as in

[3] $C_9H_{13}^+$ (121) $\rightarrow C_5H_7^+$ (67) + C_4H_6

ours, the peak *m/e* 121 has very low relative intensity (<0.5%). It is much more likely that one or both of the fragmentations *m/e* 81 → *m/e* 55 and *m/e* 41 → *m/e* 39 (for which metastable ion peaks at *m/e* 37.4 and 37.1, respectively, are calculated) give rise to this metastable peak.

It should be noted here that the mass spectrum of 2-methylthioadamantane (**2***b*) also has its base peak at *m/e* 135 and is at *m/e* < 135 almost identical with that of **1** and **2***a*. It shows metastable ion peaks corresponding to the transformations numbered 1, 2, and 4–9 in Table 1, and to the loss of $CH_3S^\cdot$ from the molecular ion at *m/e* 100.2 (calculated for M(*m/e* 182) → M-CH_3S(*m/e* 135) : *m/e* 100.1). A peak at *m/e* 134 (relative intensity 3.5%) indicates that elimination of CH_3SH occurs as well, analogous to the loss of H_2S from **2***a*.

The compounds **1**, **2***a* and **2***b* give rise to an abundant even-electron ion $C_{10}H_{15}^+$ which may or may not be the same in all three cases, but which appears to give identical fragmentations. Apparent intramolecular 1,2-hydride shifts in adamantanes have very recently been shown to be intermolecular processes (8) *in solution*. At this time it is not known whether the energetically unfavorable twisted transition state for such an intramolecular 1,2-hydride shift (8) can occur in an adamantyl cation in a state of high energy *under conditions which exclude an intermolecular process*. Very recently reported results (9) of the study of electron-impact fragmentation of various deuterated bicyclic alcohols indicate that very rapid hydride and C—C bond shifts occur in these systems while H_2O elimination takes place. At the present time 1,2-hydride shifts in adamantyl carbonium ions of high energy, such as occur in electron-impact fragmentation reactions, cannot be discounted.

2-Adamantanol and 2-Adamantanamine

The striking similarity of the mass spectra (Fig. 2) of 2-adamantanol (**2***c*) and 2-adamantanamine (**2***d*) is apparent at first glance. The amine gives a much more abundant molecular ion and shows a large number of peaks of considerable relative intensity (nine peaks with more than 40% relative intensity). The base peak for **2***c* and the second most intense peak in the spectrum of **2***d* (both at *m/e* 134) represent loss of H_2O and NH_3 from the molecular ions **6** and **7**, respectively (Scheme 1).

The presence of a metastable peak at *m/e* 118.2

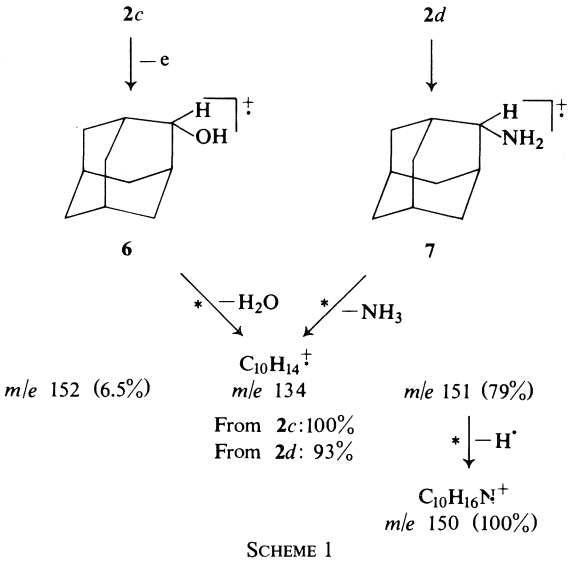

SCHEME 1

Can. J. Chem. Downloaded from www.nrcresearchpress.com by 210.87.254.5 on 09/05/12
For personal use only.

Can. J. Chem. Downloaded from www.nrcresearchpress.com by 210.87.254.5 on 09/05/12
For personal use only.

(calcd. 118.1) for the transformation **6** (*m/e* 152) → $[C_{10}H_{14}]^{+\cdot}$, and at *m/e* 118.9 (calcd. 118.9) for the transformation **7** (*m/e* 151) → $[C_{10}H_{14}]^{+\cdot}$ indicates that 18 and 17 mass units, respectively, are lost as a single group. These metastable peaks occur also in spectra run at low ionizing energy (12 eV). The loss of NH_3 appears to be one of the major fragmentation processes of 2-adamantanamine and the M-17 peak is in fact the second strongest peak (relative intensity 57%) in its 12 eV mass spectrum. The facility with which this fragmentation occurs is surprising as loss of NH_3 from primary amines is an uncommon reaction (10). A 1,3-elimination, for which the spatial relationship is favorable, would give rise to the molecular ion (**8**) of 2,4-dehydroadamantane (tetracyclo-[3.3.1.$1^{3,7}$. $O^{2,4}$]decane (11)).

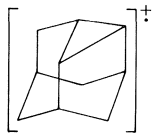

8

The source of the hydrogen atoms in the dehydration of cyclohexanols as a result of electron impact has been thoroughly investigated (12, 13). The main course for which good evidence is available in the case of cyclohexanol is a 1,4-elimination involving *cis*-oriented groups (13). An example has been reported (14) where 1,4-elimination was impossible (as it is in 2-adamantanol). In this case a diaxial 1,3-elimination occurred exclusively. In cyclohexanol it has been demonstrated that the hydroxyl-bearing carbon atom does not supply also the hydrogen for the dehydration (12). This finding has been corroborated recently (9) in the case of several bicyclic alcohols, where evidence for rapid 1,3-hydride shifts and/or C—C bond shifts was obtained. The adamantane skeleton would permit analogous 1,3-hydride shifts but these would result in identical cations. Stabilization may occur ultimately by loss of a hydrogen atom. We tentatively interpret the formation of radical ion **8** from either **6** or **7** as resulting from this process.

In the mass spectrum (Fig. 2) of **2***c* M-1 and M-2 peaks occur with a relative intensity slightly lower than that of the molecular ion peak.

Loss of a hydrogen atom from the molecular ion (**7**) of 2-adamantanamine gives rise to the most abundant species $C_{10}H_{16}N^+$ (*m/e* 150) in its 70 eV spectrum (Fig. 2*a*) and to a strong metastable peak at *m/e* 149.1 for the transformation M → M-1 (calcd. *m/e* 149.0). It is the fragmentation of **7** and of $C_{10}H_{16}N^+$ with retention of nitrogen in the fragment ions which probably gives rise to the main differences between the spectra of **2***c* and *d*. It is surprising that these differences are still so minor (in view of the fact that $C_{10}H_{16}N^+$ (*m/e* 150) causes the base peak) except for the very intense (75%) peak at *m/e* 30, representing the fragment $CH_2{=}\overset{+}{N}H_2$, a frequently occurring abundant species in the spectra of many primary amines. No metastable peak could be found for a fragmentation involving this ion.

The metastable peaks assigned to transformations of $C_{10}H_{14}^{+\cdot}$ (*m/e* 134) and its smaller fragments as they occur in the spectra of **2***c* (Fig. 2*a*) and *d* (Fig. 2*b*) are listed in Table 2. Apart from the peak at *m/e* 30 and the very intense M and M-1 peaks in the spectrum of **2***d*, the most characteristic difference between Figs. 2*a* and *b* is the presence of a peak at *m/e* 108 (relative intensity 20%) in the spectrum of the amine. This ion may be directly derived from the molecular ion $C_{10}H_{17}N^{+\cdot}$ (**7**) or from ion $C_{10}H_{16}N^+$ by elimination of $C_3H_7^{\cdot}$ (eq. 4) and C_3H_6 (eq. 5), respectively.

[4] $C_{10}H_{17}N^{+\cdot}$ (*m/e* 151) → $C_3H_7^{\cdot}$ + $C_7H_{10}N^+$ (*m/e* 108)

[5] $C_{10}H_{16}N^+$ (*m/e* 150) → C_3H_6 + $C_7H_{10}N^+$ (*m/e* 108)

If the first fragmentation [4] would give rise to a metastable peak one would expect it at *m/e* 77.3. The mass spectrum of **2***d* shows indeed a metastable peak at *m/e* 77.2, but this has been tentatively assigned to transformation number 10 in Table 2, as it occurs also in the spectrum of **2***c*.

Cleavage of the carbon–carbon bond adjacent to the nitrogen after electron impact is the preferred reaction of amines and elimination of a hydrogen atom does not normally result in an abundant species (15). The fact that the M-1 ion gives rise to the base peak in the case of the amine and that NH_3 elimination occurs to such an extent must be considered as additional evidence that the adamantane skeleton resists fragmentation (16).

It was one of the original goals of this investigation to see whether it would be possible to distinguish easily between 1- and 2-substituted adamantane isomers by means of low-resolution mass spectroscopy. Our 70 eV spectra of 1-

TABLE 2. Metastable ion peaks (*m/e*) for transformations $A^+ \rightarrow B^+ + C$ involving $C_{10}H_{14}^{\cdot+}$ and smaller fragments in the 70 eV spectra of **2***c* and *d*

Transformation no.	A(*m/e*)	B(*m/e*)	C	*m/e*		
				2*c*	**2***d*	Calculated
1	$C_{10}H_{14}^{\cdot+}$(134)	$C_{10}H_{13}$(133)	$H^{\cdot}$	—	132.1	132.0
2	$C_{10}H_{14}^{\cdot+}$(134)	C_9H_{11}(119)	$CH_3^{\cdot}$	105.6	105.8	105.7
3	$C_{10}H_{14}^{\cdot+}$(134)	$C_8H_{10}^{\cdot+}$(106)	C_2H_4	—	83.9	83.9
4	$C_{10}H_{14}^{\cdot+}$(134)	C_8H_9(105)	$C_2H_5^{\cdot}$	82.3	82.4	82.3
5	$C_{10}H_{14}^{\cdot+}$(134)	$C_7H_8^{\cdot+}$(92)	C_3H_6	63.1	63.2	63.2
6	C_9H_{11}(119)	C_7H_7(91)	C_2H_4	—	69.7	69.6
7	C_7H_9(93)	C_7H_7(91)	H_2	89.1	89.0	89.0
8	$C_7H_8^{\cdot+}$(92)	C_7H_7(91)	$H^{\cdot}$	90.0	90.0	90.0
9	C_7H_7(91)	C_5H_5(65)	C_2H_2	—	46.5	46.4
10	C_6H_7(79)	$C_6H_6^{\cdot+}$(78)	$H^{\cdot}$	77.1	77.2*	77.0

*See text regarding this assignment.

adamantanol and 1-adamantanamine agree closely with those reported by Dolejšek *et al.* (1) and with one exception we agree with their findings and tentative interpretations which need not be discussed again. It was reported (1) that in the spectrum of 1-adamantanamine a metastable peak was present at *m/e* 21.5, corresponding to transformation [6]. In our work this peak was not

[6] $C_{10}H_{17}N^{\cdot+}$ (*m/e* 151) $\rightarrow C_3H_7N^{\cdot+}$ (*m/e* 57) + C_7H_{10}

observed, but instead there was a metastable peak at *m/e* 22.4 which was assigned to transformation [7]. For fragmentation [7] a metastable peak is

[7] $C_{10}H_{17}N^{\cdot+}$ (*m/e* 151) $\rightarrow C_3H_8N^{+}$ (*m/e* 58) + $C_7H_9^{\cdot}$

expected to occur at *m/e* 22.3. It was also found in the 12 eV spectrum and at that ionizing energy the peak *m/e* 58 (relative intensity 8%) is the third strongest in the spectrum after those at *m/e* 151 (base peak) and 94. It is characteristic for the 1-substituted adamantane compounds of group II as defined by Dolejšek *et al.* (1)) to which 1-adamantanol and 1-adamantanamine belong, that they retain their substituent in the main fragmentation of the molecular ion, with the formation of an M-57 ion (after loss of $C_4H_9^{\cdot}$), which gives rise to the base peak. This behavior is so different from that of the secondary alcohol (**2***c*) with the base peak at *m/e* 134, and 2-adamantanamine (**2***d*) with base peak at *m/e* 150, that no confusion between the identity of the isomers seems possible. This situation contrasts sharply with that of the two isomeric thiols, which were found to give almost identical spectra.

The financial support of this work by the National Research Council of Canada is gratefully acknowledged.

1. Z. DOLEJŠEK, S. HÁLA, V. HANŮS, and S. LANDA. Coll. Czech. Chem. Commun. **31**, 435 (1966).
2. H. W. GELUK and J. L. M. A. SCHLATMANN. Tetrahedron, **24**, 5361 (1968).
3. H. W. GELUK and J. L. M. A. SCHLATMANN. Tetrahedron, **24**, 5369 (1968).
4. J. R. GEIGY A-G. Belg. Pat. 629370 (1963); Chem. Abstr. **60**, 9167*c* (1964).
5. J. W. GREIDANUS. Can. J. Chem. **48**, 3593 (1970).
6. A. M. DUFFIELD, W. CARPENTER, and C. DJERASSI. Chem. Commun. 109 (1967).
7. K. BIEMANN. Mass spectrometry. McGraw-Hill Book Co., Inc., New York, N.Y., 1962. pp. 87–88.
8. P. v. R. SCHLEYER, L. K. M. LAM, D. J. RABER, J. L. FRY, M. A. MCKERVEY, J. R. ALFORD, B. D. CUDDY, V. G. KEIZER, H. W. GELUK, and J. L. M. A. SCHLATMANN. J. Am. Chem. Soc. **92**, 5246 (1970).
9. H. KWART and T. A. BLAZER. J. Org. Chem. **35**, 2726 (1970).
10. H. BUDZIKIEWICZ, C. DJERASSI, and ر. H. WILLIAMS. Mass spectrometry of organic compounds. Holden-Day, Inc., San Francisco, California, 1967. p. 299; F. W. MCLAFFERTY. Interpretation of mass spectra. W. A. Benjamin, Inc., New York, N.Y., 1966. pp. 132 and 145.
11. A. C. UDDING, J. STRATING, and H. WYNBERG. Chem. Commun. 657 (1966).
12. C. G. MACDONALD, J. S. SHANNON, and G. SUGOWDZ. Tetrahedron Lett. 807 (1963); H. BUDZIKIEWICZ, Z. PELAH, and C. DJERASSI. Monatsh. **95**, 158 (1964).
13. R. S. WARD and D. H. WILLIAMS. J. Org. Chem. **34**, 3373 (1969).
14. J. KARLINER, H. BUDZIKIEWICZ, and C. DJERASSI. J. Org. Chem. **31**, 710 (1966).
15. R. S. GOHLKE and F. W. MCLAFFERTY. Anal. Chem. **34**, 1281 (1962).
16. R. C. FORT, JR., and P. v. R. SCHLEYER. Chem. Rev. **64**, 277 (1964).

Can. J. Chem. Downloaded from www.nrcresearchpress.com by 210.87.254.5 on 09/05/12
For personal use only.

Can. J. Chem. Downloaded from www.nrcresearchpress.com by 210.87.254.6 on 09/05/12
For personal use only.

Nuclear Magnetic Resonance Spectra, Conformations, Spin Coupling Mechanisms, and INDO Molecular Orbital Calculations for the Monofluorobenzaldehydes and some Derivatives

R. WASYLISHEN[1] AND T. SCHAEFER

Chemistry Department, University of Manitoba, Winnipeg, Manitoba

Received May 17, 1971

Precise analyses of the proton and some fluorine magnetic resonance spectra in acetone solution are reported for the three monofluorobenzaldehydes as well as for 2-chloro-6-fluorobenzaldehyde and for 4-fluoro-2-nitrobenzaldehyde. The conformational dependence of the coupling parameters allows the measurement of energy differences between the *O-cis* and *O-trans* conformations. The energy differences are in better agreement with the INDO predictions than they are with energies derived from i.r. data. Dipole moments are computed reliably and their measurement is suggested as a good guide to conformational preferences for molecules of this kind. The spin–spin coupling constants between the aldehyde proton and the ring protons and fluorine nuclei are computed for benzaldehyde and the three monofluorobenzaldehydes by the INDO and CNDO molecular orbital approximations. In many instances the agreement between calculated and observed couplings is quantitative.

Les analyses détaillées des spectres de résonnance magnétique du proton et du fluor en solution dans l'acétone sont rapportées pour les trois monofluorobenzaldéhydes ainsi que pour le chloro-2 fluoro-6 benzaldéhyde et le fluoro-4 nitro-2 benzaldéhyde. La relation entre les paramètres de couplage et la conformation permet de mesurer la différence d'énergie entre les conformations *O-cis* et *O-trans*. Les différences énergétiques sont en meilleur accord avec les prévisions données par la méthode INDO qu'avec celles obtenues à partir des données i.r. Les moments dipolaires sont calculés avec certitude et leur mesure constitue un bon exemple de préférence conformationnelle pour des molécules de ce type. Les constantes de couplage spin–spin entre le proton aldéhydique et les protons du cycle et le noyau du fluor sont calculées pour le benzaldéhyde et les trois monofluorobenzaldéhydes par les approximations INDO et CNDO d'orbitales moléculaires. Dans plusieurs cas, l'accord entre les couplages calculés et observés est quantitatif.

Canadian Journal of Chemistry, **49**, 3216 (1971)

Introduction

The spin–spin coupling constants over six bonds between ring protons and methyl protons in toluene derivatives are dominated by π electron contributions, which are also important in the analogous couplings to ortho and meta ring protons (1). In benzaldehyde, on the other hand, the coupling between the aldehydic protons and the para ring protons is not sensibly different from zero (2) but the coupling over five bonds to the meta protons is strongly stereospecific and is probably dependent on a σ electron mechanism (3–5).

The spin–spin coupling constants between fluorine nuclei and methyl protons in derivatives of the fluorotoluenes depend primarily on a π electron mechanism, their signs being opposite to the analogous ring proton – methyl proton couplings in the toluenes. The sign opposition has its reasonable origin in the signs of the hyperfine interaction constants: $Q_{CF} > 0$ and $Q_{CH} < 0$ (6).

[1]Holder of an NRCC Scholarship, 1971–1972.

In brief, ${}^{4,6}J_{o,p}{}^{H,CH_3} < 0$, ${}^{4,6}J_{o,p}{}^{F,CH_3} > 0$, ${}^{5}J_{m}{}^{H,CH_3} > 0$, ${}^{5}J_{m}{}^{F,CH_3} < 0$, ${}^{5}J_{m}{}^{H,CHO} > 0$, ${}^{6}J_{p}{}^{H,CHO} = 0$, where left superscripts give the number of bonds intervening between the coupled nuclei, indicated in the right superscript. In the right subscripts, *o*, *m*, and *p* signify ortho, meta, and para positions of the substituents relative to the fluorine or proton ring positions.

A recent sign determination gave ${}^{6}J_{p}{}^{F,CHO} < 0$ in *p*-fluorobenzaldehyde (7) suggesting a negative *Q* value for an aldehyde group coplanar with the ring if this is indeed a π electron coupling. On the other hand, the sign sequence of fluorine–proton couplings in pentafluorobenzaldehyde (8) is evidently the same as in the fluorotoluene derivatives (6) but with a much larger magnitude of ${}^{5}J_{m}{}^{F,CHO}$ than of ${}^{5}J_{m}{}^{F,CH_3}$. A resolution of this apparent contradiction and a base for the more general study of the coupling mechanisms in benzaldehyde derivatives (9) demands reliable coupling data for the three monofluorobenzaldehydes. A careful analysis of the p.m.r. spectra of these compounds, as well as of two of their

Can. J. Chem. Downloaded from www.nrcresearchpress.com by 210.87.254.6 on 09/05/12
For personal use only.

derivatives, is reported in this paper. Fluorine spectra are reported where necessary.

The model in which σ and π electron mechanisms for the couplings are separately considered is very successful for the toluene (1), fluorotoluene (6, 10), and fluoropicoline (11) derivatives. In this model ring substituents affect spin couplings between ring protons, and between ring protons and ring fluorine substituents, primarily via a polarization of the σ system (12, 13); while their effect on long-range couplings between side-chain nuclei and ring protons or fluorine substituents is much less marked. It is of interest to discover whether such a simple model can also be used in discussing the couplings in benzaldehyde derivatives. Therefore, INDO and CNDO molecular orbital methods (13–15) are used to compute the long-range couplings between the aldehyde proton and the ring protons and fluorine nuclei. The differences between the couplings found by the two methods are an indication of the π electron contribution to the couplings (14).

Conformational preferences are deduced from the observed long-range couplings over five bonds.

Experimental

The compounds were obtained commercially and were used without further purification, except for the nitro derivative from which ferromagnetic dust had to be removed. Thirty mole percent solutions in acetone-d_6, containing tetramethylsilane (TMS) as an internal reference, were degassed by the freeze–pump–thaw technique. Other solvents that were tried gave very tightly coupled spectra and made an accurate analysis difficult at 100 MHz. At 60 MHz even the acetone solutions did not allow completely reliable analyses in one or two cases.

The p.m.r. spectra were recorded in the frequency sweep mode on an HA100-D spectrometer at a probe temperature of 30 ± 1 °C. The calibration procedure is described for *m*-fluorobenzaldehyde and applies to the other compounds. The ring proton peak positions were determined by reading manual and sweep oscillator frequencies at intervals of less than 3 Hz, each peak being calibrated at least five times. Proton resonance peaks were normally less than 0.12 Hz wide at half-height. The aldehyde proton peaks were calibrated ten times. The average standard deviations of the measured peak frequencies were 0.017 Hz for the protons and 0.019 Hz for the aldehyde protons (this compares with an r.m.s. error of 0.019 Hz in the analysis, see below). Sweep rates were 0.01 Hz/s.

Some spectra were also recorded at 60 MHz on a DA-60-I spectrometer at a probe temperature of 31 ± 1 °C. Fluorine resonance spectra were measured on an A56-60 spectrometer at a probe temperature of 32 ± 1 °C. When the solutions were prepared it was not considered that fluorine spectra would be required and therefore no internal fluorine reference material was present. At any rate, the observed fluorine spectra were needed only to confirm the sign of certain coupling constants. The fluorine resonance peaks were normally less than 0.20 Hz wide at half-height.

Certain decoupling and tickling experiments were carried out in the usual way (16).

Results and Discussion

(1) Analysis of Spectra

(a) p-Fluorobenzaldehyde

The proton resonance is the $[AB]_2X$ part of an $[AB]_2XR$ spectrum and was analyzed using the computer program LAOCN3 (17) in a manner similar to the analysis recently described for *p*-fluorotoluene (10). Of the 128 calculated transitions with intensity greater than 0.01, 106 were assigned to experimental peaks. The r.m.s. error was 0.012 Hz when all parameters were allowed to vary in the iteration. The probable error in all parameters was less than or equal to 0.003 Hz. The final parameters are given in Table 1. Extensive tickling experiments (16) confirmed the negative sign of $^6J_p^{F,CHO}$.

(b) 2-Nitro-4-fluorobenzaldehyde

The analysis of the proton resonance spectrum using LAME (18) was straightforward except that the peaks from the ring proton ortho to the nitro group were somewhat broadened by incompletely relaxed coupling to the quadrupolar ^{14}N nucleus. This means that the shift of this proton, H_3, is precise to only ±0.1 Hz and that $J_o^{H_3,F}$ is known to only ±0.1 Hz. All of the 48 transitions for H_1, H_5, and H_6 were assigned. The r.m.s. error between observed and calculated transitions was 0.007 Hz. Three elements in the correlation matrix were greater than 0.05 and these lay between 0.05 and 0.17. The probable error was 0.004 Hz or less for all but the two parameters above and the error in the small $^6J_p^{H,CHO}$ is realistically put at 0.02 Hz. Final parameters are tabulated in Table 1.

(c) o-Fluorobenzaldehyde, ABCDXR

Of 183 transitions calculated to have intensity greater than 0.01, 156 were assigned to experimental peaks, yielding an r.m.s. error of 0.018 Hz when all parameters were allowed to vary in the LAOCN3 analysis. The probable errors in the parameters was less than or equal to 0.005 Hz. Parameters are given in Table 1.

No splittings attributable to $^5J_p^{HF}$ were observed in the H_5 resonance region. However, after assigning all the transitions in the low-field H_5 region a negative value of J_p^{HF} was obtained on

Can. J. Chem. Downloaded from www.nrcresearchpress.com by 210.87.254.6 on 09/05/12
For personal use only.

TABLE 1. Spectral parameters in Hz for 30 mol % solutions in acetone-d_6

Parameter*	Compound				
ν_1	1030.934	1002.39 ± 0.02	1000.540	1038.202	1024.562
ν_2	—	757.556	797.565	—	—
ν_3	724.058	—	728.877	721.070	785.5
ν_4	767.844	738.907	—	763.131	—
ν_5	731.790	758.945	728.877	732.659	765.262
ν_6	782.816	773.587	797.565	—	801.501
$^3J_o^{HH}$	[8.417(3,4) 7.389(4,5) 7.757(5,6)]	[8.268(4,5) 7.594(5,6)]	8.561	[8.474(3,4) 8.159(4,5)]	8.657
$^4J_m^{HH}$	[1.010(3,5) 1.885(4,6)]	[2.732(2,4) 1.431(2,6) 1.026(4,6)]	[2.207(2,6) 2.612(3,5)]	0.976	2.528
$^5J_p^{HH}$	0.401	0.428	0.396	—	0.329
$^3J_o^{HF}$	10.804	[8.879(2,3) 8.575(3,4)]	8.689	10.467	[7.720(4,5) 8.2 ± 0.1]
$^4J_m^{HF}$	[5.404(2,4) 7.091(2,6)]	5.352	5.502	5.849	5.601
$^5J_p^{HF}$	−0.183	0.232	—	−1.068	—
$^4J_o^{H,CHO}$	−0.152	−0.005(1,2)†; −0.116(1,6)	−0.123	—	−0.06 ± 0.02
$^5J_m^{H,CHO}$	[0.739(1,5) 0.122(1,3)]	0.391	0.442	[0.273(1,5) 0.539(1,3)]	[0.658(1,5) 0.132(1,3)]
$^6J_p^{H,CHO}$	−0.005†	0.015†	—	−0.010†	—
$^4J_o^{F,CHO}$	−0.378	—	—	−1.080	—
$^5J_m^{F,CHO}$	—	1.845 ± 0.02	—	—	—
$^6J_p^{F,CHO}$	—	—	−0.442	—	< |0.05|

*Chemical shifts, ν, are relative to internal TMS at 100 MHz.
†Not necessarily different from zero, there being no *direct* experimental evidence for their presence. Unless otherwise indicated, the probable errors are normally less than or equal to 0.005 Hz (see text).

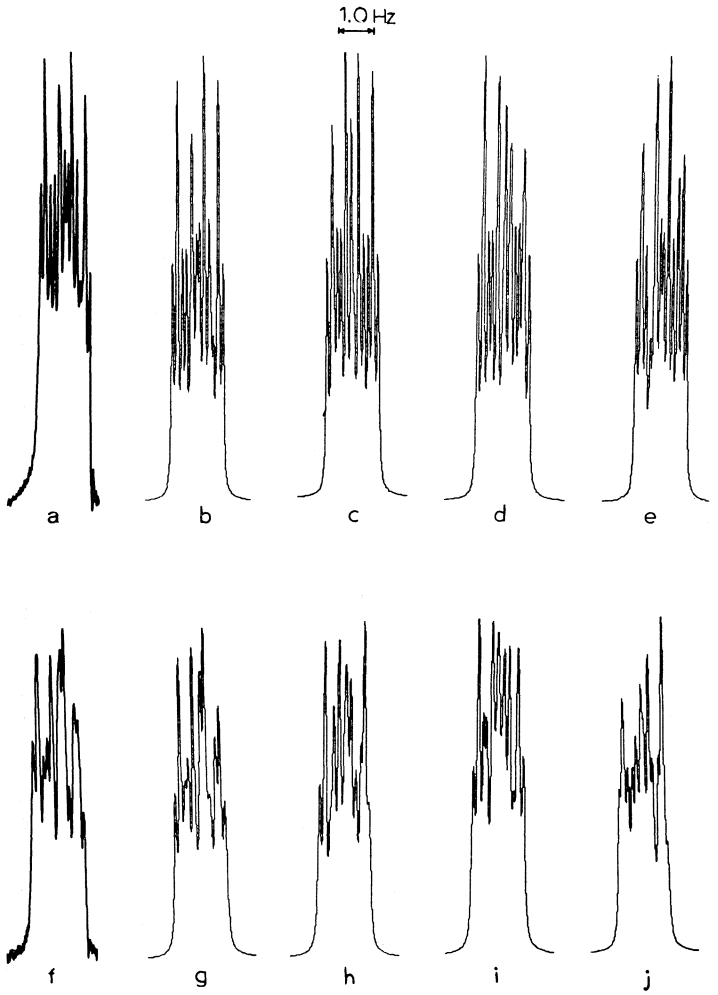

FIG. 1. The aldehyde proton magnetic resonance of *o*-fluorobenzaldehyde as a 30 mol % solution in acetone. In *a* the observed spectrum is shown at 100 MHz while in *f* the observed spectrum appears at 60 MHz. In *b* to *e* and *g* to *j* the spectra calculated with the coupling parameters in Table 1 and with the following couplings involving the aldehyde proton are shown; *b* and *g* are clearly the correct sign combinations so that the signs of all these couplings can be directly obtained from the aldehyde proton resonance.

100 MHz 60 MHz	*b* *g*	*c* *h*	*d* *i*	*e* *j*
$^4J_o^{F,CHO}$	−0.378	0.378	−0.378	−0.378
$^5J_m^{H_3,CHO}$	0.122	0.122	0.122	−0.122
$^5J_m^{H_5,CHO}$	0.739	0.739	0.739	0.739
$^4J_o^{H_6,CHO}$	−0.152	−0.152	0.152	−0.152

iteration. The negative sign was clearly confirmed by comparison of the observed ^{19}F resonance spectrum with calculated spectra using various sign combinations. Weak irradiation experiments confirmed the negative sign of $^4J_o^{F,CHO}$, as did the observed ^{19}F spectrum. The ring proton resonance spectrum was *not* sensitive to the sign of $^4J_o^{F,CHO}$.

For reasons of space we give here only the observed and calculated spectra at 100 and 60 MHz of the aldehyde proton, Fig. 1 (agreements in the other regions were excellent). The correct

Can. J. Chem. Downloaded from www.nrcresearchpress.com by 210.87.254.6 on 09/05/12
For personal use only.

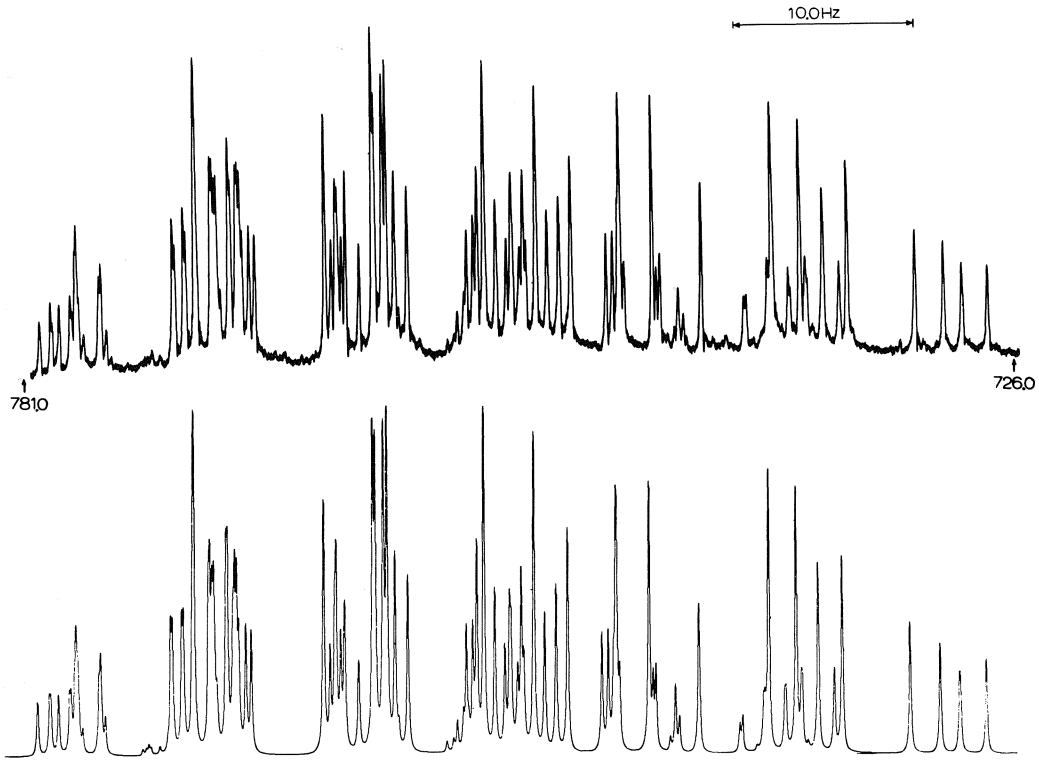

FIG. 2. The observed and calculated ring proton magnetic resonance spectra at 100 MHz of a 30 mol % solution of *m*-fluorobenzaldehyde in acetone. The calculated spectrum uses the parameters in Table 1. There are present a few impurity peaks, their presence becoming obvious only when proper assignments of peak position are complete.

There are one or two peaks which appear unresolved in the calculated spectrum, a consequence of the Lorentzian line shape. A calculated spectrum in which the right hand half of the peaks is "brought down" more sharply than for a Lorentzian, thereby simulating spectrometer conditions, showed better agreement with the observed spectrum for these peaks.

signs of all the long-range couplings to the aldehyde proton are easily found from Fig. 1 even in the absence of double resonance experiments. The effective T_2 in the calculated spectra in Fig. 1 was deliberately increased beyond the value indicated by the observed spectrum at 100 MHz because it makes comparisons more obvious without vitiating any conclusions.

(d) m-Fluorobenzaldehyde, ABCDXR

The chemical shift between H_2 and H_5 is only about 0.015 p.p.m., presenting some analysis problems. In a preliminary experiment the ring proton spectrum was calibrated twice while decoupling the aldehyde proton. Several trial and error calculations with LAOCN3, followed by some iterative runs, finally yielded the correct relative chemical shifts of H_5 and H_2. The coupling parameters so obtained agreed to within about 0.02 Hz with the results of the complete analysis to follow.

Proper calibration procedures on the complete proton spectrum, and assignment of 126 of the 137 ring proton transitions with intensities greater than 0.01, gave the parameters in Table 1. The r.m.s. error was 0.019 Hz and the probable errors varied between 0.003 and 0.006 Hz (two values). No agreement between calculated and observed ring proton spectra could be obtained unless $^4J_o^{H_6,CHO}$ was -0.116 Hz. Observed splittings in the H_6 region could not be predicted if this coupling was held at 0.00 Hz in the interaction and, furthermore, the small doublet splittings (0.1 Hz) in the H_6 region between 795 to 810 Hz (see Fig. 2) disappeared when the aldehyde protons were irradiated. One might note that at 60 MHz these splittings are *not* observable. In Fig. 2 the calculated and observed ring proton spectra are compared. Apart from a few obvious, weak impurity peaks, the agreement is quite satisfactory.

Can. J. Chem. Downloaded from www.nrcresearchpress.com by 210.87.254.6 on 09/05/12
For personal use only.

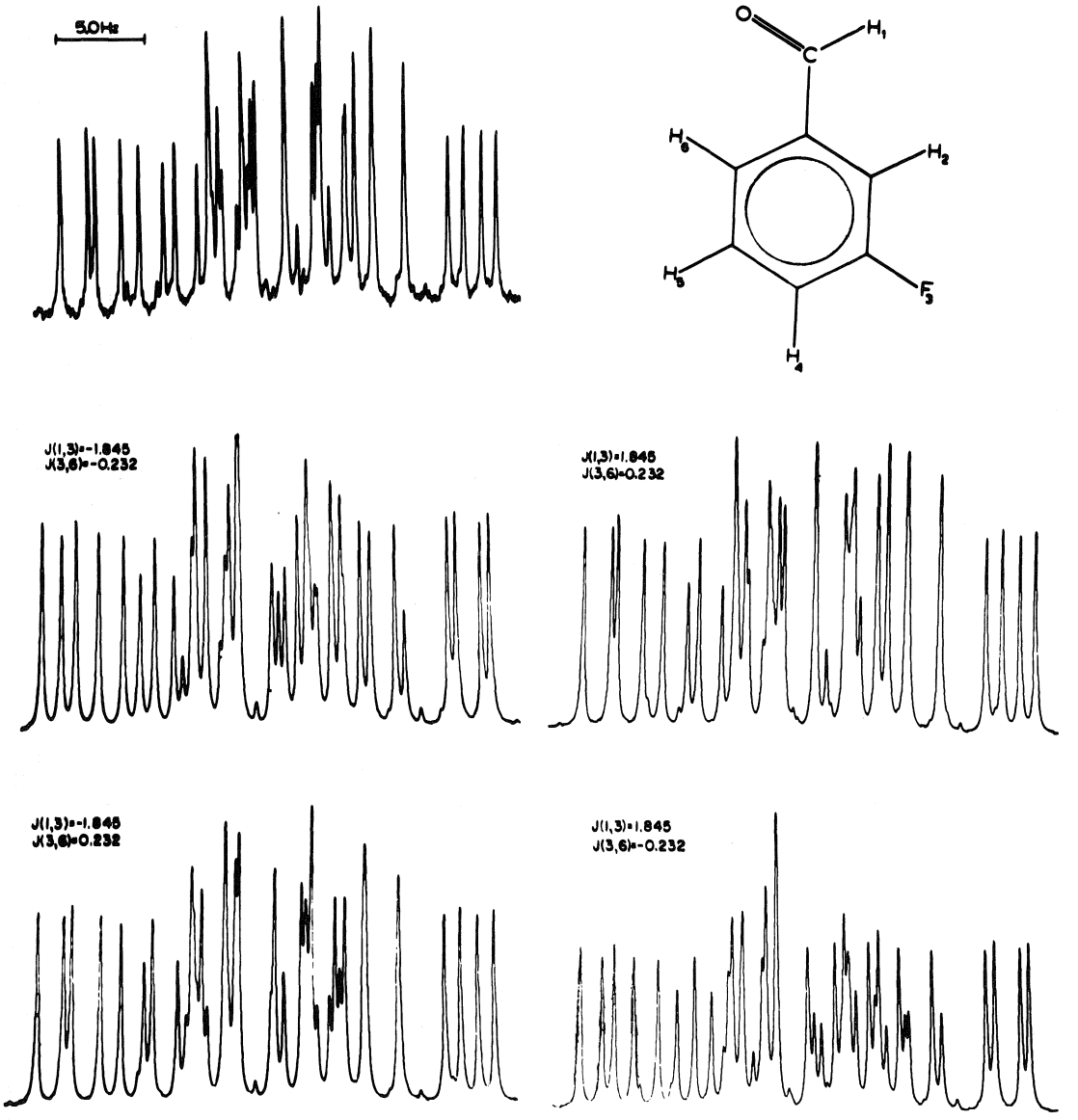

FIG. 3. The observed and calculated ^{19}F magnetic resonance spectra at 56 MHz of a 30 mol % solution of *m*-fluorobenzaldehyde in acetone. The calculated spectra use the spectral parameters in Table 1 and different sign combinations for $^5J_m^{F,CHO}$ and $^5J_p^{HF}$. There is no doubt that the calculated spectrum with both signs positive is the correct one.

The aldehyde proton resonance displayed asymmetry about its midpoint[2] and could be reproduced only by a positive value of $^5J_m^{F,CHO}$. Because a negative value could be inferred from previous work (8) it was felt necessary to compare the ^{19}F spectrum with those calculated for different signs of $^5J_m^{F,CHO}$. In Fig. 3 the various sign combinations of $^5J_m^{F,CHO}$ and $^5J_p^{HF}$ very clearly demonstrate the positive sign of these two couplings. A positive $^5J_p^{HF}$ had previously been known only in fluorobenzene itself (19) and was negative in those derivatives studied to date (10).

Finally, it might be stressed for the benefit

[2]Because of multiple degeneracies in the aldehyde proton resonance the estimated error in the *shift* of the aldehyde proton and in $^5J_m^{F,CHO}$ is 0.02 Hz.

Can. J. Chem. Downloaded from www.nrcresearchpress.com by 210.87.254.6 on 09/05/12
For personal use only.

of other analysts that the near degeneracy of the H_2 and H_5 chemical shifts allows the presence of $^4J_o^{H_6,CHO}$ to go undetected at 60 MHz.

(e) 2-Fluoro-6-chlorobenzaldehyde

The analysis of the proton resonance spectrum as an ABCX part of an ABCXR spectrum by LAOCN3 was straightforward. The negative signs of $^5J_p^{HF}$ and $^4J_o^{F,CHO}$ were confirmed by double irradiation experiments. The r.m.s. error was 0.010 Hz and probable errors were 0.004 Hz or less. Parameter values are given in Table 1.

(2) The Chemical Shifts

The chemical shifts are solvent dependent (20) and will not be discussed in detail. The relative shifts of the ring protons are consistent with the predictions (21) based on mesomeric and inductive interactions of the substituents with the aromatic ring, as modified by magnetic anisotropy effects from the carbonyl group at the ortho proton (21), for example, and by the sizeable reaction field (22) shifts caused by the polar solvent. The shifts of the aldehydic protons show some evidence for deshielding effects caused by steric interactions (21, 23) with ortho substituents.

(3) The Spin–Spin Coupling Constants in the Ring

(a) The Proton–Proton Couplings

Taking J_o^{HH} as 7.54, J_m^{HH} as 1.38, and J_p^{HH} as 0.63 Hz in benzene (24) the additivity of substituent effects on these couplings was examined by using the parameters for fluorobenzene in acetone solution (19) and for benzaldehyde in CCl_4 solution (25). The agreement between predicted and observed proton–proton couplings was perfect for *p*-fluorobenzaldehyde, deviations ranging between 0.00 and 0.04 Hz for the four values. For *m*-fluorobenzaldehyde agreement was also good, the average deviation for six values being less than 0.04 Hz. The biggest deviation was 0.07 Hz for one of the J_o^{HH} couplings.

In *o*-fluorobenzaldehyde the mean deviation between predicted and observed couplings was 0.07 Hz (six values), not quite large enough to decide whether the substituent effect of the aldehyde group depends on its conformation (24). The INDO calculations suggest no conformational dependence (13). In later sections it is shown that *m*-fluorobenzaldehyde probably exists almost equally in the *O-cis* and *O-trans* conformations whereas *o*-fluorobenzaldehyde exists predominantly in the *O-trans* conformation indicated in Table 1.

For 2-fluoro-6-chorobenzaldehyde and 2-nitro-4-fluorobenzaldehyde the average deviation rises to 0.27 and 0.11 Hz, respectively. A saturation phenomenon (26) is indicated for three substituents in that the deviations of the calculated from the observed couplings are in the direction expected if the effect of a substituent has been decreased by the presence of the other two substituents. The saturation phenomenon is evidently most marked when the three substituents are placed 1, 2, 3 on the ring.

(b) The Proton–Fluorine Couplings

The substituent effect of the aldehyde group on these coupling constants has not been previously measured. Considering the aldehyde group as more electronegative than hydrogen, the observed changes in these couplings are, with one exception, in the direction found by Goldstein and co-workers (27) for a series of fluorobenzene derivatives. The exception is $J_o^{H_2,F}$ in *m*-fluorobenzaldehyde where a decrease of 0.4 Hz relative to its value in fluorobenzene is observed instead of a predicted increase (27). It is noted that, in contrast to ring proton–proton couplings, ring proton–fluorine couplings are measurably solvent dependent (28) so that a further uncertainty is present here.

In fluorobenzene in acetone solution $^5J_p^{HF} = 0.3$ Hz and the methyl group replacement technique (6, 29) implies that σ and π contributions to this coupling are of opposite sign, resulting in a value near zero (10). Electronegative substituents decrease the positive σ electron contribution, giving rise to a negative value observed in known fluorobenzene derivatives (10, 27). A substituent placed ortho to fluorine has a markedly larger effect than one placed meta to fluorine (10). Therefore, the small negative value of J_p^{HF} (-0.18 Hz) in *o*-fluorobenzaldehyde and the small positive value in *m*-fluorobenzaldehyde (0.23 Hz) are in agreement with the known regularities, as is the larger negative value (-1.07 Hz) in 2-fluoro-6-chlorobenzaldehyde.

(4) Spin–Spin Couplings to the Aldehydic Protons

(a) To Meta Protons over Five Bonds, $^5J_m^{H,CHO}$, and Conformational Preferences

In benzaldehyde $^5J_m^{H,CHO}$ is 0.38 Hz (2), an

Can. J. Chem. Downloaded from www.nrcresearchpress.com by 210.87.254.6 on 09/05/12
For personal use only.

Can. J. Chem. Downloaded from www.nrcresearchpress.com by 210.87.254.6 on 09/05/12
For personal use only.

average of the two couplings in **1**. In a series of 4-substituted derivatives of **1** a maximum increase of 0.1 Hz is found for strongly electron donating groups like OCH_3 but $^5J_m^{H,CHO}$ is never less than 0.38 Hz, even for electron attracting groups (3). The coupling is stereospecific. In 2-hydroxybenzaldehyde (9), 2-aminobenzaldehyde,[3] 2-hydroxy-3-methoxybenzaldehyde (5*a*), all of which correspond to **2** because of hydrogen

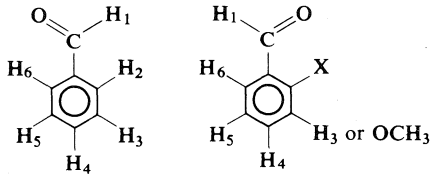

1 **2**

bonding of the carbonyl group to X, $^5J_m^{H_5,CHO}$ is undetectably small. When X = OCH_3 or Br the aldehyde group adopts a conformation in which the carbonyl oxygen and X are *trans* to one another. In these two cases $^5J_m^{H_3,CHO}$ is not detectably different from zero while $^5J_m^{H_5,CHO}$ is 0.84 and 0.77 Hz for X = OCH_3 and Br, respectively (9).

Consideration of *all* of these data strongly suggests that in benzaldehyde $^5J_m^{H_3,CHO} = 0.00$ Hz while $^5J_m^{H_5,CHO} = 0.76$ Hz when numbering as in **1**, in good agreement with theoretical models (30). Note particularly that the coupling increases in 2-methoxybenzaldehyde compared to 2-bromobenzaldehyde in a manner analogous to the 4-substituted derivatives, but that $^5J_m^{H_3,CHO}$ (non zig-zag) does *not* increase above zero.

To a very good approximation, therefore, the accurate data in Table 1 can be used to derive the proportions of the two possible conformations of each of the compounds in acetone solution.

(i) o-Fluorobenzaldehyde

One has the two possible conformations, **3** and **4**, called *O-cis* and *O-trans*, respectively.

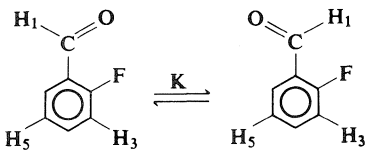

3 **4**

[3]Unpublished work in this laboratory.

On the assumption that the 1,5 coupling in **3** is zero the data in Table 1 give the populations as $P_3 = 0.14$ and $P_4 = 0.86$ or $K = 6.1$. Hence the free energy difference at 31 °C is 1.1 kcal/mol, *O-trans* more stable. This conclusion differs markedly from that reached by far i.r. torsional data in the gas phase (31), $K = 1.6$, or from that obtained by i.r. intensity measurements in solution (32), 32% *trans*, $K < 1$. On the other hand, the INDO calculations yield an energy difference of 0.94 kcal/mol, *O-trans* more stable. The entropy difference between **3** and **4** is presumably small and although the polar acetone will somewhat favor the more polar *O-cis* form, the agreement between INDO and our result is still remarkably good.[4] The only other conformational data on this system is for the radical anion, where only one conformation is observed, assigned to the *O-trans* form (33).

There is no evidence that **4**, the predominant isomer, is nonplanar; while **3** would have a maximum out-of-plane twist of 20° of the carboxyl group (34), the available coupling data on 2,6-dichloro- and 2,6-dinitro-benzaldehydes imply no measurable change in $^5J_m^{H,CHO}$ for this degree of nonplanarity (34).

(ii) m-Fluorobenzaldehyde

$^5J_m^{H,CHO}$ is 0.39 Hz, strongly implying a zero free energy difference between the two conformations. INDO computes an energy difference of 0.16 kcal/mol, *O-trans* more stable. The acetone solvent favors the *O-cis* form and therefore the agreement is quite close, INDO having $K = 1.3$ for zero entropy difference between conformations. In contrast, torsional frequency measurements in the gas phase (31) have $K = 10$, *O-cis* more stable. Band intensity measurements in the i.r. suggest 70% *O-trans* in nonpolar solvents (32), while other i.r. data for chloroform solutions give $K = 2.3$, *O-cis* more stable (31). The radical anion of this molecule contains comparable populations of two isomers (33).

(iii) 2-Fluoro-6-chlorobenzaldehyde

The procedure yields a free energy difference of 0.41 kcal/mol, *O-trans* to chlorine being more stable. The coupling constant data on 2,6-dichlorobenzaldehyde (34) suggest a maxi-

[4]Note that the assumption of a zero ^5J_m in the non zig-zag conformation (1,5 in **3**) puts a lower limit on $K = P_4/P_3$ and, therefore, on the free energy difference.

Can. J. Chem. Downloaded from www.nrcresearchpress.com by 210.87.254.6 on 09/05/12
For personal use only.

mum twist of 20° of the carbonyl group from the plane of the ring when it lies *cis* to chlorine. In that compound $^5J_m^{H,CHO}$ is 0.40 Hz, implying the validity of the population analysis above, *i.e.*, a small twist of the carbonyl group does not noticeably affect $^5J_m^{H,CHO}$.

(iv) 2-Nitro-4-fluorobenzaldehyde

The free energy difference obtained from the coupling constants is 0.87 kcal/mol, *O-trans* to the nitro group more stable. Note that the sum of the coupling constants is 0.79 Hz, almost the same as in benzaldehyde and in 2,6-dinitrobenzaldehyde, 0.78 Hz (34). The INDO energy difference is 1.64 kcal/mol, *O-trans* to nitro more stable. But the calculation was done for completely planar conformations so that 1.64 kcal/mol is very much of an upper limit. The *O-cis* to nitro form must have strong steric hindrance between the N—O and C=O bonds. Our previous measurements on 2,6-dinitrobenzaldehyde indicate a maximum twist of 25° of the carbonyl group out of the plane of the ring. No doubt the nitro group will also twist out of plane. The INDO computations were not done for nonplanar conformations of this molecule. For benzaldehyde our INDO calculations on nonplanar forms are not encouraging for standard geometries.

(v) Suggested Dipole Moment Measurements

The INDO computations on 2-fluoro- and 3-fluorobenzaldehydes predict dipole moments of 4.32 (2.95) and 3.47 (1.13) D, respectively, the *O-trans* moment being given in brackets. For benzaldehyde we calculate 2.75 D, measured values ranging from 2.8 to 3.0 D in solution (35). For *p*-fluorobenzaldehyde we calculate 1.87 D, observed being 1.98 D (35). The good agreement encourages the measurement of the dipole moments of the other two isomers as a check on the conformational information reported in this paper. We emphasize that small long-range couplings *can* be measured accurately and if this is done, we feel that relatively reliable conformational information can be obtained (complete analyses of spectra and repeated calibration of peak positions by patient personnel is absolutely essential, however).

(b) To Fluorine over Four Bonds, $^4J_o^{F,CHO}$, and Five Bonds, $^5J_o^{F,CHO}$

The population analyses in previous sections can be used in calculating values of $^4J_o^{F,CHO}$ when the C—H bond of the aldehyde group lies *cis*, J_c, and when it lies *trans*, J_t, to the fluorine. Thus, for *o*-fluorobenzaldehyde write $0.14\,J_t + 0.86\,J_c = 0.38$ Hz (Table 1) while for 2-fluoro-6-chlorobenzaldehyde write $0.66\,J_t + 0.34\,J_c = 1.08$ Hz. Then $^4J_c^{F,CHO}$ is -0.2 and $^4J_t^{F,CHO}$ is -1.6 Hz. This result is insensitive to the assumptions concerning $^5J_m^{F,CHO}$. An assumption that it is 0.1 Hz in the non ziz-zag path yields $^4J_c^{F,CHO}$ as -0.4 and $^4J_t^{F,CHO}$ as -1.4 Hz.

For 2,6-difluorobenzaldehyde one predicts $^4J_o^{F,CHO}$ to be -0.9 Hz. For pentafluorobenzaldehyde there is a report of $+1.0$ Hz for this coupling (8), a reasonable magnitude but a questionable sign. In ortho fluoro derivatives of benzalchloride a negative sign and a similar stereochemical dependence is found for $^4J_o^{F,CHCl_2}$ (36).

In *m*-fluorobenzaldehyde $^5J_m^{F,CHO}$ is $+1.84$ Hz. There is a reported value of -1.3 Hz for this coupling in pentafluorobenzaldehyde (8) and must be the mean of its values in *O-cis* and *O-trans* conformations with respect to one meta fluorine substituent. The population analysis implies 1.84 Hz as the average value for the two equally populated *O-cis* and *O-trans* forms of *m*-fluorobenzaldehyde. If $^5J_m^{F,CHO}$ has a conformational dependence similar to that of $^5J_m^{H,CHO}$ then $^5J_m^{F,CHO}$ lies between $+3$ and 4 Hz in the *O-cis* form of *m*-fluorobenzaldehyde (as actually calculated by INDO, see below). If -1.3 Hz is the correct value in pentafluorobenzaldehyde, a very large substituent effect exists in this molecule.

(c) INDO and CNDO–MO Calculations[5] of J

These were carried out on an IBM 360/65 system, using standard geometries (14). As many as 76 cycles in the s.c.f. procedure were necessary to obtain convergence of the calculated coupling constants to 0.01 Hz; as few as 50 were sufficient for CNDO. As a check the proton couplings in benzene were calculated and agreed to within less than 0.01 Hz with the values quoted in ref. 14. The $J(^{13}C—H)$ value in benzaldehyde was calculated as 159.08 Hz, in exact agreement with the value given in ref. 37.

In Table 2 the calculated coupling constants to the aldehyde proton are reported for the planar

[5]We are indebted to Dr. G. Maciel who kindly sent us a CDC listing of the finite perturbation subroutine for INDO and to a referee for a firm prod towards these calculations.

Can. J. Chem. Downloaded from www.nrcresearchpress.com by 210.87.254.6 on 09/05/12
For personal use only.

TABLE 2. Calculated aldehyde proton coupling constants in Hz in the planar conformations of benzaldehyde and the three fluorobenzaldehydes

Coupling constant (Hz)	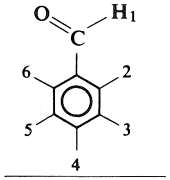		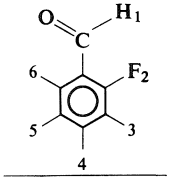		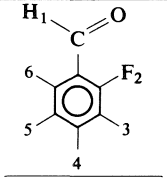		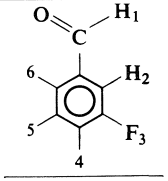		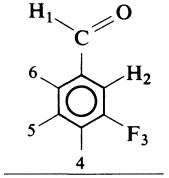		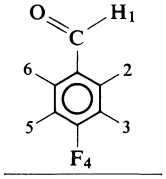	
	INDO	CNDO	INDO	CNDO	INDO	CNDO	INDO	CNDO	INDO	CNDO	INDO	CNDO
$^4J(1,2)$	0.21	0.53	0.11	0.31	0.38	0.50	0.20	0.52	−0.30	0.36	0.18	0.52
$^4J(1,6)$	−0.41	0.28	−0.37	0.30	0.16	0.51	−0.43	0.27	0.08	0.49	−0.40	0.27
$^5J(1,3)$	0.20	0.02	0.21	0.03	1.60	0.93	−0.36	0.07	3.47	2.55	0.19	0.02
$^5J(1,5)$	1.60	0.90	1.55	0.88	0.20	0.02	1.61	0.89	0.24	0.02	1.51	0.86
$^6J(1,4)$	−0.29	0.00	−0.29	0.00	−0.28	0.00	−0.31	0.00	−0.34	−0.01	0.53	0.08

TABLE 3. Comparison of calculated and observed aldehydic proton coupling constants on the basis of deduced conformation* preferences in benzaldehyde and its monofluoro derivatives

		$^4J_o^{H,CHO}$	$^5J_m^{H,CHO}$	$^6J_o^{H,CHO}$	$^{4,5,6}J_{o,m,p}^{F,CHO}$
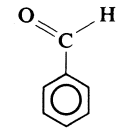	Experimental	−0.10	0.38	−0.03	—
	INDO	−0.10	0.90	−0.29	—
	CNDO	0.40	0.46	0.00	—
			H_5 / H_3		
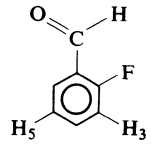	Experimental	−0.15	0.74 / 0.12	0.00	−0.39
	INDO	−0.30	1.36 / 0.40	−0.29	0.14
	CNDO	0.33	0.76 / 0.16	0.00	0.34
		H_2 / H_6			
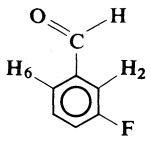	Experimental	−0.01 / −0.12	0.39	0.00	1.84
	INDO	−0.05 / −0.17	0.92	−0.32	1.56
	CNDO	0.44 / 0.38	0.46	−0.01	1.31
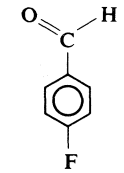	Experimental	−0.12	0.44	—	−0.44
	INDO	−0.11	0.85	—	0.53
	CNDO	0.40	0.44	—	0.08

*Benzaldehyde is planar in the gas phase (38) and it is assumed that it and *p*-fluorobenzaldehyde are planar in solution. The fractional contributions of the *O-cis* and *O-trans* forms of the *o*- and *m*-fluorobenzaldehydes are taken from section *4a*, as derived from the five-bond proton–proton coupling constants. All data are in Hz.

conformations of benzaldehyde and the three fluorobenzaldehydes. In view of the expense of these calculations, they were not done for the other two compounds in Table 1. In Table 3 the observed and calculated coupling constants are compared. All conformations are planar, benzaldehyde and *p*-fluorobenzaldehyde naturally having two equally populated forms, while the fractional populations of the *o*-fluorobenzaldehyde and *m*-fluorobenzaldehyde were taken from section *4a* above.

(i) Calculated Couplings in Table 2

Inasmuch as the INDO approximation considers one-center exchange integrals (14) it includes the π electron contribution, expected to be negative over four or six bonds and positive over five bonds. The expectation is borne out by, for example, the two sets of data for benzaldehyde in Table 2. However, it is probable that our calculations using standard geometries somewhat overestimate the π electron contributions to $^5J_m^{H,CHO}$ (see below). The data in Table 2 may well be of interest in the study of those molecules in which the carbonyl group is fixed by intramolecular hydrogen bonding. Note that the presence of the fluorine substituents has a negligible effect on the calculated magnitudes of $^5J_m^{H,CHO}$ and $^6J_p^{H,CHO}$ and probably constitutes support for the conformational arguments in section *4a*. The insensitivity to substituent *and solvent* effects of the long-range couplings between protons on a side-chain and ring protons is experimentally known for a variety of benzene derivatives (3, 6, 10).

(ii) Observed and Calculated Couplings in Table 3

A stringent comparison between observed and calculated values can be made for benzaldehyde and *p*-fluorobenzaldehyde. INDO is in excellent agreement with the observed $^4J_o^{H,CHO}$ data while CNDO yields rather too large values, indicating the importance of π electron contributions (for that matter, INDO is also in striking agreement with the two different observed $^4J_o^{H,CHO}$ values in *m*-fluorobenzaldehyde).

On the other hand, CNDO agrees quantitative-

Can. J. Chem. Downloaded from www.nrcresearchpress.com by 210.87.254.6 on 09/05/12
For personal use only.

TABLE 4. Computed aldehydic proton coupling constants in benzaldehyde and *p*-fluorobenzaldehyde for perpendicular orientations of the carbonyl group

		$^4J_o^{H,CHO}$	$^5J_m^{H,CHO}$	$^6J_p^{H(F),CHO}$
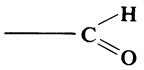	INDO	−0.43	1.01	−0.76
	CNDO	0.48	0.19	0.01
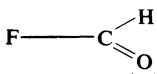	INDO	−0.49	0.98	1.45
	CNDO	0.46	0.17	0.13

ly with the $^5J_m^{H,CHO}$ measurements while INDO overestimates their magnitude substantially, suggesting that π electron contributions to $^5J_m^{H,CHO}$ are very small. This suggestion is verified by our observations on appropriate compounds that a methyl group, replacing the ring or aldehyde proton, does not couple to the remaining proton. It should couple if a π electron contribution were important (29). Furthermore, the five-bond coupling is not known for the anti-zig-zag arrangement and (in Table 2) CNDO calculates less than 0.03 Hz for this situation while INDO finds 0.2 Hz, which would be easily observed.

Again, CNDO predicts a vanishing $^6J_p^{H,CHO}$, as observed for all molecules in Table 3, while INDO overestimates this coupling by −0.3 Hz.

The agreement between calculated and observed H, F couplings in Table 3 is not terribly good, an exception being $^5J_m^{F,CHO}$ in the INDO approximation. Both methods calculate a positive $^6J_p^{F,CHO}$ in *p*-fluorobenzaldehyde, contrasting with the negative observed value. Similar disagreements for H, F couplings in other molecules are mentioned by Pople and co-workers (14).

In general the agreement between theory and experiment for the present molecules is impressive and the use of the combined CNDO and INDO theories in conjunction with precise experimental, long-range coupling data is suggested as an improved tool in conformational studies.

(d) Calculations of J for nonplanar Conformations

It has been argued (39) that, as the carbonyl group twists about the C—C bond in benzaldehyde $^6J_p^{H,CHO}$ should become large and negative, displaying an extremum when the carbonyl group lies perpendicular to the ring plane. Similarly, $^6J_p^{F,CHO}$ in *p*-fluorobenzaldehyde should become large and positive (7). In Table 4 the computed long-range couplings of the aldehydic proton in benzaldehyde and *p*-fluorobenzaldehyde are presented for conformations in which the plane of the carbonyl group lies perpendicular to the aromatic plane. The INDO calculations bear out the previous predictions as expected if, in the qualitative model (7, 39), the coupling to the para position now goes mainly via a π electron mechanism. The synthesis of the 2,6-di-*t*-butyl derivatives is suggested.

Finally, it may be remarked that the presence of a substituent distorts the benzene ring and it would be of interest to perform a systematic series of calculations in which such a distortion is introduced.

We are grateful to Dr. J. B. Rowbotham for help with the computer program and to the NRCC for financial support.

1. C. J. MACDONALD and W. F. REYNOLDS. Can. J. Chem. **48**, 1002 (1970).
2. R. J. KOSTELNIK, M. P. WILLIAMSON, D. E. WISNOSKY, and S. M. CASTELLANO. Can. J. Chem. **47**, 3313 (1969).
3. S. S. DANYLUK, C. L. BELL, and T. SCHAEFER. Can. J. Chem. **47**, 4005 (1969).
4. D. G. KOWALEWSKI and V. J. KOWALEWSKI. Mol. Phys. **9**, 331 (1965).
5. (*a*) S. FORSÉN, B. AKERMARK, and T. ALM. Acta Chim. Scand. **18**, 2313 (1964). (*b*) G. J. KARABATSOS and F. M. VANE. J. Am. Chem. Soc. **85**, 3886 (1963).
6. D. J. BLEARS, S. S. DANYLUK, and T. SCHAEFER. J. Chem. Phys. **47**, 5037 (1967).
7. T. SCHAEFER and S. S. DANYLUK. Can. J. Chem. **47**, 4289 (1969).
8. R. R. DEAN and W. MCFARLANE. J. Chem. Soc. B, 509 (1969).
9. D. G. DEKOWALEWSKI and S. CASTELLANO. Mol. Phys. **16**, 567 (1969).
10. R. WASYLISHEN and T. SCHAEFER. Can. J. Chem. **49**, 94 (1971).
11. J. B. ROWBOTHAM, R. WASYLISHEN, and T. SCHAEFER. Can. J. Chem. **49**, 1799 (1971).

Can. J. Chem. Downloaded from www.nrcresearchpress.com by 210.87.254.6 on 09/05/12
For personal use only.

12. S. CASTELLANO and R. KOSTELNIK. J. Am. Chem. Soc. **90**, 141 (1968).
13. G. E. MACIEL, J. W. MCIVER, JR., N. S. OSTLUND, and J. A. POPLE. J. Am. Chem. Soc. **92**, 4506 (1970).
14. D. L. BEVERIDGE and J. A. POPLE. Approximate molecular orbital theory. McGraw-Hill Book Company, New York, N.Y., 1970.
15. Program 141. Quantum chemistry program exchange. Indiana University, Bloomington, Indiana.
16. R. FREEMAN and W. A. ANDERSON. J. Chem. Phys. **37**, 2053 (1962).
17. S. CASTELLANO and A. A. BOTHNER-BY. Mellon Institute Publication, Pittsburgh, Pennsylvania, 1967.
18. C. W. HAIGH and J. M. WILLIAMS. J. Mol. Spectrosc. **32**, 398 (1969).
19. J. E. LOEMKER and J. H. GOLDSTEIN. Spectrosc. Lett. **1**, 153 (1968).
20. T. SCHAEFER and W. G. SCHNEIDER. J. Chem. Phys. **32**, 1218 (1960).
21. K. HAYAMIZU and O. YAMAMOTO. J. Mol. Spectrosc. **29**, 183 (1969).
22. A. D. BUCKINGHAM. Can. J. Chem. **38**, 300 (1960).
23. T. SCHAEFER, W. F. REYNOLDS, and T. YONEMOTO. Can. J. Chem. **41**, 2969 (1963).
24. S. CASTELLANO and R. KOSTELNIK. Tetrahedron Lett. 5211 (1967).
25. W. BRÜGEL. Nuclear magnetic resonance spectra and chemical structure. Academic Press. New York, N.Y., 1967.
26. T. SCHAEFER, G. KOTOWYCZ, H. M. HUTTON, and J. W. S. LEE. Can. J. Chem. **46**, 2531 (1968).
27. J. E. LOEMKER, J. M. READ, JR., and J. H. GOLDSTEIN. J. Phys. Chem. **72**, 991 (1968).
28. H. M. HUTTON, B. RICHARDSON, and T. SCHAEFER. Can. J. Chem. **45**, 1795 (1967).
29. R. HOFFMAN and S. GRONOWITZ. Arkiv Kemi, **16**, 471 (1960).
30. M. BARFIELD and B. CHAKRABARTI. Chem. Rev. **69**, 757 (1969).
31. F. A. MILLER, W. G. FATELY, and R. E. WITKOWSKI. Spectrochim. Acta, **23**A, 891 (1967).
32. A. R. KATRITZKY, M. V. SINNOTT, T. T. TIDWELL, and R. D. TOPSOM. J. Am. Chem. Soc. **91**, 628 (1969).
33. A. HUDSON and J. W. E. LEWIS. Mol. Phys. **19**, 241 (1970).
34. C. L. BELL, S. S. DANYLUK, and T. SCHAEFER. Can. J. Chem. **47**, 3529 (1969).
35. A. L. MCCLELLAN. Tables of experimental dipole moments. W. H. Freeman and Company, San Francisco, California, 1963.
36. H. M. HUTTON, J. B. ROWBOTHAM, B. H. BARBER, and T. SCHAEFER. Can. J. Chem. **49**, 2033 (1971).
37. G. E. MACIEL, J. W. MCIVER, JR., N. S. OSTLUND, and J. A. POPLE. J. Am. Chem. Soc. **92**, 1 (1970).
38. R. K. KAKAR, E. A. RINEHART, C. R. QUADE, and T. KOJIMA. J. Chem. Phys. **52**, 3803 (1970).
39. C. L. BELL, S. S. DANYLUK, and T. SCHAEFER. Can. J. Chem. **47**, 3529 (1969).

Can. J. Chem. Downloaded from www.nrcresearchpress.com by 210.87.254.6 on 09/05/12
For personal use only.

Can. J. Chem. Downloaded from www.nrcresearchpress.com by 210.87.254.5 on 09/05/12
For personal use only.

NOTES

K-Absorption Spectroscopic Investigations on Mixed Valency

H. L. NIGAM AND U. C. SRIVASTAVA
Chemistry Department, Allahabad University, Allahabad, India

Received March 10, 1971

Evidence for the existence of mixed valency Cu(I)–Cu(II) in some copper complexes has been adduced from X-ray absorption spectroscopic study. Two distinct edges K_1 and K_2 have been observed for the uni and divalent states of copper.

Des preuves concernant l'existence d'une valence mixte Cu(I)–Cu(II) dans quelques complexes avec le cuivre, sont apportées par suite d'une étude spectroscopique d'absorption aux rayons X. Deux valeurs distinctes K_1 et K_2 ont été observées pour les états mono et divalent du cuivre.

Canadian Journal of Chemistry, **49**, 3229 (1971)

The valency-dependence of the relative shifts in the position of the X-ray K-absorption discontinuity of a particular metal in its different compounds is well known (1–4). Thus Boehm *et al.* (1) and Mande and Chetal (2) have decided the valency of cobalt in vitamin B_{12} and in Co–thiomalic acid complex, respectively, on the basis of the shifts in the Co K-edge in them. However, the possibility of gaining evidence for the co-existence of two different oxidation states in the same compound from X-ray absorption spectra does not appear to have been explored hitherto. Very recently, however, Vishnoi (5) has shown that the L_{III}-edge shift for lead in Pb_3O_4 (involving Pb(II) and Pb(IV)) is intermediate between those due to PbO and PbO_2. Although, theoretically, the above possibility follows from the valency-dependence of edge-shifts, an experimental verification of the same may be feasible only in those cases where the separation between the wavelengths of the absorption edges corresponding to different valence-states can be resolved on the spectra. With this end in view, we have investigated the K-absorption edges of copper in some complexes which have been otherwise shown to involve Cu(I) and Cu(II) existing together. It may be noted that Beaman *et al.* (6) have shown from their K-absorption studies on copper salts that, in general, the $1s \rightarrow 4p$ absorption (*i.e.* the K-absorption maximum) in Cu(I) salts occurs at about 10 eV lower energy than that in Cu(II) salts.

The complexes, *viz.* Cu–thiomalic acid (Cu–TMA) and Cu–thio vanol (Cu–TV), have been prepared and studied in this laboratory using other physico-chemical methods by Nigam *et al.* (7–10). Earlier, the Cu–TMA complex has also been studied by Klotz *et al.* (11) and by Cheney *et al.* (12). Their magneto-chemical (9) and polarographic (7, 11, 12) studies have consistently shown that Cu–TMA involves a mixed-valency system (–Cu(II)–SR–Cu(I)). The complex has recently been examined in solution by Smith *et al.* (13) using electron spin resonance (e.s.r.) measurements. The broad resonance observed in the frozen aqueous solutions of the complex between p*H* 1.9 and 9.8 have been attributed to the cuprous–cupric charge delocalization. However, the delocalization envisaged does not seem to be extensive. Also, it is dependent largely on the concentration factor. The measurements described in this paper have been done in solid form. The Cu–TV complex, when freshly prepared, is a yellow powder and has been shown to involve Cu(I) (10) in a polymeric chain structure $—(—R—O—Cu(I)—S—R—)_n$. However, on long exposure to dry air or oxygen the solid slowly turns green, presumably due to the formation of Cu(II); the phenomenon is usual to copper complexes formed with reducing sulfur ligands (14).

The K-absorption spectra of these complexes have been recorded photographically using a 40 cm radius Cauchois type curved crystal spectrograph using $(\bar{2}01)$ reflection planes of mica as analyzer. The source of radiation was a

Can. J. Chem. Downloaded from www.nrcresearchpress.com by 210.87.254.5 on 09/05/12
For personal use only.

Machlett sealed tungsten-target X-ray tube which was operated at 16 kV and 12 mA. The set up, standardized by resolving $Mo\beta_{1,3}$ doublet in the first order, gave a dispersion of about 12.5 x.u. per mm. The reference lines used were $L\alpha_1$, $L\alpha_2$, $L\beta_1$, $L\beta_4$ of tungsten. Thin and uniform absorption screens were prepared by evenly spreading the substance in fine powder form on scotch tape and were placed between the X-ray tube window and the analyzing crystal. Due care was taken to keep the Cu–TV (yellow) screen air tight so as to prevent oxidation during exposure to X-rays. The exposure time varied from 15–20 h. Several spectrograms were taken for each sample. The microphotometer records were taken on a Kipp and Zonen Moll microphotometer with magnification of 25 and 8, the latter having been used for measurements. Figure 1 shows the energy *vs.* absorption coefficient ($\log I_0/I$) curve (plotted from the microphotometer traces) for Cu–TMA while Fig. 2 shows the curves for Cu–TV (*a*, for the freshly prepared sample and *b*, when exposed overnight to dry air).

It can be observed that the absorption jump in case of Cu–TMA (Fig. 1) exhibits an unusual edge-structure. The complete edge apparently consists of two edges, shown as K_1 and K_2. The low energy peak A_1 is well defined in intensity and is situated ~10 eV to the lower energy side of the main peak. Further, in case of Cu–TV no such edge-structure shows up for the freshly prepared sample (Fig. 2*a*) whereas in case of the oxidized sample the normal edge apparently splits up into two (Fig. 2*b*) as in Cu–TMA and the first absorption maximum A_1 again appears ~10 eV below the main peak. If the oxidized form is considered to form simply a separate phase with no mixed valency present, the edge structure should be, as can be seen in the literature, very different from the one observed here. It may thus appear as if the two edges K_1 and K_2 correspond to Cu(I) and Cu(II) in conformity with Beaman's observation (6) (ut supra) and that Cu(I) in Cu–TV (yellow) may have only partially oxidized to Cu(II) in the green sample.

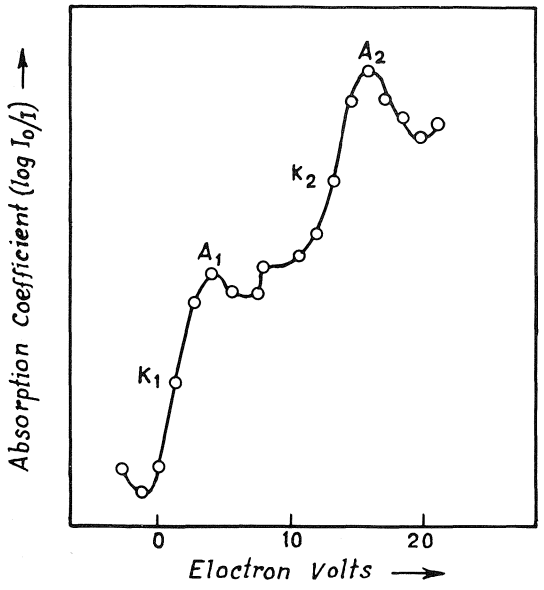

FIG. 1. K-edge of Copper in Cu–TMA.

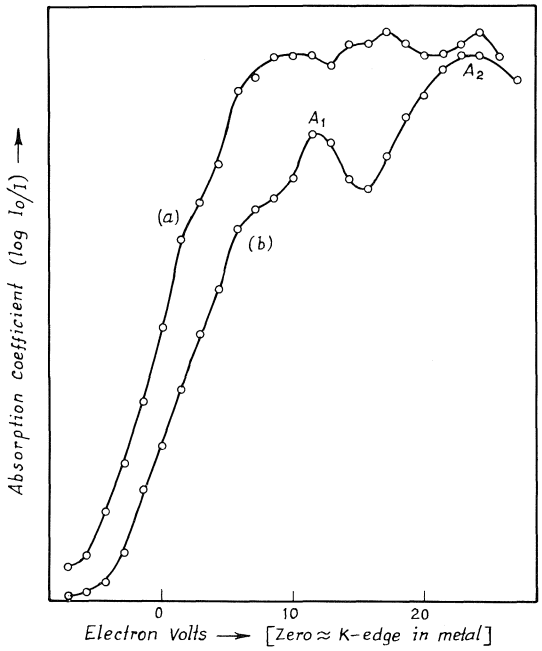

FIG. 2. K-absorption edge of copper in (*a*) Cu–TV (yellow), (*b*) Cu–TV (green).

The authors are grateful to Professor B. K. Agarwal and Dr. A. N. Vishnoi for providing laboratory facilities.

1. G. BOEHM, A. FAESSLER, and G. RITTMAYER. Z. Naturf. **96**, 509 (1954).
2. C. MANDE and A. R. CHETAL. Rontgenspektren und Chemische Bindung Vortage des Internationalem Symposium, Leipzig: Physikalich Chemishen Institute der Karl-Marx-Universitat. 1966.
3. B. K. AGARWAL and L. P. VERMA. J. Phys. C, Solid State Phys. **3**, 535 (1970).
4. Y. CAUCHOIS. Les Spectres de Rayons X et la structure Electronique de la Matiere, Paris. 1948.

5. A. N. VISHNOI. J. Phys. C. (Metal Phys.) Suppl. No. 2 S 227 (1970).
6. W. W. BEAMAN, J. FORSS, and J. N. HUMPHREY. Phys. Rev. **67**, 217 (1945).
7. H. L. NIGAM, R. C. KAPOOR, and U. KAPOOR. Vij. Par. Anu. Patrika, **4**, 359 (1961).
8. H. L. NIGAM, R. C. KAPOOR, U. KAPOOR, and S. C. SRIVASTAVA. Vij. Par. Anu. Patrika, **7**(1), 43 (1964).
9. S. C. SINHA. D.Phil. Thesis. Allahabad University, Allahabad, India. 1964.
10. H. L. NIGAM and K. B. PANDEY. Ind. J. Chem. **8**, 454 (1970).
11. I. M. KLOTZ, G. H. CZERLINSKI, and M. A. FIESS. J. Am. Chem. Soc. **80**, 2920 (1958).
12. G. E. CHENEY, Q. FERNANDO, and H. FREISER. J. Phys. Chem. **63**, 2055 (1959).
13. T. D. SMITH, C. MOORE, J. F. BOAS, J. R. PILBROW, and G. J. TROUP. J. Chem. Soc. A, 965 (1969).
14. M. B. MISHRA. D.Phil. Thesis. Allahabad University, Allahabad, India. 1967.

Can. J. Chem. Downloaded from www.nrcresearchpress.com by 210.87.254.5 on 09/05/12
For personal use only.

The Pressure Dependence of the Activation Volume

D. L. GAY
Xavier College, Sydney, Nova Scotia

Received September 8, 1970[1]

The analysis of the pressure dependence of the activation volume, $(\partial\Delta V^*/\partial P)_T$, in terms of ion-dielectric theory has been performed. The values of $(\partial\Delta V^*/\partial P)_T$ obtained on this basis are in good agreement with those found for the hydrolyses of organic halides. These results further indicate that contributions to $(\partial\Delta V^*/\partial P)_T$ arising from compression of the molecule or ion are by far more important than those arising from electrostriction of the dielectric medium. Also, the effects of quadrupole moments can be very important since the contributions from this are as great as those from dipole moments. Nevertheless it seems that ion-dielectric theory gives only a partial answer to the question of the nature and origin of $(\partial\Delta V^*/\partial P)_T$. Apparently, the contributions from solvent structure, unaccounted for on this model, cannot be ignored.

Une analyse de la dépendance du volume d'activation par rapport à la pression, $(\partial\Delta V^*/\partial P)_T$, a été réalisée en fonction de la théorie ion-diélectrique. Les valeurs de $(\partial\Delta V^*/\partial P)_T$ obtenues sur cette base, sont en bon accord avec celles trouvées pour l'hydrolyse des halogénures organiques. Ces résultats indiquent de plus que les contributions à $(\partial\Delta V^*/\partial P)_T$ provenant de la compression des molécules ou des ions sont de beaucoup plus importantes que celles provenant de l'électrostriction du milieu diélectrique. De plus, les effets des moments quadrupolaires peuvent être très importants puisque leurs contributions sont aussi grandes que celles des moments dipolaires. Néanmoins, il semble que la théorie ion-diélectrique ne donne qu'une réponse partielle à la question de l'origine et de la nature de $(\partial\Delta V^*/\partial P)_T$. Apparemment, les contributions dues à la structure du solvant, non interprétées dans ce modèle, ne peuvent être ignorées.

Canadian Journal of Chemistry, **49**, 3231 (1971)

Recently some attention has been focussed upon finding an analytical function which best expresses the pressure dependence of reaction rates (1–3). This situation is essential since the activation volume, ΔV^*, is pressure dependent (1–7). The pressure dependence of the activation volume, $(\partial\Delta V^*/\partial P)_T$, for the hydrolytic reactions of organic halides usually lies in the range 0 to +10 ml/kbar mol (1–7). This has been attributed to differences in the compression of the ground state and transition state (1, 4, 9).[2] However, this does not give as clear a picture of the factors contributing to ΔV^* and the associated parameter $(\partial\Delta V^*/\partial P)_T$ as is desirable. Benson and Berson

[1]Revision received May 10, 1971.

[2]A referee has calculated $(\partial\Delta V^*/\partial P)_T$, assuming the initial and transition state compressibilities to be the same (K), on the following basis

$$(\partial\Delta V^*/\partial P)_T = -\Delta V^* \times K$$

If $\Delta V^* = -15$ ml/mol and $K = 100 \times 10^{-6}$ bar^{-1}, then $(\partial\Delta V^*/\partial P)_T = 1.5$ ml/kbar mol. This is in the range found for the reactions being considered in this paper.

5. A. N. VISHNOI. J. Phys. C. (Metal Phys.) Suppl. No. 2 S 227 (1970).
6. W. W. BEAMAN, J. FORSS, and J. N. HUMPHREY. Phys. Rev. **67**, 217 (1945).
7. H. L. NIGAM, R. C. KAPOOR, and U. KAPOOR. Vij. Par. Anu. Patrika, **4**, 359 (1961).
8. H. L. NIGAM, R. C. KAPOOR, U. KAPOOR, and S. C. SRIVASTAVA. Vij. Par. Anu. Patrika, **7**(1), 43 (1964).
9. S. C. SINHA. D.Phil. Thesis. Allahabad University, Allahabad, India. 1964.
10. H. L. NIGAM and K. B. PANDEY. Ind. J. Chem. **8**, 454 (1970).
11. I. M. KLOTZ, G. H. CZERLINSKI, and M. A. FIESS. J. Am. Chem. Soc. **80**, 2920 (1958).
12. G. E. CHENEY, Q. FERNANDO, and H. FREISER. J. Phys. Chem. **63**, 2055 (1959).
13. T. D. SMITH, C. MOORE, J. F. BOAS, J. R. PILBROW, and G. J. TROUP. J. Chem. Soc. A, 965 (1969).
14. M. B. MISHRA. D.Phil. Thesis. Allahabad University, Allahabad, India. 1967.

The Pressure Dependence of the Activation Volume

D. L. GAY
Xavier College, Sydney, Nova Scotia

Received September 8, 1970[1]

The analysis of the pressure dependence of the activation volume, $(\partial\Delta V^*/\partial P)_T$, in terms of ion-dielectric theory has been performed. The values of $(\partial\Delta V^*/\partial P)_T$ obtained on this basis are in good agreement with those found for the hydrolyses of organic halides. These results further indicate that contributions to $(\partial\Delta V^*/\partial P)_T$ arising from compression of the molecule or ion are by far more important than those arising from electrostriction of the dielectric medium. Also, the effects of quadrupole moments can be very important since the contributions from this are as great as those from dipole moments. Nevertheless it seems that ion-dielectric theory gives only a partial answer to the question of the nature and origin of $(\partial\Delta V^*/\partial P)_T$. Apparently, the contributions from solvent structure, unaccounted for on this model, cannot be ignored.

Une analyse de la dépendance du volume d'activation par rapport à la pression, $(\partial\Delta V^*/\partial P)_T$, a été réalisée en fonction de la théorie ion-diélectrique. Les valeurs de $(\partial\Delta V^*/\partial P)_T$ obtenues sur cette base, sont en bon accord avec celles trouvées pour l'hydrolyse des halogénures organiques. Ces résultats indiquent de plus que les contributions à $(\partial\Delta V^*/\partial P)_T$ provenant de la compression des molécules ou des ions sont de beaucoup plus importantes que celles provenant de l'électrostriction du milieu diélectrique. De plus, les effets des moments quadrupolaires peuvent être très importants puisque leurs contributions sont aussi grandes que celles des moments dipolaires. Néanmoins, il semble que la théorie ion-diélectrique ne donne qu'une réponse partielle à la question de l'origine et de la nature de $(\partial\Delta V^*/\partial P)_T$. Apparemment, les contributions dues à la structure du solvant, non interprétées dans ce modèle, ne peuvent être ignorées.

Canadian Journal of Chemistry, **49**, 3231 (1971)

Recently some attention has been focussed upon finding an analytical function which best expresses the pressure dependence of reaction rates (1–3). This situation is essential since the activation volume, ΔV^*, is pressure dependent (1–7). The pressure dependence of the activation volume, $(\partial\Delta V^*/\partial P)_T$, for the hydrolytic reactions of organic halides usually lies in the range 0 to +10 ml/kbar mol (1–7). This has been attributed to differences in the compression of the ground state and transition state (1, 4, 9).[2] However, this does not give as clear a picture of the factors contributing to ΔV^* and the associated parameter $(\partial\Delta V^*/\partial P)_T$ as is desirable. Benson and Berson

[1]Revision received May 10, 1971.

[2]A referee has calculated $(\partial\Delta V^*/\partial P)_T$, assuming the initial and transition state compressibilities to be the same (K), on the following basis

$$(\partial\Delta V^*/\partial P)_T = -\Delta V^* \times K$$

If $\Delta V^* = -15$ ml/mol and $K = 100 \times 10^{-6}$ bar^{-1}, then $(\partial\Delta V^*/\partial P)_T = 1.5$ ml/kbar mol. This is in the range found for the reactions being considered in this paper.

(8) estimate a 50% change in ΔV^* over a 3 kbar range. This would result in $(\partial \Delta V^*/\partial P)_T$ in the expected range. However, this estimate takes into account only the electrostriction of the solvent and any compression of the cavity containing the initial and transition states is taken to be negligibly small. Walling and Tanner (9) have pointed out that if the transition state is not a volume extremum, pressure displaces the transition state along the reaction-coordinate. A theoretical treatment of the pressure dependence of the activation volume then becomes particularly difficult. They further state that only for a small group of non-ionic reactions will the transition state have compressibility factors of normal molecules. These conclusions have been amply refuted by Benson and Berson (10) who have shown that perturbations of the parameters ΔV^* and ΔF^* are negligibly small in the pressure ranges commonly employed, even for extremely compressible transition states. It seems, therefore, that an estimate of the pressure dependence of the activation volume taking into consideration a larger number of factors is wholly desirable. This will then allow a clearer understanding of the nature and origin of $(\partial \Delta V^*/\partial P)_T$ as well as providing useful information about the transition states involved. Results will be discussed in terms of the hydrolytic reactions of organic halides for which there is by far the largest body of accurate data.

The activation volume may be split up into two terms, $\Delta V^*(r)$ and $\Delta V^*(s)$ (11). $\Delta V^*(r)$ is the change in the van der Waals volume when the transition state is formed, that is the volume change due directly to the changing interaction of the reacting molecules with each other. The main contributions to it are due to changes in bond length, changes in the non-bonded interactions within the molecules, and changes in electron densities around nuclei. $\Delta V^*(s)$ is the volume change due directly to the changing interaction of the reacting molecules with the solvent. These changes are not all localized in the solvent but may also be localized within the molecules (11, 14, 15). As yet there is no adequate molecular theory which is both accurate and detailed enough to treat the interaction of a molecule with its solvent. By far the most applicable is that of Whalley (14). In this model the molecule is considered to be in a spherical cavity in a continuous dielectric medium. The cavity is both expansible and compressible and has a dielectric constant equal to unity. If the dielectric constant of the medium is very much greater than unity, the electrostatic volume of solvation, $\Delta V^*(s)$, due to the changing electrostatic interaction between the molecule and the dielectric (solvent) is given by eq. 1,

$$[1] \quad V^*(s) = (Nz^2e^2/2a_0)\,[(\partial \varepsilon_0^{-1}/\partial P) + (1 - 1/\varepsilon_0)(\partial \ln a_0/\partial P)] + (3N\mu^2/2a_0^3)\,[(\partial \varepsilon_0^{-1}/2\partial P) + (1 - (3/2\varepsilon_0))(\partial \ln a_0/\partial P)] + (5Nq^2/2a_0^5)\,[(\partial \varepsilon_0^{-1}/3\partial P) + (1 - (5/3\varepsilon_0))(\partial \ln a_0/\partial P)]$$

for an ion of charge ze, with point dipole (μ) and quadrupole moment (q) at the center. $\Delta V^*(s)$ is the sum of terms due to charge, dipole, and quadrupole. $\Delta V^*(s)$ can be further split up into two terms. These terms are $\Delta V^*(c)$ and $\Delta V^*(e)$. $\Delta V^*(c)$ is the change in volume of the cavity (molecule) caused by the force, resulting from the electrostatic interaction with the dielectric (solvent), exerted on it by the dielectric (solvent) and represented by terms in $(\partial \ln a_0/\partial P)$. These changes are not localized in the solvent but in the cavity (molecule). $\Delta V^*(c)$ is not an electrostriction of the cavity (molecule) which is zero if the dielectric constant is unity. $\Delta V^*(e)$ is the change in the volume of the dielectric (solvent). This change is localized in the solvent and is represented by terms in $(\partial \varepsilon_0^{-1}/\partial P)$. According to Whalley's analysis (14) compression of the cavity contributes more to the electrostatic volume of solvation than does electrostriction of the dielectric (2). Whalley was also able to show that quadrupole moments may be important in some reactions.

Let us assume that the part of the activation volume $\Delta V^*(r)$ is not significantly pressure dependent, as would be expected if a critical amount of change in the bond length(s) is needed for reaction. Then the variation of the activation volume with pressure must be explained in terms of the variation of $\Delta V^*(s)$ with respect to pressure. In fact it has long since been recognized that solvation effects can be very important in determining the effects of pressure on reaction rates (13, 16, 17). An estimate of this pressure dependence of the activation volume, $(\partial \Delta V^*/\partial P)_T$, may be obtained by differentiating Whalley's expression for $\Delta V^*(s)$, eq. 1, with respect to pressure. The resulting expression for $(\partial \Delta V^*/\partial P)_T$ ob-

TABLE 1. Factors contributing to $(\partial\Delta V^*/\partial P)_T$[a]

1. Charge	$\frac{Nz^2e^2}{2a_0}\left[\frac{\partial^2\varepsilon_0^{-1}}{\partial P^2} - 2\left(\frac{\partial \ln a_0}{\partial P}\right)\left(\frac{\partial\varepsilon_0^{-1}}{\partial P}\right) + \left(1-\frac{1}{\varepsilon_0}\right)\left(\frac{\partial^2 \ln a_0}{\partial P^2}\right) - \left(1-\frac{1}{\varepsilon_0}\right)\left(\frac{\partial \ln a_0}{\partial P}\right)^2\right]$
2. Dipole	$\frac{3N\mu^2}{2a_0^3}\left[\frac{\partial^2\varepsilon_0^{-1}}{\partial P^2} - 3\left(\frac{\partial \ln a_0}{\partial P}\right)\left(\frac{\partial\varepsilon_0^{-1}}{\partial P}\right) + \left(1-\frac{3}{2\varepsilon_0}\right)\left(\frac{\partial^2 \ln a_0}{\partial P^2}\right) - \left(1-\frac{3}{2\varepsilon_0}\right)\left(\frac{\partial \ln a_0}{\partial P}\right)^2 \times 3\right]$
3. Quadrupole	$\frac{5Nq^2}{2a_0^5}\left[\frac{\partial^2\varepsilon_0^{-1}}{\partial P^2} - \frac{10}{3}\left(\frac{\partial \ln a_0}{\partial P}\right)\left(\frac{\partial\varepsilon_0^{-1}}{\partial P}\right) + \left(1-\frac{5}{3\varepsilon_0}\right)\left(\frac{\partial^2 \ln a_0}{\partial P}\right) - 5\left(1-\frac{5}{3\varepsilon_0}\right)\left(\frac{\partial \ln a_0}{\partial P}\right)^2\right]$

[a] $(\partial^2 \ln \varepsilon_0/\partial P^2)_T = 67.28 \times 10^{-10}$, ref. 22.
$(\partial^2 \ln \varepsilon_0/\partial P)_T = 46.7 \times 10^{-6}$, ref. 22.
$\varepsilon_0 = 80.2$, ref. 22.
$(\partial \ln a_0/\partial P)_T = -5 \times 10^{-6}$ bar^{-1}, ref. 14.
$(\partial \ln a_0/\partial P^2)_T = 1.2 \times 10^{-9}$ bar^{-2}, computed from compressibility data in ref. 23.
$e = 4.8 \times 10^{-10}$ e.s.u.
$\mu = 10$ D (two point charges $+\frac{1}{2}e$ and $-\frac{1}{2}e$ about 4 Å apart).
$q = 0.2 \times 10^{-24}$ e.s.u. (two point charges each $\frac{1}{2}e$ that are 4 Å apart).
$z = 1$.
$a_0 = 3$ Å.
$N = 6.02 \times 10^{23}$ mol^{-1}.

TABLE 2. Contributions to $(\partial\Delta V^*/\partial P)_T$ from charge, dipole, and quadrupole

	Term (ml/kbar mol)				$(\partial\Delta V^*/\partial P)_T$
	1	2	3	4	(ml/mol kbar)
1. Charge	0.3	0.02	3.1	0.06	3.3
2. Dipole	0.1	0.02	5.1	0.19	5.0
3. Quadrupole	0.1	0.0	3.1	0.3	2.8

TABLE 3. Values of $(\partial\Delta V^*/\partial P)_T$ for some organic hydrolysis reactions

Substrate	Temperature (°C)	$(\partial\Delta V^*/\partial P)_T$ (ml/kbar mol)	Reference
Methyl bromide	70.0	5.5	6
Isopropyl bromide	50.0	6.0	6
Benzyl chloride	50.0	2.6	21
Allyl chloride	50.25	1.6	5
β-Methyl allyl chloride	50.25	1	5
trans-γ-Methyl allyl chloride	12.02	4.7	5

tained by this process is separated into contributions from charge, dipole, and quadrupole in Table 1 and evaluated on a term by term basis in Table 2. The calculated value of 5.0 ml/kbar mol for $(\partial\Delta V^*/\partial P)_T$ for a dipolar transition state agrees reasonably well with those for a number of hydrolytic reactions of organic halides, Table 3, whose transition states are thought to be dipolar.

The important contributions to the activation volume for the hydrolysis of organic halides probably arise from (*1*) an increase in the C—Cl bond length, (*2*) a contraction due to the possible formation of a new C—O bond to the incoming water, and (*3*) a contraction of the solvent and the transition state caused by an increased electrostatic interaction with the solvent due to the electric moments of the transition state. Contributions (*1*) and (*2*) may be equated to ΔV^*(r) and (*3*) to ΔV^*(s). In general there is no firm evidence about the relative contributions of these three factors to the overall activation volume (ΔV^*) and hence $(\partial\Delta V^*/\partial P)_T$. Baliga and Whalley (2) estimate that ΔV^* for the hydrolysis of tertiary butyl chloride in water is made up of contributions of +12 and −14 ml/mol from ΔV^*(r) and ΔV^*(s), respectively. If this is so we may estimate the value of $(\partial\Delta V^*/\partial P)_T$ on the following basis[2]

$$[2] \qquad (\partial\Delta V^*/\partial P)_T = -\Delta V^*.K$$

and

$$[3] \qquad \Delta V^* = \Delta V^*(\text{r}) + \Delta V^*(\text{s})$$

therefore

$$[4] \qquad (\partial \Delta V^*/\partial P)_T = -\Delta V^*(\mathrm{r}).K + \Delta V^*(\mathrm{s}).K$$

substituting the above values for ΔV^*(r) and ΔV^*(s) estimated by Baliga and Whalley (2), together with the assumed value of K,[2] we then have

$$[5] \qquad (\partial \Delta V^*/\partial P)_T = (-1.2 \times 10^{-3} + 1.3 \times 10^{-3}) \text{ ml/mol atm} = 0.1 \times 10^{-3} \text{ ml/atm mol}$$

This value is in the range found for this reaction in water (2). On this basis it seems that the pressure dependence of the activation volume must be viewed in terms of the compensation of the two terms in eq. 4. Also it seems likely that the pressure dependence of ΔV^*(r) may be making a significant contribution to the pressure dependence of the overall activation volume. That is to say that $(\partial \Delta V^*(\mathrm{r})/\partial P)_T \neq 0$, thus its contribution to $(\partial \Delta V^*/\partial P)_T$ may not be ruled out a priori. A theoretical analysis of the factors influencing $(\partial \Delta V^*(\mathrm{r})/\partial P)_T$ is not very straightforward and will not be attempted here. Thus further use will be made of ion-dielectric theory in trying to understand the origin and nature of $(\partial \Delta V^*/\partial P)_T$ as reflected in the behavior of $(\partial \Delta V^*(\mathrm{s})/\partial P)_T$.

There is a marked lack of sensitivity of the activation volume to temperature changes (5, 6, 24–27). Values of $(\partial \Delta V^*/\partial T)_P$ usually lie in the range 0.2 ml/mol deg for a variety of reactions. The implication of this is that $(\partial \Delta V^*/\partial P)_T$ should not be very temperature dependent, if $(\partial \Delta V^*/\partial P)_T$ is simply equal to $-\Delta V^*.K$. On the basis of ion-dielectric theory this behavior must be explained in terms of the changing interaction between the molecule(s) and the solvent with changing temperature. This would result in a change in ΔV^*(s) and ΔV^*(r), perhaps less C–Cl elongation as well as C—O formation. Thermodynamically $(\partial \Delta V^*/\partial T)_P = -(\partial \Delta S^*/\partial P)_T$. The complex behavior of $(\partial \Delta S^*/\partial P)_T$ cannot be explained in terms of ion-dielectric theory (6) as has been found for the hydrolysis of methyl and isopropyl bromide in water. Thus we can conclude also that the temperature dependence of the activation volume is difficult to explain quantitatively on this basis. Qualitatively this apparent lack of sensitivity of ΔV^* to temperature may be attributed to the fact that the initial and transition state volumes vary similarly with respect to temperature. The implication here being that water molecules are being held as tightly in the initial state as in the transition state, which is highly polar. The importance of initial state solvation and its relation to solvent structure has been quite adequately demonstrated by Arnett *et al.* in their work on the partial molal heats of solution in aqueous organic solvents (18).

If terms involving $(\partial^2 \ln a_0/\partial P^2)_T$ are by far the more important in determining the pressure dependence of the activation volume, as is evident from the results in Table 2, then it would be expected that the pressure dependence of the activation volume would be neither temperature nor pressure dependent, if the dielectric constant is very much greater than unity. In this case "a" would not be sensitive to dielectric constant. This lack of sensitivity of $(\partial \Delta V^*/\partial P)_T$ to temperature and solvent is not unknown (5, 20, 21). The temperature sensitivity of this parameter has been discussed earlier. However, the sensitivity of $(\partial \Delta V^*/\partial P)_T$ to solvent may be very large (2, 4, 7, 28), contrary to predictions of ion-dielectric theory as outlined in this paper. Thus it becomes evident that ion-dielectric theory does not totally account for all that is happening in solution under these conditions. Similar conclusions have been reached previously by Baliga and Whalley (2, 28, 29) who observed large variations in the activation volume for reactions which occur without large changes in the interactions with solvent. A detailed analysis of this large variation of the contribution of this interaction with solvent is not known in terms of ion-dielectric theory. Hence most workers have resorted to the approach of Arnett *et al.* (18) and have analyzed the effect of solvent on the activation volume in terms of the solvent effect on initial and transition state partial volumes (2, 20, 21, 32). The result of this approach is that in most cases the variation of partial volume of the initial state is more responsible for the variation of the activation volume with solvent composition than the transition state (2, 20, 30). In some cases the variation of the partial volume of the transition state may be more responsible (20). It also seems likely that when there is no variation of the activation volume with solvent that both the initial and transition state partial volumes are undergoing similar changes as solvent composition changes (21). In all cases

$(\partial \Delta V^*/\partial P)_T$ undergoes parallel changes (30). The implication of all this is that solvent structure is playing a part in influencing this kinetic behavior. This has been illustrated in other studies (18, 19, 30). However, at present a quantitative estimate of the extent of this cannot be made.

It is worthwhile to mention that in all of those studies quoted in the previous paragraph involved aqueous-organic solvent mixtures. It is known that the structural nature of these systems is quite complex. This complexity is reflected in the kinetics in these systems. However, when the variation of activation volume with solvent is related to a change from one pure solvent to another (*e.g.* ethanol, methanol, etc.), Eckert and co-workers (31–33) have found that then the variation of ΔV^* with solvent can be explained on the basis of ion-dielectric theory. All of the solvents involved in these studies are structurally similar, so structural influences are ruled out and a less complicated behavior results.

One further conclusion worth mentioning here, is the fact that the contributions to the pressure dependence of the activation volume from quadrupole moments can be quite significant and cannot be ignored. The contribution from quadrupole moments is about equal to that from dipole moments, Table 2.

To summarize, we may say that although these calculations are not very refined mainly because of the rough estimates of the parameters involved, that ion-dielectric, as applied here, does afford a clearer understanding of the nature and origin of the pressure dependence of the activation volume. Valuable information about the transition state can also be extracted on this basis. However, it may be constantly borne in mind that the contribution to ΔV^* and $(\partial \Delta V^*/\partial P)_T$ arising from structural properties of the aqueous binary solvent must be considered.

The author wishes to thank the National Research Council of Canada and the Council for Research, St. Francis Xavier University for support of this research.

1. H. S. Golinkin, W. G. Laidlaw, and J. B. Hyne. Can. J. Chem. **44**, 2139 (1966).
2. B. T. Baliga and E. Whalley. Can. J. Chem. **48**, 528 (1970).
3. J. Koskikallio and E. Whalley. Trans. Faraday Soc. **55**, 813 (1959).
4. K. J. Laidler and R. Martin. Int. J. Chem. Kinet. **1** 113 (1969).
5. A. B. Lateef and J. B. Hyne. Can. J. Chem. **47**, 1369 (1969).
6. B. T. Baliga and E. Whalley. J. Phys. Chem. **73**, 654 (1969).
7. J. B. Hyne, H. S. Golinkin, and W. G. Laidlaw. J. Am. Chem. Soc. **88**, 2104 (1966).
8 Sidney W. Benson and Jerome A. Berson. J. Am. Chem. Soc. **84**, 152 (1962).
9. Cheves Walling and Dennis D. Tanner. J. Am. Chem. Soc. **85**, 612 (1963).
10. Sidney W. Benson and Jerome A. Berson. J. Am. Chem. Soc. **86**, 259 (1964).
11. E. Whalley. Adv. Phys. Org. Chem. **2**, 93 (1964).
12. M. G. Evans and M. Polanyi. Trans. Faraday Soc. **31**, 875 (1935).
13 S. D. Hamann. Physicochemical effects of pressure. Butterworths Scientific Publications, London. 1957.
14. E. Whalley. J. Chem. Phys. **38**, 1400 (1968).
15. E. Whalley. Ber. Bunsenges. Phys. Chem. **70**, 957 (1966).
16. A. L. Th. Moesveld. Z. Phys. Chem. **105**, 455 (1923).
17. A. L. Th. Moesveld and W. A. T de Meester. Verlag Gevone Vergader Afdell Natuurk. Ned. Akad. Wetenschaf, **36**, 827 (1927).
18. E. M. Arnett, W. G. Bentrude, J. J. Burke, and P. M. Duggelby. J. Am. Chem. Soc. **87**, 1541 (1965). E. M. Arnett, P. McC. Duggelby and J. J. Burke. J. Am. Chem. Soc. **85**, 1350 (1963). E. M. Arnett, W. G. Bentrude, and P. McC. Duggelby. J. Am. Chem. Soc. **87**, 2048 (1965).
19. F. Franks and D. J. G. Ives. Q. Rev. **20**, 1 (1966).
20. Digby D. MacDonald and J. B. Hyne. Can. J. Chem. **48**, 2494 (1970).
21. D. L. Gay and E. Whalley. Can. J. Chem. **48**, 2021 (1970).
22. B. B. Owen, R. C. Miller, C. E. Miller, and H. L. Cogan. J. Phys. Chem. **65**, 2065 (1961).
23. E. A. Moelwyn-Hughes. Physical chemistry. 2nd revised ed. Pergamon Press, N.Y., 1961. pp. 323, 331.
24. C. Walling and H. S. Schugar. J. Am. Chem. Soc. **85**, 607 (1963).
25. K. J. Laidler and D. Chen. Trans. Faraday Soc. **54**, 1026 (1963).
26. J. Kiskikallio and E. Whalley. Can. J. Chem. **37**, 783 (1959).
27. Moyra J. MacKinnon, A. B. Lateef, and J. B. Hyne. Can. J. Chem. **48**, 2025 (1970).
28. B. T. Baliga and E. Whalley. Can. J. Chem. **43**, 1835 (1964).
29. B. T. Baliga, R. J. Withey, and E. Whalley. Trans. Faraday Soc. **61**, 517 (1965).
30. H. S. Golinkin, I. Lee, and J. B. Hyne. J. Am. Chem. Soc. **89**, 1307 (1967).
31. R. A. Grieger and C. A. Eckert Trans Faraday Soc. **66**, 2579 (1970).
32. C. A. Eckert. Ind. Eng. Chem. **59**(9), 20 (1967).
33. J. R. McCabe, R. A. Grieger, and C. A. Eckert. Ind. Eng. Chem. Fund. **9**(1), 156 (1970).

An Unusual Course of a Nitro Sugar Acetylation: Formation of a Crystalline Nitronic Acid – Acetic Acid Mixed Anhydride[1]

WERNER RANK AND HANS H. BAER[2]
Department of Chemistry, University of Ottawa, Ottawa, Canada

Received April 21, 1971

Whereas acetylation of methyl 4,6-*O*-benzylidene-3-deoxy-3-nitro-β-D-mannopyranoside (**1**) and its β-D-*galacto* isomer **2** with acetyl chloride and triethylamine in ether furnished the expected 2-*O*-acetylated nitro glycosides, **1***a* and **2***a*, the same method applied to the α-D-*talo* isomer **3** gave the 2-*O*-acetyl derivative of the corresponding nitronic acid – acetic acid anhydride, **4**.

L'acétylation du méthyl *O*-benzylidène-4,6 déoxy-3 nitro-3 β-D-mannopyranoside (**1**) et de son isomère β-D-*galacto* **2**, par le chlorure d'acétyle et la triéthylamine dans l'éther, conduit aux produits attendus à savoir les nitro glycosides *O*-acétylés en 2, **1***a* et **2***a*. La même méthode appliquée à l'isomère α-D-*talo* **3** conduit au dérivé *O*-acétylé en 2 d'un anhydride d'acide nitronique et acétique (**4**).

Canadian Journal of Chemistry, **49**, 3236 (1971)

Can. J. Chem. Downloaded from www.nrcresearchpress.com by 210.87.254.105 on 09/05/12
For personal use only.

The preparation of nitro sugar acetates by standard acetylation techniques is sometimes attended with difficulties due to occurrence of dehydration or dehydroacetylation and other complications that may ensue (1). Boron trifluoride catalysis (2, 3) has proved very efficient in the acetylation of various sensitive compounds, circumventing some of the difficulties mentioned, but in one recent instance it has caused acetolysis of a trityl ether function (4). This was overcome by the use of equivalent amounts of acetyl chloride and triethylamine in ether solution at 0°. The method, which involves an intermediate generation of ketene, has now been applied to methyl 4,6-*O*-benzylidene-3-deoxy-3-nitro-β-D-mannopyranoside (**1**), -β-D-galactopyranoside (**2**), and -α-D-talopyranoside (**3**).

Whereas **1** and **2** gave high yields of the expected (and known) 2-acetates **1***a* and **2***a*, respectively, the taloside **3** furnished in 92% yield an abnormal product. Elemental analysis of the crystalline material (m.p. 136–137°) corresponded to $C_{18}H_{21}NO_9$, and the n.m.r. spectrum revealed that *two* acetyl groups had entered although the benzylidene acetal as well as the anomeric methoxyl group were retained. The i.r. spectrum was free from hydroxyl absorption and showed an ester carbonyl band at 1750 cm^{-1}, but it lacked the band expected for the nitro group in the 1550 cm^{-1} region. Instead, there was a sharp peak at 1800 cm^{-1} attributable to an acid anhydride structure, and an intense band occurred at 1620 cm^{-1}, in the region where nitronic acids and their esters show strong C=N absorption (5). The product exhibited high-intensity u.v. absorption (λ_{max} 242 nm, ε 8000, in methanol) in the range in which nitronic acids and their salts are known to absorb strongly (5) in contrast to nitroalkanes that have very low absorption in

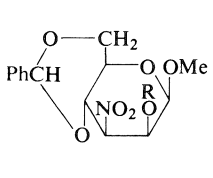

1 R = H
1*a* R = Ac

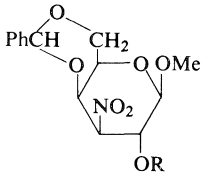

2 R = H
2*a* R = Ac

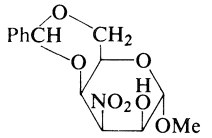

3

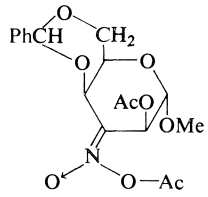

4

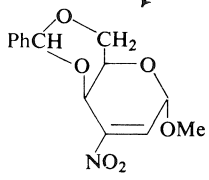

5

[1]Part XXII in a series on the reactions of nitro sugars. For Part XXI see ref. 7.

[2]Author to whom inquiries should be directed.

Can. J. Chem. Downloaded from www.nrcresearchpress.com by 210.87.254.105 on 09/05/12
For personal use only.

that range. Although the compound was remarkably stable in the crystalline state and could be recrystallized from ethyl acetate, it suffered loss of both acetyl groups when chromatographed on silica gel, giving in 85% yield the known methyl 4,6-*O*-benzylidene-2,3-dideoxy-3-nitro-α-D-*threo*-hex-2-enopyranoside (**5**). This fact demonstrated that the acetylation of **3** had masked but not irreversibly altered or removed the nitro group at C-3. On the basis of all the spectroscopic and chemical evidence we allocate to the new compound the structure **4** of a mixed nitronic acid–acetic acid anhydride. Although the chemistry of nitronic esters has been investigated extensively, only a few nitronic carboxylic anhydrides have been described in the literature, and spectral data do not seem to be available (5, 6). In nitronic esters, the occurrence of geometrical isomerism has been established, and the same may be predicted for anhydrides. This matter has not yet been examined in connection with **4**, and the formula depicted is arbitrary with respect to the C=N bond geometry.

We have recently shown that nitronate formation with base occurs in **3** much more readily than it does in **1** and **2**, and the differences in nitromethylene acidity of these and a number of similar glycosides were interpreted by stereochemical considerations (7). Apparently the unusual behavior of **3** reported here is another manifestation of the special ease with which this isomer is converted into the *aci*-nitro form.

Experimental

*Methyl 2-O-Acetyl-4,6-O-benzylidene-3-deoxy-3-nitro-β-D-mannopyranoside (**1a**)*

Triethylamine (1.93 ml, 13.8 mmol) in anhydrous ether (30 ml) was chilled in an ice water bath, and acetyl chloride (1.04 ml, 14.7 mmol) was added with magnetic stirring. A voluminous white precipitate of triethylammonium chloride occurred. After 5 min a solution of the nitro mannoside **1** (8) (206 mg, 0.66 mmol) in dry dichloromethane (4 ml) was added and the reaction mixture was stirred for 30 min at 0°. The mixture was then agitated with cold water, and after phase separation, the aqueous layer was extracted twice with ether. The combined ether solution and extract was washed three times with water, dried over sodium sulfate, and evaporated giving crystalline **1***a* (223 mg, 95%). Upon recrystallization from chloroform – petroleum ether the material (194 mg, 83%) showed m.p. 162–163°, $[\alpha]_D$ −88.7° (*c*, 0.53 in $CHCl_3$), lit. (8), m.p. 136–137° after recrystallization from aqueous ethanol; $[\alpha]_D$ not reported. Because of the melting point discrepancy the earlier acetylation procedure (8) was repeated but the product was recrystallized from chloroform – petroleum ether. The product (yield, 79%, m.p. 159–160°) was identical with that prepared by the new method according to mixed melting point, i.r. spectrum (8), and n.m.r. spectrum (100 MHz in $CDCl_3$): τ 2.6 (5-proton multiplet, phenyl), 4.13 (1-proton doublet, H-2, with $J_{2,3} = 3.5$, $J_{1,2} = 0$ Hz), 4.33 (1-proton singlet, $PhCHO_2$), 5.20 (1-proton quartet, H-3, with $J_{2,3} = 3.5$, $J_{3,4} = 10.5$ Hz), 5.48 (sharp singlet, H-1, overlapped by H-6,6′ multiplet), 6.05 (symmetrical 1-proton triplet with 10.5 Hz splitting, H-4), 6.50 (3-proton singlet, OCH_3, overlapping H-5 multiplet), 7.89 (3-proton singlet, *O*-acetyl).

*Methyl 2-O-Acetyl-4,6-O-benzylidene-3-deoxy-3-nitro-β-D-galactopyranoside (**2a**)*

The nitro galactoside **2** (8) (206 mg) was dissolved in 10 ml of dichloromethane and acetylated as described above for **1**. Upon decomposition of the reaction mixture with water, the main part of the product **2***a* (160 mg) separated as crystals which were collected, washed with cold water, and dried; m.p. 149–151°. An additional crop (43 mg, m.p. 146–148°) was obtained by work-up of the reaction mixture as described for **1**. Total yield, 87%. The i.r. spectrum was superposable with that of **2***a* prepared earlier (2).

*Methyl 2-O-Acetyl-3-(O-acetyl-aci-nitro)-4,6-O-benzylidene-3-deoxy-α-D-lyxo-hexopyranoside (**4**)*

The nitro taloside **3** (9) (103 mg, 0.33 mmol) in dichloromethane (3 ml) was treated as described above for **1** with acetylating reagent consisting of acetyl chloride (0.52 ml, 7.3 mmol) and triethylamine (0.97 ml, 6.9 mmol) in anhydrous ether (20 ml). The aforementioned work-up procedure gave 120 mg (92%) of crystals that were homogeneous on t.l.c. with carbon tetrachloride – ethyl acetate (2:3, v/v). Recrystallization from ethyl acetate gave a first crop of **4** (29 mg, m.p. 136–137°), and a second crop (83.5 mg, m.p. 132–135°) upon addition of petroleum ether to the mother liquor. For i.r. and u.v. data, see discussion. The n.m.r. data (100 MHz, in $CDCl_3$): τ 2.5–2.7 (5-proton multiplet, phenyl), 4.35 (overlapping signals with 2-proton intensity, H-2 and $PhCHO_2$), 4.9–6.2 (signals corresponding to 5 ring protons), 6.62 (3-proton singlet, OCH_3), 7.83, 7.96 (3-proton singlets, *O*-acetyl).

Anal. Calcd. for $C_{18}H_{21}NO_9$ (395.4): C, 54.65; H, 5.35; N, 3.54. Found: C, 54.61; H, 5.18; N, 3.64.

A sample of **4** (100 mg) was chromatographed on a column (1.5 × 30 cm) containing 20 g of silica gel (0.05–0.20 mm, E. Merck AG, Darmstadt, Germany) with carbon tetrachloride – ethyl acetate (2.0:1.5, v/v) as eluent. The effluent was monitored by t.l.c., and only a single compound appeared. Evaporation furnished crystalline nitroolefin **5** (63 mg, 85%), m.p. 187–188°, whose i.r. spectrum was superposable with that of an authentic sample; reported, m.p. 185–186° (9).

We thank the National Research Council of Canada for support of this work.

1. H. H. Baer. Adv. Carbohydr. Chem. Biochem. **24**, 69 (1969).
2. H. H. Baer, F. Kienzle, and F. Rajabalee. Can. J. Chem. **46**, 80 (1968).

3. H. H. BAER and F. KIENZLE. Can. J. Chem. **47**, 2819 (1969).
4. H. H. BAER, W. RANK, and F. KIENZLE. Can. J. Chem. **48**, 1302 (1970).
5. A. T. NIELSEN. *In* The chemistry of the nitro and nitroso groups. Part 1. *Edited by* H. FEUER. Interscience Publishers. New York, N.Y. 1969. p. 349.
6. S. A. SHEVELEV, V. I. ERASHKO, B. G. SANKOV, and A. A. FAINZIL'BERG. Bull. Acad. Sci. USSR, Chem. Ser. **8**, 1856 (1970).
7. H. H. BAER and W. RANK. Can. J. Chem. This issue.
8. H. H. BAER, F. KIENZLE, and T. NEILSON. Can. J. Chem. **43**, 1829 (1965).
9. H. H. BAER and F. KIENZLE. Can. J. Chem. **45**, 983 (1967).

Can. J. Chem. Downloaded from www.nrcresearchpress.com by 210.87.254.105 on 09/05/12
For personal use only.

Synthesis of 3-Deoxy-3-nitro-D-xylose[1]

JAN KOVÁŘ AND HANS H. BAER
Department of Chemistry, University of Ottawa, Ottawa, Canada

Received May 28, 1971

Crystalline 3-deoxy-3-nitro-α-D-xylose (**5**) was obtained in 40% over-all yield by periodate oxidation of 3-deoxy-1,2-*O*-isopropylidene-3-nitro-α-D-glucofuranose (**2**) followed by borohydride reduction and acid hydrolysis. In addition to the intermediate 3-deoxy-1,2-*O*-isopropylidene-3-nitro-α-D-xylofuranose (**4**), a small amount of an isomer probably having the D-*ribo* configuration was isolated. The title compound (**5**) was also obtained by hydrolysis of its methyl β-pyranoside (**1**).

Le déoxy-3 nitro-3 α-D-xylose (**5**) cristallisé, a été obtenu avec un rendement global de 40% par oxydation au periodate du déoxy-3 *O*-isopropylidène-1,2 nitro-3 α-D-glucofuranose (**2**), suivie par une réduction au borohydrure et hydrolyse acide. En plus du produit intermédiaire, le déoxy-3 *O*-isopropylidène-1,2 nitro-3 α-D-xylofuranose (**4**), une petite quantité d'un isomère ayant probablement la configuration du D-*ribo*, a été isolée. Le composé (**5**) a également été obtenu par hydrolyse de son méthyl β-pyranoside.

Canadian Journal of Chemistry, **49**, 3238 (1971)

For a study (1) on conformational and configurational equilibria in methyl 3-deoxy-3-nitropentopyranosides it was desirable to prepare the methyl β-pyranoside **1** of 3-deoxy-3-nitro-D-xylose (**5**). The glycoside was known to be a minor by-product in the nitromethane cyclization of L′-methoxydiglycolaldehyde; its formation had been revealed by isolation of the corresponding amine subsequent to catalytic hydrogenation, but the nitro glycoside itself had not been isolated (2). Although new efforts to separate **1** in crystalline condition from the products of nitromethane cyclization eventually proved successful (1), an independent synthesis of the parent sugar **5** was concurrently undertaken, and this synthesis, the first of a free nitro pentose, is recorded here.

3-Deoxy-1,2-*O*-isopropylidene-3-nitro-α-D-glucofuranose (**2**) (3) was oxidized with sodium metaperiodate and the resulting pentodialdose derivative **3**, which was not isolated, was reduced with sodium borohydride to give syrupy but sufficiently well-characterized 3-deoxy-1,2-*O*-isopropylidene-3-nitro-α-D-xylofuranose (**4**) as the main product. A crystalline by-product arose in small proportion and was revealed by analysis and spectroscopy to be an isomer of **4**. Although its configuration was not established by chemical means, it most likely was the D-*ribo* isomer, formed by alkali-catalyzed epimerization during the borohydride reduction.[2] The n.m.r. spectra of **4** and its isomer are in accord with this assumption and suggest, moreover, the T_2[3] conformation for both compounds, *i.e.* the same conformation that has been assigned (3) to the glucofuranose derivative **2**. As in the latter, the xylofuranose **4** exhibits zero coupling between H-2 and -3 and a coupling of 4 Hz between H-3 and -4. The isomer, on the other hand, shows coupling between H-2 and -3 (although its value could not be determined by first-order analysis), and it exhibits a 10 Hz coupling between H-3

[1]Part XXIV in a series on reactions of nitro sugars. For part XXIII see ref. 3.

[2]Compare the analogous, D-*gluco* → D-*allo* epimerization described in the preceding article (3).

3. H. H. BAER and F. KIENZLE. Can. J. Chem. **47**, 2819 (1969).
4. H. H. BAER, W. RANK, and F. KIENZLE. Can. J. Chem. **48**, 1302 (1970).
5. A. T. NIELSEN. *In* The chemistry of the nitro and nitroso groups. Part 1. *Edited by* H. FEUER. Interscience Publishers. New York, N.Y. 1969. p. 349.
6. S. A. SHEVELEV, V. I. ERASHKO, B. G. SANKOV, and A. A. FAINZIL'BERG. Bull. Acad. Sci. USSR, Chem. Ser. **8**, 1856 (1970).
7. H. H. BAER and W. RANK. Can. J. Chem. This issue.
8. H. H. BAER, F. KIENZLE, and T. NEILSON. Can. J. Chem. **43**, 1829 (1965).
9. H. H. BAER and F. KIENZLE. Can. J. Chem. **45**, 983 (1967).

Can. J. Chem. Downloaded from www.nrcresearchpress.com by 210.87.254.40 on 09/05/12
For personal use only.

Synthesis of 3-Deoxy-3-nitro-D-xylose[1]

JAN KOVÁŘ AND HANS H. BAER
Department of Chemistry, University of Ottawa, Ottawa, Canada

Received May 28, 1971

Crystalline 3-deoxy-3-nitro-α-D-xylose (**5**) was obtained in 40% over-all yield by periodate oxidation of 3-deoxy-1,2-*O*-isopropylidene-3-nitro-α-D-glucofuranose (**2**) followed by borohydride reduction and acid hydrolysis. In addition to the intermediate 3-deoxy-1,2-*O*-isopropylidene-3-nitro-α-D-xylofuranose (**4**), a small amount of an isomer probably having the D-*ribo* configuration was isolated. The title compound (**5**) was also obtained by hydrolysis of its methyl β-pyranoside (**1**).

Le déoxy-3 nitro-3 α-D-xylose (**5**) cristallisé, a été obtenu avec un rendement global de 40% par oxydation au periodate du déoxy-3 *O*-isopropylidène-1,2 nitro-3 α-D-glucofuranose (**2**), suivie par une réduction au borohydrure et hydrolyse acide. En plus du produit intermédiaire, le déoxy-3 *O*-isopropylidène-1,2 nitro-3 α-D-xylofuranose (**4**), une petite quantité d'un isomère ayant probablement la configuration du D-*ribo*, a été isolée. Le composé (**5**) a également été obtenu par hydrolyse de son méthyl β-pyranoside.

Canadian Journal of Chemistry, **49**, 3238 (1971)

For a study (1) on conformational and configurational equilibria in methyl 3-deoxy-3-nitropentopyranosides it was desirable to prepare the methyl β-pyranoside **1** of 3-deoxy-3-nitro-D-xylose (**5**). The glycoside was known to be a minor by-product in the nitromethane cyclization of L′-methoxydiglycolaldehyde; its formation had been revealed by isolation of the corresponding amine subsequent to catalytic hydrogenation, but the nitro glycoside itself had not been isolated (2). Although new efforts to separate **1** in crystalline condition from the products of nitromethane cyclization eventually proved successful (1), an independent synthesis of the parent sugar **5** was concurrently undertaken, and this synthesis, the first of a free nitro pentose, is recorded here.

3-Deoxy-1,2-*O*-isopropylidene-3-nitro-α-D-glucofuranose (**2**) (3) was oxidized with sodium metaperiodate and the resulting pentodialdose derivative **3**, which was not isolated, was reduced with sodium borohydride to give syrupy but sufficiently well-characterized 3-deoxy-1,2-*O*-isopropylidene-3-nitro-α-D-xylofuranose (**4**) as the main product. A crystalline by-product arose in small proportion and was revealed by analysis and spectroscopy to be an isomer of **4**. Although its configuration was not established by chemical means, it most likely was the D-*ribo* isomer, formed by alkali-catalyzed epimerization during the borohydride reduction.[2] The n.m.r. spectra of **4** and its isomer are in accord with this assumption and suggest, moreover, the T_2[3] conformation for both compounds, *i.e.* the same conformation that has been assigned (3) to the glucofuranose derivative **2**. As in the latter, the xylofuranose **4** exhibits zero coupling between H-2 and -3 and a coupling of 4 Hz between H-3 and -4. The isomer, on the other hand, shows coupling between H-2 and -3 (although its value could not be determined by first-order analysis), and it exhibits a 10 Hz coupling between H-3

[1]Part XXIV in a series on reactions of nitro sugars. For part XXIII see ref. 3.

[2]Compare the analogous, D-*gluco* → D-*allo* epimerization described in the preceding article (3).

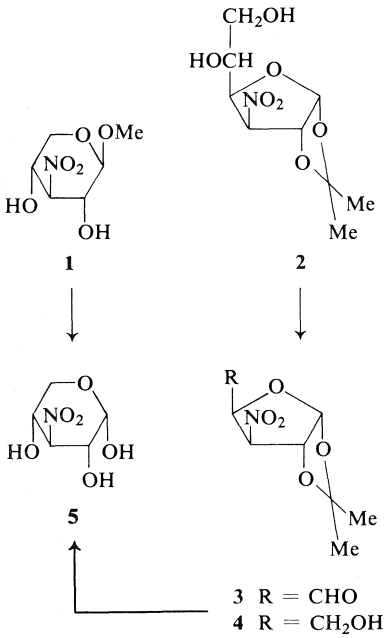

and -4. Acid hydrolysis of the main product **4** afforded **5**, the over-all yield from **2** being 40%. The reducing sugar crystallized as the downward mutarotating α-anomer. Acid hydrolysis of the previously described (1) methyl xyloside **1** furnished a sugar identical with **5**, thus ascertaining the structures of the latter as well as those of its precursors **4** and **2**.

Experimental

3-Deoxy-1,2-O-isopropylidene-3-nitro-α-D-xylofuranose (4) and Isomer

To a solution of 3-deoxy-1,2-*O*-isopropylidene-3-nitro-α-D-glucofuranose (**2**) (164 mg, 0.66 mmol) in water (7 ml) was added sodium metaperiodate (155 mg, 0.72 mmol), and the mixture was stirred at room temperature for 10 min. The excess of periodate was destroyed by ethylene glycol (2 drops), the solution was cooled in an ice water bath, and carbon dioxide gas was passed through. Sodium borohydride (45 mg) was added, followed after 15 min by another 45 mg of the same reagent. After a further 15 min the reaction solution was deionized by stirring with Dowex-1X2 (HCO_3^-) and Amberlite IR-120 (H^+) ion exchange resins. Evaporation furnished a pale yellow oil (141 mg) which exhibited 2 spots (R_f 0.53 and 0.65) on t.l.c. with chloroform – ethyl acetate (1:1). By column chromatography on silica gel (Davidson Chemical; see footnote 3 in ref. 3) with chloroform as eluent, compound **4** was obtained as a colorless oil (66 mg, 43%) that was homogeneous on t.l.c., corresponding to the faster moving spot. It distilled at 1 mm Hg at 90–95° (bath temperature) and showed $[\alpha]_D$ +61° (*c*, 0.23 in $CHCl_3$). Prominent i.r. bands in $CHCl_3$: 3600 (OH), 3000, 2950, 2910 (CH), 1558 and 1370 (NO_2), 1460, 1385, 1260, 1170, 1090, and 1025 cm^{-1}. The n.m.r. data (in $CDCl_3$): τ 3.85 (doublet, J = 3.5 Hz, H-1), 4.90 (doublet, J = 3.5 Hz, H-2), 4.95 (doublet, J = 4.0, H-3), 5.37 (quartet, J = 4.0 and 5.5 Hz, H-4), 6.18 (2-proton doublet, $J_{4,5} = J_{4,5'}$ = 5.5 Hz, H-5, -5′), 8.45, 8.62 (3-proton singlets, CH_3).

Anal. Calcd. for $C_8H_{13}NO_6$ (219.2): C, 43.85; H, 5.98; N, 6.38. Found: C, 44.11; H, 6.12; N, 6.47.

Further elution of the chromatographic column produced a crystalline *isomer* (22 mg) which melted at 74–75° after recrystallization from carbon tetrachloride; $[\alpha]_D$ +122° (*c*, 0.2 in $CHCl_3$). Prominent i.r. bands in $CDCl_3$: 3610 (OH), 3000, 2945, 2890 (CH), 1558, and 1360 (NO_2), 1455, 1385, 1380, 1310, 1255, 1220, 1165, 1135, 1110, 1030–1015 cm^{-1}. The n.m.r. data (in $CDCl_3$): τ 4.13 (doublet, J = 3.5 Hz, H-1), 4.9–5.1 (2-proton multiplet, H-2 and -3), 5.27 (sextet, $J_{3,4}$ = 10 and $J_{4,5} = J_{4,5'}$ = 2 Hz, H-4), 5.95, 6.17 (2-proton quartet of doublets due to H-5 and -5′, $J_{5,5'}$ = 13 and $J_{4,5} = J_{4,5'}$ = 2 Hz), 8.48, 8.67 (3-proton singlets, CH_3).

Anal. Calcd. for $C_8H_{13}NO_6$ (219.2): C, 43.85; H, 5.98; N, 6.38. Found: C, 43.80; H, 5.86; N, 6.36.

3-Deoxy-3-nitro-α-D-xylose (5)

From 4

The isopropylidene derivative **4** (27 mg) was refluxed for 1 h in methanol (1 ml) containing 2 drops of 2.8 *N* hydrogen chloride in dioxane. The solution was then filtered through 0.2 ml of Dowex 1X8 (acetate form, prewashed with methanol) and evaporated to give a residue that crystallized upon trituration with chloroform. The product (20.7 mg, 94%) melted at 144–145° (dec.) after recrystallization from acetone–chloroform. An n.m.r. spectrum in D_2O showed no peaks attributable to isopropylidene or methoxyl groups. $[\alpha]_D$ +90 (2 min) → +65 (12 min) → +55° (30 min, final, *c*, 0.12 in water).

Anal. Calcd. for $C_5H_9NO_6$ (179.1): C, 33.52; H, 5.06; N, 7.82. Found: C, 33.72; H, 4.91; N, 7.76.

From 1

Methyl 3-deoxy-3-nitro-β-D-xylopyranoside (**1**) (16 mg) (1) was boiled for 5 min in 1 ml of half-concentrated hydrochloric acid. The cooled solution was treated with activated charcoal, filtered, and evaporated *in vacuo*. The product (11 mg, 74%) gave an n.m.r. spectrum (in D_2O) superposable on that of **5** obtained from **4**. After recrystallization from acetone–chloroform it melted at 144–146°, undepressed on admixture of the preceding sample.

This work was supported by the National Research Council of Canada.

1. H. H. Baer and J. Kovář. Can. J. Chem. **49**. 1940 (1971).
2. H. H. Baer and H. O. L. Fischer. J. Am. Chem. Soc. **81**, 5184 (1959).
3. J. Kovář and H. H. Baer. This issue.

Can. J. Chem. Downloaded from www.nrcresearchpress.com by 210.87.254.40 on 09/05/12
For personal use only.

The Structure of the Hofmann Base Derived from Lycopodine Methiodide

N. CHIN-YOU, D. B. MACLEAN, A. PRAKASH, AND C. CALVO
Department of Chemistry, McMaster University, Hamilton, Ontario

Received June 29, 1971

A new structure, **4***a*, based on chemical and X-ray crystallographic data, is proposed for the Hofmann base derived from lycopodine.

Une nouvelle structure, **4***a*, fondée sur des données chimiques et de cristallographie au rayons-X, est proposée pour la base du type Hofmann dérivant de la lycopodine.

Canadian Journal of Chemistry, **49**, 3240 (1971)

The methiodide of lycopodine ($C_{16}H_{25}NO$, **1***a*), on treatment with potassium tertiary butoxide in boiling tertiary butyl alcohol, gives in high yield the Hofmann base ($C_{17}H_{27}NO$), to which structure **2** was assigned (1). On similar treatment the methiodide of clavolonine (**1***b*) is reported to yield a compound to which structure **3***b* was assigned (2). It seemed unlikely that lycopodine and clavolonine would yield products of different structure under the same reaction conditions and this led us to reinvestigate this reaction. It is also of mechanistic interest to clarify these structures for the formation of a compound of structure **2** from lycopodine methiodide is not in harmony with accepted views on the mechanism of displacement reactions (3).

We show here that the Hofmann base derived from lycopodine has structure **4***a* formed from lycopodine methiodide in a remarkable rearrangement. Mass spectral data indicate that its analogue derived from clavolonine has structure **4***b*.

The evidence which led to the proposal of structure **2** is now summarized. The Hofmann base did not have a double bond, had an *N*-methyl group and was tetracyclic; in its formation a carbon–nitrogen bond must have broken and a new carbon–carbon bond must have formed. The new base has only two hydrogens alpha to the carbonyl group (by deuterium exchange) in contrast to lycopodine which has three and both hydrogens are in a methylene group (i.r.). The isomer, **3***a*, was precluded since it was already known (4).

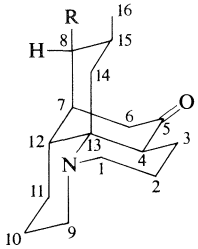

1

a R = H
b R = OH

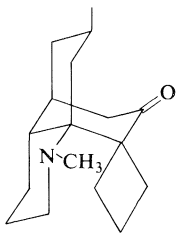

2

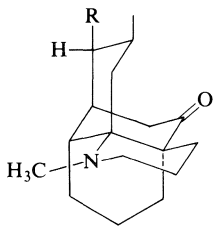

3

a R = H
b R = OH

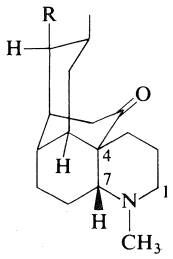

4

a R = H
b R = OH

Mass spectral evidence provided the first clue that structure **2** is untenable. The spectra of both **1***a* and **3***a* have base peaks at M-57 formed by elimination of the original bridging atoms of lycopodine and a hydrogen. The Hofmann base, however, has only a very weak ion at M-57 but has its base peak at *m/e* 57 of composition

C_3H_7N. To study the genesis of this ion we prepared the Hofmann base from lycopodine methiodide-*N*-Me-d_3 and from lycopodine methiodide -9,9-d_2.[1] There was no loss of deuterium in either reaction. In the first instance the peak at *m/e* 57 shifted completely to *m/e* 60 showing that the N—CH_3 group is a constituent of this ion while in the second case the base peak remained at *m/e* 57 (there was a small shift to *m/e* 58), a fact that precludes **2** from further consideration. The formation of the M-57 ion in lycopodine and its derivatives is thought to be initiated by fission of the C_{13}—C_{14} bond producing a stable immonium ion (5). The absence of an ion at M-57 in the spectrum of the Hofmann base implies that the N—C_{13} bond is no longer present.

The n.m.r. spectrum of the methiodide of the Hofmann base has three protons, aside from those of the two *N*-methyl groups, shifted downfield relative to their positions in the base itself suggesting the presence of three protons on carbons adjacent to nitrogen. In the spectrum of the methiodide of the Hofmann base derived from lycopodine methiodide-9,9-d_2 the low field proton at 4.65 δ is absent but those at 4.08 and 3.80 δ are present and unaltered in any way. These data suggest structure **4***a* for the Hofmann base. The configuration at C-9 is assigned on the basis of n.m.r. data since one of the two *N*-methyl groups of **4***a* methiodide appears at 2.90 δ (the other at 3.50) and must be situated in the shielding cone of the carbonyl group.

We suggest that **4***a* is formed by the sequence shown in Scheme 1. The enolate **5**, formed from lycopodine methiodide, undergoes solvolysis to **6** which stabilizes itself by hydride transfer from C-9 to -13 to give the immonium ion **7**. The latter then cyclizes as shown to **4***a*. Since there is no loss of deuterium in the reaction of the 9,9-d_2 derivative, the hydrogen transferred must come from C-9. This is not unexpected since 1,5 hydride transfer in 10-membered rings is well documented (6). The possibility that fission of the N—C_{13} bond occurs homolytically and that a hydrogen radical transfer occurs cannot be ruled out. Radical mechanisms have been demonstrated in nitrogen ylide rearrangements (7) and transannular hydrogen atom transfers have been observed (8).

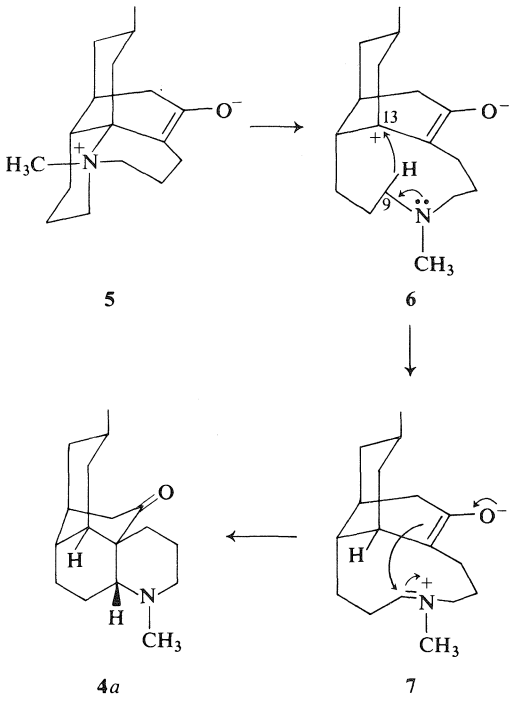

SCHEME 1

The final structure has been verified by an X-ray crystallographic study of the hydrobromide of **4***a* which was purified by recrystallization from a methanol–ether mixture. The orthorhombic crystals proved to have space group $P2_12_12_1$ with a = 12.10(1), b = 7.06(1), c = 19.68(3) Å, and Z = 4. The structure was solved from the Patterson projections of the [100] and [001] zones using data measured from integrated precession photographs taken with MoKα radiation. The structure was refined using the intensities of 2647 independent reflections measured with the Syntex P1 automatic diffractometer of which 1264 were sufficiently intense to be measured, and a full matrix least squares computer program written for the CDC 6400. The model contained independent positional and isotropic thermal parameters for all the light atoms except the hydrogen atoms and positional and anisotropic thermal parameters for the Br. The final value agreement index,

[1]Lycopodine-9,9-d_2 was obtained by reduction of the corresponding lactam with lithium aluminum deuteride and oxidation of the dihydrolycopodine-5,9,9-d_3 so obtained with Jones reagent.

$$R = \frac{\sum ||F_o| - |F_c||}{\sum |F_o|}$$

is 0.078 while the weighted reliability index,

$$R_w = \left\{\frac{\sum W(|F_o| - |F_c|)^2}{\sum WF_o^2}\right\}^{1/2}$$

is 0.085. Weights were chosen so that the local value of F_o would be independent of the magnitude of F_o. All the individual bond distance and angles are those expected for structure **4***a*.

This work was supported by grants from the National Research Council of Canada.

1. W. A. HARRISON, M. CRUCUMELLI-RODOSTAMO, D. F. CARSON, L. R. C. BARCLAY, and D. B. MACLEAN. Can. J. Chem. **39**, 2086 (1961).
2. R. H. BURNELL and D. R. TAYLOR. Tetrahedron, **15**, 173 (1961).
3. L. TENUD, S. FAROOK, J. SEIBL, and A. ESCHENMOSER. Helv. Chim. Acta, **53**, 2059 (1970).
4. D. B. MACLEAN, WON-RYUL SONG, and W. A. HARRISON. Can. J. Chem. **38**, 528 (1960).
5. D. B. MACLEAN. Can. J. Chem. **41**, 2654 (1963).
6. V. PRELOG and K. SCHENKER. Helv. Chim. Acta, **35**, 2044 (1952); V. PRELOG. Angew. Chem. **70**, 145 (1958).
7. D. HELMLINGER and G. OURISSON. Ann. **686**, 19 (1965).
8. J. E. BALDWIN, J. E. BROWN, and R. W. CORDELL. Chem. Commun. 31 (1970).

Can. J. Chem. Downloaded from www.nrcresearchpress.com by 210.87.254.6 on 09/05/12
For personal use only.

Canadian Journal of Chemistry

Published by THE NATIONAL RESEARCH COUNCIL OF CANADA

VOLUME 49 OCTOBER 15, 1971 NUMBER 20

The Solvolysis of 5,5-Diphenylcyclononyl *p*-Toluenesulfonate. A Reinvestigation

JOHN M. MCINTOSH,[1] M. H. MISKOW,[2] AND GORDON WOOD

Department of Chemistry, University of Windsor, Windsor, Ontario

Received June 8, 1971

Reinvestigation of the acetolysis of 5,5-diphenylcyclononyl tosylate (**1**) has confirmed the absence of any transannular processes and deamination of the corresponding amine **16** gave a similar result. Trifluoroacetolysis of **1** caused extensive transannular hydride migration but no phenyl migration. The former may be due to secondary acid-catalyzed rearrangements.

Une étude concernant l'acétolyse du tosylate du diphényl-5,5 cyclononyle (**1**) a confirmé l'absence de tout processus *trans* annulaire; la désamination de l'amine **16** correspondante conduit à un résultat similaire. La trifluoroacétolyse de **1** provoque une forte migration *trans* annulaire d'hydrure mais aucune migration de phényle. Ceci peut être dû à une transposition acido catalysée secondaire.

Canadian Journal of Chemistry, **49**, 3243 (1971)

The facility with which transannular rearrangements occur in medium-sized ring compounds is well documented (1, 2). However, in spite of the efforts made by several groups, the only established case of transannular migration of a group *other than hydride* in such compounds is found in the formation (1%) of 1,5-diphenylcyclooctene from 5,5-diphenylcyclooctyl tosylate in trifluoroacetic acid (3). The lack of other examples is intriguing when considered in the light of data for 1,2-migrations where phenyl migration is a more facile reaction than that involving hydride (4).

A maximum on the graph of total ring strain *vs.* ring size (5) indicates that a nine-membered ring might be expected to provide the most favorable situation for rearrangement in the medium-ring series. The solvolytic behavior of cyclononyl tosylate has been well investigated (1, 6) and Blomquist and Hallam have reported the kinetics and product distribution obtained from the acetolysis of 5,5-diphenylcyclononyl tosylate (**1**) (7). It was concluded by these workers that the latter compound gave no products of transannular rearrangement, nor was anchimeric assistance involved in the reaction. However, the analytical techniques available at the time were such that the presence of a minor component in the solvolysis mixture could have been overlooked. In addition, the effect of solvent on the products formed from 5,5-diphenylcyclooctyl tosylate (3) suggested that a study of the effect of solvent on the solvolysis of **1** would be useful.

Many comparisons have been drawn between deamination and solvolytic reactions (8). The results of these comparisons can be summarized in part by noting that both the ratio of substitution to elimination reactions and the amount of rearrangement are found to be larger in deamination reactions. Further, since bimolecular substitution reactions with medium-ring substrates are slow compared to carbonium ion reactions, and since the only protons in the favorable *trans*-coplanar arrangement for concerted elimination in the diazonium cation intermediates are sterically inaccessible to an external base, virtually all products in the deamination of medium-ring amines are derived from carbonium ion intermediates (1). In contrast, it has recently

[1]To whom correspondence should be addressed.
[2]NRCC Scholarship holder 1966–1970.

TABLE 1. Percentage yields of products from the reactions of **1** and **16**

Compound	Conditions	2	3	4	5	12	13	14	15
1	HOAc	38	31	15	16	—	—	—	—
1	TFA*	—	—	—	9	47	17	7	15
16	HOAc/RONO	23	—	14	46†				

*Buffered with 0.3 *M* sodium trifluoroacetate.
†Analyzed as the acetate; 17% alcohol formed not analyzed.

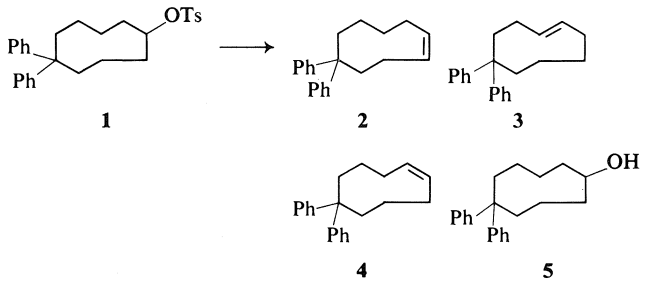

CHART 1

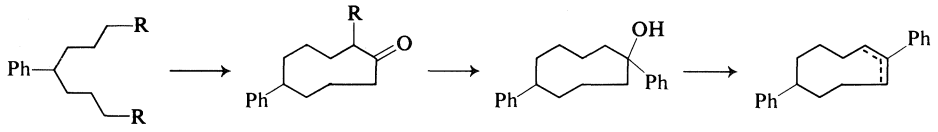

CHART 2

been noted (9–11) that partitioning of the carbonium ions in solvolysis reactions with E1 mechanisms may vary with the nature of the leaving group. It appears that a substantial portion of the proton removal from the β-carbon is effected by the counter ion, affording a route for elimination which is not available in the deamination reaction. With these concepts in mind we prepared 5,5-diphenylcyclononyl amine (**16**) and compared the products of its deamination with those of the solvolytic reactions of **1**.

Acetolysis of **1** in unbuffered acetic acid for 12 half-lives, followed by hydride reduction of the product according to the original procedure (7) afforded the products shown (Chart 1) in the amounts indicated in Table 1. These were identified by their molecular weights (mass spectra) and spectral characteristics. Gas chromatographic comparison of the acetolysis mixture with an authentic sample of 1,5- and/or 1,6-diphenylcyclononene (**6**), the expected product of phenyl migration, showed the absence of a detectable amount (1%) of **6** in the mixture. The preparation of **6** from 5-phenylazelanitrile is shown in Chart 2.

Repetition of the experiment in buffered trifluoroacetic gave the products shown in Chart 3. The yields are shown in Table 1. Again, none of the compound **6** could be detected. The results of the deamination of 5,5-diphenylcyclononyl amine (**16**) in acetic acid are summarized in Chart 4 and Table 1.

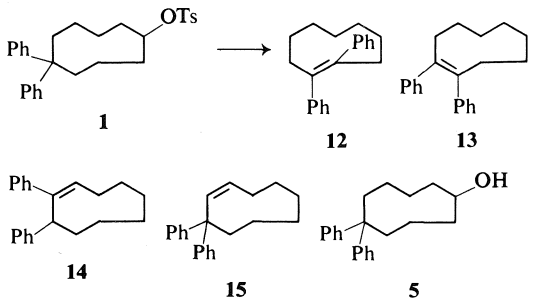

CHART 3

Can. J. Chem. Downloaded from www.nrcresearchpress.com by 210.87.254.6 on 09/05/12
For personal use only.

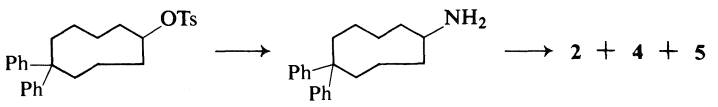

1 16

CHART 4

Discussion

The data on which the distinction between **2**, **3**, and **4** rest are worthy of some discussion. The n.m.r. spectrum of **4** shows two envelopes centered at δ 2.2 and 1.5 with relative areas of 8:4. The spectrum of **2** shows more complex and broad absorptions centered at δ 2.2 and 1.2. The chemical shift of the bulk of the high-field part of the spectrum of **2** suggests that the protons are separated from the olefinic bond and the aromatic nuclei by a larger distance than similar protons in **4**. Hence, the structural assignments were made on the basis of the relative symmetry of the two spectra and the chemical shifts of the methylene protons in the two compounds. However, when the signals near δ 2.2 were irradiated, the olefinic protons in both **2** and **3** collapsed to give singlets whereas **4** afforded two doublets (J = 11 Hz) separated by 17 Hz. It appears that the structural assignments require the reverse to be true. This olefinic non-equivalence can be rationalized by the existence of **4** mainly in an asymmetric conformation, but the same explanation may apply to the case of the methylene protons, in which case the structural assignments for **2** and **3**, and **4**, must be reversed. The remainder of the structures seem secure on the basis of their spectra.

Because of the known isomerization of olefins by acetic and trifluoroacetic acids, the stability of a mixture of olefins **2**, **3**, and **4** to the reaction conditions was determined. In acetic acid, very little isomerization was noted, but a significant amount (18%) of addition did occur. The reverse was true in trifluoroacetic acid where little addition, but significant isomerization to **12** and **13** occurred, with concurrent disappearance of **3**. Under deamination conditions, **3** was completely isomerized into **2**.

It is difficult to draw conclusions from the results in trifluoroacetic acid, since the olefins would be present initially in a homogeneous state in the reactions, whereas the isomerization experiments were heterogeneous throughout. A similar problem has been reported previously (3).

Conclusion

From the results of these experiments, it seems clear that, at least in acetic acid, the presence of the *gem*-diphenyl moiety restricts the conformations of **1** to those in which *both* hydride and phenyl transannular migrations are unfavorable. This is in agreement with the previous work (7). In trifluoroacetic acid, the results are not so clear with regard to hydride migrations since the olefin stability tests indicate that secondary rearrangements may account for the observed product distribution.

Experimental

Melting points are uncorrected. The i.r. spectra were obtained on a Beckman IR-12 in 10% (*w*/*w*) carbon tetrachloride solution. Unless otherwise noted, n.m.r. spectra were recorded on a Jeolco JNM-C60HL instrument in 10% (*w*/*v*) carbon tetrachloride solution and shifts are in δ units relative to tetramethylsilane. Small samples were accumulated on a Jeolco JRA-1 spectrum accumulator. The u.v. spectra were recorded on a Beckman DK-1 in cyclohexane. The mass spectra were obtained from Morgan Schaeffer Corp., Montreal. The g.l.c. analyses were carried out on an F and M Model 720 Gas Chromatograph utilizing one of the following columns: *A*, 10 ft × 0.25 in. XE-60 (Silicone gum nitrile); *B*, 6 ft × 0.25 in. QF-1; *C*, 6 ft × 0.25 in. Carbowax 20M; all 10% on 60–80 mesh Chromosorb W. Area measurements were made by planimeter. Except as noted the drying agent was magnesium sulfate. Liquid column chromatography was performed using Fisher certified neutral alumina, Brockman Activity 1 (80–200 mesh). Composition of mixtures are stated in terms of moles unless otherwise noted.

5,5-Diphenylcyclononanol

This compound was prepared by the published (7) procedure except that the ketone was purified by chromatography using methylene chloride followed by recrystallization from cyclohexane at −20°.

5,5-Diphenylcyclononyl Tosylate (1)

The method of Brown and Ham (12) was used and a yield of 90% based on the alcohol was common, m.p. 102–104°. This compound was relatively unstable and consequently was never heated above 30° nor kept for long periods of time; i.r.: 1360, 1170 (d), 1090 and 885 (br) cm^{-1}; n.m.r. ($CDCl_3$): 7.50 (4H, q, J = 8), 7.1 (10H, s), 4.70 (1H, m), 2.42 (3H, s), 2.4–0.9 (14H, m).

Acetolysis of 5,5-Diphenylcyclononyl Tosylate

The tosylate (1.8 g) was dissolved in 108 ml anhydrous

Can. J. Chem. Downloaded from www.nrcresearchpress.com by 210.87.254.6 on 09/05/12
For personal use only.

Can. J. Chem. Downloaded from www.nrcresearchpress.com by 210.87.254.6 on 09/05/12
For personal use only.

acetic acid and stirred at 35° for 36 h (12 half-lives) (7). The solvolysis product was quenched with 300 ml cold water and extracted with four 50 ml portions of ether. The combined ether portions were then washed with five 50 ml portions of water, two 40 ml portions of saturated sodium bicarbonate solution, and dried. After filtering and removing the ether there remained 1.16 g of an amber viscous liquid which was dissolved in 50 ml anhydrous ether, 100 mg lithium aluminum hydride added, and the mixture stirred for 3 h. Water (0.5 ml) was added dropwise, followed by magnesium sulfate (1–2 g). The mixture was stirred for 1 h, filtered, and the ether removed leaving 1.03 g of a colorless oil. This was subjected to column chromatography on 70 g alumina using petroleum ether (30–60°) (1020 ml) as eluent from which 804 mg of a white solid (fraction *1*) was obtained. The eluent was then changed to ether (1200 ml) followed by methylene chloride (1200 ml) but gave a combined total of only 39 mg of white solid (fraction *2*). Finally three methanol fractions were collected, combined, and the solvent removed. The residue was dissolved in methylene chloride, filtered in order to remove any column residue, and concentrated, to give 191 mg brown oil (fraction *3*). The total amount recovered from the column was 1.03 g.

The three fractions were analyzed by g.l.c. on column *B* (175°). Fraction *1* consisted only of compounds **2** and **3** (80%) and **4** (20%), while the second fraction contained a small amount of **5** in addition to **2**, **3**, and **4**. Fraction *3* consisted mainly of compound **5** and other small unidentified compounds (total 1%). The overall distribution was **2** + **3** (68%), **4** (15%), and **5** (16%). Sufficient quantities of **2** and **3**, **4**, and **5** were collected by g.l.c. (column *A*) for spectral examination. Fraction *1* gave only **2** when subjected to gas chromatography on an acid contaminated column *C* (205°). The n.m.r. of **3** was obtained by subtraction of the portion due to **2***a*. Compound **5** was shown by comparison of the i.r., n.m.r., and g.l.c. retention times to be identical to 5,5-diphenylcyclononanol.

Compound **2**: i.r. 1653 (w), 1580 (w), 725, 700 cm^{-1}; n.m.r. 7.18 (10H, s), 5.68 (2H, t, J = 6), 2.5–0.9 (12H, m).

Compound **3**: i.r. (in addition to those of **2**) 992 cm^{-1}; n.m.r. 7.13 (10H, s), 5.45 (2H, m), 2.5–0.8 (12H, m); u.v. (56:44 mixture of **2** and **3**) λ_{max} (C_6H_{12}) 270 (log ε 2.65), 266 sh (2.67), 263 (2.75), 259 (2.78), 254 (2.79), 249 (2.78), 244 (2.75), 218 inf (4.14) mμ; *m/e* 276 (P), 277 (P + 1, 23.2%), and the following additional prominent peaks: 193 (B), 180, 179, 178, 167, 165, 117, 91, 41.

Compound **4**: i.r. 1650 (w), 1598, 1580 (w), 700 cm^{-1}; n.m.r. 7.17 (10H, s), 6.0–5.0 (2H, m), 2.6–1.1 (12H, m); u.v. λ_{max} (C_6H_{12}) 270 (log ε 2.79), 265 sh (2.82), 263 (2.88), 259 (2.90), 254 (2.90) 249 (2.88), 244 (2.84), 219 inf (4.52) mμ; *m/e* 276 (P), 277 (P + 1, 23.2%), and the following additional prominent peaks: 205, 193, 181, 180 (B), 179, 178, 167, 165, 129, 115, 103, 91, 77, 41.

Trifluoroacetolysis of 5,5-Diphenylcyclononyl Tosylate (1)

The tosylate (4 g) was added to 35 ml trifluoroacetic acid (Eastman highest purity) containing 1.43 g (0.3 *M*) sodium trifluoroacetate and the mixture was stirred at 5° for 23 h. An aliquot taken after 18 h showed virtually no tosylate in the i.r. spectrum. The mixture was poured cautiously into 500 ml cold saturated sodium bicarbonate solution and extracted with five 50 ml portions of ether. The combined ether portions were washed twice with 25 ml of water, dried, filtered, and concentrated to give 2.16 g of a brown oil (small 1780 cm^{-1}, trifluoroacetate). This was dissolved in 150 ml dry ether, 0.15 g lithium aluminum hydride was added, and the mixture stirred magnetically for 30 min. After the dropwise addition of 1 ml of water, the solution was stirred for 30 min, a few grams of magnesium sulfate were added, the mixture filtered through Celite, and the solvent removed to give 1.9 g of an amber oil. This was chromatographed on 70 g alumina using pentane as eluent. Fraction *1* (500 ml) was 1.03 g of a yellow oil, which by g.l.c. on column *A* (180°) consisted of **12**, **13**, **14**, and **15**, (65:24:3:8). Over the next ten 100 ml fractions methylene chloride was added gradually up to 5% by volume and these fractions combined to give 0.31 g yellow oil (fraction *2*), which by g.l.c. consisted mainly of the same four compounds in the ratio 30:10:20:37 and a few other peaks (all < 1%). The eluent was then changed to 10:1 ether–methanol to give 0.36 g of a brown oil (fraction *3*), which by g.l.c. consisted of mainly **14** and **15** (7 and 17%, respectively) and 45% **5**. The total recovery was 1.70 g with the following composition: **12** (47%), **13** (17%), **15** (15%), **5** (9%), with the remainder totalling a maximum of 5% (all individually less than 1%). None of compound **6** could be detected. Sufficient quantities of compounds **12** to **15** were collected for spectral analysis:

Compound **12**: i.r., 1598, 1572 (w), 702 cm^{-1}: n.m.r. 7.01 (10H, s), 2.66 (4H, m), 1.67 (10H, br s); u.v. λ_{max} (C_6H_{12}) 246 sh (log ε 3.97) mμ; *m/e* 276 (P), 277 (P + 1, 23.4%), and the following prominent peaks: 115, 105, 91 (B), 77.

Compound **13**: i.r., 1600, 1585 (w), 1575 (w), 703 cm^{-1}; n.m.r. 7.22 (10H, s), 2.19 (4H, s), 1.48 (10H, br s); u.v. λ_{max} (C_6H_{12}) 245 sh (log ε 3.68) mμ.

Compound **14**: i.r. 1599, 1584 (w), 1574 (w) 702 cm^{-1}; n.m.r. 7.13 and 7.00 (10H), 5.79 (1H, t, J = 8.6), 4.22 (1H, m), 2.47 (2H, m), 1.71 (10H, br s); u.v. λ_{max} (C_6H_{12}) 238 sh (log ε 3.74) mμ; *m/e* 276 (P), 277 (P + 1, 23.1%), and the following additional prominent peaks: 205, 129, 117, 115, 91 (B).

Compound **15**: i.r. 1600, 702 cm^{-1}; n.m.r. 7.25 (10H, s), 5.85 (1H, d, J = 10), 3.30 (1H, m), 2.3 and 1.68 (12H); u.v. λ_{max} (C_6H_{12}) 274 (log ε 3.09), 2.67 (3.11), 260 (3.06), 254 (2.97), 224 inf (4.09) mμ; *m/e* 276 (P), 277 (P + 1, 23.4%), and the following additional prominent peaks: 205, 192, 179, 115, 91 (B).

5,5-Diphenylcyclononylamine (16)

Hydrogenation of the oxime of 5,5-diphenylcyclononanone was extremely slow, while reduction with lithium aluminum hydride gave mainly a secondary amine. To 6.2 g tosylate **1** dissolved in 120 ml dry dimethylsulfoxide was added 1.7 g sodium azide. The solution was stirred magnetically for 5 days at room temperature, poured into 250 ml cold water, and extracted with four 50 ml portions of ether. The combined ether portions were washed in turn with four 25 ml portions of water, dried over sodium sulfate, filtered, and concentrated to give 3.5 g of azide (i.r. 2100 cm^{-1}). This was dissolved in 150 ml dry tetrahydrofuran, 2.0 g lithium aluminum hydride added, and the mixture heated to reflux for 2 h,

Can. J. Chem. Downloaded from www.nrcresearchpress.com by 210.87.254.6 on 09/05/12
For personal use only.

then left stirring overnight. After the addition of 2 ml of water, 2 ml of 15% sodium hydroxide was added, followed by 6 ml of water. The resulting solid was filtered and the filtrate dried with sodium sulfate. After removal of solvent there remained 3.6 g of a colorless viscous oil. This was dissolved in 40 ml 95% ethanol and 80 ml of a saturated ethanolic picric acid solution added. The solution was heated to reflux, left overnight, and the picrate filtered and dried (dec. 236–238°).

Anal. Calcd. for $C_{27}H_{30}N_4O_7$: C, 62.06; H, 5.79; N, 10.72. Found: C, 62.15; H, 5.72; N, 10.60.

The picrate was dissolved in 400 ml of 5% sodium hydroxide solution (heated) and the amine extracted with three 100 ml portions of ether. The ether fractions were combined and washed with a small portion of 5% sodium hydroxide solution, then passed through about 50 g Rexyn 201 ion exchange resin, followed by 200 ml of ether. The ether solution was dried with sodium sulfate, filtered, and concentrated. The pure amine was dried under reduced pressure at 100° in a drying tube to give 1.45 g white solid, m.p. 95–96°, which turned brown on exposure to air. The overall yield was 38%, i.r. 3320 cm^{-1}; n.m.r. 7.27 (10H, s), 2.73 (s, 10), 3.7 (1H, m), 2.6–0.5 (16H, m).

Anal. Calcd. for $C_{21}H_{27}N$: C, 85.95; H, 9.27. Found: C, 85.73; H, 8.99.

Acetamide: m.p. 233–235° (from ethyl acetate – cyclohexane). i.r. (KBr) 3280, 2940, 1640, 1560, 1490, 1450, 750, 705 cm^{-1}; *m/e* 335 (P), 276, 206, 205, 193, 168, 167, 166, 140, 129, 127, 117, 115, 114, 100, 91 (B), 70, 60, 57, 56, 44, 43.

Anal. Calcd. for $C_{23}H_{29}NO$: C, 82.34; H, 8.71; N, 4.17. Found: C, 82.30; H, 8.49; N, 4.39.

Deamination of 5,5-Diphenylcyclononylamine

An attempt with sodium nitrite and trifluoroacetic acid gave large amounts of aromatic nitration (i.r., strong 1525 and 1350 cm^{-1}), possibly from the dinitrogen tetroxide produced. Substitution of isoamyl nitrite in trifluoroacetic acid gave an unknown solid, m.p. 190–195°, with a large increase in weight and no olefin after an hour at reflux. Hence glacial acetic acid was used. Amine **16** (0.54 g) was dissolved in 10 ml glacial acid in a 25 ml two-neck flask equipped with a septum and condenser with calcium chloride drying tube. Using a syringe, 290 μl (1.1 equiv) of freshly distilled isoamyl nitrite was added and the solution heated at reflux (bath 130°) with magnetic stirring for 5 h, then cooled and left stirring overnight. The solution was poured into 25 ml cold water, extracted with three 25 ml portions of ether, which in turn were combined and washed with two portions of water and saturated sodium bicarbonate solution, then dried. After filtration and ether removal there remained 0.8 g of a brown viscous oil (i.r., strong 1735 cm^{-1}). This was chromatographed on 40 g alumina. Fraction *1* (petroleum ether, 560 ml) gave 0.17 g of amber product which by g.l.c. (column *A*) and n.m.r. was shown to be a 62:38 mixture of compounds **2** and **4**. While slowly increasing the amount of methylene chloride up to 50%, 1050 ml were collected to give 0.25 g of an amber oil, which was identical by i.r. and n.m.r. (mixed with authentic) to 5,5-diphenylcyclononyl acetate (7) (decomposed under g.l.c. conditions). Recrystallization from petroleum ether (30–60°) gave the acetate as a white solid, m.p. 98–100°, (undepressed with authentic material). Elution with pure methylene chloride (350 ml) gave 0.1 g brown oil which by i.r. and n.m.r. was shown to be a 50:50 mixture (80:20 by weight) of 5,5-diphenylcyclononanol **5** and isoamyl alcohol. Hence, the overall yield was 0.50 g which consisted of 37% olefin, 46% acetate, and 17% alcohol.

5-Phenylazelanitrile (7)

This compound was synthesized by the method of Cope and Kinnel (13) using the reported dimethylsulfoxide method of nitrile synthesis rather than refluxing ethanol.

Dimethyl 5-Phenylazelate (8)

The dinitrile **17** (23 g) was hydrolyzed by heating at reflux for 16 h in 200 ml concentrated hydrochloric acid. The cooled solution was made basic with 15% sodium hydroxide, extracted with several portions of ether, then acidified to p*H* 2.

Extraction with ether gave 25 g of an amber liquid which was dissolved in 175 ml methanol and heated at reflux for 6 h in the presence of 10 ml concentrated sulfuric acid. The cooled solution was poured into water and extracted with three 150 ml portions of ether. The combined ethereal extracts were washed with saturated brine, dried, and evaporated. The residue was distilled and the fraction boiling from 185–191° (2.5 mm) was collected (n_D^{23} = 1.4950) to give diester **8** (21.4 g) in 67% yield.

5-Phenylcyclononanone (10)

Diester **8** (15.8 g) was cyclized in the same manner used in the preparation of **1** (7). The crude acyloin **9** (2.6 g) was isolated by distillation (b.p. 149–158° (0.2 mm)). This material was reduced by the same method used in the preparation of **1** and the product purified by column chromatography on 50 g of alumina. Elution with petroleum ether gave 0.4 g of hydrocarbon. The solvent was then changed gradually to pure methylene chloride and elution continued until a dark band was about to be eluted. Concentration of the fraction gave 0.6 g of a brown liquid which was purified by g.l.c. collection (8 ft × 0.5 in. 10% XE-60, 230°). The ketone **10** (0.34 g) was obtained in 3% yield from diester **8**. i.r.: 1704 cm^{-1}; n.m.r. 7.21 (5H, s), 2.43 (5H, m), 1.80 (10H, m).

Anal. Calcd. for $C_{15}H_{20}O$: C, 83.28; H, 9.32. Found: C, 82.98; H, 9.23.

1,5-(1,6)-Diphenylcyclononene (6)

To a solution of phenyl lithium prepared from 0.8 g each of bromobenzene and lithium wire (high sodium content) in 10 ml dry ether, 0.3 g of ketone **10** in 5 ml dry ether was added slowly. The solution was heated at reflux for 1 h, cooled and stirred for 2 h, then 15 ml water added. The aqueous layer was separated, extracted twice with 15 ml of ether, and the combined organic phases dried over sodium sulfate. After filtration and solvent removal there remained 0.5 g of a brown oil (i.r., strong OH), which was dissolved in 100 ml dry benzene containing a few crystals of iodine. The solution was heated at reflux for 26 h under a Dean–Stark water trap, then cooled and washed with 10 ml of saturated sodium thiosulfate solution, two 5 ml water portions,

and dried over sodium sulfate. The brown liquid (0.4 g) obtained was purified by preparative g.l.c. (8 ft × 0.50 in. 10% SE-30, 225°). The olefin had a retention time of about 40 min.

Compound **6**: i.r. 1665 (w), 1642 (w), 1600, 701 cm^{-1}; n.m.r. 7.27 and 7.13 (10H). 5.85 (1H, t, $J = 8.6$), 3.0–2.1 (5H, m), 1.70 (8H, m); u.v. λ_{max} (C_6H_{12}) 293 inf (log ε 2.31), 241 (3.86) mμ.

Anal. Calcd. for $C_{21}H_{24}$: C, 91.25; H, 8.75. Found: C, 90.98; H, 8.73.

Olefin Stability Tests

To 1.8 ml trifluoroacetic acid containing 70 mg (0.3 *M*) sodium trifluoroacetate and 80 mg *p*-toluenesulfonic acid (1 equiv) was added 100 mg of an olefin mixture consisting of 45% **2**, 45% **3**, and 10% **4**. This was stirred in a sealed vial for 23 h at 5° (heterogeneous throughout), poured into 15 ml saturated sodium bicarbonate solution, and extracted with ether. The ether layers were washed with water and dried over sodium sulfate. After filtration and solvent removal, the residue (i.r. small 1780 cm^{-1}) was shown by g.l.c. to consist of 27% **12**, 8% **13**, 54% **2** (no **3** in i.r.), and 11% **4**. Small amounts of **14** and **15** would have been obscured under the last two peaks and hence could not be detected.

After heating the same olefin mixture in 1 ml of glacial acetic acid containing 35 mg (1 equiv) *p*-toluenesulfonic acid at 35° for 35 h, the solution was worked-up in analogous manner. By i.r. and n.m.r. comparison of a mixture of known concentration, the product was estimated to contain 18% (23% by weight) of the acetate of **1**.

About 20 mg of the olefin **6** was dissolved 0.5 ml glacial acetic acid with 19 μl isoamyl nitrite, and the solution heated at reflux (130°) for 5 h, then left stirring overnight. After an identical work-up to that of the deamination product, the residue (i.r., strong 1740 cm^{-1}, acetate) was estimated by n.m.r. to be about 35% of the mixture.

Treatment of a 42 mg sample of the same olefin mixture used in the trifluoroacetolysis test in the same manner as the olefin **6** above resulted in complete isomerization of **3** to **2** (no **3** detectable by i.r. nor n.m.r.), with the formation of only a small amount of acetate.

The financial assistance from the National Research Council of Canada is gratefully acknowledged. We also thank Mr. D. Hill for technical assistance.

1. V. Prelog and J. G. Traynham. *In* Molecular rearrangements. Vol. 1. *Edited by* P. de Mayo. Interscience, New York, N.Y., 1963. p. 593.
2. A. C. Cope, M. M. Martin, and M. A. McKervey. Q. Rev. **20**, 119 (1966).
3. A. C. Cope, P. E. Burton, and M. L. Caspar. J. Am. Chem. Soc. **84**, 4855 (1962).
4. D. Bethel and V. Gold. Carbonium ions, an introduction. Academic Press, New York, N.Y., 1967.
5. J. B. Hendrickson. J. Am. Chem. Soc. **86**, 4854 (1964).
6. V. Prelog, H. Kagi, and E. H. White. Helv. Chim. Acta, **45**, 1658 (1962).
7. A. T. Blomquist and B. F. Hallam. J. Am. Chem. Soc. **81**, 676 (1959).
8. (*a*) E. White and D. J. Woodcock. *In* The chemistry of the amino group. *Edited by* S. Patai. Interscience, New York, N.Y., 1968. p. 440; (*b*) L. Friedman. *In* Carbonium ions. Vol. 2. *Edited by* G. A. Olah and P. R. Schleyer. Interscience, New York, N.Y. 1970. p. 655.
9. (*a*) T. Cohen and A. R. Daniewski. J. Am. Chem. Soc. **91**, 533 (1969); (*b*) M. Cocivera and S. Winstein. J. Am. Chem. Soc. **85**, 1702 (1963); (*c*) T. Cohen and E. Jankowski. J. Am. Chem. Soc. **86**, 4217 (1964).
10. C. D. Nenitzescu. *In* Carbonium ions. Vol. 1. *Edited by* G. A. Olah and P. R. Schleyer. Interscience, New York, N.Y., 1967. p. 64.
11. D. J. Cram and M. R. V. Sahyun. J. Am. Chem. Soc. **85**, 1257 (1963).
12. H. C. Brown and G. Ham. J. Am. Chem. Soc. **78**, 2735 (1956).
13. A. C. Cope and R. B. Kinnel. J. Am. Chem. Soc. **88**, 752 (1966).

Can. J. Chem. Downloaded from www.nrcresearchpress.com by 210.87.254.6 on 09/05/12
For personal use only.

Can. J. Chem. Downloaded from www.nrcresearchpress.com by 210.87.254.6 on 09/05/12
For personal use only.

Solvent Effects in Free Radical Copolymerization

A. M. CHATTERJEE[1] AND C. M. BURNS[2]
Department of Chemical Engineering, University of Waterloo, Waterloo, Ontario

Received May 13, 1971

Acrylamide and *N*-vinyl pyrrolidone were copolymerized at 60° in binary aqueous solutions containing 0, 5, 67, and 80% glycerol by weight. A marked increase in the reactivity of acrylamide relative to that of *N*-vinyl pyrrolidone was observed. This increase is interpreted in terms of the relative reactivity of monomer and polymeric radical in the reaction medium.

L'acrylamide et la *N*-vinyl pyrrolidone ont été copolymérisés à 60°, dans les solutions aqueuses binaires contenant 0, 5, 67 et 80% de glycérol en poids. Un accroissement notable de la réactivité de l'acrylamide par rapport à celle de la *N*-vinyl pyrrolidone a été observée. Cet accroissement s'interprète en termes de réactivité relative du monomère et du radical du polymère dans le milieu réactionnel.

Canadian Journal of Chemistry, **49**, 3249 (1971)

In our previous communication (1) we examined the effect of the molecular structure of the monomer on the relative reactivities of the two monomers in free radical copolymerization. We have now extended our investigations to determine what effect the solvent for the reaction can have on the relative reactivities of the two monomers.

Relative reactivities in nonaqueous media had been found to undergo very little change with varying dielectric constants (2, 3). In aqueous media, readily ionizable monomers such as methacrylic acid had relative reactivities which depended on the p*H* of the medium (4). These results were explained on the basis of different reactivities of ionized and unionized forms of the same species.

For our investigation we chose a relatively neutral aqueous medium with varying ratios of water and glycerol. For comonomers, we chose two amides, acrylamide (AA) and *N*-vinyl pyrrolidone (NVP). These two monomers, their homopolymers, and their copolymers were soluble in glycerol–water mixtures up to 80% glycerol by weight. From the analysis of the relative amounts of the two monomers assimilated into the copolymers at various relative concentrations of the two monomers, it was possible to determine the relative reactivity of the two monomers. By varying the solvent composition, the effect of solvent on the relative reactivity of the two monomers in free radical copolymerization could be determined.

Experimental

Materials

Acrylamide and *N*-vinyl pyrrolidone were purchased from Monomer-Polymer Laboratories, Philadelphia. The acrylamide was used as received; it was characterized by a melting point of 84.0 °C. *N*-vinyl pyrrolidone was purified by distillation under reduced pressure (13 mm Hg at 95 °C), using a Vigreaux column and retaining the middle fraction.

Cumene hydroperoxide (Matheson, Coleman and Bell) was stored at −5 °C and used as received. Glycerol (British Drug Houses Analar) and deionized water were used as solvents. Acetone (Fisher Scientific Company, Reagent Grade) was used for precipitation.

Polymerization Procedure

The monomers were copolymerized in glass polymerization tubes approximately 4.5 in. long by 1 in. in diameter. The comonomers, initiator, and solvent were introduced by syringe. Approximately 5 g of monomer mixture was used with 25 ml of the solvent mixture. The reaction mixture was subjected to repeated freezing and thawing under vacuum. After sealing, the tubes were immersed in a water bath maintained at 60 ± 0.1 °C. Conversions were kept below 10%.

The product was isolated after brief cooling by pouring the contents into 600 ml of acetone with stirring. Hydroquinone had been added to stop the polymerization. The copolymer which precipitated was removed by filtration and dried under vacuum. It was purified twice by redissolving in water and reprecipitating in acetone.

The homopolymer of acrylamide was prepared by the same procedure. The homopolymer of *N*-vinyl pyrrolidone was prepared by bulk polymerization at 60 °C for 12 h. The two homopolymers were purified in the same manner as the copolymers.

Analysis of the Composition of the Copolymers Formed

The composition of the AA–NVP copolymers was determined by ultraviolet absorption spectroscopy in

[1]Present address: Department of Polymer Science and Engineering, University of Massachusetts, Amherst, Massachusetts 01002, U.S.A.

[2]To whom correspondence should be addressed.

aqueous solution at room temperature, using a Bausch and Lomb Spectronic 505 Recording Spectrophotometer. Both poly (AA) and poly (NVP) were found to have an absorption maximum at 201 mμ. Absorbance at this wavelength for different concentrations of poly (AA) and poly (NVP) were determined and plotted against concentration. Beer's law was seen to be obeyed up to concentrations of 0.08 g/l for poly (AA) and 0.03 g/l for poly (NVP). Measurement of the slopes of the straight lines gave the specific extinction coefficients of 8.34 l g^{-1} cm^{-1} for poly (AA) and 26.50 l g^{-1} cm^{-1} for poly (NVP). Thus determination of the absorbance of a solution of a copolymer of known total copolymer concentration enables the relative amounts of AA and NVP in the copolymer to be determined. The composition of a copolymer determined by this photometric method was confirmed by CHN elemental analysis, to determine that possible complications in the ultraviolet analysis by interactions between groups in the same chain were not occurring.[3]

Binary Solvent Compositions

Four solvent media were used, containing 0, 5, 67, and 80% by weight glycerol.

Treatment of Data (1)

The relative reactivity of the two monomers is conveniently expressed in terms of the two reactivity ratios, r_1 (AA) and r_2 (NVP), where r_1 (AA) = k_{11}/k_{12} = the ratio of the rate constants for monomers AA and NVP adding to a polymer radical ending in AA. r_2 (NVP) = k_{22}/k_{21} = the ratio of the rate constants for monomers NVP and AA adding to a polymer radical ending in NVP. The values of r_1 and r_2 can be obtained from the copolymer composition equation which relates the copolymer composition to the comonomer composition and the reactivity ratios. Several methods including a computerized "least squares" method can be used.

Results and Discussion

The mole fraction of acrylamide assimilated into the copolymer at various comonomer compositions is shown in Fig. 1. Although there is some scatter in the data, there is a definite trend for the copolymer being formed to be more enriched in acrylamide at higher glycerol concentrations.

For copolymerization in water alone, there is a "cross-over" point beyond which at higher concentrations of acrylamide in the feed the copolymer is enriched in *N*-vinyl pyrrolidone. In this case each polymeric radical prefers the alternate monomer and the reactivity ratios are less than 1. From the linear "least squares" treatment of the data the values of r_1 and r_2 are 0.66 and 0.17,

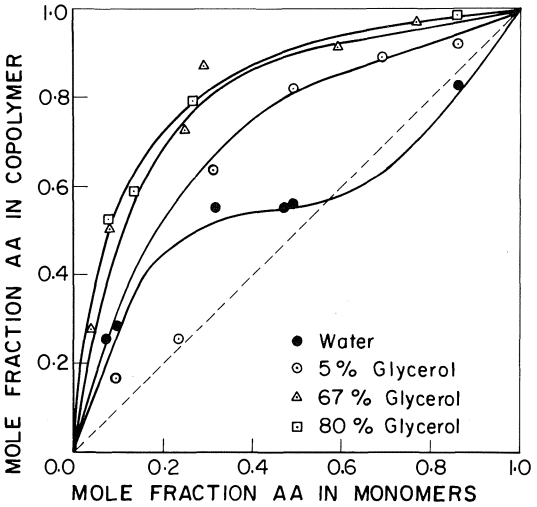

FIG. 1. Variations of copolymer composition with composition of comonomers at varying solvent compositions. AA, acrylamide. Comonomer *N*-vinyl pyrrolidone. 60°.

respectively. These values of r_1 and r_2 are consistent with the existence of a cross-over point or "azeotrope" shown in Fig. 1 since they are both less than unity (5). The linear "least squares" treatment was used to obtain the best fit of the experimental data. The standard deviations of the reactivity ratios obtained by this method are not reported, however, due to considerable controversy concerning their significance (6).

Although the reactivity ratios for this combination of monomers has not been reported before, an estimate of their reactivity ratios can be made from the Q and e values of the two monomers (7). Using average values obtained over widely varying temperatures, an estimate of r_1(AA) = 0.006 and r_2(NVP) = 0.0002 can be made. These estimates would predict an even stronger alternating tendency than was observed in this experiment. There is considerable uncertainty in the literature values of Q and e for these monomers, however, since they have not been copolymerized with monomers like styrene from which more reliable Q and e values can be obtained.

At higher glycerol concentrations in Fig. 1, there is a definite shift away from alternating behavior to increasing enrichment of the copolymer in acrylamide. The value of r_1 must be increasing with increasing glycerol concentration.

The changes in r_1 and r_2 with glycerol concen-

[3]Elemental analyses were performed in the laboratory of Alfred Bernhardt, 5251 Elbach uber Engelskirchen, Fritz-Pregl-Strasse 14–16, West Germany.

Can. J. Chem. Downloaded from www.nrcresearchpress.com by 210.87.254.6 on 09/05/12
For personal use only.

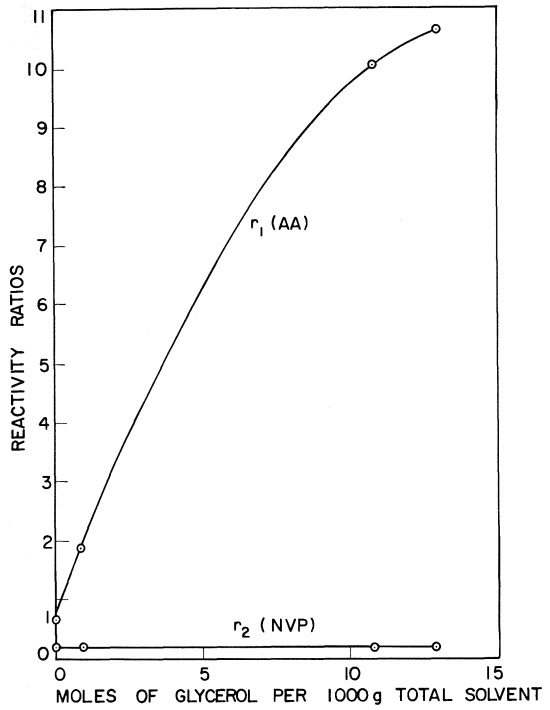

FIG. 2. Variation of reactivity ratios with composition of solvent. r_1, acrylamide; r_2, *N*-vinyl pyrrolidone.

tration can be seen more clearly in Fig. 2. A marked increase in r_1 occurs; r_2 decreases by about 35%. Each reactivity ratio represents the reactivity of the two monomers with that radical. The increase in r_1 corresponds to an increase in the relative reactivity of the acrylamide radical towards acrylamide monomer relative to *N*-vinyl pyrrolidone. The decrease in r_2 in turn corresponds to a decrease in the reactivity of the *N*-vinyl pyrrolidone radical towards *N*-vinyl pyrrolidone monomer relative to acrylamide monomer. However, r_2 only decreases from 0.17 to 0.11 while r_1 increases by a factor of 15 from 0.66 to 10.6. Thus the increase in the relative reactivity of acrylamide monomer as reflected in r_2 (or $1/r_2$) is not sufficient to account completely for the increase in r_1. Hence the presence of glycerol must also increase the reactivity of the polymeric acrylamide radical towards the acrylamide monomer in this copolymer system.

Specific influences of water have been observed earlier by DeSchryver, Smets, and Van Thielen (8). They investigated the homopolymerization of methacrylic acid in water–dioxane–ethanol mixtures and found that the rate of polymerization increased with the concentration of water at constant dielectric strength. At constant concentration of water, however, the rate of polymerization did not change with changes in the dielectric constant of the reaction medium. Using different solvents, Kerber (9) correlated the changes in the reactivity ratios of styrene and acrylic acid with associations of the solvent with acrylic acid through hydrogen bonding. Uno *et al.* (10) have concluded from a copolymerization study of acrylic esters with styrene in benzene and dioxane that the more polar solvent would break up the hydrogen bonding of the —NH and —OH groups of the monomer around the polymer. This work, then, indicates that the presence of glycerol enhances the hydrogen-bonding of acrylamide monomer to the polymer and in particular to the polymer radical ending in an acrylamide unit.

The authors gratefully acknowledge support for this research by the National Research Council of Canada and the Dean's Fund, Faculty of Engineering, University of Waterloo.

1. W. Y. LAU and C. M. BURNS. Can. J. Chem. **47**, 2057 (1969).
2. F. M. LEWIS, C. WALLING, W. CUMMINGS, E. R. BRIGGS, and F. R. MAYO. J. Am. Chem. Soc. **70**, 1519 (1948).
3. C. C. PRICE and J. G. WALSH. J. Polym. Sci. **6**, 239 (1951).
4. T. ALFREY, JR., C. G. OVERBERGER, and S. H. PINNER. J. Am. Chem. Soc. **75**, 4221 (1953).
5. P. J. FLORY. Principles of polymer chemistry. Cornell University Press, Ithaca, New York. 1953. p. 184.
6. P. W. TIDWELL and G. A. MORTIMER. Rev. Macromol. Chem. **5**, 135 (1970).
7. L. J. YOUNG. *In* Polymer handbook. *Edited by* J. Brandrup, and E. H. Immergut. Interscience, N.Y. 1966. pp. II-352, 361.
8. F. C. DESCHRYVER, G. SMETS, and J. VAN THIELEN. Polym. Lett. **6**, 547 (1968).
9. R. KERBER. Makromol. Chem. **96**, 30 (1966).
10. K. UNO, M. MAKITA, S. OOI, and Y. IWAKURA. J. Polym. Sci. (A-1) **6**, 257 (1968).

Can. J. Chem. Downloaded from www.nrcresearchpress.com by 210.87.254.6 on 09/05/12
For personal use only.

Can. J. Chem. Downloaded from www.nrcresearchpress.com by 210.87.254.105 on 09/05/12
For personal use only.

Synthesis and Reactivity of Halide Bridged, Cationic Complexes of Platinum and Palladium

K. R. Dixon and D. J. Hawke

Department of Chemistry, University of Victoria, Victoria, British Columbia

Received June 1, 1971

The chloride bridged complex, $[Pt_2Cl_2(PEt_3)_4][BF_4]_2$, reacts with C_2F_4 and H_2O or with aldehydes to yield *trans*-$[PtCl(CO)(PEt_3)_2][BF_4]$ and with HCOOH to cause catalytic decomposition of the acid to CO_2 and H_2. These reactions are of interest in mechanistic comparisons with other d^8 complexes. Similar reactions of related platinum and palladium complexes are also described, together with the synthesis of the new complexes, $[Pd_2X_2(PR_3)_4][BF_4]_2$, where X = Br or I for R = phenyl and X = Br for R = ethyl, *cis*-$[MCl(PEt_3)_2(Py)][BF_4]$ and $[MCl(PPh_3)_3][BF_4]$ where M = Pd or Pt.

Le complexe ponté chloruré, $[Pt_2Cl_2(PEt_3)_4][BF_4]_2$ réagit avec C_2F_4 et H_2O ou avec les aldéhydes pour donner $[PtCl(CO)(PEt_3)_2][BF_4]$-*trans*. Avec HCOOH le complexe provoque une décomposition catalytique de l'acide en CO_2 et H_2. Ces réactions sont intéressantes si l'on compare les mécanismes avec d'autres complexes d^8. Des réactions semblables, avec des complexes apparentés du platine et du palladium, sont également décrites. On rapporte aussi la synthèse de nouveaux complexes, $[Pd_2X_2(PR_3)_4][BF_4]_2$, où X = Br ou I pour R = phényle et X = Br pour R = éthyle, $[MCl(PEt_3)_2(Py)][BF_4]$-*cis* et $[MCl(PPh_3)_3][BF_4]$ où M = Pd ou Pt.

Canadian Journal of Chemistry, 49, 3252 (1971)

Introduction

Complexes of d^8 transition metal ions are currently the subject of intensive study and in particular many unusual reactions of $[RhCl(PPh_3)_3]$ and *trans*-$[IrCl(CO)(PPh_3)_2]$ have been described (1). Isoelectronic Pt(II) and Pd(II) systems have received less attention although the synthesis and some reactions of the *trans*-$[PtCl(CO)(PEt_3)_2]^+$ cation and related complexes have been reported (2–5).

In reactions of $[RhCl(PPh_3)_3]$ reactive intermediates are often formed by ligand substitution and we considered it possible that halogen bridged cations, $[M_2X_2(PR_3)_4]^{2+}$, where M = Pd or Pt, X = halogen and R = ethyl or phenyl, might generate similar intermediates by bridge cleavage. We therefore studied the reactivity of these species and the present paper reports their reactions with organic carbonyl compounds and a reaction with C_2F_4 and H_2O which also yields a carbonyl. No direct evidence for bridge cleavage as a first step has been obtained but the reactions appear mechanistically similar to those of Ir(I) and Rh(I) systems and represent the closest reactivity parallels yet obtained between the d^8 ions of the platinum and rhodium groups.

Results and Discussion

(1) Synthesis

The complexes, *trans*-$PdX_2(PR_3)_2$, where X = Cl, Br or I for R = phenyl and X = Cl or Br for R = ethyl, react with $AgBF_4$ (1 mol) in dry acetone to give the halogen bridged complexes, $[Pd_2X_2(PR_3)_4][BF_4]_2$, in high yield. Several studies of the synthesis of analogous platinum and palladium complexes have been reported previously, using reactions of $MX_2(PR_3)_2$ complexes with either BF_3 (2, 4) or $AgBF_4$ (6) but, of the above triethyl- and triphenylphosphine complexes of palladium, only the chlorides were known (3). We were unable to prepare $[Pd_2I_2(PEt_3)_4][BF_4]_2$ and we note that the platinum analogue is also unknown (4).

(2) Reactivity

Reactions of pyridine with $[M_2Cl_2(PEt_3)_4][BF_4]_2$, M = Pd or Pt, and of triphenyl phosphine with $[M_2Cl_2(PPh_3)_4][BF_4]_2$ give the new complexes *cis*-$[MCl(PEt_3)_2(Py)][BF_4]$ and $[MCl(PPh_3)_3][BF_4]$. The triphenylphosphine complexes are especially interesting since they are analogues of Wilkinson's complex, $[RhCl(PPh_3)_3]$, and were not accessible by the methods employed previously for the synthesis of $[MClL_3][BF_4]$ complexes (3).

Can. J. Chem. Downloaded from www.nrcresearchpress.com by 210.87.254.105 on 09/05/12
For personal use only.

(a) Reactions with Tetrafluoroethylene

Preliminary experiments with ethylene and cyclohexene gave no evidence of bridge cleavage reactions similar to the above but $[Pt_2Cl_2(PEt_3)_4][BF_4]_2$ (complex **1**) reacts with C_2F_4 at 80° in reagent grade acetone (~0.5% H_2O) to give the known complex, *trans*-$[PtCl(CO)(PEt_3)_2][BF_4]$, in high yield. $[Pt_2Cl_2(PPh_3)_4][BF_4]_2$ gives a similar reaction but palladium complexes give only degradation to palladium metal as is expected from the known instability (3) of *trans*-$[PdCl(CO)(PEt_3)_2][BF_4]$.

Similar hydrolyses have been reported previously in the reactions of $[RhCl(PPh_3)_3]$ (7) or *trans*-$[PtHCl(PEt_3)_2]$ (2) with C_2F_4 in the presence of traces of water to yield *trans*-$[RhCl(CO)(PPh_3)_2]$ or *trans*-$[PtCl(CO)(PEt_3)_2]^+$, respectively. In the rhodium reaction the π-C_2F_4 complex, *trans*-$[RhCl(C_2F_4)(PPh_3)_2]$, is an isolable intermediate but we have been unable to isolate a corresponding platinum complex in the reaction of **1**. In the absence of isolable intermediates, substituent effects or kinetic data, meaningful discussion of mechanism is not possible. However, we feel it is important to point out that the mechanism proposed[1] by Kemmitt and Nichols (7) for the hydrolysis of *trans*-$[RhCl(C_2F_4)(PPh_3)_2]$ is clearly incorrect in detail since the overall stoichiometry is

$$[RhCl(C_2F_4)(PPh_3)_2] + H_2O + H^+ \rightarrow [RhCl(CO)(PPh_3)_2] + \tfrac{1}{2}CF_2H.CF_2H + 2HF$$

The charge balance problem cannot be solved if $CF_2H.CF_2H$ is a product. In our reactions with **1**, no fluorocarbon products are detected[2] and the stoichiometry appears to be

$$[Pt_2Cl_2(PEt_3)_4]^{2+} + C_2F_4 + 2H_2O \rightarrow 2[PtCl(CO)(PEt_3)_2]^+ + 4HF$$

although the estimate is subject to error in that the two platinum complexes are difficult to separate, leading to possible error in the yield of carbonyl. We consider that the rhodium and platinum reactions are likely to have similar mechanisms and that $CF_2H.CF_2H$ is a product of some side reaction in the rhodium case. Further work is in progress to test this suggestion.

(b) Reactions with Aldehydes

1 reacts with benzaldehyde at 80° in acetone to yield *trans*-$[PtCl(CO)(PEt_3)_2][BF_4]$ and benzene. The conditions and yields for reactions of **1** with other aldehydes (Table 2) suggest that the order of reactivity is $CCl_3CHO > C_6H_5CHO > CH_3CHO > n\text{-}C_6H_{13}CHO$, although CCl_3CHO functions mainly as a chlorinating agent. $[Pt_2Cl_2(PPh_3)_4][BF_4]_2$, with more electron withdrawing phosphines than **1**, does not react with benzaldehyde at 80°.

Decarbonylation of aldehydes by $[RhCl(PPh_3)_3]$ has been extensively studied by Wilkinson and co-workers (8) who propose a mechanism involving nucleophilic attack by the metal on the carbon atom of the aldehyde, leading to oxidative addition of the aldehyde C—H bond to the metal. This mechanism should be promoted by electron withdrawing substituents on the aldehyde, and by electron donating ligands on the metal, and our results are therefore consistent with the operation of a similar mechanism with bridge cleavage replacing the initial ligand substitution step.

In reactions with other carbonyl compounds, **1** gives some decarbonylation of acetyl chloride although the main reaction is chlorination of the platinum complex giving *cis*-$[PtCl_2(PEt_3)_2]$. Reaction of **1** with acetone gives no evidence of decarbonylation.

(c) Reactions with Formic Acid

1 does not react with benzoic or acetic acid but it catalytically decomposes formic acid to CO_2 and H_2 at a rate similar to those reported previously (9) for other transition metal complexes. Degradation of the catalyst is quite rapid in our system and the products include *trans*-$[PtCl(CO)(PEt_3)_2][BF_4]$, which suggests that catalysis proceeds according to Scheme 1.

The feasibility of the scheme is confirmed by reaction of *trans*-$[PtHCl(PEt_3)_2]$ with fluoroboric acid to give **1** and H_2 in good yield. Also, the hydrolysis of *trans*-$[PtCl(CO)(PEt_3)_2]^+$ to *trans*-$[PtHCl(PEt_3)_2]$ and CO_2 is known and its mechanism has been discussed in terms of an intermediate $[PtCl(COOH)(PEt_3)_2]$ complex (5).

$[Pt_2Cl_2(PPh_3)_4][BF_4]_2$ gives a similar, but

[1]A similar mechanism has been proposed for analogous reactions of iridium complexes (17).

[2]Except C_4F_8 which is a normal trace product of heating C_2F_4.

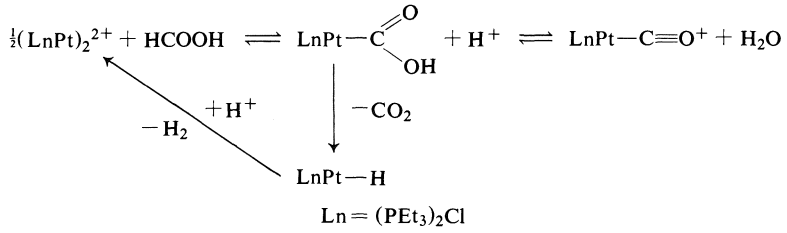

SCHEME 1

slower, catalytic decomposition of formic acid and the solid products show infrared absorptions at 3500 (wb), 2110 (s), and 1650 (sb) cm^{-1}, consistent with the presence of a carbonyl and a carboxylic intermediate. The carboxylic acid could be formed by oxidative addition to platinum of the C—H bond of the aldehyde, followed by proton loss. The oxidative addition step should be slower for more positive metal centers (1) and in agreement with this we find that $[Pt_2Cl_2(PPh_3)_4][BF_4]_2$ reacts 10 times slower than **1** and $[Pd_2Cl_2(PEt_3)_4][BF_4]_2$ shows essentially no catalytic activity. Carboxylic complexes of iridium have recently been isolated and shown to undergo pyrolysis to CO_2 and a hydride complex (10). However, formates have been shown to undergo similar reactions (11, 12) and, since the 3500 cm^{-1} infrared absorption is very weak, the possibility that the intermediate is more correctly formulated as a formate, [LnPt(HCOO)], cannot be excluded at present.

Our reactions generally gave less H_2 than CO_2 but no explanation for this is available at present.

Experimental

Reactions 1–3 below were conducted in an atmosphere of dry nitrogen and reactions 4–7 in evacuated, thick-walled Pyrex glass tubes (~50 ml capacity) or in an evacuated, stainless steel autoclave (60 ml capacity). Products were stable and were isolated and purified in the atmosphere. The solvents used for recrystallizations are included in Table 1. Where solvent pairs were used, the second solvent was added dropwise to a concentrated solution of the complex in the first solvent until crystallization began.

Complexes, *trans*-$[PdX_2(PR_3)_2]$ (3) and *trans*-$[PtHCl(PEt_3)_2]$ (13), were prepared as previously described. $[Pt_2Cl_2(PEt_3)_4][BF_4]_2$ and $[Pt_2Cl_2(PPh_3)_4][BF_4]_2$ were prepared as previously described (3) or by a procedure similar to 1(*a*) below. Solvents and organic reagents were dried over molecular sieves (type 4A) before use.

Details of the characterization of new complexes are included in Table 1. The conductance measurements were made on $\sim 10^{-3}$ *M* solutions in nitromethane using a dip-type cell connected to a conductivity bridge, Model RC16B2 of Industrial Instruments Inc. The results obtained are in the ranges expected for 1:1 or 1:2 electrolytes as appropriate (14).

Infrared spectra were recorded, with accuracy ± 5 cm^{-1} from 4000 to 250 cm^{-1}, for all products described below, using a Beckman IR 20 spectrophotometer calibrated against polystyrene film or water vapor. Where additional characterization is not given these served to identify the products. Absorptions other than those due to internal vibrations of ligands or anions are included in Table 1. Although the assignment of absorptions *ca.* 400 cm^{-1} to metal–phosphorus stretching modes has been shown to be incorrect (15), these absorptions are included in Table 1 since the number of bands in this region may still be used to assign stereochemistry, especially in complexes of triethylphosphine (16). The complexes, $[MCl(PEt_3)_2(Py)][BF_4]$, M = Pd or Pt, were assigned *cis* stereochemistry on the basis of infrared and nuclear magnetic resonance criteria as discussed previously (2).

(1) Preparation of $[Pd_2X_2(PR_3)_4][BF_4]_2$ Complexes

(*a*) A solution of *trans*-$[PdBr_2(PEt_3)_2]$ (0.50 g. 1.0 mmol) in acetone (~10 ml) was added dropwise to a stirred solution of $AgBF_4$ (0.196 g, 1.0 mmol) in acetone (~10 ml) at 25°. After stirring for 30 min, filtration gave AgBr (0.170 g, 0.90 mmol). The filtrate was evaporated under reduced pressure to small volume (~2–5 ml) and added to diethyl ether (~100 ml) giving $[Pd_2Br_2(PEt_3)_4][BF_4]_2$ (0.39 g, 0.38 mmol) as a yellow precipitate.

(*b*) A similar procedure using *trans*-$[PdI_2(PEt_3)_2]$ with $AgBF_4$ gave a more complex reaction whose products could not be characterized.

(*c*) A similar procedure using a suspension of *trans*-$[PdBr_2(PPh_3)_2]$ (0.20 g, 0.025 mmol) in acetone with $AgBF_4$ (0.056 g, 0.029 mmol) gave AgBr (0.046 g, 0.025 mmol) and $[Pd_2Br_2(PPh_3)_4][BF_4]_2$ (0.19 g, 0.012 mmol).

(*d*) A similar procedure at −10° using a suspension of *trans*-$[PdI_2(PPh_3)_2]$ (0.27 g, 0.30 mmol) in acetone with $AgBF_4$ (0.06 g, 0.30 mmol) gave AgI (0.064 g, 0.27 mmol) and $[Pd_2I_2(PPh_3)_4][BF_4]_2$ (0.22 g, 0.13 mmol). *Trans*-$[PdI_2(PPh_3)_2]$ (0.02 g, 0.02 mmol) was present in the AgI precipitate.

(*e*) Similar procedures using *trans*-$[PdCl_2(PEt_3)_2]$ or *trans*-$[PdCl_2(PPh_3)_2]$ with $AgBF_4$ gave the known complexes $[Pd_2Cl_2(PEt_3)_4][BF_4]_2$ and $[Pd_2Cl_2(PPh_3)_4][BF_4]_2$ in ~90% yield, much better than the 30–40% yields obtained previously using BF_3 instead of $AgBF_4$.

(2) Reactions with Pyridine

(*a*) **1** (0.11 g, 0.10 mmol) was heated with pyridine (0.055 g, 0.70 mmol) in acetone (5 ml) under reflux for

Can. J. Chem. Downloaded from www.nrcresearchpress.com by 210.87.254.105 on 09/05/12
For personal use only.

Can. J. Chem. Downloaded from www.nrcresearchpress.com by 210.87.254.105 on 09/05/12
For personal use only.

TABLE 1. Characterization data

Compound	Color	Melting point (°C)	Recryst. solvents	%C		%H		Molar conductance (ohm^{-1} cm^2)	Infrared ν(M—X)	(Nujol mulls), cm^{-1} 400–450 region*
				Calcd.	Found	Calcd.	Found			
$[Pd_2Br_2(PEt_3)_4][BF_4]_2$	Yellow	140–145 dec.	CH_3OH–$(C_2H_5)_2O$	28.3	28.9	5.9	6.1	197	<250	420 w 435 w
$[Pd_2Br_2(PPh_3)_4][BF_4]_2$	Yellow	~250 dec.	CH_3NO_2–$(C_2H_5)_2O$	54.2	53.9	3.8†	3.7	162	<250	445 w 415 w
$[Pd_2I_2(PPh_3)_4][BF_4]_2$	Orange	215–220 dec.	CH_3NO_2–$(C_2H_5)_2O$	51.2	51.5	3.6	3.8	165	<250	455 w 420 w
cis-$[PtCl(PEt_3)_2(Py)][BF_4]$	Colorless	212–215	$(CH_3)_2CO$–$(C_2H_5)_2O$	32.3	32.6	5.6	5.6	93	315 m	435 w 415 w
cis-$[PdCl(PEt_3)_2(Py)][BF_4]$	Colorless	203–205	$(CH_3)_2CO$–$(C_2H_5)_2O$	37.6	37.5	6.5	6.4	95	305 m	440 w 425 w
$[PtCl(PPh_3)_3][BF_4]$	Colorless	265–275 dec.	abs. CH_3OH	58.8	59.1	4.1‡	4.9	77	317 m	420 m 440 m
$[PdCl(PPh_3)_3][BF_4]$	Yellow	~230 dec.	CH_3NO_2–$(C_2H_5)_2O$	63.9	63.3	4.5	4.9	80	312 m	430 sh 420 m

*See experimental section.
†%F; Calcd., 9.5; Found, 10.3.
‡%F; Calcd., 6.9; Found, 7.3.

TABLE 2. Reactions of complexes, $[M_2Cl_2(PR_3)_4][BF_4]_2$, with R′CHO

M	R	R′	Conditions*	Results
Pt	C_2H_5	C_6H_5	80°, 48 h	65% $[PtCl(CO)(PEt_3)_2][BF_4]$
Pt	C_6H_5	C_6H_5	80°, 48 h	No reaction
Pt	C_2H_5	CH_3	80°, 48 h	20% $[PtCl(CO)(PEt_3)_2][BF_4]$
Pt	C_2H_5	*n*-C_6H_{13}	110°, 20 h Acetone solvent†	No reaction
Pt	C_2H_5	C_6H_5	100°, 3 h N_2 atmosphere	No reaction
Pt	C_2H_5	CCl_3	Reflux (98°) 3 h N_2 atmosphere	76% $[PtCl_2(PEt_3)_2]$ 10% $[PtCl(CO)(PEt_3)_2][BF_4]$
Pd	C_2H_5	C_6H_5	80°, 48 h	Degradation to metallic Pd

*Unless stated otherwise, reactions were conducted in evacuated thick-walled glass tubes without solvent.
†A reaction without solvent gave extensive decomposition of the heptanaldehyde but no evidence for $[PtCl(CO)(PEt_3)_2][BF_4]$.

8 h. Addition of the resulting solution to diethyl ether (~200 ml) gave *cis*-$[PtCl(PEt_3)_2(Py)][BF_4]$ (0.126 g, 0.199 mmol) as a white precipitate.

(*b*) A similar procedure using $[Pd_2Cl_2(PEt_3)_4][BF_4]_2$ (0.093 g, 0.10 mmol) with pyridine (0.055 g, 0.70 mmol) gave *cis*-$[PdCl(PEt_3)_2(Py)][BF_4]$ (0.095 g, 0.175 mmol).

(3) Reactions with Triphenylphosphine

(*a*) $[Pt_2Cl_2(PPh_3)_4][BF_4]_2$ (0.120 g, 0.071 mmol) was stirred in CH_3NO_2 (3 ml) with PPh_3 (0.050 g, 0.190 mmol) at 25° for 30 min. Addition of the resulting solution to diethyl ether (~100 ml) gave $[PtCl(PPh_3)_3][BF_4]$ (0.153 g. 0.139 mmol) as a white precipitate.

(*b*) A similar procedure using $[Pd_2Cl_2(PPh_3)_4][BF_4]_2$ (1.568 g, 1.04 mmol) with PPh_3 (0.61 g, 2.3 mmol) in CH_3NO_2 (20 ml) gave $[PdCl(PPh_3)_3][BF_4]$ (1.96 g, 1.93 mmol) as a precipitate from diethyl ether (~300 ml).

(4) Reactions with C_2F_4

(*a*) **1** (0.162 g, 0.147 mmol) was heated with a large excess of C_2F_4 (~10 mmol) in reagent grade acetone (3 ml) at 110° for 20 h in a thick-walled glass tube. Small amounts of CO_2 and cyclo-C_4F_8 were detected in the gaseous products. Addition of the solution to diethyl ether gave *trans*-$[PtCl(CO)(PEt_3)_2][BF_4]$ (0.155 g, 0.266 mmol) as a white precipitate which was recrystallized from benzene. M.p. 168–170° (lit. (2) 168–171°). The glass reaction tube was visibly etched suggesting that HF had been formed during the reaction.

Various similar experiments using lower temperatures and carefully dried solvents gave no evidence of an isolable intermediate olefin complex.

At lower C_2F_4 pressures the yield of carbonyl was poor but an estimate of the reaction stoichiometry was possible. For example, **1** (0.209 g, 0.189 mmol) with C_2F_4 (0.064 g, 0.64 mmol) at 85° for 20 h in a steel autoclave gave $[PtCl(CO)(PEt_3)_2][BF_4]$ (0.130 g, 0.224 mmol). Infrared and mass spectral analysis of the gaseous products showed only C_2F_4 (0.055 g, 0.55 mmol).

(*b*) A similar procedure using $[Pt_2Cl_2(PPh_3)_4][BF_4]_2$ (0.15 g, 0.09 mmol) with C_2F_4 (~50 mmol) in CH_2Cl_2 (5 ml) at 110° for 60 h in a steel autoclave gave $[PtCl(CO)(PPh_3)_2][BF_4]$ (0.07 g, 0.08 mmol).

(*c*) Preliminary experiments under similar conditions using $[Pd_2Cl_2(PEt_3)_4][BF_4]_2$ gave only degradation to palladium metal.

(5) Reactions with Aldehydes

(*a*) **1** (0.18 g, 0.16 mmol) was heated with C_6H_5CHO (4.0 ml, 39 mmol) at 80° for 48 h in a thick-walled glass tube. Excess benzaldehyde was removed under vacuum and the residue dissolved in acetone. Addition of the resulting solution to diethyl ether gave $[PtCl(CO)(PEt_3)_2][BF_4]$ (0.12 g, 0.21 mmol) as a white precipitate. After recrystallization from benzene it had m.p. 168–169° (lit. (2), 168–171°). Analysis of the excess benzaldehyde by gas–liquid chromatography showed the presence of benzene (~0.15 mmol).

(*b*) Reactions with other complexes and aldehydes were carried out in a similar manner and the results are summarized in Table 2.

(6) Reactions with Carboxylic Acids

(*a*) **1** (0.11 g, 0.10 mmol) was heated with HCOOH (2.00 g, 43.6 mmol) in acetone (5 ml) at 110° for 20 h in a steel autoclave. Separation of the volatile products by standard vacuum techniques gave CO_2 (34.6 mmol) and H_2 (26.6 mmol) which were identified by mass and infrared spectroscopy. This corresponds to a rate of acid decomposition ~0.2 mol l^{-1} h^{-1} (*cf.* ref. 9). Addition of the acetone solution to diethyl ether gave **1** (0.04 g, 0.036 mmol) whose infrared spectrum showed the presence of some $[PtCl(CO)(PEt_3)_2][BF_4]$, $\nu(C{\equiv}O)$ = 2110 cm^{-1}. Similar reactions in glass tubes using smaller quantities of HCOOH gave higher rates of catalyst recovery. For example after ~75 catalytic cycles (measured by CO_2 evolution) 70% of **1** was recovered. In some experiments the solid products showed very weak infrared absorptions at 2200 and 2160 cm^{-1}.

(*b*) A similar procedure using $[Pt_2Cl_2(PPh_3)_4][BF_4]_2$ (0.126 g, 0.075 mmol) with HCOOH (2.00 g, 43.6 mmol) gave CO_2 (~3.5 mmol) and H_2 (~3.5 mmol). The solid products (0.124 g) had infrared absorptions at 3500 (vb), 2110 (s), and 1650 (b) cm^{-1} but pure complexes could not be isolated.

(*c*) A similar procedure using $[Pd_2Cl_2(PEt_3)_4][BF_4]_2$ (0.093 g, 0.10 mmol) with HCOOH (2.00 g, 43.6 mmol) gave traces of CO_2 (~0.1 mmol) and H_2 (~0.1 mmol)

Can. J. Chem. Downloaded from www.nrcresearchpress.com by 210.87.254.105 on 09/05/12
For personal use only.

and recovery of $[Pd_2Cl_2(PEt_3)_4][BF_4]_2$ (0.090 g, 0.097 mmol) contaminated with formate ion.

(*d*) Similar procedures using **1** with benzoic or acetic acid gave no evidence of reaction except for some replacement of BF_4^- by acetate.

(7) Other reactions

(*a*) **1** (0.11 g, 0.10 mmol) was heated in acetone (15 ml) at 80° for 200 h in a thick-walled glass tube. There was no evidence for formation of *trans*-$[PtCl(CO)(PEt_3)_2][BF_4]$.

(*b*) **1** (0.11 g, 0.10 mmol) was heated in acetyl chloride (0.5 ml) at 80° for 48 h in a thick-walled glass tube. Addition of the solution to light petroleum gave *cis*-$[PtCl_2(PEt_3)_2]$ (0.09 g, 0.18 mmol) as a white precipitate. Evaporation of the filtrate gave a residue whose infrared spectrum showed the presence of *trans*-$[PtCl(CO)(PEt_3)_2][BF_4]$.

(*c*) *Trans*-$[PtHCl(PEt_3)_2]$ (0.19 g, 0.41 mmol) was heated with 48% aqueous HBF_4 (0.1 ml) in acetone (5 ml) at 70° for 90 min in a glass tube. H_2 was detected in the gaseous products by mass spectrometry. Addition of the solution to diethyl ether gave **1** (0.075 g, 0.068 mmol) as a white precipitate. The filtrate contained mainly unreacted *trans*-$[PtHCl(PEt_3)_2]$.

We thank the National Research Council of Canada and the University of Victoria for research grants and the University of Victoria for a postgraduate scholarship (to D.J.H.).

1. J. P. Collman and W. R. Roper. *In* Advances in organometallic chemistry. Vol. 7. *Edited by* F. G. A. Stone and R. West. Academic Press, New York and London. 1968. p. 53.
2. H. C. Clark, K. R. Dixon, and W. J. Jacobs. J. Am. Chem. Soc. **90**, 2259 (1968).
3. H. C. Clark and K. R. Dixon. J. Am. Chem. Soc. **91**, 596 (1969).
4. H. C. Clark, K. R. Dixon, and W. J. Jacobs. J. Am. Chem. Soc. **91**, 1346 (1969).
5. H. C. Clark and W. J. Jacobs. Inorg. Chem. **9**, 1229 (1970).
6. D. A. Duddell, P. L. Goggin, R. J. Goodfellow, M. G. Norton, and J. G. Smith. J. Chem. Soc. A, 545 (1970).
7. R. D. W. Kemmitt and D. I. Nichols. J. Chem. Soc. A, 1577 (1969).
8. M. C. Baird, C. J. Nyman, and G. Wilkinson. J. Chem. Soc. A, 348 (1968).
9. R. S. Coffey. Chem. Commun. 923 (1967).
10. A. J. Deeming and B. L. Shaw. J. Chem. Soc. A, 443 (1969).
11. K. R. Laing and W. R. Roper. J. Chem. Soc. A, 1889 (1969).
12. L. Marangoni, A. Andreatta, G. F. Terrari, and G. F. Pregaglia. Chim. Ind. **52**, 862 (1970).
13. J. Chatt and B. L. Shaw. J. Chem. Soc. 5075 (1962).
14. N. S. Gill and R. S. Nyholm. J. Chem. Soc. 3997 (1959).
15. K. Shobatake and K. Nakamoto. J. Am. Chem. Soc. **92**, 3332 (1970).
16. P. L. Goggin and R. J. Goodfellow. J. Chem. Soc. A, 1462 (1966).
17. B. Clarke, M. Green, and F. G. A. Stone. J. Chem. Soc. A, 951 (1970).

Can. J. Chem. Downloaded from www.nrcresearchpress.com by 210.87.254.105 on 09/05/12
For personal use only.

Can. J. Chem. Downloaded from www.nrcresearchpress.com by 210.87.254.105 on 09/05/12
For personal use only.

Absolute Configuration of Scopolamine *N*-Oxide and of Related Compounds[1]

CAROL SAUNDERSON HUBER
Division of Biochemistry, National Research Council of Canada, Ottawa, Canada

GABOR FODOR
Department of Chemistry, West Virginia University, Morgantown, West Virginia 26506

AND

NAGABHUSHANAM MANDAVA
U.S. Department of Agriculture, Plant Science Research Division, Agricultural Research Service, Beltsville, Maryland 20705

Received April 13, 1971

Structure analysis of (−) scopolamine *N*-oxide (**1**) hydrobromide monohydrate by X-ray crystallography has proven that the *N*-methyl group is axial and the amineoxide function is equatorial. The absolute configuration of the tropic acid residue has also been determined by anomalous scattering as being *S*, in complete agreement with chemical correlation experiments.

The *N*-stereoisomer of **1** has also been detected as a minor product **2** for the first time, as a result of using 100 MHz n.m.r. spectroscopy in the product analysis of the oxidation of (−) scopolamine with hydrogen peroxide in ethanol. A similar n.m.r. study was undertaken with atropine and tropine and correlation of chemical shifts with *N*-configuration in the *N*-oxides, **3**–**6**, was attempted. *N*-oxidation of scopolamine, and by analogy of related tropane bases, has taken a preferentially equatorial course, similar to other quaternization reactions.

L'analyse de la structure du monohydrate de l'hydrobromure du *N*-oxide (**1**) de la (−) scopolamine par cristallographie RX a prouvé que le groupe *N*-méthyle est axial et que la fonction aminéoxyde est équatoriale. La configuration absolue du résidu, l'acide tropique, a également été déterminée par diffusion anormale comme étant *S*, ce qui est en parfait accord avec les expériences de corrélation chimiques. Le *N*-stéréoisomère de **1** a été aussi détecté pour la première fois, comme un produit secondaire **2** par l'utilisation de la spectroscopie r.m.n. à 100 MHz dans l'analyse du produit provenant de l'oxydation de la (−) scopolamine par le peroxyde d'hydrogène dans l'éthanol. Une étude r.m.n. semblable a été entreprise avec l'atropine et la tropine et un essai de corrélation des déplacements chimiques avec la configuration-*N* dans les *N*-oxydes, **3**–**6**, a été fait. La *N*-oxydation de la scopolamine et par analogie avec ce qui a été fait sur le tropane a provoqué une orientation préférentiellement équatoriale, ce qui est similaire aux autres réactions de transformation en dérivés quaternaires.

Canadian Journal of Chemistry, **49**, 3258 (1971)

The steric course of electrophilic additions to nitrogen, particularly of quaternizations has been extensively studied during the last 15 years (1–7). The most adequate model chosen by one of us (G.F. and his associates (1)) was the 3-azabicyclo[3.2.$1^{1,1,5}$]octane, *i.e.* nortropane, system for three main reasons. Firstly, because it represents the skeleton of a wide-spread group of natural products of considerable practical, especially pharmacological interest. Secondly, because it is a half-rigid system where the product of quaternization closely resembles the transition state, unlike piperidines, which easily undergo conformational changes, thus making conclusions drawn from product as to transition state geometry rather risky. Thirdly, unusually high steric selectivity was observed (1, 8) when *N*-alkylating or carboxymethylating tropane bases (1). After a long-lasting polemic over equatorial (1) *vs.* axial (5) course, quite recently a critical summary paper (8) appeared on tropane quaternization. A variety of alkyl and substituted alkyl groups were used herein and the conclusions were based on X-ray structure determinations of four well-characterized major products combined with n.m.r. product analysis of quaternizations and chemical correlation between the major products. These data, along with those achieved by Bottini *et al.* (2), have proven that the major attack on nitrogen was equatorial (1, 8) in all those cases. Thus, some of the previous axial assignments (9, 10) of configuration based on empirical n.m.r. had to be revised.

The present paper deals with the structure

[1]NRCC No. 12090.

Can. J. Chem. Downloaded from www.nrcresearchpress.com by 210.87.254.105 on 09/05/12
For personal use only.

analysis of the major product of *N*-oxidation of scopolamine, itself commercially available and used as an ingredient of the sleeping pill "Sominex". It was claimed by Polonovski (11) that **1**, when heated, underwent transannular reaction to a tetrahydro 1,4-oxazol derivative "scopylium bromide", thus substantiating the axial position for the *N*-oxide function. On the other hand, the position of the *N*-methyl n.m.r. signal in both **1** and its hydrobromide seemed to be in line with N—Me equatorial position (10) due to deshielding through space by the epoxide atom (12).

In order to get the final answer to this configurational problem an X-ray study was commenced by one of us (C.S.H.) and is being described now in detail. Furthermore, a new n.m.r. investigation was carried out on a number of *N*-oxides of the tropane series.

Crystal Data

Scopolamine *N*-oxide hydrobromide monohydrate, $C_{17}H_{22}NO_5Br.H_2O$, mol.wt. = 418.3 Orthorhombic, $a = 13.115\,(10)$, $b = 21.131\,(15)$, $c = 6.740\,(6)$ Å (based on $\lambda\,(CuK\alpha_1) = 1.54051$ and $\lambda\,(CuK\alpha_2) = 1.54433$ Å). $D_m = 1.47_3$ g cm^{-3}, $Z = 4$, $D_x = 1.487$ g cm^{-3}, $V = 1867.9$ Å^3. Space group: $P2_12_12_1$. $\mu(CuK\alpha) = 35.9_9$ cm^{-1}.

Experimental

The colorless lath-shaped crystals belong to the orthorhombic system. Systematic absences $h00$ if h is odd, $0k0$ if k is odd, and $00l$ if l is odd, which were observed on preliminary Weissenberg and precession photographs, showed the space group to be $P2_12_12_1$. The density was measured by flotation in a bromobenzene–chlorobenzene mixture.

A crystal of 0.22 × 0.19 mm in cross-section was cut to a length (along b) of about 0.32 mm and mounted with b parallel to the ϕ-axis of a Picker diffractometer. Cell dimensions and relative intensities were measured at room temperature with Cu radiation, using a scintillation counter and pulse-height analyzer. A Ni filter was used for the cell dimension measurements and for remeasuring (at reduced tube current) all intensities with initial peak counts over 6000, but not for recording the weaker intensities. The adequacy of the pulse-height analyzer in discriminating against Cu$K\beta$ radiation was confirmed by checking the profiles of many low-angle reflexions; no discernable Cu$K\beta$ peak was present except in the case of a few of the strongest reflexions, all of which were included in the remeasurements. The θ–2θ scan technique was used with scan ranges varying from 2.0 to 4.0° in 2θ, and a 2θ scan speed of 2 deg min^{-1}. Background counts were accumulated for 20 s at the beginning and end of each scan. Reflexions with net count less than 10, or for which the net count was less than 1/10 of the total background count, were considered "unobserved" and were given zero weight in subsequent least-squares calculations. Of the 1845 independent reflexions with $2\theta < 130°$, 1800 were "observed". A standard reflexion was monitored at frequent intervals during the data collection, and these standard intensities were used to reduce all the intensities to the same relative scale. Appropriate Lorentz-polarization corrections were applied, and the intensities were also corrected for absorption using a Gaussian integration formula. With a grid of 6 × 10 × 6 subdivisions (parallel to ***a***, ***b***, ***c***) the calculated transmission factors varied from 0.455 to 0.589.

Structure Solution and Refinement

The coordinates of the bromine atom were obtained from an unsharpened three-dimensional Patterson map. An electron-density map phased on the Br atom showed 22 of the other 24 non-hydrogen atoms in the structure, and the remaining two atoms were revealed on a subsequent difference map. All of these atoms were entered in the block-diagonal least-squares calculations as carbon initially; the nitrogen and oxygen atoms were identified as their temperature factors dropped to anomalously low values. All but one of the hydrogen atoms were located on difference maps during the course of the refinement. Initially their contributions were included in the structure factors; later their parameters were refined also. The last hydrogen atom, belonging to the water molecule, was located only on the final difference map. Its position, however, is probably quite reliable as it forms the missing link in a very reasonable hydrogen bonding scheme, to be discussed later.

Anomalous scattering corrections (13) were introduced for the bromine atom during the analysis and structure factors were calculated for both possible absolute configurations. The ratio between the two R values, 0.0593/0.0504, is more than large enough, according to Hamilton's test (14), to establish the correctness of the configuration giving the lower R value. Continued refinement with the correct absolute configuration led to a final R value of 0.045 for all observed reflexions. During the final least-squares cycle the average ratio of parameter shift/estimated standard deviation was 0.11; the largest shift for the non-hydrogen atom parameters was 0.4 σ.

The quantity minimized in the least-squares calculations was $\sum\omega(|F_o| - |F_c|)^2$. Various weighting schemes were used successively during the refinement; these were chosen to minimize the dependence of $\sum\omega\Delta^2$ on $|F_o|$ and on $\sin^2\theta$. The final scheme was of the form

Can. J. Chem. Downloaded from www.nrcresearchpress.com by 210.87.254.105 on 09/05/12
For personal use only.

Table 1(a). Fractional coordinates, vibration tensor components ($\AA^2$) for the expression $T = \exp[-2\pi^2(U_{11}a^{*2}h^2 + \cdots\cdots + 2U_{23}b^*c^*kl + \cdots\cdots)]$, and their e.s.d.'s for the non-hydrogen atoms. All quantities × 10^4.

	X	Y	Z	U11	U22	U33	2U23	2U13	2U12
BR	8711(0)	2193(0)	292(1)	479(2)	534(2)	529(2)	-69(4)	74(4)	-244(4)
N(1)	3879(3)	7422(1)	-537(5)	521(18)	337(14)	348(17)	51(27)	-54(33)	-4(28)
C(2)	3321(3)	7120(2)	1199(6)	398(19)	418(18)	377(19)	105(36)	30(33)	63(34)
C(3)	3019(3)	6490(2)	359(7)	520(22)	509(23)	427(22)	227(40)	-235(43)	-327(37)
O(4)	2680(3)	6496(2)	-1690(6)	890(26)	604(18)	524(20)	190(34)	-696(41)	-305(38)
C(5)	3725(4)	6333(2)	-1202(6)	772(30)	362(18)	362(20)	-1(33)	-125(51)	-69(42)
C(6)	4483(4)	6866(2)	-1348(6)	661(26)	357(18)	334(21)	-56(34)	172(42)	34(38)
C(7)	5357(3)	6736(2)	52(8)	485(21)	412(20)	563(27)	56(40)	389(44)	51(34)
C(8)	5009(3)	6607(2)	2199(6)	409(19)	323(16)	432(22)	8(35)	-69(36)	11(31)
C(9)	4090(3)	6992(2)	2856(6)	468(20)	396(18)	295(19)	-16(31)	-9(34)	0(32)
O(10)	4774(2)	5931(1)	2261(4)	564(17)	328(11)	387(14)	35(24)	-153(28)	-32(24)
C(11)	4910(3)	5639(2)	4020(6)	369(18)	357(18)	351(19)	32(32)	2(33)	136(31)
O(12)	5178(3)	5898(1)	5494(5)	658(18)	486(16)	389(15)	-14(27)	-92(31)	-29(28)
C(13)	4695(3)	4932(2)	3806(7)	383(19)	299(16)	456(21)	52(33)	-30(35)	91(29)
C(14)	4415(4)	4653(2)	5830(8)	532(24)	391(20)	567(27)	309(40)	245(44)	170(37)
O(15)	3498(3)	4935(2)	6524(6)	557(17)	545(16)	693(21)	322(34)	432(34)	313(29)
C(16)	5625(3)	4595(2)	2966(7)	465(21)	310(16)	463(23)	109(35)	79(41)	-3(32)
C(17)	5542(4)	4202(2)	1368(8)	632(27)	489(23)	473(24)	-102(41)	85(47)	181(42)
C(18)	6387(5)	3857(3)	696(10)	959(42)	579(27)	671(34)	-202(52)	637(73)	135(58)
C(19)	7306(5)	3927(3)	1589(12)	674(32)	534(25)	990(46)	-7(61)	772(70)	156(49)
C(20)	7392(4)	4332(3)	3116(14)	515(28)	595(27)	1228(59)	32(74)	74(73)	167(48)
C(21)	6568(4)	4669(2)	3839(9)	491(24)	466(23)	756(33)	-271(49)	-109(49)	27(39)
C(22)	4486(4)	8005(2)	-82(8)	652(24)	305(18)	592(28)	43(37)	53(51)	-173(35)
O(23)	3165(3)	7663(2)	-1981(5)	795(23)	559(18)	475(18)	293(30)	-357(36)	37(34)
O(24)	2819(4)	4272(2)	9566(7)	1058(30)	697(23)	707(25)	483(44)	642(52)	576(45)

$$\sqrt{\omega} = \left[1 + \left(\frac{|F_o| - P_2}{P_1}\right)^2\right]^{-\frac{1}{2}}$$

$$\sqrt{\omega} = \sqrt{\omega} \times \frac{\sin^2\theta}{P_3} \quad \text{if} \quad \sin^2\theta < P_3$$

with $P_1 = 15.0$, $P_2 = 10.0$, $P_3 = 0.35$. Fifteen strong reflexions which suffered noticeably from extinction were assigned zero weight in the least-squares calculations. Without these reflexions the final R is 0.0408.

Scattering factor values were those of Cromer and Waber (15) for Br^{-1}, of Hanson *et al.* (16) for carbon, nitrogen and oxygen, and of Stewart *et al.* (17) for hydrogen. The calculations were performed on IBM 360/50 and IBM 360/67 computers at the NRC Computation Center, using programs of Ahmed *et al.* (18).

X-Ray Results and Discussion

Final coordinates and thermal parameters with corresponding e.s.d.'s are given in Table 1. The e.s.d.'s were calculated from the diagonal elements of the inverse to the normal equations matrix. Observed and calculated structure amplitudes based on the final parameters have been placed in the Depository of Unpublished Data.[2]

Table 1(b). Fractional coordinates, isotropic temperature factors (Å²) for the expression $T = \exp(-B\sin^2\theta/\lambda^2)$, and their e.s.d.'s for the hydrogen atoms

	X	Y	Z	B
H(21)	277(4)	739(2)	162(9)	3.5(1.1)
H(31)	270(3)	620(2)	119(7)	2.4(0.8)
H(51)	400(4)	588(3)	-137(10)	4.4(1.1)
H(61)	475(4)	693(3)	-272(9)	4.3(1.1)
H(71)	564(4)	634(2)	-44(9)	3.8(1.0)
H(72)	585(4)	713(2)	-9(8)	3.3(0.9)
H(81)	554(4)	667(3)	312(9)	3.9(1.1)
H(91)	374(4)	672(2)	393(8)	3.1(0.9)
H(92)	440(3)	737(2)	348(7)	2.2(0.8)
H(131)	412(3)	485(2)	281(6)	1.9(0.7)
H(141)	441(4)	420(2)	621(8)	3.4(1.0)
H(142)	496(3)	471(2)	686(7)	2.7(0.9)
H(151)	326(6)	466(4)	760(13)	7.2(1.8)
H(171)	497(6)	414(3)	64(12)	6.1(1.6)
H(181)	612(5)	359(3)	-39(10)	4.9(1.3)
H(191)	787(5)	359(5)	89(20)	10.8(2.9)
H(201)	801(5)	438(3)	386(10)	4.7(1.2)
H(211)	659(4)	498(2)	480(8)	3.1(0.9)
H(221)	412(5)	835(3)	18(11)	5.3(1.4)
H(222)	504(4)	789(2)	85(8)	3.0(0.9)
H(223)	485(6)	811(3)	-139(12)	6.0(1.5)
H(231)	278(7)	728(4)	-236(14)	7.9(1.9)
H(241)	336(9)	398(5)	989(19)	12.6(2.8)
H(242)	218(13)	437(7)	1017(28)	12.5(3.5)

[2]Photocopies may be obtained free of charge, upon request, from the Depository of Unpublished Data, National Science Library, National Research Council of Canada, Ottawa, Canada.

An agreement summary is given in Table 2. The discrepancies for the reflexions in categories 3 and 4 appear to be mainly due to extinction, and most of these reflexions were given zero weight in the least-squares calculations.

The molecular structure and absolute configuration may be seen in Fig. 1, which is a stereoscopic view of the contents of one asymmetric unit drawn by Johnson's ORTEP program (19). The numbering scheme used for the organic cation is shown in Fig. 2.

Thermal Vibration Analysis

The thermal vibration of the organic cation as a whole and of selected groups of atoms was analyzed for rigid-body motion using the program of Schomaker and Trueblood (20). This program calculates **T** (translational), **L** (rotational), and **S** (screw) tensors from the observed u_{ij} values.

The rigid-body approximation is not appropriate for the whole organic cation; the differences between observed u_{ij} values and those calculated from **T** and **L** were about twice as large as the e.s.d. 's of the observed u_{ij}'s. However, the agreement between observed and calculated u_{ij}'s was considerably better for analyses of two groups: the "aromatic" group [C(13), C(16)···C(21)], and the "bicyclic" group [N(1) ···O(10), C(22), O(23)]. Some results of these analyses are listed in Table 3.

The principal axis corresponding to maximum libration (rotational oscillation), with an r.m.s. amplitude of 8.0°, of the aromatic group is 18° from the C(13)—C(16) bond direction, indicating significant twisting of the aromatic ring about this bond. The second principal axis of libration, with r.m.s. amplitude 4.6°, is 25° from the normal to the benzene ring plane, suggesting some wagging in the plane of the ring.

The libration of the bicyclic group is less anisotropic than that of the aromatic group. The principal axis of maximum libration, 5.6°, is parallel (within 2°) to the direction C(8)···C(22). For both groups the translational vibration is fairly isotropic. Corrections for rotational vibration have been calculated for the bond lengths and angles in both the aromatic and the bicyclic groups. The corrections to the bond angles are in all cases less than the corresponding e.s.d.'s, however, and have therefore been omitted.

It seems probable that the N(1)—C(22) and

Can. J. Chem. Downloaded from www.nrcresearchpress.com by 210.87.254.105 on 09/05/12
For personal use only.

TABLE 2. Agreement summary. 1800 observed reflections ($2.7 \leq |F_o| \leq 161.9$). $R = 0.045$

Category	Limits		Number
1	$\lvert\Delta F\rvert \leq 1.0\lvert F_{th}\rvert$*	or $\lvert\Delta F\rvert/\lvert F_o\rvert \leq 0.09$	1729
2	$1.0\lvert F_{th}\rvert < \lvert\Delta F\rvert \leq 2.0\lvert F_{th}\rvert$	or $0.09 < \lvert\Delta F\rvert/\lvert F_o\rvert \leq 0.14$	56
3	$2.0\lvert F_{th}\rvert < \lvert\Delta F\rvert \leq 3.0\lvert F_{th}\rvert$	or $0.14 < \lvert\Delta F\rvert/\lvert F_o\rvert \leq 0.18$	10
4	$3.0\lvert F_{th}\rvert < \lvert\Delta F\rvert$	or $0.18 < \lvert\Delta F\rvert/\lvert F_o\rvert$	5
	45 unobserved reflections ($\lvert F_{cmax}\rvert = 3.6$)		
1	$\lvert F_c\rvert \leq 1.0\lvert F_{th}\rvert$		39
2	$1.0\lvert F_{th}\rvert < \lvert F_c\rvert \leq 1.5\lvert F_{th}\rvert$		6

*$|F_{th}|$ = threshold amplitude = 2.43 to 3.39.

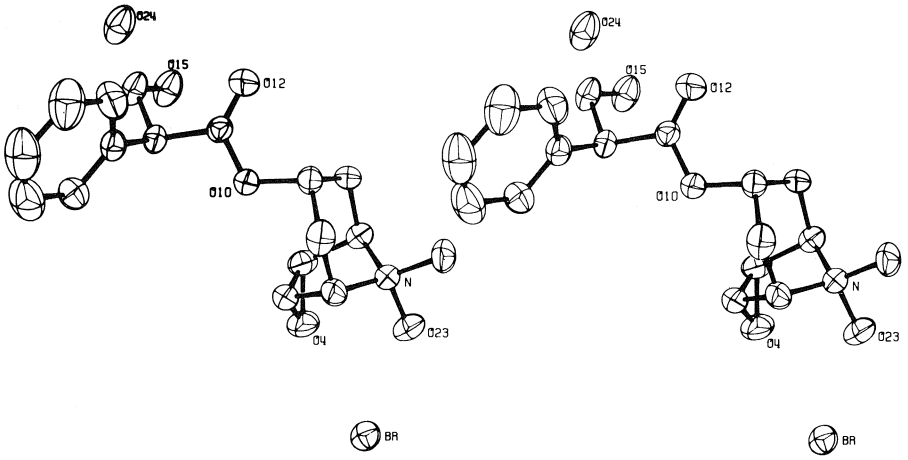

FIG. 1. Stereoscopic view of one asymmetric unit. The ellipsoids are scaled to include 50% probability.

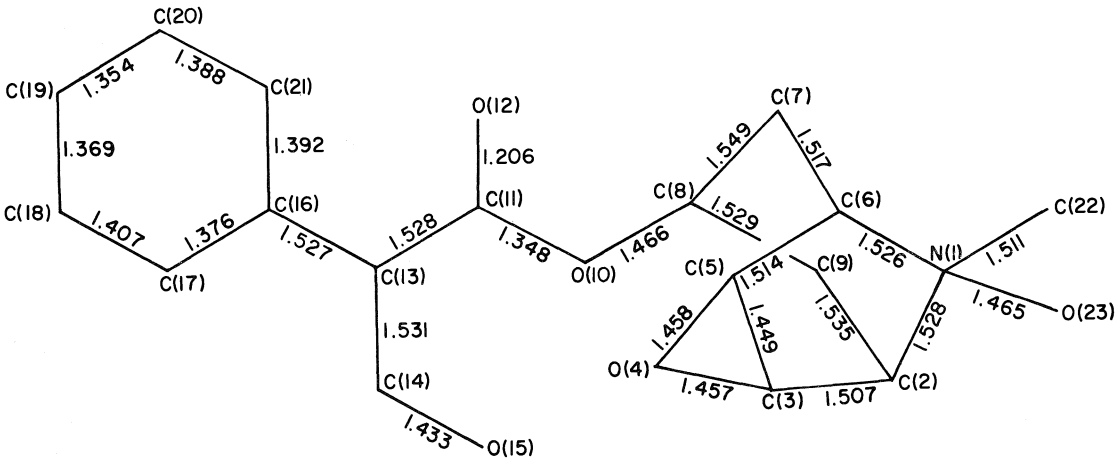

FIG. 2. Bond lengths, including libration corrections, for the non-hydrogen atoms, and the numbering scheme.

Can. J. Chem. Downloaded from www.nrcresearchpress.com by 210.87.254.105 on 09/05/12
For personal use only.

TABLE 3. Rigid-body thermal parameters*

(*a*) L × 10 (deg²)

"Bicyclic" group			"Aromatic" group		
99(12)	−22(9)	40(9)	384(100)	−216(54)	−121(42)
	266(15)	−69(10)		420(62)	53(45)
		172(13)			120(51)

(*b*) Principal axes of L

	"Bicyclic" group				"Aromatic "group			
Axis	r.m.s. amplitude (deg)	Direction cosines (× 10³)			r.m.s. amplitude (deg)	Direction cosines (× 10³)		
*L*1	5.6	−179	858	−481	8.0	679	−699	−227
*L*2	3.8	−397	−510	−763	4.6	593	703	−392
*L*3	2.8	−900	054	432	2.6	434	132	891

(*c*) Principal axes of reduced T

"Bicyclic" group				"Aromatic "group			
r.m.s. amplitude (Å)	Direction cosines (× 10³)			r.m.s. amplitude (Å)	Direction cosines (× 10³)		
0.20	−949	303	−089	0.21	−995	−071	−077
0.18	315	931	−184	0.20	−090	205	975
0.17	027	−203	−979	0.17	−054	976	−210

(*d*) Displacement of libration axes from intersecting (Å)

Direction	"Bicyclic" group	"Aromatic" group
Parallel to *L*1	0.63	−0.24
Parallel to *L*2	0.39	−0.73
Parallel to *L*3	0.25	−0.54

(*e*) Effective screw translations (Å)

Direction	"Bicyclic" group	"Aromatic" group
Parallel to *L*1	0.030	−0.004
Parallel to *L*2	−0.031	−0.007
Parallel to *L*3	−0.018	0.024

(*f*) Value of $(\overline{\Delta U_{ij}^2})^{1/2}$ (Å)²

"Bicyclic" group	"Aromatic" group
0.0022	0.0031

*Reference axes are *a*, *b*, *c*. E.s.d.'s of components of L are given after them in parentheses, in units of the least significant digit.

N(1)—O(23) bonds may be involved in non-rigid-body motion, and corrections for these bonds and for C(11)—O(12) and C(14)—O(15) have therefore been calculated assuming "riding motion", using the procedure of Busing and Levy (21). The bond lengths given in Fig. 2 and used in later discussion include the riding-motion corrections for these four bonds and the rigid-body corrections for the others except O(10)—C(11), C(11)—C(13), and C(13)—C(14) which are uncorrected.

Bond Lengths and Angles

The e.s.d.'s of the bond lengths and angles have been increased from their calculated values by 50% to allow for the omission of interaction

Can. J. Chem. Downloaded from www.nrcresearchpress.com by 210.87.254.105 on 09/05/12
For personal use only.

Can. J. Chem. Downloaded from www.nrcresearchpress.com by 210.87.254.105 on 09/05/12
For personal use only.

between atoms. The uncorrected bond lengths and angles not involving hydrogen are listed with their e.s.d.'s in Table 4. Those involving hydrogen atoms are quite normal; the C—H and O—H bond lengths vary between 0.89 and 1.12 Å.

The three N^+—C_{sp3} bonds have an average length of 1.522 Å, and none deviates significantly from this value. This average may be compared with the value 1.53 Å found in *N*-methylrhoeagenine iodide (22). The value found here for a N^+—O bond length, 1.465 Å, appears to be quite reasonable. One would expect it to be comparable to a C—O single bond, as N^+ and C are isoelectronic, and in fact it agrees very well with the C(8)—O(10) bond length, 1.466, and with C(3)—O(4), 1.457, and C(5)—O(4), 1.458 Å. The N^+—O bond length of 1.427 Å reported in the structure of sparteine-*N*(16)-oxide sesquiperchlorate (23) was not corrected for thermal motion, and its quoted e.s.d. of 0.007 Å is probably underestimated by 50% (23); the difference between it and the uncorrected value 1.443 Å found in the present analysis is not significant. The agreement of the epoxide C—O bond lengths with the corresponding value 1.47 Å quoted in International Tables (24) is satisfactory.

The C_{sp^3}—C_{sp^3} single bond C(3)—C(5) is very significantly shortened (to 1.449 Å) due to the bridging oxygen atom; any lengthening of this bond would force the C—C—O angles to even smaller values than their present average of 60.3°. The adjacent bonds, C(2)—C(3) and C(5)—C(6) are also shorter than the usual C_{sp3}—C_{sp3} bond length, 1.537 Å (25). It seems that this may be due more to the particular ring geometry than to any electronic effect of the epoxide oxygen atom; in several compounds containing 6-membered oxido-rings (26–28) the bonds adjacent to C—O are lengthened rather than shortened.

Differences between presumably equivalent bond lengths in the 6-membered heterocyclic ring might be due to the close approach of the bromide ion to H(21), H(61), H(81) and H(92), as described

TABLE 4. (*a*) Bond lengths (Å) and their e.s.d.'s

Bond	Uncorrected bond length
N(1)—C(2)	1.520(8)
N(1)—C(6)	1.518(8)
N(1)—C(22)	1.498(8)
N(1)—O(23)	1.443(8)
C(2)—C(3)	1.499(9)
C(2)—C(9)	1.529(9)
C(3)—O(4)	1.451(9)
C(3)—C(5)	1.440(10)
O(4)—C(5)	1.451(11)
C(5)—C(6)	1.507(10)
C(6)—C(7)	1.510(10)
C(7)—C(8)	1.542(10)
C(8)—C(9)	1.521(9)
C(8)—O(10)	1.461(7)
O(10)—C(11)	1.348(7)
C(11)—O(12)	1.187(8)
C(11)—C(13)	1.528(8)
C(13)—C(14)	1.531(10)
C(13)—C(16)	1.521(9)
C(14)—O(15)	1.421(9)
C(16)—C(17)	1.364(10)
C(16)—C(21)	1.379(10)
C(17)—C(18)	1.401(13)
C(18)—C(19)	1.356(15)
C(19)—C(20)	1.343(16)
C(20)—C(21)	1.382(12)

(*b*) Bond angles (deg) and their e.s.d.'s

Angle	Uncorrected value
C(2) —N(1)—C(6)	101.7(5)
C(2) —N(1)—C(22)	116.4(5)
C(2) —N(1)—O(23)	110.8(5)
C(6) —N(1)—C(22)	115.6(5)
C(6) —N(1)—O(23)	111.6(5)
C(22)—N(1)—O(23)	101.1(5)
N(1) —C(2) —C(3)	102.1(5)
N(1) —C(2) —C(9)	108.6(5)
C(3) —C(2) —C(9)	107.1(5)
C(2) —C(3) —O(4)	115.6(6)
C(2) —C(3) —C(5)	108.1(6)
O(4) —C(3) —C(5)	60.3(5)
C(3) —O(4) —C(5)	59.5(5)
C(3) —C(5) —O(4)	60.3(5)
C(3) —C(5) —C(6)	107.4(6)
O(4) —C(5) —C(6)	115.5(6)
N(1) —C(6) —C(5)	102.2(5)
N(1) —C(6) —C(7)	108.2(5)
C(5) —C(6) —C(7)	108.9(6)
C(6) —C(7) —C(8)	113.2(6)
C(7) —C(8) —C(9)	114.4(5)
C(7) —C(8) —O(10)	105.3(5)
C(9) —C(8) —O(10)	110.4(5)
C(2) —C(9) —C(8)	113.8(5)
C(8) —O(10)—C(11)	116.3(5)
O(10)—C(11)—O(12)	124.4(6)
O(10)—C(11)—C(13)	109.9(5)
O(12)—C(11)—C(13)	125.7(6)
C(11)—C(13)—C(14)	109.7(5)
C(11)—C(13)—C(16)	110.2(5)
C(14)—C(13)—C(16)	110.1(5)
C(13)—C(14)—O(15)	109.6(6)
C(13)—C(16)—C(17)	121.1(6)
C(13)—C(16)—C(21)	120.5(6)
C(17)—C(16)—C(21)	118.5(7)
C(16)—C(17)—C(18)	120.6(7)
C(17)—C(18)—C(19)	120.2(9)
C(18)—C(19)—C(20)	119.0(10)
C(19)—C(20)—C(21)	122.2(10)
C(16)—C(21)—C(20)	119.5(8)

Can. J. Chem. Downloaded from www.nrcresearchpress.com by 210.87.254.105 on 09/05/12
For personal use only.

later, but the equality of the angles C(6)—C(7)—C(8) and C(8)—C(9)—C(2), and N(1)—C(2)—C(9) and N(1)—C(6)—C(7) may be an indication that the bond length differences are not significant.

Two of the aromatic C—C bonds, C(18)—C(19), and C(19)—C(20), are significantly shorter than the usual length, 1.394 Å (25), even after rigid-body libration corrections. The most likely explanation for this is that C(19) and C(20) have extremely large u_{ij} values, as can be seen in Table 1, and probably are involved in considerable non-rigid vibration.

The rest of the bond lengths in the structure agree within experimental error with corresponding standard values and require no further comment.

The enlarged angles O(10)—C(11)—O(12), which is 124.4 instead of 120.0°, and C(11)—O(10)—C(8), which is 6.8° larger than the tetrahedral value, both contribute to relieving the O(12)····H(81) repulsion. The O(12)····H(81) distance is only 2.34 Å, and the usual O····H van der Waals separation is 2.6 Å. The C(22)—N(1)—C(2) and C(22)—N(1)—C(6) angles are also significantly larger than 109.5°, and this is probably due to repulsion between H(72) and H(222) and between H(92) and H(222). These two non-bonded interatomic distances are 2.03 and 2.25 Å respectively, while the usual H····H van der Waals contact is 2.4 Å.

Conformation

The bicyclic portion of the cation has an almost exact mirror plane of symmetry through N(1), O(4), C(8). C(2) and C(6), and C(3) and C(5) are symmetrically related within experimental error, and C(22) and O(23) are displaced only 0.009 and 0.008 Å from the plane, respectively. However, C(7) and C(9), while displaced equally from the plane, are not exactly opposite each other.

The piperidine ring N(1), C(2), C(6), C(7), C(8), C(9) is approximately chair-shaped; C(2), C(6), C(7), C(9) show small but possibly significant deviations from planarity, and N(1) and C(8) show markedly unequal displacements from the mean plane (0.873 and −1.355 Å, respectively). The enlarged angles C(6)—C(7)—C(8) (113.2°), C(7)—C(8)—C(9) (114.4°) and C(8)—C(9)—C(2) (113.8°) indicate some flattening of the ring at the unbridged end, while the reduced C(2)—N(1)—C(6) angle (101.7°) reflects the distortion introduced by the bridge. Very similar conformation is observed in the crystal structure of pseudotropine (29). O(23) is equatorial and C(22) is axial with respect to this ring. In the crystal structure of (−)hyoscine, *i.e.* scopolamine, hydrobromide (30) the *N*-methyl group is also axial, whereas in some other related structures, such as pseudotropine (29), the *N*-methyl is equatorial. The 5-membered ring is envelope-shaped, with C(2), C(3), C(5), C(6) planar and N(1) 0.64 Å out of this plane. O(4) is displaced 1.185 Å from the plane in the same direction.

The O(10), C(11), O(12), C(13) group is planar within experimental error, and C(8) is only 0.074 Å out of the plane, in keeping with the partial double-bond character of the O(10)—C(11) bond. The dihedral angle between the carboxyl group plane and the plane through N(1), O(4), C(8) is 34°. This gives a larger O(12)····H(81) distance than would a coplanar configuration, and, as mentioned earlier the observed distance is shorter than the usual van der Waals separation. The O(12)····H(91) and O(12)····H(71) distances are 2.78 and 4.15 Å, respectively.

The absolute configuration at C(13), as determined by anomalous scattering, is **S** in the notation of Cahn *et al.* (31). Fodor and Csepreghy (32) have chemically correlated (−)tropic acid with D-(−)alanine and deduced **S** absolute configuration for (−)hyoscine and (−)hyoscyamine. The torsional angle C(11)—C(13)—C(14)—O(15) is 63°, giving a staggered conformation about the C(13)—C(14) bond.

The aromatic ring shows small but possibly significant departures from planarity, and C(13) is displaced 0.10 Å from the mean plane. Equations of the various mean planes are given in Table 5.

It is of interest to compare the various non-bonded N····O distances in the present structure with those in the closely related scopolamine hydrobromide. In this structure the N····O(4), N····O(10), N····O(12), and N····O(15) distances are 2.63, 3.85, 5.46, and 7.11 Å respectively whereas in scopolamine hydrobromide the corresponding distances are 2.47, 3.88, 5.41, and 8.04 Å. These distances are similar to N····O distances in muscarinic agents (30); both scopolamine hydrobromide and scopolamine *N*-oxide hydrobromide are antagonists of the muscarinic actions of acetylcholine, but show greater ratios

TABLE 5. Mean plane equations of the form $AX + BY + CZ - D = 0$ where the coefficients of X, Y, and Z are the direction cosines of the normal to the plane relative to the unit-cell axes

Description	A	B	C	D
N(1), O(4), C(8)	0.6441	−0.2776	−0.7303	−0.0288
C(2), C(6), C(7), C(9)	0.2793	0.9594	−0.0392	15.6083
C(2), C(3), C(5), C(6)	−0.5888	0.4595	−0.6650	3.8101
O(10), C(11), O(12), C(13)	0.9574	−0.1638	−0.2378	3.5767
C(16) --- C(21)	0.2175	0.7479	−0.6272	7.6270

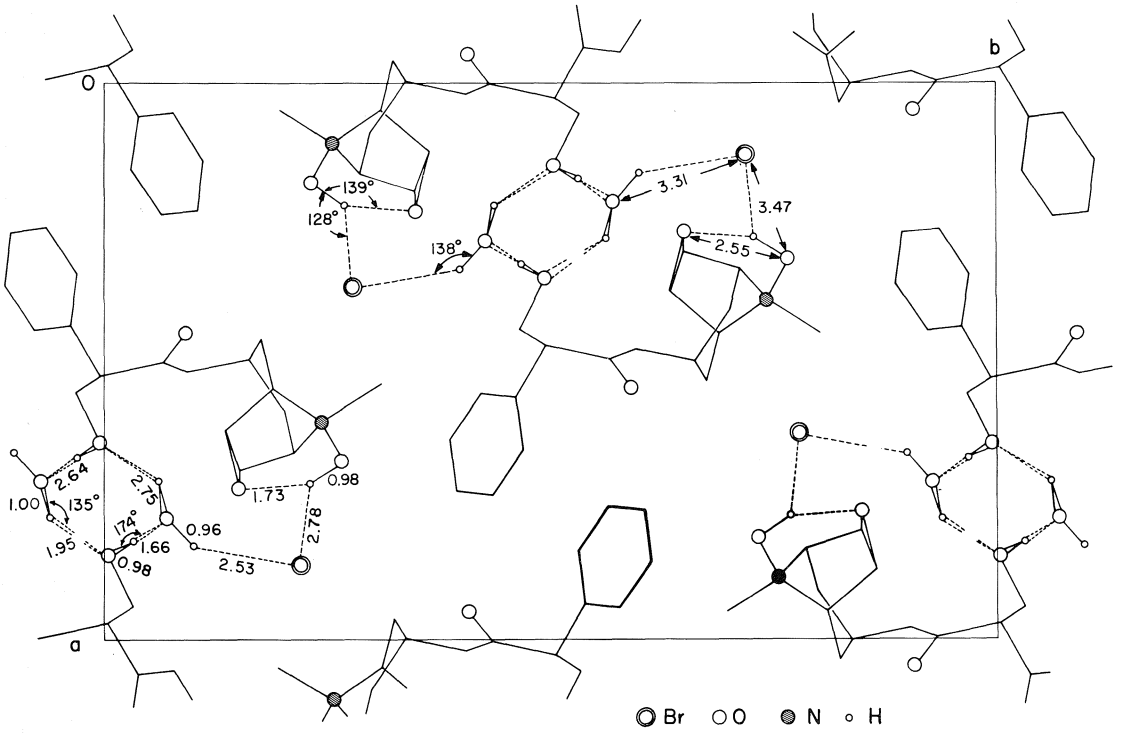

FIG. 3. Projection of the crystal structure on the (001) plane. Hydrogen bonds are indicated by broken lines.

of ganglionic blocking to post-ganglionic blocking (antimuscarinic) activity than such compounds as atropine (33).

Packing Arrangement

The organic cations are hydrogen-bonded alternately with water molecules in infinite spirals about the screw axes parallel to the Z-axis. At the same time the hydrogen bond network links the two hydroxy groups of a given molecule. The arrangement is shown in Fig. 3. The $Br^-\cdots O(23)$ distance (3.47 Å) is actually larger than the corresponding sum of van der Waals radii (3.35 Å), and is also larger than the $Br^-\cdots O(4)$ distance (3.38 Å), but the $Br^-\cdots H(231)$ distance, 2.78 Å, is 0.37 Å shorter than the usual $Br^-\cdots H$ van der Waals separation; according to Hamilton and Ibers (34) the H····heavy-atom distance is the critical factor indicating the presence of a hydrogen bond, and on this basis Br^- and O(23) should be regarded as hydrogen-bonded. The pertinent angles are also consistent with a bifurcated hydrogen bond connecting O(23) with O(4) and Br^-. In another case of a bifurcated hydrogen bond involving an intramolecular and an intermolecular contact, Cady and Larson (35) found the intermolecular hydrogen bond to be consistently weaker than the intramolecular link, as it is here. In addition to the intermolecular contacts involving

Can. J. Chem. Downloaded from www.nrcresearchpress.com by 210.87.254.105 on 09/05/12
For personal use only.

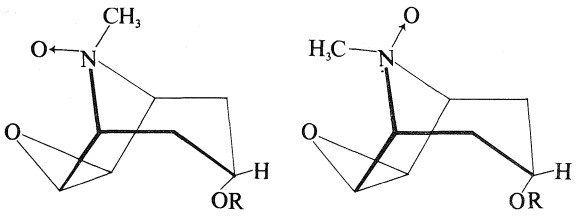

1 R=Tr

2 R=Tr

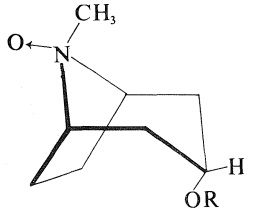

3 R=Tr
5 R=H

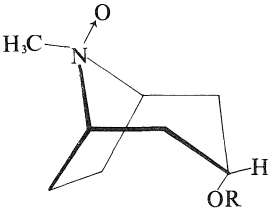

4 R=Tr
6 R=H

Tr=COCH(CH$_2$OH)C$_6$H$_5$(S)

hydrogen bonds, there are a number of others which are also shorter than the usual van der Waals separation. These include H(21)····Br$^-$ (2.88), H(61)····Br$^-$(3.05), H(81)····Br$^-$(2.97), H(92)····Br$^-$(2.91), and H(223)····Br$^-$(3.00 Å). With these in mind, inspection of Fig. 3 suggests that there is considerable Coulomb attraction between the bromide ion and the positively charged but inaccessible nitrogen atom.

Nuclear Magnetic Resonance Studies

The most vulnerable point of our previous assignments (10) was the lack of comparison of both *N*-epimer amine oxides. Therefore, we have carried out a systematic product analysis by n.m.r. of amine-oxide formation from scopolamine and a number of related bases. Unfortunately, the new technique used by Cymerman Craig and Purushotaman (36) of *N*-oxidation by *m*-chloroperbenzoic acid followed by chromatographic liberation of the free bases has not worked in our case, owing to very low reactivity of scopolamine towards that reagent. However, oxidation with hydrogen peroxide in ethanol[3] of scopolamine, atropine and tropine and the use

[3]This technique was used by Werner and his associates (37). We express our thanks for this suggestion, also for informing us of some of their related study prior to their publication.

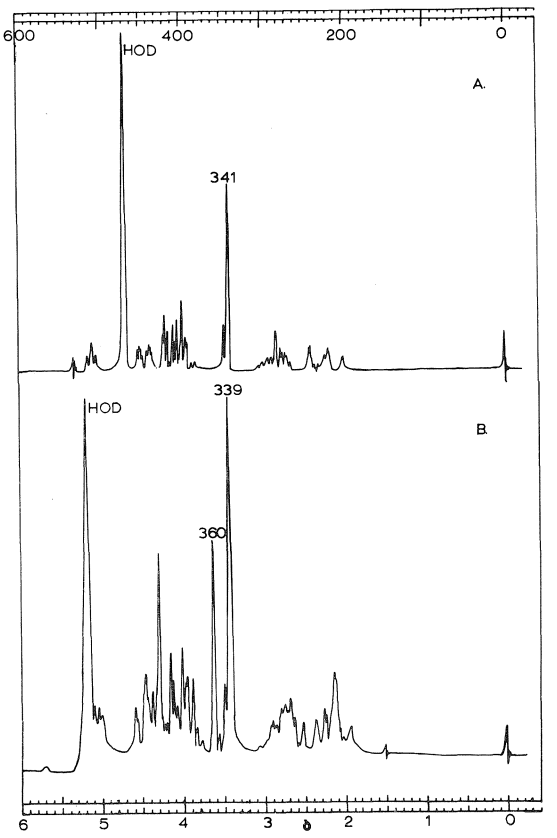

FIG. 4. Nuclear magnetic resonance (100 MHz) spectrum of *A*. scopolamine *N*-oxide hydrobromide *B*. scopolamine *N*-oxide.

of 100 MHz n.m.r. spectroscopy finally allowed us to detect two quaternary *N*-methyl signals in all three cases. Experimental details of spectra are recorded in Table 6 and Figs. 4, 5, and 6.

Scopolamine *N*-oxide (**1**) has a major *N*-methyl signal at δ 3.39 identical with that of the hydrobromide of the commercially available, *i.e.*, purified stereoisomer. The *N*-methyl protons of the minor product, **2**, resonate at 3.60 δ in much lower field than in the major product, **1**, (Fig. 4). Based on the configuration now ascertained by X-ray analysis of the major product as hydrobromide of **1** one can state that the neighboring epoxide oxygen (10, 12) has an additional deshielding effect upon the equatorial N—Me. This all fits well with our experience with n.m.r. chemical shifts in *N*,*N*-dialkyl tropanium salts (8).

On the other hand, both atropine (Fig. 5) and tropine (Fig. 6) gave a product ratio 3:1 of the *N*-oxides, the major stereoisomer showing

Can. J. Chem. Downloaded from www.nrcresearchpress.com by 210.87.254.105 on 09/05/12
For personal use only.

Can. J. Chem. Downloaded from www.nrcresearchpress.com by 210.87.254.105 on 09/05/12
For personal use only.

TABLE 6. 100 MHz nuclear magnetic resonance spectra of amineoxides, in D_2O

Formula number	Compound	N—Me	H-6,7	Chemical Shift H-1,5	H-3	H-aromatic
1 + 2	Scopolamine *N*-oxide (product analysis)	3.39(66%) 3.60(33%)	3.45(IH)(d)*J*. 36 Hz 4.08(IH)(d)*J*. 36 Hz	4.45(m)	5.1(m)	7.38(s)
1-HBr	Scopolamine *N*-oxide hydrobromide (commercial product)	3.41 —	3.46(IH)*J*. 4 Hz 4.2 (IH)*J*. 4 Hz		5.1(t)*J*, 5 Hz	7.41(s)
3 + 4	Atropine *N*-oxide (product analysis)	3.28(minor) 3.38(major)	1.6–3.0 (with H-2,4)	4.8–5.9(m) with H-3		7.38(s)
5 + 6	Tropine *N*-oxide (product analysis)	3.13(25%) 3.16(75%)		3.61(m) 3.49(m)	3.99(t)*J*, 5 Hz	
5-hydrate	Tropine *N*-oxide monohydrate (Aldrich product)	3.17(s) —		3.58(m)	4.04(t)*J*, 5 Hz	

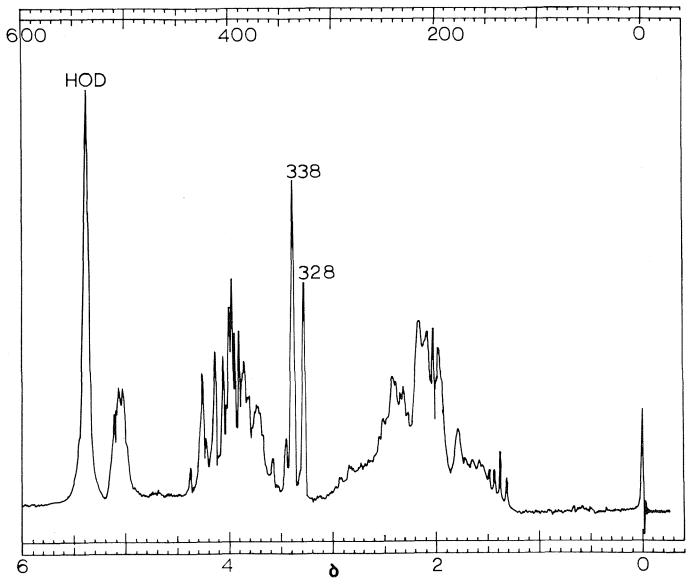

FIG. 5. Nuclear magnetic resonance (100 MHz) spectrum of atropine *N*-oxide.

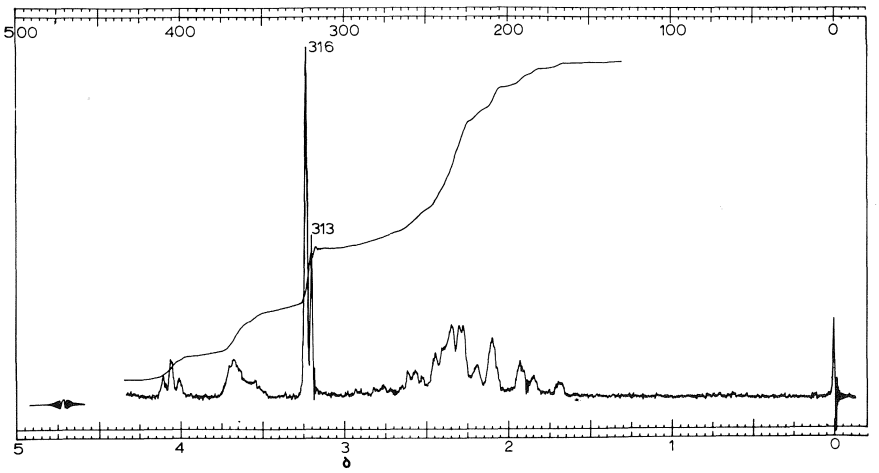

FIG. 6. Nuclear magnetic resonance (100 MHz) spectrum of tropine *N*-oxide.

$\overset{+}{N}$—Me resonance at a lower field. Our recent extensive studies (8) have shown that in epimeric *N*-deuteromethyltropanium bromides the axial $\overset{+}{N}$—Me resonates in a lower field, that is, the axial methyl is more deshielded than the equatorial one (38) unless the latter is exposed to a stronger deshielding effect, for example, by a hydroxyl or epoxide function. Based on this, "reversal" of the $\overset{+}{N}$—Me signal positions when passing from atropine *N*-oxide to scopolamine *N*-oxide can be explained. In addition, there is no reason to assume a qualitatively different steric course to operate for scopolamine than for atropine, therefore, we suggest structure of equatorial *N*-oxides **3** and **5** to the major products and **4** and **6** to their stereoisomers also in the cases of products of *N*-oxidation of atropine and tropine. We are aware of the fact that this conclusion is based on analogy, however, we don't think that there is any need to support this view by a series of further X-ray studies.

As to the explanation we can offer for preferential equatorial attack by the peroxide electrophile upon nitrogen we have to reiterate our views

Can. J. Chem. Downloaded from www.nrcresearchpress.com by 210.87.254.105 on 09/05/12
For personal use only.

Can. J. Chem. Downloaded from www.nrcresearchpress.com by 210.87.254.105 on 09/05/12
For personal use only.

expressed previously (1*c*, 8). The strong, 1,3-diaxial interaction by 2,4-placed hydrogens in the somewhat flattened (3, 8, 29, see also the present X-ray work) piperidine moiety of tropanes, which is proven by n.m.r. and X-ray data, does not give preference to a transition state involving axial attack although this would resemble the ground state of the bases that have an equatorial methyl group in a very high population (3, 29). Therefore, the transition state of lower energy would imply an attack by the solvated oxygen electrophile from the less hindered equatorial side of the molecule, even when this should put the *N*-methyl group in the more compressed axial position. However, the group already present can bear such an interaction more easily[4] than the strongly solvated and charge-separated incoming group, be the latter originally bulkier or not than the methyl. This was shown by the steric selectivity of deuteromethylation as being practically the same as of ethylation or methoxycarbonylmethylation. Hence, amineoxide formation, at least in this series, is not an exception to the general pattern of quaternization. As an extension of these studies on *N*-quaternizations in the field of *N*-methyl*trans*decahydroquinolines one of us (G.F.) and Sh. Abidi are now investigating the optimum steric course of cyanation by cyanogen bromide and $CNCl{\cdot}SbCl_5$, respectively.

Preparative Data

All melting points were taken in open capillary tubes using Thomas–Hoover capillary m.p. apparatus and are uncorrected. The n.m.r. spectra were measured on a Varian HA-100 spectrometer operated in the frequency-sweep mode with a normal probe temperature of 30 ± 1°. Deuterium oxide was used as a solvent for all of the samples (10 to 15% solution) and a 2% solution (100 μl) of 3-(trimethyl silyl)-1-propane sulfonic acid sodium salt (Tiers' salt) in D_2O was added to the samples. Benzene was used as an external lock signal for scopolamine *N*-oxide and its hydrobromide. The field-frequency lock was set on HOD peak for tropine *N*-oxide and aromatic protons singlet for atropine *N*-oxide. The signal due to methyl protons in Tiers' salt was adjusted to 0 p.p.m. before setting the field-frequency lock. Chemical shifts are expressed either on δ scale in p.p.m. or in Hz. The following letters were used for the signal splittings due to proton–proton coupling and also for the separation of signals: s, singlet; d, doublet; t, triplet; and m, multiplet. The results reported in Table 6 indicate the product analysis on all preparations before purification. The commercial sample of scopolamine *N*-oxide hydrobromide was used after several recrystallizations for n.m.r. and X-ray diffraction studies. Tropine *N*-oxide was obtained from Aldrich Chemical Company as tropine *N*-oxide dihydrate (m.p. 224° dec.) and used as such for n.m.r. measurements.

Tropine N-Oxide

To a solution of tropine (2.0 g) in 20 ml ethanol was added 30% hydrogen peroxide (20 ml) and the mixture was stirred for 2 days. The solvent was removed in vacuum at 30° to give an oil. Product analysis by n.m.r. indicated two *N*-methyl signals corresponding to two isomers in the ratio 25:75. Trituration of the oily product with acetone gave tropine *N*-oxide as white powder (1.8 g) which melted at 162° (reported (37, 10) m.p. 216 and 238° (dec.)).

Scopolamine N-Oxide

This was prepared by treatment of scopolamine with aqueous hydrogen peroxide as described below. To a stirred solution of scopolamine (2.02 g) in ethanol (25 ml) was added 30% hydrogen peroxide (20 ml) and the mixture was left at 30° with stirring for 2 days. Evaporation of solvent *in vacuo* gave scopolamine *N*-oxide as a thick syrup (2.1 g) which was submitted to product analysis by n.m.r. Trituration with acetone gave a solid which was purified by recrystallization from methanol–acetone, m.p. 130–133° (reported (10) m.p. 132–134°).

Atropine N-Oxide

This was prepared by hydrogen peroxide method following the same procedure as described for scopolamine *N*-oxide. Thus, 1.2 g of atropine in 20 ml ethanol and 20 ml 30% hydrogen peroxide gave crude atropine *N*-oxide (1.1 g) as a thick oil which was analyzed by n.m.r. Further purification yielded crystalline material, m.p. 129–131° (reported (11) m.p. 127–128°).

C.S.H. is grateful to Dr. Maria Przybylska for helpful comments on a portion of the manuscript.

1. G. Fodor. Tetrahedron, **1**, 86; Chem. Ind. London, 1500 (1961); *In* Manske, The Alkaloids, Vol. IX, 1967. Chap. 7.
2. A. T. Bottini. Stereoselectivity in quaternizations of tertiary amines. *In* Selective organic transformations. Vol. 1. *Edited by* B. S. Thyagarajan. Wiley-Interscience, New York, N.Y., 1970. pp. 89–142.
3. A. R. Katritzky *et al.* J. Chem. Soc. C, 74 (1966); 1207 (1970); 1210 (1970); 1224 (1970) and papers cited therein.
4. H. O. House *et al.* J. Org. Chem. **31**, 1068 (1966); **31**, 1073 (1966); **33**, 935 (1968); **33**, 943 (1968).
5. J. McKenna *et al.* J. Chem. Soc. B, 1184 (1967) and references cited therein.
6. K. Koczka and G. Bernáth. Chem. Ind. London, 1401 (1958) and forthcoming papers.
7. J. Kóbor, G. Bernáth, L. Radics, and M. Kajtár. Acta Chim. Budap. **60**, 255 (1969).

[4]This was suggested by D. J. Cram during a discussion of this subject at UCLA.

8. G. FODOR, R. V. CHASTAIN, JR., D. FREHEL, M. J. COOPER, N. MANDAVA, and E. L. GOODEN. J. Am. Chem. Soc. **93**, 403 (1971).
9. G. FODOR, J. D. MEDINA, and N. MANDAVA. J. Chem. Soc. D, 581 (1968).
10. N. MANDAVA and G. FODOR. Can. J. Chem. **46**, 2761 (1968).
11. M. and M. POLONOVSKI. Bull. Soc. Chim. Fr. (IV), **39**, 1161 (1926); **39**, 1162 (1926); **43**, 79 (1928).
12. K. TORI *et al.* Tetrahedron Lett. 559 (1964). R. WILLIAMS *et al.* J. Org. Chem. **33**, 509 (1968).
13. D. T. CROMER. Acta Cryst. **18**, 17 (1965).
14. W. C. HAMILTON. Acta Cryst. **18**, 502 (1965).
15. D. T. CROMER and J. T. WABER. Acta Cryst. **18**, 104 (1965).
16. H. P. HANSON, F. HERMAN, J. D. LEA, and S. SKILLMAN. Acta Cryst. **17**, 1040 (1964).
17. R. F. STEWART, E. R. DAVIDSON, and W. T. SIMPSON. J. Chem. Phys. **42**, 3175 (1965).
18. F. R. AHMED, S. R. HALL, C. HUBER, and M. E. PIPPY. NRC crystallographic programs for the IBM/360 system, world list of crystallographic computer programs, 2nd ed. Appendix p. 52 (1966).
19. C. K. JOHNSON. ORTEP: A Fortran thermal-ellipsoid plot program for crystal structure illustrations. Oak Ridge National Laboratory Report ORNL-3794, Revised (1965).
20. V. SCHOMAKER and K. N. TRUEBLOOD. Acta Cryst. B**24**, 63 (1968).
21. W. R. BUSING and H. A. LEVY. Acta Cryst. **17**, 142 (1964).
22. C. S. HUBER. Acta Cryst. B**26**, 373 (1970).
23. S. N. SRIVASTAVA and M. PRZYBYLSKA. Acta Cryst. B**25**, 1651 (1969).
24. L. E. SUTTON (*Editor*). International Tables for X-ray Crystallography, Vol. III. Kynoch Press, Birmingham, 1962.
25. Interatomic distances and configuration in molecules and ions, Supplement 1956–1959. The Chemical Society, London, 1965.
26. E. M. GOPALAKRISHNA, A. COOPER, and D. A. NORTON. Acta Cryst. B**25**, 143 (1969).
27. E. M. GOPALAKRISHNA, A. COOPER, and D. A. NORTON. Acta Cryst. B**25**, 1601 (1969).
28. E. M. GOPALAKRISHNA, A. COOPER, and D. A. NORTON. Acta Cryst. B**25**, 2473 (1969).
29 H. SCHENK, C. H. MACGILLAVRY, S. SKOLNIK, and J. LAAN. Acta Cryst. **23**, 423 (1967).
30. P. PAULING and T. J. PETCHER. Chem. Commun. 1001 (1969).
31. R. S. CAHN, C. K. INGOLD, and V. PRELOG. Experientia, **12**, 81 (1956).
32. G. FODOR and G. CSEPREGHY. J. Chem. Soc. 3222 (1961).
33. L. S. GOODMAN and A. GILMAN. The pharmacological basis of therapeutics. 3rd ed. Macmillan, New York, N.Y., 1965. p. 521–545.
34. W. C. HAMILTON and J. A. IBERS. Hydrogen bonding in solids. W. A. Benjamin, Inc., New York, N.Y., 1968.
35. H. H. CADY and A. C. LARSON. Acta Cryst. **18**, 485 (1965).
36. J. CYMERMAN CRAIG and K. V. PURUSHOTAMAN. J. Org. Chem. **35**, 1721 (1970).
37. G. WERNER and R. SCHICKFLUSS. Leibigs Annalen, **746**, 65 (1971).
38. A. T. BOTTINI and M. K. O'RELL. Tetrahedron Lett. 429 (1967).

Can. J. Chem. Downloaded from www.nrcresearchpress.com by 210.87.254.105 on 09/05/12
For personal use only.

Can. J. Chem. Downloaded from www.nrcresearchpress.com by 210.87.254.6 on 09/05/12
For personal use only.

Infrared and Raman Spectra of Potassium and Sodium Borohydride

K. B. HARVEY[1] AND N. R. MCQUAKER[2]

Department of Chemistry, University of British Columbia, Vancouver 8, British Columbia

Received April 22, 1971

Using both infrared and laser Raman techniques the low temperature vibrational spectra of KBH_4, KBD_4, $NaBH_4$, and $NaBD_4$ have been recorded. The spectra of the external lattice vibrations are consistent with the following borohydride ion site symmetries: T_d for potassium borohydride and D_{2d} for sodium borohydride. Translational frequencies are assigned and librational frequencies are inferred from absorptions tentatively assigned as second overtones. Comparison of the low and high temperature vibrational spectra suggests the following disorder–order phase changes: $O_h^5 \rightarrow T_d^2$ for potassium borohydride and $O_h^5 \rightarrow D_{2d}^9$ for sodium borohydride.

En utilisant les techniques de l'infrarouge et du laser Raman, les spectres de vibration à basse température de KBH_4, KBD_4, $NaBH_4$ et $NaBD_4$ ont été enregistrés. Les spectres de vibration du réseau externe sont consistants avec les sites de symétrie suivants pour les ions borohydrures: T_d pour le borohydrure de potassium et D_{2d} pour le borohydrure de sodium. Les fréquences de translation sont assignées et les fréquences de vibration déduites à partir des absorptions qu'il est possible d'assigner aux deuxièmes harmoniques. La comparaison des spectres de vibration à basse et haute température suggère les changements de phase désordre-ordre suivants: $O_h^5 \rightarrow T_d^2$ pour le borohydrure de potassium et $O_h^5 \rightarrow D_{2d}^9$ pour le borohydrure de sodium.

Canadian Journal of Chemistry, **49**, 3272 (1971)

Introduction

The high temperature modifications of both KBH_4 and $NaBH_4$ are known to be face-centered cubic (O_h^5-*Fm3m*) with four molecules per unit cell (1–3). Under the symmetry requirements of the O_h^5 space group the BH_4^- tetrahedra may randomly take up the two equivalent orientations possible in the lattice. This gives rise to the disordered structure known as phase *I* (4).

The heat capacity of KBH_4 has been obtained in the temperature interval 0 to 700 °K (5). An anomaly appeared at 77.2 °K and it was associated with a disorder–order transformation whose onset was identified with a broad transition from about 450 to 200 °K which appeared in the heat capacity. That the onset of the disorder–order transformation is at a higher temperature than that fixed by the anomaly is also suggested by the fact that the anomaly accounts for only 0.70 of the 1.38 e.u. expected for the excess entropy of transition in a simple disorder–order transformation. It is known that the structure of KBH_4 remains cubic down to 90 °K (6). However, no crystal studies have been undertaken below the temperature of 77.2 °K fixed by the anomaly. Thus, the structure of the completely ordered crystal is not known. The spectrum of the BH_4^- lattice vibrations should be sensitive to any change in site symmetry accompanying the transition. Accordingly, we have recorded the infrared spectra of KBH_4 and KBD_4 at 295 and at 10 °K. Raman spectra of these compounds have been recorded at 295 and 80 °K.

The mid-infrared spectrum of $NaBH_4$, at various temperatures in the interval 191 to 298 °K, has been reported by Schutte (4) and by Schutte and Ketelaar (7). These authors observed spectral changes which could be related to a phase transformation in $NaBH_4$. An anomaly in the heat capacity of $NaBH_4$ has placed this phase transformation at 189.9 °K (8). The excess entropy of transition of 1.22 e.u. suggests a simple disorder–order transformation analogous to that found in the ammonium halides (9–12). The transformation at 189.9 °K results in a contraction along what becomes the *c* axis of a body centered tetragonal structure (2). If a simple disorder–order transformation involving the orientations of the BH_4^- ions is assumed the low temperature phase *II* structure ($Z = 2$) must be consistent with the space group D_{2d}^9-$I\bar{4}m2$.

The low temperature infrared spectrum of $NaBH_4$ reported by Schutte (4) is compatible with BH_4^- ions which lie on the D_{2d} sites predicted by the D_{2d}^9 space group. As a continuation of Schutte's work we have recorded both the

[1]Dr. K. B. Harvey passed away September 27, 1970.

[2]Present address: Department of Electrical Engineering, University of Waterloo, Waterloo, Ontario.

Can. J. Chem. Downloaded from www.nrcresearchpress.com by 210.87.254.6 on 09/05/12
For personal use only.

infrared and Raman spectrum of $NaBH_4(I)$ at 295 °K and $NaBH_4(II)$ at 80 °K. A similar study has been made of $NaBD_4$.

Experimental

The KBH_4 and $NaBH_4$ were obtained from Metal Hydrides Inc. and the KBD_4 and $NaBD_4$ were obtained from Merck, Sharp and Dohme (Canada) Ltd. All compounds had an assay of not less than 98%. They were used without further purification.

In the mid-infrared (4000–500 cm^{-1}) studies the samples were prepared by mechanically depositing thin films of polycrystalline material on potassium bromide supports. This was accomplished by first grinding one surface of the polished support with a very fine emery paper (Carbimet 600 grit). A small mound of very finely divided crystalline powder, thoroughly moistened with carbon tetrachloride, was then rubbed between the ground surface of the support and the surface of a ground glass plate. The sample support was slid off the ground glass plate before "sticking" occurred. Next, any excess crystal powder was carefully brushed off the surface of the support. For studies in the region 600–50 cm^{-1} Nujol mulls and either cesium iodide or polyethylene supports were used. All samples were prepared in a dry nitrogen atmosphere provided by a glove box. While they were still in this atmosphere the sodium borohydride samples were fitted into a Hornig type low temperature cell. The potassium borohydride samples were fitted into a liquid helium cryostat, described elsewhere (13), under a stream of dry nitrogen.

The infrared spectra were recorded against a dry air background purged of CO_2. Two complementary double beam grating spectrophotometers were used: the Perkin–Elmer 421 and the Perkin–Elmer 301. The 421 was used in the region 4000–500 cm^{-1} and the 301 was used in the region 600–50 cm^{-1}. Both spectrophotometers were calibrated against known spectra (14). The error of measurement is estimated to be less than ± 2 cm^{-1}.

The samples for the Raman studies were also prepared in a dry nitrogen atmosphere. Polycrystalline material was compressed into a conical cavity at the end of a brass rod which fitted into a low temperature cell similar in design to the one described by Carlson (15). The Raman spectra were recorded with a Cary 81 spectrophotometer which was equipped with a Spectra-Physics He–Ne Laser. The instrument was calibrated with emission lines from a neon lamp and the uncertainty in the measured frequency shifts is less than ± 2 cm^{-1}.

Results and Discussion

(A) KBH_4 and KBD_4

The Lattice Vibrations and Their Combinations and Overtones

As the samples were cooled from 295 to 10 °K the absorptions appearing in the spectra of both KBH_4 and KBD_4 showed a progressive sharpening (Fig. 1) which gave no evidence of any static field (site group) splitting. The KBD_4 ν_4 absorption at 10 °K has a half-height band width of only 3.5 cm^{-1} and hence any unresolved site group splitting would have to be very small indeed. The only splittings which appear are the ^{10}B–^{11}B isotope shifts. In the case of KBD_4 these splittings (Fig. 3) are fully resolved. Since there is an absence of site group splitting at 10 °K the BH_4^- ions must lie on cubic sites in the ordered phase. If the phase transformation is effectively a simple order–disorder transformation involving the orientations of the BH_4^- ions then the low temperature modification will be consistent with the space group T_d^2-$F\bar{4}3m$. In order to distinguish this modification from the low temperature tetragonal modification of $NaBH_4$, known as phase *II* (4), we shall refer to it as phase *III*.

Under the T_d factor group the irreducible representations for the internal, optical translatory(o.t.), optical libratory(o.l.), and acoustical translatory(a.t.) KBH_4 lattice vibrations are:

$$\Gamma \text{ (internal)} = A_1 + E + 2F_2$$
$$\Gamma \text{ (o.t.)} = F_2$$
$$\Gamma \text{ (o.l.)} = F_1$$
$$\Gamma \text{ (a.t.)} = F_2$$

Only the vibrations of F_2 symmetry may appear in the infrared. Vibrations of A_1, E, and F_2 symmetries may produce Raman scattering. The borohydride ion $\nu_3(F_2)$ and $\nu_4(F_2)$ lattice vibrations show a negligible frequency shift as the temperature is lowered from 80 to 10 °K. Therefore, in Table 1 we have included the $\nu_1(A_1)$ and $\nu_2(E)$ frequencies as observed at 80 °K (Fig. 2) in the phase *III* results. On this basis the wavenumbers of the internal normal vibrations of $KBH_4(III)$ are 2314.5, 1251.5, 2281, and 1121 cm^{-1}, respectively, for $\nu_1(A_1)$, $\nu_2(E)$, $\nu_3(F_2)$, and $\nu_4(F_2)$. The corresponding $KBD_4(III)$ wavenumbers are 1199.5, 892, 1724, and 855 cm^{-1}. In the infrared spectra $KBH_4(III)$ and $KBD_4(III)$ absorptions appear at 178 and 172 cm^{-1}. The frequency ratio of 0.97 indicates that these absorptions are due to translations.

In the second order spectra of the phase *III* potassium borohydrides only three principal lines are observed. These are $2\nu_4(A_1 + E + F_2)$, $\nu_2 + \nu_4(F_1 + F_2)$, and $2\nu_2(A_1 + E)$. Enhanced intensities and/or anomalous predicted–observed frequency shifts in the second order spectra indicate that both $2\nu_4(F_2)$ and $\nu_2 + \nu_4(F_2)$ interact with $\nu_3(F_2)$. In the Raman spectrum of

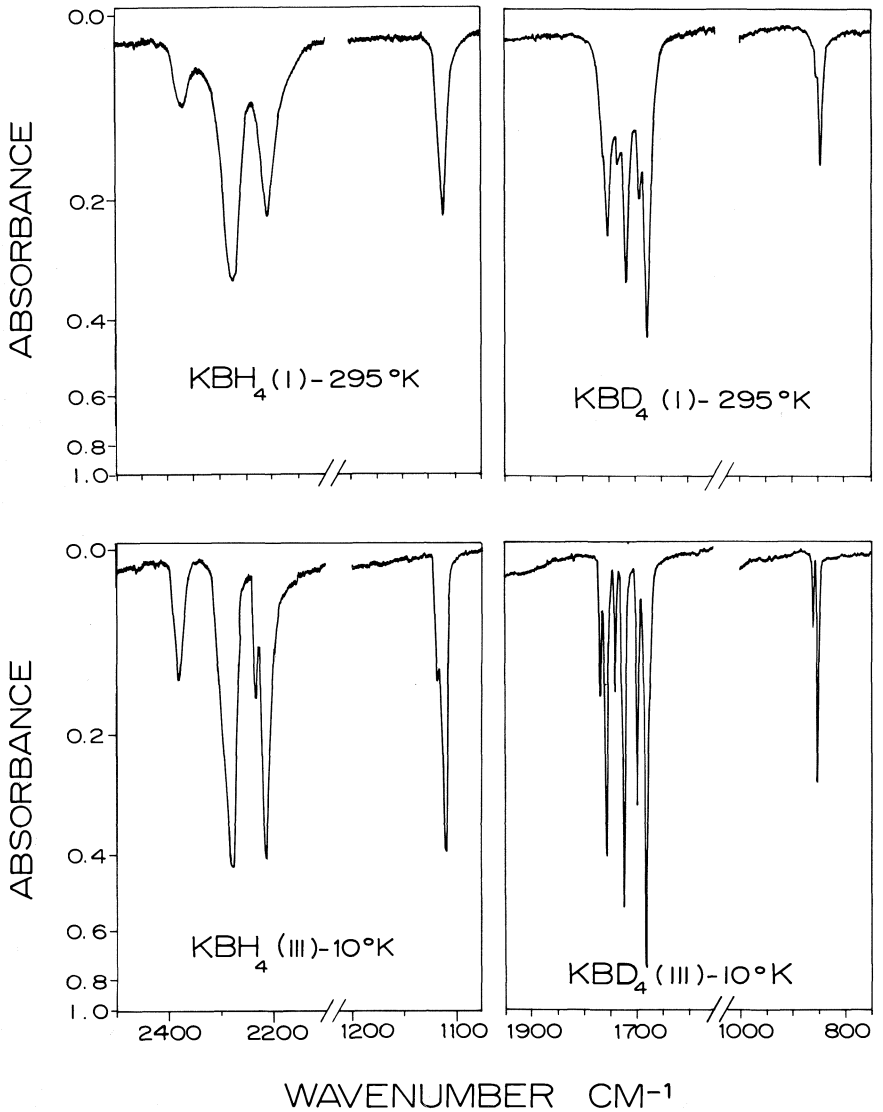

FIG. 1. The infrared spectra of KBH_4 and KBD_4 at 295 and 10 °K.

$KBH_4(III)$ the appearance of a $2\nu_4$ doublet results from a further interaction. In this case $\nu_1(A_1)$ and $2\nu_4(A_1)$ undergo Fermi resonance.

The vibrational assignments for KBH_4 and KBD_4 at 295 °K appear in Table 2.

(B) $NaBH_4$ and $NaBD_4$

Internal Lattice Vibrations and Their Combinations and Overtones

The irreducible representation for the internal fundamentals of $NaBH_4(II)$ may be summarized as follows

$$\Gamma \text{ (internal)} = 2A_1 + B_1 + 2B_2 + 2E$$

Since there is only one molecule in the primitive unit cell there are no correlation field effects. Thus, the four vibrations of the free BH_4^- ion become the precursors of 7 crystal modes which arise from a splitting of the degenerate vibrations by the static field. The correlation diagram showing this is found in Table 3. All 7 internal vibrations may produce Raman scattering. Only vibrations of B_2 and E symmetries may be infrared active.

The high and low temperature spectra (Figs. 4 and 5) indicate that $NaBD_4$ undergoes a phase transformation analogous to the one observed

Can. J. Chem. Downloaded from www.nrcresearchpress.com by 210.87.254.6 on 09/05/12
For personal use only.

TABLE 1. Low temperature infrared and Raman frequencies (in cm^{-1}) of KBH_4 and KBD_4

	KBH_4		KBD_4	
Assignment	Raman frequencies(80 °K)	Infrared frequencies(10 °K)	Raman frequencies(80 °K)	Infrared frequencies(10 °K)
$\nu_1(A_1)$	2314.5		1599.5	
$\nu_2(E)$	1251.5		892	
$^{10}\nu_3(F_2)$		2297 (sh)	1737	1739
$\nu_3(F_2)$	2291	2281	1723.5	1724
$^{10}\nu_4(F_2)$		1131		864
$\nu_4(F_2)$	1122	1121	856	855
$T_1(F_2)$		178		172
$2\nu_2(A_1 + E)$	2497		1782	
$^{10}\nu_2 + {}^{10}\nu_4(F_2)$			1770	1767
$\nu_2 + \nu_4(F_2)$	2386	2384	1757	1757
$2^{10}\nu_4(F_2)$	2238	2235	1698	1697
$2\nu_4(F_2)$	2224	2217	1682	1682
$2\nu_4(A_1)$	2185.5			

*sh = shoulder.

TABLE 2. Infrared and Raman frequencies (in cm^{-1}) of KBH_4 and KBD_4 at 295 °K

	KBH_4		KBD_4	
Assignment	Raman frequencies	Infrared frequencies	Raman frequencies	Infrared frequencies
ν_1	2310		1599	
ν_2	1248.5		890.5	
$^{10}\nu_3$			1733 (sh)	1732
ν_3		2279	1717	1717
$^{10}\nu_4$				858 (sh)
ν_4	1118	1117	851	850
T_1		173		168
$2\nu_2$	2495		1782	
$^{10}\nu_2 + {}^{10}\nu_4$				1762 (sh)
$\nu_2 + \nu_4$	2380	2377	1752.5	1752
$2^{10}\nu_4$			1694	1693
$2\nu_4$	2217	2213	1679	1677
$2\nu_4$	2181			

TABLE 3. Correlation diagram for the BH_4^- lattice vibrations of $NaBH_4(II)$

Vibration	Free ion symmetry(T_d)		Site/factor group symmetry(D_{2d})
ν_1	A_1	→	A_1
ν_2	E	→	A_1, B_1
ν_3	F_2	→	B_2, E
ν_4	F_2	→	B_2, E

in $NaBH_4$ (8). The low temperature spectra of both compounds can then be explained on the basis of the D_{2d} factor group analysis. We may note that the vibrations of compounds containing naturally occurring boron may be sensitive to ^{10}B–^{11}B isotope shifts. In the case of the sodium borohydrides this is true of ν_3 and ν_4. In order to distinguish between splittings arising from isotope shifts and splittings arising from the static field we may compare the low temperature vibrational spectra of the sodium borohydrides with that of the cubic potassium borohydrides. The appropriate ^{10}B–^{11}B isotope shifts are compared in Table 4.

Since the vibrational spectrum of $NaBD_4(II)$ is characterized by sharp well resolved lines (Figs. 4, 5, and 6) we choose this salt for a discussion of vibrational assignments. The assignments for $NaBH_4(II)$ are, for the most part, completely analogous. An intense Raman scattering at 1622 cm^{-1} in the spectrum of $NaBD_4$(II) (Fig. 5) is assigned as $\nu_1(A_1)$. The two expected components of ν_2 also appear. The scattering at 916 cm^{-1} is arbitrarily assigned as $\nu_2(A_1)$ and the 904 cm^{-1} scattering is then assigned as $\nu_2(B_1)$. (It will be seen shortly that these assignments can be con-

Can. J. Chem. Downloaded from www.nrcresearchpress.com by 210.87.254.6 on 09/05/12
For personal use only.

Can. J. Chem. Downloaded from www.nrcresearchpress.com by 210.87.254.6 on 09/05/12
For personal use only.

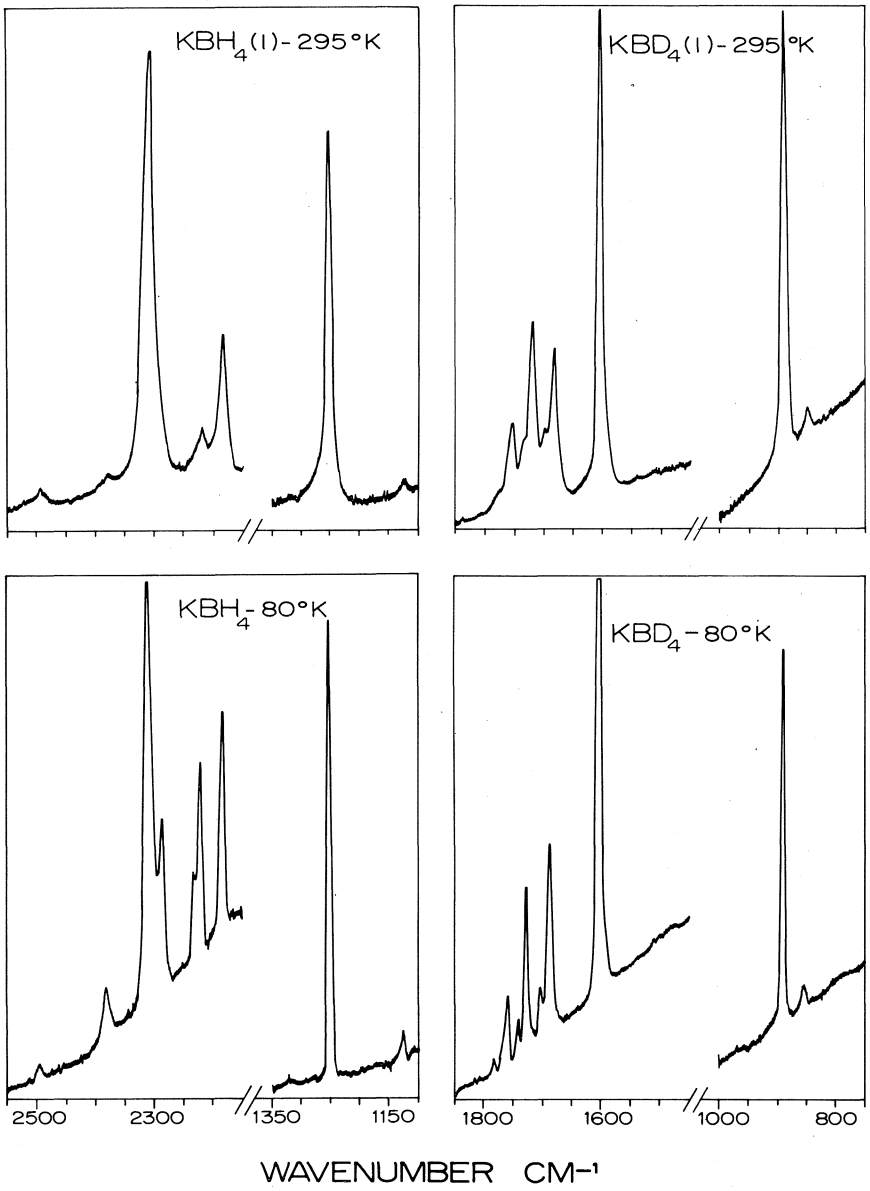

FIG. 2. The Raman spectra of KBH_4 and KBD_4 at 295 and 80 °K.

firmed when the possible combinations for $\nu_2 + \nu_4$ are considered.) In the region 800–1000 cm^{-1} four absorptions appear in the infrared (Figs. 4 and 6). The most intense absorption appearing at 854.5 cm^{-1} is assigned as $\nu_4(E)$; $^{10}\nu_4(E)$ appears at 865 cm^{-1}. This leaves two absorptions, either one of which could be assigned as $\nu_4(B_2)$. The most reasonable choice is the 870 cm^{-1} absorption since, as will be seen later, it predicts $2\nu_4$ and $\nu_2 + \nu_4$ overtones and combinations which are consistent with the observed spectral results. The assignment for the anomalous line at 877 cm^{-1} is discussed later.

The region 1650–1850 cm^{-1} is very rich in spectral information. The prominent absorption at 1735.5 cm^{-1} is assigned as $\nu_3(E)$; $^{10}\nu_3(E)$ appears at 1755 cm^{-1}. A second absorption possessing striking intensity is found at 1692

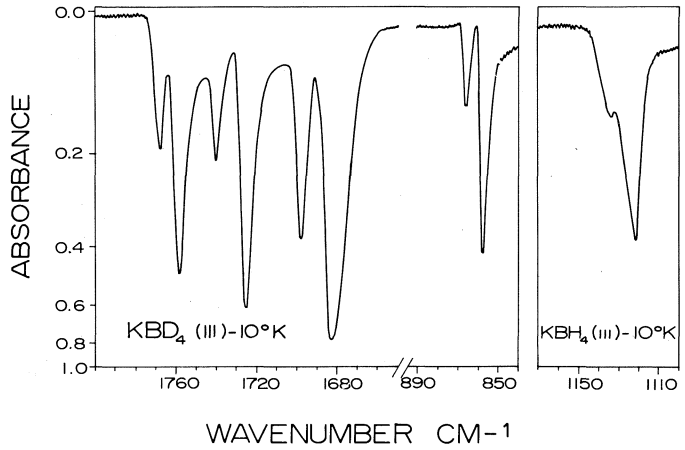

FIG. 3. Detail in the infrared spectra of KBD_4(III) and KBH_4(III).

TABLE 4. ^{10}B–^{11}B isotope shifts (in cm^{-1}) in the low temperature BH_4^- lattice vibrations of sodium and potassium borohydride

Compound	$^{10}\nu_3$	ν_3	Shift	$^{10}\nu_4$	ν_4	Shift
KBH_4	2297 (sh)	2281	26	1131	1121	10
$NaBH_4$	2334 (sh)	2303	31	1134	1122	12
KBD_4	1739	1724	15	864	855	9
$NaBD_4$	1755	1735.5	19.5	865	854.5	10.5

cm^{-1} and it is assigned to a component of $2\nu_4$. Since it is observed with such enhanced intensity it can be assumed to be undergoing Fermi resonance with $\nu_3(E)$. This selects E type symmetry and hence it must originate from the combination $\nu_4(E) + \nu_4(B_2) = 2\nu_4(E)$. The predicted–observed frequency shift of 33 cm^{-1} is also consistent with an interaction of $\nu_3(E)$ and $2\nu_4(E)$. The absorption appearing at 1715 cm^{-1} on the high frequency side of $2\nu_4(E)$ can be assigned as $2\,^{10}\nu_4(E)$. Assuming a $^{10}\nu_4(B_2)$ frequency of 880 cm^{-1} gives a predicted–observed frequency shift of 30 cm^{-1} for $2\,^{10}\nu_4(E)$. Besides $2\nu_4(E)$ there are two other possible $2\nu_4$ components. These are $\nu_4(B_2) + \nu_4(B_2) = 2\nu_4(A_1)$ and $\nu_4(E) + \nu_4(E) = 2\nu_4(A_1 + B_1 + B_2)$. The later component is expected to appear in the infrared with a predicted frequency of 1709 cm^{-1}. However, no evidence was found for its appearance. (We may note that it appears in the Raman spectrum of $NaBH_4$(*II*) as a result of interaction with $\nu_1(A_1)$ (Fig. 5).) The remaining absorption on the low frequency side of $\nu_3(E)$ at 1724 cm^{-1} is assigned as $\nu_3(B_2)$. The absorptions appearing at 1764, 1773, 1789, and 1798 cm^{-1} must be assigned to combinations of $\nu_2 + \nu_4$. There are 8 possible predicted combinations. These are

$$\begin{aligned}
\nu_2(B_1) + \nu_4(E) &= 1759(E)\\
^{10}\nu_2(B_1) + {}^{10}\nu_4(E) &= 1769(E)\\
\nu_2(A_1) + \nu_4(E) &= 1771(E)\\
^{10}\nu_2(A_1) + {}^{10}\nu_4(E) &= 1781(E)\\
\nu_2(B_1) + \nu_4(B_2) &= 1774(A_2)\\
^{10}\nu_2(B_1) + {}^{10}\nu_4(B_2) &= 1784(A_2)\\
\nu_2(A_1) + \nu_4(B_2) &= 1786(B_2)\\
^{10}\nu_2(A_1) + {}^{10}\nu_4(B_2) &= 1796(B_2)
\end{aligned}$$

The combinations of B_2 and E symmetry types will be both infrared and Raman active, while the combinations of A_2 symmetry type will be inactive. Since combinations of E symmetry can undergo Fermi resonance with $\nu_3(E)$ and those of B_2 symmetry can interact with $\nu_3(B_2)$, it can be expected that the observed combinations may have enhanced intensities and may also lie at frequencies slightly higher than those predicted. On this basis the assignments for the 1764, 1773, 1789, and 1798 cm^{-1} absorptions are $\nu_2(B_1) + \nu_4(E)$, $\nu_2(A_1) + \nu_4(E)$, $\nu_2(A_1) + \nu_4(B_2)$ and

Can. J. Chem. Downloaded from www.nrcresearchpress.com by 210.87.254.6 on 09/05/12
For personal use only.

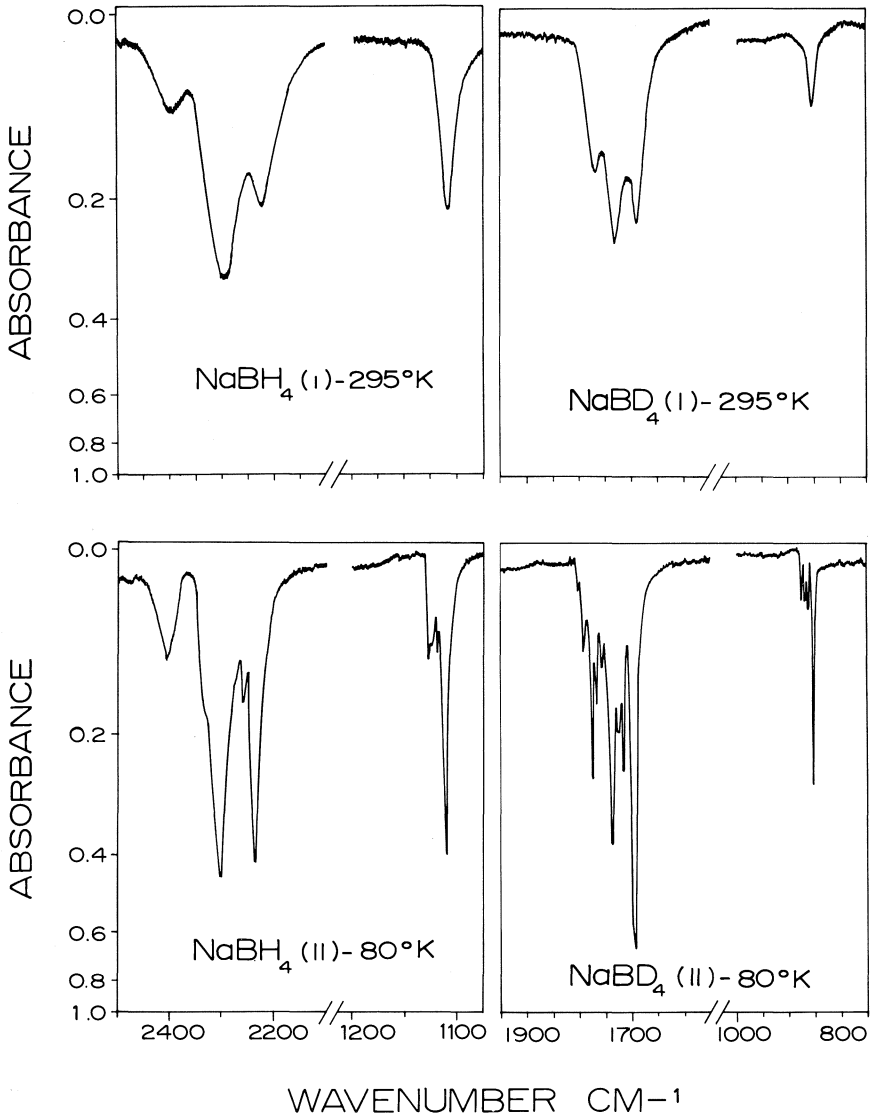

FIG. 4. The infrared spectra of $NaBH_4$ and $NaBD_4$ at 295 and 80 °K.

$^{10}\nu_2(A_1) + {}^{10}\nu_4(B_2)$. This choice of assignments is the only reasonable one and removes the arbitrariness associated with the assignments $\nu_2(A_1)$, $\nu_2(B_1)$, and $\nu_4(B_2)$.

The foregoing $NaBD_4(II)$ assignments along with those for $NaBH_4(II)$ are summarized in Table 5. The assignments for the high temperature disordered cubic phases appear in Table 6. Table 7 compares the earlier low temperature results obtained by Schutte (4) for $NaBH_4$ with those obtained in this work. A comparison of the results shows that Schutte reports two $2\nu_4$ absorptions which are not compatible with the results of this work. It is possible that the 2223 cm^{-1} absorption could be assigned as $\nu_4(E) + \nu_4(E) = 2\nu_4(B_2)$ which has a predicted frequency of 2244 cm^{-1}. However, if this is the case such a line should also be observed in the spectrum of $NaBD_4(II)$. The shoulder reported at 2197 cm^{-1} appears to be completely spurious. Also, the 2287 cm^{-1} absorption reported by Schutte does not appear in our spectra. Since it is reported as a

Can. J. Chem. Downloaded from www.nrcresearchpress.com by 210.87.254.6 on 09/05/12
For personal use only.

Can. J. Chem. Downloaded from www.nrcresearchpress.com by 210.87.254.6 on 09/05/12
For personal use only.

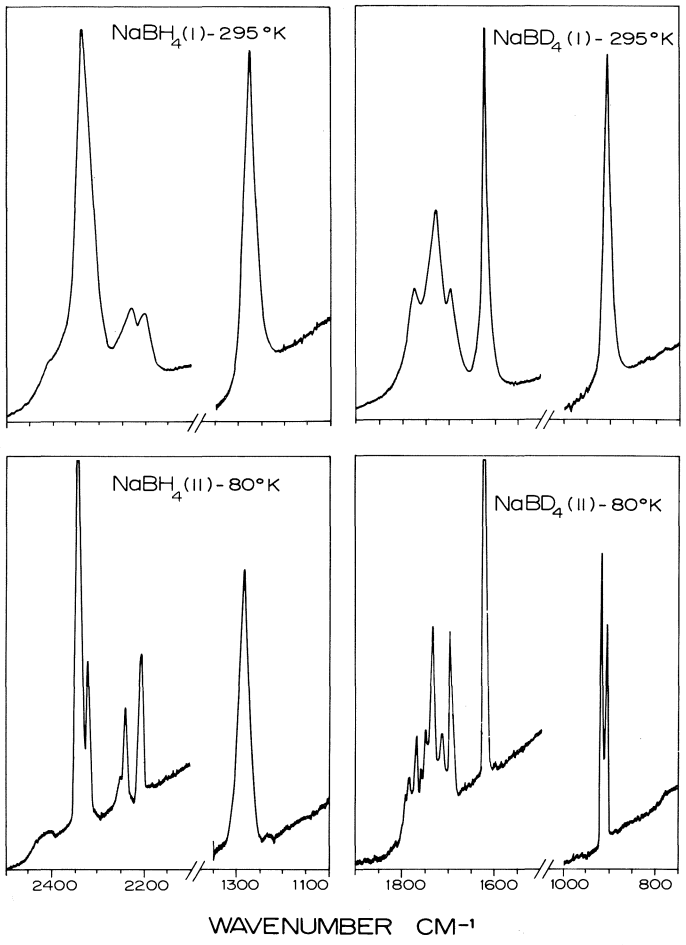

FIG. 5. The Raman spectra of $NaBH_4$ and $NaBD_4$ at 295 and 80 °K.

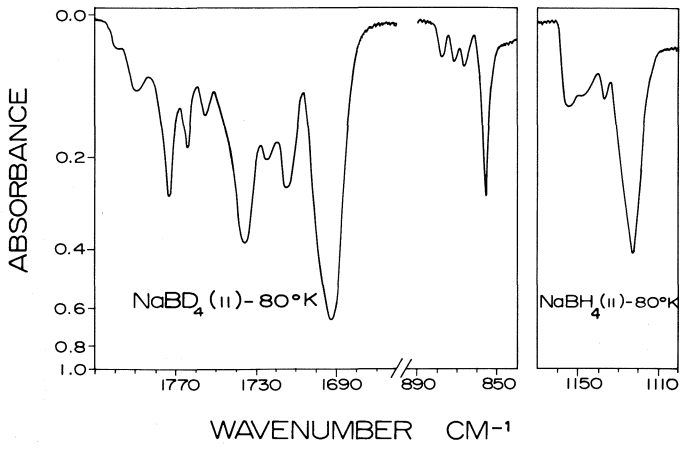

FIG. 6. Detail in the infrared spectra of $NaBD_4$(II) and $NaBH_4$(II).

Can. J. Chem. Downloaded from www.nrcresearchpress.com by 210.87.254.6 on 09/05/12
For personal use only.

TABLE 5. Infrared and Raman frequencies (in cm^{-1}) of $NaBH_4$ and $NaBD_4$ at 80 °K

Assignment	$NaBH_4(II)$		$NaBD_4(II)$	
	Raman frequencies	Infrared frequencies	Raman frequencies	Infrared frequencies
$\nu_1(A_1)$	2341		1622	
$\nu_2(A_1)$	1280		916	
$\nu_2(B_1)$			904	
$\nu_3(B_2)$		2272 (sh)		1724.5
$\nu_3(E)$	2322	2302	1740.5	1735.5
$^{10}\nu_3(E)$		2334 (sh)		1755
$\nu_4(B_2)$		1148		870
$\nu_4(E)$		1122		854.5
$^{10}\nu_4(E)$		1134		865
$\nu_L(A_2,E)$		(384)*		(292)
$\nu_T(B_2,E)$		172		167
$2\nu_2(A_1)$	2560		1821	
$^{10}\nu_2 + {}^{10}\nu_4(B_2)$			1800	1798
$\nu_2 + \nu_4(B_2)$			1791	1789
$\nu_2 + \nu_4(E)$	2408	2404	1775	1773
$\nu_2 + \nu_4(E)$			1766	1764
$2^{10}\nu_4(E)$	2257	2256	1720	1715
$2\nu_4(E)$	2244	2236	1701	1692
$2\nu_4(A_1)$	2210			
$3\nu_L$		1153		877

*The frequencies in parentheses for ν_L are inferred from $3\nu_L$.

TABLE 6. Infrared and Raman frequencies (in cm^{-1}) of $NaBH_4$ and $NaBD_4$ at 295 °K

Assignment	$NaBH_4(I)$		$NaBD_4(I)$	
	Raman frequencies	Infrared frequencies	Raman frequencies	Infrared frequencies
ν_1	2335		1618	
ν_2	1278		907.5	
ν_3		2297	1728	1729
ν_4		1119		853
ν_T		160		155
$\nu_2 + \nu_4$	2403 (sh)	2393	1772.5	1767
$2\nu_4$	2229	2222	1695	1690
$2\nu_4$	2197.5			

TABLE 7. Infrared frequencies (in cm^{-1}) of $NaBH_4(II)$

Assignment	Infrared frequencies*	
	This work	Schutte (4)
$\nu_4(E)$	1122	1123
$^{10}\nu_4(E)$	1134	1135 vw
$3\nu_L$	1148 (sh)	
$\nu_4(B_2)$	1153	1152 vw
		2197 (sh) w
		2223 s
$2\nu_4(E)$	2236	2238 s
$2^{10}\nu_4(E)$	2256	2256 m
$\nu_3(B_2)$	2272 (sh)	
		2287 vs
$\nu_3(E)$	2303	2305 vs
$^{10}\nu_3(E)$	2334 (sh)	
$\nu_2 + \nu_4(E)$	2404	2404 w

*v = very, w = weak, m = medium, s = strong, sh = shoulder.

strong distinct absorption it is difficult to associate it with the shoulder we observe at 2272 cm^{-1}. The shoulders we observe at 1148 and 2334 cm^{-1} may have been missed in the earlier work because of their low intensity. A possible explanation for the discrepancies between the results is that Schutte's samples may have been prepared while exposed to the atmosphere. Earlier work done in this laboratory[3] has shown that such exposure can allow for the occurrence of slight decomposition and possibly the formation of hydrated forms of $NaBH_4$ (16). Such introduction of impurities into the sample could easily explain the discrepancies. The point to be emphasized though is that Schutte's results, like

[3]N. R. McQuaker, unpublished results.

Can. J. Chem. Downloaded from www.nrcresearchpress.com by 210.87.254.6 on 09/05/12
For personal use only.

those of this work, show an unambiguous splitting of ν_4 which may be associated with the disorder–order phase transformation.

External Lattice Vibrations

The irreducible representations for the optical translatory (o.t.), optical libratory (o.l.), and acoustical translatory (a.t.) fundamentals of $NaBH_4(II)$ are the following

$$\Gamma(\text{o.t.}) = B_2 + E$$
$$\Gamma(\text{o.l.}) = A_2 + E$$
$$\Gamma(\text{a.t.}) = B_2 + E$$

None of the Raman active external fundamentals produced observable scattering, and in the infrared spectra of the sodium borohydrides only one absorption appears which may be associated with the external fundamentals. In the spectrum of $NaBH_4(II)$ it appears at 172 cm^{-1} and in the $NaBD_4(II)$ spectrum it appears at 167 cm^{-1}. The frequency ratio of 0.97 indicates that these absorptions are due to translations. The anomalous absorption appearing in the $NaBD_4(II)$ spectrum at 877 cm^{-1} may be associated with the anomalous $NaBH_4(II)$ absorption appearing at 1153 cm^{-1}. A tentative assignment is $3\nu_L$. The assumption of the $3\nu_L$ assignment places librations, without correction for anharmonicity, at 384 cm^{-1} for $NaBH_4(II)$ and at 292 cm^{-1} for $NaBD_4(II)$; the frequency ratio is 0.76 which compares with an expected ratio of 0.71. There is only one piece of experimental information with which to check the $3\nu_L$ assignment. Stockmeyer and Stephenson (17) using heat capacity data have estimated that ν_L for $NaBH_4(II)$ should lie at about 350 cm^{-1}. While this result does not exclude the $3\nu_L$ assignment, it does not give exceptionally strong support for it either and hence the $3\nu_L$ assignments must be regarded as only tentative.

The authors acknowledge with thanks the support o the National Research Council of Canada. One of us (N.R.M.) wishes to gratefully acknowledge the award of a National Research Council of Canada Post-graduate Scholarship.

1. A. M. SOLDATE. J. Am. Chem. Soc. **69**, 987 (1947).
2. S. C. ABRAHAMS and J. KALNAJS. J. Chem. Phys. **22**, 434 (1954).
3. E. R. PETERSON. Ph.D. Thesis. Washington State University, 1967.
4. C. J. H. SCHUTTE. Spectrochim. Acta, **16**, 1054 (1960).
5. G. T. FURUKAWA, M. L. REILLY, and J. H. PICCIRELLI. J. Res. Nat. Bur. Std. **68A**, 651 (1964).
6. P. T. FORD and H. M. POWELL. Acta Cryst. **7**, 604 (1954).
7. C. J. H. SCHUTTE and J. A. A. KETELAAR. Spectrochim. Acta, **17**, 815 (1961).
8. H. L. JOHNSTON and N. C. HALLET. J. Am. Chem. Soc. **75**, 1467 (1953).
9. C. C. STEPHENSON, L. A. LANDERS, and A. G. COLE. J. Chem. Phys. **21**, 1044 (1952).
10. C. C. STEPHENSON, R. W. BLUE, and J. W. STOUT. J. Chem. Phys. **21**, 1046 (1952).
11. M. SORAI, H. SUGA, and S. SEKI. Bull. Chem. Soc. Japan, **38**, 1125 (1965).
12. C. C. STEPHENSON and A. M. KARO. J. Chem. Phys. **48**, 104 (1968).
13. A. H. HARDEN. Ph.D. Thesis. University of British Columbia, 1970.
14. IUPAC Tables of Wavenumbers for the Calibration of Infrared Spectrophotometers. Butterworth, Washington, D.C. 1961.
15. G. L. CARLSON. Spectrochim. Acta, **24A**, 1519 (1968).
16. Sodium borohydride, a manual of techniques. Metal Hydrides Inc. 1958.
17. W. H. STOCKMEYER and C. C. STEPHENSON. J. Chem. Phys. **21**, 1311(1953).

Can. J. Chem. Downloaded from www.nrcresearchpress.com by 210.87.254.105 on 09/05/12
For personal use only.

Low Temperature Infrared and Raman Spectra of Lithium Borohydride

K. B. HARVEY[1] AND N. R. MCQUAKER[2]

Department of Chemistry, University of British Columbia, Vancouver 8, British Columbia

Received April 22, 1971

The infrared spectra of polycrystalline $LiBH_4$ and $LiBD_4$ have been recorded in the region 4000–50 cm^{-1} at 80 °K. Raman spectra of polycrystalline samples were also recorded at this temperature. The spectra of the BH_4^- and BD_4^- lattice vibrations are consistent with symmetrically equivalent borohydride ions which lie on either general positions, two-fold axes or mirror-planes. Six lattice vibrations of translatory origin appear in the infrared spectrum of $LiBH_4$ and a mode of libratory origin is inferred from an absorption tentatively assigned as a second overtone of a librational mode. Similar spectral results are obtained for $LiBD_4$. The inferred librational frequencies are 418 cm^{-1} for the BH_4^- ions and 319 cm^{-1} for the BD_4^- ions.

Les spectres infrarouges du $LiBH_4$ et du $LiBD_4$ sous la forme polycristalline ont été enregistrés dans la région de 4000–50 cm^{-1} à 80 °K. Les spectres Raman des échantillons polycristallins ont été aussi enregistrés à cette température. Les spectres de vibration dans le réseau pour BH_4^- et BD_4^- sont compatibles avec une symétrie équivalente pour les ions borohydrure qui se trouvent sur l'une ou l'autre des positions d'un axe de symétrie d'ordre deux ou des plans de symétrie. Les six vibrations du réseau dues à un mouvement de translation apparaissent dans le spectre infrarouge du $LiBH_4$ et un mode d'une origine oscillatrice qui est déduite d'une absorption peut être assigné à titre d'essai comme une seconde harmonique d'un mode d'oscillation. D'autres spectres analogues sont obtenus pour $LiBD_4$. Les fréquences oscillatrices déduites sont 418 cm^{-1} pour les ions BH_4^- et 319 cm^{-1} pour les ions BD_4^-.

Canadian Journal of Chemistry, 49, 3282 (1971)

Introduction

The room temperature mid-infrared spectrum of $LiBH_4$ was reported by Price in 1949 (1). Evidently no vibrational studies of this compound or its deuterated analog, $LiBD_4$, have been reported since. An early X-ray crystal study of $LiBH_4$ (2) indicated an orthorhombic structure (D_{2h}^{16}-*Pcmn*) with four molecules per unit cell. Under the D_{2h}^{16} space group both the lithium ions and the boron atoms lie on mirror-plane positions of multiplicity four while the hydrogen atoms lie on two independent sets of general positions of multiplicity eight. The four BH_4^- ions in the unit cell are symmetrically equivalent; *i.e.*, they are symmetrically related by a center of symmetry and two axial glide planes at $x = 1/4$ and $x = 3/4$. Heat capacity data for $LiBH_4$ (3) showed no anomalies in the temperature interval 15–303 °K. Recently, the nuclear spin lattice relaxation times, T_1, for protons and deuterons in polycrystalline $LiBH_4$ and $LiBD_4$ have been measured (4, 5). The results have been interpreted as indicating that both $LiBH_4$ and $LiBD_4$ contain borohydride ions of two crystallographically independent kinds. Thus there is an apparent discrepancy between the X-ray and nuclear magnetic resonance (n.m.r.) results.

The vibrational spectra of the BH_4^- and BD_4^- lattice vibrations should be sensitive to the geometry of the borohydride ions. Accordingly, we have recorded the infrared and laser Raman spectra of both $LiBH_4$ and $LiBD_4$. Several fundamental frequencies have been assigned. Librational frequencies for the BH_4^- and BD_4^- ions have been inferred from absorptions assigned as second overtones of librational modes.

Experimental

The $LiBH_4$ was obtained from Metal Hydrides Inc. and the $LiBD_4$ was obtained from Merck, Sharpe and Dohme (Canada) Ltd. Both compounds were of reagent grade and had an assay of not less than 98%. They were used without further purification.

In the low temperature infrared study the samples were prepared as Nujol mulls in a dry nitrogen atmosphere. Both cesium iodide and polyethylene supports were used. While still in the dry nitrogen atmosphere the samples were fitted into a Hornig type low temperature cell. For the Raman studies the sample preparation was identical to that described for KBH_4 and KBD_4 (6).

The infrared and Raman spectra were recorded at 80 °K using the instrumentation described previously (6).

Results and Discussion

Internal Lattice Vibrations

If the structure of lithium borohydride is consistent with the D_{2h}^{16}-*Pcmn* space group then the

[1]Dr. K. B. Harvey passed away September 27, 1970.

[2]Present address: Department of Electrical Engineering, University of Waterloo, Waterloo, Ontario.

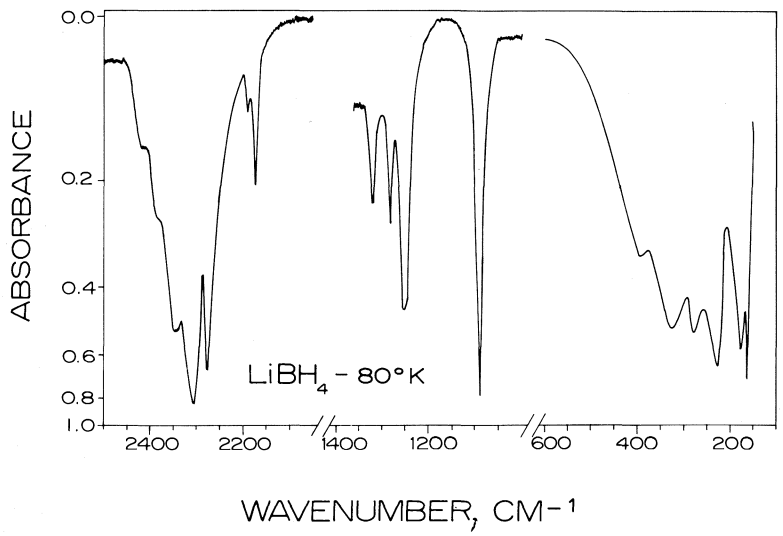

FIG. 1. The infrared spectrum of $LiBH_4$ at 80 °K.

irreducible representation for the internal fundamentals may be summarized as

$$\Gamma(\text{internal}) = 6A_g + 3B_{1g} + 6B_{2g} + 3B_{3g} + 3A_u + 6B_{1u} + 3B_{2u} + 6B_{3u}$$

These 36 internal normal vibrations may be considered to arise from the 9 normal vibrations of the BH_4^- ion through a correlation field effect resulting from the presence of four BH_4^- ions in the unit cell. The correlation diagram for the static field (site group) splitting which gives the 9 normal vibrations of the BH_4^- ion is found in Table 1. Under the D_{2h} factor group the correlation field splitting results in each A' mode giving four crystal modes of symmetries A_g, B_{2g}, B_{1u}, and B_{3u}. Similarly each A'' mode will give four crystal modes of symmetries B_{1g}, B_{3g}, A_u, and B_{2u}. Vibrations of gerade symmetry are all Raman active and vibrations of B_{1u}, B_{2u}, and B_{3u} symmetries may appear in the infrared.

In practice, it is usually found that correlation field effects do not give measurable splittings (see for example, ref. 7). Accordingly, we may make the infrared assignments according to the following scheme:

$\nu_1(B_{1u} + B_{3u})$
$\nu_2(B_{1u} + B_{3u}), \nu_2'(B_{2u})$
$\nu_3(B_{1u} + B_{3u}), \nu_3'(B_{1u} + B_{3u}), \nu_3''(B_{2u})$
$\nu_4(B_{1u} + B_{3u}), \nu_4'(B_{1u} + B_{3u}), \nu_4''(B_{2u})$

For the Raman assignments the corresponding scheme is:

$\nu_1(A_g + B_{2g})$
$\nu_2(A_g + B_{2g}), \nu_2'(B_{1g} + B_{3g})$
$\nu_3(A_g + B_{2g}), \nu_3'(A_g + B_{2g}), \nu_3''(B_{1g} + B_{3g})$
$\nu_4(A_g + B_{2g}), \nu_4'(A_g + B_{2g}), \nu_4''(B_{1g} + B_{3g})$

If the factor group splitting is small the frequencies of corresponding assignments for the two schemes will essentially coincide.

In the region 2400–2200 cm^{-1} the infrared spectrum of $LiBH_4$ (Fig. 1) has as its most prominent feature a triplet of intense absorptions which appear at 2277, 2307, and 2350 cm^{-1}. These absorptions may be associated with the broad unresolved absorption band observed by Price (1) at 2320 cm^{-1} and which he assigns to the BH_4^- stretching vibrations. With respect to the triplet we observe, the two most intense absorptions are assigned as $\nu_3(B_{1u} + B_{3u}) = 2277\ cm^{-1}$ and $\nu_3'(B_{1u} + B_{3u}) = 2307\ cm^{-1}$. The highest wavenumber component is then assigned as $\nu_3''(B_{2u}) = 2350\ cm^{-1}$. It is found that the two low wavenumber ν_3 components also appear in the Raman spectrum (Table 2). A very intense

TABLE 1. Correlation diagram for the BH_4^- lattice vibrations in $LiBH_4$

Vibration	Free ion symmetry(T_d)	Site group symmetry(C_s)
ν_1	A_1 →	A'
ν_2	E →	A', A''
ν_3	F_2 →	A', A', A''
ν_4	F_2 →	A', A', A''

Can. J. Chem. Downloaded from www.nrcresearchpress.com by 210.87.254.105 on 09/05/12
For personal use only.

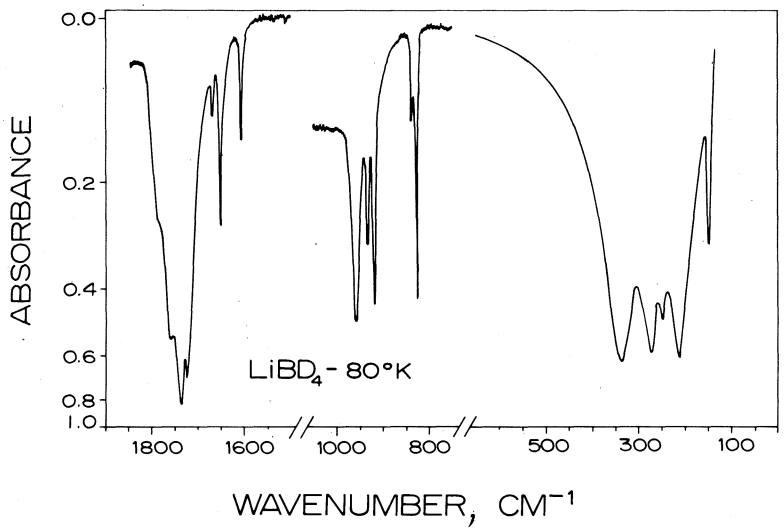

FIG. 2. The infrared spectrum of $LiBD_4$ at 80 °K.

TABLE 2. Infrared and Raman frequencies (in cm^{-1}) of $LiBH_4$ and $LiBD_4$ at 80 °K

	$LiBH_4$		$LiBD_4$	
Assignment	Raman frequencies	Infrared frequencies	Raman frequencies	Infrared frequencies
ν_1	2300		1605.5	1606
ν_2	1287	1284	923	919
ν_2'	1325	1323	937	937
ν_3	2274	2277	1721	1722
ν_3'	2309(sh)	2307	1739	1736
ν_3''		2350		1757
$^{10}\nu_4$		1099(sh)		837
ν_4		1089		828
ν_L		(418)*		(319)
T_1		391		340
T_2		324		276
T_3		274		248
T_4		232		215
T_5		175.5		149.5
T_6		162.5		
$\nu_2' + \nu_4$		2423		1785(sh)
$\nu_2 + \nu_4$		2387(sh)		
$2^{10}\nu_4$		2197		1679
$2\nu_4$		2176		1654
$3\nu_L$	1253	1254	959	957

*Frequencies in parentheses for ν_L have been inferred from $3\nu_L$.

Raman scattering at 2300 cm^{-1} is assigned as $\nu_1(A_{1g} + B_{2g})$. The presence of $\nu_1(B_{1u} + B_{3u})$ in the infrared spectrum is evidently obscured by the intense ν_3 absorptions. This is not so for $LiBD_4$ (Fig. 2). In this case ν_1 appears in the infrared at 1605.6 cm^{-1}. This compares with an intense Raman scattering observed at 1606 cm^{-1}. The structure of the ν_3 $LiBD_4$ absorptions is similar to that observed for $LiBH_4$.

In the region 1400–1000 cm^{-1} four absorptions appear in the infrared spectrum of $LiBH_4$. The lowest lying absorption which appears at 1089 cm^{-1} may be associated with the absorption Price reports at 1096 cm^{-1} and which he assigns to a BH_4^- bending vibration. In the series KBH_4, $RbBH_4$, and $CsBH_4$ ν_4 is found to appear at about 1100 cm^{-1} with ν_2 appearing some 120 cm^{-1} higher.[3] Assuming this order is preserved for

[3]N. R. McQuaker, unpublished results.

Can. J. Chem. Downloaded from www.nrcresearchpress.com by 210.87.254.105 on 09/05/12
For personal use only.

Can. J. Chem. Downloaded from www.nrcresearchpress.com by 210.87.254.105 on 09/05/12
For personal use only.

$LiBH_4$ we can assign the 1089 cm^{-1} absorption as a component of ν_4. Unexpectedly no other nearby absorptions are observed which may be assigned to the two remaining predicted components. A similar situation exists in the case of $LiBD_4$ where the ν_4 absorption appears at 828 cm^{-1}. It is very sharp and has a half-height band width of only 6 cm^{-1}. Therefore it is unlikely that more than one ν_4 component contributes to its intensity. The 837 cm^{-1} absorption appearing on the high wavenumber side of the 828 cm^{-1} ν_4 absorption is the result of a ^{10}B–^{11}B isotope shift. Since none of the ν_4 components of either $LiBH_4$ or $LiBD_4$ appear in the Raman spectra only the one component can be assigned in each case. Of the three remaining absorptions appearing in the bending region of the spectrum of each of the lithium borohydrides, two are assigned to the two predicted ν_2 components. In the spectrum of $LiBH_4$ we may associate the two sharpest absorptions with ν_2. If we choose the most intense of these absorptions as $\nu_2(B_{1u} + B_{3u})$ then the assignments are $\nu_2(B_{1u} + B_{3u}) = 1284\ cm^{-1}$ and $\nu_2'(B_{2u}) = 1323\ cm^{-1}$. The corresponding assignments for $LiBD_4$ are 919 and 933 cm^{-1}, respectively. The mean ν_2 frequencies for the crystalline BH_4^- and BD_4^- ions are 1304 and 926 cm^{-1} and the frequency ratio is 0.711. This compares with a predicted frequency ratio of 0.707 for the "free" ions. After assigning the components of ν_2 there remains an anomalous line at 1254 cm^{-1} in the spectrum of $LiBH_4$ and an anomalous line at 957 cm^{-1} in the spectrum of $LiBD_4$. The assignment for these lines is commented on later.

The spectra associated with the BH_4^- and BD_4^- lattice vibrations (Table 2) are consistent with symmetrically equivalent borohydride ions. (If there were crystallographically non-equivalent borohydride ions involved we could expect to see a set of lattice vibrations arising from each crystallographically non-equivalent ion.) The appearance of ν_1 and the two components of ν_2 in the infrared spectra allows three possibilities for the site symmetry of the borohydride ions; *i.e.*, the BH_4^- and BD_4^- ions must be on either general positions, two-fold axes or mirror-planes. This result is consistent with the symmetrically equivalent mirror-plane positions indicated by the X-ray study (2). It is likely that the rather broad minima observed for the proton and deuteron T_1 *vs.* temperature curves are due to crystallographically non-equivalent hydrogen and deuterium atoms and not crystallographically non-equivalent borohydride ions as has been suggested (4, 5).

External Lattice Vibrations

The external lattice vibrations include those of optical translatory(o.t.), optical libratory(o.l.), and acoustical translatory(a.t.) origin. The respective irreducible representations are

$$\Gamma(\text{o.t.}) = 4A_g + 2B_{1g} + 4B_{2g} + 2B_{3g} + 2A_u + 3B_{1u} + B_{2u} + 3B_{3u}$$

$$\Gamma(\text{o.l.}) = A_g + 2B_{1g} + B_{2g} + 2B_{3g} + 2A_u + B_{1u} + 2B_{2u} + B_{3g}$$

$$\Gamma(\text{a.t.}) = B_{1u} + B_{2u} + B_{3u}$$

In the vibrational Raman spectra of the lithium borohydrides none of the predicted modes of either libratory or translatory origin appear. In the infrared no modes were observed which could be assigned to libratory oscillations but 6 $LiBH_4$ and 5 $LiBD_4$ translatory vibrations were observed. In the zero wavevector limit 7 infrared active translations are predicted. These will arise from out of phase motions involving the lithium and borohydride ions. The highest wavenumber translations labelled T_1, T_2, T_3, and T_4 (Table 2) possess $LiBD_4$–$LiBH_4$ frequency ratios in the range 0.85 to 0.95. These compare with a calculated frequency ratio of 0.89. The two lowest wavenumber translations appearing in the $LiBH_4$ spectrum at 175.5 and 162.5 cm^{-1} evidently compare with the 149.5 cm^{-1} translation of $LiBD_4$. Assignments for the translations with respect to symmetry type must be reserved until a study involving single crystals and polarized radiation is made.

Combinations and Overtones

The combinations and overtones appearing in the $LiBH_4$ and $LiBD_4$ spectra which involve internal fundamentals are readily assigned to components of $2\nu_4$ and $\nu_2 + \nu_4$ (Table 2). The components of $\nu_2 + \nu_4$ are found to have higher frequencies than those predicted by the observed ν_2 and ν_4 frequencies. This may be attributed to Fermi resonance with components of ν_3.

Finally, we come to the anomalous $LiBH_4$ and $LiBD_4$ absorptions at 1254 and 957 cm^{-1}. It is likely that they have the same origin as the anomalous $NaBH_4$ and $NaBD_4$ absorptions which appear at 1153 and 877 cm^{-1} and have tentatively been assigned to second overtones of librational modes (6). If the same $3\nu_L$ assignment

is made for the lithium borohydrides, modes of libratory origin without correction for anharmonicity are placed at 418 and 319 cm^{-1} for the BH_4^- and BD_4^- ions. The frequency ratio is 0.76 which compares with an identical frequency ratio for the sodium borohydrides. The predicted frequency ratio is 0.71. In the spectra of the sodium borohydrides these absorptions appear only in the spectra of the ordered tetragonal phases. This situation is comparable with that observed for the ammonium halides (8) where absorptions involving librational modes appearing in the second order spectra suffer a striking loss in intensity as a result of a transition from an ordered phase to a disordered phase. Also with respect to the series KBH_4, $NaBH_4$, and $LiBH_4$, where the BH_4^- ions suffers a progressive distortion (from T_d to D_{2d} to C_s site symmetry), it is found that the relative intensity of $3\nu_L$, starting with zero observable intensity for KBH_4, is progressively enhanced (6). This is evidently a result of the fact that for the series KBH_4, $NaBH_4$, and $LiBH_4$ there are a progressively greater number of possible components which can contribute to the intensity of $3\nu_L$. It is expected that neutron inelastic scattering studies of the alkali-metal borohydrides will be undertaken in the near future (9). These studies will, no doubt, place the modes of libratory origin and in so doing will indicate if the assignments $3\nu_L$ are indeed correct.

The authors acknowledge with thanks the support of the National Research Council of Canada. One of us (N.R.M.) wishes to gratefully acknowledge the award of a National Research Council of Canada Postgraduate Scholarship.

1. W. C. Price. J. Chem. Phys. **17**, 1044 (1949).
2. P. M. Harris and E. P. Meibohm. J. Am. Chem. Soc. **69**, 1231 (1947).
3. N. C. Hallet and H. L. Johnston. J. Am. Chem. Soc. **75**, 1496 (1953).
4. T. Tsang and T. C. Farrar. J. Chem. Phys. **50**, 3498 (1968).
5. L. Niemela and J. Auranen. Ann. Univ. Turku, A **I**, 132 (1970).
6. K. B. Harvey and N. R. McQuaker. Can. J. Chem. This issue.
7. K. B. Harvey and N. R. McQuaker. J. Chem. Phys. **55**, 4390 (1971).
8. E. L. Wagner and D. F. Hornig. J. Chem. Phys. **18**, 296 (1950); **18**, 305 (1950).
9. T. C. Farrar. Private communication.

Can. J. Chem. Downloaded from www.nrcresearchpress.com by 210.87.254.105 on 09/05/12
For personal use only.

Can. J. Chem. Downloaded from www.nrcresearchpress.com by 210.87.254.6 on 09/05/12
For personal use only.

Ion Scavenging by Neopentane in γ-Irradiated Liquid Alkanes

J. A. STONE AND G. MATSUSHITA
Chemistry Department, Queen's University, Kingston, Ontario

Received May 7, 1971

The γ-radiolysis of low concentrations of neopentane in liquid cyclo-C_5H_{10} and C_2H_6 at 0.25 g ml^{-1} density leads to methane yields much greater than expected from the mixture compositions. In cyclo-C_6H_{12}, *n*-C_6H_{14}, cyclo-$C_6H_{11}CH_3$, and 3-methylpentane the yields are much less than expected. The effect is explained in terms of positive ion scavenging which is enhanced by added electron scavengers. The efficiency of scavenging by $C(CD_3)_4$ in C_2H_6 is equal to that of ND_3. The efficiency in cyclo-C_5H_{10} is less than that in C_2H_6 but is greater than that observed previously in this solvent.

La radiolyse-γ, à faible concentration de néopentane dans le cyclopentane et C_2H_6 à une densité de 0.25 g ml^{-1}, conduit à des rendements en méthane nettement plus grands à ceux prévus d'après les compositions du mélange. Dans le cyclohéxane le *n*-C_6H_{14}, le méthyl cyclohéxane et le méthyl-3 pentane les rendements sont inférieurs à ceux prévus. Les résultats sont expliqués par le piègage des ions positifs qui est augmenté par l'adjonction d'agents piègeurs électroniques. L'efficacité du piègage par $C(CD_3)_4$ dans C_2H_6 est la même que celle de ND_3. L'efficacité dans le cyclohéxane est moindre que dans C_2H_6 mais plus grande que celle observée précédemment dans ce solvant.

Canadian Journal of Chemistry, **49**, 3287 (1971)

Introduction

The yields of products from the radiolysis of liquid binary mixtures of saturated hydrocarbons are often non-linear functions of the constituent electron fractions (1, 2). This is usually taken to imply some form of "energy transfer" subsequent to the initial energy deposition which is assumed to occur according to the electron fraction. We have previously studied "energy transfer" by measuring HD and D_2 yields from low concentrations of perdeuterocarbons in hydrocarbon solvents (3, 4). The results obtained are interpretable in terms of positive charge transfer which is always exothermic when judged by gas phase ionization potentials. HD and D_2 yields above those expected for the electron fraction of perdeuterocarbon are obtained when the protiated solvent has the higher ionization potential and the reverse occurs when the solvent has the lower ionization potential. The reactions leading to enhanced yields may be represented by the equations

$$[1] \qquad R_1H \rightsquigarrow R_1H^+ + e$$

$$[2] \qquad R_1H^+ + R_2D \rightarrow R_1H + R_2D^+$$

$$[3] \qquad R_2D^+ + e \rightarrow D, D_2 \rightarrow HD, D_2$$

By confining ourselves to studying only hydrogen yields and using only low concentrations of perdeuterocarbon we have a sensitive technique and we avoid possible complications inherent in the measurement of liquid products such as the change in identity of radicals resulting from metathetical reactions (3, 5).

We find that charge transfer between liquid saturated hydrocarbons is an inefficient process when compared with other ion scavenging reactions such as proton transfer to ND_3 (6) or C_2H_5OD (7). For example 0.43 *M* C_2H_5OD scavenges 2.1 G ions in cyclo-C_5H_{10} whereas 0.42 *M* cyclo-C_6D_{12} scavenges only 0.5 G (8). By comparison the cycloalkane cyclo-C_3H_6, which reacts by H_2 transfer with other alkane molecular ions, is practically as efficient as NH_3 (9). However H_2 transfer to a saturated hydrocarbon is apparently peculiar to this one molecule. The reason for the relatively low efficiency of the charge transfer reaction is not known but the process becomes more efficient in a given solvent the greater the difference in gas phase ionization potential between donor and acceptor (4). In contrast H_2 transfer is favored by a closeness in ionization potentials (10).

In order to obtain more information on the charge transfer process we have used a new hydrocarbon solute, neopentane. This allows study of the formation of another gaseous product, methane, in addition to hydrogen. $G(H_2) = 2.5$ and $G(CH_4) = 3.9$ for pure liquid $C(CH_3)_4$ the latter value being little affected by up to 10 mol% N_2O (11). Some CH_4 must arise from ionic precursors and the lack of an effect of the electron scavenger on $G(CH_4)$ is due to the instability of the molecular ion. This decom-

poses in one of two ways in the liquid phase to yield CH_4 or $\cdot CH_3$ (12)

[4] $C(CH_3)_4^+ \rightarrow C(CH_3)_3^+ + \cdot CH_3$

[5] $C(CH_3)_4^+ \rightarrow i\text{-}C_4H_8^+ + CH_4$

Since most $CH_3\cdot$ radicals will abstract from the solvent at the dose rates we employ (13) the measured CH_4 yield provides information on the ion scavenging ability of $C(CH_3)_4$.

In a preliminary communication (14) we described some results obtained in the cyclo-C_5H_{10}/$C(CH_3)_4$ system. Results for other hydrocarbon solvents have now been obtained. For studies in C_2H_6, which itself yields radiolytic CH_4, $C(CD_3)_4$ has been employed with the added advantage that HD and D_2 as well as CD_4 and CHD_3 yields may be measured.

Experimental

Neopentane (Matheson CP grade) and neopentane-d_{12} (Merck, Sharpe and Dohme of Canada) were used after trap-to-trap distillation under vacuum. Cyclohexane (Fisher Spectroanalyzed), cyclopentane (Phillips Research Grade), methylcyclohexane, and 3-methylpentane (3MP) (Phillips Pure Grade) were used as received. Ethane (Phillips Research Grade) was subjected to trap-to-trap vacuum distillation. Removal of cyclopentene from cyclopentane by treatment with concentrated H_2SO_4 followed by fractional distillation did not change the results from those observed in the absence of this treatment.

All samples except those containing ethane were irradiated in Pyrex ampoules with a low vapor to liquid volume ratio. In all calculations it is assumed that the $C(CH_3)_4$ is completely in the liquid phase. Ethane samples were irradiated at a density of 0.25 g ml^{-1} at 318 °K in a stainless steel vessel of 4.2 ml volume to a dose of 1.6×10^{19} eV/g. The other samples received doses of $\sim 2 \times 10^{19}$ eV/ml. The dose rate in the γ-source (Gammacell 220) was 9.3×10^{17} eV/g min in the Fricke dosimeter.

Gases non-condensible at 77 °K (H_2, HD, D_2, and methane) were measured volumetrically and analyzed by mass spectrometry. Methane could be removed quantitatively (> 98%) from all hydrocarbon solvents except ethane by two or three freeze–pump–thaw cycles. With ethane samples two cycles were employed and the remaining methane was determined by gas–solid chromatography. The results obtained by this combined analysis are not as precise as those from the single measurement.

Results

CH_4 yields from solutions of $C(CH_3)_4$ in cyclo-C_5H_{10} and cyclo-C_6H_{12} are shown in Fig. 1, curves *I* and *III*. The non-zero intercept of 0.04 for curve *I* is the CH_4 yield from pure cyclo-C_5H_{10}. The value is in agreement with that

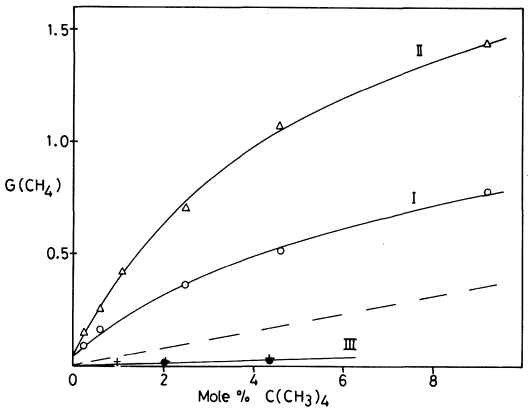

FIG. 1. Methane yields from $C(CH_3)_4$ in: *I*, cyclo-C_5H_{10}; *II*, *c*-C_5H_{10}/2.5 mol% CCl_4; *III*, cyclo-C_6H_{12}+, cyclo-C_6H_{12} + 2.5 mol% CCl_4 ●, ---- "expected" yield.

obtained by Hughes and Hanrahan (15). Yield curves for CH_4 from $C(CH_3)_4$ in *n*-C_6H_{14}, cyclo-$C_6H_{11}CH_3$, and 3MP after correction for CH_4 from the solvent alone are, within experimental error, indistinguishable from that for cyclo-C_6H_{12}. The broken line is the expected yield from direct radiolysis taking $G(CH_4) = 3.9$ for pure $C(CH_3)_4$.

The electron scavengers CCl_4 and SF_6 increase $G(CH_4)$ in the $C(CH_3)_4$/cyclo-C_5H_{10} system but slightly decrease it in *n*-C_6H_{14}, cyclo-$C_6H_{11}CH_3$ and 3MP. In cyclo-C_5H_{10} $G(CH_4)$ increases with increasing CCl_4 concentration up to ~1 mol% and then remains constant up to at least 3 mol%. Curve *II*, Fig. 1 shows the yields at 2.5 mol%. The decreased yields in cyclo-C_6H_{12} are shown by the filled symbols slightly below curve *III*.

The addition of 7 mol% C_2H_5OH to cyclo-C_5H_{10} containing 4.1 mol% $C(CH_3)_4$ and 2.3 mol% CCl_4 reduces $G(CH_4)$ by 55% while $G(H_2)$ remains constant.

The yields of CHD_3 and CD_4 from $C(CD_3)_4$ in C_2H_6 at 0.25 g ml^{-1} and 318 °K are shown in Fig. 2. No other deuterated methanes were detected ($G < 0.2$ at ~4 mol% $C(CD_3)_4$). The broken line represents the methane yield expected from the stoichiometric composition assuming that deuteration has no effect on *G*(methane). A partial confirmation of this was obtained when *G*(methane) from C_2H_6 containing 3.7 mol% $C(CD_3)_4$ and 1.05 mol% $C(CH_3)_4$ was equal to that from C_2H_6 containing 4.75 mol% $C(CD_3)_4$.

The yields of HD and D_2 from C_2H_6/$C(CD_3)_4$ in the presence and absence of SF_6 are shown in

Can. J. Chem. Downloaded from www.nrcresearchpress.com by 210.87.254.6 on 09/05/12
For personal use only.

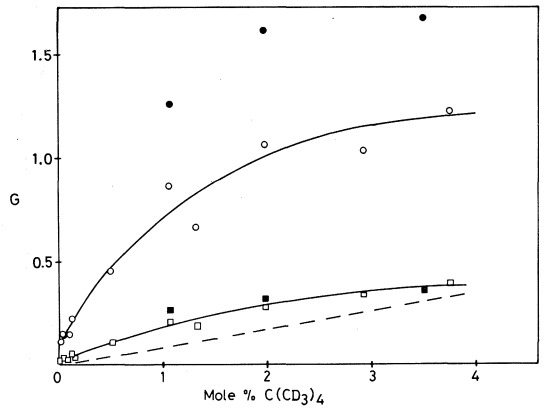

FIG. 2. Methane yields from $C(CD_3)_4$ in C_2H_6: ○, CHD_3; ●, CHD_3 with 1.1 mol% SF_6; □, CD_4; ■, CD_4 with 1.1 mol% SF_6; ---- "expected" yield.

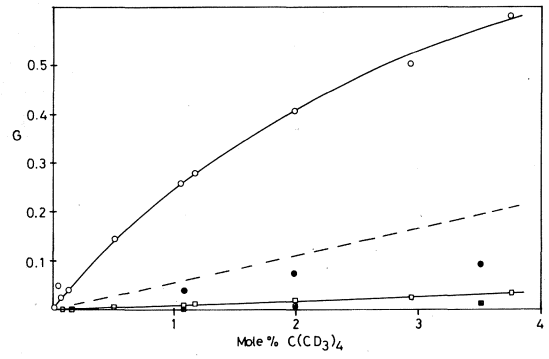

FIG. 3. ○ HD and □ D_2 yields in $C_2H_6/C(CD_3)_4$; ● HD and ■ D_2 in the presence of 1.1 mol% SF_6; ---- expected total hydrogen by direct radiolysis of $C(CD_3)_4$.

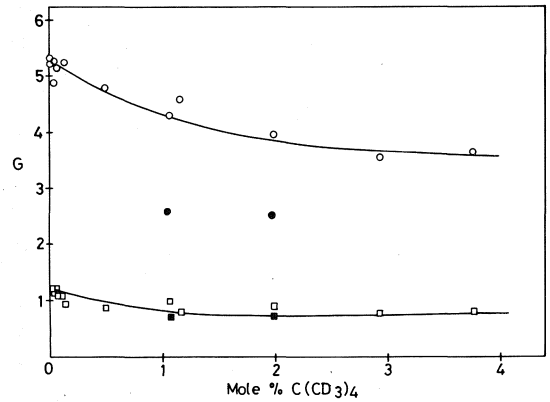

FIG. 4. ○ H_2 and □ CH_4 yields in $C_2H_6/C(CD_3)_4$; ● H_2 and ■ CH_4 in the presence of 1.1 mol% SF_6.

Fig. 3 while Fig. 4 shows the corresponding H_2 and CH_4 yields.

For purposes of comparison 1.2 mol% *n*-C_4D_{10} was irradiated in C_2H_6. G(HD) was 0.27 and $G(D_2)$ was 0.15. There was no measurable change in G(total hydrogen). Similarly 1.96 mol% cyclo-C_6D_{12} in C_2H_6 under the same conditions gave G(HD) = 0.6 and $G(D_2)$ = 0.3.

Discussion

The participation of ions in the enhancement of yields in cyclo-C_5H_{10} and C_2H_6 over those expected from the solution compositions is shown by the effects of electron and positive ion scavengers.

(*i*) $G(HD + D_2)$ in $C_2H_6/C(CD_3)_4$ is reducible to a much greater proportion by electron scavengers than is either the total hydrogen yield or the yield of H_2 in pure liquid $C(CH_3)_4$ (11).

(*ii*) While $G(HD + D_2)$ is drastically decreased by SF_6 the yield of methane ($CHD_3 + CD_4$) is increased. Hydrogen is formed subsequent to charge neutralization by an electron but not by an anion while methane is formed prior to neutralization (reactions 4 and 5). The lower mobility of the anion relative to the electron allows greater opportunity for the occurrence of ion molecule reactions before neutralization which leads to an increased methane yield. It is possible that some methane might be formed following neutralization by an anion of ions which would otherwise yield hydrogen since the observed decrease in $G(HD + D_2)$ is accompanied by an increase in $G(CHD_3 + CD_4)$. Such formation is unlikely since there is no increase in $G(CH_4)$ when N_2O reduces $G(H_2)$ in liquid $C(CH_3)_4$ (11) and the increase in $G(CH_4)$ in cyclo-$C_5H_{10}/C(CH_3)_4$ is much too large if it is assumed that the ratio of hydrogen to methane from the solute is the same as that in C_2H_6.

(*iii*) The addition of C_2H_5OH as a competitive ion scavenger to the system cyclo-C_5H_{10}/$C(CH_3)_4/CCl_4$ decreases $G(CH_4)$.

We will assume in subsequent discussion that all yields from neopentane above those expected from direct radiolysis as determined by the stoichiometric composition are a measure of the extent of ion scavenging by the neopentane.

The gas phase ionization potentials of the hydrocarbons employed are shown in Table 1, the value for neopentane referring to the production *i*-$C_4H_{10}^+ + CH_4$; the appearance potential for $C(CH_3)_3^+ + CH_3$ is 0.18 eV higher (16).

Can. J. Chem. Downloaded from www.nrcresearchpress.com by 210.87.254.6 on 09/05/12
For personal use only.

TABLE 1. Gas phase ionization potentials (ref. 23)

Alkane	Ionization potential (eV)
C_2H_6	11.65
C_4H_{10}	10.63
cyclo-C_5H_{10}	10.53
$C(CH_3)_4$	10.35
$CH_3CH_2CH(CH_3)CH_2CH_3$	10.08
cyclo-C_6H_{12}	9.88
cyclo-$C_6H_{11}CH_3$	9.85

In agreement with previous studies the "activating" solvents have a higher ionization potential than neopentane. We suggest that the enhanced yields of methane that we observe in cyclopentane and ethane are mainly due to charge transfer from the solvent molecular ion followed by prompt formation of either CH_4 or CH_3 (reaction 2 followed by 4 or 5). Two other possibilities are hydride ion transfer and proton transfer. It is unlikely that hydride ion transfer makes a major contribution since the majority of scavengeable ions in cyclo-C_5H_{10} are molecular (10) and the same appears to be true in C_2H_6 at 0.26 g ml^{-1} (17). Also there is no reason why H^- transfer by neopentane should be more facile than that by other hydrocarbons and indeed the reverse is more probable (18). For proton transfer to neopentane to play a major role the protonated molecular ion of the solvent would have to be formed in improbably high yield. $C_2H_7^+$ has been observed in the ion source of a mass spectrometer (19) but evidence for stable protonated forms of higher hydrocarbons in the gas phase is lacking. There is no direct evidence for their occurrence in the liquid phase.

In cyclo-$C_5H_{10}/C(CH_3)_4$ G(methane + hydrogen) is constant within experimental error over the mixture composition studied. In $C_2H_6/C(CD_3)_4$ there is a gradual increase with increasing $C(CD_3)_4$ concentration which is 0.2 G at 3.76 mol%. This implies that in general the neopentane ions formed by charge scavenging lead to either methane or hydrogen but the formation of two of these molecules from a single charge transfer process is a rare event. The $C_2H_6^+$ ions which charge transfer to $C(CD_3)_4$ are precursors of both CH_4 and H_2 in the absence of this solute.

Charge scavenging by $C(CH_3)_4$ in cyclo-C_5H_{10} is more efficient than that by cyclo-C_6D_{12} or cyclo-$C_6D_{11}CD_3$ (1) but not as efficient as that

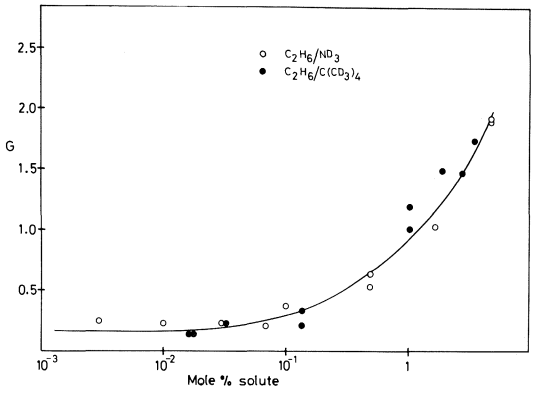

FIG. 5. Positive ion scavenging in C_2H_6 at 0.25 g ml^{-1}. ● $C(CD_3)_4$, ○ ND_3 (24).

by C_2H_5OH or NH_3 (8). However $C(CD_3)_4$ is as efficient as ND_3 in C_2H_6. This comparison is made in Fig. 5 where G(ions scavenged) is calculated as 4/3 G(HD) for C_2H_6/ND_3 (6) and as $G(HD + D_2 + CHD_3 + CD_4)$ corrected for yields from direct radiolysis for $C_2H_6/C(CD_3)_4$. This high efficiency of $C(CD_3)_4$ in C_2H_6 can be related in part to the large difference in ionization potential between it and C_2H_6. However, cyclo-C_6D_{12} and n-C_4D_{10} are not as efficient even though they are also favored by a large exothermicity in charge transfer. A contributing factor for $C(CD_3)_4$ could be the rapidity of loss of CD_3 (reaction 4) or CD_4 (reaction 5) which may occur in the period of one C—C vibration and which constitutes an efficient chemical relaxation process analogous to the protonation of ND_3. Such a chemical step prior to charge neutralization does not appear to be available to the other perdeuterocarbons and physical relaxation of the excited ion formed by charge transfer may not be rapid enough for efficient trapping. Since most of the HD and some of the D_2 in $C_2H_6/C(CD_3)_4$ is formed following neutralization it appears that either some neopentane ions are stabilized in solution or, if they do decompose, then little methane is formed but the resulting ionic fragment yields D atoms after neutralization.

The scavenging plot (Fig. 3) appears typical for positive ion scavenging (9). The limiting yield at low solute concentrations is attributable to the yield of freely diffusing ions and $G \sim 0.2$ is consistent with the value found for similar alkanes, albeit at higher phase density (20). At higher solute concentrations scavenging in the spurs takes place but the experimental points for both ND_3 and $C(CD_3)_4$ do not conform to the

Can. J. Chem. Downloaded from www.nrcresearchpress.com by 210.87.254.6 on 09/05/12
For personal use only.

Can. J. Chem. Downloaded from www.nrcresearchpress.com by 210.87.254.6 on 09/05/12
For personal use only.

usual square root relationship, the yields increasing more steeply than predicted (9). This will be discussed more fully in a succeeding communication.

The ratios of isotopic hydrogens and methanes in the $C_2H_6/C(CD_3)_4$ system are of interest. As might be expected very little D_2 is produced relative to HD. However, about 25% of the methane arising from $C(CD_3)_4$ is CD_4. This is unexpected since the mass spectrum of $C(CH_3)_4$ shows that loss of 15 mass units is twenty times as probable as loss of 16 units. This large percentage of ionic unimolecular decomposition is, however, in accord with the recent value of ~20% obtained by Collin and Ausloos (12) from a study of the radiolysis of liquid neopentane. It is possible that some of the CD_4 in our work arises from a cage disproportionation involving $CD_3\cdot$ and a deuterated ion or radical. With the present information this cannot be distinguished from reaction 5.

If the values of gas phase ionization potentials are taken to apply precisely to the liquid phase then reactions 2 and 4 are overall very slightly endothermic or thermoneutral when *c*-C_5H_{10} is the solvent. In two experiments performed with $C(CD_3)_4$ in this solvent $G(CD_4)/G(CHD_3)$ was 0.42 and 0.39 in the presence and absence of CCl_4, respectively. This implies that both reactions 4 and 5 occur but that with the lower recombination energy of cyclo-$C_5H_{10}^+$ reaction 5 assumes greater importance. Thermoneutral charge transfer is bidirectional. However, the fast decomposition of the neopentane molecular ion will provide a bias in favor of products from this ion. Such a bias will not be present in mixtures in which products are formed subsequent to ion electron combination.

In the above discussion it has been presumed that the species present in solution are the single, molecular ions. However, Ausloos and coworkers (21, 22) have shown that in the gas phase radiolysis of ethane stable dimer ions play a role. Presumably these and higher agglomerations will be of importance in the liquid phase. Reaction equations written in terms of single ions will therefore have no physical meaning. However, our present and previous studies show that the relative order of gas phase ionization potentials still holds in the liquid and can therefore be used to predict the direction of charge transfer. The actual mechanism of product formation will of course be dependent on the state of aggregation.

Conclusion

Neopentane is a highly efficient ion scavenger in C_2H_6 at 0.25 g ml^{-1} and is a fairly efficient one in liquid cyclopentane. This can be correlated with positive charge scavenging which increases in efficiency with increase in difference in ionization potential between donor and acceptor. An added factor may be the formation of the neopentane molecular ion in a repulsive state, the resulting rapid loss of $\cdot CH_3$ or CH_4 in $\sim 10^{-13}$ s enhancing the trapping efficiency.

The authors thank Atomic Energy of Canada Ltd., Commercial Products, and the National Research Council of Canada for financial support.

1. P. J. Dyne and J. Denhartog. Can. J. Chem. **40**, 1616 (1962).
2. T. J. Hardwick. J. Phys. Chem. **66**, 2132 (1962).
3. J. A. Stone. Can. J. Chem. **42**, 2872 (1964).
4. J. A. Stone, A. R. Quirt, and O. Miller. Can. J. Chem. **44**, 1175 (1966).
5. G. A. Muccini and R. H. Schuler. J. Phys. Chem. **64**, 1436 (1960).
6. F. Williams. J. Am. Chem. Soc. **86**, 3954 (1964).
7. J. W. Buchanan and F. Williams. J. Chem. Phys. **44**, 4377 (1966).
8. J. A. Stone. Can. J. Chem. **46**, 3531 (1968).
9. K. D. Asmus, J. M. Warman, and R. H. Schuler. J. Phys. Chem. **74**, 246 (1970).
10. P. Ausloos, A. A. Scala, and S. G. Lias. J. Am. Chem. Soc. **89**, 3677 (1967).
11. K. Horacek and G. R. Freeman. J. Chem. Phys. **53**, 4486 (1970).
12. G. J. Collin and P. Ausloos. J. Am. Chem. Soc. **93**, 1336 (1971).
13. R. H. Schuler and R. R. Kuntz. J. Phys. Chem. **67**, 1004 (1963).
14. J. A. Stone. Chem. Commun. 1677 (1968).
15. B. M. Hughes and R. J. Hanrahan. J. Phys. Chem. **69**, 2707 (1965).
16. B. Steiner, C. F. Giese, and M. G. Inghram. J. Phys. Chem. **34**, 189 (1961).
17. P. T. Holland and J. A. Stone. Unpublished work.
18. P. Ausloos, S. G. Lias, and A. A. Scala. *In* Advances in chemistry series 58. American Chemical Society. 1966. p. 264.
19. V. Aquilanti and G. G. Volpi. J. Chem. Phys. **44**, 2307 (1966).
20. W. F. Schmidt and A. O. Allen. J. Phys. Chem. **72**, 3730 (1968).
21. S. K. Searles, L. W. Sieck, and P. Ausloos. J. Chem. Phys. **53**, 849 (1970).
22. P. Ausloos, R. E. Rebbert, and L. W. Sieck. J. Chem. Phys. **54**, 2612 (1971).
23. K. Watanabe, T. Nakayama, and J. Mottl. U.S. Department of Commerce Office Technical Service Report, **158**, 319 (1959).
24. P. T. Holland. Unpublished results.

Can. J. Chem. Downloaded from www.nrcresearchpress.com by 210.87.254.42 on 09/05/12
For personal use only.

Epimerization of Monosaccharides Under Acetolysis Conditions

WALTER SOWA

Department of Organic Chemistry, Ontario Research Foundation, Sheridan Park, Ontario

Received May 17, 1971

Monosaccharides with a *cis*-configuration at C-2 and -3 readily undergo inversion at C-2 in an acetolysis medium composed of acetic acid, acetic anhydride, and sulfuric acid. The acetolysis-inversion reaction has been carried out with 2,3;5,6-di-*O*-isopropylidene-D-gulofuranose, 2,3;6,7-di-*O*-isopropylidene-D-*glycero*-D-*gulo*-heptose, 2,3-*O*-isopropylidene-D-ribose, D-ribose, and D-mannose using chromatography for isolation of the deacetylated epimeric products. The reaction requires a medium with a high concentration of acetic acid (*ca.* 90%) and appears to take place only with furanose structures. Inversions observed with the unsubstituted pyranoses D-ribose and D-mannose probably occur because of tautomerization to furanose forms. The epimerization proceeds in the direction which yields a smaller number of *cis*-oriented groups at C-2, -3, and -4 of the furanose forms of monosaccharides.

Les monosaccharides avec une configuration *cis* au C-2 et -3 subissent une inversion rapide au C-2 dans un mélange acétolysant composé d'acide acétique, d'anhydride acétique et d'acide sulfurique. La réaction d'acétolyse produisant une inversion a été effectuée avec le di-*O*-isopropylidène-2,3;5,6, D-gulofuranose, le di-*O*-isopropylidène-2,3;6,7 D-*glycéro*-D-*gulo*-heptose, le *O*-isopropylidène-2,3 D-ribose, D-ribose, et le D-mannose utilisant la chromatographie pour l'isolation des composés désacétylés épimères. La réaction exige un milieu avec une grande concentration d'acide acétique (*ca.* 90%) et semble fonctionner uniquement avec des structures furanosiques. Les inversions observées avec les pyranoses non substitués tel que le D-ribose et le D-mannose sont probablement dûes à la tautomérisation vers les formes furanosiques. L'épimérisation s'oriente dans la direction qui donne un plus petit nombre de groupements orientés en position *cis* au C-2, -3, et -4 des formes furanosiques des monosaccharides.

Canadian Journal of Chemistry, 49, 3292 (1971)

Introduction

Several years ago Jerkeman (1) made the unusual observation that D-glucose was formed from certain derivatives of D-mannose when they were acetolyzed. Treatment of 2,3;5,6-di-*O*-isopropylidene-D-mannofuranose, methyl β-D-mannofuranoside or 1,5,6-tri-*O*-acetyl-2,3-*O*-isopropylidene-D-mannofuranose with a mixture of acetic acid, acetic anhydride, and sulfuric acid at room temperature yielded, after deacetylation, a 4:1 mixture of D-glucose and D-mannose. No C-2 inversion was observed on acetolysis of ethyl 2,3,4,6-tetra-*O*-acetyl-β-D-mannopyranoside, methyl α-D-mannopyranoside, methyl β-D-glucopyranoside or derivatives of D-galactofuranose, D-xylofuranose, and L-arabinofuranose; phenyl β-D-glucofuranoside gave a trace of D-mannose. It was suggested that epimerization of D-mannofuranose derivatives occurs under acetolysis conditions through conversion of a *cis–trans* arrangement of three contiguous hydroxyl groups into a *trans–cis* arrangement via cyclic acetoxonium intermediates. Protonation causes the two *cis*-acyloxy groups at C-2 and -3 to join in a seven-membered ring which undergoes nucleophilic attack by an acyloxy group *trans*-situated on an adjacent carbon. The second cyclic ion which is formed then hydrolyzes to afford the epimer D-glucose. There are several related interconversions of carbohydrates which are considered to take place by similar successive neighboring acyloxy group participation. Cyclohexane polyols epimerize at elevated temperatures in 95% acetic acid – toluenesulfonic acid (2*a*), 95% acetic acid – sulfuric acid (2*b*, *c*, *d*), acetic acid – acetic anhydride – sulfuric acid (2*d*) and acetic acid – sulfuric acid (2*d*). More recently cyclopentane polyols have been isomerized in 95% acetic acid – sulfuric acid (3). Other reports describing different media include the deacylation–inversion of cyclitols (4*a*), polyhydroxytetrahydropyrans (4*b*), and aldoses (4*c*) in liquid hydrogen fluoride, and the transformations of carbohydrate acetates by antimony pentachloride (5), by zinc chloride in acetic anhydride (6), and by phosphorus pentachloride and aluminum chloride in chloroform (*cf.* 7).

Acetolysis has many valuable applications in carbohydrate chemistry (8). The general desirability of avoiding inadvertant production of artefacts made further examination of the acetolysis-inversion reaction of interest. It was highly unlikely that such epimerization was unique to D-mannofuranose derivatives. It was also of

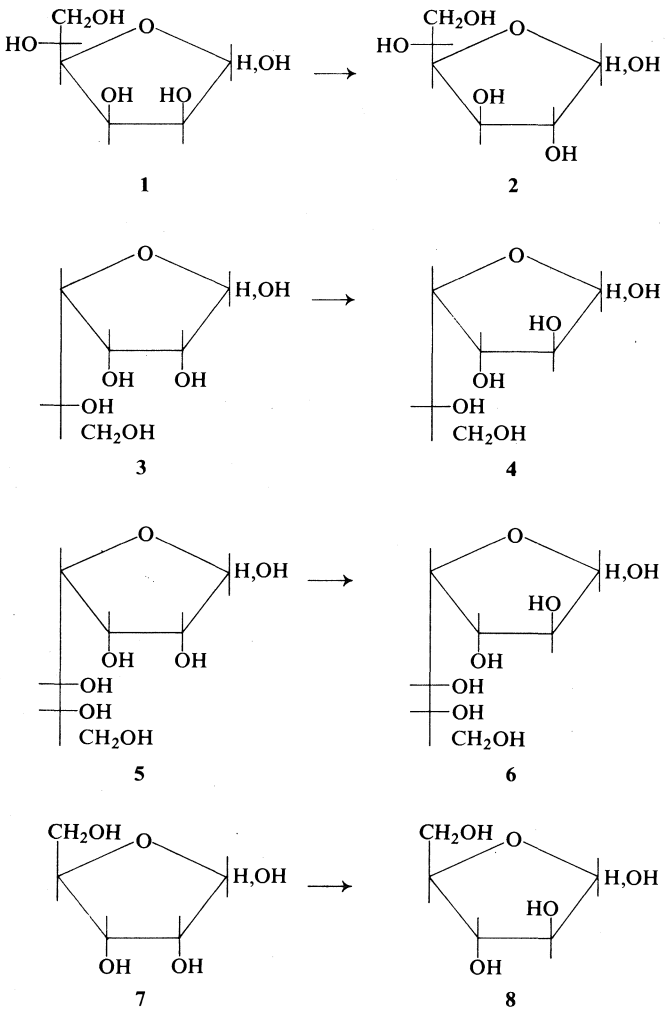

FIG. 1. Furanose structures of D-mannose (**1**), D-glucose (**2**), D-gulose (**3**), D-idose (**4**), D-*glycero*-D-*gulo*-heptose (**5**), D-*glycero*-D-*ido*-heptose (**6**), D-ribose (**7**), and D-arabinose (**8**).

interest to investigate the acetolysis-inversion reaction since, unlike the inversions mentioned above, it appeared to be confined to furanose sugars. In addition, the reaction appeared to have some value in synthesis for carrying out C-2 hydroxyl inversion without resort to the Lobry de Bruyn – Alberda van Ekenstein transformation (9) which normally requires an alkaline medium.

Results and Discussion

The close similarity between the furanose structures of D-mannose (**1**) and D-gulose (**3**) (Fig. 1) suggested that carbohydrate derivatives with the *gulo* configuration might be convertible to the *ido* by acetolysis. 2,3;5,6-Di-*O*-isopropylidene-D-gulose (10) and 2,3;6,7-di-*O*-isopropylidene-D-*glycero*-D-*gulo*-heptose (11) were each treated with the mixture of acetic acid, acetic anhydride, and sulfuric acid described by Jerkeman (1). Experiments followed by t.l.c. indicated that the maximum yield of epimers from both *gulo* sugars occurred at about 30 h. This time is one-half that reported for the conversion of D-mannose to D-glucose (1). After treatment of the reaction mixtures with triethylamine for deacetylation, the products were isolated chromatographically and weighed. From 2,3;5,6-di-*O*-isopropylidene-D-gulose, D-idose and D-gulose were obtained in a ratio of approximately 3 to 1.

Can. J. Chem. Downloaded from www.nrcresearchpress.com by 210.87.254.42 on 09/05/12
For personal use only.

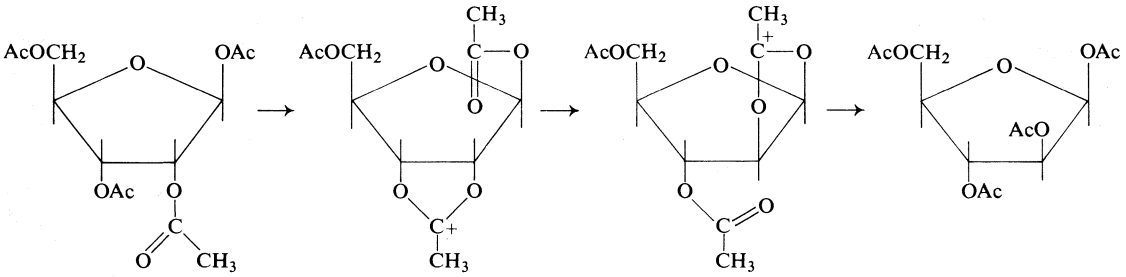

The ratio ranged between 2.5 to 1 and 3.4 to 1, possibly because of decomposition of sugars during acetolysis and variability in chromatographic recovery which in turn may have been related to the scale of the experiment. The yield of D-idose varied between 36 and 51%. The 2,3;6,7-di-*O*-isopropylidene-D-*glycero*-D-*gulo*-heptose on acetolysis gave D-*glycero*-D-*ido*-heptose and D-*glycero*-D-*gulo*-heptose in a ratio of 2 to 1; the yield of D-*glycero*-D-*ido*-heptose was 47%. The use of triethylamine for deacetylation is a procedure communicated to Jerkeman by Whelan (1). The possibility of epimerization under deacetylation conditions was investigated by deacetylation of D-*glycero*-D-*gulo*-heptose hexaacetate and examination of the product by t.l.c. No D-*glycero*-D-*ido*-heptose was detected.

Jerkeman, after finding that derivatives of D-galactose, D-xylose, and L-arabinose did not rearrange on acetolysis, suggested that C-2 inversion would be observed with the furanosidic acetates of their epimers (1). The prediction has now been confirmed for ribose. 2,3-*O*-Isopropylidene-D-ribofuranose (12) was acetolyzed at room temperature for 90 h, not necessarily the optimum time, and worked-up in the usual manner. D-Arabinose and D-ribose were isolated chromatographically in the ratio of 0.8 to 1.

An observation relating to furanoses is that acetolysis of the 1,2-*O*-isopropylidene derivatives of D-glucofuranose triacetate and D-xylofuranose diacetate leaves the sugars in the furanose form with little or no conversion to pyranose acetate taking place (1, 13). A recent synthesis of 1,2,3,5-tetra-*O*-acetyl-β-D-ribofuranose from methyl D-ribofuranoside takes advantage of the stability of the acetylated furanose structure in an acetolysis medium (14). It appeared possible that if free sugars were dissolved in an acetolyzing medium, tautomerization might occur with the formation of relatively large amounts of furanoses. The acetolysis-inversion data accumulated thus far show that derivatives of certain sugars epimerize only in the furanose form. Therefore a pyranose to furanose conversion of the free sugars should be indicated by the appearance of epimers. This expectation was borne out by results of experiments with D-ribose and D-mannose. Crystalline D-ribose, which has a pyranose structure (15), and α-D-mannopyranose were each acetolyzed for 24 h in the usual manner. From the reaction with D-ribose, D-arabinose and D-ribose were isolated in the ratio of 0.85 to 1, while D-mannose yielded a mixture of D-glucose and D-mannose in 0.3 to 1 ratio. The epimerizations are indirect evidence for the existence of furanose modifications of the two monosaccharides in the acetolysis medium which was employed.

In the original work on C-2 inversion of D-mannofuranose (1), the formation of a seven-membered cyclic acetoxonium ion as the first species was favored in conformity with a mechanism postulated for transformations of cyclitol acetates in hydrogen fluoride (4*a*). An alternative mechanism with five-membered cyclic acetoxonium ions was preferred to explain the epimerization of cyclitols in acetic acid – sulfuric acid (2*d*). More recently direct evidence for a five-membered cyclic structure has been provided from n.m.r. studies of *cis* and *trans* isomers of 1,2-diacetoxycyclohexane in hydrogen fluoride (16). The *trans* isomer was unreactive while the *cis* was quantitatively converted to a 2-methyl-1,3-dioxolenium ion and acetic acid. The cyclic ion was isolated as the crystalline tetrafluoroborate. In the case of furanoses in an acetolysis medium, inversion at the central carbon of a *cis–trans* sequence of substituents probably proceeds through a transient tricyclic system of five-membered rings in which little change in position is required for the atoms directly involved.

Can. J. Chem. Downloaded from www.nrcresearchpress.com by 210.87.254.42 on 09/05/12
For personal use only.

Can. J. Chem. Downloaded from www.nrcresearchpress.com by 210.87.254.42 on 09/05/12
For personal use only.

The data collected in the present work and that of Jerkeman (1) indicate that only monosaccharides with a *cis*-2,3 configuration epimerize in an acetolysis medium. The inversion can be related to the nonbonded repulsive interactions in the furanose forms of such monosaccharides. The initial configuration of the anomeric group is unimportant since it can be assumed to readily take up a configuration *trans* to its neighbor. It is apparent then that the C-2 inversion of monosaccharides in an acetolyzing medium proceeds in the direction which yields a smaller number of *cis*-groups at C-2, -3, and -4 of the furanose form. The conversions which have been observed and the number of groups in a *cis*-orientation are as follows: D-mannose (**1**) to D-glucose (**2**) (3 and 2), D-gulose (**3**) to D-idose (**4**) (3 and 2), D-*glycero*-D-*gulo*-heptose (**5**) to D-*glycero*-D-*ido*-heptose (**6**) (3 and 2) and D-ribose (**7**) to D-arabinose (**8**) (2 and 0). The case of furanoses with all *cis* substituents at C-2, -3, and -4 (mannose and gulose configurations) is interesting. They have comparatively high free energies and n.m.r. spectra of aqueous equilibrium solutions of D-mannose and D-lyxose show no furanose while that of D-*glycero*-D-*gulo*-heptose shows very little (17). In water the interactions between *cis* substituents on adjacent carbon atoms are relieved by a ring expansion to the pyranose form which accommodates bulky groups in equatorial positions. In an acetolysis medium of a suitable composition, an alternative device consisting of a furanose (*cis*) to furanose (*trans*) transformation by way of acetoxonium ions becomes feasible. The mild conditions under which the inversion takes place with furanoses are in remarkable contrast to similar inversions reported with other five-membered cyclic structures, the cyclopentanepolyols (3). The latter require heating in 95% acetic acid – sulfuric acid for many hours.

The easy C-2 inversion of D-ribose in an acetolyzing medium appeared to be inconsistent with the results of Reist *et al.* who acetolyzed 4-*S*-benzoyl-4-thioribopyranose derivatives to 4-thio-ribofuranose compounds without epimerization of the latter (18). When their experimental conditions were used with D-ribose, the starting material was recovered accompanied by only a trace of D-arabinose detectable by paper chromatography. The experiment was repeated maintaining the 1:1 ratio of acetic acid:acetic anhydride but in one case increasing the concentration of sulfuric acid and in another raising the temperature from 0° to room temperature. These modifications had no effect on the extent of epimerization and again only a trace of D-arabinose was detectable. Under the more vigorous reaction conditions an unidentified compound with a chromatographic mobility greater than that of D-ribose was formed. It was not examined further. Epimerization in an acetolysis medium is thus related to the concentration of acetic acid since inversion occurs in a medium of 10:1 but not 1:1, acetic acid:acetic anhydride.

The importance of acetic acid concentration explains why C-2 inversion has not been observed more often during the long history of acetolysis. Epimerization takes place in a medium of 10:1 acetic acid:acetic anhydride in the presence of sulfuric acid. In contrast the classic "isomerizing mixture" first used by Hudson and associates in 1934 (ref. 19 and refs. in 20) for anomerization and for acetolysis of glycosides, acetals, and anhydrosugars was a 3:7 or 1:2 mixture of acetic acid and acetic anhydride plus sulfuric acid. On one occasion, D-*glycero*-D-*gulo*-heptose was treated for 48 h at 20° with a 1:2 mixture of acetic acid and acetic anhydride, with 2.5% by volume of sulfuric acid (21). An 80% yield of α- and β-hexaacetates of D-*glycero*-D-*gulo*-heptose was obtained. On the other hand in the present work with an "epimerizing mixture", acetolysis of the isopropylidene derivative of the same heptose yielded the *ido* isomer as the major product. A preparation of 1,2,3,5-tetra-*O*-acetyl-β-D-ribofuranose by acetolysis of a methyl ribofuranoside mixture has been described (14). In one variation the ratio of acetic acid to acetic anhydride was 1.5 to 2 while in the other it was 30 to 7. In the latter case an unidentified component was detected by t.l.c. It is possible that this is the acetate of D-arabinose. Studies of anomerization mechanisms have not been inconvenienced by C-2 inversions since they have been conducted usually, but not always, with low acetic acid:acetic anhydride ratios of 1:1 (22) and 3:10 (23) and confined to acetylated pyranoses. For the acetolysis of polysaccharides, a valuable technique in structural investigations (8), it is customary to use mixtures containing from 0 to 50% acetic acid. It appears that, fortuitously, undesirable C-2 inversions have been avoided. The present work suggests that particular care should be taken if acetolyses are carried out for

Can. J. Chem. Downloaded from www.nrcresearchpress.com by 210.87.254.42 on 09/05/12
For personal use only.

structural analysis of polysaccharides containing furanose sugars with *cis*-2,3 configurations. The existence of such polysaccharides has been reported recently following the discovery of D-ribofuranose in antigenic lipopolysaccharides of *Salmonella* (24).

Experimental

General

Melting points were determined on a Fisher-Johns melting point apparatus and are uncorrected. Optical rotations were obtained with a Carl Zeiss photoelectric polarimeter Model 0.005° using a sodium spectral light source. Visualization reagents for paper chromatography and t.l.c. were *p*-anisidine hydrochloride (25) and silver nitrate – sodium hydroxide (26). Dibenzyl dithioacetals were prepared by treatment of the sugar with toluenethiol in the presence of trifluoroacetic acid (27) for 2 h at room temperature, followed by evaporation of the mixture to dryness.

*Acetolysis of 2,3;5,6-Di-O-isopropylidene-*D*-gulofuranose*

2,3;5,6-Di-*O*-isopropylidene-D-gulofuranose was prepared by sodium borohydride reduction of 2,3;5,6-di-*O*-isopropylidene-D-gulonolactone in ether containing acetic acid (10). Yields up to 93% were obtained by using powdered borohydride from a freshly-opened bottle and by prolonging the reaction time to *ca.* 3 days. Acetolysis was carried out as described by Jerkeman (1). Preliminary experiments followed by paper chromatography indicated that the highest ratio of D-idose to D-gulose occurred at around 30 h. The following procedure was then used. To a stirred and cooled solution of 2,3;5,6-di-*O*-isopropylidene-D-gulofuranose (200 mg) in acetic acid (6 ml) and acetic anhydride (0.8 ml) was added sulfuric acid (0.3 ml). The reaction mixture was left at room temperature for 30 h and then poured into ice-water. The aqueous solution was extracted with chloroform and the extract washed with saturated sodium bicarbonate solution followed by water. The chloroform solution was evaporated to a syrup which was deacetylated overnight by a mixture of methanol (16 ml), water (2 ml), and triethylamine (2 ml). The resulting mixture was evaporated to a syrup (80 mg) which was separated on Whatman No. 4 paper in ethyl acetate – pyridine–water (5:2:5 *v*/*v*, top layer). Appropriate zones were extracted with water to yield D-idose (50 mg, 36% yield based on di-*O*-isopropylidene-D-gulose) and D-gulose (20 mg). The ratio of D-idose to D-gulose and the yield were not constant as the scale was varied. For example, in acetolysis on a 12 g scale the ratio of D-idose to D-gulose was 3.4 to 1 after chromatography on 10 sheets (46 × 57 cm) of Whatman 3MM paper; the yield of D-idose from di-*O*-isopropylidene-D-gulose was 51%.

The syrupy D-idose, $[\alpha]_D^{22}$ +16.2° (*c* 2.5 in water), was acetylated in pyridine – acetic anhydride but the resulting acetate did not crystallize. The syrupy acetate (100 mg) was then treated with a mixture of acetic anhydride (1 ml), acetic acid (0.5 ml), and sulfuric acid (0.02 ml) for 43 h. After work-up in the usual manner there was obtained 1,2,3,4,6-penta-*O*-acetyl-α-D-idopyranose, m.p. 92–94° and $[\alpha]_D^{22}$ +54.7° (*c* 2 in chloroform). Literature values are m.p. 91–92° and $[\alpha]_D^{21}$ +54° (*c* 1.6 in chloroform) (28).

*Acetolysis of 2,3;6,7-Di-O-isopropylidene-*D*-glycero-*D*-gulo-heptose*

2,3;6,7-Di-*O*-isopropylidene-D-*glycero*-D-*gulo*-heptose, m.p. 93–95°, and $[\alpha]_D^{21}$ −29.8° (*c* 1.2 in chloroform), was prepared by condensation of acetone with D-*glycero*-D-*gulo*-heptose as described by Brimacombe and Tucker (11) except that the sulfuric acid catalyst was replaced by zinc chloride – phosphoric acid (29) and in column chromatography ether was used in place of acetone–toluene. With zinc chloride – phosphoric acid instead of sulfuric acid as acetalation catalyst, the heptose appeared to dissolve and react more readily with less formation of acetone condensation by-products.

Small scale experiments followed chromatographically were carried out to determine the duration of acetolysis for maximum formation of the *ido* epimer of the heptose. The following procedure was then used. To a cooled and stirred mixture of 2,3;6,7-di-*O*-isopropylidene-D-*glycero*-D-*gulo*-heptose (500 mg), acetic acid (15 ml), and acetic anhydride (2 ml) was added concentrated sulfuric acid (0.75 ml). After 24 h at room temperature, the reaction was worked-up and the product deacetylated as described above for the hexose. A portion (140 mg) of the syrupy mixture (320 mg) was separated by preparative t.l.c. on two plates (20 × 20 cm) of cellulose using ethyl acetate – pyridine–water (10:4:3 *v*/*v*) as developing solvent. D-*glycero*-D-*ido*-Heptose (76 mg, 49% yield based on di-*O*-isopropylidene-D-*glycero*-D-*gulo*-heptose) and D-*glycero*-D-*gulo*-heptose (36 mg) were isolated. The D-*glycero*-D-*ido*-heptose was characterized as its dibenzyl dithioacetal, m.p. 129–130° and $[\alpha]_D^{21}$ +70° (*c* 1 in pyridine). Literature values are m.p. 130–131° and $[\alpha]_D^{20}$ +71.4° (*c* 2.6 in pyridine) (30).

To test whether any epimerization occurred in the deacetylation step, a crude crystalline mixture of α- and β-D-*glycero*-D-*gulo*-heptose hexaacetates, m.p. 122–124°, was prepared from D-*glycero*-D-*gulo*-heptose and acetic anhydride using boron trifluoride etherate as catalyst. The heptose acetate was treated with trimethylamine in the same way as the acetolysis product. Only the starting sugar, D-*glycero*-D-*gulo*-heptose, was detectable by t.l.c.

*Acetolysis of 2,3-O-Isopropylidene-*D*-ribose*

2,3-*O*-Isopropylidene-D-ribose (12) (1.0 g, b.p.$_{0.1}$ 122–124°) was acetolyzed for 90 h at room temperature in a mixture of acetic acid (30 ml), acetic anhydride (4 ml), and sulfuric acid (1.5 ml). The reaction mixture was worked-up and a portion (300 mg) of the deacetylated product was separated by t.l.c. on four plates of cellulose (20 × 20 cm) developed twice in ethyl acetate – pyridine–water (8:2:1 *v*/*v*). D-Arabinose (95 mg) and D-ribose (118 mg) were isolated. The D-arabinose, on crystallization from aqueous ethanol had m.p. 158–159° and $[\alpha]_D^{22}$ −107° (*c* 2.3 in water). Literature values are m.p. 158.5–160° and $[\alpha]_D^{25}$ −105 ± 3° (equilibrium; *c* 2 in water) (31*a*). The syrupy D-arabinose also yielded *N*-(4-nitrophenyl)-D-arabinosylamine, m.p. 204°, on reaction with *p*-nitroaniline. The literature m.p. is 206° (31*a*). The recovered D-ribose crystallized with m.p. 87–89° and $[\alpha]_D^{22}$ −18.3° (*c* 2.8 in water). Literature values are m.p. 87° and $[\alpha]_D^{25}$ −19° (equilibrium; water) (31*b*).

Can. J. Chem. Downloaded from www.nrcresearchpress.com by 210.87.254.42 on 09/05/12
For personal use only.

Epimerization of D-*Ribose in an Acetolysis Mixture*

Crystalline D-ribose (1.0 g) was treated with a mixture of acetic acid (30 ml), acetic anhydride (4 ml), and sulfuric acid (1.5 ml) at room temperature for 24 h. The reaction mixture was worked-up and a portion (200 mg) of the deacetylated product (0.84 g) was separated by chromatography on a sheet of Whatman 3MM paper developed in butanol–pyridine–water (6:4:3 *v/v*). D-Arabinose (70 mg) and D-ribose (82 mg) were isolated. The D-arabinose, $[\alpha]_D^{22}$ −107° (*c* 1.8 in water), was characterized as the dibenzyl dithioacetal, m.p. 148–149° and $[\alpha]_D^{22}$ +17.8° (*c* 1.2 in pyridine). Literature values for the thioacetal are m.p. 149° and $[\alpha]_D$ +18.6° (*c* 3.88 in pyridine) (32).

Epimerization of D-*Mannose in an Acetolysis Mixture*

Crystalline D-mannose (1.0 g) was treated for 24 h at room temperature with a mixture of acetic acid (30 ml), acetic anhydride (4 ml), and sulfuric acid (1.5 ml). The reaction mixture, after work-up and deacetylation in the usual manner, yielded a syrupy product (0.8 g). A portion (300 mg) of the mixture was separated by chromatography on Whatman 3MM paper in ethyl acetate – pyridine–water (8:2:1 *v/v*). D-Glucose (53 mg), $[\alpha]_D^{23}$ +50.1° (*c* 0.78 in water) and D-mannose (189 mg), $[\alpha]_D^{23}$ +14.6° (*c* 1.1 in water), were isolated as syrups. The D-glucose was converted to its dibenzyl dithioacetal, m.p. 136–138° and $[\alpha]_D^{22}$ −97.6° (*c* 0.8 in pyridine). Literature values are m.p. 139° and $[\alpha]_D^{15}$ −98.4° (pyridine) (33). The D-mannose was characterized as its phenylhydrazone, m.p. 200–201°. The literature value is m.p. 199–200° (34).

Non-epimerization of D-*Ribose in an Acetolysis Mixture*

The acetolysis conditions used by Reist *et al.* (18) for converting 4-*S*-benzoyl-4-thio-ribopyranosides to 4-thio-ribofuranose derivatives without observable C-2 epimerization were applied to D-ribose. To an ice-cold solution of acetic acid (38 ml), acetic anhydride (38 ml), and sulfuric acid (2.3 ml) was added 0.9 g (0.06 mol) of D-ribose. The reaction mixture was kept at 0° for 48 h and then decomposed by the addition of anhydrous sodium acetate (8.5 g). The resulting mixture was evaporated to dryness *in vacuo* with the bath temperature below 30°. The residue was partitioned between water (50 ml) and chloroform (20 ml). The aqueous layer was extracted with chloroform (3 × 10 ml) and the combined chloroform extracts were dried (anhydrous sodium sulfate) and evaporated to dryness. The residue was evaporated with methanol several times and then redissolved in chloroform (20 ml). The chloroform solution was washed with saturated sodium bicarbonate solution (3 × 10 ml), dried (anhydrous sodium sulfate), and evaporated to dryness. The resulting syrup (1.27 g) was deacetylated overnight in a solution of methanol (20 ml), water (2.5 ml), and triethylamine (2.5 ml). Evaporation of the mixture yielded a syrup (0.78 g) which was examined by paper chromatography in butanol–pyridine–water (10:3:3 *v/v*). It was composed of ribose with only a trace of arabinose. The syrupy D-ribose crystallized with m.p. 85–86°, mixed m.p. 85–87°, and $[\alpha]_D^{23}$ −18.5° (*c* 1.3 in water)

The above experiment was repeated using the same conditions (0° for 48 h) except that the concentration of sulfuric acid was increased from 2.3 to 3.3 ml. The reaction mixture was worked-up and examined chromatographically. Again, the syrupy product contained mainly D-ribose with only a trace of D-arabinose, barely detectable with the *p*-anisidine and silver nitrate reagents. The mixture contained *ca.* 10% of an unidentified component giving a positive reaction with both spray reagents and having a mobility relative to D-ribose (R_{ribose}) of 1.9.

In another variation, the procedure was repeated as before (D-ribose 0.9 g, acetic acid 38 ml, acetic anhydride 38 ml, sulfuric acid 2.3 ml, time 48 h) but the temperature was room temperature (23°) instead of 0°. The product, after work-up, was examined chromatographically. D-Ribose was the major component with a trace of D-arabinose, *ca.* 30–40% of the component with R_{ribose} 1.9 and a small amount of a second unidentified component with R_{ribose} 2.2.

The author gratefully thanks Mrs. Brigitte Licht for valuable technical assistance and help with translations. This work was made possible by funds received from the Province of Ontario through the Department of Trade and Development.

1. P. JERKEMAN. Acta Chem. Scand. **17**, 2769 (1963).
2. (*a*) M. E. PITMAN. M.Sc. Thesis. University of Tasmania. 1957; (*b*) S. J. ANGYAL, P. A. J. GORIN, and M. E. PITMAN. Proc. Chem. Soc. 337 (1962); (*c*) P. A. J. GORIN. Can. J. Chem. **41**, 2417 (1963); (*d*) S. J. ANGYAL, P. A. J. GORIN, and M. E. PITMAN. J. Chem. Soc. 1807 (1965).
3. S. J. ANGYAL and D. M. LUTTRELL. Aust. J. Chem. **23**, 1831 (1970).
4. (*a*) E. J. HEDGLEY and H. G. FLETCHER, JR. J. Am. Chem. Soc. **84**, 3726 (1962); (*b*) E. J. HEDGLEY and H. G. FLETCHER, JR. J. Am. Chem. Soc. **85**, 1615 (1963); (*c*) D. PEDERSEN and H. G. FLETCHER, JR. J. Am. Chem. Soc. **82**, 945 (1960).
5. H. PAULSEN, W.-P. TRAUTWEIN, F. G. ESPINOSA, and K. HEYNS. Chem. Ber. **100**, 2822 (1967).
6. F. MICHEEL and R. BÖHM. Tetrahedron Lett. **3**, 107 (1962).
7. N. K. RICHTMYER. Adv. Carbohyd. Chem. **1**, 37 (1945).
8. R. D. GUTHRIE and J. F. MCCARTHY. Adv. Carbohyd. Chem. **22**, 11 (1967).
9. J. C. SPECK, JR. Adv. Carbohyd. Chem. **13**, 63 (1958).
10. R. K. HULYALKAR. Can. J. Chem. **44**, 1594 (1966); L. M. LERNER, B. D. KOHN, and P. KOHN. J. Org. Chem. **33**, 1780 (1968).
11. J. S. BRIMACOMBE and L. C. N. TUCKER. J. Chem. Soc. C, 562 (1968).
12. P. A. LEVENE and E. T. STILLER. J. Biol. Chem. **102**, 187 (1933).
13. H. BÖRJESON, P. JERKEMAN, and B. LINDBERG. Acta Chem. Scand. **17**, 1705 (1963); P. JERKEMAN and B. LINDBERG. Acta Chem. Scand. **17**, 1709 (1963).
14. R. D. GUTHRIE and S. C. SMITH. Chem. Ind. London, 547 (1968).
15. M. RUDRUM and D. F. SHAW. J. Chem. Soc. 52 (1965).
16. C. PEDERSEN. Tetrahedron Lett. **6**, 511 (1967).
17. S. J. ANGYAL. Angew. Chem. Int. Ed. **8**, 157 (1969).

18. E. J. REIST, D. E. GUEFFROY, and L. GOODMAN. J. Am. Chem. Soc. **86**, 5658 (1964).
19. E. MONTGOMERY and C. S. HUDSON. J. Am. Chem. Soc. **56**, 2463 (1934).
20. R. M. HANN and N. K. RICHTMYER (*Editors*). The Collected Papers of C. S. Hudson. Academic Press, Inc., New York, N.Y. 1946.
21. E. M. MONTGOMERY, N. K. RICHTMYER, and C. S. HUDSON. J. Am. Chem. Soc. **65**, 1848 (1943).
22. W. A. BONNER. J. Am. Chem. Soc. **73**, 2659 (1951); W. A. BONNER. J. Am. Chem. Soc. **81**, 1448 (1959); E. P. PAINTER. J. Am. Chem. Soc. **75**, 1137 (1953); R. U. LEMIEUX, C. BRICE, and G. HUBER. Can. J. Chem. **33**, 134 (1955).
23. J. JANSON and B. LINDBERG. Acta Chem. Scand. **14**, 877 (1960).
24. M. BERST, C. G. HELLERQVIST, B. LINDBERG, O. LÜDERITZ, S. SVENSSON, and O. WESTPHAL. Eur. J. Biochem. **11**, 353 (1969); M. SARVAS and H. NIKAIDO. J. Bacteriol. **105**, 1063 (1971).
25. L. HOUGH, J. K. N. JONES, and W. H. WADMAN. J. Chem. Soc. 1702 (1950).
26. W. E. TREVELYAN, D. P. PROCTER, and J. S. HARRISON. Nature, **166**, 444 (1950).
27. W. SOWA. Can. J. Chem. **49**, 1176 (1971).
28. L. F. WIGGINS. *In* Methods in carbohydrate chemistry Vol. I. Academic Press, Inc., New York, N.Y. 1962, p. 140.
29. O. TH. SCHMIDT. *In* Methods in carbohydrate chemistry. Vol. II. Academic Press, Inc., New York, N.Y. 1963, p. 318.
30. J. W. PRATT, N. K. RICHTMYER, and C. S. HUDSON. J. Am. Chem. Soc. **75**, 4503 (1953).
31. (*a*) R. L. WHISTLER and J. N. BEMILLER. *In* Methods in carbohydrate chemistry Vol. I. Academic Press, Inc., New York, N.Y., 1962. p. 71. (*b*) p. 81.
32. H. ZINNER, H. BRANDNER, and G. REMBARZ. Chem. Ber. **89**, 800 (1956).
33. E. PACSU. Chem. Ber. **57**, 851 (1924).
34. H. S. ISBELL and H. L. FRUSH. *In* Methods in carbohydrate chemistry Vol. I. Academic Press, Inc., New York, N.Y., 1962. p. 145.

Can. J. Chem. Downloaded from www.nrcresearchpress.com by 210.87.254.42 on 09/05/12
For personal use only.

Can. J. Chem. Downloaded from www.nrcresearchpress.com by 210.87.254.42 on 09/05/12
For personal use only.

The Reaction of 5-Unsubstituted-1,2-Dithiole-3-thiones with some Activated Acetylenes

D. M. McKINNON AND J. M. BUCHSHRIBER
Department of Chemistry, University of Manitoba, Winnipeg, Manitoba

Received May 20, 1971

5-Unsubstituted 1,2-dithiole-3-thiones undergo addition reactions with dimethyl acetylenedicarboxylate and dibenzoylacetylene to give amorphous 2-thioformylmethylene-1,3-dithioles. In certain cases these may undergo further addition of activated acetylene to give thiopyranspiro-1,3-dithioles, but may also lose sulfur to give bis-1,3-dithiolylidene-2-butenes, which are probably formed via initial dimerization of the thioformylmethylenedithioles. The stereochemistry of the products is discussed briefly.

Les dithiol-1,2 thiones-3 non substitués en -5 subissent des réactions d'addition avec l'acétylènedicarboxylate de diméthyle et le dibenzoylacétylène pour donner les thioformylméthylène-2 dithioles-1,3 amorphes. Dans certains cas, ceux-ci peuvent additionner de l'acétylène activé pour donner les bis-dithiolylidène-1,3 butènes-2; ces derniers sont probablement formés par une dimérisation initiale des thioformylméthylènedithioles. La stéréochimie des produits est discutée brièvement.

Canadian Journal of Chemistry, **49**, 3299 (1971)

While the reaction of various activated acetylenes with 1,2-dithiole-3-thiones **1** has been studied extensively (1–5), most of these reactions have involved the use of 5-substituted 1,2-dithiole-3 thiones **1***a*. The initial products of the reaction are then 3-thioacylmethylene-1,3-dithioles **2***a*, formed by addition to the thione. Likewise, the reaction of 5-unsubstituted-1,2-dithiole-3-thiones **1***b*, would provide 3-thioformylmethylene-1,3-dithioles, **3**. These, being thials, would be expected to be much less stable than the thiones **2** (6). Little is reported on this type of reaction, but 4-phenyl-1,2-dithiole-3-thione (**1***c*) reacted with dibenzoylacetylene (5) to produce an unstable adduct which was demonstrated to be a thial, and **1***c* reacted with ethyl phenylpropiolate to give a product formed via a thial intermediate (7). It seemed desirable to investigate these reactions further to identify intermediates and products. It was also interesting to determine if the initial adducts reacted with more activated acetylene to form the spiran di-adducts **4** of the type reported for other 5-substituted-1,2-dithiole-3-thiones (3, 5). Most of our studies were performed on 1,2-dithiole-3-thione (**1***d*) and 4-phenyl-1,2-dithiole-3-thione (**1***c*). The activated acetylenes were dimethyl acetylenedicarboxylate and dibenzoylacetylene, and in one case, ethyl phenylpropiolate.

1,2-Dithiole-3-thione (**1***d*) reacted with 1 equiv of dimethyl acetylenedicarboxylate at room tem-

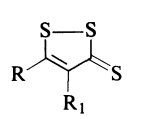

1

a R′ = H
b R = H
c R = H; R_1 = Ph
d R = R_1 = H

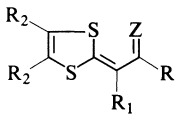

2

a Z = S
b Z = O

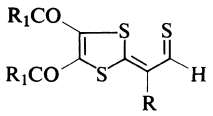

3

a R = H; R_1 = OMe
b R = H; R_1 = Ph
c R = Ph; R_1 = OMe
d R = Ph; R_1 = Ph

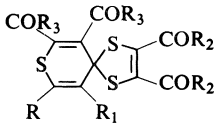

4

a R = R_1 = H; R_2 = Ph; R_3 = OMe
b R = H; R_1 = Ph; R_2 = R_3 = OMe
c R = H; R_1 = R_2 = R_3 = Ph

Can. J. Chem. Downloaded from www.nrcresearchpress.com by 210.87.254.42 on 09/05/12
For personal use only.

perature to provide two compounds, after only a short reaction time (3 h). The major component, which was not crystalline and was unstable, is probably the compound **3***a*, since its n.m.r. indicated the presence of a proton within the accepted range for thials (8).

A minor component was the only product identified when the reaction was allowed to proceed for 1 day, although then two other products were obtained as uncrystallizable glasses. This other component was probably the tetra-carboxylic ester **5***a* which could have been formed by extrusion of the thial sulfur atoms from two molecules of the thial **3***a*. Confirmation of this was achieved by heating **3***a* in benzene. From the solution **5***a* was obtained, although there were a number of other minor products. Treatment of the thione **1***d* with excess acetylenic ester gave rather similar results. Under no conditions were we able to obtain any diadduct of the type **4**.

5

a R = H; R_1 = OMe
b R = H; R_1 = Ph
c R = Ph; R_1 = OMe
d R = R_1 = Ph

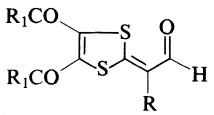

6

a R = Ph; R_1 = OMe
b R = R_1 = Ph

The compounds **5***a* could exist as two geometrical isomers with respect to the central double bond, but we are unable to distinguish what was actually formed, although the *trans* form seems more likely. This compound is probably formed by stepwise extrusion of two sulfur atoms from an initially formed dithiacyclobutane (Scheme 1). Presumably the formation of pyrylenes and dithiopyrylenes (9) from 4*H*-pyran-4-thiones and 4*H*-thiopyran-4-thiones proceeds via a similar scheme. Although the formulation "*b*" of the dimer cannot be excluded, the structure "*a*" appears more likely on the basis of results with other thiocarbonyl compounds. Such dimers are well known (10), although trimers may also be obtained. Thiaphosgene forms dimers (11, 12) and recently such intermediates have been proposed in the reaction of carbon disulfide with dimethyl acetylenedicarboxylate (13). No direct evidence appears to be available for the loss of sulfur from "*a*" to form the episulfide, but certain thiones under the influence of acetylides form both dithiacyclobutanes and episulfides (14). Possibly the former are precursors of the latter. Also, a dithiacyclobutanedioxide loses sulfur dioxide to form an episulfide (15). The last stage in the proposed scheme, the loss of sulfur from the episulfide to form the olefine, is a well-known reaction (16, 17). The geometry of the olefine would be determined by that of the initially formed dithiacyclobutane "*a*" or possibly "*b*". Although a *trans* geometry appears more likely, *cis* cannot be excluded. *Trans* products are common in many such cycloadditions (18).

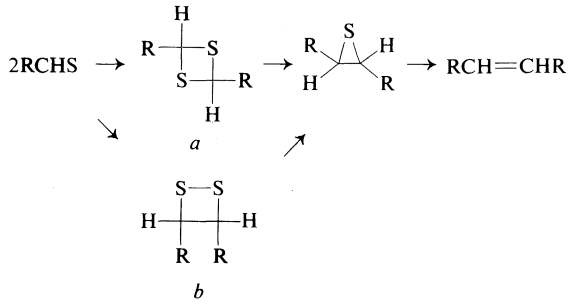

SCHEME 1

The two other non-crystalline products obtained from the reaction of the acetylenic ester with **1***d* over 1 day were not identified. Spectroscopy (i.r. and n.m.r.) indicated that they were methyl esters of carboxylic acids, but lacking analytical data no satisfactory structure can be advanced.

Very similar results were obtained by treatment of the thione **1***d* with dibenzoylacetylene. Reaction over a short time provided the thial **3***b* as an amorphous brown solid. This was the major product. No tetraketone **5***b* was obtained, but it was the major product when the reaction was performed in boiling benzene for 1 day, and **3***b* gave **5***b* on further heating in benzene. Numerous other fractions were obtained by t.l.c. in these reactions, but in only trace amounts. As in the previous case, no assignment of the geometry of **5***b* was possible. No diadduct of the type **4** was

Can. J. Chem. Downloaded from www.nrcresearchpress.com by 210.87.254.42 on 09/05/12
For personal use only.

isolated under any of the conditions tried with dibenzoylacetylenes, but when the thial **3***b* was heated with dimethyl acetylenedicarboxylate, the compound **5***b* was obtained, along with an orange oil. This could not be crystallized, but its spectroscopic properties indicated it might be the spiran **4***a*.

4-Phenyl-1,2-dithiole-3-thione (**1***c*) reacted with dimethyl acetylenedicarboxylate to give the thial mono-adduct **3***c* as a pasty brown solid. This was insufficiently stable to permit proper isolation, although evidence for the presence of a thial group was obtained. This was accompanied by a trace amount of the aldehyde **6***a* which was also obtained from the thial **3***c* by treatment with mercuric acetate. Further boiling of **3***c* in benzene or xylene gave the tetracarboxylic ester **5***c*, and treatment with more dimethyl acetylenedicarboxylate provided the spiran tetracarboxylic ester **4***b*. Compound **3***c* failed to react with ethylpropiolate. The aldehyde **6***a* was obtained in trace amounts in all these reactions, even when performed under nitrogen and in dry solvents. It appears that it is formed from unreacted thial by aerial oxidation or hydrolysis on the t.l.c. plates, prior to developing.

With dibenzoylacetylene, 4-phenyl-1,2-dithiole-3-thione (**1***c*) has been reported (5) to give an unstable thial. This reaction was further investigated to determine the products of further reaction. The thial **3***d* was obtained as a pasty solid which could not be purified satisfactorily. Refluxing it in benzene gave the tetraketone **5***d* in low yield, but better conversion was achieved in xylene. Small amounts of the spiran tetraketone **4***c* were also obtained from the reaction of the thione **1***c* with dibenzoylacetylene, and this was the major product when the thial **3***d* was treated with dibenzoylacetylene, although small amounts of the tetraketone **5***d* were also found. In all of these reactions, small amounts of the aldehyde **6***b* were obtained. As in the reaction of **1***c* with dimethyl acetylenedicarboxylate, this is probably formed by aerial oxidation of unreacted thial **3***d*.

From the above products, a sequence of reactions may be seen. Reaction of the initial 1,2-dithiole-3-thione **1***c* or *d* with the activated acetylene, first produces a thial mono-adduct, which may react in three ways. One reaction common to all studied is that producing the butendiylidenedithioles **5**. However, where the thial group is stabilized by conjugation to a phenyl group, as in **3***c* or *d*, it is possible that this reaction becomes slower, and other reactions may compete effectively with it, *i.e.* the thial may react with a suitably activated acetylene to form a di-adduct **4** or it may form the corresponding aldehyde **6** by hydrolysis or oxidation.

The n.m.r. spectra of the products derived from dimethyl acetylenedicarboxylate in deuterochloroform are interesting in that while the phenyl substituted compounds **3***c* and **5***c* demonstrate non-equivalence of the methyl groups on the ester function due to their different environments with respect to the exocyclic double bond, the methyl groups on the ester functions of **3***a* and **5***a* are equivalent. Related phenomena have been observed for the reaction products **2***a* of a variety of 1,2-dithiole-3-thiones with acetylenes (1, 4, 19–21). Where the acetylene is unsymmetrical, two geometrical isomeric products are obtained. The detection of non-equivalence or of isomers then seems to be related to the presence of a substituent α to the thiocarbonyl group in the thioacylmethylene-1,3-dithioles (originally a 4-substituent on the starting 1,2-dithiole-3-thione). However, the data for the analogous acylmethylene-1,3-dithioles **2***b* (22, 23) indicate that two isomers are present even where there is no α substituent. Interconversion of the two forms of the thioacyl compounds by isomerization about the exocyclic double bond has been suggested (21), and similar phenomena could render the ester functions equivalent in **3***a*, **5***a*, and other such derivatives of dimethyl acetylenedicarboxylate, but the magnetic equivalence of substituents seems to be merely co-incidental since the n.m.r. spectrum of **5***c* in hexadeuterobenzene, because of its solvent shift effects (24) indicated that the two ester groups had different shifts. The two isomers, however, may be interconvertible by a rate slower than the n.m.r. time scale. Unfortunately, **3***c* was insufficiently soluble in cold benzene to allow any conclusions to be made, and heating caused rapid formation of **5***c*. The aldehyde **6***a* also demonstrated non-equivalence of the ester functions.

Experimental

The i.r. spectra were performed on a Perkin–Elmer model 337 spectrophotometer, in liquid paraffin mulls except where otherwise stated. The n.m.r. spectra were obtained on a Varian Model 50/60A spectrometer, and unless otherwise stated in deuterochloroform solution using tetramethylsilane as an internal standard. Some of these were done in methylene chloride solution but peaks

Can. J. Chem. Downloaded from www.nrcresearchpress.com by 210.87.254.42 on 09/05/12
For personal use only.

were not properly resolved in this. The t.l.c. was performed on 1 mm thick layers of silica gel type D.S.F. 5 supplied by Mondray Ltd. Development of plates was carried out using benzene with increasing proportions of chloroform. Where bands were not properly separated, the separate fractions were re-chromatographed. Melting points were obtained on a Fisher-Johns apparatus. Mass spectra were obtained on a Finnegan 1015 quadrupole mass spectrometer.

Reaction of 1,2-Dithiole-3-thione with Dimethyl Acetylenedicarboxylate

1,2-Dithiole-3-thione (25)(134 mg, 1 mmol) and dimethyl acetylenedicarboxylate (142 mg, 1 mmol) in benzene (30 ml) were stirred at room temperature for 3 h. The solvent was removed in the cold under reduced pressure, and t.l.c. of the crude material gave **3***a* as a brown paste (70%) which could not be purified further.

The n.m.r. of **3***a*, 5.78 (6H singlet, two equivalent CH_3 groups), 1.55 (1H doublet, $J = 7.5$ Hz, vinyl proton), -1.65 τ (1H doublet, $J = 7.5$ Hz, thial proton). The i.r. spectrum 1725 cm^{-1} (C=O str) broad peak in methylene chloride.

Traces of **5***a* (~10 mg) were also obtained as a purple solid. A repeat of the above reaction but for 24 h, and in boiling benzene gave **5***a* as purple matted needles from nitromethane, m.p. 195–197° (42%).

Anal. Calcd. for $C_{18}H_{16}S_4O_8$: C, 44.27; H, 3.28; S, 26.23. Found: C, 44.54; H, 3.06; S, 26.33.

The n.m.r. of **5***a*, 6.20 (12H singlet, four equivalent CH_3 groups), 4.15 τ (4H multiplet, methine protons). The i.r. spectrum, 1740, 1725, 1710 cm^{-1} (C=O str). In deuterobenzene, the methyl groups were evident at 6.77 and 6.75 τ.

Two other fractions were also isolated by t.l.c. (~30 mg each). These were obtained as uncrystallizable orange glasses. The n.m.r. indicated they were methyl esters.

Similar results were obtained when the thione **1***d* was allowed to react with excess acetylenic ester.

*Conversion of Dimethyl 2-Thioformylmethylene-1,3-dithiole-4,5-dicarboxylate (**3***a*) into Tetramethyl 1,4-Butenediylidene-2,2′-bis(1,3-dithiole-4,5-dicarboxylate) (**5***a*)*

The ester **3***a* (100 mg, 0.3 mmol) in benzene (25 ml) was refluxed for 24 h. Examination of the solution gave **5***a* (40%) along with six other fractions which gave only traces of material.

Reaction of 1,2-Dithiole-3-thione with Dibenzoylacetylene

The thione (134 mg, 1 mmol) and dibenzoylacetylene (26) (234 mg, 1 mmol) in benzene (25 ml) were stirred together at room temperature for 3 h. The solvent was removed in the cold under reduced pressure, and t.l.c. of the crude material gave **3***b* as a brown solid (74%). This could not be sufficiently purified for analysis.

The n.m.r. of **3***b*, 2.17 (1H doublet, $J = 7.5$ Hz, vinyl proton), 3.03 to 2.45 (10H bands, aromatic protons), 0.78 τ (1H doublet, $J = 7.5$ Hz, thial proton). The i.r. spectrum, 1660 cm^{-1}, broad, (C=O str) in methylene chloride.

A repeat of the above reaction for 18 h in boiling benzene gave **3***b* (4%) and the tetraketone **5***b* as dark green plates m.p. 203–205° from nitromethane (38%).

Anal. Calcd. for $C_{38}H_{24}S_4O_4$: C, 67.86; H, 3.57; S, 19.04. Found: C, 68.08; H, 3.67; S, 18.97.

The n.m.r. spectrum, 4.31 to 3.70 (4H multiplet, the methine protons), 2.90 to 2.40 τ (20H bands, aromatic protons). The i.r spectrum, 1630 and 1655 cm^{-1} (C=O str).

Ten other bands were also separated, but gave only traces of products. Similar results were obtained when the thione was treated with excess dibenzoylacetylene.

*Reaction of 4,5-Dibenzoyl-2-thioformylmethylene-1,3-dithiole (**3***b*) with Dimethyl Acetylenedicarboxylate to form **4***a*

The thial (20 mg, 0.055 mmol) and the ester (7.7 mg, 0.055 mmol) in benzene (3 ml) were refluxed for 3 h. From the mixture was isolated **5***b* (60%) and a small amount (~10 mg) of an orange glass which was possibly **4***a*.

*Conversion of 4,5-Dibenzoyl-2-thioformylmethylene-1,3-dithiole-(**3***b*) into 1,4-Butenediylidene-2,2′-bis(4,5-dibenzoyl-1,3-dithiole) (**5***b*)*

The diketone (150 mg, 0.24 mmol) in benzene (30 ml) was refluxed for 18 h. Work-up of the mixture gave **5***b* (43%) and ten other minor fractions.

Reaction of 4-Phenyl-1,2-dithiole-3-thione with Dimethyl Acetylenedicarboxylate

The thione (210 mg, 1 mmol) and the ester (142 mg, 1 mmol) in benzene (30 ml) were stirred at room temperature for 1.5 h. Work-up gave **3***c* as a brown pasty solid (85%) which could not be purified satisfactorily.

The n.m.r. spectrum of **3***c*, 6.25 and 6.17 (two 3H singlets, methyl groups), 2.73 (5H singlet, aromatic protons), 0.35 τ (1H singlet, thial proton). The i.r. spectrum, 1740 cm^{-1} (C=O) broad, methylene chloride solution.

Along with this compound was obtained a trace of **6***a*.

*Conversion of Dimethyl α-Phenylthioformylmethylene-1,3-dithiole-4,5-dicarboxylate (**3***c*) into Tetramethyl 1,4-Diphenyl-1,4-butenediylidene-2,2′-bis(1,3-dithiole-4,5-dicarboxylate) (**5***c*)*

The thial (230 mg, 0.65 mmol) in benzene (30 ml) was refluxed for 24 h. Work-up gave the tetracarboxylic ester as reddish-purple needles from nitromethane, m.p. 212–216° (43%).

Anal. Calcd. for $C_{30}H_{24}S_4O_8$: C, 56.25; H, 3.75; S, 20.00. Found: C, 56.17; H, 3.75; S, 19.82.

The n.m.r. spectrum of **5***c*, 6.22 and 6.27 (two 6H singlets, methyl protons), 4.23 (2H singlet, methine protons), 2.92 to 2.42 τ (10H bands, aromatic protons). The i.r. spectrum, 1725 and 1750 cm^{-1} (C=O str).

When the reaction was performed in boiling xylene, the yield was raised to 80%. A small amount (~5 mg) of **6***a* was also obtained in the reaction.

*Preparation of Dimethyl-2-α-phenylformylmethylene-1,3-dithiole-4,5-dicarboxylate (**6***a*)*

The thial **3***c* (120 mg, 0.34 mmol) was added to a hot solution of excess mercuric acetate in acetic acid (10 ml). The dark color of the thial disappeared almost instantaneously. The solution was diluted with water and the benzene extract purified by t.l.c. The product was obtained as orange prisms, m.p. 127–129°, from ethanol:benzene 1:1 (80%).

Can. J. Chem. Downloaded from www.nrcresearchpress.com by 210.87.254.42 on 09/05/12
For personal use only.

Anal. Calcd. for $C_{15}H_{12}S_2O_5$: C, 53.53; H, 3.57; S, 19.04. Found: C, 53.61; H, 3.56; S, 19.21.

The n.m.r. of **6***a* 6.23 and 6.18 (two 3H singlets, methyl groups), 2.73 (5H singlet, aromatic protons), 0.75 τ (1H singlet, thial proton). The i.r. spectrum, 1770 and 1750 (C=O str, from ester), 1630 cm^{-1} (C=O str, from aldehyde).

Reaction of Dimethyl-2-α-phenylthioformylmethylene-1,3-dithiole-4,5-dicarboxylate (3c) with Dimethyl Acetylenedicarboxylate

The thial (274 mg, 0.78 mmol) and the ester (122 mg, 0.78 mmol) in benzene (30 ml) were refluxed for 3 h. Work-up gave the diadduct **4***b* as an uncrystallizable orange glass (40%). Mass spectrum showed a parent ion at *m/e* 494, calcd. 494, *m/e* 435 ($M-CO_2CH_3$)

The n.m.r. spectrum, 6.32 (6H singlet, two equivalent methyls on the dithiole ring), 6.18 and 6.13 (two 3H singlets, methyls on the thiopyran ring), 3.67 (1H singlet, vinyl proton), 2.78 to 2.50 τ (5H bands, aromatic protons). The i.r. spectrum 1720 cm^{-1} (C=O str) broad, in methylene chloride.

Attempted Reaction of Dimethyl α-Phenylthioformylmethylene-1,3-dithiole-4,5-dicarboxylate (3c) with Ethyl Phenylpropiolate

The thial (176 mg, 0.5 mmol) and the ester (87 mg, 0.5 mmol) in benzene (30 ml) were refluxed for 24 h. Only **5***c* was isolated from the mixture. The n.m.r. examination of all fractions indicated none with an ethyl group.

Reaction of 4-Phenyl-1,2-dithiole-3-thione with Dibenzoylacetylene

The thione (420 mg, 2 mmol) and dibenzoylacetylene (464 mg, 2 mmol) in benzene (40 ml) were stirred at room temperature for 2½ h. Work-up of the mixture gave **3***d* as a brown powder, which could not be purified sufficiently for analysis (71%).

The n.m.r. of **3***d*, 2.99 to 2.50 (15H bands, the aromatic protons), −0.65 τ (1H singlet, the thial proton). The i.r. spectrum 1655 cm^{-1} (C=O str) broad, in methylene chloride.

Compound **4***c* was also isolated as a yellow powder, m.p. 89–92° (14%).

Anal. Calcd. for $C_{41}H_{20}S_3O_4$: C, 72.57; H, 3.83; S, 14.22. Found: C, 72.47; H, 3.80; S, 14.06.

The n.m.r. spectrum of **4***c*, 3.45 (1H singlet, vinyl proton), 3.10 to 2.11 τ (25H bands, the aromatic protons). The i.r. spectrum 1675 and 1640 cm^{-1} (C=O str).

Conversion of 2-α-Phenylthioformylmethylene-4,5-dibenzoyl-1,3-dithiole (3d) into 1,4-Diphenyl-1,4-butenediylidene-2,2′-bis(4,5-dibenzoyl-1,3-dithiole) (5d)

The thial (160 mg, 0.36 mmol) in xylene (26 ml) was refluxed for 24 h. Examination of the mixture gave **5***d* as purple needles, m.p. 244–246° (51%).

Anal. Calcd. for $C_{50}H_{32}S_4O_4$: C, 72.94; H, 3.90; S, 15.54. Found: C, 72.72; H, 4.04; S, 15.39.

The n.m.r. spectrum of **5***d*, 4.10 (2H singlet, methine protons), 3.00 to 2.35 τ (30H bands, the aromatic protons). The i.r. spectrum, 1675 cm^{-1} (C=O str) broad.

Also obtained was **6***b* as an orange oil which could not be crystallized (16%). This compound was also prepared below.

The n.m.r. of **6***b*, 3.07 to 2.33 (15H bands, the aromatic protons), 0.72 τ (1H singlet, the aldehydic proton). The i.r. spectrum, 1655 and 1625 cm^{-1} (C=O str). The mass spectrum *m/e* 428 (parent peak) calcd. 428.

Preparation of 2-α-Phenylformylmethylene-4,5-dibenzoyl-1,3-dithiole (6b)

The thial **3***d* (200 mg, 0.45 mmol) in boiling acetic acid (10 ml) was treated with an excess of mercuric acetate. The solution turned yellow after 5 min and the mixture was poured into water and extracted with benzene. Evaporation gave **6***b* as an uncrystallizable oil (85%). The mass spectrum, *m/e* 428 (parent peak), 234 ($M-(PhCO\cdot C)_2$), 194; 105 ($PhCO^+$).

Reaction of 2-α-Phenylthioformylmethylene-4,5-dibenzoyl-1,3-dithiole (3b) with Dibenzoylacetylene

The thial (165 mg, 0.47 mmol) and dibenzoylacetylene (110 mg, 0.47 mmol) were refluxed in benzene (20 ml) for 18 h. Examination of the mixture gave **4***c* (70%), **5***d* (6%), and **6***b* (6%). Also isolated was 49 mg of another orange solid, m.p. 190–193°. The mass spectrum *m/e* 573 (possibly metastable peak), 105 ($PhCO^+$).

Anal. Found: C, 73.08; H, 3.88; S, 13.98. This possibly corresponds to an isomer of **4***c*.

Anal. Calcd. for $C_{41}H_{20}S_3O_4$: C, 72.57; H, 3.83; S, 14.22.

The n.m.r. spectrum of the compound, 3.05 to 2.15τ (25H bands, aromatic protons). The i.r. spectrum 1700, 1655, and 1645 cm^{-1} (probably C=O str).

The authors wish to thank Mr. R. Dickinson for the preparation of n.m.r. spectra, and Mr. M. Arneson for mass spectra. Financial support by the National Research Council of Canada is gratefully acknowledged.

1. H. BEHRINGER, D. BENDER, J. FALKENBERG, and R. WIEDENMANN. Ber. **101**, 1428 (1968).
2. H. BEHRINGER and D. DEICHMANN. Tetrahedron Lett. 1013 (1967).
3. D. B. J. EASTON and D. LEAVER. Chem. Commun. 585 (1965).
4. J. M. BUCHSHRIBER, D. M. MCKINNON, and M. AHMED. Can. J. Chem. **47**, 2039 (1969).
5. M. AHMED, J. M. BUCHSHRIBER, and D. M. MCKINNON. Can. J. Chem. **48**, 1991 (1970).
6. R. MAYER. Synthesis and properties of thiocarbonyl compounds. *In* Organosulfur chemistry. Interscience, New York, 1967.
7. D. LEAVER and D. M. MCKINNON. Unpublished results.
8. J. G. DINGWALL, S. MCKENZIE, and D. H. REID. J. Chem. Soc. C, 2532 (1968).
9. F. ARNDT, P. NACHWEY, and J. PUSCH. Ber. **58**, 1644 (1925).
10. E. CAMPAIGNE. Chem. Rev. **39**, 1 (1946).
11. J. I. JONES, W. KYNASTON, and J. L. HALES. J. Chem. Soc. 614 (1957).
12. A. SCHONBERG. Trans. Faraday Soc. **32**, 514 (1936).
13. D. L. COFFEN. Tetrahedron Lett. 2633 (1970).
14. W. RIED and H. KLUG. Ber. **94**, 368 (1961).
15. W. J. MIDDLETON. Chem. Abstr. **61**, 5612 (1964).

16. J. D. LOUDON. The extrusion of sulfur. *In* Organic sulfur compounds. Vol. I. Pergamon, New York, 1961.
17. M. SANDERS. Chem. Rev. **66**, 297 (1966).
18. R. B. WOODWARD and R. HOFFMAN. The conservation of orbital symmetry. Academic Press, New York, 1970. p. 73.
19. C. PORTAIL and J. VIALLE. Bull. Soc. Chim. Fr. 3187 (1966).
20. M. BEHRINGER, J. KILGER, and R. WIEDENMANN. Tetrahedron Lett. 1185 (1968).
21. M. BEHRINGER and R. WIEDENMANN. Tetrahedron Lett. 3705 (1965).
22. H. DAVY, M. DEMUYNCK, D. PAQUER, A. ROUESSAC, and J. VIALLE. Bull. Soc. Chim. Fr. 2057 (1968).
23. E. CAMPAIGNE and H. HAAF. J. Org. Chem. **30**, 732 (1965).
24. R. WASYLISHEN, T. SCHAEFER, and R. SCHWENK. Can. J. Chem. **48**, 2885 (1970) and references therein.
25. E. KLINGSBERG. J. Am. Chem. Soc. **86**, 5290 (1964).
26. R. E. LUTZ and W. R. SMITHEY. J. Org. Chem. **16**, 51 (1951).

Can. J. Chem. Downloaded from www.nrcresearchpress.com by 210.87.254.42 on 09/05/12
For personal use only.

Isomers of 1-(4-Chlorophenyl)-2,3-dimethylisoindoline

K. R. Freter and F. K. Hess
Pharma-Research Canada Ltd., 250 Hymus Blvd., Pointe Claire, Québec
AND
J. Sygusch and F. Brisse
Département de Chimie, Université de Montréal, Montréal, Québec

Received June 21, 1971

The chemical properties and n.m.r. data of the two isomers of 1-(4-chlorophenyl)-2,3-dimethylisoindoline are reported. The crystal structure of one of the isomers was determined by X-ray diffraction.

Les propriétés chimiques et les données r.m.n. relatives aux deux isomères du (chloro-4 phényl)-1 diméthyl-2,3 isoindoline sont rapportées. La structure cristalline de l'un des isomères a été déterminée par diffraction de rayons-X.

Canadian Journal of Chemistry, 49, 3305 (1971)

Reduction of 1-(4-chlorophenyl)-2,3-dimethylisoindole (**1**) with zinc in acetic acid gave in a good overall yield the expected isoindolines (**2***a* and *b*), which could be separated by column chromatography on silica with chloroform.

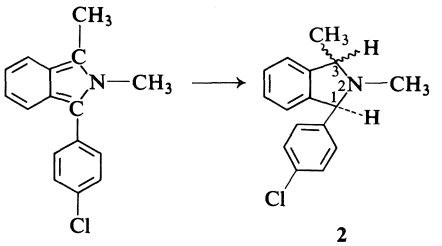

1 → **2**

a 15%
b 58%

Each isomer could be equilibrated with the other, in acetic anhydride solution in the presence of boron trifluoride. This finding corresponds with the recently published result on 1,3-dimethylisoindolines (1).

Refluxing of either of the isomers in acetic anhydride even for several days left them unchanged. This was unexpected in view of the fact, that the 3-unsubstituted isoindoline, **3**, like phenyl substituted-tetrahydrocarbolines (2) or -tetrahydroisoquinolines (3), yields the corresponding benzhydrol **4** in a matter of hours (4).

Catalytic hydrogenolysis of **2***a* or *b* on the other hand, followed smoothly the expected course yielding in both instances the same *o*-benzyl-benzylamine, **5**.

The n.m.r. signals (Table 1) for both isomers show pronounced differences. The chemical

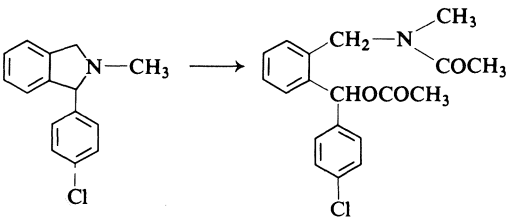

3 → **4**

shifts of the methine protons of **2***a* and *b* (as hydrochlorides) differ considerably (see Table 1). More interesting is the fact, that the signals of these protons (the H-1 singlet and the H-3 quartet), show splitting (**2***a*, J = 2.7 Hz; **2***b*, J = 2.5 Hz), when the spectra of the free bases are measured. This seems to be an example of long-range coupling "across" a non-aromatic heterocycle; the coupling constants are considerably greater than usually observed for long-range coupling along 4σ bonds (5).[1] A conclusion, however,

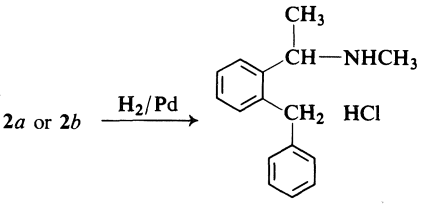

5

[1]While this work was in progress, another related example of long-range coupling in the dihydrofuran series was reported (6), where coupling constants of $J_{2,5}$ = 0.4 Hz for *cis*- and 4.0 Hz for *trans*-derivatives were found.

Can. J. Chem. Downloaded from www.nrcresearchpress.com by 210.87.254.40 on 09/05/12
For personal use only.

TABLE 1. The n.m.r. data for isoindolines **2***a* and *b*

	τ (ppm)*			
Proton	**2***a* HCl (D_2O)	**2***b* HCl (D_2O)	**2***a* Base ($CDCl_3$)	**2***b* Base ($CDCl_3$)
8H	2.1–3.0 m	2.0–2.9 m	2.7–3.5 m	2.7–3.5 m
C_1-H	3.93 s	3.61 s	5.54 d (J = 2.7)	5.14 d (J = 2.5)
C_3-H	4.84 q (J = 7)	4.64 q (J = 7)	6.30 q (J = 6.5) d (J = 2.7)	5.66 q (J = 6.5) d (J = 2.5)
N-CH_3	6.74 s	6.95 s	7.63 s	7.72 s
C-CH_3	8.00 d (J = 7)	7.98 d (J = 7)	8.53 d (J = 6.5)	8.74 d (J = 6.5)

*All J-values are Hz.

about *cis–trans* assignment on grounds of the difference in these long-range coupling constants cannot be drawn.

The same holds true for the difference in chemical shifts. Interpretation in the case of symmetrically substituted isoindolines has previously led to erroneous assignments (7), which could be corrected only by application (8) of the *N*-benzyl method of Hill and Chan (9). This, of course, is of no help in this case of unsymmetrical substitution.

The shielding and deshielding effects of the chlorophenyl ring in 1-position on the protons of the 3-methyl group and on the 3-proton are opposite for both isomers. While in **2***a* the 3-methyl signal is shifted to lower field and the H-3 signal to higher field, the reverse is true for **2***b*. A decision, in which case the 1-chlorophenyl substituent exerts its shielding or deshielding influence, rests solely on the question, which orientation this substituent takes.

We were unable to predict from model studies, whether this substituent takes a coplanar or perpendicular position, or any intermediate angle relative to the (almost) planar isoindoline system.

A recent publication (10) about similarly substituted phthalans augmented our hesitation, to predict the stereochemistry on grounds of n.m.r. studies alone.

An X-ray diffraction study was then undertaken to determine the relative stereochemistry of the substituents at C-1 and -3.

Good crystals of indoline **2***a* were obtained from methanol solutions. Precession photographs indicated that the space group is $P2_1/c$ and that there are four molecules in a monoclinic unit cell of dimensions: a = 9.071(2), b = 12.443(3), c = 11.945(4) Å and β = 93.19(10)°. Three dimensional intensity data were collected with an automatic Picker diffractometer using MoKα radiation. Of the 1851 measured reflexions, 1639 were observed. The phases of 234 reflexions with normalized structure factors E greater than 1.50 were determined by the symbolic addition procedure for non-centrosymmetric crystals as described by Germain *et al.* (13). An E-map calculated with the 234 phased reflexions yielded all the non-hydrogen atoms. The atomic parameters were refined by the least-squares procedure using the programs written by Ahmed *et al.* (11). After five cycles of isotropic temperature factor refinement followed by two cycles of anisotropic temperature factor refinement, the R-factor decreased to 9.9%.

At this stage a Fourier difference map revealed the positions of 10 hydrogen atoms which were subsequently included in the refinement. So far the refinement, still in progress, has reached an R-factor of 7.6%.

The molecular structure projected on the 100 plane is shown in Fig. 1. Indoline **2***a* can thus be said to be *cis*-1-(4-chlorophenyl)-3-methyl-2-methylisoindoline. The bond distances and angles are in good agreement with expected values. The complete results of the X-ray investigation will be published elsewhere.

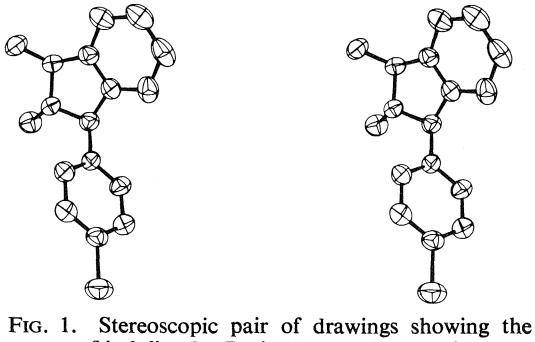

FIG. 1. Stereoscopic pair of drawings showing the structure of indoline **2***a*. Projection on the 100 plane.

Can. J. Chem. Downloaded from www.nrcresearchpress.com by 210.87.254.40 on 09/05/12
For personal use only.

Can. J. Chem. Downloaded from www.nrcresearchpress.com by 210.87.254.40 on 09/05/12
For personal use only.

Experimental

The n.m.r. spectra were determined on a Varian Associates Model T-60. Melting points were taken on a Fisher-Johns Apparatus and are uncorrected. Microanalyses were carried out by Dr. C. Daesslé, Montreal, Québec.

1-(4-Chlorophenyl)-2-methylisoindolone-(3)

2-(4-Chlorobenzoyl)benzoic acid was treated with aqueous methylamine at 180° as described for the unsubstituted phenyl compound (12); m.p. 128–129 °C; mol. wt. 257; yield 75%.

Anal. Calcd. for $C_{15}H_{12}ClNO$: C, 70.00; H, 4.67; N, 5.44; Cl, 13.74. Found: C, 70.11; H, 4.71; N, 5.65; Cl, 13.93.

1-(4-Chlorophenyl)-2,3-dimethylisoindole (1)

This compound was prepared in 60% yield, from the above isoindolone according to Theilacker and Schmidt (12) with methyl lithium solution; m.p. 124–126 °C; mol. wt. 255.7.

Anal. Calcd. for $C_{16}H_{14}NCl$: C, 75.20; H, 5.52; N, 5.48; Cl, 13.85. Found: C, 74.77; H, 5.86; N, 5.75; Cl, 13.75.

1-(4-Chlorophenyl)-2,3-dimethylisoindoline (2a and b)

The isoindole (**1**) (26.7 g) was dissolved in glacial acetic acid (150 ml) and water (100 ml), and zinc dust (25 g) was introduced under stirring in several portions. The mixture was heated to reflux for 30 min, diluted with water (200 ml), filtered to remove excess zinc, and made basic with concentrated ammonia. The basic material was extracted with ether, the combined ether extracts were washed with water, dried over magnesium sulfate, and evaporated to dryness. The oily residue (22.6 g) was separated on a silica gel column using chloroform as eluant. Two major basic fractions were obtained. The one leaving the column first (**2***a*) was a colorless oil (4g, 14.8%) which was converted to the hydrochloride by addition of ethereal hydrochloric acid. It was recrystallized from acetone/ether and had an m.p. of 210–219 °C (dec.); m.p. of the free base 87–88° (acetone–water).

The second fraction, **2***b*, 15.8 g of colorless oil (58.5%) was transformed to the hydrochloride by the same method. After recrystallization it had an m.p. of 208–218 °C (dec.); m.p. of the free base 83° (acetone–water); mol. wt. 294.2.

Anal. Calcd. for $C_{16}H_{16}ClN{\cdot}HCl$: C, 65.35; H, 5.82; N, 4.79; Cl, 24.08. Found for **2***a* (R_F 0.6): C, 65.03; H, 5.83; N, 4.89; Cl, 24.06. Found for **2***b* (R_F 0.2): C, 65.39; H, 5.41; N, 4.51; Cl, 24.08.

The R_F values refer to t.l.c. on silica, chloroform as eluant.

2-Benzyl-α,N-dimethylbenzylamine (5)

The above isoindoline (either isomer as free base) (4 g) was dissolved in ethanol (100 ml), palladium-on-charcoal (5%, prehydrogenated) (1 g) was added, and the mixture was shaken in an atmosphere of hydrogen at room temperature and atmospheric pressure.

The uptake of hydrogen came to an end, when 770 ml were consumed (calculated 750 ml). The mixture was filtered and evaporated to dryness. The residue was crystallized from ethanol and had an m.p. of 175–176 °C; 3 g (75%); mol. wt. 261.8.

Anal. Calcd. for $C_{16}H_{19}N{\cdot}HCl$: C, 73.20; H, 7.69; N, 5.35; Cl, 13.55. Found: C, 73.20; H, 7.82; N, 5.60; Cl, 13.70.

The n.m.r. (τ) in D_2O, 1.8–2.7 m (9H), 5.17 q (J = 7.0 Hz) (1H), 5.68 s (2H), 7.35 s (3H), 8.37 d (J = 7.0 Hz) (3H).

Conversion from 2b into 2a

The free base, liberated from the hydrochloride of **2***b* (2g), was dissolved in acetic anhydride (20 ml), 2 drops of boron trifluoride were added, and the mixture was heated for 2 days to reflux. The mixture was then poured on ice–ammonia, extracted with chloroform, and the residue of the chloroform extract separated as described above. An oil (0.7 g) was obtained, which was identical with respect to i.r., m.p. of hydrochloride, and t.l.c. with **2***a*.

The fact, that equilibrium could be reached by subjecting **2***a* to the same conditions, was established only by t.l.c.

The authors wish to thank Mrs. A. Thomas for her skillful assistance.

1. C. O. Bender and R. Bonnett. J. Chem. Soc. (C) 2186, (1968).
2. K. Freter, H. H. Huebner, H. Merz, H. D. Schroeder, and K. Zeile. Liebigs Ann. Chem. **684**, 159 (1965).
3. K. Freter, M. Goetz, and J. T. Oliver. J. Med. Chem. **13**, 1228 (1970).
4. K. Freter, M. Goetz, J. T. Oliver, and K. Zeile. German Patent Application (to C. H. Boehringer Sohn) B 95 987, December 22, 1967. K. Freter and M. Goetz. Can. J. Chem. **48**, 1670 (1970).
5. E. O. Bishop. Ann. Reports **58**, 55 (1961).
6. C. Barbier, D. Gagnaire, and P. Vottero. Bull. Soc. Chim. Fr. 2330 (1968).
7. L. A. Carpino. J. Am. Chem. Soc. **84**, 2196 (1962).
8. L. A. Carpino. Chem. Commun. 494 (1966).
9. R. K. Hill and T. K. Chan. Tetrahedron, **21**, 2015 (1965).
10. F. J. Petracek, N. Sugisaka, M. W. Klohs, R. G. Parker, J. Bordner, and J. D. Roberts. Tetrahedron Lett. 707–710 (1970).
11. F. R. Ahmed, S. R. Hall, M. E. Pippy, and C. P. Huber. (1966) NRC Crystallographic Programs for the IBM 360 System. World list of Crystallographic Programs. 2nd Ed. Appendix, page 52.
12. W. Theilacker and W. Schmidt. Liebigs Ann. Chem. **597**, 95 (1955).
13. G. Germain, P. Main, and M. M. Woolfson. Acta Cryst. B**26**, 274 (1970).

Can. J. Chem. Downloaded from www.nrcresearchpress.com by 210.87.254.105 on 09/05/12
For personal use only.

Hydration of CN^-, NO_2^-, NO_3^-, and OH^- in the Gas Phase

J. D. PAYZANT, R. YAMDAGNI, AND P. KEBARLE
Chemistry Department, University of Alberta, Edmonton, Alberta

Received April 14, 1971

By measuring the $A^-(H_2O)_{n-1} + H_2O = A^-(H_2O)_n$ equilibria in the gas phase and their temperature dependence, the equilibrium constants and $\Delta H_{n,n-1}$ and $\Delta S_{n,n-1}$ for some of the hydrates of NO_2^-, NO_3^-, CN^-, and OH^- were determined. Available thermochemical data are used for the evaluation of the total heats of hydration of the above ions. The total heats of hydration were then compared with the $\Delta H_{1,0}$. Relative to the total hydration energies the $\Delta H_{1,0}$ of the above ions were found larger than the $\Delta H_{1,0}$ of the halide ions.

An approximate linear correlation was found to exist between $\Delta H_{1,0}$ of negative ions and the heterolytic bond dissociation energy $D(A^- - H^+)$. With this relationship independent estimates for the electron affinities of NO_2 and NO_3 could be obtained.

The $\Delta H_{n,n-1}$ of OH^- were found in essential agreement with earlier measurements from this laboratory and in disagreements with recent measurements (Friedman) which gave much higher values.

En mesurant les équilibres $A^-(H_2O)_{n-1} + H_2O = A^-(H_2O)_n$ en phase gazeuse et leurs dépendances par rapport à la température, pour quelques hydrates de NO_2^-, NO_3^-, CN^- et OH^-, les constantes d'équilibre, $\Delta H_{n,n-1}$ et $\Delta S_{n,n-1}$ ont été déterminées. Les données thermodynamiques disponibles ont été utilisées pour évaluer les chaleurs totales d'hydratation de ces ions. Les chaleurs totales d'hydratation ont été comparées avec $\Delta H_{1,0}$. Relativement aux énergies totales d'hydratation, les valeurs $\Delta H_{1,0}$ pour ces ions sont plus importantes que les valeurs de $\Delta H_{1,0}$ pour les ions halogénés.

Une corrélation presque linéaire existe entre les valeurs de $\Delta H_{1,0}$ des ions négatifs et l'énergie de dissociation de la liaison hétérolytique $D(A^-—H^+)$. Au moyen de cette corrélation, des estimations indépendantes de l'électron affinité de NO_2 et NO_3 ont été obtenues.

Les valeurs $\Delta H_{n,n-1}$ de OH^- ainsi trouvées sont en bon accord avec les mesures obtenues antérieurement dans ce laboratoire et sont en désaccord avec des mesures récentes (Friedman) conduisant à des valeurs bien plus élevées.

Canadian Journal of Chemistry, 49, 3308 (1971)

I. Introduction

The present work is a continuation of gas phase ion equilibria studies dealing with the interaction of polar molecules with positive and negative ions. The studies consist in experimentally determining the temperature dependence of the equilibrium constant $K_{n,n-1}$ for the general reaction $(n,n-1)$ occurring in the gas phase. Van't Hoff plots of the equilibrium constants lead then to the enthalpy and entropy changes

$$A^{\pm}(B)_n = A^{\pm}(B)_{n-1} + B \qquad (n,n-1)$$

$\Delta H_{n,n-1}$ and $\Delta S_{n,n-1}$. Previous studies include the positive ions H^+ with B = H_2O (1), NH_3 (2), CH_3OH (3), the alkali ions with B = H_2O (4), the negative ions: F^-, Cl^-, Br^-, I^- with H_2O (5) and OH^- with H_2O (6).

The choice of CN^-, NO_2^-, and NO_3^- was dictated by several considerations. Firstly these ions play an important part in reactions in aqueous solutions. After the study of the spherical halide ions an investigation of some non-spherical ions seemed of interest.

The ions NO_2^-, NO_3^- and their hydrates $NO_2^-(H_2O)_n$ and $NO_3^-(H_2O)_n$ are probably of importance to the ionic chemistry in the D region of the ionosphere. The recent rocket borne mass spectrometer measurements by Narcissi (7) indicate that $NO_3^-(H_2O)_n$ is the dominant negative ion at altitudes below 90 km. Laboratory measurements of the hydration equilibria of NO_3^- thus for this reason also appeared of interest. The equilibrium constants would permit the calculation of the equilibrium concentrations of $NO_3^-(H_2O)_n$ at different water concentrations and temperatures and set limits on the $NO_2^-(H_2O)_n$ ratios that might be expected in the ionosphere. A comparison with the calculated (8) ionospheric ratios of the hydrated positive ions $H^+(H_2O)_n$ could then also be made. The equilibrium constants can be also used for the evaluation of the reverse reactions once the rate constants for the forward reactions

Can. J. Chem. Downloaded from www.nrcresearchpress.com by 210.87.254.105 on 09/05/12
For personal use only.

have been determined by laboratory measurements. In most cases the rate constants for the forward reactions have not been determined. Nevertheless the $\Delta H_{n,n-1}$ remain useful guides to the decomposition rates of the clusters n since the activation energies for the decomposition E_n should be very close to the enthalpy changes $\Delta H_{n,n-1}$. An example of a situation where a qualitative guide to the dissociation rate constants is of value is the interpretation of the rocket borne mass spectrometer data of the lower ionosphere. The ions before sampling pass through a shock front caused by the motion of the rocket. Depending on the temperature in the front some clusters might decompose while others with high $\Delta H_{n,n-1}$ values might survive. Knowledge of the $\Delta H_{n,n-1}$ values allows a check on the consistency of the mass spectral data even though they might be affected by the shock wave.

One final reason for selecting the NO_2^- and NO_3^- ions was the existence of a relationship between the hydration interaction $\Delta H_{1,0}$ and the electron affinity of the uncharged species (6). This relationship permits an estimate of the as yet not completely established values of the electron affinities of NO_2 and NO_3.

Results from this laboratory for the $\Delta H_{n,n-1}$ of the OH^- hydration were published not too long ago (6). However, a more recent investigation by Friedman and co-workers (9, 10) based on a different (non equilibrium) method reported substantially higher $\Delta H_{n,n-1}$ values. The earlier equilibrium determinations (6) were not done with a pulsed electron beam, *i.e.* the time dependence of the ion concentrations was not followed. (See Experimental section.) It was therefore thought important to repeat the equilibrium experiments with measurements of the time dependence of the ions so as to place the equilibrium data on a firmer footing.

II. Experimental

(a) Apparatus, Method of Measurement, and Experimental Data

The measurements of the equilibrium constants $K_{n,n-1}$ were made by mass spectrometric detection of the ions escaping from a reaction chamber. The pressure in the reaction chamber – ion source was in the Torr range, typically 0.5 to 5 Torr. Ionization was obtained by a 2000 V electron beam of some 10^{-8} A entering the field-free reaction chamber through a narrow slit. The ion exit slit was about 4 mm below the electron beam. For these conditions the average ion escaping through the slit had spent some 1 ms in the reaction chamber. The ion currents detected with the mass spectrometer were assumed proportional to the concentrations of the ions in the reaction chamber.

The above apparatus has been described in greater detail in a previous publication (5). In the present work data were obtained by two different procedures. In some measurements continuous electron irradiation was used and the measured ion currents were assumed to come predominantly from ions which have spent sufficiently long time in the reaction chamber to have achieved equilibrium. In other experiments the electron beam was pulsed, using a program in which the beam was on for some 10 or 50 μs and off for some 5 ms. The off time was equal to time required for the ion current to decay essentially to zero. The mass analyzed individual ion pulses, after amplification, were fed into a multiscaler where the ions were collected in different chanels according to the time of arrival after the electron pulse. The intensity–time dependence plots so obtained were used to examine whether the ion ratios become stationary with time. Constant ion ratios with time must be present if the equilibrium is achieved. The above procedure is essentially identical to the method used for kinetic studies of ion molecule reactions described in previous publications (11). The only difference is the use of the multiscaler with which the effective sensitivity is greatly increased. Figure 1 shows the time dependence of the ion intensities for NO_2^- and $NO_2^-.H_2O$. The ratio of the ion intensities is seen to be essentially independent of time. The initial history of the reaction, *i.e.* the de-

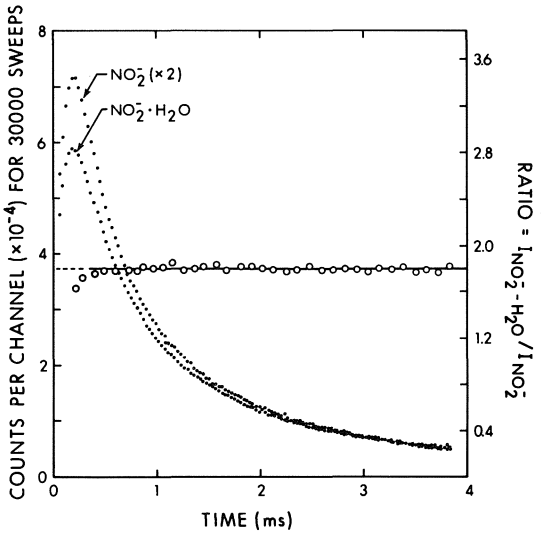

FIG. 1. Time dependence of NO_2^- and $(NO_2H_2O)^-$ ions escaping from ion source after start of short (10 μs) electron pulse. Ion source pressure 4.1 Torr H_2O vapor, temperature 164 °C. Ion intensity ratio required to be constant if equilibrium $NO_2^- + H_2O \rightleftharpoons (NO_2H_2O)^-$ is achieved.

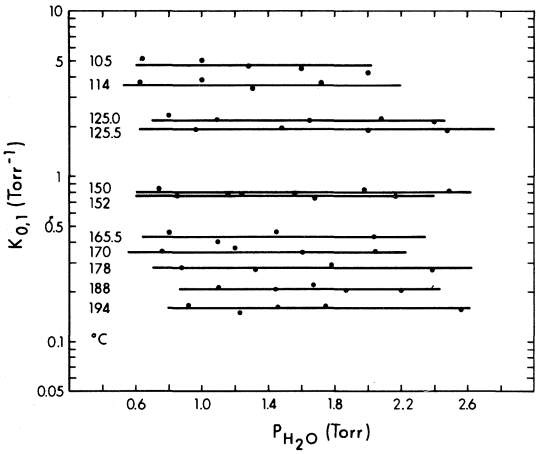

FIG. 2. Equilibrium constant $K_{0,1}$ for reaction: $CN^- + H_2O \rightleftharpoons (CNH_2O)^-$ *vs.* pressure of water in ion source.

crease of NO_2^- and the increase of $NO_2^-.H_2O$ on the approach to equilibrium, cannot be seen on the figure since concentration conditions are so selected that equilibrium is rapidly achieved. Thus the rate constant for the third body dependent forward reaction 1 should be (12) $k_1 \approx 10^{-28}$ cm^6 molecule^{-2} s^{-1}.

[1] $$NO_2^- + 2H_2O \rightleftharpoons NO_2^-.H_2O + H_2O$$

At a pressure of 4 Torr H_2O, this leads to a half-life of about 1 μs for the NO_2^- ion with regard to disappearance by the forward step of reaction 1.

Shown in Fig. 2 is the pressure independence of the equilibrium constants $K_{1,0}$ for the CN^- hydration reactions. The equilibrium constants were evaluated from the known H_2O pressure and the stationary ion ratios. Van't Hoff plots for the NO_2^-, NO_3^-, and CN^- hydration reactions are shown in Fig. 3. The present data for the NO_2^- hydration equilibrium can be compared with earlier results from this laboratory. In an earlier general survey of negative ion hydration (Kebarle, Arshadi, and Scarborough (5)) the equilibrium constants $K_{1,2} \approx 46$ and $K_{2,3} \approx 3$ (Torr^{-1}) were measured at ~292 °K. The present data in Fig. 3 extrapolated to 292 °K lead to $K_{1,2} \approx 44$ and $K_{2,3} \approx 2$. This represents fairly good agreement, considering the difference of the apparatus used, temperature and pressure measurement (the previous work was done in the presence of O_2 as the major gas component).

(b) Production of NO_2^- and NO_3^-

The NO_2^- and NO_3^- ions were produced by the addition of some 5×10^{-2} Torr of $C_2H_5ONO_2$ to the water vapor which was in the Torr range. This method of production had been used in the earlier investigation (5). Primary and secondary electrons slowed down to near thermal velocities are probably involved in dissociative electron capture by the ethyl nitrate. The products of slow electron dissociative capture and ion molecule reactions at low pressures in ethyl nitrate have been

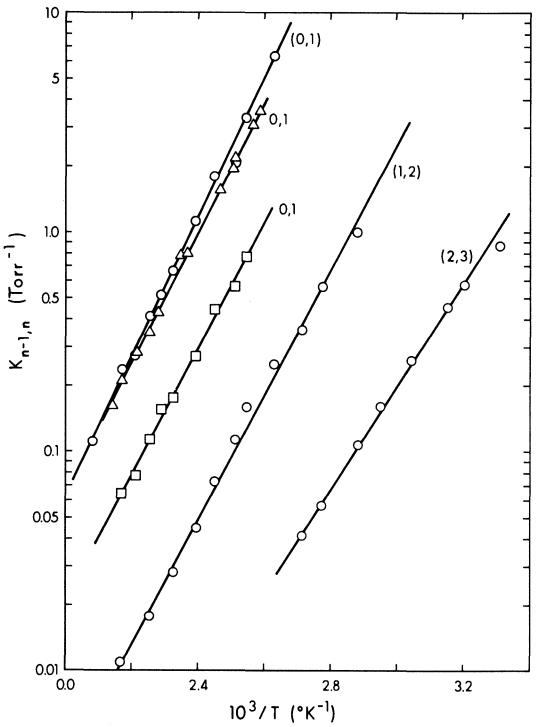

FIG. 3. Van't Hoff plot of equilibrium constants $K_{n-1,n}$ for reactions $A^-(H_2O)_{n-1} + H_2O = A^-(H_2O)_n$ in the gas phase. ○, NO_2^-; △, CN^-; □, NO_3^-.

studied by Kriemler and Buttrill (13). NO_2^- is the major product of the electron capture, $C_2H_3O^-$, $C_2H_5O^-$, OH^-, and HNO_2^- are also produced by the same process and found to yield NO_3^- by ion molecule reactions with ethyl nitrate.

The presence of NO_3^- in the present (high pressure) experiments is probably explained by the same processes. Interestingly the NO_3^- to NO_2^- yield (roughly 1:4) was found to decrease at low temperature. Near room temperature very little NO_3^- was formed. This prevented measurement of the higher hydration equilibria ($n = 2$ and 3) of NO_3^- which occur near and below room temperature.

(c) Production of CN^-

The cyanide ion was produced by the addition of some 5×10^{-2} Torr of cyanogen iodide to oxygen carrier gas (~5 Torr) containing variable pressures of H_2O (0.8–2.5 Torr). The CN^- ion is probably produced by dissociative capture, reaction 2,

[2] $$e + CNI \rightarrow CN^- + I$$

of the electrons slowed down by the gas in the reaction chamber. Reaction 2 is exothermic (with thermal electrons). Unfortunately only the 1,0 hydration equilibrium was measured. No experimental difficulties should exist for the measurement of the equilibria for the higher hydrates of this ion.

Can. J. Chem. Downloaded from www.nrcresearchpress.com by 210.87.254.105 on 09/05/12
For personal use only.

TABLE 1. Total and partial enthalpies and entropies of hydration for some single negative ions[a]

A^-	$-\Delta H_h$	$\Delta H_{1,0}$	$\Delta H_{2,1}$	$\Delta H_{3,2}$	$\Delta S^0_{1,0}$	$\Delta S^0_{2,1}$	$\Delta S^0_{3,2}$
OH^-	116.3[b]	25 (22.5)[d]	17.9 (16.4)[d]	(15.1)[d]	20.8 (19.1)	21.2 (19.3)	
F^-	113.3[c]	23	16.6	13.7	17.4	18.7	20.4
Cl^-	81.3[c]	13.1	12.7	11.7	16.5	20.8	23.2
Br^-	77.9[c]	12.6	12.3	11.5	18.4	23	24.8
I^-	64.1[c]	10.2	9.8	9.4	16.3	19	—
CN^-	78.1[b]	13.8	—	—	19.8	—	—
NO_2^-	73[b]	14.3	12.9	10.4	21	23.7	21.2
NO_3^-	68[b]	12.4	—	—	19.1	—	—

[a]All ΔH values in kcal/mol, all ΔS values in e.u. per mol, standard state 1 atm $T \simeq 300$ °K.
[b]Mode of calculation and references see section *IIb*.
[c]From Table 2 in chapter: Hydration effects and thermodynamic properties of ions. J. E. Desnoyers and C. Jolicoeur, ref. 14.
[d]Previous determination from this laboratory, ref. 6.

(d) Reproducibility and Error Estimate

Measurements under different experimental conditions and apparatus have shown that the equilibrium constants can be reproduced within 10–20% when measured on the same instrument. The error increases to ~50% if the clustering gas is a minor component of the gas mixture used. This is due to errors in the concentration determination of this component. A systematic 50% error in the equilibrium constant leads to ~0.3 kcal error in the ΔG^0 and no error in the ΔH. In practice the ΔH determinations have been found reproducible to within 5% when different instruments were used. These deviations are probably due to errors in temperature measurement. The nature of the experiments is such that no absolute error limit can be quoted.

III. Discussion of Results

(a) Hydration of CN^-, NO_2^-, and NO_3^-

The $\Delta H_{n,n-1}$ and $\Delta S^0_{n,n-1}$ obtained from the slopes of the intercepts of the Van't Hoff plots (Fig. 3) are given in Table 1. The previously determined values for the halide ions are also given in Table 1 for comparison purposes.

The total single ion heats of hydration $\Delta H_h(A^-)$ also given in Table 1 correspond to the enthalpy change for the process $A^-_{(gaseous)} \rightarrow A^-_{(aquated)}$. The values for F^-, Cl^-, Br^-, and I^- were taken from the review article of Desnoyers and Joliceur (15). The values for OH^-, CN^-, NO_2^-, and NO_3^- were calculated from the thermochemical data given in Table 2. The calculation of these values is discussed in section *IIIc*.

TABLE 2[a]

A^-	$\Delta H_f(A^-,aq)conv$	$\Delta H_f(A,g)$	e.a.(A)
OH^-	−55[b]	9.31[b]	42.5[c]
CN^-	36[b]	106.5[d]	88[d]
NO_2^-	−25[b]	7.9[b]	~55[f]
NO_3^-	−45.6[b]	16.6[e]	~90[f]

[a]All values in kcal/mol, 298 °K.
[b]Reference 15.
[c]Reference 21.
[d]Reference 22.
[e]Reference 23.
[f]See section *IIIb*.

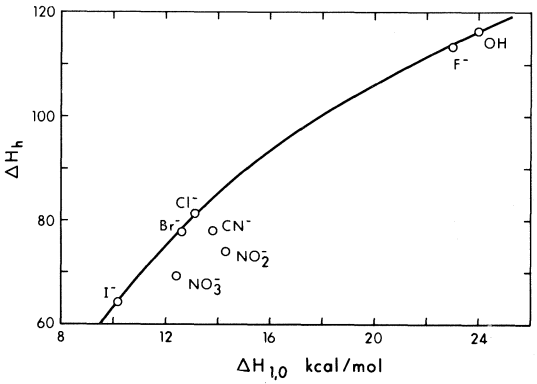

FIG. 4. Plot of total heat of hydration for negative ions A^- *vs.* $\Delta H_{1,0}$, where $\Delta H_{1,0}$ corresponds to enthalpy change for reaction $AHOH^- \rightarrow A^- + H_2O$.

The $\Delta H_{1,0}$ values are compared with the total single ion heats of hydration in Fig. 4. One finds that the halide ions give a continuous curve in this plot. The CN^-, NO_2^-, and NO_3^- ions are displaced from this curve towards relatively larger $\Delta H_{1,0}$ values than those for the halogens. The relatively stronger interactions with the initial water molecules for the unsymmetrical ions are not unexpected. They probably reflect specific hydrogen bonding to the electro negative groups (O atoms in NO_2^- and NO_3^- and N atom in CN^-).

An examination of the change of $\Delta H_{n,n-1}$ with n would be of considerable interest. Unfortunately

Can. J. Chem. Downloaded from www.nrcresearchpress.com by 210.87.254.105 on 09/05/12
For personal use only.

values up to $n = 3$ were obtained only for the NO_2^- ion (Table 1). The oxygen atoms in NO_2^- are known to form an angle of $\sim 115°$ and the N–O distance is 1.24 Å. The electronic structure of NO_2^- indicates an excess of electronic charge on the O atoms. Therefore, one would expect that the first two water molecules would hydrogen bond to the O atoms and the third one to the N atom. Furthermore the $\Delta H_{2,1}$ should only be a little smaller than $\Delta H_{1,0}$ while the $\Delta H_{3,2}$ should be appreciably lower than the $\Delta H_{2,1}$. The experimental values are 14.3, 12.9, and 10.4 kcal/mol showing a drop of 1.4 kcal between $\Delta H_{1,0}$ and $\Delta H_{2,1}$ and 2.5 kcal between $\Delta H_{2,1}$ and $\Delta H_{3,2}$. The difference of 1.4 kcal between $\Delta H_{1,0}$ and $\Delta H_{2,1}$ for the NO_2^- ion appears somewhat larger than what would be expected. Unfortunately the accuracy of the experimental determinations which is estimated at around 5% is insufficient so that one cannot be certain whether the relatively large drop of 1.4 kcal is real or not.

(b) Relationship between $\Delta H_{1,0}$ for Hydration of Negative Ions B^- and Heterolytic Bond Energy B^-—H^+

An approximate correlation of the enthalpy change $\Delta H_{1,0}$ for the (1,0) reaction: $(BHOH)^- \rightarrow B^- + HOH$ with the heterolytic bond energy $D(B^-—H^+) = D(B—H) + I_p(H) - e.a.(B)$ might be expected on the grounds that the strength of the hydrogen bond B^----HOH which is broken in reaction (1,0) should be related to $D(B^-—H^+)$ since the bridging H atom in the hydrate $(BHOH)^-$ must carry appreciable positive charge induced by the negative group B^-. A plot of $\Delta H_{1,0}$ *vs.* $D(B^-—H^+)$ is shown in Fig. 5 for $B^- = I^-, Br^-, Cl^-, F^-, OH^-$, and the newly measured NO_2^-, NO_3^-, and CN^- ions. The first group of ions can be fitted by a straight line. Of course there is no *a priori* reason that the relationship, if it exists, needs be linear. The observed deviation of Cl^- is almost certainly due to experimental error since it must be expected that the halogens should give a smooth curve. Probably the experimental $\Delta H_{1,0}$ for Cl^- is low by 0.8 to 1 kcal. The deviation of OH^- (relative to F^-) may be due to experimental error or to a real departure from the relationship due to the structural difference between F^- and OH^-. The electron affinities (e.a.) of NO_2 and NO_3 are not well established. Therefore, using the experimental $\Delta H_{1,0}$ we have placed these two ions on the

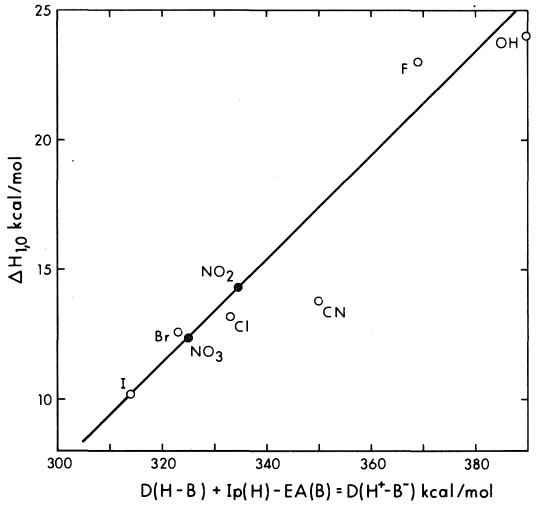

FIG. 5. Plot of $H_{1,0}$ for hydrate $(AHOH)^-$ *vs.* the heterolytic bond dissociation energy $D(H^+ — A^-)$ corresponding to process $HA \rightarrow H^+ + A^-$.

line. The values for $D(B^-—H^+)$ defined by this procedure lead to electron affinities of NO_2 and NO_3. With the supporting thermochemical data $\Delta H_f(HNO_{2,g}) = -19$ kcal (15), $\Delta H_f(HNO_{3,g}) = -32.3$ kcal (15), $\Delta H_f(NO_2) = 7.9$ kcal (15), $\Delta H_f(NO_3) = 16.6$ kcal (16) one obtains e.a.(NO_2) = 57 kcal or 2.5 eV and e.a.(NO_3) = 90 kcal or 3.9 eV. These values are close to what might be expected. Berkowitz and Chupka (17) in their recent determinations of electron affinities by endothermic charge transfer conclude that $2.1 <$ e.a.$(NO_2) < 2.3$ eV. For NO_3 Berkowitz and Chupka suggest $3.09 <$ e.a.$(NO_3) < 3.2$ eV. The present estimate of 3.9 is somewhat higher and agrees with a value based on an old lattice energy calculation (18) which need not be considered very accurate. The $\Delta H_f(NO_3) = 16.6$ kcal was determined by a somewhat questionable method. This heat of formation leads to $D(H—NO_3) = 100.6$ kcal while $D(H—NO_2) =$ 80 kcal can be evaluated from the data given above.

The difference between the two dissociation energies appears too large. A lower $D(H—NO_3)$ corresponding to a lower $\Delta H_f(NO_3)$ would lead to a lower e.a.(NO_3) which would be in better agreement with the limits of Berkowitz and Chupka quoted above.

The CN^- ion does not fit well in the plot shown in Fig. 5. The deviation is too large to be explained on the basis of experimental error in $\Delta H_{1,0}$ or the

Can. J. Chem. Downloaded from www.nrcresearchpress.com by 210.87.254.105 on 09/05/12
For personal use only.

Can. J. Chem. Downloaded from www.nrcresearchpress.com by 210.87.254.105 on 09/05/12
For personal use only.

thermochemical data used for $D(H^+—CN^-)$. The deviation probably reflects the somewhat special situation for CN. CN^- is believed to have a dipole moment with negative charge on the nitrogen. Thus on the basis of simple electrostatic arguments the water molecule should be attached to the nitrogen and not to the carbon. The heterolytic bond energy used for the plot relates to bonding to carbon. Thus it is possible that the special polarity of the CN^- ion might be responsible for the deviation from the plot.

(c) Hydration of OH^-

The experimental $\Delta H_{1,0} = 24.0$ and $\Delta H_{2,1} = 17.9$ kcal/mol for the hydration of OH^- are given in Table 1 together with the results from an earlier determination (6). The present results are higher by about 1.5 kcal. The reason for this is probably due to temperature measurement differences. The newer results were done under otherwise similar conditions to those used earlier (6) but with the pulsing technique (see section *IIa*) with which it was established that the OH^- and its hydrates have stationary concentration ratios with time. The present results are still very much lower than the data obtained by Friedman and co-workers (9, 10) $\Delta H_{1,0} = 34.5$ and $\Delta H_{2,1} = 23.0$ kcal/mol. We don't understand the reason for the discrepancy between the two sets of results, particularly since the $\Delta H_{n,n-1}$ for $H^+(H_2O)_n$ measured by the two different methods (1, 15) were in good agreement. If the present results are correct, they will also invalidate the theoretical calculations (10) and the conclusion (9) that the $\Delta H_{n,n-1}$ (for $n = 1$ to 3) of $H_3O^+(H_2O)_n$ and $OH^-(H_2O)_n$ are the same. This condition was used by Friedman and co-workers to derive a total heat of hydration for the proton (9). While this report was examined by the referees a paper by Kraemer and Diercksen (20) has come to our attention. These authors have done s.c.f.-m.o. calculations on the system $(HOHOH)^-$. The binding energy found relative to OH^- and HOH was 24 kcal/mol which is in close agreement with the present results. Earlier calculations by the above authors gave $D(H_3O^+—H_2O) = 32$ kcal which is a fairly good agreement with the experimental results of 36 kcal/mol (1, 15).

(d) Calculation of the Total Heats of Hydration of CN^-, NO_2^-, NO_3^-, and OH^-

The heats of hydration $\Delta H_h(A^-)$ corresponding to the enthalpy change for the process $A^-_{(gaseous)} \rightarrow A^-_{(aquated)}$ were calculated with the equations

$$\Delta H_h(A^-) = \Delta H_f(A^-, aq)abs - \Delta H_f(A^-, g)$$

$$\Delta H_f(A^-, aq)abs = \Delta H_f(A^-, aq)conv - \Delta H_f(H^+, aq)abs$$

$$\Delta H_f(A^-, g) = \Delta H_f(A, g) - e.a.(A)$$

where, $\Delta H_f(A^-,aq)abs$ is the absolute heat of formation of the aquated ion A^- while $\Delta H_f(A^-,aq)conv$ is the "conventional" heat of formation relative to $\Delta H_f(H^+,aq)conv = 0$. For the absolute heat of formation of the H^+ aquated ion $\Delta H_f(H^+,aq)abs = 95.6$ kcal/mol was used. This value is based on $\Delta H_f(H^+,g) = 365.6$ and $\Delta H_h(H^+) = -270$ kcal/mol. The proton hydration value of 270 kcal (Desnoyers and Jolicoeur (14)) is based on data by Randles and is consistent with gas phase hydration measurements from this laboratory (5). The uncertainties of the values quoted in Table 2 are hard to estimate. Probably the electron affinities are the least reliable with an estimated 5 kcal uncertainty. The $\Delta H_f(NO_3,g) \sim 16.6$ kcal/mol is also believed to be not very reliable. On the whole one might judge that the newly calculated ΔH_h for CN^-, NO_2^- have an error of about ± 4 kcal while the error for the $\Delta H_h(NO_3^-)$ is somewhat larger.

1. P. KEBARLE, S. K. SEARLES, A. ZOLLA, J. SCARBOROUGH, and M. ARSHADI. J. Am. Chem. Soc. **89**, 6393 (1967).
2. S. K. SEARLES and P. KEBARLE. J. Phys. Chem. **72**, 742 (1968).
3. P. KEBARLE, R. N. HAYNES, and J. G. COLLINS. J. Am. Chem. Soc. **89**, 5753 (1967).
4. I. DZIDIC and P. KEBARLE. J. Phys. Chem. **74**, 1966 (1970).
5. M. ARSHADI, R. YAMDAGNI, and P. KEBARLE. J. Phys. Chem. **74**, 1475 (1970). P. KEBARLE, M. ARSHADI, and J. SCARBOROUGH. J. Chem. Phys. **49**, 817 (1968).
6. M. ARSHADI and P. KEBARLE. J. Phys. Chem. **74**, 1483 (1970).
7. R. S. NARCISSI and W. ROTH. Advances in electronics and electron physics. Vol. 29. Academic Press Inc., New York. pp. 79–113.
8. E. E. FERGUSON and F. C. FEHSENFELD. J. Geophys. Res. Space Phys. **74**, 5743 (1969).
9. M. DE PAZ, A. GUIDONI GIARDINI, and L. FRIEDMAN. J. Chem. Phys. **52**, 687 (1970).
10. M. DE PAZ, S. EHRENSON, and L. FRIEDMAN. J. Chem. Phys. **52**, 3362 (1970).
11. D. A. DURDEN, P. KEBARLE, and A. GOOD. J. Chem. Phys. **50**, 805 (1969). A. GOOD, D. A. DURDEN, and P. KEBARLE. J. Chem. Phys. **52**, 222 (1970).

12. L. J. PUCKETT and W. C. LINENBERGER. Phys. Rev. A, **1**, 1635 (1970).
13. P. KRIEMLER and S. E. BUTTRILL, JR. J. Am. Chem. Soc. **92**, 1123 (1970).
14. J. E. DESNOYERS and C. JOLICOEUR. Modern aspects of electrochemistry. Vol. 5. *Edited by* J. O. M. Bockris and B. E. Conway. Plenum Press, N. Y. 1969.
15. National Bureau of Standards Technical Note 270–3. U.S. Department of Commerce, Washington, D.C.
16. National Bureau of Standards Circular 500. U.S. Department of Commerce, Washington, D.C.
17. J. BERKOWITZ and W. A. CHUPKA. J. Chem. Phys. To be published.
18. K. B. YATSIMIRSKII. Izvest. Akad. Nauk SSSR. Ofdel khim. Nauk, **411**, 453 (1947); J. Gen. Chem. U.S.S.R. **17**, 2019 (1947).
19. M. DE PAZ, J. J. LEVENTHAL, and L. FRIEDMAN. J. Chem. Phys. **51**, 3748 (1969).
20. W. P. KRAEMER and G. H. F. DIERCKSEN. Chem. Phys. Lett. To be published.
21. L. M. BRANSCOMB. Phys. Rev. **148**, 11 (1966).
22. J. BERKOWITZ, W. A. CHUPKA, and T. A. WALTER. J. Chem. Phys. **50**, 1497 (1969).
23. V. I. VEDENEYEV *et al.* Bond energies, ionization potentials, and electron affinities. Edward Arnold (Publishers) Ltd., London. 1966.

Can. J. Chem. Downloaded from www.nrcresearchpress.com by 210.87.254.105 on 09/05/12
For personal use only.

Can. J. Chem. Downloaded from www.nrcresearchpress.com by 210.87.254.42 on 09/05/12
For personal use only.

Nuclear Magnetic Resonance Studies of Co(II) Complexes of Thiourea and Related Ligands

D. R. Eaton and K. Zaw

Department of Chemistry, McMaster University, Hamilton, Ontario

Received May 28, 1971

A number of tetrahedral Co(II) complexes of thiourea, *N*-methyl thiourea, and *N,N'*-dimethyl thiourea have been studied by nuclear magnetic resonance (n.m.r.). All the complexes are paramagnetic and the proton resonances show large isotropic shifts in acetone-d_6 solutions. The origin of these shifts is discussed. Two sets of resonances are observed for each position and this is attributed to restricted rotation about the C—N bond. The barrier for this rotation is higher in the complexes than in the free ligands. For all complexes the exchange between free and coordinated ligand is fast at room temperature but slow below −80 °C. The complexes are dissociated to a greater or lesser extent in acetone solution and equilibrium constants and other thermodynamic data are reported for this dissociation. Entropy differences are more important than energy differences in determining the extent of dissociation. It has been demonstrated that both associative and dissociative mechanisms play a part in the ligand exchange process. The relative importance of the two mechanisms differs in the various complexes.

Un nombre de complexes tétrahédriques du cobalt(II) de la thiourée, la *N*-méthyl thiourée et de la *N,N'*-diméthyl thiourée a été étudié par r.m.n. Tous les complexes sont paramagnétiques et les protons en résonance montrent de larges déplacements isotopiques dans les solutions d'acétone-d_6. L'origine de ces déplacements est discutée. Deux séries de résonance sont observées pour chaque position et ceci est attribué à la rotation qui est limitée autour du lien C—N. La barrière pour cette rotation est plus élevée dans les complexes que dans les ligands libres. Pour tous les complexes, l'échange entre le ligand libre et le ligand complexé est rapide à la température ambiante, mais lente au-dessous de −80 °C. Les complexes sont dissociés pour une plus grande ou plus petite quantité dans une solution d'acétone et les constantes d'équilibre ainsi que les autres facteurs thermodynamiques sont donnés pour ces dissociations. Les différences d'entropie sont plus importantes que les différences d'énergie dans l'établissement du pourcentage dissocié. Il a été démontré que les deux mécanismes d'association et de dissociation jouent un rôle dans le processus d'échange des ligands. L'importance relative des deux mécanismes est différente dans plusieurs complexes.

Canadian Journal of Chemistry, **49**, 3315 (1971)

Introduction

Most transition metal complexes are labile. We define labile complexes as those for which ligand exchange occurs in a time shorter than, or comparable to, the time taken to perform an analytical experiment on the ligand distribution in the system. If proton n.m.r. is the chosen analytical method, as it is in our case, the relevant period is of the order of several minutes which represents the time needed to prepare a solution containing complex and free ligand and to obtain its n.m.r. spectrum. By this criterion Co(III) complexes and some other complexes with multidentate ligands are stable or non-labile. Most other complexes are labile, even those containing "good" bidentate ligands such as β-diketones (1, 2).

A second criterion for ligand lability is provided by the condition for "fast exchange" in a n.m.r. experiment. If the lifetime of a complexed ligand engaged in an exchange process with free ligand is small compared to $1/2\pi\Delta\nu$ (where $\Delta\nu$ is the frequency separation between the n.m.r. lines in the free and complexed environments) a n.m.r. experiment will reveal only a single resonance at the average position. For the paramagnetic complexes we are concerned with $\Delta\nu \sim 10^2$–10^3 Hz so the critical lifetime is 10^{-3}–10^{-4} s. The lifetime range of 10^{-4} to 10^2 s for ligand exchange rather nicely defines a class of complexes which can plausibly function as intermediates in homogeneously catalyzed reactions. The mechanisms of such reactions catalyzed by transition metal complexes involve a sequence of ligand exchange steps. The occurrence of a more stable complex in such a sequence will seriously impede the reaction. More labile complexes are likely to have such a transient existence that they are unimportant in determining the overall effectiveness of the reaction.

These considerations have led us to undertake some detailed studies of ligand exchange mecha-

Can. J. Chem. Downloaded from www.nrcresearchpress.com by 210.87.254.42 on 09/05/12
For personal use only.

nisms involving systems at the shorter lifetime end of the above scale. A number of additional considerations dictated our choice of systems for such studies. If the results are to have relevance to most homogeneous catalysis they should be restricted to exchange between neutral species in non-aqueous solvents. The majority of studies of ligand exchange mechanisms carried out thus far have involved charged species in aqueous solution. Thus Wilkins in a recent review (3) remarks that "the study of ligand substitution in non-aqueous solutions has barely commenced." We also require a synthetically flexible system which will enable us to vary the metal atom, the geometry of the complex, and both the exchanging and non-exchanging ligands in a fairly systematic manner. We started these studies with some prejudice (4, 5) that outer sphere complexes might play a key role in exchange mechanisms. We therefore thought it desirable to optimize the possibility of detecting such complexes by providing some hydrogen bonding sites at the periphery of the complexes. Previous experience with exchange reactions with phosphine complexes have demonstrated to us that the n.m.r. spectra of complex mixtures can become rapidly uninterpretable. We therefore prefer ligands with only one or two different types of proton. A combination of these factors has led to the choice of thiourea complexes as a basis for ligand exchange studies. In subsequent papers we shall report exchange studies of these complexes with anilines and other ligands and shall return to a detailed consideration of the role of the second coordination sphere. Thiourea and substituted thiourea complexes have been reported for most of the first row transition metal elements. They have been extensively investigated using spectroscopic and magnetic measurements (6–11) and some X-ray structural work has been reported (12–14). They have not previously been studied by n.m.r. For our purposes it is essential that we know how the lability and degree of dissociation of these complexes in solution vary from compound to compound. We also wish to know the mechanism (associative or dissociative) of the ligand exchange process. This information can be conveniently obtained by n.m.r. In the present paper we report the pertinent data for a series of Co(II) complexes.

Results

Some twelve Co(II) complexes of thiourea, *N*-methyl thiourea, and *N*,*N*′-dimethyl thiourea have been examined. All these complexes are paramagnetic. We also report data on three Zn(II) complexes, which are diamagnetic, for comparison purposes. The proton spectrum of thiourea does not appear to have been previously examined in solution although there are reports of solid state n.m.r. studies (15, 16). ^{14}N spectra have also been reported (17). A recent study discusses restricted rotation in *N*-methyl thiourea using n.m.r. as the experimental technique (18). The structures of urea and thiourea constitute a classic problem involving tautomerism but there is now a concensus of opinion that **1** rather than **2** is correct (19). The n.m.r. spectrum of thiourea

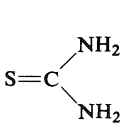

1

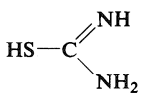

2

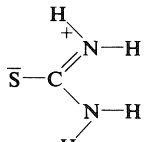

3

in acetone-d_6 (Fig. 1*A*) is consistent with structure **1**, having a single proton peak 6.33 p.p.m. to low field of TMS. On cooling to −70 °C this peak splits into a doublet of equally intense lines. This is still inconsistent with involvement of the tautomer **2** and a more reasonable explanation invokes restricted rotation about the C—N bond arising from contribution of structure **3**. Such a structure would be planar with different environments for the "inside" and "outside" hydrogens. Restricted rotation is scarcely surprising since it occurs in many other amides and the phenomenon has been widely studied by n.m.r. (20). Given this explanation the interpretation of the spectra of *N*-methyl thiourea (18) and *N*,*N*′-dimethyl thiourea (Fig. 1) follows naturally. It is interesting to note that the rotational barriers are apparently higher for methyl derivatives. This possibly represents a steric effect, although it is also consistent with the greater electron donating properties of the methyl group.

Turning to the thiourea complexes two structural conclusions have been drawn from the magnetic and spectroscopic studies of the Co(II) and Zn(II) compounds reported in the literature. It has been concluded, mostly from infrared data, that they are all bonded through the sulfur atom. They are also all thought to have tetrahedral or distorted tetrahedral geometry about the metal atom. The only cases where this has been challenged are $Co(TU)_4(NO_3)_2$ for which

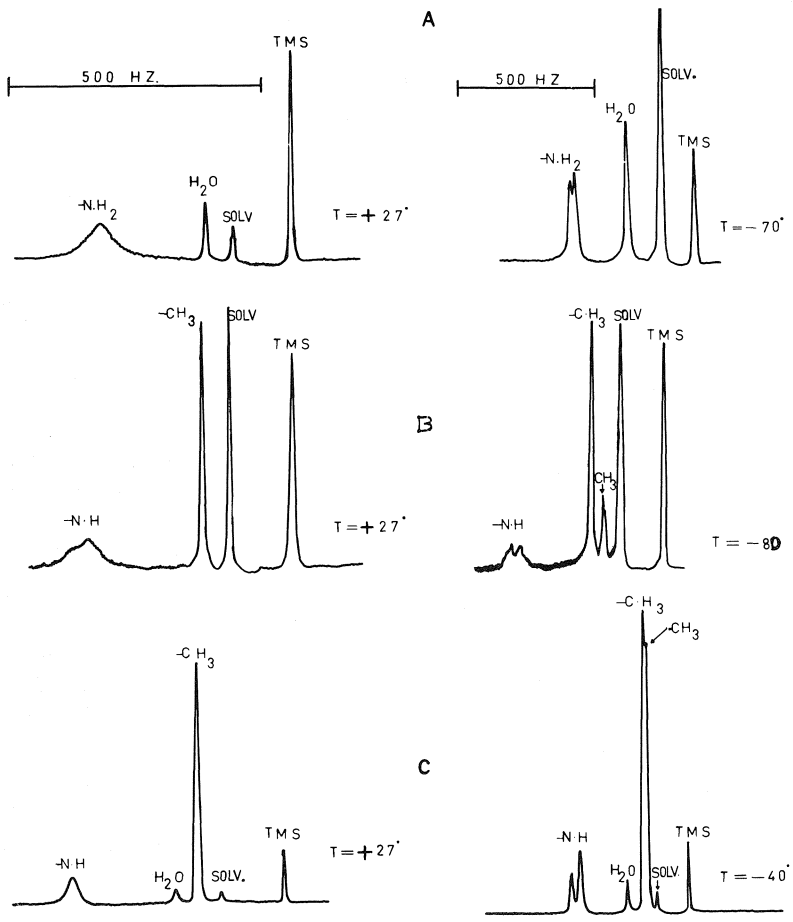

FIG. 1. Nuclear magnetic resonance spectra of thiourea ligands: *A*, thiourea; *B*, *N*-methyl thiourea; *C*, *N,N'*-dimethyl thiourea.

six coordination was suggested (6) and some complexes of stoichiometry $Co(TU)_3X_2$ for which five coordination was postulated (21). However, later workers (11, 22) have concluded that these compounds are also tetrahedral or distorted tetrahedral in solution. Spectroscopic studies have also shown that in solvents such as acetone these compounds are partly dissociated although no quantitative results have been reported. In compounds such as $Co(TU)_2Cl_2$ where there is a choice of dissociating ligands, conductivity studies indicate that it is the thiourea which dissociates. The present results are entirely compatible with all these conclusions.

Figure 2 shows the n.m.r. spectra of $Zn(TU)_2Cl_2$. The NH_2 resonance has been shifted downfield relative to free thiourea. Addition of free ligand shifts the resonance to high field indicating fast exchange. On cooling a solution of $Zn(TU)_2Cl_2$ to around 0 °C the thiourea resonance is split into a doublet, which is again attributed to restricted rotation about the C—N bond. Cooling a solution containing excess ligand to −80 °C gives no free ligand peak, *i.e.*, the ligand exchange remains fast. The spectra of $Zn(TU)_4(NO_3)_2$ and $Zn(TU)_4(ClO_4)_2$ are similar except that a temperature of ~ −25 °C is necessary to freeze out the C—N bond rotation in the nitrate and the line remains a singlet to −80 °C in the perchlorate. Chemical shift data for these complexes and for the free ligands are summarized in Table 1.

Figures 3 and 4 show some representative spectra of Co(II) thiourea complexes. As anticipated for paramagnetic compounds the shifts are much larger than those of the diamagnetic

Can. J. Chem. Downloaded from www.nrcresearchpress.com by 210.87.254.42 on 09/05/12
For personal use only.

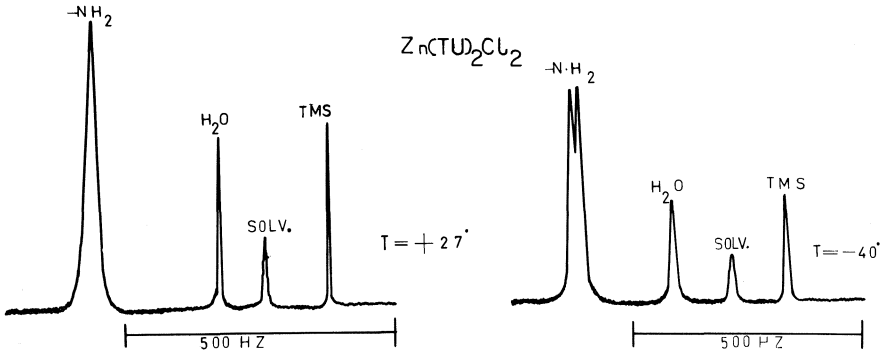

FIG. 2. Nuclear magnetic resonance spectra of $Zn(TU)_2Cl_2$.

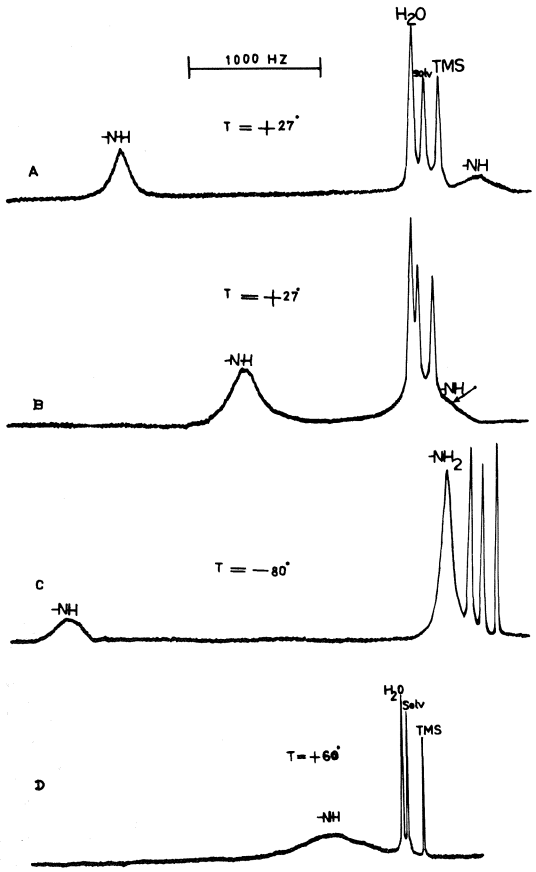

FIG. 3. Nuclear magnetic resonance spectra of $Co(TU)_2Cl_2$: *A*, room temperature; *B*, excess ligand added; *C*, as in *B*; temperature, −80 °C; *D*, as in *B*, temperature, +60 °C (NH_2 is free ligand resonance).

zinc complexes. In all cases there is a doubling of the resonances attributable as before to restricted rotation about the C—N bond. There is no collapse of any of these doublets up to the boiling point of acetone. (In view of the zinc results mentioned above the most likely cases to observe such a collapse are perhaps the perchlorates. We have however refrained from making any measurements above room temperature on these compounds out of respect for the known explosive properties of heavy metal perchlorates in organic solutions.) The large chemical shifts greatly facilitate quantitative measurements on the dissociation and ligand exchange equilibria of these compounds. Addition of free ligand to these solutions at room temperature leads to a single set of resonances at an average position demonstrating fast exchange. This is illustrated in Fig. 3*b*. Cooling a solution containing complex and free ligand leads to the appearance of both contact shifted and free ligand lines (Fig. 3*c*). The ligand exchange process has become slow. Heating such a solution averages the two N—H lines (Fig. 3*d*). Ligand dissociation has been followed by rotation about the C—N bond. The frequencies of the resonances are concentration dependent demonstrating dissociation of the thiourea. The qualitative behavior of the *N*-methyl thiourea and *N*,*N*′-dimethyl thiourea complexes is similar. Room temperature spectra are shown in Fig. 4.

Before proceeding with any quantitative analysis of these spectra we must first deal with two possible difficulties. Firstly it may be noted that all the spectra show a small resonance attributable to water present in the acetone-d_6. Since water is itself a potential ligand it could play an important role in the system. Addition of water enhances this resonance but does not affect the line due to acetone-d_5. There is therefore no fast proton exchange between water and acetone under the conditions of these experiments. The amount of water in the original solvent

Can. J. Chem. Downloaded from www.nrcresearchpress.com by 210.87.254.42 on 09/05/12
For personal use only.

TABLE 1. Chemical shifts of free ligands and zinc complexes

Compound	—NH_2		—CH_3[1]		
	Room temperature	Low temperature	Room temperature	Low temperature	Low temperature (°C)
TU	−380	−421, −410	—	—	−70
MTU	−380	−414, −389	−168	−189, −167	−30
DMTU	−398	−450, −417	−168	−167, −161	−30
$Zn(TU)_2Cl_2$	−441	−474, −457	—	—	−50
$Zn(TU)_4(NO_3)_2$	−430	−455, −438	—	—	−30
$Zn(TU)_4(ClO_4)_2$	−456	−464	—	—	−60

[1]All shifts measured in Hz relative to TMS at 56.4 MHz. Solvent, acetone-d_6.

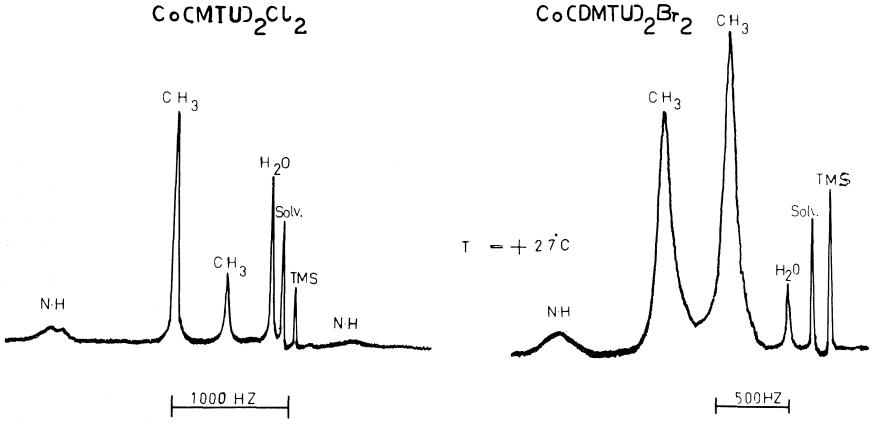

FIG. 4. Nuclear magnetic resonance spectra of $Co(MTU)_2Cl_2$ and $Co(DMTU)_2Br_2$.

can therefore be estimated from the integrated intensities of the resonances obtained by adding measured increments of water. Values of between 1 and 2% were obtained. Acetone-h_6 can be obtained somewhat drier without too much difficulty and a sample was shown to have 0.3% water by comparative integration of the acetone ^{13}C satellites. In acetone-h_6 resonances in the diamagnetic region are largely obscured by the solvent but it was shown that the isotropically shifted peaks of cobalt thiourea complexes occurred in the same positions in this solvent as in the acetone-d_6. The effect of adding increasing amounts of water on the thiourea and water resonances of $Co(TU)_2Cl_2$ and $Co(TU)_4(ClO_4)_2$ has been investigated. The thiourea resonance is not affected initially but then moves towards its diamagnetic position. The water resonance initially occurs at its diamagnetic position but is shifted to low field if a large excess of water is added. Fast exchange of both water and thiourea between coordinated and free environments is indicated. On a mole fraction basis a 40-fold excess of water is needed to displace half the thiourea of $Co(TU)_2Cl_2$ and an 8-fold excess to displace half the thiourea of $Co(TU)_4(ClO_4)_2$. At −80 °C both exchange equilibria are slow and the coordinated water appears as a broad line at about −7000 Hz from TMS. This is consistent with literature values for the shift of water complexed to Co^{2+} in other solvents (23). These results are not consistent with an equilibrium of the type

[1] $Co(TU)_2Cl_2 + H_2O \rightleftharpoons Co(TU)(H_2O)Cl_2 + TU$

with an equilibrium constant independent of

Can. J. Chem. Downloaded from www.nrcresearchpress.com by 210.87.254.42 on 09/05/12
For personal use only.

TABLE 2. Coordination numbers of Co complexes

$Co(TU)_2Cl_2$			$Co(TU)_4(ClO_4)_2$		
Total conc. TU (mg/ml)	Observed shift (Hz)*	Calcd. coord. No.	Total conc. TU (mg/ml)	Observed shift (Hz)*	Calcd. coord. No.
3.61	−2079	3.9	7.74	−1353	3.6
4.61	−1620	3.8	8.74	−1224	3.3
5.61	−1291	3.8	9.94	−1125	3.5
6.61	−1186	3.9	10.94	−964	3.3
7.61	−923	3.7	11.94	−862	3.2
			12.94	−797	3.2

*Shifts are measured relative to the free ligand.

solvent composition. For such a situation addition of excess of one of the ligands must always lead to a decrease in the average shift for that ligand whereas the water shift is increased by addition of water. The situation is rather that the complexing abilities of thiourea and water depend strongly on the nature of the solvent system. This conclusion has also been reached by Shul'man *et al.* (24) from electrochemical studies. At low concentrations of water the water is a very poor ligand and does not compete with thiourea. At higher concentrations it competes much more favorably. At the 1–2% level the observed shift from the diamagnetic position is less than 5 Hz and since the full contact shift at room temperature is ~5000 Hz and there is fast exchange a negligible amount of water is complexed. We can therefore neglect the equilibrium 1 under these conditions. A plausible rationalization of these observations is that if the cobalt is formally neutral, *i.e.*, if the chloride ion is not dissociated from $Co(TU)_2Cl_2$, water is a poor ligand. With increasing dielectric constant there is some ionization and water becomes a better ligand. Water obviously competes somewhat more favorably in the perchlorate complex which is charged. In any event we can safely disregard small percentages of water provided its resonance occurs within a few Hz of its diamagnetic position.

The second point which deserves some preliminary consideration concerns the coordination number of the cobalt. The concensus of opinion, as we have noted above, is that only four coordinated tetrahedral species are present in solutions of cobalt thiourea complexes. Swaminathan and Irving (25), however, have studied cobalt perchlorate thiourea in 95% ethanol and concluded that $Co(TU)_6^{2+}$ is an important species. If this were the case in acetone it would invalidate the analysis of the data given below. The coordination number of the cobalt in solutions containing excess thiourea can be obtained in the following manner. The limiting shift for thiourea fully complexed to cobalt can be obtained directly at low temperatures, where the exchange is slow, and indirectly at higher temperatures (see below). Given this limiting shift the fraction of thiourea complexed in any fast exchanging solution is readily obtained from the observed contact shift. Knowing the total thiourea concentration the number of moles complexed can be compared with the number of moles of cobalt present and a coordination number obtained. A series of results for $Co(TU)_2Cl_2$ and $Co(TU)_4(ClO_4)_2$ each in the presence of excess thiourea is given in Table 2. In all cases the total coordination number remains somewhat below four. There is however a possible flaw in this argument. If the limiting shift of a five or six coordinated species were substantially less than that of the four coordinated species, low apparent coordination numbers would be obtained. If this were so though, at low temperatures we would obtain a different (smaller) limiting shift in the presence of excess thiourea. Experiment shows that this does not occur and that at −80 °C excess ligand merely increases the free ligand resonance without shifting the complexed resonance. We therefore agree with the conclusions of Cotton and co-workers (6), Hall and Horrocks (22), and Maneces *et al.* (26) that five or higher coordination numbers are not important for these compounds in solution. This does not preclude the presence of small concentrations of such species which might act as intermediates in the exchange process. We will also express some reservations later about the situation at very low temperatures for one compound. However, it seems reasonable to attempt initial analysis of the data on the basis of four coordination.

Can. J. Chem. Downloaded from www.nrcresearchpress.com by 210.87.254.42 on 09/05/12
For personal use only.

Can. J. Chem. Downloaded from www.nrcresearchpress.com by 210.87.254.42 on 09/05/12
For personal use only.

On this assumption, the principle equilibrium present is

[2] $Co(TU)_2X_2 + S \rightleftharpoons Co(TU)SX_2 + TU$

(where S represents a solvent molecule). In some cases it may also be necessary to consider the further dissociation

[3] $Co(TU)SX_2 + S \rightleftharpoons CoS_2X_2 + TU$

In the fast exchange situation, if the degree of dissociation is small, the shift of the undissociated compound may be obtained by plotting the observed shifts against the reciprocal of the square root of the concentration.[1] A typical plot is shown in Fig. 5. In the slow exchange situation at low temperatures the limiting shift is obtained directly. If this analysis is correct, the limiting shifts should plot against $1/T$ throughout the temperature range. Figure 6 shows these plots for $Co(TU)_2X_2$ where X = Cl, Br, I. It may be noted that there is some indication of non-

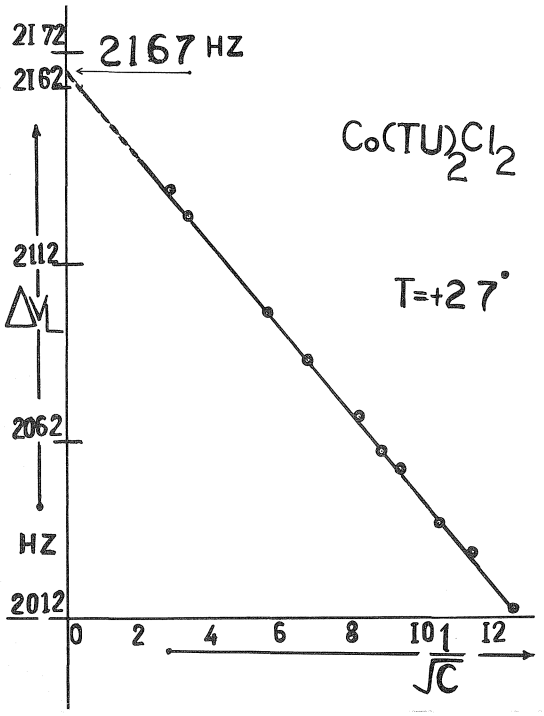

FIG. 5. Concentration dependence of NH shift of $Co(TU)_2Cl_2$.

[1]Degree of dissociation $\alpha = (k/c)^{1/2}$, $\Delta\nu_0 = \Delta\nu_L \times$ fraction complexed, hence $\Delta\nu_0 = \Delta\nu_L [1 - (1/n)(k/c)^{1/2}]$ when n is number of TU molecules in complex.

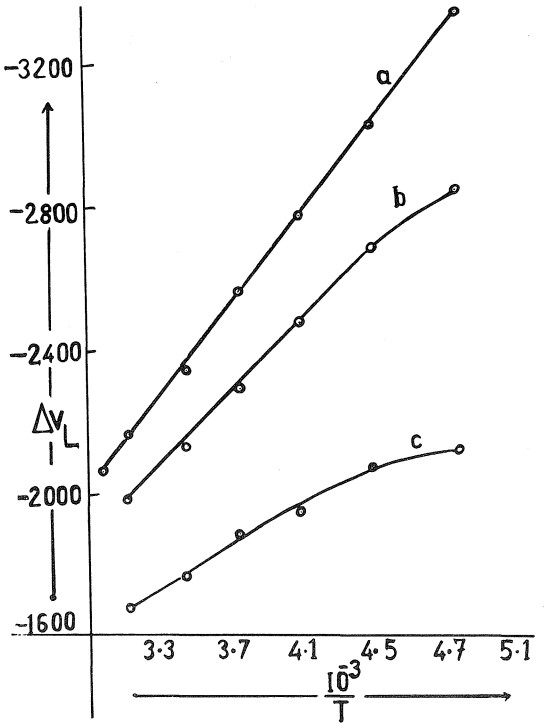

FIG. 6. Temperature dependence of limiting shifts; (*a*) $Co(TU)_2Cl_2$, (*b*) $Co(TU)_2Br_2$, (*c*) $Co(TU)_2I_2$.

linearity at the lowest temperatures for the bromide and iodide. The perchlorate and nitrate complexes show similar behavior. With one exception the MTU and DMTU complexes closely parallel the TU complexes. The exception is $Co(MTU)_2I_2$ which appears to be anomalous in both the concentration and temperature dependence of the shifts. It is believed that this discrepancy arises from poor experimental data resulting from overlap of different resonances at certain concentrations and temperatures. It is possible that the slightly anomalous shifts at low temperature indicate the formation of new and different complexes. More probably they simply represent a "normal" deviation from Curie law behavior. However, the general consistency of the high and low temperature data leads us to believe that the values obtained for the limiting shifts are reliable.

Given this reassurance we may then use the limiting shifts to calculate the degrees of dissociation and equilibrium constants for reaction 2 for all cases where we have fast exchange. The temperature dependence of the equilibrium constant

TABLE 3. Observed isotropic shifts for Co(II) complexes*

Compound	Isotropic shift			
	Inside NH—	Outside NH—	Inside N—CH_3	Outside N—CH_3
$Co(TU)_2Cl_2$	−2460	+200	—	—
$Co(TU)_2Br_2$	−2275	+820	—	—
$Co(TU)_2I_2$	−1980	+1500	—	—
$Co(TU)_4(NO_3)_2$	−1674	+244	—	—
$Co(TU)_4(ClO_4)_2$	−1746	+1333	—	—
$Co(MTU)_2Cl_2$	−2171	—	−1026	−565
$Co(MTU)_2Br_2$	−1868	+1144	−1131	−736
$Co(MTU)_2I_2$	−1552	+1868	−1223	−789
$Co(MTU)_4(ClO_4)_2$	−1378, −1175	+1459	−1750	−851
$Co(DMTU)_2Br_2$	−1831	—	−1115	−726
$Co(DMTU)_2I_2$	—	+2540	−1276	−734
$Co(DMTU)_4(ClO_4)_2$	−1078	+1723	−1697	−802

*Shifts in Hz at 56.4 MHz from TMS. All solutions 0.02 M in acetone-d_6. Temperature 27 °C.

TABLE 4. Limiting shifts and thermodynamic data for cobalt complexes

Compound	$\Delta\nu_L$*	$K_D \times 10^{-4}$ (27 °C)†	ΔH (kcal/mol)	ΔS (e.u.)
$Co(TU)_2Cl_2$	−2167	1.46	+3.5±0.4	−5.8±1.5
$Co(TU)_2Br_2$	−1982	2.82	+4.0±0.4	−2.5±1.6
$Co(TU)_2I_2$	−1684	3.86	+6.1±0.8	+4.9±2.8
$Co(TU)_4(NO_3)_2$	−1362	14.4	+4.6±0.2	+2.6±0.9
$Co(TU)_4(ClO_4)_2$	−1496	53.5	+2.9±0.4	+0.1±1.6
$Co(MTU)_2Cl_2$	−1925	1.21	+3.2±0.5	−6.6±2.1
$Co(MTU)_2Br_2$	−1646	1.29	+3.9±0.2	−4.5±0.9
$Co(MTU)_2I_2$	−1047‡	4.09	§	§
$Co(MTU)_4(ClO_4)_2$	−1638‡	31.7	+2.9±0.2	−1.7±0.6
$Co(DMTU)_2Br_2$	−997‡	2.06	+2.3±0.1	−8.9±0.5
$Co(DMTU)_2I_2$	−1120‡	3.66	+3.3±0.9	−5.1±3.6
$Co(DMTU)_4(ClO_4)_2$	−1585‡	29.4	+2.7±0.4	−2.2±1.6

*$\Delta\nu_L$ is limiting shift in Hz at 56.4 MHz measured from free ligand.
†K_D obtained from equations $\alpha = n(1 - \Delta\nu_0/\Delta\nu_L)$, $K_D = \alpha^2C/(1-\alpha)$; where α = fraction of complex dissociated, n = number of thiourea molecules in complex, $\Delta\nu_O$ = observed shift, $\Delta\nu_L$ = limiting shift
‡Limiting shift of CH_3 resonance. Other limiting shifts refer to NH.
§Line overlap leads to questionable temperature data.

gives values of ΔH and ΔS for reaction 2. Some experimental data for the cobalt complexes is given in Table 3. Limiting shifts, equilibrium constants at room temperature, and values of ΔH and ΔS for all the compounds examined are given in Table 4. The data at low concentrations was then reexamined to investigate the effect of the second dissociation (eq. 3). In all cases very small values (10^{-9}–10^{-10}) were obtained for the second dissociation constants. The differences between the values for different compounds are probably not significant and they are therefore not quoted here.

We next turn to a consideration of the rates and mechanism of the ligand exchange process. In principle rate constants can be determined from the line broadening in a fast exchange situation. In practice quantitative experiments along these lines give very questionable results. We will therefore be content with some qualitative observations. $1/2\pi\Delta\nu$ for these systems is of the order of 10^{-4} s and this gives a measure of the lifetime of free or complexed ligand. The temperature at which coalescence of free and complexed ligand signals occurs is a qualitative measure of relative exchange rates. The variation of this temperature among the different compounds is surprisingly modest (−40 to −60 °C) and we hesitate to ascribe significance to the differences. Information on the mechanism of ligand exchange can be obtained by studying the line widths of the free and complexed ligand as a function of ligand concentration in the slow exchange region. Data for two of these compounds is shown graphically in Fig. 7 and spectra for a third in Fig. 8. These results will be discussed below.

Can. J. Chem. Downloaded from www.nrcresearchpress.com by 210.87.254.42 on 09/05/12
For personal use only.

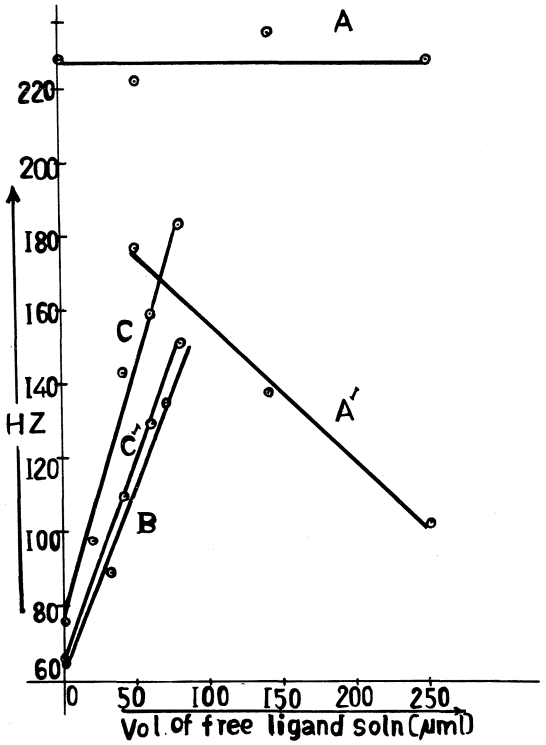

FIG. 7. Dependence of line widths on free ligand concentration: *A*, complexed TU in $Co(TU)_2Cl_2$; *A'*, free TU in $Co(TU)_2Cl_2$; *B*, complexed MTU in $Co(MTU)_2Cl_2$; *C* and *C'*, two CH_3 signals of complexed DMTU in $Co(DMTU)_2Br_2$.

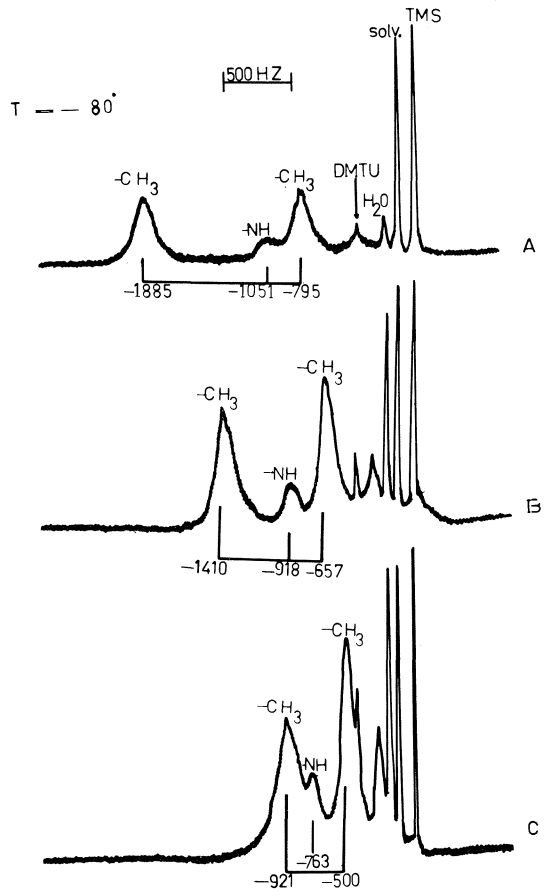

FIG. 8. Low temperature n.m.r. spectra of $Co(DMTU)_4(ClO_4)_2$ in the presence of excess ligand. *A*, *B*, and *C* represent increasing amounts of ligand.

Discussion

(a) The Nuclear Magnetic Resonance Spectra

All the n.m.r. data can be readily interpreted on the assumption that thiourea is bonded to the metal though sulfur and rotation about the C—N bond is completely restricted. Thus all TU complexes show two resonances, one shifted to high field and one to low field. The high field resonance is significantly broader than the low field resonance. Since the predominant relaxation mechanism is likely to be dipolar interaction with the unpaired electrons on the cobalt the hydrogen closer to the metal will be broader. A model gives distances of 5.88 and 4.62 Å for the "inside" and "outside" hydrogens, respectively. The high field line is therefore assigned to the "outside" position. For all DMTU complexes two hydrogens and two methyls are observed. Both methyls are shifted to low field but the less shifted line is broader. This is therefore assigned to the outer position. $Co(MTU)_2Cl_2$ and $Co(MTU)_4(ClO_4)_2$ both show two methyl resonances and three hydrogens, two to low field and one to high field, under appropriate conditions. Presumably we are distinguishing between hydrogens *a* and *b* in structure **4**.

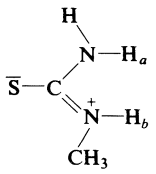

4

The relative intensities of the various lines suggest that isomers with "outside" methyl groups are preferred as might be anticipated on steric grounds. The enhanced barrier to rotation on complexing the thiourea suggests that ionic

Can. J. Chem. Downloaded from www.nrcresearchpress.com by 210.87.254.42 on 09/05/12
For personal use only.

Can. J. Chem. Downloaded from www.nrcresearchpress.com by 210.87.254.42 on 09/05/12
For personal use only.

structures such as **4** make a greater contribution when the thiourea interacts with a positively charged metal ion. This seems not unreasonable.

The origin of the isotropic shifts is not unambiguous. The choice lies between a dipolar mechanism which requires the complex to be magnetically anisotropic, a contact mechanism which requires delocalization of spin density to the ligand or a combination of the two (27). Since the ground state of tetrahedral Co(II) is orbitally non-degenerate the magnetic anisotropy might be expected to be small and the dipolar shifts correspondingly not important. This argument is, however, far from water-tight since there are low-lying excited states. We are more impressed by the observation that octahedral $Ni(TU)_6(ClO_4)_2$ also shows a large splitting between "inside" and "outside" NH protons (28). In this case significant dipolar shifts are very unlikely and the difference must arise from differing contact interactions. Thus although it is tempting to postulate that the difference in shift of the "inside" and "outside" hydrogens arises from differences in the $(3\cos^2\theta - 1)/r^3$ term in the expression for dipolar shifts, this explanation will not hold for Ni complexes and therefore seems less likely for Co complexes. We prefer the possibility that the difference reflects the difference in electronic environments resulting from differing hydrogen bonding interactions of the two hydrogens. Effects of this type do not appear to have been reported previously. It is interesting to note that Piovesana and Furlani (29) have recently suggested that the infrared spectra of these complexes provide evidence for intramolecular hydrogen bonding between an "outside" hydrogen and a halide ligand. There are possibilities of delocalizing spin into both the σ and π orbitals of the ligand. Since both high and low field shifts are observed both types of delocalization may be contributing. It is quite plausible that the relative contributions should depend critically on the energy of the N—H bonding orbital relative to that of the molecular orbital containing the unpaired electron and hence on the hydrogen bonding. It is also interesting that the contact shifts change smoothly in the series Cl, Br, and I with the low field shifts decreasing and the high field shifts increasing. Attempts have been made to explain similar trends observed in Co(II) pyridine and hexamethylphosphoramide complexes in terms of changes in the metal ligand bonding (30). The significance of this correlation has however been challenged (31) and an alternative explanation based on steric factors put forward. Either type of explanation could be applied to the present case and we do not feel that we can add much towards the resolution of this particular controversy.

(b) Ligand Dissociation

The equilibrium constants of Table 4 show that the degree of dissociation of all three series of complexes depends on the anion present and increases in the order $Cl < Br < I < ClO_4$. The differences between corresponding compounds of TU, MTU, and DMTU are relatively small but indicate that the DMTU perchlorate is least dissociated followed by MTU and TU in that order. The data of Table 4 also show that the entropy term is at least as important as the enthalpy term in determining the amount of dissociation. The indicated errors are obtained by least squares analysis on the data. The results with aqueous acetone have indicated that thiourea becomes a poor ligand if the positive charge on the cobalt atom becomes large. Presumably back donation to the π^* orbital makes a significant contribution to the bond strength. The significantly lower values of ΔH for the ionic perchlorates is consistent with this picture. We tentatively ascribe differences in ΔS to variations in the hydrogen bonding interactions which determine the structure of the second coordination sphere. This structure will be discussed in more detail in a subsequent publication.

(c) The Ligand Exchange Process

The similarity of the temperature of coalescence of free and complexed ligand resonances shows that the rates of ligand exchange for all these complexes are comparable. We doubt whether attempts at quantitative measurements of line widths would add substantially to this conclusion. We can however make some deductions regarding mechanism from the variation of the line widths with concentration. If the mechanism of ligand exchange is associative, *i.e.*

$$\text{Co complex} + \text{TU}^* \rightleftharpoons \text{Co complex TU}^* \rightleftharpoons \text{Co complex} + \text{TU}$$

it can be readily shown that

$$1/\tau_c = k[\text{TU}] \qquad 1/\tau_L = k[\text{Co complex}]$$

where τ_c and τ_L are the lifetimes of complexed

Can. J. Chem. Downloaded from www.nrcresearchpress.com by 210.87.254.42 on 09/05/12
For personal use only.

and free ligand and $1/\tau_c$ and $1/\tau_L$ are a measure of the respective line widths under conditions such that separate lines are observed for the two environments. If on the other hand we have a dissociative mechanism, it follows that

$$1/\tau_c = k$$

and

$$1/\tau_L = k[\text{Co complex}]/[\text{TU}]$$

We cannot distinguish between a dissociative mechanism involving a lower coordination number for cobalt and one in which the coordination number is maintained by substituting solvent molecules. The latter is much more likely and the observation of the second type of kinetics most probably indicates that the rate determining step for thiourea ligand exchange is

$$\text{Co complex} + \text{S} \rightleftharpoons \text{Co complex S} + \text{TU}$$

This is then followed by fast reaction of the solvent containing complex with free thiourea. It is apparent that the key experiment is to determine the behavior of the line widths as a function of free ligand concentration. The results of Fig. 7 show very clearly that both types of mechanism must be considered. Thus the lines *A* and *A'* for $Co(TU)_2Cl_2$ show that the line width of the complexed thiourea resonance is independent of free thiourea concentration whereas that of the free thiourea decreases with added ligand. On the other hand *B*, *C*, and *C'* clearly demonstrated that the linewidths of complexed MTU and DMTU increase with added ligand. For TU complexes a dissociative mechanism predominates, for MTU and DMTU complexes an associative mechanism is more important. Most probably both processes occur for all complexes and only their relative contributions are changing.

Finally we draw attention to the spectra of $Co(DMTU)_4(ClO_4)_2$ shown in Fig. 8. These spectra were obtained at -80 °C and the sharp resonances at the free ligand positions show that free ligand is not involved in fast exchange with the complex. However, addition of free ligand clearly shifts the positions of the complexed ligand lines. A fast equilibrium between complexed ligand and ligand in a fifth coordination position or an outer sphere site is indicated. We cannot distinguish between these possibilities in the present case. This is the only complex in the present series which shows this type of behavior with thiourea as the competing ligand but we shall report in a subsequent paper more substantial evidence for the existence of both types of higher coordination number complexes in exchange reactions between these compounds and aniline ligands.

Conclusions

This study has been of a preliminary nature with the objective of establishing the n.m.r. characteristics of thiourea complexes. As anticipated all the complexes studied are partly dissociated and undergo fast ligand exchange. There are significant differences in the degree of dissociation but qualitatively the rates of ligand exchange do not differ. In spite of this more than one exchange mechanism is operative. There is indirect evidence that the interactions of a complex with its surroundings, *i.e.*, the "second coordination sphere," plays an important part in determining the chemical reactivity. This is reflected in the influence of the entropy term on the degree of dissociation and in the large differences in the chemical shifts of "inside" and "outside" NH protons which are attributed to intra or intermolecular hydrogen bonding effects. We are undertaking extension of this type of study to thiourea complexes of other transition metals and to exchange reactions involving ligands other than thiourea. More detailed discussion of the factors influencing the ligand exchange mechanisms will be deferred until this additional datum has been presented.

Experimental

The following compounds were synthesized by literature methods:
$Co(TU)_2Cl_2$ (6), $Co(TU)_2Br_2$ (6), $Co(TU)_2I_2$ (11), $Co(TU)_4(NO_3)_2$ (6), $Co(TU)_4(ClO_4)_2$ (6); $Co(MTU)_2Cl_2$ (7), $Co(MTU)_2Br_2$ (7), $Co(MTU)_4(ClO_4)_2$ (7); $Co(DMTU)_2Cl_2$ (7), $Co(DMTU)_2Br_2$ (7), $Co(DMTU)_4(ClO_4)_2$ (7); $Zn(TU)_2Cl_2$ (32), $Zn(TU)_4(NO_3)_2$ (32), $Zn(TU)_4(ClO_4)_2$ (32). Starting materials were purchased from Fisher Sci. Co., Alfa Inorganics, and Pfaltz and Bauer Inc. Products were characterized by their melting points and visible spectra all of which agreed well with data in the literature. $Co(DMTU)_2Cl_2$ is very sparingly soluble in acetone and n.m.r. data is not reported for this reason.

$Co(MTU)_2I_2$ and $Co(DMTU)_2I_2$ do not appear to have been reported previously. They were prepared as follows.

$Co(MTU)_2I_2$

Stoichiometric quantities of $CoI_2.2H_2O$ and MTU were dissolved in a mixture of chloroform and alcohol 1:3 by volume and the solution heated for 30–40 min.

The hot solution was filtered and allowed to evaporate at room temperature for several days. The dark green oily liquid obtained was washed several times with ether and the remaining ether pumped off. The resulting dark green liquid was dried in vacuo over P_4O_{10} to give a crystalline solid. The melting point of the product was 80–82°. The visible spectrum shows the triplet of bands characteristic of tetrahedral Co complexes (14 800, 13 900, and 13 050 cm^{-1}).

$Co(DMTU)_2I_2$

The procedure was similar to the above except that ethyl alcohol was used as a solvent. Melting point of product was 113–115 °C; absorption bands observed at 15 500, 14 500, and 13 800 cm^{-1}. All compounds were dried over P_4O_{10} under vacuo before using. Nuclear magnetic resonance spectra were obtained with a Varian DP 60 spectrometer operating at 56.4 MHz and equipped with a variable temperature probe. Acetone-d_6 was used as purchased. Spectroscopically pure acetone-h_6 was dried over a molecular sieve and redistilled. Tetramethyl silane was used as an internal reference throughout.

We are indebted to the National Research Council of Canada for financial support of this research and to the Canadian International Development Agency for a scholarship to one of us (K.Z.).

1. T. J. Pinnavaia and R. C. Fay. Inorg. Chem. **5**, 233 (1966).
2. D. R. Eaton and K. L. Chua. Can. J. Chem. **49**, 56 (1971).
3. R. G. Wilkins. Accounts Chem. Res. **3**, 408 (1970).
4. D. R. Eaton and S. R. Suart. J. Am. Chem. Soc. **90**, 4170 (1968).
5. D. R. Eaton. Can. J. Chem. **47**, 2645 (1969).
6. F. A. Cotton, C. D. Faut, and J. T. Mague. Inorg. Chem. **3**, 17 (1964).
7. P. Askalani and R. A. Bailey. Can. J. Chem. **47**, 2275 (1969).
8. G. Yagupsky and R. Levitus. J. Inorg. Nucl. Chem. **27**, 263 (1965).
9. A. Yamaguchi, R. B. Penland, S. Mizushima, T. J. Lane, C. Curran, and J. V. Quagliano. J. Am. Chem. Soc. **80**, 527 (1958).
10. O. Piovesana and C. Furlani. J. Inorg. Nucl. Chem. **30**, 1249 (1968).
11. C. D. Flint and M. Goodgame. J. Chem. Soc. A, 1718 (1967); A, 744 (1966).
12. M. Perez-Rodriquez, M. Cubero, R. Vega, A. Morente, and J. C. Vazquez. Acta Cryst. **14**, 1101 (1961).
13. R. G. Vranka and E. L. Amma. J. Am. Chem. Soc. **88**, 4270 (1966).
14. W. A. Spofford, P, Boldrini, E. L. Amma, P. Carfagno, and P. S. Gentile. J. Chem. Soc. D, 40 (1970).
15. D. H. Smith and R. N. Cotts. J. Chem. Phys. **41**, 2403 (1964).
16. J. W. Emsley and J. A. S. Smith. Trans. Faraday Soc. **57**, 893 (1961).
17. O. W. Howarth, R. E. Richards, and L. M. Venanzi. J. Chem. Soc. 3335 (1964).
18. A. S. Tompa, R. D. Barefoot, and E. Pryce. J. Phys. Chem. **73**, 435 (1969).
19. I. T. Millar and H. D. Springall. Sidgwick's organic chemistry of nitrogen. 3rd ed. Oxford University Press. 1966. p. 421.
20. W. E. Stewart and T. H. Sidall. Chem. Rev. **70**, 517 (1970).
21. K. C. Dash and D. V. R. Rao. Z. Allgem. Chem. **345**, 217 (1966).
22. D. D. Hall and W. D. Horrocks. Inorg. Chem. 1809 (1969).
23. (*a*) B. B. Wayland and W. L. Rice. Inorg. Chem. **5**, 54 (1966). (*b*) C. C. McDonald and W. D. Phillips. J. Am. Chem. Soc. **85**, 3736 (1963).
24. V. M. Shul'man, S. V. Larionov, T. V. Kramareva, E. I. Arykova, and V. V. Yadima. Russ. J. Inorg. Chem. **11**, 580 (1966).
25. K. Swaminathan and H. M. N. Irving. J. Inorg. Nucl. Chem. **28**, 171 (1966).
26. N. Maneces, C. Piriz MacColl, and R. Levitus. Inorg. Nucl. Chem. Lett. **4**, 597 (1971).
27. D. R. Eaton and W. D. Phillips. Adv. Mag. Res. **1**, 103 (1965).
28. D. R. Eaton and K. Zaw. To be published.
29. O. Piovesana and C. Furlani. J. Inorg. Nucl. Chem. **32**, 879 (1970).
30. B. B. Wayland and R. S. Drago. J. Am. Chem. Soc. **88**, 4597 (1966).
31. G. N. LaMar. Inorg. Chem. **6**, 1939 (1967).
32. V. J. Meyer. Z. Anorg. Chem. **49**, 20 (1906).

Can. J. Chem. Downloaded from www.nrcresearchpress.com by 210.87.254.42 on 09/05/12
For personal use only.

Can. J. Chem. Downloaded from www.nrcresearchpress.com by 210.87.254.5 on 09/05/12
For personal use only.

Quasichemical Treatment of the Solubility of Reactive Gases in Fused Salts

A. Block-Bolten and S. N. Flengas

Department of Metallurgy and Materials Science, University of Toronto, Toronto 181, Ontario

Received June 2, 1971

A quasichemical model applicable to solubilities of reactive gases in fused salts has been developed. The treatment is based on local ordering effects, and accounts for next-nearest neighbor anion repulsions.

The present calculation is applicable to common ion fused salt systems where complex ions with a pronounced heat of formation do not form. The treatment allows the evaluation of structural parameters from available experimental data.

On a développé une méthode quasi-chimique applicable aux solubilités des gaz réactifs dans des sels fondus.

La méthode est fondée sur les effets locaux de classement et tient compte des répulsions provoquées par le prochain plus proche anion voisin. Cette méthode de calcul est applicable aux systèmes de sels fondus ioniques avec un ion commun où les ions complexés ayant une chaleur de formation importante ne se forment pas. Cette étude permet une évaluation des paramètres structuraux à partir de données expérimentales disponibles.

Canadian Journal of Chemistry, **49**, 3327 (1971)

Introduction

In a previous investigation the solubilities of bromine vapor in molten AgBr were reported (1). The results were interpreted as indicating the presence of Br_3^- ions in the melt. In this system, in addition to negative limiting heats of mixing, the partial molar entropies of mixing $\overline{\Delta S}_{Br_2}$ for liquid bromine were positive.

The partial molar heats of mixing, on the assumption that the $AgBr_3$ species are present, may be represented by the reaction

$$Br_{2\ (liquid)} + [(AgBr)_{m-n}\cdot(AgBr_3)_n] \rightarrow [(AgBr)_{m-n-1}\cdot(AgBr_3)_{n+1}]$$

for which

$$[1] \qquad \overline{\Delta H}_{Br_2} = \overline{\Delta H}_{AgBr_3} + \Delta H_R^0$$

where ΔH_R^0 is the heat for formation of $AgBr_3$ from pure liquid bromine and AgBr.

The formation of a Br_3^- species may be thought of as the result of attachment of the non-polar bromine molecule to a Br^- ion in the melt, by ion-induced dipole type interactions. Such species are usually described as triplets $Br^-(B^+...Br^-)$. The energy accompanying the ion-induced dipole interaction is expected to be of rather low magnitude, and therefore the term ΔH_R^0 should not constitute a significant contribution to the total energy of mixing. On the contrary, the dissolved bromine which is closely associated with the Br^- ions in the form of the Br_3^- triplet is not expected to be sufficiently polarized as to occupy distinctive anionic and cationic positions in the liquid sublattices. In this sense the dissolved bromine should occupy the same lattice site as the carrier Br^- anion. Such host Br^- ions are shielded from the surrounding Ag^+ cations by the attached bromine molecules and a volume disturbance in the local symmetry of the ionic distributions is expected to occur.

The net result should be that the next nearest neighbor repulsions of the type Br^-–Ag^+–Br^-, Br^-–Ag^+–Br_3^- and Br_3^-–Ag^+–Br_3^- are expected to be significantly different and a pronounced heat effect due to the distribution of those interactions should be the predominant factor in the heat of mixing given by eq. 1.

It also follows that the partial molar entropies of mixing reported previously (1) may be attributed to local ordering effects.

In the present quasichemical treatment the thermodynamic properties of dilute solutions of reactive gases X_2 in ionic melts AX are treated on the basis of local ordering and on the predominance of next-nearest neighbor anion type repulsions. The method for calculating local ordering is based on the statistical treatment of adsorption of gases on surfaces by Chang (2), and its application to solid solutions by Wasastjerna (3). An extension of this theory to the partial molar properties of reciprocal and simple binary fused salt systems has also been made by Block-Bolten (4). The present calcula-

Can. J. Chem. Downloaded from www.nrcresearchpress.com by 210.87.254.5 on 09/05/12
For personal use only.

tions are applicable to dilute solutions of common cation fused salt systems where complex ions having pronounced heats of formation do not form.

The calculation of the number of significant interactions by the present method depend entirely on the measured partial molar heats of mixing, and the calculated values are then used to predict accurately the partial entropies of mixing.

Quasichemical Treatment of Local Order

Considering the solubility of a gaseous species X_2 in the melt A^+X^- according to

$$[2] \qquad X_2 + A^+X^- \rightleftharpoons A^+X_3^-$$

the types of significant interactions present in the solution are the X^-–A^+–X^-, X^-–A^+–X_3^-, and X_3^-–A^+–X_3^-, where A^+ is the common cation. In general, solutions of this type represent a binary mixture AX–AY in which only next-nearest anion to anion repulsions are taken to be significant.

If a dilute solution contains n_1 g-mol of solute AX dissolved in n_2 g-mol of AY, the *real* fractions of the next-nearest neighbor pairs in the anion sublattice, of the type, X^-Y^-, X^-X^-, and Y^-Y^-, are given by λ, κ, ν, respectively. The total number of pairs in the solution are equal to $\frac{1}{2}NZ(n_1 + n_2)$, where N is the Avogadro number and Z is the coordination number.

A "local order" parameter σ is defined as the fraction of the number of ionic pairs XY present in excess of the same type of pairs calculated for a randomly distributed solution. Hence

$$[3] \qquad \sigma = \frac{P_{XY} - N_X \cdot N_Y}{N_X \cdot N_Y}$$

P_{XY}, is the probability of finding the actual pairs XY, and N_X, N_Y are the corresponding ionic fractions.

When $P_{XY} < N_X N_Y$, the system exhibits positive deviations from ideality. In the case of compound formation $P_{XY} > N_X N_Y$. Accordingly, $1 \geqslant \sigma \geqslant -1$. $\sigma = 0$ for the random solution.

By dividing the pair number for a given ion pair by the total number of significant ionic pairs in the solution given as

$$[4] \qquad \tfrac{1}{2}N(n_1 + n_2)Z(\kappa + \nu + 2\lambda)$$

where $\kappa + \nu + 2\lambda = 1$ by definition, the following expressions are readily derived

$$[5] \qquad \lambda = N_X N_Y(\sigma + 1)$$

$$[6] \qquad \kappa = N_X^2 - N_X N_Y \sigma$$

$$[7] \qquad \nu = N_Y^2 - N_X N_Y \sigma$$

The energy of the solution is also given by

$$[8] \qquad E_S = \tfrac{1}{2}N\,Z(n_1 + n_2)[\kappa\varepsilon_{XX} + 2\lambda\varepsilon_{XY} + \nu\varepsilon_{YY}]$$

where ε_{XX}, ε_{YY}, and ε_{XY} are the repulsive pair interaction energies for the ionic pairs XX, YY, and XY, respectively.

Partial differentiation of eq. 8 yields

$$[9] \qquad \overline{\Delta H}_{AX} = \left[\lambda + (n_1 + n_2)\frac{\partial\lambda}{\partial n_1}\right]RTb$$

where

$$[10] \qquad b = \tfrac{1}{2}Z\,N(n_1 + n_2)[2\varepsilon_{XY} - \varepsilon_{XX} - \varepsilon_{YY}]$$

Hence the partial molar heat of mixing for the solute AX depends upon the number of X^-Y^- pairs and on the rate of increase of such pairs with solute concentration.

The partial molar entropies of mixing may also be calculated from configurational considerations.

Per gram mole of solution the gross distribution of the number of pairs XX, XY, and YY, in the total number of available paired sites, which is $\frac{1}{2}ZN$, is given as

$$[11] \qquad \left[\frac{\left(\frac{Z}{2}N\right)!}{\left(\frac{Z}{2}\kappa N\right)!\left(\frac{Z}{2}\nu N\right)!\left[\left(\frac{Z}{2}\lambda N\right)!\right]^2}\right]^{2/Z}$$

In this calculation the fractions κ, ν, and λ are quantities to be eventually determined from the treatment of the experimental data. The permutation number $((Z/2)N)!$, however, includes many more configurations because of site overlapping. Accordingly, the distributions must be normalized by a factor giving the random distribution of pairs in paired positions where the only restriction is that each pair must contain at least one X^- or one Y^- ions. The combinatory number in such a random system is given as

$$[12] \qquad \left[\frac{\left(\frac{Z}{2}N\right)!}{\left(\frac{Z}{2}NN_X\right)!\left(\frac{Z}{2}NN_Y\right)!}\right]^{2/Z}$$

where, the $2/Z$ exponent in expressions 11 and 12

Can. J. Chem. Downloaded from www.nrcresearchpress.com by 210.87.254.5 on 09/05/12
For personal use only.

is introduced to correct the number of distributions to truly independent ones, as each central cation is surrounded by $Z/2$ pairs of anions.

The normalized combinatory number is obtained by dividing eq. 11 by eq. 12, and is given as

$$[13]\quad C=\left[\frac{\left(N\frac{Z}{2}N_X\right)!\left(N\frac{Z}{2}N_Y\right)!}{\left(N\frac{Z}{2}\kappa\right)!\left(N\frac{Z}{2}\nu\right)!\left[\left(N\frac{Z}{2}\lambda\right)!\right]^2}\right]^{2/Z}$$

This expression was first derived by Chang (2). Accordingly, the integral entropy of mixing for $n_t = n_1 + n_2$ g-moles of mixture is given as

$$[14]\quad \Delta S_M = n_t k \ln C$$

Using Stirling's approximation

$$[15]\quad \Delta S_M = n_t R \ln \frac{N_X^{N_X} N_Y^{N_Y}}{\kappa^{\kappa}\cdot\nu^{\nu}\cdot\lambda^{2\lambda}}$$

which is independent of Z.

The partial molar entropy of mixing for the solute AX is calculated from eq. 15 by partial differentiation

$$[16]\quad \overline{\Delta S}_{AX} = R \ln \frac{N_X}{\kappa^{(\kappa+(\partial\kappa/\partial n_1)n_t)}\lambda^{2(\lambda+(\partial\lambda/\partial n_1)n_t)}\nu^{(\nu+(\partial\nu/\partial n_1)n_t)}}$$

Using the transformations

$$[17]\quad \kappa + \frac{\partial\kappa}{\partial n_1} n_t = 1 - \left(\lambda + \frac{\partial\lambda}{\partial n_1} n_t\right)$$

$$[18]\quad \nu + \frac{\partial\nu}{\partial n_1} n_t = -\left(\lambda + \frac{\partial\lambda}{\partial n_1} n_t\right)$$

eq. 16 reduces to

$$[19]\quad \overline{\Delta S}_{AX} = R \ln \frac{N_X}{\kappa\left(\frac{\lambda^2}{\kappa\nu}\right)\left(\lambda + \frac{\partial\lambda}{\partial n_1} n_t\right)}$$

For the equilibrium between ion-pairs,

$$[20]\quad [XX] + [YY] \rightleftarrows 2[XY]$$

the equilibrium constant is written as

$$[21]\quad \frac{\lambda^2}{\kappa\cdot\nu} = e^{-\Delta G_R^0/RT}$$

where, ΔG_R^0 is the standard free energy for the exchange reaction 20.

If the standard entropy change for this reaction is taken to be insignificant, then the standard free energy may be approximated by the energy of the exchange reaction 20, ΔE_X^0. However, according to eqs. 8 and 9, since the pressure–volume work is also insignificant, $\Delta E_X^0 = \Delta H_X^0$, where ΔH_X^0 is the enthalpy change for reaction 20.

Combining eqs. 9, 19, and 21, the expression for the partial molar entropy of mixing becomes

$$[22]\quad \overline{\Delta S}_{AX} = R \ln \frac{N_X}{\kappa} + \frac{\overline{\Delta H}_{AX}}{T}$$

It should be noted that eq. 22 which has been derived by the quasichemical method on the assumption of local ordering only has the same form as the classical expression for entropy. Accordingly, the activity and the activity coefficient are

$$[23]\quad a_{AX} = \kappa/N_X$$

and

$$[24]\quad \gamma_{AX} = \kappa/N_X^2$$

For the "ideal" totally dissociated and random solution where $\sigma = 0$, $\kappa_{ideal} = N_X^2$. The activity coefficient is therefore given as the ratio of the real over the ideal number of pairs XX.

Application of the Theory

From previous measurements in the Br_2–AgBr system activity coefficients for the $AgBr_3$ component have been derived, as well as heat and entropy data. For this system XX, YY, and XY represent the interactions, Br_3^-–Br_3^-, Br^-–Br^-, and Br^-–Br_3^-, respectively.

The data are summarized in Table 1. Using the determined values of $\overline{\Delta H}_{AgBr_3}$, κ is given as $\kappa = \gamma_{AgBr_3}^{H}\cdot N_{Br_3^-}^2$ and the order parameter σ is evaluated from eq. 6; γ^H is the activity coefficient where Henry's Law is applicable. Similarly, ν and λ are calculated from eqs. 5, 6, 7, and 21. The partial molar entropies of mixing are then calculated directly from eq. 22 using κ and the experimentally determined partial molar heats of mixing. The results of these calculations are also included in Table 1.

Table 1 also includes the fraction κ of pairs Br_3^-–Br_3^- in the "ideal" solution which is given as $N_{Br_3^-}^2$. Comparing κ_{ideal} to κ, it is apparent that the real system contains γ^H times more Br_3^-–Br_3^- pairs than the random system.

Furthermore, λ is slightly less than the ideal fraction of Br_3^-–Br^- type pairs, which indicates that the thermodynamic properties are mainly determined by the formation of Br_3^-–Br_3^- type pairs.

Can. J. Chem. Downloaded from www.nrcresearchpress.com by 210.87.254.5 on 09/05/12
For personal use only.

TABLE 1. Structural characteristics of the $AgBr–Br_2$ system

	Measured				Calculated								
T (°K)	$N_{Br_3^-} \times 10^3$	$\overline{\Delta H}_{AgBr_3}$ (cal mol^{-1})	$\gamma^H_{AgBr_3}$	$\overline{\Delta S}_{AgBr_3}$* (e.u.)	$10^6 \kappa_{ideal} = N_{Br_3^-}{}^{-2}$	$10^3 \lambda_{ideal} = N_{Br_3^-} \times (1\text{-}N_{Br_3^-})$	$\kappa \times 10^6$	$\lambda \times 10^3$	ν	$\lambda + \frac{\partial\lambda}{\partial n_{Br_3}} n_t$	b† (cal mol^{-1})	$\sigma \times 10^3$	$\overline{\Delta S}_{AgBr_3}$ (e.u.)
Spring balance													
862 ± 2	2.22	−6410	2.564	2.84	4.928	2.215	12.635	2.207	0.9960	0.9886	−3.786	−3.61	2.83
897 ± 1	1.71	−6730	2.985	2.96	2.924	1.707	8.728	1.701	0.9966	0.9897	−3.815	−3.34	2.98
950 ± 2	1.46	−7210	3.259	3.03	2.132	1.458	6.948	1.453	0.9971	0.9905	−3.856	−3.36	3.04
Torsion balance													
790 ± 1	3.38	−5760	1.815	2.81	11.424	3.369	20.735	3.362	0.9933	0.9877	−3.706	−2.20	2.84
810 ± 2	2.97	−5940	2.084	2.76	8.821	2.961	18.383	2.952	0.9941	0.9876	−3.737	−3.17	2.77
860 ± 1	2.24	−6400	2.460	2.92	5.018	2.235	12.344	2.228	0.9955	0.9882	−3.790	−3.27	2.89
885 ± 1	1.89	−6620	2.805	2.96	3.572	1.886	10.019	1.880	0.9962	0.9894	−3.805	−3.18	2.93

*$\overline{\Delta S}_{AgBr_3} = \overline{\Delta S}^{xs}_{AgBr_3} + RT \ln N_{Br_3^-}$, where $\overline{\Delta S}^{xs}$ is given in eq. 6 of ref. 1.
†b average: −3.785.

The interaction parameter b is a property of the system and may be calculated as follows:

From $N_X - \lambda = \kappa$, for the dilute solutions

$$[25] \qquad \lambda = N_X - \gamma^H \cdot N_X^2$$

where $N_X = n_1/n_t$. By differentiation and addition,

$$[26] \quad \lambda + n_t(\partial\lambda/\partial n_1) = 1 + N_X\gamma^H(N_X - 2)$$

Combining eqs. 9 and 26 the limiting heat of mixing is given as

$$[27] \quad \overline{\Delta H}_{AX,\,lim} = RTb(1 - 2\gamma_{AX}{}^H N_X + \gamma_{AX}{}^H N_X{}^2)$$

The b values calculated from this relationship are shown in Table 1 and have an average value of, $b = -3785$ cal.

This value is reasonably constant and appears to increase slightly with temperature.

Similarly, the partial molar entropy of mixing for dilute solutions may be written as

$$[28] \quad \overline{\Delta S}_{AX} = -R \ln \gamma_{AX}{}^H \cdot N_X + Rb(1 - 2\gamma^H \cdot N_X + \gamma^H \cdot N_X{}^2)$$

where the first term has the meaning of $-\overline{\Delta G}_{AX}/T$.

The $\lambda + n_t\,(\partial\lambda/\partial n_1)$ terms have also been calculated and tabulated in Table 1. Considering the importance of the two terms in eq. 9 which determine the heats of mixing, it is evident that the *change* of the number of unlike ion pairs, with concentration, is predominant. Values of the order parameter σ are also included in this Table and are of the order of 3×10^{-3}; as incidated earlier $\sigma = 0$ for a random mixture.

In conclusion it has been shown that the thermodynamic properties of the solutions are directly related to structure and to order–disorder effects which are created because of local interactions. The treatment allows the evaluation of these parameters from available experimental data.

1. A. BLOCK-BOLTEN and S. N. FLENGAS. Can. J. Chem. **49**, 2266 (1971).
2. T. S. CHANG. Proc. Camb. Phil. Soc. **35**, 265 (1939).
3. J. A. WASASTJERNA. Soc. Sci. Fenn. Comm. Phys. Math. XIV 3, 1948.
4. A. BLOCK-BOLTEN. Thermodynamics of molten salts and slags. (in Pol.) PWN. Krakow. 1964. Chem. Abstr. 63: 1268*d* (1965).

Can. J. Chem. Downloaded from www.nrcresearchpress.com by 210.87.254.5 on 09/05/12
For personal use only.

Can. J. Chem. Downloaded from www.nrcresearchpress.com by 210.87.254.40 on 09/05/12
For personal use only.

Nuclear Magnetic Resonance Investigation of Possible Molecular Motion in Coronene, Perylene, and Triphenylene in the Solid State

C. A. FYFE
Chemistry Department, University of Guelph, Guelph, Ontario

AND

B. A. DUNELL AND J. RIPMEESTER[1]
Chemistry Department, University of British Columbia, Vancouver, British Columbia

Received May 5, 1971

Broad-line nuclear magnetic resonance (n.m.r.) and spin lattice relaxation time measurements on solid coronene indicate the presence of a molecular reorientation process at 160 °K. The activation energy for the process has been determined at 5.9 kcal/mol and the nature of the motion deduced as being reorientation in the plane of the molecule. No motional processes are observed for perylene or triphenylene.

The results are discussed with respect to thermodynamic data and the molecular structures.

La largeur de raie en r.m.n. ainsi que les mesures du temps de relaxation spin réseau de coronène solide indique la présence d'un processus de réorientation à 160 °K. L'énergie d'activation du processus a été déterminée comme étant de 5.9 kcal/mol et la nature du mouvement a été précisée comme étant une orientation dans le plan de la molécule. Aucun processus de mouvement n'a été observé pour le perylène et tryhénylène.

Les résultats sont discutés en fonction des données thermodynamiques et des structures moléculaires.

Canadian Journal of Chemistry, 49, 3332 (1971)

Introduction

Molecular motion of benzene about its molecular axes in the solid state was shown by Andrew in 1950 (1). An investigation of naphthalene and anthracene did not show any evidence for motion (2). Recently however, a similar type of motion has been observed for pyrene in the solid (3). The purpose of the present work was to investigate possible reorientation processes in a variety of large symmetrical polycyclics. Coronene, perylene, and triphenylene were chosen as they were approximately circular and planar. Their crystal structures have been determined (4–6).

Experimental

The spectrometer used was a conventional crossed-coil type previously described (7). Spin–lattice relaxation times were determined by the "adiabatic fast passage" technique (8). Calculations were carried out using Fortran IV programmes on an I.B.M. 360–50 computer. Materials were from commercial sources and gave m.p.'s consistent with literature values.

[1]Present address: School of Chemical Sciences, University of Illinois, Urbana, Illinois, U.S.A.

Results and Discussion

A. Coronene

At 100 °K coronene gives linewidth and second moment values of 9.3 ± 0.3 G and 8.5 ± 0.3 G^2, respectively. As the temperature is increased, these values drop to 1.5 ± 0.2 G and 1.2 ± 0.2 G^2, respectively (Figs. 1, 2). The linewidth transition is quite abrupt, centered at 160 °K, but the second moment transition is quite smooth. Calculation of the rigid-lattice second moment by the procedure of Van Vleck (9) using the crystal structure data of Robertson and White (4) and assuming C—H = 1.08 Å, yields a value of 7.0 G^2 in reasonable agreement with the low temperature experimental value (Table 1). The difference

TABLE 1. The observed and calculated* second moment values (G^2) for coronene, perylene, and triphenylene

Compound†	Observed	Calculated
Coronene (S)	8.5 (120 °K)	7.0
Coronene (R)	1.13 (298 °K)	1.3
Perylene (S)	8.0 (298 °K)	11.0
Triphenylene (S)	9.3 (298 °K)	10.2

*For details see text.
†(S) = stationary, (R) = rotating.

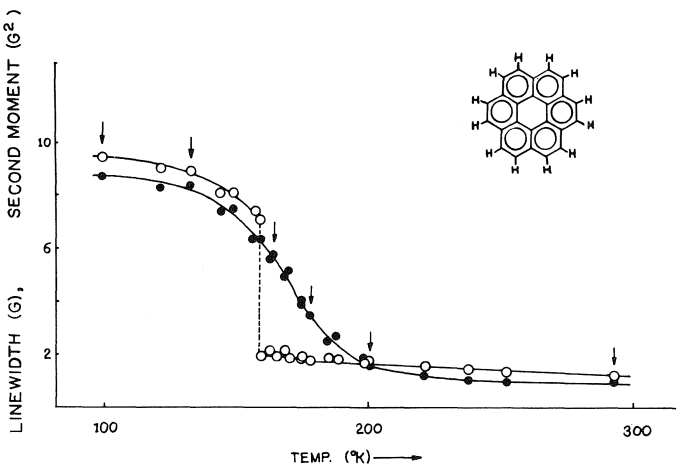

FIG. 1. The observed temperature dependence of the linewidth (open circles) and second moment values (filled circles) of the proton resonance of coronene in the solid state. The vertical arrows indicate the temperatures of the typical spectra shown in Fig. 2.

between the observed second moment of 8.5 G^2 at 120 °K and the calculated rigid lattice value of 7.0 G^2 may be due to a reduction in the lattice dimensions from the room temperature values, or to a small change in crystal structure. Coronene shows a thermal anomaly between 215 and 250 °K (12). Molecular reorientation of the molecule in the plane of the ring lowers this value to 1.3 G^2 by the formulae of Andrew and Eades (10), in agreement with the value experimentally observed. The change of second moment is attributed chiefly to reorientation of the coronene molecules about their six-fold axes. Other possible motions are excluded by the size of the molecule and the crystal structure data.

The sudden discontinuous change in linewidth with temperature may be due to a contribution from some unresolved structure in the spectrum observed at low temperatures when the lattice is rigid (adjacent hydrogen atoms on a given ring are close), or to some structural peculiarity which is present at low temperatures but which is relieved at 160 °K with the motion or the rings. It is not possible because of this asymmetry to obtain an estimate of the activation energy from the linewidth data by the B.P.P. approximation. It is also found that the variation of second moment with temperature does not lead to a straight line plot of ln ν_c *vs.* T^{-1} by use of the treatment proposed by Powles (13).

An activation energy can, however, be obtained from T_1 measurements. These are shown in Fig. 3 plotted as their logarithms against the reciprocal of absolute temperature. The gradient of the curve yields the activation energy for the process, found to be 5.8 kcal/mol. The empirical Waugh estimate based on the temperature of the linewidth transition (11) yields 5.9 kcal/mol, but the closeness of the agreement is probably fortuitous.

It is of interest to note that above $T^{-1} = 0.0047$ (below $T = 213$ °K) no values of T_1 have been given. This is because the intensity of the adiabatic rapid passage signals is very poor over the temperature range where the second moment is changing rapidly. This effect, which has been observed previously and will be reported in more detail in a separate communication, is characteristic of motional transitions which occur over a range of temperature without involving a phase change.

B. Perylene and Triphenylene

At room temperature, perylene gives a linewidth of 8.4 ± 0.3 G and a second moment of 9.3 ± 0.4 G^2. This latter value is in approximate agreement (Table 1) with the rigid lattice value calculated from the crystal structure data of Ahmed and Trotter (5). There is, however, little change in this value on raising the temperature to 520 °K. Similarly, at 298 °K triphenylene gives a linewidth of 7.6 ± 0.3 G, and the second moment of 9.3 ± 0.4 G^2 is in agreement with a

Can. J. Chem. Downloaded from www.nrcresearchpress.com by 210.87.254.40 on 09/05/12
For personal use only.

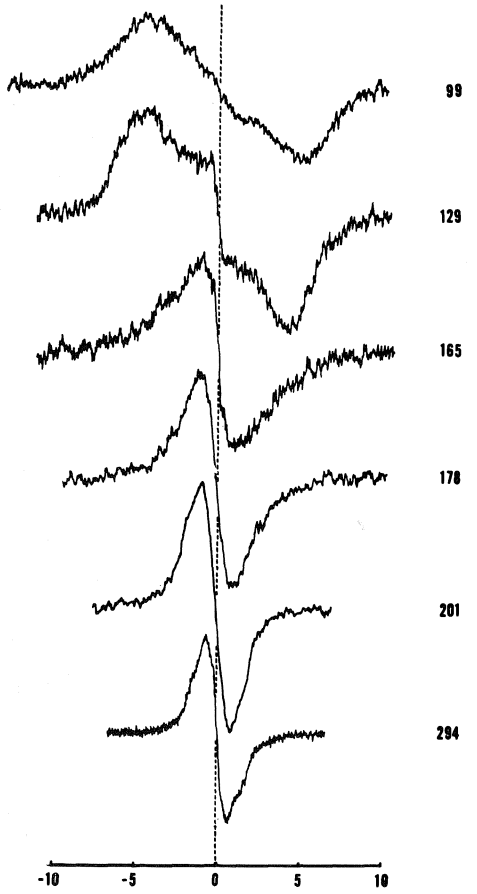

FIG. 2. Representative spectra of the ^1H n.m.r. spectrum of solid coronene recorded at the temperatures indicated. The corresponding points on the second moment curve are indicated by vertical arrows in Fig. 1. Abscissa in gauss.

calculated second moment value from the crystal structure data of Camerman and Trotter (6) (Table 1). Again there is only a slight change with temperature up to 470 °K.

The lack of exact agreement between the observed second moments and the calculated rigid lattice values is thought to be due to the fact that there are relatively large contributions to the second moments from close approaches of pairs of protons within one molecule. The exact positions of these sterically interacting atoms cannot be found with any degree of certainty, so their exact contributions to the total second moment is not known. The tendency in the molecule will be to minimize these steric interactions, so the calculated second moment will, if anything, tend to overestimate them.

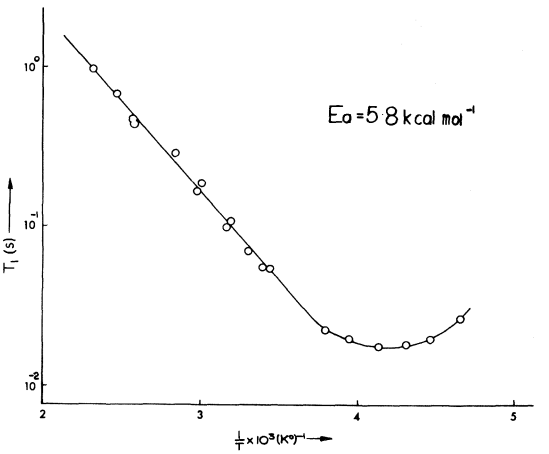

FIG. 3. The spin lattice relaxation time (T_1) of coronene in the solid state plotted on a logarithmic scale against the reciprocal of absolute temperature.

Discussion

Of the three polycyclics investigated, only one shows a motional transition (Table 1). This is in agreement with the thermodynamic data of Wong and Westrum (12), who investigated the heat capacities of a whole series of polycyclics. Of these, only pyrene and coronene showed anomalously small entropies of melting, indicative of molecular motion in the solid before melting.

A possible explanation may lie in the detailed molecular structure of the compounds in their crystal lattices. Thus, there is a small, but significant deviation of the perylene molecules from planarity (6). This is interpreted as being due to inter- rather than intra-molecular forces as no steric interactions are relieved by the distortion. The non-planarity of the molecules allows for a more favorable energy of packing. A side view is shown below.

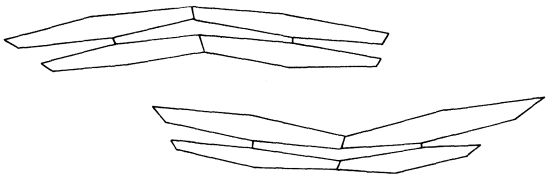

The approach between the two molecules is close, and rotation of the molecules about their

Can. J. Chem. Downloaded from www.nrcresearchpress.com by 210.87.254.40 on 09/05/12
For personal use only.

centers would increase the intermolecular contacts and would be opposed, therefore, by a heightened energy barrier. It would be possible for rotation around a two-fold axis to occur without serious intermolecular contacts if the molecules passed through a planar configuration during the motion, but this would require an increase in lattice energy equal to the stabilizing effect on the lattice of the distortion of the molecules from planarity, and the rotation would be opposed by a correspondingly higher activation energy. Considering that the activation energy for the rotation in the molecular plane of pyrene, which is of roughly the same size as perylene, is *ca.* 14 kcal/mol (3), one can see that an increase in the energy barrier produced by the above effects could prevent rotational reorientation at frequencies detected by n.m.r. at accessible temperatures.

Triphenylene also shows significant deviations from planarity, two rings being raised with respect to the plane of the center ring, and the third lowered (5). It is thought that both inter- and intra-molecular forces may contribute to this distortion. However, rotation of the molecule would necessitate either a complete rotation of the distorted molecule by 360°, or the attainment of a planar structure during the motion, with again an increase in the activation energy for the process.

Distortion from a planar structure is not found in the two complexes of perylene whose structures have been determined (14, 15), and n.m.r. measurements on these may provide a guide to the correctness of the explanation given above.

The authors would like to thank Professor C. A. McDowell for his interest in this work and Professor E. F. Westrum for the communication of the thermodynamic data quoted prior to its publication. They would also like to thank the National Research Council of Canada for a scholarship (to J.R.) and grants-in-aid of research (to C.A.F. and B.A.D.).

1. E. R. ANDREW. J. Chem. Phys. **18**, 607 (1950).
2. F. A. RUSHWORTH. J. Chem. Phys. **20**, 920 (1952).
3. C. A. FYFE, D. F. R. GILSON, and K. H. THOMPSON. Chem. Phys. Lett. **5**, 215 (1970).
4. *a.* J. M. ROBERTSON and J. G. WHITE. J. Chem. Soc. 607 (1945). *b.* J. K. FAWCETT and J. TROTTER. Proc. Roy. Soc. London. Ser. A. **289**, 366 (1966).
5. F. R. AHMED and J. TROTTER. Acta Cryst. **16**, 503 (1963).
6. A. CAMERMAN and J. TROTTER. Proc. Roy. Soc. London. Ser. A. **279**, 129 (1964).
7. B. A. DUNELL, C. A. FYFE, C. A. MCDOWELL, and J. RIPMEESTER. Trans. Faraday Soc. **65**, 1153 (1969).
8. W. R. JANZEN, T. J. R. CYR, and B. A. DUNELL. J. Chem. Phys. **48**, 1246 (1968).
9. J. H. VAN VLECK. Phys. Rev. **74**, 1168 (1948).
10. E. R. ANDREW and R. G. EADES. Proc. Roy. Soc. London. Ser. A. **216**, 398 (1953).
11. J. S. WAUGH and E. I. FEDIN. Sov. Phys. Solid State, **4**, 1633 (1963).
12. W-K. WONG and E. F. WESTRUM, JR. J. Chem. Thermodyn. **3**, 105 (1971).
13. J. G. POWLES. J. Polymer Sci. **22**, 79 (1956).
14. J. C. A. BOEYENS and F. H. HERBSTEIN. J. Phys. Chem. **69**, 2160 (1965).
15. A. W. HANSON. Acta Cryst. **16**, 1147 (1963).

Can. J. Chem. Downloaded from www.nrcresearchpress.com by 210.87.254.40 on 09/05/12
For personal use only.

The Effect of SF_6 and N_2O on the 2537 Å Photolysis of Aqueous I^- and $Fe(CN)_6^{4-}$ [1]

M. Crawford and R. Rumfeldt

Department of Chemistry, University of Windsor, Windsor, Ontario

Received May 10, 1971

The solvated electron yield from the 2537 Å photolysis of aqueous I^- containing N_2O and SF_6 is given by $\phi(e_{aq}^-) = \phi(F^-/6) + \{\phi(I_2) + \phi(N_2)\}$ with the calculated ratio $k_{e+SF_6}/k_{e+N_2O} = 2.00 \pm 0.2$. $\phi(e_{aq}^-)$ from the 2537 Å photolysis of aqueous $Fe(CN)_6^{4-}$ was measured using SF_6, N_2O, and mixtures of N_2O and SF_6 as the scavengers with the material balance being represented by $\phi(e_{aq}^-) = \phi(F^-/6) + \phi(N_2) = \phi(Fe(CN)_6^{3-})/2$. The average value obtained was $\phi(e_{aq}^-) = 0.67 \pm 0.03$ and the calculated values of k_{e+SF_6}/k_{e+N_2O} were 2.20 ± 0.2 from the product ratio's at low $[SF_6]$ and 1.86 ± 0.2 from a competition plot at higher $[SF_6]$. A mechanism is presented describing the specificity of SF_6 as a scavenger of e_{aq}^-.

Le rendement en électron solvaté, obtenu par photolyse à 2537 Å de I^- aqueux contenant N_2O et SF_6, est donné par $\phi(e_{aq}^-) = \phi(F^-/6) + \{\phi(I_2) + \phi(N_2)\}$ avec le rapport calculé $k_{e+SF_6}/k_{e+N_2O} = 2.00 \pm 0.2$. Le rendement $\phi(e_{aq}^-)$, obtenu par photolyse à 2537 Å de $Fe(CN)_6^{4-}$ aqueux, a été mesuré en utilisant SF_6, N_2O et des mélanges de N_2O et SF_6 en tant qu'agents piégeurs et avec un bilan matériel pouvant être représenté par: $\phi(e_{aq}^-) = \phi(F^-/6) + \phi(N_2) = \phi(Fe(CN)_6^{3-})/2$. La valeur moyenne obtenue est $\phi(e_{aq}^-) = 0.67 \pm 0.03$ et les valeurs calculées de k_{e+SF_6}/k_{e+N_2O} sont de 2.20 ± 0.2 à partir du rapport de produit à faible $[SF_6]$ et de 1.86 ± 0.2 à partir d'un tracé compétitif à $[SF_6]$ plus élevé. Un mécanisme est présenté pour décrire la spécificité de SF_6 en tant qu'agent piégeur de e_{aq}^-.

Canadian Journal of Chemistry, **49**, 3336 (1971)

Introduction

It has recently been demonstrated (1, 2) that the molecule SF_6 can be used quantitatively as a scavenger for solvated electrons generated either by the γ-radiolysis or photolysis of a variety of anions in aqueous solution. Whereas with the radiation chemical systems the kinetic evidence has confirmed the specificity of SF_6 as a hydrated electron scavenger, no such evidence has been offered with the photochemical systems. While it seems reasonable to assume that the rate constants or rate constant ratios should be independent of the method used to generate e_{aq}^-, it is a relatively simple matter to replace the assumption with experimental data.

The 2537 Å photolysis of aqueous I^- containing the competing solutes of SF_6 and N_2O was chosen as a model system since (*a*) the photolysis of aqueous I^- has been thoroughly studied (3) and should not present a source of anomalies, (*b*) the competing solutes are both neutral molecules thus eliminating the usual ionic strength corrections, (*c*) all the products of interest are easily and quantitatively measurable, and (*d*) the absolute rate constants and the rate constant ratios of e_{aq}^- with SF_6 and N_2O have been measured by the methods of radiation chemistry.

A second system of interest is the 2537 Å photolysis of $Fe(CN)_6^{4-}$. Although there can be no doubt that e_{aq}^- is produced, three widely differing values (1.0 (4), 0.66 (5), and 0.35 (6)) for $\phi(e_{aq}^-)$ have been reported. Since at least two of these values ($\phi(e_{aq}^-) = 0.66$ (5) and 0.35 (6)) were determined from very detailed studies of the $Fe(CN)_6^{4-}$ system, the origin of the disagreement is not obvious. Waltz and Adamson (7) have recently reported $\phi(e_{aq}^-) = 0.66$ thus tending to confirm the results of Airey and Dainton (5). However, it seems appropriate to study the effect of SF_6 on this system hopefully to substantiate, using this different scavenger, one or other of the previously reported values and, if possible, to elucidate the origin of the discrepancies.

Experimental

The apparatus and procedures are essentially the same as those described previously (2). In addition, an Oriel model C-13-62 low pressure Hg lamp operated with a stabilized power supply was used for most experiments. As a further precaution to assure the constancy of intensity, the actinometry was repeated immediately before and after each run.

All salts used in these experiments were reagent grade and used without further purification.

[1]This work was supported in part by the Defence Research Board of Canada, Grant Number 1675-08.

Can. J. Chem. Downloaded from www.nrcresearchpress.com by 210.87.254.40 on 09/05/12
For personal use only.

Can. J. Chem. Downloaded from www.nrcresearchpress.com by 210.87.254.40 on 09/05/12
For personal use only.

The iodine yields were measured as I_3^- using the spectrophotometric absorption at 353 mμ and the extinction coefficient $2.64 \times 10^4\ M^{-1}\ cm^{-1}$. The total iodine yield is given by the sum $I_3^- + I_2$ where I_2 was calculated using $742\ M^{-1}$ as the equilibrium constant for $I^- + I_2 \rightleftharpoons I_3^-$. The absorption at 420 mμ with $\varepsilon_{420\ m\mu} = 1.03 \times 10^3$ was used to calculate the $Fe(CN)_6^{3-}$ yields.

Results

(a) Photolysis of I^- Solution Containing SF_6 and N_2O

The products measured after irradiation with 2537 Å light of aqueous $5 \times 10^{-2}\ M\ I^-$ solutions containing SF_6 and N_2O were N_2, $I_2(I_3^-)$, and F^- the yields of which were linear with time for the irradiation times used. The total iodine yield is given by $\phi(I_2 + I_3^-)$, however, for convenience it shall simply be represented by $\phi(I_2)$. The relationships between the yields were $\phi(I_2) = \phi(N_2)$ and $\phi(e_{aq}^-) = \phi(F^-/6) + \phi(I_2)$, where $\phi(e_{aq}^-)$ has been determined from I^- solutions containing only SF_6 or N_2O at an equivalent concentration (see ref. 2 or 3).

The relative yields of F^- and I_2 depend upon the competing reactions depicted stoichiometrically by reactions 2 and 3.

[1] $$I^- + h\nu\ (2537\ Å) \rightarrow e_{aq}^- + I$$

[2] $$e_{aq}^- + SF_6 \rightarrow 6F^-, SO_4^{2-}, 8H^+$$

[3] $$e_{aq}^- + N_2O \rightarrow N_2, I_2, 2OH^-$$

Under the conditions used in these experiments, reaction 3 always predominated thus preventing a sufficient increase in $[H^+]$ to suppress the F^- yield. Accordingly, the pH of the photolyzed solutions were near neutral or slightly alkaline. The linear equation describing this competition

[4] $$[\phi(F^-/6]^{-1} = [\phi(e_{aq}^-)]^{-1} + [\phi(e_{aq}^-)]^{-1} k_3[N_2O]/k_2[SF_6]$$

(1) where k_2 and k_3 are the rate constants for reactions 2 and 3, respectively, requires that $\phi(e_{aq}^-)$ be constant over the range of scavenger concentrations employed, a condition not satisfied by the concentration range employed here ($[SF_6] = 1.8 \times 10^{-4}\ M$ and $[N_2O] = 1.0 \times 10^{-3}$ to $3 \times 10^{-3}\ M$ for which $\phi(e_{aq}^-)$ is known to vary).

By combining eq. 4 with the equivalent equation for $\phi(I_2)$ it is easily shown that the yield ratio is given by eq. 5.

[5] $$\phi(F^-/6)/\phi(I_2) = k_2[SF_6]/k_3[N_2O]$$

The mean value taken from six runs was $k_2/k_3 = 2.00 \pm 0.2$ and, within the limits of the experimental error, this value is in excellent agreement with that measured from the γ-radiolysis of aqueous SF_6–N_2O solutions (1). The effect of added salts on $10^{-2}\ M\ I^-$ solutions with $[SF_6] = 1.8 \times 10^{-4}\ M$ and $[N_2O] = 1.8 \times 10^{-3}\ M$ was tested using $4 \times 10^{-2}\ M$ of F^-, Cl^-, and Br^-, respectively. The yields from these solutions (including the $5 \times 10^{-2}\ M\ I^-$ solutions) differed by less than 3%, indicating no significant effect.

(b) Photolysis of $Fe(CN)_6^{4-}$ Solutions

(i) $Fe(CN)_6^{4-}$–N_2O Solutions

The main products measured on photolysis of aqueous $3.5 \times 10^{-3}\ M\ Fe(CN)_6^{4-}$ solutions containing $[N_2O] = 2 \times 10^{-2}\ M$ were N_2 and $Fe(CN)_6^{3-}$. A relatively low yield of CN^- was also measured, however, this was found to be the result of photohydrolysis which is the dominant process at exciting wavelengths longer than 2537 Å (9). The formation of $Fe(CN)_5H_2O^{3-}$ implied by the yield of CN^- would be too low to cause an error in the determination of $Fe(CN)_6^{3-}$ whose spectrum overlaps that of $Fe(CN)_5H_2O^{3-}$ at the analytical wavelength employed.

The quantum yield of N_2 was independent of the irradiation time and when the $Fe(CN)_6^{3-}$ yields were measured prior to the gas analysis, linear yield *vs.* time plots were obtained. Based on these plots the relationship and the average yield was found to be $\phi(Fe(CN)_6^{3-})/2 = \phi(N_2) = 0.64 \pm 0.04$ and independent of the lamp intensity over the range 2×10^{-4} to 6×10^{-6} einstein l^{-1} min^{-1}. These results are in excellent agreement with Airey and Dainton (5) and Waltz and Adamson (7).

The lower yields of Ohno (6) could not be reproduced although it was observed that the repeated freeze–thaw cycles employed in the gas analysis procedure caused a substantial reduction (~30%) in the optical density at 420 mμ; however, on standing the optical density slowly increased, approaching its original value.

(ii) $Fe(CN)_6^{4-}$–SF_6 Solutions

The variation of the F^- yield with irradiation time for the 2537 Å photolysis of $5 \times 10^{-3}\ M$ $Fe(CN)_6^{4-}$ solutions containing $[SF_6] = 1.4 \times 10^{-3}$ and $1.9 \times 10^{-4}\ M$ is shown in Fig. 1. The pronounced curvature in the F^- yields when $[SF_6] < 10^{-3}\ M$ is easily understood in terms of depletion of SF_6 as well as the competition for

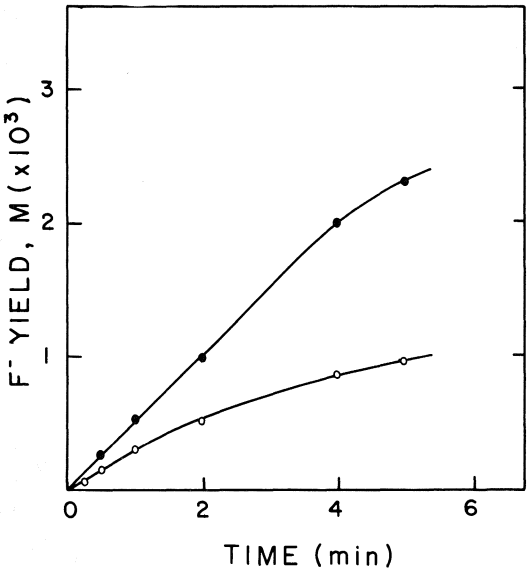

FIG. 1. The dependence of F^- yields on the irradiation time at an intensity of 1.24×10^{-4} einstein l^{-1} min^{-1} in the 2537 Å photolysis of aqueous $Fe(CN)_6^{4-}$ containing $[SF_6] = 1.9 \times 10^{-4}$ (○) and 1.4×10^{-3} *M* (●).

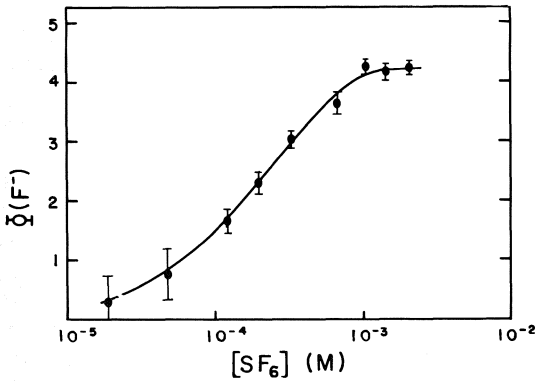

FIG. 2. The variation of $\phi(F^-)$ with $[SF_6]$ in the 2537 Å photolysis of $Fe(CN)_6^{4-}$.

e_{aq}^- by the product ions $Fe(CN)_6^{3-}$ and H^+ (the latter being indicated by a decrease in p*H*). Figure 2 illustrates the dependence of $\phi(F^-)$ on $[SF_6]$ where $\phi(F^-)$ has been determined from the initial linear portion of plots such as those in Fig. 1. When $[SF_6] < 10^{-4}$ *M* the yield *vs.* time plots exhibited continuous curvature precluding an accurate determination of $\phi(F^-)$ thus these values are necessarily only approximate. Using the plateau value of Fig. 2 and assuming a 1:6 ratio between e_{aq}^- and F^- as found in other systems then $\phi(e_{aq}^-) = \phi(F^-/6) = 0.69 \pm 0.02$. Again, good agreement is obtained with the value of Airey and Dainton (5).

In contrast to the N_2O–$Fe(CN)_6^{4-}$ system, the CN^- yields from the photolysis of SF_6–$Fe(CN)_6^{4-}$ solutions were relatively large (*i.e.* ~50% of the F^- yield) and due to the contribution of $Fe(CN)_5H_2O^{3-}$ at 420 mμ does not provide a reliable measure of the $Fe(CN)_6^{3-}$ yield. For example the apparent yield when $[SF_6] = 1.4 \times 10^{-3}$ *M* was $\phi(Fe(CN)_6^{3-}) = 1.90 \pm 0.10$. If $\phi(e_{aq}^-) = \phi(F^-/6) = \phi(Fe(CN)_6^{3-})/2$ then the material balance ratio, $\phi(F)/\phi(Fe(CN)_6^{3-})$, should be 3.0; however, values ranging from 2.5 to 1.7 were obtained depending upon $[SF_6]$ and irradiation time.

(iii) $Fe(CN)_6^{4-}$–N_2O–SF_6 Solutions

Solutions for which $[Fe(CN)_6^{4-}] = 3.5 \times 10^{-3}$ *M* and containing N_2O and SF_6 in the range $[N_2O] = 8.6 \times 10^{-4}$ to 1.5×10^{-2} *M* and $[SF_6] = 1.80 \times 10^{-4}$ to 1.4×10^{-3} *M* were photolyzed. In the experiments using $[SF_6] > 1.8 \times 10^{-4}$ *M* the high pressure cell employed was not readily attached to the gas analysis system, thus only F^- yields were measured. Since the sum $[N_2O] + [SF_6]$ was maintained sufficiently large to ensure that $\phi(e_{aq}^-)$ would be constant, eq. 4 was applicable. The appropriate plot is depicted in Fig. 3 from which the values $\phi(e_{aq}^-) = \phi(F^-/6) = 0.67 \pm 0.05$ and $k_2/k_3 = 1.85 \pm 0.2$ were calculated from the intercept and slope.

At the lower $[SF_6]$ both F^- and N_2 were determined. The p*H* of the photolyzed solutions remained near neutral and the CN^- yields were comparable to those of the $Fe(CN)_6^{4-}$–N_2O solutions, thus the absorbance at 420 mμ was

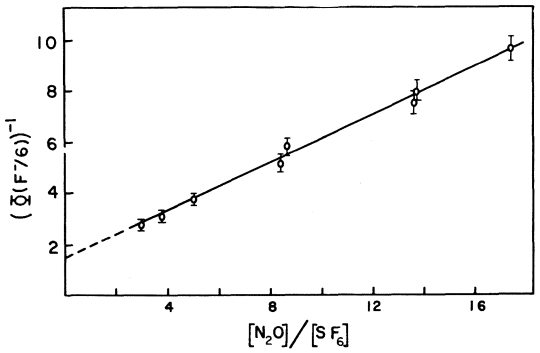

FIG. 3. The effect on $\phi(F^-/6)$ of varying $[N_2O]/[SF_6]$ in the 2537 Å photolysis of aqueous $Fe(CN)_6^{4-}$ in which $[N_2O] + [SF_6] > 10^{-3}$ *M*.

Can. J. Chem. Downloaded from www.nrcresearchpress.com by 210.87.254.40 on 09/05/12
For personal use only.

TABLE

e_{aq}^- origin	Ionic strength	k_2/k_3	Reference
2537 Å photolysis I^-	0.05	2.00±0.2	This work
2537 Å photolysis $Fe(CN)_6^{4-}$	3.5×10^{-3}*	2.20±0.2† 1.85±0.2‡	This work
γ-Radiolysis H_2O	0	1.75§	1
Pulse radiolysis	0	1.92±0.27	1, 8

*Degree of dissociation of $K_4Fe(CN)_6$ is unknown.
†Obtained using eq. 5.
‡Obtained using eq. 4.
§Error limits not quoted.

assumed to provide an acceptable measure of $Fe(CN)_6^{3-}$. The yield relationship was found to be $\phi(F^-/6) = \phi(Fe(CN)_6^{3-})/2$. Applying eq. 5 to the data from nine experiments in which $[SF_6] = 1.8 \times 10^{-4}$ *M* and $[N_2O]$ was in the range 8.6×10^{-4} to 2.9×10^{-3} *M* resulted in $k_2/k_3 = 2.20 \pm 0.20$.

Discussion

The values calculated for k_2/k_3 obtained from the photolysis of either aqueous I^- or $Fe(CN)_6^{4-}$ containing SF_6 and N_2O are seen to be in good agreement with those obtained by the techniques of radiation chemistry (Table 1). The independence of k_2/k_3 with respect to ionic strength is predictable on the basis of the Brönsted–Bjerrum theory; however, a specific ion effect which might have been anticipated was also absent. Anbar and Hart (10) have shown that the absorption maximum of e_{aq}^- is sensitive to both a change in solvent and added non-reactive solutes and have measured a substantial decrease in the rate of reaction 3 in concentrated electrolyte solutions. Unfortunately, these authors make no comment about the reduced solubility of N_2O in salt saturated solutions and by taking account of published solubility data (11) a substantial reduction in $[N_2O]$ is to be expected. Thus, it is uncertain whether the reported effect on reaction 3 is due to a reduction in $[N_2O]$ or k_3. In any event, for the photochemical systems studied k_2/k_3 was independent of the specific ionic atmosphere. It must be noted, however, that the solute concentrations may not have been sufficiently high to develop the potential effect thus the invariance observed cannot be assumed to be conclusive.

Over the range of $[N_2O]$ and $[SF_6]$ studied the material balance equations

$$[6] \quad \phi(e_{aq}^-) = \phi(F^-/6) + \{\phi(I_2) = \phi(N_2)\}$$

and

$$[7] \quad \phi(e_{aq}^-) = \phi(F^-/6) + \phi(N_2) = \phi(Fe(CN)_6^{3-})/2$$

were satisfied although the $Fe(CN)_6^{3-}$ yields cannot be assumed to be completely reliable. The evidence clearly confirms the relationship $\phi(e_{aq}^-) = \phi(F^-/6)$ despite the fact that in the I^- system there is no net oxidation while in the $Fe(CN)_6^{4-}$ system an overall oxidation of the $Fe(CN)_6^{4-}$ is indicated and which is equivalent to that obtained in the presence of N_2O alone.

The average value, $\phi(e_{aq}^-) = 0.67 \pm 0.03$, for the 2537 Å photolysis of $Fe(CN)_6^{4-}$ as determined from the three different systems ($\phi(N_2)$ from N_2O saturated solutions, $\phi(F^-/6)$ from solutions in which $[SF_6] = 2 \times 10^{-3}$ *M* and the intercept of the competition plot) provides convincing support for the value reported by Airey and Dainton (5). The larger value previously reported (4) may have resulted by not taking account of the presence of a high yield of $Fe(CN)_5H_2O^{3-}$; however, an adequate explanation for the low yields reported by Ohno (6) is not apparent and this discrepancy remains unresolved.

The special advantage of SF_6 is in the quantitative relationship $\phi(e_{aq}^-) = \phi(F^-/6)$ and in its specificity towards e_{aq}^-. Even hydrogen atoms fail to react with SF_6, suggesting that its reactions are kinetically controlled. An apparent exception to the inert character of SF_6 is the reaction with exploding metals (12). While seemingly unrelated, a similarity between these latter "reagents" and e_{aq}^- is in their low ionization potentials suggesting that reaction with SF_6 is an electron transfer process, determined in part by the high electron affinity of SF_6 and the low ionization potential of the donor species.

Can. J. Chem. Downloaded from www.nrcresearchpress.com by 210.87.254.40 on 09/05/12
For personal use only.

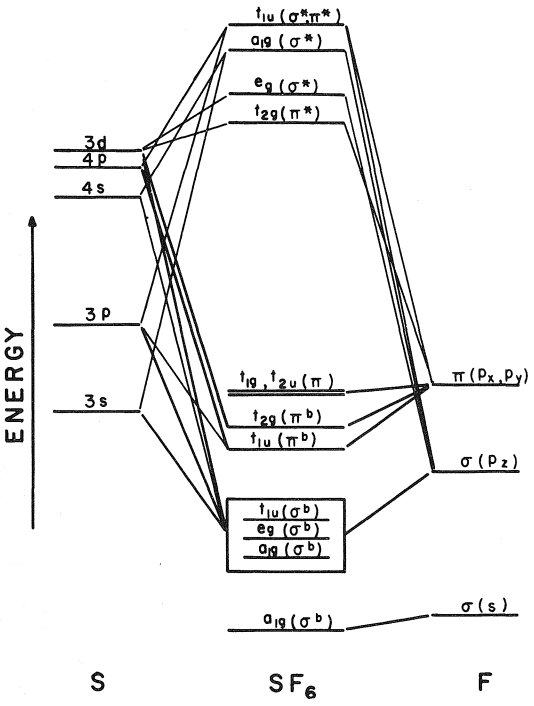

FIG. 4. Molecular orbital scheme for SF_6 based on the orbital transformation properties in O_h symmetry.

Figure 4 represents a qualitative molecular orbital diagram of SF_6 based on the orbital transformation properties in O_h symmetry. For simplicity the core approximation is made for the fluorine 2s electrons leaving a p^5 valence configuration for fluorine. It can be seen that the valence 3s and 3p electrons of sulfur would become localized on the fluorine principally through the a_{1g} and t_{1u} (σ) orbitals. Hypothetically this would leave sulfur in an extremely electron deficient state, thus some balancing of the charge density would be required and can conveniently be visualized as involving the t_{1u} and $t_{2g}(\pi)$ molecular orbitals. This partial withdrawal of charge from the fluorine through the π bonds would be augmented if there was a contraction of the nonbonding t_{1g} and t_{2u} orbitals, thereby reducing the effective nuclear charge of the fluorines. Such a scheme describes SF_6 with effectively no accessible lone pairs which would account for its lack of any discernible nucleophilic character, extremely low solubility and generally inert character. In particular this marked reduction in the availability of fluorine electrons would inhibit the formation of a transition state in possible highly exothermic abstraction reactions with reagents such as hydrogen atoms. On the other hand this scheme also describes the fluorines as being relatively electron deficient as compared to F^-, thus causing an overall high molecular electron affinity.

Further reference to Fig. 4 shows that the addition of an electron to SF_6 to yield SF_6^- would involve the use of a high energy anti-bonding orbital (presumably the $e_g(\sigma^*)$ or $t_{2g}(\pi^*)$ thus destabilizing the molecule. Dissociation of SF_6^- could follow a variety of paths (13) however, maximum π bonding would be maintained by the dissociative process

$$[8a] \qquad e + SF_6 \rightarrow SF_6^-$$

$$[8b] \qquad SF_6^- \rightarrow SF_5 + F^-$$

where SF_5 would have a trigonal bipyramidal structure. The reaction of SF_5 with an oxidizable substrate should simply parallel that proposed for SF_6 *i.e.*

$$[9a] \qquad SF_5 + A^- \rightarrow SF_5^- + A$$

$$[9b] \qquad SF_5^- \rightarrow SF_4 + F^-$$

resulting in SF_4 which also has a trigonal bipyramidal structure (14) with the lone pair being in the trigonal plane. Reactions 8*b* and 9*b* are not meant to imply the existence of SF_6^- or SF_5^- as intermediates as these species may be in repulsive states in which case reaction 8*a* with 8*b* and 9*a* with 9*b* would constitute single concerted reactions.

The hydrolysis of SF_4 has been found to yield SOF_2 (12) which further hydrolyses to SO_3^{2-}. In systems such as I^- the final redox balance would be achieved by the reduction of I_2 either by SOF_2 or SO_3^{2-} which are stoichiometrically equivalent. In the case of $Fe(CN)_6^{4-}$ material balance requires that SOF_2 must be hydrolyzed without a further increase in the oxidation state of sulfur. Unfortunately, in this system the final state of sulfur could not be determined, however, SO_3^{2-} seems the most likely product.

These mechanistic considerations can be summarized by the following general reaction scheme

$$[10] \qquad SF_6 + A^- \rightarrow SF_6^- + A$$

$$[8b] \qquad SF_6^- \rightarrow SF_5 + F^-$$

$$[9a] \qquad SF_5 + A^- \rightarrow SF_5^- + A$$

Can. J. Chem. Downloaded from www.nrcresearchpress.com by 210.87.254.40 on 09/05/12
For personal use only.

[9*b*] $$SF_5^- \rightarrow SF_4 + F^-$$

[11] $$SF_4 + H_2O \rightarrow SOF_2 + 2H^+2F^-$$

[12] $$SOF_2 + 2H_2O \rightarrow SO_3^{2-} + 4H^+2F^-$$

[13] $$SO_3^{2-} + 2A + H_2O \rightarrow SO_4^{2-} + 2H^+ + 2A^-$$

While this reaction sequence is consistent with the essential features observed in the radiation chemistry and photochemistry of aqueous solutions containing SF_6, it does not preclude the possibility of additional significant reactions. For example, from conductometric pulse radiolysis studies of aqueous SF_6 in the absence of added solutes the intermediate SF_5 was found to react directly with H_2O (15). Since reaction 14

[14] $$SF_5 + H_2O \rightarrow SF_4 + F^- + OH + H^+$$

is effectively equivalent to reaction 9*a* with 9*b*, then no change in the stoichiometry would result. Of potential greater consequence are those reactions which describe the reactivity of the product F^- in the particular medium investigated. The use of simple reagent blanks should ordinarily provide a reasonable basis for assessing the lability of F^- and consequently the validity of the relationship $\phi(e_{aq}^-) = \phi(F^-/6)$.

The financial support of the Defence Research Board and National Research Council of Canada is gratefully acknowledged.

1. K.-D. Asmus and J. H. Fendler. J. Phys. Chem. **72**, 4285 (1968).
2. R. Rumfeldt. Can. J. Chem. **49**, 1262 (1971).
3. F. S. Dainton and S. Logan. Proc. Roy. Soc. A, **287**, 281 (1965).
4. M. Shirom and G. Stein. Nature, **204**, 778 (1964).
5. P. L. Airey and F. S. Dainton. Proc. Roy. Soc. A, **291**, 340 (1966).
6. S. Ohno. Bull. Chem. Soc. Jap. **40**, 1770 (1967); **40**, 1776 (1967); **40**, 1779 (1967); **40**, 2035 (1967).
7. W. L. Waltz and A. W. Adamson. J. Phys. Chem. **73**, 4250 (1969).
8. S. Gordon, E. J. Hart, M. S. Matheson, J. Rabani, and J. K. Thomas. Discuss. Faraday Soc. **36**, 193 (1963).
9. S. Ohno. Bull. Chem. Soc. Jap. **40**, 1765 (1967).
10. M. Anbar and E. J. Hart. J. Phys. Chem. **69**, 1244 (1965).
11. A. Seidall. Solubilities of inorganic and metal organic compounds. D. Van Nostrand Co., New York. 1953. p. 1139.
12. E. Cook and B. Siegel. J. Inorg. Nucl. Chem. **29** 2739 (1967).
13. A. J. Ahearn and N. B. Hannay. J. Chem. Phys. **21**, 119 (1953).
14. H. L. Roberts. Q. Rev. **15**, 30 (1961).
15. K.-D. Asmus, W. Grunbein, and J. H. Fendler. J. Am. Chem. Soc. **92**, 2625 (1970).

Can. J. Chem. Downloaded from www.nrcresearchpress.com by 210.87.254.40 on 09/05/12
For personal use only.

Can. J. Chem. Downloaded from www.nrcresearchpress.com by 210.87.254.5 on 09/05/12
For personal use only.

Total Synthesis of DL-Glucose, 3-*O*-Methyl-DL-glucose, and 3-Deoxy-DL-*ribo*-hexopyranose from 1,6:3,4-Dianhydro-β-DL-*allo*-hexopyranose, a Product Obtained from Acrolein Dimer

U. P. SINGH[1] AND R. K. BROWN

Department of Chemistry, University of Alberta, Edmonton, Alberta

Received May 7, 1971

The reaction of butyllithium in ether with 1,6:2,3-dianhydro-4-deoxy-β-DL-*ribo*-hexopyranose (**1**), a substance obtained in five steps from acrolein dimer, gave 1,6-anhydro-3,4-dideoxy-β-DL-*erythro*-hex-3-enopyranose (**2**). The compound 1,6:3,4-dianhydro-β-DL-*allo*-hexopyranose (**3**), obtained from **2**, was converted by reaction with aqueous barium hydroxide followed by hydrolysis of the product, to DL-glucose **5**. Treatment of **3** with sodium methoxide in methanol followed by acid hydrolysis of the 1,6-anhydro intermediate **6**, gave 3-*O*-methyl-DL-glucose (**7**). The same intermediate, **6**, along with the methyl glycoside **8**, could be obtained by the acid-catalyzed reaction of **3** with methanol. Lithium aluminum hydride reacted with **3** to form 1,6-anhydro-3-deoxy-β-DL-*ribo*-hexopyranose (**9**), which was hydrolyzed readily to 3-deoxy-DL-*ribo*-hexopyranose (**10**).

Yields were excellent throughout. All products obtained from the oxirane **3** were those resulting only from *trans* diaxial opening of the oxirane ring.

La réaction du butyllithium dans l'éther avec le 1,6:2,3-dianhydro-4-déoxy-β-DL-*ribo*-hexopyranose (**1**), une substance obtenue en cinq étapes à partir du dimère de l'acroléine, a donné le 1,6-anhydro-3,4 didéoxy-β-DL-*erythro*-hex-3-énopyranose (2). On a converti le composé 1,6:3,4-dianhydro-β-DL-*allo*-hexopyranose (**3**), obtenu de **2**, en DL-glucose **5**, par la réaction avec l'hydroxyde de baryum en solution aqueuse suivie de l'hydrolyse du produit. Le 3-*O*-méthyl-DL-glucose (**7**) fut obtenu à partir de la réaction de **3** avec le méthoxyde de sodium dans le méthanol, suivie par l'hydrolyse acide de l'intermédiaire 1,6-anhydro **6**. On a pu obtenir le même intermédiaire **6**, avec le glycoside de méthyl **8**, par la réaction catalysée par les acides de **3** dans le méthanol. L'hydrure de lithium et d'aluminium a réagi avec **3** pour former le 1,6-anhydro-3-déoxy-β-DL-*ribo*-hexopyranose (**9**), qu'on a hydrolysé facilement en 3-déoxy-DL-*ribo*-hexopyranose (**10**).

Les rendements se sont avérés partout excellents. Tous les produits obtenus à partir de l'oxirane **3** étaient ceux résultant de l'ouverture *trans* diaxiale du noyau oxirane.

Canadian Journal of Chemistry **49**, 3342 (1971)

Introduction

A preliminary communication (1) from this laboratory reported the synthesis of DL-glucose from 1,6:2,3-dianhydro-4-deoxy-β-DL-*ribo*-hexopyranose (**1**), an intermediate product obtained in five steps from acrolein dimer. This note provides the experimental details for the synthesis of DL-glucose, and as well describes the conversion of **1** to 3-deoxy-DL-*ribo*-hexopyranose and to 3-*O*-methyl-DL-glucose and its methyl glycoside, thus indicating the synthetic utility of compound **1**.

Results and Discussion

The sequence of reactions and the compounds obtained are shown in Scheme 1. The 100 MHz p.m.r. spectra obtained for all of the isolated compounds are in full agreement with the structures shown. The signals for most of the protons could be determined by spin decoupling, and these provided observed couplings which clearly supported these structures and the conformations indicated.

The reaction of *n*-butyllithium readily converted **1**, in ether, to 1,6-anhydro-3,4-dideoxy-β-DL-*erythro*-hex-3-enopyranose (**2**) whose *O*-methyl and *O*-acetyl derivatives have been described elsewhere (2). The reaction of *m*-chloroperoxybenzoic acid with **2** gave only the *exo* oxirane, **3**, as expected (3), with no evidence for simultaneous formation, even in small amount, of the *endo* oxirane isomer. Opening of the oxirane ring by base gave 1,6-anhydro-β-DL-*gluco*-hexopyranose (**4**, R = H), in good yield, and this product was hydrolyzed to DL-glucose (**5**, R = H), a crystalline solid. The 100 MHz p.m.r. spectra of **5** (R = H) in D_2O and of its pentaacetate in $CDCl_3$ were identical

[1]Postdoctoral Fellow, 1970-1971.

Can. J. Chem. Downloaded from www.nrcresearchpress.com by 210.87.254.5 on 09/05/12
For personal use only.

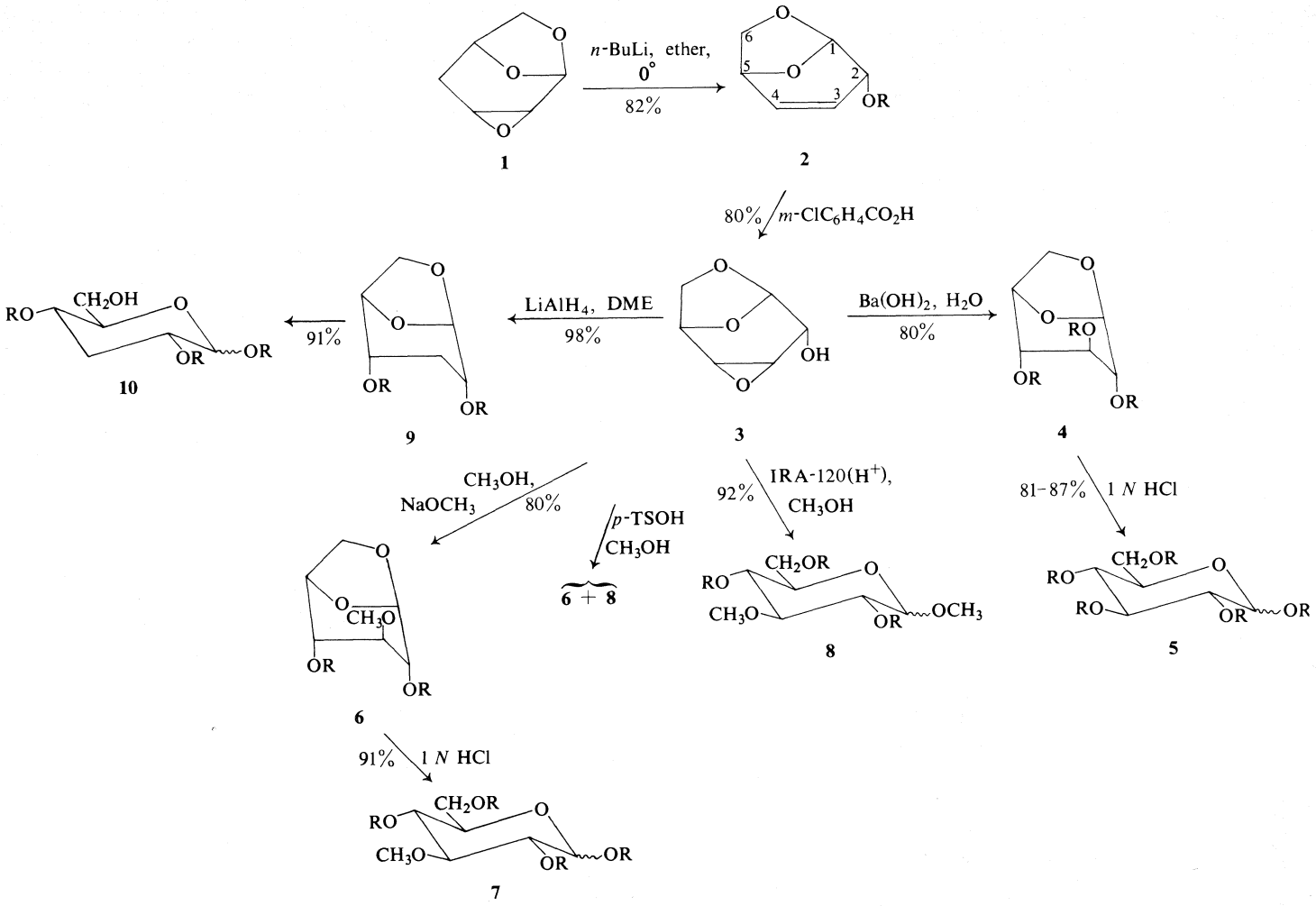

SCHEME 1

Can. J. Chem. Downloaded from www.nrcresearchpress.com by 210.87.254.5 on 09/05/12
For personal use only.

to those of authentic D-glucose and its penta-acetate.

The oxirane **3**, treated with sodium methoxide in methanol, gave a very good yield of 1,6-anhydro-3-*O*-methyl-β-DL-*gluco*-hexopyranose (**6**, R = H), a viscous oil, as the only isolable product. The p.m.r. spectra of **6** (R = H) and of its diacetate (also a viscous oil) were in accord with the assigned structures. Hydrolysis of the diacetate of **6** with 1 *N* hydrochloric acid gave an excellent yield of 3-*O*-methyl-α,β-DL-glucopyranose (**7**, R = H) whose 100 MHz p.m.r. spectrum in D_2O was identical to that of authentic 3-*O*-methyl-α,β-D-glucopyranose. Compound **6** (R = H) was also obtained as the major product when **3** was heated in methanol containing *p*-toluenesulfonic acid monohydrate. This was accompanied by the product **8** (R = H) whose formation could not be avoided. Treatment of **3** with a mixture of methanol and Amberlite IRA-120 (H^+) gave an excellent yield of what is believed to be methyl 3-*O*-methyl-α,β-DL-glucopyranoside (**8**, R = H). The 100 MHz p.m.r. spectrum of **8** (R = H) in D_2O showed two doublets ($J \sim 3.5$ and 8 Hz) in the anomeric proton region, corresponding to a mixture of the α- and β-pyranose isomers, the latter being present to the extent of ~5–10%. All the signals of the D_2O p.m.r. spectrum of authentic methyl 3-*O*-methyl-α-D-glucopyranoside (in which the anomeric proton signal for the β-isomer was absent) were found in the spectrum of the DL-glucopyranoside. However, there were additional signals present in the spectrum of the DL-glucopyranoside, but these could be due to the presence of the contaminating β-isomer. Better corroboration of the structure of **8** was found when it was converted to a crystalline triacetate, whose 100 MHz p.m.r. spectrum in $CDCl_3$ was identical to that of the triacetate of authentic methyl 3-*O*-methyl-α-D-glucopyranoside.

Treatment of a solution of **3** in tetrahydrofuran (THF) with $LiAlH_4$ gave a nearly quantitative yield of 1,6-anhydro-3-deoxy-β-DL-*ribo*-hexopyranose (**9**, R = H). Acid-catalyzed hydrolysis of **9** (R = H) gave **10** (R = H) whose p.m.r. spectrum in D_2O possessed four sets of doublets in the anomeric proton signal region, indicating that **10** (R = H) in D_2O existed as an equilibrium mixture of α- and β-pyranose and furanose structures, with the β-pyranose isomer as the major component. Acetylation of **10** (R = H) gave an excellent yield of a solid tetraacetate whose 100 MHz p.m.r. spectrum identified the structure as 1,2,4,6-tetra-*O*-acetyl-3-deoxy-β-DL-*ribo*-hexopyranose.

It is interesting that the only isolable products obtained from the reaction of **3** with each of the reagents, aqueous base, sodium methoxide in methanol, methanol containing an acid, and $LiAlH_4$ in THF, were those arising from a *trans* diaxial opening of the oxirane ring, a reaction course which has been found to take place preferentially with other oxiranes (3–6).

Experimental

Melting points and boiling points are uncorrected. Elemental analyses were made by Mrs. D. Mahlow and Mrs. A. Dunn of our microanalytical laboratory. The i.r. absorption spectra were obtained by Mr. R. Swindlehurst, of this Department, using a Perkin–Elmer Model 421 spectrophotometer. The 100 MHz p.m.r. spectra and spin decoupling experiments were made by Mr. G. Bigham and associates in this Department. Tetramethylsilane was the internal reference. Signal assignments were made with the aid of double irradiation spin decoupling. The reported coupling constants were estimated from the signal spacings where possible, and are therefore approximate values.

Column and thin layer chromatography was carried out using Silica Gel G (Merck and Co.) as adsorbent. Solvents were usually removed by rotary evaporator under vacuum, unless otherwise stated. The drying agent employed for organic solutions was anhydrous sodium sulfate.

*1,6-Anhydro-3,4-dideoxy-β-DL-erythro-hex-3-enopyranose (**2**, R = H)*

A solution of 2.56 g (0.02 mol) of the oxirane **1** (7) in 50 ml of anhydrous ether, was kept at 0° while 12 ml of a 22% solution of *n*-butyllithium (0.041 mol) in hexane was added dropwise over a 15 min period. Throughout the reaction the solutions were protected from the atmosphere by nitrogen. The yellow reaction mixture was allowed to warm slowly to room temperature and then left overnight. It was treated cautiously with water and the ether layer was then separated. The aqueous layer was extracted continuously for 24 h with dichloromethane. The combined ether layer and dichloromethane extracts were dried and freed from drying agent and solvent. The resulting yellow oil solidified when cooled, and gave after crystallization from chloroform–hexane, 2.10 g (82%) of **2** (R = H), m.p. 67–68°.

Anal. Calcd. for $C_6H_8O_3$: C, 56.25; H, 6.25. Found: C, 56.31; H, 6.60.

The i.r. spectrum in chloroform showed strong absorption at 3575 (sharp) and 3445 cm^{-1} (broad) for OH.

The 100 MHz p.m.r. spectrum in $CDCl_3$ had signals at τ 4.34 for H-1 (narrow triplet, $J_{1,2} \sim 2.0$, $J_{1,3} \sim 1.5$ Hz); 6.27–6.50 for H-2, (min.)-6_{exo} and (min.)-6_{endo} (multiplet); 4.26 for H-3 (doublet of quartets), $J_{2,3} \sim$

Can. J. Chem. Downloaded from www.nrcresearchpress.com by 210.87.254.5 on 09/05/12
For personal use only.

3.5, $J_{3,4} \sim 10.0$ Hz); 3.88 for H-4 (doublet of doublets, $J_{4,5} \sim 4.5$ Hz); 5.25–5.45 for H-5 (multiplet); 6.82 for O*H* (singlet, $w/2 \sim 6$ Hz).

*1,6:3,4-Dianhydro-*β*-*DL*-allo-hexopyranose (**3**)*

To a solution of 2.56 g (0.02 mol) of **2** (R = H) in 100 ml of dry dichloromethane was added 6.88 g (0.04 mol) of 80% *m*-chloroperoxybenzoic acid. The reaction mixture was protected from moisture while being stirred at room temperature for 24 h. The precipitated *m*-chlorobenzoic acid was removed and the filtrate stirred with excess anhydrous sodium carbonate. The solids were then removed by filtration and the filtrate freed of solvent. The crude **3**, contaminated with *m*-chlorobenzoic acid, was purified by chromatography using dichloromethane – ethyl acetate (2:1) as eluent. The first fraction contained the *m*-chlorobenzoic acid; the second contained **3** which gave colorless needles from dichloromethane – *n*-hexane, m.p. 108–109°; yield, 2.31 g (80%).

Anal. Calcd. for $C_6H_8O_4$: C, 50.00; H, 5.59. Found: C, 49.79; H, 5.25.

The i.r. spectrum in chloroform showed bands at 3515 (OH) and 1250 cm^{-1} (oxirane).

The 100 MHz p.m.r. spectrum in $CDCl_3$ showed signals at τ 4.75 for H-1 (narrow multiplet, $J_{1,2} \sim 1.0$, $J_{1,3} \sim 2.0$ Hz); 6.39 for H-2 (quartet, $J_{2,3} \sim 4.5$, $J_{2,OH} \sim 12$ Hz); 6.65 for H-3 (triplet of quartets, $J_{3,4} \sim 4.5$, $J_{3,5} \sim 0.7$ Hz); 6.77 for H-4 (doublet of doublets, $J_{4,5} \sim 1.8$ Hz); 5.28 for H-5 (complicated doublet); 6.01 for H-6_{endo} (doublet of doublets, $J_{6exo,6endo} \sim 7.5$, $J_{5,6endo} \sim 0.7$ Hz); 6.22 for H-6_{exo} (doublet of doublets, $J_{5,6exo} \sim 4.3$ Hz); 7.14 for O*H* (doublet).

*1,6-Anhydro-*β*-*DL*-glucopyranose (**4**, R = H)*

The oxirane **3** (0.5 g) was heated for 15 h under nitrogen with 10% barium hydroxide in a 2:1 water–dioxane solution. The solution was then cooled, diluted with dioxane, and neutralized with carbon dioxide. The barium carbonate precipitate was removed, and the filtrate freed of solvent, leaving 450 mg (80%) of colorless syrup.

A portion of this syrup (200 mg) was treated with a mixture of 5 ml of acetic anhydride and 5 ml of pyridine at room temperature for 24 h, giving 1,6-anhydro-β-DL-glucopyranose triacetate (**4**, R = CH_3CO) as a colorless syrup, b.p. 130–131° at 0.1 mm; yield, 325 mg (91%).

Anal. Calcd. for $C_{12}H_{16}O_8$: C, 50.00; H, 5.59. Found: C, 49.78; H, 5.29.

The i.r. spectrum in chloroform showed strong absorption at 1740 cm^{-1} (C=O).

The 100 MHz p.m.r. spectrum was identical to that of authentic 1,6-anhydro-β-D-glucopyranose triacetate.

*α,β-*DL*-Glucose (**5**, R = H)*

A quantity (200 mg) of **4** (R = H) in 10 ml of 1 *N* aqueous hydrochloric acid was heated for 5 h in an oil bath at 100°. The mixture was cooled and neutralized with Amberlite IRA-400 ($OH^{\ominus}$) and then filtered. The filtrate was freed from solvent and the residue was freeze dried, giving a colorless glassy solid which produced needles from aqueous ethanol – ether, m.p. 113–115°; yield, 190 mg (81%). Reported m.p. of a 1:1 mixture of D- and L-glucose, 112–113.5 (8).

Anal. Calcd. for $C_6H_{12}O_6$: C, 40.00; H, 6.71. Found: C, 39.60; H, 6.64.

DL-Glucose gave the same spectral characteristics shown by D-glucose and showed the presence of two anomeric proton signals in the area ratio of 1:2 for the α and β anomers.

Hydrolysis of the triacetate of **4** as above gave α,β-DL-glucose in 87% yield.

*α,β-*DL*-Glucose Pentaacetate (**5**, R = CH_3CO)*

Acetylation of 50 mg of **5** (R = H) as was done for compound **4** (R = H) above, gave a viscous liquid which deposited colorless prisms from chloroform – petroleum ether, m.p. 115–117°; yield, 97 mg (90%).

Anal. Calcd. for $C_{16}H_{22}O_{11}$: C, 49.24; H, 5.64. Found: C, 49.60; H, 5.50.

The 100 MHz p.m.r. spectrum of this material in $CDCl_3$ was identical to that of authentic fully acetylated D-glucose and showed the presence of two anomeric proton signals in the area ratio of 1:2 for the α and β anomers.

*1,6-Anhydro-3-O-methyl-*β*-*DL*-glucopyranose (**6**, R = H)*

A solution of 400 mg of the oxirane **3** in 30 ml of dry methanol, previously treated with 1.0 g of sodium metal, was heated under reflux, and meanwhile protected by a nitrogen atmosphere. The disappearance of **3** was followed by t.l.c. using 1% methanol in chloroform as solvent. The reaction was complete after 30 h. The solution was cooled, then neutralized with IRA-120 ($H^{\oplus}$) in methanol. The resin was removed and the filtrate freed from solvents to provide, after distillation, pure **6** (R = H) as a colorless syrup, b.p. 140–143° at 0.1 mm; yield, 380 mg (80%).

Anal. Calcd. for $C_7H_{12}O_5$: C, 47.73; H, 6.87. Found: C, 47.40; H, 6.66.

*2,4-Di-O-acetyl-1,6-anhydro-3-O-methyl-*β*-*DL*-glucopyranose (**6**, R = CH_3CO)*

A quantity (250 mg) of **6** (R = H) was treated with 10 ml of a 1:1 mixture of acetic anhydride and pyridine for 1 h at 60°. From this was obtained 335 mg (90%) of crude diacetate which when distilled at 100–105° at 0.1 mm gave a viscous oil.

Anal. Calcd. for $C_{11}H_{16}O_7$: C, 50.77; H, 6.20. Found: C, 51.06; H, 5.91.

The i.r. spectrum in chloroform showed strong absorption at 1735 cm^{-1} (C=O).

The 100 MHz p.m.r. spectrum in $CDCl_3$ had signals at τ 4.74 for H-1 (singlet, $w/2 \sim 3.5$, $J_{1,2} \sim 1.5$ Hz); 5.38–5.65 for H-2, (min.)-4 and (min.)-5 (multiplet, $J_{5,6endo} \sim 1.5$, $J_{5,6exo} \sim 5.5$ Hz); 6.83–6.95 for H-3 (multiplet); 6.05 for H-6_{endo} (doublet of doublets, $J_{6exo,6endo} \sim 7.5$ Hz); 6.30–6.55 for H-6_{exo} (multiplet); 6.63 for OCH_3 (singlet); 7.94 and 7.96 (singlets for two CH_3CO).

*3-O-Methyl-α,β-*DL*-glucose (**7**, R = H)*

A solution of 280 mg of **6** (R = CH_3CO) in a mixture of 10 ml of 1 *N* aqueous hydrochloric acid and 5 ml of dioxane was heated at 80° for 5 h in an oil bath. The reaction mixture was cooled and neutralized with Amberlite IRA-400 ($OH^{\ominus}$) and filtered. The solvent was removed from the filtrate and the residue was freeze-dried. The resulting colorless syrup, when crystallized from methanol–ether, gave fine hygroscopic

Can. J. Chem. Downloaded from www.nrcresearchpress.com by 210.87.254.5 on 09/05/12
For personal use only.

needles, m.p. 135–137° (shrinking at 80°); yield, 190 mg (91%). The above syrup could also be distilled at 155–157° at 0.1 mm to provide a viscous oil which crystallized when seeded.

Anal. Calcd. for $C_7H_{14}O_6$: C, 43.30; H, 7.27. Found: C, 43.31; H, 7.18.

The 100 MHz p.m.r. spectrum of **7** (R = H) in D_2O after the solution had stood 24 h to allow completion of mutarotation, was identical to that of authentic 3-*O*-methyl-α,β-D-glucose.

*Methyl 3-O-Methyl-α,β-DL-glucopyranoside (**8**, R = H)*

A solution of the oxirane, **3**, (600 mg) in 50 ml of anhydrous methanol containing 2 g of Amberlite IRA-120 ($H^{\oplus}$) was heated under reflux for 60 h. The solution was cooled, separated from the resin by filtration, and the filtrate freed from solvent. The colorless syrup so obtained (800 mg, 92%) gave a single spot on a t.l.c. plate (solvent, methanol–chloroform, 1:10), and also gave an R_f value similar to that of the corresponding authentic D compound.

The i.r. spectrum of this syrup and that of authentic methyl 3-*O*-methyl-D-glucopyranoside (both in $CHCl_3$) were identical.

The 100 MHz p.m.r. spectrum of **8** (R = H) in D_2O showed signals at τ 4.97 for H-1 of the α isomer (doublet, $J \sim 3.5$ Hz); 5.38 for H-1 of the β isomer (doublet, $J \sim 8.0$ Hz) with the α anomer in large predominance. The signal for the β isomer was absent in the spectrum of the authentic D-glucopyranoside as were several other signals found in the spectrum of the DL-substance. The origin of these extra signals is unknown, but could be due to contaminating β isomer.

Acceptable evidence for the structure was obtained by conversion of **8** (R = H) to its triacetate, isolated after work-up as a colorless syrup which crystallized from ether and petroleum ether as needles, m.p. 81–81°; yield 845 mg (87%).

Anal. Calcd. for $C_{14}H_{22}O_9$: C, 50.30; H, 6.63. Found: C, 50.30; H, 6.82.

The spectral characteristics of this triacetate were identical to those of the authentic D isomer.

*Reaction of **3** with Methanol Containing p-Toluenesulfonic Acid Monohydrate*

A solution of **3** (500 mg) in 50 ml of anhydrous methanol containing 250 mg of *p*-toluenesulfonic acid monohydrate was heated under reflux for 10 h. The disappearance of **3** during the reaction was followed by t.l.c. (solvent, ethylacetate–chloroform, 2:1). The mixture was cooled and then brought to $pH \sim 9$ with sodium methoxide. The methanol was removed and the residue was diluted with 50 ml of water and this mixture was subjected to continuous liquid–liquid extraction with chloroform for 48 h. The chloroform solution was freed from solvent and gave a syrup which showed two spots on t.l.c. (2% methanol in chloroform). The two components were separated by column chromatography. The first fraction obtained by elution with 1% methanol in chloroform gave 337 mg (60%) of material identical with product **6** (R = H). The second fraction obtained by elution with 5% methanol in chloroform gave a syrup (216 mg, 30%), which on acetylation with acetic anhydride and pyridine provided 312 mg (91%) of crystalline material, m.p. 81–82°, which was identical to the triacetate of **8** above.

*1,6-Anhydro-3-deoxy-β-DL-ribo-hexopyranose (**9**, R = H)*

A solution of 500 mg of **3** in 25 ml of dry, freshly distilled tetrahydrofuran (THF) was added slowly and dropwise to a stirred suspension of $LiAlH_4$ (400 mg) in 30 ml of dry THF at room temperature and under nitrogen. After addition was completed, the reaction mixture was stirred overnight at room temperature, and then heated to reflux for 45 min. The solution was cooled and treated with 15 ml of THF saturated with water and then with 2 ml of 15% aqueous sodium hydroxide solution. The granular precipitate was removed by filtration and the filtrate was dried. Removal of the drying agent and then the solvent gave a syrup which solidified on cooling. This material showed only one spot on t.l.c. (solvent, dichloromethane). Sublimation at 100–105° at 0.1 mm provided colorless needles, m.p. 117–119°; yield, 497 mg (98%).

Anal. Calcd. for $C_6H_{10}O_4$: C, 49.31; H, 6.90. Found: C, 49.45; H, 6.66.

The i.r. spectrum in chloroform showed absorption at 3600 and 3470 cm^{-1} (OH).

The 100 MHz p.m.r. spectrum in $CDCl_3$ showed signals at τ 4.60 for H-1 (singlet, $w/2 \sim 4$ Hz); 5.75–6.50 for H-2, (min.)-4, -6_{exo}, (min.)-6_{endo}, 20H (multiplet); 7.75–8.30 for H-3_{exo}, -3_{endo} (multiplet); 5.30–5.54 for H-5 (multiplet).

*2,4-Di-O-acetyl-1,6-anhydro-3-deoxy-β-DL-ribo-hexopyranose (**9**, R = CH_3CO)*

Treatment of 300 mg of **9** (R = H) with 10 ml of a 1:1 mixture of acetic anhydride and pyridine at 60° for 0.5 h, and the solution then left overnight at room temperature, gave a colorless solid which was sublimed at 90–95° at 0.2 mm. Colorless needles, m.p. 123–124°; yield, 357 mg (96%).

Anal. Calcd. for $C_{10}H_{14}O_6$: C, 52.19; H, 6.13. Found: C, 52.31; H, 6.11.

The i.r. spectrum in chloroform showed strong absorption at 1735 cm^{-1} (C=O).

The 100 MHz p.m.r. spectrum in $CDCl_3$ had signals at τ 4.54 for H-1 (doublet, $J_{1,2}$ 1.5 Hz); 5.20–5.45 for H-2, (min.)-4, and (min.)-5 (multiplet); 7.55–8.25 for H-3_{exo}, -3_{endo} (multiplet); 6.05–6.25 for H-6_{exo}, -6_{endo} (multiplet); 7.84 and 7.86 (two singlets for CH_3CO).

*3-Deoxy-α,β-DL-ribo-hexopyranose (**10**, R = H)*

A solution of 250 mg of **9** (R = H) in a mixture of 10 ml of 1 *N* aqueous hydrochloric acid and 5 ml of dioxane was heated at 80° for 5 h with an oil bath. The mixture was cooled and then neutralized with Amberlite IRA-400 ($OH^{\ominus}$). Removal of the solvent from the filtrate gave a residue which was freeze dried. The resulting pale yellow syrup showed only one spot on t.l.c. (solvent, 7% methanol in chloroform, or 3% methanol in ethyl acetate). Distillation at 139–145° at 0.01 mm gave **10** (R = H) as a colorless viscous oil; yield 235 mg (91%); lit. m.p. of the D isomer, 108–111° (9).

Anal. Calcd. for $C_6H_{12}O_5$: C, 43.90; H, 7.37. Found: C, 44.27; H, 7.23.

The 100 MHz p.m.r. spectrum in D_2O, taken after the compound had been in solution 48 h, showed

signals at τ 4.72 (doublet, $J \sim 4.0$ Hz), 4.91 (doublet, $J \sim 3.5$ Hz), 5.04 (doublet, $J \sim 3.0$ Hz) and 5.47 (doublet, $J \sim 8.0$ Hz) for H-1 of the α- and β-furanose and pyranose isomers, with the β-pyranose quite predominant. No change was observed in the spectrum taken again after the solution had stood for a week.

*3-Deoxy-β-DL-ribo-hexopyranose Tetraacetate (**10**, R=CH_3CO)*

Acetylation of 150 mg of **10** (R=H) as had been done for **9** (R=H) above gave a syrup from which the tetraacetate was obtained as colorless needles from ether and hexane, m.p. 114–115°; yield, 278 mg (91%).

Anal. Calcd. for $C_{14}H_{20}O_9$: C, 50.60; H, 6.07. Found: C, 50.71; H, 6.02.

The i.r. spectrum in chloroform showed strong absorption at 1745 cm^{-1} (C=O).

The 100 MHz p.m.r. spectrum in $CDCl_3$ indicated that only one compound, the β-pyranose isomer, was present. Signals occurred at τ 4.39 for H-1 (doublet, $J_{1,2} \sim 8.0$ Hz); 5.05–5.35 for H-2, (min.)-4 (multiplet); 7.30–7.55 for H-3_{endo} (multiplet); 8.10–8.60 for H-3_{exo} (multiplet); 6.10–6.40 for H-5 (multiplet); 5.75–5.95 for the two C-6 protons; 7.93, 7.97, 7.99, 8.00 (four singlets for CH_3CO).

The filtrate from the above tetraacetate provided a material which had the same i.r. spectrum and R_f value on a t.l.c. plate (solvent, chloroform) as did the tetraacetate, but the 100 MHz p.m.r. spectrum showed four doublets in the anomeric proton signal region indicating the presence of both the α- and β-furanose and -pyranose isomers with the β-pyranose isomer predominant; τ 3.70 (d, $J \sim 4.0$ Hz), 3.84 (d, $J \sim 3.80$ Hz); 3.90 ($J \sim 0$ Hz) and 4.36 (d, $J \sim 8.0$ Hz).

The authors thank the National Research Council of Canada for financial support for this work.

We thank Dr. R. U. Lemieux and Dr. T. L. Nagabhushan of this Department for a sample of 3-*O*-methyl-D-glucose.

1. U. P. SINGH and R. K. BROWN. Can. J. Chem. **48**, 1791 (1970).
2. U. P. SINGH and R. K. BROWN. Can. J. Chem. **49**, 1179 (1971).
3. H. B. HENBEST and R. A. WILSON. J. Chem. Soc. 1958 (1957).
4. A. FURST and PL. A. PLATTNER. Intern. Congr. Pure and Appl. Chem. 12th Congr. New York, N.Y., 1951. Abstr. of paper. p. 405.
5. A. S. HALLSWORTH and H. B. HENBEST. J. Chem. Soc. 3571 (1960).
6. T. P. MURRAY, U. P. SINGH, and R. K. BROWN. Can. J. Chem. **49**, 2132 (1971).
7. F. SWEET and R. K. BROWN. Can. J. Chem. **46**, 2289 (1968).
8. M. L. WOLFROM and B. H. WOOD. J. Am. Chem. Soc. **71**, 3175 (1949).
9. E. J. HEDGLEY, W. G. OVEREND, and A. A. C. RENNIE. J. Chem. Soc. 4701 (1963).

Can. J. Chem. Downloaded from www.nrcresearchpress.com by 210.87.254.5 on 09/05/12
For personal use only.

Can. J. Chem. Downloaded from www.nrcresearchpress.com by 210.87.254.5 on 09/05/12
For personal use only.

A Novel S_N1 Displacement: The Reaction of Tertiary Amines with Acetic Anhydride

R. P. MARIELLA AND K. H. BROWN[1,2]

Department of Chemistry, Loyola University, Chicago, Illinois 60626

Received September 3, 1970[3]

The action of acetic anhydride on tertiary amines at reflux may cause the displacement of one of the R groups from the amine. The groups which are displaced are benzyl, *t*-butyl, benzhydryl, trityl, and cinnamyl; the groups which are not displaced are methyl, ethyl, *n*-butyl, phenyl, α-naphthyl, *iso*-propyl, allyl, and propargyl. An S_N1 mechanism with special steric requirements is consistent with the experimental results.

L'action de l'anhydride acétique sur les amines tertiaires à reflux, peut provoquer le déplacement de l'un des groupes R de l'amine. Les groupes qui sont déplacés sont benzyle, *t*-butyle, benzhydryle, tritYle, et cinnamyle; les groupes qui ne sont pas déplacés sont méthyle, éthyle, *n*-butyle, phényle, α-naphtyle, *iso*-propyle, allyle, et propargyle. Un mécanisme S_N1 avec des conditions stériques spéciales est consistant avec les résultats expérimentaux.

Canadian Journal of Chemistry, **49**, 3348 (1971)

In the course of studying the acetylation of amines (1) we have examined the reaction of several tertiary amines with acetic anhydride. It was found that certain special tertiary amines underwent displacement of one of the groups attached to nitrogen by the acetic anhydride, while other tertiary amines were inert.

$$[1]\quad RR'R''N + (CH_3CO)_2O \xrightarrow{\text{Reflux}} RR'NCCH_3 + CH_3C{-}OR''$$

Table 1 shows the results of the reaction of the various tertiary amines with acetic anhydride at reflux (eq. 1). The results of Table 1 show that the groups displaced are benzyl, *t*-butyl, benzhydryl, trityl, and cinnamyl; and that the groups which are not displaced are methyl, ethyl, *n*-butyl, phenyl, α-naphthyl, *iso*-propyl, allyl, and propargyl. A pure S_N2 mechanism would require that methyl be most easily displaced, hence the results preclude any S_N2-like mechanism. A pure S_N1 mechanism would require that allyl and propargyl be displaced along with the others mentioned. The data, however, does not substantiate these predictions either. However, an ionization mechanism seems to be the most reasonable based on the evidence given here and on the para substitution results from the reaction of acetic anhydride with benzyldimethylamines (2).

Among the evidence which was used to choose a mechanistic pathway was the reaction of cinnamyldimethylamine. The cinnamyl group, as expected from the rule of vinylogy (3) reacts like the benzyl group, hence cinnamyldimethylamine undergoes displacement of the cinnamyl group on reaction with acetic anhydride. This reaction gave two products; 60% cinnamyl acetate, $CH_3COOCH_2CH{=}CHC_6H_5$, and 30% α-phenylallyl acetate, $CH_3COOCH(C_6H_5)$-$CH{=}CH_2$. This is a typical product spread for an allylic rearrangement in an S_N1 process (4).

The results of our experiments indicate the general mechanistic pathway shown in eq. 2 with its associated rate (eq. 3).[4]

Those amines which underwent displacement *via* C—N bond cleavage *all* have one group which can stabilize an incipient carbonium ion and *at least* one methyl group attached to nitrogen. This suggests that an ionization mechanism is taking place, but with steric requirements also present. An examination of the mechanism shown in eq. 2 and of its associated rate expression shown in eq. 3 indicates that CH_3COOR'' will not form at a reasonable rate if $K_{eq}(3)$ is very small, where $K_{eq}(3) = k_1/k_{-1}$. Also, if k_{-1}/k_2

[1]Taken from the Ph.D. Dissertation of Kenneth H. Brown, Loyola University, Chicago, Illinois, 1971.

[2]The authors wish to express acknowledgment to Professor J. W. Wilt of our Department for his discussions of the mechanistic implications of this reaction.

[3]Revision received July 16, 1971.

[4]The rate eq. 3 was obtained by the steady state treatment of the reaction mechanism shown in eq. 2.

TABLE 1. The acetylation of tertiary amines*

$$RR'R''N + (CH_3CO)_2O \rightarrow RR'NCCH_3 + CH_3C{-}OR''$$

Amines which underwent the above reaction†	Amines which failed to undergo the above reaction‡
$\underline{(CH_3)_3CN(CH_3)_2}$	$C_6H_5N(CH_3)_2$
$\underline{C_6H_5CH_2N(CH_3)_2}$	$(C_6H_5)_2NCH_3$
$\underline{C_6H_5\underset{\displaystyle CH_3}{\underset{\vert}{C}}HN(CH_3)_2}$	$(C_6H_5)_3N$
	α-$C_{10}H_7N(CH_3)_2$
$\underline{(C_6H_5CH_2)_2NCH_3}$	$(CH_3CH_2CH_2CH_2)_3N$
$\underline{C_6H_5CH_2\underset{\displaystyle CH_3}{\underset{\vert}{N}}CH_2CH_2OH}$	$(CH_3)_2CHN(CH_3)_2$
	$HC{\equiv}CCH_2N(CH_3)_2$
$\underline{C_6H_5CH{=}CHCH_2N(CH_3)_2}$§	$CH_2{=}CHCH_2N(CH_3)_2$
$\underline{(C_6H_5)_2CHN(CH_3)_2}$	$C_6H_5CH_2\underset{\displaystyle CH_2CH_3}{\underset{\vert}{N}}C_6H_5$
$\underline{(C_6H_5)_3CN(CH_3)_2}$§	$(C_6H_5CH_2)_3N$

*Except where indicated, all the amines were used as received from various chemical supply houses.
†The group displaced from each tertiary amine is indicated by being underlined.
‡In the case of unreacted amines, the starting amines were recovered quantitatively, and were not destroyed by other reactions.
§See Experimental section for preparation.

is much less than one, then the rate will be dependent only on k_1. If k_{-1}/k_2 is much greater than one, the reaction rate will be drastically diminished.

We postulate three fundamental reasons why reaction occurred or did not occur:

A. For amines with phenyl substituents, electronic considerations make k_1 rather small due to electron-withdrawal by the aromatic ring. Hence **3** is never reached.

B. For *very* sterically hindered amines, K_{eq}(**3**) is very small due to a decrease in k_1. Thus, the rate will decrease as a function of k_1.

C. For the R'' group to be displaced by C—N cleavage *via* ionization, R'' must be a good carbonium ion, *and* **3** must be bulky enough to require a collapse to product in order to lower its energy. Both of these considerations necessitate a large k_2, which makes the denominator of the rate equation unity. Thus, the rate is only a function of k_1, which is large enough for all the amines studied except the anilines and perhaps the very sterically crowded amines.

There are thus two structural requirements, electronic and steric; and it is the subtle interplay of these factors which determines whether or not C—N bond cleavage will occur. Intermediate **3** must be sterically crowded enough to undergo S_N1 displacement to products due to the release of energy associated with steric strain, but not so

[2] $$RR'R''N + (CH_3CO)_2O \underset{k_{-1}}{\overset{k_1}{\rightleftharpoons}} \left[CH_3C(=O)O\text{–}C(CH_3)(=O)\text{–}\overset{\oplus}{N}RR'R'' \right] \xrightarrow{k_2} CH_3CNRR' + CH_3C{-}OR''$$

1 2 3 4 5

[3] $$\frac{d(CH_3COOR'')}{dt} = \frac{k_1[RR'R''N][(CH_3CO)_2O]}{1 + k_{-1}/k_2}$$

Can. J. Chem. Downloaded from www.nrcresearchpress.com by 210.87.254.5 on 09/05/12
For personal use only.

TABLE 2. Structural requirements of *t*-amines in acetylation reaction*

Amines which fulfill *both* the electronic requirements and the steric requirements of the reaction		Amines which do not satisfy both the electronic requirements *and* the steric requirements of the reaction	
$(CH_3)_3CN(CH_3)_2$	(*C*)	$C_6H_5N(CH_3)_2$	(*A*)
$C_6H_5CH_2N(CH_3)_2$	(*C*)	$(C_6H_5)_2NCH_3$	(*A*)
$C_6H_5CHN(CH_3)_2$ (CH$_3$)	(*C*)	$(C_6H_5)_3N$	(*A*)
		α-$C_{10}H_7N(CH_3)_2$	(*A*)
$(C_6H_5CH_2)_2NCH_3$	(*C*)	$(CH_3CH_2CH_2CH_2)_3N$	(*B*) and (*C*)
$C_6H_5CH_2NCH_2CH_2OH$ (CH$_3$)	(*C*)	$(CH_3)_2CHN(CH_3)_2$	(*C*)
		$HC{\equiv}CCH_2N(CH_3)_2$	(*C*)
$C_6H_5CH{=}CHCH_2N(CH_3)_2$	(*C*)	$CH_2{=}CHCH_2N(CH_3)_2$	(*C*)
$(C_6H_5)_2CHN(CH_3)_2$	(*C*)	$(C_6H_5CH_2)_3N$	(*B*)
$(C_6H_5)_3CN(CH_3)_2$	(*C*)	$C_6H_5CH_2NC_6H_5$ (CH$_2$CH$_3$)	(*A*)

*The *A*, *B*, or *C* after each amine refer to the reasons set forth in the discussion. These reasons can be applied to justify the above amines as concerns their reactivities.

sterically crowded so as to prevent its formation at all; for the prevention of its formation would preclude any question of how **3** would go to product. The electronic considerations are that no groups can be present on the amine which make k_1 very small; phenyl qualifies as such a group. Also, in order for the displacement from **3** to products to occur, there must be present a potentially stable carbonium ion, one which can undergo S_N1 displacement.

Table 2 shows whether each amine can fulfill *both* the electronic *and* the steric requirements of the reaction, as detailed above. Satisfying one of the requirements is not enough for a successful reaction. The amine *must* satisfy *both* requirements in order to go to products. Those amines which satisfy both requirements were, in fact, the only ones which experimentally were found to undergo C—N cleavage (see Table 1).

The lone inconsistent result is that of allyldimethylamine. The steric requirements of cinnamyldimethylamine, in the preferred *trans* isomer, are quite the same as those of the allyldimethylamine since the vinyl group removes the phenyl ring from the reaction site. Thus, the allyl group should be displaced as is the cinnamyl group. The fact that the allyldimethylamine is inert with acetic anhydride is thus explained only on the grounds that the electronic factors for the formation of a good carbonium ion are not sufficient for the allyl group.

Besides acetic anhydride, the displacement of the benzyl group from benzyldimethylamine was successfully accomplished using trifluoroacetic anhydride. This result supports the proposed mechanism since k_1 will be larger due to the electron-withdrawing effect of the three fluorine atoms, while the steric requirements are approximately the same as the parent acetic anhydride.

Experimental

All melting points were obtained on a Fisher-Johns hot plate and are uncorrected. All boiling points were obtained using standard vacuum distillation techniques and are uncorrected. All n.m.r. spectra were taken on a Varian A-60A instrument as 50% CCl_4 solutions, using 1% TMS as internal standard, except in those cases where solubility considerations required $CDCl_3$ as solvent. All i.r. spectra were taken as neat smears (for liquids) or as KBr pellets (for solids), and were performed on a Beckman IR-5A spectrophotometer. Elemental analyses were performed by Micro-Tech Laboratories, Skokie, Illinois.

Acetylation of Tertiary Amines

Since all the reactions of the tertiary amines with acetic anhydride were nearly the same, a general procedure will be used to illustrate how each amine was reacted with the acetic anhydride.

The Reaction of Acetic Anhydride with Tertiary Amine

Tertiary amine (0.1 mol) was added dropwise to a well-stirred mixture of acetic anhydride (140 ml) and anhydrous sodium acetate (1 g). The temperature of the reaction mixture remained the same during the addition. The mixture was heated at reflux for 24 h and then rotary evaporated at 80° and 30 mm for 1 h, leaving a thick sludge. Water (100 ml) was added to the sludge and the aqueous mixture was extracted with 100 ml of ether (25 ml per extraction), and the combined ether layer was dried ($MgSO_4$), filtered, and concentrated on the rotary evaporator at reduced pressure, leaving a crude

Can. J. Chem. Downloaded from www.nrcresearchpress.com by 210.87.254.5 on 09/05/12
For personal use only.

Can. J. Chem. Downloaded from www.nrcresearchpress.com by 210.87.254.5 on 09/05/12
For personal use only.

product. The product was purified by usual techniques of distillation (for liquids) and crystallization (for solids). The i.r. and n.m.r. spectra were taken of the product and compared with the spectra of the starting material. The cases of benzyl acetate and *t*-butyl acetate were verified by comparison with authentic samples of these compounds.

Preparation of Trityldimethylamine

Dimethylamine was bubbled slowly into a 500 ml flask of benzene (100 ml) at 10° with stirring until 15 g (0.33 mol) was added. Then triphenylmethyl chloride (27.9 g, 0.1 mol) in benzene (75 ml) was added dropwise over a 20 min period to the cold (+10°) solution. The mixture was then stirred at 25° for 6 days in a well-stoppered flask. Hydrochloric acid (200 ml, 3 *N*) was added and the aqueous layer was made basic with 40% KOH. A voluminous solid precipitated out of solution. The white solid was removed from the mixture by filtration and then was extracted with ether (200 ml) four times. The combined ether layer was dried (KOH pellets), filtered, and concentrated at reduced pressure, leaving a crystalline white solid (24 g, 83%), m.p. 94.5–97.0°; mixed m.p. with trityl chloride gave a m.p. range of 80–120°; n.m.r. (CCl_4), τ 2.4–3.0 (multiplet, phenyl protons, 15H): 7.96 (singlet, methyl protons, 6H).

Anal. Calcd. for $C_{21}H_{21}N$: C, 87.81; H, 7.32; N, 4.88. Found: C, 87.74; H. 7.51; N, 5.00.

Preparation of Cinnamyldimethylamine

Dimethylamine was bubbled into a flask of cold (10°) benzene (75 ml) until 8.75 g (0.20 mol) was added. Cinnamyl chloride (8.60 g, 0.05 mol) was added dropwise over 20 min and the mixture was stirred at 25° for 4 days in a well-stoppered flask. Hydrochloric acid (200 ml, 3 *N*) was added and the aqueous layer was made basic with 40% KOH. A white solid precipitated from solution. The mixture was extracted with ether (200 ml, 50 ml per extraction), and the combined ether layer was dried (K_2CO_3), filtered, and concentrated at reduced pressure, leaving a viscous yellow liquid (8.0 g, 83%), b.p. 61–63°/0.25 mm (2); n.m.r. (CCl_4), τ 2.7 (singlet, phenyl protons, 5H); 3.5 (multiplet, vinyl protons, 2H); 7.03 (doublet, methylene protons, 2H); 7.80 (singlet, methyl protons, 6H); i.r. (neat), ν (cm^{-1}) 1370 (methyl stretch).

The Acetylation of Cinnamyldimethylamine to Cinnamyl Acetate and α-Phenylallyl Acetate (2)

Cinnamyldimethylamine (4.03 g, 0.025 mol), acetic anhydride (75 ml), and sodium acetate (0.5 g) were stirred together at reflux for 48 h. The mixture was then rotary evaporated at 80° and 5 mm for 3 h to remove the acetic anhydride. The residue was then treated with water (100 ml) and then extracted with ether (250 ml, 50 ml per extraction). The combined ether layer was dried ($MgSO_4$), filtered, and concentrated at reduced pressure, leaving 4.1 g of red liquid. The red liquid was distilled under vacuum through a 4-in. Vigreux column. Two products were distilled; first was 1.0 g of a clear white liquid, α-phenylallyl acetate (b.p. 61–65°/0.025 mm); n.m.r. (CCl_4), τ 2.71 (singlet, phenyl protons, 4.9H); 3.70 (doublet, vinyl proton alpha to phenyl, 1H); 4.00 (multiplet, vinyl proton, 1H); 4.90 (multiplet, terminal methylene, 2H); 8.06 (singlet, methyl protons, 3H); second product was a 2.0 g fraction of clear white liquid, cinnamyl acetate (b.p. 81–84°/0.025 mm); n.m.r. (CCl_4), τ 2.70 (singlet, phenyl protons, 5H); 3.40 (doublet, vinyl proton alpha to phenyl, 1H); 3.5–4.0 (multiplet, vinyl proton beta to phenyl, 1H); 5.33 (doublet, methylene protons, 2H); 8.02 (singlet, methyl protons, 3H).

The cinnamyl acetate (0.58 g) was then placed in a mixture of acetic anhydride (13 ml), acetic acid (0.5 g), and sodium acetate (0.05 g). The mixture was heated at reflux for 24 h, then worked-up as above leaving a single pure compound which had an i.r. and n.m.r. identical with cinnamyl acetate.

Product Data

The yields of the successful reactions were as follows: dimethyl-*t*-butylamine gave 50% *t*-butyl acetate; dimethylbenzylamine gave 40% benzyl acetate; *N,N*-α-trimethylbenzylamine gave 55% α-methylphenethyl acetate; dibenzylmethylamine gave 10% benzyl acetate; *N*-benzyl-*N*-methylethanolamine gave 30% benzyl acetate; dimethylcinnamylamine gave 70% of a 2:1 mixture of cinnamyl acetate and α-phenylallyl acetate; benzhydryldimethylamine gave 25% benzhydryl acetate; trityldimethylamine gave a small yield (< 10%) of trityl acetate.

1. R. P. MARIELLA and K. H. BROWN. J. Org. Chem. **36**, 735 (1971).
2. V. G. DREFAHL, H. LUCKERT, and W. KOHLER. J. Prakt. Chem. **11**, 341–344 (1960).
3. R. C. FUSON. Reactions of organic compounds. John Wiley and Sons, Inc., New York, N.Y., 1964. p. 513.
4. J. MARCH. Advanced organic chemistry: reaction, mechanism and structure. McGraw-Hill Book Co., New York, N.Y., 1968. p. 270–274.

Can. J. Chem. Downloaded from www.nrcresearchpress.com by 210.87.254.42 on 09/05/12
For personal use only.

Biosynthesis of Cernuine[1]

Y. K. Ho, R. N. Gupta, D. B. MacLean, and Ian D. Spenser
Department of Chemistry, McMaster University, Hamilton, Ontario

Received June 10, 1971

The biosynthesis of cernuine (**9**), an alkaloid of *Lycopodium cernuum*, was studied in intact plants. Specific incorporation of lysine, cadaverine, Δ^1-piperideine, and pelletierine was demonstrated. The alkaloid is not a modified dimer of pelletierine, as might have been anticipated on the basis of structural relations, since only one pelletierine unit is incorporated.

La biosynthèse de la cernuine (**9**), un alcaloide issu du *Lycopodium cernuum*, a été étudiée sur des plantes intactes. L'incorporation spécifique de la lysine, de la cadavérine, de la Δ^1-pipérideine, et de la pelletierine, a été démontrée. L'alcaloide n'est pas un dimère modifié de la pellétierine, comme on pourrait le supposer d'après les relations structurales puisque seule une unité de pellétierine est incorporée.

Canadian Journal of Chemistry, **49**, 3352 (1971)

Introduction

In our previous work on the biosynthesis of the Lycopodium alkaloids (2–5) attention was focussed on the precursors of lycopodine (**6**), the major alkaloid of the group. We now report on the origin of cernuine (**9**), a Lycopodium alkaloid whose skeletal type is exceptional in that it does not bear a simple structural relationship to lycopodine.

Lysine (**1**) (3, 4), cadaverine (**2**) (4), Δ^1-piperideine (**3**) (5), and acetate (4) were found to serve as specific precursors of lycopodine. These results lent credence to the hypothesis (Scheme 2) which prompted the work, that lycopodine and its structural relatives were modified dimers of a $C_5N—C_3$ unit, such as pelletierine (**4**), which in turn arises from lysine (Scheme 1). A dinitrogeneous species (*e.g.* **5**) is assumed to be an intermediate in the pathway to lycopodine (**6**). Other alkaloids, such as lycodine (**7**) and α-obscurine (**8**), could arise from the same intermediate. It is now known that pelletierine (**4**) cannot be the monomer unit, $C_5N—C_3$, demanded by the hypothesis, since only one intact pelletierine moiety was incorporated into lycopodine when multiply labelled pelletierine was administered to *Lycopodium tristachyum* (3, 5). It nevertheless appears likely on the basis of the mode of incorporation of the other precursors that a $C_5N—C_3$ unit related to pelletierine is implicated in the biosynthesis of lycopodine, and that a dinitrogeneous species with a lycodine–obscurine type skeleton serves as an intermediate.

Cernuine (**9**), like lycodine, can be formally dissected into, and could conceivably arise from, two $C_5N—C_3$ units (Scheme 3), but the manner in which the two units are joined is entirely different in the two systems. It is noteworthy that *L. cernuum*, the species which yields cernuine, does not elaborate alkaloids of the lycodine or the lycopodine type. It was of interest, therefore, to determine whether the substrates known to be involved in the biosynthesis of lycopodine are also implicated in cernuine biosynthesis, and, in particular, whether pelletierine (**4**) is incorporated and if so, whether it serves as a precursor of one or of both halves of the cernuine system. The work here reported leads to the conclusion that there is complete analogy in the biosynthesis of cernuine and of lycopodine.

Methods and Results

The plant used in this investigation was *Lycopodium cernuum* L., a subtropical Lycopodium species. A voucher specimen, authenticated by Dr. C. D. Adams, Department of Botany, University of the West Indies, is deposited in the University herbarium, Mona, Jamaica. Feeding experiments were carried out at the field station of the Institute of Jamaica, at Mason River.

Specifically labelled samples of lysine, cadaverine, Δ^1-piperideine, and pelletierine were administered to intact plants and also to cuttings. A summary of these experiments is presented in

[1]A preliminary account of part of this work has been published (1).

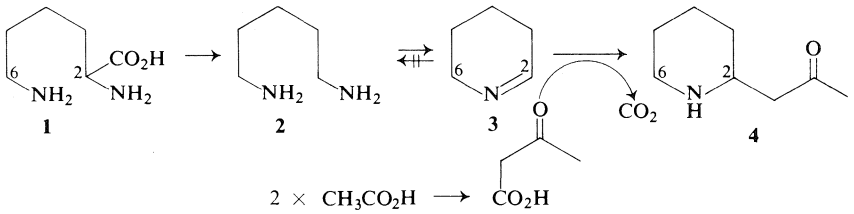

SCHEME. 1. Biosynthesis of pelletierine.

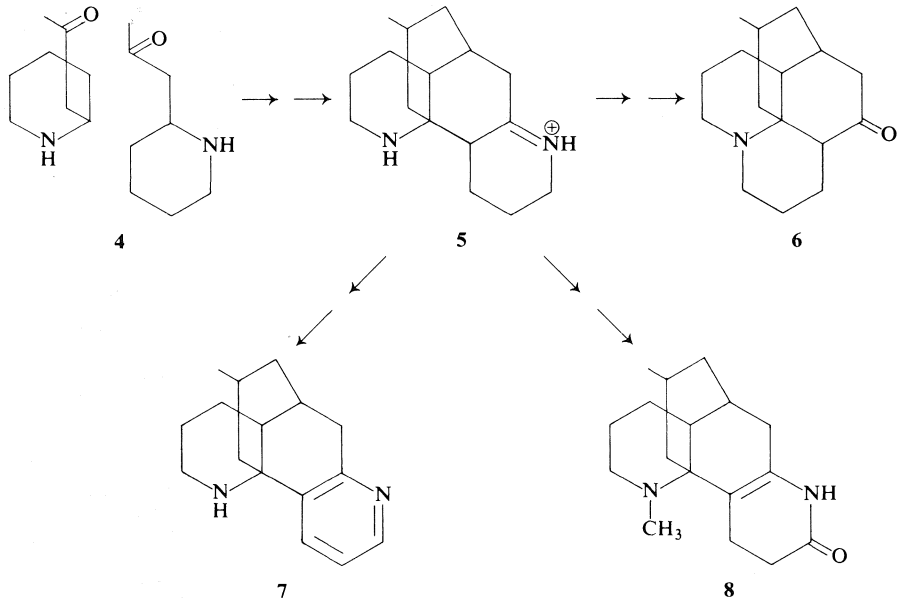

SCHEME. 2. The pelletierine hypothesis of the origin of the Lycopodium alkaloids related to lycopodine.

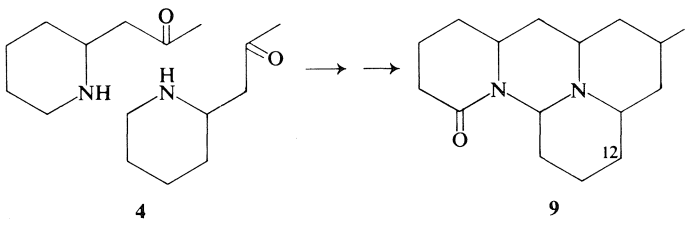

SCHEME 3. The pelletierine hypothesis of the origin of cernuine.

Table 1. In each case cernuine (**9**) isolated from the plants was radioactive, whereas lycocernuine (12-hydroxycernuine), the major alkaloidal component, contained negligible activity.

The ^{3}H:^{14}C ratio of the samples of cernuine from experiments 2 and 6 was determined by liquid scintillation counting. Whereas the ^{3}H:^{14}C ratio of the precursor was maintained in the cernuine derived from the multiply labelled pelletierine (experiment 6), approximately one-third of the tritium, relative to ^{14}C, was lost in the course of incorporation of the multiply

Can. J. Chem. Downloaded from www.nrcresearchpress.com by 210.87.254.42 on 09/05/12
For personal use only.

Can. J. Chem. Downloaded from www.nrcresearchpress.com by 210.87.254.42 on 09/05/12
For personal use only.

TABLE 1. Incorporation of precursors into cernuine

Experiment no.	Compound administered	Nominal total activity (mCi)	Nominal specific activity (mCi/mmol)	Weight of dry plant (g)	Cernuine: Yield* (mg)	Cernuine: Specific activity (counts min^{-1} $mmol^{-1}$) $\times 10^{-4}$
1	2-^{14}C-DL-Lysine†	0.1	3.3	77	12.5	32.1±1.2
2	4,5-$^{3}H_2$,2-^{14}C-DL-Lysine			77	23	16.5±0.8(^{14}C)
	from 4,5-$^{3}H_2$-DL-Lysine†	1.0	5.4×10^3			
	from 2-^{14}C-DL-Lysine†	0.1	3.3			
3	6-^{14}C-DL-Lysine‡	0.1	48	63	20	33.2±1.3
4	1,5-^{14}C-Cadaverine†	0.1	3.2	92	30	27.8±1.2
5	6-^{14}C-Δ^1-Piperideine§	0.1	0.8	92	31	15.8±0.6
	from 6-^{14}C-DL-lysine‡	0.1	48			
6	4-^{3}H,6,2′-$^{14}C_2$-Pelletierine§			164	45	17.8±0.6(^{14}C)
	from 4-^{3}H-Pelletierine§	0.6	10			
	from 6-^{14}C-Pelletierine§	0.03	1			
	from 2′-^{14}C-Pelletierine§	0.02	0.25			

*Total yield, obtained by pooling the samples isolated from wick-fed intact plants and from beaker-fed cuttings.
†New England Nuclear.
‡Commissariat à l'Energie Atomique, France.
§See Experimental.

TABLE 2. Incorporation of lysine, cadaverine, and Δ^1-piperideine into cernuine

Precursor:	2-^{14}C-Lysine		4,5-$^{3}H_2$,2-^{14}C-Lysine		6-^{14}C-Lysine		1,5-^{14}C-Cadaverine		6-^{14}C-Δ^1-Piperideine	
Experiment no.:	1		2		3		4		5	
Product	SA*	RSA†	SA	RSA	SA	RSA	SA	RSA	SA	RSA
Cernuine (9)	2.02±0.06‡	100±3	3.18±0.04‡,§	100±1	3.04±0.03‡	100±1	3.61±0.04‡	100±1	4.02±0.08‡	100±2
2-*n*-Butyl-4-methyl-6-*n*-pentylpyridine (10)	—		2.22±0.02§	70±1	2.22±0.02	73±1	2.66±0.03	74±1	2.15±0.02	54±1
β-Alanine‖(11)	0.48±0.01	24±1								
γ-Aminobutyric acid‖(12)	0.51±0.03	25±2								

*Specific activity (counts min^{-1} $mmol^{-1}$) $\times 10^{-4}$
†Relative specific activity (%) (cernuine = 100).
‡Obtained from the original sample of cernuine, whose specific activity is given in Table 1, by dilution with inactive cernuine.
§Specific activity with respect to ^{14}C.
‖Isolated as the *N*-2,4-dinitrophenyl derivative.

TABLE 3. Incorporation of ^{3}H,^{14}C-labelled precursors

Experiment no.	Precursor	^{3}H:^{14}C Ratio	
		In precursor	In cernuine
2	4,5-$^{3}H_2$,2-^{14}C-DL-Lysine	10.6±0.4	6.5±0.04
6	4-^{3}H,6,2′-$^{14}C_2$-Pelletierine	12.4±0.1	12.2±0.1

TABLE 4. Incorporation of pelletierine into cernuine

4-^{3}H,6,2′-$^{14}C_2$-Pelletierine		Cernuine	
Total activity administered (^{14}C) (d.p.m.) × 10^{-7} in		Specific activity (^{14}C) (counts min^{-1} $mmol^{-1}$) × 10^{-4}	
6-^{14}C-Pelletierine	6.77±0.01		
2′-^{14}C-Pelletierine	4.64±0.01	Kuhn–Roth acetate*	0.81±0.06
Total	11.41±0.01	Intact cernuine†	1.99±0.03
$\frac{2'\text{-}^{14}C}{\text{Total}}$	(41±1)%	$\frac{\text{Kuhn–Roth acetate}}{\text{Intact cernuine}}$	(41±1)%

*Isolated as acetyl-α-naphthylamide.
†Obtained from the cernuine, specific activity (17.8 ± 0.6) × 10^4 counts min^{-1} $mmol^{-1}$ (experiment 6) by dilution with inactive carrier.

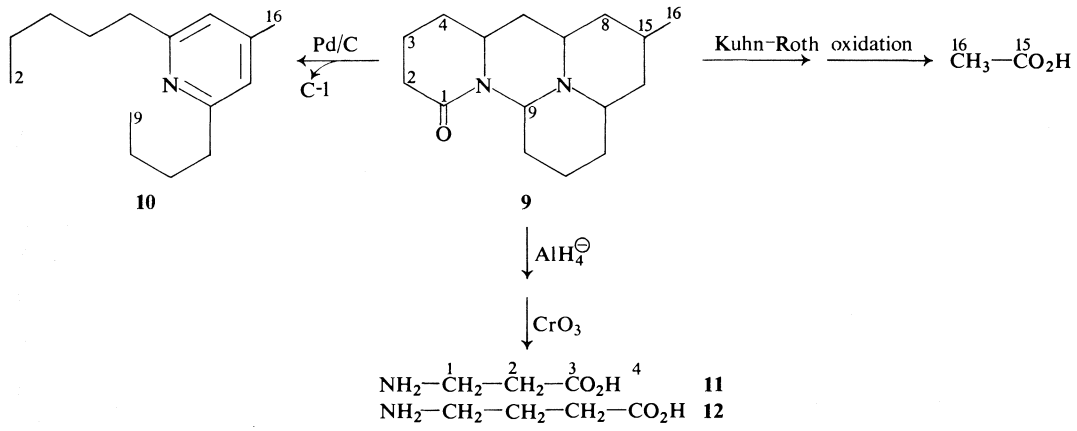

SCHEME 4. Degradation of cernuine (numbers refer to the carbon atoms of cernuine).

labelled lysine into cernuine (experiment 2) (Table 3). To determine the distribution of ^{14}C, the labelled samples of cernuine were partially degraded, by reactions to be discussed presently, into the degradation products shown in Scheme 4. The specific activities of the degradation products are listed in Tables 2 and 4. Indicated limits are standard deviation of the mean.

The samples of 2-*n*-butyl-4-methyl-6-*n*-pentylpyridine (**10**) obtained from cernuine derived from 2-^{14}C-lysine (experiment 2), 6-^{14}C-lysine (experiment 3), and 1,5-^{14}C-cadaverine (experiment 4) retained approximately three-quarters of the activity of the intact alkaloid. The pyridine derivative (**10**) from the cernuine derived from 6-^{14}C-Δ^1-piperideine (experiment 5), contained approximately one-half of the original activity. β-Alanine (**11**) and γ-aminobutyric acid (**12**), recovered from 2-^{14}C-lysine-derived cernuine (experiment 1), contained one-quarter of the original activity. Finally, the fraction of activity recovered in the acetate obtained by Kuhn–Roth

Can. J. Chem. Downloaded from www.nrcresearchpress.com by 210.87.254.42 on 09/05/12
For personal use only.

oxidation of pelletierine-derived cernuine was identical with the fraction of activity at the carbonyl carbon atom of the precursor (experiment 6) (Table 4).

Discussion

Even though degradation of cernuine was only partial and the activity of the intact molecule was not fully accounted for in terms of the activities of degradation products representing individual labelled sites, the results nevertheless support the view that the radioactive precursors were incorporated into cernuine in a manner which is completely analogous to their mode of incorporation into lycopodine.

Lysine enters each of the two C_5 units of lycopodine, C-1 to -5 and C-9 to -13, in a symmetrical manner, and with equal efficiency (2, 4). Cadaverine, a symmetrical molecule and a likely stage of the pathway, is incorporated similarly (4). Analogous entry of lysine and cadaverine into cernuine would be predicted to place activity derived from 2-^{14}C-lysine, from 6-^{14}C-lysine, and from 1,5-^{14}C-cadaverine equally into four sites, C-1, -5, -9, and -13. One quarter of the activity of cernuine, derived from 2-^{14}C-lysine (experiment 2), 6-^{14}C-lysine (experiment 3), and 1,5-^{14}C-cadaverine (experiment 4) was indeed found at C-1 (cernuine minus pyridine derivative (**10**)) (Table 2) (Scheme 5).

In experiment 1 access to C-1 was gained in another manner. Reduction of cernuine with lithium aluminum hydride followed by oxidation of the reduction product with chromic acid gave β-alanine and γ-aminobutyric acid derived, respectively, from C-1 to -3 and C-1 to -4 of cernuine. Both acids, obtained by degradation of cernuine derived from 2-^{14}C-lysine, contained one-quarter of the activity of the intact alkaloid. This result confirms those of the previous experiments in which the activity at C-1 was obtained by difference. The finding of one-quarter of the activity of cernuine at C-1 from cernuine derived from 2-^{14}C-lysine, 6-^{14}C-lysine, and 1,5-^{14}C-cadaverine is in complete analogy with the results found for lycopodine.

Δ^1-Piperideine is another substrate whose specific incorporation into lycopodine has been demonstrated (5). The precursor enters both "halves" of the alkaloid with equal efficiency. Its mode of incorporation differs from that of

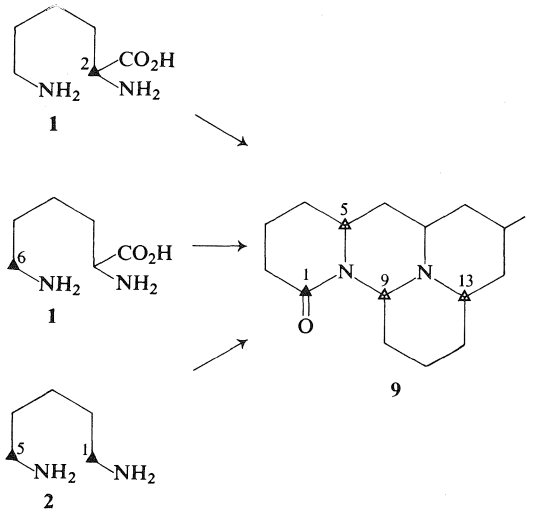

SCHEME 5. Incorporation of lysine (**1**) and cadaverine (**2**) into cernuine. Sites of activity derived from 2-^{14}C- and 6-^{14}C-lysine and from 1,5-^{14}C-cadaverine, established by degradation (▲) (~25% of total activity from each of the three substrates) or inferred (Δ).

lysine in that the individuality of C-2 and -6 of Δ^1-piperideine is preserved in the course of its route into lycopodine. Analogous entry of Δ^1-piperideine into cernuine would be predicted to place label derived from 6-^{14}C-Δ^1-piperideine equally into the two sites, C-1 and -9. In accord with this prediction C-1 of cernuine derived from 6-^{14}C-Δ^1-piperideine was found to account for approximately half the activity of the intact alkaloid (cernuine minus pyridine derivative (**10**)) (experiment 5) (Table 2) (Scheme 6).

The evidence is clearly consistent with the view that cernuine, like lycopodine, is a modified dimer of an intermediate, C_5N—C_3, whose piperidine nucleus is, in turn, derived from lysine (**1**) via

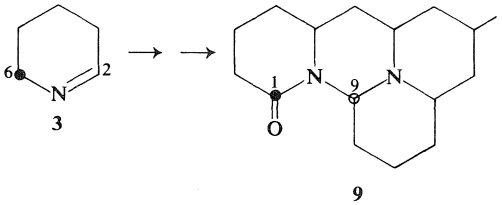

SCHEME 6. Incorporation of Δ^1-piperideine into cernuine. Sites of activity from 2-^{14}C-Δ^1-piperideine, established by degradation (●) (~50%) or inferred (○).

Can. J. Chem. Downloaded from www.nrcresearchpress.com by 210.87.254.42 on 09/05/12
For personal use only.

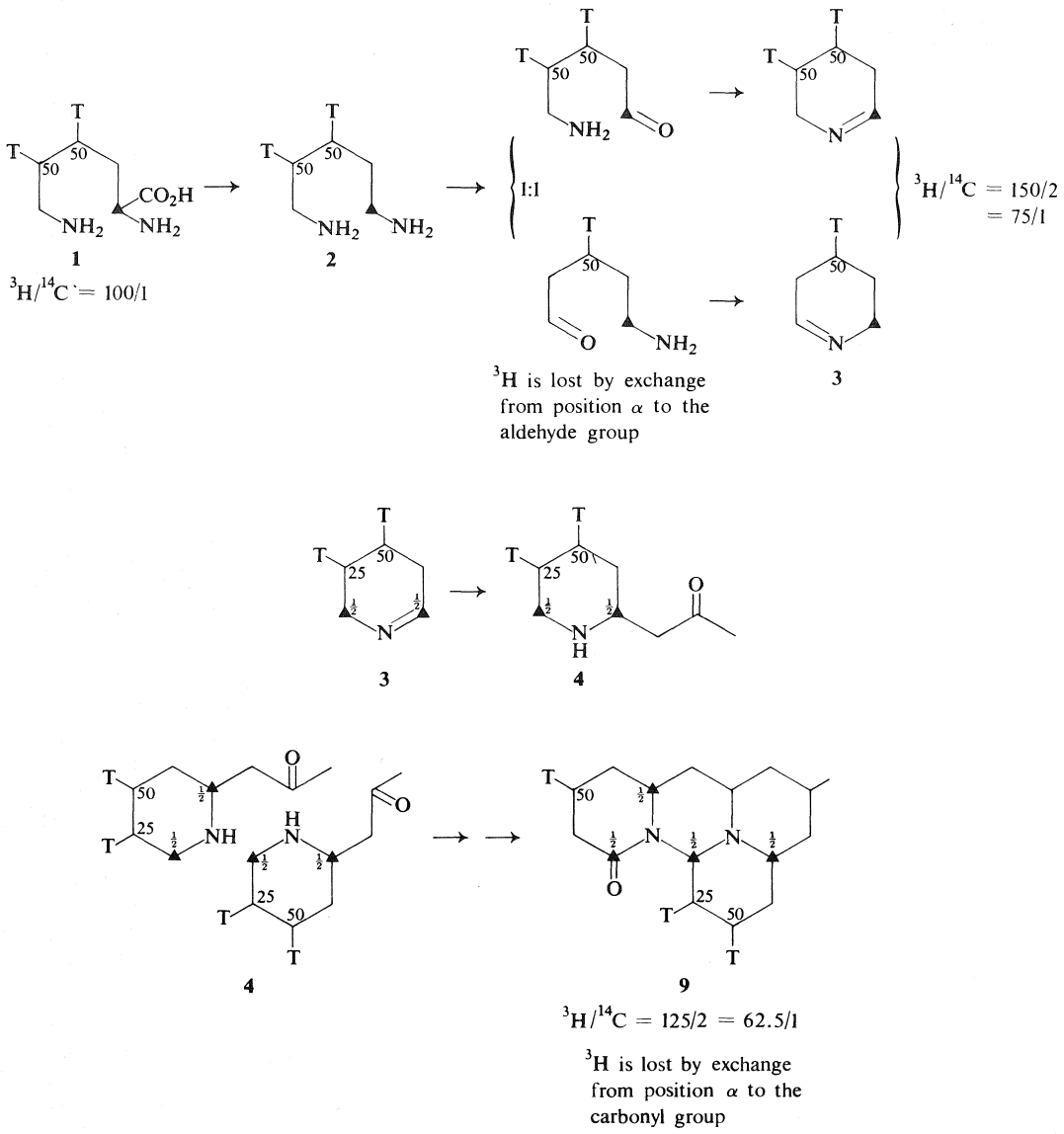

SCHEME 7. Predicted mode of incorporation of 4,5-$^3H_2$,2-^{14}C-lysine into cernuine. (Both of the two $C_5N—C_3$ units, postulated as cernuine precursors, are here arbitrarily represented as pelletierine).

cadaverine (**2**) and Δ^1-piperideine (**3**) (*cf.* Scheme 1).

Further evidence supporting this sequence to cernuine is provided by the result of the feeding experiment with multiply labelled 4,5-$^3H_2$, 2-^{14}C-lysine (experiment 2). As shown in Scheme 7, a loss of 37.5% tritium, relative to ^{14}C, is predicted by the hypothetical sequence to occur in the course of the incorporation of this lysine into cernuine. The observed loss of 39% (experiment 2) (Table 3) is in remarkable agreement with this prediction.

To throw light on the nature of the postulated intermediate, $C_5N—C_3$, a multiply labelled sample of pelletierine (**4**) of known isotope distribution was administered to *L. cernuum* (experi-

Can. J. Chem. Downloaded from www.nrcresearchpress.com by 210.87.254.42 on 09/05/12
For personal use only.

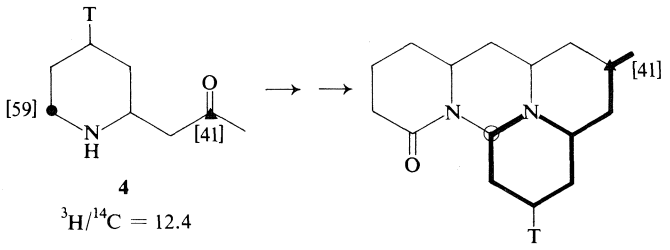

SCHEME 8. Incorporation of pelletierine into cernuine. Sites of activity established by degradation (▲) (~41% of total activity) or inferred (○, T).

ment 6). Consistent with the hypothesis (Scheme 3), that pelletierine was the intermediate whose dimerization leads to cernuine, the ^3H:^{14}C ratio of the precursor was maintained in the product (Table 3). Degradation of the cernuine showed, however, that only one intact pelletierine unit had been incorporated. The acetic acid, obtained from the C_2 unit, C-15,16, of the cernuine by Kuhn–Roth oxidation, contained 41% of the activity of the intact alkaloid, a distribution corresponding to the fraction of ^{14}C-activity within the sidechain of the precursor (Table 4). Entry of two intact pelletierine units would have led to a Kuhn–Roth acetate containing 20% of the activity of the original cernuine. An intact pelletierine moiety thus serves as the precursor of the C_8 unit, C-9 to -16, but not of the C_8 unit, C-1 to -8, of cernuine (Scheme 8). This biosynthetic relationship is entirely analogous to the mode of entry of pelletierine into lycopodine (3, 5). The problems of interpretation, raised by these experimental results, have been discussed (5).

The Chemistry of the Degradation Reactions

The methods used to degrade cernuine are outlined in Scheme 4. Kuhn–Roth oxidation gave C-15 and -16 as acetic acid which was converted to its α-naphthylamide derivative for purification and radioactive assay. Dehydrogenation of cernuine over palladium–charcoal by the method of Ayer *et al.* (6, 7) gave compound **10** which was purified and assayed as its picrolonate. Compound **10** contains all the carbons of cernuine except C-1 and thus the activity at this center is obtained by difference. The third degradation of Scheme 4 in which C-1 is isolated as β-alanine or γ-aminobutyric acid deserves further comment.

The treatment of cernuine with lithium aluminum hydride has been reported to give a single compound, dihydrodeoxycernuine (7). We obtained, however, a small amount (<7%) of an isomer, dihydrodeoxyepiallocernuine (8), in addition to the expected product. Dihydrodeoxyepiallocernuine differs in configuration at C-9 and -13 from dihydrodeoxycernuine but the mechanism by which the isomerization occurs is not known. Fission of the N—C_9 bond does not accompany the reduction of the amide as we suggested earlier (1). Since both isomers are expected to yield the same oxidation products the mixture was oxidized without further purification. β-Alanine and γ-aminobutyric acid were isolated, identified, and assayed for radioactivity as their 2,4-dinitrophenyl derivatives. As shown in Scheme 4 the carbon atoms of the amino acids are expected to be derived from C-1 to -3 and C-1 to -4 of cernuine.

To verify that the amino acids come solely from C-1 to -3 and C-1 to -4 of cernuine we prepared a mixture of dihydrodeoxycernuine-1,1-d_2 and its isomer, subjected the mixture to oxidation, and examined the amino acids for their deuterium content. Deuterium was incorporated into the dihydrodeoxy compounds by carrying out the reaction of cernuine with lithium aluminum deuteride. Two products, both of mass 250, were obtained from this treatment and the ratio of the two, determined by g.l.c., was the same as that obtained in the hydride reduction. Oxidation of the mixture gave β-alanine-d_2 and γ-aminobutyric acid-d_2 isolated as their 2,4-dinitrophenyl derivatives. The mass spectra of the 2,4-dinitro-

Can. J. Chem. Downloaded from www.nrcresearchpress.com by 210.87.254.42 on 09/05/12
For personal use only.

phenyl derivatives showed no evidence of the presence of undeuterated acids. It can be concluded that the degradation proceeds specifically as shown in Scheme 4.

Experimental

Administration of Labelled Compounds to Lycopodium cernuum

Two methods were used for the administration of tracers to *Lycopodium cernuum* L. Firstly, a solution containing the labelled compound was infused through cotton wicks into the stems of intact plants growing in their natural environment. Cotton thread was inserted into the stems and the end of each thread was placed into a small glass beaker. The tracer solution (10 ml) was divided among the beakers and was absorbed by the plants through the wicks. After the original tracer solution had been absorbed, the beakers were repeatedly refilled with glass-distilled water. The plants were kept in contact with the tracer for 48–72 h and were then harvested.

Secondly, fresh cuttings (12–18 in. high) were packed with cut stems downward into a 100 ml beaker. The labelled compound, dissolved in glass-distilled water (10 ml), was added to the beaker. Refilling and harvesting was carried out in the same manner as above.

A summary of the feeding experiments which were carried out is outlined in Table 1.

6-^{14}C-Δ^1-Piperideine (experiment 5) was prepared (5) from 6-^{14}C-DL-lysine (Commissariat à l'Energie Atomique, France). 6-^{14}C-Pelletierine and 4-^{3}H-pelletierine were synthesized by condensation of labelled Δ^1-piperideine prepared from 6-^{14}C-DL-lysine (Commissariat à l'Energie Atomique, France), and from 4-^{3}H-DL-lysine (Commissariat à l'Energie Atomique, France), respectively, with inactive acetoacetic acid (9). 2′-^{14}C-Pelletierine was obtained by condensation of 3-^{14}C-acetoacetic acid (prepared by hydrolysis of ethyl 3-^{14}C-acetoacetate (New England Nuclear)) with Δ^1-piperideine obtained from inactive lysine. An intermolecularly triply labelled sample, 4-^{3}H,6,2′-$^{14}C_2$-pelletierine (experiment 6), was obtained by mixing these samples.

Isolation of Cernuine and Lycocernuine (cf. ref. 7)

Aerial parts of *L. cernuum* were dried and ground to a fine powder in a blendor (Osterizer Galaxie 500). The powder (500 gm) was moistened with ammonia (0.6 *M*, 1 ml/gm) and was continuously extracted with chloroform for 48 h. The chloroform extract was concentrated to one-tenth of its volume and ether was added. The solution was then extracted with hydrochloric acid (0.6 *M*, 5 × 30 ml). The aqueous extract was washed twice with ether, basified with ammonia (1.2 *M*), and was then extracted with chloroform (5 × 25 ml). The chloroform extract was dried (anhydrous sodium sulfate) and concentrated almost to dryness and a small amount of acetone was added. Lycocernuine (110 mg), which precipitated, was recrystallized from acetone and melted at 228–229° (lit. 230–231°)(7).

The mother liquors from the crystallization were dissolved in benzene and applied to a column of neutral alumina, activity I (40 g). Elution with benzene and benzene–ether (1:1) gave a mixture of minor bases. Anhydrous ether then gave cernuine, and elution with chloroform gave lycocernuine. Finally, methanol gave a mixture of minor bases.

The cernuine was sublimed at 110° and 3 × 10^{-3} mm, and was recrystallized from hexane, m.p. 101–102° (lit. 103–104°)(7). In several instances, particularly in the case of radioactive samples, the cernuine was dissolved in ether and the solution was neutralized with an ethereal solution of perchloric acid. The solvent was evaporated and the cernuine perchlorate so obtained was recrystallized from water or from ethanol–ether, and melted at 110° (lit. 110°) (10).

Several variations of the isolation procedure were employed in early experiments. When ether instead of chloroform was used as extracting solvent, the extraction of alkaloids was incomplete. The alkaloid extract, on the basis of g.l.c. analysis, contained twice as much cernuine as lycocernuine whereas the reverse was true when a better solvent such as chloroform (see above) or methanol (see below) was used. Thus when ether was used, only part of the lycocernuine was extracted from the plant material.

Methanol was employed as solvent in large scale batch extraction (7). Finely ground *L. cernuum* was extracted at room temperature with methanol for 36 h and the methanolic extract was concentrated at reduced pressure. Extraction was repeated twice with fresh solvent and the combined extracts were warmed with hydrochloric acid (0.6 *M*). Acid-insoluble material was removed by filtration and was then re-extracted with hydrochloric acid. The filtrates were combined, non-basic material was extracted with ether, and the aqueous layer was made strongly basic with ammonia. The alkaloidal fraction was then extracted into chloroform and worked-up as already described.

Degradation of Cernuine

Reduction of Cernuine (7)

Cernuine (250 mg) was added to a slurry of lithium aluminum hydride (0.50 g) in anhydrous ether (20 ml, dried over sodium hydride), and the resulting mixture was refluxed for 20 h, and was then cooled in ice. Excess hydride was decomposed by dropwise addition of water (0.5 ml) followed by sodium hydroxide (4 *M*, 0.5 ml). More water (1.5 ml) was then added and the mixture was stirred for 20 min, and filtered with suction. The granular precipitate was washed thoroughly with ether and the ethereal filtrate was dried over sodium sulfate and concentrated at reduced pressure. The crystalline residue was sublimed at 100° and 4 × 10^{-3} mm. The mass spectrum of the sublimed product showed a signal, *m/e* 248, which was regarded as due to the molecular ion of the reduction product. However, two components, retention times 2.0 min and 3.2 min, were detected by g.l.c. (1% Carbowax 20 M, coated with 5% KOH on Chromosorb W, 4 ft × 0.125 in., 130–210° at 10°/min and a helium flow rate of 40 ml/min). The retention time of the minor component (< 7%) was 2 min, identical with that of an authentic sample of dihydrodeoxyepiallocernuine.[2] When a sample of the reduction product, mixed with authentic

Can. J. Chem. Downloaded from www.nrcresearchpress.com by 210.87.25.42 on 03/03/15
For personal use only.

Can. J. Chem. Downloaded from www.nrcresearchpress.com by 210.87.254.42 on 09/05/12
For personal use only.

dihydrodeoxyepiallocernuine,[2] was injected, only two components with retention times 2.0 and 3.2 min, respectively, were observed. The intensity of the peak of the minor component increased with the amount of the authentic dihydrodeoxyepiallocernuine added. The major component was regarded as dihydrodeoxycernuine. These two components were not further separated and were used for the oxidation described below. The same procedure was used to prepare the dideuterated compounds, except that lithium aluminum deuteride was substituted for the hydride.

β-Alanine and γ-Aminobutyric Acid from Cernuine

The above reduction product (192 mg) of cernuine was dissolved in hot aqueous sulfuric acid (6 *M*, 4 ml) and chromium trioxide (500 mg) in water (2 ml) was added in several portions. The mixture was heated under reflux with stirring for 48 h. The cooled mixture was extracted several times with ether. The ether layer was rejected. The aqueous layer was diluted with water (10 ml) and warmed, and hot saturated aqueous barium hydroxide solution was added until the solution was neutral. The precipitate was filtered off and washed repeatedly with hot water. The filtrate was evaporated to dryness. The residue was dissolved in water (1 ml) and aqueous sodium bicarbonate (1.2 *M*) was added until the p*H* of the solution was 9. A solution of 1-fluoro-2,4-dinitrobenzene in methanol (10%, *v/v*, 1.5 ml) was then added. The mixture was allowed to stand with occasional shaking for 1 h, the p*H* being maintained at 8–9 with additional bicarbonate solution. After 1 h, water (4 ml) and bicarbonate solution (0.5 ml) were added and excess reagent was removed by extraction with ether (2 × 6 ml). The solution was then acidified with hydrochloric acid (6 *M*) and extracted with ether (3 × 6 ml). The dried (sodium sulfate) ether extract was concentrated and the yellow dinitrophenyl (DNP) amino acids were separated by preparative t.l.c. (silica gel, developed with benzene – pyridine – acetic acid (80:20:2)).

Three yellow bands were observed. The major band showed an R_f value (R_f 0.69) identical with that of an authentic sample of *N*-2,4-dinitrophenyl-β-alanine. A second band (R_f 0.84) corresponded to *N*-2,4-dinitrophenyl-γ-aminobutyric acid. The minor band (R_f 0.28) was not further examined, but may have been *N*-2,4-dinitrophenylglycine. The amino acid derivatives were eluted separately from adsorbent with methanol. The methanolic extract of the β-alanine band (R_f 0.69) which was the most abundant was evaporated to dryness. The residue was dissolved in water (1 ml), hydrochloric acid (6 *M*, 1 ml), was added, and the mixture was extracted with ether (3 × 5 ml). The ether layer was washed with water (2 ml), dried (sodium sulfate), and evaporated to dryness. The residue was sublimed at 160–170° and 1×10^{-3} mm when the DNP derivative of β-alanine was obtained as a yellow crystalline solid; yield, 8 mg. The band of the DNP derivative of γ-aminobutyric acid (R_f 0.84) was worked-up similarly; yield, 5 mg.

The same procedure was applied to the product obtained by reduction of cernuine with lithium aluminum deuteride. The DNP derivatives of β-alanine and γ-aminobutyric acid were analyzed mass spectrometrically showing molecular ions at *m/e* 257 and 271, respectively. There were no peaks at 255 and 269 corresponding to undeuterated acid.

Kuhn–Roth Oxidation of Cernuine

A solution of chromic acid (2 g) in water (3 ml) was added to a solution of cernuine (100 mg) in sulfuric acid (2 *M*, 5 ml). The mixture was heated under reflux for 2 h. Steam was then passed through the mixture until 200 ml of distillate had been collected. The distillate was neutralized with sodium hydroxide (0.1 *M*) and evaporated to dryness. The sodium acetate so obtained was converted into acetyl-α-naphthylamide (11) which was purified by sublimation at 135° and 1×10^{-3} mm. The white sublimate was crystallized from benzene and the product resublimed. Acetyl-α-naphthylamide, m.p. 158–159°, was obtained as colorless needles.

Dehydrogenation of Cernuine (7)

Cernuine (100 mg) was dehydrogenated with 5% palladium-on-charcoal, as described by Ayer *et al.* (7), and the basic products separated by preparative t.l.c. on silica gel (0.5 mm thickness, developed with ether/ammonia (75 ml/2 drops)). The most polar component (R_f 0.65), which was the most abundant one (20 mg), was eluted from the adsorbent with chloroform and subjected to high vacuum distillation at 50° and 4×10^{-3} mm to yield 2-*n*-butyl-4-methyl-6-*n*-pentylpyridine (14 mg), identical with an authentic sample.[2] The pyridine derivative was converted into the picrolonate, which after recrystallization from ethanol–ether melted at 137–139°.

Anal. Calcd. for $C_{25}H_{33}N_5O_5$: C, 62.09; H, 6.88; N, 14.48. Found: C, 62.10; H, 6.91; N, 14.33.

It was also converted into the chloroplatinate, which was recrystallized from ethanol containing a drop of hydrochloric acid. The orange crystals so obtained melted at 186–188° (lit. 189–190°)(7). The minor components of the dehydrogenation were not examined.

Radioactivity Measurements

Radioactivity was assayed on samples of finite thickness on aluminum planchettes with a low background gas flow system (Nuclear Chicago Corporation, Model 4342). Samples were plated with the aid of a 1% solution of collodion in dimethylformamide. The usual corrections for background and self-absorption were applied. The ^3H:^{14}C ratios were measured by liquid scintillation counting (Mark I, Liquid Scintillation Computer, Model 6860, Nuclear Chicago Corporation). Radioactivity due to ^3H and ^{14}C was determined simultaneously by external standardization counting with ^{133}Ba. Samples were dissolved in benzene or methanol and the solution was dispersed in a solution of Liquifluor (Nuclear Chicago Corporation) diluted 25 times with toluene. Duplicate samples of each compound were counted under comparable conditions of quenching. The confidence limits shown in the results (Tables 1–4) are standard deviation of the mean.

We are indebted to many friends and colleagues in Kingston, Jamaica. Without their help this investigation could not have been undertaken. We owe a particular debt of gratitude to Dr. C. D. Adams, Department of

[2]We are greatly indebted to Dr. W. A. Ayer for supplying this sample.

Botony, University of the West Indies, for the taxonomic identification of the species used in our experiments; to Mr. G. R. Proctor, Institute of Jamaica, for permission to use the facilities of the field station of the Institute at Mason River; and to Dr. W. R. Chan, Department of Chemistry, University of the West Indies, and Dr. B. S. Mootoo, Government Analyst, for their unfailing help, generosity and patience. We thank Dr. C.-K. Yu and Miss T. Nguyen of this department for the preparation and analysis of the deuterated compounds.

This work was supported through grants from the National Research Council of Canada.

1. R. N. GUPTA, Y. K. HO, D. B. MACLEAN, and I. D. SPENSER. Chem. Commun. 409 (1970).
2. R. N. GUPTA, M. CASTILLO, D. B. MACLEAN, I. D. SPENSER, and J. T. WROBEL. J. Am. Chem. Soc. **90**, 1360 (1968).
3. M. CASTILLO, R. N. GUPTA, Y. K. HO, D. B. MACLEAN, and I. D. SPENSER. J. Am. Chem. Soc. **92**, 1074 (1970).
4. M. CASTILLO, R. N. GUPTA, D. B. MACLEAN, and I. D. SPENSER. Can. J. Chem. **48**, 1893 (1970).
5. M. CASTILLO, R. N. GUPTA, Y. K. HO, D. B. MACLEAN, and I. D. SPENSER. Can. J. Chem. **48**, 2911 (1970).
6. W. A. AYER, J. K. JENKINS, S. VALVERDE-LOPEZ, and R. H. BURNELL. Tetrahedron Lett. 2201 (1964).
7. W. A. AYER, J. K. JENKINS, S. VALVERDE-LOPEZ, and R. H. BURNELL. Can. J. Chem. **45**, 433 (1967).
8. W. A. AYER, J. K. JENKINS, K. PIERS, and S. VALVERDE-LOPEZ. Can. J. Chem. **45**, 445 (1967).
9. R. N. GUPTA and I. D. SPENSER. Can. J. Chem. **47**, 445 (1969).
10. L. MARION and R. H. F. MANSKE. Can. J. Res. B, **26**, 1 (1948).
11. E. LEETE, H. GREGORY, and E. G. GROS. J. Am. Chem. Soc. **87**, 3475 (1965).

Can. J. Chem. Downloaded from www.nrcresearchpress.com by 210.87.254.42 on 09/05/12
For personal use only.

Can. J. Chem. Downloaded from www.nrcresearchpress.com by 210.87.254.6 on 09/05/12
For personal use only.

The Effect of *S*-Substituent Variation on the Pyrolysis of Xanthates of Primary Alcohols[1]

R. E. GILMAN AND M. J. BOGDANOWICZ

Department of Chemistry, Rochester Institute of Technology, One Lomb Memorial Drive, Rochester, New York

Received June 10, 1971

A study of the pyrolysis of a series of *S*-substituted xanthates of cyclohexanemethanol was undertaken to determine the effect of variations in the nature of the *S*-substituent on the course of the pyrolysis of xanthates. Xanthates with the following *S*-substituents were prepared by standard reactions and pyrolyzed at 240°: *n*-hexyl, 2-phenylethyl, benzyl, phenacyl, and diphenylmethyl. Evidence is presented that supports the view that a competitive homolytic pathway becomes more significant as the stability of the free radical derived from the *S*-substituent increases. At the two extremes, the *S*-hexyl xanthate yields 90% methylenecyclohexane and no cyclohexanemethanol whereas the *S*-diphenylmethyl xanthate yields only 25% alkenes (methylenecyclohexane and 1-methylcyclohexene) along with 65% cyclohexanemethanol.

Une étude a été effectuée sur une série de xanthates de la cyclohexaneméthanol *S*-substitués afin de déterminer l'influence du *S*-substituant sur le cours de la pyrolyse des xanthates. Les xanthates avec les *S*-substituants suivants ont été préparés par des méthodes classiques et pyrolysés à 240°: *n*-hexyle, 2-phénylèthyle, benzyle, phénacyle, et diphénylméthyle. Des preuves sont présentées pour confirmer le fait qu'un processus homolytique compétitif peut devenir plus important si la stabilité du radical libre issu du *S*-substituant augmente. Aux deux extrêmes, le xanthate *S*-hexyle conduit à 90% de méthylènecyclohexane sans trace de cyclohexaneméthanol, alors que le xanthate *S*-diphénylméthyle conduit à seulement 25% d'alcène (méthylènecyclohexane et méthyl-1 cyclohexène) et à 65% de cyclohexaneméthanol.

Canadian Journal of Chemistry, **49**, 3362 (1971)

The pyrolysis of xanthate esters, the Chugaev reaction, has been primarily studied with xanthates that contain an *S*-methyl substituent (1, 2). McAlpine, who was the first to report a systematic study of xanthates with a variety of *S*-substituents, suggested that the presence of electronegative groups on the thiol sulfur decreases the thermal stability of xanthates and this results in a lower initial pyrolysis temperature (3). The order of stability of *S*-substituted xanthates of menthyl alcohol was found to be as follows:

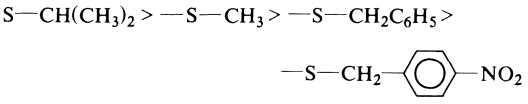

A more recent study by O'Connor and Nace indicated much the same order of stability for *S*-substituted xanthates of cholesterol (4). Kinetic studies of the pyrolysis of these xanthates showed that an increase in the electronegativity of the *S*-alkyl group decreased the stability of the xanthate in the order shown below:

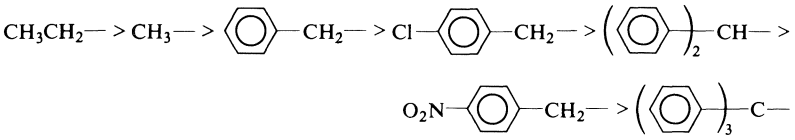

In our earlier studies of *S*-*p*-bromophenacyl xanthates of primary alcohols, we found evidence that an alternate pathway competes with the normal Chugaev elimination when the strongly electronegative *S*-*p*-bromophenacyl group is present (5). Based on a product analysis study we proposed that this alternate pathway involves an initial thermally induced homolysis of the type shown in Scheme 1.

In order to test the validity of this explanation for the formation of these non-Chugaev products, we studied a series of xanthates of cyclohexanemethanol that contained *S*-substituents that would yield homolysis intermediates of considerably different stability. If our initial postulate of a

[1]Presented at the 158th National Meeting of the American Chemical Society, New York, New York, September, 1969.

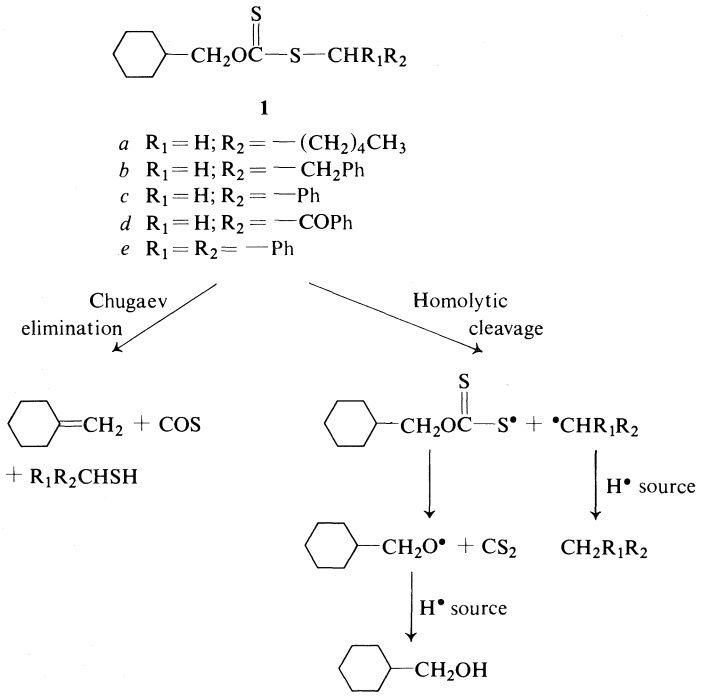

SCHEME I

free radical mechanism is correct, we should observe a direct relationship between the extent of the competitive cleavage and the stability of the free radical generated in the homolytic cleavage of the sulfur–carbon bond. The cyclohexanemethyl group was chosen as the *O*-substituent since the alkene product of the normal Chugaev elimination, methylenecyclohexane, is known to be unstable with respect to rearrangement to 1-methylcyclohexene. Furthermore, these isomeric alkenes are easily separated and analyzed by g.l.p.c. We thus could study both the extent of alkene rearrangement under the pyrolysis conditions and the ratio of Chugaev to non-Chugaev reaction. An additional question of practical interest is the extent of elimination of β-hydrogens of the *S*-alkyl group. Any elimination of this type would lead to alkenes derived from the *S*-alkyl group and be detrimental to the practical synthesis of pure alkenes from primary alcohols.

We now report the results of a study of the pyrolysis of xanthates **1***a–e* that were prepared from cyclohexanemethanol and the respective alkyl halides by standard methods (7, 8). The pyrolyses of these xanthates were carried out in a manner previously described (5) and the products were analyzed by gas chromatographic methods (see Experimental). The results are shown in Table 1. The most striking feature of these results is the overall variation in alkene and cyclohexanemethanol yields as the nature of the *S*-substituent is changed. The total yield of alkene (methylenecyclohexane plus 1-methylcyclohexene) is greatest for those *S*-substituents that would lead to the least stable free radicals if the homolytic pathway proposed in Scheme 1 were followed. Thus the total alkene yield decreases in the following order:

$$-S(CH_2)_5CH_3 \simeq -S-CH_2CH_2Ph > -S-CH_2Ph > -S-CH_2\overset{O}{\overset{\|}{C}}Ph > -S-CHPh_2$$

With the exception of the *S*-phenacyl group, for which no data concerning the relative stability of the corresponding phenacyl radical could be found, this order is the inverse of the order of stability of the free radicals derivable from the homolytic cleavage of the sulfur–carbon bond (9).

The variations in the yields of cyclohexanemethanol with change in the *S*-substituent are equally striking. In this case the alcohol yields are

Can. J. Chem. Downloaded from www.nrcresearchpress.com by 210.87.254.6 on 09/05/12
For personal use only.

TABLE 1. Products of the pyrolysis of 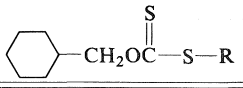

	R				
Product*	$-CH_2(CH_2)_4CH_3$	$-CH_2CH_2Ph$	$-CH_2Ph$	$-CH_2\overset{O}{\overset{\|}{C}}-Ph$	$-CHPh_2$
	89 ± 10	80 ± 15	54 ± 4	18 ± 4	20 ± 5
	3 ± 2	—	14 ± 2	15 ± 2	6 ± 4
	0–1	5 ± 1	7 ± 3	50 ± 3	63 ± 6
$Ph-CH_3$	—	—	27 ± 5	17 ± 1	15 ± 4
RSH	91 ± 3	81 ± 8	92 ± 4	—	—
1-Hexene	2 ± 1				
$PhCH=CH_2$		5 ± 2			
$CH_3\overset{O}{\overset{\|}{C}}-Ph$				76 ± 1	
Ph_2CH_2					81 ± 16

*Yields are reported as percentages of theoretical yields and are averages of results from 4 pyrolyses.

[1] 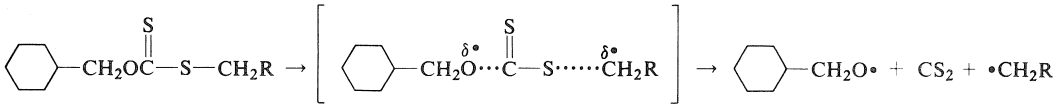

directly proportional to the order of stability of the *S*-substituents as free radicals and are inversely proportional to the order of total alkene yields. The combined variations in alkene and alcohol yields thus lend strong support to our proposal that the alternative pathway shown in Scheme 1 is correct. Whether or not the homolysis is a step-wise sequence (Scheme 1) or involves a concerted homolysis of the C—O and S—C bonds (eq. 1) cannot be determined from present data. Whether step-wise or concerted, the transition state for the homolysis must involve the formation of an incipient free radical from the *S*-substituent of the xanthate. Only in this way could the relative stability of the *S*-substituent as a free radical have such a dramatic effect on the course of the xanthate pyrolysis.

An alternative explanation for these results could involve the formation of ion pairs, rather than radical pairs. Detailed kinetic studies would be needed in order to distinguish between these possibilities (effect of solvent type on reaction rates), but our results with the *S*-phenacyl group are indicative that the radical pair is the correct choice. The formation of an ion pair with positive charge build-up on the carbon adjacent to the carbonyl carbon would be particularly unfavorable. We would thus expect the *S*-phenacyl xanthate to give a much higher yield of alkene, and correspondingly lower yield of alcohol, than the *S*-benzyl xanthate if the ion pair mechanism were operative.

The yields of toluene observed in the distillates are also dependent on the nature of the *S*-substituent. The absence of toluene in the pyrolysates of the *S*-hexyl and *S*-2-phenylethyl xanthates, that pyrolyze smoothly without tar formation, and the presence of substantial amounts in all other cases strongly suggests that toluene is formed in secondary reactions (dehydrogenation of the alkenes) that are significant only when tarry by-products are formed. In the *S*-benzyl xanthate, toluene would also be formed via homolytic cleavage of the carbon–sulfur bond followed by hydrogen abstraction from some donor species. However, since the non-Chugaev pathway is oc-

Can. J. Chem. Downloaded from www.nrcresearchpress.com by 210.87.254.6 on 09/05/12
For personal use only.

Can. J. Chem. Downloaded from www.nrcresearchpress.com by 210.87.254.6 on 09/05/12
For personal use only.

curring to only about 7% of the total reaction (as determined from the yield of cyclohexanemethanol), most of the toluene formed in this case must also be derived from the alkenes.

The phenacyl and diphenylmethyl mercaptans were not isolated. Phenacyl mercaptan would be expected to decompose under the reaction conditions in a manner similar to that found for *p*-bromophenacyl mercaptan to yield acetophenone along with considerable tar (5). The acetophenone formed in the pyrolysis of xanthate **1***d* must, therefore, be formed via both the non-Chugaev pathway (about 50% based on the yield of cyclohexanemethanol) and the thermal decomposition of the phenacyl mercaptan formed from the normal Chugaev pathway. Diphenylmethyl mercaptan would also be expected to decompose at these temperatures since diphenylmethyl disulfide is known to thermally decompose to thiobenzophenone and diphenylmethane (6). Thus the diphenylmethane formed in the pyrolysis of xanthate **1***e* probably arises from both the homolytic pathway (about 60% based on the yield of cyclohexanemethanol) and the normal Chugaev pathway.

Finally, from a practical viewpoint, the extent of alkene rearrangement and formation of alkenes derivable from the *S*-substituent of the xanthate are of importance. While the variation in alkene rearrangement is not as regular as are the variations in total alkene and alcohol yields, the trend is clear. Those xanthates that undergo clean pyrolysis without tar formation (*S*-hexyl and *S*-2-phenylethyl) yield little or no rearranged alkene (1-methylcyclohexene). Those xanthates that undergo pyrolysis by both pathways (plus tar formation) yield considerably more rearranged alkene. We have previously demonstrated that the pyrolysis residue promotes the rearrangement of methylenecyclohexane to 1-methylcyclohexene (5). Low yields of 1-hexene and styrene were observed for the two xanthates that contain *S*-substituents with hydrogens beta to the sulfur. Whether these alkenes were formed through β-elimination via the *S*-alkyl group of the xanthate or subsequent elimination of hydrogen sulfide from the mercaptan products is not known.

In view of these results, it is now apparent that the course of primary alcohol xanthate pyrolysis can be controlled by proper choice of the *S*-substituent. The use of *S*-substituents larger than methyl enables the formation of crystalline xanthates that can be purified more readily than can high boiling oils. Smooth pyrolysis to alkenes should then take place as long as the *S*-substituent does not lead to a relatively stable free radical via homolysis of the carbon–sulfur bond.

Experimental

Melting points were taken on a Fisher–Johns Melting Point Apparatus and are corrected. Boiling points are uncorrected. The i.r. spectra were recorded on a Perkin–Elmer Model 257 recording spectrophotometer. The n.m.r. spectra were recorded on a Hitachi Model R-20 spectrometer and chemical shift data are given in p.p.m. downfield (δ) from tetramethylsilane as an internal standard (multiplicity: s, singlet; d, doublet; t, triplet; m, multiplet). Elemental analyses were performed by Baron Consulting Company, Orange, Connecticut.

Sodium Cyclohexylmethyl Xanthate (2)

Cyclohexanemethanol (57 g, 0.5 mol) was added dropwise (15 min) to a suspension of sodium hydride (24.4 g, 0.6 mol of 56% oil dispersion) in 150 ml of anhydrous ether. The mixture was stirred for 15 min and then carbon disulfide (76 g, 1.0 mol) was added with stirring and cooling over a period of 45 min. Additional portions of ether (250 ml total) were added as needed to keep the suspension fluid. Stirring was continued for 30 min and then the solid product (115 g) was collected by filtration and purified in 10 g portions. The crude sodium salt (10 g) was dissolved in reagent anhydrous acetone (25 ml) and filtered to remove impurities. Concentration of this solution to 10 ml and dilution with anhydrous ether (500 ml) resulted in the formation of 5.8 g of crystalline material after refrigeration overnight. Concentration of the filtrate to 50 ml, followed by the addition of 200 ml of anhydrous ether, gave an additional 1.6 g. The total yield of 7.4 g represents an 80% conversion of the starting alcohol to crystalline sodium xanthate (**2**). This salt was used for the preparation of all of the cyclohexylmethyl *S*-substituted xanthates without characterization or further purification.

Cyclohexylmethyl S-Hexyl Xanthate (1a)

Sodium cyclohexylmethyl xanthate (**2**) (26.6 g, 0.125 mol) was dissolved in anhydrous reagent acetone (50 ml). 1-Bromohexane (18.1 g, 0.110 mol) was added rapidly to the solution and mixed for 2 h at room temperature. Ice water (200 ml) was added and the water–acetone layer decanted from the resulting oil. The oil was dissolved in ether (200 ml), dried over calcium chloride, filtered, and the ether evaporated to yield a yellow oil (27.3 g, 91%): b.p. 142°/0.5 mm; ν_{max} (neat) 2937, 2862, 1453, 1382, 1221, 1065, 972, 939, 913, 892, 846, 729 cm^{-1}; n.m.r. ($CDCl_3$), δ 0.75–2.00 (22H, broad m), 3.07 (2H, t, J = 7 Hz, SCH_2), 4.32 (2H, d, J = 6 Hz, OCH_2).

Anal. Calcd. for $C_{14}H_{26}OS_2$: C, 61.29; H, 9.55; S, 23.37. Found: C, 61.58; H, 9.25; S, 23.72.

Cyclohexylmethyl S-2-Phenylethyl Xanthate (1b)

Sodium cyclohexylmethyl xanthate (**2**) (18.5 g, 0.08 mol) was dissolved in anhydrous acetone (150 ml). 1-Bromo-2-phenylethane (14.8 g, 0.08 mol) was added

rapidly and the solution was stirred for 10 min. The addition of cold water (300 ml) yielded an oil that solidified on cooling. Recrystallization from 95% ethanol gave 16.2 g (74%) of crystalline **1***b*: m.p. 43.0–43.5°; ν_{max} (melt) 3090, 3068, 3031, 2928, 2855, 1609, 1496, 1448, 1228, 1062, 969, 934, 911, 890, 844, 828 cm^{-1}; n.m.r. ($CDCl_3$), δ 0.75–2.00 (11H, broad m), 3.09 (4H, m, SCH_2CH_2), 4.31 (2H, d, J = 6 Hz, OCH_2), 7.13 (5H, s, phenyl).

Anal. Calcd. for $C_{16}H_{22}OS_2$: C, 65.26; H, 7.53; S, 21.78. Found: C, 65.13; H, 7.49; S, 21.82.

Cyclohexylmethyl S-Benzyl Xanthate (1c)

Sodium cyclohexylmethyl xanthate (**2**) (25.0 g, 0.118 mol) was dissolved in anhydrous acetone (100 ml). Benzyl bromide (17.1 g, 0.10 mol) was added rapidly and the solution was stirred for 15 min. Cold water (350 ml) was added and the water–acetone layer was decanted from the precipitated oil. An ether solution of this oil was dried ($CaCl_2$) and evaporated to give a brilliant yellow oil (25.7 g, 92%): b.p. 175°/0.4 mm; ν_{max} (neat) 3096, 3070, 3039, 2935, 2860, 1605, 1499, 1453, 1225, 1062, 972, 936, 916, 856, 770, 700 cm^{-1}; n.m.r. ($CDCl_3$), δ 0.75–2.00 (11H, broad m), 4.19 (2H, s, SCH_2), 4.23 (2H, d, J = 6 Hz, OCH_2), 7.06 (5H, s, phenyl).

Anal. Calcd. for $C_{15}H_{20}OS_2$: C, 64.27; H, 7.19; S, 22.88. Found: C, 64.56; H, 7.34; S, 22.63.

Cyclohexylmethyl S-Phenacyl Xanthate (1d)

A solution of 1-bromoacetophenone (19.9 g, 0.10 mol) in anhydrous acetone (50 ml) was added rapidly to a solution of **2** (25.0 g, 0.12 mol) in anhydrous acetone (100 ml). The solution was stirred for 15 min and then diluted with cold water (300 ml). The oil that precipitated solidified on standing at −5°. Recrystallization from ethanol–ether gave 19.3 g (64%) of crystalline **1***d*: m.p. 36–37°; ν_{max} (melt) 3062, 2929, 2855, 1688, 1599, 1581, 1450, 1237, 1060, 988, 750, 690 cm^{-1}; n.m.r. ($CDCl_3$), δ 0.75–2.00 (11H, broad m), 4.26 (2H, d, J = 6 Hz, OCH_2), 4.55 (2H, s, SCH_2), 7.6 (5H, m, phenyl).

Anal. Calcd. for $C_{16}H_{20}O_2S_2$: C, 62.33; H, 6.54; S, 20.79. Found: C, 62.11; H, 6.39; S, 20.63.

Cyclohexylmethyl S-Diphenylmethyl Xanthate (1e)

Sodium cyclohexylmethyl xanthate (**2**) (21.2 g, 0.10 mol) and chlorodiphenylmethane (20.2 g, 0.10 mol) were placed in a 1 l flask with anhydrous reagent acetone (375 ml). This solution was refluxed on a steam bath for 22 h. Ice water (600 ml) was added and a precipitate formed. The water–acetone solution was decanted from the oil and the oil was dissolved in ether, dried ($MgSO_4$), filtered, and the ether evaporated to give a yellow–green oil. Crystallization of this oil from 95% ethanol gave 15.9 g (44%) of **1***e*: m.p. 35–37°; ν_{max} (melt) 3090, 3065, 3032, 2930, 2855, 1601, 1495, 1450, 1236, 1053, 970, 931, 911, 781, 749, 699 cm^{-1}; n.m.r. ($CDCl_3$), δ 0.75–2.00 (11H, broad m), 4.21 (2H, d, J = 6 Hz, OCH_2), 6.00 (1H, s, SCH), 7.19 (10H, s, phenyl).

Anal. Calcd. for $C_{21}H_{24}OS_2$: C, 70.77; H, 6.78; S, 17.99. Found: C, 70.59; H, 6.75; S, 18.11.

Pyrolysis of Xanthates

All pyrolyses were carried out at 240° until gas evolution stopped (2–4 h) in the apparatus that has been described in a previous publication (5).

Analysis of Pyrolysis Products

The components of the pyrolysis mixtures (distillate) were separated by preparative scale g.l.p.c. on a Varian 1520B gas chromatograph using a 10 ft × 3/8 in. column of 15% Carbowax 20M on Chromosorb W, 30–60 mesh. Comparison of the i.r. spectra of these collected compounds with those of authentic samples showed the mixture to consist of the components shown in Table 1. Quantitative gas chromatographic analysis was done with the Perkin–Elmer 800 gas chromatograph with a 12 ft × 1/8 in. column of 15% Carbowax 20M on Chromosorb W, 30–60 mesh. The area normalization method was used to compute the yields shown in Table 1.

We gratefully acknowledge financial support from the Undergraduate Research Participation Program of the National Science Foundation (Grants GY 2889 and GY 4610) and the donors of The Petroleum Research Fund (Grant 2849-B), administered by the American Chemical Society.

1. C. H. DePuy and R. W. King. Chem. Rev. **60**, 431 (1960).
2. H. R. Nace. Org. React. **12**, 57 (1962).
3. I. M. McAlpine. J. Chem. Soc. 906 (1932).
4. G. L. O'Connor and H. R. Nace. J. Am. Chem. Soc. **75**, 2118 (1953).
5. R. E. Gilman, J. D. Henion, S. Shakshooki, J. I. H. Patterson, M. J. Bogdanowicz, R. J. Griffith, D. E. Harrington, R. K. Crandall and K. T. Finley. Can. J. Chem. **48**, 970 (1970).
6. H. Wuyts. Chem. Ber. **36**, 863 (1903).
7. J. Berger and I. Uldall. Acta Chem. Scand. **18**, 1353 (1964).
8. J. D. Roberts and C. W. Sauer. J. Am. Chem. Soc. **71**, 3925 (1949).
9. W. A. Pryor. Radical reactions. McGraw-Hill, New York, N.Y., 1966.

Can. J. Chem. Downloaded from www.nrcresearchpress.com by 210.87.254.6 on 09/05/12
For personal use only.

Determination of the Bond Dissociation Energy $D(C_2H_5Hg—C_2H_5)$ by the Toluene Carrier Method

A. C. LALONDE AND S. J. W. PRICE

Department of Chemistry, University of Windsor, Windsor, Ontario

Received June 9, 1971

The pyrolysis of diethylmercury has been studied in a toluene carrier flow system from 601 to 673 °K using total pressures of 1.04 to 7.75 mm. The progress of the reaction was followed by measuring the amounts of unreacted alkyl. Partial solution of butane in the toluene condensed at the outlet of the reactor made full product analysis difficult. Complete analysis in a number of runs did yield a good material balance between alkyl decomposed and $C_4H_{10} + \frac{1}{2}(C_2H_6 + C_2H_4 +$ *n*-propylbenzene).

[1] $$Hg(C_2H_5)_2 \rightarrow HgC_2H_5 + C_2H_5$$

[3] $$C_2H_5 + C_6H_5CH_3 \rightarrow C_2H_6 + C_6H_5CH_2$$

[4] $$2C_2H_5 \rightarrow C_4H_{10}$$

[5] $$2C_2H_5 \rightarrow C_2H_4 + C_2H_6$$

The Arrhenius equation for reaction 1, $\log k_1(s^{-1}) = 15.4 - (45\,700 \pm 1\,000)/2.3\,RT$, is in excellent agreement with that estimated by Benson and O'Neal. Based on a number of simplifying approximations, $\log k_3(cm^3\ mol^{-1}\ s^{-1}) = 10.9 - (9\,300 \pm 2\,000)/2.3\,RT$. The estimated disproportionation to combination ratio, $k_5/k_4 = 0.09 - 0.12$ is in good agreement with earlier work.

Approximate correction of E_1 to absolute zero yields $D(C_2H_5Hg—C_2H_5) = 43.7$ kcal mol^{-1} and therefore by difference $D(Hg—C_2H_5) = 6.5$ kcal mol^{-1}.

La pyrolyse du diéthylmercure a été étudiée dans un système ou le courant porteur est le toluène, entre 601 et 673 °K et en utilisant des pressions totales de 1.04 à 7.75 mm. L'avancement de la réaction est suivie en mesurant la quantité d'alkyle n'ayant pas réagi. La condensation de solution de butane dans le toluène, à la sortie du réacteur, rend dificile l'analyse complète des produits. L'analyse complète sur plusieurs essais, donne un bon équilibre au point de vue produit entre la décomposition de l'alkyle et $C_4H_{10} + \frac{1}{2}(C_2H_6 + C_2H_4 +$ *n*-propylbenzène)

[1] $$Hg(C_2H_5)_2 \rightarrow HgC_2H_5 + C_2H_5$$

[3] $$C_2H_5 + C_6H_5 \rightarrow C_2H_6 + C_6H_5CH_2$$

[4] $$2C_2H_5 \rightarrow C_4H_{10}$$

[5] $$2C_2H_5 \rightarrow C_2H_4 + C_2H_6$$

L'équation d'Arrhenius pour la réaction 1, $\log k_1\ (s^{-1}) = 15.4 - (45\,700 \pm 1\,000)/2.3\,RT$, est en excellent accord avec celle estimée par Benson et O'Neal. Fondé sur un certain nombre de simplifications approximatives $\log k_3\ (cm^3\ mol^{-1}s^{-1}) = 10.9 - (9\,300 \pm 2\,000)/2.3RT$. L'estimation du rapport dismutation sur combinaison, $k_5/k_4 = 0.09 - 0.12$ est en bon accord avec un travail précédent.

L'extrapolation approximative de E_1 ou zéro absolu donne $D(C_2H_5Hg—C_2H_5) = 43.7$ kcal mol^{-1} d'où par différence $D(Hg—C_2H_5) = 6.5$ kcal mol^{-1}.

Canadian Journal of Chemistry, **49**, 3367 (1971)

Introduction

Three previous investigations of the pyrolysis of diethylmercury have been reported. In a nitrogen carrier flow system (1) over the temperature range 593–693 °K the decomposition was essentially homogeneous. Total pressures of 10 ± 1 mm were used with contact times of 0.1 to 0.3 s. Under these experimental conditions, it is unlikely that the reactant gases reached thermal equilibrium until an appreciable part of the reaction zone had been traversed. In some experiments a partial pressure of 0.4 mm of toluene was added. The presence of toluene was reported to have no effect on the rate constant, the ethane/ethylene ratio (approximation 1) or the C_4/C_2 ratio (approximation 4). These ratios were independent of temperature. The mechanism proposed both in the presence and absence of toluene involved, in addition to the decomposition steps, only the combination and disproportionation of C_2H_5.

The extent of decomposition was measured both by the mercury produced and by $C_4H_{10} + \frac{1}{2}(C_2H_4 + C_2H_6)$. Good agreement was ob-

Can. J. Chem. Downloaded from www.nrcresearchpress.com by 210.87.254.42 on 09/05/12
For personal use only.

Can. J. Chem. Downloaded from www.nrcresearchpress.com by 210.87.254.42 on 09/05/12
For personal use only.

tained between the two methods. The Arrhenius equation obtained was log k (s^{-1}) = 14.1 − (42 500/2.3 RT). If the activation energy is accepted as a reasonable measure of $D_1(C_2H_5Hg—C_2H_5)$ then by difference $D_2(C_2H_5—Hg)$ = 7.7 kcal mol^{-1} (2) (approximate correction to 0 °K would give D_1 = 40.5 kcal mol^{-1} and therefore D_2 = 9.7 kcal mol^{-1}). An earlier study (3) using essentially the same experimental procedures gave a slightly lower activation energy, 41.5 kcal mol^{-1}, but should be considered only as a preliminary investigation to the work discussed above.

A static system study (4) carried out between 496–566 °K using pressures of 1–10 mm gave log k (s^{-1}) = 14.4 − (41 900/2.3 RT). Extrapolation to higher temperatures yields rate constants about a factor of two greater than those observed in the N_2 carrier work. A zero order heterogeneous reaction with an activation energy of 22.1 kcal mol^{-1} was also reported.

Experimental

Materials

(*a*) Toluene from sulfonic acid (Eastman Organic X325) was prepared for use by refluxing over sodium under vacuum and then degassing twice by bulb-to-bulb distillation.

(*b*) Diethylmercury was prepared by a standard Grignard reaction using ethyl magnesium iodide and mercuric chloride. The resulting ether solution was dried over $CaCl_2$, fractionally distilled and the alkyl stored under its own vapor pressure. Vapor pressure data are given in Table 1. These data are in good agreement with previous data (5) and yield ΔH_{298}(vap) = 10.7 kcal mol^{-1} *cf.* the N.B.S. selected value (6) of 10.8 kcal mol^{-1}.

Apparatus and Procedure

The present work was carried out in a toluene carrier flow system using contact times selected to minimize both thermal equilibrium and diffusion errors (7, 8). In order to check for surface effects a vessel packed with quartz tubes was used. This vessel had a volume of 117 cm^3. The unpacked vessel used had a volume of 165 cm^3. The surface-to-volume ratios of the unpacked and packed vessels were respectively 1.25 and 21.2 cm^2/cc. Before use, the packing material and both vessels were treated with boiling concentrated nitric acid and vacuum baked without rinsing.

TABLE 1. Vapor pressure data for diethylmercury

t (°C)	p(mm)
0.0	0.55
14.3	1.40
21.0	2.20
44.0	8.90
62.0	22.00

Refrigerated traps at the outlet of the furnace were intended to remove toluene, unreacted alkyl, *n*-propylbenzene, dibenzyl and related compounds while allowing ethane, ethylene, butane, and other minor gaseous products to be collected in a gas burette. The products from the gas burette were analyzed using a Perkin–Elmer 154 gas chromatograph, equipped with a 1/4 in. × 6 ft silica gel column. A flow rate of He of 60 cc/min was used with a column temperature of 80 °C.

A Perkin–Elmer 800 gas chromatograph was used to analyze the condensed toluene for *n*-propylbenzene and residual alkyl. The analyses were carried out on a 0.02 in. × 150 ft polypropylene glycol open tubular column at 60 °C using a flow rate of N_2 of 10 cc/min. Following most runs the toluene in the traps was warmed to room temperature and then frozen down into a single trap to ensure collection of all residual alkyl. In selected runs where the toluene was to be analyzed for dissolved butane in addition to alkyl and *n*-propylbenzene, the toluene was allowed to warm to only −5 °C. This temperature was high enough to prevent loss of alkyl by fractional crystallization and low enough to minimize loss of butane before analysis. In these runs the 1 μl syringe used for injecting the gas chromatography sample was precooled to −10 °C.

The standard mixture needed for calibration of the gas chromatographs were prepared by standard gravimetric and volumetric procedures with the exception of the butane standard for the Perkin–Elmer 800. To prepare this standard a known weight of toluene was allowed to flow through the system and condense in a trap cooled by an acetone and Dry Ice bath in the same manner as in an ordinary run. The acetone and Dry Ice bath was replaced by a liquid N_2 bath. A known quantity of butane was distilled on to the toluene by replacing the toluene bulb with a butane vessel and allowing the butane to flow through the system in the same way as the toluene. After the distillation was complete, the liquid N_2 bath was replaced with the acetone and Dry Ice bath. About 75% of the butane then went into solution with the toluene and the remainder was collected and measured in the gas burette. The amount of butane recovered was subtracted from the initial amount distilled into the toluene. Consequently, the concentration of butane in toluene was known. This liquid standard was then removed from the system and analyzed under the same conditions as the liquid samples collected at the end of a run. It was felt that preparing and handling the standard in this way would duplicate systematic errors and lead to a more meaningful calibration.

Results and Discussion

The full experimental results are given in Table 2. They may be discussed in terms of the following mechanism.

[1] $$Hg(C_2H_5)_2 \rightarrow HgC_2H_5 + C_2H_5$$

[2] $$HgC_2H_5 \rightarrow Hg + C_2H_5$$

[3] $$C_2H_5 + C_6H_5CH_3 \rightarrow C_2H_6 + C_6H_5CH_2$$

Can. J. Chem. Downloaded from www.nrcresearchpress.com by 210.87.254.42 on 09/05/12
For personal use only.

TABLE 2. Pyrolysis of diethylmercury

Temperature (°K)	P (mm)	Time* (min)	t_c	Toluene / Alkyl (molar ratio)	Alkyl used (moles × 10^4)	Residual alkyl (moles × 10^4)	Products (moles × 10^4) C_2H_6	C_2H_4	C_4H_{10}‡	*n*-Propyl§ benzene	k_g† (s^{-1})	k_m† (s^{-1})
673	6.14	4,55,8	1.47	208/1	2.740	0.026	0.700	0.356	0.462	0.361	0.38	3.16
672	6.20	4,55,4	1.30	176/1	3.459	0.046			0.437	0.302		3.32
668	4.71	3,53,4	1.52	63/1	6.190	0.119	0.802	0.384	2.439	0.434	0.49	2.59
668	4.65	3,43,4	1.71	109/1	2.537	0.036	0.496	0.291	1.364	0.309	0.82	2.49
663	6.08	3,53,4	1.38	94/1	5.985	0.343	0.891	0.382	2.295	0.214	0.51	2.07
661	6.30	3,29,3	1.60	26/1	9.890	0.754	1.252	0.779	1.030	0.621	0.16	1.62
660	6.25	3,25,2	1.61	48/1	4.840	0.375	0.708	0.410	0.471	0.398	0.18	1.59
660	4.69	3,23,4	1.54	61/1	2.747	0.336	0.538	0.285	1.090	0.233	0.57	1.37
659	3.07	3,23,4	1.13	63/1	2.634	0.396	0.410	0.215	1.534	0.287	1.36	1.67
659	3.14	3,23,4	1.20	72/1	1.999	0.288	0.342	0.168	1.186	0.168	1.19	1.61
659	4.17	3,23,4	1.42	62/1	2.640	0.239	0.424	0.226	1.165	0.176	0.64	1.69
659	6.24	4,64,4	1.33	183/1	3.959	0.443	0.791	0.340	0.151	0.519	0.21	1.66
658	6.10	3,51,4	1.42	131/1	4.050	0.499	0.912	0.382	2.641t	0.317	1.34	1.47
657	7.00	3,43,4	1.48	142/1	3.460	0.417	0.551	0.220	1.432	0.350	0.58	1.43
657	6.42	4,40,3	1.58	52/1	7.490	0.749	0.910	0.472	0.504	0.409	0.13	1.43
656	7.75	4,50,3	1.51	61/1	10.198	1.387	1.561	0.780	0.697	0.756	0.17	1.31
656	6.14	2,26,2	1.56	57/1	4.300	0.454	0.421	0.240	0.382	0.304	0.14	1.44
654	4.72	3,52,4	1.51	81/1	4.840	0.601	0.770	0.353	1.698	0.459	0.48	1.39
654	3.51	3,23,4	1.40	73/1	1.910	0.325	0.442	0.240	1.083	0.208	1.14	1.27
654	4.75	3,53,4	1.74	64/1	5.447	0.473	0.722	0.351	2.334			1.40
654	4.39	5,30,5	1.72	54/1	3.420	0.392	0.522	0.270	1.516	0.244	0.52	1.26
654	6.00	7,52,5	1.47	170/1	3.030	0.469	0.583	0.237	1.068			1.27
653	6.14	4,64,4	1.31	223/1	3.270	0.625	0.779	0.272	0.417	0.118	0.28	1.22
652	6.14	2,26,2	1.70	58/1	3.920	0.604	0.530	0.306	0.421	0.255	0.17	1.10
650	5.56	3,73,4	1.74	86/1	6.630	0.899	1.214	0.543	3.489t	0.336	1.03	1.14
649	6.36	3,55,5	1.42	184/1	3.260	0.835	0.717	0.271	0.981			1.05
647	6.06	3,34,3	1.68	43/1	6.980	1.822	0.946	0.504	0.740	0.335	0.16	0.80
647	6.35	4,34,2	1.71	36/1	8.580	2.329	0.820	0.456	0.665	0.386	0.11	0.76
645	4.42	3,60,4	1.67	92/1	4.210	1.255	0.536	0.243	2.366t	0.185	0.67	0.72
645	6.92	5,54,4	1.60	209/1	2.750	0.950	0.427	0.066	0.735	0.086	0.29	0.67

Can. J. Chem. Downloaded from www.nrcresearchpress.com by 210.87.254.42 on 09/05/12
For personal use only.

TABLE 2. Pyrolysis of diethylmercury (*Concluded*)

Temperature (°K)	P (mm)	Time* (min)	t_c	Toluene / Alkyl (molar ratio)	Alkyl used (moles × 10^4)	Residual alkyl (moles × 10^4)	Products (moles × 10^4) C_2H_6	C_2H_4	C_4H_{10}‡	*n*-Propyl§ benzene	k_g† (s^{-1})	k_m† (s^{-1})
646	6.14	5,17,5	1.04	32/1	5.455	2.296	0.252	0.316	0.149	0.135	0.09	0.83
643	5.21	3,33,4	1.49	106/1	2.670	0.930	0.457	0.202	1.124t	0.176	0.71	0.71
640	6.35	3,40,3	1.73	48/1	7.517	3.025	0.761	0.382	0.667	0.2995	0.12	0.53
640	6.29	3,40,3	1.67	55/1	6.846	2.676	0.811	0.406	0.459	0.312	0.12	0.56
640	6.29	3,40,5	1.70	49/1	7.535	3.218	0.861	0.441	0.555	0.319	0.12	0.50P
636	5.56	3,33,4	1.42	143/1	2.280	1.220	0.287	0.114	0.631	0.049	0.33	0.43
635	5.47	2,16,2	0.88	58/1	4.300	2.966						0.43
635	4.78	3,40,4	1.72	50/1	5.630	2.633	0.374	0.187	2.308t	0.162	0.37	0.44
631	6.14	3,20,3	1.02	32/1	5.350	3.337	0.238	0.308	0.255	0.086	0.09	0.46P
630	6.14	5,40,3	1.77	57/1	6.148	3.567	0.516	0.247	0.269	0.224	0.07	0.31
630	6.14	4,40,3	1.78	34/1	10.160	5.587	0.382	0.207	0.261	0.255	0.04	0.34
627	5.21	4,42,4	1.50	94/1	3.939	2.508	0.328	0.152	1.976t	0.117	0.29	0.30
626	4.78	8,39,4	1.69	112/1	2.500	1.626	0.201	0.079	0.664t	0.079	0.24	0.25
617	4.65	4,40,4	1.73	146/1	1.890	1.479	0.142	0.061	0.249t	0.045	0.13	0.14
617	7.16	4,51,3	1.69	76/1	7.290	5.620	0.408	0.194	0.147	0.361	0.53	0.15
616	4.36	3,33,4	1.71	63/1	3.421	2.695	0.141	0.067	0.405	0.051	0.10	0.15
612	1.04	4,84,2	0.84	34/1	7.940	7.259						0.11
612	4.61	4,20,2	1.21	38/1	5.180	1.285						0.12
610	4.75	2,30,2	0.36	71/1	14.190	9.783						0.10
610	7.32	3,51,3	1.04	45/1	14.640	12.530						0.15P
609	6.40	3,45,3	1.10	69/1	6.990	6.164						0.12P
609	6.47	2,30,2	2.43	24/1	8.790	5.795						0.09
608	5.99	2,60,4	1.87	129/1	3.900	3.330						0.08
607	6.40	3,47,2	1.86	44/1	9.530	8.053						0.09
602	6.14	2,61,2	1.87	67/1	7.900	7.000						0.06
601	6.10	2,60,2	1.92	52/1	9.690	8.550						0.06

*Prerun, duration of alkyl flow, post-run.
†k_g, rate constant based on product analysis, k_m, rate constant based on alkyl analysis.
‡Except as noted, this is the butane collected with the gaseous products. P, Runs in packed vessel, surface to volume ratio 17 times that in unpacked vessel. t, Total butane, see Table 3.
§Obtained under conditions optimized for residual alkyl analyses. Possibly in error by up to ±20%.

TABLE 3. Results from runs with full butane analysis

Temperature (°K)	Butane (moles × 10^4) With gaseous products	Butane (moles × 10^4) Dissolved in toluene	k_g (s^{-1})	k_m (s^{-1})
658	2.149	0.493	1.34	1.47
650	3.490	0.995	1.03	1.14
645	1.652	0.714	0.67	0.72
643	1.124	0.208	0.71	0.71
635	1.570	0.738	0.37	0.44
627	0.970	0.206	0.29	0.30
626	0.372	0.292	0.24	0.25
617	0.124	0.249	0.13	0.14

[4] $2\,C_2H_5 \rightarrow C_4H_{10}$

[5] $2\,C_2H_5 \rightarrow C_2H_4 + C_2H_6$

[6] $C_2H_5 + C_6H_5CH_2 \rightarrow C_6H_5C_3H_7$

plus the following minor reactions

[7] $C_2H_5 \rightarrow C_2H_4 + H$

[8] $H + C_6H_5CH_3 \rightarrow CH_3 + C_6H_6$

[9] $H + C_6H_5CH_3 \rightarrow H_2 + C_6H_5CH_2$

[10] $CH_3 + C_6H_5CH_3 \rightarrow CH_4 + C_6H_5CH_2$

[11] $CH_3 + C_2H_5 \rightarrow C_3H_8$

[12] $CH_3 + C_6H_5CH_2 \rightarrow C_6H_5C_2H_5$

Reactions 8–12 are a consequence of reaction 7. The yields of methane, propane, and ethylbenzene were too low for accurate quantitative analysis, but indicated that even at the highest temperature used only about 2% of the ethyl radicals were removed by reaction 7.

Based on the proposed mechanism material balance considerations require that

$$\left[\begin{matrix}\mathrm{Hg(C_2H_5)_2}\\ \text{decomposed}\end{matrix}\right] = [C_4H_{10}] + \tfrac{1}{2}([C_2H_6] + [C_2H_4] + [C_6H_5C_3H_7])$$

Values of k_1 may therefore be calculated either from the quantity of unreacted alkyl (k_m) or from the products shown on the right side of the preceding equation (k_g). It is immediately obvious from Table 2 that gross discrepancies exist between values of k_g and k_m. The discrepancies exist because in the bulk of the work only the gaseous products were analyzed for butane. As shown by a few selected runs in which the butane in the liquid products was also analyzed (see Table 3), full analysis leads to good agreement. The slightly lower values of k_g reflect the fact that either loss of butane from solution or loss of residual alkyl tend to make $k_g < k_m$.

Because the analysis of the liquid products for butane was rather time consuming, once the agreement between k_g and k_m was established all further considerations were based on k_m. Throughout the work attempts were made to find various trap conditions that would allow the bulk of the butane to reach the gas burette. Initially two traps, both kept at −80 °C, were used. It was soon found convenient to have the second trap at −196 °C so that all products other than traces of methane and hydrogen could be frozen out. This trap was warmed to −80 °C after the run was over and the gaseous products collected. Later a third trap was installed between the furnace and the two original traps. Test runs were carried out with this trap at −20, −30, −40, −60, −65, and −70 °C. None of these tests were successful. In almost all cases $k_g \leqslant 0.5\,k_m$. In one run with the three traps at −30, −80, and −196 °C, respectively, $k_g = 0.9\,k_m$ was achieved but this result could not be reproduced. The results in Table 3 were obtained with a trap temperature sequence of −60, −80, and −196 °C.

Tests for the effect of alkyl concentration, total pressure, and contact time on k_m are shown in Tables 4, 5, and 6, respectively. The decomposition is essentially first order (Table 4). At the temperatures and pressures used the unimolecular decomposition of a molecule as complex as $Hg(C_2H_5)_2$ should be at, or near, the high pressure limit. The limited results in Table 5 tend to confirm this. The results in Table 6 indicate that significant thermal equilibrium and longitudinal diffusion errors have been avoided. As shown in Table 2, a 17-fold increase in surface-to-volume ratio produced a

Can. J. Chem. Downloaded from www.nrcresearchpress.com by 210.87.254.42 on 09/05/12
For personal use only.

Can. J. Chem. Downloaded from www.nrcresearchpress.com by 210.87.254.42 on 09/05/12
For personal use only.

TABLE 4. Effect of initial alkyl concentration

T (°K)	Initial alkyl concentration (mol/cc × 10^9)	k_m (s^{-1})
659	0.83	1.66
	1.04	1.61
	1.30	1.67
	1.65	1.69
657	1.14	1.41
	1.20	1.43
	2.60	1.52
	3.00	1.43
	3.10	1.40
617	0.82	0.14
	2.44	0.15

TABLE 5. Effect of total pressure

Temperature (°K)	Pressure (mm)	k_m (s^{-1})
659	6.24	1.66
	4.17	1.61
	3.14	1.69
	3.07	1.66
654	6.00	1.27
	4.75	1.40
	4.72	1.39
	4.39	1.26
	3.51	1.27
617	7.16	0.15
	4.65	0.14
612	4.61	0.12
	1.04	0.11

TABLE 6. Contact time variation

Temperature (°K)	t_c (s)	k_m (s^{-1})
635	1.72	0.44
	1.42	0.42
	0.88	0.43
610	2.43	0.10
	1.21	0.11
	0.37	0.10

maximum increase in k_m of 50%, indicating that the reaction in the unpacked vessel is essentially a homogeneous process.

From the Arrhenius plot of k_m shown in Fig. 1, $\log k_m$ (s^{-1}) = 15.4 − (45 700 ± 1 000/2.3 RT). As may be seen from Fig. 2, the rate constants from the present work are in basic agreement with those from previous work (1, 4). The slightly lower rate constants and the low activation energy obtained in the N_2 carrier work (1)

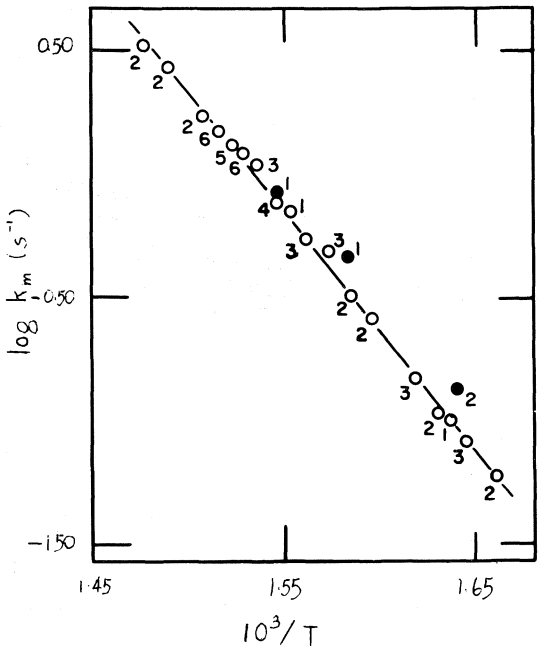

FIG. 1. Arrhenius plot for the decomposition of diethylmercury based on residual alkyl analysis. Numbers indicate number of runs averaged. ●, packed vessel; ○, unpacked vessel.

are possibly the results of thermal equilibrium problems caused by the rather short contact times used. The higher rate constants and lower activation energy from the static system work possibly reflect failure to completely isolate the homogeneous reaction. The present A factor and activation energy are in excellent agreement with the estimated "preferred" values given by Benson and O'Neal (2).

Using $D_1(C_2H_5Hg—C_2H_5) + D_2(Hg—C_2H_5)$ = 50.2 kcal mol^{-1} (2) and accepting the present activation energy as a reasonable measure of D_1 gives D_2 = 4.5 kcal mol^{-1} (approximate correction of E_1 to 0 °K would give D_1 = 43.7 kcal mol^{-1} and D_2 = 6.5 kcal mol^{-1}).

Although the total butane yield was determined in only a few runs, the material balance established allows the total butane to be estimated for all runs with full gas analysis from

$$\text{total butane} = \text{alkyl used} - \text{residual alkyl} - \tfrac{1}{2}([C_2H_6] + [C_2H_4] + [C_6H_5C_3H_7])$$

This process is somewhat inaccurate since all errors will accumulate in the calculated butane

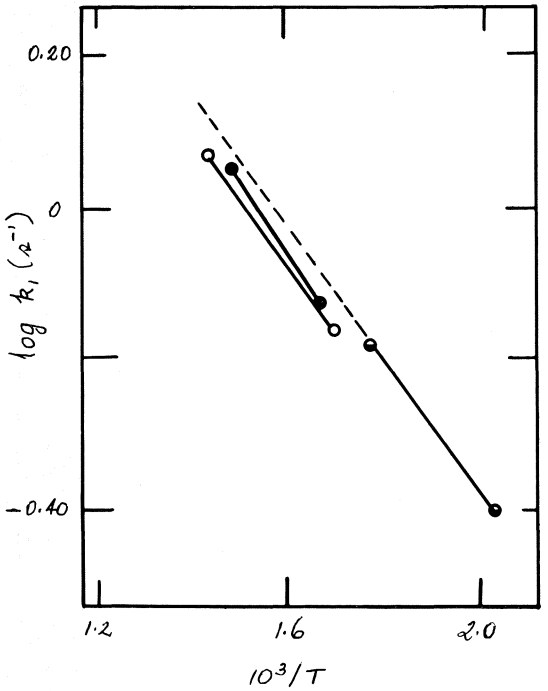

FIG. 2. Arrhenius plots for the decomposition of diethylmercury. Points indicate the temperature range studied. ○ N_2 flow system study, ◒ static system study, ● this work.

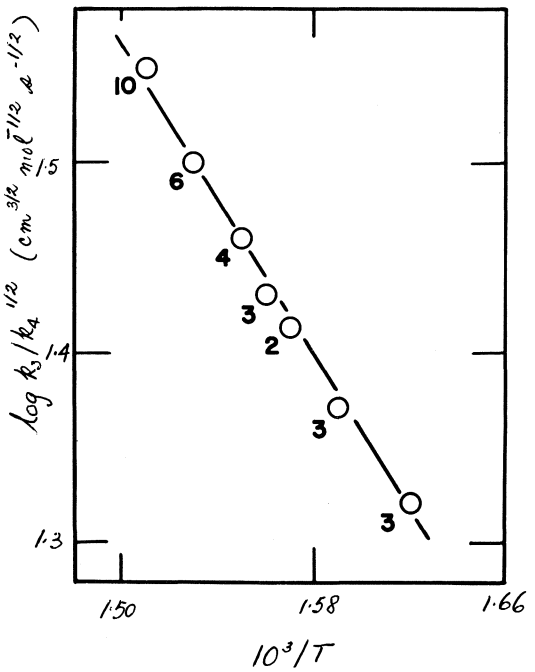

FIG. 3. Arrhenius plot of $k_3/k_4^{1/2}$. Numbers indicate number of runs averaged.

yield. However, a number of interesting tentative conclusions may be reached in this way.

First, if an approximate correction to the ethylene yield is made to allow for reaction 7 (the ethylene from reaction 7 varies from about 35% at the highest temperature used to about 10% at the lowest) this then allows values of $k_3/k_4^{1/2}$ to be calculated from

$$k_3/k_4^{1/2} = \frac{(\text{moles } C_2H_6 - \text{moles } C_2H_4)\ 760 \times 82 \times T}{(\text{moles } C_4H_{10})^{1/2}(Vt)^{1/2}P}$$

when T = run temperature (°K), V = volume of the reaction zone (cm^3), t = duration of alkyl flow (s), and P = toluene pressure (mm). The Arrhenius plot shown in Fig. 3 was constructed using values of $k_3/k_4^{1/2}$ calculated in this way. The curve obtained from the average points is quite good, but it should be noted that a scatter of up to ± 25% in $k_3/k_4^{1/2}$ occurred at the highest three temperatures. This scatter was reduced to about ±10% in the case of the lower four points. The Arrhenius equation obtained is

$\log k_3/k_4^{1/2}$ ($cm^{3/2}$ $mol^{-3/2}$ $s^{-1/2}$) = 4.62 − (9 300 ± 2 000/2.3RT).

If $\log k_4$(cm^3 mol^{-1} s^{-1}) = 12.6 at all temperatures used (9) then $\log k_3$ (cm^3 mol^{-1} s^{-1}) = 10.9 − (9 300 ± 2 000/2.3RT). Past experience with methyl radical reactions in similar systems (10) would indicate that, within the experimental temperature range, values of k_3 calculated from this equation should be reasonable. However, because of the increasing non-uniformity of radical concentrations with increasing percent decomposition, the individual Arrhenius parameters are of limited significance. Studies over a wide range of temperature using a variety of C_2H_5 sources would be required to obtain significant A and E values. If k_3 is calculated at 650 °K, a value of 0.63×10^8 cm^3 mol^{-1} s^{-1} is obtained. This value is of the same order of magnitude as the corresponding rate constants for hydrogen abstraction by methyl radicals from toluene, 2.46×10^8 cm^3 mol^{-1} s^{-1}.

It is also interesting to consider values of k_5/k_4. These are again somewhat scattered but with minor exceptions are in the range 0.10–0.15 with the majority between 0.11–0.14. No temperature dependence was noted. If an

Can. J. Chem. Downloaded from www.nrcresearchpress.com by 210.87.254.42 on 09/05/12
For personal use only.

estimated correction for C_2H_4 from reaction 7 is made the range of ratios for the majority of runs would shift to 0.09–0.12. These results are in agreement with several previous studies (11) and lend some additional support to the general conclusion that $E_5 - E_4$ is approximately zero.

Since the present results for k_1 are based to a large extent on analysis of residual alkyl, one further point of considerable importance should be considered. Based on the present value of k_3 and the literature value for k_{13} (12).

[13] $C_2H_5 + Hg(C_2H_5)_2 \rightarrow C_2H_6 + C_2H_5HgC_2H_4$

$k_{13}/k_3 = 1.5$ at 650 °K and will show little variation over the temperature range used. This leads to the conclusion that in the least favorable case in the present study, the $Hg(C_2H_5)_2$ undergoing reaction 13 is only 0.003 of that decomposing by reaction 1. The general conclusion that reaction 13 is unimportant under the present experimental conditions is supported by the failure to observe any significant variation in k_m over a wide range of toluene to alkyl ratios.

This work has been supported by a grant from the National Research Council of Canada.

1. H. V. Carter, E. I. Chappell, and E. Warhurst. J. Chem. Soc. 106 (1956).
2. S. W. Benson and H. E. O'Neal. Kinetic data on gas phase unimolecular reactions. NSRDS-NBS 21. 1970. p. 520.
3. B. G. Gowenlock, J. C. Polanyi, and E. Warhurst. Proc. Roy. Soc. Ser. A, **218**, 269 (1953).
4. W. Pastfield. Diss. Abstr. **15**, 1325 (1955).
5. C. Heitz. J. Organomet. Chem. **8**, 401 (1967).
6. Selected values of chemical thermodynamic properties. Natl. Bur. Std., U.S. Tech. Notes, No. 270-4. 1969.
7. J. J. Batten. Aust. J. Appl. Sci. **12**, 11 (1961).
8. M. F. R. Mulcahy and M. R. Pethard. Aust. J. Chem. **16**, 527 (1963).
9. S. W. Benson. 2nd International Symposium on Gas Kinetics, Swansea. 1971. To be published.
10. A. N. Dunlop, R. J. Kominar, and S. J. W. Price. Can. J. Chem. **48**, 1269 (1970).
11. (*a*) Tables of bimolecular gas reactions. NSRDS-NBS 9. 1967. p. 111. (*b*) E. Tatajezak and A. F. Trotman-Dickenson. Supplementary tables of bimolecular gas reactions. University of Wales Institute of Science and Technology, Cardiff 1971.
12. Tables of Bimolecular Gas Reactions, NSRDS-NBS 9. 1967. p. 72.

Can. J. Chem. Downloaded from www.nrcresearchpress.com by 210.87.254.42 on 09/05/12
For personal use only.

The Dissolution of Magnesium Oxide in Dilute Sulfuric Acid[1]

DIGBY D. MACDONALD AND D. OWEN
Whiteshell Nuclear Research Establishment, Research Chemistry Branch, Atomic Energy of Canada Limited, Pinawa, Manitoba

Received May 5. 1971

The kinetics of dissolution of sintered magnesium oxide pellets in dilute sulfuric acid at 4.00 and 25.00 °C have been investigated using the rotating disc technique. The rate of depletion of hydrogen ions in the bulk solution is found to be controlled by both transport through the diffusion layer and chemical reaction with the oxide surface. The chemical reaction occurring at the oxide surface has an activation energy of 13 kcal mol^{-1}. The diffusion coefficients for hydrogen ion in dilute sulfuric acid at the two temperatures of interest have been calculated. These coefficients yield an activation energy of 3.6 kcal mol^{-1} for the diffusion of hydrogen ions to the oxide surface.

Les cinétiques de dissolution de pastilles d'oxyde de magnésium fritté dans de l'acide sulfurique dilué, ont été étudiées à 4.00 et 25.00 °C, au moyen de la technique du disque tournant. La vitesse de diminution des ions hydrogène dans le volume de la solution est contrôlée à la fois par le phénomène de transport à travers la couche de diffusion et par la réaction chimique avec la surface de l'oxyde. La réaction chimique se fait à la surface de l'oxyde a une énergie d'activation de 13 kcal mol^{-1}. Les coefficients de diffusion de l'ion hydrogène dans l'acide sulfurique dilué ont été calculés pour les deux températures; ces coefficients conduisent à une énergie d'activation de 3.6 kcal mol^{-1} pour la diffusion des ions hydrogène vers la surface de l'oxyde.

Canadian Journal of Chemistry, **49**, 3375 (1971)

Introduction

The dissolution behavior of metal oxides in aqueous solution is important to many fields of chemistry and technology. A great number of studies have been reported in which the dissolution experiment is performed upon powdered samples. In view of the fact that dissolution is a heterogeneous process this technique suffers from many drawbacks. Perhaps the two most serious disadvantages are the lack of a well defined hydrodynamic or transport regime and an inherent uncertainty as to the actual (or even apparent) surface area of the sample. Accordingly, most studies of this type are reduced to qualitative interpretation.

In the present study the dissolution of magnesium oxide in dilute sulfuric acid was investigated using a rotating disc (1, 2). The rotating disc technique allows the dissolution reaction to be studied under closely controlled hydrodynamic conditions while maintaining a relatively constant surface area. The results of this study clearly demonstrate that the rates of dissolution of magnesium oxide in dilute sulfuric acid are highly reproducible and permit quantitative interpretation of the process involved.

[1]A.E.C.L. No. 4003.

Experimental

Materials

Weighed portions (1.80 g) of British Drug Houses (B.D.H.) or Anachemia reagent grade magnesium oxide powder were pressed into pellets at 7500 p.s.i.g. and sintered in air at 800 °C for 1½ h. The sintered pellets were strong, easily polished and showed no tendency to "flake" when rotated in sulfuric acid. The density of the pellets was found to be 2.00 g cm^{-3}. This figure is well below the theoretical density of 3.58 g cm^{-3} and suggests considerable porosity in the sample. However, longer sintering times (up to 4 h) did not increase the density markedly so all pellets used in this work were prepared as described above. The dissolution reaction was limited to a well defined area by painting the sides and one face of each pellet with polyurethane varnish. Pellets prepared in this manner using both the B.D.H. and Anachemia oxides gave identical results within experimental error.

Dilute sulfuric acid solutions (0.005–0.050 *M*) were prepared by diluting reagent grade concentrated sulfuric acid with deionized distilled water.

Apparatus

The rotating disc used in this study was similar to that described previously (3) and incorporated features recommended by Riddiford (2). The disc was machined from Teflon and contained an inset on the underside of sufficient size to accept a magnesium oxide pellet. Immediately before a run was started the pellet was pressed into place and the exposed face was ground down to within 0.5 mm of the surrounding Teflon surface with No. 600 silicon carbide paper. Any free magnesium oxide grindings were washed away with distilled water. The disc was screwed on to a threaded stainless steel shaft

Can. J. Chem. Downloaded from www.nrcresearchpress.com by 210.87.254.105 on 09/05/12
For personal use only.

Can. J. Chem. Downloaded from www.nrcresearchpress.com by 210.87.254.105 on 09/05/12
For personal use only.

which passed through a roller bearing assembly at the top of the reaction vessel. This bearing was designed to ensure minimum eccentricity of the disc (<1% of the pellet radius). The shaft was rotated by an adjustable speed electric motor via a pulley-belt arrangement. Rotational velocities were measured using a General Radio Type 1531-AB stroboscope. The temperature of the reaction vessel was maintained to within ±0.05 °C of the desired value using a water bath thermostat.

Method

The reaction vessel was assembled and thermostated for 1 h to ensure thermal equilibrium with the water bath. The reaction was initiated by pipetting 300 ml of prethermostated dilute sulfuric acid into the reaction vessel and starting the electric motor which had been preset at the desired rotational velocity. The underside of the disc was viewed with a mirror to ensure that no gas bubbles were trapped on the magnesium oxide surface. Aliquots (10 ml) of reaction solution were removed at regular time intervals and analyzed for magnesium ion by titration with standard disodium EDTA solution using Erichrome Black T as indicator. The duration of each run was such that more than 50% of the available hydrogen ions were consumed.

Rotational velocities were restricted to the range 10.47–104.72 rad s^{-1} (100–1000 r.p.m.). The upper limit was chosen so that the maximum Reynolds number (eq. 1),

$$[1] \qquad Re_{max} = r^2\omega/\nu$$

where ν and ω represent the kinematic viscosity and angular velocity, respectively, did not exceed the critical value (2×10^5) for transition to turbulent flow (2). Substituting r and ν equal to 0.952 cm and 8.9×10^{-3} cm^2 s^{-1} (4), respectively, into eq. 1 yields a maximum Reynolds number of 1.07×10^4, *i.e.* well below the critical value given above. The lower limit (10.47 rad s^{-1}) is sufficiently high to ensure negligible contribution to mass transport to or from the oxide surface by natural convection (2).

Results

The stoichiometry of the reaction between magnesium oxide and hydrogen ion in solution is represented by eq. 2

$$[2] \qquad MgO + 2H^+ \rightarrow Mg^{2+} + H_2O$$

In order to determine the kinetic order of the dissolution process with respect to hydrogen ion and to formulate a rate expression for the reaction, it is necessary to determine the actual concentration of hydrogen ion in solution at any given time. This can be accomplished by assuming that the first dissociation of sulfuric acid is complete and that the concentration of hydrogen ion at any given time is determined by reaction 2 and the second dissociation represented by eq. 3

$$[3] \qquad HSO_4^- \overset{K_2}{\rightleftharpoons} H^+ + SO_4^{2-}$$

The material balance equations for hydrogen and sulfate are therefore given by eqs. 4 and 5,

$$[4] \qquad \{H\}_{Total} = [H^+] + [HSO_4^-] + 2c = 2a$$

$$[5] \qquad \{SO_4\}_{Total} = [HSO_4^-] + [SO_4^{2-}] = a$$

where a denotes the number of moles of H_2SO_4 per liter of solution at zero time assuming no dissociation and c is the concentration of magnesium ion at the time of interest. Since the concentration of sulfate ion is determined by eq. 6

$$[6] \qquad [SO_4^{2-}] = \frac{K_2[HSO_4^-]}{[H^+]}$$

it is possible to eliminate $[SO_4^{2-}]$ and $[HSO_4^-]$ using eqs. 4, 5, and 6 and to express $[H^+]$ as a function of the known parameters c, K_2, and a.

$$[7] \qquad [H^+]^2 + (K_2 - a + 2c)[H^+] + 2K_2(c - a) = 0$$

or

$$[8] \qquad [H^+] = -(1/2)(K_2 - a + 2c) + (1/2)\{(K_2 - a + 2c)^2 - 8K_2(c - a)\}^{1/2}$$

In all subsequent calculations K_2 was taken as 1×10^{-2} and 2×10^{-2} M at 25 and 4 °C, respectively (5).

The kinetic order of the reaction between magnesium oxide and hydrogen ion was determined by calculating $\ln \{d[H^+]/dt\}_{t\rightarrow 0}$ graphically from plots of $[H^+]$ *vs.* time for runs differing only in the initial concentration of sulfuric acid and plotting this quantity against $\ln [H^+]_{t=0}$ as shown in Fig. 1. The solid line is drawn with a gradient equal to one. This plot clearly establishes that the dissolution reaction is first order with respect to hydrogen ion. Accordingly, the rate equation can be written as eq. 9,

$$[9] \qquad -d[H^+]/dt = (kA/V_t)[H^+]$$

where A is the projected surface area of the exposed oxide and V_t is the volume of the solution. Since the concentration of magnesium ion, c, (and therefore $[H^+]$) is determined by removing aliquots of solution, V_t must be regarded as time dependent when integrating eq. 9. This integration yields eq. 10 (6),

$$[10] \qquad -\sum V_t \ln ([H^+]_t/[H^+]_{t-\delta t}) = kAt$$

Can. J. Chem. Downloaded from www.nrcresearchpress.com by 210.87.254.105 on 09/05/12
For personal use only.

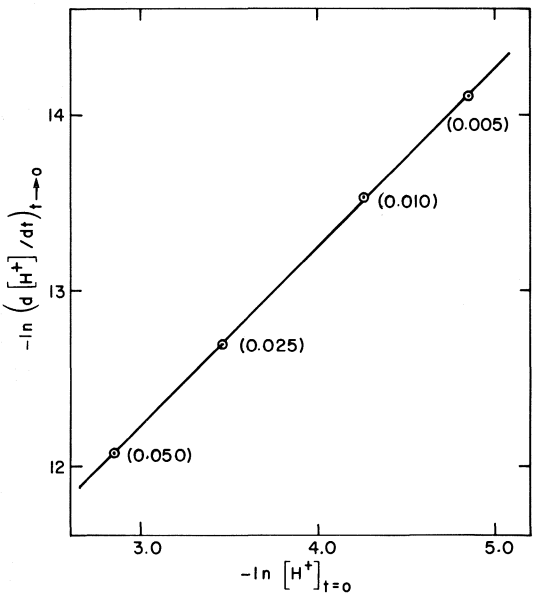

FIG. 1. Dependence of the initial rate on hydrogen ion concentration. $T = 25.00 \pm 0.05$ °C, $\omega = 31.42$ rad s^{-1}. The numbers in parentheses represent the initial concentrations of sulfuric acid.

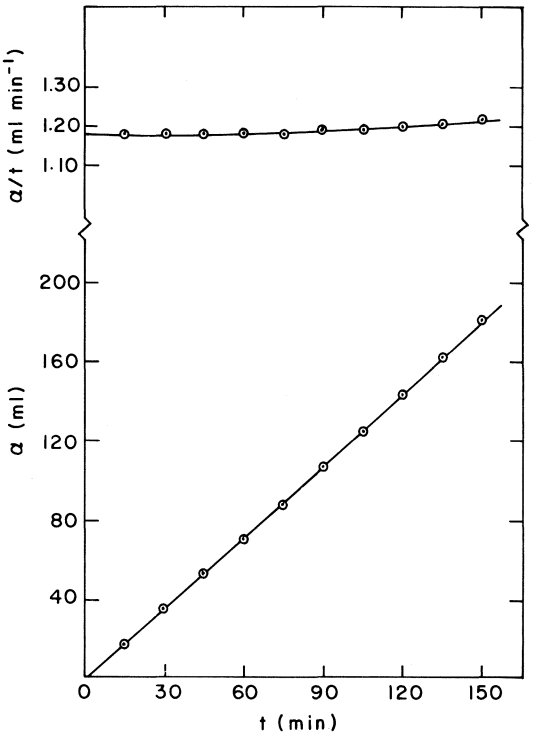

FIG. 2. Rate plot for the dissolution of magnesium oxide in dilute sulfuric acid. $a = 0.050$ M, $T = 4.00 \pm 0.05$ °C, and $\omega = 52.40$ rad s^{-1}. $\alpha = \Sigma V_i \ln \{[H^+]_{t-\delta}/[H^+]_t\}$.

where V_t is the volume of solution in the time interval $t - \delta t$ to t. A typical plot of eq. 10 is shown in Fig. 2. These plots were quite linear over most of the reaction studied. In some cases, however, and especially so for high rotational velocities, the rate plots deviated slightly from linearity near the end of the run. This phenomenon is illustrated in Fig. 2 by the plot of $\{\sum V_t \ln ([H^+]_t/[H^+]_{t-\delta t})\}/t$ *vs.* t. A strictly linear rate plot would yield a horizontal line. In practice, however, the plot "curls" upwards near the end of the run with an apparent increase in kA (see eq. 10) of 2–3%. Consequently, all rate constants were calculated from $(kA)_{t\to 0}$ and the projected area of the exposed oxide surface. The time dependence of kA most likely arises from the influence of a steadily roughening surface on the hydrodynamics of the system and possibly from the concomitant increase in surface area.

Rate constants for the dissolution of magnesium oxide in sulfuric acid are listed in Table 1. Each value represents the mean of at least three determinations. The uncertainties quoted are the average deviations from the means. These average deviations are seldom more than ±2% of the corresponding rate constants and demonstrate the high reproducibility that can be obtained by careful control of the hydrodynamics of the system.

TABLE 1. Rate constants for the dissolution of magnesium oxide in dilute sulfuric acid

ω (rad s^{-1})	$k \times 10^3$ (cm s^{-1})	
	4 °C	25 °C
10.48	4.03±0.07	7.20±0.10
20.95	5.24±0.05	9.48±0.08
31.42	6.03±0.05	11.64±0.19
41.90	6.70±0.10	12.90±0.12
52.40	7.09±0.11	14.69±0.40
73.36	7.60±0.10	17.17±0.19
104.72	8.78±0.11	19.28±0.37

Discussion

The reaction between hydrogen ion and magnesium oxide takes place in the following sequence: (*a*) transport of hydrogen ion to the oxide surface, (*b*) chemical reaction at the surface,

Can. J. Chem. Downloaded from www.nrcresearchpress.com by 210.87.254.105 on 09/05/12
For personal use only.

and (*c*) transport of the products from the surface to the bulk liquid. The transport processes, (*a*) and (*c*), are determined by the hydrodynamics of the system whereas the rate of the chemical process reflects the difference in free energy between the initial state and the transition state for the kinetic path involved. Of the three processes identified above only the first two involve the rate of depletion of hydrogen ions in the bulk solution. The role played by both of these processes in the dissolution of magnesium oxide in sulfuric acid is examined in detail in the following discussion.

According to the Nernst theory (7) for diffusion controlled reactions the rate constant for transport of hydrogen ions to the oxide surface can be expressed by eq. 11

$$[11] \qquad k_T = D/\delta$$

where D is the diffusion coefficient of the reactant (hydrogen ion) and δ is the thickness of the "ideal" Nernst diffusion layer. Solution of the Navier–Stokes equations for nonturbulent transport to the surface of a rotating disc yields eq. 12 for the transport rate constant (1, 2)

$$[12] \qquad k_T = 0.620\, D^{2/3}\nu^{-1/6}\omega^{1/2}$$

where ν and ω have been defined previously (see eq. 1). Equation 12 predicts that if the rate of depletion of hydrogen ions in the bulk solution is purely transport controlled then a plot of k_T *vs.* $\omega^{1/2}$ will be linear. Plots of this type for the dissolution of magnesium oxide in sulfuric acid at 4.00 and 25.00 °C are shown in Fig. 3. These plots are not linear and exhibit greatest curvature at the lowest temperature. The direction of curvature suggests that the observed rate constant approaches a limiting value at high rotational velocities. This indicates that over the range of rotational velocities employed in the present study both the transport and chemical processes exert some control of the overall rate of depletion of hydrogen ions in the bulk solution. Accordingly, the concentration of hydrogen ion at the oxide surface is neither effectively zero (transport control) nor equal to the concentration in the bulk solution (chemical control). Since the chemical reaction at the oxide surface is first order with respect to hydrogen ion then the rate of reaction can be written as eq. 13.

$$[13] \qquad -V_t(\mathrm{d}[H^+]/\mathrm{d}t)s = k_c A'[H^+]_s$$

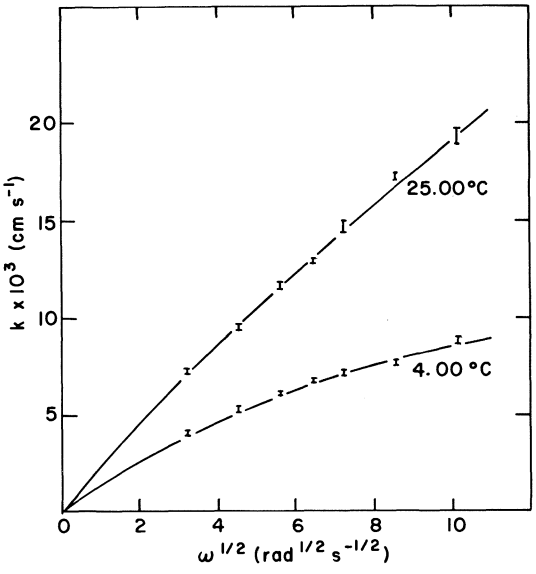

FIG. 3. The dependence of rate on rotational velocity.

where A' is the true surface area of the oxide. Similarly, the rate of transport of hydrogen ions to the surface is given by eq. 14,

$$[14] \qquad -V_t\mathrm{d}[H^+]/\mathrm{d}t = k_T A([H^+] - [H^+]_s)$$

where $[H^+]_s$ represents the hydrogen ion concentration at the oxide surface. At steady-state $\mathrm{d}[H^+]_s/\mathrm{d}t$ is identical to $\mathrm{d}[H^+]/\mathrm{d}t$ and hence $[H^+]_s$ can be expressed in terms of the bulk hydrogen ion concentration and the two rate constants k_T and k_c.

$$[15] \qquad [H^+]_s = k_T A[H^+]/(k_c A' + k_T A)$$

Substitution of eq. 15 into eq. 14 yields the following expression for the rate of depletion of hydrogen ions in the bulk solution.

$$[16] \qquad -V_t\frac{\mathrm{d}[H^+]}{\mathrm{d}t} = \left(\frac{k_T k_c \alpha}{k_T + k_c \alpha}\right) A[H^+]$$

where α is the roughness factor for the oxide surface, *i.e.* (A'/A). Comparison of eqs. 16 and 9 reveals that the observed rate constant is related to k_T and k_c by eq. 17.

$$[17] \qquad k = k_T k_c \alpha/(k_T + k_c \alpha)$$

or, by substituting eq. 12 for k_T and rearranging

$$[18] \qquad k^{-1} = (\alpha k_c)^{-1} + 1.613\, D^{-2/3}\nu^{1/6}\omega^{-1/2}$$

Plots of k^{-1} *vs.* $\omega^{-1/2}$ for the dissolution of magnesium oxide in sulfuric acid at 4.00 and

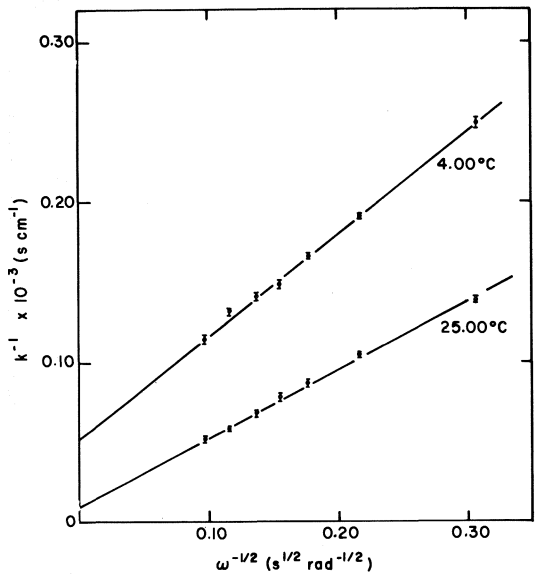

FIG. 4. Plot of reciprocal rate constant *vs.* $\omega^{-1/2}$.

25.00 °C are presented in Fig. 4. The plots are linear as predicted by eq. 18 for consecutive first order rate processes. If the dissolution process were completely transport controlled over the range of rotational velocities and temperatures studied then the lines drawn in Fig. 4 should pass through the origin. However, this is not the case and the finite intercepts at $\omega^{-1/2} = 0$ demonstrate the existence of joint transport/chemical control.

The intercepts at $\omega^{-1/2} = 0$ yield numerical values for (αk_c) of 1.92×10^{-2} cm s^{-1} and 10.0×10^{-2} cm s^{-1} at 4.00 and 25.00 °C, respectively. If it is assumed that α is independent of temperature then the (αk_c) values listed above correspond to an activation energy of 13 kcal mol^{-1} for the reaction of hydrogen ions with the magnesium oxide surface.

Vermilyea (8) has shown in a recent study that the dissolution behavior of powdered magnesium oxide is quite similar to that for the magnesium hydroxide. This led him to conclude that the magnesium oxide surface is rapidly converted to the hydroxide (eq. 19) and that this later species reacts with hydrogen ion in the dissolution reaction.

[19] $MgO + H_2O \rightleftarrows Mg(OH)_2$

$\Delta G^0 = -6.45$ kcal mol^{-1}

The calculated standard free energy change (9) for reaction 19 is sufficiently negative to support this view. In the present study, therefore, it seems reasonable to associate the chemical process occurring at the surface with the rapid hydration of MgO to produce $Mg(OH)_2$ which in turn reacts with protons in the rate determining step (eq. 20).

[20] $Mg(OH)_{2,\,s} + H^+ \xrightarrow{\text{slow}} Mg(OH)_{aq}^+ + H_2O$

[21] $Mg(OH)_{aq}^+ + H^+ \xrightarrow{\text{fast}} Mg_{aq}^{2+} + H_2O$

The proposed rate determining step is consistent with the observed activation energy.

The gradients of the k^{-1} *vs.* $\omega^{-1/2}$ plots presented in Fig. 4 permit determination of the diffusion coefficients for hydrogen ion in dilute sulfuric acid at the two temperatures of interest. The viscosity and density of dilute sulfuric acid solutions (<0.1 *M*) differ little from the corresponding quantities for pure water (10). Accordingly, the kinematic viscosities for pure water (4) at 4 °C (1.57×10^{-2} cm^2 s^{-1}) and at 25 °C (8.91×10^{-3} cm^2 s^{-1}) are used here to calculate the hydrogen ion diffusion coefficients. These calculations result in values of $4.5_1 \times 10^{-5}$ and $7.1_3 \times 10^{-5}$ cm^2 s^{-1} at 4 and 25 °C, respectively. Riddiford (2) has recently summarized previous determinations of D_{H^+} at 18–25 °C and found that the most reliable values fall in the range 2.8×10^{-5} to 1×10^{-4} cm^2 s^{-1} depending upon the solution employed. While no specific values are quoted for 0.050 *M* sulfuric acid, the diffusion coefficients reported in the present study seem very reasonable. The temperature dependence of D_{H^+} can be represented by eq. 22

[22] $$D_{H^+} = Z_D \exp(-E_D/RT)$$

where Z_D is the pre-exponential factor and E_D is the activation energy for the diffusion process. The diffusion coefficients calculated in this study yield a value of 3.6 kcal mol^{-1} for E_D. This value lies within the range 2–6 kcal mol^{-1} normally associated with diffusion of ions in aqueous solution.

The authors wish to thank Dr. S. Banerjee for his interest in this work.

1. V. G. LEVICH. Physicochemical hydrodynamics. Prentice-Hall, Inc., Englewood Cliffs, New Jersey. 1962.
2. A. C. RIDDIFORD. Advances in electrochemistry

Can. J. Chem. Downloaded from www.nrcresearchpress.com by 210.87.254.105 on 09/05/12
For personal use only.

and electrochemical engineering. *Edited by* P. Delahay. Interscience Publ. Inc., New York. **4**, 47 (1966).
3. D. D. MacDonald and G. A. Wright. Can. J. Chem. **48**, 2847 (1970).
4. Handbook of chemistry and physics. The Chemical Rubber Co., Cleveland Ohio. 50th ed. 1969.
5. D. D. Perrin. Pure Appl. Chem. **20**(2), 133 (1969).
6. R. S. Bradley. Trans. Faraday Soc. **34**, 278 (1938).
7. L. L. Bircumshaw and A. C. Riddiford. Q. Rev. **6**, 157 (1952).
8. D. A. Vermilyea. J. Electrochem. Soc. **116**, 1179 (1969).
9. Selected values of chemical thermodynamic properties N.B.S. Circular 500. Part 1. 1961.
10. M. R. Savino and V. Vitagliano. Ric. Sci. Ser. II, **2**, 341 (1962).

Can. J. Chem. Downloaded from www.nrcresearchpress.com by 210.87.254.105 on 09/05/12
For personal use only.

Can. J. Chem. Downloaded from www.nrcresearchpress.com by 210.87.254.40 on 09/05/12
For personal use only.

Preparation and Transformations of Three *p*-Menthane-3-methanesulfonyloxy-4,8-diols

G. L. Lange and M. Bosch

Department of Chemistry, University of Guelph, Guelph, Ontario

Received July 9, 1971

Three diastereomeric *p*-menthane-3-methanesulfonyloxy-4,8-diols were synthesized from (+)-pulegone. Treatment of each methanesulfonate with aqueous base resulted in a stereospecific reaction involving antiperiplanar groups to give one product: either an α-ketol by a pinacol-type rearrangement or an epoxide by an intramolecular S_N2-type reaction. Although the possibility existed for 1,3- as well as 1,2-diol monomethanesulfonate transformations, only products from the latter type of reaction were isolated.

Les trois diastéréoisomères du *p*-menthane méthanesulfonyloxy-3 diols-4,8 ont été synthétisés à partir de la (+)-pulégone. Le traitement de chaque méthanesulfonate par une base aqueuse, conduit à une réaction stéréospécifique qui implique des groupes antipériplanaires et qui donne un seul produit: soit un α-cétol par une transposition pinacolique, soit un époxyde par une réaction intramoléculaire du type S_N2. Bien qu'il existe des possibilités de transformation pour les monométhanesulfonate diols-1,3 et -1,2, seuls les produits correspondant au dernier type de réaction ont été isolés.

Canadian Journal of Chemistry, **49**, 3381 (1971)

Introduction

The literature contains numerous examples of transformations of 1,2- and 1,3-diol monosulfonates, usually tosylates or methanesulfonates (mesylates). Monosulfonates of 1,2-diols upon treatment with base commonly undergo a pinacol-type rearrangement to give a carbonyl compound (1) or they undergo an intramolecular displacement of the sulfonate to yield an epoxide (2) (eq. 1). The 1,3-diol monosulfonates may yield an oxetane (3) or fragmentation products (3, 4) (eq. 2). Of course, in both systems the sulfonate group could also undergo intermolecular displacement

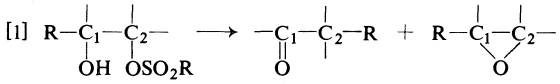

[2]

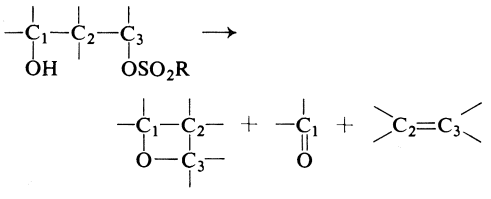

or elimination. In cyclic systems, the relative stereochemistry of the hydroxyls in the starting material and the stability of the reacting conformation are generally critical factors in determining which reaction pathway will be followed.

A 1,2,3-triol monosulfonate (*e.g.* tertiary hydroxyl, tertiary hydroxyl, secondary sulfonate) would involve competition among all the pathways described above. A compound with such a triol moiety (the sulfonate being replaced by its biological equivalent) has been suggested by Barton and Gupta (5) as a precursor to the sesquiterpene, zierone. Transformations of related triol monotosylates have been employed in the synthesis of some A-norcholesteryl derivatives (6).

This report describes the preparation and transformations of three *p*-menthane-3-mesyloxy-4,8-diols, which are examples of the triol monosulfonates discussed above. They were prepared by epoxidation of (+)-pulegone (**1**) to give the ketoepoxides **2**, followed by reduction to the hydroxyepoxides **3**, hydrolysis to the triols **4** and finally selective monomesylation. The preparation of each of these synthetic intermediates and the base-catalyzed transformations of the monomesylates **5** will be discussed in detail.

Results and Discussion

Preparation of Hydroxyepoxides (3)

(+)-Pulegone (**1**) was epoxidized with alkaline hydrogen peroxide to give pulegone oxides **2***a* and *b* (64:36%, respectively) as previously reported (7). The two stereoisomeric ketoepoxides were separated and reduced with sodium borohydride in methanol. Compound **2***a* gave a mixture of two

Can. J. Chem. Downloaded from www.nrcresearchpress.com by 210.87.254.40 on 09/05/12
For personal use only.

hydroxyepoxides, **3***a* and *b* (47:53%, respectively), which were separated by spinning band distillation, while **2***b* gave only one product, **3***c*.

Infrared and n.m.r. spectroscopy were conclusive in establishing the assigned configurations and major conformations for the three hydroxyepoxides (Scheme 1). An i.r. study of hydrogen bonding in dilute carbon tetrachloride solutions revealed the presence of intramolecular hydrogen bonding (3565, 3602 cm^{-1}) in **3***a* where the epoxide and the C-3 hydroxyl are *cis*, while in **3***b* where these functional groups are *trans* and the hydroxyl is axial, only free hydroxyl absorption (3628 cm^{-1}) was observed. Compound **3***c* showed intramolecular hydrogen bonding (3583 cm^{-1}) which is consistent with the *trans* orientation of the epoxide and the equatorial hydroxyl.

The n.m.r. spectra of the hydroxyepoxides, particularly the resonances of the C-3 hydrogens and hydroxyls, were quite instructive. Analysis of the C-3 hydrogens in both **3***a* and *c* was complicated by intramolecular hydrogen bonding of the C-3 hydroxyl with the epoxide oxygen, which slowed the rate of OH exchange sufficiently to allow the observation of H—C—O—H coupling. Fraser *et al.* (8) recently devised a Karplus-type equation to calculate these vicinal coupling constants (eq. 3). If one assumes the C-3 hydroxyl

$$[3]\quad J_{HCOH} = 10.4\cos^2\phi - 1.5\cos\phi + 0.2$$

is directed towards the epoxide oxygen, Dreiding models of the conformations depicted in Scheme 1 give H—C—O—H dihedral angles of 140 and 95° for **3***a* and *c* respectively. Calculation of the coupling constants using these angles gives the following comparison with the values actually observed for the hydroxyl coupling: for **3***a*, $J_{calcd.} = 5.3$; $J_{obs.} = 7$ Hz; and for **3***c*, $J_{calcd.} = 0.2$, $J_{obs.} = 2$ Hz. Considering the limitations of the method (8) and the possibility of steric interactions between the hydroxyl and the C-10 methyl, the calculated and observed values agree reasonably well.

Exchange of the C-3 hydroxyl with deuterium oxide simplifies the analysis of the C-3 hydrogen as it eliminates the H—C—O—H coupling. The half-band width ($w/2$) of hydrogens α to the hydroxyl (H_α) is very useful in determining the axial or equatorial nature of these hydrogens. The axial H_α would be expected to have a relatively broad half-band width (~15 Hz) because of the large axial–axial vicinal coupling while $w/2$ for the equatorial H_α would be narrower (~6 Hz) because of the smaller equatorial–equatorial and equatorial–axial coupling constants (9). In **3***a* the H_α appears at τ 6.25 as a distorted quartet ($w/2$ = 15 Hz) while in **3***c* it appears at τ 6.15 again as a quartet ($w/2$ = 15 Hz). Consequently both these hydroxyepoxides must possess an axial hydrogen and an equatorial hydroxyl at C-3.

The H_α in **3***b*, where there is no complication with intramolecular hydrogen bonding, exhibits a multiplet (τ 6.40, $w/2$ = 7 Hz) characteristic of an equatorial hydrogen, and thus an axial hydroxyl. The chemical shift of this equatorial hydrogen is an unusual feature of this spectrum as it appears at higher field than the corresponding axial hydrogens in **3***a* and *c* (τ 6.25 and 6.15 respectively). Normally axial hydrogens appear at higher field than equatorial in cyclohexane (10). This upfield shift may be due to the shielding effect of the C-10 methyl or the epoxide ring (11) on this equatorial hydrogen, which is situated directly above the plane of the epoxide. Shielding by a cyclopropane ring has been invoked to explain the upfield position of an equatorial H_α relative to an axial H_α (12).

Examination of Dreiding models for the two ketoepoxides **2***a* and *b* provides support for the product distribution obtained upon borohydride reduction. Compound **2***a* does not exhibit any significant difference in the steric environment of the carbonyl group from either the α- or the β-face and this is reflected in the 47:53% distribution obtained for hydroxyepoxides **3***a* and *b*. Compound **2***b* exhibits considerably less hindrance on the α-face and borohydride attack from this side gives the β-alcohol, **3***c*, which is the only product detected.

Hydroxyepoxides **3***a* and *c* were previously prepared by another route (13). There are some differences in the physical constants reported for **3***a* while **3***c* and the *p*-nitrobenzoate derivatives for both show good agreement (see Experimental).

*Preparation of Triols (**4**) and Monomesylates (**5**)*

Treatment of the hydroxyepoxides with aqueous acid afforded one triol in each case: **3***a* → **4***a*, **3***b* → **4***b* and **3***c* → **4***c* (Scheme 1). The insolubility of the triols in solvents used for obtaining solution i.r. spectra precluded a study of hydrogen bonding but n.m.r. spectra run in hexadeuterioacetone provided useful information. When interpreting these spectra it was assumed the very

Can. J. Chem. Downloaded from www.nrcresearchpress.com by 210.87.254.40 on 09/05/12
For personal use only.

bulky dimethylcarbinol group at C-4 would be in the equatorial position. The half-band width of the H_α was then used to determine the configuration at C-3. In **4***a*, the broad signal for this hydrogen (τ 6.12, $w/2 = 17$ Hz) indicates an axial hydrogen and an equatorial hydroxyl. The narrow signals for H_α in **4***b* (τ 6.05, $w/2 = 7$) and **4***c* (τ 6.05, $w/2 = 8$) indicate the presence of axial hydroxyls at C-3. The structural assignments for the three triols are consistent with this n.m.r. data and with the transformations to be described later. During the acid-catalyzed opening of the epoxide ring, the protonated epoxide intermediate must have undergone attack by water at the less hindered C-8 position in preference to C-4 (14).

Attempts to effect selective monotosylation of the triols **4** at the C-3 secondary hydroxyl were unsuccessful presumably because of the considerable steric hindrance of the neighboring groups. But preparation of the monomesylates **5** was successful in all three cases. Mesylation has been shown to proceed via the less sterically demanding sulfene intermediate (15). Mesylate **5***a* was stable and was fully characterized while **5***b* and *c* were unstable and the crude material was used in the next step. With the desired *p*-menthane-3-mesyloxy-4,8-diols in hand, it was then possible to examine the base-catalyzed transformations of these diastereomers.

Transformation Products of Monomesylates (5)

Treatment of pure monomesylate **5***a* with dilute aqueous base afforded a 90% yield of one compound as analyzed by g.l.c. and t.l.c. The i.r. spectrum of this substance indicated a carbonyl group (1705 cm^{-1}) and an intramolecularly hydrogen bonded hydroxyl (3500 cm^{-1}), features characteristic of α-ketols (16). The n.m.r. spectrum included a six-proton peak (τ 8.64) appropriate for the methyl groups in the moiety $(CH_3)_2C(HO)-C(=O)-$. A structure consistent with these data and its derivation from **5***a* is 1-[3-(R)-methylcyclopentyl]-2-hydroxy-2-methyl-1-propanone (**6**).

The structure was confirmed by an unambiguous synthesis. The Grignard reagent of 3-(R)-methylcyclopentyl chloride was prepared by the following route: (+)-pulegone → 3-(R)-methyladipic acid (17) → 3-(R)-methylcyclopentanone (17) → 3-(R)-methylcyclopentanol → 3-(R)-methylcyclopentyl chloride (presumably a mixture of diastereomers). This Grignard reagent was reacted with the cyanohydrin of acetone (eq. 4) to yield ketol **6** (35%), identical with the product from **5***a*, and an alcohol (23%) which was not fully characterized but presumably is **7** by analogy with similar displacements in cyanohydrin–Grignard reactions (18). The intermediate imine in this reaction was very stable in aqueous acid and could be extracted from an ether solution of the crude reaction mixture with 1 *N* hydrochloric acid, thus separating the imine and the alcohol (**7**). Hydrolysis of the imine in 0.1 *M* sodium hydroxide solution proceeded readily to give the ketol (**6**) as the only product. The imine could also be hydrolyzed by heating to reflux in 0.5 *N* hydrochloric acid for 16 h but some dehydration occurred under these conditions to give an α,β-unsaturated ketone (1670, 1615 cm^{-1}) (30% by g.l.c.) in addition to the ketol (70%). As both the synthetic ketol and that formed by rearrangement of **5***a* were prepared under alkaline conditions, epimerization at the cyclopentyl position adjacent to the carbonyl group would be expected. The g.l.c. analysis of the ketol indicated only one symmetrical peak while the n.m.r. spectrum exhibited two methyl doublets (τ 8.90, $J = 6$ Hz; τ 8.98, $J = 6$ Hz) of approximately equal area for the 3-methyl group on the cyclopentyl ring.

[4] $(CH_3)_2C(OH)-CN$ + ClMg–(cyclopentyl)–H → **6** + $(CH_3)_2C(OH)$–(cyclopentyl)–H (**7**)

Examination of conformation **5***a* (Scheme 1) shows the antiperiplanar (180°) (19) relationship of the C-3 mesyloxy group and the C_4—C_5 bond, the preferred orientation for a pinacol-type rearrangement, which would result in displacement of the mesyloxy group and formation of the ring contracted product **6**.

Treatment of crude mesylate **5***b* with dilute base gave 83% (based on **4***b*) of hydroxyepoxide **8***a*. This structure is based on spectral data, comparison with an authentic sample and examination of its mode of formation. The i.r. spectrum showed an intramolecularly hydrogen bonded

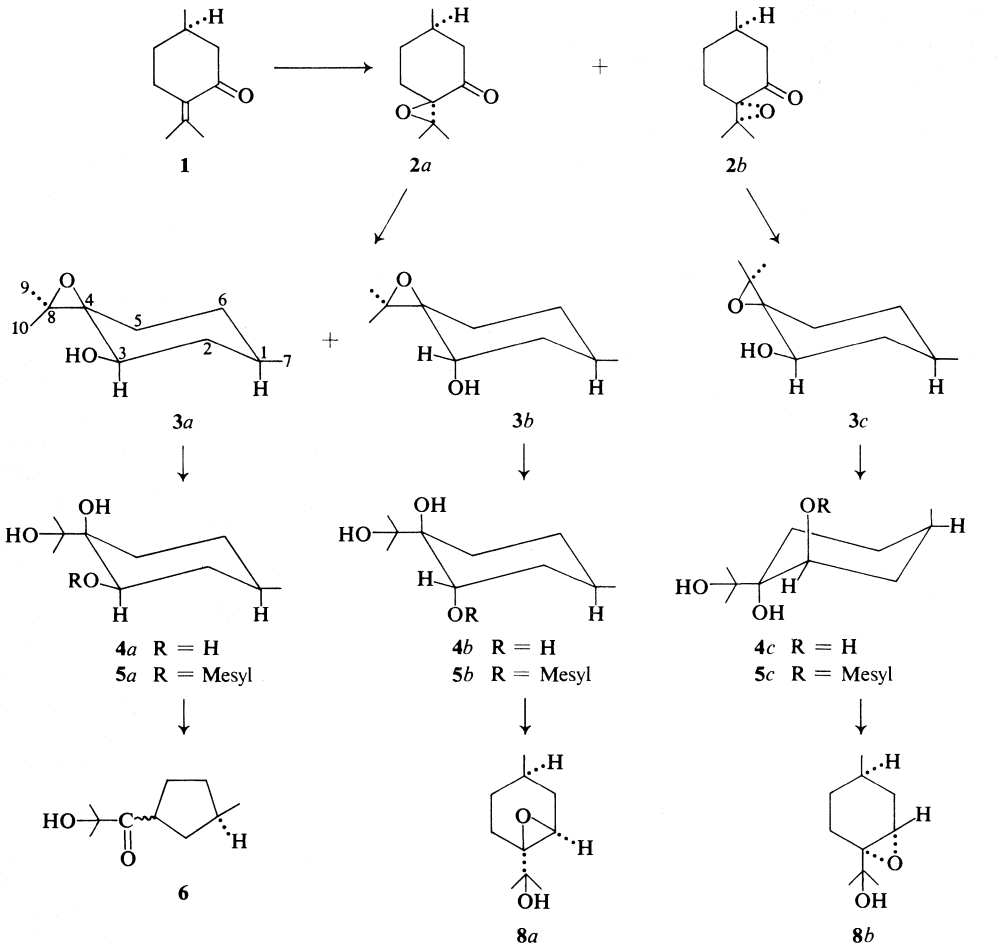

SCHEME 1

hydroxyl (3552 cm^{-1}) and bands characteristic of an epoxide (800–950 cm^{-1}) (20) while the n.m.r. spectrum indicated a dimethyl carbinol group (three-proton singlets at τ 8.82 and 8.83) and a trisubstituted epoxide (τ 6.78, 1H). In DMSO the hydroxyl appeared as a singlet at τ 5.85 indicating the alcohol was tertiary (21).

The reaction of 3-*p*-menthen-8-ol (22) with *m*-chloroperbenzoic acid gave a mixture of two hydroxyepoxides, **8***a* (30%) and *b* (70% by g.l.c.). Rickborn and Lwo have shown in the case of 4-methylcyclohexene (23) that the methyl substituent exerts only a slight steric effect in favor of the *trans* product (53.6-46.4%) and thus the dimethyl carbinol group must be exerting some additional influence in favor of the *trans* product **8***b*. The minor component in the epoxidation, **8***a*, was identical to the product obtained from mesylate **5***b*. Analysis of the resonance for the C-3 hydrogen in the n.m.r. spectra of **8***a* and *b* was conclusive in distinguishing between these two epoxides. In **8***a* this hydrogen appeared as a doublet (τ 6.78, J = 5 Hz) while in **8***b* it was a narrow multiplet (τ 6.74). Coupling constants for the C-3 hydrogens were calculated using Tori's revised Karplus equation (24) for 1,2-epoxycyclohexanes (eq. 5). The following dihedral angles (ϕ) between the C-3 and the two C-2 hydrogens were

$$[5] \qquad J = 5.1 \cos^2 \phi$$

measured from Dreiding models: for **8***a*, ϕ = 17 and 103°; and for **8***b*, ϕ = 65 and 55°. These angles predict $J_{calcd.}$ = 4.7 and 0.3 Hz, respectively, for **8***a* and $J_{calcd.}$ = 0.9 and 1.7 Hz, respectively, for

Can. J. Chem. Downloaded from www.nrcresearchpress.com by 210.87.254.40 on 09/05/12
For personal use only.

8*b*. Thus one would expect the C-3 hydrogen in **8***a* to be a doublet with a coupling constant of about 5 Hz while in **8***b* this hydrogen would be expected to be a narrow unresolved multiplet. These predictions are in good agreement with the observed values and support the structures proposed for **8***a* and *b*.

In the conformation proposed for **5***b* the C-3 mesyloxy and C-4 hydroxyl groups are in a *trans* diaxial orientation. Displacement of the mesyloxy by the hydroxyl in an S_N2-type reaction would lead directly to **8***a*.

Crude monomesylate **5***c* upon treatment with aqueous base gave **8***b* as the only product in 74% yield (based on **4***c*). The assignment was also based on spectral data, comparison with an authentic sample, and its mode of formation. The major product (70%) from epoxidation of 3-*p*-menthen-8-ol (see above) was identical to transformation product **8***b*. An S_N2-type displacement of the axial mesyloxy group by the C-4 hydroxyl in **5***c* would give this α-epoxide.

Treatment of the triols (**4**) themselves under the basic conditions employed in the transformation of the mesylates (**5**) resulted in complete recovery of starting triol indicating the necessity of the mesyloxy group in these transformations.

Summary

The two types of reactions common to the 1,2-diol monosulfonate systems, namely pinacol-type bond migration and epoxide formation, were the only reactions observed with the triol monomesylates investigated. In these transformations the group antiperiplanar to the departing mesyloxy group was always involved in the reaction. A probable reason for the lack of any 1,3-diol monosulfonate reactions (*i.e.* fragmentation and oxetane formation) in these systems is the thermodynamic instability of the conformations in which the bulky dimethylcarbinol group must assume an axial position if the reaction is to proceed.

In one reported example of a 1,2,3-triol monomesylate transformation in the steroid field (6*b*), it was suggested that the monomesylate **9** first undergoes fragmentation to give diketone **10** which then gives the dehydrated aldol product **11** under the basic conditions of the reaction. By analogy to the rearrangement of our mesylate **5***a*, another plausible mechanism would be a pinacol-type rearrangement to give ring-contracted product **12** followed by dehydration to **11**.

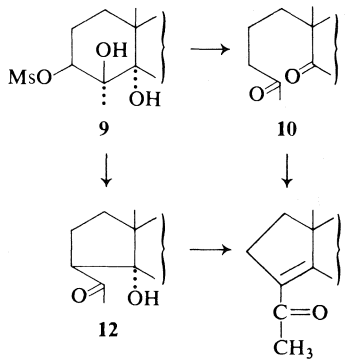

Experimental

The i.r. spectra were recorded on a Beckmann IR5A spectrometer with the exception of the hydrogen bonding spectra which were run on a Beckmann IR12 spectrometer using *ca.* 0.005 *M* carbon tetrachloride solutions in a variable path length cell. The n.m.r. spectra were determined on a Varian A-60A spectrometer using tetramethylsilane as internal standard. Optical rotations were measured on a Bellingham and Stanley polarimeter. The g.l.c. analyses and separations were carried out on a Model A-700 "Autoprep" using a 1/4 in. × 6 ft column with 20% Carbowax 20 M on 60/80 Chromosorb W operating at 120° with a He flow rate of 75 cc/min. For analytical t.l.c., a 0.25 mm thickness of GF-254 Silica Gel was employed while for preparative t.l.c., a 1.0 mm thickness of PF-254 Silica Gel was used, both with the solvent system 40:60 ethyl acetate – benzene. Spinning band distillations were carried out on a Nester–Faust 117 apparatus with a column length of 18 in. Melting points were determined on a Gallenkamp apparatus and are uncorrected. Microanalyses were performed by A. G. Gygli, Toronto, Ontario, and H. S. McKinnon, Department of Chemistry, University of Guelph, Guelph, Ontario.

The pulegone used in these experiments was Bakers, practical grade, $[\alpha]_D^{25}$ + 26° (neat).

p-Menthane-4,8-epoxy-3-ols (3)

The pulegone oxides (**2**) were prepared from (+)-pulegone and separated according to a procedure described (*7a*). To an ice-cooled stirred solution of **2***a* (33.2 g, 0.20 mol) in 200 ml methanol was added dropwise over 15 min a solution of sodium borohydride (7.5 g, 0.20 mol) in 40 ml water and 200 ml methanol. After stirring for an additional 30 min at room temperature the reduction mixture was poured into 800 ml water and extracted with ether (4 × 250 ml). The combined extracts were washed with water and brine and dried (Na_2SO_4). Removal of the solvent *in vacuo* gave a colorless oil (30.9 g, 91%), shown by g.l.c. to contain two components, **3***a* and *b*, in a ratio of 47:53 respectively. Spinning band distillation of the oil separated the two components: (−)-4,8-epoxymenthol (**3***a*); b.p. 110–111°/4 mm; i.r. (CCl_4) 3450, 2875, 1455, 1378, 1138, 1100, 1052, 854, 652 cm^{-1}, hydroxyl region at 0.005 *M*, 3602, 3565 cm^{-1}; n.m.r. (CCl_4) τ 8.93 (3H, d, J = 6 Hz), 8.68 (3H, s), 8.52 (3H, s), 7.39 (1H, d, J = 7 Hz, disappeared on addition of D_2O),

Can. J. Chem. Downloaded from www.nrcresearchpress.com by 210.87.254.40 on 09/05/12
For personal use only.

Can. J. Chem. Downloaded from www.nrcresearchpress.com by 210.87.254.40 on 09/05/12
For personal use only.

6.25 (1H, dd, $w/2 = 15$ Hz); $[\alpha]_D^{25}$ −35° (*c*, 2 in methanol) (lit. (13) +34°); *p*-nitrobenzoate derivative, m.p. 128.5–129.0° (lit. (13) 134–135°), $[\alpha]_D^{25}$ −61° (*c*, 2 in chloroform) (lit. (13) −65°).

Anal. Calcd. for $C_{17}H_{21}NO_5$ (*p*-nitrobenzoate derivative): C, 63.94; H, 6.63. Found: C, 64.03; H, 6.81.

(+)-4,8-Epoxyneomenthol (**3***b*); b.p. 116–117°/4 mm, m.p. 51.5–52.5°; i.r. (CCl_4) 3580, 3420, 2900, 1450, 1430, 1375, 1095, 1032, 960, 878, 688 cm^{-1}, hydroxyl region at 0.005 *M*, 3628 cm^{-1}; n.m.r. (CCl_4) τ 9.07 (3H, d, $J = 6$ Hz), 8.75 (3H, s), 9.70 (3H, s) 8.28 (1H, s, disappeared on addition of D_2O), 6.40 (1H, m, $w/2 = 7$ Hz); $[\alpha]_D^{25}$ +50° (*c*, 2 in methanol); *p*-nitrobenzoate derivative, m.p. 165.5–166.5, $[\alpha]_D^{25}$ +63° (*c*, 2 in chloroform).

Anal. Calcd. for $C_{10}H_{18}O_2$ (**3***b*): C, 70.55; H, 10.65. Found: C, 70.94; H, 11.01.

Sodium borohydride reduction of pulegone oxide **2***b* (23.1 g, 0.14 mol) as described above for **2***a* gave a colorless oil, (−)-4,8-epoxyneoisomenthol (**3***c*), b.p. 85–87°/0.65 mm (21.4 g, 91%) which exhibited only one peak on g.l.c. analysis; i.r. (CCl_4) 3400, 2900, 1450, 1370, 1112, 1055, 868, 650 cm^{-1}, hydroxyl region at 0.005 *M*, 3628 (vw), 3583 cm^{-1}; n.m.r. (CCl_4) τ 8.97 (3H, d, $J = 6$ Hz), 8.67 (3H, s), 8.46 (3H, s), 7.34 (1H, d, $J = 2$ Hz, disappeared on addition of D_2O), 6.12 (1H, dd, $w/2 = 15$ Hz); $[\alpha]_D^{25}$ −4° (*c*, 2 in methanol) (lit. (13) +1°); *p*-nitrobenzoate derivative, m.p. 125.5–127.0° (lit. (13) 128–129°), $[\alpha]_D^{25}$ −15° (*c*, 2 in chloroform) (lit. (13) −16°).

Anal. Calcd. for $C_{10}H_{18}O_2$ (**3***c*): C, 70.55, H, 10.65. Found: C, 70.17; H, 10.77.

*p-Menthane-3,4,8-triols (**4**)*

(*a*) To hydroxyepoxide **3***a* (2.0 g, 12 mmol) was added a solution of 2 drops concentrated sulfuric acid in 20 ml water and the suspension was heated over a steam bath for 5 min with vigorous agitation. The reaction mixture was cooled and extracted with ether (3 × 30 ml) and the combined extracts were washed with water (2 × 25 ml), brine (1 × 25 ml), and dried (Na_2SO_4). Removal of the solvent *in vacuo* gave a colorless oil (2.0 g, 91%). The t.l.c. indicated the product contained a major component (R_f 0.18) and two impurities (R_f's 0.25 and 0.49). Isolation of the major band by preparative t.l.c. afforded the crystalline (+)-4,8-dihydroxymenthol (**4***a*); m.p. 66.0–67.5°; i.r. (CCl_4) 3425, 2940, 1380, 1180, 1138, 1100, 1040, 1020, 858 cm^{-1}; n.m.r. (CCl_4) τ 9.03 (3H, d), 8.85 (3H, s), 8.71 (3H, s), 6.92, 6.50, 6.35 (total of 3H, disappeared on addition of D_2O), 6.12 (1H, m, $w/2 = 17$ Hz); $[\alpha]_D^{25}$ +16° (*c*, 2 in chloroform)

Anal. Calcd. for $C_{10}H_{20}O_3$: C, 63.80; H, 10.71. Found: C, 63.66; H, 10.65.

(*b*) Hydroxyepoxide **3***b* (2.0 g, 12 mmol) was treated with aqueous sulfuric acid as described above to give a white precipitate. Extraction with ether gave a crude product which upon crystallization from chloroform gave 1.98 g (90%) of (+)-4,8-dihydroxyneomenthol (**4***b*); m.p. 166.5–167.0°; i.r. (KBr) 3225, 2900, 1455, 1420, 1370, 1170, 1138, 1112, 1068, 1002, 985, 975, 954, 917, 845 cm^{-1}; n.m.r. (CD_3COCD_3) τ 9.16 (3H, d, $J = 5$ Hz), 8.82 (3H, s), 6.68 (3H, s), 7.16, 6.85, 5.80, 5.60, 5.56 (total of 3H, disappeared on addition of D_2O), 6.05 (1H, m, $w/2 = 7$ Hz); $[\alpha]_D^{25}$ +22° (*c*, 2 in methanol).

Anal. Calcd. for $C_{10}H_{20}O_3$: C, 63.80; H, 10.71. Found: C, 64.01; H, 10.97.

(*c*) Hydroxyepoxide **3***c* (2.0 g, 12 mmol) after treatment with aqueous sulfuric acid as described above, work-up, and crystallization from chloroform gave (−)-4,8-dihydroxyneoisomenthol (**4***c*) (1.55 g, 70%); m.p. 165.0–166.0°; i.r. (KBr) 3350, 2900, 1425, 1375, 1210, 1180, 1145, 1070, 1012, 955, 915 cm^{-1}; n.m.r. (CD_3COCD_3) τ 8.88 (3H, d, $J = 6$ Hz), 8.80 (3H, s), 8.72 (3H, s), 7.22, 6.80, 5.79, 5.55, 5.00 (total of 3H, disappeared on addition of D_2O) 6.05 (1H, m, $w/2 = 8$ Hz); $[\alpha]_D^{25}$ −27° (*c*, 2 in methanol).

Anal. Calcd. for $C_{10}H_{20}O_3$: C, 63.80; H, 10.71. Found: C, 63.78; H, 11.00.

*p-Menthane-3-methanesulfonyloxy-4,8-diols (**5**)*

(*a*) To a stirred solution of triol **4***a* (3.0 g, 16 mmol) in 40 ml dry pyridine at 5° was added dropwise methanesulfonyl chloride (2.1 g, 18 mmol). After stirring for 24 h at 5° (precipitate of pyridinium chloride), the reaction mixture was combined with 80 ml water and the aqueous phase was extracted with ether (3 × 100 ml). The combined extracts were washed with cold 6 *N* hydrochloric acid (2 × 50 ml), saturated sodium bicarbonate solution (1 × 50 ml), water (2 × 50 ml), and brine (1 × 50 ml) and then dried (Na_2SO_4). Removal of the solvent gave a yellow oil (2.96 g, 70%) which was crystallized from 2:1 pentane–ether to give the pure mesylate **5***a*; m.p. 66.5–67.5°; i.r. ($CHCl_3$) 3500, 2950, 1350, 1250, 1210, 1175, 952, 918, 880, 693 cm^{-1}; n.m.r. (CCl_4) τ 9.00 (3H, d), 8.85 (3H, s), 8.64 (3H, s), 7.59, 6.80 (each 1H, disappeared on addition of D_2O), 6.97 (3H, s), 5.10 (1H, m).

Anal. Calcd. for $C_{11}H_{22}O_5S$: C, 49.60; H, 8.30. Found: C, 49.28; H, 8.15.

(*b*) Similarly, to a stirred solution of triol **4***b* (1.4 g, 7.4 mmol) in 20 ml dry pyridine at 5° was added dropwise methanesulfonyl chloride (1.1 g, 9.6 mmol) and after stirring for 24 h at 5° the reaction was worked-up as described above. Removal of the solvent gave crude mesylate **5***b* which was unstable and was used directly in the next step [see (*b*) of following section].

(*c*) A solution of triol **4***c* (1.8 g, 9.6 mmol) in 25 ml dry pyridine was reacted with methanesulfonyl chloride (1.4 g, 12 mmol) as described above and then worked-up to give crude mesylate **5***c* which was unstable and was used directly in the next step [see (*c*) of following section].

*Transformations of Mesylates (**5**)*

(*a*) A solution of mesylate **5***a* (2.96 g, 11.1 mmol) in 8 ml dioxane and 8 ml 0.45 *M* sodium hydroxide solution was stirred at 65° under nitrogen for 2 h. The reaction mixture was cooled, poured into 30 ml water and extracted with ether (3 × 75 ml). The combined extracts were washed with water (2 × 25 ml), brine (1 × 25 ml), and dried (Na_2SO_4). Removal of the solvent *in vacuo* gave a pale yellow oil (1.70 g, 90%) which exhibited only one spot on t.l.c. and one peak on g.l.c. An analytical sample was prepared by preparative g.l.c. The compound was shown to be 1-[3-(R)-methylcyclopentyl]-2-hydroxy-2-methyl-1-propanone (**6**); i.r. (film) 3500, 2950, 2850, 1705, 1460, 1170, 1070, 970 cm^{-1}, hydroxyl region at 0.005 *M* in CCl_4, 3500 cm^{-1}; n.m.r. (CCl_4) τ 8.64 (6H,s), 8.98, 8.90 (total 3H, two d, $J = 6$ Hz in each case), 6.60 (1H, broad m), 6.20 (1H, s, disappears on addition of D_2O); $[\alpha]_D^{25}$ −9° (*c*, 2 in chloroform).

Anal. Calcd. for $C_{10}H_{18}O_2$: C, 70.55; H, 10.65. Found: C, 70.61; H, 10.69.

Can. J. Chem. Downloaded from www.nrcresearchpress.com by 210.87.254.40 on 09/05/12
For personal use only.

(*b*) Crude mesylate **5***b* (prepared from 1.4 g, 7.4 mmol of **4***b*) was dissolved in 4 ml dioxane and 4 ml 0.45 *M* sodium hydroxide solution and stirred at 65° under nitrogen for 4 h. Work-up as described previously gave a yellow oil (1.05 g, 83% based on **4***b*) which exhibited only one spot on t.l.c. and one peak on g.l.c. (retention time 14.3 min). An analytical sample was prepared by preparative g.l.c. The compound was shown to be *trans-p*-menthan-3,4-epoxy-8-ol (**8***a*); i.r. (CCl_4) 3552, 2925, 1450, 1365, 1340, 1195, 1155, 1125, 975, 955, 875, 855, 845 cm^{-1}; n.m.r. (CCl_4) τ 9.12 (3H, d, $J = 5$ Hz), 8.83 (3H, s), 8.82 (3H, s), 8.29 (1H, s, disappeared on addition of D_2O), 6.78 (1H, d, $J = 5$ Hz); n.m.r. (DMSO) τ 5.85 (1H, s, disappeared on addition of D_2O).

Anal. Calcd. for $C_{10}H_{18}O_2$: C, 70.55; H, 10.65. Found: C, 70.46, H, 10.72.

(*c*) Similarly, crude mesylate **5***c* (prepared from 1.8 g, 9.6 mmol of **4***c*) was dissolved in 4 ml dioxane and 4 ml 0.45 *M* sodium hydroxide solution and stirred at 65° under nitrogen for 4 h. Work-up as described above gave a yellow oil (1.22 g, 75% based on **4***c*) which exhibited only one spot on t.l.c. and one peak on g.l.c. (retention time 13.4 min). An analytical sample was prepared by preparative g.l.c. The compound was shown to be *cis-p*-menthan-3,4-epoxy-8-ol (**8***b*); i.r. (CCl_4) 3552, 2900, 1450, 1365, 1340, 1180, 1160, 1125, 1085, 1025, 955, 920, 905, 848 cm^{-1}; n.m.r. (CCl_4) τ 9.13 (3H, d, $J = 5$ Hz), 8.85, (6H, s), 8.23 (1H, s, disappeared on addition of D_2O), 6.74 (1H, narrow m).

Anal. Calcd. for $C_{10}H_{18}O_2$: C, 70.55; H, 10.65. Found: C, 70.58; H, 10.73.

Preparation of Authentic Samples

(a) 1-[3-(R)-Methylcyclopentyl]-2-hydroxy-2-methyl-1-propanone (6)

3-(R)-Methylcyclopentanone (17) after reduction with sodium borohydride gave 3-(R)-methylcyclopentanol, which upon reaction with calcium chloride in concentrated hydrochloric acid (25) gave 3-(R)-methylcyclopentyl chloride, b.p. 54–56°/55 mm. A solution of 3-(R)-methylcyclopentyl chloride (7.1 g, 0.06 mol) in 30 ml dry ether was added dropwise to magnesium turnings (1.46 g 0.06 g atm) under nitrogen at a rate to maintain reflux. The reaction was completed by heating to reflux for an additional 30 min. The Grignard solution was cooled in an ice bath and stirred mechanically while a solution of acetone cyanohydrin (2.55 g, 0.03 mol) (26) in 10 ml ether was added dropwise. The resultant slurry was stirred and heated at 35° for 3 h. The reaction mixture was cooled and a solution of ammonium chloride (3.2 g, 0.06 mol) in 25 ml water was added with stirring. The two phases were separated and the aqueous phase was extracted with ether (6 × 25 ml). The combined organic phases were extracted with 1 *N* hydrochloric acid (5 × 20 ml) (retained), saturated sodium bicarbonate solution (1 × 20 ml), brine (1 × 20 ml), and dried ($MgSO_4$). Removal of the solvent gave a colorless oil (1.0 g, 23%), which was >90% one compound by g.l.c. and was tentatively formulated as 3-(R)-methylcyclopentyldimethylcarbinol (7); i.r. (film) 3350, 2860, 1455, 1375, 1295, 1265, 1250, 935 cm^{-1}; n.m.r. (CCl_4) τ 9.02, 8.98 (total of 3H, two d, $J = 6$ Hz in each case), 8.88 (6H, s), 8.45 (1H, s, disappeared on addition of D_2O); $[\alpha]_D^{25}$ +2° (c, 2 in chloroform).

The 100 ml of the hydrochloric acid phase from above, which contains the imine salt, was basified with 4.4 g sodium hydroxide to give a solution *ca.* 0.1 *M* in sodium hydroxide and 10 ml ethanol was added to promote dissolution of the organic compound. The solution was heated to reflux for 4 h, cooled, saturated with sodium chloride, and extracted with ether (5 × 50 ml). The extract was washed with brine (2 × 25 ml), dried ($MgSO_4$), and the solvent removed to give a colorless oil (1.78 g, 35%) which exhibited only one peak on g.l.c. at the same retention time as the transformation product **6** from mesylate **5***a*. The i.r. and n.m.r. spectra were identical to **6** (see above) and $[\alpha]_D^{25}$ −10° (*c*, 2 in chloroform).

Hydrolysis of the imine could also be effected in 0.5 *N* hydrochloric acid solution heated under reflux for 16 h. Work-up gave a yellow oil shown by g.l.c. to be a mixture of two components (30:70), the latter having the same retention time as **6**; i.r. of mixture (CCl_4) 3500, 2950, 1705, 1670, 1615, 1160, 970 cm^{-1}.

(b) cis- and trans-p-Menthan-3,4-epoxy-8-ols (8)

To a stirred solution of 3-*p*-menthen-8-ol (1.0 g, 6.5 mmol) (22) in 10 ml dichloromethane at room temperature was added dropwise a solution of *m*-chloroperbenzoic acid (1.8 g, 10.5 mmol) in 20 ml dichloromethane. The reaction was stirred for 20 min and a 10% sodium sulfite solution was added to destroy the excess peracid. The organic layer was washed with saturated sodium bicarbonate solution (1 × 10 ml) and brine (1 × 10 ml) and dried ($MgSO_4$). Removal of the solvent *in vacuo* gave a colorless oil (0.99 g, 90%), which was shown by g.l.c. to be a 70:30 mixture of two components with retention times of 13.4 and 14.3 min, respectively. These compounds were separated by preparative g.l.c. and shown to be identical to **8***b* and *a* (see above) respectively, the transformation products of mesylates **5***c* and *b*, respectively.

The authors wish to thank the National Research Council of Canada for financial support of this research.

1. (*a*) E. J. Corey, M. Ohno, R. B. Mitra, and P. A. Vatakencherry. J. Am. Chem. Soc. **86**, 478 (1964). (*b*) G. Büchi and J. A. Carlson. J. Am. Chem. Soc. **91**, 6470 (1969). (*c*) T. Hirata and T. Suga. J. Org. Chem. **36**, 412 (1971).
2. (*a*) E. E. Royals and J. C. Leffingwell. J. Org. Chem. **31**, 1937 (1966). (*b*) R. G. Carlson and J. K. Pierce. Tetrahedron Lett. 6213 (1968).
3. (*a*) R. B. Clayton, H. B. Henbest, and M. Smith. J. Chem. Soc. 1982 (1957). (*b*) M. Matsui and D. K. Fukushima. J. Org. Chem. **35**, 561 (1970).
4. (*a*) P. S. Wharton and G. A. Hiegel. J. Org. Chem. **30**, 3254 (1965). (*b*) J. A. Marshall and S. F. Brady. J. Org. Chem. **35**, 4068 (1970).
5. D. H. R. Barton and G. S. Gupta. Proc. Chem. Soc. 308 (1961).
6. (*a*) A. F. Thomas, K. Heusler and J. M. Müller. Tetrahedron, **16**, 264 (1961). (*b*) S. Julia, J.-P. Lavaux, S. R. Pathak, and G. H. Whitham. J. Chem. Soc. 2633 (1964). (*c*) R. M. Moriarty and K. Bhamidipaty. J. Org. Chem. **35**, 2297 (1970).
7. (*a*) J. Katsuhara. J. Org. Chem. **32**, 797 (1967). (*b*) W. Reusch and P. Mattison. Tetrahedron, **24**, 4933 (1968).
8. R. R. Fraser, M. Kaufman, P. Morand, and G. Govil. Can. J. Chem. **47**, 403 (1969).

9. (*a*) N. S. BHACCA and D. H. WILLIAMS. Applications of n.m.r. spectroscopy in organic chemistry. Holden–Day, San Francisco, California, 1964. p. 79. (*b*) G. BERTI, B. MACCHIA and F. MACCHIA. Tetrahedron, **24**, 1755 (1968).
10. L. M. JACKMAN. Applications of n.m.r. spectroscopy in organic chemistry. Pergamon Press, Oxford, 1959. p. 116.
11. K. TORI, K. AONO, K. KITAHONOKI, R. MUNEYUKI, Y. TAKANO, H. TANIDA, and T. TSUJI. Tetrahedron Lett. 2921 (1966) and references therein.
12. J. TADANIER and W. COLE. J. Org. Chem. **27**, 4610 (1962).
13. W. TAGAKI and T. MITSUI. J. Org. Chem. **25**, 1476 (1960).
14. R. E. PARKER and N. S. ISAACS. Chem. Rev. **59**, 737 (1959).
15. J. F. KING and T. DURST. J. Am. Chem. Soc. **87**, 5684 (1965).
16. R. N. JONES, P. HUMPHRIES, F. HERLING, and K. DOBRINER. J. Am. Chem. Soc. **74**, 2820 (1952).
17. E. J. EISENBRAUN and S. M. MCELVAIN. J. Am. Chem. Soc. **77**, 3383 (1955).
18. M. S. KHARASCH and O. REINMUTH. Grignard reactions of nonmetallic substances. Prentice–Hall, New York, N.Y., 1954. pp. 777 and 783.
19. W. KLYNE and V. PRELOG. Experientia, **16**, 521 (1960).
20. K. NAKANISHI. Infrared absorption spectroscopy. Holden–Day, San Francisco, California, 1962. p. 36.
21. O. L. CHAPMAN and R. W. KING. J. Am. Chem. Soc. **86**, 1256 (1964).
22. E. H. ESCHINASI. J. Org. Chem. **35**, 2010 (1970).
23. B. RICKBORN and S.-Y. LWO. J. Org. Chem. **30**, 2212 (1965).
24. K. TORI, T. KOMENO and T. NAKAGAWA. J. Org. Chem. **29**, 1136 (1964).
25. W. A. YARNALL and E. S. WALLIS. J. Org. Chem. **4**, 284 (1939).
26. R. F. B. COX and R. T. STORMONT. Organic syntheses. Coll. Vol. 2. John Wiley and Sons, New York, N.Y., 1943. p. 7.

Can. J. Chem. Downloaded from www.nrcresearchpress.com by 210.87.254.40 on 09/05/12
For personal use only.

Can. J. Chem. Downloaded from www.nrcresearchpress.com by 210.87.254.5 on 09/05/12
For personal use only.

Radiolysis of Trifluoroacetic Acid

J. BETTS[1] AND E. A. CHERNIAK[2]

Department of Chemistry, Carleton University, Ottawa, Canada

Received November 6, 1970[3]

The gaseous products of the ^{60}Co-γ radiolysis of liquid CF_3COOH at 23 °C and solid CF_3COOH at −196 °C have been identified and their *G*-values have been determined. The products and *G*-values are, for the radiolysis of liquid CF_3COOH; CO_2(7.1), CO(0.71), CF_3H(0.27), C_2F_6(1.36), H_2(0.031) and, for the radiolysis of solid CF_3COOH; CO_2(2.5), CF_3H(0.30), C_2F_6(0.39). CO and H_2 are not produced in the radiolysis of solid CF_3COOH and CF_4 and C_2F_4 are not produced in the radiolysis of solid and liquid CF_3COOH. The mechanisms of gaseous product formation in the radiolysis of solid and liquid CF_3COOH are compared.

Les produits gazeux provenant de la radiolyse par le ^{60}Co-γ de CF_3COOH liquide à 23 °C et de CF_3COOH solide à −196 °C ont été identifiés et leurs valeurs de *G* ont été déterminées. Les produits et les valeurs de *G* sont pour la radiolyse de CF_3COOH liquide, : CO_2(7.1), CO(0.71), CF_3H(0.27), C_2F_6-(1.36), H_2(0.031) et pour la radiolyse de CF_3COOH solide: CO_2(2.5), CF_3H(0.30), C_2F_6(0.39). CO et H_2 ne sont pas produits dans la radiolyse de CF_3COOH solide et CF_4 et C_2F_4 ne sont pas produits dans la radiolyse de CF_3COOH solide et liquide. Les mécanismes de la formation de produit gazeux dans la radiolyse de CF_3COOH solide et liquide sont comparés.

Canadian Journal of Chemistry, **49**, 3389 (1971)

Although considerable progress has recently been made in understanding the radiation chemistry of acetic acid (1), very little is known about the effects of ionizing radiation on trifluoroacetic acid. An electron spin resonance (e.s.r.) study[4] has shown that the only transient species trapped at −196 °C, in the γ-radiolysis of polycrystalline CF_3COOH, was $\cdot CF_3$ and that by −175 °C the disappearance of this species was complete. By contrast, the only transient species trapped at −196 °C in the γ-radiolysis of polycrystalline CH_3COOH, was the radical anion, $CH_3\dot{C}\bar{O}OH$ (1). The disappearance of this anion was complete by −86 °C and beyond that temperature, the species trapped were $\cdot CH_2COOH$ and $CH_3\dot{C}O$. The radical anion, $CF_3\dot{C}\bar{O}OH\cdots NH_3$, has been detected at −196 °C in γ-irradiated single crystals of $CF_3COO^- NH_4^+$ but it is unstable and by −78 °C it has transformed completely into $\cdot CF_2CO\bar{O}\ NH_4^+$ and F^- (2). Both $\cdot CF_2CO\bar{O}\ NH_4^+$ and the radical $CF_3C\dot{O}O$ are products of the room temperature γ-radiolysis of single crystals of $CF_3COO^-NH_4^+$ (2).

In this study the gaseous products of the ^{60}Co-γ radiolysis of liquid CF_3COOH at room temperature and of polycrystalline CF_3COOH at −196 °C have been identified and their *G*-values have been measured. Comparison of yields of gaseous products obtained from CF_3COOH at two greatly different temperatures and from two different phases provides useful information on the mechanism of radiolysis.

Experimental

Eastman Kodak White Label CF_3COOH was refluxed with a small quantity of concentrated sulfuric acid, distilled, treated with anhydrous sodium sulfate, de-aerated by trap-to-trap distillation *in vacuo* and sealed into Pyrex vials at −196 °C. These vials were cleaned with chromic acid, a mixture of dilute nitric acid and hydrogen peroxide, hot tap water and triply distilled water and then were baked out on the vacuum line. All taps and joints were lubricated with Apiezon grease as CF_3COOH vapor was adsorbed on silicone grease.

Approximately 5 ml samples were irradiated in a 100 Ci ^{60}Co-γ "well" source at about 23 °C. Two irradiations at −196 °C were performed in a 600 Ci ^{60}Co-γ "cave" source. Electron density corrected Fricke dosimetry was used to obtain absorbed doses.

After irradiation the contents of the vials were distilled, through a breakseal, into a −196 °C trap and then into a −131 °C trap. The volatile products were divided into fractions which were non-condensible at −210 and −145 °C, using a solid N_2 trap and Ward-LeRoy still, and then were measured in a gas buret and analyzed mass spectrometrically. The volatile products from a few

[1]NRCC Postdoctoral Fellow (1964–1965). Present address: Department of Chemistry, Kingston Polytechnic, Kingston-upon-Thames, Surrey, England.

[2]Present address: Department of Chemistry, Brock University, St. Catharines, Ontario.

[3]Revision received June 30, 1971.

[4]P. B. Ayscough, private communication.

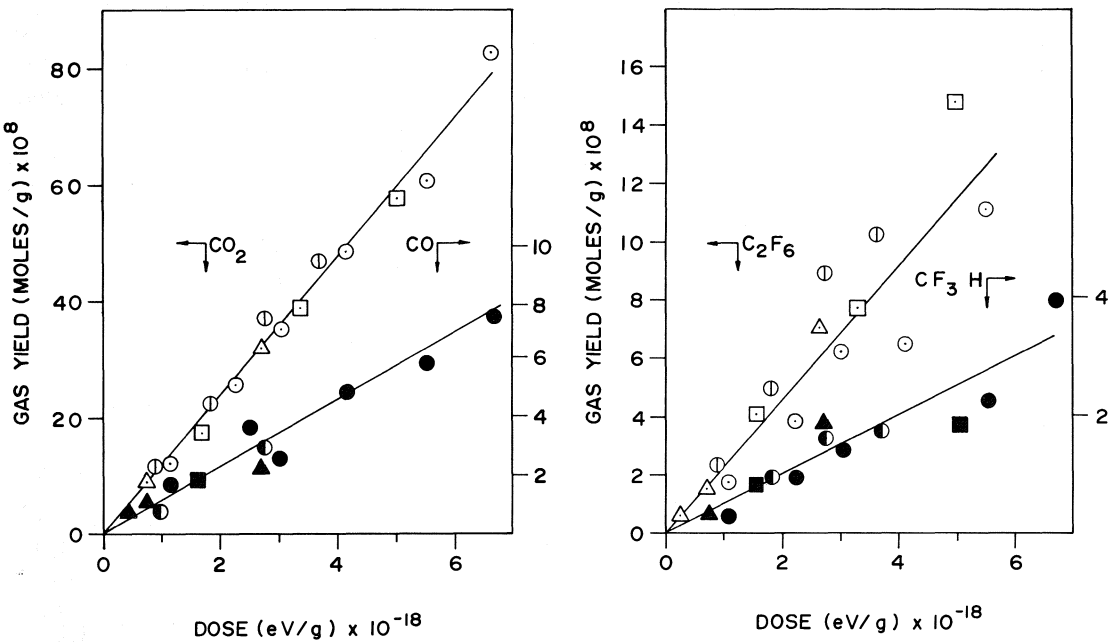

FIG. 1. CO_2, CO, CF_3H, and C_2F_6 yields as a function of dose and dose rate in the radiolysis of liquid CF_3COOH at 23 °C. Dose rates (units of 10^{14} eV g^{-1} s^{-1}): □, ■ 14.0; ⊙, ● 9.27; ◑, ◐ 2.57; △, ▲ 1.07.

TABLE 1. *G*-values of gaseous products for ^{60}Co-γ radiolysis of CF_3COOH and CH_3COOH

System	*G*-values (molecules/100 eV)						
	CO_2	CO	CF_3H	C_2F_6	H_2	CF_4	Reference
CF_3COOH liquid, 23 °C	7.1±0.3	0.71±0.20	0.27±0.06	1.36±0.30	0.031±0.008	0	This work
CF_3COOH solid, −196 °C	2.5±0.4	≃0	0.30±0.04	0.39±0.02	≃0	0	This work
CH_3COOH liquid, 27 °C	6.0	0.73	3.34 (CH_4)	0.62 (C_2H_6)	0.35		3

samples were examined by gas–solid chromatography, using a 10 ft alumina column at 0 °C, hydrogen carrier gas and a hot wire detector. No attempt was made to analyze the products which were condensible at −145 °C.

Results and Discussion

Mass spectrometric analysis of the volatile products showed that the fraction which was non-condensible at —210 °C, consisted of H_2 and CO, while the fraction which was non-condensible at −145 °C, consisted of CF_3H, C_2F_6, and CO_2. Gas–solid chromatographic analysis showed that CF_4 was not a radiolysis product. Mass spectrometric analysis showed that C_2F_4 was not a radiolysis product and that SiF_4 was not present in the gases analyzed.

The dependence of gaseous product yields on absorbed dose and dose rate, in the radiolysis of liquid CF_3COOH, is shown in Figs. 1 and 2. These yields are independent of dose rate in the range (1.07–14.0) × 10^{14} eV g^{-1} s^{-1}. Gaseous product *G*-values, obtained from Figs. 1 and 2, are compared, in Table 1, with analogous gaseous product *G*-values obtained by Johnsen (3) in studies on the ^{60}Co-γ radiolysis of liquid CH_3COOH at a dose rate of 5 × 10^{15} eV g^{-1} s^{-1}. Table 1 also contains average gaseous product *G*-values obtained in the radiolysis of solid CF_3COOH at −196 °C at a dose rate of 1.85 × 10^{14} eV g^{-1} s^{-1}.

The data in Table 1 show that in the radiolysis of liquid CF_3COOH at 23 °C, the gaseous products are CO_2, CO, CF_3H, C_2F_6, and H_2, which are identical to those found by Mearns and Back (4) in their study of the continuous (low pressure mercury arc) photolysis of CF_3COOH vapor in the temperature range 90 to 190 °C. In the radiolysis of solid CF_3COOH at −196 °C, the gaseous products are CO_2,CF_3H, and C_2F_6. The gases

Can. J. Chem. Downloaded from www.nrcresearchpress.com by 210.87.254.5 on 09/05/12
For personal use only.

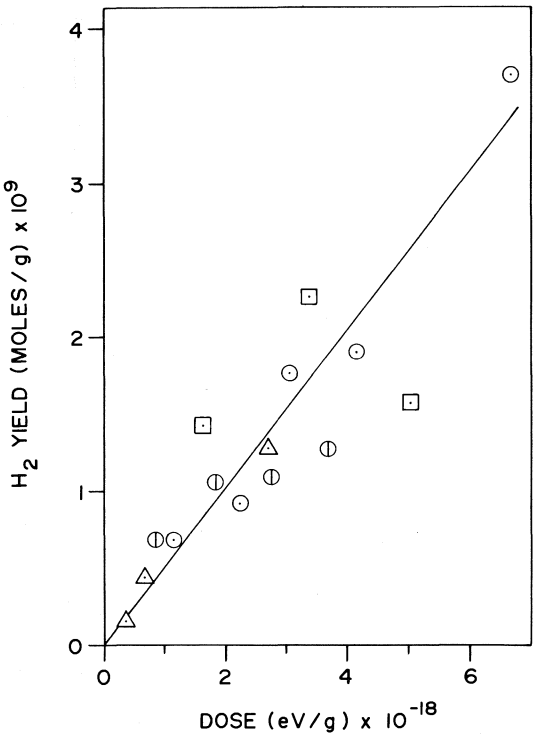

FIG. 2. H_2 yields as a function of dose and dose rate in the radiolysis of liquid CF_3COOH at 23 °C. Dose rates (units of 10^{14} eV g^{-1} s^{-1}): ⊡ 14.0, ⊙ 9.27, ◑ 2.57, △ 1.07.

SiF_4, C_2F_4, and CF_4 are not produced in the radiolysis of either liquid or solid CF_3COOH. Thus, in the γ-radiolysis of liquid and solid CF_3COOH, HF and $:CF_2$ are not radiolysis products and disproportionation reactions involving pairs of $\cdot CF_3$ radicals as well as abstraction of F atoms by H· and $\cdot CF_3$ do not occur. The species $:CF_2$ is a known transient in the isothermal flash photolysis of CF_3COOH vapor (5) and C_2F_4 (as well as C_2F_6) are final products of both the flash and (high pressure xenon arc) photolyses of CF_3COOH vapor (6).

The data in Table 1 also show that $G(CO_2)$ (liquid) = (2.9 ± 0.6) × $G(CO_2)$(solid), $G(C_2F_6)$ (liquid) = (3.6 ± 1.0) × $G(C_2F_6)$(solid) and $G(CF_3H)$(liquid) = $G(CF_3H)$(solid), within the limits of experimental error. Also, if an oxygen atom balance is assumed, considerable losses of H and F atoms have taken place. For H the losses are 96% (liquid) and 88% (solid) and for F the losses are 60% (liquid) and 57% (solid). Approximately 28% of the C atoms remain unaccounted for in the radiolysis of the liquid and the solid. These figures suggest that in the γ-radiolysis of liquid and solid CF_3COOH considerable numbers of H and F atoms have been incorporated into non-gaseous products.

The fact that $G(CO_2)$(liquid)/$G(CO_2)$(solid) ≃ $G(C_2F_6)$(liquid)/$G(C_2F_6)$(solid) implies that CO_2 and C_2F_6 have a common precursor. This may be the radical cation, $CF_3\dot{C}\overset{+}{O}OH$, which is formed in the primary ionization [1] and which is consumed exclusively in the very rapid proton transfer reaction 2. Reaction 2 is facilitated by hydrogen bonding which exists in gaseous CF_3COOH (7), in liquid CF_3COOH (8, 9) and, by inference, in solid CF_3COOH, since the crystal structure of this solid, unlike that of solid CH_3COOH (10), is not known. In reactions 1 and 2 CF_3COOH, $CF_3\dot{C}\overset{+}{O}OH$, and $CF_3COOH_2^+$ represent segments in long hydrogen bonded chains of parent molecules.

$$[1] \qquad CF_3COOH \rightsquigarrow CF_3\dot{C}\overset{+}{O}OH + e^-$$

$$[2] \qquad CF_3\dot{C}\overset{+}{O}OH + CF_3COOH \rightarrow \cdot CF_3 + CO_2 + CF_3COOH_2^+$$

$\cdot CF_3$ radicals and CO_2 molecules produced in reaction 2 are hot species as ΔH[3] is approximately −15 kcal/mol.[5] Because $G(CO_2) \gg G(C_2F_6)$, in both phases, a very large number of $\cdot CF_3$ radicals do not recombine

$$[3] \qquad CF_3C\dot{O}O \rightarrow \cdot CF_3 + CO_2$$

to form C_2F_6. Further reactions of this species are reactions 4 to 7, inclusive. Reaction 4 probably occurs in spurs and involves hot $\cdot CF_3$ radicals as Mearns and Back (4) have shown that reaction 4 does not occur in the gas phase. Since the probability of escape of hot $\cdot CF_3$ radicals from spurs in the liquid is greater than the probability of escape of these radicals from spurs in the solid, the yield of CF_3H from reaction 4 is expected to be less in

$$[4] \quad \cdot CF_3 + CF_3COOH \rightarrow CF_3H + \cdot CF_3 + CO_2$$

$$[5] \quad \cdot CF_3 + \cdot COOH \rightarrow CF_3H + CO_2$$

[5] $\Delta H_f^\circ(CF_3C\dot{O}O) = -193$ kcal/mol was obtained from the expression: $D(CF_3COO{-}H) = \Delta H_f^\circ(CF_3C\dot{O}O) + \Delta H_f^\circ(H\cdot) - \Delta H_f^\circ(CF_3COOH)$ where $D(CF_3COO{-}H) \simeq D(CH_3COO{-}H) = 111$ kcal/mol (11) and $\Delta H_f^\circ(H\cdot) = 52$ kcal/mol (12). The group additivity method of Benson (13) was used to obtain $\Delta H_f^\circ(CF_3COOH) = -252$ kcal/mol. $\Delta H_f^\circ(\cdot CF_3) = -114$ kcal/mol and $\Delta H_f^\circ(CO_2) = -94$ kcal/mol are from ref. 12.

Can. J. Chem. Downloaded from www.nrcresearchpress.com by 210.87.254.5 on 09/05/12
For personal use only.

Can. J. Chem. Downloaded from www.nrcresearchpress.com by 210.87.254.5 on 09/05/12
For personal use only.

[6] $\cdot CF_3 + CF_3COOH \rightarrow CF_3\dot{C}(OH)OCF_3$

[7] $\cdot CF_3 + CF_3\dot{C}(OH)OCF_3 \rightarrow (CF_3)_2C(OH)OCF_3$

liquid than in the solid. However, the yield of CF_3H from reaction 5 is expected to be greater in the liquid than in the solid, where recombination to yield CF_3COOH is more probable. Thus reaction 5, which is an important source of CF_3H in the photolysis of CF_3COOH vapor (4), together with reaction 4, can be used to explain the observed lack of dependence of $G(CF_3H)$ on temperature and phase. The ·COOH radical is a product of one of two probable neutral dissociation processes, [8] and [9], which occur in the radiolysis.

[8] $CF_3COOH \dashrightarrow \cdot CF_3 + \cdot COOH$

[9] $CF_3COOH \dashrightarrow CF_3\dot{C}O + \cdot OH$

The dissociation of CF_3COOH to H· and $CF_3C\dot{O}O$ is considered unimportant because of the magnitude of $D(CF_3COO—H)$[5] and the very small $G(H_2)$ obtained in this study.

The addition of $\cdot CF_3$ to carbonyl groups is well established (6, 14). Gordon (15) has shown that the activation energy for the addition of $\cdot CF_3$ to CF_3COCF_3 is 9.7 kcal/mol, the activation energy for the dissociation of $(CF_3)_2\dot{C}OCF_3$ to $\cdot CF_3$ and CF_3COCF_3 is 30.6 kcal/mol and $\cdot CF_3$ and $(CF_3)_2\dot{C}OCF_3$ combine readily to form perfluoro *t*-butyl methylether. For the non-gaseous product of reaction 7, C:F:H is 1:2.3:0.3. The C:F:H values for atoms which are unaccounted for in the radiolysis of solid CF_3COOH is 1:2.0:3.0 and in the radiolysis of liquid CF_3COOH is 1:2.1:4.2. Thus reactions 6 and 7 are important in the radiolysis of both solid and liquid CF_3COOH and other mechanisms for H atom loss exist.

Various products of the interaction of electrons, released in reaction 1, with $CF_3COOH_2^+$ and CF_3COOH are possible. Processes 10 to 13 inclusive are consistent with the absence of H_2 in

[10] $CF_3COOH_2^+ + e^- \rightarrow CF_3\dot{C}O + H_2O$

[11] $CF_3COOH_2^+ + e^- \rightarrow CF_3CHO + \cdot OH$

[12] $CF_3COOH + e^- \rightarrow \cdot CF_3 + HCOO^-$

[13] $CF_3COOH + e^- \rightarrow CF_3\dot{C}O + OH^-$

the radiolysis of solid CF_3COOH and the very small $G(H_2)$ observed in the radiolysis of liquid CF_3COOH, the indirect evidence for the absence of HF, the absence of CO in the radiolysis of solid CF_3COOH and the F and H atom losses noted in this work.

The activation energy for reaction 14 is estimated to be $E_{14} = 17$ kcal/mol.[6] Amphlett and

[14] $CF_3\dot{C}O \rightarrow \cdot CF_3 + CO$

Whittle (17) have obtained a lower limit to E_{14} which is 10 kcal/mol and have shown that the frequency factor for reaction 14 is abnormally low. Thus, in the radiolysis of solid CF_3COOH at −196 °C, no CO is expected and $CF_3\dot{C}O$ radicals are likely to recombine or to react with other radicals (*e.g.* ·OH, $\cdot CF_3$) to form non-gaseous products. In the radiolysis of liquid CF_3COOH at 23 °C some $CF_3\dot{C}O$ radicals will decompose to CO and the remainder will form non-gaseous products, as in the solid. Non-gaseous products (HCOOH and H_2O) will also be formed in the reactions of $HC\dot{O}O$ and OH^- with $CF_3COOH_2^+$.

We thank the National Research Council of Canada for financial support and for providing one of us (J.B.) with a National Research Council Postdoctoral Fellowship. We also thank Dr. F. P. Lossing and Mr. R. Pilon for assistance with the mass spectrometric analyses and the Defence Research Board of Canada for the use of their irradiation facilities.

1. P. B. Ayscough, K. Mach, J. P. Oversby, and A. K. Roy. Trans. Faraday Soc. **67**, 360 (1971).
2. F. D. Srygley and W. Gordy. J. Chem. Phys. **46**, 2245 (1967).
3. R. H. Johnsen. J. Phys. Chem. **63**, 2041 (1959).
4. A. M. Mearns and R. A. Back. Can. J. Chem. **41**, 1197 (1963).
5. J. P. Simons and A. J. Yarwood. Nature, **192**, 943 (1961).
6. J. R. Majer and J. P. Simons. Advances in photochemistry. Vol. 2. Interscience Publ. New York. 1964.
7. J. Karle and L. O. Brockway. J. Am. Chem. Soc. **66**, 564 (1944).
8. G. C. Pimentel and A. McClellan. The hydrogen bond. W. H. Freeman, San Francisco. 1960.

---

[6] $E_{14} = \Delta H[14] + E_{-14} = 17$ kcal/mol. $\Delta H_f^0(CF_3\dot{C}O) = -152$ kcal/mol was obtained from the expression: $D(CF_3CO—OH) = \Delta H_f^0(CF_3\dot{C}O) + \Delta H_f^0(\cdot OH) - \Delta H_f^0(CF_3COOH)$ where $D(CF_3CO—OH) \simeq D(CH_3CO—OH) = 109$ kcal/mol (11), $\Delta H_f^0(\cdot OH) = 9$ kcal/mol (12) and $\Delta H_f^0(CF_3COOH) = -252$ kcal/mol.[5] $\Delta H_f^0(CO) = -26$ kcal/mol is from (12). It is assumed that E_{-14} is the same as the activation energy (5 kcal/mol) for $\cdot CH_3 + CO \rightarrow CH_3\dot{C}O$, obtained by Kerr and Calvert (16). $D(CF_3—\dot{C}O) = 12$ kcal/mol has also been estimated from the relation: $D(CF_3CO—OH) + D(CF_3—\dot{C}O) = \Delta H_f^0(\cdot OH) + \Delta H_f^0(CO) + \Delta H_f^0(\cdot CF_3) - \Delta H_f^0(CF_3COOH)$.

9. T. S. S. R. MURTY and K. S. PITZER. J. Phys. Chem. **73**, 1426 (1969).
10. R. E. JONES and D. H. TEMPLETON. Acta Crystallogr. **11**, 484 (1960).
11. J. G. CALVERT and J. N. PITTS, JR. Photochemistry. J. Wiley. New York. 1966.
12. D. D. WAGMAN, W. H. EVANS, V. B. PARKER, I. HALOW, S. M. BAILEY, and R. H. SCHUMM. N.B.S. Technical Note 270–3, U.S. Department of Commerce. 1968.
13. S. W. BENSON. Thermochemical kinetics. J. Wiley. New York. 1966.
14. J. M. TEDDER and J. C. WALTON. Progress in reaction kinetics. Vol. 4. Pergamon, Oxford. 1967.
15. A. S. GORDON. J. Chem. Phys. **36**, 1330 (1962).
16. J. A. KERR and J. G. CALVERT. J. Phys. Chem. **69**, 1022 (1965).
17. J. C. AMPHLETT and E. WHITTLE. Trans. Faraday Soc. **63**, 80 (1967).

Can. J. Chem. Downloaded from www.nrcresearchpress.com by 210.87.254.5 on 09/05/12
For personal use only.

Can. J. Chem. Downloaded from www.nrcresearchpress.com by 210.87.254.6 on 09/05/12
For personal use only.

NOTES

Lignin and Related Compounds. III. An Improved Synthesis of 3-(4-Hydroxy-3-methoxyphenyl)-1-propanol and 3-(4-Hydroxy-3,5-dimethoxyphenyl)-1-propanol

J. M. Pepper, G. S. Sundaram, and G. Dyson

Department of Chemistry and Chemical Engineering, University of Saskatchewan, Saskatoon, Saskatchewan

Received June 7, 1971

3-(4-Hydroxy-3-methoxyphenyl)-1-propanol (dihydroconiferyl alcohol) (**1**) and 3-(4-hydroxy-3,5-dimethoxyphenyl)-1-propanol (dihydrosinapyl alcohol) (**2**) have been synthesized in good yields from 4-allyl-2-methoxyphenol (eugenol) and 4-allyl-2,6-dimethoxyphenol by means of the hydroboration reaction.

L'(hydroxy-4 méthoxyphényl-3)-3 propanol-1 (alcool dihydroconiferyle) (**1**) et l'(hydroxy-4 diméthoxyphényl-3,5)-3 propanol-1 (alcool dihydrosinapyle) (**2**) ont été synthétisés avec un bon rendement à partir de l'allyl-4 méthoxy-2 phénol (eugénol) et l'allyl-4 diméthoxy-2,6 phénol au moyen d'une réaction d'hydroboration.

Canadian Journal of Chemistry, **49**, 3394 (1971)

Introduction

Studies in these laboratories on the catalytic hydrogenolysis of spruce and aspen lignins (1, 2) have shown that significant quantities of 3-(4-hydroxy-3-methoxyphenyl)-1-propanol (dihydroconiferyl alcohol) (**1**) and 3-(4-hydroxy-3,5-dimethoxyphenyl)-1-propanol (dihydrosinapyl alcohol) (**2**) may be obtained. In order to study the properties and potential uses of these compounds it was necessary to synthesize them in adequate amounts. Previously reported syntheses involved

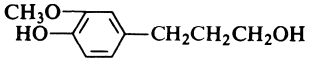

1

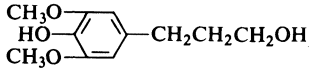

2

the ultimate reduction of ethyl dihydroferulate or ethyl dihydrosinapate using either sodium in alcohol or lithium aluminum hydride (3–5). The preparation of these esters from the available starting materials, vanillin and syringaldehyde, involved several steps resulting in low overall yields.

This note reports the direct conversion by hydroboration and subsequent alkaline oxidation of the commercially available compounds, 4-allyl-2-methoxyphenol (eugenol) and 4-allyl-2,6-dimethoxyphenol, into **1** and **2** respectively. The required primary alcohol isomer is the major product representing ninety percent of the total. Separation of the two isomers may be achieved by repeated recrystallization from carbon tetrachloride – chloroform (5:1) mixture to give white crystals of the desired products **1** and **2** in approximately 80 and 75% yields, respectively. The success of the synthesis is dependent on the use of rigorously anhydrous conditions.

The characterization of the products was confirmed through their n.m.r. and mass spectra.

Experimental

Synthesis of 3-(4-Hydroxy-3-methoxyphenyl)-1-propanol (1)

Eugenol (9.7 g), obtained by fractional distillation (b.p. 78–80°/1 mm), was added to a 500 ml, three-necked flask which had been dried for 1 h at 110°. The flask was immediately fitted with a thoroughly dry pressure equating dropping funnel, a calcium chloride drying tube, and an inlet for dry nitrogen. Tetrahydrofuran (50 ml) previously dried over calcium hydride for 12 h and redistilled from $LiAlH_4$, was added to the flask which was then stoppered.

Borane (1 *M* in tetrahydrofuran) (60 ml) was added dropwise (30 drops per min) through the funnel to the

stirred solution in the flask which was maintained at 0° by an ice bath. The solid, substituted borane separated near the end of the addition. Stirring was continued for an extra 30 min, at which time water (20 ml) was added to decompose the excess borane. This was followed by the addition of 3 *M* NaOH (24 ml), after which the mixture was allowed to warm to room temperature and 30% H_2O_2 (14 ml) added carefully and stirring continued for 1.5 h. The resulting pale yellow solution was extracted with diethyl ether (6 × 50 ml), saturated with NaCl, acidified with HCl (50 ml 2 *M*) and further extracted with ether (3 × 50 ml). The combined ether extracts were dried and concentrated to leave a yellow oil which slowly crystallized on standing at −15 °C. A gas chromatographic analysis (using a 6 ft, 1/8 in. stainless steel column packed with 10% SE30 on Chromosorb W, programmed from 100 °C at 4°/min) showed the two isomeric alcohols separated by 6.2 min.

Two crystallizations from carbon tetrachloride – chloroform (5:1) gave 3-(4-hydroxy-3-methoxyphenyl)-1-propanol (**1**), 8.7 g, (81%), m.p. 64–65° (reported m.p. 63–65° (4)).

Synthesis of 3-(4-Hydroxy-3,5-dimethoxyphenyl)-1-propanol (2)

Using the same procedure as described above, 4-allyl-2,6-dimethoxyphenol (10.7 g) was converted into 3-(4-hydroxy-3,5-dimethoxyphenyl)-1-propanol (**2**), 9.0 g (77%) m.p. 75–76° (reported m.p. 75–76.5° (4)).

This work was supported by an EMR grant from the Department of Forestry and Fisheries for which grateful acknowledgment is made.

1. J. M. Pepper and Y. W. Lee. Can. J. Chem. **47**, 723 (1969)
2. R. Fleming. Master's Thesis. University of Saskatchewan, Saskatoon, Saskatchewan, 1969.
3. C. P. Brewer, L. Cooke, and H. Hibbert. J. Am. Chem. Soc. **70**, 57 (1948).
4. C. J. Coscia, W. J. Schubert, and F. F. Nord. J. Org. Chem. **26**, 5091 (1961).
5. I. A. Pearl. J. Org. Chem. **24**, 740 (1959).

Can. J. Chem. Downloaded from www.nrcresearchpress.com by 210.87.254.6 on 09/05/12
For personal use only.

An Approach to Stereochemical Analysis by Ion Cyclotron Resonance. Distinguishing *exo*- and *endo*-Norborneol

Maurice M. Bursey[1] and Michael K. Hoffman
Venable Chemical Laboratory, The University of North Carolina, Chapel Hill, North Carolina 27514

Received March 8, 1971

The ion cyclotron resonance spectra of mixtures of biacetyl and *exo*- or *endo*-norborneol show differences in the acetylation of the alcohol by the *m/e* 129 ion formed from biacetyl. The differences may be interpreted as a difference by a factor of four in rates of acetylation; a steric effect is proposed as the cause of the difference.

Les spectres de résonance cyclotron-ion de mélanges de biacétyle et d'*exo*- ou d'*endo*-norbornéol, montrent des différences dans l'acétylation de l'alcool, par l'ion *m/e* 129 qui se forme à partir du biacétyle. Les différences peuvent être interprétées comme une différence dans les vitesses d'acétylation par un facteur de quatre; il est suggéré qu'un effet stérique est la cause de cette différence.

Canadian Journal of Chemistry, **49**, 3395 (1971)

The reaction rates of *exo*- and *endo*-norborneol with acetylated biacetyl in the gaseous phase (eq. 1) differ by a factor of 4.

[1] $C_7H_{11}OH + C_6H_9O_3^+ \rightarrow C_7H_{11}O(H)OC_2H_3^+ + C_4H_6O_2$

We have proposed that ion–molecule reactions studied by ion cyclotron resonance (i.c.r.) may be of use in the identification of organic functionality (1). Thus, 2,3-butanedione undergoes an ion–molecule reaction with itself (eq. 2) to give a species ("triacetyl", **1**) capable of transferring a specific (2) acetyl group to most oxygen- and nitrogen-containing functional groups (eq. 3). Our purpose in pursuing such studies is to explore the possibilities for reactions capable of distinguishing epimers, a problem which has been

[1]Research Fellow of the Alfred P. Sloan Foundation, 1969–1971.

stirred solution in the flask which was maintained at 0° by an ice bath. The solid, substituted borane separated near the end of the addition. Stirring was continued for an extra 30 min, at which time water (20 ml) was added to decompose the excess borane. This was followed by the addition of 3 *M* NaOH (24 ml), after which the mixture was allowed to warm to room temperature and 30% H_2O_2 (14 ml) added carefully and stirring continued for 1.5 h. The resulting pale yellow solution was extracted with diethyl ether (6 × 50 ml), saturated with NaCl, acidified with HCl (50 ml 2 *M*) and further extracted with ether (3 × 50 ml). The combined ether extracts were dried and concentrated to leave a yellow oil which slowly crystallized on standing at −15 °C. A gas chromatographic analysis (using a 6 ft, 1/8 in. stainless steel column packed with 10% SE30 on Chromosorb W, programmed from 100 °C at 4°/min) showed the two isomeric alcohols separated by 6.2 min.

Two crystallizations from carbon tetrachloride – chloroform (5:1) gave 3-(4-hydroxy-3-methoxyphenyl)-1-propanol (**1**), 8.7 g, (81%), m.p. 64–65° (reported m.p. 63–65° (4)).

Synthesis of 3-(4-Hydroxy-3,5-dimethoxyphenyl)-1-propanol (2)

Using the same procedure as described above, 4-allyl-2,6-dimethoxyphenol (10.7 g) was converted into 3-(4-hydroxy-3,5-dimethoxyphenyl)-1-propanol (**2**), 9.0 g (77%) m.p. 75–76° (reported m.p. 75–76.5° (4)).

This work was supported by an EMR grant from the Department of Forestry and Fisheries for which grateful acknowledgment is made.

1. J. M. Pepper and Y. W. Lee. Can. J. Chem. **47**, 723 (1969)
2. R. Fleming. Master's Thesis. University of Saskatchewan, Saskatoon, Saskatchewan, 1969.
3. C. P. Brewer, L. Cooke, and H. Hibbert. J. Am. Chem. Soc. **70**, 57 (1948).
4. C. J. Coscia, W. J. Schubert, and F. F. Nord. J. Org. Chem. **26**, 5091 (1961).
5. I. A. Pearl. J. Org. Chem. **24**, 740 (1959).

Can. J. Chem. Downloaded from www.nrcresearchpress.com by 210.87.254.6 on 09/05/12
For personal use only.

An Approach to Stereochemical Analysis by Ion Cyclotron Resonance. Distinguishing *exo*- and *endo*-Norborneol

Maurice M. Bursey[1] and Michael K. Hoffman
Venable Chemical Laboratory, The University of North Carolina, Chapel Hill, North Carolina 27514

Received March 8, 1971

The ion cyclotron resonance spectra of mixtures of biacetyl and *exo*- or *endo*-norborneol show differences in the acetylation of the alcohol by the *m/e* 129 ion formed from biacetyl. The differences may be interpreted as a difference by a factor of four in rates of acetylation; a steric effect is proposed as the cause of the difference.

Les spectres de résonance cyclotron-ion de mélanges de biacétyle et d'*exo*- ou d'*endo*-norbornéol, montrent des différences dans l'acétylation de l'alcool, par l'ion *m/e* 129 qui se forme à partir du biacétyle. Les différences peuvent être interprétées comme une différence dans les vitesses d'acétylation par un facteur de quatre; il est suggéré qu'un effet stérique est la cause de cette différence.

Canadian Journal of Chemistry, **49**, 3395 (1971)

The reaction rates of *exo*- and *endo*-norborneol with acetylated biacetyl in the gaseous phase (eq. 1) differ by a factor of 4.

[1] $C_7H_{11}OH + C_6H_9O_3^+ \rightarrow C_7H_{11}O(H)OC_2H_3^+ + C_4H_6O_2$

We have proposed that ion–molecule reactions studied by ion cyclotron resonance (i.c.r.) may be of use in the identification of organic functionality (1). Thus, 2,3-butanedione undergoes an ion–molecule reaction with itself (eq. 2) to give a species ("triacetyl", **1**) capable of transferring a specific (2) acetyl group to most oxygen- and nitrogen-containing functional groups (eq. 3). Our purpose in pursuing such studies is to explore the possibilities for reactions capable of distinguishing epimers, a problem which has been

[1]Research Fellow of the Alfred P. Sloan Foundation, 1969–1971.

[2] $$CH_3COCOCH_3^{+\cdot} + CH_3COCOCH_3 \rightarrow \underset{\mathbf{1}}{CH_3C(=O)-C(=O^+COCH_3)CH_3} + CH_3CO^{\cdot}$$

[3] $$\mathbf{1} + R-O-R \rightarrow \begin{matrix} R \\ \diagdown \\ O^+ \\ \diagup \\ R \end{matrix}\!\!-C(=O)-CH_3 + CH_3COCOCH_3$$

[4] 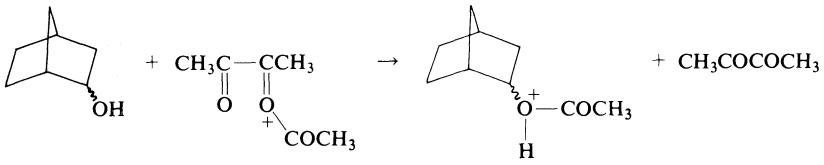

1 2

[5] $$\frac{k_{exo}}{k_{endo}} = \left\{\frac{P_s}{(P_s + 1.44P_p)[B]}\right\}_{exo} \Big/ \left\{\frac{P_s}{(P_s + 1.44P_p)[B]}\right\}_{endo}$$

explored by conventional mass spectrometry for many systems (3) but whose general solution by this technique is not satisfactory from the viewpoint of establishing predictive rules.

The epimers *exo*- and *endo*-norborneol appeared to offer an especially attractive case for detecting large differences in reactivity. These types of systems have been studied for many years, beginning with the study of acetolysis of the tosylates and brosylates, where a ratio of rate constants equal to 350 was observed (4).[2] For the present case, the well known controversy over the nature of the intermediate carbonium ion in such systems is not pertinent. One school of thought presents the observed differences in reactivity in similar systems as the result of steric interference (6), while the other group claims that σ delocalization is responsible (7). The differences in steric environment of the alcohol function in *exo*- and *endo*-norborneol, in any event, are well known.

At an ionizing energy of 13 eV and pressures of *ca.* 2×10^{-5} Torr each of 2,3-butanedione and *exo*- or *endo*-norborneol, the only ion–molecule reaction product observed (other than "triacetyl," **1** and the irrelevant ions protonated biacetyl, and a self-reaction of norborneol at *m/e* 138) occurs at *m/e* 155. This mass corresponds to the addition of 43 mass units to the molecular weight of norborneol. Double-resonance experiments demonstrate that this ion originates entirely from **1** (eqs. 1, 4) and that the reaction occurs only in the analyzer section of the i.c.r. cell.[3] The reaction is therefore interpreted as a transfer of the acetyl ion from "triacetyl," **1**, to the alcohol, analogously to examples we have studied before (1, 2).

Prior experience and consideration of the relative rates for reactions of the epimeric alcohols would lead to the thought that under similar conditions the same amount of acetylated product would be produced from each of the epimers. Solution chemistry proves a better guide than prior experience in gas-phase ionic chemistry here, however, since the *exo* isomer forms the acetylated product approximately four times as rapidly as the *endo* isomer.

Examination of one formulation (8) of the derivation of the rate constant for the decomposi-

[2]This ratio refers to formation of the carbonium ion, not that of the oxonium ion generated here, of course. Studies of the carbonium ion by i.c.r. have been reported (5).

[3]Since the precursor **1** is a secondary ion, production of *m/e* 155 from it should occur to a greater extent in the analyzer than the source, where secondary ions have not yet formed to so great an extent from the primary ions. The precursor of **1** $(CH_3COCOCH_3)^{+\cdot}$, is observed as a precursor of *m/e* 155 to a very small extent only in the analyzer but this is a result of its role in the formation of **1**.

Can. J. Chem. Downloaded from www.nrcresearchpress.com by 210.87.254.6 on 09/05/12
For personal use only.

tion of a precursor ion to one non-decomposing secondary ion, in the absence of competing reactions of the precursor,[4] leads to the approximation [5] where P_s is power absorption by the secondary ion **2**, P_p is the power absorption by the precursor ion **1**, [B] is the concentration of norborneol in the chamber, and 1.44 is the factor $155^2/129^2$. Note that **1**, "triacetyl," is the same in both cases.[5]

Evaluation of several sets of data in the total pressure range 1×10^{-5} to 3×10^{-5} Torr for each isomer leads to a factor of approximately 4 for k_{exo}/k_{endo} for the pair of compounds. The initial consideration of ion–dipole interaction (11) suggests very similar rates for these reactions; even inclusion of the additional term (12) brought in by the locked-dipole model (13) does not suggest a difference of more than a few percent, since the dipole moments of the two compounds differ only by 6% (14).

The differences in relative rates are considerably smaller than the large differences observed in solution chemistry, but still are impressive for gas-phase ionic chemistry, where previous experience has shown similar cross-sections for similar functionalities. Presumably the difference in rates, and cross-sections, may be explained by differences of the steric environment of the *exo* and *endo* hydroxyl group. For the *endo* isomer, the bulkiness of the "triacetyl ion" appears to prevent attack from the hindered underside, so that fewer collisions can result in transfer than in the *exo* isomer, where attack of the "triacetyl ion" appears possible on either side of the alcohol molecule. It appears possible that other, more selective acylating agents can be devised, such as the selective nitryl transfer agents described recently (15). Thus the value of 4 is only a preliminary estimate of the difference in reactivity to be found with acyl transfer reactions, since the ability of "triacetyl" to acetylate most oxygen and nitrogen functionalities points to its great lack of discrimination. We are exploring other species for improvement of the k_{exo}/k_{endo} ratio so that obvious identification of hydroxyl stereochemistries may eventually be made on the basis of *a priori* reasoning.

[4]The acetylated product **2** is formed only from **1**, by ion cyclotron double resonance. Although there is an *m/e* 95 peak in the spectrum, corresponding to the norbornyl cation, which might be considered a product of loss of acetic acid from **2**, it is partially the result of unimolecular decomposition of the molecular ion of norborneol and otherwise the result of a reaction of *m/e* 86 (biacetyl) or 87 (protonated biacetyl) with norborneol. Ion ejection experiments (9) indicated a barely detectable dependence on **1** in one of several experiments performed, but never a dependence on **2**. Hence our assumptions are justified.

[5]An expression for the rate constant differing in coefficients of residence times, which cancel in the derivation from ref. 8, has been proposed as an approximate solution to the general equation (10). No tests have been performed, to our knowledge, to distinguish between the expressions of refs. 8 and 10.

Experimental

Kleinfelter and Schleyer's procedure for the preparation of *exo*-norborneol (16) was used: m.p. 126–127°, reported m.p. 127–128°. Toivonen's procedure was used (17) for the preparation of the *endo* isomer: m.p. 148–149°, reported m.p. (18), 149–150°. The 2,3-butanedione sample was freshly drawn each day (Aldrich Chemical Co., Inc.).

The i.c.r. techniques employed here, except for ion ejection double resonance (9), were those described by Henis (19). Our ionizing current was 0.05 μA; total ion current, < 10 pA; typical cell voltages were: trap, 0.48 V; analyzer, split (20), 0.24 and 0.26 V; source drift, split (20), −0.11 and +0.35 V; magnetic field sweep, 10 min; response, 0.1 s; field modulation amplitude, 10 G. The fixed frequency (130.53 kHz) defined 85 G/a.m.u.; its r.f. level was 0.6 μA. Pressure readings were monitored by a VacIon pump used for ultimate pumping of the cell.

This study was supported by the National Institute of General Medical Sciences (GM 15 994), the National Science Foundation (GP 8096, GU 2059), and the Advanced Research Projects Agency (Contract SD-100 with the University of North Carolina Materials Research Center). The ICR-9 spectrometer was purchased through support by Hercules, Inc., the Shell Companies Foundation, the National Science Foundation (GU 2059), and the North Carolina Board of Science and Technology (159).

1. M. M. Bursey, T. A. Elwood, M. K. Hoffman, T. A. Lehman, and J. M. Tesarek. Anal. Chem. **42**, 1370 (1970).
2. M. K. Hoffman, T. A. Elwood, T. A. Lehman, and M. M. Bursey, Tetrahedron Lett. 4021 (1970).
3. S. Meyerson and A. W. Weitkamp. Org. Mass Spectrom. **1**, 659 (1968).
4. S. Winstein and D. S. Trifan. J. Am. Chem. Soc. **71**, 2953 (1949).
5. F. Kaplan. J. Am. Chem. Soc. **92**, 1445 (1970).
6. H. C. Brown. The transition state. The Chemical Society, London, 1962. p. 140.
7. G. D. Sargent. Q. Rev. **20**, 301 (1966).
8. G. C. Goode, R. M. O'Malley, A. J. Ferrer-Correia, R. I. Massey, K. R. Jennings, J. H. Futrell, and P. M. Llewellyn. J. Mass. Spectrom. Ion Phys. **5**, 393 (1970).
9. J. Beauchamp and J. Armstrong. Rev. Sci. Instrum. **40**, 123 (1969).
10. S. E. Buttrill. J. Chem. Phys. **50**, 4125 (1969).

Can. J. Chem. Downloaded from www.nrcresearchpress.com by 210.87.254.6 on 09/05/12
For personal use only.

11. G. GIOUMOUSIS and D. P. STEVENSON. J. Chem. Phys. **29**, 294 (1958).
12. S. K. GUPTA, E. G. JONES, A. G. HARRISON, and J. J. MYHER. Can J. Chem. **45**, 3107 (1967).
13. T. F. MORAN and W. H. HAMILL. J. Chem. Phys. **39**, 1413 (1963).
14. H. KRIEGER. Suomen Kemistilehti, **31B**, 348 (1958).
15. W. B. NIXON and M. M. BURSEY. Tetrahedron Lett. 4389 (1970).
16. D. C. KLEINFELTER and P. v. R. SCHLEYER. Org. Synth. **42**, 79 (1962).
17. A. TOIVONEN. Ann. Acad. Sci. Fennicae, Ser. A, II, No. 72 (1956).
18. K. ALDER and H. F. RICKERT. Ann. Chem. **543**, 1 (1939).
19. J. M. S. HENIS. J. Am. Chem. Soc. **90**, 844 (1968).
20. T. A. ELWOOD, J. M. TESAREK, T. A. LEHMAN, and M. M. BURSEY. 18th Annual Conference on Mass Spectrometry and Allied Topics. San Francisco, California, June 14–19, 1970.

Can. J. Chem. Downloaded from www.nrcresearchpress.com by 210.87.254.6 on 09/05/12
For personal use only.

Pulse Radiolysis of Formamide and Formamide–Water Mixtures

D. C. WALKER AND S. C. WALLACE[1]
Chemistry Department, University of British Columbia, Vancouver, British Columbia

Received June 7, 1971

From the optical absorption spectrum observed by a sub-nanosecond pulse radiolysis method it is concluded that irradiated pure liquid formamide (dielectric constant = 109) does not yield solvated electrons with lifetimes $>10^{-11}$ s. In formamide–water mixtures the hydrated electron is formed in low yield and the position of the absorption band of e_{aq}^- is not altered by changing the composition. Apparently formamide reacts much more rapidly with thermalized electrons than it does with hydrated electrons. The latter may be formed in formamide–water mixtures due to aggregates of water molecules.

Le spectre d'absorption optique observé par la méthode de radiolyse avec une pulsation en dessous de la nanoseconde a permis de conclure que la formamide liquide pure irradiée (constante diélectrique = 109) ne donne pas d'électrons solvatés avec des temps de vie supérieurs à 10^{-11} s. Dans les mélanges formamide–eau, l'électron hydraté se forme avec un faible rendement et la position de la bande d'absorption de e_{aq}^- n'est pas altérée par un changement de composition. Apparemment, la formamide réagit beaucoup plus rapidement avec des électrons chauffés qu'elle ne le fait avec des électrons hydratés qui pourraient se former dans les mélanges formamide–eau, par suite des conglomérats de molécules d'eau.

Canadian Journal of Chemistry, **49**, 3398 (1971)

For a wide range of liquids (*e.g.* hydrocarbons, ethers, amines, alcohols, water)[2] there is, in general, an increase in both the radiation yield and the energy of the optical absorption band maximum of solvated electrons with increasing static dielectric constant (1, 2). Thus the pulse radiolysis of formamide ($HCONH_2$) is of interest because it has an exceptionally high dielectric constant (109 at 20 °C). On the basis of polaron theory and the fact that the positive end of the molecule is dispersed over an NH_2 group, one would anticipate an absorption band for electrons solvated in this medium to be in the visible or near i.r. region of the spectrum.

We present data on the sub-nanosecond pulse radiolysis absorption spectrum of pure liquid formamide and various formamide–water mixtures, taken by measuring the reabsorption of the system's own Cerenkov light when subjected to an intense 3 ns pulse of 500 kV electrons from a Febetron accelerator. We have demonstrated the qualitative potentiality of this technique (3) and will deal with the quantitative assessment of data elsewhere (4). It will be shown that for absorbing species whose mean lifetime exceeds the pulse duration (thus their concentration builds up throughout the pulse whereas the light intensity has the same time profile as the pulse) and when using spectrographic detection the relationship [1] should be used.

$$[1] \qquad I_0/I_t = G\varepsilon\,(23.03\ D/N)$$

[1]Present address: Radiation Laboratory, University of Notre Dame, Indiana 46556, U.S.A.

[2]Note added in proof: the dipolar aprotic solvents DMSO and HMPA are exceptions to their trends.

11. G. GIOUMOUSIS and D. P. STEVENSON. J. Chem. Phys. **29**, 294 (1958).
12. S. K. GUPTA, E. G. JONES, A. G. HARRISON, and J. J. MYHER. Can J. Chem. **45**, 3107 (1967).
13. T. F. MORAN and W. H. HAMILL. J. Chem. Phys. **39**, 1413 (1963).
14. H. KRIEGER. Suomen Kemistilehti, **31B**, 348 (1958).
15. W. B. NIXON and M. M. BURSEY. Tetrahedron Lett. 4389 (1970).
16. D. C. KLEINFELTER and P. v. R. SCHLEYER. Org. Synth. **42**, 79 (1962).
17. A. TOIVONEN. Ann. Acad. Sci. Fennicae, Ser. A, II, No. 72 (1956).
18. K. ALDER and H. F. RICKERT. Ann. Chem. **543**, 1 (1939).
19. J. M. S. HENIS. J. Am. Chem. Soc. **90**, 844 (1968).
20. T. A. ELWOOD, J. M. TESAREK, T. A. LEHMAN, and M. M. BURSEY. 18th Annual Conference on Mass Spectrometry and Allied Topics. San Francisco, California, June 14–19, 1970.

Can. J. Chem. Downloaded from www.nrcresearchpress.com by 210.87.254.40 on 09/05/12
For personal use only.

Pulse Radiolysis of Formamide and Formamide–Water Mixtures

D. C. WALKER AND S. C. WALLACE[1]
Chemistry Department, University of British Columbia, Vancouver, British Columbia

Received June 7, 1971

From the optical absorption spectrum observed by a sub-nanosecond pulse radiolysis method it is concluded that irradiated pure liquid formamide (dielectric constant = 109) does not yield solvated electrons with lifetimes $>10^{-11}$ s. In formamide–water mixtures the hydrated electron is formed in low yield and the position of the absorption band of e_{aq}^- is not altered by changing the composition. Apparently formamide reacts much more rapidly with thermalized electrons than it does with hydrated electrons. The latter may be formed in formamide–water mixtures due to aggregates of water molecules.

Le spectre d'absorption optique observé par la méthode de radiolyse avec une pulsation en dessous de la nanoseconde a permis de conclure que la formamide liquide pure irradiée (constante diélectrique = 109) ne donne pas d'électrons solvatés avec des temps de vie supérieurs à 10^{-11} s. Dans les mélanges formamide–eau, l'électron hydraté se forme avec un faible rendement et la position de la bande d'absorption de e_{aq}^- n'est pas altérée par un changement de composition. Apparemment, la formamide réagit beaucoup plus rapidement avec des électrons chauffés qu'elle ne le fait avec des électrons hydratés qui pourraient se former dans les mélanges formamide–eau, par suite des conglomérats de molécules d'eau.

Canadian Journal of Chemistry, **49**, 3398 (1971)

For a wide range of liquids (*e.g.* hydrocarbons, ethers, amines, alcohols, water)[2] there is, in general, an increase in both the radiation yield and the energy of the optical absorption band maximum of solvated electrons with increasing static dielectric constant (1, 2). Thus the pulse radiolysis of formamide ($HCONH_2$) is of interest because it has an exceptionally high dielectric constant (109 at 20 °C). On the basis of polaron theory and the fact that the positive end of the molecule is dispersed over an NH_2 group, one would anticipate an absorption band for electrons solvated in this medium to be in the visible or near i.r. region of the spectrum.

We present data on the sub-nanosecond pulse radiolysis absorption spectrum of pure liquid formamide and various formamide–water mixtures, taken by measuring the reabsorption of the system's own Cerenkov light when subjected to an intense 3 ns pulse of 500 kV electrons from a Febetron accelerator. We have demonstrated the qualitative potentiality of this technique (3) and will deal with the quantitative assessment of data elsewhere (4). It will be shown that for absorbing species whose mean lifetime exceeds the pulse duration (thus their concentration builds up throughout the pulse whereas the light intensity has the same time profile as the pulse) and when using spectrographic detection the relationship [1] should be used.

$$[1] \qquad I_0/I_t = G\varepsilon\,(23.03\ D/N)$$

[1]Present address: Radiation Laboratory, University of Notre Dame, Indiana 46556, U.S.A.

[2]Note added in proof: the dipolar aprotic solvents DMSO and HMPA are exceptions to their trends.

Can. J. Chem. Downloaded from www.nrcresearchpress.com by 210.87.254.40 on 09/05/12
For personal use only.

where I_0 is the number of Cerenkov light photons per pulse when there is no reabsorption, I_t that obtained when there is partial reabsorption, G is the 100 eV radiation yield of absorbing species, ε the absorption coefficient at a particular wavelength, D the incident dose per pulse (in eV cm^{-2}) measured using a calorimeter thick enough to completely stop the high energy electrons, and N Avagadro's number. The I_0 data was obtained from concentrated solutions of H^+ and other scavengers and the relative intensity agreed with that theoretically predicted (5) from other compounds and mixtures. For any spectrum so obtained (23.03 D/N) is a constant but does change from pulse to pulse due to slight variations in the electron pulse intensity. In fact, because the characteristic curves for the film sensitivity as a function of wavelength were established by a multiple pulse method (4), these variations were averaged out and the relative magnitude of $G\varepsilon$ for the various solutions should be quite reliable.

Figure 1 shows the absorption spectra for pure formamide, 20% H_2O, 36% H_2O, 50% H_2O, and pure H_2O within the wavelength range 300 to 900 nm.[3] Because of a fairly rapid decay of the band centered at 680 nm in the formamide–water mixtures ($k = 3.5 \times 10^8\ s^{-1}$ in the 50% solution, see later) very small corrections (< 10%) were applied to the $G\varepsilon$ values given in Fig. 1 to account for the diminished lifetimes in the mixtures (4).)

High concentrations of H^+ (2 M) completely removed the band centered at 680 nm in all the water-containing solutions and also eliminated the weak band seen as a shoulder at ~520 nm in the pure formamide. The long wavelength edge of the u.v. band in pure formamide was also somewhat reduced by the presence of H^+.

Several features of these spectra are important. (*i*) For the case of pure formamide, only a very weak absorption band in the range 400–500 nm seems to be related to species formed by thermalized-electron capture. Since the yield of long-lived ($> 10^{-8}$ s) free-ions in irradiated pure formamide has been shown by N_2O scavenging to be 3.3 ± 0.3 (6), commensurate with its high dielectric constant, then the absorption band at $\lambda \sim 520$ nm must have $\varepsilon \sim 300\ M^{-1}\ cm^{-1}$ if it is to be attributed to the species responsible for the free-ion yield. Although we cannot measure the lifetime of the species absorbing at 520 nm others have reported bands in the range 400–550 nm with lifetimes of microseconds and longer (7–9) so that the 520 nm band does not appear to arise from a very short lived ($\sim 10^{-11}$ s) strongly absorbing species.

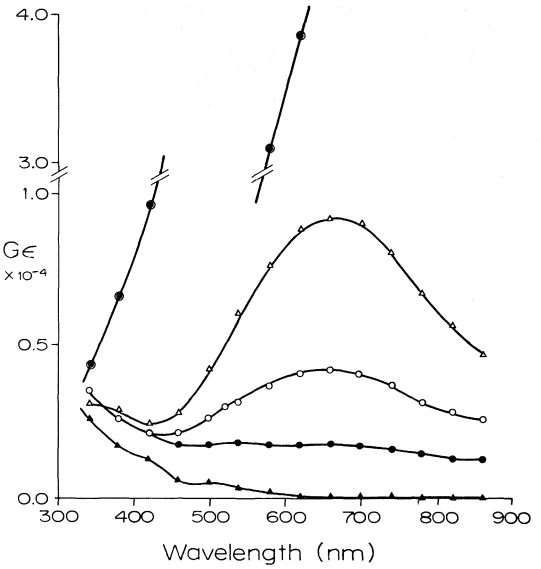

FIG. 1. Absorption spectra of pulse irradiated formamide and formamide–water mixtures. ▲, pure formamide; ●, 20% H_2O; ○, 36% H_2O; △, 50% water; and ◉, pure H_2O (% by volume).

For the wavelength range 600–900 nm there is no detectable absorption, which means $G\varepsilon < 500\ M^{-1}\ cm^{-1}\ (100\ eV)^{-1}$ for species with lifetimes > 3 ns. By conventional pulse radiolysis methods using 40 ns pulses this has been shown to continue out to 2000 nm (9). We can also conclude that $G\varepsilon < 4 \times 10^3$ for species having lifetimes $\sim 10^{-10}$ s, or $G\varepsilon < 4 \times 10^4$ if the lifetimes were $\sim 10^{-11}$ s.

Solvated electrons in formamide would be expected to have a broad and intense absorption band with ε in the range (1.5–3) $\times 10^4\ M^{-1}\ cm^{-1}$ at λ_{max} by analogy with other solvents

[3]The spectra in Fig. 1 are somewhat different to the preliminary oral presentation of this work at the Marianské Lazné Discussion (13) for two reasons. Firstly, those spectra showed the optical density of the film divided by the gamma of the film, which subsequent analysis shows to be proportional to log ($G\varepsilon$). Secondly, the absorption containing distinct peaks at ~500 nm for 10 and 20% solutions are artifacts arising from reciprocity law failure in a region of low film sensitivity. In the work reported in the current paper this problem was overcome by establishing characteristic curves for the photographic film using a multiple pulse method and working to constant film density (4).

Can. J. Chem. Downloaded from www.nrcresearchpress.com by 210.87.254.40 on 09/05/12
For personal use only.

and thus we conclude that solvated electrons with lifetimes $>10^{-11}$ s are not formed in pure liquid formamide. Perhaps the weak band at $\lambda \sim 520$ nm arises from solvent anions, or decomposition fragments, because it is eliminated by acids.

(*ii*) For all solutions containing large quantities of water a single absorption band centered at ~680 nm was observed, in addition to the u.v. band of formamide and perhaps the shoulder at 520 nm. This main band corresponds very closely in position and shape to that of the hydrated electron. There is no evidence of any shift in the band position or its shape on changing the composition of the mixture. (In this respect they are somewhat analogous to solutions of alcohols in hydrocarbons (10).) This suggests that the solvation shells of the solvated electrons formed in these solutions consist almost entirely of H_2O molecules and are not representative of potential well depths (or solvation energies) intermediate between pure H_2O and pure formamide.

Using the technique of kinetic laser photometry (11) it was shown that the decay of the species responsible for absorption at 632.8 nm proceeds by a pseudo-first order process giving a rate constant for the reaction

$$e_{aq}^- + HCONH_2 \rightarrow \text{Products}$$

of $k = (1.8 \pm 0.2) \times 10^7\ M^{-1}\ s^{-1}$, which is independent of formamide concentration over the range studied, 2.5 to 12.6 M. This k must be compared with values of 4×10^7 (12) and ~$10^6\ M^{-1}\ s^{-1}$ (7) obtained at concentrations of formamide ~$10^{-2}\ M$ in H_2O by microsecond pulse radiolysis methods.

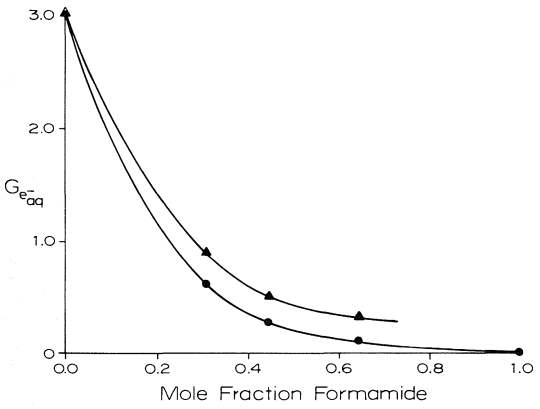

FIG. 2. Plot of $G(e_{aq}^-)$ as a function of mole fraction of formamide. ●, $G(e_{aq}^-)$ values were obtained from the spectra of Fig. 1 taking $\varepsilon(e_{aq}^-)_{580} = 1.1 \times 10^4\ M^{-1}\ cm^{-1}$. ▲, the values of $G(e_{aq}^-)$ divided by the mole fraction of water.

(*iii*) By taking $\varepsilon\ (e_{aq}^-)_{580} = 1.1 \times 10^4\ M^{-1}\ cm^{-1}$ one can plot the value of $G(e_{aq}^-)$ observed as a function of the mole fraction of the mixture, as in Fig. 2 (lower line). If these values of $G(e_{aq}^-)$ are divided by the mole fraction of water then the upper line of Fig. 2 is obtained. These data suggest that formamide molecules are in competition with aggregates of water molecules (perhaps 4 or 6) for the capturing of thermalized electrons formed by the radiolysis. A detailed knowledge of oligomer formation in these solutions would be required to extend this argument to a quantitative level. However, it is quite evident that formamide reacts much more rapidly (by several orders of magnitude) with the precursors of the hydrated electrons than it does with hydrated electrons, once formed.

Our conclusions are that formamide does not form solvated electrons but that it reacts rather rapidly with thermalized electrons, perhaps to give solvent anions which then represent the "free-ion" species which may reduce several electron scavengers (6). In formamide–water mixtures the solvated electrons formed have solvation shells consisting only of water molecules.

We are most grateful to Dr. Geraldine Kenney-Wallace for kind assistance with the laser photometry experiments and to the National Research Council of Canada for financial support.

1. (*a*) R. A. HOLROYD. *In* Fundamental processes in radiation chemistry. *Edited by* P. Ausloos. Interscience Publishers. 1968. p. 413. (*b*) G. R. FREEMAN and J. M. FAYADH. J. Chem. Phys. **43**, 86 (1965).
2. (*a*) L. M. DORFMAN. Adv. Chem. Ser. **50**, 36 (1965). (*b*) L. M. DORFMAN. Presented at the Herrenalb Discussion on Solvated Electrons. 1971. To be published.
3. D. C. WALKER and S. C. WALLACE. Chem. Phys. Lett. **6**, 111 (1970).
4. S. C. WALLACE and D. C. WALKER. To be published.
5. I. M. FRANK and I. TAMM. Dokl. Acad. Nauk SSSR, **14**, 109 (1937).
6. D. A. HEAD and D. C. WALKER. Can. J. Chem. **48**, 1657 (1970).
7. N. S. FEL', P. I. DOLIN, and V. I. ZOLOTAREVSKII. Khim. Vys. Energ, **1**, 154 (1967).
8. (*a*) A. MATSUMOTO and N. N. LICHTIN. Oral presentation to the International Conference on Radiation Chemistry. Argonne National Lab.,

Illinois. 1968. (*b*) N. N. LICHTIN. Private communication.
9. H. A. GILLIS, N. V. KLASSEN, and D. C. WALKER. Unpublished data.
10. T. J. KEMP, G. A. SALMON, and P. WARDMAN. *In* Pulse radiolysis. *Edited by* M. Ebert *et al.* Academic Press. 1965. p. 255.
11. G. A. KENNEY and D. C. WALKER. J. Chem. Phys. **50**, 4074 (1969).
12. E. J. HART, E. M. FIELDEN, and M. ANBAR. J. Phys. Chem. **71**, 3993 (1967).
13. D. C. WALKER, D. A. HEAD, and S. C. WALLACE. *In* Progress and problems in contemporary radiation chemistry. *Edited by* J. Teply. Prague. 1971. p. 250.

Can. J. Chem. Downloaded from www.nrcresearchpress.com by 210.87.254.40 on 09/05/12
For personal use only.

Crystal and Molecular Structure of the 1:1 Complex of Chloral Hydrate and 7-Bromo-2,3-dihydro-1-methyl-5-phenyl-1,4-benzodiazepin-2-one

R. F. DUNPHY AND H. LYNTON
Department of Chemistry, University of New Brunswick, Fredericton, New Brunswick

Received March 11, 1971

The structure of a 1:1 complex of chloral hydrate and 7-bromo-2,3-dihydro-1-methyl-5-phenyl-1,4-benzodiazepin-2-one has been determined by the heavy atom method. The complex crystallizes in the orthorhombic system, space group *Pbca*, with unit cell dimensions $a = 13.45(1)$, $b = 26.74(2)$, $c = 11.23(1)$ Å and 8 molecules in the unit cell. The 1:1 complex of chloral hydrate and diazepam, 7-chloro-2,3-dihydro-1-methyl-5-phenyl-1,4-benzodiazepin-2-one, is isomorphous with the above compound and has unit cell dimensions $a = 13.43(1)$, $b = 26.60(2)$, $c = 11.20(1)$ Å. The final atomic parameters have been obtained from a block-diagonal least squares refinement using anisotropic thermal parameters. The final agreement residual for 575 observed reflections is $R = 0.079$.

The structure consists of chains of chloral hydrate and Br-diazepam molecules linked by hydrogen bonds.

La structure d'un complexe 1:1 entre l'hydrate de chloral et le bromo-7 dihydro-2,3 méthyl-1 phényl-5 benzodiazépin-1,4 one-2 a été déterminée par la méthode de l'atome lourd. Le complexe cristallisé dans le système orthorhombique, groupe d'espace *Pbca*. La maille élémentaire, contenant 8 molécules, a pour dimensions: $a = 13.45(1)$, $b = 26.74(2)$ et $c = 11.23(1)$ Å. Le complexe 1:1 entre l'hydrate de chloral et le diazépam, chloro-1 dihydro-2,3 méthyl-1 phényl-5 benzodiazépin-1,4 one-2, est isomorphe du composé précédent et la maille élémentaire a pour dimensions: $a = 13.43(1)$, $b = 26.60(2)$ et $c = 11.20(1)$ Å. Les paramètres atomiques ont été affinés par moindre carrés (diagonalisation par blocs) en utilisant des facteurs thermiques anisotropes. L'indice d'accord final est $R = 0.079$ pour 575 réflexions observées.

La structure est constituée par des chaines d'hydrate de chloral et de molécules de Br-diazépam liées par liaisons hydrogène.

Canadian Journal of Chemistry, 49, 3401 (1971)

Introduction

Diazepam (Fig. 1*a*), which has found medicinal use as a tranquilizer and skeletal muscle relaxant, forms a 1:1 complex with chloral hydrate, $CCl_3CH(OH)_2$. The bonding between these two molecules was thought to be hydrogen bonding but the exact nature of the molecular packing was not known.

The structural determination was done on a complex containing the similar bromine compound (Fig. 1*b*) and chloral hydrate. This com-

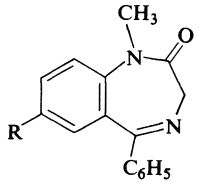

(*a*) R = Cl
(*b*) R = Br

FIG. 1. Structure of diazepam and a similar bromine compound.

Illinois. 1968. (*b*) N. N. LICHTIN. Private communication.
9. H. A. GILLIS, N. V. KLASSEN, and D. C. WALKER. Unpublished data.
10. T. J. KEMP, G. A. SALMON, and P. WARDMAN. *In* Pulse radiolysis. *Edited by* M. Ebert *et al.* Academic Press. 1965. p. 255.
11. G. A. KENNEY and D. C. WALKER. J. Chem. Phys. **50**, 4074 (1969).
12. E. J. HART, E. M. FIELDEN, and M. ANBAR. J. Phys. Chem. **71**, 3993 (1967).
13. D. C. WALKER, D. A. HEAD, and S. C. WALLACE. *In* Progress and problems in contemporary radiation chemistry. *Edited by* J. Teply. Prague. 1971. p. 250.

Can. J. Chem. Downloaded from www.nrcresearchpress.com by 210.87.254.6 on 09/05/12
For personal use only.

Crystal and Molecular Structure of the 1:1 Complex of Chloral Hydrate and 7-Bromo-2,3-dihydro-1-methyl-5-phenyl-1,4-benzodiazepin-2-one

R. F. DUNPHY AND H. LYNTON
Department of Chemistry, University of New Brunswick, Fredericton, New Brunswick

Received March 11, 1971

The structure of a 1:1 complex of chloral hydrate and 7-bromo-2,3-dihydro-1-methyl-5-phenyl-1,4-benzodiazepin-2-one has been determined by the heavy atom method. The complex crystallizes in the orthorhombic system, space group *Pbca*, with unit cell dimensions $a = 13.45(1)$, $b = 26.74(2)$, $c = 11.23(1)$ Å and 8 molecules in the unit cell. The 1:1 complex of chloral hydrate and diazepam, 7-chloro-2,3-dihydro-1-methyl-5-phenyl-1,4-benzodiazepin-2-one, is isomorphous with the above compound and has unit cell dimensions $a = 13.43(1)$, $b = 26.60(2)$, $c = 11.20(1)$ Å. The final atomic parameters have been obtained from a block-diagonal least squares refinement using anisotropic thermal parameters. The final agreement residual for 575 observed reflections is $R = 0.079$.

The structure consists of chains of chloral hydrate and Br-diazepam molecules linked by hydrogen bonds.

La structure d'un complexe 1:1 entre l'hydrate de chloral et le bromo-7 dihydro-2,3 méthyl-1 phényl-5 benzodiazépin-1,4 one-2 a été déterminée par la méthode de l'atome lourd. Le complexe cristallisé dans le système orthorhombique, groupe d'espace *Pbca*. La maille élémentaire, contenant 8 molécules, a pour dimensions: $a = 13.45(1)$, $b = 26.74(2)$ et $c = 11.23(1)$ Å. Le complexe 1:1 entre l'hydrate de chloral et le diazépam, chloro-1 dihydro-2,3 méthyl-1 phényl-5 benzodiazépin-1,4 one-2, est isomorphe du composé précédent et la maille élémentaire a pour dimensions: $a = 13.43(1)$, $b = 26.60(2)$ et $c = 11.20(1)$ Å. Les paramètres atomiques ont été affinés par moindre carrés (diagonalisation par blocs) en utilisant des facteurs thermiques anisotropes. L'indice d'accord final est $R = 0.079$ pour 575 réflexions observées.

La structure est constituée par des chaines d'hydrate de chloral et de molécules de Br-diazépam liées par liaisons hydrogène.

Canadian Journal of Chemistry, 49, 3401 (1971)

Introduction

Diazepam (Fig. 1*a*), which has found medicinal use as a tranquilizer and skeletal muscle relaxant, forms a 1:1 complex with chloral hydrate, $CCl_3CH(OH)_2$. The bonding between these two molecules was thought to be hydrogen bonding but the exact nature of the molecular packing was not known.

The structural determination was done on a complex containing the similar bromine compound (Fig. 1*b*) and chloral hydrate. This com-

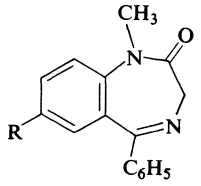

(*a*) R = Cl
(*b*) R = Br

FIG. 1. Structure of diazepam and a similar bromine compound.

TABLE 1. Final parameters (e.s.d.'s) (x, y, $z \times 10^4$; $U_{ij} \times 10^3$)*
T.F. = exp $[-2\pi^2(a^{*2}h^2U_{11} \cdots + 2b^*c^*klU_{23} + \cdots)]$

Atom	x	y	z	U_{11}	U_{22}	U_{33}	U_{23}	U_{13}	U_{12}
Br	1063(4)	0471(2)	0754(5)	100(6)	167(6)	211(7)	−41(7)	−4(6)	31(6)
Cl(*1*)	−5448(9)	2940(4)	1120(10)	183(18)	154(17)	101(15)	−25(14)	−52(14)	22(15)
Cl(*2*)	−5304(11)	3918(5)	2061(11)	332(26)	142(17)	118(18)	17(14)	−69(17)	5(18)
Cl(*3*)	−6882(8)	3301(5)	2807(12)	111(16)	205(19)	207(20)	−26(17)	−53(16)	34(16)
O(*1*)	−3543(17)	2282(8)	2535(26)	109(34)	120(32)	162(38)	12(36)	−19(32)	−11(29)
O(*2*)	−5219(18)	2635(10)	3658(21)	138(35)	140(39)	80(34)	13(30)	20(31)	−24(32)
O(*3*)	−5078(16)	3407(10)	4384(22)	77(32)	176(42)	110(37)	−13(32)	−19(30)	35(31)
N(*1*)	−2296(20)	1732(10)	2748(28)	75(38)	83(39)	159(47)	−15(38)	−5(38)	38(34)
N(*2*)	−3195(21)	1498(10)	0363(23)	85(37)	90(40)	35(37)	11(31)	−5(30)	−8(35)
C(*1*)	−2889(28)	1976(15)	2031(33)	104(59)	96(54)	140(59)	−59(49)	50(47)	−83(45)
C(*2*)	−2832(26)	1973(13)	0747(28)	121(54)	60(48)	63(46)	81(43)	−65(43)	−14(42)
C(*3*)	−2640(23)	1121(12)	0574(31)	58(44)	49(43)	90(48)	29(42)	−17(41)	55(36)
C(*4*)	−1703(22)	1144(9)	1207(25)	101(43)	78(35)	57(41)	−80(25)	17(33)	−83(31)
C(*5*)	−0941(25)	0825(12)	0786(33)	38(44)	34(40)	153(56)	74(44)	31(48)	−14(39)
C(*6*)	−0026(19)	0879(10)	1338(23)	51(36)	53(38)	33(39)	−35(31)	64(31)	95(28)
C(*7*)	0157(27)	1168(14)	2367(36)	118(52)	99(52)	72(50)	−14(49)	−42(46)	−36(47)
C(*8*)	−0640(27)	1452(13)	2764(32)	146(57)	102(50)	54(51)	−36(44)	−9(44)	29(47)
C(*9*)	−1571(21)	1428(11)	2166(27)	36(38)	50(39)	50(41)	−38(32)	72(28)	0(34)
C(*10*)	−3054(28)	0602(15)	0192(29)	67(51)	122(60)	45(46)	−17(42)	29(40)	−37(43)
C(*11*)	−3489(28)	0566(15)	−0939(35)	104(56)	148(57)	106(55)	−25(51)	−67(49)	−57(48)
C(*12*)	−3842(29)	0085(15)	−1257(36)	109(53)	120(58)	179(66)	−36(51)	−15(54)	18(49)
C(*13*)	−3839(29)	−0300(14)	−0409(37)	128(58)	104(57)	195(70)	−86(51)	70(54)	11(53)
C(*14*)	−3385(27)	−0275(14)	0706(37)	50(45)	127(57)	163(62)	−28(52)	21(48)	3(44)
C(*15*)	−2910(22)	0188(12)	1015(33)	46(47)	40(45)	149(56)	10(46)	58(45)	−34(39)
C(*16*)	−2376(30)	1741(16)	4094(32)	163(62)	187(68)	80(55)	−71(52)	−3(52)	−21(56)
C(*17*)	−5604(18)	3268(11)	2424(25)	102(43)	99(48)	135(46)	−88(37)	127(29)	−45(40)
C(*18*)	−4869(33)	3102(13)	3371(33)	236(72)	42(49)	75(50)	1(41)	−78(51)	−17(49)

plex is isomorphous with the other and offers the advantage of a heavy atom in the structure.

Crystal Structure Analysis

Crystal data are as follows:

$C_{16}H_{13}BrN_2O \cdot C_2H_3Cl_3O_2$ f.w. = 494.6
Orthorhombic, a = 13.45(1), b = 26.74(2), c = 11.23(1) Å, V = 4038.9 Å^3, ρ_0 = 1.60(3), z = 8, ρ_c = 1.627 (20 °C, MoK$\bar{\alpha}$, λ = 0.71069 Å).

$C_{16}H_{13}ClN_2O \cdot C_2H_3Cl_3O_2$ f.w. = 450.2
Orthorhombic, a = 13.43(1), b = 26.60(2), c = 11.20(1) Å, V = 4001.1 Å^3, ρ_0 = 1.47(3), z = 8, ρ_c = 1.445 (20 °C, MoK$\bar{\alpha}$, λ = 0.71069 Å).

The unit cell dimensions and their estimated standard deviations for both complexes were obtained from least squares evaluations of the positions of 12 independent reflections. In both cases the space group is *Pbca* (D_{2h}^{15}), No. 61 in ref. 1. X-Ray powder patterns for both complexes show similar intensity distributions.

Intensity data for the bromo complex were collected on a Picker computer-controlled four-angle diffractometer using a $\theta/2\theta$ scan with β-filtered MoKα radiation and a scintillation detector. The *hkl* octant was explored to the maximum limit of measurable intensity, $2\theta = 30°$. Of the 830 accessible reflections in this region, 575 were considered observed. The threshold was taken as 10% of the total background count or 18 counts, whichever was greater. The specimen used for intensity data was a colorless needle-shaped crystal 0.48 mm long and 0.24 mm in cross section, the long direction being parallel to the a axis. This crystal was sealed in a glass capillary tube and mounted with the a axis parallel to the ϕ direction of the diffractometer. The linear absorption coefficient for MoKα radiation is 25.5 cm^{-1}. No absorption or extinction corrections were applied.

The position of the bromine atom was established from a three dimensional Patterson synthesis and the remaining atoms, with the exception of the hydrogens, from successive Fourier syntheses. All atoms occupy general positions. The quantity $R_2 = \sum w(|F_o| - |F_c|)^2$ was minimized for the observed reflections only by successive cycles of block-diagonal least squares using 3 × 3 matrices for the positional parameters and 6 × 6 matrices for the anisotropic thermal parameters of each atom. The weighting function used was $w = \{1/(1 + [(|F_o| - P_2)/P_1]^4)\}$ with P_1 = 65 and P_2 = 75. Scattering factor

Can. J. Chem. Downloaded from www.nrcresearchpress.com by 210.87.254.6 on 09/05/12
For personal use only.

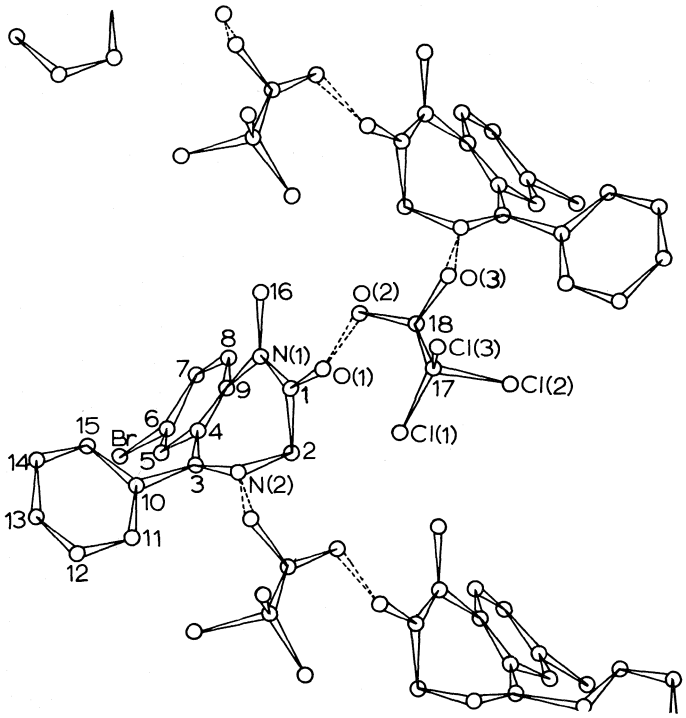

FIG. 2. The structure of the complex as projected along the *a* axis.

curves for Br, Cl, O, N, and C were those given in ref. 2. The bromine scattering curve was corrected for anomalous dispersion (3).

The final agreement residual $R = \sum(||F_o| - |F_c||)/\sum|F_o|$ was 0.079. In the last cycle no parameter shift exceeded 0.3 times the estimated standard deviation. A difference synthesis showed a small amount of remaining electron density no where greater than $0.5e$ Å^{-3}, probably due to the hydrogens, but the resolution was not sufficient to determine their positions. A set of structure factors for the final parameters given in Table 1 has been placed in the Depository of Unpublished Data.[1]

Discussion

The numbering scheme used in this paper and the general structure of the complex are shown in Fig. 2. Each Br–diazepam molecule is hydrogen bonded through the carbonyl group oxygen, O(*1*) and the nitrogen atom N(*2*) to the two hydroxy groups, O(*2*) and O(*3*), of two different chloral hydrate molecules. The hydroxy groups of each chloral hydrate molecule are thus hydrogen bonded to two different Br-diazepam molecules. This results in four staggered chains through the cell in the *c* direction. The hydrogen bonding is evidenced by the relatively short O(*1*) · · · O(*2*) and N(*2*) · · · O(*3*) distances 2.75(3) and 2.77(4) Å (4, 5, 7).

The bond lengths and angles, although of low accuracy (e.s.d.'s 0.03–0.05 Å), are comparable with those for many organic structures found in the literature. The structure of the chloral hydrate molecule is similar to that found by Ogawa (6). The structure of diazepam shown in Fig. 1 is confirmed.

We wish to thank Dr. C. Podesva of Delmar Chemicals Limited, La Salle, Quebec for suggesting the problem and supplying samples of the complexes, Mr. M. J. R. Clark for the determination of the preliminary crystallographic data, Dr. F. R. Ahmed of the "Biochemistry Laboratory", NRCC for use of his computer programs, and the National Research Council of Canada for financial support.

[1]Photocopies may be obtained free of charge, upon request, from the Depository of Unpublished Data, National Science Library, National Research Council of Canada, Ottawa, Canada K1A 0S2.

Can. J. Chem. Downloaded from www.nrcresearchpress.com by 210.87.254.6 on 09/05/12
For personal use only.

1. International Tables for X-Ray Crystallography. Vol. 1. The Kynoch Press, Birmingham, England. 1965. Sect. 4.3.
2. International Tables for X-Ray Crystallography. Vol. III. The Kynoch Press, Birmingham, England. 1962. Table 3.3.1A.
3. International Tables for X-Ray Crystallography. Vol. III. The Kynoch Press, Birmingham, England. 1962. Table 3.3.2C.
4. W. FULLER. J. Phys. Chem. **63**, 1705 (1959).
5. G. C. PIMENTEL and A. L. MCCLELLAN. The hydrogen bond. Freeman, San Francisco. 1960. Chap. 9.
6. K. OGAWA. Chem. Soc. Jap. Bull. **36**, 610 (1963).
7. W. C. HAMILTON and J. A. IBERS. Hydrogen bonding in solids. W. A. Benjamin, Inc., New York. 1968. Chap. 5.

Can. J. Chem. Downloaded from www.nrcresearchpress.com by 210.87.254.6 on 09/05/12
For personal use only.

Reactions of Some Fluorinated Acetylenes with Tetrakis(triphenylphosphine)platinum(0)

W. R. CULLEN AND F. L. HOU

Chemistry Department, University of British Columbia, Vancouver 8, British Columbia

Received June 23, 1971

The reactions of tetrakis(triphenylphosphine)platinum(0), (**1**) with 3,3,3-trifluoropropyne and 3,3,4,4,4-pentafluorobutyne produce *cis*-$(P(C_6H_5)_3)_2Pt(C{\equiv}CCF_3)_2$ and $(P(C_6H_5)_3)_2Pt(C{\equiv}CC_2F_5)_2$, respectively. The analogous reaction between (**1**) and hexafluoro-2-butyne yields the known $(P(C_6H_5)_3)_2Pt(F_3CC_2CF_3)$.

Les réactions du tétrakis (triphénylphosphine) de platine(0), (**1**) avec le trifluoro-3,3,3 propyne et le pentafluoro-3,3,4,4,4 butyne conduisent respectivement au *cis*-$(P(C_6H_5)_3)_2Pt(C{\equiv}CCF_3)_2$ et $(P(C_6H_5)_3)_2Pt(C{\equiv}CC_2F_5)_2$. Une réaction analogue entre (**1**) et l'hexafluoro butyne-2 donne le composé connu $(P(C_6H_5)_3)_2Pt(F_3CC_2CF_3)$.

Canadian Journal of Chemistry, **49**, 3404 (1971)

Although a number of platinum–acetylene complexes have been prepared (1–8), only a few platinum acetylides are known. Chatt and Shaw (2) first prepared some acetylides of the type *trans*-$(P(C_2H_5)_3)_2Pt(C{\equiv}CR)_2$ (R = H, CH_3, C_6H_5) by the reaction of the sodium acetylide with *cis*-$(P(C_2H_5)_3)_2PtCl_2$ in liquid ammonia. A similar bisacetylide, *trans*-$(P(C_2H_5)_3)_2Pt(C{\equiv}CCF_3)_2$, was isolated by Stone and co-workers (4) from the reaction of *trans*-$(P(C_2H_5)_3)_2PtCl_2$ with trifluoropropynylmagnesium iodide. Recently, Roundhill and co-workers (5) also prepared a platinum bisacetylide hydride by the reaction of tetrakis(triphenylphosphine)platinum(0), (**1**), with 1-ethynylcyclohexanol.

Harbourne and Stone (3) have reported that 3,3,3-trifluoropropyne reacts with (**1**) to yield the π-bonded complex $(P(C_6H_5)_3)_2Pt(CF_3C_2H)$. We wish to report that this reaction affords the σ-bonded complex *cis*-$(P(C_6H_5)_3)_2Pt(C{\equiv}CCF_3)_2$ (**2**) in low yield if excess propyne is used and if the reactants are left for longer periods. A similar product $(P(C_6H_5)_3)_2Pt(C{\equiv}CC_2F_5)$ (**3**) is obtained when (**1**) and 3,3,4,4,4-pentafluorobutyne react at 20°.

The structure of (**2**) follows from its infrared and ^{19}F nuclear magnetic resonance (n.m.r.) spectra. The former shows absorptions at 2115 and 2060 cm^{-1} which are characteristic of $C{\equiv}CCF_3$ groups σ-bonded to a metal (4, 9, 10). The presence of two $C{\equiv}C$ stretching frequencies suggests that the fluorocarbon groups are *cis* to each other in this compound. The ^{19}F n.m.r. spectrum confirms this stereochemistry and shows a triplet of doublets centered at 44.2 p.p.m. [$J_{^{195}Pt-CF_3}$ 29.8 Hz; J_{P-CF_3} 3.8 Hz]. The chemical shift and ^{195}Pt–CF_3 coupling constant are similar to those found for analogous bisacetylide *trans*-$(P(C_2H_5)_3)_2Pt(C{\equiv}CCF_3)_2$ (4), which shows, however, a triplet of triplets in its ^{19}F n.m.r. spectrum because the fluorocarbon groups are *trans* to each other. The spectrum of (**2**) arises because only *one* phosphorus atom is significantly coupled to the CF_3 group. Since it has been found (3, 6, 11) that

1. International Tables for X-Ray Crystallography. Vol. 1. The Kynoch Press, Birmingham, England. 1965. Sect. 4.3.
2. International Tables for X-Ray Crystallography. Vol. III. The Kynoch Press, Birmingham, England. 1962. Table 3.3.1A.
3. International Tables for X-Ray Crystallography. Vol. III. The Kynoch Press, Birmingham, England. 1962. Table 3.3.2C.
4. W. FULLER. J. Phys. Chem. **63**, 1705 (1959).
5. G. C. PIMENTEL and A. L. MCCLELLAN. The hydrogen bond. Freeman, San Francisco. 1960. Chap. 9.
6. K. OGAWA. Chem. Soc. Jap. Bull. **36**, 610 (1963).
7. W. C. HAMILTON and J. A. IBERS. Hydrogen bonding in solids. W. A. Benjamin, Inc., New York. 1968. Chap. 5.

Can. J. Chem. Downloaded from www.nrcresearchpress.com by 210.87.254.105 on 09/05/12
For personal use only.

Reactions of Some Fluorinated Acetylenes with Tetrakis(triphenylphosphine)platinum(0)

W. R. CULLEN AND F. L. HOU

Chemistry Department, University of British Columbia, Vancouver 8, British Columbia

Received June 23, 1971

The reactions of tetrakis(triphenylphosphine)platinum(0), (**1**) with 3,3,3-trifluoropropyne and 3,3,4,4,4-pentafluorobutyne produce *cis*-$(P(C_6H_5)_3)_2Pt(C{\equiv}CCF_3)_2$ and $(P(C_6H_5)_3)_2Pt(C{\equiv}CC_2F_5)_2$, respectively. The analogous reaction between (**1**) and hexafluoro-2-butyne yields the known $(P(C_6H_5)_3)_2Pt(F_3CC_2CF_3)$.

Les réactions du tétrakis (triphénylphosphine) de platine(0), (**1**) avec le trifluoro-3,3,3 propyne et le pentafluoro-3,3,4,4,4 butyne conduisent respectivement au *cis*-$(P(C_6H_5)_3)_2Pt(C{\equiv}CCF_3)_2$ et $(P(C_6H_5)_3)_2Pt(C{\equiv}CC_2F_5)_2$. Une réaction analogue entre (**1**) et l'hexafluoro butyne-2 donne le composé connu $(P(C_6H_5)_3)_2Pt(F_3CC_2CF_3)$.

Canadian Journal of Chemistry, **49**, 3404 (1971)

Although a number of platinum–acetylene complexes have been prepared (1–8), only a few platinum acetylides are known. Chatt and Shaw (2) first prepared some acetylides of the type *trans*-$(P(C_2H_5)_3)_2Pt(C{\equiv}CR)_2$ (R = H, CH_3, C_6H_5) by the reaction of the sodium acetylide with *cis*-$(P(C_2H_5)_3)_2PtCl_2$ in liquid ammonia. A similar bisacetylide, *trans*-$(P(C_2H_5)_3)_2Pt(C{\equiv}CCF_3)_2$, was isolated by Stone and co-workers (4) from the reaction of *trans*-$(P(C_2H_5)_3)_2PtCl_2$ with trifluoropropynylmagnesium iodide. Recently, Roundhill and co-workers (5) also prepared a platinum bisacetylide hydride by the reaction of tetrakis(triphenylphosphine)platinum(0), (**1**), with 1-ethynylcyclohexanol.

Harbourne and Stone (3) have reported that 3,3,3-trifluoropropyne reacts with (**1**) to yield the π-bonded complex $(P(C_6H_5)_3)_2Pt(CF_3C_2H)$. We wish to report that this reaction affords the σ-bonded complex *cis*-$(P(C_6H_5)_3)_2Pt(C{\equiv}CCF_3)_2$ (**2**) in low yield if excess propyne is used and if the reactants are left for longer periods. A similar product $(P(C_6H_5)_3)_2Pt(C{\equiv}CC_2F_5)$ (**3**) is obtained when (**1**) and 3,3,4,4,4-pentafluorobutyne react at 20°.

The structure of (**2**) follows from its infrared and ^{19}F nuclear magnetic resonance (n.m.r.) spectra. The former shows absorptions at 2115 and 2060 cm^{-1} which are characteristic of $C{\equiv}CCF_3$ groups σ-bonded to a metal (4, 9, 10). The presence of two $C{\equiv}C$ stretching frequencies suggests that the fluorocarbon groups are *cis* to each other in this compound. The ^{19}F n.m.r. spectrum confirms this stereochemistry and shows a triplet of doublets centered at 44.2 p.p.m. [$J_{^{195}Pt-CF_3}$ 29.8 Hz; J_{P-CF_3} 3.8 Hz]. The chemical shift and ^{195}Pt–CF_3 coupling constant are similar to those found for analogous bisacetylide *trans*-$(P(C_2H_5)_3)_2Pt(C{\equiv}CCF_3)_2$ (4), which shows, however, a triplet of triplets in its ^{19}F n.m.r. spectrum because the fluorocarbon groups are *trans* to each other. The spectrum of (**2**) arises because only *one* phosphorus atom is significantly coupled to the CF_3 group. Since it has been found (3, 6, 11) that

Can. J. Chem. Downloaded from www.nrcresearchpress.com by 210.87.254.105 on 09/05/12
For personal use only.

$J_{P\ trans\text{-}CF_3}$ is usually greater than $J_{P\ cis\text{-}CF_3}$ it seems reasonable to assign the coupling in (**2**) to the interaction between the CF_3 groups and the phosphorus atoms *trans* to them. However, the value of 3.3 Hz found for *trans*-$(P(C_2H_5)_3)_2Pt(C{\equiv}CCF_3)_2$ (4) makes this assignment less certain.

Although $(P(C_6H_5)_3)_2Pt(C{\equiv}CC_2F_5)_2$ (**3**) shows only one C≡C stretching absorption at 2125 cm^{-1}, this is not sufficient evidence to assign a *trans* structure. Unfortunately, the ^{19}F n.m.r. spectrum was not obtainable due to its low solubility. Since (**3**) was made by the same procedure as (**2**) a *cis* geometry seems more likely.

Additional evidence that (**3**) is formulated correctly is provided by its mass spectrum which shows a parent multiplet at $m/e = 1000 \pm 10$. The calculated parent multiplet, $m/e = 1005$, for (**3**) is well within counting error. Furthermore, the observed relative intensities of the parent multiplet are in good agreement with the calculated values as shown in Table 1. Additional multiplets are observed in the spectrum indicating that the molecule fragments by loss of triphenylphosphine, fluorocarbon and phenyl groups.

The reaction of hexafluorobutyne-2 with (**1**) produces $(P(C_6H_5)_3)_2Pt(F_3CC_2CF_3)$, (**4**) which has been obtained previously by different routes (6, 7). This compound in which the acetylene moiety is π-bonded was identified by microanalysis, and by its infrared and n.m.r. spectra.

Experimental

All reactions were carried out under a nitrogen atmosphere and volatile reagents were manipulated in a standard vacuum system. Melting points were determined in evacuated capillaries and are uncorrected. Infrared spectra were recorded on a Perkin–Elmer 457 spectrophotometer, mass spectra on an AEI MS-9 spectrometer, and n.m.r. spectra on Varian T-60 and HA-100 spectrometers. Chemical shifts are given in p.p.m. downfield from external TMS and upfield from external $CFCl_3$. Microanalyses were performed by Mr. P. Borda of this department.

TABLE 1. Relative intensities in the parent multiplet of the mass spectrum of $(P(C_6H_5)_3)_2Pt(C{\equiv}CC_2F_5)_2$

	Relative intensity	
m/e	Observed	Calculated
1002	2.2	1.55
1003	2.4	0.77
1004	61	65.71
1005	100	100
1006	91	91.89
1007	35	34.55
1008	22	21.92
1009	8.7	8.29

3,3,3-Trifluoropropyne was prepared by the dechlorination of 1,1,2-trichloro-3,3,3-trifluoropropene with zinc dust in dimethylformamide (12). 3,3,4,4,4-Pentafluorobutyne was a gift from Dr. M. C. Waldman. Hexafluorobutyne-2 was purchased from Peninsular ChemResearch Inc. and potassium tetrachloroplatinite from Platinum Chemicals, Inc.

Preparation of cis-$(P(C_6H_5)_3)_2Pt(C{\equiv}CCF_3)_2$ (2)

Tetrakis(triphenylphosphine)platinum(0), (**1**), was prepared by the action of an aqueous solution of 0.4 g of sodium borohydride on an aqueous alcoholic solution of triphenylphosphine (2.1 g, 8 mmol) and potassium tetrachloroplatinite (0.83 g, 2 mmol). The precipitated complex, (**1**) was filtered under nitrogen, dissolved in 50 ml of hot benzene, and transferred into a Pyrex tube 3,3,3-Trifluoropropyne (1.4 g, 15 mmol) was then condensed into the Pyrex tube. After 5 months at room temperature, the tube was opened and the solvent and excess alkyne were removed under reduced pressure. The residue was washed with pentane and ethanol and the crude product was crystallized twice from diethyl ether at −78° to give white solid *cis*-$(P(C_6H_5)_3)_2Pt(C{\equiv}CCF_3)_2$ (0.16 g, 9%), m.p. 180° (dec.).

Anal. Calcd. for $C_{42}H_{30}F_6P_2Pt$: C, 55.7; H, 3.3; F, 12.6. Found: C, 55.4; H, 3.3; F, 12.4.

The ^1H n.m.r. spectrum (acetone solution) showed a multiplet at 7.00 p.p.m. and the infrared spectrum ($CHCl_3$ solution) showed the following absorptions: 2990 (br), 2115 (s), 2060 (sh), 1590 (w), 1480 (w), 1435 (w), 1420 (sh), 1335 (w), 1300 (sh), 1220 (br), 1097 (s), 1030 (sh), 998 (w), 905 (w), 867 (w), 610 (w), 522 (m), 504 (sh), 435 (w) cm^{-1}.

Preparation of $(P(C_6H_5)_3)_2Pt(C{\equiv}CC_2F_5)_2$ (3)

A benzene solution of 3,3,4,4,4-pentafluorobutyne (2.2 g, 16 mmol) and (**1**) (2.5 g, 2 mmol) was sealed in a Pyrex tube. The tube was left at room temperature for 5 months. After opening the tube, the solvent and excess alkyne were removed under reduced pressure. The residue was washed with methanol. Crystallization from dichloromethane at −78° gave a white solid $(P(C_6H_5)_3)_2Pt(C{\equiv}CC_2F_5)_2$ (0.10 g, 5%), m.p. 220° (dec.).

Anal. Calcd. for $C_{44}H_{30}F_{10}P_2Pt$: C, 52.5; H, 3.0; F, 18.9. Found: C, 52.4; H, 2.9; F, 18.6.

It showed a multiplet at 7.17 p.p.m. in its ^1H n.m.r. spectrum and infrared absorptions ($CHCl_3$ solution) at: 3000 (br), 2125 (m), 1585 (w), 1480 (w), 1435 (w), 1338 (w), 1176 (s), 1098 (m), 1072 (m), 1028 (m), 1000 (w), 520 (s), 510 (sh), 434 (w) cm^{-1}.

Preparation of $(P(C_6H_5)_3)_2Pt(CF_3C_2CF_3)$ (4)

Hexafluorobutyne-2 (2.6 g, 16 mmol) and (**1**) (2.5 g, 2 mmol) in benzene were reacted for 14 days at 20°. After removal of solvent and excess alkyne the crude residue was extracted with dichloromethane and crystallized at −78° to yield white crystals of $(P(C_6H_5)_3)_2Pt(F_3CC_2CF_3)$ (0.70 g, 40%), m.p. 216° (lit. value (6) 215–216°).

Anal. Calcd. for $C_{40}H_{30}F_6P_2Pt$: C, 54.5; H, 3.4. Found: C, 54.8; H, 3.3.

We thank the National Research Council of Canada for financial support, Dr. M. C. Waldman for the gift of 3,3,4,4,4-pentafluorobutyne, and Mr. J. E. H. Ward for technical assistance.

1. J. CHATT, G. A. ROWE, and A. A. WILLIAMS. Proc. Chem. Soc. 208 (1957).
2. J. CHATT and B. L. SHAW. J. Chem. Soc. 4020 (1959).
3. D. A. HARBOURNE and F. G. A. STONE. J. Chem. Soc. A, 1765 (1968).
4. M. I. BRUCE, D. A. HARBOURNE, F. WAUGH, and F. G. A. STONE. J. Chem. Soc. A, 356 (1968).
5. J. H. NELSON, H. B. JONASSEN, and D. M. ROUNDHILL. Inorg. Chem. **8**, 2591 (1969).
6. J. L. BOSTON, S. O. GRIM, and G. WILKINSON. J. Chem. Soc. 3468 (1963).
7. E. O. GREAVES, C. J. L. LOCK, and P. M. MAITLIS. Can. J. Chem. **46**, 3879 (1968).
8. A. D. ALLEN and C. D. COOK. Can. J. Chem. **42**, 1063 (1964).
9. W. R. CULLEN and W. R. LEEDER. Inorg. Chem. **5**, 1004 (1966).
10. W. R. CULLEN and M. C. WALDMAN. J. Fluorine Chem. **1**, 41 (1971/72).
11. B. CLARKE, M. GREEN, R. B. L. OSBORN, and F. G. A. STONE. J. Chem. Soc. A, 167 (1967).
12. W. G. FINNEGAN and W. P. NORRIS. J. Org. Chem. **28**, 1139 (1963).

Can. J. Chem. Downloaded from www.nrcresearchpress.com by 210.87.254.105 on 09/05/12
For personal use only.

Molecular Screening in Helium Molecular Ion[1]

C. M. WANG AND B. MUSULIN
Department of Chemistry, Southern Illinois University, Carbondale, Illinois 62901

Received May 3, 1971

Variational energy calculations for He_2^+ were performed and the results were used to evaluate a semi-empirical method for choosing orbital exponents in quantum chemical calculations.

Des calculs relatifs aux variations d'énergie de He_2^+ ont été effectués, et les résultats ont été utilisés pour évaluer une méthode semi-empirique pour le choix de la représentation des orbitales dans les calculs de chimie quantique.

Canadian Journal of Chemistry, **49**, 3406 (1971)

Introduction

Harriss *et al.* (1) have demonstrated that the use of a molecular screening parameter may be used to simplify the variational energy calculations of the LiH and Li_2 problems in the valence electron approximation, *i.e.*, the calculations were treated as two-electron problems through the neglect of core-electrons. In this method the exponential parameter occurring in molecular wave functions is given by

$$[1] \qquad Z = Ae^{-R} + B$$

where Z is the exponential paramter, R is the diatomic internuclear distance, and A and B are arbitrary parameters to be determined from the screening constants of the united and separated atoms. In the aforementioned test calculations, the results depended not only upon the concept of a distance dependent screening constant but also upon the method of averaging used to determine A and B in eq. 1.

For example, in the case of He_2^+, the separated atoms are He and He^+ for which the atomic screening constants, according to Slater's (2) rules, are 1.70 and 2.00, respectively. The average values of the screening constant which is the value of B ($\lim_{R\to\infty} Z$) in eq. 1 is 1.80. Likewise the united atom, Be^+, has electrons, with screening constants 3.70 and 2.30, whose average value is 3.23. Since $\lim_{R\to 0} Z = A + B$, the value of A for He_2^+ is found to be 1.43. The purpose of this investigation is to determine the distance dependence of the orbital parameter in energy calculations of a diatomic molecule containing only electrons which are in 1s orbitals in the separated atoms, *i.e.*, He and He^+. The results are compared to those predicted by eq. 1 in order to test the propriety of the averaging assumption.

[1]Presented in part before the First Canadian Theoretical Symposium on Quantum Chemistry, University of Alberta, Edmonton, Alberta, August 23–27, 1965.

We thank the National Research Council of Canada for financial support, Dr. M. C. Waldman for the gift of 3,3,4,4,4-pentafluorobutyne, and Mr. J. E. H. Ward for technical assistance.

1. J. CHATT, G. A. ROWE, and A. A. WILLIAMS. Proc. Chem. Soc. 208 (1957).
2. J. CHATT and B. L. SHAW. J. Chem. Soc. 4020 (1959).
3. D. A. HARBOURNE and F. G. A. STONE. J. Chem. Soc. A, 1765 (1968).
4. M. I. BRUCE, D. A. HARBOURNE, F. WAUGH, and F. G. A. STONE. J. Chem. Soc. A, 356 (1968).
5. J. H. NELSON, H. B. JONASSEN, and D. M. ROUNDHILL. Inorg. Chem. **8**, 2591 (1969).
6. J. L. BOSTON, S. O. GRIM, and G. WILKINSON. J. Chem. Soc. 3468 (1963).
7. E. O. GREAVES, C. J. L. LOCK, and P. M. MAITLIS. Can. J. Chem. **46**, 3879 (1968).
8. A. D. ALLEN and C. D. COOK. Can. J. Chem. **42**, 1063 (1964).
9. W. R. CULLEN and W. R. LEEDER. Inorg. Chem. **5**, 1004 (1966).
10. W. R. CULLEN and M. C. WALDMAN. J. Fluorine Chem. **1**, 41 (1971/72).
11. B. CLARKE, M. GREEN, R. B. L. OSBORN, and F. G. A. STONE. J. Chem. Soc. A, 167 (1967).
12. W. G. FINNEGAN and W. P. NORRIS. J. Org. Chem. **28**, 1139 (1963).

Can. J. Chem. Downloaded from www.nrcresearchpress.com by 210.87.254.42 on 09/05/12
For personal use only.

Molecular Screening in Helium Molecular Ion[1]

C. M. WANG AND B. MUSULIN
Department of Chemistry, Southern Illinois University, Carbondale, Illinois 62901

Received May 3, 1971

Variational energy calculations for He_2^+ were performed and the results were used to evaluate a semi-empirical method for choosing orbital exponents in quantum chemical calculations.

Des calculs relatifs aux variations d'énergie de He_2^+ ont été effectués, et les résultats ont été utilisés pour évaluer une méthode semi-empirique pour le choix de la représentation des orbitales dans les calculs de chimie quantique.

Canadian Journal of Chemistry, **49**, 3406 (1971)

Introduction

Harriss *et al.* (1) have demonstrated that the use of a molecular screening parameter may be used to simplify the variational energy calculations of the LiH and Li_2 problems in the valence electron approximation, *i.e.*, the calculations were treated as two-electron problems through the neglect of core-electrons. In this method the exponential parameter occurring in molecular wave functions is given by

$$[1] \qquad Z = Ae^{-R} + B$$

where Z is the exponential paramter, R is the diatomic internuclear distance, and A and B are arbitrary parameters to be determined from the screening constants of the united and separated atoms. In the aforementioned test calculations, the results depended not only upon the concept of a distance dependent screening constant but also upon the method of averaging used to determine A and B in eq. 1.

For example, in the case of He_2^+, the separated atoms are He and He^+ for which the atomic screening constants, according to Slater's (2) rules, are 1.70 and 2.00, respectively. The average values of the screening constant which is the value of B ($\lim_{R\to\infty} Z$) in eq. 1 is 1.80. Likewise the united atom, Be^+, has electrons, with screening constants 3.70 and 2.30, whose average value is 3.23. Since $\lim_{R\to 0} Z = A + B$, the value of A for He_2^+ is found to be 1.43. The purpose of this investigation is to determine the distance dependence of the orbital parameter in energy calculations of a diatomic molecule containing only electrons which are in 1s orbitals in the separated atoms, *i.e.*, He and He^+. The results are compared to those predicted by eq. 1 in order to test the propriety of the averaging assumption.

[1]Presented in part before the First Canadian Theoretical Symposium on Quantum Chemistry, University of Alberta, Edmonton, Alberta, August 23–27, 1965.

Can. J. Chem. Downloaded from www.nrcresearchpress.com by 210.87.254.42 on 09/05/12
For personal use only.

Method

In calculations associated with He_2^+, three atomic orbital wave functions are used. Within the framework of the valence bond method (3), there have been three variation calculations of increasing complexity, *viz.*, a single orbital exponent (4), different exponents for the orbitals of He and He^+ (5), and distinct exponents for each of the three orbitals (6). In each of these calculations, a variation was performed so as to obtain the best value(s) of the orbital parameter(s) at the equilibrium (experimental or theoretical) internuclear distance.

The present calculation was also performed within the framework of the valence bond method, *i.e.*, the trial wave function was a linear combination of Slater determinantal wave functions representing the ground state configuration. The optimum value(s) for the orbital parameter(s) in, first, a Pauling-type calculation, and in, second, a Weinbaum-type calculation, for various values of the internuclear distance, R, was (were) determined. The spacing of R values was finer in the region of the experimental equilibrium distance, R_e. The original Pauling and Weinbaum calculations were reproduced in order to both test the computer programs and obtain potential curves for comparison purposes.

The calculations were performed on an IBM 1620 computer with 40K storage utilizing programs written in FORTRAN II. The subroutine for the exponential integral, $-Ei(-x)$, was based upon the Hastings approximation (7).

Results and Discussion

Table 1 presents sample results of the present Pauling-type calculation along with results of similar calculations for comparison purposes. Corrections to the original Pauling calculation (8) have been verified. The most striking fact shown in Table 1 is that the energy curve obtained from a complete variation of Z is so little different from that found by Pauling using the value of Z obtained at R_e. The difference never is as great as 1 kcal. Also surprising is the fact that the optimum value of Z is not a monotonic function of R. Apparently for He_2^+ the optimum value of Z at each R is fairly close to the value at R_e. The near accordance results from the facts that the optimum value of Z is a slowly varying function of R and that the optimum value of Z passes through a maximum not too far from the Pauling value and then decreases towards the Pauling value. As a result, the energy values obtained by the two methods are very close.

Although the three orbital average does not have the monotonic functional form assumed by eq. 1, the semi-empirical results are superior at large R to the results obtained with the Pauling constant orbital exponent. Relative to experimental values, discrepancies in calculations with only 1s orbitals (He_2^+) are less than discrepancies in calculations averaging 1s and 2s orbitals (LiH and Li_2). This result substantiates the limitations on eq. 1 suggested by Empedocles (9). The Pauling-type results do not warrant any comments concerning the method of assigning values to A and B in eq. 1.

Table 2 presents sample results of the present Weinbaum-type calculation along with results of the Weinbaum calculation for comparison purposes. As expected there is improvement for every R value except at R_e where the two methods coincide. The most important fact in Table 2 is that one of the orbital parameters does exhibit

TABLE 1. Ground state energies and screening parameters using a single orbital exponent

	Z		$-E$ (hartree)		
R (bohr)	From eq. 1	This work	From Z (eq. 1)	Pauling*	This work
0.4	2.76	1.93	−2.2961	−1.1375	−1.1179
0.5	2.67	1.97	0.0908	0.8539	0.8862
0.7	2.51	1.99	2.5759	2.9504	2.9886
1.0	2.33	1.96	4.0501	4.2198	4.2446
1.5	2.12	1.89	4.7411	4.8146	4.8196
2.0	1.99	1.84	4.8673	4.9051	4.9051
2.5	1.92	1.81	4.8707	4.8886	4.8896
3.0	1.87	1.79	4.8526	4.8596	4.8620

*$Z = 1.833$.

TABLE 2. Ground state energies and screening parameters using separate screening for He and He^+

	Z − He	Z − He^+	$-E$ (hartree)	
R (bohr)	(This work)	(This work)	Weinbaum*	This work
0.4	2.83	2.3772	−11.5065	−3.7500
0.5	2.50	2.1750	−2.4667	−0.1827
0.7	2.17	2.0181	2.4261	2.7681
1.0	1.98	1.9998	4.1423	4.2072
1.5	1.84	2.0240	4.8137	4.8236
2.0	1.75	2.0300	4.9254	4.9257
2.5	1.71	2.0349	4.9183	4.9190
3.0	1.69	2.0111	4.8930	4.8953

*$Z(He) = 1.734$, $Z(He^+) = 2.029$.

TABLE 3. First excited state energies and screening parameter using a single orbital exponent

R (bohr)	Z (This work)	$-E$(hartree) Pauling*	This work
0.5	1.42	−2.1585	−1.7904
1.0	1.69	2.7393	2.7686
1.5	1.78	4.0481	4.0518
2.0	1.80	4.5002	4.5016
2.5	1.80	4.6755	4.6768
3.0	1.80	4.7494	4.7509

*Z = 1.833.

the monotonic decreasing form of eq. 1 while the second parameter approximates the same functional form. The implication is that in many-electron systems the number of orbital parameters used must correspond to the number which, in a variational calculation, allows each exponent to assume what appears to be the normal monotonically decreasing form.

The present work also demonstrates that a semi-empirical method, like *ab initio* methods, may be chosen according to the complexity required or allowed. The use of a single semi-empirical exponent yielded results comparable only to the Pauling calculation and in no way as accurate as the Weinbaum calculation. On the other hand, the use of the semi-empirical exponent economizes the calculation by eliminating the variation of the exponent. Even if two semi-empirical exponents were used to obtain a calculation corresponding to the Weinbaum calculation, the effort would be correspondingly less than the true variation calculation.

Table 3 presents the results of a Pauling-type calculation for the first excited state. Unlike the ground state, the orbital exponent is a monotonically increasing function. The results substantiate the theorem given by Harriss and Frost (10) that the optimum Z for the first excited state is always lower than the optimum Z for the ground state. With the modification of functional form, the semi-empirical techniques used in this investigation can be extended to excited states.

Computing facilities available precluded any attempt to extend the Csavinsky (6) calculation with three distinct orbital exponents.

One of us (C.M.W.) acknowledges a fellowship from the Graduate School of Southern Illinois University. We are indebted to the Computing Center of Southern Illinois University.

1. D. K. HARRISS, C. W. MITCHELL, and B. MUSULIN. Theoret. Chim. Acta (Berl.), **1**, 93 (1963).
2. J. C. SLATER. Phys. Rev. **36**, 57 (1930).
3. H. EYRING, J. WALTER, and G. E. KIMBALL. Quantum chemistry. John Wiley & Sons, Inc., New York. 1944.
4. L. PAULING. J. Chem. Phys. **1**, 56 (1933).
5. S. WEINBAUM. J. Chem. Phys. **3**, 547 (1935).
6. P. CSAVINSKY. J. Chem. Phys. **31**, 178 (1959).
7. C. HASTINGS, JR. Applications for digital computers. Prentice-Hall, Inc., New Jersey. 1963.
8. P. N. REAGAN, J. C. BROWNE, and F. A. MATSEN. Phys. Rev. **132**, 304 (1963).
9. P. EMPEDOCLES. J. Chem. Phys. **46**, 4474 (1967).
10. D. K. HARRISS and A. A. FROST. Theoret. Chim. Acta (Berl.), **3**, 174 (1965).

Erratum: Studies on Acyl Alkyl Diimides

THOMAS R. LYNCH, FREDERICK N. MACLACHLAN, AND YUM KUEN SIU
Chemistry Department, Scarborough College, University of Toronto, West Hill, Ontario

Received July 29, 1971

(Ref. Can. J. Chem. **49**, 1598 (1971))

Canadian Journal of Chemistry, **49**, 3408 (1971)

In the preparation of compounds **2***e–g* and **4***e–g*, the presence of 1 equiv of sulfuric acid was inadvertently omitted from the Experimental, although mentioned in the Results and Discussion. Thus on p. 1602, column 2, line 8 should read "...added) containing sulfuric acid (0.5 mol). The combined..."

Can. J. Chem. Downloaded from www.nrcresearchpress.com by 210.87.254.42 on 09/05/12
For personal use only.

Can. J. Chem. Downloaded from www.nrcresearchpress.com by 210.87.254.105 on 09/05/12
For personal use only.

Infrared Spectra of Hydroxyl Groups on the Surface of Platinum

B. A. MORROW AND P. RAMAMURTHY
Department of Chemistry, University of Ottawa, Ottawa, Canada

Received July 12, 1971

Infrared spectroscopy has been used to show that two types of PtOH species exist on the surface of silica-supported platinum. One of these is produced when O_2 is allowed to react with hydrogen covered platinum (ν(OH) = 3497 cm^{-1}) and the other is produced when H_2O reacts with a reduced platinum oxide (ν(OH) = 3544 cm^{-1}).

La spectroscopie infrarouge a été utilisée pour montrer qu'il existe deux types d'espèce PtOH sur la surface du platine fixée sur un support en silice. L'une d'elles est produite lorsqu'on laisse O_2 réagir avec le platine recouvert d'hydrogène (ν(OH) = 3497 cm^{-1}) et l'autre est produite lorsque H_2O réagit avec un oxyde de platine réduit (ν(OH) = 3544 cm^{-1}).

Canadian Journal of Chemistry, **49**, 3409 (1971)

There have been many recent investigations of the gas phase reactions of hydrogen, oxygen, and water on platinum catalysts (1–3) but at no time has there been any evidence for the existence of surface PtOH groups, nor is this species generally considered in discussions of this subject. On the other hand, electrochemists have for a number of years postulated that surface PtOH groups play an important role in many electrochemical processes (4–6). In this communication we present the first spectroscopic evidence for the existence of hydroxyl groups on the surface of platinum.

Silica-supported samples were prepared by standard techniques (3, 7) involving the slurrying of sufficient silica (Cab-O-Sil, H-5) with H_2PtCl_6 in acetone (or water), such that after pressing 200 mg of the dried powder into thin discs and reducing in H_2 at 350 °C for several hours, 16% by weight of Pt was incorporated. The silica had been previously heated in air at 800 °C in order that a minimum residual band in the 3700–3300 cm^{-1} region due to hydrogen-bonded surface silanol groups would be present. A typical background spectrum in the 4000–3000 cm^{-1} region is given by curve (*a*) in Fig. 1 showing the well known infrared band due to non-interacting silanol groups at 3749 cm^{-1} (8, 9).

All attempts to detect PtOH surface species by adsorbing H_2O on freshly reduced platinum proved futile. Only the well known broad featureless absorption between 3700–3400 cm^{-1} could be detected (9) and a similar band could be produced using silica alone. However, when O_2 was

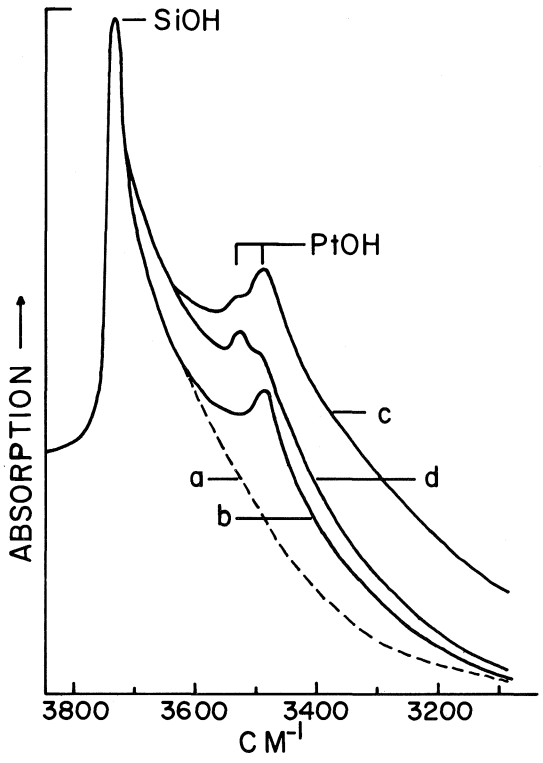

FIG. 1. (*a*) Background spectrum of fully reduced silica-supported platinum showing the SiOH absorption at 3749 cm^{-1}; (*b*) spectrum obtained after adding O_2 to (*a*); (*c*) spectrum obtained after adding O_2 to a sample which had been pretreated with H_2 and H_2O; (*d*) spectrum obtained after degassing (*b*) at 400 °C (background same as in (*a*)) followed by the addition of H_2O vapor.

Can. J. Chem. Downloaded from www.nrcresearchpress.com by 210.87.254.105 on 09/05/12
For personal use only.

added to a "hydrogen covered" (7) platinum sample, the spectrum shown in Fig. 1 curve (*b*) was obtained in which there is an additional sharp absorption band at 3497 cm^{-1}. Hydrogen covered platinum was prepared by first cooling the sample in hydrogen to 20 °C after reduction (or regeneration) and then evacuating the hydrogen for 5 min until the pressure was less than 10^{-3} Torr (7). Upon addition of O_2 to a sample which was covered with both H_2 and H_2O, curve (*c*) was obtained in which an additional weak feature at 3544 cm^{-1} is present. Regardless of the method of production, neither band changed in intensity after prolonged evacuation at 20 °C, but the intensity of both bands slowly diminished on heating under vacuum at 100–200 °C, the lower wavenumber band decreasing at the faster rate, and then disappeared entirely leaving a clear background spectrum if evacuated at 400 °C for 2 h. Finally, upon addition of H_2O after the above mentioned type of evacuation procedure (400 °C), curve (*d*) was obtained in which both bands are present, but the 3544 cm^{-1} absorption is the more intense. The above effects were not observed when pure silica alone was utilized.

These spectra strongly indicate that two types of PtOH groups are probably formed under these conditions on silica-supported platinum. The OH stretching frequency in $(CH_3)_3PtOH$ is reported to be at 3559 cm^{-1} (10), and in the model compound $Ag_2[PtCl_5OH]$ synthesized by ourselves as a confirmation of this expected wavenumber region, the OH stretching frequency is at 3512 cm^{-1}. Both bands of the adsorbed species show the appropriate isotopic shifts characteristic of OH species when deuterium (either D_2 or D_2O) is substituted (2609 and 2580 cm^{-1}) and the 3544 cm^{-1} band shifts 11 cm^{-1} to lower wavenumber when $H_2{}^{18}O$ is used. The latter is the same shift previously reported for ^{18}O silanol groups (8).

We do not consider that these bands are due to physically adsorbed water (which might result from some particular metal-support interaction) because adsorption of water alone on a freshly reduced Pt sample does not produce these bands, nor is there any evidence for the growth of a band near 1600 cm^{-1} due to the HOH deformation mode. The same bands cannot be detected using alumina-supported platinum because of the almost total absorption due to the support hydroxyl groups in this region, but again, under similar reaction conditions, no band near 1600 cm^{-1} is observed.

As further evidence that these bands are probably attributable to PtOH species, when ethylene or ethylene-^{13}C is added, the PtOH bands immediately disappear and a spectrum of adsorbed ^{12}CO or ^{13}CO is observed near 2050 cm^{-1}. No such reaction occurs when water alone is present on silica-supported platinum.

The reason for two types of PtOH species is obscure at the moment. One possible explanation is that there may be several types of surface site, for example (111) and (100) crystal planes, but this would not readily account for the differences in the conditions required to produce these groups. Since heating under vacuum at 400 °C after admission of O_2 is likely to lead to a more reduced platinum oxide surface, the most probable explanation is that the 3497 cm^{-1} band is due to PtOH on a fully oxidized surface, whereas the 3544 cm^{-1} band would correspond to a PtOH on a more reduced surface. Further investigations of this aspect of the problem are underway.

In conclusion, this work provides the first direct confirmation of the views of the electrochemists concerning the possible existence of surface PtOH groups. Further, the fact that they are formed when O_2 is added to hydrogen covered platinum has important consequences in connection with the H_2/O_2 titration reaction on platinum. Thus, several recent controversies (1, 2) concerning the stoichiometry of these reactions may have to be re-examined in the light of this work.

The financial support of Atomic Energy of Canada Ltd. is gratefully acknowledged.

1. G. R. Wilson and W. K. Hall. J. Catal. **17**, 190 (1970).
2. N. Giordane and E. Moretti. J. Catal. **18**, 228 (1970).
3. D. D. Eley, D. M. Moran, and C. H. Rochester. Trans. Faraday. Soc. **64**, 2168 (1968).
4. D. Gilroy and B. E. Conway. Can. J. Chem. **46**, 875 (1968).
5. A. K. Vijh. Can. J. Chem. **49**, 78 (1971).
6. H. Wroblowa, M. L. B. Rao, A. Damjanovic, and J. O'M. Bockris. J. Electroanal. Chem. **15**, 139 (1967).
7. B. A. Morrow and N. Sheppard. Proc. Roy. Soc. London, Ser. A, **311**, 391 (1969).
8. B. A. Morrow and A. Devi. Can. J. Chem. **48**, 2454 (1970).
9. A. J. Tyler, F. H. Hambleton, and J. A. Hockey. J. Catal. **13**, 35 (1969).
10. M. N. Hoechstetter. J. Mol. Spectrosc. **13**, 407 (1964).

Canadian Journal of Chemistry

Published by THE NATIONAL RESEARCH COUNCIL OF CANADA

VOLUME 49 NOVEMBER 1, 1971 NUMBER 21

The Specific Activity of Silica Supported Platinum for the Catalysis of Hydrogen – Water Deuterium Exchange[1,2]

N. H. SAGERT AND R. M. L. POUTEAU

Research Chemistry Branch, Whiteshell Nuclear Research Establishment, Atomic Energy of Canada Limited, Pinawa, Manitoba

Received April 26, 1971

Some rate data are reported for deuterium exchange between water and hydrogen using a series of platinum–silica catalysts. Three different methods of preparing catalysts were used to give different series of metal particle sizes. Within each series, the particle size was increased by sintering batches in air, at temperatures up to 700 °C. These methods produced platinum particles ranging from 5 to 250 Å in diameter. Metal surface areas and particle sizes were measured by hydrogen chemisorption, X-ray diffraction, and electron microscopy.

The specific rates, *i.e.*, rates per unit surface area of platinum varied by a factor of three within each series, reaching a maximum for sintering temperatures of about 500 °C. These maximum rates, measured at 127 °C with a water-to-hydrogen ratio of 0.31, varied from 1.9×10^{-8} to 5×10^{-8} mol D_2 cm^{-2} s^{-1}. Thus no effect of particle size on rate was observed, and the differences noted are ascribed to other effects of the methods of preparing the catalysts.

Certaines données de vitesse sont reportés pour l'échange du deutérium entre l'eau et l'hydrogène lorsqu'on utilise une série de catalyseurs platine–silice. Trois méthodes différentes de préparation des catalyseurs ont permis d'obtenir différentes séries de taille de particule métallique. Dans chaque série, la taille de la particule a été augmentée par frittage dans l'air à des températures supérieures à 700 °C. Ces méthodes ont donné des particules de platine dont la gamme des diamètres varie de 5 à 250 Å. Les aires de surfaces métalliques et les tailles des particules sont mesurées par chimisorption de l'hydrogène, par diffraction aux rayons-X et par microscopie électronique.

Les vitesses spécifiques, c'est-à-dire les vitesses par unité de surface du platine, varient avec un facteur de trois dans chacune des séries, atteignant un maximum pour des températures de frittage de l'ordre de 500 °C. Ces vitesses maximales mesurées à 127 °C avec un rapport eau-hydrogène de 0.31, varient de 1.9×10^{-8} à 5×10^{-8} mol D_2 cm^{-2} s^{-1}. Par contre, aucun effet de la taille des particules n'a été observée et les différences notées sont assignées aux autres effets des méthodes de préparation des catalyseurs.

Canadian Journal of Chemistry, 49, 3411 (1971)

Introduction

Because supported metal catalysts are industrially important, they have been studied for many years. Two types of studies are specific to such catalysts. These are investigations of the role of metal-support interaction and, for a given metal and support, the effect of the degree of metal dispersion. Such investigations have only become possible in recent years because methods have been developed for measuring the surface area of exposed metal in the presence of supports with surface areas perhaps hundreds of times larger than those of the metal (1).

Changes in the metal particle size might be expected to affect rates in two ways. As the particle size is decreased the fraction of edge and corner atoms rises markedly (2). This will affect reactions requiring certain geometries. Secondly, as the particle size decreases, the electronic properties of the particles must change from those of the

[1]A.E.C.L. No. 4004.

[2]Presented in part at the 4th Canadian Symposium on Catalysis, Halifax, Nova Scotia, June 1971.

Can. J. Chem. Downloaded from www.nrcresearchpress.com by 210.87.254.5 on 09/05/12
For personal use only.

Can. J. Chem. Downloaded from www.nrcresearchpress.com by 210.87.254.5 on 09/05/12
For personal use only.

bulk metal to, ultimately, those of a single atom (3).

Both metal-support and metal-dispersion effects have been observed, but their relative importance is still debatable. For a number of hydrogenation reactions, the specific activity, *i.e.*, the activity per unit surface area of metal, has been shown to remain constant with changes in the support and with metal particle size (4–7). On the other hand, it has been shown for nickel on silica catalysts that the specific activity for hydrogenolysis of ethane remained constant with changing nickel particle size (8), whereas for nickel on silica–alumina, the specific activity varied with particle size (9, 10). It was also much lower than for nickel on silica. Dorling *et al.* (11) found, for the hydrogenation of ethylene on platinum–silica catalysts, that the methods used to create differences in particle size led to differences in specific activity. However, they found the difference in activity arose from factors such as poisoning and chlorine content of the catalyst.

We have studied the effect of platinum particle size on the hydrogen – water deuterium isotope exchange. This reaction is of interest to the nuclear industry as a means of obtaining enriched deuterium. In addition, it has several practical advantages. The products differ only isotopically from the reactants, so that no chemical changes occur in the catalyst–reagent system with time, or along the catalyst bed. Furthermore, the heat of reaction is negligible, so that the heat effects in the bed can be neglected. If the amount of D_2O in the water is kept low then only reaction 1

$$[1] \qquad HDO + H_2 \rightleftarrows H_2O + HD$$

need be considered, and the kinetics are considerably simplified (12). The reaction is conveniently followed by measuring the amount of HD formed. Early work on the kinetics of the reaction has been summarized by Bond (13). No attempt was made in this work to study mechanistic details.

Experimental Procedures

Kinetic Studies

Rate measurements were carried out in a flow system at atmospheric pressure. The hydrogen stream was saturated at 63.5 °C with water vapor containing 4.0% D_2O. The stream was then passed downward through the reactor which contained from 25 to 200 mg of catalyst mixed with glass beads to give a constant volume of catalyst bed. The catalyst bed was 0.5 cm in diameter and 1.5 cm long. It was kept at constant temperature (±0.5 °C) in a furnace. After the gas stream left the reactor, water was stripped out using a Dry Ice – acetone trap. Glass–teflon stopcocks were used throughout the system to avoid contamination by grease.

The amount of HD in the gas stream was determined gas chromatographically using a 1 m activated charcoal column at 25 °C and a thermal conductivity detector. Hydrogen containing about 100 p.p.m. deuterium was used as the carrier gas and the signal obtained was proportional to the difference in HD content between the reactor gas stream and the carrier gas (12). The chromatograph was calibrated at regular intervals by analyzing the HD mass spectrometrically on a Consolidated 21–130 mass spectrometer, and by using large amounts of catalyst to give the equilibrium amount of HD from water containing 1, 2, and 4% D_2O. Flow rates were controlled by regulators and precision needle valves. The flows were measured either with rotameters which had been calibrated with a positive displacement meter, or with a linear mass flowmeter which had been similarly calibrated. Temperatures were measured with an iron–constantan thermocouple.

Unless otherwise noted, prior to rate measurements, the catalysts were evacuated to 10^{-5} Torr for at least 1 h while the temperature was raised to 350 °C. They were then reduced at that temperature for 12 h in a hydrogen stream and cooled to reaction temperature in flowing hydrogen. Catalysts were often slowly deactivated, losing at most 5% of their activity per day. As measurements on any given catalysts were made within 2 or 3 days, corrections for loss of activity were small. Calculations based on equations given by Satterfield (14) showed that the efficiency factor for pore diffusion was close to unity and that the linear velocity through the bed was high enough to ensure plug flow.

Materials

(i) Reagents

Ultra High Purity hydrogen (99.999% min) was passed through a Deoxo unit to remove traces of oxygen, and through a cold trap to remove water. The 4% D_2O in water was made by adding D_2O to deionized, distilled water.

(ii) Catalysts

The catalysts used contained about 1% platinum by weight on porous chromatographic grade silica gel (40–60 mesh). Before adding the platinum, the gel was calcined at 600 °C for 16 h. Platinum was then put on the gel by ion exchanging with $Pt(NH_3)_4(OH)_2$, by impregnating with H_2PtCl_6, or by impregnating with $Pt(NH_3)_2(NO_2)_2$.

Catalysts prepared with $Pt(NH_3)_4(OH)_2$ were made by following the procedure of Benesi *et al.* (15). The hydroxide was prepared from $Pt(NH_3)_4Cl_2$ by ion exchange with the hydroxide form of a strong base resin. A solution 10^{-2} *M* in hydroxide and 10^{-3} *M* in chloride was added dropwise to a stirred suspension of the silica gel, keeping the p*H* between 7.5 and 9. The product was filtered, dried overnight at 120 °C, sieved, and pre-reduced in 15 g lots in a stream of hydrogen at 200 °C. Portions were then sintered in air for 5 h at temperatures up to 700 °C.

Catalysts prepared with H_2PtCl_6 were made by wetting the gel with a solution containing the required amount of platinum, followed by evaporation to dryness with stirring.

Catalysts prepared from $Pt(NH_3)_2(NO_2)_2$ were made

Can. J. Chem. Downloaded from www.nrcresearchpress.com by 210.87.254.5 on 09/05/12
For personal use only.

by dissolving sufficient compound in hot water, and evaporating to dryness with the gel.

All catalysts were then dried, sieved, pre-reduced, and sintered as described before. The actual amount of platinum on the catalysts was determined by atomic absorption spectrometry (16).

Surface Area and Particle Size Measurements

Total surface areas were measured by adsorption of nitrogen at 77 °K using a standard volumetric B.E.T. apparatus, and assuming the surface area of the nitrogen molecule to be 16.2 Å^2. Platinum surface areas were calculated from hydrogen chemisorption isotherms measured at 25 °C, following procedures of Dorling *et al.* (17), except that a commercial quartz spiral bourdon gage was used as a manometer. It was assumed that one hydrogen atom was adsorbed per exposed platinum atom, and that the surface area of the platinum atom was 8.9 Å^2 (17). Catalysts were subjected to the same reduction as those used for kinetic studies, and were then evacuated to 2×10^{-6} Torr overnight at 300 °C before isotherms were measured.

For samples with crystallites in the larger size ranges the size of the platinum crystallites was determined from the broadening, B, of X-ray diffraction lines. A Phillips counter diffractometer, fitted with a step-scanning attachment, was used to measure the position and profile of the (111) line of platinum. Filtered copper radiation was used, and the Kα doublet was resolved by a graphical method (18). Corrections for instrumental broadening were made from Warren's expression

$$[2] \qquad \beta^2 = B^2 - b^2$$

where b is the half width of the instrumental broadening and β is the true half width. The crystalline size, D, was obtained from the Scherrer expression

$$[3] \qquad D = K\lambda/\beta \cos\theta$$

where λ is the wavelength, θ the Bragg angle, and K the classical Scherrer constant, taken as 0.9 (18).

Electron microscopy was done with an Hitachi HU 200E microscope using a high resolution stage. Samples were prepared by mulling the catalyst in ethyl alcohol. After the coarse particles had settled, a portion of the supernatant liquid was deposited on a carbon substrate supported on a 200 mesh copper grid, using a special atomizer. Micrographs were obtained at a plate magnification of 100 000 ×, and were magnified photographically for particle size counting.

Results

The reaction rate, k, given as moles of D_2 transferred per gram of catalyst per second was calculated (12) from eq. 4.

$$[4] \qquad k = \frac{F}{(\alpha + \gamma)W} \ln \frac{n_e - n_0}{n_e - n}$$

Here, F is the hydrogen flow rate in mol/s, W is the weight of the catalyst in g, α is the reciprocal of the equilibrium constant for reaction 1, γ is the ratio of the partial pressure of hydrogen to water, n_0 and n are the deuterium concentrations in the hydrogen before and after reaction respectively, and n_e is the equilibrium concentration of deuterium in the hydrogen after reaction. The value of n_e is calculated (12) from eq. 5

$$[5] \qquad n_e = \frac{N_0 + \gamma n_0}{\alpha + \gamma}$$

where N_0 is the deuterium concentration of the water vapor from the saturator. The value of α was calculated (19) from eq. 6.

$$[6] \qquad \log_{10}\alpha = \frac{205}{T(°K)} - 0.129$$

Thus k may be calculated from the initial slope of a plot of $\ln (n_e - n_0)/(n_e - n)$ against W/F. Such a plot is shown in Fig. 1 for a 0.75% platinum on silica catalyst prepared by $Pt(NH_3)_4^{2+}$ exchange. The catalyst temperature is 80 °C and γ is 3.18. The rate is $2.6_1 \times 10^{-4}$ mol D_2/g s and the yield is linear to quite high conversions. Rates were reproduced to within ±5% and are probably accurate to within ±10%.

The temperature dependence of the rates is shown in Fig. 2, plotted in the Arrhenius form, for catalysts prepared from $Pt(NH_3)_4^{2+}$. At temperatures above 100 °C, a reasonably linear relationship was obtained, and the apparent activation energy corresponded to 9.3 ± 0.5 kcal/mol. At temperatures below 100 °C, catalysts of lower metal surface area tended to show a decrease in rate from the Arrhenius dependence, while those with the larger areas actually showed an increase in rate at lower temperatures. Catalysts made from H_2PtCl_6 and from $Pt(NH_3)_2$-

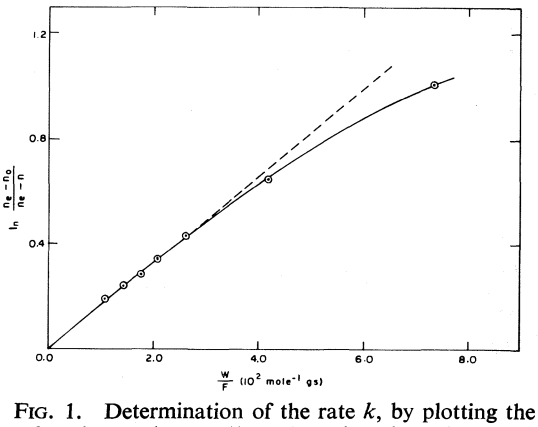

FIG. 1. Determination of the rate k, by plotting the rate function, $\ln (n_e - n_0)/(n_e - n)$, against the reciprocal of the flow. Catalyst: 0.75% Pt prepared from $Pt(NH_3)_4^{2+}$ and unsintered. Reaction temperature 80 °C.

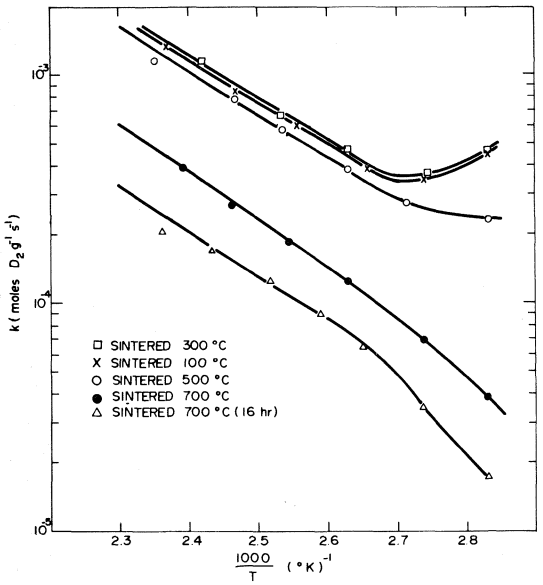

FIG. 2. Arrhenius plot for catalysts containing 0.75% Pt prepared from $Pt(NH_3)_4^{2+}$ and sintered at various temperatures.

$(NO_2)_2$ gave straight lines or showed slight downward deviations from Arrhenius behavior at lower temperatures. Some less well reduced catalysts prepared from H_2PtCl_6 gave upward deviations from Arrhenius behavior at low temperatures. Apparent activation energies for the catalysts prepared with H_2PtCl_6 were in the range 7.5 ± 1 kcal/mol except for a value of 9.6 for the catalyst sintered at 700 °C. Apparent activation energies for catalysts prepared from $Pt(NH_3)_2(NO_2)_2$ were in the range of 9 ± 1 kcal/mol.

The B.E.T. surface area of the silica gel after air drying at 600 °C was 323 m^2/g. Some typical hydrogen chemisorption isotherms are shown in Fig. 3 for catalysts prepared with $Pt(NH_3)_4^{2+}$ and sintered at various temperatures. Under these conditions, hydrogen adsorption on the silica gel itself was negligible. The linear portion of the isotherm at higher pressure was extrapolated to zero pressure and this adsorbed volume was used to calculate the metal surface area assuming monolayer coverage. From this area an average particle size can be calculated, assuming a geometry for the particle. We assumed the crystallites were spheres exposing their entire surface. The average size obtained is equivalent to $\sum n_i d_i^3 / \sum n_i d_i^2$ (15), *i.e.*, an area averaged diameter, where d_i is the diameter of the ith particle.

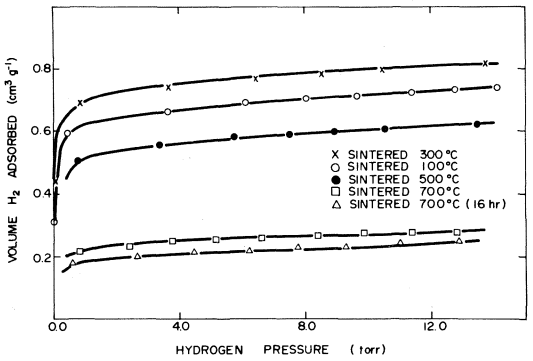

FIG. 3. Hydrogen adsorption isotherms for catalysts with 0.75% Pt prepared from $Pt(NH_3)_4^{2+}$ and sintered at various temperatures.

The X-ray method gives a volume averaged diameter $\sum n_i d_i^4 / \sum n_i d_i^3$ and furthermore measures "crystallite size" rather than particle size (20). However, twinning has been shown to be of minor importance for most supported catalysts (21). From the electron micrographs a true average diameter $\sum n_i d_i / \sum n_i$, as well as the other two averages, can be calculated. Table 1 compares the three methods of obtaining particle sizes for catalysts prepared by H_2PtCl_6. Table 2 shows the different types of particle diameter averages obtained by electron microscopy compared with the same type obtained by other methods, where possible. The agreement shows that the particle

TABLE 1. Particle diameters for H_2PtCl_6 catalysts

Sintering temperature (°C)	Particle diameter (Å)		
	Electron microscopy	X-Ray	Adsorption
100	32.5		26.1
250			26.1
400	36.0	32.5	29.5
500		36.8	37.6
600		74.8	67.7
700	97.5	90.7	97.0

TABLE 2. Particle diameter averages for H_2PtCl_6 catalysts sintered at 400 °C

Average	Particle diameter (Å)		
	Electron microscopy	X-Ray	Adsorption
$\Sigma n_i d_i / \Sigma n_i$	36.0	—	—
$\Sigma n_i d_i^3 / \Sigma n_i d_i^2$	39.2	—	29.5
$\Sigma n_i d_i^4 / \Sigma n_i d_i^3$	42.0	32.5	—

Can. J. Chem. Downloaded from www.nrcresearchpress.com by 210.87.254.5 on 09/05/12
For personal use only.

size distribution is reasonably narrow, for this catalyst at least.

Neither electron microscopy nor X-ray diffraction were suited to the smaller ranges of particle size of the catalysts prepared by ion exchange. However, for catalysts prepared in this way and sintered to high temperatures these methods did show that the particle size distribution was probably at least bimodel since there seemed to be at least a few particles of quite large size (~100 Å). For the catalysts prepared by $Pt(NH_3)_2(NO_2)_2$ impregnation, good agreement was obtained between adsorption methods and electron microscopy, although the number of particles counted was necessarily small. The X-ray diffraction results gave poorer agreement, probably because of the large corrections for instrumental broadening.

From a knowledge of k, and the metal surface area, the specific rate is obtained. Figure 4 shows some specific rates at 127 °C as a function of particle size as measured by hydrogen chemisorption. Within each catalyst series, a maximum specific rate is obtained for sintering temperatures of about 500 °C. The variations in specific rate within each catalyst series are greater than the variations between the three series, and no well-defined variation in specific rate solely with particle size is observed.

A series of catalysts containing 0.12 to 0.75% platinum was prepared by $Pt(NH_3)_4^{2+}$ exchange. These catalysts were not sintered and were reduced *in situ* at 350 °C. Specific rates were in the range $3.0 \pm 0.8 \times 10^{-8}$ mol D_2/cm^2 Pt s, and apparent activation energies were in the range 8.8 ± 1.0 kcal/mol. Rather larger errors were involved in measuring surface areas at the lowest platinum concentrations. However, the approximately constant specific rates and apparent activation energies confirm that pore diffusion is relatively unimportant in this system (14). They also confirm that our results are not changed by the slightly different platinum loadings used.

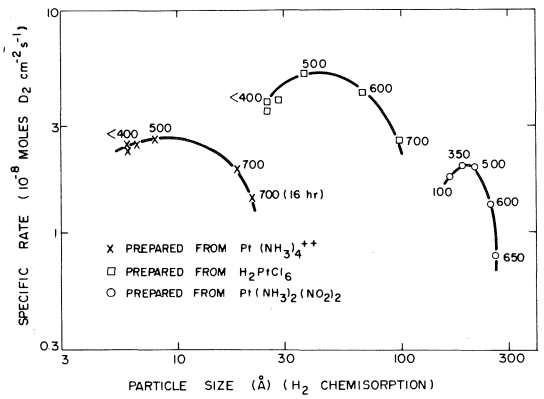

FIG. 4. Specific rates measured at 127 °C for the catalysts studied. The figures beside points give the sintering temperature.

Discussion

From Fig. 2, it is apparent from the changes in the Arrhenius slope that the reaction shows complex behavior below 100 °C. A number of possibilities suggest themselves as explanations for this behavior. For example, if the water adsorption characteristics of the support are important, it should be noted that at 80 °C, with a saturation temperature of 63.5 °C, the relative pressure of water is about 0.5. Hence the water adsorption isotherms may be quite complex. However, a study of the complicated behavior below 100 °C was not within the scope of this work. Further discussion will be confined to the region above 100 °C where reasonably straight Arrhenius plots and nearly constant activation energies were obtained.

We have noted above that no clear effect of particle size on the specific rate at 127 °C has been demonstrated. This observation was somewhat surprising. Both theoretical and experimental work have indicated that electronic properties undergo drastic changes in going from atomic dispersion to the bulk metal (22–24). For platinum the first ionization potential of the atom is 9.0 eV (25), whereas the work function of metallic platinum is 5.4 eV (26). At least part of the change from atomic to metallic properties should occur in going from 6 to 300 Å particles, and yet no gross effects on the specific rates are noted over this range. Thus, the hydrogen–water isotopic exchange seems insensitive to changes in electronic properties of the metal catalyst. It joins a growing list of reactions for which varying platinum particle size does not change the specific rate. These include hydrogen–deuterium exchange (4), various hydrogenation reactions (4–7), dehydrogenation of cyclohexane and isopropanol (27), and hydrogenolysis of cyclopentane (27).

Certain reactions, the best example of which is the isomerization of neopentane (28), show sensitivity to changes in the metal particle size.

Can. J. Chem. Downloaded from www.nrcresearchpress.com by 210.87.254.5 on 09/05/12
For personal use only.

Can. J. Chem. Downloaded from www.nrcresearchpress.com by 210.87.254.5 on 09/05/12
For personal use only.

These have been termed "demanding" reactions by Boudart, and the major factor making them demanding is thought to be a requirement for a definite geometric arrangement of surface atoms (28). The isomerization of neopentane is thought to require triadsorption of neopentane at triple adsorption sites. For the simpler reactions, such as the exchange reaction considered here, apparently there is no strict geometrical requirement.

There appears to be some variation of specific activity with the method of catalyst preparation. Some of this may be illusory. The $Pt(NH_3)_4^{2+}$ exchanged catalyst adsorbed sufficient hydrogen that, for the most highly dispersed catalysts, the ratio of H-to-Pt was almost 1.5. Similar behavior was noted by Poltorak and Boronin (29) and, to a lesser extent, by Benesi *et al.* (15). The results given in Fig. 4 are presented in terms of particle size, based on the assumption that one H atom is adsorbed per platinum atom. There is evidence that, for particles 15 Å in diameter and larger, this is a good assumption (17), but if, with very small particles, more than one H atom is taken up per platinum atom, the actual surface areas will be smaller than measured and hence the specific rates will be larger. A 50% decrease in measured areas would bring the $Pt(NH_3)_4^{2+}$ catalyst rates close to those from H_2PtCl_6 catalysts. Other differences between the series are the acidity of the medium in which the platinum is deposited, and the chlorine content. There is evidence that chloride acts as a promoter for hydrogenation reactions (11).

There also appears to be a very characteristic variation in specific rate within each series of catalysts. That is, a maximum in specific rate is observed for each series for catalysts sintered about 500 °C. In some cases, the small decreases observed at lower sintering temperatures may not be real, but the decreases at higher temperatures definitely are. Three possible explanations suggest themselves for this behavior, although no definite conclusions can be reached. The heats of adsorption of water on silica gel vary from 5 to 1 kcal/mol for gels degassed at 150 and 810 °C, for 50 mg water adsorbed per g of gel (30). Thus the gels degassed at higher temperatures are less hydrophilic, and, if water adsorbed on the gel plays any part in the kinetics, lower rates may result. On the other hand, a very high coverage of water molecules may slightly inhibit diffusion of water to the platinum, lowering the specific rate. Another possibility is that when platinum crystallites are heated much above 480 °C, the low energy (111) face will be preferentially developed (4). It is possible that this face has a lower specific activity. Thirdly, a maximum in oxidation–reduction activity has been observed for alumina and silica–alumina heated to about 600 °C (31). Although this type of activity has not been observed for silicas, it is possible that oxidation–reduction activity, too low to form the cations and anions studied by Flockhart *et al.* (31) can effect the properties of the platinum in this system. In any case, the fact that the curves in Fig. 4 have the same shape suggests that platinum particle size has relatively little to do with the rate of exchange.

Although a true kinetic study was not undertaken, some comments on the reaction mechanism can be made. In several places in the foregoing discussion we have alluded to the possible effects of the silica support. Thus, non-linear adsorption of water was suggested as being responsible for the behavior at reaction temperatures less than 100 °C. Furthermore, whatever the source and size of the platinum particles, maximum specific rates were obtained for silicas heated to about 500 °C. When the silicas were heated to high temperatures the specific rate fell, and it was suggested that the hydrophobic character of the silicas is responsible. It is noted that the maximum specific rate occurs where the gel is about half covered with surface hydroxyls (32). These observations suggest that the silica support plays an important role in the catalysis, and that this role is far more important than the platinum particle size. It is tentatively suggested that water vapor is adsorbed on the support, and that this adsorbed water reacts with hydrogen at the platinum particles. If the rate at which water can be transferred to the platinum is indeed important then it is not surprising that no effect of particle size was noted. However, any real discussion of the role of the support must await a thorough study of this factor.

Generally reactions which involve hydrogen transfer are facile reactions, as noted above. However, Poltorak and Boronin found very large changes in specific rates for reactions involving oxygen (29), and this was attributed to the loss of metallic character when small particles of platinum have a high coverage of oxygen atoms. Now one type of mechanism for hydrogen–water

exchange (33) is the following sequence

[7] $$HDO + Pt \rightarrow HD + PtO$$

[8] $$H_2 + PtO \rightarrow H_2O + Pt$$

Our results suggest that, if this is the mechanism, the coverage of oxygen atoms remains low during reaction.

We would like to thank S. C. Cribbs for doing the platinum analyses, D. Faulkner and E. E. Sexton for taking the electron micrographs, and A. Sawatzky and A. M. Duclos for measuring the X-ray diffraction patterns. Discussions with G. G. Strathdee and E. A. Symons are gratefully acknowledged.

1. M. Boudart. Adv. Catal. **20**, 153 (1969).
2. G. C. Bond. *In* IV International Congress on Catalysis. *Compiled by* J. W. Hightower, Rice University Printing Department. 1969. p. 1217.
3. P. B. Weisz. Ann. Rev. Phys. Chem. **21**, 175 (1970).
4. O. M. Poltorak and V. S. Boronin. Zhur. Fiz. Khim. **39**, 2491 (1965).
5. T. A. Dorling and R. L. Moss. J. Catal. **5**, 111 (1966).
6. P. C. Aben, J. C. Platteeuw, and B. Stouthamer. *In* IV International Congress on Catalysis. *Compiled by* J. W. Hightower, Rice University Printing Department. 1969. p. 543.
7. M. Boudart, A. Aldag, J. E. Benson, N. A. Dougharty, and C. G. Harkins. J. Catal. **6**, 92 (1966).
8. D. J. C. Yates, W. F. Taylor, and J. H. Sinfelt. J. Am. Chem. Soc. **86**, 2996 (1964).
9. W. F. Taylor, D. J. C. Yates, and J. H. Sinfelt. J. Phys. Chem. **68**, 2962 (1964).
10. J. L. Carter, J. A. Cusamano, and J. H. Sinfelt. J. Phys. Chem. **70**, 2257 (1966).
11. T. A. Dorling, M. J. Eastlake, and R. L. Moss. J. Catal. **14**, 23 (1969).
12. P. Margineanu and A. Olariu. J. Catal. **8**, 359 (1967).
13. G. C. Bond. Catalysis by metals. Academic Press, London. 1962. pp. 217–220.
14. C. N. Satterfield. Mass transfer in heterogeneous catalysis. M.I.T. Press, Cambridge, Mass. 1970.
15. H. A. Benesi, R. M. Curtis, and H. P. Studer. J. Catal. **10**, 328 (1968).
16. M. M. Schnepfe and F. S. Grimaldi. Talanta, **16**, 591 (1969).
17. T. A. Dorling, C. J. Burlace, and R. L. Moss. J. Catal. **12**, 207 (1968).
18. H. P. Klug and L. E. Alexander. X-Ray diffraction procedures. John Wiley and Sons, New York. 1954. pp. 491–538.
19. J. A. Ayres. Production of heavy water status report. BNWL report 884 Battelle Memorial Institute Pacific Northwest Laboratory, Richland, Washington, 1969. p. 64.
20. C. R. Adams, H. A. Benesi, R. M. Curtis, and R. G. Meisenheimer. J. Catal. **1**, 336 (1962).
21. N. R. Avery and J. V. Sanders. J. Catal. **18**, 129 (1970).
22. G. Rienacker and N. Hansen. Z. Eleckrochem. **60**, 887 (1956).
23. R. Suhrmann, G. Kruger, G. Wedlev, and F. Nene. Z. Phys. Chem. **30**, 1 (1961).
24. R. F. Baddour and M. C. Deibert. J. Phys. Chem. **70**, 2173 (1966).
25. V. I. Vedeneyev, L. V. Gurvich, V. N. Kondrat'yev, V. A. Medvedev, and Ye L. Frankevich. Bond energies, ionization potentials, and electron affinities. Edward Arnold Publishers Ltd., London, 1966. p. 152.
26. C. W. Oatley. Proc. Phys. Soc. **51**, 318 (1938).
27. O. M. Poltorak and V. S. Boronin. Zhur. Fiz. Khim. **40**, 2671 (1966).
28. M. Boudart, A. W. Aldag, L. D. Ptak, and J. E. Benson. J. Catal. **11**, 35 (1968).
29. O. M. Poltorak and V. S. Boronin. Zhur. Fiz. Khim. **39**, 1476 (1965).
30. N. K. Nair and J. M. Thorp. Trans. Faraday Soc. **61**, 975 (1965).
31. B. D. Flockhart, I. R. Leith, and R. C. Pink. Trans. Faraday Soc. **66**, 469 (1970).
32. N. H. Sagert and P. J. Dyne. Can. J. Chem. **45**, 615 (1967).
33. J. H. Rolston. Private communication.

Can. J. Chem. Downloaded from www.nrcresearchpress.com by 210.87.254.5 on 09/05/12
For personal use only.

Can. J. Chem. Downloaded from www.nrcresearchpress.com by 210.87.254.5 on 09/05/12
For personal use only.

Crystal and Molecular Structure of Dichlorobis(4-methylpyridine)zinc(II), $Zn(4\text{-}CH_3Py)_2Cl_2$

H. Lynton and M. C. Sears

Department of Chemistry, University of New Brunswick, Fredericton, New Brunswick

Received May 12, 1971

Crystals of dichlorobis(4-methylpyridine)zinc(II), $Zn(4\text{-}CH_3Py)_2Cl_2$, are monoclinic, space group $P2_1/c$, with $a = 14.294(13)$, $b = 7.885(8)$, $c = 13.473(11)$ Å, $\beta = 100.60(5)°$ and 4 molecules in the unit cell. The final atomic parameters were obtained from a block-diagonal least squares refinement using anisotropic thermal parameters. The hydrogen atom positions were established but the parameters were not refined. The final agreement residual for 1348 observed reflections is $R = 0.043$. The zinc atom is tetrahedrally coordinated.

Les cristaux de dichloro bis-(méthyl-4 pyridine) zinc(II), $Zn(CH_3\text{-}4\ Py)_2Cl_2$, cristallisent dans le système monoclinique, groupe d'espace $P2_1/c$.

La maille élémentaire contenant 4 molécules d'eau a pour dimensions $a = 14.294(13)$, $b = 7.885(8)$, $c = 13.473(11)$ Å, $\beta = 100.60(5)°$. Les paramètres atomiques ont été affinés par moindre carrés (diagonalisation par blocs) en utilisant des facteurs thermiques anisotropes. La position des atomes d'hydrogène a été établie mais les paramétres n'ont pas été affinés. L'indice d'accord final pour 1348 réflexions observées est $R = 0.043$. L'atome de zinc est coordonné d'une façon tétrahédrique.

Canadian Journal of Chemistry, 49, 3418 (1971)

Introduction

Previous papers (1, 2) published in this laboratory reported the stereoconfigurations for $Zn(4\text{-}CH_3Py)_2Cl_2$, $Hg(4\text{-}CH_3Py)Cl_2$, and $Cd(4\text{-}CH_3Py)Cl_2$, as determined by infrared spectroscopy and a normal coordinate analysis. In order to confirm the stereochemistry, crystal structure determinations of the above complexes were attempted. Crystals of the Cd(II) complex were not sufficiently large and crystals of the Hg(II), while adequate in size, were found to be extensively twinned. The analogous bromide complexes yielded similar results. However, good single crystals of the Zn(II) complex were obtained and the crystal structure determined.

Crystal Structure Analysis

Crystal data are as follows:

$C_{12}H_{14}N_2ZnCl_2$ f.w. = 322.5

Monoclinic, $a = 14.294(13)$, $b = 7.885(8)$, $c = 13.474(11)$ Å, $\beta = 100.60(5)°$, $v = 1492.5$ Å^3, $\rho_0 = 1.42(2)$, $z = 4$, $\rho_c = 1.435$ (20 °C, MoK$\bar{\alpha}$, $\lambda = 0.71069$ Å).

The unit cell dimensions and their estimated standard deviations (in parentheses) were obtained from a least squares evaluation of the positions of 12 independent reflections. The space group is $P2_1/c$ (C_{2h}^5), No. 14 in *International Tables for X-ray Crystallography*, Vol. I (3).

Intensity data were collected on a Picker computer-controlled four-angle diffractometer using a $\theta/2\theta$ scan with β-filtered MoKα radiation and a scintillation detector. The two octants hkl and $\bar{h}kl$ were explored to a maximum 2θ of 45°. There were 1960 accessible reflections in this region of which 1348 were considered observed. The threshold was taken as $0.10\times$ the background count or 36 counts, whichever was greater. The specimen was plate-like, with dimensions $0.35 \times 0.30 \times 0.17$ mm, the shortest diagonal being parallel to the b axis. The b axis of the crystal was mounted parallel to the ϕ direction of the diffractometer. The linear absorption coefficient for MoKα radiation is $\mu = 19.9$ cm^{-1}. No absorption or extinction coefficients were applied.

The position of the zinc atom was established from a three-dimensional Patterson synthesis. All of the carbon, nitrogen, and chlorine atoms were then located from successive three-dimensional Fourier syntheses. All atoms occupy general positions. The method of refinement was by successive cycles of block-diagonal least squares, using 3×3 matrices for the positional parameters and 6×6 matrices for the anisotropic thermal parameters of each atom. The quantity minimized was $\sum w(|F_o| - |F_c|)^2$ for observed reflections only, using the weighting function $w = 1/(1 + [(|F_o| - P_2)/P_1]^4)$

Can. J. Chem. Downloaded from www.nrcresearchpress.com by 210.87.254.5 on 09/05/12
For personal use only.

TABLE 1. Final parameters* T.F. = exp $[-2\pi^2(a^{*2}h^2U_{11} \ldots + 2b^*c^*klU_{23} + \ldots)]$

Atom	x	y	z	U_{11}	U_{22}	U_{33}	U_{23}	U_{13}	U_{12}
Zn	2528(1)	1978(1)	1994(1)	111(1)	98(1)	78(1)	−4(1)	15(1)	4(1)
Cl(1)	2068(1)	4656(2)	1817(2)	153(2)	98(2)	144(2)	0(2)	25(2)	21(2)
Cl(2)	2595(2)	0609(3)	3431(1)	231(3)	147(3)	76(2)	13(2)	27(2)	8(2)
N(1)	3843(4)	1885(7)	1601(4)	113(6)	92(6)	89(6)	4(5)	7(5)	14(6)
N(2)	1748(3)	0617(7)	0841(4)	93(6)	101(6)	74(5)	2(5)	21(5)	7(5)
C(1)	4563(5)	0964(11)	2086(6)	143(10)	155(11)	122(9)	21(9)	6(7)	27(9)
C(2)	5425(5)	0823(12)	1776(7)	99(9)	199(13)	203(13)	16(11)	24(8)	44(9)
C(3)	5578(5)	1655(9)	0936(6)	93(8)	125(10)	179(11)	−56(8)	32(7)	−7(7)
C(4)	4851(5)	2614(10)	0430(6)	134(9)	143(10)	155(10)	−19(8)	66(8)	−17(8)
C(5)	3995(5)	2732(10)	0785(5)	123(8)	130(9)	120(8)	2(8)	16(7)	13(8)
C(6)	6495(6)	1514(12)	0557(8)	131(10)	188(14)	258(17)	−67(12)	73(10)	−12(9)
C(7)	1642(5)	−1063(9)	0899(5)	115(8)	109(8)	97(8)	8(7)	23(6)	−4(7)
C(8)	1213(5)	−2026(9)	0096(5)	127(8)	115(8)	109(8)	−13(7)	30(7)	−22(8)
C(9)	0865(4)	−1240(10)	−0827(5)	77(7)	158(10)	98(8)	−30(7)	26(6)	−6(7)
C(10)	0965(5)	0465(10)	−0881(5)	113(8)	150(10)	75(7)	0(7)	12(6)	4(8)
C(11)	1405(5)	1384(9)	−0049(5)	114(8)	114(9)	84(7)	18(6)	19(6)	9(7)
C(12)	0422(6)	−2274(12)	−1737(6)	155(10)	211(14)	115(9)	−58(9)	11(8)	−44(10)

*Estimated standard deviations in parentheses; $x, y, z \times 10^4$; $U_{ij} \times 10^3$.

TABLE 2. Parameters for the hydrogen atoms × 10^3
T.F. = exp $[-8\pi^2 U(\sin\theta/\lambda)^2]$

Atom		x	y	z	U (Å^2)
C(1)	H(1)	434	041	268	63
C(2)	H(2)	603	018	220	63
C(4)	H(3)	513	348	−014	63
C(5)	H(4)	335	342	032	63
C(6)	H(5)	670	021	063	101
	H(6)	645	232	−004	101
	H(7)	708	198	108	101
C(7)	H(8)	194	−170	156	63
C(8)	H(9)	101	−322	028	63
C(10)	H(10)	068	112	−155	63
C(11)	H(11)	165	276	−013	63
C(12)	H(12)	012	−188	−245	101
	H(13)	012	−335	−134	101
	H(14)	−034	−183	−166	101

TABLE 3. Intramolecular distances and angles (e.s.d.'s in parentheses)

Bond		Distance (Å)	Bonds		Angle (degrees)
Zn—Cl(1)		2.211(2)	Cl(1)—Zn—Cl(2)		121.8(1)
Zn—Cl(2)		2.204(2)			
			Cl(1)—Zn—N(1)		106.0(2)
Zn—N(1)		2.046(5)	Cl(1)—Zn—N(2)		108.0(2)
Zn—N(2)		2.042(5)	Cl(2)—Zn—N(1)		108.5(2)
			Cl(2)—Zn—N(2)		109.9(2)
N(1)—C(1)		1.329(9)			
N(1)—C(5)		1.338(9)	N(1)—Zn—N(2)		100.6(2)
N(2)—C(7)		1.337(9)			
N(2)—C(11)		1.351(8)	Zn—N(1)—C(1)		123.9(5)
			Zn—N(1)—C(5)		119.4(5)
			Zn—N(2)—C(7)		121.9(4)
C(1)—C(2)	side	1.377(11)	Zn—N(2)—C(11)		119.9(4)
C(4)—C(5)	side	1.396(11)			
C(7)—C(8)	side	1.371(10)	C(1)—N(1)—C(5)		116.7(6)
C(10)—C(11)	side	1.385 (9)	C(7)—N(2)—C(11)		117.9(5)
			N(1)—C(1)—C(2)		123.4(7)
C(2)—C(3)	top	1.360(12)	N(1)—C(5)—C(4)		122.2(7)
C(3)—C(4)	top	1.362(11)	N(2)—C(7)—C(8)		122.8(6)
C(8)—C(9)	top	1.396(10)	N(2)—C(11)—C(10)		121.4(6)
C(9)—C(10)	top	1.355(11)			
			C(1)—C(2)—C(3)		120.2(8)
C(3)—C(6)		1.496(11)	C(3)—C(4)—C(5)		120.1(7)
C(9)—C(12)		1.512(11)	C(7)—C(8)—C(9)		119.4(6)
			C(9)—C(10)—C(11)		120.8(6)
			C(2)—C(3)—C(4)	top	117.4(7)
			C(8)—C(9)—C(10)	top	117.7(6)
			C (2)—C(3)—C(6)		122.2(7)
			C (4)—C(3)—C(6)		120.4(7)
			C (8)—C(9)—C(12)		120.7(6)
			C(10)—C(9)—C(12)		121.6(6)

with $P_1 = 25$ and $P_2 = 30$ (14). This weighting function gives almost equal weights in the middle range of $|F_o|$ but reduced weights for the higher and lower values. Scattering factor curves used were those for Zn, Cl, N, C, and H given in *International Tables for X-ray Crystallography*, Vol. III (4). The real and imaginary dispersion corrections were applied to the scattering curves of zinc and chlorine (5).

The final agreement residual $R = \sum(||F_o| - |F_c||)/\sum|F_o|$ for all atoms except hydrogen was 0.056. A difference synthesis at this point showed the positions of all the hydrogens as peaks with electron density between 0.4–0.5 e Å^{-3}, and no other residual electron density greater than 0.25 e Å^{-3}. The hydrogens were assigned isotropic thermal parameters by the following scheme: for hydrogens on methyl

Can. J. Chem. Downloaded from www.nrcresearchpress.com by 210.87.254.5 on 09/05/12
For personal use only.

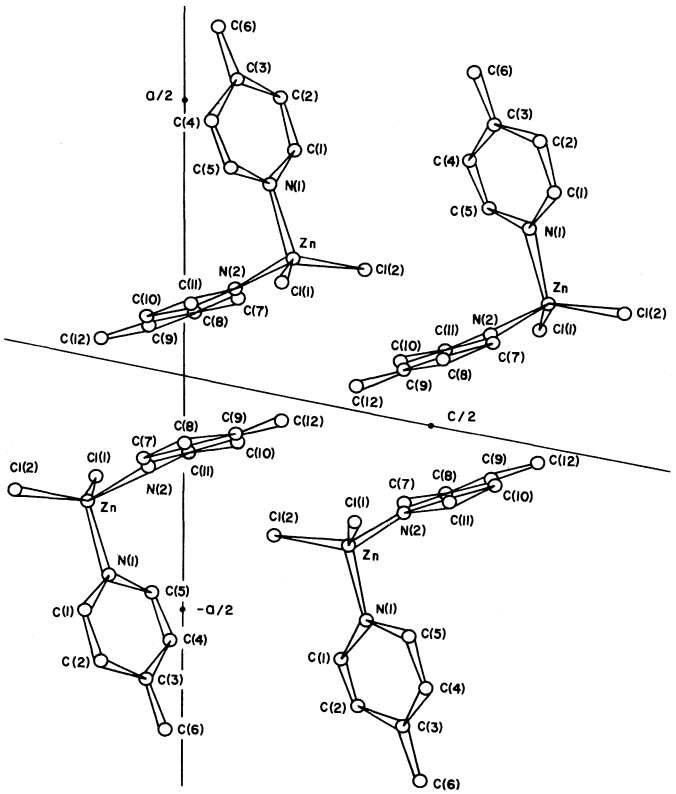

FIG. 1. Stereochemistry of the molecule and packing in the unit cell.

groups, $B = 8.00$; and for hydrogens on ring carbons, $B = 5.00$ Å^2. The positional and thermal parameters for the hydrogens were not refined during subsequent least squares cycles. The final agreement residual for all atoms was $R = 0.043$. Hamilton's significance test on the crystallographic R factor was applied and at a significance level of 0.01(1%) the reduction in the R factor from 0.056 to 0.043 was significant. A set of structure factors for the final parameters given in Tables 1 and 2 has been placed in the Depository of Unpublished Data.[1]

Discussion

The intramolecular bond distances and angles are given in Table 3. The stereochemistry of the molecule, the packing in the unit cell, and the numbering scheme are shown in Fig. 1.

The coordination about the zinc atom is distorted tetrahedral. The large Cl–Zn–Cl angle 121.8(1)° may be attributed to repulsions between nonbonding electrons on adjacent chlorine atoms. Similar large values have been reported for this angle in $Zn(Py)_2Cl_2$ (6) (121.0°), dichloro-(2,9-dimethyl-1,10-phenanthroline)zinc(II) (7) (121.2°), and dichlorobis(1-methyltetrazole) zinc(II) (8) (118.4°).

The Zn—N bond distances of 2.046(5) and 2.042(5) Å are not significantly different. There are few precise values of the Zn—N and Zn—Cl bond lengths reported in the literature for comparison with this study. A recent summary of Zn—N and Zn—Cl bond distances, in a number of complexes where zinc is tetrahedrally coordinated, is given by Baenziger and Schultz (8). The Zn—N distances fall in the range 1.99–2.10 Å. The Zn—N bond lengths found in this investigation fall well within this range and agree, within experimental error, with the Zn—N distances of 2.04(1) and 2.06(1) Å determined for dichlorobis(1-methyltetrazole)zinc(II), and are similar to the corresponding distances of 2.02(4) and 1.99(4) Å reported for $Zn(Py)_2Cl_2$.

[1]Photocopies may be obtained upon request from the Depository of Unpublished Data, National Science Library, National Research Council of Canada, Ottawa K1A 0S2, Canada.

Can. J. Chem. Downloaded from www.nrcresearchpress.com by 210.87.254.5 on 09/05/12
For personal use only.

Can. J. Chem. Downloaded from www.nrcresearchpress.com by 210.87.254.5 on 09/05/12
For personal use only.

TABLE 4. Mean bond lengths (Å) in pyridine and substituted pyridines

	Bond length (Å)				
Bond	$Zn(4\text{-methylpyridine})_2Cl_2$	Pyridine (microwave)	$Zn(Py)_2Cl_2$	$Ni(3,5\text{-dimethylpyridine})_4(ClO_4)_2$	4-Methylpyridine in $[HBrB(4\text{-methylpyridine})N(CH_3)]^+PF_6^-$
C—N	1.339	1.3402	1.35	1.341	1.36
C—C (side)	1.383	1.3945	1.39	1.370	1.36
C—C (top)	1.368	1.3944	1.34		1.39
$C—CH_3$	1.504	—	—	1.513	1.51

TABLE 5. Mean bond angles in pyridine and substituted pyridines

Bonds	Bond angle (degree)		
	$Zn(4\text{-methylpyridine})_2Cl_2$	4-Methylpyridine in [HBrB(4-methylpyridine) $N(CH)_3]^+PF_6^-$	Pyridine (microwave)
C—N—C	117.3	117.3	116.8
N—C—C	122.5	122.1	121.3
C—C—C	120.3	120.9	118.5
C—C—C (top)	117.5	116.3	118.3

TABLE 6. Best mean plane through the rings (e.s.d.'s in parentheses)

Atom	Distance from plane in (Å)
Ring 1	
equation $-0.245X - 0.789Y - 0.563X + 3.625 = 0^a$	
N(1)	0.009(5)
C(1)	−0.002(8)
C(2)	−0.003(9)
C(3)	0.001(8)
C(4)	0.006(8)
C(5)	−0.011(8)
Ring 2	
equation $-0.951X - 0.130Y - 0.279Z - 1.800 = 0^a$	
N(2)	0.004(5)
C(7)	−0.003(7)
C(8)	−0.001(7)
C(9)	0.004(6)
C(10)	−0.002(7)
C(11)	−0.002(7)

[a]Referred to an orthogonal set of axes, X along a, Y along b, and Z along c^*.

The Zn—Cl bond distances of 2.211(2) and 2.04(2) Å are possibly significantly different ($t = 2.47$) according to Cruickshank's criterion (9). In the Baenziger–Schultz summary, the Zn—Cl distances lie between 2.18 and 2.30 Å. The Zn—Cl bond lengths in this work are quite close to the Zn—Cl distances of 2.06(5) and 2.198(5) Å reported for dichlorobis(1-methyltetrazole)zinc(II), and 2.19(1) and 2.18(1) Å determined for $Zn(Py)_2Cl_2$.

An examination of chemically equivalent bonds in the two 4-methylpyridine rings suggests that the C(8)—C(9) bond distance is significantly different ($t = 2.68$) from one of its three equivalent bond distances and possibly different ($t = 2.28$ and $t = 2.30$) from the other two. However, the C(8)—C(9) distance is not significantly different from the mean value of 1.368 Å. There are no distinguishing features of the environment about this particular bond which would explain this result. The remaining chemically equivalent distances are not significantly different from each other.

Table 4 compares the mean bond distances in the 4-methylpyridine rings with those given for the microwave study of pyridine (10), the pyridine ligand in the $Zn(Py)_2Cl_2$ structure (6), the 3,5-dimethylpyridine ligand in the Ni(3,5-dimethylpyridine)$_4(ClO_4)_2$ structure (11) and the 4-methylpyridine ligand in the structure of (+)-4-methylpyridinetrimethylaminebromohydroboronhexafluorophosphate (12). Within limits of accuracy, the bond lengths in the above ligands agree quite well with this investigation, the exception being that the C—C (top) distances (adjacent to the methyl group) in this structure are somewhat lower than the pyridine microwave study. In addition, the C—CH_3 average value of 1.504 Å is in excellent agreement with the average value of 1.505(5) Å for a number of bonds between tetrahedral carbon atoms and aromatic rings (13).

Comparable bond angles in the 4-methylpyridine rings are not significantly different. Table 5 compares the means of the ring angles in this study and some of the ligands mentioned

Can. J. Chem. Downloaded from www.nrcresearchpress.com by 210.87.254.5 on 09/05/12
For personal use only.

above. The ring angles in the recently reported 4-methylpyridine complex are in good agreement with this work. Within experimental error, the 4-methylpyridine rings are planar (see Table 6).

The closest approach distance between two molecules in this structure is 3.560(7) Å between Cl(1) of one molecule and C(8) of the molecule in the next cell along the *b* direction.

We wish to thank Dr. D. G. Brewer of the University of New Brunswick for suggesting the problem, Dr. F. R. Ahmed of the Biochemistry Laboratory, National Research Council of Canada for use of his computer programs and the National Research Council of Canada for financial support.

1. D. G. Brewer, P. T. T. Wong, and M. C. Sears. Can. J. Chem. **46**, 3137 (1968).
2. M. C. Sears, W. V. F. Brooks, and D. G. Brewer. Can. J. Chem. **48**, 3786 (1970).
3. International Tables for X-ray Crystallography. Vol. I. The Kynoch Press, Birmingham, England. 1965. Sect. 4.3.
4. International Tables for X-ray Crystallography. Vol. I. The Kynoch Press, Birmingham, England. 1962. Table 3.3.1. A.
5. International Tables for X-Ray Crystallography. Vol. III. The Kynoch Press, Birmingham, England. 1962. Table 3.3.2. C.
6. Yu. A. Sokolova, L. O. Atovmyan, and M. A. Porai-Koshits. Zh. Struct. Khim. **7**, 855 (1966)
7. H. S. Preston and C. H. L. Kennard. Chem. Commun. 708 (1967).
8. N. C. Baenziger and R. J. Schultz. Inorg. Chem. **10**, 661 (1971).
9. D. W. J. Cruickshank and A. P. Robertson. Acta Cryst. **6**, 698 (1953).
10. B. Bak, L. Hansen-Hygard, and J. Rastup-Anderson. J. Mol. Spectry. **2**, 361 (1958).
11. F. Madaule-Aubry and G. M. Brown. Acta Cryst. B**24**, 745 (1968).
12. G. Allegra, E. Benedetti, C. Pedone, and S. L. Holt. Inorg. Chem. **10**, 667 (1971).
13. Interatomic Distances Supplement (1965). Special Publication No. 18, London: The Chemical Society. p. S15S.
14. F. R. Ahmed, P. Singh, and W. H. Barnes. Acta Cryst. **B24**, 316 (1969).

Can. J. Chem. Downloaded from www.nrcresearchpress.com by 210.87.254.5 on 09/05/12
For personal use only.

Complexes of Cu(II), Co(II), and Ni(II) with "QPyNO"

MARIE TONG AND D. G. BREWER
Department of Chemistry, University of New Brunswick, Fredericton, New Brunswick

Received June 1, 1971

A new ligand, 2,3-di(2-pyridine *N*-oxide) quinoxaline and its complexes with copper(II), cobalt(II), and nickel(II), have been prepared. A detailed investigation of the magnetic and spectral properties of these compounds has led to some tentative suggestions as to their structures.

Un nouveau ligand, le di-(pyridine-2 *N*-oxyde)-2,3 quinoxaline et ses complexes avec le cuivre(II), le cobalt(II) et le nickel(II), ont été préparés. Une étude détaillée sur les propriétés magnétiques et spectrales de ces composés a permis de faire certaines suggestions quant à la structure de ces composés.

Canadian Journal of Chemistry, **49**, 3425 (1971)

Can. J. Chem. Downloaded from www.nrcresearchpress.com by 210.87.254.6 on 09/05/12
For personal use only.

Introduction

The coordination properties and the complexes of pyridine *N*-oxide (1, 2) and quinoxaline (3, 4) have been studied extensively. The present paper reports the results of an investigation on the complexes of a new ligand, 2,3-di(2-pyridine *N*-oxide) quinoxaline, with some metals of the first transition series, *viz.*, Cu(II), Co(II), and Ni(II).

The ligand 2,3-di(2-pyridine *N*-oxide) quinoxaline (hereafter called QPyNO), with the structure **1**, contains both coordinating oxygen and nitrogen atoms, and can act as a chelating agent with the formation of a six-membered ring with the metal ion. Since this ligand has two similar sites, it is capable of functioning either as mono-bidentate or a bis-bidentate chelating agent.

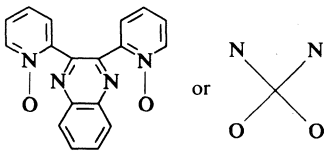

1

The complex, QPyNO–ICl, in which QPyNO can only act as a unidentate agent, due to the linear bonding requirement for the iodine atom (5), was prepared using the method described by Kauffman and Stevens (6). The large differences between the i.r. spectra of all the metal complex compounds in this study and that of QPyNO–ICl suggests that QPyNO is not acting as a unidentate ligand.

A molecular model of QPyNO was constructed and shows that the most probable geometry, involving the ligand in a six-membered ring with the metal ion, would place two pyridine *N*-oxide rings parallel and about 45° to the plane of the quinoxaline ring. This kind of arrangement leaves one oxygen atom above, and the other oxygen atom below, the plane of the quinoxaline ring. This arrangement is consistent with the structure proposed by Geary for the 2,3-di(2-pyridyl) quinoxaline complexes (7).

Experimental

Starting Materials

Analytical grade metal salts were used without further purification.

o-Phenylene diamine was purified by sublimation.

2,2′-Pyridil 1,1′-dioxide was prepared and purified according to the method described by Daihei Oda (8).

2,3-di(2-Pyridine *N*-oxide) quinoxaline was prepared by refluxing equimolar quantities of 2,2′-pyridil 1,1′-dioxide and *o*-phenylene diamine in ethanol until all the 2,2′-pyridil 1,1′-dioxide had been dissolved (approximately 2 h). Ethanol was removed by evaporation. The product was recrystallized from ethanol, m.p. = 268 °C.

Anal. Calcd. for $C_{18}H_{12}N_4O_2$: C, 68.34; N, 17.72; O, 10.13; H, 3.80. Found: C, 68.14; N, 17.70; O, 10.31; H, 3.68.

Preparation of Complexes

All the complexes except $Ni_3Cl_6(QPyNO)_4 \cdot 4H_2O$ were prepared by mixing stoichiometric molar quantities of ligand and metal salt in ethanol and refluxing for 1 h. Complexes were formed either immediately after mixing or upon heating. The precipitates were separated by filtration, washed thoroughly with ethanol, and were dried in a desiccator.

The complex $Ni_3Cl_6(QPyNO)_4 \cdot 4H_2O$ was prepared by mixing equimolar quantities of ligand and nickel chloride in ethanol without heating. The green precipitate was separated by filtration, washed thoroughly with ethanol, and dried in a desiccator.

Analytical data are given in Table 1.

Magnetic Measurements

Magnetic susceptibilities of all the complexes were obtained at room temperature, using a Gouy type balance equipped with a Newport 1½ in. Electromagnet

TABLE 1. Analytical data of complexes

Complex	Color	Found %			Calculated %		
		M	X	C	M	X	C
$CuCl_2$–(QPyNO)	Blue-green	13.95	15.67	48.15	14.10	15.76	47.94
$CuBr_2$–(QPyNO)	Yellow-brown	11.66	29.59	39.94	11.78	29.66	40.03
$CoCl_2$–(QPyNO)·$1\frac{1}{2}H_2O$	Green	12.27	14.98	45.82	12.47	15.02	45.68
$CoBr_2$–(QPyNO)·H_2O	Green	10.39	28.76	39.40	10.66	28.94	39.07
CoI_2–(QPyNO)·H_2O*	Green	8.90	38.98	33.59	9.11	39.26	33.39
Ni_3Cl_6–$(QPyNO)_4$·$4H_2O$	Green	10.22	12.38	49.71	10.21	12.35	50.08
Ni_5Cl_{10}–$(QPyNO)_4$·$4H_2O$	Yellow	15.08	18.10	43.80	14.79	17.89	43.54
$NiBr_2$–$(QPyNO)_2$·H_2O	Yellow	6.50	18.29	49.93	6.76	18.42	49.73
NiI_2–$(QPyNO)_2$·H_2O	Yellow	6.17	26.48	44.75	6.10	26.38	44.87

*Prepared under N_2, this compound is easily decomposed under moisture.

TABLE 2. Infrared frequencies of complexes

Complexes	N—O stretching (cm^{-1})*	N—O bending (cm^{-1})*	M—O stretching (cm^{-1})*
QPyNO	1254; 1238	862; 848	—
$CoCl_2$(QPyNO)·$1\frac{1}{2}H_2O$	1230(sh); 1215; 1209	844; 837	373
$CoBr_2$(QPyNO)·H_2O	1233(sh); 1219; 1205	844; 837	373
CoI_2(QPyNO)·H_2O	1230(sh); 1218; 1205	845; 837	370
$CuCl_2$(QPyNO)	1249; 1192	843; 825	392
$CuBr_2$(QPyNO)	1248; 1188	841; 822	388
$Ni_3Cl_6$$(QPyNO)_4$·$4H_2O$	1239(sh); 1226; 1213	847; 838	370
$Ni_5Cl_{10}$$(QPyNO)_4$·$4H_2O$	1234; 1229(sh); 1214	847; 839	373
$NiBr_2$$(QPyNO)_2$·$H_2O$	1235(sh); 1229(sh); 1220	846; 840(sh); 835(sh)	371
$NiI_2$$(QPyNO)_2$·$H_2O$	1232(sh); 1215(sh); 1208	844; 840	377

*sh = shoulder.

Type C. $Ni(en)_3S_2O_3$ was used for the calibration (en = ethylenediamine).

Spectrophotometric Measurements

The infrared spectra were recorded on a Beckman IR-12 filter/grating spectrophotometer, using Nujol mull.

The electronic spectra were recorded on a Hitachi Ratio Recording spectrophotometer, model EPS-3T, using Nujol mull.

Results and Discussion

Infrared Spectra

The infrared spectra of all the complexes are very complicated, and no meaningful structure correlation can be deduced from them alone. The i.r. spectra of the complexes and that of the ligand are quite similar. However, in the 1200–1300 and 800–900 cm^{-1} regions, a noticeable shift is observed. These are listed in Table 2. These assignments are made by comparing the i.r. spectra of pyridine *N*-oxide and 2,2′-bipyridine 1,1′-dioxide complex compounds (9, 10) with the QPyNO complexes.

All the hydrated complexes show a broad band around 3400 cm^{-1}. However, from the i.r. data alone, it is not possible to determine whether the water molecule is coordinated to the metal or not.

The complexes $CoCl_2$(QPyNO)·$1\frac{1}{2}H_2O$, $CoBr_2$(QPyNO)·H_2O, CoI_2(QPyNO)·H_2O, $Ni_3Cl_6$$(QPyNO)_4$·$4H_2O$, $NiBr_2$$(QPyNO)_2$·$H_2O$, and $NiI_2$$(QPyNO)_2$·$H_2O$ in which the ligand is mono-bidentate, all have a strong absorption band around 455 cm^{-1}, and it is likely that this band can be associated with mono-bidentate QPyNO.

Nickel Complexes

The electronic spectra and magnetic moments (Table 3) clearly indicate that all the nickel complexes are octahedral (11). For the complexes $NiBr_2$$(QPyNO)_2$·$H_2O$ and $NiI_2$$(QPyNO)_2$.$H_2O$, it is obvious that an octahedral structure can be formed when each of the QPyNO acts as a mono-bidentate ligand (**2**). (The *trans* arrangement of the ligands is tentatively proposed due to its reduced steric hindrance.)

Nickel chloride easily forms complexes with

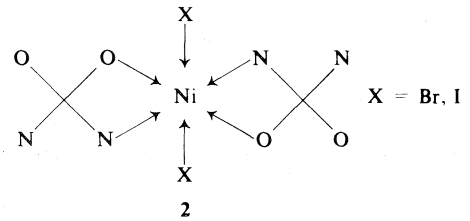

2

Can. J. Chem. Downloaded from www.nrcresearchpress.com by 210.87.254.6 on 09/05/12
For personal use only.

TABLE 3. Magnetic moment and electronic spectra of complexes

Complexes	μ (B.M.)	Electronic spectra (nm)*
$CoCl_2(QPyNO)\cdot 1\frac{1}{2}H_2O$	4.76	614; 634; 679; 1615
$CoBr_2(QPyNO)\cdot H_2O$	4.30	630(sh); 676; 1220(vw); 1545; 1720
$CoI_2(QPyNO)\cdot H_2O$	4.45	670(sh); 716; 1740; 1910
$CuCl_2$–(QPyNO)	1.81	362; 450(sh); 700(sh); 865(br)
$CuBr_2$–(QPyNO)	1.86	360; 430(sh); 780(sh); 920(br)
Ni_3Cl_6–$(QPyNO)_4\cdot 4H_2O$	3.44	400(sh); 660; 1330
Ni_5Cl_{10}–$(QPyNO)_4\cdot 4H_2O$	3.37	420(sh); 730; 800; 1439
$NiBr_2$–$(QPyNO)_2\cdot H_2O$	3.14	420(sh); 714; 1250; 1400(sh)
NiI_2–$(QPyNO)_2\cdot H_2O$	3.16	683; 1200; 1460

*sh = shoulder, vw = very weak, br = broad.

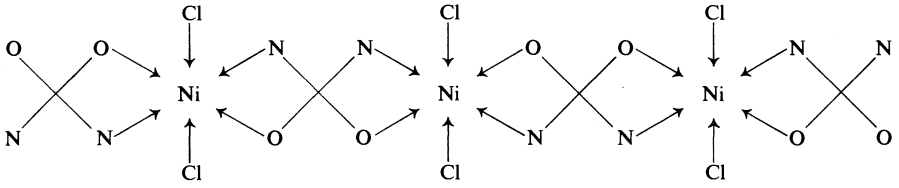

3

QPyNO. When prepared at room temperature, a green complex, $Ni_3Cl_6(QPyNO)_4\cdot 4H_2O$, is obtained. The structure of this compound is proposed as **3**.

In this arrangement, two QPyNO are acting as bis-bidentate ligand, whereas the other two are acting as mono-bidentate ligand. A more stable yellow complex, $Ni_5Cl_{10}(QPyNO)_4\cdot 4H_2O$, is obtained, when nickel chloride and QPyNO are refluxed together in ethanol. In this compound, two more metal atoms are coordinated to the two "free" ends of the $Ni_3Cl_6(QPyNO)_4\cdot 4H_2O$ complex and four water molecules also enter into coordination to give the structure **4**.

The insolubility of these two nickel chloride complexes in ordinary organic solvents, makes it very difficult to study their properties in more detail.

Cobalt Complexes

According to the electronic spectra and magnetic data (Table 3), cobalt halides form tetrahedral complexes with the mono-bidentate QPyNO (12). The visually estimated center of gravity of the ν_2 and ν_3 modes are used to calculate the values of D_q and B (13). These are listed in Table 4. During this study, a paper was published on the complexes of the 2,3-di(2-pyridyl) quinoxalines (7). By comparing the two sets of B values, an increase in stability and electronic delocalization in our system over the 2,3-di(2-pyridyl) quinoxaline system is indicated (14).

TABLE 4. D_q and B values of cobalt complexes

Complexes	ν_2 (cm^{-1})	ν_3 (cm^{-1})	D_q	B
$CoCl_2(QPyNO)\cdot 1\frac{1}{2}H_2O$	6 192	14 728	357	679
$CoBr_2(QPyNO)\cdot H_2O$	6 472	14 793	374	668
$CoI_2(QPyNO)\cdot H_2O$	5 747	13 967	331	652
$CoCl_2(DPYQ)$*	5 510	16 200	315	820
$CoBr_2(DPYQ)$*	5 390	16 000	310	810

*From ref. 7.

Copper Complexes

The visible spectra of the $CuCl_2$ and $CuBr_2$ complexes show a single broad band around 800–900 nm and are characteristic of six-coordinate copper. Thus, a tetragonal structure is

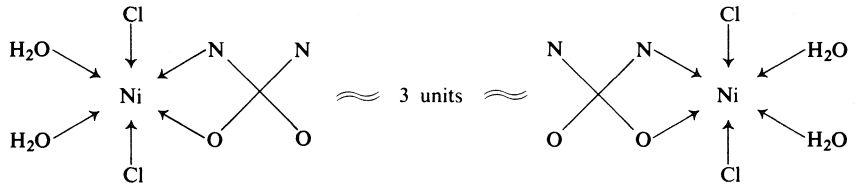

4

Can. J. Chem. Downloaded from www.nrcresearchpress.com by 210.87.254.6 on 09/05/12
For personal use only.

expected in the complexes, with the QPyNO coordinating as a bridging bis-bidentate ligand. The insolubility of these two complexes in organic solvents is also an indication of their polymeric nature.

We thank the National Research Council of Canada for support of this work.

1. J. V. QUAGLIANO, J. FUJITA, G. FRANZ, D. J. PHILLIPS, J. A. WALMSLEY, and S. Y. TYREE. J. Am. Chem. Soc. **83**, 3770 (1961).
2. R. L. CARLIN. J. Am. Chem. Soc. **83**, 3773 (1961).
3. D. E. BILLING and A. E. UNDERHILL. J. Chem. Soc. A, **5**, 8 (1968).
4. (*a*) D. E. BILLING, A. E. UNDERHILL, D. M. ADAMS, and D. M. MORRIS. J. Chem. Soc. A, 902 (1966). (*b*) A. E. UNDERHILL. J. Chem. Soc. A, 4336 (1965).
5. MAX. T. ROGERS and W. K. MEYER. J. Phys. Chem. **66**, 1397 (1962).
6. G. B. KAUFFMAN and K. L. STEVENS. Inorg. Syn. **7**, 176 (1963).
7. W. J. GEARY. J. Chem. Soc. A, 71 (1969).
8. DAIHEI ODA. Nippon Kagaku Zasshi, **82**, 480 (1961).
9. Y. KAKIUTI, S. KIDA, and J. V. QUAGLIANO. Spectrochim. Acta, **19**, 201 (1963).
10. A. VINCIGUERRA, P. G. SIMPSON, Y. KAKIUTI, and J. V. QUAGLIANO. Inorg. Chem. **2**, 286 (1963).
11. A. B. P. LEVER. Inorganic electronic spectroscopy. Elsevier Publishing Company, New York. 1968.
12. B. N. FIGGIS and J. LEWIS. Prog. Inorg. Chem. **6**, 37 (1964).
13. A. B. P. LEVER. J. Chem. Ed. **45**, 711 (1968).
14. L. E. ORGEL. An introduction to transition-metal chemistry. John Wiley and Sons, Inc., New York. 1962.

Can. J. Chem. Downloaded from www.nrcresearchpress.com by 210.87.254.6 on 09/05/12
For personal use only.

Can. J. Chem. Downloaded from www.nrcresearchpress.com by 210.87.254.5 on 09/05/12
For personal use only.

Stereochemistry of Dehydrogenation by D-Galactose Oxidase[1]

A. MARADUFU,[2] G. M. CREE,[3] AND A. S. PERLIN
Department of Chemistry, McGill University, Montreal, Quebec

Received June 1, 1971

The stereochemistry of dehydrogenation of the primary carbinol group of D-galactose by D-galactose oxidase has been determined. Using D-galactose-6-*d* and methyl β-D-galactopyranoside-6-*d*, it has been established that the reaction involves removal of the *pro-S* 6-hydrogen atom. This conclusion is based on product analysis, and on the relative impact of the deuterium isotope effect on oxidation rates of substrates having different *R*:*S* deuteration patterns. The absolute configurations at C-6 of these substrates have been determined by selective chemical transformations to products of known configuration. The rotational conformation of the 6-carbinol group of D-galactose and its possible relationship to the specificity of the enzyme are discussed, as well as the stereochemistry of reductive deuteration of *aldehydo* sugar derivatives.

On a déterminé la stéréochimie de déshydrogénation du groupement carbinol primaire du D-galactose par le D-galactose oxydase. Il a été établi, en utilisant le D-galactose-6-*d* et le méthyl β-D-galactopyranoside-6-*d*, que la réaction implique le départ de l'atome d'hydrogène-6 *pro-S*. Cette conclusion se base sur le produit d'analyse et sur l'impact relatif de l'effet de l'isotope deutérium sur les vitesses d'oxydation des substrats ayant des modèles différents de deutération *R*:*S*. Les configurations absolues en C-6 de ces substrats ont été déterminées par des transformations chimiques sélectives en produits de configuration connue. La conformation rotationnelle des groupements carbinole-6 du D-galactose et sa relation possible avec la spécificité de l'enzyme sont discutées, de même que la stéréochimie de deutération réductive des dérivés *aldéhydo* des sucres.

Canadian Journal of Chemistry, **49**, 3429 (1971)

D-Galactose oxidase from *Polyporus circinatus* (1, 2) (D-galactose oxireductase) catalyzes the reaction

$$\text{D-Galactose} + O_2 \rightarrow \text{DL-Galactohexodialdose} + H_2O_2$$

that is, it converts the primary carbinol group of D-galactose to an aldehyde. D-Galactopyranosides and unsubstituted D-galactopyranosyl residues of various oligo and polysaccharides also are oxidized by the enzyme (2–4), but attack is inhibited or retarded by the introduction of substituents at secondary positions of the D-galactopyranosyl moiety (5).

It was assumed *a priori* that D-galactose oxidase must effect a stereospecific removal of one of the C-6 hydrogen atoms, as is true for several dehydrogenases that have been examined (6–9), and this was subsequently found to be the case. To examine the precise stereochemistry involved, the well-established approach of utilizing a partially deuterated substrate of known configuration (6–11) was adopted.

The chirality of the 6-carbinol group may be described *e.g.*, as for methyl β-D-galactopyranoside (**1**), in terms of replacement of a hydrogen atom by deuterium (9, 12, 13). That is, H_S is designated as the *pro-S* hydrogen (deuterium in this position would confer an *S* configuration upon the carbinol group as in **2**) and H_R, the *pro-R* hydrogen as in the *R* diastereomer **3**. From the correlations of absolute configuration described below, it is concluded that the *pro-S* hydrogen is removed specifically by D-galactose oxidase.

Samples of methyl β-D-galactopyranoside[4] monodeuterated at position-6 (**1***a* and *b*) were prepared as substrates for this study by reaction sequences involving, as the key step, reduction of 1,2:3,4-di-*O*-isopropylidene-α-D-galactohexodialdose-1,5-pyranose (**4***a*) (14) with sodium borodeuteride (for **1***a*), and reduction of the dialdose-6-*d* **4***b* with sodium borohydride (for **1***b*)[5] (Scheme 1). Analysis of **1***a* (below) showed that the distribution of deuterium in the 6-car-

[1]Presented at the 54th Canadian Chemical Conference and Exhibition, C.I.C., Halifax, Nova Scotia, May 31–June 2, 1971.

[2]C. B. Purves Scholarship Holder, 1970–1971.

[3]Harold Hibbert Memorial Fellow, 1967–1968.

[4]This glycoside, which is one of the most reactive substrates of D-galactose oxidase (3), proved to be more satisfactory in some respects than D-galactose itself. However, the stereochemistry of the reaction with D-galactose was found to be the same, as shown below.

[5]An attempt to achieve stereospecific deuteration by reduction with yeast (15) was unsuccessful: although the yeast culture rapidly reduced benzaldehyde, it had no noticeable effect on the deuterated *aldehydo* sugar derivative **4***b*.

Can. J. Chem. Downloaded from www.nrcresearchpress.com by 210.87.254.5 on 09/05/12
For personal use only.

ERRATUM

3429

Erratum: Stereochemistry of Dehydrogenation by *D*-Galactose Oxidase

A. MARADUFU, G. M. CREE, AND A. S. PERLIN
Department of Chemistry, McGill University, Montreal, Quebec

Received December 6, 1971
(Ref.: Can. J. Chem. **49**, 3429 (1971))

Canadian Journal of Chemistry, **50**, 768 (1972)

On p. 3429, right-hand column, lines 5 and 6, the numbers **2** and **3** should be interchanged, *i.e.* the lines should read:

"... upon the carbinol group as in **3**) and H_R, the *pro-R* hydrogen as in the *R* diastereomer **2**. From ..."

On. p. 3430, left-hand column, lines 10 and 11, Scheme 1 should read Scheme 2, *i.e.*:

"... configurational correlations illustrated on Scheme 2."

FOR ERRATA SEE
Vol. 50 ... 1972 ... P. 768 .....

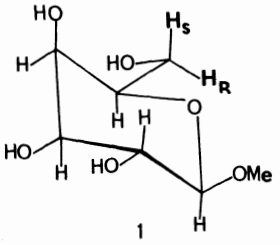

1

a 2+3 (3·6:1)
b 2+3 (1:3)

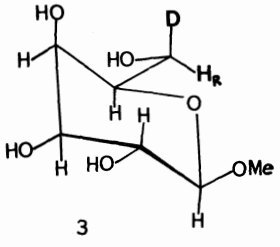

3

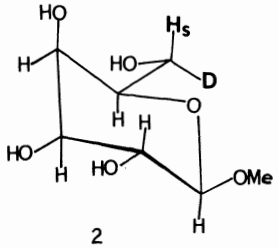

2

binol group corresponded to a mixture of 3.6 parts of the *R*-diastereomer and 1 part of the *S*-diastereomer; *i.e.*, 3.6 of **2**: 1 of **3**. In **1***b*, the distribution of isotope constituted a diastereoisomeric mixture of 1 part of (*R*)(**2**) to 3.0 parts of (*S*)(**3**). The stereochemistry of these reductions is considered further below.

These stereochemical descriptions of the C-6 chiral centers in **1***a* and *b* were obtained *via* the configurational correlations illustrated in Scheme 1.[6] D-Galactose-6-*d* (**5***a* or *b*), obtained in the course of synthesis of **1***a* or *b*, respectively, was degraded to D-threose-4-*d* by oxidation with lead tetraacetate (16) and the tetrose, then acetylated to give crystalline tri-*O*-acetyl-α-D-threofuranose-4-*d* (**6***a* or *b*) respectively. The absolute configuration at the 4-position of **6** was then deduced by reference to tri-*O*-acetyl-α-D-threofuranose-4-*d* (**6***c*) prepared from D-xylose-5-*d* of known absolute configuration (11). This latter sequence (Scheme 2) comprised *O*-benzoylation of 1,2-*O*-isopropylidene-α-D-xylofuranose-5-*d*, hydrolysis, lead tetraacetate oxidation of 3,5-di-*O*-benzoyl-D-xylofuranose-5-*d*, and finally, conversion of the latter to **6***c*. A comparison of the isotope distribution at C-4 of **6***a*, *b*, and *c* was readily carried out by measuring the relative intensities of the well-separated H-4 signals in the p.m.r. spectrum of each of these products (Fig. 1). This showed that **6***a* and *c* are virtually indistinguishable but strikingly different from **6***b*. Since the configuration at C-5 of the D-xylose-5-*d* utilized as a reference point is predominantly *R*[7] (11), it follows that the configuration of D-galactose-6-*d* (**5***a*) also is predominantly *R*, and hence **5***b* predominantly *S*, as indicated above.

Glycosides **1***a* and *b* having been characterized, they were then used as substrates for D-galactose oxidase. The 6-aldehydo products (**7***a* and *b*, respectively) of these oxidations were acetylated in pyridine, with concomitant β-elimination, which afforded the known (18) unsaturated aldehyde, *i.e.*, methyl 2,3-di-*O*-acetyl-α-L-*threo*-4-deoxy-hex-4-enodialdopyranoside-6-*d* (**8***a* and *b* respectively). Measurements of the residual 6-deuterium and 6-protium contents of **8** and its dinitrophenylhydrazone by mass spectrometry and p.m.r. spectroscopy concurred in showing that the enzymatic dehydrogenation of **1***a* had involved loss of 80% of a 6-hydrogen present originally, whereas in **1***b* 75% of the corresponding 6-hydrogen remained. That is, in both instances the results demonstrate a specific removal of the *pro-S* 6-hydrogen atom.

This same stereospecificity for D-galactose oxidase has been deduced by comparing oxidation rates for D-galactose, D-galactose-6-*d* (**5***a* and *b*), and D-galactose-6,6′-d_2 (Table 1). Firstly, the relative rates for D-galactose and the dideuterio compound show that the dehydrogenation is subject to a kinetic isotope effect of about 7.7. Accordingly, **5***a* and *b* show intermediate, and substantially different, oxidation rates that reflect the relative proportions of hydrogen and deuterium removed in the process. Moreover, there is good agreement between the observed rates and those calculated, indicating that there is no substantial secondary kinetic isotope effect. Since **5***b* experiences a slower rate than **5***a*, and possesses a correspondingly higher proportion of the *S*-diastereomer, these results also demonstrate that the oxidative attack on D-galactose

[6]It is assumed that in all of these reactions the new chiral centers generated within the primary carbinol group by deuteration are unaffected.

[7]D-Xylose-5-*d* prepared in the current (and also in an earlier (17)) study contains a slightly higher preponderance of the *R* diastereomer than does D-xylose-5-*d* described initially by Lemieux and Howard (11); the current procedure differs in using sodium borodeuteride – water in place of lithium aluminum deuteride – ether.

Can. J. Chem. Downloaded from www.nrcresearchpress.com by 210.87.254.5 on 09/05/12
For personal use only.

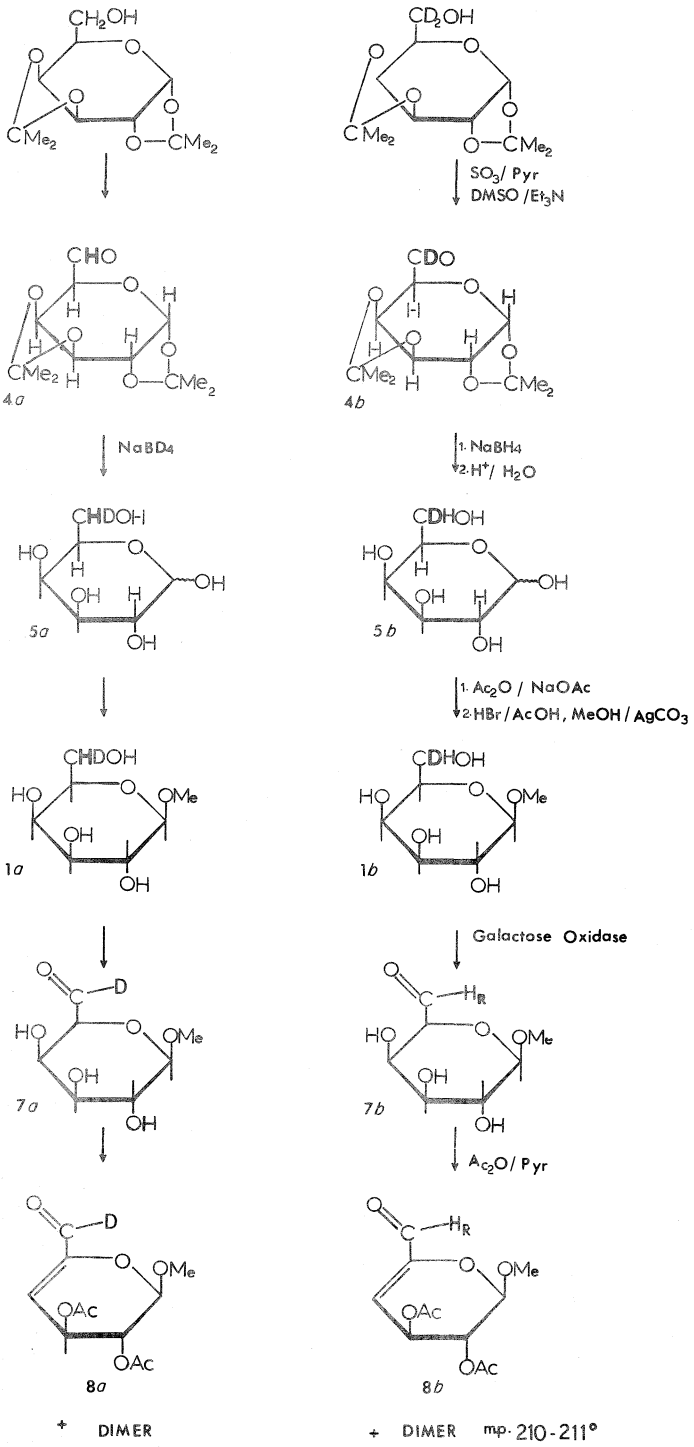

SCHEME 1. Synthesis of methyl β-D-galactopyranoside-6-*d* (1*a* and *b*) and examination of its oxidation by D-galactose oxidase.

Can. J. Chem. Downloaded from www.nrcresearchpress.com by 210.87.254.5 on 09/05/12
For personal use only.

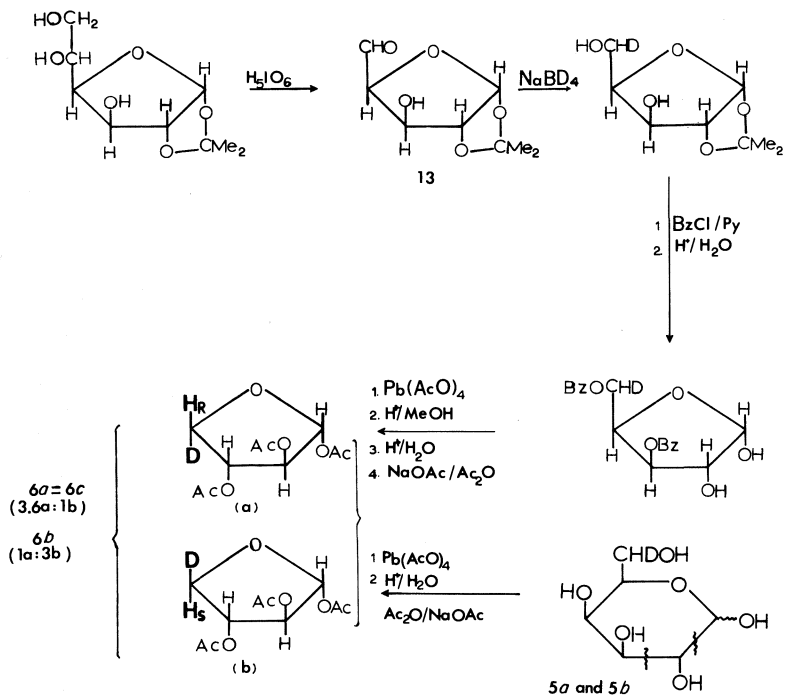

SCHEME 2. Sequence of reactions used in determining the absolute configuration of the 6-carbinol group in methyl β-D-galactopyranoside-6-*d* (**1***a* and *b*).

involves stereospecific abstraction of the *pro-S* 6-hydrogen atom.

Not only is the axial 4-hydroxyl group of D-galactose essential to the enzymatic oxidation, but substitution of its H atom (with methyl or glycosyl (5)) inhibits the reaction. By contrast, similar blocking of the 2- or 3-hydroxyl group has only a retarding effect on the rate, and modification at the 1-position influences rate even less. Evidence from the p.m.r. spectra of D-galactopyranose peracetates (19, 20) and spectral information provided below, suggests that a favored rotational conformation of the 6-carbinol group is one in which the *pro-S* hydrogen and the 4-hydroxyl group stand in a *cis*-1,3 relationship with respect to each other, as illustrated in **1**. It may be pertinent that in such an arrangement, the approaching enzyme would find the specificity-determining 4-hydroxyl group, the *pro-S* 6-hydrogen that is to be removed and the 6-hydroxyl group all in close spatial proximity to each other on the same face of the D-galactose substrate.[8] Perhaps an orientational relationship such as this accounts for the contrasting action of D-galactose oxidase with respect to ethanol dehydrogenase (from yeast (6) and liver (9)) or glycolic acid dehydrogenase (from plants (8)). That is, these latter enzymes remove H_R rather than H_S from the primary carbinol group.

Some information about how the 6-carbinol group of D-galactose derivatives is oriented has been deduced from H-5, H-6 coupling constants (19, 20): the two observed values of 7 and 5.5–6.0 Hz have been attributed to the *trans*–diaxial and *gauche* arrangements, respectively, of **9** or **10**. Rotamer **11** is unfavorable because it would involve eclipsing between OH-6 and axial OH-4 (19, 20). Examination of selectively deuterated acetates **1***a* and *b* at 220 MHz (Fig. 2) shows clearly that the larger spacing (7.2 Hz) arises from coupling between H-5 and H_S-6 (*i.e.*, as in **1** and **9**, though not as in **10**); at this higher frequency, the H-5, H_R-6 spacing is 6.3 Hz. These data may be interpreted most directly by assuming that in by far its most favorable orientation, the 6-carbinol group is close to **9** but rotated about 25° clockwise; which, incidentally, minimizes the O-4, H_S-6 eclipsing interaction, as found in **1**.

[8]However, no information is as yet available concerning the geometry of the active site of D-galactose oxidase, and the "favorableness" of such an arrangement of groups cannot be assessed.

Can. J. Chem. Downloaded from www.nrcresearchpress.com by 210.87.254.5 on 09/05/12
For personal use only.

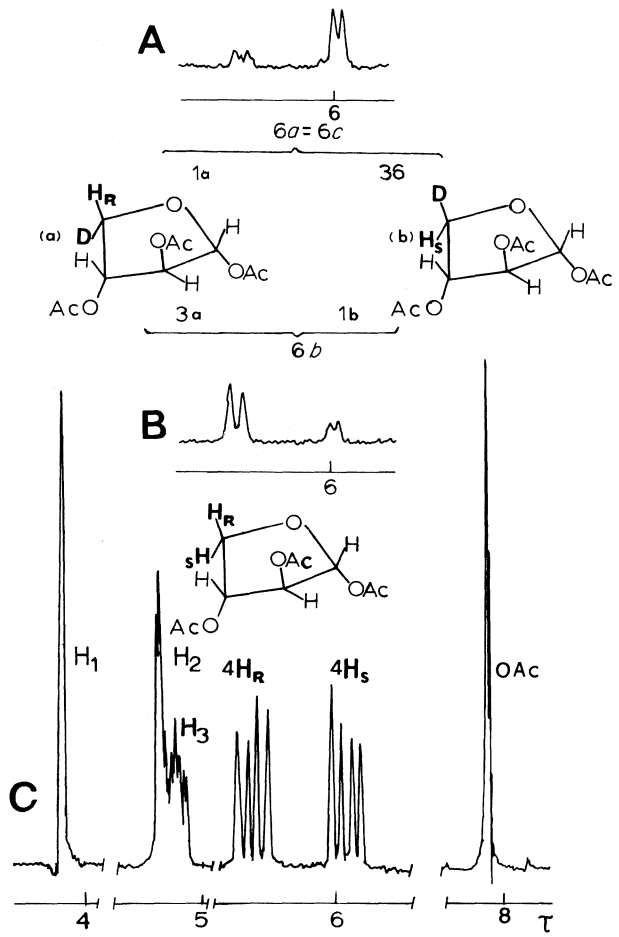

FIG. 1. The p.m.r. spectra at 100 MHz (in deuterochloroform), of 1,2,3-tri-*O*-acetyl-α-D-threofuranose and partially 4-deuterated specimens of this tetrose derivative (**6***a* and *b*); (*A*) H_4 signals of **6***a* and *c*, (*B*) H_4 signals of **6***b*, (*C*) the total spectrum of the undeuterated compound, with the acetoxyl proton signal (OAc) being recorded at about 2/3 relative intensity. The conformations depicted are taken to be approximately representative of the spectral information (unpublished results).

TABLE 1. Rates of oxidation of D-galactose and deuterated D-galactoses by D-galactose oxidase*

Substrate	Rate† (observed)	Contribution due to C—H	Contribution due to C—D	Rate (calculated)
D-Galactose	0.77	—	—	—
D-Galactose-6-*d* (3.6*R*:1*S*)	0.66	0.60	0.02	0.62
D-Galactose-6-*d* (1*R*:3*S*)	0.28	0.19	0.08	0.27
D-Galactose-6,6′-d_2	0.10	—	—	—

*Colorimetric assay at 420 nm (Experimental).
†Slope of the plot of optical density *vs.* reaction time from 2 to 12 min; during this initial period each plot was virtually a straight line.

According to the Karplus curve (21), the expected couplings then are $J_{5,6(S)}$ 7.5 and $J_{5,6(R)}$ 6.0 Hz, which are close to the splittings observed. Nevertheless, it is reasonable to expect that a mixed population of rotamers exists, in which energy differences are relatively small. In this event, the large coupling shown to take place between H-5 and H_S-6 indicates that **9** should be an important contributor to the rotational itinerary.

The stereochemistry of hydride reduction of the

Can. J. Chem. Downloaded from www.nrcresearchpress.com by 210.87.254.5 on 09/05/12
For personal use only.

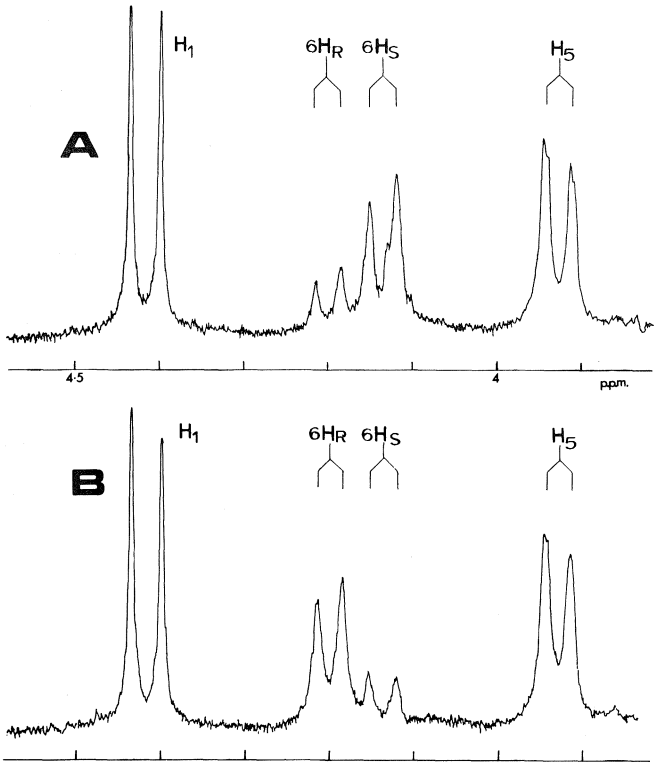

FIG. 2. Partial p.m.r. spectrum at 220 MHz (in deuterochloroform) of methyl 2,3,4,6-tetra-*O*-acetyl-β-D-galactopyranoside-6-*d* (**1***a* (*A*) and *b* (*B*)).

6-*aldehydo* compound **4** merits comment. A predominance of the *R* carbinol product, as found, is accounted for most readily by a topology in which the hydride ion approaches from the least hindered, *re*-face (12, 22–24), and by assuming (24, 25) that the stereochemistry of the starting material and product are closely similar. According to the p.m.r. spectrum of **4**, which shows that H-6 is not coupled with H-5, the C=O group appears to be oriented preferably *gauche* with respect to the C_4—C_5 bond (as in **12**); this deviates somewhat from the Karabatsos model (24) in which the C=O group would be eclipsed with one of the C-5 substituents. From the alternative possibility, *i.e.*, C=O *gauche* with respect to the C_5—O_5 bond, a predominantly *S* carbinol should be formed, contrary to the result obtained. Conceivably, however, O-5 might participate in stabilizing the transition complex, as in the "cyclic model" of Cram *et al.* (22, 23), but then could lead to a predominantly *R* product only if attack from the *more* hindered *si*-face were facilitated in the complex. The slightly lower

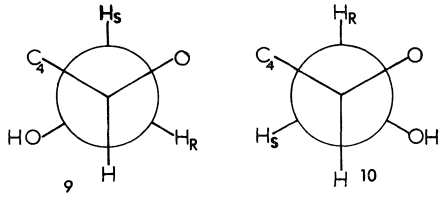

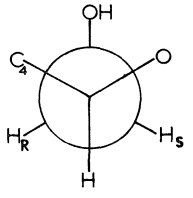

11

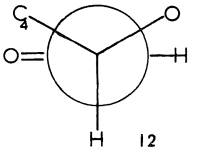

12

Can. J. Chem. Downloaded from www.nrcresearchpress.com by 210.87.254.5 on 09/05/12
For personal use only.

Can. J. Chem. Downloaded from www.nrcresearchpress.com by 210.87.254.5 on 09/05/12
For personal use only.

degree of stereoselectivity in the reduction of **4***b* than of **4***a* is attributable possibly to a slower transfer of a deuteride (26, 27), than of a hydride, anion with a concomitant increase in 'the randomness of the reaction. Reduction of the 5-*aldehydo* pentose derivative **13** with aqueous borohydride presumably involves a topology similar to that for **4**, because of the similar diastereomeric makeup of both products, despite the fact that **13** exists as a *gem* diol (in deuterium oxide (17)). More directly comparable with **4** as an *aldehydo* compound is the 3-*O*-benzyl derivative of **13** which, when reduced with lithium aluminum deuteride, also gives rise predominantly to the corresponding *R* carbinol (11), as already noted.

Experimental

Melting points were taken with a Fisher–Johns hot-plate apparatus and are uncorrected. The i.r. spectra were recorded using KBr discs or in solution with a Unicam Sp-200 G spectrometer. Electronic spectra were recorded with a Unicam Ultraviolet spectrometer. Mass spectra were recorded with a double-focusing AEI spectrometer; the energy of ionization was 70 eV. The n.m.r. spectra were recorded with a Varian 100 MHz HA-100 spectrometer using an internal TMS lock signal, or a Varian A60 spectrometer. Spectra at 220 MHz were provided by the Canadian 220 MHz NMR Centre, Sheridan Park, Ontario.

Column chromatography was performed using cellulose powder for aqueous systems and silica gel (Macherey, Nagel and Co.) for non-aqueous systems. The t.l.c. plates were prepared from silica gel G according to Stahl and were dried in a 100 °C oven for 1 h, and cooled in a vacuum desiccator. Descending chromatography on Whatman No. 1 was used for all paper chromatography work; reducing sugars were detected with silver nitrate (28) or with aniline oxalate (29). Solvents for paper chromatograms were butanol:ethanol:water (4:1:5 upper layer) (28) or *n*-propanol:acetic acid:water (6:1:2) (3), unless otherwise specified. Visualization of t.l.c. plates was effected with 5% concentrated sulfuric acid in ethanol or 2,4-dinitrophenylhydrazine in phosphoric acid and ethanol; with both reagents, carbohydrates and derivatives showed up as dark spots on a lighter background; α, β-unsaturated aldehydes and benzoates were also visualized with a u.v. lamp.

*1,2:3,4-Di-O-isopropylidene-α-D-galactohexodialdose-1,5-pyranose (**4a**)*

1,2:3,4-Di-*O*-isopropylidene-α-D-galactopyranose (prepared by de-*O*-acetylation of the crystalline 6-acetate, m.p. 109–110° (30)) was oxidized with methyl sulfoxide in the presence of triethylamine – sulfur trioxide as described previously (14). The diketal (1.5 g) was dissolved in methylsulfoxide (10 ml), triethylamine (3 ml) was then added, followed by a solution of sulfur trioxide – pyridine (2.8 g) in methylsulfoxide (10 ml). On shaking, the mixture rapidly became warm and darkened (reaction was complete within a few minutes, as indicated by t.l.c.) (benzene:ether (1:1)). It was then cooled in acetone–CO_2 and slowly diluted with chloroform (200 ml), then washed successively with 2 *N* hydrochloric acid, water, dilute sodium bicarbonate, water (2 ×). The dried chloroform solution was concentrated to a syrup (1.0 g), which was chromatographed on a column of silica gel with benzene:ether (1:1) as eluant to separate the aldehyde **4** (1.0 g) from a small amount (50 mg) of accompanying 1,2:3,4-di-*O*-isopropylidene-6-*O*-(methylthio)-methyl-α-D-galactopyranose.

6-O-Acetyl-1,2:3,4-di-O-isopropylidene-α-D-galactopyranose-6-d (3.6 R : 1 S)

To a stirred solution of 1,2:3,4-di-*O*-isopropylidene-α-D-galactohexodialdose-1,5-pyranose (**4***a*) (1.0 g) in ice-cold ethanol:water (1:1(15 ml), a solution of sodium borodeuteride (0.2 g) in ice water (5 ml) was slowly added, and stirring was continued for 30 min (reduction complete as shown by t.l.c.). Excess of Amberlite IR-120 resin was added, the solution was evaporated to dryness, and boric acid was removed by repeatedly dissolving the residue in methanol, followed by concentration to dryness. The reduction product (0.9 g) was acetylated with acetic anhydride (2.5 ml) in pyridine (5 ml), affording crystalline 6-*O*-acetyl-1,2:3,4-di-*O*-isopropylidene-α-D-galactopyranose-6-*d* (0.7 g); m.p. 107–108°.

*Methyl β-D-Galactopyranoside-6-d (**1a**)*

1,2:3,4-Di-*O*-isopropylidene-α-D-galactopyranose-6-*d* (prepared from the above 6-acetate) (1.0 g) was dissolved in 0.1 *N* sulfuric acid (40 ml), the solution was heated at 95° for 45 min, cooled, and neutralized with barium carbonate. Filtration was facilitated by use of Celite, the filtrate was treated with Amberlite IR-120 resin, then concentrated, and the residue was crystallized with cold methanol; yield of α-D-galactose-6-*d* (**5***a*) 0.5 g, m.p. 164–166°. The sugar (1.0 g) was converted successively by well-established procedures (31–33) to 1,2,3,4-6-penta-*O*-acetyl-β-D-galactopyranose-6-*d*, 2,3,4,6-tetra-*O*-acetyl-α-D-galactopyranosyl-6-*d*-bromide, methyl tetra-*O*-acetyl-α-D-galactopyranoside-6-*d* and, finally, to methyl β-D-galactopyranoside-6-*d* (**1***a*) m.p. 176–177° (0.3 g).

6-O-Acetyl-1,2:3,4-di-O-isopropylidene-α-D-galactopyranose-6,6′-d_2

1,2:3,4-Di-*O*-isopropylidene-α-D-galacturonic acid (34) (m.p. 158.5–159.5°) was converted to the methyl ester with diazomethane. The ester (7.5 g) in ether (100 ml) was reduced with lithium aluminum deuteride (1.0 g) dissolved in ether (150 ml), the deuteride being added over a period of 30 min with good stirring and under gentle reflux. Ethyl acetate (2 ml) and water (50 ml) were added in succession, followed by acidification with 2 *N* hydrochloric acid and dilution with water (100 ml). The aqueous layer was extracted with chloroform, and the combined chloroform and ether solutions (after washings with sodium bicarbonate and water) were dried and concentrated. Acetylation of the residue (6.1 g), as above, afforded 6-*O*-acetyl-1,2:3,4-di-*O*-isopropylidene-α-D-galactopyranose-6,6′-d_2 (6.5 g), m.p. 110°.

*Methyl β-D-Galactopyranoside-6-d (**1b**)*

1,2:3,4-Di-*O*-isopropylidene-α-D-galactopyranose-6,6′-d_2 (5.2 g) (prepared from the 6-acetate, previous section) was oxidized to the 6-deuterio dialdose (**4***b*) as

described for **4***a* above;[9] yield, 4.0 g. This syrupy aldehyde, in ethanol:water (1:1)(30 ml) was reduced at 10° with sodium borohydride (0.4 g), the product was purified by chromatography on silica gel (benzene:ether (1:1) as eluant) (yield, 2.8 g), and then acetylated with acetic anhydride – pyridine to give 6-*O*-acetyl-1,2:3,4-di-*O*-isopropylidene-α-D-galactopyranose-6-*d*; m.p. 109–110°. The latter was deacetylated and hydrolyzed, and the D-galactose-6-*d* (**5***b*) (0.9 g) obtained was converted via the acetobromo derivative, as described above, to methyl β-D-galactopyranoside-6-*d* (**1***b*) (0.3 g); m.p. 167°.

*1,2,3-Tri-O-acetyl-α-D-threofuranose-4-d (**6***a and b)*

D-Galactopyranose-6-*d* (**5***a* or *b*) was oxidized in acetic acid solution with 2 mol of lead tetraacetate per mole (16). The syrupy formate ester obtained was hydrolyzed, and the product acetylated with acetic anhydride – sodium acetate, yielding 1,2,3-tri-*O*-acetyl-α-D-threofuranose-4-*d* (**6***a*, m.p. 120–121°, $[\alpha]_D$ +35° ($CHCl_3$); or **6***b*, m.p, 120–121°, $[\alpha]_D$ +37° ($CHCl_3$)).

*1,2,3-Tri-O-acetyl-α-D-threofuranose-4-d (**6***c)*

1,2-*O*-Isopropylidene-α-D-xylofuranose-5-*d* (17) (6.0 g) was converted to 3,5-di-*O*-benzoyl-D-xylofuranose-5-*d*, using conditions for benzoylation and partial hydrolysis described by Baker and Schaub (35). The syrupy dibenzoate obtained (5.6 g), dissolved in acetic acid (300 ml), was oxidized for 1 h with a solution of lead tetraacetate (8.5 g) in acetic acid (250 ml), and after removal of most of the solvent the product was extracted into benzene; yield, 4.5 g of syrup. Methanolysis of this syrup was effected with methanol (200 ml) containing acetyl chloride (1.6 ml), under reflux for 18 h, the solution was neutralized with silver carbonate, concentrated, and the product was hydrolyzed with 0.1 *N* sulfuric acid (30 ml) at 95° for 1 h. The hydrolysate, after neutralization with barium carbonate and Amberlite IR-120 resin, was found by chromatography to consist mainly of threose; a small proportion of xylose was detected, as well as some other minor, unidentified, components. By column chromatography on cellulose (eluant: one-quarter saturated butanol), the threose was separated out (0.3 g) and then was acetylated to yield, finally, 1,2,3-tri-*O*-acetyl-α-D-threofuranose-4-*d* (**6***c*); m.p. 118–120°.

*Oxidation of Methyl β-D-Galactopyranoside-6-d (**1***a and b) with D-Galactose Oxidase*

In a typical experiment, the substrate (40 mg) was dissolved in phosphate buffer (4 ml; 0.2 *M*, p*H* 7.0) and incubated with D-galactose oxidase (5 mg, 125 units) and catalase (5 mg) at 37 °C for 3 h (t.l.c examination showed the presence of a major product (R_f 0.63 as compared with R_f 0.47 for the intact glycoside), and two minor products (R_f 0.75 and 0.46, respectively)). A mixture of Amberlite IR-120 (H^+) and Dowex-1 (bicarbonate) was added to the digest with stirring, the suspension was filtered, the filtrate concentrated, and then lyophilized. The product (36 mg) was treated with pyridine (0.8 ml) and acetic anhydride (0.4 ml) at room temperature for 18 h, the reaction mixture was concentrated, and the syrupy residue chromatographed on a column of silica gel (eluant, benzene:ether (9:1)). This afforded methyl 2,3-di-*O*-acetyl-α-L-*threo*-4-deoxy-hex-4-enodialdopyranoside (**8***a* or *b*)[10] (10 mg) followed by methyl 2,3,4,6-tetra-*O*-acetyl-β-D-galactopyranoside (3 mg from the undeuterated glycoside; 7 mg from **1***a*; 12 mg from **1***b*). The subsequent use of benzene:ether (1:4) caused elution of a third component which has been characterized (unpublished results), as a dimer originating from the aldehydic oxidation product having R_f 0.46.

2,4-Dinitrophenylhydrazone of Methyl 2,3-Di-O-acetyl-α-L-threo-4-deoxyhex-4-enodialdopyranoside

The α,β-unsaturated aldehyde (10 mg) was dissolved in ether (0.5 ml) and to this solution was added 2,4-dinitrophenylhydrazine (0.1 *M* in phosphoric acid – ethanol (36) (3–4 drops). Orange–yellow crystals which soon formed on standing, were washed with ethanol and ether; m.p. 148–152°, undepressed on admixture with a specimen prepared from an authentic sample of the α,β-unsaturated aldehyde (18). The n.m.r. and mass spectra of the two hydrazones were indistinguishable. A higher melting form of this hydrazone (m.p. 167°) which, however, is indistinguishable from the current product by n.m.r. and mass spectrometry also has been obtained (18).

Measurement of Reaction Rates for D-Galactose Oxidase

Kinetic measurements were carried out using "Galactostat" (Worthington). The "Galactostat" solution consisted of D-galactose oxidase (20 units), peroxidase (2.5 mg), and the chromogen *o*-tolidene (2.5 mg) in 0.01 *M* phosphate buffer (50 ml; p*H* 7.0). Two milliliters of this solution were added to the substrate (*ca.* 50 mg in 2 ml of water), the reaction mixture was incubated at 37 °C and absorbance was monitored at 420 nm with a Gilford automatic recording spectrophotometer. In some experiments the absorbance at a given time was checked after stopping the reaction by addition of glycine buffer (6 ml; 0.25 *M*, p*H* 9.7).

The authors gratefully acknowledge the generous financial support of the Pulp and Paper Research Institute of Canada and the National Research Council of Canada. The p.m.r. spectra at 100 MHz were kindly recorded by Dr. H. J. Koch and R. Simoneau, and the 220 MHz spectra by Dr. A. Grey at the Canadian 220 MHz NMR Centre, Sheridan Park, Ontario.

1. J. A. D. Cooper, W. Smith, M. Bacila, and H. Medina. J. Biol. Chem. **234**, 445 (1959).
2. G. Avigad, C. Asensio, D. Amaral, and B. L. Horecker. Biochem. Biophys. Res. Commun. **4**, 474 (1961).
3. G. Avigad, D. Amaral, C. Asensio, and B. L. Horecker. J. Biol. Chem. **237**, 2736 (1962).
4. S. M. Rosen, M. J. Osborn, and B. L. Horecker. J. Biol. Chem. **239**, 3196 (1964).

[9]In this reaction the proportion of 6-*O*-methylthiomethyl ether was much higher (almost 1/4) than in the oxidation of the undeuterated carbinol.

[10]Examination of the reaction mixture prior to acetylation showed that most of this product is formed during the acetylation procedure. The minor product having R_f 0.75 (above) is, in fact, the corresponding, unacetylated, α,β-unsaturated aldehyde (unpublished results).

Can. J. Chem. Downloaded from www.nrcresearchpress.com by 210.87.254.5 on 09/05/12
For personal use only.

5. R. A. SCHLEGEL, C. M. GERBECK, and R. MONTGOMERY. Carbohydr. Res. **7**, 193 (1968).
6. F. A. LOEWUS, F. H. WESTHEIMER, and B. VENNESLAND. J. Am. Chem. Soc. **75**, 5018 (1953).
7. H. R. LEVY, F. A. LOEWUS, and B. VENNESLAND. J. Am. Chem. Soc. **79**, 2949 (1957).
8. I. A. ROSE. J. Am. Chem. Soc. **80**, 5835 (1958).
9. D. ARIGONI and E. L. ELIEL. Topics in stereochemistry. Vol. 4, *Edited by* N. L. Allinger and E. L. Eliel. Interscience, New York, N.Y., 1969. p. 127.
10. A. STREITWIESER, JR. J. Am. Chem. Soc. **75**, 5014 (1953).
11. R. U. LEMIEUX and J. HOWARD. Can. J. Chem. **41**, 308 (1963).
12. K. R. HANSON. J. Am. Chem. Soc. **88**, 2731 (1966).
13. IUPAC Tentative rules for the nomenclature of organic chemistry. Section E. Fundamental stereochemistry. J. Org. Chem. **35**, 2849 (1970).
14. G. M. CREE, D. M. MACKIE, and A. S. PERLIN. Can. J. Chem. **47**, 511 (1969).
15. V. E. ALTHOUSE, K. UEDA, and H. S. MOSHER. J. Am. Chem. Soc. **82**, 5938 (1960).
16. A. S. PERLIN and C. BRICE. Can. J. Chem. **34**, 541 (1956).
17. A. S. PERLIN. Can. J. Chem. **44**, 1757 (1966).
18. A. S. PERLIN, D. M. MACKIE, and C. P. DIETRICH. Carbohydr. Res. **18**, 185 (1971).
19. R. U. LEMIEUX and J. D. STEVENS. Can. J. Chem. **43**, 2059 (1965).
20. L. D. HALL, J. F. MANVILLE, and N. S. BHACCA. Can. J. Chem. **47**, 1 (1969).
21. (*a*) M. KARPLUS. J. Chem. Phys. **30**, 11 (1959). (*b*) F. A. L. ANET. Can. J. Chem. **39**, 789 (1961).
22. D. J. CRAM and F. A. ABD ELHAFEZ. J. Am. Chem. Soc. **74**, 5828 (1952).
23. D. J. CRAM and D. R. WILSON. J. Am. Chem. Soc. **85**, 1245 (1963).
24. G. J. KARABATSOS. J. Am. Chem. Soc. **89**, 1367 (1967).
25. D. Y. CURTIN. Record Chem. Progr. (Kresge-Hooker Sci. Lib.) **15**, 111 (1954).
26. G. E. DUNN and J. WARKENTIN. Can. J. Chem. **34**, 75 (1956).
27. D. NASIPURI, C. K. GHOSH, and R. J. L. MARTIN. J. Org. Chem. **35**, 657 (1970).
28. S. M. PARTRIDGE. Nature, **158**, 270 (1946).
29. R. M. HORROCKS. Nature, **164**, 444 (1949).
30. H. OHLE and G. BEREND. Ber. **58**, 2585 (1925).
31. C. S. HUDSON and H. O. PARKER. J. Am. Chem. Soc. **38**, 1223 (1916).
32. H. OHLE, W. MARECEK, and W. BOURJAU. Ber. **62**, 849 (1929).
33. J. K. DALE and C. S. HUDSON. J. Am. Chem. Soc. **52**, 2534 (1930).
34. O. SCHIER and E. WALDMAN. Mh. Chem. Bd. **88**, 847 (1957).
35. B. R. BAKER and R. E. SCHAUB. J. Am. Chem. Soc. **77**, 5900 (1955).
36. C. D. JOHNSON. J. Am. Chem. Soc. **73**, 5888 (1951).

Can. J. Chem. Downloaded from www.nrcresearchpress.com by 210.87.254.5 on 09/05/12
For personal use only.

Can. J. Chem. Downloaded from www.nrcresearchpress.com by 210.87.254.6 on 09/05/12
For personal use only.

Effect of Solvent Upon the Vicinal Proton Coupling Constants of Complex Substituted Ethanes. III. 1,2-Dihaloalkanes

D. A. DAWSON[1] AND W. F. REYNOLDS
Department of Chemistry, University of Toronto, Toronto 5, Ontario

Received November 20, 1970[2]

The n.m.r. spectra of eight 1,2-dihaloalkanes have been determined in solvents of differing polarity. The relative rotamer stabilities for each compound have been deduced from the variation of the difference and sum of vicinal coupling constants with solvent. Variations in geminal and long range coupling constants with solvent are also attributed to conformational changes.

Les spectres de r.m.n. de huit dihalogéno-1,2 alkanes ont été déterminés dans des solvants de polarité différente. Les stabilités relatives des rotamères de chaque composé ont été déterminées en fonction des variations de la différence et de la somme des constantes de couplage vicinale selon le solvant. Les variations, selon le solvant, des constantes de couplage geminale et à longue distance sont également attribuables aux modifications conformationnelles.

Canadian Journal of Chemistry, 49, 3438 (1971)

Introduction

Abraham and co-workers have developed an electrostatic theory which allows one to predict energy differences, ΔE, between rotational isomers (rotamers) of substituted ethanes with two or more polar substituents in media of different dielectric constants, ε (1–3). This theory has been successfully applied to the investigation of a number of simple substituted ethanes in which two of the three rotamers are degenerate in energy (4).

We have been interested in the determination of ΔE values for tri-substituted ethanes of type **1**

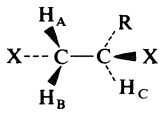

1

where X is a polar group and R is non-polar (5). In these compounds, all three rotamers have different energies. In principle, it is possible to determine ΔE values from the variation of vicinal coupling constants with ε (3). In practice, this is impossible for this system since there are eight unknowns (two ΔE values and six non-equivalent coupling constants) to be determined from the variation of two (averaged) coupling constants with solvent.

An alternative, more qualitative, approach has been described which allows one to determine relative rotamer energy levels for **1** from the variation of vicinal coupling constants with solvent (5). If rotamer 1 is more stable than rotamer 2 (see Fig. 1), then $J_{AC} > J_{BC}$ and $|J_{AC} - J_{BC}|$ decreases with increasing ε while if $E_1 > E_2, J_{BC} > J_{AC}$ and $|J_{AC} - J_{BC}|$ increases with increasing ε. Therefore, the sign of ΔE_{2-1} can be determined from the variation of $|J_{AC} - J_{BC}|$ with ε. Rotamer 3 is generally less stable than the other two since it has the maximum steric interaction. Any increase in the fractional population, p_3, of rotamer 3 with ε should lead to a decrease in $J_{AC} + J_{BC}$. However, if $E_3 \gg E_1, E_2; p_3 \approx 0$, and $J_{AC} + J_{BC}$ will remain essentially constant. Assumptions involved in this approach have been previously discussed (5). The fundamental assumption that more polar rotamers will be relatively stabilized in solutions of higher ε appears to hold for all of the dihaloethane derivatives which have been investigated (4, 5), provided that aromatic (2, 5,

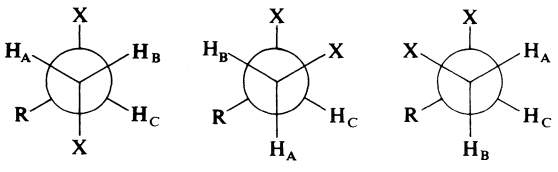

FIG. 1. Possible staggered rotamers for 1,2-dihaloalkanes (X = Cl, Br; R = CH_3, CH_2CH_3, $CH(CH_3)_2$, $C(CH_3)_3$).

[1]NRCC Bursary Holder, 1969–1970; NRCC Scholarship Holder, 1970–1972.

[2]Revision received August 10, 1971.

TABLE 1. Coupling constants (in Hz) for 1,2-dibromo and 1,2-dichloro-3,3-dimethylbutanes (0.2 *M* solutions unless otherwise stated)

Solvent	J_{AB}	J_{AC}	J_{BC}	$J_{BC} - J_{AC}$	$J_{AC} + J_{BC}$	r.m.s.*
		(a) 1,2-Dibromo-3,3-dimethylbutane				
CCl_4	−11.37	3.17	9.11	5.94	12.28	0.01
CCl_4†	−11.37	3.16	9.13	5.97	12.29	0.01
CCl_4‡	−11.38	3.14	9.17	6.03	12.31	0.01
C_6H_6	−11.50	2.75	9.65	6.90	12.40	0.01
CS_2	−11.32	3.12	9.17	6.05	12.29	0.01
$CDCl_3$	−11.45	2.73	9.70	6.97	12.43	0.01
$(CH_3)_3CCl$	−11.51	2.75	9.64	6.89	12.39	0.01
$(CD_3)_2C{=}O$	−11.72	2.42	9.98	7.56	12.40	0.01
$(CH_3)_2S{=}O$	−11.83	2.34	10.13	7.79	12.47	0.01
		(b) 1,2-Dichloro-3,3-dimethylbutane				
CCl_4	−11.88	2.97	9.06	6.09	12.03	0.01
C_6H_6	−11.99	2.60	9.56	6.96	12.16	0.01
$CDCl_3$	−11.95	2.58	9.61	7.03	12.19	0.01
$(CD_3)_2C{=}O$	−12.19	2.34	9.81	7.47	12.15	0.01

*Root mean square error (in Hz) between experimental and calculated peak positions.
†0.3 *M* solution.
‡0.5 *M* solution.

TABLE 2. Coupling constants (in Hz) for 1,2-dibromo and 1,2-dichloro-3-methylbutanes (0.3 *M* solutions)

Solvent	J_{AB}	J_{AC}	J_{BC}	$J_{AC} - J_{BC}$	$J_{AC} + J_{BC}$	r.m.s.
		(a) 1,2-Dibromo-3-methylbutane				
CCl_4	−10.33	11.10	4.69	6.41	15.79	0.01
C_6H_6	−10.43	10.36	5.02	5.34	15.38	0.01
$CDCl_3$	−10.38	10.32	5.01	5.31	15.33	0.01
$(CD_3)_2C{=}O$	−10.68	9.01	5.53	3.48	14.51	0.02
		(b) 1,2-Dichloro-3-methylbutane				
CCl_4	−11.28	9.03	5.29	3.74	14.32	0.03 (0.01)*
C_6H_6	−11.49	7.59	5.91	1.68	13.50	0.03 (0.01)
$CDCl_3$	−11.45	7.97	5.68	2.29	13.65	0.05 (0.03)
$(CD_3)_2S{=}O$	−11.85	6.77	5.47	1.30	12.24	0.03 (0.01)

*Long-range coupling to the methine proton split A and B protons into very poorly resolved doublets. Corrected r.m.s. values were obtained by treating both experimental and computer-generated peak positions as singlets.

6) or hydroxylic (2) solvents are avoided. However, the assumption may not hold in systems where strong specific hydrogen bonding can occur (7, 8). Consequently, these systems should be avoided.

It has been concluded that it should be possible to determine relative rotamer stabilities for a series of closely related compounds of type **1**, using this approach (5). In order to test this conclusion, we have determined the n.m.r. spectra of a series of eight 1,2-dihaloalkanes (X = Cl, Br; R = CH_3, CH_2CH_3, $CH(CH_3)_2$, $C(CH_3)_3$)in different solvents.

Experimental

1,2-dihalopropanes were obtained commercially. Other 1,2-dihaloalkanes were prepared by the halogenation of the appropriate olefins. All reactions were carried out in CCl_4 in the dark. Products were fractionally distilled before use and purities were checked by n.m.r. spectroscopy. Compounds were dissolved in freshly distilled ACS grade solvents with 5% tetramethylsilane added as lock and reference signal. Solutions of 1,2-dihalopropanes and butanes were degassed and sealed under vacuum before use. Other samples were not degassed since their spectra contained less fine structure. Spectra were recorded on a Varian HA-100 spectrometer operated in frequency sweep mode at a sweep rate of 0.01–0.05 Hz/s. Calibration procedures were identical to those previously reported (5).

Results

1,2-dibromo- and 1,2-dichloro-3,3-dimethylbutane (R = *t*-butyl) gave ABC spectra with negligible coupling to the *t*-butyl group. Spectra were analyzed using the exact method (9). Results are given in Table 1.

The computer programs which were available

Can. J. Chem. Downloaded from www.nrcresearchpress.com by 210.87.254.6 on 09/05/12
For personal use only.

TABLE 3. Coupling constants (in Hz) for 1,2-dibromobutane and 1,2-dichlorobutane (0.3 *M* solutions)

Solvent	J_{AB}	J_{AC}	J_{BC}	$J_{AC} - J_{BC}$	$J_{AC} + J_{BC}$	r.m.s.
		(a) 1,2-Dibromobutane				
CCl_4	−10.16	10.76	4.19	6.55	14.95	0.01
$(CD_3)_2C{=}O$	−10.48	8.61	4.78	3.83	13.39	0.02
		(b) 1,2-Dichlorobutane				
CCl_4	−11.12	8.74	4.76	3.98	13.50	0.03

to us did not allow total spectral analysis for 1,2-dihalo-3-methylbutanes (R = isopropyl) and 1,2-dihalobutanes (R = ethyl). The spectra of the first two compounds were analyzed as ABCD spectra, using the iterative computer program LAOCN3 (10). Only a chemical shift was assigned for D (the methine proton of the isopropyl group), based upon the weight average position of the D multiplet. Calculated coupling constants were completely insensitive to minor (10 Hz) variations in ν_D since the spectra were close to the ABCX limit ($\nu_C - \nu_D/J_{CD} \approx 70$). Results are given in Table 2. The spectra of the 1,2-dihalobutanes were analyzed as ABCDE spectra using a similar approach (spectra were nearly ABCXY). Results are given in Table 3. 1,2-Dichlorobutane was only run in CCl_4 since in polar solvents, $\nu_A - \nu_B \approx 0$, making it impossible to determine J_{AC} and J_{BC} accurately.

1,2-Dihalopropanes gave $ABCD_3$ spectra which were analyzed using LAOCN3. Signs of long-range coupling constants were determined by spin-tickling experiments, using standard techniques (11). Results are given in Table 4.

Only coupling constant data are presented. Chemical shift data have been deposited in the Depository of Unpublished Data, National Research Council of Canada, Ottawa, Canada, K1A 0R6.

Discussion

(A) Vicinal Coupling Constants

The difference in vicinal coupling constants increases with increasing ε for 1,2-dibromo- and 1,2-dichloro-3,3-dimethylbutane.[3] This establishes that rotamer 2 is more stable than rotamer 1 in both compounds and that the larger coupling constant is J_{BC}. In both cases, $J_{AC} + J_{BC}$ remains constant, indicating $p_3 \approx 0$. Consequently, the order of energy levels is $E_3 \gg E_1 > E_2$. The similar values of J_{AC} and J_{BC} suggest that there is little difference in conformational preference between the two compounds.

This energy level order corresponds to that deduced by Buza and Snyder (12) from the vicinal coupling constant of a specifically deuterated derivative of the dibromo compound. The coupling constants of both compounds in CCl_4 are in good agreement with those reported by Jackman and Kelly (13). Finally, Altona and Hageman concluded (from dipole moment measurements) that for the dibromo compound, p_2 is 0.73 in CCl_4 and 0.83 in C_6H_6 and that $p_3 \approx 0$ in both solvents (6). Assuming reasonable values of J_{trans}(rotamer 2) = 11.5 and J_{gauche}(rotamer 1) = 2.0 Hz (based upon low temperature n.m.r. measurements (14)) and $p_3 = 0$, our values of 9.11 and 9.65 Hz for J_{BC} in CCl_4 and C_6H_6 correspond to $p_2 = 0.75$ and 0.81 respectively, in good agreement with previous results (6).

For the remaining compounds which were run in two or more solvents, $|J_{AC} - J_{BC}|$ decreased with increasing ε, establishing that $E_2 > E_1$ and $J_{AC} > J_{BC}$. $J_{AC} + J_{BC}$ decreased in all cases, implying that p_3 is not negligible in these compounds. $J_{AC} + J_{BC}$ is smallest and most solvent sensitive for 1,2-dichloropropane. Therefore, we believe that p_3 is greater in this compound than in any of the other compounds investigated. Since rotamer 3 is known to be the least stable rotamer for 1,2-dichloropropane in both the gas phase and the neat liquid (15), we conclude that in all of the six methyl, ethyl, and isopropyl derivatives the energy level order is $E_3 > E_2 > E_1$.

In these six compounds, $J_{AC} - J_{BC}$ is larger for the dibromo compounds than for the dichloro compounds. While this might in part reflect the effect of electronegativity upon vicinal coupling constants (16), we believe that the differences are primarily due to changes in conformational preference. Rotamer 2 should be relatively less stable in the dibromo compounds because of greater

[3]Results in C_6H_6 suggest an increased stabilization of polar rotamers beyond that expected from ε. Similar "benzene effects" have been noted in previous investigations (2, 5, 6).

Can. J. Chem. Downloaded from www.nrcresearchpress.com by 210.87.254.6 on 09/05/12
For personal use only.

Can. J. Chem. Downloaded from www.nrcresearchpress.com by 210.87.254.6 on 09/05/12
For personal use only.

TABLE 4. Coupling constants (in Hz) for 1,2-dibromopropane and 1,2-dichloropropane (0.4 *M* solutions)

Solvent	J_{AB}	J_{AC}	J_{BC}	$J_{AC} - J_{BC}$	$J_{AC} + J_{BC}$	J_{AD}	J_{BD}	J_{CD}	r.m.s.
				(a) 1,2-Dibromopropane					
CCl_4	−9.92	10.87	4.04	6.83	14.91	−0.19	0.50	6.57	0.02
C_6H_6	−10.05	9.95	4.32	5.63	14.27	−0.12	0.40	6.56	0.03
$CDCl_3$	−10.03	10.19	4.26	5.93	14.45	−0.16	0.45	6.58	0.03
$(CD_3)_2C{=}O$	−10.26	8.81	4.63	4.18	13.44	0.0	0.31	6.57	0.02
				(b) 1,2-Dichloropropane					
CCl_4	−10.87	9.09	4.57	4.52	13.66	−0.15	0.37	6.50	0.03
C_6H_6	−11.09	7.81	5.04	2.77	12.85	−0.10	0.26	6.53	0.03
$CDCl_3$	−11.10	8.03	4.97	3.06	13.00	0.0	0.28	6.54	0.02
$(CD_3)_2C{=}O$	−11.43	6.43	5.39	1.04	11.82	0.0	0.19	6.56	0.01

Can. J. Chem. Downloaded from www.nrcresearchpress.com by 210.87.254.6 on 09/05/12
For personal use only.

halogen–halogen steric interactions, resulting in an increase in p_1 and $J_{AC} - J_{BC}$. This contrasts with the behavior when R = *t*-butyl where no difference in conformational preference was noted. In the latter case, *t*-butyl – halogen steric interactions are presumably much larger than halogen–halogen steric interactions. Consequently, a decrease in halogen size should decrease both steric interactions to a similar extent.

There are much smaller changes in $J_{AC} - J_{BC}$ when R is changed from methyl to isopropyl, but the changes do occur in a regular manner. For example, for the dibromo derivatives in CCl_4, $J_{AC} - J_{BC}$ is 6.83, 6.57 and 6.41 Hz for methyl, ethyl, and isopropyl derivatives respectively. It seems reasonable to attribute these differences to changes in rotamer populations since the electronic effects of the alkyl substituents should be similar. A decrease in $J_{AC} - J_{BC}$ corresponds to a decrease in p_1, which can be attributed to increased alkyl–halogen repulsions in rotamer 1. The changes are small, however, reflecting the ability of ethyl and isopropyl groups to minimize steric interactions by adopting their most favorable conformations, *i.e.* with the methyl group(s) rotated away from the halogen.

Our energy level order is consistent with previous results for 1,2-dibromo- and 1,2-dichloropropane (15, 17). Coupling constants for these compounds differ by an amount greater than the experimental error from those reported by Finegold (17), probably because the latter measurements were made at higher concentrations. Little data is available for the other compounds.

(B) Geminal and Long-range Coupling Constants

Geminal coupling constants vary with substituent within a given series. For example, for the dibromo series in CCl_4, J_{AB} is respectively -9.92, -10.16, -10.33, and -11.37 Hz for methyl, ethyl, isopropyl, and *t*-butyl derivatives. J_{AB} is also solvent dependent. Changes in J_{AB} with R substituent and solvent closely parallel the corresponding changes in vicinal coupling constants, even to the extent of showing anomalous results for C_6H_6. This strongly suggests that the changes in J_{AB} discussed above are primarily due to conformational changes, although the variation of J_{AB} with solvent could be partly due to reaction field effects (18). The results suggest that J_{AB} is significantly more negative in rotamer 2 than rotamer 1, since p_2 should increase at the expense of p_1 as the size of R or ε increases. The difference in J_{AB} for the two *t*-butyl derivatives may reflect electronegativity effects.

The long range coupling constants in 1,2-dihalopropanes are similar to those previously reported (17). Changes in J_{AD} and J_{BD} with solvent also appear to reflect conformational changes, assuming that the long-range coupling constant to the methyl group is positive when the methyl group is *trans* to a methylene proton and negative when it is in a *gauche* orientation.

Conclusions

The effect of solvent upon the sum and difference of vicinal coupling constants in compounds of type **1** can be used to determine the order of rotamer energies. It is also possible to deduce changes in conformational preference within a series of compounds of type **1**, provided that the electronic effects of substituents do not change markedly from compound to compound.

Financial support from the National Research Council of Canada is gratefully acknowledged.

1. R. J. Abraham, L. Cavalli, and K. G. R. Pachler. Mol. Phys. **11**, 471 (1966).
2. R. J. Abraham and M. A. Cooper. J. Chem. Soc. B, 202 (1967).
3. R. J. Abraham. J. Phys. Chem. **73**, 1192 (1969).
4. R. J. Abraham and R. H. Kemp. J. Chem. Soc. B, 1240 (1971) and references therein.
5. W. F. Reynolds and D. J. Wood. Can. J. Chem. **47**, 1295 (1969).
6. C. Altona and H. J. Hageman. Rec. Trav. Chim. **87**, 279 (1968).
7. W. F. Reynolds and D. J. Wood. Can. J. Chem. **49**, 1209 (1971).
8. R. J. Abraham and K. G. R. Pachler. Mol. Phys. **7**, 165 (1964).
9. (*a*) S. Castellano and J. S. Waugh. J. Chem. Phys. **35**, 1900 (1961). (*b*) J. R. Cavanaugh. J. Chem. Phys. **39**, 2378 (1963).
10. S. Castellano and A. A. Bothner-By. LAOCN3, Mellon Institute, Pittsburgh, Pennsylvania, 1966.
11. R. A. Hoffman and S. Forsen. *In* Progress in nuclear magnetic resonance spectroscopy. Vol. 1. Pergamon Press, New York, N.Y., 1966.
12. M. Buza and E. I. Snyder. J. Am. Chem. Soc. **88**, 1161 (1966).
13. L. M. Jackman and D. P. Kelly. J. Chem. Soc. B, 110 (1970).
14. D. A. Dawson and W. F. Reynolds. Unpublished results.
15. S. Mizushima. Pure Appl. Chem. **7**, 1 (1963).
16. R. J. Abraham and G. Gatti. J. Chem. Soc. B, 961 (1969).
17. H. Finegold. J. Chem. Phys. **41**, 1808 (1964).
18. P. Laszlo. *In* Progress in nuclear magnetic resonance spectroscopy. Vol. 3. Pergamon Press, New York, N.Y., 1968.

Can. J. Chem. Downloaded from www.nrcresearchpress.com by 210.87.254.105 on 09/05/12
For personal use only.

Reactions of Carbonyl Ylides

J. W. Lown and K. Matsumoto[1]

Department of Chemistry, University of Alberta, Edmonton 7, Alberta

Received June 22, 1971

2,3-Diphenylindenone oxide **1** undergoes thermal 1,3-dipolar cycloadditions via a carbonyl ylide with symmetrical olefinic dipolarophiles to give (*i*) with *cis* addends mixtures of *endo* and *exo* adducts in which *endo* adducts generally predominate in agreement with results obtained with 1-cyclohexyl-6-(cyclohexylimino)-1*a*-phenylindano[1,2-*b*]aziridine and (*ii*) with *trans* addends adducts in which the 2-*exo*-3-*endo* product predominates. The pyrilium oxide **4** is efficiently trapped with benzyne. 1,3-Diphenylisobenzofuran reacts with *cis*-addends to give *endo–exo* mixtures in which the *endo* adducts generally predominate. 2-Acetyl-5,5-pentamethylene-2-phenyl-Δ^3-1,3,4-oxadiazoline undergoes regiospecific cycloaddition via a carbonyl ylide with unsymmetrical olefinic dipolarophiles in accordance with substituent electronic effects, and with 1,4-naphthoquinone a previously postulated type of intermediate adduct is isolated.

L'oxyde de diphénylindenone-2,3 **1** peut réagir pour donner des cycloadditions dipolaires-1,3 thermiques, par l'intermédiaire d'une ylure de carbonyle possédant des dipolarophiles oléfiniques symétriques. On obtient ainsi (*i*) avec des mélanges *endo* et *exo* des produits *cis*, des produits d'addition où la forme *endo* prédomine habituellement, en accord avec les résultats obtenus avec le cyclohexyl-1 (cyclohexylimino)-6 phénylindano-1*a* aziridine[1,2-*b*] et (*ii*) avec les produits *trans*, des produits d'addition où la forme *exo*-2-*endo*-3 prédomine. L'oxyde de pyrilium **4** peut être recueilli efficacement dans le benzène. Le diphénylisobenzofuranne réagit avec les produits *cis* pour donner des mélanges *endo–exo*, où les produits d'addition *endo* prédominent généralement. Le 2-acétyl-5,5 pentamethylène-2 phényl-Δ^3-1,3,4-oxadiazoline peut réagir pour donner des cycloadditions régiospécifiques, via une ylure de carbonyle possédant des dipolarophiles oléfiniques non-symétriques, selon les effets électroniques du substituant; avec la naphthoquinone-1,4, on isole un produit d'addition intermédiaire postulé précédemment.

Canadian Journal of Chemistry, **49**, 3443 (1971)

Introduction

Examination of the orbital symmetry controlled generation of azomethine ylides from aziridines and exploration of their synthetic potential via 1,3-dipolar cycloaddition to a wide variety of multiple and heteromultiple bonds has recently proved extremely fruitful (1–18). The isoelectronic carbonyl ylides which are of equal importance have not received as much attention (19–29). Strong evidence has been obtained for the predicted (30) thermal conrotatory (27) and the photochemical disrotatory (26, 27) opening of suitable oxirane precursors to carbonyl ylides. We report an examination of the cycloaddition reactions of certain carbonyl ylides with reference to their stereochemistry, regiospecificity (31), steric, and electronic requirements.

The model compounds chosen as carbonyl ylide precursors were **1**, **2**, and **3**, affording an opportunity to examine these dipoles under as wide a range of reaction conditions as possible. The thermally induced tautomerization of **1** to **4** was reported by Ullmann and Milks (22) and

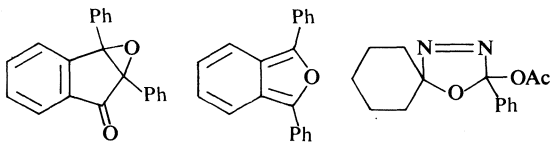

1 **2** **3**

species **4** was shown to react as a carbonyl ylide in 1,3-dipolar cycloaddition to give, with norbornadiene, an adduct which was assigned the *exo* structure **5**.

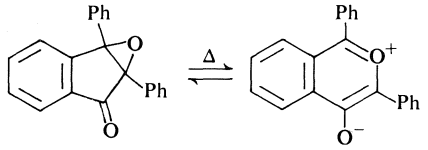

1 **4**

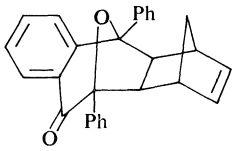

5

[1]NRCC Postdoctorate Fellow, 1969 to present.

Can. J. Chem. Downloaded from www.nrcresearchpress.com by 210.87.254.105 on 09/05/12
For personal use only.

The isoelectronic 1-cyclohexyl-6(cyclohexylimino)-1*a*-phenylindano[1,2-*b*]aziridine (**6**) was recently shown by Lown and Matsumoto (32) to undergo valence tautomerization both thermally and photochemically to the isoquinolinium imine **7**. The azomethine ylide species **7**

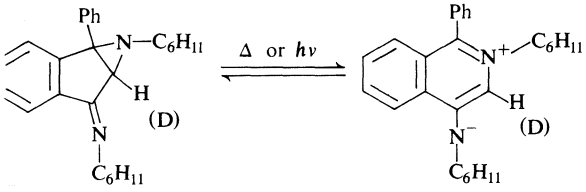

6 **7**

was trapped efficiently by olefinic dipolarophiles to give exclusively *endo* adducts, *e.g.* **8**. The

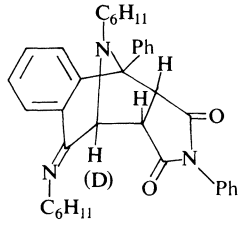

8

diametrically opposed configurational results obtained with **1** and **6** posed the questions of (*i*) whether this reflected a fundamental difference in properties of the apparently similar species of carbonyl ylides and azomethine ylides or whether (*ii*) other factors operating in **7** (*e.g.* steric hindrance from the *N*-substituent) accounted for the differences observed. However since identical results, *i.e.* exclusively *endo* adducts, are obtained with N—CH_3 analogs of **6** the problem required further investigation. Also in view of the controversy attending the mechanism of the Diels–Alder reaction it was of interest to determine if a trend towards general *endo* adduction also obtains in the related 1,3-dipolar cycloaddition reaction.

Results and Structural Assignments

Unlike the situation with **6**, wherein specific deuterium labelling allowed an unambiguous assignment of configuration by examination of the n.m.r. coupling constants (33) a similar method could not be applied to the adducts of **1**. Although diphenylisobenzofuran is normally regarded as a diene, contribution of resonance forms such as those shown below allow one to regard it as a

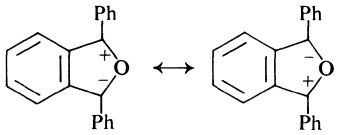

masked carbonyl ylide (28). Accordingly several 1,3-dipolar cycloaddition adducts were prepared in parallel from **1** and **2** for comparison and to aid in the n.m.r. assignments. The cycloaddition of dienophiles to **2** has been observed to give predominantly *endo*-adduction with pyracyclo-quinone and pyracyclene (33); *exo*-addition with cyclopropene (34), norbornadiene and norbornene (35), and predominantly *exo*-addition with chlorocyclopropene (36). In the latter case, which has been substantiated by Battiste and Sprouse (34), *endo* protons in the adducts were shielded by the benzene ring relative to the *exo* protons which is consistent with n.m.r. observations in other similar bicyclic adducts (37). The stereochemistry of the adducts of **2** have been assigned on this basis.

A number of other relationships became apparent upon examining the n.m.r. spectra of many adducts of **1** and **2**.

(*1*) For adducts of **2**: (protons) δ *exo* > *endo*; and (methylester) δ *endo* > δ *exo*.

(*2*) For adducts of **1**: (*i*) *J cis* (2-*exo*-3-*exo*) > *J cis* (2-*endo*-3-*endo*); (*ii*) *J trans* (2 *endo*-3-*exo*) > *J trans* (2 *exo*-3-*endo*); (*iii*) from protons, δ 3-*exo* > δ 3-*endo*; δ 2-*exo* > δ 2-*endo*; (*iv*) For *trans* adducts of **1**, Δ(δ 2-*endo*-3-*exo*) > Δ(δ 2-*exo*-3-*endo*) (see Table 3).

While these observations are empirical they serve as a check for internal consistency in the stereochemical assignment.

To obtain an accurate determination of isomeric proportion in the products, n.m.r. spectra were taken on the initially obtained mixtures before attempted purification.

Reaction of **2** separately with *cis*- and *trans*-1,2-dichloroethylene gave one adduct in each case, the product of the former being assigned the *endo* structure **9***a*. Similarly only one adduct **10***a* was obtained upon addition of *cis*-1,2-dichloroethylene with **1**.

Addition of *trans*-1,2-dichloroethylene afforded an isomeric mixture of **10***b* and *c* in the ratio of 1:4 in which the 2-*exo*-3-*endo* product predominates. Comparison of the methine proton chemical shifts and coupling constants with those of **9***a* and *b* allows assignments to be made and shows no evidence of epimerization indicating

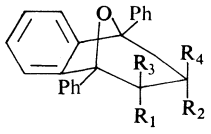

9

a $R_1 = R_2 = Cl$; $R_3 = R_4 = H$
b $R_1 = R_4 = H$; $R_2 = R_3 = Cl$
c $R_1 = R_2$ = 1,8-naphthyl; $R_3 = R_4 = H$
d $R_1 = R_2 = H$; R_3, R_4 = 1,8-naphthyl
e $R_1, R_2 = OCOO$; $R_3 = R_4 = H$
f $R_1 = R_2 = H$; $R_3, R_4 = OCOO$
g $R_1, R_2 = CONPhCO$; $R_3 = R_4 = H$
h $R_1 = R_4 = H$; $R_2 = R_3 = CO_2CH_3$
i $R_1 = R_2 = CO_2CH_3$; $R_3 = R_4 = H$
j $R_1 = R_4 = H$; $R_2 = R_3 = CN$
k $R_1 = R_4 = H$; $R_2 = R_3 = COPh$
l $R_1 = CN$; $R_2 = CH_3$; $R_3 = R_4 = H$

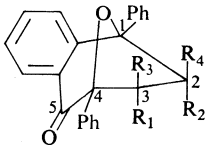

10

a $R_1 = R_2 = Cl$; $R_3 = R_4 = H$
b $R_1 = R_4 = H$; $R_2 = R_3 = Cl$
c $R_1 = R_4 = Cl$; $R_2 = R_3 = H$
d R_1, R_2 = 1,8-naphthyl; $R_3 = R_4 = H$
e $R_1 = R_2 = H$; R_3, R_4 = 1,8-naphthyl
f $R_1, R_2 = OCOO$; $R_3 = R_4 = H$
g $R_1 = R_2 = H$; $R_3, R_4 = OCOO$
h $R_1, R_2 = COOCO$; $R_3 = R_4 = H$
i $R_1, R_2 = CONPhCO$; $R_3 = R_4 = H$
j $R_1 = R_4 = CO_2CH_3$; $R_2 = R_3 = H$
k $R_1 = R_4 = H$; $R_2 = R_3 = CO_2CH_3$
l $R_1 = R_2 = H$; $R_3 = R_4 = CO_2CH_3$
m $R_1 = R_2 = CO_2CH_3$; $R_3 = R_4 = H$
n $R_1 = R_4$ = Ph; $R_2 = R_3 = H$
o $R_1 = R_4 = H$; $R_2 = R_3$ = Ph
p $R_1 = R_4 = CN$; $R_2 = R_3 = H$
q $R_1 = R_4 = H$; $R_2 = R_3 = CN$
r $R_1 = R_4 = COPh$; $R_2 = R_3 = H$
s $R_1 = R_2$ = Ph; $R_3 = R_4 = H$
t $R_1 = R_2 = H$; $R_3 = R_4$ = Ph
u $R_1 = CN$; $R_2 = CH_3$; $R_3 = R_4 = H$
v $R_1 = CN$; $R_2 = R_3 = R_4 = H$
w $R_1, R_2 = CONHCO$, $R_3 = R_4 = H$

stereospecific cycloadditions. The *cis*-configuration of **10***a* was confirmed by the facile *trans*-elimination of hydrogen chloride upon recrystallization to give **11** in which the direction of elimination is not determined. Compounds **10***b* and *c* in contrast were quite stable to heating and showed no tendency to eliminate hydrogen chloride.

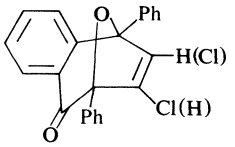

11

Diphenylisobenzofuran **2** reacted with acenaphthylene to give an isomeric mixture of the *endo* and *exo* adducts **9***c* and *d* in the ratio of 3:1. Trost recently reported reaction of **2** with the closely analogous pyracycloquinone to give an *endo*:*exo* ratio of 3:1 (33). The *exo* methine protons in the latter case resonate at δ 5.42 closely comparable with the analogous protons in **9***c* at 5.12, supporting the structural assignments. The indenone oxide **1** afforded with acenaphthylene a mixture of the analogous adducts **10***d* and *e* in the *endo*:*exo* proportion of 3:2 suggesting **2** is a good analog of **1**.

Vinylene carbonate adds to **2** to form adducts in which the ratio of the *endo* to *exo*–*cis* adducts **9***e* to *f* is 6:1. The indenone oxide similarly affords the *endo* and *exo* adducts **10***f* and *g* in a ratio of 3:1.

Exclusive formation of the endo adducts of **1** was observed with maleic anhydride **10***h* and with *N*-phenylmaleimide **10***i*.

In the addition of **1** to dimethyl maleate and dimethyl fumarate all four possible stereoisomeric adducts were observed allowing a closer comparison of chemical shifts, coupling constants, and the steric requirements of the cycloadditions. With dimethyl fumarate for example two isomeric adducts **10***j* and *k* were obtained in a ratio of 3:1 and assigned by comparison with the single adduct **9***h* of unambiguous structure obtained from **2**. Similarly two isomeric adducts **10***l* and *m* in the proportion of 3.6:1 were obtained by reaction of **1** with dimethyl maleate.

The assignments of **10***l* and *m* were proven by mild acid hydrolysis of the *endo*-maleic anhydride adduct **10***h* to the *cis-endo*-diacid **12** (see Scheme 1). A single diacid was obtained indicating that epimerization had not occurred. Treatment of **12** with diazomethane in ether gave **10***m* in quantitative yield. Direct reaction of diazomethane in ether on **10***h* also gave **10***m* in quantitative yield.

trans-Stilbene afforded two isomeric adducts **10***n* and *o* in the ratio of 5:2. Similarly *trans*-1,2-dicyanoethylene gave rise to two isomeric adducts **10***p* and *q* in the ratio of 7:1 in which assignments were made by comparison with the

Can. J. Chem. Downloaded from www.nrcresearchpress.com by 210.87.254.105 on 09/05/12
For personal use only.

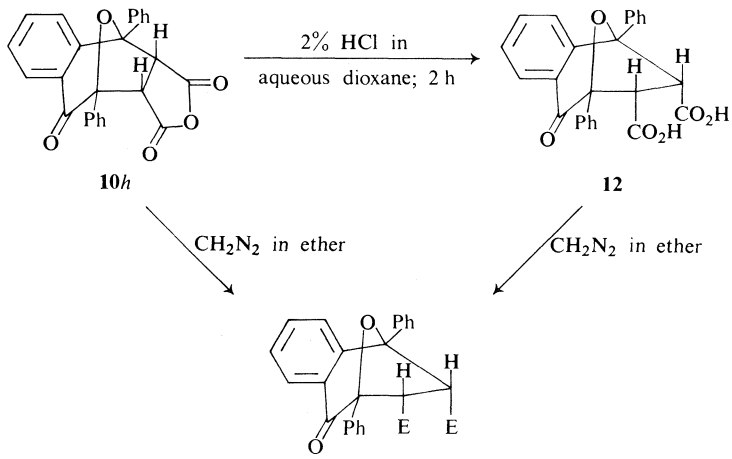

10*h* **12** **10***m*

SCHEME 1

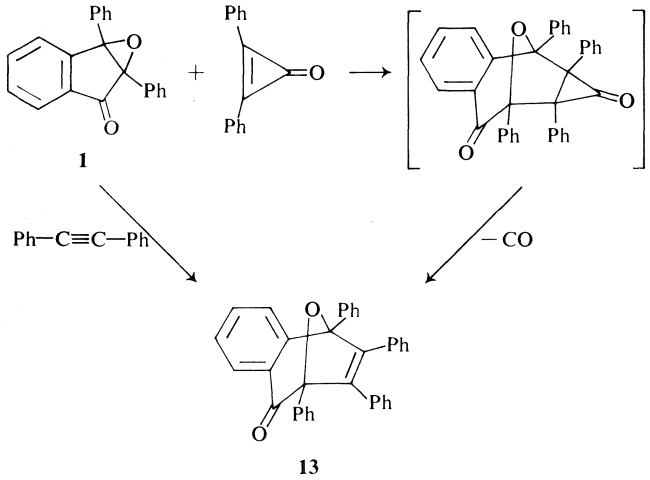

1 **13**

SCHEME 2

adduct **9***j* obtained from **1**. With very bulky groups like benzoyl on the addend one observes exclusive formation of the 2-*exo*-3-*endo* isomer as in **10***r* obtained from *trans*-dibenzoylethylene. *cis*-Stilbene gives rise to mixtures of *endo* and *exo* adducts **10***s* and *t* in the ratio of 2:3.

A result which parallels observations made with the indanoaziridine **6** (38) was that although commercial crotonitrile consists of a *cis–trans* mixture, reaction with both **1** and **2** gave exclusively *endo* adducts **10***u* and **9***l* respectively, corresponding only to addition of the *cis*-isomer in an *endo* direction. Comparison of the proton–proton coupling with those in the ABC analysis of the methine protons in the adduct **10***v* obtained from acrylonitrile, confirm the *cis* assignments in **10***u* and **9***l*.

In the reaction of **1** with diphenylcyclopro-

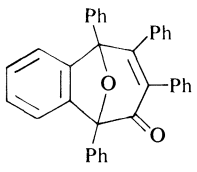

14

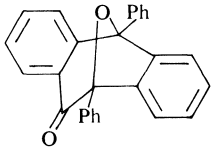

15

Can. J. Chem. Downloaded from www.nrcresearchpress.com by 210.87.254.105 on 09/05/12
For personal use only.

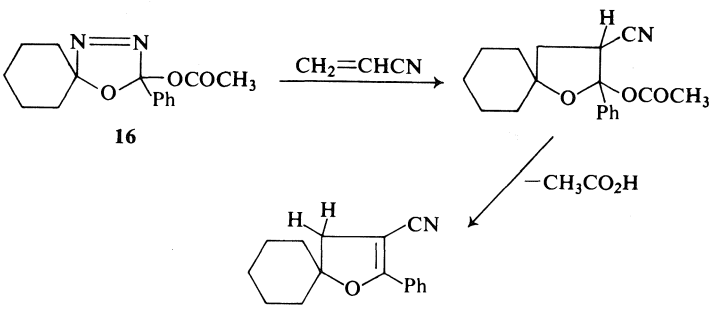

SCHEME 3

penone (see Scheme 2), cycloaddition of the carbonyl ylide takes place to the carbon–carbon double bond. Subsequent spontaneous loss of the carbon monoxide from the intermediate produces **13** which is also obtained directly with diphenylacetylene. The behavior of diphenylcyclopropenone towards **2** is quite different and involves instead initial attack at the carbonyl bond to form **14** (39).

Species **4** can also be trapped with the reactive "acetylenic" dipolarophile benzyne, generated *in situ* from diphenyliodonium-2-carboxylate to give **15**.

Δ^3-1,3-4-Oxadiazolines provide convenient precursors for acyclic carbonyl ylides. Recently prepared by Hoffman and Luthardt (24) they have been shown by these authors and by Rajagopalan and Advani (23) to cleave at moderate temperatures to carbonyl ylides which may be trapped by acetylenic dipolarophiles.

2-Acetyl-5,5-pentamethylene-Δ^3-1,3,4-oxadiazoline (**16**) reacted with acrylonitrile regiospecifically to give a single product **17** (see Scheme 3). In common with the experience of other workers (23, 24) acetic acid was eliminated from the initial product of cycloaddition. The single orientation represented by **17** was proven by the absence of a vinylic absorption in the n.m.r. spectrum. The identical regiospecificity of addition was exhibited in the cycloaddition of **16** to methyl acrylate and to crotonitrile to give **18** and **19** respectively as the only products. The orientation of addition is obvious from the n.m.r. spectra, that of **18** shows a two proton singlet at δ 2.83, and that of **19** shows a methyl group doublet at δ 1.20. Identical products **20** are obtained from both dimethyl maleate and dimethyl fumarate, corresponding to the elimination of acetic acid. Fumaronitrile affords a single adduct **21** in good yield in which acetic acid has also been eliminated during the reaction. Dibenzoylethylene reacted with **16** to give adduct **22**. The previously suggested intermediate (23) in the 1,3-dipolar cycloadditions of olefinic dipolarophiles to carbonyl ylides of this type was isolated in the case of 1,4-naphthoquinone as adduct **23**.

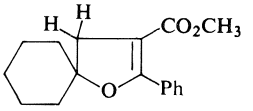

18

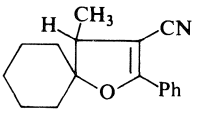

19

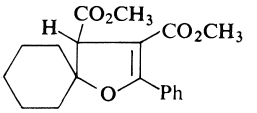

20

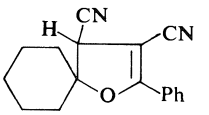

21

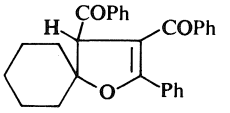

22

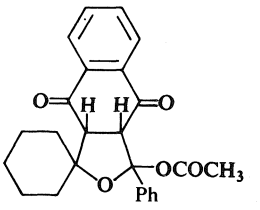

23

Discussion

Numerous attempts have been made to account for the Alder *endo* addition rule (40) in the Diels–Alder reaction. Recently the rule has been reinterpreted in quantum mechanical terms by Hoffmann and Woodward who note that the *endo* transition state is stabilized relative to the

Can. J. Chem. Downloaded from www.nrcresearchpress.com by 210.87.254.105 on 09/05/12
For personal use only.

Can. J. Chem. Downloaded from www.nrcresearchpress.com by 210.87.254.105 on 09/05/12
For personal use only.

exo transition state by symmetry controlled secondary orbital interaction (41). This view was supported by Herndon and Hall with extended Hückel calculations (42) but more recently these authors have concluded that such secondary orbital interactions may be relatively unimportant and that geometrical overlap relationships of the π-orbitals at only the primary bonding center need be considered (43). Other interpretations have been made in terms of inductive forces (44), charge-transfer interactions (45), and dipole–dipole interactions (46).

While the related (4 + 2)π 1,3-dipolar cycloaddition reaction might be expected to involve similar secondary effects leading to preferential *endo* addition, no systematic study has been undertaken. Woller and Cromwell have reported one example of cycloaddition to an aziridine, the direction of which appears to be dictated by maximum overlap of the π-orbitals of the two components (47).

Orientation phenomena in 1,3-dipolar cycloadditions reactions have been interpreted as an interplay of steric and electronic factors (48). Examination of the stereochemistry of addition of symmetrical dipolarophiles to the indenone oxide should minimize electronic factors. The stereospecificity observed in such additions noted above is in agreement with recent conclusions derived from intramolecular isotope effects on the concerted nature of 1,3-dipolar cycloadditions of tetracyanoethylene oxide to allenes (25). Two tendencies are apparent from the above results. First a general preference under these conditions for *endo* additions of *cis*-addends to **1** and **2** but exceptions are noted in the case of dimethyl maleate and *cis*-stilbene. This is in agreement with other reported examples in the case of **2** (33). Arnold and Karnischky have recently shown that the carbonyl ylide derived from the thermal cleavage of 5-oxabicyclo[2,1,0]-pentane forms a mixture of *exo* and *endo* adducts with maleonitrile (27). The *endo* preference for **1** is in agreement with the results obtained with the indanoaziridine **6** (32, 38) and removes the apparent discrepancy between the hitherto observed orientation of additions to **1** and **6**.

A second tendency is apparent during the cycloaddition of *trans*-addends to **1** for the two substituents to adopt 2-*exo*-3-*endo* positions. Although the adducts obtained from **1** appear to be configurationally stable under their conditions of preparation, however, until it is demonstrated that the product distribution in these reactions is kinetically controlled (in view of the high temperatures that must be used), any attempts to formulate a general *endo* rule for such 1,3-dipolar cycloadditions is premature.

Electronic effects might be expected to play a significant role in determining the regiospecificity of addition of unsymmetrical dipolarophiles to **1** and **2**. Ullmann and Milks have reported in the addition of unsymmetrical addends to **1** a regiospecificity to place the substituents remote from the 1-phenyl group (22) *e.g.* **28**, **29**, **30**.

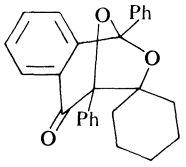

28

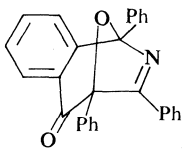

29

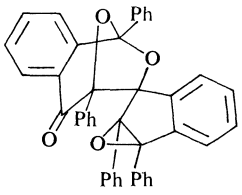

30

While steric hindrance factors will contribute here the orientation of all three additions is consonant with electronic directional effects.

Electronic factors may similarly be predominant in producing the regiospecificity observed in the additions to the acyclic ylide derived from **3** *i.e.*., in **17**, **18**, and **19** all of which correspond to the structures expected on the basis of electronic effects.

Experimental

The m.p.'s. were determined with a Fisher–Johns apparatus. The i.r. spectra were recorded with a Perkin–Elmer model 421 spectrophotometer. The n.m.r. spectra were recorded with Varian A-60 and A-100 spectrometers for *ca.* 5–10% (w/v) solutions and were taken on the initially obtained reaction mixtures to obtain an accurate determination of isomeric ratios; line positions are reported in p.p.m. from tetramethylsilane. Mass spectra were determined with an A.E.I. MS12 double-focusing high-resolution mass spectrometer (ionization energy usually 70 eV). Peak measurements were made by comparison with perfluorotributylamine at a resolving power of 15 000. In those cases where mixtures of isomers were

Can. J. Chem. Downloaded from www.nrcresearchpress.com by 210.87.254.105 on 09/05/12
For personal use only.

obtained, peak measurements were determined on the analytical samples and no attempts were made to separate the isomers. Kieselgel DF-5 (Camag, Switzerland) and Eastman Kodak precoated silica sheets were used for t.l.c. Microanalyses were carried out by Mrs. D. Mahlow of this department.

Preparation of Substrates

2,3-Diphenylindenone oxide and 1,3-diphenylisobenzofuran were prepared by the methods of Weitz and Scheffer (49) and of Newman (50) respectively.

General Procedure for 1,3-Dipolar Cycloadditions

The following experiments are representative of the reaction conditions employed throughout, thereafter the results are summarized in tabular form.

Reaction of 2,3-Diphenylindenone Oxide with Dimethyl Fumarate

A solution of 0.893 g (3 mmol) of 2,3-diphenylindenone oxide and 0.432 g (3 mmol) of dimethyl fumarate in 30 ml of dry toluene was heated to 135° in a sealed tube for 12 h under nitrogen. Evaporation of the solvent *in vacuo* and trituration of the residue with 95% ethanol afforded a mixture of adducts **10***k* and *j* in a ratio of (1:3) as shown by the n.m.r. spectrum, 1.22 g (92% yield), m.p. 188–189° as colorless crystals (from 95% ethanol).

Anal. Calcd. for $C_{27}H_{22}O_6$ (mol. wt. 442.1416): C, 73.3; H, 5.0. Found (442.1410 (mass spectrum)): C, 73.25; H, 5.0.

The i.r., spectrum ν_{max} ($CHCl_3$) 1734, 1705 cm^{-1} (C=O). The n.m.r. spectrum δ_{TMS} ($CDCl_3$) 3.20; 3.39 (4.5H, s, CO_2CH_3 (**10***j*)); 3.32, 3.59 (1.5H, s, CO_2CH_3 (**10***k*)); 4.03, 4.19 (0.5H, ABq, J = 4 Hz (**10***k*) methines); 4.04, 4.57 (1.50H, ABq, J = 5.5 Hz (**10***j*) methines); 6.8–8.3 (14H, m, aromatic protons).

Reaction of 2,3-Diphenylindenone Oxide with Dimethyl Maleate

A solution of 0.596 g (2 mmol) of 2,3-diphenylindenone oxide and 0.576 g (4 mmol) of dimethyl maleate in 25 ml of dry toluene was heated at 135° for 48 h in a sealed tube under nitrogen. Evaporation of the solvent *in vacuo* and trituration of the residue with 50% ethanol afforded a mixture of adducts **10***l* and *m* in the ratio of (3.6:1) as shown by the n.m.r. spectrum 0.82 g (94% yield), m.p. 155–158° as colorless crystals (from 50% aqueous ethanol).

Anal. Calcd. for $C_{27}H_{22}O_6$: (mol. wt. 442.1416): C, 73.3; H, 5.0. Found (442.1409 (mass spectrum)): C, 73.2; H, 4.9.

The i.r. spectrum ν_{max} ($CHCl_3$) 1745, 1714 cm^{-1} (C=O). The n.m.r. spectrum δ_{TMS} ($CDCl_3$) 3.27, 3.40 (4.68 H, s, CO_2CH_3(**10***l*)); 3.50, 3.59 (1.29H, s, CO_2CH_3 (**10***m*)); 3.84, 3.96 (1.56H, ABq, J = 9 Hz, (**10***l*) methines); 4.13, 4.31 (0.43H, ABq, J = 11.5 Hz (**10***m*) methines); 6.8–8.3 (14H, m, aromatic protons).

Reaction of 2,3-Diphenylindenone Oxide with cis-Dichloroethylene

A solution of 0.596 g (2 mmol) of 2,3-diphenylindenone oxide and 15 ml of *cis*-1,2-dichloroethylene in 15 ml of dry toluene was heated to 135° for 12 h under nitrogen. Evaporation of the solvent and excess of dichloroethylene *in vacuo* and trituration of the residue with 95% ethanol afforded **10***a* 0.566 g (72% yield), m.p. 129–131° as colorless crystals; δ ($CDCl_3$) 4.88, 5.05 (2H, ABq, J = 9 Hz, methines). Recrystallization of **10***a* from 95% ethanol or chromatography on alumina afforded the dehydrochlorinated product **11**, m.p. 130–131°, as a pale yellow crystalline solid (from 95% ethanol) in quantitative yield.

Anal. Calcd. for $C_{23}H_{15}O_2{}^{35}Cl$ (mol. wt. 359.0842): C, 77.0; H, 4.2; Cl, 9.8. Found (359.0842 (mass spectrum)): C, 77.4; H, 4.4; Cl, 9.3.

The i.r. spectrum ν_{max} ($CHCl_3$) 1710 cm^{-1} (C=O).

Reaction of 1,3-Diphenylisobenzofuran with cis-1,2-Dichloroethylene

A solution of 1.08 g (4 mmol) of 1,3-diphenylisobenzofuran and 15 ml of *cis*-1,2-dichloroethylene in 15 ml of dry benzene was heated under reflux at 100° for 12 h. Evaporation of the solvent and excess of dichloroethylene *in vacuo* and trituration of the residue with 95% ethanol afforded **9***a* 1.06 g (73% yield), m.p. 138–140°, as colorless crystals (from ether – 95% ethanol).

Anal. Calcd. for $C_{22}H_{16}O^{35}Cl_2$ (mol. wt. 366.0579): C, 71.95; H, 4.4; Cl, 19.3. Found (366.0570 (mass spectrum)): C, 71.8; H, 4.4; Cl, 19.3.

The n.m.r. spectrum δ_{TMS} ($CDCl_3$) 4.90 (2H, s, methines); 7.0–8.1 (14H, m, aromatic protons).

Reaction of 2,3-Diphenylindenone Oxide with Diphenyliodonium-2-carboxylate

A mixture of 0.894 g (3 mmol) of 2,3-diphenylindenone oxide and 2.0 g (6 mmol) of diphenyliodonium-2-carboxylate (51) in 40 ml of *sym*-trimethylbenzene was rapidly raised to reflux temperature and then heated under reflux with stirring for 3 h at which time no remaining 2,3-diphenylindenone oxide could be detected by t.l.c. Evaporation of the filtered solution to remove excess of solvents *in vacuo* gave a yellow oil which was subjected to chromatography on 100 g of alumina. Elution with *n*-pentane removed aromatic by-products, while the main fraction was obtained by elution with benzene, the main portion of which was a pale yellow oil which crystallized from 95% ethanol to give **15**, 0.869 g (80% yield), as a pale yellow solid, m.p. 78–80° (from 95% ethanol).

Anal. Calcd. for $C_{27}H_8O_2$ (mol. wt. 374.1306): C, 86.6; H, 4.85. Found (374.1300 (mass spectrum)): C, 86.7; H, 4.9.

The i.r. spectrum ν_{max} ($CHCl_3$) 1704 cm^{-1} (C=O). The n.m.r. spectrum δ_{TMS} ($CDCl_3$) 6.6–8.2 (m, aromatic protons).

*Relation of the Configuration of the Adducts of 2,3-Diphenylindenone Oxide with (a) Maleic Anhydride **10***h* and (b) Dimethyl Maleate **10***m*

(*A*) A mixture of 0.04 g (1 mmol) of adduct **10***h* and a 2% solution of hydrochloric acid in 15 ml of 25% aqueous dioxane was heated under reflux gently for 2 h. After cooling the solid which had precipitated was collected representing the diacid **12**, 0.341 g (82% yield), m.p. 150°, which was shown by t.l.c. and n.m.r. to consist of only one isomer.

A solution of 0.2 g (0.5 mmol) of **12** in 20 ml of methanol was treated with a solution of diazomethane prepared from 0.82 g (4 mmol) of *p*-toluenesulfonylmethylnitrosamide (Diazald) and the mixture stirred for 12 h. Removal of the solvents *in vacuo* and recrystallization of the residual solid from aqueous methanol afforded the diester **10***m*, 0.21 g (95% yield), m.p. 160–161°. The

Can. J. Chem. Downloaded from www.nrcresearchpress.com by 210.87.254.105 on 09/05/12
For personal use only.

TABLE 1. 1,3-Dipolar cycloaddition adducts of 2,3-diphenylindenone oxide with olefinic dipolarophiles

10	R_1	R_2	R_3	R_4	Melting point (°C)	Yield (%)	Isomer ratio*	Calculated (%) C	H	N	Cl	Found (%) C	H	N	Cl	Mass spectra Calculated	Found
b	H	Cl	Cl	H	132	69	17:83	69.8	4.1	—	17.9	69.6	4.2	—	17.6	394.0528($C_{23}H_{16}O_2{}^{35}Cl_2$)	394.0528
c	Cl	H	H	Cl													
d	-[1,8-naphthyl]-		H	H	219	93	62:37	88.0	4.9	—	—	87.3	4.8	—	—	450.1619($C_{33}H_{22}O_2$)	450.1610
e	H	H	-[1,8-naphthyl]-														
f	—OCOO—		H	H	218	87	75:25	75.0	4.1	—	—	74.97	4.19	—	—	384.0998($C_{24}H_{16}O_5$)	384.0990
g	H	H	—OCOO—														
h	—COOCO—		H	H	227	89	100:0	75.8	4.1	—	—	75.75	4.2	—	—	396.0998($C_{25}H_{16}O_5$)	396.0990
i	—CONPhCO—		H	H	261	93	100:0	78.1	4.5	3.00	—	78.1	4.5	2.7	—	471.1471($C_{31}H_{21}O_4N$)	471.1465
j	CO_2CH_3	H	H	CO_2CH_3	188	92	75:25	73.3	5.0	—	—	73.25	5.0	—	—	442.1416($C_{27}H_{22}O_6$)	442.1410
k	H	CO_2CH_3	CO_2CH_3	H													
l	H	H	CO_2CH_3	CO_2CH_3	157	94	22:78	73.3	5.0	—	—	73.2	4.9	—	—	442.1416($C_{27}H_{22}O_6$)	442.1409
m	CO_3CH_3	CO_2CH_3	H	H													
n	Ph	H	H	Ph	193	93	70:30	87.8	5.5	—	—	88.0	5.5	—	—	478.1933($C_{35}H_{26}N_2O_2$)	478.1930
o	H	Ph	Ph	H													
p	CN	H	H	CN	203	85	87:13	—	—	7.0	—	—	—	7.3	—	376.1213($C_{25}H_{16}N_2O_2$)	376.1207
q	H	CN	CN	H													
r	COPh	H	H	COPh	216	88	100:0	83.1	4.9	—	—	82.8	4.9	—	—	534.1831($C_{37}H_{26}O_4$)	534.1824
s	Ph	Ph	H	H	68	72	40:60	87.8	5.5	—	—	87.9	5.5	—	—	478.1933($C_{35}H_{26}O_2$)	478.1933
t	H	H	Ph	Ph													
u	CN	CH_3	H	H	191	80	100:0	82.2	5.2	3.8	—	82.4	5.3	4.00	—	365.1416($C_{25}H_{19}NO_2$)	365.1410
v	CN	H	H	H	179	98	100:0	82.0	4.9	4.0	—	82.1	4.8	3.75	—	351.1259($C_{24}H_{17}NO_2$)	351.1255
w	—CONPhCO—		H	H	275	93	100:0	75.9	4.3	3.5	—	75.4	4.3	3.3	—	395.1157($C_{25}H_{17}NO_4$)	395.1151

*Determined by integration of n.m.r. spectra.

Can. J. Chem. Downloaded from www.nrcresearchpress.com by 210.87.254.105 on 09/05/12
For personal use only.

TABLE 2. Adducts of 1,3-diphenylisobenzofuran

9	R_1	R_2	R_3	R_4	Melting point (°C)	Yield (%)	Isomer ratio*	Calculated (%) C	H	N	Cl	Found (%) C	H	N	Cl	Mass Spectra Calculated	Found
a	Cl	Cl	H	H	138	73	100:0	71.95	4.4	—	19.3	71.8	4.4	—	19.3	366.0579($C_{22}H_{16}O^{35}Cl_2$)	366.0570
b	H	Cl	Cl	H	142	73	—	71.95	4.4	—	19.3	71.8	4.5	—	19.4	366.0579($C_{22}H_{16}O^{35}Cl_2$)	366.0576
c	-[1,8-dinaphthyl]-		H	H	† 178	83	75:25										
d	H	H	-[1,8-dinaphthyl]-														
e	—OCOO—		H	H	‡ 218	86	85:15	77.5	4.5	—	—	77.8	4.5	—	—	—	—
f	H	H	—OCOO—														
g	—CONPhCO—		H	H	148	82	100:0	81.25	4.8	3.2	—	81.7	4.8	2.9	—	443.1521($C_{30}H_{21}NO_3$)	443.1515
h	H	CO_2CH_3	CO_2CH_3	H	148	67	—	75.35	5.35	—	—	74.95	5.3	—	—	414.1467($C_{26}H_{22}O_5$)	414.1472
i	CO_2CH_3	CO_2CH_3	H	H	114	76	100:0	75.35	5.35	—	—	75.35	5.35	—	—	414.1467($C_{26}H_{22}O_5$)	414.1472
j	H	CN	CN	H	190	84	—	82.7	4.6	8.0	—	83.0	4.5	7.9	—	348.1262($C_{24}H_{16}N_2O$)	348.1254
k	H	COPh	COPh	H‡	145	86	—	85.35	5.2	—	—	85.4	5.35	—	—		
l	CN	CH_3	H	H	140	67	100:0	85.4	5.7	4.2	—	85.2	5.7	4.1	—	337.1467($C_{24}H_{19}NO$)	337.1455

*Determined by integration of n.m.r. spectra.
†Reference 52.
‡Molecular ion too small for accurate peak measurement.

TABLE 3. Methine and alkyl group chemical shifts and coupling constants for adducts of 2,3-diphenylindenone oxide (**10**) and diphenylisobenzofuran (**9**)

Compound no.	Chemical shifts (δ)				Coupling constants (Hz)				
	R_1	R_2	R_3	R_4	J_{12}	J_{14}	J_{23}	J_{34}	J_{13}
10*a*	—	—	5.05, d	4.88, d				9	
b	4.89, d	—	—	4.95, d		1.5			
c	—	4.72, d	5.08, d	—			4.2		
d	—	—	5.28, d	5.08, d				8.5	
e	4.75, d	4.55, d	—	—	7.5				
f	—	—	5.57, d	5.37, d				8.5	
g	5.46, d	5.36, d	—	—	6.6				
h	—	—	4.49, d	4.35, d				10	
i	—	—	4.38, d	4.23, d				10	
j	3.39*	4.04, d	4.57, d	3.20*			5.5		
k	4.03, d	3.59*	3.32*	4.19, d		4			
l	3.96, d	3.84, d	3.27*	3.40*	9				
m	3.50*	3.59*	4.31, d	4.13, d				11.5	
n	—	3.76, d	4.16, d	—			8.5		
o	3.94, d	—	—	4.07, d		6			
p	—	3.93, d	4.18, d	—			6.5		
q	4.07, d	—	—	4.07, d					
r	—	4.75, d	5.65, d	—			7.5		
s	—	—	4.73, d	4.48, d				12.5	
t	4.48, d	4.16, d	—	—	8.8				
u	—	1.30†	4.04, d	3.2, d				11	
v	—	—	—	—		4		10	11.5
9*a*	—	—	4.90, s	4.90, s					
b	4.42, d	—	—	4.86, d		2.5			
c	—	—	5.12, s	5.12, s					
d	4.35, d	4.35, d	—	—					
e	—	—	5.26, s	5.26, s					
f	5.13, s	5.13, s	—	—					
g	—	—	4.18, s	4.18, s					
h	3.59, d	3.49*	3.30*	4.31, d		4.5			
i	3.49*	3.49*	4.13, d	4.13, d					
j	3.49, d	—	—	3.82, d		4.5			
k	4.52, d	—	—	5.11, d		5			
l	—	1.00†	3.72, d	3.0, d				10	

*CO_2CH_3.
†CH_3.

spectral properties of this material were identical with those of the minor component obtained by direct addition of **1** to dimethyl maleate.

(*B*) The identical product was obtained directly by reaction of **10***h* with a solution of diazomethane in ether in 87% yield.

By the above general procedures a series of adducts of **1** and **2** were prepared. Their analytical and spectral data are summarized in Tables 1–3.

Reaction of 2-Acetyl-5,5-pentamethylene-2-phenyl-Δ³-1,3,4-oxadiazoline with Acrylonitrile

A solution of 1.37 g (5 mmol) of 2-acetyl-5,5-pentamethylene-2-phenyl-Δ³-1,3,4-oxadiazoline and 10 ml of acrylonitrile in 20 ml of dry benzene was heated under gentle reflux for 6 h. Evaporation of the solvent and excess of acrylonitrile *in vacuo* gave a brown oil which was subjected to chromatography on 90 g of B.D.H. alumina. Elution with benzene first removed epoxide by-product while elution with chloroform gave **17** as a pale brown solid which was purified by recrystallization from petroleum ether (b.p. 40–60°) 0.628 g (53% yield), m.p. 107–110°.

Anal. Calcd. for $C_{16}H_{17}NO$ (mol. wt. 239.1310): N, 5.85. Found 239.1310 (mass spectrum)): N, 5.9.

The i.r. spectrum ν_{max} ($CHCl_3$) 2197 cm^{-1} (CN). The n.m.r. spectrum δ_{TMS} ($CDCl_3$) 1.0–2.4 (10H, m, C_6H_{11}); 3.42 (2H, s, methylene); 7.1–8.2 (5H, m, aromatic hydrogens).

Reaction of 2-Acetyl-5,5-pentamethylene-2-phenyl-Δ³-1,3,4-oxadiazoline with Dimethyl Fumarate

A solution of 1.37 g (5 mmol) of 2-acetyl-5,5-pentamethylene-2-phenyl-Δ³-1,3,4-oxadiazoline and 0.729 g (5 mmol) of dimethyl fumarate in 30 ml of dry benzene was heated under gentle reflux for 4 h when the evolution of nitrogen ceased. Evaporation of the solvent *in vacuo* gave a yellow oil which was subjected to chromatography on 90 g of B.D.H. alumina. Elution successively with hexane, hexane/benzene (9:1), and hexane/benzene (4:1) removed a small amount of epoxide by-product. Elution with benzene gave the main fraction **20** as a colorless solid 1.63 g (73% yield), m.p. 70° (from ether–pentane).

Anal. Calcd. for $C_{19}H_{22}O_5$ (mol. wt. 330.1467): C, 69.1; H, 6.7. Found (330.1460 (mass spectrum)): C, 69.3; H, 6.6.

The i.r. spectrum ν_{max} ($CHCl_3$) 1700 (br) (C=O). The n.m.r. spectrum δ_{TMS} ($CDCl_3$) 1.0–2.4 (10H, m, C_6H_{11}); 3.63, 3.72 (3H each, s, CO_2CH_3), 7.2–8.0 (5H, m, aromatic protons).

Can. J. Chem. Downloaded from www.nrcresearchpress.com by 210.87.254.105 on 09/05/12
For personal use only.

Can. J. Chem. Downloaded from www.nrcresearchpress.com by 210.87.254.105 on 09/05/12
For personal use only.

TABLE 4. 1,3-Dipolar cycloadditon products of 2-acetyl-5,5-pentamethylene-2-phenyl-Δ^3-1,3,4-oxadiazoline with olefinic dipolarophiles

Compound no.	R_1	R_2	R_3	Melting point (°C)	Yield (%)	Calculated C	Calculated H	Calculated N	Found (%) C	Found (%) H	Found (%) N	Mass spectra Calculated	Mass spectra Found	Nuclear magnetic resonance spectra R_1	R_2	$R_3(\delta)$ J(Hz)
17	CN	H	H	110	53	—	—	5.85	—	—	5.9	239.1310($C_{16}H_{17}NO$)	239.1310			4.05
18	CO_2CH_3	H	H	oil	65	—	—	—	—	—	—	294.1256($C_{19}H_{18}O_3$)	294.1252	3.69*	2.83	2.83
19	CN	CH_3	H	oil	43	—	—	—	—	—	—	253.1467($C_{17}H_{19}NO$)	253.1463		1.20, d	2.96,q 7
20	CO_2CH_3	CO_2CH_3	H	70	76	69.1	6.7	—	69.3	6.6	—	330.1467($C_{19}H_{22}O_5$)	330.1460	3.72*	3.63*	3.83
21	CN	CN	H	115	64	77.25	6.10	10.6	76.9	5.8	10.5	264.1263($C_{17}H_{16}N_2O$)	264.1262			3.94
22	PhCO	PhCO	H	68	83	74.24	5.98	—	74.06	6.06	—	422.1882($C_{29}H_{26}O_3$)	422.1876			5.13
24	—CONHCO—		H	200	88	72.1	6.05	4.9	72.05	5.9	5.0	283.1208($C_{17}H_{17}NO_3$)	283.1210			4.05

*CO_2CH_3.

Can. J. Chem. Downloaded from www.nrcresearchpress.com by 210.87.254.105 on 09/05/12
For personal use only.

An identical product was obtained by reaction of 2-acetyl-5,5-pentamethylene-2-phenyl-Δ^3-1,3,4-oxadiazoline with dimethyl maleate.

Reaction of 2-Acetyl-5,5-pentamethylene-2-phenyl-Δ^3-1,3,4-oxadiazoline with 1,4-Naphthaquinone

A solution of 1.10 g (4 mmol) of 2-acetyl-5,5-pentamethylene-2-phenyl-Δ^3-1,3,4-oxadiazoline and 0.63 g (4 mmol) of 1,4-naphthaquinone in 40 ml of dry benzene was heated under reflux for 5 h when a dark red solution was obtained. Evaporation of the solvent *in vacuo* gave a dark red oil which was subjected to chromatography on 90 g of B.D.H. alumina. Elution successively with 200 ml of hexane and 300 ml of (3:2) hexane/benzene removed some epoxide by-product and unreacted 1,4-naphthaquinone, while elution with 200 ml of benzene afforded the main fraction. Evaporation of the solvent gave a yellow–green oil, trituration of which with 95% ethanol gave **23** as a pale-green solid 0.63 g (40% yield), m.p. 169–171° (from 95% ethanol).

Anal. Calcd. for $C_{25}H_{24}O_5$ (mol. wt. 404.1624): C, 82.4; H, 6.2. Found (404.1616 (mass spectrum)): C, 82.05; H, 6.5.

The i.r. spectrum ν_{max} ($CHCl_3$) 1672, 1753 cm^{-1} (C=O). The n.m.r. spectrum δ_{TMS} ($CDCl_3$) 1.3–2.4 (10H, m, C_6H_{11}), 1.87 (s, 3H, CH_3); 5.76, 6.65 (2H, ABq, J = 10.5 Hz, methin 6.7–8.2 (9H, m, aromatic protons).

By the above procedures a series of adducts of **16** were prepared. Their analytical and mass spectral data are summarized in Table 4 in which the numbered groups refer to the following structure

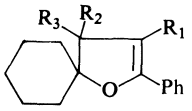

This research was supported by the National Research Council of Canada and the Chemistry Department of the University of Alberta.

1. P. B. Woller and N. H. Cromwell. J. Heterocycl. Chem., **5**, 579 (1968).
2. H. W. Heine and R. Peavy. Tetrahedron Lett. 3123 (1965).
3. R. Huisgen, W. Scheer, G. Szeimies, and H. Huber. Tetrahedron Lett. 397 (1966).
4. A. Padwa and L. Hamilton. Tetrahedron Lett. 4363 (1965).
5. H. W. Heine, A. B. Smith, and J. D. Bower. J. Org. Chem. **33**, 1097 (1968).
6. H. W. Heine, R. E. Peavy, and A. J. Durbetaki. J. Org. Chem. **31**, 3924 (1966).
7. A. Padwa and L. Hamilton. J. Heterocycl. Chem. **4**, 118 (1967).
8. A. Padwa and W. Eisenhardt. Chem. Commun. 380 (1968).
9. R. Huisgen, W. Scheer, and H. Huber. J. Am. Chem. Soc. **89**, 1753 (1967).
10. S. Oida and E. Ohki. Chem. Pharm. Bull. Jap. **16**, 764 (1968).
11. H. W. Heine and R. P. Henzel. J. Org. Chem. **34**, 171 (1969).
12. J. W. Lown, G. Dallas, and T. W. Maloney. Can. J. Chem. **47**, 3557 (1969).
13. J. W. Lown, J. P. Moser, and R. Westwood. Can. J. Chem. **47**, 4335 (1969).
14. J. W. Lown, R. K. Smalley, and G. Dallas. Chem. Commun. 1543 (1968).
15. J. W. Lown, R. K. Smalley, G. Dallas, and T. W. Maloney. Can. J. Chem. **48**, 89 (1970).
16. G. Dallas, J. W. Lown, and J. P. Moser. J. Chem. Soc. 2383 (1970).
17. J. W. Lown and J. P. Moser. Can. J. Chem. **48**, 2227 (1970).
18. J. W. Lown and K. Matsumoto. Can. J. Chem. **48**, 3399 (1970).
19. W. J. Linn and R. E. Benson. J. Am. Chem. Soc. **87**, 3657 (1965).
20. W. J. Linn. J. Am. Chem. Soc. **87**, 3665 (1965).
21. P. Brown and R. C. Cookson. Proc. Chem. Soc. 185, (1964).
22. E. F. Ullmann and J. E. Milks. J. Am. Chem. Soc. **86**, 3814 (1964).
23. P. Rajagopalan and B. G. Advani. Tetrahedron Lett. 2689 (1967).
24. R. W. Hoffmann and H. J. Luthardt. Chem. Ber. **101**, 3851 (1968).
25. W. R. Dolbier and S. H. Dai. Tetrahedron Lett. 4645 (1970).
26. Thap Do-Minh, A. M. Trozzolo, and G. W. Griffin. J. Am. Chem. Soc. **92**, 1402 (1970).
27. D. R. Arnold and L. A. Karnischky. J. Am. Chem. Soc. **92**, 1404 (1970).
28. R. Huisgen. Angew. Chem. Int. Ed. Engl. **2**, 591 (1963).
29. J. M. Dunston and P. Yates. Tetrahedron Lett. 505 (1964).
30. R. B. Woodward and R. Hoffmann. The conservation of orbital symmetry. Academic Press, New York, N.Y., 1970. p. 87.
31. A. Hassner. J. Org. Chem. **33**, 2684 (1968).
32. J. W. Lown and K. Matsumoto. Chem. Commun. 692 (1970).
33. B. M. Trost. J. Am. Chem. Soc. **91**, 918 (1969).
34. M. A. Battiste and C. T. Sprouse. Tetrahedron Lett. 4661 (1970).
35. M. P. Cava and F. M. Scheel. J. Org. Chem. **32**, 1304 (1967).
36. R. Breslow, G. Ryan, and J. T. Groves. J. Am. Chem. Soc. **92**, 988 (1970).
37. (*a*) K. B. Wiberg and W. J. Bartley. J. Am. Chem. Soc. **82**, 6375 (1960). (*b*) M. A. Battiste. Tetrahedron Lett. 3795 (1964). (*c*) G. L. Closs, L. E. Closs, and W. A. Boll. J. Am. Chem. Soc. **85**, 3796 (1963). (*d*) M. A. Battiste. J. Am. Chem. Soc. **85**, 2175 (1963). (*e*) D. C. F. Law and S. W. Tobey. J. Am. Chem. Soc. **90**, 2376 (1968).
38. J. W. Lown and K. Matsumoto. J. Org. Chem. **36**, 1405 (1971).
39. J. W. Lown, T. W. Maloney, and G. Dallas. Can. J. Chem. **48**, 554 (1970).
40. K. Alder and G. Stein. Angew. Chem. **50**, 510 (1937).
41. R. Hoffmann and R. B. Woodward. J. Am. Chem. Soc. **87**, 4388 (1965).
42. W. C. Herndon and L. H. Hall. Theoret. Chim. Acta, **7**, 4 (1967).
43. W. C. Herndon and L. H. Hall. Tetrahedron Lett. 3095 (1967).

44. (*a*) A. WASSERMANN. Diels–Alder reactions. Elsevier Publishing Co., New York, N.Y., 1965. (*b*) A. WASSERMANN. J. Chem. Soc. 828, 1511 (1935); 432 (1936).
45. R. W. WOODWARD and H. BAER. J. Am. Chem. Soc. **66**, 645 (1944).
46. J. A. BERSON, A. REMANICK, and W. A. MUELLER J. Am. Chem. Soc. **82**, 5501 (1960).
47. P. W. WOLLER and N. H. CROMWELL. J. Org. Chem. **35**, 888 (1970).
48. (*a*) R. HUISGEN. Angew. Chem. Int. Ed. Engl. **2**, 565 (1963). (*b*) R. HUISGEN. J. Org. Chem. **33**, 2291 (1968).
49. E. WEITZ and A. SCHEFFER. Chem. Ber. **54**, 2327 (1921).
50. M. S. NEWMAN. J. Org. Chem. **26**, 2630 (1961).
51. F. M. BERINGER and S. J. HUANG. J. Org. Chem. **29**, 445 (1964).
52. E. BERGMAN. J. Am. Chem. Soc. **74**, 1075 (1952).

Can. J. Chem. Downloaded from www.nrcresearchpress.com by 210.87.254.105 on 09/05/12
For personal use only.

Cyclic Imides. II. Silylsuccinimides

A. F. JANZEN AND E. A. KRAMER
Department of Chemistry, University of Manitoba, Winnipeg, Manitoba

Received June 1, 1971

A number of silylsuccinimides containing silicon substituents —H, —CH_3, —C_2H_5, —$CH{=}CH_2$, —$CH_2CH{=}CH_2$, —C_6H_5, as well as disuccinimides, have been prepared and characterized by i.r., n.m.r., and mass spectrometry. The results are compared with previous studies of silylphthalimides.

On a préparé et caractérisé par i.r., r.m.n., et spectre de masse un certain nombre de silylsuccinimides contenant des substituants du silicium, tels —H, —CH_3, —C_2H_5, —$CH{=}CH_2$, —$CH_2CH{=}CH_2$, —C_6H_5, ainsi que des disuccinimides. On compare les résultats avec des études antérieures sur les silylphthalimides.

Canadian Journal of Chemistry, **49**, 3456 (1971)

We have previously reported the preparation and characterization by i.r. and mass spectrometry of a number of silylphthalimides (1). As a continuation of this study we now describe a variety of silylsuccinimides **1–9** listed in Table 1. Silicon substituents include —H, —CH_3, —C_2H_5, —$CH{=}CH_2$, —$CH_2CH{=}CH_2$, —C_6H_5, and compounds **8** and **9** are disuccinimides. Although a number of silylsuccinimides have been prepared previously[1] few details of their spectral properties or synthetic applications have been reported.

Silylsuccinimides **1–9** were conveniently prepared from the corresponding chlorosilane and potassium succinimide and purified by vacuum distillation or recrystallization. In general, silylsuccinimides appeared more susceptible to hydrolysis than silylphthalimides, in particular disuccinimides, and they were handled in a vacuum system or nitrogen atmosphere. All compounds were liquids or low melting solids and, on the basis of i.r. and n.m.r. studies, compounds **1–9** are *N*-silylated and no evidence was found for *O*-silylation.

The i.r. spectra were examined in the region 4000–400 cm^{-1}. Two bands were found in the carbonyl region. The more intense band was found in the region 1696 $\pm$ 4 cm^{-1} and may be assigned to the vibrationally coupled asymmetric mode of vibration (3) analogous to the situation in silylphthalimides where C=O (asymmetric) bands were found in the region 1700 $\pm$ 7 cm^{-1} (1). The symmetric mode was of weaker intensity and appeared at higher frequency, in the region 1764 $\pm$ 4 cm^{-1}. Values of C=O (asymmetric) and C=O (symmetric) are recorded in Table 1. Typical i.r. spectra recorded as liquid films, clearly showing two bands in the carbonyl region, are reproduced in Fig. 1.

Splitting of the C=O bands due to vibrational interactions is consistent with the presence of two equivalent carbonyl groups (4) and therefore *N*-silylation, rather than *O*-silylation, must have occurred.

Compounds **3** and **4** showed Si—H stretching vibrations at 2201 and 2199 cm^{-1}, respectively, in the region expected for silicon–hydrogen bonds (5).

A band of strong intensity was found for all silylsuccinimides in the region 1165–1178 cm^{-1}, illustrated in Fig. 1, and this band may tentatively be assigned to a Si—N vibration. Wallwitz *et al.* have previously assigned a strong band in the region 1170–1180 cm^{-1} to a Si—N vibration in *N*-silylheterocycles (6).

The n.m.r. spectra at 40° of silylsuccinimides **1–9** showed a single sharp peak in the region −2.66 to −2.54 p.p.m. assigned to the succinimido hydrogens. The succinimido hydrogens must therefore be equivalent, consistent with *N*-silylation, and the possibility of isomeric structures resulting from the addition of silicon–hydrogen (7) or silicon–nitrogen (8) bonds across the carbonyl bond is eliminated.

The equivalence of the succinimido hydrogens is of significance with regard to the stereochemistry at the nitrogen atom. If the succinimido ring defines a plane of symmetry then the hydrogens will be equivalent if the silicon atom is in the plane of the succinimido ring or if rapid nitrogen inversion is occurring. On the other hand, pyramidal geometry at the nitrogen atom, or slow

[1]For the preparation of *N*-(trimethylsilyl)succinimide see *e.g.* ref. 2.

Can. J. Chem. Downloaded from www.nrcresearchpress.com by 210.87.254.105 on 09/05/12
For personal use only.

TABLE 1. The i.r. data of silylsuccinimides

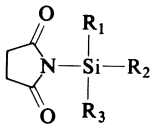

No.	R_1	R_2	R_3	Infrared (cm^{-1})* C=O (asymmetric)	C=O (symmetric)	Si—H
1	CH_3	CH_3	CH_3	1696	1761	
2	C_2H_5	C_2H_5	C_2H_5	1697	1763	
3	CH_3	CH_3	H	1700	1764	2201
4	CH_3	C_6H_5	H	1699	1766	2199
5	CH_3	CH_3	C_6H_5	1692	1761	
6	CH_3	C_6H_5	C_6H_5	1694	1764	
7	CH_3	CH_3	$CH_2CH{=}CH_2$	1699	1768	
8	Succ†	CH_3	CH_3	1698	1764	
9	Succ	CH_3	$CH{=}CH_2$	1698	1768	

*Band positions are accurate to ± 2 cm^{-1}. Compounds 5 and 6 were dissolved in Nujol; all others were neat liquid films.
†Succ = succinimido.

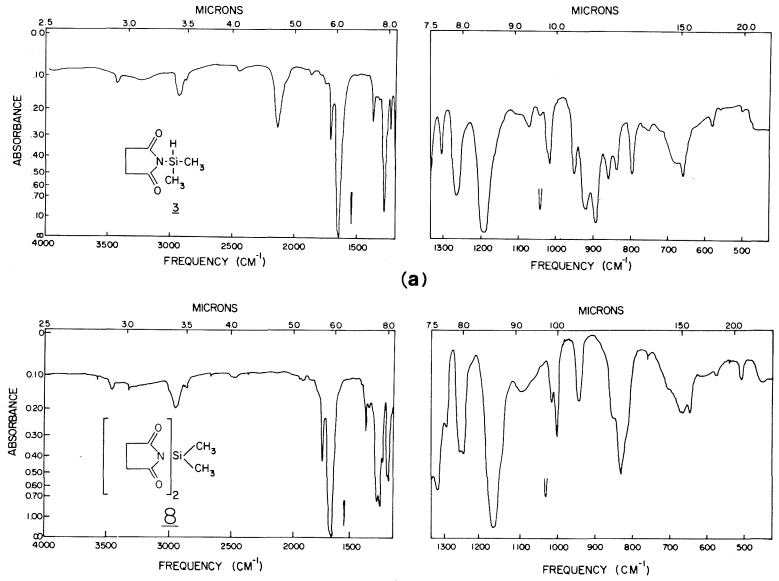

FIG. 1. Typical i.r. spectra: (*a*) *N*-(dimethylsilyl)succinimide (**3**) and (*b*) *N*-(*N'*-succinimidodimethylsilyl)succinimide (**8**) recorded as neat liquid films.

pyramidal inversion, would destroy the equivalence and a complex spectrum would be expected.

Since all compounds **1–9** showed single sharp peaks at $+40°$, therefore changing substituents on silicon has no effect on the equivalence of the succinimido hydrogens nor does the introduction of a second succinimido ring.

The n.m.r. spectrum of *N*-(triethylsilyl)succinimide (**2**) in $CHCl_3$ was recorded down to $-80°$ with the aim of establishing temperature dependent inversion. Although the succinimido peak is somewhat broadened relative to the sharp singlet triethylsilyl peak, the effect is small, and at $-80°$ silylsuccinimides must still be undergoing rapid inversion as has previously been found for *N*-substituted imines (9).

Attempts to slow down the rate of inversion at room temperature by forming complexes with $SnCl_4$ (10) and thereby introducing steric hindrance via carbonyl–metal complexing were unsuccessful. In a similar experiment, $AlCl_3$ was added to **2** and the n.m.r. spectrum recorded down

Can. J. Chem. Downloaded from www.nrcresearchpress.com by 210.87.254.105 on 09/05/12
For personal use only.

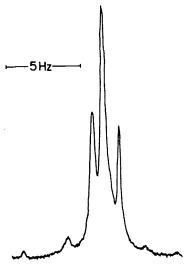

FIG. 2. The ^1H n.m.r. spectrum of *N*-(triethylsilyl)-succinimide (**2**) in benzene showing triethylsilyl region only.

to $-80°$, but the line broadening was not greater than without added $AlCl_3$.

It was noted above that the spectrum of *N*-(triethylsilyl)succinimide (**2**) in $CHCl_3$ solution gave a sharp singlet assigned to the triethylsilyl group. To confirm that the singlet was due to an A_3B_2 type of spectrum expected for an ethyl group, the sample was re-run in benzene solution and the complex pattern shown in Fig. 2 was obtained, consistent with an A_3B_2 spectrum (11).

Mass Spectra

Silylsuccinimides generally showed weak molecular ions *a* and the most prominent peaks resulted from loss of alkyl, aryl, or hydrogen,

[1] 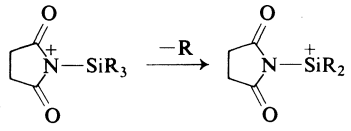

a *b*

R = CH_3, C_2H_5, C_6H_5, H

$a \xrightarrow{-R} b$ (eq. 1). If methyl and phenyl substituents, or if methyl and hydrogen substituents were present, then in both cases loss of methyl gave the more abundant peak.

There were no peaks in the mass spectra of silylsuccinimides which could be assigned to CO_2 elimination. This was rather interesting in view of the prominent loss of CO_2 observed in silylphthalimides (1) (eq. 2). The loss of CO_2 must therefore be characteristic of the phthalimido group, since *N*-alkyl- and *N*-silylphthalimides readily lose CO_2 (12, 13) whereas *N*-alkyl- and *N*-silylsuccinimides do not (13, 14).

Loss of CO has been observed in *N*-alkylsuccinimides and is also found in *N*-silylsuccinimides. For example, the ion *d*, of 23% relative abundance, in the mass spectrum of *N*-(dimethylsilyl)-

[2] 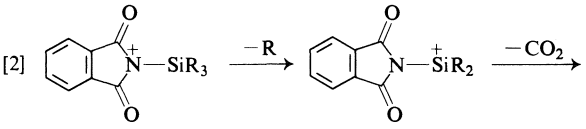

[3] 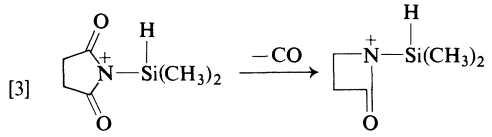

c, m/e 157 (8%) *d*, m/e 129 (23%)

succinimide **3** (eq. 3) may result from loss of CO, by analogy with the loss of CO from *N*-methylsuccinimide (eq. 4). The latter process was confirmed by high resolution mass spectrometry and the presence of a metastable ion (14).

[4] 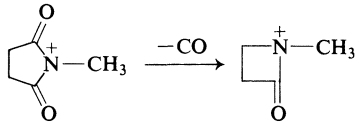

Silylsuccinimides showed peaks of varying intensity assigned to $R_3SiO\overset{+}{S}iR_2$, $R_2\overset{+}{S}iOH$, and R_3Si^+. These peaks may originate in the hydrolysis and condensation of silyl derivatives (eq. 5),

[5] 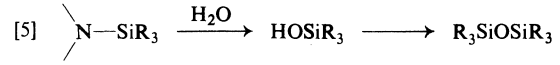

as has been noted before in mass spectral studies (15). As a further possibility siloxanes may result from skeletal rearrangements as has been found for trimethylsilyl ethers (16).

Additional peaks found at *m/e* 56, 55, 28 have also been found in *N*-alkylsuccinimides (13, 14) and must be characteristic of the succinimido ring.

Experimental

General

All compounds were manipulated in a conventional vacuum manifold or under dry nitrogen atmosphere. Organochlorosilanes were purchased from Peninsular Chemresearch and succinimide from Aldrich Chemical Co. Solvents were dried and distilled prior to use. Elemental analyses were carried out by A. Bernhardt, West Germany.

The i.r. spectra were determined on a Perkin–Elmer 337 spectrophotometer using KBr windows and calibrated against polystyrene film. Mass spectra were obtained on a Finnigan 1015 quadrupole or Hitachi Perkin–Elmer RMU-6D mass spectrometer at 50 eV. Proton n.m.r. spectra were obtained on a Varian A-56/60A spectrometer at 60 MHz in 10% (v/v) $CDCl_3$ solutions using a small amount of $CHCl_3$ as internal standard. Chemical shifts are reported relative to external tetramethylsilane

Can. J. Chem. Downloaded from www.nrcresearchpress.com by 210.87.254.105 on 09/05/12
For personal use only.

TABLE 2. Elemental analyses, boiling points, and n.m.r. data

	Elemental analyses (%)			Chemical shift (p.p.m.)*		
	Calculated	Found	Boiling point (melting point) (°C)			
	C H	C H		Succ	CH_3	H
1	49.09 7.65	49.25 8.03	120 at 10^{-2} mm	−2.62, s	−0.40, s	
2	56.29 8.98	55.92 9.08	150 at 10^{-2} mm	−2.62, s		
3	45.83 7.05	45.93 7.35	120 at 10^{-2} mm	−2.66, s	−0.42, d J = 3.5 Hz	−4.68, sep J = 3.5 Hz
4	60.24 5.98	60.41 6.49	200 at 10^{-2} mm	−2.63, s	−0.78, d J = 3.7 Hz	−5.01, q J = 3.7 Hz
5	61.76 6.48	62.33 6.43	(47–49)	−2.56, s	−0.69, s	
6	69.11 5.80	68.85 5.83	(88–90)	−2.54, s	−0.97, s	
7	54.78 7.66	55.18 8.04	170 at 10^{-2} mm	−2.62, s	−0.38, s	
8	47.22 5.55	46.73 5.70	100 at 10^{-4} mm	−2.61, s	−0.69, s	
9	—†		100 at 10^{-4} mm	−2.62, s	−0.78, s	

*s = singlet; d = doublet; q = quartet; sep = septet; succ = succinimido.
†Reactivity of **9** prevented satisfactory elemental analysis.

(TMS) using the formula δ p.p.m. ($CHCl_3$ internal) − 7.23 p.p.m. = δ p.p.m. (TMS external). All chemical shifts were found to be downfield from TMS.

Preparation of N-(Triethylsilyl)succinimide (2)

Triethylchlorosilane (4.50 g, 29.9 mmol) was slowly added to potassium succinimide (4.10 g, 29.9 mmol), prepared from potassium metal and succinimide in tetrahydrofuran, at 0° under nitrogen atmosphere. Potassium chloride was filtered off and solvent and unreacted triethylchlorosilane pumped off leaving a pale yellow liquid. Vacuum distillation gave a clear colorless liquid identified as *N*-(triethylsilyl)succinimide.

The typical procedure outlined for *N*-(triethylsilyl)succinimide was repeated for each silylsuccinimide. Products were purified by vacuum distillation, with the exception of **5** and **6** which were recrystallized from benzene, and the yield of purified product was about 25–35% for compounds **1**–**7** and 10–15% for **8** and **9**.

The i.r. data for **1**–**9** are reported in Table 1 and elemental analyses, boiling points or melting points, and n.m.r. data are reported in Table 2.

The financial assistance of the National Research Council of Canada is gratefully acknowledged. We thank the University of Manitoba for a Manitoba Graduate Fellowship (to E. A. K.).

1. A. F. JANZEN and E. A. KRAMER. Can. J. Chem. **49**, 1011 (1971).
2. L. BIRKOFER and H. DICKOPP. Chem. Ber. **101**, 2585 (1968); A. E. PIERCE. Silylation of organic compounds. Pierce Chemical Co., Rockford, Illinois, 1968.
3. L. J. BELLAMY. Advances in infrared group frequencies. Methuen, London, 1968. p. 129.
4. H. K. HALL, JR. and R. ZBINDEN. J. Am. Chem. Soc. **80**, 6428 (1958).
5. B. J. AYLETT. Advan. Inorg. Chem. Radiochem. **11**, 249 (1968).
6. U. WALLWITZ, H. SCHMIDT, and W. GOSDA. J. prakt. Chem. **32**, 274 (1966).
7. A. F. JANZEN and C. J. WILLIS. Can. J. Chem. **43**, 3063 (1965).
8. M. F. LAPPERT and B. PROKAI. Advan. Organomet. Chem. **5**, 225 (1967).
9. A. T. BOTTINI and J. D. ROBERTS. J. Am. Chem. Soc. **80**, 5203 (1958).
10. S. C. JAIN and R. RIVEST. J. Inorg. Nucl. Chem. **31**, 399 (1969).
11. J. W. EMSLEY, J. FEENEY, and L. H. SUTCLIFFE. High resolution nuclear magnetic resonance spectroscopy. Pergamon Press, 1965. p. 355, 675.
12. R. A. W. JOHNSTONE, B. J. MILLARD, and D. S. MILLINGTON. Chem. Commun. 600 (1966); T. W. BENTLEY and R. A. W. JOHNSTONE. J. Chem. Soc. C, 2354 (1968); C. M. ANDERSON, R. N. WARRENER, and C. S. BARNES. Chem. Commun. 166 (1968).
13. J. H. BOWIE, M. T. W. HEARN, and A. D. WARD. Aust. J. Chem. **22**, 175 (1969).
14. A. M. DUFFIELD, H. BUDZIKIEWICZ, and C. DJERASSI. J. Am. Chem. Soc. **87**, 2913 (1965).
15. H. BUDZIKIEWICZ, C. DJERASSI, and D. H. WILLIAMS. Mass spectrometry of organic compounds. Holden-Day, San Francisco, California, 1967. p. 476.
16. J. DIEKMAN, J. B. THOMSON, and C. DJERASSI. J. Org. Chem. **33**, 2271 (1968).

Can. J. Chem. Downloaded from www.nrcresearchpress.com by 210.87.254.105 on 09/05/12
For personal use only.

Can. J. Chem. Downloaded from www.nrcresearchpress.com by 210.87.254.6 on 09/05/12
For personal use only.

Enthalpies and Excess Enthalpies of Transfer of *n*-Alkylamine Hydrobromides from H_2O to D_2O at 25 °C

J. E. Desnoyers, R. Francescon, P. Picker and C. Jolicoeur
Department of Chemistry, University of Sherbrooke, Sherbrooke, Quebec

Received June 1, 1971

Differences in heats of solution and in heats of dilution of electrolytes in H_2O and D_2O were measured directly with a previously described cell-type differential microcalorimeter. In addition to NaCl and NaBr, most of the homologous salts RNH_3Br were studied from R = methyl to R = *n*-octyl. The results of the two simple salts are in excellent agreement with the best literature values.

The enthalpies of transfer at infinite dilution, ΔH_{tr}^0 ($H_2O \rightarrow D_2O$), are mainly a measure of the structural ion–solvent interactions and of the exchange reaction

$$RNH_3^+(D_2O) + 3\,D_2O \rightarrow RND_3^+(D_2O) + 3HDO$$

Up to R = *n*-propyl, the relative apparent molal enthalpies of transfer, $\Delta\phi_L(H_2O \rightarrow D_2O) = \Delta H_{tr}^{EX}$, are negative, approximately zero for *n*-butyl and positive for the higher members. This gradual change in the excess enthalpies of transfer is interpreted in terms of the increasing importance of hydrophobic interactions between the cations. When association occurs through micelle formation (R = *n*-octyl), there is a rapid increase in $\Delta\phi_L(H_2O \rightarrow D_2O)$ which results from hydrophobic bonding.

On a mesuré directement la différence entre les chaleurs de solution et entre les chaleurs de dilution d'électrolytes dans H_2O et D_2O, au moyen d'un microcalorimètre différentiel de type cellule. En plus de NaCl et NaBr, la plupart des sels homologues RNH_3Br ont été étudiés à partir de R = méthyle à R = *n*-octyle. Les mesures sur les deux sels simples sont en excellent accord avec les valeurs de la littérature.

Pour les bromohydrate de *n*-alcoylamine, les enthalpies de transfert à dilution infinie, ΔH_{tr}^0 ($H_2O \rightarrow D_2O$), sont surtout une mesure des interactions structurales entre les ions et le solvant et de la réaction d'échange.

$$RNH_3^+(D_2O) + 3D_2O \rightarrow RND_3^+(D_2O) + 3HDO$$

Jusqu'à R = *n*-propyle, les enthalpies apparentes molaires relatives de transfert, $\Delta\phi_L(H_2O \rightarrow D_2O) = \Delta H_{tr}^{EX}$, sont négatives, approximativement nulles pour le n-butyle et positives pour les autres. Ce changement graduel dans les enthalpies d'excès de transfert reflète l'importance croissante des interactions structurales entre les cations. Lors de l'association des cations, sous forme de micelles, il y a un accroissement rapide de $\Delta\phi_L(H_2O \rightarrow D_2O)$ indiquant la formation de liens hydrophobes.

Canadian Journal of Chemistry, **49**, 3460 (1971)

Introduction

Most properties of aqueous solutions reflect to some extent the structural changes of the solvent in the vicinity of the solute (1, 2). However, the contribution to the thermodynamic functions or excess thermodynamic functions, arising from changes in the hydrogen bond distribution in the water, are not easily separated from the more classical solute–solvent and solute–solute interactions. The H_2O/D_2O isotope effect has often been useful in this respect; because of the similarity in the dipole moment, dielectric constant, and variation of the dielectric constant with temperature of both liquids (3), first order solute–solvent and solute–solute interactions will be equal in both solvent system (4). On the other hand, because of the zero-point energy effect on the hydrogen bond, there is more structural order in D_2O than in H_2O (5). This structure is unstable and, as a result, any perturbation of the solvent structure will be more pronounced in D_2O than H_2O. Moreover, the isotopic effect on thermodynamic and transport properties, which are sensitive to structural effects, is generally larger at low temperature and pressure (6). Studies of conductance (7, 8), densities (9), and thermochemical properties (4, 10–15) show that structural changes caused by solutes are usually larger in D_2O.

The study of excess enthalpies of transfer requires very accurate heats of dilution in each solvent (11). However, it is now possible, using a differential microcalorimeter recently described (17), to measure directly the difference between heats of solution or heats of dilution in the two solvents. Thus, the transfer enthalpies and excess transfer enthalpies from H_2O to D_2O can be obtained with reasonably high accuracy.

The chosen system to initiate this study was the

Can. J. Chem. Downloaded from www.nrcresearchpress.com by 210.87.254.6 on 09/05/12
For personal use only.

homologous series *n*-alkylamine hydrobromides. Previous studies (13, 18–22) had shown that this model system was very informative in the study of hydrophobic interactions and bonding (micelle formation). Since the physical distance of closest approach between the ionic head and the counterion remains essentially constant, it is reasonable to assume that the variation in the excess functions as the chain length is increased will reflect mostly the interactions of the alkyl group with itself and with the anion. The study of the solvent isotope effect should confirm the previous propositions (19, 20) on the structural nature of these interactions.

Experimental

The heavy water (99.8%) was obtained from Stohler Isotope Chemicals and was used without further purification. The H_2O content was checked periodically by n.m.r. before and after use and was found to be within specifications. The water was doubly distilled from an alkaline permanganate solution. The alkylammonium salts were prepared and purified as previously described (19). Most manipulations were made in dry (Nalgen) plastic ware to minimize contamination of the D_2O with H_2O.

The twin-cell isothermal microcalorimeter has been described elsewhere (17); the cells used to measure differential heats of dilution were also described earlier (17) while those required for heats of solution measurements are detailed in Fig. 1. In the inverted position, the inner cell (*A*) is filled with salt and closed with a Teflon stopper (*D*) fixed to a rod (*E*). This inner cell is inserted in the main cell (*B*), which is partially filled with mercury. The outer compartment is then filled with the solvent and closed with a Teflon plug (*F*). Once the cells are fixed on the supports, the inner stopper (*D*) is lowered by means of the central rod (*E*). Mixing is prevented by the mercury which traps the salt in the inner cell. The calorimeter is then closed and evacuated; once equilibrium conditions are reached (~10 min), mixing is obtained by tipping the calorimeter.

To achieve true differentiation in the heat of solution measurements, the same weight of salt and the same number of moles of solvent were placed in each cell. The final concentrations were then at the same aquamolality (*m* mol of salt per 55.51 mol of solvent).

For differential measurements of heats of dilution, the salt solutions were prepared by weighing the salt in stoppered Nalgen bottles and then adding the calculated weight of D_2O or H_2O with a syringe. The weight of the concentrated solution and of the pure solvent were controlled so as to keep equal number of moles of salt and equal aquamolalities in both cells before and after the dilution.

Test Procedures

To verify the procedure for measurement of differential heats of solution, five experiments were performed with equal amounts of NaCl in H_2O in both cells, and, within experimental uncertainty, the resulting heat was negligible.

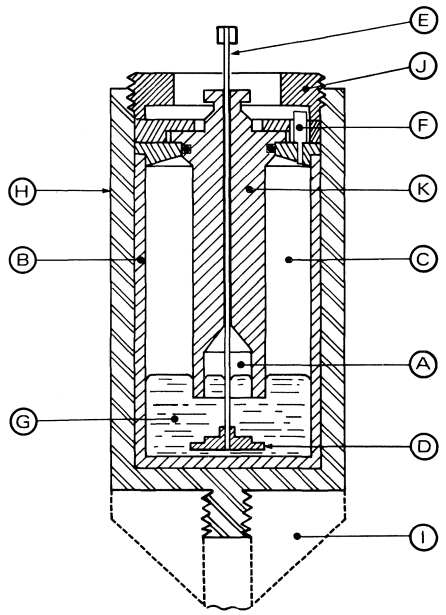

FIG. 1. Cell for heat of solution measurements: *A*, inner cell; *B*, Teflon main cell; *C*, outer compartment; *D*, Teflon inner stopper; *E*, stainless steel central rod; *F*, Teflon plug; *G*, mercury seal; *H*, copper outer cell; *I*, copper cell support; *J*, nylon ring; *K*, removable assembly.

As a test for differential measurements of excess enthalpies, the difference in the heats of dilution of NaCl and KCl in water from 1 to 0.5 *m* were measured. The average of four experiments gave $\Delta\phi_{L(KCl)}^{0.5 \rightarrow 1.0\ m} - \Delta\phi_{L(NaCl)}^{0.5 \rightarrow 1.0\ m}$ equal to 6.68 ± 0.10 cal mol^{-1} which can be compared with 8 ± 2 cal mol^{-1} obtained from Parker's data (23).

Results

The enthalpies of transfer from water to heavy water, $\Delta H_{tr}(H_2O \rightarrow D_2O)$, are derived directly from the difference in the integral heats of solution,

$$[1] \quad \Delta H_{tr}(H_2O \rightarrow D_2O) = \Delta H_{IS}(D_2O) - \Delta H_{IS}(H_2O)$$

which is also equal to the measured heat divided by the total number of moles of solute. The standard enthalpy of transfer, $\Delta H_{tr}^0(H_2O \rightarrow D_2O)$, is obtained by correcting ΔH_{tr} for the difference in the integral heats of dilution to zero concentration.

Wood *et al.* (11) have shown that the excess enthalpies of transfer are often a quadratic function of the aquamolality. Therefore, defining the transfer function from H_2O to D_2O, the excess

TABLE 1. Parameters k_1 and k_2 of eq. 2 for the excess enthalpies of transfer of NaCl and NaBr from H_2O to D_2O at 25 °C*

	k_1		k_2	
Salt	This work	Reference 11	This work	Reference 11
NaCl	−51.4	53.6	7.7	−7.1
NaBr	−50.0	51.3	7.2	−7.1

*The units of k_1 and k_2 refer to heats in calories and to concentrations in number of moles of solute per 55.51 moles of solvent.

enthalpy of transfer, ΔH_{tr}^{EX}, is given by the difference between the relative apparent molal enthalpy of the solute in D_2O and H_2O, *i.e.*

$$[2] \quad \Delta H_{tr}^{EX} = \Delta\phi_L(H_2O \rightarrow D_2O) = k_1 m + k_2 m^2$$

where m is the aquamolality. ΔH_{tr}^{EX} is therefore an integral and not a differential heat. For a given dilution experiment between the initial and final aquamolalities, m_i and m_f, the difference in the integral heats of dilution is given by the experimental heat q divided by the number of moles of salt, *i.e.*

$$[3] \quad \Delta H = (q/n)\left\{\begin{matrix} H_2O \rightarrow D_2O \\ m_i \rightarrow m_f \end{matrix}\right\} = \Delta\phi_L(m_f) - \Delta\phi_L(m_i) = k_1(m_f - m_i) + k_2(m_f^2 - m_i^2)$$

Dividing both sides by $m_f - m_i$,

$$[4] \quad \Delta H/(m_f - m_i) = k_1 + k_2(m_f + m_i)$$

Then by plotting the left-hand side of eq. 4 against $m_f + m_i$, the two constants k_1 and k_2 are obtained as the intercept and slope, respectively.

As a further test, the enthalpies of transfer and excess enthalpies of transfer of NaCl and NaBr were measured at 25 °C. The constants k_1 and k_2 derived from the data below 3 m are given in Table 1. All heats are expressed in absolute calories (4.184 J). The constants k_1 and k_2 are well within the uncertainty of Wood's data (11). Our constants have signs opposite to those of Wood since he defines the transfer process from D_2O to H_2O.

The enthalpies of transfer, corrected to the standard state of infinite dilution with the excess enthalpies of transfer, are given in Table 2. The agreement with the data of Davies and Benson (24) and Lange and Martin (25, 26) is such that we do not expect our data to be in error by more than a few cal mol^{-1}. From the present work, the difference $\Delta H_{tr}^0(Br^-) - \Delta H_{tr}^0(Cl^-)$ is 102 ± 3 cal mol^{-1}; this value should be preferred to the value 135 suggested by Arnett and McKelvey (16).

TABLE 2. Enthalpies of transfer of NaCl and NaBr from H_2O to D_2O at 25 °C

Solute	m_i	ΔH_{tr} (cal mol^{-1})	ΔH_{tr}^0 (cal mol^{-1})
NaCl	0.5000	525	549
	0.5000	521	545
	0.5000	524*	548
			Ave. 547†
NaBr	0.4085	629	648
	0.2380	639	650
			Ave. 649‡

*Reference 24: 524 at 0.5 m.
†Reference 25: 510; ref. 26: 560.
‡Reference 25: 650.

The actual uncertainties in ΔH_{tr}^0 and ΔH_{tr}^{EX} depend to a large extent on the magnitude of the heats of solution or dilution in each solvent. With the systems in the present study, we believe ΔH_{tr}^0 within 1 or 2 cal mol^{-1}, while ΔH_{tr}^{EX} should be reliable to 0.2 cal mol^{-1}.

The differences in integral heats of dilution ΔH of the homologous salts *n*-alkylamine hydrobromides are given in Table 3. From these data, $\Delta H/(m_f - m_i)$ were calculated and plotted against $m_f + m_i$ in Fig. 2. The large variation of the differential heats of dilution of *n*-octylamine hydrobromide at low concentrations makes the extrapolation very difficult. However, a plot of k_1 *vs.* the number of carbon atoms, n, in the chain is linear for n equals 3 to 6 (Fig. 3). Therefore, it is possible to obtain k_1 of the *n*-octyl salt by extrapolation in Fig. 3.

The derived parameters k_1 and k_2 and the limit of applicability of eq. 2 for ΔH_{tr}^{EX} of *n*-alkylamine hydrobromides are given in Table 4. The enthalpies of transfer ΔH_{tr} of most of these salts are given in Table 5 along with the values corrected to infinite dilution ΔH_{tr}^0.

These standard enthalpies of transfer can be compared with the data of Krishnan and Friedman (13) on the *n*-alkylamine hydrochlorides. The difference between the bromides and the chlorides varies between 80 to 90 cal mol^{-1} while the difference between NaBr and NaCl was 102

Can. J. Chem. Downloaded from www.nrcresearchpress.com by 210.87.254.6 on 09/05/12
For personal use only.

TABLE 3. Differences in heats of dilution from H_2O to D_2O of the *n*-alkylamine hydrobromides at 25 °C

Salt	m_i	m_f	ΔH^*	Salt	m_i	m_f	ΔH^*
$MeNH_3Br$	3.000†	1.500	39.9	*n*-$HexNH_3Br$	3.000	1.500	−5.40
			40.0				−5.51
			40.2				−5.76
			40.0				−5.55
	2.000	1.000	31.7		2.000	1.000	−28.9
			31.5				−29.0
			31.4				−28.8
			31.5				−28.9
	1.000	0.500	18.4		1.000	0.500	−29.3
			18.3				−29.0
			18.6				−29.1
			18.4				−29.1
$EtNH_3Br$	3.000	1.500	20.8		0.500	0.250	−11.1
			20.9				−11.0
			20.8				−10.9
			20.8				−11.0
	2.000	1.000	16.7		0.200	0.100	−2.37
			16.6				−2.24
			16.5				−1.98
			16.6				−2.19
	1.000	0.500	9.90	*n*-$PrNH_3Br$	3.000	1.500	9.10
			9.65				9.20
			9.75				9.25
			9.73				9.18
n-$OctNH_3Br$	1.000	0.500	−23.8		2.000	1.000	5.70
			−23.5				5.85
			−23.6				5.90
			−23.6				5.81
	0.500	0.250	−54.3		1.500	0.750	5.38
			−54.3				5.40
			−54.7				5.33
			−54.4				5.37
	0.300	0.150	−58.3		1.000	0.500	4.55
			−58.0				4.51
			−58.1				4.68
			−58.1				4.58
	0.200	0.100	−14.0	*n*-$BuNH_3Br$	3.000	1.500	−7.20
			−13.8				−7.08
			−14.1				−7.14
			−13.9				
	0.200	0.080	−15.8		2.000	1.000	−0.87
			−15.6				−1.08
			−15.7				−0.98
	0.150	0.075	−6.80		1.000	0.500	1.14
			−6.47				1.08
			−6.43				1.11
			−6.56		0.500	0.250	0.87
							1.17
							1.02

*ΔH is defined by eq. 3, in cal mol^{-1}.
†Actual experimental concentrations.

Can. J. Chem. Downloaded from www.nrcresearchpress.com by 210.87.254.6 on 09/05/12
For personal use only.

Can. J. Chem. Downloaded from www.nrcresearchpress.com by 210.87.254.6 on 09/05/12
For personal use only.

TABLE 4. Parameters k_1 and k_2 of eq. 2 for the *n*-alkylamine hydrobromides at 25 °C*

Salt	k_1	k_2	Maximum concentration aquamolality
$MeNH_3Br$	−42.0	3.30	3
$EtNH_3Br$	−21.6	1.80	3
n-$PrNH_3Br$	−12.0	2.00	2
n-$BuNH_3Br$	−4.80	1.80	2
n-$HexNH_3Br$	12.0	51.5	0.5
n-$OctNH_3Br$	(29.2)	(260)	—

*Values in parentheses are extrapolated values.

TABLE 5. Enthalpies of transfer from H_2O to D_2O of some *n*-alkylamines hydrobromides at 25 °C

Salt	m_f	$\Delta H_{tr}(H_2O \rightarrow D_2O)$ (cal mol^{-1})	$\Delta H_{tr}^0(H_2O \rightarrow D_2O)$* (cal mol^{-1})
$MeNH_3Br$	0.8804	30	64
		32	66 (82)
n-$PrNH_3Br$	0.4938	−31	−26
		−32	−27 (−8)
n-$BuNH_3Br$	.1603	−68	−67 (−58)
	.1769	−66	−65
n-$OctNH_3Br$	0.1233	−207	−214
		−207	−214 (−188)

*Numbers in parentheses are values of Krishnan and Friedman (13) corrected for the Br–Cl difference of 102 taken from Table 2.

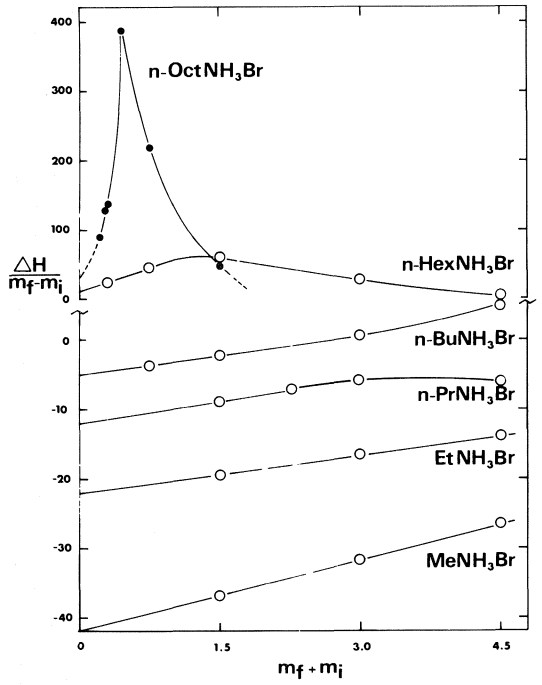

FIG. 2. Evaluation of the parameters k_1 and k_2 of eq. 2 for the excess enthalpies of transfer of *n*-alkylamine hydrobromides from H_2O to D_2O at 25 °C.

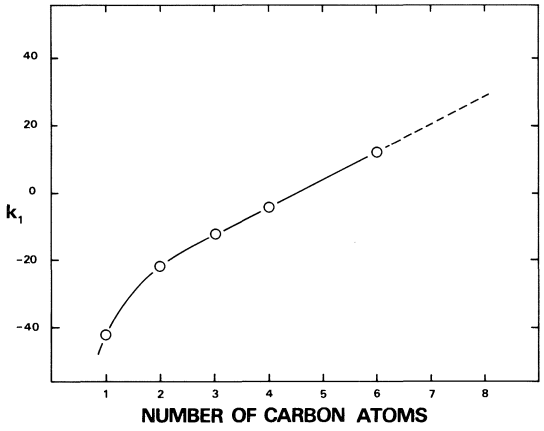

FIG. 3. Variation of k_1 with chain length.

cal mol^{-1}. This agreement is excellent in view of the uncertainty of 30 cal mol^{-1} quoted by Krishnan and Friedman.

Discussion

It is possible to interpret the data on ΔH_{tr}^0 and ΔH_{tr}^{EX} through structural changes affecting both the solute–solvent and solute–solute interactions. However, this interpretation is meaningful only if the assumptions made are clearly stated. For the

Can. J. Chem. Downloaded from www.nrcresearchpress.com by 210.87.254.6 on 09/05/12
For personal use only.

enthalpy of transfer from H_2O to D_2O, three basic assumptions are required.

(1) Water is a structured liquid and the presence of solutes will increase or decrease its structure. Knowledge of the exact nature of the water structure is not required for the present purpose; only shifts in the hydrogen bond distribution or changes in the number of bonded and unbonded species are needed.

(2) D_2O is more structured than H_2O and its structure is more sensitive to any perturbation (T, P or solutes). For interpretation of thermodynamic properties, it is immaterial if the number of bonds is larger or if the bonds are stronger in D_2O. The important point is that structural changes are more important in D_2O and that the isotope effect decreases with increasing temperature (4–7).

(3) The H_2O/D_2O transfer functions mostly reflect structural changes. This assumption is reasonable in view of the similarity in the dielectric constant, variation in the dielectric constant with temperature and dipole moment, and since differences between H_2O and D_2O are largest in those properties which are most sensitive to slight structural differences (6). Evidence for the correctness of this assumption is also obtained from a comparison with transfer functions in other systems such as propylene carbonate → water and dimethylsulfoxide → water (13).

These assumptions are sufficient to interpret thermodynamic transfer functions such as ΔH_{tr}^0, ΔS_{tr}^0, and ΔV_{tr}^0, but with properties such as heat capacities, which depend on the second derivative of the chemical potential with respect to temperature, further assumptions must be made regarding the variation of the strength of the hydrogen bonds with respect to temperature and pressure (27, 28).

The structural changes caused by a solute molecule can best be represented by an imaginary co-sphere, as suggested by Gurney (29), and the concentration effect as an overlap of these co-spheres. The larger structural change in D_2O solutions can be symbolized by a larger co-sphere. In the framework of assumptions *1–3*, the signs of the three functions, enthalpy, entropy, and volume, are easily predicted by assuming that some ice has melted in the co-sphere of structure breakers and that some water has frozen near structure makers (assumption *1*). From assumption *3*, it is clear that the transfer functions from H_2O to D_2O always have the same sign as the structural change in either co-sphere. Therefore ΔH_{tr}^0 should be positive for structure breakers and negative for structure makers. Structure maker is used here exclusively in the sense of hydrophobic ions and not hydrophilic ions such as F^-, Li^+, and Na^+. In most cases where sufficiently reliable data exists in the literature, the above predictions are verified: *e.g.* enthalpies and entropies (16) and volumes (9).

With the alkylamine hydrobromides, the standard enthalpies of transfer ΔH_{tr}^0 always include the exchange reaction

[4] $RNH_3^+(D_2O) + 3D_2O \rightarrow RND_3^+(D_2O) + 3HDO$

and there is no simple way of measuring this heat separately. If the deuterate ammonium salt was used for the heat of solution in D_2O, the exchange reaction would not be involved, but the reference state (pure solid) would not cancel out since both salts would be different. Krishnan and Friedman (13), by comparing their results for RNH_3^+ with R_4N^+, have estimated this heat to be -50 cal mol^{-1}. Correcting our results for this exchange heat would indicate that the three lower members of the series are net structure breakers (positive ΔH_{tr}^0), *n*-octylamine hydrobromide is a net structure maker (negative ΔH_{tr}^0), and *n*-butylamine hydrobromide is a weak structure maker.

While it is sufficient to consider two types of interactions when discussing properties at infinite dilution, a minimum of four different structural interactions are required when excess functions are considered (30). Such a model was suggested earlier (30) from an examination of the concentration dependence of the thermodynamic functions ($\bar{G}$, $\bar{H}$, $\bar{S}$, and $\bar{V}$) of electrolytes in aqueous solution. The qualitative description arrived at can also be applied to excess transfer functions. Since solvent structural modifications are larger in D_2O than in H_2O (assumption *2*), their contribution to excess thermodynamic functions can also be expected to be larger. Schematically, this can be represented as a larger overlap of co-spheres. Therefore, if the transfer is defined from H_2O to D_2O, the sign of the excess transfer function will be the same as that of the structural contribution to the total excess function in either solvent. By analogy with the model previously described (30), the predicted signs of ΔH_{tr}^{EX}, ΔS_{tr}^{EX}, and ΔV_{tr}^{EX} for interactions between different solutes can be summarized as follows:

Nature of interaction	ΔH_{tr}^{EX}	ΔS_{tr}^{EX}	ΔV_{tr}^{EX}
(1) hydrophobic–hydrophobic	+	+	−
(2) hydrophobic–hydrophilic	+	+	−
(3) hydrophilic–hydrophilic (same sign)	+	+	−
(4) hydrophilic–hydrophilic (opposite sign)	−	−	+

Because of the accuracy required and the limited data available in the literature, this extension of the original model cannot be verified thoroughly. Still the heats of dilution of Wood *et al.* (11) and of Snell and Greyson (15, 31) and the apparent molal volume of Conway and Laliberté (9) are in agreement with the model.

The present excess transfer data on *n*-alkylamine hydrobromides are now readily explained. This is best seen by plotting ΔH_{tr}^{EX} against the aquamolality (Fig. 4). The low concentration enthalpies were calculated directly from the constants k_1 and k_2, while, at the higher concentrations, ΔH_{tr}^{EX} were obtained directly from the experimental data (Table 3). For the three first members of the series, ΔH_{tr}^{EX} is negative indicating that the predominant structural interaction is the one between the $-NH_3^+$ group and the Br^- ion. As the chain length increases this interaction remains essentially constant, but the interaction involving the hydrophobic R-groups steadily increases. With *n*-$BuNH_3Br$, it seems that all interactions nearly cancel out, but with the higher members, hydrophobic interactions prevail. Hydrophobic–hydrophobic and hydrophobic–hydrophilic interactions both exist, but the former certainly predominates with *n*-octylamine hydrobromide, since the rapid increase in

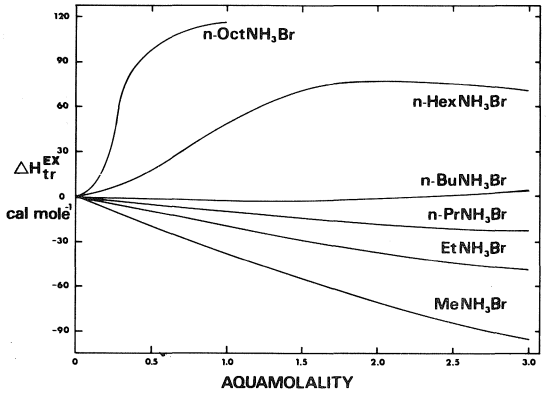

FIG. 4. Excess enthalpies of *n*-alkylamine hydrobromides from H_2O to D_2O at 25 °C.

ΔH_{tr}^{EX} corresponds to the region where micelles are formed (19, 20). Even if we consider micelle formation as a limiting case of hydrophobic interactions, some distinction between these situations may be expected from the shape of the concentration dependence. Hydrophobic interactions depend on the extent of co-sphere overlap and, as a first approximation, are linear in concentration (4); on the other hand, association or aggregation may often vary differently with concentration, as in the case of *n*-octylamine and *n*-hexylamine hydrobromides. Therefore a sharp increase in ΔH_{tr}^{EX} at some concentration is probably always related to hydrophobic bonding.

The concentration dependence of ΔH_{tr}^{EX} of the RNH_3Br salt is similar to the deviation from the Debye–Hückel theory of the relative apparent molal enthalpies (32), which confirms the above statement that the transfer excess functions have the same sign as the structural interactions in either liquid.

The present results are in excellent agreement with those of Snell and Greyson (15) on ΔH_{tr}^{EX} of the sodium salts of carboxilic acids. As in the present case, ΔH_{tr}^{EX} are negative for chain lengths up to sodium isobutyrate and positive from there on. They have suggested that the sign of ΔH_{tr}^{EX} should always be opposite that of ΔH_{tr}^{0}. If this is correct, a salt which has no net ΔH_{tr}^{0} should also have no excess transfer function. If ΔH_{tr}^{0} of RNH_3Br were plotted against k_1 (not shown), ΔH_{tr}^{0} would be equal to -70 cal mol^{-1} when $k_1 = 0$, and this would then be the heat of the exchange reaction (eq. 4). This value is of the same order of magnitude as that evaluated by Krishnan and Friedman (13). However, we should bear in mind that, with RNH_3Br salts, it is incorrect to say that one particular salt has no structural influence on the solvent. In actual fact, the amount of structure broken by the $-NH_3^+$ group and Br^- ion just balances out the increase in structure near the R-group. It is not at all obvious that similar cancellations would also affect the solute–solute structural interactions. Therefore, this analogy can at best be taken as an indication that the heat of the exchange reaction (eq. 4) is of the order of -50 to -70 cal mol^{-1}.

In the above discussion it was implied that the exchange reaction had no effect on ΔH_{tr}^{EX}. This would be true if the exchange was complete at all concentrations and if the heat of the exchange reaction was not concentration dependent.

Can. J. Chem. Downloaded from www.nrcresearchpress.com by 210.87.254.6 on 09/05/12
For personal use only.

Neither assumptions are probably correct. Therefore, the concentration dependences of the true ΔH_{tr}^{EX} should all be more negative by a small but unknown amount.

Structural interactions offer a simple explanation for solvent isotope effects in aqueous solutions. However, it should be noted that some data in the literature cannot be readily interpreted. The ΔH_{tr}^{0} of halide ions vary differently with their size than the alkali metal ions (12), F^- appears as a structure maker while divalent cations are structure breakers (31). This probably reflects the zero-point energy difference between the $F^- \cdots$ HOH and the $F^- \cdots$ DOD interactions, obscuring structural effects beyond the first coordination shell of the ions. However, it is quite possible that, in other transfer properties, the structural changes in the solvent and the solute–water interactions (or hydrogen bond distribution) will have different relative contributions. Further work on $H_2O \rightarrow D_2O$ transfer are therefore desirable, particularly with different sensitive properties such as expansitivities, compressibilities and heat capacities. The latter should also provide critical tests of the qualitative picture used presently to interpret the heat measurements.

Grateful acknowledgement is made to the Defence Research Board of Canada for financial support of this project.

1. J. E. Desnoyers and C. Jolicoeur. Modern aspects of electrochemistry. Vol. 5. *Edited by* J. O'M. Bockris and B. E. Conway. Plenum Press, New York. 1969. p. 1.
2. M. J. Blandamer. Q. Rev. London, **24**, 169 (1970).
3. C. A. Vidulich, D. F. Evans, and R. L. Kay. J. Phys. Chem. **71**, 656 (1967).
4. Y. C. Wu and H. L. Friedman. J. Phys. Chem. **70**, 166 (1966).
5. C. G. Swain and R. F. W. Bader. Tetrahedron, **10**, 183 (1960).
6. G. Némethy and H. A. Scheraga. J. Chem. Phys. **41**, 680 (1964).
7. R. L. Kay and D. F. Evans. J. Phys. Chem. **69**, 4216 (1965).
8. R. L. Kay. Adv. Chem. Ser. **73**, 1 (1968).
9. B. E. Conway and L. H. Laliberté. Trans. Faraday Soc. **66**, 3032 (1970).
10. G. C. Kresheck, H. Schneider, and H. A. Scheraga. J. Phys. Chem. **69**, 3132 (1965). G. C. Kresheck. J. Chem. Phys. **52**, 5966 (1970).
11. R. H. Wood, R. A. Rooney, and J. N. Braddock. J. Phys. Chem. **73**, 1673 (1969).
12. C. V. Krishnan and H. L. Friedman. J. Phys. Chem. **74**, 2356 (1970).
13. C. V. Krishnan and H. L. Friedman. J. Phys. Chem. **74**, 3900 (1970).
14. J. Greyson. J. Phys. Chem. **73**, 2210 (1969).
15. H. Snell and J. Greyson. J. Phys. Chem. **74**, 2148 (1970).
16. E. M. Arnett and D. R. McKelvey. *In* Solute–solvent interactions. *Edited by* J. F. Coetzee and C. D. Ritchie. M. Dekker. 1969.
17. P. Picker, C. Jolicoeur, and J. E. Desnoyers. Rev. Scient. Instrum. **39**, 676 (1968).
18. J. E. Desnoyers, G. E. Pelletier, and C. Jolicoeur. Can. J. Chem. **43**, 3232 (1965).
19. J. E. Desnoyers and M. Arel. Can. J. Chem. **45**, 359 (1967).
20. J. E. Desnoyers, M. Arel, and P. A. Leduc. Can. J. Chem. **47**, 547 (1969).
21. B. Lindman, H. Wennerström, and S. Forsen. J. Phys. Chem. **74**, 754 (1970).
22. C. Jolicoeur and H. L. Friedman. Ber. Bunsenges. Phys. Chem. **75**, 248 (1971).
23. V. B. Parker. Natl. Std. Ref. Data Ser. Natl. Bur. Std. 1965. No. 2.
24. D. H. Davies and C. G. Benson. Can. J. Chem. **43**, 3100 (1965).
25. H. E. Lange and W. Martin. Z. Elektrochem. **42**, 662 (1936).
26. H. E. Lange and W. Martin. Z. Phys. Chem. Leipzig, **A180**, 233 (1937).
27. A. Ben-Naim. Trans. Faraday Soc. **66**, 2749 (1970).
28. P. R. Philip and J. E. Desnoyers. To be published.
29. R. W. Gurney. Ionic processes in solution. McGraw-Hill, New York, 1953.
30. J. E. Desnoyers, M. Arel, G. Perron, and C. Jolicoeur. J. Phys. Chem. **73**, 3346 (1969).
31. J. Greyson and H. Snell. J. Phys. Chem. **73**, 4423 (1969).
32. J. E. Desnoyers, P. A. Leduc, J. L. Fortier, and P. Picker. To be published.

Can. J. Chem. Downloaded from www.nrcresearchpress.com by 210.87.254.6 on 09/05/12
For personal use only.

Can. J. Chem. Downloaded from www.nrcresearchpress.com by 210.87.254.5 on 09/05/12
For personal use only.

The Effect of *N*-Substitution on the Rates of Saponification of Some Amino Acid Esters[1]

JOCELYN E. PURDIE AND N. LEO BENOITON[2]
Department of Biochemistry, University of Ottawa, Ottawa, Canada

Received May 25, 1971

The saponification rates (measured at 25° by a titrimetric method) of the unprotonated forms of the methyl esters of glycine, alanine, leucine, valine, and phenylalanine were compared with those of the *N*-methyl, the *N*-acetyl, and the *N*-acetyl,*N*-methylamino acid analogues. *N*-Acetylation slightly increased or decreased the rate but *N*-methylation caused a reduction by as much as a factor of ten, depending on the complexity of the side-chain. The esters of the *N*-acetyl,*N*-methylamino acids, which exist as *cis* and *trans* isomers, were saponified at rates intermediate between those of the esters of the *N*-acetylamino acids and *N*-methylamino acids. Activation parameters were obtained for the phenylalanine and leucine derivatives. *N*-Methylation resulted in an increase in $\Delta H^{\ddagger}$ and $\Delta S^{\ddagger}$ which was attributed in part to solvation effects. The hydrolysis of the cationic esters of glycine and alanine was still evident at p*H* 11.0. *N*-Methylation had little effect on the rates of saponification of the charged forms.

On a comparé les vitesses de saponification (mesurées à 25° au moyen d'une méthode titrimétrique) des formes non-protonées des esters méthyliques des acides aminés tel que la glycine, l'alanine, la leucine, la valine, et la phénylalanine avec celles obtenues en utilisant les analogues *N*-méthyle, *N*-acétyle et *N*-méthyle,*N*-acétyle des mêmes acides aminés. On constate une légère augmentation ou diminution de la vitesse dans le cas de la *N*-acétylation, mais la *N*-méthylation occasionne une réduction de cette vitesse par un facteur allant jusqu'à dix, dépendant de la complexité de la chaîne latérale. Les esters de la forme *N*-acétyle,*N*-méthyle des acides aminés, qui sont des isomères *cis* et *trans*, ont été saponifiés à des vitesses intermédiaires entre celles obtenues pour les dérivés *N*-acétyle et *N*-méthyle des acides aminés. On a calculé les paramètres d'activation pour les dérivés de la phénylalanine et de la leucine. La *N*-méthylation a causé une augmentation du $\Delta H^{\ddagger}$ et du $\Delta S^{\ddagger}$, ce qu'on attribue en partie aux effets de solvation. L'hydrolyse des esters cationiques de la glycine et de l'alanine était encore évidente à p*H* 11.0. On remarque peu d'effet causé par la *N*-méthylation sur les vitesses de saponification des formes chargées.

Canadian Journal of Chemistry, **49**, 3468 (1971)

Introduction

Amino acid esters and their *N*-acylated derivatives are widely used as enzyme substrates and in peptide synthesis. *N*-Methylamino acids occur in peptides of bacterial origin. The chemical synthesis of peptides of *N*-methylamino acids presents problems due to 'steric hindrance' and a marked tendency of the dipeptides to cyclize (1). We have recently devised a new method for the synthesis of *N*-methylamino acid derivatives (2). During the course of this work, difficulties were encountered with the saponification of esters. From this arose the present study which is concerned with the effect of *N*-substitution on the rates of saponification of amino acid esters with side-chains of graduated complexity.

Experimental

The amino acid and sarcosine methyl esters were the hydrochlorides obtained from the amino acids (General Biochemicals) using hydrogen chloride/methanol. The *N*-methylamino acid methyl esters were the hydrobromides already described (2). *N*-Acetylamino acid esters were prepared from the *N*-acetylamino acids (Nutritional Biochemicals) using diazomethane (3). All were crystalline except for alanine which was an oil. The *N*-acetyl,*N*-methylamino acid methyl esters were prepared from the *N*-acetylamino acids using sodium hydride/methyl iodide as previously described (2) except for the following modifications. After the work-up, the methylation was repeated and the products were purified by distillation at 80°/5 mm for alanine, 98°/1.2 mm for leucine, and 95°/1.8 mm for valine. In addition, for alanine, because of the solubility of the derivative in water, the reaction mixture was not washed with water at any time. The products showed no i.r. absorbance at 1521 and 3280 cm^{-1} (2).

Ester hydrolysis was followed titrimetrically in thermostatted reaction vessels using a Radiometer p*H*-stat type PHM 26c/TT11a/SBUI/SBR2/TTA3 as described previously (4) except that a special slow delivery tube was used (Radiometer). The titrant was 0.1 *N* NaOH standardized with potassium hydrogen phthalate. The syringe was calibrated by weighing the water delivered for various distances of piston travel. The electrodes were glass, type G202B and calomel, type K401. The system was standardized before, after, and once during a day's run with the primary standard buffers borate p*H* 9.18 at 25° and phthalate p*H* 4.01 at 25°. The iso p*H* adjustment together

[1]Supported by a grant from the Medical Research Council of Canada.

[2]Associate of the Medical Research Council of Canada.

Can. J. Chem. Downloaded from www.nrcresearchpress.com by 210.87.254.5 on 09/05/12
For personal use only.

with the calibrated adjustment for electrode sensitivity were used to compensate for the fact that the electrode sensitivity is less than 100%. When the electrode sensitivity had decreased below 98% or the response time had noticeably increased, the electrode was discarded. For temperatures above 25°, the electrodes were kept continuously at the experimental temperature to avoid any drifting caused by hysteresis of the calomel electrode. All solutions and rinsing water were likewise kept at the experimental temperature.

Solutions were prepared and kept under nitrogen and titrations were carried out under a stream of nitrogen saturated with water. Solutions (~2.5 mM) of esters were made up in 0.1 M NaCl just before use. *N*-Acetyl,*N*-methyl-DL-valine methyl ester and the leucine analogue presented solubility problems, the solutions showing the Tyndall effect.

The apparent pK' for the dissociation of an amino acid or its ester is defined by the following equation:

$$RNH_3^+ \rightleftharpoons RNH_2 + H^+$$

$$K' = a_{H^+} \frac{[RNH_2]}{[RNH_3^+]}$$

The pK's were determined in 0.1 M NaCl by applying the Henderson–Hasselbalch equation to various points on the corrected titration curve. If the pK values obtained at various degrees of neutralization varied by more than 0.01 units the data were not used.

For following the rate of saponification 20 ml of ester solution were quickly brought to the required pH by manual addition of 0.1 N NaOH and the subsequent uptake of alkali due to hydrolysis was recorded on the SBR2 recorder as a function of time. The increase in volume of the reaction mixture during a run was about 0.5 ml. Above pH 11.0, it was necessary to correct for this; the additional alkali consumed to titrate this water was found from solvent titration curves. At 25° runs were not made at pH > 11.25. At higher pH's stronger titrant is required and hence more concentrated ester solutions are necessary thus introducing the risk of diketopiperazine formation. Also the electrode system is less stable at higher pH especially in runs of long duration. At 40 and 55° the buffering of the solvent was evident at lower pH's because the pK_w of water decreases.

For the first order log plots the observed rates were corrected for the ionization of the amino acid produced (correction for ester ionization was not necessary at pH > 10) using the apparent pK. The following expression was used:

$$2.303 \log_{10} \left[\frac{V_\infty}{V_\infty - V_{t_{corr}} f} \right] = k_{obs} t$$

where V_∞ = NaOH equivalent of ester
$V_{t_{corr}}$ = volume of NaOH added at time t and corrected for increase in volume of reaction mixture;
f = [1 + antilog (pK' − pH)]

For fast runs such as with *N*-acetylglycine methyl ester, Guggenheim plots (5) were used as this avoided the initial time error (and hence the error in V_t). pK' was not needed for this treatment, but as the reaction must be followed for more than two half-lives, this introduced errors due to 'drifting' in slow reactions. In such cases, log plots tended to be concave upwards and the V_∞ calculated from a Guggenheim plot was larger than expected from the initial ester concentration. Thus, where possible, both types of plots were made and the results discarded if the derived rate constants did not agree within an acceptable limit.

The concentration of hydroxide ions in the reaction mixture was determined from the pH and a curve of pH *vs.* concentration of NaOH, constructed from the titration of solvent (0.1 M NaCl) at the experimental temperature. The first order constant was divided by the concentration of alkali to give the second order constant k_2* on a concentration basis. $\Delta H^\ddagger$ and $\Delta S^\ddagger$ were calculated from the transition state theory equation

$$k_2^* = \frac{kT}{h} e^{\Delta S^\ddagger/R} e^{-\Delta H^\ddagger/RT}$$

A plot of $\log_{10} [k_2^*/T]$ *vs.* $[1/T]$ was linear for each ester but $\Delta H^\ddagger$ was obtained by using the k_2* values in three combinations, evaluating the error on each from the error in the k_2* values. A weighted mean value of $\Delta H^\ddagger$ was then calculated and this was used to obtain a value of $\Delta S^\ddagger$ at each temperature and its weighted mean was evaluated.

Results

The apparent or 'mixed' pK's of the amino acids and their esters are shown in Table 1. These are not thermodynamic quantities and were used on an empirical basis for correcting the observed titrimetric rates.

In the saponification mixtures the initial ester concentration was about 2.5 mM. This was considered a reasonable compromise between the sensitivity of the titrimetric method and the hazard of diketopiperazine formation. The latter is necessarily a bimolecular process so it was hoped that at 2.5 mM ester the reaction with hydroxide ion would predominate. Only leucine, *N*-methylleucine, and their methyl esters were detected by t.l.c. of partial hydrolysates. However, *N*-methylated diketopiperazines are difficult to detect. After saponification of *N*-methylalanine methyl ester at pH 11.0 and immediate neutralization, the hydrolysate gave only the titration curve of the amino group of an equivalent amount of *N*-methylalanine. Furthermore, consistent deviation from first order kinetics was not detected for any ester. Glycine (up to 2.5 mM) had no effect on the rate of alkali consumption in the hydrolysis of glycine methyl ester at pH 11.0. Thus we concluded that saponification of the ester was the only significant reaction occurring.

The results at 25° are shown in Table 2. For the unsubstituted esters the order of reactivities was that found by Hay *et al.* (6–8). *N*-Acetylation had

TABLE 1. Apparent pK's of amino acid derivatives

Compound[a]	pK'[b] 25°	40°	55°
L-Phenylalanine	9.180	8.91±0.01	8.565
N-Methyl-L-phenylalanine	9.315	9.06±0.01	8.832
L-Phenylalanine methyl ester	7.150		
N-Methyl-L-phenylalanine methyl ester	7.150		
L-Leucine	9.691	9.39±0.01	9.019
N-Methyl-L-leucine	9.746		
L-Leucine methyl ester	7.663		
N-Methyl-L-leucine methyl ester	7.737		
L-Valine	9.670		
L-Valine methyl ester	7.632		
N-Methyl-L-valine methyl ester	7.715		
L-Alanine	9.872		
N-Methyl-L-alanine	10.04		
DL-Alanine methyl ester	7.896		
N-Methyl-L-alanine methyl ester	8.000		
Glycine	9.700		
Sarcosine	10.131		
Glycine methyl ester	7.704		

[a]2.2–2.4 mM in 0.1 M NaCl.
[b]Average of 4–8 determinations with standard deviation ±0.005, except where otherwise indicated.

TABLE 2. Saponification of methyl esters of amino acids and their *N*-substituted derivatives at 25.0°[a]

Amino acid	*N*-Substituent	pH	k_2* (M^{-1} s^{-1})	
Glycine	—	11.200	1.11±0.02	(21)[b]
		10.830	1.135	
		10.500	1.185	
	—$COCH_3$	10–11	1.72±0.07	(9)
	—CH_3	11.0	~0.7	(3)
Alanine	—	11.200	1.04±0.015	(16)
		10.700	1.12	
		10.600	1.16	
		10.500	1.19	
	—$COCH_3$	10.3–11.0	0.94±0.02	(13)
	—CH_3	11.230	0.245	(6)
		11.009	0.279	(4)
		10.802	0.328	(2)
		10.616	0.391	(2)
		10.528	0.420	(2)
	—CH_3, —$COCH_3$	10.8–11.0	0.455±0.03	(4)
Leucine	—	11.200	0.45±0.005	(6)
	—$COCH_3$	10–11	0.43±0.02	(15)
	—CH_3	11.0–11.2	0.045±0.04	(4)
	—CH_3, —$COCH_3$	11.0–11.1	0.255±0.01	(4)
Valine	—	11.230	0.078±0.005	(6)
	—$COCH_3$	10.9–11.2	0.096±0.005	(7)
	—CH_3, —$COCH_3$	11.1–11.2	~0.055	(2)
Phenylalanine	—	10.6–11.1	0.60±0.02	(9)
	—$COCH_3$	10.5–11.1	1.075±0.02	(13)
	—CH_3	11.1–11.2	0.055±0.002	(4)

[a]In 0.1 M NaCl.
[b]Number of determinations.

Can. J. Chem. Downloaded from www.nrcresearchpress.com by 210.87.254.5 on 09/05/12
For personal use only.

Can. J. Chem. Downloaded from www.nrcresearchpress.com by 210.87.254.5 on 09/05/12
For personal use only.

little effect on the rate for alanine and leucine, a slight enhancement for valine, and a marked increase for glycine and phenylalanine. In contrast, *N*-methylation reduced the rate by an order of magnitude for phenylalanine and leucine and by a factor of five for alanine; the reduction for glycine was less again but as sarcosine methyl ester was never obtained free of amino acid it was not subjected to more detailed studies. Somewhat unexpectedly the rates for the esters of *N*-acetyl, *N*-methylleucine, -valine, and -alanine fell between those of the unsubstituted and the *N*-methylated esters. It was not certain however that true solutions were obtained, especially for the valine and leucine derivatives so the reported rates may be lower than the rate in a homogeneous aqueous solution.

As observed by Hay *et al.* (7, 8) and Wright (9) for glycine and alanine, below p*H* 11.2 the second order rate constant increased as the p*H* decreased (the results with valine were not precise enough to see this effect). This was attributed to the hydrolysis of the charged form of the ester (7, 9) which proceeds about 100 times faster than the uncharged form. In principle, both rate constants can be obtained from the following equation developed by Hay and Porter (7):

$$k_2^* [[H^+] + K_E] = k_2^+ [H^+] + k_2 K_E$$

where k_2^* = observed second order rate constant
k_2^+ = second order rate constant for charged form
k_2 = second order rate constant for uncharged form
K_E = acid dissociation constant of the ester

At p$H > 10$, $[H^+] \ll K_E$, thus a plot of k_2^* *vs.* $[H^+]$ has slope k_2^+/K_E and intercept k_2. For *N*-methyl-L-alanine methyl ester such a plot gave

$$k_2^+ = 70 \pm 6\ M^{-1}\ s^{-1}$$
$$k_2 = 0.20 \pm 0.01\ M^{-1}\ s^{-1}$$

For calculating $[H^+]$, the value of 0.83 was used for the activity coefficient of hydrogen ion, at ionic strength 0.1 *M* (10).

It is difficult to determine the rate constant for the charged form by using a titrimetric technique because of the slow overall rate at the lower p*H*'s necessarily studied and because of the buffering of the amino acid product (p*K* 9–10). For example, for *N*-methylalanine methyl ester at p*H* 10, the observed rate was one half of the true rate. Thus, although this rate constant is very desirable the accuracy with which it can be determined by this technique is rather low (*vide* lack of agreement between $\Delta H^{\ddagger}$ and $\Delta S^{\ddagger}$ values for glycine esters (7, 9)). Phenylalanine and its esters have relatively low p*K*'s and no variation in k_2^* was detected at 25° above p*H* 10.6, so phenylalanine was selected for a more detailed study. As the rates of saponification at 25° of the methyl esters of phenylalanine and *N*-acetylphenylalanine differed relative to those of leucine methyl ester and *N*-acetylleucine ester, the activation parameters were also obtained for the latter pair.

The results with *N*-methylalanine methyl ester showed that the cationic form was hydrolyzed about 350 times faster than the uncharged form. Because of this and the higher p*K*'s of *N*-methylated esters, it is likely that k_2^* would contain a contribution from k_2^+ at the highest p*H* consistent with the required degree of reproducibility of the titrimeter. Also, because of the slow reaction rates a greater number of runs were required to obtain reliable values. For this reason only *N*-methyl-L-phenylalanine ester was studied at higher temperatures. The saponification of the *N*-acetyl,*N*-methylamino acid esters was not studied at higher temperatures because their lower solubilities precluded a quantitative study in a purely aqueous environment, within the sensitivity limits of the titrimetric method.

At this juncture it should be emphasized that the main advantages of the automatic p*H*-stat method for our work are speed and the absence of buffer ions. The latter is important because esters activated in the acyl moiety are subject to general base-catalyzed hydrolysis (11).

The activation parameters for the saponification of the leucine and phenylalanine derivatives are given in Table 3.

Discussion

pK's of Amino Acids and their Esters

The α-amino group of an ester is a stronger acid than that of the parent amino acid by about two orders of magnitude. This can be qualitatively explained by the differences in inductive and electrostatic effects and in solvation between the acidic and basic forms. The ester cation resembles the monoalkyl ammonium ions whereas the acidic form of the amino acid is a zwitterion with

Can. J. Chem. Downloaded from www.nrcresearchpress.com by 210.87.254.5 on 09/05/12
For personal use only.

TABLE 3. Activation parameters for the saponification of the methyl esters of *N*-substituted phenylalanine and leucine derivatives in 0.1 *M* NaCl

Amino acid	*N*-Substituent	$k_2^*(M^{-1}\ s^{-1})^a$ 25.0°	40.0°	55.0°	ΔH^* (kcal mol^{-1})	ΔS^* (cal $mol^{-1}\ deg^{-1}$)
Phenylalanine	—	0.60±0.02	1.39±0.05	2.96±0.03	9.7±0.3	−27.0±0.8
	—$COCH_3$	1.075±0.02	2.40±0.03	5.08±0.16	9.3±0.2	−27.1±0.6
	$-CH_3$	0.055±0.002	0.185±0.09	0.48±0.01	13.9±0.4	−17.7±1.2
Leucine	—	0.45±0.005	1.03±0.01	2.25±0.01	9.8±0.1	−27.2±0.3
	—$COCH_3$	0.43±0.02	1.00±0.02	2.35±0.02	10.6±0.2	−24.6±0.7

[a]Five determinations were done for each derivative at 40 and 55°. For 25°, see Table 2.

Can. J. Chem. Downloaded from www.nrcresearchpress.com by 210.87.254.5 on 09/05/12
For personal use only.

the positive and negative substituents on adjacent carbon atoms.

The values shown in Table 1 are 'mixed' constants containing the activity coefficients of the acidic and basic forms of the amino acid or its ester. As it is difficult to assign values to the activity coefficients of zwitterions no attempt was made to convert pK' to the thermodynamic values. However this probably does not invalidate the observation that with the exception of glycine, *N*-methylation of the α-amino group causes similar shifts in pK' to those reported for the monomethyl- and dimethylamines (12) (pK = 10.62 and 10.77, respectively, at 25°). *N*-Methylation should increase the basicity of the nitrogen but would change the pattern of solvation. The resulting change in ΔG may be small due to compensation behavior and an isokinetic relationship (13, 14).

Saponification of the Esters

The saponification of esters of carboxylic acids is considered to be a nucleophilic reaction proceeding through a tetrahedral intermediate whose rate of formation is the rate-limiting step (eq. 1). The evidence for this mechanism has been reviewed recently (15). Electron-withdrawing substituents in R^1 or R^2 enhance the rate of formation of the intermediate by reducing the charge density on the carbonyl carbon.

[1] $$R^1\text{—}\overset{\overset{O}{\|}}{C}\text{—}OR^2 + OH^- \rightleftharpoons R^1\text{—}\overset{\overset{O^-}{|}}{\underset{\underset{OH}{|}}{C}}\text{—}OR^2 \rightarrow R^1\text{—}\overset{\overset{O}{\|}}{C}\text{—}OH + R^2O^-$$

Influence of the Amino Acid Side-chain

For the unsubstituted esters we found the order of reactivities to be valine ≪ leucine < phenylalanine < alanine ~ glycine. This is in agreement with Hay *et al.* (6–8) except that the absolute values differ somewhat. Using Taft σ* values, and alanine methyl ester as reference compound, they found that the saponification rates of most amino acids followed the Taft equation (16) but the slope was very shallow (ρ* = 0.65). This means that the polar effect of the side-chain is minor (unless an isokinetic relationship exists with a compensation temperature near 25°). Valine and isoleucine which have branching on the β-carbon atom were much less reactive and did not follow the Taft relationship. Peptide bonds at the valine carbonyl are notoriously resistant to acid hydrolysis (17, 18). This was attributed to steric hindrance of the peptide bond to access by reagent. Long and Lillycrop (Purdie) have shown that the rate of acid-catalyzed hydrolysis of the Leu—Gly and Gly—Leu bonds in di- and tripeptides can be explained by solvation effects (19). This aspect of the effect of alkyl groups is considered in more detail below.

Effect of N-Methylation

The slow hydrolysis of the *N*-methylamino acid esters at 25° is at first sight rather surprising. The polar effect of the —$NHCH_3$ group would be slightly less favorable than that of the —NH_2. In terms of the shielding of the carbonyl carbon from attack by OH^-, the —$NHCH_3$ group is much more effective than the —NH_2, but the —N-$(CH_3)COCH_3$ should be at least as effective in this respect, which is not reflected in the relative rates. Hence other factors must be operative.

In the transition state for the formation of the tetrahedral intermediate there is a partial bond between the OH^- and the polarized carbonyl carbon of the ester. The reaction site has an overall unit negative charge in place of the dipolar condition of the ground state, leading to stronger solvation. This would cause a further decrease in $\Delta S^{\ddagger}$ (over that due to the formation of one entity from two). On the other hand the transition state will be stabilized by solvation which will be reflected in a lower $\Delta H^{\ddagger}$. For several reaction series and processes occurring in water, changes in ΔG and $\Delta G^{\ddagger}$ are much less marked than the changes in ΔH and $\Delta H^{\ddagger}$ and ΔS and $\Delta S^{\ddagger}$. That is, compensatory changes occur in the enthalpy and entropy so that the free energy change is minimized. This has been attributed by Laidler (20) to solvation and to the properties of liquid water (14).

In the amino acid esters, β-alkyl substituents would tend to antagonize the orientation of the water molecules around the negatively charged area and promote 'iceberg' formation. An α-*N*-methyl group would considerably intensify this effect because then both front and back of the carbonyl group would be partially shielded (depending on the relative population of the conformers). Thus by changing the pattern of solvation around the carbonyl group, *N*-methylation could lead to an increase in $\Delta H^{\ddagger}$ and a less nega-

tive $\Delta S^{\ddagger}$. This is the case with L-phenylalanine methyl ester and its *N*-methyl analogue. The less negative $\Delta S^{\ddagger}$ does not compensate at room temperature for the increase in $\Delta H^{\ddagger}$ but at higher temperatures there is less disparity in saponification rates. For alanine, the ratio of saponification rates for the ester of the *N*-methylated acid to the unsubstituted acid is $\sim$1:5 compared to 1:10 for the phenylalanine and leucine pairs. For sarcosine and glycine the ratio is greater than 1:3. These figures reflect the lack of interference from β-substituents in the glycine and alanine derivatives.

Effect of N-Acetylation

At 25°, *N*-acetylation causes a 50–60% increase in rates for glycine and phenylalanine, a slight enhancement for valine and a small decrease for leucine and alanine. Charton's 'inductive' substituent constants σ′ (21) for $-CH_2NH_2$ and $-CH_2NHCOCH_3$ are 0.08 and 0.07 respectively so the purely polar effects of these substituents are very similar.

The peptide (or amide) bond is a rigid planar system due to the interaction of —NH and —CO groups to produce a resonance hybrid with considerable double bond character. This leads to *cis–trans* isomerism as illustrated below:

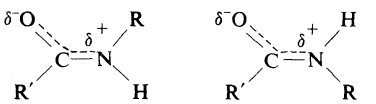

trans *cis*

Normally, in open-chain compounds, the *trans* form is the energetically more favorable. *N*-acetylleucine ethyl ester exists almost exclusively in the *trans* form in the solid state and in solution in chlorinated hydrocarbons (22). In this isomer, the $-CH_3$ of the acetyl group is distal to the ester bond with the polar peptide linkage in between. Thus the *trans* *N*-acetyl group *per se* should not greatly affect solvation of the transition state although it may interact with the alkyl side-chains to cause a less favorable conformation to be adopted.

Apart from the effects mentioned above, the ambident nucleophilic character of the peptide bond raises the possibility of anchimeric assistance or of an intramolecular nucleophilic reaction. The latter reaction has been implicated in the very rapid alkaline hydrolysis of 'active' esters of *N*-acylated glycine in which the cyclic oxazolinones were shown to occur as intermediates (23). However, no build-up of oxazolinone was detected during the saponification of the 'stable' ester methyl hippurate which is not hydrolyzed much faster than glycine methyl ester (rate constants 1.7 M^{-1} s^{-1} and 1.3 M^{-1} s^{-1} respectively (24)). Thus it is unlikely that this mechanism is important in the saponification of the esters of the *N*-acetylamino acids described here.

For the peptide bond to provide anchimeric assistance, it must stabilize the transition state of the rate-determining step (25). Assuming again that this state occurs in the formation of the tetrahedral intermediate, it can be represented as

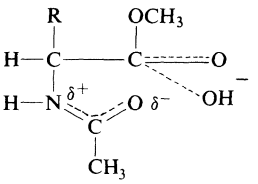

Dreiding models show that H-bonding of the *N*-acetyl oxygen to the hydroxyl group of the intermediate is sterically possible. Whether such an interaction could occur and stabilize the transition state would depend on the extent of bond formation to (and hence, charge transfer from) the incoming hydroxyl ion. There may also be a detrimental electrostatic interaction between the hydroxide ion and the *N*-acetyl oxygen. However, whichever factors are operating, *N*-acetylation of the α-amino group has a relatively small net effect on the observed rate of saponification and on the related activation parameters. The latter quantities perhaps suggest that solvation effects are of most importance in the case of the leucine esters.

N-Methylation of the *N*-acetyl derivative increases the proportion of the *cis* isomer at room temperature. Evidence for this has been obtained from n.m.r. studies of sarcosine methyl ester (26), *N*-methylalanine methyl ester (27), acetyl-D-alanyl-*N*-methyl-D-alanine methyl ester (28), and several *N*-acetyl,*N*-methylamino acids (29, 30). For sarcosine methyl ester the *trans* form is predominant while for the alanine dipeptide ester up to 20% *cis* isomer was observed. The n.m.r. spectra in $CDCl_3$ of *N*-acetyl,*N*-methylglycine, -alanine, -valine, -leucine, and -isoleucine showed splitting of the *N*-CH_3 and α-CH resonances. The ratio of the integrals for major to minor peaks ranged from 5.4 for glycine to 2.0 for isoleucine.

Can. J. Chem. Downloaded from www.nrcresearchpress.com by 210.87.254.5 on 09/05/12
For personal use only.

Can. J. Chem. Downloaded from www.nrcresearchpress.com by 210.87.254.5 on 09/05/12
For personal use only.

Insufficient data were available for assignment of the individual peaks to *cis* or *trans* forms but the ratio is probably different for the esters in aqueous solution.

From n.m.r. data on the hindered rotation of *N*,*N*-dimethylacetamide (31) and other *N*-substituted acetamides (32), it is likely that the rates of interconversion of our esters are very much greater than their rates of saponification at 25°. As there will be different transition states for each isomer the observed rate constant for saponification is

$$k_{obs} = \frac{k_{trans}}{1 + K} + \frac{k_{cis}}{1 + K} K$$

where K is the equilibrium constant [*cis*]/[*trans*].

Molecular models show that the *N*-methyl group is about the same distance from the ester carbonyl in both isomers, but the positions of *C*-methyl and —CO differ. In the *cis* isomer the *C*-methyl is always directed towards, and the oxygen of the —CO group away from the main chain. The position of these groups are interchanged in the *trans* isomer so that the ester carbonyl is less 'hindered'. On this basis the higher the proportion of *cis* isomer the more slowly the ester would be saponified. This also implies that according to the observed rates, *N*-methylation does not greatly reduce the rate of saponification of the *trans* isomer. The positive inductive effect of the *N*-methyl group will tend to increase the partial negative charge on the *N*-acetyl oxygen. In the *trans* isomer, the distal *N*-methyl group would not sterically prevent anchimeric assistance. Also, the polar peptide bond in the *trans* conformation could offset to some extent the promotion of 'ice-berg' formation by the *N*-methyl group. Both these effects would be enhanced by the increased negative charge on the acetamido oxygen and perhaps offer a partial explanation of the faster saponification of the esters of the *N*-methyl,*N*-acetylamino acids than of their *N*-methyl analogues.

Effect of N-Protonation

N-Protonation produces by far the greatest effect on the rate of saponification. Some literature values for glycine and alanine esters together with those from the present work are shown in Table 4.

Holmquist and Bruice (33) have shown that for a series of *o*-nitrophenyl esters of XCOOH where X contained neutral and positively charged groups, electrostatic facilitation of hydroxide-ion catalysis is not important. Bell and Coller (34) obtained a linear plot of log k_{OH} *vs.* pK for a series of substituted acetic acid esters including betaine and glycine esters. Apparently the favorable inductive effect of the positive charge far outweighs any adverse effect of the *N*-methyl groups, in the case of glycine and alanine esters. This is also illustrated by the greater enhancement of rate when *N*-methylalanine ester is protonated than is the case for the non-methylated derivative; there is little difference between the k_2 values for the charged forms of alanine methyl ester and *N*-methylalanine ester (Table 4). It would be of interest to study the betaines of other amino acids to see whether the rate enhancement is maintained in the presence of bulky side-chains.

TABLE 4. Saponification rates of esters of *N*-methylated glycine and alanine at 25°[a]

Ester	pK_1 of amino acid	Reference	k_2^+ or k_2 (M^{-1} s^{-1})	Reference
$\overset{+}{N}(CH_3)_3 \cdot CH_2 \cdot COOCH_3$	1.83	34	60.8	38
			79.4	39
$\overset{+}{N}H(CH_3)_2 \cdot CH_2 \cdot COOCH_3$	2.08	35	20.6	39
$\overset{+}{N}H_3 \cdot CH_2 \cdot COOCH_3$	2.35	36	28 ±3	7
$NH_2 \cdot CH_2 \cdot COOCH_3$	(3.7)	40	1.28	7
			1.13	This work
$\overset{+}{N}H_3 \cdot CH(CH_3) \cdot COOCH_3$	2.3	37	80 ±7	8
$NH_2 \cdot CH(CH_3) \cdot COOCH_3$			1.11±0.05	8
			1.04±0.02	This work
$\overset{+}{N}H_2(CH_3) \cdot CH(CH_3) \cdot COOCH_3$	2.22	37	70 ±6	This work
$NH(CH_3) \cdot CH(CH_3) \cdot COOCH_3$			0.20±0.01	This work

[a]Ionic strength 0.1 *M*.

The expert technical assistance of Mrs. Ruth Demayo in the synthetic work is gratefully acknowledged.

1. J. RUDINGER. Fifth European peptide symposium, Oxford, 1962. Pergamon Press, New York, N.Y., 1963. p. 154.
2. J. R. COGGINS and N. L. BENOITON. Can. J. Chem. **49**, 1968 (1971).
3. A. I. VOGEL. Practical organic chemistry. 3rd Ed. Longmans, London, 1964. p. 971.
4. J. E. PURDIE and N. L. BENOITON. Can. J. Biochem. **48**, 1058 (1970).
5. E. A. GUGGENHEIM. Phil. Mag. **2**, 538 (1926).
6. R. W. HAY, L. J. PORTER, and P. J. MORRIS. Austral. J. Chem. **19**, 1197 (1966).
7. R. W. HAY and L. J. PORTER. J. Chem. Soc. B, 1261 (1967).
8. R. W. HAY and P. J. MORRIS. J. Chem. Soc. B, 1577 (1970).
9. M. R. WRIGHT. J. Chem. Soc. B, 1265 (1967).
10. R. G. BATES. Electrometric pH determinations. Wiley and Sons, New York, N.Y., 1954. p. 52.
11. W. P. JENCKS and J. CARRIUOLO. J. Am. Chem. Soc. **83** 1743 (1961).
12. D. H. EVERETT and W. F. K. WYNNE-JONES. Proc. Roy. Soc. A, **177**, 499 (1941).
13. C. D. RITCHIE and W. F. SAGER. Progress in physical organic chemistry. Vol. 2. Interscience, New York, N.Y., 1964. p. 323.
14. R. LUMRY and S. RAJENDER. Biopolym. **9**, 1125 (1970).
15. S. L. JOHNSON. Advances in physical organic chemistry. Vol. 5. Academic Press, New York, N.Y., 1967. p. 237.
16. R. W. TAFT. *In* Steric effects in organic chemistry. *Edited by* M. S. Newman. Wiley and Sons, New York, N.Y., 1956. Chapt. 13.
17. R. L. M. SYNGE. Biochem. J. **39**, 351 (1945).
18. M. MURUMATU, R. HIROHATA, Y. KANDA, and S. SHIBUYA. Z. Physiol. Chem. **332**, 256 (1963).
19. D. A. LONG and J. E. LILLYCROP (PURDIE). Trans. Faraday Soc. **59**, 907 (1963).
20. K. J. LAIDLER. Trans. Faraday Soc. **55**, 1725 (1959).
21. M. CHARTON. J. Org. Chem. **29**, 1222 (1964).
22. K. BLÁHA, I. FRIČ, and J. SMOLÍKOVÁ. Coll. Czech. Chem. Commun. **33**, 3170 (1968).
23. J. DE JERSEY, P. WILLADSEN, and B. ZERNER. Biochem. **8**, 1959 (1969).
24. R. W. HAY and P. J. MORRIS. Chem. Commun. 663 (1967).
25. B. CAPON. Quart. Rev. XVIII, 45 (1964).
26. F. A. BOVEY, J. J. RYAN and F. P. HOOD. Macromol. **1**, 305 (1968).
27. M. GOODMAN and M. FRIED. J. Am. Chem. Soc. **89**, 1264 (1967).
28. V. F. BYSTROV, S. L. PORTNOVA, V. I. TSETLIN, V. T. IVANOV, and Y. A. OVCHINNIKOV. Tetrahedron, **25**, 493 (1969).
29. N. L. BENOITON and J. R. COGGINS. Proceedings 2nd American peptide symposium, Cleveland, 1970, Gordon and Breach, New York, N.Y., 1971. In press.
30. J. R. COGGINS. Ph.D. Thesis. University of Ottawa, Ottawa, Ontario, 1970.
31. A. CALZOLARI, F. CONTI, and C. FRANCONI. J. Chem. Soc. B, 555 (1970).
32. R. M. HAMMAKER and B. A. GUGLER. J. Mol. Spectrosc. **17**, 356 (1965).
33. B. HOLMQUIST and T. C. BRUICE. J. Am. Chem. Soc. **91**, 2982 (1969).
34. R. P. BELL and B. A. W. COLLER. Trans. Faraday Soc. **60**, 1087 (1964).
35. F. BASOLO and Y. T. CHEN. J. Am. Chem. Soc. **76**, 953 (1954).
36. E. J. KING. J. Am. Chem. Soc. **67**, 2178 (1945).
37. W. COCKER and J. O. HARRIS. J. Chem. Soc. 1290 (1940).
38. M. R. WRIGHT. J. Chem. Soc. B, 548 (1968).
39. G. AKSNES and P. FRØYEN. Acta Chem. Scand. **21**, 1507 (1967).
40. R. P. BELL and B. A. W. COLLER. Trans. Faraday Soc. **61**, 1445 (1965).

Can. J. Chem. Downloaded from www.nrcresearchpress.com by 210.87.254.5 on 09/05/12
For personal use only.

The Configuration Dependent Cyclization of β-2-Hydroxyaroylacrylic Acids

P. C. Arora and P. Brassard
Département de Chimie, Université Laval, Québec, Québec

Received June 14, 1971

Several alleged chromanone-2-carboxylic acids were reexamined. Some were found to have the assigned structures but others are in fact 2-coumaranonylacetic acids. Diagnostic proof was obtained by analysis of the n.m.r. spectra of the corresponding reduced substances. Useful correlations of the spectra with the structures of the keto acids are proposed.

L'étude des présumées carboxy-2 chromanones a été reprise. Les attributions de structure ont été confirmées dans certains cas mais plusieurs substances sont en fait des acides coumaranonyl-2 acétiques. Les preuves de structure ont été obtenues par l'analyse des spectres de r.m.n. des composés réduits correspondants. Des corrélations utiles entre les spectres et les structures des deux groupes d'acides sont proposées.

Canadian Journal of Chemistry, **49**, 3477 (1971)

Can. J. Chem. Downloaded from www.nrcresearchpress.com by 210.87.254.40 on 09/05/12
For personal use only.

The ambiguities associated with the cyclization of β-2-hydroxyaroylacrylic acids have been pointed out by Barr *et al.* (1). However the factors invoked (mainly steric effects) in the formation of 2-coumaranonylacetic acids and the method suggested for the determination of ring size (the evaluation of dissociation constants) do not appear to be unequivocal. Indeed the aluminum chloride catalyzed reaction between citraconic anhydride and 1,4-dimethoxybenzene gave rise, among other products, to 2-methyl-5-methoxy-2-coumaranonylacetic acid (**13**) (2). This unexpected result strongly suggested that a reexamination of some chromanone-2-carboxylic acids should be undertaken.

Syntheses of alleged chromanone-2-carboxylic acids have been affected or attempted by various means (3–5); however the conclusion has been reached (1) that one of the compounds isolated from the Friedel–Crafts condensation of 3,5-xylenol with maleic anhydride is in fact a coumaranone (**9**), whereas the colorless compounds obtained under similar conditions from β-naphthol and resorcinol as well as the one resulting from a triethylamine catalyzed cyclization of methyl β-[2-hydroxy-3,5-dimethylbenzoyl]-acrylate are claimed to be chromanones.

The syntheses of most of the known substances of these two types of oxygen-ring compounds have been repeated. It was found moreover, while attempting to degrade some β-2-hydroxybenzoylacrylic acids with aqueous barium hydroxide (6), that most of these compounds cyclize readily, thus contradicting fragmentary evidence to the contrary in the literature as to their behavior toward strong base (Jarowski *et al.* (3) found that chromanone-2-carboxylic acid yielded the corresponding 2-hydroxybenzoylacrylic acid while it has been observed (1) that β-(2-hydroxy-3,5-dimethylbenzoyl)-acrylic was not affected).

In particular, 2-hydroxy-5-methyl, *trans*-2-hydroxy-3,5-dimethyl, and 2,4-dihydroxybenzoylacrylic acids all cyclize readily to oxygen-ring compounds in the presence of barium hydroxide. *cis*-β-(2-Hydroxy-3,5-dimethylbenzoyl)-acrylic acid does not yield a monomeric compound under these conditions but can be cyclized by the use of weaker bases such as triethylamine. Moreover the oxygen-ring compounds obtained directly from *p*-cresol and resorcinol by Friedel–Crafts condensations are respectively identical to those obtained by base-catalyzed cyclizations of the corresponding benzoylacrylic acids.

Nuclear magnetic resonance spectroscopy seemed to be the most reliable method of resolving the problems of structure in these systems. Examination of the spectra of these oxygen-ring compounds revealed that they could be separated into two well defined groups. The aliphatic protons of group A (eventually found to be coumaranones) present a typical ABX pattern while those of group B (chromanones) give a more simple spectrum, *i.e.* there is no discernible splitting due to coupling of the geminal protons (Tables 1 and 2). This last pattern has also been observed in a nitrogen analog, kynurenine yellow (7). Another characteristic feature of the two groups of isomers was the difference in the chemical shifts of the methine protons. A quadruplet centered at about 5.0 p.p.m. appeared in the

TABLE 1. The n.m.r. data for coumaranones and *coumaranols*

Compound: Coumaranonyl-2-acetic acid or *3-hydroxycoumaranyl-2-acetic acid lactone*	Solvent	δ, p.p.m. (*J*, Hz) 2-CH or -CH_3	α-CH_2	3-CH
5,7-Dimethyl- (**7**)	$(CD_3)_2CO$	4.90 (q) (4.5; 6.6)	2.88; 2.98 (oct) (4.5; 6.6; 17.0)	
4,6-Dimethyl- (**9**)	$(CD_3)_2CO$	4.83 (q) (4.3; 7.0)	2.82; 2.92 (oct) (4.3; 7.0; 16.9)	
4,6-Dimethyl- (**16**)	$CDCl_3$	5.19 (m) (3.5; 5.0; 6.0)	2.85; 2.92 (oct) (3.5; 5.0; 18.0)	6.10 (d) (6.0)
6-Hydroxy- (**10**)	$(CD_3)_2CO$	4.89 (q) (4.3; 7.2)	2.83; 2.89 (oct) (4.3; 7.2; 17.0)	
4,5-Benzo- (**11**)	$(CD_3)_2CO$	5.09 (q) (4.5; 7.0)	2.98; 3.08 (oct) (4.5; 7.0; 17.0)	
Methyl ester of **11**	$CDCl_3$	5.07 (q) (4.0; 8.3)	2.93; 3.03 (oct) (4.0; 8.3; 16.9)	
4,5-Benzo- (**17**)	$CDCl_3$	5.41 (q) (4.0; 5.3; 6.6)	2.96; 3.04 (oct) (4.0; 5.3; 18.0)	6.30 (d) (6.6)
2-Methyl-5-methoxy- (**13**)	$CDCl_3$	1.44 (s)	2.93 (s)	
2-Methyl-5-methoxy- (**20**)	$CDCl_3$	1.57 (s)	2.76; 3.01 (q) (18.0)	5.42 (s)

TABLE 2. The n.m.r. data for chromanones and *chromanols*

Compound: Chromanone-2-carboxylic acid or *chromanol-2-carboxylic acid*	Solvent	δ, p.p.m. (*J*, Hz) 2-CH or -CH_3	3-CH_2	4-CH
6-Methyl- (**6**)	$(CD_3)_2CO$	5.29 (q) (5.8; 6.8)	3.04; 3.05* (5.8; 6.8)	
6-Methyl- (**15**)	$(CD_3)_2CO$	4.89 (q) (5.9; 7.4)	(m)	4.83 (q) (4.3; 8.0)
6,8-Dimethyl- (**8**)	$(CD_3)_2CO$	5.26 (q) (5.9; 6.8)	3.00; 3.01* (5.9; 6.8)	
2-Methyl-6-methoxy- (**12**)	$CDCl_3$	1.71 (s)	2.87; 3.17(q) (17.0)	
2-Methyl-6-methoxy- (**18**)	$(CD_3)_2CO$	1.54 (s)	2.22; 2.30 (oct) (4.6; 4.8; 14.0)	4.67 (q) (4.6; 4.8)
Lactone of 2-methyl-6-methoxy- (**19**)	$CDCl_3$	1.66 (s)	2.31; 2.36 (oct) (3.0; 3.5; 13.0)	5.16 (q) (2.0; 3.5)

*Pair of superimposed doublets.

spectra of all members of group A whereas it was observed at about 5.3 p.p.m. in the others. A somewhat analogous difference for methine protons at C-2 has been reported for flavanones and benzylcoumaranones (8).

These superficial distinctions are obviously not valid indications of particular structures nor are they even proof that two types of heterocycles are present since both isomers could conceivably give either (or both) type of spectra and moreover the difference in the chemical shifts for methine protons is small. However the validity of this original classification was eventually borne out by incontrovertible proof of structure. This evidence was obtained by examination of the n.m.r. spectra of the corresponding reduction products. Chromanones have been reduced to chromanols by a variety of agents which usually yield benzofurans when applied to coumaranones. However sodium borohydride was found to reduce both types of heterocycles to the corresponding alcools; the compound tentatively considered to be 7-hydroxy-2-coumaranonyl-acetic acid proved resistant to this reagent.

Can. J. Chem. Downloaded from www.nrcresearchpress.com by 210.87.254.40 on 09/05/12
For personal use only.

Can. J. Chem. Downloaded from www.nrcresearchpress.com by 210.87.254.40 on 09/05/12
For personal use only.

The compounds of group A (coumaranones) again were found to have the same general characteristics. They yielded only lactones without identifiable traces of hydroxy acids. Their n.m.r. spectra revealed that the coupling of the newly introduced methine proton resulted in the appearance of doublets at about 5.4–6.3 p.p.m.; on the other hand, the compounds of group B (chromanones) gave only or mainly hydroxy acids and the resulting methine protons appeared at about 4.7–5.2 p.p.m. as quartets in the n.m.r. spectra (Scheme 1).

Conclusions

The evidence presented here indicates that, in the case where both the *cis*- and *trans*-isomers of a β-2-hydroxyaroylacrylic acid are available, they can be cyclized respectively to a coumaranonylacetic acid and a chromanonecarboxylic acid. The reduction of some of these two types of heterocycles demonstrates unequivocally that the compound variously considered as 5,7-dimethyl-2-carboxychromanone (4) or as 4,6-dimethyl-2-coumaranonylacetic acid (1) is indeed a coumaranone while those described as 6,8-dimethyl, 5,6-benzo, and probably also 7-hydroxy 2-carboxychromanones are in fact the corresponding coumaranones. The structure of 6-methyl-2-carboxychromanone was confirmed and those of a few new compounds were also definitely established.

The cyclization of the *trans*-acids to chromanones is fairly straight-forward and follows from basic electronic considerations known to prevail in molecules of this type. However, in the case of the *cis*-acids, it is debatable whether a different mode of cyclization results from a difference in stereochemistry or whether it proceeds through the lactol tautomer. Most *cis*-β-aroylacrylic acids show a definite tendency to exist in varying degrees in the lactol form (9), a preference which however is not shown by the *o*-hydroxylated congeners (these compounds are highly colored and show i.r. bands quite characteristic of the acyclic forms). It would seem possible then that under mildly basic catalysis, the strong hydrogen bond which prevents lactol formation is disrupted giving rise to the cyclic tautomer and thence exclusively to the coumaranones (strong bases are known to produce acyclic anions) (9). The isolation of the compound now thought to be 7-hydroxy-2-coumaranonylacetic acid would indicate that electronic effects may in certain cases take precedence over configurational ones as would be expected particularly in this instance (1). These two last aspects of the mechanism involved are now being actively investigated (Scheme 2).

The reduction of three 2-coumaranonylacetic acids indicated rather surprisingly that the action of sodium borohydride is completely stereoselective. The attack occurs from the side opposite to the carboxylic group and yields lactones even when the substrate was 2,2-disubstituted. These reductions would then seem to illustrate a particularly effective case of "electrostatic shielding" (10) or of the "electrostatic influence or remote substituent dipoles" (11).

On the other hand, only two chromanone-2-carboxylic acids were reduced. In one case (**6**) a hydroxy acid was found to be the sole product formed either by borohydride reduction or by catalytic hydrogenation. The large values obtained for $|J_{ax} + J_{bx}|$ and $|J_{am} + J_{bm}|$, 12.3 and 13.3 Hz, from the n.m.r. spectrum establish that both substituents are equatorial and therefore *cis* (12). The other keto acid which was 2,2-disubstituted gave mainly a hydroxy acid (and a small amount of lactone). From the n.m.r. spectrum it can be deduced that the hydroxyl group is probably equatorial ($|J_{ax} + J_{bx}| = 9.6$ Hz), but the relative positions of the two substituents in the heterocycle have not yet been determined with certainty although they are assumed to be *cis* by analogy with the other compounds in these series.

Experimental

All melting points were taken in capillary tubes with a calibrated thermometer (Thomas–Hoover Apparatus). The i.r. spectra were recorded with a Beckman IR-4 spectrometer. The n.m.r. spectra were determined with a Varian A-60 spectrometer using tetramethylsilane as internal standard. (All values for AB patterns are corrected; for the sake of consistency all chemical shifts and coupling constants in more complex patterns are apparent and not corrected.)

(A) Preparation of Starting Materials

The following compounds were prepared according to known methods or by the authors in another context:

β-(2-Hydroxy-5-methylbenzoyl)-acrylic acid (**1**), m.p. 172–173.5° (lit. 173–174° (4)); δ ($(CD_3)_2CO$) 2.44 (s) (methyl), 7.10 (d), and 8.22 (d) (olefinic protons, $J =$ 15.5 Hz).

cis-β-(2-Hydroxy-3,5-dimethylbenzoyl)-acrylic acid (**2**), m.p. 152–155.5° (lit. 149–153° (5)); $\lambda_{max}(CHCl_3)$ 6.13, 5.82, 3.33 μ; δ ($(CD_3)_2CO$) 2.32 (s) and 2.35 (s) (methyl), 6.47 (d), and 7.22 (d) (olefinic protons, $J = 12.2$ Hz).

Can. J. Chem. Downloaded from www.nrcresearchpress.com by 210.87.254.40 on 09/05/12
For personal use only.

2 $R_1 = R_2 = CH_3$

7 $R_1 = R_2 = R_4 = H$; $R_3 = R_5 = CH_3$
9 $R_1 = R_3 = R_5 = H$; $R_2 = R_4 = CH_3$
10 $R_1 = R_2 = R_3 = R_5 = H$; $R_4 = OH$
11 $R_1 = R_4 = R_5 = H$; $R_2, R_3 =$ Benzo
13 $R_1 = CH_3$; $R_2 = R_4 = R_5 = H$; $R_3 = OCH_3$

16 $R_1 = R_3 = H$; $R_2 = R_4 = CH_3$
17 $R_1 = R_4 = H$; $R_2 = R_3 =$ Benzo
20 $R_1 = CH_3$; $R_2 = R_4 = H$; $R_3 = OCH_3$

1 $R_1 = R_2 = R_3 = R_5 = H$; $R_4 = CH_3$
3 $R_1 = R_3 = R_5 = H$; $R_2 = R_4 = CH_3$
4 $R_1 = R_2 = R_4 = R_5 = H$; $R_3 = OH$
5 $R_1 = CH_3$; $R_2 = R_3 = R_5 = H$; $R_4 = OCH_3$

6 $R_1 = R_3 = H$; $R_2 = CH_3$
8 $R_1 = H$; $R_2 = R_3 = CH_3$
12 $R_1 = CH_3$; $R_2 = OCH_3$; $R_3 = H$

15 $R_1 = H$; $R_2 = CH_3$
18 $R_1 = CH_3$; $R_2 = OCH_3$

19

SCHEME 1

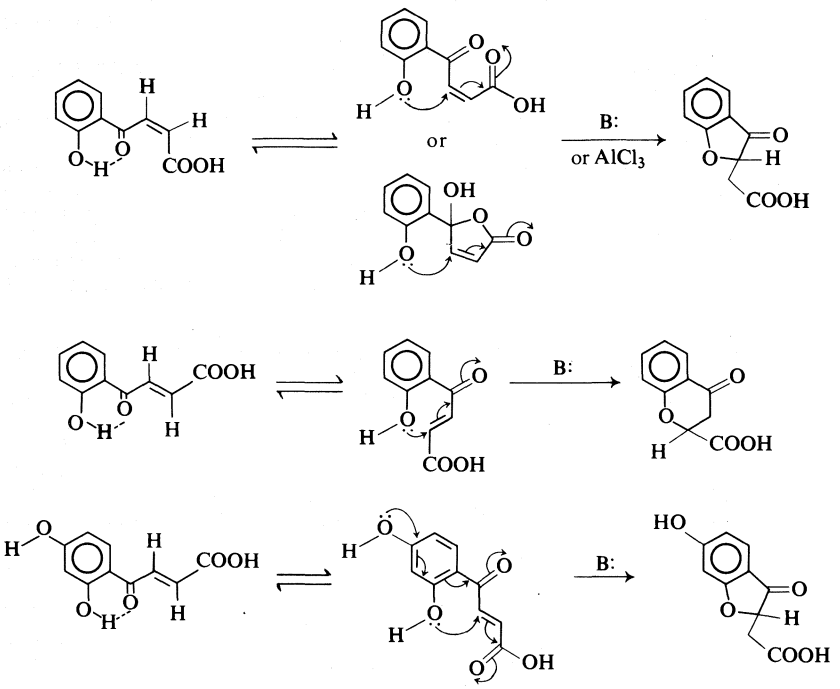

SCHEME 2

trans-β-(2-Hydroxy-3,5-dimethylbenzoyl)-acrylic acid (**3**), m.p. 135–136.5° (lit. 134–136° (5)); $\lambda_{max}(CHCl_3)$ 6.21, 6.08, 5.82, 3.33 μ; δ ($(CD_3)_2CO$) 2.32 (s) and 2.41 (s) (methyl), 7.02 (d), and 8.23 (d) (olefinic protons, J = 15.5 Hz).

β-(2,4-Dihydroxybenzoyl)-acrylic acid (**4**), m.p. 205–206° (lit. 206–208°) (1); δ ($(CD_3)_2CO$) 6.84 (d), and 7.97 (d) (olefinic protons, J = 15.0 Hz).

trans-α-Methyl-β-(2-hydroxy-5-methoxybenzoyl)-acrylic acid (**5**), m.p. 150.5–151° (13); δ ($(CD_3)_2CO$) 2.28 (d) (methyl, J = 1.5 Hz), 3.93 (s) (methoxyl), 7.93 (q) (olefinic proton, J = 1.5 Hz).

4,6-Dimethyl-2-coumaranonylacetic acid (**9**), m.p. 144–145.5° (lit. 143–144° (1)); $\lambda_{max}(CHCl_3)$ 6.25, 6.15, 5.81, 3.29 μ.

6-Hydroxy-2-coumaranonylacetic acid (**10**), m.p. 222–223° (lit. 222° (1)).

4,5-Benzo-2-coumaranonylacetic acid (**11**), m.p. 179–180° (lit. 169° (1)); methyl ester (CH_3OH, H_2SO_4), m.p. 88–89° (lit. (CH_2N_2) m.p. 102–103°).

Anal. Calcd. for $C_{15}H_{12}O_4$: C, 70.30; H, 4.72. Found: C, 70.04; H, 4.62.

(B) The Base-catalyzed Cyclization of β-2-Hydroxybenzoylacrylic Acids

The β-2-hydroxybenzoylacrylic acid (1.0 g) in an aqueous solution (25 ml) of barium hydroxide (1.0 g; 1.75 g for the dihydroxy compound) was stirred for several hours then acidified with hydrochloric acid and extracted with methylene chloride (all compounds gave negative ferric chloride tests).

6-Methylchromanone-2-carboxylic acid (**6**) from **1** (40%), m.p. 156.5–157.5° (chloroform and petroleum ether).

Anal. Calcd. for $C_{11}H_{10}O_4$: C, 64.07; H, 4.89. Found: C, 63.89; H, 4.92.

6,8-Dimethylchromanone-2-carboxylic acid (**8**) from **3** (33%), m.p. 185–186° (methylene chloride) (lit. 166–170° (dec.) (1)).

6-Hydroxy-2-coumaranonylacetic acid (**10**) from **4** (40%), m.p. and mixture m.p. 223–224.5°.

2-Methyl-6-methoxychromanone-2-carboxylic acid (**12**) from **5** (75%), m.p. 130–131° (benzene and petroleum ether).

Anal. Calcd. for $C_{12}H_{12}O_5$: C, 61.01; H, 5.12; O, 33.87. Found: C, 61.30; H, 4.83; O, 34.01.

(C) The Aluminum Chloride-catalyzed Cyclization of β-2-Hydroxybenzoylacrylic Acids

β-2-Hydroxy-5-methylbenzoylacrylic acid (1.0 g) was added to a molten mixture of aluminum chloride (10.0 g) and sodium chloride (1.5 g) at 170–180°. The melt was stirred at this temperature for 15 min then cooled and decomposed with ice and hydrochloric acid. Extraction with methylene chloride yielded 6-methylchromanone-2-carboxylic acid (**6**) which was identical (m.p., mixture m.p., and i.r. spectrum) with the compound prepared by the base-catalyzed cyclization. Prolonged heating (1 h) gave 4-hydroxy-7-methyl-3-oxoindane-1-carboxylic acid (0.3 g) by the usual method, m.p. 143.5–145° (water) (lit. 149–150° (4)) (positive ferric chloride test: dark blue); δ ($CDCl_3$) 2.30 (s) (methyl), 2.96 (d) (methylene, J = 5.0 Hz), 4.24 (t) (methine, J = 5.0 Hz), 6.80 (d) and 7.38 (d) (aromatic protons, J = 8.5 Hz), and 10.25 (carboxyl).

Can. J. Chem. Downloaded from www.nrcresearchpress.com by 210.87.254.40 on 09/05/12
For personal use only.

(D) The Triethylamine-catalyzed Cyclization of cis-β-2-Hydroxybenzoylacrylic Acids

Triethylamine (5 ml) was added to a solution of *cis*-β-(2-hydroxy-3,5-dimethylbenzoylacrylic acid (0.5 g) in ether (50 ml) and the mixture was allowed to stand for 48 h. After evaporation, acidification with dilute hydrochloric acid, and extraction with ether, 5,7-dimethyl-2-coumaranonylacetic acid was obtained, m.p. 164–165.5° (methylene chloride) (80%).

Anal. Calcd. for $C_{12}H_{12}O_4$: C, 65.44; H, 5.49. Found: C, 65.14; H, 5.48.

(E) The Reduction of Oxygen-ring Keto Acids with Sodium Borohydride

The chromanone-2-carboxylic acid or 2-coumaranonylacetic acid (1.0 g) was dissolved in dioxane (25 ml) and absolute ethanol (5 ml); sodium borohydride (0.25 g) was added and the mixture was stirred at room temperature for 24 h. The solvents were evaporated under vacuum, the residue acidified with dilute hydrochloric acid, and extracted with ether. The ether extract after washing with a 5% solution of sodium bicarbonate yielded the lactone while the hydroxy acids were recovered in the usual way from the bicarbonate extract.

cis-4-Hydroxy-6-methylchroman-2-carboxylic acid (**15**) from **6** (60%), m.p. 160.5–161.5° (acetone – petroleum ether).

Anal. Calcd. for $C_{11}H_{12}O_4$: C, 63.45; H, 5.81. Found: C, 63.79; H, 5.92.

cis-3-Hydroxy-4,6-dimethyl-2-coumaranylacetic acid lactone (**16**) from **9** (70%), m.p. 135–136° (methanol).

Anal. Calcd. for $C_{12}H_{12}O_3$: C, 70.57; H, 5.92. Found: C, 70.60; H, 5.95.

cis-3-Hydroxy-4,5-benzo-2-coumaranylacetic acid lactone (**17**) from **11** (80%), m.p. 207–208° (chloroform).

Anal. Calcd. for $C_{14}H_{10}O_3$: C, 74.33; H, 4.46. Found: C, 74.32; H, 4.43.

cis(?)-2-Methyl-4-hydroxy-6-methoxychroman-2-carboxylic acid (**18**) from **13** (63%), m.p. 155.5–156.5° (acetone – petroleum ether).

Anal. Calcd. for $C_{12}H_{14}O_5$: C, 60.50; H, 5.92. Found: C, 60.85; H, 5.94.

The corresponding lactone (**19**) (9%), m.p. 105–105.5° (chloroform – petroleum ether).

Anal. Calcd. for $C_{12}H_{12}O_4$: C, 65.44; H, 5.49. Found: C, 65.72; H, 5.43.

cis-2-Methyl-3-hydroxy-5-methoxy-2-coumaranylacetic acid lactone (**20**) (75%) from 2-methyl-5-methoxy-2-coumaranonylacetic acid (**13**) (obtained from the condensation of 1,4-dimethoxybenzene and citraconic anhydride (2)), m.p. 70.5–71° (80% methanol or isooctane).

Anal. Calcd. for $C_{12}H_{12}O_4$: C, 65.44; H, 5.49. Found: C, 65.65; H, 5.67.

1. K. P. Barr, F. M. Dean, and H. D. Locksley. J. Chem. Soc. 2425 (1959).
2. P. C. Arora and P. Brassard. To be published.
3. C. I. Jarowski, W. J. Moran, and B. J. Cramer. J. Am. Chem. Soc. **71**, 944 (1949).
4. G. Baddeley, S. M. Makar, and M. G. Ivinson. J. Chem. Soc. 3969 (1953).
5. W. Cocker, D. H. Hayes, and W. R. N. Williamson. J. Chem. Soc. 824 (1955).
6. R. E. Lutz and R. J. Taylor. J. Am. Chem. Soc. **55**, 1168 (1933).
7. T. Tokuyama, S. Senoh, T. Sakan, K. S. Brown, Jr., and B. Witkop. J. Am. Chem. Soc. **89**, 1017 (1967).
8. J. Massicot and J. P. Marthe. Bull. soc. chim. Fr. 1962 (1962).
9. R. E. Lutz, P. S. Bailey, Chi-Kang Dien, and J. W. Rinker. J. Am. Chem. Soc. **75**, 5039 (1953).
10. D. M. S. Wheeler and M. Wheeler. Chem. Ind. (London), 463 (1961).
11. H. Kwart and T. Takeshita. J. Am. Chem. Soc. **84**, 2833 (1962).
12. B. J. Bolger, A. Hirwe, K. G. Marathe, E. M. Philbin, M. A. Vickers, and C. P. Lillya. Tetrahedron, **22**, 621 (1966).
13. P. C. Arora and P. Brassard. Can. J. Chem. **45**, 67 (1967).

Can. J. Chem. Downloaded from www.nrcresearchpress.com by 210.87.254.40 on 09/05/12
For personal use only.

Can. J. Chem. Downloaded from www.nrcresearchpress.com by 210.87.254.105 on 09/05/12
For personal use only.

The Meyer Reaction of Phenylnitromethane in Acid. I. The Reactions of Phenyl-*aci*-nitromethane in Acid[1]

J. T. EDWARD AND P. H. TREMAINE
Department of Chemistry, McGill University, Montreal, Quebec

Received December 14, 1970[2]

Phenyl-*aci*-nitromethane reacts in aqueous sulfuric acid at room temperature to form phenylnitromethane and benzohydroxamic acid. The relative amounts of these two products depend on the concentration of the acid. Benzohydroxamic acid is formed by reaction of the intermediate, benzonitrile oxide, with water.

Solvent effects, substituent effects, and isotope effects have been studied to determine mechanisms for these reactions of phenyl-*aci*-nitromethane.

Le phényl-*aci*-nitrométhane au contact de l'acide sulfurique à température ambiante, donne deux produits: le phénylnitrométhane et l'acide benzohydroxamique. Un changement dans la concentration de l'acide sulfurique fait varier la proportion des deux produits. L'acide benzohydroxamique provient de la réaction de l'intermédiaire, l'oxyde de benzonitrile, avec l'eau.

L'influence du solvant et des substituants et les effets isotopiques ont été étudiés dans le but de découvrir le mécanisme de ces réactions.

Canadian Journal of Chemistry, **49**, 3483 (1971)

Introduction

Primary nitroalkanes in hot concentrated mineral acids give a carboxylic acid and hydroxylamine. This reaction was first reported by Meyer and Wurster in 1873 (1), and is now used commercially for the production of hydroxylamine.

It has been claimed (2, 3) that the rate-determining step in the Meyer reaction (illustrated in eqs. 1–3 for a phenylnitromethane) is the acid-catalyzed formation of the *aci*-form **2** of the nitroalkane **1**

[1] $$\underset{\mathbf{1}}{ArCH_2NO_2} \rightarrow \underset{\mathbf{2}}{ArCH{=}\overset{+}{N}\begin{matrix}O^-\\OH\end{matrix}}$$

[2] $$\underset{\mathbf{2}}{ArCH{=}\overset{+}{N}\begin{matrix}O^-\\OH\end{matrix}} \xrightarrow[H_2O]{H^+} \underset{\mathbf{3}}{ArC\begin{matrix}O\\NHOH\end{matrix}}$$

[3] $$\underset{\mathbf{3}}{ArCONHOH} + H_2O \rightarrow \underset{\mathbf{4}}{ArCO_2H} + NH_2OH$$

(eq. 1), followed by its rapid transformation into a hydroxamic acid **3** (eq. 2), which is then hydrolyzed to a carboxylic acid **4** and hydroxylamine (eq. 3). However, the nature of the steps involved in the transformation summarized in eq. 2 has remained obscure. Recently Cundall and Locke (3) have investigated the kinetics of the hydrolysis of nitromethane, and have proposed two possible mechanisms (one involving a nitrile oxide intermediate). However, they were unable to distinguish between these two alternatives.

In this and the following two papers we report on our studies of the mechanism of the Meyer reaction of phenylnitromethane, which in hot concentrated acid is converted into benzoic acid and hydroxylamine (4). The presence of the phenyl group makes it possible to study this reaction conveniently by u.v. spectrophotometry. In this paper we report on the mechanism of the reactions of phenyl-*aci*-nitromethane (**2**; Ar = Ph) and substituted phenyl-*aci*-nitromethanes; *i.e.*, on the mechanism of some of the reactions summarized by eq. 2, and the mechanism of **2** → **1**, the reverse of eq. 1.

Experimental

Materials

Phenylnitromethane was prepared by alkaline nitration of phenylacetonitrile (5). Nitration of phenylnitromethane with fuming nitric acid was used to prepare *m*-nitrophenylnitromethane, m.p. 96–97.5 °C (lit. 92–94 °C (6)). *p*-Methylphenylnitromethane, b.p. 76–78 °C/2 mm (lit. 99 °C/3 mm) was prepared by the reaction of α-chloro-*p*-xylene with silver nitrite in diethyl ether (7). *o*-Methylphenylnitromethane, b.p. 86–89 °C/2 mm (lit. 137–139 °C/23 mm) was synthesized in a similar manner from

[1]The research for this paper was supported in part by the Defence Research Board of Canada, Grant number 9530-57.

[2]Revision received July 21, 1971.

Can. J. Chem. Downloaded from www.nrcresearchpress.com by 210.87.254.105 on 09/05/12
For personal use only.

α-chloro-*o*-xylene, and characterized by formation of the benzal derivative, m.p. 93.5–94 °C (lit. 92 °C (8)).

The sodium salt of phenylnitromethane was prepared by addition of a methanol solution of phenylnitromethane to an equivalent amount of sodium methoxide in methanol. The solution was partially evaporated to precipitate the *aci*-salt, filtered, and the precipitate washed well with anhydrous ether. The white powder obtained was dried *in vacuo*. A stock solution of the sodium salt of phenylnitromethane was prepared by dissolving 7.5 mg of the salt in 0.01 *N* sodium hydroxide solution (10 ml).

The salts and the stock solutions of *m*-nitrophenylnitromethane, *p*-methylphenylnitromethane, and *o*-methylphenylnitromethane were prepared by a similar procedure.

Kinetic Runs

For each run, a 1.00 ml aliquot of the *aci*-salt stock solution at the reaction temperature was added to 25.00 ml of dilute sulfuric acid at the reaction temperature. After mixing, a spectrophotometer cell was rinsed with the reaction mixture, was then filled, and was placed in the temperature-controlled cell block of a Unicam SP800 spectrophotometer. After an equilibration period of 1 min, the u.v. spectra of the cell contents were obtained as a function of time by scanning at intervals. "Infinity" readings were obtained after at least seven half-lives. The pseudo-first-order rate constant (k_ψ) was calculated from the data for the optical density *vs.* time by a least-squares computer program. The concentration of the sulfuric acid was determined by titration of the reaction mixture with standard sodium hydroxide solution.

Phenyl-aci-nitromethane-α-d

Phenylnitromethane (194 mg) was dissolved in 2.5 *N* sodium deuteroxide in deuterium oxide (1 ml). The progress of the exchange was followed by p.m.r. spectroscopy. After heating to 70 °C for 6 h, the resonance from the α-proton (τ 2.9) had been reduced to 10% of the starting value. A 4 μl aliquot of this solution was added to 25.00 ml of dilute sulfuric acid and the kinetics were followed as above.

Isolation of Benzonitrile Oxide

A solution of 100 mg of the sodium salt of phenylnitromethane in 0.01 *N* sodium hydroxide solution (2 ml) was added to 3.5 *M* sulfuric acid (8 ml), resulting in a 2.8 *M* concentration of sulfuric acid. Ninety seconds after mixing, the solution was shaken with an equal volume of carbon tetrachloride; the organic layer was separated and cursorily dried over magnesium sulfate. The i.r. spectrum of the carbon tetrachloride solution was found to be identical with the spectrum of a solution of authentic benzonitrile oxide, prepared by the procedure of Wiley and Wakefield (9).

A similar extraction, carried out only 30 s after mixing, showed only a small peak at 2280 cm^{-1}, where benzonitrile oxide absorbs strongly, and a peak at 1650 cm^{-1} due to the *aci*-nitro group (10).

The first procedure above was repeated for the isolation of *m*-nitrobenzonitrile oxide from *m*-nitrophenyl-*aci*-nitromethane, but the medium used was 6.2 *M* sulfuric acid instead of 2.8 *M*. The i.r. spectrum of *m*-nitrobenzonitrile oxide in carbon tetrachloride showed characteristic absorptions at 2295, 1538, 1380, and 1350 cm^{-1}; these were observed also in the spectrum of authentic *m*-nitrobenzonitrile oxide (9).

Results and Discussion

Effect of Acid Concentration

Kornblum and Graham (11) isolated phenylnitromethane in 81% yield after addition of an excess of 20% hydrochloric acid to a strongly basic solution of phenylnitromethane at 5 °C, and Kornblum and Brown (12) isolated *p*-nitrophenylnitromethane in 93% yield after the *aci*-form had been allowed to react with 3.5 *N* sulfuric acid for 45 min. However, when the sodium salt of *p*-nitrophenylnitromethane was added to 85% sulfuric acid at room temperature, an 86% yield of *p*-nitrobenzohydroxamic acid was isolated after a few minutes. Alkylhydroxamic acids have frequently been isolated from the Meyer reaction in concentrated acid, in which their hydrolysis to a carboxylic acid and hydroxylamine is slow (13).

It is evident, then, that phenyl-*aci*-nitromethane in acid can give either phenylnitromethane or the Meyer reaction products, depending on whether the acid is dilute or concentrated.

Branch and Jaxon-Deelman (14) studied the transformation of phenyl-*aci*-nitromethane (**2**; Ar = Ph) to phenylnitromethane (**1**; Ar = Ph) in weak aqueous acid at 0 °C. They came to the conclusion that the tautomerization proceeds by ionization of the *aci*-form (**2**) to the anion (**5**) (eq. 4) which is then C-protonated by the solvent to form the nitro tautomer (**1**) (eq. 5)

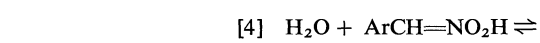

[4] $H_2O + \underset{\mathbf{2}}{ArCH{=}NO_2H} \rightleftharpoons \underset{\mathbf{5}}{ArCH{=}NO_2^-} + H_3O^+$

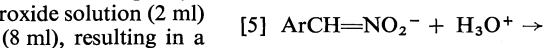

[5] $\underset{\mathbf{5}}{ArCH{=}NO_2^-} + H_3O^+ \rightarrow \underset{\mathbf{1}}{ArCH_2NO_2} + H_2O$

We studied the kinetics of the disappearance of phenyl-*aci*-nitromethane in acid by u.v. spectroscopy at 274 nm. The rate of disappearance of the *aci*-form increased with increasing acidity (Table 1). It was evident from the u.v. spectra (Fig. 1) that the nitro-form was not the only product from the reaction in 2 *M* sulfuric acid at 25.1 °C. The spectra showed clearly the decay of the *aci*-form (λ_{max} 274 nm), the formation and subsequent decay of an intermediate having a u.v. peak at 241 nm, and finally the formation of benzohydroxamic acid, having a peak at 230 nm. Phenylnitromethane, the other

Can. J. Chem. Downloaded from www.nrcresearchpress.com by 210.87.254.105 on 09/05/12
For personal use only.

TABLE 1. Rate constants for reactions of phenyl-*aci*-nitromethane in sulfuric acid at 25.1 °C

H_2SO_4 concentration (M)	10^4k_ψ* (s^{-1})	10^4k_{-1}† (s^{-1})	10^4k_2‡ (s^{-1})
0.010	23.4	20±1	3±1
0.520	27.5	22±1	6±1
1.45	35.2	18±2	17±2
1.70	37.9	16±2	22±2
1.99	44.1	14±3	30±3
2.51	66.	13±3	53±3
2.92	102.	15±5	87±5
3.14	113.	10±5	103±5
3.82	263.	10±10	258±15
4.01	325.	25±18	300±18

*Pseudo-first-order rate constant for disappearance of the *aci*-form.
†Pseudo-first-order rate constant for formation of the nitro-form.
‡Pseudo-first-order rate constant for formation of benzonitrile oxide.

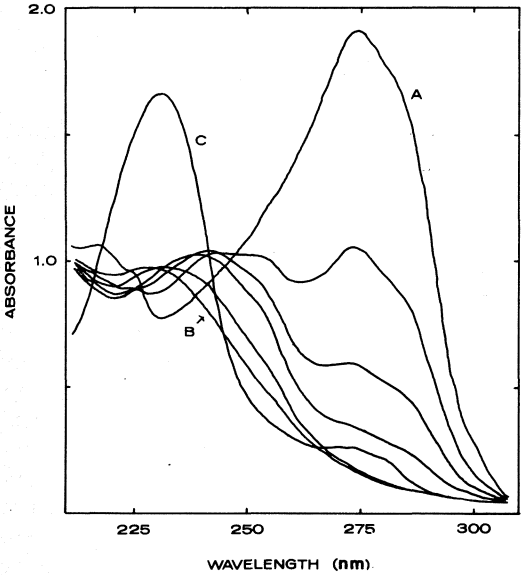

FIG. 1. The u.v. spectra recording the reaction of 0.00018 *M* phenyl-*aci*-nitromethane in 1.99 *M* sulfuric acid, after 60 s at 25.1 °C (*A*), after 3000 s at 25.1 °C (*B*), and after 2 days at 70° (*C*).

product from the *aci*-form, showed only end-absorption. On heating the reaction mixture to 70 °C for 2 days, both benzohydroxamic acid and phenylnitromethane were converted to benzoic acid (λ_{max} 230 nm), so that the peak at 230 nm increased by about 50%. Using the extinction coefficients at 230 nm of phenylnitromethane, benzohydroxamic acid, and benzoic acid, it was possible to calculate the rates of formation of phenylnitromethane (k_{-1}) and of the intermediate leading to benzohydroxamic acid (k_2) (15) (Table 1 and Fig. 2).

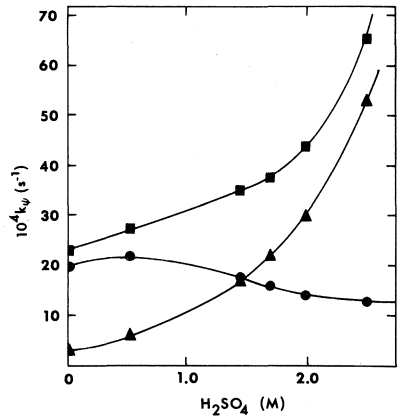

FIG. 2. Rate profiles (k_ψ) for the reaction of phenyl-*aci*-nitromethane in sulfuric acid at 25.1 °C: ■, pseudo-first-order rate constants for the disappearance of the *aci*-form; ●, pseudo-first-order rate constants for the formation of the nitro-form; ▲, pseudo-first-order rate constants for the formation of benzonitrile oxide.

The intermediate was extracted from a more concentrated reaction mixture into carbon tetrachloride and identified as benzonitrile oxide (9) by i.r. spectroscopy. It is shown in a following paper that benzonitrile oxide is hydrolyzed in acid cleanly to benzohydroxamic acid under the conditions of temperature and acid concentration employed in the present study.

Two mechanisms may be postulated (Scheme 1) for the conversion of phenyl-*aci*-nitromethane (**2**) to benzonitrile oxide (**9**). Cundall and Locke (3) proposed path *B*, without any experimental evidence to support the proposal, as well as another path not involving a nitrile oxide. However, an alternative pathway (*A*) to benzonitrile oxide may be envisaged. These two paths *A* and *B* are discussed below, and a choice between them is made. For the present it is sufficient to note that both mechanisms involve the formation of the protonated *aci* compound **6**, and hence both require acid-catalysis for the formation of the nitrile oxide **9**, as is observed (Fig. 2).

On the other hand, the formation of phenylnitromethane from phenyl-*aci*-nitromethane is inhibited by high acidities (Fig. 2). This evidence is in accord with the mechanism proposed in eqs. 4 and 5 (14, 16), high acidities preventing the formation of the anion **5** and hence the nitro compound **1**.

Isotope Effects

In an attempt to discriminate between the two

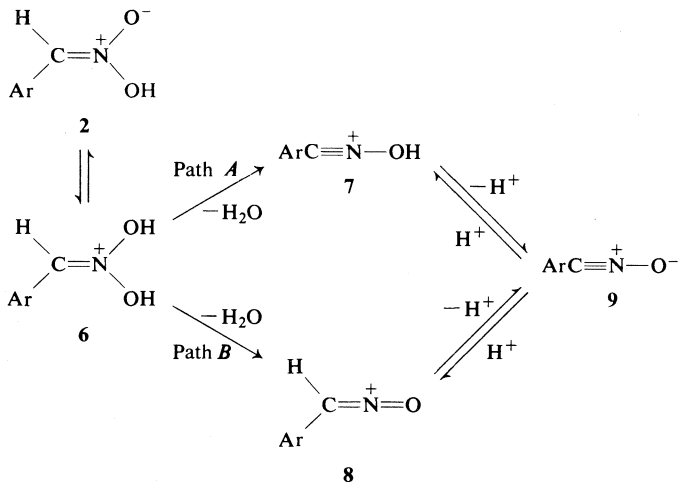

SCHEME 1

possible paths *A* and *B* in the formation of the nitrile oxide **9** from the *aci* compound **2**, we have determined the rates for the reactions of α-deuterio-*aci*-phenylnitromethane in acid solution. Significant stretching of the carbon–deuterium bond in the rate-controlling step would cause at least a two-fold decrease in the reaction rate (17). The results (Table 2) indicate that the α-hydrogen bond is not stretched in the transition state for the rate-determining step in the formation of the nitrile oxide. These results would seem to exclude path *A*, since the step **6** → **7** would certainly be the slow step in this mechanism. The evidence can be construed as evidence in support of reaction path *B* if the dehydration **6** → **8** is the slow step in the reaction.

No primary isotope effect would be expected for the tautomerization **2** → **1**, if it proceeds by the mechanism of eqs. 4–5, and none is found (Table 2).

Substituent Effects

The rate of disappearance of *m*-nitrophenyl-*aci*-nitromethane in sulfuric acid at room temperature was followed by u.v. spectrophotometry at 285 nm (Table 3 and Fig. 3). In dilute acid, the disappearance of this substituted *aci*-form was faster than the disappearance of the unsubstituted *aci*-form. Cooke and Macbeth (16) observed a similar increase in tautomerization rates of other substituted phenyl-*aci*-nitromethanes in water when the substituents were electron-withdrawing. This can be understood in terms of the mechanism of eqs. 4 and 5, if the effect of the electron-withdrawing substituent in making the substituted *aci*-form a stronger acid, and hence increasing the concentration of the anion **5** (eq. 4) is more important than its effect in decreasing the rate of protonation of **5** to form **1** (eq. 5).

In dilute acid, the *m*-nitro group can be expected not only to accelerate the conversion

TABLE 2. Isotope effects for reactions of phenyl-*aci*-nitromethane in sulfuric acid at 25.1 °C

Compound	H_2SO_4 concentration (*M*)	$10^4 k_\psi$* (s^{-1})	$10^4 k_{-1}$† (s^{-1})	$10^4 k_2$‡ (s^{-1})
$C_6H_5CD{=}NO_2H$	0.520	27.5±0.4	21±1	7±1
$C_6H_5CH{=}NO_2H$	0.520	27.5±0.4	22±1	6±1
$C_6H_5CD{=}NO_2H$	2.09	46.4±1.6	18±3	28±3
$C_6H_5CH{=}NO_2H$	2.09§	46.8±1.6	14±3	33±3

*Pseudo-first-order rate constant for disappearance of the *aci*-form.
†Pseudo-first-order rate constant for formation of the nitro-form.
‡Pseudo-first-order rate constant for formation of benzonitrile oxide.
§Value interpolated from rate data in Table 1.

Can. J. Chem. Downloaded from www.nrcresearchpress.com by 210.87.254.105 on 09/05/12
For personal use only.

Can. J. Chem. Downloaded from www.nrcresearchpress.com by 210.87.254.105 on 09/05/12
For personal use only.

TABLE 3. Pseudo-first-order rate constants (k_ψ) for disappearance of substituted phenyl-*aci*-nitromethanes in sulfuric acid at 25.4 °C

H_2SO_4 concentration (M)	*p*-Methyl 10^4k_ψ (s^{-1})	*o*-Methyl 10^4k_ψ (s^{-1})	*m*-Nitro 10^4k_ψ (s^{-1})
0.010	12.3	30.9	138.
0.520	18.4	40.5	—
1.12	27.2	50.	—
1.45	34.7	54.	—
1.73	—	67.	—
2.09	54.	82.	—
2.37	74.	97.	124.
2.69	101.	—	—
2.92	—	188.	104.
3.14	146.	—	—
4.01	—	—	78.
4.83	—	—	78.
5.69	—	—	108.
6.49	—	—	270.

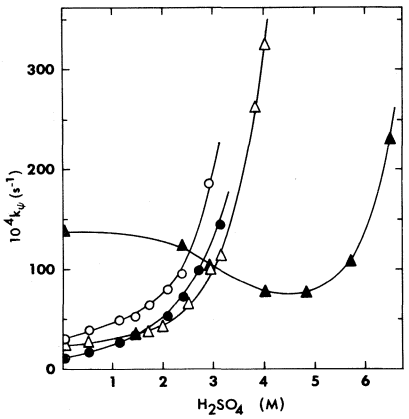

FIG. 3. Rate profiles (k_ψ) for the disappearance of phenyl-*aci*-nitromethanes in sulfuric acid: △, phenyl-*aci*-nitromethane (25.1 °C); ○, *o*-methylphenyl-*aci*-nitromethane (25.4 °C); ●, *p*-methylphenyl-*aci*-nitromethane (25.4 °C); ▲, *m*-nitrophenyl-*aci*-nitromethane (25.4 °C).

of the *aci*-form **2** to the nitro form **1**, but to retard the formation of *m*-nitrobenzonitrile oxide **9** (and thence of *m*-nitrobenzohydroxamic acid) by making the *aci*-form **2** a weaker base in the reaction **2** → **6** (Scheme 1). For these reasons, no *m*-nitrobenzonitrile oxide or *m*-nitrobenzohydroxamic acid are observed as products in dilute acid (<4 *M*). However, at high enough acid concentrations the rate of formation of the nitro compound is sufficiently depressed (by repression of reaction 4), and the rate of formation of the nitrile oxide sufficiently enhanced (by protonation of **2** → **6**), for *m*-nitrobenzonitrile oxide (λ_{max} 243 nm) to become apparent in the reaction mixture. It rapidly adds water to form *m*-nitrobenzohydroxamic acid (λ_{max} 215 nm). Some *m*-nitrobenzonitrile oxide was extracted from a concentrated solution of the *aci*-compound in 6.2 *M* sulfuric acid, and identified by its i.r. spectrum.

The rates of disappearance of *p*-methylphenyl-*aci*-nitromethane and *o*-methylphenyl-*aci*-nitromethane in sulfuric acid were determined by following the decay of their absorption peaks at 280 nm (Table 3 and Fig. 3). Even in 1 *M* sulfuric acid, some *o*- and *p*-methylbenzonitrile oxide is observed during the reaction of both substituted *aci*-forms, so the observed rate of disappearance is a combination of the rate of tautomerization to the nitro-form and the rate of dehydration to *o*- and *p*-methylbenzonitrile oxide. It is evident from the results that both of these reactions are accelerated by the proximity of the methyl group to the reaction site. The molecular model of the ortho-substituted *aci*-form shows some crowding, which is relieved on dehydration by path *A* or *B* of Scheme 1. The strain is also relieved on tautomerization to the nitro-form. A steric acceleration of the tautomerization in water has already been observed for *o*-chloro- and *o*-bromophenyl-*aci*-nitromethane (16).

Activation Parameters

The entropies of activation calculated for the disappearance of phenyl-*aci*-nitromethane in acid are negative (Table 4) over a range of acid concentration. It must be kept in mind that the disappearance of the *aci*-form takes place by two paths: tautomerization to the nitro-form and dehydration to benzonitrile oxide. As the acid concentration is increased, the increase in the entropy of activation is due to the greater contribution of the dehydration path to the disappearance. Such a process would be expected to have a higher entropy of activation than the proton transfer necessary for tautomerization (18).

There is little change in the enthalpy of activation for the disappearance of the *aci*-form as the acid concentration is increased, demonstrating the equality of the energy barriers for the two competing modes of disappearance. This indicates that for a particular acid concentration,

TABLE 4. Activation parameters for disappearance of phenyl-*aci*-nitromethane in sulfuric acid

Temperature (°C)	H_2SO_4 concentration (M)	$10^4 k_\psi$ (s^{-1})	$\Delta H^\ddagger$ (kcal/mol)	$\Delta S^\ddagger$ (e.u.)*
25.1	0.520	27.5	17±1	−15±3
34.2	0.520	63.7		
25.1	1.70	37.9	19±1	−10±3
34.2	1.70	96.		
25.1	2.51	65.7	18±1	−10±3
34.2	2.51	165.		

*1 *M* standard state.

the ratio of the rates of the two reactions (tautomerization and dehydration) would remain approximately constant as the temperature is raised.

Conclusions

This study has shown that the pseudo-first-order rate constant (k_ψ) for the disappearance of phenyl-*aci*-nitromethane (**2**) in acid is made up of two rate constants: k_{-1} for the tautomerization to the nitro form (**1**), and k_2 for the dehydration to benzonitrile oxide (**9**) (eq. 6) The mechan-

$$[6]\quad \underset{\mathbf{1}}{ArCH_2NO_2} \underset{k_{-1}}{\overset{k_1}{\rightleftharpoons}} \underset{\mathbf{2}}{ArCH{=}NO_2H} \overset{k_2}{\rightarrow} \underset{\mathbf{9}}{ArC{\equiv}\overset{+}{N}{-}O^-} + H_2O$$

isms of these reactions have been discussed, and account for the fact that while in dilute acid $k_{-1} > k_2$, in strong acid $k_2 \gg k_{-1}$. The activation parameters indicate that the relative rates would not change greatly with temperature.

Kinetic isotope studies indicate that benzonitrile oxide is formed from the protonated *aci*-form by slow elimination of water from the two hydroxyls attached to nitrogen, followed by rapid proton loss from carbon.

For work in this and the following two papers, we are pleased to acknowledge the skillful technical assistance of James Tong, the grant of a McConnell Fellowship by McGill University (to P.H.T.) for 1968–1970, and the financial support of the Defence Research Board of Canada.

1. V. MEYER and C. WURSTER. Ber. **6**, 1168 (1873).
2. P. A. S. SMITH. The chemistry of open-chain organic nitrogen compounds. Vol. II. Benjamin Press, New York, N.Y., 1960. p. 399.
3. R. CUNDALL and A. LOCKE. J. Chem. Soc. B, 98 (1968).
4. E. BAMBERGER and E. RUST. Ber. **35**, 45 (1902).
5. A. H. BLATT (Editor). Org. Syntheses. Coll. Vol. II, 512 (1942).
6. L. F. FIESER and M. GATES. J. Am. Chem. Soc. **68**, 2249 (1946).
7. N. KORNBLUM, R. A. SMILEY, R. K. BLACKWOOD, and D. C. IFFLAND. J. Am. Chem. Soc. **77**, 6269 (1955).
8. J. MEISENHEIMER and J. LINK. Ann. **468**, 217 (1929).
9. R. H. WILEY and B. J. WAKEFIELD. J. Org. Chem. **25**, 546 (1960).
10. J. P. FREEMAN and K. S. MCCALLUM. J. Org. Chem. **21**, 472 (1956).
11. N. KORNBLUM and G. E. GRAHAM. J. Am. Chem. Soc. **73**, 4041 (1951).
12. N. KORNBLUM and R. A. BROWN. J. Am. Chem. Soc. **87**, 1742 (1965).
13. S. B. LIPPINCOTT and H. B. HASS. Ind. Eng. Chem. **31**, 118 (1939).
14. G. K. BRANCH and J. JAXON-DEELMAN. J. Am. Chem. Soc. **49**, 1765 (1927).
15. A. A. FROST and R. G. PEARSON. Kinetics and mechanism. John Wiley and Sons, New York, N.Y., 1961. p. 160.
16. R. G. COOKE and A. K. MACBETH. J. Chem. Soc. 1024 (1938).
17. F. H. WESTHEIMER. Chem. Revs. **61**, 265 (1961).
18. L. L. SCHALEGER and F. A. LONG. *In* Advances in physical organic chemistry. Vol. I. *Edited by* V. Gold, Academic Press, New York, N.Y., 1963. p. 1.

Can. J. Chem. Downloaded from www.nrcresearchpress.com by 210.87.254.105 on 09/05/12
For personal use only.

Can. J. Chem. Downloaded from www.nrcresearchpress.com by 210.87.254.40 on 09/05/12
For personal use only.

The Meyer Reaction of Phenylnitromethane in Acid. II. Reactions in Acid of Benzonitrile Oxide and Benzohydroxamic Acid[1]

J. T. EDWARD AND P. H. TREMAINE
Department of Chemistry, McGill University, Montreal, Quebec

Received December 14, 1970[2]

The kinetics of the transformation of benzonitrile oxide in dilute sulfuric acid into benzohydroxamic acid have been followed by u.v. spectrophotometry at a temperature near room temperature. A mechanism is proposed on the basis of the effects of substituents and sulfuric acid concentration.

The rate profile for the hydrolysis of benzohydroxamic acid in hot dilute sulfuric acid has been obtained.

The results of these studies are applied to the detailed mechanism of the Meyer rearrangement – hydrolysis of phenylnitromethane in acid.

La cinétique de formation de l'acide benzohydroxamique à partir de l'oxyde de benzonitrile dans l'acide sulfurique a été étudiée à la température ambiante. Afin de proposer un mécanisme pour cette réaction on a étudié l'influence de divers substituants et de différentes concentrations d'acide.

La vitesse de l'hydrolyse de l'acide benzohydroxamique a été étudiée à 68.8 °C en variant la concentration de l'acide sulfurique.

Les conclusions de ces études sont appliquées au mécanisme de la réaction de Meyer sur le phénylnitrométhane.

Canadian Journal of Chemistry, **49**, 3489 (1971)

Introduction

In an example of the Meyer reaction, phenylnitromethane forms benzoic acid and hydroxylamine when heated in mineral acid (1). The slowest step in the reaction sequence is the formation of phenyl-*aci*-nitromethane (eq. 1) (2), and in the preceding paper (3) we have studied the rate at which phenyl-*aci*-nitromethane reverts to phenylnitromethane (k_{-1} of reaction 1) and the rate at which it is dehydrated to benzonitrile oxide (k_2 of reaction 2). It is already know that benzonitrile oxide in acid solution adds water to form benzohydroxamic acid (eq. 3) (4) (which has been isolated in small yield from the reaction of phenylnitromethane in hot acid (5)), and that benzohydroxamic acid is hydrolyzed to benzoic acid and hydroxylamine (eq. 4) (6), but no kinetic studies have been reported for these reactions. We now report these, as a part of an overall study of the Meyer reaction of phenylnitromethane described in this and two accompanying papers (3, 7).

$$[1] \quad ArCH_2NO_2 \underset{k_{-1}}{\overset{k_1}{\rightleftharpoons}} ArCH{=}NO_2H$$

$$[2] \quad ArCH{=}NO_2H \xrightarrow[k_2]{} ArC{\equiv}\overset{+}{N}{-}O^- + H_2O$$

$$[3] \quad ArC{\equiv}\overset{+}{N}{-}O^- + H_2O \rightarrow ArCONHOH$$

$$[4] \quad ArCONHOH + H_2O \rightarrow ArCO_2H + NH_2OH$$

Experimental

Preparation of Benzonitrile Oxide

Benzohydroximoyl chloride (m.p. 50–52 °C) was prepared by the chlorination of benzaldoxime in hydrochloric acid (8). A solution of 30 mg of benzohydroximoyl chloride in 5 ml of carbon tetrachloride was shaken with 5 ml of water, the organic layer was drawn off and dried with magnesium sulfate at 0 °C. The i.r. spectrum of this solution showed the same distinctive absorptions at 2290, 1368, 1096, and 1029 cm^{-1} that are found in the spectrum of authentic benzonitrile oxide prepared using sodium carbonate solution (8). The carbon tetrachloride solution was extracted with water and the u.v. spectrum of the extract showed an absorption at 245 nm with a slight shoulder at 253 nm. This is identical with the spectrum of authentic benzonitrile oxide in water.

The addition of aqueous sodium carbonate to this solution of benzonitrile oxide in the spectrophotometer cell initiated a change in the u.v. spectrum, which passed with an isosbestic point from an absorption with λ_{max} 245 nm to one with λ_{max} 268 nm. The product was identified as benzohydroxamate anion on the basis of its u.v. spectrum and the spectrum of benzohydroxamic acid obtained on acidification (λ_{max} 230 nm).

Kinetic Runs on the Benzonitrile Oxides

(1) From Benzohydroximoyl Chloride

A 10^{-3} *M* stock solution of benzonitrile oxide was prepared by dissolving 15 mg benzohydroximoyl chloride in 25 ml distilled water. A 1 ml aliquot of this stock solu-

[1]The research for this paper was supported in part by the Defence Research Board of Canada, Grant number 9530–57.

[2]Revision received July 21, 1971.

Can. J. Chem. Downloaded from www.nrcresearchpress.com by 210.87.254.40 on 09/05/12
For personal use only.

tion at the reaction temperature was added to 25.00 ml dilute sulfuric acid, which was pre-equilibrated at the reaction temperature. After mixing, a 1 cm spectrophotometer cell was rinsed with the reaction mixture, was then filled, and placed in the temperature-controlled cell block of a Unicam SP800 spectrophotometer. After an equilibration period of at least 1 min, the u.v. spectrum was scanned at recorded time intervals. The spectrum at "infinite" time was recorded after at least seven half-lives. The optical densities (A) were measured from the spectra at 243 nm, and the first-order rate constant was obtained from a computer-calculated least-squares plot of ln $(A_t - A_\infty)$ *vs.* time. The concentration of the sulfuric acid solution was determined after the run by titration of the reaction mixture with standard alkali. A similar procedure was used for preparation of *m*-nitrobenzonitrile oxide from *m*-nitrobenzohydroximoyl chloride for the kinetic experiments in dilute sulfuric acid.

(2) From Phenyl-aci-nitromethane

The procedure used to determine the rate of reaction of phenyl-*aci*-nitromethane in acid solution has been described in the preceding paper (3). At some acid concentrations, the u.v. spectra still show the presence of benzonitrile oxide after at least 90% of the phenyl-*aci*-nitromethane has reacted. The disappearance of this benzonitrile oxide has been followed by repetitive scanning at recorded time intervals with an equilibrium reading taken after at least seven half-lives. The data for the optical density *vs.* time were treated as above to obtain the first-order rate constant.

A similar procedure was used to follow the reactions of *m*-nitrobenzonitrile oxide at 245 nm, *o*-methylbenzonitrile oxide at 250 nm, and *p*-methylbenzonitrile oxide at 256 nm.

Hydrolysis of Benzohydroxamic Acid

One milliliter of an aqueous stock solution of benzohydroxamic acid was added to 25.00 ml of dilute sulfuric acid to produce a final concentration of benzohydroxamic acid of 0.0007 *M*. Two milliliter aliquots of this reaction mixture were measured into screw-capped glass vials. These sample tubes were heated in a thermostatted water bath to 68.8 °C. After an equilibration period of 45 min, tubes were removed at different time intervals, cooled in ice, and quenched with 3 ml of cold 9 *N* sodium hydroxide solution. The samples were then scanned with the Unicam SP800 to determine benzohydroxamate anion at 270 nm. The sample for determination at "infinite" time was withdrawn after at least seven half-lives. The data for the optical density and time were treated as above to obtain the first-order rate constant.

Results and Discussion

(A) Preparation of Benzonitrile Oxide and Substituted Derivatives

In concentrated solution, unhindered benzonitrile oxides dimerize quickly to form furoxans (9). Dilute solutions of unhindered benzonitrile oxides are stable enough for their i.r. spectra to be recorded (8). We have found that 10^{-3} *M* solutions of benzonitrile oxide in water are stable for hours, but that they react rapidly to form benzohydroxamic acid on addition of sulfuric acid. The addition of sodium carbonate to an aqueous solution of benzonitrile oxide results in the formation of benzohydroxamate anion in a few minutes.

A stock solution of benzonitrile oxide was prepared by dissolving benzohydroximoyl chloride in water; water is sufficiently basic to bring about the immediate formation of benzonitrile oxide from benzohydroximoyl chloride under these conditions. An aliquot of the stock solution was added to a sulfuric acid solution and the disappearance of benzonitrile oxide was followed by u.v. spectrophotometry.

In the same manner, it was possible to prepare a stock solution of *m*-nitrobenzonitrile oxide from *m*-nitrobenzohydroximoyl chloride. However, it was found more convenient to prepare this nitrile oxide by allowing *m*-nitrophenyl-*aci*-nitromethane to react in strong acid solution. The products of this reaction are *m*-nitrophenylnitromethane, which is stable (under the conditions of the reaction), and *m*-nitrobenzonitrile oxide, which reacts further to form *m*-nitrobenzohydroxamic acid. The latter reaction can be followed by u.v. spectrophotometry.

Both *p*-methylbenzonitrile oxide and *o*-methylbenzonitrile oxide were prepared in similar fashion from the corresponding methylphenyl-*aci*-nitromethanes.

(B) The Reaction in Acid of the Benzonitrile Oxides.

Effect of Acid Concentration

In sulfuric acid, benzonitrile oxide reacts cleanly to form benzohydroxamic acid. This is shown by the u.v. spectra, which during the reaction exhibit a sharp isosbestic point at a wavelength between those of the absorption peaks of starting material at 245 nm and of product at 228 nm. Increasing the acid concentration of the medium causes an increase in the rate of the reaction (Table 1). This marked effect of acid concentration suggests an equilibrium protonation (eq. 5) preceding the nucleophilic attack by water (eq. 6) The carbonyl form of benzohydrox-

[5] $$ArC\equiv\overset{+}{N}—O^- + H_3O^+ \rightleftharpoons ArC\equiv\overset{+}{N}—OH + H_2O$$

[6] $$ArC\equiv\overset{+}{N}—OH + 2H_2O \rightarrow \left[ArC\begin{matrix}OH\\ \diagdown\!\!\diagup\\ NOH\end{matrix} \right] + H_3O^+$$

Can. J. Chem. Downloaded from www.nrcresearchpress.com by 210.87.254.40 on 09/05/12
For personal use only.

TABLE 1. Pseudo-first-order rate constants (k_ψ) for the reaction of benzonitrile oxide in sulfuric acid

Temperature (°C)	H_2SO_4 concentration (M)	$10^4 k_\psi$ (s^{-1})
20.6	1.45	5.0*
	2.51	11.8*
	3.36	22.7*
	4.07	39.6*
25.1	1.45	7.8†
	1.70	8.8†
	1.99	12.6†
	2.51	19.7†
	4.01	46.0†
35.0	0.195	2.09*
	1.45	19.2*

*Benzonitrile oxide prepared from benzohydroximoyl chloride (see Experimental).
†Benzonitrile oxide prepared from phenyl-*aci*-nitromethane.

[7] 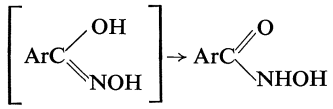

amic acid has already been identified, by u.v. and i.r. spectroscopy (10, 11), as the stable tautomer (hence eq. 7).

Over the range of acid concentrations studied, the rates of reaction of benzonitrile oxide are slightly slower than the rates of its formation from the *aci*-form. This accounts for the observation of benzonitrile oxide as an intermediate during the reaction of the *aci*-form, as described in the preceding paper (3).

Substituent Effects

With increasing acid concentration, *m*-nitrobenzonitrile oxide exhibits an increase in the rate of reaction (Table 2). However, compared to unsubstituted benzonitrile oxide, the onset of the rapid increase in the rate of reaction is delayed until higher acid concentrations. This behavior may be explained by reference to eqs. 5 and 6: the electron-withdrawing group makes the *m*-nitrobenzonitrile oxide less basic than unsubstituted benzonitrile oxide, requiring a more strongly acidic medium to form the same concentration of protonated substrate. On the other hand, the rate of reaction 6 is subject to an increase when Ar is substituted with an electron-withdrawing group, because of the enhanced electrophilicity of the substituted compound. The two effects (on reactions 5 and 6) are in opposition, but in the present instance the effect of the *m*-nitro group on reaction 5 is greater than its effect on reaction 6, so that a slower reaction results. A similar result has been reported for the acid-catalyzed hydrolysis of benzalanilines (12) and benzamides (13). Jencks (14) has recently discussed this balance between the substituent effects for a rate-determining step and a preceding equilibrium.

Up to a concentration of at least 9 M sulfuric acid, the rate of destruction of *m*-nitrobenzonitrile oxide is slower than its rate of formation from the *aci*-form, so *m*-nitrobenzonitrile oxide should be observed spectroscopically if it is an intermediate during the reaction of *m*-nitrophenyl-*aci*-nitromethane in acid. Consequently, failure to observe *m*-nitrobenzonitrile oxide during the reaction of *m*-nitrophenyl-*aci*-nitromethane in sulfuric acid of less than 4 M concentration (3) indicates that in these acid concentrations $k_{-1} \gg k_2$.

TABLE 2. Pseudo-first-order rate constants (k_ψ) for the reaction of *m*-nitrobenzonitrile oxide in sulfuric acid

Temperature (°C)	H_2SO_4 concentration (M)	$10^4 k_\psi$ (s^{-1})
20.6	1.45	2.32*
	4.07	7.1*
	4.53	10.0*
	5.69	14.6*
25.4	5.69	23.4†
	6.49	35.9†
	7.33	56.6†
	9.18	136. †

**m*-Nitrobenzonitrile oxide prepared from *m*-nitrobenzohydroximoyl chloride (see Experimental).
†*m*-Nitrobenzonitrile oxide prepared from *m*-nitrophenyl-*aci*-nitromethane.

Steric Effects

The rate profiles for *p*-methylbenzonitrile oxide and *o*-methylbenzonitrile oxide (Table 3) illus-

TABLE 3. Pseudo-first-order rate constants (k_ψ) for the reaction of methylbenzonitrile oxides with sulfuric acid at 25.4 °C

H_2SO_4 concentration (M)	*p*-Methyl $10^4 k_\psi$ (s^{-1})	*o*-Methyl $10^4 k_\psi$ (s^{-1})
0.520	—	5.5
1.12	9.2	6.7
1.45	12.7	7.4
1.73	—	8.9
2.09	20.4	12.4
2.37	31.5	16.4
2.69	38.6	—
2.92	—	25.0
3.14	55.6	—

Can. J. Chem. Downloaded from www.nrcresearchpress.com by 210.87.254.40 on 09/05/12
For personal use only.

TABLE 4. Pseudo-first-order rate constants (k_ψ) for hydrolysis of benzohydroxamic acid in sulfuric acid at 68.8 °C

H_2SO_4 concentration (M)	$10^5 k_\psi$ (s^{-1})
.195	2.32
.520	6.39
1.12	12.2
1.73	17.4
2.37	24.6
3.14	37.1
4.53	32.0

trate the rate decrease caused by the proximity of a methyl group to the reaction site. The steric effect lends support to the designation of reaction 6 as the rate-determining step in the hydrolysis of nitrile oxides, since the formation of *o*-methylbenzohydroxamic acid would be slowed by hindrance to nucleophilic attack by water.

Activation Parameters

The rates of reaction of benzonitrile oxide in 1.45 M sulfuric acid at 20.6, 25.1, and 35.0 °C (Table 1) have been used to calculate the approximate enthalpy and entropy of activation for the reaction: $\Delta H^{\ddagger} = 17$ kcal/mol, and $\Delta S^{\ddagger} = -19$ e.u. The entropy of activation is negative, as expected for a nucleophilic attack of water in the rate-determining step (15). Similar values are obtained from the data in Table 2 for *m*-nitrobenzonitrile oxide in 5.69 M sulfuric acid: $\Delta H^{\ddagger} = 17$ kcal/mol, and $\Delta S^{\ddagger} = -19$ e.u.

(C) The Hydrolysis of Benzohydroxamic Acid

The rates of hydrolysis of benzohydroxamic acid in sulfuric acid were obtained at 68.8 °C by quenching aliquots of the reaction mixture in base (Table 4). This procedure permitted determination of the resulting benzohydroxamate anion by u.v. spectrophotometry at 270 nm, where benzoate anion does not interfere (10). Over the range of acid concentrations, the rates observed are greater than the rates of the Meyer rearrangement – hydrolysis of phenylnitromethane at 68.8 °C (7); this accounts for the failure under these conditions to observe benzohydroxamic acid as an intermediate. The rate of hydrolysis of benzohydroxamic acid, like that of benzamide (16), passes through a maximum as the acid concentration is increased, and probably involves a similar mechanism (16, 17), given in eqs. 8 and 9.

[8] $C_6H_5C(=O)NHOH + H_3O^+ \rightleftharpoons C_6H_5C(=\overset{+}{O}H)NHOH + H_2O$

[9] $C_6H_5C(=\overset{+}{O}H)NHOH + H_2O \rightarrow C_6H_5C(=O)OH + NH_3OH^+$

1. S. GABRIEL and M. KOPPE. Ber. **19**, 1145 (1886).
2. P. A. S. SMITH. The chemistry of open-chain organic nitrogen compounds. Vol. II. Benjamin Press, New York, N.Y., 1960. p. 399.
3. J. T. EDWARD and P. H. TREMAINE. Can. J. Chem. This issue, preceding paper.
4. H. WIELAND. Ber. **40**, 1667 (1907).
5. E. BAMBERGER and E. RUST. Ber. **35**, 45 (1902).
6. Y. INOUE and H. YUKAWA. J. Agr. Chem. Soc. Jap. **16**, 504 (1940). Chem. Abstr. **35**, 730 (1941).
7. J. T. EDWARD and P. H. TREMAINE. Can. J. Chem. This issue, following paper.
8. R. H. WILEY and B. J. WAKEFIELD. J. Org. Chem. **25**, 546 (1960).
9. R. HUISGEN. Angew. Chem. Int. Ed. **2**, 565 (1963).
10. R. E. PLAPINGER. J. Org. Chem. **24**, 802 (1959).
11. D. HADZI and D. PREVORSEK. Spectrochim. Acta, **10**, 38 (1957).
12. A. V. WILLI and R. E. ROBERTSON. Can. J. Chem. **31**, 361 (1953).
13. I. MELOCHE and K. J. LAIDLER. J. Am. Chem. Soc. **73**, 1712 (1951).
14. W. P. JENCKS. Catalysis in chemistry and enzymology. McGraw-Hill, New York, N.Y., 1969. p. 481.
15. L. L. SCHALEGER and F. A. LONG. *In* Advances in physical organic chemistry. Vol. I. *Edited by* V. Gold. Academic Press, New York, N.Y., 1963. p. 1.
16. J. T. EDWARD and S. C. R. MEACOCK. J. Chem. Soc. 2000 (1957).
17. K. YATES and J. C. RIORDAN. Can. J. Chem. **43**, 2329 (1965).

Can. J. Chem. Downloaded from www.nrcresearchpress.com by 210.87.254.42 on 09/05/12
For personal use only.

The Meyer Reaction of Phenylnitromethane in Acid. III. The Tautomerization to the *aci*-Form[1]

J. T. Edward and P. H. Tremaine
Department of Chemistry, McGill University, Montreal, Quebec

Received December 14, 1970[2]

The rate-acidity profiles for the Meyer rearrangement–hydrolysis of phenylnitromethane in sulfuric, perchloric, and hydrochloric acid show a maximum near 3 *M* acid. Ring-substituted phenylnitromethanes also show a maximum in their rate profiles, at slightly different acid concentrations. These maxima arise because the slow formation of the *aci*-form is followed by two competing reactions: fast tautomerization back to the nitro-form, and fast rearrangement–hydrolysis to the Meyer products. The rearrangement is rate-limiting in dilute acid and is acid-catalyzed, causing the rate increase. In more concentrated acid, the rate-limiting step is the nitro to *aci* tautomerization, which is not acid-catalyzed, and which goes more slowly as the activity of water decreases.

The tautomerization was studied by means of primary and solvent deuterium isotope effects, and was found to occur through proton abstraction by water, through a transition state closely resembling the products.

En variant la concentration d'acide sulfurique, hydrochlorique, ou perchlorique, on obtient un maximum aux environs de 3 *M* acide dans la vitesse de la réaction de Meyer sur le phénylnitrométhane. Avec les phénylnitrométhanes substitués on obtient aussi un maximum de vitesse, mais à de différentes molarités d'acide.

La présence de ce maximum peut être expliquée par ce schéma de réaction: la formation lente de la forme *aci*, suivie par deux réactions rapides et concurrentes: une réaction de tautomérisation redonnant la forme nitro, et une réaction de réarrangement menant finalement aux produits Meyer. Au-dessous du maximum, la réaction de réarrangement, catalysée par l'acide, contrôle la vitesse de la réaction globale menant aux produits Meyer. Au-dessus du maximum, la réaction de tautomérisation redonnant la forme nitro est supprimée par l'acide, de sorte que la vitesse de la réaction globale de Meyer est contrôlée par la formation lente de la forme *aci*. Celle-ci est ralentie à mesure qu'on augmente la concentration de l'acide.

Afin d'éclaircir le mécanisme de la formation lente de la forme *aci*, on a étudié les effets produits par une substitution de deutérium dans le solvant ou dans le phénylnitrométhane. Les resultats indiquent que l'abstraction du proton α par l'eau passe par un état de transition ressemblant fortement aux produits.

Canadian Journal of Chemistry, **49**, 3493 (1971)

Introduction

The work done up to 1955 on the Meyer reaction (1) (a rearrangement–hydrolysis) has been reviewed by Noland (2), who proposed the formation of the *aci*-nitroalkane (eq. 1) as the slow step, followed by a series of rapid reactions in the acidic medium. This mechanism was based on the work of Junell (3), who showed that the rate of hydrolysis of nitroethane in 1 *N* hydrochloric acid was the same as its rate of bromination. Our study of the reaction of phenyl-*aci*-nitromethane in acid (4) has shown that, at least for phenylnitromethane in dilute acid, this reaction scheme must be modified by the addition of a fast back-reaction from phenyl-*aci*-nitromethane to phenylnitromethane (eq. 2). The identification of benzonitrile oxide formed by the mechanism of eqs. 3–5, as an intermediate in the rearrangement of phenyl-*aci*-nitromethane to benzohydroxamic acid was also reported at that time. The mechanism of the

$$[1] \qquad RCH_2NO_2 \xrightarrow{k_1} RCH{=}NO_2H$$

$$[2] \qquad RCH{=}NO_2H \xrightarrow{k_{-1}} RCH_2NO_2$$

$$[3] \qquad H_3O^+ + RCH{=}NO_2H \rightleftharpoons RCH{=}\overset{+}{N}\begin{matrix}OH\\OH\end{matrix} + H_2O$$

$$[4] \qquad RCH{=}\overset{+}{N}\begin{matrix}OH\\OH\end{matrix} \rightarrow RCH{=}\overset{+}{N}{=}O + H_2O$$

$$[5] \qquad H_2O + RCH{=}\overset{+}{N}{=}O \rightleftharpoons RC{\equiv}\overset{+}{N}{-}O^- + H_3O^+$$

$$[6] \qquad RC{\equiv}\overset{+}{N}{-}O^- + H_3O^+ \rightleftharpoons RC{\equiv}\overset{+}{N}{-}OH + H_2O$$

[1]The research for this paper was supported in part by the Defence Research Board of Canada, Grant number 9530-57.

[2]Revision received July 21, 1971.

Can. J. Chem. Downloaded from www.nrcresearchpress.com by 210.87.254.42 on 09/05/12
For personal use only.

[7] $2H_2O + RC{\equiv}\overset{+}{N}{-}OH \rightarrow RCONHOH + H_3O^+$

[8] $H_3O^+ + RCONHOH \rightarrow RCOOH + NH_3OH^+$

hydration of benzonitrile oxide (eqs. 6 and 7), and of the hydrolysis of benzohydroxamic acid (eq. 8) were discussed in a second paper (5). In the present paper we consider reaction 1, the rate-determining step under some (but as it will be shown, not all) conditions of the reaction.

The details of this rate-determining step may be tested by following the dependence of the overall reaction rate on the acidity of the medium. Cundall and Locke (6) found that the rate profile for the Meyer reaction of nitromethane in hydrochloric acid passed through a maximum at 4 *M* hydrochloric acid. After a slight decline, the rate continued to increase with increasing acidity up to 10*M* hydrochloric acid, the highest concentration studied. A possible explanation for the maximum at 4 *M* acid in the rate profile could have been the essentially complete protonation of nitromethane at that acidity; however, Gillespie (7) had already reported that nitromethane is only 21% protonated in 100% sulfuric acid. Alternatively, the maximum could be explained by the essentially complete formation of a hydrogen-bonded complex (8–11), in 4 *M* acid:

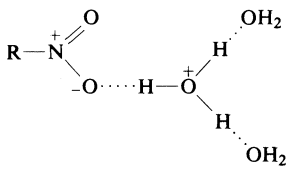

Similar hydrogen-bonded complexes of ketones in moderate concentrations of acid have been proposed (12), and may be intermediates in the enolization of ketones in acid (13). However, Haldna *et al.* (8) have presented evidence that the formation of a hydrogen-bonded complex of nitromethane does not affect the rate of bromination of nitromethane in dilute sulfuric acid, and we show in this paper that the maximum in the rate of formation of Meyer products from phenylnitromethane also is not explained by formation of such a complex.

Experimental

Materials

The preparation of phenylnitromethane, *m*-nitrophenylnitromethane, *p*-methylphenylnitromethane, and *o*-methylphenylnitromethane has been described in a previous paper (4). *p*-Nitrophenylnitromethane, m.p. 89–91.5 °C (lit. 89–90.5 °C) (14) and *p*-chlorophenylnitromethane, m.p. 31–31.5 °C (lit. 33 °C) (15), were prepared by reaction of the substituted benzyl halide with silver nitrite in diethyl ether. 2,4,6-Trimethylphenylnitromethane, m.p. 74–74.5 °C, was prepared from 2,4,6-trimethylbenzyl chloride and silver nitrite in diethyl ether (14) and was characterized by its i.r. spectrum (1550 and 1367 cm^{-1}) and its p.m.r. spectrum (singlet 3.17 for 2 protons, singlet 4.60 for 2 protons, and two singlets 7.68 and 7.75 τ with total 9 protons).

Anal. Calcd. for $C_{10}H_{13}NO_2$: C, 67.02; H, 7.31. Found: C, 67.19; H, 7.35.

All the phenylnitromethanes were stored at −20 °C until used.

Deuteriosulfuric acid (99% D) of spectroscopic quality was obtained from Merck, Sharp and Dohme of Canada, Limited.

Phenylnitromethane-α,α-d_2 was prepared by the exchange of phenylnitromethane in alkaline deuterium oxide (16). After acidification with deuteriosulfuric acid, the deuterated phenylnitromethane was extracted out with carbon tetrachloride. The organic solution was dried and evaporated. Analysis for residual hydrogen in the deuterated phenylnitromethane by p.m.r. spectroscopy showed an isotopic purity of 97% D at the α-position.

Procedures for Kinetic Runs

(*A*) Sufficient phenylnitromethane was dissolved in water or 50% ethanol to give a 0.003 *M* solution. A 4 ml aliquot of this stock solution was added to 100.0 ml of dilute mineral acid in a stoppered flask. The flask was then immersed in a thermostatted water bath (±0.05 °C) and allowed to warm up for 45 min. (Separate experiments showed that thermal equilibrium was reached in less than this time.) Five milliliter aliquots were withdrawn at recorded time intervals, cooled in ice, and scanned with a Unicam SP800 spectrophotometer. The aliquot for "infinite" time was withdrawn after at least seven half-lives.

Alternatively, the reaction mixture was subdivided into screw-capped vials before heating to the reaction temperature.

The optical densities (*A*) at the wave length of λ_{max} for the (substituted) benzoic acid produced were measured. An exception to this general procedure was made for 2,4,6-trimethylphenylnitromethane, the reaction of which was followed at 244 nm, since mesitoic acid shows only end absorption in dilute acid.

The pseudo-first-order rate constants were calculated by a computer-assisted least-squares plot of ln $(A_\infty - A_t)$ *vs.* time.

The concentration of the mineral acid solutions was determined after the runs by titration with standard alkali.

(*B*) The runs in deuteriosulfuric acid were carried out by adding 10 µl of a 1 volume % solution of phenylnitromethane in ethanol to 10 ml dilute deuteriosulfuric acid and transferring, after mixing, to a u.v. cell. The cell was kept in a thermostatted cell block at the reaction temperature (±0.1 °C) for 1 h, and then removed at recorded time intervals for optical density determination at a fixed wavelength near λ_{max} for benzoic acid. The readings were made in the heated cell compartment of a Beckman DB spectrophotometer. The data were treated as above.

Can. J. Chem. Downloaded from www.nrcresearchpress.com by 210.87.254.42 on 09/05/12
For personal use only.

Comparative runs were made at the same time under the same conditions with protiosulfuric acid.

Determination of Distribution Coefficients

A stock solution of the phenylnitromethane to be studied was made in *n*-hexane, with optical density approximately 2.0 at a chosen wavelength near λ_{max}. A 10 ml aliquot of this solution was shaken with a measured aliquot of dilute sulfuric acid in a flask held at 25.0 °C in a water bath. The amount of dilute sulfuric acid used was varied to obtain approximately 50% partition. The hexane layer was withdrawn and scanned with a Unicam SP800 spectrophotometer to determine the concentration of the phenylnitromethane present. The distribution coefficient, *D*, was calculated (17) using the equation:

$$D = nA/(A_0 - A)$$

where A_0 is the optical density of the hexane solution before equilibration with the sulfuric acid solution, A is the optical density after equilibration, and n is the ratio of the volumes used (aqueous/organic).

An estimate of the distribution coefficient in pure water (D_{aq}) was made by extrapolation from dilute acid solutions, and used to calculate the aqueous activity coefficient (f_s) of the phenylnitromethane (18) in different concentrations of acid:

$$f_s = D/D_{aq}$$

Formation of Benzaldehyde from Phenylnitromethane

A mixture of 200 mg phenylnitromethane and 50 ml 11.5 *M* sulfuric acid was heated with frequent mixing to 80 °C for 3 h. A brown gas was visible over the reaction mixture during this time. After cooling, the reaction mixture was poured over 100 g crushed ice and extracted with carbon tetrachloride. The extract was dried with magnesium sulfate and evaporated. The i.r. and p.m.r. spectra indicated that the product was a mixture of 80% phenylnitromethane and 20% benzaldehyde.

Results and Discussion

Effect of Acid Concentration

The kinetics of the Meyer reaction of phenylnitromethane were studied in hot sulfuric, perchloric, and hydrochloric acids (Table 1). In each case, the rate profile passed through a maximum at an acid concentration far below that required to protonate most of the phenylnitromethane.

The rates of the rearrangement-hydrolysis of *p*-methylphenylnitromethane, *p*-chlorophenylnitromethane, and *m*- and *p*-nitrophenylnitromethane in sulfuric acid at 68.8 °C were also determined (Table 2 and Fig. 1). The rate profile for each of these compounds exhibited a maximum at a slightly different acid concentration.

The rate of the reaction of *o*-methylphenylnitromethane was considerably slower than that of *p*-methylphenylnitromethane (Table 2). The rate for 2,4,6-trimethylphenylnitromethane was even slower. Since the rate of reaction of the *aci*-form is actually increased by ortho substituents (4, 15), these steric effects must be operative in the transition state leading to the *aci*-form.

TABLE 1. Pseudo-first-order rate constants (k_ψ) for formation of benzoic acid from phenylnitromethane in acid

Temperature (°C)	Acid	Acid concentration (*M*)	$10^5 k_\psi$ (s^{-1})
68.8	H_2SO_4	.85	4.30
		1.54	5.80
		2.56	6.82
		3.23	5.00
		4.20	3.44
		5.69	1.68
		7.18	1.18
74.8	$HClO_4$	.235	2.96
		.494	4.93
		.75	6.18
		1.09	7.6
78.6		1.03	9.7
		1.84	9.1
		2.91	5.68
		3.80	3.27
		4.64	1.95
		5.45	1.42
		7.12	.69
68.8	HCl	.469	2.46
		1.14	4.08
		3.04	4.21
		4.82	3.20
		7.78	2.15

Reaction in Very Concentrated Acid

In sulfuric acid from 7–13 *M*, and in perchloric acid from 7–11 *M*, a different reaction of phenylnitromethane was observed at 78.6 °C: the formation of benzaldehyde. Within this acidity range, the rate of formation of benzaldehyde increased rapidly with increasing acid concentration. Above 11 *M* perchloric acid and 13 *M* sulfuric acid, undetermined brown reaction products were also formed.

The formation of benzaldehyde does not take place via the *aci*-form. The reaction of the sodium salt of *aci*-phenylnitromethane with acid in this concentration range produces only benzohydroxamic acid from a cold and benzoic acid from a hot solution.

Both hot perchloric acid and hot sulfuric acid in this concentration range are oxidizing agents (19, 20). The observation of a brown gas, probably nitrogen tetroxide, during the formation of benzaldehyde, lends support to the hypothesis that oxidation of the methylene group takes place as in eq. 9. This reaction was not studied further.

[9] $PhCH_2NO_2 \rightarrow PhCHOHNO_2 \rightarrow PhCHO \rightarrow HNO_2$

TABLE 2. Pseudo-first-order rate constants (k_ψ) for the rearrangement–hydrolysis of substituted phenylnitromethanes in sulfuric acid at 68.8 °C

Substituent	H_2SO_4 concentration (M)	$10^5 k_\psi$ (s^{-1})
p-Methyl-	0.51	3.95
	1.11	5.84
	1.40	6.17
	2.69	4.98
	3.36	3.95
p-Chloro-	1.40	4.27
	2.69	8.5
	3.36	8.3
	4.01	6.5
	4.83	4.51
	5.69	3.10
m-Nitro-	0.85	0.65
	1.54	1.20
	2.56	3.32
	3.23	5.30
	3.74	6.41
	5.62	5.98
	7.45	2.59
p-Nitro-	3.36	6.4
	4.01	11.2
	4.83	15.0
	5.69	13.8
	6.47	11.6
	7.33	7.4
o-Methyl-	0.52	0.97
	1.73	1.47
	2.37	1.52
2,4,6-Trimethyl-	0.52	0.82*
	2.32	1.09*

*Rates measured at 70.0 °C.

Activity Coefficient Changes

A decrease in substrate activity coefficient with increasing acid concentration ("salting-in") has been presented as part of the explanation for a maximum in the rate profile for the hydrolysis of some carboxylic anhydrides (21) and some aryl phosphates (22). The aqueous activity coefficients of phenylnitromethane and of some substituted derivatives were determined at room temperature in sulfuric acid solutions by partition between the acid solutions and *n*-hexane (18). It was found that the variation of log f_s with the molarity of sulfuric acid was not linear. An initial increase above zero ("salting-out") was followed by a later decrease ("salting-in") as the medium became more acidic. Similar behavior has been observed with many other organic compounds in sulfuric acid (17).

Phenylnitromethane and *p*-methylphenylnitromethane showed an increase in activity coefficient up to a maximum in 3 M sulfuric acid, followed by a smooth decrease. In 6M sulfuric acid, the activity coefficient had dropped below that in pure water. The nitro-substituted phenylnitromethanes were "salted-in" in 2 M sulfuric acid. Since the nitro-substituted phenylnitromethanes show a maximum in the rate profile for the Meyer reaction at a higher acidity than unsubstituted phenylnitromethane, we must conclude that "salting-in" of the substrate cannot account for the rate decrease observed after the maximum in the rate profile. Rodima and Haldna have reported that the formation of a hydrogen-bonded complex with nitro groups in acid does not cause an abnormal change in activity coefficients for these compounds (23).

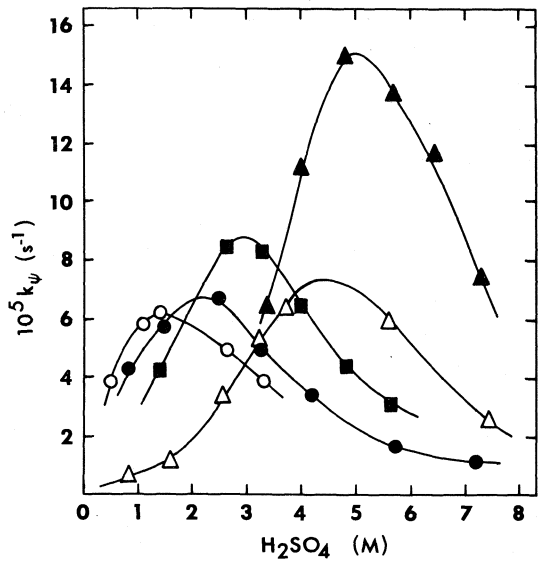

FIG. 1. Rate profiles (k_ψ) for formation of benzoic acids from phenylnitromethanes in sulfuric acid at 68.8 °C: ●, phenylnitromethane; ○, *p*-methylphenylnitromethane; ■, *p*-chlorophenylnitromethane; △, *m*-nitrophenylnitromethane; ▲, *p*-nitrophenylnitromethane.

Bunnett–Olsen Plot

Bunnett and Olsen (24) have tested a linear free energy relationship applicable to reactions of weakly basic substrates in acid. An estimate of the involvement of water in the transition state of such reactions is provided by the slope, ϕ, obtained from a plot of (log $k_\psi + H_0$) *vs.* (H_0 + log [H^+]). The parameter, ϕ, was shown to assume a value less than zero when water was not involved in the transition state, from 0 to 0.33 when water was acting as a nucleophile, and above 0.58 when water was taking part as a proton trans-

Can. J. Chem. Downloaded from www.nrcresearchpress.com by 210.87.254.42 on 09/05/12
For personal use only.

TABLE 3. Bunnett–Olsen plots for the rearrangement–hydrolysis of phenylnitromethanes at 68.8 °C

Substituent	Acid range	ϕ-Value	Correlation coefficient
Unsubstituted	0.85–7.2 *M* H_2SO_4	1.68	.9987
	1.0 –5.5 *M* $HClO_4$*	2.06	.9976
	0.45–4.8 *M* HCl	1.99	.9984
p-Methyl-	0.5 –3.4 *M* H_2SO_4	1.95	.9996
p-Chloro-	2.69–5.69 *M* H_2SO_4	1.73	.9989
m-Nitro-	3.23–7.45 *M* H_2SO_4	1.42	.9982
p-Nitro-	4.83–7.33 *M* H_2SO_4	1.45	.9994

*Rates measured at 78.6 °C.

fer agent. The Bunnett–Olsen plots of our results for the rearrangement–hydrolysis of phenylnitromethane and *p*-methylphenylnitromethane are linear and give ϕ values greater than 0.58 (Table 3). The plots for the other substituted phenylnitromethanes are linear at high acidity, but show a deviation from linearity at low acidity. Bunnett predicted such deviations from linearity when a side-reaction competes with the reaction being studied. In paper I of this series (4), we reported a parallel reaction of phenyl-*aci*-nitromethanes in acid: the rearrangement to benzohydroxamic acid, which is the predominant reaction of phenyl-*aci*-nitromethane in concentrated acid (>3 *M*), is surpassed in rate in more dilute acid by the tautomerization to phenylnitromethane. It was also found that an electron-withdrawing group assisted the tautomerization and inhibited the rearrangement, until a higher acidity was reached. This predominance of tautomerization at low acid concentrations for phenylnitromethanes having electron-withdrawing substituents is the cause of the deviations from linearity in the Bunnett–Olsen plots.

The Nitro–Aci Tautomerization

In paper I of this series (4), the tautomerization rates and the rearrangement rates of phenyl-*aci*-nitromethane were determined over a range of acid concentration at 25.1 °C. In the Meyer rearrangement–hydrolysis of phenylnitromethane, phenyl-*aci*-nitromethane is formed slowly, then undergoes two fast competing reactions, as in eq. 10. A similar reaction scheme has been

$$10] \quad ArCH_2NO_2 \underset{k_{-1}}{\overset{k_1}{\rightleftharpoons}} ArCH{=}NO_2H \xrightarrow{k_2} \text{Products}$$

analyzed by Rocek and co-workers (25) who called the reaction characterized by k_2 the "rate-limiting" step, the last step in the reaction sequence that affects the overall rate. Although this step is faster than the initial step (k_1), the rate of the reaction depends on both k_1 and k_2, because of the very fast back-reaction (k_{-1}) that is competing.

In the case of phenylnitromethane, it was found that the ratio k_2/k_{-1} was relatively insensitive to temperature changes (4). Applying this ratio to the overall rate (k_ψ) observed for the Meyer reaction of phenylnitromethane at 68.8 °C, it is possible to determine the rate k_1 of the nitro–*aci* tautomerization (26), *i.e.* eq. 11. The results of

$$[11] \quad k_1 = k_\psi \times (k_2 + k_{-1}/k_2)$$

these calculations (Table 4) show the inhibiting effect of increasing sulfuric acid concentration in the range 0.85–7.18 *M* on the tautomerization of phenylnitromethane to phenyl-*aci*-nitromethane.

It has often been proposed that tautomerization between nitro and *aci* forms (like the tautomerization between keto and enol forms) is acid-catalyzed (5, 27, 28). However, there is much experimental evidence that dilute acids *inhibit* the tautomerization of the *aci* to the nitro form (eq. 2) (15, 29–31), and so, on the principle of microscopic reversibility, inhibit the reverse reaction 1.

TABLE 4. Pseudo-first-order rate constants for tautomerization (k_1) of phenylnitromethane to phenyl-*aci*-nitromethane in sulfuric acid at 68.8 °C

H_2SO_4 Concentration (*M*)	$10^5 k_1$ (s^{-1})
.85	16.
1.54	11.
2.56	8.5
3.23	4.6
4.20	3.3
5.69	1.7
7.18	1.2

Can. J. Chem. Downloaded from www.nrcresearchpress.com by 210.87.254.42 on 09/05/12
For personal use only.

Can. J. Chem. Downloaded from www.nrcresearchpress.com by 210.87.254.42 on 09/05/12
For personal use only.

Direct evidence for the effect of acid in inhibiting reaction 1 has been produced by Haldna *et al.* (8), and is confirmed by the present work. Haldna showed that the rate of bromination (k_r) of nitromethane in sulfuric acid up to 5.3 *M* decreased with decreasing water activity (a_{H_2O}) according to eq. 12, where k_0 is constant.

$$k_r = k_0 a_{H_2O}{}^4 \quad [12]$$

Our results for the tautomerization of phenylnitromethane (Table 4) follow a similar correlation with the fourth power of the water activity over the range 1.5–5.7 *M* sulfuric acid, indicating the involvement of water as a proton acceptor (8).

Further information about the tautomerization was obtained from a study of the Meyer reaction in an acidity range where the tautomerization alone is the rate-determining step ($k_1 \simeq k_\psi$). It is shown below that this condition is fulfilled at acid concentrations above those required for the maximum in the rate profile. In these concentrations the large negative entropy of activation (Table 5) indicates a mechanism in which there is a large increase in solvent ordering in the transition state (32), as would be required for the abstraction of a proton by water.

Explanation of Maxima in Rate Profiles

It now becomes possible to explain the maxima in the rate profiles shown in Fig. 1. We have seen previously (4) that in dilute acid $k_{-1} > k_2$, so that eq. 11 becomes eq. 13. Both k_1 (Table 4) and

$$k_\psi \simeq k_1 k_2 / k_{-1} \quad [13]$$

k_{-1} (ref. 4) decrease slowly with increasing concentration of acid, and their ratio remains about constant; however, k_2 increases rapidly, so that the net effect is an increase in k_ψ with increasing concentration of acid. But in acid concentrations beyond that required for the maximum rate, $k_2 > k_{-1}$, and eq. 11 becomes eq. 14, so that now k_ψ

$$k_\psi \simeq k_1 \quad [14]$$

decreases with increasing concentration of acid. Equation 14 shows that it is only in sulfuric acid more concentrated than about 4 *M* that the rate of the Meyer reaction of phenylnitromethane becomes equal to its rate of tautomerization to the *aci* form. This contrasts with the behavior of nitroethane (3) cited above.

Primary Isotope Effect

The reaction of phenylnitromethane-α,α-d_2 was studied in 2.92 and 4.68 *M* sulfuric acid (Table 6). In 2.92 *M* acid $k_2/k_{-1} > 10$ (from extrapolation of Fig. 2 in ref. 4), and so exchange of deuterium for protium cannot be important in the first few half-lives of the reaction; it must be even less important in the more concentrated acid. In both concentrations the reaction of the deuterated compound was found to be less than that of the undeuterated compound, as would be expected if the rate-determining step is the tautomerization (eq. 1), which involves stretching of a carbon–hydrogen bond. The maximum primary isotope effect (k_H/k_D) expected at 78 °C is 5, corresponding to a transition state with departing hydrogen symmetrically disposed between the carbon and the abstracting oxygen (33). The lower values observed for phenylnitromethane tautomerization indicate a transition state in which the departing hydrogen is bound more strongly to either the carbon or the oxygen. In view of the instability of the *aci*-phenylnitromethane in acid,

TABLE 5. Activation parameters for the rearrangement–hydrolysis of phenylnitromethane in sulfuric acid

Acid concentration (*M*)	Temperature (°C)	$10^5 k_\psi$ (s^{-1})	$\Delta H^\ddagger$ (kcal/mol)	$\Delta S^\ddagger$ (e.u.)*
2.92	63.1	3.66		
	63.1	3.75		
	72.1	8.7		
	78.3	14.6	21±1	−20±1
	78.3	14.7		
	88.5	33.6		
	88.5	34.6		
4.68	63.1	1.79		
	78.3	7.97	22±1	−22±2
	88.5	16.8		

*1 *M* standard state.

TABLE 6. Kinetic isotope effects on the rearrangement–hydrolysis in sulfuric acid at 78.3 °C

Compound	Acid concentration (M)	$10^5 k_\psi$ (s^{-1})	k_H/k_D
$C_6H_5CH_2NO_2$	2.92	14.6	2.6±0.1
$C_6H_5CD_2NO_2$		5.6	
$C_6H_5CH_2NO_2$	4.68	8.0	2.5±0.1
$C_6H_5CD_2NO_2$		3.3	

TABLE 7. Solvent isotope effects on the rearrangement–hydrolysis of phenylnitromethane at 74.8 °C

Acid	Concentration (M)	$10^5 k_\psi$ (s^{-1})	k_{H_2O}/k_{D_2O}
H_2SO_4	0.51	5.25	0.63
D_2SO_4		8.35	
H_2SO_4	1.11	10.5	1.07
D_2SO_4		9.8	
H_2SO_4	1.71	12.8	1.46
D_2SO_4		8.74	
H_2SO_4	2.31	12.4	1.71
D_2SO_4		7.26	
H_2SO_4	3.00	10.5	1.79
D_2SO_4		5.88	
H_2SO_4	4.00	7.05	1.86
D_2SO_4		3.79	
H_2SO_4	5.30	3.84	1.96
D_2SO_4		1.96	

application of the Hammond postulate (34, 35) to this system would predict a transition state close to the *aci*-form or its anion: *i.e.* predict that the departing hydrogen is bound more strongly to oxygen.

Solvent Isotope Effect

The effect of carrying out the Meyer reaction of phenylnitromethane in deuteriosulfuric acid varies greatly, depending on the concentration of the acid (Table 7).

These isotope effects cannot be due to differential solvation of the initial state, since we have determined distribution coefficients of phenylnitromethane in isooctane/sulfuric acid and isooctane/deuteriosulfuric acid. The isotope effect ($f_s(H_2O)/f_s(D_2O)$) on the activity coefficient of the starting material in 4.0 M acid is 1.03. An isotope effect of 1.06 ($f_s(H_2O/f_s(D_2O)$) has been reported on the activity coefficient of nitromethane in water (36).

At high acid concentrations, the solvent isotope effect influences the rate-determining tautomerization of phenylnitromethane to phenyl-*aci*-nitromethane. Here the reaction is slowed in deuterated solvent by the lower basicity of deuterium oxide, which makes it less effective in proton abstraction (37). Swain and Rosenberg (38) pre-

Can. J. Chem. Downloaded from www.nrcresearchpress.com by 210.87.254.42 on 09/05/12
For personal use only.

Can. J. Chem. Downloaded from www.nrcresearchpress.com by 210.87.254.42 on 09/05/12
For personal use only.

dicted values for the solvent isotope effect (k_{H_2O}/k_{D_2O}) on a proton abstraction from a carbon acid such as ketones and nitroalkanes: 1.0 for zero transfer of the proton in the transition state, 1.4 for half-transfer, and 2.0 for complete transfer of the proton to water in the transition state. Bunton and Shiner (35) calculated a solvent isotope effect of 1.4 for a symmetrical "free-proton" transition state for enolization of a ketone. The relatively large values (up to 1.96) obtained for the tautomerization of phenylnitromethane indicate a transition state with considerable proton transfer, close to hydronium ion and the *aci*-form or its anion.[3]

The reaction scheme is more complex in dilute acid. Here the *aci*-form is formed slowly, but is transformed back into the nitro-form more quickly than into the Meyer reaction products. The rate-limiting step now for the Meyer reaction is the loss of water from the protonated *aci*-form (eq. 4) (4). Reactions with a protonation equilibrium prior to the rate-limiting step are usually faster in deuterated solvent because of the increased acidity of deuteronium ion, and this is observed in the Meyer reaction, as shown in Table 7.[4] As the rate-limiting step changes over to tautomerization (eq. 1) in more concentrated acid, the value of the isotope effect changes to approach the value found for the tautomerization.

Conclusion

The Meyer rearrangement–hydrolysis of phenylnitromethane in acid proceeds through tautomerization to phenyl-*aci*-nitromethane. In dilute acid, the tautomerization is followed by a rate-limiting acid-catalyzed reaction of the *aci*-form (eq. 4), which causes the observed increase in rate with increasing acidity. As the medium is made more acidic, the rate-limiting step changes to the tautomerization (eq. 1), which is inhibited in acid, so that the rate decreases with increasing acidity. The tautomerization is not acid-catalyzed, and proceeds by proton abstraction from the α-carbon by water, through a transition state closely resembling the products.

We are grateful to a referee of this paper for several helpful suggestions.

[3]A referee has pointed out that if the reaction is not acid-catalyzed the intermediate close to the transition state must be the *aci* anion, unless water is acting simultaneously as an acid and a base in some cyclic transition state. Such a mechanism could account for the entropies of activation.

[4]In the three most dilute D_2SO_4 solutions of Table 7, exchange to form $PhCHDNO_2$ and $PhCD_2NO_2$ must be significant ($k_2 = k_{-1}$ in 1.5 *M* sulfuric acid). This exchange would contribute to an increase in the observed k_{H_2O}/k_{D_2O} ratio, so that the true values of k_{H_2O}/k_{D_2O} should be smaller than those recorded in Table 7. The argument of this paragraph, however, is not changed.

1. V. Meyer and C. Wurster. Ber. **6**, 1168 (1873).
2. W. E. Noland. Chem. Revs. **55**, 137 (1955).
3. R. Junell. Arkiv Kemi, Miner. Geol. **11B**, No. 30 (1934).
4. J. T. Edward and P. H. Tremaine. Can. J. Chem. This issue.
5. J. T. Edward and P. H. Tremaine. Can. J. Chem. This issue.
6. R. Cundall and A. Locke. J. Chem. Soc. B, 98 (1968).
7. R. J. Gillespie. J. Chem. Soc. 2542 (1950).
8. U. Haldna, H. Kuura, H. Laaneste, and R. Puss. Russ. J. Phys. Chem. **38**, 469 (1964).
9. U. Haldna, and R. Puss. Russ. J. Phys. Chem. **38**, 1529 (1964).
10. U. Haldna, H. Kuura, and R. Puss. Report of Tartu State University, Tartu, Estonia, U.S.S.R. Organic reactivity. Vol. II. No. 4, p. 91 (1965).
11. W. F. Baitinger, P. Schleyer, T. S. S. R. Murty, and L. Robinson. Tetrahedron, **20**, 1635 (1964).
12. H. J. Campbell and J. T. Edward. Can. J. Chem. **38**, 2109 (1960).
13. V. A. Palm, U. Haldna, A. I. Tal'vik, and A. E. Mei. Russ. J. Phys. Chem. **36**, 1357 (1962).
14. N. Kornblum, R. A. Smiley, R. K. Blackwood, and D. C. Iffland. J. Am. Chem. Soc. **77**, 6269 (1955).
15. R. G. Cooke and A. K. Macbeth. J. Chem. Soc. 1024 (1938).
16. R. P. Bell and D. M. Goodall. Proc. Roy. Soc. London, Ser. A, 273 (1966).
17. E. M. Arnett, C. Y. Wu, J. N. Anderson, and R. D. Bushick. J. Am. Chem. Soc. **84**, 1674 (1962).
18. F. A. Long and W. F. McDevit. Chem. Revs. **51**, 119 (1952).
19. G-M. Schwab and O. Neuwirth. Ber. **90**, 567 (1957).
20. G. F. Smith. Anal. Chim. Acta, **17**, 175 (1957).
21. C. A. Bunton and J. H. Fendler. J. Org. Chem. **31**, 3764 (1966).
22. C. A. Bunton, S. J. Farber, and E. J. Fendler. J. Org. Chem. **33**, 29 (1968).
23. T. K. Rodima, and U. Haldna. Report of Tartu State University. Organic reactivity. Vol. IV. No. 1, p. 181 (1967).
24. J. F. Bunnett and F. P. Olsen. Can. J. Chem. **44**, 1917 (1966).
25. J. Rocek, F. H. Westheimer, A. Eschenmoser, L. Moldovanyi, and J. Scheiber. Helv. Chim. Acta, **45**, 2554 (1962).
26. A. A. Frost and R. G. Pearson. Kinetics and mechanism. J. Wiley and Sons, New York, N.Y., 1961. p. 195.

27. H. FEUER and A. T. NIELSEN. Tetrahedron, **19**, Suppl. **1**, 67 (1963).
28. P. A. S. SMITH. The chemistry of open-chain organic nitrogen compounds. Benjamin Press, New York, N.Y., 1966. p. 400.
29. E. P. KOHLER and J. F. STONE, JR. J. Am. Chem. Soc. **52**, 761 (1930).
30. S. H. MARON and V. K. LA MER. J. Am. Chem. Soc. **61**, 692 (1939).
31. V. M. BELIKOV, S. G. MAIRANOVSKII, T. B. KORCHEMNAYA, S. S. NOVIKOV, and V. A. KLIMOVA. Izvest. Akad. Nauk S.S.S.R., Otdel. Khim. Nauk, 1675 (1960). Chem. Abst. **55**, 8325 (1961).
32. L. L. SCHALEGER and F. A. LONG. *In* Advances in physical organic chemistry. Vol. I. *Edited by* V. Gold. Academic Press, New York, N.Y., 1963. p. 1.
33. F. H. WESTHEIMER. Chem. Revs. **61**, 265 (1961).
34. G. S. HAMMOND. J. Am. Chem. Soc. **77**, 334 (1955).
35. C. A. BUNTON and V. J. SHINER, JR. J. Am. Chem. Soc. **83**, 3214 (1961).
36. I. B. RABINOVITCH, V. D. FEDOROV, N. P. PASHKIN, M. A. AUDESNYAK, and N. Y. PIMENOV. Dokl. Akad. Nauk S.S.S.R. **105**, 108 (1955).
37. K. B. WIBERG. Chem. Revs. **55**, 713 (1955).
38. C. G. SWAIN and A. S. ROSENBERG. J. Am. Chem. Soc. **83**, 2154 (1961).

Can. J. Chem. Downloaded from www.nrcresearchpress.com by 210.87.254.42 on 09/05/12
For personal use only.

Can. J. Chem. Downloaded from www.nrcresearchpress.com by 210.87.254.42 on 09/05/12
For personal use only.

Reactions of Amine Oxides and Hydroxylamines with Sulfur Dioxide

J. T. Edward and Josephine Whiting[1]
Department of Chemistry, McGill University, Montreal, Quebec

Received January 15, 1971[2]

Strychnine *N*-oxide (**8**; X = H) reacts with sulfur dioxide in benzene to form the sulfitoamine **9** (X = H), which rearranges in boiling water to the substituted sulfamic acid **10** (X = H) by a free-radical mechanism. The sulfamic acid **10** (X = H) is also formed by reaction of strychnine *N*-oxide with cold aqueous sulfur dioxide, and may be an intermediate in the reduction of the amine oxide by sulfur dioxide in hot water. With aqueous sulfur dioxide at 0°, *N*,*N*-dimethylbenzylamine *N*-oxide gives tertiary amine by reduction and secondary amine and aldehyde by a Polonovski-type reaction; however, *N*,*N*-dimethylaniline *N*-oxide gives tertiary amine, *o*- and *p*-dimethylaminobenzene sulfonic acids, but no appreciable amount of secondary amine. The sulfonic acids are probably formed by a free-radical mechanism, since their formation is largely suppressed by the addition of hydroquinone. The reactions of hydroxylamine and of β-phenylhydroxylamine with sulfur dioxide in water have also been studied.

La réaction de l'oxide de strychnine (**8**; X = H) avec la dioxide de soufre en benzène fournit le composé **9** (X = H). En eau bouillante celle-ci réarrange a l'acide sulfamique **10** (X = H) par un mécanisme radicalaire. L'acide sulfamique est probablement l'intermédiaire quand l'oxide est réduit par la dioxide de soufre dans l'eau chaude. La dioxide de soufre réagit avec l'oxide de *N*,*N*-diméthylbenzylamine a 0° pour fournir en partie l'amine tertiaire, et en partie aldéhyde et une amine secondaire; avec l'oxide de *N*,*N*-diméthylaniline elle fournit en partie l'amine tertiaire, en partie les acides *o*- et *p*-diméthylaminobenzène sulfoniques, mais rien d'amine secondaire. Les acides sulfoniques sont probablement formées par un mécanisme radicalaire, parce qu'on peut les supprimer par l'addition de hydroquinone à la réaction. On a étudié aussi les réactions de hydroxylamine et de β-phénylhydroxylamine avec la dioxide de soufre dans l'eau.

Canadian Journal of Chemistry, **49**, 3502 (1971)

The reduction of amine oxides (**1**) to tertiary amines (**3**) has commonly been effected by aqueous sulfur dioxide (1–3), and has been assumed to take place by hydrolysis of an intermediate sulfamic acid[3] derivative **2** (route *A* in Scheme 1) (1). However, no mechanism has been advanced for the reaction **1** → **2**, in which an N—O bond becomes replaced by an N—S bond. Sometimes the reaction yields a secondary amine (**6**) and an aldehyde (**7**) (route *B*) in addition to products of route *A*. It has been postulated (5, 6) that route *B* products result from the decomposition of an intermediate sulfitoamine **4** via a Polonovski-type reaction (7) to give the iminium ion **5**, which would then be expected to hydrolyze rapidly to **6** and **7**. Thus Lecher and Hardy (5) found that the sulfitoamine **4** (R = Me, R′ = H), obtained by reaction of trimethylamine oxide (**1**; R = Me, R′ = H) with sulfur dioxide in dry benzene, decomposed in cold water to give dimethylamine (**7**; R = Me) and formaldehyde (**8**; R′ = H). The latter products were also obtained in more than 50% yield when trimethylamine oxide in aqueous solution was treated with sulfur dioxide, again presumably *via* the sulfitoamine **4** (R = Me, R′ = H), while route *A* products (**3**; R = Me, R′ = H: 15–20% yield, and **2**; R = Me, R′ = H: less than 5% yield) were obtained in smaller amounts. Wiewiorowski and Baranowski (6) found that reaction of sparteine N_{16}-oxide and lupanine *N*-oxide with aqueous sulfur dioxide went about 20% by route *A* and 80% by route *B*, while reaction of α-isosparteine *N*-oxide and sparteine N_1-oxide went 100% by route *A*. In the latter two cases the ring systems are such that the unsaturated intermediate **5** would be considerably strained, and the Polish authors suggested that for this reason route *B* was avoided and route *A* followed exclusively.

A possible route to sulfamic acids **2** and subsequent products would be by rearrangement of sulfitoamines **4** (reaction *a* of Scheme 1)

[1]Née Josephine Jaworska; holder of NRCC Studentship, 1966–1970.

[2]Revision received July 20, 1971.

[3]Sulfamic acid has the zwitterionic structure $H_3\overset{\oplus}{N}-\overset{\ominus}{SO_3}$ (4).

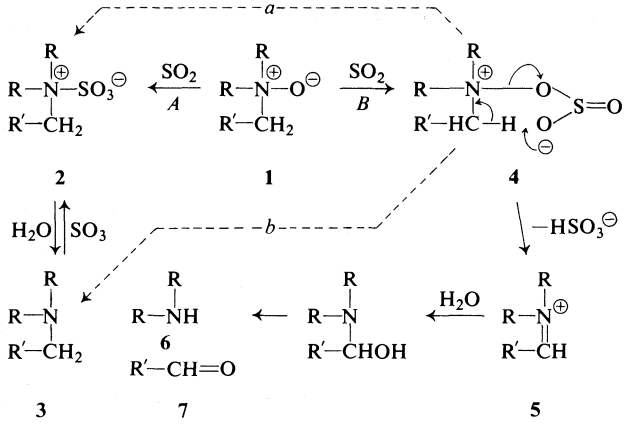

SCHEME 1

and we have investigated this possibility by studying the reactions of the sulfitoamines **9** (X = H and X = OMe), obtained by reaction of strychnine *N*-oxide (**8**; X = H) or brucine *N*-oxide (**8**; X = OMe) in benzene solution with sulfur dioxide. Because of the bridgehead position of the quaternary nitrogen atom, these sulfitoamines would not be expected to react by route *B*, and in fact in cold water they were stable. Furthermore, they showed no tendency to react with an excess of amine oxide to furnish the sulfatoamines **11** (X = H and OMe). In contrast, Lecher and Hardy (5) obtained triethylammonio sulfate (**13**) from the reaction of triethylamine oxide with sulfur dioxide in benzene, triethylammonio sulfite (**12**) presumably being an intermediate in the reaction (eq. 1). The sulfatoamines **11** (X = H and OMe) could be obtained by reaction of the amine oxides **8** (X = H and OMe) with pyridine – sulfur trioxide complex. They were hydrolyzed in water or in alkaline solution to sulfate ion and the amine oxide. (Under these conditions, **13** gave diethylamine, acetaldehyde, and sulfate ion (5) by a Polonovski-type reaction.)

In boiling water the sulfitoamine **9** (X = H) isomerized to the sulfamic acid **10** (X = H), m.p. 265–275°. This compound has been prepared previously (8), but by a route which left its structure uncertain; we have confirmed the

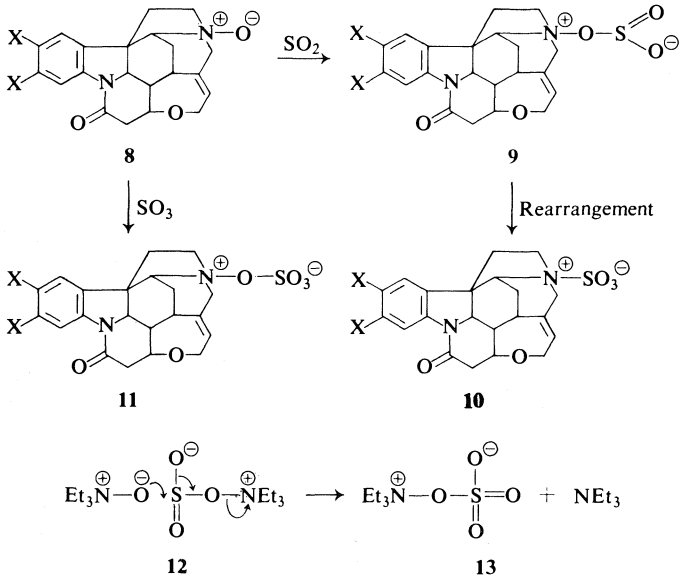

[1]

Can. J. Chem. Downloaded from www.nrcresearchpress.com by 210.87.254.42 on 09/05/12
For personal use only.

Can. J. Chem. Downloaded from www.nrcresearchpress.com by 210.87.254.42 on 09/05/12
For personal use only.

sulfamic acid structure by preparing it also by reaction of strychnine with pyridine – sulfur trioxide complex (a reaction of the type **3** → **2**). A third method of preparing **10** (X = H and OMe) was from the reaction of strychnine or brucine with sodium dithionate in boiling water. This reaction probably involved nucleophilic attack of the tertiary amines on sulfur (eq. 2).

[2] 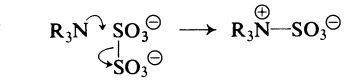

Its generality was demonstrated by preparing also the derivatives **14** (X = H) from cinchonine, **14** (X = OMe) from quinine, **15** from harmine, **16** from 6-methoxyquinoline, and **17** from 2-phenyl[1, 2-*a*]imidazopyridine. All of these are

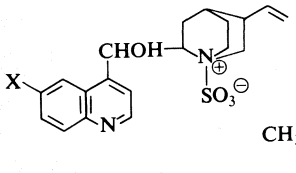

14

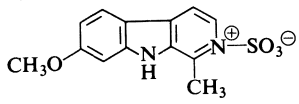

15

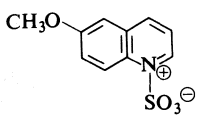

16

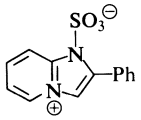

17

new compounds. Their sulfamic acid structures were demonstrated by preparing them also by reaction of the amines with pyridine – sulfur trioxide complex (used for **14** (X = H and OMe) and **15**), or with sulfur trioxide in 1,2-dichloroethane or chlorosulfonic acid in chloroform (used for **16** and **17**).[4]

The mechanism of the isomerization of the sulfitoamine **9** (X = H) into the sulfamic acid **10** (X = H) in boiling water may now be considered. After the rearrangement no sulfate ion can be detected in the solution, so that it is unlikely that the isomerization proceeds by eq. 3 (a route, furthermore, which would be disfavored by a polar solvent like water (10)). A more plausible route involves dissociation of the sulfitoamine into ion-radicals (11), followed by recombination (eq. 4). This mechanism is supported by the observation that in boiling water in the presence of the radical trap hydroquinone (11) only 25% of **9** (X = H) is isomerized to **10** (X = H), and 60% is reduced to strychnine and sulfite ion (eqs. 5 and 6).

We may now consider the confused literature on the reaction of strychnine *N*-oxide with sulfur dioxide in water. The reaction in hot water (exact temperature unspecified) was first reported by Pictet and Mattison (12), who obtained strychnine and sulfate ion. However, Polonovski and Polonovski (13) and Leuchs and Räck (14) claimed that the sulfamic acid **10** (X = H), m.p. > 330°, was also formed, while Leuchs and Boit (15) claimed a similar sulfamic acid from brucine *N*-oxide. Oesterlin (8) claimed to obtain exclusively the sulfamic acid **10** (X = H), m.p. 260–265°, from the reaction of strychnine *N*-oxide with sodium bisulfite in cold methanol, but exclusively strychnine and sulfate ion from its reaction with sodium bisulfite in water at 60°.

We have confirmed Oesterlin's observations on the effect of temperature: strychnine *N*-oxide reacts with an excess of sulfur dioxide in water at 60–65° to give strychnine (95% yield), but at 0° to give the sulfamic acid **10** (X = H),

[3] 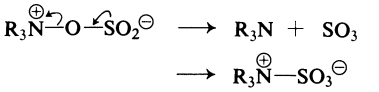

[4] 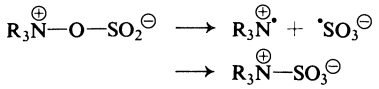

[5] 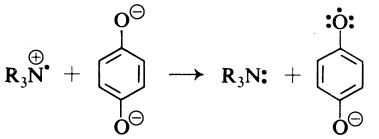

[6] 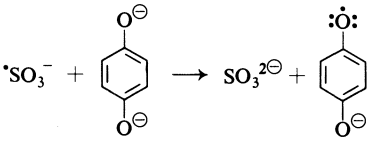

[4]The structures **14** (X = H or OMe) for the products from cinchonine or quinine, expected on general grounds to be preferred over the alternative structures having sulfur trioxide complexed to the quinoline nitrogen (9), were supported by the u.v. absorption and n.m.r. characteristics of the compounds. The structure **15** for the product from harmine was supported by similar evidence, while the structure **17** for the product from 2-phenyl[1,2-*a*]imidazopyridine seemed most plausible because it allowed maximum delocalization of the positive charge.

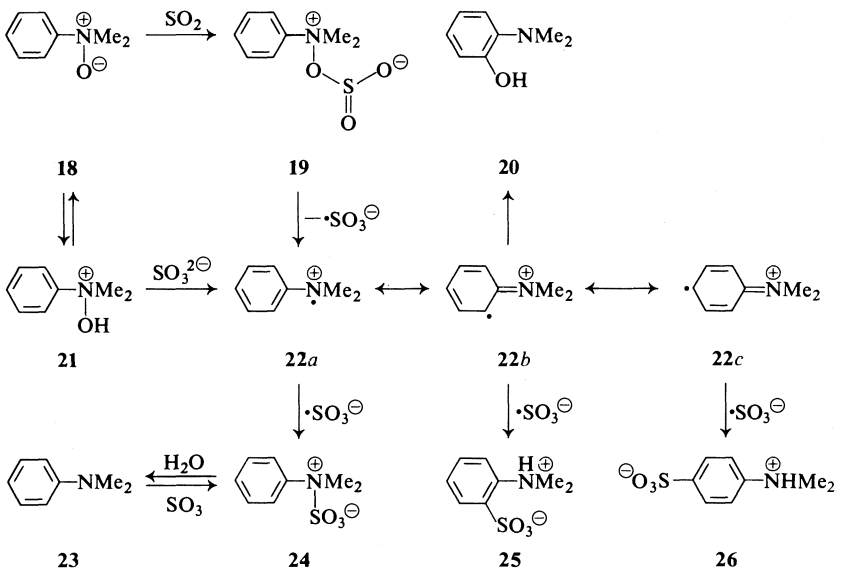

SCHEME 2

m.p. 265–275° (85% yield). This compound is fairly stable in hot water, but is rapidly hydrolyzed in dilute acid or alkali to strychnine and sulfate ion. At 65° even sulfur dioxide in water is sufficiently acidic to effect rapid hydrolysis. The sulfamic acid is consequently a possible (though not a necessary) intermediate in the formation of strychnine from strychnine *N*-oxide. (Another possible intermediate is the sulfitoamine **9** (X = H) (reaction *b* of Scheme 1): in aqueous acid or alkali it also is hydrolyzed rapidly to strychnine and sulfate ion (eqs. 7 and 8).) Sulfur dioxide in water is able to effect complete hydrolysis of **9** (X = H) within 15–20 min at 65–70°).

[7] 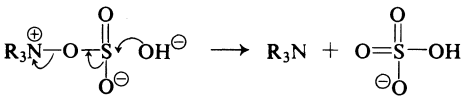

While we have demonstrated the isomerization in water of the sulfitoamine **9** (X = H) into the sulfamic acid **10** (X = H) (reaction *a* of Scheme 1), it proceeds too slowly to account for the formation of the sulfamic acid (85% yield in 15 min) from the reaction of strychnine *N*-oxide with aqueous sulfur dioxide at 0°; even at 100°, rearrangement of **9** (X = H) into **10** (X = H) is only about 50% complete in 15 min. Consequently, it seems likely that the sulfamic acid is formed from the *N*-oxide by the union of two radical ions produced by reaction 9. This one-electron oxidation–reduction reaction finds analogy in the reduction of amine oxides to aminium radical-ions by the one-electron reducing agent, iron(II) (16), and is supported by the observation that the formation of the sulfamic acid **10** (X = H) can be suppressed completely when strychnine *N*-oxide reacts with sulfur dioxide in water at 0° in the presence of hydroquinone.

Further evidence for free-radical intermediates was found in a study of the reaction of *N*,*N*-dimethylaniline oxide (**18**) with sulfur dioxide (Scheme 2). In benzene the unstable sulfitoamine **19** was formed; however, in water this decomposed to give no appreciable quantities of route *B* products, but only the products to be expected from eq. 4. These products are shown in Scheme 2, and their yields are given in Table 1.

[8] 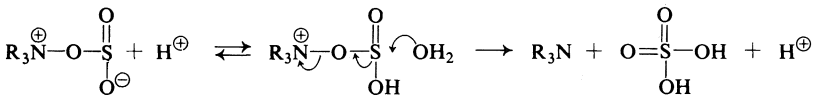

[9] 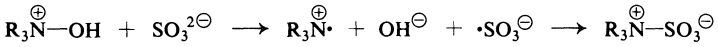

Can. J. Chem. Downloaded from www.nrcresearchpress.com by 210.87.254.42 on 09/05/12
For personal use only.

TABLE 1. Yields (%) of products in Scheme 2

Reaction	Products			
	20	**23**	**25**	**26**
18 + aqueous SO_2 at 0° (ref. 18)	0.6	22	60	20
18 + aqueous SO_2 at 0° (this work)	0.5	20	56	18
N,N-Diethylaniline *N*-oxide + aqueous SO_2 at 0°	1.0*	30*	45*	15*
19 in water at 0–20°	0.5	20	58	20
19 in water at 70–80°	2.9	51	34	9.7

*Et in place of Me in products.

[10] $$\cdot SO_3^{\ominus} \leftrightarrow {}^{\ominus}O-\underset{\underset{O}{\|}}{S}-O\cdot \xrightarrow{22b} \text{(C}_6\text{H}_4\text{)}(NMe_2)(OSO_2H) \xrightarrow{-SO_2} \mathbf{20}$$

Besides the tertiary amine **23**,[5] the ortho- (**25**), and para-sulfonic (**26**) acids were obtained along with a trace of the *o*-aminophenol **20**. The latter may have come via an unstable sulfite ester (eq. 10). None of the sulfamic acid zwitterion **24** was isolated, because even at 0° this compound (unlike corresponding aliphatic zwitterions such as **10**) is extremely readily hydrolyzed by water alone.

The predominance of route *A* products from the reaction of this amine oxide is perhaps explained by the resonance stabilization of the aminium ion **22**, which makes homolytic fission of **19** according to reaction 4 much more facile than the competing reaction **4** → **5** of route *B*.[6] The facilitation of reaction 4 is further shown by the fact that in water the sulfitoamine **19** underwent reaction within a few hours at 0°, while during this time the sulfitoamine **9** had not isomerized completely even at 100°.

About the same yields of products **20**, **23**, **25**, and **26** were obtained by treating the amine oxide **18** with sulfur dioxide in water at 0° (a reaction studied by Bamberger and Tschirner (18) more than 70 years ago), as shown in Table 1. This may indicate that Bamberger's reaction also involves the sulfitoamine **19** as an intermediate, although the alternative pathway (**18** → **21** → **22** → products), based on eq. 9, cannot be excluded at the moment. Either pathway involves the intermediacy of the aminium ion **22**; this accords with the observation that in the presence of a radical scavenger, hydroquinone, the yields of **25** and **26** from the reaction of *N,N*-dimethylaniline oxide with aqueous sulfur dioxide are reduced about six-fold, with a corresponding increase in the yield of **23**.

The reaction of *N,N*-diethylaniline *N*-oxide with sulfur dioxide in water at 0 °C gave the same types of products, and their yields are given in Table 1. Again, there were no appreciable quantities of route *B* products. The reaction was followed by n.m.r. measurements to see if there was any evidence of chemically induced dynamic nuclear polarization (c.i.d.n.p.) (19) caused by free radical intermediates. No obvious emission or enhanced absorption could be observed in the ethyl signals of diethylaniline, which after 2 h made up roughly 20% of the reaction product. However, no evidence of c.i.d.n.p. from dialkylanilinium ion radical intermediates has yet been reported; it is possible that if the relaxation time for depolarization is fast no effect will be seen. Attempts to demonstrate by e.s.r. the presence of radicals in the reaction of *N,N*-dimethylaniline *N*-oxide with aqueous sulfur dioxide were also fruitless. However, to date most *N,N*-dialkylaniline cation-radicals have eluded physical detection because of their rapid

[5]A referee has pointed out that the tertiary amine could also arise by reduction of the aminium ion by SO_3^{2-}

$$\mathbf{22} + SO_3^{2\ominus} \rightarrow \mathbf{23} + \cdot SO_3^{\ominus}$$

[6]In contrast to the sulfitoamine **19**, the sulfatoamine **27** does not rearrange in water to the aminophenyl sulfate **28**, but hydrolyzes to the amine oxide and sulfuric acid.

$$\text{(C}_6\text{H}_4\text{)}(\overset{\oplus}{N}Me_2)(O-SO_3^{\ominus}) \not\rightarrow \text{(C}_6\text{H}_4\text{)}(NMe_2)(OSO_3^{\ominus})$$

27 **28**

This result disqualifies **27** as a possible intermediate in the Boyland–Sims reaction of dimethylaniline with alkaline persulfate to give **28** (*cf.* Discussions in ref. 17).

Can. J. Chem. Downloaded from www.nrcresearchpress.com by 210.87.254.42 on 09/05/12
For personal use only.

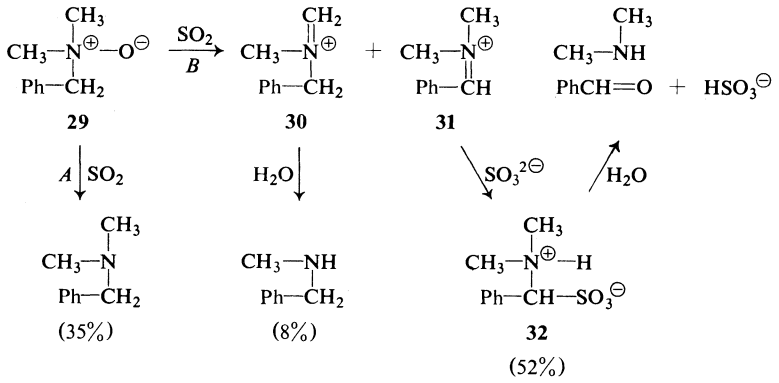

SCHEME 3

coupling reactions with themselves, solvent, or other radicals (20), and the negative results from c.i.d.n.p. and e.s.r. cannot be considered to exclude the possibility of radical intermediates.

While the reaction of *N*,*N*-dimethylaniline oxide with sulfur dioxide in water gave no route *B* products, the reaction of *N*,*N*-dimethylbenzylamine oxide (**29**) gave predominantly route *B* products, as shown by the yields indicated in Scheme 3.[7] The structure of the aminosulfonic acid **32** was inferred from its analysis, i.r. spectrum, and decomposition to benzaldehyde (and presumably dimethylamine and sulfurous acid) on attempts to crystallize it from water or 95% ethanol. The effect of the phenyl group would be expected to favor route *B* over route *A*, and to favor formation of the unsaturated intermediate **31** over **30**, in accordance with the results noted.

Finally, the reactions of β-phenylhydroxylamine and of hydroxylamine with aqueous sulfur dioxide were studied briefly. β-Phenylhydroxylamine is protonated in weakly acidic solution to give the ion **33**, analogous to protonated *N*,*N*-dimethylaniline oxide (**21**), and so might be expected to react with aqueous sulfur dioxide in similar fashion. In fact Illuminati

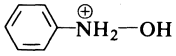

33

(21) has already reported the formation of orthanilic acid, aniline, and phenylsulfamic acid in varying amounts depending on the composition of the solvent (water, ethanol, and 60% ethanol). We have confirmed and extended Illuminati's results, as shown in Table 2. It is apparent that the course of the reaction is considerably more complex than that of dimethylaniline *N*-oxide; it is difficult, for example, to devise a plausible mechanism for the formation of metanilic acid. Furthermore, the failure of hydroquinone to affect the course of the reaction makes it unlikely that radicals are intermediates of any importance. On the other hand, it seems likely that the protonated form **33** of β-phenylhydroxylamine is required for reaction; when sodium bisulfite or sodium sulfite was used in place of sulfur dioxide, the rate of reaction became very slow.

In anhydrous ether sulfur dioxide reacted with β-phenylhydroxylamine to form the anilinium salt of phenylsulfamic acid in fairly good yield, instead of the expected sulfitoamine zwitterion. We have no plausible explanation for this result.

The reaction of hydroxylamine itself with sulfur dioxide in water gives sulfamic acid and small amounts of ammonium bisulfate (22–24). The rate of the reaction is maximal at about neutral p*H* values, but the ratio of sulfamic acid to ammonium bisulfate in the product is unaffected by p*H*. It has thence been concluded (22) that the transition complexes for both reactions have the same composition (SO_2, NH_2OH, ψH_2O); but these results are equally compatible with a transition complex made up of the ions of eq. 11. A possible route to sulfamic

[11] $NH_2OH + H_2SO_3 \rightleftarrows H_3\overset{\oplus}{N}—OH + HSO_3^{\ominus}$

acid and ammonium bisulfate would then be

[7]Hydroquinone had no appreciable effect on the yields of the different products, indicating that free radical intermediates are unlikely to be involved in the reactions of route *B*.

Can. J. Chem. Downloaded from www.nrcresearchpress.com by 210.87.254.42 on 09/05/12
For personal use only.

TABLE 2. Effect of solvent and of the presence of hydroquinone (S) on the yields (%) of the products from the reaction of phenylhydroxylamine with sulfur dioxide

Solvent	Aminobenzenesulfonic acids			Aniline	Phenylsulfamic acid
	ortho-	meta-	para-		
EtOH	35	5	10	45	1–2
EtOH (+S)	35	5	10	45	1–2
60% EtOH	20	3–5	15	40	10–15
60% EtOH (+S)	20	3–5	12	42	10–15
Water	15–20	1–3	12	20	40
Water (+S)	15–20	1–3	12	20	40

a reaction of these ions to give the radicals $H_3N^{\oplus}$ and $\cdot SO_3H$ (*cf.* reaction 9). However,

[12] $$H_3\overset{\oplus}{N}—OH + HSO_3^{\ominus} \rightarrow H_3\overset{\oplus}{N}\cdot + OH^- + \cdot SO_3H \rightarrow$$

$$H_2O + H_3\overset{\oplus}{N}\cdot + \cdot SO_3^{\ominus} \rightarrow H_3\overset{\oplus}{N}—SO_3^{\ominus}$$

Electron transfer ↓

$$NH_3 + SO_3 \xrightarrow{H_2O} \text{Ammonium bisulfate}$$

we have found the ratio of the products in this reaction to be unaffected by the presence of hydroquinone, which would have been expected to reduce the ion-radicals of eq. 12, and hence to favor the formation of ammonium ion at the expense of sulfamic acid. An intramolecular rearrangement of sulfitoammonium ion (*cf.* ref. 25) is accordingly indicated.

Experimental

The i.r. spectra were recorded with a Perkin–Elmer Model 337 spectrophotometer, n.m.r. spectra with a Varian A-60 spectrophotometer. Molecular weights were determined using a Mechrolab Model 301A osmometer. All melting points are uncorrected. Analyses were done by Dr. C. Daesslé of Montreal, Quebec, and Dr. Alfred Bernhardt of Elbach über Engelskirchen, West Germany.

(N_b-Strychninio) Sulfite[8] (**9**; *X = H)*

Strychnine *N*-oxide hydrate (26) was dehydrated by azeotropic distillation with benzene: m.p. 215–217° (lit. 216–217° (27)), ν_{max} (KBr) 958 cm^{-1} (ν N—O). Sulfur dioxide was bubbled through a stirred suspension of the anhydrous *N*-oxide (2.4 g) in benzene (100 ml) for 4 h, by which time all suspended solids had gone into solution. Concentration of the solution to 18–20 ml resulted in the separation of a white solid, which crystallized from absolute ethanol as white crystals (1.6 g, 60%), blackening at 194–196°, decomposed at 225°, ν_{max} (KBr) 1315, 1285, 1110, 1060, 990, 590 cm^{-1}.

[8]All nomenclature based on International Union of Pure and Applied Chemistry, Nomenclature of Organic Chemistry, Definitive Rules for Section *C*, Butterworths, London, 1965. p. 69.

Anal. Calcd. for $C_{21}H_{22}O_5N_2S$ (mol. wt. 414): C, 60.9; H, 5.3; N, 6.8; S, 7.7. Found (410 ± 10 (in benzene, by vapor pressure osmometry)): C, 61.0; H, 5.1; N, 6.8; S, 7.7.

*(N_b-Brucinio) Sulfite (**9**; X = OMe)*

The same procedure, applied to the anhydrous *N*-oxide of brucine (27), gave the sulfitoamine, blackening at 195 °C, decomposed at 220–225 °C, ν_{max} (KBr) 1315, 1284, 1110, 1060, 990, 590 cm^{-1}.

Anal. Calcd. for $C_{23}H_{26}N_2O_7S$: C, 58.2; H, 5.5; N, 5.9; S, 8.7. Found: C, 58.3; H, 5.4; N, 6.0; S, 8.8.

*Alkaline Hydrolysis of (N_b-Strychninio) Sulfite (**9**; X = H)*

(N_b-Strychninio) sulfite (0.12 g), swirled with 0.2 *N* sodium hydroxide (15 ml), went into solution, and in 1–2 min a white precipitate separated. This was removed by filtration, washed with cold water, and identified as strychnine (0.08 g, 88%), m.p. and mixed m.p. 284–287 °C. The filtrate, acidified with HNO_3 and treated with $BaCl_2$, gave a positive sulfate test.

*Acid Hydrolysis of (N_b-Strychninio) Sulfite (**9**; X = H)*

Sulfur dioxide was bubbled slowly for 15–20 min through a solution of (N_b-strychninio) sulfite (100 mg) in water (5 ml) at 65–70°. The solution, treated with sodium bicarbonate, deposited strychnine (76 mg, 90%), identified by m.p. and i.r. spectrum.

*(N_b-Strychninio) Sulfate (**11**; X = H)*

Pyridine – sulfur trioxide complex (0.27 g) was added to anhydrous strychnine-*N*-oxide (0.6 g) in dry pyridine (25 ml), and stirred for 5 min. The white solid (0.6 g, 83%) that separated was removed by filtration and freed from pyridine by pumping at 2 mm. It blackened at 200–202 °C, melted at 228–230 °C, ν_{max} (KBr) 1335, 1295, 1120, 1060, 710, 622 cm^{-1}.

Anal. Calcd. for $C_{21}H_{22}O_6N_2S$: C, 58.6; H, 5.2; N, 6.5; S, 7.4. Found: C, 58.6; H, 5.4; N, 6.5; S, 7.4.

*(N_b-Brucinio) Sulfate (**11**; X = OMe)*

The same procedure applied to brucine-*N*-oxide gave **11** (X = OMe), blackening 205–207 °C, melts at 235–236 °C, ν_{max} (KBr) 1334, 1295, 1129, 1060, 710, 622 cm^{-1}.

Anal. Calcd. for $C_{23}H_{26}O_8N_2S$: C, 56.3; H, 5.3; N, 5.7; S, 6.5. Found: C, 56.3; H, 5.4; N, 5.7; S, 6.3.

Alkaline Hydrolysis of (N_b-Strychninio) Sulfate

(N_b-Strychninio) sulfate (0.1 g), swirled with 0.2 *N*

Can. J. Chem. Downloaded from www.nrcresearchpress.com by 210.87.254.42 on 09/05/12
For personal use only.

Can. J. Chem. Downloaded from www.nrcresearchpress.com by 210.87.254.42 on 09/05/12
For personal use only.

sodium hydroxide (10–15 ml), went into solution. Repeated extraction with chloroform (10 × 25 ml) removed strychnine *N*-oxide hydrate (55 mg, 64%) (identified by m.p., i.r. spectrum, and t.l.c.). The aqueous phase, acidified with nitric acid and treated with barium chloride, gave a positive sulfate test.

Preparation of N-Ammonium Sulfonates

(a) By Reaction of the Amine with Sulfur Trioxide

A mixture of strychnine (0.5 g), dissolved in dry pyridine (40 ml), and pyridine – sulfur trioxide complex (0.24 g) was stirred for 15 min at room temperature. A white solid separated, which was removed by filtration, washed with pyridine, and dried under reduced pressure at room temperature. The solid **10** (X = H) (0.5 g) melted at 265–275 °C (dec.) (Oesterlin (8) reported m.p. 260–265 °C); ν_{max} (KBr) 1250, 1000, 700, 575 cm^{-1}.

By essentially the same procedure the complex **10** (X = OMe) was obtained from brucine, **14** (X = OMe) from quinine, **14** (X = H) from cinchonine, and **15** from harmine. The complexes **16** and **17** were obtained by the reaction of the parent amines with equivalent amounts of sulfur trioxide dissolved in 1,2-dichloroethane at 0° (*cf.* ref. 28) or by reaction of the parent amines with half-molar quantities of chlorosulfonic acid in chloroform at 0° (*cf.* ref. 29). The melting points and some i.r. peaks of these compounds are listed in Table 3 and their combustion analyses in Table 4. The u.v. absorption and n.m.r. spectra of these compounds were obtained, and did not differ essentially from the spectra of the analogous *N*-ammonium-*S*-thiosulfate compounds already reported (9).

(b) By Reaction of the Amine with Dithionate

A suspension of strychnine (1 g) in a solution of sodium dithionate (4 g) in water (90 ml) was refluxed for 5 h. The hot reaction mixture was filtered to remove unreacted strychnine and cooled. White crystals separated and were removed, washed with water and chloroform, and recrystallized from water or ethanol. The solid thus obtained (1.1 g, 95%), m.p. 265–275° (dec.), had an i.r. spectrum identical with that of material prepared above.

By essentially the same procedure, the following sulfamic acids were obtained from the free bases in the yields indicated: **10** (X = OMe), 83%; **14** (X = OMe), 80%; **14** (X = H), 95%; **15**, 80%; **16**, 60%; **17**, 96%.

The following amines failed to give any crystalline product after reaction with dithionate: triethylamine, *N,N*-dimethylaniline, imidazole, benzimidazole, 4-phenylpyridine, benzothiazole, and neostrychnine.

*Strychninium-N_b-sulfonate (**10**; X = H)*

(a) By Reaction of Strychnine-N-oxide with Sulfur Dioxide in Aqueous Solution

Sulfur dioxide was bubbled into a solution of strychnine *N*-oxide (1 g) in water (60 ml) at 0° for 15 min. A white solid (1 g, 85%), m.p. 265–275 °C (dec.), separated which proved identical (i.r. spectrum) with the product of the reaction of strychnine with sulfur trioxide.

TABLE 3. Melting points and i.r. peaks (cm^{-1}) of *N*-ammonium sulfonates in KBr

Compound	Melting point (°C)*	ν_{asym} (SO_3)	ν_{sym} (SO_3)	ν (S—N)	δ (SO_3)
10; X = H	265–275	1250	1000	700	575
10; X = OMe	238–240	1225	990	710	580
14; X = H	230–233	1240	990	720	575
14; X = OMe	210–215	1245	990	720	575
15	220–225	1230	1010	730	570
16	183–185	1250	1015	755	590
17	208–210	1225	990	755	570

*All melting points involved decomposition of the sample.

TABLE 4. Analyses of *N*-ammonium sulfonates

Compound	Empirical formula		%C	%H	%N	%S	Molecular weight*
10; X = H	$C_{21}H_{22}N_2O_5S$	Calcd.	60.9	5.3	6.8	7.7	414
		Found	60.6	5.5	6.8	7.5	410±10
10; X = OMe	$C_{23}H_{26}N_2O_7S$	Calcd.	58.2	5.5	5.9	8.7	
		Found	58.4	5.6	5.8	8.7	
14; X = H	$C_{18}H_{22}N_2O_4S$	Calcd.	60.9	5.9	7.5	8.5	
		Found	60.7	6.1	7.5	8.5	
14; X = OMe	$C_{19}H_{24}N_2O_5S$	Calcd.	59.4	6.0	6.9	7.9	
		Found	59.1	5.9	7.2	8.2	
15	$C_{13}H_{12}N_2O_4S$	Calcd.	53.4	4.1	9.6	10.9	
		Found	53.5	4.4	9.4	11.0	
16	$C_{10}H_9NO_4S$	Calcd.	50.2	3.8	5.9	13.4	239
		Found	50.0	3.7	5.8	13.4	235±10
17	$C_{12}H_{10}N_2O_3S$	Calcd.	56.9	3.7	10.2	11.7	274
		Found	56.7	3.5	9.9	11.5	270±10

*Determined by vapor phase osmometry using a Mechrolab Model 301A osmometer and ethanol as solvent.

Can. J. Chem. Downloaded from www.nrcresearchpress.com by 210.87.254.42 on 09/05/12
For personal use only.

*(b) By rearrangement of (N_b-Strychninio) Sulfite (**9**; X = H)*

The sulfitoamine **9** (X = H) (0.28 g) was boiled in water (40 ml) for 24 h. The solution was cooled and the precipitate that separated (0.23 g, 83%) was collected: m.p. 265–275° (dec.), ν_{max} (KBr) 1250, 1000, 700, 575 cm^{-1}. The product was shown to be identical with **10** (X = H) prepared above by m.p., i.r. spectral comparison, and combustion analysis.

Anal. Calcd. for $C_{21}H_{22}O_6N_2S$: C, 60.8; H, 5.3; N, 6.7; S, 7.7. Found: C, 60.6; H, 5.5; N, 6.7; S, 7.5.

When the time of the reaction was reduced to 15 min impure **10** (X = H), m.p. 260–268° (50% yield) crystallized from the solution on cooling, and impure **9** (X = H), blackening at 189–192°, decomposing at 210–220° (50% yield), was obtained by evaporation of the filtrate at reduced pressure.

Reaction of Strychnine N-Oxide with Aqueous Sulfur Dioxide at 60–65 °C

Sulfur dioxide was bubbled into a solution of strychnine *N*-oxide (100 mg) in water (50 ml) at 60–65 °C for 15 min. A white precipitate formed within the first 5 min and redissolved as the addition of sulfur dioxide was continued for 10 min. The solution, on treatment with sodium bicarbonate, precipitated strychnine (85 mg; 95%) identified by comparison of m.p. and i.r. spectrum with those of an authentic sample.

*Rearrangement of (N_b-Strychninio) Sulfite (**9**; X = H) in the Presence of Hydroquinone*

The sulfitoamine **9** (X = H) (0.60 g) was refluxed in water (100 ml) containing hydroquinone (0.17 g) for 24 h. The solution was cooled and extracted with ether (4 × 60 ml). The ether extracts were dried and evaporated to give residue *A* (0.14 g). The aqueous layer (p*H* ~ 5) was neutralized with sodium bicarbonate. A fine white solid separated and was extracted with chloroform (2 × 50 ml). The chloroform extract was dried and evaporated to give strychnine (0.29 g; 60%); after recrystallization from ethanol, m.p. 286–288° (dec.), undepressed by admixture with an authentic sample of strychnine. The aqueous layer was partially evaporated (25 ml). White needles separated and were collected (0.15 g, 23%), m.p. 265–275°, and were found to be identical with **10** (X = H) by mixed m.p. The aqueous filtrate gave a positive test for sulfite with $BaCl_2$ (0.17 g $BaSO_3$, 53%). Water (40 ml) was added to residue *A*, and the mixture was warmed on a steam bath for a few minutes, then cooled. The insoluble yellow material (90 mg) was removed by filtration and recrystallized from ethanol, giving slightly impure benzoquinone, m.p. and mixed m.p. 112–115°. The aqueous filtrate was evaporated and the solid residue (50 mg) recrystallized from ethanol to give needles of hydroquinone, m.p. and mixed m.p. 169–170°.

Reaction of Strychnine N-Oxide with Aqueous Sulfur Dioxide in the Presence of Hydroquinone

Sulfur dioxide was bubbled into a solution of strychnine *N*-oxide (0.34 g) and hydroquinone (0.10 g) in water (40 ml) at 0° for 10 min, during which time a white precipitate separated, redissolved, and then a yellow solid separated. The yellow solid after recrystallization from ethanol, had m.p. 113–115°, undepressed by admixture of the sample with an authentic sample of 1,4-benzoquinone. The aqueous solution was extracted with ether (3 × 25 ml) to remove a trace of hydroquinone, and then concentrated to 20 ml, and neutralized with sodium bicarbonate. White needles (0.26 g, 85%), separated; m.p. 286–288° (dec.) after recrystallization from ethanol, and identified by mixed m.p. as strychnine.

Strychnine *N*-oxide was not reduced to strychnine by hydroquinone in water at 0°.

*Acid Hydrolysis of Strychninium-N_b-sulfonate (**10**; X = H)*

(a) 6 N Hydrochloric Acid

Hydrolysis to strychnine (90% yield) and sulfate ion was complete within 2 min at room temperature.

(b) 0.5 N Hydrochloric Acid

Hydrolysis was complete in about 30 min at room temperature or 1 min at 100°.

(c) Aqueous Sulfur Dioxide

Hydrolysis was inappreciable after many hours at room temperature, but was complete (95% yield of strychnine) after 15 min at 65–70°.

*Alkaline Hydrolysis of Strychninium-N_b-sulfonate (**10**; X = H)*

Strychninium-N_b-sulfonate (0.15 g), swirled with 0.02 *N* sodium hydroxide (18.15 ml), deposited almost immediately strychnine (0.12 g); m.p. 286–288 °C (dec.) (identical by i.r. with an authentic sample of strychnine). The filtrate, acidified with nitric acid and treated with barium chloride, gave a positive sulfate test. Hydrolysis was almost instantaneous with aqueous ammonia and sodium carbonate but was inappreciable with aqueous sodium bicarbonate.

*N,N-Dimethylaniline N-Oxide (**18**)*

The following procedure is a modification of those in the literature (18, 30). Freshly distilled *N,N*-dimethylaniline (50 g) was stirred with 10% hydrogen peroxide (450 ml) at 60–70 °C for 10 h. The reaction mixture was cooled and extracted with ether (4 × 100 ml) to remove excess *N,N*-dimethylaniline. The aqueous layer was partially evaporated under reduced pressure at room temperature. A layer of benzene (100 ml) was added, and the mixture was treated with Linde Molecular Sieves Type 3A (250 g) until there was no positive peroxide test (15 h). The mixture was filtered and the benzene was evaporated. The pale-yellow solid residue was washed with cold benzene, removed by filtration, and dried at reduced pressure. It weighed 38 g (67%) and had m.p. 152–153 °C (lit. 152–153 °C (30)), ν_{max} (KBr) 965 cm^{-1} (ν N—O) (lit. 960 cm^{-1} (30)).

*(N,N-Dimethylanilinio-N) Sulfite (**19**)*

A solution of *N,N*-dimethylaniline oxide (3.02 g) in anhydrous benzene (100 ml) was saturated with sulfur dioxide. The solution turned yellow–orange, and a dark yellow gum precipitated on the walls of the flask. The benzene solution was decanted. Gradually (10 min) a white solid (18 mg) formed in the benzene solution and was removed by filtration. It had m.p. 95–98°, and an i.r. spectrum identical with that of an authentic sample of *N,N*-dimethylanilinium-*N*-sulfonate (24) prepared below.

Can. J. Chem. Downloaded from www.nrcresearchpress.com by 210.87.254.42 on 09/05/12
For personal use only.

The benzene solution was evaporated under reduced pressure at room temperature. An acid wash of the benzene distillate removed *N,N*-dimethylaniline (0.75 g, 27%), having an i.r. spectrum identical with an authentic sample.

The oily residue in the flask (3.1 g, 70%) was identified as the sulfitoamine **19** by its characteristic i.r. spectrum (film between KBr plates: ν_{max} 1320, 1200, 1060, 1010, 780, 695, 580 cm^{-1}). It was very hygroscopic and was not analyzed.

*Rearrangement of the Sulfitoamine **19** in Water*

The sulfitoamine (3.1 g) was dissolved in water (80 ml) and the solution was kept in an ice-bath for 2 h, or was heated to 70–80° for 30 min. The solution was then worked-up by the procedure of Bamberger and Tschirner (18). Results are given in Table 1.

*N,N-Dimethylanilinium Sulfonate (**24**)*

Excess sulfur trioxide in 1,2-dichloroethane was added to dry *N,N*-dimethylaniline (2 g) in 1,2-dichloroethane (50 ml) at 0°. The reaction mixture was stirred for 1 h. The white solid was removed by filtration and dried under reduced pressure: 2.5 g, m.p. 95–99 °C, (lit. (31) m.p. 85–90°) ν_{max} (KBr) 1295, 1240, 1200, 1060, 1000, 750, 690, 575 cm^{-1}. The material was very hygroscopic and was hydrolyzed in cold water to *N,N*-dimethylaniline and sulfate almost instantaneously.

Reaction of N,N-Dimethylaniline Oxide with Aqueous Sulfur Dioxide

(a) Without Hydroquinone

Sulfur dioxide was bubbled for 45 min into a solution of the oxide (9.98 g) in water (75 ml) at 0°. The resultant emerald-green solution was stirred for 2 days and then worked-up according to Bamberger and Tschirner (18). Results are given in Table 1. Identity of the various products was confirmed by combustion analysis and by their i.r. and n.m.r. characteristics.

(b) With Hydroquinone

The reaction was carried out as above, except that hydroquinone (9 g) was added to the solution of the oxide in water before the introduction of sulfur dioxide. (In a separate experiment, it was shown that hydroquinone did not react with *N,N*-dimethylaniline oxide in water.) After 2 days reaction, the solution was acidified with 2 *N* sulfuric acid (4.7 ml), and benzoquinone and excess hydroquinone removed by extraction with ether. The solution was then worked-up according to the procedure of Bamberger and Tschirner (18), and gave *N,N*-dimethylaniline (80% yield), *N,N*-dimethylamino-*o*-benzenesulfonic acid (10%), *N,N*-dimethylamino-*p*-benzenesulfonic acid (3%), and *N,N*-dimethylamino-*o*-phenol (1.5%).

*(N,N-Dimethylanilinio) Sulfate (**27**)*

Pyridine – sulfur trioxide complex (0.68 g) was stirred for 30 min with anhydrous *N,N*-dimethylaniline *N*-oxide (0.6 g) dissolved in dry pyridine (30 ml). The t.l.c. on alumina then showed that no *N*-oxide (R_f 0.75 in $CHCl_3$/EtOH 80/20) remained. An oily gum formed on the walls of the flask. The solution was decanted, and the residual gum, dried under reduced pressure, set to a pale yellow solid (0.9 g), very hygroscopic. The i.r. spectrum (ν_{max} (KBr) 1340, 1275, 1110, 1030, 755, 685, 615 cm^{-1}) was similar to that of (strychninio-N_b) sulfate.

Anal. Calcd. for $C_8H_{11}O_4NS$: C, 44.2; H, 5.1; N, 6.4; S, 14.7. Found: C, 44.4; H, 5.3; N, 6.4; S, 14.5.

Hydrolysis of (N,N-Dimethylanilinio) Sulfate in Water

The sulfate (0.9 g) in water (25 ml) was heated on a steam bath for 10 min. The solution was neutralized with sodium bicarbonate, and was extracted with chloroform (10 × 40 ml). The extracts were dried and evaporated to give *N,N*-dimethylaniline-*N*-oxide (0.45 g) ν_{max} ($CHCl_3$) 965 cm^{-1}, R_f 0.75 by t.l.c. The acidified aqueous solution gave a positive test for sulfate (0.95 g $BaSO_4$; 98%). Picric acid added to the aqueous solution gave a yellow precipitate (0.17 g) of *N,N*-dimethylaniline oxide picrate, m.p. 136–138° (lit. m.p. 136° (18)).

Reaction of N,N-Diethylaniline Oxide with Aqueous Sulfur Dioxide

The monohydrate of *N,N*-diethylaniline *N*-oxide was obtained as a pale yellow solid, m.p. 89–92 °C (lit. 96° (32)), in 50% yield.

Sulfur dioxide was bubbled for 45 min into a solution of the *N*-oxide hydrate (10 g) in water (75 ml) at 0 °C. The resultant green solution was stirred for 2 days and then worked-up according to Bamberger and Tschirner (18). Yields are given in Table 1. *o-N,N*-Diethylaminophenol had m.p. < 20 °C (lit. 8–9 °C (33)), b.p. 216–219 °C (lit. 219–220 °C (33)), ν_{max} (KBr) 3400 (ν O—H), 1390 (δ O—H), 1220–1230 (ν C—O), 748 cm^{-1} (ortho-substituted). *o-N,N*-Diethylaminobenzenesulfonic acid darkened at about 275 °C and decomposed above 270 °C (34)), ν_{max} (KBr) 2650 (N^+—H), 1245 (ν_{asym} SO_3) 1080 (ν_{sym} SO_3), 765 (ortho-substituted), 590 cm^{-1} (δ SO_3); n.m.r. in D_2O: 1.20, 6H (CH_3, triplet), 4.02 4H(CH_2, quartet), 7.85 δ, 4H (aromatic, broad multiplet).

Anal. Calcd. for $C_{10}H_{15}NSO_3$: C, 52.4; H, 6.6; N, 6.1; S, 14.0. Found: C, 52.6; H, 6.7; N, 6.0; S, 13.9.

p-N,N-Diethylaminobenzenesulfonic acid darkened at 270 °C and decomposed at 285–300 °C (lit.: darkened at 250 °C, decomposed above 270 °C (34)), ν_{max} (KBr) 2650 (ν N^+—H), 1210 (ν_{asym} SO_3), 1035 (ν_{sym} SO_3), 832 (para-substituted), 590 cm^{-1} (δ SO_3); n.m.r. in D_2O: 1.20, 6H(CH_3, triplet); 4.02, 4H(CH_2, quartet); 7.85 δ, 4H (aromatic, broad multiplet).

Anal. Calcd. for $C_{10}H_{15}NSO_3$: C, 52.4; H, 6.6; N, 6.1; S, 14.0. Found: C, 52.0; H, 6.5; N, 6.0; S, 14.2.

In a second experiment, the reaction was followed by n.m.r. In acidified D_2O the n.m.r. spectrum of diethylaniline consists of a triplet at 1.45, 6H(CH_3), a quartet at 3.25, 4H(CH_2), and a broad multiplet at 7.85 δ, 5H (aromatic). The spectrum of the *N*-oxide in D_2O consists of a triplet at 1.20, 6H(CH_3), a quartet at 4.02, 4H(CH_2), and a broad multiplet at 7.85 δ. 5H (aromatic). The alkyl and aryl protons of the ortho- and para-sulfonic acids had virtually the same chemical shifts as those in the *N*-oxide.

Sulfur dioxide was bubbled into a solution of the *N*-oxide at 0 °C, and the spectrum was scanned every few minutes for the first hour and then intermittently for 2 days. There was no obvious emission or enhanced absorption in the alkyl resonances at any time. For the first 20 min the reaction was strongly exothermic so that thermal equilibrium was not established in the

probe, and mixing was imperfect (color not homogeneous), so that during this time the resonances were not well resolved. As the reaction proceeded a well-resolved quartet appeared at 3.25 and a triplet at 1.45 δ (slightly obscured by the CH_3 at 1.20 of the *N*-oxide). After 2 h the quartet at 3.25 integrated to approximately 20% of the quartet at 4.02 δ. The spectrum did not significantly change after this time.

*Reaction of N,N-Dimethylbenzylamine N-Oxide (**29**) with Aqueous Sulfur Dioxide at 0 °C*

Sulfur dioxide was bubbled into a solution of *N,N*-dimethylbenzylamine *N*-oxide (12 g of 50% solution) at 0° for 15 min. The reaction was strongly exothermic. A sticky white precipitate of **32** was removed, washed with ether, and dried at 80° and 1 mm: white powder, ν_{max} (KBr) 2660 (ν N^+—H), 1290 (ν_{asym} SO_3), 1200, 1055 cm^{-1} (ν_{sym} SO_3).

Anal. Calcd. for $C_9H_{13}NO_3S$: C, 50.2; H, 6.1; N, 6.2; S, 14.9. Found: C, 49.9; H, 6.1; N, 6.6; S, 14.4.

Attempts to recrystallize **32** from water or 95% ethanol resulted in decomposition, and a quantitative yield of benzaldehyde, ν_{max} (neat) 1695 cm^{-1}, was obtained; its 2,4-dinitrophenylhydrazone melted at 236–237°.

In a second experiment, the reaction mixture was diluted with water (25 ml) to keep **32** in solution. After reaction the solution was boiled for 5 min to remove sulfur dioxide, cooled, and extracted with ether (3 × 40 ml). The combined ether extracts were dried ($MgSO_4$) and distilled to give benzaldehyde (2.2 g, 52%). The aqueous solution was made strongly alkaline and extracted again with ether (3 × 40 ml). The combined extracts were dried ($MgSO_4$) and concentrated, and the residue chromatographed on alumina. Elution with benzene separated first *N,N*-dimethylbenzylamine (1.9 g, 35%); n.m.r. spectrum showing singlet (6H) at 2.9, and a singlet (2H) at 7.35 δ. Next came *N*-methylbenzylamine (0.4 g, 8%), ν_{max} ($CHCl_3$) 3300 cm^{-1} (ν N—H), forming a *p*-toluenesulfonamide, m.p. 93–95° (reported m.p. 95°).

When the reaction was carried out in the presence of hydroquinone (4.5 g), the yields of benzaldehyde (50%), *N,N*-dimethylbenzylamine (37%), and *N*-methylbenzylamine (8%) were almost unchanged.

Phenylsulfamic Acid

Phenylsulfamic acid was prepared by the procedure of Traube (35), and was isolated as the phenylammonium salt, melting with sublimation at 180°, ν_{max} (KBr) 2560 (ν NH_2^+), 1200 (ν_{asym} SO_3), 1010 (ν_{sym} SO_3), 750 and 690 (monosubstituted benzene), 695 (ν S—N), 575 cm^{-1} (δ SO_3); or as the barium salt, ν_{max} (KBr) 1200 (ν_{asym} SO_3), 1060 (ν_{sym} SO_3), 750 and 690 (monosubstituted benzene) 670 (ν S—N), 580 cm^{-1} (δ SO_3). Acidification of the barium salt resulted in hydrolysis to aniline bisulfate.

Reaction of Hydroxylamine with Aqueous Sulfur Dioxide

Sulfur dioxide was bubbled into 1 *M* aqueous hydroxylamine hydrochloride (50 ml) for 30 min at 0 °C, and the solution was stirred for another 60 min. Evaporation of the solution to dryness gave a white crystalline residue (4.9 g), ν_{max} (KBr) 3100–2600 (ν NH_4^+ and NH_3^+), 1540 (δ_{deg} NH_3^+), 1445 (δ_{sym} NH_3^+), 1300 (ν_{deg} SO_3) 1160 (ν_{asym} SO_3) in HSO_4^-), 1065 (ν_{sym} SO_3), 842 (ν S—O (H) in HSO_4^-), 688 cm^{-1} (ν S—N). The relative intensities of the sulfamic acid peak at 688 (36) and the bisulfate peak at 842 cm^{-1} (37), by comparison with those of known mixtures of sulfamic acid and potassium bisulfate, indicated an approximately 9:1 ratio of sulfamic acid:ammonium bisulfate, in agreement with results in the literature (22). The ratio was not affected when the reaction was repeated in the presence of hydroquinone (5.6 g), which was removed after the reaction by extraction with ether.

Reaction of Phenylhydroxylamine with Sulfur Dioxide

Through a solution of phenylhydroxylamine (5 g) in absolute alcohol (60 ml) at 10–25 °C, dry sulfur dioxide was passed for 1–2 h with stirring. A white crystalline solid was gradually formed and the color of the solution changed from light tan to brown. The flask was stoppered and allowed to stand for 3–30 h at 10° (different times caused no significant difference in yields). The mixture was filtered and the collected solid was found by i.r. examination to be a crude mixture of orthanilic and sulfanilic acids. This mixture was separated by fractional crystallization from water. The para isomer was crystallized first; it decomposed above 270° (lit. 288° (30)) and its i.r. spectrum (ν_{max} (KBr) 1220–1170 cm^{-1} (ν_{asym} SO_3) 1035 (ν_{sym} SO_3), 815 (para-substituted benzene), 565 cm^{-1} (δ SO_3)) was identical with that of an authentic sample of sulfanilic acid. The ortho isomer was obtained from the mother liquors by fractional crystallization; it decomposed above 180° (lit. 188° (33)) and its i.r. spectrum (ν_{max} (KBr) 1230–1180 (ν_{asym} SO_3), 1025 (ν_{sym} SO_3), 770 and 705 (ortho-substituted benzene), 560 cm^{-1} (δ SO_3)) was identical with that of an authentic sample of orthanilic acid.

The original mother liquor from the *o*- and *p*-isomers was made alkaline with potassium hydroxide and was extracted with ether (4 × 50 ml). The ether extracts contained aniline, which was identified by comparison of its i.r. spectrum and its chromatographic properties on alumina with those of an authentic sample. The extracted aqueous layer was neutralized with dilute hydrochloric acid and evaporated to give a brown solid, This was extracted with hot absolute alcohol (4 × 50 ml). then with hot 90–95% alcohol (4 × 50 ml), after which the residue consisted of inorganic material only. Evaporation of the absolute alcohol extracts gave a dark-colored solid which was recrystallized from water (charcoal) to give white crystals of metanilic acid, decomposing above 210°, ν_{max} (KBr) 1240–1150 (ν_{asym} SO_3), 1025 (ν_{sym} SO_3), 790 and 700 (meta-substituted benzene), 560 cm^{-1} (δ SO_3), identical with the spectrum of an authentic sample. From the 90–95% alcohol extracts, white crystals separated whose i.r. spectrum (ν_{max} (KBr) 1210–1160 (ν_{asym} SO_3), 1055 (ν_{sym} SO_3), 750 and 690 (mono-substituted benzene), 675 (ν S—N), 580 cm^{-1} (δ SO_3)) showed them to be potassium phenylsulfamate, by comparison with the spectrum of an authentic specimen of the barium salt. Potassium phenylsulfamate was readily soluble in cold water to give a neutral solution which gave no test for sulfate ion; when this solution was made acid and heated, complete hydrolysis of the product was effected, so that addition of barium chloride yielded an abundant precipitate of barium sulfate, and neutralization of the

Can. J. Chem. Downloaded from www.nrcresearchpress.com by 210.87.254.42 on 09/05/12
For personal use only.

Can. J. Chem. Downloaded from www.nrcresearchpress.com by 210.87.254.42 on 09/05/12
For personal use only.

aqueous phase with sodium bicarbonate and extraction with ether removed aniline quantitatively.

The same procedure was followed with other solvents (water and 60% ethanol) for the reaction. The yields of the various products are reported in Table 2.

Reaction of Phenylhydroxylamine with Sulfur Dioxide in the Presence of Hydroquinone

The same procedure as above was followed, except that hydroquinone (6 g) was added at the start of the reaction. Both the white solid formed initially and the filtrate from it were extracted with ether to remove a cream-colored solid (5.6 g, 93%), m.p. 169–171°, which was mainly hydroquinone (lit. m.p. 171–172°). A trace of benzoquinone (about 5%), was detected by comparing the chromatographic properties of the product on silica gel with the properties of known mixtures of hydroquinone and benzoquinone.

Reaction of Phenylhydroxylamine with Sulfur Dioxide in Anhydrous Ether

Dry sulfur dioxide was bubbled into a solution of phenylhydroxylamine (2.5 g) in anhydrous ether (50 ml) at 0 °C for 45 min. In the first few seconds a white precipitate formed, which then darkened to an orange oil and then (within a few minutes) to a black gum. The mixture was stirred for 8–10 h, by which time the black gum had solidified on the walls of the flask and a greyish powder was suspended in the ether. The grey powder (1.4 g, 42%), collected by filtration, sublimed at about 180°, and was identified as anilinium phenylsulfamate by comparison of its i.r. spectrum (ν_{max} (KBr) 2560 (ν NH_2^+), 1200 (ν_{asym} SO_3), 1010 (ν_{sym} SO_3), 750 and 690 (mono-substituted benzene), 625 (ν S—N), and 575 cm^{-1} (δ SO_3)) with the spectrum of an authentic specimen.

Anal. Calcd. for $C_{12}H_{14}N_2O_3S$: C, 54.1; H, 5.3; N, 10.5; S, 12.0. Found: C, 54.3; H, 4.9; N, 10.3; S, 12.4.

The powder (1 g) was heated with 2 *N* hydrochloric acid to 75° for 10 min and the resultant solution then neutralized with sodium bicarbonate and extracted with ether, removing aniline (0.55 g, 90%). The aqueous layer, acidified with nitric acid, gave a positive test for sulfate with barium chloride.

The ether filtrate was evaporated to give slightly impure aniline (25 mg, 1.5%), identified by comparison of i.r. characteristics and chromatographic properties on alumina with those of an authentic sample of aniline. The black sticky solid deposited on the walls (1.8 g, 54%) was identified by its i.r. spectrum as impure anilinium phenylsulfamate.

Reaction of Phenylhydroxylamine with Sodium Bisulfite in 60% Alcohol

A solution of sodium bisulfite (5 g) and phenylhydroxylamine (2.5 g) in 60% alcohol (80 ml) was stirred for 4 days at room temperature away from contact with air. Crystals gradually formed (0.3 g, 7.5%), and were identified as a mixture of orthanilic and sulfanilic acids by i.r. spectrum. Alcohol was removed from the filtrate by evaporation, and the aqueous layer was extracted with ether (4 × 75 ml). The combined ether extracts were dried and evaporated to give phenylhydroxylamine (2.2 g, 88%), m.p. 80–81°, and a trace of aniline.

Reaction of Phenylhydroxylamine with Sodium Sulfite in 60% Alcohol

A mixture of phenylhydroxylamine (2.5 g) and sodium sulfite (6 g) in 60% alcohol (100 ml) was stirred out of contact with air for 4 days at room temperature (sodium sulfite was not completely soluble). The reaction mixture was filtered, and the solid residue was extracted with hot alcohol (4 × 60 ml). Evaporation of the alcohol extracts gave a mixture of orthanilic and sulfanilic acids (0.2 g, 5%), contaminated by a trace of sodium sulfite. Alcohol was removed from the filtrate by evaporation, and the aqueous solution was extracted with ether (4 × 75 ml). The combined ether extracts were dried and evaporated to give a crude product (2.3 g) containing phenylhydroxylamine, aniline, azoxybenzene, and unidentified products, as shown by comparison of the chromatographic properties of alumina with those of authentic samples.

The financial support of Abbott Laboratories and of the National Research Council of Canada is gratefully acknowledged.

1. C. C. J. Culvenor. Rev. Pure Appl. Chem. **3**, 83 (1953).
2. E. C. Taylor and N. E. Boyer. J. Org. Chem. **24**, 275 (1959).
3. F. A. Daniher and B. E. Hackley. J. Org. Chem. **31**, 4267 (1966).
4. A. Kanda and A. J. King. J. Am. Chem. Soc. **73**, 2315 (1951). A. Asasi, H. Todokoro and I. Nitta. Bull. Chem. Soc. Jap. **28**, 524 (1955).
5. H. Z. Lecher and W. B. Hardy. J. Am. Chem. Soc. **70**, 3789 (1948).
6. M. Wiewiorowski and P. Baranowski. Bull. Acad. Polon. Sci. Ser. Sci. Chim. **10**, 549 (1962).
7. M. Polonovski and M. Polonovski. Bull. Soc. Chim. Fr. [4], **41**, 1190 (1927).
8. M. Oesterlin. Ber. **76**, 224 (1943).
9. J. T. Edward and J. Whiting. Can. J. Chem. **48**, 337 (1970).
10. C. K. Ingold. Structure and mechanism in organic chemistry. Bell, London, 1953. p. 345.
11. W. A. Waters. The chemistry of free radicals. Clarendon Press, Oxford, 1948. pp. 67, 74, 235.
12. A. Pictet and M. Mattison. Ber. **38**, 2782 (1905).
13. M. Polonovski and M. Polonovski. Bull. Soc. Chim. Fr. [4], **39** 1147 (1926).
14. H. Leuchs and F. Räck. Ber. **73**, 731 (1940).
15. H. Leuchs and H. G. Boit. Ber. **73**, 885 (1940).
16. J. P. Ferris, R. D. Gerwe, and G. R. Gapski. J. Org. Chem. **33**, 3493 (1968); J. Am. Chem. Soc. **89**, 5270 (1967).
17. E. Boyland, D. Manson, and P. Sims. J. Chem. Soc. 3623 (1953). E. J. Behrman. J. Am. Chem. Soc. **85**, 3478 (1963). E. J. Behrman and J. O. Edwards. *In* Progress in physical organic chemistry. Vol. 4. *Edited by* A. Streitwieser and R. W. Taft. Interscience Publishers, Inc., New York, N. Y., 1967. p. 108. E. J. Behrman. J. Am. Chem. Soc. **89**, 2424 (1967). N. Venkatasubramanian and S. Sabesan. Can. J. Chem. **47**, 3710 (1969).

18. E. BAMBURGER and F. TSCHIRNER. Ber. **32**, 1882 (1899).
19. H. FISCHER and J. BARGON. Acc. Chem. Res. **2**, 110 (1969).
20. R. N. ADAMS. Acc. Chem. Res. **2**, 175 (1969).
21. G. ILLUMINATI. J. Am. Chem. Soc. **78**, 2603 (1956).
22. D. S. BRACKMAN and W. C. E. HIGGINSON. J. Chem. Soc. 3896 (1953).
23. H. H. SISLER and L. F. AUDRIETH. J. Am. Chem. Soc. **61**, 3389 (1939).
24. R. T. M. FRASER. J. Chem. Soc. 1747 (1965).
25. R. T. M. FRASER. J. Chem. Soc. 5233 (1965).
26. A. S. BAILEY and SIR R. ROBINSON. J. Chem. Soc. 703 (1948).
27. A. PICTET and G. JENNY. Ber. **40**, 1172 (1907).
28. J. F. SCULLY and E. V. BROWN. J. Org. Chem. **19**, 894 (1954).
29. H. H. SISLER and L. F. AUDRIETH. Inorg. Syn. **2**, 173 (1946).
30. S. OAE, T. KITAO, and Y. KITAOKA. J. Am. Chem. Soc. **84**, 3366 (1962).
31. O. W. WILLCOX. Am. Chem. J. **32**, 4446 (1904). J. A. MOEDE and C. CURRAN. J. Am. Chem. Soc. **71**, 852 (1949).
32. R. HUISGEN, F. BAJERLEIN, and W. HEYDKAMP. Ber. **92**, 3223 (1959).
33. M. FORSTER. J. Prakt. Chem. **21**, 341 (1880).
34. A. MICHAELIS and E. GODCHAUX. Ber. **23**, 553 (1890).
35. W. TRAUBE. Ber. **23**, 1653 (1890).
36. O. I. NAKAGAWA, S. I. MIZUSHIMA, A. J. SARACENO, T. J. LANE, and J. V. QUAGLIANO. Spectrochim. Acta, **12**, 239 (1958).
37. N. B. COLTUP, L. H. DALY, and S. E. WIBERLEY. Introduction to infrared and Raman spectroscopy. Academic Press, New York, N. Y., 1964. p. 280.

Can. J. Chem. Downloaded from www.nrcresearchpress.com by 210.87.254.42 on 09/05/12
For personal use only.

Can. J. Chem. Downloaded from www.nrcresearchpress.com by 210.87.254.5 on 09/05/12
For personal use only.

Preparation de quelques cyclohexène-2 diones-1,4 et de leurs dérivés

J. Y. Savoie et P. Brassard
Département de Chimie, Université Laval, Québec, Québec

Reçu le 2 septembre 1970[1]

Nous avons obtenu pour la première fois, à notre connaissance, les monomères des dihydroxy-5,6(*cis*) cyclohexène-2 diones-1,4 à partir de quinones lors d'oxydations catalysées par l'acide osmique. La toluquinone et l'*o*-xyloquinone donnent un mélange de deux isomères possibles. L'analyse des spectres de r.m.n. suggère qu'en général ces nouvelles substances ont une plus grande souplesse conformationnelle que les dihalogénures de quinones. La transformation de cyclohexène-2 diones-1,4 en oximes permet en outre de déterminer facilement toutes les constantes importantes de couplage.

The osmic acid catalyzed oxidation of quinones has yielded for the first time to our knowledge the monomers of some *cis*-5,6-dihydroxycyclohex-2-ene-1,4-diones. Toluquinone and *o*-xyloquinone give mixtures of the two possible isomers. Observation of the n.m.r. spectra suggests that this new class of compounds are in general conformationally more mobile than quinonedihalides. The conversion of cyclohex-2-ene-1,4-diones into oximes allows the easy evaluation of all the important coupling constants.

Canadian Journal of Chemistry, **49**, 3515 (1971)

Grâce à la découverte récente de dihydro-2,3 quinones naturelles (1–4) et de leurs produits de réduction (5–7) on a réalisé des progrès considérables dans la synthèse de cyclohexène-2 diones-1,4 (8–13). Pour notre part, nous nous sommes intéressés tout particulièrement à leurs dérivés halogénés et hydroxylés en tant qu'intermédiaires de synthèse. On connaît depuis longtemps (14) les halogénures de quinones, mais leur configuration *trans* d'abord proposée (15), a ensuite été mise en doute (16), puis réaffirmée (17). En 1926, Terry et Milas (18) croyaient avoir préparé la première dihydroxy-5,6 cyclohexène-2 dione-1,4 par l'action du chlorate de sodium sur la *p*-benzoquinone en présence d'acide osmique. Cette substance a été reconnue depuis ce temps comme un dimère qui a fait l'objet de deux études de structure (19, 20).

Synthèse

Appliquée à l'*o*-xyloquinone, la méthode originale n'a permis, après 10 jours, que de récupérer la substance de départ. Nous sommes maintenant en mesure de communiquer la première synthèse de cyclohexènediones hydroxylées en 5,6 à la suite de modifications apportées à ce procédé (voir tableau 1 et partie expérimentale). L'hydroxylation n'est d'ailleurs pas aussi spécifique que la plupart des réactions des quinones puisqu'on obtient parfois des mélanges des isomères *a* et *b* (sauf pour l'α-naphtoquinone et la phénylbenzoquinone). Par contre, les diols dérivés de la

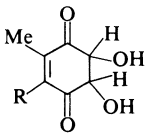

1*a* R = H
2*a* R = CH_3

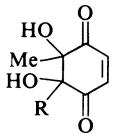

1*b* R = H
2*b* R = CH_3

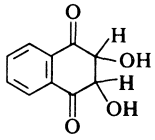

3

toluquinone et de l'*o*-xyloquinone ne montrent déjà plus de tendance à se dimériser. La chloroquinone donne un mélange complexe de monomères et de dimères, mais à partir de la *p*-benzoquinone, en interrompant l'expérience avant la fin de la réaction, nous avons pu isoler et identifier le plus simple de ces diols. La formation de l'acétonide du composé **2***a* et le fait que les diacétates de **1***b*, **2***b*, et **3** et les produits d'acétolyse des époxydes correspondants sont différents, confirment la stéréospécificité de la réaction et démontrent que l'oxydation donne bien les diols *cis*.

Les dihydroxy-5,6 cyclohexène-2 diones-1,4 sont très solubles dans l'eau, mais s'isolent du milieu réactionnel par extraction répétée avec de l'éther. Les rendements relatifs des deux isomères **1***a*, *b* et **2***a*, *b*, varient quelque peu suivant les conditions expérimentales, mais en général ceux des isomères "*a*" sont respectivement de l'ordre de 60 à 70% et d'environ 80% pour la toluquinone et l'*o*-xyloquinone. La séparation des isomères **2***a* et *b* s'effectue facilement par chromatographie sur gel de silice. Il est par contre préférable d'isoler les isomères **1***a* et *b* sous la forme d'acétate par la même méthode après acétylation du mélange car ces isomères sont peu stables en présence de cet adsorbant.

[1]Revision reçue le 9 juillet 1971.

Can. J. Chem. Downloaded from www.nrcresearchpress.com by 210.87.254.5 on 09/05/12
For personal use only.

TABLEAU 1. Hydroxylation des quinones

Quinone (0.1 mol)	Solvant	Volume (ml)	Catalyseur	Oxydant	Température (°C)	Temps	Diols (g)
p-Benzo	Eau	50	OsO_4	$NaClO_3$	25	8 jours	6.1*
	Eau	50	OsO_4	$NaClO_3$	25	48 h	3.4*, 1.4†
	Tétrahydrofuranne	50	OsO_4	$NaClO_3$	25	48 h	déc.
Tolu-	Eau–dioxanne	50:10	OsO_4	$NaClO_3$	25	74 h	7.6
	Eau–dioxanne	20:80	OsO_4	H_2O_2	25	4 h	10.3‡
o-Xylo	Eau	60	OsO_4	$NaClO_3$	25	23 jours	6.0
	Tétrahydrofuranne	60	OsO_4	$NaClO_3$	25	7 jours	7.0
	Eau–dioxanne	70:20	OsO_4	$NaClO_3$	25	50 h	15.4
	Eau–dioxanne	20:70	OsO_4	$NaClO_3$	25	40 h	11.5
	Eau–dioxanne	10:50	SeO_2	H_2O_2	65	40 h	6.8
α-Naphto-	Eau	50	OsO_4	$NaClO_3$	25	6 jours	0.1
	Eau–dioxanne	20:80	OsO_4	$NaClO_3$	25	10 jours	10.5
	Eau–dioxanne	80:20	OsO_4	$NaClO_3$	25	12 jours	17.5
	Acide acétique	80	WO_3	H_2O_2	70	24 h	déc.

*6.1 g et 3.4 g sont les poids du dimère isolé.
†1.4 g de monomère.
‡10.3 g de produit brut contenant du diol et d'autres produits.

Can. J. Chem. Downloaded from www.nrcresearchpress.com by 210.87.254.5 on 09/05/12
For personal use only.

Spectroscopie

Les études antérieures de r.m.n. sur un petit nombre de cyclohexène-2 ones naturelles et de cyclohexène-2 diones-1,4 semblent indiquer une nette prédominance d'un des conformères possibles (5, 7, 20–23). Norris et Sternhell (21) ont déduit la conformation des dibromures des méthyl-2 et bromo-2 benzoquinones et obtenu des résultats fragmentaires concernant quelques autres dérivés. Nous avons tenté d'obtenir directement des données plus générales par l'étude des monoximes correspondants (comme prévu, l'oximation d'un carbonyle ne semble pas perturber la situation conformationnelle).

Les dichloro- et dibromo-5,6 méthyl-2 cyclohexène-2 oximido-4 ones-1 donnent directement en première approximation des constantes de couplage vicinal ($J_{5,6}$) de 2.6 à 3.0 Hz et à longue distance ($J_{3,5}$) de 1.7 à 1.9 Hz, tout-à-fait comparables aux résultats antérieurs. Les spectres des mêmes dérivés de la *p*-benzoquinone elle-même permettent de plus d'évaluer toutes les constantes de couplage importantes ($J_{2,3}$, $J_{2,6}$, $J_{3,5}$, et $J_{5,6}$) et confirme l'orientation diaxiale des substituants (voir tableau 2). Dans cette partie de l'étude, nous nous sommes évertués à obtenir des échantillons purs et avons délibérément négligé les problèmes de l'isomérie *syn–anti* des substrats (le dichlorure de la toluquinonacétoxime en particulier se comporte comme un mélange d'isomères).

Il est bien connu que les époxy-5,6 cyclohexénones et cyclohexènediones adoptent de préférence la conformation "O-axiale" (5, 23, 24). Quoique Rashid et Read (11) n'aient observé que deux singulets dans le spectre de r.m.n. de l'époxybenzoquinone, nos spectres révèlent bien les deux triplets attendus pour une telle conformation (25). La valeur de $|J_{ax} + J_{a'x}|$ s'obtient donc directement et, puisque $J_{a'x}$ doit être très petit, nous obtenons une valeur de J_{ax} qui est en accord avec celle prédite. L'oxime de l'époxybenzoquinone permet encore une fois de mesurer les quatre constantes de couplage principales qui concordent bien avec les valeurs prévues pour le conformère O-axial.

Les dihydroxy-5,6 cyclohexènediones (*cis* et *trans*) présentent un problème conformationnel un peu plus délicat car, sous la forme monomère, elles montrent rarement, dans leurs spectres de r.m.n., de couplage à longue distance alors que ceux-ci sont très évidents dans le cas des dimères monohémiacétal (20). Les autres constantes de couplage peuvent parfois être mises en évidence par l'emploi de substituants convenablement situés (*i.e.* dans **1***b*) ou dans le cas de **2***a* par la formation d'un monoacétate.

Les résultats préliminaires obtenus à partir de la toluquinone et de l'*o*-xyloquinone semblaient confirmer que ces diols, comme beaucoup d'autres cyclohexènediones, adoptent une conformation particulière mais que celle-ci serait "bateau". En effet l'abaissement de la température à $-50°$ n'apporte aucune modification des spectres de r.m.n.

Le choix de substrats appropriés a toutefois permis de réjeter cette possibilité d'ailleurs peu probable. Ainsi les seuls diols, qui montrent un couplage à longue distance dans leur spectre de r.m.n. sont ceux qui dérivent des phényl et di-*t*-butyl-2,6 quinones. Dans ces deux cas, une conformation qui ne peut être que "chaise" prédomine et s'explique par des considérations élémentaires d'interaction de dipôles ou d'effets stériques. Dans les autres exemples, aucun facteur ne semble susceptible de stabiliser l'une des formes et on doit donc en conclure que l'on a affaire à des équilibres rapides de conformères "chaise".

Applications

L'énolisation de la dihydroxy-5,6(*cis*) diméthyl-2,3 cyclohexène-2 dione-1,4 dans l'éther saturé d'acide bromhydrique ou bien du diacétate correspondant dans le méthanol contenant de l'acide chlorhydrique a donné le tétrahydroxy *o*-xylène (avec un rendement de 70% à partir de l'*o*-xyloquinone). L'oxydation de cette hydroquinone par l'oxygène atmosphérique en milieu faiblement basique a aussi permis d'effectuer une synthèse de l'aurantiogliocladine beaucoup plus facile que celles publiées (26–28). D'ailleurs nous n'avons jamais pu répéter celle de Pettersson (28) en dépit de nombreuses tentatives; la réaction de Thiele sur l'hydroxy *o*-xyloquinone ne nous a jamais donné la moindre trace de tétraacétoxy *o*-xylène. De plus, cette dernière substance préparée par nous a un point de fusion de 174.0–174.5° au lieu de 97° que donne Pettersson (sans mention de rendement). D'autre part, toutes les tentatives en vue de transformer le tétrahydroxy *o*-xylène en dihydroxy-2,3 diméthyl-5,6(*trans*) cyclohexène-2 dione-1,4 (dont l'éther méthylique est la glioroséine) par les méthodes de Mayer et Weiss (29) se sont toutes soldées par des échecs.

Can. J. Chem. Downloaded from www.nrcresearchpress.com by 210.87.254.5 on 09/05/12
For personal use only.

TABLEAU 2. Spectres r.m.n. des dihalogénures des quinonemonoximes

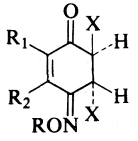

	Déplacements chimiques (p.p.m. p/r au TMS)*					Constantes de couplage (Hz)			
	C_2	C_3	C_5	C_6	R	2,3	5,6	2,6	3,5
X = Cl $R_1 = R_2 = H$ R = Ac	6.48 q	7.30 q	5.69 q	4.45 q	2.35 s	10.5	2.7	1.4	1.9
X = Cl $R_1 = CH_3$ $R_2 = H$ R = Ac	2.09 d	7.07 m	5.56 q	4.47 d	2.30 s	1.5	3.0	—	1.9
X = Br $R_1 = R_2 = H$ R = Ac	6.46 q	7.23 q	5.68 q	4.66 q	2.35 s	10.2	2.6	1.3	1.8
X = Br $R_1 = CH_3$ $R_2 = H$ R = Ac	2.11 d	7.40 m	5.37 q	4.81 d	2.32 s	1.5	2.8	—	1.8
X = Br $R_1 = R_2 = CH_3$ R = H	2.05 s	2.18 s	5.80 d	4.66 d	8.98 s		2.7		

*q: quadruplet, d: doublet, s: singulet, m: multiplet.

Can. J. Chem. Downloaded from www.nrcresearchpress.com by 210.87.254.5 on 09/05/12
For personal use only.

Partie expérimentale

Les points de fusion ont été déterminés en tube capillaire à l'aide d'un thermomètre calibré (appareil Thomas–Hoover). Les spectres i.r. ont été réalisés sur un appareil Beckman, modèle IR-4. Les spectres de r.m.n. ont été enregistrés sur un appareil Varian A 60; les déplacements chimiques sont mesurés en δ par rapport au tétraméthyl silane (δ = 0) et ne sont pas corrigés.

(I) Méthodes générales de préparation des dihydroxy-5,6 (cis) cyclohexène-2 diones-1,4 à partir des p-benzoquinones correspondantes

Méthode A (Méthode principale)

A une solution de chlorate de sodium (10.0 g) dans l'eau (50 ml) contenant de l'acide osmique (1.3 ml d'une solution aqueuse à 1%), on ajoute de l'acide chlorhydrique concentré (1 ml) puis la quinone (0.1 mol) et on maintient le milieu réactionnel sous forte agitation à 25°. La fin de la réaction est généralement indiquée par la disparition de la couleur jaune caractéristique des quinones.[2] On sature alors la solution avec du chlorure de sodium et on extrait avec de l'éther de pétrole pour éliminer les dernières traces de quinone. On extrait ensuite les eaux-mères avec plusieurs portions successives d'éther (environ 2 l au total).

Méthode B (Méthode de Milas)

A une solution de chlorate de sodium (20.0 g) dans l'eau (50 ml) contenant de l'acide osmique (1.3 ml d'une solution aqueuse à 1%), on ajoute de l'acide chlorhydrique concentré (1 ml) puis lentement de l'hydroquinone (0.1 mol) en maintenant le milieu réactionnel sous forte agitation à 0°. L'addition trop rapide de l'hydroquinone empêche, par la formation de quinhydrone, une agitation suffisante, ce qui entraîne une élévation de température et la formation de produits de décomposition. Après la disparition de la quinhydrone (1 à 2 h), on laisse le milieu réactionnel se réchauffer à 25° et on procède comme par la méthode A.

Modifications des méthodes A et B

Voir tableau 1.

(II) Hydroxylation de la p-benzoquinone

On obtient par la méthode A, à partir de 10.8 g de *p*-benzoquinone dans 50 ml d'eau, après 48 h de réaction, 3.6 g du dimère.

Dihydroxy-5,6(cis) cyclohexène-2 dione-1,4

Le précipité obtenu du mélange réactionnel est lavé avec de l'eau froide (10 ml) et le filtrat est ajouté aux eaux-mères. On sature la solution avec du chlorure de sodium et on extrait avec de l'éther de pétrole jusqu'à disparition de la couleur jaune. On extrait alors avec de l'éther et on évapore sous vide à une température inférieure à 30°. On isole ainsi 3.2 g d'une huile jaune pâle très instable. Cette substance ne cristallise pas et ne résiste pas à la chromatographie sur gel de silice. Spectre de r.m.n. ($(CD_3)_2CO$): trois singulets d'égale intensité à δ 4.60, 5.93 et 6.85 (CH 5,6, OH 5,6, et CH 2,3 respectivement).

Diacétoxy-5,6(cis) cyclohexène-2 dione-1,4

L'acétylation immédiate de l'huile isolé dans l'extraction précédente par l'anhydride acétique en présence d'une trace d'acide sulfurique donne une huile incolore après hydrolyse, extraction à l'éther, séchage et évaporation. Le produit obtenu est aussi instable que le diol correspondant. Spectre de r.m.n. (CCl_4): un singulet à δ 2.07 correspondant à six protons ($OCOCH_3$ en 5,6), un singulet à 5.75 (CH 5,6), et un troisième singulet à 6.85 (CH 2,3).

(III) Hydroxylation de la toluquinone

On obtient par la méthode B, à partir de 25.0 g (0.2 mol) de toluhydroquinone dans 80 ml d'eau et 20 ml de dioxanne après 70 h de réaction, 15.2 g (50%) d'une huile incolore. L'huile est immédiatement chromatographiée sur gel de silice. Toutefois la séparation complète des isomères est beaucoup plus facile si l'on procède d'abord à une acétylation du mélange.

Dihydroxy-5,6(cis) méthyl-5 cyclohexène-2 dione-1,4 (1b)

L'élution au chloroforme donne dans les premières fractions une huile incolore (3.5 g) qui cristallise en aiguilles de l'éther de pétrole (p.é. 30–60°), p.f. 103–103.5°. Après deux recristallisations du benzène, la dihydroxy-5,6-(*cis*) méthyl-5 cyclohexène-2 dione-1,4 fond à 106.5–107.0°. Spectre i.r. ($CHCl_3$): bandes à 2.80 et 2.85 (OH), 3.30 (C═CH), et 5.85 μ (C═O). Spectre de r.m.n ($CDCl_3$): un singulet à δ 1.51 (CH_3 6), un singulet à 4.10 (OH 6), un doublet centré à 4.13 (OH 5), un doublet centré à 4.35 (CH 5) et un singulet (deux protons) à 6.90 (CH 2,3).

Anal. calc. pour $C_7H_8O_4$: C, 53.84; H, 5.16. Trouvé: C, 53.62; H, 5.16.

Diacétoxy-5,6 méthyl-5 cyclohexène-2 dione-1,4

L'acétylation du diol par l'anhydride acétique en présence d'une trace d'acide sulfurique ou d'acide perchlorique donne avec un rendement quantitatif la diacétoxy-5,6(*cis*) méthyl-5 cyclohexène-2 dione-1,4 qui, après deux cristallisations d'un mélange d'acétate d'éthyle et d'éther de pétrole (p.é. 66–70°), fond à 117–117.5°. Spectre i.r. ($CHCl_3$): bandes à 5.69 ($OCOCH_3$), 5.80 μ (C═O). Spectre de r.m.n. ($CDCl_3$): un singulet à δ 1.58 (trois protons; CH_3 6), un singulet à 2.02 (trois protons; $OCOCH_3$ 6), un singulet à 2.28 (trois protons; $OCOCH_3$ 5), un singulet à 5.47 (CH 5), et deux doublets centrés à 6.76 et 6.90, J = 10.2 Hz.

Dihydroxy-5,6(cis) méthyl-2 cyclohexène-2 dione-1,4 (1a) et diacétoxy-5,6(cis) méthyl-2 cyclohexène dione-1,4

Les fractions subséquentes de cette chromatographie donne une huile incolore contenant un mélange des deux diols isomères. Tous les essais de cristallisation sont demeurés infructueux même pour les dernières fractions contenant presqu'exclusivement de la dihydroxy-5,6(cis) méthyl-2 cyclohexène-2 dione-1,4 identifié par son spectre de r.m.n. ($CDCl_3$): un doublet centré à δ 2.05, J = 1.8 Hz (CH_3 2), plusieurs pics dans la région de 4.3 à 4.8 correspondant à quatre protons (CH 5,6; OH 5,6), et un multiplet à 6.71 (CH 3).

Une séparation plus efficace des deux isomères a été essayé par l'emploi d'éluants moins polaires ou par des

[2]Souvent la préparation n'est pas tout à fait reproductible et donne naissance à des produits secondaires fortement colorés qui empêchent de déceler la fin de la réaction. L'extraction avec le benzène devient alors nécessaire pour éliminer l'excès de la quinone. La perte en produit dihydroxylé causée par cette extraction est assez faible.

Can. J. Chem. Downloaded from www.nrcresearchpress.com by 210.87.254.5 on 09/05/12
For personal use only.

quantités d'absorbant plus grandes. Ces modifications n'améliorent pas le résultat car la décomposition des produits augmente avec le temps de contact sur gel de silice.

L'acétylation des dernières fractions par la méthode habituelle donne le diacétoxy-5,6(*cis*) methyl-2 cyclohexène-2 dione-1,4 qui cristallise de l'acétate d'éthyle, p.f. 105–105.5°. L'échantillon analytique, obtenu après deux recristallisations d'un mélange de benzène et de *n*-hexane fond à 105–105.5°. Spectre de r.m.n. ($CDCl_3$): un doublet centré à δ 2.10 (CH_3 2), un singulet à 2.14 (six protons; $OCOCH_3$ 5,6), un singulet à 5.83 (deux protons; CH 5,6), et un multiplet à 6.78 (CH 3).

Anal. calc. pour $C_{11}H_{12}O_6$: C, 55.00; H, 5.04. Trouvé: C, 55.37; H, 5.11.

Dans cette réaction d'oxydation on obtient donc 15.2 g de produits dihydroxylés contenant approximativement 35% de dihydroxy-5,6(*cis*) méthyl-5 cyclohexène-2 dione-1,4 et 65% de l'autre diol (**1***a*) (détermination faite par spectroscopie de r.m.n.). Du mélange 3.5 g (12%) du diol (**1***b*) et 7.2 g (15%) du diacétoxy-5,6(*cis*) méthyl-2 cyclohexène-2 dione-1,4 ont pu être isolé sous forme cristalline.

(IV) Hydroxylation de l'o-xyloquinone

On obtient par la méthode A, à partir de 13.6 g (0.1 mol) d'*o*-xyloquinone dans 70 ml d'eau et 20 ml de dioxanne après 50 h de réaction 15.3 g (93%) d'une huile incolore. L'huile cristallise en présence d'éther et fournit 7.8 g de cristaux incolores, p.f. 117–118°.

Le résidu (7.5 g) est chromatographié sur gel de silice.

*Dihydroxy-5,6(cis) diméthyl-5,6 cyclohexène-2 dione-1,4 (**2***b*)*

L'élution au benzène donne dans les premières fractions 3.0 g d'une huile qui cristallise en aiguilles de l'éther de pétrole (p.é. 30–60°), p.f. 82–84°. Ce produit a été identifié comme étant la dihydroxy-5,6(*cis*) diméthyl-5,6 cyclohexène-2 dione-1,4. Après trois recristallisations de l'éther de pétrole (p.é. 30–60°) il fond à 84–85°. Spectre i.r. ($CHCl_3$): 2.84 (OH), 3.29 (C═CH), 5.81 (C═O), 6.22 (C═C). Spectre de r.m.n. ($CDCl_3$): trois singulets à δ 1.35 (CH_3 5,6), à 3.52 (OH 5,6), et à 6.87 (CH 2,3).

Anal. calc. pour $C_8H_{10}O_4$: C, 56.46; H, 5.92. Trouvé: C, 56.92; H, 5.89.

Diacétoxy-5,6(cis) diméthyl-5,6 cyclohexène-2 dione-1,4

L'acétylation de ce diol (**2***b*) par l'anhydride acétique catalysée par une trace d'acide sulfurique donne avec un rendement quantitatif la diacétoxy-5,6(*cis*) diméthyl-5,6 cyclohexène-2 dione-1,4. Après trois recristallisations de l'acétate d'éthyle ce diacétate fond à 106–106.5°. Spectre i.r. ($CHCl_3$): 3.30 (C═CH), 5.69 ($OCOCH_3$), 5.80 C═O), et 8.18 μ (C—O). Spectre de r.m.n. ($CDCl_3$): trois singulets à δ 1.61 (six protons; CH_3 5,6), à 2.08 (six protons; $OCOCH_3$ 5,6), et à 6.73 (deux protons; CH 2,3).

*Dihydroxy-5,6(cis) diméthyl-2,3 cyclohexène-2 dione-1,4 (**2***a*)*

Lors de cette même chromatographie, le benzène élue dans les fractions subséquentes 4.1 g de dihydroxy-5,6(*cis*) diméthyl-2,3 cyclohexène-2 dione-1,4 qui cristallise facilement en présence d'éther. Ce produit est identique à celui (7.8 g) isolé directement de l'huile extraite du mélange réactionnel. On obtient ainsi un rendement total de ce diol de 11.9 g (70%). L'échantillon analytique, obtenu après deux recristallisations du benzène, fond à 119–119.5°. Spectre i.r. ($CHCl_3$): 2.86 (bande large, OH), 5.89 (C═O), 6.17 μ (C═C). Spectre de r.m.n. ($CDCl_3$): trois singulets à δ 2.07 (CH_3 2,3), à 3.50 (OH 5,6), et à 4.60 (CH 5,6).

Anal. calc. pour $C_8H_{10}O_4$: C, 56.46; H, 5.92. Trouvé: C, 56.17; H, 5.97.

Diacétoxy-5,6(cis) diméthyl-2,3 cyclohexène-2 dione-1,4

A une solution du diol **2***a* dans l'anhydride acétique (10 ml), on ajoute une trace d'acide sulfurique. On obtient de cette façon après hydrolyse, filtration, lavage avec de l'eau et séchage, la diacétoxy-5,6(*cis*) diméthyl-2,3 cyclohexène-2 dione-1,4 presque pure, p.f. 124–125°. Pour analyse élémentaire, un échantillon a été recristallisé trois fois d'un mélange d'éther et de *n*-hexane, p.f. 126.5–127.5°. Spectre i.r. (KBr): 5.65 ($OCOCH_3$), 5.82 et 5.93 (C═O), 6.18 (C═C), 8.13 et 8.26 μ (C—O). Spectre de r.m.n. ($CDCl_3$): trois singulets à δ 2.07 et 2.13 (CH_3 2,3; $OCOCH_3$ 5,6) et à 5.82 (CH 5,6).

Anal. calc. pour $C_{12}H_{14}O_6$: C, 56.68; H, 5.55. Trouvé: C, 56.72; H, 5.69.

Acétonide de la dihydroxy-5,6(cis) diméthyl-2,3 cyclohexène-2 dione-1,4

A une solution d'acétone anhydre (20 ml) contenant de l'acide *p*-toluènesulfonique (5 mg) et du sulfate de cuivre (500 mg) on ajoute la dihydroxy-5,6(*cis*) diméthyl-2,3 cyclohexène-2 dione-1,4 (**2***a*) (1 g) et on laisse reposer pendant 5 jours à l'obscurité. On traite ensuite le mélange réactionnel avec un excès de bicarbonate de sodium (solution aqueuse saturée) pour éliminer l'excès d'acide, le diol qui n'a pas réagi et les produits d'énolisation. Par extraction à l'éther, on obtient, après séchage sur sulfate de sodium anhydre et évaporation sous vide, une huile que l'on chromatographie sur gel de silice avec du benzène comme éluant.

On obtient ainsi 0.9 g de l'acétonide qui cristallise de l'éther de pétrole (p.é. 66–70°) en aiguilles jaune pâle, p.f. 98–99°. L'échantillon analytique est recristallisé deux fois de l'éther de pétrole (p.é. 66–70°) p.f. 98.5–99.0°. Spectre i.r. (KBr): 3.34 et 3.36 (—$C(CH_3)_2$), 5.90 (C═O), 6.18 μ (C═C). Spectre de r.m.n. ($CDCl_3$): des singulets à δ 1.41 et 1.46 (*gem*-diméthyles), à 2.07 (CH_3 2,3) et à 4.71 (CH 5,6).

Anal. calc. pour $C_{11}H_{14}O_4$: C, 62.84; H, 6.71. Trouvé: C, 62.65; H, 6.78.

Acétoxy-5 hydroxy-6(cis) diméthyl-2,3 cyclohexène-2 dione-1,4

On dissout 0.85 g (0.02 mol) de dihydroxy-5,6(*cis*) diméthyl-2,3 cyclohexène-2 dione-1,4 dans une quantité minimale d'acide acétique (2 ml) et on ajoute l'anhydride acétique (1.2 ml) et une trace d'acide sulfurique. On laisse réagir pendant 3 min, on hydrolyse et on extrait à l'éther. Le résidu après évaporation est chromatographié sur gel de silice. Le benzène élue une huile blanche que nous n'avons pas réussi à cristalliser. Le spectre de r.m.n. de cette substance correspond à celui de l'acétoxy-5 hydroxy-6 diméthyl-2,3 cyclohexène-2 dione-1,4. L'énolisation de ce produit par de l'acide chlorhydrique dans le méthanol donne le tétrahydroxy *o*-xylène.

(V) Hydroxylation de l'α-naphtoquinone et des diméthyl-2,6, ditertiobutyl-2,6 et phényl p-benzoquinones

*Dihydroxy-2,3(cis) dioxo-1,4 tétrahydro-1,2,3,4 naphtalène (**3**)*

On obtient par la méthode A, à partir de 15.8 g de naphtoquinone-1,4 dans 80 ml d'eau et 20 ml de dioxanne après 12 jours de réaction, 12.2 g d'un précipité blanc que

Can. J. Chem. Downloaded from www.nrcresearchpress.com by 210.87.254.5 on 09/05/12
For personal use only.

l'on filtre et lave avec de l'eau froide (20 ml). L'extraction du filtrat avec de l'éther (2 l) donne 4.2 g d'une huile incolore qui cristallise facilement (les deux produits sont identiques). On isole ainsi 16.4 g (85%) de dihydroxy-2,3(*cis*) dioxo-1,4 tétrahydroxy-1,2,3,4 naphtalène qui fond à 170–172° après deux cristallisations du chloroforme. Spectre i.r. (KBr): 2.96 (OH), 5.86 à 5.90 (C═O), 6.30 μ (C═C). Spectre de r.m.n. ($(CD_3)_2CO$): deux singulets à δ 5.0 et 2.9 respectivement (OH 2,3), un singulet à 4.83 (deux protons; CH 2,3), et un multiplet centré à 8.0 (quatre protons; CH aromatiques).

Anal. calc. pour $C_{10}H_8O_4$: C, 62.50; H, 4.20. Trouvé: C, 62.88; H, 4.22.

Diacétoxy-2,3 dioxo-1,4 tétrahydro-1,2,3,4 naphtalène

L'acétylation de ce diol de la façon habituelle donne quantitativement la diacétoxy-2,3 dioxo-1,4 tétrahydro-1,2,3,4 naphtalène, p.f. 116.0–116.5°. Après trois cristallisations de l'acétate d'éthyle, ce diacétate fond à 117.0–117.5°. Spectre i.r. ($CHCl_3$): 5.67 ($OCOCH_3$), 5.79 et 5.84 (C═O), 6.25 (C═C) et 8.30 μ (bande large, C—O). Spectre de r.m.n. ($CDCl_3$): un singulet à δ 2.14 (six protons; $OCOCH_3$ 2,3), un singulet à 6.01 (deux protons; CH 2,3), et un multiplet centré à 8.0 (quatre protons; CH aromatiques).

Dihydroxy-5,6(cis) diméthyl-2,6 cyclohexène-2 dione-1,4

On obtient par la méthode A, à partir de 6.8 g (0.05 mol) de diméthyl-2,6 *p*-benzoquinone dans 10 ml d'eau et 50 ml de dioxanne, après 72 h, 7.4 g (87%) de dihydroxy-5,6(*cis*) diméthyl-2,6 cyclohexène-2 dione-1,4, p.f. 140.5–141° (chloroforme). Spectra i.r. (KBr): 2.91 (OH), 5.90 à 5.97 (C═O), 6.15 μ (C═C). Spectre de r.m.n. ($(CD_3)_2CO$): un singulet à 1.44 (CH_3 6), un doublet à 2.01, J = 1.5 Hz (CH_3 2), un singulet à 4.37 (deux protons; OH 5,6), un singulet à 4.67 (CH 5) et un quadruplet à 6.78, J = 1.5 Hz (CH 3).

Diacétoxy-5,6(cis) diméthyl-2,6 cyclohexène-2 dione-1,4

Cette substance s'obtient à partir du composé précédent de la façon habituelle, p.f. 129.5–130° ($CHCl_3$). Spectre i.r. (KBr): 5.68 et 5.73 ($OCOCH_3$), 5.80 et 5.88 (C═O), et 6.18 μ (C═C). Spectre de r.m.n. ($(CD_3)_2CO$): un singulet à 1.54 (CH_3 6), un doublet à 2.03, J = 1.5 Hz (CH_3 2), deux singulets à 1.96 et 2.20 ($OCOCH_3$ 5,6), un singulet à 5.53 (CH 5), et un quadruplet à 6.61, J = 1.5 Hz (CH 3).

Dihydroxy-5,6(cis) ditertiobutyl-2,6 cyclohexène-2 dione-1,4

On obtient par la méthode A, à partir de 4.4 g (0.02 mol) de ditertiobutyl-2,6 *p*-benzoquinone dans 10 ml d'eau et 25 ml de dioxanne, après 72 h, le dihydroxy-5,6(*cis*) ditertiobutyl-2,6 cyclohexène-2 dione-1,4 avec un rendement presque quantitatif, p.f. 124.5–125° (eau–méthanol). Spectre i.r. (KBr): 2.89 (OH), 5.90 à 5.94 (C═O) et 6.24 μ (C═C). Spectre de r.m.n. ($CDCl_3$): deux singulets à 0.96 et 1.33 ($C(CH_3)_3$ 2,6), un doublet à 4.46, J = 2.0 Hz (CH 5), et un doublet à 6.75, J = 2.0 Hz (CH 3).

Diacétoxy-5,6(cis) ditertiobutyl-2,6 cyclohexène-2 dione-1,4

Par la méthode habituelle, p.f. 164.5–165° ($CHCl_3$). Spectre i.r. (KBr): 5.68 et 5.72 ($OCOCH_3$), 5.84 et 5.89 (C═O) et 6.21 μ (C═C). Spectre de r.m.n. ($CDCl_3$): deux singulets à 1.03 et 1.29 ($C(CH_3)_3$ 2,6), deux singulets à 2.08 et 2.17 ($OCOCH_3$ 5,6), un singulet à 5.79 (CH 5), et un singulet à 6.70 (CH 3).

Dihydroxy-5,6(cis) phényl-2 cyclohexène-2 dione-1,4

On obtient par la méthode A à partir de 9.20 g (0.05 mol) de phényl-*o*-benzoquinone dans 10 ml et 50 ml de dioxanne après 65 h, 7.7 g (72%) de dihydroxy-5,6 phényl-2 cyclohexène-2 dione-1,4, p.f. 123.5–124° ($CHCl_3$). Spectre i.r. (KBr): 2.89–3.04 (OH), 5.83 et 6.01 (C═O), et 6.07 μ (C═C). Spectre de r.m.n. ($(CD_3)_2CO + D_2O$): un doublet de doublets à 4.85, J = 3.0, 1.0 Hz (CH 5), un doublet à 5.04, J = 3.0 Hz (CH 6), un doublet à 7.07, J = 1.0 Hz (CH 3), et un multiplet à 7.45 (C_6H_5).

Diacétoxy-5,6(cis) phényl-2 cyclohexène-2 dione-1,4

Préparé de la façon habituelle (n'a pas cristallisé). Spectre de r.m.n. (CCl_4): deux singulets à 2.08 et 2.11 ($OCOCH_3$), un singulet à 5.80 (deux protons; CH 5,6), un singulet à 7.09 (CH 3) et un multiplet à 7.48 C_6H_5).

(VI) Tétrahydroxy o-xylène

Méthode A: à partir de la dihydroxy-5,6(cis) diméthyl-2,3 cyclohexène-2 dione-1,4

A une solution d'éther anhydre (100 ml) saturée d'acide bromhydrique, on ajoute le diol ***2a*** (1 g) et on laisse réagir pendant 1 h à 25°. On évapore ensuite le solvant à sec et on obtient de cette façon des cristaux blancs du tétrahydroxy *o*-xylène que l'on filtre et lave avec du chloroforme froid (25 ml). Les rendements sont quantitatifs. Le tétrahydroxy *o*-xylène fond à 177–179° après deux cristallisations du chloroforme. Spectre i.r. (KBr): 2.85 à 3.12 (bande très large, OH), 6.12, 6.61 et 6.66 (C═C), et 7.46 à 8.33 μ (bande très large, C—O). Spectre de r.m.n. ($(CD_3)_2CO$): un singulet à δ 2.08 (CH_3 5,6) et une bande très large de 3.5 à 6.7 correspondant à quatre protons et disparaissant par deutériation (OH 1,2,3,4).

Méthode B: énolisation et hydrolyse de la diacétoxy-5,6-(cis) diméthyl-2,3 cyclohexène-2 dione-1,4

On laisse reposer le diacétate (1 g) dans du méthanol (20 ml) contenant de l'acide chlorhydrique concentré (1 goutte) pendant 30 h à la température ambiante. On évapore alors l'alcool et on dissout l'huile résiduelle dans du chloroforme (10 ml) et on laisse cristalliser. On filtre les cristaux et on lave avec un peu de chloroforme froid (5 ml). On isole de cette façon 0.55 g du tétrahydroxy *o*-xylène (80%), p.f. 177–179°. Le point de fusion d'un mélange avec le produit obtenu par la méthode précédente est identique. Les spectres i.r. et de r.m.n. sont aussi identiques.

Tétraacétoxy o-xylène

Par acétylation de 0.9 g du tétrahydroxy *o*-xylène dans l'anhydride acétique contenant une trace d'acide sulfurique, on obtient après hydrolyse, extraction au chloroforme, séchage et évaporation 1.6 g du tétraacétoxy *o*-xylène, p.f. 173–174°.

L'échantillon analytique obtenu après deux recristallisations de l'acétate d'éthyle fond à 174.0–174.5°. Spectre i.r. (KBr): 5.62 ($OCOCH_3$) et 8.33 μ (bande large, C—O). Spectre de r.m.n. ($(CD_3)_2CO$): un singulet à δ 2.08 (CH_3 5,6) et deux singulets à 2.22 et 2.29 ($OCOCH_3$ 1,2,3,4). Les trois singulets sont d'égale intensité.

Anal. calc. pour $C_{16}H_{18}O_8$: C, 56.80; H, 5.36. Trouvé: C, 56.96; H, 5.39.

Dihydroxy-5,6 diméthyl-2,3 benzoquinone

Méthode A: à partir du tétrahydroxy o-xylène

On dissout 1 g de tétrahydroxy *o*-xylène dans 50 ml

Can. J. Chem. Downloaded from www.nrcresearchpress.com by 210.87.254.5 on 09/05/12
For personal use only.

d'une solution faiblement basique (p*H* 8–9) et on y fait barboter de l'air pendant 1 h. On acidifie alors à p*H* 3 la solution refroidie dans la glace et on filtre le précipité rouge vin (0.7 g) de dihydroxy *o*-xyloquinone. L'extraction à l'éther des eaux-mères donne en plus 0.25 g de dihydroxy quinone (rendement total 95%). Si l'oxydation se fait à un p*H* supérieur à 9 elle est plus rapide mais les rendements sont beaucoup plus faibles.

La dihydroxy-5,6 diméthyl-2,3 benzoquinone cristallise de l'éthanol (95%) en feuilles rouge vin, p.f. 214–215° (rapide) (litt. 182, déc.). Spectre i.r. (KBr): 2.98 (OH), 6.11 (C═O), 7.75 et 8.26 μ (C—O). Spectre de r.m.n. ($(CD_3)_2CO$): deux singulets à δ 1.97 et 2.80 correspondant respectivement à six et deux protons. (CH_3 2,3; OH 5,6).

Anal calc. pour $C_8H_8O_4$: C, 57.14; H, 4.80. Trouvé: C, 57.21; H, 5.01.

Méthode B: à partir de la dihydroxy-5,6 diméthyl-2,3 cyclohexène-2 dione-1,4

On dissout 1 g du diol dans une solution de bicarbonate de sodium (p*H* 9) et on procède de la manière décrite dans la méthode A en laissant toutefois barboter le courant d'air pendant 3 h pour permettre une énolisation complète. On recueille ainsi 0.6 g (60%) de la quinone dihydroxylée identique à celle obtenue par la méthode A p.f. 213° (rapide), p.f. de mélange 213–215° (rapide). Cette méthode permet de passer directement de la dihydroxy-5,6 cyclohexène-2 dione-1,4 à la quinone dihydroxylée. Toutefois les rendements (60%) sont inférieurs à ceux de la méthode A précédente.

Diméthyl-2,3 diméthoxy-5,6 benzoquinone (aurantiogliocladine)

A une solution de dihydroxy *o*-xyloquinone (1.68 g) dans l'éther anhydre (10 ml) on ajoute 0.5 g de diazométhane. On laisse réagir jusqu'à la disparition de l'effervescence et on évapore l'éther. On chromatographie l'huile jaune orange sur gel de silice avec du benzène comme éluant. On obtient 1.85 g d'aurantiogliocladine (94%) qui cristallise en aiguilles (assez difficilement) de l'éther de pétrole (p.é. 30–60°), p.f. 61.0–61.5° (litt. 64° (30)). L'échantillon analytique a été obtenu après deux recristallisations dans le *n*-hexane suivies d'une sublimation à 40°, p.f. 62.0–62.5°. Spectre i.r. (KBr): 6.02 (C═O), 6.20 μ (C═C). Spectre de r.m.n. ($CDCl_3$): deux singulets d'égale intensité à δ 2.00 et 4.00 respectivement (CH_3 2,3; OCH_3 5,6).

Anal. calc. pour $C_{10}H_{12}O_4$: C, 61.21; H, 6.17. Trouvé: C, 61.20; H, 6.36.

(VII) Autres dérivés

Epoxy-5,6 cyclohexène-2 oximido-4 one-1

A une solution de chlorhydrate d'hydroxylamine (0.25 g) dans du méthanol (15 ml, solution aqueuse à 80%) on ajoute de l'acétate de sodium (0.23 g). Par addition d'acide chlorhydrique dilué, on ajuste le p*H* de la solution à 5. On ajoute alors 0.5 g d'époxy-5,6 cyclohexène-2 dione-1,4 et on laisse réagir pendant 2 h. On note l'apparition rapide d'une forte coloration rouge. La réaction terminée, on ajoute 10 ml d'eau et on évapore l'alcool sous vide à 40 °C. On isole ainsi 0.1 g de l'oxime qui cristallise très lentement dans les eaux-mères, p.f. 136° (déc.). Cet oxime, assez stable à l'état solide, se décompose rapidement en solution. Spectre de r.m.n. ($CDCl_3$): quatre quadruplets respectivement à δ 3.66, J = 3.7, 2.0 Hz (CH 6), 4.78, J = 3.7, 2.2 Hz (CH 5), 6.10, J = 10.0, 2.0 Hz (CH 2) et 6.97, J = 10.0, 2.2 Hz (CH 3), et un singulet à 11.89 (NOH).

Diacétoxy-5,6(trans) méthyl-5 cyclohexène-2 dione-1,4

A 0.5 g d'époxy-5,6 méthyl-5 cyclohexène-2 dione-1,4 dissous dans 5 ml d'acide acétique on ajoute 5 ml d'anhydride acétique et 1 ml d'acide sulfurique concentré et on chauffe sur un bain-marie pendant 5 min. On refroidit et on ajoute 15 g de glace. La diacétoxy-5,6(*trans*) méthyl-5 cyclohexène-2 dione-1,4 précipite du mélange réactionnel et on isole après filtration, lavage, et séchage 0.45 g de cristaux blancs, p.f. 197–198°. Après deux recristallisations de l'acétate d'éthyle ce diacétate fond à 198–199°. Spectre i.r. ($CHCl_3$): 3.28 (C═CH), 3.39 ($OCOCH_3$), 5.67 (C═O), 5.82 (C═C) et 8.00 avec épaulement à 8.26 μ (C—O). Spectre de r.m.n. ($CDCl_3$): cinq singulets à δ 1.43 (trois protons; CH_3 5), à 2.07 (trois protons; $OCOCH_3$ 5), à 2.25 (trois protons; $OCOCH_3$ 6), à 6.50 (un proton; CH 6), et à 7.02 (deux protons; CH 2,3).

Diacétoxy-5,6(trans) diméthyl-5,6 cyclohexène-2 dione-1,4

L'ouverture de 0.5 g de l'époxy-5,6 diméthyl-5,6 cyclohexène-2 dione-1,4 par la même méthode donne 0.55 g de la diacétoxy-5,6(*trans*) diméthyl-5,6 cyclohexène-2 dione-1,4, p.f. 185–187°. Ce produit cristallise de l'acétate d'éthyle en aiguilles blanches, p.f. 187.0–187.5°. Spectre i.r. (Nujol): 5.71 ($OCOCH_3$), 5.82 (C═O) et 8.28 μ (C—O). Spectre de r.m.n. ($(CD_3)_2CO$): trois singulets à δ 1.60 (six protons; CH_3 5,6), à 1.93 (six protons; $OCOCH_3$ 5,6) et 6.67 (deux protons; CH 2,3).

Diacétoxy-2,3(trans) dioxo-1,4 tétrahydro-1,2,3,4 naphtalène

Le dioxo-1,4 époxy-2,3 tétrahydro-1,2,3,4 naphtalène (1.0 g) donne par la même méthode 0.9 g de diacétoxy-2,3(*trans*) dioxo-1,4 tétrahydro-1,2,3,4 naphtalène, p.f. 211–212°. Un échantillon analytique, obtenu après deux recristallisations de l'acétate d'éthyle, fond à 215.0–215.5° (litt. 193–194° (21)). Spectre i.r. (KBr): 3.47 (acétates; vibration CH), 5.70 ($OCOCH_3$), 5.88 (C═O), 6.28 (aromatique), et 8.10 μ (bande large, C—O). Spectre de r.m.n. ($(CD_3)_2CO$): un singulet à 2.18 ($OCOCH_3$ 2,3), un singulet à 6.16 (CH 2,3) et un multiplet à 8.05 (quatre protons; CH aromatiques).

Anal. calc. pour $C_{14}H_{12}O_6$: C, 60.87; H, 4.38. Trouvé: C, 61.34; H, 4.33.

Bromo-2 dioxo-1,4 hydroxy-3 tétrahydro-1,2,3,4 naphtalène

A 10 ml d'une solution aqueuse d'acide bromhydrique à 48%, on ajoute 0.5 g de dioxo-1,4 époxy-2,3 tétrahydro-1,2,3,4 naphtalène et on agite pendant 10 min. On note alors l'apparition d'un précipité que l'on filtre aussitôt. On lave les cristaux avec 10 ml d'une solution diluée de sulfite de sodium (5%) puis avec 10 ml d'eau. On isole 0.45 g de bromo-2 dioxo-1,4 hydroxy-3 tétrahydro-1,2,3,4 naphtalène qui après deux recristallisations du chloroforme, fond à 190.00–190.5° (déc.). Cette bromohydrine est très instable, surtout en solution. Spectre i.r. (KBr): 2.86 (OH), 3.30 (CH), 3.44, 5.85 (C═O), 6.27 (C═C), et 7.91 μ (C—O). Spectre de r.m.n. ($(CD_3)_2CO$): un doublet à δ 4.81, J = 7.5 Hz, un doublet

à 5.16, J = 7.5 Hz, un multiplet à 8.00 (quatre protons: CH aromatiques).

Addition du brome ou du chlore aux oximes de quinones

L'addition du brome ou du chlore aux oximes (ou aux acétates correspondants) de quinones par les méthodes déjà décrites (17) donnent avec des rendements excellents les composés suivants dont les spectres r.m.n. sont décrits dans le tableau 2.

Dichloro-5,6 cyclohexène-2 acétoximido-4 one-1. Le p.f. 134° (déc.).

Dichloro-5,6 méthyl-2 cyclohexène-2 acétoximido-4 one-1. Le p.f. 154° (déc.).

Dibromo-5,6 cyclohexène-2 acétoximido-4 one-1. Le p.f. 135° (déc.).

Dibromo-5,6 méthyl-2 cyclohexène-2 acétoximido-4 one-1. Le p.f. 154° (déc.).

Dibromo-5,6 diméthyl-2,3 cyclohexène-2 oximido-4 one-1. Le p.f. 160° (déc.).

1. P. W. Brian, P. J. Curtis, S. R. Howland, E. G. Jeffreys, et H. Raudnitz. Exper. **7**, 266 (1951).
2. J. C. Sheenan, W. B. Lawson, et R. J. Gaul. J. Am. Chem. Soc. **80**, 5536 (1958).
3. Y. Yamamoto, K. Nitta, et A. Jimbo. Chem. Pharm. Bull. Jap. **15**, 427 (1967).
4. G. A. Ellestad, M. P. Kunstmann, H. A. Whaley, et E. L. Patterson. J. Am. Chem. Soc. **90**, 1325 (1968).
5. A. Closse, R. Mauli, et H. P. Sigg. Helv. Chim. Acta, **49**, 204 (1966).
6. S. Marumo, K. Sasaki, K. Ohkuma, K. Anzai, et S. Suzuki. Agr. Biol. Chem. **32**, 209 (1968).
7. G. Read, A. Rashid, et L. C. Vining. J. Chem. Soc. C, 2059 (1969).
8. K. Alder, F. H. Flock, et H. Beumling. Chem. Ber. **93**, 1896 (1960).
9. E. W. Garbisch, Jr. J. Am. Chem. Soc. **87**, 4971 (1965).
10. H. W. Moore. J. Org. Chem. **32**, 1996 (1967).
11. A. Rashid et G. Read. J. Chem. Soc. C, 1323 (1967).
12. A. J. Birch et K. A. M. Walker. Tetrahedron Lett. 3457 (1967).
13. D. D. Chapman, W. J. Musliner, et J. W. Gates, Jr. J. Chem. Soc. C, **124** (1969).
14. T. H. Clark. Am. Chem. J. **14**, 553 (1892).
15. O. Dimroth, H. Eber, et K. Wehr. Ann. Chem. **446**, 132 (1926).
16. A. P. ter Borg. Rec. Trav. Chim. **73**, 5 (1954).
17. J. Y. Savoie et P. Brassard. Can. J. Chem. **44**, 2867 (1966).
18. E. M. Terry et N. A. Milas. J. Am. Chem. Soc. **48**, 2647 (1926).
19. H. A. Anderson et R. H. Thomson. J. Chem. Soc. C, 2152 (1967).
20. J. Y. Savoie et P. Brassard. Can. J. Chem. **47**, 733 (1969).
21. R. K. Norris et S. Sternhell. Austr. J. Chem. **19**, 617 (1966).
22. G. Read. J. Chem. Soc. 6587 (1965).
23. C. Djerassi, W. Klyne, T. Norin. G. Ohloff, et E. Klein. Tetrahedron, **21**, 163 (1965).
24. A. Rashid et G. Read. J. Chem. Soc. C, 2053 (1969).
25. R. J. Abraham et H. J. Bernstein. Can. J. Chem. **39**, 216 (1961).
26. W. Baker, J. F. W. McOmie, et D. Miles. J. Chem. Soc. 820 (1953).
27. T. R. Seshadri et G. B. Venkatasubramanian. J. Chem. Soc. 1660 (1959).
28. G. Pettersson. Acta Chem. Scand. **18**, 2309 (1964).
29. W. Mayer et R. Weiss. Angew. Chem. **68**, 680 (1956).
30. E. B. Vischer. J. Chem. Soc. 815 (1953).

Can. J. Chem. Downloaded from www.nrcresearchpress.com by 210.87.254.5 on 09/05/12
For personal use only.

An Electron Spin Resonance Study of the 9,10-Dihydrophenanthrene Radical Anion

F. C. ADAM

Departments of Chemistry, University of Calgary, Calgary, Alberta and University of Sydney, Sydney, New South Wales, Australia

Received December 12, 1967[1]

The e.s.r. spectrum of 9,10-dihydrophenanthrene radical ion has been obtained in ether solvents at a number of temperatures between −106 and +51 °C. In dimethoxyethane–tetrahydrofuran mixtures below −80 °C, six triplet splittings are found with mean coupling constants of 5.36, 3.36, 2.66, 0.70, 0.26 and 0.15 oe. Above this temperature broadening occurs with some lines of the hyperfine spectrum due to motion resulting from the interconversion between the two equivalent conformers of the non-planar molecule ion. While the ring proton coupling constants are not strongly dependent on temperature, those due to the four methylene protons are, and interconversion between the conformers broadens the lines so that a 1:4:1 triplet is observed at low temperatures with a coupling of 2.97 oe. This is the sum of the axial and equatorial methylene proton splittings of a particular conformer. Near room temperature the motion is sufficiently rapid to give exchange narrowed lines and the process has an activation energy of 4.5 kcal/mol^{-1}. From these observations it was possible to assign the coupling constants to specific protons in the molecule and to determine the dihedral angle between the rings as 21°.

Le spectre de r.p.e. de l'ion radicalaire du 9,10-dihydrophénanthrène a été obtenu dans l'éther à différentes températures entre −106 et +51 °C. Dans un mélange diméthoxyéthane tétrahydrofuranne à une température inférieure à −80 °C, on observe six triplets avec des écarts hyperfins moyens de 5.36, 3.36, 2.66, 0.70, 0.26 et 0.15 oe. A température plus élevée, il se produit un élargissement de certaines raies du spectre hyperfin causé par une interconversion entre deux conformères équivalents de la molécule ion non-polaire. Même si les écarts hyperfins des protons des noyaux ne varient sensiblement pas avec la température, ceux dûs aux protons méthyléniques le sont, et l'interconversion entre conformères élargit les raies de telle sorte qu'à basse température on observe un 1:4:1 triplet avec un couplage de 2.97 oe. C'est la somme des écarts hyperfins des protons méthyléniques axial et équatorial de chaque conformère. Aux environs de la température ambiante, le mouvement moléculaire est suffisamment rapide pour que le phénomène d'échange produise un rétrécissement des raies et ce processus a une énergie d'activation de 4.5 kcal/mol. Grâce à ces observations, il a été possible d'assigner des écarts hyperfins à certains protons dans la molécule et de déterminer que l'angle dihèdre entre les noyaux est de 21°.

Canadian Journal of Chemistry, **49**, 3524 (1971)

Introduction

In the course of an investigation of a series of diphenyl radical anions, the spectrum of 9,10-dihydrophenanthrene reduced with different alkali me als was studied in a variety of solvents. The molecule has the carbon skeleton of diphenyl with two methylene groups bridging two of the ortho positions of the diphenyl rings. Molecular models show the molecule exists in two equivalent configurations in which the aromatic rings are held at approximately 20° relative to each other by the saturated bridge. In both conformers, each methylene group has an "axial" bond, which projects very nearly at right angles to the plane of the adjacent phenyl ring, while an "equatorial" bond lies very near to the phenyl plane. If one of the conformers is converted to the other, the equatorial proton and geminal axial proton of each methylene group exchange positions.

The numbering scheme used to identify the protons is as follows:

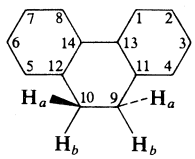

wherein H_a represents an axial proton and, H_b represents an equatorial proton.

Methyl (or methylene) groups attached to a carbon 2pπ orbital containing an unpaired electron spin have been shown (1) to give rise to isotropic proton hyperfine coupling constants

[1]Revision received June 18, 1971.

Can. J. Chem. Downloaded from www.nrcresearchpress.com by 210.87.254.5 on 09/05/12
For personal use only.

Can. J. Chem. Downloaded from www.nrcresearchpress.com by 210.87.254.5 on 09/05/12
For personal use only.

which follow a relationship given by

$$[1] \qquad a_{CH} = \rho(B_0 + B_2 \cos^2 \theta)$$

where $B_0 = 3.2$ oe, and $B_2 = 43.6$ oe, while θ is the dihedral angle that the C—H bond displays to the $2p\pi$ orbital axis as viewed down the C—C bond; ρ is the spin density in the $2p\pi$ orbitals. As a result of this angular dependence it is expected that the methylene protons in the axial and equatorial positions of the 9,10-dihydrophenanthrene anion will exhibit markedly different hyperfine coupling constants. Interconversion between the two conformers will result in modulation of these coupling constants with concomitant broadening at low interconversion rates, or with exchange-averaging of the hyperfine constants at higher rates (2).

The parent hydrocarbon species has been investigated using the technique of n.m.r. It is found that while 9,10-dihydrophenanthrene gives rise to a single narrow methylene proton absorption (3*a*), other derivatives give either a broadened methylene line, or a doublet when progressively larger groups are substituted in the remaining ortho positions of the diphenyl skeleton (3*b*) or in the bridge positions (3*c*). In particular, an activation energy of 23.1 kcal/mol is found for the 1,8-dimethyl 9,10-dihydrophenanthrene derivative, as estimated from the breadth of the n.m.r. lines observed as a function of temperature. The failure to observe line broadening in the case of 9,10-dihydrophenanthrene itself was taken to mean that the interconversion between the two conformers is extremely rapid (>100 Hz), due to a much lower barrier to conversion (<9 kcal/mol), even at the lowest temperature studied (-90 °C).

Although the diamagnetic compound studied by n.m.r. cannot be studied by e.s.r., the singly-reduced species can, and interconversion frequencies in the range 20 kHz to 100 mHz can be studied using analogous hyperfine line broadening techniques. It is not expected that the rotational energy barriers will be markedly different between the anion and the neutral hydrocarbon species, except that in the anion, the bond order of the central interannular bond is probably slightly higher. This would presumably decrease the energy required for interconversion so that an estimate of the activation energy obtained by e.s.r. would correspond to a lower limit for the neutral species. This paper describes a study of the temperature effects in the e.s.r. spectrum of the anion and an attempt to ascertain the rates of interconversion.

Experimental

9,10-Dihydrophenanthrene (DHP) was obtained from Aldrich Chemical Company, and repeated recrystallizations from ethanol were carried out followed by chromatography on alumina to make sure no phenanthrene or diphenyl remained. The purified compound was reduced by sodium metal in dimethoxyethane (DME) under high vacuum conditions. Potassium reduction gave essentially the same spectrum, and no metal splittings were observed with either metal in this solvent. Temperatures were reliable to about ± 2 °C. Cold nitrogen gas was transmitted through a conventional Dewar train to a quartz insert in the dual rectangular cavity of both a modified Strand-Labs X-band spectrometer employing a 12 in. Harvey–Wells magnet, and a Varian 4502 system. The field was calibrated with diphenyl reduced by potassium in dimethoxyethane wherein the para coupling constant of the diphenyl anion so obtained was taken to be 5.26 oe at room temperature.

Spectra of DHP anion were also taken using a 2:1 mixture of tetrahydrofuran (THF), with DME. Each solvent had been distilled from lithium aluminum hydride and stored over sodium–potassium alloy, under vacuum.

Results

Because of the similarity in structure one would expect the u.v. and e.s.r. spectra of the anion of 9,10-dihydrophenanthrene (DHP) to be analogous to biphenyl negative ion. The similarity in their u.v. spectrum has already been pointed out by Velhorst and Hoijtink (4). The solutions of DHP in DME are deep blue-green in color throughout the temperature range studied. Eloranta (5) has reported that these same green solutions are unstable and eventually lead to formation of an orange coloration. This was not the case with our preparations and both the blue-green color and the e.p.r. spectrum of solutions have remained unchanged in sealed sample tubes for a period of over three years. Biphenyl anion solutions are blue and phenanthrene, which appears to be the major impurity, produces olive green solutions. Each compound has its own characteristic e.p.r. spectrum and these have been well characterized over the temperature range of interest and in the various solvent compositions investigated. Only the spectrum of DHP exhibits the marked temperature dependence to be described. At the very lowest temperatures obtained before the onset of viscos-

Can. J. Chem. Downloaded from www.nrcresearchpress.com by 210.87.254.5 on 09/05/12
For personal use only.

ity broadening, at −110 °C in 2-to-1 THF-DME mixtures, the proton hyperfine spectra are well resolved with peak to peak widths of the order of 0.070 oe. Below −80 °C one obtains six triplet hyperfine coupling constants with mean magnitudes of 5.36, 3.36, 2.66, 0.70, 0.26, and 0.15 oe, each with more or less normal 1:2:1 intensity distributions. By virtue of the fact that these splittings are so grouped as being either quite large or quite small, a multiplet composed of the smaller splittings is separated from the remainder of the hyperfine spectrum. This group is not precisely symmetrical with respect to its center, and this asymmetry increases as the temperature is lowered. Between −70 and −50 °C this group resolves to a triplet of triplets, with a shifted center line. At −70 °C in DME the coupling constants were observed to be 5.40, 3.40, 0.71, and 0.16 oe with 1:2:1 intensity distribution, and a fifth triplet which has a separation of 2.97 oe and 1:4:1 intensities. The first four coupling constants appear to decrease slightly as the temperature approaches −50 °C, then increase slightly again at higher temperatures. The total variation is only about 5% over the entire temperature range. These couplings are ascribed therefore to the ring protons. When the temperature is further raised, near −20 °C the entire spectrum appears to be superimposed on a second hyperfine spectrum characterized by broader lines and a splitting interval of about 0.74 oe. The smallest splitting of the fine line spectrum is difficult to resolve much above room temperature and near the boiling point of DME, only the broad spectrum is obtained. Characteristic spectra are shown in Fig. 1 at various temperatures. The absorption maxima (derivative zeros) of many of the lines in the broad spectrum appear to coincide in field with the main lines of the narrow line spectrum. This suggests that the absorbing species have similar *g*-values and hyperfine couplings. In addition the 1:4:1 triplet structure noted above strongly suggests the existence of an interconversion process in which some of the lines are broadened by exchange.

Discussion

Assuming the anion to be non-planar, as the n.m.r. studies show the neutral compound to be, and to have a high barrier to inversion so that the ions exist as either one conformer or the other, then the inequivalence between the pairs of axial and equatorial protons should give rise to a triplet of triplets in the hyperfine spectrum. The couplings will be referred to as a_{CH_a} and a_{CH_b}, respectively. On the other hand a very low barrier would allow rapid interconversion between the conformers and an averaged 1:4:6:4:1 quintuplet would be observed with a coupling of $\frac{1}{2}(a_{CH_a} + a_{CH_b}) = \bar{a}$. With barriers of modest height and intermediate rates of conversion, the $M = \pm 1$ and part of the $M = 0$ line of he quintet would be broadened so that a 1:4:1 triplet would be obtained with, in this case, a splitting of $2\bar{a}$. Here $M = M_a + M_b$ and $M_a = m_{9a} + m_{10a}$, $M_b = m_{9b} + m_{10b}$ where m is the quantum number I_z. At fairly high rates of conversion, the widths of the lines are given (2*b*) by $T_2^{-1} = T_{2,0}^{-1} + j_{aa}(0)(M_a - M_b)^2$ where $T_{2,0}^{-1}$ is the natural line half width and $j_{aa}(0) = \gamma^2\tau \langle(\delta a)^2\rangle$ is the spectral density function, τ the correlation time and δa the fluctuation in the hyperfine coupling constant, $(a(t) - \bar{a})$, wherein $a(t)$ is the instantaneous value of the coupling constant. Of course the barrier to interconversion is fixed in this case and the rate ofinterconversion depends solely on temperature. The observed 1:4:1 triplet corresponds to an intermediate rate of conversion. The splitting is $2\bar{a} = a_{CH_a} + a_{CH_b} = 2.97$ oe. As the temperature is raised, the more rapid exchange between the conformers begins to narrow the broadened $M = \pm 1,0$ lines so as to give the quintuplet with hyperfine separations of $\bar{a} = 1.48$ oe. As this is approximately twice one of the ring coupling constants, an eleven line multiplet forms due to these particular protons, and the observed separation for the broad-line spectrum of about 0.74 oe is obtained. The smallest coupling constant is neglected. In particular, the multiplet structure goes from a 1:2:1:0:4:8:4:0:1:2:1 distribution at lower temperatures to 1:2:5:8:10:12:10:8:5:2:1 at higher temperatures. In the total broad-line hyperfine spectrum, the outermost few lines follow these ratios exactly. The two extreme lines of the spectrum are unaffected by the exchange process while the fourth line has a width determined by the frequency of exchange and hence is a function of temperature. A plot of the square root of the ratios of the peak-to-peak heights of the derivative spectra *vs.* $1/T$ gives an energy of activation of 4.6 kcal/mol. This value is rather larger than the 2.3 kcal/mol calculated from u.H.f.-s.c.f. computations made for the unsub-

Can. J. Chem. Downloaded from www.nrcresearchpress.com by 210.87.254.5 on 09/05/12
For personal use only.

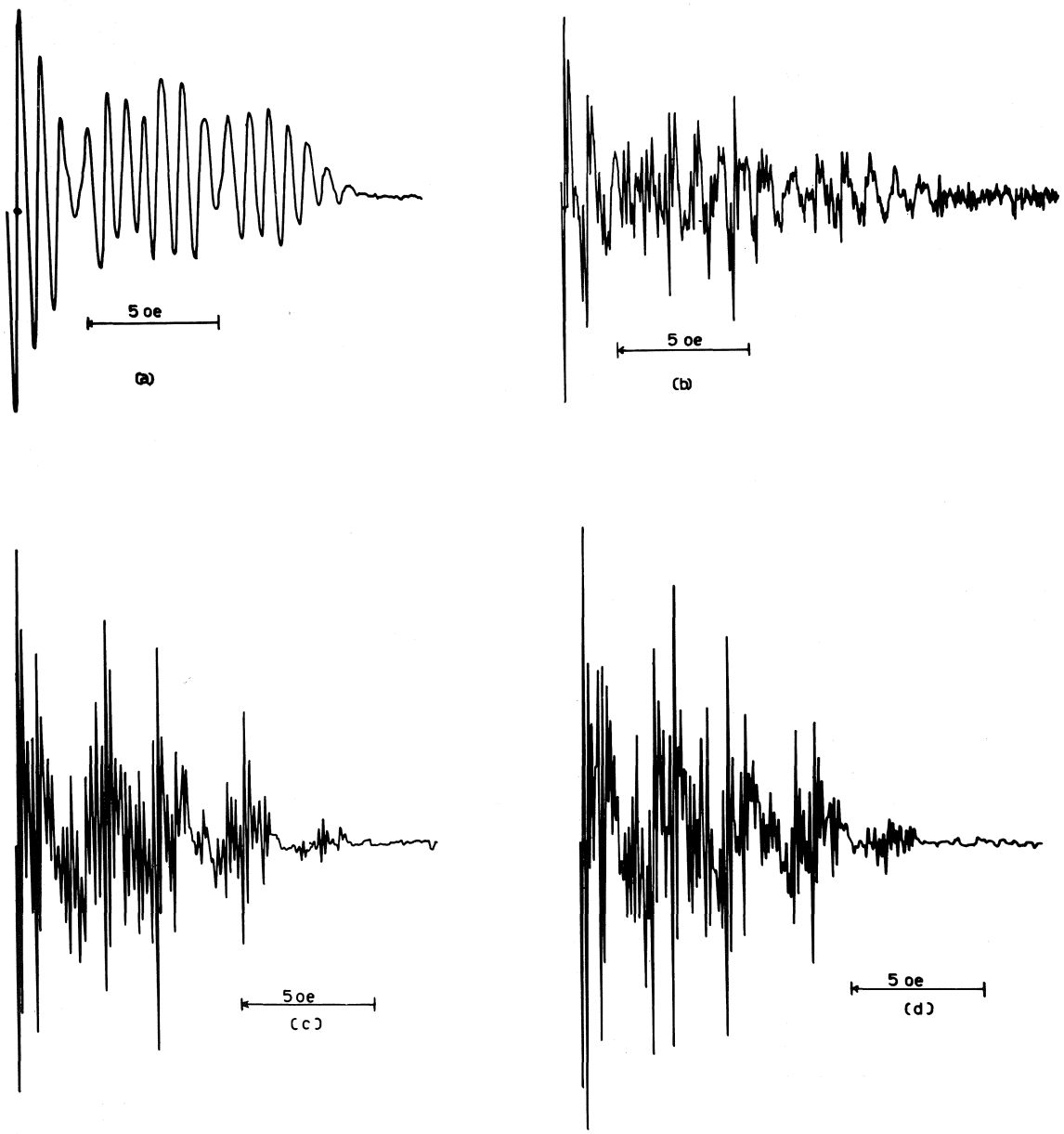

FIG. 1. Downfield half of the proton hyperfine spectrum of 9,10-dihydrophenanthrene anion in dimethoxyethane: (*a*) broad line spectrum at 51 °C; (*b*) superposition of broad and narrow line spectrum at 30 °C; (*c*) spectrum showing symmetrical low field grouping and 1:4 intensity anomaly with remaining lines, at −63 °C; (*d*) spectrum showing unsymmetrical low field grouping, at −83 °C.

stituted biphenyl anion (6), which suggests that the barrier to inversion in DHP anion arises from the energy requirements for distortion of the six-membered partly saturated ring, and is not determined by the size of the ring substituents as is the case in the n.m.r. studies (3). On the other hand this value may be compared to the difference in resonance energy between fluorene and biphenyl which is determined from thermochemical data to be 5 kcal/mol (7) and can be inter-

Can. J. Chem. Downloaded from www.nrcresearchpress.com by 210.87.254.5 on 09/05/12
For personal use only.

preted as he energy required to make the rings of diphenyl coplanar, as in fluorene, and overcome the repulsive energy of the protons in the ortho positions. In either case the barrier height determined here seems to be consistent with the other estimates of this quantity.

It is substantially lower than the estimates made from n.m.r. studies on the neutral compounds (*3a,c*), as expected, so that interconversion between the conformers of DHP itself must lie between about 5 kcal/mol and the upper limit of 9 kcal/mol cited earlier (*3a*).

Most of the coupling constants in the hyperfine spectrum can be assigned to specific positions in the DHP anion molecule by consideration of their temperature dependence, and by comparison to the spectrum of diphenyl anion which has the same π-electron system. Thus the low temperature splittings of 2.66 and 0.27 oe may be assigned to the axial and equatorial protons, respectively, of the methylene groups. At higher temperatures and exchange rates, their sum becomes the 2.97 oe splitting under the conditions of maximum broadening of the $M = \pm 1,0$ lines so as to give the anomalous 1:4:1 triplet. Eventually, at still higher temperatures and exchange rates, the normal quintuplet with the averaged 1.5 oe splitting is obtained. It is also clear that the outside group of lines of the low temperature spectrum is unsymmetrical because the exchange rate is still sufficiently high as to determine the line width for those hyperfine components which shift during conformer interconversion. This affects the lines on the inner side of the group, but not the outer and gives rise to the observed asymmetry as depicted in Fig. 1.

Since the diphenyl anion has coupling constants of $a_p = 5.26$, $a_o = 2.62$, and $a_m = 0.41$ oe, then by analogy, the large couplings for DHP anion can be assigned as $a_3 = a_6 = 5.26$, $a_1 = a_8 = 3.36$. Finally the two small splittings can be assigned by comparison to u.H.f.-s.c.f. results (8) or by use of a valence bond superposition method (9), and by analogy to other diphenyl compounds that have been deuterated or methylated in these positions (9, 10). Thus an assignment of $a_2 = a_7 = 0.70$ oe and $a_4 = a_5 = 0.15$ oe is consistent with all available data from other sources.

The methylene coupling ratio can be used with eq. 1 in the introduction to find that the spin density on the 11 and 12 positions is 0.065 and that the equatorial proton lies out the plane of the adjacent phenyl ring by 8°, while the axial proton lies 22° from the normal to the plane. If the bond lengths of 1.48, 1.39, and 1.54 Å are assumed for the interannular, ring, and bridge C—C bonds, respectively, and no distortion of the valency angles is presumed, then the dihedral angle between the two phenyl rings can be computed to be 21°. This value is at the low end of the range calculated (5) for unsubstituted diphenyl wherein the energy minimum is obtained considering both π-energies and ortho-hydrogen repulsions as a function of interplanar angle. This value also agrees well with measurements made from molecular models.

The author would like to thank Mr. Glen Smith for his technical assistance in carrying out the experiments, the National Research Council of Canada for financial assistance, and the University of Sydney, Australia, for the use of their spectrometer during sabbatical there.

1. A. Horsfield, J. R. Morton, and D. H. Whiffen. Mol. Phys. **4**, 425 (1961).
2. (*a*) J. A. Pople, W. G. Sneider, and H. J. Bernstein. High resolution magnetic resonance. McGraw-Hill, 1959. (*b*) G. Fraenkel. J. Phys. Chem. **71**, 139 (1967).
3. (*a*) D. M. Hall and M. M. Harris. J. Chem. Soc. 490 (1960). (*b*) M. Oki, H. Iwamura, and N. Hayakawa. Bull. Chem. Soc. Jap. **37**, 1865 (1964). (*c*) P. B. Rabideau, R. G. Harvey, and J. B. Stothers. Chem. Commun. 1005 (1969).
4. N. H. Velthorst and G. J. Hoijtink. J. Am. Chem. Soc. **89**, 209 (1967).
5. J. Eloranta and M. Vuolle. Suom. Kem. **B38**, 151 (1965).
6. W. G. Laidlaw and R. B. Flewwelling. Can. J. Chem. **48**, 2158 (1970).
7. G. W. Wheland. Resonance in organic chemistry. John Wiley. 1955.
8. R. B. Flewwelling. M.Sc. thesis, University of Calgary, Calgary, Alberta. 1969.
9. F. C. Adam and C. R. Kepford. Can. J. Chem. This issue.
10. K. Ishizu. Bull. Chem. Soc. Jap. **36**, 938 (1963); **37**, 1093 (1964).

A Paramagnetic Resonance Study of Unhindered Biphenyl Anion Radicals (III)

F. C. ADAM AND C. R. KEPFORD[1]

Department of Chemistry, University of Calgary, Calgary, Alberta

Received December 12, 1967[2]

The radical anions of biphenyl and some of its bridged derivatives have been studied by e.s.r. It is found that the proton hyperfine coupling constants change monotonically through the series of radical anions derived from biphenyl, 9,10-dihydrophenanthrene, fluorene, dibenzothiophene, and dibenzofuran. Deuterations have been carried out for the latter two compounds and the hyperfine coupling constants are assigned to specific positions in these anions. The data are displayed in the form of a correlation diagram from which assignments for other bridged biphenyl anions can be made.

Les anions radicalaires du biphényl et des dérivés pontés ont été étudiés par r.p.e. Il a été trouvé que les écarts hyperfins de protons changent graduellement dans la série des anions radicalaires dérivés du biphényl, 9,10-dihydrophénanthrène, fluorène, dibenzothiophène et du dibenzofuranne. Des deutérations ont été effectuées pour les deux derniers composés et les écarts hyperfins ont été assignés à des positions spécifiques pour ces anions.

Les résultats sont représentés sous forme de diagramme de corrélation au moyen duquel des valeurs de couplages d'autres anions hyperfins pontés peuvent être obtenues.

Canadian Journal of Chemistry, **49**, 3529 (1971)

Can. J. Chem. Downloaded from www.nrcresearchpress.com by 210.87.254.6 on 09/05/12
For personal use only.

Introduction

In previous papers in this series (1, 2) the spectra of hindered diarylmethyl radicals were obtained and some insight was gained into the internal configuration of such molecules from a study of the proton hyperfine structure. The ideas behind this work have been extended to the biphenyl series of compounds. It has been suggested that biphenyl itself is not planar, and that steric interactions between the ortho protons prevent the two rings from assuming a perfectly coplanar arrangement. The results of gas phase electron diffraction studies suggest the rings are oriented at an angle of 42° to each other (3) while X-ray studies on the crystal suggest the rings are coplanar, but are connected by a rather long bond (for an aromatic) of 1.50 Å (4). The barrier to internal rotation cannot be too high, because optically active derivatives of biphenyl racemize very readily, unless bulky hindering groups are substituted at the positions ortho to the interannular bond (5). The long wavelength absorption of biphenyl in the ultraviolet region occurs near that of benzene, and apart from the difference in vibrational structure and intensity, the spectra are rather similar. These considerations all indicate that the π-electron interaction between the two rings is small, and, as a result, the dihedral angle between the rings may well be established by relatively weak repulsive interactions between the ortho protons.

Structural information about the radical anion of biphenyl is completely lacking, though simple valence considerations would suggest the interannular bond has somewhat more π-character than in the case of biphenyl, and will, as a consequence, tend more toward the planar configuration, steric forces notwithstanding. To determine whether the higher bond order of the central bond is sufficient to overcome residual steric forces is the purpose of the present research. The aim is simple; it is to study a series of biphenyl-type radicals which are bridged in the 2,2′ (ortho) positions and thereby forced to assume a planar configuration. The hyperfine spectra can then be compared. Changes in the electron spin distribution can be followed by changes in the coupling coefficients (a_i) of the hyperfine spectrum through the McConnell relationship,

$$a_i = Q\rho_i$$

wherein a_i is the ring proton hyperfine coupling constant, ρ_i is the spin density at the adjacent carbon, and Q is a proportionality constant with a value of about -22.5 oe.

Experimental

The chemicals which have been used appear in Table 1, along with the abbreviations used, and the proton hyperfine coupling constants obtained from the e.s.r. spectra

[1]Present address: Pennsylvania State University, York Campus, 1031 Edgecomb, York, Pennsylvania 17403.

[2]Revision received June 29, 1971.

Can. J. Chem. Downloaded from www.nrcresearchpress.com by 210.87.254.6 on 09/05/12
For personal use only.

of their anions. Most of the parent compounds in Table 1 were obtained from Eastman Chemicals but the 9,10-dihydrophenanthrene came from the Aldrich Chemical Company and diphenylacetylene from The British Drughouses Limited. All were research grade chemicals except fluorene and dibenzofuran. The latter two were technical grade and were purified by repeated recrystallizations from 95% ethanol, with final melting points of 116 and 87 °C, respectively. The numbering scheme used for biphenyl is the usual ortho, meta, para nomenclature while the bridged compounds are indexed according to the following diagrams; in the first instance X = CH_2, S, O for fluorene (Fl), dibenzothiophene (DBT), and dibenzofuran (DBF), respectively, while the second diagram is appropriate to 9,10-dihydrophenanthrene.

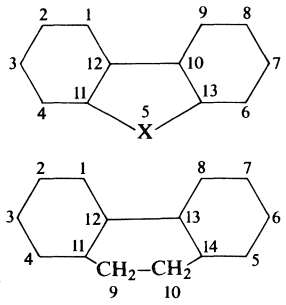

Thus the para positions of biphenyl correspond to the 3,7 positions of the furan and thiophene compounds, or to the 3,6 positions of the phenanthrene derivative, and so on.

The deuterium labelled compounds in Table 1 were obtained from the corresponding bromides by standard magnesium Grignard procedures. The 2,8-dibromo derivative of dibenzothiophene was obtained by direct bromination of the parent compound in glacial acetic acid, following the method of Neymoyer and Amstutz (6). The product melted at 225–226 °C (lit. 226–228 °C). The 3,7-dibromo derivative was prepared through direct bromination of the sulfone of dibenzothiophene which was obtained from hydrogen peroxide oxidation of dibenzothiophene in glacial acetic acid (7). The resulting 3,7-dibromobenzothiophene sulfone (m.p. 310 °C) was reduced using lithium aluminum hydride in ether to give 3,7-dibromodibenzothiophene (m.p. 180 °C). The $3d_1$-dibenzofuran was obtained through the following sequence; dibenzofuran was nitrated (8) to give 3-nitrodibenzofuran (m.p. 180 °C), which was then reduced (m.p. 94 °C), diazotized, and treated with Cu_2Br_2 to give 3-bromodibenzofuran (m.p. 110 °C). The bromide was converted to the Grignard and treated with D_2O to give the desired product.

All compounds were reduced using standard high vacuum techniques, with potassium as reductant and dimethoxyethane (DME) as solvent. The spectra were taken on a modified Strand Labs X-band spectrometer. The spectra were obtained at reduced temperature (generally at $\sim -40°$) in a conventional Dewar train using cold nitrogen gas as a refrigerant, and all couplings reported were obtained by comparison against biphenyl anion in DME at room temperature. The results as quoted should therefore be internally consistent although there remains an error of about ± 0.02 oe in the coupling constants determined from erstwhile identical samples. The temperature variation of the ring proton coupling constants is also of this magnitude. For reasons to become apparent later, we also attempted to reduce diphenyl ether and diphenyl sulfide. These compounds decomposed, however, and we could not obtain the desired spectra.

Results

The results of an analysis of the hyperfine structure of the various spectra are as listed in Table 1. The assignments were made on the basis of the spectra of the deuterated derivatives, along with the assumption that the perturbations arising from the substitutions do not change the order of the hyperfine coupling constants. It is necessary to make one exception to this in order to explain the spectra of the deuterated dibenzothiophene (DBT^-) and dibenzofuran (DBF^-) compounds. As with biphenyl anion, the largest coupling constant in DBT^- is due to the 3,7 protons but in DBF^- the largest splitting is due to the 1,9 protons. Thus the relative magnitudes of the spin

TABLE 1. Bridged biphenyl derivatives investigated and the assigned proton hyperfine constants of their anions

Parent compound	Coupling constants (oe)				
	$a_1(o)$	$a_2(m)$	$a_3(p)$*	$a_4(m)$	a_{CH_2}
Dibenzofuran (DBF)	4.90	0.93	4.74	1.95	
Dibenzothiophene (DBT)	4.43	0.91	4.94	1.41	
Fluorene (Fl)	4.27	0.88	5.02	1.26	3.85
9,10-Dihydrophenanthrene (DHP)	3.36	0.70	5.36	0.15	2.66, 0.26
Biphenyl (Bp)	2.63	0.41	5.26	0.41	
$3d_1$-Dibenzofuran	4.90	0.93	0.74(d)	1.95	
$3,7d_2$-Dibenzothiophene	4.43	0.91	0.78(d)	1.42	
$2,8d_2$-Dibenzothiophene	4.43	0.14(d)	4.94	1.42	
$3,3'd_2$-Biphenyl	2.62	< 0.08(d)	5.24	0.41	
$4d_1$-Biphenyl	2.62	0.41	5.24(0.82, d)	0.41	
Diphenylacetylene (DPA)	2.65	0.71	4.75	0.71	

*d indicates deuterium coupling constants.

densities at the ortho and para positions have become inverted, or "crossed over" between these two compounds. In this respect these conclusions differ slightly from those due to Gerdil and Lucken (9) who assigned the coupling constants of DBT^- and DBF^- by comparison of the spectra of their methyl derivatives. In this particular case there was some ambiguity in the results, but the present deuteration experiments show unequivocally that the largest splitting in DBF^- is in fact due to the 1,9 ring protons (*i.e.* the ortho positions of biphenyl).

The deuterated biphenyl compounds allow the assignments given in Table 1 to be made. They agree with those of Lapp *et al.* (10) who used a different set of derivatives to obtain their assignments.

Some of the coupling constants in the remaining compounds are also known with certainty. Two of the triplets of the 9,10-dihydrophenanthrene anion may be ascribed to methylene protons by virtue of their temperature dependence (11). This ion is not planar and interconverts between two equivalent conformers with resulting modulation of the methylene coupling constants but not those due to ring protons. The spectrum for Fl^- obtained here corresponds to that reported for the mononegative radical anion (12) and not to the fluorenyl dianion species which has an entirely different e.p.r. spectrum (13) or to the ketyl which may be produced in electrolytic systems (14). The coupling constants for Fl^- can be seen from Table 1 to be very similar to those of DBT^-; it is known from the spectrum of the bridge methylated fluorene anion that the methylene coupling constant is about 4 oe (12*b*). The spectrum obtained from diphenyl acetylene clearly corresponds to the anion monomer (not the dimer) and agrees with the results of other workers (15) who have investigated this species.

Discussion

With the exception of diphenylacetylene, the compounds of Table 1 have similar π-electron systems and their hyperfine coupling constants under normal circumstances would be expected to show corresponding similarities. However, when one compares the anions of Bp, DHP, Fl, DBT, and DBF, some of the coupling constants show considerable variation, especially those assigned to the 1 and 4 positions. These changes cannot be simply accounted for by resonance or inductive parameters of the bridging group since one of the most sensitive sites is ortho while the other is meta to the substitution. Other factors which might contribute to the observed variance are that the first two members of the series are not planar, while the remainder are; there are also geometrical factors which remove the symmetry between the ortho protons and between the meta protons of the biphenyl anion. These occur with the loss of inversion symmetry. Analogous asymmetry has been observed, for example, with the stilbene anion (16) and with the anion of acetaldehyde (17) where markedly different coupling constants are observed for the ortho positions and to a lesser extent, the meta positions. The asymmetry is attributed to coulombic interaction between the off-axis group and the different positions in the perturbed phenyl group. Clearly this effect will increase through the series of compounds considered here, since the electronegativity of the bridging group increases monotonically through the series. This does not necessarily imply an increased spin density in the bridging element, however, as both carbazole and fluorenyl dianions (13) have small spin densities at this position. Furthermore, a large spin density at the heteroatoms in DBF^- and DBT^- would result in different *g*-values for these two compounds (18) but experimentally the centers of their spectra are found at the same field. In any case, it appears as if the electronic distribution in the rings is eventually controlled by competition between the effects of the interannular bond and those of the bridging substituent. In this respect it resembles the situation found in the substituted benzene anion radicals. The extreme sensitivity of the spin distribution to chemical substitution in the latter systems has been qualitatively explained by Carrington (19) as resulting from the manner in which the inductive effect of the substituent removes the orbital degeneracy of the benzene anion. In the case of Bp^- the degeneracy has already been lifted by the presence of the other ring, but the possibility must be considered that further substitutions in the ring, such as those represented by the bridging groups studied here, might produce perturbations every bit as large as the effect produced by the neighboring ring. Such might account for the extreme sensitivity of the wave functions which can be inferred from the variation in hyperfine coupling constants. An analogous situation is

Can. J. Chem. Downloaded from www.nrcresearchpress.com by 210.87.254.6 on 09/05/12
For personal use only.

Can. J. Chem. Downloaded from www.nrcresearchpress.com by 210.87.254.6 on 09/05/12
For personal use only.

found with disubstituted benzene anions, where a wide variety of compounds have been correlated with a very simple "valence bond superposition" method formalized by Karplus and co-workers (20). Briefly, these authors suggest that the wave function for any disubstituted benzene anion can be represented by the linear superposition of the wave functions of two monosubstituted benzene anions which contain the two groups appropriate for the superposition. For dissimilar substitutions, the resulting electron distribution depends upon the fractional contribution of each fragment to the superposition. A description of the *p*-methyl benzonitrile anion would be given by the superposition of the toluene and benzonitrile anionic functions with suitable weighting factors. These ideas can be extended to the bridged biphenyl anions in the following way: any compound in the series can be looked upon as the linear superposition of

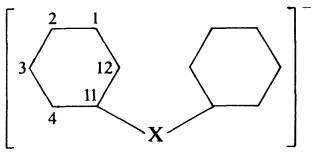

(A)

and

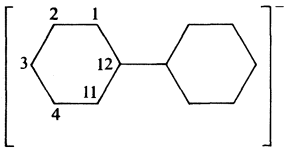

(B)

Unfortunately, the electronic structure of neither of these compounds is known, at least not in a proven planar configuration. As was noted above, attempts to produce anions of type A resulted in decomposition of the compound, rather than the formation of the mononegative ion. In the cases at hand, the spin densities of the composite molecules at the *i*th position would be given by

$$\rho_i = x\rho_i^{B} + (1 - x)\rho_i^{A}$$

where x is the fractional contribution of the planar biphenyl anion fragment B, and ρ_i^{B} and ρ_i^{A} are the spin densities at the appropriate position in the B and A fragments, respectively. While no experimental data is available for either the A or B species, it can be stated with certainty that in the limit where $x = 1$ (*i.e.* planar Bp^-), molecular symmetry requires that $\rho_1^{B} = \rho_{11}^{B}$ and $\rho_2^{B} = \rho_4^{B}$. For species A, in the other extreme, where $x = 0$, it must be assumed that $\rho_{12}^{A} = \rho_4^{A}$ and $\rho_1^{A} = \rho_3^{A}$. As mentioned earlier, this will be true only if there are no strong coulomb interactions between the two rings, although coulomb interactions with the bridging group itself do not matter. For A, the second identity is the more valid when such non-axial fields obtain. Accordingly, the most reasonable procedure to follow in correlating the data of Table 1 is to note that

$$\rho_1 = x\rho_1^{B} + (1 - x)\rho_1^{A}$$

and

$$\rho_3 = x\rho_3^{B} + (1 - x)\rho_3^{A}$$

The difference, $\rho_3 - \rho_1 = x(\rho_3^{B} - \rho_1^{B})$, using the above assumption. Alternatively, the difference in the coupling constants is proportional to the contribution of the biphenyl fragment to any composite molecule between the planar extremes represented by A and B, or $(a_3 - a_1) = xk$ wherein k is a constant. Accordingly the spin densities corresponding to the data of Table 1 have been plotted against $a_3 - a_1$ for the ring protons of each compound. The results appear in Fig. 1 taking $Q = -22.5$ oe. The "cross-over" of a_1 and a_3 between DBT^- and DBF^- is indicated. As may be seen, the points for ρ_1, ρ_2, ρ_3, and ρ_4, respectively, correlate linearly. The ordinates where $a_3 = a_1$ in Fig. 1 represent A, the hypothetical ϕ_2X^- species. It has a spin distribution such that $\rho_1^{A} = \rho_3^{A} = 0.215$, as defined by the cross-over, and at the same abscissa, $\rho_2^{A} = -0.041$ and $\rho_4 = 0.081$. By assumption $\rho_4^{A} = \rho_{12}^{A}$ at this point while from the normalization condition, $\rho_{11}^{A} = -0.047$, if use is made of the fact that the spin density on the heteroatom is zero, or at most, small. This gives the four spin densities needed for A.

The extrapolated tie lines in the correlation diagram must also satisfy the spin density distribution in the planar species, B. The lines representing ρ_1 and ρ_{12} must meet when $x = 1$, as must those representing ρ_2 and ρ_4. Accordingly the latter tie lines have been extended back to define this point. The same abscissa defines ρ_1 and hence ρ_{11} for B and a straight line is drawn between this point and ρ_{11} of A. The last spin density for B, ρ_{12}, is found from normalization, and the last tie line drawn in. The spin densities of the hypothetical B are $\rho_1^{B} = \rho_{11}^{B} = 0.120$,

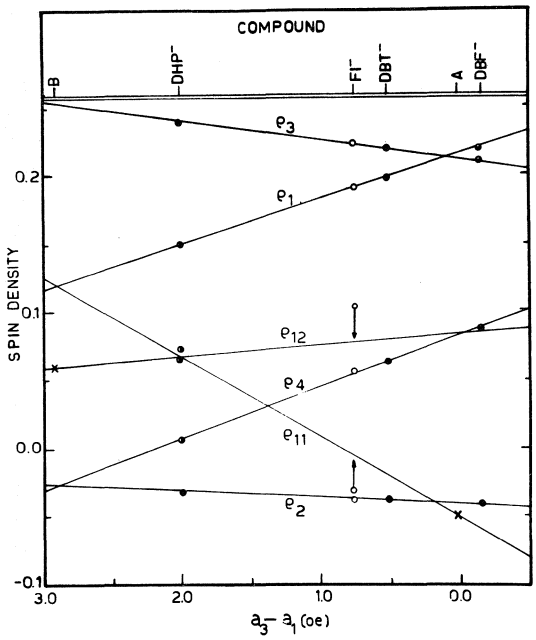

FIG. 1. Correlation diagram for the bridged triphenyl radical anions. The ordinates are spin densities of the compounds computed from Table 1, $Q = -22.5$ oe. The abscissa for each of the indicated compounds is determined by the difference in the coupling constants for positions 3 and 1. A and B are hypothetical compounds mentioned in the text, and X indicates spin densities computed using the normalization condition.

$\rho_2^B = \rho_4^B = -0.026$, $\rho_{12}^B = 0.058$ and $\rho_3 = 0.254$.

The internal consistency of this scheme can be checked in two cases. Both DHP^- and Fl^- have methylene proton splitting which may be considered to arise from spin density ρ_{11} on the ring position adjacent to the bridge. For DHP^-, an estimate of this spin density may be found if $a_{CH_2} = Q\rho_i$ and Q is taken to be $Q = 3.2 \pm 43.6 \cos^2\theta$ for these protons (see ref. 21 as presented in ref. 11). For the larger methylene splitting ($a = 2.66$ oe) and using a dihedral angle of 22° (11), one obtains the result that $\rho_{11} = 0.065$ which is so indicated in Fig. 1. The methylene protons in Fl^- are slightly different in that these protons are adjacent to two sites of unpaired electron density. The situation is analogous to that found in the cyclohexadienyl radical which exhibits coupling constants of 47.71 oe for the methylene protons, and 8.99 oe splittings for the protons on the adjacent sp^2 carbon atoms (22). Using the same proportionality, a spin density of ± 0.032 is obtained for ρ_{11} in Fl^-. This fits the diagrammed data in Fig. 1 if the sign is taken to be negative. It also implies (23) that the phase of the l.c.a.o.-m.o. coefficients at these positions in the two rings must be the same. This means that the singly occupied m.o. is symmetrical to that reflection plane of the molecule which contains the methylene protons. This agrees with Hückel m.o. expectations. The estimates of spin density from the methylene protons can be compared to the line drawn for ρ_{11} in Fig. 1.

An estimate of the cumulative errors in the analysis may now be obtained by determination of the spin densities for ρ_{12} in these two compounds.

From the normalization condition these are determined to be the relevant points indicated in Fig. 1. The value for DHP^- is slightly high, for Fl^- even more so. The worst fit is obtained for ρ_{11} of Fl^- where the expected value is too small. In a sense the correlation shown in Fig. 1 is not the best possible and other choices of Q for the ring and methylene protons could have been chosen to reduce the existing discrepancies. Alternatively, the tie lines could have been chosen so as to best fit the data presented, in which case an estimate of the inter-ring coulomb interactions involving positions 4 and 12, and the spin density in the bridging element of A could have been determined. It rather depends how much reliance one wishes to place on such linear correlations, and upon the particular molecular parameters chosen. Considered in this light, the correlation diagram of Fig. 1 can be considered to be a plot of the experimental data and may in point of fact not be as dependent on any conceptual model as has been indicated in the above development (24). As such, the diagram should be extremely useful in assigning the coupling constants of any radical which has the bridged biphenyl skeleton. Apparently therefore, the coupling constants at the positions 2, 3, and 12 are relatively insensitive to substitution while those at positions 1, 4, and 11 depend markedly on the particular substituent in the bridge. Both of the latter constants change sign through the series and accordingly may have very small values in some derivatives.

There are other features of interest brought out by these data. One of these is that the inter-annular interactions in biphenyl are not decisive, while the relatively small perturbations in the

Can. J. Chem. Downloaded from www.nrcresearchpress.com by 210.87.254.6 on 09/05/12
For personal use only.

Can. J. Chem. Downloaded from www.nrcresearchpress.com by 210.87.254.6 on 09/05/12
For personal use only.

bridging group produce large changes in the electron distribution in the molecule. This possibility was indicated in the Introduction and appears borne out by the experiments. If the extracyclic perturbations were indeed small by comparison, then according to the present interpretation, the plots for the molecules would be bunched to the left of Fig. 1, rather than evenly distributed along the horizontal axis. The insensitivity of proton coupling constants to the angle between the two rings is demonstrated by the fact that DHP^-, which is non-planar and has phenyl rings oriented at an angle of some 20° to each other, correlates with the data for the remaining planar species very well. Further evidence of the relative unimportance of planarity in these systems may be obtained by comparing the spin distribution of the "planar" species B of Fig. 1 with the values obtained experimentally for the presumably non-planar Bp^-, and those for the diphenylacetylene anion (DPA^-), the data for which are found in Table 1. This latter compound probably retains its linear configuration in the anionic form, as its spectrum is not at all similar to that of the stilbene anion (16). As a result there is little steric interaction between the ring protons, and it is unlikely the rings will have any preferred orientation relative to each other because of the cylindrical symmetry of the intervening "triple" bond. In any case the spin densities have been computed, and scaled up so that the net density in each ring is 1/2. One obtains $\rho_1 = 0.133$, $\rho_2 = -0.035$, $\rho_3 = 0.236$. This may be compared to the values of 0.12, −0.03, and 0.25 for the hypothetical planar B, and the experimental results of 0.116, −0.018, and 0.233 for the non-planar Bp^-. These are relatively small differences compared to the changes found for the remaining compounds. Calculations have been made on the biphenyl anion systems which show the spin density distribution only begins to change significantly when the interplanar angles exceed 35–40° (25). This further suggests that the resonance stabilization of the planar form is not marked enough to study the steric repulsive forces in these compounds using the present e.p.r. technique. The case of Bp^- is distinct in comparison to, say, the benzophenone anion, where ring substitutions do not materially affect the spin distribution in the rings, while changing the attitude of these rings produces relatively large effects (1, 25).

The success of the correlation diagram depends upon the correct choice of signs for the coupling constants. In particular, the meta coupling constants of Bp^- are found to be negative. The choice of opposite sign does not correlate at all and would not fit the superposition theory even in the limit of small perturbation. The McLachlan theory predicts negative spin densities at the meta position in accord with this (26) as do more refined open-shell calculations (27). On the other hand valence bond calculations such as those carried out by Schug *et al.* (28) for the naphthalene negative ion have also been carried out for Bp^- using a basis set of four structures. The results suggest that positive spin densities should be found at every carbon atom. The l.c.a o.-s.c.f. treatment proposed by Adam and Laidlaw (29) also predicts positive spin densities throughout the molecule in planar Bp^-. These latter calculations were extended to the case of DBT^-, and while pointwise agreement with the observed spin densities was still poor, the following trends were predicted: ρ_1 is predicted to increase markedly comparing DBT^- to Bp^-, ρ_2 becomes negative, ρ_3 decreases only slightly, while ρ_4 increases. These duplicate the trends found in Fig. 1. Similar trends were found by Gerdil and Lucken (30) who used McLachlan's method, and as far as DBT^- and DBF^- are concerned, were substantiated both as to direction and approximate magnitude using the u.h.f. method followed by spin annhilation (31). While these latter results do not predict the observed cross-over between DBT^- and DBF^-, they do suggest approximate equality of a_1 and a_3 in the latter compound. Furthermore, since these calculations contain coulomb repulsion effects explicitly, agreement with the correlation diagram of Fig. 1 may be taken to mean that the valence bond superposition model can be used to describe in a simple way the direction and magnitude of such effects in these molecules.

The diagram also suggests some interesting problems, the determination of the signs of the coupling constants for the meta protons, and the methylene protons in Fl^- being cases in point. Even lacking immediate experimental corroboration, Fig. 1 can be useful in assigning the proton coupling constants of other compounds with the biphenyl skeleton.

The authors would like to express their thanks to Mr. M. Williams of the Computing Centre, and to Dr. W. G.

Laidlaw for the programming assistance given. Thanks are also due to the National Research Council of Canada for financial assistance.

1. H. R. Falle and F. C. Adam. Can. J. Chem. **44**, 1387 (1966).
2. F. C. Adam and H. R. Falle. Can. J. Chem. **44**, 1397 (1966).
3. O. Bastiansen. Acta Chem. Scand. **3**, 408 (1949).
4. A. Hargreaves and S. H. Rivzi. Acta Cryst. **15**, 365 (1961).
5. R. Adams and H. C. Yuan. Chem. Rev. **12**, 261 (1933).
6. C. K. Neumoyer and E. D. Amstutz. J. Am. Chem Soc. **69**, 1920 (1947).
7. N. M. Cullinane, C. G. Davies, and G. I. Davies. J. Chem. Soc. 1435 (1936).
8. H. Gilman, W. G. Bywater, and P. T. Parker. J. Am. Chem. Soc. **57**, 885 (1935).
9. R. Gerdil and E. A. C. Lucken. J. Am. Chem. Soc. **87**, 213 (1965).
10. T. W. Lapp, J. G. Burr, and R. B. Ingalls. J. Chem. Phys. **43**, 4183 (1965).
11. F. C. Adam. Can. J. Chem. This issue.
12. (*a*) E. G. Janzen, W. B. Harrison, and B. Pickett. J. Organomet. Chem. **16**, 48 (1969). (*b*) D. Casson and B. J. Tabner. J. Chem. Soc. B, 888 (1969).
13. N. L. Bauld and J. H. Zoeler, Jr. Tetrahedron Lett. **10**, 885 (1967).
14. R. Dehl and G. K. Fraenkel. J. Chem. Phys. **39**, 1793 (1963).
15. (*a*) J. G. Broadhurst and E. Warhurst. J. Chem. Soc. A, 351 (1966). (*b*) R. E. Soida, D. O. Cowan, and W. S. Koski. J. Am. Chem. Soc. **89**, 230 (1967).
16. R. Chang and C. S. Johnson, Jr. J. Chem. Phys. **41**, 3272 (1964).
17. N. Steinberger and G. K. Fraenkel. J. Chem. Phys. **40**, 723 (1964).
18. H. C. Heller. J. Am. Chem. Soc. **89**, 4288 (1967).
19. A. Carrington. Quart. Rev. **17**, 67 (1965).
20. J. Shug, T. H. Brown, and M. Karplus. J. Chem. Phys. **37**, 330 (1967).
21. A. Horsfield, J. R. Morton, and D. H. Whiffen. Mol. Phys. **4**, 425 (1967).
22. R. W. Fessenden and R. H. Schuler. J. Chem. Phys. **38**, 773 (1963).
23. D. H. Whiffen. Mol. Phys. **6**, 223 (1963).
24. A. H. Maki and D. H. Geske. J. Am. Chem. Soc. **83**, 1852 (1961).
25. R. B. Flewwelling. M.Sc. thesis, University of Calgary, Calgary, Alberta. 1969.
26. A. D. McLachlan. Mol. Phys. **3**, 233 (1960).
27. L. C. Snyder and T. Amos. J. Chem. Phys. **42**, 3670 (1965).
28. J. C. Shug, T. H. Brown, and M. Karplus. J. Chem. Phys. **35**, 1873 (1961).
29. F. C. Adam and W. G. Laidlaw. Aust. J. Chem. **19**, 897 (1966).
30. R. Gerdil and E. A. C. Lucken. Proc. Chem. Soc. 144 (1963).
31. N. K. Ray and P. T. Narasimhan. Theoret. Chim. Acta, **11**, 156 (1968).

Can. J. Chem. Downloaded from www.nrcresearchpress.com by 210.87.254.6 on 09/05/12
For personal use only.

Can. J. Chem. Downloaded from www.nrcresearchpress.com by 210.87.254.40 on 09/05/12
For personal use only.

The Photolysis and Radiolysis of Simple Mercaptans in Dilute Glassy Matrices

J. SKELTON[1] AND F. C. ADAM
Department of Chemistry, University of Calgary, Calgary, Alberta

Received March 4, 1971

The e.p.r. spectrum of thiyl radicals is obtained when dilute solutions of aliphatic mercaptans are photolyzed in a xenon matrix at 77 °K. No proton hyperfine structure is observed at low concentrations of thiol but it appears at higher concentrations due to the reaction of hot hydrogen atoms with solute mercaptan molecules. When small amounts of the thiols are dissolved in glassy hydrocarbon matrices such as 3-methylpentane, there is produced after photolysis hyperfine structure characteristic of the solvent as well as the thiyl resonance. The e.s.r. absorption due to the solvent species disappears when the matrix is warmed a few degrees above 77 °K but thiyl radicals are stable up to the melting point of the glass. The corresponding γ-irradiated glasses do not give thiyl absorption, but two other species are produced along with solvent radicals. No thiyl radicals are observed following radiolysis, or upon photobleaching the new species. The spatial distribution of the neutral radicals in the glasses is discussed in view of these results.

Le spectre de r.p.e. de radicaux thiyl est obtenu lors de la photolyse de solutions diluées de mercaptans aliphatiques dans une matrice de xénon à 77 °K. On n'observe pas la structure hyperfine du proton en utilisant de faibles concentrations de thiol, mais elle apparaît lorsqu'on utilise des concentrations plus élevées à cause de la réaction des atomes d'hydrogène chauds avec les molécules de mercaptan en solution. Si on dissout de petites quantités de thiol dans des matrices d'hydrocarbure vitreuses, tel le méthylpentane-3, il se produit après photolyse, une structure hyperfine qui est caractéristique du solvant aussi bien que de la résonance du thiyl. L'absorption r.p.e. due à l'espèce solvant disparaît quand la matrice est chauffée à quelques degrés au-dessus de 77 °K, mais les radicaux thiyl demeurent stables jusqu'au point de fusion du verre. Les verres irradiés aux rayons-γ ne donnent pas d'absorption thiyl, mais deux autres espèces sont produites en même temps que les radicaux de solvant. On n'observe pas de radicaux thiyl après radiolyse, ou pendant la photodécoloration des nouvelles espèces. On discute de la distribution spatiale des radicaux neutres dans les verres pour arriver à ces résultats.

Canadian Journal of Chemistry, 49, 3536 (1971)

Introduction

Studies carried out in the vitreous (1, 2) or crystalline state (3) have yielded a great deal of information concerning the processes which occur during photolysis or during ionizing radiolysis of organic materials. This is partly due to the fact that reactive intermediates are held immobilized in the medium and thus restrained from further reaction, and as long as the matrix remains rigid the labile species may be studied at leisure by their u.v. and visible absorption spectra (4) in transparent media, by their e.p.r. spectrum in the case of paramagnetic species (5), or by their conductivity in the case of charged particles (6). These reactive intermediates may also be sensitive to changes in chemical environment such as occur in different solvents (7), or when small amounts of certain additives are present (8). Postradiative treatment such as photolytic bleaching of the intermediates (9), or changing the physical nature of the matrix by warming the samples (10) may also affect the different species in a variety of ways, serving to characterize, or perhaps to identify, the particular molecules under observation.

In the process of studying the γ-radiolytic decomposition of mercaptan solutions we have had occasion to study the photolytic decomposition of simple thiols in dilute solid solutions of various matrices at 77 °K. The effect of radiation or of photolytic absorption on the pure mercaptans has been extensively studied in the gaseous state (11, 12), in the solid polycrystalline state (13, 14), and in single crystals such as cysteine (15, 16). The metastable intermediates of chemical oxidation in dilute aqueous solutions have also been studied using fast flow techniques (17, 18), flash photolysis (19), or pulse radiolysis methods (20), but until recently not much work had been done on the radiolysis and photolysis of thiols in dilute rigid solutions using inert or chemically indifferent organic matrices. We wish to report on some of the work done in this direction

[1]Present address: Department of Chemistry, Oakland City College, Oakland City, Indiana 47560.

Can. J. Chem. Downloaded from www.nrcresearchpress.com by 210.87.254.40 on 09/05/12
For personal use only.

and to discuss the relationship between the intermediates of photolysis and those resulting from γ-irradiation of the same dilute solutions.

Photolytic decomposition of thiols in the gas phase involves the rupture of the S—H bond (21), with the production of a thiyl radical and a hydrogen atom which may have kinetic energy in excess of thermal. The maximum value of this excess energy is the difference between the energy of the excitation photon and the S—H bond energy of 88 kcal. In this case the low pressure mercury resonance line at 2537 Å was used for photolysis and the excess energy may be as large as 24 kcal. This excess energy may be lost by subsequent lattice collisions, until the atoms are "thermalized". As formed, however, the hydrogen atoms are "hot" and may be able to follow reaction paths requiring an energy of activation but which would not be observed with atoms which had been thermalized at 77 °K. In the present situation the most important nonthermal process is that of hydrogen atom abstraction, in which a free radical is produced along with molecular hydrogen.

The experiments to be described concern the photolytic absorption of thiols and the production of hot hydrogen atoms and their subsequent thermalization in a completely inert matrix of solid xenon. The procedure was to study the reactions of thermalized hydrogen atoms in very dilute thiol–xenon matrices, and then to raise the concentration of thiol in the xenon matrix upwards until the point was found where the products due to hot hydrogen atom attack on nearby solute molecules could be detected. These results give a rough indication of the range that hot hydrogen atoms have in a rigid matrix before becoming effectively thermalized and hence incapable of abstracting hydrogen from the CH bonds of an organic molecule. Corresponding experiments were then carried out using a rigid hydrocarbon matrix in which the solvent molecules can undergo reactions with hot hydrogen atoms quite independently of solute concentration. The various metastable species which were produced in these systems were characterized by their color and by their e.p.r. spectra and then compared to the intermediates obtained when similar glasses were subjected to γ-radiolysis.

Experimental

Matheson, Coleman and Bell were the suppliers of the solvent, 3-methylpentane (3MP), and ethanethiol, while 2,2-dimethylethanethiol (*t*-butyl mercaptan (*t*-BuSH)) was obtained from K and K Laboratories. 3MP was purified by standard techniques (1) and stored over sodium–potassium alloy under vacuum. Ethanethiol (EtSH) was distilled and stored in a dark bottle. Xenon gas was used as obtained from Air Reduction Corporation. The required amount of ethanethiol was introduced from a pipette into a clean cell which was then attached to a mercury-free high vacuum line, frozen, and evacuated to a pressure of 10^{-5} Torr. Solvent was then distilled in, and freeze–pump–thaw cycling followed until the residual pressure at 77 °K was less than 10^{-5} Torr. The cell was sealed off from the vacuum line, the sample was shaken until a homogeneous solution resulted and then refrozen preparatory to irradiation or photolysis. Xenon solutions were made up by freezing the appropriate amount of xenon on top of the degassed thiol. The resulting mixture was warmed in a petroleum ether – liquid nitrogen slurry at a temperature between −110 and −115 °C until the xenon liquified. With a melting point of −140 °C, EtSH is also a liquid at this temperature. The resulting mixture was well shaken then refrozen for photolysis.

Irradiations were carried out in a Gammacell 220 unit from Atomic Energy of Canada Ltd. Hanovia 87A45 low pressure mercury lamps were used for the photolyses.

Hydrogen yields were measured using the method of Johnson and Allen (22) except that palladium thimble rather than a combustion apparatus was used for disposal of the hydrogen gas. Electron spin resonance spectra were taken on a modified X-band Strand-Laboratory spectrometer using a 12 in. Harvey–Wells magnet system.

Results

A. Photolysis

Photolysis of the xenon–ethanethiol mixtures at 2537 Å gives rise to a yellow coloration which remains until the matrix is melted. Similar results are found with 3MP–EtSH mixtures, both dilute and concentrated, and with photolyzed pure solid EtSH. The e.p.r. spectrum of a 0.13 *M* EtSH–Xe solution at 77 °K consisted of a single unsymmetrical line near $g = 2.0$. However, the same illumination of a 0.270 *M* solution shows that this is only the high field line of three e.p.r. peaks which correspond to anisotropic g values of 2.063, 2.027, and 1.999 as shown in Fig. 1(*a*). Photolysis of higher concentrations of EtSH in xenon (>0.4 *M*) gives some proton hyperfine structure in addition to the three line spectrum, as is seen in Fig. 1(*b*). The proton hyperfine structure is characteristic of an odd-line spectrum, if it is assumed to arise from an aliphatic hydrocarbon radical with a g value near that of the free electron, and a hyperfine splitting of ~23 oe, as suggested by the larger high field lines.

The unsymmetrical three line spectrum and yellow color are ascribed to the EtS· radical, in agreement with the u.v. absorption work of

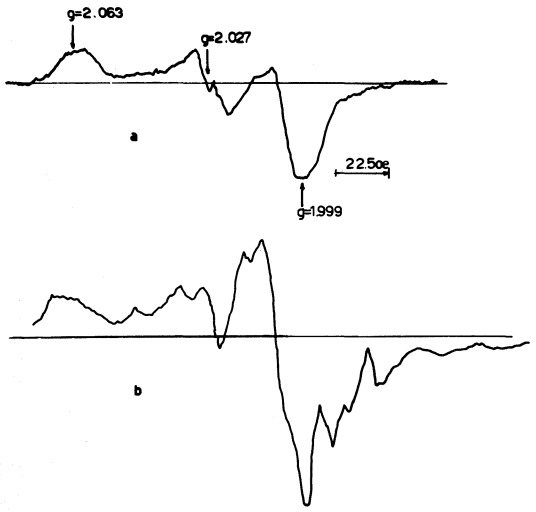

FIG. 1. First derivative e.s.r. spectra of photolyzed ethanethiol in xenon at 77 °K: (*a*) concentration 0.27 *M*; (*b*) 0.41 *M*. Corresponding positions along the horizontal axes are at the same field value.

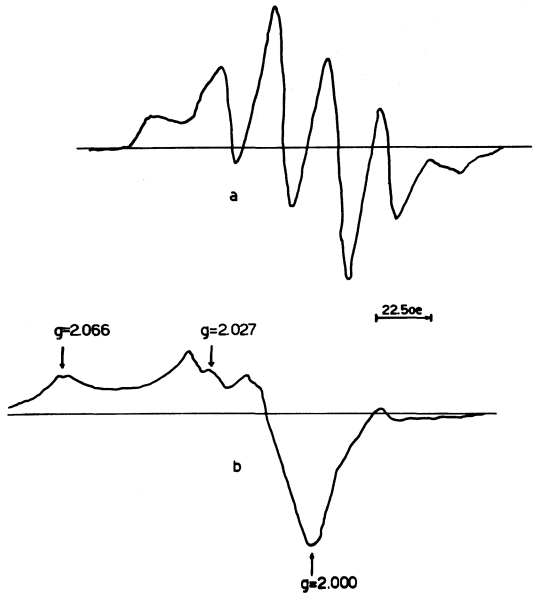

FIG. 2. First derivative e.s.r. spectra of photolyzed 0.1 *M* ethanethiol in 3 methylpentane: (*a*) temperature 77 °K, photolysis time 3 h; (*b*) temperature 91 °K, photolysis time 2 h.

Rosengren (23) and the e.p.r. work of Henriksen (24) and Kurita (25). By way of comparison, Kurita obtained principle **g**-tensor values of 2.0552, 2.0246, and 2.0032 from a single crystal study of an analogous organic thiyl radical.

As with the pure xenon matrix, illumination of the pure 3MP glass with 2537 Å radiation at 77 °K gave neither e.p.r. signal nor coloration. However, the photolysis of a 0.03 *M* solid solution of EtSH in 3MP gave an intense even-line e.p.r. spectrum with at least six hyperfine components. This is entirely different from the unsymmetrical spectrum described above and is attributed to the 3-methylpentyl radical (3MP·) because of its similarity to the hyperfine spectrum observed in glasses of this solvent after γ-radiolysis (26) and after photolysis of rigid 3MP solutions containing HI (27).

Photolysis of slightly higher concentrations (0.07 *M*) yields, in addition to the proton hyperfine structure, the low field absorption of EtS· corresponding to the *g* value of 2.06. It is significant that on warming these solid solutions to about 81 °K, the six line hyperfine structure disappears, leaving the same unsymmetrical three line as observed in the xenon matrix at lower EtSH concentrations. The corresponding spectra are shown in Fig. 2 (*a*) and (*b*). These e.p.r. signals disappear when the glass is heated to the melting point near 90 °K.

Photolysis of 0.09 *M* *t*-butyl mercaptan in a 3MP glass lends added assurance that the proton spectrum indeed arises from the 3MP solvent molecules, and not from fragmented solute molecules such as might arise through loss of HS·, for instance. This is because *t*-BuSH gives the same six line proton hyperfine spectrum as does EtSH, with the same *g* value, and on warming to ~81°K, the spectrum also fades so as to expose an analogous unsymmetrical three line spectrum due to the *t*-butyl thiyl radical. It has anisotropic *g* values of 2.060, 2.030, and 2.003, is yellow, and is also stable up to the temperature of fusion of the glass.

Similar results are obtained with solutions up to about 1 *M* in EtSH, but the intensity of the e.p.r. signals does not increase proportionately at higher concentrations. These photolyzed glasses were observed to be intense yellow at the front surface, but practically colorless deeper in the solutions. In view of this it is likely the thiyl radicals and the other products of photolysis strongly absorb the 2537 Å radiation of the source. Rosengren's (23) results for the absorption spectra of these solid solutions appear to bear out this conclusion, and as such, could explain the fact that the product yields do not increase linearly

Can. J. Chem. Downloaded from www.nrcresearchpress.com by 210.87.254.40 on 09/05/12
For personal use only.

Can. J. Chem. Downloaded from www.nrcresearchpress.com by 210.87.254.40 on 09/05/12
For personal use only.

with time of illumination, contrary to what is observed in the liquid and vapor phase photolyses for corresponding yields of product.

B. Radiolysis

Rigid hydrocarbon glasses, both with and without added mercaptan, have also been γ-irradiated. In agreement with other workers (2), the labile e.p.r. singlet and blue coloration of the "solvated electron" are observed in pure radiolysed 3MP at 77 °K. This species saturates easily at high r.f. powers and decays in a matter of minutes at any temperature above that of liquid nitrogen. The even-line proton hyperfine spectrum of 3MP· is also observed and this too will disappear slowly if the matrix is warmed a few degrees above the boiling point of nitrogen. The glasses appear to be still solid under these circumstances, and in view of the stability of the thiyl radicals in the corresponding photolyzed system it would appear that the much larger 3MP· radicals must be disappearing by some process other than those involving molecular diffusion of the radicals.

When increasing amounts of EtSH are added to the 3MP matrix, the color of the irradiated glass changes from the original blue, through green, to the orange coloration found at higher concentrations of EtSH. The e.p.r. spectrum still consists of a single line near $g = 2$ but is considerably different from the solvated electron signal in that it is much more stable at temperatures above 77 °K and can in fact be observed at temperatures beyond which the 3MP· spectrum has faded. It is considerably broader and may be observed at high microwave powers. Glasses which have been thermally annealed to remove the 3MP· and solvent trapped electrons reveal a slightly unsymmetrical singlet e.p.r. absorption with ΔH_{pp} of 26 oe and $g = 2.011$. The glass is yellowish green. An i.r. bleach with $\lambda \sim 700$ mμ gives a yellow glass and a reduced e.p.r. signal which has structure which may be attributed to a radical with $g_1 = 2.002$, $g_2 = 2.012$, and $g_3 = 2.025$. The width between extreme peaks is ~38 oe. Exposure of the glass to 420 mμ light does not regenerate the green coloration, but prolonged exposure (> 1 h) will bleach the yellow coloration. The u.v. and visible absorption spectra of the glasses (28) show the presence of transitions at 420 mμ and at 700–900 mμ. The latter is readily removed by bleaching but not the former. Only the 420 mμ absorption is obtained for EtSH in 2-methyltetrahydrofuran glasses which accounts for its yellow coloration. A broad e.p.r. spectrum has also been detected for this system and has been attributed to the radical anion $EtSH^-$ (29).

Some idea of the ability of EtSH to act as an electron scavenger in 3MP glasses may be determined by irradiation of solutions containing small amounts of other known electron scavengers. For instance, addition of CO_2 to 3MP produces an anion which is characterized by a narrow e.p.r. line near $g = 2.0$ (30). This line is not bleached by i.r. or visible light. On the other hand irradiation of the ternary mixture of 3MP with equimolar (0.02 *M*) EtSH and CO_2 at 77 °K produces a clear yellow glass which clearly exhibits the proton hyperfine structure of 3MP· in the e.p.r. spectrum, but no narrow unbleachable CO_2^- line. It appears as if it is the EtSH rather than the CO_2 which has scavenged the available electrons to produce the broad $EtSH^-$ absorption which lies under the 3MP· spectrum. The yellow coloration of the glass substantiates this conclusion. The unbleachable CO_2^- line will reappear if the concentration of EtSH is substantially reduced below that of CO_2. These effects are to be seen in Fig. 3.

The unsymmetrical spectrum of EtS· in 3MP was not observed at any time before, during, or after photobleaching, nor during the warming up of the γ-irradiated EtSH/3MP mixture to 85 °K. Nor did photobleaching at 77 °K produce any additional signal which could be attributed to the formation of additional 3MP· radical, in either pure 3MP or the thiol glasses.

Irradiation of 0.1 *M* EtSH for extended times (~10^{20} eV/g) does not materially affect the above described situation.

Products were analyzed by v.p.c. using ampoules in which the irradiated glass had been melted and brought to room temperature. Samples were withdrawn by syringe through a rubber septum at the top of the ampoule. While some fragmentation of solvent molecules is found in both the photolyzed and radiolyzed systems, the greatest changes occur with photolysis due to the formation of thioethers and ethyl disulfide. Somewhat less disulfide and no thioethers were detected in the γ-radiolyzed system. Ultraviolet absorption of the liquid solutions bear out these conclusions insofar as the photolyzed samples absorb more strongly in the disulfide region near 250 mμ than do the γ-radiolyzed samples. H_2S was detected in neither system using g.l.c.

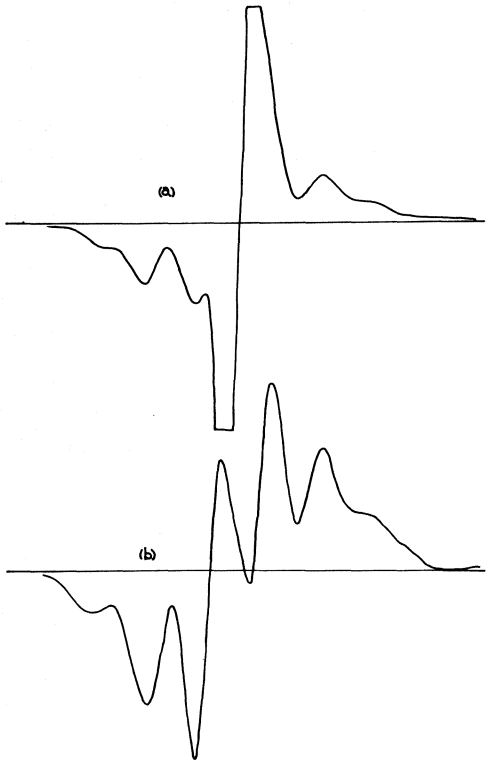

FIG. 3. First derivative e.s.r. spectra of γ-irradiated 3 methylpentane glass at 77 °K (dose 2×10^{19} eV g^{-1}): (*a*) 0.01 *M* in CO_2 (gain × 1); (*b*) 0.01 *M* in CO_2 and 0.01 *M* in ethanethiol (gain × 2).

Hydrogen gas appears to be the major product in both photolysis and radiolysis. The exposure times are such that roughly the same amount of decomposition occurs by each process. Compared to pure 3MP, the actual yields are only slightly reduced (by ~5%) for dilute solutions of EtSH in 3MP (0.01 – 0.05 *M*). The amount of hydrogen gradually increases as the concentration of EtSH is increased beyond these concentrations. A more complete report will be given on these analyses at a later date.

Discussion

A. Photolysis

The photolysis of EtSH in dilute xenon solutions produces the thiyl radical EtS· as a majority product in spite of the fact that the C—S and not the S—H bond is the weakest in the molecule (11, 29). This finding is in agreement with sulfhydryl photolysis experiments carried out in the vapor phase (11). The absence of ethyl or sulfhydryl radicals in the e.p.r. spectrum of dilute thiol solutions in xenon further indicates that the primary photolytic process must be similar in both the vapor and the glassy state. This may be true for 2537 Å mercury excitation alone, since it has been shown in the vapor phase with the use of higher photon energies, that C—S bond rupture becomes the more probable decomposition route (19).

The processes occurring in photolysis are thus best described by the reactions

[1] $$EtSH \xrightarrow{2537\ Å} EtS\cdot + H\cdot^{*}$$

[2] $$H\cdot^{*} + M \rightarrow H\cdot + M + \text{lattice energy}$$

[3] $$H\cdot^{*} + CH_3CH_2S\cdot \rightarrow CH_3CH{=}S + H_2$$

[4] $$H\cdot^{*} + CH_3CH_2SH \rightarrow \cdot CH_2CH_2SH + H_2$$
$$\rightarrow CH_3\dot{C}HSH + H_2$$

[5] $$H\cdot + CH_3CH_2SH \rightarrow CH_3CH_2S\cdot + H_2$$

Here H·* is a hydrogen atom with excess kinetic energy and M is a matrix molecule. Reaction 3 represents one of the various possible cage abstractions while reaction 4 represents the hot atom reactions occurring outside of the solvent cage. The observed hyperfine structure in Fig. 1(*b*) is what might be expected from radicals of the form given in reaction 4.

The activation energy for reaction 5 is believed to be quite small since this reaction has been shown (12) to compete favorably in the vapor phase with the olefin addition reactions which are already known to require only small energies of activation (32). On the other hand, abstractions as in reaction 4 require activation energies of about 8 kcal (2, 33). Since the photolytically produced hydrogen atoms may have energies well in excess of this, in hydrocarbon matrices one has in addition to the thermalization reaction 2

[6] $$H\cdot^{*} + C_6H_{14} \rightarrow C_6H_{13}\cdot + H_2$$

The radical so produced should therefore be close to the original site of absorption, and the resulting geminal pair may combine by the reaction

[7] $$CH_3CH_2S\cdot + \cdot C_6H_{13} \rightarrow CH_3CH_2SC_6H_{13}$$

Only slight relaxation of the matrix is required for this process, and this may explain why all 3MP· radicals produced by photolysis vanish when the matrix is warmed to 81 °K. The abstraction process 6 cannot prevail to the complete

Can. J. Chem. Downloaded from www.nrcresearchpress.com by 210.87.254.40 on 09/05/12
For personal use only.

Can. J. Chem. Downloaded from www.nrcresearchpress.com by 210.87.254.40 on 09/05/12
For personal use only.

exclusion of reaction 2 so that isolated pairs of thiyl radicals are still found resulting from reactions 2 and 5. These are the species which produce the thiyl e.p.r. signal and yellow coloration which remain up to the melting point of the glass near 95 °K, whereupon

[8] $2CH_3CH_2S\cdot \rightarrow CH_3CH_2SSCH_2CH_3$

The major products obtained by g.l.c. and hydrogen analysis support this simple scheme.

B. Radiolysis

The results of the γ-radiolysis experiments are not as clear cut as those for the photolysis, but since many of the products expected or purported to be formed (13, 14, 34) in γ-radiolysis are the same as those found in the photolysis experiment, one can proceed with a certain amount of confidence using the knowledge of the properties of those radicals which are common to both systems and which have been prepared in similar molecular environments. The effects of γ-irradiation on glasses such as 3MP have recently been reviewed (2). The reactions which best explain the experimental observations are as follows

[9] $C_6H_{14} \rightsquigarrow C_6H_{14}^*$

[10] $C_6H_{14} \rightsquigarrow C_6H_{14}^+ + e_m^-$

[11] $e_m^- + M \overset{h\nu}{\rightleftharpoons} M^-$

or

[12] $C_6H_{14}^+ + M \rightleftharpoons C_6H_{14} + M^+$

Following this will be neutralization as, for instance,

[13] $C_6H_{14}^+ + e_m^- \rightarrow C_6H_{14}^*$

In these equations, e_m^- is the mobile electron, M is some molecule in the matrix, and $C_6H_{14}^*$ is a solvent molecule in one of its excited electronic states. Following this, the excited molecule can be considered to decompose by two main routes

[14] $C_6H_{14}^* \rightarrow$ diamagnetic fragmentation products

or

[15] $\rightarrow C_6H_{13}\cdot + H\cdot^*$ or other paramagnetic products

Hot atoms produced in reaction 15 can undergo subsequent transformations such as abstraction by reaction 6, thermalization as in reaction 2 or in the presence of EtSH, any of the reactions 3, 4, and 5. In the pure 3MP glass, however, γ-irradiation gives rise to only the solvent trapped electron and 3MP· as detected by e.p.r. or visible absorption spectroscopy. Photobleaching and thermal treatment produce no additional 3MP· which implies that diamagnetic products are the sole result of the neutralization process, reaction 13, and that most probably this paramagnetic species arises only during the actual irradiation, and results from the superexcited states depicted in reaction 9. It is unlikely that small amounts of added solutes would have any effect on this direct process. On the other hand, a compound such as EtSH would be expected to act as a trap for some of the ensuing secondary products. The photolysis experiments demonstrate the ability of EtSH to act as a trap for mobile radical carriers such as hydrogen atoms. It has also been shown above that it acts as a fairly good scavenger for mobile electrons. Because its ionization potential (9.28 eV) (35) is lower than that of the solvent (10.02 eV), it might also be expected to scavenge positive charge from ionized 3MP molecules. As a result EtSH intercepts the normal matrix neutralization reaction 13 and the ensuing reaction 14 which may give rise to some of the fragmented, unsaturated, and isomerized solvent molecules which are found in the products. Such would produce $EtSH^-$ and $EtSH^+$ in the first instance; these ions are analogous to those found by Truby in the γ-radiolysis of aliphatic disulfides (36). The present experiments show that post radiative photolysis or thermal annealing of EtSH/3MP glasses produce no new radical species such as 3MP·, H·*, EtS·, H·, Et· in anything but a transitory way, and that if formed at all, then their decomposition is such as to give rise to only diamagnetic and uncolored products. Finally it should be noted that the odd-line hyperfine structure due to solute molecules is not observed in any but the xenon matrices which suggests that the range of hot hydrogen atoms is very restricted in hydrocarbon solvents.

C. Comparison of Photolyzed and Irradiated Glasses

Both photolysis and γ-radiolysis of EtSH–3MP glasses produce 3MP· radicals during the primary excitation process, but not during subsequent photochemical or thermal treatment. On the other hand EtS· radicals are produced only by photolysis and are not found in the γ-irradiated system regardless of the post-radiative treatment. In

Can. J. Chem. Downloaded from www.nrcresearchpress.com by 210.87.254.40 on 09/05/12
For personal use only.

both systems the hyperfine structure due to 3MP· fades when the temperature is raised a few degrees above 77 °K. In the γ-irradiated systems signal due to charged species remains, while in the photolyzed samples signals due to EtS· are observed until the matrix is melted. Compared to the thiyl radical, the instability of the hydrocarbon species appears to arise either from differences in the spatial distribution of these radicals in the matrix, or by some spin diffusion property characteristic to 3MP·. Molecular diffusion may be ruled out on the basis of size and the fact that EtS· is quite stable in the same matrix. The resonant hydrogen transfer reaction

[16] $C_6H_{13}\cdot + C_6H_{14} \rightarrow C_6H_{14} + C_6H_{13}\cdot$

would be specific to 3MP· in a 3MP matrix, and would allow migration of only this particular species away from the actual site of formation. Such a process would also be favored in a less-than-completely-rigid lattice and might therefore be expected to have the temperature dependence displayed by the fading 3MP· signal. The decrease observed would then result from radical–radical annihilation reactions such as reaction 7 or reaction 17

[17] $2C_6H_{13}\cdot \rightarrow$ diamagnetic products

However, in systems containing modest amounts of EtSH, the "repair" reaction

[18] $C_6H_{13}\cdot + C_2H_5SH \rightarrow C_6H_{14} + C_2H_5S\cdot$

is much more favorable than radical–radical recombinations and the fading of the 3MP· signal should therefore be accompanied by a gain in the EtS· signal. Such a gain was observed in neither of the systems studied. This suggests that no mobile radical carrier, including 3MP· and thermal hydrogen atoms, is produced subsequent to the original excitation process in γ-irradiated systems.

The alternative to the spin diffusion process has already been suggested; reaction 1 or reaction 14 produce hot hydrogen atoms that may proceed by the abstraction reaction 6 to produce a geminal pair of radicals that are restrained from reacting only by virtue of the rigidity of the matrix. However, in photolysis the intrinsically lower energies involved allow for some of the hydrogen atoms to be thermalized and give rise to a diffuse population of thiyl radicals at spacings determined by the initial concentration of EtSH. These radicals cannot react except by molecular diffusion and as a result may be detected until the matrix becomes fluid at higher temperatures. Since no such residual signal for 3MP· occurs in the γ-irradiated glasses, it must be presumed that no "isolated" 3MP· radicals are produced in the original excitation through the simultaneous production of thermal hydrogen atoms. Each act that results in the production of a 3MP· radical must also result in the production of a second, geminal partner that reacts by reaction 17 when relaxation of the matrix occurs.

The scheme outlined above for radical formation requires that decay of the 3MP· radicals should be a first order or a composite first order reaction. It has been reported that the decay is second order at 77 °K (2). We have been unable to check this result since we do not have adequate enough temperature control between 77 and 81 °K to ascertain whether the decay process is also second order in this critical temperature range.

The authors would like to express gratitude to the National Research Council of Canada, the Defence Research Board of Canada, and the United States Institute of Health, without whose financial aid this work could not have been finished. Thanks for time and help are also due to Mr. Glen Smith, Mr. David Oseen, and members of Technical Services at the University of Calgary.

1. W. H. HAMILL. *In* Radical ions. *Edited by* E. T. Kaiser and L. Kevan. Interscience. 1968.
2. J. E. WILLARD. *In* Fundamental processes in radiation chemistry. *Edited by* P. Ausloos. Interscience. 1969.
3. H. C. BOX and H. G. FREUND. J. Chem. Phys. **44**, 2345 (1966).
4. T. SHIDA and W. H. HAMILL. J. Am. Chem. Soc. **88**, 5371 (1966).
5. T. ICHIKAWA and P. K. LUDWIG. J. Am. Chem. Soc. **91**, 1023 (1969).
6. B. WISEALL and H. E. WILLARD. J. Chem. Phys. **46**, 4387 (1967).
7. S. ARAI and M. C. SAUER, JR. J. Chem. Phys. **44**, 2297 (1966).
8. D. W. SKELLY, R. G. HAYES, and W. H. HAMILL. J. Chem. Phys. **43**, 2795 (1965).
9. P. J. DYNE and O. A. MILLER. Can. J. Chem. **43**, 2696 (1965).
10. D. TIMM and H. E. WILLARD. J. Phys. Chem. **73**, 2403 (1969).
11. R. P. STEER and A. R. KNIGHT. J. Phys. Chem. **72**, 2145 (1968).
12. R. P. STEER and A. R. KNIGHT. Can. J. Chem. **47**, 1335 (1969).
13. S. B. MILLIKEN, K. MORGAN, and R. H. JOHNSON. J. Phys. Chem. **71**, 3238 (1967).

14. D. H. VOLMAN, J. WOLSTENHOLME, and S. G. HADLEY. J. Phys. Chem. **71**, 1798 (1967).
15. H. C. BOX, H. G. FREUND, and E. E. BUDZINSKI. J. Chem. Phys. **45**, 809 (1966).
16. K. AKASAKA. J. Chem. Phys. **43**, 1182 (1965).
17. W. A. ARMSTRONG and W. G. HUMPHRIES. Can. J. Chem. **45**, 2589 (1967).
18. C. NICOLAU and H. DERTINGER. Rad. Res. **42**, 62 (1970).
19. A. B. CALLEAR and D. R. DICKSON. Trans. Faraday Soc. **66**, 1987 (1970).
20. W. KARMANN, A. GRANZOW, G. MEISSNER, and A. HENGLEIN. Int. J. Radiat. Phys. Chem. **1**, 395 (1969).
21. J. G. CALVERT and J. N. PITTS. Photochemistry. John Wiley and Sons. 1966.
22. E. R. JOHNSON and A. O. ALLEN. J. Am. Chem. Soc. **71**, 1147 (1952).
23. K. J. ROSENGREN. Acta Chem. Scand. **16**, 1418 (1962).
24. T. HENRIKSEN. *In* Free radicals in biological systems. *Edited by* M. S. Blois. Academic Press. 1961.
25. Y. KURITA. Bull. Chem. Soc. Jap. **40**, 94 (1967).
26. K. FUEKI and Z. KURI. J. Am. Chem. Soc. **87**, 923 (1965).
27. S. ADITYA and J. E. WILLARD. J. Am. Chem. Soc. **88**, 229 (1966).
28. F. C. ADAM. To be published.
29. A. TORIKAI, S. SAVVADA, K. FUEKI, and Z. KURI. Bull. Chem. Soc. Jap. **43**, 1617 (1970).
30. P. M. JOHNSON and A. C. ALBRECHT. J. Chem. Phys. **44**, 1845 (1966).
31. J. A. KERR. Chem. Rev. **66**, 465 (1966).
32. K. YANG. J. Phys. Chem. **67**, 562 (1963).
33. B. A. THRUSH. Reactions of hydrogen atoms in the gas phase. *In* Progress in reaction kinetics, Vol. III, *Edited by* G. Porter, Pergamon Press, 1965.
34. J. J. J. MYRON and R. H. JOHNSON. J. Phys. Chem. **70**, 2951 (1966).
35. Handbook of Chemistry and Physics. 50th ed., chemical Rubber Co. 1970.
36. F. K. TRUBY. J. Chem. Phys. **40**, 2768 (1964).

Can. J. Chem. Downloaded from www.nrcresearchpress.com by 210.87.254.40 on 09/05/12
For personal use only.

Can. J. Chem. Downloaded from www.nrcresearchpress.com by 210.87.254.6 on 09/05/12
For personal use only.

The Analytical Reduction of Porphyrins to Pyrroles[1]

R. A. CHAPMAN,[2] M. W. ROOMI,[3] T. C. MORTON,[4] D. T. KRAJCARSKI, AND S. F. MACDONALD
Biochemistry Laboratory, National Research Council of Canada, Ottawa, Canada

Received June 21, 1971

When porphyrins or related pigments are reduced by HI–AcOH, their meso-substituents (R = H or alkyl) appear as α-CH_2R groups in the resulting pyrroles. The identification of the pyrroles, as by g.l.p.c., defines and orders the meso-substituents flanking each pair of peripheral substituents in the porphyrin. If one meso-substituent differs from the others, all the substituents about the two adjacent pyrrole nuclei are then ordered.

The pyrroles can be reductively alkylated *in situ*, and symmetry then reduces their number when the aldehyde used (R.CHO) corresponds to a bridge and its meso-substituent. This may simplify the pyrrole mixtures, identify meso-substituents, or make pyrroles distinguishable by g.l.p.c.

The critical pyrrole – propionic acids are separable as methyl esters by g.l.p.c. Desoxophylloerythrin and pyrophaeophorbides (the latter first reduced with potassium borohydride) are reduced to cyclopenteno-pyrroles which reveal the isocyclic rings and the 5-substituents. The r.r.t.'s of relevant pyrroles are reported.

La réduction des porphyrines et des pigments du même genre par HI–AcOH fait que les substituants méso (R = H ou alkyle) apparaissent sous forme de groupements CH_2R en α des pyrroles résultants. L'identification des pyrroles par c.p.l.g., par exemple, définit et classe les substituants méso qui se trouvent à côté de chaque paire de substituants périphériques dans la porphyrine. Si un des substituants méso diffère des autres, tous les substituants autour des deux noyaux pyrroles adjacents sont alors classés.

L'alkylation réductive *in situ* des pyrroles peut réduire par symétrie le nombre de pyrroles lorsque l'aldéhyde utilisé (R.CHO) correspond au pont et au substituant méso de la porphyrine initiale. Ceci peut simplifier le mélange des pyrroles, identifier les substituant méso et différentier les pyrroles par c.p.l.g.

Les acides critiques pyrrole – propioniques sont séparables de leurs esters méthyliques par c.p.l.g. La désoxophylloérythrine et les pyrophaephorbides (ces dernières d'abord réduites par le borohydrure de potassium) sont réduites en cyclopenténo-pyrroles, ce qui révèle les noyaux isocycliques et les substituants en 5. Les données t.r.r. des pyrroles correspondants sont rapportées.

Canadian Journal of Chemistry, **49**, 3544 (1971)

The pairs of peripheral substituents on porphyrins and related pigments are now usually determined by identifying the maleinimides or the pyrrole-2,5-dicarboxylic acids resulting when the pigments are oxidized with chromic acid or with permanganate, respectively. The maleinimides have been separated and identified by g.l.p.c., by g.l.p.c. and mass spectra, t.l.c., or by t.l.c. and mass spectra (1–3, 60), the pyrrole-2,5-dicarboxylic acids by paper chromatography (4). Chromic acid is usually preferred because it gives much higher yields and these can be significant when two identical pairs of peripheral substituents are present. However, permanganate has advantages: while permanganate degrades isocyclic rings to carboxyl, chromic acid destroys the pyrrole ring bearing either of these groups. The reference pyrrole-2,5-dicarboxylic acids are also more generally available synthetically than are the corresponding maleinimides.

To the same end, the pigments had been reduced by HI–AcOH at 100° to mixtures of homologous pyrroles, meso-substituents being absent or ignored (Scheme 1, $R^1 = R^2 = H$). This method was abandoned for the yields were divided among homologues, complex mixtures of labile pyrroles had to be separated by fractionating the picrates, and some pyrroles do not form picrates. Although some of the purely alkyl pyrroles were recently separated by g.l.p.c., the chromic acid method was more suitable for more complex pigments (1). The chief disadvantage of the HI–AcOH reduction had been avoided by reducing the pigments and *C*-methylating the pyrroles in one step with KOMe—MeOH at 220° (*5a*, *b*). One tetra-alkyl pyrrole then replaced four homologues (Scheme 1), but propionic acid side-chains were partially replaced by methyl (6).[5]

[1]NRCC No. 12141.
[2]NRCC Postdoctorate Fellow 1967–1969.
[3]NRCC Postdoctorate Fellow 1968–1970.
[4]NRCC Postdoctorate Fellow 1970.

[5]This suggests a reversed Michael addition followed by methylation. The analogous thermal fission of 2,4-dimethyl-5-carbethoxy-3-(2,2-dicarboxyethyl)-pyrrole dihydrazide to 2,4-dimethyl-5-carbethoxy-pyrrole (7) is interesting because perhaps facilitated by the formation of a pyrazolidone.

Can. J. Chem. Downloaded from www.nrcresearchpress.com by 210.87.254.6 on 09/05/12
For personal use only.

Although chromic acid oxidation is unique in revealing the reduced pyrrole ring in chlorins and phaeophorbides as a succinimide (1, 8), the HI–AcOH reduction had potential advantages. It was unnecessary to reduce α-hydroxyethyl side-chains to prevent further degradations. The reagent was an excellent solvent, used in indefinite excess, and easily removed. The total yields were also competitive and the products more volatile. Three considerations (9) then made the reductive method more attractive: reference pyrroles were now more easily available, the pyrrole mixtures could be simplified by reductive methylation *in situ*, avoiding KOMe—MeOH at 220°, and it was possible that meso-substituents in the pigments might be retained on the pyrroles. The implications of these are developed in Scheme 1, where the rôle of alkylation is rationalized and extended. It should be noted that vinyl or α-hydroxyethyl groups are converted to ethyl, and that ring carbethoxy or acetyl groups are split off by HI–AcOH.

Scheme 1 assumes that all and only the indicated C—C fissions will take place. The only experimental evidence here lay in the pyrroles obtained by reducing porphyrins lacking meso-substituents, particularly hemin, and in the reduction of meso-methyl-dipyrrylmethanes to α-free and α-ethyl-pyrroles (10). Not all the expected pyrroles were obtained from coproporphyrin (5*b*), but the methods of isolation were presumably inadequate.

The assumption in Scheme 1 differs only in emphasis from what was apparently Küster's interpretation of the reduction of hemin: that it was reduced to monopyrroles because α,α-dipyrrylmethane bridges, but only these, would undergo reductive fission (11). Although this led him to the correct structure for the porphin nucleus in 1912, the central 16-membered ring was unacceptable at that time (12*a*), and only synthetic evidence for the structure (symmetry) of the nucleus was acceptable much later (5*f*).

In the meantime Küster's idea was apparently regarded as an *ad hoc* assumption supporting an impossible structure. However, analogous reductions had previously been correctly interpreted in the same way by Boehm (13): the reductive fission of linear methylene-bis-phloroglucin derivatives in male fern by zinc and alkali. More generally, the reduction of porphinogens, the intermediates in the HI–AcOH reduction of porphyrins, is analogous to many reductive fissions of C—O, C—N, and C—C bonds:

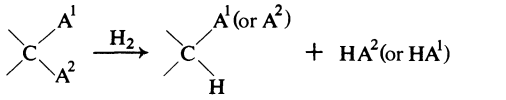

where A^1 = or ≠ A^2, and both are such that A^- and are usually regarded as stabilized; in porphinogens, here represents a bridge.

Küster's assumption was confirmed (although its reasonableness was denied) when a 1,2-di-(α-pyrryl)-ethane, unlike dipyrrylmethanes, proved stable to HI–AcOH (14). It was then concluded that the α-pyrryl residues in hemin could hardly be linked through two carbon atoms, but the result was not used to eliminate the two rival porphyrin structures (5*f*) and a third which arose later (5*g*). All three would require that the porphyrins reduce to derivatives of two pyrroles and a 1,2-dipyrrylethane. The confusion is further illustrated by an apparent attempt to find a hydrocarbon, representing the γ-substituent or the γ-bridge, among the reduction products of phylloporphyrin (15). However, in a return to Küster's interpretation and its implications, the absence of α-ethyl derivatives among the pyrroles was somewhat tentatively cited as evidence for the absence of meso methyl groups in hemin (16). Ironically, α-ethyl pyrroles from hemin had been reported (5*b*); although the methods then current were probably inadequate to decide their existence, hindsight had rejected them as unlikely (17).

The presence of meso-substituents in a pigment has been inferred from a missing methine C*H* signal in the n.m.r. spectrum, or by degrading the pigment to a porphyrin with a "phyllo-type" visible spectrum. The substituent was then identified and located by identifying the porphyrin with a synthetic one. Similarly, although the pairs of peripheral substituents in a pigment could be determined analytically, their further ordering depended ultimately upon the identification of an analytical with a synthetic porphyrin. In both cases the possible structures might be limited by empirical rules governing spectra etc. or by biogenetic ideas. However, the former could be misleading if based on an unforeseeably in appropriate model, *cf.* (18, 19), and the relevance of the latter may be in question, *cf.* petroporphyrins (20).

Can. J. Chem. Downloaded from www.nrcresearchpress.com by 210.87.254.6 on 09/05/12
For personal use only.

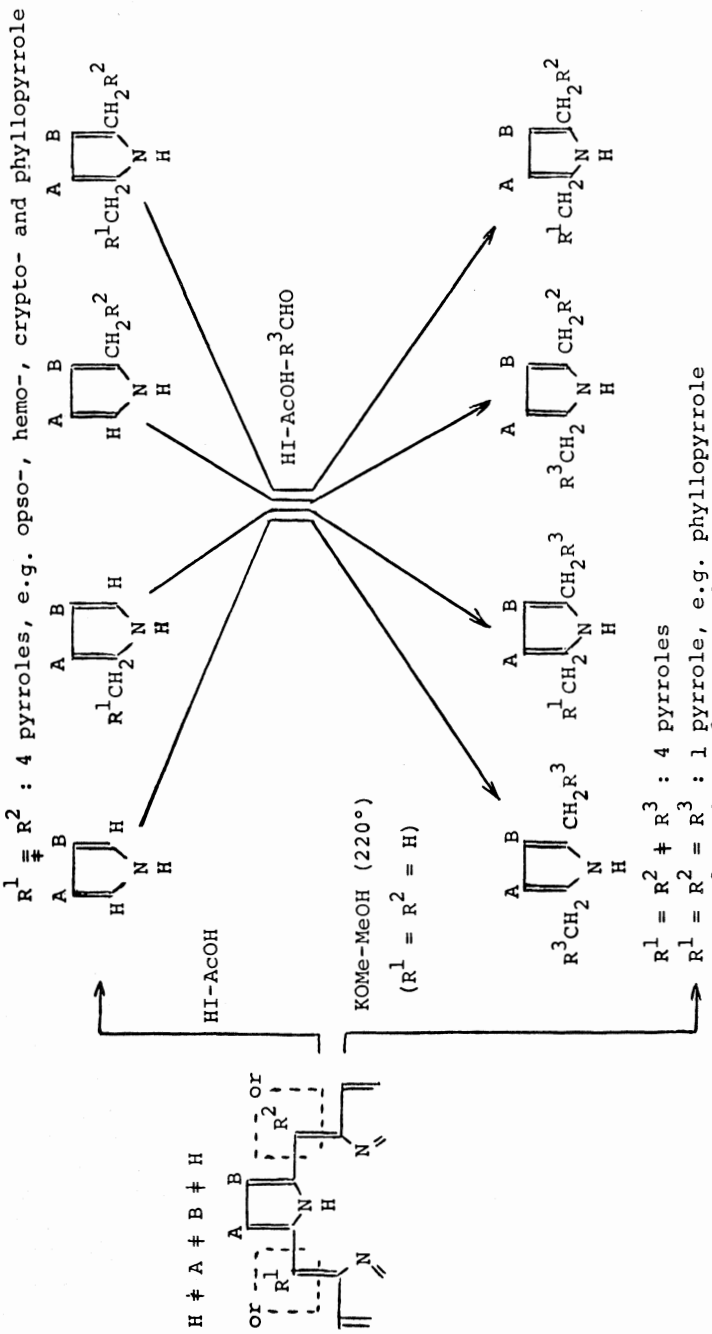

SCHEME 1. Pyrroles expected from one pyrrole nucleus in a porphyrin.

Can. J. Chem. Downloaded from www.nrcresearchpress.com by 210.87.254.6 on 09/05/12
For personal use only.

Scheme 1 implies that the identification of the pyrroles obtained by reduction will identify and locate the meso and peripheral substituents about a pyrrole nucleus in a pigment and, if any meso-substituent (R^2) is different from the others, all the substituents about the two adjacent pyrrole nuclei:

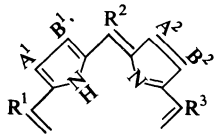

On the other hand, methylation will be fully effective in simplifying the pyrrole mixtures only in the absence of meso-substituents in the pigment. Some further implications of Scheme 1 are inescapable; these will be illustrated by the examples in Tables 1 and 2.

Tables 1 and 2 show the products expected from the pyrrole nuclei of typically substituted porphyrins. The products are those required by Scheme 1 but some represent special cases wherein a peripheral position is unsubstituted (A or B = H, becoming CH_2R^3 after alkylation), or one of the meso-substituents (X) is sufficiently large that the pyrroles bearing it do not appear with the others on g.l.p.c. The products from the reduced ring 4 of phorbins and chlorins should be unreduced pyrroles (15), the same as those from ring 4 of the corresponding porphyrins. Examples (*i*), (*j*), and (*k*) in Table 2 with large meso-substituents (X) will then represent the simplest model for ring 4 of pyrophaeophorbides and desoxophylloerythrin. The relative retention times (r.r.t.) in the tables were determined with reference pyrroles (see below), and the logarithmic scale suggests the separabilities, *e.g.* the pyrroles **2** and **3**, like **21** and **23**, could be distinguished by their r.r.t.'s but ran together under one peak.

Ignoring the r.r.t.'s in these examples, the following information could be obtained merely by counting the pyrroles and by noting whether or not the highest pyrrole homologue obtained by reduction was unchanged by alkylation, *i.e.* was a tetra-alkylpyrrole. A large meso-substituent would be recognized, but only as such, when reduction gave two pyrroles as in examples (*i*), (*j*), and (*k*). All other meso-substituents would be identified by the aldehyde used when the number of pyrroles was reduced from four to one as in

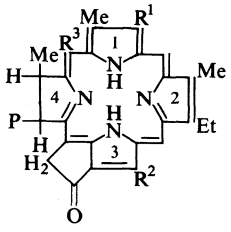

Pyrophaeophorbides

R^1 = $CH{:}CH_2$; R^2 = Me; R^3 = H:
Pyrophaeophorbide-*a*
R^1 = $CH(OH)CH_3$; R^2 = Et; R^3 = H:
Chlorobium phaeophorbide 650 fraction 4
R^1 = $CH(OH)CH_3$: R^2 = Et; R^3 = Me:
Chlorobium phaeophorbide 660 fraction 5

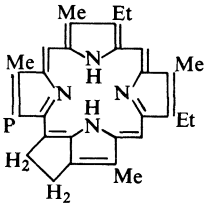

Desoxo-phylloerythrin

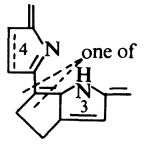

Assumed fissions

(*a*), (*b*), (*c*), (*d*), and (*g*), from three to one (see below), from four to two as in (*e*), (*f*), and (*h*), or from two to one as in (*i*) and (*j*). In the absence of a large meso-substituent (more than two pyrroles on reduction), no pyrrole common to the three chromatograms would show that one or both of the peripheral positions was unsubstituted as in (*c*), (*d*), and (*f*). The peripheral substituents would not be further defined unless the meso-substituents were identical. If they were, reduction would give three pyrroles if A = B (*cf.* Scheme 1; no examples in Tables 1 and 2); A and B would then be an alkyl group if there was a pyrrole common to the three chromatograms, H if not, and the aldehyde defining the meso-substituents here would convert the three pyrroles to one. If the meso-substituents were identical and A = H, B = alkyl as in (*c*) and (*d*), B would usually be identifiable. In (*d*), the general case, one aldehyde would identify the meso-substituents as usual by converting four pyrroles to one in which the 2- and 5-substituents were identical, and another aldehyde would identify B by converting four pyrroles to three in which the 3- and 4-substituents were B. In (*c*), the degenerate case wherein B (Me) is the next higher homologue of the meso-substituent (H), B could not be identified because the aldehyde identifying the meso-

Can. J. Chem. Downloaded from www.nrcresearchpress.com by 210.87.254.6 on 09/05/12
For personal use only.

TABLE 1. Alkyl pyrroles expected from the pyrrole nuclei of typical porphyrins, and their r.r.t.'s at 75°

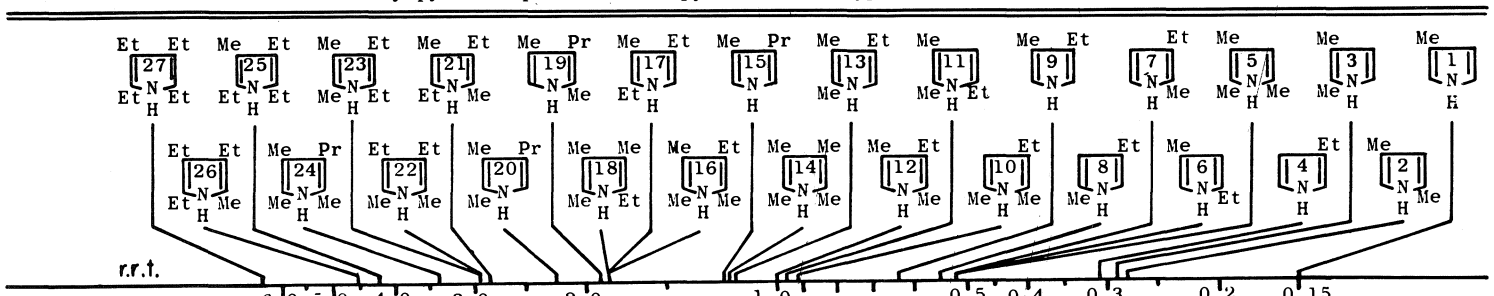

Pr = nC$_3$H$_7$

(a)	HI									16		13	12		9									
	HI-H_2CO									16														
	HI-MeCHO				25		23,21			16														
(b)	HI					24		20	19			15												
	HI-H_2CO					24																		
(c)	HI														5		3,2		1					
	HI-H_2CO											14												
	HI-MeCHO				25		23,21			16														
(d)	HI												10		8,7		4							
	HI-H_2CO									16														
	HI-MeCHO	27		26		22																		
(e)	HI						21			17			12		9									
	HI-H_2CO						21			16														
	HI-MeCHO				25		21																	
(f)	HI												11		6		3		1					
	HI-H_2CO									18		14												
	HI-MeCHO				25		23																	

TABLE 2. Pyrrole esters expected from the pyrrole nuclei of typical porphyrins, and their r.r.t.'s at 135°

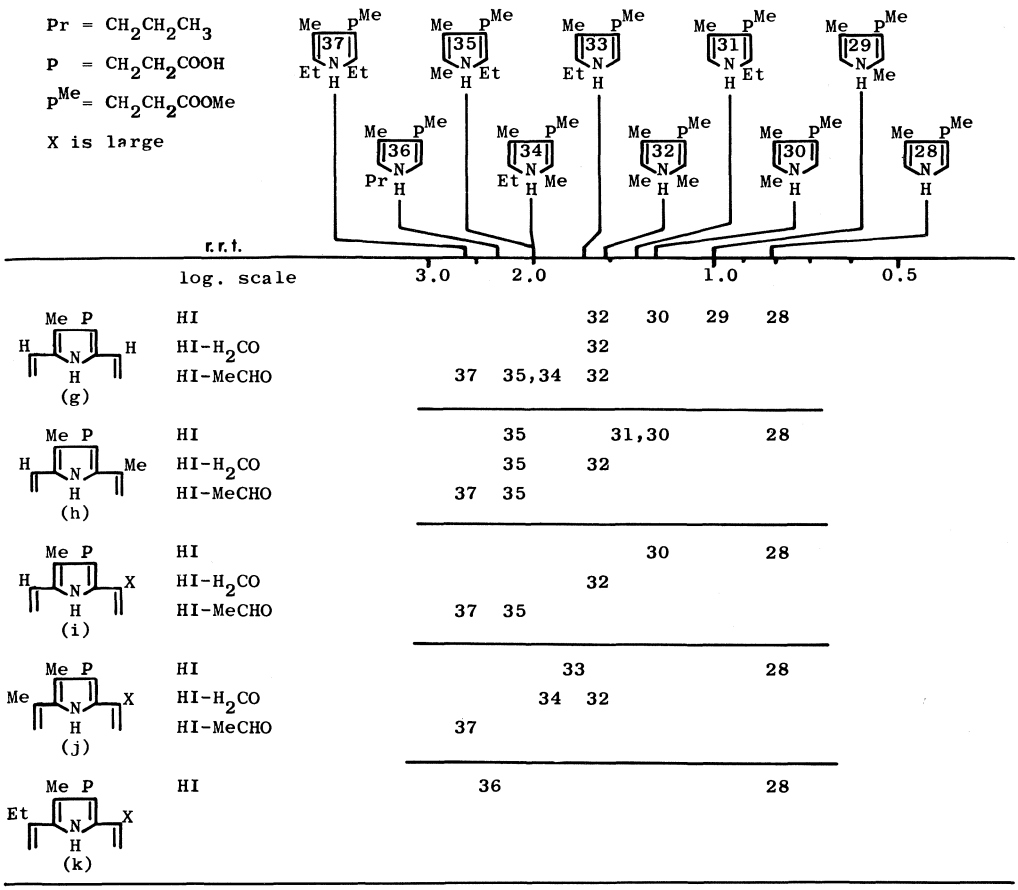

(g)	HI			32	30	29	28
	HI-H_2CO			32			
	HI-MeCHO	37	35,34	32			
(h)	HI		35		31,30		28
	HI-H_2CO		35	32			
	HI-MeCHO	37	35				
(i)	HI				30		28
	HI-H_2CO			32			
	HI-MeCHO	37	35				
(j)	HI			33			28
	HI-H_2CO		34	32			
	HI-MeCHO	37					
(k)	HI	36					28

substituents would also make the 3- and 4-substituents on the pyrroles identical.

The practicability of the methods suggested here depends, although in varying degrees, on the extent to which all and only the expected pyrroles are formed and are distinguishable. The following was clear from the behavior of reference pyrroles (see below). All the pyrroles expected from naturally substituted porphyrins were sufficiently stable in HI–AcOH at 110°, although opsopyrrole–carboxylic acid, **28**, unlike phyllopyrrole–carboxylic acid, **32**, was reportedly destroyed at 130° (15). This is fortuitous, for the instability of some pyrroles expected from unnaturally substituted porphyrins would result in missing pyrroles or extra ones. There was also no evidence that the pyrroles were alkylated significantly in HI–AcOH through scavenging. It may be significant here that cryptopyrrole was unchanged in hot HI–HCOOH, although we had expected that it would be converted into the dipyrrylmethene and thence into the fully methylated phyllopyrrole, *cf.* dipyrrylmethenes from pyrroles and HBr–HCOOH (5*h*). The methylations and ethylations were also clean. On the other hand, it was clear from the r.r.t.'s of the reference pyrroles that overlapping peaks would limit the usefulness of counting methods, *e.g.* the situation in example (*c*) would be confused with that in (*d*) because the pyrroles **21** and **23** appear under one peak.

The assumption in Scheme 1 governing the reduction remained to be tested. Twelve typical porphyrins of known structure were reduced in HI–AcOH at 110° and the products were submitted to g.l.p.c. before and after alkylation, the latter being effected by adding paraformaldehyde or paraldehyde to the mixture and continuing the heating. Mass spectra were used only occasionally for they do not readily distinguish

Can. J. Chem. Downloaded from www.nrcresearchpress.com by 210.87.254.6 on 09/05/12
For personal use only.

Can. J. Chem. Downloaded from www.nrcresearchpress.com by 210.87.254.6 on 09/05/12
For personal use only.

isomeric alkyl pyrroles with the same substituents (21). Chromatograms like those in Charts 1 and 2 were obtained only after several sources of extraneous peaks had been eliminated; this was our major effort. The peaks to the right of the ester peaks in Chart 2 correspond to incompletely removed alkyl pyrroles and become more obvious when shifted by alkylation. The numbers identifying the pyrroles correspond to those of the pyrroles in Tables 1 and 2.

The validity of the assumption (Scheme 1) may be judged by the extent to which the chromatograms represent the examples (Tables 1 and 2) or composites thereof. A subjective element exists here whenever the base lines depart from the horizontal, but the following general remarks apply equally to the chromatograms not reproduced here. There were no peaks in the chromatograms not attributable to pyrroles even when the yields were low, and although the g.l.p.c. detector is less specific than the diazonium salt or chlorine-benzidine used in the paper chromatography of pyrrole dicarboxylic acids or the t.l.c. of maleinimides. In particular, reduced pyrroles were not detected, *cf.* (12*b*). An unexpected pyrrole peak appeared among the esters from pyrophaeophorbides, and others appeared among the alkyl pyrroles if these pigments were first reduced with potassium borohydride (see below). Otherwise all the definite peaks were anticipated. This was surprising if only because any "scrambling" of the porphinogens in hot acid[6] would result in the loss of translocation of bridges.

[6]"Scrambling" refers to intermolecular redistribution reactions of porphinogens in hot acid leading to new porphinogens in which the pyrrole nuclei are randomized (22) and added formaldehyde may form the bridges (23). Analogous reactions have been observed in dipyrrylmethanes (24) and in their meso-alkyl derivatives (25); the latter may also lose their bridges with KOMe—MeOH at 220° (6, 26). It will be clear from the following expressions that the reductive C—C fissions and "scrambling" have the same structural requirements, and that the latter is analogous to many more familiar reactions:

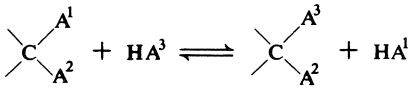

a special case of which is

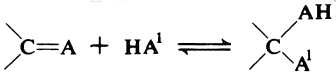

where A, A^1, A^2, A^3 are defined as above. Syntheses of unsymmetrical dipyrrylmethanes and dipyrrylmethenes may give symmetrical products in the same way.

The chromatograms also showed significant peaks corresponding to all the expected pyrroles. Although this was meaningless when a peak represented more than one pyrrole, some components appeared alone when other porphyrins were reduced, and some others could be identified unambiguously after the pyrroles were alkylated (see comments on the chromatograms below). In the absence of evidence to the contrary, it may reasonably be assumed that all the expected pyrroles will appear on the chromatograms, and some significance may be attributed to their absence. Incidentally, stoichiometry requires equal amounts of 2,5-dialkylpyrroles and 2,5-free pyrroles except from phaeophorbides, and the somewhat larger amounts of the former may reflect their greater stability.

Aside from the extra peaks mentioned above, the assumption underlying Scheme 1 appears to be justified, and the chromatograms can be inferred from the structures of the porphyrins. However, the structural information available from the chromatograms is limited by overlapping or ambiguous peaks and by other factors. When less than four differently substituted nuclei are found, qualitative data will not show when this is because two or more are identically substituted, and awkward possibilities then arise unless it can be assumed that large substituents are absent and all the products appear on the chromatograms. For this reason, and because the peripheral substituents would not all be ordered unless there were four different meso-substituents, the structures of more complex porphyrins will be more completely determined. The following discussion of the chromatograms will illustrate this and introduce some variations in the method.

The chromatograms of the alkyl pyrroles and pyrrole esters from hemin (Charts 1 and 2) and the r.r.t.'s of the reference pyrroles (Tables 1 and 2) define all the substituents about two pyrrole nuclei as those in examples (*a*) and (*g*). Ignoring the r.r.t.'s in each case, the patterns before and after methylation indicate unambiguously two different peripheral substituents, neither H, and no meso alkyl substituents. Only two differently substituted pyrrole nuclei are identified but the peripheral substituents on a third are also as in example (*a*) because the yields of the alkyl pyrroles were 64% of 2 mol before methylation and 70% after; the yield of the esters was 42%, 35% after methylation and 18% after

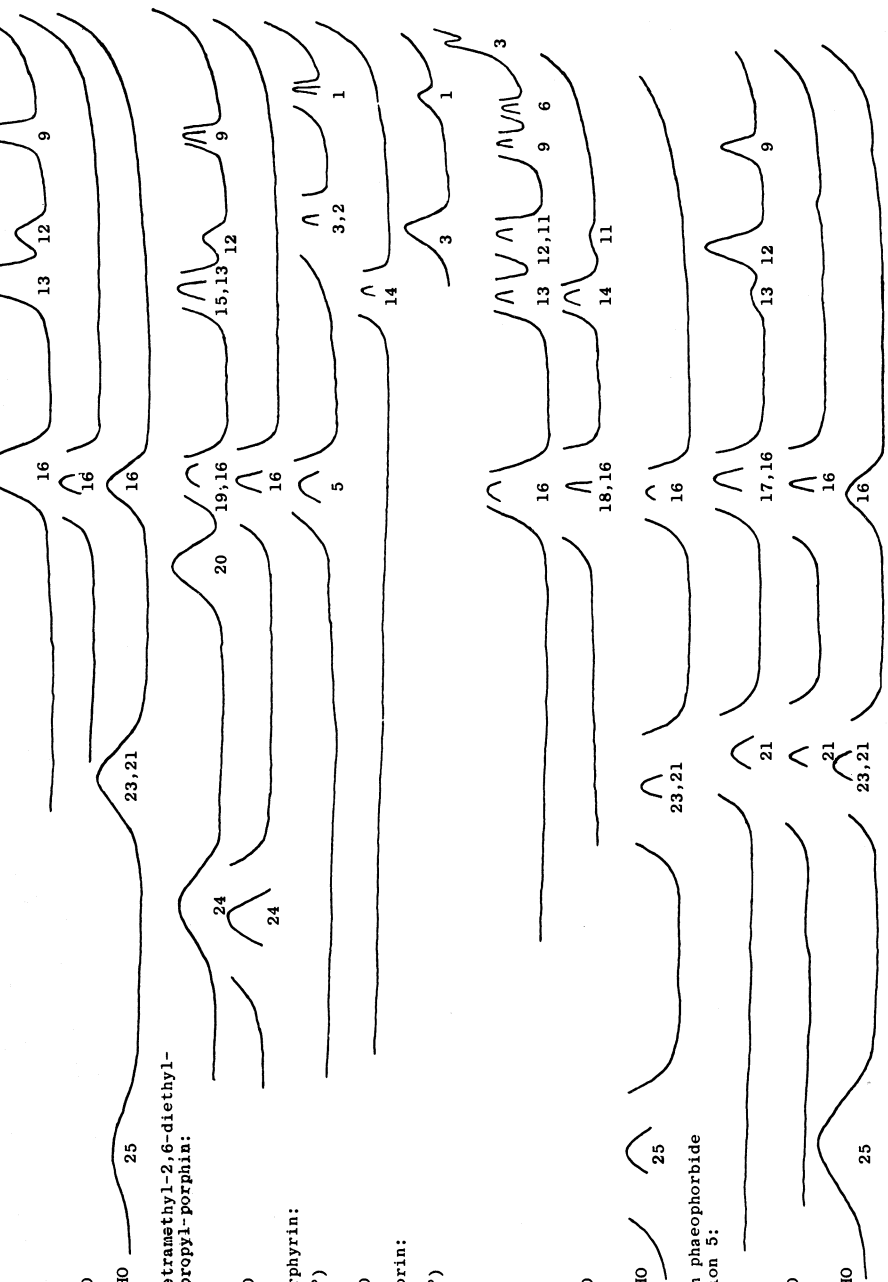

CHART 1. The g.l.p.c. of alkyl pyrroles from porphyrins, at 75° unless specified.

Can. J. Chem. Downloaded from www.nrcresearchpress.com by 210.87.254.6 on 09/05/12
For personal use only.

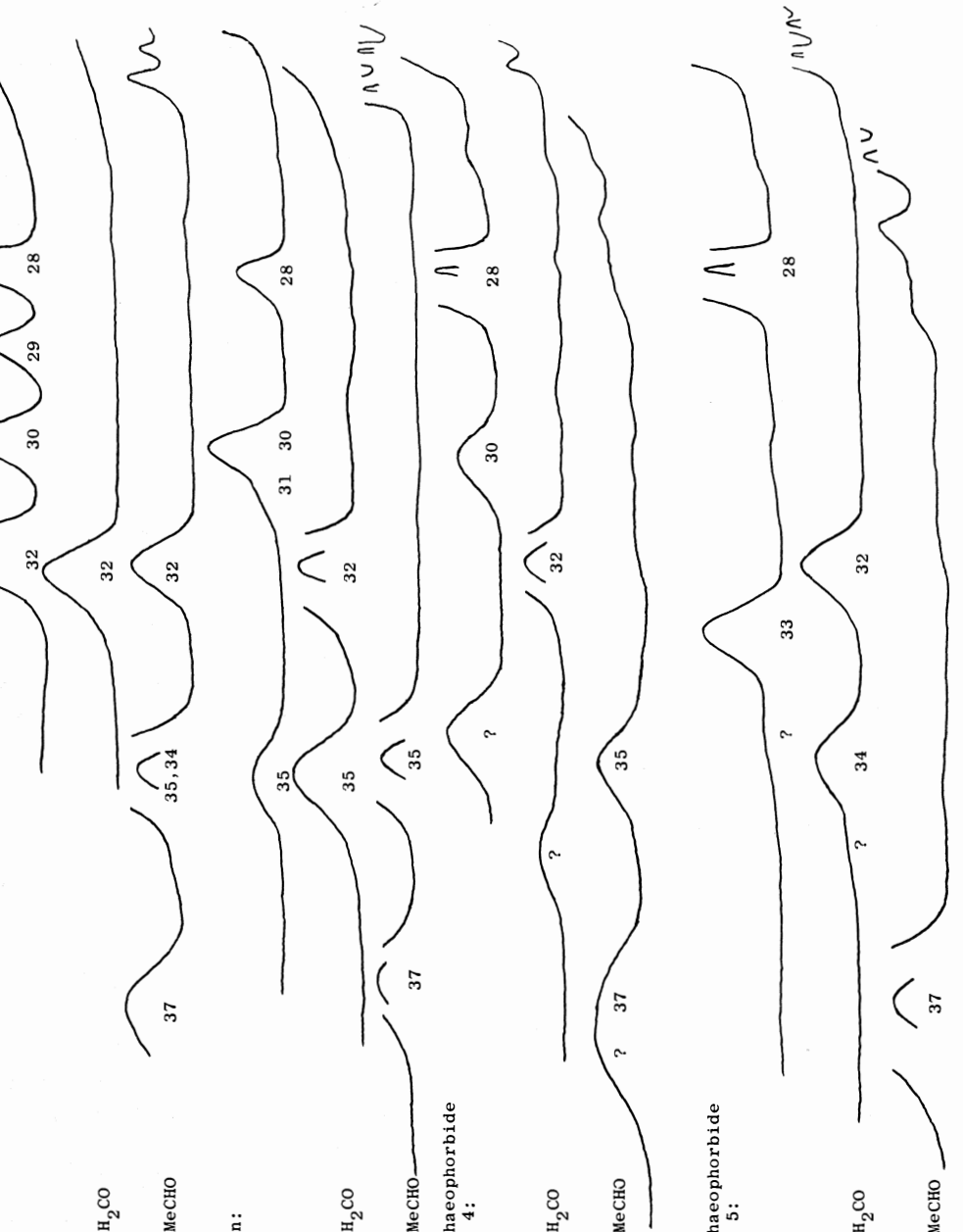

CHART 2. The g.l.p.c. of pyrrole esters from porphyrins at 135°.

Can. J. Chem. Downloaded from www.nrcresearchpress.com by 210.87.254.6 on 09/05/12
For personal use only.

Can. J. Chem. Downloaded from www.nrcresearchpress.com by 210.87.254.6 on 09/05/12
For personal use only.

ethylation. Largely because only two differently substituted nuclei are identified, the chromatograms would not exclude a structure with three nuclei as in (*a*) and one as in (*g*), or a large substituent, but a meso methyl or ethyl group is excluded. The chromatograms of the alkyl pyrroles from hemin, etioporphyrin *1*, pyrophaeophorbide-*a*, and Chlorobium chlorophyll 650 fraction 4 were essentially the same, as were those of the pyrrole esters from hemin, coproporphyrin *3*, and deuteroporphyrin *9*.

The peaks in the chromatograms from 1,3,5,7-tetramethyl-2,6-diethyl-4,8-di-*n*-propyl-porphin are identified by their r.r.t.'s as the pyrroles from (*a*) and (*b*). The composite pattern alone is ambiguous but it illustrates the simplification of pyrrole mixtures and one method for the resolution of composite peaks by alkylation.

The chromatograms of the alkyl pyrroles from deuteroporphyrin *9* and the r.r.t.'s of the reference pyrroles identify a nucleus substituted as in (*c*). The unmethylated pyrroles were run at a lower temperature here to reveal 3-methylpyrrole. After ethylation, the chromatogram (not shown) was like that of the ethylated pyrroles from hemin. The pattern alone correctly shows the unsubstituded meso positions and peripheral hydrogen. However, as the pyrroles **2** and **3** run together as do **21** and **22** (see the chromatograms from hemin), the pattern is that of a nucleus without meso or peripheral substituents. The chromatograms of the alkyl pyrroles from deuteroporphyrin *9* and from methyl 1,4,5,8-tetramethylporphin-2,3,6,7-tetracarboxylate were essentially the same.

The chromatograms of the alkyl pyrroles from diacetyl-deuteroporphyrin *9* were like those from deuteroporphyrin *9*, the acetyl groups being lost. However, their presence was evident when diacetyl-deuteroporphyrin was first reduced with potassium borohydride to hematoporphyrin. When the latter was reduced with HI–AcOH, the chromatogram showed the peaks of **12**, **13**, **16** together with unidentified peaks with higher r.r.t.'s, but no peaks of **2**, **3**, or **5**.

The r.r.t.'s of the alkyl pyrrole peaks from phyllochlorin except those marked **1**, **3**, **6**, and **14**, identify a nucleus substituted as in (*a*). Their yield was 49% of 2 mol as **9**, **13**, and **16**, aside from the contribution of **12**. This requires a second nucleus with peripheral substituents as in (*a*) wherein one meso-substituent might be a large alkyl group but not methyl. The remaining alkyl peaks and the ester peaks then each represent a single nucleus. The pyrrole **1** is identified unambiguously, the distinctive peak of 2-ethyl-3-methylpyrrole (r.r.t. 0.46) is absent, and alkyl groups moderately higher than ethyl would be evident after alkylation. The other set of alkyl pyrrole peaks is then either **1**, **3**, **6**, and **11** as indicated, or **1**, **2** with **3**, and **5**; these represent nuclei substituted as in (*f*) or (*c*), respectively. In principle, the two sets could be distinguished by propylation: were **5** present, it would appear among the products as the distinctive peak of 2,4,5-trimethyl-3-*n*-propylpyrrole; the data are in Table 3. The method is not yet practicable because a small peak coinciding with this one has not yet been eliminated from the propylation blank. Another way of distinguishing the two sets appears to have been found. When **11** and **12** are methylated to **18** and **16**, respectively, **11** disappears in 70 min, **12** in 25 min; **6** is equivalent to **11** here, to which it is even more rapidly methylated. The persistence of the **12**/**11** peak after methylation (1 h but not much longer) can then be attributed to **11** and **6**, and there is a nucleus substituted as in (*f*). A fourth nucleus is identified as in (*h*) by the chromatograms of the esters. As the latter represent only one nucleus, a favorable situation typical of many chlorophyll derivatives, their pattern alone would identify the meso-substituents. The following nuclei are then determined.

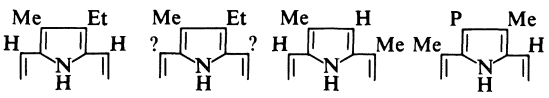

(*a*) (*f*) (*h*)

The meso-substituents on the second of these must be H, the only one allowed (see above) which has counterparts on the other three nuclei. The nuclei may be assembled in only four ways. One represents the skeleton of phyllochlorin, and the other three differ in the order of the peripheral substituents (Me and Et) on rings 1 and 2. The chromatograms from γ-phylloporphyrin *15* differed from these only in being cleaner, in having the shoulder of **31** better developed, and in the higher yields (alkyl pyrroles 70%, esters 39%).

Chromic acid oxidation will reveal the reduced ring 4 in phyllochlorin as a succinimide but it will not distinguish between 120 skeletons, *i.e.* 96

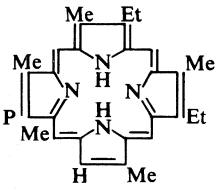

γ-Phylloporphyrin **15**

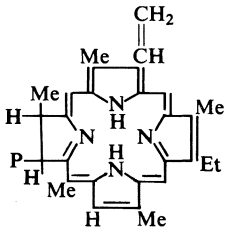

Phyllochlorin

phylloporphyrins, and 24 pyrroporphyrins which lack the meso methyl group. Not only is the meso methyl group easily identified and located by reduction, but its presence allows the structure of the porphyrin to be more completely determined, for the substituents on the two flanking nuclei can then be ordered.

From pyrophaeophorbides (see above), Scheme 1 requires the usual number of pyrroles from rings 1 and 2 but not from rings 3 and 4. One mode of fission between the latter would yield only four non-volatile derivatives of 1-(3-pyrryl)-3-(2-pyrryl)-propanone-1. The other fission would yield two pyrrole esters from ring 4, as in examples (*i*), (*j*), (*k*) (Table 2), and two ketocyclopenteno-pyrroles from ring 3. Presumably the higher r.r.t.'s of the last two would prevent their appearance with the alkyl pyrroles, and no serious attempt was made to detect them. Despite the threat of fissions about the carbonyl group, the chromatograms from the pyrophaeophorbides conform to this model except that an extra peak (r.r.t. 1.91 before alkylation) appears with the esters. As the same peak appeared whether the 5-position on ring 3 bore methyl or ethyl groups, it presumably represents ring 4. However, it has not yet been identified with any of several pyrrole – 2-propionic acids and pyrrole – 3-propionic acids made for the purpose. In the interpretation of the chromatograms, it can only be ignored in the hope that its ultimate identification will be revealing rather than confusing, *cf.* other extra peaks discussed below. It was most obvious among the peaks of the pyrrole esters from pyrophaeophorbide-*a*, least so among those from Chlorobium phaeophorbide 660 fraction 5.

We have studied only three pyrophaeophorbides, the Chlorobium phaeophorbides 660 fraction 5 and 650 fraction 4, and pyrophaeophorbide-*a*; no phaeophorbides bearing the 10-carbomethoxy group were examined. Chlorobium phaeophorbide 660 fraction 5 provides a model for the identification of the meso alkyl groups in the higher Chlorobium phaeophorbides 660, and for the confirmation of their location on the δ-positions. The structures of the lower members, fractions 5 and 6, had been determined, in part, by degrading them to δ-phylloporphyrins. This method was impracticable with the higher members because their degradations involved progressively lower yields, and some of these fractions occurred in relatively small amounts. The comparison of the results from the Chlorobium phaeophorbides 660 fraction 5 and 650 fraction 4, or from the latter and pyrophaeophorbide-*a*, were instructive because the two former differ only on the δ-position and the latter two differ significantly only on ring 3. The results from Chlorobium 650 fraction 4 and from pyrophaeophorbide-*a* suffice for these comparisons, but they are limited by the availability of the former, and by the yield of pyrroles from the latter: alkyl pyrroles 45% of 2 mol, esters 9% before methylation and 7% after.

As expected, the chromatograms from Chlorobium phaeophorbide 650 fraction 4 and from pyrophaeophorbide-*a* were the same. The 2-substituents on both were reduced to ethyl, and the pyrroles from ring 3 were not represented. The chromatograms of the alkyl pyrroles, the same as those of the alkyl pyrroles from hemin, identified one nucleus substituted as in example (*a*), but the yields were not high enough to reveal the second. It is typical of this method that no such difficulty would arise were rings 1 and 2 differently substituted as in all the higher Chlorobium phaeophorbides. Provided the anomalous peaks are ignored, the chromatograms of the esters and the r.r.t.'s of the reference pyrroles require a nucleus substituted as in (*i*), and the absence of a meso-substituent on the δ-position is revealed by the pattern alone.

The chromatograms of the alkyl pyrroles from Chlorobium phaeophorbide 660 fraction 5 (yield 75% of 2 mol) require a nucleus as in example (*a*) giving rise to the pyrroles **9**, **12**, **13**, **16**, and a second nucleus with the same peripheral substituents giving rise to **21** (as indicated) or **23**. All the cognates of **21**, *i.e.* **9**, **12**, and **17** from a nucleus as in (*e*), would be accommodated under the other peaks. All those of **23** would not, for 2,3-diethyl-4-methylpyrrole would be a distinct peak of r.r.t. 1.62. In the absence of this pyrrole, propylation confirmed **17** unambiguously (Chart 3 and the r.r.t.'s in Table 3), and thus the second

Can. J. Chem. Downloaded from www.nrcresearchpress.com by 210.87.254.6 on 09/05/12
For personal use only.

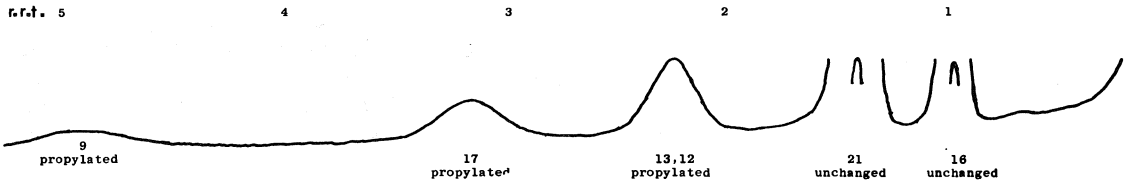

CHART 3. The g.l.p.c. of propylated alkyl pyrroles from Chlorobium phaeophorbide 660 fraction 5 at 100°.

TABLE 3. The r.r.t.'s of pyrroles*

Temperature (°C)	Substituents 5	4	3	2 H	2 Me	2 Et	2 n-C_3H_7
50	H	H	H	0.28	0.49 (43)	0.97[a]	
	H	H	Me	0.53[i] (44)	1.07 (45)		
	Me	”	”	*1.00* (5*a*)	2.21[d] (9)		
	H	Me	Et	2.74 (5*a*)	4.50[e] (46)		
	Me	”	”	5.56[b] (33)			
75	Me	H	H		0.28 (28)	0.49[c] (33)	
	Et	”	”			0.85[c,a]	
	H	H	Me	0.15[i] (44)	0.29 (45)	0.46[e] (33)	
	Me	”	”	0.28[f] (5*c*)	0.52[d] (9)	0.83[d] (46)	
	Et	”	”	0.52[f] (5*c*)	0.96[d,a]	1.46[d] (28)	
	H	H	Et	0.31[f] (47)	0.52[a]	1.10[e,a]	
	Me	”	”	0.55[d] (33)	0.92[d] (28)	1.48[d] (9)	
	Et	”	”	0.99[f] (5*c*)	1.69[d] (33)	2.50[d] (33)	
	H	Me	Me	0.32[h] (28)	0.62[e] (9)	0.98[e] (33)	
	Me	”	”		1.18[a] (5*d*)	1.86[c,a]	
	Et	”	”			2.76[b] (33)	
	H	Me	Et	0.64 (5*a*)	*1.00*[e] (46)	1.62[e] (28)	2.81[e] (36)
	Me	”	”	1.16[b] (33)	1.85[e] (46)	2.95[j] (28)	5.04[c] (33)
	Et	”	”	1.85[b] (33)	2.84[e] (46)	4.27[c] (28)	7.11[b] (33)
	H	Et	Et	1.26[h] (48)	1.96[e,a]	2.96[e,a]	
	Me	”	”		2.92[k] (5*d*)	4.60[d] (9)	
	Et	”	”			6.94[l,a]	
	H	Me	n-C_3H_7	1.21[h,a]	1.90[e] (28)	2.92[e,a]	4.98[e,a]
	Me	”	”	2.22[b,a]	3.41[b,a]	5.24[e,a]	8.77[e,a]
	Et	”	”	3.44[b,a]			
	n-C_3H_7	”	”	5.76[b,a]			
	H	Me	i-C_3H_7		1.61[e] (28)		
	Me	”	”		2.99[e] (28)		
	H	Me	n-C_4H_9		3.72[e] (28)		
	H	Me	i-C_4H_9	1.76[h,a]	2.73[e] (9)	4.14[e,a]	
	Me	”	”	3.10[b] (28)	4.86[e] (9)		
	Et	”	”	4.61[b,a]			
	H	Me	*sec*-C_4H_9		2.63[e,a]		
	Me	”	”		4.68[e,a]		
	—$CH_2CH_2CH_2$—		Me	2.00[b] (49)	3.74[b] (49)		
	—$CH_2CH_2CH_2$—		Et	3.84[b,a]	6.27[b,a]		
100	Me	Me	Et		*1.00*[e] (46)		2.35[e] (36)
	Et	”	”		1.43[e] (46)		3.15[b] (33)
	n-C_3H_7	”	”		2.26[e] (46)		4.95[e] (36)
	Me	Me	n-C_3H_7		1.68[e] (28)	2.48[e,a]	3.91[e,a]
	n-C_3H_7	”	”		3.80[b,a]	5.10[b,a]	8.00[e,a]
135	H	Me	Et		0.62[e] (46)		1.33[e] (36)
	Me	”	”	0.71[b] (33)	*1.00*[e] (46)		
	Et	”	”		1.38[e] (46)		
	n-C_3H_7	”	”	1.50[b,a]	2.00[b,a]		
	H	Me	n-C_3H_7		1.00[e] (28)	1.38[e,a]	2.00[e,a]
	Me	”	”	1.12[b,a]	1.58[e] (28)	2.12[e,a]	2.96[e,a]
	H	Me	i-C_3H_7		0.92[e] (28)		
	Me	Me	i-C_3H_7		1.38[e] (28)		
	H	Me	n-C_4H_9		1.67[e] (28)		

Can. J. Chem. Downloaded from www.nrcresearchpress.com by 210.87.254.6 on 09/05/12
For personal use only.

TABLE 3.—*Concluded*

Temperature (°C)	Substituents 5	4	3	2 H	2 Me	2 Et	2 n-C_3H_7
	H	Me	i-C_4H_9	0.96[h,a]	1.38[e] (9)	1.83[e,a]	2.59[e,a]
	Me	"	"	1.50[b] (28)	2.00[b] (28)	2.71[e,a]	3.79[e,a]
	H	Me	sec-C_4H_9		1.25[e,a]		
	Me	"	"		1.92[e,a]		
135	Me	H	P^{Me}	0.75[f] (50)			
	H	Me	P^{Me}	0.81[h] (35)	*1.00*[e] (34)	1.35[e] (36)	1.93[e,a]
	Me	"	"	1.25[b] (35)	1.52[e] (34)	2.02[e] (36)	2.83[e,a]
	Et	"	"	1.65[b] (51)	2.00[b] (51)	2.59[b] (51)	3.56[e,a]
	n-C_3H_7	"	"	2.29[b] (51)	2.73[b] (51)		
	H	Me	P	1.24[h] (35)	1.33[e] (34)		
	Me	"	"	1.86[b] (35)			

*The substituents on a pyrrole are defined by the position of its r.r.t. in the Table. In each temperature group the r.r.t.'s are relative to the R_f of the pyrrole whose r.r.t. (1.00) is in italics. A single note or reference appended to an r.r.t. refers to the preparation of the pyrrole in quantity. The first of two indicates the precursor from which the pyrrole was prepared *in situ* as described in the Experimental; the second gives the source of the precursor. (*a*) See Experimental, (*b*) from the corresponding 2-carbethoxypyrrole, (*c*) from the 3-carbethoxypyrrole, (*d*) from the 4-carbethoxypyrrole, (*e*) from the 5-carbethoxypyrrole, (*f*) from the 2,4-dicarbethoxypyrrole, (*g*) from 2,4-dimethyl-3-carbethoxypyrrole, (*h*) from the 2-carboxy-5-carbethoxypyrrole, (*i*) from 2-carbethoxy-3-methyl-4-bromo-5-carboxypyrrole, (*j*) from 2,3-dimethyl-5-carbethoxypyrrole, (*k*) from 2,5-dimethyl-3-carbethoxypyrrole, (*l*) from 2,5-diethyl-3-carbethoxypyrrole. P = CH_2CH_2COOH, P^{Me} = CH_2CH_2COOMe.

nucleus is as in (*e*). Mass spectra across the **17**/**16** peak gave no indication that it was even partially resolved. The anomalous peak is much reduced in the chromatograms of the esters here. These (yield 25%), with the r.r.t.'s of the reference pyrroles, identify a third nucleus as in (*j*); the pattern alone would indicate the meso-substituents. The pyrrole ester **33** was further identified under its g.l.p.c. peak by its mass spectrum, in which the mass peaks were those calculated and in the ratio found with the reference pyrrole: M = 195, $M - CH_3$, $M - CH_2COOMe$, $M - CH_2$-CH_2COOMe. As the **33** peak was undiminished when the HI–AcOH used had previously been heated with cryptopyrrole, it did not arise through scavenging (see under Reference Pyrroles below).

In connection with these chromatograms, it should be noted that propylation also confirmed **16** and **21** as tetraalkyl pyrroles by a method which, unlike methylation or ethylation, could not produce them from lower homologues. Further, if the analytical problem is only that of the meso alkyl group, the identification of **16** excludes its presence on the α-position. Finally, the δ-methyl group here is even more favorably situated than the γ-methyl group in phyllochlorin, for the derived pyrrole esters are better separated by g.l.p.c. Presumably there should be no difficulty in identifying and locating the meso alkyl groups in small amounts of the higher Chlorobium phaeophorbides 660.

Analytically, the isocyclic ring in chlorophylls has been identified only indirectly, and its presence prevents the identification of ring 3 by chromic acid oxidation. The indirect methods, except successive degradations, may be capriciously invalidated by other structural features. For example, the characteristic visible spectrum associated with the isocyclic ring in phylloerythrin is shared by cyclic lactones, but is not evident in phylloerythrin derivatives if the carbonyl group is reduced or if there is a δ-methyl substituent. *A priori*, the identification of the isocyclic ring and ring 3 as a cyclopentenopyrrole, after HI–AcOH reduction, appeared more promising with desoxo-phylloerythrin than with pyrophaeophorbides wherein the isocyclic ring might be labilized by the keto group. As other analytical methods take advantage of the keto group in one way or another, the reduction of desoxo-phylloerythrin was also interesting because its analogues among the petroporphyrins involve the same analytical problem.

The chromatograms of the alkyl pyrroles from desoxo-phylloerythrin showed the peak of **39** before (Chart 4 and the r.r.t.'s of the reference pyrroles in Table 3) and after methylation, as well as the usual alkyl pyrroles from rings 1 and 2. To make the pyrophaeophorbides amenable to this method, conveniently and on the same scale, their keto groups were first reduced with potassium borohydride to carbinole groups (27) which would be reduced to methylene by HI–AcOH, *cf.* the reduction of 9-hydroxy-desoxo-phyllo-

Can. J. Chem. Downloaded from www.nrcresearchpress.com by 210.87.254.6 on 09/05/12
For personal use only.

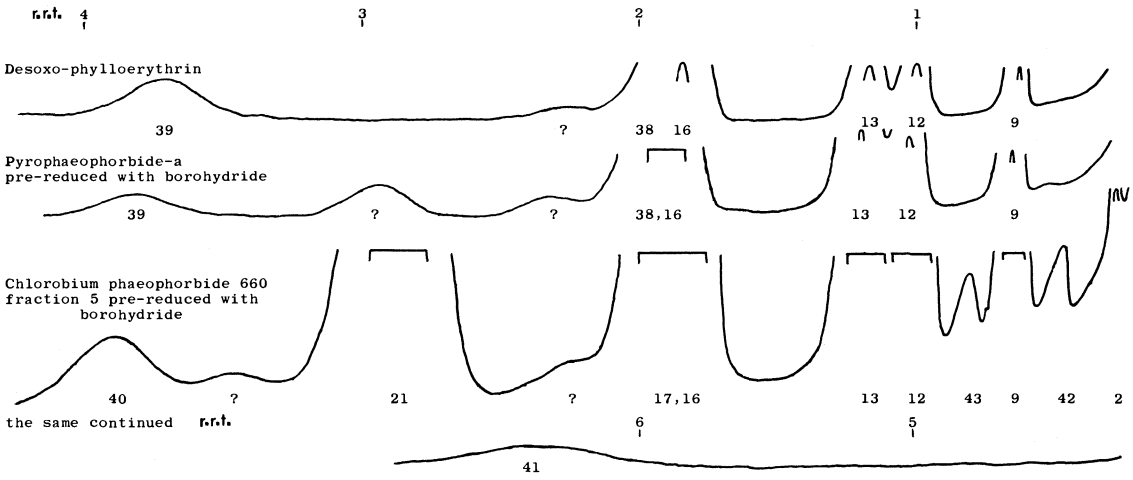

CHART 4. The g.l.p.c. of cyclopenteno-pyrroles and alkyl pyrroles from desoxo-phylloerythrin and from pre-reduced pyrophaeophorbides at 75°.

erythrin (*5i*). The chromatograms of the alkyl pyrroles from the modified pyrophaeophorbide-*a* then showed the peak of **39** before and after methylation. Those from the modified Chlorobium phaeophorbide 660 fraction 5 showed the peaks of **40** and **41** before methylation, and **41** after; this distinguishes **40** from **39**. Two of these pyrroles were also identified under their g.l.p.c. peaks by their mass spectra, in which the mass peaks were those calculated and in the ratios found with the reference pyrroles: **39** from desoxo-phylloerythrin (*M* = 135, *M*−*1*, *M*−*15*); **40** from the phaeophorbide 660 (*M* = 135, *M*−*1*, *M*−*15*, *M*−*29*). When the alkyl pyrroles from both the modified and unmodified Chlorobium phaeophorbide 660 fraction 5 were chromatographed at 135°, minimal amounts of **40** and **41** were also apparent in the latter, about 1/40 of the amounts in the former, and not enough to be detected in chromatograms run at 75°. In view of the contrasting results before and after borohydride reduction, but ignoring the possibility of other labile groups on the isocyclic rings, the nucleus (1) is determined in pyrophaeophorbide-*a* and (*m*) in Chlorobium phaeophorbide 660 fraction 5.

The remaining peaks (Chart 4), like the anomalous peak among the esters, differ from all others previously discussed. Although definitely located, they are not always present, and their absence may then have no significance. Those identified below arise through side-reactions not contemplated in Scheme 1, without firm precedents, and apparently dependent on structural factors remote from the groups involved. Further, they represent by-products and thus a second set of pyrroles from one nucleus.

The r.r.t.'s of three peaks in the chromatogram from Chlorobium phaeophorbide 660 fraction 5 (Chart 4 and Table 3) identify the pyrroles **43**,

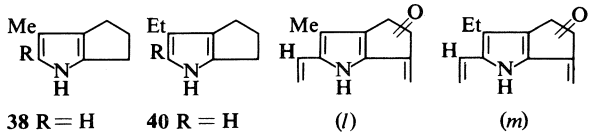

38 R = H
39 R = Me

40 R = H
41 R = Me

(*l*)

(*m*)

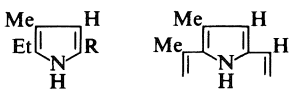

42 R = H
43 R = Me

(*n*)

(*o*)

Can. J. Chem. Downloaded from www.nrcresearchpress.com by 210.87.254.6 on 09/05/12
For personal use only.

Can. J. Chem. Downloaded from www.nrcresearchpress.com by 210.87.254.6 on 09/05/12
For personal use only.

42, and thus **2** rather than **3**. A second reduction showed the peak of **42** better developed but neither **43** nor **2**; a third confirmed these as **14** after methylation. If the pigment was not first reduced with potassium borohydride, these peaks were barely noticeable or absent. The three pyrroles require the nucleus (*n*), and this must result from the partial loss of a labile C_2 group (the α-hydroxy-ethyl group on ring 1) from a precursor of (*e*). If two carbons of the isocyclic ring were lost, pyrroles isomeric with the above would be formed from ring 3 but their r.r.t.'s would be different. The identification of (*n*) through a set of peaks here is more convincing than it would be through a single peak, *e.g.* of a maleinimide.

The behavior of pyrophaeophorbide-*a* suggests that vinyl groups may also be partially lost. About half the chromatograms from this pigment, whether or not it was prereduced with borohydride, showed very small but sometimes sharp peaks of **5** and **2** or **3**. These might arise from ring 1 if the vinyl group were lost, or from ring 3 if two carbons of the isocyclic ring were lost; the latter is unlikely, particularly in view of the behavior of Chlorobium phaeophorbide 660 fraction 5.

Presumably vinyl groups and α-hydroxy-ethyl groups would behave similarly here in the strong acid and, in contrast to acetyl groups (*cf.* diacetyldeuteroporphyrin *9*), they are both largely reduced to ethyl if not completely so (*cf.* hemin). More evidence is required, but it seems that these side-chains will be identified but not distinguished by their partial loss, provided that other structural factors are favorable. If this be so, the nuclei in Chlorobium phaeophorbide 660 fraction 5 identified as (*e*) and (*n*) are derived from (*o*); the other nuclei present were defined as (*a*), (*m*), and (*j*). The assembly of these yields the skeleton of the pigment except for the order of the substituents on ring 2. It also identifies a modified ethyl group on ring 1 and a carbonyl group in the isocyclic ring (see Fig. 1).

Aside from the question of the meso-substituent in Chlorobium chlorophyll 660 fraction 5, purely analytical methods had not ordered the substituents on rings 1, 2, or 4, and the evidence for the isocyclic ring was more indirect than usual. However, although the reductive method would have shown to its best advantage here, it would not have solved the essential analytical problem: the unspecified order of the substituents on ring

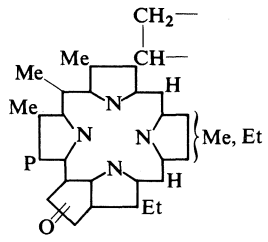

FIG. 1. The skeleton of Chlorobium phaeophorbide 660 fraction 5 derived by reductive degradations.

2 would have necessitated the degradation of the pigment to a phylloporphyrin or, the meso-substitution being known, a pyrroporphyrin for comparison with synthetic material.

These reductions suggest an alternative to a second component, in addition to porphobilinogen, in some studies of the biosynthesis of porphyrins. The abundance of the parent ions in the mass spectra of the pyrroles from a pigment would show which, if either, of the nuclei adjacent to a bridge was derived from the porphobilinogen contributing that bridge. This would require that the pigment was formed from a mixture of natural and doubly labelled porphobilinogen (*e.g.* from δ-aminolevulinic acid-5-^{13}C), and that the pyrroles were sufficiently distinguished by their β-substituents.

The Reference Pyrroles and Their Relative Retention Times

Table 3 gives the r.r.t.'s of most of the pyrroles expected from the chlorophylls, of some isomers from which these pyrroles should be distinguished, and of all the *C*-methyl, *C*-ethyl, and *C*-methyl-ethyl pyrroles. The pyrrole – propionic acids were chromatographed as their methyl esters; a few of the free acids were run for comparison but they had longer retention times and their peaks showed tailing. The pyrrole esters from uroporphyrin, and higher alkyl pyrroles such as the 2,3- and 3,5-dimethyl-4-*n*-octadecylpyrroles can be chromatographed at 180–210° but are not reported here.

We had made few alkyl pyrroles on a preparative scale, and these had usually been stored as their more stable carbethoxy derivatives. Consequently, with few exceptions, the alkyl pyrroles were prepared from carbethoxy derivatives (1 mg) by decarboxylating the latter in HI–AcOH at 110°. If the product was to be alkylated, an aldehyde was added and the mixture was heated again

Can. J. Chem. Downloaded from www.nrcresearchpress.com by 210.87.254.6 on 09/05/12
For personal use only.

before being worked-up for chromatography. The same procedure was used to reduce the porphyrins and chromatograph their pyrroles. It should be noted that β-alkyl pyrroles may be obtained from their tricarboxylic acid-diesters in HI–AcOH at the dilution used here. We had first decarboxylated the latter to dicarboxylic esters in the belief that tricarboxylic acids would not be decarboxylated (see Table 3).

The general reliability of decarboxylations in HI–AcOH is implicit in much of Fischer's work, *cf.* (*5b*), and the alkylations were restricted to types which had offered no difficulty (28). However, the usual controls on the identities of the products were impracticable here and it was assumed that the chromatograms would reveal any anomalous products. In some cases the identities of the pyrroles were confirmed chromatographically by comparison with bulk products, or with the same pyrroles from different precursors; all the important pyrroles were also obtained by reducing porphyrins.

The only apparent failures obviously arose from the instability of the pyrroles in HI–AcOH. Pyrrole itself is decomposed in HI–AcOH, and its 2,5-dialkyl derivatives are not sufficiently stable in the acid at temperatures above 90°; in neither case do the decomposition products appear on the chromatograms. In other cases only the side-chains are degraded. As *t*-butyl groups are easily split off from aromatic nuclei (29, 30), it was not surprising that HI–AcOH converted 2,4-dimethyl-3-*t*-butyl-5-carbethoxypyrrole into 2,4-dimethylpyrrole. Neither *i*-propyl nor *sec*-butyl groups were lost from analogous pyrroles, but the *sec*-butyl group was degraded to ethyl etc. though to a negligible extent. As noted above, none of these unstable pyrroles would be expected from natural porphyrins.

In about 75% of the decarboxylations only one pyrrole appeared on the chromatogram and its r.r.t. was consistent with those of its homologues. In the remaining decarboxylations, which usually involved 3- or 4-carbethoxypyrroles, there were in addition one or two unidentified peaks which usually represented <5% of the product. However, a second peak representing 20% of the product accompanied that of 2-ethyl-5-methylpyrrole.

When precautions were taken (see Experimental), neither methylation nor ethylation introduced further complications but extra peaks were often noted after propylations, and these also appeared in the blank.

The purification of the ether used eliminated some extra peaks. Others arose during the esterification of the pyrrole – propionic acids with diazomethane. Some of the latter were eliminated when the diazomethane was prepared from *N*-nitroso-*p*-toluenesulfonylmethylamide rather than from *N*-nitroso-methylurea, *cf.* (31), but two further peaks of r.r.t. 2.0 and 2.2 were only eliminated when the ethereal diazomethane was purified by washing it with concentrated aqueous ammonia; ammonia does not interfere with the esterification, *cf.* (32). Other extra peaks were finally traced to the *C*-methylation of the pyrrole – propionic acids (but not their esters) by ethereal diazomethane when catalyzed by traces of water or, more effectively, the solution from which the acids had been extracted. This was most obvious when the peak of methyl phyllopyrrole-carboxylate accompanied the expected peak of methyl cryptopyrrole-carboxylate. This *C*-methylation was prevented by drying the ether solution of the acids with $MgSO_4$, an excess of which lowered the yield. The esterifications were also slower in the absence of water. A possible source of extra peaks was eliminated when it was found that diazomethane would not bring about the base catalyzed trans-esterification of the pyrrole methyl esters in the presence of ethanol or ethyl acetate.

Although we had anticipated the alkylation of pyrroles in HI–AcOH through scavenging, it was demonstrated in only one case. When crystalline opsopyrrole-carboxylic acid was esterified by diazomethane in dry ether, the chromatogram showed only the one expected peak of **28**. If it was esterified in wet ether, a small peak of the *C*-methyl derivative **30** was also evident. If it was first heated in HI–AcOH, a third and smaller peak corresponding to **33** appeared in heavily loaded chromatograms; this peak did not appear if the HI–AcOH used had first been heated with cryptopyrrole. Evidently this alkylation is both insignificant and easily eliminated.

Some of the carbethoxypyrroles were obtained in roundabout ways merely because the materials were at hand. Aside from this, the more important ones were obtained as follows, *cf.* (33).

The Knorr synthesis gave **44** (R = COOEt, $COCH_3$, or CH_2CH_2COOEt (34)), thence successively **44** (R = COOEt → COOH → H →

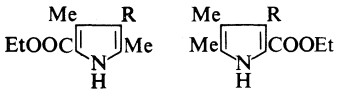

44 **45**

alkyl), but **44**, (R = $COCH_3$ → Et). If higher acylacetates or diethyl β-ketoadipate were used in the ring synthesis, the methyl groups were replaced by others.

The pyrroles **45** (R = H or Et) were obtained via the Hantzsch synthesis, thence **45** (R = H → alkyl) (33). If a higher acylacetate was used in the ring synthesis, the α-methyl group was replaced by another.

The α-methyl groups in **44** and **45** were converted successively to COOH, halogen or H (35), and alkyl; alternatively to CH_2Br then CH_2R (36). Pyrroles with higher α-alkyl groups were thus obtained without the use of higher acylacetates in the ring synthesis.

The only unconventional pyrrole ring synthesis used represents a further extension of the Hantzsch synthesis wherein acetylacetone (as its imine) replaces the acylacetate

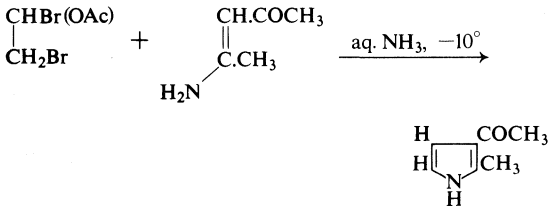

A list of Hantzsch syntheses given earlier (33) did not include that of 2-methyl-3-cyanopyrrole from diacetonitrile (37) or that of 2-(α-pyridyl)-3-carbethoxypyrrole from α-pyridoylacetic ester (38). A third such synthesis (39) had given a low-melting 2,5-dimethyl-4-ethyl-3-carbethoxypyrrole, *cf.* (28), from questionable 3-chloropentanone-2 (40). We regret that our demonstration (33) that the 2,3-dimethyl-5-carbethoxypyrrole of Fischer and Fink (41) was contaminated with the 4-methyl derivative had been anticipated (42).

Experimental

The ether used was reagent grade anhydrous ether, washed twice with acidified aqueous ferrous sulfate, three times with water, then stirred 15 min with anhydrous $MgSO_4$; it was then distilled and the center 60% was stored < 10 days in the dark at 0°.

Diazomethane: distilled ethereal diazomethane, from *N*-nitroso-*p*-toluenesulfonylmethylamide using Carbitol (52), was stirred magnetically at 0° with 1/2 volume of concentrated aqueous ammonia for 20 min. The ether layer was stored at 0° in the dark over KOH (1 pellet/2 ml) for less than 1 week, but > 24 h if it was essential to avoid *C*-alkylation. Solutions < *ca.* 0.5 *M* gave lower yields of esters.

The paraformaldehyde gave no trouble but some lots of paraldehyde were rejected because they gave peaks in the blank; no specimens of propionaldehyde or parapropionaldehyde were consistently satisfactory in this respect. Hemin (Eastman) was converted into deuterohemin, thence into deuteroporphyrin, or into diacetyldeuterohemin and diacetyl-deuteroporphyrin (5). Etioporphyrin *I* (51), 1,3,5,7-tetramethyl-2,6-diethyl-4,8-di-*n*-propylporphin (51), desoxo-phylloerythrin (51), methyl 1,4,5,8-tetramethylporphin-2,3,6,7-tetracarboxylate (53), and coproporphyrin *3* (35) had been made previously. Pyrophaeophorbide-*a*, phylloporphyrin (54), and phyllochlorin (55) were from H. Fischer's collection, the Chlorobium phaeophorbides (56, 57) were from A. S. Holt's.

The Borohydride Reduction of Chlorobium Phaeophorbide 660 Fraction 5

The pigment (1 mg) was dissolved in 2 drops of pyridine. Methanol (50 ml) was added then potassium borohydride (100 mg) in methanol (1 ml) was dropped in. The solution was stirred for 1 h then shaken with ether and 4% HCl. The pigment in the acid layer was brought into fresh ether. This was washed with water, dried ($MgSO_4$), and evaporated.

The Reduction of Porphyrins or the Decarboxylation of Carbethoxypyrroles

As the chromatograph was not programmed, separate reductions were carried out to furnish the alkyl pyrroles and the pyrrole esters from the pigments. Here and in subsequent steps the specified heating times and temperatures must not be exceeded, and the pyrroles should be protected as far as possible from light; otherwise the yields suffer.

Acetic acid (Anachemia reagent, 1.0 ml) then hydriodic acid (AnalaR 66%, stored at 0° but not decolorized, 0.5 ml) were added to the pigment (1 mg, higher concentrations lower the yield) or the carbethoxypyrrole (1 mg) in a 1.5 ml flask fitted with a stirring bar and a reflux condenser. The flask was then placed in a pre-heated oil-bath and stirred magnetically. Carbethoxy derivatives of the sensitive 2,5-dialkylpyrroles were heated 45 min at 90°; pyrophaeophorbides, desoxo-phylloerythrin, and diacetyl-deuteroporphyrin were heated 3 h at 105–110°; all other compounds 1.5 h at 105–110°.

The Alkylation of the Products

If the products were to be alkylated, 3 mg of paraformaldehyde or 0.01 ml of paraldehyde (or other aldehyde) were added to the cooled mixture; if paraformaldehyde was added before the pigments were reduced, extra peaks appeared in the chromatograms. The mixture was then heated again at 105–110° for 30 min or, when β-free pyrroles present were difficult to alkylate, 1 h. However, if methylated pyrrole esters were to be chromatographed, the mixture was heated for 30 min at 50°; a higher temperature resulted in lower yields and sometimes in an extra peak (r.r.t. 2.25) in the chromatograms.

Can. J. Chem. Downloaded from www.nrcresearchpress.com by 210.87.254.6 on 09/05/12
For personal use only.

Can. J. Chem. Downloaded from www.nrcresearchpress.com by 210.87.254.6 on 09/05/12
For personal use only.

The Extraction of the Alkyl Pyrroles

This procedure was the same whether or not the pyrroles were alkylated and whether alkyl pyrroles or esters were to be chromatographed.

The solution was decolorized with the minimum amount of phosphonium iodide (a few mg) (9), starting the reaction by returning the flask to the oil-bath for a few seconds. The solution was then colorless, very pale orange, or green (hemins); the turbidity, if any, was very slight.

The flask was fitted with a reflux condenser modified to trap the distillate, cooled, and placed in a 20° oil-bath. The solvent was removed at 5–10 mm with magnetic stirring as the bath was raised to 65–70° over 30 min. Only a film or a very little oil should remain on the walls of the flask or the yield will be lowered. When the products had been propylated, some extra peaks were minimized when the residue at this stage was kept 1 h at 65° and 0.05 mm. The flask was cooled in ice, and NaOH (1 ml of 10%) was added. The alkyl pyrroles were then extracted with 3 × 1 ml of ether at p*H* > 10.

If the alkyl pyrroles were to be chromatographed, the ether extracts were placed in a chilled tube and centrifuged (5 min), transferred to a 10 ml conical flask, and swirled at intervals over 15 min with anhydrous $MgSO_4$ (40 mg). The ether was transferred to a pear-shaped flask and removed at room temperature under a partial vacuum; unless care is taken, the more volatile pyrroles may be lost here. The residue was dissolved in ether: 1.0 ml if the product was derived from a carbethoxypyrrole, 0.10 ml if from a pyrophaeophorbide or desoxophylloerythrin, 0.25 ml if from another porphyrin and the products had been ethylated, 0.5 ml in all other cases. In every case, 2 μl of the ether solution was applied to the column.

The Preparation of the Pyrrole Esters

If the pyrrole esters were to be chromatographed, the flask containing the alkaline aqueous layer was placed in an ice-bath and stirred magnetically. Phosphoric acid (*ca.* 1 ml of 1 vol 85%:4 vol of water) was added until the mixture just began to turn congo red to black, and the pyrrole acids were extracted with 3 × 1 ml ether at p*H* 4.0. The extract was centrifuged for 10 min then transferred to a 10 ml conical flask.

When it was not essential to minimize *C*-methylation, 1 ml of ethereal diazomethane was added to the extract which was then kept in the dark for 45 min. To minimize *C*-methylation, the extract was stirred for 15 min in the dark with 40 mg of anhydrous $MgSO_4$, transferred to another flask, and esterified as above. In either case, the evaporation of the ether solution followed that of the alkyl pyrroles. The residue was dissolved in ether: 0.10 ml if the esters were derived from a pyrophaeophorbide or desoxo-phylloerythrin, or if the pyrroles had been ethylated; otherwise 0.5 ml. In all cases 5 μl were applied to the column.

Chromatography

A Pye Argon Chromatograph was used with glass columns packed with 0.5 × 117 cm of Chromosorb G (acid washed and treated with DMCS) with 5% SE-30. Unlike other columns (45), these do not separate the 2- and 3-methylpyrroles. Low-temperature column: 50 ± 0.1°, flow rate 171 ml/min, *ca.* 10.5 p.s.i., R_t of the 2,4-dimethylpyrrole standard 6.8 min; 75°, 171 ml/min, *ca.* 12.1 p.s.i., R_t of the cryptopyrrole standard 8.0. High-temperature column: 100°, 158 ml/min, *ca.* 16 p.s.i., R_t of the phyllopyrrole standard 5.4; 135°, 80 ml/min, *ca.* 10.1 p.s.i., R_t of the phyllopyrrole standard for alkyl pyrroles 2.4, R_t of the methyl cryptopyrrole-carboxylate standard for pyrrole esters 11.0. The sample was injected quickly through the open top of the column and as close to the packing as possible while the gas flow was interrupted; sophisticated methods gave poorer results. The R_t's were measured from the start of the ether peak. Yields were calculated from the areas under the peaks, assuming that the response of the detector was molar; bulk samples of cryptopyrrole and of methyl cryptopyrrole-carboxylate were used in calibrating for alkyl pyrroles and pyrrole esters, respectively, immediately before every determination of a yield.

2-Methyl-3-acetylpyrrole

Crude dibromovinyl acetate (from 43 g of vinyl acetate and 27.5 ml of bromine (43)) and 50 g of acetylacetoneimine were stirred into 400 ml of 28% aqueous ammonia at −10°. Stirring was continued for 18 h while the temperature rose slowly to 20°. The mixture was heated to 90°, cooled, and evaporated (rotary, 25 mm, 50° bath). The residue was mixed with 100 ml of water and made acid to congo red with hydrochloric acid then extracted with ether (4 × 200 ml). The extract was evaporated, the residue distilled (to 135°, 0.01 mm), and the distillate was crystallized from 100 ml of water (Darco) giving 6.1 g of colorless prisms, m.p. 95.5–96.5°. For analysis it was recrystallized from pentane (thimble) as colorless prismatic rods, m.p. 94.5–95.5° (lit. (58) 94–95°).

Anal. Calcd. for C_7H_9ON: C, 68.27; H, 7.37; N, 11.37. Found: C, 68.43; H, 7.48; N, 11.40.

To confirm its structure, it was methylated in HI–AcOH–paraformaldehyde to 2,4,5-trimethyl-3-acetylpyrrole (9), identified by m.p. and mixed m.p.

2-Methyl-3-ethylpyrrole

2-Methyl-3-acetylpyrrole (0.03 mol) was reduced with $LiAlH_4$ by the method given for 3-carbethoxy-pyrroles (33). The product was distilled (65°, 15 mm) as a colorless oil (78%).

Anal. Calcd. for $C_7H_{11}N$: C, 77.01; H, 10.16; N, 12.83. Found: C, 77.18; H, 10.32; N, 12.98.

Ethyl α-Oximinopropionylacetate

The crude oil (59) crystallized at 0° overnight. It was dried on tile, sublimed (60°, 1 × 10^{-4}), crystallized from pentane (thimble), and resublimed. Yield 7 g, m.p. 60–63° (lit. (49) 62°).

Anal. Calcd. for $C_7H_{11}O_4N$: C, 48.55; H, 6.40; N, 8.09. Found: C, 48.21; H, 6.58; N, 8.27.

2-Carbethoxy-3-ethyl-4,5-cyclopentenopyrrole

This was obtained like the 3-methyl analogue (49) using 6 g of ethyl α-oximinopropionylacetate, 10 g of cyclopentanone, 40 ml of AcOH, and 12 g of zinc dust. After the supernatant was diluted with 400 ml of water, the crude product separated at 0°. It was dried on tile, sublimed (85°, 1 × 10^{-4} mm), and crystallized thrice from absolute ethanol as colorless plates (138 mg), m.p. 113–115°.

Can. J. Chem. Downloaded from www.nrcresearchpress.com by 210.87.254.6 on 09/05/12
For personal use only.

Anal. Calcd. for $C_{12}H_{17}O_2N$: C, 69.54; H, 8.27; N, 6.76. Found: C, 69.51; H, 8.43; N, 6.87.

2-n-Propyl-4-methyl-5-carbethoxypyrrole

2-*n*-Propyl-4-methyl-3,5-dicarbethoxypyrrole was obtained by the Knorr synthesis from 11 g of crystalline ethyl α-oximinoacetoacetate, 11 g of ethyl *n*-butyrylacetate, AcOH, and zinc dust at 65°. It formed colorless needles (38%), m.p. 115–118°, from ethanol. This ester (2 g) was converted into the 3-carboxylic acid in 20 ml concentrated H_2SO_4 at 40° for 35 min (*cf.* 2,4-dimethyl-5-carbethoxypyrrole (5*e*)). The acid was decarboxylated in refluxing ethanolamine (15 ml) for 40 min and the mixture was poured into ice-water. The product was extracted into ether, the extract was washed with water and the ether was evaporated. The residue was sublimed as colorless needles (44%), m.p. 55–57°. It was analyzed after conversion to the 3-*n*-propyl derivative (see below).

2,4-Di-n-propyl-5-carbethoxypyrrole

2,4-Di-*n*-propyl-3,5-dicarbethoxypyrrole (5*c*) was converted to the 3-carboxylic acid in concentrated H_2SO_4 as usual. The acid was decarboxylated in refluxing ethanolamine, and the product was precipitated by water. After sublimation it melted at 47–50°; yield from the diester 58%. It was analyzed as the 4-methyl derivative (see below).

2,3-Dimethyl-5-ethyl-4-carbethoxypyrrole

The Knorr synthesis was carried out with 2,3-butanedione monoxime, ethyl propionylacetate, and zinc dust in AcOH at 65°. The product was precipitated by water and crystallized from ethanol as needles, m.p. 102–103.5° (lit. (33) 99–101°).

2-Ethyl-5-acetyl-3-carbethoxypyrrole

Acetyl chloride (1.2 ml) in 2 ml of CS_2 was slowly added to a stirred mixture of 2-ethyl-3-carbethoxypyrrole (1 g (33)), powdered anhydrous $AlCl_3$ (0.8 g), and CS_2 (20 ml) at 0°. The mixture was then stirred for 4 h at 20° then poured into ice-water. This was extracted with ether and the extract was washed with 5% aqueous NaOH and with water. The extract was evaporated and the residual product was sublimed (105°, 1×10^{-4} mm), m.p. 119–122°; yield 70%.

2,5-Diethyl-3-carbethoxypyrrole

The corresponding 5-acetylpyrrole (above) was hydrogenated in ethanol over Raney nickel (120°, 1700 p.s.i., 4 h). The product was distilled as an oil (140–150°, 15 mm). The structure was confirmed by reductive alkylation to 2,5-diethyl-4-methyl-3-carbethoxypyrrole, m.p. and mixed m.p. 101–103° (lit. (28) 101–103°).

2-Ethylpyrrole and 2-Ethyl-5-carbethoxypyrrole

2-Ethyl-3-carbethoxypyrrole (33) was heated with 10% aqueous NaOH at 170° for 20 h in a Teflon lined screw-capped metal vessel. The resulting 2-ethylpyrrole (5*a*) was an oil (79%), b.p. 12 mm 59–61°. Using phosgene, just as with 2-methylpyrrole (43), this was converted to 2-ethyl-5-carbethoxypyrrole (70%), b.p. 15 mm 130°, m.p. 50–51° (lit. (5*e*) 48°).

Anal. Calcd. for $C_9H_{13}O_2N$: C, 64.65, H, 7.84; N, 8.38. Found: C, 64.60; H, 7.77; N, 8.38.

2-Ethyl-3-acetyl-5-carbethoxypyrrole

A solution of 2-ethyl-5-carbethoxypyrrole (2 g) and anhydrous stannous chloride (2 g) in 10 ml of acetic anhydride was heated to the boiling point, filtered hot, cooled, and mixed with excess 5% aqueous NaOH. The precipitate was distilled (120°, 1×10^{-4} mm), yield 47%, m.p. 100–101°.

2,3-Diethyl-5-carbethoxypyrrole

The corresponding 3-acetylpyrrole (above) was hydrogenated in ethanol over Raney nickel (170°, 1800 p.s.i., 6 h) and the product was distilled (60°, 1×10^{-4} mm); yield 53%, m.p. 60–62°.

Anal. Calcd. for $C_{11}H_{17}O_2N$: C, 67.66; H, 8.78; N, 7.17. Found: C, 67.83; H, 8.94; N, 7.33.

2-Carboxy-3-n-propyl-4-methyl-5-carbethoxypyrrole

The corresponding 2-methyl pyrrole (28) in dry ether was treated with sulfuryl chloride (3.3 mol) and the solution was then refluxed 1 h. The ether was evaporated at 20°, more ether was added and then evaporated, and hot aqueous sodium acetate was added to the residue. The mixture was boiled 10 min, cooled, and extracted with ether. The product was extracted from the ether into aqueous Na_2CO_3, and precipitated from the latter with acid. It formed needles (35%) from ethanol, m.p. 208–210°.

Anal. Calcd. for $C_{12}H_{17}O_4N$: C, 60.24; H, 7.16; N, 5.85. Found: C, 59.97; H, 7.04; N, 5.72.

2-Carboxy-3-i-butyl-4-methyl-5-carbethoxypyrrole

The corresponding 2-methyl pyrrole (9) was treated with sulfuryl chloride like the 3-*n*-propyl pyrrole above. The product was sublimed (130°, 1×10^{-4} mm) and crystallized twice from aqueous ethanol; yield 12%, m.p. 198–199°.

Anal. Calcd. for $C_{13}H_{19}O_4N$: C, 61.64; H, 7.56; N, 5.53. Found: C, 61.82; H, 7.44; N, 5.42.

2,4-Dimethyl-3-t-butyl-5-carbethoxypyrrole

A solution of 0.5 g of isobutylene in 0.5 g of concentrated H_2SO_4 was added to a stirred solution of 2,4-dimethyl-5-carbethoxypyrrole in 5 ml of acetic acid at 75° over 1/2 h. After a further 2 h at 75°, the mixture was poured into ice-water which was then brought to p*H* 8 with aqueous NaOH. The precipitated product was sublimed. The cubic crystals in the sublimate were separated manually and recrystallized twice from aqueous methanol, m.p. 108–110°, yield 6%.

Anal. Calcd. for $C_{13}H_{21}O_2N$: C, 69.92; H, 9.48; N, 6.27. Found: C, 69.73; H, 9.31; N, 6.45.

2-Carbethoxy-3-n-propyl-4,5-dimethylpyrrole

Hydriodic acid (*d* 1.95, 10 ml) was slowly added to 10 ml of stirred and cooled acetic acid; hypophosphorous acid (50%, 2 ml) was then added. 2-Carbethoxy-4,5-dimethylpyrrole (0.004 mol (28)) was added to the mixture at room temperature followed by propionaldehyde (0.008 mol). The solution was stirred 2½ h at *ca.* 25° then poured into 200 ml of water. This was made alkaline with ammonia, extracted with ether, and the ether was evaporated to leave the crude product. This was an oil which solidified after distillation (1×10^{-4} mm). It was recrystallized from aqueous ethanol then from ethanol, m.p. 101–104° (lit. (5*e*) 102°), yield 40%.

Can. J. Chem. Downloaded from www.nrcresearchpress.com by 210.87.254.6 on 09/05/12
For personal use only.

Anal. Calcd. for $C_{12}H_{19}O_2N$: C, 68.86; H, 9.15; N, 6.69. Found: C, 68.79; H, 9.02; N, 6.54.

2-Carbethoxy-3-n-propyl-4-methyl-5-ethylpyrrole

The crude product, obtained as above but using 2-carbethoxy-4-methyl-5-ethylpyrrole (33), was an oil which largely solidified after distillation (75°, 1×10^{-4} mm). It was dried on tile then crystallized from ethanol as long colorless needles (19%), m.p. 73–74°.

Anal. Calcd. for $C_{13}H_{21}O_2N$: C, 69.91; H, 9.48; N, 6.27. Found: C, 69.77; H, 9.32; N, 6.42.

2-Carbethoxy-3-i-butyl-4-methyl-5-ethylpyrrole

The crude product, obtained as above but using 2-carbethoxy-4-methyl-5-ethylpyrrole and isobutyraldehyde, solidified at 0° after distillation (70°, 1×10^{-4} mm). It was recrystallized twice from methanol, m.p. 53–55° (12%).

Anal. Calcd. for $C_{14}H_{23}O_2N$: C, 70.85; H, 9.77; N, 5.90. Found: C, 70.83; H, 9.86; N, 6.06.

2-Carbethoxy-3-ethyl-4-methyl-5-n-propylpyrrole

The crude product, obtained as above but using 2-carbethoxy-4-methyl-5-*n*-propylpyrrole (33) and paraldehyde, was crystallized from aqueous ethanol, sublimed, recrystallized and resublimed, m.p. 58–59.5°.

Anal. Calcd. for $C_{13}H_{21}O_2N$: C, 69.92; H, 9.48; N, 6.27. Found: C, 69.75; H, 9.50; N, 6.45.

2-n-Propyl-3-(2-carbethoxy-ethyl)-4-methyl-5-carbethoxypyrrole

3-(2-Carbethoxy-ethyl)-4-methyl-5-carbethoxypyrrole (0.4 g (35)), 5 ml of hydriodic acid, 5 ml of acetic acid, 1 ml of hypophosphorous acid and 0.23 ml of propionaldehyde were reacted as above. The solution was poured into 60 ml of water which was then brought to p*H* 5 with ammonia. The precipitate (of the partially hydrolyzed product) was esterified in 5 ml of 5% ethanolic HCl. The solvent was evaporated and the residue was distilled then recrystallized from pentane (0.1 g), m.p. 61.5–63.5° (lit. (36) 63–64°).

Anal. Calcd. for $C_{16}H_{25}O_4N$: C, 65.08; H, 8.53; N, 4.74. Found: C, 65.19; H, 8.40; N, 4.90.

2-Methyl-3,4-diethyl-5-carbethoxypyrrole

Acetic anhydride (20 ml) was stirred into 5 ml of concentrated hydrochloric acid with cooling. 2-Methyl-4-ethyl-5-carbethoxypyrrole ((5*e*), 0.004 mol), paraldehyde (0.008 mol), and zinc amalgam (20 mesh, 10 g) were added at 25° and the mixture was stirred 1/2 h. The solution was decanted into 200 ml of water, this was made alkaline with ammonia and the crude product was filtered off. It was purified by sublimation, m.p. 76–77° (lit. (5*e*) 75°). Yield 20%.

Anal. Calcd. for $C_{12}H_{19}O_2N$: C, 68.86; H, 8.96; N, 6.67. Found: C, 68.83; H, 9.15; N, 6.87.

2-Ethyl-3-n-propyl-4-methyl-5-carbethoxypyrrole

The crude product, obtained as above but using 2-ethyl-4-methyl-5-carbethoxypyrrole (5*e*) and propionaldehyde, was sublimed (80°, 1×10^{-4} mm), m.p. 86–87° (50%).

Anal. Calcd. for $C_{13}H_{21}O_2N$: C, 69.92; H, 9.48; N, 6.27. Found: C, 70.14; H, 9.31; N, 6.48.

2-Ethyl-3-i-butyl-4-methyl-5-carbethoxypyrrole

The crude product, obtained as above but using 2-ethyl-4-methyl-5-carbethoxypyrrole and isobutyraldehyde, was sublimed (80°, 1×10^{-4} mm) and recrystallized from aqueous ethanol, m.p. 94–96° (44%).

Anal. Calcd. for $C_{14}H_{23}O_2N$: C, 70.85; H, 9.77; N, 5.90. Found: C, 70.95; H, 9.59; N, 6.07.

2,4-Di-n-propyl-3-methyl-5-carbethoxypyrrole

The crude product, obtained as above but using 2,4-di-*n*-propyl-5-carbethoxypyrrole (above) and paraformaldehyde, was extracted with ether then sublimed (65°, 1×10^{-4} mm), m.p. 78–80° (17%).

Anal. Calcd. for $C_{14}H_{23}O_2N$: C, 70.85; H, 9.77; N, 5.90. Found: C, 70.72; H, 9.74; N, 5.98.

2,3-Di-n-propyl-4-methyl-5-carbethoxypyrrole

The crude product, obtained as above but using 2-*n*-propyl-4-methyl-5-carbethoxypyrrole (above) and propionaldehyde, was distilled (80°, 1×10^{-4} mm). The partially solidified distillate was dried on tile then recrystallized twice from aqueous ethanol as colorless needles (20%), m.p. 84–87°.

Anal. Calcd. for $C_{14}H_{23}O_2N$: C, 70.85; H, 9.77; N, 5.90. Found: C, 70.68; H, 9.53; N, 6.05.

2-n-Propyl-3-i-butyl-4-methyl-5-carbethoxypyrrole

The crude product, obtained as above using 2-*n*-propyl-4-methyl-5-carbethoxypyrrole (0.65 g) and isobutyraldehyde (0.5 g), was repeatedly sublimed (65°, 1×10^{-4} mm) and recrystallized to remove starting material which was evident in the g.l.p.c.; yield, 30 mg, m.p. 78–79°.

Anal. Calcd. for $C_{15}H_{25}O_2N$: C, 71.67; H, 10.03; N, 5.57. Found: 71.49; H, 10.21; N, 5.68.

2,4-Dimethyl-3-sec-butyl-5-carbethoxypyrrole

The crude product, obtained as above but using 2,4-dimethyl-5-carbethoxypyrrole with 2-butanone and stirring at 30–35°, was sublimed then thrice recrystallized from ethanol as colorless plates (130 mg), m.p. 102–104°.

Anal. Calcd. for $C_{13}H_{21}O_2N$: C, 69.92; H, 9.48; N, 6.27. Found: C, 70.08; H, 9.31; N, 6.26.

2,3,4-Triethyl-5-carbethoxypyrrole

The crude product, obtained as above but using 2,4-diethyl-5-carbethoxypyrrole (5*e*) with paraldehyde, was this time extracted by ether. The ether was evaporated and the residue was distilled. The distillate partially solidified at 0°. It was dried on tile at 0°, recrystallized from aqueous methanol and again distilled (30%), m.p. 47–49°.

Anal. Calcd. for $C_{13}H_{21}O_2N$: C, 69.92; H, 9.48; N, 6.27. Found: C, 70.00; H, 9.42; N, 6.12.

The authors are grateful to Dr. A. S. Holt and Professor A. Treibs for gifts of specimens, and to Dr. R. F. Pottie for the mass-spectra and their interpretation.

1. H. V. Morley and A. S. Holt. Can. J. Chem. **39**, 755 (1961).
2. M. Grassl, U. Coy, R. Seyfert, and F. Lynen. Biochem. Z. **338**, 771 (1963).
3. R. K. Ellsworth and S. Aronoff. Arch. Biochem. Biophys. **124**, 358 (1968).

Can. J. Chem. Downloaded from www.nrcresearchpress.com by 210.87.254.6 on 09/05/12
For personal use only.

4. R. A. NICOLAUS, L. MANGONI, and L. CAGLIOTI. Ann. Chim. (Rome), **46**, 793 (1956); R. A. NICOLAUS, L. MANGONI, and R. NICOLETTI. Ann. Chim. (Rome), **47**, 178 (1957).
5. H. FISCHER and H. ORTH. Die chemie des pyrrols. Johnson Reprint Corp. New York, N.Y., 1968. Vol. 1. (*a*) pp. 33ff, (*b*) pp. 270ff, (*c*) pp. 255ff, (*d*) pp. 245ff, (*e*) pp. 237ff; Vol. 2/1, (*f*) pp. 161–162, (*g*) p. 347, (*h*) p. 3; Vol. 2/2, (*i*) p. 199.
6. H. FISCHER and E. BARTHOLOMÄUS. Z. Physiol. Chem. **83**, 50 (1913).
7. H. FISCHER and E. THURNHER. Z. Physiol. Chem. **204**, 68 (1931).
8. H. FISCHER and H. WENDEROTH. Ann. Chem. **545**, 140 (1940).
9. B. V. GREGOROVICH, K. S. Y. LIANG, D. M. CLUGSTON, and S. F. MACDONALD. Can. J. Chem. **46**, 3291 (1968).
10. H. FISCHER and E. BARTHOLOMÄUS. Z. Physiol. Chem. **87**, 255 (1913).
11. W. KÜSTER. Z. Physiol. Chem. **82**, 467 (1912).
12. R. WILLSTÄTTER and A. STOLL. Untersuchungen über chlorophyll. Springer, Berlin, 1913. (*a*) p. 37, (*b*) p. 383.
13. R. BOEHM. Ann. Chem. **318**, 253 (1901).
14. H. FISCHER and P. HALBIG. Ann. Chem. **447**, 124 (1926).
15. H. FISCHER, E. MERKA, and E. PLÖTZ. Ann. Chem. **478**, 283 (1930).
16. A. H. CORWIN. *In* Organic chemistry. *Edited by* H. Gilman. 2nd ed. Wiley, New York, N.Y., 1943. p. 1271.
17. BEILSTEIN. Handbuch der organischen chemie. 4th ed. Supp. 1. Vol. 22. Springer, Berlin, 1935. p. 501, footnote 2.
18. A. S. HOLT, D. W. HUGHES, H. J. KENDA, and J. W. PURDIE. J. Am. Chem. Soc. **84**, 2835 (1962).
19. J. W. MATHEWSON, W. R. RICHARDS, and H. RAPOPORT. J. Am. Chem. Soc. **85**, 364 (1963).
20. E. EISMA and J. W. JURG. *In* Organic geochemistry. *Edited by* G. Eglington and M. T. J. Murphy. Springer Verlag, Berlin, 1969. p. 695.
21. D. G. WHITTEN, K. E. BENTLEY, and D. KUWADA. J. Org. Chem. **31**, 322 (1966).
22. H. FISCHER and A. ROTHHAAS. Ann. Chem. **484**, 85 (1930).
23. D. MAUZERALL. J. Am. Chem. Soc. **82**, 2601 (1960).
24. H. FISCHER and H. J. RIEDL. Z. Physiol. Chem. **207**, 193 (1932).
25. A. TREIBS and H. G. KOLM. Ann. Chem. **614**, 199 (1958).
26. H. FISCHER and E. BARTHOLOMÄUS. Z. Physiol. Chem. **83**, 50 (1913).
27. A. S. HOLT. Plant Physiol. **34**, 310 (1959).
28. M. W. ROOMI and S. F. MACDONALD. Can. J. Chem. **48**, 139 (1970).
29. S. DAVID and P. RÉGENT. Bull. Soc. Chim. Fr. 101 (1964).
30. B. M. DUBININ. J. Gen. Chem. (USSR), **18**, 2145 (1948); Chem. Abstr. **43**, 3804 (1949).
31. H. IRIE, T. KISHIMOTO, and S. UYEO. J. Chem. Soc. C, 1645 (1969).
32. M. FRANKEL and E. KATCHALSKI. J. Am. Chem. Soc. **66**, 764 (1944).
33. M. W. ROOMI and S. F. MACDONALD. Can. J. Chem. **48**, 1689 (1970).
34. E. BULLOCK, A. W. JOHNSON, E. MARKHAM, and K. B. SHAW. J. Chem. Soc. 1430 (1958).
35. F. MORSINGH and S. F. MACDONALD. J. Am. Chem. Soc. **82**, 4377 (1960).
36. S. F. MACDONALD and A. MARKOVAC. Can. J. Chem. **43**, 3247 (1965).
37. A. STRAIN. Ann. Chem. **499**, 40 (1932).
38. J. P. WIBAUT. Rec. Trav. Chim. Pays-Bas, **45**, 657 (1926).
39. G. KORSCHUN. Bull. Soc. Chim. Fr. (4), **3**, 539 (1908).
40. BEILSTEIN. Handbuch der organischen chemie. Ed. 4, Supp. 3, **1**, Part 3. Springer, Berlin, 1959. p. 2804.
41. H. FISCHER and E. FINK. Z. Physiol. Chem. **283**, 152 (1948).
42. P. S. CLEZY and A. W. NICHOL. Aust. J. Chem. **18**, 1977 (1965).
43. A. TREIBS and W. OTT. Ann. Chem. **615**, 137 (1958).
44. R. A. NICOLAUS and L. MANGONI. Ann. Chim. (Rome), **46**, 847 (1956).
45. R. L. HINMAN and S. THEODOROPULOS. J. Org. Chem. **28**, 3052 (1963).
46. F. K. SINAIGO and H. ADKINS. J. Am. Chem. Soc. **58**, 709 (1936).
47. R A. NICOLAUS and R. NICOLETTI. Ann. Chim. (Rome), **47**, 167 (1957).
48. U. EISNER, A. LICHTAROWICZ, and R. P. LINSTEAD. J. Chem. Soc. 734 (1957).
49. A. TREIBS and D. DINELLI. Ann. Chem. **517**, 152 (1935).
50. S. F. MACDONALD. J. Chem. Soc. 4176 (1952).
51. J. L. ARCHIBALD, D. M. WALKER, K. B. SHAW, A. MARKOVAC, and S. F. MACDONALD. Can. J. Chem. **44**, 345 (1966).
52. T. J. DE BOER and H. J. BACKER. Org. Synth. Coll. Vol. **4**, 250 (1963).
53. G. P. ARSENAULT, E. BULLOCK, and S. F. MACDONALD. J. Am. Chem. Soc. **82**, 4384 (1960).
54. A. TREIBS and E. WIEDEMANN. Ann. Chem. **471**, 146 (1929).
55. H. FISCHER and S. F. MACDONALD. Ann. Chem. **540**, 211 (1939).
56. J. W. PURDIE and A. S. HOLT. Can. J. Chem. **43**, 3347 (1965).
57. A. S. HOLT, J. W. PURDIE, and J. W. F. WASLEY. Can. J. Chem. **44**, 88 (1966).
58. J. W. CORNFORTH and M. E. FIRTH. J. Chem. Soc. 1091 (1958).
59. R. DUSCHINSKY and L. A. DOLAN. J. Am. Chem. Soc. **68**, 2350 (1946).
60. W. RÜDIGER. Z. Physiol. Chem. **350**, 1291 (1969).

Can. J. Chem. Downloaded from www.nrcresearchpress.com by 210.87.254.42 on 09/05/12
For personal use only.

Ferrocene Studies. VII. 1,2-Disubstituted Ferrocenes[1]

E. Bradley Moynahan and Frank D. Popp
Department of Chemistry, Clarkson College of Technology, Potsdam, New York 13676

Received June 28, 1971

Further examples of the utility of the 2-lithiation of *N,N*-dimethylaminomethylferrocene are presented.

L'action du lithium sur la *N,N*-diméthylaminoéthylferrocène a été discutée (1). Cette réaction appliquée à d'autres exemples, constitue une voie d'accès importante aux ferrocènes disubstitués en −1,2.

Canadian Journal of Chemistry, **49**, 3565 (1971)

The lithiation of *N,N*-dimethylaminomethylferrocene has been discussed (1). We now report on further examples of this reaction as an important route to 1,2-disubstituted ferrocenes.

Earlier we reported (2) that the reaction of ferrocenyllithium with aromatic aldehydes gave aryl ferrocenyl ketones. The lithio derivative of *N,N*-dimethylaminomethylferrocene behaves in a similar manner with benzaldehyde to give the ketone **1** as a red oil which was characterized as its methiodide. Ketone **1** was previously obtained by another route (1) as a red oil characterized as its picrate. Reduction of the ketone **1** gave the alcohol **2**. Although treatment of the methiodide of **1** with potassium hydroxide yielded only decomposition products, a similar reaction of the methiodide of **2** gave rise to the diol **3**.

Reaction of ethylene oxide with the lithio derivative of *N,N*-dimethylaminomethylferrocene gave the alcohol **4** which was characterized as its hydrochloride.

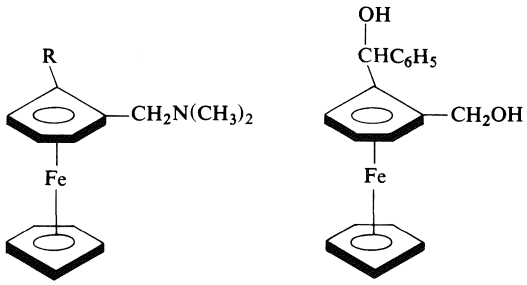

3

1 R = $-\overset{\overset{O}{\|}}{C}-C_6H_5$

2 R = $-\overset{\overset{OH}{|}}{CH}-C_6H_5$

4 R = $-CH_2CH_2OH$

Experimental

2-Benzoyl-N,N-dimethylaminomethylferrocene (1)

To 20.0 g (84.2 mmol) of *N,N*-dimethylaminomethylferrocene in 100 ml of diethyl ether was added over a 10 min period at room temperature 42 ml of *n*-butyllithium in hexane solution (105 mmol). After stirring for 1 h, 26.8 ml of freshly distilled benzaldehyde was added dropwise. After further stirring at room temperature under nitrogen, 30 ml of water was added and the ether layer removed. The ether layer was washed with water, dried over magnesium sulfate, and concentrated *in vacuo* to give an oil. Chromatography of the oil on Grade II alumina gave 14.7 g of starting material eluted with benzene – Skelly solve B and 6.9 g of a red oil, **1**, eluted with chloroform–methanol; i.r. (neat): 1640, 1115, 1010 cm^{-1}. Addition of methyl iodide to an ether solution of the red oil gave a crystalline orange methiodide, m.p. 153° (with sintering from 100°); i.r. (KBr): 1630, 1110, 1005 cm^{-1}.

Anal. Calcd. for $C_{21}H_{24}FeINO$: C, 51.56; H, 4.95; N, 2.86. Found: C, 51.49; H, 4.90; N, 2.84.

2-(α-Phenylhydroxymethyl)-N,N-dimethylaminomethylferrocene (2)

2-Benzoyl-*N,N*-dimethylaminomethylferrocene (**1**) (1.5 g) in 20 ml of diethyl ether was added dropwise to 0.5 g of lithium aluminum hydride in 20 ml of diethyl ether. The mixture was then refluxed for 2 h and the excess lithium aluminum hydride was decomposed with water and base. The ether layer was extracted with 1:10 phosphoric acid which was then added dropwise to a stirred solution of saturated sodium carbonate. The resultant oil was extracted with ether, dried, and concentrated to give 1.22 g of yellow solid which was chromatographed on Grade II alumina using Skelly solve B – chloroform and recrystallized from Skelly solve B to give m.p. 108–109°; i.r.(KBr): 3060, 2975–2780, 1600, 1102, 1005 cm^{-1};

[1]For Part VI, see ref. 3.

n.m.r.: 2.32 (s, $2CH_3$), 3.57 (q, CH_2), 4.20 (m over s, 8FcH), 5.89 (s, CH), 6.37 (m, OH), 7.95 δ (m, 5 benzene H).

Anal. Calcd. for $C_{20}H_{23}FeNO$: C, 68.78; H, 6.64; N, 4.01; Fe, 15.99. Found: C, 68.74; H, 6.63; N, 3.97; Fe, 16.20.

2-(α-Phenylhydroxymethyl)-1-(hydroxymethyl)ferrocene (3)

The methiodide of **2** (0.322 g) was placed in 35 ml of 1 *N* potassium hydroxide solution, refluxed for 5 h, and filtered hot. After cooling, the solution was extracted with ether and the ether layer was washed with water, dried, and concentrated to give **3**, m.p. 117–118° from benzene–heptane; i.r. (KBr): 3325, 1115, 1005 cm^{-1}.

Anal. Calcd. for $C_{18}H_{18}FeO_2$: C, 67.10; H, 5.63. Found: C, 67.35; H, 5.81.

2-(β-Hydroxyethyl)-N,N-dimethylaminomethylferrocene (4)

N,N-Dimethylaminomethylferrocene (20.0 g, 82.4 mm) in 100 ml of diethyl ether was lithiated with 41.0 ml (103 mm) of *n*-butyllithium in hexane. After lithiation was complete, 14.4 g (0.33 mol) of ethylene oxide in 25 ml of diethyl ether was added dropwise with cooling. After the addition was complete the reaction mixture was allowed to warm to room temperature and stirred for 9 h. Water and 10% sodium thiosulfate solution were added and a large amount of polymeric material separated. The ether layer and ether washes of the reaction mixture were combined and extracted with 1:10 phosphoric acid. The acid extracts were added dropwise to 20% sodium carbonate solution and the resultant oil extracted with ether. The dried ether extract was concentrated to give an oil which was chromatographed on alumina to give 6.85 g of starting ferrocene and 5.86 g of *4* as a yellow oil; i.r. (neat): 3400, 3100, 1110, 1005 cm^{-1}. The yellow oil gave a hydrochloride, m.p. 165° (darkens from 145°); i.r. (KBr): 3300, 3100, 2650, 1110, 1005 cm^{-1}.

Anal. Calcd. for $C_{15}H_{22}ClFeNO$: C, 55.66; H, 6.85; N, 4.33. Found: C, 55.77; H, 6.92; N, 4.30.

1. D. W. Slocum, B. W. Rockett, and C. R. Hauser. J. Am. Chem. Soc. **87**, 1241 (1965).
2. F. D. Popp and E. B. Moynahan. J. Org. Chem. **34**, 454 (1969).
3. F. D. Popp and E. B. Moynahan. J. Heterocycl. Chem. **7**, 739 (1970).

Can. J. Chem. Downloaded from www.nrcresearchpress.com by 210.87.254.42 on 09/05/12
For personal use only.

Revisions of Structural Assignments for 1-Methyl-(3 and 5)-amino-4-nitropyrazoles and Related Compounds

Misbahul Ain Khan and Brian M. Lynch
Organic Chemistry Laboratory, St. Francis Xavier University, Antigonish, Nova Scotia

Received July 5, 1971

Amino proton chemical shifts recorded for the compounds described as 5-amino-1-methyl-4-nitropyrazole and the 3-amino isomer (3) are inconsistent with charge densities calculated from simple H.m.o. treatments.

Unequivocal synthesis of 5-amino-1-methyl-4-nitropyrazole from 5-amino-1-methylpyrazole proves that the assignments should be interchanged; the structures of compounds derived from these aminonitropyrazoles are revised accordingly.

Les déplacements chimiques des protons amino du composé décrit comme étant l'amino-5 méthyl-1 nitro-4 pyrazole ainsi que de l'isomère amino-3 (3), ne sont pas compatibles avec les densités de charge calculées par simple traitement H.m.o.

Une synthèse sans ambiguité possible de l'amino-5 méthyl-1 nitro-4 pyrazole à partir de l'amino-5 méthyl-1 pyrazole, prouve que les attributions doivent être interchangées; les structures des composés qui dérivent de ces aminonitropyrazoles ont été corrigées en conséquence.

Canadian Journal of Chemistry, **49**, 3566 (1971)

Introduction

In earlier papers (1, 2) we have pointed out that simple Huckel molecular-orbital (H.m.o.) π-electron densities at amino nitrogen are linearly related to the chemical shifts of amino protons for aromatic amines in hydrogen-bond-acceptor solvents. We suggested also that these computationally trivial calculations could be used to predict chemical shifts.

The present note reports an example of such prediction, resulting in the proposed interchange of the structures assigned to 5-amino-1-methyl-4-nitropyrazole (**1**) and to 3-amino-1-methyl-4-nitropyrazole (**2***a*) by Brown and co-workers (3).

n.m.r.: 2.32 (s, $2CH_3$), 3.57 (q, CH_2), 4.20 (m over s, 8FcH), 5.89 (s, CH), 6.37 (m, OH), 7.95 δ (m, 5 benzene H).

Anal. Calcd. for $C_{20}H_{23}FeNO$: C, 68.78; H, 6.64; N, 4.01; Fe, 15.99. Found: C, 68.74; H, 6.63; N, 3.97; Fe, 16.20.

2-(α-Phenylhydroxymethyl)-1-(hydroxymethyl)ferrocene (3)

The methiodide of **2** (0.322 g) was placed in 35 ml of 1 *N* potassium hydroxide solution, refluxed for 5 h, and filtered hot. After cooling, the solution was extracted with ether and the ether layer was washed with water, dried, and concentrated to give **3**, m.p. 117–118° from benzene–heptane; i.r. (KBr): 3325, 1115, 1005 cm^{-1}.

Anal. Calcd. for $C_{18}H_{18}FeO_2$: C, 67.10; H, 5.63. Found: C, 67.35; H, 5.81.

2-(β-Hydroxyethyl)-N,N-dimethylaminomethylferrocene (4)

N,N-Dimethylaminomethylferrocene (20.0 g, 82.4 mm) in 100 ml of diethyl ether was lithiated with 41.0 ml (103 mm) of *n*-butyllithium in hexane. After lithiation was complete, 14.4 g (0.33 mol) of ethylene oxide in 25 ml of diethyl ether was added dropwise with cooling. After the addition was complete the reaction mixture was allowed to warm to room temperature and stirred for 9 h. Water and 10% sodium thiosulfate solution were added and a large amount of polymeric material separated. The ether layer and ether washes of the reaction mixture were combined and extracted with 1:10 phosphoric acid. The acid extracts were added dropwise to 20% sodium carbonate solution and the resultant oil extracted with ether. The dried ether extract was concentrated to give an oil which was chromatographed on alumina to give 6.85 g of starting ferrocene and 5.86 g of *4* as a yellow oil; i.r. (neat): 3400, 3100, 1110, 1005 cm^{-1}. The yellow oil gave a hydrochloride, m.p. 165° (darkens from 145°); i.r. (KBr): 3300, 3100, 2650, 1110, 1005 cm^{-1}.

Anal. Calcd. for $C_{15}H_{22}ClFeNO$: C, 55.66; H, 6.85; N, 4.33. Found: C, 55.77; H, 6.92; N, 4.30.

1. D. W. Slocum, B. W. Rockett, and C. R. Hauser. J. Am. Chem. Soc. **87**, 1241 (1965).
2. F. D. Popp and E. B. Moynahan. J. Org. Chem. **34**, 454 (1969).
3. F. D. Popp and E. B. Moynahan. J. Heterocycl. Chem. **7**, 739 (1970).

Can. J. Chem. Downloaded from www.nrcresearchpress.com by 210.87.254.40 on 09/05/12
For personal use only.

Revisions of Structural Assignments for 1-Methyl-(3 and 5)-amino-4-nitropyrazoles and Related Compounds

Misbahul Ain Khan and Brian M. Lynch
Organic Chemistry Laboratory, St. Francis Xavier University, Antigonish, Nova Scotia

Received July 5, 1971

Amino proton chemical shifts recorded for the compounds described as 5-amino-1-methyl-4-nitropyrazole and the 3-amino isomer (3) are inconsistent with charge densities calculated from simple H.m.o. treatments.

Unequivocal synthesis of 5-amino-1-methyl-4-nitropyrazole from 5-amino-1-methylpyrazole proves that the assignments should be interchanged; the structures of compounds derived from these aminonitropyrazoles are revised accordingly.

Les déplacements chimiques des protons amino du composé décrit comme étant l'amino-5 méthyl-1 nitro-4 pyrazole ainsi que de l'isomère amino-3 (3), ne sont pas compatibles avec les densités de charge calculées par simple traitement H.m.o.

Une synthèse sans ambiguité possible de l'amino-5 méthyl-1 nitro-4 pyrazole à partir de l'amino-5 méthyl-1 pyrazole, prouve que les attributions doivent être interchangées; les structures des composés qui dérivent de ces aminonitropyrazoles ont été corrigées en conséquence.

Canadian Journal of Chemistry, **49**, 3566 (1971)

Introduction

In earlier papers (1, 2) we have pointed out that simple Huckel molecular-orbital (H.m.o.) π-electron densities at amino nitrogen are linearly related to the chemical shifts of amino protons for aromatic amines in hydrogen-bond-acceptor solvents. We suggested also that these computationally trivial calculations could be used to predict chemical shifts.

The present note reports an example of such prediction, resulting in the proposed interchange of the structures assigned to 5-amino-1-methyl-4-nitropyrazole (**1**) and to 3-amino-1-methyl-4-nitropyrazole (**2***a*) by Brown and co-workers (3).

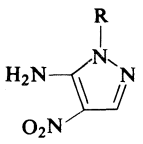

1

R = Me

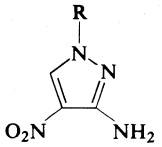

2

a R = Me
b R = H

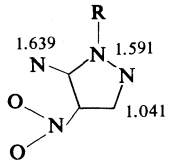

4

R = Me

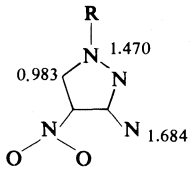

5

R = Me

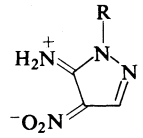

3

R = Me

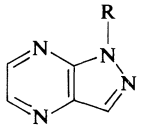

6

a R = Me
b R = H

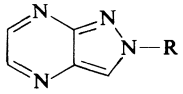

7

R = Me

and confirmation of the proposal by unambiguous synthesis of compound **1**.

Discussion and Results

Brown's group discovered that 4-methoxy-5-nitropyrimidine was converted into 3-amino-4-nitropyrazole (**2***b*) by hydrazine, and they obtained two products of respective m.p. 200 and 265–266° when the pyrimidine was treated with an excess of ethanolic methylhydrazine. The p.m.r. spectra of these products in dimethylsulfoxide-d_6 showed amino proton signals at δ 7.17 and 7.49, and they were assigned structures **1** and **2***a* respectively. However, simple resonance concepts suggest that the electron density at the 5-amino nitrogen in **1** should be significantly less than in **2***a*, in view of contributions from the form **3** (the charge displacement corresponding to **3** explains the extreme downfield position of the amino proton signal in *ortho*-nitroaniline (1)); no similar contribution is possible for structure **2***a*. Thus, qualitative considerations would indicate that **1** should have the lowfield amino proton signal at δ 7.49, and **2***a* the higher field signal at 7.17. This qualitative indication is confirmed by H.m.o. calculations on models of **1** and **2***a*, with results illustrated as **4** and **5**. The difference between the high and low field signals and the low and high charge densities indicates a response to electron density variations of *ca.* 7 p.p.m./electron, in agreement with previous work (1, 2). Further, the methyl proton signals of the compounds of m.p. 200 and 265–266° are at δ 3.65 and 3.57, and the pyrazole ring proton signals are at δ 8.42 and 7.82, respectively. If the compound of m.p. 265–266° is reassigned as **1**, and the compound of m.p. 200° as **2***a*, then the orders of the appropriate pairs of chemical shifts are in agreement with all previous charge-density/chemical shift correlations (4–7). The chemical shift patterns of the reassigned products are also consistent with the proton chemical shifts of the closely related isomeric amino-1-methyl-pyrazole-4-carbonitriles, whose structures are firmly established (8, 9). The shifts are compared in Table 1. Final confirmation of the validity of this interchange is afforded by nitration of 5-amino-1-methylpyrazole, which forms 5-amino-1-methyl-4-nitropyrazole, m.p. 266° (p.m.r. spectrum in dimethylsulfoxide-d_6: δ 3.60 (s, 3H (1-Me)); 7.60 (s, br, 2H (5-NH_2)); 7.87 (s, 1H (3-H)). Similar nitration of 5-amino-1-phenylpyrazole also afforded the 4-nitration product, 5-amino-4-nitro-1-phenylpyrazole, m.p. 154–156°, whose p.m.r. spectrum in hexadeuterodimethyl sulfoxide resembled that of **1**: δ 7.30 (s, br, 2H (5-NH_2)); 7.75 (s, 5H (1-Ph)); 8.20 (s, 1H (3-H)). The upfield shift of the amino signal as compared with **1** reflects ring-current shielding by the 1-phenyl substituent.

In view of the exchange of structural assignments for the amino-1-methyl-4-nitropyrazoles, assignments of structure for compounds derived from these species should be revised appropriately. For example, the compound described (3) as 4,5-diamino-1-methylpyrazole is actually 3,4-diamino-1-methylpyrazole, and the compound described as 1-methylpyrazolo(3,4-*b*)pyrazine (**6***a*) is the 2-methyl isomer **7**. This corrects a discrepancy between the coupling constants J_{56} for

Can. J. Chem. Downloaded from www.nrcresearchpress.com by 210.87.254.40 on 09/05/12
For personal use only.

TABLE 1. Proton chemical shifts for aminopyrazoles*

Literature structure	Correct structure	Proton shifts 1-Me	3-H	5-H	Amino
3-Amino-1-methyl-4-nitropyrazole (m.p. 265–266°)	5-Amino-1-methyl-4-nitropyrazole	3.57	7.82	—	7.49
	5-Amino-1-methylpyrazole-4-carbonitrile	3.57	7.57	—	6.57
5-Amino-1-methyl-4-nitropyrazole (m.p. 200°)	3-Amino-1-methyl-4-nitropyrazole	3.65	—	8.42	7.17
	3-Amino-1-methylpyrazole-4-carbonitrile	3.60	—	8.00	5.53

*In p.p.m from TMS, in dimethyl sulfoxide-d_6. Values for the aminonitro compounds from ref. 3.

1*H*-pyrazolo(3,4-*b*)pyrazine (**6***b*) and for the supposed **6***a* (the respective values are 3.0 and 1.8 Hz). With the revised assignment, the smaller coupling in the quinonoid ring of **7** is consistent with expectation from established bond order/coupling constant relationships (10, 11).

Finally, other structural revisions required include: 2,5,6- for 1,5,6-trimethylpyrazolo(3,4-*b*)pyrazine; 11- for 10-methyldibenzo(*f*,*h*)pyrazolo(3,4-*b*)quinoxaline; 3- for 5-diacetylamido-1-methyl-4-nitropyrazole; 3- for 5-acetamido-1-methyl-4-nitropyrazole; and 3- for 5-acetamido-4-amino-1-methylpyrazole.

Experimental

General

The p.m.r. measurements were made using a Varian A-60D spectrometer. Combustion analyses were carried out by Mrs. M. Petranovic of this laboratory using a Hewlett–Packard Model 185 CHN Analyzer. The H.m.o. calculations were made using a standard program (1), and with the following heteroatom parameters: pyrrole and nitro nitrogen, and oxygen, $h = +1$; pyridine and amino nitrogen, $h = +\frac{1}{2}$.

Reference Samples and Starting Materials

3-Amino-1-methylpyrazole-4-carbonitrile, m.p. 135–136°, was prepared using the method of Schmidt and co-workers (8); 5-amino-1-methylpyrazole-4-carbonitrile, m.p. 224–225°, was prepared following Cheng and Robins' method (9). 5-Amino-1-phenylpyrazole was a commercial sample (Aldrich Chemical Company) and was used without further purification.

5-Amino-1-methylpyrazole

5-Amino-1-methylpyrazole-4-carbonitrile (30 g) was dissolved cautiously in 85% w/w aqueous sulfuric acid (100 ml) and heated under reflux for 12 h. The mixture was cooled and added to crushed ice (500 g), basified with aqueous ammonia, and left overnight at 5°. The mixture was filtered and the filtrate extracted five times with 200 ml portions of chloroform. The chloroform extract was dried ($MgSO_4$) and the solvent was removed under reduced pressure, yielding 5-amino-1-methylpyrazole (19.9 g, 84%), m.p. 69° (lit. (12) m.p. 71–72°); p.m.r. spectrum in dimethylsulfoxide-d_6: δ 3.52 (s, 3H (1-Me)); 5.00 (s, br, 2H (5-NH_2)); 5.27 (d, $J = 2$ Hz, 1H (4-H)); 7.00 (d, $J = 2$ Hz, 1H (3-H)).

5-Amino-1-methyl-4-nitropyrazole

5-Amino-1-methylpyrazole (5.00 g) was dissolved in ice-cold 36 *N* sulfuric acid (10 ml) and 70% nitric acid (5 ml) and allowed to stand for 3 h. The reaction mixture was basified with aqueous ammonia and extracted with chloroform (200 ml) followed by ethyl acetate (5 × 100 ml). Evaporation of the ethyl acetate followed by crystallization from methanol yielded 5-amino-1-methyl-4-nitropyrazole (1.6 g, 23%), m.p. 266°.

Anal. Calcd. for $C_4H_6N_4O_2$: C, 33.81; H, 4.26; N, 39.42. Found: C, 33.80; H, 4.17; N, 39.30.

5-Amino-4-nitro-1-phenylpyrazole

5-Amino-1-phenylpyrazole (1.00 g) was dissolved in acetic anhydride (10 ml) and the solution was cooled to 0°. To the cold, stirred solution was added 90% nitric acid (2 ml); the temperature was maintained between −5 and 0° by addition of dry ice. After addition of the acid was complete, the reaction mixture was stirred for a further 5 min, and was added with stirring to crushed ice (100 g). The precipitate was collected and crystallized from ethanol, yielding 5-amino-4-nitro-1-phenylpyrazole (1.20 g, 92%), m.p. 154–156°.

Anal. Calcd. for $C_9H_8N_4O_2$: C, 52.94; H, 3.95; N, 27.44. Found: C, 53.10; H, 3.79; N, 26.90.

This research was supported by the National Cancer Institute of Canada and the National Research Council of Canada. We acknowledge Dr. D. J. Brown's courtesy in discussion of our results.

1. B. M. LYNCH, B. C. MACDONALD, and J. G. K. WEBB. Tetrahedron, **24**, 3595 (1968).
2. B. M. LYNCH. Tetrahedron Lett. 1357 (1969).
3. M. E. C. BIFFIN, D. J. BROWN, and Q. N. PORTER. J. Chem. Soc. C, 2159 (1968).
4. G. FRAENKEL, R. E. CARTER, and A. MCLACHLAN. J. Am. Chem. Soc. **82**, 5846 (1960).
5. T. SCHAEFER and W. G. SCHNEIDER. Can. J. Chem. **41**, 966 (1963).
6. B. M. LYNCH and H. J. M. DOU. Tetrahedron Lett. 2627 (1966).

Can. J. Chem. Downloaded from www.nrcresearchpress.com by 210.87.254.40 on 09/05/12
For personal use only.

7. B. M. LYNCH, A. J. ROBERTSON, and J. G. K. WEBB. Can. J. Chem. **47**, 1129 (1969).
8. P. SCHMIDT, K. EICHENBERGER, M. WILHELM, and J. DRUEY. Helv. Chim. Acta, **42**, 743 (1959).
9. C. C. CHENG and R. K. ROBINS. J. Org. Chem. **21**, 1240 (1956).
10. N. JONATHAN, S. GORDON, and B. P. DAILEY. J. Chem. Phys. **36**, 2443 (1962).
11. W. B. SMITH, W. H. WATSON, and S. CHIRANJEEVI. J. Am. Chem. Soc. **89**, 1438 (1967).
12. H. DORN, G. HILGETAG, and A. ZUBEK. Angew. Chem. **76**, 920 (1964).

Isomerization of 1-*exo*-4,5,6,7,8,8-Heptachloro-2,3-*endo*-epoxy-3*a*,4,7,7*a*-tetrahydro-4,7-methanoindane with Base

W. P. COCHRANE AND M. A. FORBES[1]

Analytical Services Section, Plant Products Division, Canada Department of Agriculture, Ottawa, Canada

Received June 8, 1971

Treatment of the title compound, **2**, with excess sodium methoxide produced an unsaturated secondary alcohol, **3**. Structure elucidation was achieved by MnO_2 oxidation followed by $CrCl_2$ reductive dechlorination to give as the major product 2-oxa-4,5,6,7,8,8-hexachloro-3*a*,4,7,7*a*-tetrahydro-4,7-methanoindane.

Le composé, **2**, donné dans le titre, traité avec un excès de méthylate de sodium a conduit à un alcool secondaire insaturé **3**. La recherche de la structure a été menée à bien par une oxydation avec MnO_2 suivie d'une déchloration réductive par $CrCl_2$ pour donner comme produit principal l'oxa-2 hexachloro-4,5,6,7,8,8-tétrahydro-3*a*,4,7,7*a* méthano-4,7 indane.

Canadian Journal of Chemistry, **49**, 3569 (1971)

In connection with previous work on polychlorinated cyclodiene pesticides it was observed that the action of base on the biological metabolite of heptachlor,[2] namely heptachlor epoxide **1**, resulted in preferential epoxide isomerization, yielding an α,β-unsaturated alcohol (1). Molecules containing the required configuration *i.e.*, a *trans* coplanar arrangement of one of the carbon–oxygen bonds of the epoxide ring and a hydrogen on an adjacent carbon, apparently undergo transformation readily (2). In heptachlor epoxide the *cis*-arrangement of the epoxy ring to the C-1 chlorine atom resulted in initial abstraction of the C-1 proton (1). As an extension to this work it was of interest to study the isomeric compound **2** in which the epoxy group is *trans* to the C-1 chlorine atom (3).

Accordingly, a solution of *trans*-epoxide **2** in methanol was treated under reflux with an excess of sodium methoxide. Reaction occurred readily to yield, after water–hexane partition, an oil which was purified by distillation, b.p. 130–132°/0.1 mm. The molecular formula $C_{10}H_5Cl_7O$ was established by elemental analysis and mass spectrometry. The i.r. spectrum indicated a bonded hydroxyl, 3380 cm^{-1} together with a double bond at 1595 cm^{-1}. Previously, an isomeric hydroxyl-containing product had been formed from the *cis*-epoxide **1**. The n.m.r. spectrum substantiated the presence of only one olefinic proton and one hydroxyl proton whose signals appeared at τ 3.95 and 7.21 respectively. Consideration of the foregoing data and the

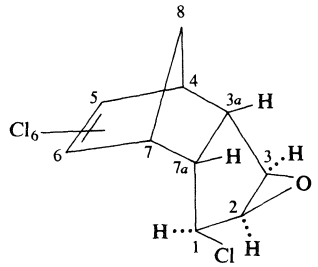

1

[1]Present address: Inland Waters Branch, Department of Energy, Mines and Resources, Federal Building, Moncton, New Brunswick.

[2]Heptachlor is the common name for the insecticidal compound 1-*exo*-4,5,6,7,8,8-heptachloro-3*a*,4,7,7*a*-tetrahydro-4,7-methanoindene.

Can. J. Chem. Downloaded from www.nrcresearchpress.com by 210.87.254.40 on 09/05/12
For personal use only.

7. B. M. LYNCH, A. J. ROBERTSON, and J. G. K. WEBB. Can. J. Chem. **47**, 1129 (1969).
8. P. SCHMIDT, K. EICHENBERGER, M. WILHELM, and J. DRUEY. Helv. Chim. Acta, **42**, 743 (1959).
9. C. C. CHENG and R. K. ROBINS. J. Org. Chem. **21**, 1240 (1956).
10. N. JONATHAN, S. GORDON, and B. P. DAILEY. J. Chem. Phys. **36**, 2443 (1962).
11. W. B. SMITH, W. H. WATSON, and S. CHIRANJEEVI. J. Am. Chem. Soc. **89**, 1438 (1967).
12. H. DORN, G. HILGETAG, and A. ZUBEK. Angew. Chem. **76**, 920 (1964).

Isomerization of 1-*exo*-4,5,6,7,8,8-Heptachloro-2,3-*endo*-epoxy-3*a*,4,7,7*a*-tetrahydro-4,7-methanoindane with Base

W. P. COCHRANE AND M. A. FORBES[1]

Analytical Services Section, Plant Products Division, Canada Department of Agriculture, Ottawa, Canada

Received June 8, 1971

Treatment of the title compound, **2**, with excess sodium methoxide produced an unsaturated secondary alcohol, **3**. Structure elucidation was achieved by MnO_2 oxidation followed by $CrCl_2$ reductive dechlorination to give as the major product 2-oxa-4,5,6,7,8,8-hexachloro-3*a*,4,7,7*a*-tetrahydro-4,7-methanoindane.

Le composé, **2**, donné dans le titre, traité avec un excès de méthylate de sodium a conduit à un alcool secondaire insaturé **3**. La recherche de la structure a été menée à bien par une oxydation avec MnO_2 suivie d'une déchloration réductive par $CrCl_2$ pour donner comme produit principal l'oxa-2 hexachloro-4,5,6,7,8,8-tétrahydro-3*a*,4,7,7*a* méthano-4,7 indane.

Canadian Journal of Chemistry, **49**, 3569 (1971)

In connection with previous work on polychlorinated cyclodiene pesticides it was observed that the action of base on the biological metabolite of heptachlor,[2] namely heptachlor epoxide **1**, resulted in preferential epoxide isomerization, yielding an α,β-unsaturated alcohol (1). Molecules containing the required configuration *i.e.*, a *trans* coplanar arrangement of one of the carbon–oxygen bonds of the epoxide ring and a hydrogen on an adjacent carbon, apparently undergo transformation readily (2). In heptachlor epoxide the *cis*-arrangement of the epoxy ring to the C-1 chlorine atom resulted in initial abstraction of the C-1 proton (1). As an extension to this work it was of interest to study the isomeric compound **2** in which the epoxy group is *trans* to the C-1 chlorine atom (3).

Accordingly, a solution of *trans*-epoxide **2** in methanol was treated under reflux with an excess of sodium methoxide. Reaction occurred readily to yield, after water–hexane partition, an oil which was purified by distillation, b.p. 130–132°/0.1 mm. The molecular formula $C_{10}H_5Cl_7O$ was established by elemental analysis and mass spectrometry. The i.r. spectrum indicated a bonded hydroxyl, 3380 cm^{-1} together with a double bond at 1595 cm^{-1}. Previously, an isomeric hydroxyl-containing product had been formed from the *cis*-epoxide **1**. The n.m.r. spectrum substantiated the presence of only one olefinic proton and one hydroxyl proton whose signals appeared at τ 3.95 and 7.21 respectively. Consideration of the foregoing data and the

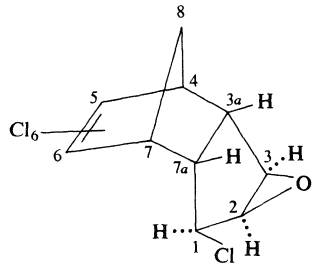

1

[1]Present address: Inland Waters Branch, Department of Energy, Mines and Resources, Federal Building, Moncton, New Brunswick.

[2]Heptachlor is the common name for the insecticidal compound 1-*exo*-4,5,6,7,8,8-heptachloro-3*a*,4,7,7*a*-tetrahydro-4,7-methanoindene.

Can. J. Chem. Downloaded from www.nrcresearchpress.com by 210.87.254.42 on 09/05/12
For personal use only.

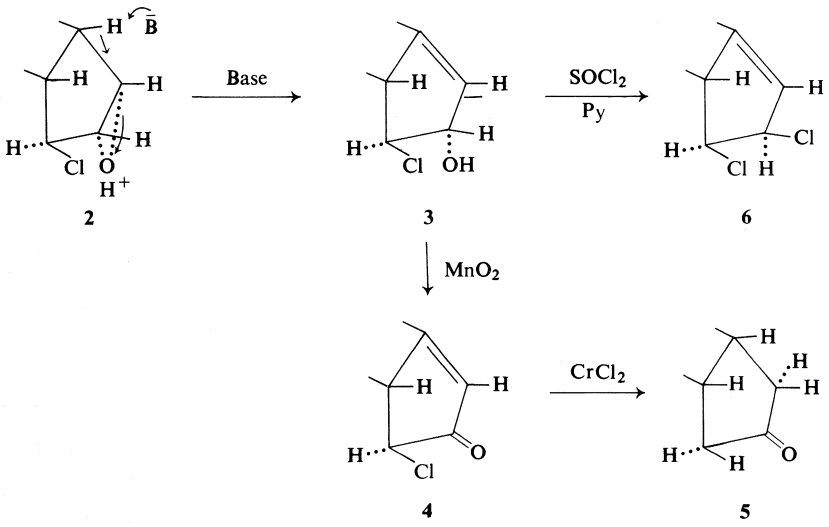

SCHEME 1

lack of characteristic ions in the mass spectrum due to retro-Diels–Alder fragmentation (4) suggested the reaction product to be the α,β-unsaturated alcohol, 2-*endo*-hydroxy-1-*exo*-4,5,6,7,8,8-heptachloro-4,7-methanoisoindene (**3**).

Oxidation of **3** with active MnO_2 gave a keto compound **4** which exhibited both i.r. carbonyl, 1745 cm^{-1}, and double bond absorptions, 1638 and 1595 cm^{-1}. Multiplets at τ 3.54 and 6.0, equivalent to 1 and 2 protons respectively, were observed in the n.m.r. spectrum which together with the i.r. and mass spectra are consistent with structure **4**. Treatment of **4** with aqueous $CrCl_2$ solution resulted in reductive dechlorination of the C-1 chloro atom and the addition of two protons to the unhindered double bond as observed from the mass spectral fragmentation pattern. This together with n.m.r. analysis, which displayed only two signals at τ 6.5 and 7.0 corresponding to 2 and 4 protons respectively, indicated the compound contained a saturated pentacyclic ring ketone group. Comparison of the i.r. spectrum, which lacked the 1638 cm^{-1} peak observed in **4**, with the two previously reported keto compounds[3] which have the carbonyls situated at C-1 or -2 in the cyclopentane ring, proved the $CrCl_2$ product to have structure **5**. The replacement of halogen by hydrogen in allylic halides, α-haloketones and *vic*-dihalides by Cr^{2+} reagents has been reported (5, 6). Reduction of multiple bonds by Cr^{2+} reagents has also been observed to occur in acidic solution but, so far, only when the olefin forms part of an enedione or an α,β-unsaturated ketone attached to an aromatic ring.

The *endo*-configuration of the C-2 hydroxyl group in **3** was confirmed by the failure of the octachloro derivative **6**, formed by reaction of **3** with PCl_3, to reconvert to **3** on treatment with aqueous alcoholic Ag_2CO_3 (1, 8). The latter reaction, monitored by g.l.c., produced only one peak which, on silylation, gave a single derivative with a different retention time to that for the silyl ether of **3**. Presumably the octachloro intermediate **6** is formed with inversion at C-2. Such a process occurs during the chlorination of *endo*-hydroxyl groups in similar polychlorinated cyclodiene compounds (9, 10).

The possible mechanism for the formation of **3** is given in Scheme 1. It is thought to be similar to that for heptachlor epoxide but, in this instance, involves initial nucleophilic attack on the *trans*-proton situated on the C-3*a* ring-junction position. The *cis* and *trans*-epoxides each gave their respective isomeric products with *t*-BuOK/t-BuOH as when NaOMe/MeOH or NaOEt/EtOH were used as the basic media, indicating the general nature of this base catalyzed isomerisation. Lack of evidence for attack at position C-2 or -3 is explained by the large steric

[3]Through the courtesy of Dr. G. T. Brooks, Unit of Invertebrate Chemistry and Physiology, The Chemical Laboratory, The University of Sussex, Brighton, U.K.

Can. J. Chem. Downloaded from www.nrcresearchpress.com by 210.87.254.42 on 09/05/12
For personal use only.

effect of the *exo*-chloro atom at C-1, inhibiting methoxide ion approach, since it has been observed that heptachlor is resistant to both peracid epoxidation and chlorine addition. Recently polychlorinated cyclodiene compounds possessing ring-junction double bonds have been prepared by the action of KOH on decachlorodicyclopentadiene (11).

Experimental

Melting points were determined on a Fisher–Johns hotstage and are uncorrected; i.r. spectra were recorded on a Beckman IR-7 spectrophotometer; n.m.r. spectra were measured in $CDCl_3$ using a Varian T-60 spectrometer with tetramethylsilane as internal standard; mass spectra were determined on a Bendix time-of-flight spectrometer, Model 12101, with the continuous ionization modification, operating at 40 eV, ambient temperature and 10^{-6} Torr, and are reported based on the ^{35}Cl fragmentation pattern. Microanalyses were determined by G. Morris, Research Branch, Canada Department of Agriculture, Ottawa.

*2-endo-Hydroxy-1-exo-4,5,6,7,8,8-heptachloro-3a,4,7,7a-tetrahydro-4,7-methanoisoindene (**3**)*

The *trans*-epoxide **2** (2.5 g) and sodium methoxide (5 g) were dissolved in methanol (50 ml), and the resulting solution was heated under reflux for 2 h and then cooled. Distilled water (300 ml) was added and the aqueous mixture extracted with chloroform (total 150 ml) which provided a brown oil (2.25 g) on evaporation. Distillation under vacuum yielded the product **3** as a colorless oil 1.97 g (80% yield), b.p. 130–132°/0.1 mm; i.r. bands (liquid film) at 3380 (broad hydroxyl) and 1595 cm^{-1} (ClC=CCl double bond); n.m.r.: τ 3.95 (dd, 1H, H-3, $J_{3,7a}$ = 1.5, $J_{2,3}$ = 7 Hz), 5.0 (m, 1H, H-2), 6.25 (dd, 1H, H-1, $J_{1,3}$ = 7, $J_{1,7a}$ = 9 Hz), 6.65 (dd, 1H, H-7*a*, $J_{7a,3}$ = 1.5, $J_{7a,1}$ = 9 Hz), 7.2 (s (broad), 1H, OH); 386 (M^+), 351 (M-Cl), 314 (M-2HCl), 287, 280, 251, 217, 181, 115.

Anal. Calcd. $C_{10}H_5Cl_7O$: C, 30.8; H, 1.3; Cl, 63.9. Found: C, 30.73; H, 0.98; Cl, 63.84.

*1-exo-4,5,6,7,8,8-Heptachloro-2-oxa-3a,4,7,7a-tetrahydro-4,7-methanoisoindene (**4**)*

Compound **3** (1.1 g) dissolved in acetone (50 ml) was stirred for 2 h at room temperature with activated MnO_2 (11 g; prepared according to Attenburrow *et al.*) (12). Filtration and evaporation of the solvent yielded a yellow semi-solid which was crystallized from ether–hexane to give prismatic crystals, m.p. 144–145 °C, 0.93 g (85% yield); n.m.r.: τ 3.5 (d, 1H, H-3, $J_{3,7a}$ = 1.5 Hz), 5.98 (s, 2H); 384 (M^+), 349 (M-Cl), 321 (M-Cl—CO), 314 (M-2Cl), 285, 279 (M-3Cl), 251 (M-Cl—CO—2Cl) 214, 181.

Anal. Calcd. for $C_{10}H_3Cl_7O$: C, 31.00; H, 0.78: Cl, 64.23. Found: C, 31.03; H, 0.48; Cl, 64.41.

*1-exo-2-exo-4,5,6,7,8,8-Octachloro-3a,4,7,7a-tetrahydro-4,7-methanoisoindene (**6**)*

Compound **3** (1.7 g), thionyl chloride (2 ml), and pyridine (5 drops) in benzene (50 ml) were refluxed for 3 h. Evaporation resulted in a dark brown viscous oil (1.77 g) which was partitioned between hexane–water. The organic phase was washed, treated with decolorizing charcoal (4 g), filtered, evaporated, and the residue crystallized from hexane to give needles, 1.2 g (68% yield), m.p. 159–160°. The i.r. ν_{max} (Nujol) 1595 cm^{-1} (ClC=CCl); n.m.r.: τ 3.69 (dd, 1H, H-3, $J_{3,7a}$ = 2, $J_{2,3}$ = 4 Hz), 5.12 (m, 1H, H-2), 5.75 (dd, 1H, H-7*a*, $J_{7a,3}$ = 2, $J_{7a,1}$ = 8 Hz), 6.18 (dd, 1H, H-1, $J_{1,7a}$ = 8, $J_{1,2}$ = 4 Hz); 404 (M^+), 369 (M-Cl), 333 (M-Cl—HCl) 298 (M-2Cl—HCl) 285, 263 (M-2Cl—HCl), 251, 228, 217.

Anal. Calcd. for $C_{10}H_4Cl_8$: C, 29.4; H, 1.0; Cl, 69.66. Found: C, 28.9; H, 0.81; Cl, 70.05.

2-oxa-4,5,6,7,8,8-Hexachloro-3a,4,7,7a-tetrahydro-4,7-methanoindane

Compound **4** (100 mg) was dissolved in acetone (5 ml), aqueous $CrCl_2$ solution (3 ml of 1 *N*) added, and the mixture placed in a water bath maintained at 55–60°. The g.l.c. analysis showed the reaction was complete after 15 min and resulted in two products. The mixture was extracted with hexane (50 ml) and evaporated to small volume. Crystallization afforded the major product as long needles, 75 mg (82% yield) m.p. 192–193° (lit. (9) m.p. about 180°). Identification was based on comparison of the i.r. spectrum with that of a previously reported sample (9); n.m.r.: τ 6.5 (m, 2H, HC—CH), 7.0 (m, 4H, $2CH_2$); 352 (M^+), 317 (M-Cl) 289 (M-Cl—CO) 270 (C_5Cl_6), 253, 235 ($C_5Cl_5^+$), 217, 183.

We wish to thank E. C. Martelock for technical assistance and P. Elliott, Food Research Institute, Canada Department of Agriculture, Ottawa, for mass spectroscopic data.

1. W. P. Cochrane and A. S. Y. Chau. Chem. Ind. 1696 (1968).
2. J. K. Crandall and L. C. Lin. J. Org. Chem. **32**, 435 (1967).
3. British Patent 714 869 (to Arvey Corp.). September 1, 1954; C. A. **50**, 402*i* (1956).
4. J. N. Damico, R. P. Barron, and J. M. Ruth. Org. Mass Spectrosc. **1**, 331 (1968).
5. W. C. Kray Jr., and C. E. Castro. J. Am. Chem. Soc. **86**, 4603 (1964).
6. J. K. Kochi, D. M. Singleton, and L. J. Andrews. Tetrahedron, **24**, 3503 (1968).
7. J. R. Hanson and E. Premuzic. Angew. Chem. **7**, 247 (1968).
8. W. P. Cochrane and A. S. Y. Chau. J. Assoc. Offic. Anal. Chem. **51**, 1267 (1968).
9. K. H. Büchel, A. E. Ginsberg, and R. Fischer. Chem. Ber. **99**, 405 (1966).
10. G. T. Brooks and A. Harrison. Life Sci. **6**, 1439 (1967).
11. K. Mackenzie and P. R. Young. J. Chem. Soc. C, 1242 (1970).
12. J. Attenburrow, A. F. B. Cameron, J. H. Chapman, R. M. Evans, B. A. Hems, A. B. A. Jansen, and T. Walker. J. Chem. Soc. 1094 (1952).

Can. J. Chem. Downloaded from www.nrcresearchpress.com by 210.87.254.42 on 09/05/12
For personal use only.

A Novel Phenolic Zwitterion

M. J. NYE[1] AND E. F. V. SCRIVEN[2]
Department of Chemistry, University of Guelph, Guelph, Ontario

Received June 24, 1971

Two examples (2-ammonio-3′,5′-dibromo-4′-oxidoacetophenone (**4***a*) and 2-pyridinio-3′,5′-dibromo-4′-oxidoacetophenone (**4***b*)) of a new type of phenolic zwitterion have been synthesized and their i.r., u.v., and p.m.r. spectra are discussed.

Deux exemples (l'ammonio-2 dibromo-3′,5′ oxydo-4′ acétophénone (**4***a*) et la pyridinio-2 dibromo-3′,5′ oxydo-4′ acétophénone (**4***b*)) d'un nouveau type de zwitterion phénolique ont été synthétisés et leurs spectres i.r., u.v., et r.m.p. discutés.

Canadian Journal of Chemistry, 49, 3572 (1971)

Can. J. Chem. Downloaded from www.nrcresearchpress.com by 210.87.254.5 on 09/05/12
For personal use only.

Introduction

3,5-Dibromotyrosine (**1***a*), 3,5-diiodotyrosine (**1***b*), and certain related compounds such as thyroxine have been found in corals (1), sponges (2), seaweeds (3), thyroid glands (4), and human blood serum (5). We were interested in synthesizing related compounds of general formula **2**, which are also internal salts, but are of a hitherto unknown type. This new type of structure is vinylogously related to the normal zwitterionic tautomer of the α-amino carboxylic acids (**3**).[3] Thus the system was of interest from the points of view of both structural novelty and the relationship to naturally occurring materials.

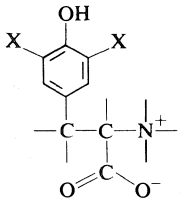

1

a X = Br,
b X = I

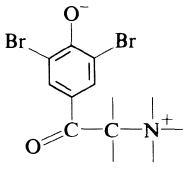

2

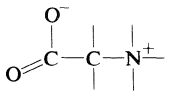

3

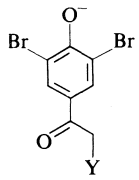

4

a Y = NH_3^+
b Y = $C_5H_5N^+$
c Y = Br K^+
d Y = Br NH_4^+
e Y = Br $C_5H_5NH^+$
f Y = NH_2 Na^+

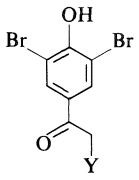

5

a Y = NH_3^+ Cl^-
b Y = $C_5H_5N^+$ Cl^-
c Y = Br
d Y = NH_2

This note reports the preparation and spectral properties of 2-ammonio-3′,5′-dibromo-4′-oxidoacetophenone (**4***a*) and 2-pyridinio-3′,5′-dibromo-4′-oxidoacetophenone (**4***b*).

Preparation

The internal salt **4***b* was prepared in good yield by heating 2-bromo-3′,5′-dibromo-4′-hydroxyacetophenone (**5***c*) with excess pyridine in methanol. Lower concentrations of pyridine or less severe heating conditions gave rise quantitatively to the pyridinium salt **4***e*.

Reaction of 2-bromo-3′,5′-dibromo-4′-hydroxyacetophenone (**5***c*) with ammonia likewise yielded its ammonium salt, **4***d*, under mild conditions, and the internal salt, **4***a*, under rigorous conditions. The conditions were somewhat critical since overheating led to complex mixtures of self-condensation products.

Structure

The structures of the ammonia and pyridine reaction products were deduced mainly by tabulation of their spectral data together with the spectral data of 2-bromo-3′,5′-dibromo-4′-hydroxyacetophenone (**5***c*) and its potassium salt. Table 1 shows that the i.r., u.v., and p.m.r. spectra fall into two distinctly different, self-consistent categories having general formulae **4** and **5**. In the i.r. spectra the carbonyl band of **4** absorbs at 1642–1675 cm^{-1}, whereas that of **5** absorbs at

[1]To whom correspondence should be addressed.
[2]Present address: Department of Chemistry, University College, London, England.
[3]Kende (6) has discussed a similar vinylogous relationship in cyclopropenone chemistry.

TABLE 1. Spectral data

Compound	The i.r. (Nujol mull) cm^{-1}; C=O stretch	The p.m.r (DMSO solution) τ; aromatic 2CH	and aliphatic CH_2	The u.v. (95% ethanol solution) nm (ε); bands above 220 nm
5*c*	1686	1.86	5.66*	286 (11000)
a	1695	1.77	5.44	282 (9900)
b	1689	1.78	3.57†	281 (14000)
4*c*	1642	2.16	5.58	253 (8500), 342 (27000)
a	1661	2.07	5.72	255 (6900), 346 (21000)
b	1664, 1675	2.05	3.80	259 (9800), 350 (26000)
d	1650	2.11	5.54	261 (6200), 355 (18000)
e	1669			
f				253 (7500), 339 (19000)

*$CDCl_3$ solvent. Unstable in DMSO.
†Acetic acid solvent.

1686–1695 cm^{-1}. The u.v. spectra reveal that **4** has two bands at 253–261 (ε 6200–9800) and 339–355 nm (ε 18 000 – 27 000), and **5** has a single band at 281–286 nm (ε 9900 – 14 000). In the p.m.r. spectra the aromatic protons fall at 2.05–2.16 τ for **4** and 1.77–1.86 τ for **5**, a shift of about 0.3 p.p.m.

It is of interest that the zwitterionic structure **4***a* is the preferred tautomer in DMSO and the solid state, rather than the uncharged form **5***d*, which behavior is also usually the case with the α-amino carboxylic acids. Further evidence for the predominance of zwitterionic tautomer **4***a* is given by pK_a measurements. One can predict that the pK_a (proton gained) for the neutral compound (**5***d*) should be *ca.* 7.5 by analogy to glycine methyl ester (pK_a = 7.59). The observed[4] pK_a was 3.81, nearly four units different from that predicted, indicating tautomer **5***d* to be incorrect.

Concerning the products arising from pyridine, **6** was initially considered as a possible structure for the compound now known to be **4***b*, since this structure places the compound into the known class of pyridinium benzoylmethylids (8). However the structure was rejected since the p.m.r. spectrum in DMSO shows two aliphatic protons rather than one. Nevertheless the presence of the ylid **6** in trace amounts in solutions of **4***b* is inferred by the observation that the aliphatic protons of **4***b* exchange rapidly in acetic acid solutions. The p.m.r spectrum in acetic acid-d_4 shows that exchange is virtually complete within 10 min at 37 °C.

A further point of interest concerning the compounds of general formula **4** was the question of whether resonance structure **7** contributes much to the resonance hybrid. The i.r. data indicate that the resonance contribution is small, since the carbonyl bond at 1642–1669 cm^{-1} is less than 5% lower than that of **5** which falls at 1686–1695 cm^{-1}. This conclusion is also supported by the observation of only a single sharp aromatic absorption in the p.m.r. spectrum at 37 °C indicating that free rotation of the aryl group around an essentially single bond is occurring.

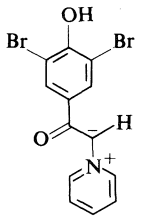

6

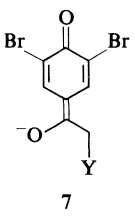

7

Experimental

Melting points were determined on a Meltemp apparatus and are uncorrected. Microanalyses were carried out by Dr. C. Daesslé, Organic Microanalyses, Montreal, Quebec. The reported i.r. data give only the principle sharply defined peaks. The n.m.r. spectra are reported in τ units relative to internal tetramethylsilane.

2,3′,5′-Tribromo-4′-hydroxyacetophenone was prepared by the method of Priestley and Moness (9). The product was recrystallized from methanol/water mixture three times to give a constant m.p. of 128°, ν_{max} (Nujol): 3333, 1686, 1580, 1555, 1307, 1252, 861, 776, 732, 721 cm^{-1}.

Pyridinium Salt of 2,3′,5′-Tribromo-4′-hydroxyacetophenone (4e)

2,3′,5′-Tribromo-4′-hydroxyacetophenone (**5***c*) (3.7 g) was dissolved in a minimum of methanol and pyridine (0.9 ml) was added. The mixture was boiled for 5 min. On cooling, 2.9 g (65%) of the white solid **4***e* precipitated. Removal of solvent gave a further 1.6 g (35%) of product. The two crops were combined and recrystallized from

[4]We thank Dr. M. J. O'Hare of this department for kindly determining this pK_a for us, using the method of Albert and Serjeant (7).

Can. J. Chem. Downloaded from www.nrcresearchpress.com by 210.87.254.5 on 09/05/12
For personal use only.

Can. J. Chem. Downloaded from www.nrcresearchpress.com by 210.87.254.5 on 09/05/12
For personal use only.

methanol; m.p. 230° (dec.); ν_{max} (Nujol): 3205–3012, 2381–2273, 1669, 1580, 1321, 1295, 1250, 1219, 1200, 1144, 689 cm^{-1}.

Anal. Calcd. for $C_{13}H_{10}O_2NBr_3$: C, 34.51; H, 2.21; N, 3.10. Found: C, 34.40; H, 2.41; N, 3.31.

2-Pyridinio-3′,5′-dibromo-4′-hydroxyacetophenone Chloride (5b)

2,3′,5′-Tribromo-4′-hydroxyacetophenone (**7***c*) (3.7 g) was dissolved in the minimum volume of methanol, pyridine (1.8 ml) was added, and the solution refluxed for 10 min. On removal of most of the solvent, a yellow precipitate of 2-pyridinio-3′,5′-dibromo-4′-oxidoacetophenone (**4***b*) was formed in almost quantitative yield. This was filtered off and ground with an excess of dilute hydrochloric acid. The white solid produced was crystallized from water to give **5***b* in 95% yield; m.p. 245° (dec.); ν_{max} (Nujol): 3571, 1689, 1248, 756, 688 cm^{-1}; τ (acetic acid): 0.95–1.42 (3H multiplet, pyridinium), 1.60–1.98 (2H multiplet, pyridinium), 1.78 (2H singlet aromatic), and 3.57 (2H singlet, CH_2).

Anal. Calcd. for $C_{13}H_{10}Br_2ClNO_2$: C, 38.35; H, 2.46; N, 3.44; Cl, 8.82; Br, 39.30. Found: C, 38.59; H, 3.04; N, 3.21; Cl, 8.82; Br, 39.21. (The H analysis was high; however, the H analysis of this compound's conjugate base (**4***b*) was acceptable.)

2-Pyridinio-3′,5′-dibromo-4′-oxidoacetophenone (4b)

2-Pyridinio-3′,5′-dibromo-4′-hydroxyacetophenone chloride (**5***b*) was dissolved in water and aqueous solution of an equivalent amount of sodium bicarbonate was added. The yellow precipitate was washed with water and methanol. The yield of **4***b* was quantitative; m.p. 225° (dec.); ν_{max} (Nujol): 1678, 758, 714, 685 cm^{-1}; τ (DMSO): 0.98–2.16 (5H multiplet, pyridinium), 2.04 (2H singlet, aromatic), and 3.80 (2H singlet, CH_2).

Anal. Calcd. for $C_{13}H_9Br_2NO_2$: C, 42.05; H, 2.43; N, 3.77; Br, 43.10. Found: C, 42.17; H, 2.61; N, 3.51; Br, 43.12.

2-Ammonio-3′,5′-dibromo-4′-oxidoacetophenone (4a)

2,3′,5′-Tribromo-4′-hydroxyacetophenone (2 g) was dissolved in diglyme (10 ml) and concentrated ammonia solution (90 ml) was added. This solution was evaporated to one third its volume in an open beaker on a hot plate over a 20 min period. It was then allowed to stand at room temperature for 18 h. The grayish-yellow precipitate which was crude 2-ammonio-3′,5′-dibromo-4′-oxidoacetophenone (**4***a*) (1.4 g, 87%) was filtered off and washed with water and ether. It was then boiled for 15 min with vigorous stirring in concentrated hydrochloric acid (80 ml). The undissolved solid was removed using a sintered-glass filter. The filtrate was neutralized by adding solid sodium bicarbonate, which caused **4***a* to precipitate (1.2 g). Further purification was effected by filtering off the solid, redissolving it in hydrochloric acid, filtering the solution and reprecipitating with sodium bicarbonate. The m.p. 230° (dec.); ν_{max} (Nujol): 2300–2650, 1661, 1250, 869, 786, 750, 719 cm^{-1}; τ ($CHCl_3$-*d*): 1.84 (2H singlet, aromatic), 5.36 (2H singlet, CH_2), and 6.46 (3H singlet NH_3^+).

Anal. Calcd. for $C_8H_7Br_2NO_2$: C, 31.20; H, 2.26; Br, 51.60; N, 4.54. Found: C, 31.35; H, 2.68; Br, 51.71; N, 4.70. (The H analysis was high; however, the H analysis of its hydrochloride salt **5***a* was acceptable).

2-Ammonio-3′,5′-dibromo-4′-hydroxyacetophenone Chloride (5a)

Compound **5***a* may be prepared by dissolving 2-ammonio-3′,5′-dibromo-4′-oxidoacetophenone (**4***a*) in the minimum amount of boiling dilute hydrochloric acid and allowing the product to crystallize. The m.p. 220° (dec.); ν_{max} (Nujol): 2620, 1690, 1253, 1142, 869, 736 cm^{-1}; τ (DMSO): 1.46 (1H broad, OH), 1.76 (2H singlet, aromatic), 5.42 (2H broad, CH_2), and 6.22 (3H broad, NH_3^+).

Anal. Calcd. for $C_8H_8Br_2ClNO_2$: C, 27.80; H, 2.32; Br, 46.40; Cl, 10.03; N, 4.06. Found: C, 28.00; H, 2.38; Br, 46.64; Cl, 10.05; N, 4.04.

Potassium Salt of 2,3′,5′-Tribromo-4′-hydroxyacetophenone (4c)

2,3′,5′-Tribromo-4′-hydroxyacetophenone (**5***c*) (1 g) was dissolved in the minimum of methanol (*ca.* 10 ml) and potassium hydroxide pellets (3 g) were added. A precipitate formed after 2 min. After 2 h the potassium hydroxide had dissolved and the remaining precipitate of **4***c* was filtered off and recrystallized from methanol, m.p. 265° (dec.); ν_{max} (Nujol): 1642, 1567, 1250, 1124, 962, 895, 809, 806, 747, 714, 665 cm^{-1}; τ (DMSO): 2.20 (2H singlet, aromatic) and 5.57 (2H singlet, CH_2).

Addition of acid to a solution of **4***c* reconverts it to **5***c*.

Ammonium Salt of 2,3′,5′-Tribromo-4′-hydroxyacetophenone (4d)

2,3′,5′-Tribromo-4′-hydroxyacetophenone (**5***c*) (3.7 g) was dissolved in benzene (40 ml) that had been dried over sodium sulfate, and excess ammonia gas (dried over potassium hydroxide pellets) was passed through this solution for 10 min. Immediately a greenish-yellow precipitate formed. After 1 h the precipitate was filtered off, washed with benzene and ether, and dried in a vacuum desiccator; yield 3.0 g (77%). The product was purified by vacuum sublimation, m.p. 120° (dec.); ν_{max} (Nujol) 3155–3030, 1650, 1563, 1334, 1274, 1198, 1176, 725 cm^{-1}; τ (DMSO): 2.14 (2H singlet, aromatic), 5.56 (2H singlet, CH_2), and 6.65 (singlet band of H_2O impurity in solvent probably hides NH_4^+).

Addition of acid to a solution of **4***d* reconverts it to **5***c*.

Financial support of the National Research Council of Canada is acknowledged.

1. C. R. Mörner. Z. Physiol. Chem. **88**, 138 (1913).
2. G. M. Sharma and P. R. Burkholder. Tetrahedron Lett. 4147 (1967).
3. J. Roche and Y. Yagi. Compte. Rende. Soc. Biol. **146**, 643 (1952).
4. M. Henze. Z. Physiol. Chem. **51**, 64 (1907).
5. R. J. Block, S. C. Werner, R. H. Mandl, V. V. Row, and I. Radichevich. Arch. Biochem. Biophys. **88** 98 (1960).
6. A. S. Kende. J. Am. Chem. Soc. **85**, 1882 (1963).
7. A. Albert and E. P. Sergeant. Ionization constants of acids and bases. Methuen and Co. Ltd., London, 1962. p. 69.
8. A. W. Johnson. Ylid chemistry. Academic Press, New York, N.Y., and London, 1966. p. 251.
9. H. M. Priestley and E. Moness. J. Org. Chem. **5**, 358 (1940).

Free Energy Barrier to Rotation of the Amino Group in 2-Aminoacetophenone

R. WASYLISHEN[1] AND T. SCHAEFER
Department of Chemistry, University of Manitoba, Winnipeg, Manitoba

Received July 5, 1971

The free energy of activation for hindered rotation of the amino group about the *N*-aryl bond in 2-aminoacetophenone is found to be 10.6 ± 0.5 kcal/mol in toluene solution at 233 ± 10 °K. Separate amino p.m.r. peaks are observed at low temperatures and these are strongly broadened by incompletely relaxed spin–spin coupling to the quadrupolar ^{14}N nucleus, making a more accurate determination of activation parameters impractical. Some INDO molecular orbital calculations are performed in an attempt to rationalize the barrier magnitude.

L'énergie libre d'activation pour la rotation empêchée du groupe amine autour de la liaison *N*-aryle dans l'amino-2 acétophénone est de 10.6 ± 0.5 kcal/mol dans une solution de toluène à 233 ± 10 °K. Des pics séparés, relatifs à la r.m.p. de l'amine, sont observés à basses températures; ceux-ci s'élargissent beaucoup par suite d'une relaxation incomplète du couplage spin–spin au noyau quadrupolaire de ^{14}N. De ce fait, une détermination précise des paramètres d'activation n'est pas pratique. Dans le but de rationaliser la grandeur de la barrière, des calculs INDO d'orbitales moléculaires ont été effectués.

Canadian Journal of Chemistry, 49, 3575 (1971)

The barrier to rotation about the amino nitrogen – ring carbon bond in *N*-alkyl derivatives of 2,6-dinitro- and 2,4,6-trinitroanilines is evidently determined mainly by hydrogen bonding of the N—H proton to the nitro group, repulsion between the *N*-alkyl group and the other, adjacent, nitro group being less important (1–3). The barriers are found by following the temperature dependence of the n.m.r. spectra of the ring protons, which are non-equivalent at low temperatures. A barrier was not detected by n.m.r. methods in *N*-unsubstituted and *N*,*N*-dimethyl derivatives (1).

If hydrogen bonding is the determining factor, a barrier should be detectable in *N*-unsubstituted aniline derivatives and observation of non-equivalent amino protons is then a direct indication of hindered rotation about the *N*-aryl bond.

When a 15 mol % solution of 2-aminoacetophenone (**1**) in toluene-d_8 is cooled to −70 °C, two broad amino p.m.r. peaks are observed. Their separation is 336 ± 10 Hz at 100 MHz and 200 ± 10 Hz at 60 MHz. The coalescence temperature is −37 ± 10 °C at 100 MHz; −43 ± 10 °C at 60 MHz. It follows (4) that the free energy of activation, $\Delta G^{\ddagger}$ for the hindered rotation at the coalescence temperatures is 10.58 ± 0.48 kcal/mol at 100 MHz and 10.54 ± 0.50 kcal/mol at 60 MHz.

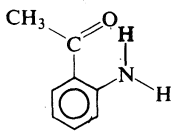

1

The broadness of the amino proton peaks (~30 Hz) arises from incompletely relaxed scalar coupling to the quadrupolar ^{14}N nucleus and therefore a proper line-shape analysis will only be possible on the ^{15}N labelled compounds; unless, of course, decoupling facilities for nitrogen are available.

At room temperature, where rotation of the amino group is rapid on the time scale defined by the low-temperature peak separation, characteristic spin–spin coupling (5) of 0.3 Hz over five bonds between the amino protons and ring protons is observed, showing that any intermolecular amino proton exchange is unimportant in these experiments.

The well-known aromatic solvent induced shifts (6) are temperature dependent and must be allowed for in accurate rate studies by proton resonance measurements (7). Calibration of the shifts of the amino proton peaks as a function of temperature at temperatures substantially below coalescence demonstrated that any difference in the temperature coefficients of the solvent effects on the chemical shifts of the two peaks caused an error whose magnitude was much less than that quoted above for $\Delta G^{\ddagger}$.

By measuring the two-bond proton–deuterium coupling in the H–N–D group of monodeutero-2-

[1]NRCC Scholarship, 1971–1972.

Can. J. Chem. Downloaded from www.nrcresearchpress.com by 210.87.254.105 on 09/05/12
For personal use only.

Cl-aniline-^{15}N, we have shown that the coupling of the protons in the amino group is 1 ± 1 Hz in magnitude (8). This parameter is therefore also unimportant in the experiments described above.

Molecular orbital calculations in the INDO approximation (9) predict that the conformation in which the amino group defines a plane perpendicular to the benzene ring is 15.0 kcal/mol less stable than a conformation in which a planar amino group has one N—H bond approaching the carbonyl group. In this hydrogen-bonded conformation the molecule is taken as completely planar, apart from the methyl hydrogens. Two C—H bonds of the methyl group are assumed to be staggered relative to the ortho C—H bond of the benzene ring. A planar amino group is a reasonable approximation in the hydrogen-bonded situation because the spin–spin coupling between the amino protons and the ring protons six bonds removed from them is apparently less than 0.1 Hz in magnitude (see ref. 5 for the arguments which allow for this conclusion).

Standard bond lengths and angles (9) were assumed in the INDO computations. Considering the many other approximations involved, *e.g.* the carbonyl group is kept coplanar with the benzene ring, the amino group is assumed planar in both conformations, the solvent may play a role and so on; the predicted barrier is reasonably close to the experimental one. A proper calculation would no doubt minimize the energy of the molecule as a function of bond lengths and angles at successive stages in the rotation of the amino group but the expense incurred would hardly be justifiable at this time.

We are pursuing the syntheses of appropriate ^{15}N-aniline derivatives with a view to finding accurate entropies of activation for the rotation of the amino group and to studying the changes in electron distribution in the N—H bond brought about by hydrogen-bonding, as detected by coupling constant variations.

Experimental

The solution of 15 mol % 2-aminoacetophenone in toluene-d_8 was carefully degassed by the freeze–pump–thaw technique. Tetramethylsilane served as internal reference. The p.m.r. spectra at 60 MHz were recorded on an A56-60 spectrometer, a methanol sample serving as a temperature calibrator. The spectra at 100 MHz were taken in the frequency sweep mode on an HA100-D spectrometer. Sample temperatures were known to at least 1 °K at 100 MHz but in view of the data given previously their accuracy is not crucial in this experiment.

Rate-dependent spectra approximating as closely as possible to observed line-widths and shifts were computed for a two-site exchange process by a program written by one of us (R.W.). Assurance was thereby obtained that the coalescence temperatures quoted above were known to at least the stated accuracy, the latter being rather a pessimistic estimate.

The INDO computations (10) were performed on an IBM 360/65 computer as were the line-shape simulations.

We are grateful for financial support from the National Research Council of Canada.

1. J. HEIDBERG, J. A. WEIL, G. A. JANUSONIS, and J. K. ANDERSON. J. Chem. Phys. **41**, 1033 (1964).
2. J. A. WEIL, A. BLUM, A. H. HEISS and J. K. KINNAIRD. J. Chem. Phys. **46**, 3132 (1967).
3. J. v. JOUANNE and J. HEIDBERG. Ber. Bunsenges. physik. Chem. **75**, 261 (1971).
4. G. BINSCH. *In* Topics in stereochemistry. *Edited by* E. L. Eliel and N. L. Allinger. Vol. 3. Interscience Publishers, New York, N.Y., 1968.
5. R. WASYLISHEN and T. SCHAEFER. Can. J. Chem. **48**, 1263 (1970).
6. R. WASYLISHEN, T. SCHAEFER, and R. SCHWENK. Can. J. Chem. **48**, 2885 (1970).
7. J. PEELING, B. W. GOODWIN, T. SCHAEFER, and C. M. WONG. Can. J. Chem. **49**, 1489 (1971).
8. R. WASYLISHEN and T. SCHAEFER. Can. J. Chem. In press.
9. J. A. POPLE and D. L. BEVERIDGE. Approximate molecular orbital theory. McGraw-Hill Book Co., Inc., New York, N.Y., 1970.
10. Program No. 141. QCPE. Indiana University, Bloomington, Indiana.

Can. J. Chem. Downloaded from www.nrcresearchpress.com by 210.87.254.105 on 09/05/12
For personal use only.

Magnetic Field Effect on Electrochemiluminescence of Carbazole

K. S. V. SANTHANAM

Chemical Physics Group, Tata Institute of Fundamental Research, Bombay 5, India

Received May 4, 1971

Effect of magnetic field on electrochemiluminescence of carbazole has been studied in *N,N* dimethylformamide. The emission intensity increases with increasing applied field with a tendency to decrease at high magnetic fields. An explanation involving perturbation of triplet–triplet annihilation rate is proposed.

L'effet d'un champ magnétique sur l'électro-chimioluminescence du carbazole a été étudié dans la *N,N*-diméthylformamide. L'intensité de l'émission augmente si l'intensité du champ appliqué augmente avec cependant une tendance à la diminution à des champs magnétiques élevés. Une explication impliquant la vitesse d'annihilation triplet–triplet est proposée.

Canadian Journal of Chemistry, **49**, 3577 (1971)

Can. J. Chem. Downloaded from www.nrcresearchpress.com by 210.87.254.40 on 09/05/12
For personal use only.

The generation of electrochemiluminescence of carbazole during the reduction of carbazole in *N,N* dimethylformamide (DMF) at −2.7 V *vs.* saturated calomel electrode has been reported (1, 2). The emission spectrum during this reduction has a maximum at 450 nm with shoulders at 420 and 470 nm. The electrochemiluminescence spectrum thus differs considerably from the photoexcited carbazole which has a maximum at 346 nm in fluid solutions and around 440 nm in rigid medium (corresponding to phosphorescence). The nature of the excited state could not be conclusively arrived at in the earlier studies. However, the close resemblance of the phosphorescent emission with electrochemiluminescent emission suggested the possible involvement of triplet carbazole in the emission process. Although our attempts to obtain unambiguous evidence of the triplet state by studying the half field transition in electron spin resonance have not yielded fruitful results, nevertheless during these studies the application of magnetic field changed the electrochemiluminescent intensity significantly. In this note the results of the effect of magnetic field on electrochemiluminescent intensity and the probable reasons for the change in the intensity are discussed.

Experiments were conducted by holding the potential of the mercury pool cathode at −2.7 V in DMF containing $(C_4H_9)_4NI$ as the supporting electrolyte in the conventional cell (2). The cell was rigidly mounted between the pole pieces of Varian Magnet (V 4500) of 9 in. diameter with a Fieldial power supply. The light output was monitored by a photomultiplier tube 1P 28 with an S_5 spectral response which was placed about 50 cm away from the magnet to avoid any field effects leading to stray emission. The field near the location of the photomultiplier tube was tested with a Gaussmeter and found to be negligible. The output from the photomultiplier was amplified through a pre-amplifier and fed to a HP *X–Y* recorder (Model 135 AM). In some experiments the preamplifier output was connected to a voltage to frequency (HP 2212 A) converter whose frequency was measured by a counter.

The change in the emission intensity after subtracting the dark current values is shown in Fig. 1. The intensity change is negligible up to 500 G and showed a significant increase at higher fields. The intensity showed a tendency to decrease at fields greater than 3000 G. It should be pointed out that the intensity fluctuations were similar both in the presence and the absence of the field.

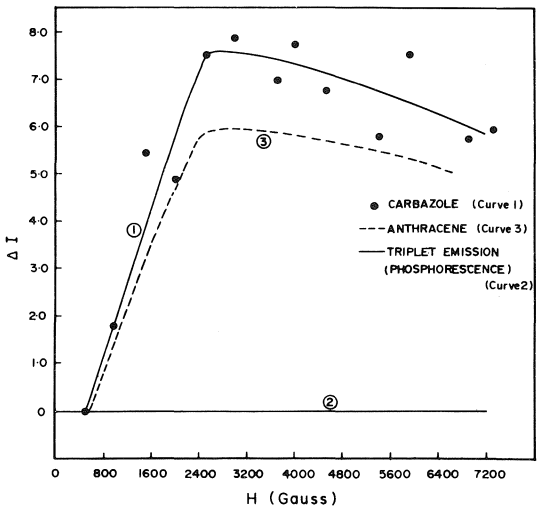

FIG. 1. Variation of emission intensity with field.

The zero field intensity was measured every time before the magnetic field was turned on and the zero field values were highly reproducible. The zero field values were restored generally within 10 s of the removal of the magnetic field.

In Fig. 1 is also shown the emission intensity behavior in the magnetic field of a system where triplet–triplet annihilation is involved (anthracene) in one of the rate determining steps of electrochemiluminescence. The curve *3* in the figure was obtained by carrying out the electrochemiluminescence of anthracene in the presence of *p*-phenylenediamine. The excited state is formed by reaction of anthracene anion with *p*-phenylene diamine cation through triplet–triplet annihilation. The absence of perturbation in the emission intensity in the magnetic field of triplet emission (3) (phosphorescence) is also shown by curve *2* in the figure.

The emission intensity enhancement in the magnetic field could arise if there is increased production of the radical in the field. The reduction of carbazole (A) to form the carbazole radical anion (A^-) is diffusion controlled and hence the reduction current is not altered in the magnetic field, suggesting the absence of increased formation of A^-. This is in agreement with the observations of Faulkner and Bard (4). The other possibility would involve mixing up of paramagnetic energy states (triplets) with singlet states resulting in population changes of the singlet emitting state. The singlet level of carbazole and its derivatives are placed about 1 eV above the triplet (5) and the zero field splitting value is of the order of 0.10 cm^{-1} (6). Hence mixing up of states in small magnetic fields seems to be remote.

It is established experimentally that the emission arising from triplet–triplet annihilation is influenced by a magnetic field. This process is understood theoretically in the case of solid state luminescence by Merrifield and co-workers (7, 8). The fact that the same magnetic field dependence is observed in the electrochemiluminescence of carbazole in solution indicates that triplet–triplet annihilation occurs after the electrochemical process. Thus the mechanism appears to be

$$A + e \rightarrow A^-$$

$$A^- + X \rightarrow {}^3F + X^-$$

$$^3F + {}^3F \rightarrow {}^*F + F$$

and accounts for the emission at 450 nm.

The author wishes to thank Dr. B. Venkataraman for helpful discussions and Mr. V. R. Bhagat, Mr. Pachauri, and Mrs. Shah for technical assistance.

1. K. S. V. Santhanam, R. N. O'Brien, and A. D. Kirk. Can. J. Chem. **47**, 1356 (1969).
2. A. J. Bard, K. S. V. Santhanam, S. Cruser, and L. Faulkner. *In* Fluorescence. *Edited by* G. G. Guilbault. Marcel Dekker, Inc., New York, N.Y. 1967. Chap. 14.
3. D. Wyrsch and H. Labhart. Chem. Phys. Lett. **8**, 217 (1971).
4. L. Faulkner and A. J. Bard. J. Am. Chem. Soc. **91**, 6495 (1969).
5. G. N. Lewis and M. Kasha. J. Am. Chem. Soc. **66**, 2100 (1944).
6. S. P. McGlynn, T. Azumi, and M. Kinoshita. The triplet state. Prentice Hall, Inc., New Jersey. 1969. p. 363.
7. R. C. Johnson, R. E. Merrifield, P. Avakian, and R. B. Flippen. Phys. Rev. Lett. **19**, 285 (1967).
8. R. C. Johnson and R. E. Merrifield. Phys. Rev. **1B**, 896 (1970).

Can. J. Chem. Downloaded from www.nrcresearchpress.com by 210.87.254.40 on 09/05/12
For personal use only.

Can. J. Chem. Downloaded from www.nrcresearchpress.com by 210.87.254.105 on 09/05/12
For personal use only.

Crystal Structure of *cis*-Dithiocyanatobis(1,10-phenanthroline)mercury(II), a Six-coordinate Mercury Complex

A. L. Beauchamp, B. Saperas, and R. Rivest
Département de Chimie, Université de Montréal, Montréal, Québec

Received June 24, 1971

cis-Dithiocyanatobis(1,10-phenanthroline)mercury(II) is a six-coordinate monomeric molecule with a distorted octahedral geometry.

Le *cis*-dithiocyanatobis(1,10-phenanthroline)mercure(II) est une molécule monomère où le mercure hexacoordonné possède un environnement octaédrique déformé.

Canadian Journal of Chemistry, **49**, 3579 (1971)

In the crystals of $HgCl_2$, $Hg(CN)_2$, $K_2HgCl_4.H_2O$, HgO and many other compounds (1), the mercury atom occupies the center of an approximate octahedron of donor atoms. However, the metal does not interact to the same extent with all of its six neighbors. In $HgCl_2$, for instance, mercury forms only two short Hg—Cl bonds of 2.25 Å and the crystal is best described in terms of discrete Cl—Hg—Cl molecules. The environment of mercury is completed through weaker interaction with two more pairs of chlorine atoms on neighboring molecules, at 3.34 and 3.63 Å, respectively. According to the classification proposed by Grdenic (1), the mercury atoms in such a compound would have an *effective* coordination number of six, but a *characteristic* coordination number of two.

Several neutral ligands have been reported to form $[HgL_6]^{2+}$ or $[Hg(L—L)_3]^{2+}$ monomeric complex ions in which mercury would achieve a characteristic coordination number of six (2). However, detailed information on the geometry and bond lengths in such species appears to be missing at the present time (1). On the basis of the infrared spectrum, the adduct $Hg(SCN)_2.2Phen$ (where Phen = 1,10-phenanthroline) was recently described as potentially six-coordinate (3). Preliminary results on the crystal structure of the latter compound definitely confirm this assumption.

The crystal belongs to the space group $P\bar{1}$ with two $Hg(SCN)_2Phen_2$ molecules per unit cell: $a = 13.25$ Å, $b = 11.08$ Å, $c = 8.44$ Å, $\alpha = 105° 12'$, $\beta = 83° 15'$, $\gamma = 90° 55'$, $D_m = 1.95$ g cm^{-3} and $D_c = 1.99$ g cm^{-3}. The intensity data were collected with a Picker FACS-1 automatic diffractometer using Ni-filtered CuKα radiation. A total of 1763 independent observed reflexions within a halfsphere of $2\theta \leqslant 120°$ were used to solve the structure by means of the heavy atom method. At the present time, all atoms, except hydrogens, have been located and the refinement has been carried out with individual isotropic thermal parameters to a conventional R factor of 0.116.

The crystal consists of discrete monomeric molecules. Two thiocyanato groups *cis* to each other and four nitrogen atoms from phenanthroline molecules acting as bidentate ligands achieve an approximately octahedral environment about mercury. Optical isomerism is expected for *cis*-$MX_2(L—L)_2$ octahedral complexes and the crystal actually is a racemic mixture, the enantiomorphs being related by the inversion center of the unit cell.

The fixed spacing of the nitrogen atoms within the rigid phenanthroline ligand involves certain constraints on the geometry of the complex. Thus, the nitrogen–metal–nitrogen angles in the chelate rings and the corresponding metal–nitrogen bond lengths become fully correlated. In *cis*-$Hg(SCN)_2Phen_2$, the small N—Hg—N angles (66 and 69°) appear reasonable in regard to the Hg—N bonds ranging from 2.37 to 2.53 Å, where the large mercury atom is involved. A still smaller value of 63° has been obtained for the N—Tl—N angle in $[Tl(CH_3)_2Phen]ClO_4$, where the Tl—N distances are 2.57 Å (4). The values

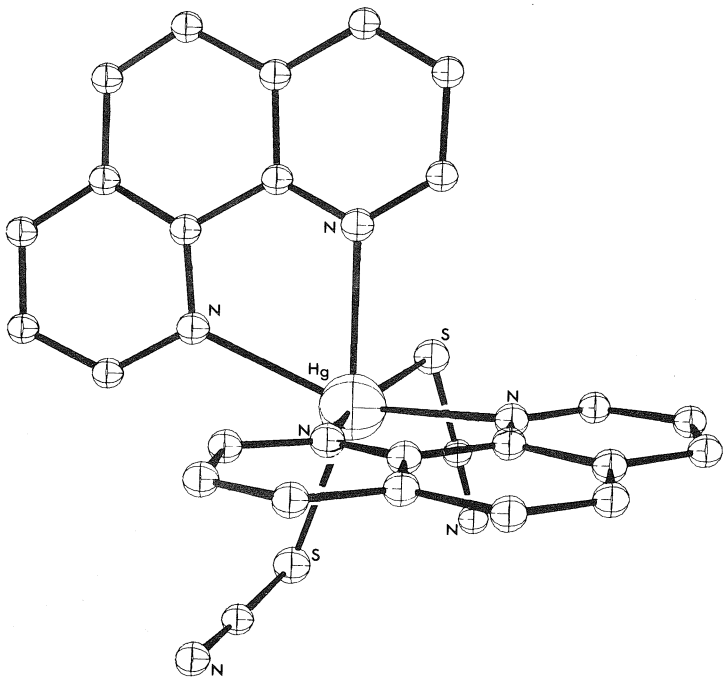

FIG. 1. Projection of the molecule. Unlabeled circles are carbon atoms.

stated above for the Hg—N bond lengths are similar to those reported for the mercurous complex salt $[Hg_2Phen](NO_3)_2$ (2.30 and 2.48 Å) (5). The Hg—N distances reported for the adducts $HgCl_2$.2Pyridine (2.60 Å) (1) and $HgCl_2$.Collidine (2.18 Å (6)) differ considerably from each other in spite of the close similarity of the ligands. Consequently, the lack of sufficient structural data on mercuric complexes with pyridine-type ligands precludes any significant conclusion at this time as to the specific effects of the rigid phenanthroline ligands in mercury compounds.

Coordination of the thiocyanato group through the sulfur atom is quite common for mercury (1). The available data on the mercury-thiocyanato compounds indicate a trend of decreasing Hg—S bond lengths with decreasing characteristic coordination number. Thus, in this six-coordinate complex, Hg—S distances of 2.58 and 2.62 Å are observed. In a series of compounds containing the tetrahedral four-coordinate $[Hg(SCN)_4]^{2-}$ unit, the Hg—S bonds average 2.52 Å (2), while the linear two-coordinate molecules ClHgSCN, BrHgSCN (7), and $Hg(SCN)_2$ (8) show still shorter bonds of 2.31, 2.32, and 2.38 Å, respectively.

We wish to thank the National Research Council of Canada for financial support.

1. D. GRDENIC. Q. Rev. **19**, 303 (1965).
2. A. A. SCHILT and R. C. TAYLOR. J. Inorg. Nucl. Chem. **9**, 211 (1959). R. L. CARLIN, J. ROITMAN, M. DANKLEFF, and J. O. EDWARDS. Inorg. Chem. **1**, 182 (1962). K. KRISHNAN and R. A. PLANE. Inorg. Chem. **5**, 852 (1966).
3. S. C. JAIN and R. RIVEST. Inorg. Chim. Acta, **4**, 291 (1970).
4. T. L. BLUNDELL and H. M. POWELL. Chem. Commun. 54 (1967).
5. R. C. ELDER, J. HALPERN, and J. S. POND. J. Amer. Chem. Soc. **89**, 6877 (1967).
6. S. KULPE. Z. Anorg. Allg. Chem. **349**, 314 (1967).
7. Z. V. ZVONKOVA and G. S. ZHDANOV. Zhur. Fiz. Khim. **26**, 586 (1952).
8. A. L. BEAUCHAMP and D. GOUTIER. To be published.

Can. J. Chem. Downloaded from www.nrcresearchpress.com by 210.87.254.105 on 09/05/12
For personal use only.

Exchange Averaging of Methylol Groups Attached to Phosphorus

S. E. ELLZEY, JR., W. J. CONNICK, JR., AND GORDON J. BOUDREAUX
Southern Regional Research Laboratory,[1] *New Orleans, Louisiana 70179*

Received June 21, 1971

Variable temperature ^1H n.m.r. spectra of pyridine solutions of tetrakis(hydroxymethyl)phosphonium chloride indicate that chemical exchange of methylol groups of the salt with those of the small amount of tris(hydroxymethyl)phosphine formed is the cause of their magnetic equivalence at elevated temperatures. Triethylamine transforms the salt into the phosphine and at least two other phosphorus species which may result from reaction of formaldehyde at oxygen of the phosphine.

Des spectres r.m.n. ^1H à différentes températures de solutions de chlorure de tetrakis (hydroxyméthyl) phosphonium dans la pyridine indiquent que l'échange chimique des groupements méthylol du sel avec ceux provenant d'une petite quantité de tris (hydroxyméthyl) phosphine formée, est la cause de leur équivalence magnétique à température élevée. La triéthylamine transforme le sel en phosphine et en au moins deux autres produits contenant du phosphore, qu'on pourrait attribuer à la réaction de la formaldéhyde avec l'oxygène de la phosphine.

Canadian Journal of Chemistry, **49**, 3581 (1971)

Reaction of aqueous or alcoholic alkali hydroxide (1) or anhydrous triethylamine (2) with tetrakis(hydroxymethyl)phosphonium chloride (**1**) yields tris(hydroxymethyl)phosphine (**3**) as the isolable product. In a recent report (3) employing ^1H and ^{31}P n.m.r. in a study of the reaction of **1** with sodium hydroxide, it was concluded that in addition to **3**, hemiformals of **3** [*e.g.*, $(HOCH_2)_2PCH_2OCH_2OH$] were also formed.

$$[1]\quad \underset{\mathbf{1}}{(HOCH_2)_4\overset{+}{P}\overset{-}{Cl}} + B \rightleftharpoons \underset{\mathbf{2}}{(HOCH_2)_3\overset{+}{P}CH_2\overset{-}{O}} + H\overset{+}{B} + \overset{-}{Cl} \rightleftharpoons \underset{\mathbf{3}}{(HOCH_2)_3P} + CH_2O$$

Evidence has now been obtained from variable temperature ^1H n.m.r. spectra of **1** in pyridine that the CH_2OH groups of **1** and **3** can become magnetically equivalent through chemical exchange. This exchange is an example of a rather rare reorganization involving C—P bonds at quadruply-connected phosphorus (4). In a solvent of higher base strength, such as triethylamine, in which the phosphonium salt is completely neutralized, attack of the liberated formaldehyde at phosphorus of the phosphine is somewhat slower than in pyridine and is apparently accompanied by attack at oxygen.

In Table 1 are summarized the results of a ^1H n.m.r. study of the phosphonium salt **1** dissolved in pyridine or triethylamine, either dry or in the presence of D_2O. In pyridine, as the temperature was raised from 33°, the doublets for **3** and **1**, in turn, collapsed to singlets before these merged into the composite singlet at δ 5.13 (Fig. 1) in the range 84–100°. The small amount of tris(hydroxymethyl)phosphine oxide (**4**) which is present was then readily seen. The coalescence was completely reversible with a change in temperature and after cooling the solution from 100° to 33°, K_{eq} was about 5×10^{-4}. In pyridine–D_2O, the signal for the phosphine **3** was already a singlet at 22°. The position of equilibrium (5), judging from the shifts of **1** (δ 4.92 at 0°), **3** (δ 4.28), and the composite signal in the aqueous medium, appears to be about the same as in neat pyridine.

These reversible effects are compatible with chemical exchange averaging of the CH_2OH groups of **1** and **3** according to eq. 1. Reversible neutralization of **1** leads to a small amount of **3**, probably through **2**. Since the overall equilibrium involves breaking and making of all P—C bonds, methylene doublets for **1** and **3** will not be observed when the overall rate is somewhat greater than J_{PCH} for a component. Coalescence of the separate signals to a *composite singlet* takes place when the rate exceeds the difference (in Hz) in chemical shift for **1** and **3**. The lower coalescence temperature of these signals (faster rate) in the more polar aqueous medium is consistent, moreover, with involvement of an ionic species, such

[1]One of the laboratories of the Southern Marketing and Nutrition Research Division, Agricultural Research Service, U.S. Department of Agriculture.

Can. J. Chem. Downloaded from www.nrcresearchpress.com by 210.87.254.6 on 09/05/12
For personal use only.

Can. J. Chem. Downloaded from www.nrcresearchpress.com by 210.87.254.6 on 09/05/12
For personal use only.

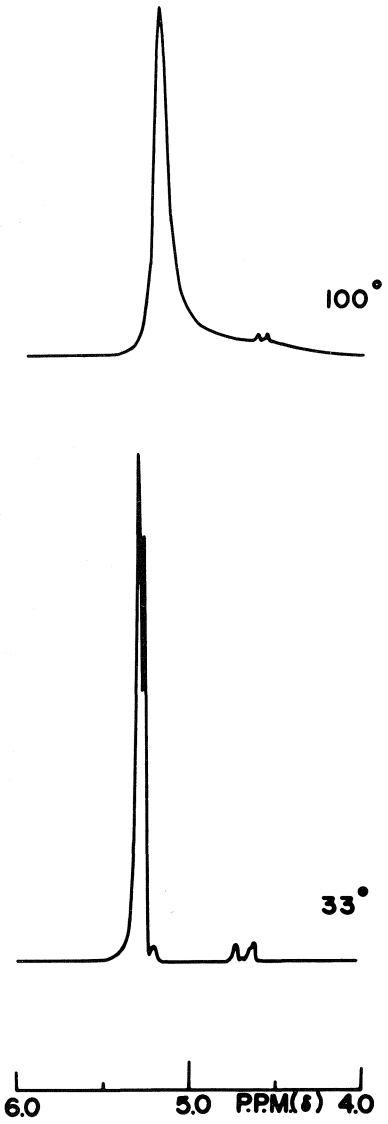

FIG. 1. The ^1H n.m.r. spectra of 20% solution of **1** in pyridine at 33 and 100°.

as **2**. The influence of formaldehyde on the rate was demonstrated by collapse to a singlet of the phosphine doublet upon addition of gaseous formaldehyde to a pyridine solution of the salt **1** at room temperature.

The complex spectrum of a triethylamine solution of **1** (amine hydrochloride filtered) is reversibly simplified at higher temperature (Fig. 2), but complete coalescence to a singlet is not achieved at 85°. Coalescence of the doublet in the triethylamine–D_2O solution is nearly complete at 33° and the position of this signal, as well as the lack of a signal for **1** at low temperature, indicates complete conversion of the salt. The numerous lines noted in the δ 4.1 region for the neat triethylamine solution are not seen in the D_2O solution. It is tentatively suggested that in dry triethylamine reversible attack of formaldehyde at phosphorus is rather slow on the n.m.r. time scale and the predominant reaction may be reversible formation of hemiformals (3), cyclic (6) or even linear formals, together with averaging of all existing PCH couplings into one doublet (P—C bonds preserved) at high temperature. As with pyridine–D_2O, addition of D_2O to triethylamine brings about faster attack of formaldehyde at phosphorus, resulting in loss of PCH coupling.

Results of an n.m.r. study of the neutralization of **1** with aqueous sodium hydroxide (7) will be reported later.

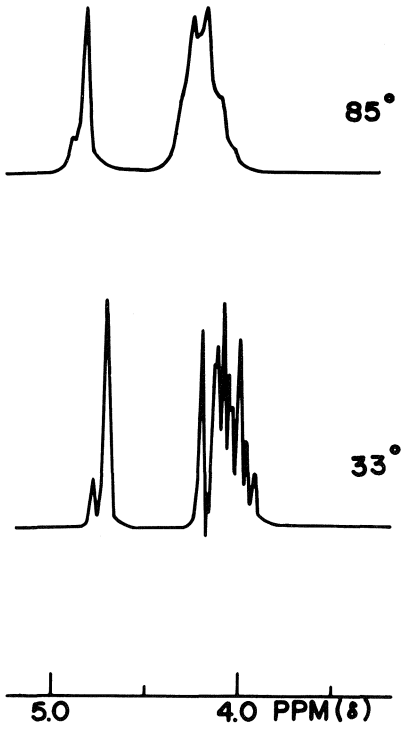

FIG. 2. The ^1H n.m.r. spectra of 20% solution of **1** in triethylamine at 33 and 85°.

TABLE 1. The ^1H n.m.r. data for $(HOCH_2)_4P$ Cl in various solvents*

Solvent	Temperature (°C)	δ, p.p.m. (J_{PCH}, Hz) 1	3	4	Other
Pyridine	33	5.27 (1.5)†	4.68 (6.2)‡	4.68 (3.0)	5.20§
"	100	5.12,‖ s($w_{1/2}$ 5.5 Hz)¶		4.53 (3.0)‖	
Pyridine (1.3 mol) in D_2O	33	4.96, s	4.33, s		
"	85	4.81, s($w_{1/2}$ 7.5 Hz)		4.37 (3.1)	5.02§
Triethylamine	33	—	7–8 lines near 4.05**		4.72, 4.79
"	85	—	4.15, broad		4.75, 4.83
Triethylamine (1.1 mol) in D_2O	0	—	4.12 (5.5), broad		4.83, 4.90
"	85	—	4.16, s($w_{1/2}$ 4.5 Hz)		4.84

*Spectra at 60 MHz, TMS, or DSS reference; 20% solutions under argon.
†The ^{31}P n.m.r. spectrum (24.3 MHz, 85% H_3PO_4 external reference) showed signal only for **1** at −27.3 p.p.m.
‡$K_{eq} = [3][CH_2O][BH^+]/[1]$, estimated from integration, is about 6×10^{-4}.
§Probably formaldehyde; the gas in pyridine – pyridine hydrochloride gave a singlet at δ 5.25.
‖Signals of authentic **3** and **4** shifted 0.14 p.p.m. upfield at 100°; doublet of **1** shifted 0.09 p.p.m. upfield at 70°.
¶Width at half-height.
The ^{31}P spectrum gave signals at +26.0 (3**), +30.9, and +35.7 p.p.m.

The ^{31}P n.m.r. spectra were kindly supplied by Dr. R. H. Dinius, Nuclear Science Center, Auburn University, Auburn, Alabama.

1. M. GRAYSON. J. Am. Chem. Soc. **85**, 79 (1963).
2. K. A. PETROV, V. A. PARASHINA, and M. B. LUZANOVA. Zh. Obshch. Khim. **32**, 553 (1962); Chem. Abstr. **58**, 5714 (1963).
3. W. J. VULLO. J. Org. Chem. **33**, 3665 (1968).
4. J. R. VAN WAZER and J. H. LETCHER. *In* Topics in phosphorus chemistry. Vol. 5. P^{31} Nuclear magnetic resonance. M. Grayson and E. J. Griffith, Eds. Interscience Publishers, New York, N.Y., 1967. p. 172.
5. J. A. POPLE, W. G. SCHNEIDER, and H. J. BERNSTEIN. High-resolution nuclear magnetic resonance. McGraw-Hill Book Co., Inc., New York, N.Y., 1959. Ch. 10.
6. S. A. BUCKLER. J. Am. Chem. Soc. **82**, 4215 (1960).
7. S. E. ELLZEY, JR., W. J. CONNICK, JR., G. J. BOUDREAUX, and H. KLAPPER. Abstracts of Papers, Southeast-Southwest Regional ACS Meeting, New Orleans, Louisiana, December 4, 1970.

Can. J. Chem. Downloaded from www.nrcresearchpress.com by 210.87.254.6 on 09/05/12
For personal use only.

Can. J. Chem. Downloaded from www.nrcresearchpress.com by 210.87.254.5 on 09/05/12
For personal use only.

Canadian Journal of Chemistry

Published by THE NATIONAL RESEARCH COUNCIL OF CANADA

VOLUME 49 NOVEMBER 15, 1971 NUMBER 22

Dimethylsulfoxidepentaammineruthenium(II) Hexafluorophosphate. A Spectroscopic Study

C. V. SENOFF, E. MASLOWSKY, JR., AND R. G. GOEL

Department of Chemistry, University of Guelph, Guelph, Ontario

Received May 6, 1971

The infrared spectra of $[Ru(NH_3)_5(CH_3)_2SO]X_2$, $[Ru(ND_3)_5(CH_3)_2SO]X_2$, $[Ru(NH_3)_5(CD_3)_2SO]X_2$, and $[Ru(ND_3)_5(CD_3)_2SO]X_2$ where $X = PF_6^-$ have been examined in detail between 4000–200 cm^{-1}. These data, together with the ^1H n.m.r. spectrum of $[Ru(NH_3)_5(CH_3)_2SO](PF_6)_2$ in D_2O, suggest that dimethyl sulfoxide is bonded to ruthenium *via* the sulfur atom in spite of the fact that the ν_{SO} frequency is not very different from that observed for uncoordinated dimethyl sulfoxide.

Les spectres infrarouges de $[Ru(NH_3)_5(CH_3)_2SO]X_2$, $[Ru(ND_3)_5(CH_3)_2SO]X_2$, $[Ru(NH_3)_5(CD_3)_2SO]X_2$ et $[Ru(ND_3)_5(CD_3)_2SO]X_2$ où $X = PF_6^-$, ont été examinés en détail entre 4000 et 200 cm^{-1}. Ces données, ainsi que le spectre r.m.n. de $[Ru(NH_3)_5(CH_3)_2SO](PF_6)_2$ dans D_2O, suggèrent que le diméthyle sulfoxyde est lié au ruthénium *via* un atome de soufre et ceci en dépit du fait que la fréquence ν_{SO} n'est pas très différente de celle observée dans le diméthyle sulfoxyde non-coordonné.

Canadian Journal of Chemistry, 49, 3585 (1971)

During the course of investigating the chemical reactions of $[Ru(NH_3)_5N_2](PF_6)_2$, it was found that this dinitrogen complex would react with dimethyl sulfoxide to form $[Ru(NH_3)_5DMSO](PF_6)_2$ where DMSO = $(CH_3)_2SO$ (1, 2). Further interest was generated by this compound by virtue of the fact that the ν_{SO} vibration in the infrared remained virtually unchanged from that observed for free dimethyl sulfoxide. At present, all known compounds containing coordinated DMSO have been reported to exhibit a shift in the ν_{SO} vibration to *higher* frequency when DMSO is bonded to the metal *via* the sulfur atom and to *lower* frequency when bonding occurs through the oxygen atom (3, and references cited therein). Consequently, it was decided to study this ruthenium(II) complex further in order to determine the nature of the DMSO–Ru bond. The initial approach has involved a detailed examination of the infrared and ^1H n.m.r. spectra of the complex. The results of this investigation are herein presented.

Results and Discussion

The infrared spectral data are presented in Table 1, together with the assignments for the observed absorption bands.[1]

(a) NH_3 Vibrations (4000–600 cm^{-1})

Band assignments for the various NH_3 modes occurring in this region were made by comparison with the spectra of other ammine complexes of ruthenium (4); this procedure was facilitated by the infrared spectra of the *N*-deuterated derivatives (Table 1). As expected, the NH_3 vibrations were not very different from those recorded for other pentaammineruthenium(II) complexes (2, 5, 6).

(b) $(CH_3)_2SO$ Vibrations (4000–600 cm^{-1})

The various CH_3, SO, and CS vibrational modes are expected to occur in this region. The CH_3 and CS modes were assigned by taking into account the previous assignments for DMSO and DMSO-d_6 (7, 8). Comparison with the spectra of the *C*- and *N*-deuterated derivatives provided a useful internal check for these band assignments.

[1]Photocopies of the spectra may be obtained free of charge, upon request, from the Depository of Unpublished Data, National Science Library, National Research Council of Canada, Ottawa, Canada.

Can. J. Chem. Downloaded from www.nrcresearchpress.com by 210.87.254.5 on 09/05/12
For personal use only.

TABLE 1. Vibrational frequencies (cm^{-1}) for the absorption bands of the complexes $[Ru(NH_3)_5(CH_3)_2SO](PF_6)_2$, $[Ru(ND_3)_5(CH_3)_2SO](PF_6)_2$, $[Ru(NH_3)_5(CD_3)_2SO](PF_6)_2$, and $[Ru(ND_3)_5(CD_3)_2SO](PF_6)_2$ between 4000-200 cm^{-1}.

Frequency (cm^{-1})				
$[Ru(NH_3)_5(CH_3)_2SO](PF_6)_2$	$[Ru(ND_3)_5(CH_3)_2SO](PF_6)_2$	$[Ru(NH_3)_5(CD_3)_2SO](PF_6)_2$	$[Ru(ND_3)_5(CD_3)_2SO](PF_6)_2$	Assignment
3367 s[a]	2510 s (1.34)[c]	3367 s	2510 s (1.34)	
3299 s	2402 m (1.37)	3299 s	2402 m (1.37)	ν(NH)[b] or ν(ND)
3219 m[a]	2350 m (1.37)	3219 m	2358 m (1.37)	
3040 w[a]	3036m	2278 w (1.33)	2277 w (1.33)	
2949 w	2949 m	2151 w (1.37)	2152 w (1.37)	ν(CH) or ν(CD)
2938 w	2938 m	2143 w (1.37)	2142 w (1.37)	
2858 w	2860 w	2040 w (1.40)	[e]	
1638 s	1200 m (1.36)	1638 s	1200 m (1.36)	$\delta_d(NH_3)$[b] or $\delta_d(ND)$
1465 vw[a]	1465 vw	1040 m (1.41)	1040 m (1.41)	
1436 m	1437 m	1031 m (1.39)	1033 m (1.39)	$\delta_d(CH)$[b] or $\delta_d(CD)$
1423 m	1428 m	1014 s (1.38)	1015 s (1.38)	
[d]	1327 m	[e]	[e]	$\delta_s(CH)$[b] or $\delta_s(CD)$
[d]	1309 m	[e]	[e]	
1345 w		1345 w		
1321 s	1014 s (1.30)	1321 s	1015 s (1.30)	
1311 s	1001 s (1.31)	1311 s	1001 s (1.31)	$\delta_s(NH)$ or $\delta_s(ND)$
1290 sh[a]	990 sh (1.30)	1292 sh	990 sh (1.31)	
1045 s	1049 s	1056 s (1.09)	1059 s (1.08)	ν(SO)
1023 sh	1020 sh	783 w (1.31)	780 w (1.31)	
1014 s	[d]	[d]	[d]	
963 m	963 m	[e]	[e]	$\rho_r(CH)$[b] or $\rho_r(CD)$
910 m	910 w	[e]	[e]	
845 vs[a]	845 vs	845 vs	845 vs	PF_6^-
755 w	600 w (1.26)	760 w	600 w (1.27)	$\rho_r(NH)$ or $\rho_r(ND)$
744 m	744 m	744 w	744 m	PF_6^-
692 m	694 s	635 m (1.09)	642 (1.08)	ν(CS)
561 s	561 s	561 s	560 s	PF_6^-
472 w	472 w	472 w	472 w	PF_6^-
446 m	445 m	411 m (1.09)	411 m (1.09)	δ_s[b](CSO)
389 m	385 m	364 m (1.09)	362 m (1.09)	δ_{as}(CSO)
[g]	420 w	450 w (1.07)	[g]	ν(RuN)
[g]	402 w	430 sh (1.07)	[g]	ν(RuN)

[a]sh, shoulder band; w, weak; m, medium; s, strong; vs, very strong.
[b]ν, stretching; δ, deformation; δ_d, degenerate deformation; δ_s, symmetric deformation; δ_{as}, asymmetric deformation; ρ_r, rocking.
[c]Numbers in parentheses refer to the isotopic ratios, ν_{NH}/ν_{ND} or ν_{CH}/ν_{CD}. Simple theory predicts 1.37 for ν_{NH}/ν_{ND}, ν_{CH}/ν_{CD} and 1.09 for $\nu_{M-NH_3}/\nu_{M-ND_3}$.
[d]Peak hidden by NH or ND absorptions.
[e]Not observed.
[f]Peak hidden by PF_6^- absorption.
[g]Peak hidden by δ_s (CSO) absorption.

Can. J. Chem. Downloaded from www.nrcresearchpress.com by 210.87.254.5 on 09/05/12
For personal use only.

Absorption bands which did not shift with *C*- and/or *N*-deuteration were assigned to PF_6^- vibrations.

The SO stretching vibration was of particular interest since its position has been found useful to ascertain the nature of the DMSO—metal bond, *i.e.*, to determine whether oxygen or sulfur is the donor atom (3 and references cited therein). The ν_{SO} vibration for $[Ru(NH_3)_5DMSO](PF_6)_2$ was observed at 1045 cm^{-1} as a strong, sharp band and between 1049–1059 cm^{-1} for the *C*- and or *N*-deuterated derivatives (Table 1). It is of interest to note that the position of this band is not very different from that reported for uncoordinated DMSO where ν_{SO} has been reported to occur at 1045 cm^{-1} in nitromethane (9) and in the vapor phase at 1102 cm^{-1} (7).

In spite of the fact that the ν_{SO} mode for DMSO and its complexes is not a pure S—O stretching vibration, it has been claimed that it is possible to determine the nature of the donor atom (O or S) from $\Delta\nu_{SO}$ *i.e.*, (ν_{SO} (ligand) $-$ ν_{SO} (complex)) (3). This generalization appears to be violated by the infrared spectrum of $[Ru(NH_3)_5DMSO](PF_6)_2$ since $\Delta\nu_{SO} \sim 0$ for this particular complex (Table 1).

Ruthenium(II) would be classified as a "soft" acid according to Pearson's concept of "hard and soft acids and bases" (10, 11). Consequently, it would be anticipated that sulfur would be the donor atom in $[Ru(NH_3)_5DMSO](PF_6)_2$ since "soft" acids have an affinity for "soft" donor atoms (oxygen is a "hard" donor atom). This "$\Delta\nu_{SO}$ rule" has received support from several single crystal X-ray diffraction studies. For example, the S—O bond length in *trans*-$PdCl_2(DMSO)_2$ (12, 13) and *cis*-$Pd(NO_2)_2(DMSO)_2$ (14), in both of which sulfur is the donor atom, is shorter than the S—O bond length reported for DMSO itself (15). Hence this particular bond length has been noted to reflect the increase in ν_{SO} observed in the infrared spectra of these complexes (13) (two ν_{SO} vibrations have been reported for *cis*-$Pd(NO_2)_2(DMSO)_2$ (14)). Also, the observed S—O bond length in those complexes where DMSO is bonded to the metal *via* the oxygen atom is significantly longer than that for free DMSO (12, 16). This observation parallels the shift in ν_{SO} to lower frequency when oxygen is the donor atom. If this trend is followed, one would expect little difference between the S—O bond length in free DMSO and that in the complex $[Ru(NH_3)_5DMSO](PF_6)_2$.

Thus, it would appear that in view of the infrared data for $[Ru(NH_3)_5DMSO](PF_6)_2$ presented here, ν_{SO} by itself is not a suitable criterion for determining the nature of the donor atom. Although the infrared data do not provide an unambiguous indication of the donor atom in this complex, ^1H n.m.r. (*vide infra*) add support to the suggestion that sulfur is the donor atom.

(c) Far Infrared Spectra (600–200 cm^{-1})

This region of the spectrum is of interest because it is here where the metal–ligand vibrations are expected to occur. Unfortunately, DMSO vibrations also occur in this region (17) but the spectra of the *C*- and *N*-deuterated derivatives in this region (Fig. 1) may be used to clarify some of the metal–ligand vibrations. No bands which could be readily assigned to metal–ligand vibrations were observed in the spectrum of $[Ru(NH_3)_5(CH_3)_2SO](PF_6)_2$. On the other hand, the spectrum of $[Ru(NH_3)_5(CD_3)_2SO](PF_6)_2$ in this region exhibited two new weak bands at 450 and 420 cm^{-1} as a result of the isotopic shifting of the δ_{CSO} vibrations (Table 1). These new bands have been assigned to metal–nitrogen stretching modes and are shifted to 420 and 402 cm^{-1} respectively in the spectrum of $[Ru(ND_3)_5(CH_3)_2SO](PF_6)_2$. No bands which could be assigned to ν_{RuN} were observed in the spectrum of the completely deuterated complex, $[Ru(ND_3)_5(CD_3)_2SO](PF_6)_2$. The strong band occurring at 279 cm^{-1} in the spectrum of $[Ru(NH_3)_5(CH_3)_2SO](PF_6)_2$ has been assigned to a Ru–N bending mode. This assignment must be considered tentative since the band absorbs near the lower end of the instrument used.

(d) ^1H n.m.r. Spectra

The ^1H spectra of several DMSO and related complexes have been recently investigated (3, 18, 19). From these studies it has been observed that the methyl proton resonance of DMSO shifts downfield by *ca.* 1 p.p.m. from free DMSO when S is the donor atom but scarcely shifts when O is the donor atom. The ^1H n.m.r. data for $[Ru(NH_3)_5DMSO](PF_6)_2$, DMSO, and $[(CH_3)_3SO]I$ in D_2O are presented in Table 2. The chemical shift for the NH_3 protons was not examined in detail. It has been suggested that S-coordination results in more deshielding of the CH_3 pro-

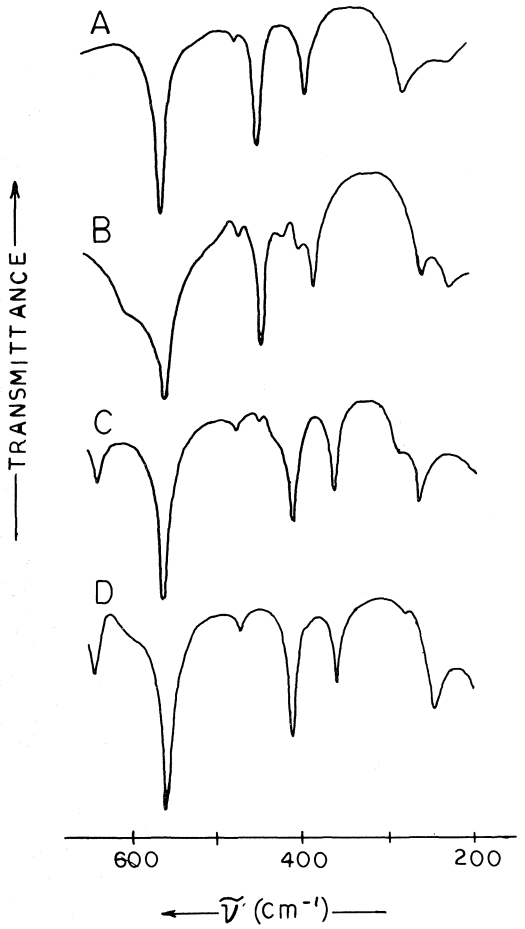

FIG. 1. Infrared spectra (600–200 cm^{-1}) of Nujol mulls of (*A*) $[Ru(NH_3)_5DMSO](PF_6)_2$, (*B*) $[Ru(ND_3)_5DMSO](PF_6)_2$, (*C*) $[Ru(NH_3)_5DMSO\text{-}d_6](PF_6)_2$, and (*D*) $[Ru(ND_3)_5DMSO\text{-}d_6](PF_6)_2$.

TABLE 2. ^{1}H n.m.r. spectra in D_2O

Compound	$\delta(CH_3)^a$	$\Delta[\delta(CH_3)]^b$
$(CH_3)_2SO$	2.70	—
$[Ru(NH_3)_5DMSO](PF_6)_2$	3.28	0.58
$[(CH_3)_3SO]^+I^-$	3.83	1.13

[a]Chemical shift quoted in p.p.m. downfield from DSS.
[b]$\Delta[\delta(CH_3)] = \delta(CH_3)_{complex} - \delta(CH_3)_{DMSO}$.

tons as compared to O-coordination because of the fewer number of bonds between the metal and the CH_3 protons in the former instance compared to the latter (18). Therefore, if it is assumed that this is a general phenomenon, then the n.m.r. data presented for $[Ru(NH_3)_5DMSO](PF_6)_2$ are consistent with the suggestion that sulfur is the donor atom. As expected, the CH_3 protons are less shielded for $[(CH_3)_3SO]I$ than $[Ru(NH_3)_5DMSO](PF_6)_2$ relative to free DMSO.

After completion of the spectroscopic investigation reported herein, preliminary results of a single crystal X-ray diffraction study became available and unambiguously show that sulfur is indeed the donor atom in $[Ru(NH_3)_5DMSO](PF_6)_2$. Complete details are presented in the following paper (20).

In conclusion, the spectroscopic data presented herein indicate that the "$\Delta\nu_{SO}$ rule" must be used with caution and must not be regarded as an infallible generalization.

Experimental

Dimethylsulfoxidepentaammineruthenium(II) hexafluorophosphate, $[Ru(NH_3)_5(CH_3)_2SO](PF_6)_2$

To an aqueous slurry of nitrogenpentaammineruthenium(II) hexafluorophosphate (5) (0.53 g in 3 ml of water) was added 1 ml of dimethyl sulfoxide and the resulting mixture was refluxed until a clear solution developed. The solution was filtered hot. From the cooled filtrate, pale yellow crystals of the complex were collected and washed with a small amount of ice-cold water, ethanol, and ether. Yield, 0.30 g (49%). The complex was recrystallized from the minimum amount of hot water as very pale yellow crystals. After washing as before, the complex was dried *in vacuo* at 78 °C in the presence of P_4O_{10}.

Anal. Calcd. for $C_2H_{21}F_{12}N_5OSRu$: C, 4.33; H, 3.82. Found: C, 4.86; H, 3.86.

Dimethylsulfoxidepentaammine-d_{15}-ruthenium(II) hexafluorophosphate, $[Ru(ND_3)_5(CH_3)_2SO](PF_6)_2$

Nitrogenpentaammineruthenium(II) hexafluorophosphate (5) was prepared using D_2O (99.8%) rather than H_2O as the solvent. The procedure used to prepare $[Ru(NH_3)_5(CH_3)_2SO](PF_6)_2$ was then followed except that D_2O was used in place of water. The crude product was dissolved in the minimum amount of D_2O and then refluxed for *ca.* 30 min. The solution was filtered hot, allowed to cool, and the yellow crystals which were deposited were collected and washed with ethanol and ether. This crop of crystals were then refluxed again with more D_2O, the resulting solution filtered hot, allowed to cool, and the product collected and washed as before. The ammine ligands were more than 90% deuterated as estimated from the intensity of the ν_{NH} bands in the infrared. No exchange of the methyl protons of DMSO were observed.

Dimethylsulfoxide-d_6-pentaammineruthenium(II) hexafluorophosphate, $[Ru(NH_3)_5(CD_3)_2SO](PF_6)_2$

The procedure used to prepare $[Ru(NH_3)_5DMSO](PF_6)_2$ was followed except that DMSO-d_6 was used in place of DMSO.

Dimethylsulfoxide-d_6-pentaammine-d_{15}-ruthenium(II) hexafluorophosphate, $[Ru(ND_3)_5(CD_3)_2SO](PF_6)_2$

The procedure used to prepare $[Ru(ND_3)_5DMSO]$-

Can. J. Chem. Downloaded from www.nrcresearchpress.com by 210.87.254.5 on 09/05/12
For personal use only.

$(PF_6)_2$ was followed except that DMSO-d_6 was used in place of DMSO.

Trimethylsulfoxonium iodide, $[(CH_3)_3SO]I$

A solution of DMSO (6.75 ml), methyl iodide (1.75 ml), and diethyl ether (10 ml) was refluxed for 3 days, after which a white solid was produced. This was filtered off, washed several times with ether, and air-dried.

Anal. Calcd. for C_3H_9IOS: C, 16.37; H, 4.12. Found: C, 16.33; H, 4.32.

Microanalyses were carried out by A. B. Gygli, Toronto, Ontario. Infrared spectra were recorded with a Beckman IR-12 infrared spectrophotometer as Nujol or halocarbon mulls between NaCl or CsI discs. Nuclear magnetic resonance spectra were recorded with a Varian A60 spectrometer in D_2O with DSS (sodium 2,2-dimethyl-2-silapentane-5-sulfonate) as internal standard.

The authors wish to acknowledge their appreciation for financial support from the National Research Council of Canada and the Department of University Affairs of the Province of Ontario.

1. A. D. Allen and C. V. Senoff. Chem. Commun. 621 (1965).
2. A. D. Allen, F. Bottomley, R. O. Harris, V. P. Reinsalu, and C. V. Senoff. J. Am. Chem. Soc. **89**, 5595 (1967).
3. W. Kitching, C. J. Moore, and D. Doddrell. Inorg. Chem. **9**, 541 (1970).
4. A. D. Allen and C. V. Senoff. Can. J. Chem. **45**, 1337 (1967).
5. A. D. Allen, T. Eliades, R. O. Harris, and P. Reinsalu. Can. J. Chem. **47**, 1605 (1969).
6. J. A. Stanko and T. W. Starinshak. Inorg. Chem. **8**, 2156 (1969).
7. W. D. Horrocks, Jr. and F. A. Cotton. Spectrochim. Acta, **17**, 134 (1961). M. T. Forel and M. Tranquille. Spectrochim. Acta, **26A**, 1023 (1970).
8. F. A. Cotton, R. Francis, and W. D. Horrocks, Jr. J. Chem. Phys. **64**, 1534 (1960).
9. W. R. Currier and J. H. Weber. Inorg. Chem. **6**, 1539 (1967).
10. R. G. Pearson. J. Chem. Ed. **45**, 581 (1968).
11. R. G. Pearson. J. Chem. Ed. **45**, 643 (1968).
12. M. J. Bennett, F. A. Cotton, and D. L. Weaver. Nature, **212**, 286 (1966).
13. M. J. Bennett, F. A. Cotton, D. L. Weaver, R. J. Williams, and W. H. Watson. Acta Cryst. **23**, 788 (1967).
14. D. A. Langs, C. R. Hare, and R. G. Little. Chem. Commun. 1080 (1967).
15. R. Thomas, C. B. Shoemaker, and K. Eriks. Acta Cryst. **21**, 12 (1966).
16. M. J. Bennett, F. A. Cotton, and D. L. Weaver. Acta Cryst. **23**, 581 (1967).
17. B. F. G. Johnson and R. A. Walton. Spectrochim. Acta, **22**, 1853 (1966).
18. W. Kitching and C. J. Moore. Inorg. Nucl. Chem. Lett. **4**, 691 (1968).
19. S. Thomas and W. L. Reynolds. Inorg. Chem. **8**, 1531 (1969).
20. F. C. March and G. Ferguson. Can. J. Chem. This issue.

Can. J. Chem. Downloaded from www.nrcresearchpress.com by 210.87.254.5 on 09/05/12
For personal use only.

Can. J. Chem. Downloaded from www.nrcresearchpress.com by 210.87.254.6 on 09/05/12
For personal use only.

The Crystal Structure of Dimethylsulfoxidepentammineruthenium(II) Hexafluorophosphate

FRANK C. MARCH AND GEORGE FERGUSON
Department of Chemistry, University of Guelph, Guelph, Ontario

Received May 6, 1971

The crystal structure of dimethylsulfoxidepentammineruthenium(II) hexafluorophosphate ($[Ru(NH_3)_5DMSO]^{2+}$ $2PF_6^-$) has been determined from three-dimensional X-ray data. The crystals are monoclinic, space group $P2_1/c$, with four formula units in a unit cell of dimensions $a = 8.805(2)$, $b = 17.335(5)$, $c = 12.373(2)$ Å, $\beta = 94.24(2)°$. The structure has been refined by full matrix least-squares methods to a final residual R of 0.054 for 1987 reflections greater than 3σ. The DMSO ligand coordinates through the sulfur atom and the S—O bond distance (1.527(7) Å) is considerably longer than that found for other sulfur–donor complexes of the ligand. The Ru—S bond distance is 2.188(3) Å.

La structure cristalline de l'hexafluorophosphate de diméthylsulphoxydepentammineruthénium (II) ($[Ru(NH_3)_5DMSO]^{2+}$ $2PF_6^-$) a été déterminée par diffraction de rayons-x à partir des données tridimensionnelles. Ce sel cristallise dans le système monoclinique, groupe d'espace $P2_1/c$, avec quatre unités formulaires dans une maille de dimensions: $a = 8.805(2)$, $b = 17.335(5)$, $c = 12.372(2)$ Å et $\beta = 94.24(2)°$. La structure a été affinée par moindres-carrés (matrice complète) jusqu'à un facteur d'accord $R = 0.054$ pour les 1987 réflexions considérées observées. Le ligand DMSO est coordonné à l'atome de soufre et la longueur de la liaison S—O (1.527(7) Å) est considérablement plus grande que celles rencontrées dans d'autres complexes de ce ligand ou le soufre est donneur. La distance Ru—S est de 2.188(3) Å.

Canadian Journal of Chemistry, 49, 3590 (1971)

Introduction

The results of an infrared and ^1H n.m.r. spectral investigation of some ruthenium complexes of dimethylsulfoxide (DMSO) are presented in a previous paper (1). It was inferred from this study that the DMSO ligand coordinates through the sulfur atom, however, the ν_{SO} vibration did not show a shift to higher frequency on complex formation as would be expected for a sulfur coordinated species. A single crystal X-ray diffraction investigation was undertaken to determine if sulfur was in fact the donor atom, and to find the effect of coordination on the length of the S—O bond.

Experimental

Crystal Data for Dimethylsulfoxidepentammineruthenium-(II) hexafluorophosphate[1]

$C_2H_{21}F_{12}N_5OP_2RuS$ f.w. = 554.3

Monoclinic $a = 8.805(2)$, $b = 17.335(5)$, $c = 12.373(2)$ Å, $\beta = 94.24(2)°$, $V = 1883.4$ Å^3, $\rho_o = 1.958 \pm 5$, $Z = 4$, $\rho_c = 1.955$, (20 °C; MoKα, $\lambda = 0.71069$ Å). Space group $P2_1/c$ (C_{2h}^5, No. 14) from systematic absences. Linear absorption coefficient for X-rays ($\lambda = 0.71069$ Å) $\mu = 10.0$ cm^{-1}.

[1]Numbers in parentheses are the estimated standard deviations in the least significant digits, which are generally derived from the inverse matrix in non-linear least-squares calculations.

Preliminary precession and Weisenberg photographs indicated monoclinic symmetry, while the systematically absent intensities for $h0l$ (l odd) and $0k0$ (k odd) gave space group $P2_1/c$ uniquely. The cell dimensions were obtained from least-squares refinement of the setting angles of 12 reflections. The crystal chosen for the data collection was a rectangular prism with approximate dimensions $0.5 \times 0.2 \times 0.2$ mm^3. Intensity data were collected to a maximum Bragg angle (θ) of 24° on a Hilger and Watts Y290 computer controlled 4-circle diffractometer. The $\theta/2\theta$ scan technique was used, with a symmetric scan of 0.8° and a scan rate of 1.667 deg/min. Stationary crystal/stationary counter background counts of 10 s duration were measured at each end of the integrated scan. Two standard reflections were monitored at approximately three hourly intervals throughout the data collection. The maximum variation in the intensity of the standard reflections was less than 3.4%.

Each intensity was corrected for background and the estimated standard deviation for each intensity ($\sigma(I)$) was given by $\sigma(I) = [\text{scan} + \text{background} + (p.\text{intensity})^2]^{1/2}$ where p is a factor introduced to avoid over weighting of the intense reflections (2). A value of 0.05 for p gave an adequate weighting of data. A total of 2757 independent reflections were accessible, of which 1987 were greater than three times their e.s.d.'s. The data were corrected for Lorentz and polarization factors, but not for absorption or extinction.

Structure Solution and Refinement

The x, y, and z coordinates of the Ru atom were obtained by inspection of a three dimensional Patterson distribution. One cycle of least-squares refinement on F (with $\sigma(F) = 0.5\ \sigma(F^2)/F$) in which the scale and positional and isotropic temperature parameters of the

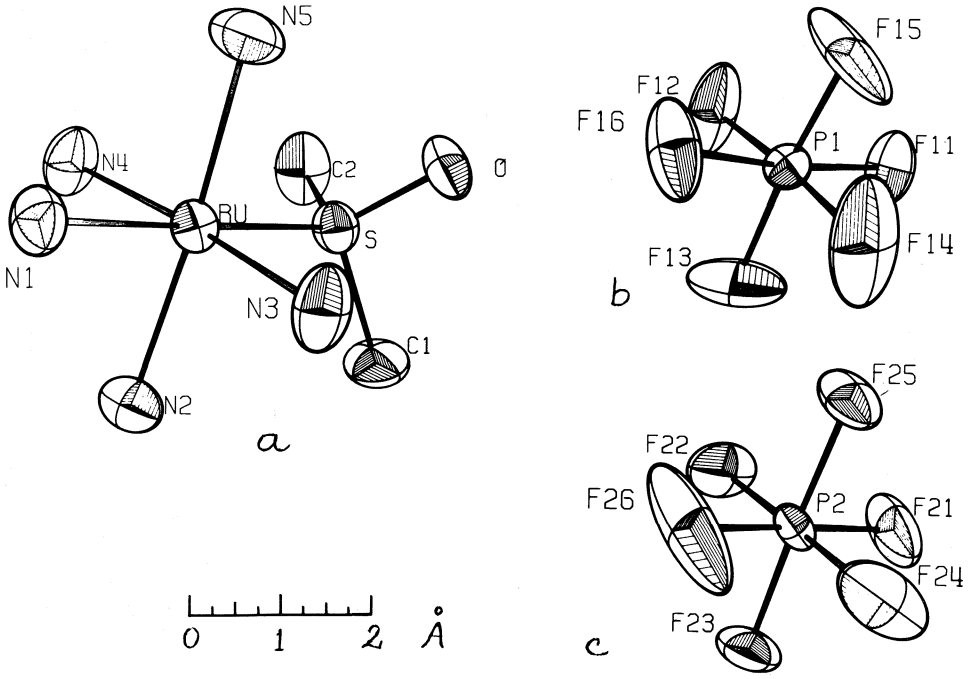

FIG. 1. View of the cation (*a*) and the anions, (*b*) and (*c*), drawn to the same linear scale. The ellipsoids in (*a*) are scaled to represent envelopes of 50% probability, while those in (*b*) and (*c*) represent envelopes of 20% probability.

ruthenium were varied yielded $R_1 = \Sigma| |F_o| - |F_c| |/ \Sigma|F_o|$ and $R_2 = [\Sigma\omega(F_o - F_c)^2/\Sigma\omega F_o^2]^{1/2}$ of 0.388 and 0.457, respectively. In all calculations of F_c the usual atomic scattering factors for C, N, O, F, S and Ru (3) were used. Corrections for anomalous dispersion for Ru were included at later stages of the refinement. Only 1987 reflections greater than 3σ were included in the least-squares calculations, and the function minimized was R_2 (above). Absolute weights (based on $\sigma(F_o)$) were used throughout the refinement. Successive difference maps of electron density distributions eventually gave all the non-hydrogen atoms. Four cycles of full matrix refinement of the model with isotropic atoms converged with $R_1 = 0.108$. At this stage all the fluorine atoms had high isotropic temperature factors (U_{iso} ranging from 0.09 to 0.22 Å^2); however, an F_o electron density map calculated using phases from all the non-fluorine atoms did not reveal any evidence of disorder of the fluorines about the phosphorus atoms. The model was refined for seven more cycles with first the ruthenium, sulfur, and phosphorus atoms allowed to vibrate anisotropically followed by all the non-fluorine atoms, and finally with all atoms allowed anisotropic vibration. The refinement converged with $R_1 = 0.054$ and $R_2 = 0.072$. On the last cycle the maximum shift in any of the positional parameters was less than 1 e.s.d., and that for the thermal parameters was less than 1.5 e.s.d.'s. The final atomic positional and thermal parameters are listed in Table 1.

A difference map calculated using the F_c values from the positional and thermal parameters given in Table 1 contained a number of small peaks (highest 1.2 e/Å^3). Many of the peaks appeared in positions corresponding to methyl and ammine hydrogen atoms, however, no attempt was made to include these in any calculations.

The final error in an observation of unit weight calculated over all "observed" data was 1.55, and ranged from 1.41 to 1.71 over 10 ranges of intensity, indicating that the relative weighting of the data was good. A table of final values of the structure amplitudes, $|F_o|$, $|F_c|$ and $\sigma(F_o)$ (the standard deviations from which the weights employed in the refinement were derived), is placed with the Depository of Unpublished Data.[2] The final values of the agreement factors for all data including those less than 3σ are: $R_1 = 0.073$ and $R_2 = 0.078$.

Discussion

The structure consists of discrete $[Ru(NH_3)_5DMSO]^{2+}$ cations and PF_6^- anions. The ranges of closest contacts between groups which are not bonded to common atoms are given in Table 2. Coordination about the Ru atom is octahedral, and the DMSO ligand is coordinated through the sulfur as inferred (1). Figure 1 shows a view of the cation and anions drawn to the same scale, showing the atomic numbering scheme. Figure 2 is a packing diagram of the structure with the unit

[2]Photocopies of the table of observed and calculated structure factors may be obtained free of charge, upon request, from the Depository of Unpublished Data, National Science Library, National Research Council of Canada, Ottawa, Canada K1A 0S2.

Can. J. Chem. Downloaded from www.nrcresearchpress.com by 210.87.254.6 on 09/05/12
For personal use only.

Can. J. Chem. Downloaded from www.nrcresearchpress.com by 210.87.254.6 on 09/05/12
For personal use only.

TABLE 1. Atomic positional* and thermal† parameters

Atom	x/a	y/b	z/c	U_{11}	U_{22}	U_{33}	U_{12}	U_{13}	U_{23}
Ru	29439(8)	84041(4)	20354(4)	0324(4)	0304(5)	0271(4)	0010(4)	0027(3)	0019(3)
S	1721(3)	8294(1)	3505(2)	037(1)	035(1)	027(1)	001(1)	006(1)	000(1)
P(1)	7293(4)	6576(2)	1046(3)	049(2)	052(2)	064(2)	011(2)	007(2)	−002(2)
P(2)	7745(4)	10056(2)	1556(3)	044(2)	053(2)	060(2)	007(2)	012(2)	022(2)
F(11)	7703(10)	6105(5)	0010(8)	087(6)	121(7)	119(7)	−004(5)	027(5)	−056(6)
F(12)	8764(17)	7037(8)	0986(9)	240(14)	205(12)	127(8)	−162(11)	100(10)	−073(9)
F(13)	8224(19)	6060(8)	1829(12)	245(18)	147(11)	215(15)	067(11)	007(13)	107(10)
F(14)	5927(17)	6068(12)	1182(14)	140(12)	381(24)	214(15)	−156(15)	074(12)	−116(17)
F(15)	6249(28)	7015(11)	0286(11)	516(31)	273(17)	130(8)	318(20)	−181(16)	−099(12)
F(16)	6856(12)	7113(8)	1984(8)	097(7)	214(12)	118(8)	059(7)	−016(5)	−093(8)
F(21)	8120(20)	9980(6)	0387(7)	341(21)	108(8)	064(6)	−018(10)	026(9)	013(5)
F(22)	9394(11)	9891(6)	1915(10)	082(6)	102(7)	218(12)	001(5)	−057(7)	030(7)
F(23)	7469(12)	9155(5)	1618(9)	117(8)	068(5)	178(9)	−029(5)	−018(7)	049(6)
F(24)	6097(13)	10153(9)	1090(18)	066(7)	231(15)	457(26)	−023(8)	−063(12)	220(18)
F(25)	8036(12)	10941(4)	1426(7)	175(9)	044(4)	102(6)	009(5)	030(6)	001(4)
F(26)	7304(27)	10128(8)	2678(10)	563(35)	145(10)	129(9)	122(15)	207(16)	051(8)
C(1)	−0220(11)	7934(7)	3283(9)	029(5)	090(8)	054(6)	−020(6)	001(5)	005(6)
C(2)	1358(15)	9169(6)	4240(8)	098(9)	039(6)	047(6)	007(6)	020(7)	−009(5)
N(1)	4283(9)	8433(5)	0601(6)	039(4)	047(5)	034(4)	001(4)	012(4)	006(4)
N(2)	0989(9)	8405(5)	0878(6)	038(4)	056(5)	038(4)	003(4)	−001(4)	−004(4)
N(3)	3027(11)	7166(4)	1893(7)	071(7)	027(4)	054(5)	006(4)	020(5)	004(4)
N(4)	2960(11)	9644(4)	1982(7)	073(7)	029(4)	053(5)	−006(5)	016(5)	−004(4)
N(5)	5062(9)	8383(6)	3028(7)	036(4)	097(7)	036(4)	−008(5)	−006(4)	004(5)
O	2474(8)	7773(4)	4365(5)	049(4)	048(4)	038(4)	010(4)	−002(4)	015(3)

*Fractional coordinates $\times 10^5$ for Ru, $\times 10^4$ for other atoms.
†T.F. = exp $[-2\pi^2(U_{11}h^2a^{*2} + U_{22}k^2b^{*2} + U_{33}l^2c^{*2} + 2U_{12}hka^*b^* + 2U_{13}hla^*c^* + 2U_{23}klb^*c^*)]$, U_{ij} in Å^2 $\times 10^4$ for Ru, $\times 10^3$ for other atoms.

TABLE 2. Interatomic distances (Å) and angles (deg)*

(*a*) Bonded distances

Bond	Distance (Å) Uncorrected	Corrected†	Average‡	Bond	Distance (Å) Uncorrected	Corrected†
Ru—S	2.188(3)	—	—	P(1)—F(11)	1.58(1)	1.63(1)
				P(1)—F(12)	1.53(2)	1.65(2)
Ru—N(1)	2.203(8)	2.209(8)	—	P(1)—F(13)	1.52(2)	1.65(2)
				P(1)—F(14)	1.51(2)	1.69(2)
Ru—N(2)	2.156(8)	2.165(8)		P(1)—F(15)	1.48(2)	1.75(2)
Ru—N(3)	2.155(8)	2.170(8)		P(1)—F(16)	1.56(1)	1.64(1)
Ru—N(4)	2.151(8)	2.166(8)		P(2)—F(21)	1.51(1)	1.62(1)
Ru—N(5)	2.156(8)	2.175(8)	2.169(5)	P(2)—F(22)	1.51(1)	1.59(1)
				P(2)—F(23)	1.58(1)	1.65(1)
S—O	1.512(7)	1.527(7)	—	P(2)—F(24)	1.53(1)	1.73(2)
				P(2)—F(25)	1.57(1)	1.62(1)
S—C(1)	1.821(11)	1.846(11)		P(2)—F(26)	1.47(2)	1.70(2)
S—C(2)	1.810(11)	1.834(11)	1.840(8)			
				Average‡	1.530(37)	1.660(46)

*Estimated standard deviations are derived from the e.s.d.'s. of atomic positional and thermal parameters and include errors in the cell parameters.

†Thermal corrections are applied using the riding model approximation.

‡Average e.s.d.'s are calculated using the expression $\sigma_{ave} = [\Sigma_m(l - \bar{l})^2/(m - 1)]^{1/2}$ where m is the number of values averaged and $(l - \bar{l})$ is the difference between each value and the average.

(*b*) Valence angles

Bonds	Angle (deg)	Bonds	Angle (deg)	Bonds	Angle (deg)
S—Ru—N(1)	175.4(2)	F(11)—P(1)—F(12)	89.2(6)	F(21)—P(2)—F(22)	89.5(8)
S—Ru—N(2)	97.7(2)	F(11)—P(1)—F(13)	93.9(7)	F(21)—P(2)—F(23)	90.3(6)
S—Ru—N(3)	90.2(3)	F(11)—P(1)—F(14)	91.2(8)	F(21)—P(2)—F(24)	85.2(1.0)
S—Ru—N(4)	96.7(3)	F(11)—P(1)—F(15)	85.4(8)	F(21)—P(2)—F(25)	86.5(5)
S—Ru—N(5)	89.1(2)	F(11)—P(1)—F(16)	174.1(6)	F(21)—P(2)—F(26)	177.3(1.1)
		F(12)—P(1)—F(13)	85.4(8)	F(22)—P(2)—F(23)	87.0(5)
N(1)—Ru—N(2)	85.1(3)	F(12)—P(1)—F(14)	174.3(9)	F(22)—P(2)—F(24)	173.4(9)
N(1)—Ru—N(3)	86.2(3)	F(12)—P(1)—F(15)	101.0(1.0)	F(22)—P(2)—F(25)	93.1(6)
N(1)—Ru—N(4)	87.0(3)	F(12)—P(1)—F(16)	88.9(7)	F(22)—P(2)—F(26)	93.1(1.0)
N(1)—Ru—N(5)	88.1(3)	F(13)—P(1)—F(14)	88.9(9)	F(23)—P(2)—F(24)	89.0(7)
N(2)—Ru—N(3)	88.7(3)	F(13)—P(1)—F(15)	173.6(1.1)	F(23)—P(2)—F(25)	176.8(6)
N(2)—Ru—N(4)	89.2(3)	F(13)—P(1)—F(16)	91.6(7)	F(23)—P(2)—F(26)	89.2(7)
N(2)—Ru—N(5)	173.1(3)	F(14)—P(1)—F(15)	84.7(1.1)	F(24)—P(2)—F(25)	90.6(7)
N(3)—Ru—N(4)	173.0(3)	F(14)—P(1)—F(16)	91.3(8)	F(24)—P(2)—F(26)	92.1(1.2)
N(3)—Ru—N(5)	89.8(4)	F(15)—P(1)—F(16)	89.5(9)	F(25)—P(2)—F(26)	94.0(6)
N(4)—Ru—N(5)	91.6(4)	Ru—S—O	114.9(3)		
		Ru—S—C(1)	114.8(4)		
		Ru—S—C(2)	117.4(4)		
		O—S—C(1)	105.0(5)		
		O—S—C(2)	103.4(4)		
		C(1)—S—C(2)	99.4(6)		

(*c*) Closest distances between groups not bonded to common atoms

Groups	Range	Number of contacts
Fluorine–ammine	2.99–3.35	10
Fluorine–methyl	3.30–3.50	5
Fluorine–fluorine	3.23–3.59	3
Fluorine–oxygen	3.34	1
Ammine–oxygen	2.98–3.13	4
Ammine–methyl	3.33–3.69	3

cell projected down the *a* axis. Interatomic distances and angles are listed in Table 2, and the r.m.s. displacements of the thermal ellipsoids along the principle axes are given in Table 3.

The high degree of thermal vibration found for the fluorine atoms of the PF_6^- anions probably reflects considerable dynamic disorder of these groups in the crystalline lattice, which is not un-

Can. J. Chem. Downloaded from www.nrcresearchpress.com by 210.87.254.6 on 09/05/12
For personal use only.

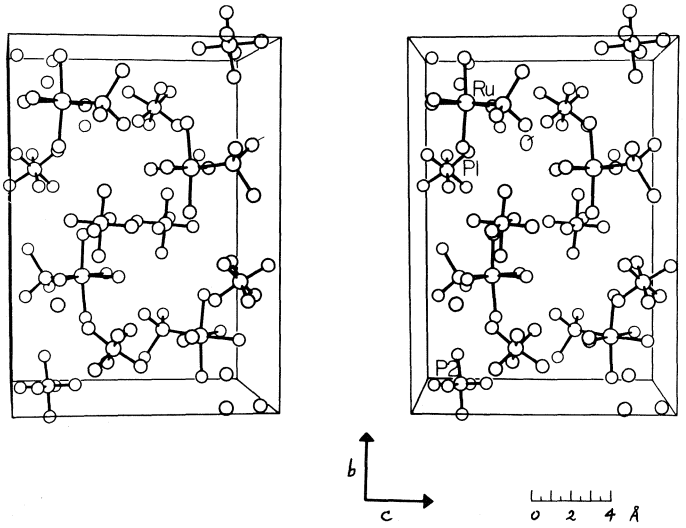

FIG. 2. Stereo diagram of the contents of the unit cell viewed along the *a* axis.

TABLE 3. Root-mean-square amplitudes (Å × 10^3) thermal displacement along the ellipsoid principal axes

Atom			
Ru	162(1)	175(1)	182(1)
S	160(4)	186(4)	195(4)
P(1)	197(5)	248(4)	253(4)
P(2)	185(5)	202(5)	283(3)
F(11)	239(17)	298(11)	422(9)
F(12)	237(32)	289(18)	648(11)
F(13)	232(28)	496(19)	555(13)
F(14)	248(33)	396(23)	712(16)
F(15)	193(57)	288(28)	911(16)
F(16)	233(23)	289(13)	544(11)
F(21)	242(13)	333(12)	586(18)
F(22)	236(16)	316(11)	507(12)
F(23)	208(16)	330(12)	463(10)
F(24)	229(20)	321(29)	782(16)
F(25)	207(10)	309(11)	424(10)
F(26)	219(34)	335(19)	806(19)
C(1)	152(19)	231(14)	312(13)
C(2)	172(20)	226(15)	318(14)
N(1)	160(16)	206(12)	224(11)
N(2)	185(12)	201(14)	240(11)
N(3)	161(14)	210(16)	283(11)
N(4)	168(14)	218(14)	280(11)
N(5)	168(14)	209(13)	314(12)
O	154(14)	225(11)	246(9)

expected (4). The average P—F distance, uncorrected for thermal motion, is 1.53(4) Å, which is not significantly shorter than distances in previously determined structures, *e.g.* 1.55(2) Å (5), 1.58 Å (6). Correction for thermal motion increases the P—F bond lengths greatly (average corrected distance 1.66(5) Å). Since a high degree of rigid body motion is present, we doubt if such corrections are meaningful in this case. It seems probable that the true value lies between the two extremes, and close to previously determined values.

The structure found for the cation is consistent with the results of the infrared study carried out by Senoff, Maslowsky, and Goel (1). Two similar structures in which DMSO is complexed to a second row transition metal (palladium) have been reported. The Ru—S distance (2.188(3) Å) is considerably shorter than the Pd—S distance found for either *trans*-$PdCl_2(DMSO)_2$ (2.299(2) Å) (ref. 7) or *cis*-$Pd(NO_3)_2(DMSO)_2$ (2.231(3), 2.253(3) Å) (ref. 8), while the S—O distance (1.527(8) Å) is longer than that found for either of the Pd complexes (1.476(5) (ref. 7) 1.463(7) (ref. 8)).[3] The principal resonance structures for these complexes may be represented as

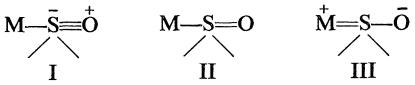

The present structure indicates that a relatively higher proportion of structure III is present for the Ru complex compared with either of the Pd complexes, with a consequently greater degree of metal → ligand π-interaction. This results in a lower S—O bond order, which is consistent with

[3]All bonded distances quoted in the body of the paper and referring to the present structure are corrected for thermal motion except for those of P—F and Ru—S.

Can. J. Chem. Downloaded from www.nrcresearchpress.com by 210.87.254.6 on 09/05/12
For personal use only.

the observed low value for the ν_{SO} bond stretching frequency compared with that found for other S-bonded DMSO complexes (1), including those of palladium discussed above. The greater extent of metal → ligand π-interaction for the present complex is presumably due to the absence of competing groups in the Ru coordination sphere for the available π-donor orbitals.

Two determinations of the crystal structure of free DMSO (9) have yielded S—O distances of 1.471 (determined at −60 °C) and 1.531 (determined at +5 °C). It has been suggested (7) that the latter value is more reliable for comparison with structures determined at room temperature. It is probably coincidental that the S—O distance is similar for the Ru complex and free DMSO as found in the second of the two determinations; however, this is consistent with the observation that the ν_{SO} frequency for the Ru complex is close to that found for free DMSO.

The S—C distance in the Ru complex (1.84(1) Å) is longer than that found for free DMSO (1.80–1.82 Å) (ref. 9) or for the Pd complexes (1.78(1) Å (ref. 7), 1.79(1) Å (ref. 8)). The Ru—N distances (2.169(5), 2.209(8) Å) are longer than normal for single Ru—N bond lengths (2.10–2.14 Å) (ref. 5). The nitrogen *trans* to the sulfur atom is significantly further from the ruthenium than the other four nitrogens. This reflects a "bond weakening" effect due to the sulfur bonded DMSO ligand, which has been found to have a considerable *trans* effect (10).

It is a pleasure to acknowledge the crystallographers and groups who have made their computer programs available to us. These include Dr. F. R. Ahmed and Mrs. M. E. Pippy at the National Research Council of Canada for the suite of IBM 360-50 programs, and the crystallography group at the University of Canterbury, New Zealand for data reduction routines and for modifications of Zalkin's Fourier program (FORDAP), the Busing–Levy full matrix least-squares (ORFLS) and function and error (ORFFE) programs. The diagrams were prepared with the assistance of Johnston's ORTEP.

We wish to thank Dr. E. Maslowsky, Jr. for supplying crystals of the ruthenium complex, Dr. C. V. Senoff for helpful discussions and the National Research Council of Canada for an operating grant (No. 576-34 to G.F.).

1. C. V. Senoff, E. Maslowsky, Jr., and R. G. Goel. Can. J. Chem. This issue.
2. P. W. R. Corfield, R. J. Doedens, and J. A. Ibers. Inorg. Chem. **6**, 197 (1967).
3. International Tables for X-Ray Crystallography. (1965). Tables 3.3.1A, 3.3.1B, 3.3.2C.
4. G. R. Miller and H. S. Gutowsky. J. Chem. Phys. **39**(8), 1983 (1963).
5. B. R. Davis and J. A. Ibers. Inorg. Chem. **9**(12), 2768 (1970) and references contained therein.
6. H. Bode and H. Clausen. Z. Anorg. Chem. **265**, 229 (1951).
7. M. J. Bennett, F. A. Cotton, D. L. Weaver, R. J. Williams, and W. H. Watson. Acta Cryst. **23**, 788 (1967).
8. D. A. Langs, C. R. Hare, and R. G. Little. Chem. Commun. 1080 (1967).
9. W. L. Reynolds. Progress in inorganic chemistry. *Edited by* S. J. Lippard. John Wiley and Sons, Inc. **12**, 1 (1970) (and references contained therein).
10. Y. N. Kukushkin, M. A. Kuz'mina, and A. F. V'yugina. Radiokhimiya. **10**(4), 470 (1968).

Can. J. Chem. Downloaded from www.nrcresearchpress.com by 210.87.254.6 on 09/05/12
For personal use only.

Can. J. Chem. Downloaded from www.nrcresearchpress.com by 210.87.254.42 on 09/05/12
For personal use only.

Photocyclization Reactions of Aryl Polyenes. IV.[1] The Syntheses of Isatogens and Isatogen-like Compounds

CLIFFORD C. LEZNOFF AND ROGER J. HAYWARD
Department of Chemistry, York University, Downsview, Ontario

Received June 22, 1971

Photochemical reactions of 1-*o*-nitrophenyl-4-phenyl-1,3-butadiene, 1,4-di-*o*-nitrophenyl-1,3-butadiene, 1-*o*-nitrophenyl-6-phenyl-1,3,5-hexatriene, and 1,6-di-*o*-nitrophenyl-1,3,5-hexatriene all gave the appropriate 2-substituted isatogen. The related *m*- and *p*-nitrophenyl polyenes were inert to the irradiation conditions. A six-membered ring isatogen-like compound, 2-phenyl-3-oxo-benzo[*d,e*]quinoline-*N*-oxide was prepared by irradiation of 1-[1′-(8′-nitronaphthyl)]-2-phenylacetylene. A seven-membered ring isatogen-like compound, 6-phenyl-7-oxo-dibenzo[*b,d*]azepine-*N*-oxide, was prepared by heating 1-[2-(2′-nitrobiphenyl)]-2-phenylacetylene.

Les réactions photochimiques de *o*-nitrophényle-1 phényle-4 butadiène-1,3, du di-*o*-nitrophényle-1,4 butadiène-1,3, de l'*o*-nitrophényle-1 phényle-6 hexatriène-1,3,5, et du di-*o*-nitrophényle-1,6 hexatriène-1,3,5 donnent toutes les isatogènes appropriées substituées en 2. Les *m*- et *p*-nitrophényle polyènes correspondants sont inertes, s'ils sont soumis à une irradiation. Un composé cyclique à six chaînons du type isatogène, l'oxyde-*N* de la phényle-2 oxo-3 benzo[*d,e*]quinoline a été préparé par irradiation du [(nitro-8′ naphtyle)-1′]-1 phényle-2 acétylène. Un composé cyclique à sept chaînons du type isatogène, l'oxyde-*N* de phényle-6 oxo-7 dibenzo[*b,d*]azépine a été préparé en chauffant le [(nitro-2′ biphényle)-2]-1 phényle-2 acétylène.

Canadian Journal of Chemistry, 49, 3596 (1971)

Introduction

The photocyclization and oxidation of substituted stilbenes have been shown to give substituted phenanthrenes (1), provided one of the substituents is not a nitro group (2). The photocyclization–oxidation reaction of 1,4-diaryl-1,3-butadienes, where the aryl groups are phenyl or substituted phenyl groups, gave mixtures of substituted 1-phenylnaphthalenes (3, 4). It was thought that the irradiation of 1-*m*- and 1-*p*-nitrophenyl-4-phenyl-1,3-butadienes (**1** and **2**) may give 1-*m*- and 1-*p*-nitrophenylnaphthalenes respectively, since photocyclization in this case can occur to a phenyl ring not substituted by a nitro group. In any case, irradiation of **1** and **2** gave no reaction. It has been shown that irradiation of 1,6-diphenyl-1,3,5-hexatriene gives chrysenes (3) but 1-*m*- and 1-*p*-nitrophenyl-6-phenyl-1,3,5-hexatrienes (**3** and **4**) are inert to photochemical reaction conditions (see Experimental).

The irradiation of 1-*o*-nitrostilbene gave 2-phenylisatogen (5), a reaction which can be more readily explained in the photochemistry of the nitro group (5, 6) than in the photocyclization–oxidation of the diaryl polyene.

Isatogens are an interesting group of compounds in that a number of them have shown marked anti-microbiological activity (7) and thus it was decided to examine the syntheses of isatogens in more detail. It was of interest to know whether the extended conjugated system of 1-*o*-nitrophenyl-4-phenyl-1,3-butadiene (**5***a*) and 1-*o*-nitrophenyl-6-phenyl-1,3,5-hexatriene (**5***b*) would influence the photochemical formation of 2-substituted isatogens (Scheme 1).

Results and Discussion

Thus, irradiation of 3.8×10^{-3} *M* solutions of **5***a* and 7.9×10^{-3} *M* iodine in dry benzene under nitrogen gave, after 3 days, a 12% yield of red crystals of 2-styrylisatogen (**6***a*). The structure of **6***a* was confirmed by comparison with a sample synthesized by another route (8).

Irradiation of 3.6×10^{-3} *M* solutions of **5***b* and 8.0×10^{-3} *M* iodine in dry benzene under nitrogen gave, after 3 days, a dark red product, 2-(4-phenylbuta-1,3-dien-1-yl)isatogen (**6***b*) in a 25% conversion from **5***b*. In addition, 60% of the starting material was recovered.

The photochemical reaction of *o,o*′-dinitrostilbene gave 2-(*o*-nitrophenyl)isatogen (5). The analogous photo-reactions of 1,4-di-*o*-nitrophenyl-1,3-butadiene (**5***c*) and 1,6-di-*o*-nitrophenyl-1,3,5-hexatriene (**5***d*) were attempted to determine the affect of the additional nitro group

[1]For Part III, see ref. 23.

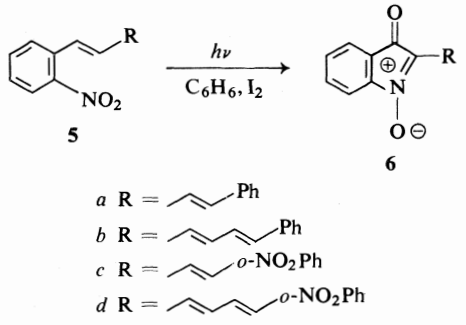

5 6

a R = Ph
b R = Ph
c R = o-NO2Ph
d R = o-NO2Ph

SCHEME 1

on the photochemical formation of isatogens and to explore the possibility of formation of bis isatogens (Scheme 1).

Thus, the photo reaction of a 3.4×10^{-3} *M* solution of **5***c* and 8.0×10^{-3} *M* iodine in dry benzene under nitrogen for 3 days gave a 30% yield of 2-(*o*-nitrostyryl)isatogen (**6***c*). Similarly irradiation of **5***d* gave a 9.1% conversion to 2-(4-*o*-nitrophenylbuta-1,3-dien-1-yl)isatogen (**6***d*) and a 30% recovery of starting material. On the other hand, 1,6-di-*m*- and 1,6-di-*p*-nitrophenyl-6-phenyl-1,3,5-hexatrienes (**7** and **8**) respectively were inert to the irradiation conditions.

Isatogens **6***c* and *d* were purified by preparative t.l.c. and irradiated. No further reactions occurred and no bis isatogens were formed.

The structures of isatogens **6***a–d* were determined primarily from spectroscopic data. The i.r. spectra were especially informative and showed —C=O— stretching vibrations at 1710 cm^{-1} and —$\overset{+}{N}$—$O^{\ominus}$—absorption peaks at 1170 cm^{-1} typical of the isatogen structure. The mass spectra of isatogens **6***a–d* showed parent ions and were consistent with the fragmentation pattern of the published mass spectra of known isatogens (9). All isatogens were dark red compounds and had correct elemental analyses. The n.m.r. spectra of **6***a* and *b* were uninformative and simply showed multiple absorption peaks between 6.5 and 7.5 p.p.m.

Isatogen-like compounds containing six- and seven-membered rings have not been prepared and it was thought that the photochemical reactions of suitable nitrostilbene derivatives could lead to the appropriate isatogen analog. Recently, however, Bond and Hooper (10) have shown that isatogens can be synthesized through tolan intermediates and it was decided to attempt the syntheses of isatogen-like compounds by this method.

The reaction of 1-iodo-8-nitronaphthalene (**9**) with cuprous phenylacetylide in pyridine for 72 h gave a mixture of 1-[1′-(8′-nitronaphthyl)]-2-phenylacetylene (**10**) and starting iodo **9**. The presence of **10** was shown by a sharp band in the i.r. spectrum of **10** at 2242 cm^{-1}, characteristic of the —C≡C— stretching frequency. The crude acetylene **10** was irradiated for 72 h in dry benzene under nitrogen to give, after purification by preparative t.l.c., a 15% yield of the dark red, 2-phenyl-3-oxo-benzo[*d,e*]quinoline-*N*-oxide (**11**), a six-membered ring isatogen analog (Scheme 2). The i.r. spectrum of **11** was characteristic of an isatogen-like compound and showed absorption peaks at 1710 and 1723 cm^{-1} (—C=O) and a weak absorption at 1173 cm^{-1} due to the $\overset{+}{N}$—$O^{\ominus}$ group. The n.m.r. spectrum of **11** showed an absorption peak at 8.96 p.p.m. due to the two ortho protons of the 2-phenyl substituent. The two ortho protons of the phenyl substituent of 2-phenylisatogens are known to be shifted downfield relative to the other protons attached to an aromatic ring (10).

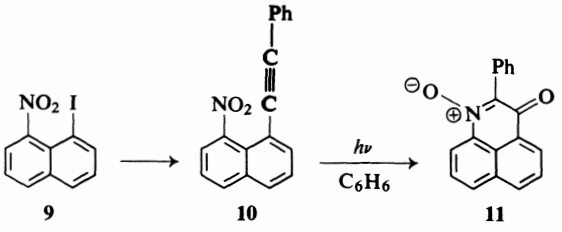

9 10 11

SCHEME 2

The reaction of 2-iodo-2′-nitrobiphenyl (**12**) with cuprous phenylacetylide in pyridine under reflux for 72 h gave a mixture of *o*-(2′-nitrophenyl)tolan (**13**) and starting iodo **12**. The mixture was heated further for 72 h with excess cuprous acetylide to give a 2.6% yield of a dark-brown product, 6-phenyl-7-oxo-dibenzo[*b,d*]azepine-*N*-oxide (**14**), a seven-membered ring isatogen-like compound (Scheme 3). The i.r. spectrum of **14** showed typical carbonyl absorption at 1712, 1721, and 1728 cm^{-1} and a weak (—$\overset{+}{N}$—$O^{\ominus}$) absorption peak at 1187 cm^{-1}. The n.m.r. spectrum of **14** showed peaks at 8.38 p.p.m. due to the ortho protons of the 6-phenyl substituent.

The spectral data of all the compounds are consistent with the assigned structures.

The mechanism of formation of isatogens from the photoreaction of *o*-nitrostilbenes has been discussed by other workers (5, 6) but firm

Can. J. Chem. Downloaded from www.nrcresearchpress.com by 210.87.254.42 on 09/05/12
For personal use only.

Can. J. Chem. Downloaded from www.nrcresearchpress.com by 210.87.254.42 on 09/05/12
For personal use only.

TABLE 1. Spectral characteristics of substituted-nitrophenyl polyenes

Compound	Substituent	The u.v. spectra (benzene) λ_{max} (nm) (ε)	The i.r. spectra (KBr) $\nu(cm^{-1})$	Mass spectra *m/e* M^+(% of base peak)
1	*m*-Nitro	336.5 (65 400), 328 (62 200)	1540, 1353, 995	251 (18.1)
2	*p*-Nitro	370 (22 900), 284 (17 600)*	1608, 1535, 1351, 998	251 (35)
3	*m*-Nitro	352 (75 700), 349 (71 600)	1539, 1355, 1004	277 (12.5)
4	*p*-Nitro	402 (32 700), 324 (18 700), 313 (19 000)	1521, 1351, 1003	277 (100)
5*a*	*o*-Nitro	311 (33 900)*	1622, 1610, 1521, 1350, 991	251 (20)
5*b*	*o*-Nitro	333.5 (32 700)	1602, 1522, 1349, 989	277 (59)
5*c*	Di-*o*-nitro	340 (11 600), 278 (18 800)*	1604, 1511, 1345, 974	296 (100)
5*d*	Di-*o*-nitro	390.5 (17 400), 370 (19 400), 326 (20 600)	1603, 1512, 1340, 997	322 (49)
7	Di-*m*-nitro	355 (17 000), 347 (16 900)	1533, 1355, 997	322 (100)
8	Di-*p*-nitro	3950 (24 200)	1541, 1346, 996	322 (73)

*Solvent 95% ethanol.

TABLE 2. Physical properties of isatogens and isatogen-like compounds

Compound	Yield (%)	Melting point (°C)	Formula	Analysis					
				Calculated			Found		
				C	H	N	C	H	N
6*a*	12	186–188*	$C_{16}H_{11}NO_2$	73.00	4.18	10.63	73.37	4.39	10.31
6*b*	25	175–176	$C_{18}H_{11}NO_2$	78.52	4.73	5.09	78.24	4.67	4.97
6*c*	30	229–230	$C_{16}H_{10}N_2O_4$	65.31	3.42	9.52	65.20	3.40	9.30
6*d*	9.1	204–206	$C_{18}H_{12}N_2O_4$	67.48	3.75	8.75	67.21	3.64	8.51
11	15	183–185	$C_{18}H_{11}NO_2$	79.14	4.03	5.12	79.34	4.23	5.43
14	2.6	239–240	$C_{20}H_{13}NO_2$	80.26	4.35	4.68	80.59	4.66	4.47

*Literature 180–183° (8).

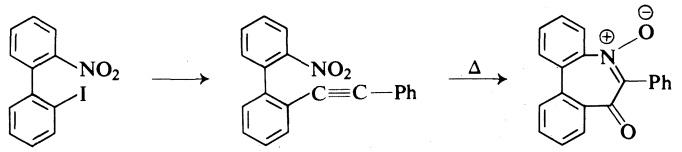

12 **13** **14**

SCHEME 3

evidence regarding postulated intermediates is lacking. The formation of **11** and **14** by photochemical and thermal means respectively is significant in the fact that the steric requirements necessary for the formation of isatogens (five-membered ring) is *not* stringent and the formation of six and seven-membered ring isatogen-like compounds is readily achieved.

Experimental

All melting points were determined on a Kofler hot stage and are uncorrected. The i.r. spectra were recorded on a Perkin–Elmer 257 i.r. spectrometer using KBr discs. The u.v. spectra were measured using a Cary 14 u.v. spectrometer and benzene as a solvent. The n.m.r. spectra were measured on a Varian A60 spectrometer using tetramethylsilane as an internal standard ($\delta = 0$ p.p.m.) and deuterochloroform as solvent. Mass spectra were recorded on a Hitachi–Perkin–Elmer RMU-6 mass spectrometer. Silica gel was used for thin- and thick-layer chromatography. All photochemical reactions were carried out in a Rayonet photochemical reactor using RPR 3500 Å lamps. Microanalyses were performed by A. B. Gygli of Toronto.

Synthesis of 1-Nitrophenyl-4-phenyl-1,3-butadienes

A typical example is given for the preparation of 1-*o*-nitrophenyl-4-phenyl-1,3-butadiene (**5***a*). To a mixture of 3.43 g (0.026 mol) of cinnamaldehyde and 12.0 g (0.025 mol) of *o*-nitrobenzyltriphenylphosphonium chloride in 100 ml methanol, was added 130 ml of 0.2 *M* lithium methoxide. The mixture was allowed to crystallize overnight after which crystals of **5***a* were obtained in 30% yield; m.p. 96–97° (lit. 98–99° (11)).

1-m-Nitrophenyl-4-phenyl-1,3-butadiene (1)

The m.p. 145–146° (lit. 145–146° (12)); yield 46%.

1-p-Nitrophenyl-4-phenyl-1,3-butadiene (2)

The m.p. 180–181° (lit. 181.5–182° (13)); yield 36%.

Synthesis of 1,4-Di-o-nitrophenyl-1,3-butadiene (5c)

1,4-Di-*o*-nitrophenyl-1,3-butadiene (**5***c*) was prepared by reacting *o*-nitrobenzyltriphenylphosphonium chloride and *o*-nitrocinnamaldehyde by the Wittig procedure identical to that given above. Product **5***c* was obtained in 49% yield; m.p. 219–220° (lit. 210–220° (14)).

Preparation of 1-Nitrophenyl-6-phenyl-1,3,5-hexatrienes

A typical example is given for the preparation of 1-*o*-nitrophenyl-6-phenyl-1,3,5-hexatriene (**5***b*). To a mixture of 2.0 g (0.0126 mol) of 5-phenylpenta-2,4-dien-1-al (15) and 6.0 g (0.0126 mol) of *o*-nitrobenzyltriphenylphosphonium chloride in 30 ml methanol was added 50 ml of 0.4 *M* lithium methoxide. The mixture was allowed to crystallize overnight after which crystals of **5***b*, m.p. 104–105°, were obtained in 17% yield.

Anal. Calcd. for $C_{18}H_{15}NO_2$: C, 77.98; H, 5.42; N, 5.04. Found: C, 78.19; H, 5.21; N, 5.14.

1-m-Nitrophenyl-6-phenyl-1,3,5-hexatriene (3)

The m.p. 184–185° (lit. 184–185° (13)); yield 54%.

1-p-Nitrophenyl-6-phenyl-1,3,5-hexatriene (4)

The m.p. 194–195° (lit. 194–196° (16)); yield 63%.

Preparation of 1,6-Di-nitrophenyl-1,3,5-hexatrienes

A typical example is given for the preparation of 1,6-di-*o*-nitrophenyl-1,3,5-hexatriene (**5***d*). To a mixture of 2.25 g (0.015 mol) of *o*-nitrobenzaldehyde and 3.25 g (0.007 mol) of 2-butene-1,4-bis(tri-*n*-butylphosphonium chloride) (17) in 50 ml methanol was added 60 ml of 0.2 *M* lithium methoxide. The mixture was allowed to crystallize overnight after which crystals of **5***d*, m.p. 232–233°, were obtained in 64% yield.

Anal. Calcd. for $C_{18}H_{14}N_2O_4$: C, 67.08; H, 4.38; N, 8.69. Found: C, 67.01; H, 4.75; N, 8.37.

1,6-Di-m-nitrophenyl-1,3,5-hexatriene (7)

The m.p. 165–166°; yield 83%.

Can. J. Chem. Downloaded from www.nrcresearchpress.com by 210.87.254.42 on 09/05/12
For personal use only.

Can. J. Chem. Downloaded from www.nrcresearchpress.com by 210.87.254.42 on 09/05/12
For personal use only.

TABLE 3. Spectral characteristics of isatogens and isatogen-like compounds

Compound	The u.v. spectra (benzene) λ_{max} (nm) (ε)	The i.r. spectra (KBr) $\nu(cm^{-1})$	Mass spectra *m/e* M^+(% of base peak)
6*a*	485 (3110), 321.5 (30 400)	1721, 1709, 1178, 980	249 (13)
6*b*	511 (4310), 372 (34 400), 355 (35 300), 342 (31 700)	1714, 1172, 989	275 (6.5)
6*c*	485 (4240), 322.5 (31 700)	1703, 1518, 1352, 1173, 979	294 (15)
6*d*	487 (4120), 325.5 (36 800)	1727, 1523, 1352	320 (4.5)
11	489 (4100), 327 (35 700)	1710, 1723, 1173	273 (21)
14	491 (3400), 331 (38 200)	1728, 1721, 1712, 1187	299 (31.4)

Can. J. Chem. Downloaded from www.nrcresearchpress.com by 210.87.254.42 on 09/05/12
For personal use only.

Anal. Calcd. for $C_{18}H_{14}N_2O_4$: C, 67.08; H, 4.35; N, 8.69. Found: C, 67.24; H, 4.22; N, 8.54.

*1,6-Di-p-nitrophenyl-1,3,5-hexatriene (**8**)*

The m.p. 218–219° (lit. 218–219° (17)); yield 62%.

Spectral Properties of the Substituted-nitrophenylpolyenes

The spectral data of these compounds are given in Table 1.

Synthesis of Mono-nitrobenzyltriphenylphosphonium Halides

The mono-nitrobenzyltriphenylphosphonium halides were prepared by a procedure identical to that given previously (4).

o-Nitrobenzyltriphenylphosphonium Chloride

The m.p. 233–234° (lit. 230° (18)).

m-Nitrobenzyltriphenylphosphonium Bromide

The m.p. 260–262° (lit. 261° (19)).

p-Nitrobenzyltriphenylphosphonium Bromide

The m.p. 279–279.5° (lit. 275–275.5° (13)).

Irradiation of Nitrophenyl Polyenes

The general techniques of irradiation on a preparative scale have been described previously (4). The photocyclization reaction products were isolated by preparative thick layer chromatography (t.l.c.) using hexane:benzene (1:2) as eluant. All the photocyclization products moved slower than the starting *o*-nitrophenyl polyenes on t.l.c. Since, in general, the results have already been mentioned, only details of identification are given (see Tables 2 and 3).

*Preparation of 1-Phenyl-2-[1′(8′-nitronaphthyl)]-acetylene (**10**)*

A mixture of 0.5 g (0.0167 mol) of 1-iodo-8-nitronaphthalene (20) and 0.275 g (0.0167 mol) of cuprous phenylacetylide (21) in 50 ml of dry pyridine was heated under reflux for 72 h in a nitrogen atmosphere. The pyridine was removed under reduced pressure and the residue was extracted with a benzene:water (1:1) mixture. The benzene layer was purified by preparative t.l.c. to give an inseparable mixture of what appeared to consist of the starting material 1-iodo-8-nitronaphthalene and the tolan (**10**). The i.r. spectrum of the mixture showed an absorption peak at 2242 cm^{-1}.

The Irradiation Product of 1-Phenyl-2-[1′(8′-nitronaphthyl)]-acetylene

The isatogen-like analog 2-phenyl-3-oxo-benzo[*d,e*]-quinoline-*N*-oxide was identified by its physical and spectral properties given in Tables 2 and 3 and by its n.m.r. spectrum which showed signals at 8.96 for H-2 (doublet) and 8.12–8.64 p.p.m. for H-9 (multiplet).

*Preparation of 6-Phenyl-7-oxo-dibenzo[b,d]azepine-N-oxide (**14**)*

A mixture of 1.0 g (0.0036 mol) of 2-iodo-2′-nitrobiphenyl (22) and 0.5 g (0.00306 mol) of cuprous phenylacetylide (20′) in 50 ml of dry pyridine was heated under reflux for 72 h in an atmosphere of nitrogen. Then the pyridine was removed under reduced pressure and the residue was extracted with benzene:water (1:1) mixture. The benzene layer was purified by preparative t.l.c. to give two products. The first consisted of a mixture of what appeared to be 2-iodo-2′-nitrobiphenyl (**12**) and *o*-(2′-nitrophenyl)tolan (**13**) (the i.r. spectrum of the mixture showed an absorption peak at 2226 cm^{-1}). The other product, a dark brown compound, was found to be 6-phenyl-7-oxo-dibenzo[*b,d*]azepine-*N*-oxide (**14**) identified by its physical and spectral properties (Tables 2 and 3) and by its n.m.r. spectrum which showed signals at 8.38 for H-2 (doublet) and 7.58–7.18 p.p.m. for H-11 (multiplet).

The authors are grateful for the support of this research by the National Research Council of Canada and to Professor R. L. Letsinger for some helpful discussions.

1. C. O. Parker and P. E. Spoerri. Nature, **166**, 603 (1950); F. R. Stermitz. *In* Organic photochemistry. I. O. L. Chapman. *Editor*. Dekker, New York, N.Y., 1967. p. 247; E. V. Blackburn and C. J. Timmons. Q. Rev. **23**, 482 (1969).
2. F. B. Mallory, C. S. Wood, and J. T. Gordon. J. Am. Chem. Soc. **86**, 3094 (1964).
3. G. J. Fonken. Chem. and Ind. 1327 (1962); C. C. Leznoff and R. J. Hayward. Can. J. Chem. **48**, 1842 (1970).
4. A. Santiago and R. S. Becker. J. Am. Chem. Soc. **90**, 3654 (1968).
5. J. S. Splitter and M. Calvin. J. Org. Chem. **20**, 1086 (1955).
6. R. Huisgen. Angew. Chem. Intern. Ed. **2**, 565 (1963).
7. M. Hooper, D. A. Patterson, and D. G. Wibberley. J. Pharm. Pharmacol. **17**, 734 (1965).
8. F. Kröhnke, G. Kröhnke, and I. Vogt. Chem. Ber. **86**, 1500 (1953).
9. D. R. Eckroth. Chem. Commun. 465 (1970).
10. C. C. Bond and M. Hooper. J. Chem. Soc. C, 2453 (1969).
11. G. B. Bachmann and R. I. Hoaglin. J. Org. Chem. **8**, 300 (1943).
12. F. Bergmann and D. Schapiro. J. Org. Chem. **12**, 57 (1947).
13. R. N. McDonald and T. W. Campbell. J. Org. Chem. **24**, 1969 (1959).
14. H. Wolf and O. Westphal. Ann. **657**, 52 (1962).
15. A. Lüttringhaus and G. Schill. Chem. Ber. **93**, 3048 (1960).
16. B. M. Miknikov and G. S. Ter-Sarkisyan. Zhur. Obshchei Khim. 30, 2521 (1960).
17. H. Heitman. Synthesis of symmetrical polyenes by Wittig reactions. PhD Thesis. University of Amsterdam, Amsterdam,Holland. 29 (1965).
18. N. N. Melnikov, A. E. Kietov, and B. I. Mel′tser. J. Gen. Chem. (U.S.S.R.). **7**, 461 (1937).
19. F. Kröhnke. Chem. Ber. **83**, 291 (1950).
20. H. Hodgson and J. Walker. J. Chem. Soc. 1620 (1933).
21. R. D. Stephens and C. E. Castro. J. Org. Chem. **28**, 3313 (1963).
22. J. A. Cade and A. Pilbeam. J. Chem. Soc. 114 (1964).
23. R. J. Hayward and C. C. Leznoff. Tetrahedron, In press.

Can. J. Chem. Downloaded from www.nrcresearchpress.com by 210.87.254.40 on 09/05/12
For personal use only.

Cyclopentadienylidenecarbonyl: the Major Primary Thermolytic Fragment of Salicylaldehyde

O. A. MAMER

Division of Clinical Biochemistry, Department of Experimental Medicine, McGill University, Montreal, Quebec

Received July 5, 1971

The thermal fragmentation of salicylaldehyde was studied from two aspects. Firstly, the temperature dependence of the intensity of the thermolytic fragment molecular ions was observed at 11 eV in the effluent from a helium flow thermal reactor attached through a helium separator to the ion source of a mass spectrometer. Secondly, the products of the thermolysis on a semi-preparative scale under trapping conditions were determined by coupled gas chromatographic – mass spectrometric analysis.

The title compound is the major primary thermal fragment in this study and was trapped with methanol as carboxymethylcyclopentadiene.

On a étudié la fragmentation thermique de la salicylaldéhyde sous deux aspects. On a observé premièrement la dépendance de la température sur l'intensité des fragments thermolytiques d'ions moléculaires obtenus à 11 eV dans un réacteur thermique à courant d'hélium, fixé dans un séparateur à hélium à la source d'ions d'un spectromètre de masse. On a déterminé deuxièmement les produits de la thermolyse sur une échelle semi-préparative par une analyse combinée c.p.g.–s.m.

Le composé mentionné dans le titre de l'article est le fragment thermique primaire principal obtenu dans cette étude et fut recueilli avec le méthanol sous forme de carboxyméthylcyclopentadiène.

Canadian Journal of Chemistry, 49, 3602 (1971)

In the course of a preliminary investigation into the relationships between the electron impact fragmentation of some ortho-substituted phenols it became of interest to study the thermolysis (1)[1] of salicylaldehyde (**1**). It was thought that the presence of an odd electron, even mass number peak *m/e* 76, 19% (2) in the spectrum of **1** might suggest a facile thermolytic preparative method for benzyne (Scheme 1) in much the same way as the thermolysis of phthalic anhydride is known to yield benzyne (3).

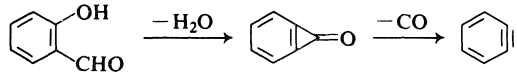

1

SCHEME 1

Surprisingly, the primary major thermolytic fragment of **1** was eventually shown to be the title compound **2** by trapping it with methanol (Scheme 2) as **4**, the methyl ester of cyclopentadienecarboxylic acid, by a modification of a method recently reported for the same compound (4). Rearrangement of **3** to the more highly conjugated **4** has been previously reported (5).

The thermolytic behavior of **1** was studied with two furnaces. Furnace A, Fig. 1, is a low pressure

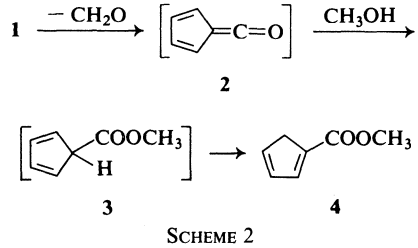

SCHEME 2

quartz flow reactor capable of reaching a temperature in excess of 1100° with a helium carrier. Furnace effluent is split in a ratio which determines in part the furnace pressure, one part going to the pumps, the second through the Becker–Ryhage helium separator (6) to the ion source of the LKB 9000 coupled gas chromatograph–mass spectrometer (g.c.–m.s.) used for the study.

By employing low ionizing energy (11 eV typically) we could sort out the molecular ions of thermolytic fragments and observe their behavior while varying the furnace temperature. Figure 2 shows the temperature dependence of the significant mass numbers in the thermolysate of **1**.

As *m/e* 122 decomposes, a thermal fragment with *m/e* 92 is produced which also decomposes with increasing temperature, probably into fragments of *m/e* 64 and 28. At very high temperatures as the yield of 92 begins to greatly diminish, 64

[1]As opposed to "pyrolysis".

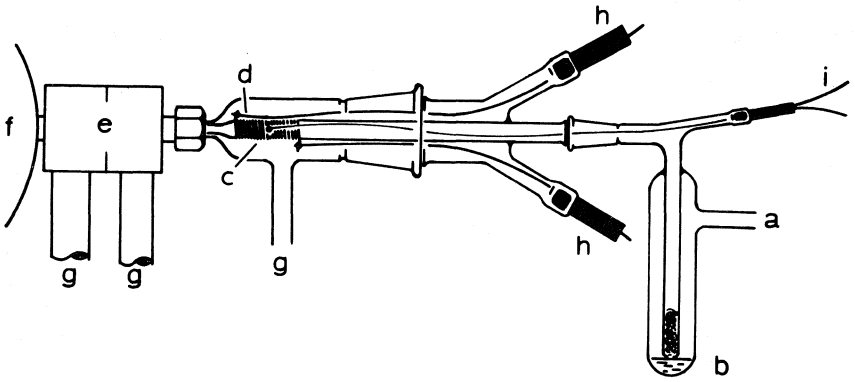

FIG. 1. Furnace A. Quartz reactor for flash thermolysis in a low pressure helium flow; (*a*) helium inlet (0.01–0.1 Torr); (*b*) sample; (*c*) Chromel–Alumel thermocouple junction; (*d*) nichrome windings on quartz furnace; (*e*) Becker–Ryhage separator; (*f*) ion source; (*g*) to pumping system; (*h*) furnace electrical leads soft-soldered through Kovar seals; (*i*) thermocouple leads in a single 1.6 mm diameter Inconel sheath soft-soldered through Kovar seal. Furnace effluent is stripped of most of the helium carrier by the separator allowing thermolysate molecular ion detection at greater concentrations in the ion source. A glass wool plug between the sample and furnace is needed to reduce the introduction of aerosols or dusts into the furnace.

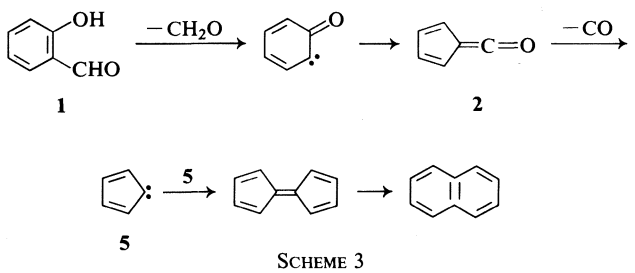

SCHEME 3

appears to fall off due to a dimerization reaction yielding 128. No significant increase at *m/e* 76 could be detected to support the occurrence of benzyne in this thermolysis.

Scheme 3 is proposed to account for the ion intensity *vs.* temperature data of Fig. 2 in the pyrolysis of **1**. A similar scheme has been proposed for the thermolysis of *o*-phenylene carbonate (4) involving **2** as an intermediate based on product analysis. A competing process in this last work is the elimination of two molecules of CO to yield cyclopentadienone which was detected as the dimer.

Furnace B, Fig. 3, was used to thermolyze **1** in such a way as to enable the trapping of reactive intermediates by bubbling them at a high rate in the argon carrier through the trapping methanol. The furnace pressure in B is necessarily higher than in furnace A because a hydrostatic head of approximately 1 to 2 mm of methanol must be overcome for bubbling to occur.

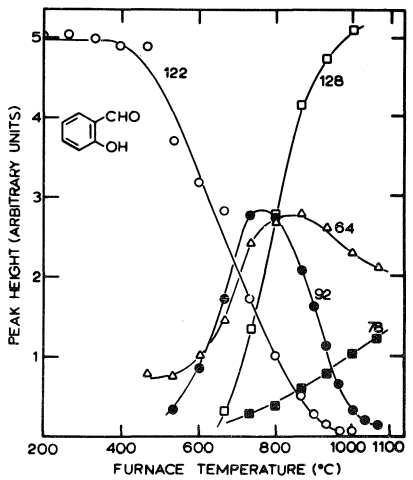

FIG. 2. Thermolysis of salicylaldehyde. Variation of significant *m/e* values with temperature of furnace A.

Thermal fragment assignments are: ○, *m/e* 122, **1**; ●, *m/e* 92, **2**; △, *m/e* 64, **5**; □, *m/e* 128, naphthalene; ■, *m/e* 78, benzene.

Can. J. Chem. Downloaded from www.nrcresearchpress.com by 210.87.254.40 on 09/05/12
For personal use only.

Can. J. Chem. Downloaded from www.nrcresearchpress.com by 210.87.254.40 on 09/05/12
For personal use only.

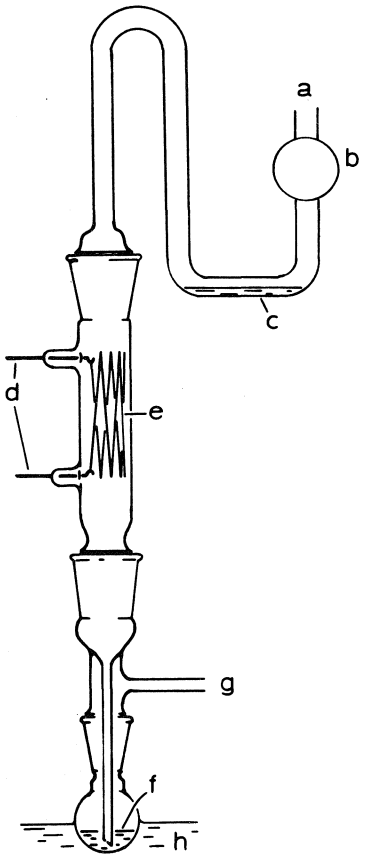

FIG. 3. Furnace B. Semi-preparative thermolysis reactor arranged for trapping experiments; (*a*) argon supply (1 atm); (*b*) flow moderating needle value; (*c*) sample; (*d*) furnace electrical leads; (*e*) nichrome filaments; (*f*) trapping reagent; (*g*) to pumping system; (*h*) cooling bath (acetone – Dry Ice).

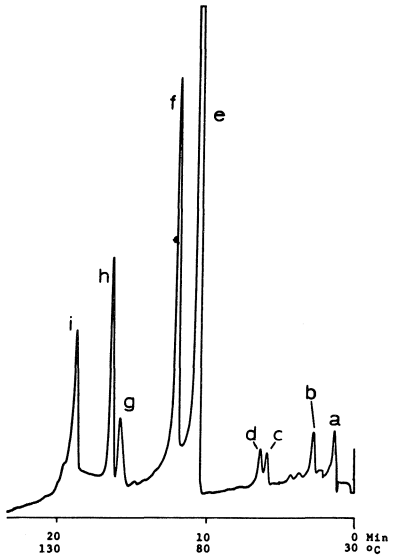

FIG. 4. Gas chromatogram of thermolysate–methanol solution prepared with furnace B; (*a*) benzene; (*b*) toluene; (*c*) phenylacetylene; (*d*) styrene; (*e*) carboxymethylcyclopentadiene; (*f*) salicylaldehyde; (*g*) unknown; (*h*) naphthalene; (*i*) salicylaldehyde dimethylacetal. The height of peak *e* (**4**) is approximately 5.5 times the recorder limits. Apparent baseline drift is due to slow decomposition of salicylaldehyde dimethylacetal on the column.

By keeping the trapping methanol at $-78°$, the methanolysis of the ketene moiety appears complete while the Diels–Alder dimerization reaction through the cyclopentadiene ring is inhibited to the extent that the sample may be stored for several days at this temperature relatively unchanged (5).

Figure 4 is the gas chromatogram obtained on analysis of the trap contents immediately after the conclusion of the thermolysis. Each eluting peak in the g.c. record was scanned at high speed with the mass spectrometer. Each spectrum and retention time was compared with those for authentic samples when available to make the identifications indicated in Fig. 4. The mass spectrum of carboxymethylcyclopentadiene (**4**) is reproduced in Fig. 5. The isotopic distribution pattern in the molecular ion requires the formula $C_7H_8O_2$ and the spectrum is consistent with the structural assignment indicated. It is also consistent with what might be considered that part of the spectrum reported (7) for dimeric **4** arising from a retro-Diels–Alder monomerization in the ion source.

When ethanol is used as the trapping agent the corresponding ethyl ester is obtained in similar yields and has a mass spectrum consistent with this assignment (molecular ion 138, $C_8H_{10}O_2$ by isotopic distribution).

DeJongh and Brent (4*b*) propose that **2** dimerizes under thermolytic conditions to yield a tricyclic diketene intermediate which in turn suffers loss of C_2O and CO and re-arrangement to indene. No trace of indene could be detected in our thermolysate possibly because rapid quenching and methanolysis may compete more successfully for **2** than dimerization.

The other significant thermolytic product de-

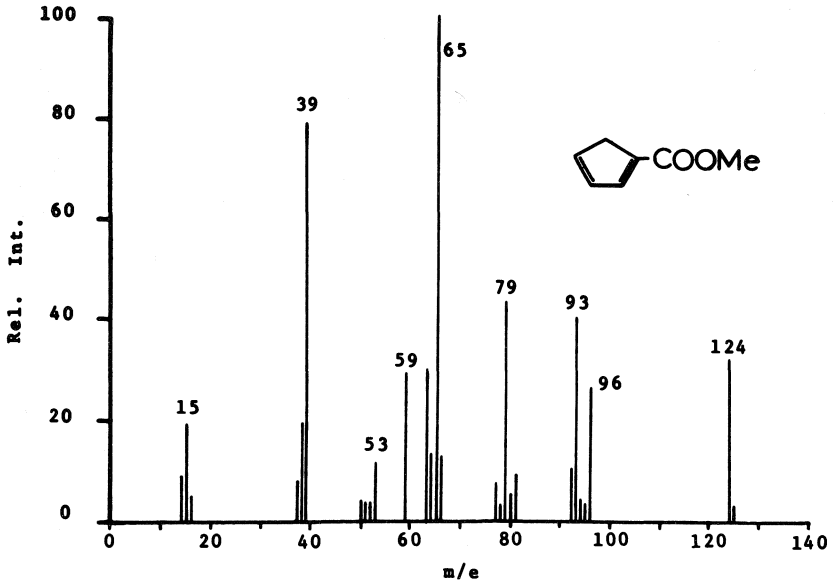

FIG. 5. Mass spectrum of **4** "on the fly" in the thermolysate gas chromatogram (Fig. 4, peak *e*). Presumed molecular ion *m/e* 124, formula $C_7H_8O_2$ by isotopic distribution.

tected was naphthalene which supports that part of the pathway of Scheme 3 earlier proposed in the *o*-phenylene carbonate pyrolysis (4*b*).

The relatively minor amounts of benzene, toluene, phenylacetylene, and styrene probably arise from the recombination of small fragments like acetylene and ethylene (8) or radical hydrocarbons formed by direct contact of heavier fragments or **1** at the incandescent nichrome wire.

Salicylaldehyde dimethylacetal is probably formed by the condensation of surviving thermally excited **1** with methanol in the trap. The mass spectrum of this peak is identical with the authentic compound (9).

Our data strongly suggest that Scheme 3 is the main thermolytic pathway of **1** and that under proper conditions cyclopentadienylidenecarbonyl can be generated from **1** in useful concentrations as a highly reactive intermediate for synthetic or trapping purposes.

Experimental

The thermolyses were conducted on salicylaldehyde as received from the supplier (British Drug Houses). Gas chromatographic retention times and mass spectra of commercially available compounds were used to establish the identity of most of the thermolytic products. An LKB 9000 combined g.c.–m.s. was used for the study in two modes as explained below.

Thermolytic Experiments

Furnace A (Fig. 1)

Before an experiment, the system was equilibrated by allowing a few milligrams of **1** to evaporate slowly from the sample holder into the helium flow over a period of about 30 min with the furnace set at about 250° and the helium flow rate adjusted to that required for the experiment. Several heating and cooling cycles of the furnace were made immediately prior to a run to ensure against ion source pressure increases due to volatilization of any condensed material from the cooler parts of the furnace.

After each furnace temperature increment, a 2 min thermal re-equilibration period was observed. Increasing the length of this period had no apparent effect on the data. Following re-equilibration, a slow scan (20 s) of the mass range *m/e* 10–250 was made with the detector output heavily filtered to reduce amplifier noise at the top of the mass peaks. Peak heights were then measured from the u.v. oscillograph tracing corresponding to each furnace temperature. Figure 2 summarizes this data. The operating conditions were: ionizing energy, 11 eV at 60×10^{-6} A; accelerating potential, 3.5 kV; source temperature, 290°; separator temperature 280°; electron multiplier output filter cutoff at 20 Hz; source slit, 0.15 mm; detector slit 0.5 mm; furnace pressure, 30 μ.

Furnace B (Fig. 3)

Thermolysis with furnace B was carried out with methanol (0.5 ml) in the trap at −78°, the nichrome filaments at approximately 800°, and an argon carrier flow rate moderated with the needle valve to maintain a rapid and violent bubbling in the trap (40 ml min^{-1} argon measured at room temperature and pressure at the pump outlet). Contact time was calculated to be 50 ms. Cooling the

Can. J. Chem. Downloaded from www.nrcresearchpress.com by 210.87.254.40 on 09/05/12
For personal use only.

furnace with a draught of ambient air was necessary to prevent softening and collapse of the Pyrex walls. Thermolysis was allowed to proceed for approximately 15 min and then the furnace was cooled and the system brought to room pressure by closing off the pumping system and increasing the argon flow.

The trap containing the methanol solution of the thermolysate (pale yellow) was disconnected and kept at Dry Ice temperature. Aliquots of the mixture were withdrawn by syringe and analyzed with the m.s. in the g.c. coupled mode: injector 300°; column, 2 m × 6 mm glass containing 3% SE 30 Ultraphase on Chromosorb W, High Performance (Pierce Chemical), temperature programmed from 30–200° at 5° min^{-1}; helium flow rate, 30 ml min^{-1}; separator, 280°; ion source, 290°, ionizing energy 70 eV scan mode (20 eV g.c. detection mode) at 60 × 10^{-6} A; scan range *m/e* 10–250 in 3 s. The gas chromatogram with peaks identified is shown in Fig. 4.

Integration of the peak areas in Fig. 4 indicates that **4** amounts to 78% of the volatile components of the thermolysate (excluding methanol).

Storage of the thermolysate solution at room temperature caused a reduction of the size of the peak for **4** to near extinction in a day or two and a simultaneous increase in a broad peak having a mass spectrum similar to that reported (7) for the dimer of **4**.

The LKB 9000 g.c.–m.s. used in this study was granted by the Medical Research Council of Canada (#ME 3720) to the Faculty of Medicine of McGill University. The author also wishes to acknowledge the general assistance in this work of Miss S. S. Tjoa. The author is especially indebted to Dr. F. P. Lossing for his suggestions and interest in the progress of this work. A useful discussion with Dr. I. P. Fisher on the design and coupling of furnace A through the Becker–Ryhage separator is gratefully recognized.

1. J. F. King, P. de Mayo, C. L. McIntosh, K. Piers, and David J. H. Smith. Can. J. Chem. **48**, 3704 (1970), footnote 3.
2. F. W. McLafferty. Interpretation of mass spectra. W. A. Benjamin, New York, N.Y. p. 166.
3. (*a*) S. Meyerson. Rec. Chem. Progr. **26**, 257 (1965); (*b*) E. K. Fields and S. Meyerson. Chem. Commun. 474 (1965); (*c*) E. K. Fields and S. Meyerson. J. Org. Chem. **31**, 3307 (1966); (*d*) R. F. C. Brown, D. V. Gardner, J. F. W. McOmie, and R. K. Solly. Aust. J. Chem. **20**, 139 (1967).
4. (*a*) D. C. DeJongh, R. Y. Van Fossen, and A. Dekovich. Tetrahedron Lett. **58**, 5045 (1970); (*b*) D. C. DeJongh and D. A. Brent. J. Org. Chem. **35**, 4204 (1970).
5. David Peters. J. Chem. Soc. 1761 (1959).
6. R. Ryhage. Arkiv Kemi. **26**, 305 (1967a).
7. D. Brent. Ph.D. Dissertation. Wayne State University, Detroit, Michigan, 1970. p. 67.
8. (*a*) M. Berthelot. Ann. Chim. Phys. **9**, 445 (1866); (*b*) G. M. Badger. Progr. Phys. Org. Chem. **3**, 1 (1966), and references cited therein.
9. R. D. Haworth and A. Lapworth. J. Chem. Soc. **121**, 76 (1922).

Can. J. Chem. Downloaded from www.nrcresearchpress.com by 210.87.254.40 on 09/05/12
For personal use only.

Isolation and Structure of a Dilignol Rhamnoside From the Leaves of *Thuja plicata* Trees

GARY D. MANNERS[1]

Faculty of Forestry, University of British Columbia, Vancouver, British Columbia

AND

ERIC P. SWAN[2]

Department of the Environment, Western Forest Products Laboratory, and Faculty of Forestry, University of British Columbia, Vancouver, British Columbia

Received June 24, 1971

The isolation of a series of dilignol glycosides from the leaves of western red cedar trees is described. The structure of the first member of this series was determined by chemical degradation reactions and n.m.r. and mass spectra of its derivatives. It is 1-(3′-methoxy-4′-hydroxyphenyl)-2-*O*-1′′-[2′′-hydroxy-4′′-(propane-3′′′-*O*-α-L-rhamnopyranoside)phenyl]-propane-1,3-diol (**1**). The novel features of this compound are discussed, together with its possible roles in the leaves.

On décrit l'isolement d'une série de glycosides de dilignol à partir des feuilles du cèdre rouge de l'ouest. La structure du premier membre de cette série fut déterminée par des réactions de dégradation chimique, par résonance magnétique nucléaire et par spectrométrie de masse de ses dérivés. Il s'agit du 1-(3′-méthoxy-4′-hydrophényl)-2-*O*-1′′-[2′′-hydroxy-4′′-(propane-3′′′-*O*-α-L-rhamnopyranoside)phényl]-propane-1,3 diol (**1**). On discute des caractéristiques de ce composé, de même que des fonctions possibles qu'il peut occuper dans les feuilles.

Canadian Journal of Chemistry, **49**, 3607 (1971)

Studies of western red cedar (*Thuja plicata* Donn) extractives from these laboratories have dealt mainly with heartwood. We now describe some phenolic compounds in leaves. The only previous work on these compounds from this species was on the biflavonoids (1). However, two glycosides of guaiacylglycerol were identified in leaves of another softwood (*Pinus sylvestris* L.) (2). These compounds are the only ones germane to this paper, other studies on softwood leaf tissues having been concerned with carbohydrate content.

Compound **1** was obtained as an amorphous solid from a sequence of column chromatographic separations of the ethyl acetate fraction from leaf extract. Attempts to crystallize the compound from organic solvents were unsuccessful. On the basis of the following results, compound **1** was identified as 1-(3′-methoxy-4′-hydroxyphenyl)-2-*O*-1′′-[2′′-hydroxy-4′′-(propane-3′′′-*O*-α-L-rhamnoside)phenyl]-propane-1,3 diol.

The color reaction of **1** with diazotized sulfanilic acid (bright orange) and its positive reaction with Gierer's reagent (6) were characteristic of an α-hydroxyguaiacyl derivative. Schroeder's reaction (7), for the detection of dihydroxy groups, was negative. Since alkaline nitrobenzene oxidation of **1** gave vanillin and protocatechualdehyde, the test with Schroeder's reagent showed that one of the hydroxyl groups on the pyrocatechol nucleus must be etherified. Hydrolysis of the compound showed several phenolic products and L-rhamnose.

Ethanolysis gave the Hibbert's ketones 1-guaiacyl-2-ethoxypropan-1-one and 1-guaiacylpropan-2-one, and an uncharacterized pyrocatechol derivative indicated by color reactions. Another ethanolysis of the fully methylated derivative of compound **1** yielded dihydroconiferyl alcohol and 1-verartryl-2-ethoxypropan-1-one. The free aromatic hydroxyl group of dihydroconiferyl alcohol established the unusual 4′′-*n*-propan-3′′′-ol side chain and the 2-4′′ alkyl–aryl ether linkage in **1**. The free aliphatic hydroxyl group established the point of attachment of the L-rhamnose in the molecule.

Proof that the arrangement of pyrocatechol and L-rhamnose groups were as shown and not interchanged, or that the substitution was as

[1]Graduate student; present address: U.S. Department of Agriculture Laboratory, Berkeley, California.

[2]Part-time Associate Professor at University of British Columbia; to whom enquiries should be sent at: Western Forest Products Laboratory, 6620 N. W. Marine Drive, Vancouver 8, British Columbia.

Can. J. Chem. Downloaded from www.nrcresearchpress.com by 210.87.254.6 on 09/05/12
For personal use only.

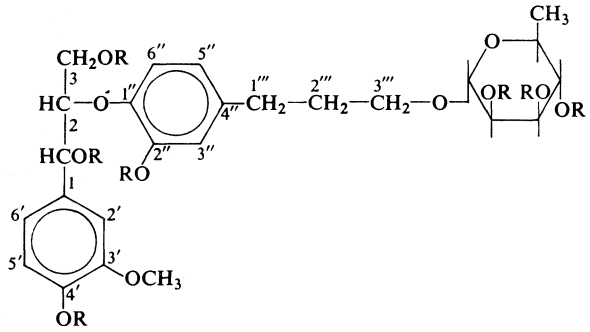

1 R = H
2 R = Ac
3 R = CH_3

a β-aryl ether rather than γ- etc. was obtained from the following experiment. Periodate oxidation of diazomethane methylated (aromatic hydroxyls C-4′ and -2′) compound **1** showed an uptake of exactly 2 mol per mol of starting compound. This 2 mol consumption of periodate was solely from the L-rhamnose moiety and showed the absence of any other vicinal diol in compound **1**. Lack of a bathochromic shift of the u.v. maximum of the oxidized product in base was evidence that the glycosidic bond did not occur through an aromatic hydroxyl.

The low melting point of the acetate derivative **2** (m.p. 48–50°) suggested that the parent **1** was a mixture of *erythro-* and *threo*-isomers. Since t.l.c. (silica and cellulose) in several solvent systems had indicated purity for both **1** and **2**, n.m.r. was necessary to confirm that **1** was indeed a mixture of isomers.

Mass spectral determination of the molecular weight of **2** gave 804, with a calculated empirical formula (from M + 1/M ratio) of $C_{39}H_{48}O_{18}$, supported by carbon and hydrogen analyses. The u.v. $\Delta\varepsilon$ value (8.04×10^3) of **1** showed the existence of two phenolic hydroxyl groups. The i.r. data substantiated the existence of aromatic nuclei, a large number of hydroxyl groups, and the absence of carbonyl. The n.m.r. spectral analyses, including double resonance experiments, were primarily done on **2** and confirmed the above structure. All the expected features of spectrum of **2** were present: six aromatic protons equally divided amongst two rings, an α-L-rhamnopyranoside moiety, an *n*-propyl side chain, a glycerol side chain, one methoxyl, two phenolic acetates, and five aliphatic acetates; with no other unexpected features present and the correct proton integral for the above. The glycerol side chain was responsible for the mixture of *erythro-* and *threo*-isomers mentioned above. The chemical shift data and nature of the n.m.r. spectrum of **2** is in agreement with similar data recorded for 1-(3,4-dimethoxyphenyl)-2-(2′-methoxyphenoxy)-propane-1,3 diol acetate reported by Ludwig *et al.* (8), and by Hemmer and Liaaen–Jensen for methyl-α-L-rhamnopyranoside triacetate (4).

Similarly, the mass spectrum of **2** shows the parent ion at *m/e* = 804 and other features expected from its fragmentation. The rhamnose triacetate moiety corresponded to the published data on the mass spectrum of methyl α-L-rhamnopyranoside triacetate (4). Several other features of the acetylated guaiacylglycerol part of **2** can be illustrated through probable formulae related to major ions *m/e* 323, 201, 221, 179, and 153, and of the acetylated *n*-propylcatechol part of **2** to *m/e* 331, 169, and 123.

Several characteristics of compound **1** are novel and require comment. First, this compound constitutes the first isolation and characterization of a free dilignol (9) glycoside. Second, the compound exists as an unusual rhamnoside rather than more commonly observed glucosides. Third, the rhamnoside is connected to the compound through a previously unreported aliphatic hydroxyl position rather than the expected aromatic hydroxyl position. Fourth, the existence of a saturated propyl side chain is unreported among other dilignols which were isolated using hydrolytic conditions, and is biosynthetically unusual. Finally, the existence of a pyrocatechol group is unreported among dilignols previously isolated and characterized.

The structure of **1** suggests the possibility of its hydrolysis and polymerization into a lignin molecule. The occurrence of pyrocatechol groupings in bark lignins (10) substantiates this, but translocation much beyond local environs of aromatic (particularly dimeric) lignin precursors is unlikely. Thus, either **1** is destined to incorporation into leaf lignin, or it may be representative of extractives which exist as free dilignols with secondary physiological functions, for example, protection mechanisms in the leaves. Since injury or disease reactions may occur in leaves, then the rhamnosidic linkage of the dilignol rhamnoside may be

Can. J. Chem. Downloaded from www.nrcresearchpress.com by 210.87.254.6 on 09/05/12
For personal use only.

Can. J. Chem. Downloaded from www.nrcresearchpress.com by 210.87.254.6 on 09/05/12
For personal use only.

cleaved to make the aglycone available for participation in detoxification or sealing-off activities.

The unusual structure of **1** suggests its participation in the less intensively studied bark or leaf lignin. A study of western red cedar bark using n.m.r. (11) has shown a lower methoxyl content and more aliphatic character than wood lignin. Thus **1** may act as precursor to lignin different in character than that observed in the wood. Such lignin may contain aryl–aryl bonded lignin polymers, which originate from coupling ortho to the *n*-propyl side chain of dilignol activated by the free pyrocatechol hydroxyl grouping. Further research on leaf lignin structure is planned.

The separation of several other related compounds isolated with **1** was accomplished. Their n.m.r. and mass spectra showed that they were also dilignol rhamnosides, but they were incompletely characterized so that structures for them are not reported here. All other compounds isolated were similar to **1**, but hydrolysis experiments gave D-glucose and L-arabinose as well as L-rhamnose. Work on their structures is continuing and will be reported later.

Experimental

Melting points (uncorrected) were taken on a Fisher–Johns apparatus. The i.r. spectra were obtained from KBr disks on a Perkin–Elmer 521; u.v. were obtained of ethanol solutions on a Beckman DK-2; n.m.r. spectra were obtained in deuterated solvents (tetramethylsilane $\tau = 10$ internal standard) on a Varian HA-100; mass spectra were obtained from Morgan-Schaeffer Corp., Montreal. Elemental analyses were obtained from Galbraith Laboratories Inc., Knoxville, Tennesee.

Paper chromatography and t.l.c. on cellulose were run with the solvents: 2% aqueous acetic acid (AA); *n*-butanol, chloroform, acetic acid, water (BCAW, 4:1:1:1); lower layer chloroform, acetic acid, water (CAW, 4:6:3). Detecting reagent was diazotized sulfanilic acid (DSA). The t.l.c. on silica used the solvents: chloroform, methanol (CM, 4:1) and benzene, ethanol (BE, 9:1). Detecting reagent was mixed nitric – sulfuric acids. Column chromatography was on Sephadex LH-20 (Pharmacia) and deactivated silicic acid (Fisher). The pressure pump was a Milton-Roy 196-47 and the eluant u.v. monitor was a Gilson UV 280 IF.

Isolation of Compounds

Yields of 1.47 g (0.76%, o.d. basis) of ethyl ether solubles and 23.8 g (3.86%) of ethyl acetate solubles were obtained from 1.5 kg (58.6% moisture) of fresh comminuted western red cedar leaves. The methanol-soluble chloroform-insoluble leaf extracts were partitioned first between ether–water and then the water fraction between ethyl acetate – water to obtain the above fractions, all others were discarded. The crude ethyl acetate extract contained at least five phenolic compounds giving the distinctive yellow–orange color with DSA characteristic of α-hydroxy guaiacyl groups. These compounds were separated from other material by two-stage column chromatography on LH-20 (gradient elution), and the major compound **1** was separated from its relatives by a similar procedure on silica gel. Approximate yields: **1**, 0.15 g; other relatives (orange–yellow with DSA), 0.35 g (o.d. basis) from the leaves.

Compound 1

The R_f values on cellulose were 0.76, 0.63, and 0.50 for AA, BCAW, and CAW, and on silica were 0.14 and 0.29 for BE and CM. A white amorphous powder, **1** had λ_{max} 279 shifting to 289.5 nm in base with $\Delta\varepsilon_{max}$ 8.04×10^3, indicating two phenolic hydroxyl groups. The i.r. bands: 3400 (s, strong), 2928 (s), 1770 (w, weak), 1605 (s), 1505 (s), 1449 (m, medium), 1429 (m), 1370 (m), 1270 (s), 1230 (m), 1207 (m), 1123 (s), 1089 (s), 1042 (s), 978 (2), 909 (w), 877 (w), 805 (w), 781 (w) cm^{-1}.

The n.m.r. (deutero-dimethyl sulfoxide τ numbers) 6H multiplet at 2.9–3.61, two singlets (1.30, 2.5, phenolic OH) 12–14H multiplet at 6.1–6.8 (aliphatic OH), singlet at 5.07 (1H, benzyl proton), 1H (methine) at 6.00 (determined by nuclear magnetic double resonance (n.m.d.r.)) and 2H multiplet at 8.18 (methylene); total integral 30–35H.

Compound **1** reacted to give a positive Gierer (6) test for benzyl hydroxyl group and a negative Schroeder (7) test for *o*-dihydroxyphenyl group. Alkaline nitrobenzene oxidation showed (t.l.c) vanillin and protocatechualdehyde as the products.

Catalytic hydrogenolysis (1 atm, room temperature) of **1** (10 mg in 10 ml ethanol) was run with $PdCl_2$–$BaSO_4$ (10 mg), a catalyst (3) highly reactive in the reduction of benzyl hydroxyl groups. The product, which was also not crystalline, gave a negative Gierer test.

Hydrolysis of **1** was very difficult. Enzymatic hydrolysis gave a very low yield of probable aglycone (low R_f in CM). More vigorous hydrolyses (2% aqueous oxalic acid or 6% methanolic hydrogen chloride at 100° for 2 h) were unsuccessful because of the formation of several phenolic compounds, none of which was the aglycone (high R_f in CM). This was probably due to the side reactions of the benzyl alcohol group. L-Rhamnose was determined by paper chromatography in the hydrolysates.

Methylation

Aromatic hydroxyl methylation of **1** used diazomethane in methyl alcohol – ether. Silica t.l.c. (CM) of the product showed two compounds (R_f 0.45, 0.55); the R_f 0.55 was the desired compound. The R_f 0.45 compound was considered to be a singly methylated derivative, because remethylation of it (separated by column chromatography) gave the higher R_f compound, aromatically methylated **1**. The n.m.r. of this product showed 9H at $\tau = 6.21$ (3 methoxyl). This product (20 mg) in ethanol (2 ml) was reacted with 0.01 *N* sodium periodate, according to the procedure of Dyer (5). Aliquots of the reaction mixture were titrated with

Can. J. Chem. Downloaded from www.nrcresearchpress.com by 210.87.254.6 on 09/05/12
For personal use only.

excess sodium arsenite (0.005 *M*) after 1 and 2 h. Consumption of periodate showed 2 mol consumed per mol of compound used after 1 h and no further after 2 h. The remainder of the reaction mixture was reacted with excess sodium arsenite, the p*H* was adjusted to 4.0 and the reaction product was taken into ethyl acetate by extraction (3 × 10 ml) in a separatory funnel. The combined ethyl acetate solutions were dried, filtered and the solvent was then removed *in vacuo*. The product (7 mg) was taken up in ethanol (100 ml) and its u.v. spectrum had λ_{max} 283 nm, unshifted in 0.01 *N* sodium methoxide. This showed that no new phenolic hydroxyl group was formed after the periodate cleaved the L-rhamnose.

Compound **1** (125 mg) was dissolved in dimethylformamide (5 ml) – methyl iodide (1 ml) and silver oxide (100 mg) was added. The reaction mixture (under nitrogen) was stirred overnight at room temperature, and then filtered and the volatile reactants removed *in vacuo*. The residue was added under nitrogen to a solution of sodium hydride (100 mg) in dimethylsulfoxide (10 ml) and, after a few minutes, methyl iodide (1 ml) was added. The reaction proceeded as before and was worked-up in the same way. The product was purified by preparative t.l.c. with BE solvent (R_f 0.10). The purified product was taken up in chloroform (1 ml) and added to petroleum ether (6 ml) – ether (2 ml) and set aside at about 5° to crystallize. The product **3** (light yellow crystals) had m.p. 54–58°, yield 22 mg.

Anal. Calcd. for $C_{32}H_{48}O_{11}$: C, 63.14; H, 7.95. Found: C, 63.17; H, 7.94.

Ethanolyses

Compound **1** (10 mg) was dissolved in 3% ethanolic hydrogen chloride (1 ml) under nitrogen in a sealed tube and heated at about 100° for 2 h. After cooling, the product was neutralized with sodium bicarbonate and shown to contain 1-guaiacyl-2-ethoxypropane-1-one (cellulose t.l.c. with butyl alcohol saturated with ammonia solvent).

The fully methylated derivative **3** (16 mg) was also subjected to ethanolysis using the same amounts and conditions as above. The product was neutralized with sodium bicarbonate, and shown to contain (t.l.c. and comparative i.r. spectra) dihydroconiferyl alcohol and 1-verartryl-2-ethoxypropan-1-one.

Acetylation to Compound 2

Compound **1** (25 mg) was treated at about 70° with pyridine (2 ml) and acetic anhydride (2 ml). After one h the volatile reactants were removed *in vacuo* and the residue was triturated with petroleum ether (65–110°) to give **2** (0.44 mg) as off-white microcrystals, m.p. 48–50°.

Anal. Calcd. for $C_{39}H_{48}O_{18}$: C, 58.20; H, 6.01. Found: C, 57.98; H, 5.85.

The n.m.r. (deutero-chloroform, τ numbers); 6H multiplet at 3.04–3.30, 3H singlet at 6.22 (methoxyl), two 3H singlets at 7.73 and 7.77 (aromatic acetates), 15H multiplet at 7.9–8.4 (aliphatic acetates); total integral 47–49. Rhamnose moiety: the anomeric H of an α-L-rhamnopyranoside is a singlet at 5.36 (4). A high field 3H doublet at 8.83 originated from C-6 coupling with the C_5-H (J = 6.5 Hz). The C_2–C_4 protons were at: H-2, 4.79 ($J_{2,3}$ = *ca.* 1 Hz); H-3, 4.77 ($J_{2,3}$ = 1.5, $J_{3,4}$ = *ca.* 10 Hz); H-4, 5.0 ($J_{4,5}$ = 4.5 Hz). The C-5 proton at 6.21 was not shifted through acetylation, as shown by n.m.d.r.

A 1H double doublet at 4.00 was assigned to the benzyl proton of a glycerol grouping. These doublets at 3.97 ($J_{1,2}$ = 7.0 Hz) and 4.05 ($J_{1,2}$ = 4.0 Hz) were attributed to a diastereomeric pair of β-guaiacylglycerol isomers. Since the C_2-H was associated with an ether-bonded carbon, it should have appeared in the region 4.5–6.0 (8). Using n.m.d.r. techniques, the 4.5–6.0 region was scanned while monitoring the low field doublet. The C_2-H resonance was located at 5.38, hidden beneath the anomeric proton resonance. The n.m.d.r. of the C_2-H caused the C_1-H doublets to collapse to two singlets at 3.97, 4.05. This irradiation of the C_2-H also clarified the multiplets in the region 5.6–6.1, indicating the C_3-(2H) resonance associated with the multiplet in this range.

The triplet (2H) at 7.37 (J = 3.7 Hz) and the multiplet (2H) at 8.18 were characteristic of the C-1‴ and C-2‴ protons of the *n*-propyl chain. When the resonance at 8.18 (under the aliphatic acetate envelope) was irradiated, the triplet at 7.37 collapsed to a singlet, thereby establishing it as the $C_{1'''}$-H resonance, and the 8.18 resonance as the $C_{2'''}$-H resonance. Irradiation of the C-2‴ resonance simplified the multiplet at 6.30–7.75 to an AB quartet 6.5 (τ_A = 6.35, τ_B = 6.65, $J_{(gem)}$ = 10.0 Hz). This resonance was from $C_{3'''}$-(2H). The chemical shift of the AB quartet suggested that they were methylene H associated with an ether bond which would occur at 5.5–6.0, rather than an ester bond. The AB nature of the spin–spin coupling of the geminal H of the methylene group indicated non-equivalence and suggested restricted rotation at the $C_{2'''}$—$C_{3'''}$ bond due to the bulky L-rhamnose moiety. Mass spectrum: *m/e* at 804 (1), 762 (7), 702 (8), 660 (2), 600 (3), 556 (2), 440 (8), 331 (8), 323 (20), 287 (10), 273 (38), 221 (24), 213 (12), 179 (19), 169 (45), 153 (80), 123 (24), 111 (49), 109 (32), 91 (33), 43 (100), figures in parentheses are percent heights of the base *m/e* of 43. Six acetate decomposition transitions were seen, two were accompanied by metastable ions:

$$804 \xrightarrow{m^* = 722.2} 762 + CH_2{=}C{=}O$$

and

$$762 \xrightarrow{m^* = 621} 702 + CH_3{-}COOH.$$

The others were:

$$702 \longrightarrow 642 + CH_3{-}COOH$$

$$642 \longrightarrow 600 + CH_2{=}C{=}O$$

$$702 \longrightarrow 660 + CH_2{=}C{=}O$$

and

$$660 \longrightarrow 600 + CH_3{-}COOH$$

The rhamnoside triacetate moiety was shown in the occurrence of an *m/e* = 273 and the ions 273, 213, 153, 111, and 109 are part of the fragmentation pathway (4).

Other Components

Several other compounds, with the same DSA color reaction as **1**, were isolated. Two in particular, **4** (R_f 0.73, 0.95 in BCAW, CAW) and **5** (R_f 0.73, 0.84),

were characterized sufficiently (n.m.r., mass spectra) to show they were closely related (dilignol rhamnosides) to **1**. Thus **4** had the same R_f as hydrogenated **1**, and mild hydrolysis of **4** gave **5**. Work on them is continuing. Other compounds gave D-glucose and L-arabinose on hydrolysis, but all had the same DSA color reaction.

We thank Dr. J. F. Manville for his generous help in interpreting the n.m.r. and n.m.d.r. spectra.

1. M. TAKABASHI, T. ITO, A. MIZUTANI, and K. ISAI. Yakugaku Zasshi. **80**, 1488 (1960).
2. O. THEANDER. Acta Chem. Scand. **19**, 1792 (1965).
3. E. ADLER and J. MARTON. Acta Chem. Scand. **15**, 357 (1961).
4. E. HEMMER and S. LIAAEN-JENSEN. Acta Chem. Scand. **24**, 3019 (1970).
5. J. R. DYER. Meth. Biochem. Anal. **3**, 111 (1956).
6. J. GIERER. Acta Chem. Scand. **8**, 1319 (1954).
7. H. A. SCHROEDER. J. Chrom. **30**, 537 (1967).
8. C. H. LUDWIG, B. J. NIST, and J. L. MCCARTHY. J. Am. Chem. Soc. **86**, 1186 (1964).
9. K. FREUDENBERG and A. C. NEISH. Constitution and biosynthesis of lignin. Springer-Verlag, New York. N.Y., 1968. p. 129.
10. T. HIGUCHI, Y. ITO, M. SHIMADA, and I. KAWAMURA. Cell. Chem. Tech. **1**, 585 (1967).
11. E. P. SWAN. Pulp Paper Mag. Can. **67**, T456 (1966).

Can. J. Chem. Downloaded from www.nrcresearchpress.com by 210.87.254.6 on 09/05/12
For personal use only.

The Trifluoroacetic Acid Solvent System. Part III. The Acid, $HB(OOCCF_3)_4$, and the Solvent Autoprotolysis Constant

M. G. HARRISS AND J. B. MILNE[1]

Department of Chemistry, University of Ottawa, Ottawa 2, Canada

Received June 25, 1971

The limiting equivalent conductivities, Λ^0, of the acids, $HB(OOCCF_3)_4$ and $HSbF_5(OOCCF_3)$, and the salt, $CsB(OOCCF_3)_4$, have been measured and found to be 22.34, 18.77, and 48.56 ohm^{-1} cm^2 $equiv^{-1}$, respectively. Calculation of the solvent autoprotolysis constant gives the value: 4×10^{-14} mol^2 l^{-2}. The salt, $CsB(OOCCF_3)_4$ is readily prepared but the parent acid, $B(OOCCF_3)_3$ could not be isolated.

Les conductivités equivalentes limites, Λ^0, des acides $HB(OOCCF_3)_4$ et $HSbF_5(OOCCF_3)$, et du sel, $CsB(OOCCF_3)_4$, ont été mesurés et determinées comme étant 22.34, 18.77 et 48.56 ohm^{-1} cm^2 $equiv^{-1}$ respectivement. Le calcul de la constante autoprotolytique du solvant a donné la valeur: 4×10^{-14} mol^2 l^{-2}. Le sel $CsB(OOCCF_3)_4$ est facilement preparé mais l'acide correspondant $B(OOCCF_3)_3$ ne peut pas être isolé.

Canadian Journal of Chemistry, 49, 3612 (1971)

Introduction

Trifluoroacetic acid is a moderately strong acid in water (1) but as a bulk solvent it is weakly acidic and does not protonate even water (2, 3). As a base trifluoroacetic acid is very weak, being a non-electrolyte in 100% sulfuric acid (4). Several studies of acids in pure trifluoroacetic acid have been made (5–7) but the hygroscopic nature of the solvent and the low concentrations of solute that must be studied to avoid complication from higher ion aggregates ($< 10^{-4}$ M) make such studies difficult (7). Any water present in the solvent will react with an acid solute, HA, to give $H_3O^+A^-$ which will produce spurious results. Even the most carefully dried trifluoroacetic acid contains $\sim 10^{-3}$ M water (3). To avoid interference from water, trifluoroacetic acid anhydride may be added in small amounts ($\sim 0.5\%$) without seriously affecting the dielectic constant and viscosity of the solvent. However, the anhydride is found to react with many of the common strong acids (7). Two acids which may be studied in the presence of anhydride are $HSbF_5(OOCCF_3)$ (7) and $HB(OOCCF_3)_4$. The electrical conductivity of these acids and the cesium salt of the latter acid, $CsB(OOCCF_3)_4$ as well as the determination of the solvent autoprotolysis constant are the subject of this paper.

Experimental Section

The experimental methods and the extrapolation procedure for the conductivity measurements have been described in Part I (3). More recently, the first fractions (~500 ml) of doubly distilled trifluoroacetic acid (b.p. 71–72 °C) were used to rinse out the conductivity cell before collecting the fraction for conductivity studies. This procedure was followed without disconnecting the cell from the distillation apparatus by using a siphon arrangement. In this way pure acid with a conductivity one fifth of that previously reported (3) was obtained ($K_{sp} = 0.0064$ μmho cm^{-1}).

Solutions of $HB(OOCCF_3)_4$ for additions to the conductivity cell were made up in trifluoroacetic acid from stoichiometric quantities of boric acid (Analar) and trifluoroacetic acid anhydride. Several days were required for the boric acid to dissolve. The anhydride was prepared from trifluoroacetic acid and phosphorus pentoxide (3). A solution of $CsB(OOCCF_3)_4$ for conductivity studies was made up by dissolving a 1:1:3 mole ratio of $B(OH)_3$/$CsOOCCF_3$/$(CF_3CO)_2O$ in trifluoroacetic acid. A small excess of anhydride was present (~0.5%) in these solutions to maintain anhydrous conditions. All insoluble material dissolved within hours at room temperature. The procedures followed are essentially those used for the alkali metal trifluoroacetates (3).

The cesium salt, $CsB(OOCCF_3)_4$, was isolated from the solution as prepared for conductivity studies by removal of trifluoroacetic acid under vacuum to the point of crystallization. The crystals were then filtered out, washed with anhydride, and dried.

Anal. Calcd. for $CsB(OOCCF_3)_4$: B, 1.81; Cs, 22.27; ratio of acidic (CF_3CO_2) groups to B, 3. Found: B, 1.81; Cs, 22.26; ratio of acidic (CF_3CO_2) groups to B, 2.99.

The compound $B_2O(OOCCF_3)_4$ was isolated in several procedures while attempting to prepare $B(OOCCF_3)_3$. In one instance the analysis approached that of $B(OOCCF_3)_3$ but this compound was never obtained pure.

(*a*) Boric acid was mixed with trifluoroacetic acid anhydride slightly in excess of that required for the formation of $B(OOCCF_3)_3$. The insoluble material dissolved after several weeks at room temperature. The solution was then evaporated to the point of crystallization, filtered, washed with anhydride and dried.

[1]To whom all correspondence should be addressed.

Can. J. Chem. Downloaded from www.nrcresearchpress.com by 210.87.254.6 on 09/05/12
For personal use only.

Can. J. Chem. Downloaded from www.nrcresearchpress.com by 210.87.254.6 on 09/05/12
For personal use only.

Anal. Calcd. for $B_2O(OOCCF_3)_4$: B, 4.4; (CF_3CO_2), 92.3. Found: B, 4.3; (CF_3CO_2), 90.5.

(*b*) For the reaction of BCl_3 and $HOOCCF_3$ in *n*-pentane the procedure of Gerrard *et al.* (8) was followed. In one experiment the reactants were mixed at −60 °C, the mixture was allowed to warm up to 20 °C overnight and then all volatile material was removed at water aspirator pressure. The product analyzed as for $B_2O(OOCCF_3)_4$: % (CF_3CO_2), observed, 91.8; theoretical, 92.3. When the acid was added dropwise to the *n*-pentane solution at 20 °C the product analyzed as a mixture of 56 mol% $B(OOCCF_3)_3$ and the remainder $B_2O(OOCCF_3)_4$.

Anal. Calcd. for mixture: B, 3.68; (CF_3CO_2), 94.9. Found: B, 3.63; (CF_3CO_2), 94.7.

(*c*) The reaction of 100 mmol of BCl_3 with 300 mmol of $(CF_3CO)_2O$ in 20 ml *n*-pentane gave after filtration and drying, $B_2O(OOCCF_3)_4$.

Anal. Calcd. for $B_2O(OOCCF_3)_4$: B, 4.42; (CF_3CO_2), 92.3. Found: B, 4.40; (CF_3CO_2), 92.1.

A computer program was written to calculate the conductimetric titration curve from Λ^0 and K_a for the acid, base, and salt. From the known association constants, the composition of the mixture, assuming reaction 5 to be complete, and the activity coefficients calculated from the extended Debye–Hückel expression used for the Fuoss extrapolations (3), the concentrations of all ionic species present were calculated by an iterative procedure. The distance of closest approach, "*a*", used in the expression for the activity coefficient was a weighted average of the "*a*" values for the electrolytes present, according to the concentrations of the electrolyte ions present. From the concentrations of the ions present and the equivalent conductivities as calculated from the simple Debye–Hückel–Onsager relation for the respective ionic strengths, the specific conductance for each experimental point was calculated.

Results and Discussion

Conductivity Studies

Antimony pentafluoride is known to act as an acid in acidic solvents such as HF (9) and HSO_3F (10). Fluorine-19 nuclear magnetic resonance studies show that it behaves similarly in $HOOCCF_3$ (7).

[1] $$HOOCCF_3 + SbF_5 \rightarrow HSbF_5OOCCF_3$$

The reaction of boric acid with sulfur trioxide in sulfuric acid gives a strong acid in 100% H_2SO_4 (11) and the analogous reaction in trifluoroacetic acid would be

[2] $$B(OH)_3 + 3(CF_3CO)_2O \rightarrow HB(OOCCF_3)_4 + 2HOOCCF_3$$

The results of conductivity studies on $HSbF_5(OOCCF_3)$ and $HB(OOCCF_3)_4$ are given in Table 1. The runs give good Fuoss plots and the equivalent conductivities, Λ^0, association constants, K_a, and standard % errors on Λ^0 are given in Table 2. As discussed below, attempts to isolate

TABLE 1. Specific conductances (K_{sp}) at 25 °C

Solvent	10^3C (mol l^{-1})	10^6K_{sp} (ohm^{-1} cm^{-1})
SbF_5	0.02799	0.2849
(Initial solvent K_{sp}	0.04085	0.3693
$= 0.0761 \times 10^{-6}$	0.05395	0.4433
ohm^{-1} cm^{-1}	0.07027	0.5236
	0.08131	0.6042
	0.09962	0.6774
	0.1178	0.7420
	0.1345	0.7979
	0.1498	0.8493
$HB(OOCCF_3)_4$	0.02971	0.1264
(Initial solvent K_{sp}	0.04882	0.1660
$= 0.00734 \times 10^{-6}$	0.07596	0.2126
ohm^{-1} cm^{-1}	0.09765	0.2432
	0.1156	0.2661
	0.1337	0.2883
	0.1483	0.3056
	0.1615	0.3208
$CsB(OOCCF_3)_4$	0.01726	0.5190
(Initial solvent K_{sp}	0.03778	0.9316
$= 0.0064 \times 10^{-6}$	0.06054	1.296
ohm^{-1} cm^{-1}	0.08517	1.633
	0.1081	1.907
	0.1282	2.130
	0.1496	2.351
	0.1710	2.556

$B(OOCCF_3)_3$ from solutions of $HB(OOCCF_3)_4$ yielded $B_2O(OOCCF_3)_4$. This behavior is like that of boric acid in water which is present as $B(OH)_4^-$ at low concentrations but forms condensed ions at higher concentrations. The complex acid, $HB(HSO_4)_4$, behaves similarly in H_2SO_4 (11). In order to further establish that $HB(OOCCF_3)_4$ was the electrolyte present at low concentrations and not the acid produced from $B_2O(OOCCF_3)_4$, a Fuoss extrapolation was carried out assuming that $B_2O(OOCCF_3)_4$ was present and that it behaved as a monobasic acid according to

[3] $$B_2O(OOCCF_3)_4 + 2HOOCCF_3 \rightarrow H_2OOCCF_3^+B_2O(OOCCF_3)_5^-$$
$$H_2OOCCF_3^+B_2O(OOCCF_3)_5^- \rightleftarrows H_2OOCCF_3^+ + B_2O(OOCCF_3)_5^-$$

If the acid were dibasic the second dissociation would be expected to be small and unlikely to be important in a low dielectric constant solvent. The extrapolation yielded $\Lambda^0 = 42.9$ ohm^{-1} cm^2 equiv^{-1} and $K_a = 1.5 \times 10^6$ mol l^{-1}. The value of Λ^0 is more than double that for $HSbF_5(OOCCF_3)$. It is doubtful in view of the relative sizes of the two anions, that $B_2O(OOCCF_3)_5^-$ should be more mobile than $SbF_5(OOCCF_3)^-$

TABLE 2. Limiting equivalent conductivities (Λ^0) and association constants (K_a)

Solute	Λ^0 (ohm^{-1} cm^2 equiv^{-1})	% Std. error on Λ^0	$10^{-5}K_a$ (mol l^{-1})	$10^8 a$ (cm)
SbF_5	18.77	5.5	0.57	5.70
$B(OOCCF_3)_3$	22.34	3.2	8.2	4.40
$CsB(OOCCF_3)_4$	48.56	6.6	0.58	5.70
$CsOOCCF_3$*	52.41	0.41	1.0	5.35

*From ref. 3.

TABLE 3. Conductimetric titration of $HB(OOCCF_3)_4$ with $CsOOCCF_3$

10^3C (mol l^{-1})		10^6K_{sp} (ohm^{-1} cm^{-1})	
$HB(OOCCF_3)_4$	$CsOOCCF_3$	Observed	Calculated
0.1615	0	0.366	—
0.1580	0.02238	0.739	0.741
0.1528	0.05587	1.226	1.252
0.1489	0.08083	1.556	1.574
0.1453	0.1034	1.831	1.837
0.1420	0.1248	2.067	2.066
0.1379	0.1512	2.266	2.302
0.1344	0.1731	2.425	2.456
0.1305	0.1985	2.598	2.625
0.1266	0.2234	2.753	2.783
0.1240	0.2399	2.860	2.884
0.1207	0.2612	2.988	3.011
0.1169	0.2854	3.126	3.150
0.1131	0.3098	3.262	3.285

and the presence of $HB_2O(OOCCF_3)_5$ is unlikely for this reason.

It is interesting that the association constant for $HSbF_5(OOCCF_3)$ is ~15 times smaller than that for $HB(OOCCF_3)_4$. Considering the similar size of the two anions, one would expect comparable K_a. For this reason it would appear that $B(OOCCF_3)_3$ produces a weaker acid than SbF_5 and the formation of the ion pair according to

[4] $B(OOCCF_3)_3 + 2HOOCCF_3 \rightleftarrows H_2OOCCF_3^+ B(OOCCF_3)_4^-$

is not as extensive as for SbF_5.

The results of a conductivity experiment with $CsB(OOCCF_3)_4$ are given in Table 1, and the Λ^0 and K_a values in Table 2. The results of the conductimetric titration of $HB(OOCCF_3)_4$ with $CsOOCCF_3$ are given in Table 3 and plotted in Fig. 1. A break in the titration curve is barely perceptible at the Cs/B mole ratio near unity. The plot is certainly not characteristic of the usual conductimetric titration but it may be accurately reproduced by calculation, assuming the neutralization

[5] $HB(OOCCF_3)_4 + CsOOCCF_3 \rightarrow CsB(OOCCF_3)_4 + HOOCCF_3$

Using the K_a and Λ^0 for $HB(OOCCF_3)_4$, $CsB(OOCCF_3)_4$, and $CsOOCCF_3$ and assuming that reaction 5 goes to completion, the conductimetric titration curve may be calculated. The curve fits the experimental points very well as shown in Fig. 1 and shows that reaction 5 is complete.

Solvent Autoprotolysis

From the limiting equivalent conductivities of $HB(OOCCF_3)_4$, $CsB(OOCCF_3)_4$, and $CsOOCCF_3$, Λ^0 for the hypothetical 100% dissociated trifluoroacetic acid may be calculated from

$$\Lambda^0_{H^+OOCCF_3^-} = \Lambda^0_{HB(OOCCF_3)_4} + \Lambda^0_{CsOOCCF_3} - \Lambda^0_{CsB(OOCCF_3)_4}$$

Using the Λ^0 in Table 2, $\Lambda^0_{H^+OOCCF_3^-}$ is calculated to be 26.19 ± 4.13 ohm^{-1} cm^2 equiv^{-1}.

Can. J. Chem. Downloaded from www.nrcresearchpress.com by 210.87.254.6 on 09/05/12
For personal use only.

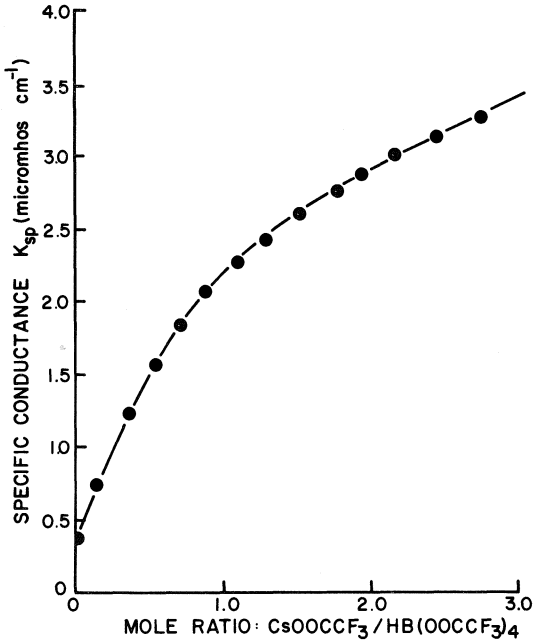

FIG. 1. Conductimetric titration of $CsOOCCF_3$ against $HB(OOCCF_3)_4$. The dots represent experimental points and the line, the calculated curve.

This is small compared to the mobilities of the alkali metal trifluoroacetates (3) and the comparison with Λ^0 for $CsB(OOCCF_3)_4$ shows that proton transfer conduction is unimportant in trifluoroacetic acid. In the simple model for ionic mobility, the low Λ^0 for small highly charged ions is accounted for by the increased effective size of the ion as a result of solvation. As the size of the ion increases solvation becomes less important and a point is eventually reached where the effect of unsolvated ion size becomes predominant and the larger ion is less mobile. In water the effect of solvation on the mobility of unipositive cations is of lesser importance than the unsolvated ion size effect at Rb^+ which is the most mobile. Trifluoroacetic acid is a more weakly solvating solvent than water and solvation is of lesser importance than the size of the unsolvated ion even for Na^+ (3). The proton is, however, strongly solvated as shown by its low mobility. The proton has a greater mobility than the sodium cation in acetic acid (12). This may indicate some contribution from a proton transfer mechanism in this solvent although many other explanations are possible.

The lowest K_{sp} we have been able to obtain for the solvent is 0.0064 μmho cm^{-1}. The concentration of autoprotolysis ions may be calculated from

$$c = 1000\, K_{sp}/\Lambda^0_{H^+OTFA^-}$$

and the autoprotolysis constant is then, $K_{ap} = c^2$. In view of the large uncertainty in $\Lambda^0_{H^+OOCCF_3^-}$, a more precise calculation employing activity coefficients and $\Lambda_{H^+OOCCF_3^-}$ adjusted for ionic strength effects is unwarranted. The solvent autoprotolysis constant is calculated to be 4×10^{-14} $(\pm 1 \times 10^{-14})$ $mol^2\, l^{-2}$.

$CsB(OOCCF_3)_4$ and $B_2O(OOCCF_3)_4$

Evaporation of an equimolar solution of $HB(OOCCF_3)_4$ and $CsOOCCF_3$ gives a crystalline solid, $CsB(OOCCF_3)_4$, the salt of the neutralization reaction. The corresponding compounds with acetic acid are known (13).

Gerrard *et al.* have reported the preparation of $B(OOCCF_3)_3$ from BCl_3 and $HOOCCF_3$ in *n*-pentane (8). They point out that the compound is unstable at its melting point (88 °C) decomposing to $B_2O(OOCCF_3)_4$. Kibbel has shown (14) that for the carboxylic acids he studied only the oxygen bridged compound was formed and not the tricarboxylate. Muetterties was unable to prepare $B(OOCCF_3)_3$ pure in his work (15). We have been unable to isolate $B(OOCCF_3)_3$ using several methods of synthesis. In all cases but one, the product was $B_2O(OOCCF_3)_4$ which appeared as colorless volatile crystals. Reaction temperature and the use of high vacuum for drying had no effect on the product obtained. In only one case the product was shown to contain some $B(OOCCF_3)_3$ (56%) in the presence of $B_2O(OOCCF_3)_4$.

The National Research Council of Canada is thanked for financial assistance and M.G.H. thanks the Council for a bursary.

1. A. J. HENNE and C. J. FOX. J. Am. Chem. Soc. **73**, 2323 (1951).
2. J. H. SIMONS and KEITH E. LORENTZEN. J. Am. Chem. Soc. **74**, 4746 (1952).
3. M. G. HARRISS and J. B. MILNE. Can. J. Chem. **49**, 1888 (1971).
4. J. BARR, R. J. GILLESPIE, and E. A. ROBINSON. Can. J. Chem. **39**, 1266 (1961).
5. Y. Y. FIALKOV and Y. Y. BOROVIKOV. Vestn. Kievski. Politekhn. Inst., Ser. Khim. Mashinostroit i Tekhnol. **6**, 66 (1965).

Can. J. Chem. Downloaded from www.nrcresearchpress.com by 210.87.254.6 on 09/05/12
For personal use only.

6. JACQUES BESSIÈRE. Bull. Soc. Chem. Fr., 3353 (1969).
7. M. G. HARRISS and J. B. MILNE. Can. J. Chem. **49**, 2937 (1971).
8. W. GERRARD, M. F. LAPPERT, and R. SHAFFERMAN. J. Chem. Soc. 3648 (1958).
9. R. J. GILLESPIE and K. C. MOSS. J. Chem. Soc. 1170 (1966).
10. R. C. THOMPSON, J. BARR, R. J. GILLESPIE, J. B. MILNE, and R. A. ROTHENBURY. Inorg. Chem. **4**, 1641 (1965).
11. R. H. FLOWERS, R. J. GILLESPIE, and J. V. OUBRIDGE. J. Chem. Soc. 607 (1956).
12. R. J. L. MARTIN. Aust. J. Chem. **15**, 409 (1962).
13. H. U. KIBBEL. Z. Anorg. u. Allgem. Chem. **259**, 259 (1968).
14. H. U. KIBBEL. Z. Anorg. u. Allgem. Chem. **259**, 203 (1968).
15. E. L. MUETTERTIES. United States Patent No. 2 782 233, Feb. 19, 1957 (Chem. Abstr. **51**, 9673a (1957)).

Can. J. Chem. Downloaded from www.nrcresearchpress.com by 210.87.254.6 on 09/05/12
For personal use only.

Association of the Butyl Alcohols and *n*-Decanol

G. E. RAJALA AND J. CROSSLEY
Chemistry Department, Lakehead University, Thunder Bay, Ontario

Received June 22, 1971

The dielectric constants at 0.1 MHz of *n*-, iso-, sec-, and *t*-butanol and *n*-decanol each at nine concentrations in the range 0.2–1.0 mole fraction in cyclohexane, *p*-dioxane, mesitylene, and *p*-xylene have been measured at 25 °C. Apparent dipole moments and Kirkwood correlation factors have been evaluated. Cyclohexane is regarded as an inert solvent in which alcohol self association alone is considered responsible for the anomalous electric polarization. The other three solvents have a disassociating effect which increases *p*-xylene $\leqslant$ mesitylene $<$ *p*-dioxane. At the lowest concentrations the alcohols have larger apparent dipole moments in these solvents than in cyclohexane. The opposite tends to be the case for the more concentrated alcohol solutions. The results suggest that alcohol association is initially dominated by the formation of small, weakly polar multimers, and eventually larger highly polar multimers predominate.

Les constantes diélectriques à 0.1 MHz du *n*-, iso-, sec-, et *t*-butanol et du *n*-décanol, chacun avec neuf concentrations dans le domaine de 0.2–1.0 mole dans le cyclohexane, *p*-dioxane, mésitylène et le *p*-xylène, ont été mesurées à 25 °C. Les moments dipolaires apparents et les facteurs de corrélation de Kirkwood ont été évalués. On considère le cyclohexane comme un solvant inerte dans lequel seule une association intermoléculaire de l'alcool est considérée comme responsable de la polarisation électrique anormale. Les trois autres solvants ont un effet de dissociation qui croît *p*-xylène $\leqslant$ mésitylène $<$ *p*-dioxane. Aux concentrations les plus basses, les alcools ont des moments dipolaires apparents plus grands dans ces solvants que dans le cyclohexane. L'inverse a tendance à se produire pour des solutions alcooliques plus concentrées. Les résultats suggèrent que l'association de l'alcool est d'abord le fait de la formation de petites multimères légèrement polaires et éventuellement une plus grande quantité de multimères hautement polaires prédomine.

Canadian Journal of Chemistry, **49**, 3617 (1971)

Can. J. Chem. Downloaded from www.nrcresearchpress.com by 210.87.254.6 on 09/05/12
For personal use only.

Introduction

Static dielectric constant, electric dipole moment, Kirkwood correlation factor, and dielectric relaxation measurements have provided useful means of examining molecular association in liquids (1–3). Hydrogen bonding in aliphatic alcohols, as the pure liquids and in dilute solution, in particular has received considerable attention. The majority of workers have been concerned with the temperature dependence of the above parameters and equilibrium constants for molecular association have been obtained (4). Relatively little work has been reported on the concentration dependence of these terms for alcohols in non-polar solvents. The powerful spectroscopic techniques have generally been limited to alcohols in dilute solution (1, 5, 6).

The nature and extent of alcohol self association are considerably influenced by the steric environment of the hydroxyl group and by changes in temperature. The former determines the geometry and size of the associated multimers, and association is favored by low temperatures. Dannhauser, in particular, has utilized these effects to study the structure of liquid alcohols (4). In solution the basicity of the solvent plays an important role in determining the extent of alcohol self association, which must compete with solute–solvent interactions (7). The electric polarization measurements appear to provide a useful method of studying molecular association in alcohols (8, 9).

In this paper we report the results of static dielectric constant measurements for several alcohol – non-polar solvent mixtures, in which the alcohol molecular size, the steric environment of the hydroxyl group, and the basicity of the solvent are variables. Cyclohexane is used as an inert reference solvent in which the self association of alcohol molecules is regarded as the only important interaction.

Experimental

Method of Measurement

The dielectric constants were measured at 0.1 MHz and 25 °C with a Wissenschaftlich-Technische Werkstatten Multi-Dekameter. No significant dielectric loss was detectable for any of the systems examined. The water jacketed WTW cells type MFLI and MFL 2/s were used for dielectric constant ranges 2–7 and 7–21, respectively. The instrument and cells were recalibrated for each set of measurements *i.e.* one solute–solvent

TABLE 1. Dielectric constants and dipole moments (in Debyes) for some alcohols at mole fraction f_2 in several solvents at 25 °C

	Cyclohexane		*p*-Xylene		Mesitylene		*p*-Dioxane	
f_2	ε	μ	ε	μ	ε	μ	ε	μ
				n-Butanol				
0.2	2.64	1.50	2.92	1.61	2.89	1.66	3.25	1.79
0.3	3.57	1.92	3.68	1.90	3.53	1.89	4.11	1.93
0.4	4.85	2.20	4.74	2.12	4.49	2.10	5.12	2.04
0.5	6.67	2.44	6.20	2.32	5.82	2.29	6.36	2.16
0.6	8.67	2.61	7.38	2.35	7.56	2.45	8.40	2.37
0.7	11.02	2.75	9.72	2.56	9.63	2.61	9.94	2.45
0.8	13.03	2.79	12.45	2.80	12.07	2.72	11.58	2.52
0.9	14.92	2.80	15.23	2.84	14.56	2.79	13.73	2.63
1.0	17.10	2.84						
				iso-Butanol				
0.2	2.59	1.43	2.98	1.66	2.89	1.66	3.26	1.80
0.3	3.32	1.77	3.58	1.87	3.58	1.90	4.03	1.89
0.4	4.69	2.15	4.55	2.05	4.37	2.06	4.09	1.98
0.5	6.49	2.42	5.94	2.28	5.58	2.25	6.05	2.10
0.6	8.33	2.55	7.74	2.45	7.31	2.43	7.63	2.25
0.7	10.77	2.72	9.75	2.58	9.37	2.58	9.36	2.38
0.8	12.91	2.79	11.96	2.69	11.74	2.69	11.52	2.52
0.9	14.88	2.82	14.67	2.79	14.28	2.78	14.13	2.68
1.0	17.12	2.85						
				sec-Butanol				
0.2	2.47	1.24	2.86	1.52	2.80	1.53	3.24	1.77
0.3	2.97	1.50	3.31	1.66	3.22	1.66	3.92	1.84
0.4	3.33	1.52	4.00	1.81	3.86	1.81	4.76	1.92
0.5	5.28	2.07	5.02	1.98	4.79	1.98	5.79	2.02
0.6	7.23	2.32	6.50	2.17	6.26	2.17	7.05	2.13
0.7	9.22	2.47	8.72	2.38	8.11	2.35	8.59	2.25
0.8	11.35	2.58	10.68	2.50	10.28	2.48	10.59	2.39
0.9	13.60	2.66	13.20	2.62	13.00	2.62	12.90	2.54
1.0	15.80	2.72						
				t-Butanol				
0.2	2.28	0.87	2.71	1.23	2.67	1.32	3.18	1.72
0.3	2.48	1.00	2.98	1.38	2.91	1.37	3.71	1.74
0.4	2.76	1.13	3.32	1.44	3.22	1.44	4.40	1.81
0.5	3.22	1.28	3.83	1.54	3.69	1.53	5.14	1.86
0.6	4.02	1.49	4.52	1.64	4.39	1.65	6.03	1.92
0.7	5.41	1.74	5.71	1.82	5.38	1.79	7.08	2.00
0.8	6.97	1.94	7.11	1.97	6.92	1.97	8.18	2.08
0.9	9.36	2.18	9.32	2.17	8.95	2.14	9.82	2.20
1.0	11.68	2.33						
				n-Decanol				
0.2	2.46	1.39	2.78	1.60	2.72	1.55	3.11	1.80
0.3	2.83	1.60	3.07	1.67	2.98	1.63	3.54	1.87
0.4	3.28	1.78	3.45	1.79	3.34	1.76	3.99	1.94
0.5	3.94	2.00	3.92	1.92	3.81	1.90	4.47	2.03
0.6	4.80	2.23	4.62	2.11	4.46	2.07	5.01	2.12
0.7	5.53	2.35	5.42	2.27	5.22	2.24	5.56	2.22
0.8	6.37	2.47	6.22	2.41	6.05	2.38	6.22	2.34
0.9	7.07	2.55	7.03	2.53	6.94	2.51	6.84	2.45
1.0	7.80	2.62						

system. Refractive index measurements at 25 °C were made for each solution at the sodium D-line.

Purification of Materials

The alcohols, solvents, and calibration liquids were all dried and fractionally distilled prior to their use.

Experimental Results

The dielectric constants ε_0 are listed in Table 1, where the concentrations in mole fraction units, which have been rounded off for convenience, differ from the actual values in the third decimal place. The evaluation of dipole moments from dielectric constant and refractive index measurements on dilute solutions often involves the approximation $\varepsilon_\infty = xn_D^2$ (x may be 1.0, 1.05, 1.1) since ε_∞, the high frequency dielectric constant, is not measured. Dielectric dispersion measurements and ε_∞ values have been reported for *n*-butanol and *n*-decanol as the pure liquids (10) and in dilute solution (7) in the solvents

Can. J. Chem. Downloaded from www.nrcresearchpress.com by 210.87.254.6 on 09/05/12
For personal use only.

Can. J. Chem. Downloaded from www.nrcresearchpress.com by 210.87.254.6 on 09/05/12
For personal use only.

employed in this study. The dielectric absorptions of the remaining butanols in *p*-xylene solution have also been reported (11). The ratio $\varepsilon_\infty / n_D^2$ is not constant for these systems, and for many solutions n_D^2 is less than the dielectric constant of the solvent. In order to attain consistency, ε_∞ values were interpolated, assuming linearity, from the pure liquid and dilute solution values. Apparent dipole moments μ were then calculated from the equation

$$\mu^2 = g\mu_0^2 = \frac{9kT(\varepsilon_0 - \varepsilon_\infty)(2\varepsilon_0 + \varepsilon_\infty)}{4\pi N\varepsilon_0(\varepsilon_\infty + 2)^2}$$

where kT is the thermal energy and N is the number of solute molecules per ml. The values are given in Table 1. Kirkwood correlation factors g were estimated with the dipole moment of the molecule in vacuum μ_0 taken to be 1.68 D.

The accuracy of the ε_0 measurements is estimated to be $\pm 0.5\%$ although the absolute error may be larger, since the values are dependent upon the dielectric constants used for the calibration liquids. The results are self consistent and plots of ε_0, μ, and g against alcohol concentration yield relatively smooth curves. Figures 1–3 are representative and compare very favorably with those obtained previously for similar systems (8, 9).

Discussion

The concentration dependence of the dielectric constant for the four butanols and *n*-decanol in cyclohexane at 25 °C is shown in Fig. 1. Similar plots are obtained for these alcohols in *p*-xylene, mesitylene, and *p*-dioxane solution and in no case is a linear relationship observed. However, the Kirkwood correlation factor g is probably a more useful parameter for examining the data for these systems in terms of molecular structure.[1] Positive and negative deviations of g from unity correspond to predominantly parallel and antiparallel alignment of near neighbor dipoles, respectively.

Figure 2 shows plots of g against alcohol mole fraction for the five alcohols in cyclohexane and mesitylene. In the absence of association g should be unity at all concentrations. The strong self association of alcohols is evident especially for the pure liquids, for which g increases *t*-butanol < *n*-decanol < sec-butanol < iso-butanol ~ *n*-butanol in accord with previous results (12). At infinite dilution all the curves must meet at $g = 1$, thus in view of the small g values for the dilute solutions ($f_2 < 0.2$) especially in cyclohexane the initial association must predominantly involve the formation of multimers having smaller dipole moments than the free monomer. These multimers could be closed or open dimers and trimers. Evidence has been presented for all these species (4, 5, 8, 13). At low temperatures the g values for some alcohols are found to be very close to zero (14) and in these cases small closed multimers must exist. It is apparent that above 0.2 mole fraction g increases with increased alcohol concentration. The majority of workers seem to favor association into linear chains as the mechanism responsible for the large g values (4, 9) although there is evidence to support the existence of highly polar cyclic multimers (6, 15). The large alkyl group in *n*-decanol and chain branching close to the hydroxyl group in sec- and *t*-butanol present steric factors which are probably responsible for a lower concentration of large multimers, and thus smaller g values, than for the relatively unhindered *n*- and iso-butanols. In alcohols such as 3-methyl-3-heptanol the hydroxyl group is so effectively screened that association is limited to small weakly polar multimers (17), and the g values for the pure liquids are less than unity (4).

Plots of g against alcohol concentration for

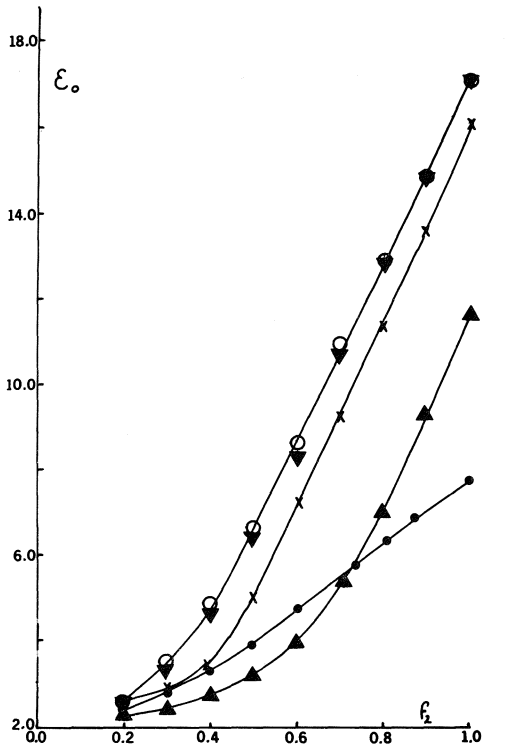

FIG. 1. Plot of the static dielectric constant ε_0 against alcohol mole fraction f_2 for *n*-butanol ○, sec-butanol ×, iso-butanol ▼, *t*-butanol ▲, and *n*-decanol ● in cyclohexane at 25 °C.

[1]See ref. 9 for a discussion of the application of the Kirkwood correlation factor to structural problems in associated liquids.

Can. J. Chem. Downloaded from www.nrcresearchpress.com by 210.87.254.6 on 09/05/12
For personal use only.

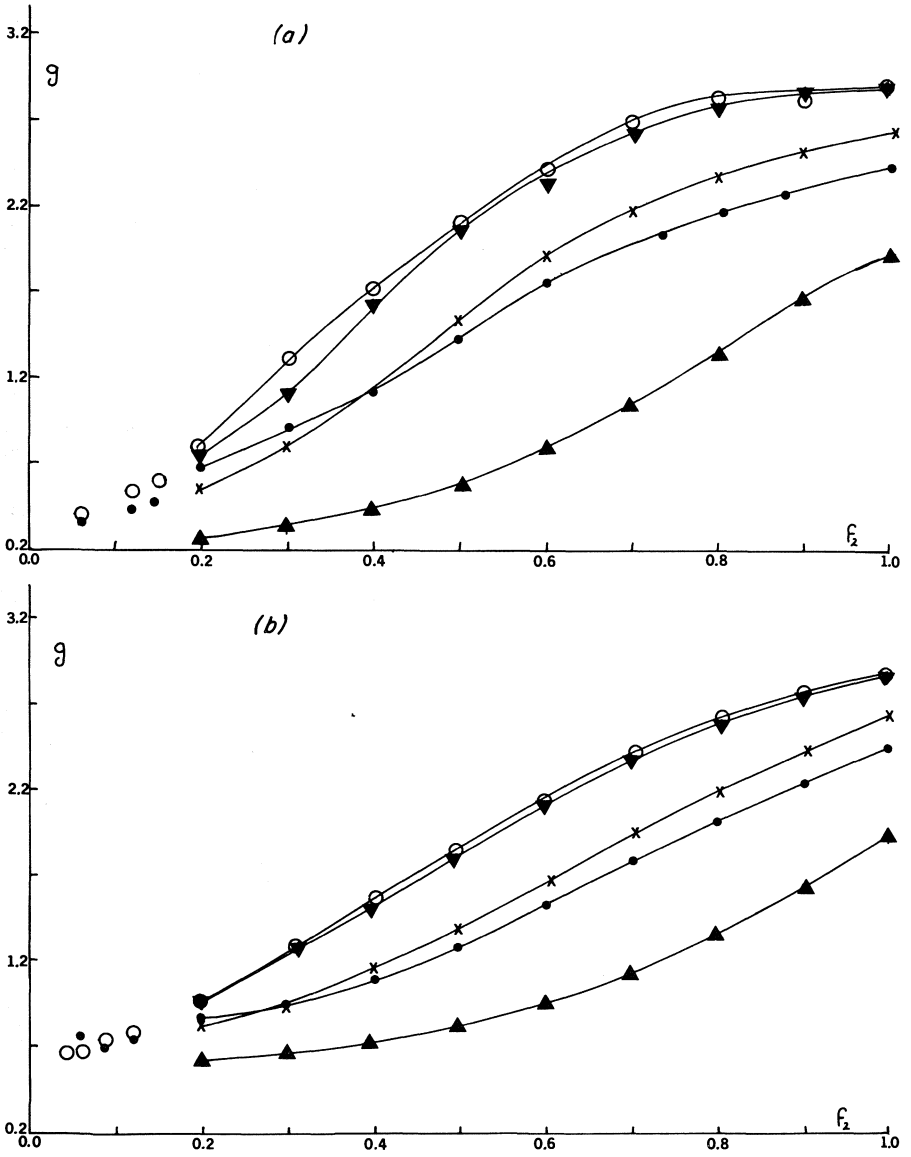

FIG. 2. Correlation factor against alcohol mole fraction in (*a*) cyclohexane and (*b*) mesitylene solution at 25 °C. The symbols have the same meaning as in Fig. 1. The points below 0.2 mole fraction for *n*-butanol and *n*-decanol are taken from ref. 7.

iso-butanol, *t*-butanol, and *n*-decanol in the four solvents are shown in Fig. 3. The two remaining butanols give curves which are similar to those for iso-butanol. For *n*-butanol, iso-butanol, sec-butanol, and *n*-decanol at 0.2 mole fraction g decreases with decreased solvent basicity *i.e.* *p*-dioxane > mesitylene ~ *p*-xylene > cyclohexane, whereas the reverse is true at 0.8 mole fraction. However, the correlation factor for *t*-butanol decreases *p*-dioxane > mesitylene ~ *p*-xylene > cyclohexane over almost the whole concentration range.

In cyclohexane solute–solvent interactions are restricted to weak van der Waals and dipole interactions (16), and the concentration dependence of g arises almost entirely from alcohol

Can. J. Chem. Downloaded from www.nrcresearchpress.com by 210.87.254.6 on 09/05/12
For personal use only.

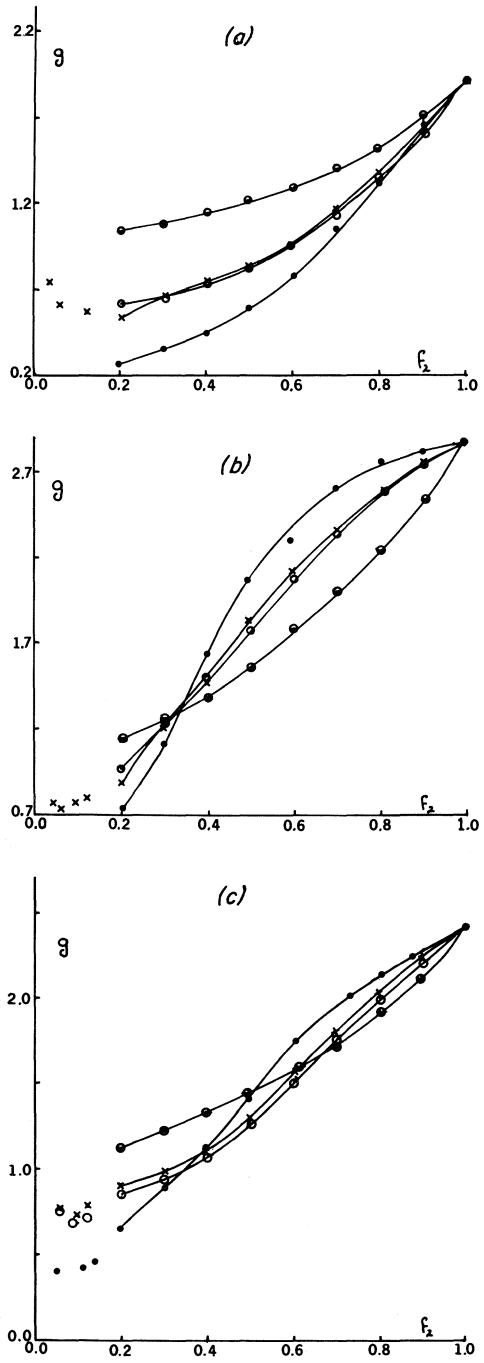

FIG. 3. Correlation factor against alcohol mole fraction in cyclohexane ●, *p*-xylene ×, mesitylene ○, and *p*-dioxane ◒ at 25 °C for (*a*) *t*-butanol, (*b*) iso-butanol, and (*c*) *n*-decanol. The points below 0.2 mole fraction for the *p*-xylene solution are taken from refs. 7 and 11.

self-association. Interactions between the hydrogen atoms of hydroxyl groups and the π-electrons of aromatic molecules or the oxygen lone pair electrons of dioxane are not negligible (11, 18). Thus, for alcohols in *p*-xylene, mesitylene, and *p*-dioxane, solute–solvent interactions will compete with solute–solute interactions. At a given concentration the proportion of self associated alcohol molecules will be less in these electron donor solvents than in the relatively inert cyclohexane. The disassociating effect produced by these solvents may be compared to that produced in the pure liquids by increased temperature (4). The extent of the disassociation should increase with the increased electron donor ability of the solvent, and a decrease in *g* with increased solvent basicity would indicate that alcohol self association involves large highly polar multimers. Conversely, for systems in which association predominantly involves small weakly polar multimers *g* should increase with increased solvent basicity. The application of this theory to the systems under discussion indicates that highly polar multimers become the most important species above about 0.3–0.5 mole fraction for *n*-butanol, iso-butanol, sec-butanol, and *n*-decanol. This alcohol concentration decreases *n*-decanol ~ sec-butanol > iso-butanol > *n*-butanol and *p*-dioxane > mesitylene ~ *p*-xylene *i.e.* with decreased degree of self association and decreased solvent basicity. Small weakly polar multimers appear to be the dominant associated species for *t*-butanol, which has the most hindered hydroxyl group, almost over the whole range of concentration. Dioxane has the largest disassociating effect which increases *n*-butanol < iso-butanol < sec-butanol < *n*-decanol < *t*-butanol.

1. G. C. PIMENTEL and A. L. MCCLELLAN. The hydrogen bond. W. H. Freeman and Co., San Francisco, California. 1960.
2. W. DANNHAUSER and A. F. FLUECKINGER. Phys. Chem. Liq. **2**, 37 (1970).
3. J. CROSSLEY. Adv. Mol. Relaxation Process. **2**, 69 (1970).
4. W. DANNHAUSER. J. Chem. Phys. **48**, 1911 (1968).
5. H. C. VAN NESS, JON VAN WINKLE, H. H. RICHTOL, and H. B. HOLLINGER. J. Phys. Chem. **71**, 1483 (1967).
6. A. N. FLETCHER and C. A. HELLER. J. Phys. Chem. **71**, 3742 (1967).
7. J. CROSSLEY. J. Phys. Chem. **75**, 1790 (1971).
8. J. MALECKI. J. Chem. Phys. **43**, 1351 (1965).
9. P. I. GOLD and R. L. PERRINE. J. Phys. Chem. **71**, 4218 (1967).

10. S. K. GARG and C. P. SMYTH. J. Phys. Chem. **69**, 1294 (1965).
11. J. CROSSLEY. Can. J. Chem. **49**, 712 (1971).
12. W. DANNHAUSER and L. W. BAHE. J. Chem. Phys. **40**, 3058 (1964).
13. J. MALECKI and Z. DOPIERALA. Acta Physica Polonica, **36**, 385, 401, 409 (1969).
14. G. P. JOHARI and W. DANNHAUSER. J. Phys. Chem. **72**, 3273 (1968); J. Chem. Phys. **48**, 5114 (1968); **50**, 1862 (1969).
15. P. BORDEWIJK, F. GRANSCH, and C. J. F. BOTTCHER. J. Phys. Chem. **73**, 3255 (1969).
16. W. G. SCHNEIDER. J. Phys. Chem. **66**, 2633 (1962).
17. J. CROSSLEY, L. GLASSER, and C. P. SMYTH. J. Chem. Phys. **52**, 6203 (1970).
18. J. CROSSLEY and C. P. SMYTH. J. Am. Chem. Soc. **91**, 2482 (1969).

Can. J. Chem. Downloaded from www.nrcresearchpress.com by 210.87.254.6 on 09/05/12
For personal use only.

Can. J. Chem. Downloaded from www.nrcresearchpress.com by 210.87.254.42 on 09/05/12
For personal use only.

Studies on Microcapsules. XII. Preparation and Characterization of Carboxylated Polyphthalamide Microcapsules

YOSHIMICHI SHIGERI, MICHIKO TOMIZAWA, KIKUKO TAKAHASHI, MASUMI KOISHI, AND TAMOTSU KONDO[1]

Faculty of Pharmaceutical Sciences, Science University of Tokyo, Funagawara-machi, Shinjuku, Tokyo, Japan

Received July 6, 1971

Carboxylated polyphthalamide microcapsules were prepared by utilizing the interfacial polycondensation reaction between basic amino acids in water and *p*-phthaloyl dichloride in organic solvent. The yield of the microcapsules was found to be dependent on the concentration of emulsifier in the organic solvent and temperature. The microcapsules moved towards the anode in an electric field irrespective of the p*H* of the medium owing to the presence of carboxylic groups in the membranes. Cation binding experiments indicated an increasing order, $Al^{3+} > Mg^{2+} > Cs^{+} > K^{+}, NH_4^{+}, Na^{+} > Li^{+}$, for the binding of these cations to the microcapsules.

On a préparé des microcapsules de polyphthalamide carboxylé en utilisant une réaction de polycondensation interfaciale entre des acides aminés basiques dans l'eau et le dichlorure de *p*-phtaloyle dans un solvant organique. Le rendement des microcapsules dépend de la concentration d'émulsifiant dans le solvant organique et de la température. Les microcapsules se déplacent vers l'anode dans un champ électrique, indépendamment du p*H* du milieu, à cause de la présence des groupements carboxyliques dans les membranes. Les expériences d'attachement de cation indiquent un ordre croissant, $Al^{3+} > Mg^{2+} > Cs^{+} > K^{+}, NH_4^{+}, Na^{+} > Li^{+}$, pour l'attachement de ces cations aux microcapsules.

Canadian Journal of Chemistry, **49**, 3623 (1971)

Introduction

In earlier papers (1, 2) of this series, the preparation and characterization of sulfonated polyphthalamide microcapsules have been reported. The principle of preparing sulfonated microcapsules had previously been described by Chang *et al.* (3). Those microcapsules were easily dispersible in water to form a quite stable dispersion owing to the presence of strongly acidic sulfonic groups in their membranes.

On the other hand, microcapsules with weakly acidic carboxylic groups in their membranes are very interesting because this kind of microcapsule may serve as a model for biological cells (3, 4) in view of the fact that many biological cells are known to have electrokinetic properties characteristic of the surface with carboxylic groups (5–7).

This paper describes the preparation and characterization of carboxylated polyphthalamide microcapsules. These microcapsules could be prepared by utilizing the interfacial polycondensation reaction between basic amino acids and *p*-phthaloyl dichloride.

[1]To whom all inquiries should be addressed.

Experimental

Materials

Basic amino acids used in this work were L-arginine, L-citrulline, L-cystine, L-histidine, and L-lysine. These amino acids were of highest purity available purchased from Ajinomoto Co. Ltd., Tokyo. Inorganic salts used for binding experiments were chlorides of aluminum, magnesium, lithium, sodium, potassium, cesium, and ammonium. All of these salts had a purity of more than 99.5%. Other chemicals employed were of reagent grade.

Preparation of Microcapsules

Carboxylated polyphthalamide microcapsules were prepared in the same way as that described in the previous paper (1) except that basic amino acids were used as diamine.

The carboxylated polyphthalamide microcapsules thus prepared are as follows: poly-L-arginine phthalamide (PAPA), poly-L-citrulline phthalamide (PCitPA), poly-L-cystine phthalamide (PCysPA), poly-L-histidine phthalamide (PHPA), and poly-L-lysine phthalamide (PLPA) microcapsules.

Partition of Amino Acids between Aqueous and Organic Phases

In the interfacial polycondensation reaction, the transfer of water soluble reactant to organic phase is a prerequisite for the reaction to occur since it has been demonstrated that polymers are formed on the organic side of interface (8). Therefore, the partition of the amino acids between the aqueous and the organic phases was determined under the conditions similar to those used in the preparation of the microcapsules.

TABLE 1. Relative partition coefficients of amino acids

Temperature (°C)	Concentration of Span 85 (%, v/v)	Relative partition coefficient		
		L-Arginine	L-Histidine	L-Citrulline
3	15	1.00	1.00	1.00
3	10	0.46	0.61	0.48
30	15	0.64	0.35	0.43

To 3 ml of a 0.4 *M* solution of amino acid in aqueous 0.45 *M* Na_2CO_3 solution in a 100 ml round bottom flask immersed in a constant temperature bath controlled at 3 and 30 °C was added 30 ml of the mixed solvent containing 10 or 15% (v/v) Span 85. The mixture was then mechanically agitated with the Chemistirrer at 620 r.p.m. for 5 min. In each case an emulsion was formed, which was centrifuged to completely separate it into two liquid layers. The amount of amino acid transferred into the aqueous phase was determined colorimetrically by making use of the color reaction with ninhydrin. The partition coefficient of an amino acid was defined as the ratio of the amount of the amino acid in the organic phase to that in the aqueous phase.

Electrophoretic Mobility

Electrophoretic mobility measurements on the carboxylated polyphthalamide microcapsules were conducted in a quartz flat microelectrophoretic cell at room temperature. For each measurement 40 microcapsules were timed in each direction to eliminate the polarization effect of the electrodes.

The dispersion media were the following buffer solutions (p*H* 3.9–9.9) of constant ionic strength (2×10^{-3}): CH_3COOH–CH_3COONa (p*H* 3.9 and 5.3), NaH_2PO_4–Na_2HPO_4 (p*H* 6.8 and 7.9), and $NaHCO_3$–Na_2CO_3(p*H* 9.9). The ionic strength of the media was adjusted by the addition of NaCl.

The microcapsule dispersion was dialyzed against distilled water before use in the same way as described in the previous paper (2). The samples for electrophoresis measurement were prepared by pipeting a few drops of the dialyzed microcapsule dispersion into a large volume of the above-mentioned dispersion media.

In view of the size of the microcapsules (*ca.* 3 μ in diameter) and the ionic strength of the dispersion media (2×10^{-3}), mobilities were converted into zeta-potentials, ζ, by means of the simple Smoluchowski equation,

$$\zeta = 4\pi\eta u/D \quad [1]$$

where u is the mobility in cm/s/V/cm, η and D are the viscosity and dielectric constant of dispersion medium.

Cation Binding

The binding of various cations to the carboxylated polyphthalamide microcapsules was measured by the method reported in the earlier paper (2). In all binding experiments of cations, the H form PLPA microcapsules, which were obtained by treating the dialyzed Na form microcapsules with hydrochloric acid, followed by dialysis against distilled water, were used. To a known volume of the redialyzed H form microcapsule dispersion in a beaker was added an equal volume of salt solution, and the mixture was allowed to react for 1 h with continuous shaking. At the end of this period, the mixture was centrifuged to remove the microcapsules. The supernatant liquid was then analyzed chelatometrically (Al^{3+} and Mg^{2+}) or potentiometrically (monovalent cations). The amount bound of Al^{3+} or Mg^{2+} was given by the difference between the cation concentrations before and after mixing with the microcapsule dispersion. The hydrogen ion concentrations liberated from the microcapsules in the supernatant liquid directly gave the amount bound of the monovalent ions.

Results and Discussion

Formation of Microcapsules

The formation of the carboxylated polyphthalamide microcapsules was affected by the concentration of Span 85 in the organic solvent and temperature. That is, the yield of microcapsules was high when they were prepared under the conditions of high Span 85 concentration and low temperature. These conditions were found to be favorable to the transfer of amino acids into the organic phase. Table 1 shows this situation, in which typical examples of relative partition coefficient of amino acid are given.

A rise in temperature or a fall in the Span 85 concentration caused a decrease in the partition coefficient. This may be due to the increased solubility of amino acid in the aqueous phase at high temperature or at low Span 85 concentration.

Electrophoresis of Microcapsules

The carboxylated polyphthalamide microcapsules moved towards the anode in an electric field irrespective of the p*H* of the medium, showing the disappearance of isoelectric point of amino acid through the reaction with *p*-phthaloyl dichloride.

In Fig. 1 are given the zeta-potentials of the microcapsules calculated from the mobility data by using eq. 1 as a function of the p*H* of the medium. The fact that the zeta-potentials become more negative as the p*H* of the medium increases will indicate the increase in the dissociation of carboxylic groups on the microcapsule surface with increasing p*H*. Figure 1 also seems to show that the carboxylic groups of all microcapsules dissociate in the same way independently of the kind of amino acid used in view of the experi-

Can. J. Chem. Downloaded from www.nrcresearchpress.com by 210.87.254.42 on 09/05/12
For personal use only.

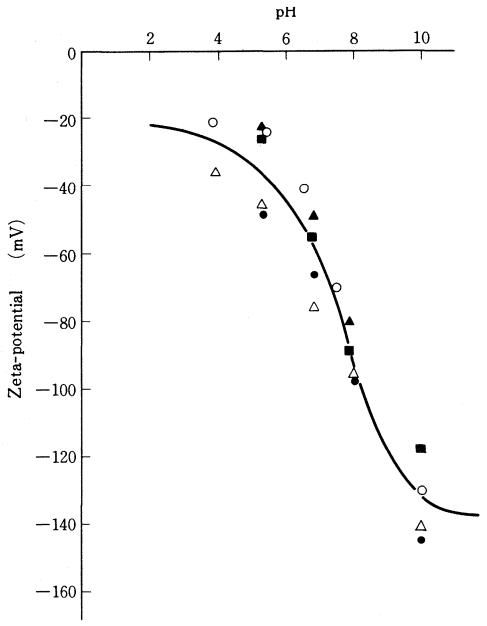

FIG. 1. Zeta-potential against p*H* for: -○-, PAPA; -△-, PCitPA; -■-, PCysPA; -●-, PHPA; -▲-, PLPA microcapsules.

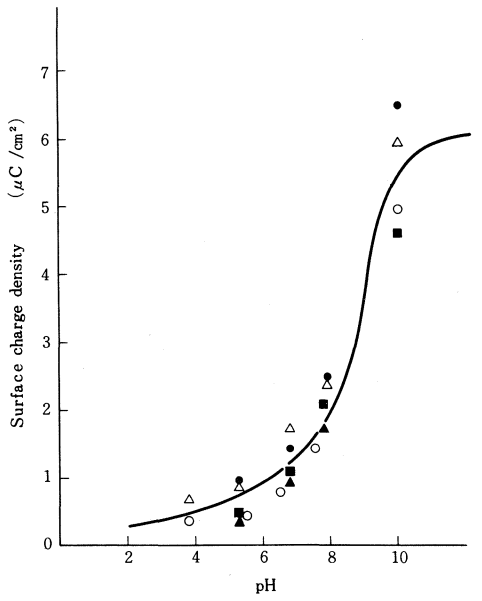

FIG. 2. Electrophoretic surface charge density against p*H* for: -○-, PAPA; -△-, PCitPA; -■-, PCysPA; -●-, PHPA; -▲-, PLPA microcapsules.

mental errors involved in the electrophoretic measurements.

The surface charge densities in the electrokinetic plane of shear, σ, were calculated from the zeta-potentials using the Gouy–Chapman relationship for a flat double layer in the form

$$[2] \quad \sigma = (1 + \sqrt{1-\alpha})\sqrt{\frac{Dn_0kT}{2}}\sinh\frac{ze\zeta}{2kT}$$

where n_0 is the number of ions per unit volume in bulk, D the dielectric constant of the medium, T the absolute temperature, k the Boltzmann constant, z the valency of the counter ion, e the electronic charge, ζ the zeta-potential of microcapsules, and α the fraction of the total space within the microcapsule surface which is not available to the counter ion (9). The factor α was introduced in eq. 2 to account for the fact that the microcapsule membranes are semipermeable (10, 11) and was arbitrarily assumed to be 0.5 (7). The calculated surface charge densities are plotted in Fig. 2 against the p*H* of the medium.

It will be of much interest to note here that the surface charge densities of the microcapsules are comparable to those of red blood cells from various animal species (6, 7). This may demonstrate the feasibility of using the carboxylated polyphthalamide microcapsules as a model for biological cells.

Cation Binding of Microcapsules

The binding isotherms for Al^{3+} and Mg^{2+} and for Li^+, Na^+, K^+, Cs^+, and NH_4^+ at 20 °C are illustrated in Figs. 3 and 4, respectively.

In these figures the amount bound of cations is expressed in terms of the number of carboxylic groups occupied by the cations in unit volume of the microcapsules (2). This quantity does not necessarily give the true amount adsorbed of the cations to the microcapsules because the binding is likely to be accompanied by the occlusion of the cations by the polymer chains of microcapsule membranes. However, the ion-exchanging ability of the carboxylated polyphthalamide microcapsules will be assured by the liberation of hydrogen ions from the microcapsules on the addition of the cations.

A remarkable effect of valency can be seen on the amount of the cations to the microcapsules. Namely, the higher the valency, the larger the amount bound to the microcapsules. This is reasonable since the cations are bound to the microcapsules by the electrostatic field of the carboxylic groups in the microcapsule membranes.

The difference in the amount bound among the monovalent cations used in this work is not

Can. J. Chem. Downloaded from www.nrcresearchpress.com by 210.87.254.42 on 09/05/12
For personal use only.

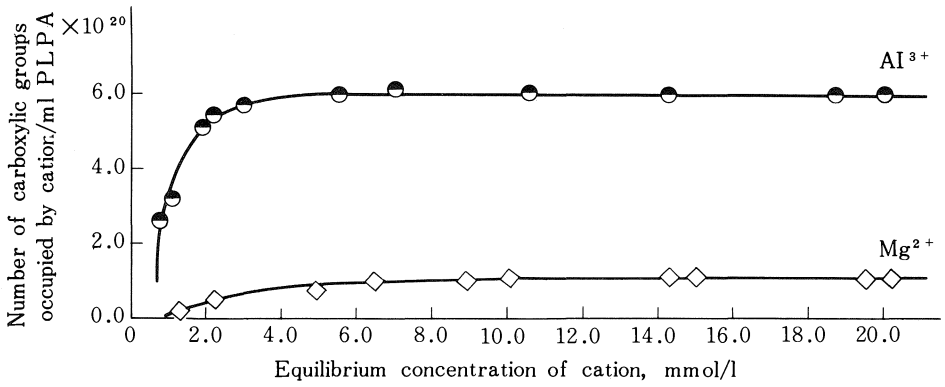

FIG. 3. Cation binding isotherms for PLPA microcapsules at 20 °C.

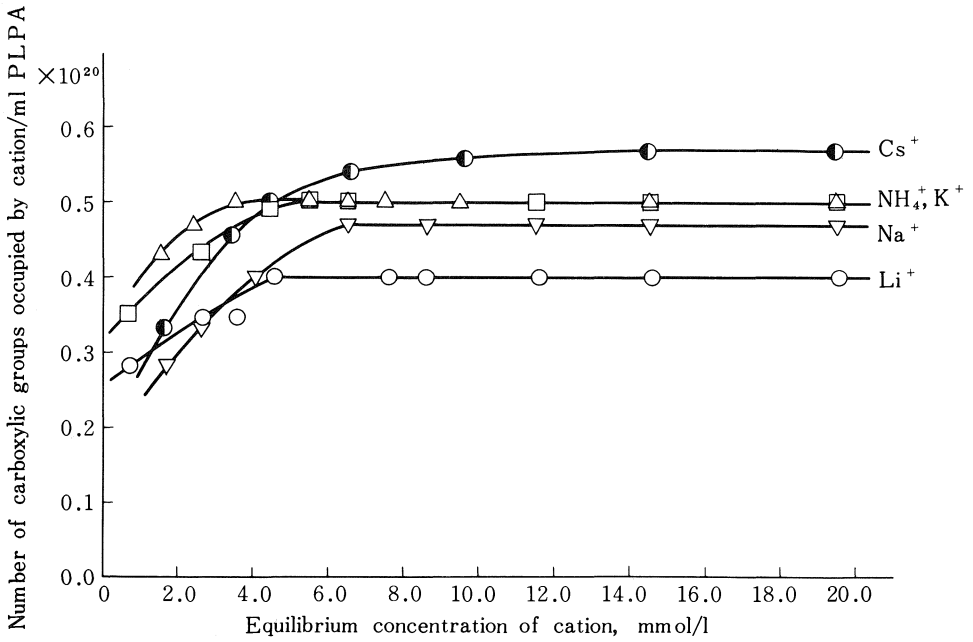

FIG. 4. Cation binding isotherms for PLPA microcapsules at 20 °C.

great enough to draw the conclusion about the exact order of these cations in the binding to the microcapsules. However, it will be safe to say that Cs^+ can be bound more strongly than Li^+.

The authors wish to express their sincere thanks to the Eisai Co., Ltd., Tokyo, for its financial aid to this work.

1. M. KOISHI, N. FUKUHARA, and T. KONDO. Can. J. Chem. **47**, 3447 (1969).
2. K. TAKAHASHI, M. KOISHI, and T. KONDO. Can. J. Chem. **48**, 3520 (1970).
3. T. M. S. CHANG, F. C. MACINTOSH, and S. G. MASON. Can. J. Physiol. Pharmacol. **44**, 115 (1966).
4. T. M. S. CHANG, L. J. JOHNSON, and O. J. RANSOME. Can. J. Physiol. Pharmacol. **45**, 709 (1967).
5. D. J. WILKINS, R. H. OTTEWILL, and A. D. BANGHAM. J. Theoret. Biol. **2**, 165 (1962).
6. E. D. EYLAR, M. A. MADOFF, O. V. BRODY, and J. L. ONCLAY. J. Biol. Chem. **237**, 1992 (1962).
7. G. V. F. SEAMAN and G. UHLENBRUCK. Arch. Biochem. Biophys. **100**, 493 (1963).
8. P. W. MORGAN and S. L. KWOLEK. J. Polym. Sci. **40**, 299 (1959).
9. D. A. HAYDON. Biochim. Biophys. Acta, **50**, 450 (1961).
10. T. M. S. CHANG and M. POZNANSKY. J. Biomed. Mater. Res. **2**, 187.
11. K. TAKAMURA, M. KOISHI, and T. KONDO. Kolloid-Z. u. Z. Polym. In press.

Can. J. Chem. Downloaded from www.nrcresearchpress.com by 210.87.254.42 on 09/05/12
For personal use only.

Proton Magnetic Resonance Spectrum of 2-Chloroaniline-^{15}N. Long-range Coupling Constants to Amino Protons from all Ring Protons

R. WASYLISHEN[1] AND T. SCHAEFER

Department of Chemistry, University of Manitoba, Winnipeg, Manitoba

Received June 10, 1971

The p.m.r. spectra of 2-chloroaniline and 2-chloroaniline-^{15}N in benzene and toluene solutions are analyzed at 60 and 100 MHz under conditions where the amino protons are exchanging intermolecularly and also where they are not exchanging. The spectrum of 2-chloroaniline-H^{15}ND in the absence of amino proton exchange is observed between −48 and 80 °C. In all situations fast rotation about the C—N bond evidently occurs. Long-range couplings of the amino protons to all ring protons are observed and their signs are determined. The nonplanarity of the amino group is discussed in terms of the long-range couplings, of the one-bond ^{15}N–H couplings, and of the two-bond H–H couplings in the amino group. The signs and magnitudes of the coupling constants between the ring protons and ^{15}N are also determined.

Les spectres de r.m.p. des 2-chloroaniline et 2-chloroaniline ^{15}N dans des solutions de benzène et toluène sont analysés à 60 et 100 MHz dans des conditions telles que l'échange intermoléculaire des protons de l'azote ait lieu, ainsi qu'en absence d'échange. Le spectre de la 2-chloroaniline-H^{15}ND en l'absence d'échange est observé entre −48 et 80 °C. Dans tous les cas, la rotation rapide autour de la liaison C—N est mise en évidence. Les couplages à longue distance entre les protons de l'azote et tous les protons du cycle sont déterminés avec leurs signes. La non-planéarité du groupement amine est discutée en termes de couplages à longue distance, de couplage ^{15}N–N et de couplages H–H à travers deux liaisons dans le groupement amine. Le signe et la valeur des constantes de couplages entre les protons du cycle et le noyau ^{15}N sont aussi déterminés.

Canadian Journal of Chemistry, **49**, 3627 (1971)

Can. J. Chem. Downloaded from www.nrcresearchpress.com by 210.87.254.105 on 09/05/12
For personal use only.

Introduction

Spin–spin coupling between protons on side-chains like methyl or aldehyde functions and protons or fluorine nuclei on the benzene ring have been extensively investigated and discussed in terms of σ and π electron coupling mechanisms (1–5). Less is known about the coupling between phenolic or amino protons with ring protons in phenol or aniline derivatives (6–10). Apparently problems of intermolecular exchange of these protons make observation of their coupling patterns difficult. When phenolic protons are held in the plane of the molecule for periods of seconds or more by intramolecular hydrogen bonds, coupling over five bonds with ring protons via the familiar zig–zag path is observed (6–8). Similar couplings are known for amino protons (9, 10).

Whenever the bond holding the proton in the side-chain lies apparently in the plane of the aromatic ring no coupling occurs over six bonds to the para proton. This rule holds for H—C=O, H—CCl_2, H—O, and H—N—R sidechain functions and is taken to mean that a σ electron mechanism does not operate over six bonds and that the π electron mechanism comes into play only when the X—H bond of the side-chain moves out of plane and thereby undergoes hyperconjugative interaction with the π electron system of the ring. In contrast, the coupling over five bonds is dominated by σ electron contributions.

In this paper a full analysis of the p.m.r. spectrum of 2-chloroaniline and of 2-chloroaniline-^{15}N is presented with a view to finding the signs and magnitudes of the long-range couplings of the amino protons to all ring protons. Our methods of stopping amino proton exchange unfortunately do not as yet allow a similar study of aniline-^{15}N itself, although the exchange rate has now been decreased to within a factor of 5 of the value necessary for such a study.

Experimental

(1) Spectra at 60 MHz

A 10 mol % solution of 2-chloroaniline (Aldrich) in benzene-d_6, to which internal tetramethylsilane was added as an internal reference and locking material, was degassed by the freeze–pump–thaw technique (degassing was carried out for all samples). The p.m.r. spectra were taken in the frequency sweep mode on a

[1]Holder of NRCC Bursary, 1970–1971.

Can. J. Chem. Downloaded from www.nrcresearchpress.com by 210.87.254.105 on 09/05/12
For personal use only.

DA60I spectrometer on a scale of 1 Hz/cm and at a sweep rate of 0.02 Hz/s. Each of 43 peaks in the ring proton region was calibrated at least five times by reading frequencies of the sweep and manual oscillators. Coupling between the amino protons and the ring protons meta to the amino group was clearly resolved. Coupling between the amino protons and the ortho and para ring protons (H-4 and -6) appeared as a marked broadening of the peaks due to these ring protons. Decoupling of the amino protons caused a marked increase of the H-4 and -6 peak heights, and some of these were measured repeatedly in the presence and absence of the decoupling field.

(2) Spectra at 100 MHz

A technique of stopping intermolecular proton exchange in benzene solutions of 2-chloroaniline was found. It was applied to solutions of 2-chloroaniline-^{14}N and 2-chloroaniline-^{15}N (96.47 atom % ^{15}N from Merck, Sharp and Dohme of Canada). A typical experiment was performed as follows. A 10 mol % solution in benzene-d_6 was left overnight in a small vial containing several NaOH pellets. The solution was then transferred to a thin-walled n.m.r. tube (ordinary thick-walled tubes cause swirling and loss of resolution in this case) containing some basic alumina and was then degassed. Such samples gave peaks whose line-widths at half-height were often less than 0.1 Hz. All clearly resolvable peaks, numbering between 60 and 85 in the different solutions, were calibrated at frequency intervals of less than 2.2 Hz at a sweep rate of 0.01 Hz/cm on an HA100D spectrometer.

Solutions of the ^{15}N compound in benzene were also studied in the presence of exchange so that comparison with nonexchanging solutions allowed a clear distinction between long-range couplings involving amino protons and ^{15}N.

A nonexchanging 20 mol % solution of the ^{15}N compound in toluene-d_8 was studied at -60 °C but the amino protons are magnetically and probably chemically (see below) equivalent even at this temperature.

(3) Deuteration Experiments

A 20 mol % nonexchanging solution in toluene-d_8 containing the ^{15}NHD group was prepared as follows. In a vial, 1.72×10^{-3} mol of D_2O were mixed with 1.32×10^{-3} mol of 2-chloroaniline-^{15}N. The mixture was shaken for 10 min and then several pellets of NaOH were added. The solution was transferred to another vial containing more pellets of NaOH, where it was left overnight. It was transferred to an n.m.r. tube containing basic alumina and was then degassed. The spectrum showed the presence of molecules containing $^{15}NH_2$ and ^{15}NHD groups in the ratio of about 8 to 3. The amino protons were not exchanging, either at -48 or at 80 °C.

(4) Double Resonance Experiments

Dozens of weak irradiation experiments (11) on all these solutions leave no doubt about the signs of the coupling constants given in Table 1. Some experiments necessitated the irradiation of a peak only 0.2 Hz displaced from another. The question then arises of how much the "unwanted" peak is being affected by the second radio-frequency field, *i.e.*, general double irradiation phenomena may occur (11). To insure the validity of the sign determinations a computer program in Fortran IV was written for the double resonance Hamiltonian of a first-order, three spin 1/2 system. Double resonance spectra were computed for various sensible choices of spectral parameters and of the intensities and frequencies of the second radio-frequency field. In this way one may show unequivocally that the weak irradiation experiments yield valid sign determinations.[2]

Results and Discussion

(1) Analyses of Spectra

(a) 10 mol % of 2-Chloroaniline in Benzene-d_6 at 60 MHz, $ABCDX_2$

Initial coupling parameters within the ring were taken from Smith *et al.* (12) and were used in a preliminary noniterative run using LAOCN3 (13). Several iterative runs in which up to 60 transitions were assigned in the ring proton region, while allowing all parameters to vary except the amino proton shift and the coupling between the amino protons and the ring protons in the ortho and para positions, gave the parameters in Table 1. The r.m.s. deviation of calculated from observed transitions was 0.012 Hz. The indicated difference between the amino proton couplings to the two meta protons is real.

The coupling between amino protons and ring protons in the ortho (H-6) and para (H-4) positions was inferred from the broad peaks for these two protons and from the narrow peaks obtained on decoupling of the amino protons. Four proximate peaks belonging to H-4 and -6 were studied in considerable detail as follows. Calculated spectra were plotted on a Calcomp plotter taking $^4J_o^{H,NH_2} = {}^6J_p^{H,NH_2} = 0.00$ Hz (decoupled spectra) with effective T_2 values chosen to reproduce the observed spectra (Lorentzian line-shapes). The two couplings were then increased in magnitude until the undecoupled observed spectra matched the calculated spectra as closely as possible. Considering the uncertainties (± 0.5 s) in the assumed T_2 values, the fact that the peaks need not have the same natural line-widths (14, 15) and the inherent uncertainties in intensity measurements, it was concluded that $^4J_p^{H,NH_2}$ and $^6J_o^{H,NH_2}$ remained uncertain to within 0.03 Hz. Their "best" magnitudes are given in Table 1.

[2]The doubting reader is assured that many cases were simulated and reproduced experimentally, including those in which the "offset" second r.f. field causes "shifting" instead of symmetrical "splittings" of peaks.

TABLE 1. Chemical shifts* and spin–spin coupling constants† of 2-chloroaniline

Parameter	60 MHz(^{14}N)‡	100 MHz(^{14}N)§	100 MHz(^{15}N)‖
ν_3	425.227 (7.087)	708.949 (0.002)	708.685 (0.003)
ν_4	385.214 (6.4202)	642.035 (0.002)	642.115 (0.003)
ν_5	407.353 (6.789)	679.006 (0.002)	678.985 (0.003)
ν_6	374.832 (6.247)	624.208 (0.002)	624.634 (0.003)
ν_{NH_2}	203.7 (3.39)	337.7	
$^3J_o^{HH}(3,4)$	8.004 (0.003)	7.992 (0.004)	7.984 (0.004)
$^3J_o^{HH}(4,5)$	7.359 (0.002)	7.346 (0.004)	7.352 (0.004)
$^3J_o^{HH}(5,6)$	8.032 (0.002)	8.015 (0.004)	8.034 (0.004)
$^4J_m^{HH}(3,5)$	1.460 (0.003)	1.476 (0.004)	1.461 (0.004)
$^4J_m^{HH}(4,6)$	1.504 (0.002)	1.502 (0.004)	1.508 (0.004)
$^5J_p^{HH}(3,6)$	0.334 (0.003)	0.326 (0.004)	0.333 (0.004)
$^4J_o^{H,NH_2}$	±0.12±0.03	−0.122 (0.004)	$^3J(^{15}N,H_6)$¶ = −1.984 (0.005)
$^5J_m^{H,NH_2}(H_3)$	0.335 (0.004)	0.351 (0.005)	$^4J(^{15}N,H_3)$ = −0.787 (0.005)
$^5J_m^{H,NH_2}(H_5)$	0.284 (0.004)	0.306 (0.003)	$^4J(^{15}N,H_5)$ = −0.362 (0.005)
$^6J_p^{H,NH_2}$	±0.095±0.03	−0.108 (0.004)	$^5J(^{15}N,H_4)$ = 0.166 (0.005)

*In Hz to low field of internal tetramethylsilane.
†In Hz, probable errors given in parentheses.
‡10 mol % solution in benzene-d_6.
§10 mol % solution in benzene-d_6, but not the same sample as for the 60 MHz spectrum.
‖10 mol % solution in benzene-d_6, amino protons exchanging.
¶$^1J(^{15}N–H) = -82.3 \pm 0.2$ Hz, signs of other $^{15}N,H$ couplings being relative to this.

Their magnitudes agree with the precise values obtained later from resolved spectra.

(b) 2-Chloroaniline-^{15}N and ^{14}N at 100 MHz

As mentioned above, nonexchanging and exchanging solutions were prepared and their spectra examined. The spectral analyses using LAME (16) gave the parameters in Table 1. All observable ring proton transitions were assigned, the r.m.s. errors lying between 0.0094 and 0.0125 Hz. Allowing all parameters to vary gave all but one of the elements in the correlation matrix as less than 0.15. There was a correlation of 0.387 between $^5J_p^{HH}$ and $^5J_m^{H_3,NH_2}$. Numerous tickling experiments allowed the unambiguous sign determinations reported in Table 1.

Calculated spectra agreed very well with observed spectra. For reasons of space only parts of these are illustrated in Figs. 1 and 2. In Fig. 1 the observed and calculated spectra are shown for the H-4 and -6 protons of 2-chloroaniline-^{15}N in the presence of amino proton intermolecular exchange. Many of the observed peaks are less than 0.1 Hz wide at half-height and very clearly demonstrate the 0.17 Hz coupling between ^{15}N and H-4 over five bonds (doublets with smallest splittings). The calculated spectrum has a line-width, $\Delta\nu_{1/2} = 0.11$ Hz, a little too high compared to the observed spectrum but it nevertheless illustrates the reliability of the relevant parameters in Table 1.

In Fig. 2 are given the observed and calculated spectra for H-4 and -6 of 2-chloroaniline-^{14}N in the absence of amino proton exchange. There is now no observable coupling to nitrogen but the triplets arising from coupling to the amino protons are clearly present. The smallest such coupling occurs with H-4 and the observed spectrum indicates the non-Lorentzian nature of the triplet peaks but sweeping in the opposite direction again resolves the weaker member on the opposite side of the triplet. The amino proton coupling to H-3 and -5 is, of course, large (0.3 Hz) and is resolved to the base line in spectra not shown here. Weak irradiation of these peaks (see Experimental) unequivocally splits the expected components of the triplets in the H-4 and -6 regions and the irradiation intensities can now be kept small enough not to perturb peaks 0.3 Hz removed from the second radio-frequency field (the reverse experiments confirm the results). The $\Delta\nu_{1/2}$ in the calculated spectrum of Fig. 2 was 0.07 Hz.

(c) 2-Chloroaniline-^{15}NHD, nonexchanging

The ring proton spectrum displayed a multiplicity of peaks arising from the mixture of NH_2, NHD, and ND_2 molecules and was not analyzed. The isotope shift of the N–H proton resonance was 0.0255 ± 0.0020 p.p.m. to high field at 31 °C. At −48 °C, where rapid spin–lattice relaxation of the deuterium nucleus occurs (17), the line-widths of the NHD and NH_2 protons were the same within experimental error. At 80 °C the proton resonance width of the NH_2 group was at least 80% of the NHD proton resonance. Assuming that quadrupolar relaxation of the deuterium nuclei is ineffective at this

Can. J. Chem. Downloaded from www.nrcresearchpress.com by 210.87.254.105 on 09/05/12
For personal use only.

Can. J. Chem. Downloaded from www.nrcresearchpress.com by 210.87.254.105 on 09/05/12
For personal use only.

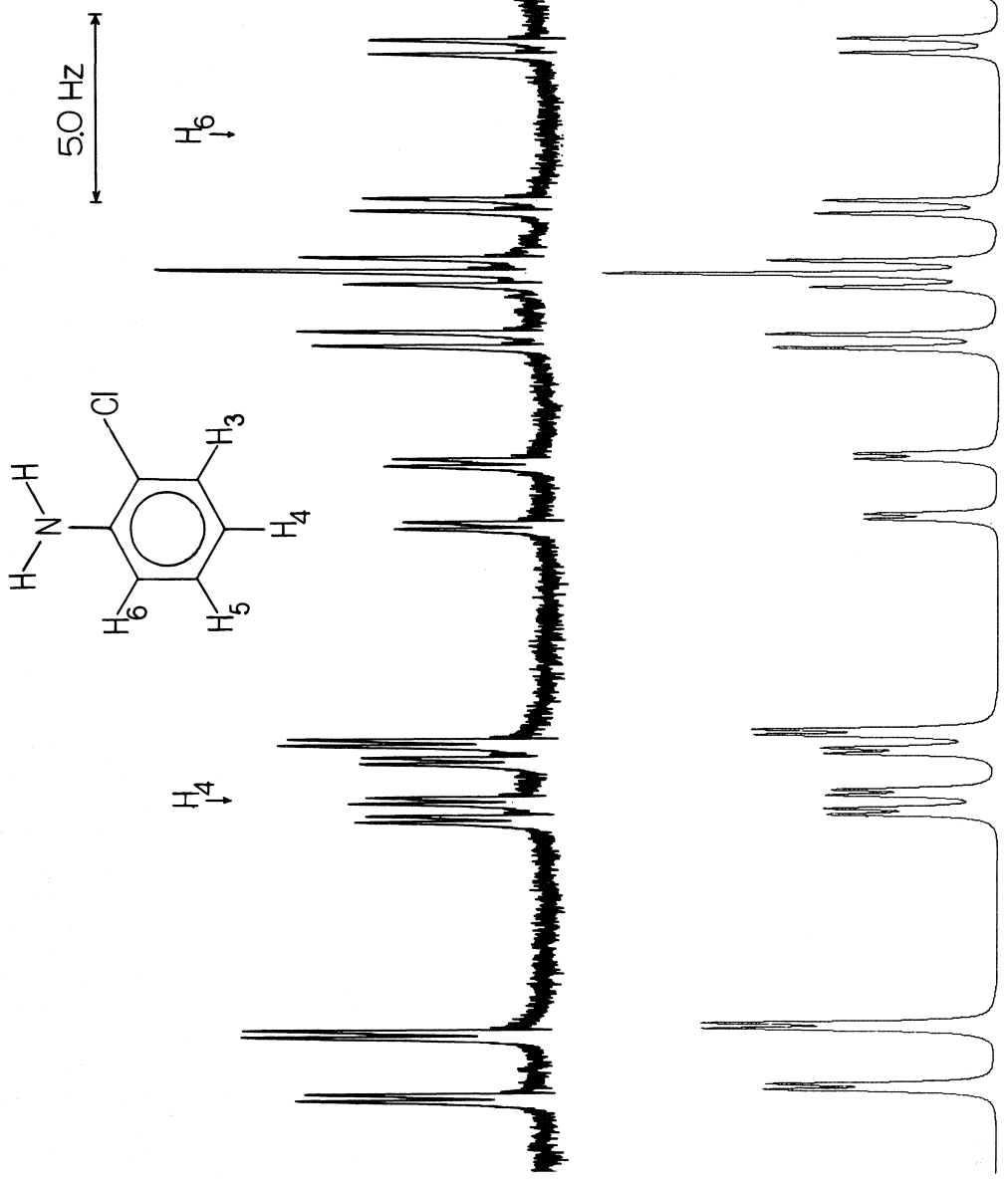

FIG. 1. The p.m.r. spectrum at 100 MHz of the H-4 and -6 protons in 2-chloroaniline-^{15}N as a 10 mol % solution in benzene-d_6. The shifts of H-4 and -6 are indicated by vertical arrows. The smallest doublet spacings in the H-4 region are about 0.17 Hz and arise from coupling to ^{15}N. The calculated spectrum uses the parameters in Table 1 with $\Delta\nu_{1/2} = 0.11$ Hz. In the observed spectrum fast intermolecular exchange of the amino protons is occurring.

Can. J. Chem. Downloaded from www.nrcresearchpress.com by 210.87.254.105 on 09/05/12
For personal use only.

temperature (17), and knowing the ratio of the nuclear moments of ^1H and ^2H, it follows that $|^2J^{H,NH}|$ is probably less than 1 Hz.

(2) Nonplanarity of the Amino Group

(a) Long-range Proton-Proton Couplings

The relative magnitudes and signs of the coupling between the amino protons and the ring protons fall into the general pattern for side-chain protons described in the introduction if it is assumed that the amino protons lie out of the plane of the ring. The coupling to the para proton, H-4, over six bonds has not been previously observed in an aniline derivative. In 2,6-dibromoaniline such a coupling is not observed (10) suggesting a lower degree of nonplanarity of the amino group in this compound, likely caused by hydrogen bonding.

The barrier to rotation about the C—N bond is evidently quite low (10) in 2,6-disubstituted anilines and the equivalence of the amino proton shifts in 2-chloroaniline at −48 °C suggests a barrier to rotation in 2-chloroaniline of less than 10 kcal/mol when it is considered that shift difference of 1 p.p.m. (18) is expected between the two amino protons if no rotation is occurring. Alternative assumptions can now be made concerning the conformation of the amino group.

If the N—H bond *cis* to the chlorine lies in the plane of the ring, as it will if strong hydrogen bonding occurs, then the calibration procedures previously described (10) lead to an angle of 25° between the plane of the ring and the plane defined by the fragment H—N—C containing the N—H bond *trans* to the chlorine (rapid rotation about C—N on the time scale defined by the reciprocals of the chemical shifts and coupling constants is assumed, of course). If, on the other hand, the N—H bonds are symmetrically arranged then an average angle of 17.5° (as defined above) may be estimated.

If the coupling from the amino protons to the ortho and para ring protons is π electron dominated then (as in toluene (1)) the ortho coupling should be slightly larger in magnitude than the para coupling, as observed (see Fig. 2 and Table 1). The coupling between the amino protons and the meta ring protons, evidently slightly substituent dependent, behaves as expected on the basis of the couplings measured for other side-chain protons (1–5).

The estimated degree of nonplanarity is in broad agreement with the microwave data for aniline itself in the gas phase (19), but there is no doubt that the estimate is not very reliable.

(b) The Coupling Between Amino Protons and ^{15}N

A check on the semiquantitative conclusions above may be available from the value of −82.3 Hz for $^1J^{15N,H}$ in 2-chloroaniline-^{15}N. It has recently been established that this coupling in aniline, anilinium ion, and their 4-substituted derivatives, is a reliable measure of the hybridization at nitrogen (20). However, there are marked solvent effects on the coupling and calibrations of hybridization in one medium must be used with circumspection in another. Furthermore, although there is little doubt (20, 21) that the nitrogen in, say, pyrrole is trigonally hybridized (and the ^{15}N–H coupling also indicates as much), an equation (22) of the type (% s character of nitrogen orbital used for bonding to hydrogen) $= aJ^{15N,H} + b$, where a and b are constants, should be parameterized using very similar compounds if semiquantitative predictions are going to be made with reasonable validity.

Of the various possibilities, the following was finally judged to be most reliable. The ^{15}N–H coupling in aniline in DMSO is −82.6 Hz while in $CDCl_3$ it is −78.6 Hz (23), reasonably close to our unpublished value of −78.8 Hz in benzene-d_6 solution (the accuracy of all these values is probably 0.2 to 0.4 Hz). In anilinium ion in H_2SO_4 one has a value of −76.0 Hz (20) which compares with −74.8 Hz in ammonium ion dissolved in acidified water (24). The phenyl carbon therefore does not cause a large change in the coupling and sp^3 hybridization in the anilinium ion can be reasonably assumed. For the coupling in an sp^2 hybridized system we do not choose an indole or pyrrole derivative because of the unknown substituent effects (alteration of effective nuclear charge at nitrogen (25)), but choose to use the gas phase value of the HNH angle of 114° in aniline as a calibration point. From the equation, s character $= \cos\theta/(\cos\theta - 1)$, where θ is the HNH angle, the s character of the nitrogen orbital used in bonding to hydrogen is then 0.29. In benzene solution, where strong hydrogen bonding of the N–H bond to solvent molecules is not expected this result is probably reasonable.

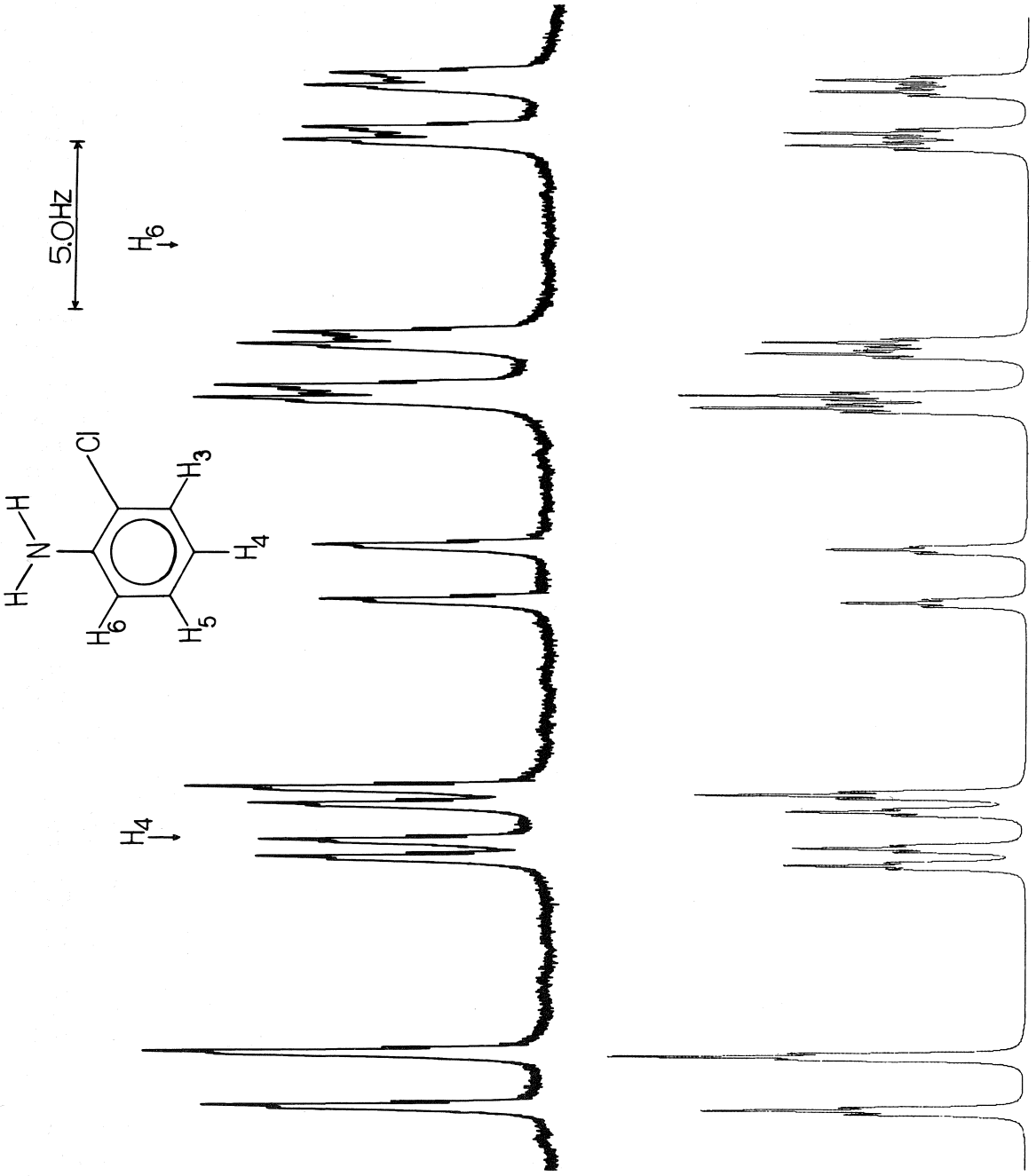

Can. J. Chem. Downloaded from www.nrcresearchpress.com by 210.87.254.105 on 09/05/12
For personal use only.

Can. J. Chem. Downloaded from www.nrcresearchpress.com by 210.87.254.105 on 09/05/12
For personal use only.

In going from DMSO solution to $CDCl_3$ solution, the coupling decreases in magnitude from 3 to 4 Hz (23) for aniline derivatives. If this correction is applied to the above value for anilinium ion, the aniline calibration point of 0.29 s character together with 0.25 s character for anilinium yields the relationship: s character $= -0.59\,J(^{15}N,H) - 17._5$.

For 2-chloroaniline-^{15}N, the coupling of -82.3 Hz then predicts an HNH angle of 116.7°. This value is hardly reliable to more than 1°, but is clearly compatible with the dihedral angle obtained from $^6J_p^{H,NH}$ above and with the idea of a nonplanarity of the amino group.[3] In addition to the errors in the coupling and the approximate nature of the correction for solvent effects, there is also the question of the direct effect of the ortho chlorine substituent on the coupling. The synthesis of a series of relevant derivatives of aniline-^{15}N is indicated.

(c) The Geminal Coupling Between the Amino Protons, $^2J^{H,NH}$

This coupling is likely less than 1 Hz in magnitude in 2-chloroaniline. In ammonium ion (27, 28) the coupling is -12.4 Hz, and is $+2.3$ Hz in formamide in aqueous solution (24). These values compare with a geminal proton coupling of -12.4 Hz in methane (29) and $+2.4$ Hz in ethylene (30). There is a striking similarity between the couplings and the probable s character of the nitrogen and carbon orbitals in these compounds.

In formamide (24) there exists a marked effect of the carbonyl group on $^1J(^{15}N,H)$. The coupling for the N—H bond lying *trans* to the C=O bond, *i.e.*, the one which will be most strongly polarized by the electric field from the C=O dipole, is 4.5 Hz larger in magnitude than the coupling for the N–H bond lying *cis* to the carbonyl group, which is -86.9 Hz. Nevertheless, if the mean value of these two couplings is decreased by 4 Hz to account for solvent effects the s character calculated from the equation above is 0.33, implying sp^2 hybridization at the nitrogen.[4]

If an HNH angle of 116 to 117° is assumed in 2-chloroaniline, the indicated proportionalities imply a value of -2.6 ± 2 Hz for $^2J^{H,H}$ in this compound, again compatible with the observed magnitude of 1 Hz or less. The uncertainty of 2 Hz in the estimated values derives from the total uncertainty of about 1 Hz in the couplings in the ammonium ion and formamide and from the uncertainty of about 1° in the HNH angle.

Although the amino group is in many respects different from a CH_2 fragment, a qualitative application of the theory of geminal proton coupling of Pople and Bothner-By (32) indicates a small positive shift of $^2J^{H,H}$ in aniline relative to ammonia, inasmuch as the H,H line is parallel to the plane of the ring.

In summary, the three rough estimates of the nonplanarity of the amino group in 2-chloroaniline are self consistent to within experimental error and suggest the measurement of the three coupling parameters in a series of aniline derivatives.

(3) Molecular Orbital Calculations in the CNDO/2 Approximation

(a) Dipole Moments and Relative Energies

Because CNDO/2 and INDO molecular orbital calculations (33, 34) yield reliable charge distributions and therefore dipole moments of relatively large molecules, *e.g.*, for fluorobenzene (33) and *p*-fluorobenzaldehyde,[5] CNDO/2 computations were done on 2-chloroaniline for various conformations of the amino group in an attempt to confirm or reject the tentative conclusions reached above. For aniline we calculate 1.56 D, the experimental value being 1.53 D (35). Although these calculations allow d orbital participation for the chlorine, the calculated dipole moment of chlorobenzene is 4.05 D,

[3]It is interesting to note that angles of 111.7 and 113.7° have been derived from solution i.r. data (26) for aniline and 2-chloroaniline, respectively.

[4]In the gas phase, the N—H bond *trans* to C=O is 0.01 Å shorter than the other and the HNH angle is 119°, the H_2N—C fragment forming a shallow pyramid (31).

[5]We calculate 1.87 D compared to the observed value at 1.98 D (35).

FIG. 2. The p.m.r. spectrum of the H-4 and -6 protons of a 10 mol % solution in benzene-d_6 of 2-chloroaniline when the amino protons are not exchanging. The small triplet splittings, less than 0.1 Hz in the H-4 region, arise from coupling to the equivalent amino protons. In the H-3 and -5 regions these couplings are large, about 0.3 Hz, and are resolved to the base line. The calculated spectrum uses the parameters in Table 1 with $\Delta\nu_{1/2} = 0.07$ Hz.

Can. J. Chem. Downloaded from www.nrcresearchpress.com by 210.87.254.105 on 09/05/12
For personal use only.

compared to the observed value in solution of 1.58 D (35). Therefore these computations were not pursued further.

(b) s-Bond Orders in the N—H Bonds

In view of the statements in section 2 concerning substituent effects on the ^{15}N–H coupling, the change in this coupling due to substituents should be reflected in change in the square of the s-bond order between ^{15}N and H (36–39). In aniline we calculate at N–H s-bond order of 0.4957 while in non-planar conformations of 2-chloroaniline the s-bond order increases by amounts sufficient to increase its square by as much as 8%. The observed increase in the magnitude of the ^{15}N–H coupling on substitution by chlorine is at most 6%, in rough agreement with the prediction (the reduced coupling is, of course, positive (40) because the gyromagnetic ratio of ^{15}N is negative).

(4) Coupling of ^{15}N to the Ring Protons

Immediately apparent from Table 1 is the substituent effect on $^4J(^{15}N,H)$. Allowing for the negative gyromagnetic ratio of ^{15}N, the effect has the same sign as that experienced by $^4J^{H,H}$ in **1** (41), where X is more electronegative

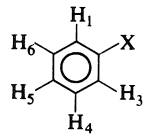

1

than hydrogen. In **1**, J^{H_1,H_3} is larger than, and J^{H_1,H_5} is smaller than, $^4J^{H,H}$ in benzene itself. In aniline-^{15}N one may then expect $^4J(^{15}N,H) \simeq -0.5$ Hz and, again by analogy to what is known for **1**, a smaller magnitude of $^5J(^{15}N,H)$ in 2-chloroaniline indicates a coupling of either sign in aniline-^{15}N.

We thank Dr. F. E. Hruska for a suggestion concerning the mono-deuteration of the amino group and are grateful to the National Research Council of Canada for financial support. We thank a referee for very useful criticisms.

1. C. J. Macdonald and W. F. Reynolds. Can. J. Chem. **48**, 1002 (1970).
2. D. J. Blears, S. S. Danyluk, and T. Schaefer. J. Chem. Phys. **47**, 5037 (1967).
3. M. P. Williamson, R. Kostelnik, and S. M. Castellano. J. Chem. Phys. **49**, 2218 (1968).
4. R. Wasylishen and T. Schaefer. Can. J. Chem. **49**, 94 (1971).
5. C. L. Bell, S. S. Danyluk, and T. Schaefer. Can. J. Chem. **47**, 3529 (1969).
6. T. Schaefer and G. Kotowycz. Can. J. Chem. **46**, 2865 (1968).
7. S. Forsén, B. Åkermark, and T. Alm. Acta Chem. Scand. **18**, 2313 (1964).
8. S. Forsén and R. A. Hoffman. J. Mol. Spectrosc. **20**, 168 (1966).
9. J. A. Weil, A. Blum, A. H. Heiss, and J. K. Kinnaird. J. Chem. Phys. **46**, 3132 (1967).
10. R. Wasylishen and T. Schaefer. Can. J. Chem. **48**, 1263, 1343 (1970).
11. R. A. Hoffman and S. Forsén. *In* Progress in nuclear magnetic resonance spectroscopy. Vol. 1. *Edited by* J. W. Emsley, J. Feeney, and L. H. Sutcliffe. Pergamon Press, Oxford, 1966.
12. W. B. Smith, A. M. Ihrig, and J. L. Roark. J. Phys. Chem. **74**, 812 (1970).
13. S. Castellano and A. A. Bothner-By. J. Chem. Phys. **41**, 3863 (1964).
14. R. Freeman and S. Wittekoek. J. Mag. Res. **1**, 238 (1969).
15. R. Freeman, S. Wittekoek, and R. R. Ernst. J. Chem. Phys. **52**, 1529 (1970).
16. C. W. Haigh and J. M. Williams. J. Mol. Spectrosc. **32**, 398 (1969).
17. R. M. Moriarty, J. P. Kim, and S. J. Druck. Tetrahedron, 25, 1261 (1969).
18. T. Yonemoto, W. F. Reynolds, H. M. Hutton, and T. Schaefer. Can. J. Chem. **43**, 2668 (1965).
19. D. G. Lister and J. K. Tyler. Chem. Commun. 152 (1966).
20. T. Axenrod, M. J. Wieder, G. Berti, and P. L. Barili. J. Am. Chem. Soc. **92**, 6066 (1970).
21. E. Rahkamaa. J. Chem. Phys. **48**, 531 (1968).
22. G. Binsch, J. B. Lambert, B. W. Roberts, and J. D. Roberts. J. Am. Chem. Soc. **86**, 5564 (1964).
23. T. Axenrod, P. S. Pregosin, M. J. Wieder, and G. W. A. Milne. J. Am. Chem. Soc. **91**, 3681 (1969).
24. R. J. Chuck, D. G. Gillies, and E. W. Randall. Mol. Phys. **16**, 121 (1969).
25. D. M. Grant and W. Litchman. J. Am. Chem. Soc. **87**, 3994 (1965).
26. P. J. Krueger. Can. J. Chem. **40**, 2300 (1962).
27. G. Fraenkel, Y. Asahi, H. Batiz-Hernandez, and R. A. Bernheim. J. Chem. Phys. **44**, 4674 (1966).
28. W. McFarlane and R. R. Dean. J. Chem. Soc. 1535 (1968).
29. M. Karplus, D. H. Anderson, T. C. Farrar, and H. S. Gutowsky. J. Chem. Phys. **27**, 597 (1957).
30. R. M. Lynden-Bell and N. Sheppard. Proc. Roy. Soc. (Lond.) **A269**, 385 (1962).
31. C. C. Costain and J. M. Dowling. J. Chem. Phys. **42**, 1339 (1965).
32. J. A. Pople and A. A. Bothner-By. J. Chem. Phys. **42**, 1339 (1965).
33. J. A. Pople and D. L. Beveridge. Approximate molecular orbital theory. McGraw-Hill Book Co., New York, N.Y., 1970.

34. Program No. 141. QCPE. Chemistry Department, Indiana University, Bloomington, Indiana 47401.
35. A. L. McCLELLAN. Tables of experimental dipole moments. W. H. Freeman and Co., San Francisco, California, 1963.
36. H. M. McCONNELL. J. Chem. Phys. **24**, 460 (1956).
37. G. E. MACIEL, J. W. McIVER, JR., N. S. OSTLUND, and J. A. POPLE. J. Am. Chem. Soc. **92**, 1 (1970).
38. M. BARFIELD and M. KARPLUS. J. Am. Chem. Soc. **91**, 1 (1969).
39. T. YONEZAWA, I. MORISHIMA, and M. FUJII. Bull. Chem. Soc. (Jap.) **39**, 2110 (1966).
40. W. McFARLANE. Q. Revs. **22**, 187 (1969).
41. S. CASTELLANO, R. KOSTELNIK, and C. SUN. Tetrahedron Lett. **46**, 4635 (1967).

Can. J. Chem. Downloaded from www.nrcresearchpress.com by 210.87.254.105 on 09/05/12
For personal use only.

Can. J. Chem. Downloaded from www.nrcresearchpress.com by 210.87.254.40 on 09/05/12
For personal use only.

The Effect of Some 3-Oxygen Functions on the Simmons–Smith Methylenation of 5,6-Unsaturated Steroids

J. F. Templeton and C. W. Wie
Faculty of Pharmacy, University of Manitoba, Winnipeg 19, Manitoba

Received July 2, 1971

The effect of 3α- and 3β-hydroxy, 3α- and 3β-acetoxy, 3-ethylene acetal, and 3α-methoxy derivatives of 5-cholestene on the addition of the Simmons–Smith reagent to the steroidal 5,6-double bond has been investigated. Reaction occurred only with *epi*-cholesterol to yield chiefly 3α-hydroxy-5,6α-cyclopropano-5α-cholestane. The 3α-ethyl ether, 3α-acetate, and a dialkoxymethane have been identified as byproducts. The p.m.r. and mass spectral data are given.

L'effet des dérivés hydroxy en 3α et 3β, acétoxy en 3α et 3β, éthylène acétal en 3, et méthoxy en 3α du cholestène-5 sur l'addition du réactif de Simmons–Smith sur une double liaison en 5,6 stéroidique a été étudié. La réaction se fait seulement avec l'*epi*-chlorestérol pour donner principalement l'hydroxy-3α cyclopropano-5,6α cholestane-5α. L'éthyl éther en 3α, l'acétate en 3α et un dialcoxyméthane ont été identifiés comme sous produits. Des données de r.m.p. et de spectrométrie de masse sont rapportées.

Canadian Journal of Chemistry, **49**, 3636 (1971)

Introduction

Since the introduction of the iodomethylzinc iodide reagent by Simmons and Smith (1–4), prepared from a zinc–copper couple and diiodomethane, it has been extensively used in organic synthesis to prepare methylene containing cyclopropane derivatives from olefins. Simmons *et al.* (4) have shown that the reagent is best represented as an equilibrium between the following species:

$$2\,ICH_2ZnI \rightleftarrows (ICH_2)_2Zn\cdot ZnI_2$$

with possible solvent stabilization. It has been suggested (3–5) that the bis-compound is the reacting molecule in a one step addition of methylene to the olefin. An important extension of the synthetic application of this reaction followed from the discovery (6, 7) that the presence of neighboring electron-donating oxygen functions was capable of both accelerating the rate of reaction and maintaining steric control over the products in a *cis* sense (8). This effect is initiated by an interaction between the electron-donating group with the metal, prior to transfer of methylene, through formation of a zinc–oxygen bond (3) or by coordination (7).

The object of the present study has been to determine the effect of various 3-oxygen functions on the addition of the iodomethylzinc iodide reagent to the steroidal 5,6-double bond.

Results and Discussion

Addition of the iodomethylzinc iodide reagent to the steroidal 5,6-double bond would be expected to be accelerated and stereochemically controlled by an increased rate of addition to the α-face of the molecule by the presence of a 3-axial oxygen function capable of coordination or reaction with the metal. Alternatively, the rigid steroid structure would hold a 3-equatorial oxygen in such a position that any zinc oxygen interaction would leave the reagent spacially removed from the double bond, and sterically hindered by the 19-methyl group, from approaching the double bond from the β-face. An axial conformation which has been postulated (9) as the reacting conformation for homoallylic alcohols is not possible in the rigid steroid molecule containing a 3-equatorial oxygen.

When cholesterol (**1***a*) was treated with the Simmons–Smith reagent in refluxing ether, only starting material was recovered. However, when *epi*-cholesterol (**1***b*) was similarly treated, the product contained no starting material by t.l.c. and after chromatographic separation several products were obtained. The major product in 60% yield was a cyclopropane containing alcohol, the spectral properties of which are consistent with those of the expected 3α-hydroxy-5,6α-cyclopropano-5α-cholestane (**2***a*). The p.m.r. spectrum no longer showed the vinylic proton of *epi*-cholesterol but had typical high-field cyclopropane ring hydrogen resonance and a hydrogen having a band width at half height characteristic of a 3-equatorial hydrogen (10). The i.r. spectrum showed a weak absorption characteristic of cyclopropyl C—H stretching. By analogy

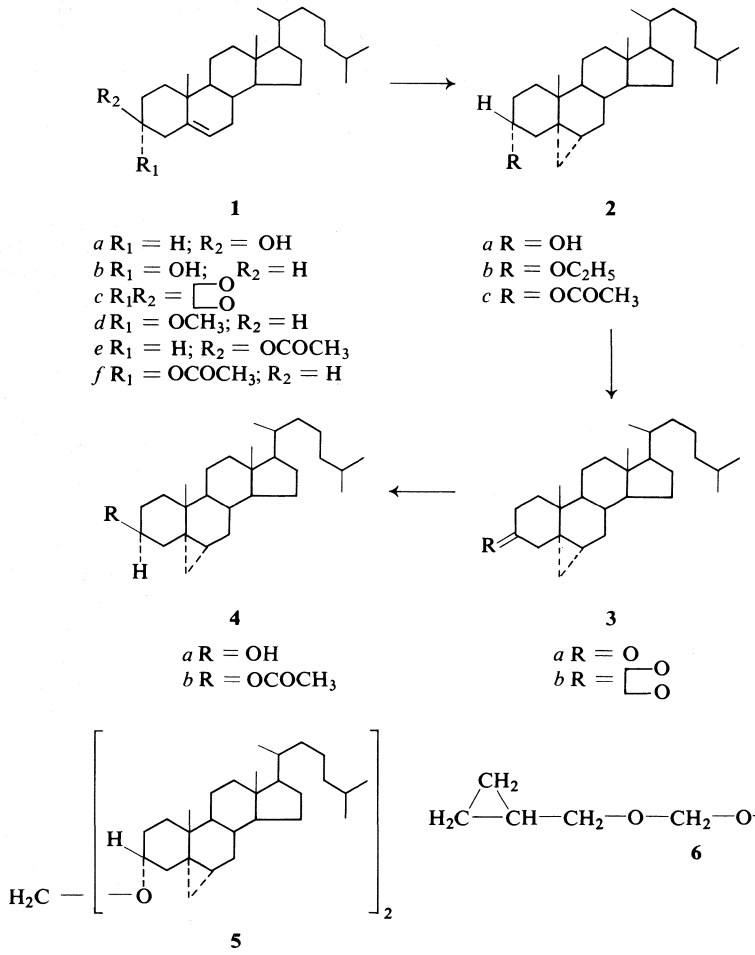

(11, 12) with other homoallylic steroidal alcohols, methylenation is concluded to have occurred *cis* to the hydroxyl group. Molecular rotation differences, which have been shown to be similar for corresponding epoxide and cyclopropane derivatives (13), are also consistent with the 5α,6α structure for **2***a*.

Chromic acid oxidation (14) of this alcohol **2***a* yielded a saturated ketone **3***a* which still contained the cyclopropane ring. Treatment of this ketone with perchloric acid in glacial acetic acid gave the known 6α-methyl-4-cholesten-3-one (15). Reduction of the ketone **3***a* with lithium tritertiary butoxyaluminum hydride (16) gave an epimeric alcohol **4***a* further characterized as its acetate **4***b*. Treatment of **4***a* with ethylene glycol and *p*-toluenesulfonic acid in refluxing benzene yielded the ethylene acetal **3***b*.

A dialkoxymethane **5** analogous to those reported (17) as a byproduct of the Simmons–Smith reaction with several low molecular weight allylic alcohols was also isolated. Bis(5,6α-cyclopropano-5α-cholestan-3α-oxy)methane (**5**) showed p.m.r. and i.r. spectra in agreement with the structure indicated. The mass spectrum of **5** has a weak signal corresponding to the molecular ion as does bis(cyclohexoxy)methane (18). This is in contrast to simple alicyclic dialkoxymethane derivatives which do not show a molecular ion peak (17–19). Signals corresponding to R^+, RO^+, and $ROCH_2^+$ ions are indicative of a structure of this type where cleavage of the ether bonds would be more favored than partial fragmentation of the hydrocarbon structure. The formation of this substance from a homoallylic alcohol suggests that there is a similar intermediate in the addition of the iodo-

Can. J. Chem. Downloaded from www.nrcresearchpress.com by 210.87.254.40 on 09/05/12
For personal use only.

Can. J. Chem. Downloaded from www.nrcresearchpress.com by 210.87.254.40 on 09/05/12
For personal use only.

methylzinc iodide to both allylic and homoallylic alcohols. The equivalent unsymmetrical formal intermediate suggested by Majerski and Schleyer (17) **6** for the allylic dialkoxymethane is unlikely because the 3-ethylene acetal **1***c* and 3α-methyl ether **1***d* derivatives of 5-cholestene (see below) fail to react under the same reaction conditions.

The presence of ethoxy derivatives has previously been noted (11) with the suggestion that they arise through formation of hydriodic acid which cleaves the ethyl ether solvent to form ethyl iodide, their formation being suppressed if the reaction mixture were first concentrated by distillation. From this reaction small quantities of 3α-ethoxy-5,6α-cyclopropano-5α-cholestane (**2***b*) have been isolated although the reaction was distilled during addition of the ethereal solution of the steroidal alcohol. Even when the zinc–copper couple was carefully washed with dry ether to remove acetic acid, it was possible to isolate 5,6α-cyclopropano-5α-cholestan-3β-yl acetate (**2***c*). This substance was also prepared by acetylation of the alcohol **2***a* and was identical in all respects with that product.

Joska *et al.* (20) state that reaction occurs between the Simmons–Smith reagent at 3-oxygen substituted 5,6-unsaturated B-norsteroids at 100°, with the 3α- and 3β-acetates giving much higher yields of methylene addition products than could be obtained from the corresponding alcohols. However, complete stereochemical control of addition was lost and principally addition from the α-face occurred irrespective of the stereochemistry at C-3. Stereochemical control in the 3β-derivatives is undoubtedly due to normal addition to the α-face, caused by hindrance from the C-10 methyl group and not because of complex formation. For the 3α-derivatives both steric hindrance and complex formation may operate.

Cholesteryl acetate (**1***e*), in contrast, was unreactive at 75° for 18 h. The p.m.r. spectrum of the crude reaction mixture did not indicate any high field resonance characteristic of the cyclopropyl protons shown by **4***b*. These findings are consistent with the decreased rate of reaction of tri-substituted six-membered olefins compared to the five-membered system as shown by the rate measurements of Rickborn and Chan (21). When cholesteryl acetate was treated under the conditions used by Joska *et al.* (20) cholesta-3,5-diene (22) was isolated. No cyclopropane derivatives were obtained. *epi*-Cholesteryl acetate (**1***f*) was recovered unchanged after refluxing overnight with the Simmons–Smith reagent.

Because of the relative difficulty of preparing 3α-hydroxy-5,6-unsaturated steroids (23), it was hoped to take advantage of the established ketalization of the steroidal 4-en-3-one system to place an oxygen atom in the 3-axial position of a steroidal 5-ene. Treatment of 5-cholesten-3-one ethylene acetal (**1***c*) with the Simmons–Smith reagent in refluxing ether gave no cyclopropane containing products as determined by p.m.r. spectroscopy and only a good yield of starting material was recovered. Six days refluxing in ether gave a crude product containing no high field resonance which corresponded to the signals of **3***b* as well as giving no corresponding acetal signals. Recently it has been suggested (9) that iodomethylzinc iodide addition to homoallylic alcohols, unlike allylic alcohols, is accelerated and sterically controlled when reaction of the alcohol and the iodomethylzinc iodide reagent occurs prior to methylenation. This mechanism rules out acceleration by an ethereal oxygen in this case. *epi*-Cholesteryl methyl ether (**1***d*) was also unreactive under refluxing ether conditions. However, in the similar case of 1-(*o*-methoxyphenyl)-propene, acceleration by an oxygen function did occur (2).

Of the 3-oxygen substituted 5-cholestene derivatives studied, only in the presence of the 3α-hydroxy function did reaction of the iodomethylzinc iodide reagent with the 5,6-double bond occur.

Experimental

Unless otherwise stated the following instruments and procedures have been used.

Melting points were carried out on a Thomas–Hoover capillary apparatus and are uncorrected. Optical rotations were measured in chloroform solution at 23° on a Bellingham and Stanley (Model A) Polarimeter (concentration range 0.4–1.5%). The i.r. spectra were determined on a Beckman Model 8 spectrophotometer using carbon tetrachloride as solvent. The u.v. spectra were recorded on a Beckman DU Model 2400 spectrophotometer using 1 cm silica cells. For p.m.r. spectra a Varian A60 instrument was used with deuterochloroform as solvent and tetramethylsilane as an internal standard. Mass spectra were determined on an A.E.I. MS12 instrument at 70 eV using a direct probe method by the Chemistry Department, University of Alberta, Edmonton. Elemental analyses were performed by Pascher and Pascher, Microanalytical Laboratory, Bonn, West Germany. Petroleum ether refers to the fraction boiling within the range of 60 to 80°. The t.l.c. was carried out on silica gel coated glass plates, developed with 10–25% v/v ethyl acetate in petroleum

Can. J. Chem. Downloaded from www.nrcresearchpress.com by 210.87.254.40 on 09/05/12
For personal use only.

ether, visualized by spraying with 4% v/v concentrated sulfuric acid in ethanol followed by heating at approximately 100°. Silver nitrate treated plates were prepared by spraying the above plates with 0.1 *N* silver nitrate and drying at 100° for 30 min before use.

Simmons–Smith Reaction

Zinc–Copper Couple

A 1.85% w/w zinc–copper couple was freshly prepared essentially by the method of LeGoff (24) as follows: zinc dust (15 mmol) was added to a hot (bath temperature 130°) stirred solution of copper acetate monohydrate (0.28 mmol) in glacial acetic acid (2 ml). The reaction was quickly removed from the heat and excess acetic acid removed by pipette. The residue was washed with acetic acid (2 ml) followed by dry ether (3 × 20 ml) to remove all acetic acid.

Iodomethylzinc Iodide Reagent

To the freshly prepared couple in dry ether (20 ml) was added dry methylene iodide (10 mmol) m.p. 5–6°, in dry ether (10 ml). Refluxing usually occurred spontaneously and the reaction was refluxed for 30–60 min.

Reaction with the Unsaturated Steroid

The steroid (1 mmol) was dissolved in dry ether (10–25 ml), added to the reagent (10 mmol), and the mixture refluxed. In reactions carried out with a steroid containing a hydroxyl group the steroid was added dropwise over 20–30 min while ether was distilled at a rate slightly greater than the addition. Dry ether was added if required to maintain the volume.

Reaction Work-up

The reaction was poured into excess saturated aqueous sodium bicarbonate and the resulting slurry extracted with ether. The ether solution was washed with water, brine, dried over anhydrous sodium sulfate, filtered, and evaporated at reduced pressure to give the crude reaction product.

Simmons–Smith Reagent with epi-Cholesterol (1b)

epi-Cholesterol (10 mmol) was treated as described above and small aliquots removed and worked-up at intervals. The t.l.c. on $SiO_2/AgNO_3$ plates indicated no starting material after 6 h. Reactions run up to 18 h gave analogous results. Chromatography of the crude reaction product on alumina gave, on elution with petroleum ether, a fraction (806 mg) which on crystallization from ether gave bis(5,6α-cyclopropano-5α-cholestan-3α-oxy)-methane (**5**), recrystallization gave 287 mg; m.p. 221–222°; $[\alpha]_D$ −40°; i.r. ν_{max} 3060 (cyclopropyl C—H stretching), 1027 (C—O stretching) cm^{-1}; p.m.r. δ 4.61 (s, 2H, dialkoxymethylene), 3.90 (unresolved multiplet, 2H, width at half height, 7 Hz, 3-equatorial hydrogen), 1.04 (s, C-19 methyl), 0.60 (s, C-18 methyl), 0.42 (s, 2H, cyclopropyl hydrogen) p.p.m.; mass spectrum, strong signal at *m/e* 383 (R^+), moderately strong signals at 399 (RO^+) and 413 ($ROCH_2^+$), weak signal at 429 ($ROCH_2O^+$), no signals greater than 429 except near the very weak M^+ at 812.

Anal. Calcd. for $C_{57}H_{96}O_2$: C, 84.17; H, 11.90. Found: C, 84.12; H, 12.10.

The mother liquor on crystallization from methanol yielded 3α-ethoxy-5,6α-cyclopropano-5α-cholestane (**2b**) (66 mg); m.p. 117.5; $[\alpha]_D$ −43°; i.r. ν_{max} 3060 (cyclopropyl C—H stretching) cm^{-1}; p.m.r. δ 3.76 (1H, unresolved triplet, band width at half height 7.5 Hz, 3-equatorial proton); 3.60 (2H, quartet, $J = 7$ Hz, ethoxymethylene protons), 0.46 (broad singlet, 2H, cyclopropyl proton) p.p.m.; mass spectrum, strong signals at *m/e* 382 (M^+ − EtOH), moderately strong peaks at 227 (M^+ − EtOH-42-17β-sidechain), 329 (cleavage of C-1 to C-10 and C-4 to C-5), 428 (M^+).

Anal. Calcd. for $C_{30}H_{51}O$: C, 84.24; H, 12.01. Found: C, 84.05; H, 12.21.

Elution with 5% benzene petroleum ether gave 5,6α-cyclopropano-5α-cholestan-3α-yl acetate (**2c**) (420 mg), recrystallized from methanol, m.p. 131–132°; mixed m.p. was not depressed and the i.r. spectrum (KBr) was identical with the acetate of a **2a** (see below).

Elution with benzene gave 3α-hydroxy-5,6α-cyclopropano-5α-cholestane (**2a**) (2.4 g), recrystallized from acetone m.p. 120–121°; $[\alpha]_D$ −65°; i.r. ν_{max} 3600 (free O—H stretching), 3050 (cyclopropyl C—H stretching) cm^{-1}; p.m.r. δ 4.00 (unresolved multiplet, 1H, half band width, 8.5 Hz, 3-equatorial hydrogen), 1.05 (C-19 methyl), 0.61 (C-18 methyl), 0.49 (broad singlet, 2H, cyclopropyl) p.p.m.; mass spectrum, strong peaks at 382 ($M^+ - H_2O$) and 400 (M^+); moderately strong peaks at *m/e* 227 ($M^+ - H_2O - 42 - 17\beta$-sidechain).

Anal. Calcd. for $C_{28}H_{48}O$: C, 83.93; H, 12.07. Found: C, 84.27; H, 12.10.

In some experiments the alcohol **2a** could be crystallized from acetone directly from the crude reaction mixture in 50% yield.

Cholesterol (**1a**), cholesteryl acetate (**1e**), *epi*-cholesteryl acetate (**1f**), cholest-5-ene-3-one ethylene acetal (**1c**), and 3α-methoxy-5-cholestene (**1d**) were treated separately with the Simmons–Smith reagent as described for *epi*-cholesterol (**1b**), starting materials were recovered in high yields (identified by mixed m.p. and i.r.). Spectroscopic examination (i.r., p.m.r.) of the mother liquor gave no indication of cyclopropyl C—H absorption. The t.l.c. did not indicate any of the expected methylene addition products.

A similar result was obtained when cholesteryl acetate (**1e**) was treated as above with the reagent for 18 h at 75°.

Cholesteryl acetate (**1e**) (1.5 g) was subjected to Simmons–Smith reaction under conditions described by Joska *et al.* (20). The crude reaction product showed three major spots on t.l.c. Chromatography on alumina gave on elution with petroleum ether a fraction (586 mg) which on recrystallization from acetone yielded cholesta-3,5-diene, m.p. 78–79°; $[\alpha]_D^{24}$ −56°; i.r. ν_{max} 3020 (vinyl C—H stretching) cm^{-1}; u.v. λ_{max} (hexane): 244 (ε 11 040), 237 (ε 18 700), 229 (ε 15 880) nm; mass spectrum *m/e* 368 (M^+); [lit. (22) m.p. 79–80°; $[\alpha]_D$ ($CHCl_3$) −65°]. The remaining two spots corresponded to starting material and cholesterol. Elution with benzene–ether–methanol (15:4:1, v/v) gave cholesterol (**1a**) (315 mg) identified by mixed m.p. and i.r.

5,6α-Cyclopropano-5α-cholestan-3α-yl Acetate (2c)

3α-Hydroxy-5,6α-cyclopropano-5α-cholestane (**2a**) (142 mg) was acetylated in pyridine acetic anhydride (2:1) overnight at room temperature. Recrystallization from methanol afforded the acetate **2c** (125 mg); m.p. 133°; $[\alpha]_D$ −44°; i.r. (KBr) ν_{max} 3050 (cyclopropyl C—H stretching), 1730 (acetate carbonyl stretching), 1280–1180

Can. J. Chem. Downloaded from www.nrcresearchpress.com by 210.87.254.40 on 09/05/12
For personal use only.

(acetate C—O stretching) cm^{-1}, p.m.r. δ 5.04 (1H, triplet, J = 2.7 Hz, half band width, 7 Hz, 3-equatorial proton), 2.00 (s, acetate methyl protons), 1.06 (s, C-19 methyl), 0.62 (s, C-18 methyl), 0.40–0.46, (m, 2H, cyclopropyl protons) p.p.m.; mass spectrum, weak peaks at 442 (M^+) and 287 ($M^+ - 42 - 17\beta$-sidechain), strong peaks at 382 ($M^+ -$ HOAc), moderately strong peaks at *m/e* 227 ($M^+ -$ HOAc $- 42 - 17\beta$-sidechain).

Anal. Calcd. for $C_{30}H_{50}O_2$: C, 81.02; H, 11.79. Found: C, 81.13; H, 11.52.

5,6α-Cyclopropano-5α-cholestan-3-one (3a)

3α-Hydroxy-5,6α-cyclopropano-5α-cholestane (**2***a*) (2.35 g) was dissolved in acetone (250 ml) and oxidized with Jones reagent (14). The crude product showed one faster spot on t.l.c. Recrystallization from methanol afforded 2.2 g; m.p. 144°; $[\alpha]_D$ −10°; i.r. ν_{max} 3050 (cyclopropyl C—H stretching), 1715 (carbonyl stretching) cm^{-1}; p.m.r. δ 3.15, 3.17 (pair of doublets, J = 1 and 16 Hz, C-4 methylene hydrogen), 1.28 (C-19 methyl), 0.65 (C-18 methyl), 0.32, 0.18 (unresolved multiplet, 2H, cyclopropyl hydrogens) p.p.m.; mass spectrum, strong peak at *m/e* 398 (M^+), moderately strong signal at *m/e* 243 ($M^+ - 42 - 17\beta$-sidechain).

Anal. Calcd. for $C_{28}H_{46}O$: C, 84.35; H, 11.63. Found: C, 84.46; H, 11.94.

6α-Methyl-4-cholestan-3-one

5,6α-Cyclopropano-5α-cholestan-3-one (**3***a*) (260 mg) was treated with glacial acetic acid (26 ml) containing 60% w/v perchloric acid (3 ml) for 15 min at 100°. The reaction was poured into water and extracted with ether. The crude product (264 mg) was recrystallized from methanol (140 mg), m.p. 125–126°; $[\alpha]_D^{23}$ (dioxane) +61°; i.r. ν_{max} (KBr) 1675, 1630 (conjugated carbonyl stretching) cm^{-1}; u.v. λ_{max} (hexane) 231 nm (ε 15 100); [lit. (15) m.p. 127°; $[\alpha]_D$ +60°; λ_{max} (EtOH) 241 nm (ε 16 650)].

3β-Hydroxy-5,6α-cyclopropano-5α-cholestane (4a)

5,6α-Cyclopropano-5α-cholestan-3-one (**3***a*) (800 mg) and lithium tri-*t*-butoxyaluminum hydride (560 mg) in dry ether (80 ml) were stirred at room temperature for 20 h. The reaction was poured into saturated ammonium chloride and extracted with ether. The crude residue showed three spots on t.l.c. which after column chromatography on alumina were separated. Elution with 20–40% benzene – petroleum ether gave starting material (195 mg); mixed m.p. 144°; identical i.r. spectrum with **3***a*.

Elution with 50–100% benzene – petroleum ether gave 3α-hydroxy-5,6α-cyclopropano-5α-cholestane (**2***a*) (88 mg); mixed m.p. 120–121°; i.r. spectrum was identical to the previous compound.

Elution with 2–15% ethyl acetate – benzene gave 3β-hydroxy-5,6α-cyclopropano-5α-cholestane (**4***a*) (500 mg). Recrystallization from petroleum ether yielded needles (458 mg); m.p. 155–156°; $[\alpha]_D$ −52°; i.r. ν_{max} 3600 (free OH stretching), 3050 (cyclopropyl C—H stretching) cm^{-1}; p.m.r. δ 3.70 (m, 1H, half band width, 21 Hz, 3-axial proton), 1.16 (C-19 methyl), 0.60 (C-18 methyl), 0–0.47 (m, 3H, cyclopropyl protons) p.p.m.; mass spectrum, strong signals at *m/e* 329, moderately strong peaks at 400 (M^+), 245 ($M^+ - 42 - 17\beta$-sidechain) and 227 ($M^+ - H_2O - 42 - 17\beta$-sidechain).

Anal. Calcd. for $C_{28}H_{48}O$: C, 83.93; H, 12.07. Found: C, 83.85; H, 11.96.

5,6α-Cyclopropano-5α-cholestan-3β-yl Acetate

3β-Hydroxy-5,6α-cyclopropano-5α-cholestane (**4***a*) (250 mg) was acetylated in dry pyridine – acetic anhydride by the same method as compound **2***a*. Crude product showed a single spot on t.l.c. Recrystallizations from methanol yielded the acetate **4***b* (250 mg), m.p. 117–118°; $[\alpha]_D$ −53°; i.r. ν_{max} 3050 (cyclopropyl C—H stretching), 1730 (acetate carbonyl stretching), 1230 (acetate C—O stretching) cm^{-1}; p.m.r. δ 4.84 (1H, half band width 23 Hz, 3-axial proton), 2.00 (3H, s, acetate methyl protons), 1.12 (C-19 methyl), 0.62 (C-18 methyl), 0.36 (m, cyclopropyl protons) p.p.m.; mass spectrum, strong peak at *m/e* 382 ($M^+ -$ HOAc), moderately strong signals at 287 ($M^+ - 42 - 17\beta$-sidechain), 227 ($M^+ -$ HOAc $- 42 - 17\beta$-sidechain), and a weak parent peak at 442 (M^+).

Anal. Calcd. for $C_{30}H_{50}O_2$: C, 81.02; H, 11.79. Found: C, 81.09; H, 11.81.

5,6α-Cyclopropano-5α-cholestan-3-one Ethylene Acetal (3b)

The ketone (**3***a*) (300 mg) was added to a mixture of benzene (50 ml) and ethylene glycol (1 ml), and refluxed for 40 min with a Dean–Stark apparatus. *p*-Toluenesulfonic acid monohydrate (2 mg) was added, and refluxing continued for a further 3 h. The resulting mixture was washed with excess saturated sodium bicarbonate solution and water. The benzene solution was filtered through anhydrous sodium sulfate and evaporated. The crude reaction product (328 mg) showed a single spot on t.l.c. Recrystallization from methanol gave **3***b* (300 mg), m.p. 117–118°; $[\alpha]_D$ −50°; i.r. ν_{max} 3070 (cyclopropyl C—H stretching), 1090 (C—O stretching) cm^{-1} p.m.r. δ 3.76 (4H, s, ethylene acetal protons), 1.09 (C-19 methyl protons), 0.62 (C-18 methyl protons), 0.36–0.45 (m, cyclopropyl protons) p.p.m.; mass spectrum, strong peak at *m/e* 99, moderately strong signal at *m/e* 442 (M^+) and a weak signal at *m/e* 343 ($M^+ - 99$).

Anal. Calcd. for $C_{30}H_{50}O_2$: C, 81.45; H, 11.31. Found: C, 81.69; H, 11.21.

We wish to thank Dr. D. R. Dalton, Chemistry Department, Temple University, Philadelphia, Pennsylvania for helpful comments on the manuscript. We also thank Miss Marylin Calman and Mrs. Helga Block of the Faculty of Pharmacy for their technical assistance. Financial assistance from the Faculty of Graduate Studies, Research Board, University of Manitoba, is gratefully acknowledged.

1. H. E. Simmons and R. D. Smith. J. Am. Chem. Soc. **80**, 5323 (1958).
2. H. E. Simmons and R. D. Smith. J. Am. Chem. Soc. **81**, 4256 (1959).
3. E. P. Blanchard and H. E. Simmons. J. Am. Chem. Soc. **86**, 1337 (1964).
4. H. E. Simmons, E. P. Blanchard, and R. D. Smith. J. Am. Chem. Soc. **86**, 1347 (1964).
5. G. Wittig and K. Schwarzenbach. Agnew. Chem. **73**, 27 (1961).

6. S. WINSTEIN, J. SONNENBERG, and L. DEVRIES. J. Am. Chem. Soc. **81**, 6523 (1959).
7. W. G. DAUBSEN and G. H. BEREZIN. J. Am. Chem. Soc. **85**, 468 (1963).
8. C. D. POULTER, E. C. FRIEDRICH, and S. WINSTEIN. J. Am. Chem. Soc. **91**, 6892 (1969).
9. J. H. H. CHAN and B. RICKBORN. J. Am. Chem. Soc. **90**, 6406 (1968).
10. A. HASSNER and C. HEATHCOCK. J. Org. Chem. **29**, 1350 (1964).
11. R. GINSIG and A. D. CROSS. J. Am. Chem. Soc. **87**, 4629 (1965).
12. R. REES, D. P. STRIKE, and H. SMITH. J. Med. Chem. **10**, 783.
13. R. C. COOKSON, D. P. G. HAMON, and J. HUDEC. J. Chem. Soc. 5782 (1963).
14. K. BOWDEN, I. M. HEILBRON, E. R. H. JONES, and B. C. L. WEEDON. J. Chem. Soc. 39 (1946).
15. R. B. TURNER. J. Am. Chem. Soc. **74**, 5362 (1952).
16. H. C. BROWN and C. J. SHOAF. J. Am. Chem. Soc. **86**, 1079 (1964).
17. Z. MAJERSKI and P. R. SCHLEYER. J. Org. Chem. **34**, 3215 (1969).
18. P. BROWN, C. DJERASSI, G. SCHROLL, H. J. JAKOBSEN, and S. O. LAWESSON. J. Am. Chem. Soc. **87**, 4559 (1965).
19. E. S. WAIGHT, J. E. HERZ, and Y. SANTOYO. Org. Mass Spectrom. **5**, 359 (1971).
20. J. JOSKA, J. FAJKOS, and F. SORM. Coll. Czech. Chem. Commun. **33**, 2049 (1968).
21. B. RICKBORN and J. H. H. CHAN. J. Org. Chem. **32**, 3576 (1967).
22. A. E. SOBEL and M. J. ROSEN. J. Am. Chem. Soc. **63**, 3536 (1941).
23. J. WEINMAN and S. WEINMAN. Steroids, **6**, 683 (1965).
24. E. LEGOFF. J. Org. Chem. **29**, 2048 (1964).

Can. J. Chem. Downloaded from www.nrcresearchpress.com by 210.87.254.40 on 09/05/12
For personal use only.

Can. J. Chem. Downloaded from www.nrcresearchpress.com by 210.87.254.40 on 09/05/12
For personal use only.

Autoxidation of 2,3-Dialkylindoles

STEWART MCLEAN AND G. I. DMITRIENKO
Department of Chemistry, University of Toronto, Toronto, Ontario

Received June 28, 1971

Autoxidation of 2,3-dimethylindole leads to the formation of an oxidized dimer **6***a*, and 2-methyl-3-ethylindole gives rise to the corresponding product **6***c* under the same conditions. In contrast, 2-ethyl-3-methylindole resembles 2,3-diethylindole in behavior and forms 2-acetyl-3-methylindole via the 3-hydroperoxyindolenine, which is an isolable intermediate. Some of the side reactions which occur under autoxidative conditions have been studied, and an attempt has been made to give a satisfactory unified rationalization of our results and those obtained for related autoxidations by numerous other workers.

L'autoxydation du diméthyl-2,3 indole conduit à la formation d'un dimère oxydé **6***a* et celle du méthyl-2 éthyl-3 indole conduit, sous les mêmes conditions, au produit correspondant **6***c*. Au contraire, l'éthyl-2 méthyl-3 indole ressemble par son comportement au diéthyl-2,3 indole et conduit à l'acétyl-2 méthyl-3 indole via l'hydroperoxy-3 indolénine qui est un intermédiaire isolable. Certaines réactions secondaires qui se font sous les conditions de l'autoxydation ont également été étudiées. Ces résultats, ainsi que ceux d'autres auteurs concernant des réactions d'autoxydation analogues ont été rationalisés d'une façon satisfaisante.

Canadian Journal of Chemistry, 49, 3642 (1971)

The autoxidation of indoles and related oxidations by peroxy compounds have led to results of chemical interest and biochemical significance. The oxidation of 2,3-disubstituted indoles (**1**) has led to a variety of products, the nature of which has been shown to depend on the reaction conditions and the nature of the substituents (1–7). Isolable products from the autoxidation of compounds of general formula **1** have included 3-hydroperoxyindolenines (**2**), 3-hydroxyindolenines (**3**), compounds (**4**) in which the substituent at C-2 has been oxidized (corresponding products have been obtained from indoles carrying a heteroatom at C-2), and compounds (**5**) in which the heterocyclic ring has been opened oxidatively, as well as rearrangement, condensation, or cleavage products derived from these. It is widely accepted that a common reaction pathway starts with the conversion of the indole (**1**) to the 3-hydroperoxyindolenine (**2**), frequently isolable, which then leads on to the other products listed; there is, however, a considerable range of opinion about the details of the latter steps.

In 1954 Beer *et al.* (1*a*) showed that the simplest dialkylindole of this class, 2,3-dimethylindole (**1***a*), on autoxidation formed the hydroperoxide (**2***a*) and a second non-peroxidic product of higher molecular weight. Leete (2*a*) reported that the corresponding hydroperoxy derivative (**2***b*) could be obtained from 2,3-diethylindole (**1***b*) under specified autoxidation conditions, while 2-acetyl-3-ethylindole (**4***b*) was isolated under other conditions. Since **2***b* could be converted to **4***b* thermally it was implicated as an intermediate, and an intramolecular mechanism for this conversion, requiring a cyclic or quasi-cyclic intermediate, was proposed. He noted that, in contrast, the dimethyl analog **2***a* failed to undergo the corresponding reaction. This interpretation was criticized by Taylor (2*b*) who pointed out that the transformation represented a special case of a family of reactions in which a substituent at C-3 in an enamine tautomer (such as **2′**) was displaced by an external nucleophile. (In this proposal, although the enamine tautomer was a key intermediate, it was invoked only to effect allylic activation at C-3.) He showed, furthermore, that a small amount of the aldehyde **4***a* could, in fact, be isolated in the dimethyl case; it followed that the same pathway was, therefore, open in the dimethyl series as in the diethyl series, but the enamine tautomer was less readily formed in the former case since it lacked the stabilization of an alkyl substituent. An alternative mechanism proposed by Wasserman and Floyd (3) also required the enamine intermediate, but utilized its nucleophilic character to attack the hydroperoxy substituent intramolecularly.

Our interest in this area was aroused when we observed that a sample of 2,3-dimethylindole

Can. J. Chem. Downloaded from www.nrcresearchpress.com by 210.87.254.40 on 09/05/12
For personal use only.

(**1***a*) which had been stored in air for some time had become contaminated with a considerable amount of an impurity which, on isolation and purification, appeared to be the non-peroxidic autoxidation product originally described by Beer *et al.* (1*a*). From its analysis, mass spectrum, and other spectroscopic characteristics, which have now been described in detail elsewhere (1), we concluded that the product corresponded in composition to two molecules of **1***a* plus two oxygen atoms, that it was a bisindoline in which one methyl group of the original four had become a methylene bridge, the remaining three being tertiary in the product, and that two NH groups and one OH group were present, the second oxygen being, therefore, disubstituted and probably part of a bridge. These data strongly suggested that the product had structure **6***a* (without the stereochemical implications represented), but other structural possibilities could be envisaged and the stereochemistry was by no means established. Although the recent work of Dave and Warnhoff (1*d*) shows that our pessimism was unwarranted, we originally considered that it would be difficult, if not impossible, to establish unequivocally the structure and stereochemistry of this molecule on chemical and spectroscopic grounds since we expected it to be particularly susceptible to rearrangement. We turned, therefore, to X-ray analysis and, with the collaboration of our colleagues in crystallography, established the total structure **6***a* by direct methods which dispensed with the necessity of preparing a heavy atom derivative or perturbing the molecule in any way (1*c*).

One observation, which, as we noted in our preliminary communication (1*c*), caused us some concern, was that the n.m.r. signal for the bridge methylene protons was a singlet in a variety of solvents and at a range of temperatures when determined at 60 or 100 MHz; even the addition of tris(dipivalomethanato)europium did not cause the signal to split.[1] We can now report, however, that at 220 MHz the protons do appear as an AB pattern with a coupling constant of 13 Hz, but even here the internal chemical shift is only 6.5 Hz, and as a consequence the multiplet is near the practical limits of resolution.

It is abundantly clear that **6***a* results from a reaction sequence quite different from any followed by 2,3-diethylindole, and there is good evidence to suggest that the difference can be attributed to the presence of a 2-methyl substituent in the precursor **1***a*. In order to probe the generality of the proposal that the autoxidation of 2,3-dialkylindoles follows a distinctive pathway when the substituent at C-2 is a methyl rather than an ethyl or other alkyl group, we have studied the behavior of the isomers 2-methyl-3-ethylindole (**1***c*) and 2-ethyl-3-methylindole (**1***d*).

When a solution of **1***c* in benzene was stirred in air, **1***c* slowly underwent autoxidation to afford a single isolable product which we have identified as **6***c*, the analog of the dimeric product, **6***a*, obtained on autoxidation of 2,3-dimethylindole. The i.r. and u.v. spectra of **6***c*, $C_{22}H_{26}N_2O_2$, m.p. 157–160°, were very similar to those of **6***a*, and the n.m.r. spectra differed in the manner expected: seven aromatic protons of **6***c* appear as a complex pattern between τ 2.6 and 3.3 and one is more highly shielded, appearing as a doublet, $J \simeq 8$ Hz (with further fine splitting), at τ 3.63, the unsplit methyl signal is at τ 8.60, the methylene protons show an extremely close correspondence to those of **6***a*, appearing in the 100 MHz spectrum as a singlet at τ 7.62, and the protons of the ethyl groups appear as two three-proton triplets, each with $J \simeq 8$ Hz, at τ 8.90 and 9.09 and a complex pattern, corresponding to four protons in the region τ 7.8 to 8.5, recognizable as two overlapping methylene quartets which have been further split because of the diastereotopic relationship between each pair of protons.

In contrast, the 2-ethyl-3-methyl isomer **1***d* as a solution in benzene appeared to undergo autoxidation more rapidly than **1***c* under the same conditions and afforded in good yield a product identified as the hydroperoxy derivative **2***d*. The compound, $C_{11}H_{13}NO_2$, m.p. 109–111°, showed the spectroscopic characteristics appropriate for its structure and the expected close correspondence to the values reported for **2***b* (2*a*). In ethyl acetate containing acetic acid **2***d* was transformed into 2-acetyl-3-methylindole (**4***d*), a reaction completely analogous to that of 2,3-diethylindole (**2***a*). When the hydroperoxy compound **2***d* was first reduced to the hydroxyindolenine **3***d* and this compound was subjected to further autoxidation, we isolated 3-methyl-3-

[1]We thank Dr. Marie L. Roy for this determination.

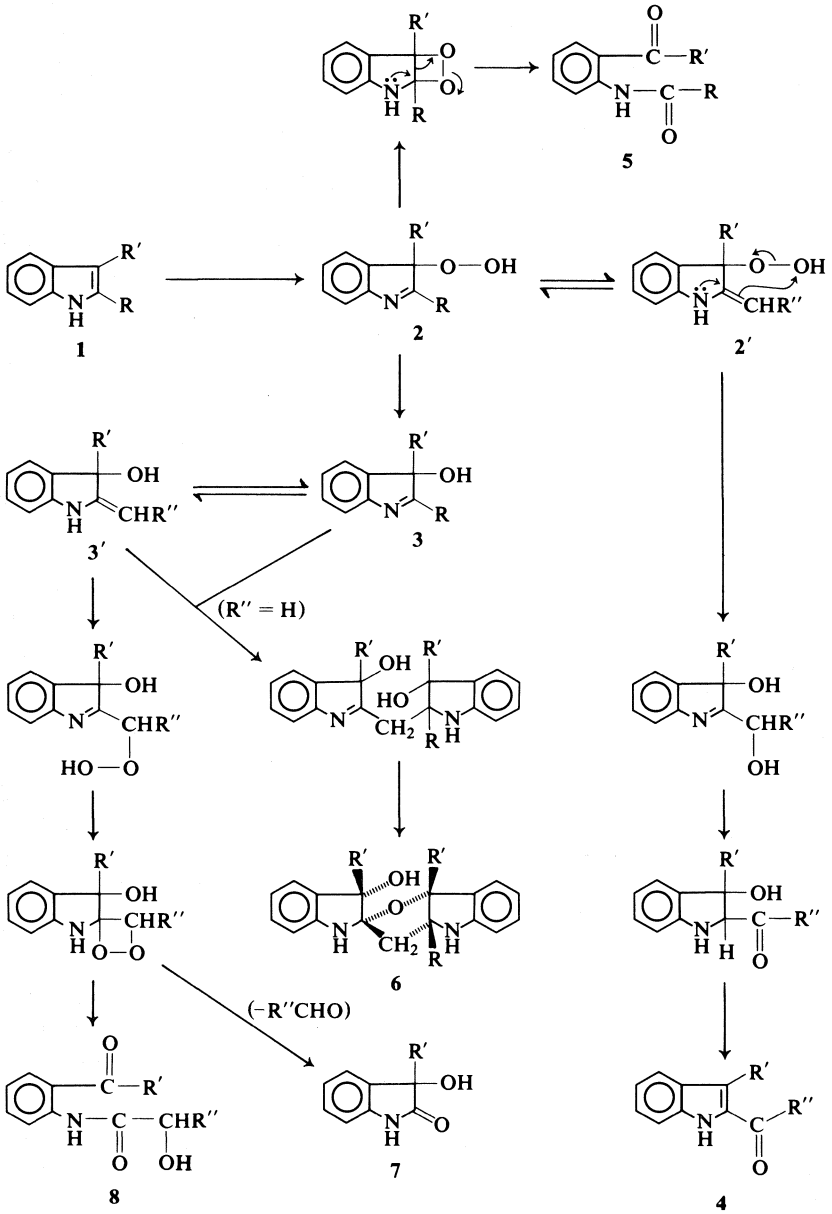

	R	R′	R″
a	Me	Me	H
b	Et	Et	Me
c	Me	Et	H
d	Et	Me	Me

CHART 1

Can. J. Chem. Downloaded from www.nrcresearchpress.com by 210.87.254.40 on 09/05/12
For personal use only.

Can. J. Chem. Downloaded from www.nrcresearchpress.com by 210.87.254.40 on 09/05/12
For personal use only.

hydroxyoxindole (**7***d*), a product obtained previously by Wasserman and Floyd (3) from the autoxidation of 2-isopropyl-3-methylindole. Our present result shows that **7***d* is formed from **3***d* rather than directly from the hydroperoxy compound **2***d*, and arises from a further, and essentially independent autoxidation reaction.

It is clear that the autoxidation of 2,3-dialkylindoles leads to a diverse array of products, the outcome of any specific oxidation being strongly dependent on variables related to structure and reaction conditions. Nevertheless, we believe that it is now possible to account for all of the observed products in a unified manner and in mechanistic terms which consistently assign nucleophilic character to enamines and electrophilic character to the carbon atom of imines (see Chart 1). There appears to be little doubt that the 3-hydroperoxy compound **2** is the initial product in all of these autoxidations and is the key intermediate leading to all observed products; it clearly arises by electrophilic attack of oxygen on the "enamine" **1**. A reaction that may ensue is the reduction of the hydroperoxy group to the hydroxy group of **3**, perhaps coupled with oxidation of a molecule of **1** to afford a further molecule of **3**. Products of formula **4** can be satisfactorily accounted for in the manner proposed by Wasserman and Floyd (3); this requires the formation of the enamine tautomer (**2′**) of **2**, followed by intramolecular electrophilic attack of the terminal oxygen of the hydroperoxy group on the enamine, leading to transfer of a hydroxyl group, and then tautomerism and dehydration as shown. Products of formula **5**, which are commonly found as reaction products, particularly when an acid catalyst is present, are best explained by the intramolecular nucleophilic attack of the terminal oxygen of the hydroperoxy group of **2** on the imine function (perhaps protonated), leading to the peroxide shown which can then open, with the assistance of the electrons on nitrogen, to afford **5**. (It is worth noting that the O—O bond of a peroxide, besides being able to break homolytically, may cleave heterolytically in either direction and the terminal oxygen of a hydroperoxy group may be either electrophilic or nucleophilic.) On the basis of the evidence we presented earlier, the formation of products of formula **7** is explained as resulting from the further autoxidation of **3**, the reduction product of **2**, by electrophilic attack of oxygen on its enamine tautomer **3′** leading to the hydroperoxy intermediate which then undergoes cyclization and cleavage in the manner shown, a sequence which is the complete analog of that leading to **5**. This route is different in detail from the one proposed by Wasserman and Floyd (3), but is consistent with the pattern of behavior we have described for other reactions in this series and provides a ready explanation for the isolation of compounds of type **8** reported by these authors if it is supposed **7** and **8** arise from a common peroxide intermediate which is cleaved in the first case with the assistance of electrons on nitrogen, and in the second case, leading to **8**, with the assistance of electrons on the 3-hydroxy function. It may be noted further that intermolecular electrophilic attack at the exocyclic double bond of an enamine such as **2′** or **3′** is, of course, a route that is always open (6), but in compounds of formula **1** the indole is effectively the exclusive "enamine" tautomer available and reaction occurs at C-3, and when the hydroperoxy function is present as in **2′**, intramolecular attack, transferring a *hydroxyl* group to the enamine is the preferred reaction mode (and leads on to **4**). It is when neither of the latter situations prevails, as is the case in **3**, that intermolecular electrophilic attack on the C-2 substituent becomes a significant reaction, leading to the introduction of a *hydroperoxy* function in the present case, and to the sequence of reactions which afford **7** and **8**. The obvious and generally accepted route to dimeric products of form **6** requires the coupling of tautomers **3** and **3′**, utilizing the nucleophilic character of the latter, followed by intramolecular nucleophilic attack by a hydroxyl group on the imine function (possibly protonated) formed in the intermediate. As written, this sequence implies the initial reduction of **2** to **3**, but the chronology is not obligatory since the corresponding coupling between the tautomers **2** and **2′** could occur first and be followed by the reduction and cyclization steps. Dave and Warnhoff (1*d*) have reported results which suggest that the route requiring initial reduction of **2** is favored, but do not establish this point conclusively. In any event, there is no evidence for the formation of dimeric products of type **6** except when the

Can. J. Chem. Downloaded from www.nrcresearchpress.com by 210.87.254.40 on 09/05/12
For personal use only.

2-substituent is methyl. Previous explanations for the difference between the autoxidation behavior of 2,3-dialkylindoles (**1**) where the 2-substituent is methyl and that of analogs where the 2-substituent is some other alkyl moiety, although they have differed in mechanistic details, have all depended on assumptions regarding the relative readiness with which intermediates such as **2** and **3** form their enamine tautomers. The above discussion suggests that these explanations must be at best incomplete since at least some enamine tautomer must be present to generate **6**. The more attractive explanation that presents itself in the light of all of the above evidence is that the bimolecular coupling process is inhibited when the substituent (R) on the imine is larger than methyl and the substituent (R″) on the enamine is consequently larger than hydrogen. As a result, alternative pathways, particularly those resulting from intramolecular processes, prevail when the 2-substituent in **1** is larger than methyl, and only 2-methyl derivatives lead to dimeric products of type **6**.

We believe that the course of all of the reactions within the category we have been concerned with can now be accounted for with the minimum of mechanistic assumptions. It is clear that other reaction pathways may also be available in specific cases, and that the products we have described may themselves be subject to further autoxidation, one illustration being provided in the very recent work of Dave and Warnhoff (1*d*).

Experimental

Melting points were determined on a Thomas–Kofler micro hot stage. Spectrometers used routinely were: a Perkin–Elmer Model 237B for i.r. spectra (carbon tetrachloride solvent unless otherwise indicated) and the wavelengths (in μ) of significant peaks are reported; a Unicam SP. 800 for u.v. spectra (methanol solvent) and wavelengths (in mμ) of absorption bands are reported, followed by the extinction coefficient (ε) in parentheses; a Varian HA-100, A-60, or T-60 for n.m.r. spectra (chloroform-*d* solvent unless otherwise indicated) and chemical shifts are reported on the τ scale, followed in parentheses by an account of the multiplicity and number of protons concerned; a CEC 21-490 for mass spectra and the *m/e* values of significant peaks are reported, followed in parentheses by their relative intensities. An AEI MS-902 mass spectrometer was used to make accurate mass measurements. The 220 MHz spectrum was recorded on the Varian HR-220 at the Canadian 220 MHz N.M.R. Center.

Autoxidation of 2-Methyl-3-ethylindole (1c)

The preparation of 2-methyl-3-ethylindole was based on the method of Pikl and Julian (8*a*): the phenylhydrazone of 2-pentanone was heated with a catalytic amount (*ca.* 1%) of cuprous chloride at 180–200° for 4 h, and 2-methyl-3-ethylindole was obtained as an oil (in 22% yield from 2-pentanone) by vacuum distillation of the reaction mixture. It showed: i.r. ($CHCl_3$) 2.89; n.m.r. 2.20–3.05 (complex; 5), 7.28 (q, J = 7 Hz; 2), 7.73 (s; 3), 8.80 (t, J = 7 Hz; 3). Picrate m.p. 154–157° (lit. (8*b*) m.p. 148–150°).

A 4% solution of 2-methyl-3-ethylindole in benzene was stirred in an open beaker and fresh solvent was added periodically to keep the volume approximately constant. After 1 week the product was precipitated as a white powder by the addition of petroleum ether; the yield corresponded to about 13% conversion and the mother liquor contained principally unchanged **2***c*. The product, **6***c*, was recrystallized three times from a benzene–hexane solution and obtained as colorless prisms, m.p. 157–160° (prior sublimation).

Anal. Calcd. for $C_{22}H_{20}N_2O_2$: C, 75.40; H, 7.48; N, 7.99. Found: C, 75.11; H, 7.60; N, 8.08.

Mass spectrum: 350 (8), 332 (1), 191 (4), 160 (32), 159 (100), 144 (38); i.r. 2.80, 2.94, 6.20; u.v. 244 (14 500), 297 (4300); n.m.r. 2.6–3.3 (complex; 7), 3.63 (d, $J \simeq 8$ Hz, with further fine splitting; 1), 6.72 (s; 1), 7.62 (s; 2), 7.8–8.5 (complex; apparently two overlapping quartets, $J \simeq 8$ Hz, with further splitting; 4), 8.60 (s; 3), 8.90 (t, J = 8 Hz; 3), 9.09 (t, J = 8 Hz; 3).

Autoxidation of 2-Ethyl-3-methylindole (1d)

2-Ethyl-3-methylindole was prepared by a method similar to that described for **1***c*: the phenylhydrazone of 3-pentanone was heated under nitrogen with a catalytic amount of cuprous chloride to 100–140° for 3 days and the reaction mixture was vacuum distilled. After recrystallization from 60–70° petroleum ether, the product (**1***d*) was obtained in 50% yield as crystals m.p. 64–68° (lit. (9) m.p. 66°); i.r. 2.87; n.m.r. 2.20–3.10 (complex; 5), 7.26 (q, J = 7 Hz; 2), 7.78 (s; 3), 8.78 (t, J = 7 Hz; 3).

A 1% solution of 2-ethyl-3-methylindole in benzene was stirred in the manner described above. After 1 day the solid (corresponding to 70% conversion) which had precipitated was collected on a filter, washed, and dried. This material, m.p. 109–111° after recrystallization from acetone, was identified as 2-ethyl-3-hydroperoxy-3-methylindolenine (**2***d*); mass spectrum: 191 (38), 173 (100); u.v. 219 (17 000), 225 (inflection; 12 500), 259 (3300).

Anal. Calcd. for $C_{11}H_{13}NO_2$: C, 69.09; H, 6.85; N, 7.33. Found: C, 69.16; H, 6.84; N, 7.25.

A 1% solution of **2***d* in 20 ml ethyl acetate containing 2 ml acetic acid was kept in the absence of air for 2 days. Solvent was removed under reduced pressure and the brown residue was dissolved in methylene chloride and washed free of acetic acid. The solid obtained from the methylene chloride was chromatographed on a column of neutral alumina and eluted with benzene. This afforded a crystalline product (yield corresponding to 45% conversion), which was recrystallized from benzene and obtained as colorless needles, m.p. 150–152°, identified

as 2-acetyl-3-methylindole (lit. (10) m.p. 146.5°); i.r. 2.89, 6.05; u.v. 237 (15 000), 310 (19 500); n.m.r. 0.77 (broad; 1), 2.1–3.0 (complex; 4), 7.40 (s; 6; in presence of benzene this signal moved upfield and split into two singlets of equal intensity).

*Autoxidation of 2-Ethyl-3-hydroxy-3-methylindole (**3d**)*

2-Ethyl-3-hydroxy-3-methylindole was prepared by shaking an ethereal solution of the hydroperoxy compound **2***d* (1.00 g) with a solution of sodium hydrosulfite (2.6 g) in 30 ml of 10% aqueous sodium hydroxide for 50 min. Evaporation of the ether layer afforded a yellow solid (0.71 g) which, after two recrystallizations from acetone–hexane, formed colorless needles, m.p. 79–83°; i.r. 2.77, 3.15 (weak); u.v. 219 (19 000), 224 (inflection), 256 (3600); n.m.r. 2.3–3.0 (m; 4), 6.35 (broad; 1), 7.53 (q, J = 7 Hz; 2), 8.53 (s; 3), 8.83 (t, J = 7 Hz; 3); the high resolution mass spectrum showed the molecular ion of mass 175.0996 (Calcd. for $C_{11}H_{13}NO$: 175.0997), but combustion analysis gave poor and unreproducible results, the best of which was:

Anal. Calcd. for $C_{11}H_{13}NO$: C, 75.40; H, 7.48; N, 7.99. Found: C, 75.76; H, 7.04; N, 8.04.

A solution of 2-ethyl-3-hydroxy-3-methylindolenine (0.25 g) in 200 ml of benzene was stirred in an open beaker for 36 h. After a small amount of amorphous precipitate had been removed by filtration, evaporation of the benzene left a brown tar from which 3-hydroxy-3-methyloxindole (**7***d*) (40 mg; 18%), m.p. 159–165° (lit. m.p. 161.5–162.5° (3); 163–165° (11)), was recovered by crystallization from benzene and recrystallization from benzene–acetone; i.r. ($CHCl_3$) 2.80, 2.91, 5.78; u.v. 252 (6000), 286 (1350); n.m.r. (acetone-d_6) 2.5–3.3 (complex; 4), 8.53 (s; 3).

We thank the National Research Council of Canada for an operating grant in support of this research and for a scholarship (to G.I.D.).

1. (*a*) R. J. S. Beer, T. Donavanik, and A. Robertson. J. Chem. Soc. 4139 (1954). (*b*) G. Berti, A. Da Settimo, G. Di Colo, and A. Nannipieri. J. Chem. Soc. C, 2703 (1969). (*c*) S. McLean, E. K. Strøm-Gundersen, K. S. Dichmann, J. K. Fawcett, and S. C. Nyburg. Tetrahedron Lett. 2645 (1970). (*d*) V. Dave and E. W. Warnhoff. Can. J. Chem. **49**, 1911, 1921 (1971).
2. (*a*) E. Leete. J. Am. Chem. Soc. **83**, 3645 (1961). (*b*) W. I. Taylor. Proc. Chem. Soc. 247 (1962).
3. H. H. Wasserman and M. B. Floyd. Tetrahedron Lett. 2009 (1963).
4. B. Witkop, J. B. Patrick, and M. Rosenblum. J. Am. Chem. Soc. **73**, 2641 (1951).
5. (*a*) E. Leete and F. Chen. Tetrahedron Lett. 2013 (1963). (*b*) S. Ghosal and S. K. Dutta. Indian J. Chem. **7**, 135, 1095 (1969).
6. M. Nakagawa, H. Yamaguchi, and T. Hino. Tetrahedron Lett. 4035 (1970).
7. H. I. Kesswani. Can. J. Chem. **48**, 689 (1970).
8. (*a*) J. Pikl and P. L. Julian. Proc. Indiana Acad. Sci. **45**, 145 (1936). (*b*) B. Oddo. Gazz. Chim. Ital. **63**, 239 (1933).
9. G. Plancher. Gazz. Chim. Ital. **28**, 388 (1898).
10. B. Oddo. Gazz. Chim. Ital. **43** II, 190 (1913).
11. B. Mills and K. Schofield. J. Chem. Soc. 5558 (1961).

Can. J. Chem. Downloaded from www.nrcresearchpress.com by 210.87.254.40 on 09/05/12
For personal use only.

Can. J. Chem. Downloaded from www.nrcresearchpress.com by 210.87.254.42 on 09/05/12
For personal use only.

Kinetic Study of the Acetate-catalyzed Aldol Reaction Between Chloral and Alkyl Methyl Ketones

B. C. MENON AND EBERHARD KIEHLMANN
Department of Chemistry, Simon Fraser University, Burnaby 2, British Columbia

Received July 6, 1971

A kinetic study of the acetate-catalyzed crossed aldol reaction of chloral with butanone, 2-heptanone, and 4-methyl-2-pentanone, respectively, in glacial acetic acid at 60° has been carried out. A comparison of the condensation rates with those for the acetate-catalyzed deuterium exchange of the ketones in glacial acetic acid at 60° indicates that the carbon—carbon bond formation in the aldol reaction is the rate-determining step. The relative rate constants for the crossed aldol reaction and the deuterium exchange of the corresponding ketones are best interpreted in terms of steric rather than polar effects.

On a entrepris une étude cinétique de la réaction aldolique catalysée par acétate, du chloral avec la butanone, l'heptanone-2, et la méthyl-4 pentanone-2, respectivement dans l'acide acétique glacial à 60°. Une comparaison des vitesses de condensation avec celles obtenues pour l'échange de deutérium catalysé par acétate des cétones dans l'acide acétique glacial à 60° indique que la formation du lien carbone—carbone dans la réaction aldolique est l'étape déterminante. Les constantes de vitesse relative pour la réaction aldolique et l'échange de deutérium des cétones correspondantes sont mieux interprétées en termes d'effets stériques que polaires.

Canadian Journal of Chemistry, 49, 3648 (1971)

The mechanistic aspects of aldol reactions have been the subject of intensive studies by various investigators. The fundamental studies by Bonhoeffer and Walters (1) and Bell and Smith (2, 3) firmly established the two-step enolization–addition mechanism through kinetic and deuterium exchange experiments with acetaldehyde.

Although the aldol reaction is catalyzed by acids and bases, the latter are more frequently employed. The base-catalyzed mechanism (4–6) may be described by eqs. 1 to 5. For the formation of aldols in concentrated solutions of acetaldehyde (7), propanal (8), and butanal (9), the proton abstraction step 1 is rate-limiting ($k_1 < k_2$). On the other hand, the formation of the new carbon—carbon bond [2] is the rate-limiting step ($k_1 > k_2$) in many aldol reactions involving ketones, for example the ethoxide-catalyzed condensation of aromatic aldehydes with acetophenones (10), the formation of diacetone alcohol from acetone (3), the condensation of benzaldehyde and acetone (11), and the condensation of formaldehyde with acetone (12).

As a continuation of our interest in the crossed aldol reaction between chloral and alkyl methyl ketones in glacial acetic acid – acetate medium (13), we have now carried out a kinetic study of the aldol reaction of chloral with butanone, 2-heptanone, and 4-methyl-2-pentanone, respectively, in glacial acetic acid – acetate medium, as well as the deuteration of these ketones under conditions similar to the aldol reaction. A comparison of these two sets of rate constants should settle, among other things, the question of the rate-limiting step in the crossed aldol reaction.

Experimental

Reagents

The commercially available ketones were purified by fractional distillation. Pure anhydrous chloral (b.p. 98°) was obtained by distillation of commercially available material (Chloral, Practical, MCB) from phosphorus pentoxide (14). Acetic acid-d_4 (minimum isotopic purity 99.5%) was obtained from Mallinckrodt Chemical Works and used without further purification. Anhydrous sodium carbonate was heated to 125° for 20 h and subsequently cooled in a desiccator.

Rate Measurements

Deuterium Exchange

A weighed amount of anhydrous sodium carbonate was placed in a 5.0-ml volumetric flask and dissolved by introducing a small volume of acetic acid-d_4. A weighed amount of the ketone was then added followed by additional acetic acid-d_4 until the volume of the solution reached the calibration point. After thorough shaking, 0.5-ml samples were transferred by syringe to each of a number of 2.0-ml glass ampoules. The ampoules were sealed and placed in a constant-temperature bath at 60 ± 0.1°. Individual ampoules were withdrawn at various time intervals, the reaction was stopped by cooling in ice–water, and the contents of the ampoules were transferred into dry n.m.r. tubes.

[1] 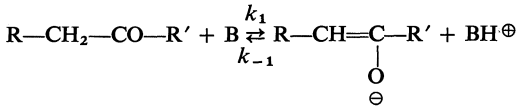

R and R′ = alkyl or aryl

[2] 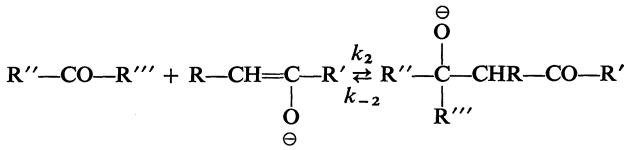

R″ and R‴ = alkyl, aryl or hydrogen

[3] 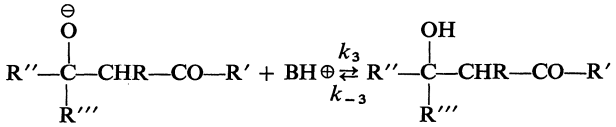

[4] 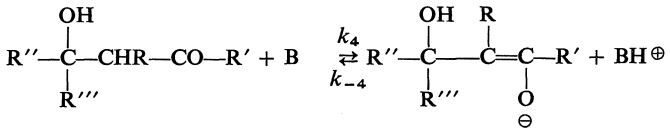

[5] 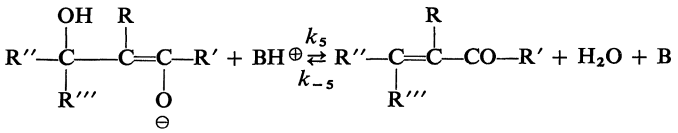

Exchange was followed to approximately one to two half-lives by integrating the proton signals of the reacting sites in question, using the peak areas of the β- or γ-proton signals as internal standard.[1] Each signal was integrated three times and an average was taken. The variation in individual integrations is ±15%, a common observation in this type of rate measurements (15–18).

Aldol Reaction

A weighed amount of anhydrous sodium carbonate was dissolved in a small volume of glacial acetic acid in a 5.0-ml volumetric flask, and known amounts of ketone and chloral were added, followed by more acetic acid until the volume of the solution reached the calibration point. After thorough shaking, 0.5 ml of the solution was transferred by syringe into each of several glass ampoules. The ampoules were sealed and placed in a constant temperature bath at 60 ± 0.1°. Individual ampoules were withdrawn at appropriate time intervals, and the concentration of the ketols formed by condensation at C-1 and -3, respectively, was determined by several integrations of the respective g.l.c. peak areas (SE-52 at 120°) and reference to a calibration curve prepared from pure product samples at known concentrations. As discussed in a previous paper (13), the crossed aldol reaction of chloral with alkyl methyl ketones under these reaction conditions is irreversible and not accompanied by dehydration. Hence the rate of the reaction can be monitored by measuring the concentration of ketol as a function of time.

[1]In the case of 4-methyl-2-pentanone a correction has been made for the partial overlap of the highly split methine signal with both the methylene peak and the α-methyl peak. See ref. 15 for details.

Results and Discussion

Rates of Deuterium Exchange

Pseudo-first-order rate constants were obtained by fitting experimental values to eq. 6 by

[6] $$N_H^t = N_H^0 \, e^{-kt}$$

means of a linear, least-squares program for the IBM 360/50 computer. In eq. 6 N_H^t and N_H^0 represent, respectively, the number of α-hydrogens at a given reacting site at time t and at time zero, relative to the internal standard, the non-exchanging β- or γ-hydrogens. In all cases studied, good fits were obtained for exchanges followed to one or two half-lives (Fig. 1), thereafter the scatter became serious. Table 1 lists the pseudo-first-order rate constants obtained for the acetate-catalyzed deuterium exchange of butanone, 2-heptanone, and 4-methyl-2-penta-

Can. J. Chem. Downloaded from www.nrcresearchpress.com by 210.87.254.42 on 09/05/12
For personal use only.

TABLE 1. Rate data for the deuterium exchange of CH_3COCH_2R, catalyzed by CD_3COONa in CD_3COOD at 60°

R	Concentration of CD_3COONa (M)*	$k_{obsd}^{CH_2}(\times 10^7\ s^{-1})$†	$k_{obsd}^{CH_3}(\times 10^7\ s^{-1})$†
CH_3‡	0.2615	11.70	8.64
	0.5132	18.85§	15.76§
	1.0000	28.00	22.90
$CH_3(CH_2)_3$‖	0.2615	14.87¶	15.31¶
	0.5132	19.84	19.94
	1.0000	28.33	28.86
$(CH_3)_2CH$**	0.2615	7.54	10.50
	0.5283	11.16	18.03
	1.0000	17.90¶	20.31¶

*Stoichiometric concentration.
†Rate constants per hydrogen.
‡[Ketone] = 1.40 M.
§Average of three runs.
‖[Ketone] = 0.87 M.
¶Average of two runs.
**[Ketone] = 1.00 M.

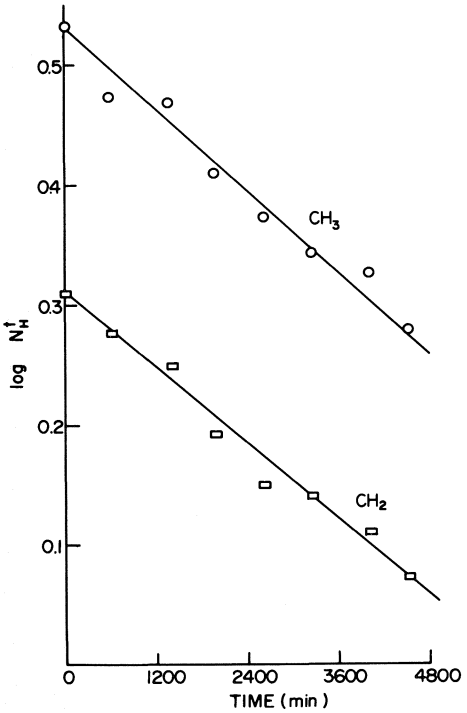

FIG. 1. Kinetics of deuterium exchange of 2-heptanone in CD_3COOD–CD_3COONa at 60°; [CD_3COONa] = 0.5132 M.

none. The rate constants are reproducible with an error of ±7%.

The observed first-order rate constants for all the ketones varied with the acetate concentration according to eq. 7. For all ketones k_0 was substantial, pointing to considerable acid-catalyzed exchange.

$$[7] \qquad k_{obsd} = k_0 + k_{AcO^{\ominus}}(AcO^{\ominus})$$

It is interesting to compare our results on deuterium exchange with those obtained in different solvent/catalyst systems by previous workers. The value of $k^{CH_2}/k^{CH_3} > 1$ for butanone is in line with that obtained by Warkentin and Cox (16) for the acetate-catalyzed deuterium exchange of butanone in aqueous solution. The high reactivity of the methylene protons of butanone has been explained by Warkentin and Barnett (15) as being due to a polar effect which overcomes the steric effect resulting in rate acceleration. For 2-heptanone our $k^{CH_2}/k^{CH_3} \approx 1.00$ is quite different from the value ($k^{CH_2}/k^{CH_3} < 0.3$) reported by Rappe and Sachs (17) for the sodium carbonate-catalyzed deuterium exchange in aqueous solution. A possible explanation for this discrepancy may be that given by Warkentin and Cox (16), who have suggested that the enolization is dependent on the nature of the catalyzing base, in close similarity to bimolecular eliminations in which product ratios have been found to depend on the base employed. The highly diminished reactivity of methylene relative to methyl protons in 4-methyl-2-pentanone is obviously due to a preponderance of steric effects controlling the course of the reaction (18).

As has been stated before, the observed rate constants contain a term due to considerable

Can. J. Chem. Downloaded from www.nrcresearchpress.com by 210.87.254.42 on 09/05/12
For personal use only.

TABLE 2. Rate data for the crossed aldol reaction between CH_3COCH_2R and chloral in acetic acid – acetate at 60°

R	Concentration of CH_3COONa (M)	$k_{obsd}^{CH_2}$($\times 10^4\ M^{-1}\ h^{-1}$)	$k_{obsd}^{CH_3}$($\times 10^4\ M^{-1}\ h^{-1}$)
CH_3*	0.5132	1.96	1.33
$CH_3(CH_2)_3$†	0.5132	0.42	1.97
$(CH_3)_2CH$‡	0.5132	~0	3.41

*[Ketone] = 1.4500 M; [chloral] = 1.2720 M.
†[Ketone] = 0.8722 M; [chloral] = 0.6750 M.
‡[Ketone] = 1.129 M; [chloral] = 0.8202 M.

acid-catalyzed exchange. As reported by Rappe and Sachs (18), the reactivity sequence found for the acid-catalyzed exchange of the methyl protons of methyl alkyl ketones containing various alkyl groups is opposite to that for the base-catalyzed deuteration rates of the corresponding ketones. Consequently, the lack of a pronounced reactivity trend for deuterium exchange in our acetic acid – acetate medium may be due to a partial cancellation of the polar and/or steric effects which are responsible for the reactivity trends observed by Rappe in acidic and basic medium, respectively.

Rates of Aldol Reaction

The experimental data for the acetate-catalyzed crossed aldol reaction between chloral and alkyl methyl ketones were found to fit the second-order rate expression [8] where a, b, and

$$[8] \qquad t = \frac{2.303}{k(a-b)} \log \frac{b(a-x)}{a(b-x)}$$

x are the concentrations in mol/l of ketone, chloral, and ketol, respectively (Fig. 2). The second-order rate constants for the reaction of chloral with butanone, 2-heptanone, and 4-methyl-2-pentanone, respectively, in glacial acetic acid – acetate medium, obtained by fitting the experimental data to eq. 8 by means of a linear least-squares program, are listed in Table 2.

The acetate-catalyzed crossed aldol reactions between chloral and alkyl methyl ketones in glacial acetic acid were found to be very slow and accompanied by discoloration of the reaction mixture on prolonged heating. As a result of these limitations the kinetics were followed to only about 15 to 20% completion of the reaction. Although the absolute uncertainty in rate constants is not known, the rate ratios observed are reliable and give valuable information regarding the orientation of the aldol reaction.

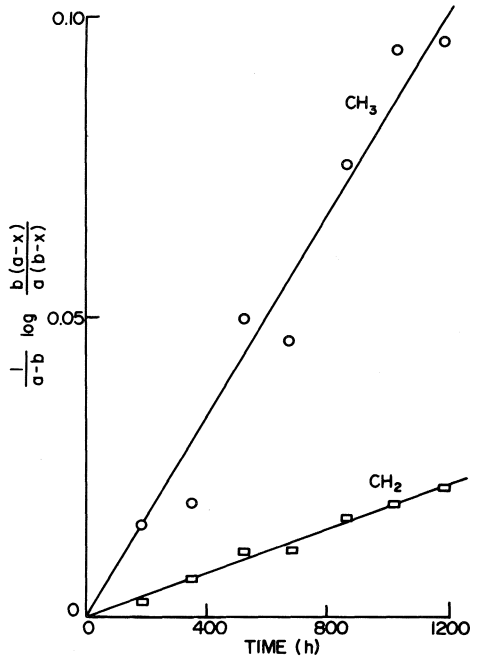

FIG. 2. Kinetics of the crossed aldol reaction of chloral with 2-heptanone in CH_3COOH–CH_3COONa at 60°; [CH_3COONa] = 0.5132 M.

A comparison of the rates of deuteration of the investigated ketones with those of their aldol reactions with chloral under the same conditions of catalyst concentration shows the rates of deuteration, and hence the enolization step, to be much faster than the rates of aldol reaction (Tables 1 and 2). This is a strong indication that the rate-limiting step in these crossed aldol reactions under the conditions employed is the step involving the carbon—carbon bond formation rather than the enolization step.

It is apparent that the major factor that

Can. J. Chem. Downloaded from www.nrcresearchpress.com by 210.87.254.42 on 09/05/12
For personal use only.

determines the relative reactivities of the two sites in the same molecule is steric hindrance which in turn could be a conglomerate of internal, nonbonded interactions and solvation (Table 2). With the exception of butanone the aldol reaction rate is greater on the methyl side than on the methylene side. In 4-methyl-2-pentanone the steric hindrance due to the isopropyl group on the methylene side is so pronounced that no observable reaction takes place at this site. The greater reactivity of the methylene group in butanone parallels its behavior during the deuteration and may be explained on similar grounds (see above).

The relative reactivities of the methyl groups show a marked increase as one goes from butanone and 2-heptanone to 4-methyl-2-pentanone. The high reactivity observed in the latter case may be due to the intermediate possessing some carbanion character (as opposed to enol character) as a result of steric hindrance to enolization and/or to solvation[2] by the sec-butyl group. The slower rates of deuteration in the case of 4-methyl-2-pentanone relative to 2-heptanone could be taken as support for this explanation (Table 1).

The results of the present investigation support conclusions arrived at from product studies of the crossed aldol reactions (13). Under identical experimental conditions of the aldol reaction, it has been reported that methyl condensation becomes more facile in the order 4-methyl-2-pentanone (61% ketol yield) > 2-heptanone (40.8%) > butanone (31.7%), and that the reactivity of the methylene group in alkyl methyl ketones drops off rapidly with increasing bulk of the alkyl groups, for example from butanone (40.3% ketol yield) via 2-heptanone (12.2%) to 4-methyl-2-pentanone (0%).

[2]The authors are indebted to one of the referees for suggesting solvation as an alternate explanation.

The financial support of these investigations by the National Research Council of Canada, Ottawa, Canada, is gratefully acknowledged.

1. K. F. Bonhoeffer and W. D. Walters. Z. Physik. Chem. **A181**, 441 (1938).
2. R. P. Bell. J. Chem. Soc. 1637 (1937).
3. R. P. Bell and M. J. Smith. J. Chem. Soc. 1691 (1958).
4. C. K. Ingold. Structure and mechanism in organic chemistry. Cornell University Press, Ithaca, New York, N.Y., 1953. p. 676–699.
5. A. A. Frost and R. G. Pearson. Kinetics and mechanism. 2nd Ed. John Wiley and Sons, Inc., New York, N.Y., 1961. p. 335–350.
6. A. T. Nielsen and W. J. Houlihan. Org. React. **16**, 4–13 (1968).
7. R. P. Bell. The proton in chemistry Cornell University Press, Ithaca, New York, N.Y., 1959. p. 137.
8. J Jiminez and A. Broche. Bull. Soc. Chim. Fr. 1499 (1961).
9. S. E. Rudakova and V. V. Zharkov. Zh. Obshch. Khim. **33**, 3617 (1963); CA. **60**, 7883 (1964).
10. E. Coombs and D. P. Evans. J. Chem. Soc. 1295 (1940).
11. D. S. Noyce and W. L. Reed. J. Am. Chem. Soc. **81**, 624 (1959).
12. S. Nagase. Kogyo Kagaku Zasshi, **64**, 1008 (1961); CA. **57**, 2064 (1963).
13. E. Kiehlmann and P. W. Loo. Can. J. Chem. **49**, 1588 (1971).
14. W. Reeve and E. Kiehlmann. J. Org. Chem. **31**, 2164 (1966).
15. J. Warkentin and C. Barnett. J. Am. Chem. Soc. **90**, 4629 (1968).
16. J. Warkentin and R. A. Cox. J. Org. Chem. **33**, 1301 (1968).
17. C. Rappe and W. H. Sachs. J. Org. Chem. **32**, 4127 (1967).
18. C. Rappe and W. H. Sachs. J. Org. Chem. **32**, 3700 (1967); Tetrahedron Lett. 2317 (1968).

Can. J. Chem. Downloaded from www.nrcresearchpress.com by 210.87.254.42 on 09/05/12
For personal use only.

Isolation of 2(*S*)-Dichloroacetamido-3-(*p*-acetamidophenyl)propan-1-ol from a Chloramphenicol-producing *Streptomyces* Species[1]

CHI-KIT WAT,[2] V. S. MALIK,[3] AND L. C. VINING

Atlantic Regional Laboratory, National Research Council of Canada and Department of Biology, Dalhousie University, Halifax, Nova Scotia

Received July 22, 1971

Cultures of a chloramphenicol-producing *Streptomyces* to which 2(*S*)-amino-3(*R*)(*p*-nitrophenyl)-propan-1,3-diol (*p*-nitrophenylserinol) was added produced a new metabolite which has been identified as 2(*S*)-dichloroacetamido-3-(*p*-acetamidophenyl)propan-1-ol (**1**). The structure was confirmed by chemical synthesis. No radioactivity was incorporated into **1** when ^{14}C-labeled *p*-nitrophenylserinol was used, suggesting that **1** is formed not by metabolism of the supplement but by diversion of intermediates normally used for chloramphenicol biosynthesis.

Des cultures de *Streptomyces* produisant du chloramphénicol, auxquelles ont avait ajouté du 2(*S*)-amino-3(*R*) (*p*-nitrophényl) propan-1,3-diol (*p*-nitrophénylsérinol) ont produit un métabolite nouveau, identifié comme étant le 2(*S*)-dichloroacétamido-3-(*p*-acétamidophényl) propan-1-ol (**1**). On a confirmé la structure par synthèse chimique. On n'a pas remarqué l'incorporation de radioactivité dans **1** lors de l'utilisation de *p*-nitrophénylsérinol marqué au ^{14}C, ce qui suggère que **1** est formé, non pas par métabolisme du supplément mais par diversion des intermédiaires utilisés normalement dans la biosynthèse du chloramphénicol.

Canadian Journal of Chemistry, **49**, 3653 (1971)

Under some culture conditions *Streptomyces* 3022a, a chloramphenicol-producing actinomycete, metabolizes its own antibiotic. The first product formed is *p*-nitrophenylserinol which may then be *N*-acetylated or degraded further to *p*-nitrobenzyl alcohol or *p*-nitrobenzoic acid (1). In experiments where *p*-nitrophenylserinol was added to cultures of the actinomycete we observed the formation of an additional metabolite. This has been isolated and shown to have structure **1** (Scheme 1).

The t.l.c. of the neutral extract from cultures supplemented with *p*-nitrophenylserinol showed a zone which absorbed u.v. light but differed in R_f value from similar zones given by known metabolites of *Streptomyces* species 3022a. The substance was not formed when *p*-nitrophenylserinol was omitted from the culture. It was isolated by preparative t.l.c. and purified. The mass spectrum showed a molecular ion at *m/e* 318.0524. Prominent M + 2 (65% of M^+) and M + 4 (12%) ions indicated that the molecule contained two atoms of chlorine and should have the composition $C_{13}H_{16}N_2O_3Cl_2$. The presence of a *p*-acylaminophenylalkyl moiety was deduced from the following evidence.

The u.v. spectrum with λ_{max} 245 nm closely resembled that of acetanilide (λ_{max} 240 nm) except for the bathochromic displacement which could be attributed to alkyl substitution of the benzene ring. The base peak at *m/e* 106.0662 in the mass spectrum of the compound corresponded to an ion of composition C_7H_8N to which structure *c* (Scheme 2) was assigned. The i.r. absorption maxima occurred at 1610 (ring C=C stretching), 3090–3310 (OH or NH stretching), 1685 and 1670 (amide C=O), and at 1542 and 1515 cm^{-1} (amide N–H deformation).

The number and position of peaks in the 1500–1800 cm^{-1} region of the spectrum suggested that the molecule contained two amide but no ester or carboxyl groups. The p.m.r. spectrum of the compound in acetone-d_6 indicated the presence of a 1,4-disubstituted benzene ring (4H; AA′BB′ system; centered at τ 2.63, which is appreciably upfield from the value, τ *ca.* 2.1, found for *p*-nitrophenylalkyl derivatives). It also showed a single hydrogen (multiplet; τ 5.98) attached to a carbon atom vicinal to a hydroxymethyl (2H; doublet; spacing 4.8 Hz; τ 6.41) and a benzylic methylene (2H; doublet; spacing 6.5 Hz; τ 7.13) group, and characteristic signals for an acetamidomethyl (3H; singlet; τ 7.95) and a dichloroacetyl (1H; singlet; τ 3.70) group. A moderately abundant fragment ion in the mass spectrum at *m/e* 287, corresponding to the loss

[1]Issued as NRCC No. 12172.

[2]NRCC Postdoctorate Fellow, 1969–71.

[3]Present address: Department of Microbiology, Baylor College of Medicine, Houston, Texas 77025.

Can. J. Chem. Downloaded from www.nrcresearchpress.com by 210.87.254.42 on 09/05/12
For personal use only.

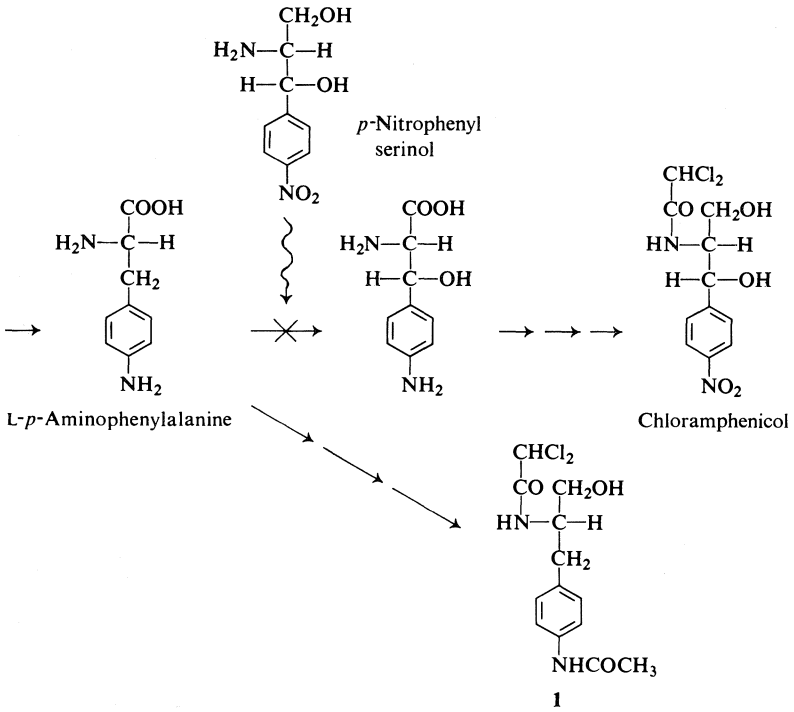

SCHEME 1. Suggested biogenetic relationship between chloramphenicol and 2(*S*)-dichloroacetamido-3-(*p*-acetamidophenyl)propan-1-ol in cultures of *Streptomyces* species 3022a supplemented with *p*-nitrophenylserinol.

of CH_3O from the molecular ion was consistent with a hydroxymethyl group being at C-1. Ions derived by expulsion of 31 mass units were prominent in the mass spectra of chloramphenicol and other phenylserinol derivatives. Absence of hydroxyl substitution at C-3 can also be deduced from the mass fragmentation pattern. Phenylalkyl compounds with this feature show a strong M-18 ion and the molecular ion is weak or absent.

This evidence establishes the basic structure as 2-amino-3-(*p*-aminophenyl)propan-1-ol. One amino group is blocked by an acetyl and the other by a dichloroacetyl substituent. The only remaining uncertainty is the location of the two acyl substituents, and the configuration at the asymmetric carbon. The acetyl group is placed at the *p*-position and the dichloroacetyl at position-2 to account for the principal ions in the mass spectral fragmentation pattern (Scheme 2). To confirm the structural assignments and establish the configuration at C-2, structure **1** was synthesized.

L-*p*-Aminophenylalanine was acetylated with acetic anhydride in glacial acetic acid to give the acetanilide, then converted with dichloroacetyl chloride in aqueous alkali to the 2-*N*-dichloroacetyl derivatives. The p.m.r. spectrum of this intermediate showed characteristic signals of the ABX system expected for a dichloroacetamido substituted carbon bearing a single hydrogen and vicinal to a benzylic methylene. The carboxyl group was reduced with diborane and the product, recovered and purified by preparative t.l.c., was shown to be identical in all respects with the natural compound. The manner of synthesis establishes that the product possesses an asymmetric center at C-2 which requires that the five aliphatic hydrogens on C-1, -2, and -3 constitute an ABMXY system. The simplicity of the p.m.r. spectrum given by the natural product is thus deceptive.

When ^{14}C-*p*-nitrophenylserinol was added to cultures of the actinomycete neither **1** nor chloramphenicol was labeled. Each must have been made *de novo* by the organism rather than by metabolism of *p*-nitrophenylserinol. The absence of **1** in unsupplemented cultures suggests that *p*-nitrophenylserinol inhibits one of the steps leading to chloramphenicol, probably the hydroxylation of *p*-aminophenylalanine to *p*-aminophenylserine (Scheme 1). The accumulated

Can. J. Chem. Downloaded from www.nrcresearchpress.com by 210.87.254.42 on 09/05/12
For personal use only.

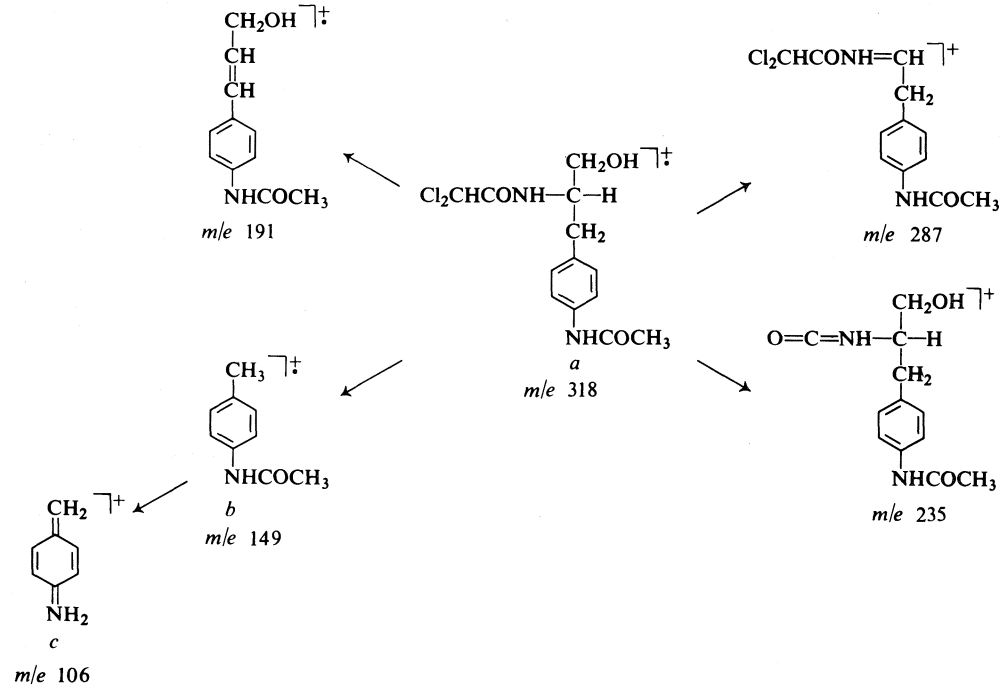

SCHEME 2. Suggested fragmentation of 2(*S*)-dichloroacetamido-3-(*p*-acetamidophenyl)propan-1-ol in the mass spectrometer.

p-aminophenylalanine could then be modified by dichloroacetylation and reduction as in the chloramphenicol pathway (2), but would undergo acetylation instead of oxidation at the *p*-amino group.

Experimental

Melting points were measured on a Fisher–Johns hot plate and are uncorrected. The p.m.r. spectra were recorded with a Varian Associates A-60A spectrometer. Mass spectra were obtained with a Consolidated Electrodynamics Corporation model 21-110B double-focusing instrument used in the electrical detection mode with 8 kV accelerating voltage and 70 eV electron energy. The sample was vaporized directly into the ion source by raising the source block temperature to 200–220°. Accurate mass measurements were made by the peak-matching method using a perfluorokerosene reference.

Culture

A single spore isolate (strain 13*s*) of *Streptomyces* sp. 3022a was used. Its history and methods used to maintain and culture it have been described (1). Cultures were grown in GNY medium (25 ml), consisting of glycerol (2%), Difco dehydrated nutrient broth (0.8%), Difco dehydrated yeast extract (0.3%), and K_2HPO_4 (0.5%) in distilled water, dispensed in 125 ml Erlenmeyer flasks. *p*-Nitrophenylserinol (2.5 mg per flask) was added before autoclaving.

Isolation

Cultures were centrifuged and the supernatant solution at p*H* 8.5 extracted with ethyl acetate. The concentrated extract was applied to 20 × 50 cm preparative t.l.c. plates spread with a 2 mm thick layer of silica gel HF_{254} (E. Merck & Co., Darmstadt) and chromatographed in chloroform–methanol (7:1). The quenching zone (R_f 0.43) located between chloramphenicol (R_f 0.50) and *N*-acetyl-*p*-nitrophenylserinol (R_f 0.34) was scraped from the plate and the adsorbent was leached with acetone. The eluted substance was taken up in hot ethyl acetate and crystallized as prisms. After recrystallization from water it was obtained as fine needles which melted initially at 167–168°, then crystallized and remelted at 177.5°; $[\alpha]^{26°}$ in methanol (*c*, 0.725) 20.3° at 365 nm, 3.31° at 436 nm; −1.65° at 546 nm, −1.79° at 578 nm, −1.65° at 589 nm; λ_{max} (MeOH) 245 nm (log ε 4.26); ν_{max} (KBr) 3310, 3240, 3130, 3090, 3000, 1685, 1670, 1610, 1542, 1515, 1445, 1410, 1370, 1322, 1270, 1224, 1208, 1140, 837, 826, 810 cm^{-1}; $M^{\pm}$ at *m/e* 318 (2% of most abundant peak) and characteristic fragment ions at *m/e* 287 (2%), 235 (2%), 191 (78%), 149 (60%), and 106 (100%). Accurate mass measurement of selected ions gave *m/e* 318.0524 ($C_{13}H_{16}N_2O_3Cl_2$ requires 318.0538), 191.0945 ($C_{11}H_{13}NO_2$ requires 191.0946), and 106.0662 (C_7H_8N requires 106.0657).

Synthesis

p-Amino-L-phenylalanine (3 g) prepared as described by McGrath *et al.* (2), was acetylated with acetic anhydride (1.5 ml) in glacial acetic acid (25 ml) under the conditions described by Weichert for the racemic amino acid (3). *p*-Acetamido-L-phenylalanine, m.p. 234–237°, was obtained in 62% yield. To a well-stirred and cooled (ice bath) solution of the product (2.22 g) in 0.5 *N* sodium

Can. J. Chem. Downloaded from www.nrcresearchpress.com by 210.87.254.42 on 09/05/12
For personal use only.

hydroxide (20 ml), dichloroacetyl chloride (1.7 ml) was added drop by drop. The p*H* was maintained above 8 by periodic addition of sodium hydroxide solution and stirring was maintained for 30 min after all of the dichloroacetyl chloride was added. The reaction mixture was brought to p*H* 3 with dilute hydrochloric acid and the precipitate (1.5 g) collected. It was chromatographed on a column (3 × 50 cm) of Sephadex G-25 (fine) using the solvent system benzene – ethyl acetate – ethanol – acetic acid – water (4 : 1 : 2 : 1 : 3). The eluate was collected in 5 ml fractions and the material from fractions 94–145 contained the product. It was recrystallized from water to give *p*-acetamido-α-*N*-dichloroacetyl-L-phenylalanine (3) as prisms (0.8 g) m.p. 105–111°; $\alpha_D^{26°}$ + 72.4° (*c*, 0.29 in methanol; λ_{max}(MeOH) 245 nm (log ε, 4.26); ν_{max}(KBr) 1710, 1670, 1542, 1505 cm^{-1}; τ (acetone-d_6) 7.93 (acetyl CH_3) 4.42 (dichloroacetyl CH), AA′BB′ system centered at 2.73, ABX system with AB and X nuclei centered at 6.85 and 5.20 respectively (calcd. J_{AB} = 14.4, J_{AX} = 8.0, J_{BX} = 5.0 Hz). Double irradiation of the A, B, and X signals confirmed the couplings.

Anal. Calcd. for $C_{13}H_{14}O_4N_2Cl_2$: C, 46.86; H, 4.23; N, 8.41; Cl, 21.28. Found: C, 46.67; H, 4.12; N, 8.34; Cl, 21.36.

The acid (0.67 g) was added to a solution of diborane (0.16 mmol/ml) in tetrahydrofuran prepared as described by Brown *et al.* (4) from boron trifluoride etherate (7.1 ml) and sodium borohydride (0.627 g) in tetrahydrofuran (60 ml), and cooled to 0°. After 2 h acetone (5 ml) was added drop by drop to destroy excess diborane, then water (20 ml). Solvent was removed *in vacuo* and the products separated by preparative t.l.c. 2-Dichloroacetamido-3-(*p*-acetamidophenyl)propan-1-ol crystallized from water as needles (12 mg) which melted at 166°, became solid, and remelted at 179.5°. It had $[\alpha]^{26°}$ in methanol (*c*, 0.72) 20.6° at 365 nm, 3.33° at 436 nm, −1.53° at 546 nm, −1.80° at 578 nm, and −1.66° at 589 nm, did not depress the m.p. of the natural sample on admixture, and showed no differences from it in u.v., mass, p.m.r., or i.r. absorption spectra.[4]

Anal. Calcd. for $C_{13}H_{16}N_2O_3Cl_2$: C, 48.92; H, 5.05; N, 8.78; Cl, 22.21. Found: C, 49.09; H, 4.94; N, 8.68; Cl, 22.05.

We thank Mr. D. J. Embree and J. Van Ingen for determining mass and p.m.r. spectra. We are also grateful to Dr. W. D. Jamieson and Dr. A. G. McInnes for assistance in interpreting the spectra.

1. V. S. Malik and L. C. Vining. Can. J. Microbiol. **16**, 173 (1970).
2. R. McGrath, L. C. Vining, F. Sala, and D. W. S. Westlake. Can. J. Biochem. **46**, 587 (1968).
3. R. Weichert. Arkiv. Kemi, **25**, 231 (1966).
4. H. C. Brown, P. Heim, and N. M. Yoon. J. Am. Chem. Soc. **92**, 1637 (1970).

[4]The i.r. spectra of **1** have been placed in the Depository of Unpublished Data, National Research Council of Canada, Ottawa, Canada K1A 0S2.

Can. J. Chem. Downloaded from www.nrcresearchpress.com by 210.87.254.42 on 09/05/12
For personal use only.

Can. J. Chem. Downloaded from www.nrcresearchpress.com by 210.87.254.42 on 09/05/12
For personal use only.

Yields of Free Ions in the X Radiolysis of Some Simple Saturated and Unsaturated Hydrocarbon Liquids: Effects of Molecular Structure and Temperature[1]

M. G. Robinson, P. G. Fuochi,[2] and G. R. Freeman
Chemistry Department, University of Alberta, Edmonton 7, Alberta

Received July 5, 1971

Pulse techniques were used at temperatures ranging from 120 to 293 °K. A quasifree electron conductance transient (k/u overshoot) was observed in liquid methane, but not in ethane, propane, cyclopropane, ethylene, propylene or butene-1. The free ion yield in methane, $G_{fi} = 0.8$ at 120 °K, is much larger than those in the other liquids, which at 183° K are: ethane, 0.13; propane, 0.076; cyclopropane, 0.04; ethylene, 0.017; propylene, 0.04; butene-1, 0.027. The activation energies of free ion formation are, in kcal/mol: ethane, 0.6; propane, 0.8; ethylene, 0.5; propylene, 1.0; butene-1, 1.0. The results are interpreted in terms of the coulombic interaction model. The distances that the secondary electrons penetrate the liquid away from their parent ions are greater when the hydrocarbon molecules are more sphere-like, and are reduced by the presence of a π bond in the molecule. Cyclopropane behaves somewhat like an olefin in this regard, a fact that is explained by the unusual bonding in the C_3 ring. In the present liquids the only ionization events that contribute appreciably to the free ion yield are those in which the electron penetrates $\gtrsim 100$ Å from the parent ion.

Les techniques de radiolyse pulsée ont été utilisées à des températures allant de 120 a 293 °K. Une conductance éphémère due à des électrons quasi libres a été observée dans le méthane liquide; l'éthane, le propane, le cyclopropane, l'éthylène, le propylène ni le butène-1 ne présentent de phénomène similaire. Le rendement en ions libres, G_{fi}, déterminé pour le méthane à 120 °K a une valeur de 0.8; pour les autres liquides, ce rendement vaut à 180 °K: 0.13 pour l'éthane, 0.076 pour le propane, 0.04 pour le cyclopropane, 0.04 pour le propylène et 0.027 pour le butène-1. L'énergie d'activation, en kcal/mol, concernant la formation d'ions libres est respectivement de 0.6 pour l'éthane, 0.8 pour le propane, 0.5 pour l'éthylène, 1.0 pour le propylène et 1.0 pour le butène-1. Les résultats sont interprétés sur la base du modèle d'interaction coulombique. La distance qu'un électron secondaire parcourt depuis l'ion parent est plus grande lorsque les molécules d'hydrocarbures sont d'autant plus spheroïdes; par ailleurs la présence d'orbitales π dans les molécules d'hydrocarbures réduit la pénétration d'un électron secondaire. A ce point de vue, le cyclopropane qui possède un genre particulier de liens C—C se comporterait plutôt comme une oléfine. Pour les liquides étudies, les ionisations qui contribuent d'une façon appréciable au rendement en ions libres sont celles pour lesquelles les distances de pénétration des électrons sont au moins de 100 Å.

Canadian Journal of Chemistry, 49, 3657 (1971)

Introduction

The influence of molecular structure on the radiation-induced free ion yield in liquid hydrocarbons has been demonstrated by both conductivity and scavenging studies (1–5). However, the precise nature of the effect is not understood. Liquids that are made up of sphere-like molecules, such as argon and neopentane, give high yields of free ions. Associated with the high yield of free ions is a short lived (μs) conductance transient, believed to be due to quasifree electrons, that is observed by a pulse radiolysis technique (2, 3). Liquids comprised of nonspherical molecules, such as *n*-hexane and *n*-pentane, have low yields of free ions and do not exhibit the short lived radiation induced transient.

In an earlier communication the prediction that liquid methane, which has nearly spherical molecules, should have a high free-ion yield was confirmed (6). A striking difference between the yields in the liquids methane and ethane was observed. The detailed results for these hydrocarbons are presented here together with data obtained for propane, some simple mono-olefins and the pseudo olefin, cyclopropane.

Recent studies have shown that electron scavenging in ethylene and propylene is much less efficient than that in ethane and propane (7). The smaller scavenging efficiencies seem to

[1]Financial assistance was received from the National Research Council of Canada.

[2]Present address: Consiglio Nazionale delle Ricerche, Laboratorio di Fotochimica e Radiazioni d'Alta Energia, Bologna, Italy.

Can. J. Chem. Downloaded from www.nrcresearchpress.com by 210.87.254.42 on 09/05/12
For personal use only.

reflect smaller ion–electron separation distances in the spurs in the π-bonded systems compared to those in the alkanes. Theory predicts that the free ion yields in the olefins should be correspondingly small, and this expectation is confirmed by the present work.

Experimental

Materials

The ethane, ethylene, propane, propylene, and butene-1 were Phillips Research Grade. Cyclopropane and methane were obtained from Matheson, the methane being Ultra Pure Grade. Each compound was purified by vacuum distillation retaining the middle fraction, and freeze–thaw–pump cycles. Prior to use the hydrocarbons were electrolyzed as liquids at 183 °K (120 °K for methane) for 2 h at 800 V/cm. Each sample was then distilled into a side-bulb attached to the conductance cell, frozen at 77 °K, and the cell-unit was sealed off with a flame.

Equipment and Technique

(a) Conductance Cell

The conductance cell was similar to that used by Tewari and Freeman (3). It was modified for ease of removal from the Dewar and to give a better seal in the Dewar by using O-rings, and making a Kovar seal around the collector lead (Fig. 1). The collector lead was insulated with heat-shrink polyethylene tubing and the Kovar was filled with paraffin wax to prevent condensation of moisture inside it.

The electrode spacing in each cell used was 5 mm and the effective area of the collecting electrode was 1.14 cm^2. The cell constants were measured using standard KCl solutions.

(b) The Quasifree Electron Conductance Transient

The height of the quasifree electron conductance transient is critically affected by traces of electron scavenging impurities such as oxygen (2, 3). However, traces of oxygen can be removed from hydrocarbons by preirradiating the sample in the conductance cell to a dose of 10^{18}–10^{19} eV/g (2). A ^{60}Co source was used for preirradiations. The presence of the quasifree electron transient in the sample after a 1 μs pulse of 1.7 MeV X-rays was sought using the circuit shown in Fig. 2*a*. The sensitivity of this circuit was much greater than that used earlier (3), and enabled currents down to 1 nA to be measured with a response time of 2 μs.

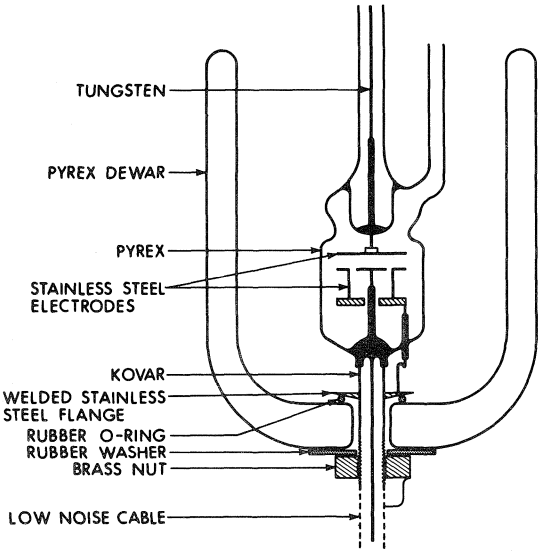

FIG. 1. Conductance cell.

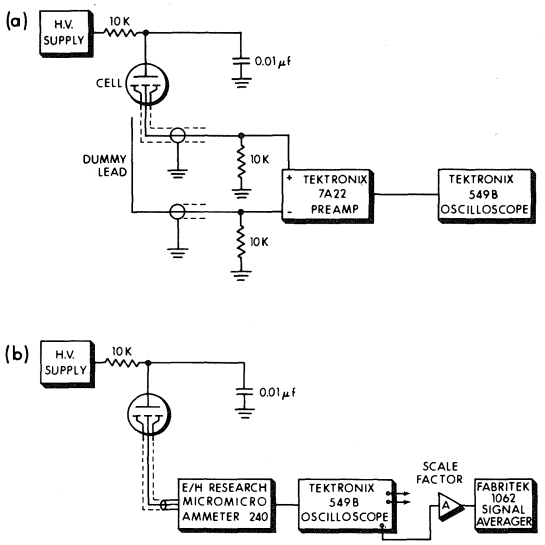

FIG. 2. Schematic diagrams of the circuits used in the measurement of: (*a*) quasifree electron conductance transient (response time 2 μs). (*b*) k/u for ion–ion neutralization (response time ≤0.2 s). Blank and beam pulse control and current monitoring same as in Fig. 3.

(c) Measurement of (k/u) for Ion-Ion Neutralization

The ion–ion neutralization reactions had half lives of the order of magnitude of a second. The decay of the conductance after a 1 ms pulse of X-rays was measured with the circuit shown in Fig. 2*b*. For each run sixteen alternate signals and blanks (no pulse from the Van de Graaff) were measured, averaged and subtracted by the Fabritek 1062 Signal Averager. Currents ≥0.1 pA were measured with response time ≤0.2 s, the response time being shorter for larger currents. Values of the ratio of the neutralization rate constant k to the sum of the charge mobilities u were calculated from the current decay curves (2).

(d) Determination of the Free-ion Yield

The free-ion yields were measured by the charge clearing method (1, 2). The circuit used was similar to that described by Tewari and Freeman (3) but modified to give a greater sensitivity. A schematic diagram of the improved circuit is shown in Fig. 3. Signals were generated by 1 μs pulses of 1.7 MeV X-rays. Alternate signals and blanks were fed into a low drift, high sensitivity integrator (Fig. 3*b*) and averaged with the Fabritek 1062. Normally the clearing field (0.3 to 6 kV) was applied for 1.7 s, beginning approximately 5 μs after the X-ray pulse, and the resulting radiation-induced current

TABLE 1. Densities, dielectric constants, and dipole moments of the hydrocarbons

Compound	T (°K)	d (g/cm³) (ref. 8)	$\frac{dd}{dT} \times 10^3$ (g/cm³ deg) (ref. 8)	ε*	$\frac{d\varepsilon}{dT} \times 10^{3}$* (deg^{-1})	μ (debye) (ref. 11)
CH_4	120	0.415		1.67†	1.9†	0.00
C_2H_4	183	0.550	1.52	1.75	2.7	0.00
C_2H_6	183	0.551	1.08	1.80‡	2.0	0.00
C_3H_6-1	183	0.662§	~1.2§	2.24§	~5.5§	0.36
c-C_3H_6	183	0.748	1.27	2.00	2.2	0.00
C_3H_8	183	0.637	1.20	1.90	2.3	0.084
C_4H_8-1	183	0.746§	~1.2§	2.31§	~5.5§	0.34

*Calculated as described in the text.
†Reference 25.
‡Assumed.
§See Fig. 4.

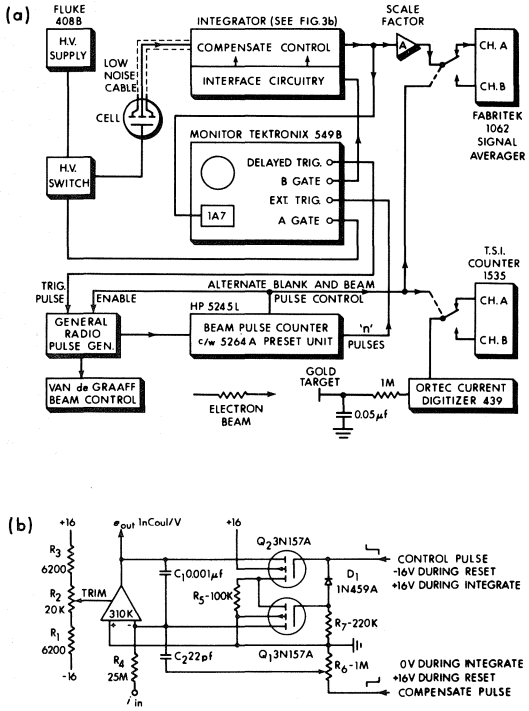

FIG. 3. (*a*) Circuit used for the measurement of the free ion yields. (*b*) Low drift, high sensitivity integrator with mosfet reset switch (detail of integrater in Fig. 3*a*). C_1 and C_2 are polystyrene. R_2 is adjusted for zero drift during integrate with input open. R_6 is adjusted for zero reset offset.

was integrated. A Tektronix 549B oscilloscope with a type 1A7 plug-in monitored the signals and provided suitable delays. Sensitivities as high as 0.125×10^{-12} C/cm were achieved with this system.

For methane the X-ray pulse was applied after the beginning of the clearing field pulse, to prevent the possible loss of quasifree electrons by neutralization during the 5 μs period between the X-ray and voltage pulses in the normal technique.

Dosimetry

A measurement of the dose per X-ray pulse for each hydrocarbon was effected by correlating the charge collected at the gold target and corresponding thermoluminescent dosimetry measurements. An Ortec model 439 Current Digitizer was used to monitor the charge collected from the gold target for, typically, 100 pulses. The same X-ray pulses irradiated several lithium fluoride crystals which were placed in front of and behind the Dewar which contained the conductivity cell. The dose absorbed by these crystals was measured with a Harshaw model 2000 Thermoluminescence Analyzer. Calibration of the lithium fluoride crystals was effected by γ-radiolysis and comparison of the thermoluminescence response (nC) with the dose from the γ-source, measured by Fricke dosimetry (eV ml^{-1}). The dose per pulse was varied between 1 and 3 (10^{10} eV/ml).

Physical Properties of the Hydrocarbons

The densities of the hydrocarbons at the different temperatures were obtained from ref. 8, those at the lowest temperatures by extrapolation. The density of butene-1 at 118 °K was measured and found to be 0.81 g/cm³, which indicated that all densities obtained by extrapolation were accurate to within 3% and most, obtained by shorter extrapolations, would be within 1% of the true value. The dielectric constants were calculated from the Debye equation (9), using appropriate densities, refractive indices (10), and dipole moments (11). The physical properties are summarized in Table 1 and Fig. 4.

Results

Quasifree Electron Conductance Transient

A quasifree electron conductance transient, previously called a k/u overshoot (2, 3) was observed in liquid methane (Fig. 5*a*). The magnitude of the transient increased as the sample was irradiated up to a dose of 1×10^{18} eV/ml, then remained constant at 6.3×10^{-19} mho cm³/eV. The height of the conductance peak was proportional to field strength from 6 to 200 V/cm. The 2 μs response time of the measuring circuit was too slow to permit meaningful k/u measurements to be made.

Can. J. Chem. Downloaded from www.nrcresearchpress.com by 210.87.254.42 on 09/05/12
For personal use only.

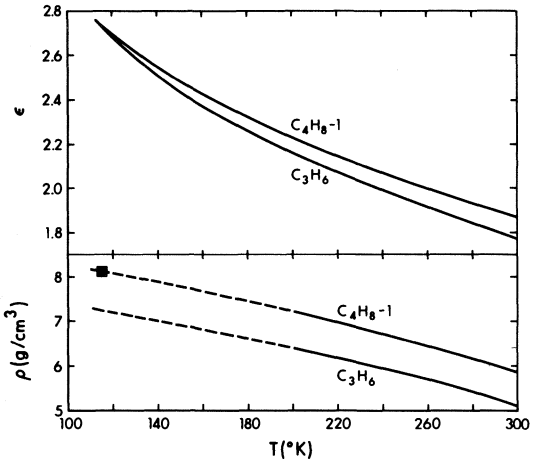

FIG. 4. Densities and dielectric constants of propylene and butene-1 as functions of temperature. ρ:— from ref. 8; --- estimated; ■ measured. ε: calculated from the Debye equation.

A quasifree electron transient was not observed in any of the other liquids, either before or after γ-radiolysis, at sensitivities down to 1 nA/cm and field strengths up to 2000 V/cm (Fig. 5*b*). The magnitude of the transient in the liquids ethane, propane, cyclopropane, ethylene, and propylene at 183 °K was $<3 \times 10^{-23}$ mho/cm³ eV, at least four orders of magnitude smaller than that in methane at 120 °K.

k/u for Ion–Ion Neutralization at 183 °K

The apparent value of k/u increased with increasing applied voltage, probably due to the neutralization of progressively larger fractions of the ions at the electrodes. In ethane the apparent values at 10 and 220 V/cm were 1.6 and 10 (10^{-6} V cm), respectively; in propane the corresponding values were 1.5 and 8 (10^{-6} V cm), respectively. The values at zero field strength would therefore be near to the theoretical value 1.0×10^{-6} V cm in both liquids.

The induced conductances of ethylene, propylene, and cyclopropane were too small to permit the measurement of k/u in those liquids. However, the apparent value in cyclopropane at 200 V/cm was 8×10^{-6} V cm, similar to those in ethane and propane at the same field strength.

The measurement of low conductances was complicated by the existence of a voltage hysteresis in the cell, presumably due to polarization of the glass envelope in the combined electric and radiation fields. The effect of the hysteresis was minimized by giving a few pulses of radiation to the cell at each new voltage, before taking readings.

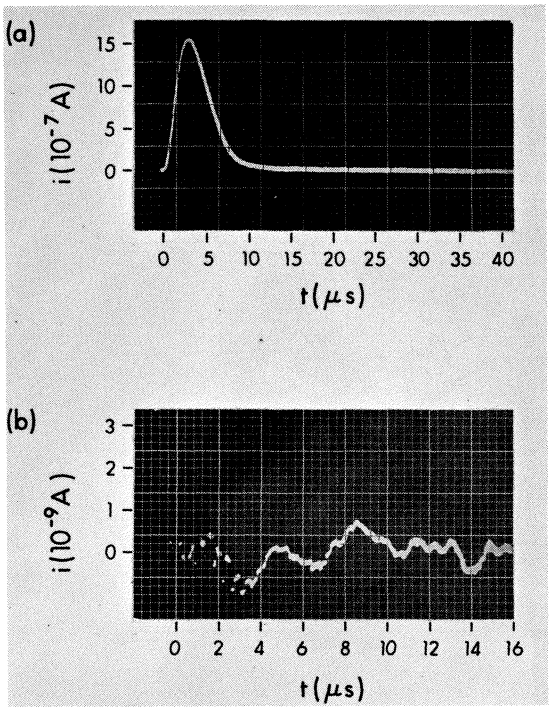

FIG. 5. (*a*) Oscilloscope trace of current *vs.* time for the quasifree electron conductance transient in methane at 120 °K. The X-ray pulse duration was 1 μs and the sample dose was 2.2×10^{10} eV/ml. Applied field 206 V/cm. (*b*) Corresponding oscilloscope trace for ethane at 183 °K. Sample dose (1 μs) $\approx 3 \times 10^{10}$ eV/ml. Applied field = 2000 V/cm.

Free Ion Yields

In Fig. 6 are shown typical yields of ions collected at the electrodes as functions of applied voltage in methane, ethane, propane, and ethylene. The curves obtained for the C_2–C_4 hydrocarbons contained plateaus; cyclopropane, propylene, and butene-1 gave curves similar to that shown for ethylene in Fig. 6. The plateaus correspond to the free ion yields. No plateau was obtained for methane, because in this case the electric field was present during the radiation pulse, and the free ion yield increases with increasing applied field strength (12, 13). The free ion yield in methane in the absence of an applied field at 120 °K, obtained by extrapolation (13), is $G_{fi} = 0.8 \pm 0.1$.

The values of G_{fi} obtained in the different liquids at several temperatures are listed in Table 2. In a given hydrocarbon the yield increases with increasing temperature. At a given tempera-

Can. J. Chem. Downloaded from www.nrcresearchpress.com by 210.87.254.42 on 09/05/12
For personal use only.

Can. J. Chem. Downloaded from www.nrcresearchpress.com by 210.87.254.42 on 09/05/12
For personal use only.

TABLE 2. Ion yields and ion–electron separation distance parameters

Liquid	G_{tot}*	T (°K)	G_{fi}†	b (Å)	bd‡ (10^{-8} g/cm²)	Liquid	G_{tot}*	T (°K)	G_{fi}†	b (Å)	bd‡ (10^{-8} g/cm²)
CH_4§	3.7	120	0.8	500	210	C_2H_4	3.9	120	0.009	84	54
								148	0.013	76	46
C_2H_6	4.0	120	0.06	129	81			181	0.017	71	39
		148	0.08	118	69						
		183	0.13	118	65	C_3H_6	4.0	148	0.013	58	40
								183	0.04	65	43
C_3H_8	4.1	120	0.026	97	69			230	0.06	64	39
		148	0.043	94	64						
		183	0.076	93	59	C_4H_8-1	4.1	120	0.009	59	48
		230	0.12	90	52			148	0.019	60	47
								181	0.027	58	43
c-C_3H_6	4.1‖	183	0.04	73	55			230	0.054	60	41
								293	0.105	64	38

*Assumed equal to the average of the gas phase values reported by refs. 26, 27 and 28.
†Free ion yield at zero field strength.
‡Product of the Gaussian parameter b and the liquid density d.
§Displays a quasifree electron conductance transient.
‖Assumed equal to that in propane, because their ionization potentials are equal (29).

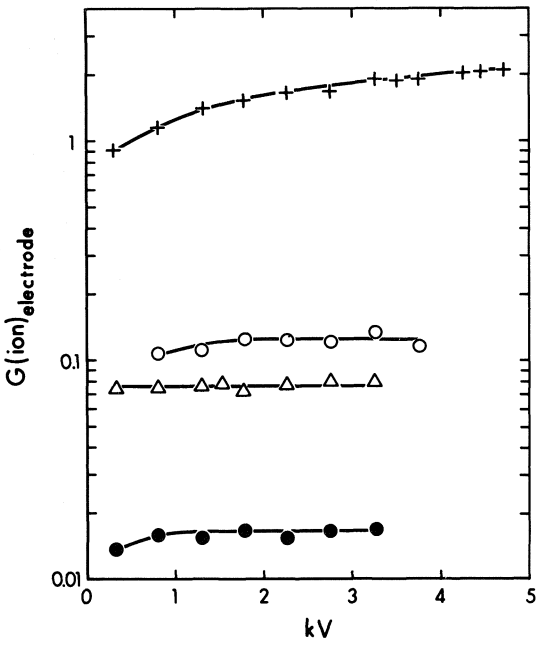

FIG. 6. Typical values of G(negative ion) collected at the anode as functions of the applied voltage. +, methane, 120 °K; ○, ethane, 183 °K; ●, ethylene, 181 °K; △, propane, 183 °K. The electrode spacing was 5 mm.

ture the yields in the liquids decrease in the order $CH_4 \gg C_2H_6 > C_3H_8 > c\text{-}C_3H_6 \approx C_2\text{-}C_4$ olefins.

The free ion yields in ethylene were the most difficult to measure because they were the lowest. However, repeated runs on three samples showed that the values were reproducible within ± 0.002 G units over the temperature range studied.

Discussion

Quasifree Electron Transient

The only liquid in the present series that displayed the quasifree electron conductance transient was methane. This conforms to the previously noted correlation between the magnitude of the transient (k/u overshoot) and the sphericity of the molecules (2, 3). The correlation exists for nonpolar compounds that do not scavenge electrons.

Free Ion Yields

The liquid that displays the quasifree electron conductance transient gives a much larger free ion yield than those that do not display the transient, under similar irradiation conditions (Table 2). This agrees with earlier observations on other systems (2, 3).

Free ion yields calculated from the coulombic interaction model (14), using the semi-empirical distribution of thermalized electron–ion separation distances (14, 15), are in reasonable agreement with the experimental results for ethane and propane. However, the calculated value for methane is too low and those for cyclopropane and the olefins are too high. The semiempirical distribution is apparently suitable for saturated compounds whose molecules are distinctly not sphere-like, but is unsuitable for liquids made up of sphere-like molecules or unsaturated compounds. Sphere-like molecules give rise to longer ion–electron separation distances, while double bonds shorten the separation distances. Different distributions must therefore be devised.

A simple form of distribution function that is convenient to use (4, 16) is the single parameter three dimensional Gaussian

$$[1] \quad N(y)/N_0 = (4y^2/\pi^{1/2}b^3) \exp(-y^2/b^2)$$

where $N(y)/N_0$ is the fraction of the ion–electron pairs that have an initial distance y between the ion and the thermalized electron, and the parameter b is the most probable value of y. The free ion yield G_{fi} is then given by eq. 2

$$[2] \quad G_{fi} = G_{tot} \int_0^\infty \left(\frac{4y^2}{\pi^{1/2}b^3}\right) \times \exp\left(-\frac{y^2}{b^2} - \frac{\xi^2}{\varepsilon y k T}\right) dy$$

where G_{tot} is the total ionization yield, ξ is the electronic charge, ε is the dielectric constant of the liquid, k is Boltzmann's constant, and T is the absolute temperature. By substituting values of G_{fi}, G_{tot}, ε, and T into eq. 2 one obtains a value of b.

Relative values of b in different liquids reflect, in an approximate way, the relative ranges of the secondary electrons in the liquids. The initial energy distributions of the secondary electrons in the different liquids are probably similar to each other, so the relative values of b allow one to compare rates of energy loss by the electrons in the different liquids. The comparison is only qualitative, because the Gaussian might not be an exact description of the electron range distribution.

Values of b for the present liquids at the different temperatures are given in Table 2. For purposes of comparison the product of the electron range b and the density d of the medium has

Can. J. Chem. Downloaded from www.nrcresearchpress.com by 210.87.254.42 on 09/05/12
For personal use only.

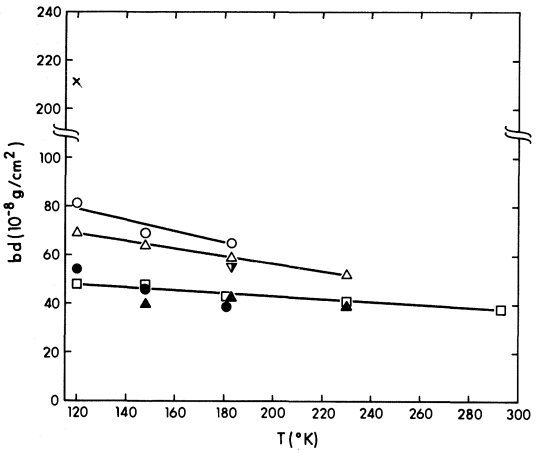

FIG. 7. Values of *bd* as functions of temperature for the different liquids. ×, CH_4; ○, C_2H_6; ●, C_2H_4; △, C_3H_8; ▲, C_3H_6; ▽, *c*-C_3H_6; □, C_4H_8-1.

more theoretical significance than does the range alone (4, 14, 17). Values of *bd* are listed in Table 2 and plotted in Fig. 7.

The values of *bd* decreased somewhat with increasing temperature (Fig. 7). The decrease might simply indicate that the Gaussian function is sharper than the real distribution function, the latter having a longer tail towards higher *y* values. A power function might be more suitable than the Gaussian (18). However, values of *bd* at the same temperature can be meaningfully compared. One can see from Fig. 7 that the relative values of *bd* are in the order $CH_4 \gg C_2H_6 > C_3H_8 > c\text{-}C_3H_6 >$ olefins. The progressively decreasing values of *bd* for the C_1-C_3 alkanes correlate with a sequence of molecular properties. Methane is relatively sphere-like and is almost isotropically polarizable; ethane is much less sphere-like than methane and it is not isotropically polarizable; propane is still less sphere-like, is not isotropically polarizable, and has a small dipole moment (Table 1). The significance of this correlation of *bd* with molecular properties is not understood. The correlation might be partly due to the effect of the molecular properties on the packing and relative orientation of the molecules in the liquid.

The presence of a π bond in the molecule decreases the value of *bd* further (Fig. 7). The π bond apparently increases the secondary electron energy loss cross section of the molecules, or increases the ease of formation of a localized state of the electron in the liquid, or both.

The behavior of cyclopropane falls between those of propane and propylene (Fig. 7). The partial olefinic nature of cyclopropane is well known in organic chemistry (19) and has been observed in radiation chemistry through its charge scavenging reactions and kinetics (7). An unusual type of bonding accounts for the chemical properties of the three-membered ring (20–22), and probably also accounts for the strength of the electron–molecule energy transfer interaction (at low energies) and for the H_2 transfer reaction with alkane positive ions observed by Ausloos and Lias (23).

Temperature Coefficients of the Free Ion Yields

Consider the following general mechanism for the ionic reactions in a radiation-induced conductance system.

[3] $\quad A \rightarrow [B^+ + C^-]$

[4] $\quad [B^+ + C^-] \rightarrow$ Products (geminate neutralization)

[5] $\quad [B^+ + C^-] \rightarrow B^+ + C^-$ (free ions)

[6] $\quad B^+ + C^- \rightarrow$ Products (random neutralization)

[7] $\quad B^+ \rightarrow$ electrode

[8] $\quad C^- \rightarrow$ electrode

The square brackets around products or reactants indicate that the species are in a spur. Only the free ions contribute to the induced conductance. Measurement of the free ion yield gives information about the competition between reactions 4 and 5.

The Arrhenius temperature coefficient of the free ion yield has little direct significance (*cf.* eq. 2), but it allows us to fit the present temperature effects into the framework of a chemist's experience. Arrhenius plots of the free ion yields in ethane, propane, ethylene, propylene, and butene-1 are shown in Fig. 8. In all these liquids at the temperatures studied $G_{fi} \leq 0.03 G_{tot}$ (Table 2), so the ratio of "rate constants" of reactions 4 and 5 is approximately proportional to G_{fi}

$$[9] \quad \frac{k_5}{k_4} = \frac{\text{rate of [5]}}{\text{rate of [4]}} \approx \frac{\text{rate of [5]}}{\text{rate of [4] + [5]}} \approx G_{fi}/G_{tot} \propto G_{f_1}$$

Thus, from the slopes of the curves in Fig. 8 one obtains $E_5 - E_4$, which equals E_5 because E_4 is presumably zero. The "activation energy" E_5

Can. J. Chem. Downloaded from www.nrcresearchpress.com by 210.87.254.42 on 09/05/12
For personal use only.

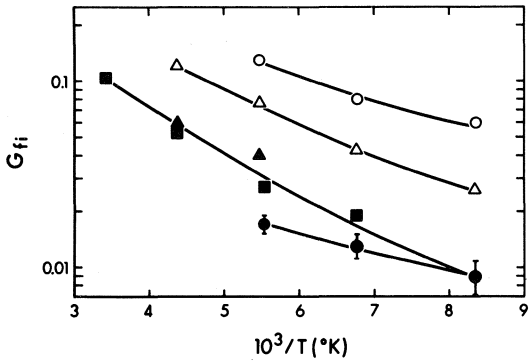

FIG. 8. Effect of temperature on the free ion yield. Arrhenius plots for: ○, ethane; ●, ethylene; △, propane; ▲, propylene; and ■. butene-1. The error bars drawn through the ethylene points were estimated from repeated runs on three samples.

seems to increase gently with increasing temperature (Fig. 8). The average values in the liquids at the temperatures studied are listed in Table 3. They range from 0.5 to 1.0 kcal/mol and are only 2–3 times the mean values of RT, which were 0.3–0.4 kcal/mol.

The coulombic attraction energy E_b between the ion and electron at separation distance b, the most probable value of y in a Gaussian $N(y)$ distribution, is about 2 kcal/mol in each of the liquids (Table 3).

$$[10] \qquad E_b = N_A\xi^2/\varepsilon b$$

where N_A is Avogadro's number. This energy is 2–3 times greater than the observed value of E_5 (Table 3) and is further evidence that the free ions originate from the long range tail of the $N(y)$ distribution.

The distances at which the ion–electron coulombic attraction energies equal E_5 range from 140 Å in butene-1 to 360 Å in ethylene (Table 3). Thus the competition between reactions [4] and [5] is only effective at distances $\gtrsim$100 Å under the present conditions. At smaller distances reaction 4 occurs to the virtual exclusion of reaction 5. The same conclusion was derived for free ion formation in *n*-hexane (24) and is in agreement with earlier expectations (12, 14).

TABLE 3. Activation energies of free ion formation

Liquid	E_5*	RT*	E_b*†	$\frac{E_b}{E_5}$	y_{E_5} (Å)‡
C_2H_6	0.6	0.3	1.5	2.5	300
C_3H_8	0.8	0.3	1.8	2.3	210
C_2H_4	0.5	0.3	2.3	4.6	360
C_3H_6	1.0	0.4	2.3	2.3	150
C_4H_8-1	1.0	0.4	2.4	2.4	140

*Average value over the temperature range studied; kcal/mol.
†Ion–electron coulombic attraction at separation distance b.
‡Distance at which the ion–electron coulombic attraction equals E_5.

We are grateful to the staff of the Radiation Research Center for aid with the electronic equipment.

1. W. F. SCHMIDT and A. O. ALLEN. J. Phys. Chem. **72**, 3730 (1968).
2. P. H. TEWARI and G. R. FREEMAN. J. Chem. Phys. **49**, 4394 (1968).
3. P. H. TEWARI and G. R. FREEMAN. J. Chem. Phys. **51**, 1276 (1969).
4. W. F. SCHMIDT and A. O. ALLEN. J. Chem. Phys. **52**, 2345 (1970).
5. K. HORACEK and G. R. FREEMAN. J. Chem. Phys. **53**, 4486 (1970).
6. M. G. ROBINSON P. G. FUOCHI, and G. R. FREEMAN. Can. J. Chem. **49**, 984 (1971).
7. M. G. ROBINSON and G. R. FREEMAN. J. Chem. Phys. In press.
8. R. W. GALLANT. Physical properties of hydrocarbons. Vol. 1, Gulf Publishing Co., Houston, Texas. 1968; Vol. 2, 1970.
9. G. M. BARROW. Physical chemistry. 2nd ed. McGraw-Hill, New York. 1966. p. 432.
10. Handbook of chemistry and physics. 50th ed. Chemical Rubber Publishing Co., Cleveland, Ohio, 1969.
11. R. D. NELSON, JR., D. R. LIDE, JR., and A. A. MARYOTT. Selected values of electric dipole moments for molecules in the gas phase. NSRDS-NBS 10 (1967).
12. G. R. FREEMAN. J. Chem. Phys. **39**, 1580 (1963).
13. J.-P. DODELET, M. G. ROBINSON, P. G. FUOCHI, and G. R. FREEMAN. To be published.
14. G. R. FREEMAN and J. M. FAYADH. J. Chem. Phys. **43**, 86 (1965).
15. G. R. FREEMAN. J. Chem. Phys. **46**, 2822 (1967).
16. A. MOZUMDER. J. Chem. Phys. **48**, 1659 (1968).
17. D. E. LEA. Actions of radiations on living cells. University Press, Cambridge. 1955. Chap. 1.
18. J.-P. DODELET and G. R. FREEMAN. Can. J. Chem. **49**, 2643 (1971).
19. L. F. FIESER and M. FIESER. Organic chemistry. Reinhold, New York. 1956. p. 295.
20. A. D. WALSH. Trans. Faraday Soc. **45**, 179 (1949).
21. R. HOFFMAN. J. Am. Chem. Soc. **90**, 1475 (1968).
22. K. F. REID. Properties and reactions of bonds in organic molecules. Longmans, London. 1968. p. 60.
23. P. AUSLOOS and S. G. LIAS. J. Chem. Phys. **43**, 127 (1965).
24. J. A. LEONE and W. H. HAMILL. J. Chem. Phys. **49**, 5304 (1968).
25. J. R. PARTINGTON. An advance treatise on physical chemistry. Vol. 5. Longmans, London. 1962. p. 349.
26. G. G. MEISELS. J. Chem. Phys. **41**, 51 (1964).
27. P. ALDER and H. K. BOTHE. Z. Naturforsch **20a**, 1700 (1965).
28. R. COOPER and R. M. MOORING. Aust. J. Chem. **21**, 2417 (1968).
29. R. W. KISER. Introduction to mass spectrometry and its applications. Prentice-Hall, Inc., Englewood Cliffs, N.J. 1965. pp. 310, 316.

Can. J. Chem. Downloaded from www.nrcresearchpress.com by 210.87.254.42 on 09/05/12
For personal use only.

Kinetic Solvent Isotope Effect for the Spontaneous Solvolysis Acetic and Propionic Anhydrides

R. E. ROBERTSON, B. ROSSALL,[1] AND W. A. REDMOND[2]

Department of Chemistry, The University of Calgary, Calgary, Alberta

Received March 11, 1971

The large kinetic solvent isotope effects for the neutral hydrolysis of acetic and propionic anhydride show unusual temperature dependency; the former passing through a maximum at about 15°, the latter showing a minimum at 30°. This unusual temperature dependency is the consequence of widely different values of the apparent ΔC_p^* in H_2O and D_2O: the value for acetic anhydride in H_2O being -74 ± 2 cal deg^{-1} mol^{-1} but -32 ± 4 in D_2O. The corresponding values for propionic anhydride being -31 ± 2 in H_2O but -94 ± 10 in D_2O. The implications of these differences are discussed.

L'importance des effets isotopiques cinétiques dans l'hydrolyse en milieu neutre d'anhydride acétique et propionique dépend étrangement de la température; le premier passe par un maximum à environ 15° tandis que le dernier présente un minimum à 30°. Cette dépendance inhabituelle par rapport à la température est la conséquence des valeurs très différentes du ΔC_p^* apparent dans H_2O et D_2O: la valeur pour l'anhydride acétique dans H_2O étant de -74 ± 2 cal deg^{-1} mol^{-1} mais de -32 ± 2 dans D_2O. Les valeurs correspondantes pour l'anhydride propionique sont de -31 ± 2 dans H_2O mais -94 ± 10 dans D_2O. Les conséquences de ces différences sont discutées.

Canadian Journal of Chemistry, 49, 3665 (1971)

Can. J. Chem. Downloaded from www.nrcresearchpress.com by 210.87.254.6 on 09/05/12
For personal use only.

Introduction

The spontaneous hydrolysis of carboxylic acid anhydrides have been widely studied (1–10). The reaction is characterized by large kinetic solvent isotope effects (k.s.i.e. $= k_{H_2O}/k_{D_2O}$) and large negative entropies of activation ($\Delta S^{\ddagger}$). Such results were interpreted as being consistent with the requirements of a general base catalyzed mechanism, BAc2, and were taken to imply (11) that more than one water molecule was tightly constrained in the transition state. Our interest in the effect of temperature on solvolytic rates led initially to an investigation of the temperature dependency of the large kinetic solvent isotope effect for acetic anhydride.

The experimental problem simply required that we extend the careful investigation of Gold (5) over a wide temperature range and obtain a complementary set of rate data in D_2O. The results were so surprising that we were led to extend our investigation to study the hydrolysis of propionic anhydride and to other anhydrides. In this paper we report our findings for the hydrolysis of acetic and propionic anhydride.

Experimental

Commercial samples of acetic anhydride and propionic anhydride were refluxed over magnesium turnings for 24 h. The anhydrides were fractionated and collected at b.p. 140–140.5° for acetic anhydride and b.p. 162–163° for propionic anhydride. Water was purified by preliminary distillation, ion exchange over Rexyn R 208-1-300 H—OH resin and finally distilled in a CO_2-free silica glass still. A specific conductance of 3×10^{-6} ohm^{-1} cm^{-1} at 20° was readily obtained. Heavy water was obtained from Merck, Sharpe and Dohme or A.E.C. of U.S.A. The D_2O was distilled off NaOH (0.001 M) into a Stuart-Wormwell still (12) including a quartz condenser and fractionated under pure nitrogen. D_2O was collected with a specific conductance below 5×10^{-7} ohm^{-1} cm^{-1} at 10°. Mole% D was determined by density measurement (pycnometry) (13) and found to exceed always 99.7 mol% D.

Potassium chloride (approximately 10^{-4} M) was added as backing electrolyte to the water to produce a reaction solution with a cell resistance of about 50 000 ohm. The conductance cell, nearly filled with this backing electrolyte, was held at constant temperature to better than ±0.002°. To a further 20 ml of thermostated backing electrolyte was added 3 μl of reactant and then vigorously shaken. It was found that 2–3 ml of this "concentrated" reactant solution added to the backing electrolyte in each cell (cell constant ~0.2) produced optimal initial resistance readings. Conductance–time data were collected by the Auto-RAM system (14) and pseudo first order rate constants were calculated as follows.

Calculation

Solvolysis of an acid anhydride molecule produces only the parent acid as product (4).

$$(RCO)_2O + H_2O \xrightarrow{k_{obs}} 2RCO_2H \xrightarrow{K_a} 2RCO_2^- + 2H^+$$

If the product were a strong acid then Onsager

[1]NRCC Postdoctorate Fellow, 1968–1970.
[2]NRCC Postdoctorate Fellow, 1965–1967.

TABLE 1. Empirical constants for the rate temperature relation 6 for solvolysis of acetic anhydride and propionic anhydride

Substrate	Solvent	A_1	$-A_2$	$-A_3$	$n_{T_1}{}^{T_2}$
Acetic anhydride	H_2O	110.42086	6925.2658	36.2782	$29_2{}^{25}$
	D_2O	48.94343	4276.5775	15.2112	$34_5{}^{40}$
Propionic anhydride	H_2O	47.32806	4110.1487	14.6943	$33_1{}^{39}$
	D_2O	138.76453	8233.3958	46.2346	$24_{12}{}^{49}$

conductance behavior could be assumed but acetic and propionic acids are weak electrolytes. The following conductance equations provided a satisfactory analysis of the conductance–time data (5, 15, 16). Ostwald's dilution law expressed in conductance terms represents the variation in conductance with concentration of the weak electrolyte. At the substrate concentrations used ($\sim 10^{-4}$ M) this was considered to be reliable.

$$[1] \qquad K_a = \Lambda^2 c/\Lambda_0(\Lambda_0 - \Lambda)$$

where K_a is the acid ionization equilibrium constant, c is the electrolyte concentration, Λ is the equivalent conductance, and Λ_0 the limiting equivalent conductance. By definition

$$[2] \qquad \Lambda = 10^3 C_K/Rc$$

where C_K is the cell constant and R is the resistance of the cell (ohms). Combining eqs. 1 and 2, one gets

$$[3] \qquad c = \frac{10^3 C_K}{\Lambda_0 R}\left\{1 + \frac{C_K}{K_a \Lambda_0 R}\right\}$$

Equation 3 relates the experimental resistance to the electrolyte concentration c provided the constants C_K, Λ_0, and K_a are known or can be estimated ($\pm 10\%$) reliably.

The Guggenheim equation (17) for calculation of first order rate constant is[3]

$$[4] \qquad C_{t+\Delta} - C_t = \frac{C_0}{2}\cdot(1 - e^{-k\Delta})\cdot e^{-kt}$$

where C_0 = stoichiometric concentration of anhydride at time, $t = 0$; C_t = concentration of acid at time t; $C_{t+\Delta}$ = concentration of acid at time $t + \Delta$; Δ = constant time interval, approximately $2\cdot t_1/2$; k^0 = observed first order rate constant.

Combining eqs. 3 and 4 and manipulating gives

$$[5] \quad \log\left\{\frac{1}{R_{t+\Delta}} - \frac{1}{R_t}\right\} + \log\left[1 + \frac{10^3 C_K}{\Lambda_0 K_a}\left\{\frac{1}{R_{t+\Delta}} + \frac{1}{R_t}\right\}\right] = \log\left[\frac{C_0\Lambda_0}{2.10^3 C_K}(1 - e^{-k\Delta})\right] - \frac{k^0 t}{2.3026}$$

Resistance data were collected in pairs, at the constant time interval Δt apart. Then rate constant k^0 was calculated by a linear least squares fit to eq. 5. For solvolysis of acetic anhydride and propionic anhydride in H_2O and D_2O; the cell constants were known, Λ_0 was calculated from available values of limiting ionic equivalent conductances (18, 19), K_a values were available for acetic acid in H_2O (20), acetic acid in D_2O (21), propionic acid in H_2O (22). K_a for ionization of propionic acid in D_2O was estimated by interpolation of ΔpK_a from the ΔpK_a *vs.* pK_a (H_2O) plot Robinson, Paabo, and Bates (23).

Excellent first order kinetic behavior was observed over five half-lives and the observed rate constant was calculated over a period of four half-lives. A precision in the rate constant, estimated by the standard deviation in k^0 for individual runs was $\pm 0.25\%$. Kinetic runs were made in quadruplicate as a further test of reproducibility; the differences between the four rate constants rarely exceeded $\pm 0.5\%$.

TABLE 2. Kinetic solvent isotope effect as a function of temperature

Temperature (°C)	Acetic anhydride	Propionic anhydride
0	2.837	3.188
5	2.892	3.024
10	2.927	2.903
15	2.941	2.818
20	2.937	2.764
25	2.916	2.737
30	2.878	2.736
35	—	2.757
40	—	2.801
45	—	2.866
50	—	2.954

[3]Number 2 is included in eq. 4 for correctness and does not affect value of k in eq. 5.

Can. J. Chem. Downloaded from www.nrcresearchpress.com by 210.87.254.6 on 09/05/12
For personal use only.

TABLE 3. Pseudothermodynamic parameters of activation for solvolysis of acetic anhydride and propionic anhydride

Substrate	Solvent	Temperature (°C)	10^3k^0 (s^{-1})	$\Delta H^{\ddagger}$ (cal mol^{-1})	$-\Delta S^{\ddagger}$ (cal deg^{-1} mol^{-1})	$-\Delta C_p^{\ddagger}$ (cal deg^{-1} mol^{-1})
Acetic anhydride	H_2O	15	1.435	10 342±10	35.59±0.03	74±2
		25	2.663	9 601±31	38.12±0.11	74±2
Acetic anhydride	D_2O	15	0.487_8	10 286±32	37.93±0.11	32±4
		25	0.913_3	9 963±33	39.03±0.11	32±4
Propionic anhydride	H_2O	25	1.522	9 508±14	39.54±0.05	31±2
		35	2.626	9 196±31	40.57±0.10	31±2
Propionic anhydride	D_2O	25	0.556_0	9 687±99	40.94±0.33	94±10
		35	0.952_3	8 749±53	44.04±0.17	94±10

Rate constants were measured[4] over the largest attainable temperature range in order to fit the rate constant – temperature data to an accurately reproducible curve using the kinetic modification of the Clarke and Glew equation (24, 25).

$$\log_{10} k^0 = A_1 + A_2/T + A_3 \log_{10} T + A_4 \cdot T + \cdots$$

Empirical parameters, A_1, A_2, A_3 for a three term fit to eq. 6 enabled recalculation of rate constants agreeing within the experimental error, see Table 1, with the observed rate constants. Rate constants were interpolated at 5° intervals over the experimental temperature range for the solvolysis in both solvents. Hence the kinetic solvent isotope effect and its temperature effect are presented in Table 2 as the ratio of the smoothed curve values of the observed first order rate constants ($k_{H_2O}{}^0/k_{D_2O}{}^0$); see Fig. 1.

Assuming the applicability of the transition state theory, the approximation: $d\Delta C_p^{\ddagger}/dT = 0$ and that the observed rate constant can be treated as that of a single rate determining step, then pseudo-thermodynamic parameters, $\Delta G^{\ddagger}$, $\Delta H^{\ddagger}$, $\Delta S^{\ddagger}$, and $\Delta C_p^{\ddagger}$ can be formally derived from parameters A_1, A_2, and A_3. These data are presented in Table 3.

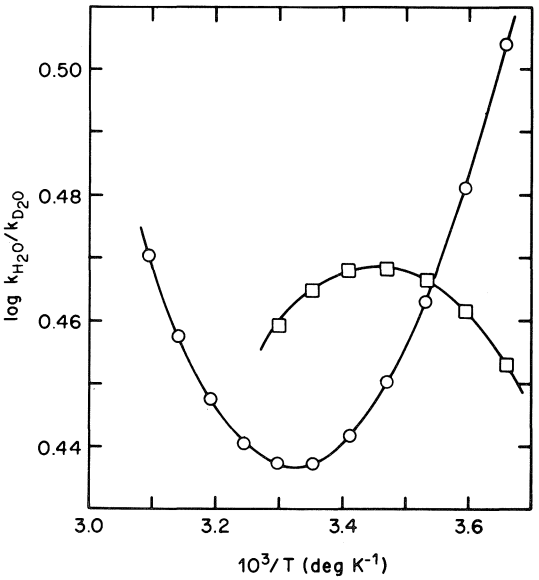

FIG. 1. Temperature dependence of k.s.i.e. for the hydrolysis of acetic anhydride (○) and proprionic anhydride (□).

Discussion

The neutral hydrolysis of acetic anhydride has been regarded as reacting by the BAc2 mechanism (7, 9, 11, 26, 27) given formal representation as

$$(RCO)_2O + 2H_2O \underset{k_2}{\overset{k_1}{\rightleftharpoons}} [\ ] \xrightarrow{k_3} 2CH_3COOH$$

where the bracketed intermediate is isomeric with

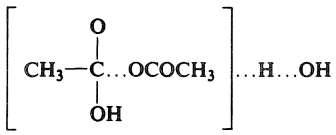

or there may be a further equilibrium involved with a correspondingly more complex rate equation. In the presence of acids or stronger bases still other rate equations will apply. The postulated transition state admits of a large number of variations (5), the simplest kinetic expression for the

[4]Rate determinations were made in randomized order of increasing and decreasing temperatures.

Can. J. Chem. Downloaded from www.nrcresearchpress.com by 210.87.254.6 on 09/05/12
For personal use only.

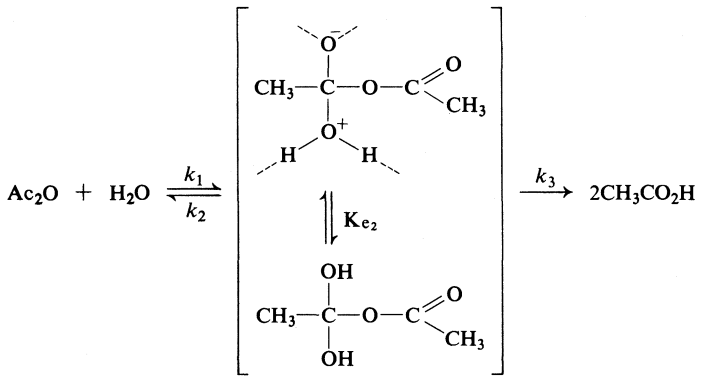

SCHEME 1

observed rate in terms of a steady state approximation being

$$[7] \qquad k^0 = \frac{k_1 k_3}{k_2 + k_3} = \frac{k_1}{1 + \alpha}$$

where $\alpha = k_2/k_3$ and the corresponding kinetic isotope effect is given by

$$[8] \qquad \frac{k^0(H_2O)}{k^0(D_2O)} = \frac{k_1(H_2O)\,(1 + \alpha(D_2O))}{k_2(D_2O)\,(1 + \alpha(H_2O))}$$

If the equilibrium term is significant (Scheme 1), further terms must be included in the k.s.i.e. In 60% dioxane/water, Bunton *et al.* (9) showed by ^{18}O exchange studies that $\alpha = 0.007$ at 25 °C where $\alpha/2 = k_e/k_h$ and k_e was the rate of exchange and k_h the rate of hydrolysis.[5] Where α is small as in the above instance, the formation of the intermediate is the rate controlling step and hence eq. 3, above, reduces to $k_0 = k_1$. In that event no complexity would be expected in the temperature dependence of k.s.i.e. or in $\Delta C_p^{\ddagger}$. Similar values of α were reported for benzoic anhydride and camphoric anhydride (9) but for no anhydride were the ^{18}O exchange for benzoyl chloride relative to the rate of hydrolysis increased markedly as the proportion of water in an organo–water mixture increased (29). Hence, Bunton's oxygen exchange data cannot be taken to exclude the possibility that α approximates unity under our conditions. Bender and Heck (30) have reported that the corresponding value of α in 25% acetonitrile/water mixture for the hydrolysis of ethyl trifluoracetate approximated to unity while the corresponding value of k.s.i.e. in water is 3.6 and $\Delta S^{\ddagger}$ is -35 cal mol^{-1} deg^{-1}. These derived data are consistent with the formation of an intermediate in which the transfer of the proton is advanced: in the limiting case α is large and $k_{obs} = K_e k_3$. While the k.s.i.e. is a little larger than found for the anhydrides, the $\Delta S^{\ddagger}$ values are about the same as shown in Table 3.

It is perhaps significant in the present comparison that the temperature dependence of the k.s.i.e. for methyl trifluoroacetate (32) and for ethyl and isopropyl trifluoroacetate (32) all appear to decrease linearly. The results obtained for acetic and propionic anhydrides show marked departure from such simple temperature dependency and is different in the two examples (Fig. 1). Such differences in temperature dependency greatly weakens any deductions based on the similarity of $\Delta S^{\ddagger}$ or the k.s.i.e. Granted the simple kinetic expression (equation 7) is satisfactory, differences in the temperature dependence of k.s.i.e. would be expected if k_2/k_3 were not too far removed from unity and the difference $\Delta H_2 - \Delta H_3$ is less than 1 kcal. The contrast between the temperature dependence of the k.s.i.e. for the two anhydrides and for the trifluoroacetates which presumably react by the same general mechanism may be attributed to a difference in the value of this ratio.

Further evidence that limiting conditions cannot be applied to the hydrolysis of the anhydrides

[5]Bunton has noted (28) that in order to obtain significant values of α from oxygen exchange experiments two conditions must be satisfied: (*1*) that an intermediate returns (*2*) that the lifetime is sufficient for the oxygens to become equivalent by proton transfer. He notes that there are a number of experimental facts which can be interpreted as casting doubts as to the attainment of the second criterion.

Can. J. Chem. Downloaded from www.nrcresearchpress.com by 210.87.254.6 on 09/05/12
For personal use only.

TABLE 4. Kinetic solvent isotope effects as pseudothermodynamic differences*

Substrate	Temperature (°C)	$\delta_I\Delta H^{\ddagger}$ (cal mol^{-1})	$\delta_I\Delta S^{\ddagger}$ (cal deg^{-1} mol^{-1})	$\delta_I\Delta C_p^{\ddagger}$ (cal deg^{-1} mol^{-1})
Acetic anhydride	15	-74 ± 42	-2.34 ± 0.14	42 ± 6
	25	362 ± 64	-0.91 ± 0.22	42 ± 6
Propionic anhydride	25	179 ± 113	-1.40 ± 0.38	-63 ± 12
	35	-447 ± 84	-3.47 ± 0.27	-63 ± 12

*$\Delta X_{D_2O} - \Delta X_{H_2O} = \delta_T\Delta X$.

is evident in the unprecedent differences in the values of $\Delta C_p^{\ddagger}$ for the two anhydrides in H_2O and D_2O (Table 3). The large value of $\delta_I\Delta C_p$ found in this study and the fact that the differences had opposite signs for small differences in structure underlines the complexity of the rate controlling processes. We do not have, as yet, comparable values for $\Delta C_p^{\ddagger}$ for the trifluoroacetates, but Bates and Robinson and co-workers have published a study of the temperature dependence of the ionization of acetic acid (33) in H_2O and D_2O and the corresponding data for the autoprotolysis of the two waters (34). For acetic acid $\delta_I\Delta F = 758$ cal; $\delta_I\delta H$ 400 cal/mol; $\delta_I\Delta S = -1.3$ cal deg^{-1} mol^{-1}, and $\delta_I\Delta C_p = 2$ cal deg^{-1} mol^{-1}. Since the latter term is small, $\delta_I\Delta H$ does not change markedly over the experimental range. In the autoprotolysis of water $\delta_I\Delta C_p = -8.2$ cal deg^{-1} mol^{-1} but in this case we are comparing different species in different environments. In the hydrolysis of acetic anhydride, $\Delta H^{\ddagger}$ is less in D_2O than in H_2O at 15 °C but greater at 25 °C. Just the opposite trend is found for the hydrolysis of propionic anhydride.

These derived parameters do not provide a basis for deciding the kind of mechanistic complexity involved but are good indicators that such complexity is present. The simplest hypothesis would seem to be that for hydrolysis in water α approximates to unity. Scott and Robertson (35) have shown in a recent paper that for a rate sequence equivalent to eq. 9 the apparent heat capacity is a complex term

$$[9]\quad \Delta C_p^{\ddagger} = \Delta C_{p_1}^{\ddagger} + \frac{\alpha}{1+\alpha}(\Delta C_{p_1}^{\ddagger} - C_{p_2}^{\ddagger}) \times \frac{\alpha}{(1+\alpha)^2}(\Delta H_2^{\ddagger} - \Delta H_3^{\ddagger})^2/RT$$

where the last term on the r.h.s. of eq. 9 is spurious and necessarily positive. Given the above possibility and in the absence of information as to the value and temperature dependence of k_2/k_3 it will be apparent that the derived values of $\Delta C_p^{\ddagger}$ do not admit of a simple interpretation in terms of solvent reorganization.

1. A. C. D. RIVETT and N. V. SIDGWICK. J. Chem. Soc. 732 (1910).
2. B. H. WILSDON and N. V. SIDGWICK. J. Chem. Soc. 1959 (1913).
3. M. KILPATRICK. J. Am. Chem. Soc. **50**, 2891 (1928).
4. S. E. VLES. Rec. Trav. Chim. Pays-Bas. **52**, 809 (1933).
5. V. GOLD. Trans. Faraday Soc. **44**, 506 (1948).
6. J. KOSKIKALLIO. Acta Chem. Scand. **13**, 665 (1959).
7. A. R. BUTLER and V. GOLD. J. Chem. Soc. 2305 (1961).
8. A. R. BUTLER and V. GOLD. J. Chem. Soc. 2212 (1962).
9. C. A. BUNTON, N. A. FULLER, S. G. PERRY, and V. J. SHINER. J. Chem. Soc. 2918 (1963).
10. F. P. CAVASINO and S. D'ALESSANDRO. Ric. Sci **7**, 421 (1964).
11. S. L. JOHNSON. Adv. Phys. Org. Chem. **5**, 237 (1967).
12. J. M. STUART and F. WORMWELL. J. Chem. Soc. 85 (1930).
13. I. KIRSCHENBAUM. Physical properties and analysis of D_2O. McGraw-Hill, New York. 1951. p. 14.
14. R. E. ROBERTSON and S. E. SUGAMORI. J. Am. Chem. Soc. **91**, 7254 (1969).
15. D. J. G. IVES. J. Chem. Soc. 731 (1933).
16. J. G. WINTERS and J. M. W. SCOTT. Can. J. Chem. **46**, 2887 (1968).
17. E. A. GUGGENHEIM. Phil. Mag. **2**, 538 (1926).
18. R. A. ROBINSON and R. H. STOKES. Electrolyte solutions. Butterworths, London. 1968. p. 463.
19. A. GIERER. Z. Naturforsch. **5A**, 581 (1950).
20. H. S. HARNED and R. W. EHLERS. J. Am. Chem. Soc. **55**, 652 (1933).
21. C. K. RULE and V. K. LAMER. J. Am. Chem. Soc. **60**, 1974 (1938).
22. H. S. HARNED and R. W. EHLERS. J. Am. Chem. Soc. **55**, 2379 (1933).
23. R. A. ROBINSON, M. PAABO, and R. G. BATES. J. Res. Nat. Bur. Stand. **73A**, 299 (1969).
24. E. C. W. CLARKE and D. N. GLEW. Trans. Faraday Soc. **62**, 539 (1966).

Can. J. Chem. Downloaded from www.nrcresearchpress.com by 210.87.254.6 on 09/05/12
For personal use only.

25. L. J. BRUBRACHER, L. TREINDL, and R. E. ROBERTSON. J. Am. Chem. Soc. **90**, 4611 (1968).
26. M. L. BENDER. Chem. Rev. **60**, 53 (1960).
27. A. QUEEN. Can. J. Chem. **45**, 1619 (1967).
28. C. A. BUNTON. Private communication, Nov. 23, 1971.
29. C. A. BUNTON, T. A. LEWIS, and D. R. LLEWELLYN. Chem. Ind. London, 1154 (1954).
30. M. L. BENDER and H. D'A. HECK. J. Am. Chem. Soc. **89**, 1211 (1967).
31. B. ROSSALL and R. E. ROBERTSON. Unpublished work.
32. J. M W. SCOTT and J. G. WINTERS. Can. J. Chem. **46**, 2887 (1968).
33. M. PAABO, R. G. BATES, and R. A. ROBINSON. J. Phys. Chem. **70**, 540 (1966).
34. A. K. COVINGTON, R. A. ROBINSON, and R. G. BATES. J. Phys. Chem. **70**, 3820 (1966).
35. J. M. W. SCOTT and R. E. ROBERTSON. Can. J. Chem. To be published.

Can. J. Chem. Downloaded from www.nrcresearchpress.com by 210.87.254.6 on 09/05/12
For personal use only.

Nuclear Magnetic Resonance Studies of Multi-site Chemical Exchange. II. Hindered Rotation in *N,N*-Dimethyl Carbamyl Fluoride

L. W. Reeves and K. N. Shaw

Department of Chemistry, University of Waterloo, Waterloo, Ontario

Received March 1, 1971

The matrix formulation of the Bloch equations including chemical exchange reported earlier is extended to include indirect spin–spin coupling in first-order spectra. The ABX ($J_{AB} = 0$) spin system is treated in detail and particular attention is paid to the determining effect on the nuclear magnetic resonance (n.m.r.) lineshapes of the relative signs of the coupling constants J_{AX} and J_{BX}. The hindered rotation for *N,N*-dimethyl carbamyl fluoride in CCl_4 as solvent has been studied using a complete ^1H n.m.r. lineshape analysis and the activation parameters obtained are: $\Delta G^{\ddagger} = 18.1 \pm 0.6$ kcal mol^{-1}, $\Delta H^{\ddagger} = 17.7 \pm 0.6$ kcal mol^{-1}, and $\Delta S^{\ddagger} = -1.4 \pm 2.1$ cal deg^{-1} mol^{-1} at 25 °C.

The complete lineshape fits give very precise values of the relative shifts (16.5 mol% in CCl_4) of the methyl groups and of the coupling constants J_{AX} (0.30 ± 0.05 Hz) and J_{BX} (0.80 ± 0.05 Hz) at all temperatures. A 40% change in J_{BX} (1.10 ± 0.05 Hz) is observed in neat DMCF from a lineshape fit at −15 °C. The origin of changes in chemical shifts with temperature and J_{BX} with solvent is discussed.

La forme matricielle des équations de Bloch appliquée à l'échange chimique et rapportée précédemment est développée pour tenir compte des couplages spin–spin indirects dans les spectres au premier ordre. Le système de spin ABX (avec $J_{AB} = 0$) est traité en détail, en portant une attention particulière à l'effet déterminant des signes relatifs des constantes de couplage J_{AX} et J_{BX} sur la forme des raies du spectre r.m.n.

L'étude de la rotation restreinte du fluorure de *N,N*-diméthyle carbamyle en solution dans CCl_4 par une analyse complète de forme de raies r.m.n. du proton a donné les paramètres d'activation: $\Delta G^{\ddagger} = 18.1 \pm 0.6$ kcal mol^{-1}, $\Delta H^{\ddagger} = 17.7 \pm 0.6$ kcal mol^{-1} et $\Delta S^{\ddagger} = -1.4 \pm 2.1$ cal deg^{-1} à 25 °C.

Le calcul complet des formes de raies donne des valeurs très précises pour les déplacements relatifs (16.5 mol% dans CCl_4) des groupes méthyles et les constantes de couplage J_{AX} (0.30 ± 0.05 Hz) et J_{BX} (0.80 ± 0.05 Hz) à toutes les températures. Une variation de 40% de J_{BX} (1.10 ± 0.05 Hz) est observée dans le DMCF pur d'après un calcul de forme de raies à −15 °C. L'origine des variations de déplacement chimique avec la température et de J_{BX} avec le solvant est discutée.

Canadian Journal of Chemistry, **49**, 3671 (1971)

Introduction

The Bloch equations (1) have been modified to include chemical exchange effects (2–4), in first-order spectra, and have allowed a simple phenomenological description of n.m.r. lineshape characteristics. In the first paper in this series (5), a concise matrix formulation of the modified Bloch equations has been presented as a basis for a series of experimental studies of a wide range of chemical systems. This formulation accommodates a general first-order *n*-site exchange system and a complete description of all rate processes is contained in a single $n \times n$ matrix. Such a theoretical approach allows an efficient routine analysis for rate constants and activation parameters.

The effect of chemical exchange on spin–spin multiplets in first-order n.m.r. spectra was recognized in the original work of Gutowsky *et al.* (2, 6), and various approximate analytical expressions have been developed to derive kinetic data for specific cases (7–10). Only recently, however, have complete lineshape analyses been applied to multi-site exchange systems with *J*-coupling (11–15). Inconsistent analyses are still appearing in the literature, however, and very little reliable kinetic data is available. Thus this paper outlines the inclusion of *J*-coupling for the representative ABX ($J_{AB} = 0$) spin system. It is shown that, from a complete lineshape analysis in the first-order limit, the detailed form of chemical exchange and additional relaxation processes and also the relative signs of indirect spin–spin coupling constants may be readily determined. The experimental case chosen, namely the hindered rotation in *N,N*-dimethyl carbamyl fluoride (DMCF), is particularly problematical because of a very small chemical shift between two environmental sites and relatively small J_{AX} and J_{BX} values.

A unified theory of exchange modified n.m.r. lineshapes has been presented by Binsch (16). This theory using the Liouville operator formalism is inclusive of the cases discussed in this

Can. J. Chem. Downloaded from www.nrcresearchpress.com by 210.87.254.6 on 09/05/12
For personal use only.

Can. J. Chem. Downloaded from www.nrcresearchpress.com by 210.87.254.6 on 09/05/12
For personal use only.

paper, but a detailed description of the lineshapes for first-order spectra (of the form observed for *N,N*-dimethyl amides) is included here to allow a lucid illustration of the inclusion of *J*-coupling and, in particular, to emphasize the effects of the relative signs of the coupling constants as discussed briefly in an earlier paper (12). The matrix formulation presented here follows directly from the stochastic exchange model discussed in the first paper in this series (5) and all the equations used are also applicable to second-order (tightly coupled) spin systems. That is, the diagonal matrix $\mathbf{\Omega}$, *cf.* eq. 19 in ref. 5, defining the Larmor frequencies for spin-sites in the first-order limit is replaced by an off-diagonal matrix with elements formally derived in terms of a superoperator (17–19) in a simple product function basis; and the intensity and population vectors $\boldsymbol{I}$ and $\boldsymbol{P}$, respectively, *cf.* eq. 20 in ref. 5, have zero elements corresponding to combination transitions. This independently developed matrix formulation is particularly amenable to numerical lineshape calculations and has been used for efficient iterative lineshape fitting, similar to that described in this paper, and will be discussed for specific examples of multi-site chemical exchange involving second-order spin systems in future publications.

Hindered rotation about the N—C bond in amides has been the subject of numerous n.m.r studies (20); but to date, reliable data for closely related chemical systems are very limited. Thus *N,N*-dimethyl carbamyl fluoride has been studied as a member of a series of halo-substituted amides to allow a correlation of the barriers to rotation with bonding parameters from molecular orbital calculations. Also, although this compound is well known as a specific enzyme inhibitor (21, 22), no information is available on its electronic structure as compared with other amides of importance in biological systems (23). The parent compound carbamyl fluoride is stable only at a low temperature (24) and hence the barrier to rotation cannot be measured for this particular amide, as is the case for other carbamyl halides and carbamyl pseudo-halides. The electronic interactions of interest, namely those between the carbonyl and amide groups and a given C-substituent X in the general structures

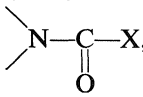

characteristics for the parent amides and a corresponding *N,N*-dimethyl amide series. As the latter amides are readily accessible, this particular series has been chosen for a quantitative comparison of bonding characteristics in C-substituted amides.

Chemical Exchange Spin-sites, ABX Spin System

A normal multi-site n.m.r. exchange system, in the first-order limit, is considered in terms of distinct sites (2, 5) of differing Larmor frequency, ω_i, such that each site may be associated with a specific molecular electronic environment and corresponding relative chemical shift, Ω_i. This concept of exchange sites may now be extended to spin systems including *J*-coupling. As the simple first-order ABX ($J_{AB} = 0$) spin system includes all the features of a general analysis, and is applicable to a study of hindered rotation in *N,N*-dimethyl carbamyl fluoride, this particular system will be considered in detail. The spin Hamiltonian for this system may be expressed in the form

$$[1]\quad H = H_0 + H_\Omega + H_J^{(1)} = -\omega_0[I_{zA} + I_{zB} + I_{zX}] + \Omega[I_{zA} - I_{zB}] + \Omega_X I_{zX} + J_{AX} I_{zA} I_{zX} + J_{BX} I_{zB} I_{zX}$$

H_0 is a generalized Zeeman term and ω_0 is a reference Larmor frequency (rad s^{-1}). An independent frequency variable x may now be defined as $x = \omega - \omega_0$ (5), where ω is the frequency of the irradiating r.f. magnetic field. H_Ω is the chemical shift term in which $\Omega_A = -\Omega$ and $\Omega_B = \Omega$ with $\omega_0 = (1/2)(\omega_A - \omega_B)$ and $\Omega_A = \omega_A - \omega_0$. $H_J^{(1)}$ is the *J*-coupling term as $H_J^{(2)} = (1/2)\{J_{AX}[I_A^+ I_X^- + I_A^- I_X^+] + J_{BX}[I_B^+ I_X^- + I_B^- I_X^+]\}$ may be neglected in a first-order ($J_{ij} \ll |\Omega_i - \Omega_j|$) determination of spectral transition frequencies and intensities (25). The $H_J^{(2)}$ term, however, has been shown to give rise to a spin–spin relaxation mechanism which may be described by Bloch type equations for a weakly coupled spin system (26). The effect of such a relaxation in addition to chemical exchange is not included in the present work. In the usual I_Z-representation with simple product basis functions, ϕ_l, the Hamiltonian given in eq. 1 is diagonal and hence all terms correspond to secular energies determining the transition frequencies listed in Table 1. As is well known, two relative sign combinations are possible for J_{AX} and J_{BX} (25) and thus it is initially assumed that $J_{AX} > 0$ and $J_{BX} > 0$. The AB-part of the ABX spectrum consists of the four transitions (each

TABLE 1
(*a*) Transition frequencies for ABX ($J_{AB} = 0$) spin system

Transition number*	Transition type	Energy levels†	Frequency x
1	A	(1,3), (2,4)	$-\Omega-\frac{1}{2}J_{AX}$
2	A	(5,7), (6,8)	$-\Omega+\frac{1}{2}J_{AX}$
3	B	(1,2), (3,4)	$\Omega-\frac{1}{2}J_{BX}$
4	B	(5,6), (7,8)	$\Omega+\frac{1}{2}J_{BX}$
1	X	(1,5)	$-\Omega_X-J_+$‡
2	X	(3,7)	$-\Omega_X-J_-$
3	X	(2,6)	$-\Omega_X+J_-$
4	X	(4,8)	$-\Omega_X+J_+$

*These transition numbers correspond to those used in Figs. 1 and 3.
†The bracket (l,m) refers to energy levels E_l and E_m, and corresponding eigen-functions ϕ_l and ϕ_m.
‡ $J_\pm = (1/2)(J_{BX} \pm J_{AX})$; $J_{BX} > J_{AX} > 0$.

(*b*) Basis (eigen) functions (ϕ_l) for ABX spin system, $I = 1/2$ nuclei

l	ϕ_l	l	ϕ_l
1	ααα	5	ααβ
2	αβα	6	αββ
3	βαα	7	βαβ
4	ββα	8	βββ

of which is doubly degenerate for $J_{AB} = 0$) shown in Fig. 1(*a*), where the *J*-couplings with the X-spin determine effective Larmor frequencies $x = -\Omega \pm (1/2)J_{AX}$ and $x = \Omega \pm (1/2)J_{BX}$. These frequencies may be associated with four distinct exchange sites, analogous to the two environmental sites with Larmor frequencies $x = \pm\Omega$. Thus in general, in the presence of exchange, a basic environmental (chemical shift) site with an associated X-spin state may be referred to as *spin site-j*, with Larmor frequency x_j. In this manner, for the couplings as given above, spin site-1 corresponds to a basic A-site associated with an α X-spin state as shown by the eigenfunctions corresponding to the energy levels determining the transition frequency $x_1 = -\Omega - (1/2)J_{AX}$: (ααα, βαα) and (αβα, ββα). For a molecular system not having a preferred conformation (equal population exchange system) all transition intensities in the AB-part of the spectrum are equal, as are those in the X-part, in the absence of exchange. The X-part of the ABX spectrum consists of the four transitions shown in Fig. 3(*a*).

In terms of a stochastic theory (3, 27) for exchange effects in a first-order spin system, the nuclear magnetization associated with spin site-*j* may be considered in terms of a spin isochromat (28) $M(x_j,\phi_j)$ with Larmor frequency x_j and phase ϕ_j (27) and a magnitude proportional to

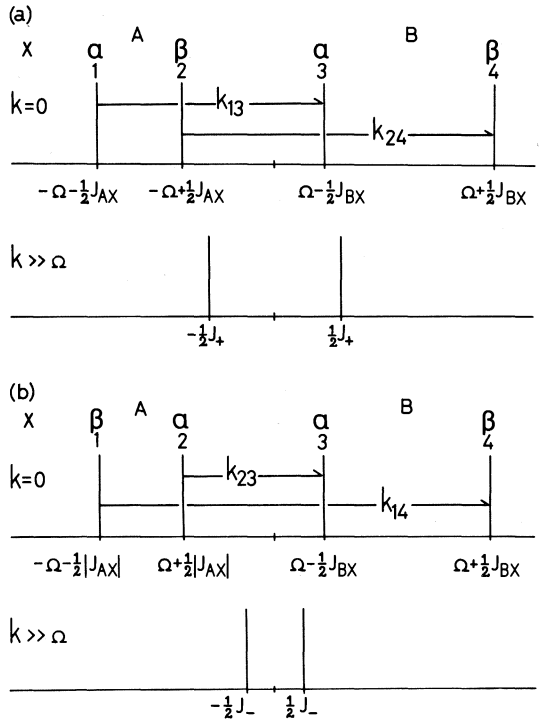

FIG. 1. AB-part of first-order ABX ($J_{AB} = 0$) spectrum in the limits of no exchange and fast exchange ($k \gg \Omega$): (*a*) $J_{BX} > J_{AX} > 0$ and $J_+ = (1/2)(J_{BX} + J_{AX})$; (*b*) $J_{BX} > 0$, $J_{AX} < 0$ with $J_{BX} > |J_{AX}|$ and $J_- = (1/2)(J_{BX} - |J_{AX}|)$. The basic A and B environmental sites are indicated along with the X-spin state corresponding to each AB-exchange spin-site.

the fractional population P_j (5). In the absence of exchange, these spin isochromats precess independently about the direction of the static applied magnetic field and a transverse relaxation time T_{2j} describes the coherent isochromat dephasing (28), and Lorentzian distribution of Larmor frequencies about x_j, associated with local magnetic field inhomogeneity. In the presence of chemical exchange, characterized by a rate constant k, individual spin isochromats are involved in a random transfer between spin-sites. Conversely, it may be considered that each spin isochromat experiences a randomly fluctuating local magnetic field with a fundamental frequency component k rad s^{-1}. Thus an exchange process gives rise to an incoherent isochromat dephasing and a modulation of the Larmor frequencies x_j. The assumptions inherent in a stochastic description of exchange effects may now be summarized as follows:

(*i*) the isochromat $M(x_j,\phi_j)$ remains in spin

Can. J. Chem. Downloaded from www.nrcresearchpress.com by 210.87.254.6 on 09/05/12
For personal use only.

Can. J. Chem. Downloaded from www.nrcresearchpress.com by 210.87.254.6 on 09/05/12
For personal use only.

site-j with a mean lifetime τ_j until a random instantaneous transfer to a different site takes place due to a chemical exchange process, such that precessional effects in the transfer interval may be neglected;

(*ii*) the site lifetime τ_j is independent of the associated spin–spin and spin–lattice relaxation times, T_{2j} and T_{1j}, respectively;

(*iii*) individual spin isochromats relax independently except for site transfer effects; and

(*iv*) for $M(x_j,\phi_j)$ in spin site-j there is a constant probability per unit time, k_{ji}, for transfer *from site-j into site-i*, this probability being inversely proportional to the fractional site population P_j.

Under these assumptions, the spin-site lifetime τ_j and associated rate constants are related by

$$[2] \qquad \sum_i k_{ji} = \tau_j^{-1}$$

where i ($i \neq j$) includes all allowed transfer sites connected with site-j, and $\tau_j > T_{1j}$. Also, in accordance with the principle of detailed balance for rate processes, spin-site populations and rate constants for any two sites satisfy the condition

$$[3] \qquad P_i k_{ij} = P_j k_{ji}$$

In terms of this stochastic model, an intramolecular mutual exchange in an ABX spin system (for example, hindered internal rotation) is described by a single first-order rate constant and will be assumed to give a transfer of nuclear magnetization between *spin-sites* distinguished by the chemical shifts for A- and B-spins, $-\Omega$ and $+\Omega$, respectively. All possible transfers between the four AB spin-sites may be represented by

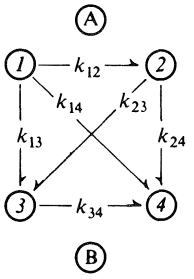

In accordance with assumption (*i*) above, it must be assumed that the X-spin state is *unchanged* during an AB spin-site transfer and hence the allowed transfers are $1 \leftrightarrow 3$ and $2 \leftrightarrow 4$ as readily seen by comparison of the eigen-functions associated with the transitions *1*, *3* and *2*, *4* in Table 1. That is, transitions *1* and *3* are A- and B-spin transitions, respectively, where all eigen-functions involved have an α X-spin part as shown in Fig. 1(*a*). For a mutual intramolecular exchange, this stochastic model is consistent with a quantum-mechanical treatment (29, 30) in that it may be considered that the molecular system following a nuclear spin-site transfer has a spin Hamiltonian differing only in interchanged magnetic properties for the A- and B-spins. An exchange operator E defined by $E|\alpha\alpha\xi_X\rangle = |\alpha\alpha\xi_X\rangle$ and $E|\alpha\beta\xi_X\rangle = |\beta\alpha\xi_X\rangle$, where ξ_X is the X-spin part of the product basis function, then determines exactly those transitions involved in AB spin-site transfers as allowed above. In an intramolecular exchange, the nuclear spin states for an individual molecule following a spin-site transfer are determined completely by the original states. This is actually the fundamental difference between such a process and an intermolecular exchange in which the overall state of an individual molecule following spin transfer depends upon the original state of this molecule and also the state of the interacting molecule. Therefore, if the X-spin undergoes an intermolecular exchange all AB spin-site transfers as depicted above are allowed as the X-spin state may now be *changed* in this exchange process. For example, spin-sites *1* and *2* differ only in the X-spin state as shown in Fig. 1(*a*). Such a spin-site transfer may also be considered to correspond to a spin–lattice relaxation mechanism for the X-spin; and in particular, the correlation time τ_C for a quadrupolar relaxation process may be comparable to the AB spin-site lifetime τ_j. Such a mechanism also leads to the effective transfers $1 \leftrightarrow 4$, $2 \leftrightarrow 3$, and $3 \leftrightarrow 4$. The effect of this additional relaxation process will depend upon the parameters $(\tau_C J_{AX})^{-1}$ and $(\tau_C J_{BX})^{-1}$, and hence in many first-order spin systems in the liquid phase such an effect may be described by a pseudo-secular contribution to the transverse relaxation time T_{2j}.

General lineshape characteristics for chemical exchange in the AB-part of a first-order ABX spectrum are concisely described through a 4×4 rate matrix, $\mathbf{K}$, as defined in the first paper of this series (5). In the zero saturation limit, a complex lineshape function $G(x)$ may then be expressed in the form

$$[4] \qquad G(x) = A\, \boldsymbol{I}.\mathbf{S}.[\mathbf{\Lambda} + (1/T_2 + ix)\mathbf{I}]^{-1}.\mathbf{S}^{-1}.\boldsymbol{P}$$

Can. J. Chem. Downloaded from www.nrcresearchpress.com by 210.87.254.6 on 09/05/12
For personal use only.

in which $\mathbf{\Lambda}$ is the diagonal matrix corresponding to a matrix $[\mathbf{K} - i\mathbf{\Omega}]$, the diagonal matrix $\mathbf{\Omega}$ being defined by the spin-site Larmor frequencies, x_j, in terms of the independent frequency variable x. $\mathbf{S}$ is the matrix which diagonalizes $[\mathbf{K} - i\mathbf{\Omega}]$, *viz.*, $\mathbf{\Lambda} = \mathbf{S}^{-1}.[\mathbf{K} - i\mathbf{\Omega}].\mathbf{S}.\boldsymbol{P}$ is the spin-site fractional population column vector and $\boldsymbol{I}$ is a transition intensity row vector. It has been implicitly assumed that T_{2j} is the same for all spin-sites in defining the relaxation matrix $\mathbf{T}_2$ as the scalar matrix $(1/T_2)\mathbf{I}$, where $\mathbf{I}$ is the 4×4 unit matrix. This simplification is usually valid in that non-secular relaxation processes (26, 29), as described by off-diagonal elements in $\mathbf{T}_2$, are negligible. However, it is to be noted that the relaxation processes associated with the J-coupled X-spin, and considered in terms of effective spin-site transfers above, are equivalently described by such off-diagonal elements. In this manner, quadrupolar relaxation effects are very simply incorporated in to eq. 4.

The matrix $\mathbf{K}$ describing intramolecular exchange effects in the AB-part of the equal population ABX ($J_{AB} = 0$) spin system with $J_{BX} > J_{AX} > 0$, and spin-sites as ordered in Fig. 1(*a*), is given (5) in terms of the rate constant k s^{-1} as

$$\mathbf{K} = \begin{pmatrix} k & 0 & -k & 0 \\ 0 & k & 0 & -k \\ -k & 0 & k & 0 \\ 0 & -k & 0 & k \end{pmatrix}$$

In accordance with eq. 2, the diagonal element K_{jj} is equal to the inverse spin-site lifetime τ_j^{-1}. The elements of the diagonal $\mathbf{\Omega}$ matrix are simply the transition frequencies listed in Table 1, and the vectors $\boldsymbol{P}$ and $\boldsymbol{I}$ have equal elements 0.25 and 1.0, respectively. Equation 4 now allows a very efficient computation of the steady-state n.m.r. absorption mode lineshape function, $V(x)$, as the real part of $G(x)$. Lineshapes have been calculated for the AB-part of the ABX spectrum defined by: $\Omega = 4.0$ Hz, $J_{AB} = 0$, $J_{AX} = 2.0$ Hz, $J_{BX} = 5.0$ Hz, and $T_2 = 0.64$ s (0.5 Hz full width at half-maximum), and are shown in Fig. 2(*a*) for rate constants in the range $0 \leqslant k \leqslant 200$ s^{-1}. These lineshapes are normalized independently of k, through the constant A in eq. 4, and the spectrum limits are ± 20 Hz. In the limit of fast exchange ($k \gg \Omega$) the spectrum reduces to a doublet. This feature is characteristic of an A_2X spin system

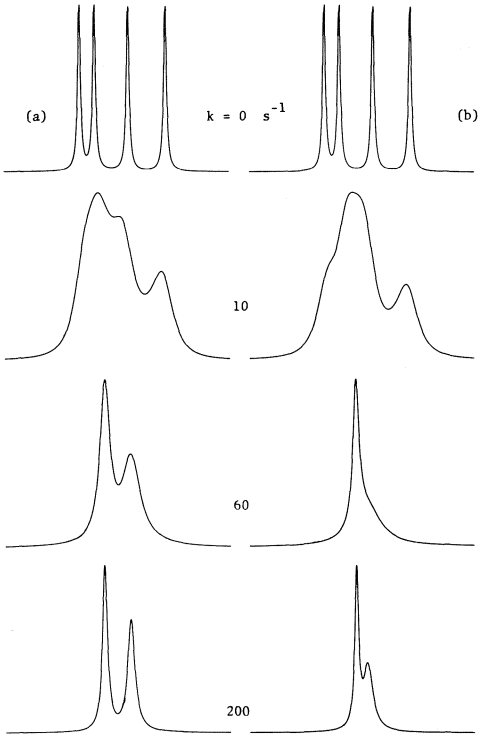

FIG. 2. Intramolecular exchange lineshape function, $V(x)$, for the AB-part of first-order ABX ($J_{AB} = 0$) spectrum; (*a*) $J_{BX} > J_{AX} > 0$; (*b*) $J_{BX} > 0$, $J_{AX} < 0$ and $J_{BX} > |J_{AX}|$.

and is consistent with the expectation that in this limit basic A- and B-sites become equivalent. As shown in Fig. 1(*a*), for J_{AX} and J_{BX} of the *same sign* the doublet splitting is J_+, where $J_+ = (1/2)(J_{BX} + J_{AX})$.

Now for a spin system with J_{AX} and J_{BX} of *different sign*, the spin–spin coupling term in the Hamiltonian given in eq. 1 may be expressed as $-|J_{AX}|I_{zA}I_{zX} + J_{BX}I_{zB}I_{zX}$, where it is assumed that $J_{AX} < 0$ and $J_{BX} > 0$. The allowed transition frequencies are defined by substituting $-|J_{AX}|$ for J_{AX} in Table 1; and the AB-part of the spectrum for this spin system is shown in Fig. 1(*b*), in which the ordered transitions *1* and *2* now correspond to β and α X-spin states, respectively. In this case, the matrix $\mathbf{K}$ is

$$\mathbf{K} = \begin{pmatrix} k & 0 & 0 & -k \\ 0 & k & -k & 0 \\ 0 & -k & k & 0 \\ -k & 0 & 0 & k \end{pmatrix}$$

Can. J. Chem. Downloaded from www.nrcresearchpress.com by 210.87.254.6 on 09/05/12
For personal use only.

and this matrix determines the lineshapes shown in Fig. 2(*b*) for the parameters previously given. In the region of coalescence ($k \sim \Omega$) and in the fast exchange limit, for a given rate constant k, these lineshapes are distinctly different from those for J_{AX} and J_{BX} of the same sign, *cf.* Fig. 2(*a*). Therefore, in general, the *relative signs* of J_{AX} and J_{BX} may be determined directly by lineshape fitting of an exchange modified ABX spectrum. To date, this feature has apparently only been recognized in a few instances (12, 31). Of course, a further consequence of J_{AX} and J_{BX} having different signs is that the doublet splitting in the fast exchange limit is J_-, where $J_- = (1/2)(J_{BX} - |J_{AX}|)$ for $J_{BX} > |J_{AX}|$, as shown in Fig. 1(*b*).

The corresponding rate matrices, **K**, for a more general unequal population exchange system have elements determined by the relationship given in eq. 3. Thus for $J_{BX} > J_{AX} > 0$ it follows that $K_{31} = -k$ and $K_{13} = -(P_A/P_B)k$, where k is the first-order rate constant for transfer from spin-site *1* and P_A is the sum of fractional populations for the spin-sites associated with the A-type basic environmental exchange site. In this manner the doublet in the fast exchange limit is centered at $x = (1 - 2P_A)\Omega$ and it has a splitting given by $(1 - 2P_A)J_- + J_+$, which is equivalent to the weighted average coupling $P_AJ_{AX} + P_BJ_{BX}$. For $J_{BX} > 0$ and $J_{AX} < 0$, this doublet is centered as above but the splitting is now given by $(1 - 2P_A)J_+ + J_-$, where J_+ and J_- are as previously defined.

Exchange effects in the X-part of the ABX ($J_{AB} = 0$) spectrum under consideration are also described by 4 × 4 matrices **K** and **Ω** analogous to those already discussed. The X-part spectra in the absence of exchange and in the fast exchange limit ($k \gg J_{\mp}$) are represented as shown in Fig. 3. The corresponding absorption mode lineshapes (for the particular set of parameters previously defined) are shown in Fig. 4, and again the relative signs of J_{AX} and J_{BX} give rise to marked differences in the computed lineshapes. An example in the literature closely related to the ABX spin system is ^{15}N-formamide analyzed as an ABXY ($J_{AB} \neq 0$) system (32). Inspection of the X-part of the experimental spectrum at 75 °C clearly shows that J_{AX} and J_{BX} have the same sign, as now verified by double resonance methods (33, 34).

With respect to experimental n.m.r. lineshape fitting, an analysis of *both* the AB- and X-parts of an ABX spectrum allows a check on the internal consistency of the fitting procedure used to obtain rate constants for a given exchange process. Also, in general, lineshape fitting is most reliable in the region of coalescence. Now the coalescence condition for the AB-part of the spectrum is determined by the chemical shift difference 2Ω, whereas the same condition for the X-part is determined by the parameter $J_- = (1/2)(J_{BX} - J_{AX})$ (or $J_+ = (1/2)(J_{BX} + |J_{AX}|)$); and hence, if J_- (or J_+) and 2Ω differ significantly, a dual analysis may allow an accurate measurement of the specific rate constant k over an extended temperature range, which is critical in the determination of reliable activation parameters from the usual Arrhenius plot.

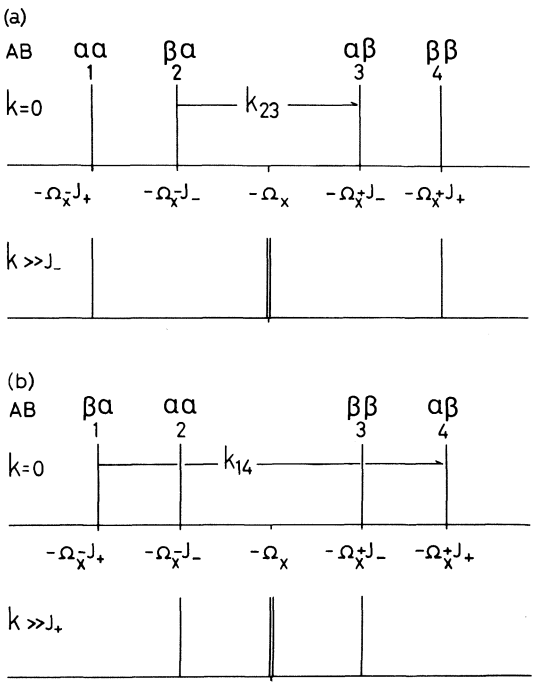

FIG. 3. X-part of first-order ABX ($J_{AB} = 0$) spectrum in the limits of no exchange and fast exchange ($k \gg J_{\mp}$): (*a*) $J_{BX} > J_{AX} > 0$ and $J_{\pm} = (1/2)(J_{BX} \pm J_{AX})$; (*b*) $J_{BX} > 0$, $J_{AX} < 0$ with $J_{BX} > |J_{AX}|$ and $J_{\pm} = (1/2)(J_{BX} \pm |J_{AX}|)$. The AB-spin states corresponding to each of the X-spin sites are shown for the ordered transitions.

Experimental

(A) Preparation of N,N-Dimethyl Carbamyl Fluoride (DMCF)

This compound was prepared by an exchange reaction between equimolar amounts of *N,N*-dimethyl carbamyl

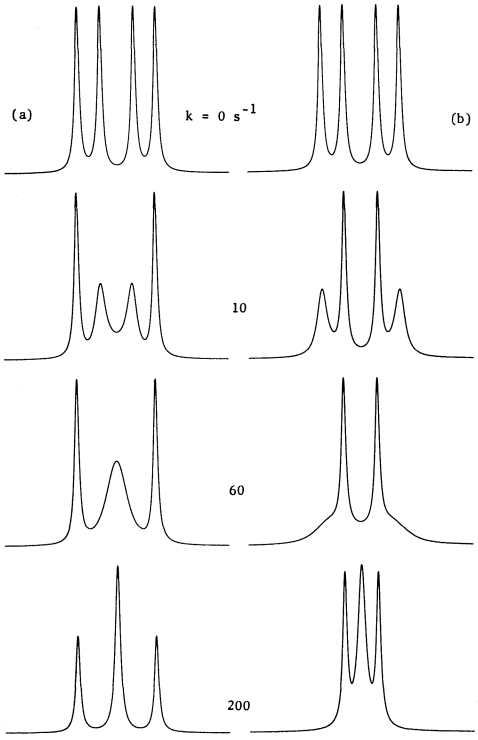

FIG. 4. Intramolecular exchange lineshape function, $V(x)$, for the X-part of an ABX ($J_{AX} = 0$) spectrum: (*a*) $J_{BX} > J_{AX} > 0$; (*b*) $J_{BX} > 0$, $J_{AX} < 0$, and $J_{BX} > |J_{AX}|$.

bromide (DMCB) and AgF, using acetonitrile as solvent, at room temperature. The yield was low (~15%), however, and hence use of SbF_3 as a fluorinating agent (35) allows a more efficient preparation. DMCB was obtained by saturating ~10 g of *N,N*-dimethyl carbamyl chloride with HBr (36) at 0 °C. A N_2 stream was used to remove any HCl or Cl_2 formed and significantly increased the product yield. DMCF was purified by a spinning-band column distillation at 760 mm and 121 °C, the final product giving the elemental analysis: C 39.81 (39.58), H 6.58 (6.59) and F 20.68 (20.88), the values in parentheses being the calculated mole percentages for C_3H_6NOF.

(B) Variable Temperature Nuclear Magnetic Resonance Spectra

The ^1H n.m.r. spectra were obtained at 100 MHz with a Varian HA-100 spectrometer equipped with a V-6031 variable-temperature probe and temperature controller. The V-6031 controller maintains a preset temperature for the N_2 gas heating or cooling the sample, and the gas temperature is sensed at about 5 cm from the sample volume in the spectrometer receiver coil. Thus the sample temperature was measured before and after recording a spectrum using a standard methanol (or glycol) sample and interpolation of the —OH chemical shifts obtained in HA-mode using the data of Van Geet (37). The temperature thus determined is estimated to be accurate to ±0.3 °C and was shown to be stable, within these limits, over a period of about 20 min. The spectra were recorded at sweep rates of 0.02 or 0.05 Hz s^{-1} to best approximate steady-state conditions, and with a low amplitude r.f. field (~0.02 mG) to minimize lineshape distortion due to saturation effects (5). At each temperature, to ensure reproducibility, at least four spectra were digitized and stored using a Fabritek FT-1074 computer interfaced with the HA-100. The interface unit, constructed in our laboratory, consists of a high input impedence differential amplifier for isolation of the A-D converter, logic circuitry for direct frequency calibration of the digital data and a digital/analog read-out for control of the HA-100 recorder. All frequencies were measured, using the V-4315 counter, with reference to TMS as an internal standard. An optimum H_0 field homogeneity was maintained over the temperature range −20 to 80 °C corresponding to a 0.4 Hz resolution (T_2 = 0.8 s) and a reference lineshape that best approximated a symmetrical Lorentzian shape. Dioxane (~2 mol%) was used to give an internal reference line, at a convenient frequency with respect to DMCF, and this linewidth was used to define the effective transverse relaxation time in the absence of chemical exchange, T_2, for DMCF. Wilmad PS-505 5 mm thin-walled sample tubes were used to attain reproducible spinning characteristics and field homogeneity control.

Lineshape measurements were made for DMCF as a 16.5 mol% solution in CCl_4. this solvent being chosen to minimize solvent–solute interactions (38). Solute–solute interactions are minimized in dilute solution. A dilution of DMCF is limited, however, by a decrease in the already small *N*-methyl chemical shift difference, 2Ω, for solute concentrations below the above value. The n.m.r. sample was degassed by the usual freeze–pump–thaw method, and sealed under N_2 at ~1 atm to prevent refluxing at the elevated temperatures required.

(C) Computation of Lineshapes

The ^1H n.m.r. spectrum of DMCF corresponds to the A_3B_3 part of a first-order A_3B_3X ($J_{AB} = 0$) spectrum and hence may be analyzed as the AB-part of an ABX ($J_{AB} = 0$) system, as described in detail in the preceding section.

A Fortran-IV program designated GPLONK has been developed for the efficient iterative fitting of theoretical absorption mode multi-site exchange lineshapes to digital data. This program is based upon eq. 22*a* of ref. 5, which follows directly from the matrix formulation of the complex lineshape function, $G(x)$, *cf.* eq. 4 above. The input consists of (*i*) N experimental intensities (40–100) with arbitrary indexing, (*ii*) frequency calibration data, (*iii*) a baseline correction parameter, (*iv*) a specific normalization data point, (*v*) the linewidth of the internal reference line, and (*vi*) data defining the initial matrices K and Ω, and also the vectors $\boldsymbol{P}$ and $\boldsymbol{I}$, in eq. 4 above. The iterative fitting relies upon a rapidly convergent search using optimized parameter increments, where the rate matrix is varied following the general procedure outlined in ref. 5. An optional variation of spin-site frequencies is available, for the checking of temperature dependence. "Best fit" parameter values correspond to the usual sum of squares of deviations (39), while the

Can. J. Chem. Downloaded from www.nrcresearchpress.com by 210.87.254.6 on 09/05/12
For personal use only.

Can. J. Chem. Downloaded from www.nrcresearchpress.com by 210.87.254.6 on 09/05/12
For personal use only.

lineshape fitting error is most conveniently considered as $\varepsilon = (1/N)\Sigma^{N}_{i=1}\,[V'(x_i) - V(x_i)]/V|x$, where $V'(x_i)$ and $V(x_i)$ are the normalized experimental and theoretical intensities, respectively, for the frequency x_i. For the 4 spin-site DMCF exchange system, the time for a complete fit and setting up of control arrays for a CALCOMP plotter on an IBM 360/75 system is less than 6 s, and this time is essentially independent of the number of data points involved as it is governed by the 4 × 4 matrix diagonalization and inversion in eq. 4 above.

(D) Calculation of Activation Parameters

The activation energy, E_a, for the hindered rotation in DMCF was determined from a least-squares fit to the usual Arrhenius equation

$$\log k = -E_a/2.303\,RT + \log A \qquad [5]$$

where k is the first-order rate constant describing the rotation at temperature T and A is the frequency factor for the rate process. A thermodynamical formulation of reaction rates (40) shows that the enthalpy and entropy of activation are given as

$$\Delta H^{\ddagger} = E_a - RT \qquad [6]$$

and

$$\Delta S^{\ddagger} = R\,[2.303 \log (Ah/kT) - 1] \qquad [7]$$

respectively, assuming E_a to be temperature independent. In eq. 7 h is Planck's constant and k is the Boltzmann constant. The free energy of activation, $\Delta G^{\ddagger}$, is then determined as $\Delta G^{\ddagger} = \Delta H^{\ddagger} - T\Delta S^{\ddagger}$ at 298 °K. The overall errors quoted for the activation parameters have been estimated from the statistical limits of 95% confidence for E_a and A (39) and a study of the systematic errors (41, 42) involved in the determination of the k values used in eq. 5.

Results and Discussion

In the A_3B_3 part of the A_3B_3X spectrum for DMCF the methyl group *trans* to the carbonyl oxygen, A_3, is assigned to low field of the B_3 group; as the former methyl group, in the planar molecular ground state, is within a shielding region associated with the magnetically anisotropic carbonyl group (43). A similar assignment for DMF (12) has been shown to be correct through use of the nuclear Overhauser effect (44); and also, the magnitude of the *trans* coupling constant, J_{BX} according to the above assignment, is shown to be greater than that of the *cis* coupling, J_{AX}, which is normal (33, 45) for substituted amides. The couplings determined for a dilute solution of DMCF in CCl_4 are $J_{AX} = 0.30 \pm 0.05$ Hz and $J_{BX} = 0.80 \pm 0.05$ Hz, the corresponding values for DMF being 0.35 and 0.06 Hz. Comparison with the related acetyl compounds CH_3CFO (J_{HF} = 7.6 Hz (42)) and CH_3CHO (J_{HH} = 2.9 Hz) shows the effects of the interposed N atom and the N—C partial double bond character, due to delocalization of the N lone pair electrons, in the amide systems. Assuming the hybridization (s-character) to be similar for π-bonding in DMCF and DMF, the relative magnitudes of J_{BX} and changes with respect to the acetyl systems may be considered to be directly related to the detailed form of the π-bonding in the 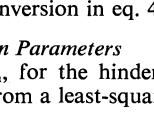 and 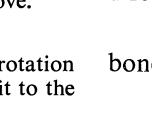 groups.

Thus it is seen that the N–C double bond character is significantly greater for DMF, as $J_{BX}(DMF)/J_{HH} = 4.8$ and $J_{BX}(DMCF)/J_{HF} = 9.5$, and hence the barrier to hindered rotation about this bond is predicted to be higher in DMF. In fact, this is shown to be the case as the activation energy for hindered rotation in DMF is 20.8 ± 0.6 kcal mol^{-1} (12) and the activation energy for DMCF has now been determined as 18.3 ± 0.6 kcal mol^{-1}, *cf.* Table 3.

The couplings J_{AX} and J_{BX} in DMCF are temperature independent within ±0.05 Hz, as defined by the iterative lineshape fitting procedure; and for the 16.5 mol% CCl_4 solution, these couplings averaged to 0.55 ± 0.05 Hz at 78.2 °C in excellent agreement with the value expected for an A_6X spectrum in the fast exchange limit. Furthermore, the observed exchange modified lineshapes unambiguously lead to the conclusion that the signs of these couplings are the same. For example, in the region of coalescence at 44.9 °C the "best-fit" errors for the same and different signs were 1.2 and 2.0%, respectively, exemplifying the precision that may be attained through a total lineshape analysis. A typical experimental lineshape at this temperature is shown along with the corresponding "best-fit" theoretical lineshape in Fig. 5. At this point, it should be mentioned that the spin–spin couplings between methyl protons and the ^{14}N spin have been neglected in the lineshape analysis. Although a ^1H–$\{^{14}N\}$ double resonance study of N-substituted amides indicated that these couplings were negligibly small, the data available from further studies using ^{15}N-amides (34) leads to the ^{14}N coupling constants J_{NA} and J_{NB} of 0.7 and 0.8 Hz, respectively. However, it may safely be assumed that the methyl protons are completely decoupled by the quadrupolar ^{14}N spin–lattice relaxation process (46, 47).

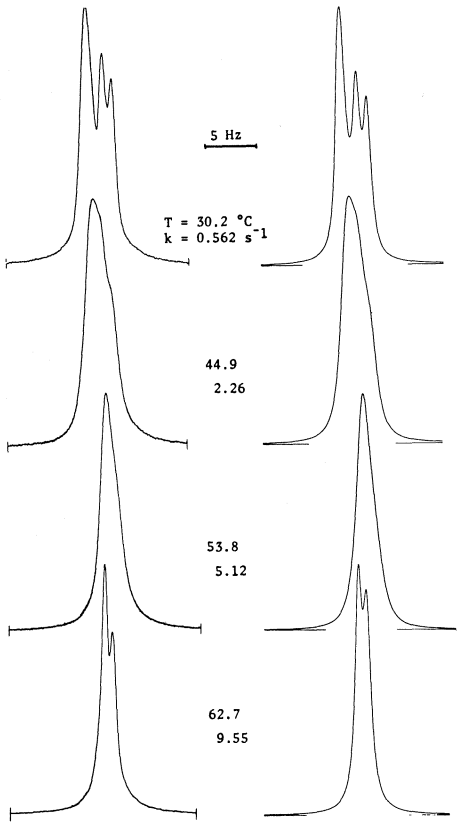

FIG. 5. Comparison of experimental and theoretical exchange lineshapes for DMCF.

In general, indirect spin–spin couplings are relatively insensitive to intermolecular interactions. In the case of a highly polar amide such as DMCF (μ = 4.02 D (48)) in a non-polar solvent, however, electrostatic solute–solute interactions may stabilize the polarized ground-state resonance form $\overset{\oplus}{N}{=}C(O^-)—F$. An increased contribution from this structure then leads to an enhanced coupling between the ^{19}F spin and methyl protons due to the change in N—C double bond character. Such an effect has been observed in that J_{BX} = 1.10 ± 0.05 Hz for neat DMCF, as determined from a complete lineshape fit at −15 °C. This is an increase of about 40% over the same coupling for dilute CCl_4 solutions *cf.* Table 2, and thus it appears that the CCl_4 solvent breaks down a specific solute–solute interaction, probably leading to a simple dimeric form (11), between DMCF molecules. As this coupling constant is unchanged on further dilution, as shown in Table 2, it may be assumed that the dimer concentration is minimal for the 16.5% solution chosen for an accurate determination of kinetic parameters.

TABLE 2. ^1H n.m.r. data for DMCF, $(H_3C)_2NCF$ (O)

(*a*) 16.5% solution in CCl_4

Temperature (°C)	ω_0 (Hz)*	2Ω (Hz)†
−15.2	−295.15±0.05‡	2.20±0.05‡
−5.5	−294.75	2.10
8.3	−294.40	2.00
15.6	−294.10	1.90
30.2	−293.55	1.75
44.9	−293.15	1.70
53.8	−292.80	1.60
62.7	−292.60	1.50
−78.2	−292.15	1.40

J_{BX} = 0.80 ± 0.05, J_{AX} = 0.30 ± 0.05 Hz‡

*$\omega_0 = (1/2)(\omega_A + \omega_B)$, determined with respect to TMS internal reference at 100 MHz and constant field.
†$2\Omega = \omega_B - \omega_A$, see text and ref. 5.
‡These error bounds are those used in the iterative lineshape fitting procedure.

(*b*) 7.5% solution in CCl_4

2Ω = 3.6 ± 0.1 Hz (220 MHz) at 22 °C
= 1.6 ± 0.1 (100 MHz) 24 °C
J_{BX} = 0.8, J_{AX} = 0.3 Hz

(*c*) Neat DMCF

2Ω = 1.2 ± 0.1 Hz (100 Hz) 30 °C
J_{BX} = 1.1, J_{AX} = 0.4 Hz

Chemical shifts are usually more sensitive to intermolecular interactions, and indeed the chemical shifts for the methyl groups in DMCF (and the shift difference 2Ω) are solvent-, concentration-, and temperature-dependent, as shown in Table 2 and Fig. 6. These chemical shifts are predominantly due to the combined effect of the magnetic susceptibility anisotropies associated with the C—F and C=O bonds. It may be considered that the NCO and NCF bond angles are both close to 120° for approximately regular sp^2 hybridization of the C atom,[1] and thus the small methyl chemical shift difference (~0.01 p.p.m.)

[1]The structure of DMCF has not been determined experimentally, but comparison of the structural data available for formamide (49), acetaldehyde (50), and acetyl fluoride (51) leads to ∠NCO = 128° and ∠NCF = 112.5°. These bond angles also correspond to a minimum energy configuration in the CNDO/2 s.c. approximation (52).

Can. J. Chem. Downloaded from www.nrcresearchpress.com by 210.87.254.6 on 09/05/12
For personal use only.

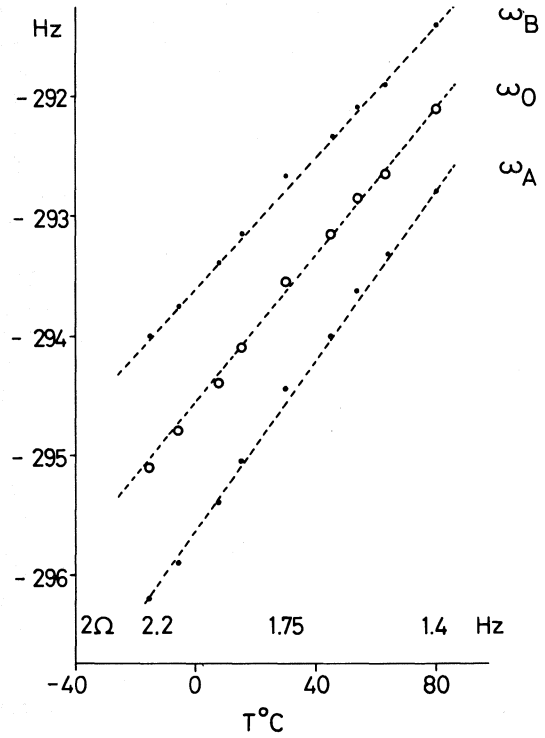

FIG. 6. Temperature dependence of *N*-methyl chemical shifts for DMCF, 16.5% in CCl_4, at 100 MHz.

implies that the charge distributions localized in these two bonds are of similar forms as the methyl groups *cis* and *trans* to the carbonyl group are in shielding regions having very nearly identical characteristics. This is to be compared with the shielding regions for the methyl groups in DMF, due to a carbonyl group only, giving $2\Omega = 17.5$ Hz at 100 MHz ($\sim$0.2 p.p.m.). As the C=O magnetic anisotropy is due to the axially asymmetric π-electron distribution in this group, it follows that delocalization of fluorine $2p\pi$-electrons, as represented by the resonance form N—C(O$^-$)=$\overset{\oplus}{F}$, may be significant in the ground-state of DMCF. The small temperature dependence of 2Ω may be ascribed to an intermolecular dipolar association which affects the magnetic anisotropies of the C=O and/or C—F groups and which varies to a small extent with temperature. It should be noted that this temperature dependence, as determined from the complete lineshape analysis for DMCF in CCl_4, is only 0.008 p.p.m. over the temperature range -15.1 to 78.2 °C. All chemical shift variations, within $\pm$0.05 Hz, were shown to be regular and reproducible over multiple lineshape fits, *cf.* Fig. 6.

The first-order rate constants, k s^{-1}, describing the hindered rotation about the N—C bond for DMCF as a 16.5 mol% solution in CCl_4 are listed in Table 3. These rate constants are average values obtained from multiple complete lineshape fits at each temperature. The corresponding temperature dependent chemical shifts are those given in Table 2, while the couplings J_{AX} and J_{BX} were assumed to be temperature independent. Because of the very small chemical shift difference 2Ω involved, the temperature interval for reliable k determinations is reduced to 66 °C and the overall k variation is only of the order of 200. The errors for the representative lineshape fits shown in Fig. 5 are maximal for very slow and very fast exchange[2] as accurately reproducible spectra for the DMCF four-site exchange system are very difficult to obtain in these limits, even with the stability afforded by a field-frequency locked spectrometer. For example, the average k value at 30.2 °C is 0.550 s^{-1} whereas six lineshape fits at this temperature gave values ranging

TABLE 3. Kinetic data for DMCF, $(H_3C)_2NCF$ (O)

Temperature (°C)	k (s^{-1})	Error*
12.2	0.076	4.4
15.6	0.159	4.2
30.2	0.550	3.7
32.5	0.692	4.1
37.6	1.99	2.2
44.9	2.29	1.2
46.5	2.57	1.3
53.8	5.11	1.3
62.7	9.55	3.9
78.2	26.3	4.6

$E_a = 18.3 \pm 0.6$ kcal mol^{-1}
$\log_{10} A = 12.9$
$\Delta H^{\ddagger} = 17.7 \pm 0.6$ kcal mol^{-1}
$\Delta S^{\ddagger} = -1.4 \pm 2.1$ cal deg^{-1} mol^{-1}
$\Delta G^{\ddagger} = 18.1 \pm 0.6$ kcal mol^{-1}

*Percentage error for iterative lineshape fit, see text.

[2]These deviations may also arise from inherent inadequacies in the formulation of the lineshape function $V(x)$, such as the assumption of equal transverse relaxation times for all spin-sites in the absence of exchange. These relaxation times may be modified by time-dependent anisotropic chemical shift and anisotropic dipole–dipole interactions (54) and also by a cross-relaxation arising from these two interactions in DMCF.

Can. J. Chem. Downloaded from www.nrcresearchpress.com by 210.87.254.6 on 09/05/12
For personal use only.

Can. J. Chem. Downloaded from www.nrcresearchpress.com by 210.87.254.6 on 09/05/12
For personal use only.

from 0.362 to 0.944 s^{-1} with fitting errors of 3.5–6.2%. The resultant Arrhenius plot, however, is most satisfactory and is shown in Fig. 7. The activation parameters derived from the temperature independent Arrhenius constants, E_a and log A, and evaluated at 25 °C are given in Table 3.

For hindered rotations in amides the entropy of activation $\Delta S^{\neq}$ derived through complete n.m.r. lineshape analyses is normally relatively small; and in general, as increasing care is taken to remove systematic errors in obtaining kinetic data for a given rate process using n.m.r. methods the values of E_a and log A tend to increase (12, 41) leading to a value of $\Delta S^{\neq}$ close to zero. This entropy change is most probably due to a difference in the solvation structures, formed by dipolar solute–solvent association, for the ground and transition states of an amide. Such an association between the strongly polar DMCF and CCl_4 is possible, to some degree, through induced polarization of the solvent molecules. Therefore, if a solvation effect is dominant, a small increase in entropy is expected on formation of the transition state in amides as the dipole moment for this state is smaller than the moment for the ground state (52). For example, the calculated dipole moments, using s.c. theory, for the ground and transition states of carbamyl fluoride in minimum energy configurations are 3.98 and 3.41 D, respectively, which may be compared with the experimental value of 4.06 D (24). The entropy of activation determined here for DMCF, $\Delta S^{\neq} = -1.4 \pm 2.1$ cal deg^{-1} mol^{-1}, is formally negative but may only be considered to be very small. For the hindered rotation under consideration, a free energy change is expected to be determined primarily by intramolecular effects and hence this activation parameter is much simpler to interpret than the energy of activation which is sensitive to intermolecular effects. It is well known that there is a general tendency in rate processes in solution for enthalpy and entropy changes to compensate each other (53) so that the effective change in free energy is reduced and hence becomes less sensitive to external effects. The free energy of activation for DMCF has been determined as $\Delta G^{\neq} = 18.2 \pm 0.6$ kcal mol^{-1} and this particular parameter will be used in a forthcoming correlation of the bonding characteristics in a complete series of C-substituted *N*,*N*-dimethyl amides.

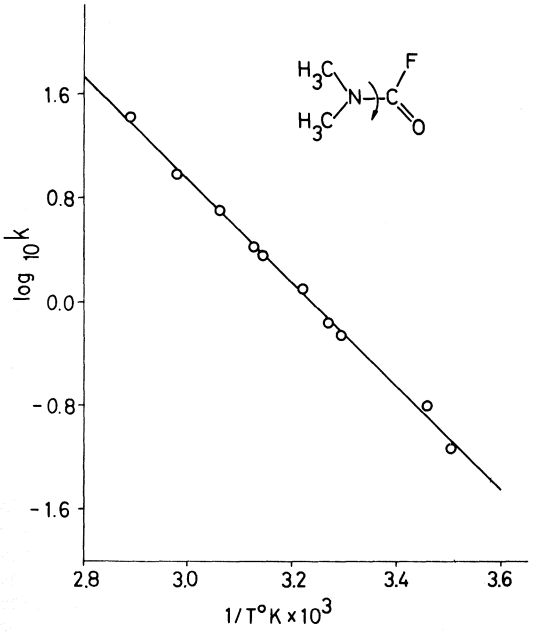

FIG. 7. Arrhenius plot for hindered rotation in DMCF, 16.5 mol% in CCl_4.

This work was supported by the National Research Council of Canada in grants to L.W.R. One of us (K.N.S.) gratefully acknowledges the financial support provided by a N.Z. Trust Lands Trust Overseas Scholarship and a British Columbia Sugar Refining Co. Scholarship while part of this work was undertaken at the University of British Columbia. We thank Mr. E. A. Allan for the preparation of DMCF.

1. F. BLOCH. Phys. Rev. **7**, 460 (1946).
2. H. S. GUTOWSKY, D. W. MCCALL, and C. P. SLICHTER. J. Chem. Phys. **21**, 279 (1953).
3. H. M. MCCONNELL. J. Chem. Phys. **28**, 430 (1958).
4. H. S. GUTOWSKY and C. H. HOLM. J. Chem. Phys. **25**, 1228 (1956).
5. L. W. REEVES and K. N. SHAW. Can. J. Chem. **48**, 3641 (1970).
6. H. S. GUTOWSKY and A. SAIKA. J. Chem. Phys. **21**, 1688 (1953).
7. E. GRUNWALD, A. LOEWENSTEIN, and S. MEIBOOM. J. Chem. Phys. **27**, 639 (1957).
8. A. LOEWENSTEIN and S. MEIBOOM. J. Chem. Phys. **27**, 1967 (1957).
9. M. TAKEDA and E. O. STEJSKAL. J. Am. Chem. Soc. **82**, 25 (1960).
10. M. T. ROGERS and J. C. WOODBURY. J. Chem. Phys. **66**, 549 (1962).
11. R. C. NEUMAN, D. N. ROARK, and V. JONAS. J. Am. Chem. Soc. **89**, 3142 (1967).
12. P. T. INGLEFIELD, E. KRAKOWER, L. W. REEVES, and R. STEWART. Mol. Phys. **15**, 65 (1968).
13. A. PINES and M. RABINOVITZ. Tetrahedron Lett. **31**, 3529 (1968). M. RABINOVITZ and A. PINES. J. Am. Chem. Soc. **91**, 1585 (1969).

14. K. I. DAHLQVIST and S. FORSEN. Acta Chem. Scand. **24**, 662 (1970).
15. C. J. CRESWELL and R. K. HARRIS. J. Mag. Res. **4**, 99 (1971).
16. G. BINSCH. J. Am. Chem. Soc. **91**, 1304 (1969).
17. C. N. BANWELL and H. PRIMAS. Mol. Phys. **6**, 225 (1963). U. FANO. Rev. Mod. Phys. **29**, 74 (1957).
18. G. BINSCH. Mol. Phys. **15**, 469 (1968).
19. S. M. COHEN. J. Chem. Phys. **52**, 234 (1970).
20. H. KESSLER. Angew Chem. (Int. Ed.) **9**, 219 (1970).
21. I. B. WILSON. J. Biol. Chem. **235**, 2312 (1960); **236**, 2292 (1961).
22. H. P. METZER. J. Biol. Chem. **238**, 3432 (1963).
23. H. A. SCHERAGA. Adv. Phys. Org. Chem. **6**, 193 (1968). Academic Press, N.Y.
24. J. S. RIGDEN and R. H. JACKSON. J. Chem. Phys. **45**, 3646 (1966).
25. P. L. CORIO. Chem. Rev. **60**, 363 (1960).
26. I. SOLOMON. Phys. Rev. **99**, 559 (1955).
27. M. BLOOM, L. W. REEVES, and E. J. WELLS. J. Chem. Phys. **42**, 1615 (1964).
28. E. L. HAHN. Phys. Rev. **80**, 589 (1950).
29. A. G. REDFIELD. I.B.M. J. Res. Dev. **1**, 19 (1957).
30. J. I. KAPLAN. J. Chem. Phys. **29**, 462 (1958). S. ALEXANDER. J. Chem. Phys. **37**, 967 (1962).
31. K. I. DAHLQVIST and S. FORSEN J. Phys. Chem. **69**, 4062 (1965).
32. L. M. PIETTE and W. G. SCHNEIDER. Can. J. Chem. **38**, 681 (1960).
33. A. J. R. BOURNE and E. W. RANDALL. Mol. Phys. **8**, 567 (1964).
34. R. J. CHUCK, D. G. GILLIES, and E. W. RANDALL. Mol. Phys. **16**, 121 (1969).
35. G. SCHRADER. British Intelligence Obj. Subcommittee Final Report No. 714 B.I.O.S. London. 1945.
36. Z. ARNOLD. Coll. Czech. Chem. Comm. **24**, 760 (1959).
37. A. L. VAN GEET. Anal. Chem. **40**, 2227 (1968).
38. A. D. BUCKINGHAM, R. SCHAEFER, and W. G. SCHNEIDER. J. Chem. Phys. **32**, 1227 (1960).
39. L. G. PARRALT. Probability and experimental error. J. Wiley and Sons, N.Y. 1961. p. 126.
40. K. J. LAIDLER. Chemical kinetics. McGraw-Hill, N.Y. 1965. p. 67.
41. A. ALLERHAND, H. S. GUTOWSKY, J. JONAS, and R. A. MEINZER. J. Am. Chem. Soc. **44**, 3185 (1966).
42. T. DRAKENBURG, K. I. DAHLQVIST, and S. FORSEN. Acta Chem. Scand. **24**, 694 (1970).
43. D. L. HOOPER and R. KAISER. Can. J. Chem. **43**, 2363 (1965); J. W. APSIMON, P. V. DEMARCO, D. W. MATHIESON, W. G. CRAIG, A. KARIM, L. SAUNDERS, and W. B. WHALLEY. Tetrahedron, **26**, 119 (1970).
44. F. A. L. ANET and A. J. R. BOURNE. J. Am. Chem. Soc. **87**, 5250 (1965).
45. E. W. RANDALL and J. D. BALDESCHWEILER. J. Mol. Spectrosc. **8**, 365 (1962).
46. S. BROWNSTEIN and V. BYSTROV. Can. J. Chem. **48**, 243 (1970).
47. J. A. POPLE. Mol. Phys. **1**, 158 (1958).
48. E. BOCK and D. IWACHA. Can. J. Chem. **46**, 523 (1968).
49. R. J. KURLAND and E. BRIGHT-WILSON, JR. J. Chem. Phys. **27**, 585 (1957).
50. R. W. KILB, C. C. LIN, and E. BRIGHT-WILSON, JR. J. Chem. Phys. **26**, 1695 (1957).
51. L. PIERCE and L. C. KRISHNER. J. Chem. Phys. **31**, 875 (1959).
52. K. N. SHAW and L. W. REEVES. Unpublished results.
53. J. E. LEFFLER. J. Org. Chem. **20**, 1202 (1955).
54. A. ABRAGAM. The principles of nuclear magnetism. Clarendon Press, Oxford. 1962. Chap. 8.

Can. J. Chem. Downloaded from www.nrcresearchpress.com by 210.87.254.6 on 09/05/12
For personal use only.

Nuclear Magnetic Resonance Studies of Multi-site Chemical Exchange. III. Hindered Rotation in Dimethylacetamide, Dimethyl Trifluoroacetamide, and Dimethyl Benzamide

L. W. Reeves, R. C. Shaddick, and K. N. Shaw
Department of Chemistry, University of Waterloo, Waterloo, Ontario

Received March 16, 1971

The experimental application of a multi-site exchange theory developed recently has been made to three restricted rotation barriers in amido-type systems. Inclusion of 8 spin-sites in the analyses of the line shapes for spectra of *N,N*-dimethyl trifluoroacetamide and dimethyl acetamide leads to improved values for the activation parameters. Variation of chemical shifts with temperature is included in the iterative fitting procedure. The determination of the relative signs of long range couplings and the inclusion and measurement of unresolved couplings has been accomplished. The barrier for hindered rotation in *N,N*-dimethyl benzamide has been re-investigated including the effect of relatively large chemical shift changes with temperature. The internal consistency of the measurements from all aspects indicates that systematic errors common in the determination of energy barriers by steady-state nuclear magnetic resonance (n.m.r.) have been largely eliminated and hence the activation parameters obtained form a reliable addition to a compilation of experimental data pertaining to the bonding in a related series of simple C-substituted amides.

L'application expérimentale d'une récente théorie de l'échange entre plusieurs sites a été faite pour trois barrières de rotation restreinte dans des structures du type amide.

L'analyse des formes de raies d'un système à huit sites des spectres de la *N,N*-diméthyle trifluroacétamide et de la diméthyle acétamide conduit à des valeurs plus précises des paramètres d'activation. Le procédé d'ajustement par iteration tient compte de la variation du déplacement chimique avec la température. Les signes relatifs des constantes de couplage à longue distance ont été déterminés, en incluant les couplages non résolus qui ont été mesurés.

La barrière de rotation restreinte du *N,N*-diméthyle benzamide a été réexaminée en tenant compte de la variation assez importante du déplacement chimique avec la température.

La consistance interne des différentes mesures indique que les erreurs systématiques communes à la détermination des barrières d'énergie par r.m.n. ont été fortement réduites. Les paramètres d'activation ainsi obtenus constituent donc une contribution sérieuse à l'ensemble des données expérimentales se rapportant au mode de liaison dans une série d'amides simples C-substituées.

Canadian Journal of Chemistry, 49, 3683 (1971)

Can. J. Chem. Downloaded from www.nrcresearchpress.com by 210.87.254.6 on 09/05/12
For personal use only.

Introduction

Although long range spin–spin couplings present in amido-type structures have been measured for some time in high resolution n.m.r. (1, 2), until very recently these couplings have been either ignored, eliminated by double irradiation decoupling (1, 6), or treated by approximate methods (3–5) in kinetic studies of the hindered rotation about the amide N—C bond. Since the chemical shifts modulated by the internal rotation are usually quite small in these molecules, the neglect of long range *cis* and *trans* coupling constants across the N—C bond can, in principle, lead to serious errors in rate constants describing the rotation. Under steady-state n.m.r. decoupling conditions, the lineshape distortion associated with the decoupling process is difficult to assess quantitatively and hence kinetic studies using this method are usually unreliable. For example, a recent double resonance study of dimethyl formamide and a normal n.m.r. study of the corresponding d_1 compound under similar solvent and concentration conditions gave free energies of activation of 21.7 and 23.0 kcal mol^{-1}, respectively, even though it is widely recognized that this particular activation parameter is least sensitive to intermolecular interactions and systematic experimental errors (3, 5). These values are to be compared with results obtained independently from complete lineshape analyses which are consistent within the experimental errors involved, namely, 20.8 ± 0.6 (7) and 20.5 ± 0.6 (8) kcal mol^{-1} at the same temperature 298 °K. In the former lineshape analysis, the hindered rotation was represented by two spin transfer processes between 4 sites defined by the chemical shift difference for the *N*-methyl protons and the *cis* and *trans* couplings to the

Can. J. Chem. Downloaded from www.nrcresearchpress.com by 210.87.254.6 on 09/05/12
For personal use only.

formyl proton. It was also recognized that the relative signs of these coupling constants could be determined through the lineshape analysis, but a conclusive experimental verification of this point (and vindication of the exchange model used) was precluded by the very small couplings involved. The initial papers in this series (9, 10) present a complete matrix formulation of general multi-site chemical exchange in first-order spin systems. Through the definition of spin-sites long range couplings are simply incorporated into the lineshape analysis. This matrix formulation of exchange has been applied to the study of n.m.r. line shapes for the methyl group signals of *N,N*-dimethyl carbamyl fluoride (10). The chemical shift difference for *cis* and *trans* methyl protons is very small and varies from 2.2 to 1.4 Hz at 100 MHz at different temperatures. Temperature dependent chemical shifts in amido type systems are not uncommon (11) and must be allowed for in accurate kinetic studies. The further complication of *cis* and *trans* coupling to the extent of 0.3 and 0.9 Hz made the line shape fitting procedure difficult. However, it was possible not only to determine relative signs of these coupling constants, but also by iterative fitting to reliably reproduce relative spin-site positions to ± 0.05 Hz. In two of the three molecules studied in this work long range coupling is present, and in one case, was not resolved under the best operating conditions of the spectrometer. Thus a full rate matrix corresponding to 8 spin-sites is required to compute and fit the lineshapes for these molecules to obtain reliable primary kinetic data.

The aim of the present series of papers thus far is to study the hindered rotation in a related series of simple C-substituted amides, using complete lineshape analyses of steady-state n.m.r. spectra, in an attempt to compile reliable data that may be used in conjunction with that available from semi-empirical s.c.f.-l.c.a.o.-m.o. calculations and other spectroscopic techniques to develop a more complete description of the electronic charge distributions and bonding characteristics in these molecules. Although a large amount of kinetic data has appeared in the literature following the initial study by Holm and Gutowsky on *N,N*-dimethyl formamide, as has already been pointed out (4, 10), until very recently little of these data can be used in semi-quantitative correlations and many of the simpler molecules have yet to be studied. Along with the data now appearing from other laboratories using total lineshape analyses, it is hoped that in the near future a meaningful and detailed correlation of the activation parameters with bonding characteristics of a series of related amides in liquids may be presented.

Experimental

All n.m.r. spectra were recorded on a Varian HA-100 spectrometer with the lock channel activated at the tetramethylsilane (TMS) or hexamethyldisiloxane (HMDS) proton resonance, (added to the extent of ~1% to all solutions). Careful checks on the line width and shape (ideally Lorentzian) in the absence of chemical exchange ensured a line width at half height of less than 0.5 Hz, but often it was as low as 0.2 Hz. Spectra were recorded on a 50 to 100 Hz sweep width and 1000 s sweep time. Each recording of a spectrum was in the limit of negligible saturation as verified by changing r.f. power and noting changes in signal amplitude.

The variable temperature equipment, standard on the HA-100 spectrometer, was used at temperatures other than ambient (30°). The V-6031 controller maintains a preset temperature for the N_2 gas heating or cooling the sample and the gas temperature is sensed at about 5 cm from the sample volume in the spectrometer receiver coil. Thus the temperature was determined before and after recording a spectrum by using a standard methanol or glycol sample and measuring the methyl to —OH and methylene to —OH chemical shifts, respectively, and the calibration data of Van Geet (12). The temperature thus determined is estimated to be accurate to ± 0.3 °C and was shown to be stable, within these limits, over a period of about 20 min. By using standardized sample tubes and constant optimized tube spinning and N_2 gas flow rates, the effects of thermal gradients as indicated by the line shapes symmetry across the small sample volume within the receiver coil are minimal.

N,N-dimethyl benzamide was purchased from K and K Laboratories. *N,N*-dimethyl acetamide was obtained from Aldrich Chemicals and purified by distillation under reduced pressure. *N,N*-dimethyl trifluoroacetamide was prepared by bubbling dimethyl-amine into ~10 g of methyl trifluoro-acetate kept at 0 °C. The saturated solution was allowed to stand for 12 h to complete the reaction and the trifluoroacetamide was distilled from the reaction mixture at 760 mm and 134 °C in 85% yield. The product was further purified by distillation under reduced pressure. In all cases the purity was checked by n.m.r. spectra taken at high gain. No impurities greater than ~0.5% by volume were detected in any sample used for study.

The matrix formulation of the Bloch equations including chemical exchange reported earlier has been used to generate the steady-state n.m.r. line shapes in the absence of saturation. A computer program GPLONK incorporates these equations to iteratively fit the experimental intensities for at least 60 digital data points, including enough base line to reliably define zero intensity. The absorption mode line shape function is given by the imaginary part of

$$G(x) = -i\omega_1 M_0 I[\mathbf{R}_2 + i\mathbf{w}]^{-1}.\boldsymbol{P}$$

which occurs as eq. 18 in ref. 9. $\mathbf{R}_2$ includes a spin-site

Can. J. Chem. Downloaded from www.nrcresearchpress.com by 210.87.254.6 on 09/05/12
For personal use only.

transfer rate matrix **K** as previously defined (10), **w** is an ($n \times n$) diagonal frequency deviation matrix, ***P*** is a site population ($n \times 1$) vector, and ***I*** is a row vector with each of the ($1 \times n$) elements unity. The independent variable x for describing frequency appears only in the diagonal matrix **w**, and complete diagonalization of the matrix $[\mathbf{R}_2 + i\mathbf{w}]$ allows the rapid numerical evaluation of the imaginary part of $G(x)$ by procedures previously outlined.

The activation energy, E_a, for hindered rotation is determined from a least-squares fit to the usual Arrhenius equation

$$\log k = -E_a/2.303\ RT + \log A$$

where k is the first-order rate constant describing the rotation at temperature T and A is the frequency factor. The enthalpy and entropy of activation are then given by (13)

$$\Delta H^* = E_a - RT$$

and

$$\Delta S^* = R[2.303 \log Ah/kT - 1]$$

respectively, where h is Planck's constant and k is the Boltzmann constant. The free energy of activation, ΔG^*, is then determined as $\Delta G^* = \Delta H^* - T\Delta S^*$ at 298 °K. The overall errors quoted for the activation parameters have been estimated from the statistical limits of 95% confidence for E_a and log A and a study of the systematic errors involved in the determination of the k values and the temperature T used in the Arrhenius equation.

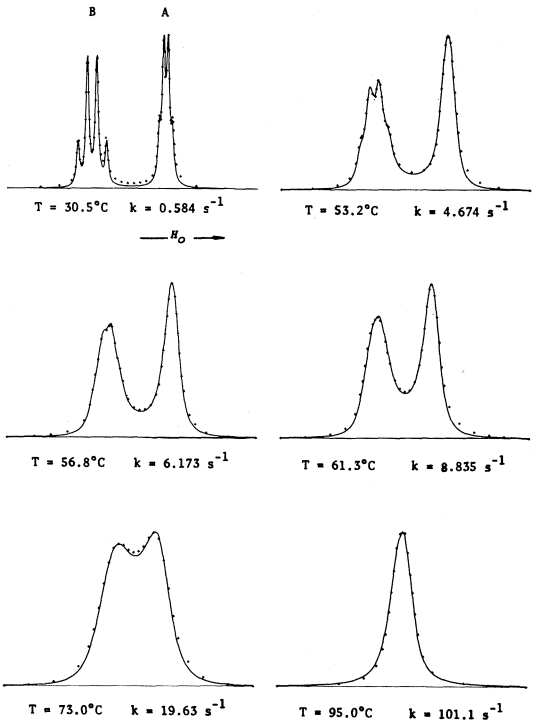

FIG. 1. Line shape fits of the methyl group spectra of DMTFA at a series of temperatures. The solid lines are computed spectra, with the rate constants given below each plot, and the dots are experimental intensities from normalized spectra.

Results and Discussion

Dimethyl Trifluoroacetamide

The molecule *N,N*-dimethyl trifluoroacetamide (DMTFA) has a proton magnetic resonance spectrum which, in the slow exchange limit, consists of two chemical shifted quadruplet signals. This is shown in Fig. 1. The quadruplet signals arise from long range coupling from the $-CF_3$ group to the *trans* and *cis* methyl groups. The spectrum is the A_3B_3 part of an $A_3B_3X_3$ system of nuclei, but with $J_{AB} = 0$. The methyl group *trans* to the carbonyl oxygen (*cis* to $-CF_3$), A_3, is expected to show a smaller coupling J_{AX} as compared with the *trans* coupling, J_{BX}, as is normal for substituted amides (7, 14, 15). On this basis, as shown in Fig. 1 at $T = 30.2$ °C, the A_3 methyl group is assigned to high field of the B_3 group. Such an assignment is opposite to those made for *N,N*-dimethyl formamide (DMF) (7) and *N,N*-dimethyl carbamyl fluoride (DMCF) (10). The very small methyl proton chemical shift difference for DMCF has been interpreted in terms of similar magnetic shielding cones for the C=O and C—F groups, which are approximately symmetrically placed with respect to the N—C bond and reduce the effective shielding in the region about the methyl group *cis* to the carbonyl oxygen. Hence, the reversal of the methyl chemical shifts in DMTFA may be considered as due to the particular form of the magnetic anisotropy of the C—CF_3 group giving rise to a shielding region about the methyl group *trans* to the carbonyl oxygen. Such a reversal is consistent with each of the C—F bonds having a significant anisotropy, as already shown in DMCF, and the removal of substituent symmetry about the N—C bond. It is possible that, due to the close proximity of $-CH_3$ and $-CF_3$ groups, a through-space coupling could increase the magnitude of J_{AX} such that $J_{AX} > J_{BX}$. Such a mechanism has been proposed for the coupling of H and F nuclei separated by five bonds (16). However, the measured coupling constants for DMTFA are 1.5 and 0.7 Hz and these may be compared with those for DMF: $J_{AX} = 0.4 \pm 0.1$ and $J_{BX} = 0.9 \pm 0.1$ Hz (7) and therefore the through-bond coupling ratios J_{trans}/J_{cis} are the same for the above assignments. Similar ratios of coupling constants have also been determined for *N*-methyl, *N*-alkyl trifluoroacetamides (17); an example being $J_{AX} = 0.8$ and $J_{BX} = 1.6$ Hz

Can. J. Chem. Downloaded from www.nrcresearchpress.com by 210.87.254.6 on 09/05/12
For personal use only.

for N—CH_3, N—$(CH_2)_3$—RH_3. Very recently (18), the coupling J_{BX} has been measured for trifluoroacetamide in acetone as 1.8 Hz, with $J_{AX} < 0.2$ Hz. These couplings may be compared with those for ^{15}N-formamide in acetone $J_{AX} = 1.45 \pm 0.05$ Hz and $J_{BX} = 13.35 \pm 0.05$ Hz, and again all ratios are consistent with the assumption that $J_{BX} > J_{AX}$ for DMTFA. The hindered rotation process about the N—C bond modulates the chemical shift difference between the *cis* and *trans* methyl groups and the rotation involves all 8 spin-sites represented by the individual components of the spin multiplets. Labelling sites 1 to 8 from low to high field, the population vector has elements [1/16, 3/16, 3/16, 1/16, 1/16, 3/16, 3/16, 1/16]. These elements allow for the equal population environmental sites (10). Since the spin states of the —CF_3 group are long lived (T_1 long), the labels of the spin-sites 1 to 4 (and 5 to 8), which correspond to the spin states of the —CF_3 group with appropriate statistical weights persist during the chemical exchange. The chemical exchange therefore, via the hindered rotation, permutes the frequencies of 1 and 5, 2 and 6, 3 and 7, and 4 and 8 if J_{AX} and J_{BX} have the same sign; or, 1 and 8, 2 and 7, 3 and 6, and 4 and 5 if J_{AX} and J_{BX} are opposite in sign. The line shapes generated by the multi-site exchange theory are quite different and a relative sign determination can be made from the experimental fit. In the fast exchange limit the remaining quadruplet has a splitting (1/2) ($J_{AX} + J_{BX}$) if the couplings have the same sign or (1/2) ($|J_{BX}| - |J_{AX}|$) for $|J_{BX}| > |J_{AX}|$ if they have opposite signs. The former result is observed experimentally.

The transfer rate matrix defined in eq. 3*a* of the earlier paper (9) is explicitly written out below

$$\begin{array}{c|cccccccc} & 1 & 2 & 3 & 4 & 5 & 6 & 7 & 8 \\ 1 & k & & & & -k & & & \\ 2 & & k & & & & -k & & \\ 3 & & & k & & & & -k & \\ 4 & & & & k & & & & -k \\ 5 & -k & & & & k & & & \\ 6 & & -k & & & & k & & \\ 7 & & & -k & & & & k & \\ 8 & & & & -k & & & & k \end{array}$$

The transverse relaxation times, in the absence of rotation, are assumed to be equal for all sites and to be directly related to the half width taken from a sharp peak in the spectrum added as a line shape reference (dioxane). The rate matrix written out above assumes that J_{AX} and J_{BX} have the same sign, while the corresponding matrix for opposite relative signs is written out below

$$\begin{array}{c|cccccccc} & 1 & 2 & 3 & 4 & 5 & 6 & 7 & 8 \\ 1 & k & & & & & & & -k \\ 2 & & k & & & & & -k & \\ 3 & & & k & & & -k & & \\ 4 & & & & k & -k & & & \\ 5 & & & & -k & k & & & \\ 6 & & & -k & & & k & & \\ 7 & & -k & & & & & k & \\ 8 & -k & & & & & & & k \end{array}$$

In the computation of lineshapes determined by the above rate matrices, the numerical procedure is based upon a single diagonalization of a complex matrix and an inversion of the associated transformation matrix. To increase the efficiency of the large number of computations involved in an iterative line shape fitting, these 8 × 8 matrices may be converted to block-diagonal form. The overall diagonalization then reduces to that for four 2 × 2 matrices, one such matrix being defined by the elements (1,1), (1,5), (5,1), and (5,5) of the matrix for J_{AX} and J_{BX} of the same sign. The population vector corresponding to this particular sub-matrix is now [1/16, 1/16]. Of course, this factoring of the rate matrix is due to the methyl groups exchanging between the two basic environmental (chemical shift) sites. In this manner, the cycle time for iterative fitting of the 8-site exchange line shape is of the order of 0.4 s on an IBM 360-75 computer.

The experimental line shapes at all temperatures are reproduced by the matrix which assumes that J_{AX} and J_{BX} have the same sign. In Fig. 1, the continuous line is the computed line shape and the data points were obtained from a normalized experimental spectrum. The values of J_{AX} and J_{BX} are 0.70 ± 0.05 and 1.50 ± 0.05 Hz, respectively, with no temperature or discernable solvent dependence. The error limits correspond to the minimum increment for these parameters in the line shape fitting. Fits for multiple spectra at the lower temperatures were reproducible within these limits. The effective positions of all 8 lines in the absence of exchange, used in the iterative line shape fit, are plotted as Fig. 2 to illustrate the consistency of the data and to obtain the temperature dependence of the chemical

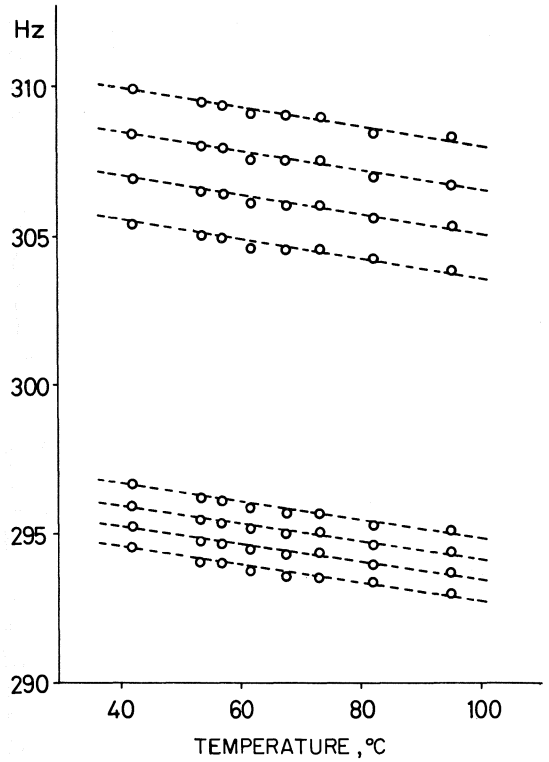

FIG. 2. Peak positions of the methyl proton signals in DMTFA as a function of temperature from the complete line shape fit data. These peak positions are measured in Hz from internal TMS.

TABLE 1. Kinetic data for DMTFA

T (°C)	$k^*(s^{-1})$	k†	k‡	k§
30.5	0.584			
41.8	1.936			
53.2	4.674			
56.8	6.173			
60.0	(7.74)		4.20	4.72
61.3	8.835			
62.1	(9.71)	4.98		
64.5	(10.9)		9.10	9.00
67.3	13.93			
70.0	(17.0)		12.90	14.54
70.2	(17.6)	6.53		
73.0	19.63			
75.0	(23.8)		17.30	19.80
75.4	(24.4)	9.22		
76.5	(26.0)	8.23		
79.6	(31.6)	9.45		
80.3	(32.8)		18.40	28.82
82.0	39.73			
82.5	(42.2)	10.7		
85.7	(54.6)		35.70	44.72
86.5	(56.2)	12.6		
89.9	(61.5)	14.4		
90.5	(62.2)		47.0	81.39
95.0	101.1			
95.3	(102.0)		88.70	103.1

$E_a = 17.37 \pm 0.26$ kcal mol^{-1}
$\Delta S^{\ddagger} = -4.26 \pm 0.77$ cal deg^{-1} mol^{-1}
$\Delta H^{\ddagger} = 16.78$ kcal mol^{-1}
$\Delta G^{\ddagger} = 18.05$ kcal mol^{-1} (298.2 °K)

*This work, 11.25 mol% in CCl_4, values in parentheses were obtained by interpolation from the Arrhenius plot (Fig. 7).
†Steady-state, ref. 1.
‡Spin-echo, computer-calculated $\sinh^{-1} F$ fit, ref. 21.
§Spin-echo, least-squares analysis using short τ approximation, ref. 21.

shifts. The solvent was CCl_4 and the concentration of DMTFA was 11.25 mol%, with 1.9% dioxane and 1% TMS.

The rate constants and kinetic parameters obtained for the hindered internal rotation in DMTFA are given in Table 1 using the reaction rate theory described in the experimental section. All activation parameters are calculated at 298.2 °K and the Arrhenius plot is shown on a composite diagram, see Fig. 7. The rate constants determined using an approximate analysis (1) have been included in Table 1, and it is seen that there is a discrepancy of a factor of 2–4 in these constants as compared with the complete line shape study. This systematic error in the primary data leads to a very low energy of activation $E_a = 9.3 \pm 0.6$ kcal mol^{-1}. The spin-echo method (19, 20) is an alternative and independent technique for the study of chemical exchange, and the rate constants previously determined (21) for DMTFA are also listed in Table 1. Again there are discrepancies, although certainly reduced, and in this case the rate constants are low in both the slow and fast exchange limits. This is contrary to the error characteristics previously discussed for a spin-echo study of DMF (3), but may be due to the use of a simplified two-site theory to fit the DMTFA data in that the heteronuclear couplings J_{AX} and J_{BX} (J_{BX} comparable with 2Ω in determining site Larmor frequencies) should be included in a complete description of the modulation of the Carr–Purcell echo train (17, 22). It should be noted, however, that the free energies of activation derived from complete line shape analysis, approximate line shape analysis, and spin-echo decay are 18.05 ± 0.30, 18.0 ± 0.6, and 17.6 ± 1.5 kcal mol^{-1}, respectively, while the activation energies vary from 9.3 to 20.6 kcal mol^{-1}. Once again the compensation of effective $\Delta H^{\ddagger}$ and $\Delta S^{\ddagger}$ values, corresponding to large systematic experimental errors in the determination of rate constants, leads to an approximately constant $\Delta G^{\ddagger}$ value (5).

Can. J. Chem. Downloaded from www.nrcresearchpress.com by 210.87.254.6 on 09/05/12
For personal use only.

Can. J. Chem. Downloaded from www.nrcresearchpress.com by 210.87.254.6 on 09/05/12
For personal use only.

Dimethyl Acetamide

A solution which contained 14.9 mol% of *N*,*N*-dimethyl acetamide (DMA) in CCl_4 as solvent was prepared with 1.7 mol% dioxane as a line shape standard and 1% hexamethyl disiloxane for a lock signal. A number of previous studies have been made of the hindered rotation barrier in this molecule (1, 4, 23–27), and the results show the usual inconsistencies some of which have been discussed in detail (4). The deviations in the values obtained for the free energies of activation from independent studies with similar solvents and solute concentrations are well outside the quoted experimental error bounds. Such deviations, however, are not unexpected in view of the fact that *cis* and *trans* scalar couplings between the *N*-methyl and $-CH_3$ groups have either been ignored or reduced by specific deuteration and the only total lineshape study (4) relies upon an approximate two-site model for the double quadruplet A_3B_3 part of an $A_3B_3X_3$ spectrum with $J_{AB} = 0$. In organic solvents, these couplings are not resolved as multiplets under the best operating conditions of the spectrometer. The most obvious spectral feature which reveals the presence of these long range couplings is the difference in apparent line width of the two methyl peaks in the region where exchange is minimal (very slow rotation).

They can be readily included, however, as distinct Larmor frequencies corresponding to a full 8 spin-site rate matrix and the generated line shapes may then be used to determine the unresolved couplings to a high degree of precision. The rate matrix has the same form as the case of DMTFA, with the relative sign ambiguity for J_{AX} and J_{BX}. In this case it is very difficult to decide relative signs because of the very small couplings, but more consistent line shape fits were obtained for J_{AX} and J_{BX} of the same sign. These features are illustrated by the experimental points and computed line shapes which are presented in Fig. 3. The methyl group *trans* to the carbonyl oxygen, A_3, is assigned to low field of the B_3 group. Such an assignment is consistent with that for DMF (7). The relatively small magnetic anisotropy of the C—H bond (28), and hence the $-CH_3$ group, is not expected to significantly modify the form of the magnetic shielding in the *N*-methyl region due to the C=O group. This is shown by the *N*-methyl chemical

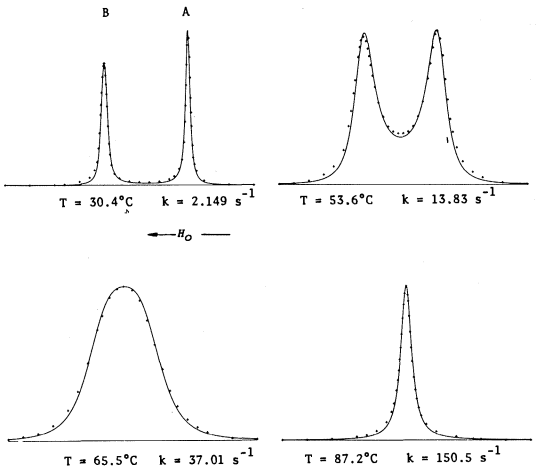

FIG. 3. Line shape fits of the methyl group proton spectra of DMA. Inequality in the heights of the methyl peaks is indicative of unresolved long range coupling. The inclusion of these unresolved couplings in a full 8 site analysis enables the values to be determined.

shift differences for CCl_4 solutions of DMF and DMA: 17.5 and 17.0 Hz, respectively, at 100 MHz and $T = 30$ °C. A temperature dependence of these chemical shifts was required for minimal error in the fits and is illustrated in Fig. 4. In the fast exchange region the extrapolation of the chemical shifts *vs.* temperature from the slow exchange region sufficed to obtain excellent consistency between the experimental and com-

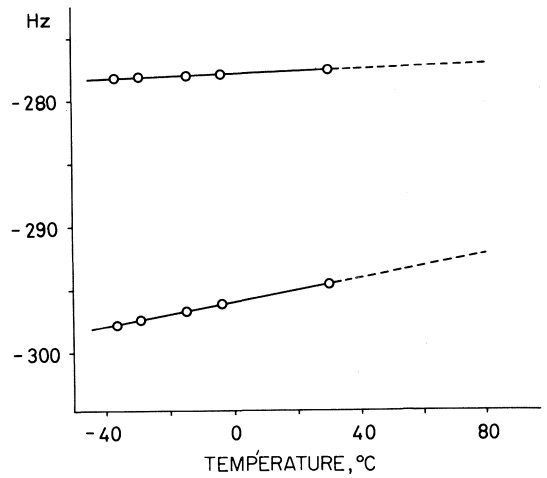

FIG. 4. Chemical shift of the methyl protons in DMA as a function of temperature (TMS internal standard). The dotted lines indicate the chemical shift data for the fast exchange limit, used to complete the line shape fits in this region.

Can. J. Chem. Downloaded from www.nrcresearchpress.com by 210.87.254.6 on 09/05/12
For personal use only.

puted spectra. The best fit data also give the values $J_{AX} = 0.10 \pm 0.05$ Hz (*cis*) and $J_{BX} = 0.40 \pm 0.05$ Hz (*trans*) at all temperatures. The J_{AX} coupling has been determined for the first time, while the J_{BX} value may be compared with that for aqueous solutions of DMA and *N*-methyl acetamide (29): $J_{trans} = 0.5$ Hz.

The kinetic data for DMA is given in Table 2. The energy of activation is 16.85 ± 0.41 kcal mol^{-1} and this value is to be compared with the values determined by recent less rigorous analyses (4, 27) for dilute solutions of DMA: $E_a = 20.6 \pm 0.3$ and 22 ± 1 kcal mol^{-1}. The increase in the former energy of activation (and free energy of activation 18.6 as compared with 17.3 kcal mol^{-1}) may be due to a relatively strong dipolar association of the amide with the solvent dimethyl sulfoxide. The latter increased value, however, is apparently a direct consequence of the particular analysis as all kinetic parameters previously determined by this method (24) are consistently high.

Dimethyl Benzamide

The methyl signals of *N*,*N*-dimethyl benzamide (DMB) are especially solvent-, concentration-, and temperature-dependent, but there is no long range coupling involving the *N*-methyl groups to complicate the line shape fits. There is a serious lack of consistent data on this barrier (1, 30) and only estimates of $\Delta G^{\ddagger}$ from coalescence of the methyl signals (3) can be made. DMBA was dissolved in CS_2 at a concentration of 2 mol% and 2% of $CHCl_3$ was added for a line shape standard, while the lock signal was provided by ~1% TMS.

TABLE 2. Kinetic data for DMA (14.9 mol% in CCl_4)

Temperature (°C)	k (s^{-1})
30.4	2.149
35.6	3.350
42.4	5.623
53.6	13.83
65.5	37.01
68.3	40.74
72.8	59.57
75.4	92.94
77.2	95.82
87.2	150.5

$E_a = 16.85 \pm 0.41$ kcal mol^{-1}
$\Delta S^{\ddagger} = -3.59 \pm 1.23$ cal deg^{-1} mol^{-1}
$\Delta H^{\ddagger} = 16.26$ kcal mol^{-1}
$\Delta G^{\ddagger} = 17.33$ kcal mol^{-1} (298.2 °K)

The rate matrix is trivial in this equal population two-site case, but the variation of Larmor frequencies required that total chemical shifts be selected and iterated to improve the final fits of the experimental to theoretical line shapes. The variation in chemical shifts with temperature is presented as Fig. 5 and typical line shape fits as Fig. 6. The best kinetic parameters are shown in Table 3.

Figure 7 is a composite diagram of Arrhenius plots for the three molecules studied here.

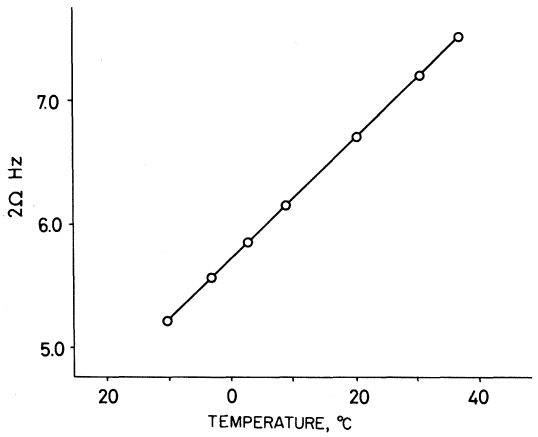

FIG. 5. Relative chemical shifts in DMBA as a function of temperature in the solutions studied. These shift differences were obtained by iterative fitting of the full line shape with chemical exchange.

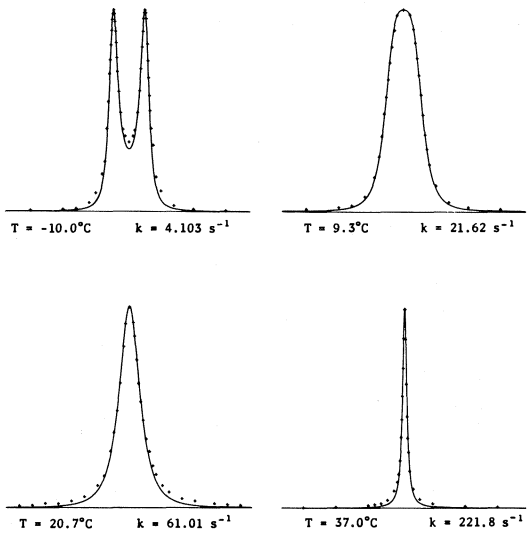

FIG. 6. Complete line shape fits for DMBA at several temperatures with adjusted chemical shifts.

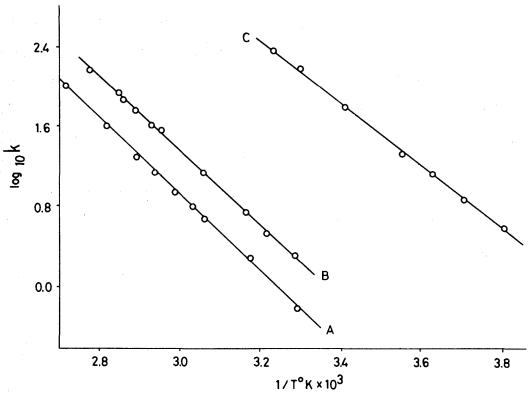

FIG. 7. Arrhenius plots for the rate constants for (*A*) DMTFA (*B*) DMA, and (*C*) DMBA for solutions described in the text.

TABLE 3. Kinetic data for DMBA (1.9 mol% in CS_2)

Temperature (°C)	k (s^{-1})
37.0	221.8
30.8	146.6
20.7	61.01
9.3	21.62
3.0	13.01
−2.9	7.589
−10.0	4.103

E_a = 14.00 ± 0.25 kcal mol^{-1}
$\Delta S^{\ddagger}$ = −4.69 ± 0.88 cal deg^{-1} mol^{-1}
$\Delta H^{\ddagger}$ = 13.40 kcal mol^{-1}
$\Delta G^{\ddagger}$ = 14.80 kcal mol^{-1} (298.2 °K)

Conclusion

The general problem of the factors which influence the barriers to rotation in an amido system is obviously complex. The role of steric as well as electronic factors are difficult to separate and indeed the reliability of energies of the transition state for comparative purposes, other than at infinite dilution in the gase phase is suspect. The recent review of Kessler (5) points out the factors which, qualitatively speaking, seem to be important. In dilute solution, and hence in the absence of appreciable intermolecular effects for a range of non-polar solvents, it is possible to correlate $\Delta G^{\ddagger}$ with parameters describing the electronic charge distribution in amides and the interaction of a C-substituent with the N—C═O bonding system (31). A similar correlation with parameters describing substituent inductive effects and steric interactions of a bulky substituent has already been attempted (4). In this present series of papers, the precision of the line shape fit data does begin to place some degree of confidence in the values of $\Delta H^{\ddagger}$ and $\Delta S^{\ddagger}$. When more related amido systems have been studied to give precise line shape fit data over a range of solvents, the interpretation of these activation parameters in terms of solvation of the ground and transition state can be attempted (32). It may then be possible to develop a more general model for the structure of amides in solution by comparison of the free energies of activation $\Delta G^{\ddagger}$, which may be considered to describe intramolecular interactions to a good approximation, and $\Delta H^{\ddagger}$ and $\Delta S^{\ddagger}$ which are expected to give more detailed information on intermolecular interactions.

This work was supported by the National Research Council of Canada in grants to L. W. Reeves.

1. M. T. ROGERS and J. C. WOODBURY. J. Phys. Chem. **66**, 540 (1962).
2. V. J. KOWALEWSKI and D. G. DEKOWALEWSKI. J. Chem. Phys. **33**, 1794 (1960); R. C. NEUMAN and L. B. YOUNG. J. Phys. Chem. **69**, 1777 (1965); K. I. DAHLQVIST and S. FORSEN. J. Phys. Chem. **69**, 4062 (1965).
3. A. ALLERHAND, H. S. GUTOWSKY, J. JONAS, and R. A. MEINZER. J. Am. Chem. Soc. **88**, 3185 (1966) and references therein.
4. R. C. NEUMAN and V. JONAS. J. Am. Chem. Soc. **90**, 1970 (1968).
5. M. KESSLER. Angew. Chem. (Int. Ed.) **9**, 219 (1970); W. E. STEWART and T. H. SIDALL. Chem. Rev. **70**, 517 (1970).
6. F. CONTI and W. VON PHILIPSBORN. Helv. Chim. Acta, **50**, 603 (1967).
7. P. T. INGLEFIELD, E. KRAKOWER, L. W. REEVES, and R. STEWART. Mol. Phys. **15**, 65 (1968).
8. M. RABINOVITZ and A. PINES. J. Am. Chem. Soc. **91**, 1585 (1969).
9. L. W. REEVES and K. N. SHAW. Can. J. Chem. **48**, 3641 (1970).
10. L. W. REEVES and K. N. SHAW. Can. J. Chem. This issue.
11. H. G. WHITTAKER and S. SIEGAL. J. Chem. Phys. **42**, 3320 (1965); H. S. GUTOWSKY, J. JONAS, and T. H. SIDALL. J. Am. Chem. Soc. **89**, 4300 (1967); M. RABINOVITZ and A. PINES. J. Chem. Soc. B, 1110 (1968); C. H. BUSHWELLER, J. W. O'NEIL, M. H. HALFORD, and F. H. BISSETT. J. Am. Chem. Soc. **93**, 1471 (1971).
12. A. L. VAN GEET. Anal. Chem. **40**, 2227 (1968).
13. K. J. LAIDLER. Chemical kinetics. McGraw-Hill, N.Y. 1965. p. 67.
14. E. W. RANDALL and J. D. BALDESCHWIELER. J. Mol. Spectrosc. **8**, 365 (1962).
15. A. J. R. BOURNE and E. W. RANDALL. Mol. Phys. **8**, 576 (1964).

Can. J. Chem. Downloaded from www.nrcresearchpress.com by 210.87.254.6 on 09/05/12
For personal use only.

16. D. R. DAVIS, R. P. LUTZ, and J. D. ROBERTS. J. Am. Chem. Soc. **83**, 246 (1960).
17. M. J. SEWELL. Unpublished results.
18. H. AKIYAMA, F. YAMAUCHI, and K. OUCHI. Chem. Commun. 355 (1970).
19. M. BLOOM, L. W. REEVES, and E. J. WELLS. J. Chem. Phys. **42**, 1615 (1965).
20. A. ALLERHAND and H. S. GUTOWSKY. J. Chem. Phys. **42**, 1587 (1965).
21. K. H. ABRAMSON, P. T. INGLEFIELD, E. KRAKOWER, and L. W. REEVES. Can. J. Chem. **44**, 1685 (1966).
22. H. S. GUTOWSKY, R. L. VOLD, and E. J. WELLS. J. Chem. Phys. **43**, 4107 (1965).
23. H. S. GUTOWSKY and C. M. HOLM. J. Chem. Phys. **25**, 1228 (1956).
24. C. W. FRYER, F. CONTI, and C. FRANCONI. Ric. Sci. Chim. **8**, 788 (1965).
25. D. G. GEHRING, W. A. MOSHER, and G. F. REDDY. J. Org. Chem. **31**, 3436 (1966).
26. R. C. NEUMAN and L. B. YOUNG. J. Phys. Chem. **69**, 1777 (1965).
27. A. CALZOLARI, F. CONTI, and C. FRANCONI. J. Chem. Soc. B, 860 (1970).
28. W. T. RAYNES and T. A. SUTHERLEY. Mol. Phys. **18**, 129 (1970).
29. A. BERGER, A. LOEWENSTEIN, and S. MEIBOOM. J. Am. Chem. Soc. **81**, 62 (1959).
30. G. SCHWENKER and H. ROSSWAY. Tetrahedron Lett. 4237 (1967).
31. L. W. REEVES and K. N. SHAW. Unpublished results.
32. K. N. SHAW and L. W. REEVES. Chem. Phys. Lett. **10**, 89 (1971).

Can. J. Chem. Downloaded from www.nrcresearchpress.com by 210.87.254.6 on 09/05/12
For personal use only.

Can. J. Chem. Downloaded from www.nrcresearchpress.com by 210.87.254.105 on 09/05/12
For personal use only.

The Penetrating Power of β-Decay Recoils of Epithermal Energies in Organic Matter

N. H. SHAFRIR

Department of Nuclear Science, Technion, Israel Institute of Technology, Haifa, Israel

Received May 5, 1971

A method for the measurement of the extent of dislocation of the β-decaying nucleus from its equilibrium position is described. An ionized layer formed at the surface of an aqueous solution of an ionic surface-active substance served as a source of β-disintegrating atoms. The primary adsorbed surface-active ions give rise to an electrical double layer within the liquid phase. When the solution contains β-active ions, some will join the electrical double layer near the surface as counter ions. It was found that radioactive β-recoils arising in an adsorbed surface layer are able to leave the surface, collected on a negatively charged plate, and counted. In order to reach the gas phase, the β-recoils have to penetrate the primary organic adsorption layer. When the expanded adsorption layer is gradually compressed, particles of lower energy are stopped, resulting in decreased recoil activity. Extrapolation to zero β-recoil activity gives an approximate value for the mass per unit area of organic material which stops completely atoms of certain initial energy. For particle energies between 2 to 22 eV, a linear dependence is found between the maximum β-recoil energy and the "penetrating power". The corresponding organic stopping layers for this energy region are between 1.0 to about 1.6×10^{-7} g/cm^2.

On décrit une méthode pour mesurer l'étendue de déplacement du noyau altérant β à partir de sa position d'équilibre. On s'est servi d'une couche ionisée formée à la surface d'une solution aqueuse d'une substance ionique de surface active comme source d'atomes désintégrants β. Les ions à surface active adsorbés en premier lieu causent la formation d'une double couche électrique au sein de la phase liquide. Quand la solution contient des ions actifs β, quelques uns d'entre eux vont se joindre à la double couche électrique près de la surface sous forme de contre-ions. On a découvert que les particules radioactives de recul β naissant dans une couche superficielle adsorbée peuvent quitter la surface, être recueillis sur une plaque chargée négativement et ensuite comptés. Pour se rendre à la phase gazeuse, les particules de recul β doivent d'abord pénétrer la première couche d'adsorption organique. Quand la couche étendue d'absorption est comprimée graduellement, les particules de plus faibles énergies sont arrêtées, causant une diminution d'activité pour la particule de recul. On obtient par extrapolation à activité nulle de la particule de recul β, une valeur approximative pour la masse par unité de surface, de matériel organique capable d'arrêter complètement les atomes possédant une certaine énergie initiale. On trouve une dépendance linéaire entre l'énergie maximale de la particule de recul β et le pouvoir pénétrant pour des particules dont l'énergie se situe entre 2 et 22 eV. Les couches d'arrêt organiques correspondant à cette région d'énergie se situent approximativement entre 1.0 et 1.6×10^{-7} g/cm^2.

Canadian Journal of Chemistry, 49, 3692 (1971)

Introduction

One of the important primary effects of nuclear transformations is the subsequent motion of the transmuted atom, in accord with the conservation of momentum and energy. The recoil energy involved can in many cases be calculated exactly. The extent of dislocation of the reaction product from its original equilibrium position depends on the fraction of the kinetic recoil energy spent for internal excitation and ionization, and on the range–energy relationship for the reaction products in the medium in question.

In the case of β-disintegration, the resulting decay products will be in the epithermal region. At present there appear to be no experimental data on the penetrating power of atoms in the eV energy region. Previous relevant measurements concerning neutrino studies (1–3), studies of surface processes by means of recoil atoms from β-decay and K-capture (4), and separation of β-decay products by recoil (5), gave only very vague information about the stopping of these particles. A few years ago some preliminary results on the penetrating power of atoms in the eV region in organic matter were reported by us (6). In these measurements a soluble ionized layer formed at the surface of an aqueous solution of an ionic surface-active substance served as a source for β-disintegrating atoms. The primary adsorbed surface active ions gave rise to an electrical double layer within the liquid phase. Ions of opposite charge were collected near the

Can. J. Chem. Downloaded from www.nrcresearchpress.com by 210.87.254.105 on 09/05/12
For personal use only.

surface. When some of the normal counter ions were replaced by β-disintegrating ions, they partly join the electrical double layer near the surface. It was found that β-recoils originating from this layer were able to leave the surface and could then be collected under atmospheric pressure. In order to reach the gas phase the β-recoils have to penetrate the primary organic adsorption layer. The thickness of the organic stopping layer can be changed gradually by alternating the adsorption conditions. Organic surface layers of the order of 0.1 $\mu g/cm^2$ are thus obtained, which are suitable for the stopping of heavy β-decay recoils in the eV region. These measurements were refined and extended to a number of β–γ disintegrating nuclides with maximum recoil energies between 2 and 22 eV.

The experiments were performed under conditions which almost completely exclude any energy-sharing processes. Thus the whole initial kinetic energy of the recoil particle remained as translational energy.

Principle of the Method

Aqueous solutions of ionic surface-active substances form an ionized surface layer at the solution–air interface. The primary adsorbed surface-active ions charge the surface electrically, giving rise to an electrical double layer. In this way counter ions of opposite sign are coadsorbed at the surface. When the solution contains β active ions of opposite charge to those of the surface active species, some of them will join the secondary adsorption side of the electrical double layer near the surface. The extent of coadsorption of the radioactive ions relative to that of the normal, non-isotopic counter ions, will depend on the physico-chemical characteristics of the radioactive ions. These values were previously determined in connection with adsorption and coadsorption studies of ionic surface-active substances at the water–air interface by means of α-disintegration recoils (7, 8).

In the preliminary experiments (6) it could be shown that a certain fraction of β-disintegration recoils arising in an ionized adsorbed surface layer are able to leave the surface and enter the gas phase even if their initial kinetic energy is only of the order of 1 eV. When leaving the liquid surface, a certain fraction of β-recoils will carry a positive charge which can then be collected on a negatively charged plate under atmospheric pressure. Choosing for the experiments β-decay systems which result in radioactive decay products, the β-recoils arriving at the collector plate can be determined by their decay characteristics.

The usual solid β-disintegration recoil source is a monoatomic film adsorbed on a cleavage plane or on a polished, carefully cleaned and degassed metal surface. In this case the adsorption energy of the atoms will be of the order of 1 eV. Thus, in the case of recoils with kinetic energies of a few eV, they will, on escaping from the surface, lose an appreciable fraction of their energy, and their original energy distribution will therefore be seriously distorted.

On the other hand, the energy of escape from the electrical double layer is small in comparison with the energies of a large part of the β recoil spectrum so that most of the recoil atoms are able to leave their place of formation, losing only a small fraction of their initial kinetic energy.

In order to reach the gas phase, the β-recoils have to penetrate the primary organic adsorption layer. The thickness, or mass per unit area of the organic stopping layer can be changed gradually by alternation of the composition of the solution. This results in changes in the primary adsorption conditions at the surface of the solution. An expanded primary adsorption layer can be compressed by raising the ionic strength of the solution at constant concentration of the surface active substance, or by raising the bulk concentration of the surface-active substance in the region below the critical micell concentration at constant ionic strength. As a result of this compression, an increase in the mass per unit area of the organic stopping layer occurs. In Fig. 1 a schematic representation of the electrical double layer formed at the surface of the solution of an ionic-surface active substance is shown.

Figure 1*A* shows the case of a fully expanded surface layer. Adsorption conditions can be controlled so that, although the organic ions cover the surface in horizontal positions, their density at the surface is high enough to cover the surface completely, not leaving any empty islands between them. Under these conditions a minimum stopping layer is obtained. Figure 1*B* illustrates an intermediate stage of compression, resulting in an intermediate stopping layer. Figure 1*C* gives a schematic representation of a

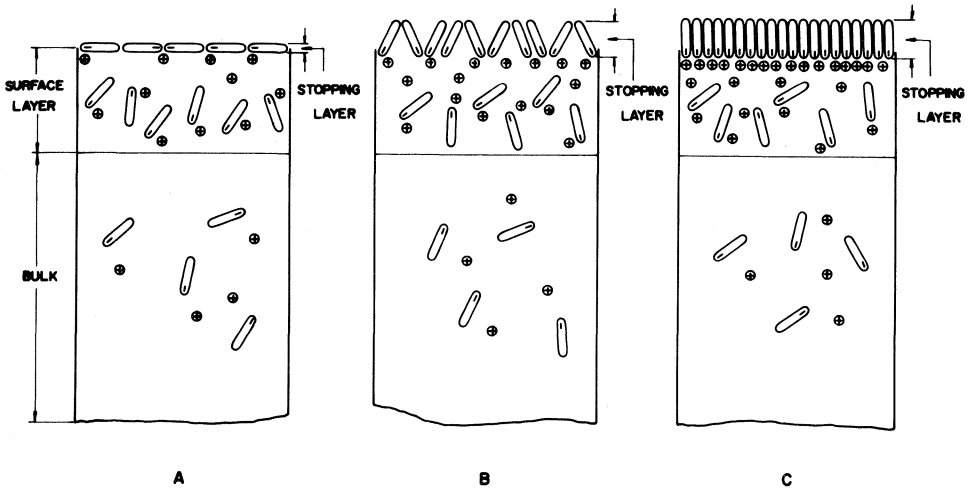

FIG. 1. Schematic representation of an electrical double layer formed at the surface of an aqueous solution of an ionic surface-active substance. A, fully expanded surface layer; B, intermediate stage of compression at surface layer; C, fully compressed surface layer.

fully compressed layer where the organic ions are closely packed and cover the whole surface in vertical position. In this case maximum stopping thickness is obtained.

Electrical double layers of this kind can, to a good approximation, be described by using the Stern picture (9), which is a combination of the rigid Helmholtz layer and the diffuse Gouy–Chapman layer (10, 11). According to this picture the charge at the surface will have a plane distribution, whereas the charge within the solution will be distributed partly parallel to this plane at a distance of the order of one atom and partly toward the bulk of the solution at depths up to a number of molecular layers in a diffusive way.

The surface concentration of the primary adsorbed organic ions and molecules which constitute the stopping layer is determined by measuring the surface tension of the solution *vs.* the concentration of the aqueous solution of the surface-active substance at various ionic strengths. From these results the surface excess of the surface-active substance (Γ) can be calculated by means of a suitably modified Gibbs adsorption equation. Because of the strong adsorption, the surface excess can in fact be taken to be equal to the surface concentration, *i.e.* $C_S = \Gamma(\text{mol/cm}^2)$. As a change in the primary adsorption conditions results in a change in the amount of coadsorption, a suitable normalization of the collector activity, which represents the number of recoils which have reached the collector, has to be made before the results of the individual measurements can be compared. The method of normalization depends on the type of system under investigation.

Experimental

The experimental arrangement used was essentially a modification of an apparatus used for the study of adsorption at ionized surface layers of aqueous solutions of surface-active substances (7, 8, 12–14), as shown in Fig. 2. A is a 5 mm deep lucite cell which contains the solution. On the bottom of the cell is a circular platinum wire B with a connection to the outside. B is connected to the positive pole of a d.c. voltage source. One mm above the liquid surface and the top of the cell, a stainless steel ring C is placed to which a negative potential is applied. In this way edge effects could be neglected. Thus only those β-recoil atoms which leave the surface within the inner edge of the stainless steel ring reach the stainless steel collector D. D is connected to the negative pole of a d.c. supply. The potential between the solution and the collector was 1100 V in order to ensure saturation collection (see Fig. 3), whereas the potential of the ring with respect to the solution was always one third of this value; thus a homogeneous field was maintained. In one experimental series where the half life of the β-recoil was extremely short, so that no effective collection could be performed, a thin window proportional counter was used instead of the collector. In this case β-recoils reaching the counter were detected directly by their α-decay characteristics.

The solution, at the surface of which the β-recoil source was coadsorbed, was 10^{-3} *N* nitric acid containing as ionic surface active substance, an extremely pure, specially synthesized sample of sodium dodecyl sulfate (12–14).

Can. J. Chem. Downloaded from www.nrcresearchpress.com by 210.87.254.105 on 09/05/12
For personal use only.

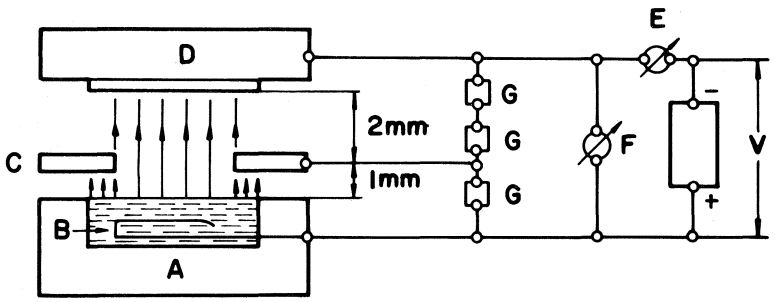

FIG. 2. Experimental arrangement. A, lucite cell containing the solution; B, circular platinum wire; C, collimating ring; D, collector plate; E, microammeter; F, voltmeter; G, 10 MΩ resistors.

TABLE 1. Disintegration characteristics of the β-decaying nuclides and their recoils, used in the stopping experiments

β-decaying nuclide			β-decay recoil		
Nuclide	$E_{max}(\beta^-)$ (MeV)	Half life	Nuclide	E_{max}(recoil) (eV)	Half life
^{212}Pb	0.589	10.6 h	^{212}Bi	2.38	60.6 min
^{210}Bi	1.16	5.01 day	^{210}Po	6.4	138.4 day
^{211}Pb	1.39	36.1 min	^{211}Bi	8.5	2.12 min
^{212}Bi	2.25	60.6 min	^{212}Po	21.3	3.10^{-7} s

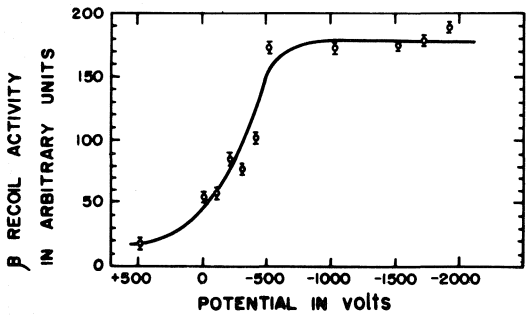

FIG. 3. β-recoil activity *vs.* collector potential.

The β-decaying nuclides and their respective recoils used in the stopping experiments are summarized in Table 1. The maximum β-energies given in this table are for highest energy β-transitions. The respective maximum recoil energies in the table are calculated from the following expression derived directly from the principle of momentum conservation

$$[1] \qquad E_{max}(\text{Recoil}) = \frac{m_0 E_0}{m_R} + \frac{E_0^2}{2m_R c^2}$$

where E_0 is the maximum β-energy, m_R the recoil mass, m_0 the rest mass of the electron, and c the velocity of light.

The β-decay processes of all the nuclides used in this work are accompanied by γ-emission, which imparts recoil momentum to the daughter nucleus in two ways: first, a small amount by direct recoil; and second, a much greater amount by internal conversion. In all the transitions listed, the nuclear excited states have half-times of the order of 10^{-10} to 10^{-13} s. However, if the atoms undergoing the γ-decay have escaped from the surface as a result of the preceding β-decay, they will be away from the surface of the solution by a distance of the order of tens of Å, thus the penetrating power of the recoils through the organic surface layer will not be influenced by the additional recoil energy.

The effect of γ-emission on the recoiling atom well away from the surface will only be to scatter a certain percentage away from the collector, thus lowering the collection yield.

Activities of the respective beta decaying nuclides were dissolved in extremely pure 10^{-3} *N* nitric acid after which the chosen amount of sodium dodecyl sulfate was dissolved in the radioactive solution. ^{212}Pb and ^{211}Pb were introduced into the system by dissolution of the activities from the collecting cathode of a ^{228}Th emanation chamber or a ^{227}Ac emanation chamber, respectively. Collection experiments were started after transient equilibria between ^{212}Pb or ^{211}Pb and their respective decay products were reached.

The collection of the ^{212}Bi atoms above the solution was continued for 2 h. In this way about 75% of the maximum collectable ^{212}Bi activity was accounted for. During that time, and in fact after the first 20 min, secular equilibrium is established between ^{208}Tl, which becomes enriched on the collector in appreciable amounts, and the transient equilibrium activities of the solution. It is a well known fact that ^{208}Tl$^+$ is able to reach the collector under these conditions because of the recoil energy associated with it as a result of the α-decay branching of ^{212}Bi and because of its positive charge (7, 8, 12, 13).

Can. J. Chem. Downloaded from www.nrcresearchpress.com by 210.87.254.105 on 09/05/12
For personal use only.

Can. J. Chem. Downloaded from www.nrcresearchpress.com by 210.87.254.105 on 09/05/12
For personal use only.

After removal of the collector, its total activity was measured over a definite time interval. After the 3.1 min activity of ^{208}Tl had decayed, the activity of the collector was followed for a further hour and identified as ^{212}Bi by its half life. From this result the β-recoil activity (^{212}Bi) was calculated for a certain reference time.

For normalization of the β-recoil activity with respect to changes in the coadsorption conditions, the simultaneous measurement of the above mentioned α-recoil activity was found to be suitable. As the highest values of the mass per unit area of the stopping layers used are negligible in comparison with the range of ^{208}Tl in the solution which in water is of the order of 10^{-5} g/cm^2 (15, 16), changes in the α-recoil activity indicate changes in the adsorption conditions and are not influenced by alterations in the thickness of the stopping layer. Thus the ^{208}Tl activity on the collector indicates the amount of coadsorbed $^{212}Bi^{3+}$ ions as a result of variation of the primary adsorption conditions. Consequently this dependence can be used directly for the normalization of the β^--recoil activities (^{210}Po, ^{212}Po) resulting from the β^--decay of coadsorbed Bi^{3+} ions, with respect to changes in adsorption conditions. For the normalization of the β^--recoil activities ^{211}Bi and ^{212}Bi, which result from the β^--decay of coadsorbed Pb^{2+} ions the same procedure is applied, but an additional correction is made for the relative coadsorptions of Pb^{2+} ions with respect to Bi^{3+} ions. This correction is based on the preferential ionic adsorption factor which has been determined experimentally for similar systems (12–14). Thus measurement of the α-recoil activity (^{208}Tl) for all the adsorption conditions used in the experiments served for the normalization of the measured β-recoil activities for the case of all four nuclides.

^{211}Bi atoms were collected above the solution for 15 min, thus reaching their saturation activity. The β-recoil activity (^{212}Bi) was determined by α-spectroscopy using a Si solid state detector in conjunction with a 256 channel pulse height analyzer.

The preparation of the ^{210}Bi and ^{212}Bi activities to be introduced into the solution was somewhat different. Both nuclides were collected in vacuum on a negatively charged platinum plate from extremely thin deposited layers of ^{210}Pb and ^{212}Pb, respectively, by making use of the β-recoil properties. The activities thus collected were then dissolved in 10^{-3} *N* nitric acid and used in the experiments as described previously.

The collection of ^{210}Pb atoms above the solution was continued for one day, and the collected activity determined by α-spectroscopy using a Si detector. The recoils obtained from the β-disintegration of ^{212}Bi were counted directly above the solution as mentioned before, when reaching the detector, by α-counting using an end window proportional counter.

The surface tension of the solutions of various concentrations of sodium dodecyl sulfate was measured with a du Noüy tensiometer. The ionic strength of the solution was controlled by additions of sodium nitrate; thus no new species were added to the system.

All the experiments were performed in a gloved box giving several advantages in addition to prevention of radioactive contamination. Dust would be well excluded, excellent air thermostation could be achieved by making the inner walls of the box thermal conducting and the relative humidity was kept high, thus minimizing surface evaporation. The evaporation was furthermore kept low by the small gas space over the surface in the experimental apparatus, which was about 2.4 cm^3. The box was thermostated at 25.0 ± 0.5 °C.

Results

Collection Experiments

In the preliminary series of measurements, collection conditions and the charge on the ^{212}Bi recoils were investigated under the experimental conditions described above. In this series the β-recoil activity was measured as a function of the collector potential under constant adsorption conditions. The concentration of sodium dodecyl sulfate was 10^{-4} mol/l, the nitric acid content of the solution 10^{-3} mol/l and the ionic strength 3×10^{-3} mol/l. Under these conditions the organic stopping layer had a thickness of 2.1×10^{-10} mol/cm^2.

The results of these measurements are shown in Fig. 3. From this it can be seen that saturation collection of the positively charged fraction of the β-recoils is reached at approximately −500 V under these experimental conditions, *i.e.*, at a field strength of approximately 1600 V/cm.

The number of β-recoils which reach the collector at zero collecting potential represents the overall amount of β-recoils which are able, under these experimental conditions, to reach the collector by a pure diffusion mechanism. These recoils consist of charged and uncharged species.

The number of β-recoils which reach the collector at the maximum applied retarding potential of +500 V represents the fraction of uncharged β-recoils, since the maximum applied retarding potential is very large in comparison with the most energetic β-recoil. It can be seen from these results that about one-third of the β-recoils are uncharged, whereas about two-thirds of them are positively charged. The fraction of negatively charged β-recoils can be assumed to be negligible.

Furthermore, it can be seen from Fig. 3 that the efficiency of collection of β-recoils when saturation has been achieved by a sufficient negative potential is three to four times as large as the collection efficiency by diffusion alone.

Stopping Layer Thickness

The thickness of the organic stopping layer which is practically identical with the excess of the dodecyl sulfate species (DS) at the surface, can be

Can. J. Chem. Downloaded from www.nrcresearchpress.com by 210.87.254.105 on 09/05/12
For personal use only.

calculated with the aid of a suitably modified Gibbs adsorption equation from surface tension/conc. measurements. The Gibbs equation for the system under investigation can be written as

$$[2] \quad -d\gamma/RT = \Gamma_{Na^+}\, d\ln a_{Na^+} + \Gamma_{DS^-}\, d\ln a_{DS^-} + \Gamma_{H_3O^+}\, d\ln a_{H_3O^+} + \Gamma_{HDS}\, d\ln a_{HDS^+} + \Gamma_{NO_3^-}\, d\ln a_{NO_3^-} + \Gamma_{Rad^{n+}}\, d\ln a_{Rad^{n+}} + \Gamma_{OH^-}\, d\ln a_{OH^-}$$

where γ = surface tension in dyn/cm, a = molar activity, Γ = surface excess in mol/cm^2, and T = absolute temperature. The symbol Rad^{n+} represents the added radioactive species. The contribution of the sixth term (Rad^{n+}) is negligible, because of the extremely low concentration of the cations. As the surface adsorption of NO_3^- relative to that of the surface-active anions is extremely small, the fifth term may be omitted too. If the ionic strength and the pH are kept constant, the first (Na^+), the third (H_3O^+), and the last (OH^-) terms of the Gibbs equation become zero, and

$$[3] \quad d\ln a_{DS^-} = d\ln a_{HDS}$$

At 25 °C the adsorption isotherm reduces, therefore, to

$$[4] \quad -d\gamma/RT = (\Gamma_{DS^-} + \Gamma_{HDS})(1 - 0.585\sqrt{m_{DS^-}})\, d\ln m_{DS}$$

where m is molarity. For very dilute solutions

$$[5] \quad -d\gamma/RT = (\Gamma_{DS^-} + \Gamma_{HDS})\, d\ln C_{DS^-}$$

and $d\ln C_{DS} = d\ln C_{DS^-}$ are valid. After denoting the sum of the surface excesses of the two existing dodecyl sulfate species by Γ_{DS}, the final result is obtained

$$[6] \quad -d\gamma/RT = \Gamma_{DS}\, d\ln C_{DS}$$

From eq. 6 the surface concentration $C_s \simeq \Gamma_{DS}$ in mol DS/cm^2 can be found and translated into g/cm^2.

Stopping Measurements

In a series of stopping measurements the β-recoil activity was determined as a function of the moles per unit area of the stopping layer. The smallest number of moles per unit area with which stopping experiments could be made was limited by the lowest value of the ionic strength which was permissible. The lower limit of this value is determined by the pH of the solution. Because of the appreciable radiocolloid formation which would occur (8), pH values higher than three are not permissible.

The mass per unit area of the stopping layer was varied according to the β-recoil under investigation, between 2.1 to 6.1 × 10^{-10} mol DS/cm^2, which corresponds to about 0.6 to 1.6 × 10^{-7} g/cm^2. A value of 10^{-4} mol/l was chosen for the sodium dodecyl sulfate concentration of the solution: thus even at the highest ionic strength used, the measurements are still made below the critical micell concentration.

The number of moles DS per unit area was calculated from the surface tension/conc. measurements, making use of eq. 6. The results obtained were found in good agreement with the values given by Matijevic *et al.* (17).

As an illustration, the results of the β-recoil stopping measurements for the system ^{212}Pb/^{212}Bi are shown in Fig. 4. From this it can be seen that when the mass per unit area is raised, the normalized β-recoil activity decreases continuously. This can be explained by the complete stopping of the lower energy part of the β-recoil spectrum. From extrapolation of the curve to

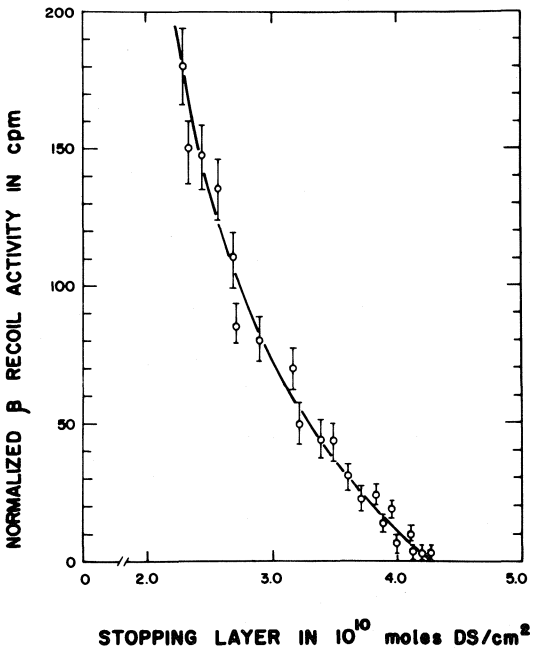

FIG. 4. Normalized β-recoil activity obtained from the system ^{212}Pb/^{212}Bi *vs.* the number of mol DS/cm^2 of the stopping layer.

Can. J. Chem. Downloaded from www.nrcresearchpress.com by 210.87.254.105 on 09/05/12
For personal use only.

TABLE 2. Experimentally determined organic stopping thicknesses for very heavy β-recoils in the energy domain 2 to 22 eV

β-decay recoil	E_{max}(recoil) (eV)	Organic stopping layer thickness	
		10^{10} mol/cm^2	10^7 g/cm^2
^{212}Bi	2.38	4.15–4.37	1.10–1.16
^{210}Po	6.4	4.6–4.85	1.22–1.29
^{211}Bi	8.5	4.7–4.95	1.25–1.31
^{212}Po	21.3	5.85–6.15	1.55–1.63

zero β-recoil activity an approximate value can be found for the number of moles of dodecyl sulfate per unit area which completely stops atoms of maximum β^--recoil energy 2.38 eV. These atoms may be said to have the shortest path through the organic stopping layer and to originate from the uppermost coadsorbed layer only. The stopping value seems to lie approximately between 4.15 to 4.37 $\times$ 10^{-10} mol DS/cm^2, which corresponds to about 1.10 to 1.16 $\times$ 10^{-7} g/cm^2 or organic material.

In Table 2 the results of the stopping measurement performed in a similar way, for all the four β-recoils under investigation are given.

Discussion

The energy loss of heavy particles with velocities $v < e^2/\hbar = 2.2 \times 10^8$ cm/s is accompanied by a quasiadiabatic interpenetration of the respective electron fields and most of the energy is transferred by nearly elastic collisions. The most successful approach to the nuclear stopping mechanism has been made by Lindhard *et al.* (18) who brought the theoretical predictions very close to the experimental results (15, 16) by introducing a screened potential based on a statistical model of the interacting atoms. Their treatment is based on a universal nuclear stopping cross section due to shielded nuclear collisions, calculated from a Thomas–Fermi model of the interaction between an ion and an atom. However, at extremely low energies, *i.e.* for values of the dimensionless Lindhard energy parameter $\varepsilon < 10^{-2}$, the Thomas–Fermi treatment is a crude approximation, when the ion and the atom do not come close to each other and thus the nuclear scattering and stopping becomes uncertain. For still lower velocities, as in the case of β-decay recoils, studied in this investigation where the initial particle velocity is of the order of 10^{-3} $e^2/\hbar$, the effective collision cross section will tend to coincide with the gas kinetic cross section, corresponding to a rate of energy loss proportional to the energy of the recoil.

The only semiquantitative treatment of this problem has been made by Jacobsen, who because of the complexity of the problem neglected the deviation of the particle path from a straight line (19). Unfortunately under these conditions no comparison between this approach and experiment can be made.

Because of the diffusion-like phenomenon of the penetration of particles through material in this extremely low energy domain the usual definition of range is not applicable. Instead we prefer to call the approximate layer of material through which the particles are able to dislocate themselves the "extent of dislocation" of the β-recoils. In Fig. 5 the results obtained for maximum β-recoil energies between 2 and 22 eV are given. It is seen that in this energy domain a nearly linear dependence between recoil energy and dislocation distance in organic matter as represented by the stopping layer thickness was found.

In the light of the considerations mentioned it seems to be safe to conclude that, under the physical and experimental circumstances which have been described, atoms resulting from β-decay which leave the surface of the solution do so only as a result of their β-recoil energy.

Another possibility which should be discussed is that some of the atoms obtained in the solution as a result of α-decay, *e.g.* ^{208}Tl, having initial kinetic energies of the order of 100 keV, could transfer their kinetic energy by a central collision more or less completely to a β-recoil atom, which

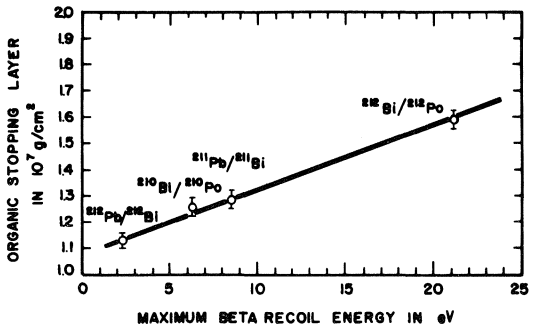

FIG. 5. Dislocation distance of heavy β-recoils in organic material as a function of particle energy.

could then be ejected from the solution. This seems to be quite improbable for two reasons. Firstly, if this mechanism should have some quantitative importance, it should in a similar way eject some of the coadsorbed β-disintegrating ions, *e.g.* ^{212}Pb. However, such activities could not be detected on the collector. Secondly, if one calculates the mean distance between the β-recoil atoms, *e.g.* ^{212}Bi-ions at the surface, knowing their specific activity in the solution, their preferential ionic adsorption at the surface layer relative to the adsorption of hydrogen and sodium ions (12, 13), and the general adsorption conditions used, one finds that this distance is of the order of 10^3–10^5 Å. This means that the direct collision mechanism is rather improbable.

Finally, it may be said that the method described here proved to be suitable for measurements of the stopping of β-recoils. Experiments using surface-active ions with greater chain lengths as well as insoluble ionized surface films are in progress.

The technical assistance of F. Lichtenstern and E. Mionis and the crew of the technical service of the Department is acknowledged.

1. C. W. SHERWIN. Phys. Rev. **75**, 1799 (1949).
2. C. W. SHERWIN. Phys. Rev. **82**, 52 (1951).
3. J. S. ALLEN. *In* The neutrino. Princeton University Press. 1958.
4. H. FRAUENFELDER. Helv. phys. acta, **23**, 347 (1950).
5. H. MUNDSCHENK. Dissertation. Mainz. 1962.
6. I. TAMIR and N. H. STEIGER (SHAFRIR). *In* Chemical effects of nuclear transformations. I.A.E.A. Vienna. 1961.
7. G. ANIANSSON and N. H. STEIGER (SHAFRIR). J. Chem. Phys. **21**, 1299 (1953).
8. N. H. STEIGER (SHAFRIR) and G. ANIANSSON. J. Phys. Chem. **58**, 228 (1954).
9. O. STERN. Z. f. Elektrochemie, **30**, 508 (1924).
10. G. GOUY. J. Ann. d. Phys. (9) **7**, 129 (1917).
11. D. L. CHAPMAN. Phil. Mag. (6) **25**, 475 (1913).
12. M. AVRAHAMI and N. H. STEIGER (SHAFRIR). *In* Radioisotopes in the physical sciences and industry. I.A.E.A. Vienna. 1962.
13. M. AVRAHAMI and N. H. STEIGER (SHAFRIR). J. Coll. Sci. **18**, 863 (1963).
14. M. AVRAHAMI. D.Sc. Thesis, Technion, Israel Institute of Technology, Haifa, Israel, 1960.
15. J. LEON and N. H. STEIGER-SHAFRIR. Can. J. Phys. **49**, 1004 (1971).
16. J. LEON and N. H. STEIGER-SHAFRIR. Can. J. Phys. **49**, 2106 (1971).
17. E. MATIJEVIC and B. A. PETHICA. Trans. Faraday Soc. **54**, 1382 (1958).
18. J. LINDHARD, M. SCHARFF, and H. E. SCHIØTT. Mat. Fys. Medd. Dan. Vid. Selsk. **33**, No. 14 (1963).
19. J. G. JACOBSEN. Nature, **117**, 858 (1928).

Can. J. Chem. Downloaded from www.nrcresearchpress.com by 210.87.254.105 on 09/05/12
For personal use only.

Can. J. Chem. Downloaded from www.nrcresearchpress.com by 210.87.254.105 on 09/05/12
For personal use only.

Etude des oxydes mixtes de lanthanides et de vanadium(V)

H. Brusset, F. Madaule-Aubry, B. Blanck, J. P. Glaziou, et J. P. Laude

Institut de Chimie, École Centrale des Arts et Manufactures, Grande Voie des Vignes, 92–Chatenay-Malabry, France

Reçu le 23 septembre 1970[1]

Ce travail présente une étude par voie sèche d'oxydes mixtes de vanadium(V) et de lanthanides. L'étude a porté sur tous les éléments de terres rares à l'exclusion du cérium et du prométhium.

Tous les orthovanadates TVO_4 ont été préparés et leurs paramètres de maille redéterminés. Des composés nouveaux ont été synthétisés: $4T_2O_3.V_2O_5$ pour tous les lanthanides étudiés, $5T_2O_3.V_2O_5$ pour les éléments allant du samarium à l'ytterbium et $6T_2O_3.V_2O_5$ pour le praséodyme et le néodyme. L'identification de ces composés a été menée par diffractométrie de rayons X.

This work presents a study of the mixed oxides of vanadium(V) and lanthanides by dry methods. The study includes all elements of the rare earth group except cerium and promethium.

All orthovanadates of the formula TVO_4 were prepared and their lattice parameters redetermined for all lanthanides. New materials were synthesized: lanthanides $4T_2O_3.V_2O_5$, for elements from samarium to ytterbium the compounds $5T_2O_3.V_2O_5$. and for praseodymium and neodymium the compounds $6T_2O_3.V_2O_5$. Identification of these materials was carried out by X-ray diffraction.

Canadian Journal of Chemistry, 49, 3700 (1971)

Dans le cadre d'une étude systématique des oxydes doubles contenant un élément de terre rare (1–4) nous nous sommes intéressés aux vanadates de lanthanides.

En effet, si sont bien connus les orthovanadates TVO_4 (où T représente l'un quelconque des lanthanides) et si quelques composés polyvanadiques ont été préparés à partir de solutions aqueuses (5, 6), la littérature ne mentionne aucun résultat concernant des études faites par voie sèche et correspondant à des mélanges d'oxydes T_2O_3 et V_2O_5 en proportions autres qu'équimoléculaires.

Nous avons entrepris l'étude de tous les systèmes binaires T_2O_3–V_2O_5, où T représente l'un des éléments suivants: lanthane, praséodyme, néodyme, samarium, gadolinium et dysprosium; l'existence de composés nouveaux analogues à ceux mis en évidence pour les éléments ci-dessus a été vérifiée pour les autres terres rares, à l'exclusion du prométhium et du cérium, c'est à dire l'europium, le terbium, l'holmium, le thulium et le lutécium. Nous avons laissé de côté le prométhium parce qu'il ne présente pas d'isotope stable; quant au cérium, seul l'orthovanadate a pu être préparé: l'oxyde Ce_2O_3, en effet, se réoxyde spontanément dès la température ambiante et l'étude de ce système aurait nécessité une autre technique que celle que nous avons employée pour les autres. Des traitements thermiques de mélanges CeO_2–V_2O_5 n'ont pas permis d'obtenir d'autres composés que $CeVO_4$.

[1]Revision reçue le 7 juin 1971.

Produits de départ et techniques expérimentales

Nous avons utilisé l'hémipentoxyde de vanadium V_2O_5 pur à 99.9%, livré par Riedel–Dehaën, et les sesquioxydes de terres rares T_2O_3 purs à 99.9% de chez Touzart et Matignon, sauf dans le cas du praséodyme où nous disposions du peroxyde Pr_6O_{11} et du terbium où il s'agissait de Tb_5O_9.

Nous avons vérifié par fluorescence X (spectromètre Philips PW 1200, anticathode de tungstène, cristal analyseur LiF) que les oxydes de terres rares ne contenaient pas, en petite quantité, d'autre lanthanide, ce qui s'est avéré exact dans tous les cas, sauf celui de l'oxyde d'erbium dont le spectre de fluorescence X a montré des pics d'intensité très faible correspondant aux raies $L\alpha_1$ du thulium, de l'holmium et du fer.

Nous disposons pour l'identification des phases cristallines d'un diffractomètre à poudres Philips PW 1310 utilisé avec un tube à anticathode de cuivre et un filtre de nickel. Les pointés des angles concernent la radiation $K\alpha_1$ du cuivre, $\lambda = 1.5405$ Å.

Tous les diffractogrammes des oxydes de départ ont été réalisés et sont en bon accord avec ceux donnés par l'ASTM (7); le pentoxyde de vanadium se présente sous sa seule forme cristalline connue, orthorhombique. Il en est de même pour les sesquioxydes (cubiques) de dysprosium, holmium, erbium, thulium, ytterbium, lutécium.

Le sesquioxyde de samarium se présente comme un mélange des formes monoclinique et cubique. Après chauffage pendant 24 h à 1500 °C les raies de la forme cubique ont toutes disparu.

Can. J. Chem. Downloaded from www.nrcresearchpress.com by 210.87.254.105 on 09/05/12
For personal use only.

Les sesquioxydes d'europium et de gadolinium qui peuvent cristalliser sous forme cubique et monoclinique apparaissent sous la seule forme cubique.

Les peroxydes Pr_6O_{11} et Tb_5O_9 après chauffage pendant 6 h sous courant d'hydrogène, ont donné naissance aux sesquioxydes correspondants: Pr_2O_3 hexagonal et Tb_2O_3 cubique.

Nd_2O_3 se présente comme un mélange de formes hexagonale et cubique, cette dernière en faible proportion et disparaissant après chauffage à 800 °C.

Quant au sesquioxyde de lanthane, commercial, c'est un mélange de La_2O_3 hexagonal et d'hydroxyde $La(OH)_3$ (provenant de l'hydratation de l'oxyde par la vapeur d'eau atmosphérique). Celui-ci disparait après chauffage à 600 °C pendant 15 h. Dans l'étude du système concernant le lanthane, nous avons utilisé du sesquioxyde préalablement chauffé à 800 °C et conservé à l'étuve ainsi que les échantillons de mélanges d'oxydes.

Les systèmes binaires ont tous été étudiés de la même façon: les mélanges d'oxydes, préalablement broyés finement, ont été effectués au sein de l'acétone; cette technique s'est montrée plus rapide et plus efficace que le passage au broyeur-mélangeur, l'acétone s'évaporant avant tout traitement ne modifie pas les résultats. Les mélanges ainsi obtenus ont été chauffés pendant des durées variables (généralement 24 h) à des températures comprises entre 600 et 1500 °C dans des creusets de platine fermés (mais non scellés) pour les mélanges riches en oxyde de vanadium.

Le refroidissement des produits de réactions s'est fait à la vitesse de refroidissement propre des fours, ceux-ci ne permettant pas d'opérations de trempe.

Nous avons utilisé un four à moufle Paris-Labo pour les chauffages à l'air jusqu'à 1100 °C, et, pour les températures supérieures, un four à moufle de la Compagnie Industrielle des Fours, à résistance de superkanthal équipé d'un programme de chauffe dont la température maximale de fonctionnement est 1500 °C. Pour les traitements effectués sous atmosphère contrôlée (azote, hydrogène), nous avons utilisé deux fours tubulaires: un petit four de laboratoire Leune jusqu'à 900 °C, à tube de quartz, un four Hermann Moritz jusqu'à 1600 °C utilisant des résistances de carbure de silicium. Nous ne nous en sommes servis que pour des chauffages sous azote, avec un tube en mullite.

Après refroidissement, tous les produits obtenus ont été examinés par diffraction des rayons X au moyen du diffractomètre Philips.

Les sesquioxydes de praséodyme et terbium pouvant donner lieu à des dioxydes, les traitements thermiques qui les concernent ont été menés sous atmosphère inerte d'azote.

Les conditions expérimentales avec lesquelles nous avons opéré ne nous ont pas permis de constituer les diagrammes d'équilibres des systèmes binaires T_2O_3–V_2O_5, mais plutôt de déterminer les conditions d'apparition de phases nouvelles figurant dans ces diagrammes. Néanmoins, comme les oxydes de terres rares sont réfractaires et que les composés nouveaux sont apparus du côté des mélanges riches en terres rares, et donc qui n'ont pas fondu lors du traitement, il est probable qu'après un refroidissement relativement rapide, étant donnée la lenteur des réactions entre solides, l'examen des phases cristallines donne une bonne idée des phases en équilibre à la température maximale de chauffe.

Résultats

Les premiers résultats, concernant les systèmes relatifs au gadolinium et à l'erbium, ont été publiés par ailleurs (1).

Dans tous les cas, on observe la formation de l'orthovanadate TVO_4 et d'un composé défini nouveau, contenant quatre atomes de terre rare pour un atome de vanadium, dont la formule dualistique peut s'écrire $4T_2O_3.V_2O_5$. Nous désignerons ce type de composé sous le nom de "composés A".

D'autre part, les systèmes se classent en deux catégories: (*i*) ceux qui font intervenir le praséodyme et le néodyme montrent en outre la formation de composés de formule globale $6T_2O_3.V_2O_5$ ("composés B"). (*ii*) les autres systèmes, à l'exception de celui du lanthane, présentent la formation de composés de formule globale $5T_2O_3.V_2O_5$ ("composés C"), sauf peut-être dans le cas du lutécium.

Dans aucun des systèmes étudiés nous n'avons observé la formation de solution solide.

a Composés formés

(1) Orthovanadates

Dans tous les cas, nous avons préparé l'orthovanadate TVO_4 par chauffage des mélanges équimoléculaires T_2O_3–V_2O_5 à 1500 °C pendant 24 h, mais la réaction est complète dès des températures inférieures à 800 °C. Une étude par analyse thermique différentielle des phénomènes observés lors du chauffage et du refroidissement du mélange équimoléculaire Gd_2O_3–V_2O_5 montre (Fig. 1), à l'échauffement, un pic exothermique vers 668 °C, et aucun phénomène au refroidissement. Le produit final est constitué uniquement par de l'orthovanadate $GdVO_4$. La netteté et la reproductibilité du phénomène observé, qui se produit à une température voisine de la température de fusion, déterminée dans les mêmes conditions, de l'oxyde V_2O_5 (673 ± 5 °C) laissent supposer que la réaction de formation de l'orthovanadate de gadolinium se fait, non pas entre deux solides, mais entre un solide (Gd_2O_3) et un liquide (V_2O_5). La réaction s'effectuerait brusquement dès homogénéïsation du mélange par la fusion de V_2O_5.

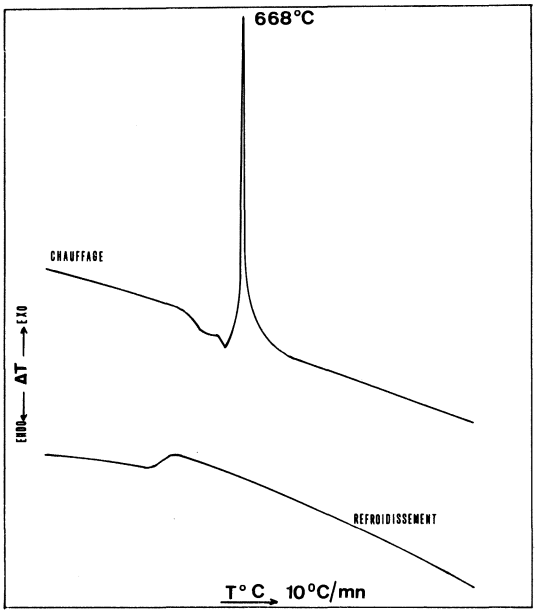

FIG. 1. Etude de la formation de l'orthovanadate de gadolinium par analyse thermique différentielle.

Or, comme nous le montrent les Figs. 4, 5 et 6, dans tous les systèmes étudiés, l'orthovanadate se forme d'abord lors des chauffages à basses températures, les composés définis nouveaux se formant ensuite (ou à température supérieure) par réaction entre l'orthovanadate et l'oxyde en excès. Le phénomène décrit ci-dessus permettrait d'expliquer cette formation privilégiée.

De même, alors que dans le cas du cérium nous n'avons pu mettre en évidence aucun composé nouveau à partir des mélanges CeO_2–V_2O_5, nous avons toujours observé la formation de $CeVO_4$. En particulier, le mélange $2CeO_2.V_2O_5$ mène à $CeVO_4$ pur pour un chauffage de 800 °C pendant 24 h.

Orthovanadates quadratiques

Les orthovanadates de terres rares, du cérium au lutécium, forment une série isomorphe, cristallisant avec la structure du zircon dans le système quadratique, groupe d'espace $I4_1/amd$ et ont été étudiés par Milligan et Vernon (8), et plus récemment par Schwarz (9) ou Aïa (10). Certains diagrammes (Nd, Ce, Eu, Dy, Ho) ont été publiés par le National Bureau of Standards (11).

Tous nos diagrammes sont en bon accord avec ceux mentionnés ci-dessus, sauf pour ceux de Milligan et Vernon (8) qui présentent un décalage angulaire systématique se traduisant par un écart sur les paramètres de maille. Le Tableau 1 donne, à titre d'exemple, le diffractogramme relatif à $SmVO_4$.

TABLEAU 1. Diffractogramme relatif à $SmVO_4$

hkl	*I**	*d* (Å)
101	m	4.802
200	Max	3.636
211	f	2.897
112	F	2.715
220	m	2.570
202	m	2.399
301	f	2.266
103	f	2.043
321	f	1.192
312	m	1.866
400	f	1.816
213	f	1.783
411	f	1.699
420	f	1.623
303	f	1.596
332	f	1.510
204	f	1.463
501	f	1.415
224	f	1.358
512	f	1.302

*F, raies de forte intensité; f, raies de faible intensité; m, raies d'intensité moyenne; Max, raie d'intensité maximale.

Nous avons procédé, dans tous les cas, à un affinement par moindres carrés des paramètres cristallins a et c à partir du diagramme indicé, chaque distance réticulaire d étant affectée d'un coefficient de pondération $w = 1/\tau^2$ où τ est l'écart type (12); nous avons choisi $\tau = \Delta d/0.798$, assimilant Δd (erreur expérimentale) à la déviation moyenne. Δd a été calculée à partir de l'évaluation de l'erreur expérimentale sur les angles 2θ; nous avons choisi $\Delta(2\theta) = 0.05°$ d'après la reproductibilité des mesures. Cet affinement a été fait au moyen d'un programme général d'affinement des paramètres de maille à partir des diagrammes de poudres écrit par l'un de nous (F.M.) pour ordinateur IBM 1130. La convergence était généralement réalisée après un ou deux cycles d'affinement.

Le Tableau 2 donne les résultats obtenus, ainsi que, pour chaque orthovanadate, les valeurs données par l'article le plus récent.

Les erreurs données sont calculées comme la déviation moyenne sur les paramètres, soit $0.798\,\tau$ si τ est l'écart-type, obtenu par la méthode des moindres carrés.

Can. J. Chem. Downloaded from www.nrcresearchpress.com by 210.87.254.105 on 09/05/12
For personal use only.

TABLEAU 2. Orthovanadates de terres rares

	Nos résultats		Résultats les plus récents de la littérature		
	a (Å)	*c* (Å)	*a* (Å)	*c* (Å)	Référence
$CeVO_4$	7.399±0.002	6.496±0.002	7.398±0.003	6.496±0.003	9
$PrVO_4$	7.364±0.002	6.465±0.003	7.367±0.003	6.468±0.003	9
$NdVO_4$	7.328±0.002	6.435±0.002	7.3290	6.4356	10
$SmVO_4$	7.264±0.002	6.388±0.002	7.266±0.003	6.394±0.003	9
$EuVO_4$	7.232±0.002	6.362±0.002	7.2365±0.0002	6.3675±0.0003	10
$GdVO_4$	7.216±0.002	6.351±0.003	7.218	6.353	11
$TbVO_4$	7.171±0.002	6.323±0.003	7.179±0.003	6.324±0.003	9
$DyVO_4$	7.147±0.002	6.305±0.003	7.1434	6.313	10
$HoVO_4$	7.117±0.002	6.284±0.003	7.2114±0.0002	6.2926±0.0005	10
$ErVO_4$	7.101±0.002	6.274±0.003	7.100	6.279	9
$TmVO_4$	7.062±0.002	6.252±0.003	7.071±0.003	6.263±0.003	9
$YbVO_4$	7.046±0.002	6.249±0.003	7.043±0.003	6.248±0.003	9
$LuVO_4$	7.025±0.002	6.233±0.002	7.01	6.23	8

Orthovanadate de lanthane

Il n'appartient pas à la série isomorphe quadratique, mais est voisin du phosphate de lanthane, qui, lui, cristallise dans le système monoclinique avec la structure de la monazite. Une étude structurale de ce composé est en cours au laboratoire (par Boursier). Des monocristaux de $LaVO_4$ ont été obtenus par le refroidissement du mélange $4V_2O_5.La_2O_3$, maintenu pendant 5 h à 1100 °C (13). Cette méthode est d'ailleurs tout à fait en accord avec les résultats que nous avons obtenus pour le système La_2O_3–V_2O_5 (*cf.* plus bas).

Des clichés de diffraction des rayons X par les méthodes de Weissenberg et de précession ont montré que le cristal appartient au groupe d'espace $P2_1/n$, avec des paramètres de maille tout à fait en accord avec les valeurs trouvées par Aïa (10). Si on fait un changement de coordonnées de façon à se trouver dans les conditions des tables internationales de cristallographie, on obtient le groupe d'espace $P2_1/c$.

Le diagramme de poudres du composé obtenu par chauffage du mélange équimoléculaire $La_2O_3.V_2O_5$, identique à celui obtenu après broyage des monocristaux préparés suivant la méthode ci-dessus, a alors été indicé au moyen d'un programme, écrit par l'un de nous (F.M.) pour IBM 1130, qui, à partir des paramètres de maille et des extinctions systématiques, génère tous les triplets d'indices possibles à l'intérieur des limites données et les attribue aux raies observées en tenant compte des incertitudes expérimentales.

Le Tableau 3 donne ce diffractogramme indicé; un affinement par moindres carrés mène ensuite aux valeurs des paramètres

	a (Å)	*b* (Å)	*c* (Å)	β (deg)
Groupe $P2_1/c$	6.716±0.003	7.267±0.005	8.388±0.004	125.83±0.03
Groupe $P2_1/n$	7.036±0.003	7.267±0.005	6.716±0.003	104.88±0.04
Données de Aïa	7.07	7.26	6.61	102.6

(2) Composés A: $4T_2O_3.V_2O_5$

On les observe pour tous les éléments.

Les diffractogrammes de ces composés sont voisins, sans que l'on puisse retrouver exactement le même nombre de raies, ce qui permettrait de conclure à une série isomorphe. Il semble que les structures de ces produits soient voisines mais le passage d'un élément au suivant s'accompagne de déformations modifiant les symétries cristallines. Cette symétrie est en tout cas basse, car des essais systématiques d'indiçage ont échoué pour les systèmes cubique, quadratique, hexagonal et orthorhombique, en utilisant entre autres les méthodes de Bjurström (15) et Ito (16), dans le cas du composé de l'erbium.

Toutefois, dans le cas du lutécium, un chauf-

Can. J. Chem. Downloaded from www.nrcresearchpress.com by 210.87.254.105 on 09/05/12
For personal use only.

Can. J. Chem. Downloaded from www.nrcresearchpress.com by 210.87.254.105 on 09/05/12
For personal use only.

TABLEAU 3. Diagramme indicé de $LaVO_4$

d_{obs} (Å)	I	$P2_1/C$
5.440	f	100
4.954	f	011
4.825	f	−111
4.354	f	110
4.177	f	−102
3.630	m	−112
3.398	F	002
3.203	Max	021
3.077	m	012
2.984	m	−211
2.962	F	−212
2.723	m	200
2.548	m	210
2.509	f	−213
2.482	f	022
2.268	m	−131
2.235	m	−302
2.225	m	112
2.185	f	−123
2.014	m	−214
1.972	f	032
1.949	m	−231
1.925	f	−304
1.860	f	−314
1.841	f	221
1.816	m	300
1.796	f	−233
1.757	f	041
1.697	f	202
1.656	f	014
1.623	f	−404
1.602	f	141
1.525	f	−423

fage à 1500 °C (température maximum que nous pourrons atteindre) pendant 96 h n'a pas permis d'obtenir le composé A pur. Le diffractogramme du produit obtenu montre les raies caractéristiques de $LuVO_4$, de Lu_2O_3 et des raies nouvelles qui ne peuvent être attribuées qu'au composé A; le diagramme correspondant est donc sans doute incomplet. L'ensemble des diagrammes de diffraction obtenus (ainsi que celui du composé analogue de l'yttrium que nous avons aussi préparé, le diagramme donné par Levin (14) n'étant pas suffisamment détaillé) figurent dans un tableau déposé en archives.[2]

La Fig. 2 présente un schéma récapitulatif des spectres de diffraction de tous les composés A étudiés, qui met en évidence les ressemblances et les différences de ces spectres. On constate que ces composés peuvent se classer par groupes de

[2]Les photocopies des documents archivés peuvent être obtenues, sur demande adressée aux archives des documents non publiés, à la Bibliothèque scientifique nationale, au Conseil national de recherches du Canada à Ottawa.

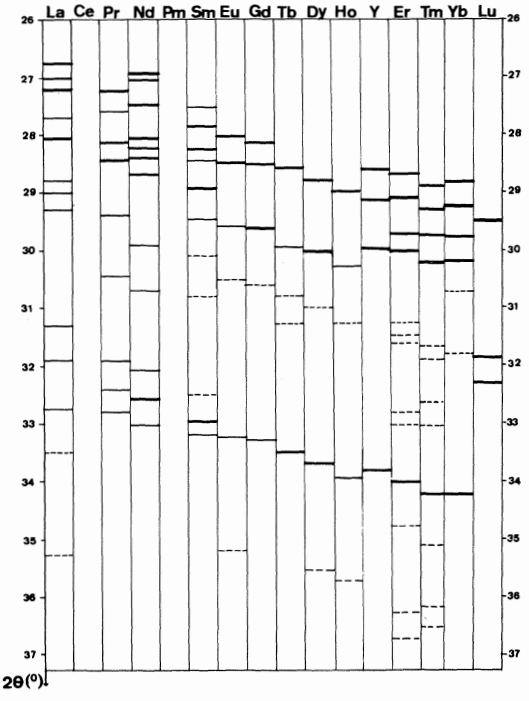

FIG. 2. Caractéristiques générales des spectres de diffraction des composés A: ▬ raies intenses; — raies moyennes; --- raies faibles.

deux ou trois fort voisins: (*i*) composés de l'europium et du gadolinium; (*ii*) composés du terbium, du dysprosium et de l'holmium; (*iii*) composés de l'erbium, du thulium et de l'ytterbium.

Les autres éléments étudiés conduisent à des composés riches en raies, difficiles à classer.

Le rapport atomique $T/V = 4$ a été vérifié par fluorescence X.

(3) Composés B: $6T_2O_3.V_2O_5$

Ces composés n'ont pu être préparés que pour le praséodyme et le néodyme. Les deux diagrammes de diffraction obtenus sont présentés Fig. 3 et peuvent être obtenus au dépôt des données non publiées.[2]

Bien qu'ils présentent certaines analogies en ce qui concerne les positions angulaires des raies intenses, le diagramme relatif au néodyme est beaucoup plus riche en raies moyennes et faibles que celui qui concerne le praséodyme et on ne peut conclure à l'isomorphisme.

(4) Composés C: $5T_2O_3.V_2O_5$

On les observe pour tous les éléments, du samarium à l'ytterbium. Leurs diffractogrammes

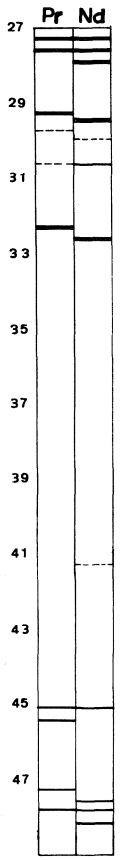

FIG. 3. Caractéristiques générales des spectres de diffraction des composés B: ▬ raies intenses; — raies moyennes; --- raies faibles.

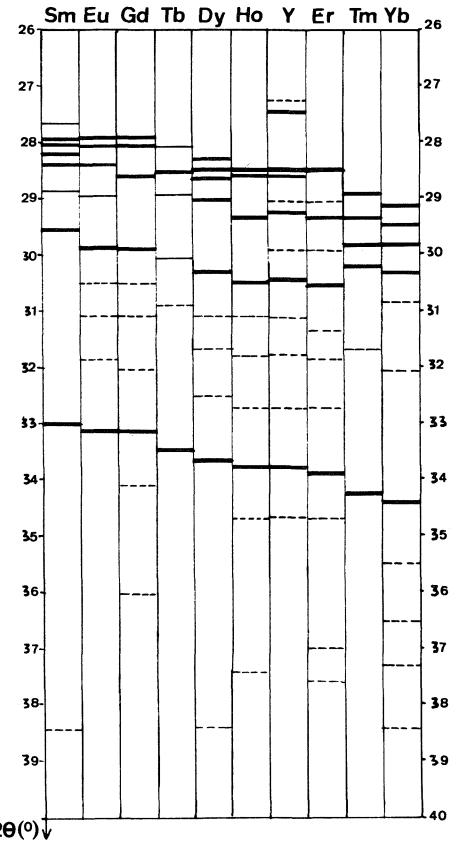

FIG. 4. Caractéristiques générales des spectres de diffraction des composés C: ▬ raies intenses; — raies moyennes; --- raies faibles.

ainsi que celui concernant l'yttrium (14) sont récapitulés par la Fig. 4, ils peuvent être obtenus au dépôt des données non publiées.[2] Il n'apparait pas plus de similitudes entre ces diagrammes qu'entre ceux qui concernent les composés A, en particulier en ce qui concerne le nombre de raies intenses.

La symétrie cristalline ici aussi est probablement basse: les raies sont nombreuses et des essais d'indiçage n'ont pas abouti. Dans le cas du lutécium, il est probable qu'il se forme complètement à une température supérieure à 1500 °C. Quelques raies nouvelles (outre les raies de $LuVO_4$ et de Lu_2O_3) apparaissent dans le diffractogramme du mélange $5Lu_2O_3.V_2O_5$ chauffé à 1500 °C pendant 96 h.

Dans le cas des trois types de composés A, B, C, seule la préparation de monocristaux permettrait de résoudre le problème posé par leur structure, puisqu'ils ne sont analogues à aucun des types classiques d'oxydes mixtes.

La teneur en vanadium est faible, et ces oxydes qui se présentent sous forme de céramiques sont réfractaires et difficilement attaquables. D'autre part, il n'est pas certain que le nombre d'atomes d'oxygène soit exactement celui qui correspond à la stoechiométrie. En effet, des études à partir de l'oxyde Pr_6O_{11} ont mené à des composés A′ et B′ correspondant à des rapports Pr/V respectivement de 4 et 6, mais dont les diagrammes de diffraction, quoique très voisins de ceux des composés A et B obtenus à partir de Pr_2O_3, ne leur sont pas tout à fait identiques, en ce qui concerne le nombre et l'intensité relative des raies. Ceci laisse prévoir la possibilité de teneurs en oxygène variables pour un même nombre T/V.

b Description des systèmes binaires

Les Figs. 5, 6, et 7 résument les résultats

Can. J. Chem. Downloaded from www.nrcresearchpress.com by 210.87.254.105 on 09/05/12
For personal use only.

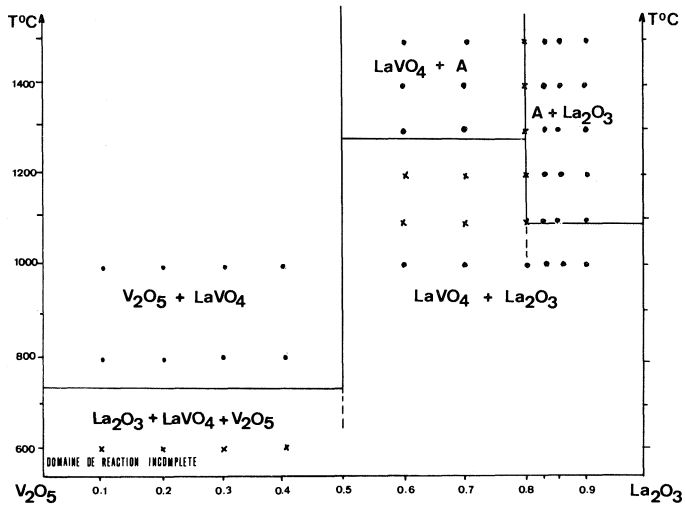

FIG. 5. Phases observées dans le système La_2O_3–V_2O_5; ● représente une expérience; × indique un produit qui contient 3 phases (réaction incomplète).

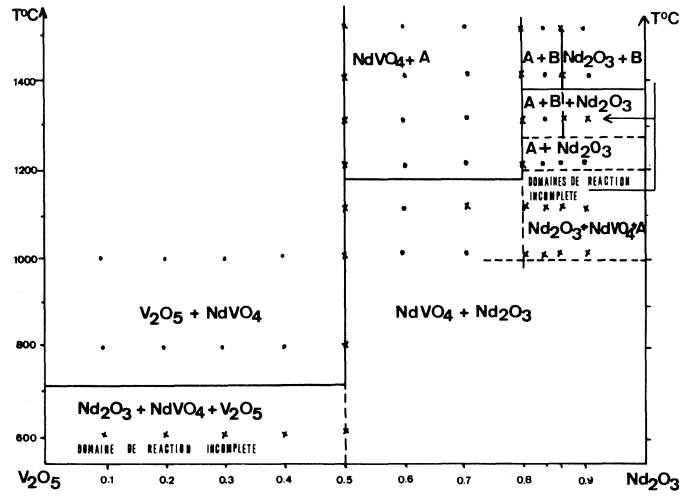

FIG. 6. Phases observées dans le système ND_2O_3–V_2O_5; ● représente une expérience; × indique un produit qui contient 3 phases (réaction incomplète).

obtenus. On observe trois types de systèmes: Fig. 5, La_2O_3–V_2O_5; Fig. 6, Nd_2O_3–V_2O_5 analogue à Pr_2O_3–V_2O_5; Fig. 7, Yb_2O_3–V_2O_5 typique des systèmes des éléments au-delà du samarium (et semblable à celui de Levin (14) pour l'yttrium).

Dans tous les cas on observe: (*i*) la facile formation de l'orthovanadate TVO_4, généralement dès les premières températures étudiées (600 °C); (*ii*) l'absence de toute solution solide; (*iii*) l'absence de tout composé défini dans le sous-sytème TVO_4–V_2O_5. Le bas point de fusion de V_2O_5 justifie alors son emploi comme fondant pour la préparation de monocristaux d'orthovanadates (13); (*iv*) la présence, dans les domaines riches en oxydes de terres rares, d'échantillons présentant trois phases cristallines, ce qui montre une réaction incomplète.

La température pour laquelle la formation des composés A est totale varie entre 1100 et 1400 °C sans que l'on puisse mettre en évidence une variation de cette température avec le numéro atomique. Dans le cas du lutécium cette température est supérieure à 1500 °C.

Can. J. Chem. Downloaded from www.nrcresearchpress.com by 210.87.254.105 on 09/05/12
For personal use only.

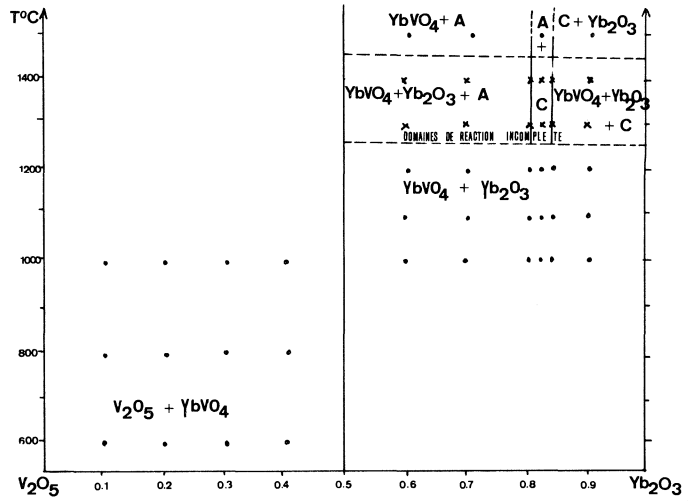

FIG. 7. Phases observées dans le système Yb_2O_3–V_2O_5; ● représente une expérience; × indique un produit qui contient 3 phases (réaction incomplète).

Les composés B se forment à une température supérieure à celle des composés A, tandis que les composés C se forment à une température voisine de celle des composés A, ou plus basse (cas du samarium, du dysprosium, de l'erbium).

Enfin le système relatif au gadolinium (1) présente un domaine de plus à cause de l'existence des deux variétés allotropiques, cubique et monoclinique de Gd_2O_3. Il en est de même du samarium, mais l'oxyde utilisé pour préparer les échantillons de départ étant un mélange des deux formes, nous avons observé la présence de ces deux formes après les traitements à basse température.

Conclusion

En conclusion, nous avons réalisé l'étude dans tout le domaine de composition des huit systèmes binaires: La_2O_3–V_2O_5, Pr_2O_3–V_2O_5, Nd_2O_3–V_2O_5, Sm_2O_3–V_2O_5, Gd_2O_3–V_2O_5, Dy_2O_3–V_2O_5, Er_2O_3–V_2O_5, Yb_2O_3–V_2O_5 et montré l'existence de composés définis nouveaux de formule globale $4T_2O_3.V_2O_5$ dans le cas de tous les éléments de terres rares sauf le cérium et le prométhium, de formule $6T_2O_3.V_2O_5$ pour le praséodyme et le néodyme, de formule $5T_2O_3.V_2O_5$ pour tous les éléments allant du samarium à l'ytterbium (groupe yttrique). Cette formation est probable, au-dessus de 1500 °C, dans le cas du lutécium.

Ces composés, de basse symétrie cristalline, ont été identifiés par leur diffractogramme de poudre, et l'étude s'en poursuit actuellement au laboratoire. Nous nous attachons, en particulier, à déterminer la symétrie cristalline des composés du type A, qui sont représentés pour l'ensemble des lanthanides, par essais d'indiçage dans le système monoclinique et par formation de solutions solides entre deux tels composés, ce qui perme tra de déterminer combien de séries isomorphes ils constituent.

1. H. BRUSSET, F. MADAULE-AUBRY, B. BLANCK et A. DEBOICHET. Bull. Soc. Chim. 15 (1969).
2. H. BRUSSET, H. GILLIER-PANDRAUD et J. L BERDOT. Bull. Soc. Chim. 2886 (1967).
3. H. BRUSSET, H. GILLIER-PANDRAUD et J. L. BERDOT. Bull. Soc. Chim. 1206 (1967).
4. H. BRUSSET, H. GILLIER-PANDRAUD et M. C. SAINE. Bull. Soc. Chim. 2244 (1969).
5. E. A. ARBIT et V. V. SEREBRENNIKOV. Zh. Néorgan. Khim. **10**, 410 (1965).
6. P. GLAZYRIN et A. IVAKIN. Kristallografiya, **9(6)**, 927 (1964).
7. A.S.T.M. Index to the powder diffraction file. Philadelphia, 1965.
8. W. D. MILLIGAN et L. W. VERNON. J. Phys. Chem. **56**, 145 (1952).
9. H. SCHWARZ. Z. Anorg. Allg. Chem. **323**, 44 (1963).
10. M. A. AÏA. J. Electrochem. Soc. **114**, 367 (1967).
11. U.S. National Bureau of Standards, Monograph 25, Sec. 4, 1965.
12. J. S. ROLLETT. Computing methods in crystallography. Pergamon Press, 1965.
13. L. H. BRIXNER et E. ABRAMSON. J. Electrochem. Soc. **112**, 70 (1965).
14. E. M. LEVIN. J. Amer. Ceram. Soc. **50**, 318 (1967).
15. T. BJURSTRÖM. Z. Phys. **69**, 346 (1931).
16. T. ITO. X-Ray studies on polymorphism. Mazuren G. Ltd, Tokyo, 1950.

Can. J. Chem. Downloaded from www.nrcresearchpress.com by 210.87.254.105 on 09/05/12
For personal use only.

Can. J. Chem. Downloaded from www.nrcresearchpress.com by 210.87.254.105 on 09/05/12
For personal use only.

An *ab initio* Molecular Orbital Study of Bonding in Fluorocarbonium Ions[1]

N. C. Baird and R. K. Datta
Department of Chemistry, University of Western Ontario, London, Ontario

Received June 7, 1971

Ab initio molecular orbital calculations are reported for the series of carbonium ions $(CH_3)^+$, $(FCH_2)^+$, and $(F_2CH)^+$ and for their neutral molecule counterparts CH_4, CH_3F, and CH_2F_2. The energies and wavefunctions for the carbonium ions have been calculated both with and without including the carbon $2p_\pi$ orbital in the minimal basis set in order to unravel the inductive destabilization and resonance stabilization due to fluorine substitution. The increase in bonding energy with multiple fluorine substitution is less than linear, due primarily to nonadditivity in the dative carbon–fluorine π bonding. The "saturation" effect noted previously for the hydride abstraction reaction enthalpies is shown to be due primarily to stability effects in the neutral molecules themselves rather than to energetic effects of the carbonium ions.

Des calculs d'orbitale moléculaire *ab initio* sont rapportés pour une série d'ions carboniums $(CH_3)^+$, $(FCH_2)^+$ et $(F_2CH)^+$ ainsi que pour leurs molécules neutres correspondantes CH_4, CH_3F et CH_2F_2. Les énergies et les fonctions d'onde pour les ions carboniums ont été calculées à la fois en incluant ou non l'orbitale du carbone $2p_\pi$ dans l'ensemble de base minimum afin de démêler la déstabilisation inductive et la stabilisation de résonance dues à la substitution du fluor. L'accroissement de l'énergie de liaison avec la substitution multiple du fluor est moins que linéaire; ceci est dû en premier à la non-additivité dans la liaison π dative carbone–fluor. Il est montré que l'effet de "saturation" noté auparavant pour les enthalpies de réaction d'abstraction de l'hydrure est dû en premier à des effets de stabilité dans les molécules neutres en soi plutôt que des effets énergétiques des ions carboniums.

Canadian Journal of Chemistry, 49, 3708 (1971)

Introduction

The thermochemical stabilities of organofluorine molecules and ions is of both theoretical curiosity and of experimental importance, since the bonding energies in such systems are distinctly nonadditive with respect to multiple fluorine substitution. For example, perfluorobenzene is some 37 kcal/mol *less* stable than that extrapolated from the change in the heat of formation (ΔH_f) in benzene compared to fluorobenzene, whereas the stabilities of the fluoromethanes *increase* upon multiple fluorine substitution (1). In addition to these nonadditivity effects in neutral molecules, some unusual trends are encountered in the closed-shell positive and negative hydrocarbon ions which contain fluorine. Given that the electronegativity of fluorine is much greater than that of carbon, one would expect fluorine substitution to destabilize carbonium ions and to stabilize carbanions. In actual fact, the opposite effects are often encountered, presumably because the p_π lone pair electrons of fluorine can stabilize the π bonding in carbonium ions, whereas the same electrons destabilize the π bonding in carbanions (2, 3).

In this paper, the electronic and geometrical structure of the fluoromethyl carbonium ion $(FCH_2)^+$ and the difluoromethyl carbonium ion $(F_2CH)^+$ are investigated by *ab initio* molecular orbital calculations in an attempt to unravel the stabilizing and destabilizing effects. These ions have been studied in some detail experimentally, since, together with $(F_3C)^+$, they appear predominant in the mass spectrum of many fluorocarbons (4).

Method of Calculation

All calculations reported herein have been obtained using the nonempirical ("*ab initio*") s.c.f.-l.c.a.o.-m.o. theory of Roothaan (5). Each molecular orbital is expanded as a linear combination of a minimal basis set (1s orbitals centered on hydrogen; 1s, 2s, and 2p orbitals centered on carbon and fluorine) of Slater-type orbitals (STOs). All integrals over the STOs are computed using the STO-3G expansions of Pople and co-workers (6), in which each STO is expanded as a linear combination of 1s or 2p Gaussian-type orbitals (GTOs). The computer

[1]Research supported by the National Research Council of Canada.

Can. J. Chem. Downloaded from www.nrcresearchpress.com by 210.87.254.105 on 09/05/12
For personal use only.

program used on a CDC-6600 computer to execute the calculations employs subroutines from the POLYATOM system[2] to compute integrals over the GTOs.

The following "standard" geometry information is used except where indicated otherwise: angles about tetravalent carbon (neutral molecules), tetrahedral; angles about trivalent carbon (carbonium ions), 120°; C—H bond distance, 1.083 Å; C—F bond distance, 1.360 Å. For the neutral molecules considered, the s.t.o. exponents used for the orbitals of C and H are those deduced as optimum for CH_4 by Pople and co-workers (7), whereas in all positive ions, the exponents for the σ orbitals of C and H are those optimum for $(CH_3)^+$ (see Table 1) (7). The values recommended by Pople and co-workers (7) for the $n = 1$ and $n = 2$ orbitals are used for all F atom orbitals in neutral compounds, and for the σ orbitals in the positive ions (Table 1). The exponents for the p_π orbitals of C and of F in the fluorocarbonium ions (Table 1) are partially optimized by calculations for $(FCH_2)^+$ using an assumed C—F distance of 1.25 Å. Simple energy minimization of the F $2p_\pi$ exponent (with no π orbital on C) leads to the value 2.53 (Table 1). Using the latter as a starting value, two sets of successive reoptimizations of first the C $2p_\pi$ exponent followed by the F $2p_\pi$ leads to the values reported in Table 1 which are probably accurate to ±0.02.

TABLE 1. Slater-type orbital exponents used in calculations

Atom	Orbital	Exponent value: Carbonium ions	Exponent value: Neutral molecules
C	1s	5.67	5.67
	2s, $2p_\sigma$	1.77	1.75
	$2p_\pi$	1.44	1.75
H	1s	1.33	1.18
F	1s	8.65	8.65
	2s, $2p_\sigma$	2.56	2.56
	$2p_\pi$	2.63	2.56
		2.53*	

*Used only for $(FCH_2)^+$ at 1.38 Å in the calculation with no C $2p_\pi$ orbital (see text).

Results and Discussion

Given the unusual geometry effects encountered in neutral fluorocarbons (8) (small FCX bond angles and short C—F bond distances), a geometry search was first executed for $(FCH_2)^+$ using the energy minimization criterion. Since variation of the FCH bond angles led to an optimum value within 2° of the "expected" 120° value, the latter value was employed in all subsequent calculations. Next the C—F bond distance and $2p_\pi$ orbital exponents of both C and F were simultaneously varied in a "brute force" minimization procedure, yielding the optimum values of 1.44, 2.63, and 1.26 Å, respectively.

The calculated carbon–fluorine bond length of 1.26 Å is very short for a linkage of this type (the average value in neutral fluoroethylenes and in fluorobenzenes being 1.33 Å (8)) and is indicative of relatively strong dative π bonding from F to C in the positive ion, as represented symbolically by the resonance structures

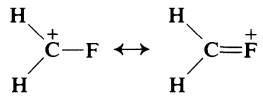

A measure of the strength of this π bonding was obtained by recalculating the wavefunction and energy for $(FCH_2)^+$ using the same molecular geometry and orbital exponents but eliminating the carbon atom $2p_\pi$ orbital from the basis set. The optimum energy calculated for this species, in which the fluorine $2p_\pi$ lone-pair of electrons is forced to remain localized on fluorine and the π bonding artificially "destroyed", is −136.1837 a.u., or some 75.1 kcal/mol less stable than the structure in which π bonding is active. A similar calculation for the difluoromethyl carbonium ion $(F_2CH)^+$, with the same bond angles, bond lengths, and orbital exponents as that for $(FCH_2)^+$ yields energies of −233.7933 and −233.5845 a.u. with and without the carbon $2p_\pi$ orbital included; thus the π bonding energy in (F_2CH^+) of 131.0 kcal/mol is less than double that in the monofluoro ion by some 19 kcal/mol. Note that these π energies are much larger than those found in the isoelectronic boron fluorides (9).

A somewhat more realistic evaluation of the π bond strength in $(FCH_2)^+$ is obtained by

[2]Available as program 47A from the Quantum Chemistry Program Exchange, Indiana University, Bloomington, Indiana, U.S.A.

TABLE 2. Mulliken population analyses for $(FCH_2)^+$ wavefunctions

Atom	Orbital*	Population† (electrons) Calculation *A*	Calculation *B*	Calculation *C*
C	1s	1.994	1.994	1.994
	2s	1.259	1.299	1.340
	$2p_\sigma$	1.213	1.216	1.207
	$2p_{\sigma'}$	0.795	0.947	0.964
	$2p_\pi$	0.394	0	0
	Total	5.654	5.456	5.505
H	1s	0.746	0.747	0.743
F	1s	1.999	1.999	1.999
	2s	1.938	1.944	1.962
	$2p_\sigma$	1.965	1.950	1.974
	$2p_{\sigma'}$	1.346	1.155	1.075
	$2p_\pi$	1.606	2.000	2.000
	Total	8.854	9.048	9.010

*The coordinate axis is such that the $2p_{\sigma'}$ orbitals on C and F lie along the C—F bond axis.
†Calculation *A* refers to the ion with C $2p_\pi$ included at $R_{CF} = 1.26$ Å; calculations *B* and *C* are for the ion without the C $2p_\pi$ orbital at $R_{CF} = 1.26$ Å and $R_{CF} = 1.38$ Å, respectively.

TABLE 3. Total energies and excess atomic charges for molecules and ions

Species	Calculation type*	Total energy (a.u.)	Excess charges (*e*) C	H	F
CH_4	—	−39.73139	−0.114	+0.028	—
CH_3F	—	−137.14671	+0.054	+0.029	−0.138
CH_2F_2	—	−234.63097	+0.242	+0.022	−0.142
$(CH_3)^+$	—	−38.79167	+0.265	+0.245	—
$(FCH_2)^+$	*A*	−136.30343	+0.346	+0.254	+0.146
	B	−136.18373	+0.544	+0.253	−0.048
	C	−136.20798	+0.495	+0.258	−0.010
$(F_2CH)^+$	*A*	−233.79331	+0.516	+0.272	+0.106
	B	−233.58453	+0.820	+0.266	−0.043

*See notes to Table 2 for details.

comparing the ion energy obtained with C $2p_\pi$ included at its optimum geometry ($R_{CF} = 1.26$ Å) and π exponents (Table 1) with the ion energy calculated without the C $2p_\pi$ orbital and using the optimum C—F distance and F $2p_\pi$ exponent. Energy minimization for this species yields an optimum energy of —136.2080 a.u. at $R_{CF} = 1.38$ Å and a F $2p_\pi$ exponent of 2.53; thus the ability of the $2p_\pi$ orbital on carbon to conjugate with the fluorine $2p_\pi$ lone pair yields an ion which is 60 kcal/mol more stable and has a bond length which is 0.12 Å shorter than the "imaginary" species in which the π electrons are localized on fluorine.

Further insight into the nature of the bonding in such carbonium ions is provided by the Mulliken population analysis (10) of the *ab initio* wavefunctions (Tables 2 and 3). Note first that the C—H bonds in the set of carbonium ions $(CH_3)^+$, $(FCH_2)^+$, and $(F_2CH)^+$ are all polar in the sense $C^{\delta-}H^{\delta+}$ to almost the same degree, since the hydrogen atom net charges all lie in the range $+0.27 \pm 0.02\,e$ (+0.25, +0.25, and +0.29 *e*, respectively).

Although each hydrogen atom bound to carbon carries about $\frac{1}{4}$ of the positive charge regardless of environment, the net charges and individual orbital populations associated with carbon and with fluorine are influenced substantially by the number of fluorine substituents and by the extent of π bonding permitted. When no $2p_\pi$ orbital is available on carbon in $(FCH_2)^+$, the population of each fluorine orbital except $2p_{\sigma'}$ is essentially equal to two (2.00, 1.96, 1.97, and 2.00 for the 1s, 2s, $2p_\sigma$, and $2p_\pi$ orbitals, respectively). The electrons in the C—F σ bond in this case are almost equally shared, since the $2p_{\sigma'}$ population on F is 1.08 *e* and the fluorine

Can. J. Chem. Downloaded from www.nrcresearchpress.com by 210.87.254.105 on 09/05/12
For personal use only.

Can. J. Chem. Downloaded from www.nrcresearchpress.com by 210.87.254.105 on 09/05/12
For personal use only.

net charge $-0.01\ e$. The σ bond reorganizes to become quite polar in the sense $C^{\delta+}F^{\delta-}$ when the C $2p_\pi$ orbital is available, although the net increase in electron density of all the σ orbitals of fluorine of $0.24\ e$ only partially compensates for the flow of 0.39 π electrons from F to C, yielding a net *positive* charge on fluorine of $+0.15\ e$. A similar phenomenon occurs in the difluoromethyl ion, in which the net charge of $-0.04\ e$ for each F drops to $+0.11\ e$ when π bonding occurs. Thus the polarization of the C—H σ electrons and the C—F π electrons toward carbon ensures a "delocalization" of the positive charge, and the net charges on carbon in the series $(CH_3)^+$, $(FCH_2)^+$, and $(F_2CH)^+$ are +0.26, +0.35, and $+0.52\ e$, all well below the "classical" +1 electron description.

At first glance, the net transfer of only $0.39\ e$ from F to C in the $(FCH_2)^+\pi$ network seems incompatible with the high energy calculated for this π bond. In fact, the following argument shows that *substantial polarization of an electron pair does not lead to a correspondingly low covalent bond strength.* If the polarization or ionicity i of a two-electron two-center bond is defined as the difference between the population q_u of an orbital ϕ_u, and the value 1.0, then

$$i = |q_u - 1|$$

$$q_u = 2(C_u^2 + C_uC_vS_{uv})$$

where S_{uv} is the overlap integral between the orbitals, and the values of C_u and C_v are interconnected by the normalization condition

$$C_u^2 + C_v^2 + 2C_uC_vS_{uv} = 1$$

In contrast, the covalent bond strength is the bond order $2C_uC_v$ relative to the completely covalent value of $1/(1 + S_{uv})$; *i.e.*

$$B = 2C_uC_v/(1 + S_{uv})$$

The essential point is that B is not linearly related to i; for small S values,[3]

$$B \sim \sqrt{1 - i^2}$$

which illustrates that even when the ionic character is large, the covalent bond strength remains quite high. In the case of $(FCH_2)^+$, for which i is 61%, the covalent bond strength B is a little over 70%. It is interesting that this B value is in good agreement with the bond shortening of 0.12 Å calculated above, since the latter corresponds to a π bond character of ~67% if one assumes that the bond order – bond length derivative established for carbon–carbon bonds applies also to carbon–fluorine linkages.[4] The analogy between carbon–carbon and carbon–fluorine π bonding also extends to the effects of multiple substitution, *i.e.* the total π energy in $(F_2CH)^+$ is significantly less than twice that in $(FCH_2)^+$, in the same way that the π energy in the allylic anion is much less than twice that in ethylene.

Although the discussion above has centered upon the ability of fluorine atoms to stabilize a carbonium ion by dative π bonding, the energetic destabilization due to the inductive effect is also of great importance in determining the overall behavior of the substituent. Unfortunately it is not possible to "turn off" the inductive effect in m.o. calculations to determine its energetic effect, so that the energetic consequences of the inductive effect can be deduced only on a relative basis. To this end, the total molecular energies (in atomic units) of $(CH_3)^+$, $(FCH_2)^+$, and $(F_2CH)^+$, all calculated using the same geometries and exponents and *without* the presence of the carbon $2p_\pi$ orbital are compared below:

$(CH_3)^+$	$E = -38.7917$	$\Delta E = -97.3920$
$(FCH_2)^+$	$E = -136.1837$	$\Delta E = -97.4008$
$(F_2CH)^+$	$E = -233.5845$	

Note in particular that the energy increase in going from $(FCH_2)^+$ to $(F_2CH)^+$ is almost identical to the difference between $(CH_3)^+$ and $(FCH_2)^+$; the small difference of 0.0088 a.u. (~5.5 kcal/mol) indicates that, whatever the magnitude of the inductive destabilization of

[3]See ref. 11 for the plot of B *vs.* i when S is included; the value of ~70% for B when $i \sim 61\%$ is taken from this plot.

[4]The rate of change of bond length with bond order is about 0.18 for $C(sp^2)$–$C(sp^2)$ linkages; see ref. 12. As a referee has pointed out, the fact that the transferability of the bond order – bond length derivative works here does not imply that this will be true for all fluorocarbon systems.

Can. J. Chem. Downloaded from www.nrcresearchpress.com by 210.87.254.105 on 09/05/12
For personal use only.

one fluorine atom, the net effect for two such units is only slightly *less* than double that for one.

In contrast, the increase in π bond energy in the transition $(FCH_2)^+$ to $(F_2CH)^+$ is 19.2 kcal/mol less[5] than for the pair $(CH_3)^+$ to $(FCH_2)^+$, and this larger change in the resonance effect dominates the variations in the overall energy changes. In terms of the total energies (with the C $2p_\pi$ orbital "active"),

$$\left.\begin{array}{ll}(CH_3)^+ & E = -38.7917\\ (FCH_2)^+ & E = -136.3034\end{array}\right\} \Delta E = -97.5117$$

$$\left.\begin{array}{ll}(FCH_2)^+ & E = -136.3034\\ (F_2CH)^+ & E = -233.7933\end{array}\right\} \Delta E = -97.4899$$

The decrease in the overall ΔE by difluoro substitution compared to monofluoro substitution of 0.0218 a.u. or 13.7 kcal/mol is in excellent agreement with the corresponding decrease in the experimental heat of formation change of 11 kcal/mol for this series:

$$\left.\begin{array}{ll}(CH_3)^+ & \Delta H_f = +261^6\\ (FCH_2)^+ & \Delta H_f = +197^3\end{array}\right\} \Delta\Delta H_f = 64 \text{ kcal/mol}$$

$$\left.\begin{array}{ll}(FCH_2)^+ & \Delta H_f = +197^3\\ (F_2CH)^+ & \Delta H_f = +144^3\end{array}\right\} \Delta\Delta H_f = 53 \text{ kcal/mol}$$

Both the calculated and the experimental results predict that the inherent stability of the methyl carbonium ion itself is increased by substitution of a second fluorine atom, although the energy gain is not quite as large as that obtained upon introduction of the first fluorine. This interpretation is in marked contrast to that given by Martin, Lampe, and Taft (2) who concluded that a "saturation effect" occurs, with the result that the total stabilization for $(F_2CH)^+$ is slightly *less* than that for $(FCH_2)^+$, and that for $(F_3C)^+$ is much less than for either the monofluoro or difluoro ions. This discrepancy occurs because Martin *et al.* did not really compare the energies of the ions themselves to each other, but rather compared the energy changes in the hydride abstraction reactions

$$CH_{4-n}F_n \rightarrow (CH_{3-n}F_n)^+ + H^-$$

In fact, their conclusion that the stabilization energy of the ion decreases with multiple fluorine substitution does not reflect any energetic property of the ions themselves, but rather is due to the *increasing stability of the neutral molecules* $CH_{4-n}F_n$ as n increases. In summary, the failure of the enthalpy change for the hydride abstraction reaction to increase continuously with n is due mainly to the greater than additive increase with n of the bonding energy of the neutral molecules $CH_{4-n}F_n$ with only a minor contribution due to the less than additive increase in bonding energy of the $(CH_{3-n}F_n)^+$ carbonium ions. It is interesting to note that both trends are reproduced by the *ab initio* energies (Table 3).

Since no correlation energy effects are included and only a minimal basis set of orbitals is employed in the present calculations, it would not be surprising if the absolute energies calculated for each of the hydride abstraction reactions above were greatly in error. In actual fact, the values obtained for ΔH (259, 198, and 195 kcal/mol for $n = 0$, 1, 2, respectively) are in fair agreement with the experimental results (262, 236, and 234 kcal/mol, respectively) if the experimental energy for the hydride ion[7] is used rather than the theoretical value; the latter is well-known to be quite inaccurate when a minimal basis set is used.

In conclusion, it appears that minimal basis set *ab initio* calculations are well-suited to the analysis of substituent effects in carbonium ions, both in terms of predicting overall trends in stability and in terms of decomposing the energy into contributions from inductive and resonance effects. Similar calculations on substituent effects in carbanions are currently in progress.

1. J. D. Cox and G. Pilcher. Thermochemistry of organic and organometallic compounds. Academic Press, New York. 1970.
2. R. H. Martin, F. W. Lampe, and R. W. Taft. J. Am. Chem. Soc. **88**, 1353 (1966).
3. A. Streitwieser, Jr. and F. Mares. J. Am. Chem. Soc. **90**, 2444 (1968).
4. J. R. Majer. Adv. Fluorine Chem. **2**, 55 (1961).

[5]Previous calculations indicate that energy differences of this order are meaningful in s.t.o. calculations when a similar series of molecules is considered. See ref. 6 and subsequent parts of the same series.

[6]Calculated using the spectroscopic ionization potential of 9.84 eV (see ref. 13) and the ΔH_f of +34 kcal/mol (see ref. 14) for the methyl radical.

[7]The experimental electron affinity of a hydrogen atom was taken as 0.75 eV (15).

5. C. C. J. ROOTHAAN. Rev. Mod. Phys. **23**, 69 (1951).
6. W. J. HEHRE, R. F. STEWART, and J. A. POPLE. J. Chem. Phys. **51**, 2657 (1969).
7. W. J. HEHRE, R. F. STEWART, and J. A. POPLE. Symp. Faraday Soc. **2**, 15 (1968).
8. L. E. SUTTON. (*Editor*) Tables of interatomic distances and configurations in molecules and ions. Special Publications 11 and 18, The Chemical Society, London, 1959 and 1965.
9. M. E. SCHWARTZ and L. C. ALLEN. J. Am. Chem. Soc. **92**, 1466 (1970).
10. R. S. MULLIKEN. J. Chem. Phys. **23**, 1833 (1953).
11. N. C. BAIRD and R. K. DATTA. Inorg. Chem. In press.
12. N. C. BAIRD. Mol. Phys. **18**, 39 (1970).
13. G. HERZBERG. Molecular spectra and molecular structure. Vol. III. D. Van Nostrand Co. Inc., Princeton, N.J. 1967. p. 609.
14. D. M. GOLDEN and S. W. BENSON. Chem. Rev. **69**, 125 (1969).
15. G. KLOPMAN. J. Am. Chem. Soc. **86**, 4550 (1964).

Can. J. Chem. Downloaded from www.nrcresearchpress.com by 210.87.254.105 on 09/05/12
For personal use only.

Can. J. Chem. Downloaded from www.nrcresearchpress.com by 210.87.254.105 on 09/05/12
For personal use only.

Axial:Equatorial Rate Ratios. 1. Eliminations Leading to the Exocyclic Methylene Group

J. F. KING AND M. J. COPPEN
Department of Chemistry, University of Western Ontario, London, Ontario

Received June 18, 1971

Phenyl *cis*-4-*t*-butylcyclohexanemethyl sulfoxide (**4**) thermolyzes to 1-*t*-butyl-4-methylenecyclohexane (**5**) at 116 and 130° about five to six times faster than its *trans* (equatorial) epimer **6**. *cis*-4-*t*-Butylcyclohexanemethyl bromide (**7**) undergoes elimination with potassium *t*-butoxide in *t*-butyl alcohol at 100° about nine times faster than its *trans* (equatorial) epimer **8**. The rate difference found for the sulfoxides **4** and **6** is the first clear demonstration of steric acceleration (without any contribution from any reagent repulsion effect) in the formation of an exocyclic carbon–carbon double bond in a simple anchored cyclohexane system. The faster elimination from **7** (*vs.* **8**) is ascribed primarily to steric acceleration; the experiment neither requires nor excludes the influence of non-bonding repulsions between the substrate and the attacking base.

Le phényl *t*-butyl-4 *cis* cyclohexaneméthyl sulfoxyde (**4**) se transforme par thermolyse à 116 et 130° en *t*-butyl-1 méthylène-4 cyclohexane (**5**); la vitesse est de cinq à six fois plus grande que pour l'épimère (équatorial) *trans* **6**. Le *t*-butyl-4 bromométhyl-1 cyclohexane (**7**) subit une réaction d'élimination sous l'action du *t*-butoxyde de potassium dans l'alcool *t*-butylique à 100° et la vitesse est de neuf fois plus grande que pour l'épimère (équatorial) *trans* **8**. La différence de vitesse trouvée pour les sulfoxydes **4** et **6** constitue la première preuve d'une accélération stérique (sans aucune contribution d'effets de répulsion du réactif) dans la formation d'une double liaison carbone–carbone exocyclique appartenant à un système cyclohexanique rigide. L'élimination plus rapide dans **7** (*vs.* 8) est due principalement à une accélération stérique; les résultats obtenus n'impliquent et n'excluent pas l'influence des répulsions de non-liaison entre le substrat et la base qui vient d'attaquer.

Canadian Journal of Chemistry, 49, 3714 (1971)

Introduction

Since the appearance of Barton's pioneering paper two decades ago (1), conformational analysis has become part of the very fabric of organic chemistry, being used routinely to explain or predict both the products and relative rates of reactions. Rationalization of relative rates in conformational terms requires some kind of description of the geometry of transition states, and it seemed to us that if we only knew enough about how conformational factors affect reaction rates, we could apply this knowledge to learn about transition state geometry, *i.e.* as a tool in the general problem of elucidating reaction mechanisms.

We have begun our attempts to apply conformational phenomena to mechanistic study using reactions of substituted cyclohexyl compounds because these appeared to be the best understood of any in conformational terms. In this, the first paper of a projected series, we describe our experiments on reactions of the type **1** → **2** ← **3**, as in Scheme 1.[1] Prior to this study, what was known about the system **1** → **2** ← **3** derived from study of the chromic acid oxidation of cyclohexanols (3–8). The work described in this account was done primarily to see if the analysis that had evolved from the cyclohexanol oxidations was general, *i.e.* could be extended to include reactions in which the central atom of A, A‡, and A′ was something other than oxygen. We also sought

[1]We use the symbol (**i**) below to indicate a rigid or anchored (2) cyclohexane ring. This symbol makes it easy to dépict reaction schemes involving anchored six-membered rings without further specifying the structure, *i.e.* whether it is part of a simple *trans*-decalin, a more complex fused ring (*e.g.* steroid), or 4-*t*-butylcyclohexyl system. At the same time the symbol (**i**) diminishes the likelihood of misunderstanding by clearly distinguishing between a simple cyclohexyl system, which is normally readily converted to the other chair conformation, from an anchored cyclohexyl system, which is not.

(**i**)

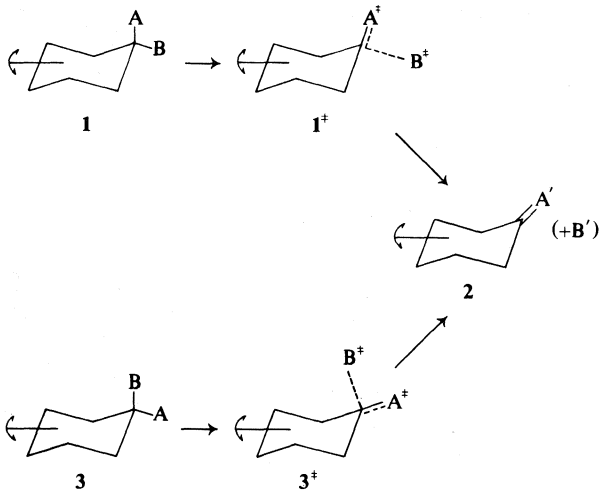

SCHEME 1

to obtain clear demonstration of the "steric acceleration effect" in a simple axial cyclohexyl compound in which the only other axial functions are hydrogens, and in addition to determine the significance, if any, of the "reagent repulsion effect" (see below). The second, and accompanying paper demonstrates the application of this "method of axial:equatorial rate ratios" to a reaction in which we have been interested, for entirely independent reasons, for some time, namely the formation of sulfenes by dehydrohalogenation of sulfonyl chlorides.

As is mentioned above, the oxidation of cyclohexanols with chromic acid has been studied extensively (3–8). It was found that axial alcohols react faster than their equatorial epimers, and further, that, except for an extremely hindered hydroxyl group (8), the greater the steric compression on the hydroxyl group the faster the reaction (4). This was explained (4) as deriving from a *steric acceleration effect*, which may be described in terms of the structures in Scheme 1. When A = OH and B = H, **1** has higher energy than **3** (*i.e.* $G(\mathbf{1}) > G(\mathbf{3})$), because of the higher total non-bonding interaction energy associated with the axial disposition of the hydroxyl function compared with the equatorial. On going from the starting material to the transition state, the non-bonding interaction energy difference, $G(\mathbf{1}^{\ddagger}) - G(\mathbf{3}^{\ddagger})$, is reduced as the geometries of $\mathbf{1}^{\ddagger}$ and $\mathbf{3}^{\ddagger}$ approach that of the product **2**; *i.e.* $G(\mathbf{1}^{\ddagger}) - G(\mathbf{3}^{\ddagger}) < G(\mathbf{1}) - G(\mathbf{3})$. Hence $G(\mathbf{1}^{\ddagger}) - G(\mathbf{1}) < G(\mathbf{3}^{\ddagger}) - G(\mathbf{3})$, or, since $G(\mathbf{1}^{\ddagger}) - G(\mathbf{1})$ is simply $\Delta G_1^{\ddagger}$, the free energy of activation for **1**, and $G(\mathbf{3}^{\ddagger}) - G(\mathbf{3})$ is $\Delta G_3^{\ddagger}$, the free energy of activation for **3**, this is more simply stated: $\Delta G_1^{\ddagger} < \Delta G_3^{\ddagger}$, *i.e.* the axial isomer **1** reacts faster than its equatorial epimer **3**.

Barton (1) had previously pointed out that "if the rate determining step is attack upon the carbon–hydrogen bond rather than upon the carbon–oxygen bond" then reaction of axial alcohols would be subject to smaller steric hindrance than that of the equatorial epimers. In terms of Scheme 1 (A = OH, B = H, and $B^{\ddagger}$ = a hydrogen partially bonded to the hydrogen-abstracting reagent), this would mean that in the process $\mathbf{3} \rightarrow \mathbf{3}^{\ddagger}$, the total non-bonding energy increases more than it does in process $\mathbf{1} \rightarrow \mathbf{1}^{\ddagger}$. This basic notion has been applied in numerous contexts for some time; for the purposes of specific reference in this paper we shall call this the *reagent repulsion effect*. As data on the cyclohexanol oxidation became available it grew apparent that for that reaction at least, the steric acceleration effect was definitely the more important, and perhaps the only significant, steric effect. In general, however, until the magnitude of the putative reagent repulsion effect in all reactions of the type $\mathbf{1} \rightarrow \mathbf{2} \leftarrow \mathbf{3}$ can be estimated, it would appear advisable to keep it in mind as a possibility which requires consideration. Alternatively, of course, one could design a system in which reagent repulsion is clearly impossible or

Can. J. Chem. Downloaded from www.nrcresearchpress.com by 210.87.254.105 on 09/05/12
For personal use only.

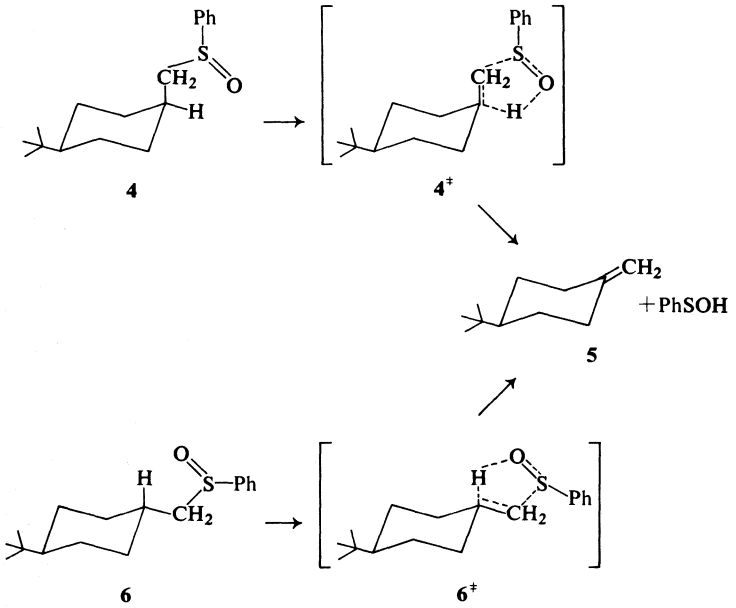

SCHEME 2

obviously of no consequence. This is, in fact, the approach adopted in the first of the reactions discussed in this paper.

Evidence available when this work was begun (9–12), and added to subsequently (13–15), strongly indicates that the thermolysis of simple alkyl (or aryl alkyl) sulfoxides with at least one β-hydrogen atom leads to the olefin and the sulfenic acid via a cyclic concerted process in which the sulfoxide oxygen acts as the proton-abstracting agent. Reactions **4** → **5** ← **6** in Scheme 2 illustrate the specific example of the sulfoxide thermolysis corresponding to the general system in Scheme 1. The transition states for the *cis*-sulfoxide **4** and the *trans*-sulfoxide **6** are depicted by **4**‡ and **6**‡, respectively. It is evident that the contribution of any reagent repulsion effect in this system would be inconsequential, whereas the steric acceleration effect would be predicted to show up undiminished. On the basis of the foregoing analysis it would be expected that relative rates of the thermolysis of **4** and **6** would be a direct measure of the steric acceleration in this system, and hence could give some notion of the significance of this effect in the general system **1** → **2** ← **3** in which the central atom of A and A′ is carbon.

A second system of the general type **1** → **2** ← **3** was also studied briefly, namely the dehydrohalogenation of the axial and equatorial cyclohexanemethyl bromides **7** and **8** to 1-*t*-butyl-4-methylenecyclohexane (**5**). It was hoped that in addition to providing another example of the Scheme 1 system in which A is carbon and B is hydrogen, that it might also lead to definite information concerning the reagent repulsion effect.

After our work was well underway another effect relevant to our study of axial:equatorial rate ratios was suggested in order to account for the products of hydride reduction and Grignard addition to carbonyl compounds (16, 17); for the specific example of additions to cyclohexanones this would be an example of the reaction **1** ← **2** → **3**, *i.e.* the *reverse* of the general reaction that we are concerned with in this paper. Felkin and co-workers (16–18) have postulated the existence of torsional strain in the transition state between the partial bond joining the attacking nucleophile to the erstwhile carbonyl carbon and any bonds to the α-carbons that eclipse (or nearly eclipse) this partial bond. This hypothesis, which we shall call the "Felkin postulate", was used to account, among other things, for the well-known predominance of the equatorial alcohol in the hydride reduction of unhindered anchored cyclohexanones, the torsional strain in this instance being between the hydride hydrogen to carbon bond and the two C—H bonds between the α-carbons

Can. J. Chem. Downloaded from www.nrcresearchpress.com by 210.87.254.105 on 09/05/12
For personal use only.

TABLE 1. Rates of thermolysis of the phenyl *cis*- and *trans*-4-*t*-butylcyclohexanemethyl sulfoxides (**4** and **6**) in benzene

Compound	Configuration	Temperature (°C)	$k \times 10^6$ (s^{-1})	k_{Ax}/k_{Eq}
cis-**4**	Axial	129.9	32	5.4
trans-**6**	Equatorial	129.9	5.9	
cis-**4**	Axial	116.4	6.4	5.8
trans-**6**	Equatorial	116.4	0.11	

and their axial hydrogens. These authors specifically suggest that the torsional strain is significant even in transition states in which the partial bond is weak; in terms of Scheme 1 this refers to that situation in which $\mathbf{1}^{\ddagger}$ is close to **2** on the reaction coordinate.

In the present context the Felkin postulate would suggest that as $\mathbf{1}^{\ddagger}$ and $\mathbf{3}^{\ddagger}$ become more and more like **2** (as one changes the reaction conditions or the nature of A or B), the energy difference between $\mathbf{1}^{\ddagger}$ and $\mathbf{3}^{\ddagger}$ will not become negligible because of the differences in torsional strain. If this be the case then the axial:equatorial rate ratio will not reduce to a simple reflection of the difference in energy between the two starting materials ($G(\mathbf{1}) - G(\mathbf{3})$).

The work described in this paper neither alters the status of the Felkin postulate nor makes specific use of it. The topic is mentioned as a possible effect which could influence axial:equatorial rate ratios in general and also as an illustration of the complexities and uncertainties that may still surround even semi-quantitative theoretical interpretation of axial:equatorial rate ratios. We wish to emphasize that application of the method of axial:equatorial rate ratios at present is an essentially empirical procedure in which the validity of the argument is directly related to the similarity between the unknown and model systems. In order to make non-trivial application of the method, the unknown and model reactions must be chemically different but sterically analogous. Obviously, enough must be known of the important factors governing axial:equatorial rate ratios to be sure that unknown and model reactions are really sterically analogous and that the unknown system will not be controlled by a hitherto unknown effect. The primary aim of our study (which is described in part in this paper) was to assemble an array of carefully chosen model systems for comparison with reactions of unknown course. It was hoped that we might also either uncover any further influences of importance in anchored cyclohexyl systems, or else reduce the likelihood of their existence to the point that useful mechanistic conclusions could be drawn by applying the method of axial:equatorial rate ratios.

Results and Discussion

Thermolysis of cis and trans Phenyl 4-t-Butylcyclohexanemethyl Sulfoxides (4 and 6)

The axial and equatorial sulfoxides **4** and **6** were obtained in a straightforward manner from the corresponding 4-*t*-butylcyclohexylcarbinols, via the methanesulfonates and the phenyl sulfides (see Experimental). Model experiments with phenyl cyclohexanemethyl sulfoxide showed that thermolysis in benzene at 130° gave, in addition to methylenecyclohexane, a second material (perhaps 1-methylcyclohexene) running slightly more slowly on v.p.c.; formation of this second material was completely suppressed by addition of calcium carbonate to the reaction. The rates of the thermolyses were followed by v.p.c. determination of the 1-*t*-butyl-4-methylenecyclohexane (**5**). The reactions were found to be cleanly first order to >60% reaction; variation in the amount of calcium carbonate had no effect on the rate.

As may be seen in Table 1, the axial sulfoxide **4** reacts five to six times faster than its equatorial epimer **6** in benzene solution in the temperature range 116–130°. By way of comparison it should be noted that Eliel and co-workers (7) found that the oxidation of *cis*-4-*t*-butylcyclohexanol with chromic acid in 75% acetic acid at 25° proceeds 3.23 times faster than the *trans* (equatorial) epimer. The increase in the ratio k_{Ax}/k_{Eq} on going from 129.9 to 116. 4° with the sulfoxides suggests that the ratio at 25° might well be distinctly greater than 6; the data, however, are probably not accurate enough to justify extrapolation to lower temperatures (or estimation of enthalpies and entropies of activation).

Can. J. Chem. Downloaded from www.nrcresearchpress.com by 210.87.254.105 on 09/05/12
For personal use only.

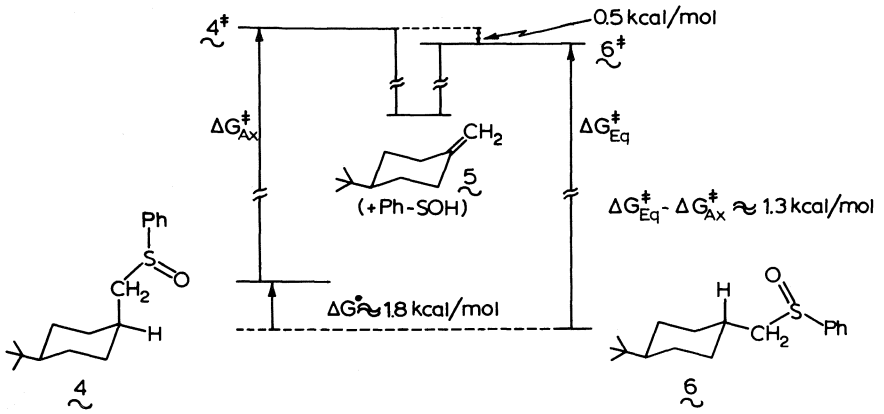

FIG. 1. Energy diagram for the thermolyses of the *cis*- and *trans*-phenyl 4-*t*-butylcyclohexanemethyl sulfoxides (**4** and **6**) at 130°.

The approximate relative free energies in the thermolyses of the sulfoxides **4** and **6** are summarized in Fig. 1. The $\Delta G°$ value (*i.e.* $G_{Ax} - G_{Eq}$) for the —CH_2SO—Ph group is assumed to be about 1.8 kcal/mol, *i.e.* comparable to that found with other —CH_2X groups, *e.g.* —CH_2CH_3, 1.75 kcal/mol (19) and CH_2OCH_3, 1.80 kcal/mol (20); it is also further assumed that the value is not much different at 130°. At that temperature the rate ratio, k_{Ax}/k_{Eq}, is 5.9, corresponding to a difference in free energy of activation ($\Delta G^{\ddagger}_{Eq} - \Delta G^{\ddagger}_{Ax}$) of 1.3 kcal/mol, indicating a roughly 0.5 kcal/mol difference in energy between the two transition states **4**‡ and **6**‡.

For any reaction in which the rate difference between two epimers derives exclusively from steric acceleration as defined here, it is evident from Fig. 1 that the rate difference cannot be greater than ΔG^0, the difference in the free energies of the starting materials; *i.e.* as the two transition states approach the same energy, $\Delta G^{\ddagger}_{Eq} - \Delta G^{\ddagger}_{Ax}$ tends toward $\Delta G°$, or, taking the Felkin postulate into account, $\Delta G°$ less the energy of the torsional strain difference. With the sulfoxide thermolysis the maximum possible difference in $\Delta G^{\ddagger}$ would be ~1.8 kcal/mol, whereas the difference that is actually observed is 1.3 kcal/mol or about 70% of this value. For the chromic acid oxidation of cyclohexanols the rate ratio of 3.23 at 25° quoted earlier corresponds to a difference in $\Delta G^{\ddagger}$ of about 0.7 kcal/mol or about 80% of 0.87 kcal/mol, the $\Delta G°$ value for the hydroxyl groups in hydroxylic media (19). If the extent of the reaction in the transition state in the thermolysis and oxidation reactions should happen to be roughly comparable, then the difference in rate between the axial and equatorial alcohols in chromic acid oxidation would seem almost entirely ascribable to steric acceleration, with little or no room for contribution by reagent repulsion. Alternatively the difference between $\Delta\Delta G^{\ddagger}$ and $\Delta G°$ could be ascribed entirely to Felkin's torsional strain in the transition state **1**‡; this would still leave very little leeway for any effect of reagent repulsion.

E2 Reaction of cis- and trans-4-t-Butylcyclohexanemethyl Bromides (7 and 8)

With the aim of obtaining further data on k_{Ax}/k_{Eq} for exocyclic eliminations, we briefly investigated the reaction of the *cis*- and *trans*-4-*t*-butylcyclohexanemethyl bromides (**7** and **8**) with strong base. These compounds were readily prepared from the cyclohexylcarbinols via the *p*-nitrobenzenesulfonate esters (see Experimental).

Each bromide was found to react with potassium *t*-butoxide in *t*-butyl alcohol at 100°. As shown in Scheme 3 the axial bromide (**7**) gave 1-*t*-butyl-4-methylenecyclohexane (**6**) (~80% yield) with no sign of any of the *t*-butyl ether. The equatorial isomer (**8**) however, gave a mixture estimated to contain about 30% of **6** and about 70% of *t*-butyl 4-*t*-butylcyclohexanemethyl ether (**9**) (total yield of this mixture also 80%), the product of a presumed S_N2 displacement at the equatorial primary carbon. As will be described in a subsequent paper in this series, we have observed that the formation of **8** from the *p*-nitrobenzenesulfonate takes place about 20 times faster than

Can. J. Chem. Downloaded from www.nrcresearchpress.com by 210.87.254.105 on 09/05/12
For personal use only.

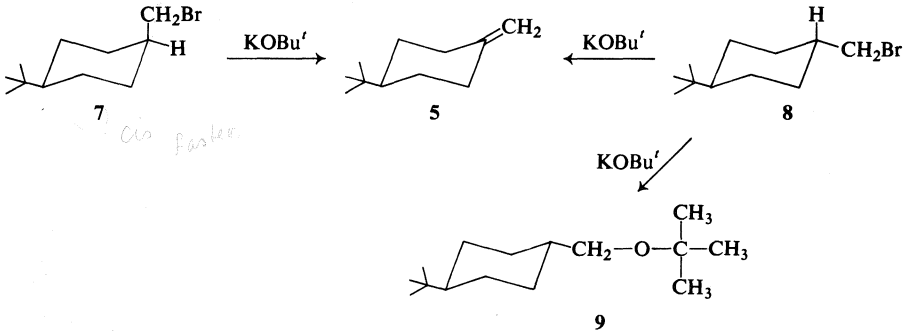

SCHEME 3

that of the axial isomer **7** under the conditions studied. For the S_N2 reaction of **7** and **8** with potassium *t*-butoxide we estimate $k_{Ax}/k_{Eq} < 0.3$; only an upper limit was obtainable because of the absence of any detectable amount of the ether from **7**.

The rate of the reaction of the bromides **7** and **8** with a large excess of potassium *t*-butoxide was obtained by following the rate of release of bromide ion. With **7** this gives the rate of elimination directly, but with **8** this yields the sum of the rates of substitution and elimination. At 100° with a base concentration of 0.76 *M* in *t*-butyl alcohol the rate of bromide ion release from the axial bromide **7** corresponded to a second order rate constant of 9.4×10^{-4} l mol^{-1} s^{-1}. With the equatorial bromide (**8**) the corresponding rate constant was 3.5×10^{-4} l mol^{-1} s^{-1}, which, from the product ratio given above, corresponds to a second order rate constant for the *elimination* of 1.1×10^{-4} l mol^{-1} s^{-1}. To show that the reaction rate depended on base concentration, another pair of determinations was carried out with the solution 0.41 *M* in potassium *t*-butoxide; this led to rate constants for the elimination of 9.0×10^{-4} and 1.0×10^{-4} l mol^{-1} s^{-1} for **7** and **8** respectively.

Approximate though these measurements are, they clearly show that the axial bromide **7** undergoes elimination (evidently bimolecular) distinctly more rapidly than its equatorial epimer **8**, by about nine times, in fact. This value corresponds to a difference in $\Delta G^{\ddagger}$ of about 1.6 kcal/mol, which is close to, but still less than, the maximum difference derivable exclusively from steric acceleration, which may be estimated as detailed above to be about 1.8 kcal/mol. It had been hoped that the considerable bulk of the *t*-butoxide ion might lead to a difference in $\Delta G^{\ddagger}$ of more than 1.8 kcal/mol, thereby requiring the postulation of another effect, *viz.* reagent repulsion, in addition to steric acceleration. In the absence of further data it is not unreasonable to ascribe the faster elimination of the axial bromide (**7**) primarily to steric acceleration; reagent repulsion is neither required nor entirely excluded.

Experimental

Melting points, which were determined on a Kofler hot stage, and boiling points are uncorrected. Unless otherwise stated, i.r. and n.m.r. spectra were determined in carbon tetrachloride solution (Fisher Spectranalyzed grade), and were determined on a Beckman IR-10 instrument and a Varian A-60 spectrometer, respectively; the chemical shifts are recorded in p.p.m. downfield from internal tetramethylsilane. The u.v. spectra were determined on a Jasco model O.R.D./U.V.5 spectropolarimeter. The t.l.c. was carried out using Camag silica gel DF 5. The refractive indices were determined with a thermostatically controlled Bausch and Lomb refractometer. Organic extracts were dried with anhydrous magnesium sulfate. The silica gel used for column chromatography was B.D.H. (for Chromatographic Adsorption). Dry ether refers to ether (Mallinckrodt anhydrous) freshly distilled from lithium aluminum hydride (Metal Hydrides). Petroleum ether refers to the fraction of b.p. 30–60°. The v.p.c. was carried out on F and M model 700 apparatus; *I* refers to injector temperature, *O* to oven temperature, and *D* to detector temperature; helium (40 ml/s) was used as the carrier gas. The degassing and sealing of Carius tubes was carried out according to the following procedure. Then tube was placed in liquid nitrogen until the sample was frozen, and then evacuated with a vacuum pump (10^{-2}–10^{-3} mm). The direction connection to the pump was closed and the sample removed from the liquid nitrogen and allowed to thaw and let stand for about 10 min with occasional gentle shaking. The tube was then put back in the liquid nitrogen, pumped, warmed, shaken as before, and then cooled and evacuated for a third time, after which the tube was sealed off at the torch.

cis-4-t-Butylcyclohexanemethyl Methanesulfonate

cis-4-*t*-Butylcyclohexylcarbinol (2.3 g) prepared as described by Buchanan *et al.* (21), and methanesulfonyl

Can. J. Chem. Downloaded from www.nrcresearchpress.com by 210.87.254.105 on 09/05/12
For personal use only.

Can. J. Chem. Downloaded from www.nrcresearchpress.com by 210.87.254.105 on 09/05/12
For personal use only.

chloride (1.3 ml, Eastman, redistilled) were dissolved in methylene chloride (15 ml, Fisher Spectranalyzed grade) and cooled in an ice bath. To this cooled solution, triethylamine (3 ml, Fisher Reagent grade, redistilled) in methylene chloride (5 ml) was added slowly. The reaction mixture was left standing at room temperature for 10 min, then poured into water, and extracted twice with methylene chloride. The combined methylene chloride layers were washed successively with water, sulfuric acid (10%) and water, and dried. Evaporation of the methylene chloride gave a white solid (2.1 g). Crystallization from methylene chloride – pentane gave *cis*-4-*t*-butylcyclohexanemethyl methanesulfonate as fine plates, m.p. 45.5–46°. The i.r. bands were found at ν_{max} 1370 (s), 1350 (s), 1250 (vw), 1180 (s), 990 (sh), 970 (sh), 950 (s), 940 (sh) cm^{-1}. The n.m.r. spectrum had bands at 0.84 (s, $-C(CH_3)_3$), 2.90 (s, $-OSO_2CH_3$), and 4.12 p.p.m. (d, $-CH_2OSO_2CH_3$, J 7.5 Hz).

Anal. Calcd. for $C_{12}H_{24}O_3S$: C, 58.01; H, 9.74; S, 12.89. Found: C, 57.82; H, 9.93; S, 13.05.

trans-4-Butylcyclohexanemethyl Methanesulfonate

This was prepared from *trans*-4-*t*-butylcyclohexylcarbinol (21) by the same procedure as for *cis*-4-*t*-butylcyclohexanemethyl methanesulfonate. Crystallization from methylene chloride – pentane gave *trans*-4-*t*-butylcyclohexanemethyl methanesulfonate as large plates, m.p. 71.5–72°. The i.r. bands were found at ν_{max} 1370 (s), 1350 (s), 1240 (vw), 1180 (s), 995 (sh), 980 (sh), 950 (s), 910 (vw) cm^{-1}. The n.m.r. spectrum had bands at 0.84 (s, $-C(CH_3)_3$), 2.85 (s, $-OSO_2CH_3$), and 3.90 p.p.m. (d, $-CH_2OSO_2CH_3$, J 5.5 Hz).

Anal. Calcd. for $C_{12}H_{24}O_3S$: C, 58.01; H, 9.74; S, 12.89. Found: C, 58.20; H, 9.88; S, 12.98.

Cyclohexanemethyl Methanesulfonate

This was prepared from cyclohexylcarbinol (Aldrich) by the same procedure as for *cis*-4-*t*-butylcyclohexanemethyl methanesulfonate. Crystallization from methylene chloride – pentane gave cyclohexanemethyl methanesulfonate as needles, m.p. 45–46.5°. The i.r. bands were found at ν_{max} 1350 (vs), 1180 (s), 980 (s), 945 (s), 900 (m) cm^{-1}. The n.m.r. spectrum had bands at 2.96 (s, $-OSO_2CH_3$) and 3.92 p.p.m. (d, $-CH_2OSO_2CH_3$, J 6 Hz).

Anal. Calcd. for $C_8H_{16}O_3S$: C, 49.97; H, 8.39; S, 16.67. Found: C, 50.14; H, 8.32; S, 16.56.

Phenyl cis-4-t-Butylcyclohexanemethyl Sulfide

cis-4-*t*-Butylcyclohexanemethyl methanesulfonate (1.3 g) was dissolved in dioxane (5 ml, Fisher Reagent grade, redistilled) and added to a solution of sodium thiophenoxide prepared by mixing sodium (0.5 g), ethyl alcohol (15 ml, 95%), thiophenol (2.5 g, Fisher Reagent grade) in dioxan (50 ml). This mixture was refluxed for 12 h under a nitrogen atmosphere and then poured into a mixture of ether and 5% aqueous sodium hydroxide. The ethereal layer was washed with 10% sulfuric acid (until the washings were acidic), then with water, and dried. Evaporation of the ether gave a white solid (1.3 g). Crystallization from pentane gave phenyl *cis*-4-*t*-butylcyclohexanemethyl sulfide as spars, m.p. 48–49°. The i.r. bands were found at ν_{max} 3060 (vw), 1585 (w), 1240 (w), 1090 (vw), 1030 (w) cm^{-1}. The n.m.r. spectrum had bands at 0.82 (s, $-C(CH_3)_3$), 2.86 (d, $-CH_2SC_6H_5$, J 7.5 Hz), and 7.1 p.p.m. (m, $-SC_6H_5$).

Anal. Calcd. for $C_{17}H_{26}S$: C, 77.79; H, 9.99; S, 12.21. Found: C, 78.01; H, 10.18; S, 12.16.

Phenyl trans-4-t-Butylcyclohexanemethyl Sulfide

This was prepared from *trans*-4-*t*-butylcyclohexanemethyl methanesulfonate by the same procedure as for phenyl *cis*-4-*t*-butylcyclohexanemethyl sulfide. Crystallization from pentane gave phenyl *trans*-4-*t*-butylcyclohexanemethyl sulfide as fine needles, m.p. 40–41°. The i.r. bands were found at ν_{max} 3060 (vw), 1585 (w), 1270 (vw), 1240 (vw), 1090 (vw), 1070 (sh), 1030 (vw) cm^{-1}. The n.m.r. spectrum had bands at 0.82 (s, $-C(CH_3)_3$), 2.70 (d, $-CH_2SC_6H_5$, J 6 Hz), and 7.1 p.p.m. (m, $-SC_6H_5$).

Anal. Calcd. for $C_{17}H_{26}S$: C, 77.79; H, 9.99; S, 12.21. Found: C, 78.04; H, 10.10; S, 12.18.

Phenyl Cyclohexanemethyl Sulfide

This was prepared from cyclohexanemethyl methanesulfonate by the same procedure as for phenyl *cis*-4-*t*-butylcyclohexanemethyl sulfide. Crystallization from pentane gave phenyl cyclohexanemethyl sulfide as spars m.p. 19–21°. The i.r. bands were found at ν_{max} 3070 (w), 1585 (m), 1260 (w), 1240 (w), 1090 (w), 1070 (sh), 1030 (w) cm^{-1}. The n.m.r. spectrum had bands at 2.70 (d, $-CH_2SC_6H_5$, J 6 Hz) and 7.1 p.p.m. (m, $-SC_6H_5$).

Phenyl cis-4-t-Butylcyclohexanemethyl Sulfoxide (4)

To a solution of phenyl *cis*-4-*t*-butylcyclohexanemethyl sulfide (2.9 g) in glacial acetic acid (200 ml) at 15° was added aqueous hydrogen peroxide (10 ml, 30%). The reaction mixture was left standing at 15° for 1 h and then poured into water. The resulting mixture was extracted twice with ether. The combined ethereal layers were washed with water and then with a saturated solution of sodium bicarbonate and dried. Evaporation of the ether gave an oil (3.0 g). Crystallization from pentane gave phenyl *cis*-4-*t*-butylcyclohexanemethyl sulfoxide (4) as fine needles, m.p. 60–61°. The i.r. bands were found at ν_{max} 3060 (vw), 1580 (vw), 1370 (m), 1240 (w), 1090 (m), 1070 (sh), 1050 (vw), 1025 (sh), 1000 (sh) cm^{-1}. The n.m.r. spectrum had bands at 0.84 (s, $-C(CH_3)_3$), 2.70 (m, $-CH_2SOC_6H_5$), and 7.5 p.p.m. (m, $-SOC_6H_5$).

Anal. Calcd. for $C_{17}H_{26}OS$: C, 73.31; H, 9.41; S, 11.51. Found: C, 73.61; H, 9.59; S, 11.71.

Phenyl trans-4-t-Butylcyclohexanemethyl Sulfoxide (6)

This was prepared from phenyl *trans*-4-*t*-butylcyclohexanemethyl sulfide by the same procedure as for phenyl *cis*-4-*t*-butylcyclohexanemethyl sulfoxide (4). Crystallization from methylene chloride – pentane gave phenyl *trans*-4-*t*-butylcyclohexanemethyl sulfoxide (6) as fine plates, m.p. 107–108°. The i.r. bands were found at ν_{max} 3060 (vw), 1580 (vw), 1370 (m), 1260 (w), 1240 (w),1090 (m), 1070 (sh), 1050 (vs), 1030 (sh), 1000 (sh) cm^{-1}. The n.m.r. had bands at 0.84 (s, $-C(CH_3)_3$), 2.50 (m, $-CH_2SOC_6H_5$), and 7.5 p.p.m. (m, $-SOC_6H_5$).

Anal. Calcd. for $C_{17}H_{26}OS$: C, 73.31; H, 9.41; S, 11.51. Found: C, 73.63; H, 9.45; S, 11.50.

Phenyl Cyclohexanemethyl Sulfoxide

This was prepared from phenyl cyclohexanemethyl sulfide by the same procedure as for phenyl *cis*-4-*t*-

Can. J. Chem. Downloaded from www.nrcresearchpress.com by 210.87.254.105 on 09/05/12
For personal use only.

butylcyclohexanemethyl sulfoxide (**4**). Crystallization from methylene chloride – pentane gave phenyl cyclohexanemethyl sulfoxide as fine needles, m.p. 56–57°. The i.r. bands were found at ν_{max} 3060 (w), 1580 (vw), 1270 (vw), 1100 (sh), 1080 (m), 1070 (sh), 1050 (s), 1020 (sh), 1000 (sh) cm^{-1}. The n.m.r. spectrum had bands at 2.71 (d, $—CH_2SOC_6H_5$, J 6 Hz) and 7.5 p.p.m. (m, $—SOC_6H_5$).

Anal. Calcd. for $C_{13}H_{18}OS$: C, 70.20; H, 8.16; S, 14.41. Found: C, 70.38; H, 8.09; S, 14.37.

1-t-Butyl-4-methylenecyclohexane (5)

This was prepared from 4-*t*-butylcyclohexane following the general procedure of Greenwald *et al.* (22). The i.r. bands were found at ν_{max} 3080 (w), 1650 (m), 1370 (m), 1245 (w), 1225 (w), 990 (w), 910 (sh), 900 (s) cm^{-1}. The n.m.r. spectrum had bands at 0.86 (s, $—C(CH_3)_3$) and 4.5 p.p.m. (broad s, $C{=}CH_2$).

Measurement of the Rate of the Reaction of the Pyrolysis of Phenyl cis- and trans-4-t-Butylcyclohexanemethyl Sulfoxides (4 and 6)

The phenyl 4-*t*-butylcyclohexanemethyl sulfoxide (*ca.* 250 mg) and naphthalene (*ca.* 140 mg, B.D.H. laboratory reagent, added as a standard for the v.p.c. assay) were weighed and dissolved in benzene (Fisher Spectranalyzed Grade, freshly distilled from calcium hydride) and the resulting solution made up to 10 ml at 25 °C. Aliquots (1 ml) of this solution with solid calcium carbonate (*ca.* 20 mg) were degassed and sealed under vacuum. These aliquots were then put into an oil bath whose temperature was controlled by a Fisher "Proportional Temperature Control" thermostat to ±0.2°. Timing was started at the time of immersion in the oil bath. After an appropriate time interval the aliquot was removed from the oil bath and placed under rapidly running cold water. The aliquot was then cooled in Dry Ice – acetone and opened. The thawed solution was then poured down a column of silica gel (*ca.* 5 g) and the column washed with 10 ml of benzene – *n*-pentane (1:1). This short column removed any unpyrolysed sulfoxide but did not alter the ratio of 1-*t*-butyl-4-methylenecyclohexane to naphthalene (known mixture ratios being the same before as after the above work-up). The resulting solution was then analyzed by v.p.c. using a 10% silicon rubber GE.SE.33 on Chromosorb WAW.DMSC 80–100 mesh column (6′ × ¼″ diameter) v.p.c. *I*, 165°; *O*, 120°; *D*, 178°). The amount of 1-*t*-butyl-4-methylenecyclohexane produced in the reaction was estimated by a comparison of the areas under the peak corresponding to naphthalene. This ratio was compared to ratios of known composition analyzed under the same conditions.

Two samples, one of the *cis*-sulfoxide **4**, the other of the *trans*-epimer **6** were sealed in ampoules as described above (except that the naphthalene was omitted), heated at 130° for 50 h, chromatographed as above, and the solvent evaporated. The n.m.r. spectra of the two materials were identical with that of an authentic specimen of 1-*t*-butyl-4-methylenecyclohexane (**5**) except for the presence of a small amount of an impurity containing hydrogens on an aromatic ring.

cis-4-t-Butylcyclohexanemethyl p-Nitrobenzenesulfonate

cis-4-*t*-Butylcyclohexylcarbinol (3.0 g) was dissolved in pyridine (5 ml, redistilled) and the resulting solution cooled in an ice bath. To this cooled solution *p*-nitrobenzenesulfonyl chloride (4.0 g, Eastman Organic) in dry pyridine (5 ml) was added slowly. The resulting solution was left standing in the ice bath for 20 min. The mixture was then poured into water and extracted twice with methylene chloride. The combined methylene chloride layers were washed with 10% sulfuric acid until the washings were acidic and then washed with water and dried. Evaporation of the methylene chloride gave a yellow solid. Crystallization from methylene chloride – carbon tetrachloride gave *cis*-4-*t*-butylcyclohexanemethyl *p*-nitrobenzenesulfonate as yellow needles, m.p. 108–109°. The i.r. bands were found at ν_{max} 3100 (vw), 1605 (w), 1535 (s), 1405 (sh), 1380 (vs), 1365 (vs), 1350 (vs), 1315 (m), 1240 (vw), 1185 (vs), 1100 (m), 1020 (vw), 975 (m), 950 (s), 930 (sh), 900 (sh), 685 (m), 615 (m) cm^{-1}. The n.m.r. spectrum had bands at 0.78 (s, $—C(CH_3)_3$), 4.20 (d, $—CH_2OSO_2—$, J 8 Hz), and 8.10 to 8.55 (q, $—OSO_2-C_6H_4NO_2$, J_{AB} 9 Hz, δ_A 8.22, δ_B 8.47).

Anal. Calcd. for $C_{17}H_{25}NO_5S$: C, 57.44; H, 7.09; N, 3.94; S, 9.02. Found: C, 57.47; H, 7.04; N, 3.88; S, 8.91.

trans-4-t-Butylcyclohexanemethyl p-Nitrobenzenesulfonate

This was prepared from *trans*-4-*t*-butylcyclohexylcarbinol by the same procedure as for *cis*-4-*t*-butycyclohexanemethyl *p*-nitrobenzenesulfonate. Crystallization from methylene chloride – carbon tetrachloride gave *trans*-4-*t*-butylcyclohexanemethyl *p*-nitrobenzenesulfonate as fine needles, m.p. 138–139°. The i.r. bands were found at ν_{max} 3100 (vw), 1650 (w), 1535 (s), 1360 (sh), 1350 (s), 1310 (m), 1230 (w), 1185 (vs), 1095 (m), 985 (w), 950 (s), 685 (m), 615 (m) cm^{-1}. The n.m.r. had bands at 0.81 (s, $—C(CH_3)_3$), 3.98 (d, $—CH_2OSO_2—$, J 6 Hz), and aromatic absorption from 8.0 to 8.53 analyzed as an AB quartet: δ_A 8.15, δ_B 8.45 p.p.m. (J_{AB} 9 Hz).

Anal. Calcd. for $C_{17}H_{25}NO_5S$: C, 57.44; H, 7.09; N, 3.94; S, 9.02. Found: C, 57.35; H, 7.16; N, 3.93; S, 9.08.

cis-4-t-Butylcyclohexanemethyl Bromide (7)

cis-4-*t*-Butylcyclohexanemethyl *p*-nitrobenzenesulfonate (2.0 g) was dissolved in dry acetone (100 ml). Lithium bromide (1.5 g) and calcium carbonate (1.0 g) were added to the solution and the resulting mixture refluxed for 24 h. The reaction mixture was then poured into water and extracted twice with petroleum ether and the extract dried. Evaporation of the petroleum ether gave an oil (1.3 g). The oil was adsorbed onto silica gel (40 g). Elution with petroleum ether afforded the crude bromide as an oil. Distillation (b.p. 58–60°/0.6 mm) gave *cis*-4-*t* butylcyclohexanemethyl bromide as an oil, n_D^{25} 1.5900. The i.r. bands were found at ν_{max} 1300 (w), 1240 (sh), 1230 (m), 1030 (broad, w), 960 (w), 680 (m) cm^{-1}. The n.m.r. spectrum had bands at 0.85 (s, $—C(CH_3)_3$) and 3.41 p.p.m. (d, $—CH_2Br$, J 8 Hz).

Anal. Calcd. for $C_{11}H_{21}Br$: C, 56.66; H, 9.08; Br, 34.27. Found: C, 56.65; H, 9.16; Br, 34.31.

trans-4-t-Butylcyclohexanemethyl Bromide (8)

This was prepared from *trans*-4-*t*-butylcyclohexanemethyl *p*-nitrobenzenesulfonate by the same procedure as for *cis*-4-*t*-butylcyclohexanemethyl bromide, except

Can. J. Chem. Downloaded from www.nrcresearchpress.com by 210.87.254.105 on 09/05/12
For personal use only.

that the reaction mixture was refluxed for only 2 h. Column chromatography (silica gel, elution with petroleum ether) followed by distillation (b.p. 58–60°/0.6 mm) gave *trans*-4-*t*-butylcyclohexanemethyl bromide as an oil, n_D^{25} 1.4858. The i.r. bands were found at ν_{max} 1300 (w), 1255 (m), 1235 (m), 1200 (vw), 1150 (vw), 980 (w), 900 (w), 655 (m) cm^{-1}. The n.m.r. spectrum had bands at 0.84 (s, $-C(CH_3)_3$) and 3.29 p.p.m. (d, $-CH_2Br$, J 5.5 Hz).

Anal. Calcd. for $C_{11}H_{21}Br$: C, 56.66; H, 9.08; Br, 34.27. Found: C, 56.67; H, 9.31; Br, 34.38.

t-Butyl trans-4-t-Butylcyclohexanemethyl Ether (9)

trans-4-*t*-butylcyclohexanemethyl bromide (215.5 mg) was dissolved in potassium *t*-butoxide – *t*-butyl alcohol (0.412 *M*, 20 ml) and the resulting solution degassed three times and sealed under vacuum (.001 mm). This sealed ampoule was then left standing at 100° for 24 h. The reaction mixture was poured into water and extracted with methylene chloride and then with ether. The methylene chloride and ether layers were neutralized with 2% sulfuric acid, washed with water, combined, and then dried. Evaporation of the solvent gave an oil (152 mg). Separation (t.l.c. cyclohexane–ether (4:1)) gave the crude ether (100 mg) as a solid. Recrystallization from pentane gave *t*-butyl *trans*-4-*t*-butylcyclohexanemethyl ether as fine needles, m.p. 31–32°. The i.r. bands were found at ν_{max} 1230 (w), 1200 (s), 1075 (m), 1020 (w) cm^{-1}. The n.m.r. spectrum had bands at 0.84 (s, $-C(CH_3)_3$), 1.10 (s, $-OC(CH_3)_3$), and 3.30 p.p.m. (d, $-CH_2OC(CH_3)_3$, J 5 Hz).

Anal. Calcd. for $C_{15}H_{30}O$: C, 79.58; H, 13.36. Found: C, 79.29; H, 13.20.

Measurement of the Rate of the Reaction of cis- and trans-4-t-Butylcyclohexanemethyl Bromide (7 and 8) with Potassium t-Butoxide in t-Butyl Alcohol at 100°

(a) Titration of the Bromide Ion Produced

Potassium *t*-butoxide was prepared by dissolving freshly cut potassium (free of the oxide crust and washed three times in pentane) in *t*-butyl alcohol (freshly distilled from calcium hydride) under a nitrogen atmosphere. The solution was standardized by titration with hydrochloric acid (0.1 *N*, B.D.H., concentrated Volumetric Solution). The *cis*- or *trans*-4-*t*-butylcyclohexanemethyl bromide solution was prepared by weighing the bromide (*ca.* 200 mg) and dissolving it in *t*-butyl alcohol (freshly distilled from calcium hydride) and making the solution up to 50 ml at 30°.

To a solution of the bromide (5 ml) was added the *t*-butoxide solution (5 ml), this mixture was then degassed three times and sealed under vacuum. The sealed solutions were then thoroughly mixed and placed in an oil bath whose temperature was controlled by a Fisher "Proportional Temperature Control" thermostat to 100.0 ± 0.2°. Timing was started at the time of immersion in the oil bath. After an appropriate time interval the aliquot was removed from the oil bath and placed in an ice bath. The sample was then opened and poured into water containing nitric acid (5 ml, 6 *N*) and the bromide ion titrated with silver nitrate. The pseudo first order rate constant was calculated from the slope of a plot of log (100 − % reaction) *vs.* time for six such determinations varying from <20 to >60% reaction; the apparent second order rate constant for bromide ion formation was obtained by dividing the pseudo first order rate constant by the potassium *t*-butoxide concentration. The apparent second order rate constants so obtained for the reaction of the *cis* bromide **7** were 9.4×10^{-4} l mol^{-1} s^{-1} ($KOBu^t$ 0.76 and substrate 1.96×10^{-2} *M*) and 9.0×10^{-2} l mol^{-1} s^{-1} ($KOBu^t$ 0.41 and substrate 1.66×10^{-2} *M*); for the *trans* bromide **8** the apparent second order rate constants for bromide ion release were 3.2×10^{-4} ($KOBu^t$ 0.41 and substrate 1.81×10^{-2} *M*) and 3.5×10^{-4} l mol^{-1} s^{-1} ($KOBu^t$ 0.76 and substrate 1.96×10^{-2} *M*).

(b) Product Analysis of the Reaction of cis- and trans-t-Butylcyclohexanemethyl Bromide with Potassium t-Butoxide

The bromide (*ca.* 250 mg) was dissolved in the *t*-butoxide solution (20 ml, 0.412 *M*), degassed three times, sealed under vacuum, and left at 100° for 24 h. The ampoule was cooled, opened, poured into water, and extracted with methylene chloride and ether. The methylene chloride and ethereal layers were neutralized with 2% sulfuric acid, washed with water, combined, and dried.

cis-4-*t*-Butylcyclohexanemethyl bromide (250 mg) gave an oil (130 mg), the n.m.r. spectrum of which showed a band at 4.45 ($C{=}CH_2$) and no bands in the region 2.5–4.4 p.p.m. ($-CH_2Br$ and $-CH_2OC(CH_3)_3$). *trans*-4-*t*-Butylcyclohexanemethyl bromide (215.5 mg) gave an oil (152 mg), the n.m.r. spectrum of which showed bands at 3.03 (d, $-CH_2OC(CH_3)_3$) and 4.45 ($C{=}CH_2$) in the ratio of 2.24:1 (*i.e.* 69:31%), but no band at 3.38 p.p.m. (CH_2Br). The apparent second order rate constants for the bromide ion formation from the *cis*-bromide (**7**) were therefore taken directly as the rate constants for the bimolecular elimination. The rate constants for the bimolecular elimination for the *trans*-bromide **8** were taken as 31% of the rate constants for the bromide ion release *i.e.* 1.0×10^{-4} and 1.1×10^{-4} l mol^{-1} s^{-1}, respectively.

This work was supported by grants from the National Research Council of Canada and the Alfred P. Sloan Foundation.

1. D. H. R. Barton. Exper. **6**, 316 (1950).
2. J. F. King and A. D. Allbutt. Can. J. Chem. **47**, 1445 (1969).
3. G. Vavon and C. Zaremba. Bull. Soc. Chim. Fr. 1853 (1931).
4. J. Schreiber and A. Eschenmoser. Helv. Chim. Acta, **38**, 1529 (1955).
5. S. Winstein and N. J. Holness. J. Am. Chem. Soc. **77**, 5562 (1955).
6. F. Šipoš, J. Krupička, M. Tichý, and J. Sicher. Coll. Czech. Chem. Commun. **27**, 2079 (1962).
7. J. C. Richer, L. A. Pilato, and E. L. Eliel. Chem. and Ind. (Lond.), 2007 (1961).
8. J. Roček, F. H. Westheimer, A. Eschenmoser, L. Moldoványi, and J. Schreiber. Helv. Chim. Acta, **45**, 2554 (1962).
9. C. A. Kingsbury and D. J. Cram. J. Am. Chem. Soc. **82**, 1810 (1960).

10. D. N. JONES and M. A. SAEED. Proc. Chem. Soc. 81 (1964).
11. S. I. GOLDBERG and M. S. SAHLI. Tetrahedron Lett. 4441 (1965).
12. J. F. KING, K. ABIKAR, D. M. DEAKEN, and R. G. PEWS. Can. J. Chem. **46**, 1 (1968).
13. D. W. EMERSON, A. P. CRAIG, and I. W. POTTS, JR. J. Org. Chem. **32**, 102 (1967).
14. J. R. SHELTON and K. E. DAVIS. J. Am. Chem. Soc. **89**, 718 (1967).
15. D. W. EMERSON and T. J. KORNISKI. J. Org. Chem. **34**, 4115 (1969).
16. M. CHÉREST, H. FELKIN, and N. PRUDENT. Tetrahedron Lett. 2199 (1968).
17. M. CHÉREST and H. FELKIN. Tetrahedron Lett. 2205 (1968).
18. M. CHÉREST and H. FELKIN. Tetrahedron Lett. 383 (1971).
19. J. A. HIRSCH. *In* Topics in stereochemistry. Vol. 1. *Edited by* N. L. Allinger and E. L. Eliel. Interscience, New York, N.Y., 1967. p. 199.
20. G. W. BUCHANAN and J. B. STOTHERS. Chem. Commun. 1250 (1967).
21. G. W. BUCHANAN, J. B. STOTHERS, and S. WU. Can. J. Chem. **47**, 3113 (1969).
22. R. GREENWALD, M. CHAYKOVSKY, and E. J. COREY. J. Org. Chem. **28**, 1128 (1963).

Can. J. Chem. Downloaded from www.nrcresearchpress.com by 210.87.254.105 on 09/05/12
For personal use only.

Can. J. Chem. Downloaded from www.nrcresearchpress.com by 210.87.254.6 on 09/05/12
For personal use only.

Axial:Equatorial Rate Ratios and the Mechanism of Formation of Sulfenes by Dehydrohalogenation of Alkanesulfonyl Chlorides[1]

J. F. KING AND T. W. S. LEE

Department of Chemistry, University of Western Ontario, London, Ontario

Received June 18, 1971

The method of axial: equatorial rate ratios has been applied to the study of the mechanism of formation of sulfenes via the reaction of alkanesulfonyl chlorides with base. The axial *trans*-2-decalinsulfonyl chloride (**6**) and the equatorial *trans*-2-decalinsulfonyl chloride (**8**) were synthesized. The axial sulfonyl chloride **6** was found to react 71 times faster than the equatorial epimer **8** with triethylamine in the presence of aniline at $-25°$, a reaction which evidently proceeds via the sulfene **7**. With water at 50° without added base (a reaction believed to take place by direct attack on the sulfur atom) **8** reacts about 14 times faster than **6**. It is concluded that the formation of the sulfene **7** from **6** by the action of triethylamine cannot take place by a mechanism involving a slow S_N2 reaction followed by a fast bimolecular elimination, and that the most likely route for **6**, and other alkanesulfonyl chlorides as well, is the E2 reaction.

La méthode des rapports de vitesse axial:équatorial a été utilisée pour étudier le mécanisme de la formation des sulfènes via la réaction des chlorures d'alkanesulfonyles avec une base. Le chlorure de la *trans*-2-décalinsulfonyle axiale (**6**) et le chlorure de la *trans*-2-décalinsulfonyle équatoriale (**8**) ont été synthétisés. Le chlorure de sulfonyle axial **6** réagit 71 fois plus vite que l'épimère équatorial **8** avec la triéthylamine en présence d'aniline à $-25°$ (réaction qui se fait via le sulfène **7**). Dans l'eau à 50°, sans l'adjonction d'une base, (réaction supposée se faire par une attaque directe sur l'atome de soufre) le composé **8** réagit environ 14 fois plus vite que le composé **6**. Ces résultats prouvent que la formation du sulfène **7** à partir de **6**, par l'action de la triéthylamine, ne peut se faire par un mécanisme impliquant une réaction S_N2 lente suivie d'une élimination bimoléculaire rapide. A partir du composé **6**, et d'autres chlorures d'alkanesulfonyle, le mécanisme le plus probable est celui faisant intervenir une réaction E2.

Canadian Journal of Chemistry, **49**, 3724 (1971)

Introduction

The work described in the accompanying paper (1) was started in the hope of ultimately using the relative rates of axial *vs.* equatorial epimers in the study of reaction mechanisms. It seemed that the method of axial:equatorial rate ratios might be applied to a problem already being studied in our laboratory, namely the mechanism of formation of sulfenes by dehydrohalogenation of alkanesulfonyl halides, eq. 1.

[1] $$RR'CHSO_2Cl + R_3''N \rightarrow RR'C{=}SO_2 + R_3''\overset{+}{N}H\ Cl^-$$

Accordingly, we have synthesized a pair of anchored axial and equatorial sulfonyl chlorides and measured their rates of reaction. A preliminary account which includes other aspects of the study of the mechanism of sulfene formation via eq. 1 has been published (3); it will be necessary in this account to refer to the other phases of this investigation (mainly kinetic studies) but full discussion of these will be taken up in a subsequent paper.

Among the possible mechanisms for sulfene formation according to eq. 1, two appeared particularly likely: (*i*) a one-step concerted elimination, *i.e.* E2 reaction, and (*ii*) substitution of chloride by the tertiary amine followed by elimination. The second mechanism though less obvious, and perhaps less probable than the first, cannot be dismissed out of hand; evidently the same first step, *i.e.* displacement of chloride by the tertiary base, is found in the pyridine catalyzed hydrolysis of benzenesulfonyl chloride (4). Since mechanism (*ii*) has two steps, it is possible, in principle, for either step to be rate controlling. That version of mechanism (*ii*) in which the intermediate sulfonammonium ion is formed rapidly and is attacked in the slow step by tertiary base to give the sulfene, would be *second* order in the tertiary amine; the reaction has been found to show only first order dependence on the tertiary amine concentration (3), thereby excluding that possibility. The kinetic data, however, do not

[1]Axial:Equatorial Rate Ratios Part 2, and Organic Sulfur Mechanisms Part 10. References 1 and 2 are respectively parts 1 and 9 of these series.

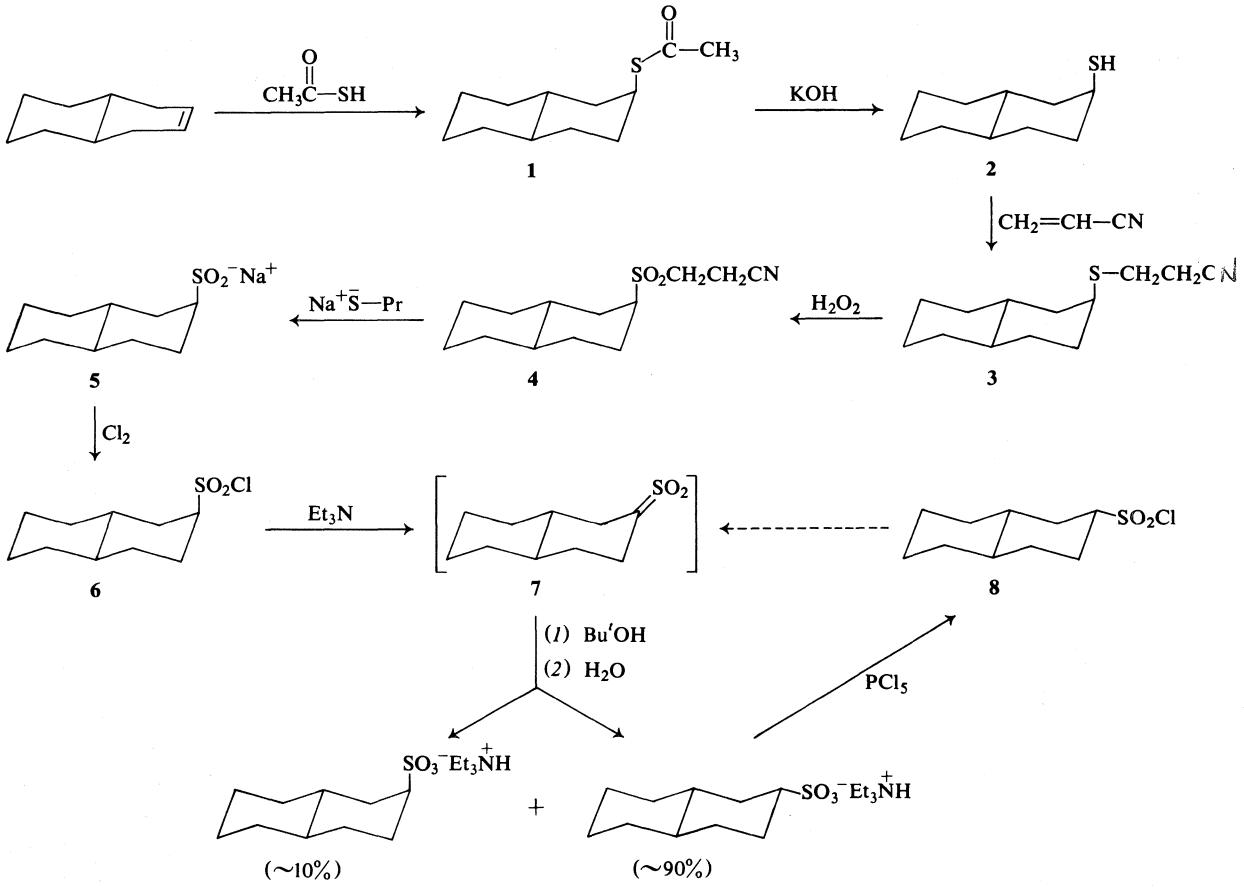

SCHEME 1

distinguish between mechanism (*i*) and the version of mechanism (*ii*) in which the attack of the tertiary amine in the sulfonyl chloride is slow and the subsequent elimination rapid. The problem of distinguishing between these possible mechanisms would appear to be quite simple by the method of axial:equatorial rate ratios.

As was shown in the accompanying paper (1) the actual formation of a double bond exocyclic to a cyclohexane ring has been found to be faster from an axial precursor than from its equatorial epimer. One would therefore predict that formation of the sulfene from a substituted cyclohexanesulfonyl chloride by a direct E2 mechanism would be distinctly faster from the axial sulfonyl chloride than from the equatorial isomer. On the other hand if the rate-controlling step were a substitution reaction, the reaction would be slower for the axial than for equatorial compound. The latter conclusion can be supported by relevant examples which will be detailed in the discussion of the mechanism section.

To apply this method it was necessary to obtain a pair of anchored axial and equatorial sulfonyl chlorides. A convenient route to the stereospecific synthesis of an axial sulfonyl chloride was suggested by the observation of Bordwell *et al.* (5) that free radical addition of thioacetic acid to anchored cyclohexenes gave apparently exclusively the axial thiolester. Of the various possible anchored cyclohexane systems that might be synthesized taking advantage of the stereospecificity of the thioacetic acid addition, the 2-substituted *trans*-decalin system was chosen because the symmetry of the olefinic starting material (Δ^2-*trans*-octalin) was such that attack onto either face of the double bond would lead to the same product.

Can. J. Chem. Downloaded from www.nrcresearchpress.com by 210.87.254.6 on 09/05/12
For personal use only.

Can. J. Chem. Downloaded from www.nrcresearchpress.com by 210.87.254.6 on 09/05/12
For personal use only.

Results and Discussion

Synthesis of the Axial and Equatorial trans-2-Decalinsulfonyl Chlorides (6 and 8)

The synthesis of the axial and equatorial sulfonyl chlorides (**6** and **8**) is summarized in Scheme 1. *trans*-Δ^2-Octalin, prepared by the recipe of Johnson *et al.* (6), when treated with thioacetic acid, gave a high yield of the axial thiolacetate **1**. The usual analytical and spectroscopic data were in full agreement with the assigned structure. Of particular significance was a band at 3.98 p.p.m. in the n.m.r. spectrum appropriate to the methine bearing the acetylthio function; the relatively narrow half-width (8 Hz) of this band clearly shows the proton to be equatorial (7, 8).

Attempts to generate **6** by direct chlorination of the thiolester **1** or the corresponding mercaptan **2** gave products which from their i.r. spectra evidently contained a sulfonyl chloride but from which we were unable to obtain **6** in anything like pure form. We thereupon took advantage of the useful procedure of Truce and Roberts (9) for converting a mercaptan to the corresponding sulfinic acid. This involved formation of the acrylonitrile adduct **3**, oxidation to the sulfone **4**, and finally elimination to form the sodium sulfinate **5**; **5** on chlorination gave the axial sulfonyl chloride **6** as a fairly pure oil which after short-path distillation was obtained as a low-melting solid recrystallizable from cold pentane. Any possibility of epimerization in the process was precluded by the observation of the characteristic narrow signal for the equatorial methine proton in the n.m.r. spectrum of **6**; the analogous narrow signal also appeared in the spectrum of **3** but was obscured, presumably by the signal for the methylene group on the other side of the sulfonyl function, in the sulfone **4**.

It was anticipated that the axial sulfonyl chloride **6** would generate the sulfene **7** on treatment with base, and that trapping of the sulfene **7** would lead to a mixture of the axial and equatorial sulfonic acids (or derivatives) in which the equatorial epimer would predominate. Accordingly, **6** was treated with triethylamine in *t*-butyl alcohol presumably giving initially a mixture of the *t*-butyl sulfonate esters, which, after the addition of water and standing for an interval, gave the mixture of triethylammonium sulfonates. The salt mixture was converted to the mixture of sulfonyl chlorides (**8** and **6**), from which the equatorial isomer **8** was obtained in the form of crystals melting at 28–29°. The mode of synthesis, elemental analysis, and n.m.r. and i.r. spectra unambiguously show that this material has the equatorial sulfonyl chloride structure **8**. The axial methine hydrogen in **8** appears as a broad hump (half-width 25 Hz) around 3.5 p.p.m., in contrast to the much sharper peak at 3.9 p.p.m. found in the spectrum of **6**. The i.r. spectrum of **8**, though in general rather similar to that of **6**, shows a characteristic strong sharp band at 600 cm^{-1}; **6** on the other hand has a similar band at 645 cm^{-1}. These bands proved useful in determining the relative quantities of **6** and **8** in mixtures of these materials; the relative intensities of the 645 and 600 cm^{-1} peaks were simply compared with those found with mixtures of known composition prepared from pure samples of **6** and **8**. In this way it was possible to show that the mixture of **6** and **8** obtained from **6** via the reaction of triethylamine and *t*-butyl alcohol followed by treatment with water (as in Scheme 1) consisted of about 90% of **8** and 10% of **6**. *t*-Butyl alcohol was used as the sulfene trap in this reaction because it was hoped that its greater bulk might lead to the formation of a smaller proportion of the axial product than would be formed using a smaller sulfene trap, *e.g.* water. In agreement with this simple notion, it was found that reaction product when water was used as the trap was apparently somewhat smaller (80:20); one cannot be certain, however, that the apparent difference, even if real, derives from the relative rates of formation of the equatorial and axial products from the sulfene and does not have some other source, *e.g.* differences arising in the formation of the sulfonyl chlorides from the salt mixture.

Kinetic and Product Analysis Studies on the Axial and Equatorial Sulfonyl Chlorides (6 and 8)

As has been mentioned already, the present study is part of our investigation of the mechanism of formation of sulfenes via dehydrohalogenation of alkanesulfonyl chlorides, as in eq. 1. In the other part of this work (which is at least partly accessible elsewhere (3, 10)) it was found that alkanesulfonyl chlorides react smoothly with tertiary amines in 1,2-dimethoxyethane, and that the extent of reaction is easily determined by potentiometric titration of the chloride ion produced. A temperature of −25° was convenient, or even necessary, for some of the reactions studied, *e.g.* phenylmethanesulfonyl chloride and triethylamine; other reactions, *e.g.* **6** and **8** with triethyl-

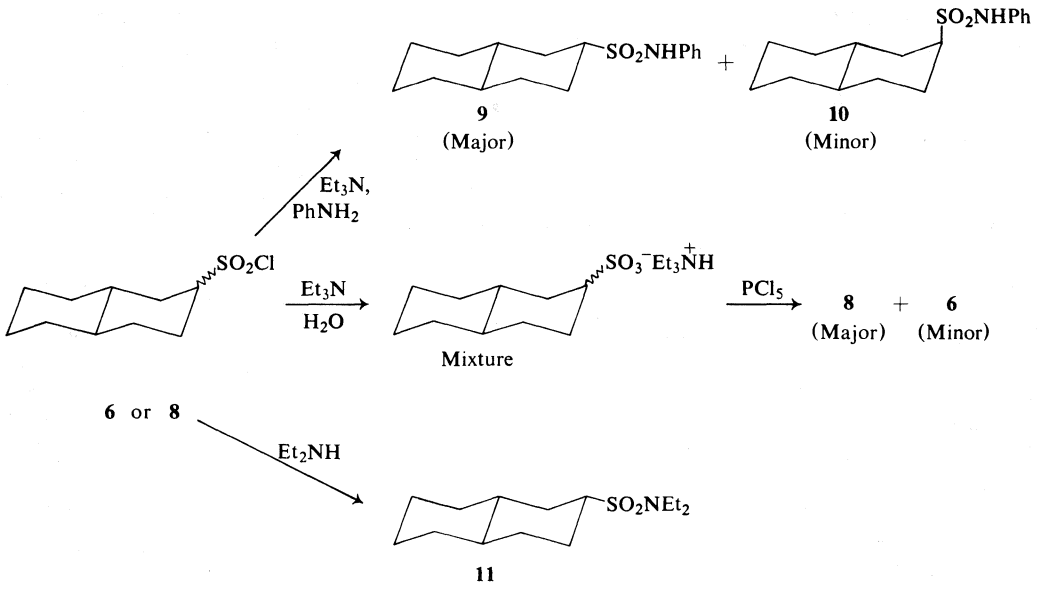

SCHEME 2

amine, were measured at that temperature for comparison, even though their rates are also readily measurable at room temperature. With a 20-fold excess of triethylamine and a 100-fold excess of aniline as the sulfene trap, the reaction showed satisfactory pseudo first order kinetics to >80% reaction. Under these conditions the axial sulfonyl chloride **6** reacts 71 times faster than its equatorial epimer **8**.

Though a substantial body of evidence now available indicates that the action of triethylamine on alkanesulfonyl chlorides bearing at least one α-hydrogen yields the sulfene, it was felt that it was of some importance to have specific evidence that the sulfene **7** was in fact being generated from the sulfonyl chlorides **6** and **8**. Since there is only one α-hydrogen in **6** and **8**, we thought that a deuterium-labelling experiment would be much less conclusive than it has been with other substrates (11, 12), and we therefore turned to another experiment to demonstrate the intermediacy of the sulfene **7**.

A classic test to determine if an intermediate is common to two reactions is to see if the two reactions give product mixtures of identical composition when the reaction conditions are identical. Accordingly both **6** and **8** were treated with triethylamine and aniline in dimethoxyethane using the same relative amounts of the reagents as in the kinetic runs but with the mixture 30 times more concentrated. The product from **6**, obtained in about 80% yield, was evidently a mixture of the equatorial and axial sulfonanilides (**9** and **10**, respectively, as in Scheme 2). Unfortunately we were able to obtain only the axial isomer **10** in crystalline form, though the sample of the presumed equatorial epimer **9** that was isolated from t.l.c. showed the spectroscopic features expected for that structure (see Experimental). In the mixture from the axial sulfonyl chloride **6**, the anilides **9** (presumed) and **10** were estimated to be present in the ratio 60 to 40; similar treatment of the equatorial sulfonyl chloride **8** gave a 75% yield of a mixture estimated to be 65% **9** and 35% **10**.

The use of water rather than aniline as the sulfene trap gave a mixture of the triethylammonium sulfonates which was converted to the mixture of the sulfonyl chlorides (**6** and **8**) so that its composition could be estimated by i.r. spectroscopy as described earlier. The sulfonyl chloride mixture obtained from **6** (in 83% yield) was estimated to consist of 20% of **6** and 80% of **8**, whereas that from **8** (88% yield) was evidently about 30% **6** and 70% **8**. When **6** or **8** was treated with diethylamine the product (obtained in 86 and 81% yields, respectively) was apparently more or less entirely the equatorial *N*,*N*-diethylamide **11**.

The similarity of the product mixtures obtained from either the axial sulfonyl chloride **6** or its equatorial epimer **8** in the reactions summarized

Can. J. Chem. Downloaded from www.nrcresearchpress.com by 210.87.254.6 on 09/05/12
For personal use only.

Can. J. Chem. Downloaded from www.nrcresearchpress.com by 210.87.254.6 on 09/05/12
For personal use only.

in Scheme 2 is regarded as good evidence for the existence of a common intermediate, *viz.* the sulfene **7**. One likely source of the slight discrepancies (*e.g.* 80:20 *vs.* 70:30 in the reaction with water) is experimental uncertainty; in this example the difference might well derive, for example, from a somewhat less efficient conversion of the axial sulfonate to the sulfonyl chloride with the material from the reaction of **6** with triethylamine and water. It is also possible, however, that the differences noted are real, though small. Such a circumstance is perfectly consistent with the sulfene mechanism if the sulfene is attacked by the trap before the initially-formed sulfene – triethylammonium chloride aggregate has either dispersed or equilibrated. Under such circumstances the sulfene trap might be attacking in the one case a sulfene with the triethylammonium ion still more or less in the axial position, and in the other a sulfene with the cation on the other side of the plane of the sulfene grouping; in that event a measurable difference in the stereochemistry of the products would not be surprising. The possibility of very rapid attack on sulfenes before the medium has fully equilibrated has been mentioned previously to account for small deviations from strict stoichiometry in the deuteration experiments (11).

Another feature of the deuteration study just referred to was that the action of tertiary amines led to the incorporation of one deuterium atom when the reaction was carried out in the presence of a deuterated sulfene trap, *i.e.* that the base invariably led to sulfene formation (11). When the sulfonyl chloride was treated with D_2O or methanol-*d* in the *absence* of base, however, no deuterium was taken up, and it was inferred that another mechanism of hydrolysis was operating under these conditions, presumably direct displacement of the chloride by water or the alcohol. It was therefore expected that if the analogous situation were to obtain in the hydrolysis of **6** and **8**, an entirely different axial:equatorial rate ratio would be observed in the absence of base. The reactions of **6** and **8** with water without added base were found to be extremely slow and to follow first order kinetics only to about 40 to 50% of completion. Even so, however, it was possible to obtain at least a rough idea of the relative rates of reaction of **6** and **8**; for the hydrolysis at 50° the value so obtained was $k_{Ax}/k_{Eq} \approx 0.07$, *i.e.* about 1/1000 of the ratio found with the triethylamine induced reaction at −25°.

The Mechanism of the Dehydrohalogenation of Alkanesulfonyl Chlorides

For the reasons presented in detail in the accompanying paper, we would expect that a concerted bimolecular elimination (E2 reaction) of hydrogen chloride would be distinctly faster with the axial sulfonyl chloride **6** than with its equatorial epimer **8**. This has of course been found, the ratio in fact being substantially larger than those discussed in the other paper (1). These results are therefore consistent with the E2 mechanism of sulfene formation, in the reaction of triethylamine with the axial sulfonyl chloride **6**, at the very least. The large axial:equatorial rate ratio for the sulfonyl chlorides probably derives primarily from the relatively large conformational free energy of the chlorosulfonyl group, taken with an evidently "product-like" transition state for the reaction (3).

Another possible mechanism which was mentioned in the introduction involves slow substitution of the chloride by direct attack of the tertiary amine, followed by rapid bimolecular elimination from the intermediate sulfonylammonium ion to form the sulfene. In such a reaction the bulky chlorosulfonyl group, in which the sulfur is tetrahedrally substituted, would become in the transition state an even bulkier group in which five substituents would be placed roughly at the apices of a trigonal bipyramid. From the following evidence it can be concluded that such a mechanism would lead to $k_{Ax}/k_{Eq} < 1$.

It would appear to be a general phenomenon that those reactions exocyclic to a cyclohexane ring, which involve expansion of the function on going from starting material to transition state, proceed more readily with the equatorial compound than with its axial epimer. The hydrolysis of esters of cyclohexanecarboxylic acids and the formation and saponification of esters of cyclohexanols are examples which have been extensively studied (see ref. 13). Of the few other examples which have been reported, one seems exceptional. The reaction of an axial amino group with 2,4-dinitrochlorobenzene apparently goes about 50% faster than that of its equatorial epimer, an observation that has been suggested to owe its origin to relatively strong hydrogen bonding in the equatorial amino function (14).

This apparent exception, as well as other considerations, suggested that our general study of axial:equatorial rate ratios and their application to the study of reaction mechanisms should

Can. J. Chem. Downloaded from www.nrcresearchpress.com by 210.87.254.6 on 09/05/12
For personal use only.

include an investigation of reactions exocyclic to the cyclohexane ring. As has been mentioned in the accompanying paper (1), we have in fact already looked at some examples involving change in the coordination number of an exocyclic atom; the details will be described in a subsequent account. The particular observations relevant to the present discussion concern the relative rates of S_N2 reactions of cyclohexanemethyl bromides and *p*-nitrobenzenesulfonates. In the one case k_{Ax}/k_{Eq} was estimated (1) as <0.3 and in the other k_{Ax}/k_{Eq} for the reaction of the *p*-nitrobenzenesulfonates with lithium bromide in acetone at 45° was found to be about 0.05 (15). Both sets of results strongly suggest that a direct displacement reaction at the sulfonyl sulfur of **6** and **8** would lead to $k_{Ax}/k_{Eq} \ll 1$.

The closest analogue of the hypothetical slow S_N2 reaction followed by rapid elimination mechanism, however, was obtained directly from the sulfonyl chlorides **6** and **8** themselves. Hydrolysis of **6** and **8** in the absence of base, which, as has been mentioned above, is believed to proceed by direct displacement on the sulfur, showed just the sort of axial:equatorial rate ratio expected: $k_{Ax}/k_{Eq} \approx 0.07$.

The above examples lead to a conclusion which we suggest is inescapable, namely that if the sulfene formation from the axial sulfonyl chloride **6** were proceeding by a rate-determining attack on the sulfur atom followed by a rapid elimination to form the sulfene, then it would have to take place more slowly than the same reaction with the equatorial compound **8**. Since the opposite is, in fact, observed experimentally we must conclude that the reaction of **6** does not proceed via "S_N2 plus E" mechanism.

These data taken by themselves do not *require* the E2 mechanism for the reaction of the equatorial isomer or of any other sulfonyl chloride. The following pieces of evidence of a totally different kind, however, are also in agreement with the E2 mechanism: (*a*) the formation of mono-exchanged products with diethylamine (11) and *n*-butylamine (16), (*b*) the distinctly negative ρ value obtained from a Hammett plot for the reaction of substituted phenylmethanesulfonyl chlorides with pyridine (3, 10), and (*c*) a linear Brønsted-type relationship in the reaction of a number of sterically different tertiary amines with methanesulfonyl chloride (16). These observations when taken with the axial:equatorial rate ratios combine to suggest very strongly that the E2 mechanism is the general mode of formation of sulfenes by the action of amines on alkanesulfonyl halides.

As a final note we wish to point out that in addition to illuminating the specific problem of the mechanism of sulfene formation, the present study serves as an illustration of the potential usefulness of the method of axial:equatorial rate ratios in the study of reaction mechanisms.

Experimental

The general experimental procedures were as described in the accompanying paper (1), with the following additions. 1,2-Dimethoxyethane (DME) (Eastman, "white label") was refluxed over lithium aluminum hydride and distilled before use, triethylamine (Eastman, "white label") was distilled from calcium hydride before use. Pentane and acrylonitrile (Eastman, "yellow label") were distilled before use. Aniline (McArthur Chemical Co. Ltd.) was distilled from zinc dust.

1,2α,3,4,4aα,5,6,7,8,8aβ-Decahydro-2-naphthyl Thiolacetate (1)

Thioacetic acid (7 g, 0.092 mol) was added to *trans*-Δ^2-octalin (10 g, 0.077 mol prepared by the method of Johnson and co-workers (6)) and the reaction mixture was stirred vigorously for 15 min. The reaction was complete after another 30 min at 50°. The excess of thioacetic acid was removed by distillation under reduced pressure. The oily residue was distilled *in vacuo* to give the thiolacetate **1** (15 g, 96%), b.p. 94° (0.8 mm), $n_D^{25.6}$ 1.5152. The n.m.r. spectrum (CCl_4) showed a broad and partially resolved band at 0.8–2.0, a singlet at 2.24, and a narrow band at 3.98 p.p.m. (half-width 8 Hz). The i.r. spectrum ($CHCl_3$) showed very strong absorption at 1670 cm^{-1}; other major bands below 1600 cm^{-1} were: 1446 (s), 1351 (m), 1120 (s), 955 (m), 874 (w), 835 (w), 641 cm^{-1} (m).

Anal. Calcd. for $C_{12}H_{20}SO$: C, 67.88; H, 9.49; S, 15.10. Found: C, 67.87; H. 9.50; S, 15.09.

1,2α,3,4,4aα,5,6,7,8,8aβ-Decahydro-2-naphthalenethiol (2)

The axial thiolacetate **1** (10 g), ethyl alcohol (50 ml), and 20% aqueous potassium hydroxide (50 ml) were mixed and allowed to reflux for 1 h. The reaction mixture was then acidified with acetic acid and the oily thiol extracted three times with ether. The ethereal phase was washed twice with water, dried, and evaporated. The residue obtained was distilled *in vacuo* to yield the axial mercaptan **2** (7.2 g, 90%), b.p. 54–55° (0.5 mm), n_D^{26} 1.5144. The n.m.r. spectrum (CCl_4) showed a partially resolved broad band at 0.8–2.0 and a narrow band at 3.5 p.p.m. (half-width, 11 Hz). The i.r. spectrum (CH_2Cl_2) showed major peaks below 1600 cm^{-1} at 1450 (s), 1355 (m), 1245 (m), 1144 (m), 1058 (w), 974 (m), 940 cm^{-1} (m).

The axial mercaptan **2** was characterized as the phenylurethane which was obtained by mixing a sample of **1** (0.5 g) with phenylisocyanate (0.35 g) and allowing the reaction to stand overnight. The product was obtained as white needles, m.p. 170–171°.

Anal. Calcd. for $C_{17}H_{23}NSO$: C, 70.54; H, 8.01; N, 4.84; S, 11.08. Found: C, 70.54; H, 8.08; N, 4.86; S, 11.10.

Can. J. Chem. Downloaded from www.nrcresearchpress.com by 210.87.254.6 on 09/05/12
For personal use only.

3-(1,2α,3,4,4aα,5,6,7,8,8aβ-Decahydro-2-naphthylthio)-propionitrile (3)

Acrylonitrile (10 g) was added dropwise with stirring and ice-bath cooling to axial mercaptan **2** (6.5 g, 0.38 mol) which had been mixed with a small quantity of sodium methoxide (0.05 g). The resulting reaction mixture was then stirred at room temperature for 1 h. Any precipitate formed at this point was filtered off and the filtrate distilled under reduced pressure to remove the excess acrylonitrile. Distillation of the resulting residue *in vacuo* yielded the product **3** (8.3 g, 97.5%), b.p. 120–121° (0.01 mm), n_D^{25} 1.5186. The n.m.r. spectrum (CCl_4) showed a broad band at 0.8–2.0, a multiplet centered at 2.62, and a narrow band at 3.24 p.p.m. (half-width, 8 Hz). The i.r. spectrum (CH_2Cl_2) showed an absorption band at 2260 cm^{-1} due to the cyano group and other major peaks below 1600 cm^{-1} at: 1450 (s), 1355 (m), 1245 (m), 1145 (w), 948 (w), 840 cm^{-1} (w).

Anal. Calcd. for $C_{13}H_{21}NS$: C, 69.80; H, 9.48; N, 6.27; S, 14.35. Found: C, 69.77; H, 9.48; N, 6.38; S, 14.31.

3-(1,2α,3,4,4aα,5,6,7,8,8aβ-Decahydro-2-naphthylsulfonyl)propionitrile (4)

To a solution of the axial sulfide **3** (2 g) in acetic acid (2.5 ml), hydrogen peroxide (30%, 2.6 g) was added slowly. The reaction mixture was allowed to stand at room temperature for 1 week. When the reaction was completed, the viscous reaction mixture was poured into water and the product extracted three times with methylene chloride. The combined organic phase was then washed with dilute sodium bicarbonate solution, twice with water, and dried. Removal of methylene chloride yielded the product **4** which was recrystallized from pentane (2.02 g, 86%), m.p. 97–98°. The n.m.r. spectrum ($CDCl_3$) showed a broad band at 0.8–2.7 and a multiplet at 2.7–3.5 p.p.m. The i.r. spectrum (CH_2Cl_2) showed a peak due to the cyano group at 2250 (m) and strong absorption bands of the sulfonyl group at 1310 (vs) and 1130 (vs); other major i.r. peaks below 1600 cm^{-1} were 1145 (m), 845 (w), 660 cm^{-1} (w).

Anal. Calcd. for $C_{13}H_{21}NSO_2$: C, 61.15; H, 8.29; N, 5.48; S, 12.55. Found: C, 61.01; H, 8.14; N, 5.46; S, 12.59.

Sodium 1,2α,3,4,4aα,5,6,7,8,8aβ-Decahydro-2-naphthalenesulfinate (5)

A solution of sodium propanethiolate was prepared by dissolving metallic sodium (0.18 g, 7.5 mmol) in a mixture of 1-propanethiol (0.495 g, 7.5 mmol) and absolute alcohol (5 ml). This solution was then added slowly to a stirred solution of the axial sulfone **4** (2 g) dissolved in absolute alcohol (30 ml). The resulting reaction mixture was allowed to reflux for 5 h, after which the alcohol was evaporated under reduced pressure. The salt obtained was washed twice with dry ether and dried to give the sodium sulfinate (1.4 g, 70%). The i.r. spectrum (Nujol) of the salt showed major bands below 1600 cm^{-1} at 1001 (s), 960 (s), 750 cm^{-1} (w).

1,2α,3,4,4aα,5,6,7,8,8aβ-Decahydro-2-naphthalenesulfonyl Chloride (6)

The axial sulfinate salt **5** (1.3 g) was dissolved in water (40 ml) with a little acetic acid (0.05 ml) added. Methylene chloride (40 ml) was also added to the solution to form a lower layer. This two-phase solution was then cooled in an ice-bath before passing in the chlorine gas. The chlorination was evidently complete when the aqueous phase became clear and the organic phase turned greenish yellow. The two layers were then separated and the aqueous phase extracted twice with methylene chloride. The combined methylene chloride phase was washed successively with dilute sodium bisulfite solution, sodium bicarbonate solution, and twice with water. Drying and evaporating of the organic phase yielded the axial sulfonyl chloride **6** (1.1 g, 80%). Purification of the compound was carried out by short-path distillation *in vacuo* followed by recrystallization from pentane, m.p. 31–32°. The n.m.r. spectrum (CCl_4) showed absorption at 0.8–2.8 (diffuse broad band) and 3.91 p.p.m. (narrow band of equatorial proton at C-2, half-width 10 Hz). The i.r. spectrum (KBr cell, CH_2Cl_2) showed major peaks below 1600 cm^{-1} at: 1450 (s), 1360 (vs), 1300 (w), 1230 (w), 1210 (m), 1165 (vs), 1142 (m), 1120 (m), 1055 (m), 1025 (w), 980 (w), 970 (w), 932 (m), 845 (m), 645 (s), 565 (s), 550 (m), 490 (m), 460 (m), 440 (w), 420 (m), 360 cm^{-1} (w).

Anal. Calc. for $C_{10}H_{17}SO_2Cl$: C, 50.73; H, 7.24; S, 13.54; Cl, 14.97. Found: C, 50.63; H, 7.22; S, 13.60; Cl, 15.03.

1,2β,3,4,4aα,5,6,7,8,8aβ-Decahydro-2-naphthalenesulfonyl Chloride (8)

To a mixture of the axial sulfonyl chloride (**6**) (10 g) and tert-butyl alcohol (30 g) in methylene chloride (25 ml), triethylamine (25 ml) was added with stirring. The resulting reaction mixture was then allowed to stand overnight at room temperature and then extracted three times with water. The aqueous phase was then evaporated under reduced pressure and dried to yield the sulfonate salt mixture (11 g). This was mixed with phosphorus pentachloride (20 g) and dry benzene (200 ml) and allowed to reflux for 1 h with constant stirring. After cooling, the reaction mixture was filtered and the filtrate washed with several portions of ice-water. Drying and evaporating the benzene phase yielded the crude product (4.1 g, 41%). This product contained a trace of impurity which was removed by t.l.c. (benzene:ether, 9:1). The product **8** was further purified by distillation *in vacuo* and recrystallization from pentane; m.p. 28–29°. The n.m.r. (CCl_4) showed absorption at 0.8–2.7 (diffuse broad band) and 3.5 p.p.m. (broad band of axial proton at C-2, half-width, 25 Hz). The i.r. (KBr cell, CH_2Cl_2) showed major peaks below 1600 cm^{-1} at 1450 (s), 1360 (vs), 1310 (w), 1240 (w), 1210 (m), 1165 (vs), 1145 (m), 1120 (w), 1055 (m), 1020 (w), 970 (m), 930 (m), 880 (w), 845 (w), 600 (s), 585 (w), 560 (m), 555 and 545 (s), 495 (m), 475 (m), 450 (sh), 440 (m), 360 cm^{-1} (w).

Anal. Calcd. for $C_{10}H_{17}SO_2Cl$: C, 50.73; H, 7.24; S, 13.54; Cl, 14.97. Found: C, 50.98; H, 7.16; S, 13.55; Cl, 15.09.

The Reaction of the Axial Sulfonyl Chloride (6) with Triethylamine and Aniline

Triethylamine (4 ml) was added quickly to a solution of the axial sulfonyl chloride **6** (0.3 g) and aniline (15 g) dissolved in 1,2-dimethoxyethane (10 ml). The reaction mixture was allowed to stand at room temperature for 2 h before it was acidified with dilute hydrochloric acid solution. Evaporation of the 1,2-dimethoxyethane under

Can. J. Chem. Downloaded from www.nrcresearchpress.com by 210.87.254.6 on 09/05/12
For personal use only.

reduced pressure was followed by extraction of the organic product with methylene chloride. The organic phase was dried and evaporated to give an oily material. Purification of the product as well as separation of the compound into two epimeric sulfonanilides were carried out by t.l.c. (benzene:ether, 9:1); of the total purification product (0.34 g, 78%), 40% was the axial sulfonanilide **10** and 60% evidently the equatorial sulfonanilide **9**.

The sulfonanilide **10** was further purified by recrystallization from methanol, m.p. 141°. The n.m.r. spectrum ($CDCl_3$) showed a complex broad band at 0.8–2.6, a narrow band due to the equatorial proton at 3.4 (half-width, 10 Hz) and multiplet of aromatic protons at 7.18–7.52 p.p.m. The major i.r. peaks below 1700 cm^{-1} were: 1600 (s), 1500 (s), 1450 (m), 1400 (m), 1340 (s), 1220 (s), 1150 (vs), 1032 (w), 912 cm^{-1} (s).

Anal. Calcd. for $C_{16}H_{23}NSO_2$: C, 65.50; H, 7.90; N, 4.77; S, 10.93. Found: C, 65.68; H, 8.05; N, 4.90; S, 11.09.

The equatorial sulfonanilide **9** was not obtained crystalline. It was purified by t.l.c. The n.m.r. spectrum ($CDCl_3$) showed complex broad band at 0.8–2.5, a relatively broad band appropriate to the axial proton at 3.15 (half-width, 16 Hz) and an aromatic absorption band at 7.18–7.52 p.p.m. The i.r. spectrum (CH_2Cl_2) also showed peaks at positions similar to that of the epimeric compound: 1600 (s), 1500 (s), 1450 (m), 1400 (m), 1340 (s), 1220 (m), 1150 (vs), 1035 (w) and 925 cm^{-1} (s).

*The Reaction of the Equatorial Sulfonyl Chloride **8** with Triethylamine and Aniline*

The above reaction was repeated with the equatorial sulfonyl chloride **8** as the substrate. The reaction mixture was allowed to remain at room temperature for 24 h before the isolation of products. The products were identified and compared by t.l.c. with the pure products obtained from the preceding experiment. The yield of the product was 75% and the ratio of axial sulfonanilide **10** to equatorial sulfonanilide **9** was estimated to be 35:65.

*The Reaction of the Axial Sulfonyl Chloride **6** with Diethylamine*

Diethylamine (1.5 ml) was added into a solution of **6** (0.3 g) in methylene chloride (10 ml). The reaction mixture was allowed to remain at room temperature for 1 h before it was washed with dilute hydrochloric acid and water and dried. Removal of solvent yielded the sulfonamide **11** as an oily material (0.34 g, 86%) which was recrystallized from pentane to give white plates, m.p. 62–63°. The n.m.r. spectrum (CCl_4) showed a broad band at 0.8–2.2 as well as a triplet at 1.2(J = 7.0 Hz) and a quartet at 3.28 p.p.m. (J = 7.0 Hz). The i.r. spectrum (CH_2Cl_2) showed major bands below 1600 cm^{-1} at 1450 (s), 1380 (m), 1350 (m), 1315 (vs), 1200 (s), 1130 (vs), 1053 (m), 1018 (s), 935 (s), 845 (w), 785 cm^{-1} (m).

Anal. Calcd. for $C_{14}H_{27}NSO_2$: C, 61.50; H, 9.95; N, 5.12; S, 11.73. Found: C, 61.64; H, 9.70; N, 5.11; S, 11.84.

*The Reaction of the Equatorial Sulfonyl Chloride **8** with Diethylamine*

The above reaction was repeated under the same conditions, with **8** (0.3 g) except that the reaction time was 2 h. The product obtained was again an oily material which was purified by recrystallization from pentane to give **11** as white plates (0.32 g, 81%), m.p. 62–63°; mixed m.p. with the sample of **11** from the preceding reaction 62–63°. The n.m.r. spectrum (CCl_4) and i.r. spectrum (CH_2Cl_2) were also identical with those of **11** obtained from the preceding reaction.

*The Triethylamine-catalyzed Reaction of the Axial Sulfonyl Chloride **6** with Water*

A mixture of triethylamine (4 ml) and water (3 ml) was added to a solution of **6** (0.3 g) dissolved in dioxane (10 ml). The reaction mixture was allowed to stand at room temperature for 30 min before it was evaporated to dryness under reduced pressure. The residue was dissolved in water, washed twice with ether, and the aqueous phase evaporated to dryness. The product obtained was then mixed with phosphorus pentachloride (1.5 g) and refluxed in dry benzene (20 ml) for 1 h. The reaction mixture was filtered and the filtrate washed several times with ice-cold water and dried. Evaporation of benzene yielded a mixture of the epimeric sulfonyl chlorides (**6** and **8**) (0.25 g, 83%) which was partially purified by t.l.c. (benzene:ether, 9:1); the two epimeric compounds could not be separated. The n.m.r. spectrum ($CDCl_3$) showed diffuse broad band at 0.8–2.75 and multiplet at 3.4–4.2 p.p.m. The i.r. spectrum (KBr cell, CH_2Cl_2) also showed the characteristic absorption bands of **6** and **8**, especially the 645 cm^{-1} peak of axial epimer **6** and the 600 cm^{-1} peak of equatorial epimer **8**. The ratio of **6** to **8** in the product mixture was estimated to be 2:8 by comparing the i.r. spectrum of the product mixture with those of known mixtures of the pure sulfonyl chlorides.

*The Triethylamine-catalyzed Reaction of the Equatorial Sulfonyl Chloride **8** with Water*

The above reaction was repeated with **8** (0.3 g) as the substrates; the reaction was allowed to run for 12 h. The product obtained was again a mixture of epimeric sulfonyl chlorides (0.265 g, 88%). The i.r. spectrum (KBr cell, CH_2Cl_2) of the purified mixture was found to be almost identical with that of a mixture of 30% of **6** and 70% of **8**.

*Measurement of the Rates of Reaction of the Axial and Equatorial Sulfonyl Chlorides (**6** and **8**) with Triethylamine and Aniline*

A stock solution of the sulfonyl chloride ($\sim 4.0 \times 10^{-3}$ M) in DME (250 ml) was prepared, and the concentration determined by allowing the solution to react with triethylamine for at least 10 half-lives and titrating the chloride ion as described below; the value so obtained was at least 98% of that expected from the weight used in making up the stock solution. A stock solution of the base was prepared by dissolving triethylamine (2.020 g) and aniline (9.313 g) in DME.

To determine the pseudo first order rate constant 25 ml portions of each stock solution were precooled and mixed (as described below), the reaction allowed to run at $-25.0 \pm 0.2°$ for an appropriate time interval whereupon the reaction was quenched by the addition of the calculated amount of dilute nitric acid solution. The resulting solution was then transferred to a 150 ml beaker and the free chloride ion titrated potentiometrically with 0.005 N $AgNO_3$ using a Radiometer PHM 25 pH meter; during the titration the beaker was cooled in ice water. The pseudo first order rate constant was obtained from

the slope (as determined by the method of least squares) of a plot of the logarithm of the concentration of unreacted substrate *vs.* time; good straight line plots of six or more points (from zero reaction to >80% reaction) were obtained by this procedure.

The precooling and mixing of the solutions was carried out as follows. The sulfonyl chloride stock solution (25 ml) was placed in a 100 ml round-bottomed flask equipped with two necks, one about 15 cm long ending in a Quickfit B24 female joint, the other about 5 cm long with a B14/23 neck. The latter was fitted with a simple adaptor consisting of a tube 12 cm long bent into an acute angle (*ca.* 60°) and bearing a male B14/23 joint at each end. The stock solution of the bases (25 ml) was pipetted into a 25 ml Erlenmeyer flask with a B14/23 neck which was then attached to the free end of the adaptor so that the contents of the Erlenmeyer flask at this stage stayed separate from the solution in the round-bottomed flask. The long neck of the larger flask was stoppered and the whole assembly almost completely immersed in the cooling liquid (ethyl alcohol) in the compartment of a Kryothermat KT-62 apparatus (Polyscience Corporation, Evanston, Ill.). After ½ h, when both solutions had reached −25°, the two solutions were mixed as quickly as possible by rotating the adaptor in the neck of the round-bottomed flask so that the base solution poured from the Erlenmeyer into the round-bottomed flask; the timing was begun from this instant.

Using the above procedure and with $[Et_3N] = 40 \times 10^{-3}$ *M*, $[PhNH_2] = 0.20$ *M*, and [**6**] $= 1.97 \times 10^{-3}$ *M*, the pseudo first order rate constant for the axial sulfonyl chloride (**6**) was found to be 1.27×10^{-4} s^{-1}. For the equatorial sulfonyl chloride **7** with [**7**] $= 2.00 \times 10^{-3}$ *M* the pseudo first order rate constant so obtained was 1.78×10^{-6} s^{-1}.

*Measurement of the Rates of Solvolysis of the Axial and Equatorial Sulfonyl Chlorides (**6** and **8**) in Aqueous Dimethoxyethane at 50.0°*

A solution (100 ml) of the sulfonyl chloride (0.010 *M*) in DME:H_2O 5:1 by volume was allowed to stand at 50.0 ± 0.1°. Aliquots were removed at intervals and the chloride ion content determined potentiometrically as above. The rate constant was obtained from the slope of a plot of log [unreacted sulfonyl chloride] *vs.* time. The plot was linear only to about 50% reaction after which the slope diminished appreciably, especially with **8** which reacts only very slowly (<35% reaction after 4 days at 50°). The first order rate constants so obtained were, for the axial sulfonyl chloride **6**, 1.1×10^{-6} s^{-1}, and for the equatorial sulfonyl chloride **8**, 1.6×10^{-5} s^{-1}.

This work was supported by grants from the National Research Council of Canada, the Petroleum Research Fund administered by the American Chemical Society, and the Alfred P. Sloan Foundation.

1. J. F. King and M. J. Coppen. Can. J. Chem. This issue.
2. J. F. King, A. Hawson, B. L. Huston, L. J. Danks, and J. Komery. Can. J. Chem. **49**, 943 (1971).
3. J. F. King and T. W. S. Lee. J. Am. Chem. Soc. **91**, 6524 (1969).
4. O. Rogne. J. Chem. Soc. B, 727 (1970).
5. F. G. Bordwell, P. S. Landis, and G. S. Whitney. J. Org. Chem. **30**, 3764 (1965).
6. W. S. Johnson, V. J. Bauer, J. L. Margrave, M. A. Frisch, L. H. Dreger, and W. N. Hubbard. J. Am. Chem. Soc. **83**, 606 (1961).
7. R. U. Lemieux, R. K. Kullnig, H. J. Bernstein, and W. G. Schneider. J. Am. Chem. Soc. **80**, 6098 (1958).
8. A. Hassner and C. Heathcock. J. Org. Chem. **29**, 1350 (1964).
9. W. E. Truce and F. E. Roberts Jr. J. Org. Chem. **28**, 593 (1963).
10. T. W. S. Lee. Ph.D. Thesis. University of Western Ontario, London, Ontario, 1969.
11. J. F. King and T. Durst. J. Am. Chem. Soc. **87**, 5684 (1965).
12. W. E. Truce and R. W. Campbell. J. Am. Chem. Soc. **88**, 3599 (1966).
13. E. L. Eliel, N. A. Allinger, S. J. Angyal, and G. A. Morrison. Conformational analysis, Interscience, New York, N.Y. 1966. pp. 72–81.
14. E. L. Eliel, E. W. Della, and T. H. Williams. Tetrahedron Lett. 831 (1963).
15. M. J. Coppen. Ph.D. Thesis. University of Western Ontario, London, Ontario, 1971.
16. E. A. Luinstra. Ph.D. Thesis. University of Western Ontario, London, Ontario, 1971.

Can. J. Chem. Downloaded from www.nrcresearchpress.com by 210.87.254.6 on 09/05/12
For personal use only.

Radiation Chemistry of Dithionates

G. S. MURTHY,[1] R. L. EAGER,[2] AND K. J. MCCALLUM

Department of Chemistry and Chemical Engineering, University of Saskatchewan, Saskatoon, Saskatchewan

Received November 25, 1970[3]

The salts $Na_2S_2O_6$, $Na_2S_2O_6.2H_2O$, $K_2S_2O_6$, BaS_2O_6, and $BaS_2O_6.2H_2O$ were irradiated at room temperature with ^{60}Co gamma rays. When the irradiated salts were dissolved in water sulfite ions, sulfate ions, and acid were found as irradiation products. The dependence of yield upon absorbed dose was studied. The *G*-values found ranged from unity to 20. Thermal annealing of the irradiated salts had only a slight effect on product yields. For BaS_2O_6 there is a large increase in product yields after a dose of 28.3×10^{22} eV per mol has been absorbed. A mechanism involving SO_3^- and $S_2O_6^-$ radical ions is proposed.

Les sels $Na_2S_2O_6$, $Na_2S_2O_6.2H_2O$, $K_2S_2O_6$, BaS_2O_6, et $BaS_2O_6.2H_2O$ furent irradiés, à la température de la pièce, avec des rayons gamma du ^{60}Co. Lorsque les sels irradiés furent dissous dans l'eau des ions sulfite, des ions sulfate et acide furent trouvés comme produits d'irradiation. La dépendance du rendement à la dose absorbée fut étudiée. Les valeurs de *G* trouvées se situaient entre 1 et 20. Le recuit thermique des sels irradiés eut seulement un petit effet sur les rendements des produits. Pour BaS_2O_6 il y a une grande augmentation des rendements des produits après l'absorption d'une dose de 28.3×10^{22} eV par mol. Un mécanisme impliquant les ions radicalaires SO_3^- et $S_2O_6^-$ est proposé.

Canadian Journal of Chemistry, 49, 3733 (1971)

Introduction

As part of a study of the radiation chemistry of inorganic sulfur compounds results are reported here on the effects of ^{60}Co gamma rays on alkali dithionates. Chantry *et al.* (1) found a single absorption line with a *g* value of 2.004 in the e.s.r. spectra of gamma irradiated single crystals of sodium dithionate. They postulated that this line was due to the SO_3^- radical ion. The presence of this species in BaS_2O_6 which had been thermally decomposed was postulated by Gilevich and Potopovich (2). To explain their results they postulated that the dithionate ion thermally decomposed to yield the radical ion SO_3^-. This species could in turn react with dithionate ions to form species such as $S_2O_5^-$, SO_4^{2-}, SO_3, and SO_2. The resulting solid upon solution in water would, therefore, yield sulfate, sulfite, and acid, which they found as products. Gilevich and Potopovich found that their thermally decomposed barium dithionate sample gave an e.s.r. spectrum consisting of a sharp peak with a *g* value of 2.011 ± 0.001 and a shoulder with a *g* value of 2.003 ± 0.001. They attributed these paramagnetic signals to the presence of SO_2^- and SO_3^- radical ions respectively.

[1]Present address: Radiation Laboratory, National Chemical Laboratory, Poona-8, India.

[2]To whom all correspondence should be addressed.

[3]Revision received July 22, 1971.

Experimental

Reagents

The hydrated dithionates were prepared from sulfur dioxide and manganese dioxide using the methods of Larson *et al.* (3) or of Brauer (4). The anhydrous salts were obtained by heating the appropriate hydrates at 105–110 °C in a hot air oven for a period of 15–20 h. The purity of the dithionates was checked by chemical tests and by comparing their infrared spectra with those reported in the literature (5, 6). The amount of water of crystallization in the hydrates was found to agree with the theoretical values. Distilled water, again distilled from alkaline permanganate and then from an alkaline acid dichromate solution, was used for dissolving the irradiated samples.

Irradiations and Dosimetry

The irradiation source was a Gamma Cell 220 ^{60}Co Irradiation Unit manufactured by Atomic Energy of Canada Limited. For the $K_2S_2O_6$ irradiations the dose rates were of the order of 1000 rad/min. For the other irradiations the dose rates were of the order of 5000 rad/min. Originally all of the samples were irradiated in screw cap bottles. For BaS_2O_6, and to a lesser extent $Na_2S_2O_6$, the odor of sulfur dioxide could be detected when the bottles were opened. Samples of $Na_2S_2O_6$ and of BaS_2O_6 were then irradiated in sealed Pyrex glass tubes. The results for $Na_2S_2O_6$ were identical for both sealed tubes and screw cap bottles. With BaS_2O_6 the sulfate yields were the same for both types of containers but the acid and sulfite yields were lower for the samples irradiated in screw cap bottles. These results indicated that for BaS_2O_6 sufficient sulfur dioxide escaped to cause a significant decrease in the sulfite and acid yields. All of the BaS_2O_6 results reported here are for irradiations in sealed tubes whereas for $Na_2S_2O_6$ most of the results were obtained using screw cap bottles. For the other salts

Can. J. Chem. Downloaded from www.nrcresearchpress.com by 210.87.254.105 on 09/05/12
For personal use only.

Can. J. Chem. Downloaded from www.nrcresearchpress.com by 210.87.254.105 on 09/05/12
For personal use only.

no odor of sulfur dioxide was detected and screw cap bottles were used for all of the irradiations. The samples were irradiated in the presence of air at a temperature of 25 ± 5 °C. The absorbed dose was measured using ferrous sulfate dosimetry assuming a *G*-value of 15.5 for the production of ferric ion. Allowance was made for the difference in the electron densities of the sample and the dosimeter.

Analytical Procedures

The irradiated salt was dissolved in deaerated triple distilled water and analyzed for sulfite, sulfate, and acid. No odor of hydrogen sulfide could be detected.

Acid was determined by a micro-titration with a standard sodium hydroxide solution using phenolphthalein as an indicator. A blank was done on a solution of the unirradiated dithionate.

Sulfate was determined by using a nephelometric method (7) in which a barium sulfate precipitate is formed. By prior treatment of the sample with hydrogen peroxide, which oxidized sulfite to sulfate, both sulfate and sulfite could be determined and the sulfite found by difference. Standard samples containing known amounts of sulfate, sulfite, and dithionate were used to prepare calibration curves.

Thermal Annealing Studies

The effect of product yields by thermally annealing the irradiated salts prior to their solution in water was studied by placing the irradiated salts in Pyrex tubes which were immersed for varying periods of time in a constant temperature bath.

Results

The anhydrous salts, $Na_2S_2O_6$, $K_2S_2O_6$, and BaS_2O_6 all showed a light brown coloration in the earlier stages of irradiation. With increasing absorbed dose the color of $Na_2S_2O_6$ did not change whereas for $K_2S_2O_6$ and BaS_2O_6 the color gradually changed to dark brown. Upon exposure to the atmosphere the light brown color of irradiated $Na_2S_2O_6$ was bleached to a white color. This latter behavior was not observed with the other irradiated salts. It was established that the bleaching effect for the $Na_2S_2O_6$ samples was due to reaction with water vapor. A sample of irradiated $Na_2S_2O_6$ was divided into two portions, one portion was placed in a desiccator containing anhydrous calcium chloride, the other portion in a desiccator containing some liquid water. The sample over the calcium chloride remained unchanged during a period of five days whereas the sample over the water started to bleach to a white color within a period of a few minutes and within 2 h no trace of the brown color was observable.

Annealing studies were made with samples of $Na_2S_2O_6.2H_2O$ and $BaS_2O_6.2H_2O$ which had received absorbed doses of 22.5×10^{22} and 23.8×10^{22} eV mol^{-1}, respectively. After annealing for 2 h at 55 °C the yellow color of both salts was unchanged. At the end of 4 h of annealing at 55 °C the color of both salts had changed to a light purple. For longer annealing periods or at higher temperatures, 85 °C for $Na_2S_2O_6.2H_2O$ and 80 °C for $BaS_2O_6.2H_2O$, the intensity of the purple color increased. The yields of products were only slightly affected by annealing. As an example, a 6 h annealing period at 85 °C reduced the sulfate, sulfite, and acid yields from the $Na_2S_2O_6.2H_2O$ sample by 2.5, 5.9, and 1.7%, respectively. For $BaS_2O_6.2H_2O$ at 80 °C the corresponding values were 1.6, 0.96, and 0.68%, respectively. Annealing experiments were not made using $Na_2S_2O_6$ and BaS_2O_6 because for these salts the evolution of SO_2 became appreciable even at 50 °C.

With BaS_2O_6 the odor of SO_2 was detected in the early stages of irradiation whereas for $Na_2S_2O_6$ the odor of SO_2 was not detected until much larger doses had been absorbed. Neither

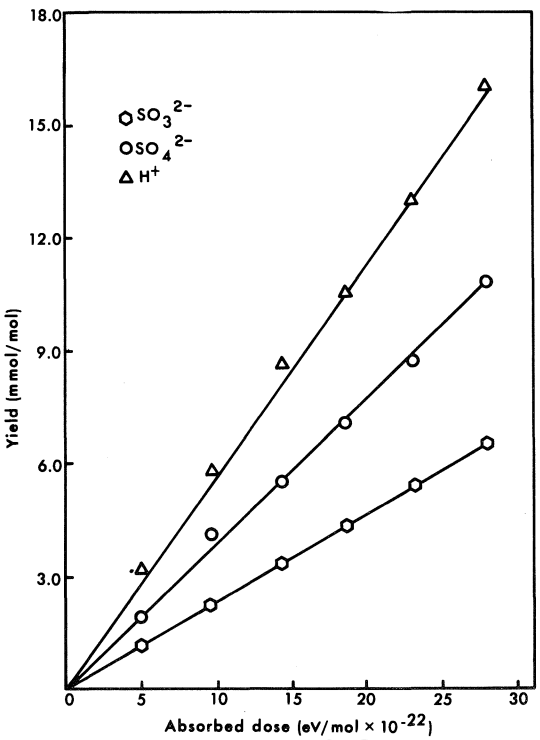

FIG. 1. Yields of SO_3^{2-}, SO_4^{2-}, and acid as a function of dose for $Na_2S_2O_6$.

TABLE 1. *G*-values of products

Compound	Dose (eV per mol × 10^{-22})	Acid	SO_3^{2-}	SO_4^{2-}
$Na_2S_2O_6$	27.6	3.45	1.45	2.30
$Na_2S_2O_6.2H_2O$	33.2	7.29	4.40	3.93
$K_2S_2O_6$	12.4	7.58	1.33	3.89
BaS_2O_6*	28.3	10.6	4.06	2.60
BaS_2O_6	41.8	—	6.85	12.87
$BaS_2O_6.2H_2O$	50.5	16.6	8.31	12.00

*At the point just before the sudden increase in yield of SO_3^{2-} and SO_4^{2-}.

$Na_2S_2O_6.2H_2O$ nor $BaS_2O_6.2H_2O$ appeared to evolve SO_2 at any time during the irradiations.

Electron spin resonance spectra were obtained from irradiated samples of the various dithionates. The samples were microcrystalline and a detailed analysis of their spectra was not made. All of the spectra indicated a paramagnetic species with a *g* value of 2.004. Irradiated BaS_2O_6 samples yielded spectra with at least six absorption peaks whose relative heights varied with the microwave power, indicating the presence of more than one paramagnetic species. With prolonged irradiations the BaS_2O_6 spectra became simpler. It may be concluded from these observations that the SO_3^- radical ion was present in all of the irradiated samples. The presence of other radical species also appears likely.

The yields of sulfite and sulfate, in mmoles, and of acid in milliequivalents, produced per mole of salt are shown plotted against absorbed dose in eV per mol in Figs. 1, 2, 3, 4, and 5 for $Na_2S_2O_6$, $Na_2S_2O_6.2H_2O$, $K_2S_2O_6$, BaS_2O_6, and $BaS_2O_6.2H_2O$, respectively. In Table 1 are given some *G*-values for the products. These were calculated from the curves given in Figs. 1–5.

Discussion

The yields of products resulting from the γ-irradiation of solid dithionates followed by solution in water shows the following behavior;

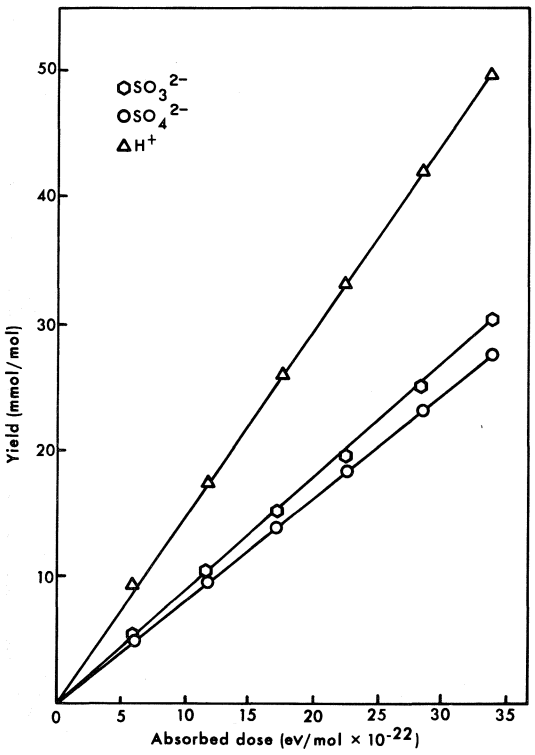

FIG. 2. Yields of SO_3^{2-}, SO_4^{2-}, and acid as a function of dose for $Na_2S_2O_6.2H_2O$.

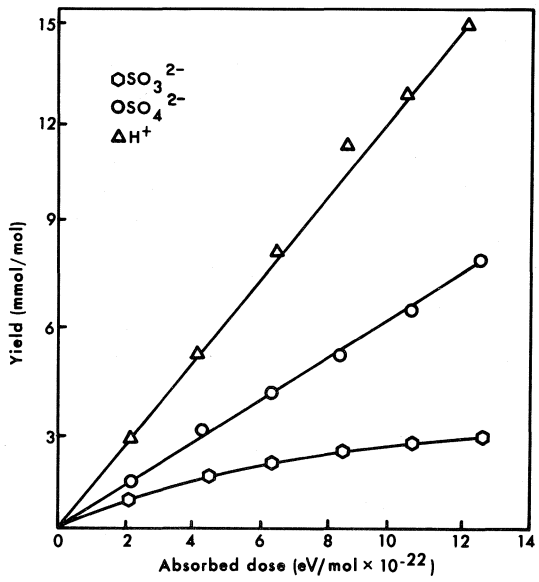

FIG. 3. Yields of SO_3^{2-}, SO_4^{2-}, and acid as a function of dose for $K_2S_2O_6$.

Can. J. Chem. Downloaded from www.nrcresearchpress.com by 210.87.254.105 on 09/05/12
For personal use only.

Can. J. Chem. Downloaded from www.nrcresearchpress.com by 210.87.254.105 on 09/05/12
For personal use only.

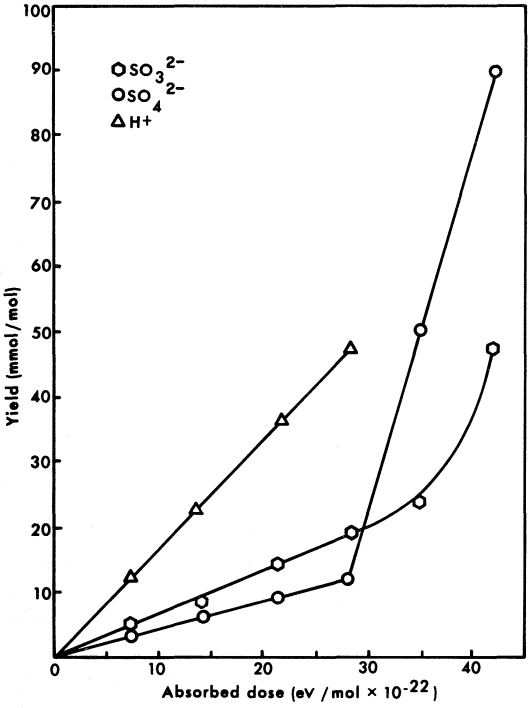

FIG. 4. Yields of SO_3^{2-}, SO_4^{2-}, and acid as a function of dose for BaS_2O_6.

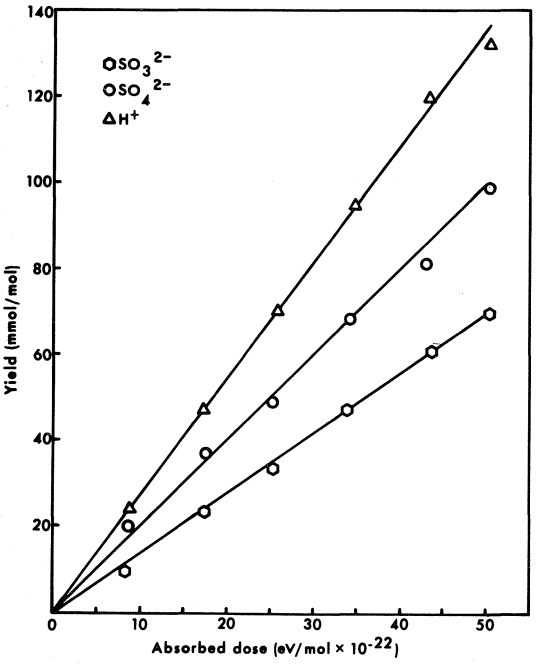

FIG. 5. Yields of SO_3^{2-}, SO_4^{2-}, and acid as a function of dose for $BaS_2O_6.2H_2O$.

the products are acid, sulfite, and sulfate; annealing of the solid salts prior to solution has little effect on the yields; for a given absorbed dose the yield of products is greater for the hydrates than for the corresponding anhydrous salts; for BaS_2O_6 there is a large increase in product yields, especially sulfate, after a dose of 28.3×10^{22} eV per mol has been absorbed.

The simplest overall reaction in which acid, sulfite, and sulfate are formed when irradiated dithionates are dissolved in water appears to be

[1] $S_2O_6^{2-} + H_2O \rightarrow 2H^+ + SO_3^{2-} + SO_4^{2-}$

Reaction 1 predicts that the ratio of sulfite to sulfate yields will be unity and that the ratio of the acid yield to the sum of the sulfite and sulfate yields will also be unity. In Table 2 the experimentally observed values of these ratios are shown, also given are the sum of the *G*-values for sulfite and sulfate. It is seen that the stoichiometry of reaction 1 is only approximately obeyed.

Possible interactions of the incident radiation with dithionate ions are

[2] $S_2O_6^{2-} \rightsquigarrow SO_3^- + SO_3^-$

[3] $S_2O_6^{2-} \rightsquigarrow S_2O_6^- + e^-$

Upon solution in water the following overall reactions would appear to be plausible

[4] $2SO_3^- + H_2O \rightarrow 2H^+ + SO_4^{2-} + SO_3^{2-}$

[5] $2S_2O_6^- + 3H_2O \rightarrow 6H^+ + SO_3^{2-} + 3SO_4^{2-}$

It is not likely that reactions of $S_2O_6^-$ and of the electron accompanying its formation will result in a yield of acid which is higher than the sum of the sulfite and sulfate yields. In the formation of the two $S_2O_6^-$ radical ions two electrons were also produced which will undergo subsequent reactions. For example, they may react with neighboring $S_2O_6^{2-}$ ions as follows

[6] $S_2O_6^{2-} + e^- \rightarrow SO_3^- + SO_3^{2-}$

Reaction 6 combined with reactions 3, 4, and 5 results in the stoichiometry represented by reaction 1.

The *G*-values found are larger than those often encountered in the irradiation of solids. This is particularly so for BaS_2O_6 and the hydrates. The increased yields from the hydrates could be due to some of the SO_3^- and $S_2O_6^-$ radical ions reacting with the water of hydration rather than undergoing the recombination reactions discussed above. It is also possible that the radiation

TABLE 2. *G*-value relationships

Compound	$G(SO_3^{2-})$ / $G(SO_4^{2-})$	$G(H^+)$ / $G(SO_3^{2-} + SO_4^{2-})$	$G(SO_3^{2-} + SO_4^{2-})$
$Na_2S_2O_6$	0.63	0.92	3.75
$K_2S_2O_6$	0.34	1.45	3.89
BaS_2O_6*	1.55	1.60	6.64
BaS_2O_6†	0.53	—	19.72
$Na_2S_2O_6.2H_2O$	1.12	0.89	8.33
$BaS_2O_6.2H_2O$	0.69	0.82	20.31

*At the point just before the sudden increase in yield of SO_3^{2-} and SO_4^{2-}.
† At maximum absorbed dose.

absorbed by the water molecules resulted in a more efficient production of final products. This might occur because the radiolytic products of the water reacted with neighboring $S_2O_6^{2-}$ ions to produce intermediate radicals which did not recombine as readily as was the case for the anhydrous salts. However, for BaS_2O_6 the only satisfactory explanation seems to be that a chain reaction can occur. The following reaction would appear to be a possibility

[7] $SO_3^- + S_2O_6^{2-} \rightarrow SO_3^{2-} + SO_3 + SO_3^-$

For $Na_2S_2O_6$ and $K_2S_2O_6$ there are two cations per anion whereas in BaS_2O_6 there is only one cation per anion. Hence for BaS_2O_6 there is a greater probability of a SO_3^- radical ion being adjacent to a dithionate ion, thus the chain lengths should be longer with a consequent higher product yield, as was found experimentally. In the hydrates the SO_3^- radical ions could also react with water molecules producing chain carriers with a resulting increase in product yields.

The small effect thermal annealing has upon product yields can be explained as follows. The pair of SO_3^- radical ions produced in reaction 2 can either remain in close proximity to one another, or as the result of acquiring sufficient kinetic energy during their formation, they may come to rest relatively far apart. If the SO_3^- radical ions which are in close proximity to one another recombine in times which are short compared to the irradiation times and to the lapse of time before the samples are dissolved in water, then only isolated SO_3^- radical ions will remain in the solid. Similarly the electron produced in reaction 3 may remain in the close proximity of the $S_2O_6^-$ radical ion with the result that they eventually recombine. Alternatively, the electron may come to rest at some distance from the $S_2O_6^-$ radical ion with the possibility of their recombination being quite small. Hence at the time of annealing only isolated intermediates are present in the dithionate substrate and consequently very little recombination can occur. *i.e.*, the effect of thermal annealing is small.

The large increase in product yields shown by BaS_2O_6 after an absorbed dose of 28.3×10^{22} eV per mol is rather unusual and an explanation is not immediately obvious. However, the following is suggested as a possibility. Reactions 2 and 3 produce the radical ion species SO_3^- and $S_2O_6^-$ which, if they survive, produce products upon solution in water, otherwise recombination reactions result in a reduced yield of products. If the extent of the recombination reaction is appreciable then a decrease in the recombination rate would result in an appreciably increased rate of production of products. In the early stages of an irradiation the probability of reactions 2 or 3 occurring in the neighborhood of a SO_3^- or $S_2O_6^-$ remaining from a previous interaction of the incident radiation with a $S_2O_6^{2-}$ ion is quite small. With increasing absorbed dose however, the probability of such a special coincidence increases.[3] Thus with increasing absorbed doses $S_2O_6^-$ radical ions formed as the result of reaction 3 occurring have an increasing probability of undergoing reactions such as the following

[8] $S_2O_6^- + SO_3^- \rightarrow SO_3^{2-} + 2SO_3$

[9] $S_2O_6^- + S_2O_6^- \rightarrow SO_3^{2-} + 3SO_3$

These newly formed $S_2O_6^-$ radical ions, as a result of undergoing reaction 8 or 9 do not have an opportunity to recombine with the electrons produced at the time of their formation and

[3]A simplified mathematical treatment leads to the conclusion that the probability is proportional to the square of the absorbed dose.

Can. J. Chem. Downloaded from www.nrcresearchpress.com by 210.87.254.105 on 09/05/12
For personal use only.

hence the yield of products is increased. Reactions 8 and 9 predict that the ratio of SO_4^{2-} to SO_3^{2-} will be greater than 1:1 in agreement with the results found in the irradiation of BaS_2O_6 when the absorbed doses are greater than 28.3×10^{22} eV per mol. At an absorbed dose of 28.3×10^{22} eV per mol the sum of the SO_3^{2-} and SO_4^{2-} yields from BaS_2O_6 is 31 mmol per mol, *i.e.*, approximately one SO_3^{2-} or SO_4^{2-} precursor species for every 32 $S_2O_6^{2-}$ ions. Using a primitive cubic structure as a simple example a given structural unit has 26 relatively close neighbors. Hence it does not seem unreasonable to expect that at these doses the newly formed $S_2O_6^-$ radical ions have a large probability of being adjacent to either SO_3^- or $S_2O_6^-$ radical ions formed earlier.

The effect was not noticed with the other salts. For $Na_2S_2O_6$ and $K_2S_2O_6$ at the largest absorbed doses given the sum of the SO_3^{2-} and SO_4^{2-} yields were 17 and 11 mmol per mol, respectively. Hence, it is conceivable that had the irradiations been carried to higher doses a sudden increase in yield of products would also have been observed. With the hydrates, $Na_2S_2O_6.2H_2O$ and $BaS_2O_6.2H_2O$ if, as proposed earlier, the reactive intermediates react with water of hydration then the extent of recombination is relatively small and there is no opportunity for a sudden increase in the rate of production of products.

A similar type of behavior had been noticed previously by Eager and Mahadevappa in the irradiation of various alkali thiosulfates except that a *falling off* in the yield of products, particularly sulfate, was observed (8). The falling off in yield occurred at approximately the same absorbed dose values which in the present work resulted in a sudden increase in yield. The explanation offered above for the increase in product yields for $Ba_2S_2O_6$ is also probably applicable for the decreased yields found with the thiosulfates. Assuming that SO_3^- radical ions are formed in the irradiated thiosulfates then if additional SO_3^- radical ions are formed in the immediate vicinity of a SO_3^- radical ion already present the two SO_3^- radical ions could react to form the dithionate ion, $S_2O_6^{2-}$. After a certain absorbed dose the probability of this happening becomes large enough so that continuing irradiation results in an appreciable decrease in the number of SO_3^- radical ions present. Since SO_3^- radical ions are likely precursors of sulfate, the observed yield of sulfate shows a sudden decrease with increasing absorbed dose.

We thank the National Research Council of Canada for financial support of this work.

1. W. G. CHANTRY, A. HORSFIELD, J. R. MORTON, J. R. ROWLANDS, and D. H. WHIFFEN. Mol. Phys. **5**, 233 (1962).
2. M. P. GILEVICH and A. K. POTOPOVICH. Vestsi Akad. Nuvuk. Belarusk. SSR. No. 2, 61 (1962).
3. D. W. LARSON, R. W. O'CONNELL, A. B. VAN CLEAVE, and R. L. EAGER. Can. J. Chem. **41**, 201 (1963).
4. G. BRAUER. (*Editor*). Handbook of preparative inorganic chemistry. 2nd ed. Vol. 1. Academic Press, New York. 1963. p. 395.
5. Y. GARNIER and C. J. DUVAL. Chromatory, **2**, 72 (1959).
6. R. M. GOLDING. J. Chem. Phys. **33**, 1666 (1960).
7. B. J. HEINRICH, M. D. GRIMES, and J. E. PUCKETT. *In* Treatise on analytical chemistry. Part II. Vol. 7. *Edited by* I. M. Kolthoff and P. J. Elving. Interscience Publishers, New York, N.Y. 1961. p. 104.
8. R. L. EAGER and D. S. MAHADEVAPPA. Can. J. Chem. **43**, 614 (1965).

Can. J. Chem. Downloaded from www.nrcresearchpress.com by 210.87.254.105 on 09/05/12
For personal use only.

On the Blue Complexes Formed in Acidic Solutions of Hexaammineruthenium(II)

F. BOTTOMLEY AND S. B. TONG
Department of Chemistry, University of New Brunswick, Fredericton, New Brunswick

Received June 18, 1971

The blue complex formed by reaction of hexaammineruthenium(II) dichloride and hydrochloric acid has been characterized by analytical, spectroscopic, electrochemical, and chemical methods as a chloro-bridged ruthenium(II)–ruthenium(III) dimer, $[Ru_2(NH_3)_6Cl_4H_2O]Cl$. With hydrobromic acid the analogous complex $[Ru_2(NH_3)_6Br_4H_2O]Br$ is formed. Reactions of the complexes with ammonia and hydrohalic acids are reported.

Le complexe bleu, obtenu en faisant réagir le dichlorure d'hexaammineruthénium(II) avec l'acide chlorhydrique a été caractérisé par des méthodes analytiques, spectroscopiques, électrochimiques et chimiques; il s'agit d'un dimère ruthénium(II)–ruthénium(III) avec un pont chloro, $[Ru_2(NH_3)_6Cl_4H_2O]Cl$. Avec l'acide bromhydrique, le complexe correspondant, $[Ru_2(NH_3)_6Br_4H_2O]Br$, est obtenu. Les réactions de ces complexes avec l'ammoniaque et les acides halogénhydriques sont rapportées.

Canadian Journal of Chemistry, **49**, 3739 (1971)

Can. J. Chem. Downloaded from www.nrcresearchpress.com by 210.87.254.105 on 09/05/12
For personal use only.

Introduction

The formation of deep blue solutions is a notable feature of ruthenium chemistry. These solutions were obtained in two distinct ways: (*a*) by reduction of chloro-complexes of ruthenium(III); (*b*) by reaction of ammine complexes of ruthenium(II) with acids. Although there are differences in the electronic state of the ruthenium in the starting material, in the ligands, and in method of preparation, it seemed possible the species responsible for the blue color was similar in all cases. Earlier investigations and discussions of the nature of the species were mainly based on solution studies (1–5). Recently two complexes have been isolated. Wilkinson and coworkers (6, 7) obtained the blue cluster anion $Ru_5Cl_{12}^{2-}$ by reduction of ruthenium(III) chloride in methanol. Lever and Powell (8) obtained a blue complex, tentatively formulated as $[Ru(NH_3)_3Cl_2H_2O]Cl$, from the reaction between hexaammineruthenium(II) dichloride and hydrochloric acid. We have reinvestigated this complex, and extended the reaction to hydrobromic acid, to determine the nature of the blue species.

Results

Hot aqueous hydrochloric acid solutions of hexaammineruthenium(II) dichloride rapidly become blue and on cooling a blue micro-crystalline material precipitates. Great difficulty was experienced in obtaining a product with reproducible chemical and physical properties. Using the criteria of maximum intensity of the absorption in the electronic spectrum and a minimum magnetic moment for the complex, the preparation was repeated under various conditions until both criteria were satisfied. The method described in the experimental section was regularly repeated and yielded deep blue micro-crystals of $[Ru_2(NH_3)_6Cl_4H_2O]Cl$. A similar procedure using hexaammineruthenium(II) dibromide and hydrobromic acid gave deep blue-green micro-crystals of $[Ru_2(NH_3)_6Br_4H_2O]Br$. Attempts to prepare a pure iodo-complex failed due to the insolubility of hexaammineruthenium(II) di-iodide in hydriodic acid.

Both the chloro- and bromo-complexes are hygroscopic and moderately air stable when dry, slightly soluble in water, methanol, and dimethylformamide (with slow decomposition), insoluble in ethanol, and decomposed by dimethylsulfoxide. The chloro-complex has a conductivity expected for a 1:1 electrolyte in DMF, but the conductivity of the bromo-complex is high (Fig. 1), possibly because this complex is decomposed by DMF more rapidly than the chloro-complex. Their infrared spectra in the region 4000–700 cm^{-1} showed absorption bands due to co-ordinated ammonia (these occurring at frequencies in the range normally observed for ruthenium(III) rather than ruthenium(II) (9)). In addition, a pronounced broad shoulder which appeared at 3430 (chloro-complex) or 3460 cm^{-1} (bromo) on the high energy side of the NH_3 band was assigned to co-ordinated water (Table 1). In the low frequency region (700–200 cm^{-1}) there were a number of

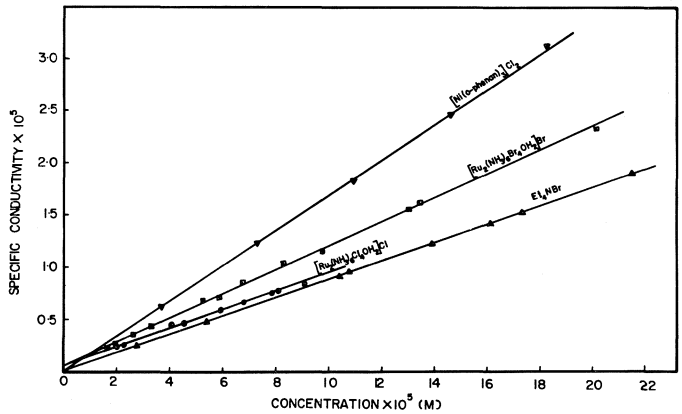

FIG. 1. Conductivity of $[Ru_2(NH_3)_6X_4H_2O]X$ (X = Cl, Br) over the concentration range 1–20 × 10^{-5} *M*.

TABLE 1. Infrared spectral data*

Complex	Frequency for assignment						
	H_2O	ν(NH)	$\delta(NH_3)_{deg}$	$\delta(NH_3)_{sym}$	ρNH_3	νRu—N	νRu—Cl
$[Ru_2(NH_3)_6Cl_4H_2O]Cl$	3430 br, sh	3260–3160 s, br	1624 s	1298 vs	808 s	—	—
$[Ru_2(NH_3)_6Br_4H_2O]Br$	3460 br, sh	3220–3150 s, br	1616 s	1296 vs	790 s	—	—
$[Ru^{III}(NH_3)_3Cl_3]$	—	3280–3220 s, br	1608 s	1325 m	786 s	467 m	311 s
				1291 vs		478 m	290 sh
						457 sh	283 s

*vs = very strong; s = strong; m = medium; br = broad; sh = shoulder.

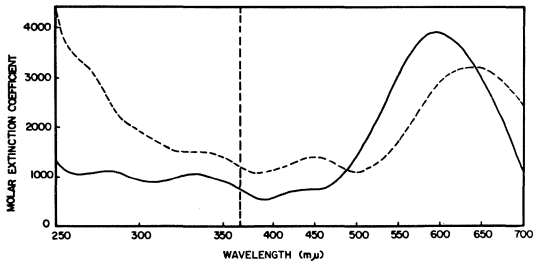

FIG. 2. Electronic spectra of $[Ru_2(NH_3)_6X_4H_2O]X$ (X = Cl, —; X = Br, ---) (aqueous solution).

bands, but no definite assignments could be made. In particular, ruthenium-chloride or bromide stretching frequencies could not be identified with certainty. The electronic spectra of the complexes (aqueous solution) are shown in Fig. 2. The three high energy absorption bands were observed in the spectra of different samples and in spectra taken as Nujol mulls and therefore are not due to impurity. This spectrum agrees with that described briefly in the literature (3).

$[Ru_2(NH_3)_6Cl_4H_2O]Cl$ has a magnetic moment of 2.05 B.M. at 21 °C and the bulk susceptibility obeys the Curie–Weiss law over the temperature range 80–294 °K with $\theta = -18.6°$. $[Ru_2(NH_3)_6Br_4H_2O]Br$ has a magnetic moment of 2.00 B.M. at 21 °C. The results are in agreement with a total of one unpaired electron per two ruthenium atoms for both complexes.

Potentiometric titration of either complex with cerium(IV) showed 50% of the ruthenium was easily oxidizable and the shape of the titration curve was similar to that for oxidation of hexaammineruthenium(II) (Fig. 3). The shape of the curve above the inflexion point indicated further oxidation took place, although no definite break was observed. Potentiometric titration of chloropentaammineruthenium(III) with cerium(IV) resulted in curves similar to the upper portion of Fig. 3. Presumably oxidation to ruthenium(IV) occurred, with loss of ammonia from the complex. Similar behavior was observed in radiolysis experiments (10). $[Ru_2(NH_3)_6Cl_4H_2O]Cl$ gave a polarographic reduction wave at −0.28 V *vs.* s.c.e. in 1 *M* hydrochloric acid, at a concentration of 3 × 10^{-4} *M*. The results were complicated by a catalytic hydrogen discharge such that the discharge appeared at potentials 0.2 V more positive than in the absence of $[Ru_2$-

Can. J. Chem. Downloaded from www.nrcresearchpress.com by 210.87.254.105 on 09/05/12
For personal use only.

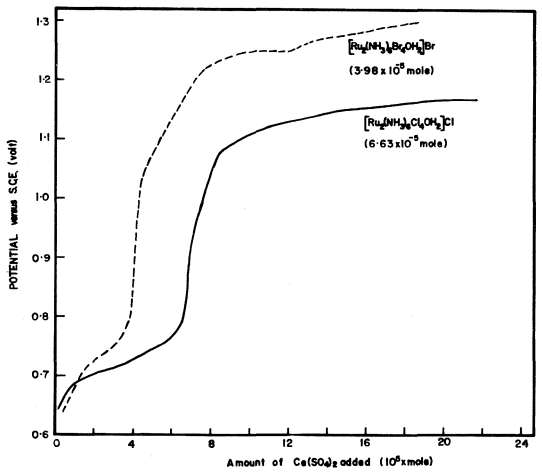

FIG. 3. Potentiometric titration curves for $[Ru_2(NH_3)_6X_4H_2O]X$ (X = Cl, —; X = Br, ---).

$(NH_3)_6Cl_4H_2O]Cl$. Under similar conditions $[Ru^{III}(NH_3)_5Cl]Cl_2$ gave a wave at −0.25 V *vs.* s.c.e. (with no catalytic hydrogen discharge). An $E_{1/2}$ of −0.27 V was reported for reduction of $[Ru^{III}(NH_3)_5Cl]Cl_2$ under conditions different from those used in this work (11). The wave height for $[Ru_2(NH_3)_6Cl_4H_2O]Cl$ corresponded to approximately 41% of the ruthenium in the complex being present as ruthenium(III) by comparison with $[Ru^{III}(NH_3)_5Cl]Cl_2$).

$[Ru_2(NH_3)_6Cl_4H_2O]Cl$ reacted with hydrochloric acid and oxygen at room temperature over several days to give a 73% yield of trichlorotriammineruthenium(III) (8). Without oxygen reaction was extremely slow. $[Ru^{III}(NH_3)_3Cl_3]$ was insoluble in all common solvents. Its infrared spectrum (Table 1) showed three absorption bands assignable to metal–nitrogen stretching frequencies and three bands assignable to metal–chlorine stretching frequencies, and the complex therefore has been assigned the *mer*-configuration, although we are aware of the error which may arise when assignment of stereochemistry is based solely on solid-state infrared data (12).

On heating $[Ru_2(NH_3)_6Cl_4H_2O]Cl$ with aqueous hydrochloric acid, ammonia was lost from the complex, but we were unable to obtain $[Ru^{III}Cl_5H_2O]^{2-}$ (8). The infrared spectrum of the product showed absorption bands assignable to co-ordinated ammonia as well as water, and microanalytical results indicated a significant nitrogen content. The bulk magnetic susceptibility was lower than expected for ruthenium(III), indicating the complex may be polymeric. At room temperature $[Ru_2(NH_3)_6Br_4H_2O]Br$ and hydrobromic acid did not give $[Ru^{III}(NH_3)_3Br_3]$, but on heating $[Ru^{III}Br_5H_2O]^{2-}$ was formed in 81% yield.

In aqueous ammonia at room temperature $[Ru_2(NH_3)_6X_4H_2O]X$ (X = Cl, Br) gave solutions having the deep wine-red color characteristic of ruthenium red (13). Addition of potassium iodide to the solution gave hexaammineruthenium(II) diiodide (30% yield), showing the presence of ruthenium(II) in the complex. Addition of the appropriate acid to the red solution regenerated the blue solution (8), and several repetitions of the ammonia/acid treatment ultimately gave chloropentaammineruthenium(III) dichloride (68%) or bromopentaammineruthenium(III) dibromide (79%). These same complexes were obtained by heating the red solution and then adding the appropriate acid. There was no reaction between $[Ru_2(NH_3)_6Cl_4H_2O]Cl$ and triphenylphosphine in refluxing methanol.

Discussion

The chemical and physical evidence presented above shows that $[Ru_2(NH_3)_6X_4H_2O]X$ (X = Cl, Br) contain halo-bridged ruthenium(II) and ruthenium(III) ions. The reason for the deep-blue color presumably lies in the presence of mixed oxidation states. Whether any particular ruthenium ion should be regarded as ruthenium(II) or ruthenium(III) is not clear. The deep color of, for example, ruthenium red, has been ascribed to "oscillating valencies", but recent results indicate that each ruthenium ion has a distinct oxidation state (14).

Assuming octahedral co-ordination about the ruthenium, the analytical and infrared results indicate the ruthenium ions are bridged by a single halide. Although this is the only formulation in agreement with all the results, it cannot be regarded as conclusive in the absence of a full structure determination. Some information on the structure of the chloro-complex may be obtained from its reactions. The high yield of $[Ru^{III}(NH_3)_3Cl_3]$ obtained from $[Ru_2(NH_3)_6Cl_4H_2O]Cl$ and hydrochloric acid means that each ruthenium ion in this complex must be co-ordinated by three ammonia molecules. Assuming the *mer*-stereochemistry assigned to $[Ru^{III}(NH_3)_3Cl_3]$ from infrared evidence is correct and no rearrangement occurred during

Can. J. Chem. Downloaded from www.nrcresearchpress.com by 210.87.254.105 on 09/05/12
For personal use only.

Can. J. Chem. Downloaded from www.nrcresearchpress.com by 210.87.254.105 on 09/05/12
For personal use only.

reaction, the three ammonia molecules will have the *mer*-configuration. Even allowing free rotation about the Ru—Cl—Ru axis, this restriction on the ammonia configuration still permits six isomers of formula $[Cl_2(NH_3)_3RuClRu(NH_3)_3ClH_2O]Cl$ and twelve isomers are possible if the two ruthenium ions have distinct, separate, oxidation states. For the bromo-complex, it is not possible to make even a partial assignment of geometry. Repeated attempts to obtain suitable crystals of either the chloro- or bromo-complex for X-ray work have not been successful to date.

Ruthenium metal was not observed in the preparation of the complexes unless solutions were heated for an extended period. It is assumed, therefore, that ruthenium(III) was formed by oxidation of ruthenium(II) by the solvent water, rather than by disproportionation, although no visible evolution of hydrogen gas was observed.

Lever and Powell (8) tentatively proposed the formula $[Ru(NH_3)_3H_2OCl_2]Cl$ for the blue chloro-complex and obtained other salts of the complex cation. We have reformulated the complex, but we find that slow evaporation of the filtrate after removal of the chloro-complex yields a small quantity of crystals with an Ru:Cl ratio of 1:3. This complex is presently under investigation.

No related mono-chloro-bridged complexes of the type discussed here are available for comparison. The only chloro-bridged ruthenium complex of known structure, $[(Bu_3^nP)_4Ru_2Cl_5]$, has a tri-chloro-bridge (15). Shilov postulated a di-chloro-bridged complex as the blue intermediate in reduction of ruthenium trichloride in tetrahydrofuran (4). The blue $Ru_5Cl_{12}^{2-}$ isolated by Wilkinson and co-workers (6, 7) is obviously unrelated to the complexes described here and hence the blue colors observed in ruthenium chemistry are not indicative of the presence of one species, but at least two unrelated complexes give blue solutions.

Experimental

Ruthenium trichloride was obtained from Johnson, Matthey and Mallory, Montreal, and used as received. All other chemicals were reagent grade. Analyses were by Bernhardt Microanalytical Laboratories, Mulheim, W. Germany. Except where indicated, all operations were carried out under argon and all solvents were deoxygenated before use.

Hexaammineruthenium(II) Dichloride and tris-o-Phenanthrolinenickel(II) Dichloride Tetrahydrate

These were prepared by literature methods (8, 16).

Anal. Calcd. for $Cl_2H_{18}N_6Ru$: Cl, 25.86; H, 6.62; N, 30.65. Found: Cl, 26.05; H, 6.36; N, 31.05.

Anal. Calcd. for $C_{36}Cl_2H_{32}N_6NiO_4$: C, 58.25; Cl, 9.55; H, 4.34; N, 11.32. Found: C, 58.38; Cl, 9.73; H, 5.00; N, 11.45.

Hexaammineruthenium(II) Dibromide and Diiodide

These were prepared by metathesis from the chloride salt.

Anal. Calcd. for $Br_2H_{18}N_6Ru$: H, 5.00; N, 23.15. Found: H, 5.06; N, 23.68.

Anal. Calcd. for $H_{18}I_2N_6Ru$: H, 3.97; N, 18.39. Found: H, 4.21; N, 18.68.

μ-Chloro-trichloroaquohexaamminediruthenium Chloride

To a solution of hexaammineruthenium(II) dichloride (0.70 g) in water (9 ml) were added 5 drops of concentrated ammonia. The solution was heated to 80 °C and concentrated hydrochloric acid (6 ml) rapidly added. The solution became blue and was filtered hot, leaving a small quantity of dark material. The filtrate was allowed to stand at 5 °C for 12 h, the blue micro-crystalline product filtered off, recrystallized from methanol at low temperature, washed with ethanol and ether, and dried in vacuo over P_2O_5. Yield 0.26 g (56%).

Anal. Calcd. for $Cl_5H_{20}N_6ORu_2$: Cl, 35.48; H, 4.03; N, 16.82. Found: Cl, 35.45; H, 4.05; N, 16.85.

μ-Bromo-tribromoaquohexaamminediruthenium Bromide

This was prepared, in 59% yield, in a similar manner to the chloro-complex, from hexaammineruthenium(II) dibromide and hydrobromic acid (48%).

Anal. Calcd. for $Br_5H_{20}N_6ORu_2$: Br, 55.34; H, 2.79; N, 11.64. Found: Br, 55.08; H, 2.78; N, 11.59.

Reaction of $[Ru_2(NH_3)_6X_4H_2O]X$ (X = Cl, Br) with Ammonia

(a) At Room Temperature

$[Ru_2(NH_3)_6Cl_4H_2O]Cl$ (0.080 g) in 1:1 aqueous ammonia (5 ml) was stirred until the solution became wine-red. To the solution was added potassium iodide, the resultant yellow precipitate of hexaammineruthenium(II) diiodide filtered off, recrystallized from dilute ammonia, washed with ethanol, and ether and dried in vacuo. Yield 0.050 g (33%).

Anal. Calcd. for $H_{18}I_2N_6Ru$: H, 3.97; N, 18.39. Found: H, 3.94; N, 18.30.

The electronic and infrared spectra of the product agreed closely with the literature (9, 17). By an analogous procedure $[Ru_2(NH_3)_6Br_4H_2O]Br$ gave $[Ru^{II}(NH_3)_6]I_2$ in 27% yield.

(b) At Elevated Temperature

A solution of $[Ru_2(NH_3)_6Cl_4H_2O]Cl$ (0.10 g) in 1:1 aqueous ammonia (9 ml) was stirred until it became wine-red and the solution gently heated for 10 min. Addition of concentrated hydrochloric acid (12 drops) gave a yellow solution which on cooling deposited yellow crystals of chloropentaammineruthenium(III) dichloride. These were removed by filtration, recrystallized from dilute hydrochloric acid, washed with ethanol and ether, and air dried. Yield 0.08 g (68%).

Can. J. Chem. Downloaded from www.nrcresearchpress.com by 210.87.254.105 on 09/05/12
For personal use only.

Anal. Calcd. for $Cl_3H_{15}N_5Ru$: H, 5.17; N, 23.93. Found: H, 5.15; N, 24.11.

The infrared and electronic spectra were in good agreement with the literature (9, 18).

In a similar manner $[Ru_2(NH_3)_6Br_4H_2O]Br$, NH_3 and HBr gave $[Ru^{III}(NH_3)_5Br]Br_2$ in 79% yield.

Anal. Calcd. for $Br_3H_{15}N_5Ru$: H, 3.55; N, 16.44. Found: H, 3.91; N, 16.55.

The infrared and electronic spectra were in good agreement with the literature (9, 18).

Reaction of $[Ru_2(NH_3)_6X_4H_2O]X$ (X = Cl, Br) with Acid

(a) At Room Temperature

Oxygen was passed through a solution of $[Ru_2(NH_3)_6Cl_4H_2O]Cl$ (0.090 g) in concentrated hydrochloric acid (20 ml) for five days at room temperature. The orange trichlorotriammineruthenium(III) was removed by filtration, washed with ethanol and ether, and air dried. The insoluble crude product was purified by warming to 60 °C in 1:1 aqueous ammonia, filtered off, washed well with water, ethanol, and ether, and air dried. Yield 0.068 g (73%).

Anal. Calcd. for $Cl_3H_9N_3Ru$: H, 3.51; N, 16.25. Found: H, 3.58; N, 16.25.

The electronic spectrum (Nujol mull) showed two bands at 297 and 375 mμ.

(b) At Elevated Temperature

A solution of $[Ru_2(NH_3)_6Cl_4H_2O]Cl$ (0.0513 g) in concentrated hydrochloric acid (10 ml) was refluxed for 1 h. The solution was filtered hot and cesium chloride added to the filtrate, giving a red precipitate, which was removed by filtration, washed with cold water, ethanol, and ether, and air dried. Yield 0.0882 g.

Anal. Found: Cl, 27.53; N, 2.58.

The electronic spectrum of the complex showed one band at 334 mμ. The infrared spectrum showed bands at 3300, 3240, 1610, 1305 (shoulder), 1292, 1273, and 780 cm^{-1} (weak), attributable to co-ordinated ammonia and at 3500 and 1650 cm^{-1}, attributable to co-ordinated water.

A solution of $[Ru_2(NH_3)_6Br_4H_2O]Br$ (0.069 g) in hydrobromic acid (48%, 10 ml) was heated until it became red. The solution was filtered hot and cesium chloride added to the filtrate. The red $Cs_2[Ru^{III}Br_5H_2O]$ was removed by filtration, washed with a little cold water, ethanol, and ether, and air dried. Yield 0.064 g (81%).

Anal. Calcd. for $Br_5Cs_2H_2ORu$: Br, 50.93. Found: Br, 50.55.

The infrared spectrum showed two broad bands in the region 3500–3650 cm^{-1} and a broad band in the region 1600–1650 cm^{-1} attributable to co-ordinated water.

Infrared spectra were recorded on a Beckman IR-12 spectrophotometer as Nujol or hexachlorobutadiene mulls between potassium bromide or polyethylene plates. Electronic spectra were recorded on a Coleman Model EPS-3T instrument. Room temperature magnetic moments were by the Gouy method. Conductivity measurements in dimethylformamide solution were made on a Beckman Model RC-18A conductivity bridge. Potentiometric titrations were carried out using a Leeds and Northrup research potentiometer, with a saturated calomel reference electrode and ceric sulfate as oxidant. Polarographic curves were recorded on a Princeton Applied Research Model 170 electrochemistry system. The analysis was carried out in a Kalousek vessel with a saturated calomel reference electrode (s.c.e.) and the dropping mercury electrode had an outflow velocity of 2.95 mg s^{-1} and a drop time of 2.97 s at a mercury column pressure of 75 cm.

We wish to thank Dr. A. B. P. Lever of York University, Ontario, for the low temperature magnetic moments, Dr. D. Barnes of this department for the polarographic measurements, the National Research Council of Canada for financial support, and Johnson, Matthey and Mallory for a generous loan of ruthenium.

1. M. G. Adamson. Aust. J. Chem. **20**, 2517 (1967).
2. M. G. Adamson. J. Chem. Soc. A, 1370 (1968).
3. J. F. Endicott and H. Taube. Inorg. Chem. **4**, 437 (1965).
4. A. K. Shilova and A. E. Shilov. Kin. i. Kat. **10**, 267 (1969).
5. P. C. Ford. Co-ord. Chem. Rev. **5**, 75 (1970).
6. J. D. Gilbert, D. Rose, and G. Wilkinson. J. Chem. Soc. A, 2765 (1970).
7. D. Rose and G. Wilkinson. J. Chem. Soc. A, 1791 (1970).
8. F. M. Lever and A. R. Powell. J. Chem. Soc. A, 1477 (1969).
9. A. D. Allen and C. V. Senoff. Can. J. Chem. **45**, 1337 (1967).
10. J. H. Baxendale, M. A. J. Rodgers, and M. D. Ward. J. Chem. Soc. A, 1246 (1970).
11. I. J. Itzkovitch and J. A. Page. Can. J. Chem. **45**, 2743 (1968).
12. J. Chatt, G. J. Leigh, and D. M. P. Mingos. J. Chem. Soc. A, 1674 (1969).
13. J. M. Fletcher, B. F. Greenfield, C. J. Hardy, D. Scargill, and J. L. Woodhead. J. Chem. Soc. 2000 (1961).
14. C. A. Clausen, R. A. Prados, and M. L. Good. Inorg. Nucl. Chem. Lett. **7**, 485 (1971).
15. G. Chioccola and J. J. Daly. J. Chem. Soc. A, 1981 (1968).
16. R. D. Feltham and R. G. Hayter. J. Chem. Soc. 4587 (1964).
17. T. J. Meyer and H. Taube. Inorg. Chem. **7**, 2369 (1968).
18. H. Hartmann and C. Buschbeck. Z. Phys. Chem. Frankfurt, **11**, 120 (1957).

Can. J. Chem. Downloaded from www.nrcresearchpress.com by 210.87.254.40 on 09/05/12
For personal use only.

Transient Phenomena in Dissociation of Diatomic Molecules[1]

R. K. BOYD
Department of Chemistry, University of Guelph, Guelph, Ontario

AND

GEORGE BURNS
Department of Chemistry, University of Toronto, Toronto 181, Ontario

Received April 30, 1971

A model suitable for studies of non-equilibrium effects in chemical reactions (13) was used to predict incubation times for the dissociation of O_2 in Ar between 2900 and 7200 °K. It was found that the model accounts satisfactorily for the experimental data. On the other hand previously used theories underestimate these incubation times by a factor of five to ten; the discrepancy is traced to assumptions used in previous investigations. When the same model is applied to the dissociation of Br_2 in Ar and Cl_2 in Ar, it correlates well a variety of experimental data, obtained over a wide temperature range.

Un modèle convenable pour les études des effets de nonéquilibre (13) a été utilisé pour prédire les temps d'incubation pour la dissociation de O_2 dans Ar entre 2900 et 7200 °K. Il a été trouvé que le modèle calculé est satisfaisant d'après les données expérimentales. D'autre part, les théories antérieurement utilisées sous-estiment ces temps d'incubation par un facteur de cinq à dix; le désaccord est retracé grâce aux suppositions utilisées dans des examens antérieurs. Lorsque le même modèle est appliqué à la dissociation de Br_2 dans Ar et de Cl_2 dans Ar, il met bien en corrélation la variété des données expérimentales obtenues audessus d'une plus grande échelle de température.

Canadian Journal of Chemistry, 49, 3744 (1971)

1. Introduction

Wray (1) showed that the dissociation of oxygen in shock waves is preceded by a measureable induction period. He proposed that such an "incubation time" (1) is due to coupling of the vibrational relaxation to dissociation of O_2. This phenomenon is predicted by the theories of Hammerling, Teare, and Kivel (2), Marrone and Treanor (3) and Heims (4). Brau, Keck, and Carrier (5) pointed out that these theories (2–4) are of a phenomenological nature, and applied their diffusion theory of dissociation reaction to predict the incubation times in oxygen. Although the Brau *et al.* calculations agreed well with the experiments (1) at very high temperatures, their predicted incubation times deviated from experiment at lower temperatures, being about five to ten times smaller than the experimental data at 5000 °K. Use of the Morse potential function instead of the truncated harmonic oscillator function in these calculations did not alter the above discrepancy. It was suggested (5) that the discrepancy may be due to experimental error, since it was relatively difficult to obtain accurate incubation times at lower temperatures (1). However, recently, Watt and Myerson (6) succeeded in obtaining accurate measurements of the incubation times and rate constants down to 2900 °K. When these new results were compared (6) with theoretical calculations of Brau *et al.* (5) the observed absolute values of incubation times were still an order of magnitude greater than calculated.

In the present work, we developed further a model for dissociation used previously (7), applied it to the O_2–Ar system below 7200 °K, and showed that the incubation times so obtained are of the order of vibrational relaxation times, and agree well with all the available experimental data (1, 6). The reaction profiles were generated, and the results compared with the previous theoretical treatments. On the other hand, when the model is used to treat the halogen recombination–dissociation reactions, it was found that it correlates well the available experimental data (7–11).

2. Non-equilibrium Dissociation–Recombination

The model for dissociation of diatomic molecules (7) assumes that the density of representative points in the vibrational phase space of n diatomic molecules, which have a total vibra-

[1]This work was supported in part by the Directorate of Chemical Sciences, Air Force Office of Scientific Research, Grant No. 69-1695.

Can. J. Chem. Downloaded from www.nrcresearchpress.com by 210.87.254.40 on 09/05/12
For personal use only.

tional energy E_v, is uniform at any given time throughout the course of the reaction. For this reason, it may be referred to as a "uniform phase density (u.p.d.) model".

If, in this model, the diatomic oscillators were in equilibrium with each other, and were unable to interact with other degrees of freedom, they could have been described by a microcanonical ensemble defined by n and E_v. The vibrational temperature, T_v, of the oscillators would have been a time independent observable. Such a microcanonical ensemble would have occupied a hypersurface of constant energy cut out of a uniform ensemble in $6n$ dimensional phase space. However, according to the model, the oscillators *do* interact with other degrees of freedom, and their total vibrational energy is a function of time. Thus, we consider a non-equilibrium ensemble, which moves through the uniform ensemble as the total energy of oscillators changes with time during the course of the reaction. It is assumed that such a non-equilibrium ensemble maintains uniform density of the representative points at any given time in phase space, and thus can be described by an "observable" T_v. The density of representative points in the vibrational phase space for such a non-equilibrium ensemble is then

$$\rho(H,t) \approx \exp\,[-H(t)/kT_v(t)]$$

The assumption that a time-dependent vibrational temperature exists (Bethe–Teller approximation) at relatively low shock wave temperatures is not unreasonable. It is commonly used if dissociation of diatomic molecules can be neglected, and it can be shown (12) that it holds exactly, within the harmonic oscillator approximation. Therefore one may expect that the u.p.d. model would describe satisfactorily some of the shock wave processes, provided that the temperature is so low that the dissociation reaction and vibrational relaxation are *weakly* coupled; this feature is discussed further below.

One expects that, during the dissociation, the uppermost levels very close to the dissociation limit would be depopulated with respect to the lower energy levels, whose distribution function is described by the assumed T_v. It is here assumed that this depopulation is limited to a very narrow energy region, and that the molecular distribution function over these levels is time-dependent during the course of reaction.

The other assumptions of the u.p.d. model were described previously (7, 13). While in the previous investigation the back reaction was neglected, in the present work both dissociation and recombination are considered. The vibrational relaxation equation now takes the form (14)

$$[1] \qquad \frac{d\varepsilon_v}{dt} = \frac{(\varepsilon_\infty - \varepsilon)}{\tau_v} - \frac{(\bar{E}_d - \varepsilon_v)}{[X_2]}\left(\frac{d[X_2]}{dt}\right)_d + \frac{(\bar{E}_r - \varepsilon_v)}{[X_2]}\left(\frac{d[X_2]}{dt}\right)_r$$

The first term on the right side of eq. 1 describes the relaxation of the unperturbed oscillator, with a characteristic vibrational relaxation time τ_v. The average vibrational energy ε_v is related to the vibrational temperature T_v via the harmonic oscillator approximation, $\varepsilon_v = R\theta/[\exp(\theta/T_v) - 1]$, where $\theta = h\nu_0/k$; ε_∞ is the value of ε_v for the special case where $T_v = T$, the instantaneous value of the translational temperature.

The subscripts $_d$ and $_r$ denote the dissociation and recombination directions, respectively; thus for example, $(d[X_2]/dt)_d$ is the rate for the dissociation of X_2, the diatomic molecule. $\bar{E}_d$ is the average energy lost by the vibrational mode when one oscillator dissociates; similarly, $\bar{E}_r$ is the average energy supplied to the vibrational mode by the recombination of two atoms. At equilibrium, detailed balance requires that $\bar{E}_d = \bar{E}_r$; in the present work, it is assumed that during the entire course of the reaction $\bar{E}_d = \bar{E}_r \simeq D$, the dissociation energy. That is to say, dissociation is considered to occur only from states very close to the top of the vibrational ladder. The second term in eq. 1 is thus the perturbation term arising from the fact that a dissociating molecule has considerably more vibrational energy than the average; as pointed out by Treanor and Marrone (14), the effect is analogous to "evaporation cooling", where only the most energetic molecules escape into the vapor phase. The last term is the "condensation heating" perturbation term.

For a closed system, the nett chemical rate may be described as the difference of the two

Can. J. Chem. Downloaded from www.nrcresearchpress.com by 210.87.254.40 on 09/05/12
For personal use only.

reaction rates

$$[2] \quad -\mathrm{d}[X_2]/\mathrm{d}t = k_d[M][X_2] - k_r[M][X]^2$$

The quantities k_d and k_r are the rate coefficients; they are, in general, functions of the internal distribution functions of the corresponding chemical species. However, in the present work, the recombinative rate coefficient is assumed to be an observable obtained from measurements after all transients have died, and thus is taken to be a time-dependent constant. This is not too unreasonable an assumption, since transient phenomena in recombinations, which have *not* been observed, involve relaxation of highly excited diatomic molecules, and are expected to be extremely fast.

The dissociative rate coefficient k_d, on the other hand, cannot be defined here by one non-zero eigenvalue, and depends on both T and T_v. The functional form of this dependence is obtained (7, 13, 15) from the two assumptions, used above in eq. 1 concerning the existence of a unique T_v and of "reactive" states X_2* very close to the dissociation limit. The fractional population of such states is given by

$$[3] \quad [X_2^*]/[X_2] = g^* \exp(-D/RT_v)/Q_v(T_v)$$

where g^* is an effective degeneracy for the reactive states, and $Q_v(T_v)$ is the vibrational partition function. The one-way rate coefficient k_d is now given by

$$[4] \quad k_d = \kappa(T)[X_2^*]/[X_2]$$

where $\kappa(T)$ is the "microscopic" rate constant describing the rate of dissociation of X_2*. Then, for given values of $[X_2]$ and of T, eqs. 3 and 4 give

$$[5] \quad k_d(T,T_v)/(k_r K_{eq}) = [Q_v(T)/Q_v(T_v)] \exp[D/R(1/T - 1/T_v)]$$

Equation 5, with $Q_v(T)/Q_v(T_v)$ replaced by the high-temperature limit (T/T_v), is the form given previously (7, 13, 15). Evaluation of the rate coefficient k_d thus requires knowledge of k_r; this problem has been discussed previously (16).

Different collision partners M, (Ar, X_2, and X), have different efficiencies for the various processes (dissociation, recombination, and relaxation). In terms of the present model, a complete description would require three values of the de-excitation collision probability P_{10} (12) which governs the value of τ_v (eq. 1), and three values of k_r. It is also necessary to know the equilibrium constant corresponding to the arbitrary "hypersurface in phase space" (17) used to distinguish reactants from products. In the present case, K_{eq} is essentially the usual equilibrium constant for the process $X_2 \rightleftharpoons 2X$.

The available experimental information is, however, far from sufficient to establish the values of six parameters, so that further simplifications had to be made. The number of independent parameters was reduced to three by making the somewhat serious approximation that, for all collision partners i,j

$$[6] \quad (P_{10})_i/(P_{10})_j = \kappa_i/\kappa_i = k_{r,i}/k_{r,j}$$

The resulting relative collision efficiencies will thus correspond to weighted averages for the relaxation and reactive processes. It should be emphasized that this approximation is *not* an essential feature of the present model, but was imposed, as a necessity, by the lack of experimental information.

Using these additional assumptions, the total chemical rate can now be expressed by a linear combination of terms

$$[7] \quad -\mathrm{d}[X_2]/\mathrm{d}t = \sum_i k_{d,i}(T, T_v) \cdot [M_i][X_2] - \sum_i k_{r,i}(T) \cdot [M_i][X]^2$$

The relaxation time τ_v in eq. 1 is now a composite function (12) of the three $(P_{10})_i$. Since each $k_{d,i}$ is a function of T_v, which is in turn a function of the concentration of all species i via eq. 1, eq. 7 does *not* represent a decomposition of the total chemical rate into separable contributions from each collision partner i, except in the limit $T_v = T$. This feature has received considerable attention (18–21). The time-dependence of the $k_{d,i}$ must be taken into account in the integration of eq. 7.

3. Method of Computation

It is the purpose of the present work to compute reaction profiles which may be directly compared with the raw experimental observations. To do this, the relaxation eq. 1 and the chemical rate eq. 7 must be integrated simultaneously with the shock conservation equations. The latter can be integrated implicitly by a modification of the iterative technique described previously (10); the modification required is a correction to the enthalpy of X_2 for the disequilibrium of the vibrational mode. This correction was calculated,

Can. J. Chem. Downloaded from www.nrcresearchpress.com by 210.87.254.40 on 09/05/12
For personal use only.

in this work, from the harmonic oscillator approximation, and was a function of the vibrational temperature.

In order to compute theoretical profiles of X_2 optical density *vs.* time, the vibrational temperature and X_2 concentration must be used, together with extrapolated or available extinction coefficient data. The integration must be performed over a rectangular slit function which is typically 1 mm wide; the resulting averaged signal should correspond to the optical density "seen" by the photomultiplier in a shock tube experiment using molecular absorption spectrophotometry. The latter must be further integrated over an RC time constant, to simulate the further distortion of the step function, at the shock front, by the amplification chain. This final profile should correspond to the profile observed on the oscilloscope screen in a typical shock-wave absorption experiment. It should agree with the experimental profile to within the accuracy of the model.

In a similar fashion, profiles of X atom concentration, two-body emission intensity (10), T, T_v, and total gas density, were computed. Further details of these computations are given in the Appendix.

4. Results

The computations were performed on an IBM 360/50 computer; ideal shock wave conservation equations were used.

(A) O_2–Ar System

In the case of oxygen, the main interest lies in the observable incubation times (1, 6). This is because the available theoretical prediction of incubation times (5) underestimates the experimental values by a factor of five to ten at temperatures below 5000 °K. Application of the present model to this problem requires knowledge of vibrational relaxation times, molecular extinction coefficients, and rate constants obtained under conditions such that relaxation is much faster than reaction.

For the case of O_2 dilute in argon, vibrational relaxation times and molecular extinction coefficients at 1470 Å have been measured (22) over the temperature range of interest. The values of $k_{r,Ar}$ were obtained from recent low-temperature recombination rate constants (23) and the results obtained by Wray (24), who studied recombination of atoms in shock-dissociated ozone. In the present work, rate constants, which were obtained (24) under such conditions that corrections for reaction

$$O + O_3 \rightarrow 2O_2$$

were necessary, were omitted. Furthermore, it was assumed that it is possible to use the data of Watt and Myerson (6) to calculate the recombination rate constants from the rate quotient law; this assumption is further discussed below. The data were combined to give the equation

$$[8] \qquad \log_{10} [k_r] = 13.4–1.70 \log_{10} T$$

over the range 200 to 5000 °K (Fig. 1); k_r is in $l^2\ mol^{-2}\ s^{-1}$.

When integrated over a 5 μs RC time-constant (6), the profile of oxygen atom concentration [O], computed for the conditions of the experiment reported in most detail (Fig. 4, ref. 6), agreed well with the experimental profile. Both incubation times and dissociation rates were in good agreement, the latter providing a check on the self-consistency of the computation. In Fig. 2, computed incubation times are plotted as a function of translational temperature. The computed values are in excellent agreement with the experimental results over the range 2900 to 7200 °K. These incubation times are three to four times longer than Camac's relaxation times (22). Our calculations indicate that up to 7200 °K, the time at which the rate of formation of oxygen atoms settles down to a steady value corresponds to practically complete relaxation (Fig. 3); that is, according to the present model, during the "normal" dissociation period (6), the fraction of O_2 in the dissociating states is very nearly at the equilibrium value. This fact justifies inclusion of the Watt and Myerson data (6) in calculation of eq. 8.

The computed profiles of optical density at 1470 Å yielded rate constants in agreement with the [O] profile values. At 5000 °K, the rate constants obtained by Wray (1) are about a factor of 2 higher than those of Watt and Myerson (6). The reason for this discrepancy is not known, but the present calculations suggest that it is *not* due to disequilibrium of internal modes, which *would* have tended to give high values from Wray's technique (7, 13). The computed incubation times for $\log (I_0/I)$, at 1470 Å, were about 20% longer than those for [O]. This qualitative trend is in agreement with the predictions of Brau, Keck, and Carrier (5).

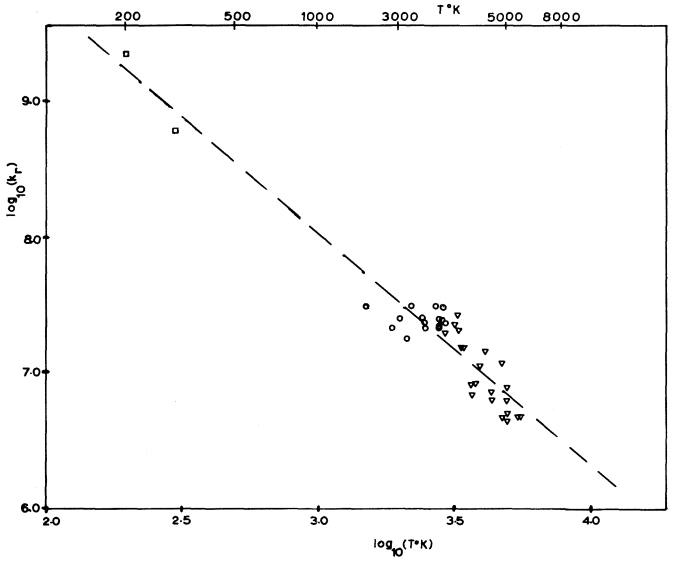

FIG. 1. Recombination rate constants $k_r(l^2\ mol^{-2}\ s^{-1})$, for O + O + Ar → O_2 + Ar. □, Campbell and Thrush, ref. 23; ○, Wray, ref. 24; △, Watt and Myerson, ref. 6.

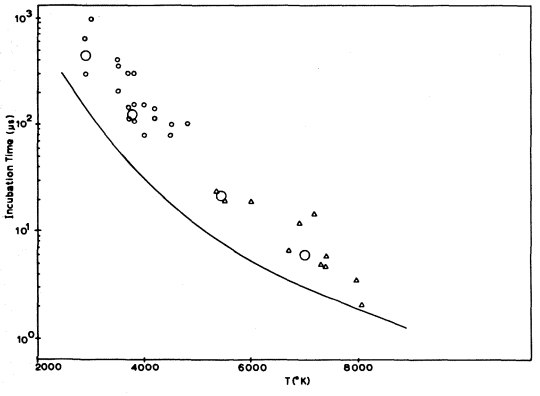

FIG. 2. Incubation times for O_2 dissociation in argon, normalized to 1.28×10^{17} molecules cm^{-1}. ○, ref. 6; △, ref. 1; ○, present work. Solid curve is the vibrational relaxation time, ref. 22.

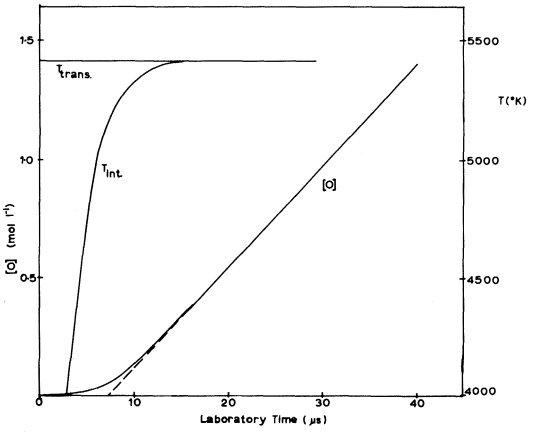

FIG. 3. Computed profiles of some gas properties. 1% O_2 in argon, total initial pressure 10^{-3} atm; shock velocity 2.45×10^5 cm s^{-1}.

(B) Br_2–Ar System

The success of the u.p.d. model in predicting well the incubation times for O_2–Ar system prompted our application of the model to other systems. Specifically the Br_2–Ar system seemed to be of particular interest. It was shown previously (7, 13) that the u.p.d. model reconciles, adequately, various experimental data on bromine dissociation–recombination reaction. However, in the past, 10% Br_2–Ar mixtures were tested; such mixtures produce extremely small experimental reaction slopes, and are thus not very useful in testing the present model. Moreover, in the past (7, 13) the back reaction has not been taken into account in calculations of dissociation profiles. In the present work both of these limitations were eliminated. For dilute mixtures, reaction profiles up to a few percent dissociation were generated; for 10% Br_2–Ar mixtures, total reaction profiles were obtained.

The high dilution (1%) data, which show least

Can. J. Chem. Downloaded from www.nrcresearchpress.com by 210.87.254.40 on 09/05/12
For personal use only.

Can. J. Chem. Downloaded from www.nrcresearchpress.com by 210.87.254.40 on 09/05/12
For personal use only.

scatter, appear to be those of Warshay (9); since these raw experimental results were not available to us, the following procedure was adopted. Seven profiles of two-body emission intensity were computed for comparison with the results obtained in Series A of ref. 10, over the range 1370 to 1900 °K; only the first few microseconds of each profile were matched, in order to define the initial slopes. The computed profiles of Br_2 optical absorption, corresponding to the best fits of the emission profiles, were then used to compute "initial slope" rate constants, for comparison with the results of Warshay (9).

The values of the relaxation time for Br_2 in Ar, and of the extinction coefficients of Br_2, were the same as used previously (7, 13). The flash-photolysis recombination rate constants, obtained (8) over the range 298 to 1300 °K, were expressed in the form

$$[9] \quad \log_{10} [k_{r,\text{flash}}] = 7.99 + 536.99/T - 3.238 \times 10^4/T^2$$

(where k_r is in $l^2\ mol^{-2}\ s^{-1}$), and extrapolated up to 1900 °K. These rate constants are believed (7, 13) to represent the contribution from argon only. The efficiency of molecular bromine is known (11), relative to that of argon, in the overall dissociation process; the efficiency of Br atoms was used as the fitting parameter.

Before integration over slit-width and electronics risetime, the computed absorption profiles showed sharp "spikes" immediately behind the shock front (7, 13). This reflects the fact that initially $T_v = 298$ °K; since the Br_2 absorption coefficient is a *decreasing* function of T_v (7, 8), these spikes are due to the relatively rapid rise of T_v, immediately behind the shock front, causing in turn a rapid decrease in the extinction coefficient. When integrated over a slit-width and rise-time, the spikes degenerate to small humps; a typical profile is shown in Fig. 4. It is difficult to eliminate subjectivity in estimating initial slopes, unless some well-defined procedure is adopted (10, 25); the procedure indicated in Fig. 4 was used in the present work. The initial slopes were converted to dissociation rate constants, and are shown in Fig. 5.

These results are similar to those obtained previously (7, 13) for mixtures containing 10% of Br_2, but involve reasonably large values of the initial slopes. The present extension of the u.p.d. model also permits matching of experimental

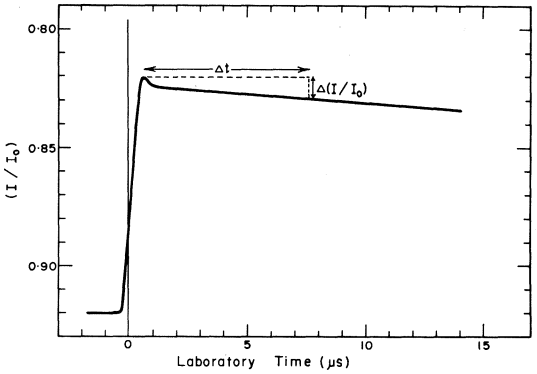

FIG. 4. Computed profile of transmitted light intensity; 1% Br_2 in argon; total initial pressure 47.6 Torr; shock velocity 1.73×10^5 cm s^{-1}; T (shock front) = 1530 °K; 0.1 cm slit width, zero time taken when shock front is at center of slit; RC time-constant = 0.1×10^{-6} s.

profiles to complete equilibrium. The most reliable data are the profiles of two-body emission obtained in Series C of ref. 10. The quality of the individual fits obtained, using the present procedure, was similar to that obtained previously (10) using a more orthodox approach. The efficiency of Br atoms, relative to that of argon, was found in the present work to be 10 ± 6, over the temperature range of the experiments (10).

Figure 6 shows the variation of the vibrational and translational temperature in a typical case. It can be seen that the two temperatures, T and T_v, approach each other as the reaction proceeds to the equilibrium. There is a maximum in the vibrational temperature, when the flow of energy into vibration from the translational heat-bath is just balanced by the loss of vibrational energy through dissociation of highly energized oscillators. In all cases studied here, this "steady state" value occurs at a time when recombination is unimportant. The concept of such a "steady state" in the vibrational distribution function was used (13) to explain the temperature dependence of the "initial slope" rate constants obtained by the shock wave emission technique, which monitors the product Br atoms. However, the use of this "steady state" assumption is not necessary in the present work, since the model yields [Br], T_v, and T directly as a function of time.

(C) Cl_2–Ar System

The temperature dependence of rate coefficients for Cl atom recombination in argon was

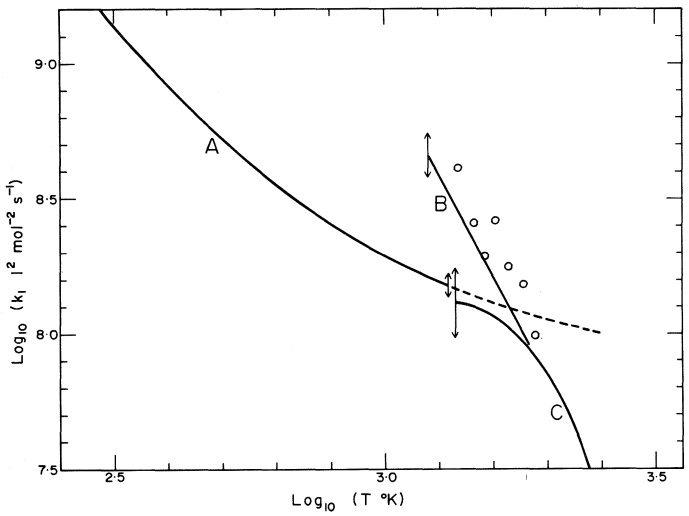

FIG. 5. Temperature dependence of rate coefficients, for $2Br + Ar \rightarrow Br_2 + Ar$. *A*: flash photolysis values of k_r, ref. 8. *B*: initial slope shock tube values of (k_d/K_{eq}), using molecular absorption spectrophotometry method, ref. 9. *C*: initial slope shock tube values of (k_d/K_{eq}) using two-body emission intensity, ref. 10. ○, present work: initial slope values of (k_d/K_{eq}) computed for absorption experiments.

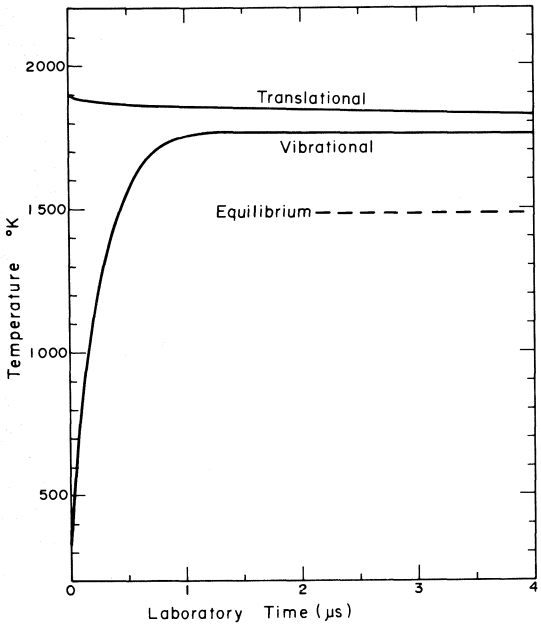

FIG. 6. Time dependence of translational and vibrational temperatures; 9% Br_2 in argon; total initial pressure 11.7 Torr; shock velocity 1.215×10^5 cm s^{-1}; Br atom efficiency, relative to argon, is 12.0.

discussed elsewhere (26, 27). It is presently assumed that Cl recombines via the "semi-relaxed" (13, 27) mechanism. The vibrational relaxation time of Cl_2 in Ar, $\tau_v(Cl_2\text{–Ar})$, was calculated using the method described elsewhere (28). Vibrational relaxation times needed for these calculations are available in the literature (22, 29). Although $\tau_v(Cl_2\text{–Ar})$ has not been measured, and thus cannot be compared to $\tau_v(Cl_2\text{–Ar})$ presently calculated, the value obtained is not unreasonable; furthermore the method (28) predicts $\tau_v(Cl_2\text{–He})$ in good agreement with experiment (30). The optical extinction coefficients for Cl_2 at 3850 and 3640 Å have been reported (31, 32). For the purposes of computation, the (unknown) total pressures were chosen in such a way that no more than 5% of dissociation occurred in the first 5 μs of the reaction. Just as in the case of Br_2 in Ar, the computed Cl_2–Ar dissociation rate coefficients display a pronounced negative temperature dependence, in agreement with experiments (31, 32) (Fig. 7).

5. Discussion

The principal finding of the present investigation is that the u.p.d. model for dissociation predicts well the observed incubation times for O_2 dissociation in argon below 7200 °K. On the other hand the previously used model (5) fails to agree with the experimental results at lower temperatures.

The dissociation of a diatomic molecule may be described by a transport matrix possessing a set of eigenvalues. However, because the signal-to-noise ratio and time resolution of shock wave data are limited, the experiment can usually be

Can. J. Chem. Downloaded from www.nrcresearchpress.com by 210.87.254.40 on 09/05/12
For personal use only.

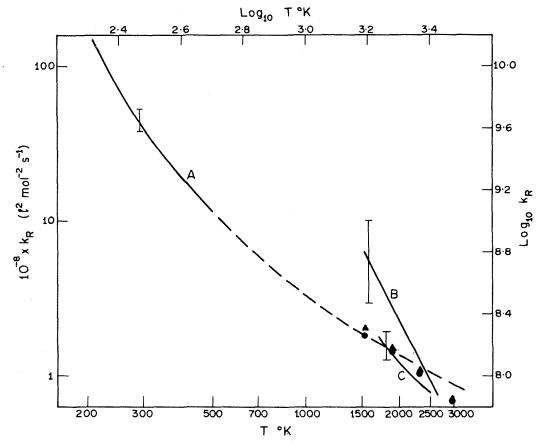

FIG. 7. Temperature dependence of rate coefficients for Cl_2 in Ar. Curve *A*, —, ref. 26; ---, calculated from "semi-relaxed" mechanism, ref. 27. Curve *B*, shock wave absorption values of k_d/K_{eq}, initial slope, ref. 31. Curve *C*, shock wave absorption value of k_d/K_{eq}, initial slope, ref. 32. △, computed values of k_d/K_{eq} from generated optical density absorption shock wave profiles at 3640 Å. ○, computed values of k_d/K_{eq} from generated optical density of absorption shock wave profiles at 3850 Å.

satisfactorily described by the *two* lowest non-zero eigenvalues, λ_1 and λ_2; certainly, from the experimental point of view, only two rate parameters (dissociation rate coefficient and internal relaxation time) are obtainable. One of the eigenvalues is associated with internal relaxation and the other with dissociation.

Commonly it is assumed that the internal relaxation is governed by the relaxation between the two lowest vibrational energy levels. In this case,

$$\lambda_2 = \lambda_{int} \simeq k_{10} + k_{01}$$

where k_{10} and k_{01} are rate constants for transitions between the lowest and first excited vibrational levels (12). For convenience in discussion, we here consider the case where recombination may be ignored, so that $\lambda_1 = \lambda_{diss} \simeq k_d$, the dissociation rate coefficient. It was emphasized in Section 2 above that a condition for the validity of the principal assumptions of the present model is that the coupling between dissociation and relaxation must be weak, *i.e.* $\lambda_1 \ll \lambda_2$. We are indebted to a referee for pointing out that this condition may be made quite explicit for the case of the modified Bethe–Teller eq. 1, used in the present model; such an equation may be shown to be valid only if λ_1 and λ_2 are well separated, and, in addition, are the only two eigenvalues of importance.

The diffusion theory of dissociation (5), which considers excitations of highly activated molecules in the dissociation limit, does not satisfactorily reproduce the experimental results under these conditions. That the theory may fail at low shock temperature was recognized by its authors (5). Specifically, in this theory, the magnitude of the vibrational relaxation transient time, and hence λ_2, depends upon the diffusion coefficient which had been defined from classical trajectory calculations within $3kT$ of the dissociation limit; it is reasonable that the diffusion time among uppermost vibrational levels be faster than k_{10}^{-1}. It is not surprising, therefore, that the incubation times obtained from the diffusion theory are smaller than those calculated in the present work, and observed experimentally, at lower temperatures.

The chief difference between the halogen and the oxygen systems is that of the negative temperature coefficients in recombination–dissociation rates. For O_2, the low temperature recombination rate coefficients agree well with those obtained in shock wave experiments, in the sense that a smooth graph of k_r (or k_d/K_{eq}) over the entire temperature range is obtained (Fig. 1). On the other hand, the negative temperature coefficients obtained for the halogens in shock waves are consistently higher than those obtained in lower temperature experiments. This discrepancy in the negative temperature coefficients is quite general, and is not limited to the few cases discussed in this work. In other examples, Br_2 in excess of He, Ne, Kr, O_2, and N_2 was similarly compared (13), and in all cases the shock wave data produced a high negative temperature dependence, while the negative temperature coefficients, obtained from flash photolysis data at lower temperatures, were considerably smaller. Similar results were obtained for iodine in a large excess of argon (33). An indirect comparison of flash and shock rate data, obtained from studies of iodine recombination over a wide pressure range of diluent argon, also predicts a discrepancy between the negative temperature coefficients (34).

For the O_2–Ar system, because the low and high temperature recombination–dissociation data are in essential agreement, the vibrational temperature decays to translational temperature within the transient time (Fig. 3). Consequently k_d, the time-dependent rate coefficient, decays, within the same time, to its time-independent value,

Can. J. Chem. Downloaded from www.nrcresearchpress.com by 210.87.254.40 on 09/05/12
For personal use only.

Can. J. Chem. Downloaded from www.nrcresearchpress.com by 210.87.254.40 on 09/05/12
For personal use only.

($k_r K_{eq}$), which in the absence of recombination may be identified with λ_1. On the other hand, the negative temperature coefficients obtained for the halogens, at low and at high temperatures, differ markedly. This would then imply that the vibrational temperature behind the shock wave reaches a "steady state", which is below the translational temperature (Fig. 6). This means that k_d, after an initial transient associated with vibrational relaxation, reaches what is almost a steady state value, obtained from shock wave results. This value of k_d is smaller than the corresponding ($k_r K_{eq}$), as can be seen from Fig. 8. This conclusion implies that for halogens in shock waves, the dissociation is governed not by one but by several nearly degenerate eigenvalues.

It must be pointed out that this interesting conclusion is based on two important assumptions: (*1*) that the available experimental data are correct and (*2*) that the extrapolation of the low temperature data into the shock wave temperature range (Figs. 5 and 7) is acceptable. We are unable to question the first of these assumptions at the present time. As to the second assumption, it could only be said that one does not anticipate the observed sharp change in the negative temperature coefficient on theoretical grounds; this is confirmed by the results of trajectory calculations on the 2Br + Ar system (35). It may be of interest to point out that the above conclusion does not depend upon detailed assumptions of the u.p.d. model; just about any other reasonable non-equilibrium model for dissociation would arrive at similar conclusions if the above two assumptions are accepted. However, the shapes of T_v *vs.* t (Figs. 3 and 6) and k_d *vs.* t (Fig. 8) are correct only to within the limitations of the u.p.d. model. We do not feel that the predicted time dependencies (Figs. 3, 6, and 8) are exact descriptions of actual phenomena: the u.p.d. model used is only a simple and approximate scheme. Nonetheless, it is highly intriguing that it predicts a variety of experimental data (Figs. 2, 3, 5, 7) with a surprising accuracy. It should also be pointed out that, in the case of *complete* reaction profiles, the scatter in the fitting parameter (Br atom efficiency), obtained using the u.p.d. model is identical to that obtained previously ($\pm 60\%$) using a more orthodox procedure (ref. 10, eq. 12).

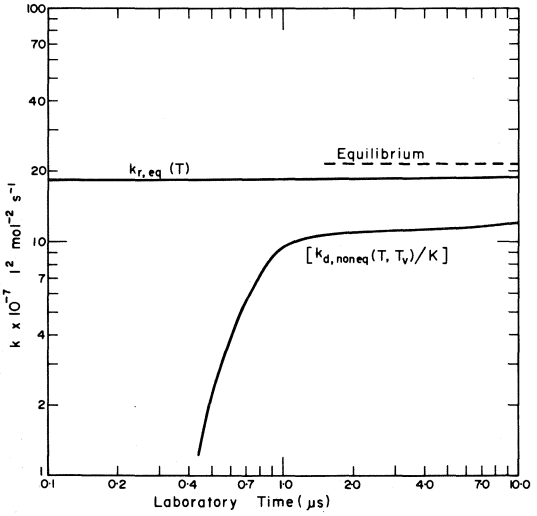

FIG. 8. Time dependence of rate coefficients for Br_2–Ar system. Conditions identical to those of Fig. 6. Variation in k_r is due to variation in the translational temperature only.

Another difference between the oxygen and halogen systems (especially bromine) is the fact that the latter display marked discrepancies in the absolute values of rate coefficients obtained using various techniques (Fig. 5). Use of the present model has permitted quantitative reconciliation of these results, but it seems worthwhile to point out here the qualitative features of the present model which led to this result. The crucial difference between the bromine and oxygen systems is one of time scales. Wray (1) discussed his results on incubation times in O_2 in terms of τ_v and τ_d, the characteristic times for relaxation and dissociation, respectively; these are inversely related to λ_2 and λ_1 above. For present purposes, a third characteristic time τ_{exp}, defining the time resolution of the experiment, is introduced; this is normally of the order of 10^{-6} s. The following very schematic diagram is useful in comparing the two systems.

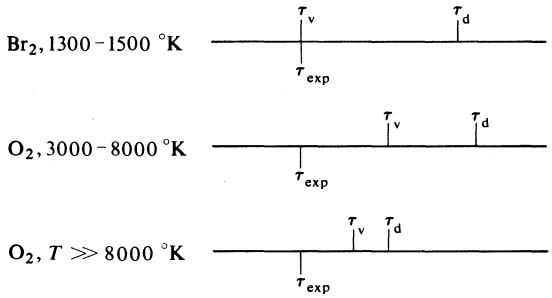

For the Br_2 system at lower temperatures, τ_v and τ_d are well separated, so that little or no coupling exists between relaxation and dissocia-

Can. J. Chem. Downloaded from www.nrcresearchpress.com by 210.87.254.40 on 09/05/12
For personal use only.

tion; thus dissociation rates obtained by monitoring two-body emission from product Br atoms agree well (10) with the flash photolysis results at their common temperature. However, τ_v and τ_{exp} are so close that an experimental technique, which is sensitive to the instantaneous vibrational distribution function of Br_2, will tend to give spurious results. Thus, since the molecular extinction coefficient is a function of T_v, this technique gives results which disagree with those of the other two independent methods (10, 13). Qualitatively (7, 13), the fact that non-equilibrium effects give apparently *high* values for the rate coefficients (9) follows from the form of the dependence of the extinction coefficient on T_v; at the wavelength used (9), the extinction coefficient decreases with increasing T_v (8, 9) behind the shock front, thus producing a spurious contribution, to the initial rate of change of optical density with time, which is of the *same* sign as that caused by dissociation of Br_2. Since the method of data reduction used (9) explicitly assumes that relaxation is effectively instantaneous within the shock front (36), this *total* initial slope is assigned entirely to the dissociation contribution. This effect is the origin of the "hump" shown in Fig. 4, and referred to in Section 4 above. When the appreciable noise levels present in such experiments are considered, it is clear that such "humps" would not be clearly observable, but would contribute to spuriously high values for the initial slopes (7, 13).

For the O_2 system, at the lower end of its temperature range, all three characteristic times are well separated. Therefore, the vibrational relaxation (22) and dissociation (1, 6) may be conveniently studied independently of one another, and observable incubation times occur. At higher temperatures, however, considerable dissociation–relaxation coupling is observed (1).

We would like to acknowledge the support of the Air Force Office of Scientific Research and the donors of the Petroleum Research Fund, administered by the American Chemical Society. This work was also supported in part by the National Research Council of Canada and by the Defence Research Board of Canada, Grant No. 9530-54. The cooperation of the Institute of Computer Science, University of Guelph, is also gratefully acknowledged.

Appendix

Computational Procedure

Let us define the rate of the dissociation reaction as $[(\partial[X_2]/\partial t)_\rho]_{r.g.t.}$, where ρ is the total density and r.g.t. refers to the real gas time, which differs from the laboratory time (l.t.) in shock wave reactions. We have

$$[A1] \qquad [X_2] = (1 - \alpha)\phi C_1/\rho_{12}$$

$$[A2] \qquad [X] = 2\alpha\phi C_1/\rho_{12}$$

$$[A3] \qquad [M] = (1 - \phi)C_1/\rho_{12}$$

where ϕ is the mole fraction of X_2 in unshocked gas, C_1 is the total molecular concentration ahead of the shock front. Furthermore, $\rho_{12}(t) = \rho_1/\rho_2(t)$, where ρ_1 is the total gas density ahead of the shock front and $\rho_2(t)$ is the total gas density behind the shock front. Then

$$[A4] \quad -[(\partial[X_2]/\partial t)_\rho]_{r.g.t.} = (\phi C_1/\rho_{12})(d\alpha/dt)_{r.g.t.}$$

which is the chemical rate described by eq. 8. Then, making the appropriate substitutions from eqs. A1 to A3, eqs. A4 and 8 give

$$[A5] \quad (d\alpha/dt)_{l.t.} = (1/\rho_{12})(d\alpha/dt)_{r.g.t.} = (C_1/\rho_{12}{}^3)k_{r,Ar}[1 + (F - 1)\phi + \alpha\phi(2E - F)][K_{eq}G(1 - \alpha)\rho_{12} - 4\phi C_1\alpha^2]$$

where E and F are the reaction efficiencies, relative to Ar, of X and X_2 respectively; G is the r.h.s. of eq. 5 and $K_{eq} = k_d/k_r$.

The vibrational relaxation equation with the assumption $(\bar{E}_d - \varepsilon_v) = (E_r - \varepsilon_v) \simeq D$ is

$$[A6] \quad (d\varepsilon_v/dt)_{r.g.t.} = [(\varepsilon_\infty - \varepsilon_v)/\tau_v + (D/[X_2])[(\partial[X_2]/\partial t)_\rho]_{r.g.t.}$$

Substituting eqs. A7 and A8 into A6

$$[A7] \qquad \varepsilon_v = R\theta/(\exp(\theta/T_v) - 1)$$

$$[A8] \qquad \varepsilon_\infty = R\theta/(\exp(\theta/T) - 1)$$

where R is the gas constant, we obtain

$$[A9] \quad (dT_v/dt)_{l.t.} = (d\varepsilon_v/dt)_{r.g.t.}(T_v/\theta)^2 \times (R\rho_{12})^{-1}(\exp(\theta/T_v))^{-1} \times (\exp(\theta/T_v) - 1)^2$$

where $(d\varepsilon_v/dt)_{r.g.t.}$ is given by eq. A6.

Since ρ_{12}, T, α, and P, the total pressure, are all functions of time behind the shock front, it is necessary to use the hydrodynamic conservation equations and the ideal gas equation of state. We have integrated eqs. A5 and A9 using a 4th order Runge–Kutta procedure. The conservation equations were integrated implicitly using an

iterative technique (10). In this way, laboratory time profiles for all relevant parameters, describing the reacting gas, were generated. Such profiles took no account of finite slit-width and electronics rise-time. For this reason appropriate integrations over known slit-width (1 mm) and electronic rise-time (0.1–0.2 $\times$ 10^{-6} s) were made.

1. K. L. WRAY. J. Chem. Phys. **37**, 1254 (1962).
2. P. HAMMERLING, J. D. TEARE, and B. KIVEL. Phys. Fluids, **2**, 442 (1959).
3. P. V. MARRONE and C. E. TREANOR. Phys. Fluids, **6**, 1215 (1963).
4. S. P. HEIMS. J. Chem. Phys. **38**, 603 (1963).
5. C. A. BRAU, J. C. KECK, and G. F. CARRIER. Phys. Fluids, **9**, 1885 (1966).
6. W. S. WATT and A. L. MYERSON. J. Chem. Phys. **51**, 1638 (1969).
7. J. K. K. IP and GEORGE BURNS. Discuss. Faraday Soc. **44**, 241 (1967).
8. J. K. K. IP and GEORGE BURNS. J. Chem. Phys. **51**, 3414 (1969).
9. M. WARSHAY. 5th International Shock Tube Symposium. White Oak, Maryland. 1965; U.S. Naval Ordnance Lab., A.D. 484600 (1966); J. Chem. Phys. **54**, 4060 (1971).
10. R. K. BOYD, GEORGE BURNS, T. R. LAWRENCE, and J. H. LIPPIATT. J. Chem. Phys. **49**, 3804 (1968).
11. R. K. BOYD, J. D. BROWN, GEORGE BURNS, and J. H. LIPPIATT. J. Chem. Phys. **49**, 3822 (1968).
12. J. F. CLARKE and M. MCCHESNEY. The dynamics of real gases. Butterworths, London. 1964. p. 298.
13. J. K. K. IP and GEORGE BURNS. J. Chem. Phys. **51**, 3425 (1969).
14. C. E. TREANOR and P. V. MARRONE. Phys. Fluids, **5**, 1022 (1962).
15. N. M. KUZNETSOV. Dokl. Akad. Nauk SSSR, **164**, 1097 (1965). (English Translation: Doklady Phys. Chem. **164**, 739 (1965)).
16. R. K. BOYD. Can. J. Chem. **49**, 1401 (1971).
17. B. WIDOM. Science, **148**, 1555 (1965).
18. S. BYRON. J. Chem. Phys. **44**, 1378 (1966).
19. GEORGE BURNS. 6th International Shock Tube Symposium. Freiburg, Germany. April, 1967; Ernst Mach Institute Wiss. Bericht **4**, 93 (1968).
20. W. C. GARDINER. Discuss. Faraday Soc. **44**, 274 (1967).
21. E. W. SCHLAG and W. G. VALANCE. J. Chem. Phys. **49**, 605 (1968).
22. M. CAMAC. J. Chem. Phys. **34**, 448 (1961).
23. I. M. CAMPBELL and B. A. THRUSH. Proc. Roy. Soc. A**296**, 222 (1967).
24. K. L. WRAY. J. Chem. Phys. **38**, 1518 (1963).
25. N. COHEN and R. R. GIEDT. J. Chem. Phys. **39**, 749 (1963).
26. M. A. A. CLYNE and D. M. STEDMAN. Discuss. Faraday Soc. **44**, 278 (1967).
27. GEORGE BURNS and R. G. BROWNE. J. Chem. Phys. **53**, 3318 (1970).
28. J. K. K. IP and G. BURNS. Discuss. Faraday Soc. **44**, 278 (1967).
29. W. D. BRESHEARS and P. F. BIRD. J. Chem. Phys. **51**, 3660 (1969).
30. E. F. SMILEY and E. H. WINKLER. J. Chem. Phys. **22**, 2018 (1954).
31. M. VAN THIEL, D. J. SEERY, and D. BRITTON. J. Chem. Phys. **69**, 834 (1965).
32. T. A. JACOBS and R. R. GIEDT. J. Chem. Phys. **39**, 749 (1963).
33. J. A. BLAKE and GEORGE BURNS. J. Chem. Phys. **54**, 1480 (1971).
34. GEORGE BURNS, R. J. LEROY, D. J. MORRISS, and J. A. BLAKE. Proc. Roy. Soc. A**315**, 81 (1970).
35. A. G. CLARKE and GEORGE BURNS. J. Chem. Phys. In press.
36. H. B. PALMER and D. F. HORNIG. J. Chem. Phys. **26**, 98 (1957).

Can. J. Chem. Downloaded from www.nrcresearchpress.com by 210.87.254.40 on 09/05/12
For personal use only.

Can. J. Chem. Downloaded from www.nrcresearchpress.com by 210.87.254.6 on 09/05/12
For personal use only.

NOTES

Methyl Cyanodithioformate as a Reactive Dienophile in Diels–Alder Reactions

D. M. VYAS AND G. W. HAY[1]

Department of Chemistry, Queen's University, Kingston, Ontario

Received June 1, 1971

A Diels–Alder reaction between cyclopentadiene and methyl cyanodithioformate afforded a 60:40 mixture of the isomers **2***a* and *b*. The n.m.r. studies of these compounds and the products of $LiAlH_4$ reduction, **3***a* and *b*, established that the major isomer, **2***a*, was 3-*exo*-cyano-3-methylthio-2-thiabicyclo-[2.2.1]hept-5-ene, and that **3***a* was the corresponding 3-*exo*-aminomethyl compound.

Une réaction de Diels–Alder entre le cyclopentadiène et le cyanodithioformate de méthyle conduit à un mélange 60:40 des isomères **2***a* et *b*. Une étude r.m.n. de ces composés et des produits de réduction par $LiAlH_4$, **3***a* et *b*, prouve que le produit majoritaire, **2***a*, est le cyano-3 *exo* méthylthio-3 thia-2 bicyclo[2.2.1]heptène-5; le produit **3***a* est l'aminoéthyl-3 *exo* correspondant.

Canadian Journal of Chemistry, **49**, 3755 (1971)

Introduction

A number of simple carbonyl compounds have been shown to function as dienophiles in the Diels–Alder reaction (1–4). However the analogous thiocarbonyl system, which has proved to be highly dipolarophilic (5), has provided very few examples of dienophilic activity. Through the pioneering research of Middleton (6), and Schonberg and König (7) the dienophilic nature of thiophosgene, thiofluorenone, perfluorothioacetone, and other fluorothiocarbonyls has been demonstrated. All of these last named compounds are highly toxic and, until recently, most were very difficult to obtain. More recent investigations have shown that thiobenzophenone (8), thioacetophenone (9), dichlorosulfine (10), and thioketene (11) react with dienes to give Diels–Alder adducts even under moderate conditions. Obviously the dienophilic potential of compounds with the carbon–sulfur double bond has been unexploited synthetically, not least because of their typical unpleasant odor and toxicity. Here presumably lies a wide field of preparative application of these compounds.

During the development of methods for the synthesis of unsaturated, deoxy sugars with sulfur in the ring, via the Diels–Alder reaction we have discovered that methyl cyanodithioformate (**1**) possesses a marked dienophilic activity. This has been demonstrated in our laboratory by the formation of Diels–Alder adducts with a wide range of dienes differing in reactivity from that of cyclopentadiene to that of 1,3-butadiene. The reagent is easily synthesized (12, 13) and is deep purple in color, a property which is useful to indicate the completion of the reaction, or to signal the occurrence of a retro-Diels-Alder reaction during the workup of the adducts. Such a dienophile has the advantage over the fluorothiocarbonyl compounds and others of introducing a potentially more useful functional group (cyano) into the product.

This paper reports the synthesis and proof of structures of stable derivatives of 2-thiabicyclo [2.2.1]hept-5-ene, synthesized via a facile Diels–Alder reaction using methyl cyanodithioformate as the dienophile.

Results and Discussion

At 0 °C, **1** reacted immediately with cyclopentadiene to give an almost quantitative yield of **2***a* and *b*[2] in a 60:40 ratio based on the peak integrations of the n.m.r. spectra. A portion of **2***a*, the major isomer, crystallized leaving a syrupy mixture (**2***ab*) which was rich in **2***b*. A slow isomerization of **2***b* to *a* was observed on standing at room temperature.

[1]To whom correspondence should be addressed.

[2]Each of **2***a*, *b*, and **3***a*, *b* was obtained as a racemic mixture. To conserve space the structural formula for only one of the enantiomers has been given in each case.

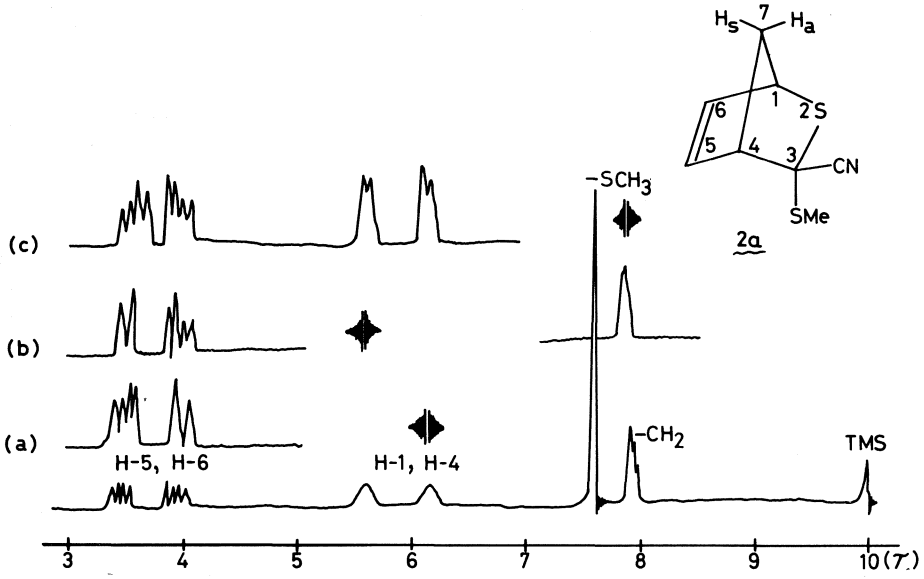

FIG. 1. The 60 MHz n.m.r. spectrum of **2***a* in deuteriochloroform with the assignments of protons as indicated. (*a*) Resonance of the H-5 and -6 protons during the simultaneous irradiation at 6.15 τ. (*b*) Resonance of the H-5, -6, and C-7 methylene protons during simultaneous irradiation at 5.61 τ. (*c*) Resonance of the H-1, -4, -5, and -6 protons during simultaneous irradiation at 7.93 τ.

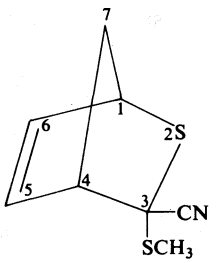

2*a*

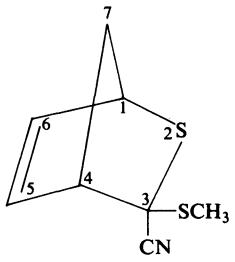

2*b*

In the 60 MHz n.m.r. spectra of **2***a* (Fig. 1) the bridgehead, methylene bridge, and vinylic protons were identified from the chemical shifts when compared to those of other Diels–Alder adducts of cyclopentadienes (8, 14), and the peak integrations. Only one of the two low-field quartets was affected by irradiation at either 6.17 or 5.63 τ (Figs. 1*a* and *b*) whereas the multiplet centered at 7.93 τ was reduced to a broad singlet by irradiation at both frequencies. Moreover, it was observed that irradiation at 7.93 τ (Fig. 1*c*) collapsed the multiplets centered at 6.15 and 5.61 τ to indistinct doublets without affecting the quartets centered at 3.50 and 3.97 τ. These data are consistent with the product being a 1,4- but not a 1,2-adduct. The latter type of compound shows significant and characteristic differences in the n.m.r. spectrum which reflect the dissimilar proton interactions inherent in such structures (15). Thus, the quartets centered at 3.50 (1H) and 3.97 τ (1H) were attributed to the resonance of the vinyl protons (H-5, -6; $J_{5,6} \simeq 6$ Hz), the multiplets centered at 5.61 (1H) and 6.15 τ (1H) were assigned to the bridgehead protons (H-1, -4; $J_{4,5} \simeq J_{1,6} \simeq 3$ Hz), and the multiplet centered at 7.93 τ (2H) was derived from the methylene bridge hydrogens. The $-SCH_3$ hydrogens gave rise to the sharp singlet at 7.64 τ (3H).

The elemental analysis, and i.r. and mass spectra, of **2***a* were consistent with the proposed structure. The mass spectrum revealed not only a distinct molecular ion ($[M]^+$) peak at *m/e* 183 but also ions with *m/e* 136, 117, 109, 66 (base peak) which, in terms of the probable fragmentation route, were attributed to $[M-SCH_3]^+$, $[H_3CSC(CN)S]^{\cdot+}$, $[M-SCH_3-HCN]^+$, and cyclopentadienyl radical cation.

The 60 MHz n.m.r. spectrum of the residual syrup, **2***ab* (Table 1), resembled that of **2***a* but was more complex; the recognizable signals from **2***a* being overlapped by others from the second component. However, two distinct, 3-proton

Can. J. Chem. Downloaded from www.nrcresearchpress.com by 210.87.254.6 on 09/05/12
For personal use only.

TABLE 1. Proton chemical shifts (τ values) of the Diels–Alder adducts **2***a* and *ab* and their $LiAlH_4$ reduction products **3***a* and *ab*

Compounds	Proton chemical shifts (τ values)*					
	H-1,H-4	H-5,H-6	H-7*a*,H-7s	$-SCH_3$	$-CH_2NH_2$	$-NH_2$
2*a*	5.61‡,6.15‡	3.50†,3.97†	7.93‡	7.64§	—	—
2*ab*	5.61‡,6.15‡ 5.71‡,6.39‡	3.32†,3.88† 3.50†	7.98‡	7.56§ 7.64§	—	—
3*a*	5.88‡,6.78‡	3.74	8.10‡	7.98§	6.95§	8.27§
3*ab*	5.88‡,6.74‡	3.50–4.20‖	8.10‡	7.98§ 7.86§	6.95§ 7.30§	8.27§

*In $CDCl_3$ with TMS as internal standard.
†Quartet.
‡Broad multiplet.
§Singlet.
‖The signals of the two vinyl protons of **3***a* and *b* overlap between these two values.

singlets were observed at 7.64 and 7.56 τ, and these were assigned to the $-SCH_3$ protons of **2***a* and *b*, respectively.

There remained the problem of establishing the stereochemistry at C-3. The shielding of *endo* ring protons or those of *endo* methyl groups in norbornene and 2-thiabicyclo[2.2.1]hept-5-ene systems as a consequence of the vinylic diamagnetic anisotropy (16) is well established (17–20) in n.m.r. studies. This effect causes the *exo* protons to resonate at a lower field than the *endo* protons. Although **2***a* lacks a hydrogen atom or a methyl group at C-3 it is evident from the chemical shifts (Table 1) that the $-SCH_3$ protons in **2***a* resonate 0.08 p.p.m. upfield to those of **2***b*. This shielding is very much smaller than that observed in comparable carbocyclic compounds (14). The Drieding model of **2***a* indicated that the $-SCH_3$ group may lie on the boundary of the shielding region of the double bond, and hence the protons, although in an *endo* position, experience a minimal diamagnetic shift.

However, for an unequivocal designation of the stereochemistry at C-3 in **2***a*, lithium aluminum hydride reduction of **2***a* to **3***a* and **2***ab* to **3***ab* was performed. The i.r. spectrum of each of **3***a* and *ab* exhibited absorption at 3.00 (broad doublet), 3.26, and 6.30 μ but not at 4.50 μ confirming that the cyano had been reduced to an amino methyl group.

Compound **3***a* gave a simple 60 MHz n.m.r. spectrum (Table 1), in which all of the proton resonances were clearly identified from their chemical shifts and peak integrations. On comparing the spectrum of **3***a* with that of **3***ab* (Table 1), the resonance signals corresponding to $-CH_2NH_2$, $-SCH_3$, and $-NH_2$ protons in **3***b* were readily identified.

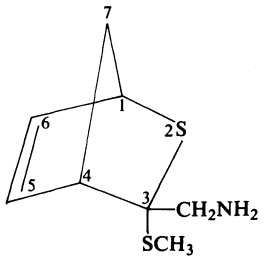

3*a*

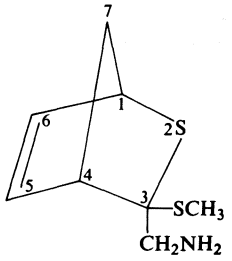

3*b*

The chemical shifts of the $-SCH_3$ protons of **3***a* and *b* are greater than those of **2***a* and *b* (Table 1), reflecting the increased shielding concommitant with the reduction of the cyano group. In each case the difference between the chemical shifts of the $-SCH_3$ protons of the major and minor isomers was not only in the same direction but also of approximately the same magnitude (**2***a*, *b*: 0.08 p.p.m.; **3***a*, *b*: 0.12 p.p.m.), indicating that the configuration at C-3 was unaffected by the reduction and that both **2***b* and **3***b* have an *exo*-SCH_3 group. This requires that the $-CH_2NH_2$ protons of **3***b* lie within the shielding zone of the ring double bond and hence, as observed (Table 1), resonate at a higher field than those of **3***a*. The difference between the chemical shifts of $-CH_2NH_2$ protons in **3***b* and *a* is 0.35 p.p.m., identical to that observed between the *endo*- and *exo*-CH_3 protons of 3-cyano-3-methylnorbornene (14).

Can. J. Chem. Downloaded from www.nrcresearchpress.com by 210.87.254.6 on 09/05/12
For personal use only.

These data lead to the conclusion that **2***a* is a racemic mixture of 3-*exo*-cyano-3-methylthio-2-thiabicyclo[2.2.1]hept-5-ene, and that **3***a* is a racemic mixture of the corresponding 3-*exo*-aminomethyl compound.

Experimental

General Conditions

All melting points were determined on a Fisher–Johns melting point block and are uncorrected. All evaporations were conducted under reduced pressure. The i.r. spectra were recorded on a Perkin–Elmer Model 180 spectrometer using the following conditions: $CHCl_3$ solution; 0.1 mm path length; scan time setting 1:1, coarse adjustment 10:1, split program 7, time constant 2. The n.m.r. spectra were obtained in $CDCl_3$ solution using either a Varian T-60 or a Bruker HX-60 60 MHz spectrometer. Mass spectra were obtained with a Jeol JMS 01SC spectrometer.

*Methyl Cyanodithioformate (**1**)*

This compound was prepared according to Simmons *et al.* (13).

*Racemic Mixture of 3-exo-Cyano-3-methylthio-2-thiabicyclo[2.2.1]hept-5-ene (**2a**)*

Compound **1** (5.88 g) in 20 ml CH_2Cl_2 was added with stirring to 4 g freshly distilled cyclopentadiene in 20 ml CH_2Cl_2 at 0 °C. An immediate loss of the deep purple color of **1** ensued. Evaporation of the solvent and excess diene gave a pale yellow syrup (9.10 g) which, after solution in a minimum volume of CH_2Cl_2 and addition of petroleum ether (b. p. 30–60 °C) to incipient cloudiness, afforded, upon cooling, 4.3 g **2***a* as colorless prisms, m.p. 85–86 °C. The n.m.r. spectrum of **2***a* as obtained on the Varian T-60 spectrometer with an internal TMS standard is given in Fig. 1. The determination of chemical shifts and peak integrations, and the decoupling experiments (Figs. 1*a–c*), were performed with the Bruker HX-60 using an internal TMS lock. The i.r. spectrum had major peaks at 3.25 (w), 3.35 (s), 3.40 (s), 3.42 (s), 3.52 (s), 4.50 (s), 6.00 (w), 7.00 (s), and 7.50 (s) μ. The mass spectrum showed major components at *m/e* 183, 136, 117, 109, and 66 (base peak).

Anal. Calcd. for $C_8H_9NS_2$: C, 52.46; H, 4.85; N, 7.46; S, 34.97. Found: C, 52.61; H, 4.85; N, 7.81; S, 34.92.

The residual syrupy mixture, **2***ab*, gave the n.m.r. spectrum (Varian T-60, internal TMS standard) which consisted of many overlapping peaks (Table 1), except two distinct singlets at 7.64 and 7.56 τ. The i.r. spectrum showed the same number and location of absorption peaks as that of **2***a*.

*Racemic Mixture of 3-exo-Aminomethyl-3-methylthio-2-thiabicyclo[2.2.1]hept-5-ene (**3a**)*

Compound **2***a* (2.2 g) in 20 ml anhydrous ethyl ether was added dropwise to 1.8 g $LiAlH_4$ in 50 ml anhydrous ethyl ether, and stirred at room temperature until the reaction subsided (45 min). The $LiAlH_4$ was destroyed in the usual fashion and the product isolated from the ether extracts by evaporation after drying over anhydrous $MgSO_4$. The yield was 1.5 g yellow–orange syrup, **3***a*, the chemical shifts of the n.m.r. spectrum (Varian T-60, internal TMS lock) of which are recorded in Table 1. The i.r. spectrum exhibited absorbance at 3.00 (m, broad doublet), 3.26 (m), 3.35 (s), 3.40 (s), 3.50 (s), 6.30 (m, broad), 6.97 (s), and 7.51 (s) μ.

A phenylurethane derivative of **3***a* was prepared according to Shriner *et al.* (21), m.p. 138–139 °C.

Anal. Calcd. for $C_{15}H_{18}N_2OS_2$: C, 58.82; H, 5.88; N, 9.12. Found: C, 58.81; H, 5.89; N, 9.33.

The mixture, **2***ab*, was reduced in the same manner. The i.r. spectrum of the product, **3***ab*, was indistinguishable from that of **3***a*. The n.m.r. spectrum (Varian T-60, internal TMS lock) data for **3***ab* is given in Table 1.

This research was supported by an Operating Grant (A1921) from the National Research Council of Canada. One author (D. M. V.) gratefully acknowledges financial assistance from Queen's University.

1. T. L. Gresham and T. R. Steadman. J. Am. Chem. Soc. **71**, 737 (1949).
2. W. J. Dale and A. J. Sisti. J. Am. Chem. Soc. **76**, 81 (1954).
3. W. J. Dale and A. J. Sisti. J. Org. Chem. **22**, 449 (1957).
4. J. F. Harris. U. S. Patent, 3 136 786 (1964).
5. R. Huisgen. Angew. Chem. **75**, 604, 742 (1963); Angew. Chem. Intern. Ed., **2**, 265, 633 (1963).
6. W. J. Middleton. J. Org. Chem. **30**, 1390 (1965).
7. A. Schonberg and B. König. Tetrahedron Lett. 3361 (1965).
8. K. Yamada, M. Yoshioka, and N. Sugiyama. J. Org. Chem. **33**, 1240 (1968).
9. A. Ohno, Y. Ohnishi, and G. Tsuchihashi. Tetrahedron. **25**, 871 (1969).
10. B. Zwanenburg, L. Thijs, and J. Strating. Tetrahedron Lett. **51**, 4461 (1969).
11. M. S. Raasch. J. Org. Chem. **35**, 3470 (1970).
12. G. Bahr and G. Schleitzer. Chem. Ber. **83**, 1771 (1955).
13. H. E. Simmons, D. C. Blomstrom, and R. D. Vest. J. Am. Chem. Soc. **84**, 4756 (1962).
14. J. C. Muller, J. P. Fleury, and U. Schiedegger. Org. Magn. Res. **2**, 77 (1970).
15. E. M. Gold, and D. Ginsburg. Angew. Chem. Intern. Ed., **5**, 246 (1966).
16. R. R. Fraser. Can. J. Chem. **40**, 78 (1962).
17. P. M. Subramanian, M. R. Emerson, and N. A. LeBel. J. Org. Chem. **30**, 2624 (1965).
18. P. Laszlo and P. R. Schleyer. J. Am. Chem. Soc. **86**, 1171 (1964).
19. Y. Kobuke, T. Fueno, and J. Furukawa. J. Am. Chem. Soc. **92**, 6548 (1970).
20. C. R. Johnson, J. E. Keisen, and J. C. Sharp. J. Org. Chem. **34**, 860 (1969).
21. R. L. Shriner, R. L. Fuson, and D. Y. Curtin. The systematic identification of organic compounds. 5th Ed. J. Wiley & Sons. New York, N. Y., 1964.

Can. J. Chem. Downloaded from www.nrcresearchpress.com by 210.87.254.6 on 09/05/12
For personal use only.

Proton Magnetic Resonance Studies of Some 1-X-2,4-Dinitrobenzenes

MICHAEL D. STEPHENS,[1] JOHN D. REINHEIMER, AND ALLAN H. KAPPELMAN
Department of Chemistry, The College of Wooster, Wooster, Ohio

Received June 11, 1971

Shaefer's additivity rules for coupling constants have been applied to trisubstituted benzenes. If a resonance interaction between substituents is possible, the observed coupling constants are larger than those predicted. For other substituents, the additivity rules are followed.

Les règles d'additivité de Shaefer, relatives aux constantes de couplage, ont été appliquées aux composés benzéniques trisubstitués. S'il y a possibilité d'une interaction de résonance entre les substituants, les constantes de couplage observées sont alors plus grandes que celles prévues. Pour les autres substituants, les règles d'additivité sont respectées.

Canadian Journal of Chemistry, **49**, 3759 (1971)

Can. J. Chem. Downloaded from www.nrcresearchpress.com by 210.87.254.105 on 09/05/12
For personal use only.

Introduction

A predictive additivity scheme for coupling constants in substituted benzene compounds has been proposed (1). The scheme has developed from correlations between substituents and coupling constants and is based specifically upon coupling parameters of mono-substituted benzene compounds. Schaefer *et al.* (2), have applied this predictive additivity scheme to a series of 1,2,4 trisubstituted benzene compounds and found very good and consistent agreement between the predicted and observed ortho coupling constants. The present study presents a series of eight 1-X-2,4-dinitrobenzene compounds and compares the observed coupling constants with the predicted.

Experimental

The 2,4-dinitrohalobenzenes and 2,4-dinitroacetanilide spectra were recorded on a Varian HA 100 n.m.r. spectrometer using an internal lock on the solvent. These and the other spectra were recorded on a Varian A 60 with an external water lock. The spectra are ABC and were analyzed using the LAOCN3 computer program of Castellano and Bothner-By (3). The compounds were recorded as both 5 and 10% solutions in acetone with no observable change in coupling constants. Acetone was the solvent for the series; 2,4-dinitrophenol was recorded in acetone, methanol, acetonitrile and CCl_4–acetone (7:3 v/v) to study coupling constant consistency in different solvent systems. A few drops of D_2O were added to samples where proton exchange was expected. All solvents were spectral grade and the compounds were obtained commercially.

Results and Discussion

The chemical shift parameters for these compounds are given in Table 1. The predicted coupling constants are determined by the following eqs. 1–3 (2), where the ΔJ values for the

$$[1]\quad J_o = J_{56} = \Delta J_{23}{}^{x} + \Delta J_{34}{}^{y} + \Delta J_{23}{}^{z} + J_o{}^{b}$$

$$[2]\quad J_m = J_{35} = \Delta J_{35}{}^{x} + \Delta J_{24}{}^{y} + \Delta J_{26}{}^{z} + J_m{}^{b}$$

$$[3]\quad J_p = J_{36} = \Delta J_{36}{}^{x} + \Delta J_{36}{}^{y} + \Delta J_{36}{}^{z} + J_p{}^{b}$$

substituents are derived from the respective monosubstituted compounds. The numbering system is somewhat confusing. In columns 1 and 2 of eqs. 1–3, the numbers refer to the tri-substituted benzene,

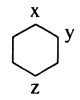

where x is regarded as C-1. The final column is the normal coupling constant for unsubstituted benzene, while columns 3, 4, and 5 are numbered from the group labelled x, y, or z. Thus, J_{56} would be J_{23} if x is on C-1, J_{34} if y is on C-1 and J_{23} if z is on C-1. The tabulated data of reference (2) place x, y, and z on C-1. The observed and predicted coupling constants are given in Table 2. McConnell's theoretical work (4) and later empirical studies (5, 6) indicate that in aromatic systems spin–spin coupling is transmitted almost exclusively through the σ bonding orbitals with the π bonding systems having a slight effect on long range coupling and accounting for approximately 0.5 Hz of the ortho coupling constant. Previous studies (5–7) of monosubstituted and disubstituted benzene compounds have shown direct correlation between substituent inductive effect and changes in coupling constants. The predictive additivity scheme has developed from

[1]NSF Undergraduate Research Participant, 1970.

TABLE 1. Chemical shift parameters of ring protons of some 1-X-2,4-dinitrobenzenes*,†

Compound	X	ν3	ν5	ν6
1	OCH_3	519.9 Hz	508.7 Hz	454.5 Hz
2	NH_2	535.4	489.8	431.3
3	OH	533.7	508.3	445.2
4	$NHNH_2$	536.8	498.3	475.2
5	$NHCOCH_3$	536.2	512.2	530.0
6	Cl	676.3‡	646.0	597.4
7	Br	527.9	506.6	494.0
8	I	523.5	495.4	510.7

*In Hz from TMS reference.
†The error in the computer calculated constants is less than 0.02 Hz for compounds **1**, **2**, **5**, **8**; less than 0.04 Hz for **3** and **7**; less than 0.06 Hz for **4** and **6**.
‡100 MHz spectrum.

these correlations and has been successfully applied to disubstituted benzenes (1, 2, 8–10) with few exceptions (1, 10). In our study the 2,4-dinitrohalobenzenes, compounds **6–8**, show very good agreement between the predicted and observed ortho and meta coupling constants. Compounds **1–3**, with OCH_3, NH_2, and OH substituents, deviate from additivity and although the necessary monosubstituted values are not available to calculate the predicted values for 4 and 5 ($NHNH_2$ and $NHCOCH_3$), a comparable deviation is expected. A deviation of 0.2 Hz for coupling constants is considered significant (1). The maximum error in the computed coupling constants is 0.06 Hz, so the observed deviations are well beyond experimental error.

What can be the causes of these deviations from the predicted coupling constants? Several possible explanations, in terms of poor ΔJ values, hydrogen bonding, or bond order may be advanced. The first possibility is not regarded as likely, because there are few cases for disubstituted benzenes in the literature where experimental and predicted results disagree (1, 10). The second explanation, that of intramolecular hydrogen bonding to the ortho nitro group, has been advanced by Castellano and Kostelnik (1). They found a deviation of 0.4 Hz for J_{56} for ortho nitrophenol. They argued that the bond lengths and bond angles of the benzene ring were distorted, causing the observed deviation. The deviations for $-NH_2$, $-OH$, $-NHNH_2$, and $NHCOCH_3$ can be explained on this basis, but no hydrogen bonding should occur with the $-OCH_3$ substituent. However, the smallest calculated deviation, 0.20 Hz occurs with this group. A change of solvent from one of small hydrogen bonding capability may effectively change the intramolecular hydrogen bond. The solvent effect of carbon tetrachloride – acetone (7:3), acetonitrile, and methanol on the spectra of 2,4-dinitrophenol was investigated. The coupling constants changed 0.05 Hz. This change is much less than 0.4–0.6 Hz deviations observed. These findings indicate that the intramolecular hydrogen bonding is not affected by the solvent, or that the intramolecular hydrogen bonding is not the correct explanation for the deviations. The third explanation, that of bond fixation, is based on the donor and acceptor nature of the substituent and nitro groups. The resonance interaction, as given in Fig. 1, increases the bond order at C_5—C_6 relative to unsubstituted benzene. Several authors (11) have drawn direct correlation between bond order and coupling constants in fused aromatic systems with coupling constants increasing as bond order increases. This indicates that those substituents for which this donor–acceptor interaction can occur should have greater coupling constants. The halogens, with their relatively small donor capacity, will not interact with the ortho or para nitro groups and this bond fixation will not occur. The deviation from additivity in the meta coupling constants cannot be easily explained by the resonance configurations. However, the data of

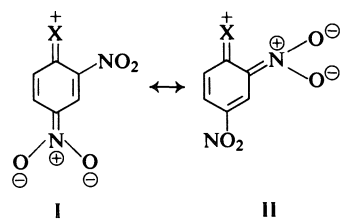

I II

FIG. 1. Resonance forms for 1-X-2,4-dinitrobenzenes.

Can. J. Chem. Downloaded from www.nrcresearchpress.com by 210.87.254.105 on 09/05/12
For personal use only.

Can. J. Chem. Downloaded from www.nrcresearchpress.com by 210.87.254.105 on 09/05/12
For personal use only.

TABLE 2. Predicted and observed coupling constants of ring protons of some 1-X-2,4-dinitrobenzenes*,†

Compound	X	J_{ortho}			J_{meta}			J_{para}		
		Observed	Predicted	Δ	Observed	Predicted	Δ	Observed	Predicted	Δ
1	OCH_3	9.28	9.08	.20	2.80	2.56	.24	.02	.16	−.14
2	NH_2	9.40	8.77	.63	2.72	2.41	.31	.28	.16	.12
3	OH	9.32	8.90	.42	2.77	2.55	.22	.17	.18	−.01
4	$NHNH_2$	9.39			2.77			.13		
5	$NHCOCH_3$	9.26			2.57			.06		
6	Cl	8.85	8.80	.05	2.49	2.48	.01	.36	.21	.15
7	Br	8.76	8.80	−.05	2.63	2.59	.04	.26	.15	.11
8	I	8.80	8.68	.12	2.54	2.56	−.02	.02	.16	−.14

*Coupling constants in Hz.
†The errors in the computer coupling constants are given in footnote † of Table 1.

Smith and Kmet (12) show the same general trend as ours; namely, that J ortho and J meta are both increased when resonance interaction between p-substituted groups can occur.

It is significant to note that Schaefer did not study compounds where a strong resonance effect could occur. As in Schaefer's study, our para coupling constants show no consistent change with change of structure.

Conclusion

Solubility considerations did not allow the use of CCl_4. The use of the additivity scheme for this series of compounds is open to challenge since the monosubstituted values used in this scheme were determined in CCl_4. Schaefer *et al.* (2) indicate that values 0.1 Hz greater than predicted will occur in an acetone solvent system. The lack of large changes in coupling constants of 2,4-dinitrophenol in different polar solvent systems indicates that an explanation involving more than intramolecular hydrogen bonding is necessary to explain the observed deviation of ortho coupling constants from the additivity scheme encountered in this study. The extent of solvent–solute hydrogen bonding will vary in these solvent systems but the small changes in coupling parameters support the resonance interpretation as a partial explanation for the observed deviations.

We would like to thank Dr. Henry Sable of Case Western Reserve for obtaining the 100 MHz spectra of the 2,4-dinitrohalobenzenes, Dr. J. Thomas Gerig of the University of California at Santa Barbara for obtaining the 100 MHz spectra of 2,4-dinitroacetanilide, and Oberlin College for the use of their Varian A-60 n.m.r. spectrometer.

This research was partially supported by NSF Grant GY-7494.

1. S. Castellano and R. Kostelnik. Tetrahedron Lett. 5211 (1967).
2. T. Schaefer, G. Kotowycz, H. M. Hutton, and J. N. S. Lee. Can. J. Chem. **46**, 2531 (1968).
3. S. Castellano and A. A. Bothner-By. J. Chem. Phys. **41**, 3863 (1964).
4. H. M. McConnell. J. Mol. Spectrosc. **1**, 11 (1957).
5. S. Castellano and C. Sun. J. Am. Chem. Soc. **88**, 4741 (1966).
6. S. Castellano, C. Sun, and R. Kostelnik. Tetrahedron Lett. 5205 (1967).
7. P. F. Cox. J. Am. Chem. Soc. **85**, 380 (1967).
8. J. M. Reed, Jr., R. W. Crecely, R. S. Butler, and J. E. Loemker. Tetrahedron Lett. 1215 (1968).
9. R. W. Crecely, R. S. Butler, J. M. Reed, and J. H. Goldstein. Spectrochim. Acta, **24A**, 685 (1968).
10. K. Hayamizu and O. Yamamoto. J. Mol. Spectrosc. **25**, 422 (1968).
11. M. Ashley Cooper and S. L. Manatt. J. Am. Chem. Soc. **91**, 6235 (1969). N. Jonathan, S. Gordon, and B. P. Dailey. J. Chem. Phys. **36**, 2443 (1962).
12. W. B. Smith and T. J. Kmet. J. Phys. Chem. **70**, 4085 (1966).

Oxygen Solubility Measurements in Liquid Paraffin[1]

D. Ruppel

Atomic Energy of Canada Limited, Whiteshell Nuclear Research Establishment Pinawa, Manitoba

Received June 11, 1971

The solubility of O_2 in liquid paraffin was determined over the temperature range from 31 to 90 °C under an O_2 pressure of 736 Torr. The solubility was also determined at 35 °C over the pressure range from 290 to 834 Torr.

La solubilité de O_2 dans de la paraffine liquide a été déterminée sur l'intervalle de température allant de 31 à 90 °C et sous une pression d'O_2 de 736 Torr. La solubilité a également été déterminée à 35 °C sur l'intervalle de pression allant de 290 à 834 Torr.

Canadian Journal of Chemistry, 49, 3762 (1971)

Introduction

In the course of flash photolysis experiments using O_2 as a triplet state quencher in viscous solutions, it became necessary to know the solubility of O_2 in liquid paraffin from approximately 30 to 90 °C, in order to determine concentrations in solution from gas pressure data.

Liquid paraffin is a colorless, transparent,

[1]A.E.C.L. No. 4010.

Can. J. Chem. Downloaded from www.nrcresearchpress.com by 210.87.254.105 on 09/05/12
For personal use only.

Smith and Kmet (12) show the same general trend as ours; namely, that J ortho and J meta are both increased when resonance interaction between p-substituted groups can occur.

It is significant to note that Schaefer did not study compounds where a strong resonance effect could occur. As in Schaefer's study, our para coupling constants show no consistent change with change of structure.

Conclusion

Solubility considerations did not allow the use of CCl_4. The use of the additivity scheme for this series of compounds is open to challenge since the monosubstituted values used in this scheme were determined in CCl_4. Schaefer *et al.* (2) indicate that values 0.1 Hz greater than predicted will occur in an acetone solvent system. The lack of large changes in coupling constants of 2,4-dinitrophenol in different polar solvent systems indicates that an explanation involving more than intramolecular hydrogen bonding is necessary to explain the observed deviation of ortho coupling constants from the additivity scheme encountered in this study. The extent of solvent–solute hydrogen bonding will vary in these solvent systems but the small changes in coupling parameters support the resonance interpretation as a partial explanation for the observed deviations.

We would like to thank Dr. Henry Sable of Case Western Reserve for obtaining the 100 MHz spectra of the 2,4-dinitrohalobenzenes, Dr. J. Thomas Gerig of the University of California at Santa Barbara for obtaining the 100 MHz spectra of 2,4-dinitroacetanilide, and Oberlin College for the use of their Varian A-60 n.m.r. spectrometer.

This research was partially supported by NSF Grant GY-7494.

1. S. Castellano and R. Kostelnik. Tetrahedron Lett. 5211 (1967).
2. T. Schaefer, G. Kotowycz, H. M. Hutton, and J. N. S. Lee. Can. J. Chem. **46**, 2531 (1968).
3. S. Castellano and A. A. Bothner-By. J. Chem. Phys. **41**, 3863 (1964).
4. H. M. McConnell. J. Mol. Spectrosc. **1**, 11 (1957).
5. S. Castellano and C. Sun. J. Am. Chem. Soc. **88**, 4741 (1966).
6. S. Castellano, C. Sun, and R. Kostelnik. Tetrahedron Lett. 5205 (1967).
7. P. F. Cox. J. Am. Chem. Soc. **85**, 380 (1967).
8. J. M. Reed, Jr., R. W. Crecely, R. S. Butler, and J. E. Loemker. Tetrahedron Lett. 1215 (1968).
9. R. W. Crecely, R. S. Butler, J. M. Reed, and J. H. Goldstein. Spectrochim. Acta, **24A**, 685 (1968).
10. K. Hayamizu and O. Yamamoto. J. Mol. Spectrosc. **25**, 422 (1968).
11. M. Ashley Cooper and S. L. Manatt. J. Am. Chem. Soc. **91**, 6235 (1969). N. Jonathan, S. Gordon, and B. P. Dailey. J. Chem. Phys. **36**, 2443 (1962).
12. W. B. Smith and T. J. Kmet. J. Phys. Chem. **70**, 4085 (1966).

Oxygen Solubility Measurements in Liquid Paraffin[1]

D. Ruppel

Atomic Energy of Canada Limited, Whiteshell Nuclear Research Establishment Pinawa, Manitoba

Received June 11, 1971

The solubility of O_2 in liquid paraffin was determined over the temperature range from 31 to 90 °C under an O_2 pressure of 736 Torr. The solubility was also determined at 35 °C over the pressure range from 290 to 834 Torr.

La solubilité de O_2 dans de la paraffine liquide a été déterminée sur l'intervalle de température allant de 31 à 90 °C et sous une pression d'O_2 de 736 Torr. La solubilité a également été déterminée à 35 °C sur l'intervalle de pression allant de 290 à 834 Torr.

Canadian Journal of Chemistry, 49, 3762 (1971)

Introduction

In the course of flash photolysis experiments using O_2 as a triplet state quencher in viscous solutions, it became necessary to know the solubility of O_2 in liquid paraffin from approximately 30 to 90 °C, in order to determine concentrations in solution from gas pressure data.

Liquid paraffin is a colorless, transparent,

[1]A.E.C.L. No. 4010.

Can. J. Chem. Downloaded from www.nrcresearchpress.com by 210.87.254.5 on 09/05/12
For personal use only.

Can. J. Chem. Downloaded from www.nrcresearchpress.com by 210.87.254.5 on 09/05/12
For personal use only.

oily liquid that is obtained from crude petroleum by refining. A high degree of refinement is indicated by freedom from unsaturated and aromatic hydrocarbons and other impurities. Existing O_2 solubility data (1) cover only a 20 °C temperature range. Also it is highly probable that variations occurred in the liquid paraffin used by different workers because its properties are dependent on its source and the techniques employed in producing it (2).

Experimental

Liquid paraffin (LP, Anachemia AC7014) as received had an average molecular weight of 390, viscosity and density at 20 °C of 126 cs and 0.871 g/cm^3, respectively, and a refractive index of 1.4748 at 21.4 °C.

The experimental method for measuring gas solubilities was based on that described by Gubbins, Carden, and Walker (3). It consisted of equilibration of the liquid with the gas phase, transfer of samples to a gas stripping cell, and subsequent analysis of the extracted gas by chromatography.

The liquid paraffin samples were prepared in a flask immersed in a constant temperature bath maintained within ±0.1 °C. The paraffin was first degassed, then O_2 was added with stirring until the pressure stabilized at 736 Torr. Solubility measurements were normally begun after approximately two hours of stirring in the O_2 atmosphere. Similar results were obtained when stirring was continued up to 16 h. Between withdrawal of successive samples, the bulk of the sample was allowed to equilibrate for ½ h.

The samples were transferred to the stripping cell by means of a gas tight syringe. As a check for air ingress during transfer, a run was performed with liquid paraffin saturated with carrier gas, and this showed negligible oxygen.

The liquid was stripped by a stream of helium carrier gas passed through the stripping cell. With liquid paraffin solvent it was necessary to heat the stripping cell to approximately 60 °C in order to reduce the viscosity and prevent a frothing problem.

The oxygen was determined gas chromatographically using a 2 meter column of "Molecular Sieve" type 5A, 40–60 mesh, at 50 °C, in conjunction with a thermal conductivity detector. The gas chromatograph was calibrated periodically by injecting measured volumes of O_2 directly on the column.

As a check on the experimental method, the solubility of O_2 in monochlorobenzene was determined.

Results

The value of the Bunsen absorption coefficient, α (cm^3 of gas at standard temperature and pressure dissolved by 1 cm^3 of solvent at the temperature of the measurement and under a partial pressure of 760 Torr), for O_2 in C_6H_5Cl at 25 °C, obtained using the described method was 0.172 ± 0.005, in good agreement with the value 0.173 found by Horiuti (1).

Table 1 gives the values of the absorption coefficient, β (cm^3 of gas at standard temperature and pressure dissolved by 1 cm^3 of solvent at the temperature and partial pressure of the measurement), measured at constant temperature for varying O_2 pressures. Henry's constant, $K_H = P/X$, where P is the partial pressure of O_2 above the solution, in Torr, and X is the mole fraction of O_2 in the solution, is also given, based on solvent average molecular weight = 390.

The data in Table 1 show that Henry's law holds over this pressure range within experimental error.

Since Henry's Law holds, the values of O_2 solubility in liquid paraffin have been given in terms of the Bunsen absorption coefficient.

Table 2 gives the experimental results.

Table 3 summarizes the results found in the literature.

TABLE 1. Absorption coefficients and Henry's constants for O_2 in Liquid Paraffin at 35 °C

P (Torr)	β	K_H (Torr)
290	0.052±0.002	2.76×10^5
397	0.068±0.002	2.90×10^5
506	0.091±0.001	2.75×10^5
631	0.112±0.001	2.80×10^5
760	0.135±0.002	2.80×10^5
834	0.150±0.001	2.76×10^5

TABLE 2. Bunsen absorption coefficients and Henry's constants for O_2 in liquid paraffin

Temperature (°C)	α	K_H (Torr)
31	0.139±0.001	2.73×10^5
35	0.137±0.001	2.75×10^5
44	0.134±0.002	2.80×10^5
57	0.135±0.001	2.74×10^5
69	0.133±0.002	2.78×10^5
79	0.133±0.002	2.76×10^5
90	0.131±0.001	2.78×10^5

TABLE 3. Comparison of Bunsen coefficients for O_2 in liquid paraffin

Temperature (°C)	α	Density	Reference
18	0.114	$d = 0.8805$	1
20	0.134	$d_{20}^4 = 0.8795$	1
24	0.134	$d_{27} = 0.868$	1
35	0.137	$d_{20} = 0.871$	This work
38	0.098	sp. gr. = 0.835	1

Discussion

The values obtained in this work for O_2 solubility in liquid paraffin are comparable to those values found by other workers, as shown in Table 3.

Baldwin and Daniel (4) measured O_2 solubilities for a series of solvent extracted mineral oils derived from the same crude, and found that the solubility decreased considerably with increasing mean molecular weight from 100 ($\alpha \simeq 0.34$) to 400 ($\alpha \simeq 0.14$) after which the decrease was slight. Values found for O_2 solubility in *n*-hexane (1), *n*-heptane (5), *n*-octane (5), and *n*-nonane (5) fit in with their results as does the value for liquid paraffin given in this work.

1. W. F. LINKE. Solubilities of inorganic and metal organic compounds. Vol. II, 4th ed. American Chemical Society, Washington, D.C. 1965. p. 1234.
2. E. MEYER. White mineral oil, petrolatum and related products. Chemical Publishing Company, Inc., New York. 1968. p. 1.
3. K. E. GUBBINS, S. N. CARDEN, and R. D. WALKER. J. Gas Chromatogr. **3**, 98 (1965).
4. R. R. BALDWIN and S. G. DANIEL. J. Inst. Petrol. **39**, 105 (1953).
5. E. S. THOMSEN and J. CHR. GJALDBAEK. Acta Chem. Scand. **17**, 127 (1963).

Erratum: The Nickel(II)–γ-Picoline–Perchlorate Complex System

M. S. SUN AND D. G. BREWER
Department of Chemistry, University of New Brunswick, Fredericton, New Brunswick

Received July 8, 1971

(Ref.: Can. J. Chem. **49**, 1502 (1971))

Canadian Journal of Chemistry, **49**, 3764 (1971)

The datum 591 nm is missing from Table 3, in the metal d and d band electronic spectra of $NiL_4(H_2O)_2(ClO_4)_2$ in Nujol.

Also on the 11th line of text (p. 1504) on the right hand column, $ClCO_4^-$ should read ClO_4^-.

Can. J. Chem. Downloaded from www.nrcresearchpress.com by 210.87.254.5 on 09/05/12
For personal use only.

Can. J. Chem. Downloaded from www.nrcresearchpress.com by 210.87.254.42 on 09/05/12
For personal use only.

A Regenerable, Solid-Phase Coupling Reagent for Use in Peptide Synthesis[1]

J. BROWN[2] AND R. E. WILLIAMS
Biochemistry Laboratories, National Research Council of Canada, Ottawa, Canada

Received August 17, 1971

The incorporation of the peptide reagent EEDQ (1) into an insoluble polymeric form is described. The utility of this reagent in peptide syntheses is investigated and its application in automated processes considered.

L'introduction du réactif peptidique EEDQ (1) sous une forme polymérique et insoluble est décrite. L'utilité du réactif dans la synthèse des peptides est étudiée et son utilisation dans une réaction automatisée est envisagée.

Canadian Journal of Chemistry, 49, 3765 (1971)

Automatic large-scale peptide syntheses have been, for the most part, hampered by the lack of a suitable reagent for carrying out the peptide bond forming step. A recent report has described an inexpensive reagent 'EEDQ' (**1**)[3] which forms the peptide bond with essentially no racemization (1). A fully automatic solid-phase synthetic sequence making use of this type of reagent is conceivable if the basic element of the reagent (the quinoline moiety) is converted to an insoluble derivative **2**. The coupling reactions could then be carried out in a solid-phase type of reaction. The spent reagent could be easily recovered by virtue of its insolubility and regenerated to be used again.

The incorporation of the quinoline nucleus into a suitable insoluble polymeric material was accomplished by the free-radical initiated polymerization of 6-isopropenylquinoline (2 parts by weight), styrene (3 parts), and divinylbenzene (0.08 parts) in benzene solution. The resulting polymer, after having been washed with petrol (30–60°) and dried, was obtained as a colorless granular powder insoluble in all common organic solvents. It contained 1.33 m*M* nitrogen (as N_2) per gram.

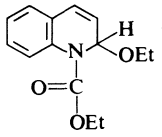

1
EEDQ

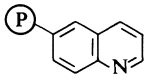

2a

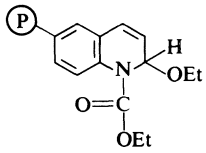

P— = Polymer

2b

The polymer was converted into the active reagent by reaction overnight in methylene chloride (6 ml/g) in the presence of a slight excess of ethyl chloroformate, triethylamine, and ethanol (2). The reagent was recovered by repeated suspensions in chloroform, washing with petrol (30–60°) and vacuum filtration. The reagent could be stored in this form for at least 3 months if protected from moisture.

Assay of the resin for the number of reagent sites available for reaction was carried out by coupling an excess of N^{α}-DNP-L-leucine and

[1]NRCC No. 12205.

[2]NRCC Postdoctorate Fellow, 1969–1971.

[3]Abbreviations: EEDQ, *N*-ethoxycarbonyl-2-ethoxy-1,2 dihydroquinoline; DCC, dicyclohexylcarbodiimide; Cbz, benzyloxycarbonyl; DNP, 2,4-dinitrophenyl; HOSu, *N*-hydroxysuccinimide. All chemicals were of reagent grade quality. All amino acid derivatives used gave satisfactory elemental analyses and suitable spectroscopic data.

glycine ethyl ester in methylene chloride. The dipeptide product (R_f 0.35) was isolated by t.l.c. (silica gel, EtOAc/C_6H_6, 2/8, v/v) and the amount formed calculated from the optical density at 340 nm of an ethanol solution (N^{α}-DNP-L-leucylglycine ethyl ester, $\varepsilon_{340} = 16\ 100$). The number of millimoles of product formed per gram of activated resin was found to be 0.20 ± 0.04.

Racemization caused by the polymeric and monomeric reagents during coupling was compared by application of the Young test (3) to each. Couplings of N^{α}-Benzoyl-L-leucine and glycine ethyl ester (released from its hydrochloride by triethylamine) were done in methylene chloride solution under identical experimental conditions. Comparison of the specific rotations of the crude neutral fractions with that of pure *N*-benzoyl-L-leucylglycine ethyl ester ($[\alpha]_D = -34.0°$ (3)) indicated the following results: the monomeric reagent (EEDQ) had produced $95.0 \pm 0.1\%$ L dipeptide, the polymeric reagent had produced $91.9 \pm 0.7\%$, and DCC with 2 equiv of HOSu[3] (4) had produced $91.1 \pm 0.1\%$. The reagent therefore seems to be slightly less effective in the polymeric form than in the monomeric form (EEDQ) but gave results at least comparable to those produced by the widely-used DCC/HOSu combination.

The use of the resin for the simplified preparation of peptides can be illustrated by this preparation: N^{α}-Cbz-L-phenylalanine (150 mg), glycine ethyl ester hydrochloride (70 mg), and triethylamine (70 μl) were mixed and shaken at room temperature for 1 h. Activated polyquinoline reagent (approximately 0.3 m*M* active reagent sites per gram) (3.3 g) was added in one portion and the mixture shaken overnight. Product isolation involved filtration of the mixture to remove the resin, washing the resin with ethyl acetate, combining the filtrates, and evaporating to dryness. The residue was taken up in ethyl acetate, filtered and evaporated to dryness (160 mg) (83.5%) (m.p. 102–105 °C, $[\alpha]_D = -16.4°$ (*c* 1.96, EtOH)). This crude residue was crystallized once from ethyl acetate – petrol (30–60°) to yield pure product (136 mg) (71.0%) m.p. 107–108 °C (uncorrected), $[\alpha]_D = -16.6°$ (*c* 1.97, EtOH)), (lit. (5), m.p. 105–106 °C, $[\alpha]_D = -16.7°$ (*c* 2.0, EtOH)). The yield (83.5%) and purity of the crude product suggests that further deblocking and coupling steps could profitably be carried out on this product if the synthesis were to be adapted to an automated synthesis of small blocked peptides.

Finally, that the reagent can be regenerated is best illustrated by the fact that all racemization tests and preparative scale experiments were carried out by repeated use and regeneration of the same 5-g sample of polyquinoline resin.

1. B. BELLEAU and G. MALEK. J. Am. Chem. Soc. **90**, 1651 (1968).
2. M. FIESER and L F. FIESER. Reagents for organic synthesis. Vol. 2. Wiley-Interscience, New York, N. Y., 1969. p. 191.
3. M. W. WILLIAMS and G. T. YOUNG. J. Chem. Soc. 881 (1963).
4. J. E. ZIMMERMAN and G. W. ANDERSON. J. Am. Chem. Soc. **89**, 7151 (1967).
5. L. E. BARSTOW and V. J. HRUBY. J. Org. Chem. **36**, 1305 (1971); R. W. Young, K. H. Wood, R. T. Joyce, and G. W. Anderson. J. Am. Chem. Soc. **78**, 2126 (1956).

Can. J. Chem. Downloaded from www.nrcresearchpress.com by 210.87.254.42 on 09/05/12
For personal use only.

Can. J. Chem. Downloaded from www.nrcresearchpress.com by 210.87.254.42 on 09/05/12
For personal use only.

Canadian Journal of Chemistry

Published by THE NATIONAL RESEARCH COUNCIL OF CANADA

VOLUME 49 DECEMBER 1, 1971 NUMBER 23

Nuclear Magnetic Resonance Studies of the Solution Chemistry of Metal Complexes. II. Protonation of the Peptide Linkages of Bis(glycylglycinato)cobaltate(III)[1]

DALLAS L. RABENSTEIN

Department of Chemistry, University of Alberta, Edmonton, Alberta

Received June 7, 1971

Protonation of bis(glycylglycinato)cobaltate(III) in acidic aqueous solutions has been investigated by proton magnetic resonance spectroscopy. Chemical shift measurements indicate that the site of protonation is the peptide oxygen rather than the Co(III)-coordinated, deprotonated peptide nitrogen as previously proposed, and that the two peptide linkages are protonated in a stepwise fashion rather than simultaneously. Equilibrium constants for the stepwise protonation equilibria have been derived from the n.m.r. data. The equilibrium constant for the first protonation step has also been determined by p*H* titration.

La protonation du cobaltate(III) du bis(glycylglycinate) en solutions acides aqueuses a été étudiée par résonance magnétique nucléaire. La mesure des déplacements chimiques indique que le site de protonation est l'oxygène du peptide beaucoup plus que l'azote du peptide déprotoné coordiné au cobalt(III) comme il a été proposé antérieurement, et que les deux liaisons peptidiques sont protonées par étapes aussi bien que simultanément. Les constantes d'équilibre de la protonation équilibrée par étapes ont été obtenues à partir des résultats de r.m.n. La constante d'équilibre pour la première étape de protonation a été également déterminée par la mesure du p*H*.

Canadian Journal of Chemistry, **49**, 3767 (1971)

Introduction

The nature of metal ion binding by peptides and proteins is of interest in view of the importance of metal ions in biological systems. Undoubtedly the specificity with which the biological functions of such molecules are influenced by metal ions is due, in part at least, to specificity in the binding of the metal ions to the potential coordination sites (2). Binding of metal ions to the peptide linkage has been the subject of much research (3–12). Binding can occur via the peptide oxygen, the protonated peptide nitrogen, and the deprotonated peptide nitrogen.

Structural studies of several bis(glycylglycinato)cobaltate(III) complexes ($Co(gg)_2^-$) have revealed that the Co(III) is bound to each peptide at the nitrogen atoms of the amino and deprotonated peptide groups and at a carboxylic oxygen atom (13).[2] Studies on the solution chemistry of $Co(gg)_2^-$ have shown that in acidic solutions the peptide linkages are protonated (14). The rapidity of the protonation reaction and the lack of any major change in the optical rotatory dispersion spectrum indicate that protonation occurs without any ligand rearrangement. It has been inferred from these results that protonation occurs at the coordinated peptide nitrogen atoms of $Co(gg)_2^-$, although McKenzie pointed out that these results are not evidence that protonation does not occur at some other site on the peptide, such as peptide oxygen or carboxyl oxygen (12).

In this paper, the results of a proton magnetic resonance study of the protonation of $Co(gg)_2^-$ in acidic aqueous solutions are reported. These

[1]For Paper I in this series, see ref. 1.

[2]Throughout this paper, fully protonated glycylglycine is abbreviated H_3gg^+, zwitterionic glycylglycine is abbreviated H_2gg, and the mono- and dianions are abbreviated Hgg^- and gg^{2-}, respectively.

Can. J. Chem. Downloaded from www.nrcresearchpress.com by 210.87.254.42 on 09/05/12
For personal use only.

results suggest that protonation of $Co(gg)_2^-$ to yield $Co(Hgg)_2^+$ is a stepwise process, and that protonation occurs at the peptide oxygen rather than the coordinated peptide nitrogen. Equilibrium constants for the stepwise protonation equilibria are derived from the n.m.r. data. While this study was in progress, the crystal structure of the $Co(Hgg)_2^+$ species was reported (15).

Experimental

Sodium bis(glycylglycinato)cobaltate(III) tetrahydrate was prepared by the method of McKenzie (12), from tris(carbonato)cobaltate(III) (16). Solutions of $NaCo(gg)_2 \cdot 4H_2O$ were prepared determinately in H_2O and D_2O, and the p*H* of these solutions was varied with concentrated HNO_3 and 13.1 *M* DCl, respectively.

The n.m.r. spectra were obtained on a Varian A56/60A spectrometer, operating at a probe temperature of 25 °C with a standard Varian variable temperature accessory. Chemical shifts are reported in Hz relative to the central resonance of the triplet of the tetramethylammonium ion (TMA) as an internal standard, negative shifts representing resonances downfield from TMA. The TMA resonance is close to the resonances of the carbon-bonded protons of $Co(gg)_2^-$, making it possible to use expanded sweep widths (100 Hz) to achieve maximum accuracy in chemical shift measurements. The central resonance of the TMA triplet is 3.17 p.p.m. downfield from sodium 3-(trimethylsilyl)-1-propane sulfonic acid (TMS*). Nuclear magnetic resonance spectra were taken of 0.5 ml solutions of known p*H* or known H^+ concentration. At p*H*'s > 0.2, samples were prepared by adding acid to solutions of $NaCo(gg)_2 \cdot 4H_2O$, and measuring the p*H* with a p*H* meter (Orion model 801) equipped with a glass electrode and a saturated calomel reference electrode. Samples were withdrawn from the solutions at the appropriate p*H* values. At p*H*'s < 0.2, samples were prepared directly in n.m.r. tubes at known H^+ concentrations by adding the appropriate amounts of $NaCo(gg)_2 \cdot 4H_2O$, solvent and acid. The H^+ concentrations of these solutions were corrected to approximately account for the H^+ consumed upon protonation of $Co(gg)_2^-$. No attempt has been made to convert all acidities to either an activity scale or a concentration scale because of the uncertainty in the ionic strengths. This approach is justified because the equilibrium constants were calculated using only data in the region where measurements were made with the p*H* meter. Even so, good agreement is obtained between the theoretical curves and the experimental points in more acidic solutions.

Results

The proton n.m.r. spectra of the α-methylene protons[3] and the β-methylene protons of $Co(gg)_2^-$ were observed over a range of acidities in both H_2O and D_2O. The spectra obtained at p*H* 9.4 are shown in Fig. 1. The resonance patterns for both methylene groups are broad at this p*H* and at the other p*H*'s studied, with the upfield pattern sharpening significantly on going from the H_2O to the D_2O solution.

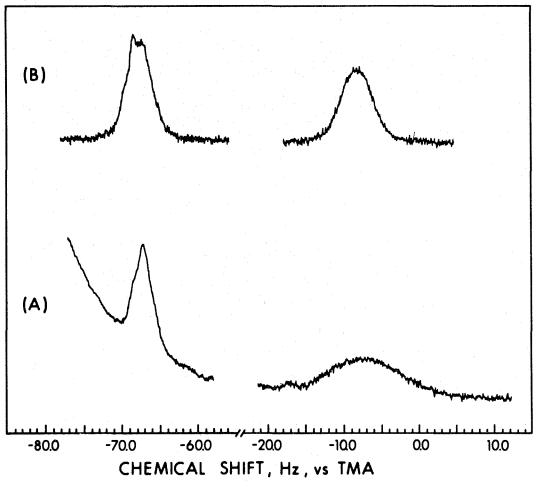

FIG. 1. 60 MHz proton n.m.r. spectra of the methylene protons of $Co(gg)_2^-$ at p*H* 9.4 in H_2O (*A*) and D_2O (*B*). 25 °C.

From the crystal structure of $Co(gg)_2^-$ (Fig. 2) (13), the spectrum of the α-methylene protons is expected to be an AB pattern due to the nonequivalent environments experienced by the two protons of each methylene group, while the spectrum of the β-methylene protons is expected to be an ABXY pattern in H_2O due to spin coupling of the non-equivalent methylene protons with the protons of the $—NH_2$ group. In D_2O the spectrum of the β-methylene protons is expected to be an AB pattern if spin coupling to the deuterium of the $—ND_2$ group is too small to observe. The multiplet patterns ob-

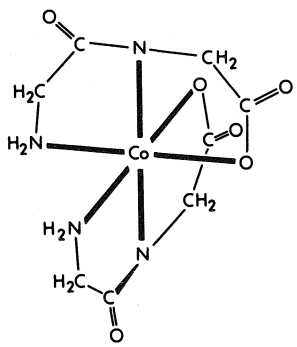

FIG. 2. Structure of $Co(gg)_2^-$ (13).

[3]The methylene groups of glycylglycine are labelled as follows: $H_2NCH_{2(\beta)}CONHCH_{2(\alpha)}CO_2H$.

Can. J. Chem. Downloaded from www.nrcresearchpress.com by 210.87.254.42 on 09/05/12
For personal use only.

served for the carbon-bonded protons, however, are more complex than simple AB patterns, possibly due to additional spin interaction with the nitrogen of the peptide ($I = 1$) or the Co(III) ($I = 7/2$) (17). Such interaction is expected to broaden the resonances as observed. In any case, the resonance pattern at higher field is significantly sharpened by changing the amino group of the peptide from $-NH_2$ to $-ND_2$, while the resonance pattern at lower field is not appreciably affected by the change. Based on the changes in the resonance patterns resulting from substitution of deuterium for the amino protons, the higher field multiplet pattern (−7.7 Hz *vs.* TMA) is assigned to the β-methylene protons of $Co(gg)_2^-$ and the lower field multiplet pattern (−67.2 Hz *vs.* TMA) to the α-methylene protons. These are the same assignments arrived at by Barnet *et al.* on the basis of the n.m.r. spectra of similar Co(III) complexes of L-alanylglycine and glycyl-L-alanine (15).

The p*H* dependence of the chemical shifts of the α- and β-methylene protons of $Co(gg)_2^-$ (measured at the center of the resonance patterns) is shown in Fig. 3. The p*H* dependence of these protons in glycylglycine is also shown for comparison. At p*H* 2.6 the resonances of the methylene protons of $Co(gg)_2^-$ start shifting downfield, indicating that some protonation has occurred at this p*H*. As the p*H* is further decreased, the resonances continue to shift downfield. At all p*H*'s, a single, averaged resonance pattern is observed for each of the methylene groups, indicating that interchange between the variously protonated forms via proton exchange is rapid on the n.m.r. time scale.

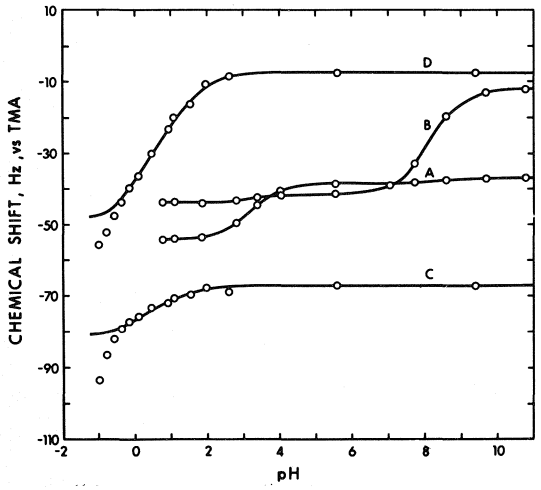

FIG. 3. Chemical shift behavior of methylene protons of glycylglycine as a function of p*H*. Curve *A*, α-methylene protons of glycylglycine; *B*, β-methylene protons of glycylglycine; *C*, α-methylene protons of $Co(gg)_2^-$; *D*, β-methylene protons of $Co(gg)_2^-$.

The observed chemical shifts in the p*H* region where protonation is occurring are the sums of the chemical shifts of the variously protonated species, weighted according to the relative concentrations of each of the species. Thus the observed shifts are a measure of the concentrations of the species present, from which the protonation equilibria can be quantitatively described. Attempts to account for the observed shifts in terms of the simultaneous protonation of both peptide linkages (eq. 1) were unsuccessful, and

[1] $$Co(gg)_2^- + 2H^+ \rightleftharpoons Co(Hgg)_2^+$$

indicated that protonation to form $Co(Hgg)_2^+$ occurs in two steps (eqs. 2 and 3).

[2] $$Co(gg)_2^- + H^+ \rightleftharpoons Co(Hgg)(gg)$$

[3] $$Co(Hgg)(gg) + H^+ \rightleftharpoons Co(Hgg)_2^+$$

These protonation equilibria are described by equilibrium constants K_{a1} and K_{a2} (eqs. 4 and 5).

[4] $$K_{a1} = \frac{[H^+][Co(gg)_2]}{[Co(Hgg)(gg)]}$$

[5] $$K_{a2} = \frac{[H^+][Co(Hgg)(gg)]}{[Co(Hgg)_2]}$$

The observed chemical shifts in this p*H* region are related to the chemical shifts of the species presented by eq. 6.

[6] $$\delta_{obs} = P_{Co(gg)_2}\delta_{Co(gg)_2} + P_{Co(Hgg)(gg)} \times \delta_{Co(Hgg)(gg)} + P_{Co(Hgg)_2}\delta_{Co(Hgg)_2}$$

where $P_{Co(gg)_2}$, $P_{Co(Hgg)(gg)}$, and $P_{Co(Hgg)_2}$ are the populations of the species indicated ($P_{Co(gg)_2} + P_{Co(Hgg)(gg)} + P_{Co(Hgg)_2} = 1$). δ_{obs} is related to equilibrium constants K_{a1} and K_{a2} by eq. 7

[7] $$(\delta_{obs} - \delta_{Co(gg)_2})\frac{1}{[H^+]^2} + (\delta_{obs} - \delta_{Co(Hgg)(gg)})\frac{1}{[H^+]K_{a1}} + (\delta_{obs} - \delta_{Co(Hgg)_2})\frac{1}{K_{a1}K_{a2}} = 0$$

which is obtained from eqs. 4, 5, and 6.

Can. J. Chem. Downloaded from www.nrcresearchpress.com by 210.87.254.42 on 09/05/12
For personal use only.

The equilibrium constants and the chemical shifts of the methylene protons in the mono- and diprotonated species were evaluated from the observed chemical shifts. The procedure involved first evaluating the chemical shift of the β-methylene protons in the Co(Hgg)(gg) species and K_{a1} from the observed β-methylene chemical shifts in the pH region where the second protonation is not extensive. The chemical shift of the β-methylene protons in the $Co(Hgg)_2^+$ species and K_{a2} were then evaluated from the observed chemical shifts at lower pH's where the diprotonated species is also present.

The chemical shift of the β-methylene protons in Co(Hgg)(gg) and K_{a1} were evaluated using eq. 8, which is obtained when the second protonation is neglected.

[8] $$(\delta_{Co(gg)_2} - \delta_{obs})/[H^+] = \delta_{obs}/K_{a1} - \delta_{Co(Hgg)(gg)}/K_{a1}$$

K_{a1} was obtained from the slope and $\delta_{Co(Hgg)(gg)}$ from the intercept of the linear portion of a plot of $(\delta_{Co(gg)_2} - \delta_{obs})/[H^+]$ *vs.* δ_{obs}. Linear behavior was obtained for the data at pH's greater than 1.4. This corresponds to the pH range over which the second protonation is not significant and, consequently, the range over which eq. 8 is valid. The chemical shift of the β-methylene protons in Co(Hgg)(gg) obtained from this plot is -24 ± 0.5 Hz and the K_{a1} is $3.5 \pm 0.25 \times 10^{-2}$ ($pK_{a1} = 1.46$).

$\delta_{Co(Hgg)_2}$ and K_{a2} were evaluated from the β-methylene chemical shifts at lower pH's from the slope and intercept respectively of a plot of $(\delta_{Co(gg)_2} - \delta_{obs})/[H^+]^2 + (\delta_{Co(Hgg)(gg)} - \delta_{obs})/K_{a1}[H^+]$ *vs.* δ_{obs} (from eq. 7). The values of $\delta_{Co(Hgg)(gg)}$ and K_{a1} determined above were used in the evaluation of $\delta_{Co(Hgg)_2}$ and K_{a2}. The chemical shift obtained in this way for the β-methylene protons in the di-protonated species is -49 ± 4 Hz and the K_{a2} is 0.8 ± 0.15 ($pK_{a2} = 0.097$).

The chemical shifts of the α-methylene protons in the mono- and di-protonated species were determined from the observed chemical shifts of the α-methylene protons using eq. 6. Populations were calculated from the previously determined equilibrium constants. The chemical shifts calculated by this procedure for the α-methylene protons in the mono- and di-protonated species are -71 and -81 Hz, respectively.

The solid curves drawn through the experimental data for the α- and β-methylene protons of $Co(gg)_2^-$ in Fig. 3 were calculated using the equilibrium constants and the chemical shifts for these protons in the mono- and di-protonated species determined above. At high acid concentrations, the experimental points deviate from the calculated curves. This is attributed to protonation of the peptides to form higher protonated species, possibly by protonation at the carboxyl oxygen.

The value of K_{a1} was also determined by a pH titration technique to check the results from the n.m.r. study. Fifty ml of 0.0491 M $NaCo(gg)_2 \cdot 4H_2O$ was titrated with 1.348 M HNO_3 to a pH of 1.00. K_{a1} was calculated from the amount of acid consumed by protonation of the complex to form Co(Hgg)(gg) at various pH's down to pH 1.00. The amount of acid required to change the pH of the solution was determined from a titration curve for 50.00 ml of H_2O. The pH titration study yielded a K_{a1} of $3.7 \pm 0.2 \times 10^{-2}$ ($pK_{a1} = 1.43$).

Discussion

Protonation of $Co(gg)_2^-$ to form $Co(Hgg)_2^+$ shifts the resonance frequency of the multiplet pattern due to the β-methylene protons by a larger amount ($\Delta\delta = 42$ Hz) than the resonance frequency of the multiplet pattern due to the α-methylene protons ($\Delta\delta = 14$ Hz), indicating that the β-methylene protons are nearer the sites of protonation. These results suggest, then, that protonation of the peptide linkage in $Co(gg)_2^-$ occurs at the peptide oxygen rather than the peptide nitrogen as previously suggested (12). While this study was in progress, it was reported that the peptide oxygens of $Co(Hgg)_2^+$ are also protonated in the crystalline state (15). Based on the n.m.r. spectra of $Co(gg)_2^-$ in 2 M $HClO_4$, these workers also concluded that the peptide oxygens are protonated in the solution phase.

Gillard *et al.* have also investigated the protonation of $Co(gg)_2^-$. The pK_a of the protonated complex, presumably for the reaction represented by eq. 1, was reported to be about 1.2 (20), although more recent n.m.r. evidence suggested a pK_a of about 0.5 (21). In the present work, it was found that the chemical shift data for protonation of $Co(gg)_2^-$ could not be fitted by a simultaneous protonation of both peptide linkages. Rather, the chemical shift data suggest a stepwise protonation of the peptide linkages of $Co(gg)_2^-$. Similar stepwise protonation behavior has also been observed for protonation

TABLE 1. Ionization constants for the peptide protons in selected metal complexes of polyglycine peptides

Equilibrium constant	$-\log K_x$	Reference
$K_{a1} = [Co(gg)_2^-][H^+]/[Co(Hgg)(gg)]$	1.46	This work
$K_{a2} = [Co(Hgg)(gg)][H^+]/[Co(Hgg)_2^+]$	0.10	This work
$K_{a1} = [Cu(gg)][H^+]/[Cu(Hgg)^+]$	4.38	6
$K_{a1} = [Cu(Hggg)][H^+]/[Cu(H_2ggg)^+]$*	5.4	7
$K_{a2} = [Cu(ggg)^-][H^+]/[Cu(Hggg)]$*	6.63	7
$K_{a1} = [Ni(Hggg)][H^+]/[Ni(H_2ggg)^+]$*	8.8	11
$K_{a2} = [Ni(ggg)][H^+]/[Ni(Hggg)]$*	7.7	11

*Glycylglycylglycine; $H_2ggg^- = H_2NCH_2CONHCH_2CONHCH_2CO_2^-$; $Hggg^{2-} = H_2NCH_2CON^-CH_2CONHCH_2CO_2^-$; $ggg^{3-} = H_2NCH_2CON^-CH_2CON^-CH_2CO_2^-$.

of the deprotonated, metal-coordinated peptide linkages in several other metal complexes of polyglycine peptides (6, 7, 11).

Other metal ions that promote the ionization of the peptide hydrogens in polyglycine peptides upon complexation include Ni(II) and Cu(II). Equilibrium constants for the ionization of the peptide protons in several Ni(II)- and Cu(II)-peptide complexes are given in Table 1. Examination of the equilibrium ionization constants listed in Table 1 reveals that the peptide protons in protonated $Co(gg)_2^-$ are much more acidic than those in the protonated Ni(II)- and Cu(II)-peptide complexes. These differences are probably due to a combination of differences in the sites of metal binding and protonation at the peptide linkage and structural changes following proton ionization. Based on evidence from the kinetics of proton-transfer between the mono- and di-protonated Cu(II)-triglycine complexes, Pagenkopf and Margerum (8) suggested that the peptide oxygen of the protonated peptide linkage is coordinated in the Cu(II)-triglycine complexes (Structure **1**), although Kim and Martell (6, 7) have reported that the protonated peptide nitrogen is coordinated in Cu(II)-polyglycine peptide complexes (Structure **2**). The peptide oxygens in the

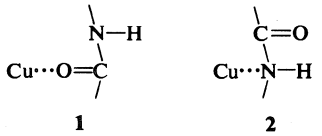

1 **2**

crystalline complex $Cu(H_2ggg)Cl{\cdot}1.5\,H_2O$, where H_2ggg^- is $H_2NCH_2CONHCH_2CONHCH_2CO_2^-$, are coordinated to the Cu(II) (Structure **1**) (18). The peptide oxygens are also coordinated in the protonated Ni(II)-triglycine complex (10, 11, 19), in contrast to $Co(Hgg)_2^-$ where protonation is at the peptide oxygen and the deprotonated peptide nitrogen is metal coordinated.

This research was supported in part by the National Research Council of Canada.

1. D. L. RABENSTEIN. J. Am. Chem. Soc. **93**, 2869 (1971).
2. H. SIGEL and D. B. MCCORMICK. Acc. Chem. Res. **3**, 201 (1970).
3. H. C. FREEMAN. Adv. Protein Chem. **22**, 258 (1967).
4. H. DOBBIE and W. O. KERMACK. Biochem. J. **59**, 246 (1955).
5. S. P. DATTA and B. R. RABIN. Trans. Faraday Soc. **52**, 1123 (1956).
6. M. K. KIM and A. E. MARTELL. Biochem. **3**, 1169 (1964).
7. M. K. KIM and A. E. MARTELL. J. Am. Chem. Soc. **88**, 914 (1966).
8. G. K. PAGENKOPF and D. W. MARGERUM. J. Am. Chem. Soc. **90**, 6963 (1968).
9. R. B. MARTIN, M. CHAMBERLIN, and J. T. EDSALL. J. Am. Chem. Soc. **82**, 495 (1960).
10. M. K. KIM and A. E. MARTELL. J. Am. Chem. Soc. **89**, 5138 (1967).
11. E. J. BILLO and D. W. MARGERUM. J. Am. Chem. Soc. **92**, 6811(1970).
12. E. D. MCKENZIE. J. Chem. Soc. A, 1655 (1969).
13. R. D. GILLARD, E. D. MCKENZIE, R. MASON, and G. B. ROBERTSON. Coord. Chem. Rev. **1**, 263 (1966).
14. R. D. GILLARD, P. M. HARRISON, and E. D. MCKENZIE. J. Chem. Soc. A, 618 (1967).
15. M. T. BARNET, H. C. FREEMAN, D. A. BUCKINGHAM, I-NAN-HSU, and D. VAN DER HELM. Chem. Commun. 367 (1970).
16. H. F. BAUER and W. C. DRINKARD. J. Am. Chem. Soc. **82**, 5031 (1960).
17. J. SUDMEIER and G. BLACKMER. J. Am. Chem. Soc. **92**, 5238 (1970).
18. T. COOPER, H. C. FREEMAN, G. ROBINSON, and J. SCHOOME. Nature, **194**, 1237 (1962).
19. H. C. FREEMAN, J. M. GUSS, and R. L. SINCLAIR. Chem. Commun. 485 (1968).
20. R. D. GILLARD and M. G. PRICE. J. Chem. Soc. A, 1813 (1969).
21. R. D. GILLARD and P. R. MITCHELL. Personal communication quoted in ref. 11.

Can. J. Chem. Downloaded from www.nrcresearchpress.com by 210.87.254.42 on 09/05/12
For personal use only.

Can. J. Chem. Downloaded from www.nrcresearchpress.com by 210.87.254.6 on 09/05/12
For personal use only.

The Crystal and Molecular Structure of $(PPh_3)_2PtO_2.2CHCl_3$

P.-T. CHENG, C. D. COOK, S. C. NYBURG, AND K. Y. WAN
Lash Miller Chemical Laboratories, University of Toronto, Toronto 181, Ontario

Received June 21, 1971

The X-ray crystal structure analysis of the chloroform adduct of the bis(triphenylphosphine) platinum di-oxygen complex $(PPh_3)_2PtO_2.2CHCl_3$ is reported. The crystals belong to the monoclinic system $a = 15.492(7)$, $b = 13.520(5)$, $c = 19.187(6)$ Å; $\beta = 98.97(6)°$. Space group $C2/c$. $Z = 4$ molecules per cell.

A total of 2740 independent X-ray reflections were measured and refinement gave a final conventional R of 6.6%.

The molecule has a two-fold axis of symmetry through the Pt atom with O—O normal to the axis. The O—O distance of 1.505(16) Å is in accord with that found with other transition elements when oxygen is taken up irreversibly to form di-oxygen complexes.

On a déterminé par diffraction de rayons-x la structure cristalline du composé d'addition du chloroforme et du dioxo bis(triphénylephosphine) platine $(PPh_3)_2PtO_2.2CHCl_3$. Ce composé cristallise avec une maille monoclinique de dimensions: $a = 15.492$ (7), $b = 13.520$ (5), $c = 19.187$ (6) Å et $\beta = 98.97$ (6)°, dans le groupe d'espace $C2/c$ avec quatre molécules par maille.

L'affinement de la structure conduit à un facteur d'accord final $R = 6.6\%$ pour les 2740 réflexions mesurées. La molécule a un axe d'ordre deux passant par l'atome de platine avec O—O perpendiculaire à cet axe. La distance O—O de 1.505 (16) Å est comparable à celles trouvées pour d'autres éléments de transition quand l'oxygène est fixé irréversiblement pour former des complexes bioxygénés.

Canadian Journal of Chemistry, 49, 3772 (1971)

Introduction

Crystallographic data are slowly accumulating on the oxygenated synthetic oxygen carriers of iridium(I) and platinum(0). Ibers and co-workers (1–5) have obtained data for three trigonal-bi-pyramidal iridium(I) complexes, $(PPh_3)_2Ir(CO)(X)(O_2)$, (X = Cl,I) and $(PPh_3)_2Ir(O_2)^+$ and have rationalized the observed variations in O—O bond lengths (Table 1) by reference to a simple three-center m.o. scheme. Kakudo and co-workers (6) have reported that the O—O bond length in the molecule $(PPh_3)_2PtO_2.1.5C_6H_6$ is 1.45 Å.

The trigonal complex $(PPh_3)_2PtO_2$ has been the subject of structural studies in these laboratories and data have been obtained for two derivatives $(PPh_3)_2PtO_2.C_6H_5CH_3$ and $(PPh_3)_2PtO_2.2CHCl_3$. Details of the former structure have already been reported (7) and although the crystallographic data were only marginal in quality, an O—O bond length of 1.26 ± 0.05 Å was indicated. This length is considerably shorter than would be anticipated for this irreversible oxygen carrier and prompted the present investigation of the complex $(PPh_3)_2PtO_2.2CHCl_3$.

Reaction of $(PPh_3)_2.Pt(C_2H_4)$ or $Pt(PPh_3)_3$ with oxygen in aromatic hydrocarbons or chlorinated alkanes as solvent (S) yields solvated complexes $(PPh_3)_2Pt(O_2)S_x$. We have determined a number of x values by integration of the ^1H or ^{19}F n.m.r. spectra of the complexes in suitably deuterated solvents. We have found that for toluene, $x = 1$ and for chloroform, $x = 2$. For the Pt complex containing tris-*p*-fluorophenylphosphine with fluorobenzene as solvent, $x = 2$.

Oxygen is taken up irreversibly by all the platinum(0) complexes we have examined and this suggests that these derivatives are more akin to the iridium(I) iodo complex $(PPh_3)_2Ir(CO)(I)(O_2)$ rather than the chloro derivative $(PPh_3)_2Ir(CO)(Cl)(O_2)$ which reacts with oxygen in a reversible manner (see Table 1). It is interesting to note that significant changes in nature of the aryl phosphine employed (*e.g.* tris-*p*-chloro, tris-*p*-fluoro, tris-*p*-methyl, and tris-*p*-methoxy) have no observable effect on the reversibility of the oxygen uptake whereas in the iridium(I) system a change in the coordinated halogen has a profound effect upon the chemical behavior and the observed bond length of the oxygen molecule.

Experimental

The ethylene adduct (8) $[(PPh_3)_2Pt.C_2H_4]$ was dissolved in oxygen-saturated chloroform. The solution was allowed to stand in an oxygen-filled desiccator when the oxygen adduct was deposited as bright orange crystals.

TABLE 1. Interatomic distances in Ir and Rh oxygen complexes*

Compound	Type	O . . . O (Å)	M . . . O (Å)	Reference
$Ir(O_2)Cl(CO)(PPh_3)_2$	TB	1.30(3)	2.09(3) 2.04(3)	Rev. 2, 3
$Rh(O_2)(diphos)_2(PF_6)$	TB	1.418(11)	2.026(8) 2.029(9)	Rev. 2
$Pt(O_2)(PPh_3)_2.1\frac{1}{2}C_6H_6$	T	1.45(4)	2.01(2) 2.01(3)	Irrev. 6
$Pt(O_2)(PPh_3)_2.2CH_3Cl$	T	1.505(16)	2.006(7)	Irrev. This work
$Ir(O_2)I(CO)(PPh_3)_2CH_2Cl_2$	TB	1.509(26)	2.035(20) 2.082(22)	Irrev. 4
$Ir(O_2)(diphos)_2(PF_6)$	TB	1.625(23)	1.961(18) 1.990(16)	Irrev. 5

*O...O in free O_2 is 1.21 Å. Diphos = $Ph_2P.CH_2.CH_2.PPh_2$, T = trigonal, TB = trigonal bipyramidal. Rev. = reversible, irrev. = irreversible.

The crystals, which are quite stable, analyze for $(PPh_3)_2PtO_2.2CHCl_3$.

Anal. Calcd. for $(PPh_3)_2PtO_2.2CHCl_3$: C, 46.07; H, 3.26; Cl, 21.48. Found: C, 49.54; H, 2.80; Cl, 21.77.

Good crystal specimens could be selected from the above preparations. These were needles having z (monoclinic as long axis and with {110} forms well developed. Unit cell dimensions were determined by measuring 2θ, χ, and ϕ settings of high angle principal reflections on an FACS-1 Picker four-circle diffractometer. The results were averaged for four crystals. The data are as follows:

$C_{38}H_{32}O_2Cl_6P_2Pt$ f.W. = 990

Monoclinic, $a = 15.492(7)$, $b = 13.520(5)$, $c = 19.187(6)$ Å, $\beta = 98.97(6)°$. $V = 3970$ Å^3, $\rho_o = 1.62(1)$, $Z = 4$, $\rho_c = 1.66$ (25 °C; CuKα, $\lambda = 1.542$ Å, μ(CuKα) = 120.2 cm^{-1}).

Intensity data were collected by automated diffractometer using CuKα radiation in 2θ scan mode at 2° min^{-1} with $4° \leqslant 2\theta \leqslant 115°$. The scanning range at low 2θ was 2° with 10 s background count at the 2θ limits. The crystals were found to be somewhat unstable under X-irradiation, reflections falling in intensity typically by 1% h^{-1}. Accordingly four separate crystals, all mounted about the z-axis were used; on average the intensity fell by about 10% during data collection from each crystal.

All the crystals were needles of volume about 0.07 mm^3 and absorption corrections were applied to all the intensity data. The weighting function used for intensity was (9)

$$\sigma^2(F^2) = (I/[(LP).A]^2) + CF^4$$

where $0.05 \leq A \leq 0.33$ is the absorption factor with C as 0.02 to allow for crystal instability. Of the 2740 independent reflections collected, 156 had $I < \sigma(I)$ and were considered unobserved.

Determination of the Structure

The three-dimensional Patterson function was used to determine the space group. Both Cc and $C2/c$ generate peaks along the line $0, 2y, \frac{1}{2}$ but only $C2/c$ has related peaks at $2x$, $2y$, $2z$ and at $2x, 0, \frac{1}{2}$. In this way the space group was established as $C2/c$ and the Pt atom coordinates found as $(0.0, 0.028, \frac{1}{4})$. Since these are of form $0, y, \pm\frac{1}{4}$ the Pt atoms lie on diad axes governing the symmetry of the molecule as a whole. (The alternative symmetry 1 in $C2/c$ for $Z = 4$ is in any case ruled out on chemical grounds.)

Refinement using the full matrix least squares programs ORFLS and XFLS (10) was routine. Scattering factors were those derived from Hartree–Fock wave functions (11) allowance being made for anomalous scattering. The conventional R factor at this stage, using isotropic temperature factors, was 9.0%. A difference Fourier map based on isotropic refinement containing all non-hydrogen atoms showed each of the three chlorine atoms of $CHCl_3$ to be disordered on two sites. We concluded that the occupancy of the chlorine atoms at these six sites was 0.5 because this gave the lowest residual, $R = 0.066$, when anisotropic refinements were completed. When the ratios were fixed at 0.4, 0.6 or 0.6, 0.4 either the residual increased or refinement could not be carried out. Final F_o and F_c values have been placed in the Depository for Unpublished Data.[1] The positional and thermal parameters with standard deviations as obtained in the least squares refinement are given in Tables 2 and 3. Since the final difference Fourier map did not show any significant peaks, all hydrogen positions were calculated using C . . . H = 1.07 Å.

The β_{ij} in Table 3 are the coefficients in the expression $\exp[-(h^2\beta_{11} + k^2\beta_{22} + l^2\beta_{33} + 2hk\beta_{12} + 2kl\beta_{13} + 2kl\beta_{23})]$.

The bond distances and angles in the molecule are shown in Fig. 1, the average standard deviations of the sp^2 carbon angles being 1°.

Discussion of the Structure

A diagram of the molecule viewed normal to the twofold axis is given in Fig. 2. Bond lengths of interest are marked in.

The twofold axis through Pt requires the oxygen molecule to lie either wholly on this axis or,

[1]Tabular data are available from the Depository of Unpublished Data, National Science Library, National Research Council of Canada, Ottawa, Canada, K1A 0S2.

Can. J. Chem. Downloaded from www.nrcresearchpress.com by 210.87.254.6 on 09/05/12
For personal use only.

TABLE 2. Fractional atomic coordinates × 10^5 (e.s.d.'s in parentheses)

Atom	x	y	z
Pt	0	2 842(4)	25 000
P	11 058(16)	13 323(17)	28 167(14)
O	4 822(45)	−10 913(50)	26 371(41)
C(11)	18 858(65)	7 970(75)	35 340(55)
C(12)	22 010(79)	12 888(88)	41 365(61)
C(13)	28 234(84)	8 565(109)	46 532(66)
C(14)	31 365(85)	− 680(106)	45 352(74)
C(15)	28 289(97)	−5 851(100)	39 256(84)
C(16)	21 973(85)	−1 356(92)	34 288(78)
C(21)	8 738(64)	25 620(69)	31 341(60)
C(22)	11 508(83)	34 107(77)	28 393(69)
C(23)	9 605(113)	43 435(105)	31 187(99)
C(24)	4 919(111)	43 783(106)	36 581(91)
C(25)	2 194(87)	35 205(121)	39 577(79)
C(26)	4 027(74)	26 056(91)	37 015(65)
C(31)	17 826(70)	15 110(73)	21 407(57)
C(32)	15 347(69)	11 707(82)	14 652(57)
C(33)	20 747(89)	12 721(102)	9 499(70)
C(34)	28 678(83)	17 459(92)	11 194(74)
C(35)	31 454(78)	20 852(85)	17 945(77)
C(36)	26 227(69)	19 695(79)	23 180(67)
Cl(1*a*)	15 463(178)	−14 013(198)	11 135(96)
Cl(1*b*)	13 725(160)	−14 086(200)	7 937(105)
Cl(2*a*)	4 095(79)	−30 891(111)	12 197(95)
Cl(2*b*)	2 507(182)	−28 589(153)	9 082(150)
Cl(3*a*)	−4 584(92)	−15 286(133)	4 408(78)
Cl(3*b*)	−1 566(121)	−8 793(149)	5 007(97)
C(01)	4 144(95)	−17 280(114)	11 051(83)
H(12)	19 586	20 179	42 042
H(13)	30 590	12 314	51 367
H(14)	36 267	−3 898	49 236
H(15)	30 715	−13 092	38 410
H(16)	19 441	−5 181	29 524
H(22)	15 044	33 470	24 048
H(23)	11 724	50 270	29 208
H(24)	3 356	50 894	38 492
H(25)	−1 364	35 651	43 919
H(26)	1 863	19 506	39 354
H(32)	9 104	8 209	13 383
H(33)	18 819	9 883	4 282
H(34)	32 730	18 516	7 221
H(35)	37 686	24 396	19 125
H(36)	28 593	22 252	28 406
H(01)	2 919	−14 759	15 969

alternatively, to lie normal to this axis through the O—O midpoint. The latter is the case. The O—O distance of 1.505(16) Å is in accord with the general observation that when oxygen is taken up reversibly by transition metal complexes the O . . . O distance is 1.3–1.4 Å but when taken up irreversibly, as here, it is about 1.5 Å. However, they cannot be compared directly since the Ir and Rh complexes are trigonal bipyramidal and the Pt complexes are trigonal (see Table 1).

In the present case the situation is somewhat complicated by what appear to be hydrogen bonds between the oxygen atoms and the neighboring carbon atoms of chloroform molecules at a C . . . O distance of 3.049(17) Å (see Fig. 2). Such short C . . . O distances are not unknown (12) and an analogous case appears in the molecular complex diethyl ether: $HCBrCl_2$ with a distance of 3.10(10) Å between the ether oxygen atom and the carbon atom of bromodichloromethane (13). In the present case, the derived H-positions for the two half-occupied chloroform molecules are virtually identical. These yield a C—H . . . O angle of 161°. The influence of this hydrogen bond, if real, on the O . . . O distance will possibly be better understood when we have recollected X-ray data for the toluene complex, since in the latter hydrogen bonding is ruled out. That

Can. J. Chem. Downloaded from www.nrcresearchpress.com by 210.87.254.6 on 09/05/12
For personal use only.

TABLE 3. Thermal parameters × 10^5 (e.s.d.'s in parentheses)

Atom	β_{11}	β_{22}	β_{33}	β_{12}	β_{13}	β_{23}
Pt	382(8)	437(10)	284(5)	0	67(2)	0
P	451(14)	414(16)	296(9)	8(10)	76(8)	−14(8)
O	481(31)	599(41)	437(27)	123(30)	36(22)	7(27)
C(11)	526(49)	577(59)	354(35)	43(45)	113(32)	−2(39)
C(12)	673(65)	821(76)	339(38)	86(57)	34(39)	−37(45)
C(13)	700(69)	1 080(102)	382(41)	184(70)	39(42)	−21(54)
C(14)	646(65)	979(90)	466(49)	−2(62)	111(44)	195(55)
C(15)	798(80)	806(80)	565(58)	53(65)	0(54)	16(57)
C(16)	531(63)	741(76)	565(51)	94(55)	−107(45)	0(51)
C(21)	455(49)	477(54)	457(40)	5(40)	−53(35)	−24(37)
C(22)	725(71)	548(63)	502(47)	−41(51)	−54(45)	0(43)
C(23)	1 001(103)	674(86)	698(75)	57(75)	−115(70)	−102(65)
C(24)	1 071(96)	774(90)	611(60)	295(75)	−181(62)	−278(61)
C(25)	647(67)	1 151(123)	556(55)	239(71)	4(46)	−220(66)
C(26)	547(57)	916(80)	430(43)	162(54)	51(39)	−184(48)
C(31)	598(55)	532(57)	359(36)	7(44)	104(34)	1(37)
C(32)	504(54)	749(69)	343(37)	−97(47)	83(34)	−47(39)
C(33)	732(74)	973(92)	445(47)	−85(66)	179(46)	−73(52)
C(34)	694(69)	783(77)	520(51)	−69(59)	258(46)	50(52)
C(35)	656(65)	689(70)	645(58)	−153(53)	306(50)	−41(52)
C(36)	509(54)	618(60)	528(46)	−214(46)	113(38)	−54(42)
Cl(1*a*)	987(79)	984(97)	744(74)	0(64)	271(67)	199(85)
Cl(1*b*)	1 006(119)	1 057(102)	963(104)	−336(91)	537(92)	−134(104)
Cl(2*a*)	671(43)	805(59)	843(55)	−158(38)	250(37)	−8(42)
Cl(2*b*)	2 636(241)	1 411(162)	1 786(189)	−1 045(155)	1 539(178)	−897(143)
Cl(3*a*)	968(74)	2 085(162)	670(51)	−40(82)	22(47)	410(76)
Cl(3*b*)	1 425(123)	2 088(188)	889(68)	141(117)	−453(75)	−94(100)
C(01)	727(78)	1 081(105)	574(58)	2(70)	211(53)	−13(62)

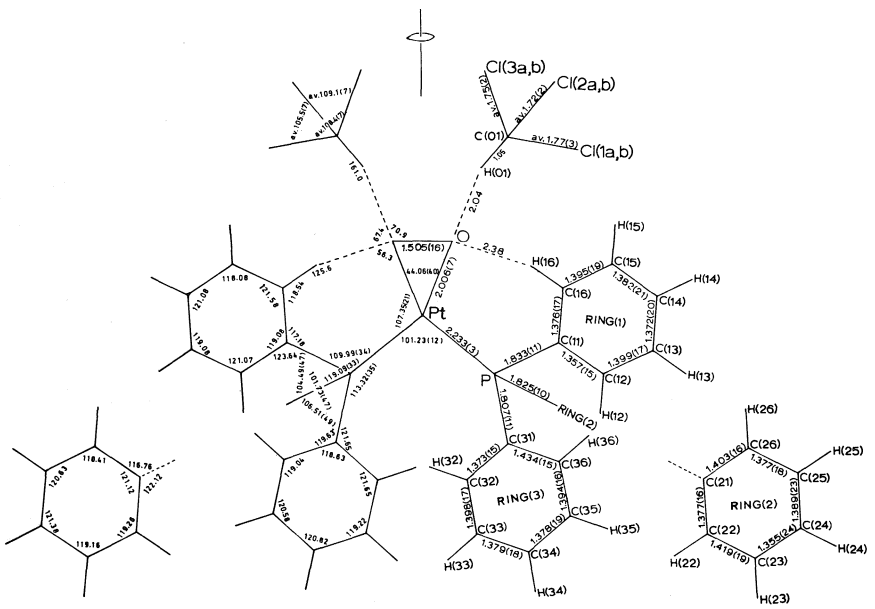

FIG. 1. Bond lengths and angles.

O . . . O is 1.45 (4) Å in the benzene complex (6) suggests that there has been some bond lengthening in the chloroform adduct. Although this lengthening is not statistically significant because of the large e.s.d. of the O . . . O bond in the benzene complex, its importance should not be underestimated. In any case, since all three complexes, when stripped of their solvent molecules, are iso-

Can. J. Chem. Downloaded from www.nrcresearchpress.com by 210.87.254.6 on 09/05/12
For personal use only.

TABLE 4. Best least squares planes of the form $AX + BY + CZ = D$ where X, Y, Z, are real orthogonal coordinates, X along x and Z along z*

(*a*) Coefficients

Plane	Description	*A*	*B*	*C*	*D*
1	Central coordination	0.3475	0.0	−0.9377	−4.7208
2	First phenyl ring	0.8024	0.4003	−0.4427	−1.0374
3	Second " "	−0.7633	0.0312	−0.6453	−4.0452
4	Third " "	−0.3899	0.8847	−0.2554	−0.0671

(*b*) *Angles between normals to planes* (deg)

Plane	2	3	4
1	46.05	70.12	83.98
2		108.32	81.12
3			60.66

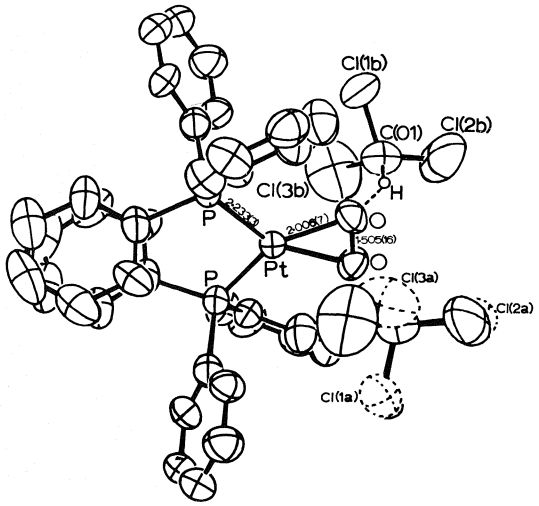

FIG. 2. Molecule of $(Ph_3P)_2PtO_2.2CHCl_3$ with 50% probability thermal ellipsoids. In order to make one of the hydrogen atoms clearly visible the corresponding $CHCl_3$ molecule has been drawn in only one of its two disordered positions. For the other $CHCl_3$ molecule both positions are given (full and broken lines, respectively).

electronic, the difference in O . . . O bond lengths must be due to the effect of solvent molecules. Ligand–solvate molecule interactions have not previously been introduced into discussions of oxygen bond lengths in complexes of this type although they may well be significant.

The Pt . . . O distance, 2.006(7) Å, is similar to that found in other platinum complexes, namely, 2.07 Å in bis(triphenylphosphine)carbonatoplatinum(II) (14), 2.01(1) in bis(triphenylphosphine)-peroxidoacetonatoplatinum(0) (15), 2.0 in potassium bis(oxalato)platinum dihydrate (16) 2.20,-2.24(3) in trimethyl (salicylaldehydato)platinum-(IV) (17), 2.01(3) in $Pt(O_2)(PPh_3)_2 1.5C_6H_6$ (6) and 2.02 in potassium bis(acetylacetonato)chloroplatinate(II) (8). With the exception of the salicylaldehydato complex, the Pt . . . O distance seems to be little affected by whether the oxygen atoms are bonded to each other or not.

The two phosphorus atoms and two oxygen atoms lie closely coplanar with the Pt atom. The angle between planes O—Pt—O′ and P—Pt—P′ is only 0.1°. Coefficients for the best least squares planes through the "central coordination moiety" and the three phenyl rings are listed in Table 4. In no case does the maximum deviation from planarity exceed 0.015 Å. There are no unusually short interatomic contacts in the crystal, except around the oxygen atoms: a close interatomic distance of 2.38 Å between O and H(16) and a close intermolecular distance of 2.39 Å between O and H(35) (at $\frac{1}{2} - x, \frac{1}{2} + y, \frac{1}{2} - z$).

Thanks are due to the National Research Council of Canada for generous financial support.

1. S. J. LAPLACA and J. A. IBERS. J. Am. Chem. Soc. **87**, 2581 (1965).
2. J. A. MCGINNETY, N. C. PAYNE, and J. A. IBERS. J. Am. Chem. Soc. **91**, 6301 (1969).
3. J. A. IBERS and S. J. LAPLACA. Science, **145**, 920 (1964).
4. J. A. MCGINNETY, R. J. DOEDENS, and J. A. IBERS. Inorg. Chem. **6**, 2243 (1967).
5. J. A. MCGINNETY and J. A. IBERS. Chem. Commun. 235 (1968).
6. T. KASHIWAGI, N. YASUOKA, N. KASAI, and M. KAKUDO. Chem. Commun. 743 (1969).
7. C. D. COOK, P -T. CHENG, and S. C. NYBURG. J. Am. Chem. Soc. **91**, 2123 (1969).
8. C. D. COOK and G. S. Jauhal. J. Am. Chem. Soc. **90**, 1464 (1968).

Can. J. Chem. Downloaded from www.nrcresearchpress.com by 210.87.254.6 on 09/05/12
For personal use only.

9. P. COPPENS. DATAP3, A single crystal X-ray absorption correction program. Crystallographic Computing. Munksgaard. 1970.
10. R. D. ELLISON. XFLS, An extensively modified version of ORFLS. (Report ORNL–TM–305, Oak Ridge National Laboratory, 1962. Unpublished.)
11. D. T. CROMER and J. B. MANN. Acta Cryst. A**24**, 321 (1968).
12. W. C. HAMILTON and J. A. IBERS. Hydrogen bonding in solids. W. A. Benjamin, New York. 1968.
13. P. ANDERSEN and T. THURMANN-MOE. Acta. Chem. Scand. **18**, 433 (1964).
14. F. CARCATI, R. Mason, G. B. ROBERTSON, and R. UGO. Chem. Commun. 408 (1967).
15. R. UGO, F. CONTI, S. CENINI, and R. MASON. Chem. Commun. 1498 (1968).
16. R. MATTES and K. KROGMANN. Z. anorg. Chem. **332**, 247 (1964).
17. M. R. TRUTER and R. C. WATLING. J. Chem. Soc. A, 1955 (1967).
18. R. MASON, G. B. ROBERTSON, and P. J. PAULING. J. Chem. Soc. A, 485 (1969).

Can. J. Chem. Downloaded from www.nrcresearchpress.com by 210.87.254.6 on 09/05/12
For personal use only.

The Catalytic Decomposition of Isopropyl Alcohol Vapor on Manganese (II) Oxide

D. G. KLISSURSKI,[1] E. F. MCCAFFREY, AND R. A. ROSS
Department of Chemistry, Lakehead University, Thunder Bay, Ontario

Received June 17, 1971

The vapor phase decomposition of isopropyl alcohol has been studied from 210 to 365 °C on manganese(II) oxide. Rates of conversion to acetone and propylene were measured with partial pressures of isopropyl alcohol from 0.3 to 22 mm. The catalyst selectivity towards dehydrogenation was around 0.80 between 320 and 365 °C while at 306 °C it was somewhat less and depended on the alcohol partial pressure. Propylene and hydrogen additions had no effect on the reaction rate while the reaction order with respect to isopropyl alcohol partial pressure was 0.4 to 0.6 except at 306 °C when it decreased with increase in the alcohol partial pressure. The effects of acetone and water additions were shown respectively to be exerted mainly on the dehydrogenation and dehydration reactions while at acetone pressures above 4 mm, considerable amounts of by-products including mesityl oxide and heavier ketones were clearly detected. The apparent activation energy of the overall decomposition as calculated from the experimental rates was 26 ± 0.5 kcal mol^{-1}. The results have been interpreted to be in general agreement with the concept that the rate-limiting step is linked to the direct interactions on the catalyst surface and it has been established that the reaction is significantly more complex than previously recognized. The physical properties of the manganese(II) oxide were determined by X-ray and nitrogen adsorption techniques while infrared, n.m.r., and gas chromatographic methods were used to analyze the products of catalysis.

On a étudié la décomposition de l'alcool isopropylique en phase vapeur, entre 210 et 365 °C, sur l'oxyde de manganèse(II). Les taux de conversion en acétone et propylène furent mesurés au moyen des pressions partielles d'alcool isopropylique entre 0.3 et 22 mm. La sélectivité du catalyseur pour la déshydrogénation se situait autour de 0.80 entre 320 et 365 °C, alors qu'à 306 °C elle était légèrement inférieure et dépendait de la pression partielle de l'alcool. Des additions de propylène et d'hydrogène n'ont eu aucun effet sur la vitesse de la réaction, alors que l'ordre de la réaction par rapport à la pression partielle d'alcool isopropylique était de 0.4 à 0.6, excepté à 306 °C où il diminuait avec l'augmentation de la pression partielle d'alcool. On a constaté que les effets de l'addition d'acétone et d'eau s'exerçaient principalement sur les réactions de déshydrogénation et de déshydratation, alors qu'à des pressions d'acétone de plus de 4 mm, des quantités considérables de produits secondaires incluant l'oxyde de mésityle et des cétones plus lourdes étaient clairement détectées. L'énergie d'activation apparente de la décomposition totale, telle que calculée à partir des vitesses expérimentales était de 26 ± 0.5 kcal mol^{-1}. Les résultats ont été interprétés comme étant en accord général avec le concept que l'étape limitante est reliée aux interactions directes à la surface du catalyseur et il a été établi que la réaction est singulièrement plus complexe qu'on l'avait prévu. Les propriétés physiques de l'oxyde de manganèse(II) ont été déterminées par les techniques de rayons-X et d'adsorption d'azote, alors qu'on a utilisé l'infrarouge, la r.m.n. et la chromatographie en phase gazeuse pour analyser les produits de catalyse.

Canadian Journal of Chemistry, 49, 3778 (1971)

Introduction

Few comprehensive kinetic studies of the heterogeneous catalytic properties of manganese(II) oxide or its mixed oxides have been reported and as a first step in an experimental assessment of these properties an examination of the catalytic decomposition of isopropyl alcohol vapor on manganese(II) oxide has been carried out. This reaction is frequently used as a model in studies of variations in catalytic activity and selectivity involving nonmetallic catalysts (1). At temperatures below 500 °C it proceeds mainly in two directions: (*a*) dehydrogenation and (*b*) dehydration.

According to current theories, catalyst activity and selectivity in this reaction may be related to lattice parameters, type of conductivity, and width of forbidden zone as well as to the acidic properties of the surface (2–5). For manganese(II) oxide in particular, a relatively high activity in the dehydrogenation of isopropyl alcohol has been reported (6) but unfortunately no data on the surface area were given and hence the specific activity cannot be estimated. At the same time, the reaction order with respect to isopropyl alcohol or any of the reaction products has not been studied and yet it is generally accepted that

[1]On leave from Academy of Sciences of Bulgaria, Sofia 13.

Can. J. Chem. Downloaded from www.nrcresearchpress.com by 210.87.254.6 on 09/05/12
For personal use only.

Can. J. Chem. Downloaded from www.nrcresearchpress.com by 210.87.254.6 on 09/05/12
For personal use only.

only dehydrogenation proceeds on the surface of this catalyst (6–8).

In the present work the activity and selectivity of manganese(II) oxide in the decomposition of isopropyl alcohol vapor have been examined from 300 to 365 °C. Reaction orders and activation energy have been measured and attention given to the more complex character of the reaction.

Experimental

Apparatus

The all-glass flow system has been described previously (9, 10). A quartz integral reactor was used and tests from 210 to 363 °C showed that isopropyl alcohol did not decompose to any detectable extent in the absence of the catalyst. High-purity nitrogen at atmospheric pressure was used as a carrier gas and the catalyst bed temperature was controlled to $\pm 0.1°$ from 300 to 400 °C by a platinum resistance thermometer connected to an expanded-scale "Sigma" proportional controller.

Reaction products were analyzed at 80 °C by a Beckman GC5 gas chromatograph using stainless steel columns, 72 in. × 0.125 in. o.d., packed with "Carbowax 1540" on "Teflon 6".

To establish the experimental conditions for which the reaction rate was not influenced by external or internal diffusion, the influence of space velocity, catalyst mass, and particle size was studied in the usual manner (9). As a result of these preliminary studies the kinetic measurements were performed at flow rates from 220 to 360 ml min^{-1} (N.T.P.) (space velocities at 342.5 °C, 300 to 500 cc gas (cc catalyst)$^{-1}$ min^{-1}).

All reaction rate measurements were made after the establishment of the steady catalyst activity level.

Materials

(a) Manganese(II) Oxide

Electrolytic grade metallic manganese, 99.999% pure, was dissolved in nitric acid to give a 4 *M* solution at p*H* 6. The solution was kept at 60 °C and 4 *M* ammonium oxalate solution added with vigorous stirring. The precipitate, $MnC_2O_4.2H_2O$, was washed with warm deionized-water until free of nitrate ions and then dried at 80 to 100 °C for 6 h. Calcination to manganese(III) oxide was carried out at 300 °C for 5 h followed by 16 h each at 400 and 600 °C (11–13). Subsequently, analysis by X-ray powder photography confirmed the α-Mn_2O_3 structure (14). Chemical analysis (15) showed 69.98% *w/w* manganese (theory 69.59%) while the specific surface area was 26 ± 2 m^2 g^{-1} (B.E.T.; N_2; −196 °C). Finally the α-Mn_2O_3 was heated for 12 h at 600 °C in a flow of hydrogen (60 ml min^{-1}) and X-ray powder photography of the product confirmed the MnO structure (14). Chemical analysis gave 76.90% *w/w* manganese (theory 77.44%) and the surface area was 23 ± 2 m^2 g^{-1}.

It was established that the specific surface area of the manganese(II) oxide samples did not change after use in the catalytic measurements.

(b) Reagents

Isopropyl alcohol and acetone were "Spectrosol" quality and their u.v. absorption characteristics, Unicam SP800A, were the same as those given on their accompanying certificates. All gaseous reagents and the nitrogen carrier (Canadian Liquid Air Ltd.) were 99.99% pure.

Results

The Effect of Temperature on the Reaction Rate and Products

Experiments were carried out with 9.72 mm partial pressure isopropyl alcohol at various temperatures from 325 to 363 °C in which the rates of conversion of the alcohol to acetone (r_1) and propylene (r_2) were measured along with the overall rate of conversion (r_3) and the selectivity ratio r_1/r_3. Within this temperature range, several other products were formed which accounted for approximately 0.1% of the total conversion. Isopropyl ether and mesityl oxide were positively identified while i.r. and n.m.r. analyses both indicated the presence of an acetylenic compound.

Although the dehydrogenation reaction was predominant, dehydration also took place simultaneously to a significant extent. The average selectivity for dehydrogenation was close to 0.80 at all temperatures with no obvious trend. Earlier it had been accepted (6) that manganese(II) oxide catalyzes the dehydrogenation reaction with a selectivity of 99–100%, a conclusion which is evidently not in agreement with the present results. However, the disagreement may be explained simply by the fact that the reaction rate previously had been measured only from the pressure changes of the gaseous products (7) or by the quantity of hydrogen evolved (6).

In Fig. 1, $\log_{10} r_3$ is plotted against the reciprocal catalyst temperature in the Arrhenius fashion. From the slope of this line the apparent activation energy, E', was calculated at 26 ± 0.5 kcal mol^{-1}. Additional measurements in the interval 210 to 300 °C confirmed this value.

For a catalytic reaction inhibited by the products it has been shown (16) that the relationship between E' and the apparent activation energy E, calculated from rate constants is given by: $E' = E/(r + 1)$, where r is the overall reaction order with respect to the inhibiting products. Because of the complexity of rate constant calculations for some reactions, it was further shown (16) that E could be obtained by plotting the temperature dependence of the flow rate at which a given degree of conversion was achieved, since then: flow rate, $V \propto k$, rate constant.

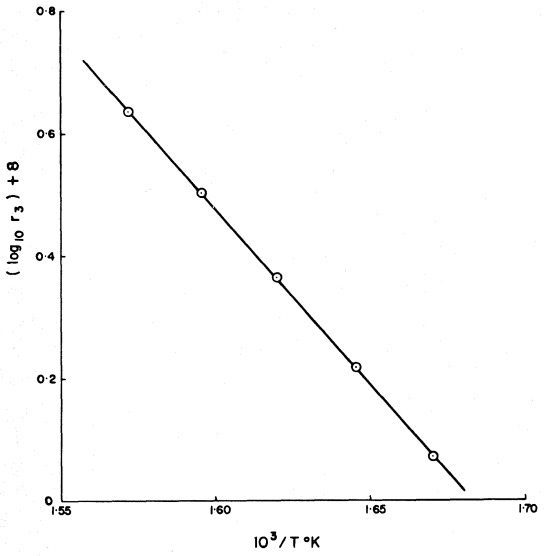

FIG. 1. Arrhenius plot of overall experimental reaction rate (r_3). Partial pressure isopropyl alcohol, 9.72 mm; flow rate, 300 ml min^{-1} (N.T.P.).

Figure 2 shows the mole fraction of isopropyl alcohol converted *vs.* the reciprocal of the flow rate at the temperatures indicated. From these data four separate Arrhenius plots of $\log_{10} V$ against $1/T$ °K were drawn for four different degrees of conversion between 15 and 30%. The plots gave an apparent activation energy of 30 ± 2 kcal mol^{-1}. The slightly higher value found for E and E' indicates the level of the product inhibition effects on the overall reaction rate.

The Effect of Isopropyl Alcohol Partial Pressure on the Reaction Rate

The partial pressure of isopropyl alcohol was varied between 0.3 and 21 mm at 306, 323, and 356 °C at 300 ml min^{-1} (N.T.P.). The results are shown in Table 1. There is a slight trend for dehydration to become more favored with decrease in temperature, particularly so at the highest isopropyl alcohol partial pressures at 306 °C. Logarithmic plots of these data indicate a reaction order for the overall decomposition from 0.4 to 0.6 with respect to isopropyl alcohol partial pressure at 323 and 356 °C. The order lay at the higher end of the range at 356 °C and at the lower end at 323 °C. Previously it has been stated (17) that the rate of reaction of isopropyl alcohol on manganese(II) oxide at "low" temperatures depends little on the alcohol partial pressure al-

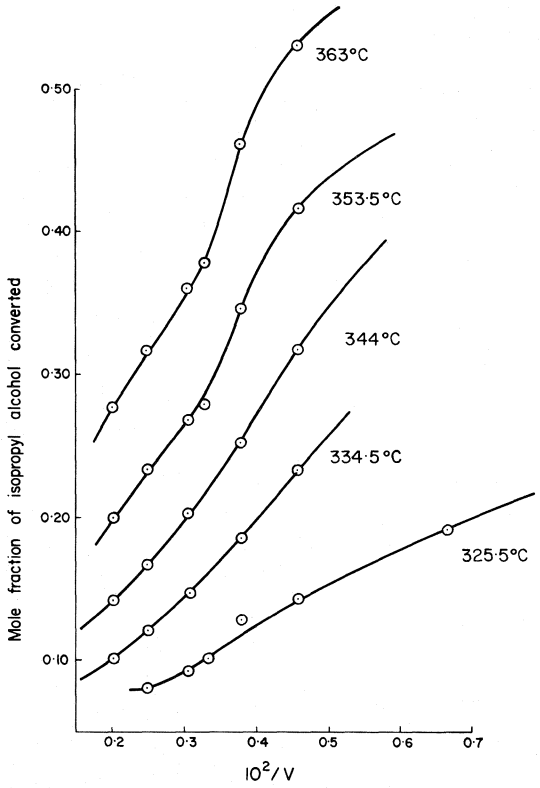

FIG. 2. Changes in mole fraction of isopropyl alcohol converted with variation in flow rate, V, at temperatures shown.

though no data were quoted. At 306 °C, the dependence of the reaction order on isopropyl alcohol partial pressure was more complex. There was a distinct tendency for the order to fall with increase in the alcohol partial pressure, *e.g.* from 0.3 to 10.0 mm the order decreased from 0.6 to about 0.2, Fig. 3. Similar effects have been observed also with $ZnO.Cr_2O_3$ catalysts (18).

The Effect of Hydrogen

In the temperature range studied with hydrogen partial pressures from 1.5 to 40 mm and an isopropyl alcohol partial pressure of 7.78 mm the reaction rate was not influenced by hydrogen partial pressure.

The Effect of Propylene

At 323 °C with 7.78 mm partial pressure isopropyl alcohol and propylene partial pressures from 0.3 to 33 mm no influence of the gas was detected on the rates of either the dehydration or dehydrogenation reactions.

Can. J. Chem. Downloaded from www.nrcresearchpress.com by 210.87.254.6 on 09/05/12
For personal use only.

TABLE 1. The effect of isopropyl alcohol partial pressure on the experimental reaction rates at flow rate 300 ml min^{-1} (N.T.P.)

Temperature (°C)	Partial pressure of isopropyl alcohol (mm)	Rate of conversion to acetone, r_1 (mol m^{-2} s^{-1}) × 10^{-8}	Rate of conversion to propylene, r_2 (mol m^{-2} s^{-1}) × 10^{-8}	Overall rate, r_3 (mol m^{-2} s^{-1}) × 10^{-8}	r_1/r_3
356.0	4.21	1.95	0.53	2.48	0.79
356.0	8.41	3.06	0.75	3.81	0.80
356.0	12.62	3.87	0.92	4.79	0.81
356.0	16.83	4.44	1.05	5.48	0.81
356.0	21.04	4.70	1.12	5.82	0.81
323.0	1.94	1.06	0.27	1.33	0.80
323.0	3.89	1.44	0.39	1.83	0.79
323.0	5.83	1.70	0.45	2.15	0.79
323.0	7.78	1.84	0.48	2.32	0.79
323.0	9.72	2.08	0.55	2.64	0.79
306.0	0.32	0.15	0.04	0.19	0.79
306.0	0.65	0.27	0.08	0.34	0.78
306.0	0.97	0.34	0.09	0.43	0.78
306.0	1.30	0.37	0.11	0.48	0.77
306.0	1.62	0.42	0.12	0.54	0.78
306.0	1.95	0.43	0.13	0.56	0.77
306.0	2.59	0.46	0.14	0.60	0.77
306.0	3.21	0.47	0.15	0.61	0.76
306.0	3.89	0.48	0.16	0.64	0.74
306.0	5.83	0.52	0.18	0.70	0.74
306.0	7.78	0.55	0.19	0.74	0.74
306.0	9.72	0.58	0.22	0.80	0.73

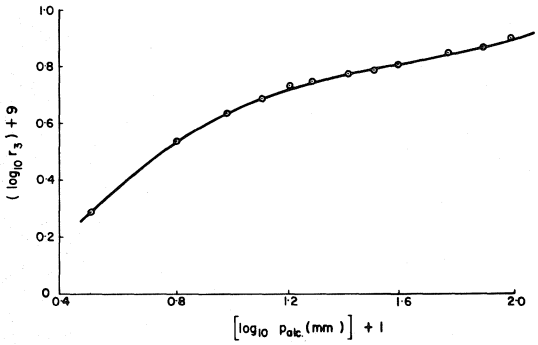

FIG. 3. Variation of overall reaction rate with initial isopropyl alcohol partial pressure at 306 °C.

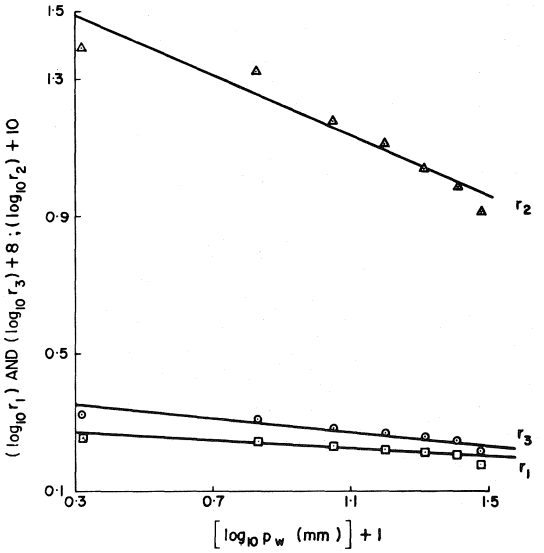

FIG. 4. The effect of the total water vapor partial pressure on r_1, r_2, and r_3 at 323 °C. Partial pressure isopropyl alcohol, 7.78 mm.

The Effect of Water Vapor

The effect of changing the water vapor partial pressure from 0.2 to 3 mm was studied at 323 and 343 °C with isopropyl alcohol partial pressures of 7.78 and 16.83 mm, respectively. At 323 °C, $r_1 \propto (p_w)^{-0.06}$, $r_2 \propto (p_w)^{-0.45}$, and $r_3 \propto (p_w)^{-0.08}$ and at 343 °C, $r_1 \propto (p_w)^{-0.05}$, $r_2 \propto (p_w)^{-0.58}$, and $r_3 \propto (p_w)^{-0.11}$. Figure 4 illustrates these effects for the experiments at 323 °C. After the removal of the added water vapor the catalyst activity recovered to its original value.

The Effect of Acetone

When 27.77 mm of acetone was passed alone over newly prepared manganese(II) oxide at 356 °C at 300 ml min^{-1} (N.T.P.), about 1% initially condensed to give mesityl oxide and six other heavier ketones. After 2 h exposure this activity had fallen to about 0.5%.

At 323 °C and isopropyl alcohol partial pressure 7.78 mm, the acetone partial pressure

Can. J. Chem. Downloaded from www.nrcresearchpress.com by 210.87.254.6 on 09/05/12
For personal use only.

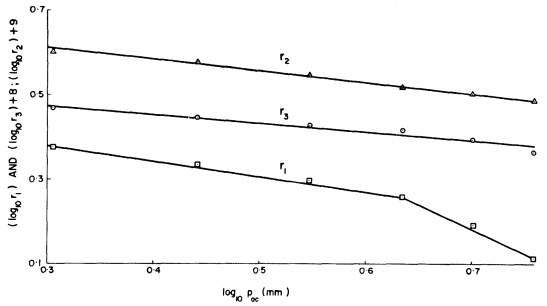

FIG. 5. The effect of the total acetone partial pressure on r_1, r_2, and r_3 at 323 °C. Partial pressure isopropyl alcohol, 7.78 mm.

was varied from 2 to 6 mm. Figure 5 shows the results obtained with respect to r_1, r_2, and r_3. The rates r_2 and r_3 are respectively $\propto (p_{ac})^{-0.06}$ and $(p_{ac})^{-0.10}$ over the entire pressure range while $r_1 \propto (p_{ac})^{-0.36}$ from 2.02 to 4.32 mm but at the higher pressures this index becomes -1.00.

Clear evidence of catalyst poisoning was obtained here. For example, when the last increment of acetone added was entirely removed at the conclusion of the experiments, r_1 was reduced by 17% and r_2 by 13% at the steady level of catalyst activity.

In this series of experiments a small trace of isopropyl ether was detected which increased in quantity with increase in acetone partial pressure but never exceeded 0.1% of the total products. Considerable amounts of other by-products including mesityl oxide principally, and two of the heavier ketones were present. These increased in amount sharply but smoothly with increase in acetone partial pressure such that they accounted for approximately 30% of the total products at 5.74 mm acetone. Their rate of formation was between first and second order with respect to the acetone partial pressure, Fig. 6.

Discussion

The decomposition of isopropyl alcohol on manganese(II) oxide involves principally dehydrogenation, dehydration, and condensation reactions. In the absence of added acetone the overall rate can be equated to the sum of the dehydrogenation and dehydration rates as the contributions of the condensation reactions are then very small. Since the selectivity ratio is almost constant at 0.80 from 320 to 365 °C, the apparent activation energy, E', of 26 ± 0.5 kcal

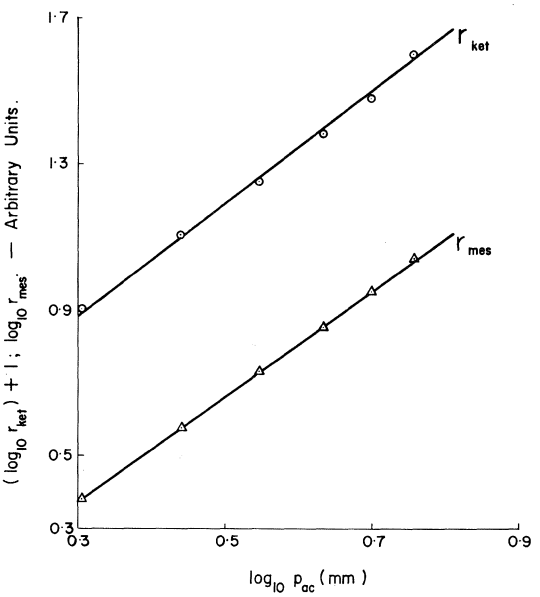

FIG. 6. Variation of the rates of ketone, r_{ket}, and mesityl oxide, r_{mes}, formation with acetone partial pressure at 323 °C. Partial pressure isopropyl alcohol, 7.78 mm.

mol^{-1} applies to both dehydrogenation and dehydration and therefore it may be compared directly with the value of Balandin *et al.* (6), 25.4 kcal mol^{-1}, for the dehydrogenation of isopropyl alcohol on manganese(II) oxide in the same temperature region. Good agreement is obtained also between the value of 30 ± 2 kcal mol^{-1} found here for E from the data of Fig. 2 and the earlier value of 31.9 kcal mol^{-1} calculated (6) from adsorption coefficients. The difference between E and E' is consistent with the effects of the products on the overall reaction rate. Balandin *et al.* interpreted their results as being consistent with desorption of acetone as the rate-controlling step. However, the complexity of the reaction was not then entirely recognized.

Although the decomposition of isopropyl alcohol has been studied frequently using a variety of catalysts (1), few papers have emphasized the kinetics of the reaction and information on the kinetic equations is limited. In dehydrogenation, the possible rate-limiting steps are (*a*) adsorption of the alcohol, (*b*) interaction on the surface, and (*c*) desorption of products. These possibilities have been discussed recently (17) for catalysis on zinc(II) oxide and a kinetic

Can. J. Chem. Downloaded from www.nrcresearchpress.com by 210.87.254.6 on 09/05/12
For personal use only.

Can. J. Chem. Downloaded from www.nrcresearchpress.com by 210.87.254.6 on 09/05/12
For personal use only.

analysis carried out. Also, in a general form the following equation has been proposed (17) for the catalytic dehydrogenation

$$[1] \qquad \text{rate} = \frac{k_1 k_3 p_{alc}}{k_1 p_{alc} + k_2 p_{ac} + k_3}$$

where k_1, k_2, and k_3 are, respectively, the rate constants for the decomposition of the alcohol, adsorption of acetone, and desorption of acetone while p_{alc} and p_{ac} are the partial pressures of isopropyl alcohol and acetone, respectively. The equation is in agreement with experimental data (18) and was derived on the assumption that at the steady state the rate of desorption of acetone is equal to its rate of adsorption plus the rate of dehydrogenation of the alcohol. By making suitable deductions in the classical manner regarding the relative weights of the component terms in the equation it can be modified (17) to explain the results of experiments with various catalysts where either (*b*) (18) or (*c*) (6, 19) was concluded to be the rate-limiting step. For the dehydration of isopropyl alcohol on metallic oxides a similar kinetic treatment (20) yields an equation for the rate like eq. 1 with rate parameters for water substituted for those of acetone.

The present results show that the order of the overall decomposition reaction with respect to isopropyl alcohol partial pressure depends on the temperature and on the pressure region, Table 1 and Fig. 3. Similar effects have been observed (18) for the reaction of 30–300 mm isopropyl alcohol at 383 °C on a $ZnO.Cr_2O_3$ catalyst. All of these data are in agreement with eq. 1, since if it is accepted (17) that $k_3 + k_1 p_{alc} \gg k_2 p_{ac}$ the equation can be transformed to

$$[2] \qquad \text{rate} = \frac{k_1}{(1/p_{alc}) + k_1/k_3}$$

Hence, with increase in the partial pressure of isopropyl alcohol the dehydrogenation reaction rate will be increasingly less affected by the isopropyl alcohol partial pressure. A similar conclusion can be obtained for the dehydration reaction. The present results show that r_1, r_2, and also r_3 are affected in this fashion by increase in the alcohol partial pressure with the major change reflected in r_1, the rate of dehydrogenation. These features are illustrated in Fig. 7 where Langmuir plots of $1/r_1$, $1/r_2$ and $1/r_3$ are given for the data obtained at 306 °C. It would be expected that

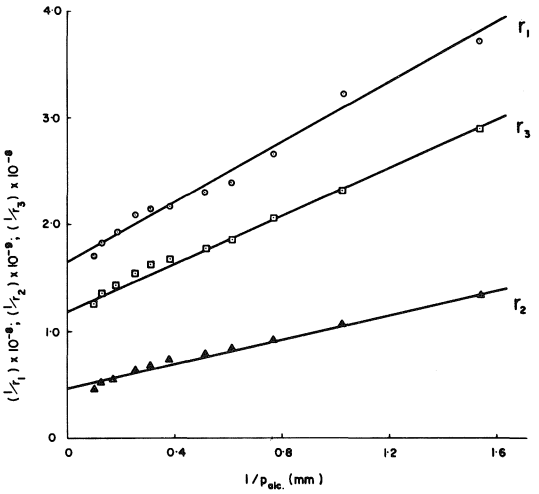

FIG. 7. Langmuir plots of r_1, r_2, and r_3 at 306 °C.

similar results would be found at the higher temperatures if higher partial pressures of isopropyl alcohol could have been used but experimental limitations were prohibitive because of the possibility of cracking reactions occurring (21). The Langmuir pattern observed at 306 °C was also noted with $ZnO.Cr_2O_3$ (18).

The zero order rate dependence of r_1, r_2, and r_3 on the partial pressure of hydrogen is interpreted in terms of a very rapid saturation of any surface sites present which might be amenable to the adsorption of the gas or alternatively that extremely rapid desorption is involved. A similar interpretation may be applied to explain the zero order kinetic relationship found with propylene.

The effect of water vapor partial pressure on the reaction rates, Fig. 4, is indicative of the accepted view (21, 22) that different surface sites are involved in the dehydrogenation and dehydration of alcohols since r_1 is only barely related to p_w while r_2 is substantially inhibited by increase of this partial pressure.

The influence of acetone partial pressure on the mechanism and rate of the reaction on manganese(II) oxide is of a significantly more complex character than has been accepted (6). The rates r_2 and r_3 are only slightly inhibited by increase in acetone partial pressure while r_1 is more significantly affected, particularly at high pressures. Indications are that inhibition of acetone formation would become almost total at acetone partial pressures around 10 mm at 323 °C. Since the rate

Can. J. Chem. Downloaded from www.nrcresearchpress.com by 210.87.254.6 on 09/05/12
For personal use only.

retardation exerted by acetone is largely concentrated on the other path of the reaction from that of the water vapor, the results can be regarded as added confirmation of the hypothesis that different surface loci are involved in the two competitive reactions. At the same time it is important to note (*i*) that at the highest acetone partial pressures a substantial increase takes place in the rates of formation of the observed secondary products such that a kinetic relationship exists between these rates and the acetone partial pressure, Fig. 6, (*ii*) that a measurable reduction in overall catalyst activity is observed after removal of this acetone, and (*iii*) that acetone itself undergoes condensation reactions on the manganese(II) oxide. Hence the intervention of additional surface reactions in these conditions occurs with complex consequences in regard to mechanistic interpretations especially involving r_1.

At present, we have been unable to develop mechanisms which completely satisfy the kinetic results. Nevertheless, some useful conclusions can be made with respect to general if not detailed reaction sequences. Thus the results show fair agreement with the concept (18) that the rate-limiting step is linked to reaction on the catalyst surface. Figure 7 supports this deduction as it expresses a proportionality between the reaction rate and the surface coverage although, taken alone, it does not imply that the slow step in the mechanisms of dehydrogenation and dehydration is reaction of the alcohol. However, some further support for this deduction is evident in the small effect of acetone and water on the overall reaction rate. Thus $r_3 \propto p_w^{-0.1}$ and $p_{ac}^{-0.1}$ but the effect of these products on the separate competitive reactions is more pronounced, $r_2 \propto p_w^{-0.5}$ and $r_1 \propto p_{ac}^{-(0.3-1.0)}$ depending on partial pressure.

The addition of water vapor hardly affects the rate of the dehydrogenation reaction and the overall relationship of r_3 with p_w is mathematically consistent with the catalyst selectivity. Isopropyl ether disappears as the water vapor pressure is increased and the catalyst recovers its original activity when the added water vapor is removed. This indicates the reversible adsorption of water on active dehydration sites and clearly shows that the surface equilibrium is very sensitive to the pressure of water vapor.

The order found with respect to acetone for r_3 when compared with that for r_1 is believed to be due to an increase in the inter-molecular reactions which produce mesityl oxide, isopropyl ether, and the heavier ketones as was observed when the acetone partial pressure was increased. Since r_3 was only slightly affected in these experiments it may be concluded that no significant change in the surface concentration of adsorbed alcohol took place. Hence the effect of added acetone is most probably exerted on a sensitive acetone adsorption/desorption equilibrium condition as the course of catalysis is considerably modified. The secondary reactions and effects present a special interest for further study.

1. O. V. KRYLOV. Catalysis by nonmetals. Academic Press, New York and London. 1970. p. 115.
2. S. Z. ROGINSKII. Zh. Fiz. Khim. **6**, 334 (1935).
3. S. Z. ROGINSKII. Dokl. Akad. Nauk. SSSR, **67**, 97 (1949).
4. K. HAUFFE. Reactions on solids and their surfaces. Russ. IL (1962).
5. G. M. SCHWAB. Adv. Catal. **2**, 229 (1952).
6. A. A. BALANDIN, A. A. TOLSTHOPYATOVA, and V. H. MATUSHEKO. Izvest. Akad. Nauk, SSSR, 1333 (1960).
7. P. SABATIER and A. MAILHE. Ann. Chim. (Paris), **8** (20), 289 (1910).
8. P. MARS. The mechanism of heterogeneous catalysis. *Edited by* J. H. de Boer *et al.* Elsevier Publishing Co., New York. 1960. p. 49.
9. R. A. ROSS and B. G. WALSH. J. Appl. Chem. **11**, 469 (1961).
10. A. B. HART, J. MCFADYEN, and R. A. ROSS. Trans. Faraday Soc. **59**, 1458 (1963).
11. T. E. MOORE, E. MARYLINN, and P. W. SELWOOD. J. Am. Chem. Soc. **72**, 856 (1950).
12. D. DOLIMORE, J. DOLIMORE, and J. LITTLE. J. Chem. Soc. A, 2946 (1969).
13. O. KADLEC and V. DANES. Coll. Czech. Chem. Comm. **32**, 1871 (1967).
14. American Society for Testing Materials, Card Index.
15. G. SCHWARZENBACH and H. FLASHKA. Complexometric titrations. Methuen and Co. Ltd., London. 1969. p. 234.
16. S. L. KIPERMAN. Introduction to the kinetics of heterogeneous catalytic reactions. (Russ.) Nauka, Moscow. 1964. p. 543.
17. O. V. KRYLOV. Russ. J. Phys. Chem. (Eng.) **39**, 1554 (1965).
18. J-E. GERMAIN, J. BIGOURD, J-P. BEAUFILS, B. GROS, and L. PONSALLE. Bull. Soc. Chim. Fr. 1777 (1961).
19. Y. DECHATRE and S. J. TEICHNER. Bull. Soc. Chim. Fr. 2804 (1967).
20. O. V. KRYLOV. Russ. J. Phys. Chem. (Eng.) **39**, 1422 (1965).
21. D. E. R. BENNETT and R. A. ROSS. J. Chem. Soc. A, 1542 (1968).
22. O. V. KRYLOV and E. A. FOKINA. Kinet. Catal. (Russ.) **1**, 421, 541 (1960).

Raman and Infrared Spectra of Crystalline OF_2

J. TREMBLAY AND R. SAVOIE

Centre de recherches sur les atomes et les molécules et Département de Chimie, Université Laval, Québec, Québec

Received June 15, 1971

Raman and infrared spectra of crystalline OF_2 indicate that this solid is not centro-symmetric and contains at least two molecules per primitive cell, on sites of symmetry C_s or C_1.

Les spectres Raman et infrarouges de OF_2 cristallin indiquent que le solide n'est pas centro-symétrique et que la maille primitive contient au moins deux molécules, situées sur des sites de symétrie C_s ou C_1.

Canadian Journal of Chemistry, 49, 3785 (1971)

Can. J. Chem. Downloaded from www.nrcresearchpress.com by 210.87.254.6 on 09/05/12
For personal use only.

Introduction

The OF_2 molecule has been shown by electron diffraction (1) and microwave measurements (2, 3) to be of C_{2v} symmetry, with bond lengths and apex angle of 1.41 Å and 103°, respectively. The infrared spectrum of the gas has also been recorded (4–6). Band contours in the ν_1 (symmetric stretch) and ν_3 (asymmetric stretch) regions have shown that the OF_2 molecule is one of the few triatomic molecules for which $\nu_1 > \nu_3$. In the condensed states, only the Raman spectrum of the liquid has been reported so far (7), which is understandable in view of the corrosive nature of this compound and its low freezing point, 49.4 °K (8).

Our main aim in undertaking the present study was to gather information on the crystal structure of the solid for which no crystallographic data are as yet available. It was expected that this type of compound would be well suited for a spectroscopic investigation since it is not contaminated by isotopic species, except by $^{18}OF_2$ at a negligible concentration of 0.2%.

Experimental

The OF_2 used in our experiments was prepared by reacting gaseous F_2 (98% pure, Matheson Co., Ltd.) with a 3% aqueous solution of NaOH which was continuously changed in the reaction vessel. The evolved gas was first purified by bubbling through distilled water and then by trap-to-trap distillation (9). Bands from probable impurities, such as CF_4 and SiF_4, were not detected in our spectra.

The infrared spectra were recorded on a carefully calibrated Perkin–Elmer (model 621) spectrophotometer and the frequencies cited later are believed to be accurate to ± 1 cm^{-1}. The far-infrared spectrum of the solid in the region 20–200 cm^{-1} was obtained on a commercial interferometer (Research and Industrial Instruments Co., model FS-720) coupled to a Fourier transform computer (FTC-100), with a theoretical resolution of 1 cm^{-1} and a probable frequency accuracy of ± 1 cm^{-1}.

The spectra were recorded using a conventional liquid helium cryostat (10), with cesium iodide or silicon backing plate. A side arm was added to the bottom part of the cryostat, making it possible to deposit the gaseous samples through a Teflon cone which could be slided in and out by a selenoid coil. This technique insured more uniform film deposits on the window and prevented samples from condensing on other cold parts of the cryostat. The temperature, measured with a calibrated carbon resistor, was controlled within a few degrees by a Teflon plug which limited the amount of liquid helium reaching the copper block to which the backing plate was attached (10). Solid films of pure OF_2 were prepared by direct deposition of the sample from a trap at liquid nitrogen temperature. (The vapor pressure of OF_2 at 77 °K is 1.44 mm Hg (9).)

The Raman spectra were recorded on a Spex (model 1400) spectrometer equipped with an argon ion laser (CRL, model 52 A) and a cooled phototube detector (Star Tracker FW-130). This instrument was calibrated with a neon discharge lamp and the frequency accuracy is estimated at ± 1 cm^{-1}. The Raman spectra of solid OF_2 proved to be difficult to obtain because of the colored nature of this compound. (The liquid is yellowish brown whereas the solid still retains a light brown coloration.) No spectrum could be obtained using the 6328 Å of a He–Ne laser (Spectra Physics, model 125) at 70 mW output power. The argon ion laser gave weak Raman spectra, especially since the power output of the laser beam had to be kept quite low (~100 mW) because part of it was absorbed, resulting in local heating of the sample.

The liquid helium cryostat used for the Raman experiments, illustrated in Fig. 1, will be described in some detail since it worked rather well and it could be of general use. The upper part of this cryostat is of conventional design, with an outer section of brass, and the liquid nitrogen and helium vessels made from stainless steel sheets joined by Heliarc welds. The tail section, of Pyrex glass (50 mm diameter) with a flat window at the end, is joined to the main body through

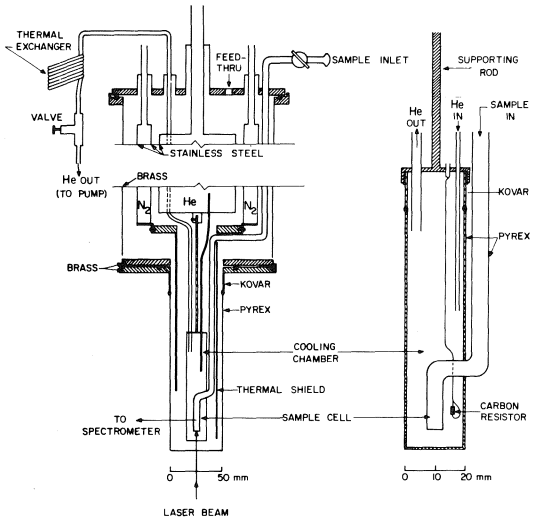

FIG. 1. Liquid helium cryostat for low-temperature Raman studies.

a Kovar seal. The copper thermal shield, bolted onto the bottom part of the liquid nitrogen pot, can be easily dismantled.

The main advantage of this cryostat is that the sample cell (of Pyrex, 6 mm diameter), as well as the sample inlet tube, contain no metal part, thus minimizing the danger of sample decomposition. The sample cell is soldered directly onto the glass cooling chamber (20 mm diameter). The temperature, measured by a carbon resistor near the sample cell, is controlled by the amount of liquid helium which is allowed to fall in the cooling compartment. When this chamber is filled with the refrigerant, the temperature of the sample is obviously close to 4.2 °K, but scattering of the laser beam occurs from the gas bubbles escaping from the liquid helium. Much better spectra can be obtained by restricting the flow of the refrigerant (this is done by partially closing the valve on the helium outlet tube) in such a way that it does not accumulate in the cooling chamber. However, the temperature of the sample is raised by a few degrees under these conditions.

Results and Discussion

The Raman and infrared spectra of crystalline OF_2 at ~10 °K are reproduced in Fig. 2 and observed frequencies are given in Table 1. Drastic changes occurred in the infrared spectrum upon annealing deposited samples by raising the temperature as near as possible to the melting point. This was particularly evident in the ν_3 region where the band at 823 cm^{-1} completely disappeared upon annealing, to be replaced by a sharp peak at 812 cm^{-1} and a very broad band extending from 815 to 850 cm^{-1}. In the ν_1 region, annealing caused each of the two components of the Fermi diad to split. In the Raman study, where the polycristalline solid was obtained by slowly cooling the melt, only minor changes in band intensities resulted from annealing the sample.

The most striking feature in the infrared spectrum of crystalline OF_2 is the broad band on the high-frequency side of the 812 cm^{-1} ν_3 peak. The fact that this band increases in relative intensity when the incident infrared beam was allowed to fall on the sample at non-normal incidence, suggested that it was due to reflection. To confirm this, we recorded the infrared reflection spectrum of a thick sample of solid OF_2, using an optical system similar to that described by Bessette and Cabana (11). A strong reflection band was indeed observed in the 815–850 cm^{-1} region. In the Raman spectrum, a sharp peak is observed at 845 cm^{-1}, its frequency being approximately coincident with the limit of the infrared reflection band. This band is too far away from the main ν_3 Raman doublet at 812/820 cm^{-1} to result from a factor-group splitting (12) of this vibration. We assign it to the longitudinal mode associated with the 812 cm^{-1} transverse vibration. We have already pointed out that transverse–longitudinal splittings are likely to occur in piezoelectric molecular crystals (13). The presence of this longitudinal mode in the Raman spectrum of solid OF_2 is a sure indication that this crystal is non-centrosymmetric (14). Furthermore, the fact that the 845 cm^{-1} Raman band occurs as a sharp peak, whose frequency remained unchanged with the various samples studied, indicates that the solid is, for reasons of symmetry or by accident, completely or nearly optically isotropic. This suggests that solid OF_2 has a cubic crystal structure.

The infrared and Raman spectra of crystalline OF_2 also give an indication as to the number of molecules per primitive cell in this solid. All of the fundamentals show at least two components (ν_1 and ν_2 in the infrared and ν_3 in the Raman), which can only result from a factor-group splitting since all these vibrations are nondegenerate in the free molecule. There are therefore at least two molecules per primitive cell in the crystal.

The far-infrared spectrum of crystalline OF_2 (Fig. 2) shows seven bands in the 40–90 cm^{-1} region, all of these having Raman-active counter-

Can. J. Chem. Downloaded from www.nrcresearchpress.com by 210.87.254.6 on 09/05/12
For personal use only.

TABLE 1. Observed frequencies (in cm^{-1}) in the infrared and Raman spectra of oxygen difluoride

Gas, infrared (ref. 5)	Liquid, Raman (ref. 7)	Solid (~10 °K) Infrared	Solid (~10 °K) Raman	Assignment
		48	47	
		56?	54	
		59	58	Lattice vibrations
		66	—	
		71	73	
		77	77 sh	
		—	82 sh	
		86	85	
		456	—	
461	461			ν_2
		461	462	
		812	812	
831	821			ν_3 transverse
		—	820	
		—	845	ν_3 longitudinal
		914	912	
	916			ν_1
		916	—	
		922 sh	922 sh	and
		925	925	
928	925			$2\nu_2$
		927	—	

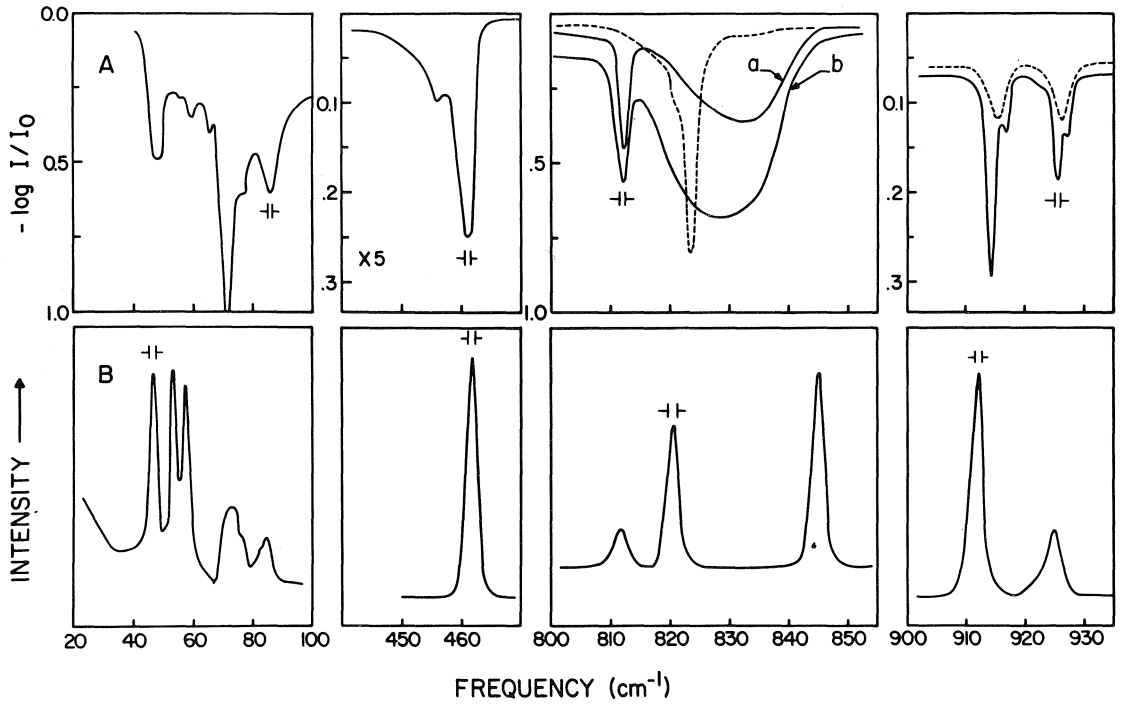

FIG. 2. Infrared (*A*) and Raman (*B*) spectra of crystalline OF_2 at ~10 °K. The dotted curve is for an unannealed sample. (*a*) and (*b*) refer to normal (90°) and oblique (60°) incidence, respectively. The band intensity has been instrumentally expanded by a factor of 5 where indicated by (× 5).

Can. J. Chem. Downloaded from www.nrcresearchpress.com by 210.87.254.6 on 09/05/12
For personal use only.

Can. J. Chem. Downloaded from www.nrcresearchpress.com by 210.87.254.6 on 09/05/12
For personal use only.

parts with almost identical frequencies. Although the number of observed lattice fundamentals is lower than the maximum of nine permissible (for $k = 0$ transitions) if the primitive cell contains two molecules, we believe that the number of molecules per primitive cell in crystalline OF_2 is in fact larger than that. This belief is based on the fact that all of the predicted active lattice modes in an infrared or Raman spectrum are seldom observed, except when the number of bands is very small. In this case, for example, since one of the moments of inertia of the OF_2 molecule is about 6 times smaller than the other two (1–3), a librational mode with frequency $\sim 200\ cm^{-1}$ should give at least one peak in either the infrared or Raman spectrum. No such band could be detected. Furthermore, seven active lattice modes in the spectra of a crystal with two molecules per primitive cell would indicate a crystal of low symmetry, which is inconsistent with the behavior of the longitudinal mode associated with the ν_3 fundamental, as mentioned above.

Although vibrational spectra of crystalline solids can seldom be interpreted on the basis of a unique choice of site and unit-cell symmetries, they usually restrict the number of such possibilities (12, 15). In this case, it is found that the site symmetry cannot be C_2 or C_{2v}, since for any possible factor group chosen thereof the ν_1 and ν_2 fundamentals should appear as singlets in the infrared spectrum, contrary to what is observed. Similarly, we can deduce that the crystal structure is not monoclinic, triclinic, or trigonal if the site symmetry is C_s, and that it is not triclinic if the site symmetry is C_1.

It seems inappropriate at this point to pursue our analysis any further, for lack of sufficient information. However, if the crystal has a cubic structure, as was suggested earlier, then a combination of C_s site and T_d crystal symmetries would certainly explain our infrared spectrum. It predicts 8 lattice bands, doublets for ν_1 and ν_2, and a singlet or doublet for ν_3, depending upon which plane of symmetry of the molecule coincides with that of the site. This type of structure, with 12 molecules per primitive cell (16), should however result in a rather complex Raman spectrum: 17 lattice bands are then predicted, whereas 4 bands should be observed in the ν_1 and ν_2 regions, and either 2 or 4 in the ν_3 region (excluding longitudinal modes).

The authors gratefully acknowledge financial support of this work by the National Research Council of Canada. One of us (J.T.) is also indebted to this organization for a graduate fellowship.

1. L. R. Maxwell. J. Opt. Soc. Am. **30**, 374 (1940).
2. L. Pierce, N. Di Cianni, and R. H. Jackson. J. Chem. Phys. **38**, 730 (1963).
3. Y. Morino and S. Saito. J. Mol. Spectry. **19**, 435 (1966).
4. Y. Morino and S. Yamamoto. J. Mol. Spectry. **23**, 235 (1967).
5. J. W. Nebgen, F. I. Metz, and W. B. Rose. J. Mol. Spectry. **21**, 99 (1966).
6. H. J. Bernstein and J. Powling. J. Chem. Phys. **18**, 685 (1950). E. A. Jones, J. S. Kirby-Smith, P. J. H. Woltz, and A. H. Nielsen. J. Chem. Phys. **19**, 337 (1951).
7. D. J. Gardiner and J. J. Turner. J. Mol. Spectry. **38**, 428 (1971).
8. P. Lebeau and A. Damiens. C. R. **188**, 1253 (1929).
9. J. G. Schnizlein, J. L. Sheard, R. C. Toole, and T. D. O'Brien. J. Phys. Chem. **56**, 233 (1952).
10. R. Savoie and A. Anderson. J. Chem. Phys. **44**, 548 (1966).
11. F. Bessette and A. Cabana Spectrochim. Acta, **25A**, 157 (1969).
12. D. F. Hornig. J. Chem. Phys. **16**, 1063 (1948).
13. R. Savoie and M. Pézolet. J. Chem. Phys. **50**, 2781 (1969).
14. R. Loudon. Adv. Phys. **13**, 423 (1964).
15. H. Winston and R. S. Halford. J. Chem. Phys. **17**, 607 (1949).
16. N. F. M. Henry and K. Lonsdale (*Editors*). International tables for X-ray crystallography. Vol. I. Kynoch Press, Birmingham, England. 1952.

The Effect of Electric Fields on the Radiolysis of Acetylene, and the Mechanism of Cuprene Formation[1]

J. P. BRIGGS[2] AND R. A. BACK

Division of Chemistry, National Research Council of Canada, Ottawa, Canada

Received June 29, 1971

Gaseous acetylene at pressures of about 200 Torr was irradiated with γ-rays at doserates between about 10^{11} and 10^{12} eV/cc s, with and without an electric field applied. The deposition of cuprene on the bottom of the reaction vessel was markedly affected by the field, but the rate of cuprene formation as measured by the pressure decrease was unchanged. Examination of the cuprene deposit with an electron microscope showed it to consist of rather uniform spheres averaging about 3000 Å in diameter, with each containing an estimated 2×10^8 molecules of acetylene. The mechanism of cuprene formation is discussed, and it is suggested that it does not proceed through a direct polymerization of acetylene, but involves a secondary polymerization of polyene intermediates, in the gas phase and after their condensation in liquid droplets.

On a irradié de l'acétylène gazeux à des pressions d'environ 200 Torr avec des rayons-γ, à des vitesses de dosage se situant entre 10^{11} et 10^{12} eV/cc s, avec et sans l'application d'un champ électrique. La formation de dépôt de cuprène au fond du récipient de réaction était grandement affectée par la présence du champ, mais la vitesse de formation de cuprène telle que mesurée par la diminution de la pression, est demeurée inchangée. Un examen du dépôt de cuprène au microscope électronique a révélé que celui-ci consiste en sphères plutôt uniformes, d'un diamètre d'environ 3000 Å, contenant chacune un nombre estimé à 2×10^8 molécules d'acétylène. On discute du mécanisme de formation du cuprène et on suggère que celle-ci ne se déroule pas selon la polymérisation directe de l'éthylène, mais qu'elle implique plutôt une polymérisation secondaire d'intermédiaires polyènes, dans la phase gazeuse et après leur condensation dans les gouttelettes liquides.

Canadian Journal of Chemistry, 49, 3789 (1971)

Can. J. Chem. Downloaded from www.nrcresearchpress.com by 210.87.254.6 on 09/05/12
For personal use only.

Superficially, the radiolysis of acetylene appears to be a simple process. The only products of importance at moderate conversions are benzene and cuprene (a $(CH)_n$ polymer) in a ratio of about 1:4 in terms of C_2H_2 consumed. The *G*-value for acetylene disappearance is about 70, approximately independent of dose, doserate, acetylene pressure, and type of radiation. Despite this apparent simplicity and despite extensive studies of the system, the mechanism is not well understood (1–7). The basic problem is an overabundance of mechanisms, as it seems clear that ions, free radicals, and excited C_2H_2 molecules are all capable of initiating polymerization and benzene formation. The difficulty is in deciding which processes in fact are important in the actual radiolysis.

Electric fields, applied during radiolysis, have been used with some success in this laboratory and elsewhere as an aid in the elucidation of mechanism (8–12). It appeared that this technique might be useful in the acetylene radiolysis, in particular in assessing the respective roles of ions, radicals, and excited molecules.

Experimental

Acetylene was irradiated in a variety of cylindrical Pyrex vessels, typically 2 or 3 cm in diameter and 5 to 10 cm long. Electrodes were made of stainless steel or of graphite deposited on the glass surface, and were either parallel plates (at each end of the cylinder) or in a coaxial configuration. Dosimetry was based on measurements of saturation ion-currents in the reaction vessels, taking $W = 25.3$ eV/ion pair (13).

Acetylene (from Matheson) was thoroughly degassed in a mercury-free vacuum line, and acetone impurity was removed by distillation from a trap at −78 °C and passage through activated charcoal. Analysis by gas chromatography showed less than 30 p.p.m. of acetone remaining. In some experiments vessels were baked, filled with acetylene, sealed with a torch and removed from the vacuum line before irradiation. In others, the vessel, mounted in the Gamma-cell, was permanently attached to the vacuum line, and the irradiation was started by the admission of purified acetylene. In these experiments, pressure was measured during the irradiation with an accuracy of about ±10 m Torr, using a Texas Instruments quartz spiral gauge. Since irradiation times were typically several days and total fractional pressure changes only a few percent, careful measurement of small

[1]NRCC No. 12171.

[2]NRCC Postdoctoral Fellow, 1968–1970. Present address: Chemistry Department, University of Alberta, Edmonton, Alberta.

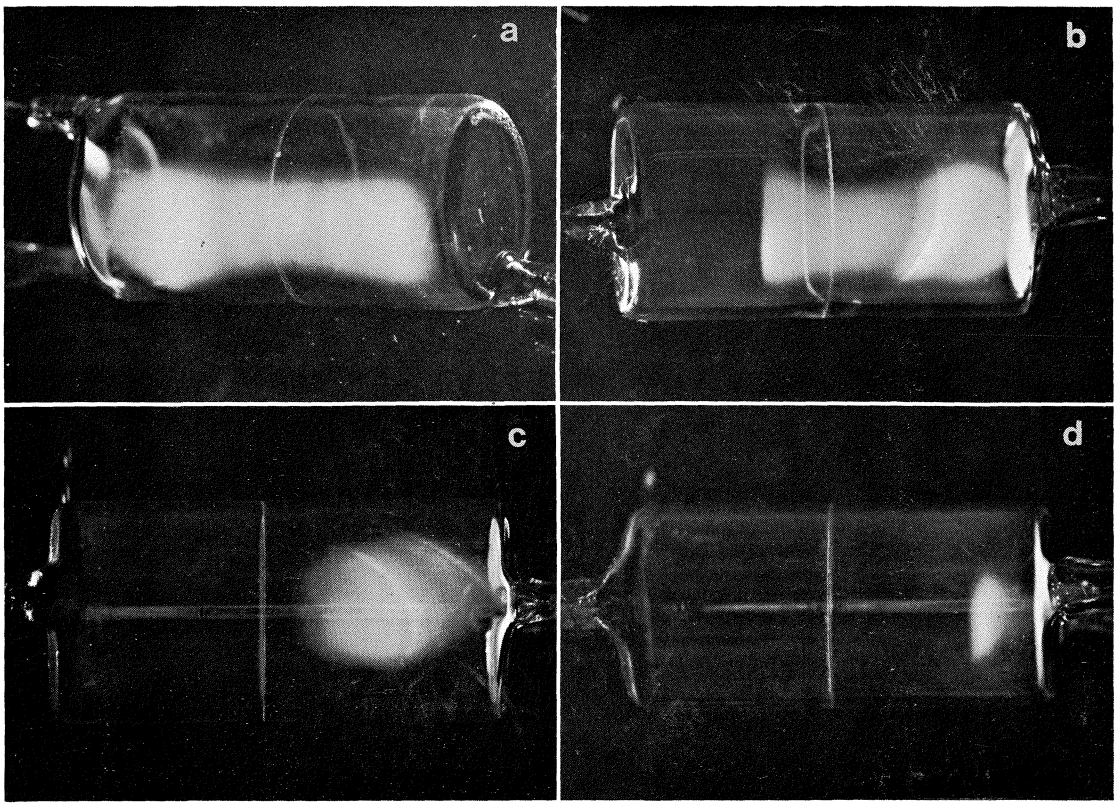

FIG. 1. The effect of applied fields on the deposition of cuprene. The anode is on the right: (*a*), no field; (*b*), 70 V, $i = 0.25\, i_{\text{saturation}}$; (*c*), 300 V, $i = 0.50\, i_{\text{saturation}}$; (*d*), 750 V, $i = 0.88\, i_{\text{saturation}}$.

changes in the temperature of the cell and connecting tubing during the experiments was essential.

Irradiations were carried out in one or the other of two AECL Gamma-cells loaded with about 500 and 9500 Ci of ^{60}Co, which with lead shields gave doserates ranging from about 10^{11} to 10^{12} eV/cc s at the acetylene pressures employed (~200 Torr).

Results

The results consist in essence of two apparently simple observations. The first was that an electric field had an obvious and marked effect on the deposition of cuprene. In the absence of a field, a thin white adherent deposit of cuprene became visible on the bottom surface of a horizontal cylindrical reaction vessel after some hours of irradiation. When a saturation voltage was applied during irradiation to parallel-plate electrodes at either end of the vessel, no such deposit of cuprene was observed, and a discoloration of the anode suggested formation of a thin film on its surface. With field strengths less than that required for saturation, the cuprene deposit did not disappear entirely, but was shifted progressively towards the anode as saturation was approached, with quite a sharp demarkation at the edge of the deposit. The photographs in Fig. 1 and the plot in Fig. 2 illustrate this behavior. These experiments were done with vessels 4.7 cm long and 2.1 cm diameter with parallel graphite electrodes at each end, acetylene pressure of 200 Torr, and a doserate of 10^{11} eV/cc s. At higher doserates, cuprene in the absence of a field was deposited less evenly, probably because of convection currents in the gas, and the effect of the field was less clear cut.

The second simple observation was that the presence of an electric field had virtually no effect on the rate of disappearance of acetylene as reflected by the change in pressure. Typical pressure–time plots are shown in Figs. 3 and 4. The more rapid initial decrease evident in the figures was shown to occur also in the absence of radiation and is presumably due to an adsorption

Can. J. Chem. Downloaded from www.nrcresearchpress.com by 210.87.254.6 on 09/05/12
For personal use only.

Can. J. Chem. Downloaded from www.nrcresearchpress.com by 210.87.254.6 on 09/05/12
For personal use only.

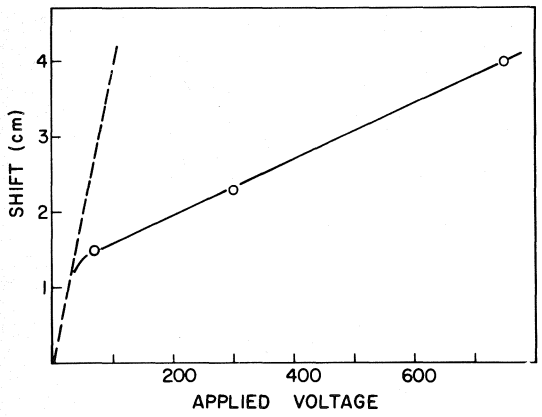

FIG. 2. Shift of the edge of the cuprene deposit towards the anode *vs.* applied voltage. The broken line is calculated on the basis of a competition between sedimentation and horizontal drift induced by the field.

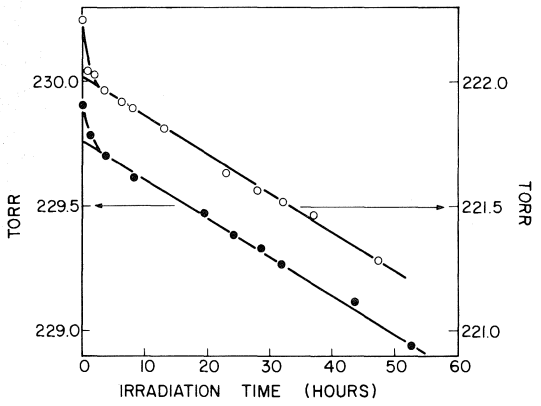

FIG. 3. Pressure–time plots for the radiolysis of acetylene: ○, no field; ●, 600 V applied.

phenomenon which appeared to be complete in about 2 h. Figure 3 represents two separate experiments under similar conditions, with and without a saturation field applied; the straight lines drawn have identical slopes. Figure 4 represents a single experiment at higher doserate, in which a field was applied, removed for a time, and reapplied. The larger absolute scatter in these data reflects a poorer temperature control than in the later experiments shown in Fig. 3. It is clear from these figures that within the experimental accuracy of perhaps $\pm 5\%$, the rate of pressure change was unaffected by the field. Other experiments under a variety of conditions including applied fields of less than saturation, and well along the saturation plateau, just short of the ion-multiplication

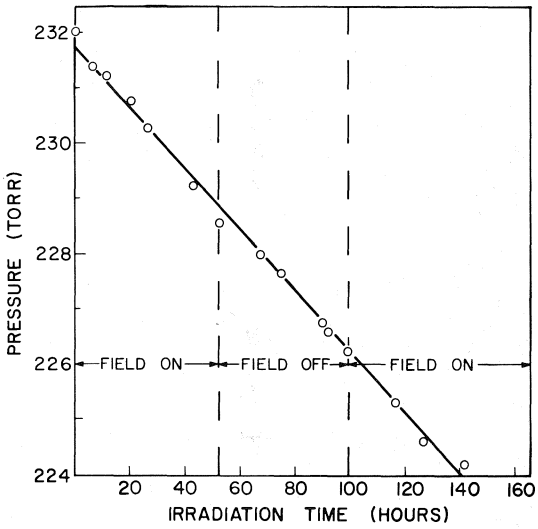

FIG. 4. Pressure–time plot for the radiolysis of acetylene.

region, also showed no effect on the rate of pressure change.

G-values for acetylene disappearance were evaluated from data such as those in Figs. 3 and 4. At an acetylene pressure of about 240 Torr and doserates of 1.1×10^{12} and 1.3×10^{11} eV/cc s, average values of $G(-C_2H_2)$ were about 90 and 125, respectively. This appears to confirm the increase in *G*-value at low intensity reported by Field (3).

Discussion

At first sight our two observations appear to be contradictory, with the first pointing to an ionic mechanism and the latter to a non-ionic one. Further consideration reveals that in fact neither observation permits any such definite interpretation. The shift of the cuprene deposit could have been caused by the action of the electric field on ionic precursors, or on cuprene particles themselves which became charged as a result of an ionic mechanism of polymerization. The particles could, however, equally well have acquired charge incidentally after polymerization by a non-ionic mechanism, as it is well known that small particles in the presence of ions or electrons readily become charged, so that the simple observation that the cuprene deposit was shifted by an applied field does not rule out a non-ionic mechanism of formation. Similarly, the lack of effect of a field on the rate of polymerization

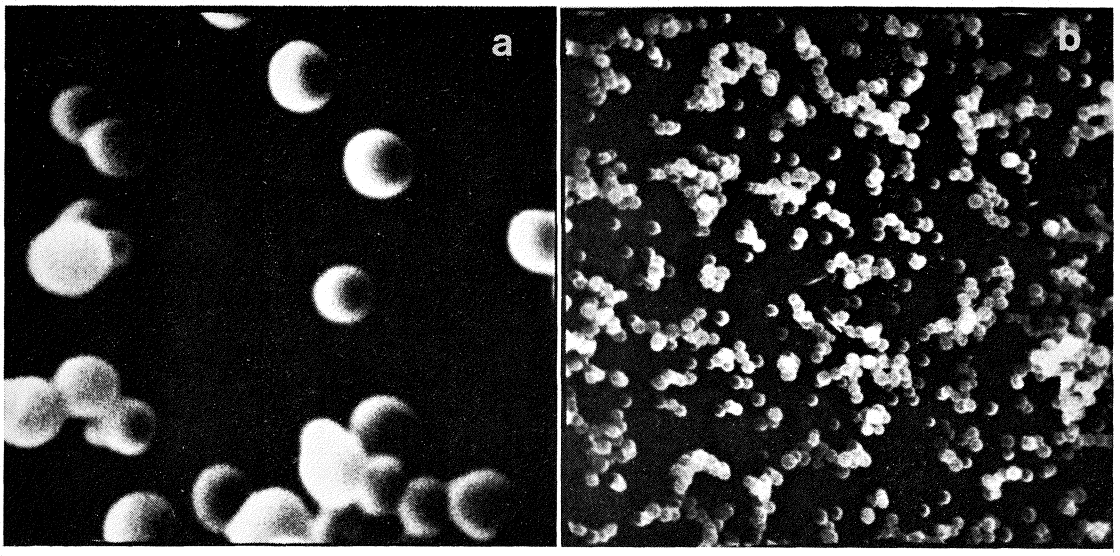

FIG. 5. Electron microscope photographs of cuprene formed in the radiolysis of acetylene. Magnifications about (*a*), 18 000; and (*b*), 3 500.

could be the consequence of a non-ionic mechanism, but is also compatible with a short-chain ionic polymerization in which chains were terminated before the ionic chain carriers could be removed to the electrodes by the field. Such behavior has been noted recently in the H_2–D_2 exchange in the presence of trace impurities (9) and the relatively low G-value for cuprene formation points to a short-chain process in the acetylene radiolysis.

The observation that electric fields approaching the ion-multiplication region caused no enhancement of the rate of polymerization indicates that low-lying excited states of acetylene do not make an important contribution to the reaction (*c.f.* Carmichael *et al.* (10)).

To gain further insight into the formation and behavior of the cuprene particles, photographs were taken with an electron microscope;[3] typical examples are shown in Fig. 5. These showed that cuprene was formed in spherical particles, fairly uniform in size, with an average diameter around 3000 Å. There were no apparent differences between particles formed in the presence and absence of an electric field or any dependence on the strength of the field. The uniform size and the lack of small particles is in accord with earlier studies of cuprene formed by α-radiation. The present photographs, however, show few connecting "stems" nor any indication that the particles were viscous liquid rather than solid, both features of the earlier studies (1, 14).

Some useful deductions can be made from the size of the particles. Assuming a typical solid hydrocarbon density of 0.7, the average particle mass is about 1×10^{-14} g, corresponding to a molecular weight of 6×10^9, and containing 2.3×10^8 molecules of C_2H_2. Taking $G(-C_2H_2)$ for cuprene formation = 80 and W = 25.3 eV/ion pair, then $M/N(-C_2H_2)$ = 20 molecules/ion-pair, so that only one cuprene particle was formed for every 10^7 ion pairs. This means that unless each particle carried an enormous multiple charge (which seems very unlikely), the cuprene particles represented a completely negligible fraction of the charge carriers in the system. This is supported by our observations that ion current measurements with both steady and intermittent fields showed no evidence for massive ions of low mobility. Lifetime measurements with the intermittent field in fact indicated that most of the negative charge carriers in the system were free electrons (15).

The simplest and most plausible explanation of the effect of the field on the deposition of cuprene appears to be a competition between the sedimentation of the particles due to gravity and the

[3]We are grateful to Dr. P. J. Blais for these photographs.

Can. J. Chem. Downloaded from www.nrcresearchpress.com by 210.87.254.6 on 09/05/12
For personal use only.

Can. J. Chem. Downloaded from www.nrcresearchpress.com by 210.87.254.6 on 09/05/12
For personal use only.

horizontal drift in the electric field. Horizontal and vertical displacements should have been equal when the force on the particle due to gravity equalled that of the electric field, which for a particle with the estimated average mass of 1×10^{-14} g and a single electronic charge should have occurred at a field strength of about 6 V/cm. Assuming that motion of the particles before attaining full size and acquiring charge was negligible, then the average horizontal drift during sedimentation at this field strength should have been about equal to the radius of the vessel, and at higher field strengths should have been proportionately larger. Calculated average horizontal drift is shown as a function of field strength in Fig. 2, together with the observed shift of the edge of the cuprene deposit. The latter is somewhat less than the former at low field strengths although considering the rough and ready nature of our calculations the agreement is not bad. As the field strength is increased, the observed shifts fall much below the calculated ones. One possible explanation of these observations is that the cuprene particles were initially neutral, and appreciable sedmentation occurred before charge was acquired by capture of a negative ion or electron. With increasing field strength, concentration of ions and electrons would be reduced by their removal at the electrodes, so that charge acquisition would be slower and the field therefore less efficient in shifting the particles. It is interesting that in a recent study of carbon formation in flames it was concluded that most of the carbon particles were initially neutral and acquired charge by collision with ions; it was also concluded that the particles each carried only a single electronic charge (16).

While the present results do not permit a decision between an ionic and a non-ionic process, some more general conclusions may be drawn about the mechanism of cuprene formation. A number of facts and observations from this and previous work point to a sequence of reactions rather than a simple direct polymerization of acetylene, and the following 4-stage mechanism is suggested:

(1) A primary polymerization of acetylene to form polyunsaturated hydrocarbons with molecular weights in the C_4 to C_{20} range. Taking a reasonable value of G(chain initiation) = 4, and $G(-C_2H_2) = 80$, appreciable chain transfer to the C_2H_2 monomer would be required to give such low molecular weights; this seems not unlikely. There is also evidence, in the relatively low G-value and its lack of a strong dependence on doserate and acetylene pressure, for some sort of self-termination of the kinetic chain, perhaps by cyclization or other rearrangement of growing polyradicals or ions to yield stabilized unreactive species.

(2) A secondary polymerization of the polyenes formed initially, which would tend to be much more reactive than acetylene. They would rapidly attain a low steady-state concentration, with their rate of formation remaining rate-controlling and the polymerization of acetylene and the polyene intermediates going on virtually as a co-polymerization. In this view of the radiolysis, benzene becomes simply one of a number of unsaturated intermediates, detectable in appreciable amounts because of the ease of formation of the aromatic ring and its relatively low reactivity. Even benzene disappears rapidly by secondary polymerization at quite low conversions (1).

(3) A physical condensation of the polyenes formed by primary and secondary polymerization. The spherical shape of the cuprene particles strongly suggests initial condensation as liquid droplets, which would require a carbon number of about 20 to permit condensation as a liquid at room temperature and a vapor pressure low enough for condensation at the very low conversions at which cuprene is observed.

(4) Rapid and extensive polymerization and cross-linking in the liquid polyene droplets, induced by radiation and leading to the final intractable cuprene product.

While we have written 4 stages in the mechanism, it should be emphasized that all four will proceed simultaneously under steady-state radiolysis. Previous authors have generally assumed, at least tacitly, a direct polymerization of acetylene to cuprene, and have tended to talk in "either-or" terms about an ionic or a non-ionic mechanism. In the more complex system that we are suggesting, it seems probable that both ions and free radicals might play a part, although one or the other might be predominant in a particular stage of the reaction. There are obvious tests of our proposed mechanism. In particular, it should be possible to detect low concentrations of polyene intermediates and to suppress cuprene formation by the removal of such intermediates at sufficiently low conversions. Experiments to do so are planned.

1. S. C. LIND. Radiation chemistry of gases. Reinhold, New York. 1961.
2. L. M. DORFMAN and F. J. SHIPKO. J. Am. Chem. Soc. **77**, 4723 (1955).
3. F. H. FIELD. J. Phys. Chem. **68**, 1039 (1964).
4. J. H. FUTRELL and L. W. SIECK. J. Phys. Chem. **69**, 892 (1965).
5. G. J. MAINS, H. NIKI, and M. H. J. WIJNEN. J. Phys. Chem. **67**, 11 (1963).
6. L. M. DORFMAN and A. C. WAHL. Rad. Res. **10**, 680 (1959).
7. S. SHIDA, M. TSUKADA, N. FUJISAKI, and T. OKA. Bull. Chem. Soc. Jap. **43**, 3314 (1970).
8. T. W. WOODWARD and R. A. BACK. Can. J. Chem. **41**, 1463 (1963).
9. T. TERAO and R. A. BACK. J. Phys. Chem. **73**, 3884 (1969).
10. H. H. CARMICHAEL, R. GORDEN, and P. AUSLOOS. J. Chem. Phys. **42**, 343 (1965).
11. I. K. LARIN, V. L. TAL'ROSE, and N. A. KULAZHENKOVA. Khimiya Vysokikh Energii, **3**, 14 (1969).
12. H. ESSEX. J. Phys. Chem. **53**, 42 (1954).
13. G. G. MEISELS. J. Chem. Phys. **41**, 51 (1964).
14. J. H. L. WATSON and K. K. KAUFMAN. J. Appl. Phys. **17**, 906 (1946); J. H. L. WATSON. J. Phys. Chem. **52**, 470 (1948).
15. R. A. BACK and J. P. BRIGGS. To be published.
16. P. J. MAYO and F. J. WEINBERG. Proc. Roy. Soc. Ser. A, **319**, 351 (1970).

Can. J. Chem. Downloaded from www.nrcresearchpress.com by 210.87.254.6 on 09/05/12
For personal use only.

Fermi Resonance of Infrared Vibrations in the —NH_2 Groups of Polynucleotides

G. ZUNDEL, W. D. LUBOS, AND K. KÖLKENBECK

Physikalisch-Chemisches Institut der Universität Muenchen, Sophienstrasse 11, 8 Muenchen 2, Germany

Received June 24, 1971

The —NH_2 group causes an intensive band pair in the i.r. spectra of DNA, r.RNA, poly (A+ U), and poly (G + C). One band occurs at 3330, another at 3180 cm^{-1}. This band pair is due to the NH stretching vibration of the hydrogen-bonded NH group as well as to the harmonic vibration of the —NH_2 bending vibration, whereby these vibrations are coupled via Fermi resonance. This follows on comparison with papers on amines. The weak shoulder in the 3500–3400 cm^{-1} range is to be assigned to the stretching vibrations of the non hydrogen-bonded NH groups. The doublet structure disappears to a large extent in the denaturated DNA, since the strength of the Fermi resonance depends on the strength of the hydrogen bonds and the hydrogen bonds are of differing strength, due to the bending and stretching. The relative intensities of the two bands are interchanged in the corresponding band pair of the —ND_2 groups, for which an explanation can also be given.

Le groupe —NH_2 provoque une paire de bandes intense dans les spectres i.r. du DNA, du r.RNA, du poly (A + U) et du poly (G + C). Une bande apparaît à 3330 et l'autre à 3180 cm^{-1}. Cette paire de bandes est due à la vibration de valence du groupe NH en liaison hydrogène aussi bien qu'à la vibration harmonique de déformation de —NH_2, ces vibrations étantes couplées grâce à la résonance de Fermi. Cela découle de la comparaison avec des publications sur les amines. Le faible épaulement dans la région 3500–3400 cm^{-1} doit être attribué à la vibration de valence des groupes NH pas liés en liaison hydrogène. La structure de doublet disparaît en cas de DNA dénaturé parce que l'intensité de la résonance de Fermi dépend de la force des liaisons hydrogène et les liaisons hydrogène sont de force différente à cause d'élongation et de déformation. Les intensités relatives des deux bandes s'interchangent dans la paire de bandes en cas des groupes —ND_2. Une explication de ce phénomène peut être également donnée.

Canadian Journal of Chemistry, 49, 3795 (1971)

Can. J. Chem. Downloaded from www.nrcresearchpress.com by 210.87.254.6 on 09/05/12
For personal use only.

The explanation of the splitting up of the bands of the —NH_2 group of the polynucleotides in the 3600–3000 cm^{-1} range is as yet most unsatisfactory. We therefore plotted spectra of films of calf thymus DNA, ribosomal RNA, poly (A + U)[1] and poly (G + C)[1] in this range. The vibrations of the —ND_2 groups of these polynucleotides were also investigated for *N*-deuteration. These spectra are shown in Fig. 1. DNA, poly (A + U) and poly (G + C) occur as a double helix under the conditions chosen (1) (see also Experimental). A considerable number of the bases are paired, too, with the r.RNA, for on warming, a high degree of u.v.-hyperchromicity (2, 3) is observed.

Broad bands, one at about 3330 and one at about 3180 cm^{-1} are observed with these polynucleotides. This band pair occurs again with interchanged relative intensities in the *N*-deuterated samples at about 2500 and 2350 cm^{-1}.

[1]The abbreviations used, A, U, G, and C, stand for the salts of polyadenylic acid, polyuridylic acid, polyguanylic acid and polycytidylic acid.

A weak shoulder is found on the slope of this band complex at about 3450 cm^{-1}.

Tsuboi (4) assigns these bands to the antisymmetric and symmetric stretching vibrations of the —NH_2 groups. He refers here to studies by Kyogoku *et al.* (5) of crystals containing 1-methylthymine and 9-methyladenine. This is a possible explanation in the case of these crystals, since according to X-ray investigations (5), both NH groups of the —NH_2 group of the 9-methyladenine are bound in the same way to O atoms of the C=O groups of the 1-methylthymine.

In DNA and the polynucleotides investigated, one NH group of the —NH_2 groups is free, that is, not linked by a hydrogen bond. Kyogoku *et al.* (6) as well as Miller and Sobell (7) investigated model substances such as 9-methyl- and 9-ethyladenine in $CDCl_3$. Here they find bands at 3517 and 3416 cm^{-1} in diluted solutions and assign these to, respectively, the antisymmetric and symmetric stretching vibrations of —NH_2 groups not bonded by hydrogen bonds. A comparison with our findings shows that the weak shoulder in the 3500–3400 cm^{-1} range should be assigned to

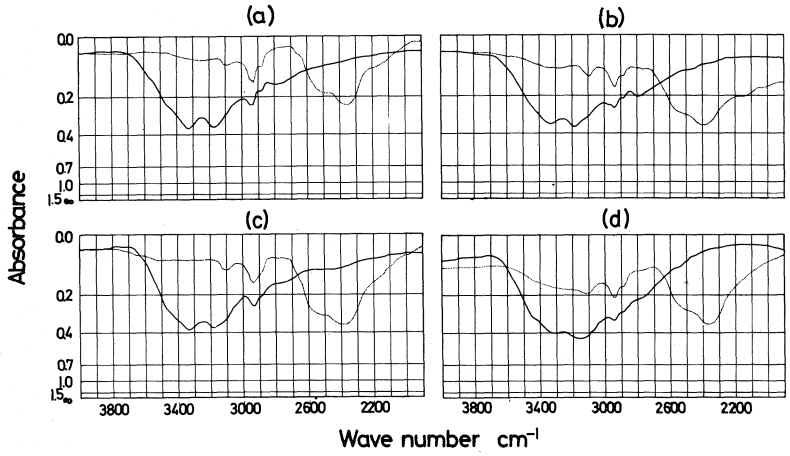

FIG. 1. The i.r. spectra of polynucleotide films: —— dried sample; ····· dried after H → D exchange; (*a*) calf thymus DNA; (*b*) r.RNA; (*c*) poly (A + U); (*d*) poly (G + C).

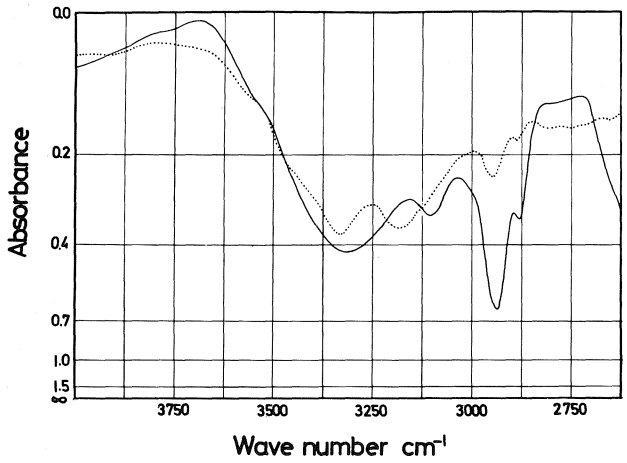

FIG. 2. The i.r. spectra of a DNA film: ····· —NHD groups present; —— —NH_2 groups present.

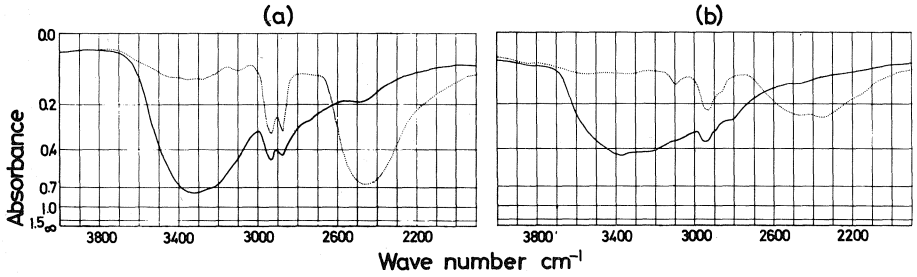

FIG. 3. The i.r. spectra of polynucleotide films: —— dried sample; ····· dried after H → D exchange; (*a*) denaturated calf thymus DNA; (*b*) poly U.

Can. J. Chem. Downloaded from www.nrcresearchpress.com by 210.87.254.6 on 09/05/12
For personal use only.

Can. J. Chem. Downloaded from www.nrcresearchpress.com by 210.87.254.6 on 09/05/12
For personal use only.

the NH stretching vibration of the NH groups not bonded by a hydrogen bond.

Which vibrations, however, cause the intensive band pair? In the case of the model substances, NH stretching vibrations of hydrogen-bonded NH groups in the 3400–3150 cm^{-1} range are observed (6, 7). It could be assumed, accordingly, that both bands are caused by NH stretching vibrations of different bases. This assignment, however, is contradicted by the findings shown in Fig. 2. The spectrum shown by the broken line is that of DNA and the spectrum shown by a continuous line is that of DNA whereby the amine groups occurred as —NHD groups. In the presence of the —NHD groups, only a broad band at about 3315 cm^{-1} is observed instead of the two bands (3333 and 3183 cm^{-1}).[2] If both bands were caused by NH stretching vibrations of different bases, the band pair would also have to be observed in the spectrum of DNA with —NHD groups.

Comprehensive papers by Wolff *et al.* (8–12*a*) give the key to the assignment of this band pair. These authors investigated the hydrogen bonds of primary amines with tertiary acceptor amines. They found a band pair which is in complete conformity with the one observed by us. Wolff *et al.* could demonstrate that this band pair comes into being through coupling of the symmetric NH stretching vibration with the harmonic vibration of the $—NH_2$ bending vibration. The harmonic vibration of the $—NH_2$ bending vibration obtains its intensity through Fermi resonance from the stretching vibration.

We can explain the band pair in the case of the polynucleotides analogously to that in the case of amines. We must only substitute the expression symmetric NH_2 stretching vibration in Wolff's explanation by stretching vibration of the hydrogen-bonded NH group and antisymmetric stretching vibration by stretching vibration of the non hydrogen-bonded NH group.

With the polynucleotides the NH bending vibration is observed in the range 1700–1600 cm^{-1}. This vibration, however, is coupled with a ring vibration and shifts this somewhat towards larger wave numbers. Thus, for instance, in the case of poly-A, when this is *N*-deuterated and thus $—ND_2$ groups are present instead of the $—NH_2$ groups, only the ring vibration Py 8a at 1630 cm^{-1} is found. When the $—NH_2$ groups are present, however, this band is shifted towards 1655 cm^{-1} and a second band is observed at 1610 cm^{-1}. Finally it should be pointed out that the coupling of the $—NH_2$ bending vibration with other ring vibrations of the base residue just like the coupling between CO stretching vibrations (12*b*), depends on the formation of the secondary structure. For when the secondary structure has formed, the transition moment of the $—NH_2$ bending vibration occurs preferably in the base ring plane. This is in part the cause of the secondary structure sensitivity of the bands at about 1700 cm^{-1}. The $—ND_2$ bending vibration should be observed at about 1210 cm^{-1}. This band is, however, masked by the intensive antisymmetric stretching vibration of the $\diagdown PO_2^- \diagup$ groups.

Hence, with the polynucleotides the band pair in the range 3400–3150 cm^{-1} is caused by the NH stretching vibration of the hydrogen-bonded NH group of the $—NH_2$ group and by the harmonic vibration of the bending vibration of the $—NH_2$ group thus coupled by Fermi resonance. The finding that only one band occurs instead of the band pair in the presence of —NHD groups (Fig. 2) is accordingly quite comprehensible, for now the harmonic vibration of the bending vibration is in a different position and can thus no longer couple with the stretching vibration. The weak band of the stretching vibration of the free NH groups, expected at about 3450 cm^{-1}, is not observed in the spectrum in the presence of the —NHD groups for this band merges with the slope of the now more intensive stretching vibration of the hydrogen-bonded NH groups.

According to Wolff and Horn (11, 12*a*), the intensity ratio in the band pair depends on the strength of the hydrogen bonds. The low-frequency band becomes more intensive, the stronger the hydrogen bond. This fact, that the strength of the Fermi resonance and thus the splitting up and intensity ratio depend on the strength of the hydrogen bond, explains the finding (Fig. 3) that

[2]The band observed at 3108 cm^{-1} in the spectrum of the sample in which the amino groups were present as —NHD groups is the stretching vibration of the CH groups of the base residues. This is all the more intensive here since the layer is approximately 10 times thicker than with the sample with the $—NH_2$ groups (see Experimental). With this sample the stretching vibrations of the aliphatic CH groups at 2957 and 2885 cm^{-1} also occur correspondingly more intensively.

Can. J. Chem. Downloaded from www.nrcresearchpress.com by 210.87.254.6 on 09/05/12
For personal use only.

with the denaturated DNA, almost no structure of the band complex can be observed. In the denaturated DNA, the hydrogen bonds vary in strength due to the stretching and bending. Thus the coupling between both vibrations also varies in strength. The doublet, therefore, becomes one broad band.

On transition from the $—NH_2$ to the $—ND_2$ band pair (Fig. 1) the two bands often interchange their intensities with the polynucleotides, in conformance with the findings with the amines. This could be caused by the fact that the stretching vibrations and the harmonic vibration of the bending vibrations shift at different degrees of strength on transition from H to D, *i.e.*, that these have somewhat different isotopic factors. Each band would then obtain, respectively, more or less stretching or bending vibration character.

Two bands at about 3380 and 3220 cm^{-1} (Fig. 3*b*) are also found with poly-U, although the latter possesses no $—NH_2$ groups. Here a different explanation applies. According to Miller and Sobell (7), the band of the stretching vibration of the free NH groups is observed at 3380 cm^{-1} with cyclohexyluracil in $CDCl_3$, whereas that of the hydrogen-bonded NH group occurs at 3180 cm^{-1}. With poly-U the band at about 3220 cm^{-1} can accordingly be assigned to the stretching vibration of the hydrogen-bonded NH groups, whereas the band at about 3380 cm^{-1} is the stretching vibration of non hydrogen-bonded NH groups, which hence do not interact so definitely with their environment. The extreme broadening of these bands is due to the fact that poly-U is present in coiled conformation (1).

Experimental

The synthetic polynucleotides were obtained by Boehringer, Mannheim (poly A, U, C), by Miles, Elkhart, Indiana (poly G), and the calf thymus DNA by theWorthington Biochemical Corporation, Freehold, N.J. The RNA is a mixture of RNA with the sedimentation constants 16S and 23S. It is produced according to the phenol extraction method (13) from escherichia coli ribosomes. Poly (A + U) and poly (G + C) were made of equimolar mixtures of aqueous solutions of the individual components. In the case of poly (G + C), the mixtures had to be tempered for 6 h at 50 °C.

Since the danger exists with DNA that the latter denaturates in distilled water already at room temperature, some samples were dried with excess salt. The excess salt was removed by repeated washing of the film with alcohol. The i.r. spectra did not differ from the samples whereby the excess salt was removed by dialysis against distilled water at 4 °C before drying. The paper by Auer and Alexandrowicz (14) provides further confirmation of the fact that under these conditions no denaturation takes place. These authors found no hyperchromicity at all in the u.v. below 20° in the case of calf thymus DNA at a concentration of 10^{-2} mol/l ($\approx$3.5 mg/ml) in an ion-free milieu. Since the DNA concentration was never less in our experiments, no denaturation occurred.

The films were dried on sample supports of Ge as described in (15) and subsequently subjected to spectroscopic investigation in the cells described in (16, 17). The spectra were plotted with photospectrometer type 221 and 325, of the Perkin–Elmer Company, Bodenseewerk, Ueberlingen, W. Germany.

In order to study the DNA with —NHD groups the film was treated with water vapor of a saturated aqueous $BaCl_2$ solution (90% D_2O + 10% H_2O). In this way approximately 10% —NHD was obtained in addition to a large number of $—ND_2$ groups and very few $—NH_2$ groups. Since in this case the number of the NH groups is considerably smaller, the film must be approximately 10 times as thick as for customary investigations, which is demonstrated by intensive CH stretching vibrations.

1. R. Steiner and D. B. S. Millar. *In* Biological polyelectrolytes. A. Veis *Editor*, Dekker New York, N.Y., 1970.
2. P. Doty, H. Boedtker, J. Fresco, R. Haselkorn, and M. Litt. Proc. Nat. Acad. Sci. **45**, 482 (1959).
3. W. M. Stanley, Jr. and R. M. Beck. Biochem. **4**, 1302 (1965).
4. M. Tsuboi. Appl. Spectrosc. Rev. **3**, 45 (1969).
5. Y. Kyogoku, S. Higuchi, and M. Tsuboi. Spectrochim. Acta, **23A**, 969 (1967).
6. Y. Kyogoku, R. C. Lord, and A. Rich. J. Am. Chem. Soc. **89**, 496 (1967).
7. J. H. Miller and H. M. Sobell. J. Mol. Biol. **24**, 345 (1967).
8. H. Wolff and D. Stachewski. Ber. Bunsenges. physik. Chem. **66**, 140 (1962).
9. H. Wolff and H. Ludwig. Ber. Bunsenges. physik. Chem. **70**, 474 (1966).
10. H. Wolff and J. Eints. Ber. Bunsenges. physik. Chem. **70**, 728 (1966).
11. H. Wolff and D. Horn. Ber. Bunsenges. physik. Chem. **71**, 467 (1967).
12. (*a*) H. Wolff and D. Horn. Ber. Bunsenges. physik Chem. **72**, 419 (1968). (*b*) F. B. Howard, I. Frazier, and H. T. Miles. Proc. Nat. Acad. Sci. **64**, 451 (1969).
13. H. Schuster, G. Schramm, and W. Zillig. Z. Naturforschg. **11b**, 339 (1956).
14. H. E. Auer and Z. Alexandrowicz. Biopolym. **8**, 1 (1969).
15. G. Zundel and J. Muehlinghaus. Z. Naturforschg. **26b**, 546 (1971).
16. G. Zundel, A. Murr, and G.-M. Schwab. Z. Naturforschg. **17a**, 1027 (1962).
17. G. Zundel. Hydration and intermolecular interaction. Academic Press New York, N.Y., 1969.

Can. J. Chem. Downloaded from www.nrcresearchpress.com by 210.87.254.40 on 09/05/12
For personal use only.

Ring–Chain Tautomerism of Hydroxyketones

JOSEPHINE E. WHITING[1] AND J. T. EDWARD
Department of Chemistry, McGill University, Montreal, Quebec

Received February 10, 1971[2]

A study of the u.v., i.r., and n.m.r. spectra of 5-hydroxy-2-pentanone and of 6-hydroxy-2-hexanone has shown that in most organic solvents there is a slight preference for the open-chain form of the hydroxyketone over the cyclic hemiketal. Increase in temperature and in polarity of solvent further favors the open-chain tautomer; in water there was no evidence of any cyclic form.

L'étude des spectres d'absorption i.r., u.v., et r.m.n. des composés 5-hydroxy-2-pentanone et 6-hydroxy-2-hexanone a montré que dans la plupart des solvants organiques la forme ouverte de l'hydroxycétone est légèrement préférée à la forme cyclique de l'hémicétal. L'augmentation de la température ainsi que de la polarité du solvant favourise l'existence de ces composés sous la forme ouverte, et dans l'eau on ne remarque que la forme ouverte.

Canadian Journal of Chemistry, 49, 3799 (1971)

It has long been known that γ- and δ-hydroxyaldehydes and ketones can react either as the straight-chain form or as the cyclic hemiacetal or hemiketal (1, 2), and an equilibrium between these forms has been assumed. However, it is only fairly recently that equilibrium constants for some of these examples of ring-chain tautomerism have been measured. Thus Hurd and Saunders (3) showed, from measurements of the u.v. absorption, that in 75% aqueous dioxane 4-hydroxybutanal and 5-hydroxypentanal exist predominantly as the cyclic hemiacetals, containing only 11.4 and 6.1% respectively of free aldehyde. (It is likely that 3–4% of the hydrated aldehyde (4) is also present.)

Substitution of the methylene hydrogens of these ω-hydroxyaldehydes by hydroxyl or hydroxymethyl groups gives the common aldopentoses and hexoses, which are known to be present in solution almost wholly in the cyclic form (5). This is to be expected on conformational grounds (6*a*, 7). The cyclic form can also be favored by being fused to other rings (8).

Although equilibrium constants have been measured for the ring–chain tautomerism of some complex hydroxyketones (*e.g.* α-(β-hydroxyethyl)-aminodesoxybenzoins (9)) and related compounds (10, 11), values for the simple hydroxyketones have been lacking. The present paper records the equilibrium constants for the ring–chain tautomerism (eqs. 1 and 2) of two of

[1] 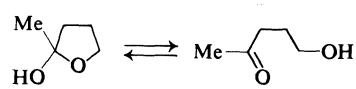

1 **2**

[2] 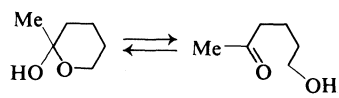

3 **4**

the simplest possible hydroxyketones, 5-hydroxy-2-pentanone (**2**) and 6-hydroxy-2-hexanone (**4**), and the effects of temperature and solvent polarity on these values. Additionally, we have looked for the possible ring–chain tautomerism of their 2,4-dinitrophenylhydrazones **5** and **6** (eqs. 3 and 4).

[3] 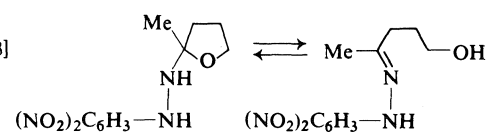

5

[4] 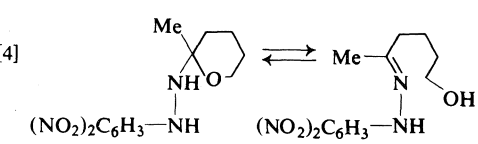

6

Cyclic structures have been postulated for the phenylhydrazones of some pyranoses (12) and for the 2,4-dinitrophenylhydrazone of a steroidal δ-hydroxyaldehyde (8), and a ring–chain tautomeric equilibrium has been demonstrated for certain hydroxyhydrazones (10).

[1]Née Josephine Jaworska, holder of an NRCC Studentship 1967–1970.

[2]Revision received August 20, 1971.

Can. J. Chem. Downloaded from www.nrcresearchpress.com by 210.87.254.40 on 09/05/12
For personal use only.

Experimental

The i.r. spectra were recorded with Perkin–Elmer Model 337 and 257 spectrophotometers for routine, and with Model 521 spectrophotometer for quantitative work. The n.m.r. spectra were recorded with a Varian A-60 spectrophotometer and u.v. spectra with a Unicam SP800 spectrophotometer equipped with a temperature-controlled cell block. Analyses were done by Dr. C. Daesslé of Montreal and Dr. A. Bernhardt of Elbach über Engelskirchen, West Germany.

Materials

Starting materials were commercial products. Wherever possible spectrograde solvents were used. For the u.v. spectra these were cyclohexane, dioxane, acetonitrile, carbon tetrachloride, chloroform, and methanol. Absolute ethanol, 95% ethanol, freshly distilled water, and freshly distilled reagent grade dimethylsulfoxide, kept over Linde Molecular Sieves Type 3A, were also used. Spectrograde carbon tetrachloride was used as solvent for the quantitative i.r. measurements. Deuterated solvents for n.m.r. were obtained from Stohler Isotopes or Merck, Sharpe, and Dohme.

5-Hydroxy-2-pentanone (2)

4,5-Dihydro-2-methylfuran (1.0 g) was refluxed for 45 min in 0.02 *N* hydrochloric acid (40 ml) until the solution was homogeneous. The solution was cooled and saturated with anhydrous potassium carbonate. The oil that separated was extracted with ether (5 × 20 ml). The combined ether extracts were dried over anhydrous sodium sulfate, filtered, and evaporated at reduced pressure at room temperature to give a pale yellow liquid (10.9 g, 90%). This product was distilled twice at 10^{-3}mm pressure and a bath temperature of 35°, and condensed on a cold finger cooled by Dry Ice – ethanol. The distillate was a clear colorless liquid, ν_{max}(neat) 3440 (ν O—H), 1720 (ν C=O), 1170 (ν C—O of **1**), and 1075 cm^{-1} (ν C—O of **2**).

Anal. Calcd. for $C_5H_{10}O_2$: C, 58.8; H, 9.9. Found: C, 58.6; H, 9.7.

The 2,4-dinitrophenylhydrazone **5**, recrystallized twice from ethanol and dried at room temperature and reduced pressure, had m.p. 150–151°, ν_{max}(KBr) 3500 (ν O—H), 3330 (ν N—H), 1625 (ν C=N), and 1130 cm^{-1} (ν C—O); λ_{max}(EtOH) 362 nm (ε 21 000), λ_{max}(acetone) 366 nm (ε 20 000); n.m.r. in DMSO-d_6: 2.1 (s, 3H, CH_3), 7.7–9.0 δ (m, 3H, Ar).

Anal. Calcd. for $C_{11}H_{14}N_4O_5$: C, 46.8; H, 5.0; N, 19.9. Found: C, 46.6; H, 5.2; N, 20.2.

6-Hydroxy-2-hexanone (4)

The hydroxy-ketone was prepared in similar fashion, in 90% yield, by hydrolysis of 2-methyl-5,6-dihydropyran-3-carboxylic acid (m.p. 118–119°, lit. 119° (1)), obtained by the method of Perkin (1). The product was a clear colorless liquid, ν_{max}(neat) 3430 (ν O—H), 1725 (ν C=O), 1095 (ν C—O of **3**), 1045 cm^{-1} (ν C—O of **4**).

Anal. Calcd. for $C_6H_{12}O_2$: C, 62.0; H, 10.4. Found: C, 62.2; H, 10.5.

The 2,4-dinitrophenylhydrazone **6**, recrystallized twice from ethanol and dried at room temperature and reduced pressure, had m.p. 94–95° (lit. 96–97° (13)), ν_{max}(KBr) 3460 (ν O—H), 3330 (ν N—H), 1618 (ν C=N), 1595 (Ar) and 1110 cm^{-1} (ν C—O); λ_{max}(EtOH) 362 nm (ε 21 000), λ_{max}(acetone) 366 nm (ε 20 000); n.m.r. in DMSO-d_6: 2.1 (s, 3H, CH_3), 7.8–9.0 δ (m, 3H, Ar).

Anal. Calcd. for $C_{12}H_{16}N_4O_5$: C, 48.6; H, 5.4; N, 18.9. Found: C, 48.7; H, 5.3; N, 19.1.

2-Methoxy-2-methyltetrahydrofuran (7)

The compound was prepared by the reported method (14) and was a colorless liquid boiling at 115–116° (lit. 114.5° (14)), ν_{max}(neat) 2849 (C—H of OMe), 1075 (ν C—O), and 1035 cm^{-1} (ν C—O); n.m.r. in CCl_4: 1.35 (s, 3H, CH_3), 3.1 δ (s, 3H, CH_3O); end absorption only in the u.v.

Anal. Calcd. for $C_6H_{12}O_2$: C, 62.0; H, 10.4. Found: C, 62.1; H, 10.3.

5-Ethoxy-2-pentanone (8)

This compound was prepared by reported methods (15). The colorless liquid, b.p. 169–170° (lit. 170–171° (15)), was purified by v.p.c. on an Aerograph 705 Autoprep with 1/12 effluent splitter. The column consisted of 30% Se-30 on Chromosorb W, 20 ft aluminum, 3/8 in. d; H_2 flow 25 ml/min, N_2 flow in detector 25 ml/min, N_2 flow in collector 300 ml/min; column temperature 175°, injector 215°, detector 250°. The liquid had ν_{max}(neat) 2875 (C—H of OEt), 1721 (ν C=O), and 1120 cm^{-1} (ν C—O); λ_{max}(cyclohexane) 278 nm (ε 17.0), λ_{max}(EtOH) 273 nm (ε 19.5), λ_{max}(H_2O) 265 nm (ε 24.6); n.m.r. in CCl_4: 1.1 (t, 3H, CH_3 of OEt), 1.8 (m, 2H, CH_2), 2.1 (s, 3H, CH_3), 2.5 (t, 2H, CH_2), 3.35 (t, 2H, CH_2), 3.4 δ (q, 2H, CH_2).

Anal. Calcd. for $C_7H_{14}O_2$: C, 64.4; H, 10.8. Found: C. 64.6; H, 10.6.

The 2,4-dinitrophenylhydrazone of **8**, recrystallized twice from ethanol and dried at reduced pressure, had m.p. 155–156°, ν_{max}(KBr) 3320 (ν N—H), 1628 (ν C=N), 1595 (Ar) and 1135 cm^{-1} (ν C—O); λ_{max}(EtOH) 362 nm (ε 21 000), λ_{max}(acetone) 366 nm (ε 20 000); n.m.r. in DMSO-d_6: 1.2 (t, 3H, CH_3 of OEt), 2.1 (s, 3H, CH_3), 7.8–9.0 δ (m, 3H, Ar).

Anal. Calcd. for $C_{12}H_{16}N_4O_5$: C, 55.3; H, 6.4; N, 9.9. Found: C, 55.5; H, 6.4; N, 9.8.

Analytical Procedures

For i.r. studies, the intensities of the carbonyl absorption at 1721 cm^{-1} of an equilibrated solution (0.005 to 0.04 *M*) of **1** ⇄ **2** in carbon tetrachloride were compared with those of a standard solution of compound **8** (compound **7** had no absorption in this region) at 22 °C.

For n.m.r. studies, 1–2 *M* solutions of **1** ⇄ **2** and **3** ⇄ **4** in carbon tetrachloride, cyclohexane-d_{12}, chloroform-*d*, acetone-d_6, ethanol-d_6, acetonitrile-d_3, dimethylsulfoxide-d_6, deuterium oxide, and formamide (for **1** ⇄ **2** only), were equilibrated at 37 ± 0.5° for 5 h (equilibrium of most samples was reached within a few minutes, in contrast to the equilibrations reported by Hurd and Saunders (3)). The spectra were recorded with probe temperature 37 ± 1°, sweep width 250 Hz. At least duplicate samples of each concentration and solvent were recorded, and the integration of each spectrum was an average of five scans. Relative concentrations of the cyclic and open-chain forms were calculated from the integrations of the two singlet methyl peaks, the one at lower field (δ_c) having a value close to that of the model compound 8 and hence

TABLE 1. Percentage of keto form **2** in different solvents

Solvent	E_T*	By n.m.r. method	By u.v. method (λ in nm)†	
(Neat liquid)		54.5		
Cyclohexane‡	30.9§	55.4	56.2	(278)
Dioxane	36.0	—	54.5	(275)
CCl_4	32.5	57.6‖	57.3	(272)
$CHCl_3$‡	39.1	55.0	57.3	(277)
Acetone‡	42.2	55.0	—	—
Ethanol‡	51.9	54.8	55.7	(274)
Methanol	55.5	—	55.4	(273)
Acetonitrile‡	46.0	55.0	56.0	(276)
DMSO‡	45.0	61.0	64.0	(278)
Water‡	63.1	100	100	(265)
Formamide	56.6	54.2	—	—

*From ref. 19.
†Measurements at 25.1°.
‡Deuterated solvents were used for n.m.r. spectra.
§E_T for *n*-hexane.
‖δ_c 125, δ_r 75 Hz.

TABLE 2. Percentage of keto form **4** in different solvents

	By n.m.r. method			By u.v. method*	
Solvent	%**4**	δ_c (Hz)	δ_r (Hz)	%**4**	λ_{max}(nm)
(Neat liquid)	54.1	115	62		
Cyclohexane†	51.4	106	56	53.5	280
Dioxane				57.4	277
CCl_4	51.2	122	70	51.0	272
$CHCl_3$†	54.0	130	77	55.1	275
Acetone†	54.8	107	55		
Ethanol†	61.8	110	57	64.7	274
Methanol				66.1	274
Acetonitrile†	55.9	107	55	62.1	276
DMSO†	54.6	119	65	56.7	278
Water†	100	130		100	278

*Spectra recorded at 25.1°.
†Deuterated solvents were used for n.m.r. spectra.

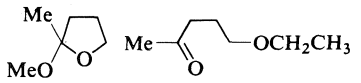

7 **8**

being assigned to the open-chain form, the one at higher field (δ_r) having a value close to that of C—Me of model **7**, and hence being assigned to the ring form. Some values of the chemical shifts δ_c and δ_r, in Hz downfield from tetramethylsilane as an internal standard, are recorded in Tables 1 and 2,[3] along with the percentage of the open-chain form obtained from n.m.r. studies.

For the u.v. study, 0.02 to 0.05 *M* solutions of **1** ⇄ **2** and **3** ⇄ **4** were equilibrated in water baths maintained at 15.0 ± 0.1, 24.8 ± 0.1, and 50.1 ± 0.1°; the temperatures of samples in the cell block (*i.e.*, the temperatures at which the spectra were recorded) were 15.4 ± 0.1, 25.0 ± 0.1, and 49.8 ± 0.2°. Samples were equilibrated for 5 h (15 min was in fact enough for most samples). The equilibria were very mobile, and no acid was required to catalyze the reaction. The hydroxyketones and model compound **8** had a band in the region 265–280 nm, depending on the solvent or solvent mixture. Compound **7**, a model for the cyclic forms, had no appreciable absorption at these wavelengths. The extinction coefficients of the hydroxyketones were compared with those of compound **8** in each solvent and solvent mixture, at each temperature. Results are recorded in Tables 1–6. At least two runs, and usually three or four, were made for each determination, and results were usually reproducible to within about 1%.

[3]In most of the solvents of Table 1 chemical shifts were found to be somewhat variable, presumably because of concentration and other effects, and are not recorded.

Results and Discussion

There are two diastereomeric conformations of the cyclic tautomers **1** and **3**; the chain tautomers may exist in a large number of different conformations, only one of which is shown in Scheme 1.

The difference in the free energy content **1***a* and *b* is probably small. The five-membered ring is quite flexible (16), and this prevents calculations

Can. J. Chem. Downloaded from www.nrcresearchpress.com by 210.87.254.40 on 09/05/12
For personal use only.

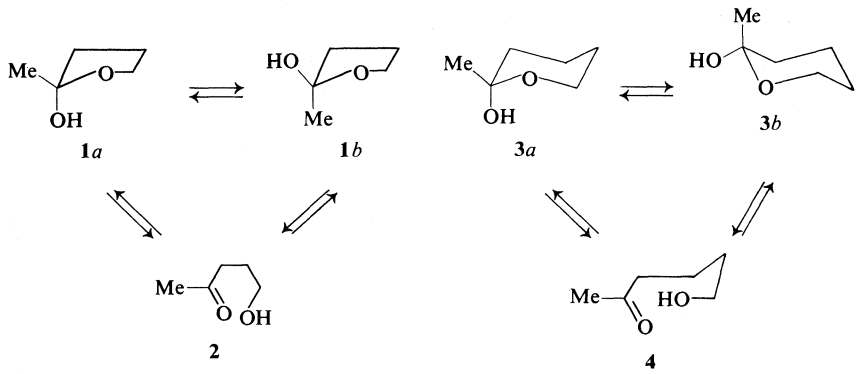

SCHEME 1

TABLE 3. Variation in amount of keto forms with mole-fraction (χ_{H_2O}) of water in dioxane–water mixtures at 25.1 °C

χ_{H_2O}	%2	χ_{H_2O}	%4
0	54.5	0	57.4
0.40	56.1	0.31	58.5
0.61	57.3	0.59	61.0
0.81	60.4	0.83	65.0
0.93	72.9	0.95	95.0
0.96	92.0	0.98	99.2
1	100	1	100

of interaction energies by the methods applicable to the more rigid chair form (6*a*) of cyclohexane. On the other hand, structure **3***a* (OH axial) should be considerably favored over **3***b* because of the anomeric effect (17), and because of the greater size of the methyl group (6*b*).

Inspection of the n.m.r. spectra of the mixtures of compounds **1** ⇄ **2** and **3** ⇄ **4** showed only two methyl signals, one for the open-chain keto form (at lower field) and one for the cyclic form. Evidently the conformational equilibrium between the cyclic forms is fast so that only a single weight average absorption is observed (6*c*). The percentages (at 37°) of the open-chain forms **2** and **4** in different solvents, calculated from the integrated areas of the different methyl signals, are given in Tables 1 and 2, respectively. In these tables are shown also the percentages (at 25°) in these solvents calculated from the u.v. absorption of the tautomeric mixtures; the lower temperature should increase the amount of the cyclic form by about 1–1.5% (see below). It is evident that the results from the two different methods are in rough agreement. Furthermore, they agree roughly with the result obtained by i.r. spectroscopy, which showed 57.7 ± 0.5% of **2** present at 22° in the mixture **1** ⇄ **2**. Because of its greater convenience, the u.v. method was used exclusively to determine the percentages of the open-chain tautomers in aqueous-organic solvents of varying composition (Tables 3, 4, and 5).

It is apparent that the hydroxyketones **2** and **4** show a much smaller tendency to cyclize than do the analogous hydroxyaldehydes studied by Hurd and Saunders (3). This is to be expected, from the lesser reactivity of ketones as compared to aldehydes.

The extent of cyclization is greatly affected by

TABLE 4. Variation in amount of keto forms with mole-fraction (χ_{H_2O}) of water in ethanol–water mixtures at 25.1 °C

χ_{H_2O}	%2	χ_{H_2O}	%4
0	55.7	0	54.8
0.20	56.0	0.26	55.6
0.42	56.2	0.45	61.1
0.61	56.5	0.58	66.5
0.64	63.5	0.78	90.0
0.82	64.5	0.90	97.8
0.85	71.5	0.96	100
0.95	95.0	1	100
1	100		

TABLE 5. Variation in amount of keto forms with mole-fraction (χ_{H_2O}) of water in dimethyl sulfoxide–water mixtures at 25.1 °C

χ_{H_2O}	%2	χ_{H_2O}	%4
0	64.0	0	61.0
0.16	67.5	0.10	66.0
0.36	77.0	0.21	72.5
0.52	87.5	0.42	87.7
0.61	92.5	0.58	100
0.72	100	0.76	100
0.97	100	1	100
1	100		

Can. J. Chem. Downloaded from www.nrcresearchpress.com by 210.87.254.40 on 09/05/12
For personal use only.

TABLE 6. Effect of temperature on percentage of keto forms **2** and **4** in various solvents

Solvent	%2			%4		
	15°	25°	50°	15°	25°	50°
Dioxane	53.9	54.5	57.2	56.7	57.4	59.7
Ethanol	54.1	55.7	57.3	62.9	64.7	67.1
Dimethyl sulfoxide	62.8	64.0	67.1	55.5	56.7	58.6
Dioxane–water	88.4*	92.0*	95.5*	91.6†	95.0†	98.5†
Dimethyl sulfoxide – water	95.6‡	97.2‡	99.0‡	92.8§	94.3§	96.5§

*Mole-fraction of water: 0.96.
†Mole-fraction of water: 0.95.
‡Mole-fraction of water: 0.75.
§Mole-fraction of water: 0.70.

the nature of the solvent, but cannot be correlated with any of the common measures of solvent polarity. This can be seen by an inspection of Tables 1 and 2, in which the solvents (other than the neat hydroxyketone) are arranged in order of increasing dielectric constant ε: on going from cyclohexane (ε ~ 2) to acetonitrile (ε = 37.5) the percentage of the keto form remains almost constant. Other measures of solvent polarity, such as Kosower's Z values (18) or Dimroth's E_T values (19) (shown in Table 1), are equally poor in correlating with the equilibrium constant: in particular, none would predict the special effect of water, and to a much lesser extent of dimethyl sulfoxide, in stabilizing the keto form. This effect is shown also in mixtures of water with organic solvents (Tables 3–5 and Fig. 1): the proportions of open-chain keto forms **2** and **4** increase rapidly with increasing proportion of water and are approximately 100% in pure water.[4] While water has the highest Z and E_T values (but not the highest dielectric constant) of the solvents in Tables 1 and 2, quantitatively its effect is out of line with these values, and stabilization of the hydroxyketones **2** and **4** by some specific solvation might seem to be indicated. Water is known to hydrogen-bond fairly strongly to the carbonyl group, but so (albeit less strongly) do methanol and ethanol (20), which are shown in Tables 1 and 2 to be comparatively ineffective in stabilizing the hydroxyketo form.

Increase in temperature favors the open-chain over the cyclic form (Table 6 and Figs. 2 and 3), indicating that the reactions **1** → **2** and **3** → **4** are endothermic (ΔH is positive: Table 7). The enthalpy and entropy changes for these reactions become much greater in the more aqueous solvents (Table 7), perhaps because of greater solvation effects. However, the solvation of **2** and **4** (in preference to **1** and **3**) would cause a decrease in entropy, and the reactions **1** → **2** and **3** → **4** are accompanied by large increases in entropy. Any explanation of the remarkable effects of water in favoring the hydroxyketo form must at the moment be highly speculative.

The furanose forms of sugars have generally been regarded as inherently less stable than the pyranose forms, and this has been in accord with the general feeling that six-membered, chair-shaped rings are always more stable than five-membered rings. However, the difference in free energy of five- and six-membered rings is not pronounced: the flexible cyclopentane has greater

TABLE 7. Thermodynamic calculations*

Solvent	ΔH^0(kcal/mol)†	ΔS^0(e.u.)‡
Equilibrium: **1** ⇄ **2**		
Dioxane–water§	5.8	23.8
DMSO–water‖	8.0	33.9
Dioxane	0.7	2.8
DMSO	1.0	4.5
Ethanol	0.7	2.8
Equilibrium: **3** ⇄ **4**		
Dioxane–water¶	9.6	38.0
DMSO–water**	4.2	19.7
Dioxane	0.7	3.1
DMSO	0.8	3.2
Ethanol	1.0	4.5

*Based on data in Table 6 and Figs. 2 and 3, in which K and T were fitted to equation: $\ln K = N(1/T) + C$.
†ΔH^0 = —NR, error approximately 5%.
‡ΔS^0 = CR, error approximately 10%.
§Mole-fraction water: 0.96.
‖Mole-fraction water: 0.75.
¶Mole-fraction water: 0.95.
**Mole-fraction water: 0.70.

[4]In contrast, 1-deoxyfructose (which differs from **4** only in having three additional hydroxyl groups) in water at 20° is only 4.5% in the open-chain form (private communication from Prof. S. J. Angyal, Sydney, Australia). The additional hydroxyl groups would be expected to favor the cyclic form both by inductive and by conformational effects, but the magnitude of combined effects is remarkable.

Can. J. Chem. Downloaded from www.nrcresearchpress.com by 210.87.254.40 on 09/05/12
For personal use only.

Can. J. Chem. Downloaded from www.nrcresearchpress.com by 210.87.254.40 on 09/05/12
For personal use only.

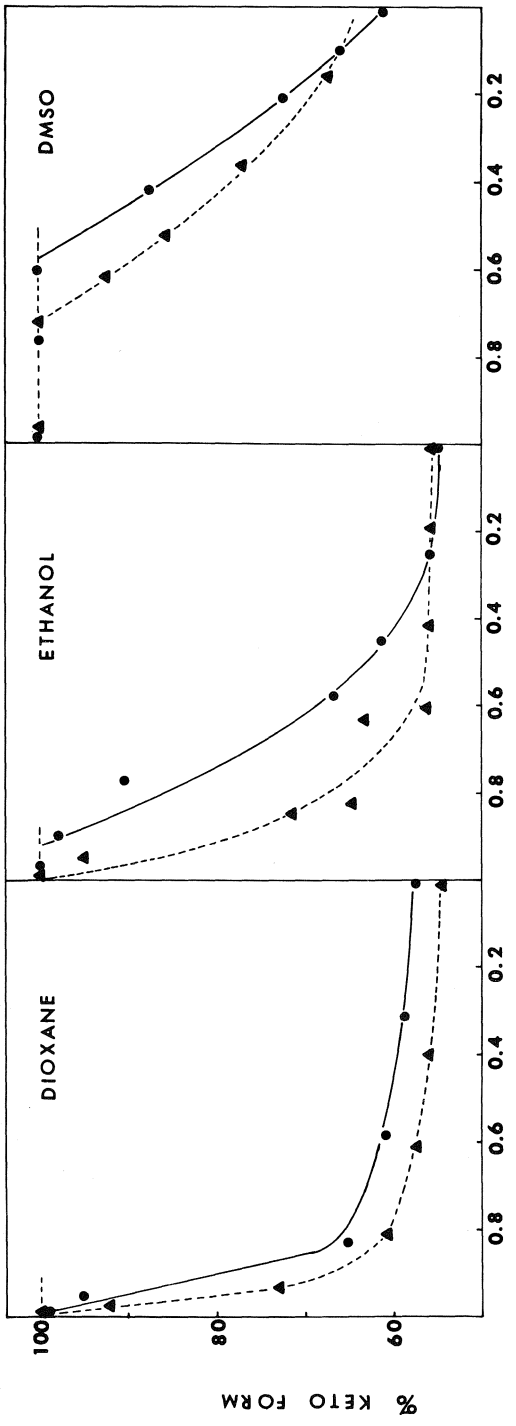

FIG. 1. Effect of mole-fraction of water in aqueous dioxane, aqueous ethanol, and aqueous dimethyl sulfoxide on the percentages of the keto forms 2 (▲) and 4 (●).

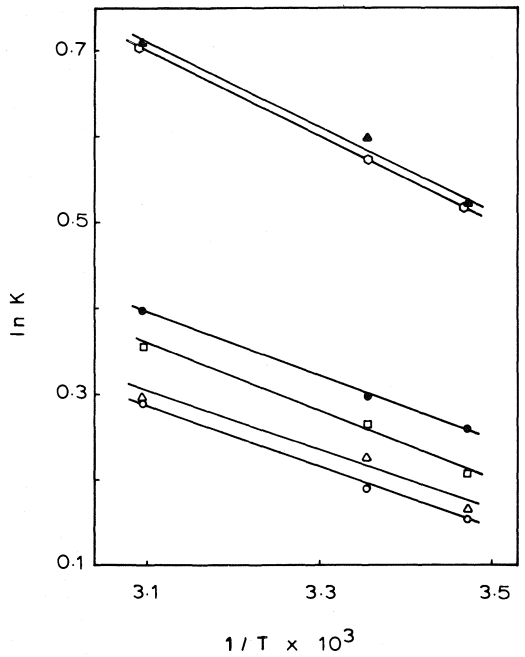

FIG. 2. Effect of temperature on equilibrium **1** ⇄ **2** in dioxane (○), ethanol (△), and dimethyl sulfoxide (⬡), and on equilibrium **3** ⇄ **4** in dioxane (●), ethanol (▲), and dimethyl sulfoxide (□).

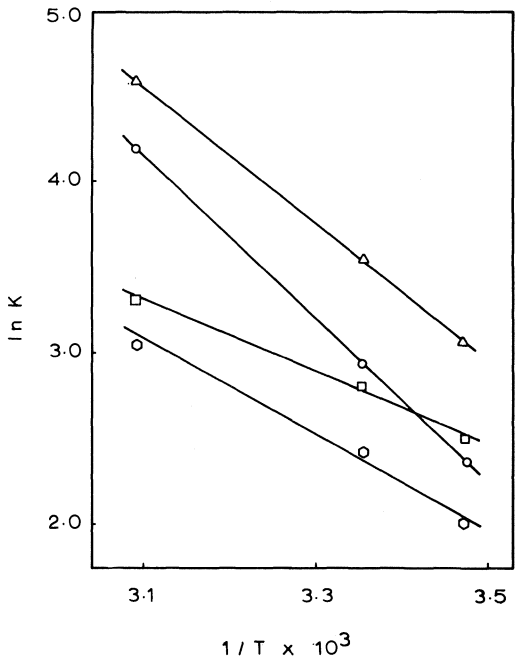

FIG. 3. Effect of temperature on equilibrium **1** ⇄ **2** in dioxane–water, 0.96 mole-fraction water (⬡) and in dimethyl sulfoxide – water, 0.75 mole-fraction water (△), and on equilibrium **3** ⇄ **4** in dioxane–water, 0.95 mole-fraction water (○), and in dimethyl sulfoxide – water, 0.70 mole-fraction water (□).

entropy than the rigid cyclohexane, and replacement of a methylene group by an oxygen atom lessens the free energy difference by reducing the eclipsed interactions in the five-membered ring (6*a*). From the data of Hurd and Saunders (3), the difference in free energy changes for the two reactions: cyclization of the hydroxyaldehydes in 75% aqueous dioxane at 25° to tetrahydropyran-2-ol (**9**), and to tetrahydrofuran-2-ol (**10**), is only 0.4 kcal/mol (13*a*). Our data for equilibrium in

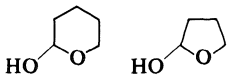

9 **10**

carbon tetrachloride show the difference in free energy changes on cyclization of the hydroxyketones to 2-methyl-2-hydroxytetrahydropyran (**3**) and to 2-methyl-2-hydroxytetrahydrofuran (**1**) to be only 0.16 kcal/mol. The difference in free energy favoring the six-membered ring is thus very small; furthermore, it is reversed in dioxane–water (~0.95 mole-fraction H_2O), the furanose form **1** then being favored by 0.3 kcal/mol. (A referee has pointed out the pertinence of the work of Trister and Hibbert (21), who found both five- and six-membered cyclic acetals formed by reaction (equilibrium-controlled) of glycerol with aldehydes. The proportion of five-membered product increased with temperature.)

If the 2,4-dinitrophenylhydrazones **5** and **6** exhibit any ring–chain tautomerism, the cyclic isomers (like **1** and **3**) could exist in two forms; additionally, the open-chain tautomer could exist in *syn* and *anti* forms. However, interconversions of *syn* and *anti* isomers of simple hydrazones can generally be induced by heat or light with relative ease (10). In fact, in DMSO-d_6 the n.m.r. spectra showed only singlets at 2.1 δ, about the value expected for the methyls of the open-chain forms **5** and **6**. The i.r. spectra of the solid hydrazones also indicated the open-chain forms only, showing substantial absorption corresponding to the hydroxyl and C=N functions. Furthermore, the 2,4-dinitrophenylhydrazones in ethanol or acetone had u.v. absorptions identical to that of the 2,4-dinitrophenylhydrazone of the model compound **8**, indicating the predominance of the

Can. J. Chem. Downloaded from www.nrcresearchpress.com by 210.87.254.40 on 09/05/12
For personal use only.

open-chain form in these solvents also. It is evident that 2,4-dinitrophenylhydrazones of hydroxy-ketones show a much smaller tendency than do the parent ketones to form the cyclic tautomer, presumably because the double bond of the hydrazone is stabilized by conjugation with the aromatic ring. In contrast, there is evidence that the 2,4-dinitrophenylhydrazone of a hydroxyaldehyde exists mainly in the cyclic form (8). This accords with the greater tendency of hydroxyaldehydes themselves to cyclize, as noted above.

We are grateful to Prof. S. J. Angyal for helpful discussion, and to a referee for thoughtful criticism and many suggestions. The financial support of the National Research Council of Canada is gratefully acknowledged.

1. W. H. PERKIN. J. Chem. Soc. **51**, 702 (1887).
2. W. CHARLTON, W. N. HAWORTH, and S. PEAT. J. Chem. Soc. 89 (1926). R. PAUL. Bull. Soc. Chem. Fr. **1**, 971 (1934). R. E. LUTZ and R. H. JORDON. J. Am. Chem. Soc. **71**, 996 (1949). D. D. WHEELER, D. C. YOUNG, and D. S. ERLEY. J. Org. Chem. **22**, 547 (1957). P. R. JONES. Chem. Rev. **63**, 461 (1963).
3. C. D. HURD and W. H. SAUNDERS. J. Am. Chem. Soc. **74**, 5324 (1952).
4. R. P. BELL. Advan. Phys. Org. Chem. **4**, 1 (1966). P. GREENZAID, Z. LUZ, and D. SAMUEL. J. Am. Chem. Soc. **89**, 749 (1967).
5. J. M. LOS, L. B. SIMPSON, and K. WIESNER. J. Am. Chem. Soc. **78**, 1564 (1956).
6. E. L. ELIEL, N. L. ALLINGER, S. J. ANGYAL, and G. A. MORRISON. Conformational analysis. Interscience Publishers, New York, N.Y., 1965. (*a*) pp. 378–380. (*b*) p. 44. (*c*) p. 153.
7. N. L. ALLINGER and V. ZALKOW. J. Org. Chem. **25**, 701 (1960).
8. J. T. EDWARD, P. F. MORAND, and I. PUSKAS. Can. J. Chem. **39**, 2069 (1961).
9. C. E. GRIFFIN and R. E. LUTZ. J. Org. Chem. **21**, 1131 (1956). R. E. LUTZ and C. E. GRIFFIN. J. Org. Chem. **25**, 928 (1960).
10. L. C. DORMAN. J. Org. Chem. **32**, 255 (1967).
11. J. V. PAUKSTELIS and R. M. HAMMAKER. Tetrahedron Lett. 3557 (1968).
12. E. G. V. PERCIVAL. Advan. in Carbohydr. Chem. **3**, 23 (1948).
13. E. G. E. HAWKINS. J. Chem. Soc. 2801 (1950). N. C. DENO, W. E. BILLUPS, K. E. KRAMER, and R. R. LASTOMIRSKY. J. Org. Chem. **35**, 3080 (1970).
14. L. E. SCHNIEPP, H. H. GELLER, and R. W. VON KORFF. J. Am. Chem. Soc. **69**, 672 (1947).
15. N. A. MILAS, S. W. LEE, C. SCHERERCH, R. O. EDGERTON, J. T. PLATI, F. X. GROSSI, and Z. WEISS. J. Am. Chem. Soc. **70**, 1594 (1948). E. P. ANDERSON, J. V. CRAWFORD, and M. L. SHERRILL. J. Am. Chem. Soc. **68**, 1294 (1946).
16. R. U. LEMIEUX. Molecular rearrangements. *Edited by* P. de Mayo. Interscience Division, John Wiley and Sons, New York, N.Y., 1963. p. 709. W. E. WILLY, G. BINSCH, and E. L. ELIEL. J. Am. Chem. Soc. **92**, 5394 (1970).
17. J. T. EDWARD. Chem. and Ind. 1102 (1955). C. B. ANDERSON and D. T. SEPP. Chem. and Ind. 2054 (1964). R. U. LEMIEUX and N. J. CHU. Abstracts of Papers. Am. Chem. Soc. **133**, 31N (1958). E. L. ELIEL and C. A. GIZA. J. Org. Chem. **33**, 3754 (1968). G. O. PIERSON and O. A. RUNQUIST. J. Org. Chem. **33**, 2572 (1968).
18. E. M. KOSOWER. J. Am. Soc. **80**, 3253 (1958). E. M. KOSOWER. An introduction to physical organic chemistry. John Wiley and Sons Inc., New York, N.Y., 1968. p. 296–305.
19. E. REICHARDT. Angew. Chem. Int. Ed. **4**, 29 (1965).
20. G. J. BREALEY and M. KASHA. J. Am. Chem. Soc. **77**, 4462 (1955). H. J. CAMPBELL, and J. T. EDWARD. Can. J. Chem. **38**, 2109 (1960). C. N. R. RAO. Ultraviolet and visible spectroscopy. Butterworths, London, 1960. p. 142.
21. S. M. TRISTER and H. HIBBERT. Can. J. Res. **14B**, 415 (1937).

Can. J. Chem. Downloaded from www.nrcresearchpress.com by 210.87.254.40 on 09/05/12
For personal use only.

Can. J. Chem. Downloaded from www.nrcresearchpress.com by 210.87.254.5 on 09/05/12
For personal use only.

Thermal Tautomerism of Crotonic Acid and Vinylacetic Acid, Neat and in Heavy Water

MARTIN B. HOCKING

Research Department, Dow Chemical of Canada, Limited, [1] *Sarnia, Ontario*

Received July 15, 1971

A distillate containing 25% vinylacetic acid has been obtained from *trans*-crotonic acid. Pure vinylacetic acid has been obtained from this by successive thermal equilibrations and distillations. Vinylacetic acid has been subjected to tautomerization conditions in acidic, neutral, and basic media, the latter in normal and in heavy water. These observations are coordinated in an attempt to arrive at plausible pathways for the various transformations observed.

A partir de l'acide crotonique-*trans*, il est obtenu un distillat contenant 25% d'acide vinylacétique. L'acide vinylacétique pur a été obtenu ultérieurement par équilibration thermique et distillation. L'acide vinylacétique a été soumis à des conditions de tautomérisation en milieu acide, neutre, et basique; cette dernière étant effectuée dans l'eau normale et dans l'eau lourde. Les observations ainsi obtenues sont réunies dans le but de déterminer les mécanismes possibles pour les différentes transformations observées.

Canadian Journal of Chemistry, 49, 3807 (1971)

Introduction

The double bond of an α,β unsaturated carboxylic acid can migrate to a position β,γ to the carbonyl. For instance, Linstead (1) has shown that thermal tautomerization of cyclohexylideneacetic acid yields an equilibrium mixture consisting largely of cyclohexene-1-acetic acid and that hydrosorbic acid in hot strong base exists as an equilibrium mixture of the α,β and β,γ tautomers (2). Similarly, Kon and Linstead (3) found that boiling 3,3-diethylacrylic acid with 60% aqueous potassium hydroxide yielded a considerable proportion of the β,γ unsaturated acid. If the α-hydrogen of the starting acid is replaced by ethyl or methyl the rate at which equilibration to the β,γ unsaturated acid can take place is severely retarded (4). The prime importance of the mobility of the hydrogen α to the carboxyl in these tautomeric changes has been demonstrated by Ives and Rydon who found that deuterium oxide exchanged rapidly with the α-hydrogens of sodium vinylacetate and much less readily with sodium *trans*-crotonate (5–7).

The *trans*-crotonic – vinylacetic tautomeric equilibrium has been shown to lie at about 98% of the former either in hot 50% sulfuric acid (8) or in hot aqueous base (9). These results have been confirmed by the isotopic exchange studies of Ives (6, 7), by the sulfur dioxide catalyzed experiments of Waterman *et al.* (10), and by our own purely thermal equilibration work (11). Butler and Small (12) reported the formation of a small proportion of methyl vinylacetate on the pyrolysis of methyl crotonate, but it was present in the starting material. During the course of this work Ozeki and Kusaka (13) reported that vinylacetic esters had been obtained on attempts to prepare crotonate esters from *trans*-crotonyl chloride via the Einhorn reaction.

The purpose of this report is to discuss our unexpected production of a 25% vinylacetic acid distillate from *trans*-crotonic acid. This work partially supplements and enlarges upon the elegant isotopic exchange studies of Ives and Rydon (5).

Experimental

Practical grade *trans*-crotonic acid was used. Analysis of the mixtures of *cis*- and *trans*-crotonic acids and vinylacetic acid was by integration of the n.m.r. resonance of the methyl double doublets (11) for the first two compounds, and of the two groups of three peaks attributed to the methylene of the latter (n.m.r. data given below). The respective multiplets were sufficiently well-separated from each other for accurate integration. Apart from convenience, this method of analysis assured no fractionation or further isomerization or tautomerization before analysis.

Vinylacetic Acid

This material, required for comparative purposes, was readily prepared by the acid hydrolysis of 3-butenenitrile (14). The n.m.r. spectrum of pure vinylacetic acid in $CDCl_3$ (chemical shifts with respect to internal tetramethylsilane, couplings in Hz measured on a multiplet expanded to 50 Hz sweep width, proton integral

[1]Contribution No. 174.

TABLE 1. Vinylacetic acid from distillation of *trans*-crotonic acid

Fraction no.	Distillate (g)	Mole percents of component acids		
		Vinylacetic	*cis*-Crotonic	*trans*-Crotonic
Todd column				
1	3.5*	—	—	—
2	15.0	10.3	55.7	34.0
3	29.0	15.7	70.8	13.5
4	30.0	17.0	71.4	11.6
5	26.0	19.3	68.6	12.1
6	23.0	21.4	69.5	9.5
Pot aliquot	—	1.9	10.9	63.8
7	46.0	—	—	—
8	21.0	20.2†	64.8†	15.0†
9	137.0	—	—	—
10	171.0	23.5	71.9	4.6
11	51.0	—	—	—
12	56.0	26.8	70.7	2.5
Pot aliquot	—	1.8	11.0	64.2
Concentric tube column				
1	23.5	19.9	67.0	13.1
2	10.0	—	—	—
3	17.0	18.2	67.5	14.3
4	3.1	—	—	—
5	1.8	18.0	80.0	1.5
6	1.6	24.6	75.6	1.5

*Fraction was mostly water.
†Results are non-uniform here because distillation was stopped for some hours between fractions 6 and 7.

TABLE 2. Effect of heating vinylacetic acid – crotonic acid mixture at 165°

Component acid	Proportions after heating		
	0 h	4 1/2 h	22 h
Vinylacetic	26.8	26.8	26.0
cis-Crotonic	70.7	48.1	20.2
trans-Crotonic	2.5	20.4	35.8
Crotonate dimer (30)	0	4.7	18.0

ratios in parentheses) was as follows: acid OH, singlet at 11.45 p.p.m. (0.95); methine proton, multiplet of 13 peaks spread over 40 Hz, centered at 5.88 p.p.m. (1.00); terminal methylene in two multiplets of 9 and 11 peaks separated by 7 Hz, centered at 5.11 p.p.m. (1.98); saturated methylene, six peaks in two groups of three, the centers of which are separated from each other by 6.7 Hz (1.0 and 1.4 Hz for lower field group, 1.3 and 1.3 Hz for higher field group). The spectrum was not amenable to first order analysis.

Vinylacetic Acid from trans-Crotonic Acid

(a) Using a "Todd" Column

trans-Crotonic acid (2.5 kg) was heated at 175° for 24 h. By raising the temperature to 187° the acids were then distilled at atmospheric pressure up a glass column (90 × 2.5 cm) packed with 1/4″ glass helices and fitted with a variable reflux head. At a reflux ratio of 100:1 and a take-off rate of about 20 ml/h the fractions given in Table 1 were obtained during a total operating time of 32 h.

The vinylacetic acid obtained was isolated by a series of thermal equilibration and distillation steps. Table 2 gives the best results obtained in a series of experiments carried out at different temperatures to determine optimum conditions for the equilibration step. The thermally equilibrated material was crystallized at 0° without solvent, and the crystallized *trans* filtered off. The initially enriched vinylacetic acid was distilled at 120 mm (b.p. range 115–120°) up a vacuum-jacketed column (70 × 2.5 cm; reflux 100:1) packed with glass helices. Table 3 outlines the results obtained by carrying out two thermal equilibrations and crystallization–distillations, on the purity and quantity of 250 g of crude vinylacetic acid obtained from crotonic acid.

(b) Using a Concentric Tube Column (15)

trans-Crotonic acid (360 g) was heated at 180° for 20 h and then distilled at atmospheric pressure at a reflux ratio of about 100:1 for a total of 48 h using completely vacuum-jacketed equipment (Table 1). Because this gave a poorer separation the product was not re-equilibrated or re-distilled.

Deuterium Exchange Experiments

Deuterium oxide (99.8%) was purchased from Atomic Energy of Canada. Vinylacetic acid was given a prelimi-

Can. J. Chem. Downloaded from www.nrcresearchpress.com by 210.87.254.5 on 09/05/12
For personal use only.

TABLE 3. Isolation of vinylacetic acid by thermal equilibration and concentration*

Components present	Proportions of components after successive treatment				
	Start	Heating 24 h at 165°	Crystallization and distillation	Heating 20 h at 165°	Final crystallization and distillation
cis-Crotonic acid	69	18	35	10	14
trans-Crotonic acid	2	34.5	5	22	2
Vinylacetic acid	29	27.5	60	57	84
Crotonate dimer (24)	0	20	0	11	0
Total mixture weight (g)	250	250	79	79	41
Vinylacetic acid content (g)	72.5	68.8	47.4	46.6	34.4

*Proportions given in mol %'s.

nary exchange treatment with heavy water to obtain carboxyl-deuterated material which was then recovered by extraction with carbon tetrachloride, dried ($MgSO_4$), and vacuum distilled (b.p. 71–73°/20 mm) before use. That only carboxyl deuteration had been effected was confirmed by n.m.r. (Table 5). The *t*-butanol used as an integral standard was dried ($MgSO_4$) and re-distilled at atmospheric pressure immediately before use.

Alkaline Conditions

Run 1 was largely exploratory. An n.m.r. tube containing vinylacetic acid (86 mg; 1 mmol), *t*-butanol (10 μl), heavy water (0.50 g), and sodium hydroxide (40 mg; 1 mmol) was cooled in an ice-water bath and sealed. Relative integrals of the initial n.m.r. spectrum bands and of those in spectra run at later intervals are given in Table 4. Runs 2, 7, and 8 were carried out in the same way as the first except that sodium metal, 41.5 (1.8 mmol), 47.2, and 43.1 mg respectively, was substituted for sodium hydroxide, and the quantity of vinylacetic acid used was raised to 145, 130, and 130 mg respectively.

Neutral and Acid Conditions

Run 3, carried out under "neutral conditions" had the same quantities of the same components as run 1, but without the sodium hydroxide. The n.m.r. tube for run 4 contained vinylacetic acid (145 mg), *t*-butanol (10 μl), heavy water (0.50 g), and concentrated sulfuric acid (8 mg).

Control Experiments

Run 5 was carried out on twice recrystallized *trans*-crotonic acid (128.8 mg; 1.5 mmol) in heavy water (0.50 g) containing *t*-butanol (10 μl) and sodium metal (43 mg; 1.9 mmol) and results are recorded in Table 6. An exchange experiment (run 6) on vinylacetic acid (145 mg; 1.7 mmol) without preliminary carboxyldeuteration, in normal water (0.50 g), was carried out in the presence of *t*-butanol (10 μl) and sodium hydroxide (71 mg; 1.8 mmol). No *cis*-crotonic acid was formed, as determined by n.m.r.

Results

Vinylacetic Acid Preparation

A distillate containing more than 25% vinylacetic acid was obtained by heating *trans*-crotonic acid for a time at 175° followed by distillation at atmospheric pressure (Table 1). The vinylacetic acid could not be isolated by distillation because of the closeness of its boiling point to that of the other main constituent, *cis*-crotonic acid, 169 and 169.3° (16) respectively. It was known (11) that *cis*-crotonic acid is readily thermally isomerized to the significantly higher boiling *trans*-isomer but that at the same time vinylacetic acid is also readily thermally tautomerized to *trans*-crotonic acid (6, 7). However, it was found that at 165° it was possible to preferentially isomerize the *cis*-crotonic acid with very little loss of the vinylacetic acid (Table 2). This mixture was then readily separable by distillation or crystallization or both (Table 3) to give reasonably pure vinylacetic acid (17), confirmed by comparison of its i.r. and n.m.r. spectra and other physical properties with those of an authentic sample (14).

Deuterium Exchange Experiments

Alkaline heavy water, at room temperature, readily exchanged deuterium with the α-hydrogens of carboxyl deuterated vinylacetic acid. After only 24 h, **1** was essentially the only

$CH_2{=}CH{-}CD_2{-}CO_2Na$

1

$CH_2D{-}CH{=}CD{-}CO_2Na$

2

species present (Table 4). The 10% drop in the integral attributed to the terminal methylenic hydrogens is accounted for by tautomerism to *trans*-crotonic acid, as seen by the nearly equivalent rise in the integral for this compound. Tautomeric equilibrium was attained after about 2 months at room temperature, or 4 h at 100°.

In either neutral or acidified heavy water vinylacetic acid was notably resistant to exchange or tautomerism. At room temperature,

Can. J. Chem. Downloaded from www.nrcresearchpress.com by 210.87.254.5 on 09/05/12
For personal use only.

TABLE 4. Vinylacetic acid deuterium exchange and tautomerization in alkaline heavy water

Total elapsed time	Relative integrals								% α-CH_2 exchanged
	CH_2	= CH —	CH_2-CO_2Na	H_2O + *t*-Bu*OH*	*t*-*Bu*OH	CH_3	— CH =	CH-CO_2Na	
Run 1, at 25°									
1 h	100	49	87	127	64	0	0	*	
27 days	61	31	0	203	63	53	19	—	
39 days	50	29	0	198	62	66	25	—	
2 h at 100°†	2.6	*	0	207	67	104	41	8	
4 h at 100°†	0	—	0	212	68	97	45	7	
6 h at 100°†	0	—	0	213	68	95	42	10	
Run 2, at 25°									
1/2 h	100	49	78	43	33	7.2	0	*	
6 h	98	53	26	89	30	11	4.0	—	
24 h	90	48	6.5	109	31	20	6.5	—	
29 h	86	47	5.0	104	30	26	11	—	
54 h	83	45	5.2	107	31	27	11	—	
149 h	63	34	2.7	110	33	50	18	—	
312 h	49	*	0	104	32	67	30	28	
56 days	2.8	—	0	111	31	111	48	7.3	
72 days	1.4	—	0	111	34	108	47	8.2	
Run 7, at 25°									
12 min	100	50	89	24	26	2.4			11
17 min	100	49	86	26	26	2.5			14
42 min	100	49	76	35	27	2.9			24
72 min	100	52	69	42	26	3.1			31
102 min	100	51	63	49	26	3.4			37
126 min	100	50	56	54	25	3.1			44
267 min	99	51	43	68	26	4.0			57
378 min	95	52	33	76	26	9.0			67
462 min	93	47	31	84	26	10.0			69
Run 8, at −5°									
11 min	100‡	50	79	‡	24	0			§
29 min	100	50	77	—	25	1.5			§
50 min	100	48	83	—	26	1.1			14
85 min	100	47	79	—	25	1.9			16
145 min	100	46	75	—	24	1.0			18
270 min	100	47	75	—	25	1.9			20
146 h	151	50	26	—	26	4.6			73
175 h	161	41	23	—	27	6.2			76
240 h	168	42	16	—	26	6.2			83

*The n.m.r. shift for α methine of crotonic acid is nearly the same as the shift of the methine of vinylacetic acid. Hence no separate integral was obtainable.
†Previous total time at room temperature, plus these times.
‡Water integral is unavoidably included with terminal methylene integral.
§Poor integrals were obtained for these two determinations because of bubbles in the viscous solution.

periods as long as 27 days under neutral conditions and 10 days when acidified, showed no exchange (Table 5). At 100°, 27% α-hydrogen exchange occurred after 66 h for the neutral experiment, and 23% in 4 h in acid, but no tautomerism was detected in either. The *t*-butanol internal standard used in the acid experiment was almost completely deuterated. As a control experiment substitution of *trans*-crotonic acid for vinylacetic acid in an alkaline heavy water run gave only about 2% terminal methyl deuterium incorporation and none at the α- and β-carbons (Table 6). Heating to 100° for 4 h brought about significant exchange at the α, about 2/3, and the terminal positions, about 1/3, but still very little exchange at the β position. In another control experiment, vinylacetic acid was heated in alkaline normal water and yielded normal *trans*-crotonic acid almost quantitatively.

Discussion

Vinylacetic Acid Formation

The *trans*-crotonic acid – vinylacetic acid tautomeric equilibrium lies about 98% on the side of the former. The high proportion of vinylacetic acid was obtained in distillates consisting largely of *cis*-crotonic acid. This is known (11) to exist in equilibrium with the *trans* and is formed via thermal cracking of the crotonate dimer **3** (Scheme 1). The 25° boiling point differential

Can. J. Chem. Downloaded from www.nrcresearchpress.com by 210.87.254.5 on 09/05/12
For personal use only.

TABLE 5. Vinylacetic acid deuterium exchange in neutral and in acidified heavy water

Total elapsed time*	Relative integrals: *t-Bu*OH	H_2O + *t*-Bu*OH*	$CH_2 = CH - CH_2CO_2D$			Crotonic methyl
Run 3, neutral						
0	28	12	46	25	45	—
27 days	29	12	46	22	46	—
27 days + 2 h at 100°	27	13	46	25	45	3
27 days + 66 h at 100°	9.5	42	47	25	32	3
Run 4, acid						
1 h	24	†	99†	37	70	4.5
6 h	24	—	99	36	70	3.5
54 h	25	—	100	37	71	3.5
246 h	25	—	100	37	70	3.8
318 h + 2 h at 100°	3.0	—	128	37	61	3.8
390 h + 4 h at 100°	1.5	—	136	38	54	4.0

*At room temperature unless otherwise stated.
†The resonance of the water hydrogens under these acid conditions coincided with the terminal methylene resonance multiplet and were integrated together.

TABLE 6. Control exchange experiments with crotonic and vinylacetic acids

Total elapsed time* (h)	Integral ratios: $CH_2 = CH - CH_2$-CO_2Na		H_2O + *t*-Bu*OH*	*t-Bu*OH	$CH_3 - CH = CH$-CO_2Na		
Run 5, crotonic acid in alkaline heavy water							
1	—	—	42	20	100	32	32
6	—	—	41	21	98	32	33
54	—	—	42	21	99	32	33
313	—	—	43	21	98	32	32
2 at 100°§	0	0	84	24	73	29	18
4 at 100°§	0	0	102	26	61	28	9.8†
Run 6, vinylacetic acid in alkaline water							
1	98	48	86	29	5.0		
2 at 100°§	10	‡	7.3	30	119	38	45
3 at 100°§	6	—	3.5	29	128	41	46

*At room temperature unless otherwise stated.
†Plus some crotonate dimer (24) began to appear.
‡See footnote †, Table 4.
§Previous elapsed time plus time indicated.

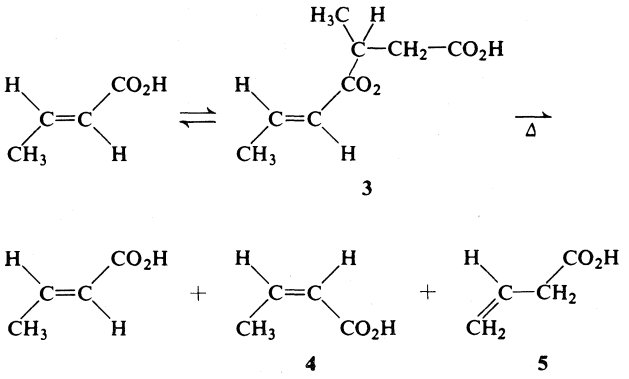

SCHEME 1

Can. J. Chem. Downloaded from www.nrcresearchpress.com by 210.87.254.5 on 09/05/12
For personal use only.

Can. J. Chem. Downloaded from www.nrcresearchpress.com by 210.87.254.5 on 09/05/12
For personal use only.

between *cis*- and *trans*-crotonic acids allows the distillation column to become highly enriched in the lower boiling *cis* isomer. *cis*-Crotonic acid (**4**), can also rapidly thermally tautomerize to vinylacetic acid (**5**) (11). The vinylacetic acid thus formed co-distils with the *cis*-crotonic acid to yield the observed 25% vinylacetic acid distillate.

Thus, *cis*-crotonic acid tautomerizes to a higher equilibrium level of vinylacetic acid than the *trans*. Of a *cis–trans* isomeric pair of α,β-unsaturated carboxylic acids, the *cis* is always the most dissociated (18). This is because there is little contribution in the *cis* acid from the resonance form **6**, due to non-coplanarity of the

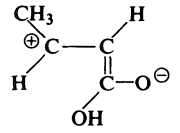

6

carboxyl carbonyl with the olefinic double bond caused by steric interactions (19). The presence of *cis* steric interactions is also supported by the 20 cm^{-1} higher i.r. frequency shown for the *cis* carbonyl *vs.* the *trans*.

The reduced olefinic conjugation conferred by the non-coplanarity, and the steric strain causing it, give two bases for easy tautomerization of *cis*-crotonic acid. A further contribution might be provided by the intramolecular 1,5 sigmatropic shift of a proton from methyl to carbonyl, for which the molecular geometry of the *cis* acid is correct. The diene gem diol intermediate formed, **7**, would readily collapse to vinylacetic acid.

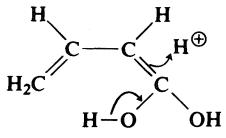

7

Vinylacetic Acid – Heavy Water Deuterium Exchange

The method of analysis used in the tautomerization experiments readily lent itself to the simultaneous determination of the extent of tautomerization and of deuterium exchange. Ives and Rydon (5–7), in their meticulous study, could not experimentally determine the position of deuterium exchange on tautomeric incorporation. Nevertheless, by an involved kinetic argument necessitating a number of assumptions they concluded that the transformations shown in Scheme 2 were occurring (6, 7). The present work proved this directly. That tautomerization to *trans*-crotonic acid occurred simultaneously to the α exchange, with incorporation of terminal deuterium, was also proven mathematically by Ives (7). We concur with these conclusions.

To determine the equilibrium ratio of incorporated deuterium, Ives (7) also evaluated the ratio $f_2/f_1 = 0.89$, where f_2 is the ratio of the rate of removal of protons to that of deuterions, and f_1 is the ratio of the rates of addition of protons and deuterons. For this evaluation it was necessary to determine rate constants k_1, the rate of deuterium exchange with light vinylacetic acid, and k_2, the rate of tautomerization of vinylacetic acid to *trans*-crotonic acid, which at 100° were found (7) to be $90 \pm 10 \times 10^{-4}$ and 58×10^{-4} min^{-1} respectively.

Plotting our 25° tautomerization data on first order coordinates, Fig. 1, yielded a rate constant k_2 of 1.55×10^{-4} min^{-1}. On attempting to fit our data to the kinetic argument used by Ives for obtaining a value for k_1 it was found that k_1 at 25° was so large relative to k_2 that k_2 was indeterminate by this method. This was probably because of the smaller Arrhenius activation energy usually shown by exchange reactions, than by isomerizations (20). Data from further room temperature (25°) and −5° exchange experiments with frequent early in-

$$\underset{\mathbf{8}}{CH_2{=}CH{-}CH_2{-}CO_2Na} \rightleftharpoons \underset{\mathbf{9}}{CH_2{=}CH{-}CHD{-}CO_2Na} \rightleftharpoons \underset{\mathbf{1}}{CH_2{=}CH{-}CD_2{-}CO_2Na}$$

$$\mathbf{8}, \mathbf{9}, \text{ or } \mathbf{1} \rightarrow \underset{\mathbf{10}}{CH_2X{-}CH{=}CX{-}CO_2Na}$$

X = H or D

SCHEME 2

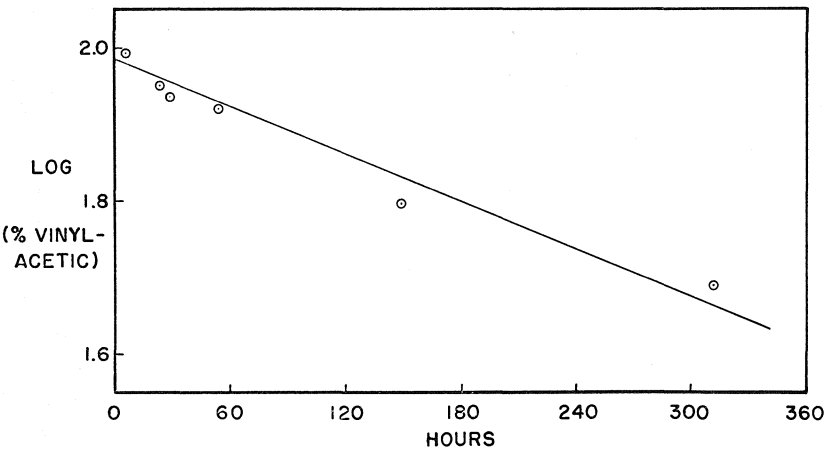

FIG. 1. First order plot of base catalyzed tautomerization of vinylacetic acid at 25°.

$$H_2C{=}CH{-}CH_2{-}X \underset{k_2}{\overset{k_1}{\rightleftharpoons}} H_2C{=}CH{=}CH{-}X \underset{k_4}{\overset{k_3}{\rightleftharpoons}} H_3C{-}CH{=}CH{-}X$$

11 (*a* X = CO_2H; *b* X = OR) — **12** (*a* X = CO_2H; *b* X = OR)

SCHEME 3

tegral determinations (Table 4) supported this suggestion and gave values for k_1 directly. Values for *initial* k_1 obtained in this way were 74×10^{-4} and 25×10^{-4} min^{-1} respectively, the former quite close to Ives' value at 100°.

Initial fast deuterium exchange α to the carboxyl in alkaline medium probably occurs via a non-classical carbanionic intermediate 12*a* (Scheme 3), as has been accepted (21, 22) for exchange reactions in allylic ethers. A proton or deuteron could add α or γ to the substituent giving exchanged starting material or tautomerized product respectively. However, allyl alkyl ethers **11***b* were found to tautomerize and γ-monodeuterate rapidly and to α-exchange only slowly, the inverse of our observations with **11***a*.

Methoxyl is inductively withdrawing and in a resonant position increases the substrate electron density by conjugation (23). Therefore, in **11***b*, alkoxyl is electron-attracting. In **12***b*, the alkoxyl is in conjugation with, and hence is raising the electron density on, the diffuse carbanion. Carboxylate anion and carboxyl have only minor changes in net inductive effect when changed from a non-conjugative to a conjugative situation (23). Thus, the overall relative electron affinity changes from $-CO_2H \gg -OR > -CO_2^{\ominus}$ to $-CO_2H > -CO_2^{\ominus} \gg -OR$ on changing from a purely inductive to an inductive plus conjugative position. The progressively greater ease of tautomerization and greater resistance to α exchange observed follow the latter order, suggesting that these substituents are affecting the allyl system conjugatively. To be conjugative this must be occurring through the intermediates **12**. The non-conjugative substitutent effect prior to the formation of **12** must only be on its rate of formation, *i.e.* slower with the ether.

The explanation for the observed difference between the ether and carboxylate now resolves itself to simply a higher γ than α electron density, and thus more ready γ protonation in the former, due to alkoxyl conjugative electron donation to the anion **12***b*, and a higher α than γ electron density in the latter **12***a* promoting α protonation. The intermediate carbanion **12***b* formed from the ether then gives alkoxyl-1-propenyl ether, rather than exchanged starting material **11**. In contrast, the sodium vinylacetate carbanion, **12***a*, gives exchanged starting material and relatively little crotonate.

Can. J. Chem. Downloaded from www.nrcresearchpress.com by 210.87.254.5 on 09/05/12
For personal use only.

The author thanks H. D. Mak for obtaining the n.m.r. spectra and C. G. Carlson and F. Johnson for helpful discussions and comments.

1. R. P. LINSTEAD. J. Chem. Soc. 1603. (1930).
2. E. N. ECCOTT and R. P. LINSTEAD. J. Chem. Soc. 2153. (1929).
3. G. A. R. KON and R. P. LINSTEAD. J. Chem. Soc. **127**, 616 (1925).
4. G. A. R. KON, E. LETON, and R. P. LINSTEAD. J. Chem. Soc. 1411 (1931).
5. D. J. G. IVES and H. N. RYDON. J. Chem. Soc. 1735 (1935).
6. D. J. G. IVES. J. Chem. Soc. 81 (1938).
7. D. J. G. IVES. J. Chem. Soc. 91 (1938).
8. E. J. BOORMAN and R. P. LINSTEAD. J. Chem. Soc. 577 (1933).
9. R. P. LINSTEAD and E. P. NOBLE. J. Chem. Soc. 614 (1934).
10. H. I. WATERMAN, J. VAN STEENIS, and J. H. DE BOER. Res. (Lond.) **2**, 583 (1949).
11. M. B. HOCKING. To be published.
12. J. N. BUTLER and G. J. SMALL. Can. J. Chem. **41**, 2492 (1963).
13. T. OZEKI and M. KUSAKA. Bull. Chem. Soc. Japan, **40**, 1232 (1967).
14. J. W. LYNN, R. L. ROBERTS, and J. R. KILSHEIMER. J. Org. Chem. **26**, 4300 (1961).
15. C. K. DONNELL and W. R. KENNEDY. Indust. Engin. Chem. **42**, 2327 (1950).
16. R. C. WEAST, *editor*. Handbook of chemistry and physics. The Chemical Rubber Co., Cleveland, Ohio, 1964.
17. M. B. HOCKING. U.S. Pat. 3 539 624 to the Dow Chemical Company. November, 10, 1970.
18. G. S. HAMMOND. *In* Steric effects in organic chemistry. *Edited by* M. S. Newman. John Wiley and Sons, Inc., New York, N.Y., 1956. p. 425.
19. L. PRATT and B. B. SMITH. Trans. Faraday Soc. **63**, 2858 (1967).
20. S. W. BENSON. The foundations of chemical kinetics. McGraw-Hill Book Company, Inc., New York, N.Y., 1960. pp. 254, 292, and 296.
21. C. D. BROADDUS. J. Am. Chem. Soc. **87**, 3706 (1965).
22. D. J. CRAM. Fundamentals of carbanion chemistry. Academic Press. New York, N.Y., 1965. pp. 54 and 58.
23. H. H. JAFFE. Chem. Rev. **53**, 222 (1953).
24. M. B. HOCKING. Can. J. Chem. **47**, 821 (1969).

Can. J. Chem. Downloaded from www.nrcresearchpress.com by 210.87.254.5 on 09/05/12
For personal use only.

Can. J. Chem. Downloaded from www.nrcresearchpress.com by 210.87.254.5 on 09/05/12
For personal use only.

Infrared Studies on Rotational Isomerism. V. 2-Nitroethanol

PAUL A. GIGUÈRE AND TOKIJI KAWAMURA
Département de Chimie, Université Laval, Québec, Québec

Received July 12, 1971

The i.r. spectra of 2-nitroethanol in the three physical states were measured between 4000 and 250 cm^{-1}. The liquid and the crystal were also studied in Raman effect. In all three states the molecules exist as *gauche* and *trans* isomers, the former being stabilized by a weak intramolecular hydrogen bond. Definite evidence for a third isomer, previously reported in dilute CCl_4 solutions, could not be ascertained from the vapor spectra as a function of temperature. On the other hand this study revealed appreciable decomposition of the vapor above 80 °C, with formation of nitroethylene and also some aldehyde. For that reason it was not possible to evaluate the enthalpy of isomerization. The difficulty of securing a pure sample of 2-nitroethanol is emphasized. Only one crystalline phase was obtained.

On a étudié en i.r. entre 4000 et 250 cm^{-1} le nitro-2 éthanol sous les trois états physiques. En outre on a étudié en Raman le liquide et le cristal. Dans les trois états les molécules existent sous forme d'isomères *trans* et *gauche*. Ce dernier est stabilisé par une faible liaison hydrogène interne. La présence d'un troisième isomère, présumément *gauche*, signalée dans les solutions diluées en solvant inerte, n'a pu être confirmée par une étude de la vapeur en fonction de la température. Celle-ci, par contre, a révélé une décomposition appréciable à partir de 80 °C avec formation de nitroéthylène et d'un peu d'aldéhyde. Pour cette raison il n'a pas été possible d'évaluer l'enthalpie d'isomérisation *gauche–trans*. On souligne la difficulté de préparer un échantillon pur de ce nitroalcool. Une seule phase cristalline a été obtenue.

Canadian Journal of Chemistry, 49, 3815 (1971)

Introduction

The existence of an intramolecular hydrogen bond between the nitro group and the hydroxymethyl group resulting in a six-membered chelate ring in 2-nitroalcohols was first postulated by Malinowski and Urbański (1). This hypothesis has been confirmed definitely by various spectroscopic studies (2–5). Claims to the contrary (6, 7) were later disproved (4). Nevertheless, the question of rotational isomerism in the nitroalcohols is not yet completely understood. For instance, 2-nitroethanol in CCl_4 solutions at high dilution has been reported to exhibit not two, but three distinct O—H stretching bands arising, presumably, from one *trans* and two *gauche* conformers (4, 5). The distinction between the latter two is not clearly established. It has been suggested to arise from two kinds of intramolecular hydrogen bonds involving respectively only one or both of the oxygen atoms of the nitro group. However, that explanation cannot account for certain other observations; in particular the fact that other β-nitroalcohols, such as 2-nitrobutanol, and 2,2-dinitropropanol, show only the two expected O—H bands at 3 μ. In the hopes of elucidating this problem we have extended the present series of investigations (8) to 2-nitroethanol. Previous work on this compound had been restricted mostly to the O—H stretching region.

Fundamentally, it is interesting to know to what extent the rather weak proton-acceptor character of the nitro group is compensated by the greater flexibility of a six-membered ring. On the other hand, introduction of a triatomic substituent leads to a significantly more complex situation than, for instance, in the 2-haloethanols because of greater possibility of coupling between the vibrations and overlapping of the bands. This is particularly true in the region of the skeleton stretching and the various CH_2 deformation modes. Experimentally, the preparation of a pure sample of the nitroalcohol is made more difficult by its thermal instability. It would seem that this aspect of the problem was not always fully appreciated in the past.

Experimental

The sample of 2-nitroethanol (Brickman and Co., Montreal) was stated to be of "practical grade". It was first dried over either sodium sulfate or molecular sieve, and then distilled[1] under reduced pressure (between 10 and 15 Torr) using a Vigreux fractionating column. The middle fraction, distilling at constant temperature (between 110 and 115 °C) was a clear, mobile liquid with, a refractive index n_D^{25} 1.4449. Now, values reported so far for this property range from a minimum of 1.4383 (9) to a maximum of 1.4497 (5), *cf.* also 1.4403^{20} (3). The most reliable seems to be n_D^{20} 1.4440 from the extensive

[1]DANGER OF EXPLOSION! Fortunately this did not materialize.

Can. J. Chem. Downloaded from www.nrcresearchpress.com by 210.87.254.5 on 09/05/12
For personal use only.

work of Burmistrov and Bashinova (10). In fact, in one instance where the distillation was carried out at rather low pressure (~0.5 Torr) and temperature (b.p. about 67°) we obtained a product of refractivity close to that reported by the Russian authors: n_D^{20} 1.4442. By comparison the brown residue of distillation had a higher refractivity; *viz.* 1.4478.

As for stability, the purified product was found, as reported before (10), to remain unaltered for periods of up to 5 or 6 months if kept in the dark. Upon exposure to daylight it took a light yellow color after a few hours, but this did not affect noticeably the i.r. spectrum of the liquid; at least not in the early stages. The spectroscopic samples were prepared as reported previously (11, 12). For the vapor spectra, because of the low volatility of the compound a 10 m folded-path absorption cell with cesium bromide windows (8) had to be used in a static system. The liquid alcohol in a side tube was kept at 10 to 20° below that of the cell enclosure. The latter, made of metal, undoubtedly catalyzed the decomposition of the vapor at temperature above 80 to 100° as revealed by our spectra. Indeed, β-nitroalcohols are known to be prone to decomposition (13) on heating with formation of nitroolefins and aldehydes. On the other hand, the Russian authors (10) found 2-nitroethanol to be stable up to 130° and even 150°, presumably in glass. Still they do recommend distilling it at low pressure (10–30 Torr).

The solid specimen were prepared either by condensation of the vapor on a support at liquid nitrogen temperature or by gradual cooling of a thin liquid film between cesium bromide discs. This always produced a glassy solid which could be devitrified easily by controlled warming. Crystallization usually occurred around −65°. Incidentally, this is well above the currently quoted melting point for 2-nitroethanol, *i.e.* −80° (14). Obviously, this datum must refer to a very impure product or a mixture of isomers. By contrast our crystals were observed to melt at about −54°. Numerous variations in the crystallization procedure, along the lines previously tried for 2-cyanoethanol (15), failed to yield a second crystalline phase. This follows naturally from the presence of both *gauche* and *trans* conformers in the normal crystal.

Discussion of Results

Interpretation of the spectra (Fig. 1) is best carried out by considering first the simplest case of the liquid, then the crystal, and finally the very complex vapor spectra. It must be emphasized again that considerable "mixing" of vibrations is expected; especially in the middle range (1600 to 800 cm^{-1}). Therefore, the assignments listed in Table 1 give an oversimplified picture.

Liquid Spectra

The broad O—H stretching band centered at about 3300 cm^{-1} is indicative of strong intermolecular hydrogen bonding. In thick samples a vague shoulder around 3550 cm^{-1} must belong to a combination tone. The OH bending expected in the neighborhood of 1350 cm^{-1} was not discernible among the NO_2 stretching and the CH_2 wagging bands. As for the OH torsion about the C—O bond, it was barely noticeable as an inflexion at 700 cm^{-1}, on the slope of the very broad band around 590 cm^{-1}. It appeared more clearly in the supercooled (at −180°) liquid.

The two stretching modes of the NO_2 group have been studied extensively in various organic compounds (16). In our spectra, both the symmetric and, to a lesser extent, the antisymmetric bands showed weak satellites. These must be due to rotational *gauche–trans* isomerism as explained before (17). The same feature accounts for the widely separated doublets of the various CH_2 deformation bands; most noticeably in the twisting and rocking bands. For the skeletal stretching and bending modes the assignments proposed here are based on the related cases of the lower nitroparaffins (18, 19), and the halogen 2-substituted ethanols (11, 12).

Crystal Spectra

The main O—H stretching band at 3220 cm^{-1} in the crystal is accompanied by a strong shoulder at 3290 cm^{-1} due, no doubt, to *trans* conformers. In very carefully annealed samples secondary maxima were visible at 3180 and 3320 cm^{-1}. From this it may be inferred that the unit cell must contain more than one molecule of each configuration. As in the liquid the OH bending mode cannot be identified clearly with any of the numerous peaks in the 7 μ region, except possibly the broader one at 1470 cm^{-1}. However, the frequency seems rather high for such an assignment. In contrast the torsional mode gives rise to a well characterized doublet with a 50 cm^{-1} separation, again due to coexistence in the crystal of *gauche* and *trans* molecules. The fact that the two components show roughly the same intensity is considered an indication that both conformers are present in equal number in the crystal lattice.

Most of the other bands exhibit multiplet structure. For instance, the CH_2 twisting modes of the isomers give rise each to a triplet; another confirmation that the unit cell contains more than one molecule of each kind, with in-phase and out-of-phase vibrations. It is noteworthy that some of the stronger components of these multiplets are shifted to *lower* frequency with respect to the liquid. Crystal field effects may be responsible for this, as well as for the much enhanced activity of certain skeletal bending bands: *v.g.* at 591, 498, 415, and 393 cm^{-1}. The presence of the

Can. J. Chem. Downloaded from www.nrcresearchpress.com by 210.87.254.5 on 09/05/12
For personal use only.

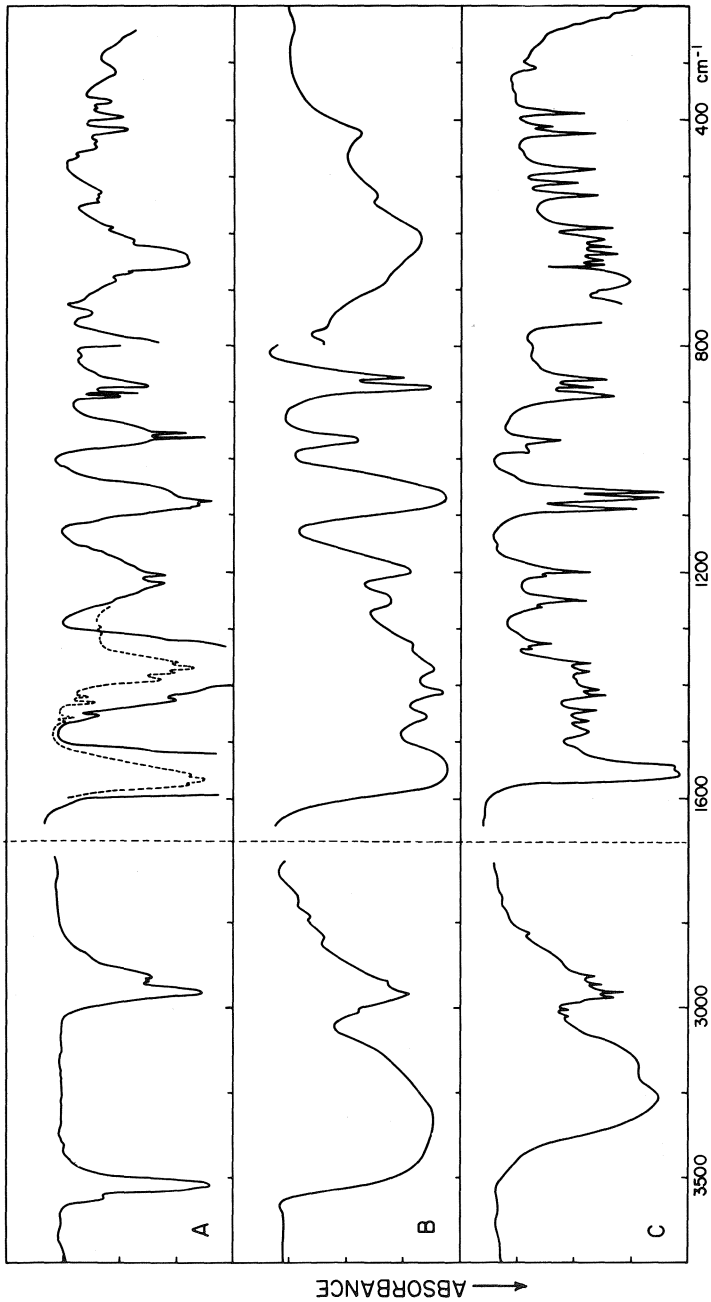

FIG. 1. The i.r. absorption of 2-nitroethanol (*A*) in the vapor at 80 °C, (*B*) in the liquid, and (*C*) in the crystalline state at −180°.

Can. J. Chem. Downloaded from www.nrcresearchpress.com by 210.87.254.5 on 09/05/12
For personal use only.

thermodynamically less stable *trans* conformer in the crystal must result from the particular situation that *inter*molecular hydrogen bonds in 2-nitroethanol are much stronger than the *intra*molecular bond of the *gauche* isomer. Indeed, the enhanced electronegativity of the oxygen atoms due to resonance among the canonical structures

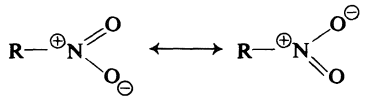

makes them better proton acceptors than, say, the halogen atoms in 2-chloro- and 2-bromoethanol. This, coupled with strong dipole–dipole interactions, leads to a high degree of molecular association in condensed phases, as reflected in the low volatility, *viz.* Table 2.

Vapor Spectra

Both the frequency and the separation of the main O—H stretching peak and its weak satellite in the i.r. spectra of the vapor are comparable with those of other 2-substituted ethanols; in particular the 2-chloro- (12). Likewise the OH torsion in the *gauche* conformer occurs at nearly the same frequency in both alcohols. From these it could be inferred that the strength of the intramolecular hydrogen bond in 2-nitroethanol is of the order of 1 kcal mol^{-1}. However, it must be

TABLE 1. Principal bands in the spectra of 2-nitroethanol (frequencies in cm^{-1})

Infrared			Raman		
Vapor*	Liquid	Crystal†	Liquid	Crystal†	Assignments
3670, 3628 ‡	3300	3290, 3220			O—H stretching
3120‡				3008, 2982	
2950		2964	2968vs	2969	
	2940	2943		2962 vs	C—H stretching
2903 ‡		2916		2943	
2892	2890	2892	2898s	2890	
2740, 2718, 2700 ‡					
1585, 1572, 1560 ‡	1562, 1550	1560, 1546, 1480	1555s	1553, 1546 m	N—O stretching (asym.)
1463, 1434	1460, 1450	1465, 1447	1458s	1458, 1445 m	CH_2 scissoring
1422, 1412	1425	1417, 1412	1425s	1418, 1404 m	
1385, 1372, 1360 ‡	1385, 1373	1392, 1373, 1361	1373vs	1388, 1372, 1362 vs	N—O stretching (sym.) OH bending
1330, 1316, 1310 ‡	1335	1336, 1325	1332m	1336, 1330, 1326 w	CH_2 wagging
1290, 1272 ‡		1267, 1262		1267	
1260, 1250	1250	1252	1254m	1255 m	CH_2 twisting (g)
1223, 1210, 1195	1200	1220, 1212, 1200	1209w	1218 m, 1199	CH_2 twisting (t)
1076	1065	1091, 1078, 1065	1074m	1089, 1075, 1061 m	C—O stretching
	1015	1035			C—C stretching
980	980	984		983	
961		973	975m	976w	C—N stretching
955‡		967		967	
894‡	890	892			CH_2 rocking (g)
886		888	889 vs	892 vs	
872	867	875	871	869	

TABLE 1—(*Concluded*)

Infrared			Raman		
Vapor*	Liquid	Crystal†	Liquid	Crystal†	Assignments
860		867			CH_2 rocking (t)
812					
800‡	800?				
787					
	700	740			
672		688			OH torsion
654‡					
639		638			
	620	625	610m	623vw	NO_2 scissoring
613		613			
589		590		594vw	NO_2 wagging
545					
533	540	536	520vw	536w	CCO bending (g)
520‡		512			
490					
480	490	489	476vw		NO_2 rocking
439		421		426	
428	435	415		417w	CCO bending (t)
		393			
		324		334	
		315		310vw	CCN bending
		280	280vw		
260?					OH torsion?

*At 80°.
†At liquid N_2 temperature.
‡Strong band in the spectrum of nitroethylene (20).

remembered that such correlations are not too reliable for strongly bent hydrogen bonds. In spite of the greater flexibility of the six-membered chelate ring there is no guarantee that the hydrogen bond in the nitroalcohol is closer to linearity than in the haloethanols.

The various other criteria used previously to evaluate the enthalpy difference between the *gauche* and the *trans* conformers are not applicable here, unfortunately. Indeed, study of the temperature dependence of the relative intensity of structure sensitive bands is precluded by decomposition upon heating. Below 50 or 60° the bands were too weak for reliable intensity measurements, even with a 10-m path. Then, beginning at about 80° dehydration of the alcohol became noticeable as revealed by appearance of the stronger bands of nitroethylene (20). It turns out that most of the conformation sensitive bands, such as the CH_2 twisting and rocking, and the C—N stretching are nearly coincident in both spectra. As for the low-frequency skeleton bending modes, they are very poorly characterized, as may be judged from Fig. 1A. Lastly, the C—O stretching frequency is not appreciably affected by changes in the azimuthal angle of the molecule.

For the same reason intensity measurements on the two O—H stretching peaks at 3670 and 3628 cm^{-1} were hampered by the strong rotational structure of the water bands which altered seriously the contour of the main nitroalcohol doublet. Still, from visual observation it appeared that the relative intensity of the *gauche* and *trans* bands did not change nearly as much with temperature as, for instance, in the 2-haloethanols. Under such conditions it was illusory to look for a third O—H stretching component corresponding to that observed in dilute CCl_4 solutions (4, 5). Conceivably this could be due to a solvent effect. At any rate the hypothesis of two *gauche* conformers involving respectively one, and the two oxygen atoms of the nitro group is not too convincing. As mentioned above it cannot account for the absence of the triplet feature in other nitroalcohols. In addition, stereochemistry shows

TABLE 2

Alcohol	Molecular weight	Boiling point (°C)
2-Nitroethanol	91	198
2-Chloroethanol	80	129
2-Bromoethanol	125	150

Can. J. Chem. Downloaded from www.nrcresearchpress.com by 210.87.254.5 on 09/05/12
For personal use only.

that rotation of the NO_2 group about its axis to bring the two oxygen atoms equidistant to the OH group will also bring the proton much closer to the nitrogen atom. The latter is a very poor acceptor in this case, due to the formal positive charge from resonance.

To complicate further the situation, another decomposition reaction occured at temperature above 120° as confirmed by emergence of a strong aldehyde band around 1720 cm^{-1}. The formation of formaldehyde from 2-nitroethanol under various influences, in particular alkylating agents, has been reported before (10). From intensity measurements on the characteristic band of nitroethylene at 800 cm^{-1} the dehydration reaction was found to be endothermic by some 5 kcal. This is only half as large as expected from bond energy considerations.

In conclusion it is clear that a quantitative study of rotational isomerism in 2-nitroethanol would require much more elaborate means than used so far in this series of investigations.

The authors are grateful to the National Research Council of Canada for a continuing research grant. The interest and cooperation of Dr. Michel Schneider were most valuable.

1. S. Malinowski and T. Urbański. Roczniki Chem. **25**, 183 (1951).
2. M. Kuhn, W. Lüettke, and R. Mecke. Z. Anal. Chem. **170**, 106 (1959).
3. Z. Eckstein, P. Gluziński, W. Sobótka, and T. Urbański. J. Chem. Soc. 1370 (1961).
4. W. F. Baitinger, P. von R. Schleyer, T. S. S. R. Murty, and L. Robinson. Tetrahedron, **20**, 1635 (1964).
5. P. J. Krueger and H. D. Mettee. Can. J. Chem. **43**, 2888 (1965).
6. H. E. Ungnade, E. D. Loughran, and L. W. Kissinger. J. Phys. Chem. **66**, 2643 (1962).
7. H. E. Ungnade and L. W. Kissinger. Tetrahedron, **19**, Suppl. 1, 121 (1963).
8. P. Buckley and P. A. Giguère. Can. J. Chem. **45**, 397 (1967).
9. W. E. Norland and P. J. Hartman. J. Am. Chem. Soc. **76**, 3227 (1954).
10. V. I. Burmistrov and V. M. Bashinova. Nefterpererab. Neftekhim. 1968, 21–3. in Chem. Abstr. **68**, 104503m (1968).
11. P. Buckley, P. A. Giguère, and D. Yamamoto. Can. J. Chem. **46**, 2917 (1968).
12. P. Buckley, P. A. Giguère, and M. Schneider. Can. J. Chem. **47**, 901 (1969).
13. N. Levy, C. W. Scaife, and A. E. W. Smith. J. Chem. Soc. 1946, 1096.
14. Handbook of chemistry and physics. 50th Ed. The Chemical Rubber Co. Cleveland, Ohio, 1969. p. C-291.
15. M. Schneider and P. A. Giguère. J. Chim. Phys. **67**, 712 (1970).
16. L. J. Bellamy. Advances in infrared group frequencies. Methuen and Co., London, 1968, p. 231.
17. G. Varsányi, S. Holly, and L. Imre. Spectrochim. Acta, **23A**, 1205 (1967).
18. T. P. Wilson. J. Chem. Phys. **11**, 361 (1943).
19. D. C. Smith, C. Y. Pan, and J. R. Nielsen. J. Chem. Phys. **18**, 706 (1950).
20. K. R. Loos and H. H. Günthard. J. Chem. Phys. **46**, 1200 (1967).

Can. J. Chem. Downloaded from www.nrcresearchpress.com by 210.87.254.5 on 09/05/12
For personal use only.

Can. J. Chem. Downloaded from www.nrcresearchpress.com by 210.87.254.6 on 09/05/12
For personal use only.

The Reaction of *trans*-Chlorocarbonylbis(triphenylphosphine)iridium(I) with Silver Nitrate

D. N. CASH AND R. O. HARRIS[1]

Scarborough College Chemical Laboratories, Department of Chemistry, University of Toronto, 1265 Military Trail, West Hill, Ontario

Received January 14, 1971[2]

The reaction of *trans*-[$Ir^{I}(CO)(PPh_3)_2Cl$] (1) with $AgNO_3$ in acetone leads to two products. If a small excess of $AgNO_3$ is present, [$Ir^{I}(CO)(PPh_3)_2(NO_3)$] is isolated; while if a larger excess of $AgNO_3$ is present, the novel compound [$Ir(CO)(PPh_3)_2(NO_3)_2Ag$] is isolated as product. The characterization, and some reactions of these complexes are discussed.

L'action du [$Ir^{I}(CO)(PPh_3)_2Cl$]-*trans* (1) sur le $AgNO_3$ dans l'acétone, conduit à deux produits. Si un léger excès d'$AgNO_3$ est présent, le composé [$Ir^{I}(CO)(PPh_3)_2(NO_3)$] est alors isolé; si par contre un plus grand excès d'$AgNO_3$ est présent, le nouveau composé isolé est alors [$Ir(CO)(Ph_3)_2(NO_3)_2Ag$]. La caractérisation ainsi que certaines réactions avec ces complexes sont discutées.

Canadian Journal of Chemistry, **49**, 3821 (1971)

Introduction

In continuing our investigation of the reactions of oxidizing metal salts, particularly nitrates, with iridium(I) complexes (1), we have examined the reaction of [$Ir(CO)(PPh_3)_2Cl$] (2) with silver nitrate, in acetone. Nyholm and Vrieze (3) have reported that this reaction produces silver metal, but gave no conditions. On the basis of our previous work, we expected reaction 1 to occur, giving [$Ir(CO)(PPh_3)_2Cl(NO_3)_2$] as product.

$$[1]\quad [Ir(CO)(PPh_3)_2Cl] + 2AgNO_3 \xrightarrow{\text{acetone}} [Ir(CO)(PPh_3)_2Cl(NO_3)_2] + 2Ag$$

Oxidation was not observed, but instead, metathesis occurred. If only a small excess of silver nitrate was present (eq. 2) the product obtained was [$Ir(CO)(PPh_3)_2(NO_3)$] (**A**). If a large excess of silver nitrate was present (eq. 3) the product [$Ir(CO)(PPh_3)_2(NO_3)_2Ag$] (**B**) was obtained.

$$[2]\quad [Ir(CO)(PPh_3)_2Cl] + AgNO_3 \xrightarrow{\text{acetone}} [Ir(CO)(PPh_3)_2(NO_3)] + AgCl$$
(A)

$$[3]\quad [Ir(CO)(PPh_3)_2Cl] + 2AgNO_3 \xrightarrow[\text{excess } AgNO_3]{\text{acetone}} [Ir(CO)(PPh_3)_2(NO_3)_2Ag] + AgCl$$
(B)

[1]Author to whom communications should be addressed.

[2]Revision received August 11, 1971.

The properties and reactions of both these complexes are discussed below.

Results and Discussion

1. [Ir(CO)(PPh$_3$)$_2$(NO$_3$)] (A)

The complex **A** is obtained (eq. 2) as a bright yellow solid, soluble in chloroform, dichloromethane, and benzene, and insoluble in alcohols, ether, and alkanes. From analysis (Table 1) and i.r. spectrum (Table 2), and from the chemical reactivity noted below, the complex is taken to be the nitrato analogue of the square planar d^8 complex *trans*-[$Ir(CO)(PPh_3)_2Cl$] (2). From the i.r. spectrum, part of which is reproduced in Fig. 1, the nitrato ligand is seen to be co-ordinated to the metal ion (4), although the exact nature of the linkage cannot be deduced by this means (5).

Complexes of d^8 iridium(I) of this type are known to react with molecular oxygen (6), sulfur dioxide (7), olefins such as tetracyanoethylene (8), cupric halides (1), halogens (9), and mercuric salts (3). Complex **A** is similarly reactive. Analysis results and i.r. spectra for all the products of the reactions discussed below are given in Tables 1 and 2, respectively. Except where noted, the i.r. spectrum of each product contained absorptions due to co-ordinated nitrato ligand.

In solution, **A** reacts irreversibly (eq. 4) with molecular oxygen to form [$Ir(CO)(PPh_3)_2(NO_3)(O_2)$] (**C**), which is unstable in solution, decomposing over a period of minutes to uncharacterized products. As a solid, **C** is stable in air for a period of days. Complex **C** reacts rapidly (eq. 5)

Can. J. Chem. Downloaded from www.nrcresearchpress.com by 210.87.254.6 on 09/05/12
For personal use only.

TABLE 1. Analysis results

	Compound	Color	Elemental analysis								
			Carbon		Hydrogen		Nitrogen		Other		
			Obsd.	Calcd.	Obsd.	Calcd.	Obsd.	Calcd.	Element	Obsd.	Calcd.
A	$[Ir(CO)(PPh_3)_2(NO_3)]$	Yellow	55.3	55.0	3.9	3.7	1.6	1.7	Cl	1.0	0
B	$[Ir(CO)(PPh_3)_2(NO_3)_2Ag]$	Brown	45.5	45.5	3.2	3.1	3.1	2.9	Ag	10.8	11.1
C	$[Ir(CO)(PPh_3)_2(NO_3)(O_2)]$	Orange	52.3	52.9	3.9	3.6	1.8	1.7			
D	$[Ir(CO)(PPh_3)_2(NO_3)(SO_4)]\cdot\frac{1}{2}CHCl_3$	Yellow	45.9	46.7	3.5	3.2	1.4	1.5	Cl	5.5	6.0
E	$[Ir(CO)(PPh_3)_2(NO_3)(SO_2)]$	Green	50.8	51.0	3.7	3.5	0.6	1.6	Cl	<0.2	0
F	$[Ir(CO)(PPh_3)_2(NO_3)(TCNE)]$	Yellow	56.4	55.2	3.5	3.2	7.0	7.5			
G	$[Ir(CO)(PPh_3)_2(NO_3)Cl_2]$	Yellow	50.2	50.6	3.8	3.4	1.6	1.6	Cl	9.1	8.1
H	$[Ir(CO)(PPh_3)_2(NO_3)Br_2]$	Yellow	45.8	45.9	3.4	3.1	1.2	1.5	Br	16.0	16.5
I	$[Ir(CO)(PPh_3)_2(NO_3)I_2]$	Orange	42.9	41.9	3.1	2.8	0.8	1.3	I	23.0	23.9
J	$[Ir(CO)(PPh_3)_2(NO_3)Cl(HgCl)]\cdot\frac{1}{2}CHCl_3$	White	38.5	39.5	3.3	2.7	1.1	1.2	Cl	10.4	10.9
K	$[Ir(CO)(PPh_3)_2(NO_3)_2(HgNO_3)]$	White	38.1	39.2	2.6	2.7	3.4	3.7	Cl	0.7	0
L	$[Ir(CO)_3(PPh_3)_2](NO_3)$	Yellow	53.7	54.2	3.7	3.5	1.6	1.6			
M	$[Ir(CO)(PPh_3)_2(NO_3)_2I]$	Orange	45.2	44.6	3.3	3.0	2.5	2.8	I	13.1	12.7
N	$[Ir(CO)(PPh_3)_2(NO_3)_2(HgCl)]$	White	39.9	40.2	2.8	2.7	2.5	2.5	Cl	4.6	3.2

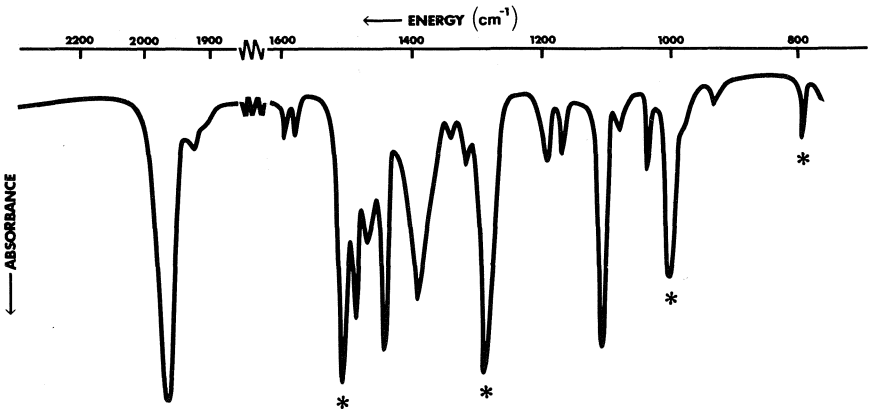

FIG. 1. Infrared spectrum of $[Ir(CO)(PPh_3)_2(NO_3)]$, * denotes a nitrato ligand absorption.

TABLE 2. Infrared absorptions (cm^{-1})[a]

	Compound	Nitrato modes[b]	Carbonyl modes[c]	Other modes
A	$[Ir(CO)(PPh_3)_2(NO_3)]$	1501 vs, sp 1281 s, sp 996 m, sp[d] 790 w, sp	1965 vvs, sp 612 mw, sp (1975 s, mbr)[i]	~310 w, br[e]
B	$[Ir(CO)(PPh_3)_2(NO_3)_2Ag]$	1499 vs, sp 1273, 1263 s, sp 995 m, sp[d] 789 w, sp	1992 vvs, sp 608 mw, sp (2005 w, sp)[i]	814 vw, sp[e] ~310 vw, vbr[e]
C	$[Ir(CO)(PPh_3)_2(NO_3)(O_2)]$	1508 vs, sp 1269 vs, sp 967 s, sp 787 w, sp	2017 vvs, sp 565 mw, sp (2031 s, sp)[i]	862 m, sp[f]
D	$[Ir(CO)(PPh_3)_2(NO_3)(SO_4)]\cdot\frac{1}{2}CHCl_3$	1549 vs, sp 1271 vs, sp 946 s, sp ~770 sh, w[d]	2067 vvs, sp	1313 s, sp[g] 1177 vs, sp[g] 887 m, sp[g] 840 m, sp[g] 673 s, sp[g]
E	$[Ir(CO)(PPh_3)_2(NO_3)(SO_2)]$	1516 vs, sp 1271 vs, sp 988, 980 m, sp 786 w, sp	~2025 vvs, br 592 m, sp	1205 s, sp[h] 1049 vs, sp[h] 335(sh315) m, br[e] 547 m, sp[e]
F	$[Ir(CO)(PPh_3)_2(NO_3)(TCNE)]$	1555 vs, sp 1281 vs, sp 948 m, sp 780 vw, sp	2067 vvs, sp 2040 w, sp[i] 579, 564 mw, sp[i]	2228 m, sp[j] ~335 mw, br[e]
G	$[Ir(CO)(PPh_3)_2(NO_3)Cl_2]$	1523 vs, sp 1283 vs, sp 985, 976 m, sp[i] 787 w, sp	2065 vvs, sp 2050 m, sp[i] 576 m, 565 mw, sp[i]	339 ms, sp[k]
H	$[Ir(CO)(PPh_3)_2(NO_3)Br_2]$	1521 vs, sp 1281 vs, sp 984(sh 974) m, sp[i] 787 w, sp	2063 vvs, sp 2051 w, sp[i] 577, 557 mw, sp[i]	
I	$[Ir(CO)(PPh_3)_2(NO_3)I_2]$	1518 vs, sp 1279 vs, sp 981(sh 969) m, sp 789 w, sp	2063 vvs, sp 579 mw, sp	545 mw, sp[e]

Can. J. Chem. Downloaded from www.nrcresearchpress.com by 210.87.254.6 on 09/05/12
For personal use only.

TABLE 2 *(Concluded)*

	Compound	Nitrato modes[b]	Carbonyl modes[c]	Other modes
J	$[Ir(CO)(PPh_3)_2(NO_3)Cl(HgCl)]\cdot\frac{1}{2}CHCl_3$	1502 vs, sp 1259 vvs, sp 986 s, sp 789 w, sp	2043 vvs, 2007 m, sp[i] 580 m, 568 mw, 551 mw, 545 ms, sp[i] (2047 vs, sp)[l]	~320 m, br[e] 278 ms, sp[e]
K	$[Ir(CO)(PPh_3)_2(NO_3)_2(HgNO_3)]$	1519 s, 1509 vs, 1494 s, sp[i] 1261, 1253 vs, sp[i] 978, 960 s, sp[i] 786 w, sp	2042 vvs, 2000 w, sp[i] 580, 554 m, sp[i] (2071 vs, sp)[l]	305 mw, br[e] 278 ms, br[e]
L	$[Ir(CO)_3(PPh_3)_2](NO_3)$	1355 vs, br[m] 829 w, sp[m]	2074 w, 2016, 2007 vvs, sp[i]	361 s, sp[e]
M	$[Ir(CO)(PPh_3)_2(NO_3)_2I]$	1526 vs, sp 1278 s, 1262 vs, sp[i] 972 ms, 964 s, sp[i] 783 mw, sp	2071 vvs, 2056 m, sp[i] 572, 553 m, sp[i]	332(sh 305) m, br[e]
N	$[Ir(CO)(PPh_3)_2(NO_3)_2(HgCl)]$	1502 vs, 1490 ms, sp[i] 1269 ms, 1255 vs, sp[i] 980 (sh 992) s, sp[i] 788 w, mbr	2054 vs, 2049 vvs, sp[i] 581 m, 557 w, 550 w, 540 vw, sp[i] (2057 vvs, sp)[l]	339 ms, sp[e] 304 m, sp[e] 269 ms, sp[e]

[a]All spectra were recorded as Nujol mulls of the solids, except as noted. All triphenylphosphine ligand modes have been omitted from the Table (19). v = very, s = strong, m = medium, w = weak, sp = sharp, br = broad, sh = shoulder.
[b]Reference 4.
[c]Reference 20.
[d]Overlaps a PPh_3 mode.
[e]Unassigned mode.
[f]Ir–O_2 mode (23).
[g]SO_4 modes (10).
[h]Ir–SO_2 modes (13).
[i]Splitting due to the presence of more than one isomer, or to correlation effects in the solid (21).
[j]Tetracyanoethylene mode (8).
[k]Ir–Cl stretching mode (22).
[l]$CHCl_3$ solution spectrum.
[m]Ionic nitrate mode (4).

in solution with sulfur dioxide gas, as do similar molecular oxygen complexes (10), to produce a bidentate sulfato complex. The product obtained from chloroform – petroleum ether was $[Ir(CO)(PPh_3)_2(NO_3)(SO_4)]\cdot\frac{1}{2}CHCl_3$ (**D**).

$$[4]\quad \underset{\textbf{(A)}}{[Ir(CO)(PPh_3)_2(NO_3)]} + O_2 \xrightarrow{CHCl_3} \underset{\textbf{(C)}}{[Ir(CO)(PPh_3)_2(NO_3)(O_2)]}$$

$$[5]\quad \underset{\textbf{(C)}}{[Ir(CO)(PPh_3)_2(NO_3)(O_2)]} + SO_2 \xrightarrow{CHCl_3} \underset{\textbf{(D)}}{[Ir(CO)(PPh_3)_2(NO_3)(SO_4)]}$$

Complex **A** reacts readily (eq. 6) in the solid state with sulfur dioxide gas, forming $[Ir(CO)(PPh_3)_2(NO_3)(SO_2)]$ (**E**) as product. The green solid **E** loses sulfur dioxide very slowly at room temperature, even under vacuum.

Complex **A** reacts in benzene (eq. 7) with the olefin tetracyanoethylene (TCNE) to give the product $[Ir(CO)(PPh_3)_2(NO_3)(TCNE)]$ (**F**). Complex **F** is soluble in chloroform and dichloromethane, but rapidly decomposes, preventing recrystallization.

$$[6]\quad \underset{\textbf{(A)}}{[Ir(CO)(PPh_3)_2(NO_3)]} + SO_2 \rightarrow \underset{\textbf{(E)}}{[Ir(CO)(PPh_3)_2(NO_3)(SO_2)]}$$

$$[7]\quad \underset{\textbf{(A)}}{[Ir(CO)(PPh_3)_2(NO_3)]} + TCNE \xrightarrow{C_6H_6} \underset{\textbf{(F)}}{[Ir(CO)(PPh_3)_2(NO_3)(TCNE)]}$$

With cupric halides in acetone, **A** reacts (eq. 8) to form the dihalonitrato complexes $[Ir(CO)(PPh_3)_2(NO_3)X_2]$ (where $X^- = Cl^-$ and Br^-). With iodine in benzene solution, **A** reacts (eq. 9) to give a similar diiodo complex.

$$[8]\quad \underset{\textbf{(A)}}{[Ir(CO)(PPh_3)_2(NO_3)]} + 2CuX_2 \xrightarrow[X^- = Cl^-, Br^-]{\text{acetone}} \underset{\textbf{(G)}\ X^- = Cl^-;\ \textbf{(H)}\ X^- = Br^-}{[Ir(CO)(PPh_3)_2(NO_3)X_2]} + 2CuX$$

Can. J. Chem. Downloaded from www.nrcresearchpress.com by 210.87.254.6 on 09/05/12
For personal use only.

Can. J. Chem. Downloaded from www.nrcresearchpress.com by 210.87.254.6 on 09/05/12
For personal use only.

[9] $[Ir(CO)(PPh_3)_2(NO_3)] + I_2 \xrightarrow{C_6H_6} [Ir(CO)(PPh_3)_2(NO_3)I_2]$
(A) (I)

In acetone, **A** reacts (eq. 10) with mercuric chloride and mercuric nitrate to give the products (when recrystallized from chloroform) $[Ir(CO)(PPh_3)_2(NO_3)Cl(HgCl)]\cdot CHCl_3$ (**J**) and $[Ir(CO)(PPh_3)_2(NO_3)_2(HgNO_3)]$ (**K**), respectively. In chloroform solution, each of these complexes displays only one carbonyl stretching absorption in the i.r. spectrum, which suggests that in each case only one isomer is present. A possible structure is shown in Fig. 3.

In chloroform or dichloromethane solution, **A** reacts readily (eq. 11) with carbon monoxide gas, losing the nitrato ligand, and forming the soluble nitrate salt of the cation $[Ir(CO)_3(PPh_3)_2]^+$. Other salts of this cation have recently been reported (11), prepared by a different route. This illustrates the relatively poor bonding which exists between the nitrato ligand and the d^8 metal ion in complex **A**. Similar reaction of the halide analogues does not result in expulsion of the anion from the co-ordination sphere (12).

[10] $[Ir(CO)(PPh_3)_2(NO_3)] + HgX_2 \xrightarrow{\text{acetone}} [Ir(CO)(PPh_3)_2(NO_3)X(HgX)]$
(A) $X^- = Cl^-, NO_3^-$ (J) $X^- = Cl^-$; (K) $X^- = NO_3^-$

[11] $[Ir(CO)(PPh_3)_2(NO_3)] + 2CO \xrightarrow[CO]{CH_2Cl_2} [Ir(CO)_3(PPh_3)_2](NO_3)$
(A) (L)

The i.r. spectrum of the solid **L** has no absorptions due to co-ordinated nitrato ligand, but does contain absorptions assigned to an ionic nitrate group.

2. [Ir(CO)(PPh$_3$)$_2$(NO$_3$)$_2$Ag] (B)

The complex **B** (eq. 3) is obtained as very small, golden brown crystals, soluble in chloroform and dichloromethane, much less so in benzene, and insoluble in alcohols, ether, and alkanes. Analysis (Table 1) supports the empirical formula given. The i.r. spectrum of the solid (Table 2), part of which is reproduced in Fig. 2, has absorptions at 1499, 1273–1263 (a partially resolved doublet), 995, and 789 cm^{-1}, which have been assigned to co-ordinated nitrato ligands, absorptions at 1992 and 608 cm^{-1} which have been assigned to carbonyl ligand, and absorptions due to triphenylphosphine ligands. A weak but sharp absorption at 814 cm^{-1} has not been assigned, but may be an additional nitrato mode. In solution in chloroform, the carbonyl stretching absorption is found at 2005 cm^{-1}. An attempt to obtain a Raman spectrum was unsuccessful as the colored complex decomposed in the laser beam.

The solid is apparently indefinitely stable in light and air. It is essentially diamagnetic at room temperature (Gouy method), and is non-conducting in dichloromethane solution ($\sim 1.5 \times 10^{-4}$ *M*). Although the complex is not sufficiently soluble for an accurate molecular weight to be determined, a molecular weight measurement (*M*) in chloroform solution ($\sim 3.5 \times 10^{-3}$ *M*) was carried out, and the value $M = 945 \pm 50$ was obtained. This compares with the value $M = 976$ for the empirical formula unit $[Ir(CO)(PPh_3)_2(NO_3)_2Ag]$. The complex is known, however, to decompose slowly in solution (see below). From these observations, complex **B** is believed to be non-ionic and monomeric in non-polar solvents such as chloroform and dichloromethane.

In acetonitrile, a molecular weight (*M*) determination (osmometric) gave the result $M = 335 \pm 20$ (Schwarzkopf, New York). This result can be explained by the dissociation in eq. 12, which produces three particles per formula unit. Acetonitrile is a solvent of high dielectric, which is, moreover, a good solvent for silver ions.

[12] $[Ir(CO)(PPh_3)_2(NO_3)_2Ag] \xrightarrow[(N_2)]{CH_3CN} [Ir(CO)(PPh_3)_2(NO_3)] + Ag^+ + NO_3^-$
(B) (A)

To further investigate the complex **B**, a series of chemical reactions was carried out, parallel to those undergone by complex **A**. The analysis results and i.r. spectra of the products of these reactions are given in Tables 1 and 2, respectively.

Complex **B** reacts in solution with molecular

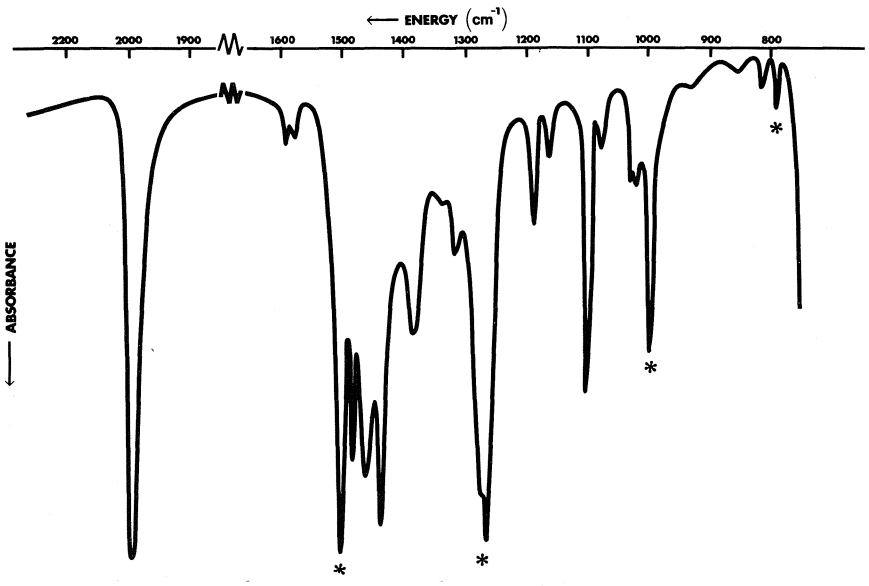

FIG. 2. Infrared spectrum of $[Ir(CO)(PPh_3)_2(NO_3)_2Ag]$, * denotes a nitrato ligand absorption.

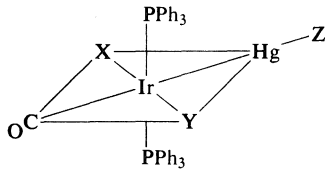

FIG. 3. Structure of one isomer of $[Ir(CO)(PPh_3)_2(X)(Y)(HgZ)]$. (*1*) X = Cl, Y = NO_3, Z = Cl; (*2*) X = NO_3, Y = NO_3, Z = NO_3; (*3*) X = NO_3, Y = NO_3, Z = Cl.

oxygen, and this reaction is slow enough that it may be followed in an open i.r. cell (0.5 mm sodium chloride cavity cell). Over a period of several minutes, absorption at 2005 cm^{-1} due to carbonyl stretching in **B** diminishes, while a new absorption at $\sim$2030 cm^{-1} appears and grows. The new band is due to carbonyl stretching in $[Ir(CO)(PPh_3)_2(NO_3)(O_2)]$ (**C**), which is the product of the reaction. This product is identical to that prepared from **A** (eq. 4). Preparatively, **C** can be prepared from **B** only in poor yield, because **C** is unstable in solution over the time scale of the reaction. It is proposed that this reaction is not a reaction of **B**, but is instead a slow dissociation (eq. 12) producing **A**, followed by the rapid reaction of **A** with molecular oxygen (eq. 4) producing **C**.

Similarly, **B** reacts with tetracyanoethylene in benzene to give a solid which has in its i.r. spectrum absorptions identical to those found for complex **F**, previously formed by the direct reaction of **A** and tetracyanoethylene (eq. 7). Complex **B** reacts in acetone with cupric halides to produce products which are identical to **G** and **H**, previously obtained by the reaction of **A** with cupric halides (eq. 8). It is assumed that all these reactions proceed by an initial dissociation (eq. 12).

As a solid, **B** does not react, however, with sulfur dioxide gas. Complexes of the type $[Ir(CO)(PPh_3)_2X]$ are known to react readily with this gas, even when dispersed as solids in potassium bromide discs (13). The lack of reaction suggests that the iridium ion in **B** is not as nucleophilic as that in **A**. Moreover, the possibility that **B** is a cocrystalline form of **A** and silver nitrate, already at variance with previous results, is further contradicted by this observation.

With iodine, and with mercuric chloride, complex **B** reacts to give products which are not identical to those produced from **A** under the same conditions. Reacting with iodine in benzene solution (eq. 13), **B** gives $[Ir(CO)(PPh_3)_2(NO_3)_2I]$ (**M**) as product, and reacting with mercuric chloride in acetone (eq. 14), **B** gives $[Ir(CO)(PPh_3)_2(NO_3)_2(HgCl)]$ (**N**) as product.

The i.r. spectrum of solid **M** contains absorptions due to co-ordinated nitrato ligands which are very similar, both in frequencies and intensities, to those observed in the i.r. spectra of a series

Can. J. Chem. Downloaded from www.nrcresearchpress.com by 210.87.254.6 on 09/05/12
For personal use only.

Can. J. Chem. Downloaded from www.nrcresearchpress.com by 210.87.254.6 on 09/05/12
For personal use only.

[13] $$[Ir(CO)(PPh_3)_2(NO_3)_2Ag] + I_2 \xrightarrow{C_6H_6} [Ir(CO)(PPh_3)_2(NO_3)_2I] + AgI$$
(B) (M)

[14] $$[Ir(CO)(PPh_3)_2(NO_3)_2Ag] + HgCl_2 \xrightarrow{\text{acetone}} [Ir(CO)(PPh_3)_2(NO_3)_2(HgCl)] + AgCl$$
(B) (N)

of similar dinitrato complexes $[Ir(CO)(PPh_3)_2(NO_3)_2X]$ (where $X^- = NCO^-$, N_3^-, NCS^-, Cl^-, and Br^-) which we have previously reported (1). The preparative route we then employed did not produce $[Ir(CO)(PPh_3)_2(NO_3)_2I]$, which is found to be stable when formed.

The solution i.r. spectrum of complex **N** contains only one carbonyl stretching absorption, indicating that only one isomer is present. A possible structure is shown in Fig. 3, emphasizing the similarity of **N** to the complexes **J** and **K** which were previously prepared from **A** (eq. 10).

The mechanism of reactions 13 and 14 is unknown. In each case, an insoluble silver halide is formed, and a product results in which there are two nitrato ligands co-ordinated to iridium. The conditions necessary for such a product to be obtained seem to be restricted. When bromine is used in place of iodine in reaction 13, the major product is found to be $[Ir(CO)(PPh_3)_2(NO_3)Br_2]$ (identical to complex **H**). When hydrogen bromide is used in place of iodine, a mixture of carbonyl hydrido-bromo complexes of iridium(III) results, which contain no co-ordinated nitrato ligand.

Reaction of **B** with mercuric nitrate in acetone (eq. 15) gives a product identical to complex **K**, prepared previously by reaction of **A** with mercuric nitrate (eq. 10).

[15] $$[Ir(CO)(PPh_3)_2(NO_3)_2Ag] + Hg(NO_3)_2 \xrightarrow{\text{acetone}} [Ir(CO)(PPh_3)_2(NO_3)_2(HgNO_3)] + AgNO_3$$
(B) (K)

The observations on **B** may now be summarized. Analysis shows the complex to have the empirical formula $[Ir(CO)(PPh_3)_2(NO_3)_2Ag]$. It may be dissolved in, and recovered unchanged from, solution in low polarity solvents such as chloroform and dichloromethane, in which it behaves as a non-ionic, monomeric solute of the formula given. In more ionizing solvents, it dissociates into three particles per formula weight (eq. 12); the postulated dissociation is supported by the chemical reactivity of the complex, which in many of its reactions gives the same products as those given by the complex **A**. In other reactions, however, **B** loses silver, but retains both nitrato groups as co-ordinated ligands.

Its i.r. spectrum shows triphenylphosphine, carbon monoxide, and nitrate to be present as ligands, there being no indication of any ionic nitrate. The absence of any large splitting of the nitrato absorptions suggests that both ligands are present in very similar, if not identical environments. The frequencies of the absorptions indicate both nitrato ligands to be co-ordinated to the iridium ion. However, some interaction of the nitrates with the silver ion is not ruled out. The position of the carbonyl stretching frequency suggests an iridium center part way between the +1 and +3 oxidation state (14).

From the above information, a tentative structure is proposed (Fig. 4). An iridium silver bond is assumed, although in the absence of a Raman spectrum or low frequency i.r. spectrum this cannot be confirmed. Several complexes containing transition metal to silver bonds are known (15); in all previous examples the silver ion is stabilized by co-ordination of some ligand or ligands. In this example, interaction of the silver ion with the

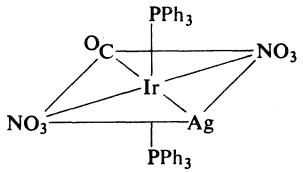

trans-bisphosphine, *trans*-dinitrato isomer

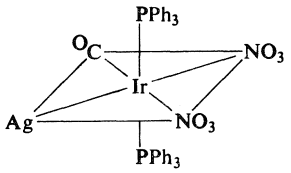

trans-bisphosphine, *cis*-dinitrato isomer

FIG. 4. Proposed structure of $[Ir(CO)(PPh_3)_2(NO_3)_2Ag]$.

Can. J. Chem. Downloaded from www.nrcresearchpress.com by 210.87.254.6 on 09/05/12
For personal use only.

nitrato ligands, or with the π-electrons of the phenyl rings of the phosphines may account for the known stability of **B**. Such interactions are not shown in Fig. 4.

The molecule of Fig. 4 can be considered to be an adduct of $[Ir(CO)(PPh_3)_2(NO_3)]$ with silver nitrate. The d^8 iridium (I) ion may act as a Lewis base towards the silver ion, forming a metal–metal bond. This type of iridium(I) complex is known to act as an electron donor towards molecules such as sulfur dioxide and nitrosonium ion (16). The resulting five co-ordinate, sixteen valence electron system is now stabilized by the addition of a nitrato ligand, forming the six co-ordinate, eighteen valence electron product. A similar product is obtained from the reaction of an iridium(I) complex with an aryldiazonium cation, in the presence of a co-ordinating anion (17).

Experimental

Reagents employed were analar grade or better, and solvents were solvent grade, unless otherwise noted. Iridium was acquired as $(NH_4)_2IrCl_6$ from Johnson Matthey Chemicals, "Specpure" grade. This was converted to $[Ir(CO)(PPh_3)_2Cl]$ (18) by a standard method. The latter was used as prepared, without recrystallization, so long as the i.r. spectrum indicated the absence of iridium(III) impurities.

All i.r. spectra were obtained using a Beckman IR 12 spectrophotometer, calibrated by polystyrene film. Molecular weights were obtained with a Mechrolab 302 osmometer, using M.C.B. spectroquality chloroform as solvent. Microanalysis was by Huffman Laboratories, Colorado.

Estimation of the silver composition of complex **B**, $[Ir(CO)(PPh_3)_2(NO_3)_2Ag]$, was carried out by suspending a preweighed sample (~0.1 g) in acetone (20 ml), to which concentrated nitric acid (2 ml) was added very slowly, with stirring, to decompose the complex. Several volumes of water were added, and the acetone distilled off. The solid residue, containing iridium as insoluble product species, was filtered off, and the filtrate and washings which contained silver nitrate in nitric acid was titrated potentiometrically against a standard bromide solution. The value of percentage silver (Table 2) is an average of several such determinations.

A. $[Ir(CO)(PPh_3)_2(NO_3)]$

Acetone (75 ml) was deoxygenated under argon, and $[Ir(CO)(PPh_3)_2Cl]$ (0.925 g) and $AgNO_3$ (0.45 g) were added. The slurry was warmed and stirred under argon for 1 h, when the yellow-brown product solid was recovered by addition of hot, deoxygenated water (150 ml). The solid was collected in air, washed with water, ethanol, and ether, and dried in air. Yield 0.685 g.

This solid contains silver chloride as well as the desired product. It darkens on standing in air, but the i.r. spectrum shows no change. This initial solid is suitable as a starting material for many of the preparations which follow, provided the further products may be recrystallized.

Complex **A** was purified by dissolving the initial product solid in a minimum of oxygen-free benzene (30 ml) under argon. The filtered bright yellow solution was diluted with several volumes of oxygen-free *n*-pentane. The bright yellow product powder was collected and dried in vacuum. Yield ~0.5 g (~50%).

B. $[Ir(CO)(PPh_3)_2(NO_3)_2Ag]$

Acetone (75 ml) was deoxygenated under argon, and $[Ir(CO)(PPh_3)_2Cl]$ (1.21 g) and $AgNO_3$ (6 g) added. The slurry was cooled in an ice bath and stirred under argon for an hour, when the product was recovered by the addition of oxygen-free water (150 ml). The orange-brown product solid was filtered off, washed well with water, ethanol, and ether, and dried in air. This solid contains silver chloride as well as complex **B**, but may be used as a starting material for the preparations which follow.

Complex **B** was recrystallized by dissolving the initial product solid in a minimum of oxygen-free chloroform (65 ml) under argon. The yellow solution was filtered, and an equal volume of oxygen-free ether added. The rapidly precipitated brown crystals were collected in air, washed with ether, and dried in vacuum. Yield 0.78 g (~60%).

C. $[Ir(CO)(PPh_3)_2(NO_3)(O_2)]$

(*i*) Complex **A** (0.25 g) was dissolved in chloroform (10 ml), and air was bubbled through the solution for several minutes. The orange solution was filtered, and diluted with petroleum ether (70 ml). The rapidly formed orange powder was collected after a few hours, washed with ether, and dried in vacuum. Yield 0.20 g (80%).

(*ii*) Complex **B** (0.1 g) was suspended in chloroform (5 ml), and methanol (25 ml) was added. After several days, dark orange crystals of product were recovered. Yield 0.03 g (30%).

D. $[Ir(CO)(PPh_3)_2(NO_3)(SO_4)]\cdot\frac{1}{2}CHCl_3$

Complex **C** (0.144 g) was dissolved in chloroform (15 ml), and sulfur dioxide gas was bubbled into the orange solution, which rapidly became pale yellow. After filtration, petroleum ether was added (35 ml). After a day at −5 °C, pale yellow crystals were obtained, which were washed with ether and dried in vacuum. Yield 0.135 g (75%).

E. $[Ir(CO)(PPh_3)_2(NO_3)(SO_2)]$

Complex **A**, under vacuum, was placed under an atmosphere of sulfur dioxide. The bright yellow powder was quantitatively converted to the lime green product solid over a period of minutes. Yield 100%.

F. $[Ir(CO)(PPh_3)_2(NO_3)(TCNE)]$

(*i*) Complex **A** (0.20 g) was added to a solution of excess tetracyanoethylene (TCNE) (0.1 g) in benzene (15 ml). The bright yellow solution deposited a pale yellow solid, which was collected in air, washed with a little benzene, then with ether, and dried in vacuum. Yield 0.10 g (~50%).

(*ii*) Complex **B** (0.1 g) was added to a solution of excess TCNE (0.05 g) in benzene (10 ml). After several minutes, the product solid was collected, washed with a little benzene and then ether and dried in air. This solid displays identical absorptions in the i.r. spectrum as the complex **F**. Yield 0.05 g (~50%).

Can. J. Chem. Downloaded from www.nrcresearchpress.com by 210.87.254.6 on 09/05/12
For personal use only.

G. [Ir(CO)(PPh$_3$)$_2$(NO$_3$)Cl$_2$]

(*i*) Complex **A** (0.20 g) was added to a slurry of excess $CuCl_2 \cdot 2H_2O$ (0.5 g) in acetone (20 ml), and stirred at room temperature. After 15 min, water (30 ml) was added, and the precipitated solid collected, washed with water, ethanol, and ether, and dried in air. The product was extracted into chloroform (3 × 5 ml), forming a pale green solution, which was filtered from a residue. Addition of methanol (35 ml) gave a pale yellow solid, which was collected after a day, washed with ether, and dried in vacuum. Yield 0.10 g (50%).

(*ii*) Complex **B** (0.20 g) was reacted in an identical manner, giving the same product. Yield 0.12 g (55%).

H. [Ir(CO)(PPh$_3$)$_2$(NO$_3$)Br$_2$]

(*i*) Complex **A** (0.20 g) was reacted with $CuBr_2$ (0.5 g) exactly as in the preparation of **G** above. The product was a bright yellow solid. Yield 0.11 g (50%).

(*ii*) Complex **B** (0.20 g) was reacted with $CuBr_2$ (0.5 g) as above, giving an identical bright yellow solid product. Yield 0.10 g (50%).

I. [Ir(CO)(PPh$_3$)$_2$(NO$_3$)I$_2$]

Complex **A** (0.13 g) was added to excess iodine (0.1 g) dissolved in benzene (15 ml). After stirring at room temperature for several minutes, the solution was filtered and diluted with ether (35 ml). The pale orange solid product was collected after one day, washed with ether, and dried in vacuum. Yield 0.07 g (40%).

J. [Ir(CO)(PPh$_3$)$_2$(NO$_3$)Cl(HgCl)]·½CHCl$_3$

Complex **A** (0.19 g) was added to excess $HgCl_2$ (0.09 g) in acetone solution (15 ml). After several minutes, the solvent was removed from the product white slurry by a water pump. The solid residue was extracted with chloroform (3 × 4 ml) to give a very pale yellow solution, which was filtered from a white residue. Addition of petroleum ether (30 ml) gave a rapidly formed white solid, which was collected after one day, washed with ether, and dried in vacuum. Yield 0.16 g (75%).

K. [Ir(CO)(PPh$_3$)$_2$(NO$_3$)$_2$(HgNO$_3$)]

(*i*) Complex **A** (0.10 g) was added to excess $Hg(NO_3)_2 \cdot H_2O$ (0.20 g) in acetone (15 ml). After stirring for several minutes, the solvent was removed by a water pump. The yellow residue was extracted with chloroform (3 × 4 ml), giving a colorless, opaque solution that was filtered from a yellow residue. The filtrate was diluted with petroleum ether (30 ml) to give a white powder as product. The product was collected, washed with ether, and dried in vacuum. Yield 0.11 g (90%).

(*ii*) Complex **B** (0.12 g) was reacted in an identical manner as (*i*) above, giving an identical product. Yield 0.12 g (90%).

L. [Ir(CO)$_3$(PPh$_3$)$_2$](NO$_3$)

Complex **A** (0.40 g) was suspended in dichloromethane (20 ml), and carbon monoxide gas was bubbled into the slurry, in the absence of oxygen. The solution was filtered after several minutes, and ether (100 ml) was added. After one day at −5 °C, the product was collected, and dried. The solid was recrystallized by dissolving in a minimum amount of ethanol (25 ml), followed by filtration and addition of ether (100 ml). The pale yellow solid product was collected after one day at −5 °C, washed with ether, and dried in vacuum. Yield 0.090 g (20%).

M. [Ir(CO)(PPh$_3$)$_2$(NO$_3$)$_2$I]

Complex **B** (0.16 g) was added to an excess of iodine (0.2 g) in solution in benzene (15 ml). After stirring for several minutes, the solution was filtered from a brown residue, and diluted with ether (75 ml). After one day at −5 °C, orange crystals of product were collected, washed with ether, and dried in vacuum. Yield 0.15 g (90%).

N. [Ir(CO)(PPh$_3$)$_2$(NO$_3$)$_2$(HgCl)]

Complex **B** (0.20 g) and $HgCl_2$ (0.09 g) were added to acetone (15 ml). The slurry rapidly became white, and after stirring for several minutes, was diluted with water (35 ml). The precipitated solid was filtered off, washed with water, and ether and dried in air. Extraction with dichloromethane (3 × 7 ml) gave a colorless solution which was filtered from a white residue, and diluted with petroleum ether (30 ml). A white powder rapidly separated, was collected, washed with ether, and dried in vacuum. Yield 0.10 g (45%).

Other Reactions of Complex B

(i) With Bromine

Complex **B** (0.10 g) was added to a solution of excess Br_2 (0.1 g) in benzene (10 ml). After several minutes, the solution was filtered from a residue, and diluted with ether (35 ml). After one day at −5 °C, bright yellow crystals were obtained, identical to complex **H** above, [Ir(CO)(PPh$_3$)$_2$(NO$_3$)Br$_2$]. Yield 0.06 g (50%).

(ii) With Hydrogen Bromide

Complex **B** (0.10 g) was added to benzene (15 ml) through which HBr gas was being slowly bubbled. After several minutes, the pale yellow solution was filtered from a residue, and diluted with petroleum ether (35 ml). After several hours, a product solid was collected. Yield 0.07 g. The product i.r. displayed no nitrato ligand absorptions, although carbonyl and metal-hydride absorptions characteristic of iridium(III) were observed.

The authors wish to thank the National Research Council of Canada for financial support of this work, and the Province of Ontario for fellowships to D.N.C.

1. D. N. Cash and R. O. Harris. Can. J. Chem. **49**, 867 (1971).
2. L. Vaska and J. W. DiLuzio. J. Am. Chem. Soc. **83**, 2784 (1961).
3. R. S. Nyholm and K. Vrieze. J. Chem. Soc. **5337** (1965).
4. K. Nakamoto. Infrared spectra of inorganic and coordination compounds. 2nd ed. J. Wiley, New York. 1970. pp. 171–173.
5. G. Topping. Spectrochim. Acta, **21**, 1743 (1965).
6. L. Vaska. Science, **140**, 809 (1963).
7. S. J. La Placa and J. A. Ibers. Inorg. Chem. **5**, 405 (1966).
8. W. H. Baddley. J. Am. Chem. Soc. **90**, 3705 (1968).
9. M. A. Bennett, R. J. H. Clark, and D. C. Milner. Inorg. Chem. **6**, 1647 (1967).
10. W. R. Horn, E. Weissberger, and J. P. Collman. Inorg. Chem. **9**, 2367 (1970).
11. M. J. Church, M. J. Mays, R. N. F. Simpson, and F. P. Stefanini. J. Chem. Soc. A, 2909 (1970).
12. L. Vaska. Science, **152**, 769 (1966).

13. E. C. MORONI, R. A. FRIEDEL, and I. WENDER. J. Organometal. Chem. **21**, P23 (1970).
14. L. VASKA. Accounts Chem. Res. **1**, 335 (1968).
15. M. C. BAIRD. Metal–metal bonds in transition metal chemistry. Prog. Inorg. Chem. Vol. 9. John Wiley and Sons, New York. 1968. pp. 114–118.
16. D. J. HODGSON and J. A. IBERS. Inorg. Chem. **8**, 1282 (1969).
17. A. J. DEEMING and B. L. SHAW. J. Chem. Soc. 1128 (1969).
18. J. P. COLLMAN, C. T. SEARS, and M. KUBOTA. Inorg. Syn. **11**, 103 (1968).
19. G. B. DEACON and J. H. S. GREEN. Spectrochim. Acta, **24A**, 845 (1968).
20. K. NAKAMOTO. Opus Cit. p. 192.
21. R. S. HALFORD. J. Chem. Phys. **14**, 8 (1946). I. R. BEATTIE and T. R. GILSON. Proc. Roy. Soc. London, Ser. A. **307**, 407 (1968).
22. J. M. JENKINS and B. L. SHAW. J. Chem. Soc. 6789 (1965).
23. J. A. MCGINNETY, R. J. DOEDENS, and J. A. IBERS. Inorg. Chem. **6**, 2243 (1967).

Can. J. Chem. Downloaded from www.nrcresearchpress.com by 210.87.254.6 on 09/05/12
For personal use only.

Can. J. Chem. Downloaded from www.nrcresearchpress.com by 210.87.254.105 on 09/05/12
For personal use only.

Metal Halide Ammines. 1. Thermal Analyses, Calorimetry, and Infrared Spectra of Cadmium Halide (Cl, Br, I) Derivatives

K. C. Patil and E. A. Secco

Chemistry Department, St. Francis Xavier University, Antigonish, Nova Scotia

Received May 26, 1971

The thermal analyses of cadmium halide hexammines reveal that decomposition occurs by loss of ammonia via the diammine and the monoammine. Calorimetric measurements along with related enthalpic values for the intermediate stable stages of the decomposition reaction are given.

The infrared spectral data of the diammines and monoammines are presented with their assignments.

Les analyses thermiques d'hexammines d'halogénure de cadmium indiquent que la décomposition se fait par perte d'ammoniaque via la diammine et la monoammine. Les mesures calorimétriques ainsi que les valeurs d'enthalpie correspondantes sont données pour les étapes intermédiaires stables.

Les données relatives aux spectres infrarouges des diamines et monoamines sont présentées avec leurs attributions.

Canadian Journal of Chemistry, 49, 3831 (1971)

Introduction

The reaction between cadmium halides (Cl, Br, I) and ammonia in aqueous solution is known to yield ammoniates or ammines of varying compositions depending on the reaction conditions, such as solution concentration and temperature (1–3). Although the kinetics of formation of cadmium halide diammines have been reported (4–6), no study of the mode of decomposition of these ammines has appeared in the literature.

The purpose of this paper is to report on the mode of decomposition, heat of decomposition, relative thermal stability, and infrared spectra of cadmium halide (Cl, Br, I), monoammines, diammines, and hexammines.

Experimental

All the halide diammines were prepared by the addition of liquor ammonia to saturated aqueous solutions ($>0.25\ m$) of the respective cadmium halide. The resulting precipitate was washed free from halide with distilled water, followed by washing with alcohol, and dried at room temperature in air. Dilute aqueous solutions ($<0.25\ m$) of cadmium halide are reported to yield basic halides with ammonia (7).

Cadmium halide hexammines were prepared by refluxing the anhydrous cadmium halide with anhydrous liquid ammonia for 3–4 h. The ammonia was Matheson compressed gas with a stated purity 99.99% grade. The apparatus consisted of a conical Pyrex flask containing a magnetic stirrer fitted to a condensor charged with an acetone – Dry Ice mixture (*ca.* −70 °C).

The heating curves recorded for differential thermal analysis, thermogravimetry, and calorimetry were obtained using the instrumentation described previously (8, 9). The infrared spectra of the compounds were recorded on a Perkin–Elmer Model−180 spectrophotometer using the standard pellet technique with KBr as the matrix material.

Results and Discussion

Thermogravimetry

The results of thermogravimetry are given in Table 1. The proposed reactions for each compound are those which best fit the observed weight loss; the intermediate and final products of decomposition were further confirmed by infrared and correlated with DTA curves.

The decomposition course of all the hexammines occurred via the following sequence

[1] $CdX_2 \cdot 6NH_{3(s)} \rightarrow CdX_2 \cdot 2NH_{3(s)} + 4NH_{3(g)}$

[2] $CdX_2 \cdot 2NH_{3(s)} \rightarrow CdX_2 \cdot NH_{3(s)} + NH_{3(g)}$

[3] $CdX_2 \cdot NH_{3(s)} \rightarrow CdX_{2(s)} + NH_{3(g)}$

[4] $CdX_{2(s)} \rightarrow CdX_{2(g)}$, where (X = Cl, Br, I).

The hexammines are relatively unstable, decomposing to the diammines after a few days in storage at room temperature.

The diammines prepared by aqueous precipitation show the corresponding steps 2, 3, and 4 in their decomposition pattern.

Differential Thermal Analysis

The results of DTA measurements are presented in Table 2 and the discussion is given to accompany the TG results.

The three endotherms corresponding to reaction eqs. 1 to 3 appeared for the bromide and iodide ammines; an additional endotherm due to

TABLE 1. Thermogravimetric analyses

Compound	Step number	Temperature range* (°C)	% of total weight lost: Observed	% of total weight lost: Calculated	Reaction
$CdCl_2 \cdot 6NH_3$	1	25–100	23.85	23.82	[1]
	2	190–240	29.81	29.78	[2]
	3	240–290	35.96	35.76	[3]
	4	>560			[4]
$CdBr_2 \cdot 6NH_3$	1	25–100	18.65	18.15	[1]
	2	175–210	22.65	22.55	[2]
	3	210–250	27.30	27.20	[3]
	4	>510			[4]
$CdI_2 \cdot 6NH_3$	1	25–110	14.91	14.50	[1]
	2	110–180	17.60	17.70	[2]
	3	180–300	21.00	21.00	[3]
	4	>400			[4]

*Onset and terminal temperatures.

TABLE 2. Differential thermal analyses

Compound	Peak number*	Peak temperature (°C)	Reaction
$CdCl_2 \cdot 6NH_3$	1	60	[1]
	2	260	[2]
	3	305	Fusion $CdCl_2 \cdot NH_3$
	4	330	[3*a*]
	5	360	[3*b*]
	6[a]	375	Crystallization $CdCl_2$
	7	590	Fusion $CdCl_2$
$CdBr_2 \cdot 6NH_3$	1	100	[1]
	2	290	[2]
	3	300	Fusion $CdBr_2 \cdot NH_3$
	4	350	[3]
	5	600	Fusion $CdBr_2$
$CdI_2 \cdot 6NH_3$	1	110	[1]
	2	160	[2]
	3	210	Fusion $CdI_2 \cdot NH_3$
	4	220	[3]
	5	380	Fusion CdI_2

*All endotherms except those marked with *a*.

the melting of the monoammine is observed in all compounds. The melting temperatures of the monoammines decrease in the order of Cl → Br → I which is interpreted in terms of stronger covalency of the Cd–N bond in going from chloride to iodide ammines.

The DTA curve of the chloride hexammine, Fig. 1, displays two endotherms attributed to steps 1 and 2 leading to the monoammine. The monoammine subsequently decomposed to the anhydrous chloride via two steps

[3*a*] $CdCl_2 \cdot NH_{3(l)} \rightarrow CdCl_2 \cdot \frac{1}{2}NH_{3(s)} + \frac{1}{2}NH_{3(g)}$

[3*b*] $CdCl_2 \cdot \frac{1}{2}NH_{3(s)} \rightarrow CdCl_{2(s)} + \frac{1}{2}NH_{3(g)}$

which accounts for the two endotherms at 330 and 360 °C, respectively. The residue after the 330 °C endotherm was determined thermogravimetrically to correspond to the composition $CdCl_2 \cdot \frac{1}{2}NH_3$. The small exotherm observed at 370 °C is attributed to crystallization of $CdCl_2$, confirmed by X-ray diffraction patterns of the residues immediately prior to the exothermic peak and immediately after this peak. The absence of a crystallization exotherm for $CdBr_2$ and CdI_2 is most likely due to the fact that these anhydrous halides result from a liquid phase decomposition reaction whereas anhydrous $CdCl_2$ results from a solid phase reaction.

Calorimetric Measurements

The calorimetric data, along with the related enthalpy values for decomposition of the halide ammines including two halide hydrates for comparison purposes, are presented in Table 3

Can. J. Chem. Downloaded from www.nrcresearchpress.com by 210.87.254.105 on 09/05/12
For personal use only.

TABLE 3. Calorimetric data

Compound	Reaction	Heat of decomposition† ΔH of compound decomposed (kcal/mol)	Heat of decomposition† ΔH per mol of NH_3 or H_2O formed (kcal/mol)	ΔH_f^0 (kcal/mol) This work‡	ΔH_f^0 (kcal/mol) Literature Value	Literature Reference
$CdCl_2 \cdot NH_3$	[5]	20.85±0.20*		−122.78	−124.79	18,19
					−122.50	20
$CdCl_2 \cdot 2NH_3$	[6]	13.50±0.50	13.50±0.50	−145.63	−152.82	18,19
					−150.50	20
$CdCl_2 \cdot 6NH_3$	[7]	31.50±0.50	8.0±0.2	−219.13	−217.70	18,19
					−236.50	20
$CdBr_2 \cdot 6NH_3$	[8]	47.2±0.2	12.0±0.2	−220.60	−218.1	20
$CdI_2 \cdot 6NH_3$	[9]	55.9±0.1	14.0±0.1	−196.90	−189.9	20
$CdCl_2 \cdot \frac{5}{2}H_2O$	[10]	16.50±0.50	6.6±0.2	−252.50	−269.9	20
$CdBr_2 \cdot 4H_2O$	[11]	60.0±0.5	15.0±0.1	−363.15	−356.30	20

*Includes ΔH (fusion) of $CdCl_2 \cdot NH_3$ which overlaps the decomposition reaction.
†All determinations were done in duplicate; ΔH values accompanied by average deviations.
‡ΔH_f° values of compounds used in our calculations are from ref. 3 below. The above ΔH_f° values were calculated using Kopp's Rule approximation, *i.e.* $\Delta C_p^\circ \simeq 0$.

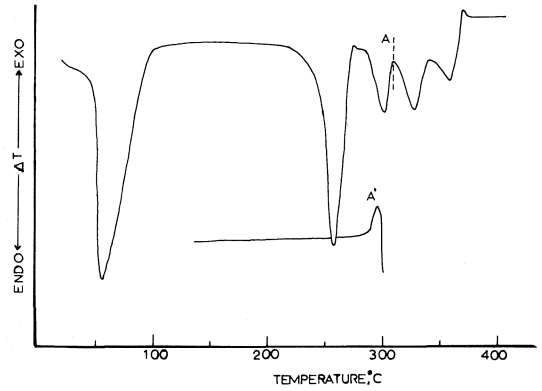

FIG. 1. Differential thermal analysis heating curve *A* for $CdCl_2 \cdot 6NH_3$ and the cooling curve *A'* from 300 °C illustrating the reversibility of the process associated with the third endotherm. The heating curve shows the additional endotherms identified with reactions 3*a* and 3*b* along with the exotherm due to crystallization.

according to the following equations showing the onset and terminal temperatures,

$$[5]\quad CdCl_2 \cdot NH_{3(s)} \xrightarrow{240\text{–}325\ ^\circ C} CdCl_{2(s)} + NH_{3(g)}$$

$$[6]\quad CdCl_2 \cdot 2NH_{3(s)} \xrightarrow{160\text{–}230\ ^\circ C} CdCl_2 \cdot NH_{3(s)} + NH_{3(g)}$$

$$[7]\quad CdCl_2 \cdot 6NH_{3(s)} \xrightarrow{25\text{–}100\ ^\circ C} CdCl_2 \cdot 2NH_{3(s)} + 4NH_{3(g)}$$

$$[8]\quad CdBr_2 \cdot 6NH_{3(s)} \xrightarrow{25\text{–}130\ ^\circ C} CdBr_2 \cdot 2NH_{3(s)} + 4NH_{3(g)}$$

$$[9]\quad CdI_2 \cdot 6NH_{3(s)} \xrightarrow{25\text{–}130\ ^\circ C} CdI_2 \cdot 2NH_{3(s)} + 4NH_{3(g)}$$

$$[10]\quad CdCl_2 \cdot 2\tfrac{1}{2}H_2O_{(s)} \xrightarrow{80\text{–}170\ ^\circ C} CdCl_{2(s)} + 2\tfrac{1}{2}H_2O_{(g)}$$

$$[11]\quad CdBr_2 \cdot 4H_2O_{(s)} \xrightarrow{25\text{–}130\ ^\circ C} CdBr_{2(s)} + 4H_2O_{(g)}$$

Our ΔH_f° values for $CdCl_2 \cdot NH_3$, $CdCl_2 \cdot 6NH_3$, and $CdBr_2 \cdot 6NH_3$ are in excellent agreement with the literature whereas a noticeable disparity is evident in the ΔH_f° values for the other compounds.

The column of values for ΔH per mole of NH_3 or H_2O formed indicates an increasing trend, $CdCl_2 \rightarrow CdBr_2 \rightarrow CdI_2$. This trend is consistent with a prediction by Chatt and co-workers (10) which suggested that the relative affinities of the halide ions for Cd^{2+} are in the direction Cl < Br < I. The order of Cd–halogen bond strength is Cl → Br → I where the difference is reported as 8–10 kcal/mol (11), thus a parallel increasing trend for the ammonia ligands is anticipated. However, in addition to the factors of ionic size and polarizability of the ligand in contributing to the stability of the metal halogen complexes (12), the role of lattice energy must also be recognized in crystalline compounds.

Infrared Spectral Data

The infrared spectra of cadmium halide hexammines (13, 14) and diammines (15, 16) already appear in the literature. In Table 4 the infrared absorption frequencies, with their

Can. J. Chem. Downloaded from www.nrcresearchpress.com by 210.87.254.105 on 09/05/12
For personal use only.

TABLE 4. Infrared absorption band frequencies*

Compound	Frequency (cm^{-1}) assignment					
	$\nu_{(NH)as}$	$\nu_{(NH)s}$	$\delta_{(NH_3)d}$	$\delta_{(NH_3)s}$	$\rho_{(NH_3)r}$	$\nu_{(M-N)}$
$CdCl_2 \cdot 2NH_3$	3350(s) 3260(s)	3160(w)	1600(m,b) 1400(w)	1220(vs,sp)	605(s) 560(s)	370(m)
$CdCl_2 \cdot NH_3$	3350(s) 3260(s)	3160(w)	1600(m,b) 1400(w)	1210(vs,sp)	600(s)	370(m)
$CdCl_2 \cdot 2ND_3$	2490(s) 2440(s)		1120(s) 1010(w)	930(s)	450(w)	350(w)
$CdBr_2 \cdot 2NH_3$	3340(s) 3250(s)	3150(w)	1600(m,b) 1400(w)	1210(vs,sp)	600(sh) 560(s)	370(m)
$CdBr_2 \cdot NH_3$	3340(s) 3250(s)	3150(w)	1600(m,b) 1400(w)	1205(vs,sp)	600(sh) 585(s,b)	370(m)
$CdI_2 \cdot 2NH_3$	3340(s) 3240(s)	3140(w)	1600(m,b) 1400(w)	1200(vs,sp)	550(s)	370(m)
$CdI_2 \cdot NH_3$	3340(s) 3240(s)	3140(w)	1600(m,b) 1400(w)	1200(vs,sp)	550(s)	370(m)
$CdI_2 \cdot 2ND_3$	2490(s) 2440(s)		1120(s) 1010(w)	925(s)	450(w)	355(w)

*vs = very strong; s = strong; m = medium; w = weak; b = broad; sp = sharp; sh = shoulder.

assignments, are presented for the diammines, monoammines, and the deuterated analogues of the diammines over the 4000–180 cm^{-1} region. The ν_H/ν_D ratios fall in the range 1.31–1.42 for the NH_3 vibrations.

The vibrational assignments are made on the basis of a simple 1:1 model (*i.e.* Cd–NH_3) where the normal modes of vibration are represented by those of a tetrahedral ZXY_3 molecule of C_{3v} symmetry.

Our data show a high degree of internal consistency for the various assignments in all ammines; the data are also in agreement with the existing literature values for the diammines. The symmetric stretching $\nu_{(NH)s}$ for the deuterated analogue is not discernible since its expected weak band at *ca.* 2320 cm^{-1} is masked by ν_3 of CO_2 present in the atmosphere. Slight shifts of 10–30 cm^{-1} are noticeable for $\nu_{(NH)s}$ and $\rho_{(NH_3)r}$ in going from $CdCl_2 \cdot NH_3 \rightarrow CdBr_2 \cdot NH_3 \rightarrow CdI_2 \cdot NH_3$.

The observation of the 370 cm^{-1} band in the monoammines confirms the $\nu_{(M-N)}$ assignment and is a step towards resolving the existing controversy (16, 17) regarding the assignment of $\nu_{(M-N)}$ and $\delta_{(N-M-N)}$ in the hexammines. The bending mode $\delta_{(N-M-N)}$ predicted to be <200 cm^{-1} was not observed in the diammines since this frequency is beyond the limits of our instrument. The slight isotopic shift evident in $\nu_{(M-N)}$, $\nu_H/\nu_D = 1.06$, suggests that this mode involves the entire NH_3 (or ND_3) mass unit; such an assumption leads to a calculated ν_H/ν_D of 1.07.

1. G. G. URAZOV and A. K. KIRAKOSYAN. Zh. Neorg. Khim. **2**, 1332 (1957).
2. A. K. KIRAKOSYAN. Russ. J. Inorg. Chem. **5**, 101 (1960).
3. A. K. KIRAKOSYAN. Russ. J. Inorg. Chem. **5**, 876 (1960).
4. M. M. PAVLYUCHENKO and T. I. TORGONSKAYA. C.A. **57**: 1599*i* (Geterongeunye Khim. Reaktsü 184 (1961)).
5. M. M. PAVLYUCHENKO and G. A. LAZERKO. Zh. Fiz. Khim. **29**, 1064 (1955).
6. G. A. LAZERKO and M. M. PAVLYUCHENKO. C.A. **51**: 16177*a*.
7. A. K. KIRAKOSYAN. Russ. J. Inorg. Chem. **7**, 1327 (1962).
8. O. K. SRIVASTAVA and E. A. SECCO. Can. J. Chem. **45**, 579 (1967).

Can. J. Chem. Downloaded from www.nrcresearchpress.com by 210.87.254.105 on 09/05/12
For personal use only.

9. P. RAMAMURTHY and E. A. SECCO. Can. J. Chem. **46**, 3605 (1968).
10. S. AHRLAND, J. CHATT, and N. R. DAVIES. Q. Rev. **12**, 265 (1958).
11. A. J. POË and M. S. VAIDYA. J. Chem. Soc. 1023 (1961).
12. A. B. BLAKE and F. A. COTTON. Inorg. Chem. **3**, 5 (1963).
13. J. M. TERRASSE, H. POULET, and J. P. MATHIEU. Spectrochim. Acta, **20**, 305 (1964).
14. L. SACCONI, A. SABATINI, and P. GANS. Inorg. Chem. **3**, 1772 (1964).
15. G. M. BARROW, R. H. KRUGER, and F. BASOLO. J. Inorg. Nucl. Chem. **2**, 340 (1956).
16. D. M. ADAMS. Metal-ligand and related vibrations. Edward Arnold Ltd., London. 1967. Chap. 6. p. 274.
17. K. NAKAMOTO. Infrared spectra of inorganic and coordination compounds. John Wiley and Sons, New York. 1963. p. 146.
18. W. BILTZ and C. MAU. Z. Anorg. Chem. **148**, 170 (1925).
19. E. TASSILLY. Ann. Chim. Phys. **17**, 38 (1899).
20. N. B. S. Circular No. 500 (1951).

Downloaded from www.nrcresearchpress.com by 210.87.254.105 on 09/05/12
For personal use only.

Can. J. Chem. Downloaded from www.nrcresearchpress.com by 210.87.254.42 on 09/05/12
For personal use only.

Electronic Spectra of Nickel Chloride in Molten Amides

M. E. Stone and K. E. Johnson,
University of Saskatchewan, Regina Campus, Regina, Saskatchewan

Received April 28, 1971

Solutions of $NiCl_2$ in molten acetamide and caprolactam have been investigated. The nature of the Ni(II) species present was found to be independent of concentration, over the concentration ranges 0.02 to 0.25 and 0.01 to 0.3 *M*, respectively; however, it was not independent of temperature. In both solvents, Ni(II) occurred mainly in octahedral environments but an increase in temperature apparently resulted in the formation of tetrahedral species.

Des mélanges de $NiCl_2$ avec l'acétamide et la caprolactame ont été étudiés. La nature des espèces Ni(II) est indépendante de la concentration sur les intervalles de concentration allant respectivement de 0.02 à 0.25 et de 0.01 à 0.3 *M*; elle n'est cependant pas indépendante de la température. Dans les deux solvants, Ni(II) se trouve principalement dans un environnement octahédrique; une augmentation de la température a cependant pour conséquence la formation d'espèces tétrahédriques.

Canadian Journal of Chemistry, **49**, 3836 (1971)

Mixtures of $NiCl_2$ with acetamide and caprolactam change color, from pale green to blue, when heated. Since color changes are often indicative of structural changes, the electronic spectra of these systems have been investigated.

Experimental

Spectra were obtained with a Cary 14H recording spectrophotometer, using a single cell. The furnace used to heat the optical cell was an adaptation of that described by Johnson, Mackenzie, and Sandoe (1). Changes included elimination of the mirror system, the light beam being passed directly through the sample. The temperature could be controlled to within ± 1 °C.

In order to correct the spectra for changes in the densities of the systems, the densities of caprolactam and acetamide were determined at various temperatures. This was done by Archimedes method, weighing a silver block in air, water, and the melts. Since the solutions expanded on heating, they decreased in molarity. In order to compare results for a constant composition, all the recorded values of optical density were divided by the density of the solvent at the temperature at which the spectrum was obtained. This treatment was based on the assumption that the densities of the solutions were the same as those of the pure solvents.

The temperature ranges used were 85 to 190 °C for acetamide and 73 to 193 °C for caprolactam; at higher temperatures the solvents discolored. The spectral range for acetamide was found to be 7.0 to 33 kK; for caprolactam it was 6.8 to 31 kK.

Results

The spectra obtained from representative $NiCl_2$/caprolactam and $NiCl_2$/acetamide mixtures by increasing the temperature are shown in Figs. 1 and 2. The densities of caprolactam and acetamide were found to be linear functions of temperature

$$p(\text{caprolactam}) = 1.0462 - 0.0005t,$$

$$p(\text{acetamide}) = 1.0763 - 0.00095t$$

In each case, a least squares fit to a straight line was computed and gave a good correlation factor (0.9645 for caprolactam taking 9 points and 0.9984 for acetamide taking 19 points).

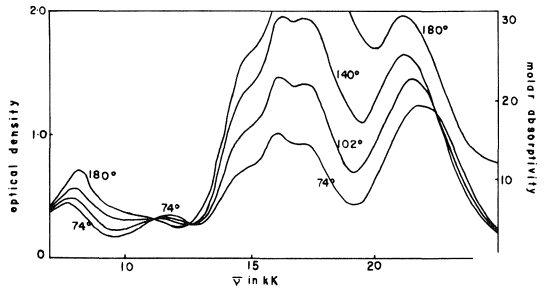

FIG. 1. Spectrum of $NiCl_2$ in molten caprolactam (0.064 *M*).

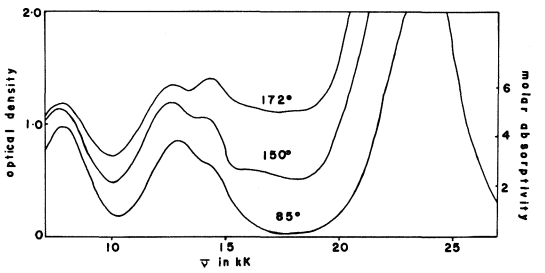

FIG. 2. Spectrum of $NiCl_2$ in molten acetamide (0.22 *M*).

TABLE 1. Electronic spectra of $NiCl_2$–caprolactam systems as results of Gaussian analyses

$NiCl_2$ in caprolactam 74 °C, 0.064 *M*		Ni $(Cap)_6Cl_2$ in EtOH room temperature (5)*		
$\bar{\nu}$ (kK)	ε ($l\,mol^{-1}\,cm^{-1}$)	$\bar{\nu}$ (kK)	ε ($l\,mol^{-1}\,cm^{-1}$)	Assignment
7.7	7	7.7	1.5	$^3T_{2g}$ (F) ← $^3A_{2g}$ (F)
11.8	5	12.7	1.5	$^3T_{1g}$ (F) ←
14.3	7	14.6	0.2	^1E (D) ←
16.0	2			
17.0	14			
		20.4	0.4	$^1T_2$ (P), $^1A_1$ (G) ←
23.1	19	23.5	4.5	$^3T_{1g}$ (P) ←

*Cap = caprolactam.

Discussion

(a) Caprolactam Solutions

Over the concentration range 0.01 to 0.3 *M*, the solutions obeyed the Bouger–Beer law that optical density is proportional to concentration. This implies that either: (*i*) a single species was present or (*ii*) there was a mixture of species whose concentration ratios remain constant when the total concentration changed.

The spectra were found to be both linear and internally linear with respect to temperature. That is (*i*) the molar absorptivity at a given wavelength was a linear function of temperature. (*ii*) each spectrum in the set could be considered as a linear combination of two other spectra in the set.

If

$$\delta = [1 - b]\varepsilon(t_1) + b\varepsilon(t_2) - \varepsilon(t_3),$$

where $\varepsilon(t)$ = molar absorptivity at a given wavelength at temperature t, then a value of b could be calculated such that δ was small compared to ε at all wavelengths.

Spectra which are both linear and internally linear with respect to temperature can arise from a single species (2). If the system under investigation had contained a single Ni(II) species, it would most likely have been a distorted octahedron, since other geometries usually correspond to spectra with higher molar absorptivities. A tetragonal distortion (D_{4h}) would have led to increased intensity and splitting of the ^3T levels, particularly $^3T_{2g}$ (F) (3). Increased intensity was observed (Table 1) but the $^3T_{1g}$ (P) ← $^3A_{2g}$ (F) and $^3T_{2g}$ (F) ← $^3A_{2g}$ (F) transitions did not appear to split.

Internal intensity can be interpreted (4) as the result of an equilibrium between two species, the spectrum of each of which is independent of temperature. As the temperature is changed, so the relative concentrations of the species change and with them the total spectrum of the mixture. However, the concentration changes arising from a chemical equilibrium are generally not linear with respect to temperature and, therefore, the total spectrum would not be expected to change linearly with temperature. Brynestad and Smith (4) have considered this problem and conclude that spectra which are both linear and internally linear with respect to temperature are not due to species in equilibrium. If they are due to a mixture, then it is a mixture of species for which the composition is independent of temperature; the extinction coefficients of the absorbing species are temperature dependent.

When the spectra of the $NiCl_2$/caprolactam solutions are compared to that of Ni$(Cap)_6Cl_2$ in ethanol at room temperature (Table 2), the former will be seen to resemble the latter in some regions but to have greater absorption in the 12–24 kK region. This absorption increases with temperature. The total spectrum of a mixture of two species should show temperature changes due to both of them. Although the weakest band (12 kK) changes little, the large increases in intensity in the bands at 8, 15, and 22 kK in the $NiCl_2$/caprolactam spectrum can be compared to those observed for octahedral Ni(II) in $KMgCl_3$ (6). Thus the mixture could have contained an octahedral species. In this case, it must also have contained a species which gave rise to the band at 17 kK. Such a band is characteristic of a tetrahedral species. However, the spectrum of tetrahedral Ni(II) in $[NiBr_4]^{2-}$ has been previously found (7) to decrease in height with increasing temperature,

Can. J. Chem. Downloaded from www.nrcresearchpress.com by 210.87.254.42 on 09/05/12
For personal use only.

TABLE 2. Electronic spectra of $NiCl_2$–acetamide systems as results of Gaussian analyses

$NiCl_2$ in acetamide 85 °C, 0.22 *M*		$[Ni(Acm)_4(H_2O)_2]Cl_2$ in EtOH room temperature (5)*		
$\bar{\nu}$ (kK)	ε (l mol^{-1} cm^{-1})	$\bar{\nu}$ (kK)	ε (l mol^{-1} cm^{-1})	Assignment
7.8	4.4	7.9	4.4	$^3T_{2g}$ (F) ← $^3A_{2g}$ (F)
12.8	3.9	12.6	4.7	$^3T_{1g}$ (F) ←
14.2	0.9	14.8	1.8	^1E (D) ←
		20.4	1.2	$^1T_2$ (P), $^1A_1$ (G) ←
23.7	10	23.7	13.7	$^3T_{1g}$ (P) ←

*Acm = acetamide.

although the results were not corrected for changes in melt density. Other tetrahedral species may behave differently but it seems unlikely that the large increase in intensity of the 17 kK band is not due to an increase in concentration.

It seems then that, in the caprolactam solutions, Ni(II) existed in an equilibrium mixture of octahedral and tetrahedral sites, the latter being favored by increasing temperature. The change in the concentration of octahderal sites would be small, leading overall to small intensity increases in the bands due to the octahedral species since the intensity of bands from each O_h site increased with temperature. In turn, these changes were modified by the sharper increase in overlapping T_d bands at ~9 kK ($^3A_2$(F) ← $^3T_1$(F)) and 17 kK ($^3T_1$(P) ← $^3T_1$(F)).

The results obtained show some similarity to those given by Angell and Gruen (8) for Ni(II) in an 11 *M* aqueous $MgCl_2$ solution at 125–180 °C. In this range, the molar absorptivity is linear with respect to temperature, although the relationship does not hold at higher temperatures (*i.e.*, up to 314 °C). The spectra were interpreted as representing a mixture of octahedral and tetrahedral complexes, so it seems that concentration changes in the Ni(II) species can be linear with respect to temperature over limited ranges.

Thus, the most plausible explanation of the spectra is that they arose from Ni(II) in a mixture of octahedral and tetrahedral environments. Since the main tetrahedral band is affected only slightly by octahedral bands, its optical density gives a measure of the concentration of the tetrahedral species. A plot of log optical density *vs.* $10^3/T$ should be linear with slope $\Delta H/2.303\bar{R}$ (9). The peaks at 14.3, 16.0 and 17.0 kK were analyzed in this way, giving the graphs shown in Fig. 3. These are linear over a region from 100 to 160 °C and are parallel to each other. The latter suggests that one tetrahedral species only is present in that temperature range. At lower temperatures, the equilibrium, if there is one, involves different species. The average value of ΔH between 100 and 160 °C is 2.2 kcal mol^{-1}. This figure is very low for an $O_h \rightarrow T_d$ Ni(II) transition, since previous workers (8, 10) obtained values of 7–17 kcal mol^{-1}. However, ΔH must vary with temperature and the type of ligand involved (see later), so the value of 2.2 kcal mol^{-1} may not be unreasonable. If the system in the 70 to 100 °C range is treated as an equilibrium mixture, then ΔH is calculated to be about 7.3 kcal mol^{-1}.

(b) Acetamide Solutions

Solutions of $NiCl_2$ in acetamide in the range of 0.02 to 0.25 molar were found to obey the Bouger–Beer Law. Unlike the caprolactam solutions, they gave spectra which were neither linear nor internally linear with respect to temperature. The spectrum obtained at 85 °C closely resembled that of $[Ni(Acm)_4(H_2O)_2]$-

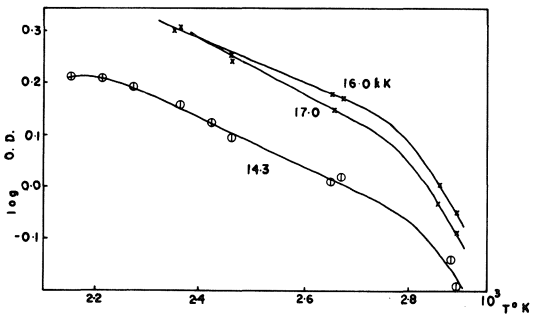

FIG. 3. Plot of $\log_{10}$ (optical density) *vs.* $10^3/T$ °A for $NiCl_2$ in caprolactam (0.064 *M*).

Can. J. Chem. Downloaded from www.nrcresearchpress.com by 210.87.254.42 on 09/05/12
For personal use only.

Cl_2 in ethanol (Table 2) and presumably corresponded to an octahedral Ni(II) site in the melt.

At higher temperatures, the spectra were similar to those obtained from the caprolactam solutions and, therefore, tetrahedral Ni(II) was probably present in the system. Since the spectra were not internally linear with respect to temperature, there could not have been a simple equilibrium between octahedral and tetrahedral species for each of which ε was independent of temperature. There could have been: (*i*) an equilibrium between octahedral and tetrahedral species for one or both of which ε varied with temperature, or (*ii*) a gradual distortion of the octahedral species toward tetrahedral symmetry. Although several octahedral $\rightleftarrows$ tetrahedral equilibria have been investigated and the temperature dependencies of the molar absorptivities have been neglected, it is possible that they are appreciable here. Temperature dependence should be greatest for centrosymmetric octahedral or pseudo-octahedral complexes, for which the transitions gain intensity by vibronic coupling. A gradual distortion would be expected to be accompanied by splitting of octahedral bands. Since this is not observed, an equilibrium is most likely.

This study does not tell us whether Cl^- is in the first coordination sphere of Ni(II) in molten amides. The ligand field parameter Δ (given by $^3A_{2g}(F) \rightarrow {}^3T_{2g}(F)$) is the same for the melts as for the compounds in EtOH solution where 6 oxygen atoms form the first links (5). The substitution of Cl which is somewhat lower in the spectrochemical series might reduce Δ a little and would also constitute a lowering of symmetry but by how much? Probably the octahedral species involve coordination by 6 amide groups and the tetrahedral species arise when a Cl substitutes for an amide, there not being enough room for 5 amides and one Cl about Ni(II). It might be interesting, within the limited temperature ranges available, to examine mixtures containing bromide instead of chloride, and alkali salts (MX).

The authors would like to thank the National Research Council of Canada for financial support.

1. K. E. JOHNSON, J. R. MACKENZIE, and J. N. SANDOE. J. Chem. Soc. A, 2644 (1968).
2. J. BRYNESTAD, C. R. BOSTON, and G. P. SMITH. J. Chem. Phys. **47**, 3179 (1967).
3. C. FURLANI and G. SARTORI. J. Inorg. Nucl. Chem. **8**, 126 (1958).
4. J. BRYNESTAD and G. P. SMITH. J. Phys. Chem. **72**, 296 (1968).
5. M. E. STONE and K. E. JOHNSON. To be published.
6. J. BRYNESTAD, H. L. YAKEL, and G. P. SMITH. J. Chem. Phys. **45**, 4652 (1966).
7. N. ISLAM. Ph.D. Thesis, New York University, New York, New York. 1968.
8. C. A. ANGELL and D. M. GRUEN. J. Amer. Chem. Soc. **88**, 5192 (1966).
9. L. I. KATZIN. J. Chem. Phys. **35**, 467 (1961).
10. D. E. SCAIFE and K. P. WOOD. Inorg. Chem. **6**, 358 (1967).

Can. J. Chem. Downloaded from www.nrcresearchpress.com by 210.87.254.42 on 09/05/12
For personal use only.

The Temperature Dependence of Transition State Volumes in Hydrolysis Reactions

MOYRA J. MACKINNON AND J. B. HYNE

Department of Chemistry, The University of Calgary, Calgary, Alberta

Received July 19, 1971

The temperature dependence of the transition state volume, $d\bar{V}^t/dT$, in a number of hydrolysis reactions is derived from pressure/rate data and partial volume temperature dependence. The values obtained for $d\bar{V}^t/dT$ vary from near zero for *p*-methylbenzyl chloride to about 0.3 ml mol^{-1} deg^{-1} for isopropyl bromide. The interpretation of the experimental and derived values for these hydrolyses is discussed in terms of charge development with accompanying solvation effects about the solute.

La dépendance du volume de l'état de transition de la température $d\bar{V}^t/dT$, dans un nombre de réactions d'hydrolyse provient de la pression/vitesse donnée et de la dépendance de la température du volume partiel. Les valeurs obtenues pour $d\bar{V}^t/dT$ varient près de zéro pour le chlorure de *p*-méthylbenzyle à environ 0.3 ml mol^{-1} deg^{-1} pour le bromure d'isopropyle. L'interprétation de ces données expérimentales pour ces hydrolyses est discutée en terme de développement de charge accompagnant les effets de solvatation autour du soluté.

Canadian Journal of Chemistry, 49, 3840 (1971)

Introduction

The temperature dependence of a transition state partial molal volume, $d\bar{V}^t/dT$, may be obtained from the temperature dependence of the activation volume, $d\bar{V}^*/dT$, and of the partial molal volume of the initial state, $d\bar{V}^g/dT$, thus

$$\frac{d\Delta V^*}{dT} = \frac{d\bar{V}^t}{dT} - \frac{d\bar{V}^g}{dT}$$

Although a few values of $d\Delta V^*/dT$ have previously been obtained experimentally (1–7), these have not been combined with partial molal volume temperature dependence data to study the transition states of these reactions. In this investigation a number of hydrolysis reactions varying in their degree of charge development in the transition state were studied and the derived values of $d\bar{V}^t/dT$ interpreted in terms of reaction mechanism.

Experimental

Materials

Water

House distilled water was passed through Illco-Way deionizing resin and then redistilled in Pyrex apparatus from which carbon dioxide was excluded. The conductivity of the water was $8 \times 10^{-7}\ \Omega^{-1}\ cm^{-1}$ at 25 °C.

Benzyl Chloride

Eastman White Label benzyl chloride was twice distilled at 10^{-3} mm Hg with collection of the middle third fraction of each distillation, $n_D^{23.0\,°C} = 1.5391$.

p-Methylbenzyl Chloride

p-Methylbenzyl chloride supplied by Aldrich Chemical Company was distilled twice at 10^{-3} mm Hg with collection of the middle third fraction each time. Analysis of the purified sample by gas–liquid chromatography showed less than 0.1% impurity, $n_D^{20} = 1.5331$.

Allyl Chloride

Matheson, Coleman and Bell allyl chloride was twice distilled under vacuum with collection of the middle third fraction each time (2), $n_D^{23.2\,°C} = 1.4155$.

n-Butyl Bromide

n-Butyl bromide supplied by Fisher Scientific Company was distilled at atmospheric pressure and a middle fraction used. Analysis by gas–liquid chromatography showed less than 0.01% impurity in the purified sample, $n_D^{23.0\,°C} = 1.4385$.

Isopropyl Bromide

Isopropyl bromide supplied by British Drug Houses was distilled at atmospheric pressure with collection of the middle third fraction, $n_D^{23.6\,°C} = 1.4251$.

Methanesulfonyl Chloride

Methanesulfonyl chloride supplied by Eastman Organic Chemicals was twice distilled under vacuum with collection of the middle third fraction each time. Analysis by gas–liquid chromatography showed less than 0.4% impurity, $n_D^{22.6\,°C} = 1.4513$.

Kinetics

The rates of hydrolysis of *p*-methylbenzyl chloride were studied in water at 1.045 and 20.00 °C over a pressure range from 1 to 2041 atm. The hydrolysis rates of *n*-butyl bromide were studied at 55.00 and 69.94 °C over a pressure range of 1 to 3402 atm. The rates for methanesulfonyl chloride were obtained at 5.00 and 21.00 °C between 1 and 2041 atm. Temperature control was maintained to ±0.01 °C in an oil bath with thermoregulator and lamp heater with an auxiliary refrigerating unit for temperatures below 20 °C.

In all reactions the rate of production of HCl resulting from the hydrolysis was followed conductimetrically, the experimental details having been previously reported (8,9). Graphical analysis of the conductivities by the Guggen-

Can. J. Chem. Downloaded from www.nrcresearchpress.com by 210.87.254.5 on 09/05/12
For personal use only.

Can. J. Chem. Downloaded from www.nrcresearchpress.com by 210.87.254.5 on 09/05/12
For personal use only.

heim method (10) yielded pseudo first-order rate constants. The high pressure systems and controls have also been previously described (8).

The hydrolysis of benzyl chloride (8), isopropyl bromide (1), and allyl chloride (2) have been studied by previous workers and their rate/pressure data were used in the determinations of $d\overline{V}^t/dT$ for these compounds.

Partial Molal Volumes

The method for determination of partial molal volumes by injection from a micro-syringe has been previously reported (11). Degassed water was used as the solvent and the temperature of the oil bath maintained to about ±0.01 °C. For temperatures below 25 °C cooling was obtained by a coil connected to an auxiliary thermostatted cryostat.

The required partial molal volumes of the reactants were obtained at two different temperatures which were as far apart as was experimentally possible for the compounds under investigation. If the upper temperature was too high it was found that the results were not reproducible due to the formation of gas bubbles.

Each determination was done at least four times. The first determination corresponded to a substrate concentration equal to that used for the kinetic runs ($\gtrsim 5 \times 10^{-4}$ *M*) where no solubility effects were found. The value of the partial molal volumes obtained with fresh solvent for each determination did not differ from those obtained with three or four repeated injections into the same solvent.

The required densities of the compounds at the temperature of injection were obtained from the literature except in the case of *p*-methylbenzyl chloride. A density value for this substrate was determined with a micro-pycnometer which had been calibrated with distilled water.

Results

Kinetics

The rate constants as a function of pressure for the hydrolysis of *p*-methylbenzyl chloride at 1.05 and 20.00 °C are presented in Table 1, and for *n*-butyl bromide at 55.00 and 69.94 °C in Table 2. Corresponding data for methanesulfonyl chloride hydrolysis at 5.00 and 21.00 °C are given in Table 3. Each rate constant is the average of at least three determinations with indicated errors being average deviations. These rate constants yield values of ΔV^* at different temperatures as shown in Table 4 together with corresponding literature values of ΔV^* for several other hydrolysis reactions. Our values of ΔV^* were obtained by fitting the rate–pressure data to a quadratic expression (12) with the indicated errors being standard deviations from this quadratic fit. In the case of isopropyl bromide, ΔV^*

TABLE 1. Rate constants for the hydrolysis of *p*-methylbenzyl chloride at 1.045 ± 0.01 and 20.00 ± 0.01 °C at various pressures

Pressure (atm)	$k \times 10^5$ s^{-1} (1.045 °C)	$k \times 10^4$ s^{-1} (20.00 °C)
1	1.463±0.020	2.377±0.012
340	1.569±0.014	—
681	1.680±0.013	2.748±0.034
1021	1.785±0.008	2.942±0.037
1361	1.909±0.011	3.082±0.020
2041	2.181±0.020	3.243±0.004

TABLE 2. Rate constants for the hydrolysis of *n*-butyl bromide at 55.00 ± 0.01 and 69.94 ± 0.01 °C at various pressures

Pressure (atm)	$k \times 10^5$ s^{-1} (55.00 °C)	$k \times 10^5$ s^{-1} (69.94 °C)
1	1.262±0.007	6.320±0.014
681	1.631±0.012	8.104±0.018
1361	2.055±0.013	10.24 ±0.10
2041	2.537±0.012	12.56 ±0.06
2722	3.094±0.023	15.39 ±0.02
3402	3.652±0.031	18.58 ±0.15

TABLE 3. Rate constants for the hydrolysis of methanesulfonyl chloride at 5.00 ± 0.01 and 21.00 ± 0.01 °C at various pressures

Pressure (atm)	$k \times 10^5$ s^{-1} (5.00 °C)	$k \times 10^4$ s^{-1} (21.00 °C)
1	1.511±0.013	1.199±0.005
340	1.765±0.014	1.388±0.013
680	2.018±0.016	1.597±0.012
1021	2.353±0.013	1.834±0.010
1361	2.718±0.008	2.070±0.024
1701	—	2.437±0.010
2041	3.684±0.024	2.736±0.010

TABLE 4. Values of ΔV^* as a function of temperture

Compound	Temperature (°C)	ΔV^*(ml/mol)
p-Methylbenzyl chloride[a]	1.05	− 4.3±0.3
	20.00	− 6.3±0.3
Benzyl chloride[b]	40.00	− 9.1±0.01
	50.25	− 9.9±0.1
	60.50	−10.3±0.2
Allyl chloride[c]	29.34	−10.2±0.7
	40.00	−10.7±0.2
	50.25	−11.4±0.1
	60.50	−12.6±0.25
n-Butyl bromide[a]	55.00	−10.5±0.1
	69.94	−10.5±0.003
Methanesulfonyl chloride[a]	5.00	− 9.6±0.3
	21.00	−10.2±0.04
Isopropyl bromide[d]	40.00	−10.7±0.02
	50.00	−10.5±0.02
	60.00	−10.2±0.0002

[a]This work.
[b]Reference 3.
[c]Reference 2.
[d]Recalculated from ref. 1.

was recalculated from the literature rate constants (1) using the quadratic expression in order that the extracted value would be comparable with the other ΔV^*'s which were obtained by this method.

Partial Molal Volumes

Table 5 presents partial molal volumes in water as a function of temperature for the same compounds for which ΔV^* data are shown in Table 4. The densities of the solutes needed in the calculation of the partial molal volumes were obtained from the literature as follows: benzyl chloride (13), allyl chloride (14), isopropyl bromide (14), *n*-butyl bromide (16), and methanesulfonyl chloride (15). The density of *p*-methylbenzyl chloride was determined at 25.1 °C = 1.06_6 g/ml, and at 23.5 °C = 1.07_0 g/ml.

Each partial molal volume in the table is the average of at least four determinations with the errors being average deviations.

Using the data in Tables 4 and 5, values of $d\overline{V}^t/dT$ may be calculated for each of the compounds under consideration by use of the equation

$$\frac{d\Delta V^*}{dT} = \frac{d\overline{V}^t}{dT} - \frac{d\overline{V}^g}{dT}$$

Table 6 presents $d\Delta V^*/dT$, $d\overline{V}^g/dT$ and $d\overline{V}^t/dT$ for the compounds in this investigation. Accumulation of uncertainties in the activation volume and the initial state partial molal volumes results in $d\overline{V}^t/dT$ values having rather large error limits. These values of $d\overline{V}^t/dT$ are shown in Fig. 1 with the required limits of uncertainty indicated for each compound. Despite the magnitude of the uncertainty in the extracted values of the temperature dependence of the transition state volume there is, nevertheless, a clear trend and a significant difference between the various hydrolyses as indicated in Fig. 1.

TABLE 5. Partial molal volumes in water at various temperatures

Compound	Temperature (°C)	Partial molal volume (ml/mol)
p-Methylbenzyl chloride	2.4	127.6±0.6
	20.4	128.1±0.6
	40.3	129.1±0.6
Benzyl chloride	20.4	112.9±0.3
	50.0	114.5±0.5
Allyl chloride	2.5	75.3±0.6
	20.4	79.1±0.4
n-Butyl bromide	20.1	105.8±0.5
	40.1	111.7±0.7
Isopropyl bromide	2.6	91.8±0.5
	40.0	102.3±0.5
Methanesulfonyl chloride	5.0	73.6±0.3
	21.0	73.6±0.3

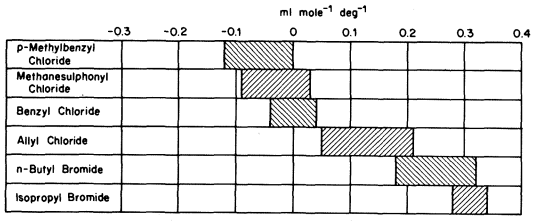

FIG. 1. Range of $d\overline{V}^t/dT$ values for transition states of several hydrolysis reactions

Discussion

A number of experimental values of $d\Delta V^*/dT$ have been previously reported (1–6) and Laidler (7) has discussed the variation of this second derivative activation parameter for several reactions involving different types of charge development or reduction in the activation process. However, since $d\Delta V^*/dT$ represents the temperature dependence of a difference, $d\overline{V}^t/dT - d\overline{V}^g/dT$, a definitive interpretation of $d\Delta V^*/dT$ variations can only be obtained through knowledge of the magnitude of the two component parts. Dissection of pseudothermodynamic parameters into their initial and transition state components has proved useful and informative in the cases of the first derivative parameters ΔH^* (17) and ΔV^* (11). Interest is currently being shown in the corresponding dissection of the second temperature derivative of the reaction rate ΔC_p^* (18) although no published data are yet available. The dissection of $d\Delta V^*/dT$ requires $d\overline{V}^g/dT$ and yields $d\overline{V}^t/dT$. This extracted value of $d\overline{V}^t/dT$ represents a further transition state property the value of which is likely to reflect the detailed nature of the solvent shell around the transition state.

Before entering into a detailed examination of the behavior of $d\Delta V^*/dT$ and its component parts, it is worth observing that despite the general utility of ΔV^* as a diagnostic probe of reaction mechanism (19), it is remarkably insensitive to changes in reaction substrate in the group of hydrolyses presented in Table 4. Apart from the one case of *p*-methylbenzyl chloride, negative ΔV^* values lie in the narrow range of −9 to −12 ml/mol for compounds with hydrolysis mecha-

Can. J. Chem. Downloaded from www.nrcresearchpress.com by 210.87.254.5 on 09/05/12
For personal use only.

TABLE 6. Values of $d\Delta V^*/dT$, $d\bar{V}^g/dT$ and $d\bar{V}^t/dT$ for the hydrolyses of several compounds

Compound	$d\Delta V^*/dT$ (ml mol^{-1} deg^{-1})	$d\bar{V}^g/dT$ (ml mol^{-1} deg^{-1})	$d\bar{V}^t/dT$ (ml mol^{-1} deg^{-1})
p-Methylbenzyl chloride	-0.10 ± 0.03	0.04 ± 0.03	-0.06 ± 0.06
Methanesulfonyl chloride	-0.03 ± 0.02	$0.0\ \pm0.04$	-0.03 ± 0.06
Benzyl chloride	-0.06 ± 0.01	0.06 ± 0.03	$0.0\ \pm0.04$
Allyl chloride	-0.08 ± 0.03	0.21 ± 0.05	0.13 ± 0.08
n-Butyl bromide	$0.0\ \pm0.01$	0.25 ± 0.06	0.25 ± 0.07
Isopropyl bromide	0.025 ± 0.001	0.28 ± 0.03	0.31 ± 0.3

nisms as different as *n*-butyl bromide and methanesulfonyl chloride. Indeed, changes in a particular ΔV^* of the same order of magnitude can be effected by *temperature* changes of some 30 to 40 °C (*vide* allyl chloride), once again emphasizing the need for caution in interpreting small changes in ΔV^* as being reflections of mechanism variations.

The experimentally determined values of $d\Delta V^*/dT$ presented in Table 6 themselves illustrate an interesting division of the hydrolysis reactions into those with negative activation volume temperature dependence and those with zero or positive temperature coefficients. Negative values for $d\Delta V^*/dT$ have commonly been associated with the development of polarity and hence electrostriction in the activation process resulting in a "tighter" transition state solvation shell whose volume is less responsive to temperature change than is the initial state. Contrariwise positive $d\Delta V^*/dT$ values have been attributed to solvation shell "loosening" in the activation process resulting from charge dispersal or decrease in polarity compared with the initial state. In all of the hydrolyses cited in Table 6 there can be little question that the transition state in the rate determining step is more polar than the initial state since in all cases the halide ion is a final product of the hydrolysis of a covalently bonded initial state. Accordingly, the zero or positive values for *n*-butyl bromide and isopropyl bromide suggest that there may well be other factors besides relative degrees of polarity or charge development in the initial and transition states involved in the determination of the temperature dependence of the volume of activation.

In discussing the results of the dissection of $d\Delta V^*/dT$ into its component parts as presented in Table 6, it must be recognized that the extracted $d\bar{V}^t/dT$ values are subject to considerable uncertainty by virtue of the accumulation of errors in the experimentally determined $d\Delta V^*/dT$ and $d\bar{V}^g/dT$ values from which the transition state parameter is derived. This question of confidence limits is always a problem with second derivative parameters and particularly so when they are obtained from the difference of two other derivatives. Despite the obvious need for caution, however, there is justification for recognizing the validity of the *trend* in $d\bar{V}^t/dT$ values demonstrated schematically in Fig. 1.

Clearly there is a trend in values from close to zero to significantly positive as the reacting substrate structure is varied from *p*-methylbenzyl chloride to isopropyl bromide. Generally speaking this order of substrate follows the decreasing degree of charge development expected in moving from the initial state to the top of the transition state energy barrier. The less developed and accessible the polarity of the system at the transition state the less tightly bound will be the solvation shell. Hence the response of the total volume of the transition state—substrate and kinetically significant solvation sheath—to temperature is expected to be greater for the less polar transition states.

A comparison of our relative values of $d\bar{V}^t/dT$ with partial molal volume temperature dependence of models such as the tetraalkylammonium bromides shows a similar trend (20). Me_4NCl with a tighter solvent shell than the larger and more hydrophobic Bu_4NBr, shows a value of $d\bar{V}^g/dT$ of about 0.11 ml mol^{-1} deg^{-1} compared to 0.25 ml mol^{-1} deg^{-1} in the case of Bu_4NBr.

The possibility of the change from chloride to bromide as the leaving anion being responsible for at least some of the change in $d\bar{V}^t/dT$ behavior must be examined. Millero and Drost-Hansen (21) compare values of $d\bar{V}^g/dT$ for tetraalkylammonium chlorides and the corresponding bromides and establish that there is no significant difference in the expansibility of the chlorides

Can. J. Chem. Downloaded from www.nrcresearchpress.com by 210.87.254.5 on 09/05/12
For personal use only.

compared to the bromides. This would seem to indicate that, within our uncertainty limits, the change from chloride to bromide is unlikely to be the major reason for the change in behavior of $d\bar{V}^t/dT$.

The effect of charge on polarity development on volumes can be modified, however, by solvent accessibility to the polar site. Attention has already been drawn to the *positive* value of $d\Delta V^*/dT$ for *n*-butyl bromide and isopropyl bromide. Despite the expected greater degree of polarization in the secondary alkyl halide compared with the primary *n*-butyl bromide, the temperature dependence of the transition state volume of isopropyl bromide is at least as great as that for the primary alkyl bromide. This may well be a reflection of the reduced solvent accessibility to the developing carbonium type center in the isopropyl case compared with the smaller but less screened positive charge character on the *n*-butyl methylene center. The fact that the temperature dependences of the initial and transition state volumes in these two cases are virtually identical also suggests that the dominant factor in determining the thermal expansivity of both states is more likely a hydrophobic type of interaction between solute and solvent. The importance of solvent accessibility to the developing polarity in the activation process is also highlighted in the data for allyl chloride particularly when compared with *n*-butyl bromide. In the allyl chloride case the developing polarity in the transition state can be delocalized over the entire hydrocarbon chain thus providing a far greater degree of solvent accessibility to the available charge than is possible in the saturated *n*-butyl chain.

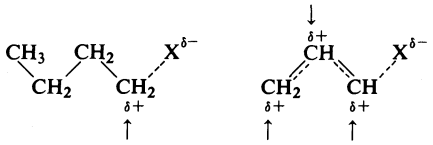

Accordingly, it might be expected that the degree of solvent electrostriction around the allyl transition state compared with the initial state would be greater than in the *n*-butyl case, leading to the relatively low value range for $d\bar{V}^t/dT$ for allyl chloride.

While *negative* values for $d\bar{V}^t/dT$ are not conclusively shown by virtue of the uncertainties associated with the first three hydrolyses in Table 6 the trend in values certainly suggests that negative values are a real phenomenon. This, of course, would mean that the volume of the transition state *decreased* with increase in temperature. It should be recalled that in hydrolyses we are dealing with a highly structured solvent, water, and that the degree of structuredness of the solvent is very temperature dependent. Any solute exerting an electrostrictive effect on water must compete with the water–water structure making interactions. As these are reduced by thermal agitation the electrostrictive effect of the solute will result in a greater degree of collapse of the environmental water "lattice" with a corresponding reduction in volume at higher temperatures. The concept of the competition between the structure making quasi crystalline field forces of liquid water and the electrostrictive attractions of a dissolved solute is, of course, a basic feature of the Frank and Wen (22) model of solvation shell structure.

Conclusion

There are now a number of good illustrations of the increased sensitivity of second derivative activation parameters to reaction mechanism variations compared with that of first derivative parameters (1, 2, 23). The principal difficulty associated with the use of these second derivatives lies in the problem of obtaining data of sufficient accuracy to permit extraction of parameters with reasonable confidence limits. The results on the second derivative parameter $d\Delta V^*/dT$ and its dissection into initial and transition state components presented here both illustrate the caution that should be exercised and the usefulness of the parameter in providing further insight into the important problem of solute–solvent interactions in the kinetics of reactions in solution.

The authors wish to thank the National Research Council of Canada for financial assistance in support of this work.

1. B. T. Baliga and E. Whalley. J. Phys. Chem. **73**, 654 (1969).
2. A. B. Lateef and J. B. Hyne. Can. J. Chem. **47**, 1369 (1969).
3. S. J. Dickson and J. B. Hyne. Can. J. Chem. **49**, 2394 (1971).
4. K. J. Laidler and D. Chen. Trans. Faraday Soc. **54**, 1026 (1958).
5. C. Walling and H. J. Shugar. J. Am. Chem. Soc. **85**, 607 (1963).
6. J. Koskikallio and E. Whalley. Can. J. Chem. **37**, 783 (1959).
7. K. J. Laidler. Discuss. Faraday Soc. **22**, 88 (1956).

Can. J. Chem. Downloaded from www.nrcresearchpress.com by 210.87.254.5 on 09/05/12
For personal use only.

8. J. B. HYNE, H. S. GOLINKIN, and W. G. LAIDLAW. J. Am. Chem. Soc. **88**, 2104 (1966).
9. MOYRA J. MACKINNON, A. B. LATEEF, and J. B. HYNE. Can. J. Chem. **48**, 2025 (1970).
10. E. A. GUGGENHEIM. Phil. Mag. (7) **2**, 538 (1926).
11. H. S. GOLINKIN, IKCHOON LEE, and J. B. HYNE. J. Am. Chem. Soc. **89**, 1307 (1967).
12. H. S. GOLINKIN, W. G. LAIDLAW, and J. B. HYNE. Can. J. Chem. **44**, 2193 (1966).
13. A. I. VOGEL. J. Chem. Soc. 644 (1948).
14. J. TIMMERMANS. Physico-chemical constants of organic chemicals. Elsevier Publ. Co. 1965.
15. O. C. BILLETER. Ber. **38**, 2015 (1905).
16. J. N. FRIEND and W. D. HARGREAVES. Phil. Mag. **34**, 647 (1943).
17. E. M. ARNETT, P. M. DUGGLEBY, and J. T. BURKE. J. Am. Chem. Soc. **85**, 1350 (1963).
18. E. M. ARNETT. Private communication.
19. W. J. LE NOBLE. Prog. Phys. Org. Chem. **5**, 207 (1967).
20. F. FRANKS and H. T. SMITH. Trans. Faraday Soc. **63**, 2586 (1967).
21. F. J. MILLERO and W. DROST-HANSEN. J. PHYS. Chem. **72**, 1758 (1968).
22. H. S. FRANK and W. Y. WEN. Discuss. Faraday Soc. **24**, 133 (1957).
23. R. E. ROBERTSON. Prog. Phys. Org. Chem. **4**, 213 (1967).

Can. J. Chem. Downloaded from www.nrcresearchpress.com by 210.87.254.5 on 09/05/12
For personal use only.

Can. J. Chem. Downloaded from www.nrcresearchpress.com by 210.87.254.42 on 09/05/12
For personal use only.

The Reaction of Active Nitrogen with Carbonyl Chloride

R. R. Baker and C. A. Winkler
Department of Chemistry, McGill University, Montreal, Quebec

Received June 22, 1971

The reaction between active nitrogen and $COCl_2$ in an unheated reaction vessel has been studied over a large range of initial reactant conditions. Analytical studies have shown CO and Cl_2 to be the only reaction products, effectively produced in equal amounts. The maximum extent of reaction corresponded to no more than 10% of the available N atoms. The reaction was found to change from first order in both N and $COCl_2$ for $[COCl_2]_0/[N]_0 < \sim 0.1$, to zero order in $COCl_2$ and second order in N, with $[COCl_2]_0/[N]_0 > \sim 0.3$. The reaction appears to be initiated by energy transfer from an excited N_2 species.

La réaction entre l'azote actif et le $COCl_2$, dans un récipient réactionnel non-chauffé, a été étudiée en fonction des conditions des corps réagissant. Des études analytiques ont montré que CO et Cl_2 étaient les seuls produits de la réaction et qu'ils se formaient en égale quantité. L'avancement maximum de la réaction correspond à 10% au plus des atomes d'azote disponibles. La réaction passe du premier ordre en N et $COCl_2$ pour $[COCl_2]_0/[N]_0 < \sim 0.1$, à l'ordre zéro en $COCl_2$ et à l'ordre deux en N pour $[COCl_2]_0/[N]_0 > \sim 0.3$. La réaction semble induite par un transfert d'énergie à partir des espèces excitées de N_2.

Canadian Journal of Chemistry, 49, 3846 (1971)

Introduction

In reactions of active nitrogen the primary step may involve the direct attack of N atoms on the additive or its acquisition of energy from an excited molecular nitrogen species (1–3). The primary step in the reaction of active nitrogen with carbonyl chloride appears to be of the latter type, followed by secondary reactions with N atoms.

Experimental

A fast flow apparatus was used, essentially similar to those described in earlier studies (*e.g.* 4–6). Active nitrogen was produced by either a microwave unit, or by a condensed discharge between electrodes, in a discharge tube so designed that the active nitrogen traversed the same path in passing from either discharge to the reaction vessel (7). A Wood's horn light trap was interposed between the discharge unit and the reaction vessel. The reaction vessels were Pyrex tubes (cleaned with HF) about 70 cm long, with internal diameters in the range 2.0 to 3.1 cm. Carbonyl chloride was introduced into the reaction vessel at points 20 to 40 cm downstream from the discharge. Temperatures in the reaction zone were measured with a thermocouple sheathed in a thin glass tube.

Nitrogen atom flow rates could be adjusted over a rather wide range by adding traces of suitable discharge catalysts (H_2, O_2, or I_2) to the N_2 before it entered the discharge tube (6). The N atom flow rate at various positions in the reaction vessel could be determined by titration with NO (8) that was added through a movable jet.

Chlorine in the reaction products was trapped over a frozen solution of KI at liquid nitrogen temperatures, and its amount estimated, after melting the solution, by titration of the liberated I_2 with standard $Na_2S_2O_3$ solution. Carbon monoxide was estimated chromatographically, using a Gow-Mac W–Ni four filament thermal conductivity detector, in samples taken from the reaction vessel with a Toepler pump.

A stream of purified (6) Linde "Bone Dry" nitrogen entered the discharge tube directly, or after it had been mixed with traces of an appropriate catalyst gas. Carbonyl chloride (Matheson, 99.0% purity) was purified by bulb-to-bulb distillation, and was stored over mercury in the dark, to avoid its possible contamination with traces of Cl_2 formed by photochemical decomposition.

Results

The reaction was accompanied by a pink emission that extended in the reaction vessel for a distance that corresponded roughly with the time required for "complete" reaction. The temperature of the reaction zone was always higher than the temperature of the Lewis–Rayleigh afterglow in the absence of $COCl_2$, and ranged from 0.2 °K higher for low reactant flow rates (N atoms, 1.5×10^{-6} mol s^{-1}; $COCl_2$, 1.0×10^{-6} mol s^{-1}) to 50 °K higher for the highest flow rates used (N atoms and $COCl_2$ each 12×10^{-6} mol s^{-1}).

Analytical Studies

Cl_2 and CO were the only detectable products from the reaction, presumably produced in equal amounts. However, from a limited number of CO analyses, it appears that the recovery of Cl_2 was always about 5–10% lower than that of CO, over a range of N atom and $COCl_2$ flow

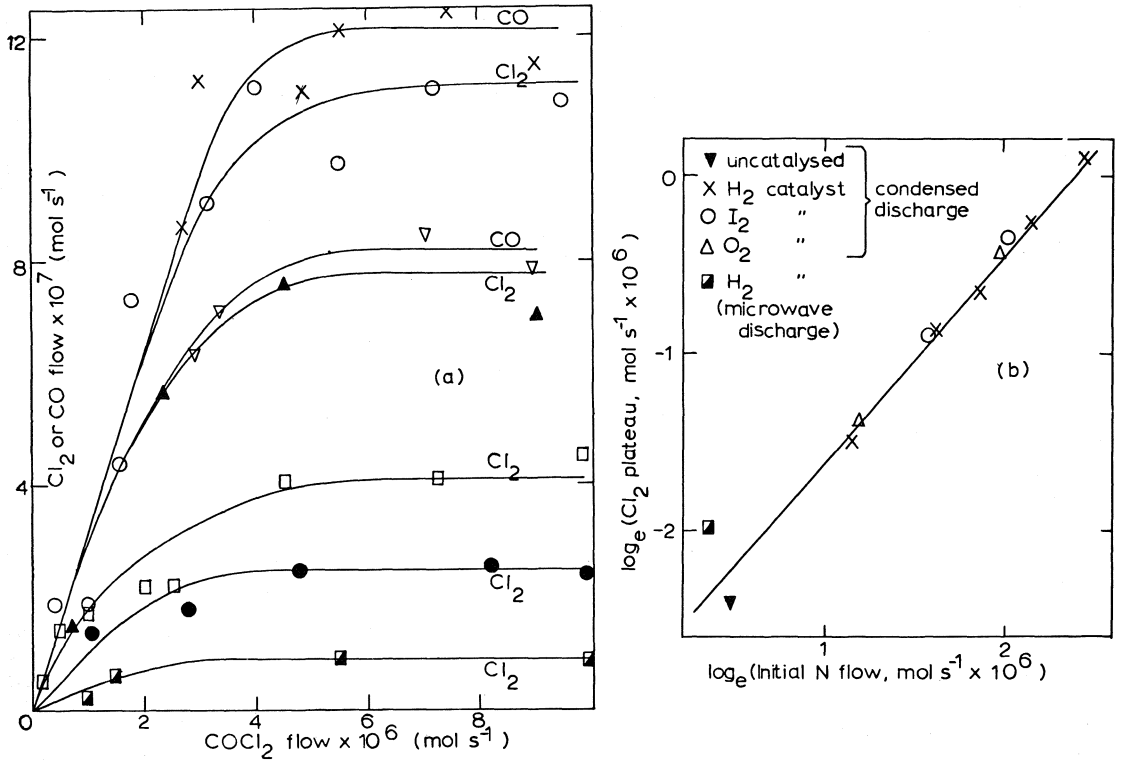

FIG. 1. (*a*) Yield of products from $COCl_2$ plus active nitrogen reaction. H_2 as catalyst: initial N atom flow = 11.7×10^{-6} mol s^{-1}, product = CO, ×; product = Cl_2, ○; initial N atom flow = 8.8×10^{-6} mol s^{-1}, product = CO, ▽; product = Cl_2, ▲. I_2 as catalyst, initial N atom flow = 4.9×10^{-6} mol s^{-1}, product = Cl_2, □. O_2 as catalyst, initial N atom flow = 3.3×10^{-6} mol s^{-1}, product = Cl_2, ●. No catalyst, initial N atom flow = 1.6×10^{-6} mol s^{-1}, product = Cl_2, ◪. These are typical data, obtained using a condensed electrode discharge, and an unheated reaction vessel of 2.0 cm internal diameter, at a total pressure of 2.3 Torr. N_2 flow = 180×10^{-6} mol s^{-1}. (*b*) Dependence of Cl_2 plateau on N atom flow rate.

rates (Fig. 1*a*). The discrepancy is thought to be due to some absorption of Cl_2 by the stopcock grease.

The plateau value for Cl_2 formation never exceeded roughly 10% of the initial N atom flow rate, independently of the nature of the discharge catalyst used and the type of discharge, for flow rates of N atoms between 1.4 and 11.7×10^{-6} mol s^{-1} (Fig. 1*b*). The least squares gradient of Fig. 1*b* is 1.1, from which it may be concluded that the maximum production of Cl_2, hence the maximum destruction of $COCl_2$, is proportional to [N]. To determine the ratio of N atom consumption, Δ[N], to Cl_2 production, $\Delta[Cl_2]$, the flow rates of N atoms, in the absence and in the presence of $COCl_2$, were determined at a point 50 cm downstream from the $COCl_2$ inlet, corresponding to a reaction time (0.10 s) in excess of that required for complete reaction. From differences in the two titrations, an average value of $\Delta[N]/\Delta[Cl_2] = 6.6 \pm 1.2$ was obtained over the range of experimental conditions used.

Kinetics Studies

The kinetics of the reaction were followed by titrating unreacted N atoms with NO (8) after various extents of reaction. The maximum loss of NO by its reaction with Cl atoms formed during the reaction was estimated from the known rate constants (3, 9) and with the assumptions that $[M] = [N_2]$ and $[Cl]_{max} = 2\Delta[Cl_2]$. A ratio of about 10^4 was calculated for the relative rates of reactions 1 and 2 for the conditions of the experiments,

[1] $$N + NO \rightarrow N_2 + O$$

[2] $$Cl + NO + M \rightarrow NOCl + M$$

Can. J. Chem. Downloaded from www.nrcresearchpress.com by 210.87.254.42 on 09/05/12
For personal use only.

The maximum loss of NO by reaction 2 would therefore be negligible during the titration.[1]

(i) Recombination of N Atoms

With a condensed electrode discharge in the absence of a dissociation catalyst, small amounts of $COCl_2$ ($<1.2 \times 10^{-6}$ mol l^{-1}) decreased the rate of N atom decay. Previous studies (11–13) have shown that, for conditions similar to those of the present study, the recombination of N atoms proceeds by first and second order heterogeneous processes, and a third order homogeneous process. Analysis of the present data (13), with corrections for the reaction of N atoms with $COCl_2$, indicated that the first order process was effectively zero, and that the presence of $COCl_2$ did not significantly alter the third order rate constant, but that it did reduce to zero the second order heterogeneous rate constant (Fig. 2).

Similar results were obtained with H_2, admitted through the discharge (Fig. 2). For these experiments, no correction was necessary for the insignificant extent to which N atoms react with H_2 at 300 °K (14–16).

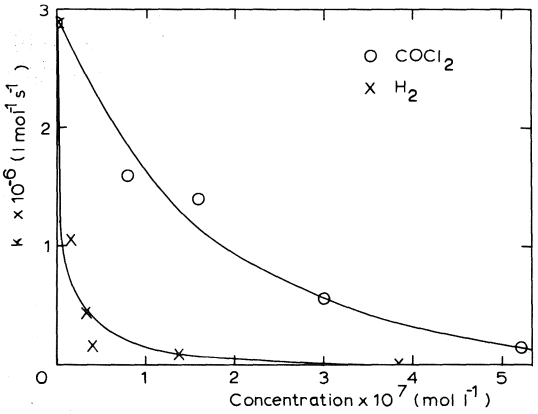

FIG. 2. Effect of $COCl_2$ and H_2 on the second order rate constant for the heterogeneous recombination of N atoms.

[1]The actual loss should be much less than the maximum, since NO will be generated by the fast reactions 3 and 4, with rate constants at 300 °K of 2 and 7×10^9 l mol^{-1} s^{-1}, respectively (10).

[3] $\quad Cl + NOCl \rightarrow NO + Cl_2$

[4] $\quad COCl + NOCl \rightarrow NO + Cl_2 + CO$

The overall effect is that reaction 2 acts mainly to catalyze the recombination of Cl atoms, or Cl and COCl radicals, with little or no net loss in NO.

(ii) Reaction of $COCl_2$

In the kinetic studies of the active nitrogen + $COCl_2$ reaction, H_2 was introduced into the discharge in sufficient quantities that the second order rate constant for the heterogeneous recombination of N atoms was zero. The presence of $COCl_2$ then increased the rate of N atom decay, as expected (typical data are shown in Fig. 3*a*). The rate of consumption of N atoms by $COCl_2$ was obtained as the difference between the decay curves in the presence and absence of $COCl_2$. A short induction period was observed in many of the reaction mixtures studied. Consumption of N atoms by $COCl_2$ was complete after about 0.06–0.08 s, leaving residual N atoms in the reaction vessel.

The orders of the reaction with respect to N atoms and $COCl_2$ were determined by plotting log (maximum rate) against log [N] and log [$COCl_2$], respectively. For a given value of $[N]_0$, the reaction order changed with the value of $[COCl_2]_0$ (Fig. 3*b*). With $[COCl_2]_0/[N]_0 < \sim 0.1$, the reaction was first order in both $COCl_2$ and N. With $[COCl_2]_0/[N]_0 > \sim 0.3$, it became zero order in $COCl_2$ and second order in N.

Discussion

Since the maximum extent of reaction, even with excess $COCl_2$, corresponded to less than 10% of the available N atoms, and the N atom decay profiles showed induction periods, it is concluded that N atoms do not attack $COCl_2$ directly. As with NH_3 and SO_2 (refs. 2, 3, and ref. 1, pp. 505–511), it is probable that the primary reaction of $COCl_2$ involves energy transfer from an excited molecular species, possibly $N_2(A^3\Sigma_u^+)$.

The observed changes in reaction order with changes in the initial concentrations of reactants (Fig. 3*b*) indicate that N and $COCl_2$ compete for some reaction intermediate, and that reaction with N predominates at low $[COCl_2]_0/[N]_0$, while reaction with $COCl_2$ predominates at high $[COCl_2]_0/[N]_0$. The kind of mechanism that would satisfy the above considerations may be represented briefly.

N_2* represents an electronically excited species produced in the discharge, $COCl_2^{+}$ represents a vibrationally excited molecule, $COCl_2$* represents an electronically excited molecule capable of dissociation, and M represents an inert molecule. The alternative reactions of $NCOCl_2$ with N

Can. J. Chem. Downloaded from www.nrcresearchpress.com by 210.87.254.42 on 09/05/12
For personal use only.

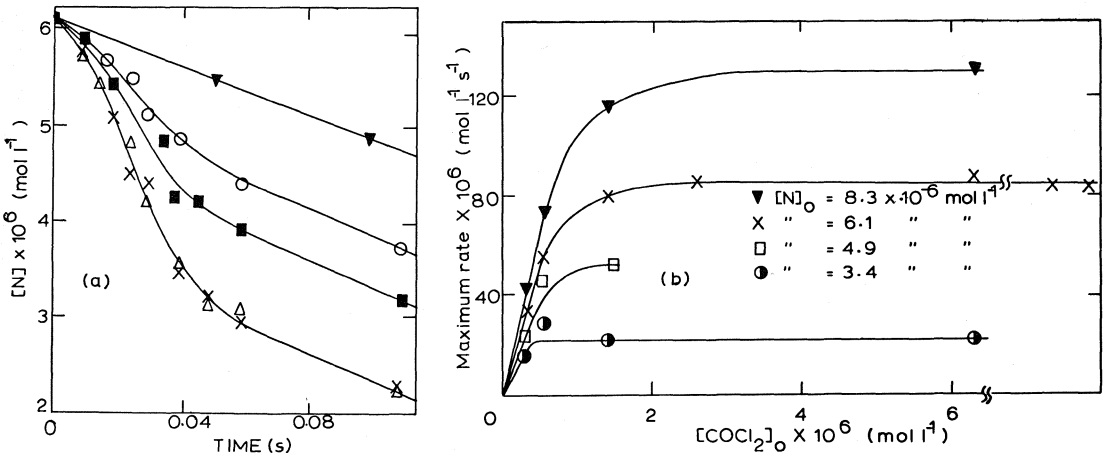

FIG. 3. (*a*) N atom decay in the presence of $COCl_2$. Typical data, obtained using a condensed electrode discharge system, catalyzed with H_2, 2.0 Torr total pressure, in a 3.1 cm internal diameter, unheated, reaction vessel. $[COCl_2]_0$ values, in mol $l^{-1} \times 10^6$, are: ▼, 0; ○, 0.31; ■, 0.55; ×, 2.6; △, 6.3. (*b*) Variation of maximum rate with $[COCl_2]_0$.

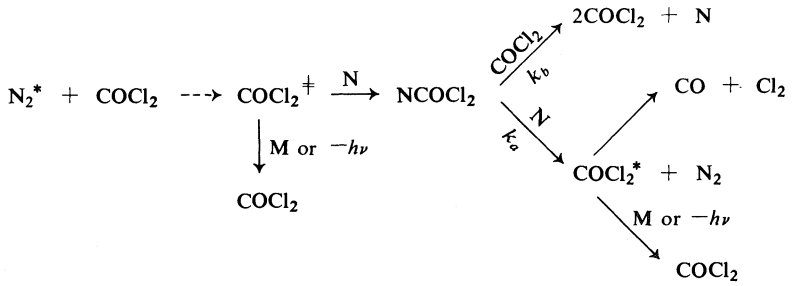

and $COCl_2$ have rate constants k_a and k_b, respectively. The observed pink reaction flame might result from emission by $COCl_2$* or, more probably, by Cl_2 ($^3\Pi_{0u}{}^+$) produced by recombination of Cl atoms (17).

If it is assumed that (*i*) the majority of $COCl_2{}^‡$ molecules are deactivated, and (*ii*) $[N_2{}^*]_0$ is constant for the different initial values of $[N]_0$ used (18–20), stationary state treatment of this mechanism yields

$$[5] \qquad \frac{d\Delta[N]}{dt} = \frac{\text{constant } [COCl_2][N]^2}{k_a[N] + k_b[COCl_2]}$$

Equation 5 is capable of predicting the observed changes in reaction order as follows.

(*i*) When $[COCl_2]_0/[N]_0$ is very small, such that $k_a[N] \gg k_b[COCl_2]$, eq. 5 reduces to

$$[6] \qquad \frac{d\Delta[N]}{dt} = \frac{\text{constant}}{k_a}[COCl_2][N]$$

and $d\Delta[N]/dt$ is first order in N and $COCl_2$, as observed when $[COCl_2]_0/[N]_0 < \sim 0.1$.

(*ii*) When $k_a[N] \ll k_b[COCl_2]$,

$$[7] \qquad \frac{d\Delta[N]}{dt} = \frac{\text{constant}}{k_b}[N]^2$$

and $d\Delta[N]/dt$ is second order in N, and zero order in $COCl_2$, as observed when $[COCl_2]_0/[N]_0 > \sim 0.3$.

The present data give a value of $2.06 \pm 0.16 \times 10^6$ l mol^{-1} s^{-1} for the constant in eq. 5, and $k_a/k_b = 0.11 \pm 0.01$.

1. A. N. WRIGHT and C. A. WINKLER. Active nitrogen. Academic Press, New York. 1968.
2. A. BROCKLEHURST and K. R. JENNINGS. Progress in reaction kinetics. Vol. 4. *Edited by* G. Porter. Pergamon, London. 1967.
3. G. R. BROWN and C. A. WINKLER. Angew. Chem. **9**, 181 (1970).
4. P. A. GARTAGANIS and C. A. WINKLER. Can. J. Chem. **34**, 1457 (1956).

Can. J. Chem. Downloaded from www.nrcresearchpress.com by 210.87.254.42 on 09/05/12
For personal use only.

5. E. M. LEVY and C. A. WINKLER. Can. J. Chem. **40**, 686 (1962).
6. R. R. BAKER, A. JACOB, and C. A. WINKLER. Can. J. Chem. **49**, 1671 (1971).
7. G. R. BROWN. Ph.D. Thesis. McGill University, Montreal, Quebec. 1970.
8. F. KAUFMAN and J. R. KELSO. J. Chem. Phys. **27**, 1209 (1957).
9. T. C. CLARK, M. A. A. CLYNE, and D. H. STEDMAN. Trans. Faraday Soc. **62**, 3354 (1968).
10. W. G. BURNS and F. S. DAINTON. Trans. Faraday Soc. **48**, 52 (1952).
11. K. M. EVENSON and D. S. BURCH. J. Chem. Phys. **45**, 2450 (1966).
12. J. M. CAMPBELL and B. A. THRUSH. Proc. Roy. Soc. Ser. A **296**, 201 (1967).
13. M. A. A. CLYNE and D. H. STEDMAN. J. Phys. Chem. **71**, 3071 (1967).
14. R. N. VARNEY. J. Chem. Phys. **23**, 866 (1955).
15. G. B. KISTIAKOWSKY and G. G. VOLPI. J. Chem. Phys. **28**, 665 (1958).
16. C. MAVROYANNIS and C. A. WINKLER. Can. J. Chem. **40**, 240 (1962).
17. M. A. A. CLYNE and D. H. STEDMAN. Trans. Faraday Soc. **64**, 1816 (1968).
18. A. JACOB, R. A. WESTBURY, and C. A. WINKLER. J. Phys. Chem. **70**, 4066 (1966).
19. A. JACOB. Ph.D. Thesis. McGill University, Montreal, Quebec. 1968.
20. J. M. ROSCOE. Ph.D. Thesis. McGill University, Montreal, Quebec. 1970.

Can. J. Chem. Downloaded from www.nrcresearchpress.com by 210.87.254.42 on 09/05/12
For personal use only.

Can. J. Chem. Downloaded from www.nrcresearchpress.com by 210.87.254.105 on 09/05/12
For personal use only.

Réaction des acétoxy-1 époxy-2,3 cyclohexanes *cis* et *trans* avec le tributylcarbéthoxyméthinephosphorane[1]

H. Favre et J. P. Lapointe
Département de Chimie, Université de Montréal, Montréal, Québec

Reçu le 9 juin 1971

La réaction de l'acétoxy-1 époxy-2,3 cyclohexane *cis* (**3**) avec le tributylcarbéthoxyméthinephosphorane conduit à quatre composés: le cyclopentène-1 carbaldéhyde (**5**), le (cyclopentène-1 yl)-3 propénoate d'éthyle (**6**), l'(acétoxy-2-*c* cyclopentyl)-3 propénoate d'éthyle *trans* (**7**), et son isomère **8** dans le rapport 8–20–12–60, avec un rendement de 70%. Un mélange 38–62 des acétoxy-époxydes **3** et **4** donne les mêmes résultats.

Four different products were obtained by the reaction of *cis*-1-acetoxy-2,3-epoxycyclohexane with tri-*n*-butyl-carbethoxymethylidenephosphorane: cyclopent-1-enaldehyde (**5**), ethyl-3-(cyclopent-1-enyl)-propeonate (**6**), *trans*-ethyl-3-(2-*c*-acetoxycyclopentyl)propeonate (**7**), and its isomer **8**, in a 8–20–12–60 ratio, with a yield of 70%. The same products were obtained when a mixing of acetoxyepoxydes **3** and **4** were used in a 38–62 ratio.

Canadian Journal of Chemistry, **49**, 3851 (1971)

Gerkin et Rickborn (1) ont montré que l'action du tributylcarbéthoxyméthinephosphorane (Bu_3-P=CHCOOEt) (2) sur l'époxyde de cyclohexène **1** conduisait principalement à l'ester α,β-éthylénique **2**. Il était intéressant d'examiner si la réaction se faisait lorsqu'un groupe acétoxy se trouvait en α de l'époxyde et de déterminer la stéréospécificité de la réaction, le cas échéant.

L'acétoxy-époxyde *cis* **3** est connu (3, 4). Sa réaction avec le tributylcarbéthoxyméthinephosphorane conduit aux quatre composés **5**, **6**, **7**, et **8** avec un rendement de 70%, dans le rapport 8–20–12–60.

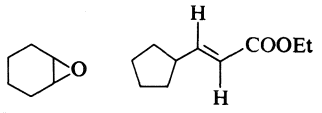

1 **2**

L'aldéhyde **5**, qui est connu (5), est caractérisé par son spectre de r.m.n.: un proton aldéhydique et un proton vinylique, et sa dinitro-2,4 phénylhydrazone.

La structure de l'ester doublement insaturé **6** découle des données spectrales suivantes. Groupe carbonyle à 1720 cm^{-1} en i.r.; en u.v., un λ_{max} à 270 mμ établit la conjugaison du groupe carbonyle et des deux doubles liaisons; le spectre de r.m.n., en plus du groupe —OEt, signale la présence des trois protons vinyliques.

Le composé principal de la réaction est l'acétoxy-ester **8**. Les spectres i.r. et de r.m.n. établissent la présence des groupes —COOEt et —OAc. Le spectre de r.m.n. indique de plus que la double liaison, conjuguée avec le groupe ester, d à 5.73 (J = 16 Hz) et dd à 6.8 (J = 16 et 7.8 Hz), est de configuration *trans*, d'après la constante de couplage de 16 Hz. Les positions respectives et la configuration *trans* des substituants portés par le cycle se déduisent de la transformation, ozona-

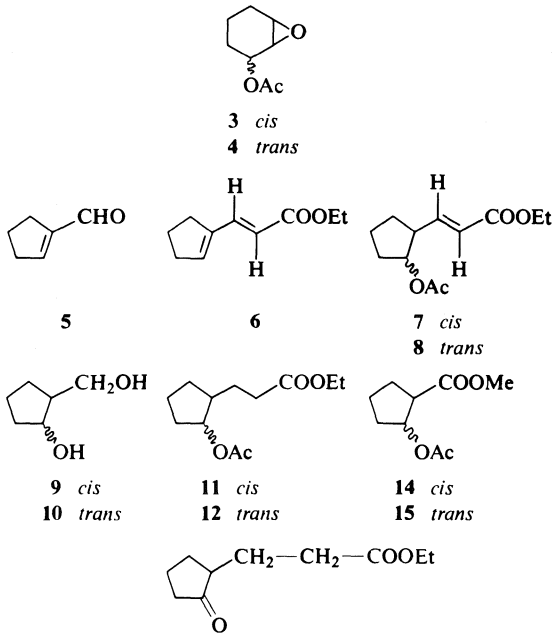

3 *cis*
4 *trans*

5 **6** **7** *cis* **8** *trans*

9 *cis* **10** *trans* **11** *cis* **12** *trans* **14** *cis* **15** *trans*

13

[1]Tiré du mémoire de maîtrise de J.P.L.

tion, suivie d'une réduction par l'hydrure de lithium et d'aluminium, du composé **8** en méthylol-2 cyclopentanol-1 *trans*, qui est connu (6).

Le quatrième composé de réaction ne s'obtient pas pur, mais en mélange avec l'acétoxy-ester **8**. L'ozonation, suivie de la réduction par l'hydrure de lithium et d'aluminium d'un mélange **7**–**8** 16–84 conduit aux deux diols **9** et **10** dans le rapport 16–84. Le spectre de r.m.n. du mélange **7**–**8**, de proportions 44–56, est semblable à celui du composé **8** pur, sauf pour une bande nouvelle à δ 5.19, attribuable à C*H*—OAc de l'isomère *cis*, à côté de la bande à δ 4.90 du composé *trans* **8**.

Nous avons préparé les diols **9** et **10** par réduction de l'éthoxycarbonyl-2 cyclopentanone par l'hydrure de lithium et d'aluminium. On sait que cette réduction conduit à des alcools insaturés et aux diols **9** et **10** (7, 8); nous montrons dans ce travail que les deux diols **9** et **10** se forment dans le rapport 23–77.

Une preuve supplémentaire de la configuration *cis*–*trans* des composés **7** et **8** repose sur la réduction du composé **8** et du mélange des composés **7** et **8** en acétoxy-esters saturés, respectivement **12** pur et un mélange de **11** et **12**. La réduction par l'hydrure de bore sodium du céto-ester **13** conduit à un mélange d'hydroxy-esters, qui par acétylation donne les acétoxy-esters **11** et **12**, dans le rapport 12–88. Le dosage, qui ne peut se faire par c.p.g., est fait par spectroscopie de r.m.n., en tenant compte des multiplets correspondant aux protons C*H*—OAc, apparaissant à δ 5.15 pour l'ester *cis* **11**, et à 4.75 pour son isomère *trans* **12**. Le composé majoritaire de réduction est l'isomère *trans*, à l'image de la réduction de la propyl-2 cyclopentanone qui donne 74% d'isomère *trans* (9). Il se trouve (tableau 1) ainsi que les trois isomères *cis* **7**, **9**, et **11** présentent, en r.m.n., une bande C*H*—OR (R = —H ou —Ac) à champ plus faible que les isomères *trans* correspondants. En revanche, les acétates de méthoxycarbonyl-2 cyclopentyles *cis* et *trans*, en mélange, ne se distinguent pas l'un de l'autre.

Un mélange 38–62 des acétoxy-époxydes **3** et **4** conduit exactement aux mêmes résultats que l'acétoxy-époxyde *cis* pur, soit aux composés **5**, **6**, **7**, et **8**, dans le rapport 10–21–10–59, et avec un rendement de 75%.

Ce travail montre que la conversion **3**–**4** → **7**–**8** se fait, et qu'elle se fait sans rétention totale de la configuration de départ. La présence de l'aldéhyde **5** dans le milieu réactionnel justifie les conclusions mécanistiques de Rickborn et Gerkin (10), formation d'aldéhyde intermédiaire.

TABLEAU 1. Déplacements chimiques du proton >C*H*— OR dans les isomères *cis*–*trans*

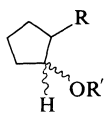

R	R′	δ *cis*	δ *trans*	Solvant
—CH=CH—COOEt	—Ac	5.19	4.90	CCl_4
—CH_2OH	—H	4.32	3.97	$CDCl_3$
—CH_2—CH_2—COOEt	—Ac	5.15	4.75	CCl_4
—COOMe	—Ac	5.40	5.40	$CDCl_3$

Partie expérimentale

Les spectres i.r. ont été mesurés à l'aide d'un spectrophotomètre Beckman IR-8 ou Perkin–Elmer 621, u.v. à l'aide d'un spectrophotomètre Spectronic 505 de Bausch and Lomb; de r.m.n. à l'aide d'appareils Jeol C 60H et JNM-4H-100, le tétraméthylsilane étant pris comme référence; de masse à l'aide d'un spectromètre Hitachi–Perkin–Elmer RMU-6D. Un appareil F and M 700 a servi à la c.p.g. Les points de fusion ont été déterminés en tubes capillaires, à l'aide d'un thermomètre étalonné avec des substances standards. Les analyses élémentaires sont de Schwarzkopf Microanalytical Laboratory, New York et de C. Daesslé, Microanalyses, Montréal.

(1) Acétoxy-1 époxy-2,3 cyclohexanes cis et trans (3 et 4)

L'isomère *cis* se prépare par époxydation du cyclohexène-2 ol-1 à la manière de Henbest et Nicholls (11). L'époxy-alcool (17.5 g) est acétylé, avec un rendement de 58%, par 175 ml d'anhydride acétique dans 175 ml de pyridine anhydre, durant 70 h. Une extraction à l'éther conduit à l'acétate **3**, qui distille à 117–118° sous 25 mm.

L'isomère *trans* **4**, en mélange avec son isomère *cis*, se prépare selon la méthode générale de Henbest et Nicholls (11), par époxydation de l'acétate de cyclohexène-2 yle, avec un rendement de 45%.

La c.p.g. (QF1 3% sur Anachrome ABS, en tube de verre de 6 m de longueur, température 162°) montre que l'isomère *cis* s'obtient pur et que le mélange des isomères *trans* et *cis* est constitué de 62% d'isomère *trans* et de 38% d'isomère *cis*.

Spectre de r.m.n. de l'isomère *cis* (CCl_4): δ 2.06 (s, 3, —OCOCH_3); 3.12 (m, 2, —C*H*—C*H*—); 5.0 (m, 1, >C*H*—OAc). Spectre de r.m.n. du mélange *cis*–*trans* (CCl_4): 2.06 et 2.08 (s, 3, —OCOCH_3); 3.15 et

Can. J. Chem. Downloaded from www.nrcresearchpress.com by 210.87.254.105 on 09/05/12
For personal use only.

Can. J. Chem. Downloaded from www.nrcresearchpress.com by 210.87.254.105 on 09/05/12
For personal use only.

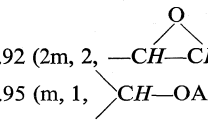

2.92 (2m, 2, —C*H*—C*H*— respectivement *cis* et *trans*); 4.95 (m, 1, C*H*—OAc).

(2) Réaction de l'acétoxy-1 époxy-2,3 cyclohexane cis avec le tributylcarbéthoxyméthinephosphorane

Dans un ballon de 500 ml à trois tubutures, muni d'un réfrigérant, d'un agitateur, d'une ampoule à brome, sous atmosphère d'azote, on met une solution de 36.9 g (0.1 mol) de bromure de tributylcarbéthoxyméthylènephosphonium, préparé selon (2), dans 140 ml de benzène anhydre. A cette solution on ajoute goutte à goutte 62.8 ml (0.1 mol) d'une solution de 1.6 *M* de butyllithium dans l'hexane. Ensuite, on ajoute rapidement 15.6 g (0.1 mol) d'acétoxy-1 époxy-2,3 cyclohexane *cis* (3). On chauffe à l'ébullition à reflux pendant 24 h. La solution refroidie est lavée trois fois avec de l'eau, séchée sur sulfate de sodium anhydre, et évaporée sous vide de 11 mm. Le résidu d'évaporation est une huile rouge, 37.5 g. Une chromatographie sur colonne de silice avec de l'éther comme éluant, permet de séparer le résidu en deux fractions: l'oxyde de tributylphosphine et les quatre composés de réaction **5**–**8**. L'analyse par c.p.g. est la suivante, sur colonne de D.E.G.S. 10% sur Chromosorb W, N. A., 3.6 m 200°: **5**, 8 ± 2%, temps de rétention 1.5 min; **6**, 20 ± 2%, 3.9 min; **7**, 12 ± 2%, 12.1 min; **8**, 60 ± 2%, 13.6 min. La distillation du résidu sous 0.35 mm permet de séparer l'aldéhyde **5** des esters **6**–**8**. L'aldéhyde **5**, très volatil, se retrouve dans une trappe à −81°, accompagné d'hexane et de benzène. Les esters **6**–**8** distillent entre 100 et 120°, sans séparation. Leur séparation se fait par chromatographie sur gel de silice; avec un mélange d'éther–hexane 25–75 comme éluant: l'ester **6** sort en premier lieu, pur, suivie de l'ester **8** pur, et finalement des esters **7** et **8** en mélange.

Cyclopentène-1 carbaldéhyde (5)

La fraction résultant de la distillation contient 45% d'aldéhyde **5**, 23% d'hexane et 32% de benzène, par dosage par c.p.g. Spectre i.r. (CCl_4): 2715, C—H de CHO; 1680 cm^{-1}, C=O. Spectre de r.m.n.: (CCl_4): δ 6.76 (s, 1, proton vinylique); 9.77 (s, 1, proton aldéhydique). L'analyse par c.p.g. (colonne de D.E.G.S. sur Chromosorb W, N.A., 3.6 m, 195°) ne donne qu'un pic pour l'aldéhyde **5** rehaussé par adjonction de l'aldéhyde authentique, préparé selon (5). Dinitro-2,4 phénylhydrazone p.f. 213–214°, seul ou en mélange avec un échantillon authentique de p.f. 215–216° (5, 12).

(Cyclopentène-1 yl)-3 propénoate d'éthyle trans (6)

Le p.éb. 110° sous 0.35 mm. Spectre u.v. (EtOH 95%) λ_{max} 270 mμ, (ε 14 400). Spectre de masse (70 éV), ion moléculaire à *m/e* 166. Spectre i.r. (CCl_4): 1720 (C=O), 1635 cm^{-1} (C=C). Spectre de r.m.n.: (CCl_4): δ 5.6 (d, 1, *J* = 16 Hz, —CH=C*H*—COOEt); 7.43 (d, 1, *J* = 16 Hz, —C*H*=CH—COOEt); 6.13 (m, 1, —CH_2—C*H*=C); 4.13 (q, 2, *J* = 6.8 Hz, —O—C*H*$_2$—CH_3); 1.26 (t, 3, *J* = 6.8 Hz, —O—CH_2—C*H*$_3$); les méthylènes du cycle apparaissent à 2.4 et 2.0 respectivement 4H et 2H.

Anal. calc. pour $C_{10}H_{14}O_2$: C, 72.26; H, 8.49. Trouvé: C, 71.99; H, 8.25.

(Acétoxy-2-t cyclopentyl)-3 propénoate d'éthyle trans (8)

Le p.éb. 110° sous 0.35 mm. Spectre i.r. (CCl_4): 1720 (C=O de COOEt); 1735 (C=O de OAc); 1650 cm^{-1} (C=C). Spectre de r.m.n. (CCl_4): δ 5.73 (d, 1, *J* = 16 Hz, —CH=C*H*—COOEt; chaque pic du doublet est dédoublé, *J* = 1.5 Hz); 6.8 (dd, 1, *J* = 16 et 7.8 Hz, −C*H*=CH—COOEt); 4.87 (m, 1, C*H*—OAc); 4.11 (q, 2, *J* = 7.2 Hz, —O—C*H*$_2$—CH_3); 2.66 (m, 1, C*H*—CH=); 2.0 (s, 3, —OCOC*H*$_3$); 1.26 (t, 3, *J* = 7.2 Hz, —OCH_2-C*H*$_3$); les méthylènes du cycle apparaissent à 2.0 et 1.76 (6H).

Anal. calc. pour $C_{12}H_{18}O_4$: C, 63.70; H, 8.02. Trouvé: C, 63.62; H, 7.95.

(Acétoxy-2-c cyclopentyl)-3 propénoate d'éthyle trans (7)

Il fut obtenu en mélange avec son isomère **8**; les proportions, déterminées par c.p.g. comme plus haut, sont de 45–55. Spectre i.r. (CCl_4): 1720 (C=O de COOEt); 1735 (C=O de OAc); 1650 cm^{-1} (C=C). Spectre de r.m.n. (CCl_4): δ 5.76 (d, 1, *J* = 16 Hz, —CH=C*H*—COOEt); 6.81 (dd, 1, *J* = 16 et 7.8 Hz, —C*H*=CH— COOEt); 4.90 et 5.19 (2m, 0.55 et 0.45 respectivement, >C*H*—OAc); 4.13 (q, 2, *J* = 7.2 Hz, —O—C*H*$_2$—CH_3); 2.69 (m, 1, >C*H*—CH=); 2.0 (s, 3, —OCOC*H*$_3$); 1.28 (t, 3, *J* = 7.2 Hz, —OCH_2C*H*$_3$); les méthylènes du cycle apparaissent à 2.03 et 1.82 (6H).

(3) Réaction d'un mélange des acétoxy-époxydes 3 et 4 avec le tributylcarbéthoxyméthinephosphorane

Le mode opératoire est décrit à la section 2, plus haut. Le mélange 38–62 des époxydes **3** et **4** décrit à la section 1, 10.9 g conduit à 10 g de composés de réaction, dosés par c.p.g.: **5**, 10 ± 2%; **6**, 21 ± 2%; **7**, 10 ± 2%; **8**, 59 ± 2%.

Les esters **6** et **8** sont obtenus purs par chromatographie sur gel de silice, de même que les esters **7** et **8** en mélange (preuves par spectroscopie de r.m.n. et i.r., ainsi que par c.p.g., à partir des échantillons authentiques décrits plus haut).

(4) Méthylol-2 cyclopentanols-1 cis et trans (9 et 10)

(a) Par réduction de l'éthoxycarbonyl-2 cyclopentanone

A une solution contenant 11 g (0.29 mol) d'hydrure de lithium et d'aluminium dans 400 ml d'éther anhydre, on ajoute goutte à goutte une solution de 21.8 g (0.14 mol) d'éthoxycarbonyl-2 cyclopentanone dans 80 ml d'éther anhydre. L'addition se fait en 1.5 h. Le mélange est ensuite porté à l'ébullition à reflux pendant 30 min, puis refroidi; l'excès d'hydrure est décomposé en ajoutant de l'eau goutte à goutte. On ajoute ensuite 200 ml d'une solution aqueuse de sel de la Rochelle à 20%. La phase éthérée est décantée et la phase aqueuse extraite deux fois par de l'éther. Les phases éthérées sont réunies, lavées avec une solution aqueuse saturée, de chlorure de sodium, séchées sur sulfate de sodium anhydre et évaporées. Après distillation, on obtient 5.2 g d'alcools insaturés, (36.5% de rendement), d'après le spectre de r.m.n. et la c.p.g. La phase aqueuse obtenue plus haut à la fin de la réaction est extraite par de l'éther d'une manière continue, durant 3 jours et permet de recueillir 5.6 g de diols **9** et **10** (rendement 34.6%).

La c.p.g. sur colonnes de (*a*) diglycérol 8% sur Chromo-

Can. J. Chem. Downloaded from www.nrcresearchpress.com by 210.87.254.105 on 09/05/12
For personal use only.

sorb W 80/100, A.W.; (*b*) Polyester de Craig 3% sur Chromosorb G 80/100, A.W. indique que les diols sont identiques avec les diols obtenus par réduction par l'hydrure de lithium et d'aluminium des acétates d'éthoxycarbonyl-2 cyclopentyle *cis* et *trans*; les configurations de ces esters sont connues à la suite des travaux de Pascual *et al.* (13, 14).[2] Les diols **9** et **10** sont dans le rapport 23–77.

Les deux diols **9** et **10** se séparent en c.p.g. préparative, sur colonne de Polyester de Craig 15% sur Chromosorb A 60/80, N.A.W. 3 m, 165°, He comme gaz porteur de débit 65 ml/min.

*Le méthylol-2 cyclopentanol-1 cis (**9**)* est homogène en c.p.g. Spectre i.r. ($CHCl_3$): 3400 cm^{-1} (—OH). Spectre de r.m.n. ($CDCl_3$): 4.32 (m, 1 C*H*—OH); 3.73 (d, 2, J = 5.8 Hz, —CH_2OH); 3.55 (s, 2, —O*H*, échangeable avec D_2O); de 1.67 à 1.94, 7, CH_2 et CH du cycle.

*Le méthylol-2 cyclopentanol-1 trans (**10**)* est homogène en c.p.g. Spectre i.r. ($CHCl_3$): 3400 cm^{-1} (—OH). Spectre de r.m.n. ($CDCl_3$): 3.97 (m, 1, C*H*—OH); 3.60 (m, 2, —CH_2OH); 3.08 (s, 2, —O*H*, échangeable avec D_2O); 1.72 (m, 7, CH_2 et autre CH du cycle).

*(b) A partir de l'ester **8***

On dissout 163 mg d'ester **8** pur dans 20 ml d'éther de pétrole (p. éb. 30–40°) et refroidit cette solution dans un bain d'acétone et de glace sèche. On ozonise jusqu'à coloration bleue persistante, puis retire le tout du bain froid. Après décoloration, on évapore le solvant sous vide de 11 mm. On reprend le résidu d'ozonides par 5 ml de tétrahydrofuranne et ajoute goutte à goutte cette solution à une solution composée de 165 mg d'hydrure de lithium et d'aluminium dans 5 ml de THF. On agite 20 min à 25°, détruit l'excès d'hydrure par addition d'eau–THF 1–1. On sature la phase aqueuse de carbonate de sodium. La phase tétrahydrofurannique se sépare de la phase aqueuse; on la décante, la sèche sur sulfate de sodium anhydre, évapore le solvant. Le résidu (110 mg) est distillé sous vide de 0.25 mm. Le méthylol-2 cyclopentanol-1 *trans* (**10**) est identique (c.p.g. i.r., r.m.n.) avec celui décrit en (*a*)).

*(c) A partir des esters **7** et **8** en mélange*

Un mélange des esters 7 et **8**, 16–84, c'est une fraction tirée de la chromatographie sur gel de silice des produits réactionnels décrits à la section 1, est ozoné et réduit comme en section (*b*) plus haut. Il conduit à un mélange des diols **9** et **10**, dans les proportions de 16–84 par dosage par c.p.g.

*(5) (Acétoxy-2 cyclopentyl)-3 propionate d'éthyle cis et trans (**11** et **12**)*

*(a) Réduction de l'ester **8***

On agite en atmosphère d'hydrogène, durant 45 min, une solution d'ester **8** (280 mg) dans 10 ml d'éthanol 95%, en présence de 25 mg d'oxyde de platine. La solution est filtrée sur de la terre de diatomée, le solvant évaporé sous vide de 11 mm. On distille le résidu et recueille 160 mg d'ester **12**, p.éb. 125° sous 1.5 mm. Spectre i.r.: (CCl_4): 1728 cm^{-1} (C=O). Spectre de r.m.n. (CCl_4): 4.80 (m, 1, >C*H*—OAc); 4.11 (q, 2, —OCH_2CH$_3$); 2.3 (m, 2, —CH_2COOEt); 2.00 (s, 3, —OCOCH_3); 1.25 (t, 3, —OCH$_2$CH_3); 1.75 (m, 9, autres H).

Anal. calc. pour $C_{12}H_{20}O_4$: C, 63.14; H, 8.83. Trouvé: C, 63.35; H, 8.60.

*(b) Réduction des esters **7** et **8** en mélange*

Comme en section (*a*), l'hydrogénation d'un mélange 46–54 des esters **7** et **8** conduit aux esters **11** et **12** dans le rapport 45–55 déterminé par spectroscopie de r.m.n. Dans le spectre de r.m.n. les bandes à 5.15 et 4.75, correspondant aux protons *cis* et *trans* C*H*—OAc, sont dans le rapport 45–55; les autres bandes du spectre sont semblables au spectre du composé *trans* pur décrit en section (*a*).

(c) Réduction de l'(oxo-2 cyclopentyl)-3 propionate d'éthyle

A une solution de 5 g d'(oxo-2 cyclopentyl)-3 propionate d'éthyle, préparé selon (15), dans 20 ml de méthanol, refroidie entre −5 et 0°, on ajoute par petites portions 1 g de borohydrure de sodium. La solution est ensuite agitée durant deux heures à cette température. On acidifie la solution par une solution aqueuse d'acide sulfurique 30%, jusqu'à coloration bleue du papier rouge Congo. On évapore le méthanol sous vide de 11 mm. On extrait plusieurs fois le résidu par de l'éther. On lave jusqu'à neutralité les solutions éthérées réunies par des lavages avec une solution saturée de chlorure de sodium. On sèche sur sulfate de sodium anhydre, évapore le solvant et traite le résidu par 35 ml de pyridine et 35 ml d'anhydride acétique durant 70 h à température de 25°. On traite par de l'eau glacée et extrait par de l'éther. On lave la solution éthérée avec une solution aqueuse d'acide chlorhydrique à 2%, puis avec une solution aqueuse saturée de bicarbonate de sodium, enfin avec une solution saturée de chlorure de sodium. On sèche sur sulfate de sodium anhydre, évapore le solvant sous vide de 11 mm et distille le résidu. On recueille 4.2 g du mélange des esters **11** et **12**, p.éb. 119° sous 1.8 mm. Spectre i.r. (CCl_4): 1730 cm^{-1} (C=O). Le spectre de r.m.n. est semblable à celui décrit en section (*b*), sauf que le rapport des bandes à δ 5.15 et 4.75, correspondant à C*H*—OAc, est de 12–88, établissant ainsi la teneur du mélange à 12% d'ester **11** et 88% d'ester **12**.

Le mélange des esters **11** et **12** ne se fractionne pas en c.p.g. sur colonnes de QF1, d'U.C.W. ou de Carbowax 20M TPA.

Nous remercions le Ministère de l'Education de la Province de Québec, le Ministère des Pêcheries et des Forêts du Canada (Comité consultatif national de

[2]Les diols **9** et **10** furent obtenus par réduction par l'hydrure de lithium et d'aluminium des éthoxycarbonyl-2 cyclopentanols *cis* et *trans* (6). Nous avons de notre côté préparé les méthoxycarbonyl-2 cyclopentanols *cis* et *trans* selon la méthode (13, 14) et réduit les acétates correspondants. Le spectre de r.m.n. d'un mélange 64–36 des acétates **14** et **15** est le suivant $CDCl_3$: 5.40 (m, 1 C*H*—OAc); 3.68 et 3.75 (2s, 3, —OCH_3 des isomères *cis* et *trans*); 2.90 (m, 1, C*H*COOMe); 2.00 et 2.03 (2s, 3, —OCOCH_3 des isomères *cis* et *trans*); 1.92 (m, 6, CH_2 du cycle); le spectre de r.m.n. de l'isomère *cis* pur sert à attribuer les pics des isomères *cis* et *trans*. La réduction de mélange *cis–trans* 64–36 par l'hydrure de lithium et d'aluminium donne un mélange des diols **9** et **10**, 63–37. Les acétates **14** et **15** se séparent en c.p.g., temps de rétention de 15.6 et 14.7 min respectivement (Polyester de Craig, 3% sur Chromosorb G 80/100, A.W., DMCS; 3.6 m, température 140°, N_2 28 ml/min.

recherche du Canada sur les ressources en eau), et les Laboratoires Ayerst, à Montréal, de leurs subventions de recherches.

1. R. M. GERKIN et B. RICKBORN. J. Am. Chem. Soc. **89**, 5850 (1967).
2. A. J. SPEZIALE et D. E. BISSING. J. Am. Chem. Soc. **85**, 3878 (1963).
3. H. B. HENBEST et R. A. L. WILSON. J. Chem. Soc. 1958 (1957).
4. P. CHAMBERLAIN, M. L. ROBERTS, et G. H. WITHAM. J. Chem. Soc. B, 1374 (1970).
5. J. C. BROWN, H. B. HENBEST, et E. R. H. JONES. J. Chem. Soc. 3634 (1950).
6. O. KOVACS, J. SZILAGYI, et G. SCHNEIDER. Magy. Kem. Folyoirat, **71**, 93 (1965).
7. E. BUCHTA et H. BAYER. Ann. **573**, 227 (1951).
8. A. S. DREIDING et J. A. HARTMAN. J. Am. Chem. Soc. **75**, 939 (1953).
9. J. B. UMLAND et B. W. WILLIAMS. J. Org. Chem. **21**, 1302 (1956).
10. B. RICKBORN et R. M. GERKIN. J. Am. Chem. Soc. **93**, 1693 (1971).
11. H. B. HENBEST et B. NICHOLLS. J. Chem. Soc. 4608 (1957).
12. I. HEILBRON, E. R. H. JONES, J. B. TOOGOOD, et B. C. L. WEEDON. J. Chem. Soc. 1827 (1949).
13. J. PASCUAL et J. CASTELLS. J. Am. Chem. Soc. **74**, 2899 (1952).
14. J. PASCUAL et F. LACASA. An. Real. Soc. Espan. Fis. Quim. Ser. B, **51**, 551 (1955).
15. G. STORK, A. BRIZZOLARA, H. LANDESMAN, J. SZMUSKOVICZ, et R. TERREL. J. Am. Chem. Soc. **85**, 207 (1963).

Can. J. Chem. Downloaded from www.nrcresearchpress.com by 210.87.254.105 on 09/05/12
For personal use only.

Can. J. Chem. Downloaded from www.nrcresearchpress.com by 210.87.254.105 on 09/05/12
For personal use only.

Kinetic Isotope Effect Studies on the Reaction of Benzyl Nitrate with Base in Various Solvents

CAROL A. POLLOCK[1] AND P. J. SMITH[2]

Department of Chemistry, Bishop's University, Lennoxville, Quebec

AND

Department of Chemistry and Chemical Engineering, University of Saskatchewan, Saskatoon, Saskatchewan

Received July 16, 1971

The role of solvent and base on the nature of the transition state for the concerted one-step carbonyl elimination reaction of benzyl nitrate has been examined using rate and kinetic isotope effect techniques. The primary hydrogen–deuterium isotope effect was found to increase with increasing strength of the abstracting base, k^H/k^D = 5.94 and 6.41 at 30° for reaction with EtO^-/EtOH and *t*-BuO^-/*t*-BuOH, respectively. The nitrogen isotope effect decreased with increasing strength of the abstracting base, 2.07, 1.82, and 1.54% for reaction with OH^-/40 vol % EtOH–H_2O, EtO^-/EtOH, and *t*-BuO^-/*t*-BuOH, respectively. The conclusion is reached that an increase in the strength of the abstracting base leads to a more reactant-like transition state with decreased rupture of both the C—H and O—N bonds. The role of solvent on the nature of the transition state was examined by determining rates and nitrogen isotope effects for reaction in various ethanol–water and ethanol – dimethyl sulfoxide mixtures. The nitrogen effect was found to remain essentially constant in solvent mixtures ranging from 65 vol % EtOH–H_2O on the one hand to 80 vol % EtOH–DMSO on the other hand where the rate constants differed by a factor of 100 fold. It is concluded that solvent plays only a very minor role in determining transition state structure for the concerted elimination reaction of a neutral substrate with base.

Le rôle du solvant et de la base sur la nature de l'état de transition pour la réaction d'élimination concertée en une étape du groupement carbonyle du nitrate de benzyle a été examiné en utilisant des techniques de vitesse et de cinétique d'effet isotopique. L'effet isotopique primaire hydrogène–deutérium croît avec la force croissante de la base qui permet l'élimination, k^H/k^D = 5.94 et 6.41 à 30° pour la réaction avec respectivement EtO^-/EtOH et *t*-BuO^-/*t*-BuOH. L'effet isotopique de l'azote décroît avec la force croissante de la base 2.07, 1.82, et 1.54% pour la réaction avec respectivement OH^-/40 vol % EtOH–H_2O, EtO^-/EtOH et *t*-BuO^-/*t*-BuOH. On arrive à la conclusion qu'un accroissement dans la force de la base d'élimination amène à un état de transition plus réactif avec une rupture décroissante de chacune des liaisons C—H et O—N. Le rôle du solvant sur la nature de l'état de transition a été examiné par détermination des vitesses et des effets isotopiques de l'azote pour la réaction dans de nombreux mélanges éthanol–eau et éthanol–diméthylsulfoxyde. On trouve que l'effet de l'azote reste essentiellement constante dans les mélanges de solvant, allant de 65 vol % EtOH–H_2O d'un côté à 80% vol EtOH–DMSO d'un autre côté, dans lesquels les constantes de vitesse diffèrent par un facteur de cent. On en conclut que le solvant ne joue qu'un petit rôle mineur dans la détermination de la structure de l'état de transition pour une réaction d'élimination concertée entre un substrat neutre et une base.

Canadian Journal of Chemistry, 49, 3856 (1971)

Introduction

It is generally accepted that the concerted one-step (E2) elimination reaction can proceed by a spectrum of transition states differing in the extent of carbon–hydrogen and carbon – leaving group bond rupture (1, 2). The nature of the transition state could range from one that is E1-like (**1**) with considerable C_α—X bond rupture and a negligible degree of C_β—H bond weakening all the way to an E1cb-like transition state (**3**) with extensive C_β—H bond rupture and very little C_α—X bond rupture. An infinite number of intermediate transition states (**2**) is considered to be possible. Furthermore, it has been proposed that the E2 mechanism can merge

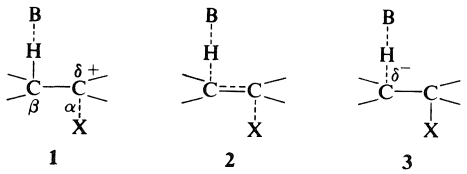

[1]Holder of an NRCC bursary 1968–1969.

[2]Author to whom all correspondence should be addressed: Department of Chemistry and Chemical Engineering, University of Saskatchewan, Saskatoon, Saskatchewan.

Can. J. Chem. Downloaded from www.nrcresearchpress.com by 210.87.254.105 on 09/05/12
For personal use only.

smoothly on the one hand to the carbonium ion mechanism (E1) and on the other hand to the carbanion mechanism (E1cb).[3]

Within recent years considerable experimental data has been accumulated from the study of several one-step processes and interpreted in the light of a variable transition state for the E2 reaction. The studies dealt mainly with the 2-phenylethyl and related systems and included eclipsing effects (4), substituent effects (5), leaving group isotope effects (6), primary hydrogen–deuterium isotope effects (7), and secondary isotope effects (8) for the reaction with OD^- in D_2O *vs.* OH^- in H_2O (k^{OD^-}/k^{OH^-}).

The determination of the relative extent of C—H and C—X bond rupture at the transition state using isotope effects is dependent on the interpretation of the magnitude of these effects in terms of the degree of decrease of the appropriate force constant(s) (bond-weakening) in going from the initial to the transition state. The interpretation of the C—X isotope effect has generally been considered to be straightforward with the magnitude of the effect being dependent upon the extent of bond rupture at the transition state. Katz and Saunders (9), however, have shown from a theoretical treatment that small isotope effects for the leaving group can be associated with reactions in which C—X bond rupture is quite far advanced at the transition state. Saunders suggests that qualitative interpretation of isotope effects should be possible, however, when systematic changes in some structural or environmental feature of a reaction are made.

Several theoretical discussions (10–12) have led to the accepted view that the magnitude of the primary hydrogen–deuterium isotope effect is at a maximum when the transition state is symmetrical and that smaller isotope effects are a result of either reactant-like or product-like transition states. A knowledge of the type of transition state from Hammett ρ or k^{OD^-}/k^{OH^-} determinations is essential, therefore, before one can interpret a small isotope effect in terms of the degree of carbon–hydrogen bond-weakening.

Westheimer's curve (plot of k^H/k^D *vs.* the degree of proton transfer to base at the transition state) has been realized by several groups of workers for entirely unrelated reaction systems. Kresge *et al.* (13) determined the isotope effect, $k^{H_3O^+}/k^{D_3O^+}$, for the hydrolysis of several vinyl ethers in aqueous solution at 25° and obtained a uniform trend when $k^{H_3O^+}/k^{D_3O^+}$ was plotted against log $k^{H_3O^+}$ with a maximum being observed. Other workers (14, 15) have realized similar behavior for base-catalyzed proton removal from carbon. For example, Longridge and Long (15) from a study of hydrogen exchange from azulenes, observed a maximum hydrogen–deuterium isotope effect when the proton was transferred between bases of similar strengths, as measured by ΔpK_a values.[4] Finally, Cockerill (7*b*), in a study of the elimination reaction of dimethyl-2-phenylethylsulfonium bromide with hydroxide ion in various water – dimethyl sulfoxide mixtures, obtained a curve with a maximum when k^H/k^D was plotted against mol % dimethyl sulfoxide.

The present available studies show that the transition state for an E2 process is dependent on leaving group (17, 7*c*), acidity of the β-hydrogen (17, 7*c*), dihedral angle (18), solvent, and base. Until very recently the latter two variables have always been changed simultaneously and it was difficult to assess the contributions of each. Recent studies (7*b*, 19), however, have been carried out on neutral and "onium" substrates in mixed solvents where the basic species was kept constant. It was found that whereas solvent plays an important role in determining transition state geometry for the reaction of the charged reactant it appears to have very little effect when the substrate is neutral.

The carbonyl elimination reaction of benzyl nitrate with ethoxide ion (eq. 1) has previously

[1] $$C_6H_5CH_2ONO_2 + {}^-OEt \rightarrow C_6H_5CHO + {}^-NO_2 + EtOH$$

been shown (6*a*) to be a concerted process by the absence of deuterium exchange with solvent and a N^{14}:N^{15} isotope effect of 2.0%. Furthermore, a recent determination (20) of the nitrogen isotope effect associated with the carbonyl elimination reaction ($E_{CO}2$) of a series of para-substituted

[3]In a recent paper (3), O'Ferrall has suggested that at the borderline between the mechanisms, a continuity of transition states need not be expected.

[4]Bordwell and Boyle (16) in two recent papers have examined the question of the use of rho values, the Bronsted, β, and hydrogen–deuterium effects as guides to transition state structures in deprotonation reactions. They conclude that these parameters are either very insensitive to large changes in transition state structure or that the transition states are essentially unaltered for widely different substrates.

TABLE 1. Nitrogen isotope effects at 30° for the $E_{CO}2$ reaction of benzyl nitrate with different bases in different solvents

Hydroxide in 40 vol % EtOH–H_2O		Ethoxide in ethanol		*t*-Butoxide in *t*-butanol	
Extent of reaction*	(k^{14}/k^{15})†	Extent of reaction*	(k^{14}/k^{15})†	Extent of reaction*	(k^{14}/k^{15})†
16.5	1.0212	10.7	1.0174	23.0‡	1.0171
22.0	1.0210	10.8	1.0180	23.5‡	1.0140
22.0	1.0206	22.1	1.0192	44.4‡	1.0153
29.4	1.0201	30.5	1.0182	44.4‡	1.0140
32.0	1.0204	42.3	1.0182	46.4‡	1.0161
	Mean 1.0207±0.0004		Mean 1.0182±0.0006		Mean 1.0154±0.0015

*Determined from yield of ammonia obtained from reduction of nitrite and nitrate.
†The limits shown are the standard deviation.
‡The amount of base corresponding to the desired extent of reaction was added.

benzyl nitrates at 20° in a solvent of 90 vol % EtOH–H_2O has shown the nitrogen effect to be appreciably sensitive to the nature of the para-substituent (2.26 and 1.62% for the *p*-CH_3 and *p*-CF_3 substituents, respectively).

Accordingly, we have carried out a study on the $E_{CO}2$ reaction of benzyl nitrate with different bases in different solvents in order to shed more light on the role of solvent and base in determining transition state geometry. The results are discussed in the light of a theory proposed by Thornton (21) which allows one to predict the effect of base strength on the nature of the transition state.

Results and Discussion

Isotope Effect Studies on the Reaction of Benzyl Nitrate with Different Bases

The nitrogen and hydrogen–deuterium isotope effects for the carbonyl elimination reaction of benzyl nitrate with hydroxide ion[5] in 40 vol % EtOH–H_2O, ethoxide ion in ethanol, and *t*-butoxide ion in *t*-butanol were determined at 30° and the results are shown in Tables 1 and 2, respectively. A summary of the isotope effects together with the pertinent rate constants is shown in Table 3.

In all the base-solvent systems studied, except for *t*-butoxide in *t*-butanol, the carbonyl elimination reaction producing nitrite ion was in competition with an S_N2 process giving nitrate ion; *i.e.* % $E_{CO}2 < 100$, Tables 2 and 5. It is possible, however, using methods described previously (6*a*) to determine both the deuterium and nitrogen isotope effects associated with the elimination process. The total rate was followed by acid–base titration and the rate constant for the carbonyl elimination reaction, k_{Eco2}, was evaluated from the relative yields of nitrite and nitrate ions determined by the selective reduction of these ions to ammonia. In all cases the ratio of nitrite to nitrate remained constant during the course of a kinetic run.

The nitrogen isotope effect for the carbonyl elimination reaction in each solvent system was obtained by comparing the N^{14}/N^{15} ratio of benzyl nitrate of natural isotopic abundance with that of nitrite ion formed in the desired elimination reaction of the ester carried to some known extent of completion. Selective reduction of the nitrite ion to ammonia accomplished the separation of the nitrogen of this ion from that of the nitrate ion formed in the simultaneous S_N2 displacement reaction (6*a*). The ammonia was then converted into nitrogen gas which was first purified and then analyzed mass spectrometrically. The isotopic abundance for the reactant was obtained by analysis of the nitrogen gas similarly formed from nitrite plus nitrate produced in a reaction which had been allowed to proceed to completion.

The isotope effect measurements, Table 3, were determined under different solvent conditions. It is reasonable to assume, however, that the abstracting base increases in strength from the aqueous medium[6] to the medium of ethoxide in ethanol and finally to the *t*-butoxide – *t*-buta-

[5]It has been shown (22) that the % base present as hydroxide is 90% in this solvent mixture.

[6]The active base in the 40 vol % EtOH–H_2O solvent could be either hydroxide ion or ethoxide ion. It is reasonable to assume that it is hydroxide since England and Burns (22) have shown that the percent base present as hydroxide in this solvent mixture is 90.

Can. J. Chem. Downloaded from www.nrcresearchpress.com by 210.87.254.105 on 09/05/12
For personal use only.

Can. J. Chem. Downloaded from www.nrcresearchpress.com by 210.87.254.105 on 09/05/12
For personal use only.

TABLE 2. Hydrogen–deuterium isotope effects at 30° for the $E_{CO}2$ reaction of benzyl nitrate with different bases in different solvents

	Hydroxide in 40 vol % ethanol–water		Ethoxide in ethanol		*t*-Butoxide in *t*-butanol	
	$C_6H_5CH_2ONO_2$	$C_6H_5CD_2ONO_2$	$C_6H_5CH_2ONO_2$	$C_6H_5CD_2ONO_2$	$C_6H_5CH_2ONO_2$	$C_6H_5CD_2ONO_2$
% $E_{CO}2$	45.8	—	87.7	60.4	100	100
10^3k_{total}*	0.079	—	0.499	0.122	481	481
$10^3k_{E_{CO}2}$*	0.028	—	0.438	0.0737	481	481
$(k^H/k^D)_{E_{CO}2}$	—			5.94±0.20†		6.41±0.24†

*k in l mol^{-1} s^{-1}.
†Estimated uncertainty based upon variation in yield of nitrite ion and variation in rate constants.

TABLE 3. Rates and isotope effects found in the $E_{CO}2$ reaction of benzyl nitrate with different bases in different solvents at 30°

Base and solvent	$10^3 k_{E_{CO}2}$	k^H/k^D	$(k^{14}/k^{15} - 1)100$
OH^-/40 vol % EtOH–H_2O	0.028	—	2.07±0.04
OEt^-/EtOH	0.438	5.94±0.20	1.82±0.06
t-BuO^-/*t*-BuOH	481.	6.41±0.24	1.54±0.15

nol solution. This view is supported by values of the *H*-function reported by Bowden (23) and is in accord with the observed rate constants for elimination ($10^3 k_{E_{CO}2}$ (30°) = 481, 0.438, and 0.028 1 mol^{-1} s^{-1} for reaction in *t*-butanol, ethanol, and 40 vol % EtOH–H_2O, respectively).

The nitrogen isotope effects decrease from a value of 2.07% obtained for the reaction in the EtOH–H_2O solvent to a value of 1.83% in EtOH and finally to 1.54% in *t*-butanol. Since the magnitude of the leaving group isotope effect depends on the extent to which the composite force constant of the O—N bond is decreased in going from the initial to the transition state (24), the largest effect associated with the reaction of benzyl nitrate with the weakest base, "hydroxide", indicates, therefore, that there is *more* O—N bond rupture in the transition state for this process than for the reactions promoted by the stronger bases, ethoxide and *t*-butoxide.

An interpretation of the magnitude of the primary hydrogen–deuterium effects, Table 3, in terms of the extent of C—H bond rupture requires a prior knowledge of the nature of the transition state with respect to the degree of proton transfer to base; *i.e.* whether the proton is *more than* or *less than* one-half transferred. The large nitrogen isotope effects observed in the three solvent systems (the theoretical maximum is approximately 3.8% at 30° (6*a*)) together with the large Hammett ρ value of +3.6 (20), measured for the ethoxide promoted reaction, suggest a transition state where the proton is more than one-half transferred, since the only way a large positive ρ can result in a reaction in which C—N bond rupture is well advanced would be for the transfer of the proton to be very well advanced as well. This conclusion receives support from the fact that the reaction of 2-phenylethyltrimethylammonium ion with ethoxide (7*c*) has similar values for ρ and the nitrogen effect. For this process Steffa and Thornton (8) have established that the proton is more than one-half transferred to base at the transition state by determining the secondary effects, k^{OD^-}/k^{OH^-}.

Consequently, the smaller value of k^H/k^D obtained for the reaction of benzyl nitrate with ethoxide than with *t*-butoxide suggests that the proton is *more transferred* to base in the transition state for the "weaker base" promoted reaction (k^H/k^D = 5.94 and 6.41 for reaction of benzyl nitrate with ethoxide and *t*-butoxide, respectively).

The nitrogen and hydrogen–deuterium isotope effects obtained for the reaction of benzyl nitrate with several bases lead to the conclusion that both the oxygen–nitrogen and carbon–hydrogen bonds are ruptured to a greater extent at the transition state for reactions promoted by bases of *decreasing* strengths. In other words, the more one bond is broken in the transition state the more also is the other. In the light of this conclusion, it is difficult to visualize a smooth transition from a carbanionic-like E2 transition state to the E1cb mechanism as visualized by Bunnett (1) for a particular reaction where substituents, base, or solvent are varied systematically since increased C—H rupture leads to an attenuated O—N bond weakening. This is in accord with the theoretical predictions of O'Ferrall (3) mentioned in the Introduction.

A theoretical treatment of Thornton (21) dealing with the effects of structural changes in the reactant on the nature of the transition state is in accord with the conclusion that a decrease in the strength of the abstracting base involved in an E2 reaction will lead to a more product-like transition state with increased C—H and O—N bond weakening. Thornton expressed the view that the geometrical change for an elimination reaction will be determined largely by the substituent effect on the parallel motion along the reaction co-ordinate where the relative lengths of the arrows below

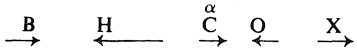

represent the relative extent to which each atom has moved when the reacting system has reached the transition state. Thornton showed that the

Can. J. Chem. Downloaded from www.nrcresearchpress.com by 210.87.254.105 on 09/05/12
For personal use only.

Can. J. Chem. Downloaded from www.nrcresearchpress.com by 210.87.254.105 on 09/05/12
For personal use only.

more difficult it is for two atoms to move apart, the greater will be the extent to which they need to separate before arriving at the state of maximum energy which separates reactants and products. With respect to the effect of base strength on the transition state geometry, it is easy to see that the weaker the base the more difficult will be the motion resulting in a transfer of the proton from carbon to base. A decrease in the strength of the base will, therefore, result in an increase in the extent of proton transfer to base and an increase in the extension of the O—N bond at the transition state since the reaction co-ordinate motion which results in the separation of hydrogen from carbon also involves a separation of nitrogen from oxygen.

The question arises concerning the relative carbanion character of the product-like transition states (increased C—H and O—N bond rupture) compared with the more reactant-like transition states. It is generally considered that for reactions characterized by large positive ρ values a decrease in ρ and an increase in k^H/k^D indicates a transition state which has less C—H bond rupture and, therefore, decreased carbanion character (5*b*). It follows from our conclusion where a decrease in C—H bond rupture is accompanied by a decrease in O—N bond rupture that the carbanion character of a transition state is dependent on the *relative* change of each of these bond lengths for a transition state where there is coupling of the motions of the bonds as illustrated by Thornton's representation of the E2 transition state. Thornton (21) considered this situation and he suggested that by making H move more relative to O, and C_α move more relative to X the transition state becomes more product-like with relatively more carbanion character at C_α than carbonium ion character at O; that is, the transition state becomes more E1cb-like.

Our conclusion that an increase in C—H bond weakening leads also to an attenuated increase in O—N bond rupture in the transition state would suggest that for a particular reaction series systematic changes in substituents, base, etc. would not lead to a changeover from the concerted to the stepwise (E1cb) mechanism for elimination. We suggest that only in those cases where coupling is poor would one expect a carbanion intermediate. The combination of a poor leaving group (25), stabilization of charge at the β-carbon (25), and a dihedral angle displaced from 180 or 0° (18) is expected to favor the formation of a carbanion intermediate involved in the elimination process.

Nitrogen Isotope Effect Studies on the Role of Solvent on Transition State Geometry for the $E_{CO}2$ Reaction of Benzyl Nitrate

The nitrogen isotope effect was determined for the carbonyl elimination reaction of benzyl nitrate at 30° in various ethanol–water and ethanol – dimethyl sulfoxide mixtures. The isotope effect results are shown in Table 4 while a summary of these effects together with the pertinent kinetic data is shown in Table 5. The overall rate constants when multiplied by the ratio $[NO_2^-]/([NO_2^-] + [NO_3^-])$, % $E_{CO}2$, give the rate constant for the elimination process, k_{Eco2}.

The rate constant for elimination is seen to decrease with increasing water content of the medium; *i.e.* k_{Eco2} = 0.438 and 0.0284 in 100% EtOH and 40 vol % EtOH–H_2O, respectively. This trend is consistent with the predicted effect (26) of an increase in solvent polarity on a reaction of an ion with a neutral substrate. Furthermore, the variation in the elimination to substitution ratio, % $E_{CO}2$, with solvent composition is also in accord with changes in polarity of the reaction solution (26). Another factor which could account for the decrease in rate constant is that the abstracting base becomes more or better solvated as the reaction mixture acquires a greater water content. This increase in solvation would make it more difficult for the base to promote elimination and hence the decrease in rate constants. This factor will be discussed in more detail below.

It is of interest to note, however, that a discontinuity exists in the plot of log k_{Eco2} *vs.* volume% EtOH–H_2O, Fig. 1, when the solvent composition is approximately 50 vol % EtOH–H_2O and the percent base present as hydroxide is greater than 80 (22). This discontinuity can be ascribed to the fact that the "abstracting" base involved in the elimination process has been changed from a "strong" base, ethoxide, to a "weaker" base, hydroxide, which becomes kinetically significant only in solutions with a composition of greater than 50% water. This view is supported by the nitrogen isotope effect results where a similar discontinuity is observed. The constancy of the nitrogen results for solvent compositions ranging from 100 vol % EtOH–H_2O to 65 vol % indicates that the abstracting base remains constant in this solvent composition region while the increase in nitrogen effect for the 50 and 40 vol % EtOH–

Can. J. Chem. Downloaded from www.nrcresearchpress.com by 210.87.254.105 on 09/05/12
For personal use only.

TABLE 4. Nitrogen isotope effect results for the $E_{co}2$ reaction of benzyl nitrate with base* in various solvent mixtures at 30°

Solvent mixture	Extent of reaction†	(k^{14}/k^{15})‡
90 vol % EtOH–H_2O	9.95	1.0171
	17.4	1.0182
	19.4	1.0188
	27.6	1.0188
		Mean 1.0183 ± 0.0008
80	10.2	1.0176
	13.5	1.0177
	26.8	1.0182
	28.4	1.0179
	41.6	1.0180
		Mean 1.0179 ± 0.0003
65	8.7	1.0180
	20.4	1.0185
	21.4	1.0192
	30.1	1.0187
	32.2	1.0178
		Mean 1.0184 ± 0.0006
50	14.8	1.0212
	15.8	1.0206
	19.8	1.0187
	22.8	1.0221
	31.1	1.0208
	36.3	1.0193
	44.7	1.0202
	46.9	1.0209
		Mean 1.0204 ± 0.0012
40	16.5	1.0212
	22.0	1.0210
	22.0	1.0206
	29.4	1.0201
	32.0	1.0204
		Mean 1.0207 ± 0.0004
95 vol % EtOH–DMSO	8.3	1.0162
	8.3	1.0171
	19.6	1.0188
	20.2	1.0181
	32.0	1.0179
		Mean 1.0176 ± 0.0010
80	23.4	1.0196
	26.6	1.0193
	28.2	1.0185
	36.5	1.0185
		Mean 1.0190 ± 0.0004

*The mixtures were prepared by diluting a solution of sodium ethoxide in ethanol with the appropriate solvent.
†Determined from the yield of ammonia obtained from reduction of nitrite and nitrate.
‡The limits shown are the standard deviation.

H_2O mixtures suggest that the abstracting base is a weaker one (21).

The only reasonable conclusion that one can draw concerning the invariance of the nitrogen isotope effect results determined for reactions carried out in solvents ranging from 100 % EtOH to 65 vol % EtOH–H_2O is that the transition state structure remains essentially constant. It should be noted that the polarity of the solvent is changed considerably over this range of solvent composition; *i.e.*, dielectric constant of EtOH and 60 vol % EtOH–H_2O is 23.2 and 44.7, respectively (27). Consequently, it appears that the effect of solvent on the nature of the transition state is negligible for reaction between an ion and a neutral molecule. A similar conclusion was reached by Cockerill *et al.* (19) who studied the elimination reaction of the 2-arylethyl bromides with potassium *t*-butoxide in *t*-butyl alcohol – dimethyl sulfoxide mixtures and found that ρ and k^H/k^D did not vary.

The possibility exists that the observed variation in rate constants and nitrogen isotope effects with solvent composition could be due to changes in base strength arising from alterations in the solvation of hydroxide ion. In other words, the discontinuities could well arise from a competi-

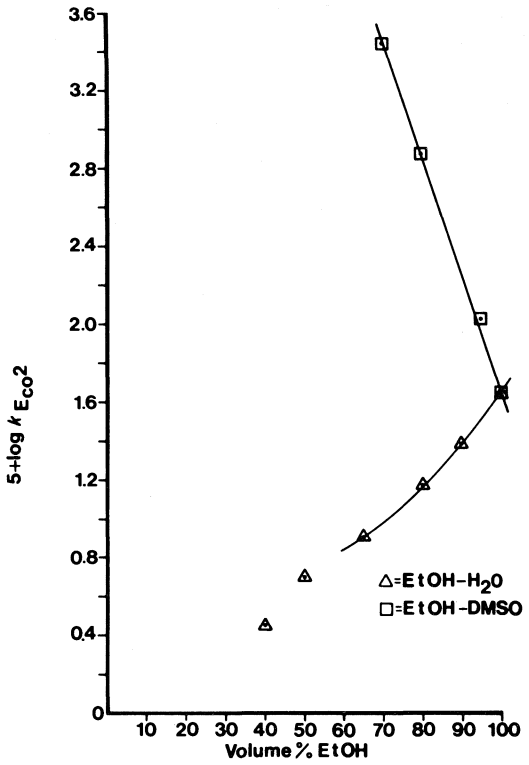

FIG. 1. Log k_{Eco2} *vs.* solvent composition for the reaction of benzylnitrate with base.

TABLE 5. Rates and nitrogen isotope effects for the $E_{CO}2$ reaction of benzyl nitrate with base* in various solvent mixtures at 30°

Solvent	$10^3 k_{overall}$†	% $E_{CO}2$	$10^3 k_{E_{CO}2}$†	$(k^{14}/k^{15} - 1)100$
100 vol % EtOH–H_2O	0.499	87.7	0.438	1.82±0.06
90	0.300	78.9	0.238	1.83±0.08
80	0.200	74.7	0.149	1.79±0.03
65	0.125	64.3	0.0800	1.84±0.06
50	0.0891	55.6	0.0495	2.04±0.12
40	0.0792	45.8	0.0284	2.07±0.04
95 vol % EtOH–DMSO	1.19	91.1	1.08	1.76±0.10
80	7.68	95.6	7.34	1.90±0.04
70	27.8	98.2	27.3	—

*The mixtures were prepared by diluting a solution of sodium ethoxide in ethanol with the appropriate solvent.
†In l mol^{-1} s^{-1}. The overall rate constants shown are the average of at least three determinations and always agreed to better than 2%.

tion of hydroxide ions of different solvation for the α-hydrogen atom. The formation of the $E_{CO}2$ transition state should require a displacement of only one solvent molecule as hydroxide ion in ethanol–water is probably solvated by a combination of two or three ethanol and water molecules.[7] Consequently, it happens that as water is added to the reaction medium the type of solvation of the partially neutralized hydroxide ion in the transition state should change; *i.e.*, as ethanol molecules are replaced by water molecules the base, hydroxide ion, would become effectively weaker. This should lead, however, to a continuous change[8] in both the second order rate constant for elimination and the nitrogen isotope effect as the solvent composition is varied which is not observed. Furthermore, it is unlikely that the nitrogen isotope effect determined in 100% EtOH, where ethoxide is base, would be the same as the isotope effect determined in 65 vol % EtOH–H_2O if the base present in the aqueous solution is a highly solvated hydroxide ion. It is concluded that the discontinuities arise due to a change in base, ethoxide ion to hydroxide ion, and are not a result of changes in base "structure", solvation of hydroxide.

In order to eliminate the problem of changing the base as well as the solvent which was encountered in the study of the reaction of benzyl nitrate with base in the ethanol–water mixtures, the nitrogen isotope effects and the rate constants associated with the reaction of benzyl nitrate with ethoxide ion[9] in various ethanol – dimethyl sulfoxide mixtures were determined, Table 5. It is seen that the rate constant for elimination increases regularly, Fig. 1, as more dimethyl sulfoxide is added to the ethanol solvent, $k_{E_{CO}2}$ is 0.000438 and 0.0273 in ethanol and 70 vol % ethanol – dimethyl sulfoxide, respectively. This variation in rate can simply be ascribed to the fact that dimethyl sulfoxide has the ability of desolvating the abstracting base, ethoxide; *i.e.*, dimethyl sulfoxide competes with the ethoxide ion for the ethanol molecules. Since the abstracting base must be partially desolvated in order to form the transition state, it follows that the variation in the ease of desolvation as influenced by additions of dimethyl sulfoxide will lead to variations in rate as observed. Once the transition state is formed, however, the base it contains is substantially the same species (a partially neutralized ethoxide ion) regardless of medium composition.

That the base is essentially constant for ethoxide in ethanol and for the several ethanol – dimethyl sulfoxide mixtures is borne out by the nitrogen isotope effect results in Table 5 where it is seen that the isotope effect remains essentially constant when the solvent composition is varied; *i.e.*, 1.82 and 1.90 in EtOH and 80 vol % EtOH–DMSO, respectively. The constancy of the nitrogen isotope effects, and hence the constancy of O–N bond rupture at the transition state, obtained under the different solvent conditions is as predicted by Thornton (21) when the base remains the same. The conclusion is reached, therefore,

[7]Hydroxide ion is believed to be hydrogen bonded to three water molecules (28).

[8]Smith and Bourns (29), in a study of the reaction of 9-fluorenyl nitrate with acetate in ethanol–H_2O mixtures, found the nitrogen isotope effect equal to 1.0091, 1.0105, 1.0131 for reaction in ethanol, 92 vol % EtOH–H_2O, 85 vol % EtOH–H_2O, respectively.

[9]It is unlikely that bases other than ethoxide; *i.e.*, nitrite or dimsyl ion, induce elimination as they are probably kinetically insignificant under the reaction conditions employed.

Can. J. Chem. Downloaded from www.nrcresearchpress.com by 210.87.254.105 on 09/05/12
For personal use only.

that the role of solvent in determining transition state structure is very minor for an elimination reaction involving a neutral substrate.

Experimental

Materials

Benzyl Nitrate and Benzyl Nitrate α-d_2

These compounds were prepared by the procedure described by Buncel and Bourns (6*a*). The benzyl nitrate α-d_2 was shown by n.m.r. to be at least 99% deuterated.

Absolute Ethyl Alcohol

This solvent was dried by the method of Lund and Bjerrum (30) and stored under anhydrous conditions.

Absolute t-Butyl Alcohol

This solvent was dried by refluxing over and distilling from sodium metal. The process was repeated twice and the *t*-butyl alcohol was stored under anhydrous conditions.

Dimethyl Sulfoxide

This solvent was distilled once from calcium hydride under reduced pressure, was filtered through a 4 ft molecular sieve (B.D.H. grade 5A) column and then fractionally redistilled under reduced pressure.

Mixed Solvents

These were prepared to give the desired solvent by per cent volume to volume.

Sodium Ethoxide and Potassium t-Butoxide

These bases were prepared by the action of the appropriate metal with the desired solvent under strictly anhydrous conditions in a nitrogen atmosphere. The base solutions in the mixed solvents were prepared by diluting the appropriate alkoxide with either dimethyl sulfoxide or water. The water used in the dilutions was CO_2 free.

Kinetic Measurements

The rate constants for the overall reactions as well as the rate constants for elimination were determined as described by Buncel and Bourns (6*a*).

Nitrogen Isotope Effects

Complete Reaction and Collection of Ammonia

A weight of benzyl nitrate and an accurately measured volume of base were allowed to react to completion. A 5 ml aliquot was extracted and added to the Kjeldahl distillation and since it is the total nitrogen that is required, the nitrite and nitrate were both distilled into the same flask containing excess sulfuric acid. The acid was back-titrated with standard alkali, using bromocresol green as indicator; followed by the immediate addition of 3 ml of 0.01 *N* sulfuric acid to prevent loss of ammonia. The titration gave the total number of moles of product formed which was usually greater than 99% of the number of moles of reactant.

Partial Reaction

A weight of benzyl nitrate was calculated so that when the reaction had proceeded to the desired extent of reaction, the nitrite produced would yield a volume of nitrogen of approximately 3 ml at standard conditions. The substrate was weighed into a reaction flask which was placed in a constant temperature bath and allowed to equilibriate. Similarly, the base of desired concentration and solvent composition was placed in the constant temperature bath. After approximately 30 min, the reactants were mixed and the reaction was allowed to proceed for a pre-determined time, as calculated from the kinetic data. The reaction flask was then removed from the bath and its contents emptied into a separatory funnel containing ice, water and diethyl ether. The aqueous layer was extracted four times with ether. The combined ether extracts were then washed four times with water and these washings were added to the aqueous layer which was then concentrated to a small volume, 25 ml, on rotary evaporator.

The concentrated solution was then added to a Kjeldahl distillation flask and the nitrite ion was converted into ammonia which was distilled into excess standard sulfuric acid and back titrated as described for the preparation of the complete samples. The resulting ammonium sulfate solution was concentrated to 3 ml in preparation for its conversion to ammonia.

In all of the partial reactions where the nitrite ion was reduced to ammonia in preparation for its conversion to nitrogen gas and mass spectrometer analysis, the amount of nitrate ion was determined by the procedure described above, so that the ratio $[NO_2^-]/([NO_2^-] + [NO_3^-])$ could be used in the evaluation of nitrogen isotope effect for the $E_{CO}2$ process.

In all cases the ammonium sulfate solutions were concentrated to 3 ml in preparation for conversion to nitrogen by the procedure described by Buncel and Bourns (6*a*).

For the reaction with *t*-butoxide in *t*-butanol, the usual method of quenching was unsatisfactory due to the fast rate of the reaction. In this case, the desired extent of reaction was achieved by adding the appropriate amount of base, corresponding to the extent of reaction required, and allowing the reaction to proceed for 30 half-lives. In these cases, the concentrations of the reactants were sufficiently low so that no more than 1% reaction occurred during the mixing of the reacting solutions.

The kinetic isotope effect was calculated by using the expression suggested by Baliga and Bourns (31)

$$\frac{k^{14}}{k^{15}} = \frac{\ln 1 - \dfrac{f'(1-p)}{1-fp}}{\ln 1 - \dfrac{rf'(1-p)}{1-f'p}}$$

where f' is the mole fraction of the ester which has undergone reaction, p is the fraction of the total reaction which is substitution and r is $(N^{14}/N^{15})_{reactant}/(N^{14}/N^{15})_{NO_2^-}$. This is a modification of an expression derived by Stevens and Attree (32), and takes into account the fact that the reactant is being consumed by reactions other than those where the isotope effect is being measured.

The N^{14}/N^{15} ratio was found to be the same for nitrate ion collected during the early stages of the reaction, 134.187 and 134.232, as for the average value found for the completes, $NO_2^- + NO_3^-$. *i.e.*, 134.212. Consequently, substitution occurs without fractionation thus making the use of f' valid.

This work was supported by the National Research Council of Canada.

Can. J. Chem. Downloaded from www.nrcresearchpress.com by 210.87.254.105 on 09/05/12
For personal use only.

The authors gratefully acknowledge both the very helpful discussions with Professor A. N. Bourns and the use of his facilities for part of the investigation.

1. J. F. BUNNETT. Angew. Chem. Int. Ed. Engl. **1**, 225 (1962).
2. J. F. BUNNETT. Surv. Progr. Chem. **5** (1969).
3. R. A. MORE O'FERRALL. J. Chem. Soc. B, 274 (1970).
4. D. J. CRAM, F. D. GREENE, and C. H. DEPUY. J. Am. Chem. Soc. **78**, 790 (1956).
5. (*a*) C. H. DEPUY and C. A. BISHOP. J. Am. Chem. Soc. **82**, 2535 (1969); (*b*) W. H. SAUNDERS, JR., D. G. BUSHMAN, and A. F. COCKERILL. J. Am. Chem. Soc. **90**, 1775 (1968); (*c*) R. BAKER and M. J. SPILLETT. J. Chem. Soc. B, 481 (1969).
6. (*a*) E. BUNCEL and A. N. BOURNS. Can. J. Chem. **38**, 2457 (1960); (*b*) W. H. SAUNDERS, JR., A. F. COCKERILL, S. AŠPERGER, L. KLASINĆ, and D. STEFANOVIC. J. Am. Chem. Soc. **88**, 848 (1966); (*c*) P. J. SMITH and A. N. BOURNS. Can. J. Chem. **48**, 125 (1970).
7. (*a*) W. H. SAUNDERS, JR., and D. H. EDISON. J. Am. Chem. Soc. **82**, 138 (1960); (*b*) A. F. COCKERILL. J. Chem. Soc. B, 964 (1967); (*c*) A. N. BOURNS and P. J. SMITH. Can. J. Chem. In preparation.
8. L. STEFFA and E. R. THORNTON. J. Am. Chem. Soc. **89**, 6147 (1967).
9. A. M. KATZ and W. H. SAUNDERS, JR. J. Am. Chem. Soc. **91**, 4469 (1969).
10. F. H. WESTHEIMER. Chem. Rev. **61**, 265 (1961).
11. R. P. BELL. Discuss. Faraday Soc. **39**, 16 (1965).
12. R. A. MORE O'FERRALL and J. KOUBA. J. Chem. Soc. B, 985 (1967).
13. A. J. KRESGE, D. S. SAGATYS, and H. C. CHEN. J. Am. Chem. Soc. **90**, 4174 (1968).
14. R. P. BELL and B. J. COX. J. Chem. Soc. B, 194 (1970).
15. J. C. LONGRIDGE and F. A. LONG. J. Am. Chem. Soc. **89**, 1292 (1967).
16. (*a*) F. G. BORDWELL and W. J. BOYLE, JR. J. Am. Chem. Soc. **93**, 511 (1971); (*b*) F. G. BORDWELL and W. J. BOYLE, JR. J. Am. Chem. Soc. **93**, 512 (1971).
17. G. AYREY, A. N. BOURNS, and V. A. VYAS. Can. J. Chem. **41**, 1759 (1963).
18. A. N. BOURNS and A. C. FROSST. Unpublished results.
19. A. F. COCKERILL, S. ROTTSCHAEFER, and W. H. SAUNDERS, JR. J. Am. Chem. Soc. **89**, 901 (1967).
20. C. A. POLLOCK and P. J. SMITH. Unpublished results.
21. E. R. THORNTON. J. Am. Chem. Soc. **89**, 2915 (1967).
22. B. D. ENGLAND and R. E. BURNS. Tetrahedron Lett. **24**, 1 (1960).
23. K. BOWDEN. Chem. Rev. **66**, 119 (1966).
24. J. BIGELEISEN and M. WOLFSBERG. Adv. Chem. Phys. **1**, 15 (1958).
25. R. A. MORE O'FERRALL and S. SLAE. Chem. Commun. 486 (1969).
26. E. S. GOULD. Mechanism and structure in organic chemistry. Henry Holt and Company, Inc., New York, N.Y., 1959. p. 488.
27. E. S. AMIS. Solvent effects on reaction rates and mechanisms. Academic Press, New York, N.Y., 1966. p. 175.
28. G. YAGIL and M. ANBAR. J. Am. Chem. Soc. **85**, 2377 (1963).
29. P. J. SMITH and A. N. BOURNS. Can. J. Chem. **44**, 2553 (1966).
30. H. LUND and J. BJERRUM. Ber. 64B, 210 (1931).
31. B. T. BALIGA and A. N. BOURNS. Can. J. Chem. **44**, 363 (1966).
32. W. H. STEVENS and R. W. ATTREE. Can. J. Res. B. **27**, 807 (1949).

Can. J. Chem. Downloaded from www.nrcresearchpress.com by 210.87.254.105 on 09/05/12
For personal use only.

Can. J. Chem. Downloaded from www.nrcresearchpress.com by 210.87.254.42 on 09/05/12
For personal use only.

Synthesis of Some Stable 7-Halo-1,4-thiazepines. Potential Substituted Penam Precursors

P. BLONDEAU,[1] R. GAUTHIER,[2] C. BERSE, AND D. GRAVEL
Department of Chemistry, University of Montreal, Montreal 101, Quebec

Received July 19, 1971

The synthesis of some new 3-carbomethoxy-5-oxoperhydro-1,4-thiazepines is described. Halogenation studies led to the preparation of three potential substituted penam ring precursors: 6,7-dibromo-3-carbomethoxy-5-oxoperhydro-1,4-thiazepine, 3-carbomethoxy-6,7-dichloro-5-oxoperhydro-1,4-thiazepine, and 3-carbomethoxy-7-chloro-6,6-dimethyl-5-oxoperhydro-1,4-thiazepine. Preliminary studies on the reactivity of these α-halothioethers showed that methanolysis to the corresponding methoxy-thiazepines may be carried out in nearly quantitative yields in the case of the first two derivatives; the third compound, on the other hand, led to an open-chain dehydrohalogenated product where C-7 is converted to the corresponding dimethyl acetal.

La synthèse de quelques nouvelles méthoxycarbonyl-3 oxo-5 perhydrothiazépines-1,4 est rapportée. Des études sur l'halogénation de ces composés ont conduit à la préparation de trois précurseurs possibles du noyau penam substitué: la dibromo-6,7 méthoxycarbonyl-3 oxo-5 perhydrothiazépine-1,4, la dichloro-6,7 méthoxycarbonyl-3 oxo-5 perhydrothiazépine-1,4, et la chloro-7 diméthyl-6,6 méthoxycarbonyl-3 oxo-5 perhydrothiazépine-1,4. Des études préliminaires sur la réactivité de ces α-halogénothioethers ont montré que, dans le cas des deux premiers dérivés, la méthanolyse pour donner les méthoxy thiazépines correspondantes peut être effectuée avec des rendements quasi-quantitatifs; le troisième composé, d'autre part, a conduit à un produit de déshydrohalogénation où le C-7 est transformé en diméthyl acétal correspondant.

Canadian Journal of Chemistry, 49, 3866 (1971)

Introduction

During the last few years several reports of total syntheses of penam[3] derivatives have appeared in the literature (1–5). In all cases the β-lactam ring was formed on either a 1,3-thiazolidine or 1,3-thiazoline ring bearing the appropriate substitution.

However, to our knowledge, there is no known synthesis of a penam ring or of a penicillanic acid[3] starting from a seven-membered cyclic precursor. Although there are reports of attempts to achieve such a goal by Knunyants and coworkers (6) and also by Leonard and Wilson (7), this synthetic approach has never been thoroughly investigated due mainly to the unavailability of stable key intermediates such as 7-halo-1,4-thiazepines. It was therefore in an attempt to overcome this limiting factor that a program was initiated first to synthesize some stable 7-halo-1,4-thiazepines and subsequently to systematically investigate the possible modes of forming the elusive 4,7-bond. The model compounds chosen were 3-carbomethoxy-6,7-dihalo-5-oxoperhydro-1,4-thiazepine (**1**) and 3-carbomethoxy-7-chloro-6,6-dimethyl-5-oxoperhydro-1,4-thiazepine (**2**) which upon cyclization could yield substituted derivatives of the penam ring system.

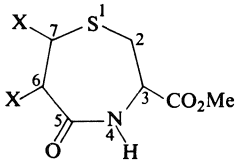

1
X = Br or Cl

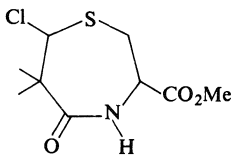

2

It could easily be gleaned from the literature that 3-carbomethoxy-7-chloro-5-oxoperhydro-1,4-thiazepines were highly unstable due to their susceptibility to dehydrohalogenate (6, 7). It was hoped, in the case of **1**, that a *trans* dihalo derivative would resist dehydrohalogenation on

[1]NRCC Predoctorate Fellow 1965–1969.
[2]NRCC Predoctorate Fellow 1968–1971.
[3]The terms "penam" and "penicillanic acid" correspond to the following ring systems and carry no stereochemical implications, as first suggested by Sheehan *et al.* (21).

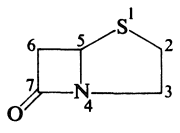

Penam

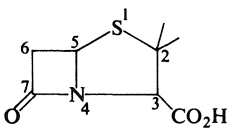

Penicillanic acid

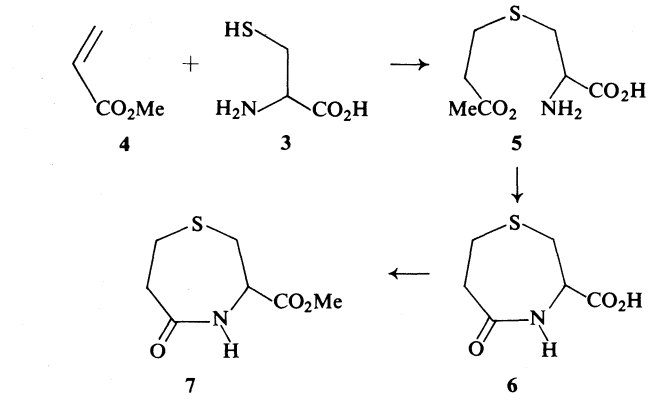

SCHEME 1

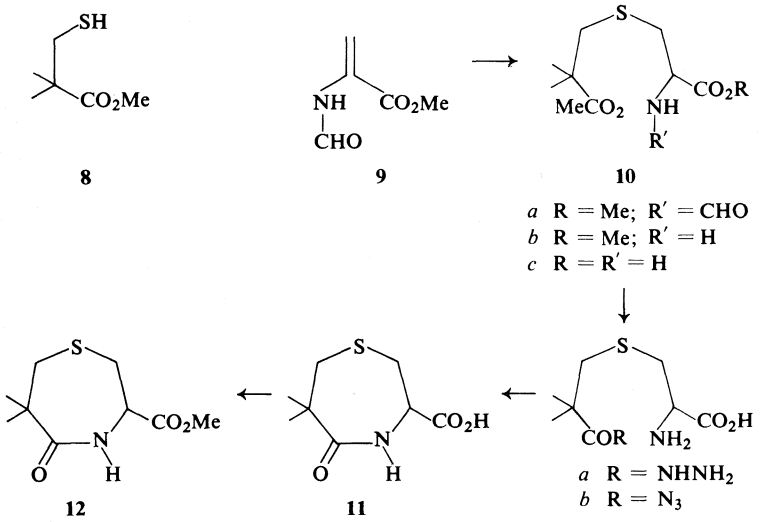

SCHEME 2

stereoelectronic grounds and in the case of **2** that the monochloro derivative would resist elimination to a certain extent due to the lack of β-hydrogens.[4]

Results and Discussion

Synthesis

Synthesis of thiazepine **7** was readily achieved by combining known methods from the literature as outlined in Scheme 1.

In a first step, L-cysteine (**3**) was condensed with methyl acrylate (**4**) following a method reported by Foldi (8) for the case of ethyl acrylate. The resulting addition product **5**, obtained in a 90% yield, was then cyclized (9, 10) in a solution of methanol saturated with ammonia to yield 49% of 3-carboxy-5-oxoperhydro-1,4-thiazepine (**6**). Esterification of the acid **6**, effected by standard treatment with ethereal diazomethane, gave a nearly quantitative yield of the desired ester **7**. (See Experimental for comment on optical purity.)

In the case of the second parent compound **12**, a synthetic approach was devised which is shown in Scheme 2.

In the first instance, synthesis of the methyl mercaptopivalate moiety **8** was achieved by standard methods (11, 12) from hydroxypivalic acid (11). This mercapto ester **8** was then condensed with methyl α-formamidoacrylate (**9**) (13)

[4]Rearrangement in an E_1 process nevertheless remained possible.

Can. J. Chem. Downloaded from www.nrcresearchpress.com by 210.87.254.42 on 09/05/12
For personal use only.

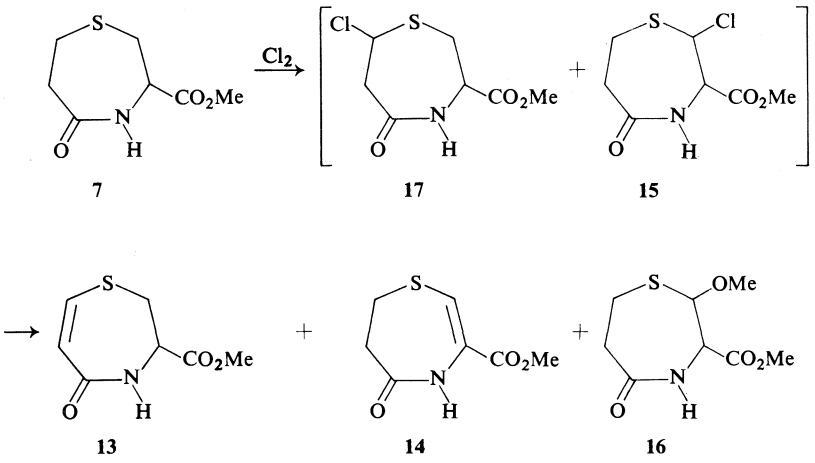

SCHEME 3

under basic conditions (8) to yield 83% of the oily diester **10***a*. Removal of the formyl protecting group was effected in high yield in methanolic hydrogen chloride to give the corresponding amino diester **10***b*. An attempt to cyclize the latter by the methanol–ammonia method (*vide supra*) completely failed as ammonolysis of the amino ester moiety took place in quantitative yield; a prolonged reaction time gave no further change.

Due to the lower reactivity of the ester group on the pivalate moiety, cyclization was achieved using the acyl azide method (14). To that effect, amino diester **10***b* was partially saponified with a sodium carbonate solution to yield 95% of the expected acid-ester **10***c*. The latter compound upon treatment with hydrazine and subsequently with nitrous acid gave the required thiazepine **11** with a 22% yield. Esterification by the usual diazomethane procedure finally gave the parent 3-carbomethoxy-6,6-dimethyl-5-oxoperhydro-1,4-thiazepine (**12**) in quantitative yield.

Halogenation

The reaction scheme expected to introduce halogen at C-6 and -7 proceeded via the 6,7-dehydro derivative **13** which, hopefully, could be halogenated on the double bond to yield the required *trans*-dihalo compound **1**.

Preparation of 3-carbomethoxy-5-oxo-2,3,4,5-tetrahydro-1,4-thiazepine (**13**) was achieved easily using a known chlorination–dehydrochlorination procedure (7). Indeed it is well known that thioethers react with chlorinating agents to give α-chloro thioethers (15) which in turn may be dehydrohalogenated. In the case of 5-oxo-perhydro-1,4-thiazepines, the α-chloro thioether intermediates are quite unstable [5] probably due to the presence of a carbonyl group at the 5-position; under the reaction conditions stipulated by Leonard and Wilson (7) the intermediate α-chloro thioether formed is dehydrohalogenated *in situ* to yield directly the 2,3,4,5-tetrahydro-1,4-thiazepine.

When the above conditions (7) were applied to perhydrothiazepine **7**, three products were obtained after chromatography on silica gel (see Scheme 3).

The desired product, 3-carbomethoxy-5-oxo-2,3,4,5,-tetrahydro-1,4-thiazepine (**13**), was formed in a 37% yield along with 19% of 3-carbomethoxy-5-oxo-4,5,6,7-tetrahydro-1,4-thiazepine (**14**) which results from the dehydrochlorination of the alternate intermediate **15**. Finally, a 1% yield of 3-carbomethoxy-2-methoxy-5-oxoperhydro-1,4-thiazepine (**16**) was obtained suggesting that intermediate **15** had, at least partially, resisted dehydrochlorination and reacted subsequently with the methanolic eluent on the chromatography column.

Concerning the introduction of two halogen atoms on the double bond of **13** in order hopefully to obtain a stable *trans*-6,7-dihalo compound, it

[5] Knunyants and co-workers (6) did report the successful preparation, by the above method, of some 7-halo-5-oxoperhydro-1,4-thiazepines; however, these were unstable and underwent dehydrohalogenation very readily. Repetition of the published procedure by Leonard and Wilson (7) did not yield the expected 7-halo-1,4-thiazepine.

Can. J. Chem. Downloaded from www.nrcresearchpress.com by 210.87.254.42 on 09/05/12
For personal use only.

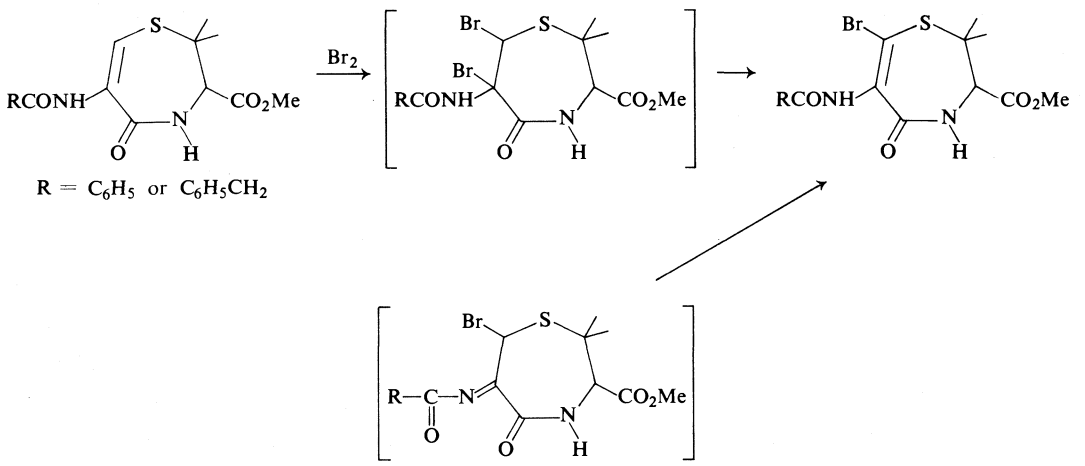

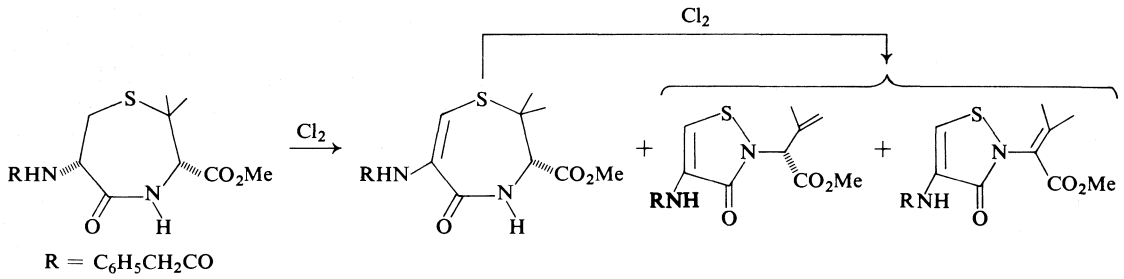

is important to note that Knunyants and coworkers (6) have carried out the bromination of a related thiazepine but without, however, succeeding to isolate the 6,7-dibromo derivative; instead there was always obtained an excellent yield of the corresponding dehydrobrominated product (see Scheme 4).

We feel, however, that this result does not militate against the presumed stability of *trans*-6,7-dihalo derivatives since dehydrohalogenation might well have gone through the corresponding acylimine (see Scheme 4) followed by tautomerization to the observed product (16).

Also of importance is the fact that Leonard and Wilson (7) in studying the chlorination at $-60°$ of a pure stereoisomer of the same thiazepine have observed, aside from the normal tetrahydrothiazepine expected, two other compounds resulting from further chlorination and rearrangement of the first reaction product (see Scheme 5).

In both cases cited above, no stable 7-halo perhydrothiazepine could be isolated. However, bromination of thiazepine **13** in dichloromethane yielded 78% of the desired 6,7-dibromo compound **18**, m.p. 133–134°. This compound could be kept for more than 1 month in dichloromethane solution but surprisingly decomposed after a few days when kept in the crystalline state.

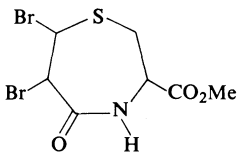

18

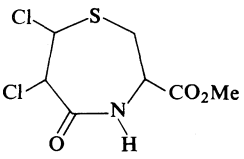

19

It is interesting to note that the 6,7-dibromo compound **18**, although slightly unstable can be obtained and kept while the 7-chloro derivative **17** could not even be isolated. This behavior could well be due to a *trans* configuration of the bromine atoms thus preventing the stereoelectronically preferred *trans*-coplanar arrangement of H and Br for a potential dehydrohalogenation.

Can. J. Chem. Downloaded from www.nrcresearchpress.com by 210.87.254.42 on 09/05/12
For personal use only.

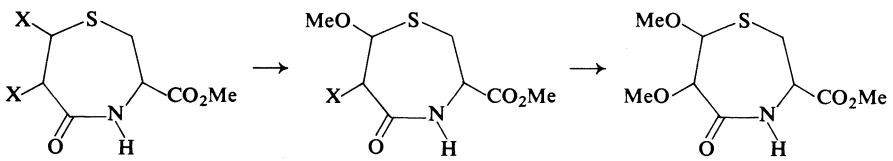

18 X = Br
19 X = Cl

21 X = Br
22 X = Cl

20

Finally, heating the dibromo derivative **18** in the presence of powdered zinc in methanol yielded the original tetrahydrothiazepine **13** quantitatively showing that bromine had been introduced without modification to the basic skeleton of the molecule.

Having succeeded in preparing the 6,7-dibromothiazepine **18** it became interesting to seek conditions whereby chlorination of the tetrahydrothiazepine **13** would occur on the double bond rather than at the sulfur atom, as illustrated previously in Scheme 5. It was expected that a *trans*-6,7-dichloro derivative could show a greater degree of stability than the corresponding dibromo compound.

In the hope of increasing the polar character of the reactants and therefore altering the normal course of the reaction, the chlorination of tetrahydrothiazepine **13** was carried out in anhydrous nitromethane rather than dichloromethane. There was thus obtained a 60% yield of a solid, m.p. 158–160°, identified as 3-carbomethoxy-6,7-dichloro-5-oxoperhydro-1,4-thiazepine (**19**). As in the previous case treatment with zinc in methanol gave the original tetrahydrothiazepine **13**.

Chlorination studies on the second model compound **12** also proved fruitful in yielding 67% of the desired 7-chlorothiazepine **2**. The position of the chlorine atom follows from the n.m.r. spectrum which shows a singlet at δ 4.90 for the C-7 methine proton; in the case of a 2-chloro derivative one would expect a doublet, unless of course the dihedral angle happened to be nearly 90° (17). However, the assigned structure **2** is strongly supported by results of the reactivity studies (see below).

Reactivity

Considering that the reported attempts (6, 7) to form a 4—7 bond starting from either a 7-halo-5-oxoperhydrothiazepine or the corresponding sulfonium ion, led only to the 6,7-dehydrohalogenated product it was necessary to seek mild conditions where elimination could be suppressed in favor of substitution by nitrogen in the 4 position.

Thus, treatment during 12 h of the 6,7-dibromothiazepine **18** in pyridine and methanol afforded an almost quantitative yield of the corresponding dimethoxy compound **20** and none of the desired penam derivative. On the other hand, the same 6,7-dimethoxy compound was obtained in 1 h when silver oxide or silver carbonate (18) was used instead of pyridine; yields were also quantitative in this case.

The action of pyridine and methanol on the 6,7-dichlorothiazepine **19** was also investigated. In this case the reaction is much slower: after 24 h of contact one can isolate a 77% yield of the monosubstitution product **22**. Examination of the fragmentation pattern in the mass spectrum corroborates the assignment made on the basis of n.m.r. data; indeed, a fragment at *m/e* 177 corresponds to the loss of methyl thioformate indicating that methanolysis takes place at C-7. This order of reactivity is also that which is expected *a priori*. Interestingly, it was later found that treatment of dibromo thiazepine **18** with silver carbonate in methanol for 20 min gave 23% of the 6-bromo-7-methoxy derivative **21**.

On the other hand, treatment of the 7-chloro-6,6-dimethyl model **2** with pyridine and methanol as above, yielded only unchanged starting material and no trace of substitution product; identical results were also observed in the case of silver oxide or silver carbonate in methanol at room temperature. However, in refluxing methanol in the presence of silver oxide or silver carbonate, a 95% yield of a new product was obtained after 1 h. The structure, which is easily derived by physical methods, corresponds to the open chain enamide **23**. A comparison of the n.m.r., i.r., and u.v. spectra of the enamide **23** to those of an authentic sample of methyl α-acetamidoacrylate was useful in confirming the assigned structure. Also in substantiation of structure **23**, the enamide was treated with a

Can. J. Chem. Downloaded from www.nrcresearchpress.com by 210.87.254.42 on 09/05/12
For personal use only.

TABLE 1. The i.r. and mass spectral data of the thiazepines

Compound	Infrared spectrum (cm^{-1}) NH	C=O ester	C=O lactam	Mass spectrum *m/e* 55*	M^+
2	3380	1750	1665	–	251
7	3380	1750	1670	+	189
12	3450	1735	1630	–	217
13	3390	1745	1650	–	187
14	3370	1710	1670	+	187
16	3420	1750	1675	+	217
18	3380	1750	1675	–	345
19	3470	1750	1680	–	257
20	3410	1750	1670	–	249
21	3380	1745	1670	–	297
22	3375	1745	1675	–	253

*An intense peak at *m/e* 55 is *characteristic of all* the 6,7-unsubstituted thiazepines reported herein, and most probably corresponds to $[CH_2{=}CH{-}C{=}O]^{\oplus}$. This fragment originates from C−5, −6, and −7 of the ring and its presence or absence is used advantageously to determine the substitution pattern in the chlorination reactions.

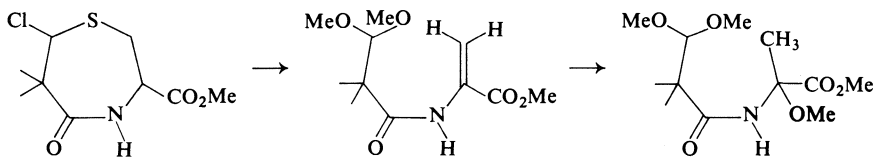

2 **23** **24**

methanol saturated with hydrogen chloride solution to give amide **24** resulting from the addition of methanol to the enamide moiety (20).

Although the desired cyclization failed to take place under both sets of conditions used, the two 7-haloperhydrothiazepine models available will now allow a systematic study of the feasibility of this particular reaction to be undertaken.

It may be of interest to add that very recently Edwards *et al.* (19) described the cyclization, under solvolytic conditions, dioxane – water – silver ion, of 5-chloro-azacyclooctan-2-one to 1-azabicyclo[3.3.0]octan-2-one.

Experimental

The i.r. spectra were determined on a Beckmann, model IR-8, spectrometer using chloroform as solvent (unless otherwise indicated). The n.m.r. spectra were determined either on a Varian A-60 or on a Jeol JNM-4H-100 spectrometer. Deuterochloroform was used as solvent unless otherwise indicated; the following abbreviations are employed: singlet (s), doublet (d), triplet (t), and multiplet (m). The u.v. spectra were measured on a Bausch and Lomb Spectronic 505 spectrometer, and the mass spectra on a Hitachi-Perkin-Elmer RMu-6D instrument. Microanalyses were by Midwest Microlab Inc., Indianapolis, Ind. Melting points are uncorrected.

S-(2-Carbomethoxyethyl)cysteine (5)

This compound was prepared following a method reported by Foldi (8) for the synthesis of *S*-(2-carboethoxyethyl)cysteine. Triethylamine (115 ml) and methyl acrylate (**4**) (51.0 g, 600 mmol) were added with stirring at 25° to a solution of *l*-cysteine hydrochloride hydrate (**3**) (87.5 g, 500 mmol) in ethanol (400 ml). The exothermic reaction which ensued was completed in a few minutes as indicated by a negative nitroprusside test. The resulting precipitate was filtered *in vacuo*, washed with boiling ethanol (2 × 100 ml), and then with ether (100 ml) to yield 90% (93 g) of a white solid melting at 208–209°; i.r. (Nujol): 3200–2000, 1730, 1610, and 1580 cm^{-1}; n.m.r. (CF_3COOH): δ 2.85 (m, 4H); 3.35 (m, 2H); 3.82 (s, 3H); 4.55 (m, 1H); 7.55 (broad m, 3H).

3-Carboxy-5-oxoperhydro-1,4-thiazepine (6)

A solution of thioether **5** (41.4 g, 200 mmol) in methanol saturated with ammonia (1.2 l) was stirred at room temperature for 7 days. The solvent was then evaporated to dryness, and the residue dissolved in water (400 ml). The solid which precipitated upon acidification to p*H* 2 with concentrated hydrochloric acid was filtered *in vacuo* and washed with cold water (50 ml). Recrystallization from acetone yielded 49% (17.1 g) of the thiazepine **6**, m.p. 218–219°. The i.r. (Nujol): 3320, 3100–2300, 1715 and 1610 cm^{-1}; n.m.r. (CF_3COOH): δ 2.8–3.4(m, 6H); 4.85 (m, 1H); 8.40 (d, 1H).

Anal. Calcd. for $C_6H_9NO_3S$: C, 41.13; H, 5.18; N, 7.99. Found: C, 41.41; H, 5.27; N, 7.73.

3-Carbomethoxy-5-oxoperhydro-1,4-thiazepine (7)

A solution of perhydrothiazepine **6** (17.5 g, 100 mmol) in methanol (200 ml) was cooled in an ice bath; an ice-cold solution of diazomethane in ether was then slowly added, until the precipitate formed was completely dissolved and evolution of nitrogen ceased. Evaporation of the solvent *in vacuo* and recrystallization of the residue

Can. J. Chem. Downloaded from www.nrcresearchpress.com by 210.87.254.42 on 09/05/12
For personal use only.

Can. J. Chem. Downloaded from www.nrcresearchpress.com by 210.87.254.42 on 09/05/12
For personal use only.

TABLE 2. The n.m.r. spectral data of the thiazepines

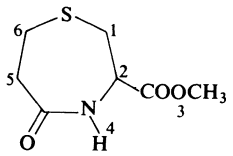

Compound	Position						
	1	2	3	4	5	6	Other
2	2.8–3.6(m)	4.70(m)	3.92(s)	6.80(m)	—	4.90(s)	1.53(6H, s)
7	2.90(m)	4.50(m)	3.82(s)	6.65(m)	2.90(m)	2.90(m)	
12	2.2–3.2(m)	4.50(m)	3.74(s)	6.40(m)	—	2.2–3.2(m)	1.20(3H, s) 1.25(3H, s)
13	3.40(m)	4.55(m)	3.82(s)	7.12(m)	6.02 (d, J = 12 Hz)	6.65 (d, J = 12 Hz)	
14	7.78(s)	—	3.85(s)	7.10(m)	3.10(m)	3.10(m)	
16	4.80 (d, J = 7 Hz)	4.32 (q, J = 7 Hz, J' = 8)	3.85(s)	6.70 (d, J = 8 Hz)	2.1–3.1	2.1–3.1	3.45(3H, s)
18	3.2(m)	5.0(m)	3.92(s)	6.85(m)	5.0 (d, J = 6 Hz)	5.30 (d, J = 6 Hz)	
19	3.20(m)	4.9(m)	3.88(s)	6.82(m)	4.9 (d, J = 6 Hz)	5.20 (d, J = 6 Hz)	
20	2.7–3.3(m)	4.42(m)	3.82(s)	6.80(m)	3.72 (d, J = 3 Hz)	4.88 (d, J = 3 Hz)	3.48(3H, s) 3.50(3H, s)
21	3.0(m)	4.82(q)	3.85(s)	6.70(m)	4.83 (d, J = 6.0 Hz)	4.50 (d, J = 6.0 Hz)	3.50(3H, s)
22	3.00(m)	4.90(m)	3.88(s)	6.80(m)	4.85 (d, J = 6.5 Hz)	4.55 (d, J = 6.5 Hz)	3.52(3H, s)

Can. J. Chem. Downloaded from www.nrcresearchpress.com by 210.87.254.42 on 09/05/12
For personal use only.

from ether gave 92% (17.3 g) of thiazepine **7**, m.p. 91–92°. The i.r.: 3380, 1750 and 1670 cm^{-1}; n.m.r.: δ 2.90 (m, 6H); 3.82 (s, 3H); 4.50 (m, 1H); 6.65 (m, 1H).

Anal. Calcd. for $C_7H_{11}NO_3S$: C, 44.42; H, 5.86; N, 7.40. Found: C, 44.54; H, 5.98; N, 7.67.

The optical purity of this compound and its derivatives has not been determined; however, following observations made in a related series where the methanol–ammonia method was used, it is probable that the compounds are at least partly racemized.

*Methyl α-Formamidoacrylate (**9**)*

Compound **9** was prepared according to the method described by Frankel and Reichmann (13); m.p. 50–52° (lit. 53° (13)). The yield for the addition of formamide on pyruvic acid was only 10%, although Frankel and Reichmann report a 20% yield for this reaction.

Bromopivalic Acid

Bromopivalic acid was prepared, as reported by Greene and Hagemeyer (11), from hydroxy pivalic acid and 48% hydrobromic acid. The yield obtained was 70%, m.p. 44° (lit. 75% yield, m.p. 46–48° (11)).

Mercaptopivalic Acid

Thiourea (47 g, 620 mmol) was added to a solution of bromopivalic acid (110 g, 608 mmol) in absolute ethanol (250 ml), and the resulting mixture heated to reflux for 12 h. Sodium hydroxide (72 g) in water (300 ml) was then added and the mixture heated to reflux under nitrogen for a further 3 h. Hydrated sodium sulfide (50 g) was then added to the reaction mixture and the solvent evaporated under vacuum until crystals began to appear. The mixture was cooled in ice, covered with ether (300 ml) and neutralized to p*H* 3 with 20% sulfuric acid. The organic layer was diluted with ether and the resulting solution washed with water saturated with sodium chloride and dried over anhydrous sodium sulfate. The ether was evaporated *in vacuo* and the remaining oil distilled under reduced pressure, to give 73% (60 g) of mercaptopivalic acid; b.p. 120°/15 mm. The i.r.: 3000, 2580, and 1700 cm^{-1}; n.m.r. (DMSO-d_6): δ 1.18 (s, 6H); 2.14 (s, 2H).

*Methyl Mercaptopivalate (**8**)*

A solution of mercaptopivalic acid (60 g, 448 mmol) in anhydrous methanol was saturated with anhydrous hydrogen chloride and then stirred at room temperature for 6 h. The solvent was evaporated to dryness and the residue taken up in ether, and washed twice with a 5% sodium bicarbonate solution. After drying over anhydrous sodium sulfate the ether was evaporated under vacuum and the remaining oil distilled under reduced pressure, yielding 62% (40 g) of methyl mercaptopivalate (**8**), b.p. 40°/0.05 mm. The i.r.: 2580 and 1730 cm^{-1}; n.m.r.: δ 1.26 (s, 6H); 1.45 (t, 1H); 2.69 (d, 2H); 3.69 (s, 3H).

Anal. Calcd. for $C_6H_{12}O_2S$: C, 48.65; H, 8.15. Found: C, 49.05; H, 8.43.

*Methyl N-Formyl S-(2-Carbomethoxy-2-methyl propyl)-cysteinate (**10a**)*

Methyl α-formamidoacrylate (**9**) (1.04 g, 8.07 mmol) was added to a solution of methyl mercaptopivalate (**8**) (1.19 g, 8.07 mmol) in methanol (25 ml). Three drops of triethylamine were then added and the mixture stirred at room temperature for 4 h. The solvent was evaporated to dryness and the residue chromatographed on silica gel using ether as eluent. The diester **10*a*** was obtained as an oil (1.85 g, 83%) which was used for the next step without further purification. The i.r. (CH_2Cl_2): 3430, 1735 and 1690 cm^{-1}; n.m.r.: δ 1.25 (s, 6H); 2.78 (s, 2H); 3.03 (d, 2H); 3.71 (s, 3H); 3.79 (s, 3H); 4.90 (m, 1H); 6.85 (m, 1H); 8.27 (s, 1H).

*Methyl S-(2-Carbomethoxy-2-methyl propyl)cysteinate (**10b**)*

Diester **10*a*** (100 mg, 3.61 mmol) was dissolved in methanol (10 ml) and the resulting solution saturated with dry hydrogen chloride and stirred at room temperature for 1 h. The solvent was then evaporated to dryness and the remaining oil taken up in ether. The organic layer was washed with a 5% sodium carbonate solution. After drying over anhydrous sodium sulfate, the ether was evaporated and compound **10*b*** (0.087 g, 95%) was obtained as a yellow oil which was used without further purification. The i.r. (CH_2Cl_2): 3400, 1730, 1380 and 1360 cm^{-1}; n.m.r.: δ 1.26 (s, 6H); 2.82 (s, 2H); 3.0 (m, 2H); 3.71 (s, 3H); 3.75 (m, 1H); 3.78 (s, 3H).

*S-(2-Carbomethoxy-2-methyl propyl)cysteine Hydrochloride (**10c**)*

Amino-diester **10*b*** (4.0 g, 16.1 mmol) was added to a 10% sodium carbonate solution (150 ml) and the resulting mixture stirred at room temperature for 1 h, after which it was acidified to p*H* 0 by careful addition of 6 *N* hydrochloric acid. The aqueous solution was then concentrated to 75 ml by evaporation under vacuum. The precipitate formed was filtered and recrystallized from 6 *N* HCl, to yield 95% (4.2 g) of the amino-diacid monoester hydrochloride **10*c***, m.p. 245° (dec.), which was used without further purification. The i.r. (Nujol): 3000, 2800, 1720 and 1700 cm^{-1}; n.m.r. (D_2O): δ 1.65 (s, 6H); 3.30 (s, 2H); 3.58 (d, 2H); 4.13 (s, 3H); 4.70 (t, 1H); 5.22 (HDO).

*3-Carboxy-6,6-dimethyl-5-oxoperhydro-1,4-thiazepine (**11**)*

A mixture of acid-ester hydrochloride **10*c*** (3.0 g, 11.1 mmol) and redistilled hydrazine hydrate (20 ml) was heated to reflux for 2 h. The excess hydrazine hydrate was evaporated to dryness; the residue was taken up in *n*-butanol (5 ml) and the solvent once again evaporated *in vacuo*. The residue was dissolved in methanol and the remaining crystals of hydrazine hydrochloride filtered. The methanolic filtrate was evaporated to dryness to yield 56% (1.45 g) of the required hydrazide as a gum.

The crude hydrazide (1.45 g, 6.18 mmol) was dissolved in 2 *N* hydrochloric acid (62 ml) at 0° and sodium nitrite (0.428 g, 6.18 mmol) added. The mixture was stirred at 0° for 15 min, and then poured into ice-cold water (3.6 l). The solution was neutralized by the addition of sodium bicarbonate (7.8 g) and kept at 4° for 40 h in the refrigerator. The mixture was then acidified to p*H* 4 with 2 *N* hydrochloric acid (about 50 ml) and the water evaporated under vacuum to a final volume of 175 ml. Crystals which appeared during the evaporation were filtered under vacuum. Recrystallization from ethanol–ether yielded 40% (495 mg) of 3-carboxy-6,6-dimethyl-5-oxoperhydro-1,4-thiazepine (**11**) m.p. 218–220°. The i.r. (Nujol);

3340, 1720 and 1555 cm^{-1}; n.m.r. (DMSO-d_6): δ 1.15 (s, 3H); 1.20 (s, 3H); 2.3–3.2 (m, 4H); 4.55 (m, 1H); 6.53 (d, 1H).

Anal. Calcd. for $C_8H_{13}NO_3S$: C, 47.27; H, 6.44. Found: C, 47.12; H, 6.87.

*3-Carbomethoxy-6,6-dimethyl-5-oxoperhydro-1,4-thiazepine (**12**)*

A solution of thiazepine **11** (1.0 g, 4.93 mmol) in methanol (10 ml) was treated with a solution of diazomethane in ether until the evolution of nitrogen ceased and the reaction mixture took on a faint yellow color. The solvent was evaporated to dryness and the residue recrystallized from ether, to yield 80% (0.85 g) of 3-carbomethoxy-6,6-dimethyl-5-oxo-perhydro-1,4-thiazepine (**12**), m.p. 89–89.5°. The i.r. (Nujol): 3450, 1735 and 1630 cm^{-1}; n.m.r.: δ 1.20 (s, 3H); 1.25 (s, 3H); 2.2–3.2 (m, 4H); 3.74 (s, 3H); 4.50 (m, 1H); 6.40 (m, 1H).

Anal. Calcd. for $C_9H_{15}NO_3S$: C, 49.85; H, 6.97. Found: C, 49.92; H, 7.04.

Reaction of 3-Carbomethoxy-5-oxoperhydro-1,4-thiazepine (7) with Chlorine

A solution of the thiazepine **7** (18.9 g, 100 mmol) in anhydrous dichloromethane (500 ml) was cooled in a mixture of Dry Ice and acetone and slowly treated (dropwise) with 1 equiv of chlorine in carbon tetrachloride (182 ml, 0.55 *M*). The resulting mixture was stirred for 2 h at −65° and, after removal of the cooling bath, allowed to warm up to room temperature, at which point evolution of hydrogen chloride could be observed. After a 2 h reflux, the solution was concentrated *in vacuo*, the oily residue dissolved in a minimum amount of chloroform and chromatographed on silica gel.

Three products were obtained by eluting successively with ether (first product) and methanol–ether (1:20) (second and third products):

(*i*) 3-Carbomethoxy-5-oxo-4,5,6,7-tetrahydro-1,4-thiazepine (**14**) (3.5 g, 19%), m.p. 88–89° (ether); u.v.: 298 mμ (ε 1700).

Anal. Calcd. for $C_7H_9NO_3S$: C, 44.91; H, 4.84; N, 7.48. Found: C, 44.71; H, 5.03; N, 7.48.

(*ii*) 3-Carbomethoxy-2-methoxy-5-oxoperhydro-1,4-thiazepine (**16**) (0.60 g, ~1%), m.p. 148–149°.

Anal. Calcd. for $C_8H_{13}NO_4S$: C, 43.82; H, 5.98; N, 6.39. Found: C, 44.15; H, 6.05; N, 6.42.

(*iii*) 3-Carbomethoxy-5-oxo-2,3,4,5-tetrahydro-1,4-thiazepine (**13**) (6.9 g, 37%), m.p. 131–132° (methanol–ether); u.v.: 227 (ε 4900) and 279 mμ (ε 7700).

Anal. Calcd. for $C_7H_9NO_3S$: C, 44.91; H, 4.84; N, 7.48. Found: C, 45.14; H, 5.02; N, 7.48.

*6,7-Dibromo-3-carbomethoxy-5-oxoperhydro-1,4-thiazepine (**18**)*

A solution of thiazepine **13** (0.935 g, 5 mmol) in anhydrous dichloromethane (100 ml) was treated (dropwise) with a solution of bromine in carbon tetrachloride (5.5 ml, 0.92 *M*). The solvent was then evaporated *in vacuo*, and the residue chromatographed on a silica gel column, eluting with dichloromethane. Recrystallization from chloroform–ether yielded 78% of dibromothiazepine **18**, m.p. 133–134°. The i.r. (CH_2Cl_2): 3380, 1750 and 1675 cm^{-1}; n.m.r.: δ 3.25 (m, 2H); 3.92 (s, 3H); 5.05 (d + m, 2H); 5.30 (d, 1H); 6.85 (m, 1H).

Anal. Calcd. for $C_7H_9Br_2NO_3S$: C, 24.22; H, 2.62. Found: C, 24.27; H, 2.52.

*Reaction of 3-Carbomethoxy-5-oxo-2,3,4,5-tetrahydro-1,4-thiazepine (**13**) with Chlorine*

A stirred solution of thiazepine **13** (1.87 g, 10 mmol) in nitromethane was slowly treated (dropwise) with chlorine in carbon tetrachloride (11 mmol; 20 ml, 0.54 *M*). Evaporation of the solvent *in vacuo* and chromatography of the residue on silica gel, eluting with dichloromethane, gave a first product in a 60% yield: 3-carbomethoxy-6,7-dichloro-5-oxoperhydro-1,4-thiazepine (**19**) (1.54 g), m.p. 158–160° (chloroform–ether).

Anal. Calcd. for $C_7H_9Cl_2NO_3S$: C, 32.57; H, 3.51. Found: C, 32.48; H, 3.63.

Further elution with dichloromethane gave 3% (340 mg) of an unseparable mixture of two products: probably a dichloro thiazepine (isomer of **19**) and the corresponding unsaturated chlorothiazepine u.v. (C_2H_5OH): 290 mμ.

*Reaction of the Dichlorothiazepine **19** with Zinc*

A mixture of the dichlorothiazepine **19** (10 mg) and zinc powder (50 mg) in methanol (10 ml) is heated to reflux for 30 min. After filtration and evaporation of the solvent, t.l.c. on silica gel using ether or methanol–ether 1:20 as eluent showed a complete transformation into 3-carbomethoxy-5-oxo-2,3,4,5-tetrahydro-1,4-thiazepine (**13**).

*Reaction of the Dibromothiazepine **18** with Zinc*

The above procedure applied to the dibromothiazepine **18** gave quantitatively the same results.

*3-Carbomethoxy-7-chloro-6,6-dimethyl-5-oxoperhydro-1,4-thiazepine (**2**)*

A solution of thiazepine **12** (1.926 g, 8.88 mmol) in methylene chloride (150 ml) was cooled to −65° in a Dry Ice – acetone bath, and treated dropwise with a solution of chlorine in carbon tetrachloride (8.8 mmol; 27 ml, 0.34 *M*). The mixture was stirred at −65° for 1 h and then heated to reflux for 20 h. The solvent was evaporated under vacuum and the residue recrystallized from carbon tetrachloride, to yield 67% (1.40 g) of chloro derivative **2**, m.p. 148.5°. The i.r. (CCl_4): 3380, 1750 and 1665 cm^{-1}; n.m.r.: δ 1.53 (s, 6H); 2.8–3.6 (m, 2H); 3.92 (s, 3H); 4.7 (m, 1H); 4.90 (s, 1H); 6.80 (m, 1H).

Anal. Calcd. for $C_9H_{14}ClNO_3S$: C, 42.94; H, 5.61. Found: C, 43.20; H, 5.69.

*3-Carbomethoxy-6-chloro-7-methoxy-5-oxoperhydro-1,4-thiazepine (**22**)*

A solution of 3-carbomethoxy-6,7-dichloro-5-oxoperhydro-1,4-thiazepine (**19**) (100 mg, 0.4 mmol) and pyridine (63 mg, 0.8 mmol) in methanol (10 ml) was stirred at room temperature for 24 h. The t.l.c. (silica gel, ether) showed the presence of two products, the dimethoxy thiazepine **20** at R_f 0.1 and the chloro-methoxy thiazepine **22** at R_f 0.5. Evaporation of the solvent and chromatography on silica gel (10 g) eluting with dichloromethane yielded 77% (75 mg) of 3-carbomethoxy-6-chloro-7-methoxy-5-oxoperhydro-1,4-thiazepine (**22**), m.p. 151–152° (chloroform–ether). The i.r.: 3375, 1745 and 1675 cm^{-1}; n.m.r.: δ 3.00 (m, 2H); 3.52 (s, 3H); 3.88 (s, 3H); 4.55 (d, 1H); 4.85 (d, 1H); 4.90 (m, 1H); 6.80 (m, 1H).

Can. J. Chem. Downloaded from www.nrcresearchpress.com by 210.87.254.42 on 09/05/12
For personal use only.

Can. J. Chem. Downloaded from www.nrcresearchpress.com by 210.87.254.42 on 09/05/12
For personal use only.

Anal. Calcd. for $C_8H_{12}NO_4SCl$: C, 37.87; H, 4.77, N, 5.52. Found: C, 37.74; H, 4.69; N, 5.46.

*3-Carbomethoxy-6,7-dimethoxy-5-oxoperhydro-1,4-thiazepine (**20**)*

Method A

A mixture of 3-carbomethoxy-6,7-dibromo-5-oxoperhydro-1,4-thiazepine (**18**) (160 mg, 0.43 mmol) and pyridine (68 mg, 0.86 mmol) in methanol (20 ml) was stirred at room temperature for 12 h. After evaporation of the solvent under vacuum, the reaction product was dissolved in a small amount of dichloromethane and chromatographed on silica gel (20 g) using ether–dichloromethane (1:20) as eluent to yield 98% (113 mg) of 3-carbomethoxy-6,7-dimethoxy-5-oxoperhydro-1,4-thiazepine (**20**), m.p. 154–155°. The i.r.: 3410, 1750 and 1670 cm^{-1}; n.m.r.: δ 2.7–3.3 (m, 2H); 3.48 (s, 3H); 3.50 (s, 3H); 3.72 (d, 1H); 3.82 (s, 3H); 4.42 (m, 1H); 4.88 (d, 1H); 6.80 (m, 1H).

Anal. Calcd. for $C_9H_{15}NO_5S$: C, 43.36; H, 6.06. Found: C, 43.49; H, 6.14.

Method B

A mixture of the dibromo thiazepine **18** (36 mg, 0.10 mmol) and silver carbonate (100 mg, 0.40 mmol) in methanol (10 ml) was stirred at room temperature for 2 h. Filtration of the solution on Celite and evaporation of the solvent under vacuum gave, after recrystallization from chloroform–ether, a nearly quantitative yield of the dimethoxy thiazepine **20**, identical in all respects to the product obtained in method A.

The same result is obtained if silver oxide is used instead of silver carbonate.

*6-Bromo-3-carbomethoxy-7-methoxy-5-oxoperhydro-1,4-thiazepine (**21**)*

A mixture of 6,7-dibromo-3-carbomethoxy-5-oxoperhydro-1,4-thiazepine (**18**) (500 mg, 1.35 mmol) and silver carbonate (1.35 g, 5.4 mmol) in methanol (50 ml) was stirred at room temperature for 20 min. The t.l.c. then showed disappearance of the starting material and the presence of two reaction products. The mixture was filtered on Celite, the solvent evaporated under vacuum and the residue chromatographed on a silica gel column (50 g) using ether as eluent. Evaporation of the first fractions yielded 23% (100 mg) of 6-bromo-3-carbomethoxy-7-methoxy-5-oxoperhydro-1,4-thiazepine (**21**) melting, after recrystallization from chloroform–ether, at 108–110°; *m/e* 296.9651; calcd. 296.9671.

The second spot observed on t.l.c. corresponds to the 6,7-dimethoxy compound **20**.

*Reaction of Thiazepine **2** with Silver Oxide and Methanol*

A mixture of 3-carboxy-7-chloro-6,6-dimethyl-5-oxoperhydro-1,4-thiazepine (**2**) (100 mg, 0.40 mmol) and silver oxide (250 mg, 1.1 mmol) in methanol (15 ml) was heated to reflux for 1 h. The mixture was then filtered on Celite, the solvent evaporated *in vacuo* and the residue chromatographed on a silica gel column (10 g) using dichloromethane as eluent. The enamide **23** (90 mg) was obtained as an oil with a 92% yield. The i.r. (CH_2Cl_2): 3330, 1720 and 1675 cm^{-1}; n.m.r.: δ 1.24 (s, 6H); 3.60 (s, 6H); 3.89 (s, 3H); 4.23 (s, 1H); 5.90 (d, 1H); 6.66 (s, 1H); 9.33 (m, 1H); *m/e*: 245.

*Reaction of Enamide **23** with Methanolic Hydrogen Chloride*

The enamide **23** (90 mg, 0.368 mmol) was dissolved in anhydrous methanol (10 ml) saturated with hydrogen chloride, and the resulting solution stirred at 25° for 3 h. The hydrogen chloride was then neutralized by careful addition of solid sodium bicarbonate, the solvent evaporated to dryness and the residue taken up in ether. The inorganic salts were filtered and the reaction products separated by preparative t.l.c. using ether as eluent, to yield 50% (50 mg) of the oily amide **24**. The i.r. (CH_2Cl_2): 3380, 1745, and 1680 cm^{-1}; n.m.r.: δ 1.16 (s, 6H); 1.70 (s, 3H); 3.24 (s, 3H); 3.55 (s, 6H); 3.83 (s, 3H); 3.18 (s, 1H); 7.60 (m, 1H).

The authors are grateful to the National Research Council of Canada for generous support of this research through grants A-2034 and A-71 to D.G. and C.B., and also through fellowships for P.B. and R.G.

1. J. C. Sheehan and K. R. Henery-Logan. J. Am. Chem. Soc. **81**, 5838 (1959) and references cited therein.
2. E. J. Corey and A. M. Felix. J. Am. Chem. Soc. **87**, 2518 (1965).
3. A. K. Bose and B. Anjaneyulu. Chem. Ind. 903 (1966).
4. A. K. Bose and I. Kgajevsky. Tetrahedron, **23**, 957 (1967).
5. B. Akermark, N. G. Johansson, and B. Sjöberg. Tetrahedron Lett. 371 (1969).
6. I. L. Knunyants, O. V. Kil'disheva, M. P. Krasuskaya, M. G. Lin'kova, V. V. Shokina, Z. V. Benevolenskaya, and L. P. Rasteikene. Bull. Acad. Sci. U.S.S.R. Div. Chem. Sci. 1702 (1959).
7. N. J. Leonard and G. E. Wilson, Jr. J. Am. Chem. Soc. **86**, 5307 (1964).
8. Z. Foldi. Acta Chim. Acad. Sci. Hung. **5**, 187 (1954).
9. B. C. Barrass and D. T. Elmore. J. Chem. Soc. 4830 (1957).
10. N. J. Leonard and R. Y. Ning. J. Org. Chem. **31**, 3928 (1966).
11. J. L. Greene, Jr. and H. S. Hagemeyer, Jr. J. Am. Chem. Soc. **77**, 3016 (1955).
12. L. C. Cheney and S. R. Piening. J. Am. Chem. Soc. **67**, 731 (1945).
13. M. Frankel and M. E. Reichmann. J. Chem. Soc. 289 (1952).
14. R. H. Wiley, C. H. Jarboe, Jr., and F. N. Hayes. Biochem. J. **68**, 528 (1958).
15. (*a*) H. Böhme, H. Fischer, and R. Frank. Ann. **563**, 54 (1949). (*b*) H. Böhme and H. J. Gran. Ann. **577**, 68 (1962). (*c*) W. E. Truce, G. H. Birum, and E. T. McBee. J. Am. Chem. Soc. **74**, 3594 (1952). (*d*) H. Böhme and H. J. Gran. Ann. **581**, 133 (1953). (*e*) F. G. Bordwell and B. M. Pitt. J. Am. Chem. Soc. **77**, 572 (1955). (*f*) G. Cilento. Chem. Rev. **60**, 147 (1960). (*g*) F. Boberg. Ann. **679**, 107 (1964). (*h*) L. A. Paquette. J. Am. Chem. Soc. **86**, 4089 (1964). (*i*) D. L. Tuleen and V. C. Marcum. J. Org. Chem. **32**, 204 (1967). (*j*) D. L. Tuleen. J. Org. Chem. **32**, 4006 (1967). (*k*) L. A. Paquette, L. S.

WITTENBROOK, and K. SCHREIBER. J. Org. Chem. **33**, 1080 (1968). (*l*) D. L. TULEEN and T. B. STEPHENS. J. Org. Chem. **34**, 31 (1969).
16. Y. HENG SUEN and H. B. KAGAN. Bull. Soc. Chim. Fr. 1460 (1965).
17. (*a*) M. KARPLUS. J. Chem. Phys. **30**, 11 (1959); (*b*) M. KARPLUS. J. Am. Chem. Soc. **85**, 2870 (1963).
18. (*a*) C. M. MCCLOSKEY and G. H. COLEMAN. Org. Synth. **3**, 434 (1955); (*b*) A. PISKALA and F. SORM. Coll. Czech. Chem. Comm. **29**, 2060 (1964); (*c*) F. MICHEEL and F. SUCKFÜLL. Ann. **507**, 138 (1933); (*d*) R. L. WHISTLER and C. S. CAMPBELL. J. Org. Chem. **31**, 816 (1966).
19. O. E. EDWARDS, J. M. PATON, M. H. BENN, R. E. MITCHELL, CHURAI WATANATADA, and K. N. VOHRA. Can. J. Chem. **49**, 1648 (1971).
20. S. W. BREUER, T. BERNATH, and D. BEN-ISHAI. Tetrahedron **23**, 2869 (1967).
21. J. C. SHEEHAN, K. R. HENERY-LOGAN, and D. A. JOHNSON. J. Am. Chem. Soc. **75**, 3292 (1953).

Can. J. Chem. Downloaded from www.nrcresearchpress.com by 210.87.254.42 on 09/05/12
For personal use only.

Can. J. Chem. Downloaded from www.nrcresearchpress.com by 210.87.254.42 on 09/05/12
For personal use only.

On the Chemistry of the Isomeric Dichlorodiphenylacetaldehydes Related to DDT. Stereoelectronic Effects in the Hydrolysis of their Cyclic Acetals

J. D. McKinney, R. E. Hawk,[1] E. L. Boozer,[1] and J. E. Suggs[1]

National Institute of Environmental Health Sciences, National Institutes of Health, Public Health Service and Department of Health, Education and Welfare, Research Triangle Park, North Carolina 27709

Received July 7, 1970[2]

The chemistry of the isomeric dichlorodiphenylacetaldehydes related to DDT was investigated to aid in delineating their possible role in the metabolism of this pesticide. In the case of the *p,p'*-isomer, the most important system under consideration, several literature syntheses were shown to be incorrect. The failure of at least one of these methods was attributed to the preferred oxidative involvement of the benzhydryl carbon via rearrangement of a β-hydroxy enol ether which normally led to the isolation of the *p,p'*-dichlorobenzophenone instead of the desired aldehyde. The *o,p'*-isomer exhibited chemistry similar to that of the *p,p'*-isomer although the steric effect of the ortho-substituted chlorine on the benzhydryl proton was notable. The *o,o'*-isomer was normal in that it did not undergo reactions involving the benzhydryl carbon. Some possible mechanistic and biological implications of the work are discussed.

La chimie des dichlorodiphénylacétaldéhydes isomères, apparentés au DDT, a été étudiée afin de délimiter leurs rôles possibles dans le métabolisme de ce pesticide. Dans le cas de l'isomère-*p,p'*, le système considéré comme le plus important, plusieurs synthèses données dans la littérature sont incorrectes. L'échec d'au moins une de ces méthodes est attribuée à l'entrée en jeu de l'oxydation préférentielle du carbone benzhydryle via une transposition d'un éther énolique β-hydroxylé qui normalement conduit au *p,p'*-dichlorobenzophénone au lieu de conduire à l'aldéhyde désiré. L'isomère-*o,p'* montre un comportement analogue à celui de l'isomère-*p,p'*, bien que l'effet stérique des substituants ortho sur le proton benzhydryle soit notable. L'isomère-*o,o'* a un comportement normal en ce sen qu'il ne subit aucune réaction impliquant le carbone benzhydryle. Certains mécanismes possibles et certaines implications biologiques de ce travail sont discutés.

Canadian Journal of Chemistry, **49**, 3877 (1971)

Today DDT is of immense biological importance, with vast quantities now distributed in the worldwide environment. However, surprisingly little work has been done toward gaining a firm theoretical understanding of its chemistry. The synthesis of the isomeric dichlorodiphenylacetaldehydes related to DDT and a study of some of their reactions were undertaken to help correct this deficiency. Investigation of their role in DDT metabolism (1) seemed essential since they are the logical intermediates in the formation of the dichlorodiphenylacetic acids which are major metabolites. Although several syntheses have been reported for these aldehydes, our attempts to reproduce some of them led to contradictory results which are theoretically interesting and may be of biological consequence.

The several syntheses reported for *bis*(*p*-chlorophenyl)acetaldehyde (**1***a*) include the rearrangement of 1,2-*bis*(*p*-chlorophenyl)ethylene glycol (**2***a*) in a sealed tube under vigorous conditions to effect a phenyl migration (2) (eq. 1); the hydrolysis of the cyclic acetal (3), 2-(*p,p'*-dichlorobenzhydryl)-1,3-dioxolane (**3***a*) (eq. 2); the reductive cleavage of the pyrazolene **4***a* (4) (eq. 3). In all three cases the aldehyde was reported as a crystalline compound varying in m.p. from 135 to 149 °C.

The synthesis of **1***a* by the hydrolysis of **3***a* appeared straightforward and was especially attractive since the starting material for synthesis of **3***a* was 2,2-dichloro-1,1-*bis*(*p*-chlorophenyl)-ethane (DDD) which is readily available. Our attempts (5) to reproduce this method afforded crystalline **3***a* whose structure confirmation conveniently eliminated structures **5***a* and **6** which are conceivable products of this reaction proposed by Riemschneider and co-workers. However, the results of our hydrolyses of **3***a* confirm that the previous workers (3) had isolated 4,4'-dichlorobenzophenone (**7**) instead of the desired aldehyde (**1***a*). The aldehyde was obtained as an oil which could not be crystallized. The crystalline material isolated by the previous workers (2–4) is characteristic of **7** in varying degrees of purity. It was later found that other workers (6) had arrived at the same conclusion since their

[1]Chamblee Toxicology Laboratory, Environmental Protection Agency, Chamblee, Georgia 30341.

[2]Revision received August 31, 1971.

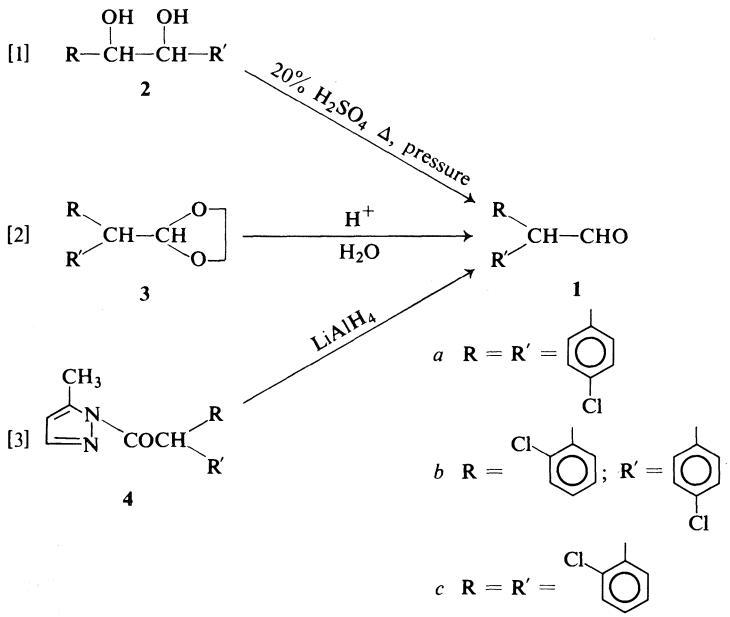

Darzens synthesis of the aldehyde had afforded an oily product. Investigation of this chemistry was undertaken since the chemistry encompassing the formation of the dichlorobenzophenone might have a bearing on its occurrence in DDT metabolism.

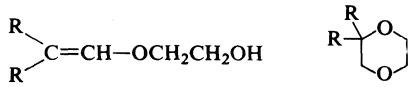

5*a*

6

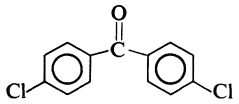

7

Based on these findings, it seemed plausible but mechanistically obscure that **1***a* might be intermediate in the formation of **7** during the hydrolysis of the acetal **3***a* under the heterogeneous conditions. However, the aldehyde was recovered in good yield when it was subjected to the conditions of hydrolysis with no appreciable conversion to dichlorobenzophenone (**7**). When the hydrolysis was carried out using mixtures of *p*-dioxane and 20% aqueous HCl (1:1 v/v), **7** was formed as the major characterizable product (30–60% yields) in 3–5 h at reflux temperature. There was no t.l.c. evidence for the intermediate formation of **1***a*. This result was supported by following the hydrolysis of **3***a* by n.m.r. under similar conditions.[3] Since the purity and structure of **3***a* have been rigorously established, an alternative route by which dichlorobenzophenone **7** can be formed from acid hydrolysis of acetal **3***a* without invoking the intermediacy of aldehyde **1***a* apparently exists. The experiments outlined in Scheme 1 were carried out with the objective of trapping or stablizing intermediates which might be responsible for the formation of **7** from acetal **3***a*.

Solvolysis of **3***a* in acetic acid in the presence of concentrated sulfuric acid at 100 °C for 1 h gave a mixture of the dichlorobenzophenone **7**, aldehyde **1***a*, and the acetoxyethanol **9***b*. These products were isolated by preparative t.l.c.[4] and

[3]The hydrolysis was carried out at 75° in *p*-dioxane-d_8 with 20% DCl. The n.m.r. scans were made at 5-min intervals for 1 h. The acetal apparently underwent immediate hydrolysis; however, there were no resonances indicating the formation of **1***a*. A control experiment had indicated that **1***a* was stable under these conditions.

[4]The acetoxyethanol **9***b* decomposed on t.l.c. to two materials; one remaining at the origin and the other near the solvent front. The latter material characteristically fluoresced light blue under short wave u.v. light. The exact nature of these products will be discussed later; however, n.m.r. studies of product mixtures of **9***b* in the presence of the n.m.r. shift reagent (7), $Eu(DPM)_3$, confirmed that the acetate group (three proton, singlet) was associated with the benzhydryl carbon and a hydroxyl group was associated with the methylene group (two proton, singlet) since the latter group experienced the largest paramagnetic shift with the reagent while the aromatic signals experienced relatively little shift.

Can. J. Chem. Downloaded from www.nrcresearchpress.com by 210.87.254.42 on 09/05/12
For personal use only.

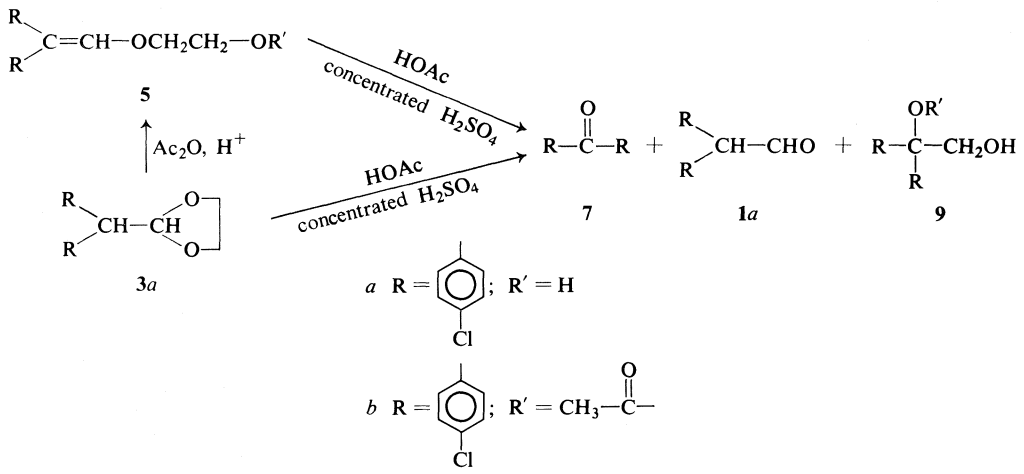

SCHEME 1

identified by their spectral properties. The benzophenone **7** constituted about 10–15% of the total along with major amounts of the aldehyde and acetoxyethanol. Solvolysis of the enol ether acetate **5***b*, which was obtained from **3***a* in good yield by treatment with acetic anhydride containing concentrated sulfuric acid, gave qualitatively but not quantitatively the same product mixture; the benzophenone **7** was formed in about 40% yield with appreciable amounts of the acetoxyethanol **9***b* and trace amounts of aldehyde **1***a*. It was also shown that neither **1***a* nor **9***b* were intermediate in the formation of **7** under the solvolysis conditions.

Since the enol acetate **5***b* affords **7** as a major product and the acetoxyethanol **9***b* is not intermediate in this conversion, the benzophenone **7** must have resulted from rearrangement of **5***b* itself or from some other yet undetected intermediate. Protonation of the enol ether acetate at the ether oxygen should activate the molecule to attack by acetate ion at the benzhydryl carbon or intramolecular attack by its own acetate group via a *quasi*-six-membered ring. The former possibility should have resulted in the diacetate **10***b*. However, this compound was not found among the products and suggested that **10***b*, if formed, possibly undergoes further cleavage at the ether oxygen to form the acetoxyethanol **9***b*, a major product of the acetic acid solvolysis reaction. Nevertheless, 2,2-*bis*-(*p*-chlorophenyl)-diethylene glycol (**10***a*) was synthesized according to the reported method (8), and its hydrolysis properties were investigated. The diethylene glycol could dehydrate in a cyclic fashion (9) to

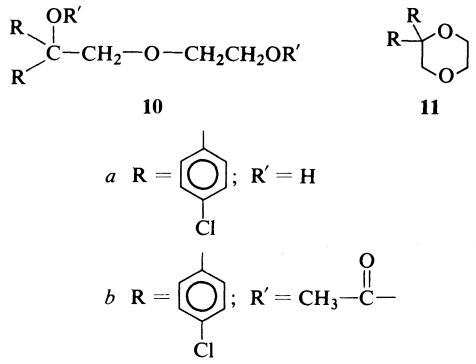

form dichlorobenzophenone **7** or dehydrate to 2,2-*bis*(*p*-chlorophenyl)-*p*-dioxane (**11**) which could possibly undergo pyrolysis to **7**. Hydrolysis experiments with **10***a* repeatedly gave mixtures as determined by t.l.c. and gas chromatography (g.c.). The mixtures consisted primarily of two materials whose chromatographic properties were reminiscent of the decomposition products[4] of the acetoxyethanol **9***b*; one material was highly polar and polymeric in nature while the other material was relatively non-polar and fluoresced light blue under u.v. light. The latter material was purified by preparative t.l.c. and identified as the symmetrical *p*-dioxane **12**. The n.m.r. spectrum of **12** revealed the non-equivalency of the methylene protons, and Drieding models show that because of the steric requirements of the bulky phenyl groups the molecule prefers a twist-boat conformation in which the methylene protons experience different environments. The mass spectrum of the compound contained a parent ion greater than 500 (*m/e*)

Can. J. Chem. Downloaded from www.nrcresearchpress.com by 210.87.254.42 on 09/05/12
For personal use only.

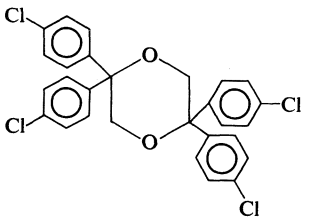

12

and was otherwise indicative of structure **12**. The dioxane **12** and polymeric products were also shown to be spontaneous decomposition products of the diethylene glycol **10***a* with or without solvent. The most plausible explanation for formation of such products would be that intramolecular hydrogen bonding may facilitate decomposition of the diethylene glycol **10***a* to the ethylene glycol **9***a* which in turn can undergo dimerization to **12** or polymerization. The dichlorobenzophenone **7** was only a minor decomposition product (<10%) of **10***a* and was detected by electron capture g.c. A small amount of dioxane **11** was also detectable among the products. Therefore, the intermediacy of **10***b* in the solvolysis of the enol ether acetate **5***b* seems likely since it would explain the presence of the acetoxyethanol **9***b* and polymeric material among the products. The formation of dichlorobenzophenone **7** from rearrangement of **5***b* is now credible and is shown in Scheme 2.[5] Invoking the intermediacy of an α-hydroxy aldehyde (**13***b*) in the formation of the dichlorobenzophenone **7** was attractive since such an intermediate would be expected to be both chemically and thermally labile and is a conceivable product in the other erroneous syntheses reported for aldehyde **1***a* by other workers. Although there is no chemical evidence to support the intermediacy of **13***a*, gas chromatography – mass spectrometry (g.c.–m.s.) confirmed its presence among the decomposition products of the enol ether acetate **5***b*. Gas chromatography on a 3% diethylene glycol succinate/2% orthophosphoric acid column at 170 °C gave eight peaks for pure enol ether acetate **5***b*, six of which were identified by their mass spectra. The first peak was the expected dichlorobenzophenone **7** in comparatively good yield having a base peak of *m/e* 139 $(R—C\equiv O)^+$ in its mass spectrum. The second peak was identified as the α-hydroxy aldehyde (**13***b*) whose mass spectrum also has a base peak of *m/e* 139 along with M (*m/e* 281), M-1 and M-HCHO (*m/e* 251) of intensities approximately 0.3% that of the base peak. The third peak was the expected aldehyde **1***a* in less than 10% yield of that of the ketone **7**. The fourth peak was a major component and was identified as the α-acetoxy aldehyde (**13***a*) although the parent molecular ion (*m/e* 313) was not discernible. However, there are prominent fragments corresponding to the loss of both HCHO (*m/e* 293) and HOAc (*m/e* 264) as well as the base peak of *m/e* 139. The presence of these fragments in the spectrum implies that both the aldehyde and acetate moieties must have been present in the original molecule. The detection of the parent ion of the α-hydroxy aldehyde (**13***b*) is probably a reflection of increased stability of this ion via hydrogen bonding. Both peaks five and seven were too weak to identify conclusively. Peaks six and eight were identified as the enol ether alcohol (**5***a*) and the enol ether acetate (**5***b*) respectively. The acidic column conditions favored decomposition since g.c. on a 3% SE-30 column at 212 °C gave smaller relative amounts of the major decomposition products. In fact, the α-acetoxy aldehyde (**13***a*) was not detectable under these conditions; however, this may also be a reflection of the poorer stability of acetate **13***a* under these conditions since the α-hydroxy aldehyde was detected. In addition, the introduction of the enol ether acetate **5***b* into the mass spectrometer by the direct probe inlet produced spectra indicating that extensive rearrangement had occurred.

In light of these data, it was suspected that similar intermediates could occur in the hydrolysis of **3***a* under aqueous acidic conditions affording dichlorobenzophenone **7**. Hydrolysis of the substituted dioxane **12** and the enol ether acetate **5***b* in *p*-dioxane and 20% HCl (1:1 v/v) gave the aldehyde **1***a* as the major product. These results are not entirely surprising since dioxane **12** might be expected to undergo cleavage and rearrangement to the aldehyde on heating with a mineral acid and, in the case of **5***b* cleavage at the ether oxygen would be expected

[5]The nature of the products from this reaction seems to clearly indicate that the normal oxonium ion resonance contribution of enol ethers, $R_2\overset{\ominus}{C}CH=\overset{\oplus}{O}—R'$, is of little importance in **5***b*. Rearrangement of **5***b* can be considered analogous to the thermal rearrangements of enolic ethers in general and allyl aryl ethers (Claisen rearrangement) producing in the case of **5***b* somewhat unexpected products because of the anomalous electronic distribution. Such thermally influenced rearrangements of this type for the most part are known (10) to proceed via first-order kinetics as depicted for **5***b* although it was not ascertained.

Can. J. Chem. Downloaded from www.nrcresearchpress.com by 210.87.254.42 on 09/05/12
For personal use only.

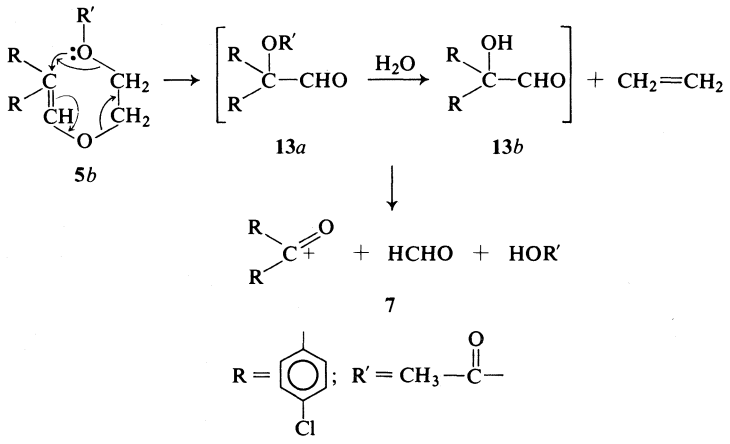

SCHEME 2

to occur more rapidly than hydrolysis of the acetate group such that an appreciable amount of the suspected "real" intermediate, the enol ether alcohol (**5***a*) is never available for rearrangement leading to dichlorobenzophenone **7**. In considering the transition state for rearranging **5***b* to **7**, the comparatively large acetate group in the vicinity of the reacting center restricts the number of configurations which may be assumed by the atoms involved, resulting in further reduction in entropy which is rate-retarding. Therefore, one would expect the enol ether alcohol (**5***a*) to rearrange as shown in Scheme 2 with a more positive entropy which would be comparatively rate-enhancing. The fact that the enol ether alcohol could not be isolated is consistent with this argument.

Variations[6] in the hydrolysis conditions of acetal **3***a* gave qualitatively but not quantitatively the same products, acetaldehyde **1***a* and dichlorobenzophenone **7**. Hydrolysis in 95% ethanol with 20% aqueous sulfuric acid (2:1 v/v) produced approximately equal quantities of **7** and **1***a*. Hydrolysis in 95% ethanol or 1,4-dioxane with concentrated sulfuric (10:1 v/v) afforded aldehyde **1***a* in good yields. Totally aqueous acidic conditions gave either no reaction or the dichlorobenzophenone **7** as the major product. These results imply that more aqueous conditions and hence more heterogeneous conditions favor production of **7**. Under more heterogeneous conditions solvolysis reactions would be minimized and intramolecular vapor phase reactions, which would be thermally influenced, become more important. This is consistent with a cyclic decomposition of **5***b* to **7** as delineated in Scheme 2. The intermediates formed in the hydrolysis of acetal **3***a* which are most tenable with our results are given in Scheme 3.

Preequilibrium protonation of **3** followed by decomposition to a resonance-stabilized carbonium ion would be expected (11). The enol ether alcohol (**5***a*) could be formed by deprotonation of this carbonium ion, and once formed, can undergo several reactions (paths *a–c*). Normal hydrolysis as in path *b* would lead to aldehyde **7**. Protonation of the enol ether oxygen followed by hydration of the double bond (path *a*) would lead to diethylene glycol **10***a* which in turn could decompose to ethylene glycol **9***a* ultimately leading to dimers and polymers. Protonation of the ether oxygen followed by intramolecular attack on the double bond and rearrangement would lead to the α-hydroxy aldehyde **13***b* which would decompose[7] to the dichlorobenzophenone **7**.

[6]Several classical methods for preparing aldehydes (Rosenmund and metal hydride reductions of the acid chloride, chromium oxide oxidation of the alcohol, etc.) were unsuccessful for **1***a*; in most cases the major isolable product was the dichlorobenzophenone **7**. The mechanistic implications of these results are not completely understood.

[7]The expected by-products of these disproportionation reactions are formaldehyde and ethylene. One would expect formaldehyde to polymerize under the reaction conditions, and attempts to trap it with various carbonyl derivatizing agents were unsuccessful. Likewise, ethylene could not be trapped as its dibromide; however, an n.m.r. hydrolysis study of **3***a* with aqueous D_2SO_4 in d_6-dimethylsulfoxide, which indicated the presence of **7** as well as trace amounts of **1***a*, showed a singlet of weak intensity at a chemical shift (τ 4.55) identical to that of authentic ethylene.

Can. J. Chem. Downloaded from www.nrcresearchpress.com by 210.87.254.42 on 09/05/12
For personal use only.

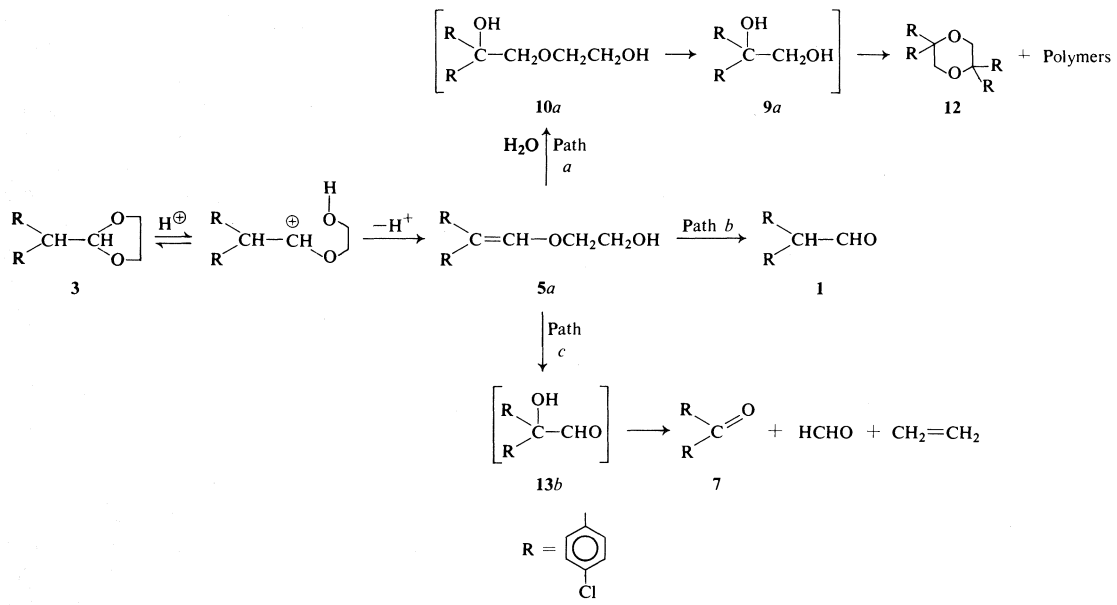

SCHEME 3

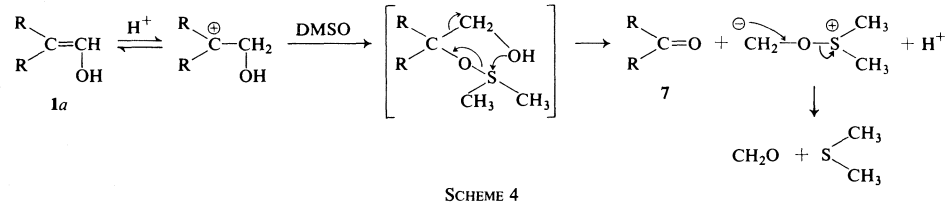

SCHEME 4

Our investigations were extended to include the *o,p'*-dioxolane **3***b* since commercial preparations of DDT contain the *o,p'*-isomer as a major component whose metabolism is qualitatively similar although quantitatively different (12). Dioxolanes **3***a* and *b* are electronically analogous and would be expected to undergo similar reactions. Under the hydrolysis conditions of **3***a* that afford only minor amounts of the expected aldehyde **1***a*, **3***b* affords quantitative yields of aldehyde **1***b*.

The anomalous hydrolysis of **3***a* seems to be manifested in the facility by which the benzhydryl carbon of this system can undergo oxidation. This reflects greater charge stabilization associated with the bis(*p*-chlorophenyl) system than with the *o,p'*-system which must be explained on the basis of steric arguments. CPK-Models[8] indicate that there are two sterically derived factors which would hinder or prevent oxidation of the benzhydryl carbon in the *o,p'*-system (**3***b*). There is steric hindrance to removal of the benzhydryl proton imposed by the *o*-chlorine,[9] and there is steric inhibition of resonance which would impair charge stabilization once the proton has been removed. Aldehyde **1***b* would be the expected hydrolysis product of **3***b* regardless of which of the two steric effects is more important in determining the course of the reaction.

Previous investigators (6) observed steric dependence in attempting to prepare the isomeric iodides from the corresponding tosylates of the

[8]Corey–Pauling–Koltun atomic models.

[9]A measure of this effect is evident from a comparison of the chemical shift of the benzhydryl proton in *p,p'*-DDT (τ 5.00) with that in *o,p'*-DDT (τ 4.25) and *o,p'*-DDD (τ 4.28); an ortho chlorine within the aromatic ring deshields the benzhydryl proton more than a para-substituted chlorine. See Keith *et al.* (13) for a discussion of the n.m.r. spectra of DDT-related compounds.

Can. J. Chem. Downloaded from www.nrcresearchpress.com by 210.87.254.42 on 09/05/12
For personal use only.

[4] 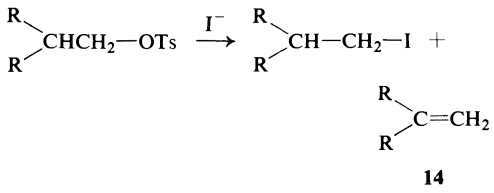

14

dichlorodiphenylethanols (eq. 4). The elimination product **14** was the sole product in the case of *p,p'*-isomer whereas the *o,p'*-isomer gave a mixture of the two products. On the other hand, the *o,o'*-isomer gave the iodide as the sole product. Steric factors are known (14) to play an important role in bimolecular elimination reactions. Steric hindrance to resonance stabilization of the product might also influence the reaction course in this case.

A steric dependence of this system was further demonstrated in our laboratory by observing the n.m.r. spectra of the aldehydes in dimethylsulfoxide (d_6-DMSO). In DMSO, **1***a*, is converted to its enol form almost quantitatively upon solution as evidenced by a decrease in the n.m.r. proton signal of the benzhydryl carbon. In most instances this enolization was accompanied by a small (<10%) conversion to the dichlorobenzophenone **7**. Crystalline material isolated from the DMSO solutions had properties identical to those of authentic **7**. The *o,p'*-isomer undergoes a slower rate of enolization as measured by n.m.r.; however, there was no evidence to indicate reactions with DMSO. It was shown using the *o,p'*-isomer that the enolization rate in DMSO could be catalyzed by the addition of either acid or base. Shaking the protio-aldehyde in chloroform-*d* with D_2O in the presence of sodium carbonate resulted in the exchange of the benzhydryl proton for deuterium while the aldehyde proton remained unchanged. The *o,o'*-isomer[10] **1***c*, however, failed to undergo enolization in DMSO at temperatures ranging from 26 to 75 °C. In comparison, diphenylacetaldehyde enolizes in DMSO to a lesser extent than did the bis(*p*-chlorophenyl)acetaldehyde. From this result one infers that the electronic effects of the chlorine substituents as well as steric factors play a role in the enolization processes. In the case of the *p,p'*-isomer, the electronic effects must also influence subsequent reactions since the dichlorobenzophenone **7** was detected in its DMSO solutions. Since enolization of **1***a* appears to be very rapid in DMSO, it is probable that formation of **7** involves the enol. Steric hindrance to removal of the benzhydryl proton would be manifested if enolization were required to form a reactive species. Although there is no compelling evidence, the following pathway is proposed (Scheme 4).[11] Preequilibrium protonation of the enol could generate the bis(*p*-chlorophenyl) carbonium ion system which is susceptible to attack by oxygen of DMSO. The resulting labile alkoxysulfonium salt could undergo intramolecular attack at sulfur to afford **7**.

This work has shown that the bis(*p*-chlorophenyl) system in conjunction with a vicinal electron deficient carbon, such as is contained in the aldehyde moiety and possibly in a trichloromethyl group,[12] can undergo rather facile reactions involving the benzhydryl carbon usually resulting in an overall oxidation at this position which may be concomitant with the loss of the adjacent group. In comparing the oxidative propensities of the *p,p'*- and *o,p'*-systems, it is evident that the requisite removal of the benzhydryl proton is subject to the stereoelectronic requirements imposed by the chlorophenyl groups. The *o*-chlorophenyl compounds have much less tendency toward oxidation and double bond formation at their benzhydryl carbons. In light of this work, the possible intermediacy of the α-hydroxy aldehyde **13***b* in the formation of dichlorobenzophenone **7** during DDT metabolism is plausible. The ease of enolization of the *p,p'*-aldehyde **1***a* could facilitate its interactions in biological systems subsequently leading to redox products such as α-hydroxy aldehyde **13***b*. Our results also lend some credence to the corollary that, if such an aldehyde were formed *in vivo*, conjugates[13] involving the hydroxy group could activate the

[10]The aldehyde **1***c*, which was obtained from Aldrich Chemical Co., Milwaukee, Wisc., exhibited no unusual reaction properties.

[11]The use of polarizing agents to promote DMSO oxidations of alcohols has been reported (15) to produce alkoxysulfonium salts which undergo base-catalyzed decomposition to carbonyl compounds. The hydroxymethylalkoxysulfonium ion which could be formed from **1***a* may constitute a special case of this in which the hydroxymethyl group acts as an internal base to effect the stepwise decomposition to two carbonyl compounds.

[12]The compound 1,1-bis(*p*-chlorophenyl)-2,2,2-trichloroethanol has been shown (16) to pyrolyze to **7** and chloroform.

[13]Previous workers (17) have shown that DDT metabolite conjugates are formed, although their exact nature is not known. However, they do not appear to be conjugated with glucuronic or sulfuric acids.

Can. J. Chem. Downloaded from www.nrcresearchpress.com by 210.87.254.42 on 09/05/12
For personal use only.

molecule as an alkylating agent.[14] Nevertheless, the occurrence of such an aldehyde would implicate a host of new and interesting metabolites which will be described elsewhere. Although, it is not surprising that the aldehyde **1***a* has not been detected in DDT metabolism, earlier work (18) has shown that 2,2-bis(*p*-chlorophenyl)-ethanol (DDOH), a known DDT metabolite (1), is a substrate of crystalline liver alcohol dehydrogenase which oxidizes DDOH to **1***a*.

Experimental

Melting points were taken on a Fisher–Johns melting point apparatus and are corrected. The i.r. spectra were obtained with Perkin–Elmer 337 and 521 spectrophotometers. The n.m.r. studies were made with a Varian T-60 and an HA-100 spectrometer equipped with a variable temperature probe using tetramethylsilane (TMS) or sodium 2,2-dimethyl-2-silapentane-5-sulfonate (DSS) as internal references. Routine gas chromatograms were obtained with a Varian Aerograph model 1868-40 chromatograph equipped with a tritium detector. The low-resolution mass spectra were obtained with an LKB 9000 gas chromatograph-mass spectrometer. Thin-layer chromatograms were run on Uniplate, Silica Gel GF plates 250 and 500 μ in thickness and were developed in methylene chloride. The bands were detected with u.v. light.

Formation of 2,2-Bis(p-chlorophenyl)acetaldehyde (1a)

(a) From Darzens Condensation

To a solution of 7.5 ml (0.077 mol) of ethyl chloroacetate and 10 g (0.04 mol) of 4,4′-dichlorobenzophenone (Eastman Organic Chemicals) in 25 ml of anhydrous benzene under nitrogen was added 6.0 g (0.12 mol) of sodium hydride (50% dispersion) with stirring over a 2 h period. The reaction mixture was stirred for 16 h at room temperature and poured into 50 ml of ice-cold 25% HCl solution. The resulting suspension was extracted with two 50-ml portions of benzene. The combined extracts were dried over anhydrous sodium sulfate and evaporated to dryness. The partially solidified residue was recrystallized from methanol, affording 9.5 g of ethyl β,β-bis(*p*-chlorophenyl)glycidate melting at 98–105°. Without further purification this material was dissolved in 40 ml of ethanol and the resulting solution was refluxed for 6 h with 15 ml of 35% aqueous potassium hydroxide solution. The ethanol was removed by rotary evaporation and the remaining mixture was diluted with 25 ml of distilled water and extracted with two 30-ml portions of ether. The aqueous phase was acidified (p*H* 4–5) with 20% hydrochloric acid, forming a milky solid suspension. The suspension was extracted with two 50-ml portions of ether and the combined extracts were washed with distilled water, dried over anhydrous sodium sulfate, and evaporated to an oily residue. Decarboxylation of the crude material was accomplished by heating in an oil bath at 140–160° under reduced pressure (water aspiration) for 30 min. The crude product **1***a* weighed 4.5 g (60%). The aldehyde was purified by dissolving in 10 ml of methanol and adding the resulting solution dropwise with stirring to 25 ml of saturated sodium bisulfite solution. The mixture was stirred at room temperature for 5 h and the solid suspension was removed by filtration. The cake was washed with water, 2-propanol, and then ether before drying under vacuum. The aldehyde was regenerated prior to use by heating portions of the bisulfite addition product with 10% sodium carbonate solution at 75° until an oil separated (15–30 min). The pure aldehyde was obtained by extraction into ether and had the following spectral properties: i.r., λ (neat) 5.80 (C=O), 3.49 (CH), 13.2 (C—Cl); n.m.r., τ (chloroform-*d*) 0.10 (doublet, J = 2.4 Hz, 1H, CHO), 3.00 (multiplet, 8H, aromatics), 5.08 (doublet, J = 2.4 Hz, 1H, benzhydryl).

The *p*-nitrophenylhydrazine derivative prepared according to the method of Shine (19) contained one molecule of methanol of crystallization and melted at 85–88°. When this material was recrystallized from ether – petroleum ether, the methanol was removed to give a crystalline compound melting at 135–138 °C: i.r., λ (Nujol) 3.03 (NH), 6.26 (C=N), 7.58, 7.72 (NO_2); n.m.r., τ (dimethylsulfoxide-d_6) 1.84, 2.95 (pair of doublets, J = 9 Hz, for *p*-nitrophenyl aromatics); 2.10, 4.82 (pair of doublets, J = 6 Hz, for azomethinyl and benzhydryl protons); 2.57 (multiplet for bis(*p*-chlorophenyl) aromatics).

The *p*-nitrophenyl hydrazone of the dichlorobenzophenone **7** was prepared according to the same procedure and melted at 213–215°: i.r., λ (Nujol) 3.02 (NH), 6.30 (C=N), 7.55, 7.90 (NO_2); n.m.r., τ (dimethylsulfoxide-d_6) 1.97 (doublet, J = 9 Hz, 2H of *p*-nitrophenyl aromatics); 2.64 (multiplet, 2H of *p*-nitrophenyl aromatics, 8H of bis(*p*-chlorophenyl) aromatics).

(b) From Hydrolysis of 2-(4,4′-Dichlorobenzhydryl)-1,3-dioxolane (3a)

To a solution of 85 mg (0.28 mmol) of dioxolane in 5 ml of 95% aqueous 1,4-dioxane was added 0.4 ml of concentrated H_2SO_4. The resulting solution was magnetically stirred and refluxed for 3 h. The 1,4-dioxane was removed by rotary evaporation and the aqueous phase doubled in volume with distilled water to 3 ml. The aqueous solution was then extracted with two 3-ml portions of anhydrous ether and the combined extracts were dried over anhydrous Na_2SO_4 containing solid Na_2CO_3. Evaporation of the ether extracts under a nitrogen stream followed by pumping *in vacuo* gave 79 mg of a mixture composed of the 2,2-bis(*p*-chlorophenyl) acetaldehyde **1***a* and starting material. The aldehyde which was purified by preparative t.l.c. (40 mg, 55% yield) was identical in every respect to aldehyde obtained via the Darzens synthesis. Longer reflux times (6–8 h) gave increasingly higher yields of aldehyde under these conditions.

Solvolysis of 2-(4,4′-Dichlorobenzhydryl)-1,3-dioxolane (3a) in Acetic Acid

To a solution of 8 ml of glacial acetic acid and 0.05 ml of concentrated H_2SO_4 was added 155 mg (0.5 mmol) of

[14]The formation of the symmetrical dioxane **12** previously discussed can be considered a head-to-tail alkylation of two molecules of the acetoxyethanol **9***b* via displacement of the acetate groups. This reaction appears to be facile since it occurs directly on a silica gel t.l.c. plate during development. This compound was also found as a reaction product of unsuccessful attempts to form amino acid Schiff bases of aldehyde **1***a*.

Can. J. Chem. Downloaded from www.nrcresearchpress.com by 210.87.254.42 on 09/05/12
For personal use only.

Can. J. Chem. Downloaded from www.nrcresearchpress.com by 210.87.254.42 on 09/05/12
For personal use only.

dioxolane **3***a*. The resulting solution was heated at 100 °C for 1 h. The acetic acid was removed by lyophilization and the residue pumped *in vacuo* over P_2O_5. The residual oil was dissolved in chloroform-*d* and examined by n.m.r. spectroscopy. The spectrum indicated a mixture of products of which the three major components were tentatively identified as 2,2-bis (*p*-chlorophenyl)acetaldehyde (**1***a*), 4,4′-dichlorobenzophenone (**7**), and 1,1-bis(*p*-chlorophenyl)-1-acetoxyethanol (**9***b*) in an approximate ratio of 3:1:3. Preparative t.l.c. of the mixture gave 45 mg of aldehyde **1***a* and 15 mg of dichlorobenzophenone **7** along with 27 mg of dimer **12** and 20 mg of polymeric material (dark brown material remaining at the origin) both of the latter materials being decomposition products of the acetoxyethanol **9***b*. A small amount (10 mg) of pure dimer **12** was obtained by repeated preparative t.l.c. and had the following properties: i.r., λ ($CHCl_3$ film) (aromatic) 6.70, 12.2; (C—O—C) 8.88, 9.18, 9.85; n.m.r., τ (chloroform-*d*) 2.99 (multiplet, aromatics), 4.65, 5.89 (doublets, J = 2.0, Hz, methylene protons); τ (benzene-d_6) 3.10 (multiplet, aromatics), 5.19, 6.17 (doublets, J = 2.0, Hz, methylene protons).

Anal. Calcd. for $C_{28}H_{20}O_2Cl_4$: C, 63.42; H, 3.77. Found: C, 63.19, H, 4.38.

1,1-Bis(p-chlorophenyl)-3-oxa-1-pentenyl-5-acetate (Enol Ether Acetate (5b))

To a solution of 20 ml of acetic anhydride and 2 ml of concentrated H_2SO_4 was added 2.0 g (65 mmol) of the dioxolane **3***a*. The resulting solution was heated at 100 °C with stirring for 0.5 h. On cooling, the reaction mixture was poured into ice water (approximately 30 ml) and extracted with two 50-ml portions of anhydrous ether. The combined extracts were washed with saturated Na_2CO_3 solution, water, and then dried over anhydrous Na_2SO_4 followed by evaporation. The residue remaining (approximately 3.2 g) was chromatographed on a column of Silcar CC-7 (40 g) using a mixture of hexane:chloroform:methanol (3:2:1) as the eluting solvent. The fractions were analyzed with t.l.c. and combined accordingly. The residue remaining on evaporation of the solvent weighed 1.87 g (91%). A portion of this material was crystallized twice from *n*-hexane affording a crystalline hygroscopic solid melting at 73–75 °C: i.r., λ (neat) (C═O) 5.75, (O—C═C) 6.20; n.m.r., τ (chloroform-*d*) 2.76 (multiplet, aromatics); 3.54 (singlet, enolic proton); 5.80 (multiplet, methylene protons); 7.97 (singlet, acetate CH_3).

Anal. Calcd. for $C_{18}H_{16}O_3Cl_2$: C, 61.56; H, 4.56; O, 13.77; Cl, 20.22. Found: C, 61.22; H, 4.74; O, 13.58; Cl, 20.04.

Formation of 4,4′-Dichlorobenzophenone (7)

(a) From Hydrolysis of 2-(4,4′-Dichlorobenzhydryl)-1,3-dioxolane (3a)

To a mixture of 10 ml of 1,4-dioxane and 10 ml of 20% aqueous HCl was added 1.0 g (3.2 mmol) of dioxolane **3***a*, and the resulting mixture was refluxed for 3.5 h. The solution after cooling to room temperature was diluted with additional water to 50 ml and extracted with two 30-ml portions of anhydrous ether. Combined ethers were washed with water, dried over anhydrous Na_2SO_4, and then evaporated. The residue was dissolved in 10 ml of methanol and gave on prolonged cooling 0.21 g (30%) crystalline material identical in every respect to authentic 4,4′-dichlorobenzophenone **7**. The mother liquor was evaporated and examined by n.m.r. spectroscopy. The remaining material (0.52 g) consisted of a mixture of dioxolane **3***a*, dichlorobenzophenone **7**, and aldehyde **1***a* (1:1:2). The total yield of **7** was approximately 57%.

(b) From Solvolysis of Enol Ether Acetate (5b)

A solution of 3 ml of glacial acetic acid and 0.1 ml of concentrated H_2SO_4 containing 83 mg (0.24 mmol) of enol ether acetate was heated at 100 °C for 1 h. The acetic acid was removed by lyophilization and pumping *in vacuo* over P_2O_5. The residual oil was examined by n.m.r. spectroscopy and consisted primarily of 4,4′-dichlorobenzophenone (**7**) and 1,1-bis(*p*-chlorophenyl)-1-acetoxyethanol (**9***b*). The oil was transferred to preparative t.l.c. plates by streaking, and the plates were developed in methylene chloride. Three major bands were detected and the middle band was removed (24 mg, 40%) and found to be identical in every respect to 4,4′-dichlorobenzophenone (**7**). The other two bands were indicative of the dimer and polymeric decomposition products of the acetoxyethanol **9***b* and were not isolated; a band was found at the origin and one near solvent front which had light blue fluorescence under short wave u.v. light.

2-(o,p′-Dichlorobenzhydryl)-1,3-dioxolane (3b)

To a solution of 6.9 g (0.028 mol) of 1-(*o*-chlorophenyl)-1-(*p*-chlorophenyl)-2,2-dichloroethane in 25 ml of ethylene glycol was added 7.05 g (0.051 mol) of powdered anhydrous potassium carbonate. The mixture was refluxed at 190–200° for 16 h and poured into ice water. The aqueous suspension was extracted with two 25-ml portions of ether, and the combined extracts were dried over anhydrous sodium sulfate and taken to dryness. The crude residue (6.2 g) afforded 4.0 g (59%) of crystalline material melting at 73–76° when crystallized from methanol: n.m.r., τ (chloroform-*d*) 2.80 (8H multiplet for aromatics); 4.54, 5.30 (2H pair of doublets, J = 4 Hz, benzhydryl proton and methinyl proton of dioxolane ring); 6.26 (4H multiplet, dioxolane ring).

2-(o-Chlorophenyl)-2-(p-chlorophenyl)acetaldehyde (1b)

A solution of 9.4 g (0.034 mol) of **3***b* in 25 ml of *p*-dioxane and 50 ml of 25% aqueous sulfuric acid was refluxed with stirring for 5 h. The reaction mixture on cooling was extracted with two 50-ml portions of ether. The combined ether extracts were extracted twice with dilute sodium bicarbonate solution and washed twice with distilled water. The ether phase was dried over anhydrous sodium sulfate and evaporated to a liquid residue weighing 9.2 g. The liquid was purified by formation of the bisulfite addition product as described for **1***a* except the stirring time was increased to 24 h. A 7.0 g portion of the addition product when decomposed with dilute sodium carbonate solution gave 5.0 g (81%) of pure aldehyde **1***b* with the following spectral properties: i.r., λ (neat) 5.75 (C═O), 6.65 (aromatic), 13.3 (C—Cl); n.m.r., τ (chloroform-*d*) 0.16 (singlet, 1H, CHO), 2.80 (multiplet, 8H, aromatics), 4.67 (singlet, 1H, benzhydryl).

1. J. E. PETERSON and W. H. ROBINSON. Toxicol. Appl. Pharmacol. **6**, 321 (1964).
2. Beilsteins Handbuch der organischem Chemie. 4th Ed., I. VIII, p. 439.

3. R. RIEMSCHNEIDER, I. ARHLE, W. COHNEN, and E. HEILMANN. Chem. Ber. **92**, 900 (1959); E. F. Riener. U. S. Pat. 2 834 708 (1958).
4. R. ENGST and M. KUJAWA. Nahrung, **12**(8), 783 (1968).
5. J. D. MCKINNEY, E. L. BOOZER, H. P. HOPKINS, and J. E. SUGGS. Exper. **25**, 897 (1969).
6. R. E. COUSELL, V. V. RANADE, L. H. LOLA, and B. H. HONG. J. Med. Chem. **11**(2), 380 (1968).
7. J. K. M. SANDERS and D. H. WILLIAMS. Chem. Commun. (D), 422 (1970).
8. R. K. SUMMERBELL, J. P. SETTLE, and M. KLAND-ENGLISH. J. Org. Chem. **23**, 932 (1958).
9. H. E. ZIMMERMAN and J. ENGLISH, JR. J. Am. Chem. Soc. **76**, 2294 (1954).
10. J. F. KINCAID and D. S. TARBELL. J. Am. Chem. Soc. **61**, 3085 (1939).
11. E. H. CORDES. In Progress in physical organic chemistry. Vol. 4. *Edited by* A. Streitwieser, Jr. and R. W. Raft. John Wiley & Sons, Inc., New York, N. Y. 1967. p. 1.
12. J. BITMAN, H. C. CECIL, S. J. HARRIS, and G. F. FRIES. Sci. **162**, 371 (1968).
13. L. H. KEITH, A. L. ALFORD, and A. W. GARRISON. J.A.O.A.C. **52**, 1074 (1969).
14. D. J. CRAM. *In* Steric effects in organic chemistry. *Edited by* M. S. Newman. John Wiley and Sons, Inc., New York, N. Y. 1956. p. 333.
15. A. H. FENSELAU and J. G. MOFFATT. J. Am. Chem. Soc. **88**(8), 1762 (1966); J. D. Albright and Leon Goldman. J. Am. Chem. Soc. **89**, 2416 (1967).
16. F. A. GUNTHER, J. H. BARKLEY, R. C. BLINN, and D. E. OTT. Pesticide Res. Bull. Stanford Research Inst. **2**(2), 3 (1962).
17. J. A. JENSEN, C. CUETO, W. E. DALE, C. F. ROTHE, G. W. PEARCE, and A. M. MATTSON. J. Agric. Food Chem. **5**, 919 (1957).
18. J. E. SUGGS, R. E. HAWK, A. CURLEY, E. L. BOOZER, and J. D. MCKINNEY. Sci. **168**, 582 (1970).
19. H. J. SHINE. J. Org. Chem. **24**(2), 252 (1959).

Can. J. Chem. Downloaded from www.nrcresearchpress.com by 210.87.254.42 on 09/05/12
For personal use only.

Can. J. Chem. Downloaded from www.nrcresearchpress.com by 210.87.254.40 on 09/05/12
For personal use only.

NOTES

Special Catalytic Power of Enzymes: Some Evidence from Model Systems

KEITH BOWDEN[1] AND A. M. LAST
Department of Chemistry, Simon Fraser University, Burnaby 2, British Columbia

Received April 28, 1971

Evidence from model systems for enzyme catalysis is discussed. These models involve neighboring group participation by carbonyl or carbon-acid groups, and indicate the important roles of proximity, strain, and orientation as potential sources of the special catalytic power of enzymes.

Nous discutons de preuves pour la catalyse enzymatique à partir de systèmes modèles. Ces modèles impliquent la participation de groupes voisins au moyen de groupes carbonyle ou carbone-acide et indiquent les rôles importants que tiennent la proximité, la contrainte et l'orientation comme sources possibles du pouvoir catalytique spécial des enzymes.

Canadian Journal of Chemistry, 49, 3887 (1971)

Several workers have discussed a number of potential sources of the special catalytic power of enzymes (1–3). Proposals indicating important roles for proximity (1, 2), strain (2), and "orbital steering" (3)[2] have been made. Our recent studies (5–8) of model systems for enzyme catalysis have enabled us to further evaluate certain of these factors.

The first model concerns the effect of a proximate formyl group on alkaline ester hydrolysis (6–8). These hydrolyses occur by initial attack of hydroxide anion on the formyl group, accompanied by intramolecular nucleophilic catalysis, in a similar way to a number of related hydrolyses (5, 9). The rate-determining step for these formyl esters appears to be either a concerted process with attack by the hydroxide anion at the formyl-carbon, synchronized with intramolecular attack at the ester carbonyl-carbon, or an intramolecular attack at the ester carbonyl-carbon, preceded by addition of the hydroxide anion to the formyl group (6–8). The rate coefficients for alkaline hydrolysis of these esters are shown in Table 1, together with the observed and "expected" rate ratios compared to their parent unsubstituted esters. These "expected" values for the formyl esters are estimated from closely related model substrates, using the known steric and polar effects of the formyl and other substituents, to give the rate ratio expected for hydrolysis by the normal direct route (6–8). Study of molecular models ("Catalin") of the three formyl esters show that both the proximity of the formyl to the ester group and internal strain increase in passing along the series, benzoate, naphthoate, and phenanthroate (Table 1). The very large rate enhancements, shown in Table 1, are a consequence of the ability of the formyl esters to employ the intramolecular catalytic route. This results from two sources. These are, firstly, the proximity of the "internal" nucleophile once formed and, secondly, internal strain. The latter, already present in the naphthoate and phenanthroate, is either increased or induced by the "primary" addition process; but is relieved as the "secondary" intramolecular attack proceeds. This process results in the formation of a cyclic intermediate. Other studies (10) of ring–chain tautomerization in both formyl- and closely related keto-carboxylic acids have shown that the formation of the ring (cyclic) tautomer is favored when internal strain caused by steric bulk interactions increase. Thus the reaction is facilitated by the induction of strain derived from the binding between substrate and the hydroxide anion. The modest rate decreases observed in passing from the benzoate to phenanthroate esters in Table 1 (attack at formyl group) are in great contrast to those expected from a comparison with the hydrolysis of 2-substituted benzoates, 8-substituted 1-naphthoates, and 5-substituted 4-phenanthroates (6, 8,

[1]Present address: Department of Chemistry, University of Essex, Cochester, Essex, England.

[2]Recently this concept has been discussed by Bruice and coworkers (4), who have presented an alternative interpretation.

TABLE 1. Rates of alkaline hydrolysis in 70% v/v aqueous dioxan at 20 °C

Methyl ester	k (l mol^{-1} s^{-1})	k/k_0 Observed	k/k_0 "Expected"
2-Formylbenzoate	271	31 900	5.0
8-Formyl-1-naphthoate	35.5	10 700	0.02
5-Formyl-4-phenanthroate	7.47	110 000	<0.01

TABLE 2. Rates of reaction with hydroxide anion in 70% v/v aqueous dioxan at 20 °C

Methyl ester	k (l mol^{-1} s^{-1})	k/k_0 Observed	k/k_0 "Expected"
2-Acetylbenzoate	6.45	760	1.0
8-Acetyl-1-naphthoate	0.533	160	0.005

11). The action, in part, of a number of esterases and allied enzymes can be related to this study. The model system described employs the addition of hydroxide anion to the formyl group to simulate the nucleophilic activity of the hydroxyl group in the unique serine residues in such enzymes.

The second model concerns the effect of a proximate acetyl group on alkaline ester hydrolysis. Methyl 2-acetylbenzoate rapidly undergoes alkaline hydrolysis, employing neighboring group participation by the carbonyl group, by the pathway described above (6). However, methyl 8-acetyl-1-naphthoate reacts by attack on the ester group by the carbanion, generated by rate-determining proton-abstraction from the acetyl group by the hydroxide anion (7). The latter cyclization process is also very rapid (Table 2). The dichotomy displayed by these two esters clearly indicates the specific control of reaction afforded by the orientation and environment of the assisting group. Study of molecular models ("Catalin") and i.r. spectroscopic investigations (8) of these two esters indicates that methyl 2-acetylbenzoate has the almost fully coplanar conformation shown (**1**) and methyl 8-acetyl-1-naphthoate has the conformation (**2**) in which the planes of the acetyl and ester groups are parallel to one another, while being perpendicular to that of naphthalene itself. The 8-acetyl-1-naphthoate reacts with intramolecular catalysis from the carbon acid. The carbanion is generated with highly favorable orientation for substitution and is closely proximate to the reaction site, the ester carbonyl-carbon. However, catalysis by the carbonyl group has distinct spatial requirements, unlike the carbon-acid process, as reaction

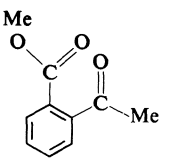

1

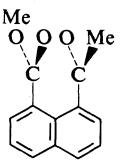

2

proceeds by a comparatively "crowded" transition state involving tetrahedral configurations at both acetyl and ester groups. The latter "crowding" is very severe in the 8-acetyl-1-naphthoate, compared to the 2-acetylbenzoate. Further the 2-acetylbenzoate has not the favorable orientation and close proximity of the methyl group for the carbon-acid path to be favored. The carbon-acid catalytic model simulates the carbon–carbon bond formation in aldolases and related enzymes.

Clearly, while an exact separation of the causes of the catalytic power of enzymes is not yet possible (12), proximity, strain, and orientation can be demonstrated in physical organic model systems to produce rate enhancements comparable to those produced by enzymes themselves.

The authors thank Dr. T. C. Bruice for a prior communication of his recent study (4).

1. T. C. BRUICE and S. J. BENKOVIC. Bioorganic mechanisms. Vol. 1. W. A. Benjamin, Inc., New York, N.Y., 1966.
2. W. P. JENCKS. Catalysis in chemistry and enzymology. McGraw-Hill Book Co., Inc., New York, N.Y., 1969.
3. D. R. STORM and D. E. KOSHLAND. Proc. Natl. Acad. Sci. **66**, 445 (1970).
4. T. C. BRUICE, A. BROWN, and D. O. HARRIS. Proc. Natl. Acad. Sci. **68**, 658 (1971).

Can. J. Chem. Downloaded from www.nrcresearchpress.com by 210.87.254.40 on 09/05/12
For personal use only.

5. K. BOWDEN and G. R. TAYLOR. Chem. Commun. 1112 (1967). K. BOWDEN and G. R. TAYLOR. J. Chem. Soc. B. 145 (1971). K. BOWDEN and M. P. HENRY. J. Chem. Soc. B. 156 (1971).
6. K. BOWDEN and G. R. TAYLOR. J. Chem. Soc. B. 149 (1971).
7. K. BOWDEN and A. M. LAST. Chem. Commun. 1315 (1970).
8. K. BOWDEN and A. M. LAST. Unpublished studies.
9. M. L. BENDER, J. A. REINSTEIN, M. S. SILVER, and R. MIKULAK. J. Am. Chem. Soc. **87**, 4545 (1965). M. L. BENDER and M. S. SILVER. J. Am. Chem. Soc. **84**, 4589 (1962). M. S. NEWMAN and S. HISHIDA. J. Am. Chem. Soc. **84**, 3582 (1962). M. S. NEWMAN and A. L. LEEGWATER. J. Am. Chem. Soc. **90**, 4410 (1968). H. D. BURROWS and R. M. TOPPING. Chem. Commun. 904 (1969). K. C. KEMP and M. L. MIETH. Chem. Commun. 1260 (1969).
10. K. BOWDEN and G. R. TAYLOR. J. Chem. Soc. B. 1390, 1395 (1971). K. BOWDEN and A. M. Last. Unpublished studies.
11. N. B. CHAPMAN, J. SHORTER, and J. H. P. UTLEY. J. Chem. Soc. 1291 (1963). D. P. EVANS, J. J. GORDON, and H. B. WATSON. J. Chem. Soc. 1430 (1937). Y. ISKANDER, R. TEWFIK, and S. WASIF. J. Chem. Soc. B. 424 (1966). J. F. CORBETT, A. FEINSTEIN, P. H. GORE, G. L. REED, and E. C. VIGNES. J. Chem. Soc. B. 974 (1969).
12. T. C. BRUICE and A. TURNER. J. Am. Chem. Soc. **92**, 3422 (1970).

Per-deuteration of *t*-Butanol in Mildly Acidic Deuterium Oxide

MARTIN B. HOCKING
Research Department, Dow Chemical of Canada, Limited,[1] *Sarnia, Ontario*

Received June 25, 1971

Heating a solution of *t*-butanol in acidified deuterium oxide under slight pressure has yielded 85% per-deuterated *t*-butanol. At atmospheric pressure normal isobutylene was produced. Isobutylene could not be hydrated in good yield by this method. A number of related alcohols were resistant to exchange by this method, but one of them, 1-methylcyclohexanol, gave nearly complete dehydration without deuterium incorporation.

En chauffant sous une légère pression une solution de *t*-butanol dans de l'oxyde de deutérium acidifié, le *t*-butanol perdeutéré est obtenu avec un rendement de 85%. Sous pression atmosphérique, l'isobutylène est obtenu. L'isobutylène, par cette méthode, ne peut pas être hydraté selon un bon rendement. Par cette méthode, un certain nombre d'alcools apparentés résistent à l'échange; cependant, l'un deux, le méthyl-1 cyclohexanol, se déshydrate presque complètement sans incorporation de deutérium.

Canadian Journal of Chemistry, **49**, 3889 (1971)

Introduction

Hydroxyl hydrogen–deuterium exchange in *t*-butanol has been shown to occur catalytically in the presence of deuterium gas at a rate of about 2% per minute at 79 °C (1) and is too fast to measure in deuterium oxide at 25° (2). Deuterium exchange of hydrogen bonded to carbon, in alcohols, has been shown to occur only to a very small extent with methanol and ethanol and not at all with isopropanol or *t*-butanol (1). Exchange of deuterium for hydrogen bonded to carbon has been achieved with the tertiary alcohol l-methylcyclohexanol in cold deuterium-enriched phosphoric acid (3), and phenolate anion has been rapidly per-deuterated in potassium deuterioamide/deuterio-ammonia (4).

We have recently discovered that *t*-butanol can be rapidly per-deuterated in mildly acidic deuterium oxide (5). The only previously reported per-deuterio-*t*-butanol synthesis was an alkylation of per-deuterio-acetone (6) and not via an exchange reaction. Hence the experimental determination of some of the parameters of this exchange, it is hoped, will be of value for future syntheses of "heavy" *t*-butanol.

Results and Discussion

Small Scale Experiments

The preliminary qualitative exchange experiments were carried out in sealed n.m.r. tubes. The progress was followed by noting the changes in the proton integrals for the respective proton groups.

A very low concentration (about 0.2 *M*) of sulfuric acid in deuterium oxide was ineffective for the alkyl hydrogen exchange of *t*-butanol at

[1]Contribution No. 192.

Can. J. Chem. Downloaded from www.nrcresearchpress.com by 210.87.254.40 on 09/05/12
For personal use only.

5. K. BOWDEN and G. R. TAYLOR. Chem. Commun. 1112 (1967). K. BOWDEN and G. R. TAYLOR. J. Chem. Soc. B. 145 (1971). K. BOWDEN and M. P. HENRY. J. Chem. Soc. B. 156 (1971).
6. K. BOWDEN and G. R. TAYLOR. J. Chem. Soc. B. 149 (1971).
7. K. BOWDEN and A. M. LAST. Chem. Commun. 1315 (1970).
8. K. BOWDEN and A. M. LAST. Unpublished studies.
9. M. L. BENDER, J. A. REINSTEIN, M. S. SILVER, and R. MIKULAK. J. Am. Chem. Soc. **87**, 4545 (1965). M. L. BENDER and M. S. SILVER. J. Am. Chem. Soc. **84**, 4589 (1962). M. S. NEWMAN and S. HISHIDA. J. Am. Chem. Soc. **84**, 3582 (1962). M. S. NEWMAN and A. L. LEEGWATER. J. Am. Chem. Soc. **90**, 4410 (1968). H. D. BURROWS and R. M. TOPPING. Chem. Commun. 904 (1969). K. C. KEMP and M. L. MIETH. Chem. Commun. 1260 (1969).
10. K. BOWDEN and G. R. TAYLOR. J. Chem. Soc. B. 1390, 1395 (1971). K. BOWDEN and A. M. Last. Unpublished studies.
11. N. B. CHAPMAN, J. SHORTER, and J. H. P. UTLEY. J. Chem. Soc. 1291 (1963). D. P. EVANS, J. J. GORDON, and H. B. WATSON. J. Chem. Soc. 1430 (1937). Y. ISKANDER, R. TEWFIK, and S. WASIF. J. Chem. Soc. B. 424 (1966). J. F. CORBETT, A. FEINSTEIN, P. H. GORE, G. L. REED, and E. C. VIGNES. J. Chem. Soc. B. 974 (1969).
12. T. C. BRUICE and A. TURNER. J. Am. Chem. Soc. **92**, 3422 (1970).

Per-deuteration of *t*-Butanol in Mildly Acidic Deuterium Oxide

MARTIN B. HOCKING
Research Department, Dow Chemical of Canada, Limited,[1] *Sarnia, Ontario*

Received June 25, 1971

Heating a solution of *t*-butanol in acidified deuterium oxide under slight pressure has yielded 85% per-deuterated *t*-butanol. At atmospheric pressure normal isobutylene was produced. Isobutylene could not be hydrated in good yield by this method. A number of related alcohols were resistant to exchange by this method, but one of them, 1-methylcyclohexanol, gave nearly complete dehydration without deuterium incorporation.

En chauffant sous une légère pression une solution de *t*-butanol dans de l'oxyde de deutérium acidifié, le *t*-butanol perdeutéré est obtenu avec un rendement de 85%. Sous pression atmosphérique, l'isobutylène est obtenu. L'isobutylène, par cette méthode, ne peut pas être hydraté selon un bon rendement. Par cette méthode, un certain nombre d'alcools apparentés résistent à l'échange; cependant, l'un deux, le méthyl-1 cyclohexanol, se déshydrate presque complètement sans incorporation de deutérium.

Canadian Journal of Chemistry, **49**, 3889 (1971)

Introduction

Hydroxyl hydrogen–deuterium exchange in *t*-butanol has been shown to occur catalytically in the presence of deuterium gas at a rate of about 2% per minute at 79 °C (1) and is too fast to measure in deuterium oxide at 25° (2). Deuterium exchange of hydrogen bonded to carbon, in alcohols, has been shown to occur only to a very small extent with methanol and ethanol and not at all with isopropanol or *t*-butanol (1). Exchange of deuterium for hydrogen bonded to carbon has been achieved with the tertiary alcohol l-methylcyclohexanol in cold deuterium-enriched phosphoric acid (3), and phenolate anion has been rapidly per-deuterated in potassium deuterioamide/deuterio-ammonia (4).

We have recently discovered that *t*-butanol can be rapidly per-deuterated in mildly acidic deuterium oxide (5). The only previously reported per-deuterio-*t*-butanol synthesis was an alkylation of per-deuterio-acetone (6) and not via an exchange reaction. Hence the experimental determination of some of the parameters of this exchange, it is hoped, will be of value for future syntheses of "heavy" *t*-butanol.

Results and Discussion

Small Scale Experiments

The preliminary qualitative exchange experiments were carried out in sealed n.m.r. tubes. The progress was followed by noting the changes in the proton integrals for the respective proton groups.

A very low concentration (about 0.2 *M*) of sulfuric acid in deuterium oxide was ineffective for the alkyl hydrogen exchange of *t*-butanol at

[1]Contribution No. 192.

Can. J. Chem. Downloaded from www.nrcresearchpress.com by 210.87.254.40 on 09/05/12
For personal use only.

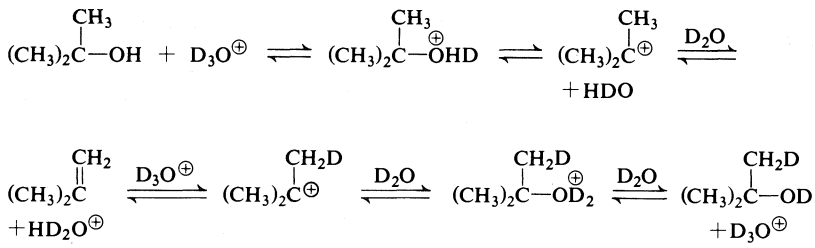

SCHEME 1

room temperature. But at 100°, 2 h were sufficient to promote exchange of 87% of the carbon-bound hydrogens and a further 2 h heating caused a further slight improvement to 93%.

Exchange was probably occurring via a succession of dehydration–hydration sequences (see Scheme 1), each sequence bringing about the exchange of one carbon-bound hydrogen for deuterium.

Preparative Scale Experiments

Attempts to carry out preparative scale exchange reactions with *t*-butanol at atmospheric pressure confirmed the intermediate formation of isobutylene. Examination of the evolved isobutylene by n.m.r. showed that no deuterium exchange had taken place, as found by Purlee and Taft (7) for the hydration of 2-methyl-2-butene in acidified deuterium oxide. Hence, the sequence of reactions leading to isobutylene must be fast relative to rate of protonation of isobutylene, the first step in its re-hydration, since the solubility limit of isobutylene in water is so readily exceeded. Additional confirmation of the slow rate of protonation of isobutylene was obtained on isolation of the residual *t*-butanol from an atmospheric pressure exchange experiment, in which it was found that only hydroxyl hydrogen–deuterium exchange had occurred. Virtually none of the isobutylene formed was retained in solution by protonation. Purlee and Taft (7) have also shown that the steps following initial protonation of 2-methyl-2-butene are extremely fast relative to the rate of protonation, and thus that any protonated isobutylene should appear as *C*-deuterated *t*-butanol.

Preparative scale deuterium exchange under pressure with a ratio of deuterium oxide:*t*-butanol of 15:1, larger than in the small scale experiments, gave 64% exchange of the methyl hydrogens. Decreasing this ratio to 10:1 decreased the extent of exchange to only 20%. If these experiments had yielded a statistical hydrogen–deuterium distribution, exchanges of 75 and 67% respectively, should have been observed. Since the small scale experiments demonstrated that 4 h was sufficient at those reagent ratios for the exchange to reach equilibrium, these too, were probably near equilibrium. However, isotope effects on the many relative rates in the steps outlined previously together with the reduced isobutylene solubility at the lower *t*-butanol/deuterium oxide ratios, could explain the discrepancies shown between the statistical and the observed deuterium distributions.

When the same preparative exchange experiments were tried with initial isobutylene, using deuterium oxide:isobutylene of 15:1, only about 3% of the theoretical hydration was achieved and this *t*-butanol was only 28% exchanged on carbon. This lack of success was possibly a consequence of the very low miscibility of the reactants. The unreacted isobutylene was not examined for its isotopic content.

Exchange Reactions with Related Alcohols

Isopropanol gave no deuterium exchange or dehydration at 25 or 100°. Anderson and Kemball (8) found that both isopropanol and *t*-butanol were resistant to catalytic vapor phase exchange of hydrogen with deuterium gas, yet ethanol and methanol were found to exchange to a very small extent.

2-Phenylisopropanol, and 1-phenylcyclohexanol were also resistant to deuterium exchange or dehydration at 25 or 100°, in agreement with that found for the former compound by Stephens and Leitch (9). In these exchange reactions methanol again was unaffected but not surprisingly (10, 11), 25% of the acetone exchanged in 3 days at room temperature, about 75% after a further hour at 100°.

Experimental

Deuterium oxide (99.8%) was purchased from Atomic Energy of Canada, Ltd. *t*-Butanol was dried ($MgSO_4$) and distilled immediately prior to use. Vinylacetic acid was used with the carboxyl hydrogen already exchanged for deuterium and dried (5). Other reagent alcohols were standard grades used as purchased from Aldrich Chemical Co. Solvent methanol was hydroxyl deuterated by

Can. J. Chem. Downloaded from www.nrcresearchpress.com by 210.87.254.40 on 09/05/12
For personal use only.

Can. J. Chem. Downloaded from www.nrcresearchpress.com by 210.87.254.40 on 09/05/12
For personal use only.

exchange with several portions of deuterium oxide, dried ($MgSO_4$), and distilled prior to use.

Determination of Isotopic Purity of Exchanged t-Butanol

Preliminary small scale experiments were carried out in sealed n.m.r. tubes. Progress of the exchange was followed by relating the initial to the subsequent integrals in the n.m.r. spectra of the peaks at 85 Hz (*t*-butyl methyls) and at about 300 Hz (H_2O). The maximum variation in the total integral for all protons present in the sealed tube was found to be ± 3% of the mean. Integrals for each proton group were normalized by a factor, when necessary, to bring the sum of the component integrals to the same value as the initial total integral.

Preparative Scale Experiments

Dry exchanged *t*-butanol contained about 4% methylene chloride on recovery. An integrated n.m.r. spectrum was obtained for this material, neat. Immediately after, using the same instrument settings, integrated spectra of pure normal *t*-butanol and pure methylene chloride were obtained, using the same washed and dried sample tube as initially. Taking the integrals observed for methyl and hydroxyl hydrogens of deuterated *t*-butanol and dividing these by the appropriately reduced (to account for CH_2Cl_2 present in deuterated sample) integrals obtained for normal *t*-butanol, gave the fractions of hydrogen still present in respective parts of the deuterated alcohol.

Small Scale Deuterium Exchanges with t-Butanol

The details of the initial experimental results with *t*-butanol and deuterium oxide under mildly alkaline conditions, and in the presence of a weak acid in sealed tubes have been reported separately (5).

Sulfuric Acid Conditions

Vinylacetic acid (130 mg), *t*-butanol (10 μl), deuterium oxide (500 μl), and concentrated sulfuric acid (8.0 mg), left 10 days at room temperature caused no change in the *t*-butyl methyl proton integral. Heating the solution for 2 h at 100°, and a further 2 h, caused reductions to 1/8 and 1/16 of the original value.

A further experiment without vinylacetic acid and using 50 l of *t*-butanol, gave 75% exchange of the *t*-butyl methyl protons after 4 h heating at 100°.

Preparative Scale Deuterium Exchange with t-Butanol

Atmospheric Pressure Attempt

Deuterium oxide (40 ml), *t*-butanol (7.4 g), and concentrated sulfuric acid (8 drops) were boiled together under reflux with protection from atmospheric moisture for 6 h, during which time isobutylene was evolved (by odor). Aliquots were removed at 4 and 6 h. Recovery of the remaining *t*-butanol (1.2 g) was accomplished by azeotropic distillation and methylene chloride extraction. Examination of this material by n.m.r. showed that no methyl proton deuterium exchange had taken place, and that the OH was 70% exchanged.

A second similar experiment was run on twice the scale through which the evolved isobutylene (7.6 g; 70%) was trapped during 6 h boiling in a U-tube cooled in Dry Ice/CCl_4/$CHCl_3$. The evolved material had a g.c. retention time at 0° and an n.m.r. spectrum identical to that of a sample of authentic isobutylene.

Pressure Deuterium Exchange

Deuterium oxide (30 ml; 1.5 mol), *t*-butanol (7.4 g; 0.1 mol), and concentrated sulfuric acid (6 drops) were placed in a 110 ml glass-lined stainless steel pressure vessel and heated in a boiling water bath for 5 h. The contents were neutralized with solid sodium carbonate and worked-up by the previous method, yielding 2.6 g of 64% carbon-deuterated (5.5 deuteriums/*t*-butyl) *t*-butanol.

The above experiment was repeated using deuterium oxide (60 ml; 3 mol), *t*-butanol (23.2 g; 0.3 mol), and concentrated sulfuric acid (16 drops). The contents were neutralized with $NaOD/D_2O$, saturated with sodium chloride, and extracted with pentane (4 × 30 ml). The combined pentane extracts yielded 15.3 g of deuterated *t*-butanol (20% carbon-deuterated; 1.8 deuteriums/*t*-butyl) after drying and distillation. Re-exchange of this partially deuterated *t*-butanol with fresh heavy water (60 ml) and concentrated sulfuric acid (12 drops) gave 10 g of 45% carbon-deuterated (4 deuteriums/*t*-butyl) *t*-butanol.

Isobutylene Hydration

Deuterium oxide (60 ml) and concentrated sulfuric acid (12 drops) were placed in the same pressure vessel and the contents cooled to 0°. Then isobutylene (11.2 g; 0.2 mol) was added. The vessel was heated at 100° for 6 h with vigorous agitation every 20 min, then cooled to −5°. The contents were neutralized with solid sodium carbonate and worked-up by the first method yielding 0.4 g of 28% carbon-deuterated *t*-butanol (2.5 deuteriums/*t*-butyl). Further extraction and examination by n.m.r. of the aqueous phase showed that no further *t*-butanol was present.

Qualitative Deuterium Exchange with Other Alcohols

Isopropanol (20 μl), 2-phenylisopropanol (20 μl), and 1-phenylcyclohexanol (53 mg; made homogeneous with 0.95 ml of hydroxyl-deuterated methanol), sealed into n.m.r. tubes with deuterium oxide (0.5, 0.5, and 0.6 ml respectively) and concentrated sulfuric acid (5.5, 8, 8 mg respectively) gave no exchange after 5 days at 25°, nor after heating at 100° for 4 h.

1-Methylcyclohexanol (40 μl, made homogeneous with 0.21 ml acetone), deuterium oxide (0.5 ml), and concentrated sulfuric acid (18 mg), when sealed into an n.m.r. tube, gave no alcohol C—H exchange during 3 days at 25°, but 25% of the acetone hydrogens had exchanged. One hour at 100° increased the extent of acetone exchange to 75% of the total and caused a colorless upper immiscible phase to appear. The b.p. of this phase was about 96° (Siwoloboff method; lit. (12) for 1-methylcyclohexene, 110°) and i.r. and n.m.r. data were consistent with a predominance of 1-methylcyclohexene together with traces of acetone and 1-methylcyclohexanol.

The author thanks H.D. Mak for the n.m.r. spectra required for this work, and for suggesting the isotopic analytical method used. He also thanks a referee for bringing his attention to ref. 9.

1. J. R. Anderson and C. Kemball. Trans. Faraday Soc. **51**, 966 (1955).
2. J. Hine and C. H. Thomas. J. Am. Chem. Soc. **76**, 612 (1954).
3. V. N. Setkina and D. N. Kursanov. Doklady Akad. Nauk. S.S.S.R. **109**, 552 (1956).
4. A. I. Shatenshtein and A. V. Vedeneev. Zhur.

Obshchei Khim. **28**, 2644 (1958). Chem. Abstr. **53**, 5836*c* (1959).
5. M. B. HOCKING. Can. J. Chem. This issue.
6. W. ZEIL, H. BUCHERT, H. HEEL, and H. PFORTNER. Z. Electrochem. **64**, 769 (1960). Chem. Abstr. **54**, 20478*h* (1960).
7. E. L. PURLEE and R. W. TAFT, JR. J. Am. Chem. Soc. **78**, 5807 (1956).
8. J. R. ANDERSON and C. KEMBALL. Trans. Faraday Soc. **51**, 966 (1955).
9. J. C. STEPHENS and L. C. LEITCH. J. Labelled Compounds, **3**, 65 (1967).
10. L. V. KARCHAGIN and M. A. PJONTKOVSKAYA. Acta Physiochim. U.R.S.S. **10**, 881 (1939).
11. S. W. BENSON and C. W. FALTERMAN. J. Chem. Phys. **20**, 201 (1952).
12. R. C. WEAST. Handbook of chemistry and physics. 45th Ed. The Chemical Rubber Publishing Co., Cleveland, Ohio, 1964. p. C 273.

Can. J. Chem. Downloaded from www.nrcresearchpress.com by 210.87.254.40 on 09/05/12
For personal use only.

Olefin Formation in the Radiolysis of *n*-Hexadecane[1]

W. E. FALCONER, W. A. SUNDER, AND L. G. WALKER[2]
Bell Telephone Laboratories, Incorporated, Murray Hill, N.J. 07974

Received June 21, 1971

Olefin production in *n*-hexadecane, irradiated both in liquid and solid states, was estimated by gas chromatography and coulometric titration. Yields of congruent olefin extrapolated to zero dose were $G = 1.6$ and 2.8 in the solid and liquid, respectively. Total olefin yields at low doses are 2.2 and 4.2 in the solid and liquid. Scission olefin yields are 0.5 and 1.0. Evidence was found for *cis* as well as *trans* hexadecene isomers. *cis*-Olefins can be lost preferentially by exposure to air.

La formation d'oléfine à partir du *n*-hexadécane, irradié à l'état liquide et solide a été estimée par c.p.g. et titrage coulométrique. Les rendements en oléfine, extrapolés à une dose de zéro, sont respectivement de $G = 1.6$ et 2.8 pour le solide et le liquide. Les rendements totaux en oléfine sont, pour de faibles doses, respectivement de 2.2 et 4.2 pour le solide et le liquide. Les rendements de scission oléfinique sont de 0.5 et 1.0. Des preuves sont apportées sur la présence des isomères *cis* et *trans* de l'hexadécène. Les oléfines *cis* se dégradent préférentiellement au contact de l'air.

Canadian Journal of Chemistry, **49**, 3892 (1971)

Introduction

In the radiolysis of paraffinic hydrocarbons, one finds two types of mono-olefin products: isomeric congruent olefins formed by the elimination of hydrogen without disruption of the hydrocarbon skeleton, and scission olefins, the result of carbon–carbon rupture. The mechanism of formation of either type may be ionic, molecular, radical, or any combination of these. In small hydrocarbons, both *cis*- and *trans*-isomers of the congruent olefin are observed, the proportions being a function of state and other variables (1, 2). By contrast, only *trans*-vinylene unsaturation is reported for polyethylene, apart from terminal vinyl groups (3, 4) and polyenes (5, 6). Unsaturation in polyethylene is usually studied by i.r. absorption at 964 cm^{-1} and 700 and 1657 cm^{-1} for *trans*- and *cis*-vinylene, respectively. Smaller extinction coefficients or spectral interference might mask small amounts of *cis*-vinylene. Alternatively, *cis*-unsaturation, if formed, could be preferentially destroyed prior to taking the spectrum.

Irradiated *n*-hexadecane has been studied as a polyethylene prototype, both in the liquid and solid phases near the melting point (7, 8). This paper discusses the formation of olefinic products of *n*-hexadecane radiolysis with the object in part of clarifying the difference between lower paraffins on the one hand and polyethylene on the other.

Experimental

Materials

Two types of *n*-hexadecane were used in this study. The first was a combination of API standard samples, 99.91% pure, which were scrubbed with sulfuric acid, washed with distilled water, dried over calcium oxide, and distilled at 157–158 °C at 15 Torr in a grease free system. The second was Humphrey Chemical Company petroleum derived olefin free grade, stated purity >99%. This

[1]Presented in part at the International Conference on Radiation Chemistry, Argonne, Illinois, August 12–15, 1968.

[2]Present address: Ryerson Polytechnical Institute, Toronto, Ontario.

Obshchei Khim. **28**, 2644 (1958). Chem. Abstr. **53**, 5836*c* (1959).
5. M. B. HOCKING. Can. J. Chem. This issue.
6. W. ZEIL, H. BUCHERT, H. HEEL, and H. PFORTNER. Z. Electrochem. **64**, 769 (1960). Chem. Abstr. **54**, 20478*h* (1960).
7. E. L. PURLEE and R. W. TAFT, JR. J. Am. Chem. Soc. **78**, 5807 (1956).
8. J. R. ANDERSON and C. KEMBALL. Trans. Faraday Soc. **51**, 966 (1955).
9. J. C. STEPHENS and L. C. LEITCH. J. Labelled Compounds, **3**, 65 (1967).
10. L. V. KARCHAGIN and M. A. PJONTKOVSKAYA. Acta Physiochim. U.R.S.S. **10**, 881 (1939).
11. S. W. BENSON and C. W. FALTERMAN. J. Chem. Phys. **20**, 201 (1952).
12. R. C. WEAST. Handbook of chemistry and physics. 45th Ed. The Chemical Rubber Publishing Co., Cleveland, Ohio, 1964. p. C 273.

Can. J. Chem. Downloaded from www.nrcresearchpress.com by 210.87.254.40 on 09/05/12
For personal use only.

Olefin Formation in the Radiolysis of *n*-Hexadecane[1]

W. E. FALCONER, W. A. SUNDER, AND L. G. WALKER[2]
Bell Telephone Laboratories, Incorporated, Murray Hill, N.J. 07974

Received June 21, 1971

Olefin production in *n*-hexadecane, irradiated both in liquid and solid states, was estimated by gas chromatography and coulometric titration. Yields of congruent olefin extrapolated to zero dose were $G = 1.6$ and 2.8 in the solid and liquid, respectively. Total olefin yields at low doses are 2.2 and 4.2 in the solid and liquid. Scission olefin yields are 0.5 and 1.0. Evidence was found for *cis* as well as *trans* hexadecene isomers. *cis*-Olefins can be lost preferentially by exposure to air.

La formation d'oléfine à partir du *n*-hexadécane, irradié à l'état liquide et solide a été estimée par c.p.g. et titrage coulométrique. Les rendements en oléfine, extrapolés à une dose de zéro, sont respectivement de $G = 1.6$ et 2.8 pour le solide et le liquide. Les rendements totaux en oléfine sont, pour de faibles doses, respectivement de 2.2 et 4.2 pour le solide et le liquide. Les rendements de scission oléfinique sont de 0.5 et 1.0. Des preuves sont apportées sur la présence des isomères *cis* et *trans* de l'hexadécène. Les oléfines *cis* se dégradent préférentiellement au contact de l'air.

Canadian Journal of Chemistry, **49**, 3892 (1971)

Introduction

In the radiolysis of paraffinic hydrocarbons, one finds two types of mono-olefin products: isomeric congruent olefins formed by the elimination of hydrogen without disruption of the hydrocarbon skeleton, and scission olefins, the result of carbon–carbon rupture. The mechanism of formation of either type may be ionic, molecular, radical, or any combination of these. In small hydrocarbons, both *cis*- and *trans*-isomers of the congruent olefin are observed, the proportions being a function of state and other variables (1, 2). By contrast, only *trans*-vinylene unsaturation is reported for polyethylene, apart from terminal vinyl groups (3, 4) and polyenes (5, 6). Unsaturation in polyethylene is usually studied by i.r. absorption at 964 cm^{-1} and 700 and 1657 cm^{-1} for *trans*- and *cis*-vinylene, respectively. Smaller extinction coefficients or spectral interference might mask small amounts of *cis*-vinylene. Alternatively, *cis*-unsaturation, if formed, could be preferentially destroyed prior to taking the spectrum.

Irradiated *n*-hexadecane has been studied as a polyethylene prototype, both in the liquid and solid phases near the melting point (7, 8). This paper discusses the formation of olefinic products of *n*-hexadecane radiolysis with the object in part of clarifying the difference between lower paraffins on the one hand and polyethylene on the other.

Experimental

Materials

Two types of *n*-hexadecane were used in this study. The first was a combination of API standard samples, 99.91% pure, which were scrubbed with sulfuric acid, washed with distilled water, dried over calcium oxide, and distilled at 157–158 °C at 15 Torr in a grease free system. The second was Humphrey Chemical Company petroleum derived olefin free grade, stated purity >99%. This

[1]Presented in part at the International Conference on Radiation Chemistry, Argonne, Illinois, August 12–15, 1968.

[2]Present address: Ryerson Polytechnical Institute, Toronto, Ontario.

sample was treated with acid as above, then purified by urea clathrate formation (7).

Radiolysis

Samples were degassed and sealed under vacuum in thin-walled Pyrex tubes prior to irradiation. They were irradiated either in an ice bath or at ~30 °C with Co^{60} γ-rays at a dose rate of $\sim 3 \times 10^{19}$ eV g^{-1} h^{-1}. Fricke dosimetry was used (9).

Analysis

Scission olefins with 6 to 14 carbon atoms were separated from each other and from the corresponding *n*-alkanes on a 40 ft by 0.125 in. o.d. stainless steel column packed with 5% Carbowax 20M on 70–80 mesh Chromosorb G, AW-DMCS. Temperature programming was used in the separation. Concentrations were monitored with a flame ionization detector.

Linear hexadecene isomers were separated isothermally on a terephthalic acid treated Carbowax 20M column, as described elsewhere (10). Although individual hexadecene isomers could be isolated only for *cis*- and *trans*-hexadecene-2, separation from the large excess of parent *n*-hexadecane was adequate to obtain analytical precision of ±5% and an accuracy of ±10% for the congruent olefin products as a group.

Total olefin yields were also determined by coulometric titration to an amperometric end point. Low solubilities of these larger hydrocarbons precluded using well-established aqueous systems for the titrations. Bromination of the olefins proved too slow to give a satisfactory end-point. Therefore a chlorination technique in dichloroacetic acid solvent was developed. To prevent loss of Cl_2 to the atmosphere, the cell shown in cutaway in Fig. 1 was designed to minimize dead volume during the titration. To determine total olefin content, 0.5 ml aliquots of irradiated *n*-hexadecane were dissolved in 30 ml of prechlorinated, redistilled dichloroacetic acid. To this, 1 ml of 30% aqueous LiCl was added, and the cell base adjusted to submerge the electrodes and minimize dead space. Chlorine was generated electrolytically using a current of 0.4 mA. Its concentration was monitored using a Heathkit Potentiostat in a three electrode configuration and a detector potential of +0.25 V.

The reliability of the technique was assessed by analysis of synthetic samples. Approximately 10^{-7} mol of olefin in a sample could be estimated to about a factor of two. The accuracy of analysis of samples containing >1 μmol of olefin was ±5%.

Results and Discussion

Yields of congruent olefin determined by gas chromatographic analysis are plotted as a function of dose in Fig. 2. The decrease in *G*(congruent olefin) with increasing dose is consistent with a mechanism in which formation of congruent olefin is linear with dose and its radiation induced removal is first order in olefin concentration. Similar behavior for *trans*-vinylene unsaturation in studies of polyethylene radiolysis has been observed by Dole *et al.* (11). The effect of state on the yield of congruent olefin is pronounced, solid

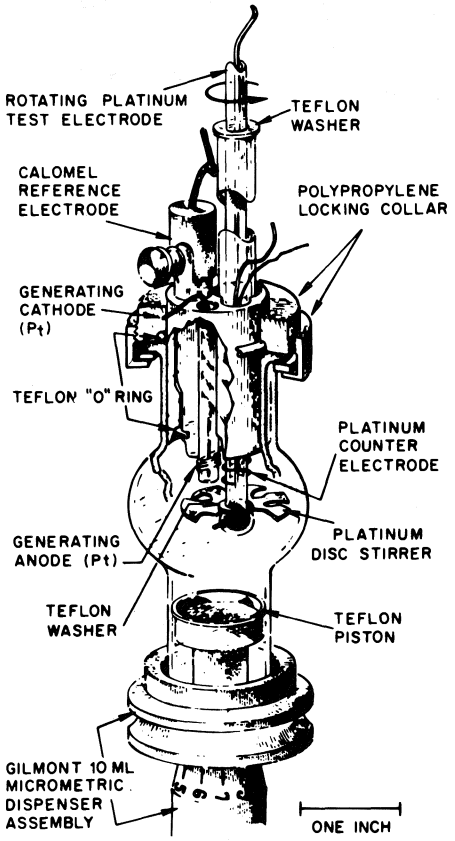

FIG. 1. Cell for coulometric titration.

state yields being about one-half those for the liquid. The incremental olefin yield in the liquid phase may result in part from the disproportionation of hexadecyl radicals with lower molecular weight scission radicals which are less abundant in the solid. The reduction in *G*(congruent olefin) with state is larger however than the change in yield of scission products. Removal of trapped hexadecyl radicals by reaction with H atoms has been suggested (7) as another factor in reducing congruent olefin yields in the solid phase. Disproportionation–combination ratios for H atoms with alkyl radicals are smaller than those between alkyl radical pairs, at least in the gas phase (12), and hence these interactions would not favor formation of olefin.

cis- and *trans*-Hexadecene-2 were examined individually. At a dose of 2×10^{19} eV g^{-1}, yields of *cis*-hexadecene-2 were $G = 0.07$ and 0.17 in the solid and liquid state, respectively, and for *trans*-hexadecene-2, $G = 0.23$ and 0.30. Dose dependence for these isomers paralleled that of the total

Can. J. Chem. Downloaded from www.nrcresearchpress.com by 210.87.254.40 on 09/05/12
For personal use only.

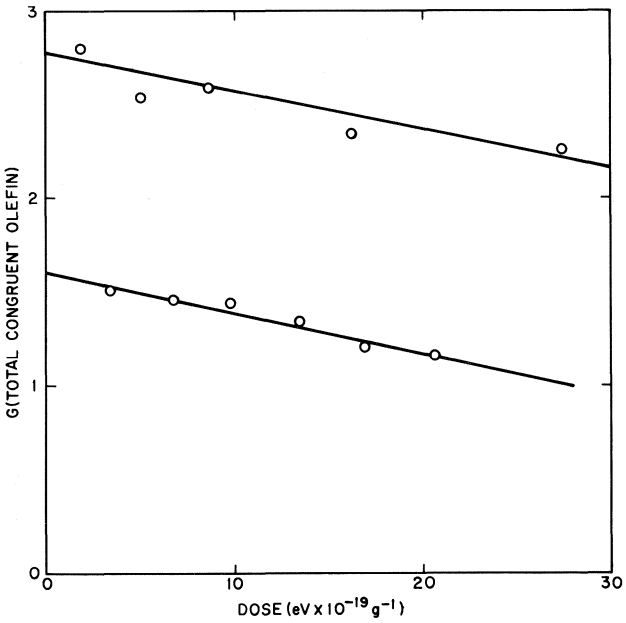

FIG. 2. Dose dependence of total yield of congruent olefin. Upper trace, liquid phase radiolysis; lower trace, solid state radiolysis.

congruent olefin shown in Fig. 2. If these *cis–trans* ratios are representative of positions other than 2, then ~25 and 35% of the congruent mono-olefin is *cis* in the solid and liquid respectively, comparable to what has been found for lower paraffins (1, 2). This finding is suggestive that one should find significant amounts of *cis*-vinylene unsaturation in irradiated polyethylene crystals or melts, which is not observed (11, 13–15). However, it was observed that *cis*-hexadecene-2 rapidly disappeared when the sample was open to air. In ~12 h its concentration fell below the limit of chromatographic detection, and the total yield of congruent olefin similarly decreased to a plateau value some 25–35% below that of a freshly opened sample. The concentration of *trans*-olefin did not appear to be affected, even on exposure to air for 2 or 3 weeks. Apparently the *cis*-isomers are preferentially air-oxidized with lower activation energies than the *trans*-olefins. A similar occurrence in polyethylene prior to i.r. examination might cause initially formed *cis*-vinylene unsaturation to escape notice, since i.r. observations were on thin polyethylene films and frequently in air (11, 13, 15). However, no evidence was found for carbonyl bands characteristic of oxidation and at least one author worked with a helium filled absorption cell (14).

The yield of *cis*- and *trans*-hexadecene-3 plus hexadecene-1, the three isomers being unresolved from each other chromatographically but separate from all other isomers, is approximately equal to that of *trans*-hexadecene-2. This places a limit on the yield of terminal olefin, which cannot be abnormally large.

In previous studies of *n*-hexadecene radiolysis (8), olefins and paraffins with the same number of carbon atoms, resulting from main chain scission were analyzed together. Total scission fraction yields were $G = 0.50$ and 1.00 for solid and liquid irradiation, respectively. Analysis of the scission olefins showed their yields to be only 20–25% of the total, *i.e.* G(scission olefin) is ~0.12 and 0.25 for solid and liquid. Comparison of product retention times with those of various olefinic standards indicates these scission olefins are all linear and probably terminal. Within the accuracy of the present analysis, the yield of each scission olefin is the same.

The total radiation induced unsaturation was determined by the coulometric titration technique, with G-values being 2.2 and 4.2 for solid and liquid respectively at doses of $\sim 10^{20}$ eV g^{-1}. This analysis indicates additional unsaturation beyond what can be accounted for in the congruent olefins and scission olefins of 0.7 and 1.3 G-units in the solid and liquid states, a difference considerably greater than the experimental un-

Can. J. Chem. Downloaded from www.nrcresearchpress.com by 210.87.254.40 on 09/05/12
For personal use only.

certainty. These differences may be associated with polyenes or with higher molecular weight unsaturated products of the radiolysis. Kang *et al.* (16) have found dienes play a significant role in the material balance of irradiated polyethylene.

In principle, a hydrogen material balance can be made by the equality

$$G(H_2) = G(\text{dimer}) + G(\text{congruent olefin}) + 2G(\text{diene}) + 3G(\text{triene}) + \ldots.$$
$$= G(\text{dimer}) + G(\text{total unsaturation}) - G(\text{scission olefin})$$

Best available values for G(dimer) at $\sim 10^{20}$ eV g^{-1} are 1.45 and 1.0 for the liquid and solid, respectively (7). For liquid phase radiolysis at this dose, $G(H_2)$ from this relationship is 5.4 compared with an observed value of 5.0 (7). For the solid the calculated $G(H_2)$ is only 3.1 compared with a measured value of 4.0. Agreement is satisfactory for the liquid, but the difference of 0.9 G-units in the solid state radiolysis suggests an unidentified source of molecular hydrogen, *i.e.* products deficient in hydrogen other than olefins and radical dimers.

1. T. GAUMANN. *In* Aspects of hydrocarbon radiolysis. T. Gaumann and J. Hoigne, *editors*. Academic Press, New York, N.Y., 1968. pp. 213–256.
2. L. KEVAN and W. F. LIBBY. J. Chem. Phys. **39**, 1288 (1963).
3. M. DOLE. *In* Crystalline olefin polymer. Part I. R. A. V. Raff and K. W. Doak, *editors*. Interscience Publishers, New York, N.Y., 1965. pp. 845–927.
4. A. CHAPIRO. Radiation chemistry of polymeric systems. Interscience Publishers, New York, N.Y., 1962.
5. M. B. FALLGATTER and M. DOLE. J. Phys. Chem. **68**, 1988 (1964).
6. D. M. BODILY and M. DOLE. J. Chem. Phys. **45**, 1433 (1966).
7. W. E. FALCONER, R. SALOVEY, W. A. SUNDER, and L. G. WALKER. Radiat. Res. **47**, 41 (1971).
8. W. E. FALCONER and R. SALOVEY. J. Chem. Phys. **44**, 3151 (1966).
9. A. G. SWALLOW. Radiation chemistry of organic compounds. Pergamon Press, New York, N.Y., 1960.
10. W. E. FALCONER and L. G. WALKER. J. Chromat. Sci. **9**, 184 (1971).
11. M. DOLE, D. C. MILNER, and T. F. WILLIAMS. J. Am. Chem. Soc. **80**, 1580 (1958).
12. A. F. TROTMAN-DICKENSON and G. S. MILNE. Tables of bimolecular gas reactions. NSRDS-NBS9 (1967).
13. M. A. CROOK and B. J. LYONS. Trans. Faraday Soc. **59**, 2334 (1963).
14. W. C. SEARS. J. Polymer Sci. **A2**, 2455 (1964).
15. P. J. FYDELOR and R. W. PEARSON. J. Appl. Polymer Sci. **5**, 171 (1961).
16. H. Y. KANG, O. SAITO, and M. DOLE. J. Am. Chem. Soc. **89**, 1980 (1967).

Sulfur Dioxide Formation in the Photo-oxidation of Methanethiol

D. M. GRAHAM AND BILLY K. T. SIE

Department of Chemistry, University of Western Ontario, London, Ontario

Received June 24, 1971

Photolysis of methanethiol in the presence of oxygen has been investigated at 228.8 and 254–265 nm. The major products detected were 2,3-dithiabutane and a liquid, tentatively identified as hydrogen peroxide. The quantum yield of sulfur dioxide was found to be small (3×10^{-5}) at 25 °C, increasing only by an order of magnitude at 125 °C. It has therefore been concluded that the reaction between CH_3S and oxygen is very slow if it occurs at all.

La photolyse du méthanethiol en présence d'oxygène a été étudiée à 228.8 nm et 254–265 nm. Les produits majoritaires détectés sont le dithia-2,3 butane et un liquide, identifié comme étant probablement du peroxyde d'hydrogène. Le rendement quantique en dioxyde de soufre est petit (3×10^{-5}) à 25 °C et n'augmente que d'un ordre de grandeur à 125 °C. Il en a été conclu que la réaction entre CH_3S et l'oxygène est une réaction très lente si elle a lieu.

Canadian Journal of Chemistry, 49, 3895 (1971)

Introduction

Determination of the relative rate constants for addition of thiyl radicals to olefins is complicated by the reversibility of the reaction over the entire temperature range available to experiment (1–3). In order to circumvent this, a method has been developed (4) which depends on the very rapid rate of reaction between the adduct radical and oxygen; under certain conditions this may compete successfully with adduct radical decom-

Can. J. Chem. Downloaded from www.nrcresearchpress.com by 210.87.254.40 on 09/05/12
For personal use only.

certainty. These differences may be associated with polyenes or with higher molecular weight unsaturated products of the radiolysis. Kang *et al.* (16) have found dienes play a significant role in the material balance of irradiated polyethylene.

In principle, a hydrogen material balance can be made by the equality

$$G(H_2) = G(\text{dimer}) + G(\text{congruent olefin}) + 2G(\text{diene}) + 3G(\text{triene}) + \ldots.$$
$$= G(\text{dimer}) + G(\text{total unsaturation}) - G(\text{scission olefin})$$

Best available values for G(dimer) at $\sim 10^{20}$ eV g^{-1} are 1.45 and 1.0 for the liquid and solid, respectively (7). For liquid phase radiolysis at this dose, $G(H_2)$ from this relationship is 5.4 compared with an observed value of 5.0 (7). For the solid the calculated $G(H_2)$ is only 3.1 compared with a measured value of 4.0. Agreement is satisfactory for the liquid, but the difference of 0.9 G-units in the solid state radiolysis suggests an unidentified source of molecular hydrogen, *i.e.* products deficient in hydrogen other than olefins and radical dimers.

1. T. GAUMANN. *In* Aspects of hydrocarbon radiolysis. T. Gaumann and J. Hoigne, *editors*. Academic Press, New York, N.Y., 1968. pp. 213–256.
2. L. KEVAN and W. F. LIBBY. J. Chem. Phys. **39**, 1288 (1963).
3. M. DOLE. *In* Crystalline olefin polymer. Part I. R. A. V. Raff and K. W. Doak, *editors*. Interscience Publishers, New York, N.Y., 1965. pp. 845–927.
4. A. CHAPIRO. Radiation chemistry of polymeric systems. Interscience Publishers, New York, N.Y., 1962.
5. M. B. FALLGATTER and M. DOLE. J. Phys. Chem. **68**, 1988 (1964).
6. D. M. BODILY and M. DOLE. J. Chem. Phys. **45**, 1433 (1966).
7. W. E. FALCONER, R. SALOVEY, W. A. SUNDER, and L. G. WALKER. Radiat. Res. **47**, 41 (1971).
8. W. E. FALCONER and R. SALOVEY. J. Chem. Phys. **44**, 3151 (1966).
9. A. G. SWALLOW. Radiation chemistry of organic compounds. Pergamon Press, New York, N.Y., 1960.
10. W. E. FALCONER and L. G. WALKER. J. Chromat. Sci. **9**, 184 (1971).
11. M. DOLE, D. C. MILNER, and T. F. WILLIAMS. J. Am. Chem. Soc. **80**, 1580 (1958).
12. A. F. TROTMAN-DICKENSON and G. S. MILNE. Tables of bimolecular gas reactions. NSRDS-NBS9 (1967).
13. M. A. CROOK and B. J. LYONS. Trans. Faraday Soc. **59**, 2334 (1963).
14. W. C. SEARS. J. Polymer Sci. **A2**, 2455 (1964).
15. P. J. FYDELOR and R. W. PEARSON. J. Appl. Polymer Sci. **5**, 171 (1961).
16. H. Y. KANG, O. SAITO, and M. DOLE. J. Am. Chem. Soc. **89**, 1980 (1967).

Sulfur Dioxide Formation in the Photo-oxidation of Methanethiol

D. M. GRAHAM AND BILLY K. T. SIE

Department of Chemistry, University of Western Ontario, London, Ontario

Received June 24, 1971

Photolysis of methanethiol in the presence of oxygen has been investigated at 228.8 and 254–265 nm. The major products detected were 2,3-dithiabutane and a liquid, tentatively identified as hydrogen peroxide. The quantum yield of sulfur dioxide was found to be small (3×10^{-5}) at 25 °C, increasing only by an order of magnitude at 125 °C. It has therefore been concluded that the reaction between CH_3S and oxygen is very slow if it occurs at all.

La photolyse du méthanethiol en présence d'oxygène a été étudiée à 228.8 nm et 254–265 nm. Les produits majoritaires détectés sont le dithia-2,3 butane et un liquide, identifié comme étant probablement du peroxyde d'hydrogène. Le rendement quantique en dioxyde de soufre est petit (3×10^{-5}) à 25 °C et n'augmente que d'un ordre de grandeur à 125 °C. Il en a été conclu que la réaction entre CH_3S et l'oxygène est une réaction très lente si elle a lieu.

Canadian Journal of Chemistry, 49, 3895 (1971)

Introduction

Determination of the relative rate constants for addition of thiyl radicals to olefins is complicated by the reversibility of the reaction over the entire temperature range available to experiment (1–3). In order to circumvent this, a method has been developed (4) which depends on the very rapid rate of reaction between the adduct radical and oxygen; under certain conditions this may compete successfully with adduct radical decom-

Can. J. Chem. Downloaded from www.nrcresearchpress.com by 210.87.254.40 on 09/05/12
For personal use only.

TABLE 1. Sulfur dioxide yields

	Temperature (°C)	Time (min)	$R(SO_2)$ $(mol\,l^{-1}\,s^{-1}) \times 10^{12}$	$\Phi(SO_2)$ $(\times 10^5)$
254–265 nm	25	302.1	1.72	2.2
$I = 7.70 \times 10^{-8}$ einstein $l^{-1}\,s^{-1}$	25	306.7	1.92	2.5
$CH_3SH = 5.00 \times 10^{-3}$ mol l^{-1}	25	606.1	2.65	3.4
$O_2 = 1.15 \times 10^{-2}$ mol l^{-1}	25	616.3	2.58	3.4
	25	630.4	3.31	4.3
	125	300.0	9.34	12
	125	300.0	10.1	13
	125	616.2	17.1	22
	125	669.8	13.4	17
228.8 nm	25	3.51	136	5.4
$I = 2.54 \times 10^{-6}$ einstein $l^{-1}\,s^{-1}$	25	3.51	138	5.4
$CH_3SH = 4.84 \times 10^{-4}$ mol l^{-1}	25	5.01	169	6.6
$O_2 = 1.46 \times 10^{-2}$ mol l^{-1}	25	7.01	154	6.1
	25	7.01	166	6.5
228.8 nm	25	30.0	205	6.3
$I = 3.24 \times 10^{-6}$ einstein $l^{-1}\,s^{-1}$	25*	30.0	220	6.8
$CH_3SH = 5.65 \times 10^{-3}$ mol l^{-1}	25*	30.0	203	6.3
$O_2 = 1.46 \times 10^{-2}$ mol l^{-1}				
228.8 nm	25	377	37	1.1
$H_2S = 5.65 \times 10^{-3}$ mol l^{-1}	25	312	43	1.3
$O_2 = 1.46 \times 10^{-2}$ mol l^{-1}	25	30.3	84	2.6

*+826 Torr CF_4.

position. In order to obtain relative reactivities, it is necessary to assume that no appreciable reaction occurs between thiyl radicals and oxygen. Some qualitative observations on the photo-oxidation of methanethiol had seemed to indicate that this was the case. However in a recent flash photolysis investigation of this reaction, strong absorptions due to SO and SO_2 were detected (5). Further, a transient absorption band at 218.5 nm, which is observed in the flash photolysis of CH_3S-containing species, disappears in the presence of oxygen. It was therefore suggested that the sulfur oxides result from oxidation of the thiyl radical. Because of the apparent disagreement between these results and our earlier work, a more careful investigation of the photo-oxidation of methanethiol was imperative.

Experimental

Methanethiol and hydrogen sulfide were purified by trap to trap distillations, using the appropriate slush baths, until the impurity level was below 0.1% as determined by g.l.c. Irradiation was carried out in quartz cells with a 100 W high pressure Hanovia SH616A lamp filtered by 1 cm of a 10% solution of 2,7-dimethyl-3,6-diazocyclohepta-1,6-diene iodide (6). This combination has maximum output intensities at 254 and 265 nm. For the short wavelength experiments, a Phillips 25 W cadmium lamp was used with no filter. Since methanethiol does not absorb at 326 nm, the effective photolysis wavelength was 228.8 nm. Analysis was performed using a mass spectrometer calibrated for each gas.

Results

The rates of formation of sulfur dioxide are given in Table 1. The absorbed light intensity was determined from the rate of hydrogen production in the photolysis of methanethiol in the absence of oxygen, assuming the quantum yield of hydrogen to be unity. This appears to be the case at 254–265 nm where the rate of hydrogen production has been shown to be equal to one-half the rate of CH_3S production, determined separately using butadiene-1,3 as a scavenger of the thiyl radical (3). Measurements, using an acetone actinometer, also indicate a hydrogen quantum yield of unity (7). At shorter wavelengths however, carbon–sulfur bond scission may become an important reaction channel (5), in which case hydrogen measurements would underestimate the absorbed light intensity.

The very low sulfur dioxide quantum yields determined are consistent with the large amounts of 2,3-dithiabutane observed. It proved impossible to determine this compound quantitatively due to its low vapor pressure and extremely strong absorption on the mass spectrometer inlet system. However it was always observed to be present in much larger quantities than sulfur dioxide. Sulfur dioxide is formed exclusively in a photolytic process, since in the absence of radiation, no reaction was observed after 10 h at 125 °C. During reaction a mist

Can. J. Chem. Downloaded from www.nrcresearchpress.com by 210.87.254.40 on 09/05/12
For personal use only.

formed on the cell walls; on warming, an explosion occurred, the only product of which appeared to be water. The mist therefore is probably hydrogen peroxide formed from the hydrogen atoms produced in the primary process. Secondary reactions involving this peroxide are likely responsible for the small increase in $\Phi(SO_2)$ as the irradiation time is increased; this effect is seen to be larger at the higher temperature.

Since the flash photolysis work was carried out in the presence of a high pressure of inert gas, two experiments were done in the presence of 826 Torr of tetrafluoromethane in order to determine if collisional stabilization is important. As is seen from the results in Table 1, addition of the inert gas had no effect. The quantum yield is also independent of thiol pressure. There is a small but significant increase in quantum yield at the shorter wavelength, and a tenfold increase in going from 25 to 125 °C.

The possibility that the low quantum yields are due to reactive disappearance of sulfur dioxide was eliminated by irradiating a mixture of methanethiol and sulfur dioxide with the mercury lamp for 10 h. No product other than 2,3-dithiabutane was detected and no change in the sulfur dioxide pressure occurred.

Since the yield of HS from carbon sulfur bond scission in the primary step is very small at 254–265 nm, and becomes appreciable at the wavelength used in the flash experiments (185–205 nm), it appeared possible that sulfur dioxide was formed from oxidation of this species. Some results obtained from irradiation of hydrogen sulfide/oxygen mixtures are given at the bottom of Table 1. The quantum yields were calculated assuming that the same amount of light is absorbed by H_2S and CH_3SH; this is reasonable since both have very high extinction coefficients at this wavelength. Only the last result approximates an initial quantum yield; in the first two the amount of photodecomposition was 40–60%. The initial sulfur dioxide quantum yield is about the same as that found for methanethiol, and it may be concluded that HS does not oxidize to any extent. This is consistent with flash photolysis observations that no sulfur dioxide is formed in the photoinitiated combustion of H_2S in the presence of high pressures of inert gas (8, 9), although it does become an important product at higher temperatures achieved under adiabatic flash conditions (8–10).

Although a definitive mechanism for the formation of sulfur dioxide cannot be ascertained from the results given here, it may be concluded that the reaction of CH_3S and HS with oxygen is extremely slow, even at 125 °C. At present it does not appear feasible to reconcile this conclusion with the flash photolysis results. The possibility exists that, even though the flash experiments were carried out in the presence of 100–200 Torr nitrogen as a temperature moderator, strictly isothermal conditions did not exist and oxidation occurred by a process analogous to the adiabatic flash combustion of H_2S (8–10).

Another possible explanation is suggested by some recent work on the partitioning of energy in the photodissociation of H_2S and CH_3SH (11). At wavelengths longer than 213.8 nm most of the available photolysis energy was observed to appear as kinetic energy of the hydrogen atom, and very little goes into internal excitation of the radical fragment. At 184.9 nm however, hydrogen atoms are produced with smaller kinetic energies than at 213.8 nm, and at the same time a large fraction of the available energy appears as internal excitation of HS and CH_3S. As the authors have suggested, this indicates a change in the primary process due either to Franck–Condon excitation to different regions of the RSH potential energy surface, or due to excitation to a different electronic state of RSH, either of which leading to dissociation into vibrationally and/or rotationally excited RS. Since the photolysis wavelength range for the flash experiments was 185–205 nm it is possible that internally excited CH_3S could have been produced, and that this internal excitation could greatly increase the rate of radical oxidation, which as we have shown does have a small activation energy. Interpretation of results obtained in the short wavelength region may also be complicated by excitation of the Schumann–Runge bands of O_2 (175–195 nm), and formation of SO_2 and SO could arise from reactions of O_2 ($^3\Sigma_u^-$) and $O(^3P)$ with CH_3S.

We are grateful to the National Research Council of Canada for financial support of this work.

1. D. M. Graham, R. L. Mieville, and C. Sivertz. Can. J. Chem. **42**, 2239 (1964).
2. D. M. Graham, R. L. Mieville, R. H. Pallen, and C. Sivertz. Can. J. Chem. **42**, 2250 (1964).
3. D. M. Graham and J. F. Soltys. Can. J. Chem. **47**, 2529 (1969).
4. D. M. Graham and J. F. Soltys. Can. J. Chem. **48**, 2173 (1969).

Can. J. Chem. Downloaded from www.nrcresearchpress.com by 210.87.254.40 on 09/05/12
For personal use only.

5. A. B. CALLEAR and D. R. DICKSON. Trans. Faraday Soc. **66**, 1987 (1970).
6. M. KASHA. J. Opt. Soc. Am. **38**, 929 (1948).
7. R. P. STEER and A. R. KNIGHT. J. Phys. Chem. **72**, 2145 (1968).
8. R. G. W. NORRISH and A. P. ZEELENBERG. Proc. Roy. Soc. **A240**, 293 (1957).
9. A. P. ZEELENBERG. 7th Symposium on Combustion, 68 (1959).
10. J. J. MCGARVEY and W. D. MCGRATH. Proc. Roy. Soc. **A278**, 490 (1964).
11. G. P. STURM JR. and JOHN M. WHITE. J. Chem. Phys. **50**, 5035 (1969).

Can. J. Chem. Downloaded from www.nrcresearchpress.com by 210.87.254.40 on 09/05/12
For personal use only.

Electron Spin Resonance Studies of Radiation Damage. Part. V. γ-Radiolysis and Photolysis of Aqueous Alkaline Glasses Containing Acetonitrile. The Photo Conversion of an Imino Radical to an Alkyl Radical at 77 °K[1, 2]

F. P. SARGENT AND M. G. BAILEY

Research Chemistry Branch, Whiteshell Nuclear Research Establishment, Atomic Energy of Canada Limited, Pinawa, Manitoba

Received June 7, 1971

The reactions of γ and photochemically produced electrons with acetonitrile in 8 *M* sodium hydroxide glasses at 77 °K have been re-investigated. The results differed from those previously reported and a novel photo-conversion of an imino radical to an alkyl radical was found. These results lead to a unified interpretation of (seemingly discrepant) observations on polar and nonpolar glasses.

Les réactions des électrons, produits par rayons gamma ou par effet photochimique, avec l'acétonitrile sur des verres d'hydroxyde de sodium 8 *M* à 77 °K ont été à nouveau étudiées. Les résultats diffèrent de ceux précédemment rapportés et une nouvelle photo-conversion d'un radical imino en un radical alkyl a été trouvée. Ces résultats permettent une interprétation unifiée des observations apparemment divergentes sur les verres polaires et non-polaires.

Canadian Journal of Chemistry, 49, 3898 (1971)

The reactions of acetonitrile with both radiation and photochemically produced electrons have received considerable attention in recent years. The radiolysis of solid acetonitrile has been extensively studied by Williams and co-workers (1)[3] and, largely due to their efforts, is reasonably well understood. The use of acetonitrile as an electron scavenger in various polar and non-polar solvents has been reported but the results seem to be in conflict with the recent work of Neta and Fessenden (2). Ayscough *et al.* (3) report that electrons produced by the γ radiolysis of aqueous 8 *M* sodium hydroxide glasses containing acetonitrile react by dissociative electron capture to produce methyl radicals. Williams and co-workers (4) have shown that electrons produced from the photolysis of tetramethylphenylenediamine (TMPD) at 366 nm in 2-methyltetrahydrofuran (MTHF) glasses also react with acetonitrile to produce methyl radicals. However, Neta and Fessenden (2) report that in their e.s.r. *in situ* irradiation experiments with aqueous solutions of acetonitrile at various p*H* values, the product was an imino radical $CH_3CHN\cdot$ characterized by an 80 G doublet. Methyl radicals were not observed. These workers performed separate experiments to determine if cyanide ion was formed. Their *G* values were in the range of 0.3 to 0.2 suggesting only about 10% of the electrons give methyl radicals by dissociative electron capture, and the majority reacted by electron capture followed by protonation to give an imino radical. We found the differences between the results in aqueous solutions and those found in glasses intriguing. We have re-examined the reactions of acetonitrile with electrons produced both photolytically and

[1]AECL No. 3937.
[2]For Part IV see ref. 7.
[3]See also refs. 4 to 8 in this reference.

5. A. B. CALLEAR and D. R. DICKSON. Trans. Faraday Soc. **66**, 1987 (1970).
6. M. KASHA. J. Opt. Soc. Am. **38**, 929 (1948).
7. R. P. STEER and A. R. KNIGHT. J. Phys. Chem. **72**, 2145 (1968).
8. R. G. W. NORRISH and A. P. ZEELENBERG. Proc. Roy. Soc. **A240**, 293 (1957).
9. A. P. ZEELENBERG. 7th Symposium on Combustion, 68 (1959).
10. J. J. MCGARVEY and W. D. MCGRATH. Proc. Roy. Soc. **A278**, 490 (1964).
11. G. P. STURM JR. and JOHN M. WHITE. J. Chem. Phys. **50**, 5035 (1969).

Can. J. Chem. Downloaded from www.nrcresearchpress.com by 210.87.254.5 on 09/05/12
For personal use only.

Electron Spin Resonance Studies of Radiation Damage. Part. V. γ-Radiolysis and Photolysis of Aqueous Alkaline Glasses Containing Acetonitrile. The Photo Conversion of an Imino Radical to an Alkyl Radical at 77 °K[1, 2]

F. P. SARGENT AND M. G. BAILEY

Research Chemistry Branch, Whiteshell Nuclear Research Establishment, Atomic Energy of Canada Limited, Pinawa, Manitoba

Received June 7, 1971

The reactions of γ and photochemically produced electrons with acetonitrile in 8 *M* sodium hydroxide glasses at 77 °K have been re-investigated. The results differed from those previously reported and a novel photo-conversion of an imino radical to an alkyl radical was found. These results lead to a unified interpretation of (seemingly discrepant) observations on polar and nonpolar glasses.

Les réactions des électrons, produits par rayons gamma ou par effet photochimique, avec l'acétonitrile sur des verres d'hydroxyde de sodium 8 *M* à 77 °K ont été à nouveau étudiées. Les résultats diffèrent de ceux précédemment rapportés et une nouvelle photo-conversion d'un radical imino en un radical alkyl a été trouvée. Ces résultats permettent une interprétation unifiée des observations apparemment divergentes sur les verres polaires et non-polaires.

Canadian Journal of Chemistry, 49, 3898 (1971)

The reactions of acetonitrile with both radiation and photochemically produced electrons have received considerable attention in recent years. The radiolysis of solid acetonitrile has been extensively studied by Williams and co-workers (1)[3] and, largely due to their efforts, is reasonably well understood. The use of acetonitrile as an electron scavenger in various polar and non-polar solvents has been reported but the results seem to be in conflict with the recent work of Neta and Fessenden (2). Ayscough *et al.* (3) report that electrons produced by the γ radiolysis of aqueous 8 *M* sodium hydroxide glasses containing acetonitrile react by dissociative electron capture to produce methyl radicals. Williams and co-workers (4) have shown that electrons produced from the photolysis of tetramethylphenylenediamine (TMPD) at 366 nm in 2-methyltetrahydrofuran (MTHF) glasses also react with acetonitrile to produce methyl radicals. However, Neta and Fessenden (2) report that in their e.s.r. *in situ* irradiation experiments with aqueous solutions of acetonitrile at various p*H* values, the product was an imino radical $CH_3CHN\cdot$ characterized by an 80 G doublet. Methyl radicals were not observed. These workers performed separate experiments to determine if cyanide ion was formed. Their *G* values were in the range of 0.3 to 0.2 suggesting only about 10% of the electrons give methyl radicals by dissociative electron capture, and the majority reacted by electron capture followed by protonation to give an imino radical. We found the differences between the results in aqueous solutions and those found in glasses intriguing. We have re-examined the reactions of acetonitrile with electrons produced both photolytically and

[1]AECL No. 3937.
[2]For Part IV see ref. 7.
[3]See also refs. 4 to 8 in this reference.

radiolytically in aqueous and other polar glasses at 77 °K; however, for brevity only the results found in aqueous 8 *M* sodium hydroxide are reported here.

We repeated the experiment of Ayscough *et al.* by γ irradiating aqueous 8 *M* sodium hydroxide glasses containing acetonitrile. Instead of the expected methyl radical the spectrum in Fig. 1(*a*) was observed. This consists of a broad trapped electron singlet flanked by two peaks separated by about 80 G. Photobleaching the trapped electrons with light of wavelength longer than 400 nm led to an increase in intensity of the doublet species. After complete removal of the singlet the spectrum in Fig. 1(*b*) was observed. We interpret this spectrum as indicated in the figure, namely, the usual methyl radical quartet together with the imino radical $CH_3CHN\cdot$, the latter being characterized by an 80 G doublet. The nitrogen $M_I \pm 1$ lines although broad, were detected at the appropriate magnetic field values (2, 5). The relative yields of the imino and methyl radicals were computed from their respective linewidths of 7.5 and 3.4 G assuming similar line shapes, binomial intensity distribution for methyl and six lines of equal area for the imino radical. This led to a relative concentration of about 10:1 *i.e.* only about 10% methyl radical. Therefore our results are in substantial agreement with those found by Neta and Fessenden.

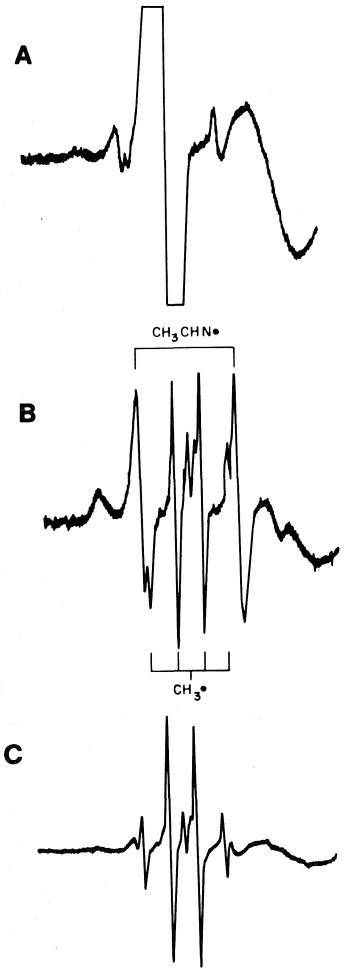

FIG. 1. Electron spin resonance spectra observed in γ irradiated aqueous 8 *M* sodium hydroxide glasses containing acetonitrile at 77 °K (*a*) examined in the dark immediately after radiolysis, gain setting 800 (*b*) followed by photobleaching λ > 400 nm, gain setting 800 (*c*) followed by photolysis at 254 nm, gain setting 250. Magnetic field increasing to left. Broad low field line is due to O^-

When the sample of Fig. 1(*b*) was further exposed to 254 nm light from a low pressure mercury resonance lamp the imino radicals were converted to methyl radicals as shown in Fig. 1(*c*). In additional experiments we were able to follow the decrease in imino radicals and the accompanying increase in methyl.

Photolysis at 254 nm of aqueous 8 *M* sodium hydroxide glasses containing acetonitrile and ferrocyanide produced spectra similar to that in Fig. 2(*a*). However, at short periods of photolysis or at reduced 254 nm light intensity spectra similar to that in Fig. 2(*b*) were obtained. This shows the presence of both methyl and imino radicals. The relative linewidths of the radicals indicate that the imino radical is present in ten-fold excess over methyl. In the absence of ferrocyanide there was a negligible amount of methyl radicals formed by photolysis.

Our results show that in aqueous 8 *N* sodium hydroxide glasses the imino radicals may be photochemically decomposed by 254 nm light to give alkyl radicals. We have found this to hold for other nitriles in polar solvents, but not in a non-polar matrix such as adamantane. Imino radicals were produced from amines in adamantane by the method of Wood *et al.* (5), but when they were photolyzed at 254 nm and 77 °K little or no conversion to alkyl radicals occurred. Therefore we suggest that the photodecomposition of imino radicals produces an alkyl radical and HCN. If the latter cannot be removed via production of cyanide ion then the reverse reaction will take place leading to no net de-

Can. J. Chem. Downloaded from www.nrcresearchpress.com by 210.87.254.5 on 09/05/12
For personal use only.

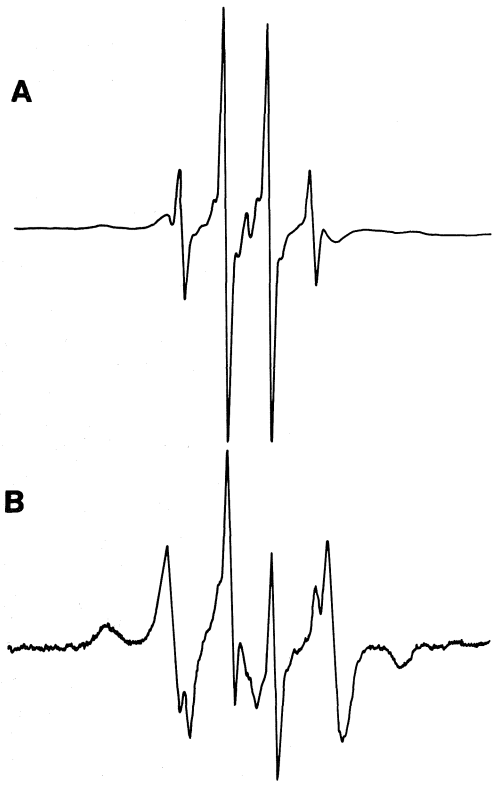

FIG. 2. Electron spin resonance spectra observed in samples of aqueous 8 *M* sodium hydroxide glasses containing acetonitrile and ferrocyanide at 77 °K photolyzed at 254 nm (*a*) 30 min at full lamp intensity, gain setting 50 (*b*) 2 min at full lamp intensity, gain setting 1250. Magnetic field increasing to left.

composition. The results presented here may be rationalized in terms of the following reaction scheme

$$[1] \quad CH_3CN + e \rightarrow (CH_3CN)^-$$

$$[2] \quad e + CH_3CN \rightarrow CH_3 + CN^-$$

$$[3] \quad (CH_3CN)^- \xrightarrow{h\nu} CH_3 + CN^-$$

$$[4] \quad (CH_3CN)^- + H_2O \rightarrow CH_3CHN\cdot + OH^-$$

$$[5] \quad CH_3CHN \xrightarrow{254\,nm} CH_3 + HCN$$

where reactions 2 and 3 only account for 10% of the radicals produced. In non-polar glasses such as MTHF the photolysis of TMPD at 366 nm is usually employed as the source of electrons. We have found that the photolysis of imino radicals is very slow at this wavelength so if imino radicals were formed they would be easily detected. Williams and co-workers report only the presence of methyl radicals (4), therefore the intermediate initially formed is probably $(CH_3CN)^-$, but in the non-polar glasses there is no source of protons to form the imino radical. The acetonitrile anion is very sensitive to light (1) and would subsequently dissociate to give methyl radicals. Although it is not possible to distinguish between methyl radicals produced by reactions 2 or 3, our results indicate that the dissociative electron capture reaction of acetonitrile in aqueous glasses is by no means as efficient as previously supposed. This conclusion is further supported by the thermodynamic data, namely the reaction 2 is endothermic in the gas phase by 0.7 ± 0.2 eV.[4]

We wish to thank R. S. Dixon for drawing our attention to the quoted thermodynamic data.

1. L. HOLLMAN, E. D. SPRAGUE, and F. WILLIAMS. J. Am. Chem. Soc. **92**, 429 (1970).
2. P. NETA and R. W. FESSENDEN. J. Phys. Chem. **74**, 3362 (1970).
3. P. B. AYSCOUGH, R. G. COLLINS, and F. S. DAINTON. Nature, **205**, 965 (1965).
4. M. A. BONIN, J. LIN, K. TSUJI, and F. WILLIAMS. Advances in chemistry. Series 82. Radiation chemistry: Vol. II. page 269.
5. D. E. WOOD, R. V. LLOYD, and D. W. PRATT. J. Am. Chem. Soc. **92**, 4115 (1970).
6. V. I. VEDENEYEV, L. V. GURVICH, V. N. KONDRAT YEV, V. A. MEDVEDEV, and YE L. FRANKEVICH. Bond energies, ionization potentials, and electron affinities. E. Arnold, London. 1966.
7. F. P. SARGENT. Can. J. Chem. **48**, 3453 (1970).

[4]Calculated from the difference of the bond dissociation energy $D(CH_3—CN)$ and the electron affinity of CN using the values given by ref. 6.

Can. J. Chem. Downloaded from www.nrcresearchpress.com by 210.87.254.5 on 09/05/12
For personal use only.

On the Existence of Free OH Groups in Liquid Water

J.-J. PÉRON,[1] C. BOURDÉRON, AND C. SANDORFY
Département de Chimie, Université de Montréal, Montréal, Québec

Received July 19, 1971

It is shown that despite the complexity of the related parts of the spectrum, vibrational overtones give evidence of the presence of free OH groups in liquid water.

Malgré la complexité du spectre on montre que l'examen des harmoniques apporte des arguments en faveur de la présence de OH libre dans l'eau liquide.

Canadian Journal of Chemistry, 49, 3901 (1971)

Can. J. Chem. Downloaded from www.nrcresearchpress.com by 210.87.254.6 on 09/05/12
For personal use only.

The presence of free OH groups in liquid water is a much debated subject. Extensive infrared and Raman work has been done including studies of vibrational overtones (1–10). Evidence for the presence of free OH groups using the fundamental was given by Walrafen (11–14), Senior and Verrall (15), and Yellin and Courchene (16). A related, and also somewhat controversial problem is whether we can apply to liquid water the so-called continuum model (4, 6, 7) or if we have to distinguish variously associated "species" in it. There has been a recent exchange of views in this respect between Schiffer (17) and Walrafen (18) which makes interesting reading.

In the present note we intend to make two points: (*a*) it is advantageous to place the problem of liquid water into the broader context of the problem of hydrogen bonded liquids and (*b*) in spite of the complexity of the overtone region it can still be used as a source of information on liquid water.

It is important in this respect to recognize the fact that the OH-stretching overtones of hydrogen bonded polymers are unusually weak compared to those of the corresponding free OH groups. This has been observed in various cases by Luck and Ditter (19), Burneau and Corset (20), and ourselves (21, 22). This weakness is likely to be due to decreased electric anharmonicity (21) and it makes it possible to observe free and oligomer vibrations, which do not show up in the fundamental region. The contribution of the free and oligomer species to the observed intensity of the overtones increases rapidly with the order of the overtones (22).

We have shown in the case of sterically hindered alcohols that such free species and oligomers can exist even at liquid nitrogen temperature in glassy matrices (21), and that in the case of liquid methanol at room temperature we also have some free and oligomeric molecules (22).

Falk and Ford (23) have cautioned against the use of overtones when dealing with the water problem. They rightly pointed out that the observed bands are likely to receive contributions from a number of other combination tones. This complexity is due to the triatomic character of the water vibrator but it is not so serious for HDO.

Worley and Klotz (24) measured the first overtone of HDO and found a band which could be assigned to a free OH group. It is followed by broader bands due to associated OH groups. This result was recently confirmed by Luck and Ditter (25) who measured the spectrum of HDO under various conditions including the critical region. When temperature is raised the intensity of the free band increases considerably. Significantly, the strongest band in this part of the spectrum is the $\nu_{OH} + \nu_{OD}$ combination band (25).

We have measured the second overtone of HDO[2] with a Cary-17 instrument using a 10 cm cell with 3× scale expansion. At room temperature we find a band at 10 400 cm^{-1} which, because of its frequency, must be the second overtone of a free OH band. It is broadened at its low frequency side. The intensity of the band increases when temperature is increased also indicating that it must belong to free or oligomer species. This implies that the polymer bands are too weak to be observed. (This conclusion is less surprising if we have examined the overtones of liquid methanol (22).) A confirmation of this assignment comes from the anharmonicity constants. For a free OH band in alcohols its value

[1]Permanent address: Laboratoire de Spectrochimie Moléculaire, Faculté des Sciences de Brest, France.

[2]Obtained from 50 ml H_2O/D_2O. See ref. 19.

Can. J. Chem. Downloaded from www.nrcresearchpress.com by 210.87.254.6 on 09/05/12
For personal use only.

is $\omega_e x_e \approx 80\ cm^{-1}$ (26). For the ν_3 band of H_2O it is only 40 cm^{-1}. Siebrand and Williams (27) have actually shown that for a single OH group this should be about double what is observed for two coupled OH groups, so in HDO we expect about 80 cm^{-1}. This is what Burneau and Corset (20) found for HDO in CCl_4 solution and this is what we find using the frequencies of the first and second overtones of the free bands as assigned above.

Turning our attention now to liquid H_2O we measured the first, second, and third overtones at temperatures varying from 20 to 80 °C (Figs. 1, 2, and 3). At 20 °C the maximum is gradually moving to higher frequencies within the respective region of absorption as we go from the first to the second and then to the third overtone. In the region of the first overtone the changes with increasing temperature are clearly due to relative intensity changes in at least two overlapping bands. The high frequency band (at 80 °C) is at 7030 cm^{-1}, the low frequency band (at 20 °C) at 6870 cm^{-1}. This region of absorption must receive contributions from both free and associated OH groups of the $2\nu_1$, $2\nu_3$, $\nu_1 + \nu_3$, $\nu_1 + 2\nu_2$, and $\nu_3 + 2\nu_2$ band of each species and possibly others (23) whose frequencies could be affected by Fermi-resonance. There is no real reason, however, why the high frequency side of the observed broad band should become more intense when temperature is raised if there is no change in the proportion of free and associated molecules. We are not going to take this for granted, since there are multiple coincidences and Fermi-resonance is possible between more than two levels. Even if we consider these pairwise, there is no insurance that the unperturbed intensity of

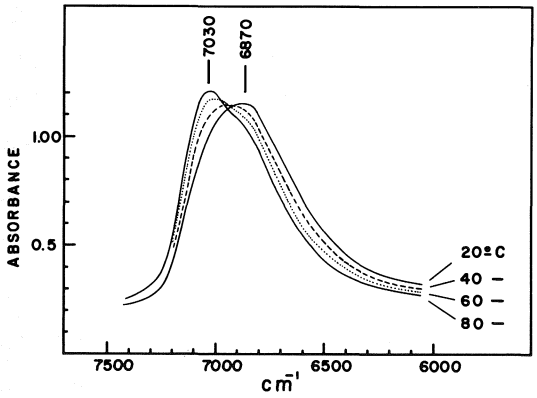

FIG. 1. The first overtone of H_2O at various temperatures (cell length 0.75 mm).

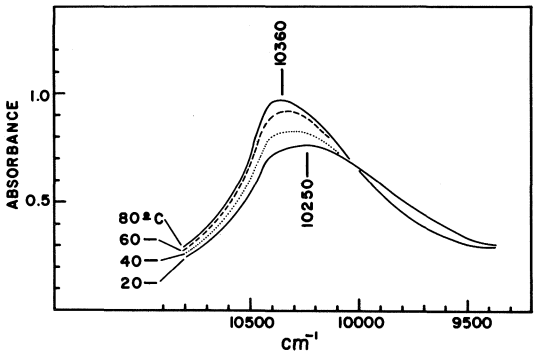

FIG. 2. The second overtone of H_2O at various temperatures (cell length 2 cm).

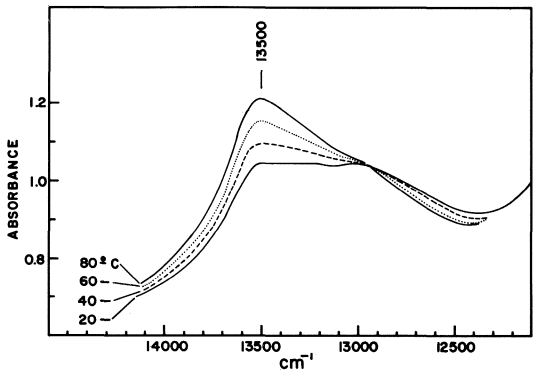

FIG. 3. The third overtone of H_2O at various temperatures (cell length 10 cm and 5 × scale expansion).

one of the interacting vibrations is negligible compared to the other, two conditions underlying the usual qualitative arguments on cases of Fermi-resonance. Under these circumstances an attempt to extract the unperturbed frequencies from the observed ones would not be justified.

The case of HDO is much clearer, however, since there is only one combination $\nu_1 + 3\nu_2$ which could have a frequency close enough to $2\nu_3$ for causing anharmonic resonance (23). Now using reasonable anharmonicity constants we can predict a difference of about 150–200 cm^{-1} between $2\nu_3$ and $\nu_1 + 3\nu_2$, a mediocre coincidence. Even more important is the fact that by far the largest perturbing term which could bring about this interaction (disregarding any possible symmetry requirement), $\langle 0,0,2|\ k_{122233} q_1 q_2^3 q_3^2 |\ 1,3,0\rangle$, would have to be a sextic term in the potential making the interaction entirely negligible. Thus we can conclude that the 7090 cm^{-1} band of HDO is a free band and not an associated band whose apparent frequency is heightened by anhar-

monic resonance. Furthermore, if the association in HDO would entirely conform to continuum theory there should be only one broad band at the level of $2\nu_3$ at all the temperatures, since no other vibration exists having similar frequencies and a non-negligible intensity. This, as we have stated, is not the case. Therefore even if the fundamental had a perfectly Gaussian or Lorentzian shape, this would be no sufficient proof for the total inexistence of "species". We also have to look at the overtones.

Now, there is a band at almost the same frequency (7030 cm^{-1}) in the spectrum of H_2O. In view of the analogy of associations in HDO and H_2O, their similar behavior when temperature is raised and the analogy between HDO and methanol (which has only one OH bond), we assign this band to molecules in which (at least) one OH group is approximately free. Then the 6870 cm^{-1} band must be due to vibrations of associated OH groups receiving intensity from both oligomers and polymers.

If these assignments are correct we have to expect that the "free" part of the higher stretching overtones becomes stronger in going from 2ν to 3ν and 4ν... This is actually what we observe. It is very significant that the effect of temperature is less and less in this order, showing that more and more of the absorbed intensity is due to the free species even at room temperature. Indeed the effect of decreased electric anharmonicity should become greater and greater in this order. The anharmonicity constant computed from the "free" overtones according to these assignments (at 80 °C) is about 75 cm^{-1}. This corresponds well to what is expected for an approximately free and uncoupled OH band. The other OH should be hydrogen bonded then so that the free OH is a part of an oligomer or polymer. If we compute the frequency of the fundamental with the above anharmonicity constant we obtain about 3600 cm^{-1} which is the free OH value obtained by Walrafen (3) in the Raman spectrum.

These observations yield a coherent picture covering the cases of alcohols, HDO, and H_2O in spite of the complexity of the water spectra. We believe that these facts add weight to the assumption that free OH groups do exist in liquid water at least at room temperature and higher temperatures. Finding "species" in liquid water is not so surprising if we have studied liquid or dissolved alcohols (21, 22) and amines (28) at low temperatures, where their bands appear clearly often even at the fundamental level. The proportion of free and oligomer species must be low, however, at least at room temperature, otherwise they would show up more strongly in the fundamental region.

We acknowledge financial help from the National Research Council of Canada.

1. D. Eisenberg and W. Kauzmann. The structure and properties of water. Oxford University Press, New York, N.Y. 1969.
2. O. Ya. Samoilov and T. A. Nosova. J. Struct. Chem. **6**, 767 (1965).
3. G. E. Walrafen. J. Chem. Phys. **47**, 114 (1967).
4. J. Schiffer and D. F. Hornig. J. Chem. Phys. **49**, 4150 (1968).
5. W. A. P. Luck and W. Ditter. J. Mol. Struct. **1**, 339 (1967–68); J. Phys. Chem. **74**, 3687 (1970).
6. G. Brink and M. Falk. J. Mol. Struct. **5**, 27 (1970).
7. H. R. Wyss and M. Falk. Can. J. Chem. **48**, 607 (1970).
8. R. Oder and D. A. I. Goring. Can. Spectry. **15**, 80 (1970).
9. A. I. Sidorova, Yu. V. Gurikov, L. V. Moiseeva, and T. G. Braginskaya. J. Struct. Chem. **10**, 681 (1969).
10. W. C. McCabe, S. Subramanian, and H. F. Fisher. J. Phys. Chem. **74**, 4360 (1970).
11. G. E. Walrafen. J. Chem. Phys. **45**, 244 (1968).
12. G. E. Walrafen. J. Chem. Phys. **50**, 560 (1969).
13. M. J. Colles, G. E. Walrafen, and K. W. Wecht. Chem. Phys. Lett. **10**, 621 (1970).
14. G. E. Walrafen and G. W. King. Private communication.
15. W. A. Senior and R. E. Verrall. J. Phys. Chem. **73**, 4242 (1969).
16. W. Yellin and W. L. Courchene. Nature, **219**, 852 (1968).
17. J. Schiffer. J. Chem. Phys. **50**, 566 (1969).
18. G. E. Walrafen. J. Chem. Phys. **50**, 567 (1969).
19. W. A. P. Luck and W. Ditter. J. Mol. Struct. **1**, 261 (1967–68).
20. A. Burneau and J. Corset. Chem. Phys. Lett. **9**, 99 (1971).
21. C. Bourdéron, J. J. Péron, and C. Sandorfy. A low temperature infrared study of sterically hindered associated alcohols. To be published.
22. C. Bourdéron. J. J. Péron, and C. Sandorfy. A vibrational overtone study of association in liquid methanol. To be published.
23. M. Falk and T. A. Ford. Can. J. Chem. **44**, 1699 (1966).
24. J. D. Worley and I. M. Klotz. J. Chem. Phys. **45**, 2868 (1966).
25. W. A. P. Luck and W. Ditter. Z. Naturforsch. **24b**, 482 (1969).
26. G. Durocher and C. Sandorfy. J. Mol. Spectry. **15**, 22 (1965).
27. W. Siebrand and D. F. Williams. J. Chem. Phys. **49**, 1860 (1968).
28. M. C. Bernard-Houplain and C. Sandorfy. A low temperature study of association in dissolved and liquid secondary amines. To be published.

Can. J. Chem. Downloaded from www.nrcresearchpress.com by 210.87.254.6 on 09/05/12
For personal use only.

Shock-Tube Study of Cr* Chemiluminescence During the Induction Period of the C_2H_2–O_2 Reaction

DAVID GUTMAN
Department of Chemistry, Illinois Institute of Technology, Chicago, Illinois 60616
AND
SHIMPEI MATSUDA
Department of Chemistry, Harvard University, Cambridge, Massachusetts 02138

Received April 14, 1971

The Cr* (a^7S–y^7P) chemiluminescence at 360 nm during the induction period of the C_2H_2–O_2 reaction was studied behind reflected shock waves. When the reaction gas mixture containing 10 p.p.m. $Cr(CO)_6$, 0.5% C_2H_2, 1.0% O_2, and 98.5% Ar was shock heated to 1650 °K, the emission intensity of Cr* grew exponentially with a growth constant equal to the chain branching constant. This observation indicates that reaction(s) leading to Cr* chemiluminescence involve only one chain carrier during the induction period of the C_2H_2–O_2 reaction. The mechanism of the chemical excitation of Cr is discussed.

La chimioluminescence de Cr*(a^7S–y^7P) à 360 nm, pendant la période d'induction de la réaction C_2H_2–O_2, a été étudiée derrière les ondes de choc réfléchies. Lorsque le mélange qazeux réactionnel, contenant 10 p.p.m. de $Cr(CO)_6$, 0.5% de C_2H_2, 1.0% de O_2 et 98.5% de Ar, est chauffé à 1650 °K, l'intensité de l'émission en Cr* croît d'une façon exponentielle et la constante de croissance est égale à la constante de fixation de chaîne. Cette observation montre que les réactions conduisant à la chimioluminescence de Cr*, impliquent uniquement un seul véhiculeur de chaîne pendant la période d'induction de la réaction C_2H_2–O_2. Le mécanisme de l'excitation chimique de Cr est discuté.

Canadian Journal of Chemistry, 49, 3904 (1971)

Introduction

It has long been observed that flames, especially the C_2H_2–O_2 and C_2H_2–air flames, containing certain additives emit intense atomic lines (1, 2). It has been shown that the excitation process is chemical rather than thermal in origin, and although the process of chemical excitation of atoms in flames has been the subject of many studies, it is not well established (1–3). This report describes the results of a kinetic study of the formation of the y^7P level of Cr as measured by the resonance emissions from 357.9 to 360.5 nm (hereafter denoted by Cr*) during the induction period of the C_2H_2–O_2 reaction in reflected shock waves.

The early part of the C_2H_2–O_2 reaction has been shown to be a highly branched chain reaction (4, 5). During the induction period of a chain branching reaction all the main chain carriers grow exponentially with the same growth constant (4, 6). If a side reaction, for example chemiluminescence and chemi-ionization in the C_2H_2–O_2 reaction, occurs between two chain carriers, products from this reaction grow according to $\exp(2\alpha t)$, where α is the chain branching constant. In general, the exponential growth constant, α^*, of a particular phenomenon is related to the chain branching constant, α, by

$$\alpha^* = n\alpha \quad [1]$$

where n is the number of chain carriers involved in the reaction leading to the phenomenon (4, 5). Since the knowledge of n in eq. 1 gives information to identify the process leading to atom excitation in flames, the exponential growth constant of Cr* emission was compared with that of the emission at 308 nm during the induction period of the C_2H_2–O_2 reaction. The emission at 308 nm has been shown to grow exponentially with a growth constant equal to the chain branching constant (7, 8).

Experimental

The 4 in. i.d. shock tube and end-on detection apparatus used in this study have been described previously (7). Two detectors (Amperex 150 UVP) were used simultaneously; one monitoring an emission at various wavelength through a monochromator (full band pass 15 nm) and the other the emission at 308 nm through an interference filter (half band pass 3 nm). Argon gas was passed through a packed column of $Cr(CO)_6$ and saturated with $Cr(CO)_6$ vapor (9).[1] The reaction gas mixture was prepared by adding the $Cr(CO)_6$ saturated Ar to C_2H_2/O_2/Ar gas mixtures. For Cr* emission

[1]For the vapor pressure of $Cr(CO)_6$, see refs. 10 and 11.

Can. J. Chem. Downloaded from www.nrcresearchpress.com by 210.87.254.40 on 09/05/12
For personal use only.

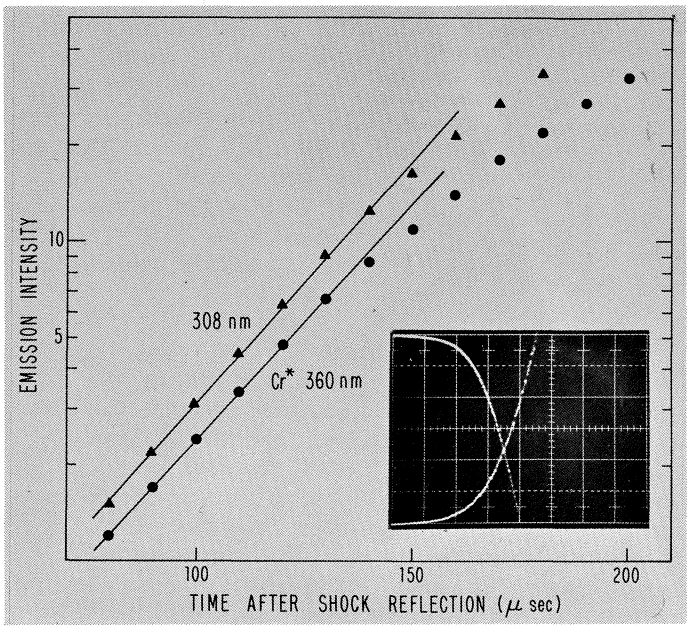

FIG. 1. Plot of emission intensity *vs.* time after shock wave reflection and oscillogram obtained in this experiment. Upper trace of the oscillogram: emission at 308 nm, 500 mV/div, lower trace: emission at 360 nm, 200 mV/div, sweep time is 50 μs/div for both traces.

measurements the gas mixture containing 10 p.p.m. $Cr(CO)_6$, 0.5% C_2H_2, 1.0% O_2, and 98.5% Ar was mainly used throughout this study. The experiment was performed at about 1650 °K and at a total concentration of 1.5×10^{-3} mol/l.

Results

It is known that there exists a continuum in the range 300–600 nm produced by the C_2H_2–O_2 reaction (1, 7, 8). Therefore, in a series of experiments the emission intensity distribution around Cr*(360 nm) was investigated in order to assure that the Cr* lines were isolated from the background continuum emission. Table 1 shows the emission intensity distribution around 360 nm for the mixture ($C_2H_2/O_2/Ar$ = 5/10/985) containing 10 p.p.m. $Cr(CO)_6$ and for the same mixture without $Cr(CO)_6$ using the emission at 308 nm as a reference. It is seen that an intense Cr* emission lies at 360 nm which is as strong as the CH*($C^2\Sigma^+$–$X^2\pi$) emission at 314 nm. It should be noted here that the CH* emission at 314 nm is much stronger in the shock heated C_2H_2–O_2 reaction than in C_2H_2–O_2 flames (7). From Table 1 it is known that the emission intensity observed at 360 nm is about 95% due to Cr* and 5% due to a background continuum.

TABLE 1. Emission intensity distribution around 360 nm (normalized at 314 nm)*

λ (nm)	I_λ/I_{308nm}	
	10 p.p.m. $Cr(CO)_6$	No $Cr(CO)_6$
370	0.05	0.05
360	0.96 (Cr*)	0.05
350	0.05	0.05
314	1.00 (CH*)	1.00 (CH*)

*Reaction gas mixture; $C_2H_2/O_2/Ar$ = 5/10/985.

The emission intensity of Cr* and the reference emission from a typical experiment is plotted against the reaction time in Fig. 1. It can be seen that both Cr* and the second emission grow exponentially with nearly the same growth constant. The exponential growth constants of Cr* and CH*(314 nm) were compared indirectly in separate experiments and found to be equal under the same experimental conditions.

Since both CH* and the reference emission grow with the same growth constant as the chain carriers (7, 8) (see Table 2), the above observations suggest that the reaction leading to Cr* excitation also involves only one chain carrier (n = 1 in eq. 1) during the induction period of the C_2H_2–O_2 reaction. When the reaction gas mixtures con-

Can. J. Chem. Downloaded from www.nrcresearchpress.com by 210.87.254.40 on 09/05/12
For personal use only.

TABLE 2. Order of reaction in chain carriers of various phenomena observed in the C_2H_2–O_2 reaction

Process	Order of reaction	Reference
CH ($A^2\Delta$–$X^2\pi$) 432 nm	1	5
($B^2\Sigma^-$–$X^2\pi$) 390 nm	1	7
($C^2\Sigma^+$–$X^2\pi$) 314 nm	1	7
Continuum 300–600 nm	1	7, 8
Cr* 360 nm	1	This study
C_2($A^3\pi_g$–$X^3\pi_u$) 515 nm	2	7
CO ($A^1\pi$–$X^1\Sigma^+$)	2	8
Chemi-ionization	2	4, 8

taining more than 25 p.p.m. $Cr(CO)_6$ were shock heated, reaction occurred extremely fast[2] and the exponential growth of the emission was no longer observed. In this case it was observed that I(Cr*)/I(308 nm) and I(314 nm)/I(308 nm) were nearly constant during the early part of the reaction. This observation also supports the result that Cr* is produced in a reaction first order in chain carriers.

Discussion

The order of reaction in chain carriers leading to the various phenomena observed in the C_2H_2–O_2 reaction is summarized in Table 2. From this table it is immediately concluded that $C_2(A^3\pi_g)$, $CO(A^1\pi)$, and chemi-ions can not be precursors of Cr* emission, because they are all formed in reactions second order in chain carriers. Several mechanisms have been proposed for metal excitation in flames.

[2] $CH + O + M \rightarrow CHO + M^*$ (ref. 3)

[3] $CH + O + M \rightarrow CO + H + M^*$ (ref. 12)

[4] $CH + OH + M \rightarrow CO + H_2 + M^*$ (ref. 13)

[5] $\begin{cases} CH(X^2\pi) + O \rightarrow CO^*(a^3\pi) + H \\ CO^* + M \rightarrow CO(X^1\Sigma^+) + M^* \end{cases}$ (ref. 1)

[6] $C + MO \rightarrow CO + M^*$ (ref. 14)

(M is a metallic element)

Reactions 2–5 involve two chain carriers, *i.e.* they are second order process in chain carriers. Consequently in the case that M is Cr, they are not consistent with the present experimental findings. In the shock tube study of $Cr(CO)_6$–O_2 and $Cr(CO)_6$–CO–O_2 reactions the formation of CrO, CrO_2, and CrO_3 has been observed by a time-of-flight mass spectrometer coupled to a shock tube (16). In the present reaction system $Cr(CO)_6$ is probably oxidized (at least partially) to CrO, CrO_2, and CrO_3. Reaction 6 is exothermic by about 150 kcal/mol in case of CrO and is able to excite Cr in the y^7P state. Thus, if there is a first order reaction or a sequence of first order reactions in chain carriers to produce carbon atoms during the induction period of the C_2H_2–O_2 reaction, reaction 6 is not inconsistent with the present experimental results.

It has been found that metal emissions are more closely related to the CH* than C_2* emission in flames (14). This observation is in agreement with the present experimental results, because both CH* and Cr* are formed in first order reactions in chain carriers while C_2* is formed in a second order process (see Table 2). Since the orders of reaction leading to Cr* and C_2* formation are different, the kinetic behaviors of Cr* and C_2* will be greatly different in flames.

In the present study it was found that Cr* together with CH* and the continuum were produced by a mechanism *first* order in chain carriers. Thus, the following processes for the Cr* emission during the induction period of the C_2H_2–O_2 reaction are suggested.

[7] $C_2H + O_2 + Cr \rightarrow Cr^* + 2CO + H$

[8] $CH + O_2 + Cr \rightarrow Cr^* + CO + OH$

Reactions 7 and 8 are exothermic by 115 and 159 kcal/mol (without Cr excitation), respectively (15). It should be pointed out that reactions 7 and 8 are kinetically indistinguishable from the two pairs of reactions,

[7*a*] $C_2H + O_2 \rightarrow CH(C^2\Sigma^+) + CO_2$

[7*b*] $CH(C^2\Sigma^+) + Cr \rightarrow CH + Cr^*$

and

[8*a*] $CH + O_2 \rightarrow OH(A^2\Sigma^+) + CO$

[8*b*] $OH(A^2\Sigma^+) + Cr \rightarrow OH + Cr^*$

Thus Cr may in fact be excited by electronic energy transfer in this system.

Since some species are excited by more than 160 kcal/mol in flames (1, 2), there arises a fundamental question over whether the excitation process is the same for all kinds of metal elements. In order to answer this question it is necessary to investigate the kinetic behaviors of various atomic emissions. Further studies related to this problem are being undertaken.

[2]The catalytic effect of $Cr(CO)_6$ on the C_2H_2–O_2 reaction will be discussed elsewhere.

Can. J. Chem. Downloaded from www.nrcresearchpress.com by 210.87.254.40 on 09/05/12
For personal use only.

The authors gratefully acknowledge financial support from the donors of the Petroleum Research Fund and from the National Science Foundation.

1. R. MAVRODINEANU and H. BOITEUX. Flame spectroscopy. John Wiley and Sons, Inc., New York. 1965.
2. J. A. DEAN and T. C. RAINS (*Editors*). Flame emission and atomic absorption spectrometry. Vol. 1. Marcel Dekker, New York. 1969.
3. T. M. SUGDEN. Ann. Rev. Phys. Chem. **13**, 369 (1962).
4. G. P. GLASS, G. B. KISTIAKOWSKY, J. V. MICHAEL, and H. NIKI. J. Chem. Phys. **42**, 608 (1965).
5. D. GUTMAN and S. MATSUDA. J. Chem. Phys. **52**, 4122 (1970).
6. J. N. BRADLEY. Trans. Faraday Soc. London, **63**, 2945 (1967).
7. I. R. SLAGLE, D. J. FIFE, S. MATSUDA, J. R. MARQUART, and D. GUTMAN. J. Chem. Phys. To be published.
8. S. MATSUDA. Ph.D. Thesis. Illinois Institute of Technology. 1970.
9. W. L. SHACKLEFORD. J. Quant. Spectry. Radiative Transfer, **5**, 303 (1965).
10. T. D. WILKERSON. Ph.D. Thesis. University of Michigan, 1962.
11. A. A. BONI. J. Electrochem. Soc. **113**, 1089 (1966).
12. H. P. BROIDA and K. E. SCHULER. J. Chem. Phys. **27**, 933 (1957).
13. J. H. GIBSON, W. E. L. GROSSMAN, and W. D. COOKE. Anal. Chem. **35**, 266 (1963).
14. P. T. GILBERT, JR. Proc. Xth Colloq. Spectrosc. Int. p. 171. Spartan Books, Washington D.C. 1963.
15. JANAF Thermochemical Table, Dow Chemical Co., Midland, Michigan. 1965.
16. S. MATSUDA and G. B. KISTIAKOWSKY. J. Chem. Phys. To be published.

Studies of the Carbonatobis(R-propylenediamine)cobalt(III) Ion

ROLAND A. HAINES AND ANTHONY A. SMITH
Department of Chemistry, University of Western Ontario, London 72, Ontario

Received July 2, 1971

The complex carbonatobis(R-propylenediamine)cobalt(III) perchlorate, $[Co(R\text{-}pn)_2CO_3]ClO_4$ has been prepared both as a mixture of isomers and as one pure optical isomer. The nature of the products is discussed and structures are assigned on the basis of c.d. and n.m.r. data.

Le complexe, perchlorate de carbonatobis (R-propylènediamine)cobalt(III), $[Co(R\text{-}pn)_2CO_3]ClO_4$, a été préparé à la fois sous forme d'un mélange d'isomères et sous forme d'un seul isomère optique. La nature des produits est discutée et les structures sont attribuées en se fondant sur les données r.m.n. et d.c.

Canadian Journal of Chemistry, 49, 3907 (1971)

There have been previous reports in the literature concerning the preparation of the carbonatobis(R-propylenediamine)cobalt(III) complex ion (1, 2). There, evidence was presented for stereoselectivity in the preparation of these complexes and the latter workers reported the isolation of a pure optically active form on the basis of o.r.d. data. However, little has been reported concerning the actual structure of the product obtained in these studies, and this is unfortunate since the synthesis could produce three possible geometric isomers, each of which has a diastereomeric mirror image. Recently it has been necessary for us to examine this system in detail while carrying out some related studies on stereoselectivity and in this paper we wish to report the results of our findings.

The traditional preparation of carbonato complexes of the type $[Co(diamine)_2CO_3]^+$ involves reaction of the corresponding *trans*-$[Co(diamine)_2Cl_2]^+$ ion with a carbonate salt. If the diamine is not itself optically active, preparation of the complex in this manner should yield equal amounts of the Λ and Δ optical isomers (3). However, the use of an optically active ligand such as R-(−)propylenediamine (R-pn) usually imposes an asymmetric bias on the synthesis and the isomers are not prepared in equal amounts. This stereoselectivity is applicable both to the formation of a particular geometric isomer and its particular optical isomer. Thus examination of the c.d. or o.r.d. spectrum of the reaction product of such a synthesis is often not too informative since such a curve would be a

Can. J. Chem. Downloaded from www.nrcresearchpress.com by 210.87.254.40 on 09/05/12
For personal use only.

The authors gratefully acknowledge financial support from the donors of the Petroleum Research Fund and from the National Science Foundation.

1. R. MAVRODINEANU and H. BOITEUX. Flame spectroscopy. John Wiley and Sons, Inc., New York. 1965.
2. J. A. DEAN and T. C. RAINS (*Editors*). Flame emission and atomic absorption spectrometry. Vol. 1. Marcel Dekker, New York. 1969.
3. T. M. SUGDEN. Ann. Rev. Phys. Chem. **13**, 369 (1962).
4. G. P. GLASS, G. B. KISTIAKOWSKY, J. V. MICHAEL, and H. NIKI. J. Chem. Phys. **42**, 608 (1965).
5. D. GUTMAN and S. MATSUDA. J. Chem. Phys. **52**, 4122 (1970).
6. J. N. BRADLEY. Trans. Faraday Soc. London, **63**, 2945 (1967).
7. I. R. SLAGLE, D. J. FIFE, S. MATSUDA, J. R. MARQUART, and D. GUTMAN. J. Chem. Phys. To be published.
8. S. MATSUDA. Ph.D. Thesis. Illinois Institute of Technology. 1970.
9. W. L. SHACKLEFORD. J. Quant. Spectry. Radiative Transfer, **5**, 303 (1965).
10. T. D. WILKERSON. Ph.D. Thesis. University of Michigan, 1962.
11. A. A. BONI. J. Electrochem. Soc. **113**, 1089 (1966).
12. H. P. BROIDA and K. E. SCHULER. J. Chem. Phys. **27**, 933 (1957).
13. J. H. GIBSON, W. E. L. GROSSMAN, and W. D. COOKE. Anal. Chem. **35**, 266 (1963).
14. P. T. GILBERT, JR. Proc. Xth Colloq. Spectrosc. Int. p. 171. Spartan Books, Washington D.C. 1963.
15. JANAF Thermochemical Table, Dow Chemical Co., Midland, Michigan. 1965.
16. S. MATSUDA and G. B. KISTIAKOWSKY. J. Chem. Phys. To be published.

Studies of the Carbonatobis(R-propylenediamine)cobalt(III) Ion

ROLAND A. HAINES AND ANTHONY A. SMITH
Department of Chemistry, University of Western Ontario, London 72, Ontario

Received July 2, 1971

The complex carbonatobis(R-propylenediamine)cobalt(III) perchlorate, $[Co(R\text{-}pn)_2CO_3]ClO_4$ has been prepared both as a mixture of isomers and as one pure optical isomer. The nature of the products is discussed and structures are assigned on the basis of c.d. and n.m.r. data.

Le complexe, perchlorate de carbonatobis (R-propylènediamine)cobalt(III), $[Co(R\text{-}pn)_2CO_3]ClO_4$, a été préparé à la fois sous forme d'un mélange d'isomères et sous forme d'un seul isomère optique. La nature des produits est discutée et les structures sont attribuées en se fondant sur les données r.m.n. et d.c.

Canadian Journal of Chemistry, 49, 3907 (1971)

There have been previous reports in the literature concerning the preparation of the carbonatobis(R-propylenediamine)cobalt(III) complex ion (1, 2). There, evidence was presented for stereoselectivity in the preparation of these complexes and the latter workers reported the isolation of a pure optically active form on the basis of o.r.d. data. However, little has been reported concerning the actual structure of the product obtained in these studies, and this is unfortunate since the synthesis could produce three possible geometric isomers, each of which has a diastereomeric mirror image. Recently it has been necessary for us to examine this system in detail while carrying out some related studies on stereoselectivity and in this paper we wish to report the results of our findings.

The traditional preparation of carbonato complexes of the type $[Co(diamine)_2CO_3]^+$ involves reaction of the corresponding *trans*-$[Co(diamine)_2Cl_2]^+$ ion with a carbonate salt. If the diamine is not itself optically active, preparation of the complex in this manner should yield equal amounts of the Λ and Δ optical isomers (3). However, the use of an optically active ligand such as R-(−)propylenediamine (R-pn) usually imposes an asymmetric bias on the synthesis and the isomers are not prepared in equal amounts. This stereoselectivity is applicable both to the formation of a particular geometric isomer and its particular optical isomer. Thus examination of the c.d. or o.r.d. spectrum of the reaction product of such a synthesis is often not too informative since such a curve would be a

Can. J. Chem. Downloaded from www.nrcresearchpress.com by 210.87.254.40 on 09/05/12
For personal use only.

Can. J. Chem. Downloaded from www.nrcresearchpress.com by 210.87.254.40 on 09/05/12
For personal use only.

resultant of contributions from all the species present.

In our work the reaction mixture for the synthesis of $[Co(R\text{-}pn)_2CO_3]^+$ yielded a c.d. curve with a predominant negative peak (530 nm) in the vicinity of the first absorption band, with a smaller positive peak at lower wavelength (470 nm). A study of the proton n.m.r. spectrum for this product, however, revealed that a mixture of species was present. The region corresponding to the resonances of the methyl groups of propylenediamine showed two doublets of unequal intensities. The predominant doublet had peaks at 1.36 and 1.31 p.p.m. downfield from sodium DSS while the other had peaks at 1.34 and 1.28 p.p.m. In addition, a minor peak occurred at 1.26 p.p.m., which was attributed to the presence of a small amount of one other isomer. A typical spectrum is shown in Fig. 1. Thus one species is predominant and will influence the resultant observed c.d. curve the most. The question remained as to the nature of this species, however, and the other major component in solution.

In order to gain further information, it was necessary to have a pure sample of one of the components and this was accomplished by making use of a variation of the stereospecific synthesis reported by Dwyer and MacDermott (2). In this way, a sample of $[Co(R\text{-}pn)_2CO_3]ClO_4$ was obtained which had a large negative c.d. peak in the region of the first absorption band (see Fig. 2) and whose proton n.m.r. spectrum showed only a single doublet with peaks at 1.37 and 1.31 p.p.m. Thus this sample corresponded to one pure optical isomer and on the basis of the sign of the predominant c.d. band (4), the Δ absolute configuration could be assigned.

A decision needed to be made, however, as to which geometric isomer was present. The n.m.r. spectrum indicated that the methyl groups of the two propylenediamine ligands were equivalent, since only one doublet was observed. Of the three possible geometric isomers, only the two shown in Fig. 3 possess a C_2 axis and hence would be consistent with the n.m.r. spectrum. It is difficult to choose between these two possibilities but the latter could be somewhat favored when one considers the structure found for the Δ isomer of $[Co(R\text{-}pn)_3]^{3+}$ from X-ray analysis (5). There the *fac*-configuration was found and the structure shown in Fig. 3(*b*) could more readily attain an

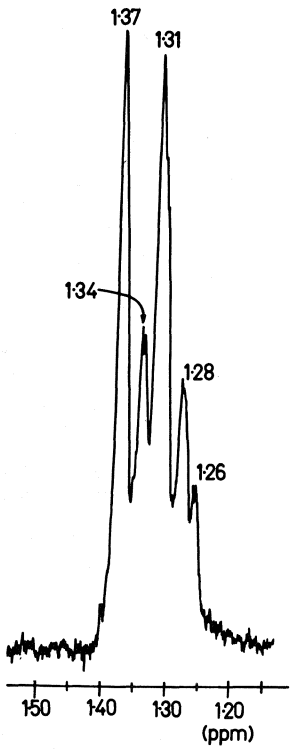

FIG. 1. Methyl region of 100 MHz n.m.r. spectrum of $[Co(R\text{-}pn)_2CO_3]ClO_4$ reaction product in D_2O.

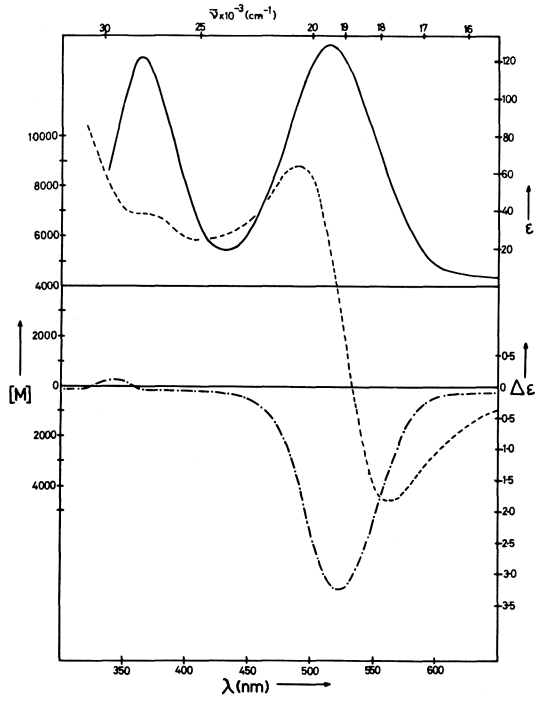

FIG. 2. Absorption (—), c.d. (·····), and o.r.d. (---) spectra of Δ-$[Co(R\text{-}pn)_2CO_3]ClO_4$.

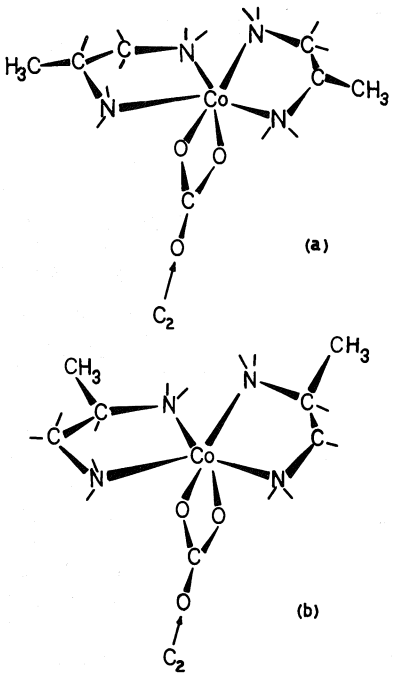

FIG. 3. Two possible geometric isomers of Δ-[Co(R-pn)$_2$CO$_3$]ClO$_4$.

intermediate leading to that configuration upon substituting CO_3^{2-} by an R-propylenediamine ligand. As illustrated, the λ conformation of each chelate ring would be expected to be found since coordination of R-pn with this conformation allows the methyl group to be equatorial and hence the complex has added stability (6).

Thus the predominant component of the original reaction mixture may be assigned to the Δ configuration of one particular geometric isomer as shown in Fig. 3(*b*). The other principal component is most likely its diastereomeric mirror image, *i.e.*, the Λ optical isomer. A comparison of the c.d. spectra of the reaction product and the pure Δ compound indicates that it is unlikely that this component corresponds to a different geometric isomer of the Δ configuration. All of the geometric isomers would be predicted to favor the Δ absolute configuration on the basis of stability arguments (6) and hence all geometric isomers would show a predominant negative c.d. band. Hence the c.d. band of the reaction product would not be expected to be too different in intensity from that of the pure Δ compound. However, such is not the case and the c.d. maximum of the Δ isomer is much more intense than that of the reaction product. These results are consistent with a cancellation effect of two isomers of opposite configurations.

Further support was provided from observations of the mother liquor obtained following filtration of the pure Δ isomer. Nuclear magnetic resonance spectra indicated that the relative proportions of the two major components had not changed significantly from that of the reaction mixture, even though a large amount of the one component had been removed. Further crops of the pure Δ isomer could be obtained from the mother liquor without changing the relative proportions. Thus the minor component must continually be converting to the pure Δ isomer to maintain an equilibrium in solution. Such a conversion is likely to occur by an intramolecular mechanism (see, for example, ref. 7) and from the n.m.r. results would be consistent with an inversion reaction without isomerization. This is due to the fact that most of the proposed intramolecular rearrangements would produce the isomer containing nonequivalent methyl groups on the pn rings. No evidence for such an isomer was observed.

Experimental

Preparation of trans-Dichlorobis(R-propylenediamine)-cobalt(III) Perchlorate, [Co(R-pn)$_2$Cl$_2$]ClO$_4$

This complex was prepared using a modification of the method of Martinette *et al.* (8), using R-propylenediamine dihydrochloride obtained from Frinton Laboratories, Vineland, N.J. The solid (12.9 g) was dissolved in ~50 ml of water and neutralized with a solution of sodium hydroxide (7.3 g) in the minimum amount of water. To this mixture was added 9.52 g of $CoCl_2.6H_2O$ in an ice bath and approximately 20 ml of 30% H_2O_2 was added slowly with stirring. After the reaction had subsided, the beaker was removed from the ice and 50 ml of concentrated hydrochloric acid was added. The dull grey solution was then concentrated to 25 ml by blowing air over the surface, keeping the temperature below 80 °C. The dark green crystals were filtered off, washed with ether and dried under a heat lamp where they crumbled to a dull green powder. This chloride salt was converted to the perchlorate salt by dissolution of the product in water followed by the addition of a slight excess of sodium perchlorate. The solid readily precipitated and was filtered off and washed on the filter with ice water until the filtrate became green. Finally, the precipitate was washed with ethanol and ether and dried under a heat lamp.

Further product could be obtained by evaporating the filtrate on a steam bath. This product was contaminated with large amounts of sodium perchlorate but could be purified by dissolving the product in acetone, filtering and reprecipitating the complex with a large excess of ether. Total yield ~6 g.

Preparation of Carbonatobis(R-propylenediamine)-cobalt(III) Perchlorate, [Co(R-pn)$_2$CO$_3$]ClO$_4$

A solution of *trans*-[Co(R-pn)$_2$Cl$_2$]ClO$_4$ (3 g) in water

Can. J. Chem. Downloaded from www.nrcresearchpress.com by 210.87.254.40 on 09/05/12
For personal use only.

(50 ml) was heated to 50 °C and an excess of solid silver carbonate (5 g) was added. The solution was stirred for 10 min, keeping the temperature at 50–55 °C. The dark red solution was allowed to cool, the silver salts were filtered off, and the filtrate was evaporated to dryness on a steam bath. The residue was dissolved in the minimum amount of boiling water, the solution was filtered and the filtrate was cooled in an ice bath to precipitate the solid.

Preparation of Δ-carbonatobis(R-propylenediamine)-cobalt(III) Perchlorate

This complex was prepared using a stereoselective method similar to that reported for the corresponding iodide salt. A quantity of the mixed complex prepared above was dissolved in a small amount of water and acetone was added until the solution turned cloudy. The flask was then stoppered and allowed to stand for a week. At the end of that time, the needle-shaped crystals were filtered, washed with acetone, and dried under a heat lamp.

Anal. Calcd. for $[Co(N_2C_3H_{10})_2CO_3]ClO_4$: C, 22.93; H, 5.50; N, 15.28; Cl, 9.67. Found: C, 22.98; H, 5.26; N, 14.92; Cl, 9.81.

General

Optical rotatory dispersion and c.d. spectra were recorded on a Durrum-Jasco ORD/UV/5 spectropolarimeter while absorption spectra were obtained on a Beckman DK-1 spectrophotometer. Nuclear magnetic resonance spectra were recorded using a Varian HA-100 instrument on solutions of the complex dissolved in D_2O and containing sodium 2,2-dimethyl-2-silapentane sulfonate (NaDSS) as internal standard.

The authors are grateful to the National Research Council of Canada for financial support of a postgraduate scholarship to A.A.S and an operating grant to R.A.H.

1. Sr. M. Martinette and J. C. Bailar. J. Am. Chem. Soc. **74**, 1054 (1952).
2. F. P. Dwyer and T. E. MacDermott. Inorg. Chem. **2**, 871 (1963).
3. This nomenclature is consistent with that suggested by IUPAC, Inorg. Chem. **9**, 1 (1970).
4. A. J. McCaffery, S. F. Mason, and B. J. Norman. J. Chem. Soc. 5094 (1965).
5. H. Iwasaki and Y. Saito. Bull. Chem. Soc. Jap. **39**, 92 (1966).
6. E. J. Corey and J. C. Bailar. J. Am. Chem. Soc. **81**, 2620 (1959).
7. F. Basolo and R. G. Pearson. Mechanisms of inorganic reactions. 2nd ed. John Wiley and Sons Inc., New York. 290.
8. Sr. M. Martinette, J. Busch, and M. Gulbinskas. J. Am. Chem. Soc. **77**, 6507 (1955).

Can. J. Chem. Downloaded from www.nrcresearchpress.com by 210.87.254.40 on 09/05/12
For personal use only.

^{35}Cl Nuclear Quadrupole Resonance of Some Phosphorus–Chlorine Compounds

J. K. B. Bishop, W. R. Cullen, and M. C. L. Gerry
Department of Chemistry, The University of British Columbia, Vancouver 8, British Columbia

Received June 2, 1971

Chlorine nuclear quadrupole resonance spectra have been observed for several compounds containing phosphorus–chlorine bonds. The compounds included some complexes of phosphorus trichloride with transition metals as well as some alkyl derivatives of thiophosphoryl chloride and phosphorus trichloride.

Les spectres de résonance quadrupolaire nucléaire du chlore ont été observés pour plusieurs composés contenant des liaisons phosphore–chlore. Ces composés incluent certains complexes du trichlorure de phosphore avec des métaux de transition ainsi que certains dérivés alkylés du chlorure de thiophosphoryle et du trichlorure de phosphore.

Canadian Journal of Chemistry, **49**, 3910 (1971)

There have been several previous reports of nuclear quadrupole resonance (n.q.r.) spectra of phosphorus–chlorine derivatives (1–9). Yet, though trivalent phosphorus halides form many complexes with transition metals there have been no previous reports of their chlorine n.q.r. spectra. We have begun a study of these, and report here the measurement of the resonances of two, namely tetrakis(trichlorophosphine)nickel, $Ni(PCl_3)_4$, and *fac*-tris(trichlorophosphine)tricarbonylmolybdenum, $Mo(CO)_3(PCl_3)_3$. We report also some further measurements of the n.q.r. spectra of compounds having general formulae $RPCl_2$ and $RPSCl_2$.

Experimental Methods

Nuclear quadrupole resonance spectra were observed using an externally quenched superregenerative spectrometer constructed in this Department. Its circuit was similar to that of Smith and Tong (10). Provision was made to permit independent variation of both pulse

(50 ml) was heated to 50 °C and an excess of solid silver carbonate (5 g) was added. The solution was stirred for 10 min, keeping the temperature at 50–55 °C. The dark red solution was allowed to cool, the silver salts were filtered off, and the filtrate was evaporated to dryness on a steam bath. The residue was dissolved in the minimum amount of boiling water, the solution was filtered and the filtrate was cooled in an ice bath to precipitate the solid.

Preparation of Δ-carbonatobis(R-propylenediamine)-cobalt(III) Perchlorate

This complex was prepared using a stereoselective method similar to that reported for the corresponding iodide salt. A quantity of the mixed complex prepared above was dissolved in a small amount of water and acetone was added until the solution turned cloudy. The flask was then stoppered and allowed to stand for a week. At the end of that time, the needle-shaped crystals were filtered, washed with acetone, and dried under a heat lamp.

Anal. Calcd. for $[Co(N_2C_3H_{10})_2CO_3]ClO_4$: C, 22.93; H, 5.50; N, 15.28; Cl, 9.67. Found: C, 22.98; H, 5.26; N, 14.92; Cl, 9.81.

General

Optical rotatory dispersion and c.d. spectra were recorded on a Durrum-Jasco ORD/UV/5 spectropolarimeter while absorption spectra were obtained on a Beckman DK-1 spectrophotometer. Nuclear magnetic resonance spectra were recorded using a Varian HA-100 instrument on solutions of the complex dissolved in D_2O and containing sodium 2,2-dimethyl-2-silapentane sulfonate (NaDSS) as internal standard.

The authors are grateful to the National Research Council of Canada for financial support of a postgraduate scholarship to A.A.S and an operating grant to R.A.H.

1. Sr. M. Martinette and J. C. Bailar. J. Am. Chem. Soc. **74**, 1054 (1952).
2. F. P. Dwyer and T. E. MacDermott. Inorg. Chem. **2**, 871 (1963).
3. This nomenclature is consistent with that suggested by IUPAC, Inorg. Chem. **9**, 1 (1970).
4. A. J. McCaffery, S. F. Mason, and B. J. Norman. J. Chem. Soc. 5094 (1965).
5. H. Iwasaki and Y. Saito. Bull. Chem. Soc. Jap. **39**, 92 (1966).
6. E. J. Corey and J. C. Bailar. J. Am. Chem. Soc. **81**, 2620 (1959).
7. F. Basolo and R. G. Pearson. Mechanisms of inorganic reactions. 2nd ed. John Wiley and Sons Inc., New York. 290.
8. Sr. M. Martinette, J. Busch, and M. Gulbinskas. J. Am. Chem. Soc. **77**, 6507 (1955).

^{35}Cl Nuclear Quadrupole Resonance of Some Phosphorus–Chlorine Compounds

J. K. B. Bishop, W. R. Cullen, and M. C. L. Gerry

Department of Chemistry, The University of British Columbia, Vancouver 8, British Columbia

Received June 2, 1971

Chlorine nuclear quadrupole resonance spectra have been observed for several compounds containing phosphorus–chlorine bonds. The compounds included some complexes of phosphorus trichloride with transition metals as well as some alkyl derivatives of thiophosphoryl chloride and phosphorus trichloride.

Les spectres de résonance quadrupolaire nucléaire du chlore ont été observés pour plusieurs composés contenant des liaisons phosphore–chlore. Ces composés incluent certains complexes du trichlorure de phosphore avec des métaux de transition ainsi que certains dérivés alkylés du chlorure de thiophosphoryle et du trichlorure de phosphore.

Canadian Journal of Chemistry, **49**, 3910 (1971)

There have been several previous reports of nuclear quadrupole resonance (n.q.r.) spectra of phosphorus–chlorine derivatives (1–9). Yet, though trivalent phosphorus halides form many complexes with transition metals there have been no previous reports of their chlorine n.q.r. spectra. We have begun a study of these, and report here the measurement of the resonances of two, namely tetrakis(trichlorophosphine)nickel, $Ni(PCl_3)_4$, and *fac*-tris(trichlorophosphine)tricarbonylmolybdenum, $Mo(CO)_3(PCl_3)_3$. We report also some further measurements of the n.q.r. spectra of compounds having general formulae $RPCl_2$ and $RPSCl_2$.

Experimental Methods

Nuclear quadrupole resonance spectra were observed using an externally quenched superregenerative spectrometer constructed in this Department. Its circuit was similar to that of Smith and Tong (10). Provision was made to permit independent variation of both pulse

Can. J. Chem. Downloaded from www.nrcresearchpress.com by 210.87.254.5 on 09/05/12
For personal use only.

Can. J. Chem. Downloaded from www.nrcresearchpress.com by 210.87.254.5 on 09/05/12
For personal use only.

length and quench frequency, the latter in the range 13–40 kHz. The carrier frequency could be swept electronically, in which case resonances were displayed on an oscilloscope, or mechanically, allowing chart presentation of resonances; in the latter case square wave Zeeman modulation at 34 Hz was used. Rough measurement of a resonance frequency (to about 50 kHz) was made by counting the oscillator, unquenched, with a Hewlett–Packard 5246L frequency counter. When resonances were strong enough to be observed on the oscilloscope accurate measurements (to between 0.5 and 5 kHz, depending on the resonance line width) were made by beating the signal from the superregenerative oscillator with that of a General Radio 1211-C oscillator, superimposing the zero beat on the resonance line, and measuring the frequency of the 1211-C oscillator with the frequency counter. Samples were cooled to a particular low temperature by immersing sample and sample coil in an appropriate bath.

Tetrakis(trichlorophosphine)nickel was prepared by the reaction of nickel carbonyl with phosphorus trichloride and was recrystallized from petroleum ether (11); its purity was checked using its Raman spectrum (12). *fac*-Tris(trichlorophosphine)tricarbonylmolybdenum was prepared by reacting h^5-cycloheptatrienetricarbonylmolybdenum, $Mo(C_7H_8)(CO)_3$, with phosphorus trichloride. The product was recrystallized from petroleum ether (13) and its purity was established from its infrared spectrum (14). Methylphosphonous dichloride, ethylphosphonous dichloride, methylphosphonothioic dichloride, and ethylphosphonothioic dichloride were all obtained from the Ethyl Corporation and used without further purification; their n.m.r. spectra were used to check their purity. The spectra of all compounds studied were obtained at 77 °K; for these measurements approximately 5 g of sample were sealed under vacuum in a glass vial. The spectrum of tetrakis(trichlorophosphine)nickel was also observed at room temperature. However, since this complex tends to decompose rather rapidly under vacuum at this temperature, the sample was sealed in the vial under nitrogen at atmospheric pressure.

Results and Discussion

In Table 1 are given the ^{35}Cl resonance frequencies measured in the present investigation, together with those of some related compounds. The frequencies for both transition metal complexes are very similar and are about 2 MHz higher than that of phosphorus trichloride but somewhat lower than those of phosphoryl chloride and thiophosphoryl chloride. Both complexes show a complicated group of lines; the magnitudes of the line separations ($\sim$0.1 MHz) suggest that the groups are due to chlorine atoms in different environments in the crystal, rather than to chemically inequivalent chlorine atoms. The resonance frequency of tetrakis(trichlorophosphine)nickel decreases by 0.5 MHz between 77 °K and room temperature, giving an approximate temperature coefficient of − 2.33 kHz/deg.

The measured molecular quadrupole coupling constants can be approximately related to that of the chlorine atom by the following relationship (15)

$$[1] \qquad eQq(\text{mol}) = (1 - s + d - I - \pi)\, eQq(\text{atom})$$

Here s and d are the degree of s- and d-hybridization of chlorine; I and π are the ionic character and pi character of the P—Cl bond. Also eQq(mol) = $-2 \times$ resonance frequency and eQq(atom) = -109.7 MHz. The internuclear parameters of tetrakis(trichlorophosphine)nickel and *fac*-tris(trichlorophosphine)tricarbonylmolybdenum have not been determined. Those of phosphorus trichloride, phosphoryl chloride, and thiophosphoryl chloride are all known (16), however, to have similar PCl_3 lengths and angles, with the P—Cl length very near the sum of the single bond radii. There is little reason to believe that the PCl_3 moieties in the complex would have a different structure. Thus s and d are expected to be essentially constant for all five compounds and π is probably very small, so that differences in the coupling constants, and hence the resonance frequencies, would be expected to reflect chiefly differences in ionic character of the PCl bond. Now, both complexes, as well as $OPCl_3$ and $SPCl_3$, have higher resonance frequencies than PCl_3, implying that their PCl bonds have evidently lower ionic character. This can be rationalized by noting that in formal terms the lone pair of electrons originally on phosphorus in PCl_3 is withdrawn toward the metal (or O or S) to form a dative bond. This in turn is reflected by withdrawal of σ-electron density from chlorine, and hence the decrease in ionic character.

The newly determined resonance frequencies of some organophosphorus compounds are also given in Table 1. Our values for methylphosphonous dichloride, CH_3PCl_2, are in good agreement with the earlier ones, whereas for ethylphosphonous dichloride, $C_2H_5PCl_2$, the agreement is poorer. The central line of the latter compound is actually a strong doublet, somewhat in disagreement with earlier work; however the spectrum showed a weak line at 25.93 MHz and probably a fourth at 25.75 MHz, in agreement with previous observations. For methylphosphonothioic dichloride, CH_3PSCl_2, the previously observed broad signal at 27.6 MHz was not found, but was replaced by a single strong line 27.859

TABLE 1. ^{35}Cl nuclear quadrupole resonance frequencies of some phosphorus–chlorine derivatives

Compound	Temperature (°K)	Resonance frequency (MHz) Present work	Earlier work (8)
PCl_3	77	—	26.104
			26.208
$Ni(PCl_3)_4$	77	27.98*	—
	295	27.47*	—
fac-$Mo(PCl_3)_3(CO)_3$	77	28.22†	—
$OPCl_3$	77	—	28.930
			28.975
$SPCl_3$	77	—	29.675
			29.800
CH_3PCl_2	77	26.078±0.001	26.078
		26.117±0.003	26.123
$C_2H_5PCl_2$	77	25.75 ±0.03	25.740
		25.826±0.005	25.805
		25.862±0.005	
		25.93 ±0.03	25.940
CH_3PSCl_2	77	27.859±0.003	27.6
$C_2H_5PSCl_2$	77	27.534±0.005	—
		27.577±0.005	
$(CH_3)_2PSCl$	77	—	26.055
$(C_2H_5)_2PSCl$	77	—	25.35
$(CH_3)(C_2H_5)PSCl$	77	—	25.85

*Frequency given is the mean of a complex band of width 0.25 MHz.
†Frequency given is the mean of a complex band of width 0.40 MHz.

MHz; evidently the crystals studied in the present work were somewhat better formed, with the chlorine atoms all in one lattice site. The magnitude of the splitting of the doublet spectrum of ethylphosphonothioic dichloride, $C_2H_5PSCl_2$, suggests that the chlorine atoms occupy two different lattice sites.

Our data confirm the report (8) that linear relationships exist between the frequencies of the alkyl derivatives of thiophosphonyl chloride, but not those of phosphorus trichloride. The relationships are

$$[2] \quad \nu(RPSCl_2) = (1/2)[\nu(R_2PSCl) + \nu(PSCl_3)]$$

$$[3] \quad \nu(RR'PSCl) = \nu(PSCl_3) - \Delta\nu(R) - \Delta\nu(R')$$

Thus from eq. 2 the frequency of the dichloroalkyl derivative is the mean of those of the trichloro and dialkylmonochloro derivative. Combination of our data with those previously published improves the validity of the relationship to the extent that it holds to within 50 kHz for both alkyl groups studied here. Equation 3 implies further that substitution of a particular alkyl group will always cause the same frequency change. Our data, combined with the earlier results, yield improved values of $\Delta\nu(CH_3) = 1.80$ MHz and $\Delta\nu(C_2H_5) = 2.14$ MHz. Table 1 shows that the frequencies of all possible methyl and ethyl derivatives can now be predicted to within 150 kHz, well within the variations expected from crystal lattice effects.

We are indebted to Mr. J. Sallos and Mr. M. Hatton for invaluable assistance and advice in the construction of the nuclear quadrupole resonance spectrometer.

We acknowledge gratefully the support of the National Research Council of Canada in the form of research grants.

1. S. NEGITA and S. SATOU. J. Chem. Phys. **24**, 621 (1956).
2. S. NEGITA and S. SATOU. Bull. Chem. Soc. Japan, **29**, 426 (1956).
3. M. A. WHITEHEAD. Can. J. Chem. **42**, 1212 (1964).
4. M. KAPLANSKY and M. A. WHITEHEAD. Can. J. Chem. **45**, 1669 (1967).
5. H. CHIHARA, N. NAKAMURA, and S. SEKI. Bull. Chem. Soc. Japan, **40**, 50 (1967).
6. R. R. HOLMES, R. P. CARTER, and G. E. PETERSON. Inorg. Chem. **3**, 1748 (1964).
7. E. A. C. LUCKEN and M. A. WHITEHEAD. J. Chem. Soc. 2459 (1961).
8. G. K. SEMIN and T. A. BABUSHKINA. Teor. Eksp. Khim. **4**, 835 (1968).
9. M. T. ROGERS and J. A. RYAN. J. Phys. Chem. **72**, 1340 (1968).

Can. J. Chem. Downloaded from www.nrcresearchpress.com by 210.87.254.5 on 09/05/12
For personal use only.

10. J. A. S. SMITH and D. A. TONG. J. Sci. Instr. ser. 2, **1**, 8 (1968).
11. J. W. IRVINE, JR. and G. WILKINSON. Science, **113**, 742 (1951).
12. H. G. M. EDWARDS and L. A. WOODWARD. Spectrochim. Acta, **26A**, 1077 (1970).
13. E. W. ABEL, M. A. BENNETT, and G. WILKINSON. J. Chem. Soc. 2323 (1959).
14. D. BENLIAN and M. BIGORGNE. Bull. Soc. Chim. Fr. **11**, 4106 (1967).
15. T. P. DAS and E. L. HAHN. Nuclear quadrupole resonance spectroscopy. Academic Press, New York. 1958.
16. T. MORITANI, K. KUCHITSU, and Y. MORINO. Inorg. Chem. **10**, 344 (1971).

Can. J. Chem. Downloaded from www.nrcresearchpress.com by 210.87.254.5 on 09/05/12
For personal use only.

OH···π Bond Enthalpy for the Phenol–Benzene Complex

DONALD BLOSER, JOSEPH MURPHY, AND J. N. SPENCER[1]
Department of Chemistry, Lebanon Valley College, Annville, Pennsylvania 17003

The OH···π hydrogen bond enthalpy for the phenol–benzene complex has been determined spectrophotometrically. Equilibrium constants for the hydrogen bonded complex are reported. The OH···π bond enthalpy was found to be -4.1 ± 0.5 kcal mol^{-1} and the entropy change -17 cal deg^{-1} mol^{-1}.

L'enthalpie de la liaison hydrogène OH···π a été déterminée par spectrophotométrie pour le complexe phénol-benzène. Les constantes d'équilibre du complexe sont rapportées. L'enthalpie de la liaison OH···π est de -4.1 ± 0.5 kcal mol^{-1} et le changement entropique de -17 cal deg^{-1} mol^{-1}.

Canadian Journal of Chemistry, **49**, 3913 (1971)

There are few spectral determinations of the magnitude of the intermolecular OH···π bond enthalpy reported in the literature. Szczepaniak and Falk (1) have determined the enthalpy difference between OH···CH_n and OH···π interactions for 2,6-diisopropyl-phenol and phenol in various solvents containing π electrons. For 2,6-diisopropyl-phenol in a 50% CCl_4–benzene mixture, the enthalpy difference between OH···CH and OH···π interactions was found to be -1.2 kcal mol^{-1}. These authors did not take into account the changes of integrated absorptivities with temperature. Powell and West (2) utilizing spectral measurements found ΔH^0 to be -1.56 kcal mol^{-1} for the OH···π bond between benzene and phenol in carbon tetrachloride solution. They further report $\Delta G_{298}{}^0$ to be 0.76 kcal mol^{-1} and ΔS^0 to be -7.8 cal deg^{-1} mol^{-1}. Murakami and Fujishiro (3) have determined OH···π enthalpies by calorimetric means and find for the system benzylalcohol–ethylbenzene–cyclohexane ΔH for the OH···π bond is -1.5 kcal mol^{-1}. For the *m*-cresol–*m*-xylene–cyclohexane system they find ΔH for the OH···π bond to be -3.1 kcal mol^{-1}. Rao, Murthy, and Bhat (4) using CNDO/2 calculations, find a theoretical OH···π enthalpy of -0.5 kcal mol^{-1}. If the equation found by Drago and Epley (5) relating OH···O and OH···N enthalpy changes and frequency shifts can be applied to OH···π systems, ΔH for the phenol–benzene adduct may be calculated to be -3.54 kcal mol^{-1} corresponding to the frequency shift for the adduct of 46 cm^{-1}. Oda, Yoshida, and Osawa (6) have reported spectrally determined free energy changes for the phenol–benzene system at 20 °C in CCl_4. However, these workers did not determine the free energy as a function of temperature and no enthalpy value could be found. The free energy change for unit concentration standard states found by these workers is 0.6 kcal mol^{-1} at 20 °C. These workers also report that a ΔH of -1.7 kcal mol^{-1} for the phenol–benzene complex was determined by Shimanouchi and Ikeda.

Experimental

Thiophene free reagent grade benzene was washed with sulfuric acid, followed by washings with water and dilute sodium hydroxide solution. After drying, benzene was

[1]To whom all correspondence should be addressed.

10. J. A. S. SMITH and D. A. TONG. J. Sci. Instr. ser. 2, **1**, 8 (1968).
11. J. W. IRVINE, JR. and G. WILKINSON. Science, **113**, 742 (1951).
12. H. G. M. EDWARDS and L. A. WOODWARD. Spectrochim. Acta, **26A**, 1077 (1970).
13. E. W. ABEL, M. A. BENNETT, and G. WILKINSON. J. Chem. Soc. 2323 (1959).
14. D. BENLIAN and M. BIGORGNE. Bull. Soc. Chim. Fr. **11**, 4106 (1967).
15. T. P. DAS and E. L. HAHN. Nuclear quadrupole resonance spectroscopy. Academic Press, New York. 1958.
16. T. MORITANI, K. KUCHITSU, and Y. MORINO. Inorg. Chem. **10**, 344 (1971).

Can. J. Chem. Downloaded from www.nrcresearchpress.com by 210.87.254.105 on 09/05/12
For personal use only.

OH···π Bond Enthalpy for the Phenol–Benzene Complex

DONALD BLOSER, JOSEPH MURPHY, AND J. N. SPENCER[1]
Department of Chemistry, Lebanon Valley College, Annville, Pennsylvania 17003

The OH···π hydrogen bond enthalpy for the phenol–benzene complex has been determined spectrophotometrically. Equilibrium constants for the hydrogen bonded complex are reported. The OH···π bond enthalpy was found to be -4.1 ± 0.5 kcal mol^{-1} and the entropy change -17 cal deg^{-1} mol^{-1}.

L'enthalpie de la liaison hydrogène OH···π a été déterminée par spectrophotométrie pour le complexe phénol-benzène. Les constantes d'équilibre du complexe sont rapportées. L'enthalpie de la liaison OH···π est de -4.1 ± 0.5 kcal mol^{-1} et le changement entropique de -17 cal deg^{-1} mol^{-1}.

Canadian Journal of Chemistry, **49**, 3913 (1971)

There are few spectral determinations of the magnitude of the intermolecular OH···π bond enthalpy reported in the literature. Szczepaniak and Falk (1) have determined the enthalpy difference between OH···CH_n and OH···π interactions for 2,6-diisopropyl-phenol and phenol in various solvents containing π electrons. For 2,6-diisopropyl-phenol in a 50% CCl_4–benzene mixture, the enthalpy difference between OH···CH and OH···π interactions was found to be -1.2 kcal mol^{-1}. These authors did not take into account the changes of integrated absorptivities with temperature. Powell and West (2) utilizing spectral measurements found ΔH^0 to be -1.56 kcal mol^{-1} for the OH···π bond between benzene and phenol in carbon tetrachloride solution. They further report $\Delta G_{298}{}^0$ to be 0.76 kcal mol^{-1} and ΔS^0 to be -7.8 cal deg^{-1} mol^{-1}. Murakami and Fujishiro (3) have determined OH···π enthalpies by calorimetric means and find for the system benzylalcohol–ethylbenzene–cyclohexane ΔH for the OH···π bond is -1.5 kcal mol^{-1}. For the *m*-cresol–*m*-xylene–cyclohexane system they find ΔH for the OH···π bond to be -3.1 kcal mol^{-1}. Rao, Murthy, and Bhat (4) using CNDO/2 calculations, find a theoretical OH···π enthalpy of -0.5 kcal mol^{-1}. If the equation found by Drago and Epley (5) relating OH···O and OH···N enthalpy changes and frequency shifts can be applied to OH···π systems, ΔH for the phenol–benzene adduct may be calculated to be -3.54 kcal mol^{-1} corresponding to the frequency shift for the adduct of 46 cm^{-1}. Oda, Yoshida, and Osawa (6) have reported spectrally determined free energy changes for the phenol–benzene system at 20 °C in CCl_4. However, these workers did not determine the free energy as a function of temperature and no enthalpy value could be found. The free energy change for unit concentration standard states found by these workers is 0.6 kcal mol^{-1} at 20 °C. These workers also report that a ΔH of -1.7 kcal mol^{-1} for the phenol–benzene complex was determined by Shimanouchi and Ikeda.

Experimental

Thiophene free reagent grade benzene was washed with sulfuric acid, followed by washings with water and dilute sodium hydroxide solution. After drying, benzene was

[1]To whom all correspondence should be addressed.

TABLE 1. Thermodynamic properties of the OH···π bond for the phenol–benzene complex

t (°C)	ε (l mol^{-1} cm^{-1})*	K†	ΔG^0 (kcal mol^{-1})	$\Delta S_{293}{}^0$ (cal deg^{-1} mol^{-1})	ΔH^0‡ (kcal mol^{-1})
20	210	0.18	0.99	−17	−4.1±0.5
30	206	0.14	1.2		
40	200	0.12	1.3		
50	191	0.085	1.6		
60	187	0.080	1.7		

*Molar absorptivity data from ref. 7.
†The standard state is unit molarity.
‡The error reported is that obtained from the error in the least square slope of the plot of Fig. 1.

refluxed over LiAlH and fractionally distilled onto activated molecular sieves. The final distillation of benzene was carried out under a dry nitrogen atmosphere. The refractive index and boiling point were used as purity criteria.

Reagent grade carbon tetrachloride was refluxed over sodium hydroxide pellets and fractionally distilled onto P_2O_5, and after drying was fractionally distilled under dry nitrogen atmosphere. A chromatogram taken before and after purification showed the procedure eliminated major impurities. Refractive index and boiling point were used as criteria for purity.

Reagent grade phenol was fractionally distilled in a three foot spinning band column under reduced pressure. The middle cut of the distillate was taken. All reagents were stored in a dry atmosphere.

All spectra were recorded on the Beckmann DK-2A recording spectrophotometer using 1 cm Teflon stoppered cells. The fundamental hydroxyl stretching frequency, 3610 cm^{-1} was used for all measurements. The solvent was carbon tetrachloride and a mixture of benzene and carbon tetrachloride served as reference. The phenol concentrations ranged from 0.003 to 0.005 M and that of benzene was 2 M in all cases. The temperature of the system was controlled to within ±1 °C with the Beckmann temperature regulator. Corrections for the change in concentrations with temperature were made by determining the density of 2 M benzene – carbon tetrachloride mixtures over the temperature range of this work. A pycnometer was used for density determinations. The densities found were 1.4876, 1.4686, 1.4495, 1.4303, and 1.4112 g ml^{-1} at 20, 30, 40, 50, and 60 °C, respectively. It was found that at the benzene concentrations used in this study, the spectral slit opened appreciably over the wavelength range of interest. Thus the extinction coefficients determined for phenol in carbon tetrachloride could not be used as a measure of the free phenol present in the ternary solution when using the absorbance mode of the DK-2A. The opening of the slit causes the peak to broaden and hence the peak absorptivity decreases. Spectra of mixtures of phenol in 2 M cyclohexane – carbon tetrachloride showed considerably different peak absorbancies from phenol spectra in CCl_4. Cyclohexane was used because its transmission in this spectral region is similar to that of benzene yet cyclohexane does not bond to phenol. Thus the DK-2A was run as a single beam instrument operated on the energy mode using manual slits. When the energy mode was used, phenol–cyclohexane – carbon tetrachloride solutions were found to have the same molar absorptivities as solutions of phenol in CCl_4.

The equilibrium constants reported are the average of a maximum of 11 determinations at 20 °C and a minimum of six determinations at 60 °C. The concentration of free phenol in the equilibrium mixture was found by using Beer's law and the temperature dependent molar absorptivities reported previously (7). The concentration of the complex was found by subtracting the free phenol concentration from the analytical concentration of phenol.

Results

The pertinent thermodynamic information and the molar absorptivity for the hydroxyl stretch of phenol is given in Table 1 and the plot log K_c *vs.* $1/T$ is shown in Fig. 1.

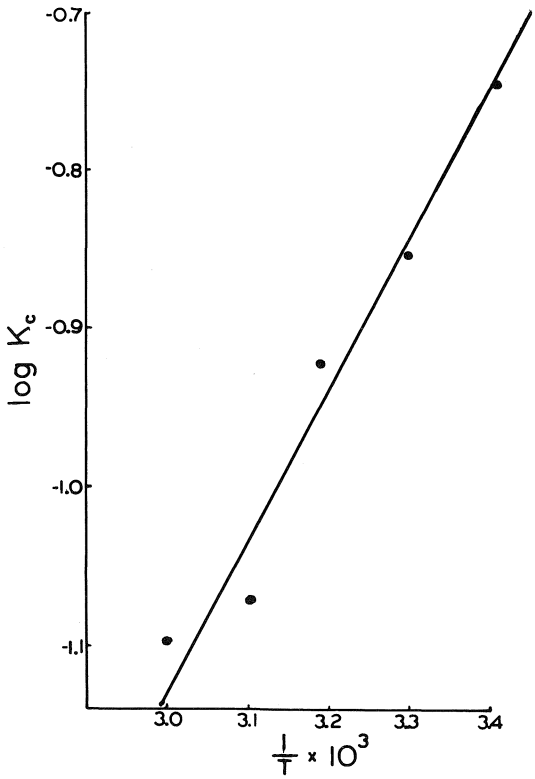

FIG. 1. Plot of log K_c *vs.* $1/T$.

Can. J. Chem. Downloaded from www.nrcresearchpress.com by 210.87.254.105 on 09/05/12
For personal use only.

The enthalpy change for the formation of the phenol–benzene OH···π bond of −4.1 kcal is larger than that previously reported (2, 6) and larger in general than the OH···π enthalpies reported for other systems. For the spectrophotometrically determined enthalpy, the discrepancy could arise from improper accounting of the effect of the temperature dependence of the molar absorptivity or neglect of the effect of changing slit width. Neglect of either of these factors could lead to apparently high free energy changes and low enthalpy changes.

The results of this work suggest that benzene is not a weak base for hydrogen bonding. Recent studies have shown that benzene is a sufficiently strong base to cause disruption of the intramolecular hydrogen bond in catechol, guaiacol, and sym-trichlorophenol (7).

1. K. Szczepaniak and M. Falk. Spectrochim. Acta, **26A**, 883 (1970).
2. D. L. Powell and R. West. Spectrochim. Acta, **20**, 983 (1964).
3. S. Murakami and R. Fujishiro. Bull. Chem. Soc. Jap. **40**, 1784 (1967).
4. A. S. N. Murthy, S. N. Bhat, and C. N. R. Rao. J. Chem. Soc. A, 1251 (1970).
5. R. S. Drago and T. D. Epley. J. Am. Chem. Soc. **91**, 2883 (1969).
6. Ryohei Oda, Zen-ichi Yoshida, and Eiji Osawa. Proc. Intern. Symp. Mol. Struct. Spectry. Tokyo. 1962. D 118/1.
7. E. A. Robinson, H. D. Schreiber, and J. N. Spencer. J. Phys. Chem. **75**, 2219 (1971).

Master Equation for the Dissociation of a Dilute Diatomic Gas. V. Effect of Energy-level Spacing

D. L. S. McElwain and H. O. Pritchard
Centre for Research in Experimental Space Science, York University, Downsview, Ontario

Received June 7, 1971

Our previous vibration–dissociation coupling calculations for H_2 have been repeated for D_2. Closer spacing of the vibrational energy levels in D_2 leads to increased translation–vibration transition probabilities, and the effect of this is to increase the rate of recombination by the vibrational mechanism at all temperatures. These numerical experiments also clarify two other issues: (*i*) that the position of the bottleneck does not necessarily occur at that level above which *direct* collisional dissociation can take place rapidly, and (*ii*) that there is no simple correspondence between the position of the bottleneck and the Arrhenius temperature coefficient for dissociation.

Nos calculs antérieurs de couplage vibration–dissociation pour H_2 ont été répétés pour D_2. L'espacement plus rapproché des niveaux d'énergie vibrationnelle dans D_2 conduit à un accroissement des probabilités de transition translation–vibration. Ceci a pour effet d'accroître la vitesse de recombinaison par le mécanisme vibrationnel à toutes les températures. Ces expériences numériques clarifient également deux autres issues (*i*) que la position du "bottleneck" n'arrive pas nécessairement à ce niveau au-dessus duquel la dissociation par collision *directe* peut avoir lieu rapidement et (*ii*) qu'il n'y a pas de correspondance simple entre la position du "bottleneck" et le coefficient de température d'Arrhénius pour la dissociation.

Canadian Journal of Chemistry, **49**, 3915 (1971)

In part III of this series (1),[1] the vibration–dissociation coupling relaxation equations were solved for H_2 at a series of temperatures, using a set of T–V transition probabilities given by eq. III (1). This equation gives an approximate prescription for the behavior of these transition probabilities as a function of the temperature and the energy gap between the levels; mass effects, except in-so-far as they enter through the diatomic vibrational characteristics, are ignored. A major drawback in our previous work, using H_2 as a model for the description of the dissociation of the general diatomic molecule, is that the vibrational energy level distribution is too sparse;

[1]Reference should be made to this and earlier papers for a full description of the details of these calculations.

Can. J. Chem. Downloaded from www.nrcresearchpress.com by 210.87.254.105 on 09/05/12
For personal use only.

The enthalpy change for the formation of the phenol–benzene OH···π bond of −4.1 kcal is larger than that previously reported (2, 6) and larger in general than the OH···π enthalpies reported for other systems. For the spectrophotometrically determined enthalpy, the discrepancy could arise from improper accounting of the effect of the temperature dependence of the molar absorptivity or neglect of the effect of changing slit width. Neglect of either of these factors could lead to apparently high free energy changes and low enthalpy changes.

The results of this work suggest that benzene is not a weak base for hydrogen bonding. Recent studies have shown that benzene is a sufficiently strong base to cause disruption of the intramolecular hydrogen bond in catechol, guaiacol, and sym-trichlorophenol (7).

1. K. Szczepaniak and M. Falk. Spectrochim. Acta, **26A**, 883 (1970).
2. D. L. Powell and R. West. Spectrochim. Acta, **20**, 983 (1964).
3. S. Murakami and R. Fujishiro. Bull. Chem. Soc. Jap. **40**, 1784 (1967).
4. A. S. N. Murthy, S. N. Bhat, and C. N. R. Rao. J. Chem. Soc. A, 1251 (1970).
5. R. S. Drago and T. D. Epley. J. Am. Chem. Soc. **91**, 2883 (1969).
6. Ryohei Oda, Zen-ichi Yoshida, and Eiji Osawa. Proc. Intern. Symp. Mol. Struct. Spectry. Tokyo. 1962. D 118/1.
7. E. A. Robinson, H. D. Schreiber, and J. N. Spencer. J. Phys. Chem. **75**, 2219 (1971).

Can. J. Chem. Downloaded from www.nrcresearchpress.com by 210.87.254.6 on 09/05/12
For personal use only.

Master Equation for the Dissociation of a Dilute Diatomic Gas. V. Effect of Energy-level Spacing

D. L. S. McElwain and H. O. Pritchard
Centre for Research in Experimental Space Science, York University, Downsview, Ontario

Received June 7, 1971

Our previous vibration–dissociation coupling calculations for H_2 have been repeated for D_2. Closer spacing of the vibrational energy levels in D_2 leads to increased translation–vibration transition probabilities, and the effect of this is to increase the rate of recombination by the vibrational mechanism at all temperatures. These numerical experiments also clarify two other issues: (*i*) that the position of the bottleneck does not necessarily occur at that level above which *direct* collisional dissociation can take place rapidly, and (*ii*) that there is no simple correspondence between the position of the bottleneck and the Arrhenius temperature coefficient for dissociation.

Nos calculs antérieurs de couplage vibration–dissociation pour H_2 ont été répétés pour D_2. L'espacement plus rapproché des niveaux d'énergie vibrationnelle dans D_2 conduit à un accroissement des probabilités de transition translation–vibration. Ceci a pour effet d'accroître la vitesse de recombinaison par le mécanisme vibrationnel à toutes les températures. Ces expériences numériques clarifient également deux autres issues (*i*) que la position du "bottleneck" n'arrive pas nécessairement à ce niveau au-dessus duquel la dissociation par collision *directe* peut avoir lieu rapidement et (*ii*) qu'il n'y a pas de correspondance simple entre la position du "bottleneck" et le coefficient de température d'Arrhénius pour la dissociation.

Canadian Journal of Chemistry, **49**, 3915 (1971)

In part III of this series (1),[1] the vibration–dissociation coupling relaxation equations were solved for H_2 at a series of temperatures, using a set of T–V transition probabilities given by eq. III (1). This equation gives an approximate prescription for the behavior of these transition probabilities as a function of the temperature and the energy gap between the levels; mass effects, except in-so-far as they enter through the diatomic vibrational characteristics, are ignored. A major drawback in our previous work, using H_2 as a model for the description of the dissociation of the general diatomic molecule, is that the vibrational energy level distribution is too sparse;

[1]Reference should be made to this and earlier papers for a full description of the details of these calculations.

molecules of interest have many more vibrational levels, and in this calculation we try to explore the likely effect of reducing the vibrational spacing[2] by repeating these calculations for D_2 which has 22 bound vibrational levels in the ground state (2) instead of the 15 in H_2.

The general pattern of behavior for D_2 at 2000 °K was very similar to that already described for H_2 at 2000 °K: an initial transient period lasting of the order of τ_{01}, the vibrational relaxation time, followed by a pseudo-steady period in which the states $v = 0$–11 were overpopulated and $v = 12$–21 were underpopulated; further, that the phenomenological rate constant and the smallest non-zero eigenvalue were related by the equation

$$d_{n-1} = -[\mathrm{M}]k_{\mathrm{d,M}}$$

as before (1). The changeover from over- to under-population occurring at $v = 11$ in D_2 is about 10 200 cm^{-1} below the dissociation limit, in contrast to the changeover at $v = 9$ in H_2, only 7000 cm^{-1} below the limit; thus it seems that, to the extent that this changeover is an indication of the presence of a bottleneck (1), the bottleneck is lower down in D_2 than in H_2. Consequently, we investigated the position of the bottleneck using our criterion (1, 3) of finding the nearest-neighbor transition to which the dissociation rate is the most sensitive. This is illustrated in Table 1, placing the bottleneck at the transition $v = 15 \leftrightarrow 16$, about 5400 cm^{-1} below the dissociation limit. In H_2, the bottleneck appeared (1, 3) to be at the transition $v = 11 \leftrightarrow 12$, about 3200 cm^{-1} below the dissociation limit, and Bauer observed (4) that this could have been due to the fact that the specific rates for direct dissociation were only significant for levels $v = 12$, 13, and 14. Since the transition probabilities used in the present calculation have the same dependence on the energy separation, the D_2 results show that the position of the bottleneck is not determined solely by whether or not there is a rapid direct dissociation channel from the levels concerned; the position of the bottleneck is determined co-operatively by much more complex factors, as we have already described (3).

[2]The wider issue of the interleaving of these vibrational states by rotational substates presents a much more severe computational problem, and work on the general rotation vibration–dissociation problem is in progress; however, at shock-tube temperatures, it is generally held that only vibration–dissociation coupling need be considered.

TABLE 1. Characterization of the bottleneck by perturbation of nearest neighbor transition probabilities. Data refer to D_2 at 2000 °K, where the standard set of transition probabilities gives $-100\,d_{n-1} = 5.757$; in this table, each transition in turn is decreased by a factor of 100

Perturbed transition	$-100\,d_{n-1}$
$7 \leftrightarrow 8$	5.737
$8 \leftrightarrow 9$	5.698
$9 \leftrightarrow 10$	5.605
$10 \leftrightarrow 11$	5.413
$11 \leftrightarrow 12$	5.087
$12 \leftrightarrow 13$	4.646
$13 \leftrightarrow 14$	4.190
$14 \leftrightarrow 15$	3.862
$15 \leftrightarrow 16$	3.804
$16 \leftrightarrow 17$	4.170
$17 \leftrightarrow 18$	4.950
$18 \leftrightarrow 19$	5.540
$19 \leftrightarrow 20$	5.717
$20 \leftrightarrow 21$	5.753

The rate of dissociation or recombination was determined as before (1) for three temperatures, 300, 1500, and 2000 °K, and the results are presented in Table 2. The following conclusions emerge.

(*i*) That at high temperatures, D_2 dissociates faster than does H_2, despite the fact that it has a slightly greater ΔE for dissociation (105.1 kcal/mol as opposed to 103.2 kcal/mol). This arises because the T–V transition probabilities fall off with increasing energy separation between the levels, and it is easier to make rapid progress in a lot of small jumps than in a few big ones; thus, as the spacings between the levels become infinitesimally small, the dissociation rate constant will approach a limit (5) of the order of a collision rate times the Boltzmann factor $\exp(-\Delta E/RT)$. Relatively few studies (6, 7) have been made on the rate of dissociation of D_2, and only in one case (7) have H_2 and D_2 been studied in the same shock tube: this was the work of Sutton, which covered the temperature range 2800–4500 °K. A relatively short extrapolation of his data to 2000 °K gives recombination rate constants for D_2 and H_2, respectively, as 4.0×10^{14} and 3.2×10^{14} mol^{-2} cm^6 s^{-1}, *i.e.* $k_r^{D_2}/k_r^{H_2} \approx 1.25$, with argon as third body. Thus, on the basis of the relatively scant evidence that exists, our conclusion that both the dissociation and recombination rates are faster for D_2 than for H_2 seems reasonable.

(*ii*) In contrast, our results for 300 °K are in direct conflict with a very substantial body of

Can. J. Chem. Downloaded from www.nrcresearchpress.com by 210.87.254.6 on 09/05/12
For personal use only.

TABLE 2. Comparison of dissociation and recombination rate constants for D_2 and H_2*

Parameter	Value at 300 °K	Value at 1500 °K	Value at 2000 °K	Unit
$K_c^{H_2}$	4.292×10^{-52}	1.630×10^{9}	9.610×10^{12}	molecules cm^{-3}
$K_c^{D_2}$	3.093×10^{-53}	1.140×10^{9}	8.173×10^{12}	molecules cm^{-3}
$K_c^{D_2}/K_c^{H_2}$	0.072	0.700	0.850	
$k_d^{H_2}$	(2.27×10^{-85})	2.516×10^{-25}	1.248×10^{-21}	molecule^{-1} cm^3 s^{-1}
$k_d^{D_2}$	(2.31×10^{-86})	2.918×10^{-25}	1.645×10^{-21}	molecule^{-1} cm^3 s^{-1}
$k_d^{D_2}/k_d^{H_2}$	0.10	1.16	1.32	
$k_r^{H_2}$	5.301×10^{-34}	1.544×10^{-34}	1.299×10^{-34}	molecule^{-2} cm^6 s^{-1}
$k_r^{D_2}$	7.469×10^{-34}	2.559×10^{-34}	2.013×10^{-34}	molecule^{-2} cm^6 s^{-1}
$k_r^{D_2}/k_r^{H_2}$	1.41	1.66	1.55	

*Values in parentheses are estimated values.

data (8–10) which shows unambiguously that H_2 recombines faster than does D_2 at 300 °K. It is believed (11, 12) that at these temperatures, recombination takes place by a rotational rather than a vibrational mechanism, and we hope to throw some light on this supposition in future work;[2] more instructive, however, would be a series of experiments between 300 and 2800 °K to detect the changeover in the ratio of $k_r^{D_2}/k_r^{H_2}$ from less-than to greater-than unity.

(*iii*) Comparison of the dissociation rates at 1500 and 2000 °K shows that the Arrhenius temperature coefficients for dissociation are D_2: 103.0 kcal/mol; H_2: 101.4 kcal/mol; *i.e.* in both cases approximately 2 kcal/mol below the spectroscopic dissociation energy. The idea that the observed Arrhenius temperature coefficient should give an indication of the position of the rate-determining step in the dissociation process has some supporters (1), but based on a visual criterion, the bottlenecks are placed at 76.0 and 83.3 kcal, respectively; alternatively, based on our criterion, such as is illustrated in Table 1, the bottlenecks are placed at 93.3 and 98.1 kcal, respectively. Clearly there is no correspondence between the Arrhenius temperature coefficient and the position of the bottleneck.

1. D. L. S. McElwain and H. O. Pritchard. Thirteenth Symposium (International) on Combustion. The Combustion Institute. 1971. p. 37.
2. W. Kolos and L. Wolniewicz. J. Chem. Phys. **43**, 2429 (1965).
3. E. Kamaratos and H. O. Pritchard. Can. J. Chem. **49**, 2617 (1971).
4. S. H. Bauer. Thirteenth Symposium (International) on Combustion. The Combustion Institute. 1971. p. 49.
5. E. Kamaratos and H. O. Pritchard. Unpublished results.
6. J. P. Rink. J. Chem. Phys. **36**, 1398 (1962).
7. E. A. Sutton. J. Chem. Phys. **36**, 2923 (1962).
8. F. S. Larkin. Can. J. Chem. **46**, 1005 (1968).
9. J. E. Bennett and D. R. Blackmore. J. Chem. Phys. **53**, 4400 (1970).
10. D. O. Ham, D. W. Trainor, and F. Kaufman. J. Chem. Phys. **53**, 4395 (1970).
11. R. E. Roberts, R. B. Bernstein, and C. F. Curtiss. J. Chem. Phys. **50**, 5163 (1969).
12. R. E. Roberts and R. B. Bernstein. Chem. Phys. Lett. **6**, 282 (1970).

Can. J. Chem. Downloaded from www.nrcresearchpress.com by 210.87.254.6 on 09/05/12
For personal use only.

Can. J. Chem. Downloaded from www.nrcresearchpress.com by 210.87.254.105 on 09/05/12
For personal use only.

Canadian Journal of Chemistry

Published by THE NATIONAL RESEARCH COUNCIL OF CANADA

VOLUME 49 DECEMBER 15, 1971 NUMBER 24

A Complex Ion Model for Molten Halides

A. D. PELTON[1]

Department of Metallurgy and Materials Science, University of Toronto, Toronto 181, Ontario

Received May 28, 1971

The formation of complex anions in molten halide systems is treated semi-quantitatively by a discrete complex anion model. The treatment is a more general application and extension of an approach reported previously by the author. By assuming the existence of discrete MY_4^{2-} tetrahalo complex anions, the model gives good agreement to experimental enthalpies and entropies of mixing and electrical conductivities in a large number of different halide systems of the general formula MY_2–AY, where M is a divalent metal, and A is an alkali. Very few adjustable parameters are required. The parameters provide semi-quantitative basicity (or acidity) scales by which molten salts and slags may be classified. The relationships of these basicity scales to ionic radii, ligand field stabilization energies, etc. are shown. General thermodynamic and mathematical aspects of the problem of complexing are discussed, particularly as regards the proper method of calculating the degree of dissociation of the complexes.

Nous avons traité de la formation d'anions complexes dans les systèmes d'halogénures fondus de façon semi-quantitative en utilisant un modèle discontinu d'anion complexe. Le traitement est une application plus générale et une extension d'une approche rapportée précédemment par l'auteur. En supposant l'existence d'anions complexes tétrahalo discontinus MY_4^{2-}, le modèle est en accord avec les enthalpies et les entropies de mélange expérimentales et les conductivités électriques pour un grand nombre de différents systèmes d'halogénures de formule générale MY_2–AY, où M est un métal divalent et A est un alcalin. Très peu de paramètres ajustables sont requis. Les paramètres fournissent des échelles semi-quantitatives de basicité (ou d'acidité) au moyen desquelles les sels fondus et les scories peuvent être classifiés. On montre les relations entre le rayon ionique, les énergies de stabilisation du champ de ligand, etc. et ces échelles de basicité. On discute aussi de la thermodynamique générale et des aspects mathématiques du problème de la formation de complexe, particulièrement en ce qui concerne la méthode appropriée pour calculer le degré de dissociation des complexes.

Canadian Journal of Chemistry, **49**, 3919 (1971)

Introduction

The concept of complex ion formation in molten salts and slags has been the subject of much recent interest. The halides, MY_2, of many divalent metals, for instance, appear to form tetrahedral anionic complexes, MY_4^{2-}, when dissolved in alkali halides. From phase diagram calculations, Lumsden (1) has shown that solutions of up to about 30 mol% of MCl_2 (where M = Mn, Mg, Fe, Zn) in KCl can be treated as ideal Temkin solutions of K^+ cations, Cl^- anions, and the complex anions MCl_4^{2-}; and similarly, solutions of up to about 20 mol% MF_2 (where M = Mn, Fe, Co, Ni, Zn, Mg, Be) in NaF can be treated as containing only Na^+, F^-, and MF_4^{2-} ions. This evidence of MY_4^{2-} anions from phase diagram calculations was first noted by Flood and Urnes (2) for the $MgCl_2$ – alkali chloride systems.

Kleppa and McCarty (3) measured enthalpies of mixing in the $MgCl_2$–ACl (where A = alkali) systems. Østvold (4) made e.m.f. measurements in these systems using glass membrane cells. By combining these data with the enthalpy data, he calculated entropies of mixing. These authors showed that their data gave evidence of tetrahedral $MgCl_4^{2-}$ complex anions. They also showed that as the alkali cation A^+ is changed

[1]Present address: Institut für theoretische Hüttenkundeder technische Universität, Clausthal-Zellerfeld, West Germany.

TABLE 1. Moles of ionic species per overall mole of solution

Ion	Complete complexing		Partial dissociation
	$X_{MY_2} \leqslant 1/3$	$X_{MY_2} \geqslant 1/3$	
M^{2+}	0	$X_{MY_2} - (2X_{MY_2} + X_{AY})/4$	$X_{MY_2}(1 - \alpha/2)$
A^+	X_{AY}	X_{AY}	X_{AY}
MY_4^{2-}	X_{MY_2}	$(2X_{MY_2} + X_{AY})/4$	$\alpha X_{MY_2}/2$
Y^-	$(X_{AY} - 2X_{MY_2})$	0	$X_{AY} + 2X_{MY_2}(1 - \alpha)$ $= (1 + X_{MY_2} - 2\alpha X_{MY_2})$
Total positive ions	X_{AY}	$(3 - X_{MY_2})/4$	$(1 - \alpha X_{MY_2}/2)$
Total negative ions	$(X_{AY} - X_{MY_2})$	$(2X_{MY_2} + X_{AY})/4$	$(1 + X_{MY_2} - 3\alpha X_{MY_2}/2)$

up the periodic table from Cs^+ to Li^+, there is apparently an increasing tendency for the complexes to dissociate into Mg^{2+} and Cl^- ions.

Pelton and Thompson (5) proposed a "discrete complex anion model", based upon the assumption of MY_4^{2-} complex anions, to account semi-quantitatively for the data in the $MgCl_2$–ACl systems. Recently, a great amount of new experimental data on halide systems of the general formulae MY_2–AY (where M = Mn, Fe, Ni, etc., and A = alkali) has become available. In the present publication, these new data will be discussed, and the applicability of the discrete complex anion model will be examined with regard to all presently available data. The basic premises of the model will also be discussed in more detail than previously (5).

A minimum of adjustable parameters is used in the model. It will be shown that these parameters provide semi-quantitative "basicity scales" for a variety of molten salts and slags. The relationship of these basicity scales to ionic radii, ligand field energies, etc. will be discussed.

Discrete Complex Anion Model, Complete Complexing

The limiting case of "complete complexing", in which dissociation of the complexes is not considered, will be discussed first. The assumption of complete complexing is, of course, thermodynamically incorrect since, as will become clear later, this assumption is inconsistent with the minimization of the free energy of the system. Partial dissociation of the complexes must occur to some greater or lesser degree. An initial examination of the simple limiting case of complete complexing will, however, make the basic physical ideas of the model much clearer than if a discussion of the complete model with partial dissociation were begun immediately.

For a molten system MY_2–AY, let X_{MY_2} and X_{AY} be the overall mole fractions of the two components. It is assumed that the only complex ions formed are the tetrahedral anions MY_4^{2-}. For $X_{MY_2} \leqslant 1/3$, and assuming complete complexing, all the M is complexed, and only the three ionic species A^+, Y^-, and MY_4^{2-} exist. The amounts of the various species in solution in this case are given in column 2 of Table 1. At $X_{MY_2} = 1/3$, only the two species A^+ and MY_4^{2-} exist, and this composition corresponds to the liquid "compound" A_2MY_4. For $X_{MY_2} \geqslant 1/3$, every M can be "complexed" only if the MY_4 tetrahedra share corners or edges through "Y-bridges". In the discrete complex anion model it is assumed that this does not happen. Discrete MY_4^{2-} anions form until all Y species are used up. The remaining M species are not preferentially bonded to any fixed number of Y's, and, for the purposes of statistical calculations, exist as independent M^{2+} cations. This assumption of two environments for an M species is taken to hold true for all compositions up to and including pure MY_2. One mole of pure MY_2, for the case of complete complexing, is considered to contain one half mole of M^{2+} cations and one half mole of MY_4^{2-} anions. This assumption will be examined later in the discussion on polymeric liquids.

The amounts of the various ionic species in solution for $X_{MY_2} \geqslant 1/3$ are given in column 3 of Table 1.

The solutions are assumed to be ideal Temkin (6) solutions of the cations A^+ and M^{2+} and of the anions Y^- and MY_4^{2-}. Of course, for the case of complete complexing, no more than three types of ions exist simultaneously.

Enthalpies

Consider the formation of a complex according to

[1] $$M^{2+} + 4Y^- \rightarrow MY_4^{2-}$$

Can. J. Chem. Downloaded from www.nrcresearchpress.com by 210.87.254.105 on 09/05/12
For personal use only.

Can. J. Chem. Downloaded from www.nrcresearchpress.com by 210.87.254.105 on 09/05/12
For personal use only.

Let the molar energy change for this process be b_1, and assume for the moment that b_1 is independent of concentration. An enthalpy of mixing term of the following form will then result due to the increase in the number of complexes which occurs when the pure components are mixed. (X_{MY_2} moles of pure MY_2 contain $X_{MY_2}/2$ moles of complexes.)

$$[2] \quad \Delta H = X_{MY_2} b_1 - \frac{X_{MY_2}}{2} b_1 = \frac{X_{MY_2}}{2} b_1 \qquad [X_{MY_2} \leqslant 1/3]$$

$$[3] \quad \Delta H = \left(\frac{2X_{MY_2} + X_{AY}}{4}\right) b_1 - \frac{X_{MY_2}}{2} b_1 = \frac{X_{AY}}{4} b_1 \qquad [X_{MY_2} \geqslant 1/3]$$

where ΔH is the molar enthalpy of mixing of X_{MY_2} moles of MY_2 and X_{AY} moles of AY. The resulting plot of ΔH *vs.* composition is shown as the upper curve in Fig. 1*a*, and is the form of a sharp peak, peaking at $X_{MY_2} = 1/3$, which is the "compound composition". This is, of course, the typical sort of curve expected for a system showing "compound formation".

The "interaction parameter" λ, defined as $\lambda = \Delta H / X_{MY_2} X_{AY}$, will have the general shape shown in Fig. 1*b*, with a pronounced "dip" at $X_{MY_2} = 1/3$ (taking b_1 to be negative).

In Figs. 2–7, the heavy lines are plots of λ for various chloride systems of the formulae MCl_2–ACl, (where A = alkali, and M = Co, Fe, Ni, Mn, Mg, Cd, Pb), as obtained calorimetrically by Papatheodorou and Kleppa (7–9), and McCarty and Kleppa (3, 10). These authors qualitatively explain the prominent dip at $X_{MCl_2} = 1/3$ in these systems along lines similar to that just discussed.

In any one of Figs. 2–7 it can be seen that for any set of systems MCl_2–ACl, λ becomes progressively less negative as A is changed up the periodic table from Cs to Li, and at the same time the dip at $X_{MY_2} = 1/3$ becomes progressively less prominent. This suggests, as discussed by McCarty and Kleppa (3, 10) and by Papatheodorou and Kleppa (7, 8), firstly that the complexes become weaker as A is changed from Cs to Li, and secondly that dissociation occurs in the less strongly complexed systems.

In the present model, the energy of formation of a complex may be taken to depend upon the environment in which it is formed. For the formation of complexes which are totally surrounded by M^{2+} cations (as in pure MY_2), let the molar energy of reaction 1 be Δe_1. For the formation of complexes which are totally surrounded by A^+ cations (as at infinite dilution in AY), let the molar energy change of reaction 1 be Δe_2. In the MCl_2–ACl systems, if A^+ is a large cation like Cs^+ with a low field strength and, therefore, good ligand donor properties, it would be expected that $\Delta e_2 < \Delta e_1$. If A^+ is a small cation like Li^+ with a high field strength, then Δe_2 would be much less negative, and could be approximately equal to or greater than Δe_1. For the general case, the energy of formation, Δe, of a mole of complex ions according to reaction 1 is taken to vary between Δe_1 and Δe_2 depending upon the cationic fractions, $N_{M^{2+}}$ and N_{A^+}, of the two cations in its first coordination shell. As a first approximation, a linear variation is assumed. That is

$$[4] \qquad \Delta e = (N_{M^{2+}} \Delta e_1 + N_{A^+} \Delta e_2)$$

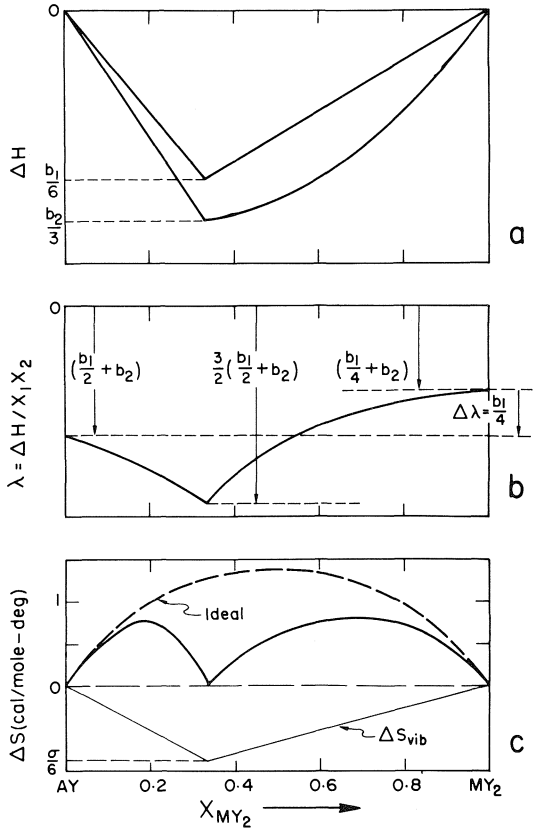

FIG. 1 (*a*) Enthalpies of mixing for complete complexing (eqs. 7 and 8). (*b*) Interaction parameter for discrete complex anion model for complete complexing. (*c*) Entropies of mixing for models.

Can. J. Chem. Downloaded from www.nrcresearchpress.com by 210.87.254.105 on 09/05/12
For personal use only.

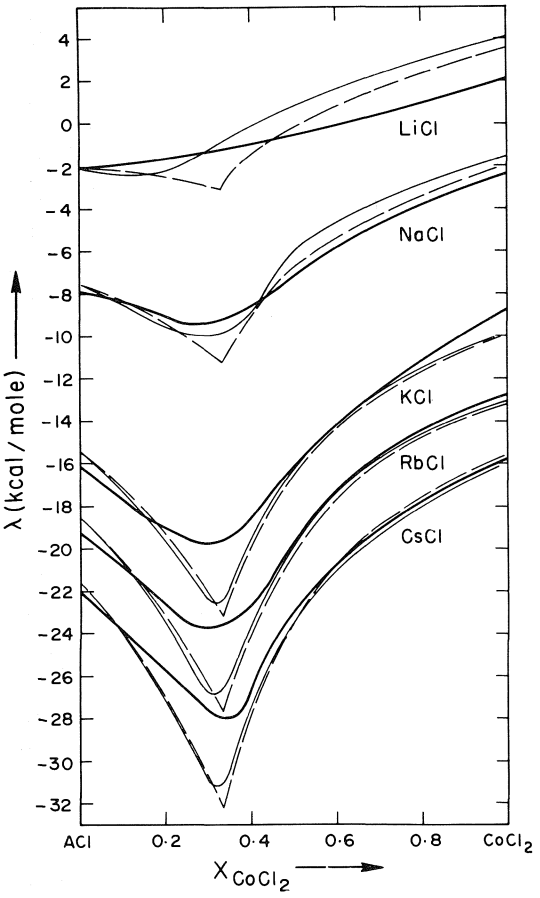

FIG. 2. Interaction parameters in $CoCl_2$–ACl systems ——— Experimental (8). - - - From model for complete complexing. ——— From model for partial dissociation.

Since the pressure–volume work of mixing is negligible, the molar enthalpy of mixing, ΔH, may be taken to be equal to the change in internal energy on mixing. Still under the assumption of complete complexing, that part of the enthalpy of mixing resulting from complex formation is now given by

$$[5]\quad \Delta H = X_{MY_2}\Delta e - \frac{X_{MY_2}}{2}\Delta e_1 \qquad [X_{MY_2} \leqslant 1/3]$$

$$[6]\quad \Delta H = \left(\frac{2X_{MY_2} + X_{AY}}{4}\right)\Delta e - \frac{X_{MY_2}}{2}\Delta e_1 \qquad [X_{MY_2} \geqslant 1/3]$$

where Δe is given by eq. 4. For $X_{MY_2} \leqslant 1/3$, $N_{A^+} = 1$, and $N_{M^{2+}} = 0$. For $X_{MY_2} \geqslant 1/3$, N_{A^+}

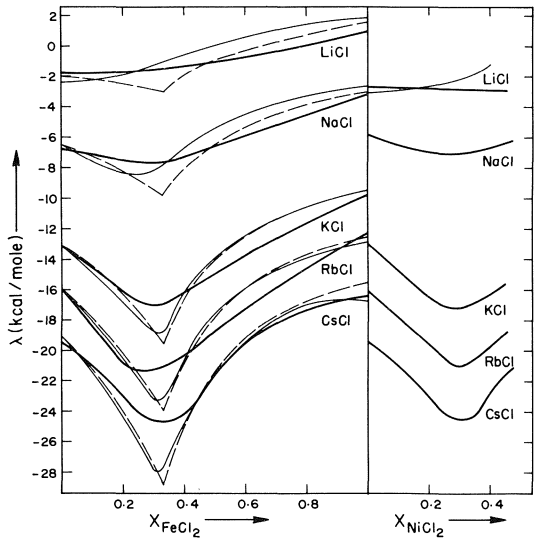

FIG. 3. Interaction parameters in $FeCl_2$–ACl and $NiCl_2$–ACl systems. ——— Experimental (7, 8). - - - From model for complete complexing. ——— From model for partial dissociation.

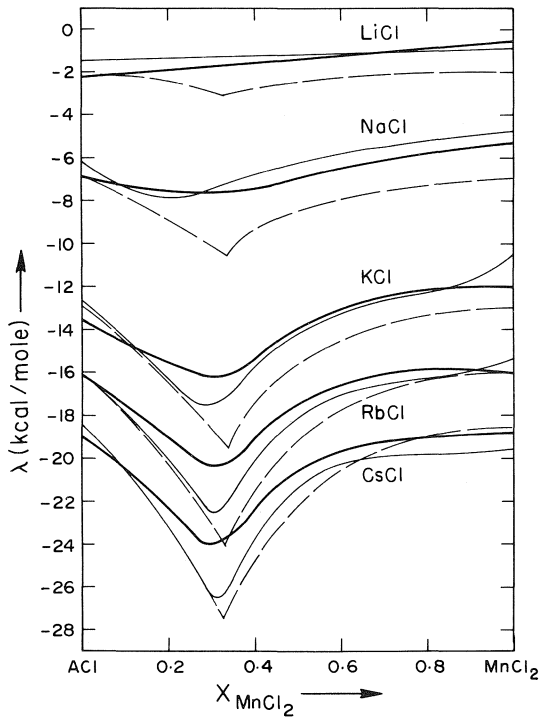

FIG. 4. Interaction parameters in $MnCl_2$–ACl systems. ——— Experimental (8). - - - From model for complete complexing. ——— From model for partial dissociation.

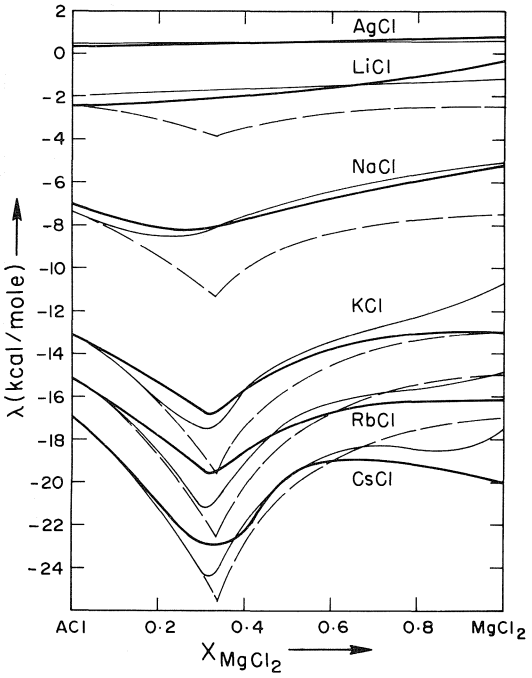

FIG. 5. Interaction parameters in $MgCl_2$–ACl systems. ——— Experimental (3). - - - From model for complete complexing. ——— From model for partial dissociation.

$= 4X_{AY}/(3 - X_{MY_2})$, and $N_{M^{2+}} = (1 - N_{A^+})$ (see Table 1). Making the substitutions in eqs. 5 and 6 and simplifying, the following equations for the case of complete complexing result

$$[7] \quad \Delta H = \frac{X_{MY_2}}{2} b_1 + X_{MY_2} b_2 \qquad [X_{MY_2} \leqslant 1/3]$$

$$[8] \quad \Delta H = \frac{X_{AY}}{4} b_1 + \frac{X_{AY}(1 + X_{MY_2})}{(3 - X_{MY_2})} b_2 \qquad [X_{MY_2} \geqslant 1/3]$$

where b_1 and b_2 are defined as

$$[9] \quad b_1 = \Delta e_1$$

$$[10] \quad b_2 = (\Delta e_2 - \Delta e_1)$$

The parameter b_1 is independent of concentration, and is a property only of the salt MY_2. It is independent of the particular MY_2–AY system. The parameter b_2 has one concentration-independent value for each MY_2–AY system. The first terms in eqs. 7 and 8 are the same as eqs. 2 and 3. The final terms in eqs. 7 and 8 give the strengthening (or weakening) effect of the A^+ ions on the complexes, and these terms are shown as the lower curve in Fig. 1*a* (b_2 is taken to be negative in Fig. 1*a*).

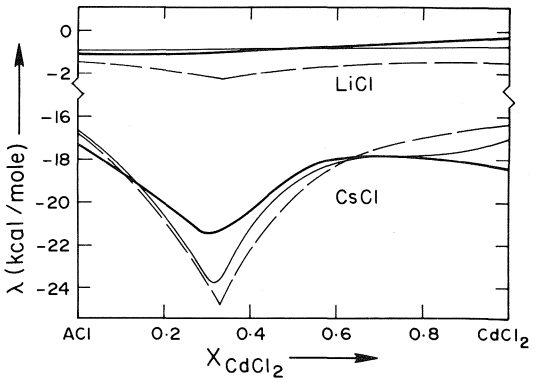

FIG. 6. Interaction parameters in $CdCl_2$–ACl systems. ——— Experimental (9). - - - From model for complete complexing. ——— From model for partial dissociation.

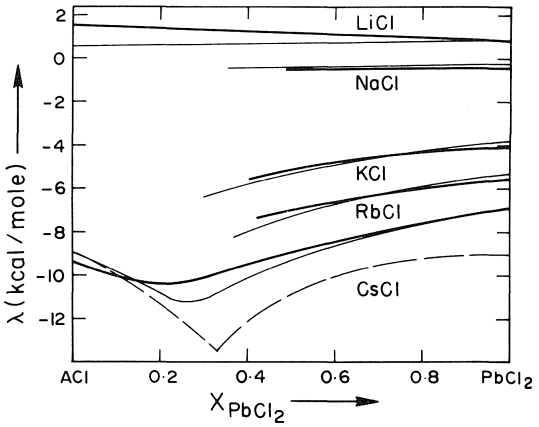

FIG. 7. Interaction parameters in $PbCl_2$–ACl systems. ——— Experimental (10). - - - From model for complete complexing. ——— From model for partial dissociation.

The overall interaction parameter which results from the combination of both enthalpy terms is shown in Fig. 1*b*. Let $\lambda_{X=1}$ and $\lambda_{X=0}$ be the values of λ when $X_{MY_2} = 1$ and $X_{MY_2} = 0$, respectively, and let $\Delta\lambda = (\lambda_{X=0} - \lambda_{X=1})$. From Fig. 1*b* it can be seen that $\Delta\lambda = b_1/4$. $\Delta\lambda$ should thus depend only on the salt MY_2, and should be constant within a group of MY_2–AY systems for a given salt MY_2. Furthermore, from the experimental value of $\Delta\lambda$, b_1 can be numerically estimated. The greater is the tendency of a salt MY_2 to form complexes, the more negative should be $\Delta\lambda$.

Can. J. Chem. Downloaded from www.nrcresearchpress.com by 210.87.254.105 on 09/05/12
For personal use only.

TABLE 2. Values of b_1 and b_2 which give best fits to experimental data

MY_2	b_1 (kcal)	AY	Temperature (°C)	b_2 (kcal)	Δe_2 (kcal)*
$CoCl_2$	−22.0	LiCl	810	+9.0	−13.0
		NaCl	810	+3.5	−18.5
		KCl	810	−4.5	−26.5
		RbCl	810	−7.5	−29.5
		CsCl	810	−10.5	−32.5
$FeCl_2$	−14.0	LiCl	810	+5.0	−9.0
		NaCl	810	+0.5	−13.5
		KCl	810	−6.0	−20.0
		RbCl	810	−9.0	−23.0
		CsCl	810	−12.0	−26.0
$NiCl_2$	−14.0	LiCl	810	+4.5	−9.5
		NaCl	810	+0.5	−13.5
		KCl	810	−6.0	−20.0
		RbCl	810	−9.0	−23.0
		CsCl	810	−12.0	−26.0
$MnCl_2$	0.0	LiCl	810	−2.0	−2.0
		NaCl	810	−7.0	−7.0
		KCl	810	−13.0	−13.0
		RbCl	810	−16.0	−16.0
		CsCl	810	−18.5	−18.5
$MgCl_2$	0.0	AgCl	730	+1.5	+1.5
		LiCl	730	−2.5	−2.5
		NaCl	810	−7.5	−7.5
		KCl	800	−13.0	−13.0
		RbCl	730	−15.0	−15.0
		CsCl	730	−17.0	−17.0
$CdCl_2$	0.0	LiCl	690	−1.5	−1.5
		CsCl	690	−16.5	−16.5
$PbCl_2$	0.0	LiCl	665	+2.5	+2.5
		NaCl	665	−1.0	−1.0
		KCl	655	−6.0	−6.0
		RbCl	660	−7.5	−7.5
		CsCl	665	−9.0	−9.0
BeF_2	−50.0	LiF	900	+20.0	−30.0
		KF	900	0.0	−50.0
		RbF	900	−3.0	−53.0

*$\Delta e_2 = b_1 + b_2$ (as in eqs. 9 and 10).

For the $CoCl_2$–ACl (8) systems in Fig. 2, $\Delta\lambda$ averages about −5.5 kcal for all the systems. The value of b_1 for $CoCl_2$ was thus taken to be −22 kcal. A value of b_2 for each individual system was then chosen to give the best fits (determined "by eye") to the data. Values of b_2 are listed in Table 2, and the fits obtained for the case of complete complexing (using eqs. 7 and 8) are shown as the dashed lines in Fig. 2. The fits appear to be quite good in all but the system with LiCl. The calculated "dip" at $X_{CoCl_2} = 1/3$ is, however, somewhat too sharp in all cases.

For the $FeCl_2$–ACl (8) systems in Fig. 3, $\Delta\lambda$ averages about −3.5 kcal for all systems. The value of b_1 for $FeCl_2$ was thus taken to be −14 kcal. The b_2 values which were chosen to give the best fits are listed in Table 2. These fits are shown in Fig. 3 as the dashed lines. The agreement is reasonable, but in the systems with LiCl and NaCl there is strong evidence for dissociation. For the $NiCl_2$–ACl systems in Fig. 3, measurements have been made (7) only over to $X_{NiCl_2} = 0.5$. The values of λ, however, are almost exactly the same at all concentrations as the values for the corresponding $FeCl_2$ systems, and so the same values of b_1 and b_2 were chosen for the $NiCl_2$ systems as for the $FeCl_2$ systems, except for the systems with LiCl, in which slightly different b_2 values were chosen in the two cases.

For the $MnCl_2$–ACl (8), $MgCl_2$–ACl (3), and $CdCl_2$–ACl (9) systems in Figs. 4–6, $\Delta\lambda$ is approximately zero for all the systems with KCl, RbCl, and CsCl (except for the $MgCl_2$–CsCl system in which $\Delta\lambda$ is actually quite positive). For the sys-

Can. J. Chem. Downloaded from www.nrcresearchpress.com by 210.87.254.105 on 09/05/12
For personal use only.

Can. J. Chem. Downloaded from www.nrcresearchpress.com by 210.87.254.105 on 09/05/12
For personal use only.

tems with NaCl and LiCl, $\Delta\lambda$ is somewhat negative, but, as shown later, this is thought to result from dissociation of the complexes. A value of $b_1 = 0.0$ was chosen for all these systems. As shown in Figs. 4–6, this results in reasonable agreement with the experimental data. The values of b_2 used are listed in Table 2.

In these less strongly complexed systems ($b_1 = 0$), the evidence for dissociation of the complexes is very strong in the systems with LiCl and NaCl, and is evident in the systems with KCl also.

For the $MgCl_2$ systems, enthalpies for the system $MgCl_2$–AgCl are available (3), and are shown in Fig. 5. This system is best fitted with $b_2 = +1.5$ kcal. The positive value may result from the fact that Ag has a tendency to form covalent bonds with chlorine and thus has a strong tendency to weaken and break up the complexes.

In the previous publication (5), a value of $b_1 = -3.0$ kcal was chosen to fit the $MgCl_2$ systems. The difference between this and the present value of 0.0 is small enough to make very little difference in the calculated curves.

For the $PbCl_2$–ACl systems (10) in Fig. 7, a value of $b_1 = 0.0$ and values of b_2 as listed in Table 2 were used. These parameters do not give good fits for the case of complete complexing, as can be seen from the dashed line for the $PbCl_2$–CsCl system in Fig. 7. However, as will be discussed later, these values do appear to give good fits when dissociation is taken into account. In the $PbCl_2$ systems there is evidence for dissociation even in the system with CsCl.

In Fig. 8*a* are plotted, as the heavy solid lines, ΔH curves for the BeF_2–LiF and BeF_2–KF systems as obtained calorimetrically by Holm and Kleppa (11). For the BeF_2–LiF system, ΔH is negative for small X_{BeF_2} and positive for large X_{BeF_2}. A plot of λ for this system is shown in Fig. 8*b*, and is of the general shape predicted by the present model. A value of $b_1 = -50$ kcal for BeF_2 gives a good fit to $\Delta\lambda$ for this system. This means that BeF_2 has a very strong tendency to form tetrahedral complexes. With a value of $b_2 = +20$ kcal for the BeF_2–LiF system, the curves calculated for complete complexing are shown as the dashed lines in Figs. 8*a*, *b*. Quite good agreement is obtained. For the BeF_2–KF system, a value of $b_2 = 0.0$ was chosen.

By comparing the fits to ΔH in Fig. 8*a* with the same fits to λ in Fig. 8*b*, it can be appreciated how small discrepancies in agreement between experimental and calculated values of ΔH are greatly magnified in the "interaction parameter" plots. This effect is particularly pronounced near the ends of the curves, as is readily seen in the curves for the BeF_2–KF system. A discrepancy between experimental and calculated values of 1.0 kcal at $X_{MY_2} = 0.9$, say, is magnified to a discrepancy of about 11.0 kcal in the plots of λ. For the chloride systems discussed previously, the interaction parameter plots of Figs. 2–7 similarly magnify discrepancies. The agreement between experiment and model in absolute values of ΔH would be more readily apparent in plots of ΔH than in the plots of λ. However, the important shape factors (the extent of the "dip" at $X_{MY_2} = 1/3$, the value of "$\Delta\lambda$", etc.) can only be seen in plots of λ.

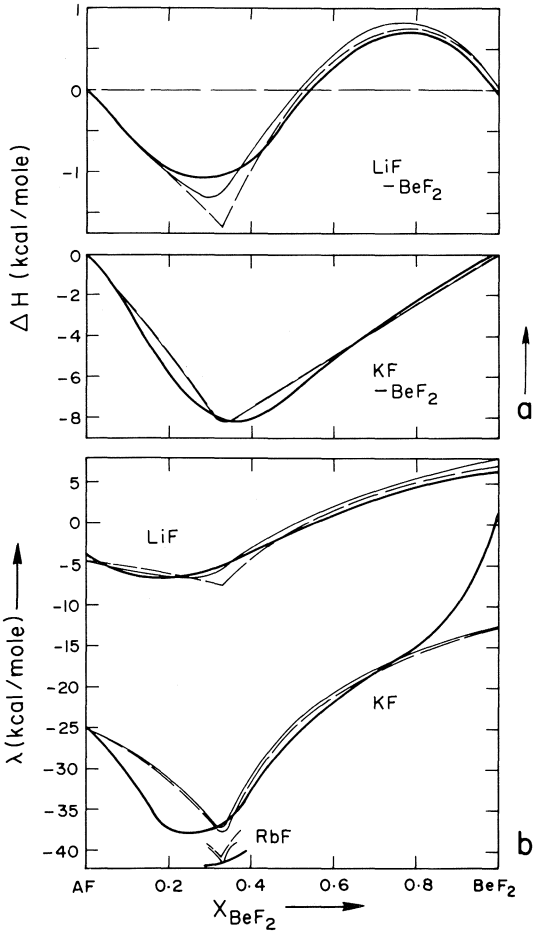

FIG. 8. Enthalpies and interaction parameters in BeF_2–AF systems. ——— Experimental (11). - - - From model for complete complexing. ——— From model for partial dissociation.

Can. J. Chem. Downloaded from www.nrcresearchpress.com by 210.87.254.105 on 09/05/12
For personal use only.

Of course, because of evidence of viscosities, electrical conductivities, etc., molten BeF_2 is generally accepted as being polymeric in nature, with BeF_4 tetrahedra sharing corners, and the assumption of discrete BeF_4^{2-} anions and Be^{2+} cations in pure BeF_2 as required by the present model is undoubtedly incorrect. This matter will be discussed at somewhat greater length later. Nevertheless, the very simple model just discussed can give surprisingly good agreement to the enthalpy of mixing data. In particular, for the BeF_2–LiF system, the existence of positive ΔH values in the BeF_2-rich concentration range, and negative values in the LiF-rich range is quite simply treated.

Entropies

The configurational entropy of mixing under the assumption of complete complexing is calculated as follows. For $X_{MY_2} \leqslant 1/3$, there is only one type of cation, A^+. The configurational entropy is then calculated by assuming a random mixture of the MY_4^{2-} and Y^- anions over $(X_{AY} - X_{MY_2})$ anion sites. For $X_{MY_2} \geqslant 1/3$, only one type of anion, MY_4^{2-}, exists, and a random mixture of the A^+ and M^{2+} cations over the $(3 - X_{MY_2})/4$ cation sites is assumed. At $X_{MY_2} = 1/3$, only A^+ cations and MY_4^{2-} anions exist and the configurational entropy is zero. Pure MY_2 contains only M^{2+} cations and MY_4^{2-} anions, and so has zero configurational entropy.

The molar configurational entropy of mixing, ΔS, is shown in Fig. 1*c* as the curve with two "humps". This is the typical sort of curve expected if the "compound" A_2MY_4 is formed, as has been discussed by Østvold (4) and by Østvold and Kleppa (12). The ideal (Raoultian) entropy of mixing is also shown in Fig. 1*c*.

Experimental partial molar entropies of mixing, $\Delta\bar{S}_{ACl}$, of ACl in the $MgCl_2$–ACl systems are shown in Fig. 9. These curves were obtained by Østvold (4), who measured the e.m.f. of concentration cells with glass membranes and combined his data with the partial enthalpies calculated from the calorimetric data (3). The ideal partial entropies, $-R \ln X_{ACl}$, are also shown in Fig. 9. The experimental curves show positive deviations from ideality for solutions concentrated in ACl, and then, near $X_{MgCl_2} = 1/3$, there is a rapid change to negative deviations. From the integral entropy of mixing curve in Fig. 1*c* it can be appreciated that this is qualitatively the predicted

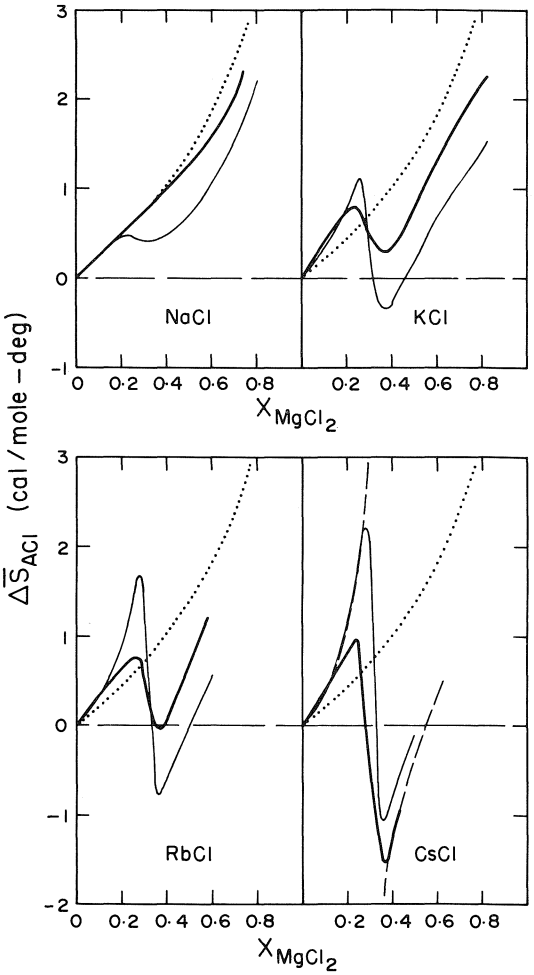

FIG. 9. Partial molar entropies of mixing of alkali chloride in $MgCl_2$–ACl systems. ——— Experimental (4). - - - From model for complete complexing. ———— From model for partial dissociation. ···· Ideal (Raoultian).

behavior of the partial entropy. In Fig. 9, in the graph for the system with CsCl, the dashed line is $\Delta\bar{S}_{ACl}$ as calculated for complete complexing. The predicted effect at $X_{MgCl_2} = 1/3$ is, of course, too drastic. As the A^+ cations become smaller, the experimentally observed effect at $X_{MgCl_2} = 1/3$ becomes less and less pronounced, again suggesting, as discussed by Østvold (4), that dissociation of the complexes occurs.

In Fig. 10 are partial excess entropies of mixing of $MnCl_2$, $\Delta\bar{S}^E_{MnCl_2}$, in $MnCl_2$–ACl systems, as calculated by Kucharski and Flengas (13) from the temperature dependences of the e.m.f.s of

Can. J. Chem. Downloaded from www.nrcresearchpress.com by 210.87.254.105 on 09/05/12
For personal use only.

formation cells, The dashed line in the graph for the system with CsCl is the curve predicted from the model for complete complexing. Positive values of $\Delta\bar{S}^{E}_{MnCl_2}$ are predicted for $X_{MnCl_2} > 1/3$, with a sudden change to negative values for $X_{MnCl_2} < 1/3$. This is in quite good agreement with the experimental curve for the $MnCl_2$–CsCl system. For smaller alkali cations, the experimentally observed effect at $X_{MnCl_2} = 1/3$ becomes less and less pronounced, again suggesting that dissociation of the complexes occurs.

Kucharski and Flengas (13) discussed the results in Fig. 10 using a similar model which was based upon the assumption of $MnCl_4^{2-}$ complexes, and which assumed complete complexing. They also included an additional term to account for vibrational entropy effects.

Discrete Complex Anion Model, Partial Dissociation

A complete discussion of the treatment of partial dissociation in the discrete complex anion model has been given previously (5).

Reaction 1 is not displaced completely to the right as was assumed in the case of complete complexing, and instead, an equilibrium is set up, with a fraction ($\alpha/2$) of the total M existing in MY_4^{2-} anionic complexes, and a fraction ($1 - \alpha/2$) existing, for the purposes of statistical calculations, as free M^{2+} cations. The amounts of the various ionic species in a mole of solution are given as functions of α in column 4 of Table 1.

Let α_{max} be the maximum permissible value of α. For $X_{MY_2} \leqslant 1/3$, $\alpha_{max} = 2$, and is that value of α for which all M is complexed. For $\alpha = 2$, column 4 of Table 1 reduces to column 2. For $X_{MY_2} \geqslant 1/3$, $\alpha_{max} = (1 + X_{MY_2})/2X_{MY_2}$, and is that value of α (see ref. 5) for which all the Y is complexed. With $\alpha = (1 + X_{MY_2})/2X_{MY_2}$, column 4 of Table 1 reduces to column 3. For $X_{MY_2} = 1$, for instance, $\alpha_{max} = 1$, and one half of the M is complexed when complete complexing occurs in pure MY_2.

The molar configurational entropy, S, of the solution at any composition is written by assuming a Temkin solution of M^{2+} and A^{+} cations and of Y^{-} and MY_4^{2-} anions. This gives S as a function of α and of composition, $S(\alpha,X)$.

Self-association of pure MY_2 must also be considered. The fact that no such model for complexing in molten salts can be thermodynamically consistent without the consideration of self-association of the pure components was first pointed out by Braunstein (14). If α^0 is the value of α in pure MY_2, then $S^0_{MY_2}$, the molar configurational entropy of pure MY_2, may be written as a function of α^0, $S^0_{MY_2}(\alpha^0)$, assuming a Temkin solution of the three ionic species M^{2+}, MY_4^{2-}, and Y^{-}. For $\alpha^0 = \alpha^0_{max} = 1$, for instance, complete complexing occurs. In this case there are only M^{2+} and MY_4^{2-} species in pure MY_2, and $S^0_{MY_2} = 0$ as discussed earlier.

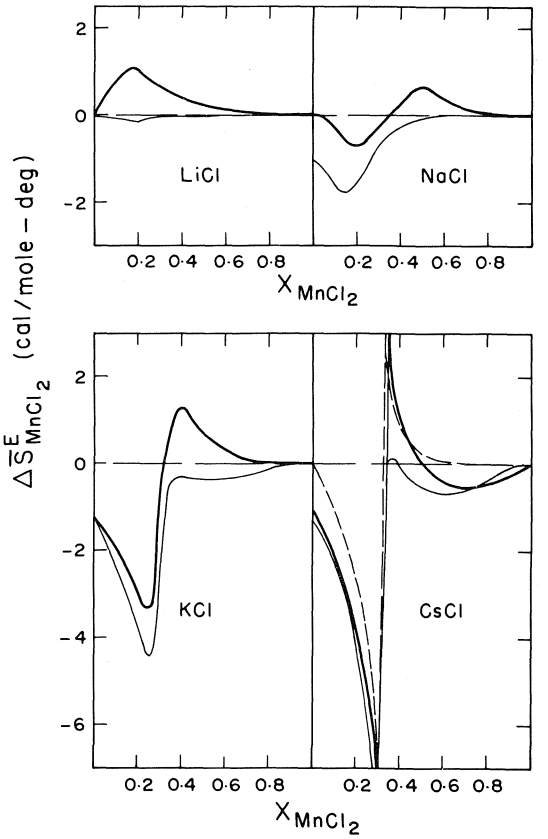

FIG. 10. Partial molar excess entropies of mixing of $MnCl_2$ in $MnCl_2$–ACl systems. ——— Experimental (13). - - - From model for complete complexing. ——— From model for partial dissociation.

The configurational entropy, S^0_{AY}, of pure AY is zero, and so the molar configurational entropy of mixing, ΔS, is given as a function of α, α^0, and composition

$$[11] \quad \Delta S(\alpha,\alpha^0,X) = S(\alpha,X) - X_{MY_2}S^0_{MY_2}(\alpha^0)$$

The explicit function has been given previously (5). For complete complexing, with $\alpha = \alpha_{max}$ and $\alpha^0 = 1$, the equation for ΔS reduces to the curve

Can. J. Chem. Downloaded from www.nrcresearchpress.com by 210.87.254.105 on 09/05/12
For personal use only.

in Fig. 1*c* for complete complexing. For $\alpha = 0$ and $\alpha^0 = 0$, the equation for ΔS reduces to the ideal (Raoultian) entropy of mixing expression.

The calculation of the enthalpy of mixing is similar to the calculation for the case of complete complexing. Δe_1 and Δe_2 are defined as before. A linear variation of Δe with the cationic fractions N_{A^+} and $N_{M^{2+}}$ as in eq. 4 is again assumed. There are $\alpha X_{MY_2}/2$ moles of complexes in solution and $\alpha^0/2$ moles in one mole of pure MY_2. That part of the enthalpy of mixing resulting from complex formation is thus given as

$$[12] \quad \Delta H = \frac{\alpha X_{MY_2}}{2}(N_{M^{2+}}\Delta e_1 + N_{A^+}\Delta e_2) - \frac{\alpha^0 X_{MY_2}}{2}\Delta e_1$$

which may be simplified to give

$$[13] \quad \Delta H = (\alpha - \alpha^0)\frac{X_{MY_2}b_1}{2} + \frac{\alpha X_{MY_2}N_{A^+}}{2}b_2$$

where b_1 and b_2 are defined as in eqs. 9 and 10. From Table 1, $N_{A^+} = X_{AY}/(1 - \alpha X_{MY_2}/2)$. Equation 13 gives an expression for ΔH as a function of α, α^0, b_1, b_2, and composition, $\Delta H(\alpha,\alpha^0,b_1, b_2,X)$. When $\alpha = \alpha_{max}$, and $\alpha^0 = 1$, the two terms of eq. 13 reduce to the two terms of eq. 7 or eq. 8 for complete complexing.

The variables α and α^0 are not independently adjustable parameters, but are uniquely determined by the values of b_1 and b_2. The values of α and α^0 actually assumed by the system are those which minimize the free energy. That is, by solving the equations $\partial(\Delta G)/\partial\alpha = 0$ and $\partial(\Delta G)/\partial\alpha^0 = 0$, where $\Delta G = \Delta H(\alpha,\alpha^0,b_1,b_2,X) - T\Delta S(\alpha,\alpha^0,X)$, α may be found as a function of b_1, b_2, and composition, $\alpha(b_1,b_2,X)$, and α^0 may be found as a function of b_1, $\alpha^0(b_1)$. Full details and explicit functions have been given previously (5). Once values of b_1 and b_2 have been chosen, values of α and α^0 at any composition may be calculated. These values may then be substituted back into the expressions for ΔS and ΔH to give unique simultaneous solutions for these properties at any composition.

Although the problem of partial dissociation could also be approached by writing an "equilibrium constant" for reaction 1, the present approach of defining α and then minimizing ΔG by setting $\partial(\Delta G)/\partial\alpha = 0$ overcomes problems of defining ionic activities and standard states, and would seem to be conceptually simpler and less subject to error. Furthermore, the fact that an equilibrium constant cannot be introduced as a third adjustable parameter, but is uniquely determined by b_1 and b_2, is emphasized by the present technique.

Since all four ionic species are simultaneously present in solution, a correction for non-random mixing must be introduced. For example, if b_2 is negative, then A^+ and MY_4^{2-} ions are favored as nearest neighbors. So the number of A^+–MY_4^{2-} and M^{2+}–Y^- nearest neighbors is increased and the number of A^+–Y^- and M^{2+}–MY_4^{2-} nearest neighbors is decreased from that predicted on the basis of random mixing. This correction has been fully discussed previously (5). The quasichemical method, as discussed by Førland (15), was used. An anion coordination number, z, must be assumed for these calculations. The value of z must lie between about 4 and 8, and it has been shown (5) that the results are quite insensitive to the value of z chosen. A value of $z = 6$ was used in the present calculations. In most systems, the correction for non-randomness is negligibly small anyway. If b_2 is small, then there is not enough driving force for non-randomization to occur to any extent. If, on the other hand, b_2 is negative enough, then the degree of complexing will be high, and α will be close to its maximum possible value. In this case, only three ionic species will exist to any extent in solution at one time (as in columns 2 and 3 of Table 1), and this type of non-randomness due to nearest neighbor "pair-exchange" cannot, of course, occur. For the systems discussed previously, the effect of non-randomness has been found to be negligible in all the systems with $CoCl_2$, $FeCl_2$, $NiCl_2$, and BeF_2. In the $MnCl_2$, $MgCl_2$, and $CdCl_2$ systems, only the systems with KCl, RbCl, and CsCl are affected, and then only in the MCl_2-rich concentration range (see ref. 5). The $PbCl_2$–CsCl system is slightly affected in the $PbCl_2$-rich concentration range. In all cases where non-randomness makes any difference, its effect is to improve the fits with the experimental data.

Comparison with Experimental Data

Using the values of b_1 and b_2 in Table 2, enthalpies and entropies of mixing were calculated for all the systems by the method just described. The calculated interaction parameters are shown in Figs. 2–8 as the light solid lines. Generally, the fits are improved over those for the complete

Can. J. Chem. Downloaded from www.nrcresearchpress.com by 210.87.254.105 on 09/05/12
For personal use only.

complexing case in all systems. In all the systems with CsCl, there is little difference between the calculated curves for complete and partial complexing, except for the weakly-complexed $PbCl_2$–CsCl system (Fig. 7) in which the consideration of partial dissociation improves the fit. For the systems with KCl, a significant difference and improvement in fit results when partial dissociation is considered in the $MnCl_2$–KCl and $MgCl_2$–KCl systems (Figs. 4 and 5). In the $CoCl_2$–KCl and $FeCl_2$–KCl systems (Figs. 2 and 3), however, b_1 is more negative than for $MnCl_2$ or $MgCl_2$, and in these systems there is little difference in λ between the cases of complete and partial complexing. In all the systems with NaCl and LiCl, however, marked dissociation can be seen to occur, except in the strongly-complexed BeF_2–LiF system (Fig. 8).

In Fig. 9 are plots of $\Delta\bar{S}_{ACl}$ for the $MgCl_2$ systems, calculated using the same b_1 and b_2 values from Table 2 which were used to fit the enthalpies. Agreement with the experimental data is reasonable, and the increasing degree of dissociation which occurs as the size of the alkali cation decreases is clearly seen. In Fig. 10 are curves of $\Delta\bar{S}^E_{MnCl_2}$ calculated from the values of b_1 and b_2 in Table 2. Agreement with experiment is reasonable, and progressive dissociation is clearly seen. Calculated values are generally somewhat too negative.

Papatheodorou and Kleppa (8) calculated partial entropies of mixing of $FeCl_2$ and $CoCl_2$ in the systems with NaCl and KCl by combining their enthalpy data with free energies calculated from vapor pressure, phase diagram, and e.m.f. data from the literature. Partial entropy curves were similar to those in Fig. 10 for the $MnCl_2$ systems, with the deviations from ideality increasing in the order Mn < Fe < Co as expected from the present model.

The effect of dissociation of the complexes upon the entropies (Figs. 9 and 10) is apparently more drastic than upon the enthalpies (Figs. 2–8). Even when dissociation is taken into account, the "dips" at $X_{MY_2} = 1/3$ in Figs. 2–8 are still generally overestimated, as is the effect at $X_{MgCl_2} = 1/3$ in Fig. 9 for the entropies. This suggests that dissociation may actually occur to a somewhat greater extent than predicted by the present treatment. Of course, the fact that only one discrete complex, MY_4^{2-}, is considered in the model would be expected to result in too "sharp" a predicted effect at $X_{MY_2} = 1/3$, since the existence of other complexes or "polymerization" would be expected to cause a "rounding off" here.

Trends in the Chloride Systems

Tetrahedral field stabilization energies (TFSE) for $MgCl_2$, $MnCl_2$, $FeCl_2$, $CoCl_2$, $NiCl_2$, and $CdCl_2$ from ref. 16 are plotted in Fig. 11. Mg, Mn, and Cd have d^0, d^5, and d^{10} configurations, respectively, and thus have zero values of the TFSE (Mg and Cd are shown in brackets in Fig. 11 to indicate that they are from different periods in the periodic table than the other elements.) In Table 2 are the values of Δe_2 used for the various systems, where Δe_2 has been defined as the energy of formation of the complexes when they are completely surrounded by A^+ cations. From eq. 10, $\Delta e_2 = b_1 + b_2$. Plots of Δe_2 for the systems of MCl_2 with various alkali chlorides are shown in Fig. 11. It can be seen that, to a first approximation, the function (Δe_2 − TFSE) is independent of the salt MCl_2, and depends mainly upon the alkali chloride alone. That is, the energy of formation of complexes when surrounded completely by alkali cations appears to be approximately equal to the TFSE plus a factor which depends only upon the cation A^+. Plots of (Δe_2 − TFSE) *vs.* r_+, the Goldschmidt radius of the alkali cation, are shown in Fig. 12 for the $CoCl_2$, $FeCl_2$, $NiCl_2$, and $MnCl_2$ systems. The curves are all quite linear, and the slopes are all nearly the same. The lines for the different MCl_2 systems still differ somewhat from each other. However, with a maximum error of only 3–4 kcal, (Δe_2 − TFSE) for all the chloride systems could be fitted by one single linear curve.

Also in Fig. 11 are plotted values of b_1 for the

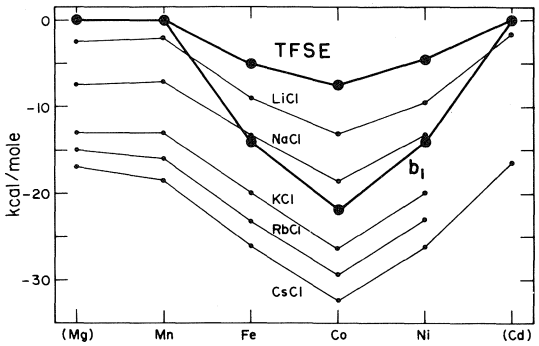

FIG. 11. Tetrahedral field stabilization energies (TFSE) and values of b_1 and Δe_2 for chloride systems from Table 2.

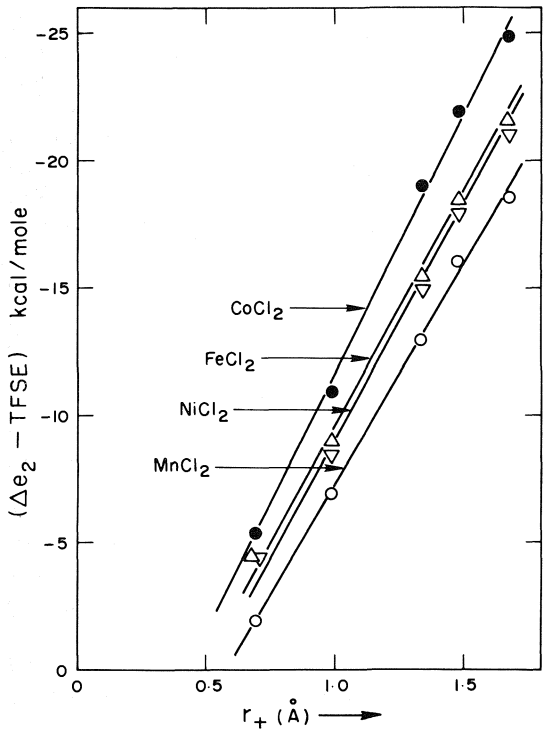

FIG. 12. (Δe_2 – TFSE) *vs.* alkali cation radius for MCl_2–ACl systems.

various systems. b_1 appears to vary approximately directly as the TFSE. (This is also the case for the $PbCl_2$ systems where TFSE = 0 and $b_1 = 0$.) No particular correlation between b_1 for the MCl_2 systems and the radius of M^{2+} is evident.

For the systems in Fig. 11, (Δe_2 – TFSE) appears to be relatively independent of the radius of M^{2+} as has just been discussed. For the $PbCl_2$ systems, however, values of Δe_2 are quite significantly less negative than for the other systems. Thus, it seems that for large enough M^{2+} ions, the strength of the complexes does begin to depend upon the M^{2+} radius.

Cantor (17) has measured freezing point depressions for additions of alkaline earth fluorides to NaF. For BeF_2 and MgF_2 additions, the liquidi are as predicted for the formation of MF_4^{2-} complexes. For CaF_2 additions, however, there are significant deviations, and for SrF_2 and BaF_2 additions, nearly ideal Raoultian liquidi are observed, thus indicating large dissociation of any complexes. This again shows that for large enough M^{2+} ions, the strength of the complexes decreases as the radius increases.

Other Experimental Data

Kucharski and Flengas (13) measured electrical conductivities and molar volumes in the $MnCl_2$–ACl systems. Experimental excess molar conductivities, Λ^E, are plotted in Fig. 13*b*, where Λ^E is defined as

$$[14] \quad \Lambda^E = \Lambda - (X_{MY_2}\Lambda_{MY_2} + X_{AY}\Lambda_{AY})$$

where Λ, Λ_{MY_2}, and Λ_{AY} are the molar conductivities of the solution and of the pure components. Note that all experimental values of Λ^E in Fig. 13*b* are negative.

Non-zero excess conductivities result from changes in number and mobility of charge carriers upon mixing. The present model permits a pre-

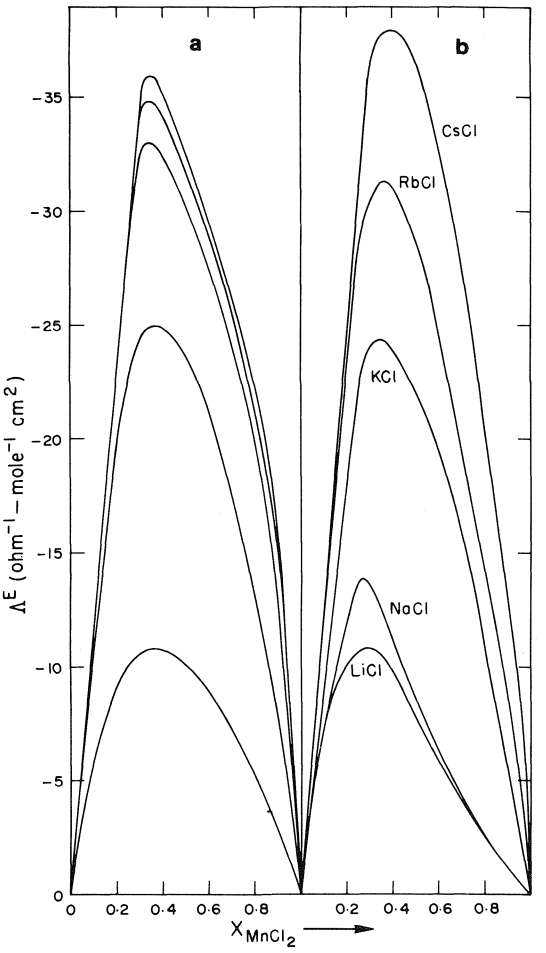

FIG. 13. (*a*) Excess molar conductivities calculated from model for $MnCl_2$–ACl systems. (*b*) Experimental (18) excess molar conductivities for $MnCl_2$–ACl systems at 800 °C.

Can. J. Chem. Downloaded from www.nrcresearchpress.com by 210.87.254.105 on 09/05/12
For personal use only.

Can. J. Chem. Downloaded from www.nrcresearchpress.com by 210.87.254.105 on 09/05/12
For personal use only.

diction of the change in the number of charge carriers which occurs when the pure components are mixed. Upon mixing, reaction 1 occurs to a certain extent, removing the relatively mobile Mn^{2+} and Cl^- ions from solution, and replacing them with the large, relatively immobile $MnCl_4^{2-}$ complexes. Let us assume that this effect is much more important than any effect due to simultaneous changes in individual ion mobilities. Since there are $\alpha X_{MnCl_2}/2$ moles of complexes in a mole of solution and $\alpha^0 X_{MnCl_2}/2$ moles in X_{MnCl_2} moles of pure $MnCl_2$, then Λ^E should, to a first approximation, be given by

$$[15] \quad \Lambda^E = \left(\frac{\alpha - \alpha^0}{2}\right) X_{MnCl_2}(2\mu_{MnCl_4^{2-}} - 2\mu_{Mn^{2+}} - 4\mu_{Cl^-})$$

where the μ_i are the individual ion mobilities, assumed independent of concentration, and the factors 2 before $\mu_{MnCl_4^{2-}}$ and $\mu_{Mn^{2+}}$ are there because these ions are doubly charged. Let us also assume that the mobilities μ_i in eq. 15 are independent not only of concentration within a given system, but are also independent of the particular $MnCl_2$–ACl system in question. (Note that μ_{A^+} does not appear in eq. 15.) Then

$$[16] \quad \Lambda^E = \left(\frac{\alpha - \alpha^0}{2}\right) X_{MnCl_2}\gamma$$

where γ is a single constant for all the $MnCl_2$ systems.

With values of α and α^0 calculated using the b_1 and b_2 parameters for the $MnCl_2$–ACl systems as in Table 2, and with $\gamma = -164$ ohm^{-1} mol^{-1} cm^2, the curves in Fig. 13*a* were calculated. The curves agree in shape quite well with the experimental curves. The peak heights for the systems with CsCl and LiCl are in good agreement with experiment, but for the other systems, the calculated values of Λ^E are rather too negative.

In Fig. 13*b*, the experimental Λ^E curves approach zero approximately linearly along nearly coincident paths as X_{MnCl_2} approaches zero. From Fig. 13*a* it can be seen that this behavior is as predicted. For the case of complete complexing, with $\alpha = \alpha_{max}$ and $\alpha^0 = 1$, eq. 16 reduces to

$$[17] \quad \Lambda^E = X_{MnCl_2}\gamma/2 \qquad [X_{MnCl_2} \leqslant 1/3]$$

$$[18] \quad \Lambda^E = X_{ACl}\gamma/4 \qquad [X_{MnCl_2} \geqslant 1/3]$$

A sharp negative peak at $X_{MnCl_2} = 1/3$ is thus predicted (as in the upper ΔH curve in Fig. 1*a*). This, of course, qualitatively explains the shape of the curves in Fig. 13. As $X_{MnCl_2} \to 0$, the model predicts that complete complexing is approached (since the equlibrium in reaction 1 is shifted to the right as the concentration of Cl^- ions increases, see ref. 5), and this explains the limiting behavior of the curves in Fig. 13 as $X_{MnCl_2} \to 0$.

In view of the simplicity of the present model and the use of only one adjustable parameter, γ, for all systems, the agreement obtained in Fig. 13 is thought to be satisfactory. Kucharski (18) discussed his measurements of Λ^E by a model assuming $MnCl_4^{2-}$ complexes and assuming complete complexing. He obtained equations for Λ^E similar to eqs. 17 and 18, thus predicting sharp peaks at $X_{MnCl_2} = 1/3$ as just discussed. A different value of γ was needed for each individual system, of course. In this case then too, all the calculated curves did not have the same limiting slope as $X_{MnCl_2} \to 0$.

Similar Λ^E curves in the $MgCl_2$–NaCl and $MgCl_2$–KCl systems have been discussed by Grjotheim, Nikolic, and Øye (19).

It has been argued that "complexes" are only a formalism for treating non-randomness in molten salts, and that complexes should not be regarded as "particles". The success of the present model in explaining the electrical conductivity, a transport property, however, supports the concept of complexes as distinct particles. Also, recent studies by Lamb (20) of transference cells containing molybdenum chloride in LiCl–KCl eutectic showed that molybdenum was transported to the anode compartment, and thus moved as a negatively charged particle, presumably an $MoCl_6^{3-}$ complex.

Excess molar volumes of mixing, ΔV^E, of the $MnCl_2$–ACl systems have been measured by Kucharski and Flengas (13), and were found to be positive. The curves are very similar in shape to the Λ^E curves of Fig. 13, with peaks at $X_{MnCl_2} = 1/3$. The peaks decrease in height from the CsCl to the LiCl system. This gives good qualitative evidence for the formation of $MnCl_4^{2-}$ complexes, and this has been discussed by the authors (13). The formation of the large complex anions appears to cause an increase in the molar volume of the solutions.

There is also, of course, a large and rapidly growing body of spectral data on molten salts

Can. J. Chem. Downloaded from www.nrcresearchpress.com by 210.87.254.105 on 09/05/12
For personal use only.

which gives strong qualitative evidence for complex anions. These data have been extensively reviewed (16, 21).

Discussion

BeF_2 and SiO_2 Systems

It was shown in Fig. 8 that the discrete complex anion model gives reasonably good fits to enthalpies in BeF_2–AF systems. For solutions rich in alkali fluoride, phase diagram calculations in the BeF_2–NaF (17) and BeF_2–LiF (22) systems support the contention that discrete BeF_4^{2-} anions are the predominant complexes.

For solutions richer in BeF_2, however, it is generally accepted that these melts are "polymeric", with the BeF_4 tetrahedra sharing corners through "fluorine bridges" in a structure similar to that of crystoballite. Molten SiO_2 is thought to have a similar structure.

For BeF_2–AF systems which are rich in BeF_2, and also for SiO_2-rich solutions of SiO_2 with basic oxides, models exist (23, 24) which attempt to explain the thermodynamic data by considering the solutions as mixtures of polymeric species such as dimers, trimers, etc. Although the ultimate explanation of the properties of these systems will undoubtedly require the consideration of such polymeric species, the success of the discrete complex anion model suggests that such an approach, in which only simple structural units are considered, can be of value and can provide insight into the melt structure.

For pure BeF_2, the discrete complex anion model is, of course, unrealistic, since even for complete complexing it assumes that only half the beryllium in pure BeF_2 is complexed. In reality, nearly all the beryllium is complexed through the sharing of fluorines. Although enthalpies are well-fitted by the simple model, entropies of mixing in solutions rich in BeF_2 are not. Experimental partial excess entropies of mixing of BeF_2 in the BeF_2-rich composition region of the BeF_2–LiF system (11) have large positive values which cannot be explained by the model, even with complete complexing. These "polymerized" melts thus appear to have a greater multiplicity than that calculated from the discrete complex anion model. Experimental $\Delta\bar{S}^E_{MnCl_2}$ values in Fig. 10 are somewhat more positive than those calculated previously, possibly giving some evidence that polymerization occurs to some extent in these systems. (Although for complete complexing, the discrete complex anion model does fit the data for the system with CsCl quite well.) McCarty and Kleppa (10) also found slight positive values of $\Delta\bar{S}^E_{PbCl_2}$ in the $PbCl_2$-rich concentration range in the $PbCl_2$–ACl systems.

Some qualitative applicability of the present model might also be expected for molten SiO_2–BO systems, where B is a divalent metal, at least in the basic melts. In the SiO_2–PbO system, for example, activities calculated from the e.m.f. data of Charette and Flengas (25) indicate that SiO_4^{4-} anions are the main complex species in the PbO-rich composition region. Østvold and Kleppa (12) measured enthalpies of mixing in this system from $X_{SiO_2} = 0$ to 0.5, and found a curve for λ similar to that in Fig. 1*b*. Curves of $\Delta\bar{S}_{PbO}$ as calculated by Østvold and Kleppa by combining their enthalpy data with activity data from the literature were qualitatively similar to those in Fig. 9.

As has been shown for the BeF_2–LiF system, a negative value of b_1 and a positive value of b_2 in an MY_2–AY system can result in positive values of ΔH for solutions rich in MY_2, and negative values for solutions rich in AY. Such an effect, if great enough, could give rise to a liquid–liquid immiscibility gap in the MY_2-rich concentration region. Such immiscibility gaps are found in many SiO_2–BO systems. (The systems where B = Mg, Ca, Sr, and Mn are examples.) Such positive b_2 values in polymeric SiO_2–BO melts could be associated with the tendency of the B^{2+} cations to polarize and distort the highly directional Si—O bonds, thus greatly weakening the network structure of the melts. As the radius of the B^{2+} cations increases, their polarizing power decreases, and less positive b_2 values occur. The large positive b_2 value in the BeF_2–LiF system can be similarly explained. The present model may thus give some qualitative insight into the reason for the existence of the immiscibility gaps in SiO_2–BO systems in the acidic region.

Vibrational Entropy

Vibrational entropy contributions have been neglected in the present treatment. Let σ be the molar vibrational entropy change associated with the formation of one mole of complexes as in reaction 1, and assume that σ is independent of composition. Then, in the discrete complex anion model, a vibrational entropy of mixing contribution, ΔS_{vib}, as shown in Fig. 1*c* should result for the case of complete complexing. This curve is similar to the upper ("b_1") curve for ΔH in

Can. J. Chem. Downloaded from www.nrcresearchpress.com by 210.87.254.105 on 09/05/12
For personal use only.

Fig. 1*a*. Such a function for ΔS_{vib} was used by Kucharski (18) in his treatment of complexing.

For partial complexing, a ΔS_{vib} term of the form:

$$[19] \qquad \Delta S_{vib} = \frac{(\alpha - \alpha^0) X_{MY_2}}{2} \sigma$$

(*cf.*: the first term in eq. 13) would result. (Again, it has been assumed that σ is independent of concentration.) If the effect of different A^+ cations is to be considered, then "σ_1" and "σ_2" parameters (analogous to the b_1 and b_2 parameters) could be defined.

If Fig. 1*c*, σ is shown as negative. However, for polymeric materials such as those containing SiO_2 or BeF_2, the formation of discrete complexes upon mixing would result in the breakdown of the ordered three-dimensional network, and positive values of σ might be expected.

Undoubtedly, vibrational entropy contributions are important in these systems. However, since the general features of the experimental data can be reasonably well-fitted by considering only the configurational entropy, and since the inclusion of the vibrational entropy terms introduces more adjustable parameters into the model, no attempt to numerically include the vibrational terms will be made at the present time.

Additional Parameters

Additional enthalpy terms could also be added to include changes in coulombic and polarization interactions upon mixing which are not accounted for in the terms in eq. 13. This has been discussed previously (5) in some detail. Extra terms to try to account for other effects such as variations in coordination number with composition could also be added. Such additional terms necessitate further adjustable parameters, however, and the justification for neglecting these terms is that the data are quite well-fitted without them.

The addition of one more adjustable parameter per system would nearly double the number of such parameters being used, and so would yield a great improvement in the agreement between experiment and theory, whether or not there were any basis whatsoever in physical fact for the reasoning which gave rise to the additional parameters.

Conclusions

For a large number of molten systems of the general formula MY_2–AY, the discrete complex anion model appears to explain quite a wide range of experimental data quite well, on the assumption of the existence of discrete MY_4^{n-} complex anions as the only complex species present.

The model can be applied to strongly complexed systems such as the $CoCl_2$ systems, and can also be applied to weakly-complexed systems such as the PbY_2 system. In the limit of zero complexing, the model reduces to the ideal Temkin model. At the other extreme, the treatment can explain some of the data for systems with strong polymerized complexes, such as systems with BeF_2 or SiO_2, although a basic limitation of the approach is that polymerization is neglected.

Molten salts such as LiCl or CsCl may be called strong bases since they are completely dissociated into A^+ and Cl^- ions. MY_2 salts in which free Y^- ions are removed from solution by an equilibrium as in reaction 1 may be called weak bases. The b_1 parameter introduced in the present treatment provides a possible quantitative basicity (or acidity) scale for molten salts and slags. Thus, $CoCl_2$, for which $b_1 = -22$ kcal, is a weaker base than $FeCl_2$ for which $b_1 = -14$; and $FeCl_2$ is a weaker base than $MnCl_2$ for which $b_1 = 0$.

For each weak base MY_2, a second basicity scale, the "b_2 scale" is also necessary for each solution of that salt with a strong base, AY, in order to account for the effect of the A^+ ions on the energy of the complexes. The situation is more complicated than the case of dilute solutions of weak protonic acids in water for which one single acidity scale suffices since there is only one solvent and only solutions in the Henrian concentration range are considered.

The relationship of the b_1 and b_2 basicity scales to such things as ionic radii and ligand field stabilization energies has been discussed.

For fused salt systems other than those discussed here, there is also strong evidence for the existence of complex ions. Spectroscopic data (16, 21) appear to indicate that tetrahedral MY_4^{n-} and octahedral MY_6^{n-} complexes may be the most common complex anions in molten halides. Many salts which are molecular liquids when pure, such as $TiCl_4$ and Al_2F_6, nevertheless form complex anions ($TiCl_6^{2-}$, AlF_4^-) when dissolved in the strongly basic alkali halides. Preferred grouping of particles to form the statistical entities called complex ions may be of prime importance in a wide variety of molten salts.

The discrete complex anion model is an attempt to classify a quite wide variety of molten salt and slag systems of the form MY_2–AY by simple quantitative "basicity scales". Undoubtedly the treatment is highly oversimplified, but the strength of the treatment lies in this simplicity and in the use of an absolute minimum of adjustable parameters. It is hoped that this type of treatment may also prove useful in classifying and understanding other more complicated complex-forming salt and slag systems.

The author wishes to thank Dr. W. T. Thompson, Dr. A. S. Kucharski, and Professor S. N. Flengas for many helpful discussions. Financial assistance from the National Research Council of Canada is also gratefully acknowledged.

1. J. Lumsden. Thermodynamics of molten salt mixtures. Academic Press, N.Y. 1966. pp. 245 and 250.
2. H. Flood and S. Urnes. Z. Elektrochem. **59**, 834 (1955).
3. O. J. Kleppa and F. G. McCarty. J. Phys. Chem. **70**, 1249 (1966).
4. T. Østvold. Acta. Chem. Scand. **23**, 688 (1969).
5. A. D. Pelton and W. T. Thompson. Can. J. Chem. **48**, 1585 (1970).
6. M. Temkin. Acta Physicochim. URSS. **20**, 411 (1945).
7. G. N. Papatheodorou and O. J. Kleppa. J. Inorg. Nucl. Chem. **32**, 889 (1970).
8. G. N. Papatheodorou and O. J. Kleppa. J. Inorg. Nucl. Chem. In press.
9. G. N. Papatheodorou and O. J. Kleppa. Inorg. Chem. In press.
10. F. G. McCarty and O. J. Kleppa. J. Phys. Chem. **68**, 3846 (1964).
11. J. L. Holm and O. J. Kleppa. Inorg. Chem. **8**, 207 (1969).
12. T. Østvold and O. J. Kleppa. Inorg. Chem. **8**, 78 (1969).
13. A. S. Kucharski and S. N. Flengas. J. Electrochem. Soc. In press.
14. J. Braunstein. J. Chem. Phys. **49**, 3508 (1968).
15. T. Førland. *In* Fused salts. *Edited by* B. Sundheim. McGraw-Hill, N.Y. 1964. Chap. 2.
16. D. M. Gruen. *In* Fused salts. *Edited by* B. Sundheim. McGraw-Hill, N.Y. 1964. Chap. 5.
17. S. Cantor. J. Phys. Chem. **65**, 2208 (1961).
18. A. S. Kucharski. Ph.D. thesis. University of Toronto, Toronto, Ontario, 1971.
19. K. Grjotheim, R. Nikolic, and H. A. Øye. Acta Chem. Scand. **24**, 489 (1970).
20. V. A. Lamb. J. Electrochem. Soc. **117**, 1269 (1970).
21. G. Mamantov. Molten salts. Marcel Dekker, N.Y. 1969.
22. R. E. Thoma, H. I. Insley, H. A. Friedman, and G. M. Hebert. J. Nucl. Mat. **27**, 166 (1968).
23. C. R. Masson, I. B. Smith, and S. G. Whiteway. Can. J. Chem. **48**, 1456 (1970).
24. C. F. Baes, Jr. J. Solid State Chem. **1**, 159 (1970).
25. G. G. Charette and S. N. Flengas. Can. Met. Q. **7**, 191 (1968).

Can. J. Chem. Downloaded from www.nrcresearchpress.com by 210.87.254.105 on 09/05/12
For personal use only.

Can. J. Chem. Downloaded from www.nrcresearchpress.com by 210.87.254.5 on 09/05/12
For personal use only.

Chaleur de dilution de solutions aqueuses d'acide polyacrylique, de son sel de sodium et de l'acide propionique

JEAN-PIERRE CARTIER[1] ET HUBERT DAOUST
Département de chimie, Université de Montréal, Montréal, Québec

Reçu le 12 juillet 1971

Des mesures de chaleur de dilution de solutions aqueuses d'acide polyacrylique et de son sel de sodium, ainsi que de l'acide propionique, ont été réalisées à l'aide d'un microcalorimètre du type Tian–Calvet à 25 °C. Les mêmes mesures ont été répétées (sauf pour le sel de sodium) en utilisant une solution aqueuse de HCl 0.2 *N* comme solvant. Les résultats obtenus pour l'acide polyacrylique sont en accord avec ceux de Silberberg, Eliassaf et Katchalsky. Les différences dans les résultats pour cet acide et son monomère "libre", l'acide propionique, sont interprétées en termes de changements de structure de l'eau induits par la longueur de la chaîne de polymère, en d'autres termes, par l'effet de chaîne. L'endothermicité de la dilution de solutions modérément concentrées du polyacrylate de sodium dans l'eau peut être expliquée à la lumière de la théorie d'Eigen et Wicke sur les solutions concentrées d'électrolytes forts.

With a Tian–Calvet microcalorimeter, heats of dilution at 25 °C have been measured for aqueous and acid (0.2 *N* HCl) solutions of polyacrylic acid and of propionic acid, and for aqueous solutions of the sodium salts of polyacrylic acid. The results are interpreted in terms of the change in structure of water resulting from the lengthening of the solute molecule. The heat of dilution of moderately concentrated solutions of sodium polyacrylate can be explained by the theory of Eigen and Wicke.

Canadian Journal of Chemistry, **49**, 3935 (1971)

Introduction

Plusieurs propriétés des polymères vinyliques solubles dans l'eau peuvent s'expliquer par la formation de liens hydrophobes entre sites ou groupements sur la chaîne (1). Ainsi, on tente d'expliquer plusieurs différences dans les propriétés physico-chimiques en solution aqueuse de l'acide poly-méthyl-méthacrylique (APMM) et de l'acide polyacrylique (APA) par le fait que ce dernier ne possède pas de groupement latéral hydrophobe. Il est bien connu que les groupements hydrophobes permettent la formation d'icebergs autour des chaînes d'hydrocarbures et favorisent ainsi une structure plus ordonnée de l'eau à l'état liquide (2, 3).

Des mesures de diffusion de la lumière par des solutions diluées d'APA et d'APMM dans HCl 0.2 *N* à différentes températures ont montré que les chaleurs de dilution sont endothermiques dans le premier cas et exothermiques dans le second (4). Par ailleurs, des travaux ont montré que le volume molal apparent du motif de base de différentes fractions d'APA dans l'eau diminue avec l'augmentation de la masse moléculaire du polymère (5).

Les résultats présentés dans le présent article confirment les résultats de Silberberg et coll. et permettent de proposer une explication pour les résultats obtenus par densimétrie (5).

[1]Nouvelle adresse: Département de chimie, Université du Québec à Montréal, Montréal, Québec.

Partie expérimentale

L'acide propionique et les produits utilisés dans la préparation des polymères étaient tous des réactifs de pureté analytique. L'eau utilisée comme solvant avait une conductivité spécifique de l'ordre de 10^{-6} mho^{-1} cm^{-1}. Deux échantillons d'APA furent utilisés dans ce travail. Le premier (APA-1) fut obtenu par la polymérisation de l'acide acrylique en s'inspirant de travaux antérieurs (6). Le sel de sodium (NaPA) fut obtenu par la neutralisation d'un échantillon d'APA-2 par de l'hydroxyde de sodium (7), l'APA-2 étant aussi préparé selon la méthode mentionnée plus haut. Chaque échantillon de polymère fut dialysé pendant au moins vingt-quatre heures puis séché par liophylisation pendant une semaine. Les masses molaires moyennes des deux échantillons d'APA furent déterminées par viscosimétrie en utilisant HCl 0.2 *N* comme solvant (4); leur valeur respective sont 270 000 et 300 000. Des titrages potentiométriques de solutions préparées gravimétriquement à partir d'échantillons séchés d'APA ont indiqué un degré de pureté de l'ordre de 92% dans les deux cas; une analyse par infrarouge de la poudre de polymère dans le nujol d'une part et en solution dans du dioxanne d'autre part, a montré que l'eau retenue par le polymère après séchage est la seule impureté détectable.

Les mesures de chaleurs de dilution furent réalisées à l'aide d'un microcalorimètre différentiel du type Tian–Calvet (8) à mille thermocouples par élément calorimétrique. Le courant produit par l'effet thermoélectrique est amplifié par un amplificateur de courant continu

TABLEAU 1. Chaleurs de dilution des solutions d'APA-1 à 25 °C

Conc. (% P/P)	m_2 (g)	n_2	Δm_1 (g)	$\bar{n}_1$ ($n_2 = 1$)	φ_2	φ_2'	ΔH_d (J)	κ_a
			Solvant: eau [$\bar{v}_2 = 0.649$ cm^3 g^{-1} (10)]					
13.080	2.505	0.0348	6.131	31.44	0.0888	0.0664	0.954	0.49
13.080	2.345	0.0325	5.866	31.61	0.0888	0.0707	0.925	0.63
9.100	1.722	0.0239	5.883	46.79	0.0609	0.0460	0.400	0.45
6.533	1.297	0.0180	6.411	67.11	0.0433	0.0325	0.223	0.46
4.581	0.828	0.0115	5.845	97.32	0.0301	0.0227	0.096	0.46
3.298	0.577	0.0080	5.890	137.88	0.0216	0.0161	0.052	0.48
2.306	0.418	0.0058	5.967	197.84	0.0150	0.0113	0.026	0.49
1.658	0.294	0.0041	5.886	276.06	0.0108	0.0081	0.009	0.33
1.166	0.210	0.0029	5.919	397.64	0.0076	0.0057	0.007	0.51
0.835	0.147	0.0021	5.839	539.69	—	—	0.005	—
0.585	0.123	0.0017	6.864	791.71	—	—	0.005	—
								$\bar{\kappa}_a = 0.48$
			Solvant: HCl 0.2 N [$\bar{v}_2 = 0.665$ cm^3 g^{-1} (10)]					
15.977	3.279	0.0455	6.752	24.97	0.125	0.0897	1.128	0.11
7.261	1.512	0.0210	6.804	59.58	0.0515	0.0381	0.186	0.10
3.668	0.775	0.0108	6.864	121.34	0.0251	0.0188	0.058	0.13
1.836	0.386	0.0054	6.670	246.66	0.0123	0.0093	0.013	0.11
0.909	0.180	0.0026	6.830	504.77	0.0062	0.0045	0.005	0.16
								$\bar{\kappa}_a = 0.12$

Leeds and Northrup modèle 9835B et enregistré à l'aide d'un enregistreur Phillips modèle RR 3216A/00. Le microcalorimètre utilisé est basculant ce qui simplifie grandement le déclanchement de la dilution et l'agitation à l'intérieur des cellules. Deux types de cellules furent utilisées pour la dilution, soit en téflon supportée par une gaine extérieure en laiton, soit en verre Pyrex, mais leur description est essentiellement la même. Elles consistent en deux tubes cylindriques concentriques fermés par le bas. Le tube extérieur a un diamètre d'environ 25 mm et une hauteur totale de 100 mm; le tube intérieur a un diamètre de 13 mm et une hauteur de 88 mm. Le tout est fermé à l'aide d'un bouchon en téflon. Un volume de 7 ml de solvant est versé dans le tube central et 21 ml de solution dans le tube extérieur. Les vapeurs des deux liquides sont séparées avant la dilution en déposant une faible quantité d'huile de paraffine légère, soit 0.2 à 0.4 ml. Cette quantité d'huile doit être maintenue la plus faible possible car le mouillage de l'huile lors de l'agitation peut produire un effet endothermique appréciable. L'agitation à l'intérieur de la cellule est assurée par l'addition de deux cent billes de verre de 1 mm de diamètre. L'étalonnage du microcalorimètre a été fait par effet Joule et vérifié par des mesures de chaleur de neutralisation de HCl par NaOH. En aucun cas l'écart entre les valeurs données pour cette réaction (9) et les valeurs calculées ne dépasse 3%.

Résultats et discussion

Les résultats obtenus sont donnés dans les Tableaux 1 à 3. Les concentrations exprimées en grammes de soluté par 100 g de solvant apparaissant dans la première colonne sont celles des solutions initiales. Dans la deuxième colonne, les masses du soluté dans les solutions sont données, tandis que dans la troisième apparaissent les nombres de moles (de motif de base dans le cas des polymères). La quantité Δm_1 est la masse de solvant ajouté lors de la dilution et $\bar{n}_1$ est le nombre moyen de moles d'eau pour une mole de soluté; φ_2 et φ_2' sont les fractions volumiques du soluté avant et après dilution. Finalement, ΔH_d est l'enthalpie de dilution telle

TABLEAU 2. Chaleurs de dilution des solutions d'acide propionique à 25 °C

Conc. (% P/P)	n_2	Δm_1 (g)	$\bar{n}_1$ ($n_2 = 1$)	ΔH_d (J)
		Solvant: eau		
80.126	0.1963	5.864	1.85	51.419
40.690	0.1175	6.916	7.63	−55.445
20.620	0.0558	6.838	19.05	−30.586
10.315	0.0293	6.843	42.20	− 8.222
5.190	0.0147	6.826	87.75	− 1.999
2.608	0.0073	6.877	180.38	− 0.441
1.317	0.0038	6.837	349.70	− 0.136
0.663	0.0019	6.825	702.58	− 0.049
0.334	0.0009	6.840	1488.72	− 0.013
		Solvant: HCl 0.2 N		
80.334	0.1983	5.919	1.84	52.741
75.047	0.2136	6.850	2.24	24.296
60.680	0.1734	6.849	3.73	−30.266
50.457	0.1436	6.889	5.33	−47.337
40.610	0.1160	6.769	7.58	−53.583
27.133	0.0777	6.813	13.38	−42.886
19.908	0.0570	6.851	19.73	−27.995
8.737	0.0249	6.855	50.20	− 6.290
4.426	0.0125	6.876	103.41	− 1.501
2.618	0.0074	6.866	177.13	− 0.462
1.327	0.0037	6.841	357.82	− 0.127
0.670	0.0019	6.876	703.16	− 0.037
0.337	0.0010	6.815	1341.05	− 0.009
0.285	0.0008	6.808	1669.94	− 0.003

Can. J. Chem. Downloaded from www.nrcresearchpress.com by 210.87.254.5 on 09/05/12
For personal use only.

Can. J. Chem. Downloaded from www.nrcresearchpress.com by 210.87.254.5 on 09/05/12
For personal use only.

TABLEAU 3. Chaleur de dilution des solutions aqueuses de NaPA à 25 °C

Conc. (% P/P)	n_2	Δm_1 (g)	$\bar{n}_1$ ($n_2 = 1$)	ΔH_d (J)
17.834	0.0375	6.475	28.85	7.641
9.330	0.0188	6.314	60.07	1.039
4.696	0.0106	6.938	124.10	−0.111
2.332	0.0052	6.933	255.90	−0.137
1.030	0.0023	6.867	584.00	−0.070
0.517	0.0011	6.929	1175.83	−0.037
0.272	0.0006	6.895	2232.26	~0

que calculée à partir des données expérimentales; ici, on peut négliger la différence entre l'enthalpie de dilution et l'énergie de dilution étant donné que les changements de volume lors de la dilution sont négligeables ou nuls (5).

Les chaleurs de dilution de l'APA dans l'eau sont endothermiques de même que dans HCl 0.2 *N* en accord avec les résultats de Silberberg et coll. Pour fins de comparaison, il est utile de définir un paramètre enthalpique apparent d'après la relation (11)

$$[1] \qquad \kappa_a = \Delta H_d / RTn_2(\varphi_2 - \varphi_2') \qquad \text{Ce paramètre est une mesure des interactions entre un soluté et un solvant; les valeurs de } \kappa_a \text{ sont données dans la dernière colonne du Tableau 1. Il y a une nette diminution de la valeur moyenne de } \kappa_a \text{ lorsque l'eau est remplacée par HCl 0.2 } N \text{ comme solvant soit de 0.48 à 0.12 et cette derniére valeur se compare assez bien avec celle donnée par la littérature (5), soit 0.0647. Lorsque les chaleurs de dilution de l'APA dans l'eau et dans HCl 0.2 } N \text{ (Fig. 1) sont comparées à celles obtenues pour l'acide propionique}$$

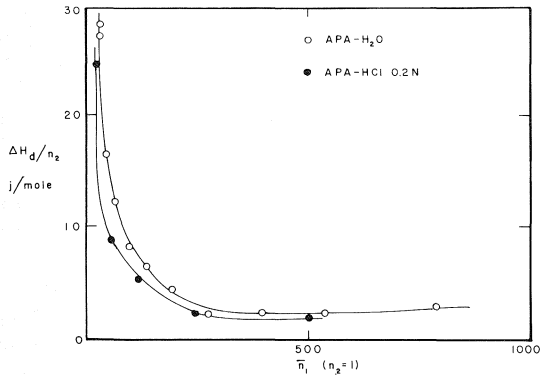

FIG. 1. Variation de l'enthalpie de dilution par mole de motif de base d'APA en fonction du nombre moyen de moles d'eau à 25 °C.

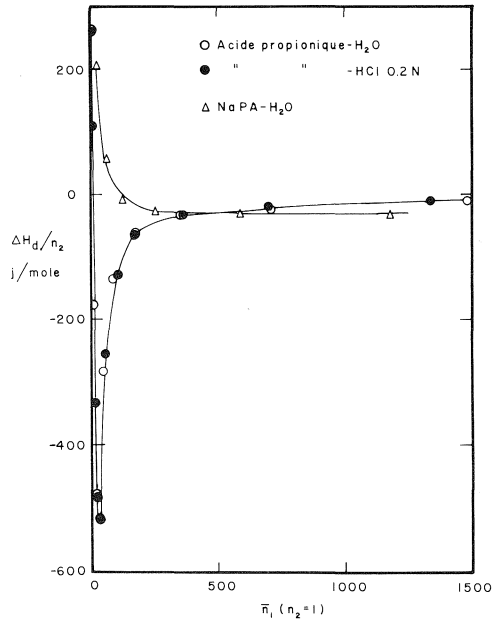

FIG. 2. Variation de l'enthalpie de dilution par mole (ou mole de motif de base) de soluté en fonction du nombre moyen de moles d'eau à 25 °C.

dans les mêmes solvants (Fig. 2), le comportement de l'APA apparait totalement différent de celui de son monomère "libre". Ces résultats peuvent être expliqués en examinant ce qui se passe à l'échelle moléculaire lors de la dilution. Les chaleurs de dilution calculées à partir des résultats de la littérature (12), montrent que la dilution d'une solution aqueuse d'acide acétique, propionique ou butyrique normal est fortement endothermique pour des solutions très concentrées pour devenir rapidement exothermique lorsque la dilution progresse et la courbe donnée dans la Fig. 2 pour l'acide propionique peut être considérée comme typique pour ces trois acides. En solution fortement concentrée, la dilution amène la rupture des ponts hydrogène persistants entre les molécules d'acide (13). La rupture des ponts hydrogène est un phénomène endothermique (2) et il est alors plus important que la solvatation des groupements COOH par intéraction dipôle–dipôle avec les molécules d'eau, phénomène qui serait exothermique d'après l'allure des résultats obtenus. Lorsque la dilution se continue, il peut y avoir formation d'icebergs autour des radicaux hydrophobes (3) et ceci pourrait expliquer le passage d'une très forte endothermicité à une très forte exothermicité

Can. J. Chem. Downloaded from www.nrcresearchpress.com by 210.87.254.5 on 09/05/12
For personal use only.

pour une augmentation relativement petite du nombre moyen de moles d'eau. Lorsque les molécules d'acide sont finalement dispersées uniformément dans la solution, pratiquement seule l'ionisation de l'acide contribue à la chaleur de dilution et globalement le phénomène d'ionisation en solution aqueuse est essentiellement endothermique (14). L'utilisation de HCl 0.2 *N* comme solvant de l'acide propionique ne modifie en rien les résultats obtenus pour les chaleurs de dilution dans l'eau pure comme le montre également la Fig. 2. Le changement de structure de l'eau que pourrait apporter l'addition de HCl n'influence donc nullement le mécanisme de dilution de l'acide propionique.

Avant de tenter d'expliquer les résultats obtenus dans le cas de l'APA, il faut savoir que: (*1*) les groupements COOH du polymère ne sont pas ionisés dans le domaine de concentration étudié ici (15); (*2*) les groupements COOH sont libres dans l'eau, *i.e.*, ils ne participent aucunement à la formation de ponts hydrogène de quelque nature que se soit d'après une étude spectroscopique récente (16). De plus, il faut accepter l'hypothèse que les effets combinés des ions H^+ (ou H_3O^+) et Cl^- sur la structure de l'eau est de briser d'importants agrégats moléculaires par solvatation des espèces ioniques pour des solutions 0.05 *m* et plus (17). A la lumière de ce qui a été écrit plus haut et des explications données à l'allure des résultats obtenus pour l'acide propionique, il faut croire que l'endothermicité de la dilution de l'APA dans l'eau ne s'explique que par un changement important dans la structure de l'eau. Les groupements COOH le long de la chaîne favorisent la dissolution de ce polymère dans l'eau par intéraction dipôle–dipôle mais afin de loger une longue chaîne dans le réseau "semi-cristallin" de l'eau, il faut briser un certain nombre d'agrégats moléculaires de dimension importante en agrégats plus petits ou en molécules libres; c'est ce qu'on peut appeler l'effet de chaîne. La rupture ou la formation de ces agrégats étant un phénomène coopératif (18), *i.e.*, que lorsqu'un lien se brise, l'agrégat tout entier se désagrège, les changements dans la structure de l'eau peuvent devenir très importants lors de la dissolution de l'APA dans l'eau ou lors de la dilution d'une solution aqueuse de cet acide. La "fusion" des agrégats peut donc expliquer la valeur positive pour l'enthalpie de dilution Lorsque HCl 0.2 *N* est employé comme solvant, il y a une nette diminution dans la valeur de cette enthalpie et ceci peut s'expliquer par le fait que les changements de structure de l'eau sont moins considérables, le nombre de gros agrégats étant moindre que dans l'eau pure.

Ce changement dans la structure de l'eau dû à l'effet de chaîne peut expliquer les résultats obtenus en densimétrie (5, 10). On remarque que la valeur de $\bar{v}_2$ pour l'APA dans l'eau est notablement plus faible que dans HCl 0.2 *N* (voir Tableau 1). En supposant que cela est entièrement dû à la différence de structure de l'eau dans les deux cas et non à celle du polymère, et sachant que la fusion des agrégats entraîne une diminution du volume spécifique de l'eau, cette diminution est plus considérable dans le cas de l'eau pure et il s'ensuit que $\bar{v}_2$ apparait plus faible dans l'eau que dans HCl 0.2 *N*. D'autre part, la diminution de φ_u^0 (= volume molaire apparent d'un motif de base d'APA non-dissocié) avec l'augmentation de la masse moléculaire du polymère peut s'expliquer par le fait qu'une longue chaîne de polymère est plus difficilement logée dans le réseau semi-cristallin du solvant qu'une courte chaîne; la transition agrégats → molécules d'eau libres devient alors plus importante dans le cas de la dissolution de longues chaînes d'APA dans l'eau d'où la valeur plus faible pour φ_u^0.

Les résultats obtenus pour les chaleurs de dilution de NaPA dans l'eau montrent que dans le cas de solutions modérément concentrées la dilution est endothermique et devient exothermique lorsque la dilution progresse (Fig. 2). En négligeant le phénomène d'hydrolyse qui existe dans ce cas, l'allure des résultats est tout à fait analogue à ceux obtenus lors de la dilution d'une solution modérément concentrée d'un électrolyte fort tel un halogénure de sodium ou de potassium. Afin d'expliquer l'endothermicité de la dilution d'une telle solution, Eigen et Wicke (19) font intervenir la dissociation qui est un phénomène typiquement endothermique. Tenant compte de ce nouvel apport d'énergie, la chaleur de dilution mesurée par mole de soluté devient la somme de deux contributions:

$$[2] \quad \Delta H_d(c) = \alpha(c)\Delta H_d^*(c) + [1 - \alpha(c)]\Delta H_\infty$$

où α est le degré de dissociation, ΔH_d^*, l'enthalpie de dilution pour l'électrolyte entièrement dissocié et ΔH_∞, l'enthalpie de dissociation complète d'une mole de soluté.

Pour les polyélectrolytes forts, comme pour les électrolytes forts ordinaires, on admet que les forces de nature électrostatique constituent la principale contribution à l'énergie libre d'interaction entre le polyion et ses ions antagonistes (20). Alors, en utilisant les bases de la théorie de Eigen et Wicke, Hosono et Ise (21) prévoient que ΔH_d^* sera exothermique en solution légèrement concentrée pour devenir endothermique en solution très diluée. Parmi les résultats rapportés dans la littérature (22–24) aucun ne donne une chaleur de dilution exothermique à haute dilution; afin de vérifier les prédictions théoriques d'Hosono et Ise, il faudrait travailler à des dilutions qui pour le moment ne sont pas accessibles aux méthodes expérimentales utilisées jusqu'ici. Une étude plus détaillée des polyélectrolytes forts fait l'objet d'une autre communication (24).

Nous tenons à remercier le Conseil National de Recherche du Canada pour l'aide financière apportée à ce projet. Nous remercions également le Service de réadaptation des handicapés physiques du Ministère de l'éducation de la Province de Québec (J.-P. C.).

1. J. ELIASSAF. J. Polymer Sci. Part B, **3**, 767 (1965).
2. G. NÉMETHY ET H. A. SCHERAGA. J. Chem. Phys. **36**, 3401 (1962).
3. G. NÉMETHY et H. A. SCHERAGA. J. Phys. Chem. **66**, 1773 (1962).
4. A. SILBERBERG, J. ELIASSAF et A. KATCHALSKY. J. Polymer Sci. **23**, 259 (1957).
5. S. FRIEDMAN, A. CAILLÉ et H. DAOUST. Macromolecules, **3**, 700 (1970).
6. S. NEWMAN, W. R. KRIGBAUM, C. LAUGIER et P. J. FLORY. J. Polymer Sci. **14**, 151 (1954).
7. A. PACKTER. J. Polymer Sci. Part A, **1**, 3021 (1963).
8. E. CALVET et H. PRAT. Microcalorimétrie et ses applications physico-chimiques et biologiques. Masson, Paris, 1956.
9. F. DANIELS, J. H. MATHEWS, J. W. WILLIAMS, P. BENDER et R. A. ALBERTY. Experimental physical chemistry. 5ième éd. McGraw-Hill, New York, N.Y. 1956.
10. S. FRIEDMAN. Thèse de maîtrise. Université de Montréal, Montréal, Québec. 1962.
11. M. A. KABAYAMA et H. DAOUST. J. Phys. Chem. **62**, 1127 (1958).
12. International Critical Tables, vol. V. 1929.
13. M. FRERI. *In* Hydrogen bonding. D. Hadzi, éd. Pergamon Press, London 1959, p. 211.
14. H. S. HARNED et B. B. OWEN. The physical chemistry of electrolytic solutions. 3ième éd. Reinhold Publishing Corp., New York, N.Y. 1958.
15. F. T. WALL et S. J. GILL. J. Phys. Chem. **58**, 740 (1954).
16. J. L. KOENIG, A. C. ANGWOOD, J. SEMIN et J. B. LANDO. J. Am. Chem. Soc. **91**, 7256 (1969).
17. S. R. GUPTA, G. J. HILLS et D. J. G. IVES. Discuss. Faraday Soc. **24**, 147 (1957).
18. H. S. FRANK et W. Y. WEN. Discuss. Faraday Soc. **24**, 133 (1957).
19. M. EIGEN et E. WICKE. J. Phys. Chem. **58**, 702 (1954).
20. S. A. RICE et M. NAGASAWA. Polyelectrolyte solutions. Academic Press, New York, N.Y. 1961.
21. M. HOSONO et N. ISE. J. Polymer Sci. **39**, 389 (1959).
22. W. SCHULZE. Z. Elektrochem. **58**, 165 (1954).
23. J. SKERJANC, D. DOLAR et D. LESKOVSEK. J. Phys. Chem. Neue Folge, **56**, 207 (1967).
24. A. HADE et H. DAOUST. À paraître.

Can. J. Chem. Downloaded from www.nrcresearchpress.com by 210.87.254.5 on 09/05/12
For personal use only.

Can. J. Chem. Downloaded from www.nrcresearchpress.com by 210.87.254.40 on 09/05/12
For personal use only.

Hydrogen Gas Solubility in the Dimethyl Sulfoxide – Water System: A Further Clue to Solvent Structure in These Media[1]

E. A. SYMONS[2]

Research Chemistry Branch, Whiteshell Nuclear Research Establishment, Atomic Energy of Canada Limited, Pinawa, Manitoba

Received July 21, 1971

The solubility of hydrogen gas in the dimethyl sulfoxide (DMSO) – water system has been measured as a function of temperature from 25 to 80 °C. A distinct minimum occurs in the solubility, as expressed on the molar scale, in the region 25–35 mol% DMSO at 25 °C. As the temperature is raised towards 80 °C the minimum becomes less pronounced. The maximum deviation from calculated "ideal" behavior is found at 32 ± 5, 35 ± 5, and 32 ± 5 mol% DMSO for 25, 50, and 80 °C, respectively.

A maximum is observed for both the partial molal entropy and heat of solution of hydrogen in the same solvent composition region. These results are discussed in terms of a changing entropy and energy of hole formation in the solvent with composition, which in turn is related to DMSO–water interaction in solution.

A temperature-dependent equilibrium between $DMSO.2H_2O$ and $DMSO.3H_2O$ complexes in solution is proposed in an attempt to correlate the considerable data which have been reported in the literature for the DMSO–water system. The second complex is thought to be present in significant quantity only at temperatures well below 25 °C.

On a mesuré la solubilité de l'hydrogène gazeux dans le système diméthyl sulfoxyde (DMSO) – eau en fonction de la température, de 25 à 80 °C. Un minimum distinct de solubilité se produit dans la région de 25 à 35 mol% de DMSO à 25 °C, tel qu'exprimé sur l'échelle molaire. Lorsqu'on élève la température aux environs de 80 °C, le minimum devient moins prononcé. On trouve la déviation maximale au comportement "idéal" calculé à des compositions de 32 ± 5, 35 ± 5 et 32 ± 5 mol% de DMSO à 25, 50 et 80 °C, respectivement.

On observe un maximum, à la fois pour l'entropie molaire partielle et pour la chaleur de dissolution de l'hydrogène dans la même région de composition de solvant. On discute de ces résultats en termes de changement d'entropie et d'énergie de formation de trous dans le solvant avec la composition, ce qui est relié à l'interaction de l'eau et du DMSO dans la solution.

On propose un équilibre dépendant de la température entre les complexes en solution $DMSO.2H_2O$ et $DMSO.3H_2O$ dans le but de faire la corrélation entre les différents résultats qui ont été rapportés en nombre considérable dans la littérature pour le système DMSO–eau. On croit que le second complexe est présent en quantité appréciable à des températures bien au-dessous de 25 °C.

Canadian Journal of Chemistry, **49**, 3940 (1971)

Introduction

The structure of dimethyl sulfoxide (DMSO) – water mixtures has been under investigation for some time (1–11). The general conclusion drawn from density, viscosity, dielectric, and thermodynamic data is that 2:1 water:DMSO association occurs to a considerable extent. However, there is evidence from phase diagram (5) and deuteron relaxation (7) studies that 3:1 association may also take place. Hydrogen bonding between DMSO and water molecules has recently been detected (6), in contrast to previous evidence to the contrary (4).

It is known that the solubility of an inert gas in a liquid can be employed as a means of examining the structure of the liquid (12–14). Since a solute gas such as hydrogen is non-polar and non-ionic, solute–solvent interaction will be small, and the effect of a changing solvent composition on its solubility should reflect mainly the relative ease of hole formation in the medium (15). This ease will depend upon the change in solvent interaction with composition.

In the present work the solubility of hydrogen gas has been measured in several DMSO–water mixtures ranging from 20.2 to 100 mol% DMSO. The temperature dependence of the solubility was determined at most compositions over the range 25.0–80.0 °C, allowing calculation of the partial molal entropies and heats of solution. These data have been combined with the results

---

[1]A.E.C.L. No. 4005.

[2]N.R.C.C. Postdoctorate Fellow, 1969–1971. Present address: Chemistry Department, Queen's University, Kingston, Ontario.

Can. J. Chem. Downloaded from www.nrcresearchpress.com by 210.87.254.40 on 09/05/12
For personal use only.

of Gubbins and co-workers (16) for pure water to provide complete coverage for this solvent system.

Experimental

Reagents

DMSO (Fisher Certified Reagent) was dried at least 48 h over Linde type 4A molecular sieves, then vacuum distilled with nitrogen bleed through a 16 in. Vigreux column. The central fraction, 38–40 °C at *ca.* 1 mm Hg, was retained for use under a nitrogen atmosphere at ambient temperature.

Deionized distilled water was used throughout.

Hydrogen gas was taken directly from a lecture bottle (Matheson, extra dry).

Tetramethylammonium hydroxide (25% aqueous solution, Matheson, Coleman, and Bell) was employed as received, the polyethylene bottle being fitted with a rubber serum cap to facilitate solution withdrawal by syringe. Samples were titrated frequently against standard sulfuric acid.

Solution Preparation

Solutions were made up in a modified 100 ml round bottom flask; the vessel is shown in Fig. 1. The side arms permitted connection of the flask to a vacuum pump and, by means of the rubber serum cap and syringe needle, to a manometer and hydrogen gas cylinder. Appropriate volumes of water and DMSO were transferred under nitrogen to the flask by pipet; where required, base solution was added by syringe.[3] The solvent composition was calculated from the number of moles of each component introduced.

The solution was cooled to minimize vaporization of the solvent, and the flask was evacuated for several minutes to remove any dissolved gas. After the vessel had been submerged in a constant temperature bath (controlled to better than ± 0.05 °C), hydrogen was introduced to a pressure equal to 1 atm plus the estimated vapor pressure of the solvent at the particular temperature. The latter pressure was obtained by extrapolation of the data of Kenttämaa and Lindberg measured at 70 °C (17). It was assumed that the shape of the vapor pressure – composition curve joining known pressures for pure water (18) and DMSO (19) at 25, 35, 50, 65, and 80 °C would be similar to that observed at 70 °C. Effects of the dissolved base on this vapor pressure were neglected.

In order to achieve equilibration of the hydrogen between the liquid and vapor phases, the solution was stirred for 5 min by means of a magnet attached to the shaft of a variable speed motor. Further stirring did not yield significant changes in measured solubility. It is apparent from the literature (see ref. 12 and references therein) that great effort is often made to ensure both complete degassing and gas equilibration, thereby allowing precision as high as 0.1%. However, the large increase necessary in analysis time to improve from 99% of the gas dissolved (typically several minutes equilibration time) to 100% (several hours) was not considered justifiable in the present case. The main reasons for this decision were the uncertainty in the solution vapor pressures and the method of analysis employed (see below).

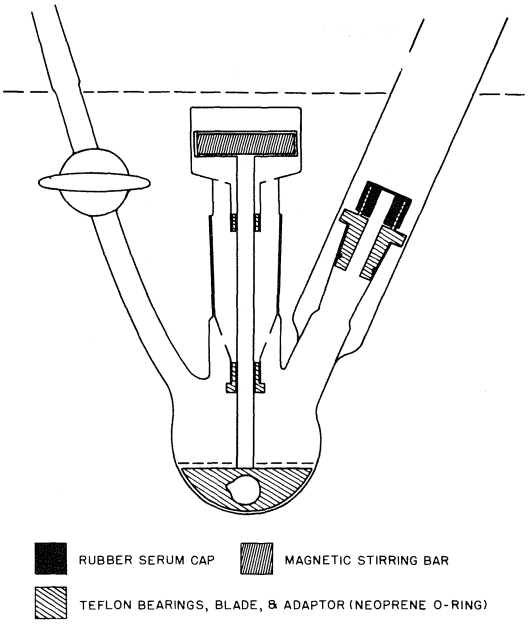

FIG. 1. Gas–liquid equilibration cell. Stiff springs hold the upper and lower sections together. The openings into the upper chamber of the stirrer unit allow free circulation of the gas.

Approximately 1 ml of solution was discarded before each main 5.0 ml sample was removed by a calibrated 5 ml syringe. It was necessary to withdraw the samples slowly in order to prevent some gas from being drawn out of solution in the syringe. Between samples, the slight pressure drop in the flask was corrected and the solution given further agitation. A total of three or four samples was normally taken per solution.

Gas Solubility Measurements

A gas chromatographic method of analysis, adapted from Gubbins and co-workers (16, 20), was utilized, wherein the dissolved gas was stripped from a solution sample by the carrier gas. The solution compartment of the gas stripping cell, shown in Fig. 2, had a capacity of 6 ml. The chromatograph, a Varian Aerograph model 1520, was operated with the thermal conductivity detector at 65 °C and the injector and column (10 ft, 1/4 in. stainless steel, 40–60 mesh 13X molecular sieve) at ambient temperature. The carrier gas was nitrogen at a flow rate of 34 ml per min. A recorder and Infotronics Corporation digital integration system were used to monitor the detector output.

Each 5.0 ml solution sample was introduced by syringe into the stripping cell at a rate which stopped the carrier gas flow until all of the sample had been added. The hydrogen was then stripped out over a period of 1–2 min. Chromatograph response was calibrated, usually

[3]The base concentrations corresponded to those employed for a reaction currently under investigation in these media, the base-catalyzed exchange of deuterium gas.

Can. J. Chem. Downloaded from www.nrcresearchpress.com by 210.87.254.40 on 09/05/12
For personal use only.

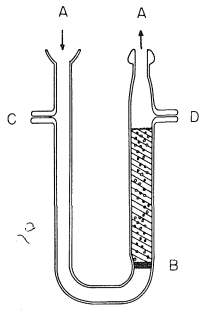

FIG. 2. Gas stripping cell for solubility analysis; overall size 5 in. × 2½ in. Points *A*, to a 4-way stopcock; *B*, medium porosity glass frit; *C*, calibration gas sample inlet; *D*, solution sample inlet. Attached at *C* and *D* were Beckman teflon ¼ in. unions whose outer ends were fitted with silicone rubber septums. The lines connecting the stopcock to the chromatograph were 1/8 in. nylon; inserted at the return side of the stopcock was a coil of 10 ft of translucent ¼ in. nylon tubing packed with 10–20 mesh indicating drierite to remove water and DMSO vapor from the gas flow.

once per solution sample, by injecting 100 μl samples of hydrogen with a 250 μl gas-tight syringe.

The complete analysis procedure was tested by determining the solubility of hydrogen in pure water and DMSO at 25.0 °C. The results, presented in Table 1, are in good agreement with literature data obtained by a method analogous to the present case (16) and by a method involving observation of the pressure drop upon equilibration of gas and liquid (21). Accuracy in the latter case was believed to be within 1%.

Results

Solubilities

The hydrogen solubilities, expressed on the molar scale, are presented in Table 2 as a function of both medium composition and temperature. They were determined by comparing the stripped gas and calibration gas integrated areas, which allowed calculation of the number of moles of gas dissolved in each 5 ml solution sample. This means of presentation was used because solubilities expressed as moles per litre were required elsewhere (see footnote 3). The corresponding mole fraction data were not included in Table 2, in order to maintain clarity.[4]

TABLE 1. A comparison of the measured and literature values for hydrogen gas solubility in DMSO and water at 25.0 °C

	H_2 solubility, $\times 10^{-5}$ mole fraction*	
Solvent	This work†	Lit. value (ref.)
Water	1.45 1.45	1.43 (16)
DMSO	7.5 7.7	7.61 (21)

*Hydrogen partial pressure of 1 atm.
†Each entry is the mean of three separate values measured for one stock solution; estimated error is ± 2%.

The solubility data are considered to be accurate to ±2%, since standard deviations for the triplicate or quadruplicate measurements leading to each entry in Table 2 varied between 0.1 and 4%, with most falling well below 2%. Within this 2% precision, smooth curves could be drawn through the data for each of the five temperatures as a function of solvent composition, as is shown in Fig. 3. The data for pure water were taken from Gubbins and co-workers (16).

The salting-out effect of added base on hydrogen solubility has been shown to be considerable for water at 25–100 °C (16). Some of the mixed media in the present study contained tetramethylammonium hydroxide in order to duplicate conditions for a related deuterium exchange study (see footnote 3). Therefore these media were examined at 65 °C to determine if a similar effect was operating in the DMSO–water mix-

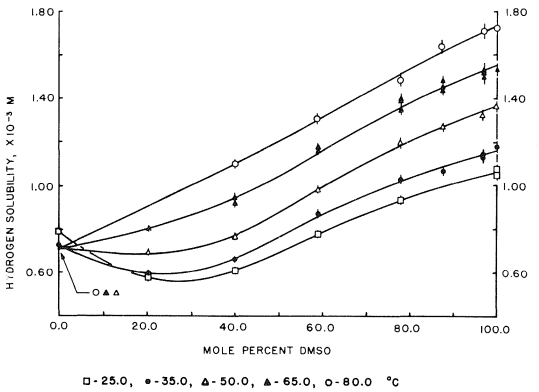

FIG. 3. Hydrogen gas solubility as a function of medium composition at the indicated temperatures. Error bars are ±2%. Data for pure water are from Gubbins and co-workers (16).

[4]The mole fraction data can be obtained by conversion of the molar values in the following manner, utilizing the density–temperature results of Cowie and Toporowski (2) for the DMSO–water system. For a chosen "moles of hydrogen per litre of solution", the litre of solution is reduced to the number of moles of DMSO plus water. The number of moles of hydrogen is negligible in comparison and can be neglected. The appropriate density yields the weight of the litre of solution, and since the relation between weight and mol% DMSO can be calculated, the individual weights of DMSO and water can be determined. Hence the number of moles of each is known, and therefore the total "moles of solvent" corresponding to the litre of mixed solvent.

TABLE 2. Solubility* of hydrogen in DMSO – water – tetramethylammonium hydroxide media† as a function of temperature

Temperature (°C)	Mole percent DMSO (base concentration, *M*)						
	100 (0)	96.9 (0.022)	87.5 (0.096)	77.9 (0.13)	59.0 (0.42)	40.1 (0.36)	20.2 (0)
25.0	1.05 1.08	—	—	0.93	0.78	0.61	0.58
35.0	1.18	1.13 1.15	1.07	1.03	0.87	0.66	0.60
50.0	1.37	1.33	1.27	1.20	0.98	0.77	0.69
65.0	1.54	1.50 1.52 1.53	1.44 1.45 1.48	1.35 1.39 1.40	1.16 1.17	0.92 0.95	0.80
80.0	1.73	1.71	1.64	1.49	1.31	1.10	—

* $\times 10^{-3}$ mol/l at 1 atm partial pressure for each temperature. Each entry is the mean of three or four separate values for one stock solution. The estimated error is ± 2%.
†See comments in text concerning the negligible effect of base concentration at this level on gas solubility. The base was not completely soluble for some solutions at 25 °C.

tures. It was found that, for 96.9, 87.5, 77.9 mol% DMSO at approximately one half and two times the listed base concentration (Table 2), and for 59.0 and 40.1% at one half the concentration, the measured solubility values were within experimental error of the mean for each set. Thus the presence of hydroxide ion in these solutions has little effect on the solubility data, and the values in Table 2 can all be considered as applying to the neutral solutions. The additional data obtained at 65 °C are included in Fig. 3 and Table 2.

Temperature Dependence

The partial molal heats of solution of hydrogen in the media were determined from the slopes of least squares plots of log (mole fraction solubility) *vs.* reciprocal absolute temperature (12). Similarly, partial molal entropies of solution were obtained from log (mole fraction solubility) *vs.* log (absolute temperature) graphs (12). In both sets of plots the least squares lines fell within 2% of all data points except two; correlation coefficients ranged from 0.997–0.999, except 0.994 at 77.9 mol% DMSO. The solubility data at 25 °C for 40.1 and 20.2 mol% DMSO were not included in these calculations, since definite upward curvature in the plots began to appear by this temperature. The results are shown in Fig. 4.

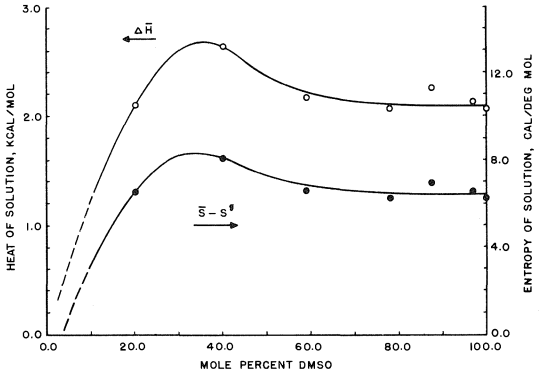

FIG. 4. Partial molal entropy (solid circles) and heat of solution (open circles) of hydrogen as a function of medium composition for 35–80 °C. The standard state for entropy is 1 atm partial pressure.

Discussion

Interpretation of Hydrogen Solubility Data

The data of Fig. 3 show a gradual disappearance of the minimum in the molar solubility – composition curve with increasing temperature. Such behavior is analogous to that for the viscosity of this solvent system (2), where the maximum in viscosity at 30–35 mol% DMSO becomes less pronounced as the temperature is raised. This viscosity effect has been ascribed to a gradual breakdown in the specific DMSO–water association (2, 6). More recently Schichman and Amey (11) have extended the viscosity measurements to lower temperatures, down to −60 °C in the region of 30 mol% DMSO. The viscosity maximum becomes even more clearly defined at the low temperatures. In Fig. 3 the position of minimum gas solubility changes with temperature from *ca.* 30 mol% DMSO at 25 °C to *ca.* 20 mol% at 50 °C.

The maximum in the partial molal entropy and heat of solution plots, Fig. 4, occurs in the same

Can. J. Chem. Downloaded from www.nrcresearchpress.com by 210.87.254.40 on 09/05/12
For personal use only.

Can. J. Chem. Downloaded from www.nrcresearchpress.com by 210.87.254.40 on 09/05/12
For personal use only.

25–35 mol% DMSO range. Hydrogen solubility in water is practically independent of temperature from about 35 to 70 °C (16), and the curves in Fig. 4 are projected towards zero for the heat of solution in water and slightly negative for the entropy.[5]

Fairly strong dipolar and/or ionic association in pure DMSO (6) must be overcome in the formation of cavities of proper size to accept the hydrogen molecules, and this is reflected in the positive heat of solution in DMSO. From 100 to *ca.* 50 mol% DMSO this function exhibits little change (Fig. 4), in agreement with the suggestion of Lindberg and Kenttämaa (1) that solvent structure remains essentially constant in this region. At the other extreme, water at lower temperatures is characterized by a relatively open structure (22–24 and references therein) which readily accepts small gas molecules; an enhanced ordering of the solvent molecules about the solute results. However, as DMSO is added to water the open structure is disrupted (6) and gradually replaced by the stronger DMSO–water complexes. The ease of accommodating the hydrogen molecules thus decreases, which leads to the observed increase in heat of solution from the value in water. Maximum energy is required in the region 25–35 mol% DMSO because intersolvent bonding is greatest at this point.

Further support for this argument comes from the energy–volume coefficient data of Macdonald and Hyne (10) for DMSO–water mixtures; their data are shown in Fig. 5. This function, the energy required per unit volume to enlarge a cavity in the solvent, is related directly to the strength of the solvent–solvent interaction. The shape of the plot in Fig. 5 resembles closely the present entropy and heat of solution curves in Fig. 4. Thus it becomes evident that the major factor controlling the solubility of hydrogen in these media lies in the structure of the mixed solvent itself.

The partial molal entropy of solution function in Fig. 4 can be interpreted in the following manner. Hildebrand and Scott consider (25) that, except for cases of specific gas–solvent interaction, the entropy of solution is comprized of two factors: (*1*) dilution of the solute on dissolution,

[5]The values for 50 °C, estimated from the data provided by Himmelblau (22), are 0.0 kcal/mol and −2.0 cal/deg mol, respectively; both become more positive with increasing temperature.

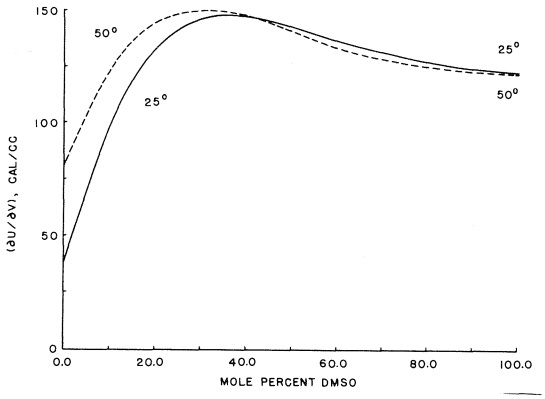

FIG. 5. Energy–volume coefficient data for the DMSO–water system at 25 and 50 °C, derived from the data of Macdonald and Hyne (10).

and (*2*) expansion of the solvent cavities in reaction to the gas molecules. Since the dilution term can be calculated directly from eq. 1, which gives the entropy change

$$[1] \qquad S_b - S_a = n \cdot R \cdot \ln (V_b/V_a)$$

for isothermal expansion of an ideal gas (26), the cavity expansion term can be obtained by difference. In eq. 1 V_a and V_b are the volumes occupied by 1 mol of gas ($n = 1$) in the vapor space and in solution, respectively; the latter value is the reciprocal of the molar gas solubility.

The results of this procedure are presented in Fig. 6 for 25, 50, and 80 °C. The figures for pure water were estimated from entropy of solution data reported by Himmelblau (22), while the gas solubilities were taken from the smooth curves of Fig. 3. Points for 40.1 and 20.2 mol% DMSO at 25 °C were not included in Fig. 6 since, due to curvature of the log (mole fraction solubility) *vs.* log (T) plots at this temperature, reliable estimates of the entropy of solution could not be made for these solvent compositions.[6] However, it appears that the maximum is not very pronounced at 25 °C.

It is apparent from a comparison of Figs. 4 and 6 that the cavity reaction term is the major contributor to the observed entropy of solution curve over the composition range from 0 to *ca.* 50 mol% DMSO. However, from 50–100 mol%

[6]The observed curvature arises from the transition in this solvent composition region from one type of temperature dependence of the solubility to another. In pure water the solubility *increases* when the temperature is *lowered* from 50 to 25 °C, whereas for solutions containing more than *ca.* 50 mol% DMSO the solubility *decreases* for the same temperature change.

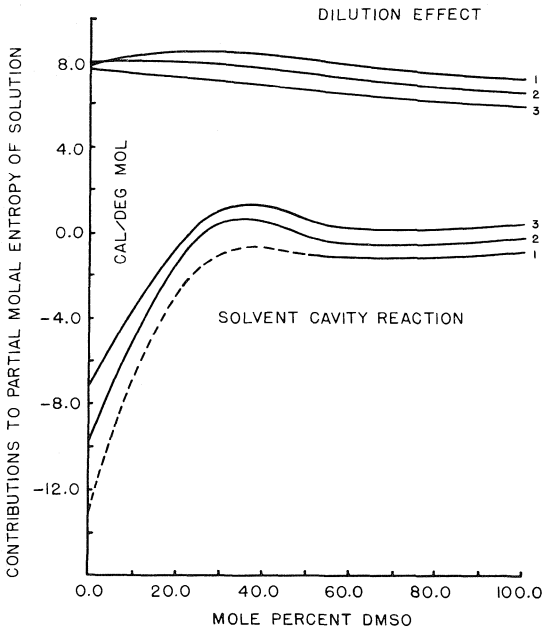

FIG. 6. A breakdown of the partial molal entropy of solution of hydrogen into contributions from dilution of the gas upon dissolution and from solvent cavity reaction to the gas molecules. Curves *1*, 25.0 °C; curves *2*, 50.0 °C; curves *3*, 80.0 °C. The standard state is 1 atm partial pressure.

DMSO, the dilution term becomes dominant, since the expansion term is now approximately zero (Fig. 6). The maximum in the net entropy near 35 mol% DMSO arises from the maximum in the expansion entropy at this point.[7] Such a result is not surprising since this region of greatest DMSO–water association is expected to be the most sensitive to perturbations such as a change of temperature (10) or introduction of an inert solute.

Similar observations to those in Fig. 4 have been made by Ben-Naim and co-workers during their investigation of the solubility of argon in several aqueous–organic systems (13, 14); their work was undertaken with a view to explaining what they considered to be the anomalously large negative heats and entropies of solution of inert gases in water. It was found in the water–methanol case (14), for example, that on changing from water to methanol the molar heat of solution of argon increased rapidly and then passed through a slight maximum before levelling off. The behavior was similar for the entropy, although no maximum was evident, in contrast to the present case. This dependence on medium composition was thought (14) to arise from a breakdown of large, hydrogen-bonded clusters of water molecules as the organic component is added. The major contribution to each function was believed to be liquid–liquid, and not gas–liquid interaction (14, 25).

DMSO–Water Complexes

Glasel (7) has discussed in some detail the experimental evidence pointing both to DMSO.$2H_2O$ and to DMSO.$3H_2O$ complexes. The excess relaxation times from his deuteron magnetic relaxation studies of DMSO–water solutions at 31 °C pass through a broad maximum at 25–30 mol% DMSO. The excess dielectric constant data of Doucet *et al.* (27) and Tommila and Pajunen (28) exhibit a similar behavior, and are interpreted by Glasel as an indication of 3:1 association. He concludes that both complexes are present in solution, and that the excess value functions for all the appropriate literature data are too flat and asymmetric to resolve a mixture of the two.

Glasel points out (7) that if the rotational reorientation time of the D_2O molecules in the 2:1 complex were considerably shorter than that for the 3:1 form, then the former complex might not be detected in a 50:50 mixture of the two. If this were the case, then even, for example, in a mixture which contains 95% of the 2:1 form the latter would probably not be observed in its true proportion, as determined from the maximum in the excess function curves arising from magnetic relaxation and dielectric constant measurements. The maximum in such curves would be strongly biased towards the 3:1 complex.

The following interpretation of complex formation in this system is put forward as a satisfactory explanation of the literature data to date. At least in the region 25–40 mol% DMSO, it is suggested that equilibria 2 and 3 are present in solution. It is clear from the DMSO–water phase

[2] $$DMSO.2H_2O = DMSO + 2H_2O$$

[3] $$DMSO.3H_2O = DMSO.2H_2O + H_2O$$

diagram (5) that at −65 °C the 3:1 form is dominant. However, at 25 °C equilibrium 3 must

[7]It should be noted that, although this maximum is believed to be real, the experimental error in the determination of the cavity entropy function is considerable, since it is obtained as the difference between two larger numbers of comparable size.

Can. J. Chem. Downloaded from www.nrcresearchpress.com by 210.87.254.40 on 09/05/12
For personal use only.

Can. J. Chem. Downloaded from www.nrcresearchpress.com by 210.87.254.40 on 09/05/12
For personal use only.

lie well to the right, since in general the various excess value functions have their maxima centered in the range 30–35 mol% DMSO (1, 2, 29). Also, the energy and entropy of activation for viscous flow for DMSO–water mixtures pass through a maximum near 30 mol% DMSO (11*a*). Since it has been demonstrated (2, 6) that the "2:1" complex is thermolabile, the proposal of the temperature-dependent equilibria 2 and 3 should overcome the problem of relating the phase diagram for this system to the various ambient temperature data (7, 11*a*).

Further evidence favoring the 2:1 complex at 25 °C and above comes from the present hydrogen solubility data, specifically from its deviation from "ideality". The "ideal" solubility has been defined for the present case as the sum of the quantities of gas which would have dissolved in the separated solvent components at each composition. These quantities were based on the hydrogen solubility in the pure liquids at each temperature. As can be seen in Fig. 7 for 25 °C, the effect of the real DMSO–water interaction is remarkable. The plots for 50 and 80 °C are similar, and show that this interaction is still fairly strong at 80 °C. The deviation functions at 25, 50, and 80 °C are quite symmetrical at the maximum, which occurs at 32 ± 5, 35 ± 5, and 32 ± 5 mol% DMSO, respectively.

It may be useful to extend the hydrogen solubility measurements to lower temperatures in order to test this two-complex hypothesis. Unfortunately, at such temperatures the DMSO–water mixtures are not in a liquid state over the full composition range (*e.g.* only from 0 to 70 mol% DMSO at 0 °C, and from *ca.* 20 to 45 mol% at −40 °C (5)), so that valuable information concerning deviation from ideality remains inaccessible (11). A shift in the maximum deviation towards 25 mol% would be predicted. However, it is interesting to note that the viscosity data recently obtained at the lower temperatures still show a maximum nearer 30 mol% (11), although the position of maximum deviation from ideality is not known. The latter would also be predicted to lie at or near 25 mol% DMSO.

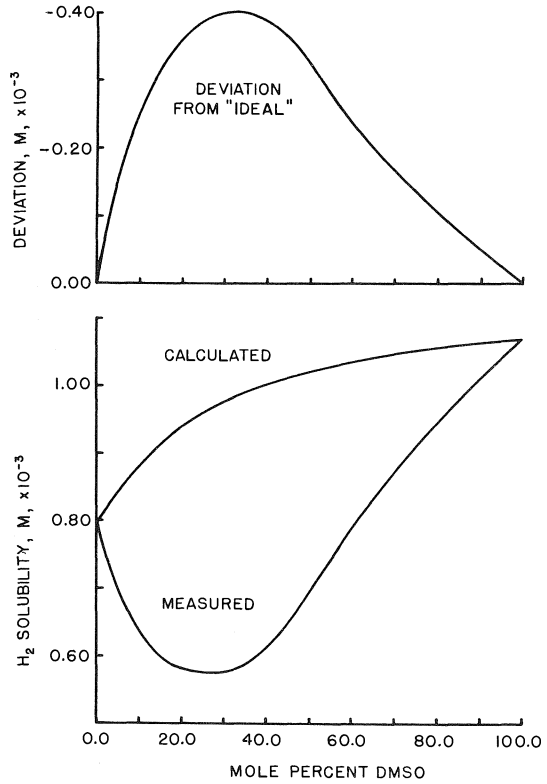

FIG. 7. The deviation from the calculated "ideal" hydrogen solubility as a function of medium composition.

The author wishes to thank Atomic Energy of Canada Limited for a fellowship, which was administered by the National Research Council of Canada, and for a very rewarding two year stay at WNRE. Valuable discussions with Dr. D. D. Macdonald, and provision of a preprint of some of their data by Dr. Macdonald and Dr. J. B. Hyne are gratefully acknowledged. The helpful comments of Drs. E. Buncel, D. A. Head, G. G. Strathdee, and N. H. Sagert on the manuscript were also appreciated.

1. J. J. LINDBERG and J. KENTTÄMAA. Suom. Kem. B**33**, 104 (1960).
2. J. M. G. COWIE and P. M. TOPOROWSKI. Can. J. Chem. **39**, 2240 (1961).
3. R. G. LEBEL and D. A. I. GORING. J. Chem. Eng. Data, **7**, 100 (1962).
4. J. J. LINDBERG and C. MAJANI. Acta Chem. Scand. **17**, 1477 (1963).
5. D. H. RASMUSSEN and A. P. MACKENZIE. Nature, **220**, 1315 (1968).
6. G. J. SAFFORD, P. C. SCHAFFER, P. S. LEUNG, G. F. DOEBBLER, G. W. BRADY, and E. F. X. LYDEN. J. Chem. Phys. **50**, 2140 (1969).
7. J. A. GLASEL. J. Am. Chem. Soc. **92**, 372 (1970).
8. K. H. JUNG and J. B. HYNE. Can. J. Chem. **48**, 2423 (1970).
9. G. BRINK and M. FALK. J. Mol. Struct. **5**, 27 (1970).
10. D. D. MACDONALD and J. B. HYNE. Can. J. Chem. **49**, 611 (1971).
11. (*a*) S. A. SCHICHMAN and R. L. AMEY. J. Phys. Chem. **75**, 98 (1971). (*b*). H. L. CLEVER and S. P. PIGOTT. J. Chem. Thermodyn. **3**, 221 (1971).
12. R. BATTINO and H. L. CLEVER. Chem. Rev. **66**, 395 (1966).

13. A. BEN-NAIM and G. MORAN. Trans. Faraday Soc. **61**, 821 (1965). A. BEN-NAIM. J. Phys. Chem. **72**, 2998 (1968).
14. A. BEN-NAIM. J. Phys. Chem. **71**, 4002 (1967).
15. D. D. MACDONALD and J. B. HYNE. Can. J. Chem. **48**, 2416 (1970).
16. S. K. SHOOR, R. D. WALKER, JR., and K. E. GUBBINS. J. Phys. Chem. **73**, 312 (1969).
17. J. KENTTÄMAA and J. J. LINDBERG. Suom. Kem. B**33**, 98 (1960).
18. Handbook of chemistry and physics. 44th ed. Chemical Rubber Publishing Co., Cleveland, Ohio. 1963.
19. Dimethyl sulfoxide technical bulletin. Crown Zellerbach Corp., Chemical Products Division, Camas, Washington 98607. 1966.
20. K. E. GUBBINS, S. N. CARDEN, and R. D. WALKER, JR. J. Gas Chromatogr. 98 (1965).
21. J. H. DYMOND. J. Phys. Chem. **71**, 1829 (1967).
22. D. M. HIMMELBLAU. J. Phys. Chem. **63**, 1803 (1959).
23. R. A. PIEROTTI. J. Phys. Chem. **69**, 281 (1965).
24. F. FRANKS and D. J. G. IVES. Q. Rev. **20**, 1 (1966).
25. J. H. HILDEBRAND and R. L. SCOTT. Regular solutions. Prentice-Hall, Inc., Englewood Cliffs, New Jersey. 1962. Chap. 4.
26. G. N. LEWIS and M. RANDELL. Thermodynamics. 2nd ed. *Revised by* K. S. PITZER and L. BREWER. McGraw-Hill Book Co., Inc., New York. 1961. p. 85.
27. Y. DOUCET, F. CALMES-PERRAULT, and M.-T. DURAND. Compt. Rend. **260**, 1878 (1965).
28. E. TOMMILA and A. PAJUNEN. Suom. Kem. B**41**, 172 (1968).
29. J. KENTTÄMAA and J. J. LINDBERG. Suom. Kem. B**33**, 32 (1960).

Can. J. Chem. Downloaded from www.nrcresearchpress.com by 210.87.254.40 on 09/05/12
For personal use only.

Can. J. Chem. Downloaded from www.nrcresearchpress.com by 210.87.254.5 on 09/05/12
For personal use only.

Proton Magnetic Resonance Studies of Ionic Solvation in Ion-exchange Resins. Part III. Multivalent Counterions

H. D. SHARMA[1] AND N. SUBRAMANIAN[2]

Department of Chemistry, University of Waterloo, Waterloo, Ontario

Received June 9, 1971

The p.m.r. spectra of Dowex AG 50W, X8, resins containing multivalent counterions have been measured. The ionic molal shifts in the exchanger phase are compared with those reported in homogeneous aqueous solutions. The spectral results are consistent with the concentrated electrolyte model of ion-exchange resins. Concentration and temperature dependence of proton chemical shifts in multivalent ionic forms of the resin suggests that ion association at high crosslinkages is more pronounced for counterions with high charge densities. The shapes of the shift-molality plots are explained by postulating that, at high crosslinkages, Mg^{2+} ion and the fixed $—SO_3^-$ group form "contact-ion pair" while the formation of "solvent-separated ion pair" is important in Be^{2+} and Al^{3+} forms of the resin. The anomalous trend in the hydration number values for magnesium and aluminum resinates can be understood as due to the long-range ordering of water structure in the presence of structure-forming ions. The p.m.r. spectra of resin–methanol system have been recorded at room temperature and at -65 °C. Failure to observe the resonance signal due to the cationic solvation shell at low temperature is attributed to the high degree of ion association under the conditions prevailing in the resin medium.

On a mesuré le spectre r.p.m. de la Dowex AG 50W, X8, résine contenant des contre-ions multivalents. On a comparé les déplacements molals ioniques dans la phase échangeuse avec ceux rapportés dans le le cas de solutions homogènes aqueuses. Les résultats spectraux sont consistants avec le modèle d'électrolyte concentré des résines échangeuses d'ions. Le fait que les déplacements chimiques des protons dépendent de la concentration et de la température dans les formes ioniques multivalentes de la résine suggère que l'association ionique à des degrés de pontage élevés est plus prononcée dans le cas de contre-ions à densité de charge élevée. On explique les formes des graphes des déplacements de molalité en postulant que, à des degrés de pontage élevés, l'ion Mg^{2+} et le groupe fixé $—SO_3^-$ forment une "paire d'ions en contact", alors que la formation de "paires d'ions séparées du solvant" est importante dans les cas où la résine a la forme Be^{2+} et Al^{3+}. On peut comprendre la tendance anormale des valeurs de nombre d'hydratation pour les résinates d'aluminium et de magnésium, connaissant l'ordre à longue portée de la structure de l'eau en présence d'ions formant la structure. On a enrégistré le spectre r.p.m. du système résine-méthanol à la température de la pièce et à -65 °C. On attribue l'insuccès à observer le signal de résonance dû à la couche de solvatation cationique à basse température, au degré élevé d'association ionique sous les conditions prévalant dans le milieu de la résine.

Canadian Journal of Chemistry, **49**, 3948 (1971)

Introduction

The n.m.r. technique is becoming increasingly useful as a means of observing directly the several phenomena connected with ion-exchange resin (1–17). Following the preliminary investigations of Gordon (1, 2) and Dinius and co-workers (3), n.m.r. has been applied to the study of a variety of problems such as electrolyte invasion (4), characterization of resin samples (6, 11), determination of rate of exchange of water protons between the internal and external phases (10), kinetics of ion exchange (12), and solvent selectivity in resin-binary aqueous solvent systems (14, 15). A report on the n.m.r. spectra of macroreticular resins has appeared very recently (17).

The main aim of the several other studies (5, 7–9, 13, 16) was to examine the structural properties of the sorbed liquid and the environments of the ionic species within the exchanger phase which are of importance in understanding the ion-exchange behavior. A systematic study of the effects of chemical structure, crosslinking, nature of counterion, inner molality and temperature on the p.m.r. spectra of several cation- and anion-exchange resins carrying monovalent counterions was reported by us earlier (8, 16). Our results as well as those from similar such studies (5, 7, 9, 13) are consistent with the model of the ion exchanger as a concentrated electrolyte

[1]To whom all correspondence should be addressed.

[2]Material in this article taken from the dissertation submitted to the University of Waterloo in partial fulfillment of the requirements for a Ph.D. degree.

Can. J. Chem. Downloaded from www.nrcresearchpress.com by 210.87.254.5 on 09/05/12
For personal use only.

solution. They also serve to indicate that ion–water interactions in the resin phase and in the homogeneous aqueous solution are closely similar, although there is increased ion association in the resin medium, especially in highly crosslinked resins. We have extended the p.m.r. spectral studies to cation-exchange resins loaded with multivalent counterions in order to obtain additional information about ionic solvation in the resin phase. The p.m.r. spectra of the exchanger suspended in a non-aqueous solvent are also reported.

Experimental

Dowex AG 50W (200–400 mesh) resins with varying nominal divinylbenzene (DVB) contents were procured from Bio-Rad Laboratories in the H^+ form. (In the case of 1% DVB resin only 50–100 mesh beads were available.) They were converted to the required ionic forms according to the recommended procedures (18). The moisture contents of the swollen resin beads were determined by the Karl Fischer titration method (19).

The capacities of the resin in the Mg^{2+} and Al^{3+} forms were estimated by the following procedure. A weighed amount of the air-dried resin in the H^+ form was placed in a column. A known volume of a standard solution of $MgSO_4$ or $Al(NO_3)_3$ followed by several bed volumes of distilled water were passed through the column. The quantities of Mg^{2+} or Al^{3+} ions used were in liberal excess of the total capacity of the resin bed to ensure complete conversion. The effluent was collected in each case and made up to a known volume. Convenient aliquot parts of the solution were titrated against standard EDTA solution using Eriochrome Black T as indicator (20). From the difference in the metal-ion concentration between the original standard solution and the effluent, the capacity of the resin for Mg^{2+} or Al^{3+} ion was calculated. The overall error in the values of the resin molalities (m) reported is expected not to exceed $\pm 4\%$.

The p.m.r. spectral measurements were made with a J.E.O.L. C-60 spectrometer. The temperature of the sample was controlled by a JES VT2 unit. A copper–constantan thermocouple placed adjacent to the sample and a Hewlett–Packard 3420A DC differential voltmeter were used to measure the temperature. The temperature of the samples could be maintained within ± 1 °C of the desired temperature. All the spectral data reported in this work are the average results of at least three separate measurements. The chemical shifts could be determined to an accuracy of ± 1 c.p.s.

Preparation of sample for the resin–methanol system was as follows. The water-swollen Dowex AG 50W resin in the particular ionic form was first air-dried and then kept at 80 °C under 1 mm pressure for 12 h. This procedure was adopted to keep the fracturing of the beads during drying to a minimum. Fisher "spectranalyzed" methanol was used without further purification. Direct titration with Karl Fischer reagent gave an upper limit of 0.05% (w/w) for water present in methanol. The anhydrous exchanger was allowed to swell in methanol for a sufficiently long time and the suspension transferred to a n.m.r. sample tube. During the preparation of the sample, care was taken to ensure minimal contact of the materials with the atmosphere.

Results

The p.m.r. spectrum of a well-settled suspension of ion-exchange resin beads in water usually shows two distinct signals attributable to the water protons inside and outside the resin particle (1–3, 8). If the interior and exterior water peaks overlap considerably, they were resolved by the use of a computer routine developed by the Computing Center, University of Waterloo (21). The shift $\Delta\nu$ c.p.s. or δ_{soln} p.p.m. represents the chemical shifts of the interior water signal with respect to the exterior water signal, a negative value signifying that the internal water peak is downfield of the external water peak.

The p.m.r. spectra of aqueous suspensions of Dowex AG 50W (X8) in the Be^{2+}, Mg^{2+}, Ca^{2+}, Sr^{2+}, Ba^{2+}, Zn^{2+}, Al^{3+}, La^{3+}, and Th^{4+} forms were recorded at a temperature of 23 ± 1 °C. The ionic molalities and the respective chemical shifts are listed in Table 1.

The effect of crosslinking on the internal water proton chemical shift was studied in Be^{2+}, Mg^{2+}, Ba^{2+}, and Al^{3+} forms of the exchanger. The δ_{soln}–m plots are shown in Fig. 1.

The influence of temperature on the p.m.r. spectrum was examined in several cases of the

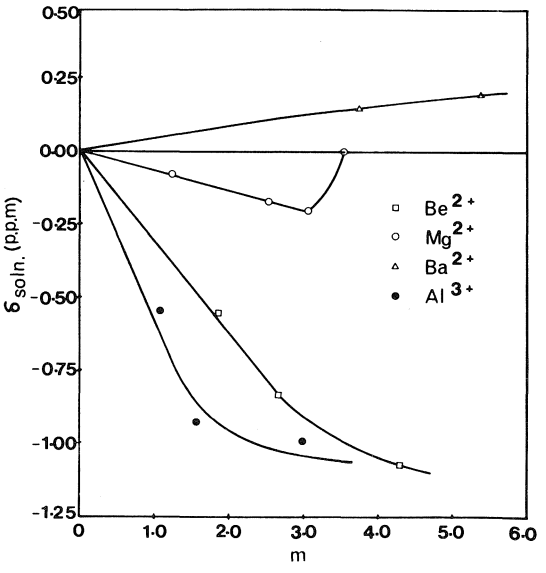

FIG. 1. δ_{soln} as a function of internal molality for multivalent ionic forms of Dowex AG 50W, at 23 °C.

Can. J. Chem. Downloaded from www.nrcresearchpress.com by 210.87.254.5 on 09/05/12
For personal use only.

TABLE 1. Comparison of ionic molal shifts in 8% crosslinked sulfonated cation-exchange resins and in homogeneous aqueous solutions

			δ_+ (p.p.m./mol)*		
			Resin phase		
Ionic form	Molality	$\Delta\nu$ (c.p.s.)	This work (23 ± 1 °C)	Reference 7 (40–42 °C)	Aqueous phase
Be^{2+}	2.7	−50.0	−0.354		−0.437†
Mg^{2+}	2.6	−10.0	−0.107	−0.08	−0.179†
Ca^{2+}	2.8	~1.0	−0.036	−0.04	−0.032†
Sr^{2+}	3.0	4.0	−0.020	−0.02	−0.005†
Ba^{2+}	3.8	9.0	~0.0	−0.02	+0.018†
Zn^{2+}	2.7	−18.0	−0.153	−0.10	−0.124‡
Al^{3+}	1.6	−56.0	−0.625		−0.519‡
La^{3+}	2.2	−17.0	−0.173		−0.239‡
Th^{4+}	—	0.0	−0.084		—

*Based on $\delta_{NH_4^+} = 0$ scale.
†Franconi and Conti (25), 27.5 °C.
‡Shoolery and Alder (26), uncorrected for bulk susceptibility.

Table 2. Hydration numbers of Dowex AG 50W resins in Mg^{2+} and Al^{3+} forms

Ion	Resin crosslinkage	Molality	$d\delta_{soln}^{ethane}/dt$ (p.p.m./°C)	h (±0.5–1.0)
Mg^{2+}	X2	1.27	0.00814	6.4
	X8	2.55	0.00676	6.4 (6.7)*
	X16	3.52	0.00538	7.0
Al^{3+}	X2	1.12	0.00742	11.9
	X8	1.60	0.00540	15.1

*Creekmore and Reilley (9).

exchanger containing di- and trivalent counterions. Some typical spectra are reproduced in Figs. 2–4. Detailed studies were carried out with Mg^{2+} (2%, 8%, and 16% DVB) and Al^{3+} (2% and 8% DVB) forms of Dowex AG 50W. In each case

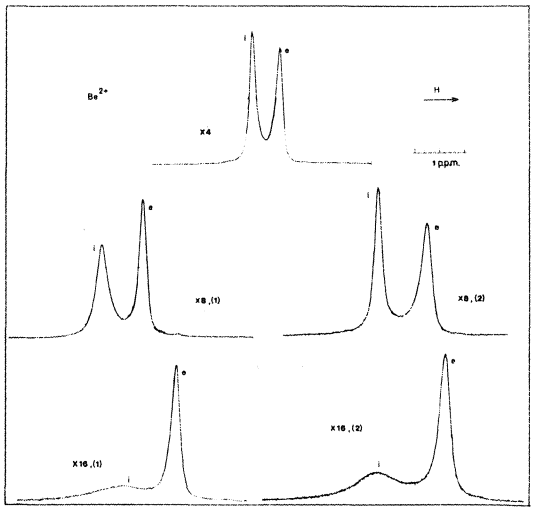

FIG. 2. Effect of crosslinking and temperature on the p.m.r. spectrum of Dowex AG 50W, Be^{2+}: (e) "external" water; (i) "internal" water; (*1*) 23 °C, (*2*) 70 °C.

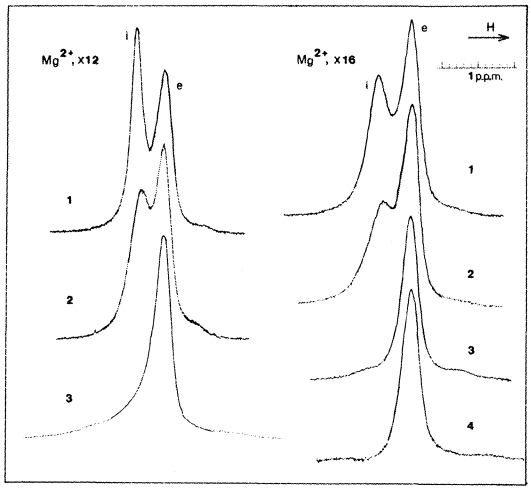

FIG. 3. Effect of temperature on the p.m.r. spectra of Mg^{2+} form of Dowex AG 50W (X12 and X16): (e) "external" water; (i) "internal" water; X12, (*1*) 70 °C, (*2*) 50 °C and (*3*) 23 °C; X16, (*1*) 78 °C, (*2*) 65 °C, (*3*) 23 °C, and (*4*) 9 °C.

the δ_{soln} value at a given temperature with respect to gaseous ethane, δ_{soln}^{ethane}, was evaluated by following the procedure described in our earlier paper (8). The slopes of the δ_{soln}^{ethane}–temperature

Can. J. Chem. Downloaded from www.nrcresearchpress.com by 210.87.254.5 on 09/05/12
For personal use only.

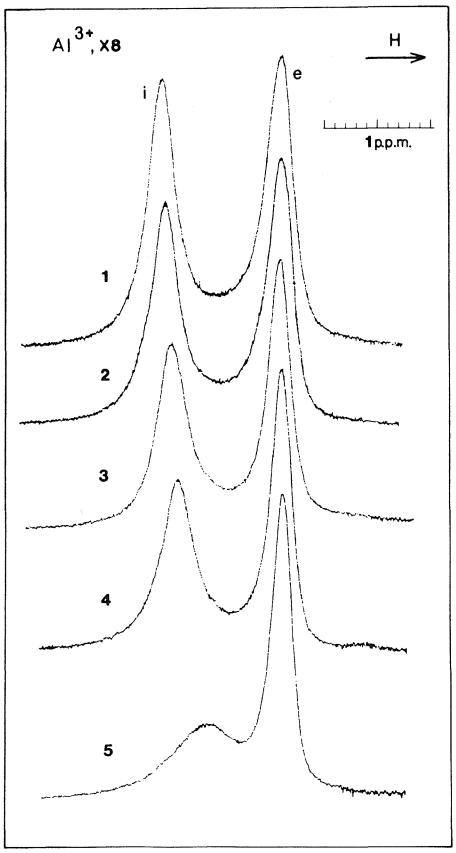

FIG. 4. Effect of temperature on $\Delta\nu$ for Dowex AG 50W (X8), Al^{3+}: (e) "external" water; (i) "internal" water; (*1*) 79 °C, (*2*) 65 °C, (*3*) 50 °C, (*4*) 34 °C, and (*5*) 9 °C.

plots, $d\delta_{soln}^{ethane}/dt$, were calculated by the method of least squares and are reported in Table 2.

The p.m.r. spectra of Dowex AG 50W resins of various crosslinkages and ionic forms in contact with methanol were recorded at 23 °C and at low temperatures. The spectra for Mg^{2+} and Al^{3+} forms of 1% crosslinked resin taken at 23 °C and at −65 °C are shown in Fig. 5.

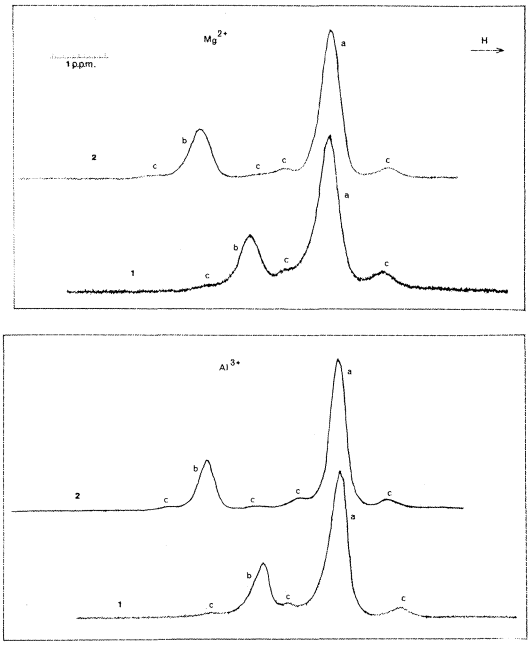

FIG. 5. Proton magnetic resonance spectra of Mg^{2+} and Al^{3+} forms of Dowex AG 50W (X1) in methanol: (*a*) methyl protons, (*b*) hydroxyl proton, and (*c*) side band; (*1*) 23 °C and (*2*) −65 °C.

Discussion

Influence of Ionic Form

It is known from p.m.r. studies of the exchanger in univalent ionic forms that the anomalous shielding effects of the aromatic rings of the resin matrix do not contribute significantly to the experimentally observed chemical shift (8, 16). Also, for the case of the spherical resin beads in contact with the solvent, corrections due to bulk susceptibility effects can be neglected (22, 23). Since the measured shifts are free from matrix and susceptibility effects, one could attribute δ_{soln} almost entirely to salt effects, *i.e.*, interactions between the sorbed water molecules and the ionic species present within the resin particle. It is then possible to divide δ_{soln} into individual ionic contributions by making an arbitrary assumption, *viz.*, $\delta_{NH_4^+}^0 = 0$ (24) ($\delta^0 = \delta/m$ as $m \to 0$). Based on this scale, a value of $\delta_{SO_3^-}^0 =$ 0.021 p.p.m./mol was obtained by us from measurements on the ammonium form of the sulfonated cation exchange resins (8). Using this value, the ionic molal shifts characteristic of the multivalent counterions studied, δ_+, were calculated. The values are compared with those obtained in homogeneous aqueous solutions in Table 1.

In both the resin and the aqueous media, the algebraic values of the molal chemical shift increase in the same order:

$$Al^{3+} \ll Be^{2+} \ll La^{3+} < Zn^{2+} < Mg^{2+} < Ca^{2+} < Sr^{2+} < Ba^{2+}$$

In a recent independent study, Howery and Kittay (7) determined the ionic molal shifts of a few divalent counterions (see Table 1). However,

Can. J. Chem. Downloaded from www.nrcresearchpress.com by 210.87.254.5 on 09/05/12
For personal use only.

their measurements were carried out at a probe temperature of 40–42 °C. It has been shown that the frequency separation between the interior and exterior water proton resonance is a function of temperature (8, 9, 16). This would explain the difference between their values and those reported in our work. The slight difference between the resin phase δ_+ values observed by us and those obtained in aqueous solutions (25) are partly due to a difference of 5 °C in the temperature of spectral measurements. Also, the aqueous solution values for Zn^{2+}, Al^{3+}, and La^{3+} are from the work of Shoolery and Alder (26) and are uncorrected for susceptibility effects. Considering these factors and the limits of experimental error involved in the measurement of molal chemical shifts, the similarity in the sign and magnitude of δ_+ values in the two systems is indeed striking. It is significant that the cation inside the resin particle exerts its "structure-making" or "structure-breaking" property to almost the same extent as in an aqueous electrolyte solution (24). This result is consistent with the earlier observations on the ion-exchange resins with univalent counterions (8, 16).

Effect of Crosslinking

Compared to the univalent ionic forms of the resin, the internal water line broadening at higher crosslinkings is generally more pronounced with multivalent counterions. For instance, the width at half-height ($W_{1/2}$) has values of 72 and 90 c.p.s., respectively, for Be^{2+} and Al^{3+} forms of 16% crosslinked resin. There is evidence for ion association at higher resin crosslinkages even among univalent counterions. Under the circumstances, one would expect the small, multiply-charged counterions like Be^{2+} and Al^{3+} to exhibit considerably greater tendencies to form ion pairs. The relatively immobile multivalent cations closely adjacent to the organic matrix hold on to the water molecules in the primary hydration sheath very tightly. This would result in large differences in the relaxation times of "free" and "bound" water. Also, the exchange between the two kinds of internal water might be expected to be relatively slow.

It can be seen from Fig. 1 that the (negative) deviation from linearity of δ_{soln}–m plots is more pronounced than in the case of monovalent counterions and occurs at lower ionic concentrations (8, 16). With increase in crosslinkage (and, therefore, molality), the interactions between counterion and resin ion are obviously enhanced to a greater extent in resins carrying multiply charged counterions. Recent p.m.r. studies in aqueous electrolyte solutions have led Vogrin and co-workers (27) to conclude that ion pairing becomes important above 2 m for bi–uni salts ($Mg(ClO_4)_2$, $CaCl_2$, $Ca(NO_3)_2$) whereas for alkali metal salts it is significant only above 5 m. It is conceivable that small multivalent ions having relatively high charge densities possess residual electrostatic free energy beyond their primary hydration sphere and therefore can interact with anions in solution. Such interactions can be expected to become more important as the dielectric constant of the medium is lowered.

It can be further observed from Fig. 1 that the δ_{soln}–m plot for Mg^{2+} resin has a maximum and that at $m = 3.52$ (corresponding to X16) δ_{soln} is actually zero. The fact that the interior and exterior water lines are buried under each other is confirmed by varying the temperature of the sample. Since the temperature coefficients of proton chemical shift are normally different for pure water and the solution, increase in temperature causes the single peak to first undergo unsymmetrical broadening and then split into two separate peaks (Fig. 3). In the case of the other three ions, δ_{soln} continues to increase up to X16, although the rate of increase is noticeably diminished at higher concentrations. Further, whereas the interior water line is considerably broadened in Be^{2+} and Al^{3+} forms of the resin, especially at X16, the line is comparatively much narrower in Mg^{2+} resin. It would seem that at crosslinking above X8, the interaction between Mg^{2+} and the fixed ionic group is enhanced to such an extent that the $—SO_3^-$ ion displaces at least one water molecule from the primary hydration shell of the cation ("contact ion pair" formation). The proportion of bulk water would correspondingly increase thereby leading to an apparent decrease in the overall effect of this cation on the structure of water. The existence of $(M—NO_3)^+$ complex in highly concentrated aqueous solutions of divalent metal nitrates has been inferred from vibrational spectral studies (28–30). Mg^{2+} is believed to exhibit contact ion pairing with NO_3^- in aqueous solutions with water to salt ratio below 6:1 (31).

On the other hand, Be^{2+} and Al^{3+} ions, by virtue of their high charge densities, tend to retain their primary hydration sphere intact and

Can. J. Chem. Downloaded from www.nrcresearchpress.com by 210.87.254.5 on 09/05/12
For personal use only.

probably bind the sulfonate anion in their second coordination shell ("solvent-separated ion pair"). Thus, with increase in concentration, these ions would have a lesser effect on the structure of water in the secondary layer while they continue to polarize the nearest-neighbor water molecules. Raman (31), infrared and n.m.r. (32) spectral evidences indicate the absence of Al^{3+}–NO_3^- contact in aqueous $Al(NO_3)_3$ solutions with concentrations comparable to those prevailing in Al^{3+} resins.

Effect of Temperature

The observed effect of temperature on $\Delta\nu$ is quite similar to that encountered in univalent ionic forms of the exchanger, *viz.*, in the case of structure-forming counterions, *e.g.*, Be^{2+}, Mg^{2+}, Zn^{2+}, Al^{3+}, La^{3+}, for which $\Delta\nu$ is negative, increase of temperature moves the peaks farther apart (*cf.* H^+, F^-); on the other hand, in the case of structure-breaking counterions, *e.g.*, Ba^{2+}, Sr^{2+}, for which $\Delta\nu$ is positive, increase of temperature decreases the separation between the two peaks (*cf.* Na^+, K^+).

Change in temperature has very little effect on the shape of the internal water line in the case of monovalent counterions (9). But for multivalent counterions, increase in temperature results in a significant sharpening of the resin phase water proton resonance (Figs. 2–4). The effect was also observed with Zn^{2+} and La^{3+} forms of the exchanger. Creekmore and Reilley (9) noted the same effect in their study of the Mg^{2+} resin. The narrowing of the internal water resonance with increase in temperature can be explained in terms of the two effects invoked above in connection with line broadening at higher resin crosslinkages, *viz.*, (*i*) the large difference in the relaxation exhibited by free and hydration water (9) and (*ii*) the lower rate of exchange between free and bound water molecules in the resin phase. Thus the observed effects of crosslinking and temperature on the internal water linewidth supplement each other.

Shoolery and Alder (26) found that the proton linewidths for aqueous electrolyte solutions were not noticeably broader than the pure water line except for Al^{3+}, Be^{2+}, and the most concentrated $ZnCl_2$ solutions. In the latter cases, lowering the temperature to slow down the proton exchange resulted only in a broadening of the line rather than a splitting of the line. It is interesting to note a similar behavior for the internal water linewidths in the resin system. It is found that $W_{1/2}$ varies within narrow limits for most ionic forms studied and has a value close to that for the H^+ form of the resin. Change in temperature has very little effect on $W_{1/2}$. But, in the case of Be^{2+} and Al^{3+} ions, lowering of temperature does result in considerable broadening of the interior water line. The observed effects within the resin phase are thus analogous to those produced by electrolytes in the homogeneous aqueous phase. This again lends support to the concept of the ion-exchange resin as a concentrated electrolyte solution.

Malinowski and co-workers (33) have developed a relationship between the "effective" hydration number of the electrolyte, h, and the temperature coefficients of proton resonance in pure water and in aqueous electrolyte solution

$$[1] \quad h = \frac{55.55}{m}\left(\frac{d\delta_{H_2O}{}^{ethane}/dt - d\delta_{soln}{}^{ethane}/dt}{d\delta_{H_2O}{}^{ethane}/dt}\right)$$

From what has been said above, it is clear that changes in temperature affect the average proton chemical shift of the interior and exterior water to different extents. The effect is identical to that observed in homogeneous electrolyte solutions. It should therefore be possible to apply eq. 1 to determine the "effective" hydration numbers of the resin salts. This has already been done in several cases involving monovalent counterions (8, 9, 16). Creekmore and Reilley (9) have estimated the h value for magnesium resinate in Dowex 50, X8, resin. We have used the $d\delta_{soln}{}^{ethane}/dt$ value listed in Table 2 to calculate the hydration numbers of Mg^{2+} and Al^{3+} forms of Dowex AG 50W. The results are included in Table 2.

Firstly, the h values for magnesium and aluminum resinates are found to be lower than those of $MgCl_2$ (34) and $Al(NO_3)_3$ (35), respectively, in aqueous solutions of comparable concentrations. Creekmore and Reilley (9) explained the lower hydration number of the magnesium resinate (X8) as due to the difference between Cl^- hydration (h = 0.6–1.0) and the resinate hydration (assumed ~0). The assumption that the hydration of the fixed sulfonate group is ~0 is not borne out by our experiments on the ammonium form of the cation exchanger (16). We attribute the observed lowering of h in the resin phase to enhanced cation–anion association

Can. J. Chem. Downloaded from www.nrcresearchpress.com by 210.87.254.5 on 09/05/12
For personal use only.

aided by the very low dielectric constant of the exchanger medium.

Secondly, the hydration numbers increase with increase in crosslinkage (or, concentration). It may be recalled here that a similar trend is also observable in the case of H^+ and F^- counterions (16). Such behavior is quite contrary to the expected effect of concentration on h. It is significant that ions exhibiting this anomalous behavior all possess the common ability to promote the structure of liquid water. In the derivation of eq. 1 it has been tacitly assumed that the ion does not perturb the secondary layer of water molecules around it. While this assumption may perhaps be reasonable for moderately large monovalent ions (*e.g.*, Na^+), it is certainly not valid for ions with high charge densities. It is therefore not surprising that for ions of the latter type, the hydration numbers determined by Malinowski's technique are rather anomalous. By taking into account the long-range ordering of water molecules in a solution containing structure-making ions, it is in fact possible to explain the observed trend in h values as a function of concentration (36).

Resin–Methanol System

Spectra at 23 °C

The p.m.r. spectrum of a suspension of the cation-exchange resin in methanol consists of two broad, unsymmetrical bands due to the methyl and the hydroxyl protons. Spinning side bands are invariably present in these spectra (2). It was observed that the spectral characteristics do not change significantly with bead size (50–100 to 200–400 mesh), resin crosslinkage (X1 to X8), or ionic form (Na^+, Be^{2+}, Mg^{2+}, and Al^{3+}). The methyl and hydroxyl proton resonances were separated by ~93 c.p.s. For all the cases studied, $W_{1/2}$ of both the peaks were ~25 c.p.s. When the solvent external to the beads was removed and the spectrum of the resin phase alone was recorded, two broad peaks ($W_{1/2} = 35$ c.p.s.) with diminished intensities and separated by 96 c.p.s. were seen in the spectrum. This shows that the interior solvent resonance is masked under the exterior solvent peaks.

According to Gordon (2), the diamagnetic anisotropy of the polystyrene matrix in cation-exchange resins can be expected to shift the carbon-bound proton resonance of the interior liquid by +14–18 c.p.s. Similar upfield shift of the methyl resonance can be expected also for the resin–methanol system. However, the interior and exterior methyl resonances are unresolved in the spectrum owing to the large peakwidth of the external solvent in this case. The broadening of the exterior liquid line increases with increasing difference in the diamagnetic susceptibility of the liquid and the solid ($\Delta\chi$) (2). Since this difference is relatively large when methanol is the solvent ($\Delta\chi = 0.221 \times 10^{-6}$ c.p.s. units), the exterior resonance is considerably broadened.

From their studies of methanolic solutions of electrolytes, Butler and Symons (37) have assigned values of −0.458 and −0.30 p.p.m. at 40 and −69 °C, respectively, for the molal shifts in the hydroxyl resonance due to Mg^{2+} ion. Based on these values, one would expect a difference of at least 30 and 70 c.p.s. between the chemical shifts of the interior and exterior hydroxyl resonances in the 1 and 8% crosslinked resins, respectively. Even greater values for this shift can be expected for the Be^{2+} and Al^{3+} forms of the exchanger. But the actually observed value has an upper limit of only 25 c.p.s. in all the cases. This could be attributed to ion pairing in the resin phase. When water is replaced by an organic solvent such as methanol, the dielectric constant of the resin medium is further lowered, thereby favoring enhanced ion association.

Spectra at Low Temperature

The spectra of the resin samples in methanol were recorded at low temperatures in an attempt to observe the resonance due to the cationic solvation shell. However, unlike in homogeneous electrolyte solutions (38), no separate signal attributable to primary shell solvent molecules appeared in the spectrum up to −70 °C. When the temperature was lowered beyond −70 °C, the sample became too viscous for any signal to be observed.

Failure to observe the cation solvation shell in the p.m.r. spectra at low temperature can be considered as evidence for the high degree of ion pairing in these resins. As mentioned earlier, strong interactions between counterions of high charge density and the fixed resin group may be expected at the low dielectric constant of the resin medium in the presence of an organic solvent. It is likely that as a consequence, the solvent molecules firmly bound in the primary shell of these cations will lose their rotational degree of freedom. Due to the resulting large

Can. J. Chem. Downloaded from www.nrcresearchpress.com by 210.87.254.5 on 09/05/12
For personal use only.

increase in the correlation time, τ_c, their resonance may be broadened beyond detection. It is interesting to note that Gordon (2) failed to observe any signal due to the counterion in the presence of anhydrous non-aqueous solvents. He considered this to reflect the very low fluidity of the resin in contact with these liquids and the consequent loss of rotational freedom of the ions. The disappearance of the ^{23}Na signal at higher resin crosslinkages has also been attributed to an increase in τ_c (9).

Ion pairing has been postulated in mixed aqueous and non-aqueous solutions of electrolytes to account for the decrease in the measured hydration number at the concentrations similar to those prevailing in the resin phase (39, 40). In contrast to the resin phase, however, cations and anions are both mobile in these systems; furthermore, the diffusion coefficients of the ionic species are also higher due to the relatively lower viscosity of the homogeneous phase. Thus, while the cationic solvation shell can be observed for these solutions in the p.m.r. spectrum at low temperatures, such is not the case for the more viscous exchanger medium, in which the anionic species is immobile. The slow rate of exchange of ions observed in 85% methanol solution can also be attributed to the immobility of ions in the resin phase (41).

The authors thank the National Research Council of Canada for providing financial support for this work and for the award of a Post-Graduate scholarship to N. Subramanian. We are grateful to Mr. W. Gilchrist for the technical assistance rendered during the spectral measurements.

1. J. E. Gordon. Chem. Ind. London, 267 (1962).
2. J. E. Gordon. J. Phys. Chem. **66**, 1150 (1962).
3. R. H. Dinius, M. T. Emerson, and G. R. Choppin. J. Phys. Chem. **67**, 1178 (1963).
4. R. H. Dinius and G. R. Choppin. J. Phys. Chem. **68**, 425 (1964).
5. D. Reichenberg and I. J. Lawrenson. Trans. Faraday Soc. **59**, 141 (1963).
6. J. P. de Villiers and J. R. Parrish. J. Polymer Sci. **A2**, 1331 (1964).
7. D. G. Howery and M. J. Kittay. J. Macromol. Sci. **A4**, 1003 (1970).
8. T. E. Gough, H. D. Sharma, and N. Subramanian. Can. J. Chem. **48**, 917 (1970).
9. R. W. Creekmore and C. N. Reilley. Anal. Chem. **42**, 570 (1970).
10. R. W. Creekmore and C. N. Reilley. Anal. Chem. **42**, 725 (1970).
11. A. Darickova, D. Doskocilovo, S. Sevicik, and J. Stamberg. Polymer Lett. **8**, 259 (1970).
12. L. S. Frankel. Anal. Chem. **42**, 1638 (1970).
13. D. G. Howery and B. H. Kohn. Anal. Lett. **3** (2), 89 (1970).
14. L. S. Frankel. Can. J. Chem. **48**, 2432 (1970).
15. D. G. Howery, G. Senum, and L. H. Madoff. Anal. Lett. **3**, (9), 483 (1970).
16. H. D. Sharma and N. Subramanian. Can. J. Chem. **49**, 457 (1971).
17. L. S. Frankel. J. Phys. Chem. **75**, 1211 (1971).
18. F. Helfferich. Ion exchange. McGraw-Hill Book Co., Inc., New York, N.Y. 1962. Chap. 9.
19. H. D. Sharma and N. Subramanian. Anal. Chem. **41**, 2063 (1969).
20. A. I. Vogel. Textbook of quantitative inorganic analysis. John Wiley and Sons, Inc., New York, N.Y. 1967.
21. A. Weerheim. Private communication.
22. J. A. Pople, W. G. Schneider, and H. J. Bernstein. High resolution nuclear magnetic resonance. McGraw-Hill Book Co., New York, N.Y. 1959.
23. K. Frei and H. J. Bernstein. J. Chem. Phys. **37**, 1891 (1962).
24. J. C. Hindman. J. Chem. Phys. **36**, 1000 (1962).
25. C. Franconi and F. Conti. *In* Nuclear magnetic resonance in chemistry. *Edited by* B. Pesce, Academic Press, New York, N.Y. 1965. p. 349.
26. J. N. Shoolery and B. J. Alder. J. Chem. Phys. **23**, 805 (1955).
27. F. J. Vogrin, P. S. Knapp, W. L. Flint, A. Anton, G. Highberger, and E. R. Malinowski. J. Chem. Phys. **54**, 178 (1971).
28. R. E. Hester and R. A. Plane. J. Chem. Phys. **45**, 4588 (1966).
29. D. E. Irish and G. E. Walrafen. J. Chem. Phys. **46**, 378 (1967).
30. A. R. Davis and D. E. Irish. Inorg. Chem. **7**, 1699 (1968).
31. D. E. Irish, G. Chang, and D. L. Nelson. Inorg. Chem. **1**, 425 (1970).
32. N. A. Matwiyoff, P. E. Darley, and W. A. Movius. Inorg. Chem. **7**, 2173 (1968).
33. E. R. Malinowski, P. S. Knapp, and B. Feuer. J. Chem. Phys. **45**, 4274 (1966).
34. R. W. Creekmore and C. N. Reilley. J. Phys. Chem. **73**, 1563 (1969).
35. E. R. Malinowski and P. S. Knapp. J. Chem. Phys. **48**, 4989 (1968).
36. H. D. Sharma and N. Subramanian. To be published.
37. R. N. Butler and M. C. R. Symons. Trans. Faraday Soc. **65**, 2559 (1969).
38. J. H. Swinehart and H. Taube. J. Chem. Phys. **37**, 1579 (1962).
39. A. Fratiello, V. M. Nishida, R. E. Lee, and R. E. Schuster. J. Chem. Phys. **50**, 3624 (1969).
40. S. A. Al-Baldawi, M. H. Brooker, T. E. Gough, and D. E. Irish. Can. J. Chem. **48**, 1202 (1970).
41. H. D. Sharma, R. E. Jervis, and L. W. McMillan. J. Phys. Chem. **74**, 969 (1970).

Can. J. Chem. Downloaded from www.nrcresearchpress.com by 210.87.254.40 on 09/05/12
For personal use only.

The Isothermal Compressibility of Organic Liquids by Ultracentrifugation. Correlation with Surface Tension

ALFRED J. RICHARD

Department of Chemistry and Pharmaceutical Chemistry, Medical College of Virginia, Health Sciences Division of Virginia Commonwealth University, Richmond, Virginia 23219

AND

KENNETH S. ROGERS

Department of Biochemistry, Medical College of Virginia, Health Sciences Division of Virginia Commonwealth University, Richmond, Virginia 23219

Received July 22, 1971

Isothermal compressibilities of seven organic liquids have been determined by analytical ultracentrifuge techniques, in good agreement with literature values obtained by other methods.

A least squares regression equation was derived that correlated the logarithmic values of isothermal compressibilities of 7 organic liquids, determined experimentally, with the liquids' surface tensions. This equation was shown to be valid for 11 other organic liquids (values obtained from literature) over a temperature range of 0° through 50°, and a surface tension range of 13 to 44 dyn per cm.

Nous avons déterminé la compressibilité isothermique pour 7 liquides organiques, avec l'ultracentrifugeuse analytique. Nos valeurs sont toujours semblables a celles déterminés par d'autres méthodes.

Une équation des moindres carrés a été déconverte entre le logarithme des valeurs des compressibilités isothermiques des 7 liquides, et de leurs tensions superficielles. Cette équation est valide pour 11 autres liquides organiques (valeurs des compressibilités obtenue dans la littérature) ayant des tensions superficielles de 13 a 44 dyn/cm et entre les températures de 0 a 50 °C.

Canadian Journal of Chemistry, **49**, 3956 (1971)

Introduction

The isothermal compressibilities (1, 2) and the isothermal piezooptic coefficients (2, 3) of liquids have been measured by ultracentrifugation. During the course of our continuing studies on the determination of isothermal compressibilities of liquids by ultracentrifugation, it was found necessary to make modifications on the schlieren optical system of the ultracentrifuge. These modifications are reported here for the Beckman Instruments Spinco E analytical ultracentrifuge.

In addition, an empirical relationship has been found between the isothermal compressibility at 1 atm and the surface tension of several liquids.

Experimental

The procedure of Dayantis (1) was followed in this work. If the refractive index (n) of a liquid at 5461 Å, and its density (ρ_0) at the temperature of choice were known, then the isothermal compressibility (β) was given by the relation:

$$\beta = \frac{(y)6n \tan\theta}{(Lam_1m_2)(n^2+2)(n^2-1)\rho_0 w^2 r_0}$$

where y was the height of the schlieren line above a baseline obtained with the same cell at a low speed, 2000–3000 r.p.m., both measured from the counter balance references, θ the schlieren bar angle, 70° for all these experiments, L the optical lever, a the cell thickness, (m_1m_2) the vertical magnification of the optical system, w the angular velocity, and r_0 the distance of the meniscus from the center of rotation. The temperature was measured before each picture was taken and was always found to be 20 ± 0.02 °C (4). The filter above the light-source was taped in place to prevent it from moving as the chamber was lowered or raised. Of great importance was the lateral position of the schlieren bar. Correct values of compressibilities were obtained only when the bar was placed relative to the slit image such that the bar image, as seen on the viewing screen, did not rise or fall as the bar angle approached 0°. Rather, the image, without tilting, should smear out symmetrically at 0°, about its position at all other angles. The bar was positioned with the chamber closed and evacuated. It was difficult to set the lateral position of the bar accurately with the counter-locking set screw arrangement on the bar holder; therefore, these screws were removed, and a micrometer was attached to the bar holder such that the micrometer abutted against the camera lens holder, thereby fixing the lateral position of the bar, see Fig. 1. Contact was maintained by spring tension. To test the effect on compressibility of the lateral position of the bar, the bar was moved 25 μ to either side of the true position at the end of a benzene determination, and a picture taken for each setting. For the displacement of the bar toward the front of the centrifuge, the compressibility was increased by 0.5% and similarly, the compressibility was decreased by 0.5% when the bar was moved toward the back of the centrifuge.

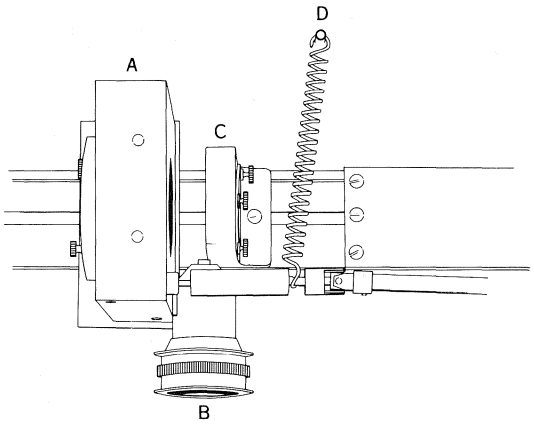

FIG. 1. View of the schlieren optical track of the ultracentrifuge, with protective cover removed. Visible components are: *A*, schlieren bar assembly; *B*, micrometer, attached to the bar assembly; *C*, camera lens mount; *D*, spring. The spring was attached to the bar assembly and to one of the support posts of the protective cover.

The cell used for these experiments had a 12 mm, 2° sector, aluminum centerpiece. Sapphire windows were necessary, but to minimize bending of even these windows, the window holders were of the older design with openings just slightly greater than the size of the sector. The clear gaskets between the windows and the window holders dissolved readily in some of the liquids used in this study, and were replaced therefore by red polyethylene gaskets normally used for the centerpiece. As a precaution, the red centerpiece gaskets were always presoaked for 2 h with the liquid under study. Cyclohexane caused some expansion of the gaskets, but the other liquids in the study did not seem to affect them. Excess grease was carefully removed from the threads and keyway of the cell body to prevent leaching.

As a check on the bar angle setting, it was found useful to place on the optical track, directly in front of the bar, an aluminum plate with the top cut to 70° to the vertical. A white card placed behind the bar, and appropriate lighting, made it possible to sight along the bar over the top of the aluminum plate. Perpendicular scribe marks on the front of the aluminum plate were also used simultaneously to check the vertical setting of the slit image. The lightsource slit width was reduced to 0.15 mm by feeler gauge, with care for the parallel alignment of the slit edges.

Each run was carried out as follows: The centrifuge was accelerated to 33 450 r.p.m. and allowed to spin there for at least 5 min. The speed was then reduced to 2095 r.p.m. and maintained there for at least 15 min at 20 °C. A picture was taken to provide the base line. The few minutes overspeed at the start of each run eliminated base line shifts that otherwise frequently occurred during centrifugation, apparently due to slight rearrangements of cell components. The final picture was taken at 23 150 r.p.m. after a minimum of 15 min at speed and at 20 °C. With benzene and cyclohexane, patterns taken 3 h after reaching speed were identical with those taken at 15 min.

All liquids studied in this work were purchased of C.P. or spectroanalyzed grade and were used with no further purification other than drying overnight with pellet KOH or $CaSO_4$ (drierite), followed by vacuum distillation to eliminate gases. The still was brought to 1 atm by the injection of He through a rubber septum on the collecting vessel; and samples, taken by syringe, were transferred quickly to the centrifuge cell that was also filled with He.

Results and Discussion

The isothermal compressibilities of seven liquids are listed in Table 1 along with available literature values.

Agreement was quite good in most cases. The values of Holder and Whalley (5) were extrapolated to 20 °C from their data at higher tem-

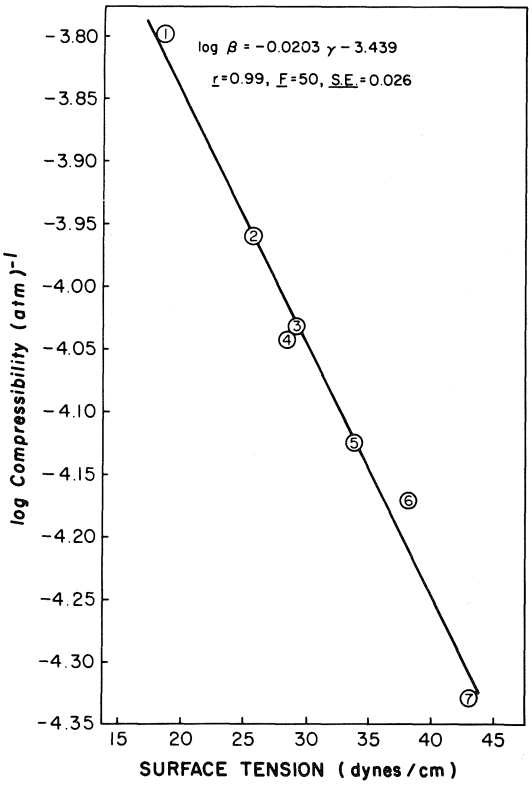

FIG. 2. Plot of the logarithm of the isothermal compressibilities (β) against the surface tensions (γ) of seven organic liquids. Values of β at 20° were determined by ultracentrifugation, values of γ also at 20° were taken from ref. 6. The liquids were: *1*, hexane; *2*, cyclohexane; *3*, benzene; *4*, toluene; *5*, chlorobenzene; *6*, pyridine; and *7*, aniline. The regression coefficient (*r*) is for the fit of experimental points to the equation given in the figure, the significance of the equation in describing the data is given by the *F*-test coefficient (*F*), and *s.e.* represents the standard error of the estimate (log β) calculated from the equation.

Can. J. Chem. Downloaded from www.nrcresearchpress.com by 210.87.254.40 on 09/05/12
For personal use only.

TABLE 1. Isothermal compressibilities of liquids at 1 atm and 20 °C

Liquid	$\beta\ 10^6(\text{atm}^{-1})$	Literature value	Reference	Difference (%)
Hexane	158.6	158.0	6	+0.4
Cyclohexane	109.4	111.0, 106.4	5,6	−0.5, +3
Benzene	92.9	94.2, 95.8	5,6	−1.3, −3
Toluene	90.6	90.8	6	−0.2
Chlorobenzene	74.9	75.0	6	−0.1
Pyridine	68.2	—	—	—
Aniline	46.8	45.9	6	+2.0

TABLE 2. Correlation of surface tension (γ) with isothermal compressibility (β) of various organic liquids at different temperatures

Compound	Temperature (°C)	γ* (dyn/cm)	$\log \beta_{obs.}$* $(\text{atm})^{-1}$	$\log \beta_{calcd.}$† $(\text{atm})^{-1}$	$\frac{\log \beta_{calcd.}}{\log \beta_{obs.}}$‡
Acetic acid	20	27.8	−4.003	−4.003	1.000
Acetic acid	50	24.8	−3.948	−3.942	0.998
Ethyl acetate	0	26.5	−4.003	−3.977	0.994
Ethyl acetate	20	23.9	−3.940	−3.924	0.996
Ethyl acetate	50	20.2	−3.824	−3.849	1.007
Acetone	20	23.7	−3.890	−3.920	1.008
Acetone	40	21.2	−3.808	−3.869	1.016
Aniline	10	44.1	−4.360	−4.334	0.994
Aniline	20	42.9	−4.337	−4.310	0.994
Aniline	50	39.4	−4.267	−4.239	0.993
Benzene	10	30.2	−4.054	−4.052	0.999
Benzene	20	28.9	−4.021	−4.026	1.001
Benzene	30	27.6	−3.987	−3.999	1.003
Chlorobenzene	20	33.6	−4.124	−4.121	0.999
Nitrobenzene	20	43.9	−4.300	−4.330	1.007
Carbon disulfide	20	32.3	−4.027	−4.095	1.017
Chloroform	20	27.1	−3.995	−3.989	0.998
Ethanol	0	24.1	−4.000	−3.928	0.982
Ethanol	10	23.6	−3.976	−3.918	0.985
Ethanol	20	22.8	−3.949	−3.902	0.988
Ethanol	30	21.9	−3.919	−3.884	0.991
n-Butanol	0	26.2	−4.085	−3.971	0.972
Methanol	0	24.5	−3.965	−3.936	0.993
Methanol	20	22.6	−3.909	−3.898	0.997
Methanol	50	20.1	−3.824	−3.847	1.006
Toluene	10	27.7	−4.069	−4.001	0.983
Toluene	20	28.5	−4.042	−4.018	0.994
Toluene	30	27.4	−4.013	−3.995	0.996
FC 78§	25	13.0	−3.605	−3.664	1.016

*Values for γ and β were obtained from ref. 6.
†Calculated from γ and the equation given in Fig. 1.
‡Ratio expresses the correlation between calculated and observed values; 1.000 is a perfect correlation.
§Fluorochemical produced by Minnesota Mining and Manufacturing Company, St. Paul, Minnesota (see ref. 2).

peratures. The value of 100×10^{-6} atm^{-1} for benzene at 20°, quoted in ref. 6, is incorrect because of an erroneous unit conversion in the transcription from the original paper (7). Dayantis (1) showed agreement with this latter value. However, there is no indication of the quality of benzene used by Dayantis, nor is it reported that the benzene was dried and degassed prior to centrifugation.

An empirical relationship was noted between β and the surface tension (γ) of the liquids in this study. As liquids became more compressible (gas-like), the surface tension decreased. A least squares equation was derived that correlated the experimental β values with literature values of γ, Fig. 2. The regression coefficient (r) for the fit of experimental points to the line was 0.99. A value of 1.00 for r would indicate a perfect fit.

A comparison of measured β values with β values calculated from the equation in Fig. 2 is presented in Table 2. All data in Table 2 were taken from literature sources, thus the equation deduced from ultracentrifugal evaluation of β

Can. J. Chem. Downloaded from www.nrcresearchpress.com by 210.87.254.40 on 09/05/12
For personal use only.

Can. J. Chem. Downloaded from www.nrcresearchpress.com by 210.87.254.40 on 09/05/12
For personal use only.

was satisfactory to represent β values obtained by other means, *e.g.*, measurement of the speed of sound through a liquid (8) or piezometry (9). Although the least square equation was obtained for data at 20 °C, the same equation was used to represent the relation between β and γ for liquids in the temperature ranges from 0–50 °C. Thus the log β and γ seem to vary in the same way with temperature.

Sinanoglu (10) has related bulk surface tension of liquids to the energy requirement for the formation of a cavity in a liquid by the displacement of the liquid's own molecules. Then solute interactions with the pre-formed cavity in the liquid were related to the interactions of various molecules of biological interest, *e.g.*, solvent denaturation of DNA, actinomyocin dimerization, and benzoquinone-hydroquinone associations in various solvents.

Surface tension values have also been related to cohesive energies of liquids (latent heat of vaporization) and as such, have been used to calculate Hildebrand and Scott solubility parameters (11). The solubility parameters have generally been useful only for regular solutions, however. For instance, the solution of aniline in water would be non-regular because of hydrogen bond interactions.

Since the energy required to form a hole, or fixed space, in a liquid was proportional to γ of that liquid (10, 12), then it was reasonable that the compressibility of the liquid was determined, at least in part, by the existence of pre-formed cavities. Thus, hydrogen bonding liquids, with considerable fixed space would be incompressible relative to ideal liquids containing little or no fixed space.

Further work is in progress to determine whether the amount of fixed space in a liquid can be determined from studying the pressure dependence of the isothermal compressibility in the ultracentrifuge.

The authors are grateful to Mrs. Annie S. Leeper for technical assistance.

1. J. DAYANTIS. Compt. Rend. Acad. Sci. Paris. Ser. C, **267**, 223 (1968).
2. A. J. RICHARD, J. GLICK, and R. BURKAT. Anal. Biochem. **37**, 378 (1970).
3. R. JOSEPS and A. P. MINTON. J. Phys. Chem. **75**, 716 (1971).
4. Technical Bulletin No. TB6003B. Beckman Instruments Inc., Palo Alto, California. p. 1.
5. G. A. HOLDER and E. WHALLEY. Trans. Faraday Soc. **58**, 2095 (1962).
6. Handbook of chemistry and physics. 49th ed. The Chemical Rubber Co., Cleveland, Ohio. 1966. pp. F-12, F-31.
7. L. A. K. STANLEY, W. TUPMAN, and K. R. HART. Trans. Faraday Soc. **51**, 323 (1955).
8. E. B. FREYER, J. C. HUBBARD, and D. H. ANDREWS. J. Am. Chem. Soc. **51**; 759 (1929).
9. M. DIAZ PENA and M. L. MCGLASHAN. Trans. Faraday Soc. **55**, 2018 (1959).
10. O. SINANOGLU. *In* Molecular associations in biology. *Edited by* B. Pullman. Academic Press, New York. 1968. pp. 427–445.
11. J. A. HILDEBRAND and R. L. SCOTT. The solubility of nonelectrolytes. Dover Publications, New York. 1964. pp. 395–434.
12. E. A. MOLEWYN-HUGHES. Physical chemistry. 2nd ed. Pergamon Press, London. 1961. p. 937.

Can. J. Chem. Downloaded from www.nrcresearchpress.com by 84.22.46.98 on 09/08/12
For personal use only.

Configurational Equilibria in Methyl 3,6-Dideoxy-3-nitro-α-L-hexopyranosides[1]

JAN KOVÁŘ, KAREL ČAPEK,[2] AND HANS H. BAER
Department of Chemistry, University of Ottawa, Ottawa, Canada

Received June 21, 1971

Epimerizations in alkaline medium, by which the methyl 3,6-dideoxy-3-nitrohexopyranosides having the α-L-*gluco* (**1**), α-L-*galacto* (**2**), α-L-*manno* (**3**), and α-L-*talo* (**4**) configurations are mutually interconverted, were investigated quantitatively by n.m.r. spectroscopy and by preparative separation of products. The epimeric equilibrium compositions obtained depend on whether an equimolar or a catalytic amount of alkali is supplied. In the first case they are governed by the thermodynamic stabilities of the nitronate anions (**4***a* > **3***a* > **2***a* ≃ **1***a*), and in the second case, by those of the free nitro glycosides (**1** > **2** ≃ **3** > **4**). The results are discussed in terms of conformational analysis, and a value of 2 kcal/mol is found for the contribution of the $A^{(1,3)}$ interaction to the conformational free energy in the nitronates. The $A^{(1,3)}$ effect strongly influences not only the product composition at the nitronate equilibrium but also the pathway of epimerization.

L'épimérisation en milieu alcalin, par laquelle les didéoxy-3,6 nitro-3 hexopyranosides de méthyle ayant les configurations α-L-*gluco* (**1**), α-L-*galacto* (**2**), α-L-*manno* (**3**), et α-L-*talo* (**4**), s'interconvertissent mutuellement, est étudiée quantitativement par r.m.n. et par séparation préparative des produits. Les compositions des équilibres épimériques obtenus dépendent des quantités de base ajoutées (équimolaire ou catalytique). Dans le cas d'une quantité équimolaire, les équilibres sont gouvernés par les stabilités thermodynamiques des anions nitronates (**4***a* > **3***a* > **2***a* ≃ **1***a*) et dans le cas d'une quantité catalytique, ils sont gouvernés par les stabilités thermodynamiques des nitro glycosides libres (**1** > **2** ≃ **3** > **4**). Les résultats sont discutés en terme d'analyse conformationnelle et une valeur de 2 kcal/mol est obtenue pour la contribution de l'interaction $A^{(1,3)}$ à l'énergie libre conformationnelle des nitronates. L'effet $A^{(1,3)}$ influence fortement non seulement la composition des produits à l'équilibre des nitronates mais également le processus de l'épimérisation.

Canadian Journal of Chemistry, **49**, 3960 (1971)

Introduction

Certain nitro glycosides and nitro cyclitols are known to undergo spontaneous epimerizations in alkaline medium (1). Two preceding investigations in this series have dealt specifically with structural, conformational, and mechanistic aspects of such reactions in methyl 3-deoxy-3-nitropentopyranosides (2) and methyl 4,6-*O*-benzylidene-3-deoxy-3-nitrohexopyranosides (3). It has been realized in those studies that the $A^{(1,3)}$ effect (4), the nonbonded interaction between a group attached by a double bond to the ring (here, $=NO_2^-$) and a vicinal, equatorial substituent (here, —OH), has a profound influence upon conformational preferences and configurational interconversions (2, 3). On the basis of free energy calculations (2) one may predict the behavior of other groups of nitro glycosides in alkaline solution, and it is the purpose of the present article to elaborate this concept by disclosing results obtained with the four available methyl 3,6-dideoxy-3-nitro-α-L-hexopyranosides.

Results

The compounds used were crystalline methyl 3,6-dideoxy-3-nitro-α-L-glucopyranoside (**1**) (5, 6) and its isomers (6) having the α-L-*galacto* (**2**), α-L-*manno* (**3**), and α-L-*talo* (**4**) configurations. In aqueous solution containing one or more equivalents of sodium hydroxide, these glycosides incur changes in optical rotation as exemplified in Fig. 1. The compounds exist, in media of sufficient alkalinity, as nitronate salts showing high intensity u.v. absorption (ε 9000–11000 in 0.01 *N* NaOH) at 248–250 nm. It was possible to distinguish the individual isomers by n.m.r. spectroscopy by virtue of differing chemical shifts in their respective *O*-CH_3 and *C*-CH_3 signals (Table 1), and to determine isomer ratios, in mixtures, by integration of these signals.

Each of the four nitro glycosides gave a spectrum corresponding to a practically uniform nitronate within the first 10 min after the addition

[1]Part XXV in a series on reactions of nitro sugars. For part XXIV see ref. 11.

[2]On leave of absence (1967–1968) from the Laboratory of Monosaccharides, Institute of Chemical Technology, Prague, Czechoslovakia.

TABLE 1. The n.m.r. data of sodium nitronates in D_2O

Compound	Chemical shifts (τ)*						Splittings (Hz)		
	H-1	H-2	H-4	H-5	O—CH_3†	C—CH_3†	$J_{1,2}$	$J_{4,5}$	$J_{5,6}$
1*a*					6.640	8.84			6.5
2*a*	——— ~5.33 ———			5.99	6.689	8.888	(<1)	2.0	6.5
3*a*	——— ~5.57 —		5.80	6.29	6.717	8.791		9.0	6.2
4*a*	——— ~5.37 ———			6.12	6.750	8.845		2.0	6.5

*Measured with acetone (τ, 7.91) as internal standard.
†Obtained from spectra of isomer mixtures, recorded at 50 Hz sweep width, by direct comparison of peak positions.

of alkali; with progressing time, epimerizations became evident by the appearance, in each case, of the signals corresponding to the other isomers (Fig. 2). The most interesting feature was that **1** and **2** gave the same initial nitronate and showed the same time-dependent changes in the resulting isomer ratios, an unexpected phenomenon that

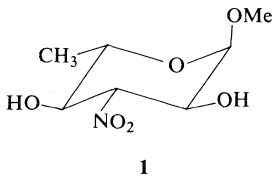

1

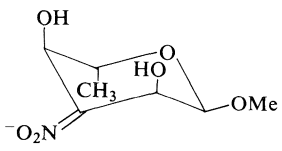

1*a*

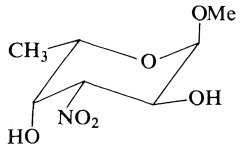

2

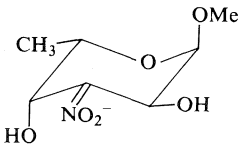

2*a*

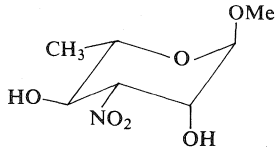

3

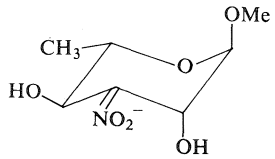

3*a*

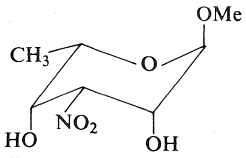

4

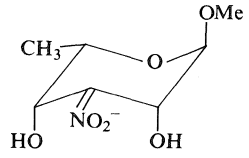

4*a*

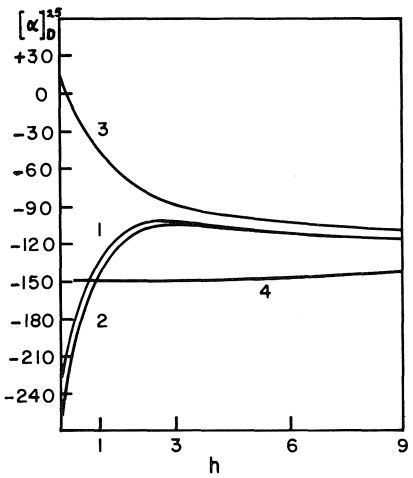

FIG. 1. Change of specific rotations of **1**–**4** (*c*, 1 in CO_2 – free water) in the presence of an equimolar amount of NaOH.

will be explained in the Discussion. The nitronate initially produced from **3** was different, but in the course of 3.5 h the composition of the mixture became nearly the same as that observed starting from **1** and **2**. The spectroscopic results thus parallel the optical rotation curves which indicated a closely similar reaction course for **1** and **2**, and attainment of a mobile equilibrium of nitronates departing from **1**, **2**, and **3**. It was found that the nitronate initially engendered from both **1** and **2** is that having the α-L-*xylo* configuration (**2***a*), *i.e.*, the nitronate corresponding to the α-L-*galacto* parent glycoside **2**. The remarkable fact that **1** did not form the α-L-*ribo* nitronate **1***a* at an early stage of the reaction was first suggested by a comparison of the *C*-CH_3 chemical shifts of the nitronates (Table 1) with those of the free nitro compounds in neutral solution (Table 2), the corresponding signals being affected very little when a given nitro glycoside is converted into its configurationally related nitronate. Def-

Can. J. Chem. Downloaded from www.nrcresearchpress.com by 84.22.46.98 on 09/08/12
For personal use only.

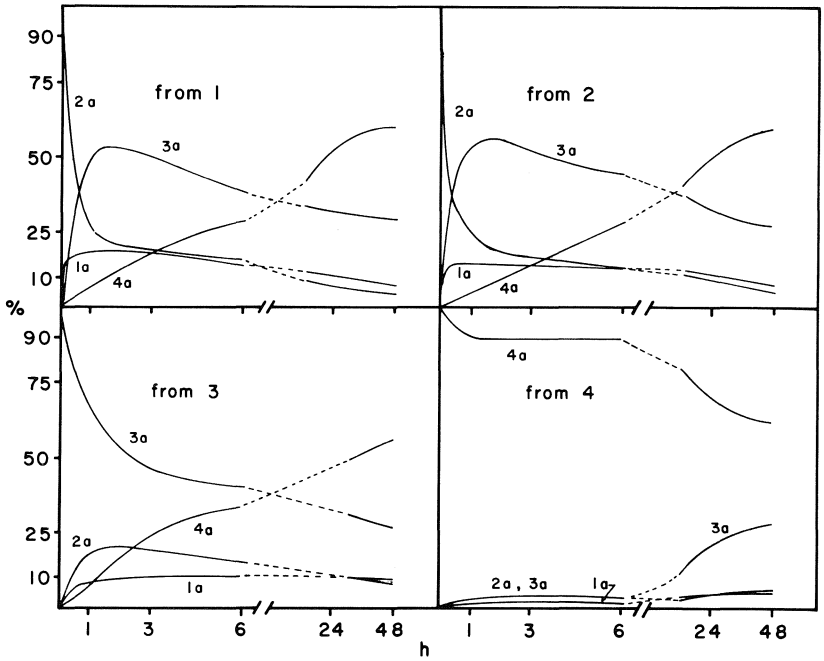

FIG. 2. Change in composition of glycoside mixtures during epimerization in the presence of excess base.

inite confirmation was provided by the preparative isolation, in 60% yield, of **2** from **1** after treatment with alkali for 1 min followed by acidification. The nitronate **1***a* did, however, constitute a component of the epimeric mixtures eventually produced from all the four nitro glycosides. The nitronate initially given by the mannoside **3** undoubtedly was the expected α-L-*arabino* salt **3***a* as was deduced from the n.m.r. data (Tables 1 and 2) and proved by the recovery of **3** in good yield upon acidification. The nitronate that initially arose from the α-L-*talo* isomer **4** had the α-L-*lyxo* configuration (**4***a*). It underwent epimerization relatively slowly so that, after the period of time when the other nitronates had reached a quasi-equilibrium among themselves (3–4 h), changes were insignificant (Figs. 1 and 2). However, after 2–3 days the reaction mixture contained **4***a* and the three isomers in the ratio of 60:40. Whereas the mixtures of nitronates obtained from **1**, **2**, and **3** contained about 20% of **4***a* at their quasi-equilibrium, they eventually assumed the same final composition, with **4***a* being the main component. From this second equilibrium we have calculated standard free energy differences for **1***a*, **2***a*, and **3***a* with respect to the thermodynamically most stable isomer, **4***a* (Table 3). It is seen that the α-L-*arabino* salt **3***a* ranks second in stability, and that the α-L-*ribo* (**1***a*) and α-L-*xylo* (**2***a*) compounds are significantly less stable and quite similar to each other. Since the equilibrium concentrations of **1***a* and **2***a* were rather small and their spectroscopic determination was, therefore, subject to a relatively large error, we also calculated the standard free energy differences for these compounds with respect to **3***a* at the quasi-equilibrium, where larger concentrations prevailed (Table 3). The latter data show the stability of **2***a* to be somewhat greater than that of **1***a*, but it is open to question whether equilibration between **1***a*, **2***a*, and **3***a* had in fact been complete at that point.

In a different series of experiments we have studied in the same way the epimerization of the nitro glycosides in the presence of a catalytic amount of base (0.05–0.1 molar equiv of NaOD) rather than in the presence of 1 molar equiv or more. Again, **1**, **2**, and **3** each underwent epimeric equilibration, and the mixtures obtained after 2 days were identical in composition within an experimental error estimated at 10% of values found (Fig. 3). As was to be expected (see Discussion), the ratio of the free nitro sugars **1**–**4** so attained was different from that of their salts

Can. J. Chem. Downloaded from www.nrcresearchpress.com by 84.22.46.98 on 09/08/12
For personal use only.

Can. J. Chem. Downloaded from www.nrcresearchpress.com by 84.22.46.98 on 09/08/12
For personal use only.

TABLE 2. The n.m.r. spectra of free nitro glycosides in D_2O

Compound	Chemical shifts (τ)*							Splittings (Hz)				
	H-1	H-2	H-3	H-4	H-5	O—CH_3	C—CH_3†	$J_{1,2}$	$J_{2,3}$	$J_{3,4}$	$J_{4,5}$	$J_{5,6}$
1	5.30	5.91	5.36	6.30	6.38	6.69	8.833	4	10	7	9–11	6
2	5.25	5.64	5.16	5.82	6.02	6.70	8.904	4	11	3.5	1.5	6.5
3	5.38	5.71	5.32	6.00	6.41	6.70	8.783	1.5	3.5	9.7	9.5	6
4	5.30	5.62 (or 5.70)	5.33	5.70 (or 5.62)	6.11	6.71	8.821	1.5	3	3	1.5	6.5

*Measured with acetone (τ, 7.91) as internal standard. Deuterium exchange of H-3 is slow enough for observing this signal.
†Obtained from spectra of isomer mixtures, recorded at 50 Hz sweep width, by direct comparison of peak positions.

TABLE 3. Configurational equilibration of nitronates at 35°

Starting compound	Products in equilibrium (%) 1*a*	2*a*	3*a*	4*a*
Final equilibrium (after 2–3 days)				
1	7	4	29	60
2	6	7	27	60
3	9	8	27	56
4	5	6	28	61
Mean*	6.75	6.25	27.75	59.25
$K_{4a/1a} = 8.80$		$-\Delta G^\circ = 1.28$ kcal/mol		
$K_{4a/2a} = 9.48$		$= 1.32$		
$K_{4a/3a} = 2.14$		$= 0.44$		
Quasi-equilibrium (after 3–4 h)				
1	10	16	49	25
2	14	18	45	23
3	15	20	50	15
Mean*	13	18	48	21
$K_{3a/2a} = 2.67$		$-\Delta G^\circ = 0.58$ kcal/mol		
$K_{3a/1a} = 3.69$		$= 0.77$ kcal/mol		

*Used for calculating *K*.

1*a*–**4***a* observed in the previous series of experiments. It is seen (Fig. 3) that the α-L-*gluco* isomer (**1**) was the preponderant component and the α-L-*galacto* (**2**) and α-L-*manno* (**3**) isomers were present as minor components in about equal proportions, the ratio being about 3:1:1. The α-L-*talo* isomer was not detected (although it is spectroscopically distinguishable from the others), but its nitronate, the α-L-*lyxo* salt **4***a*, was present to the extent of the amount of base that had been added.[3] Table 4 gives the equilibrium concentrations and standard free energy differences derived therefrom, for **2** and **3** relative to **1**.

Addition of a limited amount of base to the *talo* compound **4** also caused epimerizations (Fig. 3), but these were so slow that the approach of an epimeric equilibrium was obscured by the occurrence of side reactions which were not elucidated.

[3]This is understandable in view of the considerable differences in nitromethylene acidities. Compound **4** was found to have the lowest pK_a value (8.25) as determined potentiometrically by half-titration in water solution. The values for **1**, **2**, and **3** were 10.60, 10.45, and 9.90 respectively. (Since **1***a* is rapidly epimerized as outlined above, the value found for **1** does not represent the simple equilibrium **1** ⇌ **1***a* but a more complex equilibrium involving also **2** ⇌ **2***a*; compare a similar situation observed (2) with methyl 3-deoxy-3-nitro-β-D-xylopyranoside (2).)

TABLE 4. Configurational equilibration of nitro glycosides in the presence of a catalytic amount of NaOD at 35°

Starting compound	Products in equilibrium after 4–6 days (%) **1**	**2**	**3**	4*a*
1	59	17	16	8
2	61	13	17	9
3	60	14	18	8
Mean	60	14	17	8
$K_{1/2} = 4.28$		$-\Delta G^\circ = 0.86$ kcal/mol		
$K_{1/3} = 3.53$		$= 0.76$		

The spectroscopic studies recorded above were complemented by experiments on a preparative scale. The nitro glycosides **1**–**4** were allowed to epimerize in the presence of 1 equiv of sodium hydroxide, and samples were deionized after given periods of time. The mixtures produced were then separated by column chromatography and the epimers were isolated in crystalline form. The results are summarized in Table 5. Comparison of the ratios of glycosides isolated with the ratios of products encountered in spectroscopic experiments (Figs. 2 and 3) shows reasonable agreement, although there are some apparent discrepancies that will be discussed later on. Based on these studies, conditions have been worked out which render the *galacto* and

Can. J. Chem. Downloaded from www.nrcresearchpress.com by 84.22.46.98 on 09/08/12
For personal use only.

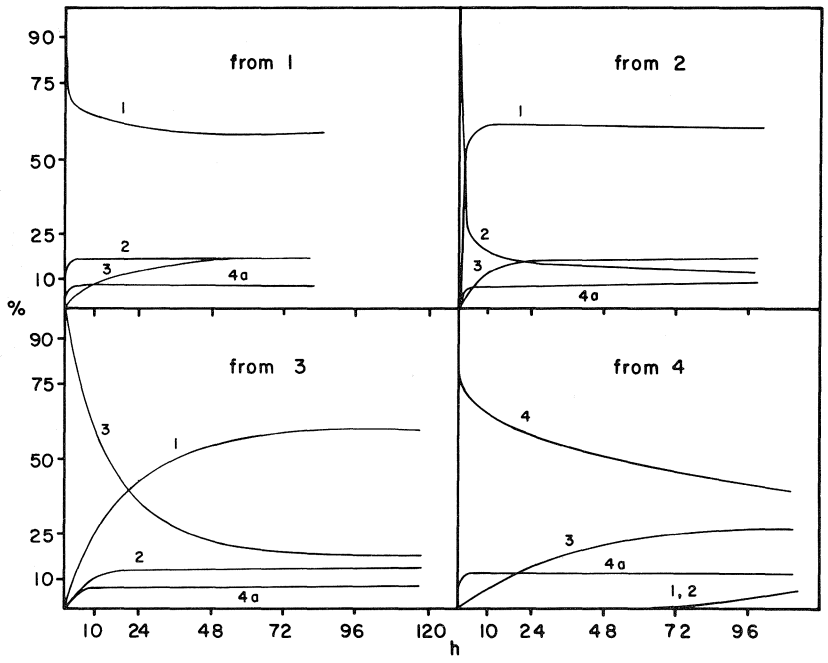

FIG. 3. Change in composition of glycoside mixtures during epimerization in the presence of a catalytic amount of base.

TABLE 5. Preparative epimerization of nitro glycosides

Starting compound	Reaction time (h)	Product composition (% of total yield) 1	2	3	4	Total yield (% recovery)
1	0.30	49	33	17	1	93
	1	23	45	25	7	85
	3	25	37	29	9	79
	5	21	30	40	8	79.5
	26	28	6	38	26	66.5
	144	6	12	32	50	60
2	0.30	24	53.5	9.5	7	90
	1	61	16	19	4	95
3	0.30	5	12	78	5	86
	1	9	18	66	7	90.5
	3	15	26	54	5	81.5
	26	12	(16)	28	44	65
4	26	———	24	———	76	66.5
	120	6	7	23	64	56

talo isomers **2** and **4** readily accessible. These isomers had previously been obtained only as minor components in the nitromethane cyclization that had afforded mainly **1** and **3** (6).

Discussion

The epimerizations occurring in the presence of an excess of base show that the order of thermodynamic stability of the nitronates is $4a >$ $3a > 2a \simeq 1a$. On the other hand, the order of stability of the free nitro glycosides as revealed by the epimerization equilibria obtained in the presence of a catalytic amount of base is $1 > 3 \simeq 2 > 4$. This is in accord with expectations based on conformational analysis as will now be outlined.

It was reasonable to assume that the free nitro glycosides **1**–**4** in aqueous solution prefer the

Can. J. Chem. Downloaded from www.nrcresearchpress.com by 84.22.46.98 on 09/08/12
For personal use only.

TABLE 6. Calculated conformational free energies (kcal/mol)*

Compound	Conformation	
	C_1^4	C_4^1
1	1.70†	
2	2.15†	
3	1.80†	
4	2.85†	
1*a*	1.25 + 2*A*	4.25
2*a*	1.70 + *A*	3.65 + *A*
3*a*	1.35 + *A*	2.75 + *A*
4*a*	2.40	2.75 + 2*A*

*The following nonbonded interaction energies were used (8): OH_a–H_a, 0.45; MeO_a–H_a, 0.45; Me_a–H_a, 0.90; OH_a–OH_a, 1.50; *gauche* OH–OH, 0.35; *gauche* OH–OMe, 0.35; *gauche* OH–Me, 0.45; anomeric effect, 1.05; Δ2 effect, 0.45.

†Plus energy of two *gauche* NO_2–OH interactions.

C_1^4 conformation, with axial anomeric methoxyl and equatorial C-3 nitro and C-5 methyl groups.[4] This assumption was confirmed by the n.m.r. spectra of **1**–**4** (Table 2). Calculation of conformational free energies using Angyal's procedure and parameters (8) and following the example of our previous work (2) gave data (Table 6) which indicated, for the C_1^4 conformers, the same order of stabilities as was found experimentally.[5]

As far as the nitronates **1***a*–**4***a* are concerned, n.m.r. spectroscopy afforded only limited information about their preferred conformations. Thus, the α-L-*xylo* salt **2***a* exhibited small coupling constants $J_{1,2}$ and $J_{4,5}$, but this feature does not permit a distinction between the C_1^4 and C_4^1 chairs in this instance. The α-L-*arabino* salt **3***a* showed a large splitting $J_{4,5}$, which agrees with the C_1^4 form and rules out the C_4^1 form. Unfortunately, the splitting of the H-1 and -2 signals, which would have confirmed this, could not be measured. In the α-L-*lyxo* salt **4***a* the splitting of H-4 and -5 was observed to be small, but this was to be expected for both chair forms. The coupling pattern of H-1 and -2 should have been able to provide a decision, but these signals were insufficiently separated to allow determination of $J_{1,2}$. However, the close spacing of the peaks tended to suggest a small rather than a large splitting, thus supporting the C_1^4 conformation. Finally, the α-L-*ribo* salt **1***a* could not be analyzed owing to its rapid epimerization; in epimeric mixtures, its presence was indicated by the OCH_3 and C—CH_3 signals, but the ring protons could not be differentiated.

Even though the n.m.r. spectral data assisted little in making conformational assignments, one may confidently assume that compounds **2***a*, **3***a*, and **4***a* prefer the C_1^4 conformation (OCH_3 axial, C—CH_3 equatorial). This follows from a comparison of the conformational free energies calculated for both chair conformations (Table 6). For computing these energies, a term (*A*) must be added for the non-bonded interaction between the nitronate grouping and an adjacent, equatorial hydroxyl group ($A^{(1,3)}$-effect) whenever this condition occurs (2). However, for **2***a* and **3***a* a numerical value of *A* is not needed for calculating the free energy differences of the chair conformers, since there is one $A^{(1,3)}$ interaction in each. The value of 1.95 kcal/mol for the calculated energy difference in the conformers of **2***a* (Table 6) corresponds to 96% of the C_1^4 form in conformational equilibrium. Similarly, for **3***a* that figure is 91.5%. In the isomer **4***a*, the C_1^4 form would be favored only moderately (by 0.35 kcal/mol) if the two $A^{(1,3)}$ interactions in the alternate, C_4^1 form were negligible. However, it is known (2) that the $A^{(1,3)}$ effect is associated with such a large energy that **4***a* will exist practically exclusively (to more than 99%) in the C_1^4 form which avoids this interaction. The fact that **4***a* in its preferred conformation is free from this strain while **2***a* and **3***a* are subject to it in either chair form accounts for the predominance of **4***a* in epimeric equilibrium. From the equilibrium ratio (2.1) of **4***a* to **3***a* it follows that the latter is higher in energy by 0.44 kcal/mol. Hence, if the conformational free energy of **4***a* is taken as 2.40 kcal/mol, that of **3***a* becomes 2.84 kcal/mol. The energy of the pure, preferred conformer of **3***a* is therefrom calculated to be 3.04 kcal/mol, accounting for the entropy change associated with conformer mixing. From this value, the *A* term in **3***a* is derived as 1.7 kcal/mol. Similar

[4]The inverse, C_4^1 form is strongly disfavored due to the anomeric effect and, particularly, due to the 3,5-diaxial interaction between the nitro and *C*-methyl groups. For the conformational symbolism see ref. 7.

[5]From the calculated, conformational free energy differences one may derive a theoretical equilibrium ratio of 2:1.5:1 for **1**, **3**, and **2**, whereas we found the ratio of 3:1:1. In view of the uncertainties inherent in both the method of determining the concentrations and the parameters used for calculating the non-bonded interactions, we consider this to be a satisfactory result. A possible source of error could be the arbitrary equating of all the *gauche* NO_2–OH interactions.

Can. J. Chem. Downloaded from www.nrcresearchpress.com by 84.22.46.98 on 09/08/12
For personal use only.

Can. J. Chem. Downloaded from www.nrcresearchpress.com by 84.22.46.98 on 09/08/12
For personal use only.

calculation using the equilibrium ratio (9.35) of **4***a* to **2***a* gave an *A* value of 2.0 kcal/mol. The latter may contain a larger error owing to the small concentration of **2***a* which probably rendered the determination of the equilibrium ratio less accurate. As far as the α-L-*ribo* isomer **1***a* is concerned, calculation shows that any *A* value exceeding 1.5 kcal/mol will make the inverted chair (C_4^1, with axial OH and C—CH_3 groups but free from $A^{(1,3)}$ strain) more stable than the normal C_1^4 chair, and from the above results one can therefore safely assume that the former preponderates considerably. This allows one to take 4.25 kcal/mol as the approximate conformational free energy of **1***a*, and it thus becomes clear why that compound is the least stable of the four epimeric salts. From our own measurements of the equilibrium compositions it follows that **1***a* exceeds **3***a* in energy by about 0.8 kcal/mol. (The value derived from the quasi-equilibrium is 0.77, and that from the final equilibrium is 0.85 kcal/mol.) These results lead to an *A* term of 2.0–2.1 kcal/mol. Analogous calculations based on the ratios of **2***a* to **1***a* found in the quasi-equilibrium (1.35) and in the final equlibrium (1.0) gave *A* values of 2.1 and 2.3 kcal/mol, respectively. Note that the calculations involving **1***a* and those involving **4***a* originated from independent measurements. The data are in excellent agreement with one another ($A = 2.0 \pm 0.3$ kcal/mol), and they are also in remarkably good harmony with the results obtained in the pentoside series (2). There, we had come to the conclusion that *A* is at least as high as 2 kcal/mol.[6] The present work thus reaffirms the magnitude of the $A^{(1,3)}$ effect and its directive power in the stereochemistry of nitro sugars where it may override such factors as the anomeric effect and the *syn*-diaxial hydroxyl group interaction. The results provide a theoretical understanding also of the epimerizations, occurring in methyl 3-deoxy-3-nitro-α-D-hexopyranosides, that had been discovered and utilized in earlier, synthetic work (9). The previous findings, which were already in good qualitative agreement with the present concept, have recently been supplemented by more reliable, quantitative data (10) revealing the configurational equilibrium of the hexoside nitronates to be fairly similar to that of their 6-deoxy analogs reported here.

Now the question must be posed as to why the nitronate which is observed immediately upon alkali addition to **1** is in fact **2***a* rather than **1***a*. Evidently a very fast epimerization takes place, at C-4, leaving behind no spectroscopically observable amount of **1** or its salt at the time of first scanning. Since the equilibrium studies have shown that **1***a* and **2***a* differ little in thermodynamic stability, it seems inconceivable that **1***a* should be formed as the first product, to be transformed completely into **2***a*, and then to be slowly regenerated as the equilibrium position demands. However, the reaction may be explained by assuming that proton abstraction from **1** involves the C-4 hydroxyl function, in significant competition with the nitromethylene group, producing an intermediate alkoxide ion through which the ensuing, rapid epimerization proceeds. This epimerization would take place by reversible ring opening between C-3 and -4, with the epimerized alkoxide being trapped, by proton transfer, to give the nitronate ion **2***a* as the kinetically favored product. Conversely, in the isomer **2** proton abstraction is more facile at the nitromethylene group so that **2***a* is readily formed and, because of paucity of the corresponding alkoxide ions in equilibrium, epimerization in the opposition direction is slow (Scheme 1). In effect, the observed reaction pattern can be attributed to differential nitromethylene acidities in **1** and **2**. Firstly, the difference in free energy between **2** and **2***a* is calculated to be smaller than that between **1** and **1***a*. Moreover, proton abstraction from C-3 in the stable C_1^4 chair of **1** would give the C_1^4 chair of **1***a* which is calculated to be the less stable conformation due to its two $A^{(1,3)}$ interactions. Therefore, in passing from **1** to the more stable C_4^1 chair of **1***a*, an energy barrier must be overcome which has no counterpart in the reaction **2** → **2***a*.

It should be recalled at this point that similar observations were made, and explanations offered, in the work on nitro pentosides (2) where the β-D-xylopyranoside underwent, in part, rapid

[6]From measurements of equilibrium constants and calculations based on chair conformations, values of 1.7 and 2.0 kcal/mol were derived. Since we found at least one of the pentoside nitronates to exist in a conformation other than the chair, we postulated that the $A^{(1,3)}$ strain that would be present in the latter contributes somewhat more energy than the figures indicated, causing the molecules to deviate from the chair form.

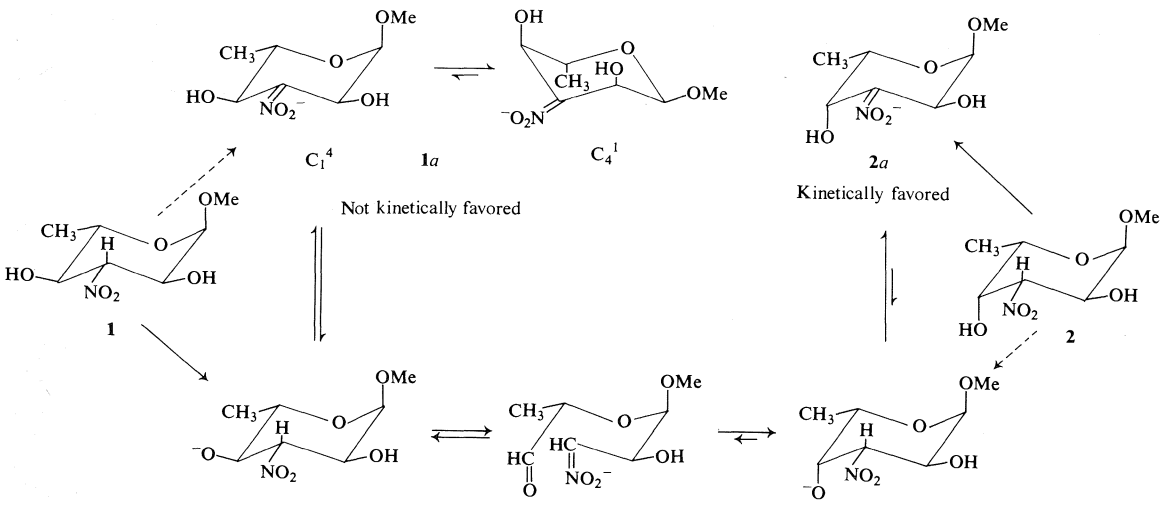

SCHEME 1

C-4 epimerization without intermediacy of its nitronate. The question as to why in that case as well as in the present one the site of preferential epimerization is C-4 rather than C-2 remains open; as a possible explanation one may invoke a lesser facility of bond cleavage between C-2 and -3 owing to an inductive, electron-pulling effect of the anomeric center.

Finally, we have to consider some of the results of the preparative epimerization experiments. While the ratios of isolated amounts of isomers starting from the α-L-*manno* and α-L-*talo* glycosides (**3** and **4**) corresponded well enough with the nitronate composition determined by spectroscopy prior to acidification, there appeared certain inconsistencies in the experiments with the α-L-*gluco* and α-L-*galacto* compounds (**1** and **2**). Starting with **1** and **2**, the ratios of isolated nitro sugars did not conform with expectations based on the distribution of nitronates in the mixtures (Table 5). Two factors may have been operative: incomplete nitronate formation owing to insufficient alkalinity of the medium from the beginning;[7] and secondly, performance of the deionization with cation exchange resin which, being a comparatively slow operation, may have caused a temporary condition of diminished alkalinity. We have demonstrated that under conditions of weak alkalinity (catalytic amount of base) the equilibrium is determined by the stabilities of the free nitro glycosides and not by those of their salts. Hence, in experiments of this kind one may obtain product compositions arising from fortuitous combinations of processes governed by both types of equilibria.

In the light of the present results the course of the nitromethane cyclization leading to **1**–**4** is readily understandable. The cyclization, as performed in alcoholic solution with sodium methoxide and an excess of nitromethane (5, 6), takes place in a medium of moderate alkalinity due to the buffer action of nitromethane. It afforded (6) mainly the glucoside **1** and the mannoside **3**. Establishment of epimeric equilibrium was not awaited, nor was completion of the cyclization ascertained, but extrapolation of the yield ratios of runs interrupted after 20 and 40 min allow the conclusion that **3** is kinetically favored and that **1** gains preponderance by virtue of epimerization that progresses concurrently with the cyclization.

Experimental

Instrumental Techniques

For all experiments, chromatographically pure, crystalline samples of the compounds **1**–**4** (6) were used. The n.m.r. spectra in the epimerization studies were obtained on a Varian T-60 instrument, using acetone as internal standard. Integration of C—CH_3 and (or) OCH_3 peaks was performed at 50 Hz sweep width, with appropriate

[7]In contrast to the spectroscopic experiments, in which an excess of base (1.2–1.5 equiv) and a higher concentration in sugar was employed, only 1 equiv was used here, and it is probably significant that aberrations occurred with the weak acids **1** and **2** and not with the stronger acids **3** and **4** (*cf.* footnote 3).

Can. J. Chem. Downloaded from www.nrcresearchpress.com by 84.22.46.98 on 09/08/12
For personal use only.

Can. J. Chem. Downloaded from www.nrcresearchpress.com by 84.22.46.98 on 09/08/12
For personal use only.

sweep offset. The chemical shifts and coupling constants listed in Tables 1 and 2 were confirmed by measurements on a Varian HA-100 instrument.

Assignments of the ring proton signals were by first-order analysis and, for the free nitro glycosides, were supported by changes in the splitting patterns observed upon deuterium exchange at C-3. All n.m.r. spectra were taken from approximately 0.17–0.25 *M* solutions (20 mg of glycoside in 0.4–0.6 ml of solution). Optical rotations were measured in a Perkin–Elmer 141 automatic polarimeter.

Preparative Epimerizations

The results assembled in Table 5 were obtained as follows. A given pure glycoside (200 mg, 0.97 mmol) was dissolved in carbon dioxide – free water (19 ml), and *N* sodium hydroxide solution (1 ml) was added. The reaction mixture was kept in a stoppered flask at 21° for the time specified (Table 5). It was then deionized by stirring with 3 ml of Rexyn 101 (H^+) cation exchange resin. After filtration the resin was washed well with water, and the combined filtrates were evaporated (bath temperature, 35°) to give a yellowish to brown syrup from which several portions of added benzene were evaporated. The syrup was then subjected to column chromatography, and the fractions eluted were examined by t.l.c., using the method previously employed for the separation of **1**–**4** (6). In the present series of experiments, the columns (2 cm in diameter) were packed with 20 g of silicic acid (Mallinckrodt analytical grade, 100 mesh), and 50-ml fractions were collected. Better separations than previously were achieved owing to the smaller amount of glycoside mixture applied. Sequential elution was performed with benzene–ethanol (99.5%) mixtures of the following compositions (v/v): *a*, 200:1; *b*, 100:1; *c*, 100:1.2; *d*, 100:1.5. Eluent *a* first produced a few milligrams of a brown oil that was inhomogeneous according to t.l.c. but did not contain any of the known glycosides. This forerun was followed by syrupy **4** containing an unknown contaminant; from later fractions, **4** crystallized spontaneously. The material was recrystallized once from ether – petroleum ether (b.p. 30–60°), if necessary with the use of a small amount of decolorizing carbon. Continuation of the chromatography with eluent *b* gave blank fractions only. Eluent *c* then gave fractions containing predominantly **3** which was accompanied by some **1**. Crystallization of these fractions from ethyl acetate – petroleum ether, with addition of a small drop of water and seeding with **3**-hydrate (6), furnished crystalline **3**. Later fractions of eluent *c* contained mainly **1** which was accompanied by residual **3**. Crystallization from chloroform – petroleum ether and seeding with **1** gave the pure compound. The mother liquors from the crystallizations of **3** and **1** were pooled and evaporated, and the residue was treated with some activated charcoal in water and then recovered. Such mixed fractions (which usually were small) showed a single spot on t.l.c., and the ratio of **1** and **3** was determined polarimetrically (6). Finally, eluent *d* produced **2** which was recrystallized from ethyl acetate – petroleum ether. A further increase in the ethanol proportion of the eluent did not give any additional amount of nitro glycoside. With few exceptions (where yields were about 5 mg or less), the data in Table 5 refer to recrystallized materials. In all cases, identity and satisfactory purity of the products were checked by t.l.c., optical rotation, and melting point. The volumes of eluents required for the chromatography depended on the composition of the glycoside mixture and varied from one separation to another.

Preparation of Methyl 3,6-Dideoxy-3-nitro-α-L-galactopyranoside (2) from 1

A solution of the glucoside **1** (100 mg) in water (2 ml) was introduced, with a syringe, into 0.75 ml of *N* sodium hydroxide solution (1.5 molar equiv). The solution was kept at 24° for 60 s and then poured into 0.05 *N* acetic acid (20 ml). The mixture was then passed sequentially through small columns of Dowex 1 × 8 (acetate form) (0.5 ml) and Rexyn 101(H^+) (5 ml), and the filtrate was evaporated to give a syrup (109 mg). Crystallization from ethyl acetate gave a first crop of **2** (23 mg, m.p. 151–153°), and recrystallization of the mother liquor material from the same solvent and some petroleum ether gave a second crop (36 mg, m.p. 147–148°); $[\alpha]_D$ −218 and −206°, respectively (*c*, 0.2 in water); reported (6): m.p. 155–158° $[\alpha]_D$ −216°. The product was identified as essentially pure **2** also by its n.m.r. spectrum. The mother liquor from the second crop (dry weight, 40 mg) was revealed by its n.m.r. spectrum to contain approximately 18 mg of **1**, 5 mg of **2**, 12 mg of **3**, and 5 mg of another component (presumably **4**).

Preparation of Methyl 3,6-Dideoxy-3-nitro-α-L-talopyranoside (4) from 1

Epimerization of **1** (200 mg) as described in a preceding section was allowed to proceed for 6 days. Elution of the chromatographic column with benzene–ethanol (200:1) gave, in fractions no. 11–14, 78 mg of crystalline **4**. Recrystallization from ether – petroleum ether afforded 60 mg (30%) of nearly pure **4**, $[\alpha]_D$ −88.1° (*c*, 1.2 in water); reported (6): −89.8°.

It also proved feasible to utilize, for preparing **4**, mother liquors that remained after the isolation of crystalline **1** in the nitromethane cyclization of L′-methoxy-L-methyldiglycolic aldehyde (5, 6). Such mother liquors had been shown (6) to contain only a small proportion of **4**. However, the proportion was increased, for example, by allowing a syrupy mixture (1.9 g) to undergo partial epimerization in an equivalent amount (9.2 ml) of aqueous *N* sodium hydroxide (22 h at room temperature). Deionization with Rexyn 101(H^+), filtration with activated charcoal, and evaporation gave a syrup that was dissolved in 5–7 ml of ether. Addition of petroleum ether to incipient turbidity and inoculation with **4** furnished crude **4** (235 mg) that was recrystallized twice in the same manner. The yield was 113 mg of pure **4**, m.p. 104–107°, $[\alpha]_D$ −89.6° (*c*, 0.8 in water). Another 240 mg of **4** (m.p. 103–107°, $[\alpha]_D$ −89.1°) was obtained from this experiment by column chromatography.

Support of this work by the National Research Council of Canada is gratefully acknowledged.

1. H. H. BAER. Advan. Carbohydr. Chem. Biochem. **24**, 67 (1969).

2. H. H. BAER and J. KOVÁŘ. Can. J. Chem. **49**, 1940 (1971).
3. H. H. BAER and W. RANK. Can. J. Chem. **49**, 3197 (1971).
4. F. JOHNSON and S. K. MALHOTRA. J. Am. Chem. Soc. **87**, 5492 (1965); R. CAPLE and W. V. VAUGHAN. Tetrahedron Lett. 4067 (1966); S. J. ANGYAL and B. M. LUTTRELL. Aust. J. Chem. **23**, 1485 (1970).
5. A. C. RICHARDSON and K. A. MCLAUCHLAN. J. Chem. Soc. 2499 (1962). K. ČAPEK, J. ŠTEFFKOVÁ, and J. JARÝ. Coll. Czech. Chem. Commun. **31**, 1854 (1966).
6. H. H. BAER and K. ČAPEK. Can. J. Chem. **47**, 99 (1969).
7. L. HOUGH and A. C. RICHARDSON. *In* Rodd's Chemistry of carbon compounds. Vol. I. Part F. *Edited by* S. Coffey. Elsevier Publishing Company, Amsterdam. 1967. p. 90.
8. S. J. ANGYAL. Aust. J. Chem. **21**, 2737 (1968).
9. H. H. BAER. J. Am. Chem. Soc. **84**, 83 (1962).
10. H. H. BAER and W. RANK. Submitted as part XXVI of this series.
11. J. KOVÁŘ and H. H. BAER. Can. J. Chem. **49**, 3238 (1971).

Downloaded from www.nrcresearchpress.com by 84.22.46.98 on 09/08/12
For personal use only.

Can. J. Chem. Downloaded from www.nrcresearchpress.com by 210.87.254.105 on 09/05/12
For personal use only.

Theory of Enthalpy of Mixing in Reactive Charge Asymmetrical Molten Salt Systems. Part I. Binary Solutions

S. N. Flengas and A. S. Kucharski

Department of Metallurgy and Materials Science, University of Toronto, Toronto 181, Ontario

Received June 15, 1971

The enthalpies of mixing for the charge asymmetrical molten salt systems; $MnCl_2$–ACl, $FeCl_2$–ACl, $CoCl_2$–ACl, $NiCl_2$–ACl, $MgCl_2$–ACl, and $CdCl_2$–ACl (where A represents Li, Na, K, Rb, and Cs) have been calculated by separating the mixing process into two parts. One part of enthalpy of mixing results from the "reaction" to form a tetrahedral complex, MCl_4^{2-}, and another part of the enthalpy of mixing arises from the "mixing" of the complexed species with the remaining free components. The "complex" species are treated as orderly configurations defined by shorter anion to cation distances within which the central metal cation interacts with the surrounding other metal cations through bridging chloride ions. The model takes into account the difference in the coordination number of the mono- and divalent components. The interaction parameters are shown to depend upon the radii of the alkali metal cations.

Les enthalpies de mélange pour des systèmes de sel fondu assymétrique tels que $MnCl_2$–ACl, $FeCl_2$–ACl, $CoCl_2$–ACl, $NiCl_2$–ACl, $MgCl_2$–ACl et $CdCl_2$–ACl (dans lesquels A représente Li, Na, K, Rb et Cs) ont été calculées en séparant le procédé de mélange en deux parties. Une partie de l'enthalpie de mélange est le résultat de la "réaction" pour former un complexe tetrahédrique, MCl_4^{2-} et une autre partie de l'enthalpie de mélange provient du "mélange" des espèces complexées avec les composants libres restants. Les espèces "complexées" sont traitées comme les configurations ordonnées définies par les plus courtes distances anion–cation à l'intérieur desquelles le cation métallique central interagit avec les autres cations métalliques environnants à travers les ions chlore pontés. Le modèle tient compte de la différence dans le nombre de coordination des composés mono- et divalents. On montre que les paramètres d'interaction dépendent des rayons des cations des métaux alcalins.

Canadian Journal of Chemistry, 49, 3971 (1971)

Introduction

Recent calorimetric measurements mainly by Kleppa and co-workers (1–3) have made available accurate determinations of the enthalpies of mixing of binary charge asymmetrical molten salt mixtures containing divalent metal chlorides and alkali chlorides. These measurements include the systems $MnCl_2$–ACl (1), $FeCl_2$–ACl (1), $CoCl_2$–ACl (1), $CdCl_2$–ACl (2), $NiCl_2$–ACl (3), and $MgCl_2$–ACl (4), where A represents alkali metal cations from Li^+ to Cs^+.

In addition the partial molar properties of the $MgCl_2$–ACl (5), the $NiCl_2$–ACl (6) and $CoCl_2$–ACl (7) systems are available from equilibrium e.m.f. studies.

Heats of mixing in these charge asymmetrical systems show pronounced deviations from regular behavior and are characterized by relatively high exothermic heat effects. In addition, the activities of the MCl_2 component indicate pronounced negative deviations from ideality.

Flood and Urnes (8) interpreted cryoscopic activities of $MgCl_2$ in the $MgCl_2$–ACl binary systems, where A = Na, K, Rb, by assuming the formation of the complex $MgCl_4^{2-}$ ions. The calculation, however, was entirely based on configurational entropies and disregarded the now known pronounced heats of mixing.

The concentration dependence of the regular solution interaction parameter defined as $\Delta H_M/X_1X_2$, where X_1 and X_2 are the mole fractions of the two components calculated from the calorimetric measurements by Papatheodorou and Kleppa (1–3) for the systems MCl_2–ACl, where, M is Mn, Fe, Co, Cd and Ni, indicates a minimum at a composition of about 33 mol% MCl_2. This behavior was interpreted as indicating that a tetrahedrally coordinated complex ionic species was present in these melts.

According to Papatheodorou and Kleppa (3) the exothermic heats of mixing in these charge asymmetrical systems is thought to originate from an enthalpy contribution assigned to the formation of the tetrahedral MCl_4^{2-} complex and by dispersion type interactions during the formation of the mixture. The treatment appears to be qualitative and the various interaction parameters are given arbitrary values to provide agreement with the experimental results. The complex ions appear to be more stable in the presence of large alkali cations like K^+ or Cs^+. Pronounced stabilization is not evident in the presence of Li^+.

Can. J. Chem. Downloaded from www.nrcresearchpress.com by 210.87.254.105 on 09/05/12
For personal use only.

Recently, Davis (9) has proposed a modified conformal solution theory for the heats of mixing in charge asymmetrical fused salt systems based on a model for an ionic melt by Reiss *et al.* (10).

If it is assumed that the interaction between the ions in the component salts and in the mixture is purely ionic, then the enthalpies of mixing may be approximated by the equation

$$[1]\quad \Delta H_M = A(X, T, \delta_{12}) - X_1[[1 + X_2(Z-1)]\, B_{12}(T, X, \delta_{12}) - B(T, \delta_{12})]\delta_{12}$$

where A, B_{12}, and B are complicated integral functions of the composition X, the coordination number Z, and the parameter $\delta_{12} = (d_1 - d_2)/d_1 \cdot d_2$, where d_1, d_2 are the sums of ionic radii in the two melts.

The Davis (9) theory for charge asymmetrical mixtures is not readily amenable to verification because of the complexity of the terms and the difficulty in making quantitative predictions regarding energetic asymmetry. In addition, in a binary mixture containing mono- and divalent cations, the coordination number cannot be expected to remain constant throughout all compositions.

Recently, Pelton and Thompson (11) calculated the concentration dependence of the heats and of the entropies of mixing in the $MgCl_2$–ACl binary systems for about 60% of the composition range using a dissociating complex ion model based on the existence of $MgCl_4^{2-}$ species. In this model, the complex anions are taken to be present even in pure liquid $MgCl_2$ and the degree of dissociation at each point is calculated by minimizing the free energy of the solution. Although the method is mathematically correct some of the physical assumptions may be considered as questionable. For example, the entropy of mixing is taken as being entirely configurational although the formation of a strong complex anion is postulated. Also, the coordination number is considered to remain constant for all compositions, and the pure salt $MgCl_2$ is calculated to consist largely of complex anions. The calculation, however, has the advantage of requiring only two adjustable parameters for each binary system, one of which is common for all five MCl_2–ACl systems.

Also, recently, Ostvold (12) has used a similar method to calculate the heats of mixing in the $MgCl_2$–ACl systems. However, in this treatment the heat of mixing was accounted for by a method outlined by Førland (13) for the mixing of mono- and divalent ions. The agreement between the theory and calculated concentration dependence of the interaction parameter is only qualitative.

In the present study the concentration dependence of the heats of mixing in binary charge asymmetrical reactive systems are calculated on the basis of a simple complex anion model. In this model, the heats of mixing are taken to originate from two sources. In the first part, the component salts react stoichiometrically to form completely a tetrahedrally coordinated anionic complex with a pronounced exothermic heat effect. The second part of the heat arises from mixing the reaction products with the unused components to form a regular type solution in which nearest or next nearest Coulombic interactions are considered to be significant. For the treatment the effects due to charge asymmetry are accounted for in terms of a variable coordination number.

The mathematical relationships derived in this manner have been applied with success to the binary mixtures of $FeCl_2$, $MgCl_2$, $MnCl_2$, $CoCl_2$, $NiCl_2$, and $CdCl_2$ with the various alkali chlorides for which experimental data are available (1–3). The theory is particularly applicable to systems which approximate the tetrahedral coordination and in which the complex anions do not dissociate to any appreciable extent. The treatment could also be adapted to take into account either linearly or octahedrally coordinated complexes.

Concept of Complex Ions in Molten Salts

The concept of complex ions in molten salts should be entirely different from that generally accepted in aqueous solutions. In dilute aqueous solutions because of the high dielectric constant of water, complex ionic species having a discrete structure may be considered to exist as well defined separate entities and the properties of the solutions may be interpreted by considering the behavior of point electrical changes in a dielectric medium.

In molten salts, the medium is totally ionic and because of the existence of strong short range electrostatic forces the requirement of local electrical neutrality is satisfied through the concept of interlocking anionic and cationic quasi-lattices.

In this sense the liquid structure is continuous and the existence of discrete complex species is conceptually difficult. It is most likely that a "complex anion" in molten salts should be best

Can. J. Chem. Downloaded from www.nrcresearchpress.com by 210.87.254.105 on 09/05/12
For personal use only.

represented by a configuration of a cation M^{n+} surrounded by anions X^- having a given coordination number within which the bond distances MX, and accordingly their energies, should be different from those expected to represent a non-complexed dissociated ionic state. It is also convenient to take the non-complexed state of the salt MX as that of the pure MX. The "complex" is expected to form only in the presence of a second salt AX which is considered to act as the ligand donor. Thus, the formation of the complex species is assumed to be the result of reactions of the type

$$MX + (n - 1)AX \rightarrow A_{n-1}MX_n$$

and the strength of the complex shall depend upon the magnitude of the competing interactions of the A^+ and M^+ cations for the same ligand anions X^-.

In a melt containing both AX and MX, it is conceivable that two kinds of MX bonds could exist: M—X bonds having the bond distance describing the "complex" state, and M—X bonds describing the "free" MX species. The pure material is expected to have only bonds of the second type.

It is also evident that the continuity of the medium imposes the restriction that the "complex" anions are not discrete isolated species but are part of the ionic liquid structure and therefore their central M cations interact with the surrounding cations through bridging X^- anions. In a melt containing MX and AX components, it is meaningless to postulate a structure based on the MX_n anions occupying single anion lattice sites in addition to other free anions and cations. The structure should still be one represented by arrays of positive and negative ions in a continuous sequence in such a manner that positive ions are always surrounded by negative ones.

Since the only characteristic of a "complex" anion is the bond distance MX, its coordination configuration, MX_n may be treated as a separate statistical entity. When MX is added to AX a "reaction" may be postulated according to the stoichiometry indicating the preferred coordination within the complex anion. For example, for a tetrahedrally coordinated complex between a divalent metal chloride and an alkali metal chloride, the reaction represented by,

$$MCl_2 + 2ACl \rightarrow A_2MCl_4$$

Regarding the preferred coordination of complex ions in fused salts, the accumulated experimental evidence indicates that such coordinations are relatively simple. Thus, mixtures of monovalent cations appear to prefer the 2-ligand configuration representing a linear or angular structure as in $Ag(CN)_2^-$ (14). Mixtures of mono- and divalent cations appear to follow the tetrahedral coordination as in $MgCl_4^{2-}$. Finally, mixtures of mono- and tetravalent cations as in the systems, $ZrCl_4$, $TiCl_4$, $HfCl_4$, with alkali chlorides (15), prefer to form octahedrally coordinated complexes of the type $ZrCl_6^{2-}$, $TiCl_6^{2-}$, and $HfCl_6^{2-}$. In these systems it has been shown that the thermodynamic properties of the solutions can be accounted for on the basis of the MCl_6^{2-} complex ion (16, 17).

From the previous discussion it follows that "complex" species in fused salts are not expected to dissociate in the same manner as their counterparts in aqueous solutions. The formation of the new type of M—Cl bond distances is initiated by the presence of the A^+ cations. Each added A^+ cation is expected to disturb one M—Cl bond and the "complex" should form "stoichiometrically."

Accordingly, the difference between the effects of various kinds of ACl ligand donors upon the same MCl_2 salt, shall be manifested as a heat effect, and the introduction of a dissociation constant is not necessary for the mathematical treatment. In a solution containing various proportions of ACl to MCl_2, the changes in the bond energies which may result from the replacement of one kind of neighboring ion by another, should result in changes in the overall heat effect of mixing and may be accounted for by assigning different values to the bond energies representing the various possible ionic combinations. Again the concept of a "dissociating complex" is not necessary.

However, if two or more "complex" coordinations are energetically favorable, then the concepts of equilibrium between "complex" species, and of dissociation, become significant.

The present treatment is applicable to salt systems which appear to conform with the concept of a single complex configuration.

Theory of Mixing of Charge Asymmetrical System Forming Complex Anions

Considering the binary mixture MCl_2–ACl over the entire composition range, from pure MCl_2 to pure ACl, the complex A_2MCl_4 is expected to form quantitatively at a composition $X_{MCl_2} = 0.333$.

TABLE 1. Mass balance for the MCl_2–ACl system*

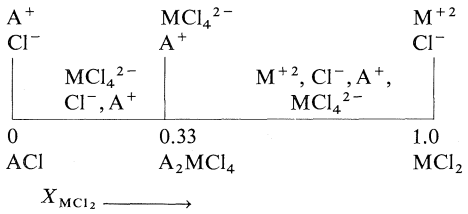

(*a*) $1.0 > X_{MCl_2} > 0.333$

$n_{MCl_2} = X_{MCl_2} - 0.5X_{ACl} = n_1$, $n_{ACl} = 0$, $n_{A_2MCl_4} = 0.5X_{ACl} = n_2$

Ionic composition	Ionic fraction
$n_{M^{2+}} = X_{MCl_2} - 0.5X_{ACl}$	$N_{M^{2+}} = \dfrac{2X_{MCl_2} - X_{ACl}}{1 + X_{MCl_2}}$
$n_{A^+} = X_{ACl}$	$N_{A^+} = \dfrac{2X_{ACl}}{1 + X_{MCl_2}}$
$n_{Cl^-} = 2X_{MCl_2} - X_{ACl}$	$N_{Cl^-} = \dfrac{4X_{MCl_2} - 2X_{ACl}}{4X_{MCl_2} - X_{ACl}}$
$n_{MCl_4^{2-}} = 0.5X_{ACl}$	$N_{MCl_4^{2-}} = \dfrac{X_{ACl}}{4X_{MCl_2} - X_{ACl}}$

(*b*) $0.333 > X_{MCl_2} > 0$

$n_{MCl_2} = 0$, $n_{ACl} = X_{ACl} - 2X_{MCl_2} = n_1$, $n_{A_2MCl_4} = X_{MCl_2} = n_2$

Ionic composition	Ionic fraction
$n_{M^{2+}} = 0$	$N_{M^{2+}} = 0$
$n_{A^+} = X_{ACl}$	$N_{A^+} = 1.0$
$n_{Cl^-} = X_{ACl} - 2X_{MCl_2}$	$N_{Cl^-} = \dfrac{X_{ACl} - 2X_{MCl_2}}{X_{ACl} - X_{MCl_2}}$
$n_{MCl_4^{2-}} = X_{MCl_2}$	$N_{MCl_4^{2-}} = \dfrac{X_{MCl_2}}{X_{ACl} - X_{MCl_2}}$

*X = the original mole fractions in the solution which is prepared by mixing the components ACl and MCl_2; n = the amount of a component in g-mol; N = ionic fractions after the complex forming reaction has taken place.

For compositions rich in ACl; namely for $0.333 > X_{MCl_2} > 0$, the melt is taken to consist of unreacted ACl and the complex compound A_2MCl_4. For compositions rich in MCl_2, namely for $1.00 > X_{MCl_2} > 0.333$, the melt may be taken to consist of unreacted MCl_2 and the complex compound A_2MCl_4.

The ionic compositions, assuming that the complex only dissociates into A^+ cations and MCl_4^{2-} anions, may be calculated from the original mole fractions by a mass balance calculation, and are given in Table 1.

For the common cation subsystem, ACl–A_2MCl_4, if the ability of the M^{2+} ions for interaction is considered as having been nearly satisfied through the formation of the "complex" anion MCl_4^{2-}, it is reasonable to expect that the species present should be randomly distributed and that only next nearest neighbor type interactions should be significant. The solutions could then be treated as regular. Thus, the bond energies to be considered in the "pure" components ACl and A_2MCl_4 are characterized by the energies of the next nearest neighbor interactions, Cl^-–A^+–Cl^- and MCl_4^{2-}–A^+–MCl_4^{2-}, respectively. The solution, in addition to the above interactions, is also characterized by interactions of the type Cl^-–A^+–MCl_4^{2-}. However, the concept of continuity in the structure of the ionic melt discussed earlier requires that the MCl_4^{2-} species be nonexistent as an isolated entity. The A^+ cations are expected to interact with the M^{2+} central cations in the "complex" species via bridging Cl^- anions. Thus it is more realistic to describe the MCl_4^{2-}

Can. J. Chem. Downloaded from www.nrcresearchpress.com by 210.87.254.105 on 09/05/12
For personal use only.

type interactions in pure A_2MCl_4 and the Cl^-–A^+–MCl_4^{2-} type interactions in the solution, as interactions between a central A^+ cation and two chloride species representing ionic arrays of the type

$$\begin{array}{ccccc} & Cl^* & & Cl^* & \\ Cl^*—M—Cl^*\cdots & A^+ & \cdots Cl^*—M—Cl^* \\ & Cl^* & & Cl^* & \end{array}$$

and

$$\begin{array}{ccc} & & Cl^* \\ Cl^-\cdots A^+\cdots & Cl^*—M—Cl^* \\ & & Cl^* \end{array}$$

where Cl^- and Cl* describe the states of the Cl^- in pure ACl and in the "complex" species, MCl_4^{2-}, respectively.

It should be noted that although the number of MCl_4^{2-} configurations in the system is fixed by stoichiometry, the two types of chloride ions in the solution can readily exchange positions so that the probability of finding a chloride species of the Cl* type in any position is taken as the fraction of the anionic positions occupied by the configuration MCl_4^{2-}.

The "significant" next nearest neighbors type interactions for the pure components and for their mixture are therefore best represented by the following energy terms. For pure ACl, the Cl^-–A^+–Cl^- type interaction is described by $E_{Cl—A—Cl}$; for pure A_2MCl_4, the Cl*—A^+—Cl* type interaction is described by $E_{Cl^*—A—Cl^*}$, and in the binary solution ACl–A_2MCl_4, the bond energies are the $E_{Cl—A—Cl}$, $E_{Cl—A—Cl^*}$, and $E_{Cl^*—A—Cl^*}$ where $E_{Cl^*—A—Cl}$ describes the new type of interaction discussed previously.

Since we are only concerned with the chloride ion coordination of the A^+ cations, the nearest neighbor coordination number for the A^+ cations should not be affected by mixing the charge asymmetric system ACl–A_2MCl_4.

In this composition range, for a melt represented by the nominal mole fractions X_{ACl} and X_{MCl_2}, respectively, the "true" composition is given in Table 1.

As the complex anions present in the mixture have originated from the reaction of X_{MCl_2} g-moles of MCl_2, the first part of the heat effect or the "reaction part" is simply proportional to the amount of complex formed, and is given by the equation

$$[2] \qquad \Delta H_1 = X_{MCl_2} b_R$$

The constant b_R represents the heat of formation per g-mol of complex according to

$$MCl_2 + 2ACl \rightarrow A_2MCl_4$$

The second part or the "mixing part" of the total heat originates by the regular solution type mixing of the charge asymmetrical mixture containing n_1 g-mol of ACl and n_2 g-mol of A_2MCl_4 according to the reaction

$$n_1ACl + n_2A_2\,MCl_4 \rightarrow (ACl)_{n_1}\,(A_2MCl_4)_{n_2}$$

This "mixing" part may be calculated by interpreting the energy of mixing as the difference between the internal energy of the solution from that of the pure components, where the previously described interactions are the only ones which are considered as being significant. Pair interactions of the same kind are taken to have the same energy in the pure components as in the solution and cancel out.

The energy change for the mixing reaction is therefore

$$[3] \qquad \Delta E_{mix}{}^{int} = E_{mix} - n_1E_{ACl} - n_2E_{A_2MCl_4}$$

The total number of next nearest neighbors interactions originating from a central A^+ cation is given by $(1/2)N(n_1 + 2n_2)Z_1$ where N is the Avogadro number and Z_1 is the coordination number for ACl. In pure ACl and A_2MCl_4, the total numbers of such interactions are $(1/2)n_1NZ_1$ and n_2NZ_1, respectively. Hence, using the above relationships and taking the probability of finding a bonded chlorine in the complex MCl_4^{2-} as being the same as that of finding the entity MCl_4^{2-}, the following expression is readily obtained according to the method which is followed for regular solutions.

$$[4] \quad \Delta E_M = \tfrac{1}{2}Z_1N(n_1 + 2n_2)\left[\frac{n_1^2}{(n_1 + n_2)^2}E_{Cl—A—Cl} + \frac{n_2^2}{(n_1 + n_2)^2}E_{Cl^*—A—Cl^*} + \frac{2n_1n_2}{(n_1 + n_2)^2}E_{Cl—A—Cl^*}\right] - \tfrac{1}{2}NZ_1n_1E_{Cl—A—Cl} - \tfrac{1}{2}NZ_12n_2E_{Cl^*—A—Cl^*}$$

$$= \frac{n_1n_2}{n_1 + n_2}\left[\frac{n_1}{n_1 + n_2}b_1 + b_2\right]$$

Can. J. Chem. Downloaded from www.nrcresearchpress.com by 210.87.254.105 on 09/05/12
For personal use only.

Introducing into this equation the expressions for n_1 and n_2, from Table 1, and performing the necessary cancellations of common terms, the following relationship is obtained

$$[4a] \qquad \Delta E_M = \frac{(X_{ACl} - 2X_{MCl_2})X_{MCl_2}}{X_{ACl} - X_{MCl_2}} \cdot \left[\frac{X_{ACl} - 2X_{MCl_2}}{X_{ACl} - X_{MCl_2}} b_1 + b_2\right]$$

where

$$b_1 = \tfrac{1}{2}NZ_1[E_{Cl^*-A-Cl^*} + E_{Cl-A-Cl} - 2E_{Cl^*-A-Cl}]$$

and

$$b_2 = \tfrac{1}{2}NZ_1[4E_{Cl-A-Cl^*} - 3E_{Cl^*-A-Cl^*} - E_{Cl-A-Cl}]$$

are parameters to be determined experimentally. Assuming that pressure–volume work is negligible eq. 4*a* can be used to represent the enthalpy of mixing ($\Delta E_M = \Delta H_M$). Thus the total enthalpy will be given by the sum of eqs. 2 and 4*a*, as shown below

$$[5] \qquad \Delta H_M = X_{MCl_2}b_R + \frac{(X_{ACl} - 2X_{MCl_2})X_{MCl_2}}{X_{ACl} - X_{MCl_2}} \cdot \left[\frac{X_{ACl} - 2X_{MCl_2}}{X_{ACl} - X_{MCl_2}} b_1 + b_2\right]$$

It should be noted that the parameter b_2 is similar to that obtained from regular solution theory for a charge symmetric mixture. The parameter b_1 is the result of charge asymmetry. Hence, the total integral heat of mixing in the reacting system is determined by the heat contribution due to the complex ion forming reaction, by a heat effect due to an exchange reaction between next nearest neighbor anions, and by asymmetry.

Considering the composition range in the subsystem MCl_2–A_2MCl_4 from $1.0 > X_{MCl_2} > 0.333$, the true composition of the solution is given in Table 1. In this range the "reaction" part of the total mixing reaction is given by

$$[6] \qquad \Delta H_1' = 0.5X_{ACl}b_R$$

Once the complex has been formed the second part of the reaction involves mixing of the unreacted MCl_2 with A_2MCl_4 according to

$$n_1MCl_2 + n_2A_2MCl_4 \rightarrow [(MCl_2)_{n_1}(A_2MCl_4)_{n_2}]$$

Again, in this system the following different kinds of chloride ions should be considered: chloride ions which surround "free" M^{2+} or A^+ cations, and chloride ions bonded in the complex ionic configuration $[MCl_4^*]^{2-}$. Also, the cation M^{2+} in the complex $[MCl_4^*]^{2-}$ is bonded to the surrounding M^{2+} or A^+ "free" cations through bridging Cl* ions. Accordingly, the system is a reciprocal salt mixture and the significant interactions in a system where the complex ion configuration is already present are given by the nearest neighbor cation to anion attractions having energy contributions given as: E_{Cl-A}, E_{Cl^*-A}, E_{Cl-M}, E_{Cl^*-M}, where the interactions E_{Cl-A} and E_{Cl-M} are also common in the pure components ACl and MCl_2. It is also expected that if the nearest neighbor coordination number of the "free" M^{2+} cations is Z_1, then the nearest neighbor coordination number of the A^+ cations should be $0.5Z_1$.

In a random system the total number of bonds which emanate from the "free" A^+ and M^{2+} ions may be calculated from the average coordination number of the solution defined as

$$[7] \qquad \bar{Z} = \frac{n_1}{n_1 + 2n_2} Z_1 + \frac{2n_2}{n_1 + 2n_2} 0.5Z_1$$

$$= \frac{n_1 + n_2}{n_1 + 2n_2} Z_1$$

The total number of significant nearest neighbor type bonds in the solution is readily calculated as,

$$\tfrac{1}{2}N(n_1 + 2n_2)\bar{Z} = \tfrac{1}{2}N(n_1 + n_2)Z_1$$

Using the same assumptions as for the ACl rich solutions, the integral energy of mixing is derived as

Can. J. Chem. Downloaded from www.nrcresearchpress.com by 210.87.254.105 on 09/05/12
For personal use only.

[8] $$\Delta E_M = \tfrac{1}{2}NZ_1(n_1 + n_2)[N_{A^+} \cdot N_{Cl^-} \cdot E_{A-Cl} + N_{A^+} \cdot N_{MCl_4^*} \cdot E_{A-Cl^*} + N_{M^{2+}} \cdot N_{Cl^-} \cdot E_{M-Cl} + N_{M^{2+}} \cdot N_{MCl_4} \cdot E_{M-Cl^*}] - \tfrac{1}{2}NZ_1 n_1 E_{M-Cl} - \frac{\tfrac{1}{2}NZ_1}{2}(2n_2)E_{A-Cl^*}$$

where the ionic fractions are given in Table 1.

From eq. 8, after performing the necessary cancellations of common terms, the following expression is derived

[9] $$\Delta E_M = \frac{(X_{MCl_2} - 0.5X_{ACl})0.5X_{ACl}}{(2X_{MCl_2} - 0.5X_{ACl})}\left[\frac{X_{MCl_2} - 0.5X_{ACl}}{X_{MCl_2} + 0.5X_{ACl}} b_1' + b_2'\right]$$

where

[9a] $$b_1' = \tfrac{1}{2}NZ_1[2E_{ACl} + 0.5E_{MCl^*} - 2E_{MCl} - 0.5E_{ACl^*}]$$

$$b_2' = \tfrac{1}{2}NZ_1[2E_{ACl} + 0.5E_{MCl^*} - E_{MCl} - 1.5E_{A-Cl^*}]$$

are interaction parameters.

The total integral heat of mixing is given as

[10] $$\Delta H_M = 0.5X_{ACl}b_R + \frac{(X_{MCl_2} - 0.5X_{ACl})0.5X_{ACl}}{(2X_{MCl_2} - 0.5X_{ACl})}\left[\frac{X_{MCl_2} - 0.5X_{ACl}}{X_{MCl_2} + 0.5X_{ACl}} b_1' + b_2'\right]$$

The second part of eq. 10 is of the form

[11] $$\Delta E_M = \frac{n_1 n_2}{2n_1 + n_2}\left[\frac{n_1}{n_1 + 2n_2} b_1' + b_2'\right]$$

and accordingly the parameter b_2' describes the regular behavior of the solution when asymmetry effects are not accounted for. The effect of variable coordination number is accounted for by the asymmetric parameter b_1'.

The above calculations indicate that the concentration dependence of the integral heat of mixing is a complex function of the concentration and that the entire heat of mixing curve may be accounted for by five parameters, b_R, b_1, b_2, b_1', and b_2'.

Determination of Energetic Parameters

The "reaction" parameter b_R can be found from an experimentally measured heat of mixing curve by substituting for $X_{MCl_2} = 0.333$ and solving either eqs. 5 and 10. Thus

[12] $$b_R = 3(\Delta H_M)_{X=0.333}$$

The parameters b_1 and b_2' may be determined from the partial molar heats of mixing.

In the ACl–A_2MCl_4 subsystem at $0.333 > X_{MCl_2} > 0$, the partial molar heats of mixing for ACl and MCl_2 may be represented by the following mixing reactions

[13] $$ACl + [(ACl)_{n_1}(A_2MCl_4)_{n_2} \rightarrow [(ACl)_{n_1+1}(A_2MCl_4)_{n_2+1}]$$

and

[14] $$MCl_2 + [(ACl)_{n_1}(A_2MCl_4)_{n_2}] \rightarrow [(ACl)_{n-2}(A_2MCl_4)_{n_2+1}]$$

The corresponding equations for the partial molar heats of mixing are derived by partial differentiation of eq. 5,

[15] $$\Delta\bar{H}_{MCl_2} = b_R + \frac{(X_{ACl}^3 - 4X_{MCl_2}^3 - 7X_{MCl_2}X_{ACl}^2 + 12X_{ACl}X_{MCl_2}^2)}{(X_{ACl} - X_{MCl_2})^3} b_1 - \frac{2X_{MCl_2}^2 - (X_{ACl} - 2X_{MCl_2})^2}{(X_{ACl} - X_{MCl_2})^2} b_2$$

Can. J. Chem. Downloaded from www.nrcresearchpress.com by 210.87.254.105 on 09/05/12
For personal use only.

$$[16] \qquad \Delta\bar{H}_{ACl} = \frac{X_{MCl_2}{}^2}{(X_{ACl} - X_{MCl_2})^2}\left[b_2 + \frac{2(X_{ACl} - 2X_{MCl_2})}{(X_{ACl} - X_{MCl_2})}\,b_1\right]$$

At $X_{ACl} = 2X_{MCl_2}$, or at the composition $X_{MCl_2} = 0.333$ eqs. 15 and 16 yield

$$[17] \qquad b_2 = (\Delta\bar{H}_{ACl})_{\text{at } X_{MCl_2}=0.333}$$

or

$$[18] \qquad b_2 = \frac{b_R - (\Delta\bar{H}_{MCl_2})_{X_{MCl_2}=0.333}}{2}$$

In the MCl_2–A_2MCl_4 subsystem at $1.0 > X_{MCl_2} > 0.333$, the mixing reactions for ACl and MCl_2 are given as

$$[19] \qquad MCl_2 + [(MCl_2)_{n_1}(A_2MCl_4)_{n_2}] \rightarrow [(MCl_2)_{n_1+1}(A_2MCl_4)_{n_2}]$$

and

$$[20] \qquad ACl + [(MCl_2)_{n_1}(A_2MCl_4)_{n_2}] \rightarrow [(MCl_2)_{n_1-0.5}(A_2MCl_4)_{n_2+0.5}$$

The partial molar heats of mixing for ACl and MCl_2 are obtained by partial differentiation of eq. 10, and are given as

$$[21] \quad \Delta\bar{H}_{MCl_2} = \frac{0.0625X_{ACl}{}^4 + 1.25X_{MCl_2}{}^2X_{ACl}{}^2 - 0.75X_{ACl}{}^3X_{MCl_2}}{((2X_{MCl_2} - 0.5X_{ACl})(X_{MCl_2} + 0.5X_{ACl}))^2}\,b_1' + \frac{X_{ACl}{}^2}{4(2X_{MCl_2} - 0.5X_{ACl})^2}\,b_2'$$

$$[22] \quad \Delta\bar{H}_{ACl} = 0.5b_R + \left[\frac{0.5X_{MCl_2}{}^2 - X_{MCl_2}X_{ACl} + 0.375X_{ACl}{}^2}{(2X_{MCl_2} - 0.5X_{ACl})(X_{MCl_2} + 0.5X_{ACl})} - \frac{0.25X_{ACl}(X_{MCl_2} - 0.5X_{ACl})^2(X_{MCl_2} - X_{ACl})}{(2X_{MCl_2} - 0.5X_{ACl})^2(X_{MCl_2} + 0.5X_{ACl})^2}\right]b_1' + \frac{(X_{MCl_2}{}^2 - X_{ACl}X_{MCl_2} - 0.125X_{ACl}{}^2)}{(2X_{MCl_2} - 0.5X_{ACl})^2}\,b_2'$$

From eq. 22, at a composition $X_{MCl_2} = 0.333$

$$[23] \qquad (\Delta\bar{H}_{ACl}) = \frac{b_R - b_2'}{2}$$

and from eq. 21,

$$[24] \qquad (\Delta\bar{H}_{MCl_2}) = b_2'$$

From eqs. 17 and 23, it follows that

$$[25] \qquad b_R = 2b_2 + b_2'$$

Hence, the parameters b_2' and b_2 may be determined directly from the experimentally obtained partial molar heats of mixing of either ACl or MCl_2 at the stoichiometric composition of $X_{MCl_2} = 0.333$,

The parameters b_1 and b_1' are determined from the equations for the integral heats of mixing 5 and 10 written in the following forms:

Can. J. Chem. Downloaded from www.nrcresearchpress.com by 210.87.254.105 on 09/05/12
For personal use only.

TABLE 2. Interaction parameters in the MCl_2–ACl system (cal/mol)

Parameter	Value when ACl = CsCl	RbCl	KCl	NaCl	LiCl
$MnCl_2$					
b_R	−15720	−13500	−10680	−4950	−1110
b_2'	−9500	−7400	−6890	−3470	−660
b_2	−3130	−3100	−1780	−750	−220
b_1'	−24300	−19800	−14650	−6900	−971
b_1	−715	+520	−974	−1080	−620
$FeCl_2$					
b_R	−16260	−13980	−11370	−5020	−972
b_2'	−10450	−8300	−6450	−3140	−430
b_2	−2900	−2850	−2480	−940	−268
b_1'	−18080	−15850	−12966	−3900	+1790
b_1	−1175	−1301	−127	−540	−666
$CoCl_2$					
b_R	−18510	−15660	−13080	−6000	−810
b_2'	−12400	−9500	−7970	−3050	+80
b_2	−3000	−3100	−2570	−1480	−450
b_1'	−9230	−7370	−3490	+916	+95
b_1	−377	−1460	−492	−908	−488
$MgCl_2$					
b_R	−15120	−12990	−10890	−5320	−1410
b_2'	−9580	−7050	−6070	−3700	−780
b_2	−2780	−2970	−2420	−870	−320
b_1'	−24680	−22200	−18100	−7990	+145
b_1	−1265	+911	−318	−1040	−339
$NiCl_2$					
b_R	−16410	−13800	−11400	−4620	−1890
b_2'	—	—	—	—	—
b_2	−3170	−2760	−2220	−950	−290
b_1'	—	—	—	—	—
b_1	+418	0	−210	−470	−340
$CdCl_2$					
b_R	−14070	—	—	—	−630
b_2'	−7290	—	—	—	+95
b_2	−3380	—	—	—	−55
b_1'	−27240	—	—	—	−500
b_1	−206	—	—	—	−332

For the composition range, $0.333 > X_{MCl_2} > 0$

$$[26] \qquad \frac{(\Delta H_M - X_{MCl_2} b_R)(X_{ACl} - X_{MCl_2})}{(X_{ACl} - 2X_{MCl_2})X_{MCl_2}} = \frac{X_{ACl} - 2X_{MCl_2}}{X_{ACl} - X_{MCl_2}} b_1 + b_2$$

which is of the linear form

$$I = Pb_1 + b_2$$

Similarly, from eq. 10,

$$[27] \qquad \frac{(\Delta H_M - 0.5X_{ACl} b_R)(8X_{MCl_2} - 2X_{ACl})}{(2X_{MCl_2} - X_{ACl})X_{ACl}} = \frac{2X_{MCl_2} - X_{ACl}}{2X_{MCl_2} + X_{ACl}} b_1' + b_2'$$

which is of the linear form

$$[28] \qquad I' = Qb_1' + b_2'$$

Because the calculations involve small differences between large numbers, it is best to obtain the parameters b_2 and b_2' from the partial molar heats of mixing, and then use the linear plots predicted by eqs. 24 and 25 to evaluate the slopes b_1 and b_1'. Alternatively, b_1 and b_1' may be calculated by solving eqs. 5 and 10, for various points along the curve where, b_R, b_2, and b_1 are known using the previously described methods.

Can. J. Chem. Downloaded from www.nrcresearchpress.com by 210.87.254.105 on 09/05/12
For personal use only.

Can. J. Chem. Downloaded from www.nrcresearchpress.com by 210.87.254.105 on 09/05/12
For personal use only.

Results and Discussion

The heats of mixing for the systems $MgCl_2$–ACl, $MnCl_2$–ACl, $FeCl_2$–ACl, $CoCl_2$–ACl, $NiCl_2$–ACl, and $CdCl_2$–ACl, which are available from calorimetric measurements by Papatheodorou and Kleppa (1–3), have been treated using the previously described expressions, and the b parameters $b_1, b_2, b_1', b_2', b_R$ for each system are summarized in Table 2.

For this calculation the parameters b_1 and b_1' were obtained both analytically and graphically.

Using the b-parameters given in Table 2, the integral heats of mixing and the regular solution interaction parameter given as $\Delta H_{mix}{}^{int}/X_{ACl}X_{MCl_2}$ can now be calculated. The plots of these interaction parameters for the MCl_2–ACl systems are shown in Figs. 1 to 6. The calculated integral heats of mixing in the MCl_2–CsCl systems are compared with the experimental values in Figs. 7 to 9. It is seen that small discrepancies between the experimental and calculated values are exaggerated in the plot of the interaction parameters, since a small error of ± 50 cal in the integral heats

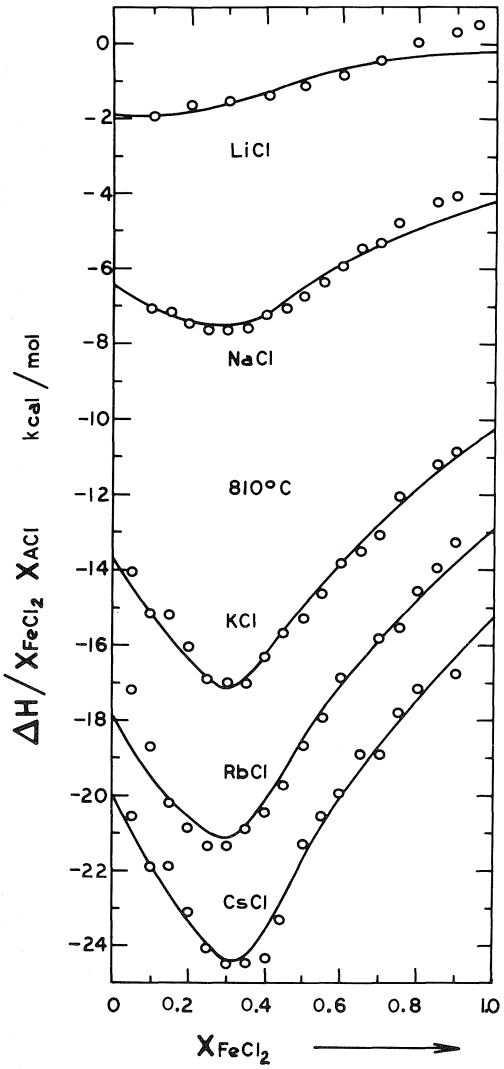

FIG. 1. Plots of $\Delta H_M/X_{ACl}\cdot X_{MCl_2}$ *vs.* X_{MCl_2} for the binary systems $FeCl_2$–ACl where A = Li, Na, K, Rb, Cs. The points represent experimental data (1). The solid line is calculated from theory using the b-values from Table 2.

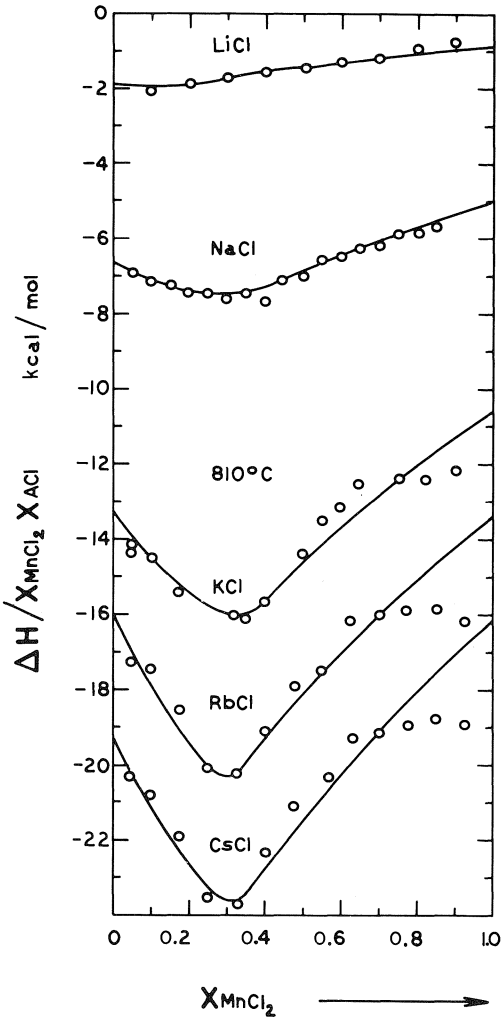

FIG. 2. Plots of $\Delta H_M/X_{ACl}X_{MCl_2}$ *vs.* X_{MCl_2} for the binary systems $MnCl_2$–ACl where A = Li, Na, K, Rb, Cs. The points represent experimental data (1). The solid line is calculated from theory using the b-values from Table 2.

Can. J. Chem. Downloaded from www.nrcresearchpress.com by 210.87.254.105 on 09/05/12
For personal use only.

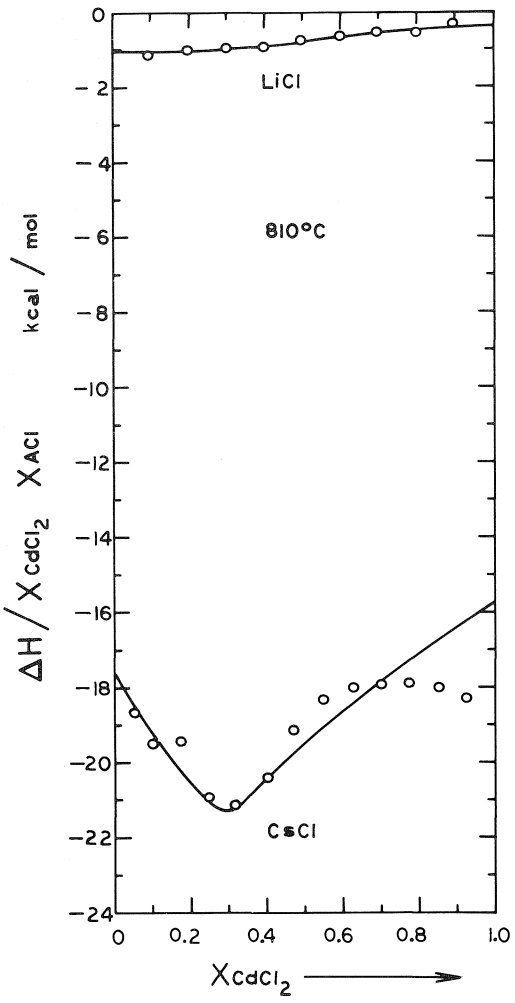

FIG. 3. Plots of $\Delta H_M/X_{ACl}X_{MCl_2}$ *vs.* X_{MCl_2}, in the binary systems $CdCl_2$–CsCl and $CdCl_2$–LiCl. The points represent experimental data (2). The solid lines are calculated from theory using the *b*-values from Table 2.

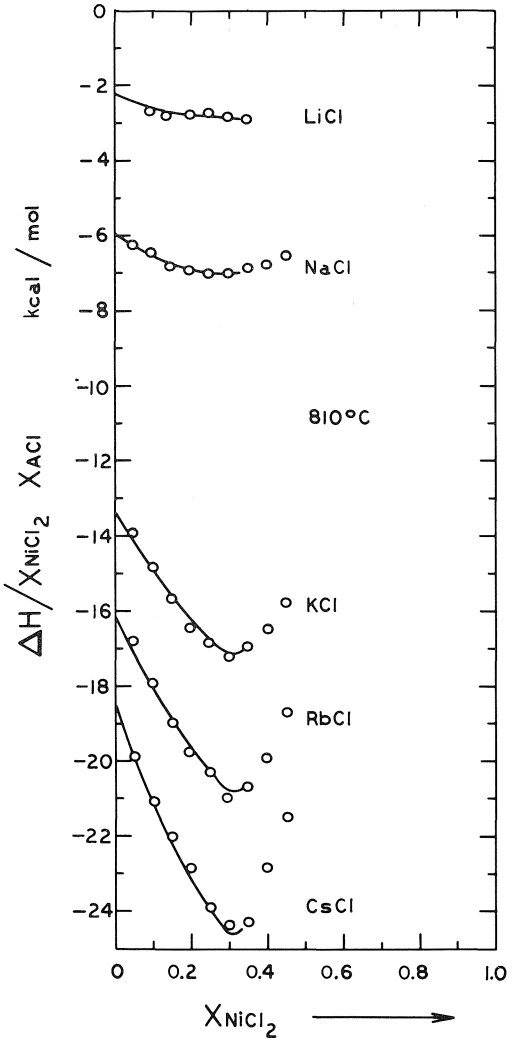

FIG. 4. Plots of $\Delta H_M/X_{ACl}X_{MCl_2}$ *vs.* X_{MCl_2} in the binary systems $NiCl_2$–ACl and where A = Li, Na, K, Rb, Cs over the available concentration range. The points represent experimental data (2). The solid lines have been calculated from theory using the *b*-values in Table 2.

of mixing leads to a large error in the value of $\Delta H_M/X_{ACl}\cdot X_{MCl_2}$.

It is significant that the interaction parameters $\Delta H_M/X_{ACl}\cdot X_{MCl_2}$ reach minimum values at a composition corresponding to the stoichiometry MCl_4^{2-}. Similarly, the integral heats of mixing reach maxima at about the same composition.

If the strength of the complex configuration MCl_4^{2-} is considered to be the result of competing interactions between the M^{2+} and the A^+ cations for the same chloride anion, it is evident that small alkali cations like Li^+ or Na^+ which create strong electrostatic fields shall have the tendency to increase the M—Cl bond distance and create weak complexes. Accordingly, the reaction parameter b_R is expected to be a function of the alkali cation radius for each MCl_2–ACl system.

Figure 10 shows the plots of b_R against r_{A^+}, for the various MCl_2–ACl binary systems. It is seen that the relationship is linear and indicates that the alkali chlorides with the largest cation size, like Rb^+ and Cs^+, form the strongest complexes, as expected.

Can. J. Chem. Downloaded from www.nrcresearchpress.com by 210.87.254.105 on 09/05/12
For personal use only.

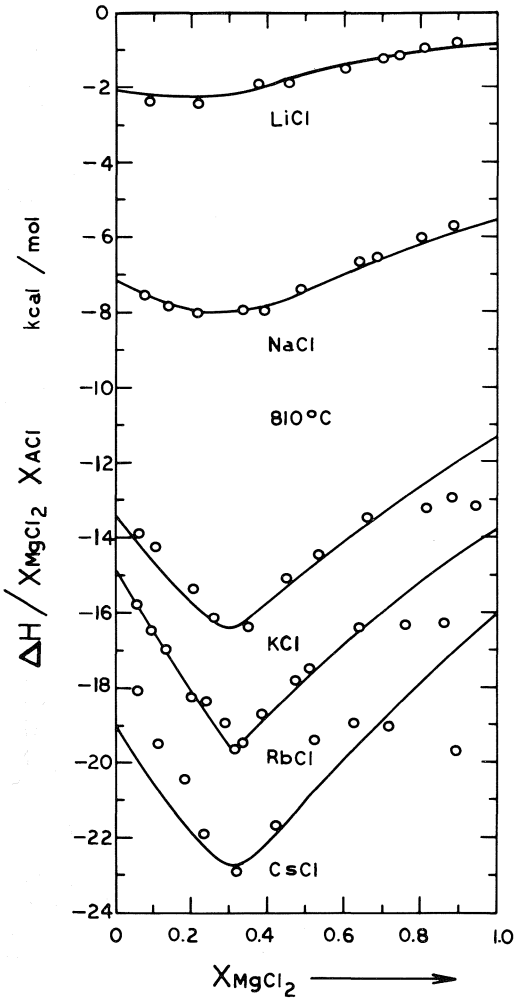

FIG. 5. Plots of $\Delta H_M/X_{ACl}X_{MCl_2}$ *vs.* X_{MCl_2} for the binary systems $MgCl_2$–ACl, where A = Li, Na, K, Rb, Cs. The points represent experimental data (4). The solid lines have been calculated from theory using the *b*-values in Table 2.

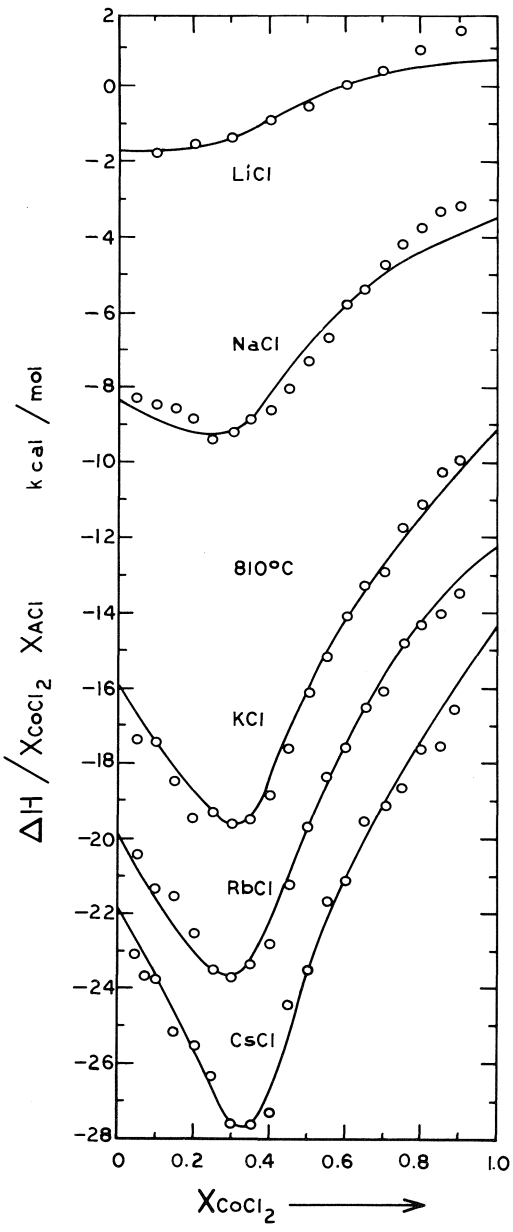

FIG. 6. Plots of $\Delta H_M/X_{ACl}X_{MCl_2}$ *vs.* X_{MCl_2} in the binary systems $CoCl_2$–ACl, where A = Li, Na, K, Rb, Cs. The points represent experimental data (1). The solid lines have been calculated from theory using the *b*-values in Table 2.

The physical significance of the parameters b_1, b_2, and b_1', b_2', is given by eqs. 4*a* and 9*a*. Although each of these parameters represent summations of energy terms which are difficult to interpret, the quantities $b_1 + b_2$ and $b_1' - b_2'$ describe the relatively simple expressions given below

$$[29]\quad b_1 + b_2 = 2(E_{Cl—A—Cl^*} - E_{Cl^*—A—Cl^*})$$

and

$$[30]\quad b_2' - b_1' = E_{M—Cl} - E_{A—Cl^*}$$

The difference in energies, shown in eq. 29, essentially describes the difference in the internal energies between a "free" chloride ion and a chloride ion bonded in a complex configuration.

Can. J. Chem. Downloaded from www.nrcresearchpress.com by 210.87.254.105 on 09/05/12
For personal use only.

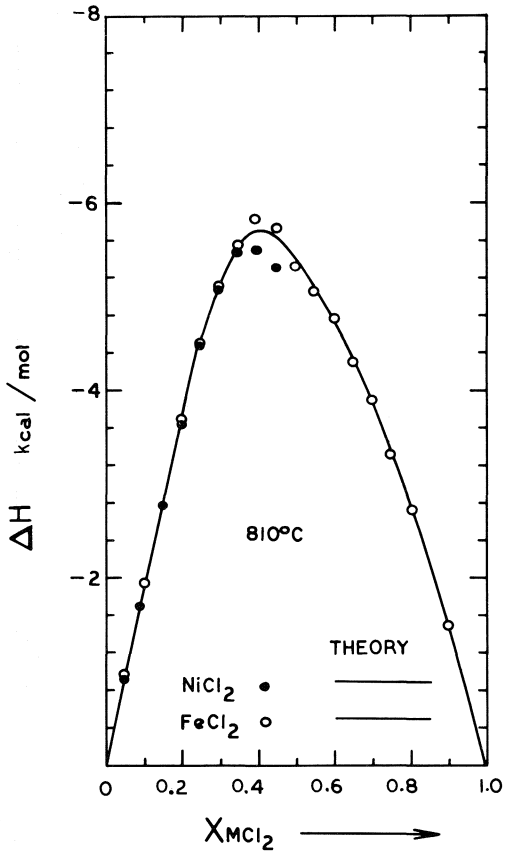

FIG. 7. Plots of the integral heats of mixing in the binary systems $NiCl_2$–CsCl and $FeCl_2$–CsCl as functions of composition. Points are experimental (3). The continuous and dashed lines represent heats calculated from theory using the *b*-parameters in Table 2.

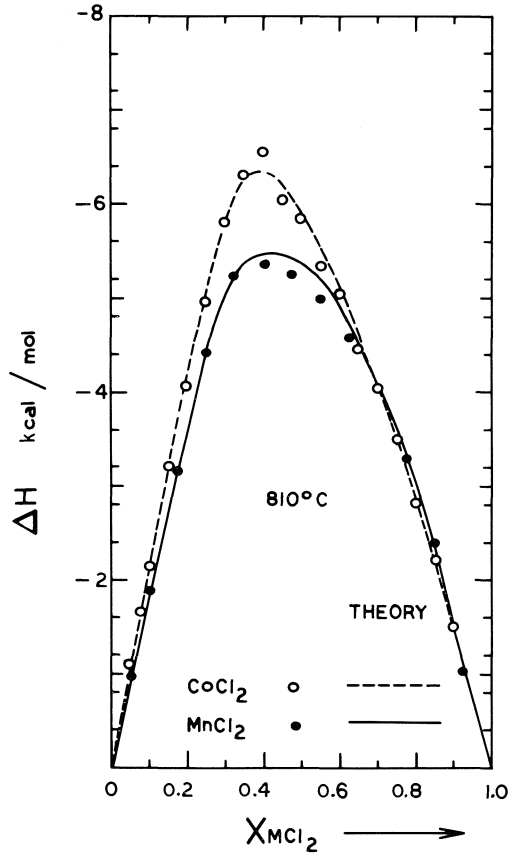

FIG. 8. Plots of the integral heats of mixing in the binary systems $CoCl_2$–CsCl and $MnCl_2$–CsCl as functions of composition. Points are experimental (1). The dashed and continuous lines are calculated from theory using the *b*-parameters in Table 2.

It follows that $b_1 + b_2$ should be proportional to the reaction parameter b_R.

Plots of $b_1 + b_2$ against b_R for the systems investigated are given in Fig. 11. It is seen that there is an almost linear relationship between $b_1 + b_2$ and b_R. Similarly, $b_2' - b_1'$ describes the difference in the interaction energies between "free" MCl and ACl*, where the Cl* refers to a chloride ion bonded in the complex. If the state of Cl* is approximated to that of the "free" chloride ions, then $b_2' - b_1'$ is expected to be proportional to the difference

$$[31] \quad \frac{1}{r_{M^{2+}} + r_{Cl^-}} - \frac{1}{r_{A+} + r_{Cl^-}} = \Delta\left(\frac{1}{d}\right)$$

The plot of $b_2' - b_1'$ against $\Delta(1/d)$ is given in Fig. 12 and indicates a nearly linear relationship within each system.

From the previously presented results it appears that the $CdCl_2$–ACl, $MgCl_2$–ACl, and $MnCl_2$–ACl systems, in which the M^{2+} ion has either no d-electrons or has a filled d^{10} or half-filled d^5 outer electronic structure, form complex species of the same approximate strength. Furthermore, the concentration dependence of the heats of mixing in $MgCl_2$ and $MnCl_2$ for solutions rich in MCl_2 cannot be predicted from the present model as accurately as with the other systems investigated. The greatest deviations are observed with the $MnCl_2$–CsCl and $MgCl_2$–CsCl binary systems, where the model is expected to hold best. It is possible that dissociation effects and the formation of more complicated complex

Can. J. Chem. Downloaded from www.nrcresearchpress.com by 210.87.254.105 on 09/05/12
For personal use only.

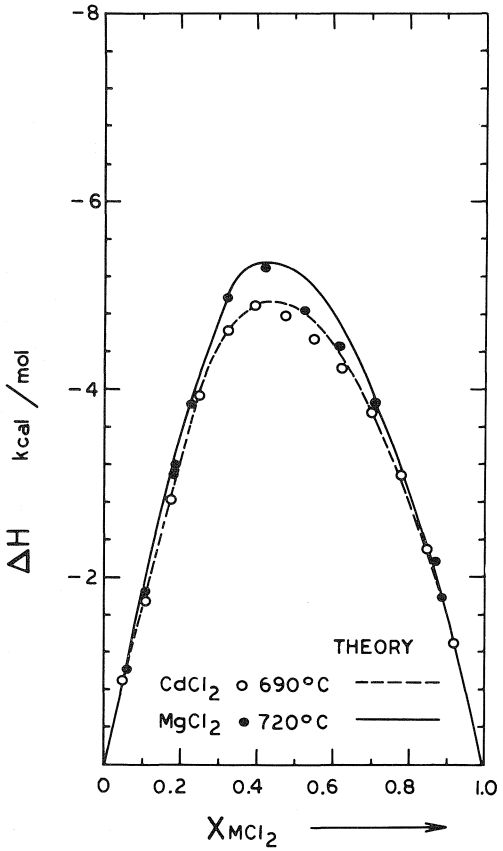

FIG. 9. Plots of the integral heats of mixing in the binary systems $CdCl_2$–CsCl and $MgCl_2$–CsCl, as functions of composition. Points are experimental (2). The lines are calculated from theory using the *b*-parameters in Table 2.

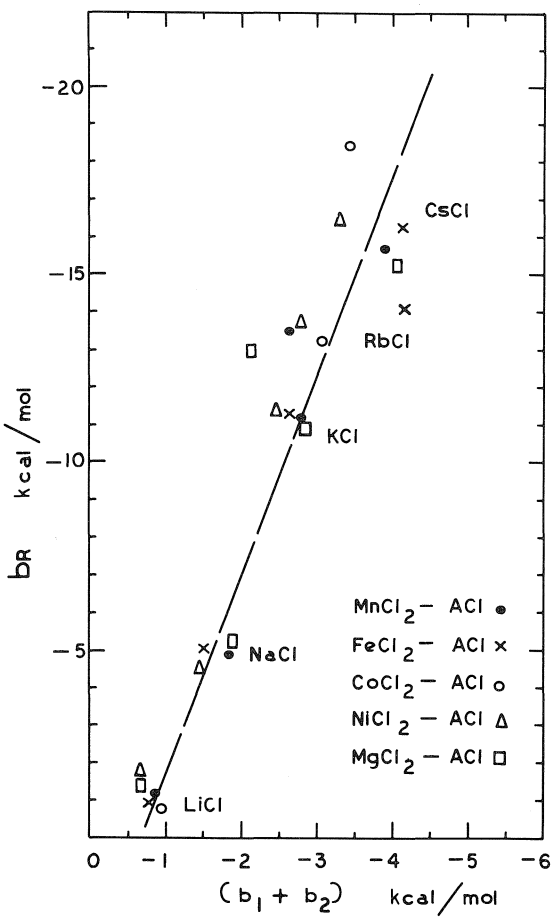

FIG. 11. Plot of the sum $b_1 + b_2$ *vs.* the reaction parameters b_R for the MCl_2–ACl systems.

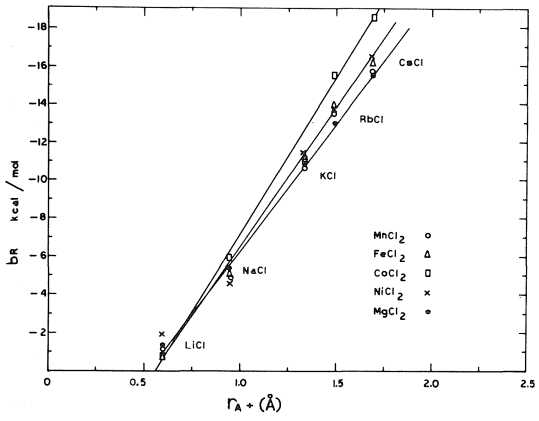

FIG. 10. Plot of the Pauling ionic radius r_{A+} of the alkali metal cations *vs.* the reaction parameter b_R for the binary systems MCl_2–ACl.

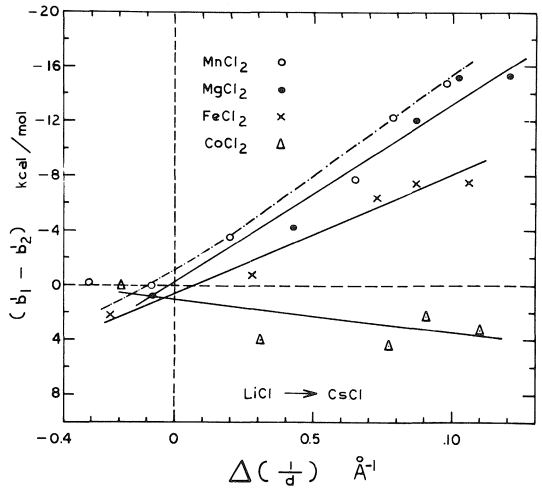

FIG. 12. Plots of the difference $b_1' - b_2'$ *vs.* $\Delta(1/d)$ for the systems MCl_2–ACl. $\Delta(1/d) = 1/(r_{M2+} + r_{Cl-}) - 1/(r_{A+} + r_{Cl-})$.

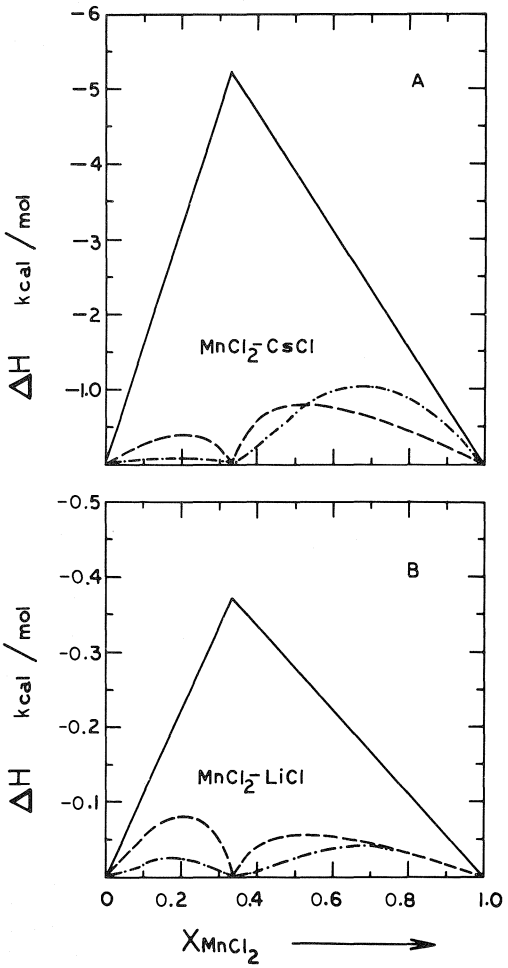

FIG. 13. (*A*) Contribution of the various *b*-parameters to the heats of mixing in the $MnCl_2$–CsCl system. ———, "reaction" part of the heat of mixing; – – –, part of the heat of mixing attributed to the parameter b_2 and b_2'; –·–·–·, part of the heat of mixing attributed to the parameters b_1 and b_1'. (*B*) Same plots for the $MnCl_2$–LiCl system.

species may take place in the metal chloride rich solutions.

It should be emphasized that although the various parameters b_1, b_2, b_1', and b_2' are large negative quantities, their contribution to the heats of mixing is much smaller than that due to the reaction parameter b_R. Figure 13 shows the contribution of the various heat effects to the total heat of mixing, for the system $MnCl_2$–CsCl.

It is evident that the heat of mixing is primarily determined by the reaction parameter b_R. For the weak complexed systems, such as the $MnCl_2$–LiCl, the contribution of the solution parameters b_1, b_2, b_1', and b_2' becomes more significant. Again the distribution of the total heat into the various contributions is shown in Fig. 13*b*.

Actually, such weakly complexed systems could also be treated as a first approximation by a simple regular solution model.

Summary

Charge asymmetrical binary systems which indicate pronounced negative heats of mixing are interpreted in terms of a model which takes into account the reaction and the asymmetry effects. The calculation accounts for the change in coordination number in a solution of mono- and divalent salts. The derived relationships predict well the concentration dependence of the heats of mixing in the systems $MnCl_2$–ACl, $FeCl_2$–ACl, $CoCl_2$–ACl, $MgCl_2$–ACl, and $NiCl_2$–ACl, where A = Li, Na, K, Rb, or Cs.

The method allows the calculation of exact equations for the partial molar heats of mixing. The parameters, b_R, b_1, b_2, b_1', and b_2', are shown to be physically meaningful as they relate to the structural characteristics of the salt components in the melt.

1. G. N. PAPATHEODOROU and O. J. KLEPPA. J. Inorg. Nucl. Chem. **33**, 1249 (1971).
2. G. N. PAPATHEODOROU and O. J. KLEPPA. Inorg. Chem. **10**, 872 (1971).
3. G. N. PAPATHEODOROU and O. J. KLEPPA. J. Inorg. Nucl. Chem. **32**, 889 (1970).
4. F. G. MCCARTY and O. J. KLEPPA. J. Phy. Chem. **70**, 1249 (1966).
5. D. E. NEIL, H. M. CLARK, and R. H. WISHALL, JR. J. Chem. Eng. Data. **10**, 21 (1965)
6. D. C. HAMBY and A. B. SCOTT. J. Electrochem. Soc. **115**, 704 (1968).
7. D. C. HAMBY and A. B. SCOTT. J. Electrochem. Soc. **117**, 319 (1970).
8. H. FLOOD and S. URNES. Z. Electrochem. **59**, 834 (1955).
9. H. T. DAVIS. J. Chem. Phy. **41**, 2761 (1964).
10. H. REISS, S. W. MAYER, and J. L. KATZ. J. Chem. Phy. **35**, 830 (1961).
11. A. D. PELTON and W. T. THOMPSON. Can. J. Chem. **48**, 1585 (1970).
12. T. OSTVOLD. Ph.D. Thesis. Institute of Phy. Chem., University of Trondheim, NTH, Norway. 1971.
13. T. FØRLAND. Norges Tek. Vclenskapsaka. Skr. **4**, 23 (1957).
14. S. N. FLENGAS and SIR ERIC RIDEAL. Proc. Roy. Soc. Ser. A. **233**, 443–454 (1956).
15. R. L. LISTER and S. N. FLENGAS. Can. J. Chem. **43**, 2947 (1965).
16. J. E. DUTRIZAC and S. N. FLENGAS. Advances in Extractive Metallurgy, Symposium. The Institution of Mining and Metallurgy, London, paper 24. 1967.
17. S. N. FLENGAS and P. PINT. Can. Met. Q. **8**, 2, 151 (1969).

Can. J. Chem. Downloaded from www.nrcresearchpress.com by 210.87.254.105 on 09/05/12
For personal use only.

Can. J. Chem. Downloaded from www.nrcresearchpress.com by 210.87.254.6 on 09/05/12
For personal use only.

Differential Thermal Analysis Studies on Ag_2CO_3[1]

G. D. NAGY, J. B. VERGETTE,[2] AND J. P. CONNOLLY
Defence Research Establishment Ottawa, Defence Research Board, Ottawa 4, Canada

Received March 1, 1971

The decomposition and phase transitions that occur during the heating and cooling of Ag_2CO_3 were studied by differential thermal analysis at heating rates of 7 to 14° per min. In helium, the Ag_2CO_3 was partially decomposed evolving CO_2 (7–35% depending upon the method of preparation) giving rise to peaks at 190 to 200°; at 350 to 400°, two endothermic peaks were observed at which CO_2 and O_2 were given off simultaneously, leaving silver metal. In CO_2 the initial partial decomposition gave rise to a peak at about 265°. The partially decomposed Ag_2CO_3 ($Ag_2O{\cdot}nCO_2$, where n is less than one) gave the same X-ray diffraction pattern as Ag_2O, which slowly converted to that for Ag_2CO_3 if left exposed to air or CO_2. The $Ag_2O{\cdot}nCO_2$ undergoes two distinct "reversible" phase transitions at 180 and 197° on subsequent reheatings. The $Ag_2O{\cdot}nCO_2$ behaves like a clathrate-type of structure in which CO_2 can be entrapped in the Ag_2O lattice.

La décomposition et les transitions de phase qui ont lieu durant le chauffage et le refroidissement du Ag_2CO_3 ont été étudiées par l'analyse différentielle thermique à une vitesse de chauffage de 7 à 14° par min. Dans l'hélium, le Ag_2CO_3 s'est décomposé partiellement (7–35% selon la manière de préparation) en dégageant du CO_2 et a occasionné des pics à une température de 190 à 200°; de 350 à 400°, deux pics endothermiques ont été observés aux températures où se sont dégagés simultanément du CO_2 et du O_2 en laissant du métal argent. Dans le CO_2, la première étape de la décomposition a occasionné un pic à une température d'environ 265°. Le Ag_2CO_3, partiellement décomposé ($Ag_2O{\cdot}nCO_2$, où n est inférieur à un), a donné le même diagramme de rayons-X que le Ag_2O; ce diagramme s'est transformé lentement en celui du Ag_2CO_3, quand le Ag_2O était exposé à l'air ou au CO_2. Le $Ag_2O{\cdot}nCO_2$ subit deux transitions "réversibles" de phase distinctes aux températures de 180 et de 197° durant des réchauffages ultérieurs. Le $Ag_2O{\cdot}nCO_2$ agit d'un type clathrate dans lequel le CO_2 peut être logé dans le réseau du Ag_2O.

Canadian Journal of Chemistry, **49**, 3986 (1971)

Introduction

The thermal decomposition of Ag_2CO_3 has been studied by other investigators as an example of a reversible chemical change involving a solid reactant giving solid and gaseous products (1–10). These studies are relevant to the development of silver oxide – silver carbonate systems used as regenerable chemisorbers for carbon dioxide (11–13) and also for silver electrodes for the reduction of oxygen (14). Our interest in Ag_2CO_3 results from the use of silver oxide electrodes in silver–zinc or silver–cadmium batteries. The silver oxides in these batteries may be converted to the carbonate by atmospheric carbon dioxide or by potassium carbonate in the potassium hydroxide electrolyte.

There is evidence that Ag_2CO_3 exists in two different forms, called active and inactive (2, 3, 7, 14). The two forms have the same chemical and crystallographic structures and are distinguished by their preparation and thermal decomposition. The active form can be precipitated from dilute aqueous equimolar solutions of silver nitrate and alkali carbonates or bicarbonates (less than 0.005 *M* for the carbonate and 0.015 *M* for the bicarbonate). It decomposes completely to Ag_2O and carbon dioxide below 200° under isothermal conditions. The inactive form can be prepared from concentrated solutions of the same salts as the active form as well as by bubbling carbon dioxide through aqueous silver bicarbonate solutions or solutions containing the silver–ammonia complex. The inactive form has been reported not to decompose at any measurable rate (7) or only to an extent of 10 to 12% below 280° (9). Above this temperature it decomposes directly to metallic silver with simultaneous evolution of carbon dioxide and oxygen. Kadlets and Dubinin (7) suggested that the 10–12% decomposition below 280° was due to the precipitation of some of the active form during the latter stages of the precipitation when the solution becomes dilute.

In previous differential thermal analysis

[1]D.R.E.O. Report No. 651. Presented in parts at the 52nd C.I.C. Conference, Montreal, May 25–28, 1969 and 2nd Annual NATAS meeting, Chicago, September 16, 1970.

[2]Present address: Algonquin College of Applied Arts and Technology, School of Technology, Ottawa, Ontario.

Can. J. Chem. Downloaded from www.nrcresearchpress.com by 210.87.254.6 on 09/05/12
For personal use only.

(DTA) work, either one or two endothermic peaks have been observed in the range 20 to 300° (8, 11, 15, 16). These have been reported to occur in the ranges 185 to 215°, and 227 to 300°. Wydeven (17) using a differential scanning calorimeter and working in a carbon dioxide atmosphere showed that, on reheating, the lower peak split into two endothermic peaks occurring at 185 and 200°. Corresponding exothermic peaks were observed at 115 and 185° on cooling. Repeated heating and cooling had little effect on these thermograms. The exothermic peak at 115° was quite broad, starting at 134° and ending at 105°. The intensity of the corresponding endothermic peak at 185° on reheating was proportional to how far into the range of the exotherm the sample was allowed to cool. Wydeven also showed that these so-called reversible peaks were not due to the reaction

[1] $$Ag_2CO_3 \rightleftarrows Ag_2O + CO_2$$

Experimental

A large proportion of the data presented here will be for commercially available Ag_2CO_3 (Mallinckrodt AR). This was prepared from $AgNO_3$ and Na_2CO_3 and can be expected to contain both forms, but predominantly the inactive form.

Attempts were made to prepare pure active and inactive forms from equimolar aqueous solutions of $AgNO_3$ and Na_2CO_3 varying from saturated solutions down to 7.5×10^{-4} *M*. In order to study the effect of coprecipitation of both forms, two preparations were made at each concentration. In one case the precipitates were filtered immediately after mixing. In the other case there were digestion periods of 24 h before filtration.

Attempts were also made to prepare the active form from dilute solutions of $AgNO_3$ and $NaHCO_3$ (7) and from carbon dioxide saturated solutions of $AgNO_3$ and $KHCO_3$ (2). We restricted our preparations to those which would be common to battery systems.

The DTA apparatus used was an R. L. Stone model with effluent gas detection (E.G.D.). The sample and reference materials were contained in platinum sample cups which rested in a Stone ring-type platinel II differential thermocouple. Helium and carbon dioxide were used as dynamic gases. At a pressure of 25 Torr above atmospheric, chemical and physical changes giving rise to temperature peaks of the order of 0.01° could be detected.

For some experiments the effluent gas was fed into a Varian Aerograph chromatograph fitted with an automatic sampler. This was used to measure the concentrations of the evolved gases in the dynamic stream. Helium was used as the carrier gas. The sensitivity was 50 p.p.m. for O_2 and 100 p.p.m. for CO_2.

X-Ray diffraction studies were done with a Philips Norelco direct-reading diffractometer. The goniometer was equipped with a high temperature stage that could be operated at reduced pressure or in a controlled gas atmosphere.

Results

(A) General Characteristics of the DTA Traces

Figure 1 shows traces of the Ag_2CO_3 and chemically precipitated Ag_2O and AgO at a heating rate of 14 °C per min. (The Ag_2O was commercially available and the AgO was prepared by the silver nitrate – potassium peroxydisulfate method (18).) Helium was used as the carrier gas except for the dashed curve for Ag_2CO_3 where CO_2 was used. The lower trace, for Ag_2O, shows a peak at 458° due to Ag_2O decomposing to silver and oxygen. The upper trace, for AgO, shows the decomposition to Ag_2O and oxygen gives rise to a peak at 210° and this Ag_2O to silver gives rise to a peak at 423°. The important things to note here are the differences in the peaks for the decomposition of normal Ag_2O and the Ag_2O from decomposed AgO. Although they have the same peak area they have different shapes and occur at different temperatures. The middle traces for commercially available Ag_2CO_3 showed three definite peaks in He, the solid curve. Carbon dioxide is evolved after the peak at 197°, in the vicinity of 200 to 220°. In a CO_2 atmosphere, the dashed curve, an additional peak is observed at 263°, at which CO_2 is evolved. Thus the discrepancy in earlier work with regard to the observance of either one or two peaks is

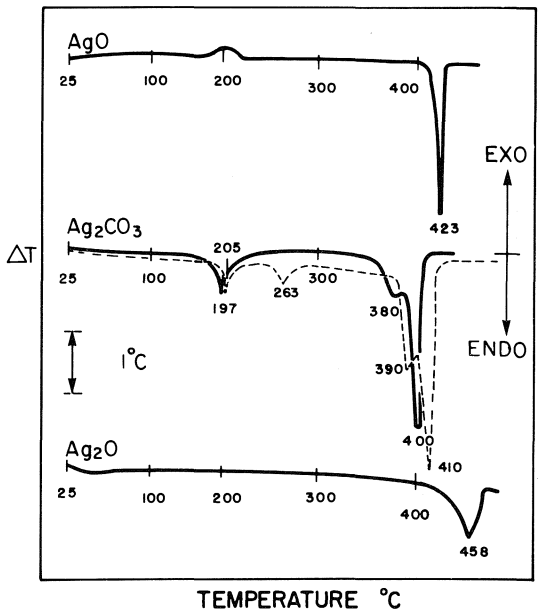

FIG. 1. DTA traces of commercially available Ag_2CO_3 and chemically precipitated AgO and Ag_2O. 14° per min. Solid lines in helium, dashed in CO_2.

Can. J. Chem. Downloaded from www.nrcresearchpress.com by 210.87.254.6 on 09/05/12
For personal use only.

due mainly to the ability of the particular apparatus to remove any evolved CO_2 and reaction 1.

The two peaks at 380 and 400° which involve decomposition to silver with the simultaneous evolution of CO_2 and O_2 occur at a considerably lower temperature than for both of the other two forms of Ag_2O shown. Carbon dioxide as the dynamic gas had less effect on these peaks than on that at the lower temperature. Here the increase was only 5 to 10° as compared to close to 70° for the lower temperature peak.

Figure 2 shows DTA traces for precipitates from various concentrations of equimolar $AgNO_3$ and Na_2CO_3 solutions. These curves do not show all of the various concentrations studied, but do show the trends. The concentrations of the solutions were: *A*, saturated with respect to Na_2CO_3; *B*, 0.1 *M*; *C*, 0.0125 *M*; *D*, 0.006 *M*; *E*, 0.0022 *M*, the lowest concentration at which enough precipitate to analyze was obtained.

There are gradual shifts in the peak temperatures as the concentration is decreased. All curves had peaks in the vicinity of 195 to 200°. Curves *A* and *E* have additional peaks at 225 and 210°. On curve *D* a peak at 210° in the form of a slight shoulder can be seen.

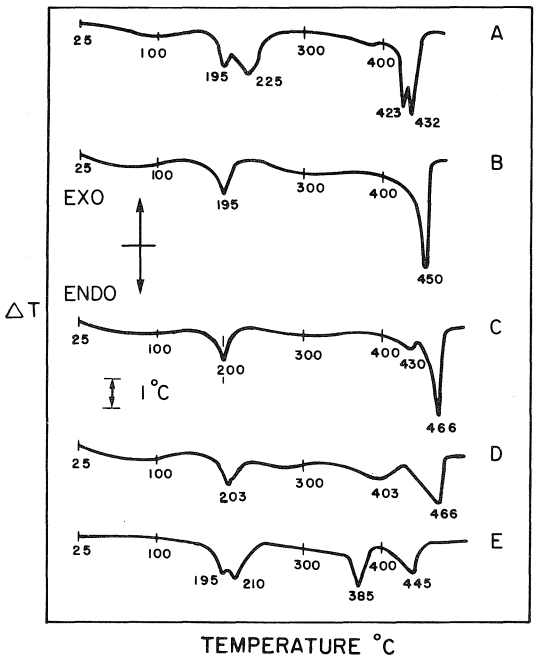

FIG. 2. DTA traces, in helium, of Ag_2CO_3 precipitated from equimolar aqueous $AgNO_3$ and Na_2CO_3 solutions. 14° per min. *A*, saturated with respect to Na_2CO_3; *B*, 0.1 *M*; *C*, 0.0125 *M*; *D*, 0.006 *M*; *E*, 0.0022 *M*.

In the temperature range of 385 to 466° two distinct peaks were observed, with the exception of the precipitates from solutions in the range of 1.0 to 0.1 *M* (see curve *B*). In these latter cases, shoulders were observed. One can see the gradual increase in the temperature of the higher peaks from curve *A* to curve *C*. A second peak begins to develop at 430° on curve *C*. The area of this new peak increases, and the temperature at which it occurs decreases as the concentration of the solutions decreases. At the same time there is a decrease in the area, and to a lesser degree, the temperature of the higher peak.

Carbon dioxide was the only gas evolved between 195 and 230°. In the case of curves *B* and *C* the gas was evolved about 10° after the peaks, but for the curves *A*, *D*, and *E*, only at the higher of the two peaks. The percentage of the total amount of CO_2 present as carbonate in the sample which was evolved below 220° increased from about 7% for curve *B* to 30% for curve *E*. About 35% of the available CO_2 was evolved for curve *A*. Vigorous stirring of the solution during precipitation decreased the amount of CO_2 evolved at these temperatures. The shift to higher peak temperatures as more CO_2 is evolved is probably due to the inhibition of the decomposition by the gaseous product. From the results of X-ray diffraction work described later, we prefer to call this partially decomposed carbonate $Ag_2O{\cdot}nCO_2$ where n is less than one.

At the peaks between 385 and 465°, CO_2 and O_2 were evolved simultaneously at each of the peaks, roughly in proportion to the amount of heat absorbed. This will be shown in more detail later.

Similarities between the precipitates for which DTA traces are shown by curves *A* and *E* were not confined to the DTA traces. The precipitates were a lemon color. The precipitate from the solution which was saturated with respect to Na_2CO_3 (curve *A*) had some medium gray powder as well. The precipitate from the 1.0 *M* solution was medium gray and the color changed through a greenish to a lemon yellow color as the concentration decreased. In all cases the precipitate blackened on exposure to light.

Digestion and aging affected only the higher temperature peaks. Typical curves are shown in

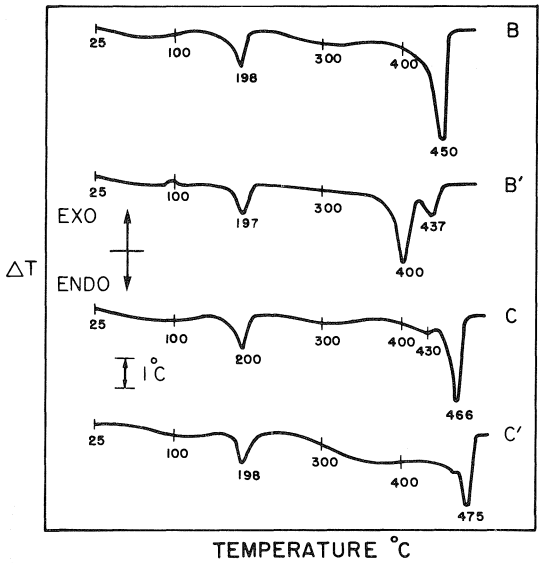

FIG. 3. DTA traces, in helium, of Ag_2CO_3, precipitated from equimolar aqueous $AgNO_3$ and Na_2CO_3 solutions. 14° per min. *B*, 0.1 *M*; *B'*, 0.1 *M*, stored 3½ months dry; *C*, 0.025 *M*, filtered immediately; *C'*, 0.025 *M*, digested 24 h.

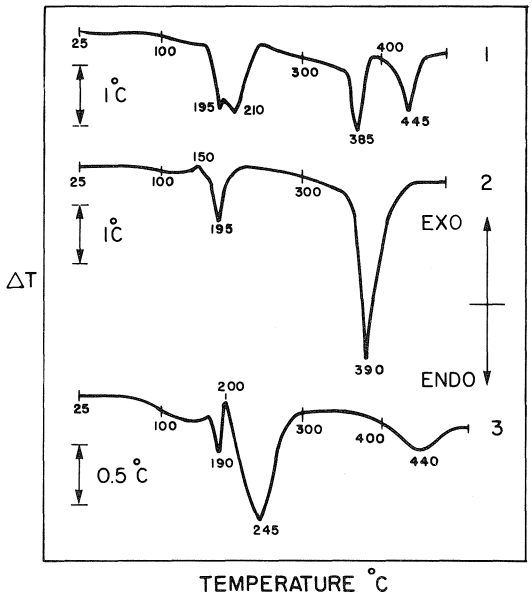

FIG. 4. DTA traces, in helium, of Ag_2CO_3 precipitates. 14° per min. (*1*) equimolar 0.0022 *M*, solutions $AgNO_3$ and $NaCO_3$; (*2*) equimolar, 0.015 *M*, solutions $AgNO_3$ and $NaHCO_3$; (*3*) equimolar 0.015 *M*, solutions $AgNO_3$ and $KHCO_3$ saturated with respect to CO_2 before mixing.

Fig. 3. Digestion increased the peak temperature. All aged material had two peaks which were observed at lower temperatures.

Figure 4 shows DTA traces of some of the precipitates made in an attempt to form the pure active form of Ag_2CO_3. The first curve is the same as curve *E* of Fig. 2. The second curve is that for the precipitate from 0.015 *M* solutions of $AgNO_3$ and $NaHCO_3$. The third curve was obtained from the precipitate resulting from mixing 0.015 *M* solutions of $AgNO_3$ and $KHCO_3$ which had been saturated with CO_2. The temperature scale on this last curve has been expanded to show some of the finer detail. In all cases the concentrations used were the lowest that gave enough precipitate to analyze. It is quite obvious that it is very unlikely that these are the same compound.

For curve *2*, gas was evolved at the exothermic peak at 150°. Carbon dioxide was evolved at the shoulder just after the peak at 195°. The amount of CO_2 was equivalent to about 15% of that available as carbonate. At the 390° peak, CO_2 and O_2 were given off simultaneously. For curve *3*, oxygen was given off at the exothermic peak at 200°. No gas was given off at the 190° peak. At 245°, about 90% of the CO_2 available as carbonate was evolved. At 440°, the gas evolved was almost entirely O_2.

It was mentioned earlier that at the peaks in the vicinity of 350 to 470°, O_2 and CO_2 were evolved simultaneously. Figures 5 and 6 show this.

In Fig. 5, the solid curve shows the average amount of carbon dioxide in the effluent gas

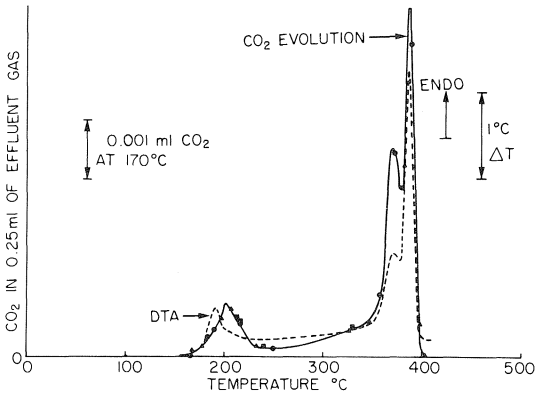

FIG. 5. Amount of CO_2 in a 0.25 ml sample of the effluent gas at 170° *vs.* temperature for commercially available Ag_2CO_3. Solid curve, CO_2 evolution; dashed curve, DTA trace in helium, 7° per min.

Can. J. Chem. Downloaded from www.nrcresearchpress.com by 210.87.254.6 on 09/05/12
For personal use only.

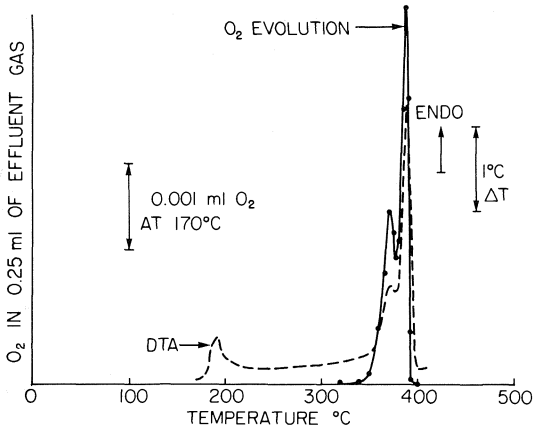

FIG. 6. Amount of O_2 in a 0.25 ml sample of effluent gas at 170° *vs.* temperature for commercially available Ag_2CO_3. Solid curve, O_2 evolution; dashed curve, DTA trace in helium, 7° per min.

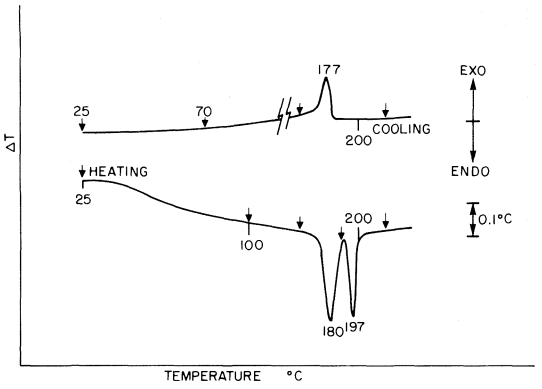

FIG. 7. DTA heating and cooling traces in helium of commercially available Ag_2CO_3 which had been previously heated to 220° and cooled to room temperature in helium. Heating rate 14° per min. Cooling rates, greater than 150°, 25° per min, less than 150°, by natural convection. The arrows refer to points at which X-ray diffraction patterns were taken.

during the course of decomposition of the commercially available Ag_2CO_3 for six runs. One-quarter milliliter samples were taken at the points indicated and about every 7 to 10 min between 230 and 250°. The dashed curve is a superimposed DTA trace.

As can be seen, about 20% of the total available, CO_2 comes off after the peak at about 195° as observed by Wydeven (17). Smaller amounts are evolved between 230 and 350°. Carbon dioxide is evolved at *both* of the peaks near 400° roughly in proportion to the heat absorbed.

Figure 6 shows curves corresponding to Fig. 5 for the case of O_2 evolution. No detectable O_2 is evolved until about 320°. Again as in the case of CO_2 evolution, O_2 is evolved at *both* peaks near 400° and roughly in proportion to the heat absorbed.

(B) Thermal Phenomena Due to Cyclic Heating and Cooling

Figure 7 shows DTA traces in helium exhibiting the so-called reversible thermal phenomena reported by Wydeven (17). The lower curve was obtained by heating $Ag_2O{\cdot}nCO_2$. In CO_2 three peaks were observed. The first two peaks were identical to those shown and the third in the range of 220 to 290° was due to decomposition of the Ag_2CO_3 formed by recombination of the $Ag_2O{\cdot}nCO_2$ and CO_2 during the cooling period.

On cooling we observed only the exotherm at 177° (Fig. 7, upper curve). Below 150°, the curve

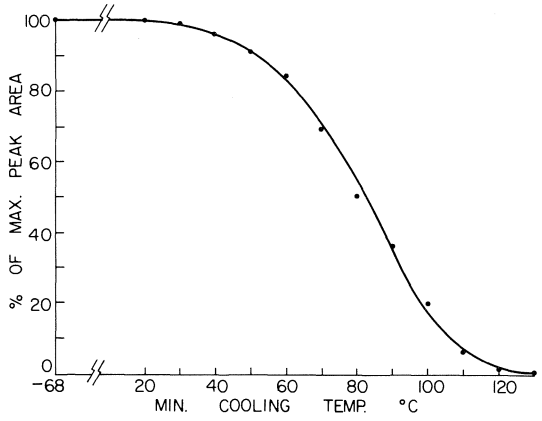

FIG. 8. Area of the 180° peak (see Fig. 7) expressed as the percentage of the maximum area observed for samples cooled to −68° as a function of the temperature to which the sample was cooled.

shown is the compressed trace. In this temperature range, the sample could only be cooled by natural convection at a rate too low to detect the presence of the low temperature transition. However, it was detected by another means as shown on Fig. 8.

In Fig. 8, the area of the 180° peak expressed as the percentage of the maximum area observed for samples which were cooled to −68° is plotted as a function of the temperature to which the sample was cooled. As can be seen the range of the transition was longer and at a lower temperature than the 105 to 134° observed by Wydeven.

Can. J. Chem. Downloaded from www.nrcresearchpress.com by 210.87.254.6 on 09/05/12
For personal use only.

Can. J. Chem. Downloaded from www.nrcresearchpress.com by 210.87.254.6 on 09/05/12
For personal use only.

Furthermore, holding the temperature at any of the temperatures in the range of the transition for up to 5 h had little effect on the area of the 180° peak on reheating. The curves were the same for He or CO_2 atmospheres.

Of the various methods used to prepare Ag_2CO_3, all precipitates with the exception of those made with CO_2 saturated solutions, exhibited this reversible phenomenon. In this latter case, where the Ag_2CO_3 is believed to have been almost pure active form, none of the reversible peaks were observed.

The recombination with carbon dioxide of the $Ag_2O{\cdot}nCO_2$ is dependent upon the thermal history and physical state of the sample. A sample which was heated to 290° and rapidly cooled in CO_2 to a temperature above 130° recombined more rapidly with CO_2 than a sample which was allowed to cool into the transition region shown on Fig. 8. In both cases the rate of recombination was much more rapid than that for normal Ag_2O.

(C) X-Ray Diffraction Studies

Ag_2CO_3 that had been heated in He to form $Ag_2O{\cdot}nCO_2$ had an X-ray diffraction pattern that was predominantly Ag_2O at 220°. On cooling to room temperature the pattern persisted. However, on exposure to air for extended periods of time the evolved CO_2 was replaced and the pattern reverted to that of Ag_2CO_3. These observations were based on the strong reflections of the 101, 130, 200, 210, 121, 031, and 150 planes of Ag_2CO_3 and the 111, 200, 220, and 311 planes of Ag_2O. Patterns of normal Ag_2O at 220° showed sharpening of the lines compared to those at room temperature observed by Rao *et al.* (15).

The arrows on Fig. 7 indicate temperatures at which X-ray diffraction patterns were taken on $Ag_2O{\cdot}nCO_2$ during the process of heating and cooling. At 100° the Ag_2O pattern began to appear and the intensity increased slowly with time. At 185°, the pattern was predominantly that of Ag_2O in less than $\frac{1}{2}$ h. At 220° the pattern was immediately predominantly that of Ag_2O. On cooling, the patterns were all that of Ag_2O.

There were six or seven additional lines observed in the Ag_2O pattern for the $Ag_2O{\cdot}nCO_2$. These were not present in the original Ag_2CO_3 pattern and could not be matched to other reported patterns for silver oxides (19–23).

It was estimated that the X-rays could completely penetrate the sample. However, to check whether or not the Ag_2O patterns observed were due to a surface layer of Ag_2O comprizing 15 to 20% of the sample, a sample, immediately after cooling to room temperature and an X-ray pattern taken, was ground, intimately mixed and another pattern taken. The pattern was still predominantly that of Ag_2O.

Discussion

Of the various methods used to form Ag_2CO_3, only the CO_2 saturated solutions gave what could be considered to be pure active form. All other preparations gave mixtures of the two forms. There is evidence that more of the active form is precipitated at high and low concentrations. The resultant mixture after partial decomposition is not a mechanical mixture. If a mechanical mixture was obtained one would expect distinct peaks at fairly distinct temperatures and not the gradual shifts as observed.

Co-precipitation of the active form with the inactive form is more subtle than just dilution of the reacting species as explained by Kadlets and Dubinin (7). If the form of the material precipitated is due to concentration alone, it is difficult to explain some of the results. First, digestion increased the temperature of the 430–460° peaks. Second, for curve *B* of Fig. 2, approximately 7% of the precipitate could be considered to be in the active form. The yield of this active form was found to be 2 mmol/l. However, for curve *E*, taking into account the solubility of Ag_2CO_3 and the concentrations of the solution, only 0.2 mmol/l of Ag_2CO_3 can be formed. Furthermore only $\frac{1}{3}$ or less than 0.1 mmol/l of this latter precipitate can be considered to be in the active form. The effect of stirring suggests that the relative quantities of the active and inactive forms are controlled by mass transfer.

The origin of the two exothermic peaks at 150 and 200° of curves *2* and *3* of Fig. 4 at which oxygen was evolved is unknown. The temperatures suggest the decomposition of AgO, but it is difficult to see how AgO can be formed under the conditions used. Since considerably more CO_2 is evolved at 245° for curve *3* compared to 210° for curve *2*, a shift in the peak temperatures is not unexpected. The high temperature peaks resemble the two different peaks observed earlier for the silver oxides both in shape and relative

Can. J. Chem. Downloaded from www.nrcresearchpress.com by 210.87.254.6 on 09/05/12
For personal use only.

temperatures. Curve *2* corresponds to that for Ag_2O formed by the decomposition of AgO and curve *3* to that for chemically prepared Ag_2O. However, we should not carry this analogy too far, since the material used for curve *2* has enough CO_2 present to be equivalent to approximately 85% carbonate.

The results shown on Figs. 5 and 6 show that the first of the two high temperature peaks observed in this work is not due only to the decomposition of the carbonate to Ag_2O and the second only to the further decomposition of the oxide to silver as might be expected. It is unlikely that the double peaks for gas evolution and DTA are due to retardation of the release of CO_2 from the interior of the sample due to a build-up of Ag_2O on the surface, as proposed by Spencer and Topley (2, 3). If this were the case, one would expect a greater effect than that observed on the peak temperatures in the CO_2 atmosphere and also O_2 evolution at only one peak. The reversible phenomena while they can be repeated on cyclic heating and cooling are not reversible in the thermodynamic sense. They can be compared to the hysteresis observed in adsorption and desorption work.

It now remains to decide how the $Ag_2O{\cdot}nCO_2$ can have the structure of Ag_2O but yet have a stoichiometry of 65–93% Ag_2CO_3. The $Ag_2O{\cdot}nCO_2$ behaves very much like clathrate-type compounds such as β-quinol (24, 25) for which CO_2 is a common enclosed molecule (26, 27). Ag_2O has an open structure. Application of extremely high pressure can convert the cubic structure to one that is hexagonal close packed and has a density 30% greater (20). It has been reported that Ag_2O can entrap O_2 (21). Silver oxide, like β-quinol, consists of two interpenetrating and identical frameworks not cross-connected by any primary bonds (28). There are other similarities between $Ag_2O{\cdot}nCO_2$ and clathrate compounds; the O_2 and entrapped CO_2 are released simultaneously when the Ag_2O cage-like structure is broken down, and the CO_2 is readily available at the time the cavity is closed.

Examination of structure of Ag_2O and also solid CO_2 (29, 30) reveals that cavities do exist in Ag_2O that could accommodate CO_2 molecules of the size in the solid form and in the quantity present in $Ag_2O{\cdot}nCO_2$. Moreover the CO_2 can be in two distinct orientations that could account for the multiple peaks observed. However, this type of structure is purely speculative at this time and any confirmation will have to await a more detailed study of the structure.

Summary

The form of Ag_2CO_3 precipitated from solutions containing $AgNO_3$ and alkali carbonate or bicarbonate is greatly dependent upon the reactant concentrations. In general, high and low concentrations and the absence of stirring tended to produce more of the active form. Only dilute CO_2-saturated bicarbonate solutions gave the relatively pure active compound.

Mixtures of active and inactive forms evolved CO_2 (7–35%) when heated to 200–265°, forming $Ag_2O{\cdot}nCO_2$ where n is less than one. This $Ag_2O{\cdot}nCO_2$ is believed to be a clathrate-type of compound which has the structure of normal Ag_2O and contains occluded CO_2 in cavities in the silver oxide. Recombination of the $Ag_2O{\cdot}nCO_2$ with carbon dioxide is dependent upon the physical state and thermal history and is much more rapid than for normal silver oxide.

The $Ag_2O{\cdot}nCO_2$ will undergo transitions at 180 and 200° on heating, with corresponding transitions, on cooling, in the ranges of 20 to 125° and 175 to 185°. The transitions are not reversible in the thermodynamic sense and none of them is due to the reaction $Ag_2CO_3 \rightleftarrows Ag_2O + CO_2$.

At temperatures above 300° two non-reversible endothermic DTA peaks have been observed. Oxygen and CO_2 are evolved simultaneously at these peaks roughly in proportion to the heat absorbed.

The assistance of Messrs. P. J. Powell and F. K. McLusky in obtaining some of the gas chromatographic results, and the Metallurgical Laboratories of Eldorado Nuclear Limited in obtaining the high-temperature X-ray diffraction patterns is gratefully acknowledged.

1. M. Tzentnershver and J. Krustinsons. Z. Phys. Chem. **124**, 225 (1926); **130**, 187 (1927).
2. W. D. Spencer and B. Topley. J. Chem. Soc. **131**, 2633 (1929).
3. W. D. Spencer and B. Topley. Trans. Faraday Soc. **27**, 94 (1931).
4. M. Watanabe. Sci. Rep. Tohoku Univ. **22**, 1229 (1933).
5. J. Zawadzki and S. Breisznajder. Z. Elektrochem. **41**, 215 (1935).
6. A. Krupkowski. Chem. Zent. II, 7 (1938).
7. O. Kadlets and M. M. Dubinin. Izv. Akad. Nauk. SSSR otd. Khim. Nauk. **3**, 390 (1961).

8. J. LEYKO and M. MACIEJEWSKI. Bull. Acad. Polon. Sci. Ser. Sci. Chem. **12**, 273 (1964).
9. T. WYDEVEN and M. LEBAN. Anal. Chem. **40**, 363 (1968).
10. P. A. BARNES and F. S. STONE. 6th Internat. Symp. on Reactivity of Solids. Schenectady, N.Y. Aug. 1968. p. 261.
11. W. J. CULBERTSON. Rep. No. AMRL-TR-64-119. Aerospace Medical Research Laboratories, Wright-Patterson AFB. Dec. 1964. AD 612021.
12. T. WYDEVEN and E. RAND. J. Catal. **12**, 271 (1968).
13. T. WYDEVEN. J. Catal. **16**, 82 (1970).
14. G. SANDSTEDE, G. WALTER, A. KOEHLING, H. KRUPP, H. RABENHORST, and K. RICHTER. German Patent 1 197 941. Aug. 5, 1965.
15. C. N. R. RAO, S. R. YOGANARASIMHAN, and M. P. LEWIS. Can. J. Chem. **38**, 2359 (1960).
16. C. NICULESCU, G. KALMUTCHI, D. HOLOHI, M. E. VASILACHE, and E. OPRESCU. Rev. Chim. (Bucharest) **18**, 671 (1967).
17. T. WYDEVEN. Aust. J. Chem. **20**, 2751 (1967).
18. J. C. BAILER, JR. Inorganic syntheses. Vol. 4. McGraw-Hill Book Co. Inc. 1953. p. 12.
19. C. P. WALES and J. BURBANK. J. Electrochem. Soc. **106**, 885 (1969).
20. S. S. KZBALINA, S. V. POPOVA, and M. R. SEREBRYAMAYA. Dokl. Akad. Nauk. SSSR, **152**, 853 (1963).
21. G. D. NAGY, W. J. MOROZ, and E. J. CASEY. Proc. Ann. Power Sources Conf. **19**, 80 (1965).
22. K. GOSSNER and H. POULE. Z. Phys. Chem. **54**, 93 (1967).
23. V. H. SABROWSKY. Z. fur. Anorg. Und. Allgam. Chem. **365**, 146 (1969).
24. H. M. POWELL. Research, **1**, 353 (1947–1948).
25. T. MOELLER. Inorganic chemistry. John Wiley and Sons, New York. 1952. p. 223.
26. D. E. DALIN and H. M. POWELL. J. Chem. Soc. 208 (1947).
27. D. E. DALIN and H. M. POWELL. J. Chem. Soc. 571 (1948).
28. A. F. WELLS. Structural inorganic chemistry. Oxford University Press, London. 1962. p. 460.
29. J. C. MCLENNAN and J. O. WILHELM. Trans. Roy. Soc. Can. Sect. 3, **19**, 51 (1925).
30. S. H. WALMSLEY and J. A. POPLE. Mol. Phys. **8**, 345 (1964).

Can. J. Chem. Downloaded from www.nrcresearchpress.com by 210.87.254.6 on 09/05/12
For personal use only.

Can. J. Chem. Downloaded from www.nrcresearchpress.com by 210.87.254.42 on 09/05/12
For personal use only.

Identification of ν(N=N) in Metal Arylazo Complexes: The Infrared and Raman Spectra of some Arylazo Complexes of Rhodium(III)

G. W. Rayner-Canham and D. Sutton[1]

Department of Chemistry, Simon Fraser University, Burnaby 2, British Columbia

Received July 8, 1971

The Raman and infrared spectra have been obtained for a series of rhodium-arylazo complexes $RhCl_2(PPh_3)_2(p\text{-}XC_6H_4N_2)$ where X = H, F, Br, CF_3, NO_2, OCH_3, NEt_2. The N=N stretching frequency ν(N=N) has been unambiguously identified from its strong appearance in the Raman spectrum and from isotopic substitution studies using ^{15}N. Trends in the value of ν(N=N) with the *p*-substituent X are discussed, in terms of the apparent degree of metal–ligand π-interaction.

Nous avons obtenu les spectres infrarouge et raman d'une série de complexes arylazo du rhodium, du type $RhCl_2(PPh_3)_2(p\text{-}C_6H_4N_2)$ où X = H, F, Br, CF_3, NO_2, OCH_3, NEt_2. La fréquence d'élongation caractéristique de la liaison N=N, ν(N=N) a été identifiée sans ambiguité à cause de sa forte intensité dans le spectre raman et des études de substitution isotopiques utilisant le ^{15}N. On discute des tendances de ν(N=N) en fonction des substituants en para, en termes de degré apparent d'interaction π métal–ligande.

Canadian Journal of Chemistry, **49**, 3994 (1971)

Introduction

Following Parshall's proposal that arylazo metal complexes may be considered as model systems of nitrogen reductase (1), we have begun a systematic study of these systems (2). Of considerable interest is the position of the N=N stretching frequency ν(N=N), since this provides a simple means of observing the effect which substituents may have on ν(N=N) and presumably on the N=N bond strength. However, to date identification of this vibration has proved difficult due to its weakness in the i.r. spectrum (3–6), an unambiguous assignment requiring the use of ^{15}N substitution (1). We have therefore undertaken to identify ν(N=N) in the Raman spectrum, and to investigate the effect of varying the *p*-substituent on the arylazo ligand. The compounds studied are those of the type originally prepared by Baird and Wilkinson (7), namely $RhCl_2(PPh_3)_2(p\text{-}XC_6H_4N_2).\frac{1}{2}CHCl_3$ (7) with X = H, NO_2, CF_3, F, Br, OCH_3, NEt_2, providing a range of electron withdrawing and donating properties (8).

Experimental

The compounds were prepared by the method of Baird and Wilkinson (7), using both chloroform and dichloromethane as solvents. All complexes were washed with acetone and ether, and vacuum dried. Analytical figures for the complexes are shown in Table 1. Analyses were performed by A. Bernhardt, Germany. ^{15}N substitution at the site adjacent to the metal was achieved (1) by using $[p\text{-}XC_6H_4{}^{14}N{\equiv}{}^{15}N]^+$ synthesized from $p\text{-}XC_6H_4{}^{14}NH_2$ and $Na^{15}NO_2$ (95% ^{15}N) obtained from Isomet Corporation, New York. Raman spectra (150–2000 cm^{-1}) of microcrystalline samples were obtained utilizing a Cary 81 Raman spectrophotometer equipped with a Spectra-Physics model 125 He/Ne laser, and calibrated using rare-gas emission lines. Decomposition of the complexes occurred with the laser power at maximum (~35 mW at sample), but the decomposition could be reduced to a negligible rate by using a defocussed beam (~10 mW at sample), except in the case of the *p*-diethylamino complex. Depolarization measurements on solutions in $CHCl_3$ and CH_2Cl_2 were not possible due to photodecomposition of the samples. Infrared spectra were obtained with a Beckman I.R. 12 spectrophotometer using Nujol and fluorolube as mulling agents.

As there are inconsistencies in reported frequencies of ν(N≡N) in solid aryl diazonium tetrafluoroborates (9, 10), we have remeasured the values of this vibration. The sharpness of the vibration in the Raman spectrum enabled accuracies of ± 1 cm^{-1} to be obtained. As in the case of the *p*-diethylamino complex, the parent diazonium salt decomposed in the laser beam.

Results

The positions of ν(N=N) in the i.r. and Raman spectra of the complexes reported here are included in Table 2. In the Raman spectra, ν(N=N) is normally a quite intense single peak, compared with the extremely weak corresponding band in the i.r. spectra. ^{15}N substitution of the co-ordinated nitrogen atom for the *p*-bromo and *p*-methoxy complexes produced isotopic shifts of ~22 cm^{-1}, only slightly smaller than the shift expected for a simple ν(N=N) vibration based on the change in reduced mass. The *p*-methoxy com-

[1]To whom all correspondence should be addressed.

Can. J. Chem. Downloaded from www.nrcresearchpress.com by 210.87.254.42 on 09/05/12
For personal use only.

TABLE 1. Analytical data for the complexes $(p\text{-}XC_6H_4N_2)RhCl_2(PPh_3)_2.yCH_2Cl_2$

		Found (%)			Calculated (%)		
X	y	C	H	N	C	H	N
F	½	58.91	4.22	3.40	59.07	4.14	3.24
Br*	½	53.96	3.80	3.05	54.19	3.75	2.97
H	1	58.44	4.26	3.08	58.12	4.20	3.15
NO_2	1	54.80	4.02	4.61	55.32	3.86	4.50
CF_3	1	55.42	3.85	3.14	55.24	3.80	2.93
OMe	1	57.65	4.08	3.34	57.53	4.28	3.05
NEt_2	½†	59.56	4.88	4.46	59.79	4.77	4.50

*% *P*, found 6.50, calculated 6.58.
†$CHCl_3$.

TABLE 2. Values of ν(N=N) for the complexes $(p\text{-}XC_6H_4N_2)RhCl_2(PPh_3)_2$ and ν(N≡N) for the corresponding diazonium tetrafluoroborate from Raman spectra

p-X	ν(N=N) (complex)	ν(N≡N) (diazonium salt)	ν(N=N)/ν(N≡N)
CF_3	1531	2309	0.662
NO_2	1524	2308	0.660
F	1527	2298	0.665
H	1525 (1504)*	2298 (2264)*	0.664 (0.664)*
Br	1515 (1493)*	2289 (2255)*	0.661 (0.662)*
OMe	1496, 1509 (1481)*	2255 (2225)*	0.667 (0.666)*
NEt_2	1471†	2157† (broad)	0.68 (approx.)

*Values for ^{15}N substituted species.
†Values obtained from i.r. spectra.

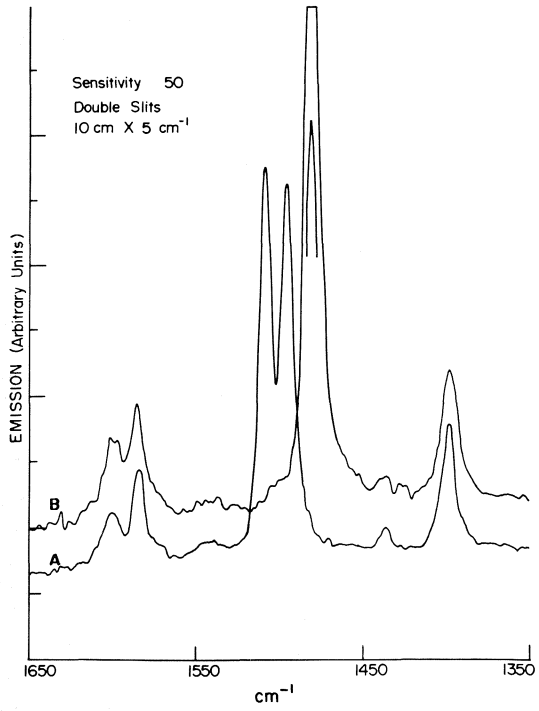

FIG. 1. Raman spectra for the complexes $(MeOC_6H_4\text{-}^{14}N{=}^{14}N)RhCl_2(PPh_3)_2$ (*A*) and $(MeOC_6H_4{}^{14}N{=}^{15}N)\text{-}RhCl_2(PPh_3)_2$ (*B*) in the ν(N=N) region.

plex was unusual in exhibiting two equal intensity peaks at 1509 and 1496 cm^{-1} in the Raman spectrum of the ^{14}N complex, but the usual single peak in the ^{15}N complex (Fig. 1). The splitting in the ^{14}N complex we attribute to Fermi resonance with a weak aromatic mode. Although Raman spectra were not obtained for the *p*-diethylamino complex, a comparison of the i.r. spectra of the ^{14}N and ^{15}N complexes showed that a weak band at 1471 cm^{-1} (^{14}N) was not present in the ^{15}N spectrum. The band is expected to shift in the ^{15}N complex into a position obscured by other absorptions, and no new band was observed.

The only other band which we have observed to shift upon isotopic substitution is the 734 cm^{-1} band in the ^{14}N *p*-bromo complex which shifted to 726 cm^{-1} (^{15}N). This band is tentatively assigned as due to the N=N—C deformation mode (11).

Discussion

The strong Raman activity of ν(N=N) in this series of compounds suggests that Raman spectroscopy is a preferred means of identifying ν(N=N) in metal azo systems, especially in view of the difficulty in distinguishing ν(N=N) from aromatic absorptions in the i.r. The position of

Can. J. Chem. Downloaded from www.nrcresearchpress.com by 210.87.254.42 on 09/05/12
For personal use only.

ν(N═N) in the present complexes is in good agreement with Parshall's assignment of bands at 1463 and 1562 cm^{-1} to this vibration in the arylazo platinum and arylazo molybdenum complexes, respectively (1). A polynuclear arylazo molybdenum system has been reported, with a band at 1550 cm^{-1} being assigned as ν(N═N) (12). Derivatives of *trans*-azobenzene (11) have ν(N═N) in the region 1400–1450 cm^{-1}.

A comparison of the values reported for the various arylazo complexes of different metals shows that they exhibit a general trend in which ν(N═N) decreases as the d^n configuration of the metal is increased. This is presumably related to a consequent increase in the electron occupancy of the π*(N═N) orbital.

As the observed isotopic shifts are only slightly less than those calculated for a pure ν(N═N) vibration, coupling with other vibrations is evidently small. According to the criteria of Fackler and Coucouvanis (13) the N═N bond order is less than two; this could be brought about by π interactions with either the metal or the aromatic ring. For the arylazo complexes, ν(N═N) decreases as the electron donating capacity of X is increased. There is also a decrease in ν(N≡N) for the corresponding diazonium salt. The near linear relationship between these effects points to the aromatic ring being predominantly responsible for the π interaction in the metal complexes. Thus, if for example, one supposes that the arylazo group withdraws π electrons from the metal, then one would expect electron withdrawing *p*-substituents (*e.g.* NO_2, F, CF_3) to give relatively larger decreases in ν(N═N) for the complexes than the decreases in ν(N≡N) observed for the corresponding diazonium salts, due to the added drain of metal electrons into the N═N function. The near constancy of the ratio ν(N═N)/ν(N≡N) indicates that in these d^6 complexes at least, the results do not appear to support such a postulate. However, for d^8 and d^4 systems, π acceptor (1) and π donor (14) properties, respectively, have been ascribed to the arylazo system.

Added support of this proposal is the observation that the d^6 metal arylazo systems reported to date (7, 15) are all pale yellow in color, irrespective of the ring substituent; whereas both the molybdenum (4) and platinum (3) complexes are intensely colored, especially when the aryl substituent is *p*-NO_2. Evidence was provided in the case of the platinum complexes that the color was due to a visible absorption band of the N═N chromophore (3) and a considerable bathochromic shift of this band relative to organic azo systems has also been observed in silylazo compounds (16). This has been shown to be a result of dπ–pπ interactions. The yellow rhodium complexes we have studied exhibit a steady increase in absorption with increasing frequency. No discrete absorption band is discernible in the visible or near u.v. range, assignable to the N═N chromophore.

The authors are grateful to the National Research Council of Canada for supporting this work through operating grants and to Mr. A. B. Gilchrist for preparation of diazonium salts and for discussions.

1. G. W. Parshall. J. Am. Chem. Soc. **89**, 1822 (1967).
2. F. W. B. Einstein, A. B. Gilchrist, G. W. Rayner-Canham, and D. Sutton. J. Am. Chem. Soc. **93**, 1826 (1971).
3. G. W. Parshall. J. Am. Chem. Soc. **87**, 2133 (1965).
4 R. B. King and M. B. Bisnette. Inorg. Chem. **5**, 300 (1966).
5. S. Trofimenko. Inorg. Chem. **8**, 2675 (1969).
6. L. Toniolo and R. Eisenberg. J. Chem. Soc. D, 455 (1971).
7. M. C. Baird and G. Wilkinson. J. Chem. Soc. A, 865 (1967).
8. A. R. Katritzky and R. D. Topsom. Angew. Chem. Int. Ed. **9**, 87 (1970).
9. R. H. Nuttall, E. R. Roberts, and D. W. A. Sharp. Spectrochim. Acta, **17**, 947 (1961).
10. B. A. Porai Koshits. Russ. Chem. Revs. **39**, 283 (1970).
11. R. Kübler. W. Lüttke, and S. Weckherlin. Z. Elektrochem. **64**, 650 (1960) and refs. therein.
12. F. J. Lalor and P. L. Pauson. J. Organomet. Chem. **25**, C51 (1970).
13. J. P. Fackler and D. Coucouvanis. Inorg. Chem. **7**, 181 (1968).
14. V. F. Duckworth, P. G. Douglas, R. Mason, and B. L. Shaw. J. Chem. Soc. D, 1083 (1970).
15. A. J. Deeming and B. L. Shaw. J. Chem. Soc. A, 1128 (1969).
16. H. Seidl, H. Bock, N. Wiberg, and M. Veith. Angew. Chem. Int. Ed. **9**, 69 (1970) and refs. therein.

Can. J. Chem. Downloaded from www.nrcresearchpress.com by 210.87.254.40 on 09/05/12
For personal use only.

Diphenylphosphinato- and Hydroxydiphenylphosphine Complexes of Platinum(II) and Palladium(II)

K. R. Dixon and A. D. Rattray

Department of Chemistry, University of Victoria, Victoria, British Columbia

Received July 16, 1971

Preparations and various interconversion reactions are described for the complexes: $[M_2X_2(PPh_2O)_2(PPh_2OH)_2]$, $[MX(PPh_2O)(PPh_2OH)_2]$, $[MX(PPh_2O)(PPh_2OH)(PEt_3)]$, and $[M(PPh_2O)_2]_n$ where M = palladium or platinum, X = chloride or bromide, Ph = phenyl, and Et = ethyl. $[Pt(PPh_2O)_2(PPh_2OH)_2]$ and $[Pt_2(PPh_2O)_4(PPh_2OH)_2]$ are also described and all the complexes are assigned structures on the basis of their infrared spectra.

Les préparations ainsi que plusieurs réactions d'interconversion sont décrites pour les complexes suivants: $[M_2X_2(PPh_2O)_2(PPh_2OH_2]$, $[MX(PPh_2O)(PPh_2OH_2)]$, $[MX(PPh_2O)(PEt_3)]$ et $[M(PPh_2O)_2]_n$ où M = palladium ou platine, X = chlore ou brome, Ph = phényle et Et = éthyle. Les complexes $[Pt(PPh_2O)_2(PPh_2OH)_2]$ et $[Pt_2(PPh_2O)_4(PPh_2)H)_2]$ sont également décrits. A partir de leurs spectres infrarouges, des structures ont été attribuées à tous les complexes.

Canadian Journal of Chemistry, **49**, 3997 (1971)

Dialkyl- or diarylphosphine oxides generally exist in equilibrium with the corresponding hydroxydialkyl- or hydroxydiarylphosphines (alternatively named dialkyl- or diarylphosphinous acids (1) and their interactions with metals are therefore of interest for the several modes of co-ordination, which are possible; namely,

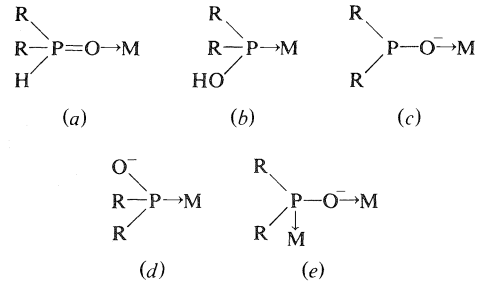

For R = phenyl, equilibrium lies strongly in favor of diphenylphosphine oxide but reactions with platinum complexes appear to proceed via a small equilibrum concentration of hydroxydiphenylphosphine. Using these reactions, and also the hydrolysis of chlorodiphenylphosphine complexes, Chatt and Heaton (2) have prepared platinum complexes containing coordination types *b*, *d*, and *e*. There is also infrared evidence (3) that suggests $Ag[PPh_2O]$ may be an example of type *c* but to our knowledge there are no examples of type *a* where R is alkyl or aryl.

In general this type of ligand has received rather little attention and we now report the results of a study of the reactions of diphenylphosphine oxide with K_2MX_4 complexes, where M = Pd or Pt and X = Cl or Br, together with studies of the structure and reactions of the products. The complexes differ from those reported by Chatt and Heaton in having both hydroxydiphenylphosphine (type *b*) and diphenylphosphinato (type *d*) ligands within the same molecule, a situation which allows very strong intramolecular hydrogen bonding.

Prior to our work, Troitskaya and co-workers (4, 5) had prepared complexes of the types $[Pt\{P(OR)_2O\}_2\{P(OR)_2OH\}_2]$ and $[Pd_2Cl_2\{P(OR)_2\}_2\{P(OR)_2OH\}_2]$ but no structures had been proposed and Pidcock and co-workers (6, 7) have recently studied this type of complex in detail by nuclear magnetic resonance spectroscopy.

Results and Discussion

The principal complexes and reactions studied are shown in Figs. 1 and 2. The structures shown are those considered most probable and they are discussed in detail below after consideration of the preparations and reactions of the complexes. For simplicity the discussion is limited to chloro complexes but their bromo analogues behave similarly.

The reactions of diphenylphosphine oxide are considered to proceed via a small equilibrium concentration of hydroxydiphenylphosphine as previously suggested (2) and the nature of our reactions and products provides further evidence for the correctness of this suggestion.

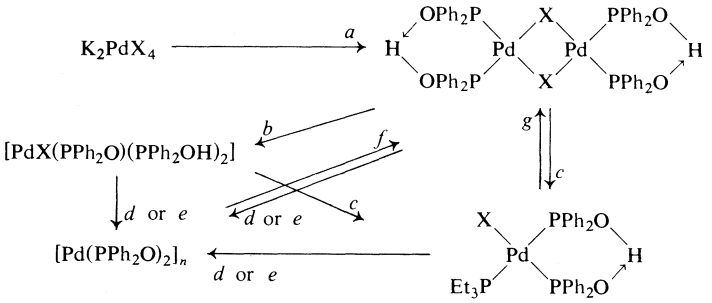

FIG. 1. Reactions of palladium complexes (X = Cl or Br, Ph = phenyl, and Et = ethyl). Reagents: (*a*) Ph_2HPO (2 mol) or Ph_2ClP (2 mol in water–acetone); (*b*) Ph_2HPO (1 mol); (*c*) Et_3P (1 mol); (*d*) NaOH; (*e*) $AgNO_3$; (*g*) HX; (*g*) 160° *in vacuo*.

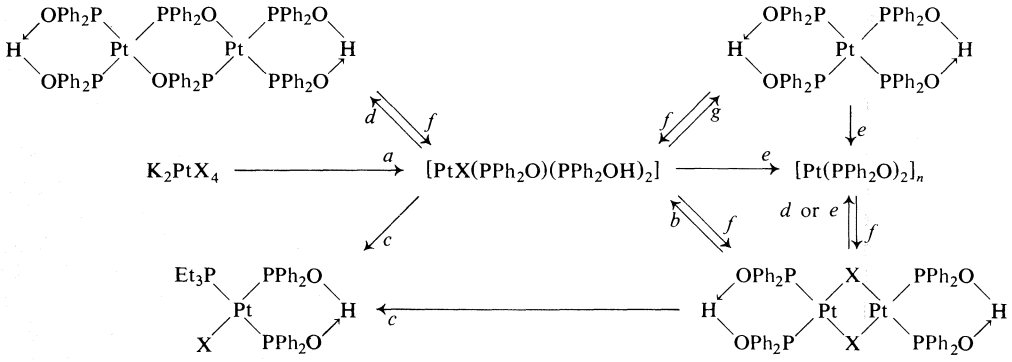

FIG. 2. Reactions of platinum complexes (X = Cl or Br, Ph = phenyl, and Et = ethyl). Reagents: (*a*) Ph_2HPO (3 mol) or Ph_3ClP (3 mol) in water; (*b*) Ph_2HPO (1 mol); (*c*) Et_3P (1 mol); (*d*) NaOH; (*e*) AgNO; (*f*) HX; (*g*) $Ag[PPh_2O]$ (1 mol).

Palladium Complexes

Diphenylphosphine oxide reacts with tetrachloropalladite(II) with elimination of hydrogen chloride according to the equation

$$2PdCl_4^{2-} + 4Ph_2HPO \rightarrow Pd_2Cl_2(PPh_2O)_2(PPh_2OH)_2 + 2HCl + 4Cl^-$$

This reaction probably proceeds via an intermediate $[PdCl_2(PPh_2OH)_2]$ complex and the reaction is thus formally similar to the reactions of tetrachloropalladite(II) with diphenylphosphine to give $[Pd_2Cl_2(PPh_2)_2(PPh_2H)_2]$ (8) and of $[PtCl_2(PPh_2OH)(PEt_3)]$ with sodium methoxide to give $[Pt_2Cl_2(PPh_2O)_2(PEt_3)_2]$ (2). However, our product is probably chloride bridged (see below) whereas the others are bridged by diphenylphosphino and diphenylphosphinato groups, respectively.

$[Pd_2Cl_2(PPh_2O)_2(PPh_2OH)_2]$ is also obtained by reaction of chlorodiphenylphosphine with tetrachloropalladite in aqueous acetone. Hydrolysis of the chlorophosphine to hydroxydiphenylphosphine may occur either before or after coordination to the metal but the reaction is otherwise similar to that of diphenylphosphine oxide.

Elimination of further hydrogen chloride from $[Pd_2Cl_2(PPh_2O)_2(PPh_2OH)_2]$ is achieved by reaction with sodium hydroxide or silver nitrate. In both cases the product is an insoluble material of empirical composition, $Pd(PPh_2O)_2$, which we believe to be a phosphinato bridged polymer (see below). Preparations of this complex are sometimes contaminated by halide but identical products are obtained from several different starting compounds (see Fig. 1), including both chloro and bromo complexes, and this leaves little doubt that the formulation is correct.

Can. J. Chem. Downloaded from www.nrcresearchpress.com by 210.87.254.40 on 09/05/12
For personal use only.

Can. J. Chem. Downloaded from www.nrcresearchpress.com by 210.87.254.40 on 09/05/12
For personal use only.

The other typical reaction of $[Pd_2Cl_2(PPh_2O)_2(PPh_2OH)_2]$, bridge cleavage by phosphine ligands, is discussed in more detail below.

Platinum Complexes

In contrast to the palladium complexes, tetrachloroplatinite(II) reacts with diphenylphosphine oxide according to the equation

$$PtCl_4^{2-} + 3Ph_2HPO \rightarrow [PtCl(PPh_2O)(PPh_2OH)_2] + HCl + 2Cl^-$$

This is the main reaction even when only 2 mol of diphenylphosphine oxide are added. This difference may be attributed to a greater stability of the chloride bridge system in palladium complexes or to a greater affinity of platinum for phosphorus ligands leading to easier cleavage of the bridges. If the chloride bridge is regarded as a relatively "hard" ligand then both factors are expected to favor the halide bridge system for palladium since this metal has more class (*a*) character (*i.e.* is "harder") (9, 10) than platinum and it is also known, for example, that $[Pd_2Br_4(SMe_2)_2]$ is bridged by bromide whereas a corresponding platinum complex, $[Pt_2Br_4(SEt_2)_2]$ has sulfur bridges (11). Various evidence from our present work supports this view. Thus the reaction

$$[M_2Cl_2(PPh_2O)_2(PPh_2OH)_2] + 2L \rightarrow [MCl(PPh_2O)(PPh_2OH)(L)]$$

proceeds easily in acetone at 25° for L = triethylphosphine or diphenylphosphine oxide for both M = Pd and Pt but for L = triphenylphosphine, reaction only occurs when M = Pt.[1] Moreover the reaction for L = diphenylphosphine oxide and M = Pd is very slow and reverses easily on recrystallization of the product, a difficulty which is responsible for the low figure obtained for the carbon analysis of $[PdCl(PPh_2O)(PPh_2OH)_2]$. Also the reaction for L = triethylphosphine and M = Pd reverses easily *in vacuo* at 160° whereas $[PtCl(PPh_2O)(PPh_2OH)(PEt_3)]$ is stable at this temperature and gives only general decomposition at higher temperatures.

The preference of palladium for a chloride bridge system is further illustrated by the following reaction

$$[Pd_2Cl_4(PEt_3)_2] + 2Ph_2HPO \rightarrow \tfrac{1}{2}[Pd_2Cl_2(PPh_2O)_2(PPh_2OH)_2] + [PdCl_2(PEt_3)_2] + HCl$$

Chatt and Heaton found that $[Pt_2Cl_4(PEt_3)_2]$ under similar conditions gave only $[PtCl_2(PPh_2OH)(PEt_3)]$ (2).

Since it is known (12) that the strength of the halogens as bridging ligands increases in the order Cl < Br < I we also investigated the reaction of tetraiodoplatinite(II) with diphenylphosphine oxide. However, even in this case, the product is $[PtI(PPh_2O)(PPh_2OH)_2]$ and not the iodide bridged, $[Pt_2I_2(PPh_2O)_2(PPh_2OH)_2]$, although we do find that the former complex reacts easily with HI to give the latter complex in high yield.[2] This is in contrast to the analogous chloro complexes where the conversion is difficult and incomplete.

The other reactions shown in Fig. 2 are similar to those of palladium complexes discussed above or require little further comment except to note that the reactions of $[PtCl(PPh_2O)(PPh_2OH)_2]$ with sodium hydroxide and $Ag[PPh_2O]$ give the new complexes $[Pt_2(PPh_2O)_4(PPh_2OH)_2]$ and $[Pt(PPh_2O)_2(PPh_2OH)_2]$, respectively. We were unable to prepare the palladium analogues since the corresponding reactions give only $[Pd(PPh_2O)_2]_n$. This is in line with the reaction of potassium tetrachloroplatinite(II) with triethylphosphite to give $[Pt\{P(OEt)_2O\}_2\{P(OEt)_2OH\}_2]$ (5) whereas tetrachloropalladite(II) gives $[Pd_2Cl_2\{P(OEt)_2O\}_2\{P(OEt)_2OH\}_2]$ and $[Pd\{P(OEt)_2O\}_2]$ (4). Moreover although Pidcock and Waterhouse (6) obtained $[Pd\{P(OPh)_2O\}_2\{P(OPh)_2OH\}_2]$ on one occasion, they were unable to repeat their preparation.

Structures

The corresponding platinum and palladium complexes have essentially identical infrared spectra and their structures are therefore considered together in the following discussion.

The complexes are characterized by elemental analysis and molecular weight measurements and by the interconversion reactions shown in Figs. 1 and 2. They are non-electrolytes in nitromethane or have small molar conductances (10–20 ohm^{-1}

[1]This reaction required only a few minutes at 25°. The product was not fully characterized but had molecular weight 862 (required for $[PtCl(PPh_2O)(PPh_2OH)(PPh_3)]$ is 896) and ν(P—O) at 1015 cm^{-1}. $[Pd_2Cl_2(PPh_2O)_2(PPh_2OH)_2]$ did not react with triphenylphosphine in 18 h at 25°.

[2]These iodo complexes were not fully characterized but had infrared spectra identical to those of their bromo analogues.

TABLE 1. Characteristic infrared absorption frequencies (cm^{-1})

Complex	ν(P—O)*	ν(M—Cl)†	Other frequencies‡
$[Pd(PPh_2O)_2]_n$	1020, 1030	—	—
$[Pt(PPh_2O)_2]_n$	990, 1010	—	—
$[Pd_2Cl_2(PPh_2O)_2(PPh_2OH)_2]$	1040	265	1300–1400, 720
$[Pd_2Br_2(PPh_2O)_2(PPh_2OH)_2]$	1030	—	1300–1400, 720
$[Pt_2Cl_2(PPh_2O)_2(PPh_2OH)_2]$	1035	280	1300–1400, 770
$[Pt_2Br_2(PPh_2O)_2(PPh_2OH)_2]$	1032	—	1300–1400, 770
$[PdCl(PPh_2O)(PPh_2OH)_2]$	970, 925, 880 m	310	2280, 1550
$[PdBr(PPh_2O)(PPh_2OH)_2]$	970, 925, 880 m	—	2270, 1550
$[PtCl(PPh_2O)(PPh_2OH)_2]$	970, 940, 900 m	310	2280, 1580
$[PtBr(PPh_2O)(PPh_2OH)_2]$	970, 940, 895 m	—	2280, 1580
$[Pt_2(PPh_2O)_4(PPh_2OH)_2]$	970	—	1300–1400, 750
$[Pt(PPh_2O)_2(PPh_2OH)_2]$	990	—	1300–1400, 750
$[PdCl(PPh_2O)(PPh_2OH)PEt_3)]$	1010	270	1300–1400, 780
$[PdBr(PPh_2O)(PPh_2OH)(PEt_3)]$	1010	—	1300–1400, 820
$[PtCl(PPh_2O)(PPh_2OH)(PEt_3)]$	1010	280	1300–1400, 800
$[PtBr(PPh_2O)(PPh_2OH)(PEt_3)]$	1010	—	1300–1400, 810

*Except for those designated medium (m) these absorptions were all strong or very strong.
†All very weak absorptions. ν(M—Br) < 250 cm^{-1}.
‡Very broad, ill-defined absorptions, see Discussion.

cm^2) which may be attributed to slight ionization of the POH groups (a typical (13) molar conductance for a 1:1 electrolyte in nitromethane is 97 ohm^{-1} cm^2). Generally the complexes are rather insoluble for nuclear magnetic resonance spectroscopy and this, together with the fact that the resonances are likely to be broadened by exchange (6), accounts for our failure to observe any resonances attributable to the hydroxylic protons.

The infrared spectra of the complexes are all generally similar and show the expected ligand absorptions. Other absorptions are shown in Table 1. The M—Cl stretching modes are assigned by comparison with spectra of the corresponding bromides but they were all very weak bands and, since ligand absorption also occurs in this region, the assignments must be approached with caution. In particular it is not possible to use them to distinguish terminal and bridging chlorines in the dinuclear complexes, since ν(M—Cl) for a chlorine *trans* to a ligand of high *trans* influence often absorbs at as low a frequency as a bridge chlorine and also from our spectra we could not distinguish with certainty between the two bands expected for a bridge system, MCl_2M, and the single band expected for a *trans* arrangement of terminal chlorines. All of the complexes have at least two very intense bands in the P—O stretching region (*ca.* 900–1100 cm^{-1} (2)). One of these, at 1100 cm^{-1}, is almost constant in frequency and corresponds to a less intense band normally observed in the spectra of phenylphosphine complexes. It is therefore assigned to a ligand absorption and the other intense bands in this region are assigned as P—O stretching in Table 1.

The complexes, $[M_2X_2(PPh_2O)_2(PPh_2OH)_2]$, $[MX(PPh_2O)(PPh_2OH)(PEt_3)]$, $[Pt(PPh_2O)_2(PPh_2O)_2]$, and $[Pt_2(PPh_2O)_4(PPh_2OH)_2]$ all show broad absorption in the 1200–1600 cm^{-1} (weak, width at half-height ~250 cm^{-1}) and 700–800 cm^{-1} (medium, width at half-height ~100 cm^{-1}) regions. There are many other absorptions in these regions and those in question, particularly the higher frequency ones, are evident only as a general rise in baseline and loss of resolution. However, the effect is quite unambiguous and is restricted to those complexes where there is a possibility of a *cis* arrangement of one diphenylphosphinato and one hydroxydiphenylphosphine ligand. We therefore consider it to be characteristic of a symmetrical hydrogen bonded system of the type

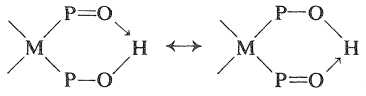

Evidence for strong hydrogen bonding involving POH groups has been obtained previously from the infrared spectra of organophosphorus acids (14) and a model of our system shows the O—O distance to be only 1.8 Å for a planar ring. Moreover the bond angles are such that the hydrogen atom could lie almost exactly on the O—O axis. Comparison of this distance with the 2.53 Å observed for the hydrogen bonds in orthophosphoric acid (15) shows that the ring is unlikely

Can. J. Chem. Downloaded from www.nrcresearchpress.com by 210.87.254.40 on 09/05/12
For personal use only.

Can. J. Chem. Downloaded from www.nrcresearchpress.com by 210.87.254.40 on 09/05/12
For personal use only.

to be planar but it does emphasize the possibility of unusually strong hydrogen bonding. If the system were not symmetrical or the ligands were not *cis* then infrared absorptions would be expected (2) for ν(P—OH) at ~880 cm^{-1}, ν(P=O) at ~1100 cm^{-1}, and ν(PO—H) at ~3200 cm^{-1} whereas the above complexes show only a single P—O stretching absorption in the range 970–1040 cm^{-1}. This is therefore consistent with a ring structure with P—O bonds intermediate between single and double bonds. Double bond character in the P—O bond of a hydrogen bonded POH group has been observed previously (15).

The absence of any infrared absorption assignable to O—H stretching is also consistent with the hydrogen bonded structure since broadening would be expected to make the absorption very difficult to observe. In agreement with this, Pidcock and Waterhouse (6) found no direct infrared evidence for the POH group in their phosphite complexes. The broad bands at 1200–1600 and 700–800 cm^{-1} in our spectra may be associated with the O—H—O system and a ring mode, respectively, but no definite assignments can be made.

On the above basis we therefore propose the structures shown in the Figs. 1 and 2 for these complexes. The $[M_2X_2(PPh_2O)_2(PPh_2OH)_2]$ complexes are consequently halide bridged in contrast to the phosphinato bridged, $[Pt_2X_2(PPh_2O)_2(PEt_3)_2]$ complexes prepared by Chatt and Heaton (2). However, the single line ^{31}P magnetic resonance spectrum of $[Pd_2Cl_2\{P(OPh)_2O\}_2\{P(OPh)_2OH\}_2]$ has been interpreted as implying a chloride bridged structure similar to our complexes (6) and we also consider that the complexes, $[Pd_2Cl_2\{P(OR)_2O\}_2\{P(OR)_2OH\}_2]$ (4), are likely to be chloride bridged and not phosphinato bridged as proposed by Chatt and Heaton (2). If the hydrogen bonded system is symmetrical then no isomers of these structures exist.

The $[MX(PPh_2O)(PPh_2OH)(PEt_3)]$ complexes have a *cis* arrangement of halide and triethylphosphine groups and again no isomers exist for a symmetrical hydrogen bond although in this case it is likely that the different *trans* influences of halide and triethylphosphine may cause an asymmetry in the hydrogen bond. There is evidence for such an asymmetry in the ^{31}P nuclear magnetic resonance spectrum of $[PtCl\{P(OMe)_2O\}\{P(OMe)_2OH\}(AsEt_3)]$ (6).

Similarly for $[Pt_2(PPh_2O)_4(PPh_2OH)_2]$, asymmetry may be induced by the different *trans* influences of oxygen and phosphorus in the phosphinato bridge. This complex is expected to show two P—O stretches assignable to the bridging and terminal systems. However, we note that ν(P—O) for the diphenylphosphinato bridge is expected at about 970 cm^{-1}. Moreover, in the series $[Pt_2Cl_2(PPh_2O)_2(PPh_2OH)_2]$, $[PtCl(PPh_2O)(PPh_2OH)(PEt_3)]$, $[Pt(PPh_2O)_2(PPh_2OH)_2]$, the ν(P—O) frequencies for the hydrogen bonded system are 1035, 1010, and 990 cm^{-1}, respectively. They therefore fall in order of increasing *trans* influence of the ligands *trans* to the hydrogen bonded system and since the diphenylphosphinato bridge has a very high *trans* influence (2) we may expect ν(P—O) for the hydrogen bonded system in $[Pt_2(PPh_2O)_4(PPh_2OH)_2]$ below 990 cm^{-1} and we consider that it is therefore not resolved from the phosphinato bridge frequency at 970 cm^{-1}.

The above *trans* influence series is also interesting as a measure of electronic effects in these molecules. The *trans* influence of phosphine ligands is due largely to σ effects (16). Thus in an $LPtP(R_2)=O$ system, a ligand, L, of high *trans* influence may be considered as weakening the Pt—P bond by electron repulsion (2) leading to a greater contribution from the structure, $LPt^+---P(R_2)—O^-$, with consequent weakening of the P—O bond.

The $[M(PPh_2O)_2]_n$ complexes have two broad absorptions *ca.* 1000 cm^{-1} which are assigned to P—O stretching modes in a diphenylphosphinato bridged polymer. The two different frequencies may be due to phosphinato groups *trans* to P or O in an irregular polymer and they are similar to the frequencies (992 and 1002 cm^{-1}) observed (2) for the diphenylphosphinato bridges in the isomers of $[Pt_2(OH)_2(PPh_2O)_2(PEt_3)_2]$.

The $[MX(PPh_2O)(PPh_2OH)_2]$ complexes do not show the typical infrared absorptions of the hydrogen bonded ring but a broad band at 2280 cm^{-1} is assigned to a hydrogen bonded OH by a deuteration experiment which shifts the frequency to 1710 cm^{-1}. Also, although there are three P—O stretches in the range 880–970 cm^{-1} which is reasonable for ν(P—O) in hydrogen bonded PO or POH groups, there is no infrared evidence for terminal PO or free POH. These results are consistent with a hydrogen bonded structure of the type

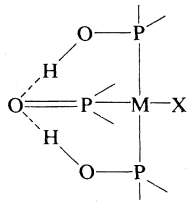

and a model shows the undistorted O—O distance to be 3.2 Å. Fairly small angular distortions could reduce this distance to a value compatible with a hydrogen bond. Although this seems the most likely structure the complexes were not sufficiently soluble for solution infrared and molecular weight studies to exclude the possibility of intermolecular hydrogen bonding.

Experimental

Chlorodiphenylphosphine was used as received from Alfa Inorganics Ltd. Diphenylphosphine oxide (2), $Ag[PPh_2O]$ (3), and $[Pd_2Cl_4(PEt_3)_2]$ (17) were prepared as previously described. Solutions of K_2MX_4 (X = Cl or Br, M = Pt or Pd) were prepared by dissolving $PdCl_2$ or K_2PtCl_4 in water containing a ten-fold excess of NaX.

Data relating to the characterization of the complexes are given in Table 2. Microanalyses were by Schwartzkopf Microanalytical Laboratory, New York. Molecular weights were determined in methylene dibromide solution at 50° using a Hitachi – Perkin Elmer Model 115 Vapor Phase Osmometer. Infrared spectra (Table 1) were recorded from 4000–250 cm^{-1} with accuracy ± 3 cm^{-1} on a Beckman IR 20 Spectrophotometer calibrated against polystyrene film and water vapor. Solid samples were examined as Nujol mulls between caesium iodide plates.

All reactions of phosphines or phosphine oxides were carried out in an atmosphere of dry nitrogen but the product complexes were stable in air. $[M(PPh_2O)_2]_n$, where M = Pt or Pd, $[PtX(PPh_2O)(PPh_2OH)_2]$, where X = Cl or Br, and $[Pt_2(PPh_2O)_4(PPh_2OH)_2]$ were too insoluble in common organic solvents for recrystallization but the other complexes were recrystallized by solution in methylene dichloride followed by addition of ethanol. The methylene dichloride was then allowed to slowly evaporate at 25° until crystals formed. Attempts to recrystallize from hot solvents generally resulted in decomposition or interconversion of complexes.

The preparations of chloro-complexes are described below. In all cases their bromo-analogues were similarly prepared in similar yield.

1. $[Pd_2Cl_2(PPh_2O)_2(PPh_2OH)_2]$

Chlorodiphenylphosphine (0.46 ml, 3.0 mmol) was added to a solution of K_2PdCl_4 (0.50 g, 1.5 mmol) in acetone (25 ml) and water (10 ml). After stirring for 5 min at 25°, filtration gave *the complex* (0.80 g, 0.73 mmol) as a yellow powder which was washed with ethanol and water and recrystallized.

A similar procedure using diphenylphosphine oxide (0.58 g, 2.9 mmol), K_2PdCl_4 (0.47 g, 1.4 mmol) in ethanol (25 ml) and water (5 ml) gave *the complex* (0.72 g, 0.66 mmol). Titration of the filtrate with 0.1 *M* NaOH solution indicated that 1.4 mmol of acid was formed during the reaction.

2. $[PdCl(PPh_2O)(PPh_2OH)_2]$

Diphenylphosphine oxide (0.61 g, 3.0 mmol) was added to a suspension of $[Pd_2Cl_2(PPh_2O)_2(PPh_2OH)_2]$ (1.63 g, 1.5 mmol) in acetone (50 ml). After stirring for 18 h at 25° the mixture was evaporated to 20 ml under reduced pressure and filtration gave *the complex* (2.20 g, 2.95 mmol) as a white powder which was washed with ethanol and recrystallized.

3. $[Pd(PPh_2O)_2]_n$

Sodium hydroxide (10.1 ml of 0.1 *M* aqueous solution, 1.01 mmol) was added to a solution of $[Pd_2Cl_2(PPh_2O)_2(PPh_2OH)_2]$ (0.55 g, 0.50 mmol) in acetone (200 ml). After stirring for 1 h under reflux, filtration gave *the complex* as a pale yellow powder (0.51 g, 1.0 mmol) which was washed with water. Addition of aqueous silver nitrate solution to the filtrate gave AgCl (0.12 g, 0.84 mmol).

Reaction of sodium hydroxide with $[Pd_2Br_2(PPh_2O)_2(PPh_2OH)_2]$ gave an identical product.

4. $[PdCl(PPh_2O)(PPh_2OH)(PEt_3)]$

Triethylphosphine (0.15 ml, 1.0 mmol) was added to a suspension of $[Pd_2Cl_2(PPh_2O)_2(PPh_2OH)_2]$ (0.50 g, 0.46 mmol) in acetone (50 ml). After stirring for 30 min at 25° the resulting solution was evaporated under reduced pressure. Diethyl ether was twice added and evaporated with final drying at 50° *in vacuo* to give *the complex* (0.57 g, 0.86 mmol) as white crystals which were washed with diethyl ether and recrystallized.

5. Reaction of $[Pd_2Cl_4(PEt_3)_2]$ with Diphenylphosphine Oxide

A suspension of $[Pd_2Cl_4(PEt_3)_2]$, (0.25 g, 0.42 mmol) in sodium dried benzene (30 ml) was stirred with diphenylphosphine oxide (0.17 g, 0.84 mmol) at 25° for 18 h. Evaporation of the benzene under reduced pressure followed by extraction of the residue with diethyl ether left $[Pd_2Cl_2(PPh_2O)_2(PPh_2OH)_2]$ (0.23 g, 0.21 mmol) as a yellow residue. Evaporation of the ether extract gave *trans*-$[PdCl_2(PEt_3)_2]$ (0.17 g, 0.41 mmol) which was identified by infrared spectroscopy (18). In a separate but identical reaction the benzene solution was extracted with water and titration of the extract with 0.1 *M* NaOH solution showed that 0.41 mmol of acid was present.

6. $[PtCl(PPh_2O)(PPh_2OH)_2]$

Chlorodiphenylphosphine (1.15 ml, 7.5 mmol) was added dropwise over a 2 h period to a solution of K_2PtCl_4 (1.05 g, 2.5 mmol) in water (75 ml) and acetone (25 ml). After stirring for a further 18 h at 25° *the complex* (1.86 g, 2.5 mmol) was filtered off and washed with water, ethanol, and methylene dichloride. Some preparations were contaminated by a yellow product which was soluble in methylene dichloride and could be converted to *the complex* by boiling in methylene dichloride containing a few drops of water. This product is still under investigation.

A similar procedure using diphenylphosphine oxide (1.54 g, 7.6 mmol) in ethanol (10 ml) and K_2PtCl_4 (1.05 g, 2.5 mmol) in ethanol (30 ml) and water (20 ml) gave *the complex* (1.90 g, 2.5 mmol) after 18 h at 25°.

Can. J. Chem. Downloaded from www.nrcresearchpress.com by 210.87.254.40 on 09/05/12
For personal use only.

Can. J. Chem. Downloaded from www.nrcresearchpress.com by 210.87.254.40 on 09/05/12
For personal use only.

TABLE 2. Characterization data

Complex	Color	Melting point (°C)	% C		% H		Molecular weight	
			Calcd.	Found	Calcd.	Found	Calcd.	Found
$[Pd(PPh_2O)_2]_n$	White	220–225	56.7	56.5	4.0	4.2	—	—
$[Pt(PPh_2O)_2]_n$	White	300–320 dec.	48.2	47.4	3.4	3.6	—	—
$[Pd_2Cl_2(PPh_2O)_2(PPh_2OH)_2]$	Yellow	225–230	52.9	53.1	3.9	4.0	1091	1133
$[Pd_2Br_2(PPh_2O)_2(PPh_2OH)_2]$	Orange	216–219	48.9	48.8	3.6	3.7	1179	1173
$[Pt_2Cl_2(PPh_2O)_2(PPh_2OH)_2]$	White	237–240	45.3	45.5	3.3	3.3	1268	1218
$[Pt_2Br_2(PPh_2O)_2(PPh_2OH)_2]$	White	235–237	42.5	42.4	3.1	3.1	1357	1369
$[PdCl(PPh_2O)(PPh_2OH)_2]$	White	235–237	57.8	56.6	4.3	4.4	—	—
$[PdBr(PPh_2O)(PPh_2OH)_2]$	White	186–187	54.6	54.0	4.1	4.1	—	—
$[PtCl(PPh_2O)(PPh_2OH)_2]$	White	246–248	51.7	51.3	3.9	4.1	—	—
$[PtBr(PPh_2O)(PPh_2OH)_2]$	White	245–246	49.1	49.1	3.7	3.9	—	—
$[Pt_2(PPh_2O)_4(PPh_2OH)_2]$	White	193–195	54.1	53.4	3.9	4.2	—	—
$[Pt(PPh_2O)_2(PPh_2OH)_2]$	White	198–201	57.5	56.5	4.2	4.6	1002	1013
$[PdCl(PPh_2O)(PPh_2OH)(PEt_3)]$	White	159–167	54.3	54.3	5.5	5.5	663	643
$[PdBr(PPh_2O)(PPh_2OH)(PEt_3)]$	White	153–162	50.9	51.0	5.1	5.1	708	689
$[PtCl(PPh_2O)(PPh_2OH)(PEt_3)]$	White	188–190	47.9	47.2	4.8	4.8	752	747
$[PtBr(PPh_2O)(PPh_2OH)(PEt_3)]$	White	181–184	45.2	45.5	4.6	4.6	797	794

*Where molecular weight measurements are not reported the complexes were too insoluble in methylene dibromide for accurate measurement.

Can. J. Chem. Downloaded from www.nrcresearchpress.com by 210.87.254.40 on 09/05/12
For personal use only.

7. [$Pt_2Cl_2(PPh_2O)_2(PPh_2OH)_2$]

HCl (3 ml of concentrated aqueous solution) was added dropwise to a suspension of $[Pt(PPh_2O)_2]_n$ (0.23 g, 0.38 mmol) in acetone (25 ml). After stirring at 40° for 3 h, water (25 ml) was added giving *the complex* (0.23 g, 0.18 mmol) as a white precipitate which was washed with water and ethanol and recrystallized.

The mixture of $[Pt(PPh_2O)_2]_n$ with AgCl which resulted from reaction of $[PtCl(PPh_2O)(PPh_2OH)_2]$ with $AgNO_3$ was also suitable for use as starting material in this reaction provided that AgCl was removed by filtration prior to addition of water. Use of this mixture was therefore the best route for preparation of $[Pt_2Cl_2(PPh_2O)_2(PPh_2OH)_2]$ from K_2PtCl_4 since the direct conversion of $[PtCl(PPh_2O)(PPh_2OH)_2]$ to $[Pt_2Cl_2(PPh_2O)_2(PPh_2OH)_2]$ (see 12(*b*) below) gave poor yields.

8. [$Pt(PPh_2O)_2]_n$

NaOH (3.0 ml of 0.1 *M* aqueous solution, 0.3 mmol) was added to a solution of $[Pt_2Cl_2(PPh_2O)_2(PPh_2OH)_2]$ (0.35 g, 0.28 mmol) in acetone (50 ml). After stirring for 3 h at 50°, filtration gave *the complex* (0.33 g, 0.55 mmol) as a white precipitate which was washed with water and ethanol. Addition of aqueous silver nitrate solution to the filtrate gave AgCl (0.078 g, 0.54 mmol).

An identical product was obtained from reaction of $[Pt_2Br_2(PPh_2O)_2(PPh_2OH)_2]$ with NaOH.

9. [$PtCl(PPh_2O)(PPh_2OH)(PEt_3)$]

Triethylphosphine (0.2 ml, 1.4 mmol) was added to a suspension of $[PtCl(PPh_2O)(PPh_2OH)_2]$ (1.02 g, 1.2 mmol) in acetone (40 ml). After stirring for 2 h at 25° the resulting solution was evaporated *in vacuo*. The residue was washed with ethanol leaving *the complex* (0.74 g, 0.98 mmol) as a white powder which was recrystallized.

10. [$Pt_2(PPh_2O)_4(PPh_2OH)_2$]

NaOH (17.5 ml of 0.1 *M* aqueous solution, 1.75 mmol) was added to a suspension of $[PtCl(PPh_2O)(PPh_2OH)_2]$ (0.90 g, 1.1 mmol) in acetone (100 ml). The resulting solution was basic to litmus and evaporation under reduced pressure to 10 ml gave *the complex* (0.87 g, 0.54 mmol) as a white precipitate. Addition of aqueous $AgNO_3$ solution to the filtrate gave AgCl (0.152 g, 1.06 mmol).

An identical product was obtained from reaction of $[PtBr(PPh_2O)(PPh_2OH)_2]$ with NaOH.

11. [$Pt(PPh_2O)_2(PPh_2OH)_2$]

$Ag[PPh_2O]$ (0.185 g, 0.60 mmol) was added to a suspension of $[PtCl(PPh_2O)(PPh_2OH)_2]$ (0.50 g, 0.60 mmol) in chloroform (100 ml). After stirring for 18 h at 25° in the dark, AgCl and unreacted starting materials were removed by filtration and the resulting solution evaporated to 10 ml under reduced pressure to give *the complex* (0.32 g, 0.32 mmol) as white crystals which were washed with acetone and recrystallized.

An identical product was obtained from reaction of $[PtBr(PPh_2O)(PPh_2OH)_2]$ with $Ag[PPh_2O]$ in methylene dibromide.

12. Other Interconversion Reactions (see Figs. 1 and 2)

With the single exception noted below, the various interconversion reactions proceeded in very high yield (80–90%).

(*a*) Conversions involving $AgNO_3$ were by dropwise addition of a small excess of aqueous $AgNO_3$ solution to a suspension or solution of the reactant complex in acetone. After stirring for 3 h at 25° the product $[M(PPh_2O)_2]_n$ complexes were obtained as precipitates mixed with silver halide. The filtrates were acid to litmus. The reactions with $[PtX(PPh_2O)(PPh_2OH)_2]$ required 20 min under reflux followed by stirring for 3 h.

(*b*) Conversions involving hydrohalic acids were by dropwise addition of excess (*cf.* expt. 7 above) concentrated aqueous acid to a suspension or solution of the reactant complex in acetone. After stirring for 3 h at 25°, addition of water precipitated the products. The reactions with $[PtX(PPh_2O)(PPh_2OH)_2]$ required a large excess of concentrated acid with heating at 50° and reaction was often incomplete making this method unsuitable for the preparation of $[Pt_2X_2(PPh_2O)_2(PPh_2OH)_2]$ complexes.

(*c*) Conversions involving sodium hydroxide were similar to reaction 3 above.

(*d*) Conversions involving triethylphosphine were similar to reactions 4 and 9 above.

(*e*) The reactions of $[PdX(PPh_2O)(PPh_2OH)_2]$ complexes with $Ag[PPh_2O]$ were similar to 12(*a*) above.

We thank the National Research Council of Canada for a research grant.

1. L. Maier. Prog. Inorg. Chem. **5**, 27 (1963).
2. J. Chatt and B. Heaton. J. Chem. Soc. A, 2745 (1968).
3. L. D. Quin and R. E. Montgomery. J. Inorg. Nucl. Chem. **28**, 1750 (1966).
4. G. A. Levishina, A. D. Troitskaya, and R. R. Shagidullin. Russ. J. Inorg. Chem. **11**, 985 (1966).
5. A. A. Grinberg and A. D. Troitskaya. Bull. Acad. Sci. USSR. 178 (1944) and T. N. Itskovich and A. D. Troitskaya. Trudy Kazan Khim. Teknol. Inst. S. M. Kivova, **18**, 59 (1953).
6. A. Pidcock and C. R. Waterhouse. J. Chem. Soc. A, 2080 (1970).
7. F. H. Allen, A. Pidcock, and C. R. Waterhouse. J. Chem. Soc. A, 2087 (1970).
8. R. G. Hayter. J. Am. Chem. Soc. **84**, 3046 (1962).
9. S. Ahrland, J. Chatt, and N. R. Davies. Q. Rev. **12**, 265 (1958).
10. R. G. Pearson. Chem. Br. **3**, 103 (1967).
11. D. L. Sales, J. Stokes, and P. Woodward. J. Chem. Soc. A, 1852 (1968).
12. J. Chatt and L. M. Venanzi. J. Chem. Soc. 3858 (1955).
13. N. S. Gill and R. S. Nyholm. J. Chem. Soc. 3997 (1959).
14. L. J. Bellamy and L. Beecher. J. Chem. Soc. 1701 (1952).
15. S. Furberg. Acta Chem. Scand. **9**, 1557 (1955).
16. J. F. Nixon and A. Pidcock. Ann. Rev. of N.M.R. Spectroscopy, **2**, 361 (1969).
17. J. Chatt and L. M. Venanzi. J. Chem. Soc. 2351 (1957).
18. P. L. Goggin and R. J. Goodfellow. J. Chem. Soc. A, 1462 (1966).

Can. J. Chem. Downloaded from www.nrcresearchpress.com by 210.87.254.40 on 09/05/12
For personal use only.

Electron Spin Resonance Studies of Reactions of Photo-generated Organic Radicals with Hydrogen Peroxide in Aqueous Solution

C. E. Burchill and P. W. Jones

Department of Chemistry, University of Manitoba, Winnipeg, Manitoba R3T 2N2

Received July 30, 1971

The reactions with H_2O_2 of free radicals derived from 2-propanol, methanol, dimethoxymethane, and tetrahydrofuran have been investigated by e.s.r. using in-cavity photolysis with acetone photosensitization to generate the radicals in flowing aqueous solutions. The variation in the concentrations of the radicals derived from a particular solute with addition of H_2O_2 is attributed to the selective oxidation of one radical by H_2O_2, propagating a secondary chain reaction, *e.g.*,

$$(CH_3)_2\dot{C}OH + H_2O_2 \rightarrow (CH_3)_2CO + H_2O + \dot{O}H$$
$$\dot{O}H + (CH_3)_2CHOH \rightarrow H_2O + (CH_3)_2\dot{C}OH$$
$$\dot{O}H + (CH_3)_2CHOH \rightarrow H_2O + \dot{C}H_2(CH_3)CHOH$$
$$\dot{C}H_2(CH_3)CHOH + H_2O_2 \not\rightarrow$$

The rate constant for the oxidation of the acetone ketyl radical ($(CH_3)_2\dot{C}OH$) by H_2O_2 is estimated to be $5 \times 10^5\ M^{-1}\ s^{-1}$.

The results and conclusions of this study are demonstrated to be consistent with the results of previous investigations employing γ-radiation, photolysis, and the reaction of Ti(III) with H_2O_2 for initiation.

Results are also reported for the direct photolysis of aqueous malonic acid in the presence of H_2O_2.

Les réactions en solution aqueuse de l'eau oxygénée sur les radicaux libres dérivés du propanol-2, méthanol, diméthoxyméthane, et du THF ont été étudiées par r.p.e., en utilisant la photolyse "interne" pour produire les radicaux avec l'acétone comme photosensibilisateur.

La variation dans les concentrations des radicaux issus d'un soluté particulier après addition d'eau oxygénée, est attribuée à l'oxydation sélective d'un radical par H_2O_2, donnant ainsi naissance à une réaction en chaîne secondaire, par exemple:

$$(CH_3)_2\dot{C}OH + H_2O_2 \rightarrow CH_3)_2CO + H_2O + \dot{O}H$$
$$\dot{O}H + (CH_3)_2CHOH \rightarrow H_2O + (CH_3)_2\dot{C}OH$$
$$\dot{O}H + (CH_3)_2CHOH \rightarrow H_2O + \dot{C}H_2(CH_3)CHOH$$
$$\dot{C}H_2(CH_3)CHOH + H_2O_2 \not\rightarrow$$

La vitesse d'oxydation par l'eau oxygénée du radical acétone cétyle ($(CH_3)_2\dot{C}OH$) est évaluée à $k = 5 \times 10^5\ M^{-1}\ s^{-1}$.

Les résultats et les conclusions de cette étude sont en accord avec d'autres précédemment obtenus par irradiation γ, photolyse et par réaction du Ti(III) sur H_2O_2 dans l'étape d'initiation.

Les résultats de la photolyse de l'acide malonique en solution aqueuse en présence d'eau oxygénée sont également mentionnés.

Canadian Journal of Chemistry, 49, 4005 (1971)

A number of techniques have been developed for the generation of free radicals directly in the cavity of an e.s.r. spectrometer, and their study under steady state conditions. These techniques include irradiation with high intensity u.v. light or a d.c. beam of high energy electrons, but the most widely employed has been the reaction of a reducing metal ion (particularly Ti(III)) with H_2O_2 to produce secondary radicals from organic substrates via hydrogen abstraction by the resulting OH radicals. All of these methods have been used to generate free radicals from organic substrates in aqueous solutions and the identity and spectral parameters of a large number of such radicals have been established. In most instances the identities of the radicals generated from a particular substrate under oxidizing conditions are independent of the mode of initiation, but the ratios of the concentrations of the radicals (when more than one is formed from a particular substrate) show significant variations.

To cite a particular example of this variability,

Can. J. Chem. Downloaded from www.nrcresearchpress.com by 210.87.254.40 on 09/05/12
For personal use only.

the reaction of OH radicals with 2-propanol produces both $(CH_3)_2\dot{C}OH$ (**1**) and $\dot{C}H_2(CH_3)$-CHOH (**2**), and the ratio of their rates of formation has been estimated to be 5.2 (1, 2).[1] Using electron beam irradiation of an aqueous solution of 2-propanol saturated with N_2O, Eiben and Fessenden (3) observed only the spectrum of **1** but indicated that the spectrum of **2**, if present at one-sixth the concentration of **1**, would have been masked by the noise band. Using direct photolysis of H_2O_2 to generate free radicals from 2-propanol Livingston and Zeldes (4) observed only the spectrum of **1** when the solvent was the neat alcohol but, with addition of water, the spectrum of **2** was observed and its concentration increased with increasing water content. In the Ti(III) initiated reaction of 2-propanol with H_2O_2 (5, 6) both **1** and **2** were observed, but the ratio of [**1**] to [**2**] was always less than the value of 5.2 found by Burchill and Thompson (2) for the primary ratio of abstraction by OH from 2-propanol. The ratio of [**1**] to [**2**] was found to increase as the initial concentration of Ti(III) was increased (6), but to decrease as the initial concentration of H_2O_2 was increased (5). Moreover this ratio was a function of the elapsed time between mixing and observation, decreasing with increasing reaction time (6).

It was proposed by Norman and West (5) that, for the Ti(III) initiated reaction, the sensitivity to initial conditions of the relative radical concentrations could be explained by a difference in their reactivity toward H_2O_2 (that radical **1** was selectively oxidized) in propagating a secondary chain reaction. James and Sicilio (6) purported to have refuted this suggestion by a study of the kinetics of the reactions of the radicals with H_2O_2. However both the qualitative arguments of Norman and West (5) and the kinetic analysis by James and Sicilio (6) include the common error of assuming that the radicals observed in the e.s.r. cavity are those generated immediately after mixing and surviving to reach the cavity (*i.e.*, that the reaction of Ti(III) with H_2O_2 is instantaneous on the time scale of the experiments). Burchill (7) has pointed out that this is not a valid assumption and that the observed time dependence of the radicals from 2-propanol could be explained by assuming a secular equilibrium within the cavity, with the ratio of [**1**] to [**2**] modified by a secondary chain reaction involving **1** and H_2O_2. It has been argued that this explanation is impossible (8) but Czapski (9) has independently offered a similar explanation of the results and, in an experimental study (10), has demonstrated that the dependence of the total radical concentrations on the initial concentrations of Ti(III) and H_2O_2 is consistent with the reaction of Ti(III) with H_2O_2 being rate controlling, and the radical concentrations being the steady state values maintained by initiation *within the cavity* and bimolecular termination of the radicals. It has also been demonstrated by Czapski (9) that the ratio of [**1**] to [**2**] could be affected, in the manner observed, by a secondary chain reaction.

The experiments reported in this paper were undertaken in an attempt to examine more directly the reactions with H_2O_2 of the radicals derived from 2-propanol and other organic substrates. It was hoped to find a basis for reconciling a number of seemingly discordant results from previous studies which used a variety of modes and rates of initiation. The method employed for generation of the radicals was high intensity photolysis in the e.s.r. cavity, with photosensitization by acetone in a manner similar to that described by Zeldes and Livingston (11). A somewhat similar study, employing biacetyl and pyruvic acid as photosensitizers, has been reported by Ayscough and Brice (12). Acetone photosensitization has recently been used in flash photolysis studies of amides in aqueous solution (13).

Experimental

The e.s.r. spectrometer used was a conventional X-band instrument (Varian E-3) operating at approximately 9.2 GHz, with 100 kHz field modulation. The resonant cavity was a Varian multi-purpose unit fitted with a slotted end plate to admit light. The light source was a medium pressure mercury arc (the inner envelope from a Westinghouse H33-1-HD 400 W street-lighting lamp). The light was focused on the cavity by a 9-in. hemispherical aluminum mirror and a single quartz condensing lens. The solutions were flowed through a flat silica cell of 0.5 mm internal depth in the light path and approximately 9 mm width. The flow rate was normally 0.5–1.0 ml/min. Control experiments demonstrated that the effects observed were independent of the flow rate over a wide range. All solutions were deoxygenated by purging

[1]A recently published report of a study of the oxidation of alcohols by Fenton's reagent (29) draws essentially the same quantitative conclusions as refs. 1, 2, and 22 concerning the ratio of α and β abstraction from alcohols by OH and the effects of deuterium substitution.

Can. J. Chem. Downloaded from www.nrcresearchpress.com by 210.87.254.40 on 09/05/12
For personal use only.

with oxygen-free nitrogen. The temperature of the solutions leaving the cell was approximately 30 °C.

Hydrogen peroxide (30%, unstabilized), acetone, 2-propanol, methanol, dimethoxymethane, tetrahydrofuran, and malonic acid were Fisher Certified Reagent grade and were used as received. In initial experiments the water used in preparing solutions was redistilled once from alkaline permanganate and once from acid dichromate. The results were then compared with those obtained using water redistilled once from a Barnstead still and, as no differences were observed, this latter source was used in all subsequent experiments.

The relative concentrations of alcohol-derived radicals produced simultaneously, and whose spectra were recorded in the same scan, were estimated by graphical double integration of their first-derivative spectra. It was established that, for a particular radical and a given modulation amplitude, there was a constant ratio of derivative peak amplitude to total intensity, and routine calculations of the ratios of radical concentrations were made using peak amplitudes. Absolute concentrations of the radicals were estimated by comparison with the double integral of spectra from aqueous solutions of the stable nitroxide, prepared by the method of Briere *et al.*

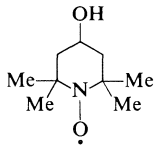

(14), and purified by repeated vacuum sublimation. Aside from the usual difficulties attending attempts at absolute concentration calibrations in e.s.r., we feel that the concentrations estimated for the photo-generated radicals must be regarded as lower limits. The standard was a homogeneous solution, completely filling the reaction cell, whereas the light source probably did not illuminate the cell uniformly. Consequently a particular *number* of spins, characterized by a particular signal intensity, might represent a higher effective *concentration* in the illuminated portion of the cell.

Results and Discussion

(1) Acetone Photosensitized Reactions

When aqueous solutions of acetone (0.68 *M*) and another organic solute (0.4–1.0 *M*) were subjected to u.v. radiation in the cavity, the spectrum of $(CH_3)_2\dot{C}OH$ (**1**) was always observed together with (usually) that of a single radical derived from the second solute.

We have assumed that the radicals are formed by reaction of a triplet excited state of acetone with the second solute. The mechanism has been described schematically by Dalton and Turro (15) (see Scheme 1). The quantum yield for intersystem crossing, ϕ_{ST}, is known to be close to unity for acetone (16), and the triplet lifetime sufficiently

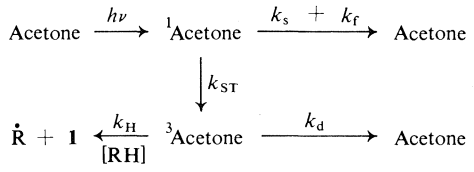

SCHEME 1

long (~10^{-5} s (17)) that the triplet may react with a good hydrogen atom donor by abstraction of H. In the absence of further secondary reactions the radicals will disappear by bimolecular reaction to yield non-radical products.

(a) 2-Propanol

With 2-propanol as substrate only the spectrum of **1** was observed. A spectrum obtained using 0.68 *M* acetone and 0.65 *M* 2-propanol is shown in Fig. 1*a*. A large modulation amplitude (1.0 G) was deliberately used to increase the signal amplitude. Under higher resolution (0.1 G modulation) the splitting due to the —OH proton and the second-order components (11) were observed (see inset Fig. 1*c*). When H_2O_2 was added, the spectrum of $\dot{C}H_2(CH_3)CHOH$ (**2**) (4–6) appeared in addition to that of **1**. As the H_2O_2 concentration was increased from zero to 0.04 *M*, the concentration of **1** decreased while that of **2** increased, but their sum remained essentially constant (see Fig. 2). Figure 1*b* shows the spectrum obtained with 0.017 *M* H_2O_2. The ratio [**2**]/[**1**] continued to increase with increasing [H_2O_2] above 0.04 *M* although the total radical concentration began to decrease. In the absence of acetone, solutions containing 0.65 *M* 2-propanol and H_2O_2 concentrations in this range did not give a useable signal. We therefore conclude that the effects of added H_2O_2 in the presence of acetone are a consequence of secondary reactions of the radicals with H_2O_2 rather than of the direct photolysis of the added H_2O_2.

The effect of varying the H_2O_2 concentration may be rationalized on the basis of the reaction scheme outlined in eqs. 1–8. We assume that, for

[1] $$^3\text{acetone} + \text{2-propanol} \rightarrow \mathbf{1} + \mathbf{1}$$

fixed concentrations of acetone and 2-propanol, the rate of reaction 1 is dependent only on the light intensity, is unaffected by the low concentrations of H_2O_2 added, and may be represented by r_i. The rate of generation of **1** will then be given by $2r_i$. It has been concluded that **1** reacts with H_2O_2 to give an OH radical which may abstract from

Can. J. Chem. Downloaded from www.nrcresearchpress.com by 210.87.254.40 on 09/05/12
For personal use only.

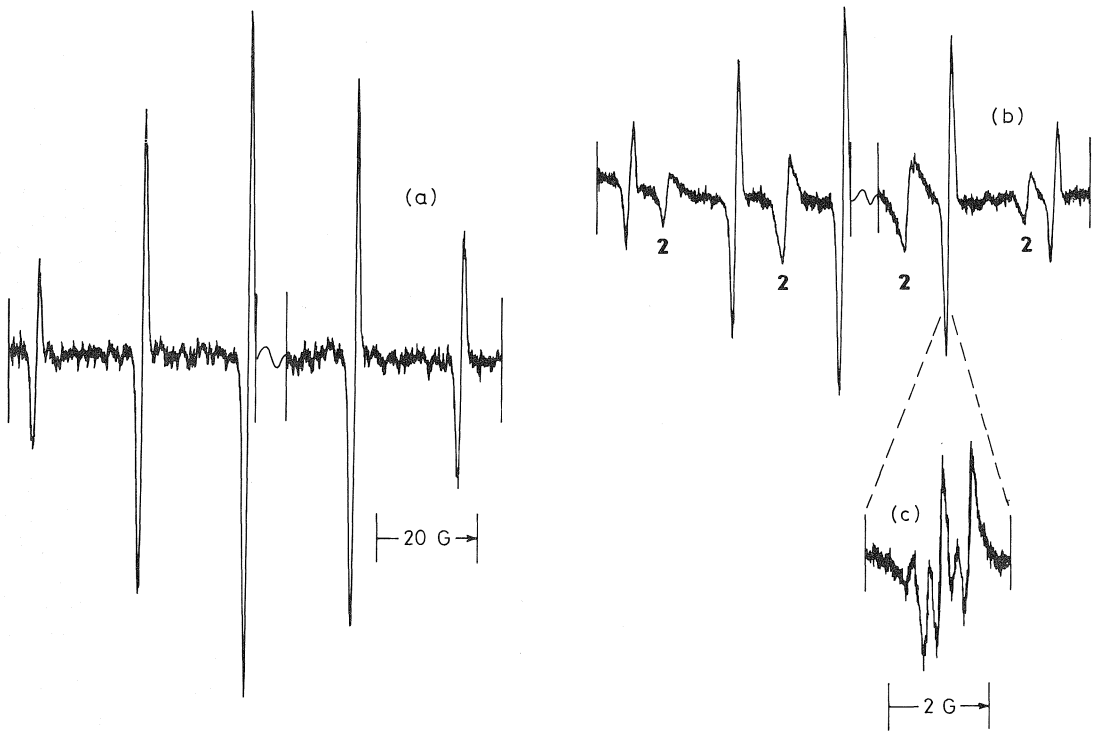

FIG. 1. The e.s.r. spectra during photolysis of aqueous solutions 0.68 *M* in acetone and 0.65 *M* in 2-propanol. The outer pair of lines in the complete spectra have been omitted. The gap in the center of each spectrum represents the region obscured by the photoinduced signal from the standard silica cell. (*a*) No H_2O_2 added. (*b*) 0.017 *M* H_2O_2 added (instrument settings the same as for (*a*)). (*c*) High resolution detail of peak above.

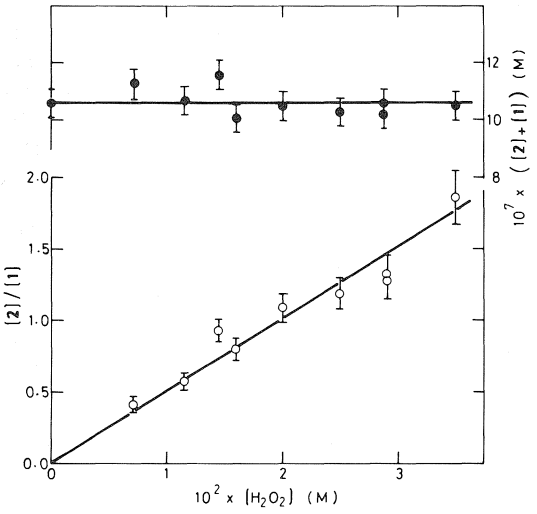

FIG. 2. Effect of added H_2O_2 on the concentrations of $(CH_3)_2\dot{C}OH$ (**1**) and $\dot{C}H_2(CH_3)CHOH$ (**2**) during photolysis of aqueous solutions 0.68 *M* in acetone and 0.65 *M* in 2-propanol.

2-propanol to give *either* **1** or **2** (reactions 2–4)

[2] $\mathbf{1} + H_2O_2 \rightarrow$ acetone $+ H_2O + \dot{O}H$

[3] $\dot{O}H$ + 2-propanol $\rightarrow H_2O + \mathbf{1}$

[4] $\dot{O}H$ + 2-propanol $\rightarrow H_2O + \mathbf{2}$

(1, 2). From the kinetics of the radiation-induced oxidation of 2-propanol by H_2O_2 it has been concluded that **2** does not react with H_2O_2 in a chain propagating reaction (1). As a consequence of the sequence of reactions 2–4 the steady state concentration of **1** would be reduced and that of **2** increased but these would not, of themselves, alter the total radical concentration since no termination is involved. In the steady state radiolysis experiments (1, 2) only one termination process was proposed (the bimolecular reaction of **2**); the assumption being that the chain length was sufficient to make [**2**] $\gg$ [**1**]. In the experiments described here, with their much greater rate of initiation and hence higher radical concentrations, the chain length would be much less. The

Can. J. Chem. Downloaded from www.nrcresearchpress.com by 210.87.254.40 on 09/05/12
For personal use only.

observed ratio [2]/[1] was, in some cases, close to unity and at least three termination processes must be considered (reactions 5–7). Reaction 8,

[5] $\mathbf{1} + \mathbf{1} \searrow$

[6] $\mathbf{1} + \mathbf{2} \longrightarrow$ non-radical products

[7] $\mathbf{2} + \mathbf{2} \nearrow$

invoked to explain the alcohol dependence of the yields in the radiation-induced oxidation of 2-propanol by H_2O_2 (1), is included in the scheme but, as demonstrated below, its rate constant is too low for this reaction to be very significant at the alcohol concentrations used in these experiments.

[8] $\mathbf{2}$ + 2-propanol → 2-propanol + $\mathbf{1}$

The rate constant for reaction 5 has been estimated as $2k_5 = 1.4 \times 10^9\ M^{-1}\ s^{-1}$ (18) and the rate constant for reaction 7 is unlikely to be significantly different since the very similar radical from *t*-butyl alcohol also has a bimolecular decay constant $2k = 1.4 \times 10^9\ M^{-1}\ s^{-1}$ (18). We have assumed that the bimolecular terminations (reactions 5-7) can be represented by a single rate constant, k_t, such that $2k_5 = k_6 = 2k_7 = k_t$. (The factor of two is not required for k_6 since this involves dissimilar radicals.) From the mechanism of eqs. 1–8, and the assumption of a steady state, eqs. 9 and 10 may be derived.

Using eq. 9, [1] + [2] = $1.06 \times 10^{-6}\ M$ (from Fig. 2), and assuming $k_t = 1.4 \times 10^9\ M^{-1}\ s^{-1}$, the calculated value of $(2r_ik_t)^{1/2}$ is $1.5 \times 10^3\ s^{-1}$. For [2-propanol] = 0.65 *M* and $k_8 = 51\ M^{-1}\ s^{-1}$ (2), k_8[2-propanol] = $33\ s^{-1}$. Thus the term involving k_8 is not significant for the conditions used and may be eliminated from eq. 10, giving eq. 11.

The proposed mechanism thus predicts that for a constant light intensity, and hence constant rate of initiation, the sum of the organic radical concentrations should be constant as the concentration of H_2O_2 is varied while the ratio of [2] to [1] should be directly proportional to [H_2O_2]. These predictions are experimentally realized as shown in Fig. 2.

[11] $$\frac{[\mathbf{2}]}{[\mathbf{1}]} = \frac{k_4k_2[H_2O_2]}{(k_3 + k_4)(2r_ik_t)^{1/2}}$$

The effect of varying light intensity, and hence r_i, was investigated by inserting a series of calibrated screens between the lamp and the e.s.r. cavity. The results are shown in Fig. 3. Equations 9 and 11 predict that the total radical concentration should vary directly with the square root of the intensity while the ratio [2]/[1] should show an inverse square root dependence.

From eq. 11, the slope of the line in Fig. 2 will be

$$\frac{k_4 \cdot k_2}{(k_3 + k_4)(2r_ik_t)^{1/2}}$$

Using the value of $(2r_ik_t)^{1/2} = 1.5 \times 10^3\ s^{-1}$ estimated above and taking $k_4/(k_3 + k_4) = 0.16$ (2), gives $k_2 = (4.8 \pm 0.3) \times 10^5\ M^{-1}\ s^{-1}$. This value may be a lower limit since, as discussed above, the concentrations estimated are probably lower limits.

The effect of H_2O_2 on solutions 0.68 *M* in acetone and 0.65 *M* in 2-propanol was also investigated in the presence of 0.1 *M* $HClO_4$. No significant difference was observed from the results in neutral solution except for the broadening of the lines for **1** as a result of proton exchange (11). A value of k_2 was estimated from the variation of [2]/[1] with [H_2O_2] and gave $k_2 = (5.1 \pm 0.5) \times 10^5\ M^{-1}\ s^{-1}$, in good agreement with the value for neutral solutions. From this we conclude that none of the rate constants involved is significantly altered in acid solution. This conclusion is also implied by the fact that the radiation-chemical yield for aqueous 2-propanol–H_2O_2 is not affected by the addition of acid (7).

To test the validity of the results and conclusions above we have checked their consequences against the experimental results from the Ti(III) initiated reaction (6) and the radiation-induced reaction (1, 2) of 2-propanol with H_2O_2.

[9] $$[\mathbf{1}] + [\mathbf{2}] = \left(\frac{2r_i}{k_t}\right)^{1/2}$$

[10] $$\frac{[\mathbf{2}]}{[\mathbf{1}]} = \frac{\frac{k_4}{k_3 + k_4} \cdot k_2[H_2O_2] + (2r_ik_t)^{1/2} + k_8[\text{2-propanol}]}{(2r_ik_t)^{1/2} + k_8[\text{2-propanol}]} - 1$$

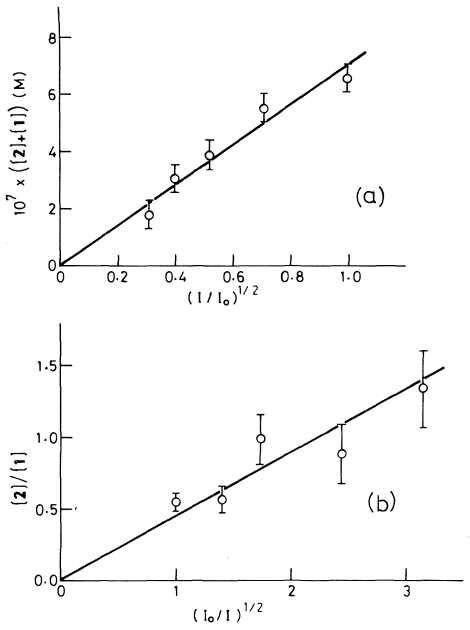

FIG. 3. Effect of varying light intensity (I) on the concentrations of $(CH_3)_2\dot{C}OH$ (**1**) and $\dot{C}H_2(CH_3)CHOH$ (**2**) during photolysis of solutions 0.68 M in acetone, 0.65 M in 2-propanol, and 0.017 M in H_2O_2. I_0 refers to the light intensity with no attenuation.

We have assumed that, in the Ti(III) system, the initiation is rate controlling and that the concentrations of the radicals observed are the steady state values maintained by the instantaneous rate of initiation *in the cavity* and bimolecular combination of the radicals (9, 10). The mechanism assumed is given by eqs. 2–7, 12. Taking k_{12} =

$$[12]\quad \text{Ti(III)} + H_2O_2 \xrightarrow{[H^+]} \text{Ti(IV)} + H_2O + OH$$

590 $M^{-1}\,s^{-1}$ for solutions in sulfuric acid,[2] $k_3/k_4 = 5.2$ (2), $k_3 + k_4 = 1.2 \times 10^9\ M^{-1}\,s^{-1}$ (19), $k_2 = 5 \times 10^5\ M^{-1}\,s^{-1}$ (above), and $k_t = 1.4 \times 10^9\ M^{-1}\,s^{-1}$, numerical integration showed that a *quasi* steady state or secular equilibrium would be reached in about 1 ms after mixing for conditions typical of those used in this type of experiment. Thus, for the mechanism and rate constants proposed, the steady state assumption would be valid for reaction times of 10 ms and greater (typical flow times between the mixer and cavity). The concentrations of the radicals derived from 2-propanol will be given by eqs. 13 and 14,

$$[13]\quad [\mathbf{1}] + [\mathbf{2}] = \left(\frac{k_{12}[\text{Ti (III)}][H_2O_2]}{k_t}\right)^{1/2}$$

$$[14]\quad \frac{[\mathbf{2}]}{[\mathbf{1}]} = \frac{k_4}{k_3}\left[k_2\left(\frac{[H_2O_2]}{k_t k_{12}[\text{Ti (III)}]}\right)^{1/2} + 1\right]$$

where [Ti(III)] and $[H_2O_2]$ refer to the concentrations of these species remaining at the time of observation. Czapski *et al.* (10) have demonstrated that the total radical concentration, observed at a fixed time after mixing, is consistent with eq. 13. We have evaluated, by numerical integration, the individual concentrations of **1** and **2** as a function of time after mixing for a solution (after mixing) 0.05 M in H_2O_2 and 0.005 M in Ti(III). Since reaction 8 was not included in the simplified mechanism the results are independent of the alcohol concentration. (Czapski *et al.* (10) experimentally observed no dependence of the ratio of [**2**] to [**1**] on the alcohol concentration up to 1.5 M.) The results of this calculation are shown in Fig. 4 and may be compared with the experimental results of James and Sicilio (Fig. 3 of ref. 6). For a system such as this, in which $[H_2O_2]_0 \gg [\text{Ti(III)}]_0$, the concentration of H_2O_2 remains roughly constant while that of Ti(III) decreases toward zero with time. As a result, the total radical concentration

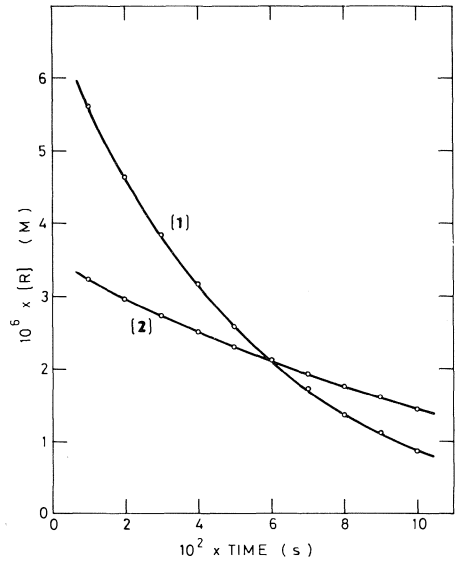

FIG. 4. Calculated time dependence of the concentrations of $(CH_3)_2\dot{C}OH$ (**1**) and $\dot{C}H_2(CH_3)CHOH$ (**2**) in the reaction of Ti(III) (5×10^{-3} M) with H_2O_2 (5×10^{-2} M) based on the mechanism and rate constants described in the text.

[2]G. Czapski, A. Samuni, and D. Meisel. Unpublished results. Private communication from G. Czapski.

Can. J. Chem. Downloaded from www.nrcresearchpress.com by 210.87.254.40 on 09/05/12
For personal use only.

Can. J. Chem. Downloaded from www.nrcresearchpress.com by 210.87.254.40 on 09/05/12
For personal use only.

decreases with time but the ratio of [**2**] to [**1**] increases, becoming greater than unity at long reaction time. This crossover point would shift to shorter times with an increase in $[H_2O_2]_0$, but to longer times with an increase in $[Ti(III)]_0$, as observed by James and Sicilio (6).

To complete the comparison with the results of James and Sicilio, we have plotted the data of Fig. 4 as log [**R**] *vs.* time after mixing, as shown in Fig. 5. Although the calculated points in Fig. 5 actually define a pair of curves, we have fitted the best straight lines through them. The "first-order rate constants" so obtained were divided by the initial peroxide concentration, giving "second-order rate constants" of 357 M^{-1} s^{-1} for **1** and 189 M^{-1} s^{-1} for **2**. These may be compared with the values of 380 and 190 M^{-1} s^{-1} experimentally obtained by such a treatment of the data (Table 1 of ref. 6). Similar calculations were carried out for a variety of initial conditions and, so long as $[H_2O_2]_0 \geq 3[Ti(III)]_0$, the time dependence of the radical concentrations could be adequately represented by first order plots and the "second-order rate constants", calculated as above, were essentially independent of the absolute values of $[Ti(III)]_0$ and $[H_2O_2]_0$ (*cf.* Table 1 of ref. 6).

The only serious disagreement between the calculated results shown here and the experimental results of James and Sicilio is in the absolute magnitudes of the radical concentrations. The concentrations reported by James and Sicilio are nearly an order of magnitude less than predicted by our mechanism. It is possible that there was a systematic error in the concentration calibration used by these authors since in an earlier study with methanol as substrate (20), in which a similar mechanism should apply, the radical concentrations reported were much greater. It has been suggested (8) that the low radical concentrations are a result of the reaction of OH with Ti(III) but this argument is untenable since the rate constant for this reaction is unlikely to be significantly greater than that for reaction of OH with 2-propanol and the concentration of the alcohol was generally fifty to one hundred times greater than the *initial* [Ti(III)].

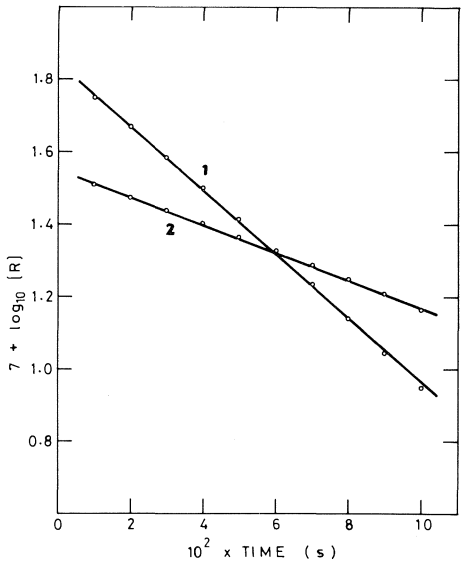

FIG. 5. First order plot of the calculated data of Fig. 4.

In the radiation-induced oxidation of 2-propanol by H_2O_2, reaction 8 was proposed to be of major importance (1). An equation analogous to eq. 10 may be derived for the steady state concentrations of the radicals in the radiation-chemical experiment (eq. 15). G_R is the sum of the primary free-radical yields for the radiolysis of aqueous solutions, and D is the dose rate in units of 6.02×10^{25} eV l^{-1} s^{-1}. For the conditions used by Burchill and Ginns (1), $(G_R.D.k_t)^{1/2} \sim 50$ s^{-1} while k_8[2-propanol] was in the range 5.0–50 s^{-1}. Thus reaction 8 is indeed not negligible at the lower rates of initiation used in the radiation-chemical study. Furthermore, for solutions 0.5 M in 2-propanol, it was found that $G(-H_2O_2)$ was independent of $[H_2O_2]$ in the range 0.05 to <0.01 M (1). This was construed as evidence that the only significant termination was bimolecular reaction of **2** (reaction 7). From eq. 15 it can be calculated that, for [2-propanol] = 0.5 M and $[H_2O_2] = 0.01$ M, [**2**]/[**1**] = 26 for a dose rate of 1.8×10^{19} eV l^{-1} s^{-1} (*i.e.*, only reaction 7 would be a significant terminating process).

In the radiation-induced oxidation of 2-propanol by H_2O_2 the chain yields were found to

$$[15] \qquad \frac{[\mathbf{2}]}{[\mathbf{1}]} = \frac{\frac{k_4}{k_3 + k_4} k_2[H_2O_2] + (G_R.D.k_t)^{1/2} + k_8[\text{2-propanol}]}{\frac{k_3}{k_3 + k_4}(G_R.D.k_t)^{1/2} + k_8[\text{2-propanol}]} - 1$$

Can. J. Chem. Downloaded from www.nrcresearchpress.com by 210.87.254.40 on 09/05/12
For personal use only.

decrease at very high alcohol concentrations (1). This phenomenon has also been reported for the photo-induced reaction (21).[3] This reduction of the yields was attributed (1) to a decrease in k_2 with decreasing dielectric constant as the solvent was varied from water to 2-propanol. To examine this proposal we have measured the concentrations of **1** and **2** for solutions containing 0.68 *M* acetone, 0.029 *M* H_2O_2, and varying concentrations of alcohol. The results are shown in Fig. 6. The initial increase in total radical concentration with increasing alcohol may be associated with increased scavenging of the acetone triplets. The decrease in [**2**]/[**1**] (from ~1.4 at low alcohol concentration to 0.13 at 0.5 mole fraction alcohol) is much too great to be accounted for by the inclusion of reaction 8 (as in eq. 10) although it would make some contribution. The most probable reason for this decrease is a decrease in k_2. In the photo-initiated reaction of H_2O_2 in pure 2-propanol (4) only the spectrum of **1** was observed, but with addition of water the spectrum of **2** became increasingly prominent. This could be accounted for by a combination of an increase in k_2 with increasing water content, thus increasing [**2**]/[**1**], and a decreasing contribution from reaction 8, which would have a similar effect.

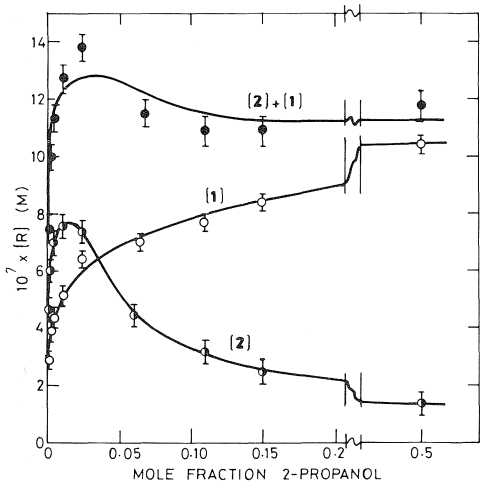

FIG. 6. Effect of varying 2-propanol concentration on the concentrations of $(CH_3)_2\dot{C}OH$ (**1**) and $\dot{C}H_2(CH_3)CHOH$ (**2**) during photolysis of solutions 0.68 *M* in acetone and 0.029 *M* in H_2O_2.

[3]Unpublished results of a re-examination of this system by C. E. Burchill and P. G. Huminicki show that the observed effects may be interpreted by a mechanism entirely analogous to that proposed for radiation initiation.

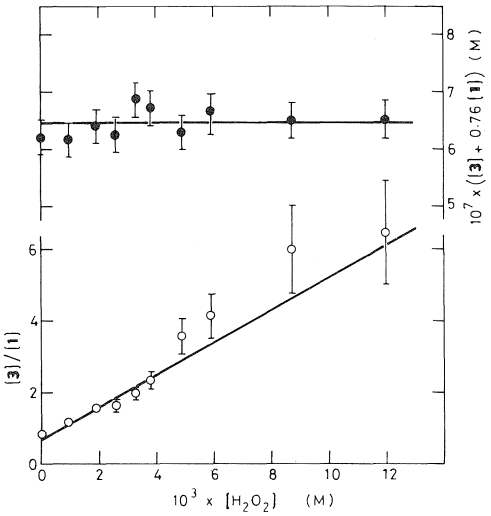

FIG. 7. Effect of H_2O_2 on the concentrations of $(CH_3)_2\dot{C}OH$ (**1**) and $\dot{C}H_2OH$ (**3**) during photolysis of solutions 0.68 *M* in acetone and 0.8 *M* in methanol.

The results and conclusions of this study are thus consistent with the mechanism proposed for the radiation-induced oxidation of 2-propanol by H_2O_2 (1, 2), and with the experimental observations from the photo-induced reaction, and e.s.r. studies using electron beam irradiation (3), photo-initiation (4, 11), and Ti(III) initiation (6, 10).

(b) Methanol

When a solution containing methanol (0.8 *M*) and acetone (0.68 *M*) was irradiated, the spectra of **1** and $\dot{C}H_2OH$ (**3**) were obtained (11). With addition of H_2O_2 the concentration of **3** increased while that of **1** decreased until, at 0.03 *M* H_2O_2, its spectrum could not be observed. The total radical concentration was essentially independent of H_2O_2 concentration while the ratio [**3**]/[**1**] increased linearly with [H_2O_2], as shown in Fig. 7. The mechanism to account for these results is outlined by eqs. 2, 5, and 16–20. Reaction 18 has been included in the mechanism since it has been shown to lead to a chain reduction of H_2O_2 (2, 22) but, as a result of the high rate constant for

[16] ^{3}acetone + $CH_3OH \rightarrow$ **1** + **3**

[2] **1** + $H_2O_2 \rightarrow$ acetone + H_2O + $\dot{O}H$

[17] $\dot{O}H$ + $CH_3OH \rightarrow H_2O$ + **3**

[18] **3** + $H_2O_2 \rightarrow H_2CO + H_2O + \dot{O}H$

[5] **1** + **1** $\rightarrow$

[19] **1** + **3** $\rightarrow$ non-radical products

[20] **3** + **3** $\rightarrow$

Can. J. Chem. Downloaded from www.nrcresearchpress.com by 210.87.254.40 on 09/05/12
For personal use only.

reaction 17 ($5 \times 10^8\ M^{-1}\ s^{-1}$ (19)), the steady state concentration of OH will be less than $10^{-8}\ M$ and the concentration of **3** will not be significantly affected by this sequence.

We have assumed that the rates of the termination processes are diffusion controlled and that the three may be represented by a composite rate constant,

$$k_t = 2k_{20} = k_{19}\left(\frac{k_{20}}{k_5}\right)^{1/2} = 2k_5\frac{k_{20}}{k_5}$$

The steady state concentrations of the organic radicals would then be given by eqs. 21 and 22, where r_i represents the rate of reaction 16.

$$[21] \qquad \left(\frac{k_5}{k_{20}}\right)^{1/2}[\mathbf{1}] + [\mathbf{3}] = \left(\frac{2r_i}{k_t}\right)^{1/2}$$

$$[22] \qquad \frac{[\mathbf{3}]}{[\mathbf{1}]} = \left(\frac{k_5}{k_{20}}\right)^{1/2} + \left(\frac{2}{r_i k_t}\right)^{1/2} k_2[H_2O_2]$$

Taking k_5/k_{20} as 1.4/2.4 (16) the observed value of [**3**]/[**1**] in the absence of H_2O_2 (0.85 ± 0.07) is in fair agreement with the predicted value of 0.76. From the peroxide dependence of [**3**]/[**1**] and a value of $k_t = 2.4 \times 10^9\ M^{-1}\ s^{-1}$ a value of $k_2 = (3.5 \pm 0.4) \times 10^5\ M^{-1}\ s^{-1}$ may be calculated, in fair agreement with that previously determined.

(c) Dimethoxymethane (Methylal)

Irradiation of an aqueous solution 0.68 *M* in acetone and 0.55 *M* in methylal gave the spectra of three radicals: **1**, $\dot{C}H(OCH_3)_2$ (**4**), and $\dot{C}H_2OCH_2OCH_3$ (**5**). The spectra of the latter radicals were identical to those obtained by Lewis and Sicilio (23). With no H_2O_2 present the concentration of **4** was significantly greater than that of **5**. With addition of H_2O_2 the intensity of the spectrum of **1** decreased toward zero, that of **4** decreased, and that of **5** increased (see Fig. 8). A quantitative treatment of this system was not attempted but the observed effects may be qualitatively understood in terms of a mechanism similar to that for 2-propanol (eqs. 2, 23–27).

[23] ^{3}acetone + methylal → **1** + **4**

[24] ^{3}acetone + methylal → **1** + **5**

[2] **1** + H_2O_2 → acetone + H_2O + $\dot{O}H$

[25] $\dot{O}H$ + methylal → H_2O + **4**

[26] $\dot{O}H$ + methylal → H_2O + **5**

As H_2O_2 is added, reaction of **1** with H_2O_2 will, via reactions 25 and 26, replace **1** with **4** and **5**.

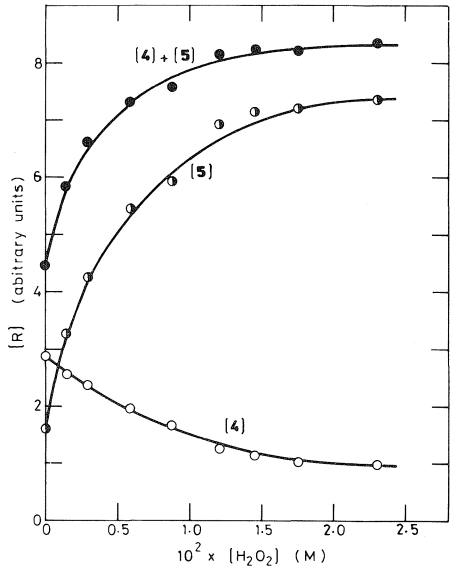

FIG. 8. Effect of H_2O_2 on the concentrations of $\dot{C}H(OCH_3)_2$ (**4**) and $\dot{C}H_2OCH_2OCH_3$ (**5**) during photolysis of solutions 0.68 *M* in acetone and 0.55 *M* in dimethoxymethane.

Thus the total concentration of radicals derived from methylal should increase as **1** decreases. The increase in [**5**] relative to [**4**] as H_2O_2 is added probably originates from a preferential oxidation of **4** by H_2O_2 to give an induced chain reaction (eq. 27). The sequence of reactions 27, 25, 26

[27] **4** + H_2O_2 → oxidized product + $\dot{O}H$ (possibly methyl formate + methanol)

could lead to an inversion of the concentrations of **4** and **5** with increased H_2O_2 in the manner observed.

This interpretation of the inversion of the concentrations of the radicals in the presence of H_2O_2 by a secondary chain reaction is consistent with the data of Lewis and Sicilio (23) for the Ti(III) initiated reaction of methylal with H_2O_2. In that study the concentrations of **4** and **5** showed a difference in time dependence, with the "rate constant" for **4** being greater than that for **5**. The rate constants themselves probably have no physical significance (as noted in a later study (6), "A plausible mechanism for a three-halves order decay is difficult to develop") since it is likely that the time dependence of the total radical concentration simply reflects the rate of initiation while the ratio of [**4**] to [**5**] decreases with decreasing rate of initiation as a result of a secondary chain reaction in a manner similar to that of 2-propanol.

Can. J. Chem. Downloaded from www.nrcresearchpress.com by 210.87.254.40 on 09/05/12
For personal use only.

To demonstrate that a free-radical chain reduction of H_2O_2 by methylal may occur we have γ-irradiated deaerated aqueous solutions of methylal and H_2O_2. For solutions 0.2 *M* in methylal and 0.01 *M* in H_2O_2, at a dose rate of 1.2×10^{19} eV l^{-1} s^{-1}, $G(-H_2O_2)$ was 22. The yield was independent of methylal concentration between 0.1 and 1.0 *M* and varied from 15 to 35 as $[H_2O_2]$ was increased from 0.005 to 0.05 *M*. These results imply a chain mechanism.

(d) Tetrahydrofuran (THF)

Irradiation of an aqueous solution 0.68 *M* in acetone and 0.55 *M* in THF gave spectra corresponding to two radicals which were identified as **1** and **6**. The latter spectrum consisted of six

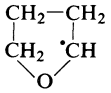

6

multiplets of relative intensity 1:1:2:2:1:1 with $a_{\dot{C}H} = 12.4$ and $a_{CH_2} = 28.3$ *G*, in agreement with previous work (24). In the presence of H_2O_2 an additional spectrum of six multiplets was observed. Two splittings of approximately 33 and 20 *G* were assigned to this spectrum and, as previously suggested (24), it is proposed that it represents radical **7**.

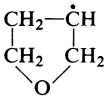

7

At low concentrations of H_2O_2 the spectrum of **1** disappeared and there was an increase in the concentration of **6** as well as the appearance of **7**. With further addition of H_2O_2 the concentration of **6** decreased while that of **7** continued to increase (see Fig. 9). It is suggested that a mechanism similar to that for methylal applies and that the initial increase in THF radicals with added H_2O_2 represents the replacement of **1** by **6** and **7**, and the inversion of the concentrations of **6** and **7** at high peroxide concentrations is a consequence of the preferential oxidation of **6** by H_2O_2 in a chain propagating reaction. The very high concentration of H_2O_2 required to bring about this inversion suggests that the rate constant for oxidation of **6** by H_2O_2 is much less than that for **1** or **4**.

When a deaerated aqueous solution 0.2 *M* in THF and 0.01 *M* in H_2O_2 was γ-irradiated at a dose rate of 1.2×10^{19} eV l^{-1} s^{-1} the $G(-H_2O_2)$ value was 29, demonstrating that an induced chain reduction of H_2O_2 by THF may indeed occur.

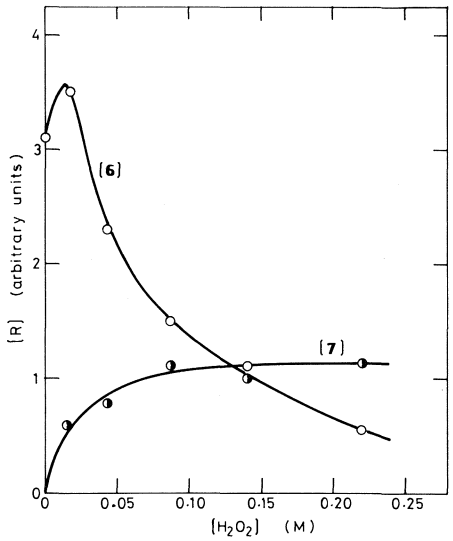

FIG. 9. Effect of H_2O_2 on the concentrations of radicals derived from tetrahydrofuran during photolysis of solutions 0.68 *M* in acetone and 0.55 *M* in THF.

6 = **7** =

(2) Direct Photolysis of Malonic Acid

Eiben and Fessenden (3) have noted that reaction of OH with malonic acid gives only the product of abstraction, $\dot{C}H(CO_2H)_2$ (**8**), whereas Dixon *et al.* (25) found only the fragment radical, $\dot{C}H_2CO_2H$ (**9**), in the Ti(III) initiated reaction with H_2O_2. In pulse radiolysis studies Simic *et al.* (26) identified the major radical species as **8** but noted a short lived transient which might have been **9**. It was thought that the qualitative differences between the results reported in refs. 3 and 25 might be traced to some reaction of the radicals with H_2O_2 which is necessarily present in the Ti(III) studies.

Malonic acid itself absorbs light in the mid u.v. and irradiation of a 1.0 *M* aqueous solution of the acid with no other additives produced a strong spectrum of **9** and a less intense spectrum of **8** (25, 3). Radical **9** is presumably formed by dissociation of an excited (possibly triplet) state of malonic acid, as has been suggested for tartaric acid (27). As in the case of tartaric acid, no

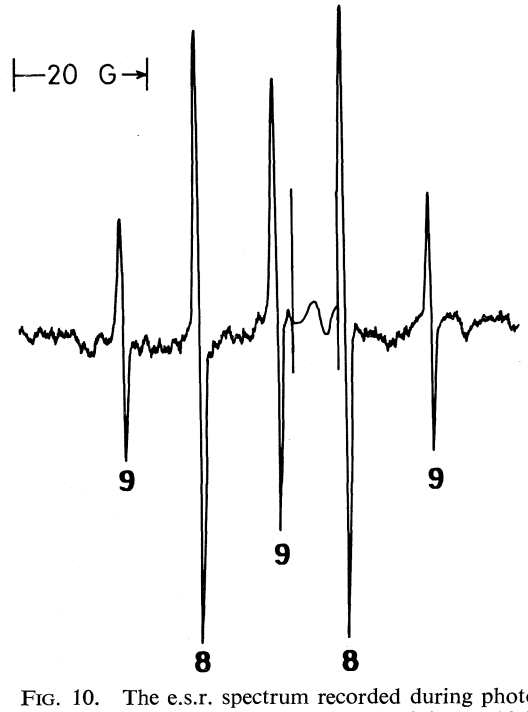

FIG. 10. The e.s.r. spectrum recorded during photolysis of aqueous 1.0 *M* malonic acid containing 0.029 *M* H_2O_2. The lines are attributed to $\dot{C}H(CO_2H)_2$ (**8**) and $\dot{C}H_2CO_2H$ (**9**).

spectrum which could be attributed to $\dot{C}O_2H$ was observed but, unlike tartaric acid, all spectra were found in absorption, nor were any intensity anomalies observed (see Fig. 10).

The origin of **8** in this system is less clear. It is possible that it is formed by abstraction of a methylene hydrogen from malonic acid by a triplet excited state of the acid, but no spectrum of the product of such a hydrogen atom addition was observed.

With the addition of H_2O_2 the spectrum of **8** increased in intensity while that of **9** remained (relatively) constant, as shown in Fig. 11. Although its spectrum was not observed, we suggest that this effect is a consequence of the reaction of $\dot{C}O_2H$ with H_2O_2. $\dot{C}O_2H$ is known to induce decomposition of H_2O_2, as in reaction 28 (28), and reaction of OH with malonic acid has

[28] $$\dot{C}O_2H + H_2O_2 \rightarrow CO_2 + H_2O_2 + \dot{O}H$$

been suggested to give only **8** (3). If the principal photo-decomposition of malonic acid is reaction 29, the subsequent reaction of $\dot{C}O_2H$ with H_2O_2 would result in the formation of **8** via reaction 30.

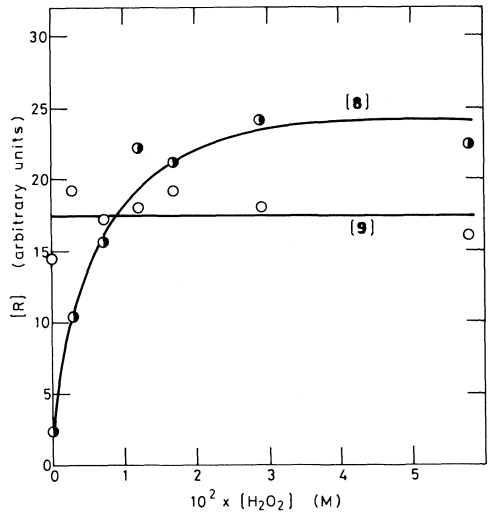

FIG. 11. Effect of H_2O_2 on the concentrations of $\dot{C}H(CO_2H)_2$ (**8**) and $\dot{C}H_2CO_2H$ (**9**) during photolysis of 1.0 *M* malonic acid.

[29] $$CH_2(CO_2H)_2 \xrightarrow{h\nu} \mathbf{9} + \dot{C}O_2H$$

[30] $$\dot{O}H + CH_2(CO_2H)_2 \rightarrow H_2O + \mathbf{8}$$

From these experiments it is clear that the presence of H_2O_2 in the Ti(III) studies is not the factor responsible for the formation of **9** from malonic acid. The explanation of this phenomenon has yet to be found.

Conclusion

This work has demonstrated that, when free radicals are generated from an organic substrate in aqueous solution, the presence of H_2O_2 may have a profound effect on the ratio of the concentrations of the radicals as a consequence of selective oxidation by H_2O_2 and induced secondary chain reactions. It has previously been shown (7, 9, 10) that, in e.s.r. studies of free radicals generated by the reaction of reducing metal ions with H_2O_2, a number of erroneous conclusions have been drawn because of the failure to recognize that the radicals observed in the flowing system are those generated *within the detector* by the rate controlling initiating step. There is therefore a need for a critical re-evaluation of all kinetic and mechanistic conclusions drawn from such studies.

This research was supported by Atomic Energy of Canada, Ltd., Commercial Products Division, to whom the authors express their gratitude. The cooperation of

Can. J. Chem. Downloaded from www.nrcresearchpress.com by 210.87.254.40 on 09/05/12
For personal use only.

Dr. H. D. Gesser in permitting the use of the spectrometer is gratefully acknowledged. The preliminary experiments in the radiation-induced reactions of ethers were carried out by Mr. R. F. Putnins. The nitroxide used for concentration calibrations was prepared by Mr. R. A. Long.

1. C. E. Burchill and I. S. Ginns. Can. J. Chem. **48**, 1232 (1970).
2. C. E. Burchill and G. F. Thompson. Can. J. Chem. **49**, 1305 (1971).
3. K. Eiben and R. W. Fessenden. J. Phys. Chem. **75**, 1186 (1971).
4. R. Livingston and H. Zeldes. J. Am. Chem. Soc. **88**, 4333 (1966).
5. R. O. C. Norman and P. R. West. J. Chem. Soc. B, 389 (1969).
6. R. E. James and F. Sicilio. J. Phys. Chem. **74**, 1166 (1970).
7. C. E. Burchill. J. Phys. Chem. **75**, 167 (1971).
8. R. E. James and F. Sicilio. J. Phys. Chem. **75**, 1326 (1971).
9. G. Czapski. J. Phys. Chem. **75**, 2957 (1971).
10. G. Czapski, A. Samuni, and D. Meisel. J. Phys. Chem. **75**, 3271 (1971),
11. H. Zeldes and R. Livingston. J. Chem. Phys. **45**, 1946 (1966).
12. P. B. Ayscough and M. C. Brice. J. Chem. Soc. B, 491 (1971).
13. M. Nakashima and E. Hayon. J. Phys. Chem. **75**, 1910 (1971).
14. R. Briere, H. Lemaire, and A. Rassat. Bull. Soc. Chim. Fr. **32**, 3273 (1965).
15. J. C. Dalton and N. J. Turro. *In* Annual review of physical chemistry **21**, 499 (1970).
16. R. F. Borkman and D. R. Kearns. J. Chem. Phys. **44**, 945 (1966).
17. P. J. Wagner. J. Am. Chem. Soc. **88**, 5672 (1966).
18. M. Simic, P. Neta, and E. Hayon. J. Phys. Chem. **73**, 3794 (1969).
19. M. Anbar and P. Neta. Int. J. Appl. Radiat. Isotop. **18**, 493 (1967).
20. R. E. Florin, F. Sicilio, and L. A. Wall. J. Phys. Chem. **72**, 3154 (1968).
21. J. Barrett, A. L. Mansell, and R. J. M. Ratcliff. Chem. Commun. 48 (1968).
22. C. E. Burchill and I. S. Ginns. Can. J. Chem. **48**, 2628 (1970).
23. E. L. Lewis and F. Sicilio. J. Phys. Chem. **73**, 2590 (1969).
24. F. Sicilio, M. Dousset, R. E. Florin, and L. A. Wall. Polym. Preprints, **6**, 956 (1965).
25. W. T. Dixon, R. O. C. Norman, and A. L. Buley. J. Chem. Soc. 3625 (1964).
26. M. Simic, P. Neta, and E. Hayon. J. Phys. Chem. **73**, 4214 (1969).
27. R. Livingston and H. Zeldes. J. Chem. Phys. **53**, 1406 (1970).
28. A. Hussain and E. J. Hart. J. Am. Chem. Soc. **87**, 1180 (1965).
29. C. Walling and S. Kato. J. Am. Chem. Soc. **93**, 4275 (1971).

Can. J. Chem. Downloaded from www.nrcresearchpress.com by 210.87.254.40 on 09/05/12
For personal use only.

Can. J. Chem. Downloaded from www.nrcresearchpress.com by 210.87.254.105 on 09/05/12
For personal use only.

The Condensation of Cyclohexanone with Furan and Pyrrole[1]

W. H. BROWN,[2] B. J. HUTCHINSON,[3] AND M. H. MACKINNON[4]
Department of Chemistry, University of Guelph, Guelph, Ontario

Received April 8, 1970[5]

Several compounds formed by the acid-catalyzed condensation of cyclohexanone with furan and pyrrole have been isolated and identified. A previously-reported structure for one of the products of the condensation of cyclohexanone with pyrrole has been shown to be incorrect.

Plusieurs composés, obtenus par la condensation acido-catalysée de la cyclohexanone avec le furanne et le pyrrole, ont été isolés et identifiés. La structure, précédemment rapportée, d'un des produits de condensation de la cyclohexanone avec le pyrrole est incorrecte.

Canadian Journal of Chemistry, **49**, 4017 (1971)

Introduction

A study of the acid-catalyzed condensation of furan with a number of acyclic carbonyl compounds has been reported in a series of papers by Brown and co-workers (1–4). In general, when ketones, such as acetone, are condensed with furan under the appropriate conditions (furan present in excess), a set of compounds **1**, **2**, **3**, and **4** whose structures are shown in Fig. 1, is obtained. However, when acetone is present in excess, only **4** is obtained. The mechanism of this set of reactions has been studied in our laboratories and will be the subject of a forthcoming communication.

Similar results have been obtained in the acid-catalyzed reaction of pyrrole with carbonyl compounds. Thus Baeyer (5) discovered the first condensation leading to such a cyclic compound; *viz.*, the condensation of pyrrole with acetone in the presence of hydrochloric acid to yield compound **5**, Fig. 1.

Investigation of this type of reaction was also undertaken by Dennstedt and Zimmerman (6) and by Chelintzev and Tronov (7). Chelintzev *et al.* (8) proposed structure **6** for the product obtained from the reaction of pyrrole with cyclohexanone. However our results indicate that this compound has a tetrazaquaterene structure **13**.

We report the products obtained from the acid-catalyzed condensation of cyclohexanone with furan and have investigated in more detail the structure of the two products formed in the condensation of cyclohexanone with pyrrole. Structures for these compounds are shown in Fig. 1. Since the structures are rather large and their names somewhat lengthy, we have used abbreviated symbols as indicated in Fig. 1. Table 1 lists the names of the compounds and their assigned numbers. These assigned numbers will be used throughout.

Results and Discussion

The Condensation of Cyclohexanone with Furan

When cyclohexanone is treated with furan in a mole ratio of 1:2 in the presence of hydrochloric acid, compounds **7** and **8** of proposed structure as shown in Fig. 1 are obtained. These products were expected on the basis of previous results (1) but no cyclic compound analogous to compound **4** was isolated from the reaction mixture. The 100 MHz proton n.m.r. spectrum of compound **7**, run neat with TMS as an internal standard, showed resonance at δ 1.42 and 2.18, relative intensity 5, which are assignable to the cyclohexyl methylene groups. The furan proton resonance occurred at δ 5.93, 6.13, and 7.13 with the following parameters: $J_{34} = 3.3$; $J_{35} = 0.8$; $J_{45} = 1.8$ Hz.

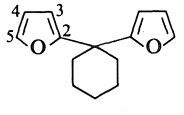

7

This is an AMX spectrum and the resulting coupling constants are in agreement with a 2-substituted furan (9).

[1]Taken in part from M.Sc. thesis of B. J. Hutchinson.
[2]Author to whom correspondence may be addressed.
[3]Present Address: Lambton College of Applied Arts and Technology, Box 969, Sarnia, Ontario.
[4]Present Address: VirChem of Canada, Ltd., 70 Hymus Boulevard, Pointe Claire, Quebec.
[5]Revision received September 10, 1971.

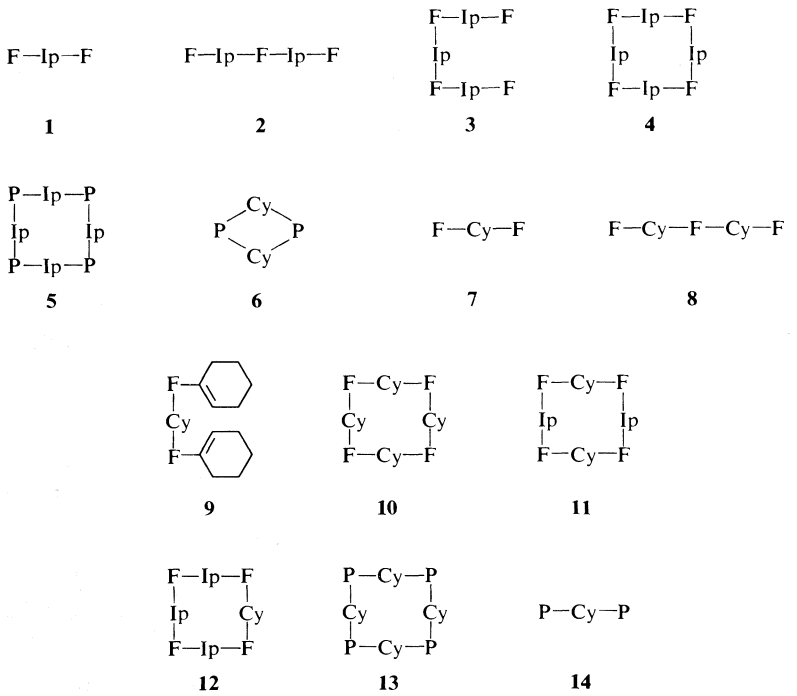

NOTE:

F represents ; P represents

Furan
(2- or 2,5-substituted)

Pyrrole
(2- or 2,5-substituted)

Cy represents ; Ip represents 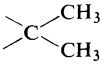

Cyclohexylidene

Isopropylidene

e.g. F—Ip—F—Ip—F represents 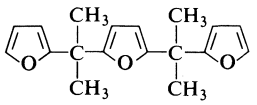

2 2

FIG. 1 Abbreviated structures for compounds referred to in text.

By analogy, the structure for **8** follows. The 60 MHz p.m.r spectrum, chemical analysis, and molecular weight are in agreement with the proposed structure.

Treatment of cyclohexanone with furan in a mole ratio of 2:1 in the presence of hydrochloric acid did not yield the expected tetroxaquaterene compound **10**. Instead a compound, corresponding to the empirical formula $C_{26}H_{32}O_2$, was isolated from the reaction mixture. Since the compound exists in good-sized, well-defined crystals it was hoped that the structure could be determined by X-ray diffraction. However, preliminary Weissenberg photographs of the orthorhombic crystals indicated the presence of excessive internal thermal motion or disorder, which ruled out further X-ray studies. A proposed structure, **9**, for the compound fits the empirical formula. If this structure is correct then **7** and **9** should react in the presence of hydrochloric acid to form **10**, as shown in eq. 1.

When this reaction was tried in dioxane satu-

Can. J. Chem. Downloaded from www.nrcresearchpress.com by 210.87.254.105 on 09/05/12
For personal use only.

TABLE 1. Nomenclature*

Compound	Name
1	2,2-Bis(2-furyl)propane
2	2,5-Bis(dimethylfurfuryl)furan
3	2,2′-Isopropylidenebis[5-(dimethylfurfuryl)furan]
4	2,2,7,7,12,12,17,17-Octamethyl-21,22,23-24-tetroxaquaterene
5	2,2,7,7,12,12,17,17-Octamethyl-21,22,23,24-tetrazaquaterene
6	Not known
7	1,1-Bis(2-furyl)cyclohexane
8	2,5-Bis(2-furylcyclohexyl)furan
9	1,1-Bis[2-{5-(1-cyclohexenyl)furyl}]cyclohexane
10	21,22,23,24-Tetroxaquaterene-2,7,12,17-tetraspirocyclohexane
11	2,2,12,12-Tetramethyl-21,22,23,24-tetroxaquaterene-7,17-dispirocyclohexane
12	2,2,7,7,12,12-Hexamethyl-21,22,23,24-tetroxaquaterene-17-spirocyclohexane
13	21,22,23,24-Tetrazaquaterene-2,7,12,17-tetraspirocyclohexane
14	1,1-Bis(2-pyrryl)cyclohexane

*For detail on the trivial name "quaterene" see refs. 13 and 14.

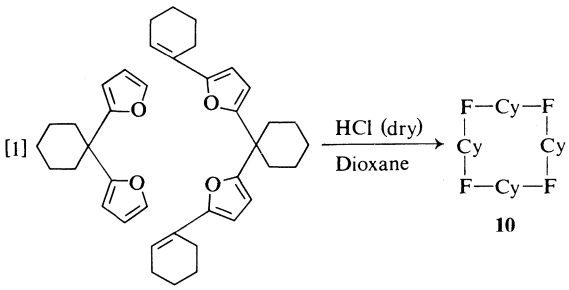

7 9 10

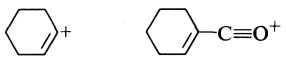

A B

rated with dry hydrogen chloride, the expected compound **10** was formed within 15 min, in 30% yield.

The 100 MHz spectrum of **9** in benzene-d_6 solution shows resonances at δ 6.37, relative intensity 1; 6.00, relative intensity 2; 2.15 and 1.49, relative intensity 13, assignable to the alkene, furan, and methylene protons respectively in the proposed structure for **9**. The resonance, assigned to the furan rings, appears as a singlet and not a multiplet as would be expected from the unsymmetrical substitution in the 2,5-positions of the furan rings in **9**. This ambiguity is fully resolved when the spectrum is run in carbon tetrachloride solution. The alkene resonance now occurs at δ 6.13 and the furan protons appear as a clear AB multiplet centered at δ 5.88, with J_{AB} = 3.2 Hz and $\nu_0\delta$ = 8.5 Hz. This confirms the unsymmetrical substitution of the furan rings in **9**.

The mass spectrum of **9** shows that the parent ion (*m/e* 376) fragments to give ions *m/e* 81 and 109. These correspond to structures **A** and **B**, which explain the alkene resonance observed in the 100 MHz n.m.r. spectrum.

The structure postulated for **10** is supported not only by its synthesis from **7** plus **9**, but also by its formation by treating **7** with cyclohexanone.

The Condensation of Cyclohexanone with Pyrrole

The product obtained from the reaction of equimolar quantities of pyrrole and cyclohexanone in the presence of hydrochloric acid has the same melting point (272–273°) as the compound reported by Chelintzev *et al.* (8). We have found this high-melting solid to have a tetrazaquaterene structure **13** rather than structure **6** previously proposed by these investigators.

The 100 MHz proton spectrum of **13** in dioxane solution shows resonances at δ 7.45, broad singlet, relative intensity 1, 5.85, doublet, relative intensity 2, J = 4.0 Hz, and multiplets at 1.93 and 1.41, total intensity 10, assignable to the pyrrole N—H, the pyrrole β-protons, and the cyclohexane protons in **13** respectively. Addition of D_2O to the solution of **13** in dioxane causes the disappearance of the resonance at δ 7.45, confirming its assignment as the pyrrole N—H and removes the doublet splitting in the resonance at δ 5.85. Since this coupling is from the N—H, the single resonance for the β-protons, which does not split to a multiplet on changing solvent, necessitates symmetrical substitution on the pyrrole rings in the 2,5-positions. Thus, together with the relative ratios of the resonances, the assignment of the structure for **13** is unambiguous. Furthermore, when **14** is treated with cyclohexanone in the mole ratio of 1:5 in the presence

Can. J. Chem. Downloaded from www.nrcresearchpress.com by 210.87.254.105 on 09/05/12
For personal use only.

Can. J. Chem. Downloaded from www.nrcresearchpress.com by 210.87.254.105 on 09/05/12
For personal use only.

of hydrochloric acid, **13** is readily formed in excellent yield. The molecular weight of **13** by Rast method is 584.

When pyrrole and cyclohexanone, in a mole ratio of 4:1, are treated with hydrochloric acid, a compound, to which structure **14** is assigned, is formed. The 100 MHz proton n.m.r. spectrum of compound **14** in benzene-d_6 showed multiplets at high field (δ 2.02 and 1.50) and at low field (δ 6.82, 6.18, and 6.06) at relative ratios of 5:3. These are assignable to the cyclohexane methylenes and the pyrrole protons respectively. The low-field multiplets of the pyrrole and its deutero analog could be completely interpreted as an AMNX spectra giving the following parameters: $J_{13} = 2.69$; $J_{14} = 2.56$; $J_{15} = 2.66$; $J_{34} = 3.41$; $J_{35} = 1.38$; $J_{45} = 2.41$ Hz.

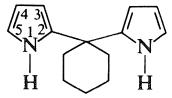

14

The values of these coupling constants require substitution of pyrrole in the 2-position as reported by Abraham and Bernstein (10) and Gronowitz *et al.* (11). Hence this interpretation makes unambiguous the assignment of structure of **14**. The n.m.r. data on substituted pyrroles have been summarized by Katritzky (12).

Experimental

Instruments used were Varian A-60-A and HA-100 n.m.r. spectrometers, a Beckman IR 5A, a Meltemp m.p. apparatus using capillary tubes (corrected thermometer), and a Varian-Mat CH-7 mass spectrometer for molecular weights. The reagents, furan, cyclohexanone, and pyrrole were reagent grade and were used without further purification.

Condensation of Cyclohexanone with Furan (Mole Ratio 1:2) to Form 7 and 8

In a three-necked 500 ml flask, fitted with a reflux condenser and stirrer, were placed 49 g (0.5 mol) of cyclohexanone, 68 g (1.0 mol) of furan, and 40 ml of absolute ethanol. To the stirred mixture was added dropwise 30 ml of 37% aqueous hydrochloric acid solution. The reaction mixture was stirred at room temperature for 24 h. When stirring was discontinued the mixture separated into two phases. The upper purple aqueous layer was separated from the lower reddish-orange organic layer. The organic phase was washed with 5% aqueous sodium bicarbonate solution until neutral, dried over anhydrous magnesium sulfate, and fractionally distilled at diminished pressure. The first fraction distilled at 94–95° (1–2 Torr) and weighed 9.23 g (8.5%). It is an oil and has $\eta_D^{25°}$ 1.5221 and $d_4^{20°}$ 1.018. Cooling to −15° for 24 h yielded crystals which melt at 13–17°.

The i.r. data λ_{max} (μ): 3.2, 3.41, 6.65, 6.89, 8.62, 9.87, 10.6, 11.28, 12.49, 13.73; n.m.r. data (δ): 7.2 (2H), 6.15 (2H), 5.90 (2H), 2.18 (4H), and 1.42 (6H).

Anal. Calcd. for $C_{14}H_{16}O_2$ (**7**) (mol. wt. 216): C, 77.76; H, 7.40. Found (216): C, 77.83; H, 7.46.

A second fraction boiled at 200–205° (1–2 Torr) and weighed 17.55 g (9.6%). The product from the distillation was a light-yellow oil which formed crystals on standing at room temperature for 12 h. The crystals were collected on a Büchner funnel and washed with cold diethyl ether to give 10.2 g of white crystals melting at 83.4–85.8°. Crystallization of the sample from hexane (8 ml/g) gave white crystals, m.p. 86.8–87.6°.

The i.r. data λ_{max} (μ): 3.2, 3.41, 6.65, 6.90, 8.21, 8.59, 9.68, 9.94, 10.32, 10.58, 12.55, 12.72, 13.55, 13.70; n.m.r. data (δ): 7.24 (2H), 6.20 (2H), 5.85 (4H), 2.14 (8H), 1.48 (12H).

Anal. Calcd. for $C_{24}H_{28}O_3$ (**8**) (mol. wt. 364): C, 79.12; H, 7.69. Found (364): C, 79.19; H, 7.60.

Condensation of Cyclohexanone with Furan (Mole Ratio 2:1) to Form 9

To a three-necked 500 ml flask, fitted with a stirrer and a reflux condenser, were added 12.8 g (0.188 mol) of furan, 37 g (0.377 mol) of cyclohexanone, and 15 ml of absolute ethanol. The solution was stirred at room temperature while 12 ml of 37% aqueous hydrochloric acid solution was added dropwise over a period of 4 min. The resulting mixture was stirred for 12 h at which time the stirrer was stopped by a sticky solid in the flask. After standing for another 12 h, the product was washed twice with 50 ml of cold water. After washing twice with 15 ml of cold hexane, a yield of 20 g (21%) of white crystals was obtained. The product was crystallized from hexane and yielded 11.5 g of white crystals. The crystals were washed twice with cold 5% aqueous sodium bicarbonate solution and once with cold water to remove any residual acid. Crystallization from absolute ethanol (40 ml/g) gave 10 g of white needles, m.p. 113.5–114.8°. An additional crystallization from the same solvent yielded white needles, m.p. 114.3–115.3°.

The i.r. data λ_{max} (μ): 3.3, 3.41, 6.55, 6.90, 8.28, 9.82, 10.86, 12.50 (shoulder), 12.85 (broad); n.m.r. data (δ): 6.18 (4H), 5.92 (6H), 2.17 (12H), 1.58 (18H). Mass spectrum: M^+ 376: *m/e* 333, M^+-C_3H_7; 320, M^+-C_4H_8; 307, M^+-C_5H_9; 295, M^+-C_6H_9; 267, M^+-O=C—C_6H_9.

Anal. Calcd. for $C_{26}H_{32}O_2$ (mol. wt. 376): C, 82.93; H, 8.57. Found (376): C, 82.48; H, 8.34.

Condensation of 9 with 7 to Form 10

Dry hydrogen chloride gas was bubbled into 10 ml of dioxane until saturated at room temperature. To this solution were added 1.5 g (0.0068 mol) of **7** and 0.85 g (0.023 mol) of **9**, while stirring. After 15 min a fine solid precipitated. After standing for an additional 15 min the solid was removed by filtration and washed on the filter with cold dioxane. The crude product had m.p. 256–262°. Crystallization from dioxane gave 0.39 g (30%) of fine white crystals, m.p. 263–264°. A mixture melting point with compound **10**, prepared by condensing **7** with cyclohexanone (see below) was not depressed.

Condensation of Cyclohexanone with 3 to Form 12

In a two-necked 200 ml flask, fitted with a reflux condenser guarded by a calcium chloride tube, were placed

Can. J. Chem. Downloaded from www.nrcresearchpress.com by 210.87.254.105 on 09/05/12
For personal use only.

3.92 g (0.01 mol) of **3**, 0.98 g (0.01 mol) of cyclohexanone, and 10 ml of absolute ethanol. Dry hydrogen chloride gas was bubbled into the mixture for 25 min by which time separation into two distinct layers had occurred. A magnetic stir bar was introduced and the mixture stirred at room temperature for 5 h. The sticky product was collected on a Büchner funnel and washed with 10 ml of absolute ethanol. The product is a white solid. Crystallization from benzene and then from ethanol–benzene gave 0.98 g (21%) of white crystals, m.p. 182.3–183.3°.

The i.r. data λ_{max} (μ): 3.38, 6.41, 7.90, 8.24, 8.62, 8.98, 9.78, 10.45, 12.88; n.m.r. data (δ): 5.82 (8H), 2.0 (4H), 1.48 (24H).

Anal. Calcd. for $C_{31}H_{36}O_4$ (mol. wt. 472): C, 78.81; H, 7.63. Found (472): C, 79.08; H, 7.69.

Condensation of Acetone with 7 to Form 11

To a 50 ml flask, fitted with a reflux condenser and stirrer, were added 1.43 g (0.007 mol) of compound **7**, 3.92 g (0.135 mol) of acetone, 10 ml of absolute ethanol, and 3 ml of 37% aqueous hydrochloric acid solution. The mixture was stirred at room temperature for 17 h. The product, a sticky solid, was removed by filtration and washed with cold hexane. A yield of 0.54 g (16%) of white crystals, m.p. 198.0–203.0° was obtained. Two crystallizations from hexane (50 ml/g) gave 0.26 g of white crystals m.p. 208.2–209.2°.

The i.r. data λ_{max} (μ): 3.38, 6.41, 6.88, 8.22, 8.95, 9.73, 10.30, 12.83, 12.93, 13.98; n.m.r. data (δ): 5.81 (8H), 2.0 (8H), 1.47 (24H).

Anal. Calcd. for $C_{34}H_{40}O_4$ (mol. wt. 512): C, 79.69; H, 7.81. Found (512): C, 79.91; H, 7.68.

Condensation of Cyclohexanone with 7 to Form 10

In a 200 ml two-necked flask were placed 4.0 g (0.018 mol) of **7**, 1.82 g (0.0185 mol) of cyclohexanone, and 20 ml of absolute ethanol. Dry hydrogen chloride gas was bubbled into the mixture for 10 min. A magnetic stir bar was placed in the flask and the mixture was stirred for 48 h. The sticky product was removed by filtration on a Hirsch funnel and then was triturated in hexane. The fine white crystals were removed by filtration and weighed 0.10 g (0.91%). Crystallization from hexane yielded 0.04 g of white amorphous substance, m.p. 267–268°. When the sample was crystallized from hexane the melting point was raised to 268–269°.

The i.r. data λ_{max} (μ): 3.41, 6.42, 6.90, 8.23, 8.86, 9.81, 10.30, 12.99; n.m.r. data (δ): 5.87 (8H), 2.0 (16H), 1.4 (24H).

Anal. Calcd. for $C_{40}H_{48}O_4$ (mol. wt. 592): C, 81.08; H, 8.11. Found (592): C, 81.09; H, 8.44.

Condensation of Cyclohexanone with Pyrrole to Form 13

A solution of 16.2 g (0.242 mol) of pyrrole and 20 ml of absolute ethanol was placed in a three-necked 500 ml flask. The flask, fitted with a stirrer and reflux condenser, was placed in an ice-bath. To the stirred solution was added dropwise 1 ml of 37% aqueous hydrochloric acid solution, followed by 23.7 g (0.242 mol) of cyclohexanone over a period of 20 min. The stirrer was stopped by the solid formed in the flask when the addition of cyclohexanone was complete. After standing at room temperature for 1 h, the product was washed with 50 ml of cold water. The solid was removed from the flask by partial dissolution in ether. The total yield of crude was 12.86 g (9.0%). Several crystallizations of the product from benzene and then from hexane gave white crystals, m.p. 272.0–272.5°. The melting point reported by Chelintzev *et al.* (8) is 272.0°.

The i.r. data λ_{max} (μ): 3.42, 6.35, 6.90, 7.05, 8.43, 9.55, 13.7 (broad), 14.15; n.m.r. data (δ): 7.45 (broad), 5.87 and 5.83 (8H), 1.93 (16H), 1.41 (24H). After deuteration (solvent, dioxane) the doublet at 5.87 and 5.83 was replaced by a singlet at 5.85.

Anal. Calcd. for $C_{40}H_{52}N_4$ (mol. wt. 588): C, 81.58; H, 8.92; N, 9.52. Found (588): C, 81.67; H, 9.00; N, 9.37.

Condensation of Cyclohexanone with Pyrrole to Form 14

A solution of 26.8 g (0.400 mol) of pyrrole and 20 ml of absolute ethanol in a three-necked 500 ml flask, fitted with a magnetic stirrer and reflux condenser, was placed in an ice-bath. While stirring, 1 ml of 37% aqueous hydrochloric acid solution was added, followed by 9.8 g (0.10 mol) of cyclohexanone, the latter being added dropwise over a period of 5 min. The solution passed through color changes from reddish-brown to dark green and finally dark brown over a period of 24 h. Two phases separated when stirring was discontinued. About 25 ml of ether was added, followed by sufficient 5% aqueous sodium bicarbonate solution to neutralize the acid. The ether layer was separated and evaporated in a current of air, leaving 19.5 g of a dark-brown thick oil. On standing for 4 days the oil partially crystallized. Purification by fractional crystallization of the mixture from dilute ethanol was tedious and wasteful. Accordingly the product was fractionally distilled, yielding 6.5 g (30%) of a pale-yellow oil, boiling at 178–185° (1 Torr). The oil crystallized to a solid, m.p. 93–100°. Crystallization from 70% aqueous ethanol yielded colorless fine needles, m.p. 105–106°. The compound deteriorates rapidly on exposure to air, heat and light.

The i.r. data λ_{max} (μ): 2.91, 3.24, 3.43, 3.50, 6.50, 6.91, 9.16, 9.70, 13.65 (broad); n.m.r. data (δ): 7.06–7.50 (broad, 2H), 6.28–6.45 (multiplet, 2H), 5.95–6.10 (triplet, 4H), 1.80–2.15 (broad, 5H), 1.33–1.70 (broad, 5H).

Anal. Calcd. for $C_{14}H_{18}N_2$ (mol. wt. 214): C, 78.45; H, 8.47; N, 13.08. Found (214): C, 78.40; H, 8.44; N, 13.12.

Condensation of Cyclohexanone with 14 to Form 13

Compound **14** (0.002 mol) was treated with 0.98 g (0.10 mol) of cyclohexanone at 0° using concentrated aqueous hydrochloric acid as catalyst. A yield of 83% of purple crystals resulted. Crystallization of the crude product from hexane and then from acetone–water gave white crystals, m.p. 272°. A mixture melting point with **13**, obtained as described above by the condensation of cyclohexanone with pyrrole, showed no depression.

B.J.H. is grateful to the National Research Council of Canada for financial assistance.

We are indebted to Dr. D. B. MacLean, Department of Chemistry, McMaster University, Hamilton, Ontario, for the determination of some mass spectra, to Dr. C. A. Fyfe for assistance with the 100 MHz proton resonance spectra, and to Mr. T. W. Hall for technical assistance in preparing some of the compounds.

Most of the microanalyses were carried out by Uniroyal Limited Research Laboratories, Guelph, Ontario.

1. R. G. ACKMAN, W. H. BROWN, and G. F. WRIGHT. J. Org. Chem. **20**, 1147 (1955).
2. R. E. BEALS and W. H. BROWN. J. Org. Chem. **21**, 447 (1956).
3. W. H. BROWN and H. SAWATZKY. Can. J. Chem. **34**, 1147 (1956).
4. W. H. BROWN and W. N. FRENCH. Can. J. Chem. **36**, 537 (1958).
5. A. BAEYER. Ber. **19**, 2184 (1886).
6. M. DENNSTEDT and J. ZIMMERMAN. Ber. **23**, 1370 (1890).
7. V. V. CHELINTZEV and B. V. TRONOV. J. Russ. Phys. Chem. Soc. **48**, 105 (1916); Chem. Abstr. **11**, 452 (1917).
8. V. V. CHELINTZEV, B. V. TRONOV, and S. G. KARMANOV. J. Russ. Phys. Chem. Soc. **48**, 1210 (1916); Chem. Abstr. **11**, 1418 (1917).
9. G. S. REDDY and J. H. GOLDSTEIN. J. Phys. Chem., **65**, 1539 (1961).
10. R. J. ABRAHAM and H. J. BERNSTEIN. Can. J. Chem. **39**, 905 (1961).
11. S. GRONOWITZ, A. HORNFELDT, B. GESTBLOM, and R. A. HOFFMAN. Arkiv. Kemi. **18**, 133 (1961).
12. A. R. KATRITZKY. Physical methods in heterocyclic chemistry. Vol. II. Academic Press, New York and London, 1963. pp. 128–133.
13. R. G. ACKMAN, WILLIAM H. BROWN, and GEORGE F. WRIGHT. J. Org. Chem. **20**, 1150 (1955).
14. A. PATTERSON, L. CAPEL, and D. WALKER. The ring index. 2nd ed. November, 1959. p. 756.

Can. J. Chem. Downloaded from www.nrcresearchpress.com by 210.87.254.105 on 09/05/12
For personal use only.

Can. J. Chem. Downloaded from www.nrcresearchpress.com by 210.87.254.105 on 09/05/12
For personal use only.

The Pyrolysis of Cumene, *p*-Cymene, and α-Methylstyrene at 800 °C

RAY F. SEVERSON, WALTER H. SCHULLER, AND RAY V. LAWRENCE
Naval Stores Laboratory,[1] *Olustee, Florida 32072*

Received July 9, 1971

Cumene, *p*-cymene, and α-methylstyrene were pyrolyzed at 800 °C on Vycor glass. The products were separated by preparative g.l.p.c. and those identified were benzene, toluene, *p*-xylene, styrene, α-methylstyrene, *p*-methylstyrene, indene, *p*,α-dimethylstyrene, naphthalene, 1- and 2-methylnaphthalene, diphenyl, 2-vinylnaphthalene, acenaphthalene, fluorene, and phenanthrene. Possible mechanisms for the formation of these compounds are discussed.

Le cumène, le *p*-cymène et l'α-méthylstyrène ont été pyrolysés à 800 °C sur du verre Vycor. Les produits obtenus ont été séparés par c.p.g.l. et identifiés comme étant le benzène, le toluène, le *p*-xylène, le styrène, l'α-méthylstyrène, le *p*-méthylstyrène, l'indène, le *p*,α-diméthylstyrène, le naphtalène, le méthyl-1 et -2 naphtalène, le diphényle, le vinyl-2 naphtalène, l'acénaphtalène, le fluorène, et le phénanthrène. Les mécanismes possibles de formation de ces produits sont discutés.

Canadian Journal of Chemistry, **49**, 4023 (1971)

In the course of our study of the thermal behavior of resin acids, we discovered that very little was known about the pyrolytic behavior of the terpene-isopropyl group at high temperature. The behavior of the isopropyl moiety in the 300–700° range on catalytic surfaces has been widely studied (1–3); however, its behavior at 800° on inert Vycor glass had not been reported. It was of interest, in connection with the pyrolysis of resin acids, to determine which of the four possible primary pyrolytic reaction pathways as illustrated in Scheme 1 is the most highly favored at 800°.

Because of the thermal stability of the phenyl nucleus, two simple aromatic terpenes, cumene and *p*-cymene, and their unsaturated analog, α-methylstyrene, were chosen for this study. If a methyl rearrangement to the ring with subsequent loss of ethylene or acetylene was important, cumene and α-methylstyrene (**2**, R = H) should fragment to give a large yield of toluene (**3**) while *p*-cymene would yield *p*- or *m*-xylene depending on whether transfer to either the α- or β-carbon of the ring was important. The elimination of methane (or $CH_3\cdot + H\cdot$) from cumene and *p*-cymene would yield known styrenes (**1**) and dehydrogenation would give α-methylstyrenes (**2**), while the direct loss of the isopropyl moiety (or fragmentation of initial dehydrogenation) would produce benzene or toluene (**4**). The loss of the equivalent of methane from 2-methylstyrenes would yield phenylacetylenes (**5**).

Experimental

Cumene, *p*-cymene, and α-methylstyrene were obtained from commercial sources and were passed through alumina to remove autooxidized material just before use.[2] Toluene, *m*-xylene, cumene, indene, and 1-methylnaphthalene for use as g.l.c. standards were purified by preparative g.l.p.c. Naphthalene, diphenyl, 1,5-dimethylnaphthalene, dibenzyl, phenanthrene, 1-methylphenanthrene, and *m*- and *p*-terphenyl for g.l.c. standards were recrystallized from 95% EtOH. Tetradecane (99%) was used as purchased.

Apparatus

The pyrolysis apparatus consisted of a vertically mounted Cenco Hevi-Duty type 70T electric combustion furnace with a 12 in. heating chamber containing a Vycor glass combustion tube (30 mm o.d. × 32 cm long with a tapered end having a 3-4 mm opening and 24/40 glass joints sealed at the top and bottom) packed with an 1/8 in. diameter Vycor rod. This tube was connected to an air condenser, an ice trap, a Dry Ice trap, a gas dispersion trap (containing 15 ml of acetone), and a final Dry Ice trap. The extensive trapping system was required to trap the aerosol which formed upon cooling of the pyrolytic gases. A Temco portable indicating pyrometer was used to measure the pyrolysis tube temperature and the temperature controller was used to maintain the temperature at 800°.

Typical Pyrolysis Run

A side arm addition funnel was placed on top of the pyrolysis tube and the desired amount of N_2 (400 ml/min), as measured by a flow meter, was allowed to pass through

[1]One of the laboratories of the Southern Marketing and Nutrition Research Division, Agricultural Research Service, U. S. Department of Agriculture.

[2]We have found this procedure to be very effective in removing autooxidation products, *i.e.*, peroxides, hydroperoxides, etc., from organic materials.

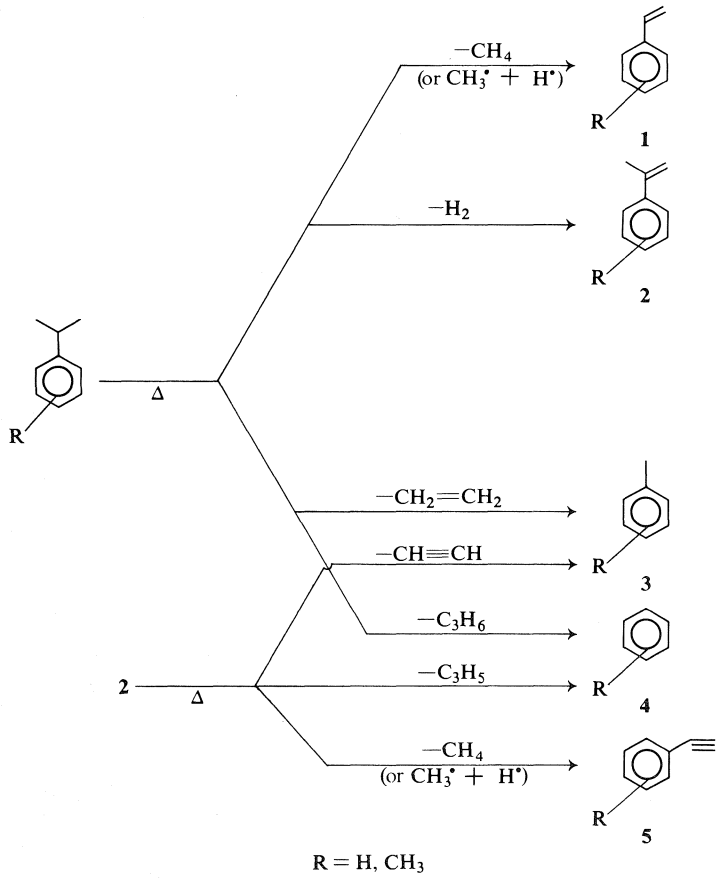

SCHEME 1

the system. When the pyrolysis temperature had stabilized, 10 g of the compound to be pyrolyzed was placed in the addition funnel and added dropwise into the pyrolysis tube. When the run was complete, the trapped material was quantitatively removed from the four traps with acetone and the samples were subjected to g.l.p.c. analysis. The last trap generally contained only acetone which had been carried over from the preceding gas dispersion trap.

Analysis of Products and Calculation of % Yield

Analytical g.l.p.c. data was obtained on an F&M 500 using a 12 ft × 1/4 in. copper column packed with 10% OV-17 on 60/70 mesh NAW Chromosorb W with a temperature program of 80–275° at 2.9°/min and He flow rate of 120 ml/min. Tetradecane was used as an internal standard and internal marker. The response factor for each product was estimated from a standard curve obtained by plotting the integration area/mg *vs.* relative retention of a standard solution of 14 representative aromatic hydrocarbons described above and tetradecane in benzene. The plot was essentially linear with a negative slope.

Identification of Products

The products identified were collected from the OV-17 column under the conditions given above. The i.r. spectra were run on a Perkin–Elmer 21, as specified. All u.v. data were obtained on a Spectronic 505 in 95% EtOH.

Benzene, 0.10 (relative retention time, tetradecane = 1.00); toluene, 0.16; *p*-xylene, 0.27; styrene, 0.33; cumene, 0.38; α-methylstyrene, 0.50; *p*-cymene, 0.52; indene, 0.64; naphthalene, 0.93; 2-methylnaphthalene, 1.13; 1-methylnaphthalene, 1.18; diphenyl, 1.31; 2-vinylnaphthalene, 1.40; acenaphthalene, 1.48; fluorene, 1.67; and phenanthrene, 2.02; all had retention times, i.r. and u.v. identical to the authentic samples.

p-Methylstyrene:[3] 0.52; i.r. and u.v. identical with literature (4).

p,α-Dimethylstyrene: 0.67; i.r. ν_{max} (CS_2) 888 (vinylidene), and 822 cm^{-1} (two adjacent ArH); u.v. λ_{max} 250 and 282–293 mμ.

Results and Discussion

Cumene, *p*-cymene, and α-methylstyrene were pyrolyzed neat at 800 °C on Vycor rod to yield

[3] *p*-Cymene and *p*-methylstyrene were not separated on OV-17 column. A 15 ft × 1/4 in. copper column packed with 10% SE-30 on 60/80 mesh NAW Chromosorb W was used to separate and identify these two components.

Can. J. Chem. Downloaded from www.nrcresearchpress.com by 210.87.254.105 on 09/05/12
For personal use only.

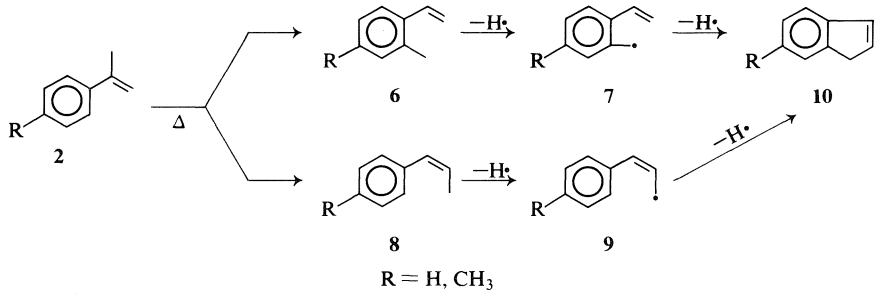

R = H, CH_3

SCHEME 2

a large number of g.l.p.c. analyzable products. Considerable gaseous and carbonaceous products were produced which were not collected or analyzed. The comparison of the yields of the 18 major products identified from this study is given in Table 1.

As shown, a fair yield of toluene and xylene was obtained. However, the amount is not substantial enough to support a methyl rearrangement mechanism. The magnitude of the yields of toluene and *p*-xylene observed in this work is generally found in the high-temperature pyrolysis of most organic materials (6–8).

However, inspection of Table 1 does give considerable information about the pyrolytic behavior of the arylisopropyl moiety at 800°. The elimination of methane[4] to yield styrenes (**1**) is greatly favored over dehydrogenation to give α-methylstyrenes (**2**) and the direct loss (or fragmentation of initial dehydrogenation) of the isopropyl group (**4**) is highly favored. The failure to isolate phenylacetylenes (**5**) would indicate that loss of methane (or its equivalent) from α-methylstyrenes is not favored or the resulting acetylene is not stable under these conditions. These observations are consistent with the relatively low yield of isopropylphenanthrenes and isopropylnaphthalenes observed in the thermal cracking of the resin acid molecule at 800° (10).

TABLE 1. Major pyrolysis products at 800 °C, contact time ≃ 3.9 s*

Compound	% Yield†		
	p-Cymene	Cumene	α-Methylstyrene
Benzene	5.8	27.0	16.2
Toluene	11.1	3.7	5.2
Xylene‡	3.1	0.6	0.6
Styrene	7.2	18.7	13.8
Cumene	—	24.2	—
α-Methylstyrene	1.7	2.8	24.3
p-Cymene	23.4	—	—
p-Methylstyrene	22.5	—	0.6
Indene	1.6	2.5	7.9
p-,α-Dimethylstyrene	4.5	—	—
Naphthalene	3.9	6.9	9.0
2-Methylnaphthalene	2.7	0.7	1.4
1-Methylnaphthalene	0.3	0.6	1.5
Diphenyl	0.3	1.1	2.6
2-Vinylnaphthalene	0.8	0.3	0.4
Acenaphthalene	0.5	0.6	1.0
Fluorene	0.2	1.2	1.6
Phenanthrene	2.1	4.0	3.8
	% g.l.c. volatile products identified		
	91.7	94.9	89.9
	% g.l.c. volatile products§		
	35.3	41.4	46.0

*Calculated according to method of Balandin and Tolstopyatov (5).
†Based on % g.l.p.c. volatile material in pyrolysate.
‡At least 90% the para isomer.
§Percent based on initial amount of compound pyrolyzed.

The relative yield of indene produced here is substantially greater than the amount observed when propylbenzene or other arylalkyl compounds are pyrolyzed (11). One possible rationale for increased indene formation is given in Scheme 2.

The dehydrogenated compound **2** would undergo methyl rearrangement to produce either the *o*-methylstyrene (**6**) or β-methyl compound **8**. Hydrogen abstraction from the arylmethyl **6** or vinyl methyl **8** would be expected to readily occur to yield intermediates **7** and **9**, which would be expected to undergo cyclization with the loss of hydrogen to give the indene **10**.

The above mechanism predicts that a substantial amount of 6-methylindene should be found during the pyrolysis of *p*-cymene. After a careful search through the pyrolysis products from *p*-cymene, the presence of the known 6-methylindene (12) could not be established. However, since the thermal stability of 6-methylindene under these conditions is not known, it would not

[4]The elimination of methane is most likely a two-step process, the first step being a loss of a methyl radical followed by the elimination or abstraction of a hydrogen atom (9).

Can. J. Chem. Downloaded from www.nrcresearchpress.com by 210.87.254.105 on 09/05/12
For personal use only.

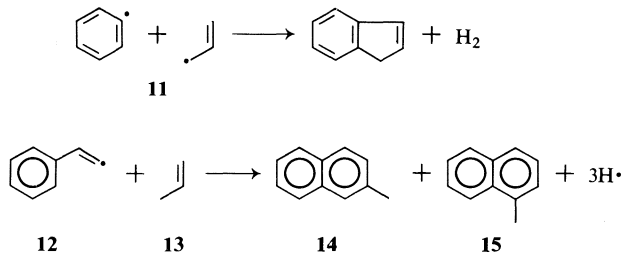

SCHEME 3

be safe to conclude that a mechanism such as Scheme 2 could not be the primary pathway for indene formation.

Another possible mode of indene formation is the attack of a C_3 unit, such as **11**, on a phenyl radical, followed by cyclization and dehydrogenation (Scheme 3). This mechanism has been previously proposed by Badger *et al.* (13) for the formation of indene during the pyrolysis of isoprene.

The high yield of naphthalene can be explained by the attack on styrene by a vinyl radical followed by cyclodehydrogenation. An analogous reaction, as shown in Scheme 3, between a styryl radical **12** and propylene **13** can be used to explain the equal yields of 2-methyl- (**14**) and 1-methylnaphthalene (**15**) obtained during the pyrolysis of α-methylstyrene and cumene. This observation of a 1:1 2-methyl- to 1-methylnaphthalene ratio, also, indicates that the main pathway for methylnaphthalene formation is via styryl propylene condensation, since it has been reported that hot tube reactions between methyl radicals and naphthalene generally greatly favor the formation of the 1-methyl compound (14).

The higher yield of 2-methyl- relative to 1-methylnaphthalene in pyrolysis products from *p*-cymene can be readily explained by the condensation of *p*-methyl styrene with a vinyl radical.

The other products in Table 1 which have not been discussed are most likely formed by coupling of pyrolysis fragments as discussed by Badger *et al.* (13) and Cohen (15).

This research was conducted while author Ray F. Severson was a National Research Council Resident Postdoctorate Research Associate, 1970. Mention of a company or product does not imply endorsement by the U.S. Department of Agriculture to the exclusion of others which may be equally suitable.

1. K. A. KOBE and R. T. ROMASN. Ind. Eng. Chem. **43**, 1755 (1943).
2. E. W. BEGRE, B. V. ROMANOVSKII, K. V. TOPCHIEVA, and HOHI THANT. Kinet. Katal. **9**, 931 (1968).
3. A. REVILLON, A. GUYOT, and Y. TRAMBOUZE. J. Chim. Phys. Physicochim. Biol. **65**, 849 (1968).
4. K. C. BRYANT, G. T. KENNEDY, and E. M. TANNER. J. Chem. Soc. 2389 (1949).
5. A. A. BALANDIN and A. A. TOLSTOPYATOV. Gen. Chem. (USSR), **17**, 2182 (1947); Chem. Abstr. **42**, 4824*i* (1948).
6. W. A. LALANDE, JR. Ind. Eng. Chem. **26**, 678 (1934).
7. E. G. HIGMAN, I. SCHMELTZ, and W. S. SCHOLOTZHAUER. Agric. and Food Chem. **18**, 636 (1970).
8. N. FRIEDMANN, H. H. BOVEE, and S. L. MILLER. J. Org. Chem. **35**, 3230 (1970).
9. J. A. KERR, A. F. TROTMAN-DICKENSON, and M. WALTER. J. Chem. Soc. 3584 (1964).
10. R. F. SEVERSON, W. H. SCHULLER, and R. V. LAWRENCE. Southeast–Southwest Regional Meeting, American Chemical Society, New Orleans, Louisiana, December 2–4, 1970; Can. J. Chem. This issue.
11. G. M. BADGER and J. M. SPOTSWOOD. J. Chem. Soc. 4420 (1960).
12. J. A. ELVIDGE and R. G. FISTER. J. Chem. Soc. 590 (1963).
13. G. M. BADGER, J. K. DONNELLY, and T. M. SPOTSWOOD. Aust. J. Chem. **19**, 1023 (1966).
14. G. P. ARMSTRONG, D. H. GROVE, D. L. HAMMICK, and H. W. THOMPSON. J. Chem. Soc. 1700 (1948).
15. S. COHEN. Progress in physical chemistry. Vol. 3. Interscience Publishers, New York, N. Y., 1965. p. 1.

Can. J. Chem. Downloaded from www.nrcresearchpress.com by 210.87.254.105 on 09/05/12
For personal use only.

The Thermal Behavior of Methyl Dehydroabietate at 600–800 °C

RAY F. SEVERSON, WALTER H. SCHULLER, AND RAY V. LAWRENCE
Naval Stores Laboratory,[1] *Olustee, Florida 32072*

Received July 9, 1971

Methyl dehydroabietate was pyrolyzed on Vycor rod at 600, 700, and 800 °C with varying contact times. Some 40–60 products were observed upon g.l.p.c. analysis, with the number of products decreasing with increasing temperature and increasing contact time at 800 °C. Considerable carbon formation was found to occur at 800 °C and long contact times. The 24 major products which could readily be separated by preparative g.l.p.c. methods were collected and identified. The high yield of naphthalene-related compounds obtained is explained by the thermal rupture of the A-ring which is initiated by elimination of the carbomethoxy moiety.

Le dihydroabiétate de méthyle a été pyrolysé sur du Vycor en tige à 600, 700, et 800 °C en faisant varier le temps de contact. Environ 40 à 60 produits ont été mis en évidence par analyse en c.p.g.l., et il a été constaté que le nombre de produits diminue lorsque la température augmente, et lorsque le temps de contact à 800 °C augmente. Des quantités de carbone importantes se forment à 800 °C lorsque le temps de contact est important. Les 24 produits majeurs qui peuvent être facilement séparés par c.p.g.l. préparative ont été obtenus et identifiés. Le rendement élevé obtenu en produits apparentés au naphtalène est expliqué en invoquant la rupture thermique du cycle-A qui est initiée par l'élimination de la partie carbométhoxy.

Canadian Journal of Chemistry, **49**, 4027 (1971)

Can. J. Chem. Downloaded from www.nrcresearchpress.com by 210.87.254.40 on 09/05/12
For personal use only.

The studies of the thermal behavior of resin acids in the past have been largely confined to relatively low temperatures (below 400 °C). It has been shown that the four conjugated dienoic resin acids and their methyl esters, neoabietic, palustric, abietic, and levopimaric, thermally isomerize, and disproportionation occurs in a slow irreversible step to yield dehydroabietic acid (1). It was thus not surprising that pot distillation decarboxylations of abietic acid and dehydroabietic acid produced the same relative mixture of hydrocarbons which retained the original phenanthrene ring system (2, 3).

In the first reported study of the reactions of resin acids under pyrolytic conditions (4), we found, at 800 °C on Vycor glass, abietic acid, levopimaric acid, dehydroabietic acid, and methyl dehydroabietate; all appeared to fragment in a similar manner to yield the same spectrum of products. In contrast to early findings at low temperature, at 800 °C, and fairly long contact times, the resin acids studied gave naphthalene derivatives as major products. No logical pyrolytic fragmentation mechanisms were deduced from the products formed under these high-temperature conditions (4).

With the assumptions that the C-ring of the dienoic resin acids would readily dehydrogenate to yield dehydroabietic acid and that methyl dehydroabietate would undergo the same pyrolytic fragmentation as the free acid, in this communication methyl dehydroabietate was pyrolyzed on Vycor glass at 600, 700, and 800 °C with varying contact times.[2] The products identified are used to propose a high-temperature pyrolytic fragmentation mechanism for conjugated dienoic resin acids.

Experimental

Methyl dehydroabietate was prepared by the reaction of the free acid with diazomethane and recrystallized from MeOH: $[\alpha]_D^{25}$ +59.8° (*c* 2.0, 95% EtOH). The pyrolysis apparatus used was the same as previously described (5). The percent yield of each product was determined by g.l.p.c. under conditions on OV-17 as reported earlier (5).

Typical Pyrolysis Run

A side-arm addition funnel was placed on top of the pyrolysis tube and the desired flow of nitrogen (400ml/min at STP), as measured by a low meter, was allowed to pass through the system. When the desired pyrolysis temperature had stabilized, 4 g of methyl dehydroabietate was melted by means of a heat lamp and added dropwise into the pyrolysis tube (the nitrogen flow was continued). When the run was complete, the trapped material was quantitatively removed with benzene and the sample was subjected to g.l.p.c. analysis.

Shorter contact times at 800 °C were obtained by

[1]One of the laboratories of the Southern Marketing and Nutrition Research Division, Agricultural Research Service, U. S. Department of Agriculture.

[2]The methyl ester was used since it can be easily pyrolyzed in the absence of solvent.

Can. J. Chem. Downloaded from www.nrcresearchpress.com by 210.87.254.40 on 09/05/12
For personal use only.

running the pyrolysis experiments at reduced pressure in the presence of nitrogen (400 ml/min at STP). A pressure regulator and a 33-l surge tank, placed after the trapping system, were used to maintain a constant pressure. The pressure readings were taken at the nitrogen inlet to the pyrolysis system. The 800° runs were run at pressures of 760 (contact time, 2.6 s), 449 (1.5 s), 104 (0.36 s), and 21 Torr (0.07 s).

Equation 1 was used to calculate contact times (τ) with the corresponding corrections being made when atmospheric pressure was not used. In eq. 1: V, free vol-

$$[1] \qquad \tau\ (s) = \frac{(60)\ (273)\ V}{(22\ 410)\ (M/t + a)\ T}$$

ume of tube in the heated area (volume of tube minus volume occupied by packing); M, moles of organic material being pyrolyzed at atmospheric pressure; t, addition time in min; a, velocity of carrier gas ml/min (nitrogen); T, absolute temperature of pyrolysis tube. All calculations were made assuming ideal gas behavior.

Preparative Gas–Liquid Phase Chromatography of Products

The products were collected in four fractions from the OV-17 column (Fraction I, OV-17 relative retention times 0.10 to 0.93; Fraction II, OV-17 relative retention times 1.13 to 1.40; Fraction III, OV-17 relative retention times 1.48 to 1.96; and Fraction IV, OV-17 relative retention times above 1.96). The products were re-collected off a 15 ft × 1/4 in. copper column packed with 10% SE-30 on 60/80 mesh NAW Chromosorb W with a flow rate of 90 ml/min of He under temperature conditions as given below.

Identification of Products

The i.r. spectra were run on a Perkin–Elmer 21 as specified. All u.v. data was obtained on a Spectronic 505 in 95% EtOH.

Mass spectra were obtained on a CEC 21-110B mass spectrometer by the direct inlet technique.

Products from Fraction I, Collected from SE-30 Column Using a Program 80–125° at 2.9°/min

Benzene

OV-17, 0.10;[3] SE-30, 2.7;[4] retention time and u.v. identical to authentic sample.

Toluene

OV-17, 0.16; SE-30, 4.5; retention time, i.r., and u.v. identical to authentic sample.

p-Xylene

OV-17. 0.27; SE-30, 5.4; retention time and u.v. identical to known compound.

Styrene

OV-17, 0.33; SE-30, 9.6; retention time, i.r., and u.v. identical to authentic sample.

α-Methylstyrene

OV-17, 0.50; SE-30, 14.0; retention time and u.v. identical to known compound.

[3]Retention time on OV-17 under conditions previously reported relative to tetradecane (relative retention time, 1.00) (5).

[4]Retention time (min) on SE-30 relative to point of injection.

Indene

OV-17, 0.64; SE-30, 16.1; retention time, i.r., and u.v. identical to authentic sample.

Naphthalene

OV-17, 0.93; SE-30, 23.6; retention time, i.r., and u.v. identical to authentic sample.

Products from Fraction II, Collected from SE-30 Column at 135°

2-Methylnaphthalene

OV-17, 1.13; SE-30, 17.8; retention time, i.r., and u.v. identical to known compound.

1-Methylnaphthalene

OV-17, 1.18; SE-30, 18.0; retention time, i.r., and u.v. identical to authentic sample.

1-Vinylnaphthalene

OV-17, 1.30; SE-30, 29.9; $\nu_{max}(CS_2)$, 983 and 914 (vinyl), 798 (three adjacent ArH), and 773 cm^{-1} (four adjacent ArH); u.v. data identical to literature (6).

2-Vinylnaphthalene

OV-17, 1.40; SE-30, 36.2; retention time, i.r., and u.v. identical to authentic sample.

Products from Fraction III, Collected from SE-30 Column at 160°

Acenaphthalene

OV-17, 1.38; SE-30, 11.8; retention time, i.r., and u.v. identical to authentic sample.

Acenaphthene

OV-17, 1.52; SE-30, 13.5; retention time, i.r., and u.v. identical to known compound.

2-Isopropenylnaphthalene

OV-17, 1.54; SE-30, 15.7; ν_{max} (CS_2), 895 (vinylidene and one ArH), 822 (two adjacent ArH), and 752 cm^{-1} (four adjacent ArH); u.v. data identical to literature (7); mass spectrum m/e, 168, 153 (M-CH_3), 152 (M-CH_4), and 141 (M-CH_2=CH).

1-Methyl-6-vinylnaphthalene

OV-17, 1.57; SE-30, 16.7; i.r. ν_{max} (CS_2), 983 and 895 (vinyl), 875 (one ArH), 827 and 833 (two adjacent ArH), and 810 and 750 cm^{-1} (three adjacent ArH); u.v. λ_{max} 238, 245, 253.5, 276, 285, and 295.5 mμ; mass spectrum m/e, 168, 152 (M-CH_3), and 141 (M-CH_2=CH). General i.r. spectra is consistent with 1,6-disubstituted naphthalene (9, 10). The u.v. spectra has the general characteristics of a 2-vinylnaphthalene (6, 7) with a slight bathochromic shift due to increased alkyl substitution (8).

1-Methyl-2-vinylnaphthalene

OV-17, 1.61; SE-30, 17.7; i.r. ν_{max} (CS_2), 984 and 897 (vinyl), 818 (two adjacent ArH), and 780 and 758 cm^{-1} (four adjacent ArH); u.v. λ_{max} 245.5, 253.5, 267, 277, 287, and 298.5 mμ; mass spectrum m/e, 168, 153 (M-CH_3), and 141 (M-CH_2=CH).

1-Methyl-6-isopropylnaphthalene

OV-17, 1.65; SE-30, 19.5; i.r. ν_{max} (CS_2), 873 (one ArH), 816 (two adjacent ArH), and 772 cm^{-1} (three adjacent ArH); u.v. λ_{max} 210, 227.5, 261–264, 271.5, 289, 293, and 300.5 mμ; mass spectrum m/e, 184, 169 (M-CH_3), 153 (169-CH_4), and 141 (M-C_3H_7).

A Substituted Vinylnaphthalene

OV-17, 1.73; SE-30, 24.0; i.r. ν_{max} (CS_2), 983 and 902 (vinyl), 840, 766, 746, 734, 272, and 683 cm^{-1}; mass

Can. J. Chem. Downloaded from www.nrcresearchpress.com by 210.87.254.40 on 09/05/12
For personal use only.

spectrum *m/e*, 184, 182, 180, 178, 169, 167, 165, 157, 155, and 153; u.v. λ_{max} 208.5, 230, 245.5, 277, 287.5, and 299 mμ; data is consistent with a 1- or 2-vinylnaphthalene derivative.

1-Ethyl-6-vinylnaphthalene

OV-17, 1.76, SE-30, 25.5; i.r. ν_{max} (CS_2), 983 and 900 (vinyl), 880 (one ArH), 808 (two adjacent ArH), and 760 cm^{-1} (three adjacent ArH); u.v. λ_{max} 246, 253, 277, 285.5, and 296 mμ; mass spectrum *m/e* 182, 180 ($M-H_2$), 178 ($M-2H_2$), 167 ($M-CH_3$), 165 ($182-CH_3$) 155 ($M-CH{=}CH_2$), 154 ($M-CH_2{=}CH_2$), and 153 ($M-CH_2CH_3$).

2,6-Divinylnaphthalene

OV-17, 1.83; SE-30, 27.5; i.r. ν_{max} (CS_2), 984 and 900 (vinyl), 888 (one ArH), and 810 cm^{-1} (two adjacent ArH); u.v. λ_{max} 232, 240–242, 254.5, 286.5, 297, and 310 mμ; mass spectrum *m/e*, 180, 178 ($M-H_2$), 154 ($M-CH{=}CH$), 153 ($M-CH{=}CH_2$), and 152 ($M-CH_2{=}CH_2$).

4-Vinylacenaphthalene

OV-17, 1.86; SE-30, 29.7; i.r. ν_{max} (CS_2), 982 and 902 (vinyl), 873 (one ArH), 763 (three adjacent ArH), and 728 cm^{-1} (*cis*, $CH{=}CH$); u.v. λ_{max} 211, 232.5, 254.5, 263–264, 323, and 334 mμ; mass spectrum *m/e*, 178, 176 ($M-H_2$), 165 (M-CH), 164 ($M-CH_2$), 163 ($M-CH_3$), 153 ($M-CH{=}C$), 152 ($M-CH{\equiv}CH$), 151 ($M-CH{=}CH_2$), and 150 ($M-CH_2{=}CH_2$).

4-Vinylacenaphthene

OV-17, 1.92; SE-30, 34.5; i.r. ν_{max} (CS_2), 983 and 900 (vinyl), 870 (one ArH), and 764 cm^{-1} (three adjacent ArH); u.v. λ_{max} 247, 256, 284, 294, 306, 330, and 345 mμ; mass spectrum *m/e*, 180, 178 ($M-H_2$), 176 ($M-2H_2$), 167 (M-CH), 166 ($M-CH_2$), 165 ($M-CH_3$), 153 ($M-CH{=}CH_2$), and 152 ($M-CH_2{=}CH_2$).

4-Isopropylacenaphthene

OV-17, 1.96; SE-30, 36.3; i.r. ν_{max} (CS_2) 862 (one ArH) and 762 cm^{-1} (three adjacent ArH); u.v. λ_{max} 231, 249, 290 (282–290 broad, unresolved), and 323 mμ; mass spectrum *m/e*, 196, 183 (M-CH), 182 ($M-CH_2$), 181 ($M-CH_3$), 180 ($M-CH_4$), 168 ($M-CH_2{=}CH_2$), 167 ($M-CH_2CH_3$), 166 ($M-CH_2{=}CH_2$, H_2), 165 ($M-CH_3$, CH_4), 154 (M-isopropenyl), and 153 (M-isopropyl).

Products from Fraction IV, Collected from 10% SE-30 Column Using a Temperature Program 215–275° at 2.9°/min

Phenanthrene

OV-17, 2.02; SE-30, 8.0; retention time, i.r., and u.v. identical to authentic sample.

1-Methylphenanthrene

OV-17, 2.11; SE-30, 10.8; retention time and u.v. identical to known compound.

Results and Discussion

Methyl dehydroabietate was pyrolyzed neat on Vycor rod at 600, 700, and 800 °C with varying contact times. Some 40–60 different products were observed upon g.l.p.c. analysis, with the number of products decreasing with increasing temperature and increasing contact time at 800 °C. Only those compounds which could be readily separated by g.l.p.c. methods and present in approximately a 1% yield were collected and identified. The 24 major products identified and their relative yields are given in Table 1. Considerable carbon formation was observed at 800 °C and long contact times.

The amount of carbonaceous products decreased with decreasing contact time and temperature. Also in the 800°, 2.9 s contact time run, the products were taken up in acetone and a 7% yield of benzene was observed.

Examination of Table 1 shows the following trends: as temperature increases and contact time at 800° increases, the products tend to fragment to the most thermally stable aromatic compounds, *i.e.*, naphthalene, acenaphthylene, and phenanthrenes,[5] and the yield of g.l.p.c. volatile products decreases.

Thus, the compounds found at 800 °C and a long contact time from the pyrolysis of abietic, levopimaric, and dehydroabietic acid (5) have resulted from considerable fragmentation of the initially formed products. However, the products identified at lower temperatures and shorter contact times do give sufficient information to allow for reasonable explanation of the pyrolytic fragmentation pathways of the dienoic resin acids and dehydroabietic acid.

The large yield of naphthalene and naphthalene derivatives must arise from cleavage in the A-ring of the parent molecule. Precedence for rupture of the A-ring is the fact that all compounds studied previously are converted to dehydroabietic acid under relatively mild conditions (1, 4, 11) and the phenyl nucleus is very stable to heat (12). Cleavage of the A-ring is most likely facilitated by the ease with which resin acids undergo decarboxylation (differential thermal analysis and thermogravimetric analysis show that resin acids began to readily decarboxylate at 275 °C (13)) since fragmentation does not appear to readily occur until the carboxylate moiety is lost. In all the high-temperature studies to date only decarboxylated products have been isolated.

The initial fragmentation of methyl dehydro-

[5]We found that at 800 °C, contact time 3.9 s, in benzene solution, 2-vinylnaphthalene yielded toluene, styrene (6%), naphthalene (27%), 2-methylnaphthalene (5%), phenanthrene (3%), and 33% unreacted; 1-methylnaphthalene yielded toluene (2%), naphthalene (17%), 2-methylnaphthalene (2%), and 72% unreacted; acenaphthene yielded naphthalene (8%), acenaphthylene (72%), and 1% unreacted. Naphthalene, acenaphthylene, and phenanthrene were very stable under the pyrolysis conditions.

TABLE 1. Products identified from the pyrolysis of methyl dehydroabietate*

	% Yield†					
Pyrolysis temperature (°C):	600	700	800			
Compound Contact time (s)(4):	2.7	2.4	2.6	1.5	0.36	0.07
Toluene	2.8	3.1	2.7	3.4	2.6	1.8
p-Xylene	0.5	1.0	0.5	0.3	0.3	0.5
Styrene	0.4	0.2	1.1	0.8	1.3	0.8
α-Methylstyrene	1.4	1.4	—	0.2	1.0	0.9
Indene	0.6	1.8	1.8	0.8	1.3	1.3
Naphthalene	0.3	2.2	20.7	22.1	15.7	4.6
2-Methylnaphthalene	0.4	2.1	5.3	4.0	3.8	1.7
1-Methylnaphthalene	0.3	1.9	2.8	1.7	2.4	1.5
1-Vinylnaphthalene	4.3	2.5	1.3	1.1	1.3	1.4
2-Vinylnaphthalene	3.7	10.0	7.3	6.2	10.4	10.8
Acenaphthylene	1.3	4.3	9.6	11.0	13.0	4.6
Acenaphthene	1.8	4.0	1.3	1.0	2.3	2.2
2-Isopropenylnaphthalene	1.3	5.2	—	—	—	3.2
1-Methyl-6-vinylnaphthalene	3.3	4.8	1.8	0.5	1.5	2.7
1-Methyl-2-vinylnaphthalene	4.5	5.9	1.4	0.3	1.7	3.9
1-Methyl-6-isopropylnaphthalene	2.6	1.6	1.1	0.9	1.0	1.7
A Vinylnaphthalene	1.8	4.7	1.2	0.8	1.6	4.7
1-Ethyl-6-vinylnaphthalene	2.7	1.7	0.9	1.1	1.8	3.1
2,6-Divinylnaphthalene	4.1	2.8	—	—	0.4	1.5
4-Vinylacenaphthalene	2.7	1.3	2.1	1.0	3.9	7.2
4-Vinylacenaphthene	4.3	5.2	—	—	1.2	4.6
4-Isopropylacenaphthene	1.0	2.4	—	—	0.6	1.5
Phenanthrene	1.7	3.0	8.3	14.0	8.1	2.2
1-Methylphenanthrene	1.0	0.2	—	—	0.2	0.6
	% g.l.c. volatile products identified					
	48.8	73.3	78.2	71.2	77.4	69
	% Methyl dehydroabietate recovered‡					
	35.7	18.6	0.8	1.75	24.7	42.2
	%Yield of g.l.c. volatile products§					
	41.3	28.6	25.0	26.2	28.7	38

*Added neat on Vycor rod.
†Based on total amount of g.l.c. volatile material in pyrolysate, excluding methyl dehydroabietate.
‡Based on initial amount of methyl dehydroabietate used.
§Based on amount of methyl dehydroabietate reacted.

abietate (**1**) as proposed by Arbuzov and Khiamatullina (2) would be expected to result in the loss of the carbomethoxy group to yield intermediate **2** (Scheme 1). The high resolution mass spectral data on methyl dehydroabietate is also in accord with the initial formation of **2**. Labeling experiments (14) have shown that elimination of carbomethoxy group via the extraction of the 5α-hydrogen to yield the 4,5-dehydro compound **2** is the most highly favored process. Compound **2** would then be expected to thermally equilibrate to yield **3** and **4**.

Hydrocarbon **2** can undergo a retro Diels–Alder (15) reaction losing ethylene to yield **5** (Scheme 2). Aromatization and other fragmentation would yield those products indicated. The A-ring fragmentation of **3** resulting in the loss of a

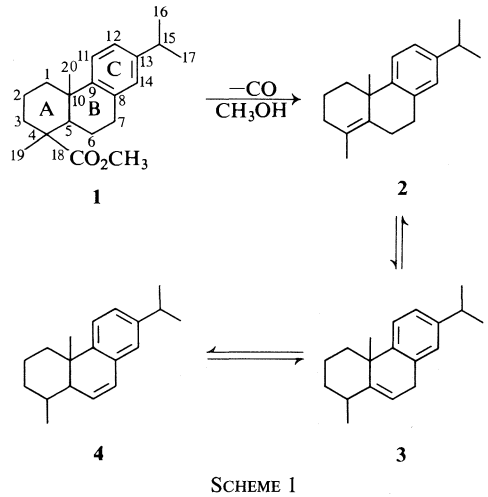

1 **2** **4** **3**

SCHEME 1

Can. J. Chem. Downloaded from www.nrcresearchpress.com by 210.87.254.40 on 09/05/12
For personal use only.

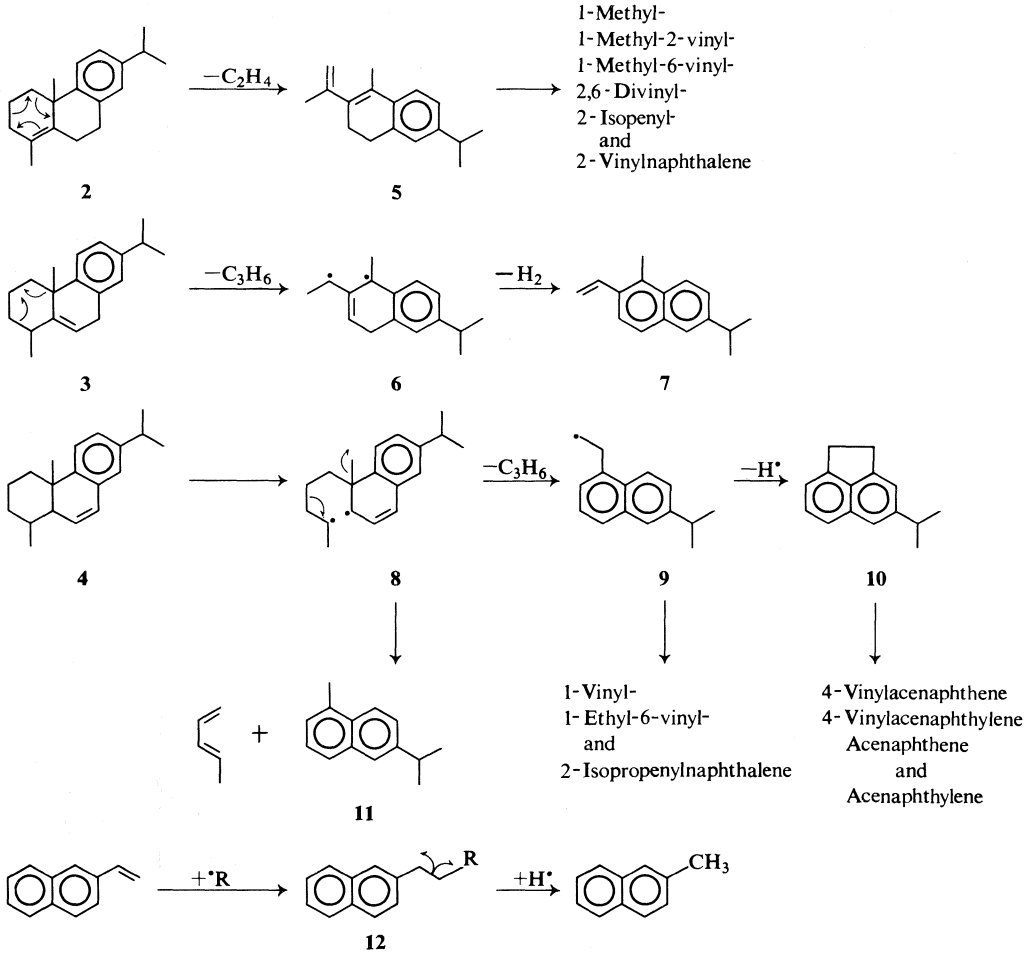

SCHEME 2

C_3H_6 fragment would yield the benzyl-allyl stabilized diradical **6**. Dehydrogenation would yield **7** which could also decompose to yield those products observed from **5**. A homolytic β-cleavage of the C_4—C_5 bond in **4** would result in the formation of the fairly stable diradical **8**. An elimination of the C-17 methyl and the loss of propene would yield 4-isopropylacenaphthene (**10**) which could continue to dehydrogenate and fragment to yield 4-vinylacenaphthene, 4-vinylacenaphthylene, acenaphthene, and acenaphthylene. β-Elimination of a hydrogen atom in **9** would give 1-vinylnaphthalene, while 1-ethyl-6-vinylnaphthalene could result from hydrogen abstraction and fragmentation of isopropyl group. The loss of ethylene from **9** and dehydrogenation of the isopropyl moiety would lead to 2-isopropenylnaphthalene. 1-Methyl-6-isopropylnaphthalene (**11**) could form directly from **8** by the elimination of a C_5 unit which could be expected to disproportionate to yield 1-methylbutadiene.

The higher yield of 2-methyl- relative to 1-methylnaphthalene was an unexpected observation. The cleavage of the A-ring of the resin acid molecule would directly lead to the 1-methyl derivative. Rearrangement of C-19 or -20 methyls to the 5 position or one of the isopropyl methyls to the 12 or 13 position would be required to produce a 2-methylnaphthalene directly from the parent molecule. Rearrangement of the C-19 or -20 methyls was not appealing since upon pyrolysis of 1-methylnaphthalene very little 2-methyl was formed and it has been reported (15) that hot

Can. J. Chem. Downloaded from www.nrcresearchpress.com by 210.87.254.40 on 09/05/12
For personal use only.

tube reactions between methyl radicals and naphthalene generally greatly favor the formation of the 1-methyl compound.

A study on the thermal behavior of cumene, *p*-cymene, and α-methylstyrene (5) also indicates that the high yield of 2-methylnaphthalene does not result from a methyl transfer from the isopropyl moiety to the ring system.

It thus appears that a mechanism such as proposed for the formation of toluene during the pyrolysis of styrene (12) is the most probable mode of which 2-methylnaphthalene is formed. The attack of a phenyl naphthyl, or some other radical on 2-vinylnaphthalene would result in the formation of a species such as **12**. β-Fission of the resulting ethylene linkage would be expected to occur readily, and the resulting radical could abstract hydrogen to give 2-methylnaphthalene. This mechanism is supported by the large yield of 2-methylnaphthalene obtained during the pyrolysis of 2-vinylnaphthalene.

Phenanthrene and 1-methylphenanthrene could be formed by complete aromatization of the resin acid molecule with loss of the required alkyl groups. The low yield of 1-methylphenanthrene could indicate that demethylation is a favored process or that the majority of the phenanthrene is formed by the reductive coupling of 2-vinylnaphthalene and styrene (12). The apparent complete lack of retene in the pyrolysate and increasing yield of phenanthrene with increasing temperature and longer contact times would also indicate that the primary route of phenanthrene formation is via 2-vinylnaphthalene.

The other products in Table 1 which have not been discussed are most likely formed by coupling of pyrolysis fragments as discussed by Badger *et al.* (16) and Cohen (12).

This research was conducted while author Ray F. Severson was a National Research Council Resident Postdoctorate Research Associate, 1970. The authors wish to thank Dr. Bernard A. Parkin, Jr., of the Naval Stores Laboratory for many helpful discussions and aid in developing the pyrolysis apparatus, Mr. Gordon S. Fisher of the Naval Stores Laboratory for assistance in interpretation of u.v. and i.r. spectra, and Mr. Verne W. Tripp and Mr. James B. Stanley of the Southern Regional Research Laboratory, SMNRD, for mass spectral analysis.

1. H. Takeda, W. H. Schuller, and R. V. Lawrence. J. Chem. Eng. Data, 89 (1969).
2. B. A. Arbuzov and A. G. Khiamatullina. Bulletin of the Academy of Sciences USSR, Div. of Chemical Science, 1520 (1961).
3. L. Ruzicka and H. Schinz. Helv. Chim. Acta, **6**, 833 (1923).
4. R. F. Severson, W. H. Schuller, and R. V. Lawrence. J. Chem. Eng. Data, In press.
5. R. F. Severson, W. H. Schuller, and R. V. Lawrence. Can. J. Chem. This issue.
6. L. H. Klemn, H. Fiffer, J. W. Sprague, and W. Hodes. J. Org. Chem. **20**, 190 (1955).
7. L. H. Klemn, W. Solomon, and A. Kohlik. J. Org. Chem. **27**, 2777 (1962).
8. R. A. Morton and J. A. de Gowcia. J. Chem. Soc., 916 (1934).
9. R. L. Werner, W. Kenard, and D. Rayson. Aust. J. Chem. **8**, 346 (1955).
10. E. E. Vago, E. M. Tanner, and K. C. Bryant. Institute of Pet. Jr. **35**, 293 (1949).
11. F. H. Max Nestler and D. F. Zinkel. Anal. Chem. **35**, 1747 (1963).
12. S. Cohen. Progress in physical chemistry. Vol. **3**, Interscience Publishers, New York, N.Y., 1965. p. 1.
13. W. H. Schuller and C. M. Conrad. J. Chem. Eng. Data, **11**, 89 (1966).
14. C. R. Enzell and I. Wahlberg. Acta Chem. Scand. **23**, 871 (1969).
15. G. P. Armstrong, D. H. Grove, D. L. Hammick, and H. W. Thompson. J. Chem. Soc. 1700 (1948).
16. G. M. Badger, J. K. Donnelly, and T. M. Spotswood. Aust. J. Chem. **19**, 1023 (1966).

Can. J. Chem. Downloaded from www.nrcresearchpress.com by 210.87.254.40 on 09/05/12
For personal use only.

Photoelectron Spectra and Bonding in Some Halosilanes

D. C. Frost, F. G. Herring, A. Katrib, and R. A. N. McLean
The Department of Chemistry, University of British Columbia, Vancouver 8, British Columbia

and

J. E. Drake and N. P. C. Westwood
Department of Chemistry, University of Windsor, Windsor, Ontario

Received June 29, 1971

The photoelectron spectra of some halosilanes, SiH_3X (X = F, Cl, Br), SiH_2X_2 (X = F, Cl), and $SiHCl_3$ have been studied, to obtain information on the bonding, especially (p → d)π back-bonding to silicon. The spectra were assigned on simple orbital overlap grounds, by comparison with the carbon analogues and by use of CNDO/2 calculations. Few discrepancies were found, but in these cases the first method was preferred. There is ample evidence from the individual ionization potentials and by comparison of the spectra with those of the analogous carbon compounds for interaction of the halogen pπ electrons with the silicon d orbitals. This is also indicated by some empirical calculations on the chlorosilanes, which also confirm the assignment of the spectra.

It can also be shown that the ionization potentials are consistent with the silicon–halogen σ bond strength decreasing through the series $H_3SiF > H_3SiCl > H_3SiBr$.

Les spectres photoélectroniques de quelques halosilanes SiH_3X (X = F, Cl, Br), SiH_2X_2 (X = F, Cl), et $SiHCl_3$ ont permis d'étudier le mode de liaison au silicium et plus particulièrement le renforcement de la liaison π(p → d). Les spectres sont attribués en considérant le simple recouvrement des orbitales par comparaison avec les analogues du carbone et en utilisant les calculs CNDO/2. Bien que les résultats soient peu divergents, on préfère dans ces cas, utiliser la première méthode. L'interaction entre les électrons pπ des halogènes et les orbitales d du silicium, est fortement mise en évidence par les potentiels d'ionisation individuels et par comparaison avec les spectres des composés analogues du carbone. Elle est montrée aussi par quelques calculs empiriques qui confirment également l'attribution de spectres.

Il est aussi possible de montrer que les potentiels d'ionisation sont en accord avec la force de la liaison entre le silicium et l'halogène, qui décroît dans la séquence: $H_3SiF > H_3SiCl > H_3SiBr$.

Canadian Journal of Chemistry, **49**, 4033 (1971)

Introduction

Many of the properties of compounds containing silicon bonded to elements with π electrons, either lone pair or bonding have been explained in terms of the interaction of the π orbital with a symmetry related d orbital on silicon to form a (p → d)π bond. A recent review gives an excellent survey of the available evidence (1), but we particularly refer to the physical properties in a series of silicon compounds, which do not conform to what would be expected by simply comparing with the carbon analogues, taking into account the electronegativity difference. Among such properties there are changes in shape and opening of bond angles, anomalously short Si—X bond lengths, bond energies which are greater than expected, low base strengths and dipole moments of silyl species, and higher transition energies in u.v. spectra (see also ref. 2).

Although (p → d)π bonding seems a reasonable explanation for most of these observations (there are some anomalies where it is not, *e.g.* n.m.r. chemical shifts (1)), there is very little real evidence that this is the cause and not any other. For example in one good calculation which shows the presence of (p → d)π bonding in trisilylamine (3), it was recognized that the "lone pair" can interact with an e orbital on the SiH_3 group which may only have a small amount of d character.

We set out therefore to use photoelectron (p.e.) spectroscopy to discover more of the nature of the π or "lone pair" electrons on the atom adjacent to silicon. One would expect on electronegativity grounds that the ionization potential (i.p.) of these π electrons would move to lower energy compared to the carbon analogue, and any deviation from this would indicate that these electrons were involved in bonding with the silicon atoms or groups including the silicon atom. Examination of the other i.p.'s of the molecule could aid with the assignment of the type of interaction involved. If the electrons on the carbon analogue were virtually non-bonding, ionization would produce a species with a very similar

Can. J. Chem. Downloaded from www.nrcresearchpress.com by 210.87.254.5 on 09/05/12
For personal use only.

Can. J. Chem. Downloaded from www.nrcresearchpress.com by 210.87.254.5 on 09/05/12
For personal use only.

Franck–Condon envelope and hence a fairly sharp band in the p.e. spectrum. Should the electrons on the silicon species be involved in some bonding there would be a change in geometry on ionization and excitation to several vibrational levels could be expected, *i.e.* a broader band would be produced.

Due to our interest in organometallic bases (4*a*), it was decided first to investigate the available methyl silicon compound with atoms of groups **5**, **6**, and **7** attached to the silicon (4*b*). However, it was soon discovered that ionization from orbitals situated mainly on the methyl groups interfered so much to make reasonable deductions difficult. It was then decided to study some simple non-methylated silyl compounds, and the most readily available of these were the halo-silanes, SiH_nX_{4-n}(n = 0–3.) The tetrahalosilanes had already been studied (5–8*a*), although only in the case of SiF_4 was any particular attention paid to the involvement of Si d orbitals (5). (More recently Bassett and Lloyd (8*b*) have also considered d orbital interactions.) In this case CNDO/2 calculations were performed with and without the inclusion of Si d orbitals in the basis set and better agreement with the observed spectrum was obtained with the former.

Two main reasons for choosing the halosilanes were that (*a*) they are the simplest species known with a "lone pair" atom attached to silicon, which should result in obtaining the maximum amount of information from the p.e. spectra and (*b*) many physicochemical studies have been carried out on them and it would be useful to compare the results of these methods with the p.e. spectra. Some of the anomalous properties of the halosilanes which it would be hoped could be rationalized are as follows (1, 2, 9): (*1*) The silicon–halogen bond lengths are less than the sum of the Pauling radii with most disagreement for the lighter halogens, but through the whole series of halosilanes there is very little change in the silicon–hydrogen bond length. (*2*) All SiH_3X species have lower dipole moments and nuclear quadrupole coupling constants than the analogous carbon compounds. (*3*) The Si–X bond energies are higher than estimated on the basis of comparison of the ratio of the energies of the silicon and carbon analogues with that of SiH_4 and CH_4. (*4*) The u.v. absorptions of SiH_3Cl are shifted to shorter wavelengths compared to CH_3Cl (10). (*5*) There is very little change in the average Si—H stretching frequency through the series SiH_3X (X = F, Cl, Br, I). (*6*) Although the proton chemical shifts for most series of halosilanes move to lower field with increasing electronegativity the opposite is true through the series SiH_3F, SiH_2F_2, $SiHF_3$.

Properties *1–4* have all been rationalized in terms of (p → d)π bonding increasing the Si—X bond order (and hence the bond length (1), bond energy (5) and the stability of the electronic ground state (6)) and decreasing the lone pair character on the halogen (and hence the dipole moment and quadrupole coupling constant). If there is as expected very little use of d orbitals in the Si—H bonds then the properties of these bonds would not vary much with the halogen as the most electronegative would have the greatest (p → d)π bonding and thus the charge at the silicon would vary little. Any interaction of the "lone pair" orbitals with Si—H σ orbitals was of course considered negligible. This would then explain properties *1* and *5*. Of course, in the days when n.m.r. chemical shifts were considered purely as a function of electronegativity this would conflict slightly with the first part of property *6*, although even here the difference through a series was not as great as in the analogous series of carbon compounds. The deviation in the fluoro series was rationalized as being due to increased (p → d)π bonding.

As many of the properties of the halosilanes depend on the postulated (p → d)π bonding we set out to use p.e. spectroscopy to try to determine how much influence it has. It was decided that a study of one whole series SiH_3X (X = F, Cl, Br, I) and at least one series SiH_nX_{4-n} (here X = Cl) would be sufficient with comparison with the previously studied carbon analogues to give the information needed. SiH_2F_2 was also studied. The interpretation of the p.e. spectra can be aided by using the results of semi-empirical calculations such as CNDO/2, although care must be exercized (11), so it was decided to perform such calculations on the molecules studied here. It would also be instructive to see the amount of d character obtained for the various molecular orbitals in these calculations.

After completion or our work a note appeared on some of the molecules studied here, *i.e.* the SiH_3X species (12). In this, the breadth of the lowest energy band in the p.e. spectra of X = Cl, Br, I, assigned to ionization of the mainly "lone pair" electrons, and the shift to higher energy compared to the carbon compounds, was cited

Can. J. Chem. Downloaded from www.nrcresearchpress.com by 210.87.254.5 on 09/05/12
For personal use only.

as evidence for (p → d)π bonding. The possibility of p → σ* (SiH_3) bonding was not considered as there was no excitation of any SiH vibration. However, there are a number of cases in which expected vibrations do not appear in the p.e. spectrum and we do not believe that there is sufficient evidence to discount the latter possibility. In fact, our calculations show that this effect is considerable and therefore we believe that some other indications must be looked for in the p.e. spectra of halosilanes to indicate (p → d)π bonding (13).

Experimental

SiH_3Cl and SiH_2Cl_2 were prepared according to the method of Hollandsworth *et al.* (14), by passing SiH_4 (Matheson Co.) over heated silver chloride about ten times, and collecting the products at −126° (methylcyclohexane slush). Pure SiH_3Cl was obtained by passing the products through a −112° trap (*n*-butyl bromide slush). Ninety-five percent pure SiH_2Cl_2 can be obtained by passing the residue in the −112° trap through a −95° trap (toluene slush), the residue in this case being $SiHCl_3$.

SiD_3Cl and SiD_2Cl_2 were prepared as above from SiD_4 and AgCl. SiD_4 was prepared (15) by the action of $LiAlD_4$ on $SiCl_4$ in diglyme *in vacuo*. The products are distilled through a −126° trap to remove $SiCl_4$ and solvent, and pure SiD_4 is collected at −196°.

SiH_3F and SiH_2F_2 were prepared by the reaction (16) of SiH_3Cl and SiH_2Cl_2 respectively with antimony trifluoride and purified by passing through a −126° trap (to remove chloro-silanes). These species especially were kept in the gas phase as short a time as possible.

SiH_3Br and SiH_2Br_2 were prepared by the reaction of a three to one excess of SiH_4 with BBr_3 at 0 °C for 6 h (17). SiH_3Br was obtained by passing the products through a −95° trap. The residue from the −95° trap yielded SiH_2Br_2 by passing through a −78° trap (acetone to solid CO_2). Again these species were always kept at −196°. No spectrum of SiH_2Br_2 was obtained as it seemed to decompose to SiH_4, HBr, and SiH_3Br in our spectrometer.

The purity of all samples was tested by comparing the n.m.r. and i.r. spectra with the literature values for the pure species (18, 19). The samples were stored at −196° until used.

The p.e. spectrometer employed a 180 degree 4 in. radius analyzer, and the 21.22 eV radiation emanated from a 2450 mHz microwave discharge in helium.

The approximate molecular orbital calculations performed in this work were as described by Santry and Segal (20) including in the basis set 3d orbitals for all the second row elements.

The bond lengths employed were obtained for each molecule as follows: H_3SiF (21), H_2SiF_2 (22), H_3SiCl (23), H_2SiCl_2 (24), and $HSiCl_3$ (25). The bond angles were assumed to be tetrahedral.

Results and Discussion

We shall discuss the p.e. spectrum and calculations for each molecule in order, and when a series has been completed *e.g.* SiH_nX_{4-n} we shall describe the trends in the discussion of the last molecule. We have referred to the studies of the halomethanes by Potts *et al.* (26) and Dixon *et al.* (31) to aid our interpretation of the p.e. spectra of the halosilanes.

H_3SiF

The p.e. spectrum of this molecule (see Fig. 1 and Table 1) has three bands of relative intensities 2:3:1 with resolved vibrational structure in the last one, and on the high energy side of the second band. This latter structure and the intensity ratios indicate two ionization processes in the second band. The first band has two components, but as this is assigned to the e(SiH_3) orbital, it is expected to have a Jahn–Teller contour. The vertical i.p.'s for the four processes are 12.80, ≈16.13, ≈16.38 (uncertain, as this only appears as a shoulder), and 19.29 eV.

The CNDO/2 calculations including 3d orbitals on Si predict four ionization potentials below 21.22 eV at 12.3, 15.75, 17.27, and 18.42 eV, corresponding to ionization from 3e(σSiH_3), 7a_1(σF—SiH_3), 2e(*n*F), and 6a_1(Si3s) orbitals respectively (major component in brackets). Considering the approximations involved, the agreement appears reasonable.

The first band, corresponding to ionization from the 3e orbital, has maxima at 12.58 and

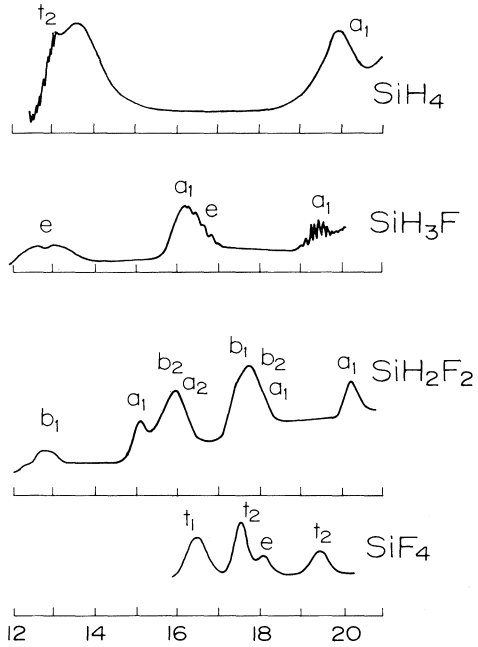

FIG. 1. Photoelectron spectra of fluorosilanes.

Can. J. Chem. Downloaded from www.nrcresearchpress.com by 210.87.254.5 on 09/05/12
For personal use only.

13.02 eV, *i.e.* a Jahn–Teller splitting of 0.44 eV which is somewhat less than that in CH_3F (0.5 eV).

The CNDO/2 calculations indicate that there is some Si—F π^* character in this mainly Si—H bonding orbital. This effect is even more obvious in CH_3F (27), and this can be seen by comparing the first i.p.'s of CH_3F and SiH_3F with those of CH_4 and SiH_4. As expected there is quite a large drop from CH_4 (13.97 eV) (27) to SiH_4 (12.60 eV) (28). However the first i.p. in CH_3F (13.04 eV) is very close to that of SiH_3F (12.80 eV); the unexpectedly large reduction in the first i.p. of CH_3F is due to the much larger π^* character compared to the SiH_3F. This in turn, could be caused by better overlap in the orbitals in CH_3F and also by the possibility of F $p\pi \rightarrow$ Si $d\pi$ interaction in SiH_3F which is not available in CH_3F.

As mentioned above, the second band extending from 15.5–16.8 eV has two components with vertical i.p.'s 16.13 and 16.58 eV, and it would appear that these correspond to the $7a_1$ and 2e orbitals predicted by CNDO/2 calculations to be at 15.75 and 17.27 eV respectively. However a Gaussian analysis of the band using the mirror image of the low energy trace to complete the curve for the first ionization process indicates relative intensities 16.13 eV curve : 16.38 eV curve of $\approx$1:1. Normally it has been observed that when two i.p.'s are close together a doubly degenerate one will have a band about twice the area of a non-degenerate one but there is no real indication of this in the present spectrum. It would have been hoped that the structure on the second component of the band would confirm the order predicted by the CNDO/2 calculations. The spacing of the five peaks of the second component are 1470, 1420, 1400, and 1340 cm^{-1}, which is most likely to correspond to a progression in the symmetric SiH_3 stretching vibration considerably reduced from 2206 cm^{-1} in SiH_3F (18). It would have been thought more likely for this mode to be excited by ionization from a_1 (mainly σ SiH_3) orbital, but if as the calculation suggests the higher energy component is the e(*n*F), then there is a considerable bonding interaction between the fluorine "lone pair" orbital and the SiH_3 bonding orbital. In fact it suggests that the 3e and 2e levels can be considered as antibonding and bonding levels respectively produced by the interaction of the fluorine $2p\pi$ and σ (SiH_3) orbitals. Although we should prefer the assignment of the structure on the basis of ionization from an a_1 orbital, it is possible to reconcile either assignment and we follow the order given by the calculation.

The 2e orbital is almost all fluorine lone pair with an almost equal small amount (5%) of Si p and d character, but from the breadth of the p.e. band this seems to be a considerable underestimation. In CH_3F the band appears to be somewhat wider and is at a higher energy ($\sim$17 eV) which is in agreement with our earlier suggestion that there is a greater interaction between the F $p\pi$ orbitals and the CH_3 moiety in CH_3F than in SiH_3F. The fact that the F lone pair electrons are at a higher orbital energy in SiH_3F than in CH_3F probably also means that there is no large stabilization of these electrons by the Si $d\pi$ orbital as is also shown in the CNDO calculations. The $7a_1$ orbital is mainly Si—H and Si—F bonding.

The third band in the spectrum consists of a progression of eight peaks from 19.10–19.81 eV with spacings of $\sim$ 800 cm^{-1}. This band is assigned to ionization from the $6a_1$ orbital in accord with the CNDO/2 calculations. The progression could be in ν_3, Si—F stretch (870 cm^{-1} in SiH_3F) or ν_2, H_3Si wag (990 in SiH_3F). As most of the bonding character in this orbital is Si—F σ bonding, one would expect the former vibration to be excited. However, this would mean a very small decrease in frequency from the molecule to the ion, which would be surprising for a bonding electron. As there is some H—F antibonding character, it is more likely that the H_3Si wag has been excited.

Purely on the evidence presented here we cannot say that there is extensive (p $\rightarrow$ d)π bonding in this molecule. Any stabilization of the F lone pair could be caused by the same type of interaction as in CH_3F.

SiH_2F_2

The p.e. spectrum of SiH_2F_2 below 21.22 eV has five distinct broad bands in the ranges (*a*) 12.3–13.4, (*b*) 14.6–15.54, (*c*) 15.54–16.67, (*d*) 16.92–18.77, and (*e*) 19.83–20.85 eV with no apparent vibrational structure. This pattern is exactly analogous to the spectrum of CH_2F_2, except that in general the bands have moved to lower energy in SiH_2F_2. Eight i.p.'s are predicted below 21.22 eV. The next i.p. is predicted to be as high as 36 eV and therefore we should expect eight

TABLE 1. Ionization potentials for SiH_3F and CH_3F

Vert.[a] i.p. (eV)	Calc. i.p. (eV)	Orbital		CH_3F (eV)
		Symmetry	Type	
12.08 (2)	12.3	e	σ(Si—H) π*(Si—F)	13.04
16.13 } (3)	15.75	a_1	σ(Si—H)	17.06
16.58 }	17.27	e	*n*(F) π(Si—F)	17.06
19.29 (1)	18.42	a_1	σ(SiH_3F)	23.40

[a]Relative intensity in brackets.

or less i.p.'s. In fact bands *c* and *d* above appear to contain two and three components respectively, as the intensity ratios for the five bands are 3:4:8:12:3 and as these have obvious shoulders. As a result eight vertical i.p.'s can be distinguished and these are listed in Table 2 along with the values obtained from the CNDO/2 calculations and assignments based on these calculations. Of course, as was shown for SiH_3F, the order of observed and calculated i.p.'s are not necessarily the same, but as there is no structure observed on the bands it is not possible to assign the spectrum otherwise.

The assignment of the first two bands to b_1 and a_1 σ(SiH_2) orbitals is essentially correct as (*a*) these orbitals are derived from the t_2 orbital of SiH_4 at ~12.60 eV (see Fig. 1) whereas the lowest energy t_1 orbital of SiF_4 is at 16.46 eV (*b*) the CNDO/2 calculations give fairly good agreement with the observed value, and the slight reduction in energies calculated is probably due to overestimation of the interaction with lower orbitals, and (*c*) the order $b_1 > a_1$ is also the order of the highest energy orbitals in CH_2F_2.

The next two lowest energy i.p.'s are calculated to be from b_2 orbitals, the lower from a F lone pair orbital and the higher a Si—F σ bonding orbital. It is surprising that these two are so close together. The a_2 orbital which is purely F lone pair in CH_2F_2 has been relatively stabilized in SiH_2F_2 and this is due to the effect of the Si 3d orbitals, and the increased distance between the F atoms (see below and ref. 13). The mainly lone pair orbitals a_2, b_1, and a_1 are all shown to be stabilized by (p → d)π bonding, and this may be the reason why they are at lower energy than the b_2 (Si—F) σ bonding orbital. Despite this explanation the position of the a_2 band is questionable as reference to Fig. 1 indicates. The a_2 orbital can only be derived from the t_1 orbital of SiF_4 and it is highly unlikely that it would move to higher energy than the t_1 orbital of SiF_4. We therefore prefer the assignment given in Fig. 1 to the calculated assignment in Table 2. All the i.p.'s of SiH_2F_2 show a slight decrease in energy compared to the analogous carbon compounds as expected, except for the lowest energy b_2 and a_2 i.p.'s. These are the lone pair orbitals which are least influenced by bonding with the σ(SiH_2) framework. If the influence of the F....F distance on the energy of these orbitals were small the relative stabilization compared to CH_2F_2 would be a better indication of (p → d)π bonding than the comparison between CH_3X and SiH_3X as these orbitals have no interaction with the σ(Si—H) system. A comparison of the spectra through the series SiH_4 → SiF_4 (see Fig. 1) should reveal some interesting points about the bonding. The bands at ~13 eV in the fluorosilanes are clearly derived from the t_2 band in SiH_4, but to get a measure of Si—H bonding it seems reasonable to try to consider the average values of all orbitals involved in mainly Si—H bonding. If we make the gross assumption that the orbitals we assign as being mainly Si—H σ bonding are purely due to this, then we can estimate the weighted average σ Si—H i.p. as SiH_4, 12.6; SiH_3F, 13.91, and SiH_2F_2, 14.03 eV. There is obviously some Si—F σ bonding involved in the a_1 orbital of the latter two, and this would cause an increase in the i.p. However as the a_1 σ(Si—F) orbital is fairly close to the lowest σ(Si—F) orbital in SiF_4 (t_2), σ(Si—F) bonding is not going to have an overwhelming effect on the lower orbital. From the figures, therefore, it is surprising that the second F atom has so little effect. The average σ M—H i.p. does not seem to give a very good indication of the bonding properties of the M—H bond, although the correct trend is indicated. For example, the average Si—H stretching frequencies (18) through the series SiH_4, SiH_3F, and SiH_2F_2 are 2189, 2201, and 2247.5 cm^{-1} which could

Can. J. Chem. Downloaded from www.nrcresearchpress.com by 210.87.254.5 on 09/05/12
For personal use only.

TABLE 2. Ionization potentials for SiH_2F_2 and CH_2F_2

Vert. i.p. (eV)	Calc. i.p. (eV)	Orbital Symmetry	Orbital Type	CH_2F_2 (eV)
12.85 (3)	12.4 (b_1)	b_1	σ(Si—H)	13.29
15.20 (4)	14.79 (a_1)	a_1	σ(Si—H)	15.25
16.07 } (8)	16.03 (b_2)	b_2	*n*(F)	15.40
16.37 }	17.16 (b_2)	a_2	*n*(F)	15.58
17.60 }	17.18 (a_2)	b_1	*n*(F), π(Si—F)	18.97
17.93 } (12)	17.58 (b_1)	a_1	*n*(F), π(Si—F)	18.97
18.30 }	18.59 (a_1)	b_1	σ(Si—F)	18.97
20.19 (3)	18.67 (a_1)	a_1	σ(Si—F)	23.9

indicate a progressive increase in Si—H bond order. A simple comparison of the lowest energy σ(Si—H) orbital also gives this expected order *i.e.* SiH_4 (12.6), SiH_3F (12.8), SiH_2F_2 (12.85 eV). Comparison of the whole series of spectra with the analogous carbon series shows almost identical positioning of the bands with respect to one another except for the relative increase in the lower b_1 and a_1 i.p.'s in SiH_2F_2. However, on the whole the bands are better resolved from ones in the silicon series. The chlorosilanes are the only series for which we have all the members $SiH_{4-n}Cl_n$(n = 0, 1, 2, 3, and 4) and the photoelectron spectra of these are shown in Fig. 2. We shall discuss each molecule separately and then compare the whole series.

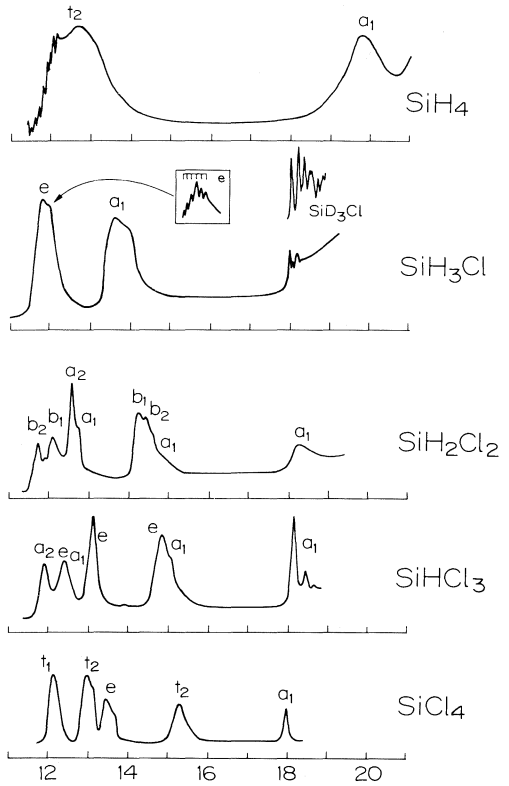

FIG. 2. Photoelectron spectra of chlorosilanes.

SiH_3Cl

SiH_3Cl has three bands below 21.2 eV in its p.e. spectrum (Fig. 2, Table 3) 11.3–12.3, 13.1–14.7, and 17.9–18.9 eV with intensity ratios 6:9:2. One expects to observe four i.p.'s below 21.22 eV corresponding to ionization from e[*n*(Cl)], a_1[σ(Si—Cl)], e[σ(SiH_3)], and a_1[σ-(SiH_3)] orbitals. The observed spectrum seems to correspond to this series if the second and third i.p.'s are together in the second band. The observed maxima for these bands are 11.65, 13.51, 13.99, and 18.23 eV respectively, and these can be compared with values of 11.42, 13.08, 13.66, and 17.16 eV obtained in a CNDO/2 calculation. However it is possible that the assignment of the second and third i.p.'s could be interchanged.

The first band has a barely resolved progression with a separation of 500 cm^{-1} which corresponds to the Si—Cl stretching vibration at 545 cm^{-1} in SiH_3Cl. This would be expected to be excited if the Cl lone pair electrons were involved in extensive bonding to the silicon. As pointed out previously (12) other indications of this influence are obvious from the spectra. Firstly, the band is much broader in SiH_3Cl (band width $w_{1/2}$ = 0.4 eV) than CH_3Cl ($w_{1/2}$ = 0.2 eV) and HCl ($w_{1/2}$ = 0.1 eV), as expected for ionization from an orbital with more bonding character. Also the band has moved to higher i.p. than in CH_3Cl, which is the opposite from what one would expect on electronegativity grounds. The CNDO/2 calculations give fairly good agreement for the energy of this i.p. but indicate that it has a high proportion of σ SiH_3 character with a fairly large π* contribution from the Cl lone pair. The major

Can. J. Chem. Downloaded from www.nrcresearchpress.com by 210.87.254.5 on 09/05/12
For personal use only.

Can. J. Chem. Downloaded from www.nrcresearchpress.com by 210.87.254.5 on 09/05/12
For personal use only.

lone pair electron density, however, is calculated to be in the second highest e orbital. This does not appear to be correct as changing the halogen atom has a much greater effect on the lower e orbital than on the upper e orbital (*cf.* SiH_3Cl and SiH_3Br below). The calculation certainly describes the orbitals correctly as the antibonding and bonding combination of Cl lone pair and $\sigma(SiH_3)$ orbitals respectively, but it appears to interchange the centers of electron density. The upper e band is broad but the components caused by Jahn–Teller distortion are not obvious as in SiH_3F and SiH_3Br, probably because of the close proximity of the a_1 band.

The a_1 band at 18.23 eV with adiabatic i.p. 18.13 eV has signs of structure. Two vibrational components separated by 1800 cm^{-1} are clearly observed but in this region the rising background and very poor signal/noise ratio prevent the assignment of further peaks. The p.e. spectrum of SiD_3Cl showed this band much more clearly and six components of separation 1320 cm^{-1} were observed (see Fig. 2). The vibration which is excited is obviously ν_1 at 2201 in SiH_3Cl and 1581 cm^{-1} in SiD_3Cl (18). The reduction in stretching frequency in the ion is as expected for the removal of an electron from a bonding orbital, which in this case is mainly $\sigma(SiH_3)$. In other respects SiD_3Cl has an almost identical spectrum to SiH_3Cl.

SiH_2Cl_2

The spectrum of SiH_2Cl_2 (see Fig. 2 and Table 4) has three distinct bands below 13 eV with maxima at 11.70, 12.09, and 12.53 eV respectively of relative intensity 1:1:2. Obviously there are two processes involved in the last band which has a shoulder at $\approx$12.76 eV. Between 13.8 and 15 eV there is a broad band three and one half times as intense as the first two bands and there is a further weak band at 18.32 eV. Eight i.p.'s are predicted below 21 eV and as a result of this and the intensity pattern three i.p.'s must be present in the broad band. Gaussian analyses revealed these components. As all the bands are structureless, comparison with CH_2Cl_2 and SiH_2F_2 CNDO/2 and empirical calculations must be used to aid assignment.

If one considers that the lone pair orbitals are not involved in bonding one would expect four low energy ionizations from a_1, b_1, a_2, and b_2 orbitals. These correspond to the in plane-out of phase, out of plane-in phase, out of plane-out of phase and in plane-in phase combinations and, as discussed earlier (26) on overlap grounds this should be the order of increasing energy. CH_2Cl_2 was assigned according to these arguments, but later reassigned with a_2 and b_1 interchanged in the basis of the empirical calculations described below. The CNDO/2 calculations do not fit well with this assignment. As can be seen from the table the calculated i.p.'s do not agree with the observed i.p.'s as well as in the other molecules particularly in the first two i.p.'s. Also the four lowest energy i.p.'s are not as clearly separated from the next set of i.p.'s as they should be. This is because the calculations predict considerable bonding character in these orbitals (see column 5 of Table 4). As discussed with SiH_3Cl, these calculations seem to sometimes overestimate the interaction between two symmetry related orbitals. In SiH_2Cl_2, this means that the b_1 and a_1 orbitals could be pushed to higher energy than the observed value and in fact we believe that this has happened in this molecule with b_1 and b_2, and a_1 and a_2 being interchanged. However, the fact that the a_2 comes at lower energy than expected compared to CH_2Cl_2 (12.22 eV) is interesting. This is the only orbital which is completely non-bonding in CH_2Cl_2 but can be stabilized in SiH_2Cl_2 by gaining some Si dπ character. The calculations also indicate that the highest b_2 orbital is mainly lone pair on the chlorine. However the highest b_2 and a_2 orbitals are calculated to have mainly σ(Si—H) character and the next highest b_1 and a_1 orbitals around 14 eV to have considerable lone pair character. This is probably too extreme but it does show that the four lowest orbitals cannot be considered as pure lone pair orbitals. The assignment we prefer for the lowest energy i.p.'s places the almost non-bonding a_2 orbital as the third band as it is the sharpest, consistent with a small change in geometry on ionization.

TABLE 3. Ionization potentials for SiH_3Cl and CH_3Cl

SiH_3Cl i.p. (eV)	Orbital		Calc. i.p. (eV)	CH_3Cl i.p. (eV)
	Symmetry	Type		
11.65 (6)	e	n(Cl) σ^*(Si—H)	11.42	11.30
13.51 } (9)	a_1	σ(Si—Cl)	13.08	14.02
13.99 }	e	σ(Si—H) π(Si—Cl)	13.66	15.40
18.23 (23)	a_1	$\sigma(SiH_3Cl)$	17.16	21.5

TABLE 4. Ionization potentials for SiH_2Cl_2 and CH_2Cl_2

Vert. i.p. (eV)	Orbital Symmetry	Orbital Type	Calc. i.p. (eV)	CH_2Cl_2
11.70 (2)	b_2	n(Cl)	10.94 (b_1)	11.40
12.09 (2)	b_1	n(Cl) σ^*(Si—H)	11.3 (b_2)	11.40
12.53 } (4)	a_2	n(Cl)	12.11 (a_1)	12.22
12.76 }	a_1	n(Cl) σ^*(Si—H)	12.58 (a_2)	12.22
14.20 }	b_2	σ(Si—Cl)	13.32 (b_2)	15.30
14.45 } (7)	a_1	σ(Si—Cl)	13.95 (b_1)	15.94
14.60 }	b_1	σ(Si—H)	14.62 (a_1)	16.77
18.32 (1:5)	a_1	$\sigma(H_2SiCl_2)$	16.56 (a_1)	20.30

TABLE 5. Ionization potentials for $SiHCl_3$ and $CHCl_3$

Obs. i.p. (eV)	Calc. i.p. (eV)	Orbital Symmetry	Orbital Type	$CHCl_3$ (eV)
11.94	10.43	a_2	n(Cl)	11.48
12.41	11.13	a_1	n(Cl)σ^*(Si—H)	11.91
12.41	11.49	e	n(Cl)	12.01
13.07	12.92	e	n(Cl)	12.85
14.75	16.64	e	σ(Si—Cl)	15.99
14.98	16.71	a_1	σ(Si—H)	16.96
18.14	16.11	a_1	$\sigma(SiHCl_3)$	19.8

The other orbitals have the same order as given by purely overlap of lone pair considerations. The preferred order is $b_2 > b_1 > a_2 > a_1$. For the mainly lone pair orbitals (b_2, a_2) the CNDO calculations give the correct order.

The 18.32 eV band is as expected an a_1 orbital being mainly Si(3s) but having (Si—H_2) and ($SiCl_2$) bonding character. The assignment of the other three i.p.'s around 14–15 eV is by no means clear. The calculation gives $b_2 > b_1 > a_1$, but it seems more reasonable for the mainly σ(Si—H) b_1 orbital to be at higher energy than the σ(Si—Cl) b_2 orbital.

$SiHCl_3$

The p.e. spectrum of $SiHCl_3$ has five distinct bands with maxima at 11.96, 12.41, 13.07, 14.75, and 18.14 eV with relative intensities 1.2:3.4:2.1:3.4:1. There is a distinct shoulder at 14.98 eV on the fourth band which is broad enough and of intensity to imply the presence of two components. We expect four low energy i.p.'s from mainly Cl lone pair orbitals, a_2, e, a_1, and e in order of increasing orbital energy. The a_1 and the first e orbital appear to be accidentally degenerate at 12.41 eV, and the intensity ratios are in good agreement with placing the a_2 at 11.94 eV and the other e at 13.07 eV. The assignment of the 11.94 eV band to the a_2 orbital is further confirmed by the narrowness of the band as this is the only pure Cl lone pair orbital, and also by the fact that the a_2 orbital is derived from the t_1 orbital of $SiCl_4$ at 12.03 eV (see Fig. 2). The shift of the a_2 band from 11.48 eV in $CHCl_3$ to 11.94 eV in $SiHCl_3$ indicates the effect of central atom size on this completely non-bonding orbital. The stabilization of this orbital in the $SiHCl_3$ shows that we cannot just consider shifts in otherwise non-bonding orbitals as an indication of (p–d)π bonding. One must consider all the "lone pair" orbitals which can possibly bond with d orbitals on the central atom. The CNDO/2 calculations also confirm the order $a_2 > a_1 > e > e$, although as for SiH_2Cl_2 the calculated i.p.'s are rather bad at lowest energy (see Table 5). The a_1 orbital is calculated to have a considerable amount of Si—H and Si—Cl bonding character as for the lowest a_1 orbital in SiH_3Cl and SiH_2Cl_2. The higher energy e orbital is mainly n(Cl) with some π (Si—Cl) whereas the lower energy e orbital has some σ(Si—Cl) character, though again it is mainly n(Cl).

The maximum at 14.75 eV is assigned as mainly the e σ(Si—Cl) and the shoulder at 14.98 to the

Can. J. Chem. Downloaded from www.nrcresearchpress.com by 210.87.254.5 on 09/05/12
For personal use only.

Can. J. Chem. Downloaded from www.nrcresearchpress.com by 210.87.254.5 on 09/05/12
For personal use only.

a_1 σ(Si—Cl) on the basis of intensity and the relation to the t_2 σ(Si—Cl) orbital of $SiCl_4$ at 15.13 eV. Although all the previous bands have had no structure, the a_1 σ($SiHCl_3$) band at 18.14 eV has three peaks separated by 2000 cm^{-1}. This progression obviously involves ν(a_1) Si—H stretch, which has a value of 2236 cm^{-1} in the neutral molecule (18). CNDO/2 calculations again indicate that this band is mainly Si(3s).

Comparison with the chloroform ($CHCl_3$) spectrum shows that the orbitals are in the same order for $SiHCl_3$ and $CHCl_3$. Again the first four bands are at lower energy in the carbon species indicating the lower bonding character of the halogen pπ electrons and greater halogen–halogen interactions. If lone pair repulsions were the only factor in determining the energy of the higher orbitals (considering them purely as lone pair orbitals) it would be expected that the range of the first four i.p.'s would be much smaller for $SiHCl_3$. In fact the separation between the first and fourth i.p. is only reduced by 0.24 eV and between first and third reduced by 0.06 eV and between the first and second it is actually increased by 0.04 eV from $CHCl_3$ to $SiHCl_3$. It can be seen that the second through fourth orbitals have been stabilized by some other means *i.e.* (p → d)π bonding compared to the non-bonding a_2 orbital. However the mainly Si—Cl σ bonding orbitals are at a higher energy (e, 14.75; a, 14.98) than the corresponding C—Cl σ bonding orbitals (e, 15.99; a, 16.96), for a weaker σ bonding system in the former case. The weighted average chlorine 'lone pair orbital' energy increases as expected on electronegativity grounds through the series; SiH_3Cl (11.65 eV), SiH_2Cl_2 (12.27 eV), $SiHCl_3$ (12.55 eV), and $SiCl_4$ (12.73 eV). The spectra of the chlorosilanes are again very similar to the corresponding series of carbon compounds, but in contrast to the fluoro compounds the bands are not as well resolved, except for the lower band of SiH_2Cl_2. As the t_2 band in SiH_4 and the lone pair bands in $SiCl_4$ occur in the same energy range (12–13.5 eV), the SiH bonding orbitals are not as well separated as in the series of fluoro compounds. However a study of the trends in Fig. 2 shows that the lowest energy i.p.'s in the chlorosilanes between 12 and 13.5 eV are mostly derived from the lone pair electrons of $SiCl_4$ and that the next set of bands (13.5–15 eV) are mainly due to σ(Si—Cl). The bands around 15 eV in SiH_2Cl_2 and $SiHCl_3$ are all derived from the t_2 band of $SiCl_4$ at 15 eV. If these bands in the halosilanes were totally due to Si—Cl σ bonding then we observe the expected decrease in the σ(Si—Cl) i.p. from $SiCl_4$ to SiH_3Cl. The bands derived from the t_2 band of SiH_4 move to lower orbital energy in the chlorosilanes (see Fig. 2) and coalesce with the bands derived from the t_2 σ(Si—Cl) orbital of $SiCl_4$. The shift to lower energy is expected on substitution of the electron withdrawing halogen atom. For example the Si—H stretching frequencies increase on substitution of a H atom. However, as there are no purely σ(SiH) bonding orbitals it is difficult to put too much stress on these arguments. One interesting point of comparison between the carbon series and silicon series is that in the former the energy separation between the highest "lone pair" i.p. and the lowest of the next set of "σ-bonding" i.p.'s is a constant 3 eV through the whole series whereas for the latter the separation is only 1.5–2 eV. This is caused by both the greater stabilization of the Cl "lone-pair" orbitals by bonding to the silicon atom, reducing the orbital energy of the lowest i.p.'s, and also by the weaker σ bonding system round the silicon atom increasing the orbital energy of the next lowest i.p.'s.

SiH_3Br

In SiH_3Br the same three bands appear as in SiH_3Cl, in this case with intensity ratios approximately 2:3:1, but the two ionization processes in the second band are better resolved (see Fig. 3). Ionization from the e(Br), a_1(SiH_3Br), e(SiH_3), and a_1(SiH_3Br) orbitals occurs at 11.00, 12.96, 13.63, and 18.04 eV respectively where the values for the two e orbitals are the average of two maxima. No CNDO/2 calculations were carried out for this molecule.

The first band of half width 0.5 eV has a spin-

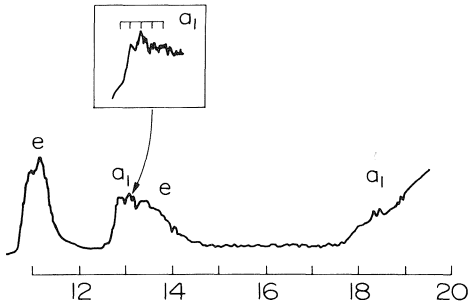

FIG. 3. Photoelectron spectrum of silyl bromide.

Can. J. Chem. Downloaded from www.nrcresearchpress.com by 210.87.254.5 on 09/05/12
For personal use only.

orbit splitting of 0.20 eV, which is more reasonable than the 0.14 eV reported previously (12), as HBr and CH_3Br have splittings of $\sim$0.30 eV (30). The half-width of the band is considerably greater than that in CH_3Br and the i.p. is 0.30 eV higher. As discussed previously, all these observations are indicative that the pπ lone pairs on the bromine atom in SiH_3Br have considerably more bonding character than those in CH_3Br. This bonding almost certainly involves the dπ orbitals on the silicon atom. There were some signs of barely resolved structure on the low energy spin-orbit component of the first band. It corresponds to a progression of $\sim$320 cm^{-1}, which seems to be too small to be the Si—Br stretch, which is at 430 cm^{-1} in the parent molecule.

Comparing the mainly lone pair i.p.'s with the carbon analogues through the series SiH_3X (X = F, Cl, Br), we observe a similar though smaller stabilization from CH_3Br (10.70 eV) to SiH_3Br (11.00 eV) as for CH_3Cl (11.30 eV) to SiH_3Cl (11.65 eV). This could be taken as an indication of slightly greater (p $\rightarrow$ d)π bonding in SiH_3Cl. Of course, as discussed earlier the lone pair orbital in SiH_3F (16.13 eV) is destabilized with respect to CH_3F (17.06 eV), as expected on electronegativity grounds, but this is probably due to greater F(pπ) $\rightarrow$ $\sigma^*(CH_3)$ bonding in the latter.

The a_1 component of the second band with maximum at 12.96 eV has three resolvable peaks with a separation of 400 cm^{-1}, corresponding to the Si—Br stretch. This is the first time structure has been observed on the a_1 band of an MH_3X system. It is rather surprising that ν(Si—Br) is excited and not $\nu(SiH_3)$ or $\delta(SiH_3)$ though evidence is possibly lost in the rest of the band, especially as the part of the band where the structure is observed has more complex structure as well as the three obvious peaks. Calculations on SiH_3Cl indicate that this orbital is nevertheless expected to be mainly Si—X σ bonding with only a small amount of Si—H_3 σ bonding, although this is less so for SiH_3F. In agreement with this, a steady decrease in this a_1 i.p. is observed through the series: SiH_3F (16.13), SiH_3Cl (13.51), SiH_3Br (12.96 eV), indicating a weakening of the σ bonding system, especially the Si—X bond, through the series. For the methyl halides a similar trend is observed except of course all of the a_1 i.p.'s are at higher energy, *viz*: CH_3F (17.06 eV), CH_3Cl (14.42 eV), and CH_3Br (13.49 eV). The overall weakening of the Si—X bond through the series can be observed from Table 6 in which we compare the Si—X bond length in SiH_3X compounds with the C—X bond length in the analogous CH_3X species (1). As the i.p.'s indicate, the Si—F bond is considerably stronger than the Si—Cl and Si—Br bonds. Multiple bonding in the Si–halogen bond is indicated by the smaller difference between r(Si—X) and r(C—X) compared to MH_3X where X = CH_3, H.

The second lowest energy e orbital ionizes to produce a band with two maxima at 13.43 and 13.83 eV *i.e.* a Jahn–Teller splitting of 0.4 eV. As can be seen in Fig. 2 this orbital is derived from the t_2 orbital in SiH_4, and ionization from this orbital produces a Jahn–Teller splitting of 0.5 eV. The splitting is not observed in SiH_3Cl as there is an overlap with the a_1 band, but in SiH_3F the splitting is 0.46 eV. These splittings are somewhat less than those observed in the analogous carbon containing compounds (0.5–0.7 eV) as would be expected for species with lower vibrational energies.

It is instructive to compare the position of this band through the series of MH_3X complexes: H_3SiF, 12.8; H_3SiCl, 13.90; H_3SiBr, 13.61; H_3CF, 13.06; H_3CCl, 15.40; H_3CBr, 15.08 eV. As expected the orbital is more stable in the silicon chloride than in the bromide and much less stable in these than in the carbon analogues. All the orbitals discussed so far are at lower energy in SiH_3Cl than in SiH_3Br. This weaker bonding possibly explains the much more ready disproportionation of the latter. The ionization potential of SiH_3F appears to be anomalously low but in this case $\sigma(SiH_3)$ is destabilized by interaction with the other low energy e orbital, the F lone pair which is at higher energy. We have already discussed the relatively lower energy of CH_3F in terms of the π contribution from the F atom. Of all the silyl halides, SiH_3F dispro-

TABLE 6. The M—X bond lengths in MH_3X species (in Å) (1)

	M		
X	C	Si	$\Delta[r(Si—X) - r(C—X)]$
F	1.384	1.595	0.211
Cl	1.781	2.048	0.267
Br	1.939	2.209	0.270
CH_3	1.534	1.867	0.333
H	1.092	1.480	0.388

TABLE 7. Ionization potentials of the non-bonding halogen orbitals[a]

Molecule	Ionic state	Ionization potentials: x–x Interaction	M—X p–pπ Interaction	M—X d–p Interaction
MH_3X	^2E	I_1	$-\gamma_1$	δ_1
MH_2X_2	$^2B_2$	$I_2+1/3(\beta_\sigma+2\beta_\pi)$	$-2/3\ \gamma_2$	$2/9\ \delta_2$
	$^2A_2$	$I_2+\beta_\pi$	-0	$4/3\ \delta_2$
	$^2B_1$	$I_2-\beta_\pi$	$-2\gamma_2$	$2/3\ \delta_2$
	$^2A_1$	$I_2-1/3(\beta_\sigma+2\beta_\pi)$	$-4/3\ \gamma_2$	$16/9\ \delta_2$
MHX_3	$^2A_2$	$I_3+1/2(\beta_\sigma+3\beta_\pi)$	0	0
	$^2E''$[b]	$I_3+1/12(\beta_\sigma+11\beta_\pi)$	$-1/6\ \gamma_3$	$57/54\ \delta_3$
	$^2E'$[b]	$I_3-1/4(\beta_\sigma+3\beta_\pi)$	$-3/2\ \gamma_3$	$3/2\ \delta_3$
	$^2A_1$	$I_3-1/6(\beta_\sigma+11\beta_\pi)$	$-8/3\ \gamma_3$	$8/9\ \delta_3$
MX_4	T_1	$I_4+1/2(\beta_\sigma+3\beta_\pi)$	0	0
	E	$I_4-1/2(\beta_\sigma-\beta_\pi)$	0	$8/3\ \delta_4$
	T_2	$I_4-1/6(\beta_\sigma+11\beta_\pi)$	$-8/3\ \gamma_4$	$8/9\ \delta_4$

[a]For full explanations of symbols see Ref. 31.
[b]These are chosen as different representatives E′ and E″ of a planar D_{3h} system. Conversion to C_{3v} produces off diagonal matrix element $-1/4(\beta_\sigma-\beta_\pi)+1/2\ \gamma_3-15/18\ \delta_3$.

TABLE 8. Comparison of calculated and observed ionization potentials for the non-bonding electrons neglecting d orbital interaction*

Molecule	Ionic state	Calculation *a* (eV)	Calculation *b* (eV)	Observed (eV)
SiH_3Cl	^2E	12.51	11.65	11.65†
SiH_2Cl_2	$^2B_2$	12.16	11.90	11.70
	$^2B_1$	12.85	12.08	12.09
	$^2A_2$	12.53	12.53	12.53†
	$^2A_1$	13.26	12.76	12.76
$SiHCl_3$	$^2A_2$	11.94	11.94	11.94†
	$^2E''$	12.54	12.24	12.41
	$^2E'$	13.22	13.07	13.07
	$^2A_1$	13.29	12.63	12.41
$SiCl_4$	$^2T_1$	12.06	12.06	12.06†
	^2E	13.43	13.44	13.44†
	$^2T_2$	13.41	12.95	12.95†

*For these results I_1, 12.51; I_2, 12.69; I_3, 12.79; I_4, 12.91; β_σ, −1.22; β_π, −0.16; γ_1, 0.86; γ_2, 0.39; γ_3, 0.25; γ_4, 0.18.
†These values were used for the calculation of the values of I_2, and β_σ(or β_π), γ_1 and γ_4.

portionates fastest, and the fact that this has the lowest energy σ-bonding electrons indicates the weaker Si—H σ bond may be the driving force behind the disproportionation.

Empirical Calculations on Chlorosilanes

After the completion of the work described in this manuscript, Dixon *et al.* (31) published a paper on the assignment of the "non-bonding" electron i.p.'s for the chloromethanes on the basis of a simple pseudo one-electron Hamiltonian. In the first approximation the matrix elements of the Hamiltonian are proportional to the overlaps between the constituent atomic orbitals and the corrections to the average chlorine "lone-pair" i.p.'s are given in terms of $\beta_\sigma = kS_{\sigma\sigma}$ and $\beta_\pi = kS_{\pi\pi}$. As this model did not give very good predictions of the observed ionization potentials, interaction with the σ bonding orbitals was included and this gave excellent agreement. The interaction was considered as being between the chlorine 2pπ orbitals and an average carbon 2p orbital and the correction to the i.p. obtained by the first model is

$$\Delta I = \frac{-x\beta_\pi^2(\mathrm{CX})}{\Delta E(\mathrm{CX})} \equiv -x_\gamma$$

where x is determined from the orbital overlaps.

Solving the equations of Table 7 without column 5 for the chlorosilanes, *i.e.* exactly analogous to the previous treatment of the chloromethanes, produces the results given in Table 8, calculation *b* (calculation *a* is the calculation including only chlorine–chlorine interaction). In these calculations, the ratio $\beta_\sigma/\beta_\pi = S_\sigma/S_\pi$ was again estimated using best atom single-zeta

Can. J. Chem. Downloaded from www.nrcresearchpress.com by 210.87.254.5 on 09/05/12
For personal use only.

Can. J. Chem. Downloaded from www.nrcresearchpress.com by 210.87.254.5 on 09/05/12
For personal use only.

Slater orbitals and a value of 7.58 was obtained. The γ_2 and γ_3 values were again obtained by interpolating $1/\gamma$ linearly between γ_1 and γ_4, although we believe this is a rather unsatisfactory procedure. All other operations were carried out as for the halomethanes. Although the agreement between calculations *b* and the observed values is good, the I values obtained are all higher than for the carbon analogues, which is impossible, as silicon is less electronegative than carbon. Also there is a small internal inconsistency in the calculations for carbon compounds, which becomes considerably greater for the silicon compounds. This arises as follows:

Dixon *et al.* calculated a value for $I_4 - I_2$ for relationship A

$$[A] \quad \tfrac{1}{2}[I(E) + I(T_1)](MCl_4) - I(A_2)(MH_2Cl_2) = I_4 - I_2$$

and the values obtained for the carbon and silicon compounds are 0.34 and 0.22 eV respectively. However, they neglected to point out that $I_4 - I_2$ can also be obtained from the relationship B

$$[B] \quad I(T_1)(MCl_4) - \tfrac{1}{2}[3I(B_2) - I(B_1)](MH_2Cl_2) = I_4 - I_2$$

and in this case the corresponding values are 0.29 and 0.56 eV respectively for the silicon series. The small error for the carbon species (0.06 eV) shows what was suspected by Dixon *et al.*, *i.e.* that the β values would not be quite constant in the series $CH_{4-n}X_n$ due to the change in electronic charge. However, we believe that this error is too small (within the error in measurement of i.p.'s) to affect the value of the method for the carbon compounds. However, along with the high I values obtained, the large difference (0.3 eV) for the silicon compounds indicates that another factor has been omitted from the equations used for the i.p.'s. It is reasonable to assume that the variation in β values through the silicon series $SiH_{4-n}X_n$ is not significantly greater than in the corresponding carbon series. The only way to obtain suitable I_n values would be to include a contribution to the i.p.'s for the interaction of the lone pairs with the silicon d orbitals. As can readily be shown, when this contribution is included (see below), relationship B for $I_4 - I_2$ is independent of this effect whereas relationship A is not. Therefore the better value of $I_4 - I_2$ is 0.56 eV.

As mentioned above the obvious improvement for the chlorosilanes would be the inclusion in the calculated i.p.'s of a term indicating d orbital participation. By analogy with the γ interaction

$$\Delta I = +x\beta_\pi{}^2 \frac{[\text{Si (3d)} - \text{Cl (2p)}]}{\Delta E[\text{Si (3d)} - \text{Cl (2p)}]} = +x\delta$$

where again x is determined by orbital overlap. The values of γ obtained are given in column 5 of Table 7. However, the inclusion of δ values presents a major problem. Without them, there were ten parameters to be found, of which three, β_π, γ_2, and γ_3 could be related to other parameters, the last two by rather a dubious process. Now there are 14 parameters and only 12 equations. Therefore more parameters have to be fixed before any predictions can be made, and additional approximations have to be made compared to the halomethanes.

First attempts were made to fix the I values at a constant ratio of the I values for the corresponding carbon species based on electronegativity differences. However it was impossible to get a suitable ratio which would give the correct value of $I_4 - I_3$, fixed at 0.12 eV and $I_4 - I_2$ fixed at 0.56 eV on our assignments. It was thought more suitable then to fix both β_σ and β_π from the carbon values, as these values principally depend on the distance between the chlorine atoms. The β values for silicon were then obtained from the carbon values by assuming k in the equations $\beta = kS$ is the same, and multiplying the carbon β values by the ratios of the appropriate overlap integrals. The calculated values for the silicon compounds were $\beta_\sigma = -0.66$, $\beta_\pi = -0.085$ (for carbon $\beta_\sigma = -1.50$, $\beta_\pi = -0.24$). This then fixes I_4, I_3, and I_2 and γ_4, δ_4, γ_2, and δ_2 can then be calculated using the T_2, $E(SiCl_4)$, A_2 and $B_1(SiH_2Cl_2)$ states respectively. The A_1 state of SiH_2Cl_2 is then predicted at 12.93 eV compared to the observed 12.76 eV. This is reasonable, but it is impossible taking intermediate values of either γ_3 or δ_3 or both, to obtain any sensible values for the i.p.'s of $SiHCl_3$. Therefore other solutions were sought with different values of $\beta_\sigma = 7.58\ \beta_\pi$.

Complete solutions are possible for $SiCl_4$ and SiH_2Cl_2 (as discussed above) and for $SiHCl_3$, by solving for γ_3 and δ_3 between the average of the E states and the A_1 state. Then the only predictions which can be made are the A_1 state of SiH_2Cl_2 and the separation of the E states in $SiHCl_3$. Larger values produced even worse results. How-

Can. J. Chem. Downloaded from www.nrcresearchpress.com by 210.87.254.5 on 09/05/12
For personal use only.

ever small values seemed much more reasonable especially as the complete solution of SiH_2Cl_2 (which is possible with four independent equations) gave $\beta_\pi \approx 0$. A satisfactory solution is obtained with $\beta_\pi = 0.05$ eV, and the results are shown in Table 8. The *I* values are now all smaller than the corresponding values for the carbon compounds, as predicted on electronegativity grounds. The δ values indicate, as expected, the dominance of the d orbitals on silicon and the decrease in δ with increasing number of chlorines per silicon reflects the decreasing ratio of available silicon d orbitals to chlorine lone pair orbitals. The γ values would also be expected to show a steady decrease with increasing number of chlorines. However the error on these values is quite large. For example, if we use the $^2A_1$ state of SiH_2Cl_2 rather than the $^2B_1$ to estimate γ_2, we obtain a value of 0.18 eV instead of 0.08 eV.

In general the error on the parameters will be quite large, not only because of the error in the measurement of the p.e. spectra (±0.1 eV) but also because of accidental degeneracy (*i.e.* for ^2E and $^2A_1$ in $SiHCl_3$ and $^2A_2$ and $^2A_1$ in SiH_2Cl_2). However, for all the calculations we have carried out varying the value of β_π from 0–(−0.15) the best and almost only reasonable assignment is that given in Tables 8 and 9 and the *I* and δ values show the same trends as the calculation of Table 9. The only possible alternative assignment which emerged was the $^2A_1$ state of $SiHCl_3$ at 13.07 eV accidentally degenerate with the $^2E_1$ state, and this was only for large values of β. Despite the many gross assumptions we believe this method gives a satisfactory description of the assignment of the p.e. spectra of the halosilanes and an indication of the importance of silicon d orbital participation.

TABLE 9. Comparison of calculated and observed ionization potentials including d orbital interaction*

Molecule	Ionic state	Calculated (eV)	Observed (eV)
SiH_3Cl	^2E	11.65	11.65
SiH_2Cl_2	$^2B_2$	11.70	11.70
	$^2B_1$	12.09	12.09
	$^2A_2$	12.53	12.53
	$^2A_1$	12.83	12.76
$SiHCl_3$	$^2A_2$	11.94	11.94
	$^2E''$	12.36	12.41
	$^2E'$	13.08	13.07
	$^2A_1$	12.41	12.41
$SiCl_4$	$^2T_1$	12.06	12.06
	^2E	13.44	13.44
	$^2T_2$	12.95	12.95

*I_1, ≈11.10; I_2, 11.77; I_3, 12.21; I_4, 12.33; β_σ, −0.38; β_π, −0.05; γ_1, ≈0.17; γ_2, 0.07; γ_3, 0.15; γ_4, −0.05; δ_1, ≈0.72; δ_2, 0.60; δ_3, 0.49; δ_4, 0.37.

Conclusions

The p.e. spectra of the halosilanes indicate that, compared to the halomethanes, the predominantly halogen "lone pair" orbitals have more bonding character. Among the evidence is the shift to higher energy of the "lone pair" i.p.'s along with the reduction in all other i.p.'s for the halosilanes, and SiH_3Cl and SiH_3Br have broader bands than the corresponding CH_3Cl and CH_3Br. For the di-, tri-, and tetra-halosilanes, the expected convergence of the "lone pair" orbitals due to reduced halogen–halogen (pπ–pπ) interaction is not observed. As a result it is postulated that some of the "lone pairs" are being stabilized more than others by bonding with the rest of the system. Although, in most cases, this can be via other than Si d orbital, in the tetrahalides this cannot be for two of the three "lone pair" orbitals. As the di- and tri-halides show similar trends to the corresponding tetrahalides we inferred that Si d orbitals are as important in the bonding in these species.

Other trends in the bonding in the silyl halides which can be deduced from the p.e. spectra, are (*1*) the strengthening of the Si—X σ bond through the series $SiH_3Br > SiH_3Cl > SiH_3F$ and (*2*) compared to the other orbitals the relatively small effect on the SiH_3 σ bonding orbital with change in the halogen. As mentioned in the introduction, this latter effect is evident in some of the physical properties of the halosilanes. A general weakening in the σ bonding system compared to the halomethanes is also evident from the lower i.p.'s for the halosilanes and, as a result, the physical properties of the halosilanes indicating stronger silicon halogen bonds must be caused by the additional (p → d)π bonding and perhaps p → σ* (SiH) bonding. There is as yet no explanation for the anomalies in the n.m.r. chemical shifts mentioned in the introduction, but as these are caused by second order effects we are not likely to get much information from p.e. spectroscopy.

The empirical one-electron Hamiltonian calculations carried out lend support to the conclusion made above that (p → d)π bonding is an important influence in stabilizing the chlorine "lone pair" orbitals of the chlorosilanes. In fact variations in silicon d orbital participation (δ) appear to have a much greater effect on these

orbitals than variations in the other silicon orbitals (γ) and interactions between the orbitals on the constituent atoms (β).

The confirmation of the assignment by the results of these calculations also evokes some observations regarding the CNDO/2 calculations. In SiH_2Cl_2 the low i.p. values obtained for the non-bonding b_1, b_2 and a_1 orbitals but not the a_2 orbital is almost certainly a consequence of the overestimation of the interaction of the former with other bonding orbitals of the same symmetry. In contrast for $SiHCl_3$ the a_2 orbital is at relatively higher energy than the other "lone pair" orbitals. In this case overestimation of silicon 3d participation has effectively cancelled the former effect. However this effect is evident in the energy separation of the two lowest e orbitals. The CNDO/2 calculations can obviously cause considerable confusion in the assignment of p.e. spectra, (8, 11, 29, 32, 33) if these effects are not taken into account.

We thank the National Research Council of Canada for financial support and Professor C. A. McDowell for his continued interest in the work. One of us (R.A.N.M.) acknowledges receipt of a Killam Fellowship from the University of British Columbia.

1. E. A. V. Ebsworth. *In* Organometallic compounds of the Group IV elements. *Edited by* A. G. McDiarmid. Marcel Dekker, New York, N.Y., 1968. p. 1.
2. B. J. Aylett. Advan. Inorg. Chem. and Radiochem. **11**, 249 (1968).
3. P. G. Perkins. Chem. Commun. 268 (1967).
4. (*a*) R. A. N. McLean and J. D. Umpleby. Can. J. Chem. **48**, 3769 (1970). (*b*) A. B. Cornford, D. C. Frost, R. A. N. McLean, and J. D. Umpleby. To be published.
5. W. E. Bull, B. P. Pullen, F. A. Grimm, W. E. Moddeman, G. R. Schweitzer, and T. A. Carlson. Inorg. Chem. **9**, 2474 (1970).
6. J. C. Green, M. L. H. Green, P. J. Joachim, A. F. Orchard, and D. W. Turner. Phil. Trans. Roy. Soc. Lond. A, 268, 111 (1970).
7. A. W. Potts, H. J. Lempka, D. G. Streets, and W. C. Price. Phil. Trans. Roy. Soc. Lond. A, 268, 59 (1970).
8. (*a*) P. J. Bassett and D. R. Lloyd. Chem. Phys. Lett. **6**, 166 (1970). (*b*) P. J. Bassett and D. R. Lloyd. J. Chem. Soc. A, 641 (1971).
9. E. A. V. Ebsworth. Volatile silicon compounds. Pergamon, Oxford. 1963, pp. 15–26, 50–58.
10. S. Bell and A. D. Walsh. Trans. Faraday Soc. 62, 3005 (1966).
11. D. C. Frost, F. G. Herring, C. A. McDowell, and I. A. Stenhouse. Chem. Phys. Lett. **4**, 523 (1970).
12. S. Cradock and E. A. V. Ebsworth. Chem. Commun. 57 (1971).
13. D. C. Frost, F. G. Herring, A. Katrib, R. A. N. McLean, J. E. Drake, and N. P. C. Westwood. Chem. Phys. Lett. **10**, 347 (1971).
14. R. P. Hollandsworth, W. M. Ingle, and M. A. Ring. Inorg. Chem. **6**, 844 (1967).
15. R. H. Herber. Inorganic isotopic syntheses. Benjamin, New York, N.Y. 1962, p. 31.
16. H. J. Emeleus and A. G. Maddock. J. Chem. Soc. 293 (1944).
17. J. E. Drake and J. Simpson. Inorg. Nucl. Chem. Lett. **2**, 219 (1966).
18. G. J. Janz and Y. Mikawa. Bull. Chem. Soc. (Jap.), **34**, 1495 (1961).
19. (*a*) E. A. V. Ebsworth and J. J. Turner. J. Chem. Phys. **36**, 2628 (1962). (*b*) E. A. V. Ebsworth and J. J. Turner. J. Phys. Chem. **67**, 805 (1963).
20. D. P. Santry and G. A. Segal. J. Chem. Phys. **47**, 158 (1967).
21. A. H. Sharbaugh. Phys. Rev. **78**, 64 (1950).
22. V. W. Laurie. J. Chem. Phys. **26**, 1359 (1957).
23. A. H. Sharbaugh. Phys. Rev. **74**, 1870 (1948).
24. L. O. Brockway and I. E. Coop. Trans. Faraday Soc. **34**, 1429 (1938).
25. R. C. Mockler, J. H. Bailey, and W. Gordy. J. Chem. Phys. **21**, 1710 (1953).
26. A. W. Potts, J. H. Lempka, D. G. Streets and W. C. Price. Phil. Trans. Roy. Soc. Lond. **A268**, 59 (1970).
27. C. R. Brundle, M. B. Robin, and H. Basch. J. Chem. Phys. **53**, 2196 (1970).
28. B. P. Pullen, T. A. Carlson, W. E. Moddeman, G. K. Schweitzer, W. E. Bull, and F. A. Grimm. J. Chem. Phys. **53**, 768 (1970).
29. For example, D. C. Frost, F. G. Herring, C. A. McDowell, M. R. Mustafa, and J. S. Sandhu. Chem. Phys. Lett. **2**, 663 (1968).
30. D. C. Frost, C. A. McDowell, J. L. Ragle, and I. A. Stenhouse. J. Chem. Phys. **53**, 178 (1970).
31. R. N. Dixon, J. N. Murrell, and B. Narayan. Mol. Phys. **20**, 611 (1971).
32. D. W. Davies. Chem. Phys. Lett. **2**, 173 (1968).
33. D. C. Frost, F. G. Herring, C. A. McDowell, and I. A. Stenhouse. Chem. Phys. Lett. **5**, 291 (1970).

Can. J. Chem. Downloaded from www.nrcresearchpress.com by 210.87.254.5 on 09/05/12
For personal use only.

Can. J. Chem. Downloaded from www.nrcresearchpress.com by 210.87.254.6 on 09/05/12
For personal use only.

Reductions with Sulfurated Borohydrides. VII. Reactions with Epoxides

J. M. Lalancette and A. Frêche
Département de Chimie, Faculté des Sciences, Université de Sherbrooke, Sherbrooke, Québec

Received August 9, 1971

The reaction of $NaBH_2S_3$ with epoxides gives symmetrical bis-(2-hydroxyethyl) disulfides. The stereochemistry of the reaction is similar to the attack of H_2S on the epoxides in basic solution. Substituted epoxides are opened from the less hindered side. The reaction proceeds with good yield and is general. An improved method of preparation of the 1,2-mercaptols is presented.

La réaction de $NaBH_2S_3$ avec les époxydes mène aux bis-(hydroxy-2 éthyl) disulfures symétriques. La stéréochimie de la réaction est semblable à celle de l'action de H_2S sur un époxyde, en milieu basique. L'époxyde est ouvert du côté le moins empêché. La réaction, qui apparaît générale, fonctionne avec de bons rendements. Une méthode améliorée de préparation des 1,2-mercaptols est présentée.

Canadian Journal of Chemistry, **49**, 4047 (1971)

The formation of sulfurated borohydrides of general formula MBH_2S_3 has been reported (1). This new type of hydride has shown distinctive reducing properties with aldehydes (2), ketones (3), oximes (4), nitro compounds, and nitriles (5). This paper completes this study and describes the reaction of different epoxides with $NaBH_2S_3$.

From previous observations of ketones, it is known that $NaBH_2S_3$ can act either as a source of hydride or sulfide ions. With the epoxide group, the reaction products indicate that the sulfide group rather than the hydride ion is involved in the reaction. The nucleophilic reaction can be illustrated by eq. 1. An attack by the hydride ion instead of the sulfide group would have led to the formation of the alcohol rather than the disulfide, as is the case with $NaBH_4$ or $LiAlH_4$.

The reaction has been observed with *cis*-stilbene oxide, *trans*-stilbene oxide, styrene oxide, 3-phenoxy-1-propene oxide, and 1-phenyl-1-methylethylene oxide. In all cases, very good yields of the corresponding disulfides were obtained, in accordance with eq. 1. The usual measurements reported in Table 1 have confirmed the structure of those new compounds. Depending on the structure of the starting epoxides, temperature and reaction time have been adjusted in order to achieve high yields of disulfides.

In order to obtain complementary information on the structure of the disulfides, they were reduced with $LiAlH_4$ to give the corresponding 1,2-mercaptols. Subsequent action of phosgene led to expected 1,3-oxathiolan-2-ones as indicated in eq. 2. The 1,2-mercaptols and their derivatives are described in Table 2. The 1,2-mercaptols obtained from *cis*- and *trans*-stilbene were also treated by Raney nickel giving a mixture of alcohol by simple desulfurization and hydrocarbon by desulfurization and hydrogenolysis.

From the structure of the disulfides, it can be noted that the opening of the epoxide ring gives the most substituted alcohols, indicating that the attack of the sulfide group takes place on the less-substituted end of the epoxide.

The Stereochemistry of the Disulfides

The reaction products of the epoxides of *cis*- and *trans*-stilbenes have been examined more closely in order to establish the stereochemistry of the corresponding disulfides and the stereochemistry of the reaction with $NaBH_2S_3$. Each disulfide having four asymetric carbons, several possible configurations have to be considered.

[1] 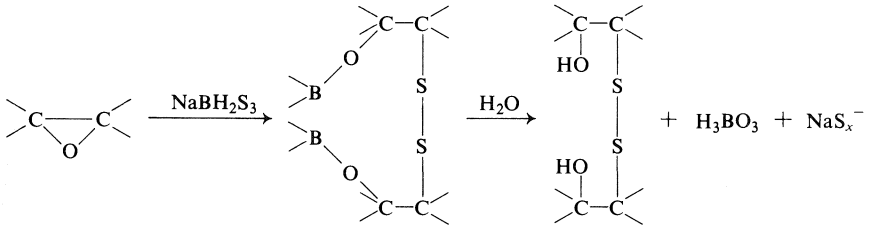

Can. J. Chem. Downloaded from www.nrcresearchpress.com by 210.87.254.6 on 09/05/12
For personal use only.

TABLE 1. Reactions of epoxides with $NaBH_2S_3$

Epoxides	Reaction temperature (°C)	Epoxide/ $NaBH_2S_3$	Duration (h)	Product	Yield (%)	Melting point (°C)	Analysis								Infrared (cm^{-1})	Mass spectrometry	Derivatives
							Calculated				Found						
							C	H	S	O	C	H	S	O			
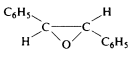 *trans*	65	1/2	34	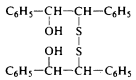	94	104									M/400 in CCl_4: 3605, 3575	334 (3%) $(C_6H_5CH_3)S_2$ 229 (1%) M/2 197 (4%) $(C_6H_5CH)_2OH$ 196 (9%) $(C_6H_5CH)_2O$ 180 (100%) $(C_6H_5CH)_2$ 167 (26%) $(C_6H_5)_2CH$ et $C_6H_5CHSSCH$ 107 (65%) C_6H_5CHOH 105 (55%) C_6H_5CO	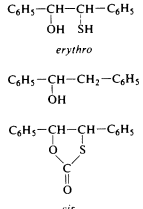 *erythro* *cis*
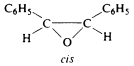 *cis*	45	1/2	20	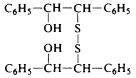	78		73.33	5.71	13.99	6.98	73.08	5.65	14.27	7.14	M/400 in CCl_4: 3597, 3520 (broad)	334 (52%) $(C_6H_5CH)_3S_2$ 229 (10%) M/2 197 (15%) $(C_6H_5CH)_2OH$ 196 (18%) $(C_6H_5CH)_2O$ 180 (100%) $(C_6H_5CH)_2$ 167 (35%) $(C_6H_5)_2CH$ et $C_6H_5CHSSCH$ 107 (25%) C_6H_5CHOH 105 (77%) C_6H_5CO	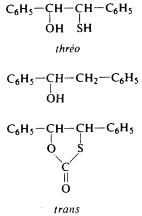 *thréo* *trans*
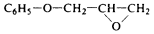	0	1/1	2	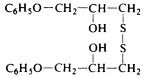	85	92	58.99	6.05	17.49	17.46	58.63	6.24	17.94	17.61	M/400 in CCl_4: 3587 (broad)	366 (2.5%) M 273 (2.5%) M—C_6H_5O 151 (6%) $C_6H_5OCH_2CHOHCH_2$ 150 (31%) $C_6H_5OCH_2CHOCH_2$ 134 (37%) $C_6H_5OCH_2CHCH_2$ 133 (29%) $C_6H_5OCH_2CHCH$ 107 (50%) $C_6H_5OCH_2$ 94 (94%) C_6H_5OH 77 (100%) C_6H_5	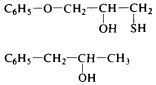
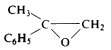	−70	1/1	5	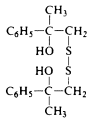	94	Liquid									M/400 in CCl_4: 3592, 3530 (broad)	150 (9%) $C_6H_5CCH_3CH_2S$ 149 (46%) $C_6H_5CCH_2CH_2S$ 121 (48%) $C_6H_5CCH_3OH$ 118 (60%) $C_6H_5CCH_3CH_2$ 105 (42%) C_6H_5CO 103 (24%) $C_6H_5CCH_2$ 43 (100%) CH_3CO	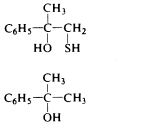
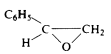	−70	1/1	5	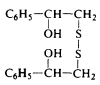	71	Liquid									M/400 in CCl_4: 3607, 3550		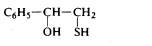

Can. J. Chem. Downloaded from www.nrcresearchpress.com by 210.87.254.6 on 09/05/12
For personal use only.

TABLE 2. Derivatives of the disulfides

α-Mercaptol	Reaction of formation: Precursor	Reaction of formation: Conditions	Yield (%)	Melting point (°C)	Analysis: Calculated C	Calculated H	Calculated S	Calculated O	Found C	Found H	Found S	Found O	Infrared (cm^{-1})	Mass spectrometry
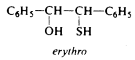 *erythro* **6**	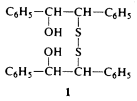 **1**	$LiAlH_4$; 3h reflux in EtOEt	91	74–75	73.00	6.13	13.92	6.95	73.05	6.15	14.06	7.13	5% CCl_4; weak band at 2570 M/100 in CCl_4; 3605, 3577	230 (1%) M 180 (52%) $(C_6H_5CH)_2$ 179 (48%) $C_6H_5CCHC_6H_5$ 178 (32%) $C_6H_5CCC_6H_5$ 123 (18%) C_6H_5CHSH 122 (12%) C_6H_5CHS 121 (22%) C_6H_5CS 107 (100%) C_6H_5CHOH 106 (16%) C_6H_5CHO 105 (30%) C_6H_5CO
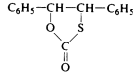 *cis* **11**	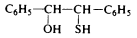	$COCl_2$; in benzene/ pyridine	89	141–142	70.25	4.72			70.09	4.79			Strong band at 1745	256 (4%) M 228 (10%) M—CO 212 (8%) M—CO_2 180 (4%) M—CO_2S 122 (100%)C_6H_5CHS 121 (40%) C_6H_5CS 106 (2%) C_6H_5CHO 105 (25%) C_6H_5CO
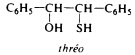 *thréo* **7**	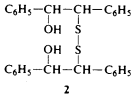 **2**	$LiAlH_4$; 12 h reflux in EtOEt	87										5% CCl_4; weak band at 2570 M/400 in CCl_4; 3607, 3500 (broad)	
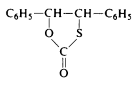 *trans* **12**	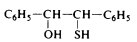	$COCl_2$; in benzene/ pyridine	84	120–121	70.25	4.72	12.51	12.48	70.37	4.70	12.63	12.75	Strong band at 1750	256 (3.5%) M 228 (16.5%)M—CO 212 (21%) M—CO_2 180 (10%) M—CO_2S 179 (16.5%)$C_6H_5CCHC_6H_5$ 178 (21%) $C_6H_5CCC_6H_5$ 122 (100%) C_6H_5CHS 121 (60%) C_6H_5CS 105 (28.5%)C_6H_5CO
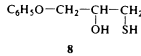 **8**	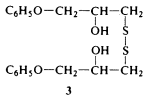 **3**	$LiAlH_4$; 4 h reflux in EtOEt	85	Liquid									5% CCl_4; weak band at 2570 M/400 in CCl_4; 3593	184 (8%) M 166 (1%) M-H_2O 133 (7.5%)M-H_2O, SH 107 (26%) $C_6H_5OCH_2$ 94 (100%) C_6H_5OH 91 (11%) $CH_2CHOHCH_2SH$ 73 (16%) CH_2CCH_2SH
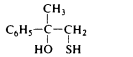 **9**	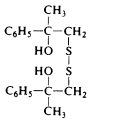 **4**	$LiAlH_4$; 18 h reflux in EtOEt	83	Liquid									5% CCl_4; weak band at 2570 M/200 in CCl_4; 3602 (medium) 3518 (strong	150 (6%) M-H_2O 135 (10%) M-SHetM-H_2O,CH_3 121 (70%) $C_6H_5COHCH_3$ 105 (31%) C_6H_5CO 103 (18%) $C_6H_5CCH_2$ 77 (33%)C_6H_5 43 (100%)CH_3CO
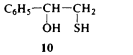 **10**	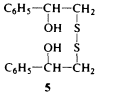 **5**	$LiAlH_4$; 9 h reflux in EtOEt	91	Liquid									5% CCl_4; weak band at 2570 M/400 in CCl_4; 3603, 3530	136 (4%) M-H_2O 121 (4.5%) $C_6H_5CHOHCH_2$ 107 (82.5%) C_6H_5CHOH 105 (16%) C_6H_5CO 104 (22.5%) $C_6H_5CHCH_2$ 103 (14%)$C_6H_5CCH_2$ 91 (16%) $C_6H_4CH_2$ 77 (56%) C_6H_5

[2] 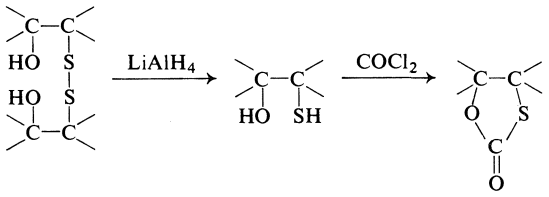

The n.m.r. of the disulfides obtained from these epoxides shows two doublets for each H—C—O and H—C—S structure, these four peaks being centered around 5 and 4 δ; those two doublets have equivalent intensities and very similar J, of the order of 6 Hz. This suggests that each of these disulfides is a mixture of two diastereoisomers in approximately equal proportions.

The n.m.r. of the corresponding 1,2-mercaptols or their 1,3-oxathiolan-2-ones cannot differentiate clearly between *threo* and *erythro* structures. In order to assign the proper configurations to the disulfides and 1,2-mercaptols, the *erythro* isomer was prepared by the action of H_2S in basic solution on the *trans*-stilbene oxide (6), this reaction being known to proceed via a Walden inversion. By comparison with the products obtained by the action of $NaBH_2S_3$ on the stilbene oxides followed by $LiAlH_4$, it was found that *trans*-stilbene oxide gave the *erythro*-1,2-mercaptol, the *threo* isomer being obtained from *cis*-stilbene oxide. It must be noted that the reaction was highly specific, each of those diastereoisomers being obtained in a pure state, after the action of $LiAlH_4$.

The stereochemistry of the reaction of each of the stilbene oxides with $NaBH_2S_3$ is represented in Figs. 1 and 2. Since a *trans* opening mechanism must be accepted, from analogy of the action of HS^- as indicated above, the attack on the (*d,l*)-*trans*-stilbene oxide gives the (*d,l*)-*erythro* isomer and the same reaction on the *meso*-stilbene oxide gives the (*d,l*)-*threo* isomer. Since the reduction of the disulfide by $LiAlH_4$ does not affect the C—S bond (7) and since only one diastereoisomer is produced by the reduction of each of the disulfides, it can be said that each disulfide contains only one type of structure, *erythro* for the disul-

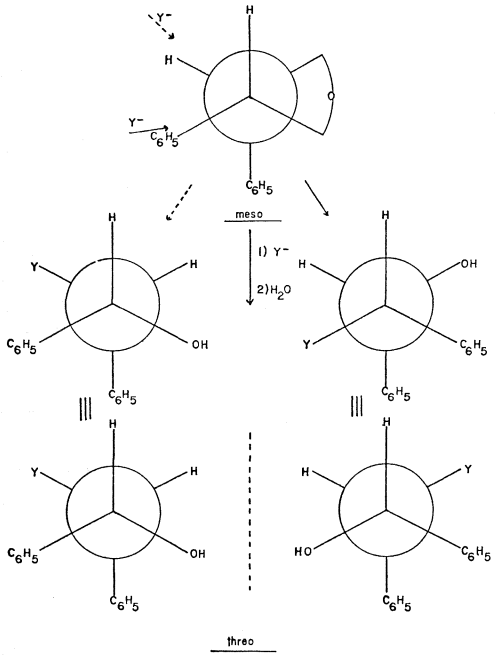

FIG. 1. Stereochemistry of the opening of *cis*-stilbene oxide.

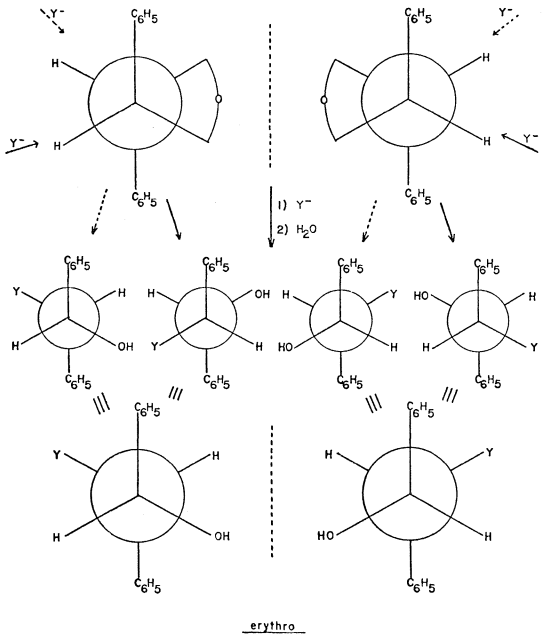

FIG. 2. Stereochemistry of the opening of *trans*-stilbene oxide.

Can. J. Chem. Downloaded from www.nrcresearchpress.com by 210.87.254.6 on 09/05/12
For personal use only.

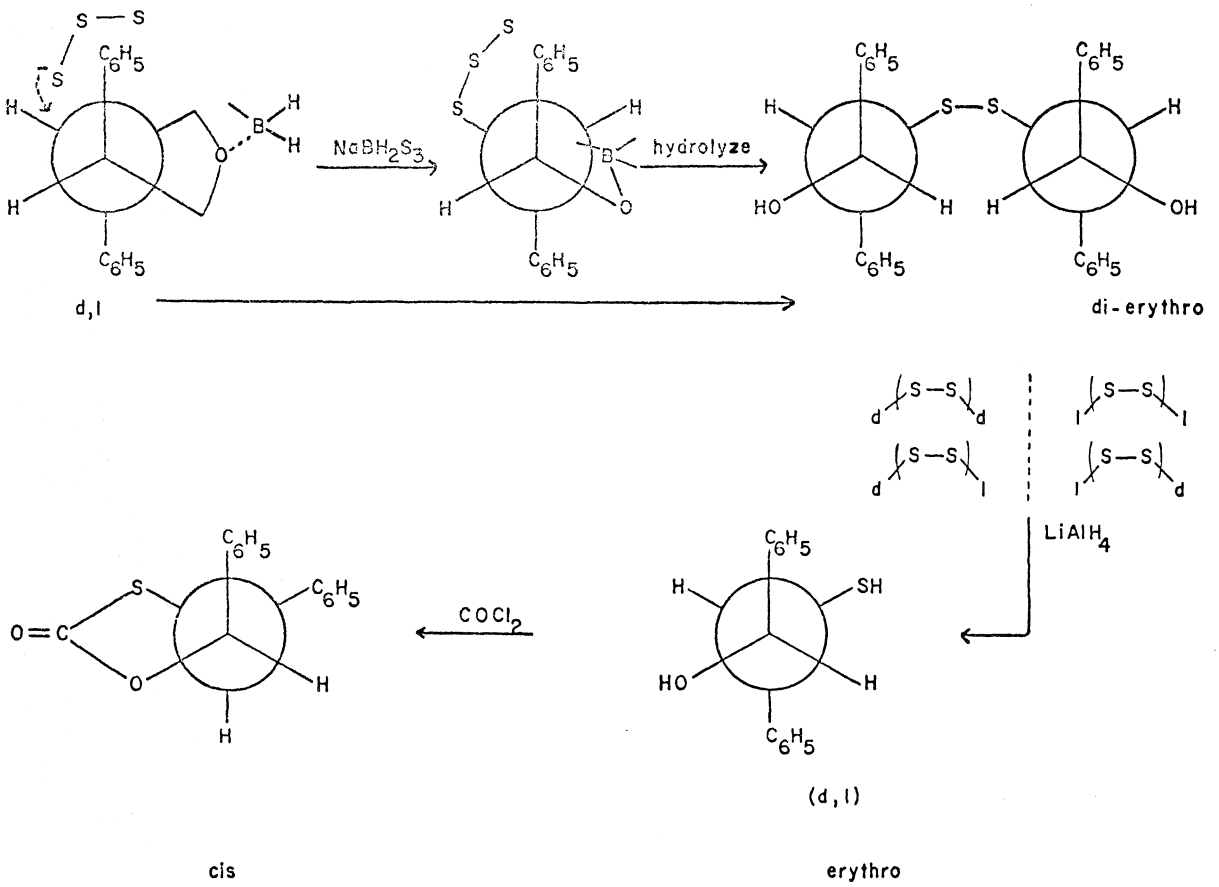

FIG. 3. Stereochemistry of the derivatives of *trans*-stilbene oxide. For sake of clarity, the staggered rather than the more probable eclipsed geometry is presented.

fide originating from the reaction of *trans*-stilbene oxide and *threo* for the disulfide originating from the reaction of the *cis*-stilbene oxide. These conclusions are in accordance with the n.m.r. measurements of the disulfides suggesting the existence of a pair of diastereoisomers in the reaction products. When the *trans* epoxide is opened by $NaBH_2S_3$ an *erythro* racemic mixture is formed and the association of two (*d,l*)-*erythro* structures in the disulfide is responsible for the formation of two pairs of stereoisomers from the four enantiomers present. This situation is illustrated in Figs. 3 and 4.

In the course of the preparation of the 1,2-mercaptols, we found that by reducing the reaction mixture obtained by the action of H_2S on an epoxide, the yields of 1,2-mercaptols were increased from the moderate values reported in the literature (8) of 25–35% to an almost quantitative value. The action of $LiAlH_4$ renders the method much more interesting since all the undesirable polysulfides are reduced to the expected 1,2-mercaptol.

The reaction of $NaBH_2S_3$ on epoxides gives a new class of compounds, the bis-(2-hydroxyethyl) disulfides and the stereochemical study of those disulfides offers clear evidence concerning the *trans* opening of the epoxide ring by the attack of $NaBH_2S_3$. How the two mercaptol fragments unite to give the disulfide remains an open question at the present time. The facile transformation of the disulfide into the 1,2-mercaptol by the action of $LiAlH_4$ offers an interesting alternate route to this class of compounds (6, 9).

Experimental

The n.m.r. measurements were made with a Varian, A60 apparatus. The i.r. measurements were made with a

Can. J. Chem. Downloaded from www.nrcresearchpress.com by 210.87.254.6 on 09/05/12
For personal use only.

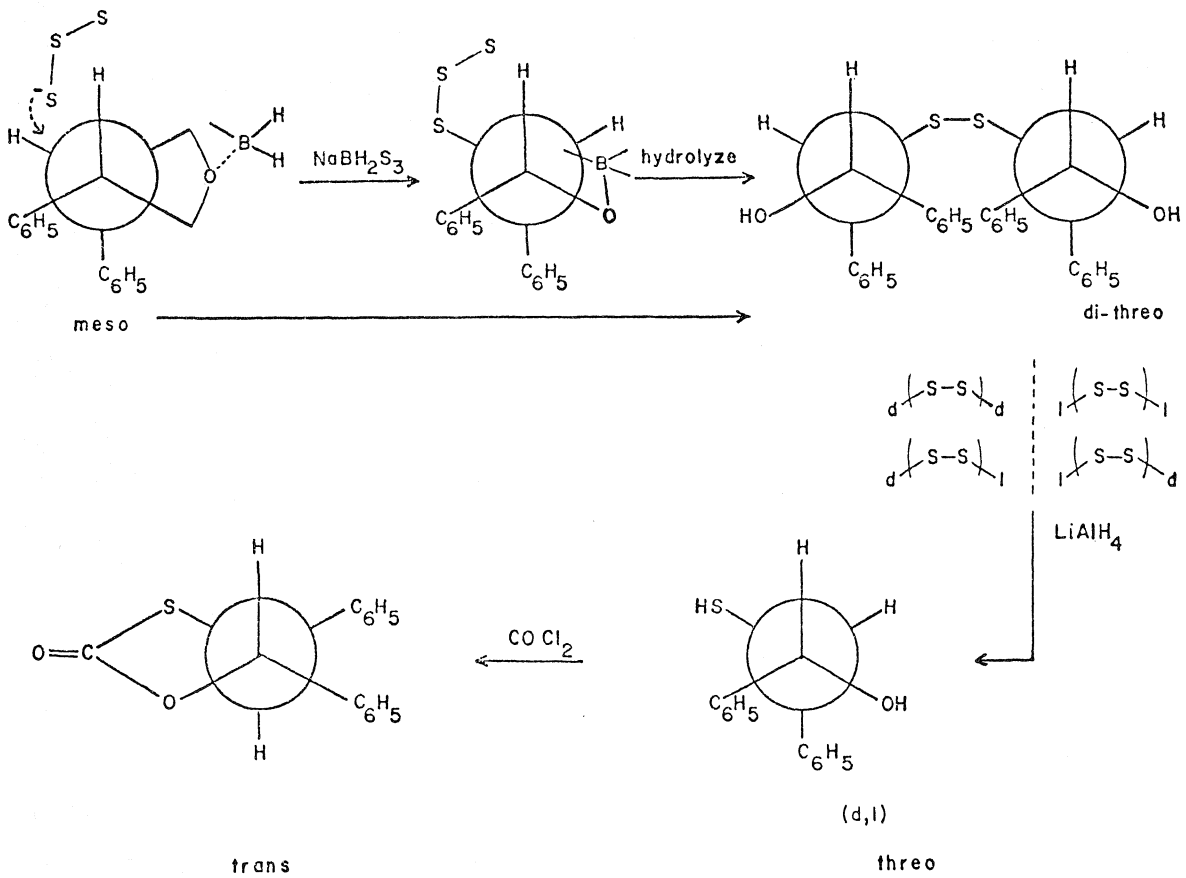

FIG. 4. Stereochemistry of the derivatives of *cis*-stilbene oxide. For sake of clarity, the staggered rather than the more probable eclipsed geometry is presented.

Perkin–Elmer, model 137 spectrophotometer. The v.p.c. measurements were made with a Microteck, model G.C.2000R apparatus, using an Se30, 4 ft column. Mass spectrometry measurements were performed on a Hitachi Perkin–Elmer instrument, model RMU-6.

(1) Reaction of $NaBH_2S_3$ with trans-Stilbene Oxides

The sulfurated borohydride was prepared as described (1) by treating a mixture of 0.050 mol (1.90 g) of $NaBH_4$ and 0.150 mol (4.8 g) of sulfur with 40 ml of anhydrous tetrahydrofuran (THF), the flask being kept cool (25–30°) with a water bath and under anhydrous conditions by circulation of nitrogen in the system. After 15 min, the initial hydrogen evolution had stopped and the sulfurated hydride was used *in situ* by addition of 4.9 g (0.025 mol) of *trans*-stilbene oxide. After a reflux of 34 h under nitrogen, the reaction mixture was cooled and hydrolyzed by 50 ml of a 10% sodium hydroxide solution. By extractions with chloroform, 5.4 g of the disulfide was obtained, the solid being recrystallized in cyclohexane. A similar procedure was used with other epoxides, the variations of experimental conditions and yields being reported in Table 1.

The n.m.r. (δ) of the various disulfides are the following (ref. Table 2): disulfide **1**: singlet at 2.40 (2H); doublet at 5.03 (1H, J = 5.5 Hz); doublet at 4.97 (1H, J = 60 Hz); doublet at 3.64 (1H, J = 5.5 Hz); doublet at 3.68 (1H, J = 6.0 Hz); multiplet at 7.1 (10H). Disulfide **2**: multiplet at 2.0 (2H); doublet at 3.93 (1H, J = 7.25 Hz); doublet at 4.01 (1H, J = 7.5 Hz); doublet at 4.93 (1H, J = 7.5 Hz); doublet at 5.02 (1H, J = 7.25); multiplet at 7.2 (10H). Disulfide **3**: multiplet at 3.0 (4H); multiplet at 4.05 (4H); multiplet at 4.30 (2H); singlet at 5.35 (2H); multiplet at 7.1 (10H). Disulfide **4**: singlet at 1.5 (6H); singlet at 2.80 (2H); multiplet between 3.08 and 3.13 (4H); multiplet around 7.15 (10H). Disulfide **5**: doublet at 2.79 (4H, J = 6 Hz); singlet at 3.80 (2H); triplet at 4.67 (2H, J = 6 Hz); multiplet at 7.1 (10H).

(2) Reduction of the Disulfides by $LiAlH_4$

The disulfide obtained from *trans*-stilbene oxide (2.3 g, 0.005 mol) was treated by an excess (0.75 g, 0.020 mol) of $LiAlH_4$ in 30 ml of anhydrous ether. After a reflux of 3 h, the reaction mixture was hydrolyzed by 1.5 g of water, filtered, and diluted by 50 ml of chloroform. After drying and evaporation of the solvents the expected 1,2-mercaptol (2.1 g, 91%) was obtained and recrystallized in CCl_4. A similar technique was used for the reduction of the other disulfides, the results being reported in Table 2.

The n.m.r. (δ) of the 1,2-mercaptols are the following:

Can. J. Chem. Downloaded from www.nrcresearchpress.com by 210.87.254.6 on 09/05/12
For personal use only.

Can. J. Chem. Downloaded from www.nrcresearchpress.com by 210.87.254.6 on 09/05/12
For personal use only.

mercaptol **4**: doublet at 4.83 (1H, J_{AM} = 7.8 Hz); double doublet at 4.17 (1H, J_{AM} = 7.8, J_{MX} = 5.1 Hz); doublet at 1.70 (1H, J_{AX} = 5.1 Hz); broad singlet at 2.60 (1H); singlet at 7.27 (10H). Mercaptol **7**: doublet at 4.76 (1H, J_{MX} = 7.5 Hz); double doublet at 4.11 (1H, J_{MX} = 7.5, J_{AM} = 5.7 Hz); doublet at 2.17 (1H, J_{AM} = 5.7 Hz); broad singlet at 3.20 (1H); singlet at 7.07 (10H). Mercaptol **8**: complex multiplet centered at 4.04 (3H); complex multiplet between 2.67 and 3.10 (2H); double doublet centered at 1.60 (1H); singlet at 3.20 (1H); multiplet at 7.0 δ (5H). Mercaptol **9**: singlet at 1.47 (3H); singlet at 3.10 (1H); double doublet at 1.03 (1H, J_{AX} = 10, J_{BX} = 7.5 Hz); two double doublets at 2.63 (2H, J_{AX} = 10, J_{BX} = 7.5 Hz) and 2.91 (J_{AB} = 13.5 Hz). Mercaptol **10**: triplet at 4.44 (1H); singlet at 3.50 (1H); multiplet between 2.70 and 2.45 (2H); double doublet at 1.25 (1H, J_1 = 8.0, J_2 = 8.5 Hz); singlet at 7.1 (5H).

(3) Reaction of the 1,2-Mercaptols with Phosgene

A 30 ml portion of a benzene solution of phosgene (obtained by bubbling $COCl_2$ through the solvent for 15 min) was mixed with a solution of 0.300 g of the 1,2-mercaptol **6** in 50 ml of the same solvent. After adding 0.5 ml of dry pyridine to the reaction mixture, the system was stirred at room temperature for 15 min. After the evaporation of the solvent, the reaction product was recrystallized in the mixture chloroform – ethyl acetate. The characteristics of the 1,3-oxathiolan-2-ones are reported in Table 2. In the n.m.r., the derivative from the *trans*-stilbene (**11**) gave a doublet at 6.14 (1H, J = 6.0 Hz) and a doublet at 5.28 δ (J = 6.0 Hz). With the derivative of the *cis*-stilbene (**12**) the n.m.r. was showing a doublet at 5.46 (1H, J = 9.0 Hz); and a doublet at 4.96 δ (1H, J = 9.0 Hz). The protons of the mercaptan, of the alcohol and of the aromatic system were also present in those spectra.

(4) Desulfurization of the 1,2-Mercaptols with Raney Nickel

A sample of 0.300 g (0.0007 mol) of the 1,2-mercaptol **6** was treated by 6 g of freshly prepared Raney nickel during 24 h at room temperature. After filtration and evaporation of the solvent, 250 mg of a yellow liquid was obtained. From n.m.r. analysis, this liquid was a mixture of 1,2-diphenylethanol (60%) and 1,2-diphenylethane (40%).

The n.m.r. of the 1,2-diphenylethanol: triplet at 4.70 (1H, J = 7 Hz); doublet at 2.88 δ (2H, J = 7 Hz). The n.m.r. of the 1,2-diphenylethane: singlet at 2.89 δ (4H). A similar method was used to characterize the 1,2-mercaptol **7**.

(5) Opening of the Epoxide of trans-Stilbene by H_2S in Basic Solution

A solution of 0.6 g (0.015 mol) of NaOH in 10 ml of CH_3OH was saturated by a stream of H_2S at 0 °C for 1 h. To this solution, 1.0 g (0.005 mol) of epoxide was added slowly, the bubbling of H_2S being maintained in the course of the addition. After a contact of 18 h, the reaction mixture was diluted with 15 ml of water, and acidified at 0° to pH 2 by H_2SO_4. The organic phase was extracted with CH_2Cl_2, washed with a solution of sodium bicarbonate, dried, and distilled. This crude product represented about 25% of the expected 1,2-mercaptol and various polysulfides. The reduction, as described in section 2, was then applied to this mixture and a yield of 94% of the 1,2-mercaptol was thus obtained. The physical properties of this *erythro*-1,2-mercaptol were identical as those observed with **6**.

The authors thank the National Research Council of Canada and the Defence Research Board of Canada (grant 9530-30) for financial assistance.

1. J. M. LALANCETTE, A. FRÊCHE, and R. MONTEUX. Can. J. Chem. **46**, 2754 (1968).
2. J. M. LALANCETTE and A. FRÊCHE. Can. J. Chem. **47**, 739 (1969).
3. J. M. LALANCETTE and A. FRÊCHE. Can. J. Chem. **48**, 2366 (1970).
4. J. M. LALANCETTE and J. R. BRINDLE. Can. J. Chem. **48**, 735 (1970).
5. J. M. LALANCETTE and J. R. BRINDLE. Can. J. Chem. **49**, 2990 (1971).
6. E. E. VAN TAMELEN. J. Am. Chem. Soc. **73**, 3444 (1951).
7. F. G. BORDWELL and W. H. MCKELLIN. J. Am. Chem. Soc. **73**, 2251 (1951).
8. L. GOODMAN, A. BENITEZ, and B. R. BAKER. J. Am. Chem. Soc. **80**, 1680 (1958).
9. C. DJERASSI, M. GORMAN, F. X. MARKLEY, and E. B. OLDENBURG. J. Am. Chem. Soc. **77**, 568 (1955).

Can. J. Chem. Downloaded from www.nrcresearchpress.com by 210.87.254.42 on 09/05/12
For personal use only.

Thiazoloisoquinolines. IV. The Synthesis and Spectra of Thiazolo[4,5-*h*]- and Thiazolo[5,4-*f*]isoquinolines. The Ultraviolet and Proton Magnetic Resonance Spectra of Some Substituted Isoquinolines[1,2]

ALFRED TAURINS AND RICHARD KANG-CHUAN HSIA[3]

Department of Chemistry, McGill University, Montreal, Quebec

Received July 21, 1971

Thiazolo[4,5-*h*]isoquinoline was synthesized from 7-aminoisoquinoline in four steps: by the reaction with potassium thiocyanate and bromine to give 7-amino-8-thiocyanoisoquinoline; cyclization of the latter with hydrochloric acid to produce 2-aminothiazolo[4,5-*h*]isoquinoline, followed by the Sandmeyer reaction to yield a 2-chloro derivative, and finally, reduction with hydriodic acid and phosphorus. Thiazolo[5,4-*f*]isoquinoline was prepared from 6-aminoisoquinoline via 6-amino-5-thiocyanoisoquinoline. The synthesis of 2,5-diaminothiazolo[5,4-*h*]isoquinoline was achieved by cyclization of 5-acetamido-8-aminoisoquinoline which was obtained from 5-aminoisoquinoline. In 5-amino-8-thiocyano- and 8-amino-5-thiocyanoisoquinolines, the thiocyano group was hydrolyzed to the thiol group with 8 *N* hydrochloric acid and ethanol (1:1).

The u.v. and p.m.r. spectra of the intermediate isoquinolines, and the i.r., u.v., and n.m.r. spectra of thiazoloisoquinolines were studied.

On a synthétisé le thiazolo[4,5-*h*]isoquinoline à partir de la 7-aminoisoquinoline en quatre étapes: par la réaction avec le thiocyanate de potassium et le brome, on obtient le 7-amino-8-thiocyanoisoquinoline; la cyclisation de ce produit avec l'acide chlorhydrique amène au 2-aminothiazolo[4,5-*h*]isoquinoline, suivi par la réaction de Sandmeyer, ce qui donne le dérivé 2-chloro dont on fait la réduction avec l'acide iodhydrique et le phosphore. On a préparé le thiazolo[5,4-*f*]isoquinoline à partir du 6-aminoisoquinoline en passant par le 6-amino-5-thiocyanoisoquinoline. On a réussi la synthèse du 2,5-diaminothiazolo-[5,4-*h*]isoquinoline qui fut obtenu à partir du 5-aminoisoquinoline. Pour les 5-amino-8-thiocyano- et le 8-amino-5-thiocyanoisoquinolines, le groupe thiocyano a été hydrolysé en thiol avec l'acide chlorhydrique 8 *N* et l'éthanol (1:1).

On a étudié les spectres ultraviolet et de r.m.p. des isoquinolines intermédiaires, de même que les spectres i.r., u.v., et r.m.n. des thiazoloisoquinolines.

Canadian Journal of Chemistry, 49, 4054 (1971)

Discussion

The program aimed at the synthesis of eight isomeric thiazoloisoquinolines was continued. Two representatives of this series, thiazolo[4,5-*c*]- and thiazolo[5,4-*c*]isoquinolines have been described in the previous papers (1–3). In this work, we report studies in the series of thiazolo[4,5-*h*]- (**1**), -[5,4-*f*]- (**2**), and -[5,4-*h*]isoquinoline (**3**). The general method for the preparation of the amino derivatives of **1**, **2**, and **3**, was the thiocyanation of the appropriate aminoisoquinolines, followed by the cyclization of the *o*-aminothiocyano derivatives.

The starting material for the preparation of thiazolo[4,5-*h*]isoquinoline (Scheme 1) was 7-aminoisoquinoline (**5**) which was thiocyanated in the 8-position with potassium thiocyanate and bromine in 95% acetic acid to give 7-amino-8-thiocyanoisoquinoline (**6**).

Treatment of **6** with alcoholic hydrochloric acid

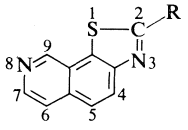

1
[4,5-*h*]

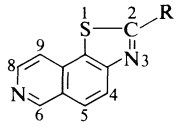

2
[5,4-*f*]

a R = NH_2
b R = Cl
c R = H

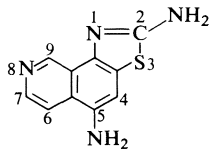

3
[5,4-*h*]

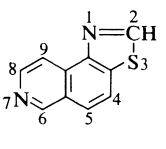

4
[4,5-*f*]

[1]For Part III, see Hall and Taurins (3).

[2]This work received financial assistance from the National Research Council of Canada, Ottawa, Canada. Taken from a portion of the Ph.D. Thesis of R. K. C. Hsia.

[3]Holder of an NRCC Studentship, 1966–1969.

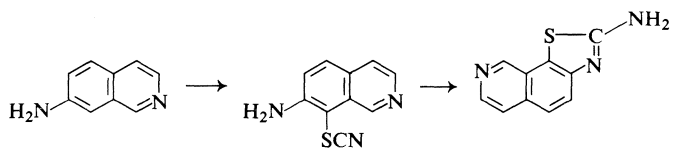

5 6 1*a*

SCHEME 1

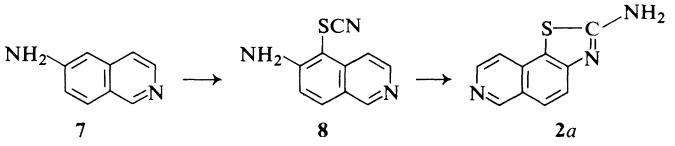

7 8 2*a*

SCHEME 2

at reflux temperature gave 2-aminothiazolo-[4,5-*h*]isoquinoline (**1***a*) in the form of a yellow crystalline substance. Diazatization of 2-amino-thiazolo[4,5-*h*]isoquinoline (**1***a*) with sodium nitrite in 70% nitric and 85% orthophosphoric acid mixture (1:4), followed by the treatment of the diazonium salt with cuprous chloride gave 2-chlorothiazolo[4,5-*h*]isoquinoline (**1***b*), which on reduction with hydriodic acid and red phosphorus gave thiazolo[4,5-*h*]isoquinoline (**1***c*). This forms colorless needles, m.p. 138–139° (*n*-hexane) and has a very low solubility in organic solvents.

In the synthesis of thiazolo[5,4-*f*]isoquinoline (**2***c*), thiocyanation of 6-aminoisoquinoline (**7**) produced the key intermediate 6-amino-5-thiocyanoisoquinoline (**8**) which was cyclized with hydrochloric acid to obtain 2-aminothiazolo-[5,4-*f*]isoquinoline (**2***a*). The further steps leading to the chloro-derivative **2***b* and the parent compound 2*c* were similar to those outlined for the [4,5-*h*] series (Scheme 2). Thiazolo[5,4-*f*]isoquinoline (**2***c*) was obtained in pure state by sublimation and recrystallization from *n*-hexane. This forms colorless needles, m.p. 170° (dec.), and has a very low solubility in organic solvents.

The preparation of 2,5-diaminothiazolo[5,4-*h*]-isoquinoline (**3***a*) is outlined in Scheme 3. To achieve the [5,4-*h*]-fusion of the thiazole and isoquinoline rings, it would be necessary to have amino and thiocyano groups in the 8- and 7-positions, respectively. To prevent the thiocyanation of the 5-position in 8-aminoisoquinoline, that position was blocked by the acetamido group. The starting material, 5-acetamidoisoquinoline (**9**), was nitrated in concentrated sulfuric acid with potassium nitrate to give 5-

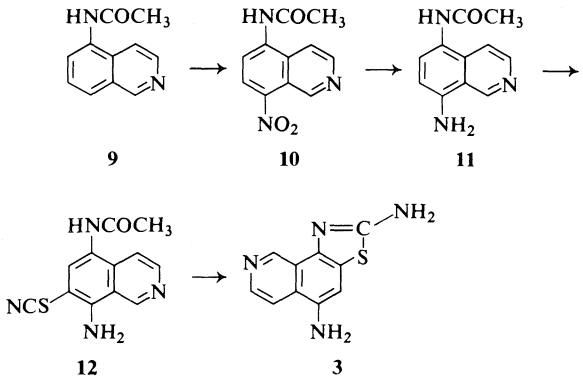

9 10 11 12 3

SCHEME 3

acetamido-8-nitroisoquinoline (**10**). Catalytic hydrogenation of **10** with hydrogen and 5% palladium-on-charcoal catalyst produced 5-acetamido-8-aminoisoquinoline (**11**), which on thiocyanation yielded 5-acetamido-8-amino-7-thiocyanoisoquinoline (**12**). The compound **12** was successfully cyclized with hydrochloric acid to give 2,5-diaminothiazolo[5,4-*h*]isoquinoline (**3**), a yellow crystalline compound. Diazatization of **3**, followed by Sandmeyer reaction, failed to produce the desired 2,5-dichloro[5,4-*h*]isoquinoline.

In order to synthesize thiazolo[4,5-*f*]isoquinoline (**4**) by the same type of cyclization reactions as mentioned previously, it was desirable to obtain 5-amino-6-thiocyanoisoquinoline from 5-amino-isoquinoline. However, the only product of the thiocyanation of 5-aminoisoquinoline was 5-amino-8-thiocyanoisoquinoline (**13**). The structure of 5-amino-8-thiocyanoisoquinoline (**13**) was obvious from its inability to cyclize with 4 *N* hydrochloric acid and ethanol (1:1) under reflux (the starting material was recovered). However,

Can. J. Chem. Downloaded from www.nrcresearchpress.com by 210.87.254.42 on 09/05/12
For personal use only.

TABLE 1. The u.v. absorption maxima and log ε values of thiazolo[4,5-*h*]isoquinoline and its derivatives (in absolute ethanol)

Compound	α-Band		p-Band		β-Band	
	λ_{max} (nm)	log ε	λ_{max} (nm)	log ε	λ_{max} (nm)	log ε
Thiazolo[4,5-*h*]isoquinoline	333	3.70	289	3.78	253	4.66
	319	3.64	279	3.78	227	4.36
	304	3.64			207	4.25
2-Chloro-	335	3.51	288	3.72	254	4.50
	323	3.47			228	4.14
					216 sh	3.95
2-Acetamido-	325–345	3.54	312	4.03	262 sh	4.56
			301	4.08	238	4.28
					207	4.27
2-Amino-	360	3.71	308	4.30	266	4.84
			296	4.28	228	4.41
					206	4.39
2-Hydroxy-	355	3.65	314	3.70	252	4.57
			297	3.92	216	4.40
			287	4.01		
			273	4.26		

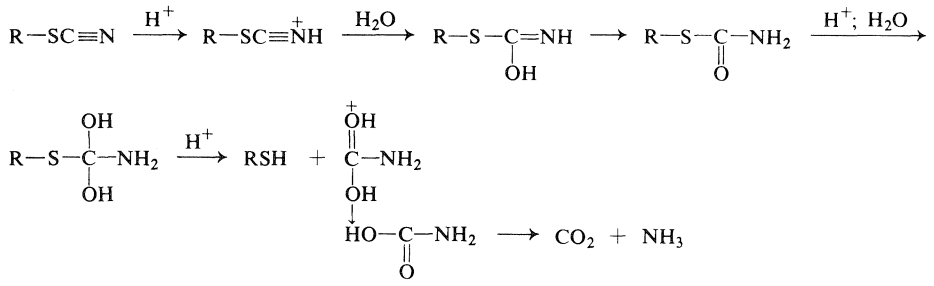

SCHEME 4

8 *N* hydrochloric acid and ethanol (1:1) hydrolyzed **13** to give 5-amino-8-mercaptoisoquinoline (**14**).

Thiocyanation of 8-aminoisoquinoline gave only a para-substituted product, 8-amino-5-thiocyanoisoquinoline (**15**). Since no ortho-substitution occurred, 8-aminoisoquinoline could not serve as the key intermediate for the preparation of thiazolo[5,4-*h*]isoquinoline.

8-Amino-5-thiocyanoisoquinoline (**15**) was also hydrolyzed with 8 *N* hydrochloric acid and ethanol (1:1) to give 8-amino-5-mercaptoisoquinoline (**16**), a kind of reaction not reported for thiocyanates. Conversion of thiocyanates to mercaptans has been usually achieved by reduction, for example, with zinc and hydrochloric acid, lithium aluminum hydride, or sulfides (4). Riemschneider (5) found that thiocyanates are transformed into thiocarbamates by treatment with sulfuric acid at 0 to 5°, but no further change was observed.

It is believed that the acidic hydrolysis of the thiocyano group proceeds through a thiocarbamate intermediate which is hydrolyzed further to give the thiol as shown in Scheme 4.

Spectra

Ultraviolet Spectra

The u.v. absorption data of thiazolo[4,5-*h*]- and -[5,4-*f*]isoquinoline and their derivatives are presented in Tables 1 and 2. The pattern of the spectra of these compounds is characteristic of the angularly fused three-ring aromatic and hetero-aromatic systems which usually display three main types of bands arising from $\pi \rightarrow \pi^*$ transitions. (In most cases, linearly fused three-ring systems show only two bands, due to the coalescing of bands.) These bands are designated as α-, p-, and β-bands by Clar (6), or as L_b, L_a, and $B_a + B_b$ bands by Platt (7). The u.v. spectra of the angular unsubstituted thiazoloisoquinolines **1***c* and **2***c*, and also of thiazolo[4,5-*c*]- and -[5,4-*c*]-

Can. J. Chem. Downloaded from www.nrcresearchpress.com by 210.87.254.42 on 09/05/12
For personal use only.

TABLE 2. The u.v. absorption maxima and log ε values of thiazolo[5,4-*f*]isoquinoline and its derivatives (in absolute ethanol)

Compound	α-Band		p-Band		β-Band	
	λ_{max} (nm)	log ε	λ_{max} (nm)	log ε	λ_{max} (nm)	log ε
Thiazolo[5,4-*f*]isoquinoline	333	3.56	286	3.72	250 sh	4.55
	319	3.53	274	3.78	244	4.66
	306	3.45			210 sh	4.04
2-Chloro-	335	3.55	278	3.76	252	4.80
	320	3.55			227	4.53
	306	3.44				
2-Acetamido-	333	3.63	295–310	3.83	272	4.63
	319	3.87			262	4.60
					240	4.24
					229 sh	4.17
					205	4.14
2-Amino-	345 sh	3.47	320	3.80	267	4.70
					245 sh	4.21
					219 sh	4.03
					206	4.03
2-Hydroxy-	290–340	3.83	273	4.17	252	4.74
					219 sh	4.28

TABLE 3. The u.v. absorption maxima and log ε values of monosubstituted isoquinolines (in absolute ethanol)

Compound	α-Band		p-Band		β-Band	
	λ_{max} (nm)	log ε	λ_{max} (nm)	log ε	λ_{max} (nm)	log ε
5-Aminoisoquinoline	335	3.64	244	4.04	208	4.26
6-Amino-	337	3.56	306	3.95	242	4.54
					206	3.88
7-Amino-	360	3.42	283	3.97	236	4.50
					214	4.16
8-Amino-	360	3.93	242	4.39	212	4.63
5-Acetamido-	320	3.86	290	3.90	220	4.62
			268	4.27		
5-Bromo-	325	3.76	286	3.82	222	4.76
			276	3.86		
5-Nitro-	330	3.72	230–235	4.02	214	4.49
	310	3.60				
6-Hydroxy-	325 sh	3.25	286	3.66	230	4.69
7-Hydroxy-	335	3.35	263	3.49	224	4.45
Isoquinoline (14)	317	3.5	266	3.6	217	4.6

isoquinoline (1, 2) are similar to those of phenanthridine (8) and benzo[*h*]isoquinoline (9).

The u.v. absorption maxima and their corresponding log ε values of the mono- and disubstituted isoquinolines, measured in ethanol, are summarized in Tables 3 and 4. The spectral data for isoquinoline (10) have been added for reference. Osburn *et al.* (11) have recorded the u.v. spectra of 2-, 3-, 4-, 5-, 6-, 7- and 8-aminoisoquinolines in neutral and strongly acidic water solutions, and determined their pK_a values. Comparison of these data with those in Table 3 shows that only 5-aminoisoquinoline has the same spectrum in water and ethanol solution, and that 6-, 7-, and 8-aminoisoquinolines in ethanol display a red shift of α- and p-bands in the order of 10 to 12 nm compared with the values obtained in water. Amino and hydroxyl groups in the 6-position produce a red shift of the β-band, as shown by the 6-amino-, 6-hydroxy-, and 6-amino-5-thio-

Can. J. Chem. Downloaded from www.nrcresearchpress.com by 210.87.254.42 on 09/05/12
For personal use only.

TABLE 4. The u.v. absorption spectra and log ε values of disubstituted isoquinolines (in absolute ethanol)

Compound	α-Band		p-Band		β-Band	
	λ_{max} (nm)	log ε	λ_{max} (nm)	log ε	λ_{max} (nm)	log ε
5-Amino-8-thiocyano-isoquinoline	390	3.99	252	4.16		
	345	3.95			214	4.41
8-Amino-5-thiocyano-	370	3.88	252	4.01	214	4.06
	325	3.74				
6-Amino-5-thiocyano-	340	3.55	302	3.72	248	4.58
			292	3.80	204	3.84
5-Amino-8-mercapto-	340	3.84	254	4.06	214	4.31
8-Amino-5-mercapto-	335	3.98	244	4.40	215	4.41
8-Amino-5-bromo-	355	3.90	238	4.05	213	4.47
	325	3.85				
5-Bromo-8-nitro-	330	3.80	296	3.78	220	4.48
5-Acetamido-8-amino-	370	3.72	248	4.13	210	4.40
5-Acetamido-8-nitro-	350	3.93	230	4.32	212	4.27

cyanoisoquinoline. It is believed that this shift is due to the resonance effect which involves the 6-amino-, or 6-hydroxy group, and the ring nitrogen; for example,

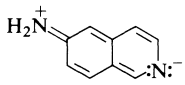

The 6-amino group in isoquinolines causes also a strong red shift of the p-band. In the majority of 5,8-disubstituted isoquinolines, the p-band shows a blue shift, and a considerable red shift of the α-band, compared with the p-band of unsubstituted isoquinoline. All 5,8-disubstituted isoquinolines have the β-band very close to 216 nm, the position of the β-band in unsubstituted isoquinoline.

Nuclear Magnetic Resonance Spectra

A survey of the literature reveals that in addition to the n.m.r. spectrum of isoquinoline (12, 13) only a few spectra of substituted isoquinolines have been studied (14–16).

In this work, we recorded the n.m.r. spectra of a number of isoquinolines with one (Table 5) or two substituents (Table 6) on the benzenoid ring. When it was possible, first-order interpretation of spectra was applied and the coupling constants were measured with an accuracy of 0.2 Hz. In 5-, 6-, 7-, and 8-aminoisoquinolines, the two doublets for H-3 and -4, are well separated from other bands, but in the rest of the compounds, with the exception of 6-hydroxyisoquinoline, the H-4 is overlapping with bands from the benzenoid ring. 5-Nitroisoquinoline represents a very special case by showing a complex multiplet including also the H-3 band.

In 5-aminoisoquinoline, the protons H-6, -7, and -8 represent an ABX system, however, the spectrum of these protons is "deceptively simple", as in a quasi A_2B system, consisting of a triplet and a doublet.

6-Aminoisoquinoline displays a spectrum of the benzenoid protons from which it is possible to measure the coupling constants $J_{5,7}$ and $J_{7,8}$. However, the coupling constant $J_{5,8}$ seems to be very small, because there is no corresponding splitting between H-5 and -8. Most of the disubstituted isoquinolines (Table 6) investigated were of the 5,8-type, and the bands for H-6 and -7 showed up as two doublets, with the exception of 5-acetamido-8-nitro- and 5-bromo-8-nitroisoquinoline where H-6 and -7 formed a singlet with the intensity of two protons.

In the n.m.r. spectrum of thiazolo[4,5-*h*]isoquinoline, the two doublets at 7.78 and 8.62 δ are assigned to H-6 and -7, and the two singlets at 9.14 and 9.40 δ to H-2 and -9, respectively (Table 7). Such an assignment to H-2 and -9 is in agreement with the n.m.r. spectra of 2-substituted thiazolo-[4,5-*h*]isoquinolines in which the band at 9.14 δ is not present. The band at 9.40 δ shows also a slight coupling with both H-6 and -7. The two remaining benzenoid ring protons H-4 and -5 also display a typical AX pattern of two doublets centered at 7.82 and 8.33 δ ($J_{4,5}$ = 9.0 Hz). However, the assignment for both H-4 and -5 is not

Can. J. Chem. Downloaded from www.nrcresearchpress.com by 210.87.254.42 on 09/05/12
For personal use only.

Can. J. Chem. Downloaded from www.nrcresearchpress.com by 210.87.254.42 on 09/05/12
For personal use only.

TABLE 5. The n.m.r. spectra of monosubstituted isoquinolines

Compound	Chemical shift (δ)*								J (Hz)	
	H-1	H-3	H-4	H-5	H-6	H-7	H-8	Other	$J_{3,4}$	Other
Isoquinoline†	9.22 s	8.52 s	(7.90	to	7.23)	m‖		—	6.0	
5-Acetamido-‡	9.30 s	8.55 d	m‖	—	(8.20	to	7.48) m‖	2.22 (CH_3)	6.0	
5-Amino-†	9.18 s	8.47 d	7.57 d	—	6.90 t		7.53 d	4.37 (NH_2)	6.0	
6-Amino-‡	8.94 s	8.14 d	7.38 d	6.83 d	—	7.11 q	7.79 d	5.98 (NH_2)	6.0	$J_{7,8}$ = 9.0 Hz $J_{5,7}$ = 2.4 Hz
7-Amino-‡	9.00 s	8.20 d	7.55 d	(7.77	to 7.00) m‖	—	m‖	4.10 (NH_2)	6.0	
8-Amino-‡	9.53 s	8.38 d	7.50 d	(7.60	to	6.78) m‖	—	6.05 (NH_2)	6.0	
5-Bromo-†	9.22 s	8.62 d	m‖	—	(8.00	to	7.42) m‖	—	6.0	
5-Nitro-‡	9.50 s	m‖	m‖	—	(8.80	to	7.73) m‖	—	—	
6-Hydroxy-‡§	9.22 s	8.43 d	7.70 d	m‖	—	(7.50	to 7.31) m‖	—	6.0	
7-Hydroxy-‡§	9.13 s	8.37 d	(7.97	to	7.42) m‖	—	m‖	—	6.0	

*Doublet, d; quartet, q; triplet, t.
†In $CDCl_3$ solution.
‡In DMSO-d_6 solution.
§After exchange of OH with D_2O.
‖Overlapping multiplets.

TABLE 6. The n.m.r. spectra of disubstituted isoquinolines

Compound	Chemical shift (δ)*							J (Hz)	
	H-1	H-3	H-4	H-6	H-7	H-8	Other	$J_{3,4}$	$J_{6,7}$
5-Acetamido-8-amino-†	9.50 s	8.39 d	7.61 d	7.44 d	6.72 d	—	3.10 (CH_3) 6.08 (NH_2)	6.0	8.5
5-Acetamido-8-nitro-†	9.90 s	8.73 d	8.30 d	8.43 s		—	3.25 (CH_3)	6.0	—
5-Amino-8-mercapto-†	9.33 s	8.43 d	8.02 d	6.71 d	7.31 d	—		6.0	8.5
8-Amino-5-mercapto-‡	9.93 s	8.30 d	8.07 d	7.70 d	6.93 d	—		6.0	8.5
5-Amino-8-thiocyano-†	9.64 s	8.66 d	8.19 d	6.97 d	7.87 d	—	6.88 (NH_2)	6.0	8.7
6-Amino-5-thiocyano-‡	9.23 s	8.53 d	8.26 d	—	7.47 d	8.16 d		6.0	‖
7-Amino-8-thiocyano-†	9.21 s	8.41 d	8.00 d	7.75 s§	—	—		6.0	—
8-Amino-5-thiocyano-†	9.64 s	8.65 d	7.95 d	7.89 d	6.60 d	—	7.10 (NH_2)	6.0	9.0
5-Bromo-8-nitro-†	10.50 s	9.58 d	8.86 d	9.00 s		—		6.0	—

*Doublet, d; singlet, s.
†In DMSO-d_6 solution.
‡In acetic acid-d_4 solution.
§Overlap with H-5.
‖$J_{7,8}$ = 9.0 Hz.

Can. J. Chem. Downloaded from www.nrcresearchpress.com by 210.87.254.42 on 09/05/12
For personal use only.

TABLE 7. The n.m.r. spectra of thiazolo[4,5-*h*]isoquinoline and its derivatives

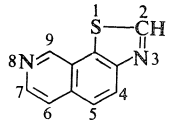

Compound	Chemical shift (δ)*							*J* (Hz)	
	H-2	H-4	H-5	H-6	H-7	H-9	Other	$J_{4,5}$	$J_{6,7}$
Thiazolo[4,5-*f*]isoquinoline†	9.14 s	7.82 d or 8.33 d	8.33 d or 7.82 d	7.78 d	8.62 d	9.40 s	—	9.0	5.9
Acetamido-‡·§	—	Overlap at 8.21	to 8.35	8.21 d	8.91 d	9.79 s	2.61 (CH_3)	—	5.8
2-Amino-‡	—	Overlap at	7.77 7.92	to	8.47 d	9.26 s	3.39 (NH_2)	—	5.8
2-Chloro-†	—	7.76 d or 8.04 d	8.04 d or 7.76 d	7.59 d	8.67 d	9.32 s	—	9.0	5.9
2-Hydroxy-‡	—	7.51 d or 8.08 d	8.08 d or 7.51 d	7.59 d	8.55 d	9.32 s	—	9.0	5.8

*Doublet, d; singlet, s.
†In $CDCl_3$ solution.
‡In DMSO-d_6 solution.
§At 160°.

TABLE 8. The n.m.r. spectra of thiazolo[5,4-*f*]isoquinoline and its derivatives

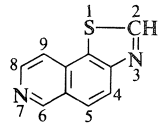

Compound	Chemical shift (δ)							*J* (Hz)	
	H-2	H-4	H-5	H-6	H-8	H-9	Other	$J_{4,5}$	$J_{8,9}$
Thiazolo[5,4-*f*]isoquinoline*	9.19 s	7.74 d or 8.12 d	8.12 d or 7.74 d	9.38 s	8.65 d	7.82 d	—	6.0	9.0
2-Acetamido-†	—	Overlap at 8.75 d		10.01 s	9.31 d	8.58 d	3.0 (CH_3)	—	5.8
2-Amino-†	—	8.10 d	7.75 d	9.32 s	8.55 d	7.73 d	‡ (NH_2)	9.0§	5.5
2-Chloro-*	—	Overlap at 7.97 d		9.30 s	8.65 d	7.73 d		—	6.5

*In $CDCl_3$ solution.
†In DMSO-d_6 solution.
‡NH_2 absorbs in the same region as H-4 and -5.
§NH_2 bands disappear after D_2O exchange. $J_{4,5}$ value is that of the deuterated compound.

Can. J. Chem. Downloaded from www.nrcresearchpress.com by 210.87.254.42 on 09/05/12
For personal use only.

possible from the first-order interpretation of the spectrum. The n.m.r. spectrum of thiazolo-[5,4-*f*]isoquinoline (Table 8) is analogous to that of thiazolo[4,5-*h*]isoquinoline.

Infrared Spectra

The i.r. spectra of thiazoloisoquinolines in the region 1700–400 cm^{-1} are presented in Table 9.

The strong bands starting from 1615–1602 to 1350 cm^{-1} are attributed to the aromatic and heteroaromatic double bond stretching vibrations. The bands in the region 1350–950 cm^{-1} are mostly moderate or weak, and they are assigned to C—H in-plane-deformation vibrations. Strong bands due to C—H out-of-plane bending motions occur in the region 950–650 cm^{-1}. All compounds in this series have strong bands between 835–810 cm^{-1}. In the far i.r. region, 650–400 cm^{-1} (ring deformation vibrations) (17) the band pattern is very sensitive to the nature of substituents.

The 2-aminothiazoloisoquinolines **1***a* and **2***a* are characterized by the bands 1650, 1660 and 1542, 1545 cm^{-1}, respectively (NH_2 group). The 2-hydroxythiazoloisoquinolines **1***d* and **2***d* exist actually in the lactam forms, as indicated by the strong carbonyl absorption bands at 1690 and 1680 cm^{-1}, respectively.

Experimental

Melting points were determined on a Gallenkamp melting point apparatus and are corrected. The u.v. spectra were recorded on a Unicam spectrophotometer model 800. Absolute ethanol was used as the solvent. The n.m.r. spectra were taken on a Varian n.m.r. spectrometer model A-60. Solvents used were acetic acid-d_4, carbon tetrachloride, deuteriochloroform, dimethylsulfoxide-d_6, and deuterium oxide. Tetramethylsilane was used as an internal standard. The i.r. spectra were recorded on a Perkin–Elmer model 521 and model 337 spectrophotometers (on KBr pellets). Elemental analyses were carried out by C. Daessle, Montreal and A. Bernhardt, Germany. The n.m.r. spectra were recorded by Mr. Victor Yu.

2-Aminothiazolo[4,5-h]isoquinoline (1a)

7-Aminoisoquinoline (**5**) (2.88 g, 0.02 mol) and potassium thiocyanate (8 g, 0.063 mol) were dissolved in 80 ml of 95% acetic acid in a 250 ml three-neck flask equipped with a mechanical stirrer, a thermometer, and a dropping funnel. Methanol (8 ml) was also added to the solution, which was cooled to 0–5°. Bromine (1.2 ml, 0.02 mol) in 10 ml of 95% acetic acid was added dropwise with stirring over a period of 20 min. The reaction mixture was poured into 100 ml of water after being stirred for an additional hour. The acid solution was neutralized with saturated sodium carbonate solution. The orange precipitate of 7-amino-8-thiocyanoisoquinoline (**6**) was collected and dried (yield 78%): i.r. (KBr): 2144 (SCN); 3445, 3365, 3230 cm^{-1} (NH_2).

A solution of 3.2 g of crude 7-amino-8-thiocyanoisoquinoline (**6**) in 150 ml of 4 *N* hydrochloric acid and 150 ml of ethanol was refluxed for 2 h. The hot solution was filtered and left to stand overnight. A yellow crystalline compound, 2-aminothiazolo[4,5-*h*]isoquinoline hydrochloride, precipitated. The salt was dissolved in water and neutralized with dilute sodium carbonate solution. The free base, 2-aminothiazolo[4,5-*h*]isoquinoline (**1***a*), precipitated (yield 90%); pale yellow needles, m.p. 303.5–305.5° (ethanol–water).

Anal. Calcd. for $C_{10}H_7N_3S$: C, 59.68; H, 3.51; N, 20.88; S, 15.92. Found: C, 59.60; H, 3.67; N, 20.74; S, 16.01.

2-Chlorothiazolo[4,5-h]isoquinoline (1b)

Cuprous chloride was prepared from 3 g of copper sulfate pentahydrate, 0.66 g of sodium chloride, 0.54 g of sodium hydrogen sulfite, and 0.36 g of sodium hydroxide, and dissolved in 10 ml of concentrated hydrochloric acid. The solution was cooled while the diazotation of the amino compound **1***a* was being carried out.

2-Aminothiazolo[4,5-*h*]isoquinoline (**1***a*) (1.2 g, 6.0 mmol) was added to 40 ml of 85% phosphoric acid with mechanical stirring. It was then cooled and maintained at 5–10° and 10 ml of 70% nitric acid was added. The resulting solution was cooled to 0–5° and sodium nitrite (0.44 g, 6.5 mmol) in 4 ml of water was added, with constant stirring, over a period of 15 min. The reaction mixture was stirred for another 15 min at this temperature, and was then added over a period of 20 min to the stirred solution of cuprous chloride in concentrated hydrochloric acid at 0–5°. The reaction mixture was stirred for another hour at room temperature. It was made basic with 20% sodium hydroxide solution. The basic mixture was extracted with three 250 ml portions of diethyl ether. The ether extract was washed with water, dried over magnesium sulfate, and filtered. The ether solution was evaporated to dryness leaving a pale yellow solid. The crude 2-chlorothiazolo[4,5-*h*]isoquinoline (**1***b*) was sublimed at 2 mm (bath temperature 98°). The sublimate (0.52 g) was recrystallized from *n*-hexane to give 0.45 g of the pure colorless chloro compound, m.p. 130–131°.

Anal. Calcd. for $C_{10}H_5N_2SCl$: C, 54.42; H, 2.28; N, 12.70; S, 14.53. Found: C, 54.33; H, 2.32; N, 12.85; S, 14.57.

Thiazolo[4,5-h]isoquinoline (1c)

2-Chlorothiazolo[4,5-*h*]isoquinoline (**1***b*) (0.5 g, 2.3 mmol) was dissolved in a mixture of 8 ml of 47% hydriodic acid, 4 ml of 95% acetic acid, and 4 ml of water, and 0.28 g of red phosphorus was added. The resulting mixture was refluxed for 3 h and filtered while hot. The volume was reduced to 6 ml and allowed to cool. The orange–red crystalline precipitate was collected, dissolved in water and neutralized with dilute sodium carbonate solution. The resulting precipitate was filtered off, washed with water, and dried. Recrystallization from *n*-hexane gave colorless needles of thiazolo[4,5-*h*]isoquinoline (**1***c*) in 58% yield, m.p. 138–139°.

Anal. Calcd. for $C_{10}H_6N_2S$: C, 64.49; H, 3.25; N, 15.05; S, 17.21. Found: C, 64.34; H, 3.32; N, 14.93; S, 17.08.

2-Acetamidothiazolo[4,5-h]isoquinoline

2-Aminothiazolo[4,5-*h*]isoquinoline (**1***a*) (0.5 g, 2.5

TABLE 9. The i.r. spectra of thiazolo[4,5-*h*]- and -[5,4-*f*]isoquinolines

1*c*	2*c*	1*a*	2*a*	1*b*	2*b*	1*d*	2*d*
						1690 vs	1685 vs
		1650 vs	1660 vs				
	1615 s		1615 s	1610 s			1615 s
1604 m	1602 s				1603 s		
1578 m	1575 w	1590 vw	1575 m			1585 s	
			1560 s		1570 w		1570 m
1528 w		1542 vs	1545 vs				
1495 m	1498 s	1500 s	1495 s		1485 m	1503 m	1505 w
	1465 s			1464 vs	1460 s		
1452 m		1440 s	1450 s			1445 m	1455 m
1437 w	1430 s	1427 w	1425 m	1428 s	1425 s		
1409 s	1400 s		1410 m			1410 m	1402 vw
1383 m		1378 m	1390 m	1385 s	1372 s	1365 m	1388 m
1347 m	1352 s	1352 m	1350 m	1347 s	1345 s	1352 s	1360 m
1308 m	1312 w	1320 s	1315 m			1310 vw	1328 vw
1298 m	1298 w	1290 w	1290 w				
	1278 s					1270 vw	
1260 vs	1265 sh	1253 m	1250 m	1250 s	1250 s	1247 s	1265 m
1226 m	1220 w			1220 w			
1214 m							
1210 m	1208 w					1202 m	1203 w
1172 w	1176 w			1180 w		1178 m	
		1163 w	1150 w		1163 w		1170 m
1140 vw		1132 w		1140 w		1135 vw	1132 w
	1127 m	1120 w			1120 vw		
			1085 m				
			1062 vw	1060 s	1060 vs		
1048 m	1040 w		1038 m			1045 m	1045 m
1027 w		1030 vw		1028 s	1025 s		1028 m
	1010 m						
968 s	983 w	975 s		985 s	983 vs	975 m	995 m
	942 w						
	928 w						
910 w		910 vw	908 shm	910 w	910 w		
			890 vs				
865 vs	858 vs						
852 m		850 shw	854 s			845 shw	842 m
825 m	828 vs	833 vs	835 s	830 w	830 wsh	830 s	
	810 vs		810 s	816 vs	810 vs		810 s
800 w	795 w	790 vw					
	768 w			770 w	770 w		765 w
728 s					738 w		
697 s	690 s			685 w	685 shw		
680 vw	685 s		680 w	680 m	680 s		682 m
		670 w		675 w	670 s		
657 vw	652 s						640 m
		630 w				630 shm	635 wsh
		610 w					
			580 m			587 s	590 s
	573 s	565 w		575 m	570 m		570 shw
532 s	530 s	545 w				545 m	
526 s				525 w	525 w		
		512 w	510 shw	510 w	510 w		512 w
505 s			502 m	490 w	490 w	500 w	
475 s			464 m				
		450 w	440 shm				
		415 w	425 m				
	400 m				385 w		

mmol) was refluxed with a mixture of 8 ml of acetic anhydride and 4 ml of pyridine for 2 h. Filtration of the cooled reaction mixture gave 0.55 g of 2-acetamidothiazolo[4,5-*h*]isoquinoline (91% yield). Colorless crystals, m.p. > 350° (absolute ethanol).

Anal. Calcd. for $C_{12}H_9N_3OS$: C, 59.24; H, 3.73; N, 17.27; S, 13.08. Found: C, 59.46; H, 3.37; N, 17.29; S, 13.29.

2-Hydroxythiazolo[4,5-h]isoquinoline

2-Chlorothiazolo[4,5-*h*]isoquinoline (**1***b*) (0.3 g, 1.48 mmol) was refluxed in 30 ml of 0.5 *N* sodium hydroxide solution for 3 h. The solution was cooled and acidified with dilute acetic acid to p*H* 6. The resulting precipitate was filtered off, washed with water and dried to give a 65% yield of 2-hydroxythiazolo[4,5-*h*]isoquinoline. Pale yellow needles, m.p. 296–297.5° (ethanol).

Can. J. Chem. Downloaded from www.nrcresearchpress.com by 210.87.254.42 on 09/05/12
For personal use only.

Can. J. Chem. Downloaded from www.nrcresearchpress.com by 210.87.254.42 on 09/05/12
For personal use only.

Anal. Calcd. for $C_{10}H_6N_2OS$: C, 59.38; H, 2.99; N, 13.85. Found: C, 59.62; H, 2.81; N, 13.96.

*6-Amino-5-thiocyanoisoquinoline (**8**)*

6-Aminoisoquinoline (**7**) (2.88 g, 0.02 mol) and potassium thiocyanate (8.0 g, 0.063 mol) were dissolved in 100 ml of 95% acetic acid. The solution was cooled to 0–5° and bromine (1.2 ml, 0.02 mol) in 10 ml of glacial acetic acid was added dropwise. The reaction mixture was poured into 100 ml of water, and neutralized with sodium carbonate solution. The orange precipitate was collected and dried (85% yield). Recrystallization from a large volume of benzene gave yellow needles of **8**, m.p. 159.5–161°.

Anal. Calcd. for $C_{10}H_7N_3S$: C, 59.68; H, 3.51; N, 20.88; S, 15.92. Found: C, 59.59; H, 3.52; N, 20.99; S, 15.76. The i.r. (KBr): 2148 (SCN); 3382, 3316, 3162 cm^{-1} (NH_2).

*2-Aminothiazolo[5,4-f]isoquinoline (**2a**)*

A solution of 6-amino-5-thiocyanoisoquinoline (**8**) (2.0 g, 0.01 mol) in 120 ml of 4 *N* hydrochloric acid and 120 ml of ethanol was refluxed for 2 h. The acid solution was evaporated in order to remove the ethanol and was neutralized with sodium carbonate solution. The yellow precipitate was collected, washed with water, and dried to give 1.82 g (91% yield) of **2a**. Recrystallization from aqueous alcoholic solution gave yellow needles, m.p. 251–253°.

Anal. Calcd. for $C_{10}H_7N_3S$: C, 59.68; H, 3.51; N, 20.88; S, 15.92. Found: C, 59.66; H, 3.61; N, 20.73; S, 15.80.

The i.r. (KBr): 3305, 3110 (broad) cm^{-1} (NH_2).

*2-Chlorothiazolo[5,4-f]isoquinoline (**2b**)*

2-Aminothiazolo[5,4-*f*]isoquinoline (1.2 g, 6 mmol) was transformed into 2-chlorothiazolo[5,4-*f*]isoquinoline (**2b**) by a procedure similar to that used for the preparation of **1b**. The crude 2-chlorothiazolo[5,4-*f*]isoquinoline (**2b**) was sublimed at 2 mm (bath temperature 110°). The sublimate (0.52 g, 38% yield) was recrystallized twice from *n*-hexane giving 0.45 g of colorless needles of the chloro compound, m.p. 170° (dec.).

Anal. Calcd. for $C_{10}H_5N_2SCl$: C, 54.42; H, 2.28; N, 12.70; Cl, 16.07. Found: C, 54.03; H, 2.70; N, 12.81; Cl, 16.10.

*Thiazolo[5,4-f]isoquinoline (**2c**)*

This compound was prepared from 2-chlorothiazolo-[5,4-*f*]isoquinoline (0.5 g, 2.3 mmol) by a method analogous to that applied for the preparation of **1c**. Colorless needles (55% yield) m.p. 174–175.5° (*n*-hexane).

Anal. Calcd. for $C_{10}H_6N_2S$: C, 64.49; H, 3.25; N, 15.05; S, 17.21. Found: C, 64.76; H, 3.29; N, 14.92; S, 17.08.

2-Acetamidothiazolo[5,4-f]isoquinoline

Colorless needles (ethanol), m.p. > 350°.

Anal. Calcd. for $C_{12}H_9N_3OS$: C, 59.24; H, 3.73; N, 17.27; S, 13.08. Found: C, 59.64; H, 3.31; N, 17.32; S, 13.33.

2-Hydroxythiazolo[5,4-f]isoquinoline

2-Chlorothiazolo[5,4-*f*]isoquinoline (**2b**) was hydrolyzed with 0.5 *N* sodium hydroxide solution and the hydroxy derivative was obtained in the form of fine yellow needles, m.p. > 350° (aqueous ethanol).

Anal. Calcd. for $C_{10}H_6N_2OS$: C, 59.38; H, 2.99; N, 13.85. Found: C, 59.41; H, 3.37; N, 13.73.

*5-Acetamido-8-aminoisoquinoline (**11**)*

5-Acetamido-8-nitroisoquinoline (**10**) (4.6 g, 0.02 mol) was reduced with hydrogen and 5% palladium-on-charcoal in absolute ethanol for 2 h. The catalyst was filtered off and the filtrate was evaporated to dryness. The resulting substance was crystallized from ethanol to give 2.4 g (85% yield) of 5-acetamido-8-aminoisoquinoline (**11**) as yellow needles, m.p. 270.5–272.5°.

Anal. Calcd. for $C_{11}H_{11}N_3O$: C, 65.67; H, 5.51; N, 20.74. Found: C, 65.77; H, 5.75; N, 20.70.

*2,5-Diaminothiazolo[5,4-h]isoquinoline (**3**)*

5-Acetamido-8-aminoisoquinoline (**11**) (3.02 g, 0.015 mol) and potassium thiocyanate (6.0 g, 0.047 mol) were dissolved in 120 ml of 95% acetic acid, and 10 ml of methanol. The resulting solution was cooled to 0–5° and bromine (0.9 ml, 0.015 mol) in 15 ml of glacial acetic acid was added dropwise over a period of 20 min. The reaction mixture was poured into 100 ml of water. The acid solution was neutralized with sodium carbonate solution. The crude orange product, 5-acetamido-8-amino-7-thiocyanoisoquinoline (**12**), weighed 3.2 g. A solution of 3 g of **12** in 150 ml of ethanol and 150 ml of 4 *N* hydrochloric acid was refluxed for 3 h. The acid solution was filtered, and the volume of the filtrate was reduced to 50 ml. The acid solution was poured onto ice and neutralized with sodium carbonate solution. The dark green precipitate was collected and recrystallized from aqueous alcoholic solution to give pale yellow needles, m.p. 274–276°. The total yield of 2,5-diaminothiazolo[5,4-*h*]isoquinoline (**3**) was 60%.

Anal. Calcd. for $C_{10}H_8N_4S$: C, 55.54; H, 3.73; N, 25.91. Found: C, 55.68; H, 3.77; N, 25.74.

The u.v. (ethanol): λ_{max} 227, 270, 382 nm; log ε 4.36, 4.27, 3.78; i.r. (KBr): 1652 m, 1550 vs, 1484 m, 1442 s, 1426 s, 1380 vs, 1202 m, 885 s, 847 s, 830 s, 802 m, 670 w, 580 m, 497 w, 460 w, 435 m, 420 m cm^{-1}.

2,5-Diacetamidothiazolo[5,4-h]isoquinoline

This compound was prepared from **3** using the procedure reported above for the acetamido derivative of **1c**. Fine colorless needles (dimethylformamide), m.p. > 350° (dec.).

Anal. Calcd. for $C_{14}H_{12}N_4O_2S$: C, 55.98; H, 4.03; N, 18.64; S, 10.68. Found: C, 55.79; H, 4.10; N, 18.78; S, 10.61.

*5-Amino-8-thiocyanoisoquinoline (**13**)*

This compound was obtained from 5-aminoisoquinoline (2.88 g, 0.02 mol) and potassium thiocyanate (8.0 g, 0.063 mol) using the procedure reported above for the preparation of **8**. The crude product (80% yield) was crystallized from a large volume of benzene to give yellow needles of **13**, m.p. 181–183°.

Anal. Calcd. for $C_{10}H_7N_3S$: C, 59.57; H, 3.51; N, 20.88; S, 15.94. Found: C, 59.6; H, 3.6; N, 20.9; S, 15.9.

*5-Amino-8-mercaptoisoquinoline (**14**)*

A solution of 2.0 g (0.01 mol) of 5-amino-8-thiocyanoisoquinoline (**13**) in 120 ml of 8 *N* hydrochloric acid and 120 ml of ethanol was refluxed for 4 h. The acid solution was evaporated to dryness on a water bath leaving a yellow solid, which was dissolved in 50 ml of water. Neutralization of the solution with sodium carbonate solution produced a precipitate which was filtered and

dried. Recrystallization from ethanol gave 1.5 g of **14** (87% yield), m.p. 260–262°.

Anal. Calcd. for $C_9H_8N_2S$: C, 61.36; H, 4.54; N, 15.91; S, 18.19. Found: C, 61.60; H, 4.48; N, 15.71; S, 18.11.

*8-Amino-5-thiocyanoisoquinoline (**15**)*

8-Aminoisoquinoline (3.35 g, 0.015 mol) and potassium thiocyanate (6.0 g, 0.047 mol) were dissolved in 90 ml of 95% acetic acid, and 6 ml of methanol. Bromine (0.9 ml, 0.015 mol) in 10 ml of 95% acetic acid was added dropwise, at 0–5°, followed by steps similar to the preparation of **8**. 8-Amino-5-thiocyanoisoquinoline (**15**) was obtained in a 79% yield (2.4 g). Recrystallization from benzene yielded yellow needles, m.p. 209–211°.

Anal. Calcd. for $C_{10}H_7N_3S$: C, 59.57; H, 3.51; N, 20.88. Found: C, 59.27; H, 3.83; N, 20.66.

*8-Amino-5-mercaptoisoquinoline (**16**)*

8-Amino-5-thiocyanoisoquinoline (**15**) was transformed into **16** by a method similar to that used for the preparation of **14**. 8-Amino-5-mercaptoisoquinoline (**16**) formed colorless needles, m.p. 244–246° (ethanol).

Anal. Calcd. for $C_9H_8N_2S$: C, 61.36; H, 4.54; N, 15.91; S, 18.19. Found: C, 61.77; H, 4.05; N, 16.09; S, 18.13.

Starting Materials and Intermediates

7-Hydroxyisoquinoline (18), m.p. 229.5–231°; lit. 229–231°. 7-Aminoisoquinoline (**5**) (19), m.p. 203–205°; lit. 204°. 6-Methoxyisoquinoline hydrochloride (19), m.p. 216°; lit. 220°. 6-Hydroxyisoquinoline (20), m.p. 220–222°; lit. 220°. 6-Aminoisoquinoline (7), m.p. 216°; lit. 211–212° (11). 5-Nitroisoquinoline (21), m.p. 106°; lit. 106–108°. 5-Aminoisoquinoline (11), m.p. 128–131°; lit. 129–131°. 5-Acetamidoisoquinoline (**9**) (22), m.p. 161–163°; lit. 166°. 5-Bromoisoquinoline (11), m.p. 82.5–84°; lit. 82–84°. 5-Bromo-8-nitroisoquinoline (23), m.p. 128–139.5°; lit. 139–141°. 8-Aminoisoquinoline (23), m.p. 172–174°; lit. 170–172°.

1. C. E. Hall and A. Taurins. Can. J. Chem. **44**, 2465 (1966).
2. C. E. Hall and A. Taurins. Can. J. Chem. **44**, 2473 (1966).
3. C. E. Hall and A. Taurins. Can. J. Chem. **46**, 691 (1968).
4. E. E. Reid. Organic chemistry of bivalent sulfur. Vol. 6. Chemical Publishing Co., Inc., New York, N.Y., 1966. p. 44.
5. R. Riemschneider. J. Am. Chem. Soc. **78**, 844 (1956).
6. E. Clar. Aromatische Kohlenwasserstoffe. 2nd Ed. Springer, Berlin, 1952.
7. J. R. Platt. J. Chem. Phys. **17**, 484 (1949).
8. H. Bruns. Spectrum No. H9/1. DMS UV Atlas of organic compounds. Vol. III. Butterworth, London and Verlag Chemie, Weinheim, 1967.
9. C. E. Loader and C. J. Timmons. Spectrum No. H22/22. DMS UV Atlas of organic compounds. Vol. IV. Butterworth, London and Verlag Chemie, Weinheim, 1967.
10. S. F. Mason. *In* Physical methods in heterocyclic chemistry. Vol. 2. A. R. Katritzky, *Editor*. Academic Press, New York, N.Y., 1963. p. 38.
11. A. R. Osburn, K. Schofield, and L. N. Short. J. Chem. Soc. 4191 (1956).
12. E. Van der Donckt, R. H. Martin, and F. Geerts-Evrard. Tetrahedron, **20**, 1498 (1964).
13. P. J. Black and M. L. Heffernan. Austr. J. Chem. **19**, 1287 (1966).
14. W. Brügel, T. Ankel, and F. Kruckeberg. Zeitschr. für Elektrochem. **64**, 1121 (1960).
15. K. Tori, M. Ogata, and H. Kano. Chem. Pharm. Bull. (Jap.). **71**, 681 (1963).
16. L. Pohl and W. Wiegrebe. Zeitschr. für Naturforschung. **20B**, 1032 (1965).
17. J. S. Steward. Far infrared spectroscopy. *In* Interpretive spectroscopy. S. K. Freeman, *Editor*. Reinhold Publishing Corporation, New York, N.Y., 1965. pp. 131–169.
18. R. B. Woodward and W. Von E. Doering. J. Am. Chem. Soc. **67**, 860 (1945).
19. R. A. Robinson. J. Am. Chem. Soc. **69**, 1939 (1947).
20. R. A. Robinson. J. Am. Chem. Soc. **69**, 1944 (1947).
21. C. G. Le Fevre and R. J. W. Le Fevre. J. Chem. Soc. 1470 (1935).
22. J. J. Craig and W. E. Cass. J. Am. Chem. Soc. **64**, 783 (1952).
23. M. Gordon and D. E. Pearson. J. Org. Chem. **29**, 329 (1964).

Can. J. Chem. Downloaded from www.nrcresearchpress.com by 210.87.254.42 on 09/05/12
For personal use only.

Can. J. Chem. Downloaded from www.nrcresearchpress.com by 210.87.254.6 on 09/05/12
For personal use only.

Electrophilic Substitution in Methyl-Substituted Naphthalenes. II. The Hyperconjugative Model of the Methyl Group in PPP- and ω-Technique Calculations

LE-KHAC HUY AND W. FORST
Department of Chemistry, Université Laval, Québec 10, Québec

Received June 25, 1971

A study of the dependence of common reactivity indices in 1,4-dimethylnaphthalene on the values of the parameters for the heteroatom model of the methyl group reveals that this model is not suitable within the Pople–Pariser–Parr formalism. However, if this model is used in conjunction with the ω-technique, two of the indices, superdelocalizability and localization energy, may give the correct order of reactive positions of 1,4-dimethylnaphthalene provided that an appropriate choice of parameter values is made.

L'étude de la variation des indices de réactivité usuels du 1,4-diméthyl naphtalène avec les valeurs des paramètres pour le modèle hétéroatome du groupement méthyle révèle que ce modèle ne convient pas au formalisme de Pople–Pariser–Parr. Cependant, si ce modèle est utilisé avec la technique ω, deux des indices, la superdélocalisabilité et l'énergie de localisation, peuvent donner le bon ordre des positions réactives de 1,4-diméthyl naphtalène advenant un choix approprié des valeurs des paramètres.

Canadian Journal of Chemistry, **49**, 4065 (1971)

Introduction

This paper deals with computational aspects of a study of electrophilic substitution reported more fully in Part III (following paper, ref. 17). The justification for a separate presentation is the desire to leave the main argument of Part III uncluttered with details of procedure, some of which is rather involved.

Exploratory calculations have shown that (*a*) it was generally difficult to obtain agreement between theory and experiment whenever substitution took place in a β-position; (*b*) not only the nature of the model for the methyl group but also numerical values of the parameters involved had substantial influence on the calculated result. Therefore before undertaking the study of all the methyl naphthalenes we have investigated first in some detail the model and parameter representation of the methyl group, using 1,4-dimethylnaphthalene as a convenient test case, one where chloromethylation and several other electrophilic substitutions all take place in a β-position; more complete experimental results (1) give the order of reactive positions[1] in this compound as $3 > 5 > 6$ for electrophilic substitution.

Since almost any result can be obtained by appropriate manipulation of parameters in a semi-empirical molecular orbital (m.o.) method, one must choose a consistent set of parameters that can correlate various types of data, *e.g.* spectral properties, reactivity, etc. quantitatively as well as qualitatively. Although we deal in this paper exclusively with the qualitative order of reactive positions in 1,4-dimethylnaphthalene, we show in Part III that parameter values chosen on this basis are in fact consistent in the sense defined above. The reason for testing parameters on reactivity first is due to the fact that the reverse procedure, *i.e.* testing parameters on spectral properties, ionization potentials and the like, before calculating reactivity, is unworkable, as will be pointed out on several occasions.

In a previous note (2), hereafter referred to as Part I, we have investigated the dependence of three representative reactivity indices q_r, S_r and L_r, defined further below, on the value of the parameter h for the *inductive* effect of the methyl group. It turned out that a given reactivity index behaves similarly, whether calculated by the ω-technique or the more expensive (in terms of computer time) Pople–Pariser–Parr (PPP) technique; in particular, only S_r, perhaps accidentally, gave the correct order of reactive positions.

[1]The following numbering is used throughout Parts II and III:

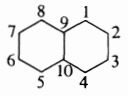

Can. J. Chem. Downloaded from www.nrcresearchpress.com by 210.87.254.6 on 09/05/12
For personal use only.

We now wish to investigate how the three reactivity indices behave as a function of parameters for the *hyperconjugative* effect of the methyl group.

Method of Calculation

The method of calculation by the ω-technique (3) has been described in Part I and will not be repeated here in detail. We only re-write eq. 1 of Part I in the slightly more general form

$$[1] \qquad \alpha_r^{t+1} = \alpha + \omega\beta\,(n_r - q_r^t)$$

where α and β are standard Coulomb and exchange integrals, respectively, q_r is electron density at atom r, n_r is the number of π-electrons made available for conjugation by atom r, and ω is an adjustable parameter. As before, the exchange integral β_{rs} is made dependent on bond length by the relation

$$[2] \qquad \beta_{rs}^{t+1} = \beta \exp[-2.683\,(0.12 - 0.18\,p_{rs}^t)]$$

where p_{rs} is the mobile bond order between atoms r and s. The superscript t in eqs. 1 and 2 represents the number of iterations.

The diagonal and off-diagonal elements in the PPP-technique (4) were also given in Part I. We present them in eqs. 3 and 4 in a slightly more general form,

$$[3] \qquad \alpha_r = (\alpha_r)_{\text{core}} + q_r\gamma_{rr} + \sum_{s \neq r} (q_s - Z_s)\gamma_{rs}$$

$$[4] \qquad \beta_{rs} = (\beta_{rs})_{\text{core}} - \tfrac{1}{2}p_{rs}\gamma_{rs}$$

where $(\alpha_r)_{\text{core}} = -W_r$ is an empirical parameter representing the sum of the π-electron kinetic energy in atomic orbital r and of potential energy due to core r only; γ_{rr} and γ_{rs} are the one- and two-center, two-electron repulsion integrals; $(\beta_{rs})_{\text{core}}$ is the resonance integral between cores r and s; Z_s is the number of electrons contributed by core s to the system.

In both the ω- and PPP-technique, the criterion of self-consistency was a variation of less than 10^{-4} in all wave function coefficients of occupied orbitals. To avoid convergence problems we have used a procedure similar to that of Ettinger (5), which consists of taking the average electron densities and mobile bond orders (eqs. 1 and 2) of two preceding iterations as input for the next iteration.

Values for the various parameters are given in Part I. Calculations were done on IBM 360/60 by means of programs written in Fortran IV.

It has been pointed out recently by Harris (6*a*) that when matrix elements of the total energy operator are dependent on net charges, this charge-dependence should be taken into account. As applied to methods used here, *i.e.* the ω- and PPP-techniques, however, it can be demonstrated (6) that the only changes are the interpretation of parameters appearing in eqs. 1–4, but not the form of the equations; hence no conclusions are affected.

Model for Methyl Group

In contrast with the inductive model, it is assumed in the hyperconjugative model for the methyl group that there is actual mixing of the aromatic ring π-orbitals with the (pseudo) π-orbital of the methyl group, leading to a flow of electrons between the methyl group and the ring, and their redistribution in the ring. Streitwieser and co-workers (3) have discussed the various theoretical representations suitable for describing the hyperconjugative effect; we select the so-called heteroatom model because it requires the least number of parameters. Briefly, the methyl group in this model is treated as a single heteroatom X contributing two electrons to the π-system; thus in eqs. 1 and 3, n_x and $Z_x = 2$ for the heteroatom and n_x, $Z_x = 1$ for all other carbon atoms.

This model has been criticized by Dewar (7) because the methyl group is made to contribute only one π-orbital, while the other antibonding orbital is neglected. In effect, this model gave the wrong prediction for behavior of electrons in the methyl group (8); however it is not likely wrong insofar as properties of electrons *in the ring* are concerned, which is the property of interest in the present study. Furthermore, inclusion of the methyl antibonding π-orbital requires the methyl group to be treated as a modified vinyl group (9), necessitating five parameters. Such large number of adjustable parameters effectively negates whatever superiority this model may have over the heteroatom model.

As applied to the ω-technique, the heteroatom model requires specification of two integrals, the heteroatom Coulomb (α_x) and exchange (β_{c-x}) integrals, which, in turn, are determined in terms of their standard values by means of two parameters, h_x and k_{c-x}:

$$[5] \qquad \alpha_x = \alpha + h_x\,\beta$$

$$[6] \qquad \beta_{c-x} = k_{c-x}\,\beta$$

Can. J. Chem. Downloaded from www.nrcresearchpress.com by 210.87.254.6 on 09/05/12
For personal use only.

In the PPP-technique, one can always choose W_x and $(\beta_{c-x})_{core}$ so as to make calculations directly comparable with the ω-technique. If we write

$$W_x = W_c - H_x\,\beta \quad [7]$$

$$(\beta_{c-x})_{core} = K_{c-x}\,\beta \quad [8]$$

where $\beta = -2.39$ eV is the standard resonance integral and $W_c = 11.16$ eV is the ionization potential of the carbon atom, then H_x and K_{c-x} are the PPP equivalents of h_x and k_{c-x}. In addition, two subsidiary parameters, the electron affinity E_x and the effective nuclear charge Z_x^{eff} of the heteroatom (to be used in Roothan's formula for calculating repulsion integrals), need to be specified. Electron affinity appears only in the one-center, two-electron repulsion integral γ_{xx}:

$$\gamma_{xx} = W_x - E_x \quad [9]$$

As W_x is allowed to change, one could always compensate for this change by choosing an appropriate value for E_x. Hence the choice of a value for E_x is by no means critical and calculations were done by taking E_x to be equal to E_c, the electron affinity of a carbon atom.

Comparison of the dashed and solid lines in Figs. 5 and 6 shows that whether calculations are done using $Z_x^{eff} = Z_c^{eff} = 2.090$, or using the relation (10)

$$\gamma_{xx} = 5.325\,Z_x^{eff} \quad [10]$$

the general trend is the same. Consequently, the initially four-parameter PPP-problem is reduced to a two-parameter problem, and calculations by the PPP-technique are directly comparable with those using ω-technique.

Reactivity Indices

For convenience, definitions of reactivity indices used in this work (q_r, S_r, and L_r) are summarized here. For completeness, we also include here definitions of two other indices, f_r and π_{rr}, which will be used only in Part III. The definitions apply to a closed-shell molecule and electrophilic substitution. If c_{jr} is the wave function coefficient of atom r in orbital j, then the total π-electron density at atom r is

$$q_r = 2\sum_{j=1}^{m} c_{jr}^2 \quad [11]$$

(sum over occupied orbitals j)

The frontier electron density f_r for an electrophilic substitution is a contribution to q_r arising from the pair of electrons occupying the highest orbital m

$$f_r = 2\,c_{mr}^2 \quad [12]$$

The mobile bond order between atoms r and s is defined as

$$p_{rs} = 2\sum_{j=1}^{m} c_{jr}c_{js} \quad [13]$$

Self-polarizability at atom r is given by

$$\pi_{rr} = 4\sum_{j=1}^{m}\sum_{k=m+1}^{m}\frac{c_{jr}^2 c_{kr}^2}{\varepsilon_j - \varepsilon_k} \quad [14]$$

where the second sum (index k) is over unoccupied orbitals and ε_j is the one-electron energy in orbital j. Superdelocalizability for an electrophilic substitution is defined as

$$S_r = 2\sum_{j=1}^{m} c_{jr}^2/\varepsilon_j \quad [15]$$

As usual, we define localization energy in electrophilic substitution as the difference in π-energy between the original molecule and a "residual molecule" in which two electrons and one carbon atom at position r of attack are taken out of conjugation. However, in contrast to some previous treatments, we have applied iterations to both the original reactant and the "residual molecule", and in the latter have carried all computations to self-consistency at each position r separately. As in Part I, superscripts ω and P are used to distinguish indices calculated by the ω- and PPP-techniques.

Results and Discussion

Since there are two parameters to contend with, cross-comparison between two techniques (ω and PPP) is somewhat complicated. Consequently, for the sake of convenience and clarity we shall discuss separately results based on the two techniques before making the comparison.

(a) ω-Technique

The results of calculations are shown in Figs. 1–3, which represent the dependence of the three reactivity indices q_r^{ω}, S_r^{ω}, and L_r^{ω} on the two hyperconjugative parameters. The effect of one parameter (h_x or k_{c-x}) in the range of its commonly used values is illustrated by keeping the other constant; these constant values were taken more or less arbitrarily[2] as $h_x = 2.5$ and $k_{c-x} = 0.7$.

[2]These values are close to the cross-over-points in Figs. 2 and 3.

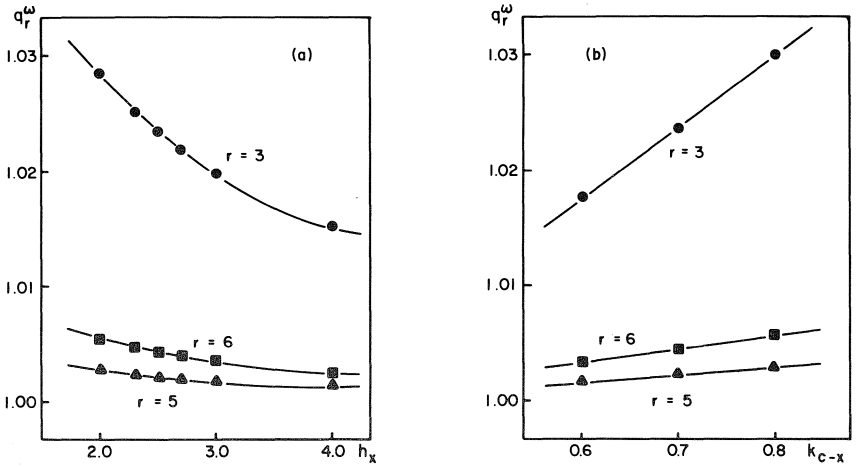

FIG. 1. Electron density of 1,4-dimethylnaphthalene at position r, calculated by the ω-technique (ω = 1.4) and using heteroatom model for representing the methyl groups: (*a*) as a function of parameter h_x (k_{c-x} = constant = 0.7) (*b*) as a function of parameter k_{c-x} (h_x = constant = 2.5).

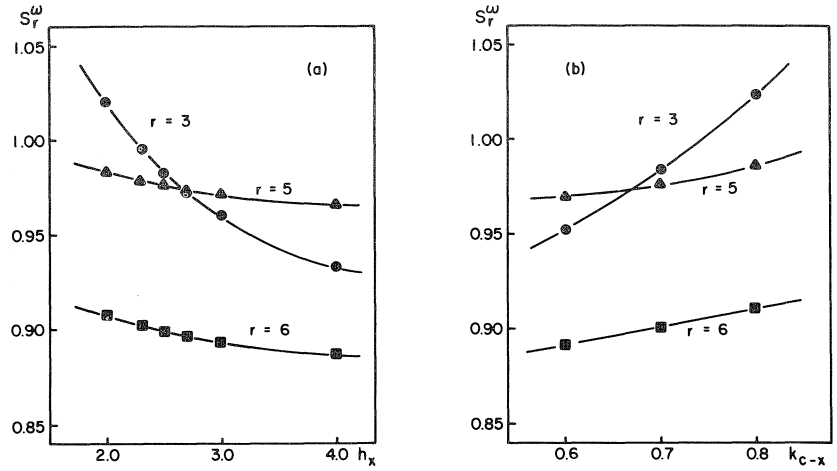

FIG. 2. Superdelocalizability of 1,4-dimethylnaphthalene at position r, calculated by the ω-technique (ω = 1.4) and using heteroatom model for representing the methyl groups: (*a*) as a function of parameter h_x (k_{c-x} = constant = 0.7) (*b*) as a function of parameter k_{c-x} (h_x = constant = 2.5).

The result for electron density q_r^ω (Fig. 1) shows that this index is relatively insensitive to both h_x and k_{c-x}, at least within the chosen range of parameter values. The most reactive position (position 3) is correctly predicted in 1,4-dimethylnaphthalene, but not the following positions. The results are thus quite analogous to those obtained in Part I for the inductive effect of the methyl group so that whatever the model used (inductive or hyperconjugative), electron density does not seem to be a good index of reactivity, a conclusion reached on other grounds by Ridd (11) and Greenwood and McWeeny (12), and corroborated by our own results (13) on other methylnaphthalenes.

The behavior of superdelocalizability S_r^ω (Fig. 2) and of localization energy L_r^ω (Fig. 3) is more interesting. S_r^ω behaves here in the same way as it did on the inductive model: cross-over points are observed in both Figs. 2*a* and *b*, so that depending on the chosen values of h_x and k_{c-x}, S_r^ω may or may not give the correct order of

Can. J. Chem. Downloaded from www.nrcresearchpress.com by 210.87.254.6 on 09/05/12
For personal use only.

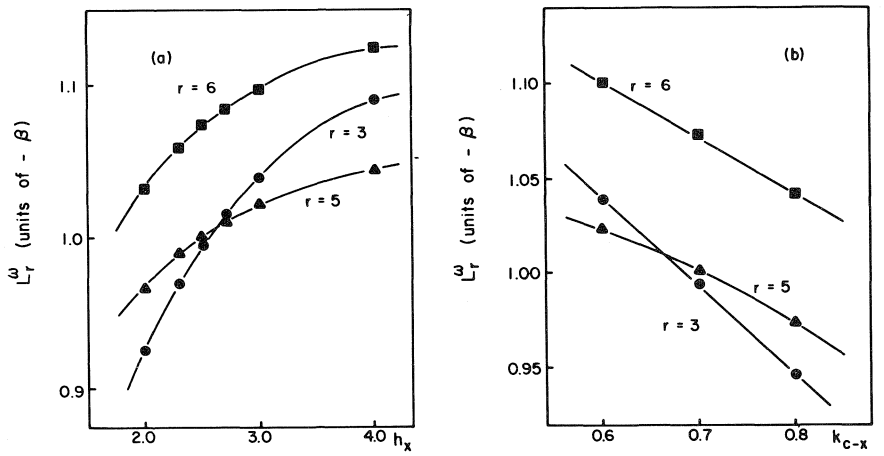

FIG. 3. Localization energy of 1,4-dimethylnaphthalene at position r, calculated by the ω-technique (ω = 1.4) using heteroatom model for representing the methyl groups: (*a*) as a function of parameter h_x(k_{c-x} = constant = 0.7) (*b*) as a function of parameter k_{c-x} (h_x = constant = 2.5).

reactive positions in 1,4-dimethylnaphthalene. The same behavior is now also displayed by L_r^ω (Figs. 3*a* and *b*), which contrasts with the behavior of L_r^ω on the inductive model (Fig. 3, Part I). Interestingly enough, the crossover points occur for both S_r^ω and L_r^ω at nearly the same value of h_x (~2.7) and k_{c-x} (~0.7).

The effect of the parameter ω on q_r^ω and S_r^ω is small, but ω influences considerably the "residual molecule", and hence also L_r^ω. Figure 4 shows the dependence of L_r^ω on ω with h_x and k_{c-x} constant at 2.0 and 0.8, respectively. The dependence on ω is linear, so that order of

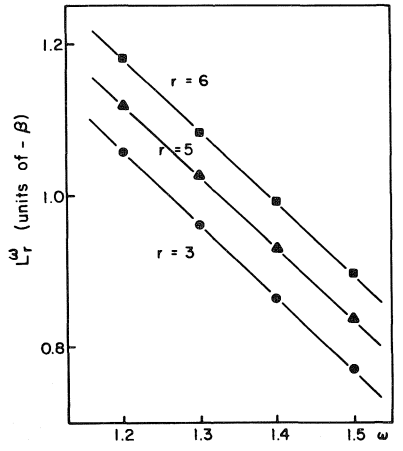

FIG. 4. Localization energy of 1,4-dimethylnaphthalene at position r, calculated using heteroatom model (h_x = 2.0, k_{c-x} = 0.8) for representing the methyl groups as a function of parameter ω

reactive positions is not affected. These findings confirm those of Part I. It is interesting to note that, with the values of h_x and k_{c-x} mentioned, L_r^ω and S_r^ω are in fairly good *quantitative* agreement with experimental results of Dallinga *et al.* (1) on the rate of hydrogen–deuterium exchange in 1,4-dimethylnaphthalene, *i.e.* are proportional to the logarithm of the rate constant (13).

(b) The PPP-Technique

Results of calculations are again given in the form of graphs (Figs. 5 and 6) representing the dependence of the reactivity indices on one parameter (W_x or $(\beta_{c-x})_{core}$) by keeping the other constant. The constant values used (W_x = 16 and $(\beta_{c-x})_{core}$ = −1.4 eV) imply $H_x \sim 2.0$ and $K_{c-x} \sim 0.7$ (*cf.* eqs. 7 and 8), and therefore correspond essentially to h_x and k_{c-x}.

The dependence of q_r^P on both parameters is the same as that of L_r^P, and hence, to conserve space, only the case of the latter will be displayed (Fig. 5). First of all, we can see that L_r^P is relatively insensitive to the values of both parameters. Furthermore, it gives the correct qualitative order of reactive positions of 1,4-dimethylnaphthalene. Quantitatively, however, the predominance of the most reactive position 3 over the other two (see Fig. 5) is somewhat larger than determined by experiment (1). Such behavior is different from that observed previously for L_r^ω in the ω-technique.

In Fig. 6, cross-over points are observed for S_r^P as a function of both parameters. However, the inversion in the order of reactive positions

Can. J. Chem. Downloaded from www.nrcresearchpress.com by 210.87.254.6 on 09/05/12
For personal use only.

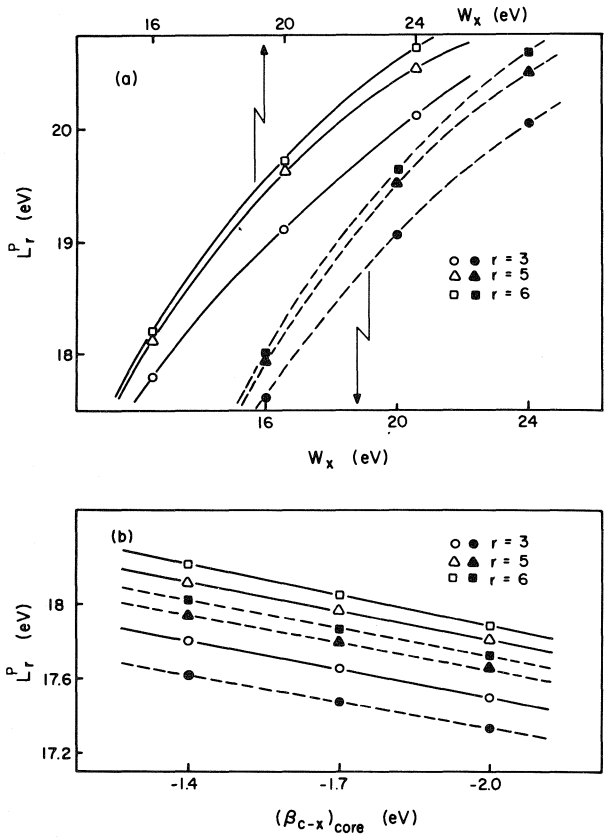

FIG. 5. Localization energy (L_r^P) of 1,4-dimethylnaphthalene at position r, calculated by the PPP-technique and using heteroatom model for representing the methyl group: (*a*) as a function of parameter W_x [$(\beta_{c-x})_{core}$ = constant = −1.4 eV] (*b*) as a function of parameter $(\beta_{c-x})_{core}$ [W_x = constant = 16 eV]. Dashed lines represent calculations where effective nuclear charge (Z_x^{eff}) was made dependent on the W_x by means of eq. 10.

now involves positions 5 and 6 and not positions 3 and 5, as in the case of the ω-technique. Levy and Berthier (14) and Ross (15), in calculations on singlet–singlet transition of propene and methyl-substituted ethylenes, respectively, have determined the parameter values as $W_x \sim 12$ and $(\beta_{c-x})_{core} \sim -1.4$ eV. With reference to Fig. 6, it is seen that these values would lead to a wrong order of reactive positions of 1,4-dimethylnaphthalene. On the other hand, S_r^P predicts, as in the case of q_r^P and L_r^P, too great a predominance of position 3 over the other two (*cf.* Fig. 6) as compared to experimental results (1), irrespective of the values used for hyperconjugative parameters.

As an important aside, we may note that the transfer of charge from the methyl group to the π-system of naphthalene in PPP calculations (~0.7 per methyl group) is very high compared with at most 0.05 per methyl group obtained in the ω-technique calculations. Such a high transfer of charge on the heteroatom model has been noted before by Levy and Berthier (14) who used PPP-technique in calculations on propene. According to recent accurate (all-valence and CNDO) calculations (16), the transfer of π-charge from the methyl group to the π-system of substituted molecule is about 0.03 per methyl group, which compares reasonably well with our ω-technique result, but not with that of the PPP-technique. If the transfer of charge is taken as a measure of perturbation, it may be questioned why the methyl group should lead to such a high perturbation in the PPP result. Thus there is some doubt about the validity of the heteroatom model within the PPP formalism.

Can. J. Chem. Downloaded from www.nrcresearchpress.com by 210.87.254.6 on 09/05/12
For personal use only.

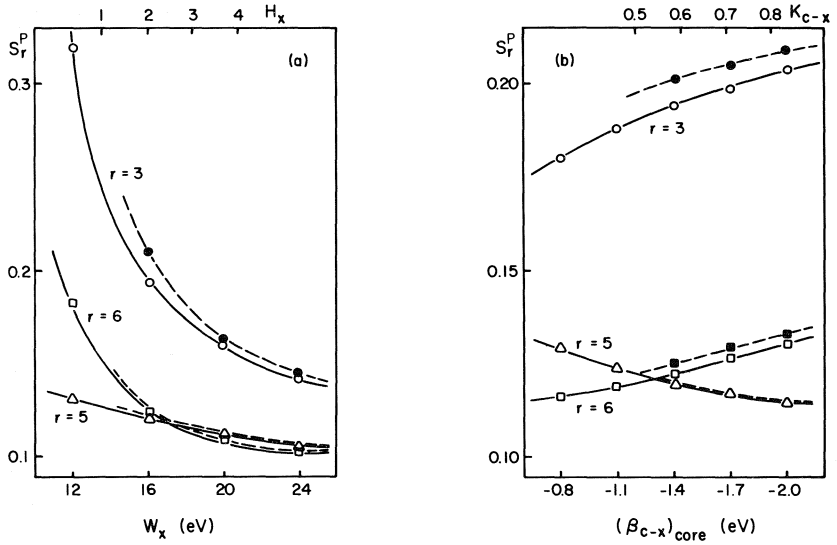

FIG. 6. Superdelocalizability (S_r^P) of 1,4-dimethylnaphthalene at position r, calculated by the PPP-technique and using heteroatom model for representing the methyl group: (*a*) as a function of parameter W_x [$(\beta_{c-x})_{core}$ = constant = -1.4 eV] (*b*) as a function of parameter $(\beta_{c-x})_{core}$ [W_x = constant = 16 eV]. Dashed lines represent calculations where effective nuclear charge (Z_x^{eff}) was made dependent on W_x by means of eq. 10.

Conclusions

Using the inductive model of the methyl group we have pointed out in Part I, where the PPP- and ω-techniques were shown to yield comparable results in reactivity calculations, that the cause of this equivalence was the chosen parametrization and the weak perturbation produced by the methyl group. In the present calculations, involving the heteroatom model for the hyperconjugative effect of the methyl group, the methyl group still produces a weak perturbation in ω-technique calculations, but a large perturbation in the PPP calculations. For this reason it is not too surprising that the ω- and PPP-techniques no longer produce comparable results; in fact, the heteroatom model is clearly unsuitable for PPP calculations.

Insofar as the ω-technique is concerned, the reactivity indices S_r^{ω} and L_r^{ω} are shown to be strongly dependent on the values of the parameters for the hyperconjugative heteroatom model of the methyl group. Both S_r^{ω} and L_r^{ω} may account qualitatively, or even quantitatively, for rates of electrophilic substitution in 1,4-dimethylnaphthalene if $h_x < 2.7$ and $k_{c-x} > 0.7$. Compared with the values $h_x = 3.0$ and $k_{c-x} = 0.7$ advocated by Streitwieser and co-workers (3) for the calculations of ionization potentials (but which would yield the wrong order of reactive positions), our values of h_x and of k_{c-x} suggest a necessity for a stronger hyperconjugative effect in reactivity calculations than in calculations of ionization potentials.

1. G. DALLINGA, P. J. SMIT, and E. L. MACKOR. Mol. Phys. **3**, 130 (1960).
2. LE-KHAC HUY and W. FORST. Theoret. Chim. Acta (Berl.) **16**, 393 (1970).
3. A. STREITWIESER, JR. and P. M. NAIR. Tetrahedron, **5**, 149 (1959). A. Streitwieser, Jr. J. Am. Chem. Soc. **82**, 4123 (1960). P. Nounou. J. Chim. Phys. **64**, 276 (1967)
4. J. A. POPLE. Trans. Faraday Soc. **49**, 1375 (1953). P. Pariser and R. G. Parr. J. Chem. Phys. **21**, 466, 767 (1953).
5. R. ETTINGER. Tetrahedron, **20**, 1579 (1964).
6. (*a*) F. E. HARRIS. J. Chem. Phys. **48**, 4027 (1968). (*b*) K. Jug. J. Chem. Phys. **51**, 2779 (1969).
7. M. J. S. DEWAR. Tetrahedron, **19**, Suppl. 2, 89 (1963); see also Hyperconjugation. The Ronald Press Co., New York, N.Y. 1962.
8. J. P. COLPA and E. DE BOER. Mol. Phys. **7**, 333 (1964).
9. R. S. MULLIKEN, C. A. RIEKE, and N. G. BROWN. J. Am. Chem. Soc. **63**, 41 (1941). N. Muller and R. S. Mulliken. J. Am. Chem. Soc. **80**, 3489 (1958). N. Muller, L. N. Pickett, and R. S. Mulliken. J. Am. Chem. Soc. **76**, 4770 (1954).

Can. J. Chem. Downloaded from www.nrcresearchpress.com by 210.87.254.6 on 09/05/12
For personal use only.

10. See, for example, R. L. Flurry, Jr. Molecular orbital theory of bonding in organic molecules. Marcel Dekker, Inc., New York, N.Y. 1968.
11. J. H. RIDD. *In* Physical methods of heterocyclic chemistry. Vol. 1. A. R. Kartrisky, Editor. Academic Press, New York, N.Y. 1963. p. 109.
12. A. H. GREENWOOD and R. MCWEENY. *In* Advances in physical organic chemistry. **4**, V. Gold, Editor. Academic Press, New York, N.Y. 1966. p. 73.
13. LE-KHAC HUY. Ph. D. Thesis, Université Laval, Quebec, Quebec, 1970.
14. B. LEVY and G. BERTHIER. J. Chim. Phys. **63**, 1375 (1966).
15. B. ROOS. Acta Chem. Scand. **21**, 2318 (1967).
16. M. D. NEWTON and W. N. LIBSCOMB. J. Am. Chem. Soc. **89**, 4261 (1967). J. A. POPLE and M. GORDON. J. Am. Chem. Soc. **89**, 4253 (1967).
17. P. CANONNE, LE-KHAC HUY, and W. FORST. Can. J. Chem. This issue.

www.nrcresearchpress.com by 210.87.254.6 on 09/05/12
For personal use only.

Can. J. Chem. Downloaded from www.nrcresearchpress.com by 210.87.254.40 on 09/05/12
For personal use only.

Electrophilic Substitution in Methyl-substituted Naphthalenes III. Correlation between Experimental Results and Molecular Orbital Calculations of Reactivity Indices

P. Canonne, Le-Khac Huy, and W. Forst
Department of Chemistry, Université Laval, Québec 10, Québec

Received June 25, 1971

Common reactivity indices (electron density q_r, self-polarizability π_{rr}, frontier electron density f_r, superdelocalizability S_r, and localization energy L_r) are calculated for electrophilic substitution in 25 methylnaphthalenes. An elementary s.c.f. method in the form of a modified ω-technique is used, using the hyperconjugative-heteroatom model for the methyl groups, with $\omega = 1.4$, $h_x = 2.0$, $k_{c-x} = 0.8$. This choice gives reasonably good ionization potentials and very good correlation for singlet transitions (p-band) in u.v. spectra of α-methylnaphthalenes. Purely static indices q_r, f_r, and π_{rr} are found to be unsuitable for predicting reactive positions for chloromethylation, while S_r and L_r are very satisfactory. On the theory that the polarizing effect of the approaching reagent is important, the index $q_r' = q_r + \pi_{rr}\,\delta\alpha_r$ may be obtained, which is also found to be very satisfactory for $\delta\alpha_r = \beta$. If the interaction is viewed as an interaction between a hard acid (chloromethyl) and soft base (methylnaphthalenes), the index $\Delta E_r = aq_r + bf_r$ is obtained, which is likewise found to be satisfactory with $a = 1$, $b = 0.15$. These results show clearly that it is insufficient to base reactivity considerations in methylnaphthalenes entirely on the properties of the isolated substrate molecule, but that even a very simple description of the substrate–reagent interaction is sufficient since the four indices S_r, L_r, q_r', and ΔE_r all have the same predictive value.

Nous avons entrepris l'étude de la substitution électrophile de 25 méthylnaphtalènes en utilisant une version modifiée de la technique Oméga pour calculer les indices de réactivité usuels (densité électronique q_r, autopolarisabilité π_{rr}, densité des électrons frontaliers f_r, superdélocalisabilité S_r et énergie de localisation L_r). Le modèle hétéroatome a été utilisé pour représenter le groupement méthyle. Notre choix des paramètres ($\omega = 1.4$, $h_x = 2.0$ et $k_{c-x} = 0.8$) nous a permis d'obtenir des valeurs raisonnables des potentiels d'ionisation et une très bonne corrélation entre l'énergie de transition singulet–singulet calculée et observée (bande p) des spectres u.v. Nous avons trouvé que les indices purement statiques q_r, f_r et π_{rr} ne réussissent pas à prédire les positions les plus réactives telles qu'obtenues expérimentalement par la chlorométhylation, tandis que S_r et L_r donnent des résultats satisfaisants. Cependant, en tenant compte de l'effet polarisateur du réactif électrophile, un nouvel indice $q_r' = q_r + \pi_{rr}\,\delta\alpha_r$ peut être défini qui conduit également à des prédictions satisfaisantes si $\delta\alpha = \beta$. D'autre part, si l'interaction substrat-réactif (électrophile) est considérée comme étant celle entre un acide dur (chlorométhyle) et une base molle (méthyl naphtalènes), l'indice ainsi obtenu $\Delta E = aq_r + bf_r$ est aussi un bon indice de réactivité si $a = 1$ et $b = 0.15$. L'ensemble de nos résultats démontre clairement qu'il est insuffisant d'étudier la réactivité chimique en se basant uniquement sur les propriétés de la molécule isolée (molécule du substrat). Cependant, même une très simple description de l'interaction substrat–réactif (électrophile) s'avère déjà suffisante car les quatre bons indices q_r', S_r, L_r, et ΔE conduisent tous à des prédictions identiques.

Canadian Journal of Chemistry, **49**, 4073 (1971)

Introduction

A simple theoretical treatment of the reactivity of conjugated organic compounds seeks a correlation between rate of reaction and some reactivity index derived from the π-molecular orbital (m.o.) representation of the ground state of the substrate molecule (1). A large number of studies have shown that the predictive value of the commonly employed reactivity indices, such as self-polarizability, free valence, reactivity number, superdelocalizability, is about equal for alternant hydrocarbons; the reason is that all ultimately relate to the same basic function (2). The same is not true of non-alternant systems (*e.g.* methylnaphthalenes), and therefore such systems promise to provide a more meaningful test of the reactivity indices. However, theoretical studies on the reactivity of non-alternant hydrocarbons (1*a*, 3, 4) are fragmentary because of the dearth of appropriate experimental results.

Experimental data are now available, mostly from P.C.'s laboratory,[1] giving the yield for chloromethylation (an electrophilic substitution) at various reactive positions of 25 different methyl-substituted naphthalenes (*cf.* Table 2);

[1]See Part IV, to be published.

Can. J. Chem. Downloaded from www.nrcresearchpress.com by 210.87.254.40 on 09/05/12
For personal use only.

there are also rate constants for H–D exchange in six symmetric dimethylnaphthalenes (4). Using this body of data, we propose to examine the problem of electrophilic substitution in methylnaphthalenes from the point of view of m.o. theory in the π-electron approximation. Inasmuch as the amount of calculations is large (an average of four reactive positions are to be calculated per compound for each of six reactivity indices), and since the results of the calculations are then compared against experimental data which give only relative order of reactive positions and not actual rate constants, elaborate s.c.f. calculations are not warranted for reasons of both cost and significance. Furthermore, the problem is considerably circumscribed theoretically in that the attacking reagent is the same in most cases, as are the solvent and reaction conditions in general, so that the only variable is the number of methyl groups in the substrate molecule; hence, to this extent, the calculations provide as much a test of the model for the methyl group as they provide a test of the reactivity indices themselves.

For comparison purposes, Table 3 summarizes experimental results for other types of attacking reagent.

Method of Calculation

We have chosen an elementary s.c.f. method in the form of the so-called "ω-technique" (1*a*), which (unlike the simple Hückel m.o. method) allows for a redistribution of electrons in the aromatic ring, an important point in connection with the hyperconjugative model for the methyl group (*vide infra*), yet requires moderate amounts of computer time. Consequently the superscript ω on reactivity indices (*cf.* Parts I and II) has been dropped as redundant.

This choice was arrived at after comparative investigation of other methods and models for the methyl group, which are described in Part I (5) and Part II (preceding paper, ref. 15) to which the reader is referred for details. On balance, the hyperconjugative-heteroatom model turned out to be the most appropriate for reactivity calculations, and therefore has been used in all calculations reported in this paper.

It is worthwhile to note that the hyperconjugative model, at least insofar as π-electrons are concerned, is supported by recent calculations (6) using more sophisticated methods (CNDO and all-valence *ab initio*) which show that there is a small transfer of charge (*cf.* Part II), accompanied by a polarizing effect (6*c* and *d*), which results in electrons being driven away from the atom to which the methyl group is attached and their redistribution in the π-system of the substrate. On the other hand, it is found by these methods that the methyl group causes *withdrawal* of σ-electrons from the ring (6*b* and *c*), which is an effect opposite to that assumed in the inductive model of the methyl group.

Within the framework of the ω-technique, the heteroatom model for the methyl group requires the specification of three parameters (*cf.* Part II): ω, h_x and k_{c-x}.

It is shown in Parts I and II that the calculated order of reactive positions in 1,4-dimethylnaphthalene, using either model for the methyl group, is independent of the value of ω, so that this choice is not at all critical. We have used throughout Streiwieser's value (1*a*) $\omega = 1.4$.

Insofar as the parameters h_x and k_{c-x} are concerned, results of Part II show that S_r and L_r give the correct order of reactive positions in 1,4-dimethylnaphthalene if $h_x < 2.7$ and $k_{c-x} > 0.7$. The values used throughout this work are $h_x = 2.0$ and $k_{c-x} = 0.8$.

The fact that these values yield the correct *relative* order of reactive positions does not necessarily make them reasonable, and therefore the calculation of the *absolute* value of some property is desirable as a check. Three checks have been made; all satisfactory:

(*1*) As mentioned in Part II, the above choice for h_x and k_{c-x} yields values of L_r that give good semi-quantitative agreement with experimental rate constants (4) for hydrogen–deuterium exchange in 1,4-dimethylnaphthalene.

(*2*) Ionization potentials for 1-methyl- and 2-methylnaphthalene, calculated by the method of Streitwieser (7*a*) with the above values of h_x and k_{c-x}, yield the values of 8.23 eV (1-methyl) and 8.37 eV (2-methyl). This compares reasonably well with the experimental (7*b*) values of 7.96 eV for 1-methyl and 8.10 eV for 2-methyl naphthalene.

(*3*) Table 1 and Fig. 1 show a correlation between the observed energy of the singlet transition in the u.v. spectra of some polymethylnaphthalenes, and $x_{m+1} - x_m$, the energy difference (in units of β) between the lowest unoccupied $(m + 1)$ and the highest occupied (m) orbital. The singlet transition is the $^1L_a \leftarrow {}^1A$ transition, or the

TABLE 1. Experimental data from the u.v. spectra of α-methylnaphthalenes and numerical values for x_m, x_{m+1}, calculated by ω-technique (ω = 1.4, h_x = 2.0, k_{c-x} = 0.8)

Molecule	λ_{max} (p-band)* mμ	eV	x_{m+1}	x_m	$x_{m+1} - x_m$	Solvent	Reference 16 for λ_{max}
Naphthalene	275	4.517	0.6683	−0.6683	1.3366	Ethanol	*a*
1-Methylnaphthalene	281	4.420	0.7088	−0.5777	1.2865	Hexane	*b*
1,4-Dimethylnaphthalene	289	4.298	0.7422	−0.4870	1.2292	Ethanol	*a*
1,5-Dimethylnaphthalene	287	4.328	0.7490	−0.5104	1.2594	Isooctane	*c*
1,8-Dimethylnaphthalene	285	4.358	0.7486	−0.5118	1.2604	Isooctane	*c*
1,4,5-Trimethylnaphthalene	292	4.254	0.7864	−0.4377	1.2241	Petrol ether	*d*
1,4,5,8-Tetramethylnaphthalene	296	4.196	0.8268	−0.3803	1.2071	Methanol	*e*

*Strictly speaking, the 0—0 band should be used, which is the longest-wavelength peak in the band. It is not always well-resolved, and therefore for consistency the maximum peak of the band is used throughout.

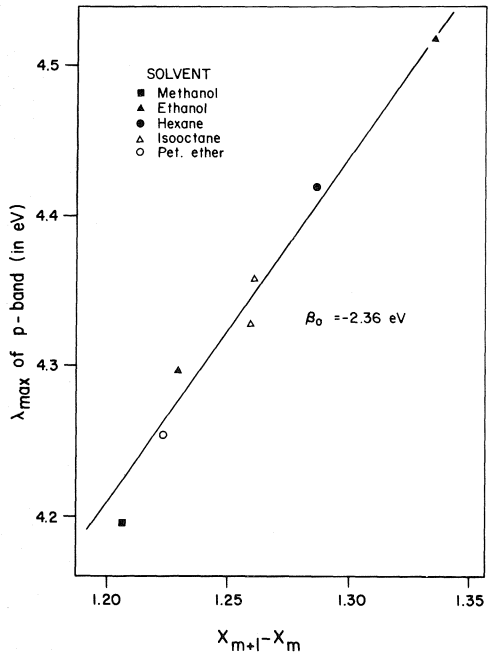

FIG. 1. Correlation between energy of singlet transition in u.v. spectra (λ_{max}) and $x_{m+1} - x_m$ of α-methylnaphthalenes. Standard error on β_0 is $\sigma = \pm 0.15$ eV.

p-band in Clar's notation (8), and it is transversely polarized *i.e.* in the direction perpendicular to the long axis of the molecule, so that methyl substitution in positions 1, 4, 5, or 8 (α-positions) extends conjugation in the transverse direction and produces a bathochromic effect. The correlation is surprisingly good if one considers that configuration interaction is ignored. The least-squares value of β_0 calculated from the slope of the straight line in Fig. 1 is $\beta_0 = -2.36$ eV, in ood agreement with the generally accepted values of −2.4 to −3.0 eV.

It is interesting to note that parameter values recommended by Streitwieser (h_x = 3.0, k_{c-x} = 0.7) (1*a*) give higher ionization potentials for 1- and 2-methylnaphthalene (8.37 and 8.48 eV, respectively), and a much higher β_0 in the correlation of Fig. 1 (−6.54 eV, to be precise).

Experimental

Since we feel that mere specification of the most reactive position is much too crude a criterion that tends to disguise important differences in reactivity, Table 2 summarizes fairly detailed experimental information on chloromethylation. Part *A* lists reactant naphthalenes that in general chloromethylate easily, *i.e.* those that are very reactive, as can be seen from the reaction medium and from reaction conditions. The last three compounds listed in part *A* are somewhat less reactive than the rest, since the reaction conditions are more severe. The chloromethylated compound, once formed, tends to be unstable and some of it ends up as bis-naphthyl methane. On the assumption that all the bis-naphthyl methane found comes from the chloromethylated compound, "yield 2" represents a rough correction for loss to bis-naphthyl methane. Part *B* of Table 2 lists reactant naphthalenes requiring more drastic reaction medium and reaction conditions, *i.e.* methylnaphthalenes significantly less reactive than those of part *A*. The yield of bis-naphthyl methane was generally about 5%, so that yields listed in part *B* should be increased by that amount to correct roughly for loss to bis-naphthyl methane.

Table 3 summarizes available experimental results on other electrophilic substitutions. A critical evaluation of each entry was not feasible, nor was it possible to reconstruct experimental conditions in as much detail as in Table 2, since the pertinent information is mostly lacking, except for the case of hydrogen–deuterium exchange in symmetric dimethylnaphthalenes where experimental data are very complete. With this exception, results listed in Table 3 will be considered as slightly suspect and will not be used to formulate important arguments. It may be noted, however, that with the exception of a few cases of succinoylation (a bulkier substituent than the rest), the most reactive positions for electrophilic substitutions of Table 3 are the same as those for chloromethylation (Table 2).

Can. J. Chem. Downloaded from www.nrcresearchpress.com by 210.87.254.40 on 09/05/12
For personal use only.

TABLE 2. Summary of experimental results* on chloromethylation of methylnaphthalenes

(A) Reaction medium: gaseous HCl, paraformaldehyde, anhydrous acetic acid

Reactant naphthalenes	Substitution at position	Yield 1† (%)	Yield 2‡ (%)	Reaction condition	
				Time (h)	Temperature (°C)
1,3-Dimethyl-	4	84	89	4	25
1,2,3-Trimethyl-	4	86	92	4	25
1,3,7-Trimethyl-	4	81	87	4	25
1,3,8-Trimethyl-	4	82	88	3	25
1,3,6,7-Tetramethyl-	4	90	96	2	25
1,3,6,8-Tetramethyl-	4	92	98	2	25
1,3,5-Trimethyl-	4	30	52	24	60
1,3,5,7-Tetramethyl-	4	27	57	24	60
1,3,5,8-Tetramethyl-	7	40 } 59	77	16	60
	6	19 }			

(B) Reaction medium: concentrated HCl, 85% H_3PO_4, paraformaldehyde anhydrous acetic acid

Reactant naphthalenes	Substitution at position	Yield (%) at indicated position	Reaction condition*	
			Time (h)	Temperature (°C)
1-Methyl-	4	76	6	60
2-Methyl-	1	86		
1,2-Dimethyl-	4	52		
1,4-Dimethyl-	2	45		
1,5-Dimethyl-	2 }	32		
	4 }	7		
1,6-Dimethyl-	4 }	57	17	30
	5 }			
1,8-Dimethyl-	4	51		
2,3-Dimethyl-	1	43		
2,6-Dimethyl-	1	72		
1,2,4-Trimethyl-	3	25		
1,2,6-Trimethyl-	4 }	65		
	5 }			
1,6,7-Trimethyl-	4 }	30		
	5 }			
2,3,6-Trimethyl-	1, 4, and 5§	93		
1,2,3,4-Tetramethyl-	6	17		
1,2,5,6-Tetramethyl-	4	21		

*See also part V (to be published).
†Yield 1: Yield (in mol% of starting compound) of substituent at position indicated.
‡Yield 2: Yield 1 plus yield of bis-naphthyl methane.
§Only isomer with substitution at position 1 isolated; existence of the other two isomers inferred from n.m.r. spectra.

Results of Calculations

To conserve space, results of the calculations are summarized in several tables of the Discussion, but actual numerical values are not quoted unless it is essential for the argument. A complete listing of numerical results is available (9).

Discussion

It is convenient to consider first a qualitative overview of all the results, and then take a more quantitative look at the more interesting reactivity indices.

(a) Qualitative Correlations

Table 4 gives a comparison between the most reactive position for chloromethylation of methylnaphthalenes as observed experimentally (column 2; *cf.* Table 2) and as predicted by the various reactivity indices (columns 3 to 7). The division into groups *A* and *B* repeats the division made in Table 2. Wrong predictions are put in parentheses.

For methyl naphthalenes of group *A*, all the reactivity indices are equally successful in correctly predicting the most reactive position in all but one case. Note that in all successfully predicted cases of this group substitution takes place at an α-position. For methylnaphthalenes of group *B*, the comparison between theory and experiment is less clear-cut, but if results for

Can. J. Chem. Downloaded from www.nrcresearchpress.com by 210.87.254.40 on 09/05/12
For personal use only.

TABLE 3. Summary of experimental data on hydrogen–deuterium exchange (*A*), nitration (*B*), bromination (*C*), and succinoylation (*D*) of methylnaphthalenes

Reactant naphthalenes	Electrophile	Most reactive position	Reference 17
1-Methyl-	*B*	4	*a, b*
	C	4	*i*
	D	4	*c, d*
2-Methyl-	*B*	1	*a, e*
	D	5 or 6	*f, g*
1,2-Dimethyl-	*B*	4	*j*
	C	4	*h*
	D	4	*c*
1,3-Dimethyl-	*B*	4	*j, n*
	C	4	*i*
	D	4	*k, j*
1,4-Dimethyl-	*A*	2	*q*
1,5-Dimethyl-	*A*	4	*q*
1,6-Dimethyl-	*D*	4	*l*
1,7-Dimethyl-	*D*	4	*l*
1,8-Dimethyl-	*A*	4	*q*
	B	4	*m*
	D	4	*t*
2,3-Dimethyl-	*A*	1	*q*
	B	1	*a, o, j*
	C	1	*i*
	D	5 or 6	*d, g, p*
2,6-Dimethyl-	*A*	1	*q*
	B	1	*r*
	C	1	*r*
	D	1	*u*
2,7-Dimethyl-	*A*	1	*q*
	D	1	*s*
1,2,3-Trimethyl-	*B*	4	*j*
	C	4	*i*
2,3,6-Trimethyl-	*D*	4	*v*
1,2,3,4-Tetramethyl-	*D*	6	*h*
1,3,5,7-Tetramethyl-	*B*	4	*j*
	C	4	*i*
1,3,6,7-Tetramethyl-	*B*	4	*j*
	C	4	*i*
1,3,6,8-Tetramethyl-	*B*	4	*j*
	C	4	*i*

groups *A* and *B* are analyzed together, three types of reactivity indices may be discerned:

(i) Type 1 or α-discriminating. Self-polarizability π_{rr} and frontier electron density f_r belong to this type. These indices invariably predict an α-position as the most reactive, and therefore they may be eliminated from further consideration as unsuitable as such.

(ii) Type 2 or β-discriminating. This is the case of electron density q_r but, unlike type 1, this index does not discriminate absolutely. Actually, with the exception of four cases, q_r correctly predicts the most reactive position for group *B* compounds of Table 4, about half of which substitute in an α-position. Three of the four exceptions are dimethylnaphthalenes, and if these are analyzed more closely by considering the order of reactive positions in a given molecule (Table 5), in four cases out of six the index discriminates in favor of a β-position. Therefore electron density is not a very promising reactivity index, a conclusion also reached in Part II.

(iii) Type 3 or non-discriminating. Indices of this type are superdelocalizability S_r and localization energy L_r which do not appear to discriminate against either α or β positions; in fact these two indices are easily the best of the lot, with wrong predictions in only two out of 25 methylnaphthalenes of Table 4. A more stringent test, such as the prediction of the *order* of reactive positions in a number of dimethylnaphthalenes (Table 5), also shows the superiority of these indices, since the correct order of reactive positions is predicted in every case, except for the 2,7-dimethyl compound where S_r inverts the importance of positions 3 and 4.

The two cases where type 3 indices fail are the 1,3,5,8- and 1,2,3,4-tetramethyl compounds. It is

Can. J. Chem. Downloaded from www.nrcresearchpress.com by 210.87.254.40 on 09/05/12
For personal use only.

TABLE 4. Comparison between most reactive positions of methylnaphthalenes as observed experimentally and as predicted by various reactivity indices†

Reactant naphthalenes	Experimental*	q_r	$\pi_{r,}$	f_r	S_r	L_r	q_r'	ΔE
1,3-Dimethyl-	4	4	4	4	4	4	4	4
1,2,3-Trimethyl-	4	4	4	4	4	4	4	4
1,3,5-Trimethyl-	4	4	4	4	4	4	4	4
1,3,7-Trimethyl-	4	4	4	4	4	4	4	4
1,3,8-Trimethyl-	4	4	4	4	4	4	4	4
1,3,5,7-Tetramethyl-	4	4	4	4	4	4	4	4
1,3,5,8-Tetramethyl-	6, 7	(4, 2)	(4)	(4)	(4)	(4)	(4)	(4)
1,3,6,7-Tetramethyl-	4	4, 2	4	4	4	4	4	4
1,3,6,8-Tetramethyl-	4	4	4	4	4	4	4	4
1-Methyl-	4	(2)	4	4	4	4	4	4
2-Methyl-	1	1	1	1	1	1	1	1
1,2-Methyl-	4	4	4	4	4	4	4	4
1,4-Dimethyl-	2	2	(5)	(5)	2	2	2	2
1,5-Dimethyl-	4	(2)	4	4	4	4	4	4
1,6-Dimethyl-	4	(2)	5	4	5, 4	4	5	5, 4
1,8-Dimethyl-	4	(2)	4	4	4	4	4	4
2,3-Dimethyl-	1	1	1	1	1	1	1	1
2,6-Dimethyl-	1	1	1	1	1	1	1	1
2,7-Dimethyl-	1	1	1	1	1	1	1	1
1,2,4-Trimethyl-	3	3	(8, 5)	(8)	3	3	3	3
1,2,6-Trimethyl-	4, 5	5	5	4	4, 5	4	5	4
1,6,7-Trimethyl-	4, 5	2, 5	5	4	4, 5, 8	4	4	4, 5, 8
2,3,6-Trimethyl-	1, 4, 5	5, 4, 1	5, 4, 1	5	1, 4, 5	4, 5	1, 4, 5	1, 4, 5
1,2,3,4-Tetramethyl-	6	6	(5)	(5)	(5)	(5)	(5)	(5)
1,2,5,6-Tetramethyl-	4	4	4	4	4	4	4	4

*Chloromethylation.
†Parentheses indicate wrong prediction.

TABLE 5. Qualitative order of reactive positions of symmetric dimethylnaphthalenes as predicted by reactivity indices and as observed experimentally for H–D exchange (4)

Naphthalene	Experimental	S_r	L_r	q_r	q_r'	ΔE
1,4-Dimethyl-	2 > 5 > 6	2 > 5 > 6	2 > 5 > 6	2 > 6 > 5	2 > 5 > 6	2 > 5 > 6
1,5-Dimethyl-	4 > 2 > 3	4 > 2 > 3	4 > 2 > 3	2 > 4 > 3	4 > 2 > 3	4 > 2 > 3
1,8-Dimethyl-	4 = 2 > 3	4 > 2 > 3	4 > 2 > 3	2 > 4 > 3	4 > 2 > 3	4 > 2 > 3
2,3-Dimethyl-	1 > 5 > 6	1 > 5 > 6	1 > 5 > 6	1 > 6 > 5	1 > 5 > 6	1 > 5 > 6
2,6-Dimethyl-	1 > 4 > 3	1 > 4 > 3	1 > 4 > 3	1 > 3 > 4	1 > 4 > 3	1 > 4 > 3
2,7-Dimethyl-	1 > 3 > 4	1 > 4 > 3	1 > 3 > 4	1 > 3 > 4	1 > 4 > 3	1 > 4 > 3

tempting to explain away the two failures by steric hindrance at positions 4 and 5, respectively. However in the 1,3,6,7-compound, position 4 would be sterically hindered to the same extent as position 5 in the 1,2,3,4-compound, and yet in one case substitution does take place at such a position, and in the other case it does not. Clearly more subtle geometrical considerations, such as non-planarity and bond lengths, seem necessary to put "steric hindrance" on a rational basis. Therefore when geometry is ignored, as in the present work, "steric hindrance" is an undefined concept of no predictive value, and cannot be invoked to explain failures of a reactivity index.

It is interesting to note that when numerical values of S_r and L_r for the most reactive position are examined, a clear gap is found between index values for groups *A* and *B* of Table 4; the more reactive compounds of group *A* all have $S_r > 1.30$, $L_r < -0.60\ \beta_0$, and the less reactive compounds of group *B* all have $S_r < 1.20$, $L_r > -0.65\ \beta_0$ (recall that highest reactivity corresponds to highest S_r but to least L_r).

(b) Quantitative Correlations

After a preliminary screening based on qualitative correlations, we now propose to subject the more promising indices to a limited quantitative correlation using rate constants for hydrogen–deuterium exchange in a number of symmetric dimethylnaphthalenes, obtained by Dallinga *et al.* (4). These studies were all done under the same

Can. J. Chem. Downloaded from www.nrcresearchpress.com by 210.87.254.40 on 09/05/12
For personal use only.

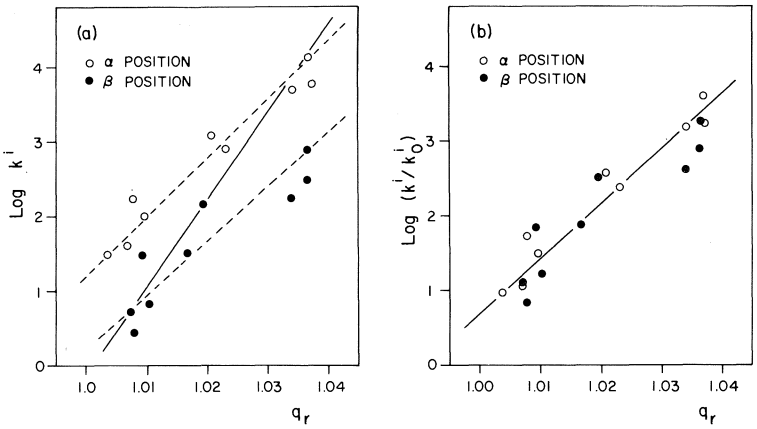

FIG. 2. Correlations between electron density q_r and absolute (*a*) and relative (*b*) rate constant for hydrogen–deuterium exchange in symmetric dimethylnaphthalenes; k^i is in units of $h^{-1} \times 10^3$. Continuous line in (*a*) and (*b*) i the least-squares line for all points (correlation coefficient 0.8 in (*a*), 0.93 in (*b*)), and the dotted lines in (*a*) are least-squares lines for α and β points taken separately (correlation coefficient 0.95 and 0.91, respectively).

experimental conditions; the reagent deuterium is here small enough to make possible steric hindrance quite negligible.

It is important to stress that when the concept of the "most reactive" position is put on a quantitative basis, this implies a correlation with the *absolute* rate constant. By contrast, Dallinga *et al.* have used two reference rate constants, one for substitution in naphthalene at an α-position (k_0^{α}), and the other at β-position (k_0^{β}), and therefore they have two kinds of relative rate constants (k^i/k_0^i, where $i = \alpha$ or β), which is useful for correlating, independently, substitutions at α or β positions, but is inappropriate for our purpose which is to seek a correlation without regard to whether a position is α or β.

(1) Electron Density (Type 2)

Figure 2*b* shows, in agreement with Dallinga *et al.*, that this index correlates with the relative rate constant and not the absolute rate constant (Fig. 2*a*), and therefore is not useful for predicting the most reactive position in a given molecule.

It is now easy to understand why q_r discriminates in favor of β positions. Suppose we have a molecule where the reactivity at an α position slightly exceeds that at β position

$$k^{\alpha} \sim k^{\beta}$$

In naphthalene, however, the two rates are significantly different: $k_0^{\alpha} > k_0^{\beta}$, so that q_r, being proportional to k^i/k_0^i, is nevertheless larger at the β position

$$[1] \qquad k^{\beta}/k_0^{\beta} > k^{\alpha}/k_0^{\alpha}$$

Thus q_r will always give the correct prediction if β is the most reactive position, but will fail to predict a most reactive α position unless $k^{\alpha} - k^{\beta}$ is sufficiently large to reverse the inequality of eq. [1].

(2) Type 3 Indices

Figures 3 and 4 show that S_r and L_r correlate with absolute rate constants, as one would expect for a "good" index, which they both are.

(3) Further Considerations

The fact that S_r and L_r, which are based on a model for the transition state, both emerge as a useful index, while all other reactivity indices derived from the properties of the isolated substrate molecule fail, must be interpreted to mean that successful treatment of reactivity in non-alternant hydrocarbons requires that the effect of the attacking reagent on the electronic structure of the substrate be taken into consideration, at least insofar as the present study is concerned.

A very simple approach along these lines consists of assuming that the field of the approaching reagent (electrophilic or nucleophilic) affects only the Coulomb integral α_r at position r of the substrate molecule. We can then write for the change in ε_{π}, the total π-electron energy

$$[2] \qquad \delta\varepsilon_{\pi} = \frac{\partial\varepsilon_{\pi}}{\partial\alpha_r}\delta\alpha_r + \frac{1}{2}\frac{\partial^2\varepsilon_{\pi}}{\partial\alpha_r^2}\delta\alpha_r^2 + \ldots$$

Since (10): $\partial\varepsilon_{\pi}/\partial\alpha_r = q_r$; $\partial^2\varepsilon_{\pi}/\partial\alpha_r^2 = \pi_{rr}$, then

$$[3] \qquad \delta\varepsilon_{\pi} \approx q_r\delta\alpha_r + (1/2)\pi_{rr}\delta\alpha_r^2$$

Can. J. Chem. Downloaded from www.nrcresearchpress.com by 210.87.254.40 on 09/05/12
For personal use only.

TABLE 6. Numerical values for q_r and q_r' of 1-methylnaphthalene as calculated by ω-technique (exact) and by approximate formula [4]

		q_r'			
		Exact ($\delta\alpha_r = \beta_0$)		Approximate formula	
Position	q_r	Hückel	ω-Technique	$\delta\alpha_r = \beta_0$	$\delta\alpha_r = 0.4\ \beta_0$
2	1.0318	1.4265	1.2695	1.4489	1.1986
3	1.0055	1.3170	1.2372	1.4090	1.1669
4	1.0201	1.4387	1.2648	1.4570	1.1950
5	1.0031	1.4108	1.2443	1.4352	1.1759
6	1.0023	1.3735	1.2345	1.4072	1.1643
7	1.0049	1.3842	1.2385	1.4116	1.1676
8	1.0006	1.3981	1.2402	1.4302	1.1724

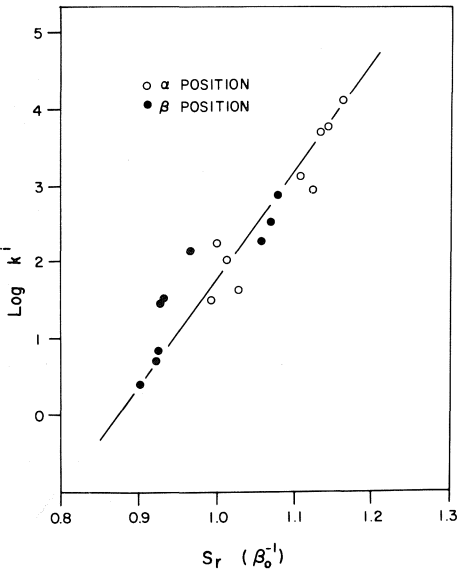

FIG. 3. Correlation between superdelocalizability and absolute rate constant (k^t) for hydrogen–deuterium exchange in symmetric dimethylnaphthalenes; k^t is in units of $h^{-1} \times 10^3$. Correlation coefficient is 0.95.

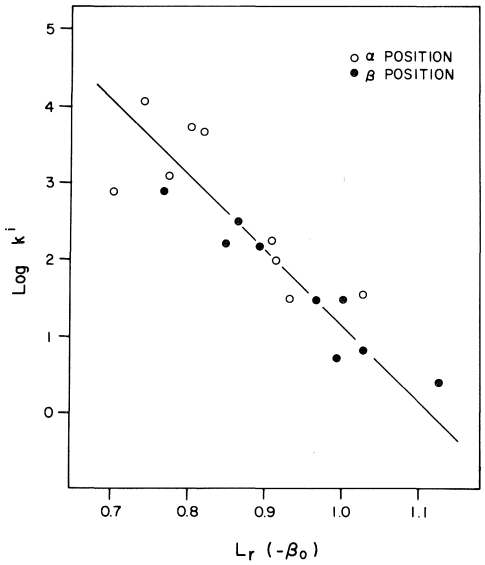

FIG. 4. Correlation between localization energy L_r and absolute rate constant (k^t) for hydrogen–deuterium exchange in symmetric dimethylnaphthalenes; k^t is in units of $h^{-1} \times 10^3$. Correlation coefficient is 0.89.

Equation 3 has been around for a long time, but its two terms are not usually considered together. Thus in alternant hydrocarbons $q_r = 1$ for all r and therefore π_{rr} is taken as the reactivity index, even if the second term of eq. 3 is believed to be much smaller than the first. In non-alternant hydrocarbons q_r is no longer the same for all r, and therefore by the above argument q_r, as part of the leading term in eq. 3, should be the reactivity index.

The failure of q_r noted earlier in the Discussion suggests that the two terms in eq. 9 are actually of comparable magnitude, which in turn implies that $\delta\alpha_r$ is not small, *i.e.* the polarizing effect of the electrophilic reagent produces an appreciable change in the Coulomb integral at position r. For example, Brown (11) has estimated that $\delta\alpha_r \sim 2$ eV at a distance ~ 5 Å, which is of the same magnitude, if not larger, than the effect of the presence of a heteroatom in the molecule (12).

Greenwood and McWeeny (12) have proposed to take the polarization effect into account by defining a new electron density q_r', still given by eq. 11 of Part II (15), but which is calculated by replacing α_r at position r by $\alpha_r + \delta\alpha_r$, and then solving the secular determinant as usual. Table 6 compares q_r and q_r' calculated with $\delta\alpha_r = \beta_0$ for 1-methylnaphthalene, one of the cases where q_r fails (*cf.* Table 4). It can be seen that q_r' tends to

Can. J. Chem. Downloaded from www.nrcresearchpress.com by 210.87.254.40 on 09/05/12
For personal use only.

Can. J. Chem. Downloaded from www.nrcresearchpress.com by 210.87.254.40 on 09/05/12
For personal use only.

discriminate less in favor of position 2, a β-position; in fact, the simple Hückel result for q_r' actually correctly predicts position 4 as the most reactive.

It is clear that with appropriate manipulation of the value assigned to $\delta\alpha_r$, q_r' can be made to yield the correct result, but such calculations are very tedious and long, since at every r and for each new value of $\delta\alpha_r$ the secular determinant must be resolved anew. However, we may write approximately

$$[4] \qquad = q_r' \approx q_r + \pi_{rr}\delta\alpha_r$$

where q_r and π_{rr} refer to the unperturbed system, so that q_r' of eq. 4 does not require any new calculations. The last two columns of Table 6 show q_r' obtained from eq. 4 and it is seen that it behaves in the same way as the exact q_r', except that it requires a smaller assigned value of $\delta\alpha_r$; this is not a serious handicap since $\delta\alpha_r$ is adjusted empirically, not for each methylnaphthalene individually but for the methylnaphthalenes as a whole

Table 4, last column but one, gives q_r' of eq. 4, with $\delta\alpha_r = \beta_0$, for all 25 methylnaphthalenes. The index fails only in the same two cases where S_r and L_r have failed. The index q_r' (again with $\delta\alpha_r = \beta_0$) also correctly predicts the order of reactive positions in dimethylnaphthalenes (Table 5, last column but one). Finally Fig. 5 shows that q_r' correlates with the absolute rate constant for H–D exchange, as a "good" index should.

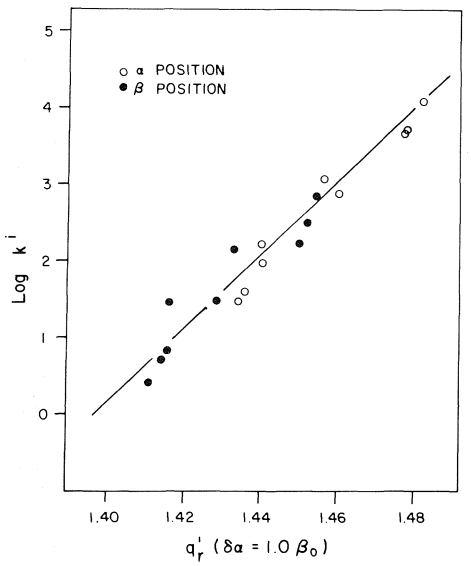

FIG. 5. Correlation between q_r' and absolute rate constant (k^i) for hydrogen–deuterium exchange in symmetric dimethylnaphthalenes; k^i is in units of $h^{-1} \times 10^3$. Correlation coefficient is 0.97.

A treatment of chemical reactivity based on a somewhat different approach is that of Klopman (13). He introduces the concept of soft and hard acids and bases and proceeds to show that reactivity is essentially determined by frontier electron density when the interaction is soft–soft, and by total charges on the two reacting partners when the interaction is hard–hard. If for the moment we confine our attention to reactions involving one and the same electrophilic agent, then relative reactivity of different substrates should be determined by indices calculated for the isolated substrate molecule, *i.e.* f_r for soft–soft interaction, and by q_r for hard–hard interaction. Our results show that neither f_r nor q_r is a good index, so that presumably we are dealing with the intermediate case of a soft–hard interaction. In fact, the two main electrophilic reagents considered here, chloromethyl and particularly deuterium, may be considered as hard acids, while the methylnaphthalenes may be regarded as soft bases.

In such an intermediate case, ΔE, the energy change due to the mutual perturbation of molecular orbitals of both reacting partners, will be given, in the zero-order approximation of Klopman's treatment, by a linear combination of q_r and f_r

$$[5] \qquad \Delta E \approx aq_r + bf_r$$

where a and b are variable parameters that measure the softness of one partner and the hardness of the other. It is noteworthy that in complete analogy with eq. 4, eq. 5 combines a type 1 index (f_r *vs.* π_{rr}) with type 2 index (q_r), although the reasoning that leads to the combination is quite different in each case.

We can therefore expect that with appropriate choice for a and b, the index ΔE should be just as good an index as q_r', or as S_r and L_r. Tables 4 and 5 (last column) and Fig. 6 show that this is indeed the case when $a = 1$, $b = 0.15$. Some degree of correspondence between ΔE and S_r is not too surprising since both are derived from concepts implicating frontier orbitals.

The theory, as presented here, treats $\delta\alpha_r$ and b as adjustable parameters; it is noteworthy, however, that the same value of $\delta\alpha_r$ (or of b) holds essentially for all the methylnaphthalene sub-

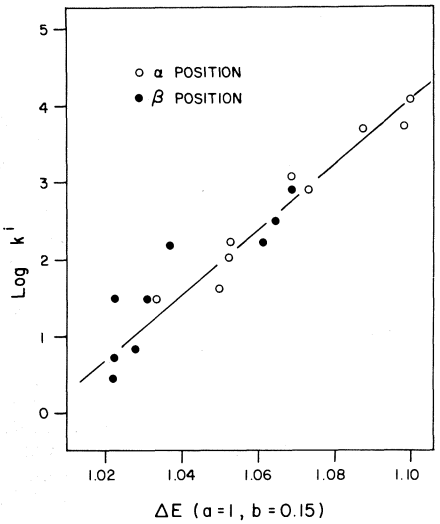

FIG. 6. Correlation between ΔE and absolute rate constant (k^i) for hydrogen–deuterium exchange in symmetric dimethylnaphthalenes; k^i is in units of $h^{-1} \times 10^3$. Correlation coefficient is 0.95.

strates, and for all the electrophilic substitutions (chloromethylation, H–D exchange, and to a less substantiated extent, also nitration and bromination) investigated. Thus $\delta\alpha_r$ and b are relatively insensitive to the details of the substrate–reagent interaction, and therefore promise to be eventually amenable to calculation.

A rather different tack has been taken recently by Daudel, Chalvet, and collaborators (14) whose treatment is somewhat similar to Fukui's but with another twist. They consider the transition state as a structure where delocalization extends from the substrate to include the attacking reagent, so that the latter may be represented by a heteroatom X characterized by the usual parameters k_{c-x}, h_x. Suitable manipulation of h_x, presumably reflecting the nature of the reagent and solvent, can then produce different order of reactive positions; it turns out that manipulation of k_{c-x} merely accentuates the difference of reactivity between different positions. These authors find[2] for electrophilic substitution in 1-methylnaphthalene with acetic anhydride as solvent, that $h_x \sim 0$. But acetic anhydride is precisely the solvent used in the chloromethylation and H–D exchange experiments which served as experimental basis for our treatment. The result $h_x = 0$ at position of attack gives support to our view that in such reactivity calculations in methylnaphthalenes the onus is on the representation for the methyl group to obtain agreement between theory and experiment.

[2]O. Chalvet, personal communication.

Conclusions

The present results show clearly that even if only the crudest correlations are intended, purely static indices q_r, π_{rr}, and f_r are insufficient to account for electrophilic reactivity in methylnaphthalenes. For an index to be successful, the effect of the attacking reagent must be included in some way, as in L_r which measures the energy required to localize two electrons of the delocalized system at site r of the substrate, or as in S_r which is based (14) on a representation where delocalization is assumed to extend to a pseudo orbital involving the attacking reagent and substrate hydrogen at site r.

Looking at the problem slightly differently, we might also say that the reactivity of a methylnaphthalene is basically determined by the reactivity toward the reagent of the parent (naphthalene) substrate, superimposed on which is the effect of the methyl substituents. The electron density q_r is different from unity only in naphthalenes with a methyl substituent, which means that q_r reflects mostly the effect of the substituents; this is also suggested by the fact that q_r is proportional to the *relative* rate constant $k^i/k_0{}^i$, where $i = \alpha$ or β. To become a successful index, q_r must therefore be combined with some quantity that reflects both the properties of the parent hydrocarbon and of the attacking reagent; in one case (q_r', eq. 4) this turns out to be π_{rr}, in the other (ΔE, eq. 5) it is f_r.

This work was done with financial assistance from the National Research Council of Canada.

1. (*a*) A. STREITWIESER. Molecular orbital theory for organic chemists. Wiley. 1961. (*b*) R. DAUDEL. Quantum theory of chemical reactivity. *In* Advances in quantum chemistry. *Edited by* P.-O. Löwdin. Academic Press. 1964. p. 191 ff. (*c*) M. J. S. DEWAR. Chemical reactivity. *In* Advances in chemical physics. Vol. VIII. *Edited by* R. Daudel. Interscience, London. 1965. p. 65 ff. (*d*) L. SALEM. Molecular orbital theory of conjugated systems. W. A. Benjamin, New York. 1966.
2. (*a*) J. KOUTECKY, R. ZAHRADNIK, and J. Čižek. Trans. Faraday Soc. **57**, 169 (1961). (*b*) K. FUKUI, T. YONEZAWA, and C. NAGATA. J. Chem. Phys. **26**, 831 (1957).

Can. J. Chem. Downloaded from www.nrcresearchpress.com by 210.87.254.40 on 09/05/12
For personal use only.

3. J. M. BONNIER, M. GELUS, and J. RINAUDO. J. Chim. Phys. **65**, 1326 (1968). A. STREITWIESER, JR., J. I. BRAUMAN, and J. B. BUSH. Tetrahedron, **19**, Suppl. 2, 379 (1963). S. CARRA, M. RAIMONDI, and M. SIMONETTA. Tetrahedron, **22**, 2673 (1966). R. B. HERMANN, Int. J. Quant. Chem. **2**, 165 (1968). P. BELTRAME, P. L. BELTRAME, and M. SIMONETTA. Tetrahedron, **24**, 3043 (1968).
4 G. DALLINGA, P. J. SMIT, and E. L. MACKOR. Mol. Phys. **3**, 130 (1960).
5. LE-KHAC HUY and W. FORST. Theoret. Chim. Acta (Berl.), **16**, 393 (1970).
6. (*a*) M. D. NEWTON and W. N. LIPSCOMB. J. Am. Chem. Soc. **89**, 4261 (1967). (*b*) W. J. HEHRE and J. A. POPLE. Tetrahedron Lett. 2959 (1970). (*c*) H. KOLLMAR and H. O. SMITH. Ang. Chemie (Int. Ed.) **9**, 462 (1970). (*d*) J. A. POPLE and M. GORDON. J. Am. Chem. Soc. **89**, 4253 (1967).
7. (*a*) A. STREITWIESER, JR. and P. M. NAIR. Tetrahedron, **5**, 149 (1959). A. STREITWIESER, JR. J. Am. Chem. Soc. **82**, 4123 (1960). (*b*) J. M. BONNIER, M. GELUS, and P. NOUNOU. J. Chim. Phys. **62**, 1191 (1965).
8. E. CLAR. Aromatische Kohlenwasserstoffe. Springer Verlag, Berlin. 1941.
9. LE-KHAC HUY. Ph.D. Thesis. Université Laval, Quebec, Quebec, 1970.
10. C. A. COULSON and H. C. LONGUET-HIGGINS. Proc. Roy. Soc. London, **A191**, 39 (1947); **A192**, 16 (1947); **A193**, 447 (1948); **A195**, 188 (1948).
11. R. D. BROWN. Tetrahedron, Suppl. 2, **19**, 337 (1963).
12. A. H. GREENWOOD and R. MCWEENY. *In* Advances in physical organic chemistry. *Edited by* V. Gold. Academic Press, New York, **4**, 736 (1966).
13. G. KLOPMAN. J. Am. Chem. Soc. **86**, 1463, 4550 (1964); **87**, 3300 (1965); **90**, 223 (1968). R. F. HUDSON and G. KLOPMAN. Tetrahedron Lett. **12**, 1103 (1967). G. KLOPMAN and R. F. HUDSON. Theoret. Chim. Acta (Berl.), **8**, 165 (1967).
14. J. BERTRAN, O. CHALVET, R. DAUDEL, T. F. W. MCKILLOP, and G. H. SCHMID. Tetrahedron, **26**, 339 (1970). O. CHALVET, R. DAUDEL, and T. F. W. MCKILLOP. Tetrahedron, **26**, 349 (1970). O. CHALVET, R. DAUDEL, G. H. SCHMID, and J. RIGAUDY. Tetrahedron, **26**, 365 (1970).
15. LE-KHAC HUY and W. FORST. Can. J. Chem. This issue.
16. (*a*) D. J. CRAM, C. K. DALTON, and G. R. KNOX. J. Am. Chem. Soc. **85**, 1088 (1963); (*b*) R. A. MORTON and J. A. GOUVEIA. J. Chem. Soc. 916 (1934); (*c*) R. A. FRIEDEL and M. ORCHIN. Ultraviolet spectra of atomic compounds. Wiley and Sons, New York, N.Y., 1951; (*d*) E. HEILBRONNER, U. FRÖHLICHER and PL. A. PLATTNER. Helv. Chim. Acta, **32**, 2479 (1949). (*e*) W. L. MOSBY. J. Am. Chem. Soc. **75**, 3348 (1953).
17. (*a*) P. R. WELLS and P. G. E. ALCORN. Aust. J. Chem. **16**, 1108 (1963). (*b*) H. W. THOMPSON. J. Chem. Soc. 2310 (1932). (*c*) R. R. HAWORTH and C. R. MAVIN. J. Chem. Soc. 20 (1932). (*d*) A. CONNU, J. ULRICH, and K. PERSAUD. Chim. Anal. **47**, 357 (1965). (*e*) H. E. FIERZ-DAVID and E. MANUHORT. Helv. Chim. Acta, **20**, 1024 (1937). (*f*) R. D. HAWORTH B. M. LETSKY, and C. R. MAVIN. J. Chem. Soc. 1784 (1932). (*g*) R. M. O. OSCULT and M. T. ROGERT. J. Am. Chem. Soc. **63**, 127 (1941). (*h*) C. L. HOWETT. J. Chem. Soc. 193 (1940). (*i*) P. CANONNE and J. M. LEGOT. Unpublished results. (*j*) P. CANONNE and A. REGNAULT. Can. J. Chem. **45**, 1267 (1967). (*k*) G. R. CLEMO and N. D. CHATYE. J. Chem. Soc. 1968 (1956). (*l*) N. P. BUU-HOÏ et G. SAINT-RUF. Bull. Soc. Chim. 2387 (1960). (*m*) L. I. DENISOVA, N. A. MOROSOVA, V. A. PLAKHOV, and A. I. TOCHILKIN. Chem. Abstr. **60**, 11957 (1964). (*n*) R. ADAMS and H. H. GIBBS. J. Am. Chem. Soc. **79**, 170 (1957). (*o*) H. WILLSTNEDT. Svensk. Kem. Tidsks, **54**, 223 (1949). (*p*) R. H. MARTIN and J. SENDERS. Bull. Soc. Chim. Belges, **64**, 221 (1955). (*q*) G. DALLINGA, P. J. SMIT, and E. L. MACKOR. Mol. Phys. **3**, 130 (1960).(*r*) N. BASKEWITCH. M.Sc. Thesis. University of Montreal, Montreal, Quebec, 1967. (*s*) G. R. CLEMO, N. D. NAWORTH, and E. WALTON. J. Chem. Soc. 2368 (1929). (*t*) J. M. GAFTS. J. Chem. Soc. 4179 (1958). (*u*) K. A. ANDIANOV, V. A. ODINETSTAND, and A. A. ZHDANOV. Chem. Abstr. **54**, 10918 (1960). (*v*) E. ADORAND and J. M. CRAFTS. Bull. Soc. Chim. Fr. **34**, 531, 1880.

Can. J. Chem. Downloaded from www.nrcresearchpress.com by 210.87.254.40 on 09/05/12
For personal use only.

Can. J. Chem. Downloaded from www.nrcresearchpress.com by 210.87.254.40 on 09/05/12
For personal use only.

Action des organomagnésiens sur les composés β-dicarbonylés V. Synthèses de β-diols bitertiaires à partir de β-hydroxycétones. Induction asymétrique 1-3[1]

JACQUELINE MICHEL[2] ET PERSÉPHONE CANONNE
Département de Chimie, Université Laval, Québec 10, Québec

Reçu le 29 décembre 1970[3]

L'action des organomagnésiens sur des β-hydroxycétones possédant un groupement inducteur en β du carbonyle conduit à des β-diols bitertiaires symétriques. Les proportions des diastéréoisomères *méso* et *thréo* obtenus dépendent surtout de la nature du groupement inducteur.

La détermination de la configuration des β-diols a été menée à bien en utilisant leurs spectres de r.m.n. dont les signaux de méthyles et du méthylène en α des hydroxyles se manifestent à des champs différents. L'étude conformationnelle des β-hydroxycétones et β-diols est réalisée au moyen de leurs spectres i.r.

Nous formulons aussi une hypothèse sur l'attaque préférentielle des organomagnésiens et sur les états de transition de cette réaction.

Addition of organomagnesium compounds to β-hydroxyketones with an asymmetric center gave a diastereoisomeric mixture of symmetric ditertiary β-diols, the ratio of *meso* and *threo* forms depending on the nature of the inductive group.

The configurations of the β-diols were determined using their respective n.m.r. spectra in which the methyl and the methylene protons have different chemical shifts.

The conformations of the β-hydroxyketones and the β-diols were studied by i.r. spectroscopy. Models for a preferred attack of the organomagnesium compounds are proposed and product-determining transition states for the reactions are also suggested.

Canadian Journal of Chemistry, **49**, 4084 (1971)

Ce mémoire expose l'étude de l'action des organomagnésiens sur des β-hydroxycétones de formule $R—C(OH)CH_3—CH_2—COCH_3$ présentant un centre asymétrique en β du groupement carbonyle.

Dans une note préliminaire (1) nous avons rapporté que cette réaction conduit à des β-diols bitertiaires constitués par un mélange de diastéréoisomères *érythro* et *thréo*, et que la proportion de chaque isomère dépend surtout de la nature du substituant *R* inducteur.

Dans le présent travail, nous décrivons les résultats obtenus sur un plus grand nombre de β-hydroxycétones dans le but d'apporter une contribution au domaine de l'induction asymétrique 1-3 auparavant entrepris par Leitereg et Cram (2, 3), Brienne *et al.* (4, 5), et Maffrand et Maroni (6, 7) sur des composés analogues et formulons une hypothèse sur l'attaque préférentielle des organomagnésiens et sur les états de transition probables qui orientent cette réaction.

Pour une approche plus aisée de cette étude, nous classons les hydroxycétones, d'après leurs analogies et propriétés respectives, en trois types (schéma 1).

Les β-hydroxycétones ont été préparées selon la méthode précédemment décrite (8) en faisant réagir 3 mol de réactif de Grignard pour 1 mol de pentadione-2,4.

L'action du réactif de Grignard (RMgX) sur la pentadione-2,4 ou sur la β-hydroxycétone substituée par le même radical R mène à une proportion identique du β-diol diastéréoisomère prépondérant (schéma 2). Ceci démontre que les β-diols bitertiaires résultent de l'addition sur la forme non énolisée de l'acétylacétone avant que celle-ci puisse se tautomériser, et que l'intermédiaire, en l'occurence le cétoalcoolate de magnésien, est le même.

Les rendements de la réaction en β-hydroxycétones figurent à la partie expérimentale. Les trois facteurs influençant cette réaction sont d'après nos expériences:

(*i*) la nature du réactif de Grignard;

(*ii*) la durée du temps d'addition: lorsqu'elle augmente, le rendement baisse car il y a accroissement des composés de clivage formés sous l'influence de l'organomagnésien en excès (9);

(*iii*) la température du mélange réactionnel: l'abaissement défavorise l'élimination de OMgX, donc la formation de produits de déshydratation.

---

[1]Cette publication recouvre une partie du mémoire qui doit être présenté par J. Michel à l'Ecole des Gradués de l'Université Laval, en vue de l'obtention du doctorat.

[2]Boursière du Conseil des Arts du Canada.

[3]Revision reçue le 3 septembre 1971.

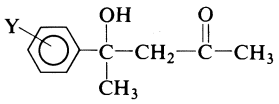

type I

1 Y = H
2 Y = *p*-CH_3
3 Y = *p*-Cl
4 Y = *m*-Cl
5 Y = *p*-OCH_3

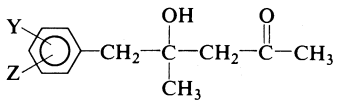

type II

6 Y = H; Z = H
7 Y = H; Z = *o*-CH_3
8 Y = H; Z = *m*-CH_3
9 Y = H; Z = *p*-CH_3
10 Y = *m*-CH_3; Z = *p*-CH_3
11 Y = *m*-CH_3; Z = *m*-CH_3

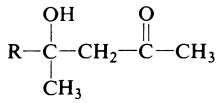

type III

12 R = C_6H_{11}
13 R = $(CH_3)_2CH$
14 R = $CH_2CH=CH_2$

SCHÉMA 1

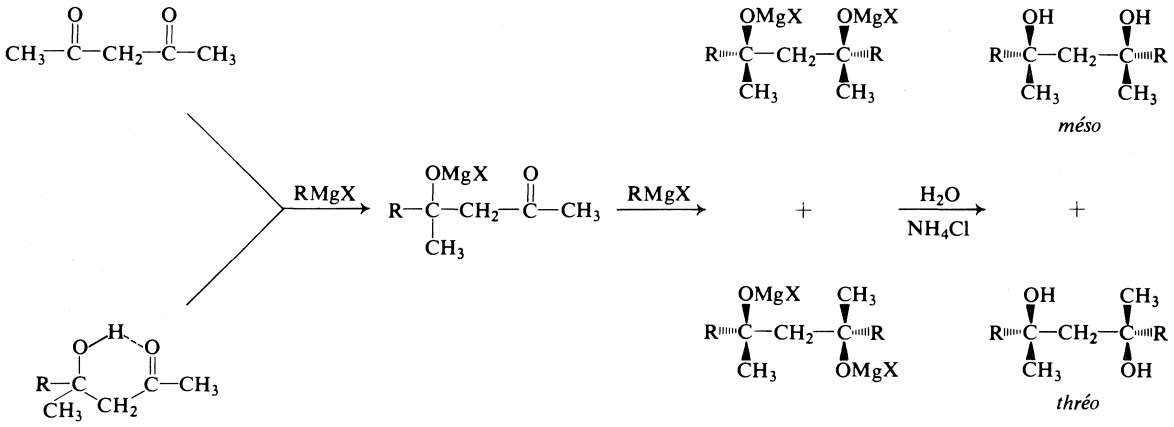

type I

21 R = C_6H_5
22 R = *p*-$CH_3C_6H_4$
23 R = *p*-ClC_6H_4
24 R = *m*-ClC_6H_4
25 R = *p*-$OCH_3C_6H_4$

type II

26 R = $C_6H_5CH_2$
27 R = *o*-$CH_3C_6H_4CH_2$
28 R = *m*-$CH_3C_6H_4CH_2$
29 R = *p*-$CH_3C_6H_4CH_2$
30 R = 3,4-$(CH_3)_2C_6H_3CH_2$
31 R = 3,5-$(CH_3)_2C_6H_3CH_2$

type III

32 R = C_6H_{11}
33 R = $(CH_3)_2CH$
34 R = $CH_2CH=CH_2$

SCHÉMA 2

Etude conformationnelle des β-hydroxycétones

Etude par i.r.

Les fréquences ν(C=O) sont rapportées à la partie expérimentale (tableau 6). Dans tous les exemples étudiés, nous vérifions l'existence d'une liaison hydrogène intramoléculaire entre l'hydroxyle et le carbonyle (tableau 1). En effet, les fréquences ν(OH) observées se trouvent dans le

Can. J. Chem. Downloaded from www.nrcresearchpress.com by 210.87.254.40 on 09/05/12
For personal use only.

TABLEAU 1. Spectres i.r.* des β-hydroxycétones
R—C(OH)CH_3CH_2—$COCH_3$ (cm^{-1})

No.	ν(OH) libre	ν(OH) lié intra	ν(OH) lié π	Δν(OH)†	Δν′(OH)‡
1	3618	3511		107	
2	3618	3508		110	
3	3614	3504		110	
4	3610	3507		103	
5	3617	3508		109	
6	3618	3531	3594	87	24
7	3619	3534	3597	85	22
8	3624	3542	3592	82	32
9	3622	3535	3590	87	32
10	3623	3532	3590	91	33
11	3624	3536	3592	88	32
12	3624	3530		94	
13	3625	3529		96	
14	3620	3531	(3592)	89	28

*En solution diluée dans le tétrachlorure de carbone (10^{-3} *M*).
†Δν(OH) = ν(OH) libre − ν(OH) lié intra.
‡Δν′(OH) = ν(OH) libre − ν(OH) lié π.

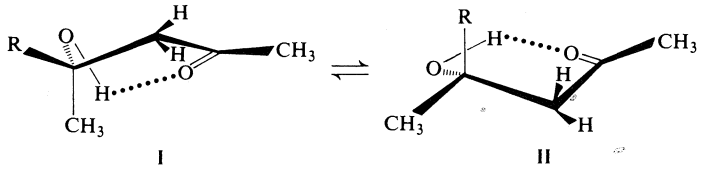

I ⇌ II

SCHÉMA 3

domaine de celles d'hydroxyles engagés dans des associations intramoléculaires 3500–3535 cm^{-1} et les intensités des bandes demeurent inchangées en faisant varier les solutions de 10^{-2} à 10^{-3} *M*. De plus, nous observons pour les β-hydroxycétones de type **II** et la β-hydroxycétone **14** une interaction intramoléculaire entre l'hydroxyle et le noyau aromatique que nous appelons liaison π. Une molécule chélatée pourra rendre compte de ces faits dans des conformations "pseudo chaises".

Les hydroxycétones **12** et **13** présentent un spectre i.r. analogue par ses caractéristiques à celui des hydroxycétones de type **I**, excepté une force moins grande de la liaison hydrogène $\Delta\nu(OH) = 90\ cm^{-1}$. L'absence de liaison π pour **1** à **5** permet de tenir pour acquis qu'il ne peut y avoir de liaison intramoléculaire entre l'hydroxyle et le noyau aromatique lorsque ces deux substituants sont géminés.

Si, à l'exemple de Kuhn (10), nous établissons une relation entre la force des liaisons intramoléculaires et Δν(OH) nous constatons pour les β-hydroxycétones du type **I** une valeur plus élevée donc une liaison hydrogène plus forte que pour celle du type **II**. Ces dernières ont l'hydrogène de l'hydroxyle alternativement lié à l'oxygène du carbonyle et au phényle: les deux conformations répondent à cette exigence (schéma 3).

Etude par r.m.n.

Les résultats donnés par la r.m.n, sont rassemblés dans le tableau 2, les signaux des hydroxyles et des aromatiques n'y sont pas rapportés. Les hydroxyles se manifestent sous la forme d'un singulet vers 3.5 p.p.m. pour les hydroxycétones des types **II** et **III** et vers 4.5 p.p.m. pour celles du type **I**. Les signaux des protons aromatiques ont des déplacements chimiques de l'ordre de 7.0–7.5 p.p.m.

Pour fin de discussion, nous nous référons aux hydroxycétones **12** et **13** car nous supposons que les substituants cyclohexyle et isopropyle influencent moins les autres protons des groupements étudiés que ne peuvent le faire le phényle et le benzyle dans les autres hydroxycétones. L'effet de champ du phényle dans les hydroxycétones de type **I** perturbe l'ensemble des protons dans la molécule et l'on observe la non équivalence magnétique des protons H_A et H_B du méthylène. Les protons méthyléniques des hydroxycétones des types **II** et **III** apparaissent sous la forme d'un singulet.

On note le blindage: 0.26 et 0.16 p.p.m. des signaux des méthyles *D* (voir la structure dans le

Can. J. Chem. Downloaded from www.nrcresearchpress.com by 210.87.254.40 on 09/05/12
For personal use only.

Can. J. Chem. Downloaded from www.nrcresearchpress.com by 210.87.254.40 on 09/05/12
For personal use only.

tableau 2) des β-cétols **1** et **6**, représentatifs des types **I** et **II**, relativement au signal de celui de **12**. En conséquence, on suppose que le méthyle *D* est situé dans le cône de blindage des phényles. Et pour que cette possibilité existe pour **1**, il faut admettre une prédominance de la conformation **II** de cette hydroxycétone (phényle en position quasi axiale par rapport au cycle "pseudo chaise"). Dans le type **I**, le blindage est moins tangible pour **3**, **4**, **5**: hydroxycétones ayant sur des phényles un substituant chlore ou méthoxyle, mais on peut remarquer que les glissements chimiques de tous les protons de ces hydroxycétones sont déplacés vers les champs faibles; cet effet est imputable au chlore et au groupe méthoxyle.

Les déplacements chimiques des hydroxycétones du type **II** et ceux du type **III** sont d'ordre de grandeur comparable eu égard à l'effet non négligeable du noyau aromatique. On déduit pour les β-cétols du type **II** et **III** une conformation "pseudo chaise" telle que le groupement R soit en position "quasi équatoriale" (conformation **I**).

Préparation des β-diols bitertiaires

Les β-diols bitertiaires symétriques de formule $RC(OH)CH_3—CH_2—C(OH)CH_3R$ sont, soit isolés du milieu réactionnel lors de la synthèse des β-hydroxycétones, soit préparés par action des organomagnésiens (RMgX) sur les hydroxycétones correspondantes.

Le rendement des réactions est fortement influencé par l'encombrement stérique; en effet, il fut impossible d'obtenir les diols correspondants aux groupements *o*-tolyle et naphtylméthyle. Trois moles d'organomagnésiens sont utilisées pour 1 mol d'hydroxycétone et donnent un mélange de deux diastéréoisomères *méso* et *thréo*. L'isomère majoritaire se purifie facilement par cristallisation fractionnée. En général, la séparation des isomères s'effectue par chromatographie sur colonne de gel de silice; leur pureté est controlée par chromatographie en phase gazeuse sur une colonne de Carbowax, par chromatographie sur couche mince et par r.m.n.

Les diols du type **II** (**26**–**31**) et les diols **33**[4] et **34**[4] du type **III** ont des temps de rétention trop voisins pour être séparés. Pour les diols du type **I** (**21**–**25**) et le diol **32** les rapports de leurs temps de rétention $T_{méso}/T_{thréo}$ sont d'environ 1.3–1.5. En considérant l'ordre d'élution d'alcools diastéréoisomères 1–2, Gault et Felkin (12) ont essayé d'élaborer une règle afin de déterminer leur configuration. Par extension, les β-diols suivent la même règle à savoir que généralement le composé *thréo* est élué le premier. La liaison hydrogène intramoléculaire est beaucoup plus forte pour ce diastéréoisomère et il est donc moins susceptible de former des liaisons intermoléculaires avec les groupes polaires de la phase stationnaire. Les temps de rétention relativement voisins pour les couples de diastéréoisomères étudiés à substituants benzyles nous permettent de supposer que les hydroxyles du *méso* et du *thréo* sont engagés également dans des associations intramoléculaires OH...π.

Etude configurationnelle et conformationnelle des β-diols

Dans certains cas (5, 7), l'étude par i.r. des liaisons hydrogène intramoléculaires peut se révéler suffisante pour déterminer à la fois la configuration et la conformation des composés, mais pour nos composés les résultats diffèrent selon les types de diols; nous avons dû avoir recours à la r.m.n. et nous nous sommes basés sur les signaux des méthyles et du méthylène en α des hydroxyles.

Etude par i.r.

Les valeurs des fréquences maximales d'adsorption se rapportant au groupe hydroxyle en solution diluée dans CCl_4 sont groupées dans le tableau 3. Les spectres i.r. des β-diols ont tous en commun une forte absorption entre 3500 et 3530 cm^{-1}, preuve de l'existence d'une conformation cyclique et une bande étroite vers 3610 cm^{-1} correspondant au signal de l'hydroxyle libre. De plus, pour les β-diols *thréo* du type **I** (**21***a*–**26***b*) et les β-diols du type **II** (**26**–**31**), nous observons une bande vers 3570 et 3590 cm^{-1} qui correspond à l'association intramoléculaire entre un hydroxyle et un phényle (liaison π).

Dans les diols du type **I** et le diol **32** les Δν(OH) (différence entre la fréquence de la bande OH libre et celle de la bande OH lié) sont plus élevés dans les isomères *thréo* que dans les isomères *méso*. En outre, le rapport (A'/A) des coefficients d'absorption intégrée des bandes OH lié (A) et OH libre (A'), calculé pour ces diols (13), montre, aux erreurs de mesure de surface près, une très légère prédominance de formes chélatées pour la configuration *méso*. Ce rapport (A'/A) a une

[4]Des essais de séparation par distillation se sont avérés également inefficaces. Des difficultés de cet ordre ont été décrites par Wolf (11).

TABLEAU 2. Spectres de r.m.n.* des β-hydroxycétones

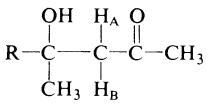

C *D*

No.	δ(CH_3) *C*	δ(CH_3) *D*	δ(CH_2)†	δ(CH_3)‡	δ(H_A)	δ(CH_2)	δ(H_B)	Δδ(AB)	*J*
1	1.42	1.89			2.66		3.04	0.38	16.0
2	1.39	1.89		2.23	2.63		2.97	0.34	16.5
3	1.45	1.99			2.78		3.02	0.24	16.0
4	1.48	2.07			2.84		3.12	0.28	17.5
5	1.42	1.98			2.71		2.97	0.26	16.5
6	1.12	2.01	2.75			2.42			
7	1.16	2.06	2.77	2.33		2.51			
8	1.07	2.01	2.74	2.27		2.43			
9	1.18	2.06	2.76	2.28		2.46			
10	1.18	2.00	2.73	2.15		2.42			
11	1.10	2.00	2.76	2.15		2.42			
12	1.11	2.16				2.54			
13	1.12	2.18				2.60			
14	1.18	2.13				2.52			

*Les déplacements chimiques sont donnés en p.p.m. et les constantes de couplage en Hz pour des solutions à 25% dans CCl_4. Le TMS sert de référence interne.
†Méthylène du groupe benzyle.
‡Méthyles aromatiques.

TABLEAU 3. Spectres i.r.* des diastéréoisomères des β-diols bitertiaires symétriques (cm^{-1})

No. diastéréoisomère†	ν(OH) libre	ν(OH) lié	γ(OH) π	Δν(OH)‡	Δν′(OH)§
21*a*	3616	3533		83	
21*b*	3614	3509	(3574)‖	105	40
22*a*	3615	(3529)		84	
22*b*	3612	3508	3572	104	40
23*a*	3615	3528		87	
23*b*	3606	3507	(3570)	99	38
24*a*	3618	3524		94	
24*b*	3609	3511		98	
25*a*	3616	3526		80	
25*b*	3614	3510	3574	104	40
26*a*	(3614)	3531	3596	83	18
26*b*	(3612)	3535	3598	77	14
27*a*	3614	3533	3594	81	30
28*a*	3614	3531	3590	83	24
29*a*	3615	3530	3592	85	23
30*a*	3614	3530	3591	84	23
31*a*	3614	3531	3589	83	25
32*a*	3624	3524		100	
32*b*	3620	3524		96	
33¶	3625	3532		93	
34¶	3620	3531	(3580)	89	40

*En solution diluée dans le tétrachlorure de carbone ($2.5\ 10^{-3}\ M$)
†*a*, *méso*; *b*, *thréo*.
‡Δν(OH) = ν(OH) libre − ν(OH) lié intra.
§Δν′(OH) = ν(OH) libre − ν(OH) lié π.
‖Les valeurs entre parenthèses correspondent à des épaulements.
¶Spectre du mélange de diastéréoisomères.

signification plus exacte lorsqu'il s'agit du couple de diastéréoisomères **32**; le rapport (A'/A) pour ces diastéréoisomères est 4.8 pour le *méso* et 4.0 pour le *thréo*. Les diols diastéréoisomères de type **I** ont leurs rapports (A'/A) encore plus similaires; et nous renonçons à conclure quelle configuration aurait une population de forme chélatée plus abondante, si ce n'est que les diastéréoisomères se trouvent probablement sous forme associée prépondérante.

Can. J. Chem. Downloaded from www.nrcresearchpress.com by 210.87.254.40 on 09/05/12
For personal use only.

Can. J. Chem. Downloaded from www.nrcresearchpress.com by 210.87.254.40 on 09/05/12
For personal use only.

Plusieurs conformations cycliques: soit "pseudo chaise" soit "pseudo croisée" peuvent être proposées (schéma 4). Les formes chélatées

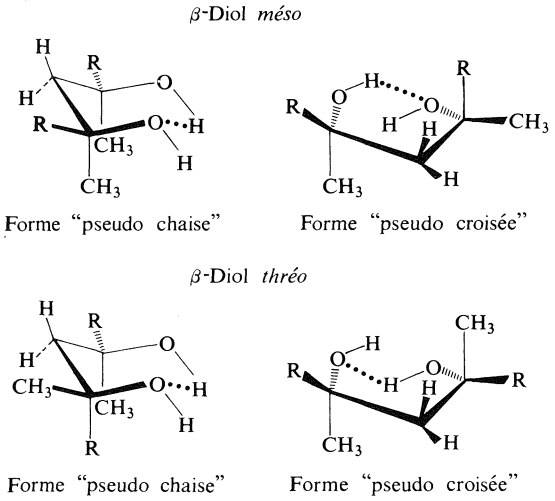

SCHÉMA 4

dans des conformations "pseudo chaises" présentent l'inconvénient pour les diastéréoisomères *thréo* d'avoir de fortes interactions 1-3; un substituant R volumineux se trouve alors en position "quasi axiale", qui est énergétiquement moins favorable que celle "quasi équatoriale" du *méso*.

Par contre une forme "pseudo croisée" peut être vraisemblablement envisagée pour l'isomère *thréo* dans laquelle les interactions 1-3 sont minimisées; les substituants encombrants adoptent une position "quasi équatoriale" plus probable (schéma 4).

Toutefois pour les isomères *thréo* des diols (**21**–**25**), un épaulement vers 3570 cm^{-1} montre l'existence d'une association intramoléculaire entre un des hydroxyles et le noyau benzénique porté par l'autre carbone asymétrique. Cette liaison π ne peut avoir lieu que lorsque le phényle est en position "quasi axiale": seule la conformation "pseudo chaise" répond à cette exigence.

Pour les diols du type **II** (**26**–**31**) et les diols **33** et **34** nous ne sommes pas en mesure de discuter systématiquement des différences entre les deux diastéréoisomères,[5] sauf pour **26***a* et **26***b*. Les trois bandes OH libre, OHπ et OH lié sont présentes pour les deux isomères, et similairement aux β-diols du type **I**, plus intenses pour le *thréo*; mais les Δν(OH) et Δν(OH′), sensiblement plus élevés quand il s'agit du *méso*, signifient selon Kuhn, des liaisons intramoléculaires plus fortes. Dans les cas des diols du type **II** des liaisons ont probablement lieu entre un hydroxyle et un noyau benzénique du groupement benzyle porté par le même carbone. Les deux hydrogènes entrant dans des associations intramoléculaires la bande OH libre est un épaulement et le rapport (A'/A) ne peut être calculé.

Etude par r.m.n.

Nous rassemblons au tableau 4 les déplacements chimiques de signaux des protons méthyliques et méthyléniques afin de déterminer la configuration et conformation des diastéréoisomères *méso* et *thréo* et procéder leur dosage.

Comme il a été déjà constaté précédemment (3 et 7) on remarque que chaque couple de dias-

TABLEAU 4. Spectres de r.m.n.* des diastéréoisomères des β-diols bitertiaires symétriques

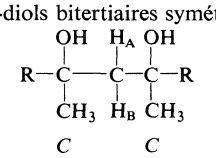

β-Diols	δ(CH₃) *C*	δ(H_A)	δ(CH₂)	δ(H_B)	Δδ	*J*
21*a*	1.50	2.40		2.53	0.13	15.0
21*b*	1.23		2.38			
22*a*	1.53	2.38		2.53	0.15	16.5
22*b*	1.21		2.33			
23*a*	1.48		2.46			
23*b*	1.22		2.30			
24*a*	1.37		2.34			
24*b*	1.21		2.31			
25*a*	1.66		2.60			
25*b*	1.28		2.39			
26*a*	1.27	1.57		1.87	0.30	15.0
26*b*	1.23		1.78			
27*a*	1.30	1.68		1.97	0.29	15.0
27*b*	1.27		1.88			
28*a*	1.23	1.44		1.76	0.32	15.0
28*b*	1.18		1.66			
29*a*	1.28	1.57		1.91	0.34	15.0
29*b*	1.24		1.80			
30*a*	1.28	1.47		1.82	0.35	15.0
30*b*	1.23		1.70			
31*a*	1.32	1.62		1.94	0.32	15.0
31*b*	1.27		1.84			
32*a*	1.30	1.50		1.70	0.20	11.0
32*b*	1.20		1.67			
33*a*	1.31	1.50		1.67	0.17	11.0
33*b*	1.20		1.66			
34*a*	1.31	1.47		1.74	0.27	9.0
34*b*	1.25		1.62			

*Les déplacements chimiques sont donnés en p.p.m. et les constantes de couplage en Hz. Le TMS sert de référence interne.

[5]Les isomères *thréo* des β-diols du type II n'ont pas été isolés. Les valeurs données dans ce mémoire pour le composé **26***b* nous ont été aimablement communiquées par M. et Mme Maroni du laboratoire de synthèse et physico-chimie organique de la Faculté des Sciences de Toulouse, France.

TABLEAU 5. Dosage* des diastéréoisomères des β-diols bitertiaires symétriques

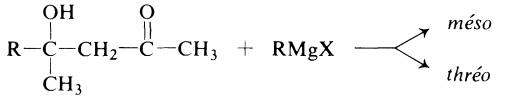

R MgX	β-Diols	Rendement (%)	*méso* %	*méso* p.f.°	*thréo* %	*thréo* p.f.°
C_6H_5MgBr	**21**	60	20	117	80	106.5
p-$CH_3C_6H_4MgBr$	**22**	52	20	133	80	106
p-ClC_6H_4MgBr	**23**	65	10	178	90	153
m-ClC_6H_4MgBr	**24**	60	25	49	75	visq.
p-$CH_5OC_6H_4MgBr$	**25**	40	25	130	75	106
$C_6H_5CH_2MgCl$	**26**†	45	80	94	20	103
o-$CH_3C_6H_4CH_2MgCl$	**27**†	29	80	71	20	‡
m-$CH_3C_6H_4CH_2MgCl$	**28**†	30	80	visq.	20	‡
p-$CH_3C_6H_4CH_6MgCl$	**29**†	40	80	104	20	‡
3,4-$(CH_3)_2C_6H_3CH_2MgCl$	**30**†	34	80	108	20	‡
3,5-$(CH_3)_2C_6H_3CH_2MgCl$	**31**†	31	80	80	20	‡
$C_6H_{11}MgCl$	**32**	31	50	113	50	85
$(CH_3)_2CH$—MgCl	**33**	48	55	liq.	45	liq.
CH_2=CH—CH_2MgBr	**34**	50	65	liq.	35	liq.

*Dosage effectué par r.m.n. avec une précision de l'ordre de 10%.
†Pour ces diols, le dosage est très approximatif et les chiffres donnés ne représentent qu'un ordre de grandeur.
‡Impur.

téréoisomères possède des signaux des protons méthyliques et méthyléniques différents.

Les signaux de méthyle se manifestent par un singulet et résonnent à des champs plus faibles pour les isomères *méso* que pour les *thréo*. Cette différence est encore plus importante pour les β-diols du type **I** (**21** à **26**).

Les signaux méthyléniques, en α des hydroxyles, suivent le même ordre et ils sont beaucoup plus déblindés pour les isomères *méso* que *thréo*. De plus on remarque une non équivalence magnétique des protons du méthylène (H_A et H_B) dans le cas des diastéréoisomères *méso* qui se traduit, pour la plupart des β-diols, par un doublet de doublet. Une équivalence magnétique apparente observée dans les cas des composés **23***a*, **24***a*, et **25***a* pour les protons méthyléniques résulterait de l'anisotropie des groupements chlore et méthoxyles substitués sur le noyau benzénique.

Un singulet caractérise les protons méthyléniques des diastéréoisomères *thréo*. De ces constatations on est amené à attribuer la conformation "pseudo chaise" aux diastéréoisomères *méso* et aux *thréo* des diols du type **I**: L'abaissement du signal des méthyles allant jusqu'à 0.38 p.p.m. pour le *thréo* (**25***b*) résulte probablement d'un blindage dû aux groupements phényles dans une conformation cyclique "pseudo chaise". Le déplacement chimique du méthyle donné par le spectre est une valeur moyenne des positions "quasi axiale" et "quasi équatoriale".

Hypothèses conformationnelles

Les données fournies par les études spectroscopiques nous amènent à prévoir une forte population de conformations chélatées cycliques de ces diols à l'image de Maskens *et al.* (14), Wolf (11), et Maffrand et Maroni (7). Nous pouvons conclure à l'existence des conformations "pseudo chaise" et "pseudo croisée" pour les isomères *thréo* et à une conformation majoritaire "pseudo chaise" pour les isomères *méso*.

Cependant, nous ne pouvons négliger la probabilité d'existence des autres conformations et, en particulier, des conformations non cycliques ouvertes. Dans cette éventualité, les groupements portés par les carbones adjacents sont en position décalée. Le schéma 4 présente les conformations cycliques les plus probables des β-diols bitertiaires étudiés dans le présent travail.

Induction asymétrique-1,3

L'examen des résultats rassemblés au tableau 5 nous mène à formuler les remarques suivantes:

(*i*) Les β-hydroxycétones de type **I** (**1–5**) qui possèdent en position 3 du carbonyle un substituant inducteur phényle conduisent à la formation d'un diol majoritaire en *thréo*.

(*ii*) Les β-hydroxycétones de type **II** (**6–11**) dont le groupement en position 3 du carbonyle est un benzyle donnent un diol diastéréoisomère prépondérant *méso*.

(*iii*) Les β-hydroxycétones de type **III** (**13–14**)

Can. J. Chem. Downloaded from www.nrcresearchpress.com by 210.87.254.40 on 09/05/12
For personal use only.

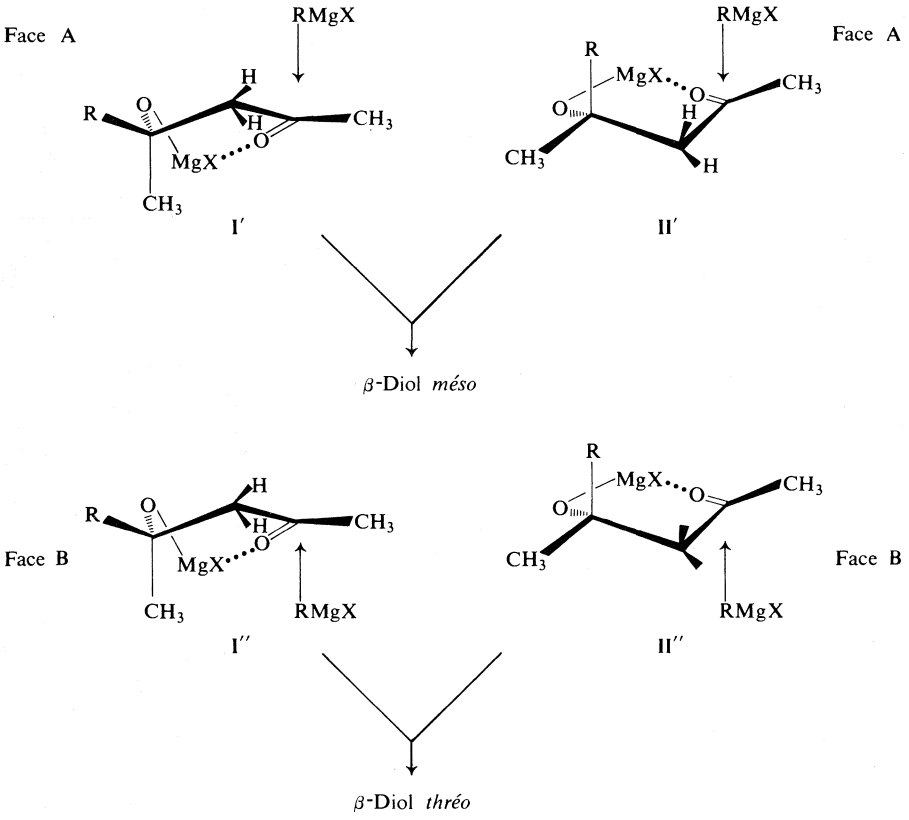

SCHÉMA 5

qui ont un groupement cyclohexyle, isopropyle ou allyle montrent une stéréosélectivité moins prononcée et favorisent la formation du diastéréoisomère *méso*.

La stéréosélectivité de cette réaction est en général très affirmée, elle est due à l'importance des volumes effectifs des groupements inducteurs et des réactifs ajoutés. Cette remarque est en accord avec la théorie de Richer fondée sur l'encombrement stérique (15–16); en effet, il a montré que, pour les cétones cycliques, la stéréosélectivité des réactions de réduction dépend de la combinaison des effets stériques du réactif et de la cétone. D'autre part, nous observons une augmentation de la stéréosélectivité lorsque les groupes R sont aromatiques et substitués par des groupements polaires. Cette hypothèse est notamment étayée par l'exemple du groupe para-chlorophényle qui, ajouté à l'hydroxycétone **3** de même groupement inducteur, augmente fortement la stéréosélectivité de la réaction. Par ailleurs, une diminution de la stéréosélectivité est constatée lorsque l'on fait réagir les groupes allyle, isopropyle, et cyclohexyle sur les hydroxycétones correspondantes **12–14**; dans ces cas, seulement, les effets stériques interviennent.

Nous supposons au premier temps la formation de cétoalcoolates de MgX possédant des conformations chélatées analogues au "modèle cyclique" préconisé par Leitereg et Cram (3). Dans chaque conformation "pseudo chaise" possible (**I** et **II**), une des faces est moins encombrée, et selon le volume de l'entité nucléophile (R^-) transférée au carbone du carbonyle se forme l'isomère *thréo* ou *méso* en prédominance (schéma 5). Dans le cas d'effet polaire, Chérest *et al.* (17) supposent que les états de transition sont favorisés dans lesquels la séparation est grande d'entre le réactif nucléophile et un groupe électronégatif.

Partie expérimentale

Les spectres i.r. ont été enregistrés sur les spectrophotomètres Beckman, modèle IR-12, et Perkin–Elmer, modèles 457 et 621, les produits ont été étudiés à l'état dissous dans le tétrachlorure de carbone (Baker), ce solvant ayant été déshydraté par passage sur tamis molécu-

Can. J. Chem. Downloaded from www.nrcresearchpress.com by 210.87.254.40 on 09/05/12
For personal use only.

Can. J. Chem. Downloaded from www.nrcresearchpress.com by 210.87.254.40 on 09/05/12
For personal use only.

laire (4 Å, 1/16″) (Baker). Les concentrations des solutions varient de 5.10^{-2} à 10^{-3} *M*. Les cellules utilisées sont constituées d'un cylindre de verre, d'une paire de fenêtres en NaCl provenant d'un même lot de polissage, et de montures en acier inoxydable; les épaisseurs des cuves sont de 5, 20, et 50 mm. Les spectres de r.m.n. ont été obtenus avec un spectrographe Varian modèle A60, le tétraméthylsilane servant de référence interne, avec des solutions à 25% dans le chloroforme deutérié. Les déplacements chimiques sont donnés en p.p.m. et les constantes de couplage en Hz. Les points de fusion ont été mesurés sur un appareil Thomas Hoover et sont donnés non corrigés. Les chromatographies sur couche mince analytique ont été effectuées sur gel de silice G (Mackerey-Nagel et Merck-Darmstadt) et ont permis le contrôle de la pureté des produits. Le solvant utilisé était un mélange éther de pétrole – éther en proportions variables suivant les produits à éluer. Les chromatographies sur colonne ont été réalisées à l'aide de gel de silice Davison Chemical grade 923.

Préparation des solutions d'organomagnésiens mixtes

Les chlorures de xylyle et de mésityle ont été préparés au laboratoire par chloration au moyen de chlorure de sulfuryle et par chlorométhylation (8).

L'appareillage comprend un ballon quadricol de 2 l pour la préparation des β-hydroxycétones et de 500 ml en ce qui concerne celle des β-diols, équipés d'un système d'agitation étanche, d'une ampoule à introduction, d'un réfrigérant ascendant avec tube de garde à chlorure de calcium, d'un thermomètre et d'une arrivée d'azote sec.

Les organomagnésiens sont obtenus par la méthode habituelle (8) à partir de tournures de magnésium (BDH) et d'halogénures d'alcoyle et d'aryle fraîchement distillés et séchés sur chlorure de calcium. Les solutions sont préparées sous atmosphère d'azote et sont dosées selon la méthode de Gilman *et al.* (18), donnant des résultats optimistes de 10%.

Synthèse des β-hydroxycétones, type ***II***

Au réactif de Grignard préparé à partir de 1.5 mol d'halogénure d'alcoyle et de 1.61 at/g de Mg (40 g) dans 1100 ml d'éther anhydre ($\simeq 1.2$ *M*) refroidi à $-15°$ par un mélange acétone–carboglace, est ajoutée en 30 min une solution de 0.5 mol d'acétylacétone (50 g) diluée dans 200 ml d'éther anhydre. L'addition terminée, le milieu réactionnel est ramené à température ambiante et laissé sous agitation pendant 18 h. On hydrolyse par une solution glacée de chlorure d'ammonium en contrôlant la température de la réaction à 5°. La phase aqueuse est extraite deux fois par 200 ml d'éther. Cette solution éthérée est jointe à la phase éthérée décantée, l'ensemble est lavé par 100 ml d'eau et séché sur sulfate de magnésium anhydre. L'évaporation de l'éther donne une huile de couleur jaune brun, qui est traitée par le réactif de Girard T, préalablement recristallisé dans un mélange méthanol – éthanol absolu (1:1), ou préparé au laboratoire selon la méthode décrite dans (19). On utilise 100 g dans 200 ml de méthanol absolu auquel on ajoute 2 g de résine cationique acide [Rexyn 102 (H)]. Après un reflux de 2 h, on évapore le méthanol, on hydrolyse le résidu visqueux par 500 ml d'eau et on extrait par 400 ml d'éther de pétrole (p.éb. 30–60°) les produits non cétoniques: hydrocarbures, alcools, et β-diols. Après addition de 50 ml d'une solution aqueuse de formaldéhyde à 36%, on extrait en continu pendant 48 h par l'éther de pétrole, la β-hydroxycétone désirée, accompagnée de cétones α,β-éthyléniques, de cétones de scission. Une distillation sous un vide de 0.1 mm de Hg permet d'obtenir un β-cétol pur (3*e* fraction). Leurs constantes physiques se trouvent rassemblées dans le tableau 6.

Synthèse des β-hydroxycétones, types ***I*** *et* ***III***

Un mode opératoire identique au précédent est suivi, à quelques modifications près. Lors de l'addition de l'acétylacétone à la solution organomagnésienne, on veillera à refrigérer celle-ci à $-25°$ afin d'éviter la formation de cétone α,β-éthylénique, les réactions avec le bromure de phénylmagnésium et surtout avec le chlorure de cyclohexylmagnésium étant plus exothermiques. La préparation est poursuivie de manière analogue mais après distillation la β-hydroxycétone est séparée de la cétone éthylénique par chromatographie. Dix grammes de cétones préalablement distillées sont adsorbés sur une colonne de 800 g de gel de silice, l'éluant est un mélange d'éther de pétrole et d'éther. Nous reportons les constantes physiques de ces hydroxycétones dans le tableau 6, et celles des cétones insaturées correspondantes dans le tableau 7.

Synthèse des β-diols

Mode opératoire ***I****: β-diols* ***21***, ***22***, ***23***, ***24***, ***25***

On ajoute en 10 min 0.02 mol d'hydroxycétone dans 50 ml d'éther anhydre au réactif de Grignard préparé à partir de 0.07 at/g de magnésium (1.68 g) et 0.06 mol d'halogénure d'alcoyle dans 100 ml d'éther anhydre. Lors de l'addition du β-cétol on maintient le mélange réactionnel à une température de 15°, après l'avoir ramené à température ambiante, on l'abandonne sous agitation pendant 18 h. On hydrolyse par 100 ml d'une solution saturée de NH_4Cl le mélange maintenu à 5°, on extrait trois fois à l'éther; après lavage à l'eau, puis séchage sur $MgSO_4$, on évapore l'éther et l'huile obtenue est chromatographiée sur gel de silice. Un mélange d'éther de pétrole (30–60°) et d'éther anhydre en proportions variables est utilisé pour éluer les produits, les conditions opératoires spécifiques seront indiquées pour chaque composé.

*Diphényl-2,4 pentanediol-2,4 (****21****)*

A la solution de Grignard préparée à partir de 9.6 g de bromobenzène, on ajoute 3.5 g de **1**, après traitement de la réaction (mode opératoire **I**), on obtient une huile (6.6 g) laquelle est chromatographiée sur 200 g de gel de silice, on élue aux différents mélanges éther de pétrole (30–60°) – éther suivants: (99:1) le biphényle, (90:10) l'acétophénone et la phényl-4 pentène-3 one-2 **1***i*, (87:13) le β-diol *thréo* (2.7 g), le β-diol *méso* (0.7 g). Après trois recristallisations dans le mélange éther de pétrole – éther (80:20) on recueille 2.5 g d'isomère *thréo* et 0.6 g de *méso*, pour un poids total de 3.1 g.

Anal. calc. pour $C_{17}H_{20}O_2$: C, 79.90; H, 7.80. Trouvé **21***a*: C, 79.51; H, 7.67. **21***b*: C, 79.62; H, 7.80.

*Di-p-tolyl-2,4 pentanediol-2,4 (****22****)*

On introduit 10.3 g de bromotoluène afin de préparer la solution de bromure de *p*-tolylmagnésium, on ajoute 3.8 g de **2**, après traitement de la réaction (mode opératoire **I**) on obtient une huile (7 g), laquelle est chromatographiée sur 700 g de gel de silice, on élue aux mélanges éther de pétrole (30–60°) – éther suivants: (95:5) le bitolyle, (85:15) la *p*-méthylacétophénone, (80:20) la *p*-tolyl-4 pentène-3-one-2 **2***i* (60:40), le β-diol *thréo*

Can. J. Chem. Downloaded from www.nrcresearchpress.com by 210.87.254.40 on 09/05/12
For personal use only.

TABLEAU 6. Propriétés physiques des β-hydroxycétones

No.	Formules β-hydroxycétones	Rendement (%)	p.éb.° (0.1 mm Hg)	Analyse en % Calc. C	Calc. H	Trouvé C	Trouvé H	Infrarouge ν et δ (cm^{-1}) ν(C—OH)	δ(O—H)	ν(C=O)	ν(O—H)†
1	$C_{11}H_4O_2$*	52	70	74.13	7.92	74.28	8.00	1177	1375	1705	3482
2	$C_{12}H_{16}O_2$	34	74	74.97	8.39	75.33	8.42	1168	1350	1704	3485
3	$C_{11}H_{13}O_2Cl$	55	98	62.10	6.16	62.37	6.11	1173	1371	1705	3481
4	$C_{11}H_{13}O_2Cl$	58	86	62.10	6.16	62.20	6.18	1180	1380	1708	3490
5	$C_{12}H_{16}O_3$	65	104	69.21	7.74	69.53	7.69	1185	1380	1704	3485
6	$C_{12}H_{16}O_2$	75	92	74.97	8.39	75.23	8.27	1171	1365	1706	3489
7	$C_{13}H_{18}O_2$	65	100	75.69	8.80	75.52	8.74	1167	1386	1719	3505
8	$C_{13}H_{18}O_2$	70	97	75.69	8.80	75.71	8.77	1173	1377	1712	3482
9	$C_{13}H_{18}O_2$	65	95	75.69	8.80	75.60	8.73	1177	1382	1711	3445
10	$C_{14}H_{20}O_2$	72	112	76.32	9.15	76.27	9.10	1175	1376	1708	3440
11	$C_{14}H_{20}O_2$	70	108	76.32	9.15	76.18	9.07	1170	1370	1710	3455
12	$C_{11}H_{20}O_2$	43	70	71.69	10.94	72.02	10.84	1177	1380	1705	3505
13	$C_8H_{16}O_2$	50	35	66.63	11.18	66.88	11.08	1180	1380	1708	3490
14	$C_8H_{14}O_2$	56	66	67.57	9.93	67.59	9.90	1178	1382	1705	3430

*Point de fusion 29°.
†Ces valeurs ont été déterminées en film (fenêtres de NaCl).

TABLEAU 7. Caractéristiques physiques des cétones α,β-éthyléniques

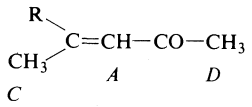

R	No.	p.éb.° (0.1 mm Hg)	Formules	Analyse en % Calc. C	Calc. H	Trouvé C	Trouvé H	Résonance magnétique nucléaire* δ(CH_3) C	δ(CH_3) D	δ(H_A)	Infrarouge (cm^{-1}) ν(C=C)	ν(C=O)
C_6H_5	**1***i*	60	$C_{11}H_{12}O$	82.46	7.55	82.26	7.51	2.10	2.12	6.50	1617	1675
p-$CH_3C_6H_4$	**2***i*	65	$C_{12}H_{14}O$	82.72	8.10	81.41	8.01	2.14	2.24	6.47	1615	1680
p-ClC_6H_4	**3***i*	80	$C_{11}H_{11}OCl$	69.45	5.69	69.80	5.80	2.10	2.13	6.12	1625	1670
p-$CH_3OC_6H_4$	**5***i*	100	$C_{12}H_{14}O_2$	75.76	7.42	75.54	7.35	2.17	2.43	6.55	1625	1680
C_6H_{11}	**12***i*	80	$C_{11}H_{18}O$	79.46	10.92	79.24	10.73	2.03	2.06	5.98	1615	1690

*Les déplacements chimiques sont donnés en p.p.m. Le TMS sert de référence interne.

Can. J. Chem. Downloaded from www.nrcresearchpress.com by 210.87.254.40 on 09/05/12
For personal use only.

(2.5 g), (50:50) le β-diol *méso* (0.9 g). Après trois recristallisations dans le mélange éther de pétrole – éther (80:20), on recueille 2.3 g d'isomère *thréo* **22***b* et 0.7 g de *méso* **22***a*, pour un poids total de 3 g.

Anal. calc. pour $C_{19}H_{24}O_2$: C, 80.24; H, 8.51. Trouvé **22***a*: C, 80.27; H, 8.60. **22***b*: C, 80.25; H, 8.60.

*Di-p-chlorophényl-2,4 pentanediol-2,4 (**23**)*

On prépare la solution de *p*-chlorophénylmagnésium à partir de 11.5 g de *p*-chlorobromobenzène, à laquelle on ajoute 4.25 g de **3**, après traitement de la réaction, selon le mode opératoire indiqué, on obtient une huile (10 g) que l'on chromatographie sur 800 g de gel de silice, on élue aux mélanges éther de pétrole (30–60°) – éther suivants: (90:10) le dichloro-4,4′-diphényle, (75:25) la *p*-chloroacétophénone, (62:38) le β-diol *thréo* (4.2 g), (40:60) le β-diol *méso* (0.4 g). On recristallise les deux diastéréoisomères séparément; le β-diol *thréo* dans le mélange éther de pétrole – éther (70:30), et le *méso* dans (40:60) et on recueille 3.9 g de *thréo* **23***b* et 0.3 g de *méso* **23***a*, soit un poids total de 4.2 g.

Anal. calc. pour $C_{17}H_{18}O_2$: C, 62.79; H, 5.58. Trouvé **23***a*: C, 61.96; H, 5.36. **23***b*: C, 62.18; H, 5.46.

*Di-m-chlorophényl-2,4 pentanediol-2,4 (**24**)*

A la solution jaune clair du bromure de *m*-chlorophénylmagnésium, préparé à partir de 11.5 g de *m*-bromochlorobenzène et de 2 g de magnésium dans 15 ml d'éther anhydre est ajouté 4.24 g d'hydroxycétone **4** diluée dans 5 ml d'éther anhydre. Un résidu pâteux peu soluble dans l'éther est hydrolysé par 250 ml de chlorure d'ammonium. Après extraction et évaporation, on obtient 7 g d'une pâte brune que l'on dépose sur 500 g de gel de silice. L'isomère *thréo* **24***b* passe à (80:20) d'éther de pétrole – éther (3.0 g) précédé par le dichloro-3,3′ diphényle, une cétone de scission et un peu de cétone α,β-éthylénique. Ce produit blanc très visqueux cristallise difficilement à cause de son bas point de fusion. Au mélange éluant (70:30), on trouve l'autre isomère **24***a* visqueux incristallisable (1.0 g).

Anal. calc. pour $C_{17}H_{18}O_2Cl_2$: C, 62.79; H, 5.58. Trouvé **24***a*: C, 61.76; H, 5.33. **24***b*: C, 61.83; H, 5.35.

*Di-p-méthoxyphényl-2,4 pentanediol-2,4 (**25**)*

p-Chloroanisole (11.22 g) et 2 g de magnésium dans 150 ml d'éther anhydre contribuent à la préparation de la solution organomagnésienne à laquelle est additionnée l'hydroxy cétone **5** selon le mode opératoire **I**. Après hydrolyse par une solution de chlorure d'ammonium et extraction à l'éther, on recueille 8 g de composé brut. Une partie de l'huile est précipitée dans un mélange de solvant éther de pétrole – éther (50:50); 1.5 g de *thréo* est obtenu après recristallisation. On chromatographie la fraction restante (6.5 g) sur une colonne de 500 g de gel de silice. Le composé *thréo* **25***b* est élué à (80:20) d'éther de pétrole – éther (0.5 g) et le *méso* **25***a* (0.5 g) à (70:30) du même mélange.

Anal. calc. pour $C_{19}H_{24}O_4$: C, 72.12; H, 7.65. Trouvé **25***a*: C, 72.40; H, 7.57. **25***b*: C, 71.92; H, 7.59.

*Mode opératoire **II**: β-diols **26–31***

On suit le mode opératoire **I** en ajoutant le β-cétol à température ambiante.

*Diméthyl-2,4 diphényl-1,5 pentanediol-2,4 (**26**)*

On utilise 7.6 g de chlorure de benzyle pour la préparation de la solution de chlorure de benzylmagnésium à laquelle on additionne 3.8 g de β-cétol **4**, la réaction est traitée selon le mode opératoire indiqué précédemment et on obtient 9.0 g d'une huile jaune pâle. La chromatographie est réalisée avec la moitié du liquide soit 4.5 g sur 120 g de gel de silice. L'éluant est un mélange éther de pétrole – éther; sortent à (98:2) le bibenzyle, à (90:10) la phénylacétone, à (82:18) un mélange de diastéréoisomères *thréo* et *méso* (p.f. 94°); le poids total des cristaux ainsi isolés est 1.3 g. L'huile restante se solidifie, on filtre les cristaux, et on recristallise dans le mélange éther de pétrole – éther (70:30). On recueille 1.3 g de composé *méso*, poids total 2.6 g.

Anal. calc. pour $C_{19}H_{24}O_2$: C, 80.29; H, 8.44. Trouvé: C, 80.11; H, 8.38.

*Diméthyl-2,4 di o-tolyl-1,5 pentanediol-2,4 (**27**)*

On utilise 8.4 g de chlorure d'*o*-xylyle pour préparer le réactif de Grignard correspondant auquel on ajoute 4.12 g de β-hydroxycétone **5**, après traitement de la réaction en se référant au mode opératoire **II** on recueille un liquide visqueux jaune clair (10.5 g) lequel est chromatographié sur 1 kg de gel de silice. On élue à différents gradients d'éther de pétrole – éther: à (97:3) le di-*o*-tolyl-1,2 éthane, à (85:15) l'*o*-tolyl acétone, à (80:20) la β-hydroxycétone non réagie, et à (60:40) une huile visqueuse. Une seconde chromatographie effectuée avec 3 g de produit sur 120 g de gel de silice permet de recueillir le diastéréoisomère *méso* **27***a* sous la forme d'une huile cristallisant lentement: 1.8 g après cristallisation de l'hexane–éther, le *thréo* **27***b* restant dans les eaux mères.

Anal. calc. pour $C_{21}H_{28}O_2$: C, 80.73; H, 9.03. Trouvé: C, 80.54; H, 8.99.

*Diméthyl-2,4 di m-tolyl-1,5 pentanediol-2,4 (**28**)*

On opère sur les mêmes quantités employées pour la synthèse de **27**: 8.4 g de chlorure de *m*-xylyle et 4.12 g de β-cétol **6** pour obtenir 10 g d'une huile jaune ocre qui est chromatographiée sur 500 g de gel de silice, l'éluant est un mélange éther de pétrole – éther qui laisse passer à (97:3) le di *m*-tolyl-1,2 éthane, à (80:20) la *m*-tolylacétone, à (70:30) la β-hydroxycétone non réagie et à (50:50) la fraction contenant le diol, celle-ci est rechromatographiée sur 120 g de gel de silice, mais le diol reste sous la forme d'un liquide clair, dont nous recueillons 1.9 g. Le spectre de r.m.n. nous indique la présence des deux diastéréoisomères, le *méso* étant prépondérant.

Anal. calc. pour $C_{21}H_{28}O_2$: C, 80.73; H, 9.03. Trouvé: C, 80.35; H, 8.90.

*Diméthyl-2,4 di p-tolyl-1,5 pentanediol-2,4 (**29**)*

On opère sur les mêmes quantités employées pour la synthèse de **27**. Le chlorure de *p*-xylyle (8.4 g) et 4.12 g de β-cétol **7** pour obtenir 8 g d'un liquide jaune, on le chromatographie sur 500 g de gel de silice et on élue les produits aux mélanges d'éther de pétrole – éther suivants: (97:3) le di *p*-tolyl-1,2 éthane, (85:15) la *p*-tolylacétone et (70:30) le β-diol (mélange des deux diastéréoisomères). Après recristallisation de l'hexane–éther nous isolons le *méso* **29***a* (2.5 g).

Anal. calc. pour $C_{21}H_{28}O_2$: C, 80.73; H, 9.03. Trouvé: C, 80.45; H, 8.98.

*Diméthyl-2,4 di (xylyl-3,4)-1,5 pentanediol-2,4 (**30**)*

On utilise 9.3 g de chlorure de diméthyl-3,4 benzyle pour préparer la solution organomagnésienne correspon-

dante à laquelle on ajoute 4.40 g d'hydroxycétone **8**, la réaction traitée, on recueille 10.5 g d'huile, laquelle est chromatographiée sur 500 g de gel de silice, on élue à des mélanges différents d'éther de pétrole et d'éther: (98:2) le di (xylyl-3,4)-1,2 éthane, (90:10) la xylyl-3,4 acétone, et (80:20) 0.5 g de mélange de diastéréoisomères (p.f. 101°), et 2.0 g de β-diol *méso* **30***a* (p.f. 108°). Après recristallisation de l'hexane–éther, on recueille 1.9 g de β-diol *méso*.

Anal. calc. pour $C_{23}H_{32}O_2$: C, 81.13; H, 9.47. Trouvé: C, 80.60; H, 9.37.

*Diméthyl-2,4 di (xylyl-3,5) pentanediol-2,4 (**31**)*

On peut se référer aux quantités utilisées dans la synthèse de **30** pour le chlorure de diméthyl-3,5 benzyle et l'hydroxycétone **9**, on obtient 11 g d'huile laquelle est chromatographiée sur 500 g de gel de silice. On sépare le di (xylyl-3,5)-1,2 éthane à (99:1) d'éther de pétrole – éther, la xylyl-3,5 acétone à (80:20), et le β-diol à (60:40). On recueille le mélange de diastéréoisomères à prépondérance *méso* et ce dernier est recristallisé, on en obtient 1.8 g.

Anal. calc. pour $C_{23}H_{32}O_2$: C, 81.13; H, 9.47. Trouvé: C, 80.68; H, 9.39.

*Synthèse des β-diols **32–34***

On suit le mode opératoire **I** pour la synthèse de ces diols.

*Dicyclohexyl-2,4 pentanediol-2,4 (**32**)*

On prépare la solution de chlorure de cyclohexylmagnésium en ajoutant 7 g de chlorure de cyclohexyle dilué dans 100 ml d'éther anhydre. (Pour initier la réaction, on chauffe le ballon contenant des tournures de magnésium et quelques millilitres d'éther anhydre, alors que sont introduites quelques gouttes de bromure de cyclohexyle pur.) On additionne l'hydroxy-4 cyclohexyl-4 pentanone-2 **12** (3.7 g) à la solution organomagnésienne refroidie à 15°. La réaction traitée de façon habituelle conduit à 6 g d'une huile jaune clair qui est chromatographiée sur 500 g de gel de silice. On élue au mélange éther de pétrole – éther: en premier, le dicyclohexyle (97:3), l'hydroxycétone non réagie (80:20), le β-diol *thréo* **32***b* (75:25) (0.7 g), et le β-diol *méso* **32***a* (70:30) (1.2 g). Après deux recristallisations dans l'hexane–éther, on recueille 0.6 g de *thréo* et 0.9 g de *méso*.

Anal. calc. pour $C_{17}H_{32}O_2$: C, 76.06; H, 12.02. Trouvé **32***a*: C, 76.08; H, 12.04. **32***b*: C, 76.15; H, 12.08.

*Tétraméthyl-2,3,5,6 heptanediol-3,5 (**33**)*

On additionne la β-hydroxycétone **13** (2.8 g) à la solution magnésienne d'isopropyle (4.7 g de chlorure d'isopropyle et 1.8 g de magnésium dans 100 ml d'éther anhydre). Après traitement de la réaction, on recueille 4 g d'une huile jaune, contenant de l'hydroxycétone non réagie et le mélange des β-diols diastéréoisomères que nous distillons sous 1 mm de Hg. La β-hydroxycétone passe à 40° et le diol entre 76 et 80° (1.8 g). Une tentative de séparation sur colonne de gel de silice (300 g) ne donne aucun résultat.

Anal. calc. pour $C_{11}H_{24}O_2$: C, 70.16; H, 12.85. Trouvé: C, 69.80; H, 12.80.

*Diméthyl-4,6 nonadiène-1,8 diol-4,6 (**34**)*

La β-hydroxycétone **14** (2.8 g) est ajoutée à la solution magnésienne d'allyle (7.26 g de bromure d'allyle et 2 g de magnésium dans 100 ml d'éther anhydre). On traite la réaction selon le mode opératoire **I** et on recueille 3.5 g d'une huile jaune. On distille le mélange sous 1 mm de Hg entre 70 et 75° et nous obtenons 1.8 g d'un liquide incolore **34**. Une tentative de séparation sur colonne de gel de silice donne un léger enrichissement d'isomère *méso*.

Anal. calc. pour $C_{11}H_{20}O_2$: C, 71.69: H, 10.94. Trouvé: C, 71.43; H, 10.85.

Nous remercions Monsieur S. Brownstein de nous avoir conseillés dans l'étude r.m.n. et Monsieur et Madame P. Maroni de nous avoir communiqué les résultats permettant de compléter ces travaux.

Nous exprimons notre reconnaissance au Conseil National de Recherches du Canada et au Conseil des Arts du Canada pour l'aide financière apportée sous forme de subventions.

1. J. MICHEL et P. CANONNE. Tetrahedron Lett. 4275 (1970).
2. T. J. LEITEREG et D. J. CRAM. J. Am. Chem. Soc. **90**, 4011 (1968).
3. T. J. LEITEREG et D. J. CRAM. J. Am. Chem. Soc. **90**, 4019 (1968).
4. M. J. BRIENNE, C. OUANNES, et J. JACQUES. Bull. Soc. Chim. 1036 (1968).
5. M. J. BRIENNE, C. FOUQUEY, et J. JACQUES. Bull. Soc. Chim. 2375 (1969).
6. J. P. MAFFRAND et P. MARONI. Tetrahedron Lett. 4201 (1969).
7. J. P. MAFFRAND et P. MARONI. Bull. Soc. Chim. 1608 (1970).
8. P. CANONNE et L. C. LEITCH. Can. J. Chem. 1761 (1967).
9. J. P. FREEMAN. J. Am. Chem. Soc. **80**, 1926 (1958).
10. L. P. KUHN. J. Am. Chem. Soc. **74**, 2492 (1952).
11. J. G. WOLF. Thèse de doctorat de spécialité. Toulouse, France. **843** (1969).
12. Y. GAULT et H. FELKIN. Bull. Soc. Chim. 742 (1965).
13. L. CAZAUX. Thèse de doctorat ès-sciences. Toulouse, France. **310** (1967).
14. K. MASKENS, D. E. MINNIKIN, et N. POLGAR. J. Chem. Soc. C, 2113 (1966).
15. J.-C. RICHER. J. Org. Chem. **30**, 324 (1965).
16. M. PERRY, Y. MARONI-BARNAUD, J.-C. RICHER, et D. CHARAS. Bull. Soc. Chim. 3981 (1970).
17. M. CHÉREST, H. FELKIN, et N. PRUDENT. Tetrahedron Lett. 2199 (1968).
18. H. GILMAN, P. D. WILKINSON, W. P. FISCHEL, et C. H. MEYERS. J. Am. Chem. Soc. **45**, 1508 (1923).
19. A. GIRARD. Org. Synth. Coll. Vol. **II**, 85 (1943).

Can. J. Chem. Downloaded from www.nrcresearchpress.com by 210.87.254.40 on 09/05/12
For personal use only.

Can. J. Chem. Downloaded from www.nrcresearchpress.com by 210.87.254.6 on 09/05/12
For personal use only.

Ions and Aggregates of Tetra-*n*-Butylammonium Picrate in Nonaqueous Solvents: A Thermodynamic Study

SAUL GOLDMAN AND G. C. B. CAVE
Department of Chemistry, McGill University, Montreal, Quebec

Received December 1, 1970[1]

Values of ΔG^0, ΔH^0, and ΔS^0 at 25 °C were obtained by distribution studies and by calorimetry, for the dimerization and trimerization of tetra-*n*-butylammonium picrate (**1**) in anhydrous benzene, chlorobenzene, and *o*-dichlorobenzene. The standard enthalpy of sublimation of **1** was calculated. The values of ΔG^0 for the ionization, dimerization, and trimerization of **1** were linear functions of the reciprocal of the dielectric constant of the solvent. The intercepts and slopes of these graphs are interpreted; partial desolvation of the ions, and of the monomers on association is invoked. A simple potential function is used with the data, in order to deduce suitable models of the dimer and the trimer of **1**.

Les valeurs de ΔG^0, ΔH^0 et ΔS^0 ont été obtenues à 25 °C, au moyen d'études de distribution et de calorimétrie, pour la dimérisation et la trimérisation du picrate de tétra-*n*-butylammonium (**1**) dans le benzène anhydre, le chlorobenzène et l'*o*-dichlorobenzène. L'enthalpie standard de sublimation de **1** a été calculée. Les valeurs de ΔG^0 pour l'ionisation, la dimérisation et la trimérisation de **1** sont des fonctions linéaires de l'inverse de la constante diélectrique du solvant. Les intersections et les pentes de ces tracés sont interprétées; la désolvatation partielle de ces ions et des monomères pendant l'association est invoquée. Avec ces données, on utilise une fonction potentielle simple de façon à déduire des modèles convenables pour le dimère et le trimère de **1**.

Canadian Journal of Chemistry, **49**, 4096 (1971)

Introduction

In a previous study (1), the values of ΔG^0 at 25 °C were determined for the ionization, dimerization, and trimerization of the tetra-*n*-butylammonium picrate monomer in anhydrous benzene, chlorobenzene, and *o*-dichlorobenzene by using a solvent-extraction method. In the present work, this study has been extended to 35 and 45 °C, in order to be able to evaluate ΔH^0 and ΔS^0 for the above-noted reactions in the same anhydrous solvents. To complement this solvent-extraction study, calorimetric measurements were also made on the nonaqueous systems.

Experimental

Apparatus

Solvent Extraction

The equilibration bottles, the water thermostat, and the apparatus for dielectric-constant measurements have previously been described (1).

Calorimeter

The calorimeter was a conventional 500-ml Dewar flask in the usual tin housing. This flask was capped with a specially constructed hollow glass cover which could be clamped firmly against a rubber gasket on the flask, in order to provide a seal. Inlet and outlet glass tubes in this cover permitted the circulation through it of thermostatted water, thereby preventing condensation of solvent vapor on its under surface. Two glass tubes were also sealed vertically through the cover, to serve as access ports to the flask. The smaller tube accommodated thermistor leads which fitted snugly; the larger tube was for the addition of salt to the solvent in the flask, and it was kept stoppered between additions.

The thermistor was a low-range type, 0 to 90 °C, sensitive to changes of 0.001 °C (Sargent S-81620 Thermometric Element). It was calibrated against a calibrated Beckmann thermometer over the required range of 20 to 50 °C.

Materials

The preparation, purification, and analysis of the tetra-*n*-butylammonium picrate (Bu_4NPi), and the purification and measured densities of the solvents benzene, chlorobenzene, and *o*-dichlorobenzene have been described elsewhere (2). Distilled water was used for the aqueous phase in the solvent-extraction experiments.

Procedures

Solvent Extraction

The preparation of stock standard solutions of Bu_4NPi, the equilibration of the two liquid phases, and the analysis for the equilibrium concentrations of Bu_4NPi in the separated phases have been described elsewhere (1).

Calorimetry

The integral heat of solution of Bu_4NPi was determined in duplicate as a function of its concentration in each of the solvents *o*-dichlorobenzene, chlorobenzene, and the binary mixture (1:1 *v*/*v*) benzene–chlorobenzene, at 25, 35, and 45 °C. Thus a known weight (~ 2 g) of Bu_4NPi

[1]Revision received July 23, 1971.

Can. J. Chem. Downloaded from www.nrcresearchpress.com by 210.87.254.6 on 09/05/12
For personal use only.

was added through the cover port to a known weight of the solvent (~ 250 g) in the calorimeter. Prior to this addition, both solute and solvent were separately brought to the same initial, known temperature. Solution of the added Bu_4NPi was effected by hand-swirling the calorimeter. The resulting drop in temperature was found from the observed change in the response of the thermistor immersed in the solution. The entire procedure was executed with the calorimeter immersed up to its cover in a water thermostat held to within 0.2 °C of the contents of the calorimeter. In addition, water from this thermostat was pumped through the hollow cover of the calorimeter. Heat leakage from the calorimeter was found to be negligible over the period of the solution process; the equilibrium temperature remained constant within 0.001 °C for several minutes.

After a constant temperature had been reached following solution of the added Bu_4NPi, the temperature of the water in the thermostat was re-adjusted until it was again within 0.2 °C of the solution's temperature. Additional lots of Bu_4NPi were then added in succession, and the entire procedure was repeated after each addition. In this way, the heats of solution were found over the required concentration range of Bu_4NPi.

Prior to the first addition of Bu_4NPi, the temperature of the pure solvent in the calorimeter was measured with a calibrated thermometer. Thereafter, the temperature of the solution was found prior to each successive addition of Bu_4NPi by subtracting the temperature drop for the preceding run, as found from the thermistor. This method of temperature measurement was necessary because the response curve of the thermistor was temperature sensitive.

The water equivalent of the calorimeter was determined at 25 °C by using KNO_3 and water. This value was assumed to apply also at 35 and 45 °C.

Results, and Treatment of the Data

Solvent Extraction

Distribution experiments at 35.1 and 45.1 °C gave the equilibrium stoichiometric concentrations of Bu_4NPi in the aqueous and in the organic phases. A least-squares fit of these data to a previously derived polynomial (1) permitted evaluation of the formation constants for the various species previously shown (1) to be derived from the Bu_4NPi monomer in the organic phase. The treatment was identical with that reported (1) for the same systems at 25.0 °C. A previous study (2) had also shown Bu_4NPi and its aggregates to be partially hydrated in the present solvents; and the hydration constants and water activities at 25.0, 35.1, and 45.1 °C had at that time been evaluated. By using those hydration constants, the formation constants found from the present distribution studies were corrected as previously described (1), to give corresponding values for the anhydrous species formed from the anhydrous monomer in the organic phase. These molar equilibrium constants for the anhydrous species are entered in Table 1, where

$$p = [Bu_4NPi]_{\text{organic solvent}}/[Bu_4NPi]_{\text{water}}$$

$$Bu_4N^+ + Pi^- \overset{k}{\rightleftharpoons} Bu_4NPi \text{ (water)}$$

$$Bu_4NPi \overset{K}{\rightleftharpoons} Bu_4N^+ + Pi^- \text{ (organic solvent)}$$

$$n\ Bu_4NPi \overset{Kn}{\rightleftharpoons} [Bu_4NPi]_n \text{ (organic solvent)}$$

i.e., p = partition coefficient of the anhydrous monomer Bu_4NPi; K = dissociation constant of the anhydrous monomer in the organic phase; k = formation constant of the monomer in water; K_2, K_3, K_6 = formation constants of the anhydrous dimer (K_2), the anhydrous trimer (K_3), and the anhydrous hexamer (K_6) from the anhydrous monomers, in the organic phase; and D is the dielectric constant of the water-saturated organic solvent.

The values of the equilibrium constants K_2 and K_3 in Table 1 are for anhydrous species in water-saturated solvents. Therefore these values were next corrected to values in anhydrous solvents, that is, the presence of unbound water in the solvents was taken into account. To do so, advantage was taken of the linear relationship found to exist between $1/D$ and each of $\log K_2$ and $\log K_3$. This relationship is illustrated in Fig. 1, by plots of ΔG_2^0 ($= -RT \ln K_2$) and ΔG_3^0 ($= -RT \ln K_3$) *vs.* $1/D$, the data being from Table 1. Then from measured values (1) of the dielectric constant of each water-saturated solvent, and literature values for the corresponding anhydrous solvents, interpolation in Fig. 1 gave the required values for K_2 and K_3 in anhydrous solvents. The corrections proved to be very small. They were not applied to K or K_6 due to the unavailability of plots similar to those in Fig. 1, but the error introduced by applying the values of K and K_6 in Table 1, to the case of anhydrous solvents is doubtless negligibly small.

The values of K, K_2, K_3, and K_6 for the anhydrous solvents were then converted from a molar to a molal basis; previously measured (2) densities were used. From the temperature dependence of these four molal equilibrium constants, the corresponding standard enthalpy changes ΔH^0, ΔH_2^0, ΔH_3^0, and ΔH_6^0 were found by least-squares, and the values are entered in Table

Can. J. Chem. Downloaded from www.nrcresearchpress.com by 210.87.254.6 on 09/05/12
For personal use only.

TABLE 1. Thermodynamic equilibrium constants for anhydrous species at three temperatures, in three solvents, from solvent-extraction data

Solvent	Temperature (°C)	D	$K \times 10^8$ (mol/l) Mean	s.d.*	$pk \times 10^{-3}$ (l/mol) Mean	s.d.*	K_2 (l/mol) Mean	s.d *	ν	$K_3 \times 10^{-2}$ (l²/mol²) Mean	s.d.*	ν	$K_6 \times 10^{-7}$ (l⁵/mol⁵) Mean	s d.*	$RT \ln K_f$† (kcal/mol)	Reference
o-Dichlorobenzene	25.0	10.07	1820	80	145	4	5.57	0.72	4	1.17	0.11	4			6.5	11, 12, 13 and this work
	35.1	9.67	1380	70	151	4	8.20	0.66	5	0.81	0.12	4				
	45.1	9.27	1280	150	137	7	6.91	0.82	5	1.04	0.19	4				
Monochlorobenzene	25.0	5.64	24.9	10.0	68.8	2.0	6.8	1.4	4	4.71	0.67	4	1.06	0.28	10.5	8
	35.1	5.48	12.0	3.9	70.3	1.3	7.9	1.1	5	3.20	0.27	4	1.35	0.18		
	45.1	5.32	7.7	4.9	67.6	1.7	8.26	0.84	5	3.32	0.43	4	1.11	0.22		
Benzene	25.0	2.28	0 5	0.39	4.68	0.59	9.8	7.7	4	286	132	3			22.8	12
	35.1	2.27	0.38	0.68	5.07	0.17	19.0	7.2	4	205	25	3				
	45.1	2.24	0.08	0.71	6.25	0.30	4.0	5.7	5	186	31	3				
m-Dichlorobenzene	25.0	5.04													11.7	8

*s.d. means standard deviation. For K and pk there were five degrees of freedon, for K_6 there were two; and for K_2 and K_3 the degrees of freedom are entered in the Table.
†$K_f = 1/K$. These values were determined from conductance data.

TABLE 2. Standard enthalpy changes at 25 °C for the dissociation and aggregation of tetra-*n*-butylammonium picrate monomer in three anhydrous solvents

Solvent	ΔH^0 (kcal/mol)		ΔH_2^0 (kcal/mol)		ΔH_3^0 (kcal/mol)		ΔH_6^0 (kcal/mol)	
	Mean	s.d.*	Mean	s.d.*	Mean	s.d.*	Mean	s.d.*
o-Dichlorobenzene	−1.36	0.13	2.91	0.85	−2.5	3.1		
Chlorobenzene			0.3	3.4	−2.6	2.6	−0.5	2.1
Benzene–chlorobenzene (1:1 *v/v*)			−2.3	6.0	−2.8	1.8		

*s.d. is the standard deviation for one degree of freedom. ΔH^0 = standard enthalpy change for the dissociation of the Bu_4NPi monomer; ΔH_2^0, ΔH_3^0, ΔH_6^0 = standard enthalpy changes for the formation of the dimer (ΔH_2^0), the trimer (ΔH_3^0), and the hexamer from the Bu_4NPi monomer.

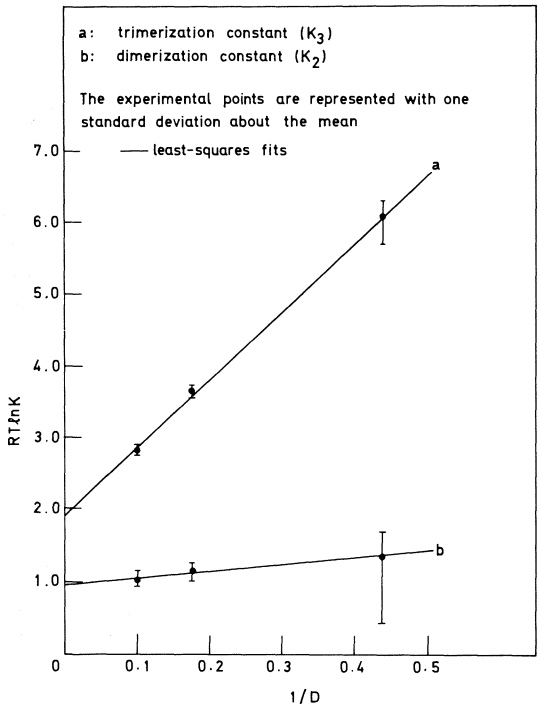

FIG. 1. The relationship between minus the standard free energy of formation of the dimer and the trimer of Bu_4NPi from the monomer, and the reciprocal of the dielectric constant of the solvent, for three solvents at 25 °C.

2. For ΔH^0, namely the standard enthalpy of dissociation of the monomer in the particular solvent, reliable values were obtained only for the *o*-dichlorobenzene system. For the binary solvent system, 1:1 *v/v* benzene–chlorobenzene, the four standard enthalpies were evaluated as follows: Each equilibrium constant K, K_2, K_3, and K_6 was interpolated at each temperature from the linear relationship between $1/D$ and the logarithm of the appropriate equilibrium constant, and the measured value of D for the binary solvent. The standard enthalpy changes were then found from the temperature dependence of the equilibrium constants.

Calorimetry

The heat of solution at each addition of Bu_4NPi to each solvent was calculated in the usual way, by using the heat capacities of the solvents and the measured water equivalent of the calorimeter. However, the heat capacity of the (1:1 *v/v*) benzene–chlorobenzene mixture was interpolated from those of the pure solvents.

The total heat of solution, $\sum\Delta H$, is given in kcal by

$$[1] \quad \sum\Delta H = W_s\left(\Delta H_s^0[m]_T + \sum_{i=1}^{n}\Delta H_i^0[m_i]\right)$$

where W_s = weight in kg of solvent in the calorimeter; ΔH_s^0 = standard enthalpy of solution of Bu_4NPi to give entirely Bu_4NPi monomers, per mole of monomers (kcal/mol); $[m]_T$ = stoichiometric molal concentration of Bu_4NPi in the calorimeter; ΔH_i^0 = standard enthalpy of formation of species X_i from the Bu_4NPi monomer, per mole of X_i (kcal/mol); $[m_i]$ = molal concentration of species X_i in the calorimeter.

The standard state of each species in solution is the conventional, hypothetical ideal one-molal solution. The solutions of the monomer and its aggregates are assumed to obey Henry's law over the concentration ranges studied.

In the present systems, the ΔH_i^0 are ΔH^0, ΔH_2^0, and ΔH_3^0, and also ΔH_6^0 in the case of chlorobenzene. These values were available (Table 2). Their large standard deviations were not unduly detrimental for the present purposes, because the values of $\sum_i\Delta H_i^0[m_i]$ were much smaller than $\Delta H_s^0[m]_T$, at most 10%, even at the highest values of $[m]_T$. The unavailability of

Can. J. Chem. Downloaded from www.nrcresearchpress.com by 210.87.254.6 on 09/05/12
For personal use only.

TABLE 3. Standard enthalpy of solution of 1 mol of Bu_4NPi monomer Bu_4NPi (solid) $\xrightarrow{\Delta H_s^0}$ Bu_4NPi (monomer in solution)

Solvent	Temperature (°C)	ΔH_s^0 (kcal/mol) Mean	Standard deviation	Degrees of freedom
o-Dichlorobenzene	25	5.71	0.02	21
	35	6.03	0.02	21
	45	6.35	0.02	21
Chlorobenzene	25	6.01	0.03	17
	35	6.36	0.02	11
	45	6.56	0.03	11
Chlorobenzene–benzene (1:1 *v/v*)	25	7.13	0.07	7
	35	7.45	0.03	7
	45	7.75	0.03	7

values of ΔH^0 (enthalpy of dissociation of Bu_4NPi) in the cases of chlorobenzene and the mixture benzene–chlorobenzene was also not detrimental because in the range of Bu_4NPi concentrations studied by calorimetry (0.01–0.1 *m*), the concentration of ions was negligibly small in those two solvents.

The $[m_i]$ in eq. 1 are the concentrations of each individual species in the equilibrium mixture in the calorimeter, namely ions, monomer, dimer, trimer, and also hexamer in the case of chlorobenzene. These values of $[m_i]$ were calculated from the known stoichiometric concentration $[m]_T$ of Bu_4NPi in the calorimeter, by using eq. 2:

$$[2] \quad [m]_T = \frac{K^{1/2}[X_1]}{(\gamma_\pm)_0} + [X_1] + 2K_2[X_1]^2 + 3K_3[X_1]^3 + 6K_6[X_1]^6$$

where $[X_1]$ = molality of the Bu_4NPi monomer (ion pair); $(\gamma_\pm)_0$ = mean ionic activity coefficient of the single ions in the organic phase.

The values of $(\gamma_\pm)_0$ were estimated by using iteratively the conventional Debye–Hückel expression. The values of K, K_2, K_3, K_6 for the anhydrous species in the anhydrous solvents were calculated from the corresponding values in Table 1, by applying the water corrections described above. The value of $[X_1]$ corresponding to a given value of $[m]_T$ was found correct to three significant figures, as follows: A range of values of $[X_1]$ was chosen with very small increments, such that the computer-calculated values of the right-hand side of eq. 2 spanned the entire range of values of $[m]_T$ used in the experiments. From this tabulation, $[X_1]$ was read off for each given $[m]_T$. From each such value of $[X_1]$, the molalities of the ions, dimers, trimers, and hexamers were found from the expressions $K^{1/2}[X_1]^{1/2}(\gamma_\pm)_0^{-1}$, $K_2[X_1]^2$, $K_3[X_1]^3$, and $K_6[X_1]^6$, respectively. Equation 2 was then recast, to give a new linear function ϕ

$$[3] \quad \phi \equiv \sum \Delta H - W_s \sum_{i=1} \Delta H_i^0 [m_i] = \Delta H_s^0 W_s [m]_T$$

A least-squares fit of eq. 3 to the data ϕ *vs.* $W_s[m]_T$ gave the values of ΔH_s^0 entered in Table 3, for each solvent system.

Standard Enthalpy of Sublimation of Bu_4NPi

The standard enthalpy of transfer (ΔH_t^0) of Bu_4NPi monomer from its standard-state solution (1 *m*) to the gas in its standard state (1 atm, 35 °C) was calculated as described below, for each solvent. Each resulting value was added to the standard enthalpy of solution of the Bu_4NPi monomer in the corresponding solvent, obtained from Table 3. Thus, three estimates were obtained, one for each solvent, for the standard enthalpy of sublimation of Bu_4NPi. The results are in Table 5.

In order to calculate ΔH_t^0 for each solvent system, this enthalpy change was considered to consist of a "non-electrostatic" contribution (ΔH_{tne}^0) and an electrostatic one (ΔH_{te}^0). These contributions were estimated separately, as follows.

Non-electrostatic Contribution

By non-electrostatic contribution is meant the

Can. J. Chem. Downloaded from www.nrcresearchpress.com by 210.87.254.6 on 09/05/12
For personal use only.

TABLE 4. The non-electrostatic contribution ΔH_{tne}^0 to the standard enthalpy of transfer of Bu_4NPi monomer from three solvents to the gas, at 35 °C

Solvent	Hildebrand solubility parameters: Solvent δ_2 ($cal^{1/2}/ml^{1/2}$)	Hildebrand solubility parameters: Bu_4NPi δ_1 ($cal^{1/2}/ml^{1/2}$)	Partial molal volume of Bu_4NPi, $\bar{V}_1$ (ml/mol)	ΔH_{tne}^0 (kcal/mol)
Benzene	9.1	8.5	404	29.8
Chlorobenzene	9.4	8.5	404	29.6
o-Dichlorobenzene	9.7	8.5	404	29.3

value that the standard enthalpy of transfer would have if there were no charges on the two ions that comprize the monomer. Simple relationships involving Hildebrand solubility parameters (3) were applied to the following two processes, where X_1 denotes the hypothetical Bu_4NPi monomer of zero dipole

$$X_1 \xrightarrow{\Delta H_I^0} X_1 \xrightarrow{\Delta H_{II}^0} X_1$$

solution; standard state 1 *m* | pure liquid; standard state | gas; standard state 1 atm, 35 °C

In general

$$\Delta H_I^0 \simeq \Delta E_I^0 = -\psi_2^2 V_1(\delta_1 - \delta_2)^2$$

and

$$\Delta H_{II}^0 = V_1\delta_1^2 + RT$$

whence

$$[4] \quad \Delta H_{tne}^0 = V_1[\delta_1^2 - \psi_2^2(\delta_1 - \delta_2)^2] + RT$$

where ψ_2 = volume fraction of solvent in the solution at T °K; V_1 = molal volume of Bu_4NPi, supercooled liquid at T °K; δ_1, δ_2 = Hildebrand solubility parameters for the Bu_4NPi monomer and the solvent, respectively; $-\Delta H_I^0$ = partial molal enthalpy of mixing (sometimes designated $\bar{H}_1^M$).

The necessary quantities, and the values calculated for ΔH_{tne}^0 are entered in Table 4. The values of δ_2 were estimated from the internal energy of evaporation of the solvents and their molal volumes. The value for δ_1 was estimated as follows: The value of δ_1 for the discharged Bu_4N^+ ion alone was taken to be similar to that of *n*-butane or *n*-pentane, namely about 7. The value of δ_1 for the discharged picrate ion was taken to be similar to that of benzene or nitrobenzene, namely about 10. Therefore δ_1 for the hypothetical Bu_4NPi monomer of zero dipole was taken to be the average of 7 and 10. The molal volume V_1 of Bu_4NPi (supercooled liquid) was taken as being equal to its partial molal volume ($\bar{V}_1$) in the organic solvents. Values of $\bar{V}_1$ for Bu_4NPi were calculated from measured densities of solutions of Bu_4NPi in the solvents (4). It is recognized that this is an approximation in that the densities were for solutions of Bu_4NPi that had charged ions. In the present case, $\psi_2 = 1$.

The values of ΔH_{tne}^0 in Table 4 must be considered as being rough estimates. Several approximations entered into the calculations. For example, this solubility-parameter approach should strictly be used only with nonpolar solvents. Moreover, the value 8.5 for δ_1 is uncertain.

Electrostatic Contribution

Plots of $RT \ln pk$ *vs.* $(1 - 1/D)$ are shown in Fig. 2; the data are in Table 1. The value of any ordinate in Fig. 2 gives $[\Delta G_{t(s-w)}^0 + RT \ln k]$, where the first term is the standard free energy of transfer of one mole of Bu_4NPi monomers into its standard-state solution (1 *m*) in water, from its standard-state solution (1 *m*) in a solvent of dielectric constant *D*. In the case of the intercept, the solvent is a hypothetical one of unit dielectric constant, and here $\Delta G_{t(s-w)}^0$ is designated as $\Delta G_{t(h-w)}^0$. In this hypothetical solvent the electrostatic interactions between solute and solvent are absent, but the "non-electrostatic" interactions are still present. Thus, the hypothetical solvent is not a vacuum. The almost negligible variation from solvent to solvent, in the values of ΔH_{tne}^0 in Table 4 is relevant to this special case.

Now it is reasonable to write

$$[5] \quad \Delta G_{te(g-s)}^0 = \Delta G_{t(h-s)}^0$$

That is, the electrostatic contribution $\Delta G_{te(g-s)}^0$ to the standard free energy of transfer for the process

Bu_4NPi (gas, s.s.) $\rightarrow$ Bu_4NPi (solution, s.s.)

Can. J. Chem. Downloaded from www.nrcresearchpress.com by 210.87.254.6 on 09/05/12
For personal use only.

TABLE 5. Standard enthalpy changes for the transfer of the Bu_4NPi monomer between phases, and the standard enthalpy of sublimation of Bu_4NPi, at 35 °C

	ΔH_{308}^0 (kcal/mol)						
			Transfer from solution to gas				
	Solution, ΔH_s^0 from Table 3		Electrostatic $\Delta H_{te(s-g)}^0$		Non-electrostatic $\Delta H_{tne(s-g)}^0$	Sublimation ΔH_{subl}^0	
Solvent	Mean	s.d.*	Mean	s.d.* $\nu = 1$	Mean	Mean	s.d.*
o-Dichlorobenzene	6.03	0.02	9.4	4.6	29.3	44.7	4.6
Chlorobenzene	6.36	0.02	8.9	4.1	29.6	44.9	4.1
Chlorobenzene–benzene (1:1 *v/v*)	7.45	0.03	8.1	3.7	29.7	45.2	3.7

*Standard deviation for ν degrees of freedom.

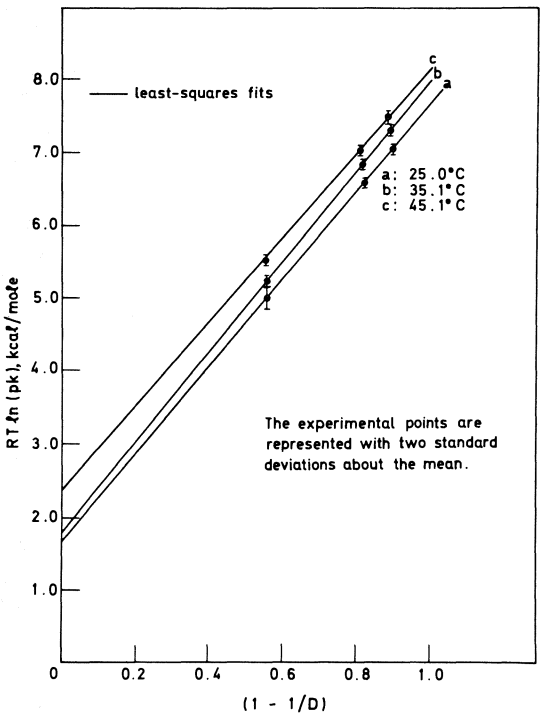

FIG. 2. The relationship between minus the standard free energy change for the transfer Bu_4NPi (water) → Bu_4NPi (org. solvent) of the monomer, and the reciprocal of the dielectric constant (D) of the organic solvent.

equals the total standard free energy of transfer for the following process

$$Bu_4NPi\,(\text{hypothetical solution}, D = 1, \text{s.s.}) \rightarrow Bu_4NPi\,(\text{solution, s.s.})$$

In that case

$$[6] \quad \Delta G_{te(g-s)}^0 = \Delta G_{t(h-w)}^0 - \Delta G_{t(s-w)}^0$$

The right-hand side of eq. 6 is just the intercept (at $D = 1$) minus the ordinate (at D) in Fig. 2.

Equation 6 was used with the data of Fig. 2, to evaluate $\Delta G_{te(g-s)}^0$ for each of the three solvents at each of the three temperatures. The resulting values of $\Delta G_{te(g-s)}^0$ varied linearly with $1/T$ over the range studied. Therefore $\Delta H_{te(g-s)}^0$ was calculated for each solvent, by least-squares. These enthalpy values are entered in Table 5.

The data in Table 5 permitted the calculation of the standard enthalpy of sublimation (ΔH_{subl}^0) of Bu_4NPi from the solid to the monomeric gas at 1 atm and 35 °C. Thus,

$$[6] \quad \Delta H_{subl}^0 = \Delta H_s^0 + \Delta H_{tne(s-g)}^0 + \Delta H_{te(s-g)}^0$$

These values calculated for ΔH_{subl}^0 were not significantly different. This conclusion suggests that the calorimetric data, from which the values of ΔH_s^0 were obtained, are consistent with the distribution data, from which the $\Delta H_{te(s-g)}^0$ data were calculated.

Discussion

The data at 25 °C in Table 1 are plotted in Figs. 1 and 2; $RT \ln K_2$ and $RT \ln K_3$ are plotted against $1/D$, and $RT \ln pk$ is plotted against $(1 - 1/D)$. Figure 3 shows a plot of $RT \ln K_f$ *vs.* $1/D$, where K_f is the formation constant of the Bu_4NPi monomer from its ions. Literature values of K_f obtained from conductance data were used in lieu of the much less precise values of K ($= 1/K_f$) reported in the present work from distribution data.

The observed linearity of all these graphs will now be interpreted.

Can. J. Chem. Downloaded from www.nrcresearchpress.com by 210.87.254.6 on 09/05/12
For personal use only.

Can. J. Chem. Downloaded from www.nrcresearchpress.com by 210.87.254.6 on 09/05/12
For personal use only.

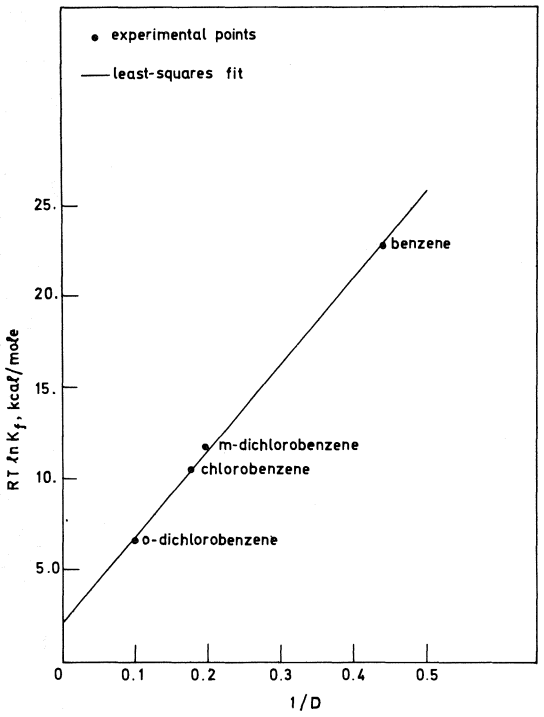

FIG. 3. The relationship between minus the standard free energy of formation of the monomer Bu_4NPi from its simple ions, and the reciprocal of the dielectric constant of the solvent, for four solvents at 25 °C.

Formation Constant K_f

A value for the "internuclear" distance of separation of the two ions in the Bu_4NPi monomer was calculated by using Rittner's formula (5) and published values (6, 7) of his parameters

$$\mu = er - \frac{r^4 e(\alpha_1 + \alpha_2) + 4re\alpha_1\alpha_2}{r^6 - 4\alpha_1\alpha_2}$$

where μ = dipole moment of Bu_4NPi, 16.2×10^{-18} e.s.u. cm (6); $e = 4.803 \times 10^{-10}$ e.s.u.; α_1, α_2 = polarizabilities of the ions: 31.2×10^{-24} ml for Bu_4N^+ (7) and 24.4×10^{-24} ml for Pi^- (7); r = "internuclear" distance of separation of the two ions in Bu_4NPi.

Three real positive roots were obtained for r, namely, 5.74, 4.42, and 1.62 Å. The value 5.74 Å was chosen for use; it agreed best with literature values (8, 9) calculated by applying a Denison–Ramsey model to conductance data for Bu_4NPi in various solvents.

Figure 3 is now interpreted by using a modified Denison–Ramsey approach (9) similar to that used by Pettit and Bruckenstein (10); but our approach avoids their (10) simplifying assumption regarding entropies.

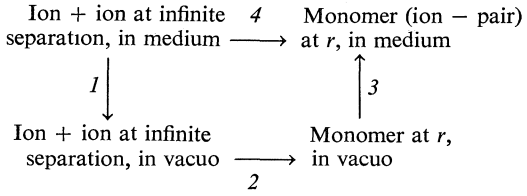

Cycle I

For Cycle I, it is assumed that the non-electrostatic (to use a conventional expression) contributions to ΔH_1 and ΔH_3 are equal and opposite. Then Pettit and Bruckenstein (10) showed that

$$[7] \quad -\Delta G_4^0 = RT \ln K_f = -\Delta V_2/D + T\Delta S_4$$

where ΔV_2 = standard free energy change for step *2* at 0 °K; T = absolute temperature; D = dielectric constant of the medium at T °K; ΔS_4 = entropy change due to translational, rotational, and vibrational changes for step *4*.

Equation 7 was accepted for use in the present treatment; but the further assumption that $\Delta S_2 = \Delta S_4$ made by Pettit and Bruckenstein (10) is unacceptable, and was not used in the present treatment. Instead, eq. 7 was fitted by least-squares to the data $RT \ln K_f$ *vs.* $1/D$, in Table 1; these data are seen in Fig. 3 to give a linear plot. The least-squares value found for the slope in Fig. 3 was $\Delta V_2 = -47.6 \pm 1.2$ kcal/mol; and the value found for the intercept was $\Delta S_4 = 6.7 \pm 1.0$ e.u. Pettit and Bruckenstein (10), by using their assumption that $\Delta S_2 = \Delta S_4$, calculated that $\Delta S_4 = -18.1$ e.u. Thus their value is 24.8 e.u. more negative than ours.

Interpretation of ΔS_4

In order to explain the small but positive entropy change (6.7 e.u.) found for step *4* of Cycle I, partial desolvation of the solvated ions when they combine is postulated. Then step *4* in Cycle I becomes

$$Bu_4N \cdot aS^+ + Pi \cdot bS^- \rightarrow Bu_4NPi \cdot (a + b - x)S + xS$$

where S is the solvent. Change in translational entropy usually provides the major contribution to the standard entropy change in reactions of this kind. Therefore a value of $x \sim 1$ would account for the small positive value found for ΔS_4^0. Moreover, ion pairing results in some

Can. J. Chem. Downloaded from www.nrcresearchpress.com by 210.87.254.6 on 09/05/12
For personal use only.

mutual neutralization of oppositely charged particles and fields, which in turn should weaken ion–solvent interaction and thereby promote desolvation. In addition, squeezing out of an intervening, bound solvent molecule would allow closer approach of the ions in the monomer.

Interpretation of ΔV_2

The postulated desolvation with $x \sim 1$ requires that Cycle I be modified as shown in Cycle II, below

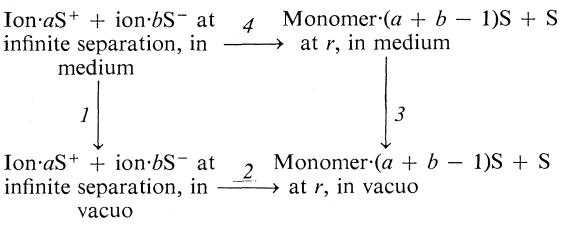

Cycle II

Equation 7 then becomes

$$[8] \quad -\Delta G_4^0 = RT \ln K_f = -\Delta V_2/D + T\Delta S_4 - \Delta H_{2,\,\text{desolv}}$$

where $\Delta H_{2,\,\text{desolv}}$ = contribution to the enthalpy change in step *2* of Cycle II at 0 °K and constant pressure, due to the desolvation.

The value of $\Delta H_{2,\,\text{desolv}}$ is considered to be small relative to the other terms. It is also assumed not to vary significantly for the four solvents. However, it is recognized that this is a questionable assumption, supported only tenuously by the fact that the graph in Fig. 3 is linear.

The value found for the intercept in Fig. 3, namely 1.99 kcal/mol, would then be attributed to $(T\Delta S_4 - \Delta H_{2,\,\text{desolv}})$, not solely to $T\Delta S_4$ as was done in the preceding section.

A value will next be calculated for ΔV_2. It proved expedient (4) to use for this purpose a simple ion–ion potential function

$$[9] \quad \Delta V_2 = -\frac{e^2}{r} + \frac{B}{r^{6.9}}$$

where r = equilibrium "internuclear" distance of separation of the two ions in the Bu_4NPi monomer; B = a constant; exponent 6.9 = a value determined empirically by Pettit and Bruckenstein (10), from experimental values of ΔV_2 for the ion pairs of gaseous alkali halides.

By setting $(d\Delta V_2/dr) = 0$ at $r = 5.74$ Å, B was found to be 6.33×10^{-63} e.s.u.^{2} cm$^{5.9}$. Substitution of these values of r and B into eq. 9 then gave $\Delta V_2 = -49.5$ kcal/mol. This calculated value agrees well with the experimental value $\Delta V_2 = -47.6 \pm 1.2$ kcal/mol (1.2 is one standard deviation). Thus, evaluation of r from the measured dipole moment and use of a simple function for the electrostatic potential permitted the calculation of a reasonable value for the slope in Fig. 3.

Partition Coefficient of Bu_4NPi *Monomer*

Figure 2 shows that plots of $RT \ln pk$ *vs.* $(1 - 1/D)$ are linear for each of the three temperatures. Now $RT \ln pk$ is equal to minus the standard free energy of transfer (ΔG_t^0) for the process

$$Bu_4N^+ + Pi^- \rightarrow Bu_4NPi$$
(in water) (in organic solvent)

The least-squares values of the slopes and intercepts of the three lines in Fig. 2 are given in Table 6. In order to interpret these data, it will be supposed that the potential function given by eq. 9, with $B = 6.63 \times 10^{-63}$ e.s.u.^{2} cm$^{5.9}$ is valid for step *3* of Cycle II. Then for the transfer process for the monomer

$$Bu_4NPi \text{ in water, dielectric constant } D_w \xrightarrow{\Delta H_t} Bu_4NPi \text{ in organic solvent, dielectric constant } D$$

it is readily shown that

$$[10] \quad (\Delta H_t)_{0\,°K,\,P} = \left(\frac{e^2}{2a_1} + \frac{e^2}{2a_2} - \frac{e^2}{r} + \frac{6.63 \times 10^{-63}}{r^{6.9}}\right)\left(\frac{1}{D} - \frac{1}{D_w}\right) + \Delta H_{tne}$$

where a_1, a_2 = radii of Bu_4N^+ and Pi^- ions, respectively, at infinite separation; r = defined under eq. 9; ΔH_{tne} = non-electrostatic contribution to the enthalpy of transfer of Bu_4NPi monomer from water to organic solvent, strictly applicable at 0 °K and constant pressure. The

TABLE 6. Least-squares values of slopes and intercepts for the linear plots (Fig. 2) $RT \ln pk$ *vs.* $(1 - 1/D)$ at 25.0, 35.1, and 45.1 °C

Temperature (°C)	Slope (kcal/mol)		Intercept (kcal/mol)	
	Mean	2 × s.d.*	Mean	2 × s.d.*
25.0	6.02	0.18	1.63	0.14
35.1	6.19	0.14	1.77	0.11
45.1	5.78	0.11	2.33	0.08

*s.d. = standard deviation for one degree of freedom. (Twice the s.d. is reported, to conform with bars in Fig. 2.)

Can. J. Chem. Downloaded from www.nrcresearchpress.com by 210.87.254.6 on 09/05/12
For personal use only.

tacit assumption that ΔH_{tne} is not a function of the dielectric constant introduces an error that is considered to be small compared to the value of the electrostatic term. Abbreviating eq. 10,

$$[11] \quad (\Delta H_t)_{0\,°K,\,P} = Z\left(\frac{1}{D} - \frac{1}{D_w}\right) + \Delta H_{tne}$$

then for a transfer between standard states at T °K, one gets

$$[12] \quad \Delta H_t^0 = (\Delta H_t)_{0\,°K,\,P} + RT^2\left[\frac{\partial \ln Q}{\partial T}\right]_p$$

and

$$[13] \quad \Delta S_t^0 = \Delta S + RT\left[\frac{\partial \ln Q}{\partial T}\right]_p$$

where ΔS includes the translational, rotational, and vibrational entropy changes at T °K that are associated with the transfer; and where Q is the ratio of the partition functions for the "product" and the "reactant".

From eqs. 11, 12, and 13

$$[14] \quad -\Delta G_t^0 = RT\ln p = Z\left(1 - \frac{1}{D}\right) + Z\left(\frac{1}{D_w} - 1\right) + T\Delta S - \Delta H_{tne}$$

whence

$$[15] \quad RT\ln pk = Z\left(1 - \frac{1}{D}\right) + Z\left(\frac{1}{D_w} - 1\right) + T\Delta S - \Delta H_{tne} + RT\ln k$$

On relating eq. 15 to Fig. 2 and the corresponding data in Table 6, it is seen that for these straight lines

$$[16] \quad \text{Slope} = Z = \left(\frac{e^2}{2a_1} + \frac{e^2}{2a_2} - \frac{e^2}{r} + \frac{6.33 \times 10^{-63}}{r^{6.9}}\right)$$

$$[17] \quad \text{Intercept} = Z\left(\frac{1}{D_w} - 1\right) + T\Delta S - \Delta H_{tne} + RT\ln k$$

Interpretation of the Slope

Statistical treatment of the values in columns 2 and 3 of Table 6 showed that the values of the slope do not depend significantly on temperature in the range tested. Inspection of the expression for Z in eq. 16 shows that Z should be essentially independent of temperature.

By assuming for Bu_4NPi spherical ions of equal radii $a = (a_1 + a_2)/2$, then on substituting into eq. 16 the mean value of $Z = 6.00$ kcal/mol from Table 6, and $r = 5.74 \times 10^{-8}$ cm from the dipole moment, $a = 5.98$ Å with a standard deviation of 0.02 Å. This value of a is for the solvated ions at infinite separation. Although the assumptions made are crude, the value 5.98 Å is a reasonable one.

Interpretation of the Intercept

In eq. 17 the term $RT\ln k$ will be neglected. It is not known for Bu_4NPi, but for Et_4NPi it is approximately 1.0 at 25 °C (14). The term ΔH_{tne} will also be considered negligibly small compared to the electrostatic contribution. The grounds for neglecting ΔH_{tne} are presently not very satisfactory, being based only on the large dipole moment (16.2 D) of Bu_4NPi. Unfortunately, the highly structured nature of water makes it impracticable to attempt a solubility-parameter approach to evaluate ΔH_{tne}. Accordingly, the following interpretation of the intercept is provisional.

By neglecting $RT\ln k$ and ΔH_{tne}, and by substituting the observed values for the intercepts and for Z (from Table 6) and the published values for D_w (15), ΔS in eq. 17 was calculated and the values are entered in Table 7.

The value of about 25 e.u. calculated for ΔS is considered to be a reasonable one. Transfer of the Bu_4NPi monomer from water into the organic solvents used would be expected to result in some desolvation, partly because water is known to form cage-like structures around organic solutes, and partly because water molecules are about one-fifth the size of the organic-solvent molecules.

Dimerization (K_2) and Trimerization (K_3) Constants

Figure 1 shows that plots of $RT\ln K_2$ and of $RT\ln K_3$ *vs.* $1/D$ are linear for each of the three temperatures. The data are in Table 1. The large standard deviations in the values of K_2 for benzene were due to the relative paucity of dimers in

TABLE 7. Values of ΔS (eq. 14) for the transfer of Bu_4NPi monomer from water into three organic solvents at three temperatures

Temperature (°C)	Dielectric constant of water, D_w (13)	ΔS (e.u.)	
		Mean	s.d.*
25.0	78.54	25.4	1.1
35.1	74.97	25.6	0.8
45.1	71.58	25.2	0.6

*s.d. = standard deviation for one degree of freedom.

TABLE 8. Least-squares values of slopes and intercepts for the linear plots (Fig. 1) of $RT \ln K_2$ and $RT \ln K_3$ *vs.* $1/D$, at three temperatures

Temperature (°C)	Dimers (kcal/mol)				Trimers (kcal/mol)			
	Slope		Intercept		Slope		Intercept	
	Mean	2 × s.d.*	Mean	2 × s.d.*	Mean	2 × s.d.*	Mean	2 × s.d.*
25.0	0.95	0.26	0.94	0.07	9.53	0.46	1.91	0.13
35.1	1.66	0.88	1.05	0.25	10.02	0.30	1.68	0.09
45.1	−1.2	1.2	1.44	0.35	9.73	0.26	1.87	0.07

*s.d. = standard deviation for one degree of freedom (twice the s.d. is reported here to conform with the bars in Fig. 1).

those solutions (always less than 10% of the stoichiometric concentration of the salt).

In order to interpret these data, equations will be derived in a manner analogous to that used above for the formation constant K_f.

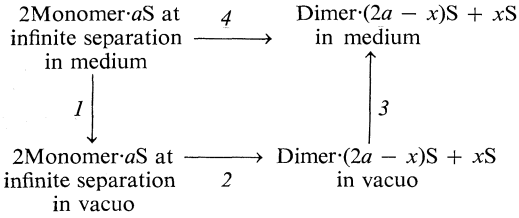

Cycle III

For Cycle III it is assumed that the non-electrostatic contributions to ΔH_1 and ΔH_3 are equal and opposite. Then for step *4* of Cycle III

$$[18] \quad -\Delta G_4^0 = RT \ln K_2 = -\frac{\Delta V_2}{D} + T\Delta S_4 + \Delta H_{2,\text{desolv}}$$

where ΔV_2 = standard free energy change for step *2* at 0 °K; $\Delta H_{2,\text{desolv}}$ = contribution to the enthalpy change in step *2* of Cycle III at 0 °K, due to the desolvation; K_2 = equilibrium constant for step *4* of Cycle III.

Similarly, for the reaction

$$\text{3Monomer·}aS \text{ at infinite separation in medium} \xrightarrow{\Delta G_4^0} \text{Trimer·}(3a - y)S + yS \text{ in medium}$$

$$[19] \quad -\Delta G_4^0 = RT \ln K_3 = -\frac{\Delta V_2}{D} + T\Delta S_4 + \Delta H_{2,\text{desolv}}$$

where ΔV_2 and $\Delta H_{2,\text{desolv}}$ now refer to a trimer cycle.

On relating eqs. 18 and 19 to the dimer and trimer plots, respectively, in Fig. 1, and to the corresponding data in Table 1, it is seen that the slopes of these straight lines in Fig. 1 give $-\Delta V_2$, and the intercepts give $(T\Delta S_4 + \Delta H_{2,\text{desolv}})$; the least-squares values of these slopes and intercepts are entered in Table 8.

Interpretation of the Intercepts

By assuming that $\Delta H_{2,\text{desolv}}$ is much smaller than $T\Delta S_4$ in eqs. 18 and 19, values for ΔS_4 were calculated for each plot in Fig. 1 by using the data in Table 8. The results are in Table 9.

These low, positive values for ΔS_4 include all translational, rotational, and vibrational entropy changes associated with step *4* of Cycle III for the dimer, and for the corresponding step for the trimer. In order to explain them, it is necessary to postulate desolvation; and this in turn is based on the presumption that the changes in translational entropy make much the largest contribution to ΔS_4. Provisionally then, it is suggested that the extent of the desolvation is approximately as follows

$$\text{2Monomer·}aS \rightarrow \text{Dimer·}(2a - 1)S + S$$
$$\text{3Monomer·}aS \rightarrow \text{Trimer·}(3a - 2)S + 2S$$

That is, there is no net change in the number of particles in the solutions.

Interpretation of the Slopes of the Dimer Plots

The slope of the straight line in Fig. 1 gives ΔV_2, the standard free energy change for the following reaction at 0 °K

$$\text{2Bu}_4\text{NPi·}aS \text{ at infinite separation in vacuo} \rightarrow \text{Dimer·}(2a - 1)S + S \text{ in vacuo}$$

provided $\Delta H_{2,\text{desolv}}$ is constant for the three solvents, thereby making it part of the intercept.

Two possible models of the solvated dimer are now considered. One is a "rigid-dipole" rectangular model, proposed by Fuoss (16–18) and by Geddes and Kraus (19). In it, the monomers have associated laterally to form the dimer, and the equilibrium internuclear distance of separa-

Can. J. Chem. Downloaded from www.nrcresearchpress.com by 210.87.254.6 on 09/05/12
For personal use only.

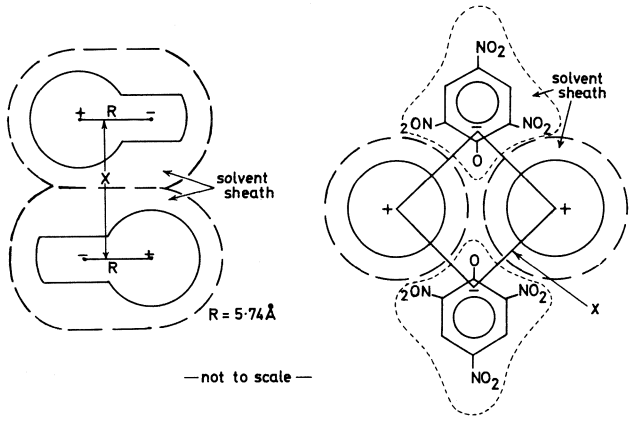

FIG. 4. Sketches of (*a*) rigid-dipole model, and (*b*) square model, for the dimer of Bu_4NPi in a low-dielectric solvent.

TABLE 9. Entropy changes for the dimerization and trimerization of Bu_4NPi monomers at three temperatures

Temperature (°C)	ΔS_4 (e.u.) Dimerization Mean	Dimerization 2 × s.d.*	Trimerization Mean	Trimerization 2 × s.d.*
25.0	3.17	0.25	6.41	0.44
35.1	3.41	0.81	5.45	0.29
45.1	4.53	1.10	5.88	0.22

*s.d. = standard deviation for one degree of freedom (twice the s.d. is reported).

tion of the ions in the monomer is unchanged by dimerization. The second model for the dimer was proposed by O'Konski and Higuchi (20). In it, the dimer is a rhombus. Such a symmetrical planar arrangement gives the most energetically favored configuration that symmetrical ions can assume.

Since the picrate ion is unsymmetrical, and the potential function given by eq. 9 is a simplified one, it is not possible to decide *a priori* which model is better for Bu_4NPi. Therefore both models have been applied to the present data, in order to make a choice.

The two models of the dimer are illustrated in Fig. 4; solvent separation of the constituents of these ionic aggregates has been presumed. Such solvent separation is suggested by at least three facts: (*i*) the "internuclear" distance of separation of the two ions in the monomer was calculated above to be 5.74 Å; (*ii*) the molar absorptivity of the monomer was found to be the same as that of the free picrate ion in the solvents used in the present work, but different from that of picric acid; (*iii*) the distance parameters calculated below for the dimer models.

Electrostatic calculations follow, for the distance parameter X_m of the two models in Fig. 4. For each model, eq. 9 was applied in order to express the potential energy of formation (ΔV_2) of the dimer from the monomers at 0 °K. The value of the exponent in the repulsion term was assumed to be −6.9; but the value of B was expected to differ from the value it had for the case of monomer formation from the two ions. The experimental value used for ΔV_2 was found as follows: statistical treatment showed for the values of the slopes in Table 8 that the variances were homogeneous, and the mean values were not significantly different. Therefore a weighted mean and a weighted standard deviation were calculated from the values at the three temperatures, to give $\Delta V_2 = -0.92$ kcal/mol with a standard deviation of 0.48.

(a) Rigid-dipole Model

Application of eq. 9 to Fig. 4(*a*) gives

$$[20]\quad (\Delta V_2)_{X=X_m} = -\frac{2e^2}{X_m} + \frac{2e^2}{(R^2 + X_m{}^2)^{1/2}} + \frac{B}{X_m{}^{6.9}}$$

whence

$$[21]\quad \left(\frac{\partial \Delta V_2}{\partial X}\right)_{X=X_m} = 0 = \frac{2e^2}{X_m{}^2} - \frac{2e^2 X_m}{(R^2 + X_m{}^2)^{3/2}} - \frac{6.9B}{X_m{}^{7.9}}$$

Can. J. Chem. Downloaded from www.nrcresearchpress.com by 210.87.254.6 on 09/05/12
For personal use only.

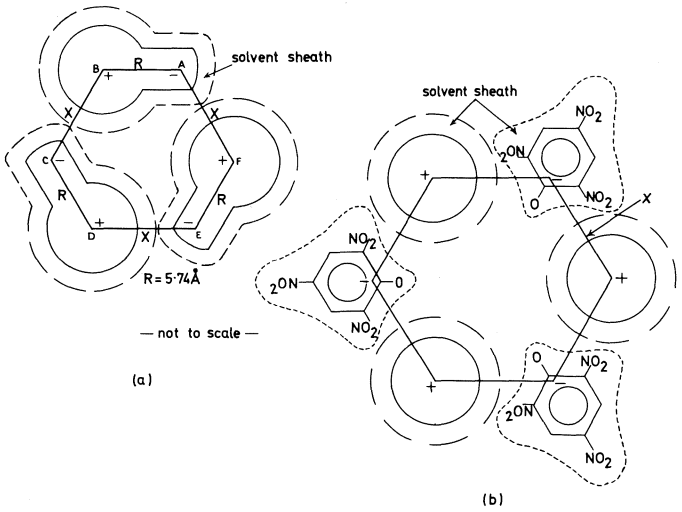

FIG. 5. Sketches of (*a*) rigid-dipole model, and (*b*) regular hexagon model, for the trimer of Bu_4NPi in a low-dielectric solvent.

Solution of eqs. 20 and 21, with $R = 5.74 \times 10^{-8}$ cm, $e = 4.803 \times 10^{-10}$ e.s.u., and $\Delta V_2 = -0.92/14.4 \times 10^{12}$ erg molecule^{-1} gave $X_m =$ 19 Å and $B = 1.70 \times 10^{-60}$ e.s.u.^{2} cm$^{5.9}$. For $\Delta V_2 = -0.92 + 0.48$ and $-0.92 - 0.48$ kcal/mol, respectively, $X_m = 24$ and 16 Å, respectively.

(b) Rhombohedral Model

Exploratory calculations by applying eq. 9 to the rhombohedral model showed that the configuration with minimum energy was a square. On considering only nearest-neighbor repulsion terms, the two simultaneous equations applicable to the square configuration are

$$[22] \quad (\Delta V_2)_{X=X_m} = -\frac{4e^2}{X_m} + \frac{\sqrt{2}e^2}{X_m} + \frac{4B}{X_m^{6.9}} + 2V_p$$

$$[23] \quad \left(\frac{\partial \Delta V_2}{\partial X}\right)_{X=X_m} = 0 = \frac{4e^2}{X_m^2} - \frac{\sqrt{2}e^2}{X_m^2} - \frac{27.6B}{X_m^{7.9}}$$

where V_p = standard free energy change for the reverse of step *2* of Cycle II, calculated above to be 49.5 kcal/mol for an "internuclear" distance of separation of 5.74 Å for the two ions in the monomer.

Solution of eqs. 22 and 23 with $\Delta V_2 = -0.92/14.4 \times 10^{12}$ erg molecule^{-1} gave $X_m = 7.4$ Å and $B = 1.76 \times 10^{-62}$ e.s.u.^{2} cm$^{5.9}$. For $\Delta V_2 = -0.92 + 0.48$ and $-0.92 - 0.48$ kcal/mol, respectively, $X_m = 7.4$, and 7.3 Å, respectively.

Interpretation of the Slopes of the Trimer Plots

The slope of the straight line in Fig. 1 gives ΔV_2, the standard free energy change for the following reaction at 0 °K

$$\underset{\text{at infinite separation in vacuo}}{3Bu_4NPi\cdot aS} \rightarrow \underset{\text{in vacuo}}{\text{Trimer}\cdot(3a-2)S + 2S}$$

provided $\Delta H_{2,\,desolv}$ is constant for the three solvents.

As with the dimer, so too for the solvated trimer two different models can be prescribed. They are illustrated in Fig. 5. One is based on the rigid-dipole approach, and is a non-regular, planar hexagonal ring. The other model is based on the symmetrical-ions approach with the constraint imposed that eq. 9 is used; this model is a regular, planar hexagonal ring.

Electrostatic calculations follow, for the dimensions X and R in Fig. 5(*a*), and X in Fig. 5(*b*). In both cases eq. 9 was used exactly as it was for the dimer calculations. The experimental value used for ΔV_2 was the mean of the three values given in Table 8 for three temperatures. The variance used for this mean was the sample variance around the mean, with two degrees of freedom. Thus $\Delta V_2 = -9.76 \pm 0.25$ kcal/mol.

(a) Rigid-Dipole Model (Non-regular Hexagon)

From Fig. 5*a*, alternate sides (X and R) are equal, and all internal angles are 120°. One

Can. J. Chem. Downloaded from www.nrcresearchpress.com by 210.87.254.6 on 09/05/12
For personal use only.

Can. J. Chem. Downloaded from www.nrcresearchpress.com by 210.87.254.6 on 09/05/12
For personal use only.

general contact electron-cloud repulsion term is considered for each dipole–dipole interaction. Then the following equations apply

$$[24]\quad (\Delta V_2)_{X=X_m} = -\frac{3e^2}{X_m} - \frac{3e^2}{(R + X_m)} + \frac{6e^2}{(R^2 + X_m{}^2 + RX_m)^{1/2}} + \frac{3B}{X_m{}^{6.9}}$$

$$[25]\quad \left(\frac{\partial \Delta V_2}{\partial X}\right)_{X=X_m} = 0 = \frac{3e^2}{X_m{}^2} + \frac{3e^2}{(R + X_m)^2} - \frac{3e^2(R + 2X_m)}{(R^2 + X_m{}^2 + RX_m)^{3/2}} - \frac{20.7B}{X_m{}^{7.9}}$$

Solution of eqs. 24 and 25, with $R = 5.74 \times 10^{-8}$ cm, and $\Delta V_2 = -9.76/14.39 \times 10^{12}$ erg/molecule gave $X_m = 11.0$ Å and $B = 1.14 \times 10^{-61}$ e.s.u.^{2} cm$^{5.9}$. On repeating the calculation but with $\Delta V_2 = -9.76 + 0.25$, and $-9.76 - 0.25$ kcal/mol, respectively, $X_m = 11.1$ and 10.9 Å, respectively.

(b) Regular Hexagon Model

On considering only nearest-neighbor electron-repulsion terms, application of eq. 9 to Fig. 5*b* gives

$$[26]\quad (\Delta V_2)_{X=X_m} = -\frac{6e^2}{X_m} - \frac{3e^2}{2X_m} + \frac{6}{\sqrt{3}}\frac{e^2}{X_m} + \frac{6B}{X_m{}^{6.9}} + 3V_p$$

$$[27]\quad \left(\frac{\partial \Delta V_2}{\partial X}\right)_{X=X_m} = 0 = \frac{6e^2}{X_m{}^2} + \frac{3e^2}{2X_m{}^2} - \frac{6}{\sqrt{3}}\frac{e^2}{X_m{}^2} - \frac{41.4B}{X_m{}^{7.9}}$$

where V_p has the same meaning as in the dimer case. Solution of eqs. 26 and 27 with $R = 5.74 \times 10^{-8}$ cm and $\Delta V_2 = -9.76/14.39 \times 10^{12}$ erg/molecule gave $X_m = 7.24$ Å and $B = 1.68 \times 10^{-62}$ e.s.u.^{2} cm$^{5.9}$. On repeating the calculation with $\Delta V_2 = -9.76 + 0.25$ and $-9.76 - 0.25$ kcal/mol, respectively, $X_m = 7.25$ and 7.23 Å, respectively.

Choice of a Model

For two reasons, the rigid-dipole models for the dimer and the trimer were considered to be less satisfactory than the regular models, namely a square for the dimer, and a regular hexagon for the trimer. First, the calculations based on rigid-dipole models gave equilibrium separation distances which intuitively seem too large (X_m = 19 Å for the dimer, 11.0 Å for the trimer); similar calculations based on the regular models gave more reasonable values (X_m = 7.4 Å for the dimer, 7.24 Å for the trimer).

Secondly, it was concluded elsewhere (2) that the value of the average hydration number of Bu_4NPi in the organic solvents was not significantly dependent on the extent to which the monomers were associated into the *i*-mers. It was proposed then (2) that the hydration site was the para-nitro group of the picrate ion. Examination of Figs. 4 and 5 reveals that this hydration site is more accessible in the regular models than it is in the rigid-dipole models, which suggests that the regular models are more consistent with this reported behavior of the average hydration number.

We are grateful to the National Research Council of Canada for financial assistance. We also thank Professor W. H. Stockmayer for very helpful suggestions on some of the theoretical aspects.

1. S. Goldman and G. C. B. Cave. Can. J. Chem. **49**, 1716 (1971).
2. S. Goldman and G. C. B. Cave. Can. J. Chem. **49**, 1726 (1971).
3. J. H. Hildebrand and R. L. Scott. The solubility of nonelectrolytes. 3rd ed. Dover Publications Inc., New York, N.Y. 1964.
4. S. Goldman. Ph.D. Thesis. McGill University, Montreal, Quebec. 1969.
5. E. S. Rittner. J. Chem. Phys. **19**, 1030 (1951).
6. W. R. Gilkerson and K. K. Srivastava. J. Phys. Chem. **65**, 272 (1961).
7. W. R. Gilkerson and J. L. Stuart. J. Phys. Chem **65**, 1465 (1961).
8. P. H. Flaherty and K. H. Stern. J. Am. Chem. Soc. **80**, 1034 (1958).
9. J. T. Denison and J. B. Ramsey. J. Am. Chem. Soc. **77**, 2615 (1955).
10. L. D. Pettit and S. Bruckenstein. J. Am. Chem. Soc. **88**, 4783 (1966).
11. H. S. Curry and W. R. Gilkerson. J. Am. Chem. Soc. **79**, 4201 (1957).
12. W. R. Gilkerson and R. E. Stamm. J. Am. Chem. Soc. **82**, 5295 (1960).
13. F. Accascina, E. L. Swarts, P. L. Mercier, and C. A. Kraus. Proc. Nat. Acad. Sci. **39**, 917 (1953).
14. F. Accascina, A. D'Aprano, and R. M. Fuoss. J. Am. Chem. Soc. **81**, 1058 (1959).
15. H. S. Harned and B. B. Owen. The physical chemistry of electrolyte solutions. 2nd ed. Reinhold Publishing Corporation, New York, N.Y. 1950. p. 118.
16. R. M. Fuoss. J. Am. Chem. Soc. **56**, 1027 (1934).
17. R. M. Fuoss. J. Am. Chem. Soc. **56**, 1031 (1934).
18. R. M. Fuoss. J. Am. Chem. Soc. **58**, 982 (1936).
19. J. A. Geddes and C. A. Kraus. Trans. Faraday Soc. **32**, 585 (1936).
20. C. T. O'Konski and W. J. Higuchi. J. Chem. Phys. **23**, 1174 (1955).

Can. J. Chem. Downloaded from www.nrcresearchpress.com by 210.87.254.5 on 09/05/12
For personal use only.

Observations on the Visible Emission from Electronically Excited CS_2

S. J. Arnold and G. H. Kimbell

Defence Research Establishment Valcartier, P.O. Box 880, Courcelette, Quebec

Received June 7, 1971

A detailed study has been made of the CS_2 afterglow emission observed when either pure CS_2 or a CS_2–Ar mixture is passed through a microwave discharge or when CS_2 is introduced into a stream of discharged argon or active nitrogen. The emission is continuous and extends from 340 to 640 nm with a maximum at 440 nm. The emitting state is thought to be the V state which is responsible for the CS_2 fluorescence.

Nous avons accompli une étude détaillée de l'émission du CS_2 après rayonnement, qu'on peut observer lorsque le CS_2 pur ou un mélange CS_2–Ar passe à travers une décharge de microonde ou lorsque CS_2 est introduit dans un courant d'argon déchargé ou d'azote actif. L'émission est continue et s'étend de 340 à 640 nm, avec un maximum à 440 nm. On croit que l'état émetteur soit l'état V, qui est responsable de la fluorescence de CS_2.

Canadian Journal of Chemistry, **49**, 4110 (1971)

Introduction

Although several reports on the visible absorption and emission spectra of gaseous carbon disulfide have appeared in the literature (1–8), a complete assignment of the various observed features remains to be achieved. Absorption studies (1–3) indicated the existence of two band systems, a relatively strong system in the region 220–150 nm and a weaker system in the region 430–290 nm. Kleman (1) made a rotational analysis of some of the bands at the long wavelength end of the near u.v. system and obtained a value of 74.9 kcal mol^{-1} for the band origin, ν_{000}. Douglas and Milton (2) then positively identified the upper state as the bent $^3A_2$ state. The remaining near u.v. absorption bands (330–290 nm) are frequently referred to as the V system.

Observations of emission spectra attributed to CS_2 were made by Herman *et al.* (5) in pure CS_2 vapor following a condensed discharge and by Westbury and Winkler (6) upon the addition of CS_2 to active nitrogen. In each case a pale blue continuous emission, which extended from 350 to 640 nm with a maximum at 470 nm, was observed; a definite emitting state was not assigned in either case. Recently, Rosenkranz and Wagner (7) and Arnold and Kimbell (8) reported the observation of a similar emission spectrum from shock-heated CS_2/Ar mixtures. Rosenkranz and Wagner attributed the emission to the $^3A_2$ state whereas Arnold and Kimbell assigned it to the previously unobserved $^3\Sigma_u^+$ state whose existence had been postulated by Mulliken (4).

Heicklen (9) and Mills and Zare (10) have observed the fluorescence of CS_2 excited by light of wavelength near 320 nm. Douglas (11) measured the lifetime of this fluorescence to be 15 μs and inferred that the V state was responsible.

In the present study an investigation was made of the afterglow observed when either pure CS_2 or a CS_2/Ar mixture was passed through a microwave discharge and when CS_2 was introduced into discharged argon or active nitrogen. The results of this work, in conjunction with the earlier work just described, suggest that the V state is responsible for the emission observed in both the afterglow and fluorescence experiments. It seems likely that the thermal emission observed in the shock tube experiments may be exclusively from the $^3A_2$ state.

Experimental

The apparatus used for these experiments is shown in Fig. 1. In the first group of experiments either pure CS_2 or a 10% mixture of CS_2 in an inert gas was passed through a 2450 MHz microwave discharge, whereas in the second group of experiments CS_2 was introduced into nitrogen or argon which had previously passed through the discharge. All experiments were conducted at a total

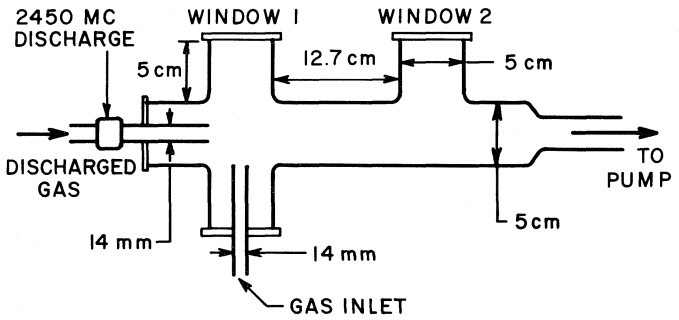

FIG. 1. Schematic of afterglow cell.

pressure of about 3.5 Torr. Emission spectra were obtained either at the inlet jet (window 1) or in the afterglow region (window 2). The detection system consisted of a McPherson Model 235 Monochromator equipped with a 300 L/mm grating having a reciprocal dispersion of 68 A/mm; an EMI 9558 QB photo-multiplier having an "S-20" response was used with an Esterline Angus recorder.

The CS_2 used was Anachemia Reagent Grade which had been dried over "Drierite" and degassed prior to use. The argon and nitrogen were "ultra high purity" grade containing less than 10 p.p.m. of impurities and were supplied by Matheson.

Results and Discussion

The results of the present series of emission measurements are summarized in Table 1. The principal emission feature which could be observed at the second window in all cases (when either pure CS_2 or a CS_2/Ar mixture was passed through a microwave discharge or when CS_2 was introduced in a stream of active nitrogen or discharged argon) was a continuum which extended from 340 to 640 nm with an energy maximum at approximately 440 nm (see Fig. 2). In all cases extensive deposits of carbon and sulfur were observed on the walls of the reaction cell.

Since the afterglow emission is practically identical in all four cases it seems reasonable to suppose that the emitting species (CS_2*) is formed in the same manner in the four systems. A probable mechanism is the three-body recombination reaction

$$[1] \qquad CS + S + M \rightarrow CS_2^* + M \rightarrow CS_2 + h\nu$$

This mechanism is supported by the fact that the afterglow could not be observed at the first window and that extensive dissociation was observed in all cases. The only alternative mechanism for the formation of CS_2* is by direct excitation in the microwave discharge, by energy transfer from metastable argon or a component of active nitrogen. If this is the case, the continuum should be observed at the first window. It is also unlikely that the spectral distribution of the continuum would be virtually identical in all cases; in addition it would be required that in the case of discharged pure CS_2 the emitting species be sufficiently long-lived to emit strongly at a distance of 1 m from the excitation region (system pressure 5 Torr). It would then be impossible to correlate the afterglow with the state responsible for the fluorescence. Consequently, it would appear to be most likely that the emitting species is formed by a recombination mechanism subsequent to dissociation either by a microwave discharge or by highly active components of discharged argon or nitrogen.

The visible emission observed when a CS_2/Ar mixture is shock heated (7, 8) has an energy distribution which is very similar to that of the afterglow continuum. When the emission spectrum shown in ref. 8 is corrected for the relative spectral sensitivity of the photographic plates used, a spectrum extending from 350 nm into the red, with a single maximum at 550 nm, is obtained.

The emission, which occurs at the shock front, is due to thermal excitation of ground state CS_2 and not to recombination. It can be adequately explained by the mechanism

$$[2] \qquad CS_2 + Ar \rightleftarrows CS_2^* + Ar$$

$$[3] \qquad CS_2^* \rightarrow CS_2 + h\nu$$

in which the transition responsible for the emis-

Can. J. Chem. Downloaded from www.nrcresearchpress.com by 210.87.254.5 on 09/05/12
For personal use only.

TABLE 1. Results of emission measurements

System	Observations
Pure CS_2 is passed through the discharge	(*a*) A pale blue afterglow which was continuous extended from 340 to 640 nm with a maximum at approximately 440 nm (Fig. 2). The afterglow was visible from the discharge inlet throughout the cell (*b*) Copious deposits of yellow sulfur formed rapidly on the cell walls (*c*) Deposits of carbon formed towards the pump
A 10% mixture of CS_2 in Ar is passed through the discharge	(*a*) An intense blue afterglow which was continuous extended from 340 to 640 nm with a maximum at approximately 440 nm. The afterglow was visible from the discharge inlet throughout the cell (*b*) A weak emission, attributable to $S_2(^3\Sigma-^3\Sigma)$, was superimposed on the continuum (*c*) Sulfur and carbon deposits were again observed on the cell walls
CS_2 is introduced into a stream of discharged argon	(*a*) A brilliant green flame formed on the discharge inlet which changed to a pale blue afterglow midway to the second window. The afterglow was visible to the pump (*b*) Bands, attributable to the $CS(A^1\Pi-X^1\Sigma)$ system, were observed at the first window (*c*) A continuum, extending from 340 to 640 nm with a maximum at approximately 440 nm, was observed at the second window (*d*) Weak emission, attributable to the (0–0) and (0–1) bands of the C_2 "Swan" system, was superimposed on the continuum (*e*) Copious sulfur deposits were observed around the discharge inlet
CS_2 is introduced into a stream of active nitrogen	(*a*) The orange-yellow Lewis–Rayleigh afterglow of active nitrogen changed gradually to a blue-green afterglow which was visible to the pump (*b*) The N_2 first positive $(B^3\Pi-A^3\Sigma)$ and the N_2 second positive $(C^3\Pi-B^3\Pi)$ systems were the only emission observed at the first window (*c*) A continuum, extending from 340 nm to 640 nm with a maximum at approximately 440 nm, was observed at the second window

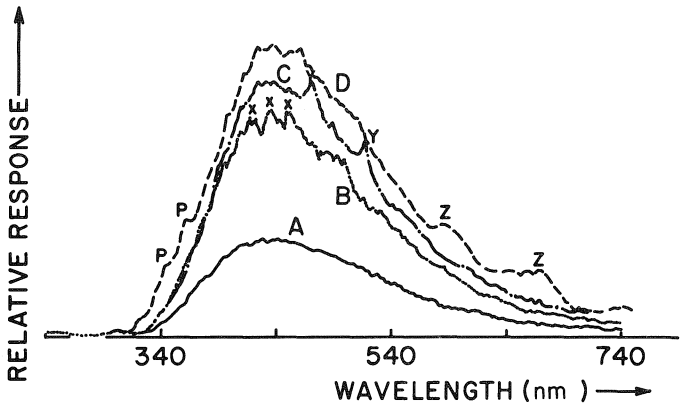

FIG. 2. Relative emission spectrum from electronically excited CS_2. When corrected for photomultiplier response and photon energy the curves broaden with maxima at approximately 440 nm. (*a*) discharged pure CS_2. (*b*) discharged CS_2(10%)–Ar(90%) mixture. *X* indicates the position of $S_2(^3\Sigma-^3\Sigma)$ bands. (*c*) CS_2 introduced into a stream of discharged Ar. *Y* indicates the position of the C_2 "Swan" (0–0) and (0–1) bands. (*d*) CS_2 introduced into a stream of active nitrogen. *Z* indicates the position of N_2 first positive bands and *P*, N_2 second positive bands.

Can. J. Chem. Downloaded from www.nrcresearchpress.com by 210.87.254.5 on 09/05/12
For personal use only.

Can. J. Chem. Downloaded from www.nrcresearchpress.com by 210.87.254.5 on 09/05/12
For personal use only.

sion is undoubtedly from an excited electronic state to the ground state of the CS_2 molecule.

It is of some interest to speculate on the states responsible for the radiation observed in the fluorescence, afterglow, and shock tube experiments. There appear to be at least two electronic states which could contribute, the $^3A_2$ state and the V state which Douglas (11) has inferred is responsible for the fluorescence. Since the afterglow emission has a spectral distribution essentially identical to the fluorescence, it may, therefore, originate in the same electronic state. Since it is probable that the afterglow emission is formed by a recombination process and since any recombination process is unlikely to involve electronically excited CS or S, it seems reasonable that the state formed on recombination is one which can correlate with ground state $CS(^1\Sigma)$ and $S(^3P)$ at 102 kcal mol^{-1} above ground (12). The $^3A_2$ state, which has a potential minimum at 74.9 kcal mol^{-1} above the ground state, can correlate with $CS(^1\Sigma)$ and $S(^3P)$ (see ref. 13 for a potential energy diagram) whereas the V state which is considered to have singlet character (11) should not. Hence, in order to reconcile these two theses it is necessary to propose (*a*) that the similarity of the fluorescence and the afterglow spectra is coincidental or (*b*) that an interelectronic level mixing process as mentioned by Douglas (11) is operative.

Douglas has suggested that the anomalously long lifetime of the fluorescence is due to interelectronic level mixing. This mixing occurs when a molecule goes back and forth between two excited states spending more of its time in the state with the high density of levels, a state from which it cannot readily radiate because this higher density state is not strongly coupled to the ground state. In the fluorescence case the molecule is thought to be initially excited to the V state which undergoes mixing, possibly with the lower $^3A_2$, accounting for its long fluorescent lifetime. In the afterglow case the molecule is formed by recombination into the $^3A_2$ state and then undergoes mixing with the V state from whence its radiates. That more than one state can be involved in the fluorescence measurements is consistent with recent measurements of Lambert and Kimbell (14) who found that the fluorescence lifetime varied slightly with the wavelength of both the exciting and fluorescing radiation.

Arnold and Kimbell (8) attributed the shock tube emission to the previously unobserved $^3\Sigma_u^+$ state (ν_{000} of 57 kcal mol^{-1}) but Rosenkranz and Wagner (15) have recently pointed out that the temperature dependence of the partition functions must be considered in determining the apparent activation energy. When this is done, the results of Arnold and Kimbell agree with those of Rosenkranz and Wagner who suggested that the emitting state had an activation energy of 74 kcal mol^{-1} and was the $^3A_2$ state previously observed by Kleman in absorption. If this is indeed the case, the question can be raised as to why the same process does not take place as in the case of the afterglow with the resultant emission from the V state. If only the lower vibrational levels of the $^3A_2$ state are populated by shock-heating, mixing with the V state which should lie 86 kcal mol^{-1} above the ground state would be less probable.

Conclusions

When either pure CS_2 or a CS_2–Ar mixture is passed through a microwave discharge, or when CS_2 is introduced into a stream of discharged argon or into active nitrogen, a pale blue afterglow is observed. This afterglow emission, which appears continuous and extends from 340 to 640 nm with a maximum at 440 nm, has a spectral distribution very similar to that observed from the fluorescence of gaseous CS_2. The excited state responsible for both the afterglow emission and the fluorescence is suggested to be the V state. The state from which the shock-heated emission occurs is the $^3A_2$ state. The latter conclusions are speculative only and undoubtedly more experimentation is necessary to unequivocally identify the emitting states.

We wish to acknowledge the assistance of Professor E. F. Greene in the reassessment of the shock tube data.

1. B. Kleman. Can. J. Phys. **41**, 2034 (1963).
2. A. E. Douglas and E. R. V. Milton. J. Chem. Phys. **41**, 357 (1964).
3. W. C. Price and D. M. Simpson. Proc. Roy. Soc. A**165**, 272 (1938).
4. R. S. Mulliken. Can. J. Chem. **36**, 10 (1958).
5. L. Herman, R. Herman, and J. Akriche. J. Quant. Spect. Rad. Transfer, **3**, 77 (1963).
6. R. A. Westbury and C. A. Winkler. Can. J. Chem. **38**, 334 (1960).
7. F. Rosenkranz and H. Gg. Wagner. Zeit. fur Physikalische Chemie Neue Folge, **61**, 302 (1968).
8. S. J. Arnold and G. H. Kimbell. J. Phys. Chem. **73**, 3751 (1969).

9. J. HEICKLEN. J. Am. Chem. Soc. **85**, 3562 (1963).
10. J. W. MILLS and R. N. ZARE. Chem. Phys. Lett. **5**, (37) (1970).
11. A. E. DOUGLAS. J. Chem. Phys. **45**, 1007 (1966).
12. V. H. DIBELER and J. A. WALKER. J. Opt. Soc. Am. **57**, 1007 (1967).
13. H. A. OLSCHEWSKI, J. TROE, and H. GG. WAGNER. Zeit. fur Physikalische Chemie Neue Folge Bd, **45**, 329 (1965).
14. C. LAMBERT and G. H. KIMBELL. Unpublished data.
15. F. ROSENKRANZ and H. GG. WAGNER. Private communication.

Can. J. Chem. Downloaded from www.nrcresearchpress.com by 210.87.254.5 on 09/05/12
For personal use only.

Comments on the Infrared Spectra of SO_2 Clathrate-hydrate Formed by Vapor Condensation

A. H. HARDIN[1] AND K. B. HARVEY[2]

Chemistry Department, University of British Columbia, Vancouver 8, British Columbia

Received August 20, 1971

Gaseous mixtures having clathrate-hydrate stoichiometries were condensed at 83 °K into an amorphous phase. Infrared spectra were recorded at a series of temperatures up to 180 °K in order to determine the transformation temperature and the nature of the annealed phase. Bands associated with the H_2O molecules began to shift position at 125 °K while those attributed to guest molecules decreased to null intensity. There was no evidence of a unique clathrate-hydrate H_2O spectrum nor of free or hindered rotation of the guest molecules.

Des mélanges gazeux, ayant une stoichiométrie de clathrate hydraté, ont été condensés à 83 °K en une phase amorphe. Les spectres infrarouges ont été enregistrés à différentes températures jusqu'à 180 °K dans le but de déterminer la température de transformation ainsi que la nature de la phase de recuit. Les bandes associées avec des molécules d'H_2O commencent à se déplacer à 125 °K alors que celles attribuées à des molécules-hôtes diminuent jusqu'à une intensité nulle. Il n'y a aucune preuve quant à la formation d'un spectre unique de clathrate hydraté H_2O ni d'une rotation libre ou empêchée des molécules-hôtes.

Canadian Journal of Chemistry, **49**, 4114 (1971)

Clathrate compounds have provided a means of studying weak intermolecular interactions whereby quantized motions of the trapped guest molecules have been suggested on the basis of infrared (1–5), microwave (6), and nuclear magnetic resonance (7–9) results. Preliminary infrared investigations were made in this laboratory on the type I clathrate-hydrates of Kr, H_2S, and SO_2 (3). Recent work (10) repeated and extended those experiments, but during the process the original results could not be reproduced under suitable experimental conditions. It is concluded that the technique of sample formation did not yield clathrate-hydrate, but an amorphous mixture of ice and guest.

The requirement of maintaining an equilibrium dissociation pressure while forming and observing films sufficiently thin to the infrared is the only difficulty met for clathrate-hydrates. Barrer and Ruzicka (11) formed non-spectroscopic samples by condensing H_2O on a glass surface at 77 °K and by then applying a relatively high pressure of guest vapor. However, guests of interest in the infrared condense at such temperatures and the high pressures needed for non-condensing guest, *i.e.* methane, would lead to a vapor phase spectrum even over a short path length.

Harvey, McCourt, and Shurvell (3) prepared samples by a modification of this method, *i.e.* condensation and annealing of stoichiometric gaseous mixtures. The method was prone to sample fractionation during condensation and/or annealing. Subsequent work attempted to overcome such fractionation by sample formation from the vapor phase in a closed, low volume sample chamber, or as low temperature mulls of crystalline clathrate-hydrates.

In view of the recent infrared results the con-

[1]Present address: School of Chemical Sciences, The University of East Anglia, Norwich, NOR 88C, U.K.
[2]Deceased September 27, 1970.

9. J. HEICKLEN. J. Am. Chem. Soc. **85**, 3562 (1963).
10. J. W. MILLS and R. N. ZARE. Chem. Phys. Lett. **5**, (37) (1970).
11. A. E. DOUGLAS. J. Chem. Phys. **45**, 1007 (1966).
12. V. H. DIBELER and J. A. WALKER. J. Opt. Soc. Am. **57**, 1007 (1967).
13. H. A. OLSCHEWSKI, J. TROE, and H. GG. WAGNER. Zeit. fur Physikalische Chemie Neue Folge Bd, **45**, 329 (1965).
14. C. LAMBERT and G. H. KIMBELL. Unpublished data.
15. F. ROSENKRANZ and H. GG. WAGNER. Private communication.

Can. J. Chem. Downloaded from www.nrcresearchpress.com by 210.87.254.105 on 09/05/12
For personal use only.

Comments on the Infrared Spectra of SO_2 Clathrate-hydrate Formed by Vapor Condensation

A. H. HARDIN[1] AND K. B. HARVEY[2]

Chemistry Department, University of British Columbia, Vancouver 8, British Columbia

Received August 20, 1971

Gaseous mixtures having clathrate-hydrate stoichiometries were condensed at 83 °K into an amorphous phase. Infrared spectra were recorded at a series of temperatures up to 180 °K in order to determine the transformation temperature and the nature of the annealed phase. Bands associated with the H_2O molecules began to shift position at 125 °K while those attributed to guest molecules decreased to null intensity. There was no evidence of a unique clathrate-hydrate H_2O spectrum nor of free or hindered rotation of the guest molecules.

Des mélanges gazeux, ayant une stoichiométrie de clathrate hydraté, ont été condensés à 83 °K en une phase amorphe. Les spectres infrarouges ont été enregistrés à différentes températures jusqu'à 180 °K dans le but de déterminer la température de transformation ainsi que la nature de la phase de recuit. Les bandes associées avec des molécules d'H_2O commencent à se déplacer à 125 °K alors que celles attribuées à des molécules-hôtes diminuent jusqu'à une intensité nulle. Il n'y a aucune preuve quant à la formation d'un spectre unique de clathrate hydraté H_2O ni d'une rotation libre ou empêchée des molécules-hôtes.

Canadian Journal of Chemistry, **49**, 4114 (1971)

Clathrate compounds have provided a means of studying weak intermolecular interactions whereby quantized motions of the trapped guest molecules have been suggested on the basis of infrared (1–5), microwave (6), and nuclear magnetic resonance (7–9) results. Preliminary infrared investigations were made in this laboratory on the type I clathrate-hydrates of Kr, H_2S, and SO_2 (3). Recent work (10) repeated and extended those experiments, but during the process the original results could not be reproduced under suitable experimental conditions. It is concluded that the technique of sample formation did not yield clathrate-hydrate, but an amorphous mixture of ice and guest.

The requirement of maintaining an equilibrium dissociation pressure while forming and observing films sufficiently thin to the infrared is the only difficulty met for clathrate-hydrates. Barrer and Ruzicka (11) formed non-spectroscopic samples by condensing H_2O on a glass surface at 77 °K and by then applying a relatively high pressure of guest vapor. However, guests of interest in the infrared condense at such temperatures and the high pressures needed for non-condensing guest, *i.e.* methane, would lead to a vapor phase spectrum even over a short path length.

Harvey, McCourt, and Shurvell (3) prepared samples by a modification of this method, *i.e.* condensation and annealing of stoichiometric gaseous mixtures. The method was prone to sample fractionation during condensation and/or annealing. Subsequent work attempted to overcome such fractionation by sample formation from the vapor phase in a closed, low volume sample chamber, or as low temperature mulls of crystalline clathrate-hydrates.

In view of the recent infrared results the con-

[1]Present address: School of Chemical Sciences, The University of East Anglia, Norwich, NOR 88C, U.K.
[2]Deceased September 27, 1970.

Can. J. Chem. Downloaded from www.nrcresearchpress.com by 210.87.254.105 on 09/05/12
For personal use only.

clusions drawn from the previous work must be revised. The previous samples were not annealed to a temperature sufficiently high to permit the desired phase transformation, even ignoring the problem of sample decomposition. For example, condensates were annealed only to 110 °K for 2–3 min and subsequent spectra had bands at 780, 1640, and 3700 cm^{-1} much as found for amorphous ice (10). More detailed infrared experiments have shown that H_2O molecules only attain sufficient energy to reorient at 125 °K (10). Typical indications of reorientation or annealing were the disappearance of the weak 3700 cm^{-1} peak and the shifting of "lattice" modes to higher wavenumber while the so-called internal modes shifted to lower wavenumber by as much as 30–40 cm^{-1}, *i.e.* as in the amorphous to crystalline ice transformation. The ice phase transformation is also accompanied by a distinct sharpening of the bands, but there is no evidence for this in the clathrate transformation reported by Harvey *et al.* The feature at 2410 cm^{-1} found by Harvey, McCourt, and Shurvell and attributed to the H_2O lattice, did not appear in the subsequent work. They found that this feature was of constant wavenumber for a variety of clathrate-hydrates (Kr, H_2S, SO_2). Upon re-examination of the original background spectra of McCourt (12) and Shurvell (13) a small amount (*ca.* 2%) of uncompensation was found between 2410 and 2240 cm^{-1} due to atmospheric CO_2. Although this was just detectable in the background of the empty cell, after sample deposition and reference beam attenuation the energy difference in this region was proportionally much larger.

These comments have some effect on the conclusions Harvey *et al.* made with respect to the SO_2 guest peaks. The strong $\nu_3(SO_2)$ band observed at 1340 cm^{-1} (78 °K) lies between the $SO_{2\ (g)}$ value (1362 cm^{-1}) and the $SO_{2\ (s)}$ value at 78 °K (1322 cm^{-1}), indicating the presence of relatively large, amorphous SO_2 agglomerates. Further, the shoulders reported on $\nu_3(SO_2)$ for clathrate at 78 °K could have arisen from SO_2 molecules possessing positional or chemical differences in the H_2O support (*e.g.* SO_2 molecular aggregates, SO_2 molecules individually in holes in the H_2O network, or as SO_2 layers between H_2O surfaces). More simply the shoulders could have arisen from changes in the relative intensities of the three features seen in the pure SO_2 solid.

In conclusion the results reported by Harvey, McCourt, and Shurvell appear to be for an amorphous SO_2–H_2O mixture. Thus the $\nu_3(SO_2)$ shoulders cannot be associated with free or hindered SO_2 rotation in a clathrate structure. Finally, the feature at 2410 cm^{-1} which was thought to indicate H_2O in a clathrate-hydrate lattice is an instrumental artifact. Since the work of Harvey *et al.* many data have been published on the various modifications of ice (14) and these indicate that for a clathrate-hydrate with disordered hydrogen bonding the spectra due to the lattice are probably of little difference from those of ice Ih.

1. R. M. Hexter and T. D. Goldfarb. J. Inorg. Nucl. Chem. **4**, 171 (1957).
2. D. F. Ball and D. C. McKean. Spectrochem. Acta, **18A**, 933 (1962).
3. K. B. Harvey, F. R. McCourt, and H. F. Shurvell. Can. J. Chem. **42**, 960 (1964).
4. M. Davies and W. C. Child. Spectrochem. Acta, **21A**, 1195 (1965).
5. C. Barthel, X. Gerbaux, and A. Hadni. Spectrochem. Acta, **26A**, 1183 (1970).
6. J. C. Burgiel, H. Meyer, and P. L. Richards. J. Chem. Phys. **43**, 4291 (1965).
7. C. A. McDowell and P. Raghunathan. Mol. Phys. **15**, 259 (1968).
8. A. W. K. Khanzada and C. A. McDowell. J. Mol. Struct. **7**, 241 (1970).
9. J. P. McTague. J. Chem. Phys. **50**, 47 (1969).
10. A. H. Hardin. Ph.D Thesis. Department of Chemistry, University of British Columbia, Vancouver, British Columbia 1970.
11. R. M. Barrer and D. J. Ruzicka. Trans. Faraday Soc. **58**, 2262 (1962).
12. F. R. McCourt. B.Sc. Thesis. Department of Chemistry, University of British Columbia, Vancouver, British Columbia 1962.
13. H. F. Shurvell. Ph.D. Thesis. Department of Chemistry, The Univeristy of British Columbia, Vancouver, British Columbia 1964.
14. E. Whalley *et al.* J. Chem. Phys. **46**, 1264 (1970) and references contained therein.

Preparation and Structural Elucidation of *cis*- and *trans*-1-Phenyl-2-methylcyclohexanol

K. G. RUTHERFORD, S. WASSENAAR, J. F. BRIEN, AND D. P. C. FUNG
Department of Chemistry, University of Windsor, Windsor, Ontario

Received July 27, 1971

The preparation of *cis*- and *trans*-1-phenyl-2-methylcyclohexanol by hydrolysis of an isomeric mixture of the corresponding hydrogen phthalate esters is described. The elucidation of the structures of the alcohols is also described.

La préparation du *cis*- et *trans*-phényl-1 méthyl-2 cyclohexanol, par hydrolyse d'un mélange isomérique des esters des phthalates d'hydrogène correspondants, est décrite. L'élucidation des structures des alcools est également décrite.

Canadian Journal of Chemistry, **49**, 4116 (1971)

Can. J. Chem. Downloaded from www.nrcresearchpress.com by 210.87.254.105 on 09/05/12
For personal use only.

In our studies on the low temperature pyrolysis of sterically hindered hydrogen phthalate esters, it was of interest to investigate the *cis*- and *trans*-1-phenyl-2-methylcyclohexanol system. In the case of our previous investigations (1, 2) on the pyrolysis of the hydrogen phthalate esters of *cis*- and *trans*-1,2-dimethylcyclohexanol, the synthesis of the isomeric alcohols was achieved by the reaction of methyl magnesium iodide with 2-methylcyclohexanone. To our surprise, Cram's rule of "steric control of asymmetric induction" (3) was followed to a greater degree than expected. Thus, from this reaction a crude isomeric mixture of the *trans*- and *cis*-alcohols was obtained in yields of *ca.* 83 and 17% respectively. Purification of the alcohols by spinning band distillation procedure proved acceptable although several large runs were necessary to prepare adequate supplies of the *cis*-alcohol.

In the case of the Grignard reaction of phenyl magnesium bromide with 2-methylcyclohexanone, an isomeric mixture of alcohols (92 and 8%) was obtained. Intuitively, one would predict the isomer obtained in 8% yield to be the *cis*-alcohol. It was found that if the hydrogen phthalate derivatives of these alcohols were first prepared according to a procedure previously described in this laboratory (4), the mixture of these derivatives could be hydrolyzed easily with sodium hydroxide. Although this procedure results in a yield of 25% olefins, the remaining portion of the reaction mixture contains *ca.* 43% of the *trans*-1-phenyl-2-methylcyclohexanol and 57% of the *cis*-isomer. Undoubtedly, the $B_{AL}1$ mechanism is conveniently operative during basic hydrolysis, thus resulting in the formation of goodly amounts of the *cis*-alcohol.

The structure of the expected *cis*-1-phenyl-2-methylcyclohexanol was elucidated by hydroboration of pure 1-phenyl-2-methylcyclohexene followed by oxidative conversion of the borane intermediate. This procedure was used previously by Brown and Zweifel (5) to prove the structure of *cis*-1,2-dimethylcyclohexanol. It follows then that the alcohol obtained in larger amounts in the Grignard reaction of phenyl magnesium bromide with 2-methylcyclohexanone is the expected *trans*-1-phenyl-2-methylcyclohexanol. Thus Cram's rule is followed to a high degree in the 2-substituted cyclohexanone system. An inspection of Fig. 1, in which are shown Newman projections of proposed transition states leading to products from the reaction of Grignard reagents with 2-methylcyclohexanone, supports the experimental results obtained. Thus, much less steric effect is observed in the transition state leading to *trans*-product than is for that which leads to the *cis*-isomer.

The hydrolytic epimerization technique described in this paper should be applicable to the synthesis of similar isomeric cyclic 1-aryl-2-alkylcyclanols.

Experimental

Melting points were determined on a Fisher–Johns apparatus and are uncorrected. The i.r. spectra were recorded on a Beckman IR-10 spectrophotometer and all solutions were w/w% in the specified solvent. Only the significant absorptions are reported (cm^{-1}). Microanalyses were determined by Midwest Microlab Inc., Indianapolis, Indiana. The n.m.r. spectra were measured

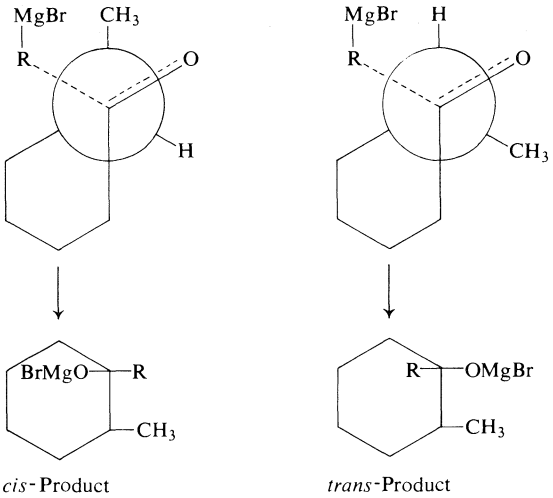

cis-Product *trans*-Product

FIG. 1. Proposed transition states for the reaction of Grignard reagents with 2-methylcyclohexanone.

with a JEOL C-60HL instrument and all solutions were w/v % in the stipulated solvent. The chemical shifts are reported in τ downfield from internal tetramethylsilane (multiplicity: s, singlet; d, doublet; t, triplet; m, multiplet; bm, broad multiplet). All g.l.c. was conducted on a Hewlett Packard (F. and M.) 720 instrument and the peak areas were determined with a disc integrator.

1-Phenyl-2-methylcyclohexene

An isomeric mixture of 1-phenyl-2-methylcyclohexanol (5.0 g, 26.3 mmol) was dehydrated with 15 ml of a 16.5% sulfuric acid – acetic acid solution (v/v) according to the method of Garbisch (6, 7). This yielded a mixture of 1-phenyl-2-methylcyclohexene and 1-phenyl-6-methylcyclohexene (3.2 g, 72.1%) and these olefins were shown to be present in the relative amounts of 87.1 and 12.9%, respectively, by means of g.l.c. analysis (LAC-728, 130°). These olefins were separated by preparative g.l.c. (LAC-728, 140°) and their physical and spectral properties compared favorably with those reported by Garbisch (7).

The 1-phenyl-2-methylcyclohexene was used to prepare *cis*-1-phenyl-2-methylcyclohexanol by the method of Brown and Zweifel (5) involving hydroboration.

cis-1-Phenyl-2-methylcyclohexanol

1-Phenyl-2-methylcyclohexene (0.800 g, 4.64 mmol) was added to a solution of sodium borohydride (0.145 g, 3.83 mmol) and 10 ml of freshly distilled tetrahydrofuran. The reaction was carried out under a nitrogen atmosphere maintaining the temperature at 20–30° with an ice bath during the addition of freshly distilled boron trifluoride etherate (1.09 g, 7.65 mmol). The solution was stirred at 25° for 1 h followed by the cautious addition of 2 ml of water. When reaction ceased, 5.6 ml of 3 *N* sodium hydroxide was added quickly followed by the rapid addition of 5.6 ml of 30% hydrogen peroxide. The solution was stirred for 1 h at 25° after which it was salted out with sodium chloride and extracted with 25 ml of ether. The ethereal layer was washed with five 10 ml portions of ice cold water, dried, and concentrated. The crude product was analyzed by g.l.c. (Carbowax 20M, 180°) and the major component (66.9%) was purified by preparative g.l.c. (Carbowax 20M, 200°). Crystallization from hexane yielded pure *cis*-1-phenyl-2-methylcyclohexanol (0.296 g, 33.4%), m.p. 61–63°. The i.r. spectrum (*ca.* 5% in CCl_4) showed characteristic bands at 3605 (free O—H stretch) and 3480 cm^{-1} (bonded O—H stretch). The n.m.r. spectrum (*ca.* 10% in $(CD_3)_2SO$) showed the following peaks (τ): 2.57 (m, 5, C_6H_5), 5.27 (s, 1, OH), 7.50–8.90 (bm, 9, $(CH_2)_4$ and CH), 9.40 (d, 3, J = 7.0 Hz, CH_3). The singlet at 5.27 disappeared on the addition of deuterium oxide which is indicative of the hydroxyl proton signal.

Anal. Calcd. for $C_{13}H_{18}O$: C, 82.06; H, 9.53. Found: C, 82.04; H, 9.56.

1-Phenyl-2-methylcyclohexanol

A solution of phenyl magnesium bromide was prepared from magnesium turnings (7.3 g, 0.30 mol), bromobenzene (42.0 g, 0.27 mol), and 200 ml of anhydrous ether. Reaction of the Grignard reagent with 2-methylcyclohexanone (28.0 g, 0.25 mol) dissolved in 100 ml of anhydrous ether yielded after distillation an isomeric mixture of 1-phenyl-2-methylcyclohexanol (31.1 g, 65.5%) as a colorless oil: b.p. 93–96° (0.38 mm); η_D^{25} 1.5363. Analysis by g.l.c. (LAC-728, 180°) showed two well-defined peaks representing the isomeric alcohols in the amounts of 92.0 and 8.0%, respectively. The isomeric alcohols were converted to the corresponding hydrogen phthalate esters (4). Saponification of the isomeric hydrogen phthalate mixture was carried out in the following manner. To an isomeric mixture of the 1-phenyl-2-methylcyclohexyl hydrogen phthalates (30.0 g, 88.8 mmol), 0.1 *N* sodium hydroxide (932.0 ml, 93.2 mmol) was added. The solution was heated at reflux temperature for 4 h. After cooling to 25°, 100 ml of chloroform was added through the condenser. The organic layer was separated, dried, and concentrated. The yellow oil (15.0 g) was distilled yielding three fractions (13.2 g). The first fraction constituted 25% of the distilled product, b.p. 25–82° (0.5 mm). The i.r. spectrum indicated olefins. The second fraction comprized 43% of the distilled reaction product, b.p. 82–93° (0.45 mm). The i.r. showed the presence of the alcohol group. The third fraction constituted 32% of the product and it solidified partially, b.p. 73–85° (0.05 mm). The i.r. showed the presence of the alcohol group. Fractions two and three were combined and g.l.c. analysis (LAC-728, 180°) indicated that the two alcohols were present in the amounts of 43.4 and 56.6%, respectively. Preparative g.l.c. (Carbowax 20M, 200°) was used to separate the alcohols. The isomer with the shorter retention time (43.4%) was a liquid, η_D^{25} 1.5355. The i.r. spectrum (30% in CS_2) showed characteristic absorption bands at 3610 (free O—H stretch) and 3500 cm^{-1} (bonded O—H stretch). The n.m.r. spectrum ($(CD_3)_2SO$, 18%) showed the following peaks (τ): 2.67 (m, 5, C_6H_5), 5.50 (s, 1, OH), 7.83–8.83 (bm, 9, $(CH_2)_4$ and CH), 9.50 (d, 3, J = 5.5 Hz, CH_3). The peak at 5.50 disappeared on the addition of deuterium oxide. This isomer was assigned the *trans*-structure.

Anal. Calcd. for $C_{13}H_{18}O$: C, 82.06; H, 9.53. Found: C, 82.15; H, 9.38.

Can. J. Chem. Downloaded from www.nrcresearchpress.com by 210.87.254.105 on 09/05/12
For personal use only.

After g.l.c. separation, the isomeric alcohol with the longer retention time (56.6%) was recrystallized from hexane, m.p. 62–64°. The n.m.r. and i.r. spectral data were identical to those of *cis*-1-phenyl-2-methylcyclohexanol prepared by the hydroboration procedure previously described. The mixed m.p. was not depressed. This isomer was assigned the *cis*-structure.

The experimental procedure described above proved amenable to much larger scale runs for the preparation of *cis*- and *trans*-alcohols without any appreciable changes. In most runs, the hydrolytic epimerization of the hydrogen phthalate mixture yielded approximately equimolar amounts of *cis*- and *trans*-alcohols.

The financial support given by the National Research Council of Canada and by the Petroleum Research Fund (Grant No. 1575-A4) administered by the American Chemical Society is gratefully acknowledged.

1. K. G. Rutherford and D. P. C. Fung. Can. J. Chem. 42, 2657 (1964).
2. K. G. Rutherford and R. M. Ottenbrite. Can. J. Chem. **45**, 679 (1967).
3. D. J. Cram and F. A. Abd Elhafez. J. Am. Chem. Soc. **74**, 5828 (1952).
4. K. G. Rutherford, J. M. Prokipcak, and D. P. C. Fung. J. Org. Chem. **28**, 582 (1963).
5. H. C. Brown and G. Zweifel. J. Am. Chem. Soc. **83**, 2544 (1961).
6. E. W. Garbisch, Jr. J. Org. Chem. **26**, 4165 (1961).
7. E. W. Garbisch, Jr. J. Org. Chem. **27**, 4243 (1962).

Can. J. Chem. Downloaded from www.nrcresearchpress.com by 210.87.254.105 on 09/05/12
For personal use only.

Can. J. Chem. Downloaded from www.nrcresearchpress.com by 210.87.254.105 on 09/05/12
For personal use only.

COMMUNICATIONS

Steric and Electronic Effects on the Stereochemistry and Molecular Structure of Nitrato Tris(diphenylmethylphosphine)Copper(I)

M. MATHEW AND G. J. PALENIK
Department of Chemistry, University of Florida, Gainesville, Florida
AND
A. J. CARTY[1]
Department of Chemistry, University of Waterloo, Waterloo, Ontario

Received August 27, 1971

A single crystal X-ray study of $(Ph_2MeP)_3CuNO_3$ revealed the presence of three different Cu—P distances and a unidentate nitrate group. Steric and electronic factors responsible for the unusual molecular dimensions of the nitrate group and the variation in Cu—P bond lengths and O—Cu—P bond angles are discussed.

Une étude aux rayons-X d'un cristal unique de $(Ph_2MeP)_3CuNO_3$ révèle la présence de trois différentes distances Cu—P et d'un groupe nitrate unidentate. Les facteurs stériques et électroniques responsables des dimensions moléculaires inhabituelles du groupe nitrate et de la variation de la longueur de liaison Cu—P ainsi que des angles des liaisons O—Cu—P sont discutés.

Canadian Journal of Chemistry, **49**, 4119 (1971)

We wish to report the X-ray crystal and molecular structure of nitrato tris(diphenylmethylphosphine)copper(I). This complex has several unprecedented structural features which are of importance to an understanding of the interplay of steric and electronic effects in d^{10} complexes, a subject which has recently attracted considerable attention (1, 2). In addition, the completion of this structure has allowed a direct comparison of accurate molecular parameters for the monodentate nitrate group (in $(Ph_2MeP)_3CuNO_3$) and the bidentate nitrate group (in $(Ph_3P)_2CuNO_3$ (3)) when the metal ion has the *same* oxidation state and coordination number. Only one other instance of such a direct comparison has been reported (4). In that case the metal had a high oxidation state and the results were entirely predictable. Our data for $(Ph_2MeP)_3CuNO_3$ are unexpected in view of current ideas (5) on metal–nitrato bonding.

Colorless crystals of L_3CuNO_3 (L = Ph_2MeP, $PhMe_2P$, $PhEt_2P$, Ph_2EtP) are obtained from the reduction of $Cu(NO_3)_2.3H_2O$ by phosphines (6). The infrared spectra of these complexes indicated that the nitrate coordination differed significantly from that found in $(Ph_3P)_2CuNO_3$ (6). Since no copper(I) complexes with a coordination number greater than four are known, the presence of unidentate nitrate in these compounds seemed likely. Therefore, a single crystal X-ray structural determination of $(Ph_2MeP)_3CuNO_3$ was undertaken.

Crystal Data
$(C_{39}H_{39}P_3CuNO_3)$

Monoclinic crystals, space group $P2_{1/n}$, a = 12.523(3), b = 20.110(6), c = 14.455(5) Å; β = 95.22(2)°; U = 3625.1 Å^3, Dm = 1.322 g/cm^3, Dc = 1.330 g/cm^3, Z = 4.

A total of 5382 independent reflections was measured ($2\theta < 130°$) using the stationary crystal – stationary counter method and $CuK\alpha_1$ (λ = 1.54051 Å) radiation. The 3391 reflections which were considered to be observed were used in the analysis. The structure was solved by the heavy atom method, with the light atoms being located in successive Fourier syntheses. The refinement was by full-matrix least-squares methods using individual isotropic thermal parameters followed by block-diagonal least-squares cycles, with anisotropic thermal parameters to yield a final R, the usual residual, of 0.081.

The stereochemistry around the copper atom together with the atomic numbering are shown

[1]To whom all correspondence to be addressed.

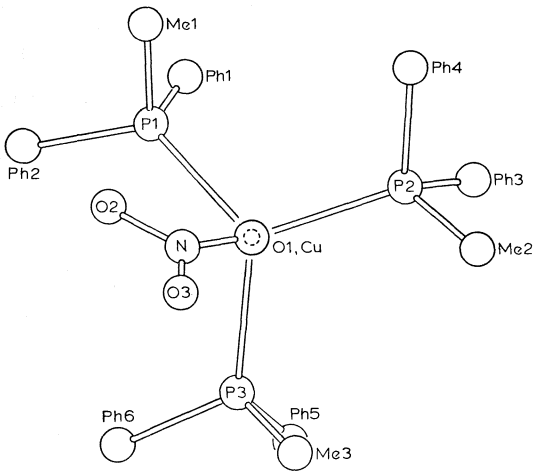

FIG. 1. A view down the O1—Cu bond in nitrato tris(diphenylmethylphosphine)copper(I) illustrating the conformation about the Cu atom and the atomic numbering. Pertinent distances are Cu—P1 of 2.259(2), Cu—P2 of 2.315(2), Cu—P3 of 2.270(2), Cu—O1 of 2.206(6), O1—N of 1.166(8), N—O2 of 1.247(8), and N—O3 of 1.209(8) Å.

in Fig. 1 which is a view down the Cu—O1 bond. The nitrate is bonded in a unidentate fashion to the Cu atom at a distance of 2.206(6) Å, compared to the non-bonded distances Cu—O(3) of 4.060(5) and Cu—O(2) of 3.249(2) Å. Surprisingly the Cu—O1 distance is not significantly different from the Cu—O distance of 2.22(1) Å found in $(Ph_3P)_2CuNO_3$(3) where the nitrate is bidentate; other studies (4) have found distinctly shorter M—O bonds in unidentate nitrate complexes. Similarly the N—O1 bond length of 1.166(8) Å is *shorter* than the N—O (coordinated) distance in $(Ph_3P)_2CuNO_3$(3) contrary to popular prediction[1] and considerably shorter than the N—O (coordinated) distances in any other complex containing unidentate nitrate.[2]

Furthermore, the N—O distances increase in the order N—O1 < N—O3 < N—O2, the opposite of that found for other unidentate nitrate species and in disagreement with π bonding arguments.[1] We believe that these results are explicable in terms of a larger than normal contribution from a resonance form of type C below to the metal–nitrato bond in order to minimize electronic charge build up on the copper atom. We are currently investigating other low valent metal nitrato complexes containing strong σ donor ligands to see whether this idea is of more general applicability.

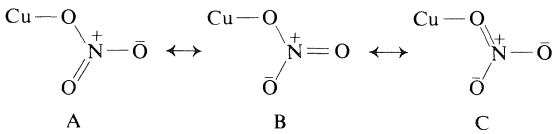

A B C

Another significant feature of the structure is the steric effect of the unsymmetrically bonded nitrate group on the P—Cu—P and P—Cu—O1 angles and Cu—P bond lengths. The P1—Cu—P2 angle of 127.8(2)° results from the orientation of the nitrate ion relative to the Cu—P bonds. In $(Ph_2MeP)_3CuCl$ (2) all the P—Cu—P angles are close to 115° in spite of severe steric crowding. Furthermore, the inequality of the P—Cu distances, Cu—P1 is 2.259(2), Cu—P2 is 2.315(2), and Cu—P3 is 2.270(2) Å, appears to be correlated with the corresponding P—Cu—O1 angle. The longest distance Cu—P2 has the smallest P—Cu—O1 angle (87.9(2)°) compared to P3—Cu—O1 (96.3(2)°) and P1—Cu—O1 (107.4(2)°). The relationship between the Cu—P distance and the P—Cu—O angle is a reflection of the s character in the Cu—P bonds which is, in turn, dependent on the angle (or vice versa) the increase in s character for a Cu—P bond corresponding to a shorter bond and larger angle. Making the realistic assumption (11) that the s character in the copper bonding orbitals is concentrated in bonds to the more electropositive (phosphorus) ligands, a weak Cu—O interaction would be predicted, and is indeed found. We have therefore an interesting example of the importance of cooperative steric and electronic effects in a d^{10} complex. This work also lends further credence to the idea that metal–phosphorus bond lengths in d^{10} complexes are sensitive to s electron character in a similar fashion to M—P bonds in complexes of the heavier transition metals (12).

---

[1]Attachment of one oxygen atom to a metal should partially restrict π bonding to the NO_2 fragment of the M—O1—N$\langle^{O2}_{O3}$ unit. Hence the N—O2 and N—O3 bond orders should increase at the expense of N—O1.

[2]Accurate X-ray data have been reported for only 5 complexes containing unidentate nitrate groups. These are: $Ni(NO_3)_2(H_2O)_4$ (7), $Cu(NO_3)_2$ (pyridine-*N*-oxide) (8), $Cu(NO_3)_2$(1,4-diazacycloheptane)$_2\cdot\frac{1}{2}H_2O$ (9), K[Au$(NO_3)_4$] (10), $VO(NO_3)_3CH_3CN$ (4). Unidentate nitrate groups have been identified in other compounds by X-ray methods (see ref. 5) but the data are either incomplete or of low precision.

Can. J. Chem. Downloaded from www.nrcresearchpress.com by 210.87.254.105 on 09/05/12
For personal use only.

We thank the National Research Council of Canada for financial support of this work.

1. E. L. Muetterties and C. W. Alegranti. J. Am. Chem. Soc. **92**, 4114 (1970).
2. G. J. Palenik and S. J. Lippard. Inorg. Chem. **10**, 1322 (1971).
3. G. G. Messmer and G. J. Palenik. Inorg. Chem. **8**, 2750 (1969).
4. F. N. B. Einstein, E. Enwall, D. M. Morris, and D. Sutton. Inorg. Chem. **10**, 678 (1971).
5. C. C. Addison, N. Logan, S. C. Wallwork, and C. D. Garner. Q. Rev. **25**, 289 (1971).
6. W. A. Anderson, A. J. Carty, G. J. Palenik, and G. Schreiber. Can. J. Chem. **49**, 761 (1971).
7. P. Gallezot, D. Weigel, and M. Prettre. Acta Cryst. **22**, 699 (1967).
8. S. Scavnicar and B. Matkovic. Acta Cryst. **25**B 2046 (1969).
9. M. S. Hussain and H. Hope. Acta Cryst. **25**B, 1866 (1969).
10. C. D. Garner and S. C. Wallwork. J. Chem. Soc. (A), 3092 (1970).
11. H. A. Bent. Chem. Rev. **61**, 275 (1961).
12. L. Aslanov, R. Mason, A. G. Wheeler, and P. O. Whimp. Chem. Commun. 30, (1970).

Can. J. Chem. Downloaded from www.nrcresearchpress.com by 210.87.254.105 on 09/05/12
For personal use only.